this document downloaded from

vulcanhammer.net

Since 1997, your complete online resource for information geotecnical engineering and deep foundations:

The Wave Equation Page for Piling

Online books on all aspects of soil mechanics, foundations and marine construction

Free general engineering and geotechnical software

And much more...

Terms and Conditions of Use:

All of the information, data and computer software ("information") presented on this web site is for general information only. While every effort will be made to insure its accuracy, this information should not be used or relied on for any specific application without independent, competent professional examination and verification of its accuracy, suitability and applicability by a licensed professional. Anyone making use of this information does so at his or her own risk and assumes any and all liability resulting from such use. The entire risk as to quality or usability of the information contained within is with the reader. In no event will this web page or webmaster be held liable, nor does this web page or its webmaster provide insurance against liability, for any damages including lost profits, lost savings or any other incidental or consequential damages arising from the use or inability to use the information contained within.

This site is not an official site of Prentice-Hall, Pile Buck, the University of Tennessee at Chattanooga, or Vulcan Foundation Equipment. All references to sources of software, equipment, parts, service or repairs do not constitute an endorsement.

Visit our companion site http://www.vulcanhammer.org

DEPARTMENT OF THE ARMY
U.S. Army Corps of Engineers
Washington, DC 20314-1000

EM 1110-2-1100

CECW-EW

Manual
No. 1110-2-1100

30 April 2002

Engineering and Design
COASTAL ENGINEERING MANUAL

1. Purpose. The purpose of the *Coastal Engineering Manual* (CEM) is to provide a comprehensive technical coastal engineering document. It includes the basic principles of coastal processes, methods for computing coastal planning and design parameters, and guidance on how to formulate coastal flood studies, shore protection, and navigation projects.

2. Applicability. This manual applies to all HQUSACE elements and all USACE commands having Civil Works and military design responsibilities.

3. Discussion. The CEM is divided into two major subdivisions: science-based and engineering-based. The science subdivision is further divided into three parts. The first part, "Coastal Hydrodynamics," leads the reader from the fundamental principles of wave theory and ocean wave generation through the process of wave transformation as the wave form approaches and reacts with the shore including water-level variations and currents. The second part, "Coastal Sediment Processes," addresses longshore and cross-shore transport as well as shelf, and wind transport processes. The third part, "Coastal Geology," covers geomorphology, coastal classification, and morphodynamic processes on sandy shores.

The engineering-based subdivision is oriented toward a project-type approach, rather then the individual structure design and is divided into two parts. The first one, "Coastal Planning and Design," provides information on the design process and selection of appropriate type of solution to various coastal problems. The second part, "Design of Coastal Project Elements," provides engineering guidance on materials, fundamentals of design, and reliability.

4. Distribution Statement. Approved for public release, distribution unlimited.

FOR THE COMMANDER:

1 Appendix
Appendix A - Glossary

ROBERT CREAR
Colonel, Corps of Engineers
Chief of Staff

This manual supersedes *Shore Protection Manual,* 1984; EC 1110-2-289, 30 September 1996; EC 1110-2-292, 31 March 1998; EM 1110-2-1004, 30 November 1993; EM 1110-2-1412, 15 April 1986; EM 1110-2-1414, 7 July 1989; EM 1110-2-1502, 20 August 1992; EM 1110-2-1616, 31 January 1991; EM 1110-2-1617, 20 August 1992; EM 1110-2-1618, 28 April 1995; EM 1110-2-2904, 8 August 1986; EM 1110-2-3301, 31 May 1995.

DEPARTMENT OF THE ARMY
U.S. Army Corps of Engineers
Washington, DC 20314-1000

CECW-EH

Manual
No. 1110-2-1100

31 July 2003

Engineering and Design
COASTAL ENGINEERING MANUAL

1. Purpose. The purpose of the *Coastal Engineering Manual* (CEM) is to provide a comprehensive technical coastal engineering document. It includes the basic principles of coastal processes, methods for computing coastal planning and design parameters, and guidance on how to formulate coastal flood studies, shore protection, and navigation projects. This Change 1 to EM 1110-2-1100, 30 April 2003, includes the following changes and updates:

a. Part I-4. Incorporates new chapter titles.
b. Part II-1. Formulas corrected.
c. Part II-2. Numerous changes to formulas, coefficients, and figures.
d. Part II-4. New findings on the subject matter have been added.
e. Part III-1. Table and figure improved.
f. Part III-2. References corrected.
g. Appendix A. Additional terms added and some definitions modified.

2. Applicability. This manual applies to all HQUSACE elements and all USACE commands having Civil Works and military design responsibilities.

3. Discussion. The CEM is divided into six parts in two major subdivisions: science-based and engineering-based. The first four parts of the CEM and an appendix were issued in 30 April 2002. These included:

Part I, "Introduction"
Part II, "Coastal Hydrodynamics"
Part III, "Coastal Sediment Processes"
Part IV, "Coastal Geology"
Appendix A, "Glossary"

The engineering-based subdivision is oriented toward a project-type approach and is divided into two parts. Part V, "Coastal Project Planning and Design," is published separately with the same date as this change. The text and figures provide information on the design process and selection of appropriate types of solution to various coastal problems. Part VI, "Design of Coastal Project Elements," which provides engineering guidance on materials, fundamentals of design, and reliability, is in preparation.

4. Distribution Statement. Approved for public release, distribution unlimited.

5. Substitute the following pages:

Chapter	Remove Page	Insert Page
I-4	I-4-2 and I-4-3	I-4-2 and I-4-3
II-1	II-1-89	II-1-89
II-2	II-2-i thru II-2-72	II-2-i thru II-2-72
II-4	II-4-i thru II-4-38	II-4-i thru II-4-40
III-1	III-1-8 and III-1-22	III-1-8 and III-1-22
III-2	III-2-103	III-2-103
Appendix A	A-1 thru A-94	A-1 thru A-94

FOR THE COMMANDER:

Barbara B. Caspell

for MICHAEL J. WALSH
Colonel, Corps of Engineers
Chief of Staff

DEPARTMENT OF THE ARMY
U.S. Army Corps of Engineers
Washington, DC 20314-1000

CECW-CE

Manual
No. 1110-2-1100

1 April 2008

Engineering and Design
COASTAL ENGINEERING MANUAL

1. Purpose. The purpose of the *Coastal Engineering Manual* (CEM) is to provide a comprehensive technical coastal engineering document. It includes the basic principles of coastal processes, methods for computing coastal planning and design parameters, and guidance on how to formulate and conduct studies in support of coastal flooding, shore protection, and navigation projects. This Change 2 to EM 1110-2-1100, 1 April 2008, includes the following changes and updates:

a. Part I-1. References were checked and some were deleted (Engineer Manuals that are no longer in the USACE inventory).
b. Part I-4. Minor changes were made in the text to better reflect the contents of subsequent parts of the CEM.
c. Part II-1. Figure II-1-9 has been revised; Equations II-1-128, II-1-160, and II-1-161 have been corrected.
d. Part II-2. Equations II-2-4, II-2-5, and II-2-32 have been corrected along with other errors reported by various users.
e. Part II-5. References were checked and some were deleted (Engineer Manuals that are no longer in the USACE inventory).
f. Part II-6. The value of "e" used in Eq. II-6-28 has been corrected.
g. Part II-7. The table of contents was corrected. A new section, II-7-11, Note to Users, Vessel Buoyancy, was added at the end of the chapter.
h. Part III-3. Corrections have been made to format and spelling. Different plots were added to Figures III-3-24 and III-3-26.
i. Part IV-1. Corrections have been made to references.
j. Part V-1. Citation of an Engineer Regulation has been corrected.
k. Part V-2. Citation of references has been changed, web pages with sources of wind and wave data have been added. Some minor text changes have also been made.
l. Part V-3. Citations of unpublished reports or personal communications have been deleted, and links to other figures or parts of the CEM have been checked and corrected.
m. Part V-4. Minor text changes, corrections to references and Figure V-4-1.
n. Part V-5. Links to other parts of the CEM that were planned but never written have been deleted.

2. Applicability. This manual applies to all HQUSACE elements and all USACE commands having Civil Works and military design responsibilities.

3. Discussion. The CEM is divided into five parts in two major subdivisions: science-based and engineering-based. The first four parts of the CEM and Appendix A compose the science-based subdivision:

Part I, "Introduction"
Part II, "Coastal Hydrodynamics"
Part III, "Coastal Sediment Processes"
Part IV, "Coastal Geology"
Appendix A, "Glossary"

The engineering-based subdivision is oriented toward a project-type approach, Part V, "Coastal Project Planning and Design."

4. Distribution Statement. Approved for public release, distribution unlimited.

5. Note to Users. Revised chapters are dated 1 April 2008. Readers need to download the entire new chapters and discard earlier versions in their possession.

FOR THE COMMANDER:

STEPHEN L. HILL
Colonel, Corps of Engineers
Chief of Staff

Table of Contents

Page

I-1-1. Purpose and Scope I-1-1

I-1-2. Applicability I-1-1

I-1-3. Definitions I-1-1

a. Coastal I-1-1
b. Coastal engineering I-1-1
c. Coastal science I-1-2

I-1-4. Bibliography I-1-2

I-1-5. References I-1-2

I-1-6. Acknowledgments I-1-4

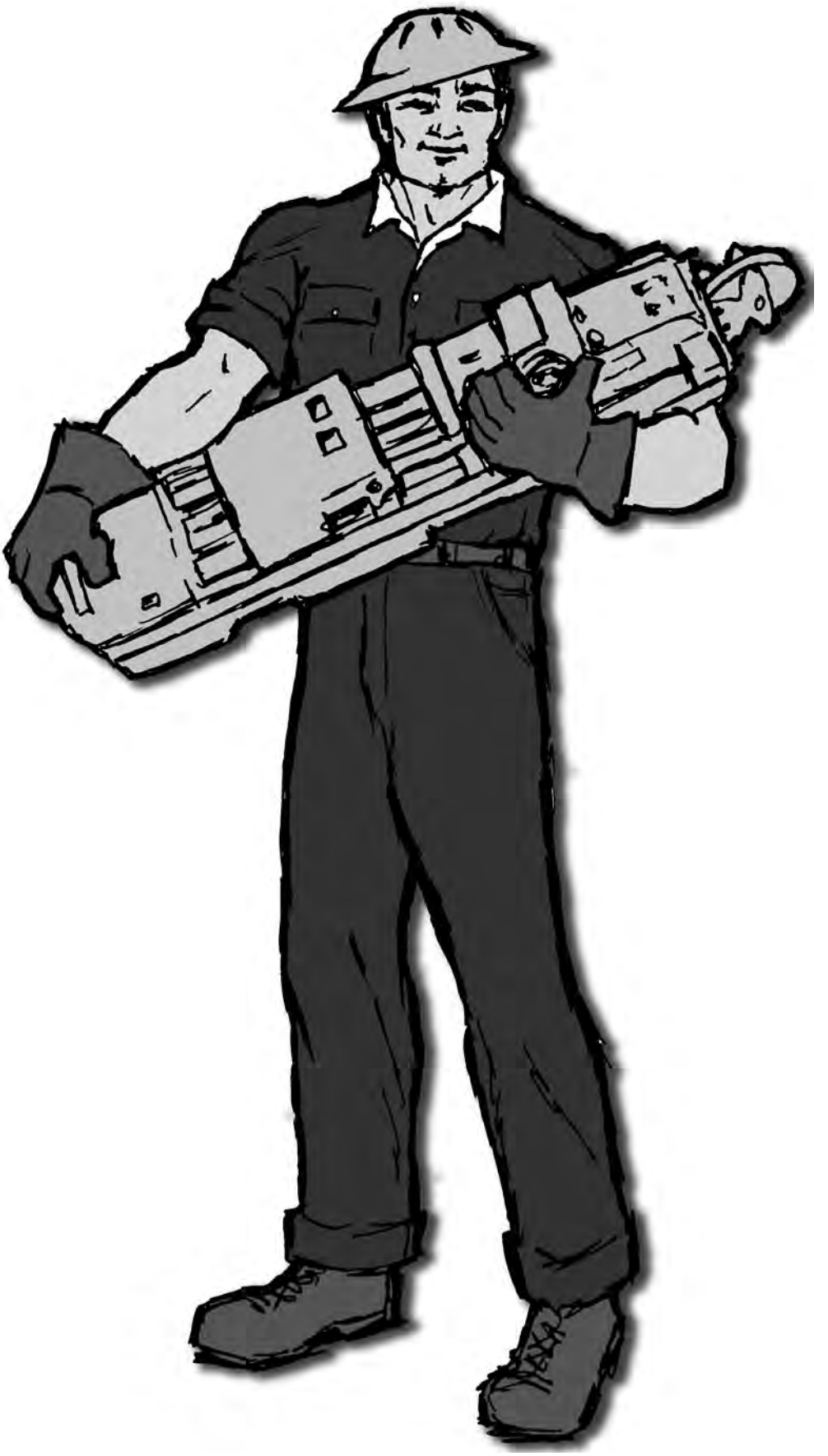

Chapter I-1
Introduction

I-1-1. Purpose and Scope

The *Coastal Engineering Manual* (CEM) assembles in a single source the current state-of-the-art in coastal engineering to provide appropriate guidance for application of techniques and methods to the solution of most coastal engineering problems. The CEM provides a standard for the formulation, design, and expected performance of a broad variety of coastal projects. These projects are undertaken to provide or improve navigation at commercial harbors, harbor works for commercial fish handling and service facilities, and recreational boating facilities. As an adjunct to navigation improvements, shore protection projects are often required to mitigate the impacts of navigation projects. Beach erosion control and hurricane or coastal storm protection projects provide wave damage reduction and flood protection to valuable coastal commercial, urban, and tourist communities. Environmental restoration projects provide a rational layout and proven approach to restoring the coastal and tidal environs where such action may be justified, or required as mitigation to a coastal project's impacts, or as mitigation for the impact of some previous coastal activity, incident, or neglect. As the much expanded replacement document for the *Shore Protection Manual* (1984) and several other U.S. Army Corps of Engineers (USACE) manuals, the CEM provides a much broader field of guidance and is designed for frequent updates.

I-1-2. Applicability

This manual is applicable to U. S. Army Corps of Engineers (USACE) Commands having civil works responsibility. It is anticipated that the comprehensive scope and instructions of this manual will warrant its use by a broad spectra of coastal engineers and scientists beyond the bounds of the USACE. Although this broad application has been considered throughout the development of the CEM, some sections are specific to the mission, authority, and operation of the USACE.

I-1-3. Definitions

Definitions are listed throughout the manual when terms are first introduced. In addition, a glossary of terms is provided in the appendix, and Table IV-1-1 lists definitions of common coastal geologic features. However, a few basic definitions will help the novice to better understand and grasp the purpose and scope of the CEM. Part IV, Chapter 2 defines types of coastal structures.

a. Coastal. Referring to the zone where the land meets the sea, a region of indefinite width that extends inland from the sea to the first major change in topography. In this manual, "coastal" will refer to shores that are influenced by wave processes (oscillatory flow dynamics). Bays, and lakes, and estuaries are included, but rivers, primarily influenced by generally unidirectional currents, are generally beyond the scope of this manual. Estuaries, including that part of rivers subject to the ebb and flow of the tide are covered by this manual.

b. Coastal engineering. One of several specialized engineering disciplines that fall under the umbrella of civil engineering. It is a composite of many physical science and engineering disciplines having application in the coastal area. It requires the rational interweaving of knowledge from a number of technical disciplines to develop solutions for problems associated with natural and human induced changes in the

coastal zone, the structural and non-structural mitigation of these changes, and the positive and negative impacts of possible solutions to problem areas on the coast. Coastal Engineers may utilize contributions from the fields of geology, meteorology, environmental sciences, hydrology, physics, mathematics, statistics, oceanography, marine science, hydraulics, structural dynamics, naval architecture, and others in developing an understanding of the problem and a possible solution. The Coastal Engineer must consider the processes present in the area of interest such as:

- Environmental processes (chemical, ecological).
- Hydrodynamics processes (winds, waves, water level fluctuations, and currents).
- Seasonal meteorological trends (hurricane season, winter storms).
- Sediment processes (sources, transport paths, sinks, and characteristics).
- Geological processes (soil and strata characteristics, stable and migrating sub-aerial and sub-aqueous features, rebounding or subsiding surfaces).
- Long-term environmental trends (sea level rise, climate change).
- Social and political conditions (land use, development trends, regulatory laws, social trends, public safety, economics).

Harbor works, navigation channel improvements, shore protection, flood damage reduction, and environmental preservation and restoration are the primary areas of endeavor.

c. Coastal science. This field is a suite of interdisciplinary technologies applied to understanding processes, environments, and characteristics of the coastal zone. Coastal Engineers use these understandings to develop physical adaptations to solve problems and enhance the human interface with the coast.

I-1-4. Bibliography

Technical and scientific literature cited in each chapter is listed in the chapter references.

I-1-5. References

The following are official USACE engineer regulations (ER), engineer manuals (EM), engineer pamphlets (EP), and technical manuals (TM) found in the bibliographies following each chapter. They are highlighted here for easy USACE use.

TM 5-850-1
Engineering and Design of Military Ports

ER 1105-2-100
Planning Guidance Notebook

EP 1165-2-1
Digest of Water Resources Policies and Authorities

EM 1110-1-1802
Geophysical Exploration for Engineering and Environmental Investigations

EM 1110-1-1804
Geotechnical Investigations

EM 1110-2-1204
Environmental Engineering for Coastal Shore Protection

EM 1110-2-1415
Hydrologic Frequency Analysis

EM 1110-2-1613
Hydraulic Design of Deep-Draft Navigation Projects

EM 1110-2-1615
Hydraulic Design of Small Boat Harbors

EM 1110-2-1906
Laboratory Soils Testing

EM 1110-2-2301
Test Quarries and Test Fills

EM 1110-2-2302
Construction with Large Stone

EM 1110-2-5025
Dredging & Dredged Material Disposal

EM 1110-2-5026
Beneficial Uses of Dredged Material

EM 1110-8-1 (FR)
Winter Navigation on Inland Waterways

I-1-6. Acknowledgments

Authors of Chapter I-1:

Joan Pope, U.S. Army Engineer Research and Development Center, Vicksburg, Mississippi.
John H. Lockhart, Jr., Headquarters, U.S. Army Corps of Engineers, Washington, DC, (retired).

Reviewer:

Andrew Morang, Ph.D., CHL

Table of Contents

Page

I-2-1. Introduction I-2-1

I-2-2. Coastal Areas I-2-1

a. Atlantic North: Glaciated coast I-2-1
b. Atlantic Central and South: Barrier and drowned valley coasts I-2-2
c. The Atlantic and Gulf of Mexico: Coral and mangrove coasts I-2-4
d. Gulf of Mexico East: Wetland mangrove, and barrier coasts I-2-4
e. Gulf of Mexico West: Barrier coast I-2-6
f. Pacific: Sea cliffs and terraced coasts I-2-7
g. The Bering and Chukchi Seas: Arctic coastal plains and barriers I-2-8
h. The Beaufort Sea: Deltaic coast I-2-9
i. Pacific: Volcanic islands I-2-9
j. Great Lakes of North America I-2-11

I-2-3. Stability I-2-13

I-2-4. Erosion I-2-14

I-2-5. Solutions I-2-16

I-2-6. References I-2-24

I-2-7. Acknowledgments I-2-26

List of Figures

Page

Figure I-2-1. Atlantic coast characteristics I-2-2
Figure I-2-2. Atlantic coast tide and wave characteristics I-2-3
Figure I-2-3. Barrier Island and bay complex, southern Rhode Island I-2-4
Figure I-2-4. New York Harbor, 1940s I-2-5
Figure I-2-5. Length of barrier islands and spits in the United States I-2-6
Figure I-2-6. Cape Hatteras, North Carolina I-2-7
Figure I-2-7. Hallandale Beach I-2-8
Figure I-2-8. Gulf of Mexico coastal characteristics I-2-9
Figure I-2-9. Gulf of Mexico tide and wave characteristics I-2-10
Figure I-2-10. East Pass Inlet, Florida I-2-11
Figure I-2-11. Morgan Peninsula, Alabama I-2-12
Figure I-2-12. Dulac, Louisiana I-2-13
Figure I-2-13. Pacific coast characteristics I-2-14
Figure I-2-14. Pacific coast tide and wave characteristics I-2-15
Figure I-2-15. Pocket beach just north of Laguna Beach, southern California I-2-16
Figure I-2-16. Mouth of the Siuslaw River, southern Oregon near the town of Florence I-2-17
Figure I-2-17. Seattle, located in sheltered Puget Sound I-2-18
Figure I-2-18. Alaska coastal characteristics I-2-19
Figure I-2-19. Hawaiian Islands wave characteristics I-2-20
Figure I-2-20. Great Lakes shoreline characteristics I-2-21
Figure I-2-21. Minnesota Point, photographed from Duluty, Minnesota, looking south I-2-22
Figure I-2-22. Calumet Harbor, Indiana I-2-22
Figure I-2-23. Duluth Canal, Minnesota I-2-23
Figure I-2-24. Bluffs about 1 km north of St. Joseph Harbor, eastern Lake Michigan I-2-24

List of Tables

Table I-2-1. Age and Sandy Shores of the Major Hawaiian Islands I-2-12

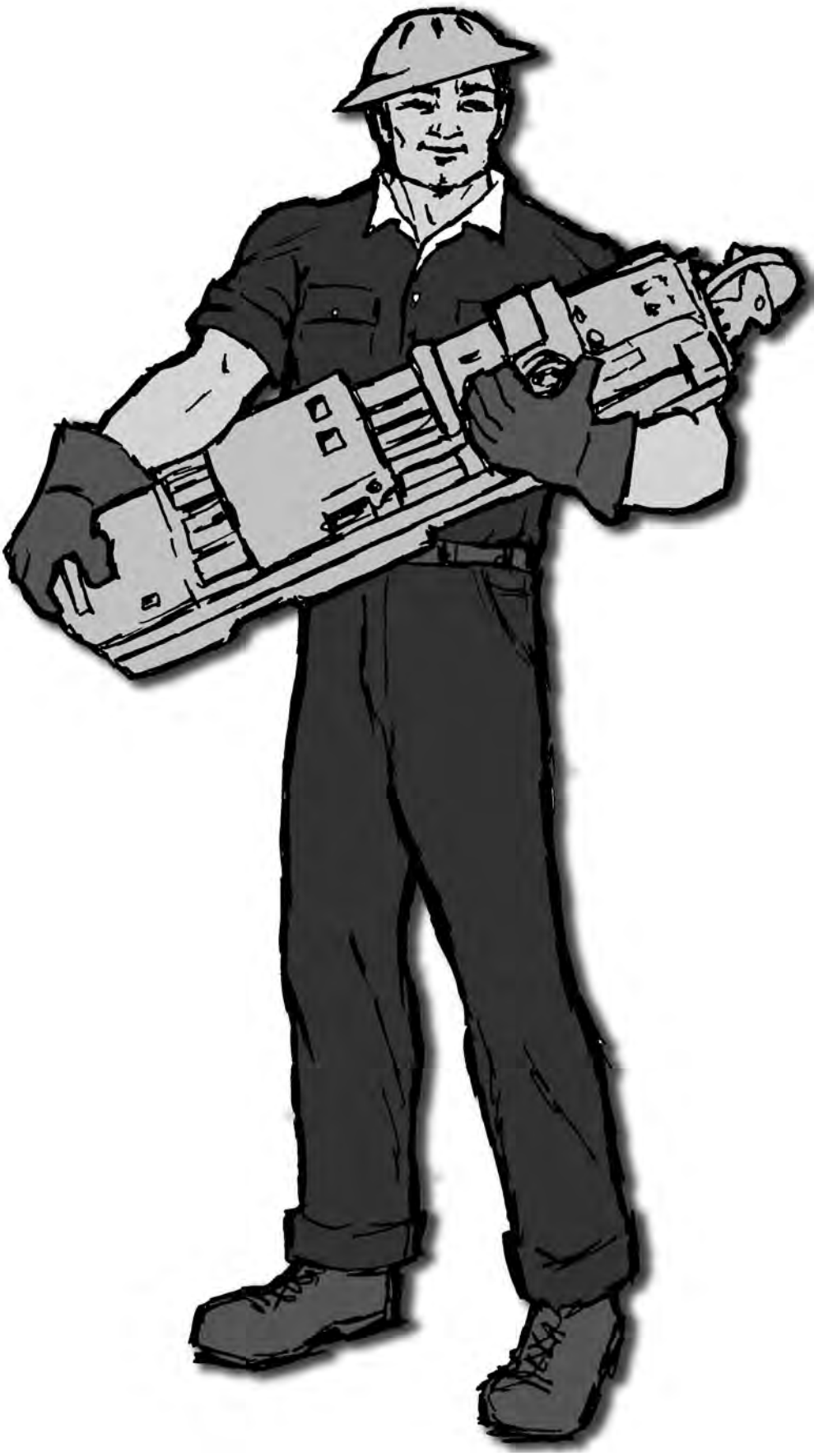

Chapter I-2
Coastal Diversity

I-2-1. Introduction

The coasts, or shores, of the world are the margins separating the 29 per cent of the earth that is land from the 71 percent that is water. By reworking and often eroding the margins of the land, the seas aid streams, subsurface water, glaciers, and the wind in wearing down the continents. Sediments derived from the land are often transient along the coasts, temporarily forming beaches, bars or islands before coming to rest on the sea floor. There is significant natural diversity in shore types throughout the United States and even greater diversity throughout the world (see Part IV for details). Consequently, engineering, development, and policy strategies need to be tailored for each unique region and need to be flexible to changes in the local condition. Coastal engineers, managers, and planners need to be aware of coastal diversity for a number of reasons:

a. The coast is dynamic and constantly evolving to a new condition.

b. The balance and interaction of processes are different in different areas - understanding diversity provides clues to the critical factors that may affect a particular study site.

c. Different settings imply different erosion and accretion sediment patterns.

d. Analytical tools and procedures may be suitable for a particular setting but totally inappropriate for another.

e. Similarly, engineering solutions may only be appropriate for certain settings where they will function properly.

Shorelines are subject to a broad range of processes, geology, morphology, and land usages. Although winds, waves, water levels, tides, and currents affect all coasts, they vary in intensity and relative significance from one location to another. Variations in sediment supply and geological setting add to this coastal diversity. A more detailed discussion and analysis of the processes at work along the United States coasts is given by Francis P. Shepard and Harold R. Wanless in their book *Our Changing Coastline* (1971).

I-2-2. Coastal Areas

The popular image of a long, straight, sandy beach with a sandy backshore and foreshore, vegetated sand dunes, and gently sloping near shore zone with rhythmic plunging breakers may be the ideal image of the zone where the land meets the sea, but is not the norm along most coasts. Not all coastal areas are sandy, nor are all shores dominated by wave action. Some coastal areas have scenic clay bluffs or rocky headlands. Others are shallow mud flats or lush wetlands. For some shores, tidal currents or river discharge dominate sediment transport and the shore character. For other shores, the effects of glaciers, marine life (coral), or volcanoes may control the geomorphology. Shore materials include transportable muds, silts, sands, shells, gravels, and cobbles, and insitu rock formations or bedrock (erosive and non-erosive). In portions of the United States, the coastal area is sinking and gradually becoming permanently inundated; in other areas, new lands are accreting or even rising out of the sea.

a. Atlantic North: Glaciated coast (Figures I-2-1, I-2-2). These coasts are normally deeply indented and bordered by numerous rocky islands. The embayments usually have straight sides and deep water as a

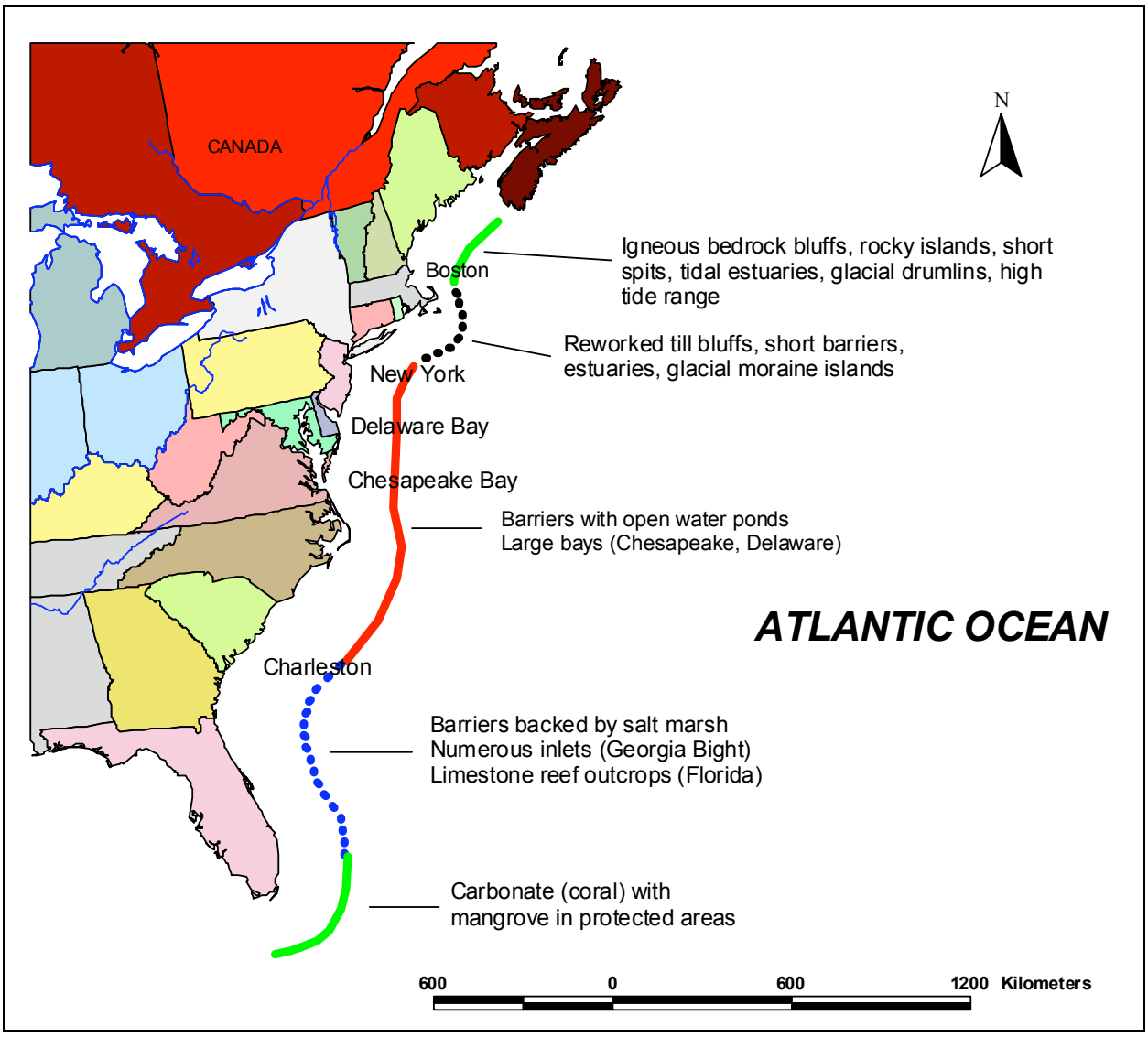

Figure I-2-1. Atlantic coast characteristics

result of erosion by the glaciers. Uplifted terraces may be common along these coasts that were formerly weighted down by ice. Abrupt changes in coastal character occur where glacial deposits and particularly glacial outwash play a dominant role, while in some rocky areas, few glacial erosion forms can be found. Moraines, drumlins, and sand dunes, the result of reworking outwash deposits, are common features. Glaciated coasts in North America extend from the New York City area north to the Canadian Arctic (Figures I-2-3, I-2-4, IV-2-8, and IV-2-9), on the west coast, from Seattle, Washington, north to the Aleutian Islands, and in the Great Lakes. (Figure IV-2-20) (Shepard 1982).

b. Atlantic Central and South: Barrier and drowned valley coasts. South of the glacial areas begins the coastal Atlantic plain, featuring almost continuous barriers interrupted by inlets and by large embayments with dendritic drowned river valleys, the largest being Delaware and Chesapeake Bays. The North American coastline is reported to include over 10,000 km of barriers, about 33 percent of all barrier coast of the world (Berryhill, Dixon, and Holmes 1969). The United States alone has a total length of 4,900 km of barriers and spits, the longest extent for a single nation (Figure I-2-5 and Table IV-2-3). Extensive wetlands and marshes

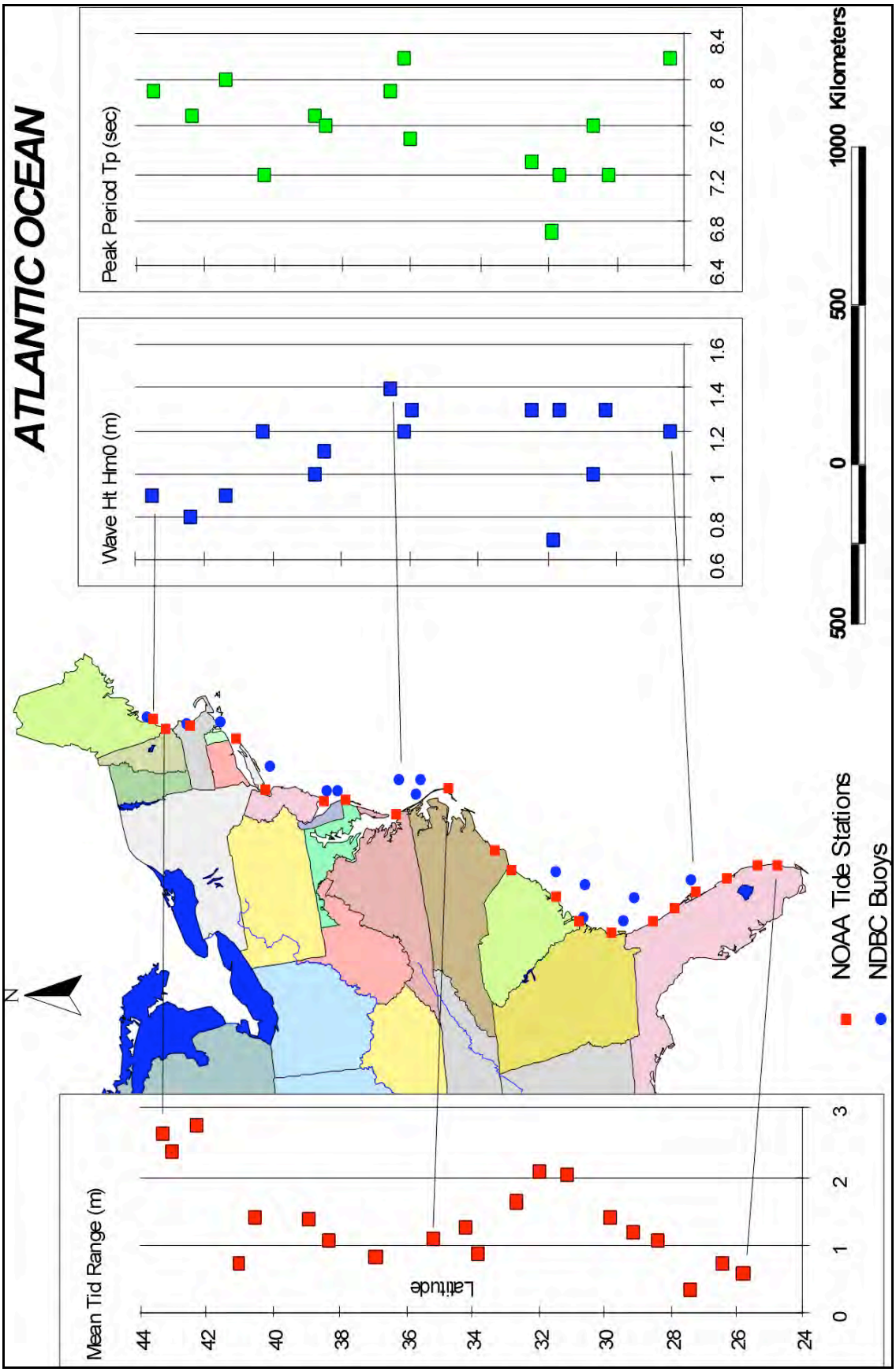

Figure I-2-2. Tide and wave characteristics of the Atlantic coasts. Wave data summarized from National Data Buoy Center buoys. H_mO and T_p averaged from hourly statistics over total period of record from statistics computed by National data Buoy Center. Tide range for indicated stations from statistics presented in NOAA Tide Tables

Figure I-2-3. Barrier Island and bay complex, southern Rhode Island. View looking west toward Quonochontaug Point, a rocky headland with bedrock outcrops. The barrier in the foreground is East Beach, with Block Island Sound to the left and Ninigret Pond to the right. Prominent overwash fans can be seen in the shallow waters of the pond (April 1977)

mark much of the coast, where sediment and marsh vegetation have partly filled the lagoons behind the barriers. Some coasts have inland ridges of old barrier islands, formed during interglacial epochs, separated from the modern barrier islands by low marshes or lagoons. The best exhibit of cuspate forelands in the world extends from the mouth of Chesapeake Bay to Cape Romain, South Carolina (Figure I-2-6). The coast is much straighter south of Cape Romain and the only cuspate foreland is that of Cape Canaveral, Florida. Barrier Islands and drowned valleys continue south to Miami, Florida (Figure I-2-7), except for a brief length of coast in the Myrtle Beach, South Carolina, area where the barriers are attached to the coastal plain. Much of the southeast coast of Florida was extensively filled, dredged, and reshaped in the early 20th century to support development (Lenček and Bosher 1998). From Miami around the tip of Florida through Alabama, Mississippi and eastern Louisiana, coastal characteristics alternate between swampy coast and white sand barriers (Shepard 1982).

c. The Atlantic and Gulf of Mexico: Coral and mangrove coasts. The barrier islands change from quartz sand south of Miami to carbonate-dominated sand, eventually transforming into coral keys and mangrove forest. The Florida Keys are remnants of coral reefs developed during a higher sea level stage of the last interglacial period. Live reefs now grow along the east and south side of the keys and the shallows of Florida Bay studded with mangrove islands extending north and west into the Everglades and the Ten Thousand Islands area that comprises the lower Florida Gulf of Mexico coast (Shepard 1982).

Figure I-2-4. New York Harbor, late 1930s. This drowned river valley system, partly sculpted by glaciers, is one of the world's finest natural harbors. The USACE has an active role dredging, clearing debris, and maintaining navigability of this great port. View looking north, with Manhattan in the center and Brooklyn to the right. Photograph from Beach Erosion Board archives

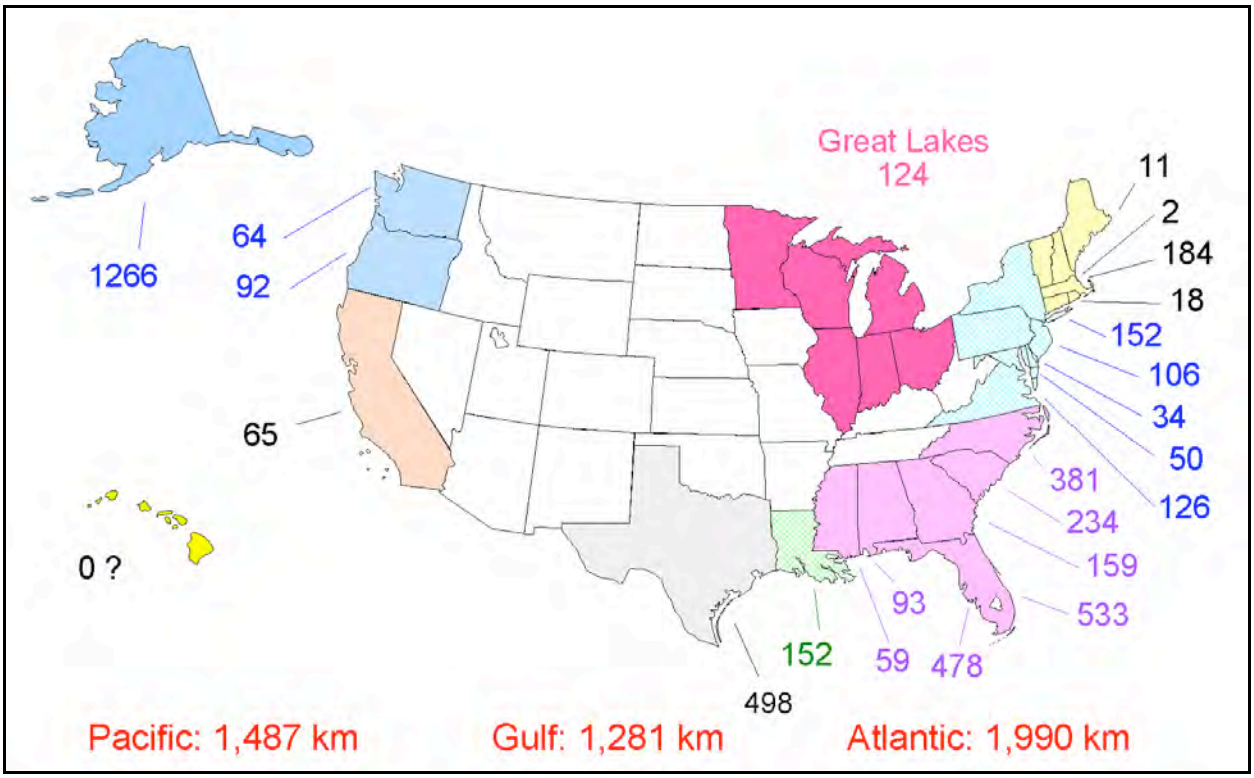

Figure I-2-5. Length (in km) of barrier islands and spits in the United States. Data measured from U.S. Geological Survey topographic maps (see Table IV-2-3 for details)

d. Gulf of Mexico East: Wetland mangrove, and barrier coasts (Figures I-2-8, I-2-9). On Florida's Gulf of Mexico coast, barrier islands begin at Cape Romano and extend north as far as Cedar Keys. Enclosed bays usually have an abundance of mangrove islands and the topography is low with many lakes and marshes. North of Cedar Keys, the barrier islands end. They are replaced by a vast marsh doted with small vegetated islands. The rock strata in this area are limestone, which, along with the low river gradients and numerous ponds or sinkholes, accounts for the absence of sand in the region. Due to its location and the large shallow water area offshore, little wave energy is present except during rare hurricanes. Some 130 km to the northwest, the swamp coast ends. Here the coastal trend changes direction from north-south to east-west, and Ochlockonee Bay, with drainage from the southern Appalachian Mountains, provides quartz sand for redevelopment of barrier islands. These sandy islands, with their various openings for access to the lowland port cities, continue westward as far as the Mississippi River delta (Figures I-2-10 and I-2-11).

Studies of the Mississippi delta indicate that the river has built a series of deltas into the Gulf of Mexico during postglacial times and that the Balize Delta (bird foot) is the latest, with an age of about 1500 years. The Bird Foot delta is southeast of New Orleans, lying among a series of old passes that extend for 300 km (186 miles) along the coast. Most of the greater Mississippi delta is marshland and mud flats, with numerous shallow lakes and intertwining channels (Figures I-2-12 and IV-3-9). The principal rivers have built natural levees along their course. These natural levees are about a meter above the normal water level, but many of them have been artificially raised to provide protection to towns and cities from floods. Aquatic plants cover the marshland, which is remarkable for the huge population of waterfowl it supports. In the areas of old delta lobes, subsidence has left only the natural levees above water in some instances.

e. Gulf of Mexico West: Barrier coast. From western Louisiana, west of the Mississippi Delta marsh coast, toward the southwest, barrier islands become the dominant coastal features. Some of the longest

Figure I-2-6. Cape Hatteras, North Carolina, view north. The Atlantic Ocean is to the right, and the bay to the left of the barrier is Pamlico Sound. The rough water in the foreground is the infamous Diamond Shoals, known as the "Graveyard of the Atlantic." The bump in the shoreline is the location of the Cape Hatteras lighthouse, which was recently moved inland away from the receding shore. A mature maritime forest has grown on the beach ridges in the central portion of the barrier. The forest indicates that this portion of the island has been stable for several hundred years. Photograph taken February 28, 1993, during the waning stage of an extratropical storm

barrier islands in the world are located along the Texas coast. Padre Island and Mustang Island, combined, extend for 208 km and feature extensive dune fields behind the broad beaches. The dunes rarely rise more than 10 m in height, and many marshy wash-over deltas have extended into the large lagoons behind the barriers. The lagoons and estuaries decrease in depth toward Mexico. A large part of Laguna Madre is only inundated during flood periods or when the wind blows water from Corpus Christi Bay onto the flats. River deltas are responsible for much of this infilling, resulting in large differences between recent chart depths and those of 100 years ago (Shepard 1982).

f. Pacific: Sea cliffs and terraced coasts (Figures I-2-13, I-2-14). Low sea cliffs bordered by terraces and a few coastal plains and deltas compose the coasts of southern California. Blocks form projections into the sea and feature a series of raised terraces such as those at Point Loma, Soledad Mountain, and the San Pedro Hills in the Los Angeles area. North of Los Angeles, the Santa Monica Mountains follow the coast. Sea cliffs in this area are actively eroding, particularly in areas where they have been cut into alluvium (Figure I-2-15). At Point Conception, the coast trends north-northwest and a different

Figure I-2-7. Hallandale Beach, an example of a popular recreation beach in an urban area on the Atlantic coast of southeast Florida. Photograph taken June 27, 1991, after the beach had been renourished using sand hydraulically pumped from an offshore source. Stakes in the beach were used as survey markers

geomorphology is evident. Despite the presence of a series of regional mountain ranges that cut across the coast, the rugged central and northern California coast is one of the straightest in the world. This area has high cliffs with raised marine terraces. A few broad river valleys interrupt the mountainous coast. Here, river sediments have been returned by the waves to the beaches and carried inland by westerly winds to form some unusually large dune fields. Monterey and San Francisco Bays, the two largest embayments, are at the mouths of the Salinas and the San Joaquin-Sacramento rivers respectively; the latter drains the great central valley of California. North of Cape Mendocino, the coast trends almost directly north, through Oregon and Washington, to the Strait of Juan de Fuca. Along this coast, lowland valleys at the mouths of large rivers alternate with short, relatively low mountainous tracts. Barriers or spits have formed at river mouths, as have large dune fields (Figure I-2-16). Many of the rivers, including the great Columbia, discharge into estuaries. This indicates that the rivers have not yet been able to fill drowned valleys created by the sea level rise when the great Pleistocene continental glaciers melted (Shepard 1982).

Because of the North Pacific Ocean's harsh wave climate, all of the major cities in Oregon and Washington were founded in sheltered water bodies. For example, Vancouver, Washington, and Portland, Oregon, are on the Columbia River. Puget Sound, a deep, sheltered, fjord-like water body in western Washington State, provides safe access for ships steaming to Tacoma, Bellingham, Everett, and Seattle (Figure I-2-17).

g. The Bering and Chukchi Seas: Arctic coastal plains and barriers (Figure I-2-18). The volcanic Aleutian Mountains trend southwest from Anchorage, Alaska, to form the Alaska Peninsula and the Aleutian Islands that extend some 2200 km (1370 miles) forming the border between the Pacific Ocean and the Bering Sea (Figure I-2-14). Beyond the Alaska Peninsula and bordering the Bering Sea, extensive coastal plains

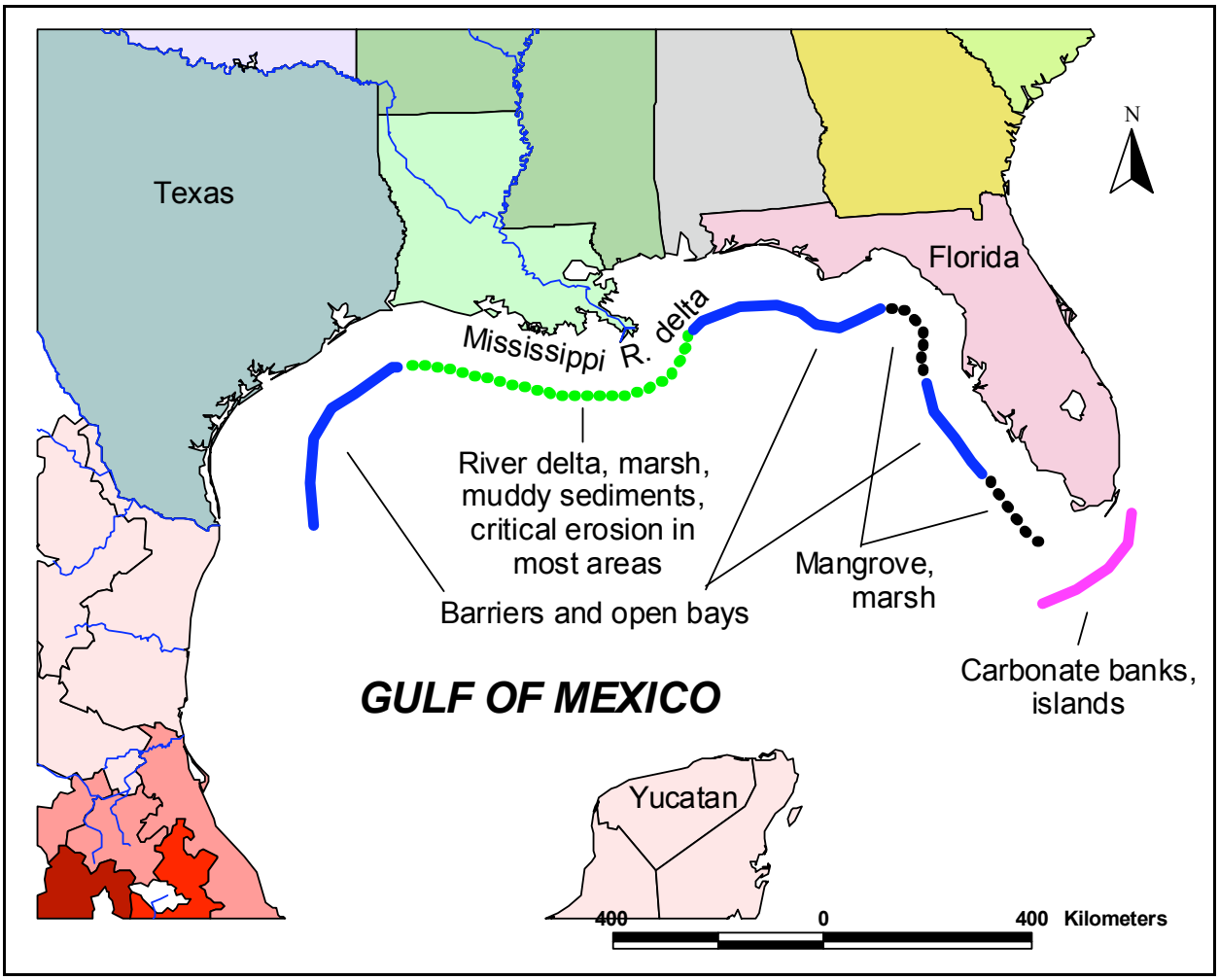

Figure I-2-8. Gulf of Mexico coastal characteristics

are found with numerous lakes and meandering streams. Only a few mountain ranges extend as points into the sea. The Yukon River has formed a large delta with many old lobes that form a vast plain connecting small, elevated tracts. The oldest is located in the now drowned mouth of the Kuskokwim River. One reason this coast differs from the glaciated southern coast of Alaska, is because it was largely ice- free during the Pleistocene era. Permafrost becomes more important to the north where it greatly increases the number of surface depressions in the summer when it melts forming *thaw lakes*. Rising above the coastal plain with mountains over 1,000 m, the Seward Peninsula with Norton Sound and the Bering Sea to the south and Kotzebbue Sound and the Chukchi Sea to the north provides a great contrast to the adjoining coasts. North of Kotzebue Sound, barriers and cuspate forelands similar to those of North Carolina border the coast. The first cuspate foreland is the unusual Point Hope. Three more cuspate forelands extend along the coast terminating with Point Barrow, the most northern point of Alaska (Shepard 1982).

h. The Beaufort Sea: Deltaic coast. East of Point Barrow, the coast is dominated by river deltas. Rivers draining the Brooks Range and father east the Mackenzie, draining the northern Canadian Rockies, built these deltas even though the rivers flow only a short period each year. Where the deltas are not actively building into the sea, extensive barrier islands can be found (Shepard 1982). One of the dominant processes in shaping beaches in Alaska is the ride-up of shore ice (Kovacs 1983).

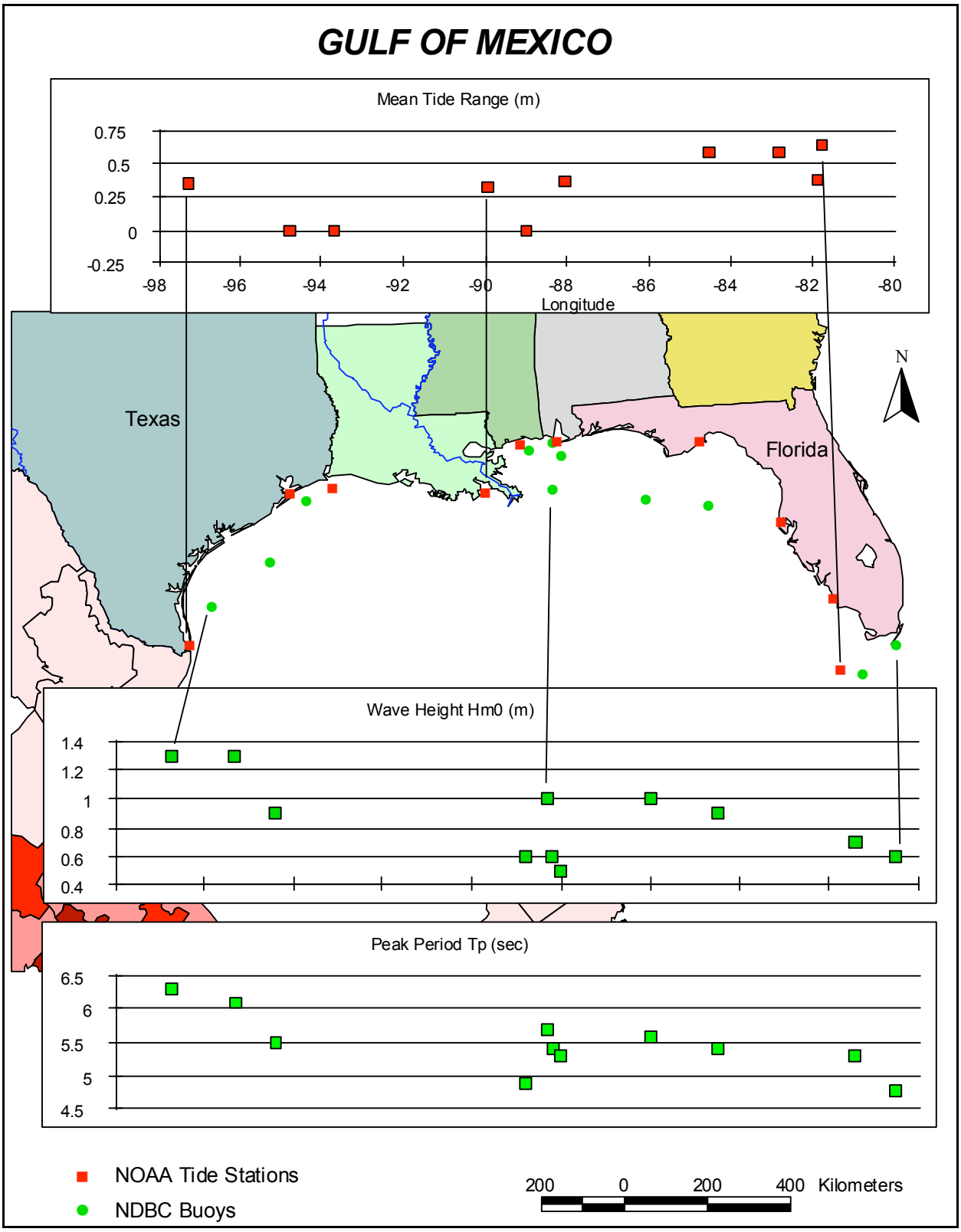

Figure I-2-9. Tide and wave characteristics of the Gulf Coast

Figure I-2-10. East Pass Inlet, Florida, View looking west towards Santa Rosa Island, with the Gulf of Mexico on the left and Choctawhatchee Bay to the right. The barrier island immediately beyond the inlet is part of Eglin Air Force Base and has remained undeveloped. The beach in the foreground is Holiday Isle, which has been heavily commercialized. This area of Florida is noted for its brilliant white quartz sand and excellent fishing. The inlet is a Federal navigation project with converging rubble-mound jetties. Photograph taken March 1991

i. Pacific: Volcanic islands (Figure I-2-19). The Hawaiian archipelago extends from the large island of Hawaii across the central Pacific Ocean northwest to tiny Kure Atoll, 2450 km away. The eight main islands of the state of Hawaii, at the southeast end of the archipelago comprise 99 percent of the land area. About 20 percent of the 1,650 km of shore on the main islands is sandy beach (USACE 1971). Aside from manmade structures, the remainder of the shore consists primarily of outcrops or boulders of lava, but also includes muddy shores, gravel beaches, beach rock, raised reefs, and lithified sand dunes. Elevations of the rocky shores vary from 1-2 m high raised reefs to 600 m sea cliffs along the Napali coast of Kauai. The Hawaiian Islands are the tops of volcanic mountains rising above the ocean floor about five km below the water surface. These volcanoes formed over a localized hot spot of magma generation. As the older volcanoes formed great shields and died, the movement of the ocean floor and crust moved them to the northwest. A higher percentage of sand shores are found on the older islands, see Table I-2-1. Beaches on Hawaiian Islands are smaller than those on the continental shores, because of the young age of the islands, the absence of large rivers to supply sediment, and the shape and exposure of the island beaches to the wave systems that affect the islands. The sand on the beaches is also different in that it is primarily calcareous and of biologic origin. The calcareous sand originates as shells and test of animals or algae that live on the fringing reefs or shallow waters adjacent to the islands. Two exceptions are some beaches near stream mouths are detritus basalt sand, and a few beaches on the island of Hawaii are black volcanic glass sand generated by the steam explosions that occur when hot lava flows into the ocean (Moberly and Chamberlain

Figure I-2-11. Morgan Peninsula, Alabama, about 10 km east of the mouth of Mobile Bay (21 April 1998). This is the back side of the barrier island, with Mobile Bay in the right side of the photograph. The dead trees clearly show that the shore has retreated within the last few years. In this portion of the Alabama shore, erosion on the back side of the barrier is a more serious threat than on the ocean side

Table I-2-1
Age and Sandy Shores of the Major Hawaiian Islands

Island	Age (million years)	Total Shoreline (km)	Sandy Shoreline (km)	Percent Sandy Shoreline
Kauai	5.1	182	80	44
Oahu	3.7 to 2.6	319	90	28
Molokai	1.5 to 1.9	170	40	24
Lanai	NA	84	29	35
Maui	1.3 to 0.9	256	54	21
Hawaii	Active	492	35	7

Based on Campbell & Moberly 1985.

Figure I-2-12. Dulac, Louisiana (March 1981). Located near the Gulf of Mexico entrance to the Houma Navigation Channel, many residents of Dulac and other towns in the Acadian parishes of southern Louisiana depend on the water for their livelihoods - shrimping, fishing, and servicing the offshore petroleum industry. Although about 25 km from the Gulf, Dulac, at an elevation of 1-2 m above sea level, is highly vulnerable to hurricanes and flooding

1964). The coastal geology of each island is derived from the erosion of the island shield and subsequent volcanic activity (Campbell and Moberly 1985).

j. Great Lakes of North America. The five Great Lakes, Ontario, Erie, Huron, Michigan, and Superior, are located along the Canadian and U.S. boundary, except that Lake Michigan is totally within the United States (Figure I-2-20). They have a combined surface area of 245,300 km^2 (94,700 $miles^2$), making them the largest freshwater body in the world. Together with the Saint Lawrence Seaway, they form a major shipping artery that is navigable inland for 3,770 km from the Atlantic by ocean-going vessels, except from about December through April when shipping is blocked by ice (Figures I-2-21, I-2-22, and I-2-23). The lakes range in elevation from about 183 m for Lake Superior (International Great Lakes Datum 1985) to about 75 m for Lake Ontario, with the largest drop in elevation, 51 m between Lakes Erie and Ontario at Niagara Falls (CCEE 1994). Geologically, the Great Lakes are relatively young, having been formed by glacial action during the Pleistocene period. Prior to the glacial age, the area occupied by Lake Superior was a broad valley and the area occupied by the other lakes was a spreading plain. During the ice period, glaciers deepened the bed of Lake Superior and gouged deep depressions forming the beds of the other lakes. As the ice sheet retreated, fingers of ice remained in the depressions, rimmed by glacial moraines and outwash plains. Lakes were formed when the ice melted. Successive advances and retreats of the ice caps changed the drainage of the lake region until about 10,000 years ago. Then, the northern part of the area up warped or rebounded causing the lakes to drain into the St. Lawrence through what is now the Niagara River.

The shores of the Great Lakes and other freshwater lakes in the United States and throughout the world are as diverse as the ocean shores, featuring high and low erosive and non-erosive cliffs and bluffs, low plains, sandy beaches, dunes, barriers and wetlands (Figure I-2-24).

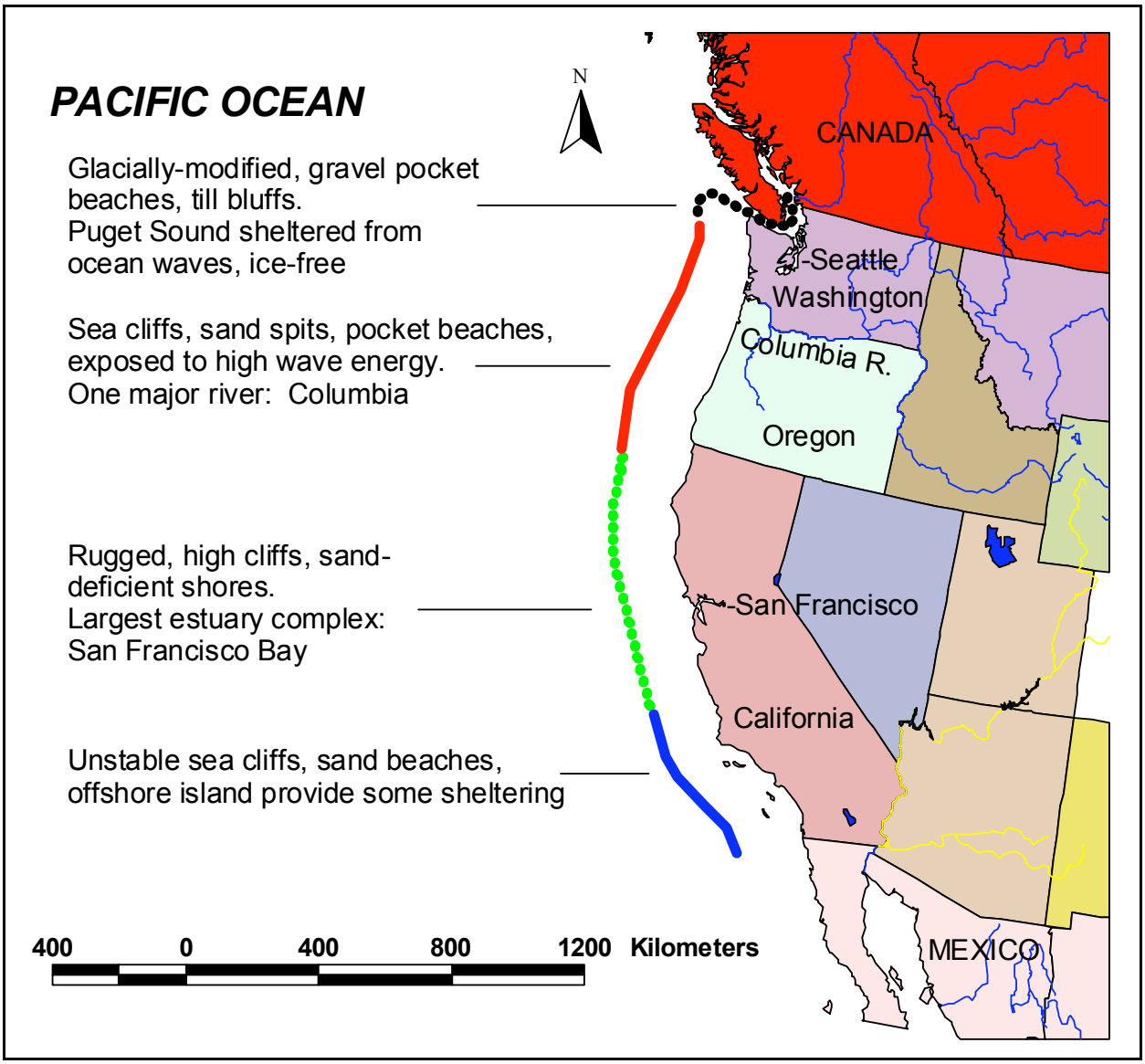

Figure I-2-13. Pacific coastal characteristics

I-2-3. Stability

Not all shores are in equilibrium with the present littoral processes. Shores with a character inherited from previous non-littoral processes (i.e., glacial or river deposited materials) maybe doomed to significant rates of erosion under present conditions, such as the Mississippi delta of Louisiana and portions of the Great Lakes. Some shores exhibit short-term seasonal or episodic event-driven cyclic patterns of erosion and accretion (e.g., the southern U.S. Atlantic coast). Other shores demonstrate long-term stability due to balanced sediment supply and little relative sea level rise influence, such as the west coast of Florida. For some shores, very little beach-building material is available, and what little is available may be prone to rapid transport, either alongshore or offshore (e.g., the Great Lakes). Shores that have been heavily modified by man's activities usually require a continuing commitment to retain the status quo. Prime examples are New Jersey, which was extensively modified during the 20th century and is now undergoing several major

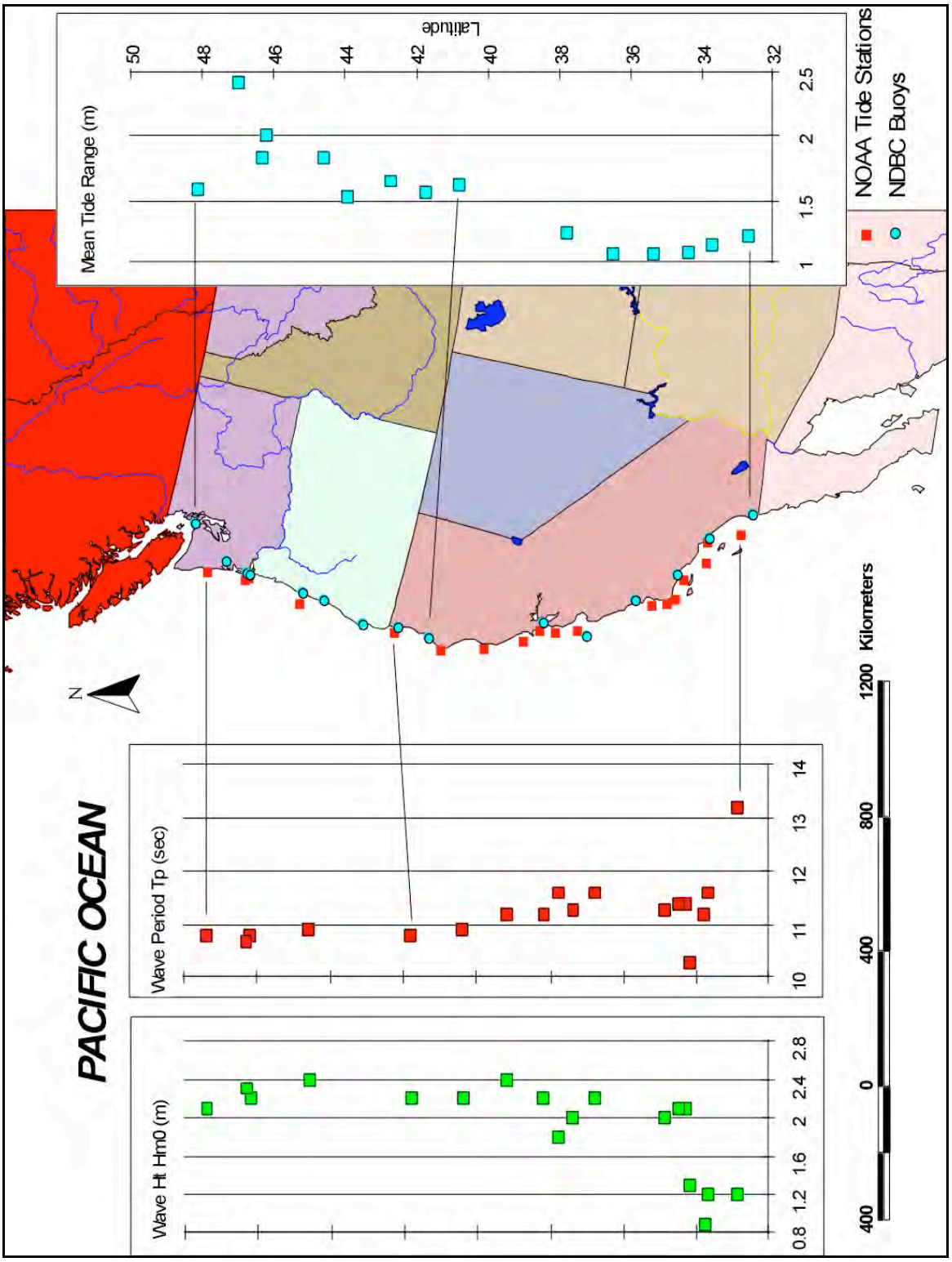

Figure I-2-14. Pacific coast tide and wave characteristics. The southernmost buoy shows high wave period because of the influence of swell waves and sheltering from wind waves provided by offshore islands

Figure I-2-15. Pocket beach just north of Laguna Beach, southern California (April 1993). Poorly consolidated sandstone and conglomerate bluffs in this area are highly vulnerable to erosion, jeopardizing exclusive residential properties. Erosion is caused by storm waves and groundwater runoff

beach fills, and numerous urban areas around the country (Los Angeles, New York, Galveston, Chicago, Miami, Palm Beach).

I-2-4. Erosion

In order for one shore to accrete, often some other shore must erode. Erosion is a natural response to the water and wind processes at the shore, but erosion is only a problem when human development is at risk. Sometimes, man-made alterations to the littoral system, including modifications to sediment sources or sinks, may contribute to the eroded condition. The National Shoreline Study (DOA 1971) found that 24 percent of the entire United States shore of 135,000 km (84,000 miles) is undergoing significant erosion where human development was threatened. If Alaska, with its 24,800 km. (15,400 miles) of shore is removed from the statistic, 42 percent of the United States shore is experiencing significant erosion!

I-2-5. Solutions

There are no absolute rules, nor absolute solutions to the problem of coastal erosion given the dynamic and the diverse character of the shoreline. No single set of regulations, or single land use management philosophy, is appropriate for all coastal situations or settings. The diversity of the coasts requires consideration of a variety of solutions when addressing problems in a particular area. Solutions can be classified into five broad functional classes of engineering or management, as listed in Table I-2-2. These options are explored in detail in Part V of the CEM.

Figure I-2-16. Mouth of the Siuslaw River, southern Oregon near the town of Florence (December 1994; view looking south). This and other Federal navigation projects on the Oregon and Washington coasts are difficult and expensive to maintain because of high wave energy and a short construction season. The scale of these Pacific projects is difficult to appreciate from aerial photographs: the Siulslaw rubble-mound jetties, first built in 1917, are 180 m apart and the north jetty is 2300 m long. The shore in this area consists of long barrier spits interrupted with rocky headlands

Table I-2-2
Alternatives for Coastal Hazard Mitigation

Functional Class	Approach Type
1. Armoring structures	Seawall
	Bulkhead
	Revetment - revetment
2. Beach stabilization structures and facilities	Breakwaters (including artificial headlands)
	Groins
	Sills vegetation
	Groundwater drainage
3. Beach restoration	Beach nourishment
	Sand passing
4. Adaptation and accommodation	Flood proofing
	Zoning
	Retreat
5. Combinations	Structural and restoration
	Structural and restoration and adaptation
6. Do nothing	(no intervention)

Abbreviated from CEM Part V, Table V-3-1

Figure I-2-17. Seattle, located in sheltered Puget Sound, is one of the world's great natural anchorages. In the 1800s Seattle was a timber town and point of embarkation for Alaska and the Orient. During the 1980s and 1990s, the port has prospered with container traffic and the export of grain and other agricultural products. Areas of the harbor need regular dredging. (Photograph July 1995)

Sometimes the solutions require the use of "hard" static structures built of rock, steel, or concrete, and sometimes the solutions involve "soft" dynamic approaches, such as adding littoral material or modifying the vegetation. Chapter V-3, "Shore Protection Projects" provides a more detailed discussion of the options and limitations available to the coastal engineer.

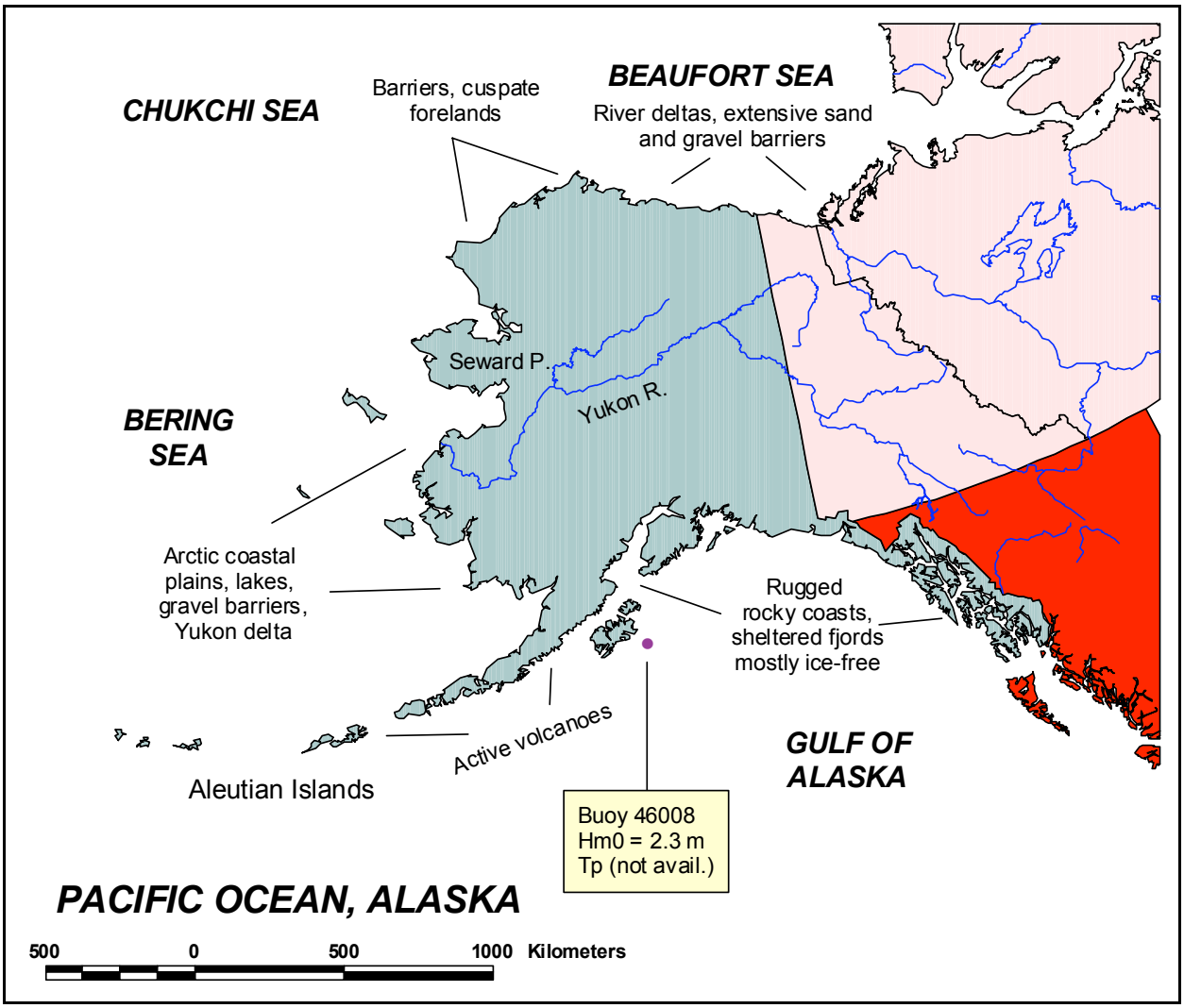

Figure I-2-18. Alaska coastal characteristics

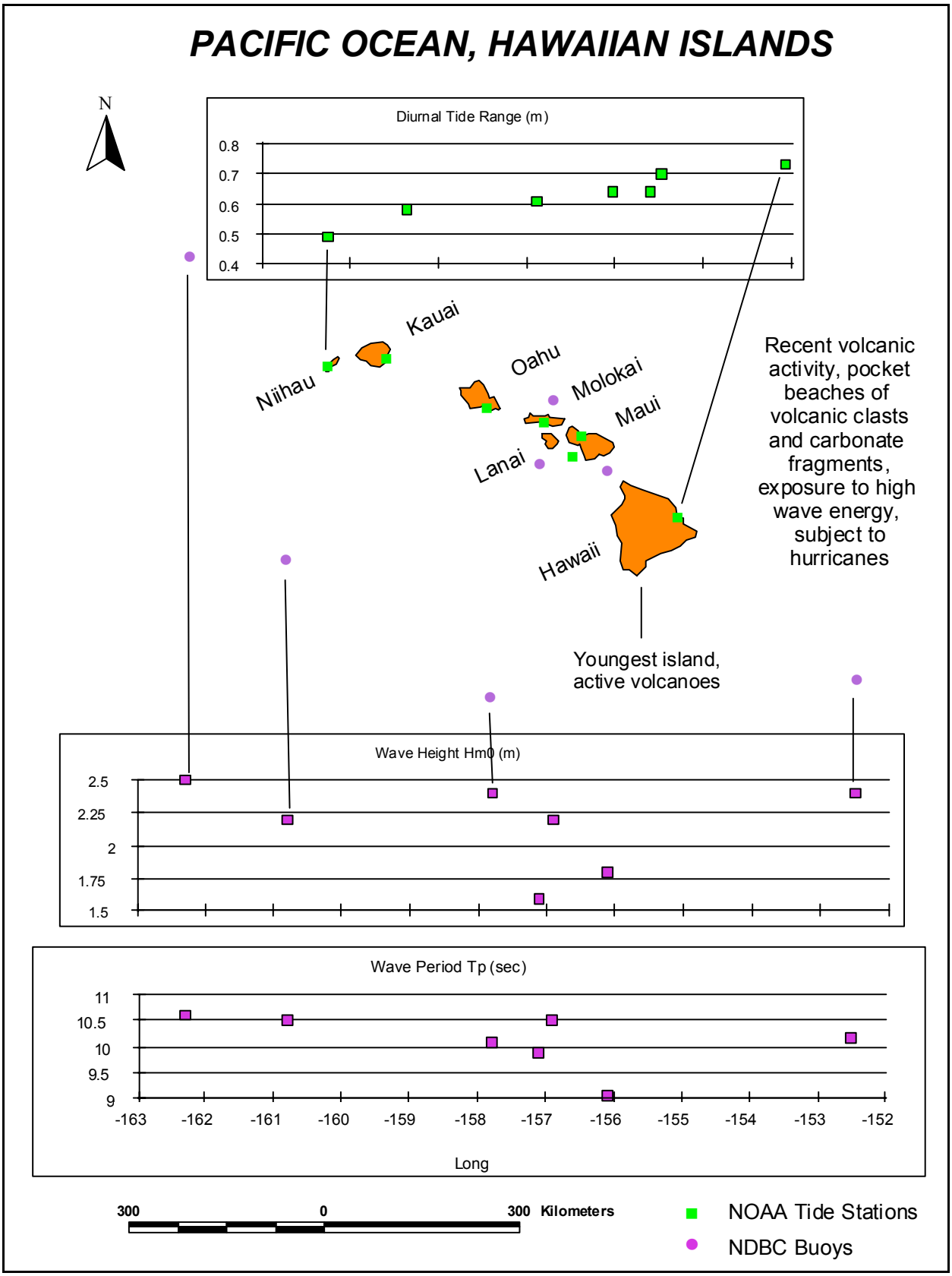

Figure I-2-19. Hawaiian Islands wave characteristics

Figure I-2-20. Great Lakes shoreline characteristics

Figure I-2-21. Minnesota Point, photographed from Duluth, Minnesota, looking south (November 1994). This bay-mouth sand spit is reputed to be the largest fresh water barrier in the world. It extends from the Wisconsin shore near Superior to the Minnesota shore at Duluth. St. Louis Bay, to the right, needs regular dredging because of silt and sand supplied by the St. Louis River. The northern part of Minnesota Point is developed with residential property. Nearby Duluth and Superior are both major industrial centers, accessible by ocean-going ships

Figure I-2-22. Calumet Harbor, Indiana (September 1985). This is an example of the industrial infrastructure found in many of the Great Lakes cities that thrived from the 1800s until the 1970s. Many of these steel mills are now closed, but some of the sites are being redeveloped for other purposes. Calumet is a Federal navigation project. The concrete cap on the breakwater in the foreground has shifted, indicating some damage to the underlying wood crib (originally built in the 1890s)

Figure I-2-23. Duluth Canal, Minnesota (November 1994). Thanks to the St. Lawrence Seaway and a network of locks, rivers, and canals, deep-draft ocean-going freighters can ship bulk commodities and goods throughout the Great Lakes. This vessel is taking iron ore from the nearby Mesabe Iron Range to some distant port. The Duluth Canal, excavated privately in 1871, is now a Federal project maintained by the USACE.

Figure I-2-24. Bluffs about 1 km north of St. Joseph Harbor, eastern Lake Michigan (November 1993). In this area, the sand and clay bluffs are receding at an average rate of between 0.3 and 0.4 m per year. They are highly vulnerable to ground water seepage and, during periods of high lake level, to wave attack. Freshly-slumped clay blocks can be seen on the bluff face in the right side of the image

I-2-6. References

Berryhill, Dickinson, and Holmes 1969
Berryhill, H. L., Dickinson, K. A., and Holmes, C. W. 1969. "Criteria for Recognizing Ancient Barrier Coastlines," *American Association of Petroleum Geologist Bulletin 53,* pp 703-707

Campbell and Moberly 1985
Campbell, J. F., and Moberly, R. 1985. "130. Hawaii," Bird, E. C. F., and Schwartz, M. L., eds., *The World's Coastline,* Van Nostrand Reinhold, New York, NY., p 1011-1022.

CCEE 1994
Concise Columbia Electronic Encyclopedia (CCEE). 1994. Columbia University Press, Encyclopedia.com—Results for Great Lakes.

DOA 1971
Department of the Army, Corps of Engineers. 1971. *Report on the National Shoreline Study,* Washington, DC. 20314, August 1971, 59 p.

Kovacs 1983
Kovacs, A. 1983. Shore ice rid-up and pile-up features, Part I: Alaska's Beaufort sea coast, CRREL Report CR-83-9-PT-1, U.S. Army Cold Regions Research and Engineering Laboratory,Hanover, NH.

Lenček and Bosker 1998
Lenček and Bosker. 1998. *The Beach: The History of Paradise on Earth.* Viking New York, 310 p.

Moberly and Chamberlain 1964
Moberly, R. and Chamberlain, T. 1964. "Hawaiian Beach Systems," *Hawaii Institute of Geophysics Report 64-2,* University of Hawaii.

Shepard and Wanless 1971
Shepard, Francis P., and Wanless, Harold R. 1971. *Our Changing Coastlines,* McGraw-Hill, New York, NY., 579 p.

Shepard 1982
Shepard, Francis P. 1982. "North America, Coastal Morphology." *Encyclopedia of Beaches and Coastal Environments, Encyclopedia of Earth Sciences,* Volume XV, Schwartz, Maurice L. Editor, Hutchinson Ross Publishing Co., 940 p, pp 593-603.

I-2-7. Acknowledgments

Authors of Chapter I-2, "Coastal Diversity:"

John H. Lockhart., Jr., Headquarters, U.S. Army Corps of Engineers, Washington, DC, (retired).
Andrew Morang, Ph.D., Coastal and Hydraulics Laboratory (CHL), Engineer Research and Development Center, Vicksburg, Mississippi.

Reviewer:

Joan Pope, CHL

Table of Contents

Page

I-3-1. Ancient World I-3-1

I-3-2. Pre-Roman Times I-3-1

I-3-3. Roman Times I-3-3

I-3-4. Modern Age I-3-4

I-3-5. Civil Engineer Era I-3-5

I-3-6. United States Army Corps of Engineers I-3-6

I-3-7. Coastal Engineering in the United States I-3-10

a. Nineteenth century projects I-3-10
b. Nineteenth century coastal engineering I-3-11
c. Early coastal development and shore protection I-3-12
d. Early 20th century beach development and the Engineering Advisory Board on Coastal Erosion I-3-13
e. American Shore and Beach Preservation Association I-3-13
f. The Board on Sand Movement and Beach Erosion I-3-15
g. The Beach Erosion Board I-3-15
h. BEB focus on basic research I-3-16
i. Dalecarlia reservation and World War II I-3-19
j. BEB accomplishments I-3-20
k. Evolution of shore protection and the shift from structures to beach nourishment I-3-21
l. The Coastal Engineering Research Center and the Coastal Engineering Research Board I-3-22
(1) Early years I-3-22
(2) Fort Belvoir I-3-22
(3) Field Research Facility I-3-23
(4) Shore Protection Manual I-3-23
(5) Waterways Experiment Station I-3-23
(6) The Coastal and Hydraulics Laboratory I-3-23

I-3-8. Coastal Engineering in the Military I-3-23

a. Amphibious operations I-3-23
b. Expedient harbors I-3-24
c. Military coastal engineering studies I-3-24
d. Port operations, Republic of Korea I-3-25
e. Port operations, Republic of Vietnam I-3-25

(1) Vung Ro I-3-26
(2) Da Rang River I-3-26
f. Temporary wharfs I-3-26
g. Rapidly Installed Breakwater System I-3-27

I-3-9. Summary I-3-28

I-3-10. References I-3-29

I-3-11. Acknowledgments I-3-36

List of Figures

Page

Figure I-3-1. Fiscal year 1997 dredging by the U.S. Army Corps of Engineers at coastal projects I-3-9

Figure I-3-2. Federally maintained deep-draft and small boat harbors with structures I-3-9

Figure I-3-3. Federal shore protection and beach erosion control projects I-3-10

Figure I-3-4. Converging jetty system designed by James B. Eads I-3-12

Figure I-3-5. Wood crib design of Great Lakes breakwaters I-3-14

Figure I-3-6. Construction of Fire Island jetty, 1940 . . . . . I-3-15

Figure I-3-7. Jetty construction, Rockaway Inlet, New York, 1932 . . . . . I-3-16

Figure I-3-8. Hurricane storm damage, Atlantic City, NJ, 1944 . . . . . I-3-17

Figure I-3-9. Construction of Manasquan Inlet jetties I-3-18

Figure I-3-10. Coney Island in 1941, on the eve of World War II I-3-19

Figure I-3-11. Jones Island State Park on July 4th holiday I-3-20

Figure I-3-12. Grass planting, beach restoration, 1930s I-3-21

Figure I-3-13. The shift from fixed structures to beach restoration and nourishment I-3-22

Figure I-3-14. Aerial photograph of the Mulberry “B” Harbor at Arromanches, France, June 1944 . . . . . I-3-25

Figure I-3-15. Operation MIKI, Waianae, Oahu, HI, October 1949 . . . . . I-3-26

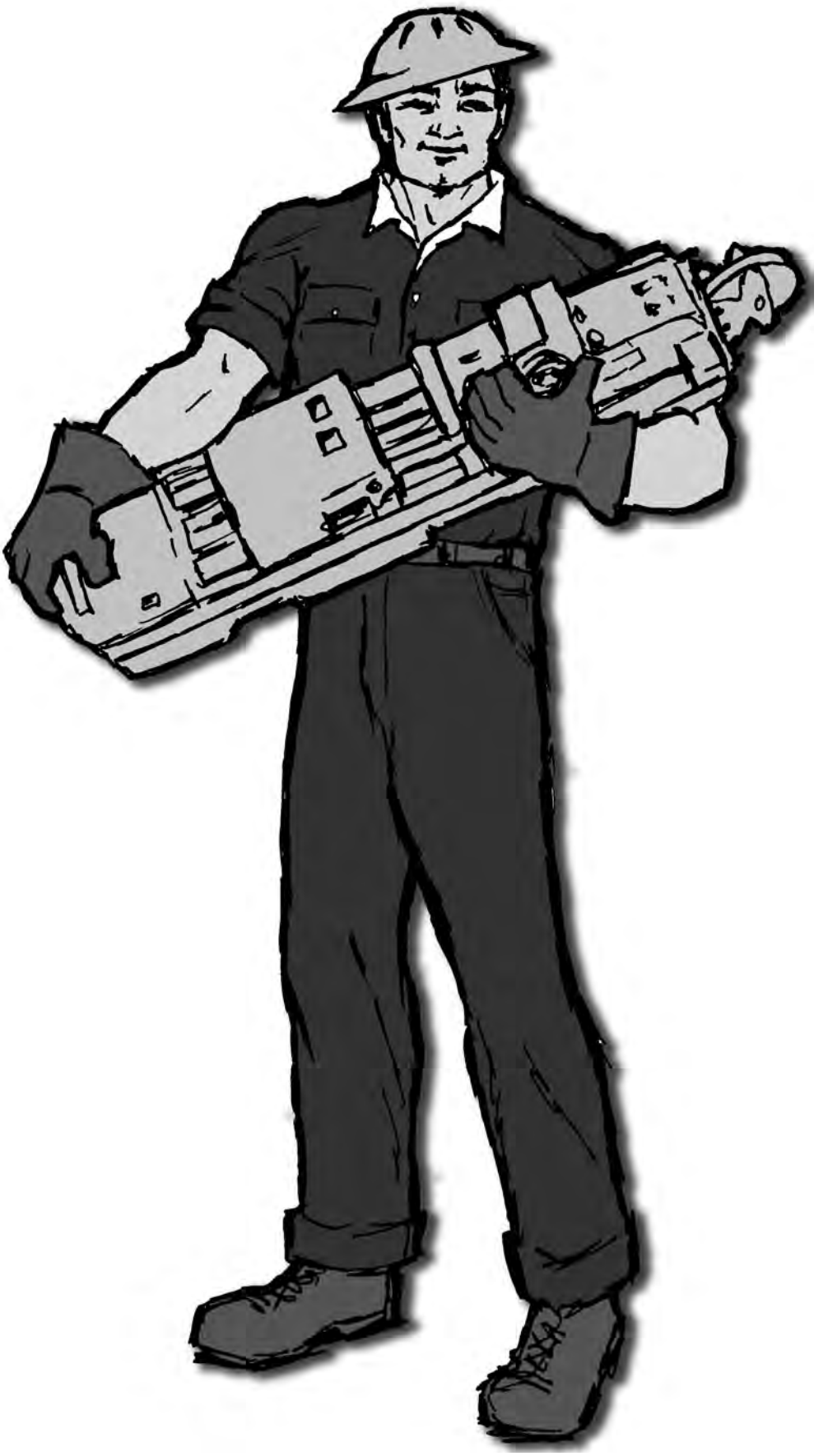

Chapter 1-3
History of Coastal Engineering

I-3-1. Ancient World

The history of coastal engineering reaches back to the ancient world bordering the Mediterranean Sea, the Red Sea, and the Persian Gulf. Coastal engineering, as it relates to harbors, starts with the development of maritime traffic, perhaps before 3500 B.C. Shipping was fundamental to culture and the growth of civilization, and the expansion of navigation and communication in turn drove the practice of coastal engineering. The availability of a large slave labor force during this era meant that docks, breakwaters, and other harbor works were built by hand and often in a grand scale similar to their monumental contemporaries, pyramids, temples, and palaces. Some of the harbor works are still visible today, while others have recently been explored by archaeologists. Most of the grander ancient harbor works disappeared following the fall of the Roman Empire. Earthquakes have buried some of the works, others have been submerged by subsidence, landlocked by silting, or lost through lack of maintenance. Recently, archaeologists, using modern survey techniques, excavations, and old documents, have revealed some of the sophisticated engineering in these old harbors. Technically interesting features have shown up and are now reappearing in modern port designs. Common to most ancient ports was a well-planned and effectively located seawall or breakwater for protection and a quay or mole for loading vessels, features frequently included in modern ports (Quinn 1972).

Most ancient coastal efforts were directed to port structures, with the exception of a few places where life depended on coastline protection. Venice and its lagoon is one such case. Here, sea defenses (hydraulic and military) were necessary for the survival of the narrow coastal strips, and impressive shore protection works built by the Venetians are still admired. Very few written reports on the ancient design and construction of coastal structures have survived. A classic treatise by Vitruvius (27 B.C.) relating the Roman engineering experience, has survived (Pollio, Rowland, and Howe 1999). Greek and Latin literature by Herodotus, Josephs, Suetonius, Pliny, Appian, Polibus, Strabo, and others provide limited descriptions of the ancient coastal works. They show the ancients' ability to understand and handle various complex physical phenomena with limited empirical data and simple computational tools. They understood such phenomena as the Mediterranean currents and wind patterns and the wind-wave cause-effect link. The Romans are credited with first introducing wind roses (Franco 1996).

I-3-2. Pre-Roman Times

Most early harbors were natural anchorages in favorable geographical conditions such as sheltered bays behind capes or peninsulas, behind coastal islands, at river mouths, inside lagoons, or in deep coves. Short breakwaters were eventually added to supplement the natural protection. The harbors, used for refuge, unloading of goods, and access to fresh water, were closely spaced to accommodate the safe day-to-day transfer of the shallow draft wooden vessels which sailed coastwise at speeds of only 3-5 knots.

Ancient ports can be divided into three groups according to their structural patterns and the development of engineering skill (Frost 1963).

a. The earliest were rock cut, in that natural features like offshore reefs were adapted to give shelter to craft riding at anchor.

b. In the second group, vertical walls were built on convenient shallows to serve as breakwaters and moles. Harbors of this type were in protected bays, and often the walls connected with the defenses of a walled town (for example, ancient Tyre on the Lebanese coast). Often these basins were closeable to traffic using chains to prevent the entry of enemy ships (Franco 1996).

c. The third group were harbors that were imposed on even unpromising coasts by use of Roman innovations such as the arch and improved hydraulic cement. Projects like this required the engineering, construction, and financing resources of a major empire.

All ancient ports had one thing in common: they had to be kept clear of silt at a time when mechanical dredging was unknown. This was accomplished by various means. One was by designing the outer parts of the harbor so that they deflected silt-bearing currents. The second was by allowing a controlled current to flow through the port or by flushing it out when necessary by means of channels. For example, at Sidon, a series of tanks (like swimming pools) were cut into the harbor side of a natural rock reef. The tanks filled with clear water that was held in place with sluice gates. When the gates were opened, currents of clear water would flush the inner harbor. Documentary and archaeological evidence show that both Tyre and Sidon were flourishing and powerful ports from the Bronze Age through the Roman era and must therefore have been kept clear of silt for over a thousand years (Frost 1963). Another method of preventing silt consisted of diverting rivers through canals so that during part or much of the year, the flow would enter the sea at location well away from the harbor.

The origins of breakwaters are unknown. The ancient Egyptians built boat basins with breakwaters on the Nile River at Zoser's (Djoser) step pyramid (ca. 2500 B.C.) (Inman 2001). The Minoans constructed a breakwater at Nirou Khani on Crete long before the explosion of Santorini (Thera) in ca. 1500 B.C. The breakwater was small and constructed of material taken from nearby dune rock quarries (Inman 1974, Figure 4). In the Mediterranean, size and sophistication of breakwaters increased over time as the Egyptian, Phoenician, Greco-Macedonian, and Roman civilizations developed and evolved. Breakwaters were built in China but generally at a later date than in the Mediterranean.

Probably the most sophisticated man-made harbor of this era was the first harbor of Alexandria, Egypt, built west of Pharos Island about 1800 B.C. by the Minoans. The main basin, built to accommodate 400 ships about 35 m in length, was 2,300 m long, 300 m wide and 6-10 m deep. Large stone blocks were used in the many breakwaters and docks in the harbor. Alexander the Great and his Greek successors rebuilt the harbor (300-100 B.C.) in monumental scale. The Island of Pharos was joined to the mainland by a 1.5 km breakwater with two openings dividing two basins with an area of 368 hectares (910 acres) and 15 km of quay front. Alexandria is probably best known for the 130m-high lighthouse tower used to guide ships on a featureless coast to the port from 50 km at sea. The multi-storied building was built with solid blocks of stone cemented together with melted lead and lined with white stone slabs. Considered one of the Wonders of the Ancient World, it eventually collapsed due to earthquakes between 1326 and 1349 (Franco 1996, Empereur 1997).

Another feature of the Greek harbors was the use of colossal statues to mark the entrances. Colossal statues of King Ptolemy, which stood at the base of the lighthouse, have been found with the lighthouse debris. Historians report the most famous harbor statue was the 30 m high Colossus of Rhodes, which stood on the breakwater heads. Three ancient windmill towers are still surviving upon the Rhodes breakwater (Franco 1996). Frost (1963) notes that the Greeks had used hydraulic cement long before the Romans.

I-3-3. Roman Times

The Romans introduced many revolutionary innovations in harbor design. They learned to build walls underwater and constructed solid breakwaters to protect exposed harbors. They used metal joints and clamps to fasten neighboring blocks together and are often credited with discovering hydraulic cement made with pozzolanic ash obtained from the volcanic region near Naples, which hardens underwater. Frost (1963) notes that the Greeks had used hydraulic cement long before the Romans. The Romans replaced many of the Greek rubble mound breakwaters with vertical and composite concrete walls. These monolithic coastal structures could be built rapidly and required little maintenance. In some cases wave reflection may have been used to prevent silting. In most cases, rubble or large stone slabs were placed in front of the walls to protect against toe scour. The Romans developed cranes and pile drivers and used them extensively in their construction. This technology also led them to develop dredges. Another advanced technique used for deep-water applications was the watertight floating cellular caisson, precursor of the modern day monolithic breakwater. They also used low, water-surface breakwaters to trip the waves before they reached the main breakwater. The peculiar feature of the vertical wall breakwater at Thapsus (Rass Dimas, Tunisia) was the presence of vents through the wall to reduce wave impact forces. This idea is used today in the construction of perforated caisson breakwaters (Franco 1996).

Using some of these techniques, the Romans built sophisticated breakwaters at Aquileia, Italy (ca. 180 B.C.), and at Caesarea, Israel (ca. 20 B.C.). The southwestern breakwater at Caesarea contained a "forebreakwater" that acted as a submerged reef that "trips" the wave causing it to break and dissipate energy before encountering the main breakwater (Inman 2001).

The largest manmade harbor complex was the imperial port of Rome; the maritime town at the mouth of the Tiber River was named Portus (The Port). It is now some four km from the sea, partly buried under Rome-Fiumicino airport. Despite its importance to the capital of the empire, (300,000 tons/year of wheat from Egypt and France), the harbor always suffered siltation from the river. Trajan, who also built the ports of Terracina and Centumcellae, built Portus' inner hexagonal basin. The port of Centumcellae was built just to serve his villa at a site with favorable rocky morphology. A grandiose engineering project between 107-106 B.C. created a sheltered bathing and boating retreat. Slaves from all parts of the empire excavated a harbor and hauled in massive stones to create an artificial harbor to dampen the force of the waves. After the decline of Portus, it became, and remains, the Port of Rome. After remaining unchanged for over 1,000 years, the inner Roman Basin, which was dredged from rock (200,000 m^3 or 260,000 yd^3), is still in use. Roman engineers also constructed harbors in northern Europe along the main waterways of the Rhine and Danube and in Lake Geneva. They became the first dredgers in the Netherlands to maintain the harbor at Velsen. Silting problems here were solved when the previously sealed solid piers were replaced with new "open"-piled jetties. In general, the Romans spread their technology throughout the western world. Their harbors became independent infrastructures, with their own buildings and storage sheds as opposed to the pre-Roman fortified city-enclosed harbors. They developed and properly used a variety of design concepts and construction techniques at different coastal cites to suit the local hydraulic and morphological conditions and available materials (Franco 1996).

The Romans also introduced to the world the concept of the holiday at the coast. The ingredients for beach holidays were in place: high population density coupled with a relatively high standard of living, a well-established economic and social elite, and a superb infrastructure of roads. From the end of the republic to the middle of the second century of the empire, resorts thrived along the shores of Latium and Capania, and an unbroken string of villas extended along the coast from the seashore near Rome to the white cliffs of Terracina. Fine roads connected these resorts to the capital, allowing both the upper crust and the masses to descend from sultry and vapor-ridden Rome to the sea. For five hundred years, the sybaritic town of Baiae reigned as the greatest fashionable beach resort of the ancient world. Seneca the Younger called Baiae a

"vortex of luxury and a harbor of vice," an alluring combination that Romans found irresistible (Lenček and Bosker 1998).

I-3-4. Modern Age

After the fall of the Western Roman Empire, a long hiatus in coastal technology and engineering prevailed throughout most of the European world with a few exceptions. Little is recorded on civil engineering achievements during the Dark and Middle Ages. The threat of attack from the sea caused many coastal towns and their harbors to be abandoned. Many harbors were lost due to natural causes such as rapid silting, shoreline advance or retreat, etc. The Venice lagoon was one of the few populated coastal areas with continuous prosperity and development where written reports document the evolution of coastal protection works, ranging from the use of wicker faggots to reinforce the dunes to timber piles and stones, often combined in a sort of crib work. Protection from the sea was so vital to the Venetians, that laws from 1282 to 1339 did not allow anyone to cut or burn trees from coastal woods, pick out mussels from the rock revetments, let cattle upon the dikes, remove sand or vegetation from the beaches or dunes, or export materials used for shore protection (Franco 1996).

In England, coastal engineering works date back to the Romans, who recognized the danger of floods and sea inundation of low-lying lands. On the Medway, for example, embankments built by the Romans as sea defense remained in use until the 18th century (Palmer and Tritton Limited 1996). The low-lying lands, consisting of recently-deposited alluvial material, were exceeding fertile but were also vulnerable to flooding from both runoff and storm surges. In the Middle Ages, the Church became instrumental in reclaiming and protecting many marshes, and monks reclaimed portions of the Fylde and Humber estuaries. In 1225, Henry III constituted by Charter a body of persons to deal with the question of drainage (Keay 1942).

Across the North Sea, the Friesland area of the Netherlands had a large and wealthy population in the period 500 - 1000 A. D., and increasing need for agricultural land led to building of sea dikes to reclaim land that previously was used for grazing (Bijker 1996). Water boards developed in response to the need for a mutual means to coordinate and enforce dike maintenance. These boards represent some of the earliest democratic institutions in the Netherlands.

Engineering and scientific skills remained alive in the east, in Byzantium, where the Eastern Roman empire survived for six hundred years while Western Rome decayed. Of necessity, Byzantium had become a sea power, sending forth fleets of merchant ships and multi-oared dromonds (swift war vessels) throughout the Black Sea and Mediterranean. When the weary soldiers of the first crusades reached Byzantium's capital city, Constantinople, in 1097, they were amazed and awed by its magnificence, sophistication, and scientific achievements. Constantinople was built on the hills overlooking the Golden Horn, a natural bay extending north of the Bosporus. Marble docks lined the waterfront, over which passed the spices, furs, timber, grain, and the treasures of an empire. A great chain could be pulled across the mouth of the Golden Horn to prevent intrusion by enemy fleets. A series of watch towers extended along the length of the Sea of Marmara, the Bosphoros, and the south shore of the Black Sea, and the approach of an enemy fleet could be signaled to the emperor within hours by an ingenious code using mirrors by day and signal fires by night (Lamb 1930).

The Renaissance era (about XV - XVI centuries) was a period of scientific and technologic reawakening, including the field of coastal engineering. While the standards for design and construction remained those developed primarily by the Romans, a great leap in technology was achieved through the development of mechanical equipment and the birth of the hydraulic sciences including maritime hydraulics (Franco 1996). "The Italian School of Hydraulics was the first to be formed and the only one to exist before the middle of the 17th century" (Rouse and Ince 1963). Leonardo da Vinci (1465-1519), with his well-known experimental method, based on the systematic observation of natural phenomenon supported by intellectual reasoning and

a creative intuition, could be considered the precursor of hydrodynamics, offering ideas and solutions often more than three centuries ahead of their common acceptance. Some of his descriptions of water movement are qualitative, but often so correct, that some of his drawings could be usefully included in a modern coastal hydrodynamics text. The quantitative definition and mathematical formulation of the results were far beyond the scientific capabilities of the era. Even so, da Vinci was probably the first to describe and test several experimental techniques now employed in most modern hydraulic laboratories. To visualize the flow field, he used suspended particles and dyes, glass-walled tanks, and movable bed models, both in water and in air. The movement from kinematics to dynamics proved impossible until the correct theory of gravitation was developed, some two centuries latter by Sir Issac Newton (Fasso 1987). The variety of hydro kinematics problems dealt with in da Vinci's notebooks is so vast that it is not possible to enumerate them all in this brief review. In the 36 folios (sheets) of the Codex Leicester (1510), he describes most phenomena related to maritime hydraulics. Richter (1970) provides an English translation of da Vinci's notebooks (Franco 1996). The scientific ideas of the Italian Renaissance soon moved beyond the confines of that country, to the European countries north of the Alps.

I-3-5. Military and Civil Engineer Era

After the Renaissance, although great strides were made in the general scientific arena, little improvement was made beyond the Roman approach to harbor construction. Ships became more sea-worthy and global navigation became more common. With global navigation came the European discovery of the Americas, Australia, New Zealand, Indonesia, and other areas of the world, soon followed by migration and colonization. Trade developed with previously unreachable countries and new colonies. France developed as the leader in scientific knowledge. The French "G'enie" officers, who, along with their military task, were also entrusted with civilian public works, are reportedly the direct ancestors of modern civil engineers. S'ebastien le Prestre de Vauban (1633-1707) was a builder of numerous fortresses and perfected the system of polygonal and star shaped fortifications. His most eminent public works project was the conversion of Dunkirk into an impregnable coastal fortress. Apart from the construction of several forts, there were extensive harbor and coastal works, including the excavation of canals and harbor basins, the construction of two long jetties flanking the entrance channel, and the erection of storehouses and workshops. A great lock, a masterpiece of civil engineering, was built at the entrance to the Inner Harbor. Vauban himself designed and supervised the lock construction. Unfortunately, no more than 30 years after its completion, the fortress was destroyed as a consequence of the Spanish War of Succession. Vauban's projects provide a good example of engineering methods and lucidity. They consisted of an explanatory memorandum, several drawings, and a covering letter. The memorandum had four sections: (1) general background of the scheme; (2) detailed descriptions of the different parts, with references to the drawings; (3) cost estimates; (4) features and advantages of the work. It was during this time that the term "Ingenieur" was first used in France, as a professional title for a scientifically-trained technician in public service.

While France enjoyed a leading position in Europe with regard to exact sciences and their applications to technical problems, a social and economic revolution later known as the "Industrial Revolution" was taking place in England. The riding-horse and the packhorse gave way to the coach, the wagon and the barge. Hard roads and canals replaced the centuries old soft roads and trails, dusty in dry weather and mud-bound during rains (Straub 1964). Steam power allowed industry to be concentrated in factories that required continuous supply of raw materials and export of manufactured goods.

In the 18th and 19th centuries, advances in navigation and mathematics, the advent of the steam engine, the search for new lands and trade routes, the expansion of the British Empire through her colonies, and other influences, all contributed to the revitalization of sea trade and a renewed interest in port works. As the volume of shipping grew, more vessels were needed and as the dimensions of the new vessels became larger,

increased port facilities were necessary. Ports of the world experienced growing pains for the first time since the Roman era, and, except for the interruption caused by two world wars, port needs continue to grow (Quinn 1972).

I-3-6. United States Army Corps of Engineers

Since the formation of the United States, Army engineers and the Corps of Engineers have been responsible for or intimately associated with a wide variety of civil projects and improvements to waterways, ports, and navigation systems. The following paragraphs summarize the history of the U.S. Army Corps of Engineers (USACE) and outline some of the Corps' early efforts in coastal and navigation improvements.

The origins of the USACE date to June of 1775, at the beginning of the American War of Independence, when the Second Continental Congress authorized General Washington to assign a "chief engineer" for the "grand army" (Parkman 1978). General Washington selected Colonel Richard Gridley, a seasoned artilleryman, who had been preparing a line of fortifications around Boston during the early weeks of the war. Military operations during the war underscored the need for an efficient body of engineers, and in March of 1779, the Continental Congress finally authorized a separate and distinct "corps of engineers," to be commanded by Louis LeBègue Du Portail, an officer recruited by the American mission in France. The corps was a vital unit of the Continental Army until disbanded in November 1783 with the arrival of peace.
When war between France and England broke out in the 1790s Congress authorized President Washington to begin construction of a system of fortifications along the coast. In 1802, in anticipation of the European belligerents signing a treaty of peace, Congress cut back and reorganized the army and created a separate corps of engineers, limited at that time to sixteen officers (Parkman 1978). The Act of March 16, 1802 had other far-reaching consequences, as it provided further that the Corps was to constitute the personnel of a military academy at West Point. Congress had recognized the almost complete absence of trained military and civil engineers in the United States, and, in effect, established a national college of engineering. West Point was the only school in the country to graduate engineers until 1824, when Rensselaer Polytechnic Institute was formed. Quickly becoming the growing nation's primary source of engineering expertise, the Corps first concentrated on constructing and maintaining strategically-placed coastal fortifications to repel naval attacks. But soon it became concerned with civil functions as it planned and executed the national internal improvement program initiated in the 1820s (Maass 1951).

Until the early 1800s, little maintenance or improvement was done to harbors or rivers, and maintaining navigability of waterways was considered the responsibility of the states or private interests. What little the Federal government had done was carried out by the Treasury Department, which had assisted navigation by erecting lighthouses, beacons, buoys, and public piers. In 1818, John C. Calhoun, then Secretary of War, recommended that the Corps of Engineers be directed to improve waterways navigation and other transportation systems because these civil works would facilitate the movement of the Army and its materials while contributing to national economic development (USACE 1978). Congress accepted Calhoun's recommendations and passed the landmark General Survey Act, which President James Monroe signed into law on April 30, 1824. It directed the President to use Army engineers to survey roads and canals. By the mid-1820s Corps of Engineers officers were busy surveying the Ohio and lower Mississippi Rivers and the Great Lakes, identifying navigation impediments, and proposing improvements and new routes.

Only a month later, on May 24, 1824, President Monroe signed the first Rivers and Harbors Act, which authorized the President to appropriate Federal monies to improve navigation on the Ohio and Mississippi Rivers. By 1829, Army engineers were using steam-powered snagboats to remove snags and floating trees and to dig out sandbars that impeded river traffic. Subsequent acts authorized a wide variety of internal improvements and assigned Army engineers to direct and manage these projects. Work soon began on a number of challenging locations that were deemed critical for the growth of a growing nation.

Hazardous navigation conditions on the Great Lakes also called for the rapid improvement of harbors. With the passage of the Rivers and Harbors Act, Congress voted a $20,000 appropriation for deepening the channel at the harbor of Presque Isle (at Erie, Pennsylvania) on Lake Erie (Drescher 1982). Signaling the beginning of federal involvement in the development of harbors on the Great Lakes, the USACE now maintains over 600 navigation projects throughout these waterways.

One of the USACE's first civil projects on an ocean coast was repairing Long Beach at Plymouth, Massachusetts. The beach was a long, narrow sand spit that formed the town's harbor. Constantly endangered by waves and wind, it had been a subject of concern to the citizens of the town as early as 1702, when they made it a crime to fell its trees or fire the grass. The congressional appropriation of $20,000 on May 26, 1824, "to repair Plymouth Beach in the state of Massachusetts, and thereby prevent the harbour at that place from being destroyed" initiated the Corps' civil works mission in New England. Corps officers supervised local agents, who built a cribwork breakwater along the beach's outer shore and erected brush fences and planted grass to stabilize the sand. Similar projects were undertaken at nearby Duxbury and other beaches in New England (Parkman 1978). The pattern whereby Corps specialists supervise local contractors has continued to this day for most civil works projects.

Over the succeeding century and a half, the USACE's role in civil works grew dramatically, in step with the growth of the nation's population and economy. To adequately cover this interesting story in the CEM would risk doubling its size, so readers are referred to a series of books that document the history of each district (Table I-3-1).

Presently, USACE officers and a large contingent of non-military government employees maintain a navigation system of more than 40,000 km (25,000 miles) and 219 locks and dams connecting large regions of the country. Of the nation's top 50 ports active in foreign waterborne commerce, over 90 percent require regular dredging (Waterborne Commerce Statistics Center 1999). Over 300 million cubic meters of dredged material are removed from navigation channels each year. In 1997, the USACE contracted for the dredging of about half this total (157 million m^3, see Figure I-3-1) at coastal sites only. This does not include inland waterways (Hillyer 1996).

Most inlets and harbors used for commercial navigation in the United States are protected and stabilized by hard structures. The USACE built most of the structures and is responsible for maintaining even a larger number since the Federal Government assumed responsibility for some state and local projects. Figure I-3-2 summarizes the locations of the Federal projects (Hillyer 1996).

Many U.S. coastal urban and recreational centers are protected by erosion control and storm damage reduction projects constructed cooperatively by the USACE, state, and local governments (Figure I-3-3). Although most of the 83 Congressionally authorized shore protection projects are in densely developed areas, some were constructed primarily for recreation and are associated with public or park beaches (Sudar et al. 1995).

Table I-3-1
Selected Bibliography of USACE History

Region	Reference
General history of USACE	USACE 1998
Alaska District	Jacobs 1976
Atchafalaya Basin	Reuss 1998
Baltimore District	Kanarek 1978
Buffalo District	Drescher 1982
Charleston District	Moore 1981
Chicago District	Larson 1979
Detroit District	Larson 1981
Galveston District	Alperin 1977
Honolulu District	van Hoften 1970
Jacksonville District	Buker 1981
Little Rock District	Rathbun 1990
Los Angeles District	Turhollow 1975
Mobile District	Davis 1975
New England Division	Parkman 1986
New Orleans District	Cowdrey 1977
New York District	Klawonn 1977
North Atlantic Division	Chambers 1980
Ohio River Division	Johnson 1992
Pacific Ocean Division	Thompson 1981
Philadelphia District	Snyder and Guss 1974
Pittsburgh District	Johnson 1979
Portland District	Willingham 1983
San Francisco District	Hagwood 1982
Savannah District	Barber 1989
Seattle District	Seattle District 1969
St. Paul District	Merritt 1979
St. Lawrence Seaway	Becker 1984
St. Louis District	Dobney 1978
Wilmington District	Hartzer 1984

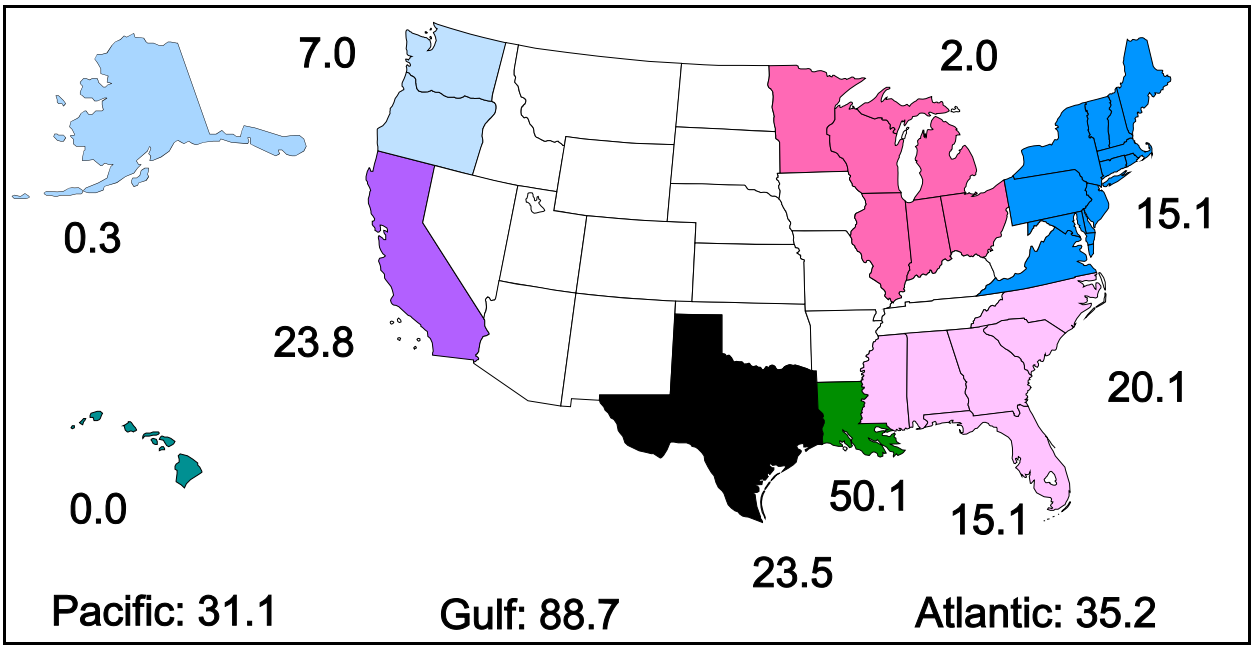

Figure I-3-1. Fiscal year 1997 dredging by the U.S. Army Corps of Engineers at coastal projects (million m^3). These totals do not include dredging of inland waterways and rivers, but do include Great Lakes ports (from Hillyer 1996)

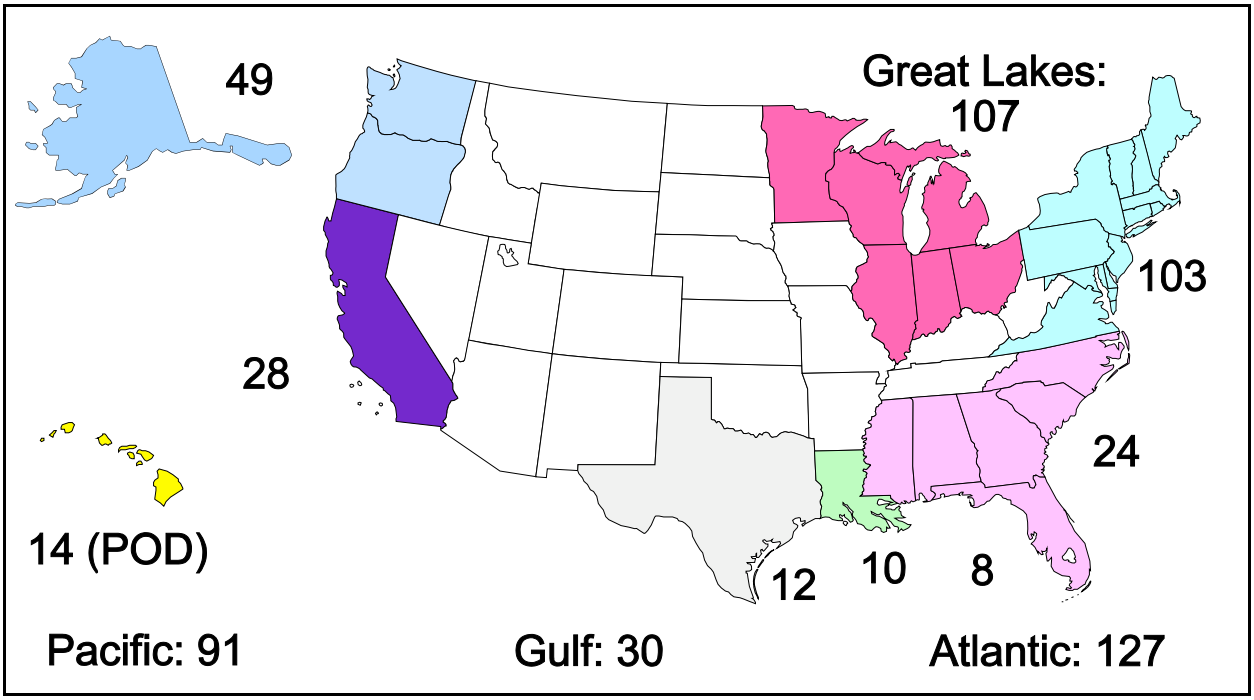

Figure I-3-2. Federally maintained deep-draft and small boat harbors with structures (from Hillyer 1996)

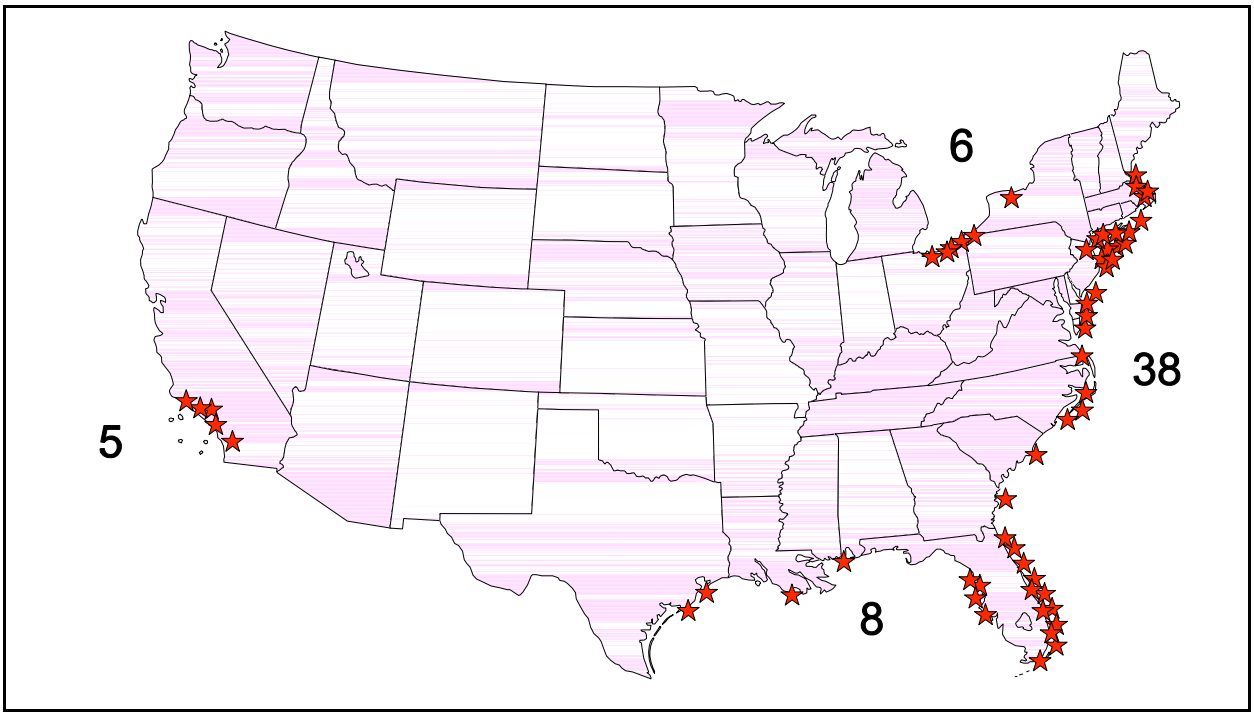

Figure I-3-3. Location of 57 large Congressionally authorized shore protection and beach erosion control projects. Some 26 small projects with limited scope and low cost (less than a few hundred thousand dollars) are not shown (from Hillyer 1996)

I-3-7. Coastal Engineering in the United States[1]

a. Nineteenth century projects. From the birth of the United States through the 18th century, local and Federal coastal projects were designed to accommodate and facilitate growth. Harbors that were usable in their natural setting in the 18th century had to be improved during the industrial age to service the 19th century's larger, steam powered, ocean-going vessels. Though the Corps' attention focused on navigation-related improvements, its coastal activities ranged from beach reconstruction to blasting better shipping channels to building new ports and lighthouses. Some of the early projects are summarized below:

(1) Currents sweeping by Sullivan's Island, South Carolina, caused substantial erosion that threatened Fort Moultrie in the 1820s. A major reclamation program was started by the USACE under its authority to solve the erosion problems of existing fortifications (Moore 1982).

(2) Congress appropriated funds in 1826 for the Corps to combat erosion of valuable sand spits protecting Duxbury and Provincetown Harbors in Massachusetts and to construct jetties at Warren River and Martha's Vineyard to prevent sand from being carried by currents into the harbors (Parkman 1978).

(3) Attention of the United States Government was first directed to Erie Harbor at the close of the War of 1812. In 1823, the Board of Engineers presented an elaborate plan for improvement of the harbor's entrance. In May of 1824, Congress authorized improvements and protection of the vulnerable Presque Isle Peninsula (Goreki and Pope 1993). Engineering work continues at Presque Isle to this day (Figure V-3-10).

[1] One of the most detailed discussions of the history of coastal engineering in the United States is Weigel and Saville 1996.

(4) In 1830, Army Engineers surveyed and made recommendations for the improvement of Baltimore Harbor, Maryland. A prolonged program of channel improvement began in 1852, and by the summer of 1872, as many as 13 dredges were engaged in the excavation of the waterway. By the time of the Spanish-American war in 1898, Baltimore had become one of the world's major ports (Kanarek 1976 pp. 41-59).

(5) Buffalo, New York, and Cleveland, Ohio, grew from frontier villages to manufacturing and commercial centers in a little over a century because of their locations at the terminus of water and rail routes connecting the grain-rich areas of the west to the eastern urban centers. The economic lives of the two cities depended on the construction and maintenance of harbor facilities such as seawalls, jetties, breakwaters, and dredged channels. As a result of successive harbor improvement projects, they have become major cities on the Great Lakes (Drescher 1982). Much of the 19th century development of the mid-West and the Great Lakes occurred as European immigrants traveled through the port of New York, along the Erie Barge Canal through Buffalo, and on to points further west.

(6) Hell Gate, a one-mile section of the East River that connected Long Island Sound with New York Harbor, had very strong currents that sliced around rocks and islands and ran back and forth because the tides in the harbor and sound did not coincide. In 1845, New York city began an effort to open the East River to navigation and in 1852, the Corps tackled the immensely difficult task of developing new technology for underwater excavation and blasting that would be required to clear Hell Gate for navigation. The project was completed 30 years later (Klawonn 1977 pp. 69-93).

(7) In 1868, Congress responded to request for assistance from California that resulted in a long productive period of Federal, State, and local cooperation. The development of the California coast with rail connections to modern, deepwater ports at San Diego, Los Angeles, San Francisco, and Oakland was the ultimate result (Turhollow 1975 pp. 20-48).

(8) Following the devastating 1900 hurricane at Galveston, Texas, which drowned over 6,000 of its citizens, the city assigned three civilian engineers the task of developing the safest and most efficient means to protect the city from similar future floods. Based on their study, the city constructed a 5,360-meter (17,600-foot) curved face concrete seawall, (Figure V-3-5). The city was elevated several meters using sand pumped from Galveston Bay onto the beach behind the seawall. At the same time, Congress authorized a connecting seawall to protect the port and military reservation at Fort Crockett. The 4,900-ft extension was constructed from 1904 to 1905 (Alperin 1977, pp. 237-244).

b. Nineteenth century coastal engineering. In 19th century United States, most engineering in the coastal area consisted of the application of principles well known to engineers accustomed to dealing with rivers. There was little concern about the unique nature of the coast, and studies of the effects of wind and waves upon the shore were sporadic, desultory, and unscientific. Trial and error, frequently accompanied by innovation was the teaching tool of the day. Improvement of the St. Johns River mouth at Jacksonville, Florida provides a good example. A continuously shifting sinuous channel through the bar made navigation difficult, so in the 1850s, a citizens group petitioned the USACE for help in dealing with the sandbar problem. One solution proposed was to put the scouring power of the current to work by constructing jetties. The USACE engineers preferred to try clearing the channel by frequent dredging and raking during the strongest phase of the ebb. These attempts failed, and in 1878 influential citizens hired Captain James B. Eads to study the problem. The 1878 Eads report recommended constructing two converging jetties to create a stable deep channel out to sea. His report contained principles of seacoast engineering, sketches of the tidal prism, and estimates of the area that could be maintained. The sophisticated technology to confirm Eads' findings would not be available well into the 20th century. Largely as a result of Eads' success constructing the jetties at the mouth of the Mississippi River, the USACE adopted a modified version of his jetty plan for improving the St. Johns River entrance (Buker 1981, pp. 69-82) (Figure I-3-4).

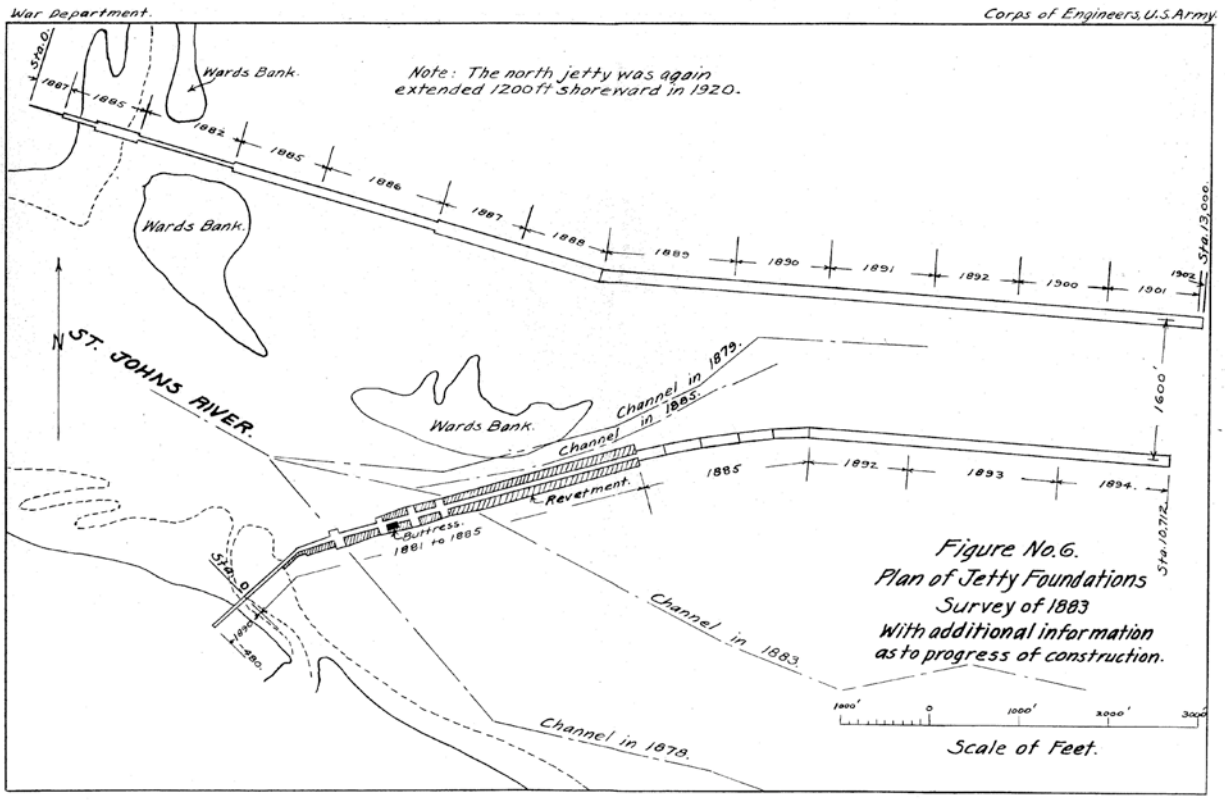

Figure I-3-4. Converging jetty system designed by James Buchanan Eads for the mouth of the St. Johns River, Florida. Figure courtesy of USAED, Jacksonville

Colonel Quincy Gillmore, familiar with Eads' plan for Jacksonville, used a similar plan to construct the jetties at Charleston Harbor, South Carolina, between 1878 and 1893. From the barrier islands on each side of the harbor entrance, the USACE constructed two converging jetties followed by a parallel section. The near shore portion of the jetties was constructed to just below the low tide water surface, thereby serving as a weir and allowing the flood tide to come in normally. During the ebb tide, the bottom currents were channeled through the parallel section (constructed higher, with the seaward quarter above high tide) toward the bar and this scouring action kept the new channel clear (Moore 1982). A similar plan was used at the mouth of the St. Mary's River at the Florida-Georgia border. Major George L. Gillespie, District Engineer in Portland, OR, submitted a plan for a dike at the mouth of the Columbia River to concentrate river currents and tides to scour a deep channel. Construction commenced on the south jetty in 1884, a project that had to overcome fierce winter storms and hazardous working conditions (Willingham 1983).

c. Early coastal development and shore protection. From the early days of settlement to the present, Americans have built in the coastal area. During the 1600 and 1700s, the original colonies owed their prosperity largely to the availability of good natural harbors, rich nearby fishing grounds, and active trade with the Caribbean and Europe. As the giant continent was explored and settled in the 1800s, rivers and the Great Lakes became the prime mode of moving goods and people to and from distant towns. In the 20th century, a new social phenomena arose that resulted in an ever-increasing interest in the coastal zone: more and more Americans achieved the economic means and leisure time to enjoy the beach for recreational purposes. Even before beaches became popular vacation destinations, engineers constructed structures to aid navigation, to halt erosion, and to protect shore front development from storm surge. They designed bulkheads, revetments, and seawalls to hold the shoreline in place. Generally, these designs were successful, with Galveston, Texas, and San Francisco, California, being two examples of early seawall construction. Other structures, such as groins and jetties, impeded longshore transport of sand. Groins are intended to

protect a finite beach section, while jetties keep sand out of the navigation channel between the jetties, define and maintains the harbor entrance channel, and provide calm water access to the harbor facilities (Figures I-3-5, I-3-6). For jetties built along uninhabited coastal areas in the 19th and early 20th centuries, the buildup of sand on the up-drift beach and the loss of sand on the downdrift beach was considered a minor consequence compared to the major benefits of ocean navigation trade (Figure I-3-7). In nearly every instance, these harbor structures interrupted the alongshore movement of sand and starved nearby downdrift beaches (USACE 1971), but it was not until the shore was developed in the later 20th century that this interruption of sand transport was regarded as a problem.

d. Early 20th century beach development and the Engineering Advisory Board on Coastal Erosion. As urbanization and congestion increased, the more affluent escaped to the seashore, where resorts arose to accommodate them. Until the age of the automobile, these resorts remained small isolated coastal enclaves tied to the hinterland by rails. The technical revolution brought electric trains, automobiles, gasoline-powered pleasure boats, labor-saving devices for the home, and a new era of leisure to a prospering nation (USACE 1971; Morison and Commager 1962). Electricity provided convenient power to energy-poor barriers. Changing morals allowed people to sunbathe and enjoy the hedonism of the beach experience. And with the growing use of the automobile, beach-goers in increasing numbers followed newly-built roads to the coast. Concern about shore erosion grew as more people acquired property and built homes and businesses, assuming a stable shoreline.

The New Jersey shore, close to the New York and Philadelphia urban areas, was one of the first highly developed shorelines (Figures I-3-8 and I-3-9). During the period 1915 to 1921, three hurricanes and four tropical storms battered the Jersey shore, causing severe beach erosion. In New Jersey, millions of dollars were spent on uncoordinated and sometimes totally inappropriate erosion control structures which often produced results that were only minimally effective, and, in some cases, counterproductive (Hillyer 1996). Engineers and city managers soon realized that individual property owners were incapable of dealing with coastal erosion and that a broader approach was necessary. In 1922, because of rapidly eroding shorelines and revenue losses to the coastal communities, the State funded and appointed an Engineering Advisory Board on Coastal Erosion. Its only recommendation was that further research was needed (Moore and Moore 1983).

In contrast to the haphazard development of the Jersey shore, some of the early large-scale coastal projects proved to be remarkably successful social and engineering accomplishments. America's first large engineered beach fill was the boardwalk and recreational beach on Coney Island in 1922 - 1923 (Farley 1923). With the completion of the project, immigrants and factory workers could escape the sweatshops of the sweltering city and enjoy a (crowded) Sunday at the beach for only a nickel subway ride (Figure I-3-10; Stanton 1999). This was followed by the ambitious construction of the Jones Beach Parkway by Robert Moses and the Long Island State Park Commission in 1926 - 1929, during which more than 30 million m^3 of sand were pumped to create Jones Island (DeWan 1999; Kana 1999) (Figure I-3-11). In Chicago, the entire waterfront was reshaped between 1920 and 1940 with the addition of over 14.2 square km of fill, resulting in one of America's premier urban parks (Chrzastowski 1999). These were city- and state-sponsored projects, with minimal input by the Federal Government.

e. American Shore and Beach Preservation Association. Delegates (85) representing 16 states met at Asbury Park, New Jersey, in 1926, to discuss their growing coastal zone problems. After the first meeting, two more, following shortly thereafter, led to the formation of the American Shore and Beach Preservation Association (ASBPA). The Association brings together a cross section of engineers, public officials, State and Federal personnel, and coastal property owners. Their aim is that "Man must come to the rescue of the beaches." Members see themselves as leaders and teachers in a conservation movement to fight shore and beach erosion (Patton 1934). Their influence in State and Federal governments and continued interest in coastal zone issues is responsible for many of the laws and actions to protect the U. S. shores and beaches.

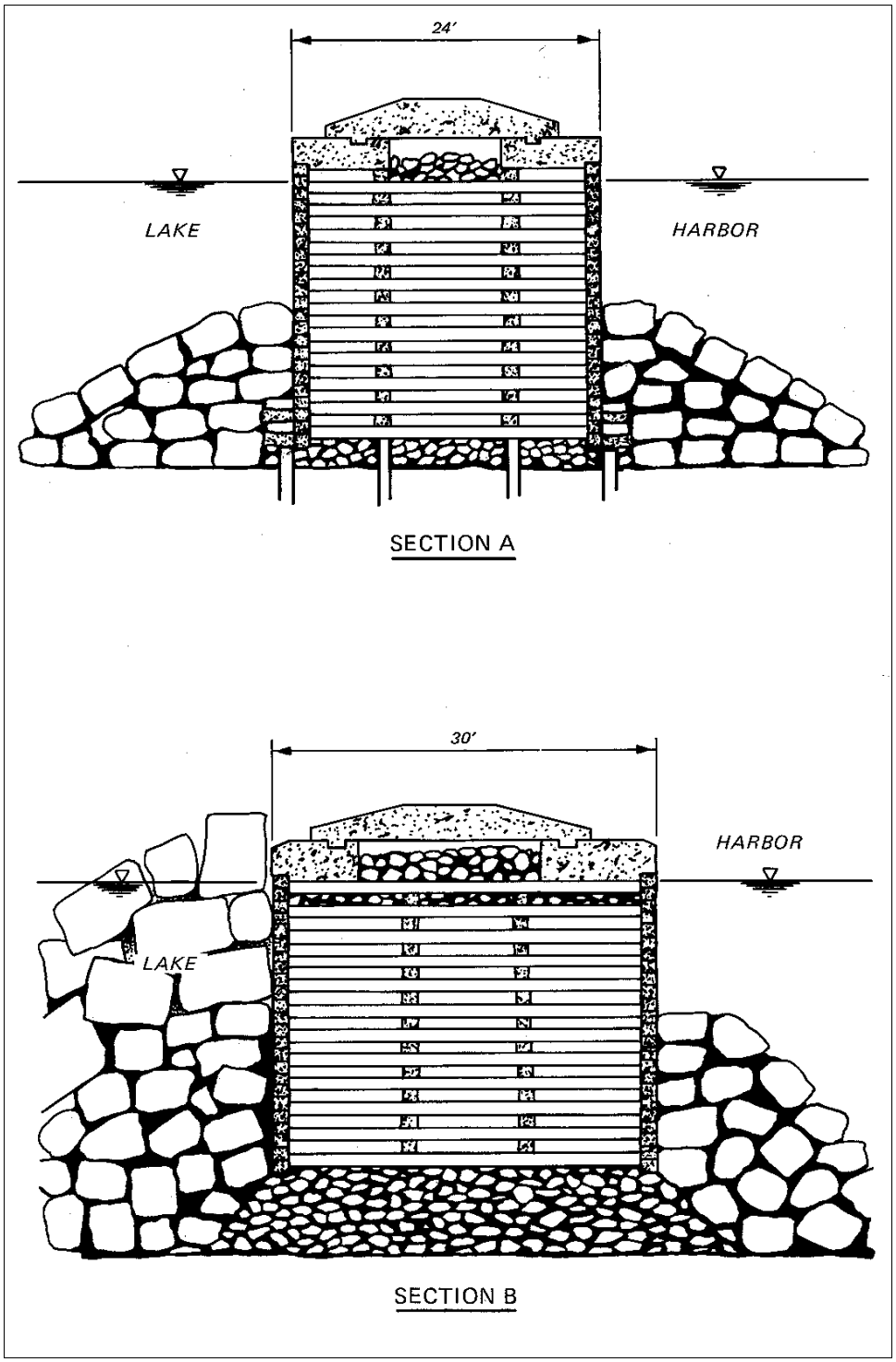

Figure I-3-5. Example of wood crib breakwater typical of the construction technique used in the Great Lakes during the late 1800's, in this case from Calumet Harbor, Illinois. Skilled wood craftsmen built the cribs on land or on a barge, floated them into place, and sank them using rock and gravel fill. Almost 1,000 of these breakwaters were built around the Great Lakes, and many of them, now a century old, need rehabilitation.

Figure I-3-6. Construction of Fire Island jetty on Democrat Point, at the west end of Fire Island, Long Island, New York. Many early USACE jetties were built from the land moving seaward using materials brought in by train. Photograph taken 3 Jan 1940, from Beach Erosion Board Archives.

f. The Board on Sand Movement and Beach Erosion. On January 29, 1929, Major General Edgar Jadwin, Chief of Engineers, USACE, issued a Special Order creating a four-officer board "to investigate and report on the subject of sand movement and beach erosion at such localities as may be designated by the Chief of Engineers." The Chief of Engineers designated Jamaica Bay, New York, and Cold Springs Inlet, New Jersey, as the first two projects for investigation by the "Sand Board" as it became familiarly known. The board employed two consultants, Dr. Douglas W. Johnson of Columbia University and Professor Thorndike Saville of the University of North Carolina. With their advice and assistance, a list of field experiments was prepared. The northern coast of New Jersey, with its area of active erosion and numerous shore protection installations was selected for conducting the experiments. Lieutenant Leland K. Hewitt was assigned to the board in April 1929, to conduct the experiments. Morrough P. O'Brien, recently returned from Freeman Scholarship studies in Europe, was borrowed from the University of California to provide expert assistance in the studies. Hewitt and O'Brien set up their headquarters in Long Branch, New Jersey, and began assembling equipment and personnel to carry out their task. Thus began a USACE research program destined to have far-reaching effects (Wilson and Eaton 1960)

g. The Beach Erosion Board. During this period, the ASBPA, under the leadership of J. Spencer Smith, its persuasive president, was engaged in a campaign to bring combined Federal, State and local effort to bear upon the U. S. beach preservation problems. After two years of Congressional hearings, Section 2 of the River and Harbor Act of 1930, authorized and directed the Chief of Engineers "to cause investigations and studies to be made in cooperation with appropriate agencies of the various states on the Atlantic, Pacific, and Gulf coasts and on the Great Lakes, and Territories, with a view of devising effective means of preventing erosion of the shores of coastal and lake waters by waves and currents . . ." The new law also provided for the creation of the Beach Erosion Board (BEB) by the provision "that there shall be organized under the Chief of Engineers, United States Army, by detail from time to time from the Corps of Engineers and from the engineers of state agencies charged with beach erosion and shore protection, a board of seven members,

Figure I-3-7. Construction of the jetty on the east side of Rockaway Inlet, Long Island, New York, 12 July 1932. The urban area on the opposite side of the inlet is the east end of Coney Island, and Jamaica Bay is in the distance. In seven decades, the fillet has filled with sand to approximately the end of the jetty seen in this image. Photograph from Beach Erosion Board Archives.

of whom four shall be officers of the Corps of Engineers and three shall be selected with regard to their special fitness by the Chief of Engineers from among the state agencies cooperating with the War Department. The board will furnish such technical assistance as may be directed by the Chief of Engineers in the conduct of such studies as may be undertaken and will review the reports of investigation made . . ." Obviously, reconsideration of the mission and need for the original Board on Sand Movement and Beach Erosion was required. Since the new law defined the functions of the BEB as being related to cooperative studies with the states, It was decided to create two boards, one known as the Shore Protection Board (SPB), that would conduct investigations and report upon problems concerning federal property shore protection and the other, the BEB to have similar responsibilities with respect to cooperative studies. Members of the SPB consisted of the military members of the BEB plus the District Engineer for the concerned locality. For the next sixteen years the two boards shared the same staff and headquarters until the SPB was abolished and its duties transferred to the BEB. (Wilson and Eaton 1960)

h. BEB focus on basic research (Willingham 1983). The Corps had, historically, not favored expenditure of Federal funds to protect private property, whether in river basins or coastal flood plains. During the 1930's, however, attitudes began to change, and Congress expanded Federal

Figure I-3-8. Atlantic City, New Jersey, at the mouth of Absecon Inlet, 15 September 1944. This is one of a series of images taken after the hurricane of 14 September, a Category 3 storm that caused 390 deaths in the northeast U.S. This photograph illustrates the degree of urban development along this coast. Photograph taken from a blimp from the U.S. Naval Air Station, Lakehurst, NJ. Official U.S. Navy Photograph (from Beach Erosion Board Archives)

participation in coastal protection. A significant legislative event was the passage in 1936 of an Act wherein it was declared the policy of the United States "... to assist in the construction where Federal interests are involved, but not the maintenance, of works for the improvement and protection of the beaches along the shores of the United States, and to prevent erosion due to the action of waves, tides, and currents, with the purpose of preventing damage to property along the shores of the United States, and promoting and encouraging the healthful recreation of the people..." The Act further authorized the Board "to publish from time to time such useful data and information concerning the protection of beaches as the Board may deem to be of value to the people of the United States..." The act also required that the Board "in making its report on any work or project relating to shore protection shall,

Figure I-3-9. Construction of Manasquan Inlet jetties, New Jersey, October 2, 1930, view looking north. Material for the jetties was supplied via an elevated roadway that extended out to sea from the land. Note that sand is already accumulating on the south (lower) side of the south jetty. The shoreline is continuous, and at this site the inlet was dredged after the jetties were completed. Other man-made openings that are now Federal navigation projects include Panama City Inlet, Florida, Duluth Cut, Minnesota, and Aransas Pass, Texas. (Photograph from Beach Erosion Board archives)

in addition to any other matters upon which it may be required to report, state its opinion as to the advisability of adopting the project; what Federal interest, if any, is involved in the proposed improvement; and what share of the expense, if any, should be borne by the United States." (Cited in Wilson and Eaton 1960).

Although there was substantial support in Congress for federal aid in coastal protection, much difficulty was encountered in determining the proper extent of such aid. The BEB, lacking more specific instructions from Congress, interpreted "federal interest" as pertaining only to the interest of the United States as a landowner of shore property. This resulted in practically no recommendations for federal aid by the BEB during the 1930s. Other Federal agencies were concerned with putting people to work during the depression and interpreted the 1936 Act differently. The Works Progress Administration built revetments, dikes, retaining walls, and jetties on North Carolina's Outer Banks at a cost more than $4 million. The Corps held back on coastal construction projects because of uncertainties about predicting conditions at individual coastal sites revealed by board survey reports. The BEB, driven by professional curiosity, undertook

Figure I-3-10. Coney Island in 1941, on the eve of World War II. For only a 5-cent subway ride, workers from the sweltering city could relax at the beach (from Beach Erosion Board archives)

scientific investigations into coastal processes despite the lack of authorization in either the 1930 or 1936 acts. By the beginning of World War II, the BEB was publishing technical reports and memoranda on its research results (Moore and Moore 1991).

i. Dalecarlia reservation and World War II. Expansion of military activities prior to our entry into World War II required the removal of the Washington Engineering District and the BEB from the Navy Building on Constitution Ave. in Washington, D.C. to a small office building on the Dalecarlia reservation in Washington. The new site was adequate for expansion of facilities, which was to follow, and admirably served the BEB's needs. Upon our entry in the war, need soon arose for intelligence to meet amphibious operations requirements and research to explore means of providing expedient harbor facilities. Logically, the Chief of Engineers called on the BEB staff for assistance on these problems. In addition, the BEB was tasked to train intelligence teams to staff the various military commands. Although these activities were directed toward military requirements, they provided much additional data and knowledge for later use in the Board's peacetime mission. Interest and activity in Congress to clarify the problem of federal aid for shore protection resumed as the war drew to a close. Public Law 166, enacted on July 31, 1945, substituted "public interest" for "Federal interest" as previously used in the 1936 Act, and a year later, Public Law 727 spelled out the conditions and limitations for federal aid for shore protection works. Only publicly owned shores were eligible and the Federal contribution could not exceed one-third of the first cost of protective works with no contribution toward maintenance cost. During the Korean War, most of the Board's staff was again diverted to military efforts. During this lull in preparation of cooperative studies, Technical Report No. 4, *Shore Protection Planning and Design*, was produced. The report was a manual of coastal engineering that summarized the knowledge gained by the BEB and representing its current technical doctrine. Cooperative studies resumed at an accelerated pace with the end of the Korean War. Congress

Figure I-3-11. Jones Island State Park, Long Island, New York, 4 July, 1958. One of the nation's premier urban beaches, Jones Beach is only 45 km from Manhattan, but traffic can be problematic on some days. The legend on the photograph states that there are 11,117 cars in the parking lots. From Beach Erosion Board archives

amended the law to permit Federal aid to privately owned shores when a public benefit resulted and to permit aid toward periodic beach nourishment costs. The 1954 and 1955 River and Harbor Acts authorized sixty-two federal aid projects, a significant increase over the five projects authorized up to that date (Wilson and Eaton 1960).

j. BEB accomplishments. In summary, the BEB made substantial progress toward establishing sound coastal engineering techniques and established a research impetus in coastal processes. It commenced the collection of a permanent record of pertinent data and provided a manual on the best techniques to address specific shore erosion problems. The presence of Murrough P. O'Brien and Thorndike Saville on the Beach Erosion Board for such an extended period provided a continuity of objective and effort unique in public service (Wilson and Eaton 1960). During its 33-year existence, the BEB reviewed 149 cooperative study reports and two Federal surveys of beach erosion problems. The BEB reviewed 114 of the cooperative studies following the 1946 legislation allowing Federal participation in construction cost and recommended 72 as Federal projects. The BEB published 135 technical memoranda and four technical reports, 130 of which were published after the 1946 legislation authorizing the BEB to make general investigations and publish technical reports (Moore and Moore 1991).

Figure I-3-12. Workers planting grass on a beach restoration project. The date and location of this image were not recorded, but the scene is likely the Outer Banks. Many dune and beach restoration efforts, sponsored by the National Park Service and other agencies during the late 1930s, also served as work relief efforts for a nation trying to recover from the Great Depression. Photograph from the Beach Erosion Board Archives

k. Evolution of shore protection and the shift from structures to beach nourishment. Prior to the 1950s, the general practice was to use hard structures to protect against beach erosion or storm damages. These structures were usually coastal armoring such as seawalls and revetments or sand-trapping structures such as groins. During the 1920s and '30s, private or local community interests protected many areas of the shore using these techniques in a rather ad hoc manner. In certain resort areas, structures had proliferated to such an extent that the protection actually impeded the recreational use of the beaches. Erosion of the sand continued, but the fixed back-beach line remained, resulting in a loss of beach area. The obtrusiveness and cost of these structures led the USACE in the late 1940s and early 1950s, to move toward a new, more dynamic, method. USACE projects no longer relied solely on hard coastal defense structures as techniques were developed which replicated the protective characteristics of natural beach and dune systems. The resultant use of artificial beaches and stabilized dunes as an engineering approach was an economically viable and more environmentally friendly means for dissipating wave energy and protecting coastal developments. Artificial beaches also had more aesthetic and recreational value then structured shores. The transition from hard structures to beach fill approaches is depicted in Figure I-3-13, which compares the percentage of Federal shore protection funds spent on beach nourishment and on coastal protection structures per decade. Since the 1970s, 90 percent of the Federal appropriation for shore protection has been for beach nourishment (Hillyer 1996).

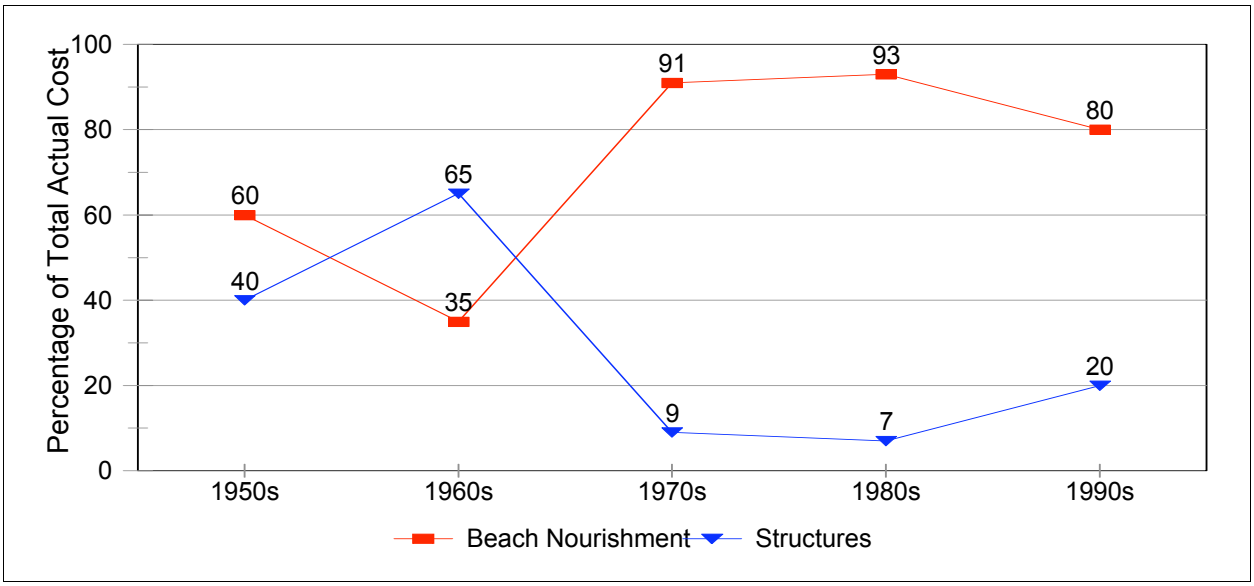

Figure I-3-13. The shift from fixed structures to beach restoration and nourishment (from Hillyer 1996)

l. The Coastal Engineering Research Center and the Coastal Engineering Research Board. In 1962, the USACE studied the merits of strengthening its coastal engineering research capabilities and the benefits from having the evaluation and reporting of coastal projects follow the same procedures as river, harbor, and flood control investigations. Responding to the recommendations of the Corps' internal study board, Congress, by approving Public Law 172 on November 7,1963, abolished the BEB and established the Coastal Engineering Research Center (CERC). CERC had the same mission as the BEB less its review function, but retained an advisory system in a "Board on Coastal Engineering Research, constituted by the Chief of Engineers in the same manner as the present Beach Erosion Board" (Moore and Moore 1991).

(1) Early years. The Coastal Engineering Research Board (CERB) and CERC followed the lead of their predecessor, the BEB, in pursuing field measurements and basic coastal processes research. The argument was that more research would produce more data, provide for more sound coastal engineering approaches, and lead to greater savings. Spurred by both increasing development and environmental awareness, CERC planned programs to quantify phenomena that previously had been only understood qualitatively. The Marine Science Council, created by the Marine Resources and Engineering Development Act of 1966, appointed the USACE as coordinating agency in a multidisciplinary, interagency effort to identify the effects of construction on the coastal zone. That same year, USACE Headquarters (HQUSACE) asked CERC to draft a program covering the Corps' long range needs in coastal engineering. This triggered a reevaluation and a program increase between 1964 and 1969 (Moore and Moore 1991).

(2) Fort Belvoir. As CERC assumed new missions, its most critical needs were office space and a shelter for the Shore Processes Test Basin (SPTB). Weather conditions limited the open-air SPTB use to the period April through October. A HQUSACE command inspection of CERC in December, 1967, concluded that there was not enough space at the Dalecarlia site for the future CERC. A plan was developed to build a research and development complex in the northwest corner of Fort Belvoir on 182 hectares (450 acres). Several USACE and Department of Army agencies would be located at the complex. CERC, the Board of Engineers for Rivers and Harbors, and the Institute for Water Resources would be located in the Kingman Building. CERC was allocated 40.5 hectares (100 acres) for the replacement of existing test facilities and future expansion.

(3) Field Research Facility. Prior to its move to Fort Belvoir, CERC had planned and budgeted to construct a Field Research Facility (FRF) to evaluate and examine coastal phenomena on prototype (full-size) scale. CERC learned that the U.S. Navy was preparing to surplus a bombing range at Duck, North Carolina, and acquired the property in 1973. On 29 August 1980, the 50th Anniversary of the creation of the Beach Erosion Board, the FRF was officially opened. The 73.7-hectare (182-acre) FRF stretches from ocean to sound, contains a 589-m (1800-foot) pier and laboratory facilities and is used for physical and biological studies (Mason 1979). Meteorological, topographical and oceanographic data are continuously recorded, and the staff conduct research projects at the site and frequently host large field experiments involving other Federal, state and local agencies, plus U.S. and foreign universities. The FRF's advantages of ocean location, research pier, sophisticated infrastructure, synoptic and continuing hydrodynamic and process database, and experienced staff are unique in the United States. Data are accessible on the Internet at the FRF's Web page: http://www.frf.usace.army.mil/frf.html

(4) Shore Protection Manual. When first established, CERC was the only Federal agency with a mission in coastal engineering and almost alone in funding studies of waves and their effects. The research programs at CERC, with their field and laboratory testing and data collection, had an immense practical value. CERC's first combined volume containing guidance on coastal science and engineering was *Shore Protection, Planning, and Design*, Technical Report No. 4 (TR-4), first issued in 1954. The USACE District and Division staffs had a need to apply the data and research results reported by CERC into useful design tools, and they often relied on TR-4 and some related Engineering Manuals published by HQUSACE for design guidance. The *Shore Protection Manual* (SPM) was first published by CERC in 1973 as the updated replacement for TR-4. CERC used the SPM as its primary technology transfer mechanism for many years, with a second edition printed in 1975, a third in 1977, and a fourth and final edition in 1984.

(5) Waterways Experiment Station. A number of events and policy changes in the early 1980's shifted CERC's emphasis into more applied research and moved the laboratory to the Waterways Experiment Station (WES) in Vicksburg, Mississippi. Despite disruptions caused by the 1983 relocation and declining research budgets, CERC prospered in Vicksburg. Reimbursable project work more than compensated for the decline. Mathematical modeling, sophisticated wave tanks and basins (part of the reason for the move), and a closer, more responsive relation with the USACE District and Division staffs all contributed to increased workload.

(6) The Coastal and Hydraulics Laboratory. In the early 1990s, due to political and policy changes, Federal funding for the beach erosion control and flood control projects was severely curtailed and closely regulated. This resulted in reduced research funding and a decrease in the number of new beach erosion control and flood control studies at CERC and the Hydraulics Laboratory. During 1996, both laboratories were combined into one new entity, the Coastal and Hydraulics Laboratory (CHL). CERC's traditional functions such as coastal engineering research, design guidance development such as this manual, and design assistance are still provided by the CHL with the advice of the CERB and a field review group of Division and District staff engineers.

I-3-8 Coastal Engineering in the Military

a. Amphibious operations. Amphibious military operations are not new. Herodotus (1992, translation) describes, in *The Histories*, how Xerxes constructed and used a floating causeway across the Hellespont (the Dardanelles) in 480 B.C. The first amphibious operation in the Americas was the 49-day siege of the French Fortress of Louisburg on Cape Breton Island, Nova Scotia, Canada, in 1745. The Chief Engineer of the operation was Richard Gridley who published that same year the first map in America, a "Plan of the City and Fortifications of Louisburg," and who later became the first Chief Engineer under Commander-in-Chief George Washington in 1775. Many amphibious operations were conducted in North Africa, Italy, France, and the Pacific during World War (W.W.) II. These exercises taught us that for a successful over-the-beach

assault, details and forecasts of changes must be acquired of coastal type, beach configuration, morphodynamics, profiles, wave conditions, tides, beach material, beach trafficability, and nearshore and offshore bottom-holding capacity for moorings and anchored ships. At the start of the war, many charts were available showing areas safe for deep-draft navigation and details of land topography, but hardly any of the nearshore areas where assault troops and supplies could be landed. Much of this type of information was collected and evaluated during the war. Of prime importance to military amphibious operations are the wave conditions that can be anticipated. Correlations among wind strength, duration, fetch, and wave height and period were developed in the United States and in the United Kingdom (U.K.) for wave forecast for planning and for operations. The state-of-the-art in military coastal engineering at the end of W.W. II was documented in the *Manual on Amphibious Oceanography*, (University of California at Berkley (UCB), Institute of Engineering Research (IER) 1952) (Wiegel 1999).

b. Expedient harbors. Expedient harbor design for the invasion of Normandy also required substantial coastal engineering effort. The design of the two Mulberry harbors ("A" at St. Laurent (Omaha Beach) and "B" at Arromanches) required information on wave and tide prediction (design tide range was 7.3 meters (24 feet)), wave diffraction, wave induced forces, bottom conditions, and placement of structures and their foundations. Wave-diffraction theory (wave transmission about the tip or through a gap between breakwaters) was developed for this project. The Mulberry Harbor was designed in two parts. The portion closest to shore, in shallow water, had a breakwater of vertical reinforced-concrete caissons (code name "Phoenix") and sunken ships protecting it, while the seaward portion was protected by moored floating breakwaters ("Bombardon"). The Bombardon had a cross section similar to a Maltese cross in shape; each unit was 61 meters (200 feet) in length, 7.6 meters (25 feet) in beam and depth with 5.8 meters (19 feet) draft. They were deployed in pairs with a 15.2 meters gap between pairs. Located inside the shallow water sheltered area were pier heads and mile-long pontoon-supported flexible bridges (causeways code named "whales"). After initial construction, a storm along the Normandy coast with gale winds blowing from the northeast generated sea conditions larger than project design waves. Operations were disrupted and delayed, with great damage to the artificial harbors, craft and ships. Mulberry "A" suffered damage beyond repair. Shown in Figure I-3-14 Is Mulberry "B" after being repaired. *The Civil Engineer in War, A Symposium of Papers on Wartime Engineering Problems, Volume 2, Docks and Harbors* (Institute of Civil Engineers 1948) provides details on the design, installation, and performance of the Mulberry Harbors (Wiegel 1999).

c. Military coastal engineering studies. After W.W. II, UCB contracted with the Office of Naval Research (ONR) to review amphibious operations reports from the war. As expected, many landing-craft and amphibious-vehicle casualties were due to enemy action, but many were related to problems with waves and currents causing capsizing, swamping, broaching, getting stuck on bars and, when the ramps were down, filling with water and sand. Another major problem was beach trafficability. Vehicles were frequently stuck in the sand. A trafficability study of beach sand characteristics, beach slope, water level, and vehicle type was made. It was observed that saturated sand near the water's edge would liquefy due to vibrations produced by the vehicular traffic. Several full-scale amphibious assault-training exercises were observed in detail and reports prepared on the observations and findings.

During the 25 October, 1949, exercise across three west coast beaches at the Waianae-Pokai Bay region of Oahu, Hawaii, long-period waves surging up the steep beach face caused substantial landing craft casualties on two of the beaches. Many of the craft broached and were shoved onto the steep beach by the surging breakers (see Figure I-3-15). Of the 20 landing craft sent ashore in 3 "waves" in the first 15 minutes of the amphibious exercise, 7 retracted and 8 were lost, some filling with water and sand when the ramps were lowered. The exercise was quickly halted and five of the craft later salvaged. Because of the problems experienced moving personnel, equipment and supplies through the surf and over the beach, the Department of Defense began the development of helicopters and air cushion vehicles (Wiegel 1999).

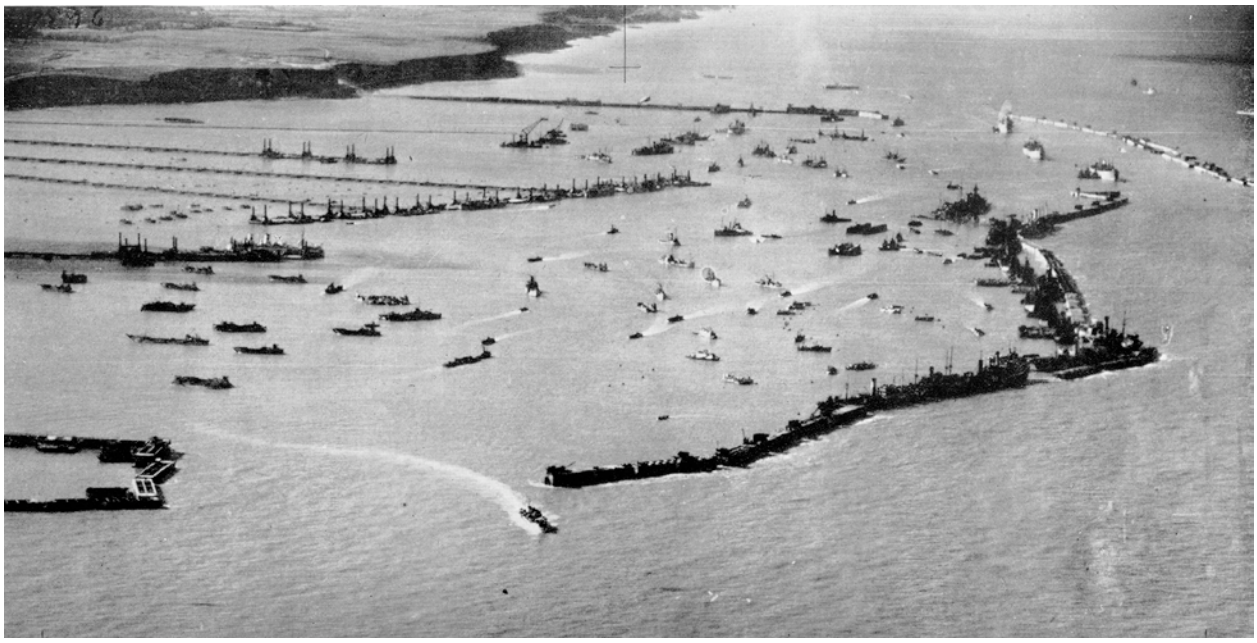

Figure I-3-14. Aerial photograph of the Mulberry "B" Harbor at Arromanches, France, June 1944 (from Institution of Civil Engineers, London, England, 1948, p. 242)

d. Port operations, Republic of Korea. One of the major amphibious operations in the Republic of Korea (ROK) was the invasion at Inchon Harbor. The east coast of the ROK is generally rocky sea cliffs, while the south and west coasts are extensive mud flats with many small conical islands. During low tide at Inchon, the tidal flats extend at least 50 km offshore and the only approach to the port is a narrow channel 1 to 2 meters deep at zero tide. Extreme tides, ranging from -0.6 meters to +9.8 meters, provided many engineers their first experience with a sea of water quickly changing into a sea of mud. After the 15 September 1950 amphibious assault, General MacArthur said ". . . conception of the Inchon landing would have been impossible without the assurance of success afforded by the use of the Seabee pontoon causeways and piers." The tidal basin and other facilities were relatively intact at the time of the invasion. However, during the U.S. evacuation in January 1951, the lock gates to the tidal basin were demolished, then rebuilt after return of the U.S. forces in February 1951 (Wiegel 1999).

e. Port operations, Republic of Vietnam. In Vietnam, the U.S. Navy Officer in Charge of Construction was responsible for Saigon-Newport and DaNang deep-water ports. Data were collected on coastal sediments, storms, tides, and waves to plan the dredging of these ports and seven other sites. The Army port construction section used these data and the Beach Erosion Board's Technical Report No. 4, *Shore Protection Planning and Design*, to prepare detailed design of port facilities. The DeLong Corporation's installation of piers, prefabricated causeway components, and use of self elevating barges also contributed to successful port facility operations. The sand on many of the Vietnamese beaches was of such character that over-the-shore operations were almost impossible. Rock, concrete, articulators, pierced-steel planking and other means attempted to stabilize the sand were serviceable for very limited periods ranging from days to two weeks. Waves on the foreshore undermined the stabilizing structures and decreased the bearing capacity, resulting in the structures sinking out of sight. Engineers, drawing on their W.W. II and subsequent experience, used draglines and blasting to dig nearby coral, crush it, and then place it in compacted layers where the foreshore had been previously excavated for the purpose. This installation lasted several months with only minor repair and was judged very satisfactory (Wiegel 1999).

Figure I-3-15. Operation MIKI, Waianae, Oahu, HI, October 1949, (Many landing craft broached and were shoved onto the beach by surging breakers) (from Wiegel and Kimberly 1949)

(1) Vung Ro. For the construction of the port of Vung Ro to support the major air base at Tuy Hoa, estimates of typhoon and monsoon waves were made and wave refraction studies used to plan the port. Port development included landing-craft ramps, a floating pontoon cube barge dock, two DeLong barge piers (183 x 24.4-meters) (600 x 80-feet) with two girder spans off a 120-meter (394-foot) rock fill causeway, tanker mooring facilities and a pipeline connecting to the tank farm south of Tuy Hoa airstrip about 15.5 km (9.6 miles) distance. Seven months after the port was completed the facilities were struck by a typhoon, but survived wave conditions exceeding the design wave criteria (Wiegel 1999).

(2) Da Rang River. The U.S. Air Force wanted a harbor closer to the air base that would be located at the mouth of the Da Rang River. The river brings a great amount of sand to the coast in this area. The USACE had recommended, based on studies by CERC and WES, a site several miles south where the 3-fathom line was much closer to shore. The Navy had funded hydraulic model studies of the entrance and jetties at the southern site. However, the Air Force pressed on at the river mouth site with a "turnkey project" contractor. After several months of pilot channel dredging, the contractor conceded that construction of a harbor at the Da Rang River mouth was impractical and the project was abandoned (Wiegel 1999).

f. Temporary wharfs. The Army has two sizes of self-elevating pier systems, known as DeLong barges. These units are honeycomb-like, welded-steel, box-girder structures consisting of plates and stiffeners that are towed to a site where a temporary harbor is being built or an existing port rehabilitated. The units are anchored on pneumatic caissons that are forced into the sea bed with air jacks. The units can

be used on noncohesive beds but are unsuitable for rock, organic materials, or wet clays and silts. The units can be installed in a variety of configurations at the site (Figure I-3-16) (Department of the Army 1990).

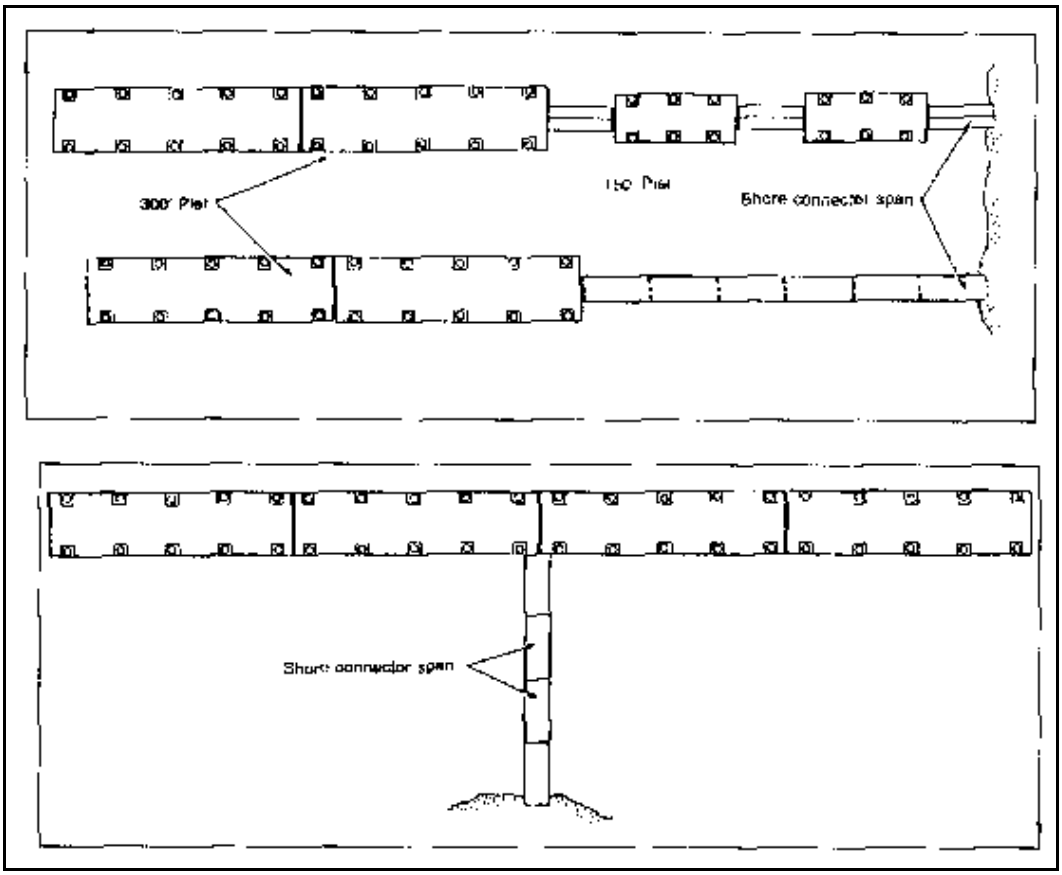

Figure I-3-16. DeLong self-elevating barge piers. Upper figure shows finger piers, lower a T-type marginal wharf (from Department of the Army 1990)

g. Rapidly Installed Breakwater System. Engineers and scientists at CHL are developing a Rapidly Installed Breakwater (RIB) system to address problems encountered by the U.S. armed forces while offloading ships during Logistics Over The Shore operations. When seas become sufficiently energetic during offloading, the capabilities of ship-based crane operators and stevedore crews are severely restricted. The RIB system, consisting of a series of floating breakwater units that are assembled in a "V" orientation, is designed to create a "pool" of calmer water where the crews will be able to continue to unload vessels even during storms. For many years, CHL had been involved with the design and deployment of floating breakwaters, primarily for application within bays or estuaries which are semi-protected from large waves. But, these structures were intended to attenuate waves with heights not exceeding 4 ft and periods not exceeding 4 sec, while in an oceanic environment, waves with heights up to 10 ft are common during storms, with associated periods up to 10 sec. To date, research efforts have concentrated on military applications for the RIB system. Potential civil applications include rescue and recovery operations, temporary small vessel shelter from energetic seas, and to protect exposed dredging and marine operations (e.g., bridge repair, rubble-mound breakwater construction),.

I-3-9. Summary

For most of the nation's history, the U.S. Army Corps of Engineers has played an active role in the coastal zone. To the mid-1800s, this role was largely confined to coastal defense and some harbor protection. But, in the mid-1800s, the USACE's mission expanded to include developing civil works projects in support of a growing nation. These responsibltiies included harbor construction, dredging and clearing waterways, building canals and channels, and protecting coastal areas threatened by erosion (*e.g.*, Presque Isle). During the second half of the 20th century, the USACE's role further expanded to include environmental restoration and preservation of threatened coastal areas. Since the 1930s, coastal-related research and development have been conducted to advance the technical foundations and basis for conducting coastal civil works.

The 20th century was witness to a large-scale evolution in the development of, use of, and interest in the coastal zone. National defense, agriculture, navigation, economic development, recreation, and environmental worth all contribute to the definition of coastal policy and action. During the early years of the 21st century there will be continuing development pressure in the coastal zone . Coastal engineers and scientists will undoubtedly be asked to play an increasing role in planning, designing, and maintaining infrastructure projects, in coastal management and environmental mitigation, and will continue their more traditional missions of navigation and flood protection.

In fiscal year 1998, the USACE and contractor-owned dredges removed 182 million cubic meters of material from Federally-constructed and maintained channels at a cost of $713 million. Dredged material is a valuable resource with numerous potential benefits, including construction of protective dunes and beaches, maintenance of beaches through bypassing to reestablish natural sediment-transport paths, and restoration and creation of wetlands and coastal habitat. Demand for dredged material usage is increasing, but environmental concerns and constraints present new engineering challenges that must be addressed.

Erosion and flooding threaten an estimated $3 trillion of development along the coast, with 80 to 90 percent of the nation's sandy beaches eroding (Hillyer 1996). Shore protection and restoration throughout the developed areas of the coast will increase, especially if the growing value of coastal property and recreation benefits are factored into the cost benefit calculations.

Because of the age of many harbor structures, improving and rebuilding jetties and breakwaters will be a major mission area. Wetlands restoration should also be growth areas, and already the USACE is involved in major restoration projects in the Everglades, in south Louisiana, and along many stretches of the intracoastal waterway.

Emergency coastal response work is also likely to be a growth area for the USACE. Many of the recent arrivals to the coastal zone have not personally experienced a major disaster like the Galveston hurricane of 1900, the 1962 Ash Wednesday storm, or the Great New England Hurricane of 1938. Much of the population is ignorant of the hazards that exist and is not prepared to respond to the aftermath of a catastrophic storm. The USACE has actively participated in disaster emergency and recovery efforts in Puerto Rico and other Caribbean islands, and many of these skills are applicable to mainland disasters.

I-3-10. References

Alperin 1977
Alperin, L. M. 1977. *Custodians of the Coast: History of the United States Army Engineers at Galveston*. Galveston District, U.S. Army Corps of Engineers, Galveston, TX, 318 p.

Barber 1989
Barber, H. E. 1989. *A History of the Savannah District, U.S. Army Corps of Engineers.* Savannah District, U.S. Army Corps of Engineers, Savannah, GA, 554 p.

Becker 1984
Becker, W. H. 1984. *From the Atlantic to the Great Lakes, a history of the U.S. Army Corps of Engineers and the St. Lawrence Seaway.* Office of the Chief of Engineers, Washington, DC. 179 p.

Bijker 1996
Bijker, E. W. 1996. History and Heritage in Coastal Engineering in the Netherlands. *History and Heritage of Coastal Engineering,* N. C. Kraus, ed., Coastal Engineering Research Council, American Society of Civil Engineers, Reston, VA, pp. 390 - 412.

Birkemeier, Dolan, Fisher 1984
Birkemeier, W. A., Dolan, R., and Fisher, N. 1984. The Evolution of a Barrier Island: 1930-1980. *Shore and Beach*, Vol. 52, No. 2, pp 2-12.

Buker 1981
Buker G. E. 1981. *Sun, Sand and Water: a History of the Jacksonville District U.S. Army Corps of Engineers, 1821-1975.* U.S. Government Printing Office, Washington, DC., 288 p.

Chambers 1980
Chambers, J. W., II. 1980. *The North Atlantic Engineers : a History of the North Atlantic Division and its Predecessors in the U.S. Army Corps of Engineers, 1775-1975.* North Atlantic Division, U.S. Army Corps of Engineers, New York, NY, 167 p.

Chrzastowski 1999
Chrzastowski, M. J. 1999. Geology of the Chicago Lakeshore, Shaping the Chicago Shoreline, poster produced by the Department of Natural Resources, Illinois State Geological Survey, Champaign, IL.

Cowdrey 1977
Cowdrey, A. E. 1977. *Land's End: a History of the New Orleans District, U. S. Army Corps of Engineers, and its Lifelong Battle with the Lower Mississippi and Other Rivers Wending Their Way to the Sea.* New Orleans District, U.S. Army Corps of Engineers, New Orleans, LA, 118 p.

Davis 1975
Davis, V. S. 1975. *A History of the Mobile District 1815 to 1971.* Mobile District, U.S. Army Corps of Engineers, Mobile, AL, 109 p.

Department of the Army 1990
Department of the Army. 1990. Port Construction and Repair. Field Manual FM 5-480, Headquarters, Department of the Army, Washington, DC.

DeWan 1999
DeWan, G. 1999. "The Master Builder, How planner Robert Moses transformed Long Island for the 20th Century and Beyond." *Long Island, Our Story.* **http://www.lihistory.com/** (18 May 2000).

Dobney 1978
Dobney, F. J. 1978. *River Engineers on the Middle Mississippi: a History of the St. Louis District, U.S. Army Corps of Engineers.* U.S. Government Printing Office, Washington, DC., 177 p.

Drescher 1982
Drescher, N. M. 1982. *Engineers for the Public Good, A History of the Buffalo District, U.S. Army Corps of Engineers,* U. S. Army Corps of Engineers, Buffalo, NY, pp 155-173, 203-235.

Empereur 1997
Empereur, J. Y. 1997. "The Riches of Alexandria." Transcript of a 1997 Interview on NOVA Online, **http://www.pbs.org/wgbh/nova/sunken/empereur.html** (28 Aug 2000).

Farley 1923
Farley, P. P. 1923. Coney Island public beach and boardwalk improvement. *The Municipal Engineers Journal*, Vol. 9, Paper 136, pp 136.1-136.32.

Fasso 1987
Fasso, C. A. 1987. "Birth of hydraulics during the Renaissance period," Hydraulics and Hydraulic Research; a Historical Review, IAHR, G. Garbrecht Editor, Balkema, pp 55-79

Franco 1996
Franco, Leopold. 1996. "History of Coastal Engineering in Italy," *History and Heritage of Coastal Engineering,* American Society of Civil Engineers, New York, NY. pp 275-335.

Frost 1963
Frost, H. 1963. *Under the Mediterranean, Marine Antiquities.* Prentice-Hall, Englewood Cliffs, N.J. p 278.

Goreki and Pope 1993
Goreki, R. J., and Pope, J. 1993. Coastal Geologic and Engineering History of Presque Isle Peninsula, Pennyslvania. Miscellaneous Paper CERC-93-8, U.S. Army Engineer Waterways Experiment Station, Vicksburg, MS.

Hagwood 1982
Hagwood, J. J., Jr. 1982. *Engineers at the Golden Gate: a History of the San Francisco District, U.S. Army Corps of Engineers, 1866-1980.* San Francisco District, U.S. Army Corps of Engineers, San Francisco, CA, 453 p.

Hartzer 1984
Hartzer, R. B. 1984. *To Great and Useful Purpose: a History of the Wilmington District U.S. Army Corps of Engineers,* Wilmington District, U.S. Army Corps of Engineers, Wilmington, NC, 172 p.

Herodotus 1992
Herodotus. 1992. *The Histories,* Written in the middle of the 5th century B.C., translation by George Rawlinson and introduction by Hugh Bowden, J. M. Dent & Sons Ltd.,London.

Hillyer 1996
Hillyer, T. M. 1996. *Shoreline Protection and Beach Erosion Control Study, Final Report: An Analysis of the U.S. Army Corps of Engineers Shore Protection Program.* IWR Report 96-PS-1, Shoreline Protection and Beach Erosion Control Task Force, Water Resources Support Center, Institute for Water Resources, U.S. Army Corps of Engineers, Alexandria, VA (prepared for the Office of Management and Budget, Washington, DC.)

Inman 1974
Inman, D. L. 1974. Ancient and Modern Harbors: a Repeating Phylogeny. *Proceedings of the 14th Coastal Engineering Conference,* Copenhagen, Denmark, June 1974, American Society of Civil Engineers, Reston, VA, pp. 2049-2067.

Inman 2001
Inman, D. L. 2001. History of Early Breakwaters. *Association of Coastal Engineers Newsletter*, Alexandria, VA.

Institute of Civil Engineers 1948
Institution of Civil Engineers. 1948. *The Civil Engineer in War. A Symposium of Papers on War-time Engineering Problems. Vol. 2, Docks and Harbors.* Papers and discussions, published by The Institution of Civil Engineers, London, United Kingdom.

Jacobs 1976
Jacobs W. A. 1976. *The Alaska District, United States Army, Corps of Engineers, 1946-1974: a History.* From a manuscript researched and compiled by Lyman L. Woodman, Alaska District, U.S. Army Corps of Engineers, Elmendorf AFB, Alaska, 145 p.

Johnson 1979
Johnson, L. R. 1979. *The Headwaters District: a History of the Pittsburgh District, U.S. Army Corps of Engineers.* Pittsburgh District, U.S. Army Corps of Engineers, Pittsburgh, PA, 380 p.

Johnson 1992
Johnson, L. R. 1992. *The Ohio River Division, U.S. Army Corps of Engineers, the History of a Central Command*. Ohio River Division, U.S. Army Corps of Engineers, Cincinnati, OH, 484 p.

Kana 1999
Kana. T. 1999. Long Island's South Shore Beaches, A Century of Dynamic Sediment Management. *Coastal Sediments '99,* Kraus, N. C., and McDougal, W. G. (eds.), American Society of Civil Engineers, Reston, VA, pp.1584-1596.

Karanek 1978
Kanarek, H. K. 1978. *The mid-Atlantic engineers: a History of the Baltimore District, U.S. Army Corps of Engineers, 1774-1974.* U.S. Government Printing Office, Washington, DC., 196 p.

Keay 1942
Keay, T. B. 1942. Coast Erosion in Great Britain, General Question of Erosion and Prevention of Damage; and the Drainage of Low-Lying Lands. *Shore and Beach,* Vol. 10, No. 2, pp. 66 - 68.

Klawonn 1977
Klawonn, Marion J. 1977. *Cradle of the Corps, A History of the New York District, U.S. Army Corps of Engineers, 1975-1975,* New York District, U.S. Army Corps of Engineers, New York, NY, 310 p.

Lamb 1930
Lamb, H. 1930. *The Crusades, Iron Men and Saints,* Doubleday, Doran & Co., Garden City, NY.

Larson 1979
Larson, J. W. 1979. *Those Army Engineers: a History of the Chicago District, U.S. Army Corps of Engineers,* Chicago District, U.S. Army Corps of Engineers, Chicago, IL, 307 p.

Larson 1981
Larson, J. W. 1981. *Essayons: a History of the Detroit District, U.S. Army Corps of Engineers.* Detroit District, U.S. Army Corps of Engineers, Detroit, MI, 215 p.

Lenček and Bosker 1998
Lenček, L., and Bosker, G. 1998. *The Beach: The History of Paradise on Earth.* Viking, New York, 310 p.

Maass 1951
Maass, A. 1951. *Muddy Waters, the Army Engineers and the Nation's Rivers.* Harvard University Press, Cambridge, MA, 306 p.

Mason 1979
Mason, Curtis. 1979. "The Coastal Engineering Research Center's Field Research Facility at Duck, North Carolina," *Shore & Beach, Journal of the American Shore and Beach Preservation Association,* Vol. 47, No. 2, pp 13-16.

Merritt 1979
Merritt, R. H. 1979. *Creativity, Conflict & Controversy : a History of the St. Paul District, U.S. Army Corps of Engineers.* U.S. Government Printing Office, Washington, DC., 461 p.

Moore 1981
Moore, 1981. *The Lowcountry Engineers: Military Missions and Economic Development in the Charleston District,* U.S. Army Corps of Engineers. U.S. Government Printing Office, Washington, DC., 140 p.

Moore and Moore 1982
Moore, Jamie W., and Moore, Dorthy P. 1982. *The Lowcountry Engineers, Military Missions and Economic Development in the Charleston District,* U.S. Army Corps of Engineers (Atlanta, GA: Government Printing Office), pp16-21

Moore and Moore 1983
Moore, Jamie W., and Moore, Dorthy P. 1983. The Corps of Engineers and Coastal Engineering, A 50 Year Retrospective,? Orville T. Magoon, ed., *Coastal Zone 83 III,* New York: ASCE, 1983, pp 1627-1639

Moore and Moore 1991
Moore, Jamie W. and Moore, Dorthy P. 1991. *History of the Coastal Engineering Research Center, 1963-1983,* U. S. Army Engineer Waterways Experiment Station, Vicksburg, MS

Morison and Commager 1962
Morison, S. E., and Commager, H. S. 1962. *The Growth of the American Republic.* Fifth Ed., Oxford University Press, New York.

Palmer and Tritton., eds. 1996
Palmer, R., and Tritton Limited (eds.). 1996. History of Coastal Engineering in Great Britain. *History and Heritage of Coastal Engineering,* N. C. Kraus, ed., Coastal Engineering Research Council, American Society of Civil Engineers, Reston, VA, pp. 214 - 274.

Parkman 1978
Parkman, Aubrey. 1978. *Army Engineers in New England, The Military and Civil Works of the Corps of Engineers, 1775-1975,* Waltham, MA, U.S. Army Engineer Division, 1978, pp34-38.

Parker 1980
Parker 1980. "Structures in the Beach Zone-To Be or Not to Be," paper presented at the American Soc. Of Civil Engineers Convention and Exposition, Florida, 27-1 Oct, 1980, ASCE Reprint No.80-648.

Patton 1934
Patton, R. S. 1934. "The Purpose of the American Shore and Beach Preservation Association," *Shore and Beach II,* Journal of the American Shore and Beach Preservation Association Oct. 1934, pp132-136.

Quinn 1972
Quinn, Alonzo DeF. 1972. *Design and Construction of Ports and Marine Structures,* Second Edition, Mc Graw-Hill Book Company, New York, N.Y., 611p.

Rathburn 1990
Rathbun, M. Y. 1990. *Castle on the Rock, 1881-1985: the History of the Little Rock District, U.S. Army Corps of Engineers.* Little Rock District, U.S. Army Corps of Engineers, Little Rock, AK, 192 p.

Reuss 1998
Reuss, M. 1998. *Designing the Bayous: the Control of Water in the Atchafalaya Basin: 1800-1995.* Office of History, U.S. Army Corps of Engineers, Alexandria, VA, 474 p.

Richter 1970
Richter, J. P. 1970. *The Notebooks of Leonardo da Vinci,* Dover Publishing, New York, NY.

Rouse and Ince 1963
Rouse, H. and Ince, S. 1963. *History of Hydraulics,* Dover, NY.

Seattle District 1969
Seattle District. 1969. *History of the Seattle District, 1896-1968 : United States Army, Corps of Engineers : 72 Years in Peace and War.* Seattle District, U.S. Army Corps of Engineers, Seattle, WA, 222 p.

Shore Protection Manual 1984
Shore Protection Manual. 1984. 4th ed., 2 Vol., U.S. Army Engineer Waterways Experiment Station, U.S. Government Printing Office, Washington, DC.

Shore Protection, Planning, and Design 1954
Shore Protection, Planning, and Design. 1954. Technical Report No. 4, U.S. Beach Erosion Board, Washington, DC, 393 p.

Snyder and Guss 1974
Snyder, F. E. and Guss, B. H. 1974. The District; a History of the Philadelphia District, U.S. Army Corps of Engineers, 1866-1971, U.S. Army Engineer District, Philadelphia, PA,
263 p.

Stanton 1999
Stanton, J. 1999. "Coney Island - Nickel Empire (1920's-1930's)." *Coney Island History Site.* North American Integration & Development Center, School of Public Policy and Social Research, University of California, Los Angeles, CA, **http://naid.sppsr.ucla.edu/coneyisland/** (16 May 2000).

Straub 1964
Straub, Hans. 1964. *A History of Civil Engineering,* English Translation by Erwin Rockwell, The M.I.T. Press, Massachusetts Institute of Technology, Cambridge, Massachusetts, 258 p.

Sudar, Pope, Hillyer, and Crumm 1995
Sudar, R. A., Pope, J., Hillyer, T., and Crumm, J. 1995. "Shore Protection Projects of the U.S. Army Corps of Engineers." *Shore and Beach*. Journal of the American Shore and Beach Preservation Association, Vol. 63, No. 2, pp. 3-16.

Thompson 1981
Thompson, E. N. 1981. *Pacific Ocean Engineers-History of the U.S. Army Corps of Engineers in the Pacific, 1905-1980.* U.S. Army Engineer Division, Pacific Ocean, Honolulu pp 460.

Turhollow 1975
Turhollow, Anthony F. 1975. *A History of the Los Angeles District, U. S. Army Corps of Engineers, 1898-1965,* Los Angeles, CA, U. S. Army Engineer District, pp 20-48.

UCB, IER 1952
University of California, Berkeley, Institute of Engineering Research. 1952. *Manual on Amphibious Oceanography,* R. L. Wiegel, Project Engineer and Editor, under contract with Office of Naval Research, Amphibious Branch, Contract N7-29535, Project No. NR 252-003, Pentagon Press, July 1952, 2 volumes.

USACE 1971
U.S. Army Corps of Engineers. 1971. National Shoreline Study: Shore Protection Guidelines. Department of the Army, Corps of Engineers, Washington, DC.

USACE 1980
U.S. Army Corps of Engineers. Army 1980. *Annual Report of Civil Works Activities of the Chief of Engineers for FY 1979, Volume 1, Summary/Highlights,* Department of the, Office of the Chief of Engineers, Washington, DC. 12 August 80, pp 44-47.

U.S. Army Corps of Engineers 1998
U.S. Army Corps of Engineers. 1998. *The History of the US Army Corps of Engineers.* Engineer Pamphlet EP 360-1-21, Washington, DC.

Waterborne Commerce Statistics Center 1999
Waterborne Commerce Statistics Center, Water Resources Support Center, Navigation Data Center, U.S. Army Corps of Engineers, Alexandria, VA. **http://www.wrsc.usace.army.mil/ndc/** (6 Dec 1999).

Wilson and Eaton 1960
Wilson, MG Walter K., Jr. and Eaton, Richard O. 1960. "A History of the Beach Erosion Board," *Shore and Beach,* Journal of the American Shore and Beach Preservation Association, Volume Twenty-eight, Number one, April 1960, pp 4-9.

Wiegel 1999
Wiegel, Robert L. 1999. *Military Examples of Coastal Engineering,* Miscellaneous Paper CHL-99-3, September 1999, Prepared for Coastal Engineering Research Board, U.S. Army Corps of Engineers Research and Development Center, Vicksburg, MS 39180-6199.

Wiegel and Kimberly 1949
Wiegel, Robert L., and Kimberly, H. L. 1949. *Operation MIKI, Hawaiian amphibious phase (ground coverage),* University of California, Berkley, Inst. Engrg. Res., Series 29, Issue 14.

Wiegel and Saville 1996
Wiegel, R. L., and Saville, T., Jr. 1996. History of Coastal Engineering in the United States. *History and Heritage of Coastal Engineering,* N. C. Kraus, ed., Coastal Engineering Research Council, American Society of Civil Engineers, Reston, VA, pp. 214 - 274.

Willingham 1983
Willingham, W. F. 1983. *Army Engineers and the Development of Oregon, a History of the Portland District U.S. Army Corps of Engineers.* Portland District, U.S. Army Corps of Engineers, Portland, OR.

van Hoften 1970
van Hoften, E. 1970. *History of the Honolulu Engineer District, 1905-1965.* U.S. Army Engineer District, Honolulu, pp 133.

Vitruvius, Rowland, and Howe, eds. 1999
Vitruvius, P., Rowland, I. D., and Howe, T. N. eds. 1999. Vitrivius: Ten Books on Architecture. Cambridge University Press, Cambridge, MA.

I-3-11. Acknowledgments

Authors of Chapter I-3, "History of Coastal Engineering:"

John H. Lockhart. Jr., Headquarters, U.S. Army Corps of Engineers, Washington, DC, (retired).
Andrew Morang, Ph.D., Coastal and Hydraulics Laboratory (CHL), Engineer Research and Development Center, Vicksburg, Mississippi.

Reviewers:

Joan Pope, CHL
Martin A. Reuss, Ph.D., Office of History, U.S. Army Corps of Engineers, Alexandria, Virginia.

Table of Contents

Page

I-4-1. Background I-4-1

a. Shore Protection Planning and Design, TR 4 . . . . . I-4-1
b. Shore Protection Manual, SPM I-4-1
c. Coastal Engineering Manual, CEM I-4-2

I-4-2. Structure I-4-2

a. Part II I-4-2
b. Part III I-4-2
c. Part IV I-4-2
d. Part V I-4-3
e. Part VI I-4-3
f. *Appendix A* I-4-3
g. Updates I-4-3

I-4-3. References I-4-3

I-4-4. Acknowledgments I-4-4

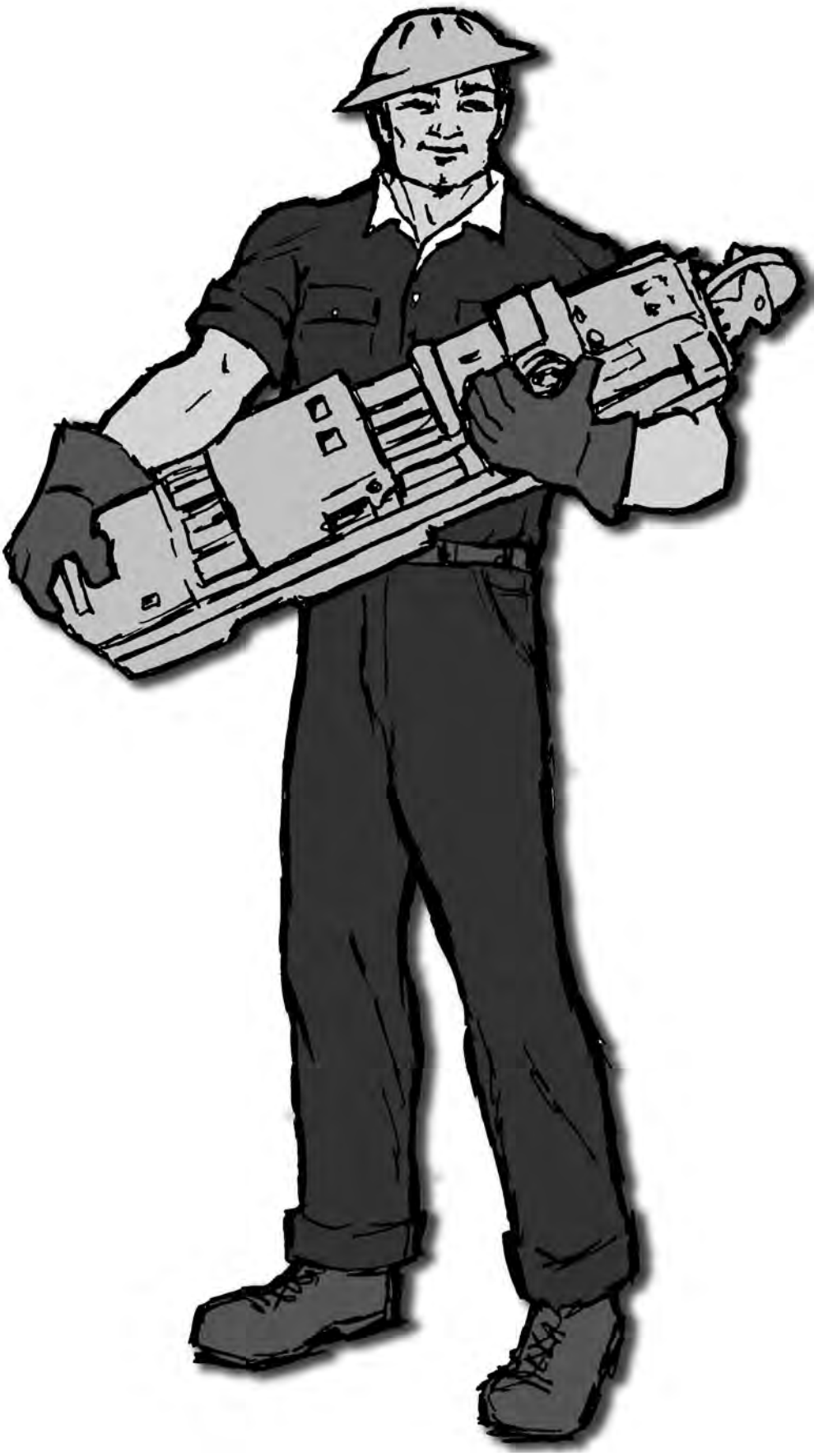

Chapter I-4
The Coastal Engineering Manual

I-4-1. Background

During the 1970s, '80s, and '90s, coastal engineering practice by the U.S. Army Corps of Engineers (USACE) and standard engineering for most coastal projects throughout the world have been based, wholly or in part, on the *Shore Protection Manual (SPM)*. Since the *SPM* was last updated in 1984, the coastal engineering field has witnessed many technical advances and increased emphasis on computer modeling, environmental restoration, and project maintenance applications. The BEB produced the first standardized guidance on coastal structure design in 1954, *Shore Protection Planning and Design*, also known as *TR-4*. This was the forerunner of the *SPM* that was first published by CERC in 1973, and revised in 1975, 1977, and 1984. These documents present the methodology that guided coastal structure and beach fill design for most of the projects constructed to date. The USACE traditionally is responsible for constructing and maintaining United States Federally authorized coastal civil works projects including harbor entrance channels, navigation channels and structures, coastal storm damage reduction and shore protection projects. Therefore, the USACE is primarily responsible for developing the principles of coastal engineering as they are practiced in the United States.

a. Shore Protection Planning and Design, TR 4. The methodologies of *TR-4* emphasized designing coastal structures for stability against wave forces. The technology available at that time provided little means to address the functional performance of structures, nor provide any guidance for predicting the performance or stability of a beach fill. Beach and dune design was only qualitatively addressed. Simple linear wave theory, static terrestrial structural engineering principles, and trail-and-error experiential data were used to develop the empirical relationships and rules-of-thumb presented in *TR-4*. Beach fills of this era were not usually designed to perform a particular function, but were typically placed as an added feature to increase the sediment supply in the area of interest and to reduce wave energy striking the protective structures (the primary project feature).

b. Shore Protection Manual, SPM. The *SPM* was a significant advancement over *TR-4* in that it used the results of physical model tests to develop principles of wave-structure interaction, advancements in wave theory, and statistics and other data from various projects. The *SPM* provided significantly more guidance in the positioning and intent of groins and breakwaters, predicting the flood control benefits of seawalls, and predicting the stability of beach fills. At 1,160 pages, the first edition of the *SPM* was almost three times the length of the 20-year-older *TR-4* (Camfield 1988). The *SPM* and beach fill projects of the 1970s and early '80s were designed around the objective of beach erosion control and recreational use. The quantity of material to be placed was computed based on the long-term recession rates, and the amount of surface area desired to support recreational needs. The *SPM* presented guidance to assist in predicting maintenance nourishment quantities based on the grain size of the placed fill and its projected stability relative to the native material grain size. Neither the *SPM* nor the projects constructed during this time concerned themselves with the performance of the beach fill template during a particular storm. At that time, beach fills were not usually designed with a primary purpose of providing flood control benefits.

The *SPM* is commonly used as a university textbook and as a training aid for apprentice engineers. It is also a convenient reference for empirical procedures to compute a particular design parameter. Approximately 30,000 copies have been sold through the U.S. Government Printing Office. Translations into other languages, including Chinese and Catalonnian (Spanish), further attest to the *SPM's* role as an international standard guidance for professional coastal engineers (Pope 1993, 1998). Even though the *SPM* is a general

coastal engineering reference, some aspects of navigation and harbor design are not included and its primary focus is shore protection.

c. Coastal Engineering Manual, CEM. The advent of numerical models, reliable field instrumentation techniques, and improved understandings of the physical relationships which influence coastal processes lead to more sophisticated approaches in shore protection design in the later 1980s and 90s. Numerous guidance and analytical tools have been developed over the last 15 years to assist the coastal engineer in predicting not only the stability of a beach fill, but also its performance during extreme events. Cross-shore and alongshore change models, hydrodynamic hind cast data bases, and stochastic statistical approaches have been developed to provide the practicing coastal engineer with procedures for quantifying the flood control benefits of a proposed design. The functional interaction of beach erosion control structures (i.e., groins and breakwaters) can be analyzed with numerical simulation. Seawalls can be designed not only for stability, but also physically modeled to predict various elements of the wave-structure interaction including scour and overtopping. A "modern" technical document incorporating all the tools and procedures used to plan, design, construct, and maintain coastal projects was needed. The USACE tasked the Coastal Engineering Research Center and, later, the Coastal and Hydraulics Laboratory with producing a new reference incorporating established science and much of this new technology, to be called the *Coastal Engineering Manual (CEM)*. Included in the *CEM* are the basic principles of coastal processes, methods for computing planning and design parameters, and guidance on how to develop and conduct studies in support of coastal storm damage reduction, shore protection, and navigation projects. Broader coverage of all aspects of coastal engineering are provided, including new sections on navigation and harbor design, dredging and dredged material placement, structure repair and rehabilitation, wetland and low energy shore protection, cohesive shores, risk analysis, numerical simulation, the engineering process, and other topics.

I-4-2. Structure

The *CEM* contains two major subdivisions: science-based parts and engineering-based parts. The science-based parts include "Part II - Coastal Hydrodynamics," "Part III – Coastal Sediment Processes," and "Part IV – Coastal Geology." These provide the scientific foundation on which the engineering-based parts rely.

a. Part II. "Coastal Hydrodynamics" is organized to lead the reader from the fundamental principles of linear and other wave theories, including irregular waves and spectral analysis, to ocean wave generation and through the process of transformation as the wave approaches and reacts with the coastline. Analysis of water level variations including astronomical tides and storm surges are presented along with the hydrodynamics of coastal inlets and harbors are included in other chapters.

b. Part III. "Coastal Sediment Processes" includes chapters on sediment properties, along shore and cross-shore transport, as well as chapters on wind transport, cohesive sediment processes and shelf transport.

c. Part IV. "Coastal Geology" includes chapters on terminology, geomorphology, and morphodynamics.

The two engineering-based parts, Part V – "Coastal Project Planning and Design" and Part VI – "Design of Coastal Project Elements" are oriented toward a project-type approach, rather than the individual structure design approach that characterized the *SPM*. The architecture and substance of the engineering-based parts is the result of an internationally-attended workshop in February 1994. A logical systems-based approach is used for the engineering structure of the *CEM*. This mirrors the engineering process with guidance in

selecting and using various planning and design tools as appropriate for the project at hand. The engineering tools are presented in a modular grouping to allow for future updates as the technology continues to advance.

d. Part V. "Coastal Project Planning and Design" starts with chapters discussing the planning and design process and site characterization. Following these general chapters are ones discussing the planning and design of shore protection projects (including coastal armoring, beach restoration, beach stabilization and coastal flood protection projects), beach fill, navigation projects (including defining the fleet, entrance channel, inner harbor elements, structures, sedimentation, maintenance, and management), and environmental enhancement projects (including laws, regulations, and authorities, issues, alternative approaches, planning, and design). A final chapter outlines conditions and regulations unique to USACE projects in the United States.

e. Part VI. "Design of Coastal Project Elements" includes chapters discussing philosophy of coastal structure design, the various types and function of coastal structures, site conditions, materials, design fundamentals, reliability, and the design of specific project elements (including a sloping-front structure, vertical-front structure, beach fill, floating structure, pile structure, and a pipeline and outfall structure.

f. Appendix A. The "Glossary of Coastal Terminology" has been compiled from numerous sources and lists terms found throughout the CEM. Note that there is no single, comprehensive list of mathematical terms and symbols. Each CEM chapter has its own symbol list.

g. Updates. The CEM is intended to be a "living document" and to be updated periodically as advances in the field render the existing chapters obsolete or inadequate. Comments and suggestions should be addressed to the Coastal and Hydraulics Laboratory, CEERD-HN-CE. Corrected or modified chapters will be posted on the CHL web page.

I-4-3. References

Camfield 1988
Camfield, F. E. 1988. "Technology Transfer – The Shore Protection Manual," *Journal of Coastal Research,* 4(3), pp 335-338.

Pope 1993
Pope, J. 1993. "Replacing the SPM: The Coastal Engineering Manual." *The State of the Art of Beach Nourishment, Proceedings, 6th Annual National Conference on Beach Preservation Technology, Florida Shore and Beach Preservation Association, Tallahassee, FL,* pp 319-334.

Pope 1998
Pope, J. 1998. "Replacing the SPM: The Coastal Engineering Manual." *PIANC Bulletin,* No. 97, pp 43-46.

USACE 1954
USACE 1954. *Shore Protection Planning and Design, Technical Report No. 4,* Beach Erosion Board, U.S. Government Printing Office, Washington, DC.

***Shore Protection Manual* 1984**
Shore Protection Manual, 4th ed., 2 Vol., U.S. Army Engineer Waterways Experiment Station, U.S. Government Printing Office, Washington, DC, 1,088 p.

I-4-4. Acknowledgments

Authors of Chapter I-4, "The Coastal Engineering Manual:"

Joan Pope, U.S. Army Engineer Research and Development Center, Vicksburg, Mississippi.
John H. Lockhart, Jr., Headquarters, U.S. Army Corps of Engineers, Washington, DC, (retired).

Reviewer:

Andrew Morang, Ph.D., CHL

Table of Contents

Page

II-1-1. Introduction II-1-1

II-1-2. Regular Waves II-1-3
a. Introduction II-1-3
b. Definition of wave parameters II-1-4
c. Linear wave theory II-1-5
(1) Introduction II-1-5
(2) Wave celerity, length, and period II-1-6
(3) The sinusoidal wave profile II-1-9
(4) Some useful functions II-1-9
(5) Local fluid velocities and accelerations II-1-12
(6) Water particle displacements II-1-13
(7) Subsurface pressure II-1-21
(8) Group velocity II-1-22
(9) Wave energy and power II-1-26
(10) Summary of linear wave theory II-1-29
d. Nonlinear wave theories II-1-30
(1) Introduction II-1-30
(2) Stokes finite-amplitude wave theory II-1-32
(3) Subsurface pressure II-1-34
(4) Maximum wave steepness II-1-35
e. Other wave theories II-1-36
(1) Introduction II-1-36
(2) Nonlinear shallow-water wave theories II-1-36
(3) Korteweg and de Vries and Boussinesq wave theories II-1-36
(4) Cnoidal wave theory II-1-37
(5) Solitary wave theory II-1-41
(6) Stream-function wave theory II-1-50
(7) Fourier approximation -- Fenton's theory II-1-50
f. Wave breaking II-1-56
g. Validity of wave theories II-1-56

II-1-3. Irregular Waves II-1-59
a. Introduction II-1-59
b. Wave train (wave-by-wave) analysis II-1-65
(1) Introduction II-1-65
(2) Zero-crossing method II-1-65
(3) Definition of wave parameters II-1-66
(4) Significant wave height II-1-68
(5) Short-term random sea state parameters II-1-68
(6) Probability distributions for a sea state II-1-70
(7) Wave height distribution II-1-74

(8) Wave period distribution II-1-75
(9) Joint distribution of wave heights and periods II-1-76
c. Spectral analysis II-1-77
(1) Introduction II-1-77
(2) Description of wave spectral analysis II-1-80
(3) Examples of frequency spectra II-1-85
(4) Wave spectrum and its parameters II-1-85
(5) Relationship between $H_{1/3}$, H_s and H_{m0} in shallow water II-1-88
(6) Parametric spectrum models II-1-88
(7) Directional spectra II-1-93
(8) Wave groups and groupiness factors II-1-95
(9) Random wave simulation II-1-97
(10) Kinematics and dynamics of irregular waves II-1-98

II-1-4. References and Bibliography II-1-99

II-1-5. Definitions of Symbols II-1-116

II-1-6. Acknowledgments II-1-121

List of Tables

Page

Table II-1-1. Classification of Water Waves II-1-8

Table II-1-2. Boundary Value Problem of Water Wave Theories (Dean 1968) II-1-50

List of Figures

Page

Figure II-1-1. Definition of terms - elementary, sinusoidal, progressive wave II-1-4

Figure II-1-2. Local fluid velocities and accelerations II-1-13

Figure II-1-3. Profiles of particle velocity and acceleration by Airy theory in relation to the surface elevation II-1-14

Figure II-1-4. Water particle displacements from mean position for shallow-water and deepwater waves II-1-17

Figure II-1-5. Variation of wave parameters with d/L_0 (Dean and Dalrymple 1991) II-1-23

Figure II-1-6. Characteristics of a wave group formed by the addition of sinusoids with different periods II-1-25

Figure II-1-7. Variation of the ratios of group and phase velocities to deepwater phase speed using linear theory (Sarpkaya and Isaacson 1981) II-1-27

Figure II-1-8. Variation of shoaling coefficient with wave steepness (Sakai and Battjes 1980) II-1-30

Figure II-1-9. Summary of linear (Airy) wave theory - wave characteristics II-1-31

Figure II-1-10. Wave profile shape of different progressive gravity waves II-1-34

Figure II-1-11. Normalized surface profile of the cnoidal wave (Wiegel 1960). For definition of variables see Part II-1-2.e.(3) II-1-40

Figure II-1-12. Normalized surface profile of the cnoidal wave for higher values of k^2 and X/L (Wiegel 1960) II-1-40

Figure II-1-13. k^2 versus L^2H/d^3, and k^2 versus $T\sqrt{g / d}$ and H/d (Wiegel 1960) II-1-41

Figure II-1-14. Relationship among L^2H/d^3 and the square of the elliptic modulus (k^2), y_c/H, y_t/H, and K(k) (Wiegel 1960) II-1-42

Figure II-1-15. Relationships among $T\sqrt{g / d}$, L^2H/d^3, and H/d (Wiegel 1960) II-1-43

Figure II-1-16. Relationship between cnoidal wave velocity and L^2H/d^3 (Wiegel 1960) II-1-44

Figure II-1-17. Functions M and N in solitary wave theory (Munk 1949) II-1-49

Figure II-1-18. Surface elevation, horizontal velocity and pressure in 10-m depth (using Fenton's theory in ACES) II-1-55

Figure II-1-19. Influence of a uniform current on the maximum wave height (Dalrymple and Dean 1975) II-1-57

Figure II-1-20. Ranges of suitability of various wave theories (Le Méhauté 1976) II-1-58

Figure II-1-21. Grouping of wind waves based on universal parameter and limiting height for steep waves II-1-59

Figure II-1-22. Radar image of the sea surface in the entrance to San Francisco Bay II-1-61

Figure II-1-23. Measured sea surface velocity in the entrance to San Francisco Bay II-1-62

Figure II-1-24. Representations of an ocean wave II-1-63

Figure II-1-25. Wave profile of irregular sea state from site measurements II-1-63

Figure II-1-26. Definition of wave parameters for a random sea state II-1-64

Figure II-1-27. Definition sketch of a random wave process (Ochi 1973) II-1-64

Figure II-1-28. Gaussian probability density and cumulative probability distribution II-1-71

Figure II-1-29. Rayleigh probability density and cumulative probability distribution ($x = \alpha$ corresponds to the mode) II-1-71

Figure II-1-30. Histograms of the normalized (a) wave heights and (b) wave periods with theoretical distributions (Chakrabarti 1987) II-1-73

Figure II-1-31. Surface elevation time series of a regular wave and its spectrum (Briggs et al. 1993) II-1-79

Figure II-1-32. Surface elevation time series of an irregular wave and its spectrum (Briggs et al. 1993) II-1-80

Figure II-1-33. Schematic for a two-dimensional wave spectrum $E(f,\theta)$ II-1-81

Figure II-1-34. Directional spectrum and its frequency and direction spectrum (Briggs et al. 1993) II-1-82

Figure II-1-35. Sketches of wave spectral energy and energy density (Chakrabarti 1987) II-1-84

Figure II-1-36. Definitions of one- and two-sided wave spectra (Chakrabarti 1987) II-1-85

Figure II-1-37. Energy density and frequency relationship (Chakrabarti 1987) II-1-86

Figure II-1-38. Comparison of the PM and JONSWAP spectra (Chakrabarti 1987) II-1-87

Figure II-1-39. Definition sketch for Ochi-Hubble spectrum (Ochi and Hubble 1976) II-1-90

Figure II-1-40. Variation of H_s/H_{mo} as a function of relative depth $\bar{d}$ and significant steepness (Thompson and Vincent 1985) II-1-91

Figure II-1-41. Identification and description of wave groups through ordered statistics (Goda 1976) II-1-96

Chapter II-1
Water Wave Mechanics

II-1-1. Introduction

a. Waves on the surface of the ocean with periods of 3 to 25 sec are primarily generated by winds and are a fundamental feature of coastal regions of the world. Other wave motions exist on the ocean including internal waves, tides, and edge waves. For the remainder of this chapter, unless otherwise indicated, the term waves will apply only to surface gravity waves in the wind wave range of 3 to 25 sec.

b. Knowledge of these waves and the forces they generate is essential for the design of coastal projects since they are the major factor that determines the geometry of beaches, the planning and design of marinas, waterways, shore protection measures, hydraulic structures, and other civil and military coastal works. Estimates of wave conditions are needed in almost all coastal engineering studies. The purpose of this chapter is to give engineers theories and mathematical formulae for describing ocean surface waves and the forces, accelerations, and velocities due to them. This chapter is organized into two sections: *Regular Waves* and *Irregular Waves*.

c. In the *Regular Waves* section, the objective is to provide a detailed understanding of the mechanics of a wave field through examination of waves of constant height and period. In the *Irregular Waves* section, the objective is to describe statistical methods for analyzing irregular waves (wave systems where successive waves may have differing periods and heights) which are more descriptive of the waves seen in nature.

d. In looking at the sea surface, it is typically irregular and three-dimensional (3-D). The sea surface changes in time, and thus, it is unsteady. At this time, this complex, time-varying 3-D surface cannot be adequately described in its full complexity; neither can the velocities, pressures, and accelerations of the underlying water required for engineering calculations. In order to arrive at estimates of the required parameters, a number of simplifying assumptions must be made to make the problems tractable, reliable and helpful through comparison to experiments and observations. Some of the assumptions and approximations that are made to describe the 3-D, time-dependent complex sea surface in a simpler fashion for engineering works may be unrealistic, but necessary for mathematical reasons.

e. The *Regular Waves* section of this chapter begins with the simplest mathematical representation assuming ocean waves are two-dimensional (2-D), small in amplitude, sinusoidal, and progressively definable by their wave height and period in a given water depth. In this simplest representation of ocean waves, wave motions and displacements, kinematics (that is, wave velocities and accelerations), and dynamics (that is, wave pressures and resulting forces and moments) will be determined for engineering design estimates. When wave height becomes larger, the simple treatment may not be adequate. The next part of the *Regular Waves* section considers 2-D approximation of the ocean surface to deviate from a pure sinusoid. This representation requires using more mathematically complicated theories. These theories become nonlinear and allow formulation of waves that are not of purely sinusoidal in shape; for example, waves having the flatter troughs and peaked crests typically seen in shallow coastal waters when waves are relatively high.

f. The *Irregular Waves* section of this chapter is devoted to an alternative description of ocean waves. Statistical methods for describing the natural time-dependent three-dimensional characteristics of real wave systems are presented. A complete 3-D representation of ocean waves requires considering the sea surface as an irregular wave train with random characteristics. To quantify this randomness of ocean waves, the *Irregular Waves* section employs statistical and probabilistic theories. Even with this approach, simplifications are required. One approach is to transform the sea surface using Fourier theory into summation of simple sine waves and then to define a wave's characteristics in terms of its spectrum. This

allows treatment of the variability of waves with respect to period and direction of travel. The second approach is to describe a wave record at a point as a sequence of individual waves with different heights and periods and then to consider the variability of the wave field in terms of the probability of individual waves.

g. At the present time, practicing coastal engineers must use a combination of these approaches to obtain information for design. For example, information from the *Irregular Waves* section will be used to determine the expected range of wave conditions and directional distributions of wave energy in order to select an individual wave height and period for the problem under study. Then procedures from the *Regular Waves* section will be used to characterize the kinematics and dynamics that might be expected. However, it should be noted that the procedures for selecting and using irregular wave conditions remain an area of some uncertainty.

h. The major generating force for waves is the wind acting on the air-sea interface. A significant amount of wave energy is dissipated in the nearshore region and on beaches. Wave energy forms beaches; sorts bottom sediments on the shore face; transports bottom materials onshore, offshore, and alongshore; and exerts forces upon coastal structures. A basic understanding of the fundamental physical processes in the generation and propagation of surface waves must precede any attempt to understand complex water motion in seas, lakes and waterways. The *Regular Waves* section of this chapter outlines the fundamental principles governing the mechanics of wave motion essential in the planning and design of coastal works. The *Irregular Waves* section of this chapter discusses the applicable statistical and probabilistic theories.

i. Detailed descriptions of the basic equations for water mechanics are available in several textbooks (see for example, Kinsman 1965; Stoker 1957; Ippen 1966; Le Méhauté 1976; Phillips 1977; Crapper 1984; Mei 1991; Dean and Dalrymple 1991). The Regular Waves section of this chapter provides only an introduction to wave mechanics, and it focuses on simple water wave theories for coastal engineers. Methods are discussed for estimating wave surface profiles, water particle motion, wave energy, and wave transformations due to interaction with the bottom and with structures.

j. The simplest wave theory is the *first-order, small-amplitude*, or *Airy* wave theory which will hereafter be called *linear theory*. Many engineering problems can be handled with ease and reasonable accuracy by this theory. For convenience, prediction methods in coastal engineering generally have been based on simple waves. For some situations, simple theories provide acceptable estimates of wave conditions.

k. When waves become large or travel toward shore into shallow water, higher-order wave theories are often required to describe wave phenomena. These theories represent *nonlinear waves*. The linear theory that is valid when waves are infinitesimally small and their motion is small also provides some insight for finite-amplitude periodic waves (nonlinear). However, the linear theory cannot account for the fact that wave crests are higher above the mean water line than the troughs are below the mean water line. Results obtained from the various theories should be carefully interpreted for use in the design of coastal projects or for the description of coastal environment.

l. Any basic physical description of a water wave involves both its surface form and the water motion beneath the surface. A wave that can be described in simple mathematical terms is called a *simple wave*. Waves comprised of several components and difficult to describe in form or motion are termed *wave trains* or *complex waves*. Sinusoidal or monochromatic waves are examples of simple waves, since their surface profile can be described by a single sine or cosine function. A wave is *periodic* if its motion and surface profile recur in equal intervals of time termed the *wave period*. A wave form that moves horizontally relative to a fixed point is called a *progressive wave* and the direction in which it moves is termed the *direction of wave propagation*. A progressive wave is called *wave of permanent form* if it propagates without experiencing any change in shape.

m. Water waves are considered *oscillatory* or *nearly oscillatory* if the motion described by the water particles is circular orbits that are closed or nearly closed for each wave period. The linear theory represents pure oscillatory waves. Waves defined by finite-amplitude wave theories are not pure oscillatory waves but still periodic since the fluid is moved in the direction of wave advance by each successive wave. This motion is termed *mass transport* of the waves. When water particles advance with the wave and do not return to their original position, the wave is called a *wave of translation*. A solitary wave is an example of a wave of translation.

n. It is important in coastal practice to differentiate between two types of surface waves. These are *seas* and *swells*. Seas refer to short-period waves still being created by winds. Swells refer to waves that have moved out of the generating area. In general, swells are more regular waves with well-defined long crests and relatively long periods.

o. The growth of wind-generated oceanic waves is not indefinite. The point when waves stop growing is termed a *fully developed sea* condition. Wind energy is imparted to the water leading to the growth of waves; however, after a point, the energy imparted to the waters is dissipated by wave breaking. Seas are short-crested and irregular and their periods are within the 3- to 25- sec range. Seas usually have shorter periods and lengths, and their surface appears much more disturbed than for swells. Waves assume a more orderly state with the appearance of definite crests and troughs when they are no longer under the influence of winds (swell).

p. To an observer at a large distance from a storm, swells originating in a storm area will appear to be almost unidirectional (i.e., they propagate in a predominant direction) and long-crested (i.e., they have well-defined and distinctly separated crests). Although waves of different periods existed originally together in the generation area (seas), in time the various wave components in the sea separate from one another. Longer period waves move faster and reach distant sites first. Shorter period components may reach the site several days later. In the wave generation area, energy is transferred from shorter period waves to the longer waves. Waves can travel hundreds or thousands of kilometers without much loss of energy. However, some wave energy is dissipated internally within the fluid, by interaction with the air above, by turbulence upon breaking, and by percolation and friction with the seabed. Short-period components lose their energy more readily than long-period components. As a consequence of these processes, the periods of swell waves tend to be somewhat longer than seas. Swells typically have periods greater than 10 sec.

II-1-2. Regular Waves

a. Introduction. Wave theories are approximations to reality. They may describe some phenomena well under certain conditions that satisfy the assumptions made in their derivation. They may fail to describe other phenomena that violate those assumptions. In adopting a theory, care must be taken to ensure that the wave phenomenon of interest is described reasonably well by the theory adopted, since shore protection design depends on the ability to predict wave surface profiles and water motion, and on the accuracy of such predictions.

b. Definition of wave parameters.

(1) A progressive wave may be represented by the variables x (spatial) and t (temporal) or by their combination (phase), defined as $\theta = kx - \omega t$, where k and ω are described in the following paragraphs. The values of θ vary between 0 and 2π. Since the θ-representation is a simple and compact notation, it will be used in this chapter. Figure II-1-1 depicts parameters that define a simple, progressive wave as it passes a fixed point in the ocean. A simple, periodic wave of permanent form propagating over a horizontal bottom may be completely characterized by the wave height H wavelength L and water depth d.

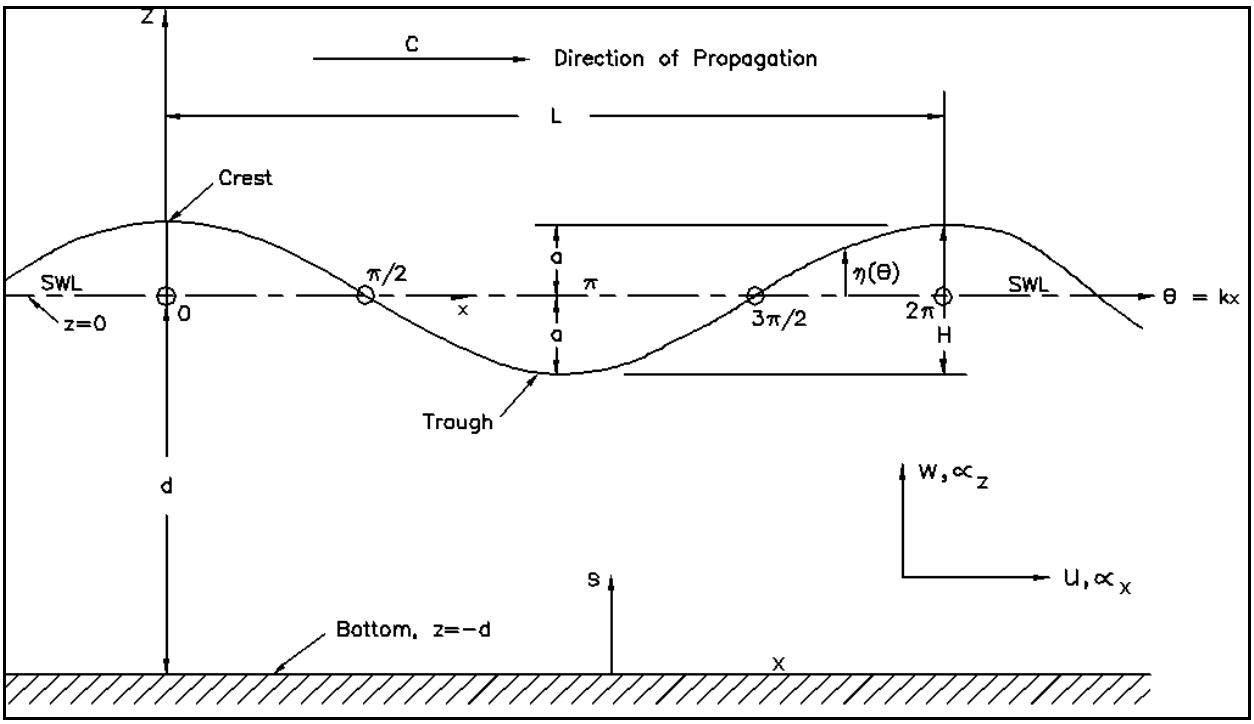

Figure II-1-1. Definition of terms - elementary, sinusoidal, progressive wave

(2) As shown in Figure II-1-1, the highest point of the wave is the *crest* and the lowest point is the *trough*. For linear or small-amplitude waves, the height of the crest above the still-water level (SWL) and the distance of the trough below the SWL are each equal to the wave amplitude a. Therefore $a = H/2$, where H = *the wave height*. The time interval between the passage of two successive wave crests or troughs at a given point is the *wave period T*. The *wavelength L* is the horizontal distance between two identical points on two successive wave crests or two successive wave troughs.

(3) Other wave parameters include $\omega = 2\pi/T$ the *angular* or *radian frequency*, the *wave number* $k = 2\pi/L$, the *phase velocity* or *wave celerity* $C = L/T = \omega/k$, the *wave steepness* $\epsilon = H/L$, the *relative depth* d/L, and the *relative wave height* H/d. These are the most common parameters encountered in coastal practice. Wave motion can be defined in terms of dimensionless parameters H/L, H/d, and d/L; these are often used in practice. The dimensionless parameters ka and kd, preferred in research works, can be substituted for H/L and d/L, respectively, since these differ only by a constant factor 2π from those preferred by engineers.

c. Linear wave theory.

(1) Introduction.

(a) The most elementary wave theory is the *small-amplitude* or *linear wave theory*. This theory, developed by Airy (1845), is easy to apply, and gives a reasonable approximation of wave characteristics for a wide range of wave parameters. A more complete theoretical description of waves may be obtained as the sum of many successive approximations, where each additional term in the series is a correction to preceding terms. For some situations, waves are better described by these higher-order theories, which are usually referred to as *finite-amplitude wave theories* (Mei 1991, Dean and Dalrymple 1991). Although there are limitations to its applicability, linear theory can still be useful provided the assumptions made in developing this simple theory are not grossly violated.

(b) The assumptions made in developing the linear wave theory are:

- The fluid is homogeneous and incompressible; therefore, the density ρ is a constant.
- Surface tension can be neglected.
- Coriolis effect due to the earth's rotation can be neglected.
- Pressure at the free surface is uniform and constant.
- The fluid is ideal or inviscid (lacks viscosity).
- The particular wave being considered does not interact with any other water motions. The flow is irrotational so that water particles do not rotate (only normal forces are important and shearing forces are negligible).
- The bed is a horizontal, fixed, impermeable boundary, which implies that the vertical velocity at the bed is zero.
- The wave amplitude is small and the waveform is invariant in time and space.
- Waves are plane or long-crested (two-dimensional).

(c) The first three assumptions are valid for virtually all coastal engineering problems. It is necessary to relax the fourth, fifth, and sixth assumptions for some specialized problems not considered in this manual. Relaxing the three final assumptions is essential in many problems, and is considered later in this chapter.

(d) The assumption of irrotationality stated as the sixth assumption above allows the use of a mathematical function termed the *velocity potential* Φ. The velocity potential is a scaler function whose gradient (i.e., the rate of change of Φ relative to the x-and z-coordinates in two dimensions where x = horizontal, z = vertical) at any point in fluid is the velocity vector. Thus,

$$u = \frac{\partial \Phi}{\partial x} \tag{II-1-1}$$

is the fluid velocity in the x-direction, and

$$w = \frac{\partial \Phi}{\partial z} \tag{II-1-2}$$

is the fluid velocity in the z-direction. Φ has the units of length squared divided by time. Consequently, if Φ(x, z, t) is known over the flow field, then fluid particle velocity components *u* and *w* can be found.

(e) The incompressible assumption (a) above implies that there is another mathematical function termed the *stream function* Ψ. Some wave theories are formulated in terms of the stream function Ψ, which is orthogonal to the potential function Φ. Lines of constant values of the potential function (equipotential lines) and lines of constant values of the stream function are mutually perpendicular or orthogonal. Consequently, if Φ is known, Ψ can be found, or vice versa, using the equations

$$\frac{\partial \Phi}{\partial x} = \frac{\partial \Psi}{\partial z} \tag{II-1-3}$$

$$\frac{\partial \Phi}{\partial z} = -\frac{\partial \Psi}{\partial x} \tag{II-1-4}$$

termed the *Cauchy-Riemann conditions* (Whitham 1974; Milne-Thompson 1976). Both Φ and Ψ satisfy the *Laplace equation* which governs the flow of an *ideal fluid* (inviscid and incompressible fluid). Thus, under the assumptions outlined above, the Laplace equation governs the flow beneath waves. The Laplace equation in two dimensions with x = horizontal, and z = vertical axes in terms of velocity potential Φ is given by

$$\frac{\partial^2 \Phi}{\partial x^2} + \frac{\partial^2 \Phi}{\partial z^2} = 0 \tag{II-1-5}$$

(f) In terms of the stream function, Ψ, Laplace's equation becomes

$$\frac{\partial^2 \Psi}{\partial x^2} + \frac{\partial^2 \Psi}{\partial z^2} = 0 \tag{II-1-6}$$

(g) The linear theory formulation is usually developed in terms of the potential function, Φ.

In applying the seventh assumption to waves in water of varying depth (encountered when waves approach a beach), the local depth is usually used. This can be justified, but not without difficulty, for most practical cases in which the bottom slope is flatter than about 1 on 10. A progressive wave moving into shallow water will change its shape significantly. Effects due to the wave transformations are addressed in Parts II-3 and II-4.

(h) The most fundamental description of a simple sinusoidal oscillatory wave is by its length L (the horizontal distance between corresponding points on two successive waves), height H (the vertical distance to its crest from the preceding trough), period T (the time for two successive crests to pass a given point), and depth d (the distance from the bed to SWL).

(i) Figure II-1-1 shows a two-dimensional, simple progressive wave propagating in the positive x-direction, using the symbols presented above. The symbol η denotes the displacement of the water surface relative to the SWL and is a function of x and time t. At the wave crest, η is equal to the amplitude of the wave a, or one-half the wave height $H/2$.

(2) Wave celerity, length, and period.

(a) The speed at which a wave form propagates is termed the *phase velocity* or *wave celerity* C. Since the distance traveled by a wave during one wave period is equal to one wavelength, wave celerity can be related to the wave period and length by

$$C = \frac{L}{T} \tag{II-1-7}$$

(b) An expression relating wave celerity to wavelength and water depth is given by

$$C = \sqrt{\frac{gL}{2\pi} \tanh\left(\frac{2\pi d}{L}\right)} \tag{II-1-8}$$

(c) Equation II-1-8 is termed the *dispersion relation* since it indicates that waves with different periods travel at different speeds. For a situation where more than one wave is present, the longer period wave will travel faster. From Equation II-1-7, it is seen that Equation II-1-8 can be written as

$$C = \frac{gT}{2\pi} \tanh\left(\frac{2\pi d}{L}\right) \tag{II-1-9}$$

(d) The values $2\pi/L$ and $2\pi/T$ are called the *wave number k* and the *wave angular frequency* ω, respectively. From Equation II-1-7 and II-1-9, an expression for wavelength as a function of depth and wave period may be obtained as

$$L = \frac{gT^2}{2\pi} \tanh\left(\frac{2\pi d}{L}\right) = \frac{gT}{\omega} \tanh\,(kd) \tag{II-1-10}$$

(e) Use of Equation II-1-10 involves some difficulty since the unknown L appears on both sides of the equation. Tabulated values of d/L and d/L_0 (SPM 1984) where L_0 is the deepwater wavelength may be used to simplify the solution of Equation II-1-10. Eckart (1952) gives an approximate expression for Equation II-1-10, which is correct to within about 10 percent. This expression is given by

$$L \approx \frac{gT^2}{2\pi} \sqrt{\tanh\left(\frac{4\pi^2}{T^2}\frac{d}{g}\right)} \tag{II-1-11}$$

(f) Equation II-1-11 explicitly gives L in terms of wave period T and is sufficiently accurate for many engineering calculations. The maximum error 10 percent occurs when $d/L \approx 1/2$. There are several other approximations for solving Equation II-1-10 (Hunt 1979; Venezian and Demirbilek 1979; Wu and Thornton 1986; Fenton and McKee 1990).

(g) Gravity waves may also be classified by the water depth in which they travel. The following classifications are made according to the magnitude of d/L and the resulting limiting values taken by the function $\tanh(2\pi d/L)$. Note that as the argument of the hyperbolic tangent $kd = 2\pi d/L$ gets large, the tanh (kd) approaches 1, and for small values of kd, tanh (kd) $\approx$ kd.

(h) Water waves are classified in Table II-1-1 based on the relative depth criterion d/L.

Table II-1-1
Classification of Water Waves

Classification	d/L	kd	tanh (kd)
Deep water	1/2 to ∞	π to ∞	≈1
Transitional	1/20 to 1/2	π/10 to π	tanh (kd)
Shallow water	0 to 1/20	0 to π/10	≈ kd

(i) In deep water, tanh (kd) approaches unity, Equations II-1-7 and II-1-8 reduce to

$$C_0 = \sqrt{\frac{gL_0}{2\pi}} = \frac{L_0}{T} \tag{II-1-12}$$

and Equation II-1-9 becomes

$$C_0 = \frac{gT}{2\pi} \tag{II-1-13}$$

(j) Although *deep water* actually occurs at an infinite depth, *tanh (kd)*, for most practical purposes, approaches unity at a much smaller *d/L*. For a relative depth of one-half (i.e., when the depth is one-half the wavelength), tanh ($2\pi d/L$) = 0.9964.

(k) When the relative depth *d/L* is greater than one-half, the wave characteristics are virtually independent of depth. Deepwater conditions are indicated by the subscript *0* as in L_o and C_o except that the period *T* remains constant and independent of depth for oscillatory waves, and therefore, the subscript for wave period is omitted (Ippen 1966). In the SI system (System International or metric system of units) where units of meters and seconds are used, the constant $g/2\pi$ is equal to 1.56 m/s^2, and

$$C_0 = \frac{gT}{2\pi} = \frac{9.8}{2\pi} T = 1.56T \ m/s \tag{II-1-14}$$

and

$$L_0 = \frac{gT^2}{2\pi} = \frac{9.8}{2\pi} T^2 = 1.56T^2 \ m \tag{II-1-15}$$

(l) If units of feet and seconds are specified, the constant $g/2\pi$ is equal to 5.12 ft/s^2, and

$$C_0 = \frac{gT}{2\pi} = 5.12T \ ft/s \tag{II-1-16}$$

and

$$L_0 = \frac{gT^2}{2\pi} = 5.12T^2 \ ft \tag{II-1-17}$$

(m) If Equations II-1-14 and II-1-15 are used to compute wave celerity when the relative depth is *d/L* = 0.25, the resulting error will be about 9 percent. It is evident that a relative depth of 0.5 is a satisfactory boundary separating deepwater waves from waves in water of *transitional depth*. If a wave is traveling in *transitional* depths, Equations II-1-8 and II-1-9 must be used without simplification. As a rule of thumb, Equation II-1-8 and II-1-9 must be used when the relative depth is between 0.5 and 0.04.

(n) When the relative water depth becomes shallow, i.e., $2\pi d/L < 1/4$ or $d/L < 1/25$, Equation II-1-8 can be simplified to

$$C = \sqrt{gd} \tag{II-1-18}$$

(o) Waves sufficiently long such that Equation II-1-18 may be applied are termed long waves. This relation is attributed to Lagrange. Thus, when a wave travels in shallow water, wave celerity depends only on water depth.

(p) In summary, as a wind wave passes from deep water to the beach its speed and length are first only a function of its period (or frequency); then as the depth becomes shallower relative to its length, the length and speed are dependent upon both depth and period; and finally the wave reaches a point where its length and speed are dependent only on depth (and not frequency).

(3) The sinusoidal wave profile. The equation describing the free surface as a function of time t and horizontal distance x for a simple sinusoidal wave can be shown to be

$$\eta = a \cos (kx - \omega t) = \frac{H}{2} \cos \left(\frac{2\pi x}{L} - \frac{2\pi t}{T} \right) = a \cos \theta \tag{II-1-19}$$

where η is the elevation of the water surface relative to the SWL, and $H/2$ is one-half the wave height equal to the wave amplitude a. This expression represents a periodic, sinusoidal, progressive wave traveling in the positive x-direction. For a wave moving in the negative x-direction, the minus sign before $2\pi t/T$ is replaced with a plus sign. When $\theta = (2\pi x/L - 2\pi t/T)$ equals 0, $\pi/2$, π, $3\pi/2$, the corresponding values of η are H/2, 0, -H/2, and 0, respectively (Figure II-1-1).

(4) Some useful functions.

(a) Dividing Equation II-1-9 by Equation II-1-13, and Equation II-1-10 by Equation II-1-15 yields,

$$\frac{C}{C_0} = \frac{L}{L_0} = \tanh \left(\frac{2\pi d}{L} \right) = \tanh kd \tag{II-1-20}$$

(b) If both sides of Equation II-1-20 are multiplied by d/L, it becomes

$$\frac{d}{L_0} = \frac{d}{L} \tanh \left(\frac{2\pi d}{L} \right) = \frac{d}{L} \tanh kd \tag{II-1-21}$$

(c) The terms d/L_o and d/L and other useful functions such as $kd = 2\pi d/L$ and $\tanh (kd)$ have been tabulated by Wiegel (1954) as a function of d/L_o (see also SPM 1984, Appendix C, Tables C-1 and C-2). These functions simplify the solution of wave problems described by the linear theory and are summarized in Figure II-1-5. An example problem illustrating the use of linear wave theory equations and the figures and tables mentioned follows.

EXAMPLE PROBLEM II-1-1

FIND:

The wave celerities C and lengths L corresponding to depths d = 200 meters (656 ft) and d = 3 m (9.8 ft).

GIVEN:

A wave with a period T = 10 seconds is propagated shoreward over a uniformly sloping shelf from a depth d = 200 m (656 ft) to a depth d = 3 m (9.8 ft).

SOLUTION:

Using Equation II-1-15,

$$L_0 = \frac{gT^2}{2\pi} = \frac{9.8\ T^2}{2\pi} = 1.56\ T^2\ m\ (5.12\ T^2\ ft)$$

$$L_0 = 1.56T^2 = 1.56(10)^2 = 156\ m\ (512\ ft)$$

For d = 200 m

$$\frac{d}{L_0} = \frac{200}{156} = 1.2821$$

Note that for values of

$$\frac{d}{L_0} > 1.0$$

$$\frac{d}{L_0} = \frac{d}{L}$$

therefore,

$$L = L_0 = 156\ m\ (512\ ft)\ (deepwater\ wave,\ since \frac{d}{L} > \frac{1}{2})$$

which is in agreement with Figure II-1-5.

By Equation II-1-7

$$C = \frac{L}{T} = \frac{156}{T}$$

$$C = \frac{156}{10} = 15.6\ m/s\ (51.2\ ft/s)$$

For d = 3 m

$$\frac{d}{L_0} = \frac{3}{156} = 0.0192$$

Example Problem II-1-1 (Continued)

Example Problem II-1-1 (Concluded)

By trial-and-error solution (Equation II-1-21) with d/L_o it is found that

$$\frac{d}{L} = 0.05641$$

hence

$$L = \frac{3}{0.05641} = 53.2\ m\ (174\ ft)\ \left(\text{transitional depth, since}\frac{1}{25} < \frac{d}{L} < \frac{1}{2}\right)$$

$$C = \frac{L}{T} = \frac{53.2}{10} = 5.32\ m/s\ (17.4\ ft/s)$$

An approximate value of L can also be found by using Equation II-1-11

$$L \approx \frac{gT^2}{2\pi}\sqrt{\tanh\left(\frac{4\pi^2}{T^2}\frac{d}{g}\right)}$$

which can be written in terms of L_o as

$$L \simeq L_0\sqrt{\tanh\left(\frac{2\pi d}{L_0}\right)}$$

therefore

$$L \simeq 156\sqrt{\tanh\left(\frac{2\pi(3)}{156}\right)}$$

$$L \simeq 156\sqrt{\tanh(0.1208)}$$

$$L \simeq 156\sqrt{0.1202} = 54.1\ m\ (177.5\ ft)$$

which compares with L = 53.3 m obtained using Equations II-1-8, II-1-9, or II-1-21. The error in this case is 1.5 percent. Note that Figure II-1-5 or Plate C-1 (SPM 1984) could also have been used to determine d/L.

(5) Local fluid velocities and accelerations.

(a) In wave force studies, the local fluid velocities and accelerations for various values of z and t during the passage of a wave must often be found. The horizontal component u and the vertical component w of the local fluid velocity are given by the following equations (with θ, x, and t as defined in Figure II-1-1):

$$u = \frac{H}{2}\frac{gT}{L}\frac{\cosh[2\pi(z+d)/L]}{\cosh(2\pi d/L)}\cos\theta \tag{II-1-22}$$

$$w = \frac{H}{2}\frac{gT}{L}\frac{\sinh[2\pi(z+d)/L]}{\cosh(2\pi d/L)}\sin\theta \tag{II-1-23}$$

(b) These equations express the local fluid velocity components any distance ($z + d$) above the bottom. The velocities are periodic in both x and t. For a given value of the phase angle $\theta = (2\pi x/L - 2\pi t/T)$, the hyperbolic functions *cosh* and *sinh*, as functions of z result in an approximate exponential decay of the magnitude of velocity components with increasing distance below the free surface. The maximum positive horizontal velocity occurs when $\theta = 0, 2\pi$, etc., while the maximum horizontal velocity in the negative direction occurs when $\theta = \pi, 3\pi$, etc. On the other hand, the maximum positive vertical velocity occurs when $\theta = \pi/2, 5\pi/2$, etc., and the maximum vertical velocity in the negative direction occurs when $\theta = 3\pi/2, 7\pi/2$, etc. Fluid particle velocities under a wave train are shown in Figure II-1-2.

(c) The local fluid particle accelerations are obtained from Equations II-1-22 and II-1-23 by differentiating each equation with respect to t. Thus,

$$\alpha_x = \frac{g\pi H}{L}\frac{\cosh[2\pi(z+d)/L]}{\cosh(2\pi d/L)}\sin\theta = \frac{\partial u}{\partial t} \tag{II-1-24}$$

$$\alpha_z = -\frac{g\pi H}{L}\frac{\sinh[2\pi(z+d)/L]}{\cosh(2\pi d/L)}\cos\theta = \frac{\partial w}{\partial t} \tag{II-1-25}$$

(d) Positive and negative values of the horizontal and vertical fluid accelerations for various values of θ are shown in Figure II-1-2.

(e) Figure II-1-2, a sketch of the local fluid motion, indicates that the fluid under the crest moves in the direction of wave propagation and returns during passage of the trough. Linear theory does not predict any net mass transport; hence, the sketch shows only an oscillatory fluid motion. Figure II-1-3 depicts profiles of the surface elevation, particle velocities, and accelerations by the linear wave theory. The following problem illustrates the computations required to determine local fluid velocities and accelerations resulting from wave motions.

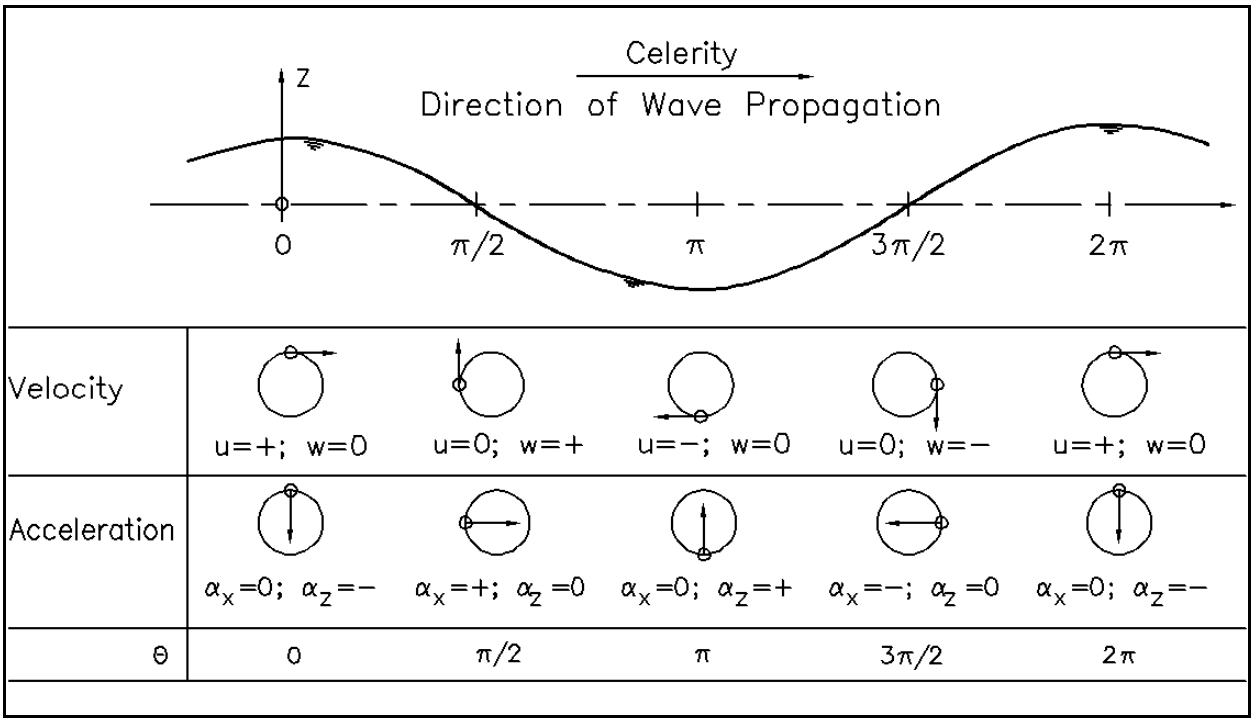

Figure II-1-2. Local fluid velocities and accelerations

(6) Water particle displacements.

(a) Another important aspect of linear wave theory deals with the displacement of individual water particles within the wave. Water particles generally move in elliptical paths in shallow or transitional depth water and in circular paths in deep water (Figure II-1-4). If the mean particle position is considered to be at the center of the ellipse or circle, then vertical particle displacement with respect to the mean position cannot exceed one-half the wave height. Thus, since the wave height is assumed to be small, the displacement of any fluid particle from its mean position must be small. Integration of Equations II-1-22 and II-1-23 gives the horizontal and vertical particle displacements from the mean position, respectively (Figure II-1-4).

(b) Fluid particle displacements are

$$\xi = -\frac{HgT^2}{4\pi L}\frac{\cosh\left(\frac{2\pi(z+d)}{L}\right)}{\cosh\left(\frac{2\pi d}{L}\right)}\sin\theta \tag{II-1-26}$$

$$\zeta = +\frac{HgT^2}{4\pi L}\frac{\sinh\left(\frac{2\pi(z+d)}{L}\right)}{\cosh\left(\frac{2\pi d}{L}\right)}\cos\theta \tag{II-1-27}$$

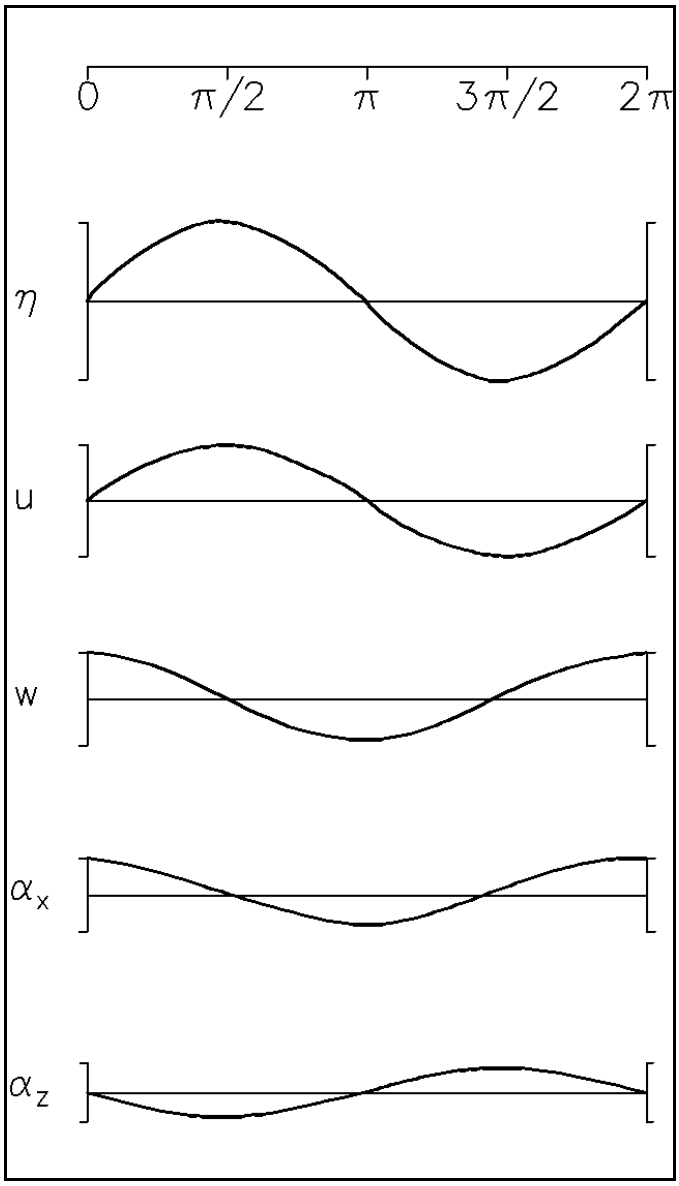

Figure II-1-3. Profiles of particle velocity and acceleration by Airy theory in relation to the surface elevation

where ξ is the horizontal displacement of the water particle from its mean position and ζ is the vertical displacement from its mean position (Figure II-1-4). The above equations can be simplified by using the relationship

$$\left(\frac{2\pi}{T}\right)^2 = \frac{2\pi g}{L} \tanh \frac{2\pi d}{L} \tag{II-1-28}$$

EXAMPLE PROBLEM II-1-2

FIND:

The local horizontal and vertical velocities u and w, and accelerations α_x and α_z at an elevation z = -5 m (or z = -16.4 ft) below the SWL when $\theta = 2\pi x/L - 2\pi t/T = \pi/3$ (or 60^0).

GIVEN:

A wave with a period T = 8 sec, in a water depth d = 15 m (49 ft), and a height H = 5.5 m (18.0 ft).

SOLUTION:

Calculate

$$L_0 = 1.56T^2 = 1.56(8)^2 = 99.8\ m\ (327\ ft)$$

$$\frac{d}{L_0} = \frac{15}{99.8} = 0.1503$$

By trial-and-error solution or using Figure II-1-5 for d/L_0 = 0.1503, we find

$$\frac{d}{L} = 0.1835$$

and

$$\cosh\frac{2\pi d}{L} = 1.742$$

hence

$$L = \frac{15}{0.1835} = 81.7\ m\ (268\ ft)$$

Evaluation of the constant terms in Equations II-1-22 to II-1-25 gives

$$\frac{HgT}{2L}\ \frac{1}{\cosh(2\pi d/L)} = \frac{5.5\ (9.8)(8)}{2\ (81.7)}\ \frac{1}{1.742} = 1.515$$

$$\frac{Hg\pi}{L}\ \frac{1}{\cosh(2\pi d/L)} = \frac{5.5\ (9.8)(3.1416)}{81.7}\ \frac{1}{1.742} = 1.190$$

Substitution into Equation II-1-22 gives

$$u = 1.515\ \cosh\left[\frac{2\pi(15\ -\ 5)}{81.7}\right]\ [\cos\ 60^0]$$

$$= 1.515\ [\cosh(0.7691)]\ (0.500)$$

Example Problem II-1-2 (Continued)

Example Problem II-1-2 (Concluded)

From the above known information, we find

$$\frac{2\pi d}{L} = 0.7691$$

and values of hyperbolic functions become

$$\cosh(0.7691) = 1.3106$$

and

$$\sinh(0.7691) = 0.8472$$

Therefore, fluid particle velocities are

$$u = 1.515(1.1306)(0.500) = 0.99\ m/s\ (3.26\ ft/s)$$

$$w = 1.515(0.8472)(0.866) = 1.11\ m/s\ (3.65\ ft/s)$$

and fluid particle accelerations are

$$\alpha_x = 1.190(1.3106)(0.866) = 1.35\ m/s^2\ (4.43\ ft/s^2)$$

$$\alpha_z = -1.190(0.8472)(0.500) = -0.50\ m/s^2\ (1.65\ ft/s^2)$$

(c) Thus,

$$\xi = -\frac{H}{2}\frac{\cosh\left(\frac{2\pi(z+d)}{L}\right)}{\sinh\left(\frac{2\pi d}{L}\right)}\sin\theta \tag{II-1-29}$$

$$\zeta = +\frac{H}{2}\frac{\sinh\left(\frac{2\pi(z+d)}{L}\right)}{\sinh\left(\frac{2\pi d}{L}\right)}\cos\theta \tag{II-1-30}$$

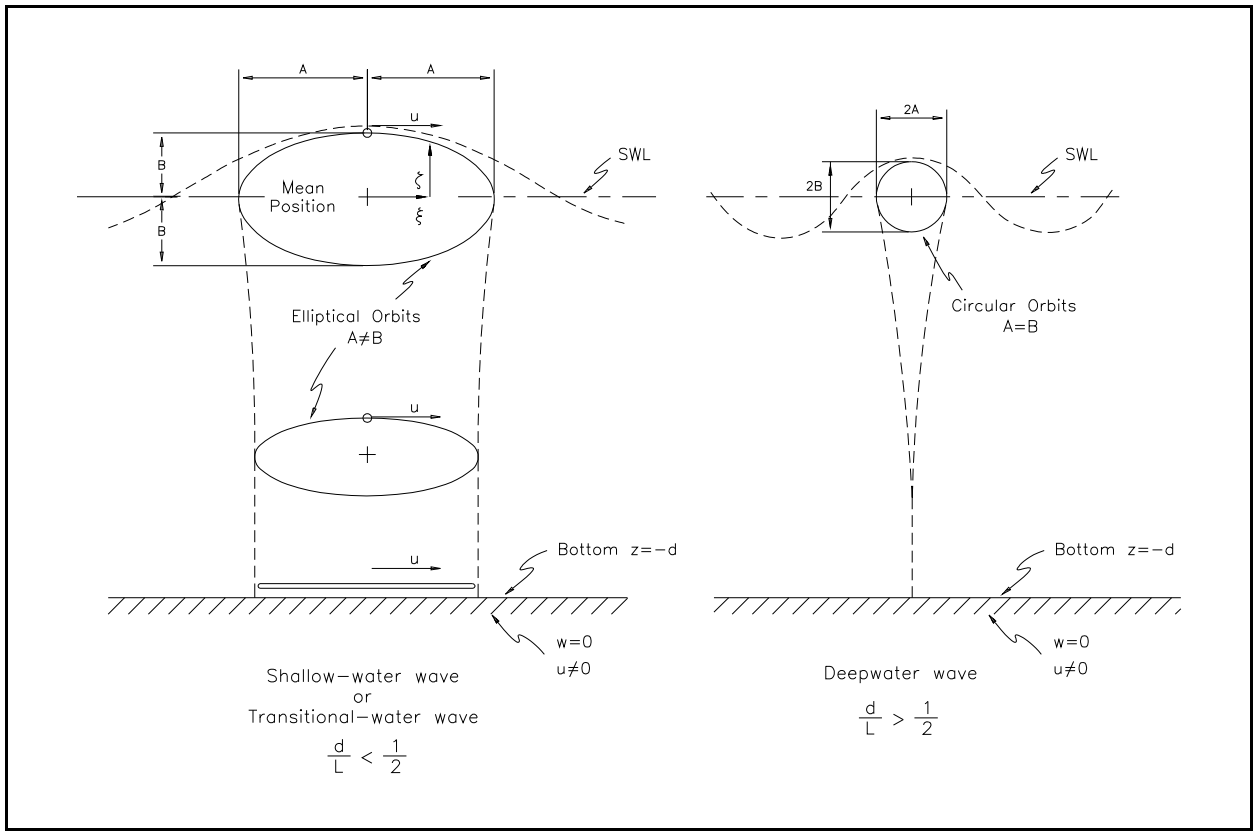

Figure II-1-4. Water particle displacements from mean position for shallow-water and deepwater waves

(d) Writing Equations II-1-29 and II-1-30 in the forms,

$$\sin^2 \theta = \left[\frac{\xi}{a} \frac{\sinh\left(\frac{2\pi d}{L}\right)}{\cosh\left(\frac{2\pi(z+d)}{L}\right)} \right]^2 \tag{II-1-31}$$

$$\cos^2 \theta = \left[\frac{\zeta}{a} \frac{\sinh\left(\frac{2\pi d}{L}\right)}{\sinh\left(\frac{2\pi(z+d)}{L}\right)} \right]^2 \tag{II-1-32}$$

and adding gives

$$\frac{\xi^2}{A^2} + \frac{\zeta^2}{B^2} = 1 \tag{II-1-33}$$

in which A and B are

$$A = \frac{H}{2} \frac{\cosh\left(\frac{2\pi(z + d)}{L}\right)}{\sinh\left(\frac{2\pi d}{L}\right)} \tag{II-1-34}$$

$$B = \frac{H}{2} \frac{\sinh\left(\frac{2\pi(z + d)}{L}\right)}{\sinh\left(\frac{2\pi d}{L}\right)} \tag{II-1-35}$$

(e) Equation II-1-33 is the equation of an ellipse with a major- (horizontal) semi-axis equal to A and a minor (vertical) semi-axis equal to B. The lengths of A and B are measures of the horizontal and vertical displacements of the water particles (see Figure II-1-4). Thus, the water particles are predicted to move in closed orbits by linear wave theory; i.e., a fluid particle returns to its initial position after each wave cycle. Comparing laboratory measurements of particle orbits with this theory shows that particle orbits are not completely closed. This difference between linear theory and observations is due to the mass transport phenomenon, which is discussed later in this chapter. It shows that linear theory is inadequate to explain wave motion completely.

(f) Examination of Equations II-1-34 and II-1-35 shows that for deepwater conditions, A and B are equal and particle paths are circular (Figure II-1-4). These equations become

$$A = B = \frac{H}{2} e^{\left(\frac{2\pi z}{L}\right)} \quad \text{for } \frac{d}{L} > \frac{1}{2} \text{ (i.e., deepwater limit)} \tag{II-1-36}$$

(g) For shallow-water conditions (d/L < 1/25), the equations become

$$A = \frac{H}{2} \frac{L}{2\pi d} \tag{II-1-37}$$

and

$$B = \frac{H}{2}\left(1 + \frac{z}{d}\right) \tag{II-1-38}$$

EXAMPLE PROBLEM II-1-3

FIND:

(a) The maximum horizontal and vertical displacement of a water particle from its mean position when z = 0 and z = -d.

(b) The maximum water particle displacement at an elevation z = -7.5 m (-24.6 ft) when the wave is in infinitely deep water.

(c) For the deepwater conditions of (b) above, show that the particle displacements are small relative to the wave height when $z = -L_0/2$.

GIVEN:

A wave in a depth d = 12 m (39.4 ft), height H = 3 m (9.8 ft), and a period T = 10 sec. The corresponding deepwater wave height is H_0 = 3.13 m (10.27 ft).

SOLUTION:

(a)

$$L_0 = 1.56T^2 = 1.56(10)^2 = 156\ m\ (512\ ft)$$

$$\frac{d}{L_0} = \frac{12}{156} = 0.0769$$

From hand calculators, we find

$$\sinh\left(\frac{2\pi d}{L}\right) = 0.8306$$

$$\tanh\left(\frac{2\pi d}{L}\right) = 0.6389$$

When z = 0, Equation II-1-34 reduces to

$$A = \frac{H}{2}\,\frac{1}{\tanh\left(\frac{2\pi d}{L}\right)}$$

and Equation II-1-35 reduces to

$$B = \frac{H}{2}$$

Thus

$$A = \frac{3}{2}\,\frac{1}{(0.6389)} = 2.35\ m\ (7.70\ ft)$$

$$B = \frac{H}{2} = \frac{3}{2} = 1.5\ m\ (4.92\ ft)$$

Example Problem II-1-3 (Continued)

Example Problem II-1-3 (Concluded)

When z = -d,

$$A = \frac{H}{2\ \sinh\left(\frac{2\pi d}{L}\right)} = \frac{3}{2(0.8306)} = 1.81\ m\ (5.92\ ft)$$

and $B = 0$.

(b) With H_0 = 3.13 m and z = -7.5 m (-24.6 ft), evaluate the exponent of e for use in Equation II-1-36, noting that $L = L_0$,

$$\frac{2\pi z}{L} = \frac{2\pi(-7.5)}{156} = -0.302$$

thus,

$$e^{-0.302} = 0.739$$

Therefore,

$$A = B = \frac{H_0}{2} e^{\left(\frac{2\pi z}{L}\right)} = \frac{3.13}{2}(0.739) = 1.16\ m\ (3.79\ ft)$$

The maximum displacement or diameter of the orbit circle would be 2(1.16) = 2.32 m (7.61 ft) when z = -7.5 m.

(c) At a depth corresponding to the half wavelength from the MWL, we have

$$z = -\frac{L_0}{2} = \frac{-156}{2} = -78.0\ m\ (255.9\ ft)$$

$$\frac{2\pi z}{L} = \frac{2\pi(-78)}{156} = -3.142$$

Therefore

$$e^{-3.142} = 0.043$$

and

$$A = B = \frac{H_0}{2} e^{\left(\frac{2\pi z}{L}\right)} = \frac{3.13}{2}(0.043) = 0.067\ m\ (0.221\ ft)$$

Thus, the maximum displacement of the particle is 0.067 m, which is small when compared with the deepwater height, H_0 = 3.13 m (10.45 ft).

(h) Thus, in deep water, the water particle orbits are circular as indicated by Equation II-1-36 (see Figure II-1-4). Equations II-1-37 and II-1-38 show that in transitional and shallow water, the orbits are elliptical. The more shallow the water, the flatter the ellipse. The amplitude of the water particle displacement decreases exponentially with depth and in deepwater regions becomes small relative to the wave height at a depth equal to one-half the wavelength below the free surface; i.e., when $z = L_0/2$.

(i) Water particle displacements and orbits based on linear theory are illustrated in Figure II-1-4. For shallow regions, horizontal particle displacement near the bottom can be large. In fact, this is apparent in offshore regions seaward of the breaker zone where wave action and turbulence lift bottom sediments into suspension. The vertical displacement of water particles varies from a minimum of zero at the bottom to a maximum equal to one-half the wave height at the surface.

(7) Subsurface pressure.

(a) Subsurface pressure under a wave is the sum of two contributing components, dynamic and static pressures, and is given by

$$p' = \frac{\rho g H \cosh\left[\frac{2\pi(z+d)}{L}\right]}{2\cosh\left(\frac{2\pi d}{L}\right)} \cos\theta - \rho g z + p_a \tag{II-1-39}$$

where p' is the total or absolute pressure, p_a is the atmospheric pressure, and ρ is the mass density of water (for salt water, ρ = 1,025 kg/m^3 or 2.0 slugs/ft^3, for fresh water, ρ = 1,000 kg/m^3 or 1.94 slugs/ft^3). The first term of Equation II-1-39 represents a dynamic component due to acceleration, while the second term is the static component of pressure. For convenience, the pressure is usually taken as the gauge pressure defined as

$$p = p' - p_a = \frac{\rho g H \cosh\left[\frac{2\pi(z+d)}{L}\right]}{2\cosh\left(\frac{2\pi d}{L}\right)} \cos\theta - \rho g z \tag{II-1-40}$$

(b) Equation II-1-40 can be written as

$$p = \rho g \eta \frac{\cosh\left[\frac{2\pi(z+d)}{L}\right]}{\cosh\left(\frac{2\pi d}{L}\right)} - \rho g z \tag{II-1-41}$$

since

$$\eta = \frac{H}{2}\cos\left(\frac{2\pi x}{L} - \frac{2\pi t}{T}\right) = \frac{H}{2}\cos\theta \tag{II-1-42}$$

(c) The ratio

$$K_z = \frac{\cosh\left[\frac{2\pi(z + d)}{L}\right]}{\cosh\left(\frac{2\pi d}{L}\right)} \tag{II-1-43}$$

is termed *the pressure response factor*. Hence, Equation II-1-41 can be written as

$$p = \rho g(\eta K_z - z) \tag{II-1-44}$$

(d) The pressure response factor K for the pressure at the bottom when z = -d,

$$K_z = K = \frac{1}{\cosh\left(\frac{2\pi d}{L}\right)} \tag{II-1-45}$$

is presented as function of d/L_0 in the tables (SPM 1984); see also Figure II-1-5. This figure is a convenient graphic means to determine intermediate and shallow-water values of the bottom pressure response factor K, the ratio C/C_0 ($=L/L_0 = k_0/k$), and a number of other variables commonly occurring in water wave calculations.

(e) It is often necessary to determine the height of surface waves based on subsurface measurements of pressure. For this purpose, it is convenient to rewrite Equation II-1-44 as

$$\eta = \frac{N(p + \rho g z)}{\rho g K_z} \tag{II-1-46}$$

where z is the depth below the SWL of the pressure gauge, and N a correction factor equal to unity if the linear theory applies.

(f) Chakrabarti (1987) presents measurements that correlate measured dynamic pressure in the water column (s in his notation is the elevation above the seabed) with linear wave theory. These laboratory measurements include a number of water depths, wave periods, and wave heights. The best agreement between the theory and these measurements occurs in deep water. Shallow-water pressure measurements for steep water waves deviate significantly from the linear wave theory predictions. The example problem hereafter illustrates the use of pertinent equations for finding wave heights from pressure measurements based on linear theory.

(8) Group velocity.

(a) It is desirable to know how fast wave energy is moving. One way to determine this is to look at the speed of wave groups that represents propagation of wave energy in space and time. The speed a group of

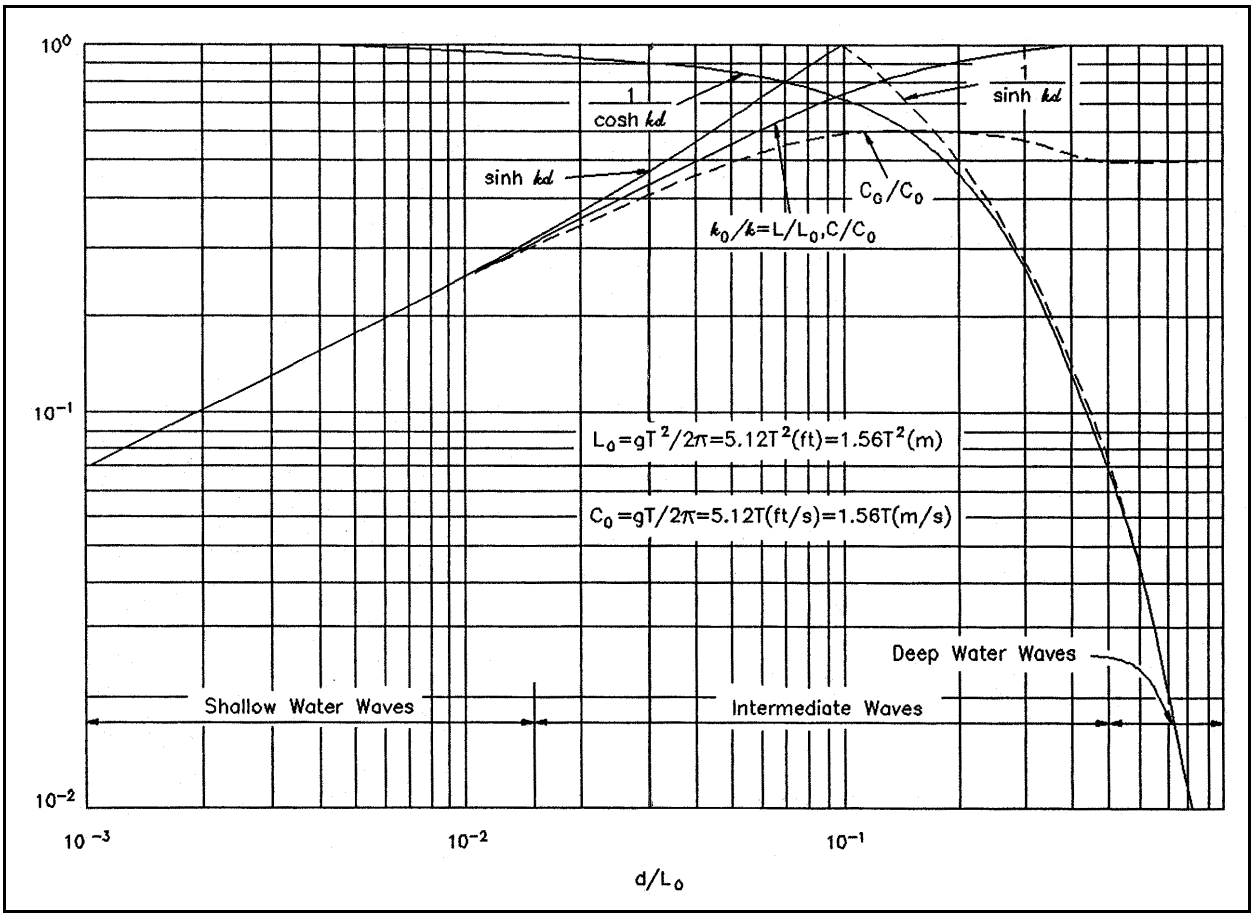

Figure II-1-5. Variation of wave parameters with d/L_0 (Dean and Dalrymple 1991)

waves or a wave train travels is generally not identical to the speed with which individual waves within the group travel. The group speed is termed the *group velocity* C_g; the individual wave speed is the *phase velocity* or *wave celerity* given by Equations II-1-8 or II-1-9. For waves propagating in deep or transitional water with gravity as the primary restoring force, the group velocity will be less than the phase velocity. For those waves, propagated primarily under the influence of surface tension (i.e., capillary waves), the group velocity may exceed the velocity of an individual wave.

(b) The concept of group velocity can be described by considering the interaction of two sinusoidal wave trains moving in the same direction with slightly different wavelengths and periods. The equation of the water surface is given by

$$\eta = \eta_1 + \eta_2 = \frac{H}{2}\cos\left(\frac{2\pi x}{L_1} - \frac{2\pi t}{T_1}\right) + \frac{H}{2}\cos\left(\frac{2\pi x}{L_2} - \frac{2\pi t}{T_2}\right) \tag{II-1-47}$$

where η_1 and η_2 are the two components. They may be summed since superposition of solutions is permissible when the linear wave theory is used. For simplicity, the heights of both wave components have been assumed equal. Since the wavelengths of the two component waves, L_1 and L_2, have been assumed slightly different for some values of x at a given time, the two components will be in phase and the wave height observed will be 2H; for some other values of x, the two waves will be completely out of phase and

EXAMPLE PROBLEM II-1-4

FIND:

The height of the wave H assuming that linear theory applies and the average frequency corresponds to the average wave amplitude.

GIVEN:

An average maximum pressure p = 124 kilonewtons per square meter is measured by a subsurface pressure gauge located in salt water 0.6 meter (1.97 ft) above the bed in depth d = 12 m (39 ft). The average frequency f = 0.06666 cycles per second (Hertz).

SOLUTION:

$$T = \frac{1}{f} = \frac{1}{(0.0666)} \approx 15\ s$$

$$L_0 = 1.56T^2 = 1.56(15)^2 = 351\ m\ (1152\ ft)$$

$$\frac{d}{L_0} = \frac{12}{351} \approx 0.0342$$

From Figure II-1-5, entering with d/L_0,

$$\frac{d}{L} = 0.07651$$

hence,

$$L = \frac{12}{(0.07651)} = 156.8\ m\ (515\ ft)$$

and

$$\cosh\left(\frac{2\pi d}{L}\right) = 1.1178$$

Therefore, from Equation II-1-43

$$K_z = \frac{\cosh\left[\frac{2\pi(z+d)}{L}\right]}{\cosh\left(\frac{2\pi d}{L}\right)} = \frac{\cosh\left[\frac{2\pi(-11.4+12)}{156.8}\right]}{1.1178} = 0.8949$$

Since $\eta = a = H/2$ when the pressure is maximum (under the wave crest), and $N = 1.0$ since linear theory is assumed valid,

$$\frac{H}{2} = \frac{N(p + \rho g z)}{\rho g K_z} = \frac{1.0\ [124 + (10.06)\ (-11.4)]}{(10.06)\ (0.8949)} = 1.04\ m\ (3.44\ ft)$$

Therefore,

$$H = 2(1.04) = 2.08\ m\ (6.3\ ft)$$

Note that the value of K in Figure II-1-5 or SPM (1984) could not be used since the pressure was not measured at the bottom.

the resultant wave height will be zero. The surface profile made up of the sum of the two sinusoidal waves is given by Equation II-1-47 and is shown in Figure II-1-6. The waves shown in Figure II-1-6 appear to be traveling in groups described by the equation of the envelope curves

$$\eta_{envelope} = \pm H \cos\left[\pi\left(\frac{L_2 - L_1}{L_1 L_2}\right)x - \pi\left(\frac{T_2 - T_1}{T_1 T_2}\right)t\right] \tag{II-1-48}$$

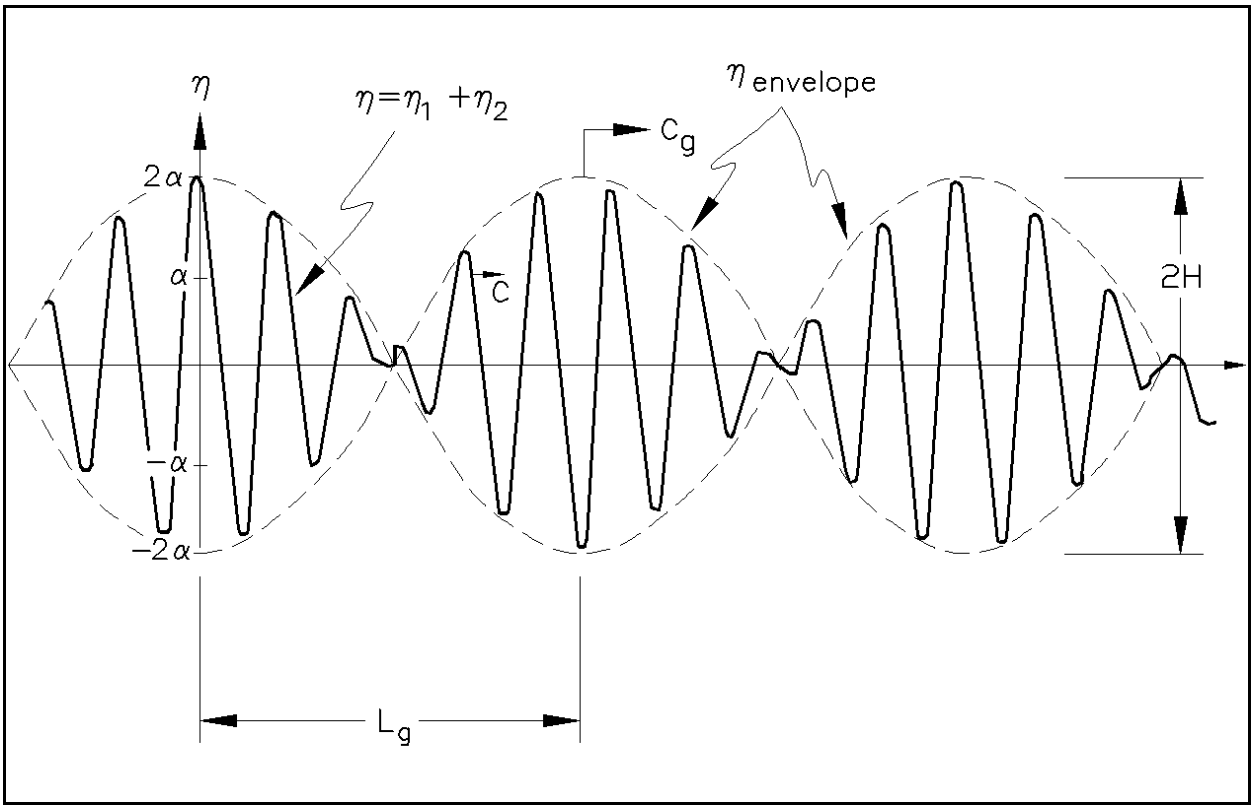

Figure II-1-6. Characteristics of a wave group formed by the addition of sinusoids with different periods

(c) It is the speed of these groups (i.e., the velocity of propagation of the envelope curves) defined in Equation II-1-48 that represents the group velocity. The limiting speed of the wave groups as they become large (i.e., as the wavelength L_1 approaches L_2 and consequently the wave period T_1 approaches T_2) is the group velocity and can be shown to be equal to

$$C_g = \frac{1}{2}\frac{L}{T}\left[1 + \frac{\frac{4\pi d}{L}}{\sinh\left(\frac{4\pi d}{L}\right)}\right] = nC \tag{II-1-49}$$

where

$$n = \frac{1}{2}\left[1 + \frac{\frac{4\pi d}{L}}{\sinh\left(\frac{4\pi d}{L}\right)}\right] \tag{II-1-50}$$

(d) In deep water, the term $(4\pi d/L)/\sinh(4\pi d/L)$ is approximately zero and $n = 1/2$, giving

$$C_{g_0} = \frac{1}{2}\frac{L_0}{T} = \frac{1}{2}C_0 \text{ (deep water)} \tag{II-1-51}$$

or the group velocity is one-half the phase velocity.

(e) In shallow water, $\sinh(4\pi d/L \approx 4\pi d/L)$ and

$$C_{g_s} = \frac{L}{T} = C \approx \sqrt{gd} \text{ (shallow water)} \tag{II-1-52}$$

hence, the group and phase velocities are equal. Thus, in shallow water, because wave celerity is determined by the depth, all component waves in a wave train will travel at the same speed precluding the alternate reinforcing and canceling of components. In deep and transitional water, wave celerity depends on wavelength; hence, slightly longer waves travel slightly faster and produce the small phase differences resulting in wave groups. These waves are said to be *dispersive* or propagating in a *dispersive medium*; i.e., in a medium where their celerity is dependent on wavelength.

(f) The variation of the ratios of group and phase velocities to the deepwater phase velocity C_g/C_0 and C/C_0, respectively are given as a function of the depth relative to the deep water wavelength d/L_0 in Figure II-1-7. The two curves merge together for small values of depth and C_g reaches a maximum before tending asymptotically toward $C/2$.

(g) Outside of shallow water, the phase velocity of gravity waves is greater than the group velocity. An observer that follows a group of waves at group velocity will see waves that originate at the rear of the group move forward through the group traveling at the phase velocity and disappear at the front of the wave group.

(h) Group velocity is important because it is with this velocity that wave energy is propagated. Although mathematically the group velocity can be shown rigorously from the interference of two or more waves (Lamb 1945), the physical significance is not as obvious as it is in the method based on the consideration of wave energy. Therefore an additional explanation of group velocity is provided on wave energy and energy transmission.

(9) Wave energy and power.

(a) The total energy of a wave system is the sum of its kinetic energy and its potential energy. The kinetic energy is that part of the total energy due to water particle velocities associated with wave motion. The kinetic energy per unit length of wave crest for a wave defined with the linear theory can be found from

$$\bar{E}_k = \int_x^{x+L}\int_{-d}^{\eta} \rho\frac{u^2 + w^2}{2}\,dz\,dx \tag{II-1-53}$$

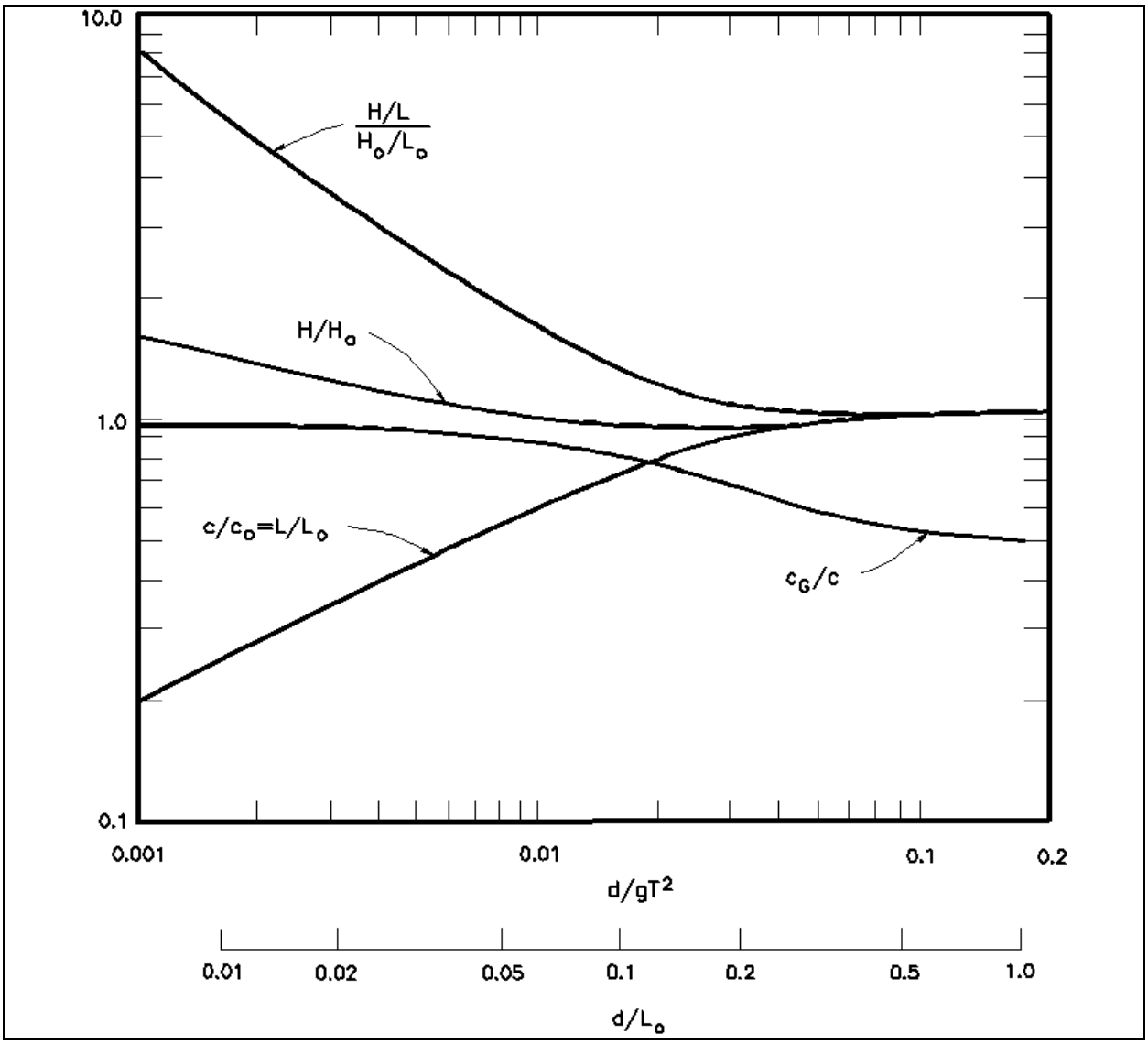

Figure II-1-7. Variation of the ratios of group and phase velocities to deepwater phase speed using linear theory (Sarpkaya and Isaacson 1981)

which, upon integration, gives

$$\bar{E}_k = \frac{1}{16} \rho g H^2 L \tag{II-1-54}$$

(b) Potential energy is that part of the energy resulting from part of the fluid mass being above the trough: the wave crest. The potential energy per unit length of wave crest for a linear wave is given by

$$\bar{E}_p = \int_x^{x+L} \rho g \left[\frac{(\eta + d)^2}{2} - \frac{d^2}{2} \right] dx \tag{II-1-55}$$

which, upon integration, gives

$$\bar{E}_p = \frac{1}{16} \rho g H^2 L \tag{II-1-56}$$

(c) According to the Airy theory, if the potential energy is determined relative to SWL, and all waves are propagated in the same direction, potential and kinetic energy components are equal, and the total wave energy in one wavelength per unit crest width is given by

$$E = E_k + E_p = \frac{\rho g H^2 L}{16} + \frac{\rho g H^2 L}{16} = \frac{\rho g H^2 L}{8} \tag{II-1-57}$$

where subscripts *k* and *p* refer to kinetic and potential energies. Total average wave energy per unit surface area, termed the *specific energy* or *energy density*, is given by

$$\bar{E} = \frac{E}{L} = \frac{\rho g H^2}{8} \tag{II-1-58}$$

(d) *Wave energy flux* is the rate at which energy is transmitted in the direction of wave propagation across a vertical plan perpendicular to the direction of wave advance and extending down the entire depth. Assuming linear theory holds, the average energy flux per unit wave crest width transmitted across a vertical plane perpendicular to the direction of wave advance is

$$\bar{P} = \frac{1}{T}\int_t^{t+r} \int_{-d}^{\eta} p\, u\, dz\, dt \tag{II-1-59}$$

which, upon integration, gives

$$\bar{P} = \bar{E} n C = \bar{E} C_g \tag{II-1-60}$$

where $\bar{P}$ is frequently called *wave power*, and the variable *n* has been defined earlier in Equation II-1-50.

(e) If a vertical plane is taken other than perpendicular to the direction of wave advance, $\bar{P} = E C_g \sin \theta$, where θ is the angle between the plane across which the energy is being transmitted and the direction of wave advance.

(f) For deep and shallow water, Equation II-1-60 becomes

$$\bar{P}_0 = \frac{1}{2} \bar{E}_0 C_o \text{ (deep water)} \tag{II-1-61}$$

$$\bar{P} = \bar{E} C_g = \bar{E} C \text{ (shallow water)} \tag{II-1-62}$$

(g) An energy balance for a region through which waves are passing will reveal that, for steady state, the amount of energy entering the region will equal the amount leaving the region provided no energy is added or removed. Therefore, when the waves are moving so that their crests are parallel to the bottom contours

$$\bar{E}_0 n_0 C_0 = \bar{E} n C \tag{II-1-63}$$

or since

$$n_0 = \frac{1}{2} \tag{II-1-64}$$

$$\frac{1}{2} \bar{E}_0 C_0 = \bar{E} n C \tag{II-1-65}$$

(h) When the wave crests are not parallel to the bottom contours, some parts of the wave will be traveling at different speeds and the wave will be refracted; in this case Equation II-1-65 does not apply (see Parts II-3 and II-4). The rate of energy transmission is important for coastal design, and it requires knowledge of C_g to determine how fast waves move toward shore. The mean rate of energy transmission associated with waves propagating into an area of calm water provides a different physical description of the concept of group velocity.

(i) Equation II-1-65 establishes a relationship between the ratio of the wave height at some arbitrary depth and the deepwater wave height. This ratio, known as the *shoaling coefficient* (see Part II-3 for detail derivation), is dependent on the wave steepness. The variation of shoaling coefficient with wave steepness as a function of relative water depth d/L_0 is shown in Figure II-1-8. Wave shoaling and other related nearshore processes are described in detail in Parts II-3 and II-4.

(10) Summary of linear wave theory.

(a) Equations describing water surface profile particle velocities, particle accelerations, and particle displacements for linear (Airy) theory are summarized in Figure II-1-9. The Corps of Engineers' microcomputer package of computer programs (ACES; Leenknecht et al. 1992) include several software applications for calculating the linear wave theory and associated parameters. Detailed descriptions of the ACES and CMS software to the linear wave theory may be found in the ACES and CMS documentation.

(b) Other wave phenomena can be explained using linear wave theory. For example, observed decreases and increases in the mean water level, termed wave setdown and wave setup, are in essence nonlinear quantities since they are proportional to wave height squared. These nonlinear quantities may be explained using the concept of radiation stresses obtained from linear theory. Maximum wave setdown occurs just seaward of the breaker line. Wave setup occurs between the breaker line and the shoreline and can increase the mean water level significantly. Wave setdown and setup and their estimation are discussed in Part II-4.

(c) *Radiation stresses* are the forces per unit area that arise because of the excess momentum flux due to the presence of waves. In simple terms, there is more momentum flow in the direction of wave advance because the velocity U is in the direction of wave propagation under the wave crest when the instantaneous water surface is high (wave crest) and in the opposite direction when the water surface is low (wave trough). Also, the pressure stress acting under the wave crest is greater than the pressure stress under the wave trough leading to a net stress over a wave period. Radiation stresses arise because of the finite amplitude (height) of the waves. Interestingly, small-amplitude (linear) wave theory can be used to reasonably approximate radiation stresses and explain effects such as wave set down, wave setup, and the generation of longshore currents.

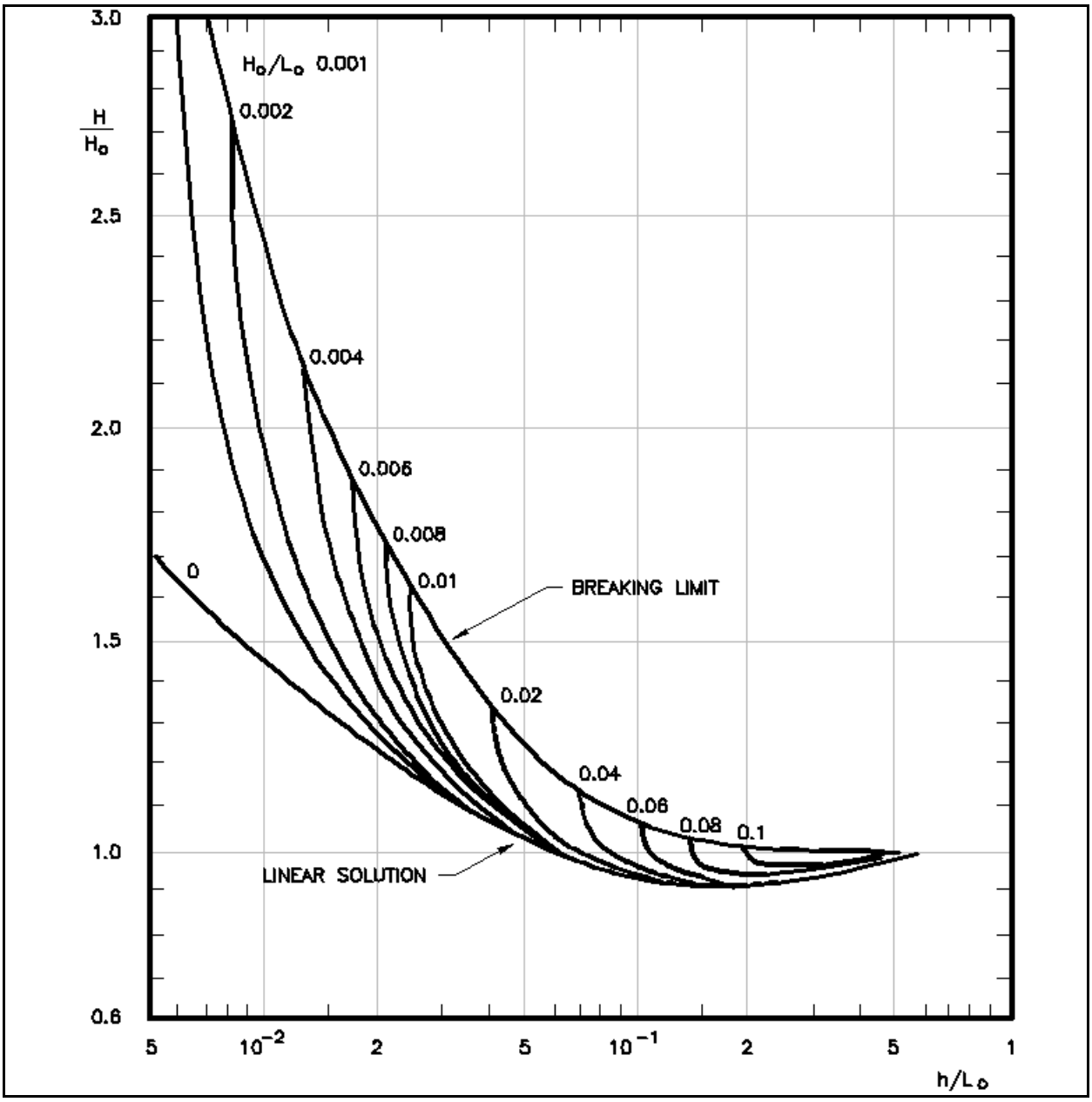

Figure II-1-8. Variation of shoaling coefficient with wave steepness (Sakai and Battjes 1980)

d. Nonlinear wave theories.

(1) Introduction.

(a) Linear waves as well as finite-amplitude waves may be described by specifying two dimensionless parameters, the wave steepness *H/L* and the relative water depth *d/L*. The relative water depth has been discussed extensively earlier in this chapter with regard to linear waves. The *Relative depth* determines whether waves are dispersive or nondispersive and whether the celerity, length, and height are influenced by water depth. *Wave steepness* is a measure of how large a wave is relative to its height and whether the linear wave assumption is valid. Large values of the wave steepness suggest that the small-amplitude

Relative Depth	Shallow Water $\frac{d}{L} < \frac{1}{20}$ $kd < \frac{\pi}{10}$	Transitional Water $\frac{1}{20} < \frac{d}{L} < \frac{1}{2}$ $\frac{\pi}{10} < kd < \frac{\pi}{2}$	Deep Water $\frac{d}{L} > \frac{1}{2}$ $kd > \frac{\pi}{2}$
1. Wave profile	Same As >	$\eta = \frac{H}{2}\cos\left[\frac{2\pi x}{L} - \frac{2\pi t}{T}\right] = \frac{H}{2}\cos\theta$	< Same As
2. Wave celerity	$C = \frac{L}{T} = \sqrt{gd}$	$C = \frac{L}{T} = \frac{gT}{2\pi}\tanh\left(\frac{2\pi d}{L}\right)$	$C = C_0 = \frac{L}{T} = \frac{gT}{2\pi}$
3. Wavelength	$L = T\sqrt{gd} = CT$	$L = \frac{gT^2}{2\pi}\tanh\left(\frac{2\pi d}{L}\right)$	$L = L_0 = \frac{gT^2}{2\pi} = C_0 T$
4. Group velocity	$C_g = C = \sqrt{gd}$	$C_g = nC = \frac{1}{2}\left[1 + \frac{4\pi d/L}{\sinh(4\pi d/L)}\right]C$	$C_g = \frac{1}{2}C = \frac{gT}{4\pi}$
5. Water particle velocity			
(a) Horizontal	$u = \frac{H}{2}\sqrt{\frac{g}{d}}\cos\theta$	$u = \frac{H}{2}\frac{gT}{L}\frac{\cosh[2\pi(z+d)/L]}{\cosh(2\pi d/L)}\cos\theta$	$u = \frac{\pi H}{T}e^{\left(\frac{2\pi z}{L}\right)}\cos\theta$
(b) Vertical	$w = \frac{H\pi}{T}\left(1+\frac{z}{d}\right)\sin\theta$	$w = \frac{H}{2}\frac{gT}{L}\frac{\sinh[2\pi(z+d)/L]}{\cosh(2\pi d/L)}\sin\theta$	$w = \frac{\pi H}{T}e^{\left(\frac{2\pi z}{L}\right)}\sin\theta$
6. Water particle accelerations			
(a) Horizontal	$a_x = \frac{H\pi}{T}\sqrt{\frac{g}{d}}\sin\theta$	$a_x = \frac{g\pi H}{L}\frac{\cosh[2\pi(z+d)/L]}{\cosh(2\pi d/L)}\sin\theta$	$a_x = 2H\left(\frac{\pi}{T}\right)^2 e^{\left(\frac{2\pi z}{L}\right)}\sin\theta$
(b) Vertical	$a_z = -2H\left(\frac{\pi}{T}\right)^2\left(1+\frac{z}{d}\right)\cos\theta$	$a_z = -\frac{g\pi H}{L}\frac{\sinh[2\pi(z+d)/L]}{\cosh(2\pi d/L)}\cos\theta$	$a_z = -2H\left(\frac{\pi}{T}\right)^2 e^{\left(\frac{2\pi z}{L}\right)}\cos\theta$
7. Water particle displacements			
(a) Horizontal	$\xi = -\frac{HT}{4\pi}\sqrt{\frac{g}{d}}\sin\theta$	$\xi = -\frac{H}{2}\frac{\cosh[2\pi(z+d)/L]}{\sinh(2\pi d/L)}\sin\theta$	$\xi = -\frac{H}{2}e^{\left(\frac{2\pi z}{L}\right)}\sin\theta$
(b) Vertical	$\zeta = \frac{H}{2}\left(1+\frac{z}{d}\right)\cos\theta$	$\zeta = \frac{H}{2}\frac{\sinh[2\pi(z+d)/L]}{\sinh(2\pi d/L)}\cos\theta$	$\zeta = \frac{H}{2}e^{\left(\frac{2\pi z}{L}\right)}\cos\theta$
8. Subsurface pressure	$p = \rho g(\eta - z)$	$p = \rho g\eta\frac{\cosh[2\pi(z+d)/L]}{\cosh(2\pi d/L)} - \rho gz$	$p = \rho g\eta e^{\left(\frac{2\pi z}{L}\right)} - \rho gz$

Figure II-1-9. Summary of linear (Airy) wave theory - wave characteristics

assumption may be questionable. A third dimensionless parameter, which may be used to replace either the wave steepness or relative water depth, may be defined as the ratio of wave steepness to relative water depth. Thus,

$$\frac{H/L}{d/L} = \frac{H}{d} \tag{II-1-66}$$

which is termed the *relative wave height*. Like the wave steepness, large values of the relative wave height indicate that the small-amplitude assumption may not be valid. A fourth dimensionless parameter often used to assess the relevance of various wave theories is termed the *Ursell number*. The Ursell number is given by

$$U_R = \left(\frac{L}{d}\right)^2 \frac{H}{d} = \frac{L^2 H}{d^3} \tag{II-1-67}$$

(b) The value of the Ursell number is often used to select a wave theory to describe a wave with given L and H (or T and H) in a given water depth d. High values of U_R indicate large, finite-amplitude, long waves in shallow water that may necessitate the use of nonlinear wave theory, to be discussed next.

(c) The linear or small-amplitude wave theory described in the preceding sections provides a useful first approximation to the wave motion. Ocean waves are generally not small in amplitude. In fact, from an engineering point of view it is usually the large waves that are of interest since they result in the largest forces and greatest sediment movement. In order to approach the complete solution of ocean waves more closely, a perturbation solution using successive approximations may be developed to improve the linear theory solution of the hydrodynamic equations for gravity waves. Each order wave theory in the perturbation expansion serves as a correction and the net result is often a better agreement between theoretical and observed waves. The extended theories can also describe phenomena such as *mass transport* where there is a small net forward movement of the water during the passage of a wave. These higher-order or extended solutions for gravity waves are often called *nonlinear wave theories*.

(d) Development of the nonlinear wave theories has evolved for a better description of surface gravity waves. These include *cnoidal*, *solitary*, and *Stokes* theories. However, the development of a Fourier-series approximation by Fenton in recent years has superseded the previous historical developments. Since earlier theories are still frequently referenced, these will first be summarized in this section, but Fenton's theory is recommended for regular waves in all coastal applications.

(2) Stokes finite-amplitude wave theory.

(a) Since the pioneering work of Stokes (1847, 1880) most extension studies (De 1955; Bretschneider 1960; Skjelbreia and Hendrickson 1961; Laitone 1960, 1962, 1965; Chappelear 1962; Fenton 1985) in wave perturbation theory have assumed the wave slope ka is small where k is the wave number and a the amplitude of the wave. The perturbation solution, developed as a power series in terms of $\epsilon = ka$, is expected to converge as more and more terms are considered in the expansion. Convergence does not occur for steep waves unless a different perturbation parameter from that of Stokes is chosen (Schwartz 1974; Cokelet 1977; Williams 1981, 1985).

(b) The fifth-order Stokes finite-amplitude wave theory is widely used in practical applications both in deep- and shallow-water wave studies. A formulation of Stokes fifth-order theory with good convergence properties has recently been provided (Fenton 1985). Fenton's fifth-order Stokes theory is computationally efficient, and includes closed-form asymptotic expressions for both deep- and shallow-water limits. Kinematics and pressure predictions obtained from this theory compare with laboratory and field measurements better than other nonlinear theories.

(c) In general, the perturbation expansion for velocity potential Φ may be written as

$$\Phi = \epsilon\Phi_1 + \epsilon^2\Phi_2 + \ldots \tag{II-1-68}$$

in which $\epsilon = ka$ is the *perturbation expansion parameter*. Each term in the series is smaller than the preceding term by a factor of order *ka*. In this expansion, Φ_1 is the first-order theory (linear theory), Φ_2 is the second-order theory, and so on.

(d) Substituting Equation II-1-68 and similar expressions for other wave variables (i.e., surface elevation η, velocities *u* and *w*, pressure *p*, etc.) into the appropriate governing equations and boundary conditions describing the wave motion yields a series of higher-order solutions for ocean waves. Equating the coefficients of equal powers of *ka* gives recurrence relations for each order solution. A characteristic of the perturbation expansion is that each order theory is expressed in terms of the preceding lower order theories (Phillips 1977; Dean and Dalrymple 1991; Mei 1991). The first-order Stokes theory is the linear (Airy) theory.

(e) The Stokes expansion method is formally valid under the conditions that $H/d \ll (kd)^2$ for $kd < 1$ and $H/L \ll 1$ (Peregrine 1972). In terms of the Ursell number U_R these requirements can be met only for $U_R < 79$. This condition restricts the wave heights in shallow water and the Stokes theory is not generally applicable to shallow water. For example, the maximum wave height in shallow water allowed by the second-order Stokes theory is about one-half of the water depth (Fenton 1985). The mathematics of higher-order Stokes theories is cumbersome and is not presented here. See Ippen (1966) for a detailed derivation of the Stokes second-order theory.

(f) In the higher-order Stokes solutions, superharmonic components (i.e., higher frequency components at two, three, four, etc. times the fundamental frequency) arise. These are superposed on the fundamental component predicted by linear theory. Hence, wave crests are steeper and troughs are flatter than the sinusoidal profile (Figure II-1-10). The fifth-order Stokes expansion shows a secondary crest in the wave trough for high-amplitude waves (Peregrine 1972; Fenton 1985). In addition, particle paths for Stokes waves are no longer closed orbits and there is a *drift* or *mass transport* in the direction of wave propagation.

(g) The linear dispersion relation is still valid to second order, and both wavelength and celerity are independent of wave height to this order. At third and higher orders, wave celerity and wavelength depend on wave height, and therefore, for a given wave period, celerity and length are greater for higher waves. Some limitations are imposed on the finite-amplitude Stokes theory in shallow water both by the water depth and amplitude nonlinearities. For steeper waves in shallow water, higher-order terms in Stokes expansion may increase in magnitude to become comparable or larger than the fundamental frequency component (Fenton 1985; Chakrabarti 1987). When this occurs, the Stokes perturbation becomes invalid.

(h) Higher-order Stokes theories include aperiodic (i.e., not periodic) terms in the expressions for water particle displacements. These terms arise from the product of time and a constant depending on the wave period and depth, and give rise to a continuously increasing net particle displacement in the direction of wave propagation. The distance a particle is displaced during one wave period when divided by the wave period gives a mean drift velocity $\bar{U}(z)$, called the *mass transport velocity*. To second-order, the mass transport velocity is

$$\bar{U}(z) = \left(\frac{\pi H}{L}\right)^2 \frac{C}{2} \frac{\cosh\,[4\pi(z + d)/L]}{\sinh^2\,(2\pi d/L)} \tag{II-1-69}$$

indicating that there is a net transport of fluid by waves in the direction of wave propagation. If the mass transport leads to an accumulation of mass in any region, the free surface must rise, thus generating a pressure gradient. A current, formed in response to this pressure gradient, will reestablish the distribution of mass.

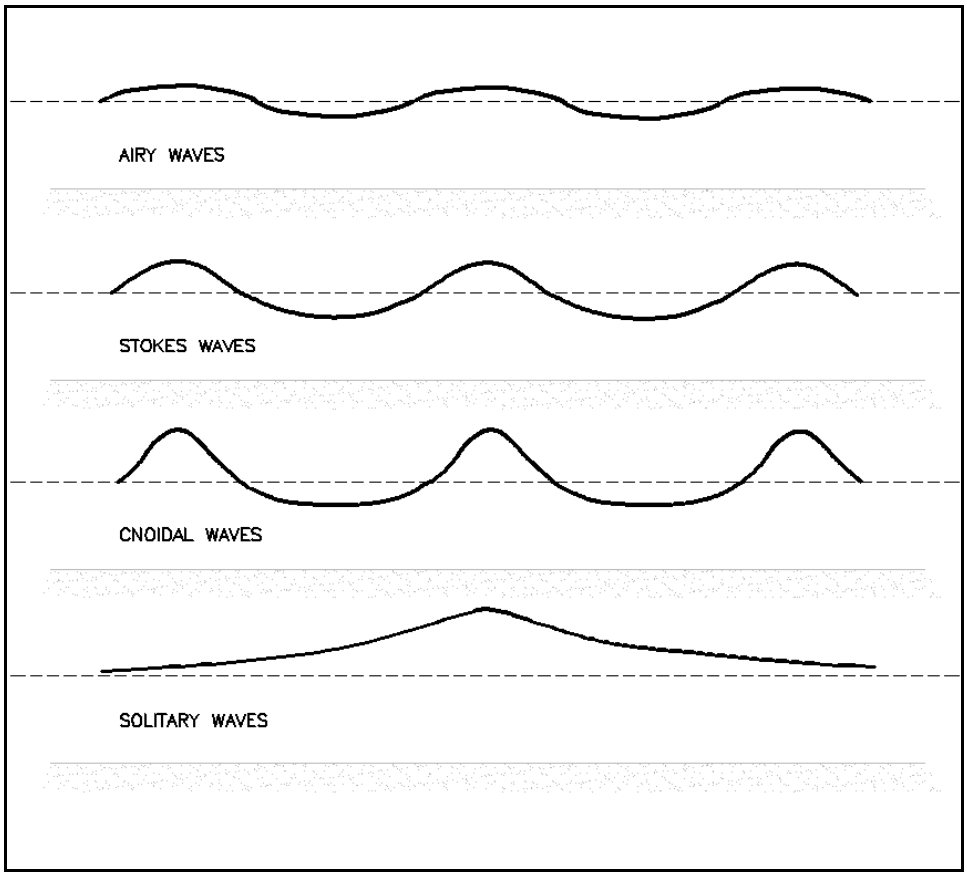

Figure II-1-10. Wave profile shape of different progressive gravity waves

(i) Following Stokes, using higher-order wave theories, both theoretical and experimental studies of mass transport have been conducted (Miche 1944; Ursell 1953; Longuet-Higgins 1953; Russell and Osorio 1958; Isaacson 1978). Results of two-dimensional wave tank experiments where a return flow existed in these studies show that the vertical distribution of the mass transport velocity is modified so that the net transport of water across a vertical plane is zero. For additional information on mass transport, see Dean and Dalrymple (1991).

(3) Subsurface pressure.

(a) Higher-order Stokes theories introduce corrections to the linear wave theory, and often provide more accurate estimates of the wave kinematics and dynamics. For example, the second-order Stokes theory gives the pressure at any distance below the fluid surface as

$$p = \rho g \frac{H}{2} \frac{\cosh[2\pi(z+d)/L]}{\cosh(2\pi d/L)} \cos\theta - \rho g z$$
$$+ \frac{3}{8}\rho g \frac{\pi H^2}{L} \frac{\tanh(2\pi d/L]}{\sinh^2(2\pi d/L} \left(\frac{\cosh[4\pi(z+d)/L]}{\sinh^2(2\pi d/L)} - \frac{1}{3} \right) \cos\ 2\theta \qquad \text{(II-1-70)}$$
$$- \frac{1}{8}\rho g \frac{\pi H^2}{L} \frac{\tanh(2\pi d/L)}{\sinh^2(2\pi d/L)} \left(\cosh \frac{4\pi(z+d)}{L} - 1 \right)$$

(b) The terms proportional to the wave height squared in the above equation represent corrections by the second-order theory to the pressure from the linear wave theory. The third term is the steady component of pressure that corresponds to time-independent terms mentioned earlier.

(c) A direct byproduct of the high-order Stokes expansion is that it provides means for comparing different orders of resulting theories, all of which are approximations. Such comparison is useful to obtain insight about the choice of a theory for a particular problem. Nonetheless, it should be kept in mind that linear (or first-order) theory applies to a wave that is symmetrical about the SWL and has water particles that move in closed orbits. On the other hand, Stokes' higher-order theories predict a wave form that is asymmetrical about the SWL but still symmetrical about a vertical line through the crest and has water particle orbits that are open (Figure II-1-10).

(4) Maximum wave steepness.

(a) A progressive gravity wave is physically limited in height by depth and wavelength. The upper limit or breaking wave height in deep water is a function of the wavelength and, in shallow and transitional water, is a function of both depth and wavelength.

(b) Stokes (1880) predicted theoretically that a wave would remain stable only if the water particle velocity at the crest was less than the wave celerity or phase velocity. If the wave height were to become so large that the water particle velocity at the crest exceeded the wave celerity, the wave would become unstable and break. Stokes found that a wave having a crest angle less than 120 deg would break (angle between two lines tangent to the surface profile at the wave crest). The possibility of the existence of a wave having a crest angle equal to 120 deg is known (Lamb 1945). Michell (1893) found that in deep water the theoretical limit for wave steepness is

$$\left(\frac{H_0}{L_0} \right)_{max} = 0.142 \approx \frac{1}{7} \qquad \text{(II-1-71)}$$

Havelock (1918) confirmed Michell's finding.

(c) Miche (1944) gives the limiting steepness for waves traveling in depths less than $L_0/2$ without a change in form as

$$\left(\frac{H}{L} \right)_{max} = \left(\frac{H_0}{L_0} \right)_{max} \tanh \left(\frac{2\pi d}{L} \right) = 0.142 \tanh \left(\frac{2\pi d}{L} \right) \qquad \text{(II-1-72)}$$

Laboratory measurements indicate that Equation II-1-72 is in agreement with an envelope curve to laboratory observations (Dean and Dalrymple 1991).

e. Other wave theories.

(1) Introduction.

(a) Extension of the Stokes theory to higher orders has become common with computers, but the mathematics involved is still tedious. Variations of the Stokes theory have been developed in the last three decades oriented toward computer implementation. For example, Dean (1965) used the stream function in place of the velocity potential to develop the stream function theory. Dean (1974) did a limited comparison of measured horizontal particle velocity in a wave tank with the tenth-order stream function theory and several other theories. Forty cases were tabulated in dimensionless form to facilitate application of this theory.

(b) Others (Dalrymple 1974a; Chaplin 1980; Reinecker and Fenton 1981) developed variations of the stream function theory using different numerical methods. Their studies included currents. For near-breaking waves, Cokelet (1977) extended the method of Schwartz (1974) for steep waves for the full range of water depth and wave heights. Using a 110th-order theory for waves up to breaking, Cokelet successfully computed the wave profile, wave celerity, and various integral properties of waves, including the mean momentum, momentum flux, kinetic and potential energy, and radiation stress.

(2) Nonlinear shallow-water wave theories.

(a) Stokes' finite amplitude wave theory is applicable when the depth to wavelength ratio d/L is greater than about 1/8 or $kd > 0.78$ or $U_r < 79$. For longer waves a different theory must be used (Peregrine 1976). As waves move into shallow water, portions of the wave travel faster because of amplitude dispersion or waves travel faster because they are in deeper water. Waves also feel the effects of frequency dispersion less in shallow water, e.g., their speed is less and less influenced by water depth.

(b) For the mathematical representation of waves in shallow water, a different perturbation parameter should be used to account for the combined influence of amplitude and frequency dispersion (Whitham 1974; Miles 1981; Mei 1991). This can be achieved by constructing two perturbation parameters whose ratio is equivalent to the Ursell parameters (Peregrine 1972). The set of equations obtained in this manner are termed the *nonlinear shallow-water wave equations*. Some common wave theories based on these equations are briefly described in the following sections.

(3) Korteweg and de Vries and Boussinesq wave theories.

(a) Various shallow-water equations can be derived by assuming the pressure to be hydrostatic so that vertical water particle accelerations are small and imposing a horizontal velocity on the flow to make it steady with respect to the moving reference frame. The horizontal velocity might be the velocity at the SWL, at the bottom, or the velocity averaged over the depth. If equations are written in terms of depth-averaged velocity $\bar{u}$ they become:

$$\begin{aligned} &\frac{\partial \eta}{\partial t} + \frac{\partial}{\partial x}(d + \eta)\bar{u} = 0 \\ &\frac{\partial \bar{u}}{\partial t} + \bar{u}\frac{\partial \bar{u}}{\partial x} + g\frac{\partial \eta}{\partial x} = \frac{1}{3}d^2\frac{\partial^3 \bar{u}}{\partial x^2 \partial t} \end{aligned} \tag{II-1-73}$$

which are termed the *Boussinesq equations* (Whitham 1967; Peregrine 1972; Mei 1991). Originally, Boussinesq used the horizontal velocity at the bottom. Eliminating $\bar{u}$ yields (Miles 1979, 1980, 1981)

$$\frac{\partial^2 \eta}{\partial t^2} - gd\frac{\partial^2 \eta}{\partial x^2} = gd\frac{\partial^2}{\partial x^2}\left(\frac{3}{2}\frac{\eta^2}{d} + \frac{1}{3}d^2\frac{\partial^2 \eta}{\partial x^2}\right) \tag{II-1-74}$$

A periodic solution to Equation II-1-74 is of the form

$$\begin{aligned} \eta &= a\, e^{i(kx - \omega t)} = a \cos\theta \\ \bar{u} &= U_0\, e^{i(kx - \omega t)} = U_0 \cos\theta \end{aligned} \tag{II-1-75}$$

which has a dispersion relation and an approximation to it given by

$$C = \frac{C_s}{\left[1 + \frac{1}{3}(kd)^2\right]^{1/2}} \approx C_s\left[1 - \frac{1}{3}(kd)^2 + \ldots\right] \tag{II-1-76}$$

The term $1/3\ (kd)^2$ in Equation II-1-76 represents the dispersion of wave motion.

(b) The most elementary solution of the Boussinesq equation is the *solitary wave* (Russell 1844; Fenton 1972; Miles 1980). A solitary wave is a wave with only crest and a surface profile lying entirely above the SWL. Fenton's solution gives the maximum solitary wave height, $H_{max} = 0.85$ d and maximum propagation speed $C^2_{max} = 1.7$ gd. Earlier research studies using the solitary waves obtained $H_{max} = 0.78$ d and $C^2_{max} = 1.56$ gd. The maximum solitary-amplitude wave is frequently used to calculate the height of breaking waves in shallow water. However, subsequent research has shown that the highest solitary wave is not necessarily the most energetic (Longuet-Higgins and Fenton 1974).

(4) Cnoidal wave theory.

(a) Korteweg and de Vries (1895) developed a wave theory termed the *cnoidal theory*. The cnoidal theory is applicable to finite-amplitude shallow-water waves and includes both nonlinearity and dispersion effects. Cnoidal theory is based on the Boussinesq, but is restricted to waves progressing in only one direction. The theory is defined in terms of the *Jacobian elliptic function*, *cn*, hence the name cnoidal. Cnoidal waves are periodic with sharp crests separated by wide flat troughs (Figure II-1-10).

(b) The approximate range of validity of the cnoidal theory is $d/L < 1/8$ when the Ursell number $U_R > 20$. As wavelength becomes long and approaches infinity, cnoidal wave theory reduces to the solitary wave theory, which is described in the next section. Also, as the ratio of wave height to water depth becomes small (infinitesimal wave height), the wave profile approaches the sinusoidal profile predicted by the linear theory.

(c) Cnoidal waves have been studied extensively by many investigators (Keulegan and Patterson 1940; Keller 1948; Laitone 1962) who developed first- through third-order approximations to the cnoidal wave theory. Wiegel (1960) summarized the principal results in a more usable form by presenting such wave characteristics as length, celerity, and period in tabular and graphical form to facilitate application of cnoidal theory.

(d) Wiegel (1964) further simplified the earlier works for engineering applications. Recent additional improvements to the theory have been made (Miles 1981; Fenton 1972, 1979). Using a Rayleigh-Boussinesq

series, Fenton (1979) developed a generalized recursion relationship for the KdV solution of any order. Fenton's fifth- and ninth-order approximations are frequently used in practice. A summary of formulas of the cnoidal wave theory are provided below. See Fenton (1979), Fenton and McKee 1990), and Miles (1981) for a more comprehensive theoretical presentation.

(e) Long, finite-amplitude waves of permanent form propagating in shallow water may be described by cnoidal wave theory. The existence in shallow water of such long waves of permanent form may have first been recognized by Boussinesq (1871). However, the theory was originally developed by Korteweg and de Vries (1895).

(f) Because local particle velocities, local particle accelerations, wave energy, and wave power for cnoidal waves are difficult to describe such descriptions are not included here, but can be obtained in graphical form from Wiegel (1960, 1964). Wave characteristics are described in parametric form in terms of the modules k of the *elliptic integrals*. While k itself has no physical significance, it is used to express the relationships between various wave parameters. Tabular presentations of the elliptic integrals and other important functions can be obtained from the above references. The ordinate of the water surface y_s measured above the bottom is given by

$$y_s = y_t + H\, cn^2 \left[2K(k) \left(\frac{x}{L} - \frac{t}{T} \right) \;,\; k \right] \tag{II-1-77}$$

where

y_t = distance from the bottom to the wave trough

H = trough to crest wave height

cn = elliptic cosine function

$K(k)$ = complete elliptic integral of the first kind

k = modulus of the elliptic integrals

(g) The argument of cn^2 is frequently denoted simply by ( ); thus, Equation II-1-77 above can be written as

$$y_s = y_t + H\, cn^2(\;) \tag{II-1-78}$$

(h) The elliptic cosine is a periodic function where cn^2 [2K(k) ((x/L) - (t/T)] has a maximum amplitude equal to unity. The modulus k is defined over the range 0 and 1. When $k = 0$, the wave profile becomes a sinusoid, as in the linear theory; when $k = 1$, the wave profile becomes that of a solitary wave.

(i) The distance from the bottom to the wave trough y_t, as used in Equations II-1-77 and II-1-78, is given by

$$\frac{y_t}{d} = \frac{y_c}{d} - \frac{H}{d} = \frac{16d^2}{3L^2} K(k)\,[K(k) - E(k)] + 1 - \frac{H}{d} \tag{II-1-79}$$

where y_c is the distance from the bottom to the crest, and $E(k)$ the complete elliptic integral of the second kind. Wavelength is given by

$$L = \sqrt{\frac{16d^3}{3H}}\, k\, K(k) \tag{II-1-80}$$

and wave period by

$$T\sqrt{\frac{g}{d}} = \sqrt{\frac{16y_t}{3H}}\, \frac{d}{y_t}\left[\frac{k\, K(k)}{1 + \frac{H}{y_t\, k^2}\left(\frac{1}{2} - \frac{E(k)}{K(k)}\right)}\right] \tag{II-1-81}$$

Note that cnoidal waves are periodic and of permanent form; thus L = CT (see Figure II-1-10).

(j) Pressure under a cnoidal wave at any elevation *y* above the bottom depends on the local fluid velocity, and is therefore complex. However, it may be approximated in a hydrostatic form as

$$p = \rho g\,(y_s - y) \tag{II-1-82}$$

i.e., the pressure distribution may be assumed to vary linearly from $\rho g y_s$ at the bed to zero at the surface.

(k) Wave profiles obtained from different wave theories are sketched in Figure II-1-10 for comparison. The linear profile is symmetric about the SWL. The Stokes wave has higher more peaked crests and shorter, flatter troughs. The cnoidal wave crests are higher above the SWL than the troughs are below the SWL. Cnoidal troughs are longer and flatter and crests are sharper and steeper than Stokes waves. The solitary wave, a form of the cnoidal wave described in the next section, has all of its profile above the SWL.

(l) Figures II-1-11 and II-1-12 show the dimensionless cnoidal wave surface profiles for various values of the square of the modulus of the elliptic integrals k^2, while Figures II-1-13 to II-1-16 present dimensionless plots of the parameters which characterize cnoidal waves. The ordinates of Figures II-1-13 and II-1-14 should be read with care, since values of k^2 are extremely close to 1.0 ($k^2 = 1 - 10^{-1} = 1 - 0.1 = 0.90$). It is the exponent α of $k^2 = 1 - 10^{-\alpha}$ that varies along the vertical axis of Figures II-1-13 and II-1-14.

(m) Ideally, shoaling computations might be performed using a higher-order cnoidal wave theory since this theory is able to describe wave motion in relatively shallow water. Simple, completely satisfactory procedures for applying cnoidal wave theory are not available. Although linear wave theory is often used, cnoidal theory may be applied for practical situations using Figures such as II-1-11 to II-1-16. The following problem illustrates the use of these figures.

(n) There are two limits to the cnoidal wave theory. The first occurs when the period of the function cn is infinite when $k = 1$. This corresponds to a solitary wave. As the wavelength becomes infinite, the cnoidal theory approaches the solitary wave theory. The second limit occurs for $k = 0$ where the cnoidal wave approaches the sinusoidal wave. This happens when the wave height is small compared to water depth and the cnoidal theory reduces to the linear theory.

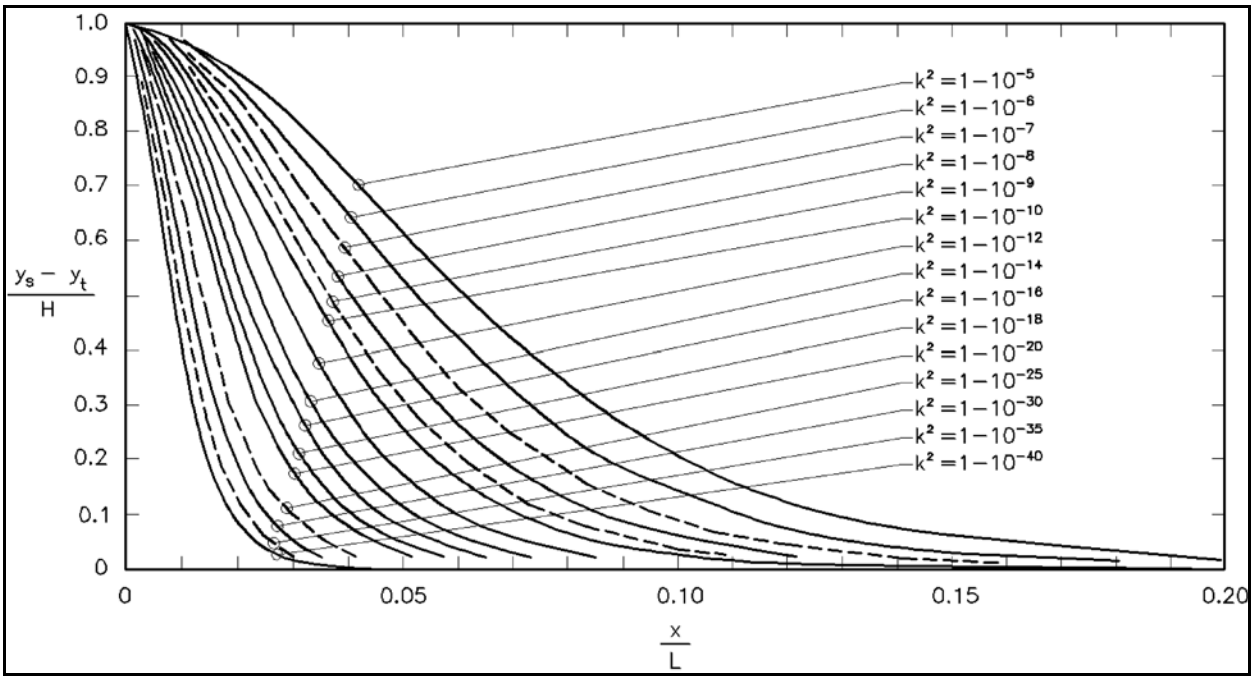

Figure II-1-11. Normalized surface profile of the cnoidal wave (Wiegel 1960). For definition of variables see Part II-1-2.e.(3)

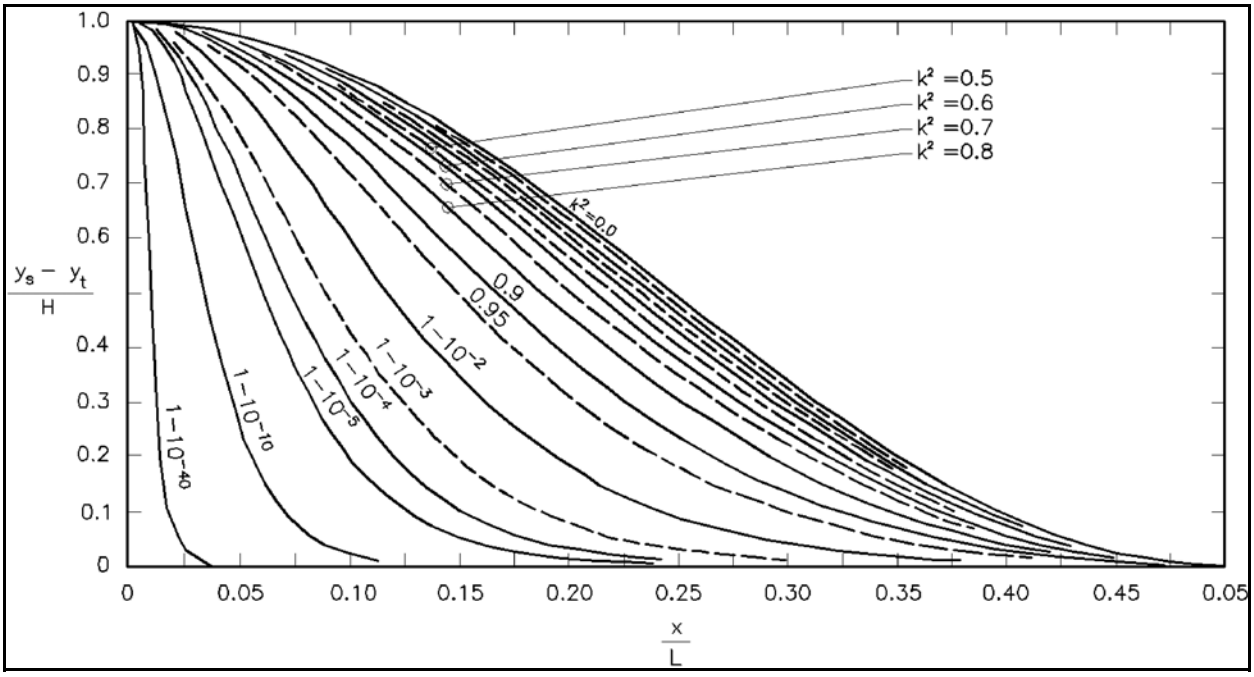

Figure II-1-12. Normalized surface profile of the cnoidal wave for higher values of k^2 and X/L (Wiegel 1960)

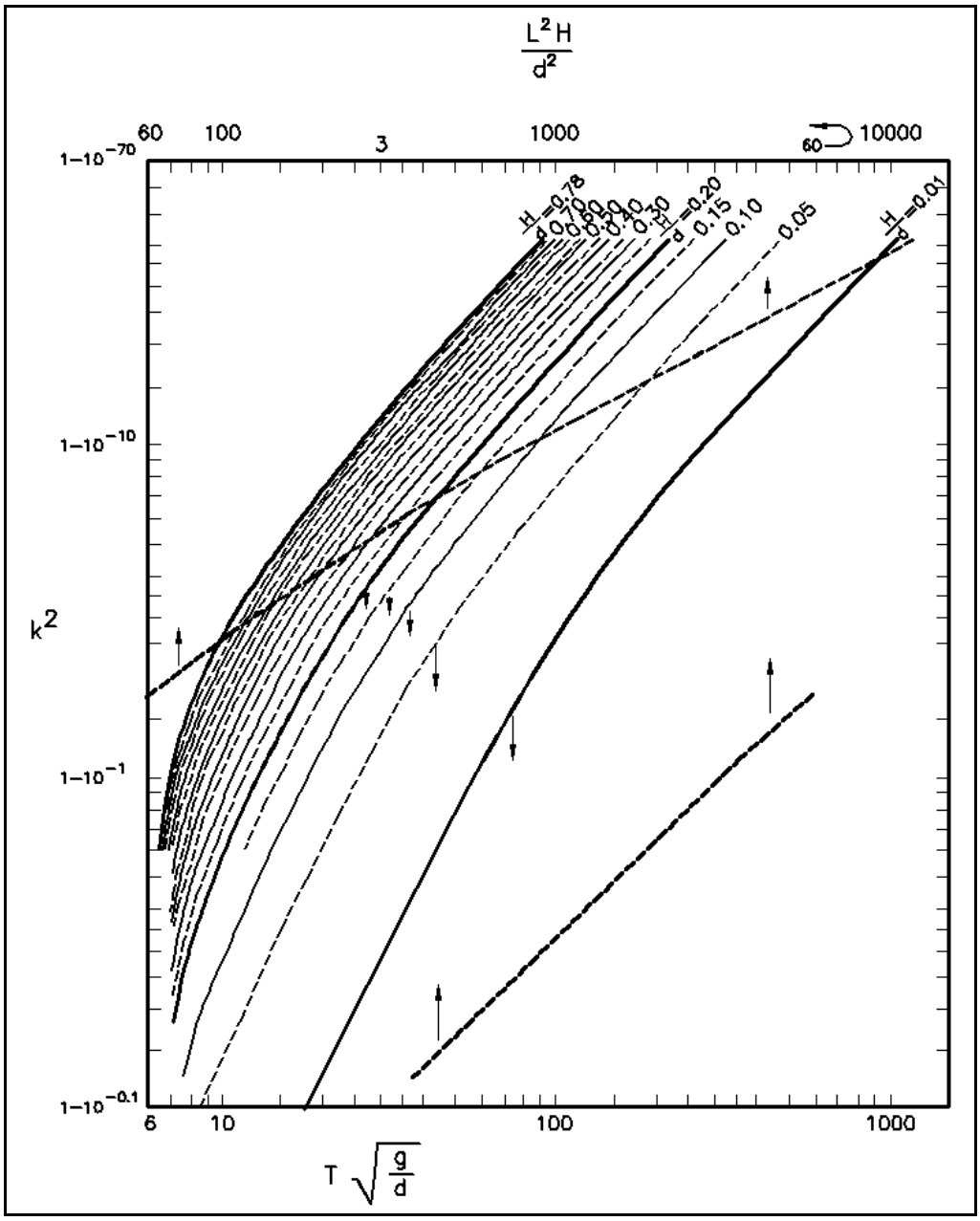

Figure II-1-13. k^2 versus L^2H/d^3, and k^2 versus $T\sqrt{g/d}$ and H/d (Wiegel 1960)

(5) Solitary wave theory.

(a) Waves considered in the previous sections were oscillatory or nearly oscillatory waves. The water particles move backward and forward with the passage of each wave, and a distinct wave crest and wave trough are evident. A solitary wave is neither oscillatory nor does it exhibit a trough. In the pure sense, the solitary wave form lies entirely above the still-water level. The solitary wave is a wave of translation because the water particles are displaced a distance in the direction of wave propagation as the wave passes.

(b) The *solitary wave* was discovered by Russell (1844). Boussinesq (1871), Rayleigh (1876), Keller (1948), and Munk (1949) performed pioneering theoretical studies of solitary waves. More recent analyses

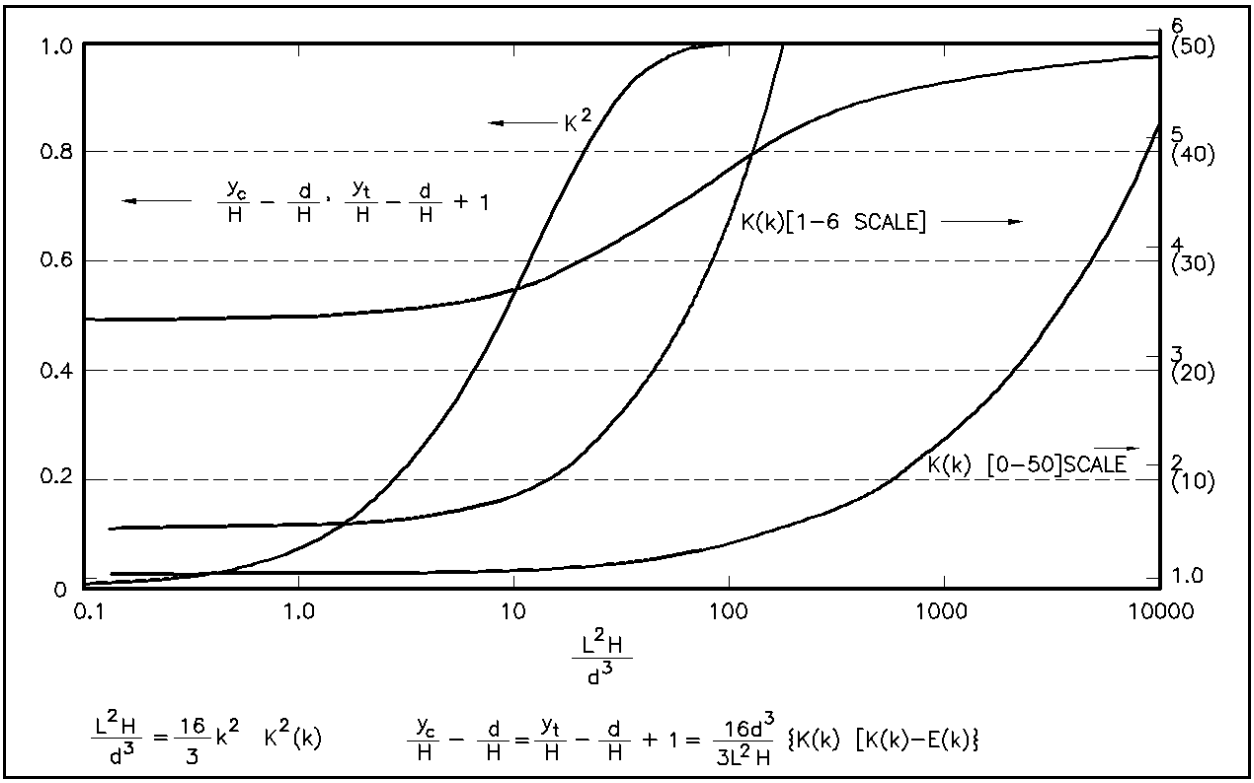

Figure II-1-14. Relationship among L^2H/d^3 and the square of the elliptic modulus (k^2), y_c/H, y_t/H, and K(k) (Wiegel 1960)

of solitary waves were performed by Fenton (1972), Longuet-Higgins and Fenton (1974), and Byatt-Smith and Longuet-Higgins (1976). The first systematic observations and experiments on solitary waves can probably be attributed to Russell (1838, 1844), who first recognized the existence of a solitary wave.

(c) In nature it is difficult to form a truly solitary wave, because at the trailing edge of the wave there are usually small dispersive waves. However, long waves such as tsunamis and waves resulting from large displacements of water caused by such phenomena as landslides and earthquakes sometimes behave approximately like solitary waves. When an oscillatory wave moves into shallow water, it may often be approximated by a solitary wave (Munk 1949). As an oscillatory wave moves into shoaling water, the wave amplitude becomes progressively higher, the crests become shorter and more pointed, and the trough becomes longer and flatter.

(d) Because both wavelength and period of solitary waves are infinite, only one parameter H/d is needed to specify a wave. To lowest order, the solitary wave profile varies as $sech^2 q$ (Wiegel 1964), where $q = (3H/d)^{1/2}\,(x\text{-}Ct)/2d$ and the free-surface elevation, particle velocities, and pressure may be expressed as

$$\frac{\eta}{H} = \frac{u}{\sqrt{gd}\,\frac{H}{d}} \tag{II-1-83}$$

$$\frac{u}{\sqrt{gd}}\,\frac{H}{d} = \frac{\Delta p}{\rho g H} \tag{II-1-84}$$

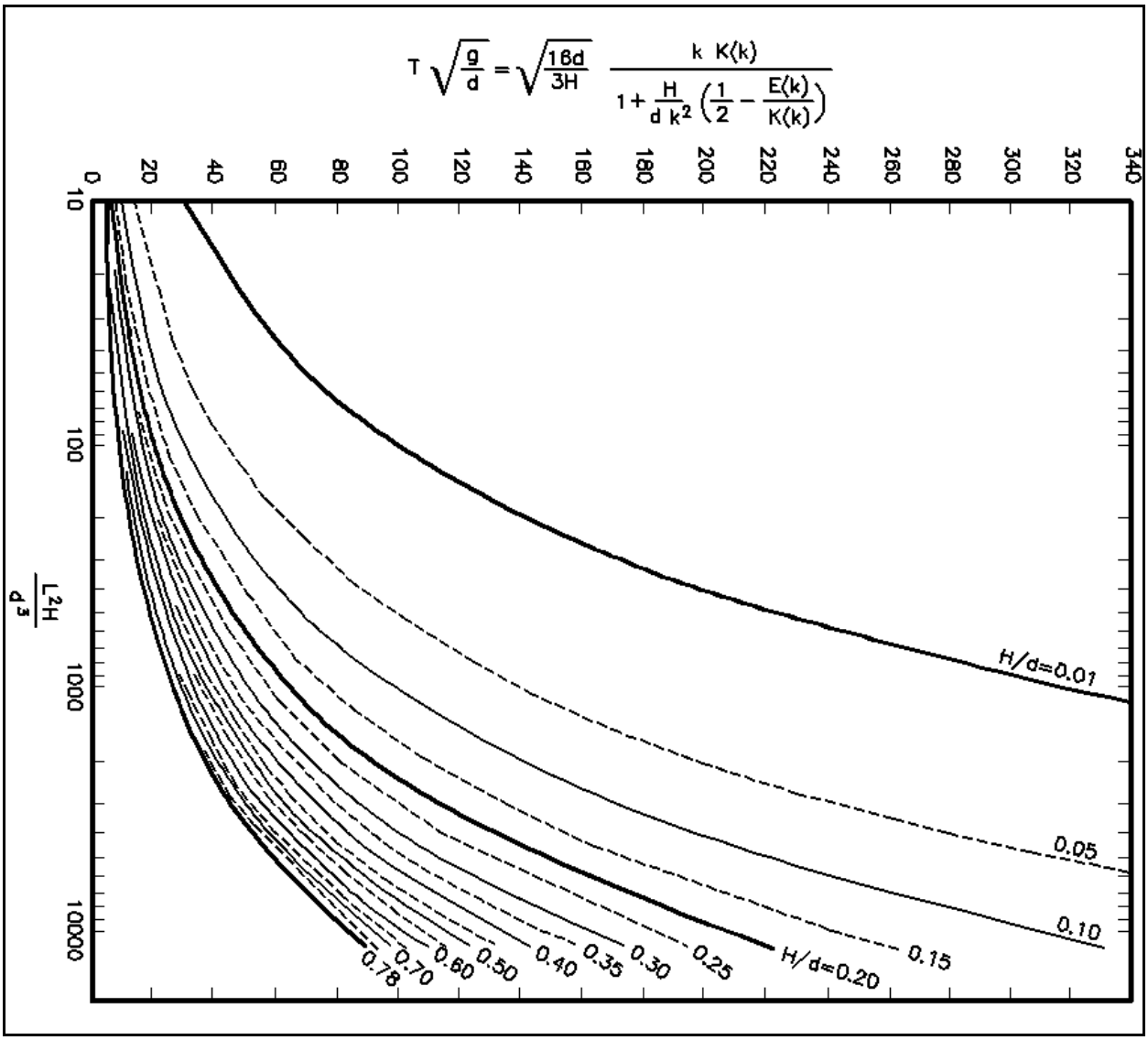

Figure II-1-15. Relationships among $T\sqrt{g/d}$, L^2H/d^3, and H/d (Wiegel 1960)

$$\frac{\Delta p}{\rho g H} = sech^2\ q \tag{II-1-85}$$

where Δp is the difference in pressure at a point due to the presence of the solitary wave.

(e) To second approximation (Fenton 1972), this difference is given by

$$\frac{\Delta p}{\rho g H} = 1 - \frac{3}{4}\frac{H}{d}\left[1 - \left(\frac{Y_s}{d}\right)^2\right] \tag{II-1-86}$$

where y_s = the height of the surface profile above the bottom. The wave height H required to produce Δp on the seabed can be estimated from

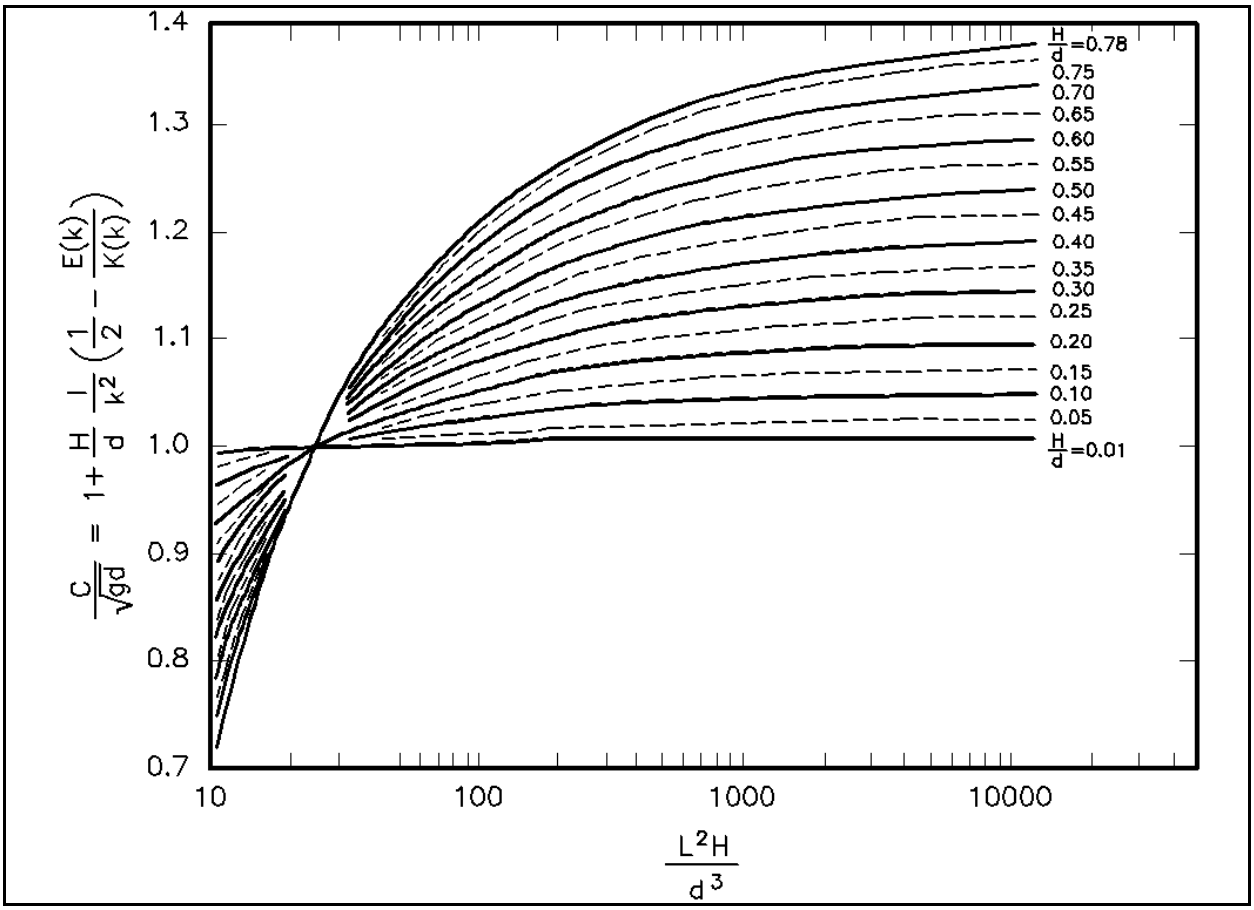

Figure II-1-16. Relationship between cnoidal wave velocity and L^2H/d^3 (Wiegel 1960)

$$\frac{\Delta p}{\rho g H} = \frac{1}{2} + \frac{1}{2}\sqrt{1 - \frac{3\Delta p}{\rho g d}} \tag{II-1-87}$$

(f) Since the solitary wave has horizontal particle velocities only in the direction of wave advance, there is a net displacement of fluid in the direction of wave propagation.

(g) The solitary wave is a limiting case of the cnoidal wave. When $k^2 = 1$, K(k) = K(1) = ∞, and the elliptic cosine reduces to the hyperbolic secant function and the water surface y_s measured above the bottom reduces to

$$y_s = d + H\,sech^2\left[\sqrt{\frac{3}{4}\frac{H}{d^3}}\,(x - Ct)\right] \tag{II-1-88}$$

(h) The free surface is given by

$$\eta = H\,sech^2\left[\sqrt{\frac{3}{4}\frac{H}{d^3}}\,(x - Ct)\right] \tag{II-1-89}$$

EXAMPLE PROBLEM II-1-5

FIND:

(a) Using cnoidal wave theory, find the wavelength L and compare this length with the length determined using Airy theory.

(b) Determine the celerity C. Compare this celerity with the celerity determined using Airy theory.

(c) Determine the distance above the bottom of the wave crest y_c and wave trough y_t .

(d) Determine the wave profile.

GIVEN:

A wave traveling in water depth d = 3 m (9.84 ft), with a period T = 15 sec, and a height H = 1.0 m (3.3 ft).

SOLUTION:

(a) Calculate

$$\frac{H}{d} = \frac{1}{3} = 0.33$$

and

$$T\sqrt{\frac{g}{d}} = 15\sqrt{\frac{9.8}{3}} = 27.11$$

From Figure II-1-13, enter H/d and T to determine the square of the modulus of the complete elliptical integrals, k^2:

$$k^2 = 1 - 10^{-5}$$

Entering both Figures II-1-13 and II-1-14 with the value of k^2 gives

$$\frac{L^2H}{d^3} = 290$$

or

$$L = \sqrt{\frac{290\ d^3}{H}} = \sqrt{\frac{290\ (3)^3}{1}}$$

Example Problem II-1-5 (Continued)

which gives L = 88.5 m (290.3 ft). The wavelength from the linear (Airy) theory is

$$L = \frac{gT^2}{2\pi} \tanh\left(\frac{2\pi d}{L}\right) = 80.6\ m\ (264.5\ ft)$$

To check whether the wave conditions are in the range for which cnoidal wave theory is valid, calculate *d/L* and the *Ursell number* = L^2H/d^3:

$$\frac{d}{L} = \frac{3}{88.5} = 0.0339 < \frac{1}{8} \qquad \text{0.K.}$$

$$\frac{L^2H}{d^3} = \frac{1}{\left(\frac{d}{L}\right)^2}\left(\frac{H}{d}\right) = 290 > 26 \qquad \text{0.K.}$$

Therefore, cnoidal theory is applicable.

(b) Wave celerity is given by

$$C = \frac{L}{T} = \frac{88.5}{15} = 5.90\ m/s\ (19.36\ ft/s)$$

while the linear theory predicts

$$C = \frac{L}{T} = \frac{80.6}{15} = 5.37\ m/s\ (17.63\ ft/s)$$

Thus, if it is assumed that the wave period is the same for cnoidal and Airy theories, then

$$\frac{C_{cnoidal}}{C_{Airy}} = \frac{L_{cnoidal}}{L_{Airy}} \approx 1$$

(c) The percentage of the wave height above the SWL may be determined from Figure II-1-11 or II-1-12. Entering these figures with $L^2H/D^3 = 290$, the value of $(y_c - d)/H$ is found to be 0.865, or 86.5 percent. Therefore,

$$y_c = 0.865\ H + d$$

$$y_c = 0.865(1) + 3 = 0.865 + 3 = 3.865\ m\ (12.68\ ft)$$

Example Problem II-1-5 (Continued)

Example Problem II-1-5 (Concluded)

Also from Figure II-1-11 or II-1-12,

$$\frac{(y_t - d)}{H} + 1 = 0.865$$

thus,

$$y_t = (0.865 - 1)(1) + 3 = 2.865\ m\ (9.40\ ft)$$

(d) The dimensionless wave profile is given in Figures II-1-11 and II-1-12 for $k^2 = 1 - 10^{-5}$. The results obtained in (c) above can also be checked by using Figures II-1-11 and II-1-12. For the wave profile obtained with $k^2 = 1 - 10^{-5}$, the SWL is approximately 0.14H above the wave trough or 0.86H below the wave crest.

The results for the wave celerity determined under (b) above can now be checked with the aid of Figure II-1-16. Calculate

$$\frac{H}{y_t} = \frac{(1)}{2.865} = 0.349$$

Entering Figure II-1-16 with

$$\frac{L^2 H}{d^3} = \frac{(1)}{2.865} = 0.349$$

and

$$\frac{H}{y_t} = 0.349$$

it is found that

$$\frac{C}{\sqrt{g\ y_t}} = 1.126$$

Therefore,

$$C = 1.126\ \sqrt{(9.8)(2.865)} = 5.97\ m/s\ (19.57\ ft/s)$$

The differences between this number and the 5.90 m /sec (18.38 ft/s) calculated under (b) above is the result of small errors in reading the curves.

where the origin of x is at the wave crest. The volume of water within the wave above the still-water level per unit crest width is

$$V = \left[\frac{16}{3} d^3 H\right]^{\frac{1}{2}} \tag{II-1-90}$$

(i) An equal amount of water per unit crest length is transported forward past a vertical plane that is perpendicular to the direction of wave advance. Several relations have been presented to determine the celerity of a solitary wave; these equations differ depending on the degree of approximation. Laboratory measurements suggest that the simple expression

$$C = \sqrt{g(H + d)} \tag{II-1-91}$$

gives a reasonably accurate approximation to the celerity of solitary wave.

(j) The water particle velocities for a solitary wave (Munk 1949), are

$$u = CN \frac{1 + \cos(My/d) \cosh(Mx/d)}{[\cos(My/d) + \cosh(Mx/D)]^2} \tag{II-1-92}$$

$$w = CN \frac{\sin(My/d) \sinh(Mx/d)}{[\cos(My/d) + \cosh(Mx/D)]^2} \tag{II-1-93}$$

where M and N are the functions of H/d shown in Figure II-1-17, and y is measured from the bottom. The expression for horizontal velocity u is often used to predict wave forces on marine structures situated in shallow water. The maximum velocity u_{max} occurs when x and t are both equal to zero; hence,

$$u_{max} = \frac{CN}{1 + \cos(My/d)} \tag{II-1-94}$$

(k) Total energy in a solitary wave is about evenly divided between kinetic and potential energy. Total wave energy per unit crest width is

$$E = \frac{8}{3\sqrt{3}} \rho g H^{\frac{3}{2}} d^{\frac{3}{2}} \tag{II-1-95}$$

and the pressure beneath a solitary wave depends on the local fluid velocity, as does the pressure under a cnoidal wave; however, it may be approximated by

$$p = \rho g (y_s - y) \tag{II-1-96}$$

(l) Equation II-1-96 is identical to that used to approximate the pressure beneath a cnoidal wave.

(m) As a solitary wave moves into shoaling water it eventually becomes unstable and breaks. A solitary wave breaks when the water particle velocity at the wave crest becomes equal to the wave celerity. This occurs when (Miles 1980, 1981)

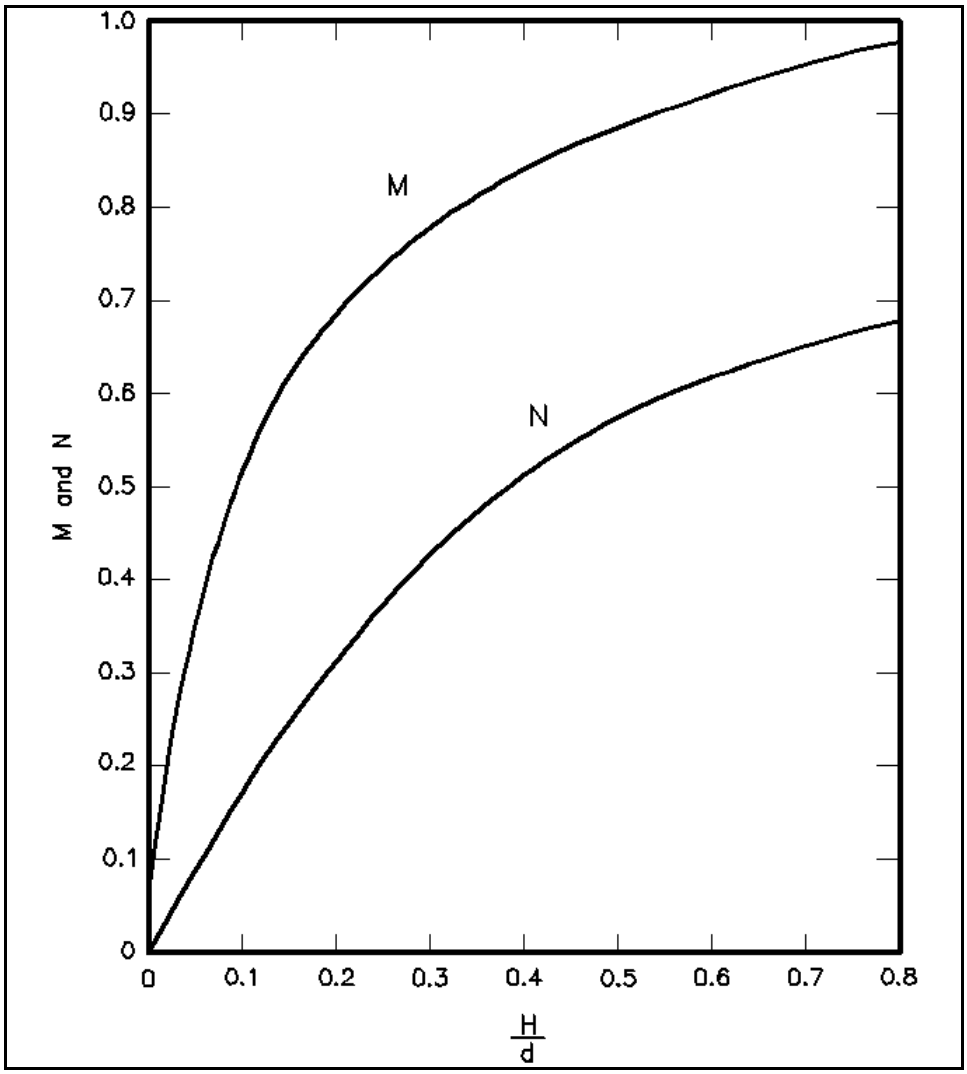

Figure II-1-17. Functions M and N in solitary wave theory (Munk 1949)

$$\left(\frac{H}{d}\right)_{max} = 0.78 \tag{II-1-97}$$

(n) Laboratory studies have shown that the value of $(H/d)_{max} = 0.78$ agrees better with observations for oscillatory waves than for solitary waves and that the nearshore slope has a substantial effect on this ratio. Other factors such as bottom roughness may also be involved. Tests of periodic waves with periods from 1 to 6 sec on slopes of $m = 0.0$, 0.05, 0.10, and 0.20 have shown (SPM 1984) that H_b/d_b ratios are approximately equal to 0.83, 1.05, 1.19, and 1.32, respectively. Tests of single solitary waves on slopes from $m = 0.01$ to $m = 0.20$ (SPM 1984) indicate an empirical relationship between the slope and the breaker height-to-water depth ratio given by

$$\frac{H_b}{d_b} = 0.75 + 25m - 112m^2 + 3870m^3 \tag{II-1-98}$$

in which waves did not break when the slope m was greater than about 0.18 and that as the slope increased the breaking position moved closer to the shoreline. This accounts for the large values of H_b/d_b for large slopes; i.e., as $d_b \rightarrow 0$. For some conditions, Equations II-1-97 and II-1-98 are unsatisfactory for predicting breaking depth. Further discussion of the breaking of waves with experimental results is provided in Part II-4.

(6) Stream-function wave theory. Numerical approximations to solutions of hydrodynamic equations describing wave motion have been proposed and developed. Some common theories and associated equations are listed in Table II-1-2. The approach by Dean (1965, 1974), termed a *symmetric, stream-function theory*, is a nonlinear wave theory that is similar to higher order Stokes' theories. Both are constructed of sums of *sine* or *cosine* functions that satisfy the original differential equation (Laplace equation). The theory, however, determines the coefficient of each higher order term so that a best fit, in the least squares sense, is obtained to the theoretically posed, dynamic, free-surface boundary condition. Assumptions made in the theory are identical to those made in the development of the higher order Stokes' solutions. Consequently, some of the same limitations are inherent in the stream-function theory, and it represents an alternative solution to the equations used to approximate the wave phenomena. However, the stream-function representation had successfully predicted the wave phenomena observed in some laboratory wave studies (Dean and Dalrymple 1991), and thus it may possibly describe naturally occurring wave phenomena.

Table II-1-2
Boundary Value Problem of Water Wave Theories (Dean 1968)

		Exactly Satisfies			
Theory		**DE**	**BBC**	**KFSBC**	**DFSBC**
Linear wave theory		X	X	-	-
Third-order Stokes		X	X	-	-
Fifth-order Stokes		X	X	-	-
First-order cnoidal		-	X	-	-
Second-order cnoidal		-	X	-	-
Stream function theory	numerical wave	X	X	X	-

DE = Differential equation.
BBC = Bottom boundary condition.
KFSBC = Kinematic free surface boundary condition.
DFSBC = Dynamic free surface boundary condition.
X = Exactly satisfies.

(7) Fourier approximation -- Fenton’s theory.

(a) Fenton's Fourier series theory, another theory developed in recent years (Fenton 1988), is somewhat similar to Dean's stream function theory, but it appears to describe oceanic waves at all water depths better than all previous similar theories.

(b) The long, tedious computations involved in evaluating the terms of the series expansions that make up the higher order stream-function theory of Dean had in the past limited its use to either tabular or graphical presentations of the solutions. These tables, their use, and their range of validity may be found elsewhere (Dean 1974).

(c) Stokes and cnoidal wave theories yield good approximations for waves over a wide range of depths if high-order expansions are employed. Engineering practice has relied on the Stokes fifth-order theory (Skjelbreia and Hendrickson 1961), and the stream function theory (Dean 1974). These theories are

applicable to deepwater applications. An accurate steady wave theory may be developed by numerically solving the full nonlinear equations with results that are applicable for short waves (deep water) and for long waves (shallow water). This is the Fourier approximation method. The method is termed *Fenton's theory* here. Any periodic function can be approximated by Fourier series, provided the coefficients of the series can be found. In principal, the coefficients are found numerically. Using this approach, Chappelear (1961) developed a Fourier series solution by adopting the velocity potential as the primary field variable. Dean (1965, 1974) developed the stream function theory. The solutions by both Chappelear and Dean successively correct an initial estimate to minimize errors in the nonlinear free-surface boundary conditions.

(d) A simple Fourier approximation wave theory was introduced by Rienecker and Fenton (1981) and was subsequently improved by Fenton (1985, 1988; Fenton and McKee 1990). It is an improved numerical theory that has a range of applicability broader than the Stokes and cnoidal theories. Details of the theory are given by Reinecker and Fenton (1981) and Fenton (1985, 1988; Fenton and McKee 1990). Sobey et al. (1987) recasted Fenton's work into a standardized format including currents in the formulation up to fifth order. The theory has been implemented to calculate wave kinematics and the loading of offshore structures (Demirbilek 1985). For coastal applications, a PC-based computer code of Fenton's theory is available in the Automated Coastal Engineering System (ACES) (Leenknecht, Szuwalski, and Sherlock 1992). A brief description of Fenton's theory is given here; details are provided in ACES.

(e) Fenton's Fourier approximation wave theory satisfies field equations and boundary conditions to a specified level of accuracy. The hydrodynamic equations governing the problem are identical to those used in Stokes' theory (Table II-1-2). Various approximations introduced in earlier developments are indicated in the table. Like other theories, Fenton's theory adopts the same field equation and boundary conditions. There are three major differences between Fenton's theory and the others. First, Fenton's theory is valid for deep- and shallow-water depths, and any of the two quantities' wave height, period or energy flux can be specified to obtain a solution. Second, the Fourier coefficients are computed numerically with efficient algorithms. Third, the expansion parameter for the Fourier coefficients is $\epsilon = kH/2$ rather than $\epsilon = ka$, which is used in Stokes theories. The coefficients are found numerically from simultaneous algebraic equations by satisfying two nonlinear free-surface boundary conditions and the dispersion relationship. Finding the coefficients requires that wave height, wave period, water depth, and either the Eulerian current or the depth-averaged mass transport velocity be specified.

(f) In Fenton's theory, the governing field equation describing wave motion is the two-dimensional (x,z in the Cartesian frame) Laplace's equation, which in essence is an expression of the conservation of mass:

$$\nabla^2 \Psi = \frac{\partial^2 \Psi}{\partial x^2} + \frac{\partial^2 \Psi}{\partial z^2} = 0 \tag{II-1-99}$$

where Ψ is the stream function. Ψ is a periodic function that describes wave motion in space and time, which also relates to the flow rate.

(g) Wave motion is a boundary-value problem, and its solution requires specifying realistic boundary conditions. These boundary conditions are usually imposed at the free surface and sea bottom. Since the seabed is often impermeable, flow rate through the sea bottom must be zero. Therefore, the bottom boundary condition may be stated in terms of Ψ as

$$\Psi(x, -d) = 0 \quad \text{at } z = -d \tag{II-1-100}$$

(h) Two boundary conditions, *kinematic* and *dynamic*, are needed at the free surface. The kinematic condition states that water particles on the free surface remain there, and consequently, flow rate through the surface boundary must be zero. The net flow Q between the sea surface and seabed may be specified as

$$\Psi(x,\eta) = -Q \qquad \text{at } z = \eta \tag{II-1-101}$$

where η is the sea surface elevation. The dynamic free-surface boundary condition is an expression of specifying the pressure at the free surface that is constant and equal to the atmospheric pressure. In terms of the stream function Ψ this condition may be stated as

$$\frac{1}{2}\left\{\left(\frac{\partial \Psi}{\partial x}\right)^2 + \left(\frac{\partial \Psi}{\partial z}\right)^2\right\} + g\eta = R \qquad \text{at } z = \eta \tag{II-1-102}$$

in which R is the Bernoulli constant.

(i) The boundary-value problem for wave motion as formulated above is complete. The time-dependency may be removed from the problem formulation by simply adapting a coordinate system that moves with the same velocity as the wave phase speed (Fenton 1988; Fenton and McKee 1990; Sobey et al. 1987). This is equivalent to introducing an underlying current relative to which the wave motion is measured. The current (also called *Stokes' drift velocity* or *Eulerian current*) causes a Doppler shift of the apparent wave period measured relative to a stationary observer or gauge. The underlying current velocity must therefore also be known in order to solve the wave problem in the steady (moving) reference frame.

(j) Fenton's solution method uses the Fourier cosine series in kx to the governing equations. It is clearly an approximation, but very accurate, since results of this theory appear not to be restricted to any water depths. $\epsilon = kH/2$ is the expansion parameter replacing ka in the Stokes wave theory. The dependent variable is the stream function Ψ represented by a Fourier cosine series in kx, expressed up to the Nth order as

$$\Psi(x,z) = -\bar{u}(z+d) + \left(\frac{g}{k^3}\right)^{\frac{1}{2}} \sum_{j=1}^{N} B_j \frac{\sinh jk(z+d)}{\cosh jkd} \cos jkx \tag{II-1-103}$$

where the B_j are dimensionless Fourier coefficients. The truncation limit of the series N determines the order of the theory. The nonlinear free-surface boundary conditions are satisfied at each of $M+1$ equi-spaced points on the surface. Wave height, wave period, water depth, and either the mean Eulerian velocity or the Stokes drift velocity must be specified to obtain a solution.

(k) The solution is obtained by numerically computing the N Fourier coefficients that satisfy a system of simultaneous equations. The numerical solution solves a set of $2M+6$ algebraic equations to find unknown Fourier coefficients. The problem is uniquely specified when $M = N$ and overspecified when $M > N$. Earlier wave theories based on stream function consider the overspecified case and used a least-squares method to find the coefficients. Fenton was the first to consider the uniquely specified case and used the collocation method to produce the most accurate and computationally efficient solution valid for any water depth.

(l) An initial estimate is required to determine the $M+N+6$ variables. The linear theory provides this initial estimate for deep water. In relatively shallow water, additional Fourier components are introduced. An alternative method is used in the shallow-water case by increasing the wave height in a number of steps. Smaller heights are used as starting solutions for subsequent higher wave heights. This approach eliminates the triple-crested waves reported by others (Huang and Hudspeth 1984; Dalrymple and Solana 1986).

(m) Sobey et al. (1987) compared several numerical methods for steady water wave problems, including Fenton's. Their comparison indicated that accurate results may be obtained with Fourier series of 10 to 20 terms, even for waves close to breaking. Comparisons with other numerical methods and experimental data (Fenton and McKee 1990; Sobey 1990) showed that results from Fenton's theory and experiments agree

consistently and better than results from other theories for a wide range of wave height, wave period, and water depth. Based on these comparisons, Fenton and McKee (1990) define the regions of validity of Stokes and cnoidal wave theory as

$$\frac{L}{d} = 21.5\, e^{\left(-1.87\frac{H}{d}\right)} \tag{II-1-104}$$

(n) The cnoidal theory should be used for wavelengths longer than those defined in this equation. For shorter waves, Stokes' theory is applicable. Fenton's theory can be used over the entire range, including obtaining realistic solutions for waves near breaking.

(o) In water of finite depth, the greatest (unbroken) wave that could prevail as a function of both wavelength and depth is determined by Fenton and McKee (1990) as

$$\frac{H}{d} = \frac{0.141063\frac{L}{d} + 0.0095721\left(\frac{L}{d}\right)^2 + 0.0077829\left(\frac{L}{d}\right)^3}{1.0 + 0.078834\frac{L}{d} + 0.0317567\left(\frac{L}{d}\right)^2 + 0.0093407\left(\frac{L}{d}\right)^3}\text{a} \tag{II-1-105}$$

(p) The leading term in the numerator of this equation is the familiar steepness limit for short waves in deep water. For large values of L/d (i.e., shallow-water waves), the ratio of cubic terms in the above equation approaches the familiar 0.8 value, a limit for depth-induced breaking of the solitary waves. Therefore, the above equation may also be used as a guide to delineate unrealistic waves in a given water depth.

(q) The formulas for wave kinematics, dynamics, and wave integral properties for Fenton's theory have been derived and summarized (Sobey et al.1987; Klopman 1990). Only the engineering quantities of interest including water particle velocities, accelerations, pressure, and water surface elevation defined relative to a Eulerian reference frame are provided here.

(r) The horizontal and vertical components of the fluid particle velocity are

$$u(x,z) = \frac{\partial \Psi}{\partial z} = -\bar{u} + \left(\frac{g}{k}\right)^{\frac{1}{2}} \sum_{j=1}^{N} jB_j \frac{\cosh jk(z+d)}{\cosh jkd} \cos jkx \tag{II-1-106}$$

$$w(x,z) = -\frac{\partial \Psi}{\partial x} = \left(\frac{g}{k}\right)^{\frac{1}{2}} \sum_{j=1}^{N} jB_j \frac{\sinh jk(z+d)}{\cosh jkd} \sin jkx \tag{II-1-107}$$

(s) Fluid particle accelerations in the horizontal and vertical directions are found by differentiating the velocities and using the continuity equation. These component accelerations are

$$a_x(x,z) = \frac{Du}{Dt} = u\frac{\partial u}{\partial x} + w\frac{\partial u}{\partial z}$$
$$a_z(x,z) = \frac{Dw}{Dt} = u\frac{\partial w}{\partial x} + w\frac{\partial w}{\partial z} = u\frac{\partial u}{\partial z} - w\frac{\partial u}{\partial x} \tag{II-1-108}$$

where

$$\frac{\partial u}{\partial x} = -\left(\frac{g}{k}\right)^{\frac{1}{2}} \sum_{j=1}^{N} j^2 B_j \frac{\cosh jk(z+d)}{\cosh jkd} \sin jkx \tag{II-1-109}$$

$$\frac{\partial u}{\partial z} = \left(\frac{g}{k}\right)^{\frac{1}{2}} \sum_{j=1}^{N} j^2 B_j \frac{\sinh jk(z+d)}{\cosh jkd} \cos jkx \tag{II-1-110}$$

(t) The instantaneous water surface elevation $\eta(x)$ and water particle pressure are given by

$$\eta(x) = \frac{1}{2} a_N \cos Nkx + \sum_{j=1}^{N-1} a_j \cos jkx$$

$$p(x,z) = \rho(R - gd - gz) - \frac{1}{2}\rho(u^2 + w^2) \tag{II-1-111}$$

(u) Integral properties of periodic gravity waves, including wave potential and kinetic energy, wave momentum and impulse, wave energy flux and wave power, and wave radiation stresses obtained by Klopman (1990) and Sobey et al. (1987) are listed in the Leenknecht, Szuwalski, and Sherlock (1992) documentation.

(v) A computer program developed by Fenton (1988) has recently been implemented in the ACES package. The ACES implementation facilitates use of Fenton's theory to applications in deep water and finite-depth water. It uses Fourier series of up to 25 terms to describe a wave train and provides information about various wave quantities. The output includes wave estimates for common engineering parameters including water surface elevation, wave particle kinematics, and wave integral properties as functions of wave height, period, water depth, and position in the wave form.

(w) The wave is assumed to co-exist on a uniform co-flowing current, taken either as the mean Eulerian current or mean mass transport velocity. At a given point in the water column, wave kinematics are tabulated over two wavelengths, and vertical distribution of the selected kinematics under the wave crest are graphically displayed. ACES implementation of Fenton's theory and its input/output requirements, computations, and examples are described in detail in the ACES documentation manual (Leenknecht, Szuwalski, and Sherlock 1992).

(x) Figure II-1-18 illustrates the application of Fenton's theory. This case represents shallow-water (10-m) conditions and wave height and period of 5 m and 10 sec, respectively. Surface elevation, horizontal velocity, and pressure over two wavelengths is shown graphically in Figure II-1-18. The ACES documentation includes guidance on proper use of Fenton's theory.

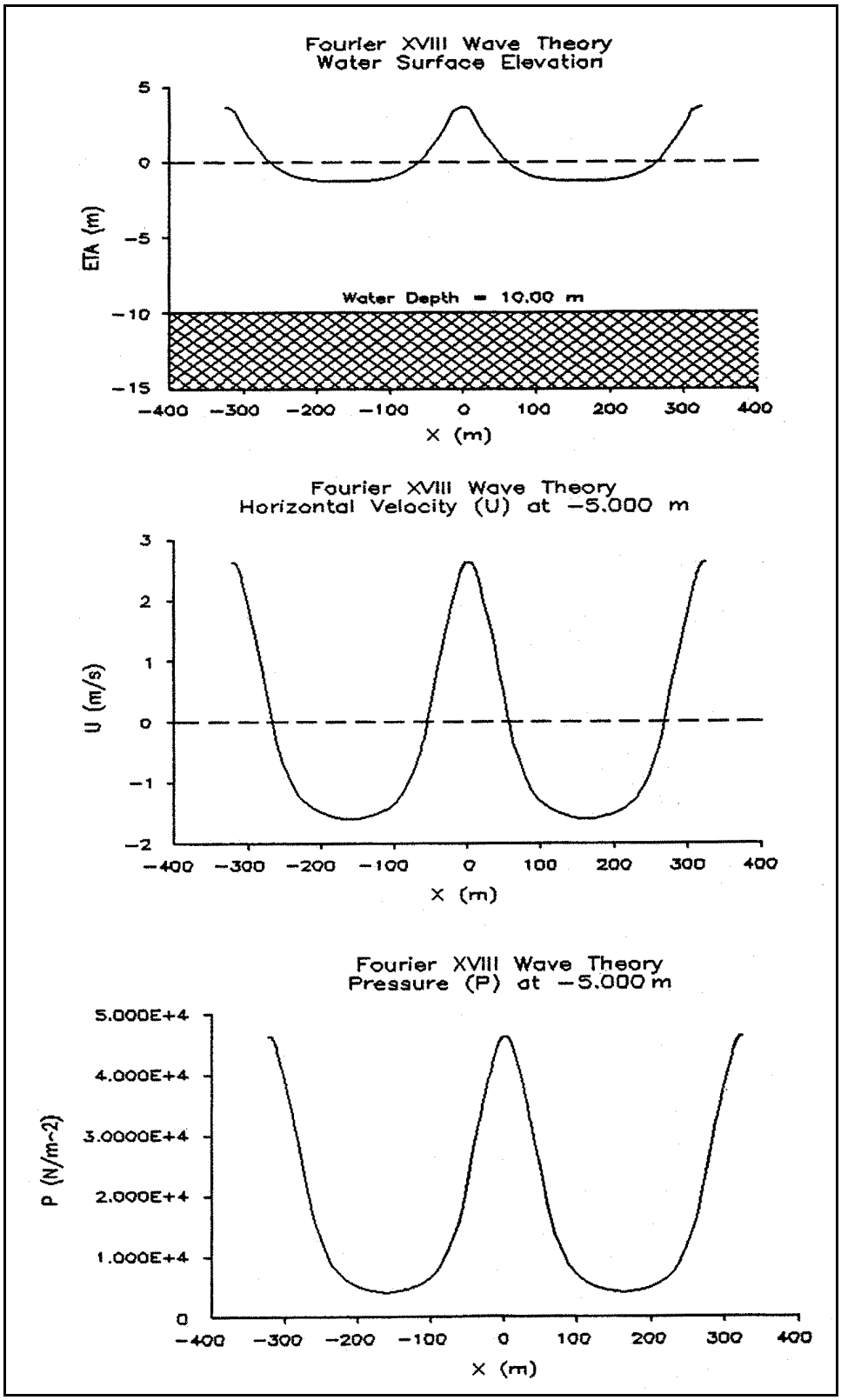

Figure II-1-18. Surface elevation, horizontal velocity, and pressure in 10-m depth (using Fenton's theory in ACES)

f. Wave breaking.

(1) Wave height is limited by both depth and wavelength. For a given water depth and wave period, there is a maximum height limit above which the wave becomes unstable and breaks. This upper limit of wave height, called *breaking wave height*, is in deep water a function of the wavelength. In shallow and transitional water it is a function of both depth and wavelength. Wave breaking is a complex phenomenon and it is one of the areas in wave mechanics that has been investigated extensively both experimentally and numerically.

(2) Researchers have made some progress over the last three decades in the numerical modeling of waves close to breaking (Longuet-Higgins and Fenton 1974; Longuet-Higgins 1974; 1976; Schwartz 1974; Dalrymple and Dean 1975; Byatt-Smith and Longuet-Higgins 1976; Peregrine 1976; Cokelet 1977; Longuet-Higgins and Fox 1977; Longuet-Higgins 1985; Williams 1981; 1985). These studies suggest the limiting wave steepness to be $H/L = 0.141$ in deep water and $H/d = 0.83$ for solitary waves in shallow water with a corresponding solitary wave celerity of $c/(gd)^{1/2} = 1.29$.

(3) Dalrymple and Dean (1975) investigated the maximum wave height in the presence of a steady uniform current using the stream function theory. Figure II-1-19 shows the influence of a uniform current on the maximum wave height where T_c is the wave period in a fixed reference frame and U is the current speed.

(4) The treatment of wave breaking in the propagation of waves is discussed in Part II-3. Information about wave breaking in deep and shoaling water and its relation to nearshore processes is provided in Part II-4.

g. Validity of wave theories.

(1) To ensure their proper use, the range of validity for various wave theories described in this chapter must be established. Very high-order Stokes theories provide a reference against which the accuracy of various theories may be tested. Nonlinear wave theories better describe mass transport, wave breaking, shoaling, reflection, transmission, and other nonlinear characteristics. Therefore, the usage of the linear theory has to be carefully evaluated for final design estimates in coastal practice. It is often imperative in coastal projects to use nonlinear wave theories.

(2) Wave amplitude and period may sometimes be estimated from empirical data. When data are lacking or inadequate, uncertainty in wave height and period estimates can give rise to a greater uncertainty in the ultimate answer than does neglecting the effect of nonlinear processes. The additional effort necessary for using nonlinear theories may not be justified when large uncertainties exist in the wave data used for design. Otherwise, nonlinear wave theories usually provide safer and more accurate estimates.

(3) Dean (1968, 1974) presented an analysis by defining the regions of validity of wave theories in terms of parameters H/T^2 and d/T^2 since T^2 is proportional to the wavelength. Le Méhauté (1976) presented a slightly different analysis (Figure II-1-20) to illustrate the approximate limits of validity for several wave theories, including the third- and fourth-order theories of Stokes. In Figure II-1-20, the fourth-order Stokes theory may be replaced with more popular fifth-order theory, since the latter is often used in applications. Both Le Méhauté and Dean recommend cnoidal theory for shallow-water waves of low steepness, and Stokes' higher order theories for steep waves in deep water. Linear theory is recommended for small steepness H/T^2 and small U_R values. For low steepness waves in transitional and deep water, linear theory is adequate but other wave theories may also be used in this region. Fenton's theory is appropriate for most of the wave parameter domain. For given values of H, d, and T, Figure II-1-20 should be used as a guide to select an appropriate wave theory.

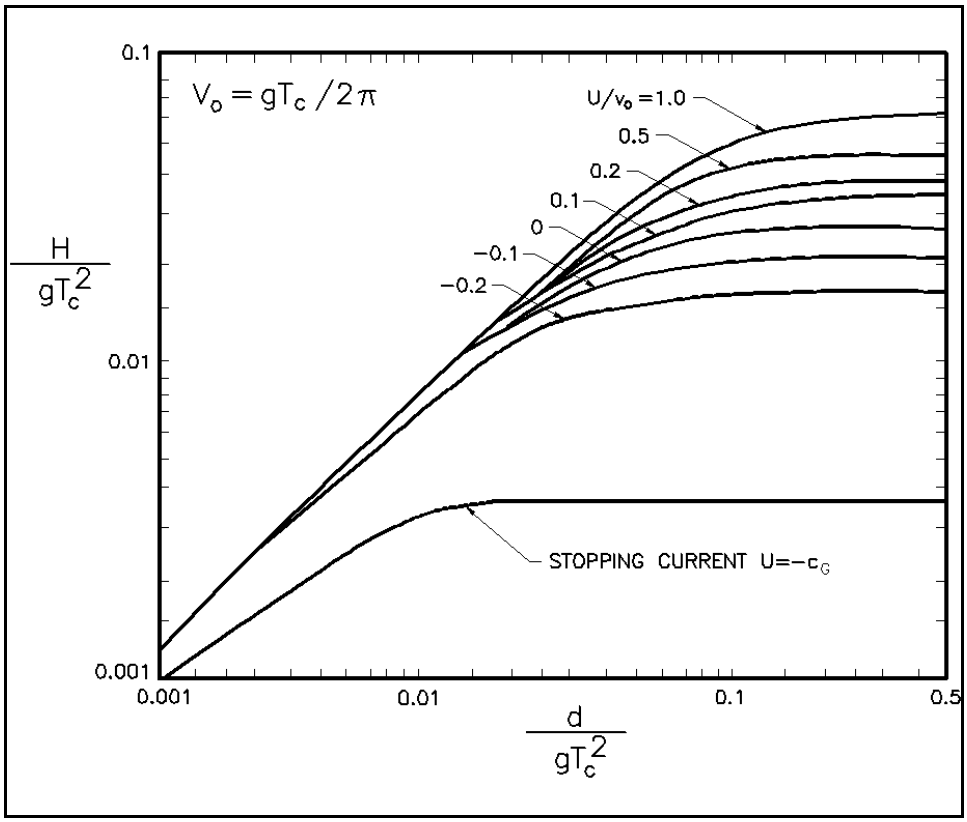

Figure II-1-19. Influence of a uniform current on the maximum wave height (Dalrymple and Dean 1975)

(4) It is necessary to know the limiting value of wave heights and wave steepness at different water depths to establish range of validity of any wave theory that uses a Stokes-type expansion. This is customarily done by comparing the magnitude of each successive term in the expansion. Each should be smaller than the term preceding it. For example, if the second term is to be less than 1 percent of the first term in the Stokes second-order theory, the limiting wave steepness is

$$\frac{H}{L} \leq \frac{1}{80} \frac{\sinh^3 kd}{\cosh kd \,(3 + 2\sinh^2 kd)} \tag{II-1-112}$$

(5) If the third-order term is to be less than 1 percent of the second-order term, the limiting wave steepness is

$$\frac{H}{L} \leq \frac{1}{7} \frac{\sinh^3 kd}{\sqrt{1 + 8\cosh^3 kd}} \tag{II-1-113}$$

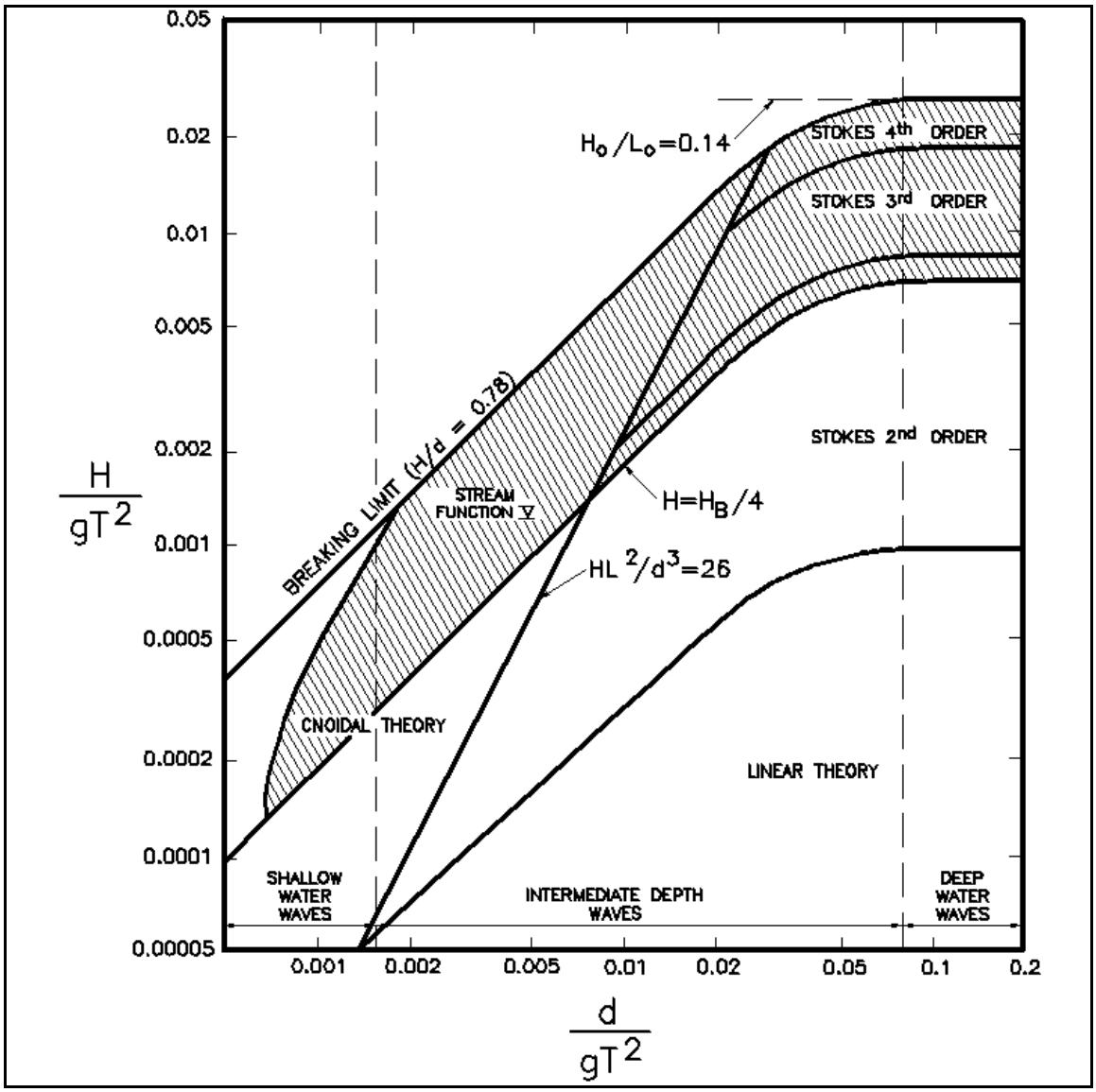

Figure II-1-20. Ranges of suitability of various wave theories (Le Méhauté 1976)

(6) Similarly, using the fifth-order expansion, the asymptotes to Stokes third-order theory are $H/L_0 < 0.1$ and $H/d < 3/4(kd)^2$ for deep water and shallow water, respectively. This allows the range of Stokes' theory to be expanded by adding successively smaller areas to the domain of linear theory in Figure II-1-20 until the breaking limit is reached. The fifth-order Stokes theory gets close enough to the breaking limit, and higher order solutions may not be warranted. Laitone (1962) suggests a shallow-water limit on Stokes' theory by setting the Ursell number U_R equal to 20. For an Ursell number of approximately 20, Stokes' theory approaches the cnoidal theory.

(7) The magnitude of the Ursell number U_R (sometimes also called the *Stokes number*) shown in Figure II-1-20 may be used to establish the boundaries of regions where a particular wave theory should be used. Stokes (1847) noted that this parameter should be small for long waves. An alternative, named the *Universal parameter* (U_p), has recently been suggested (Goda 1983) for classification of wave theories.

(8) Limits of validity of the nonlinear (higher-order) wave theories established by Cokelet (1977) and Williams (1981), are shown in Figure II-1-21. Regions where Stokes waves (short waves) and cnoidal and solitary waves (long waves) are valid are also shown in this figure. The breaking limit for solitary waves $H_b^W = 0.833$ established by Williams (1981) and the limiting height designated as H_b^F determined by Cokelet (1977) are also shown on Figure II-1-21. The line between short and long waves corresponds to a value of the Ursell number $U_R \approx 79$. This theoretical partition agrees with data from Van Dorn (1966).

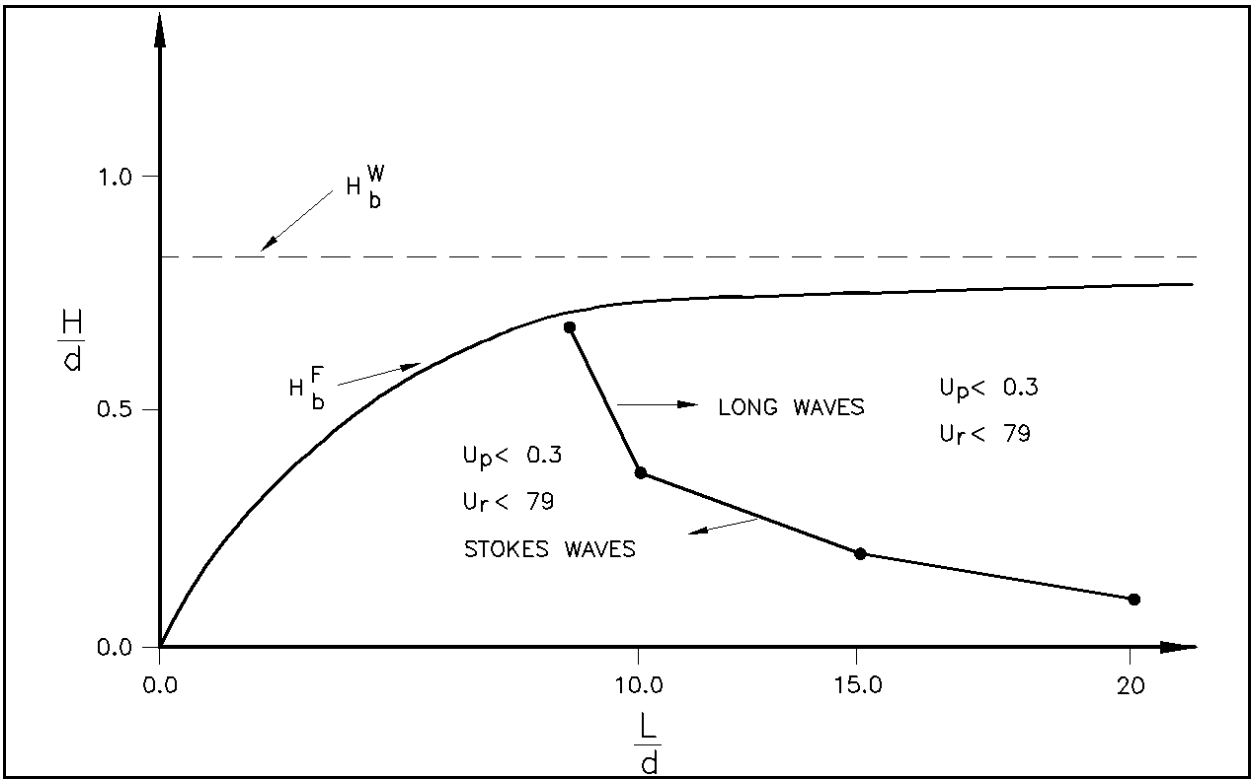

Figure II-1-21. Grouping of wind waves based on universal parameter and limiting height for steep waves

II-1-3. Irregular Waves

a. Introduction.

(1) In the first part of this chapter, waves on the sea surface were assumed to be nearly sinusoidal with constant height, period and direction (i.e., monochromatic waves). Visual observation of the sea surface (as in the radar image of the entrance to San Francisco Bay in Figure II-1-22) and measurements (such as in Figure II-1-23) indicate that the sea surface is composed of waves of varying heights and periods moving in differing directions. In the first part of this chapter, wave height, period, and direction could be treated as deterministic quantities. Once we recognize the fundamental variability of the sea surface, it becomes necessary to treat the characteristics of the sea surface in statistical terms. This complicates the analysis but more realistically describes the sea surface. The term *irregular waves* will be used to denote natural sea states in which the wave characteristics are expected to have a statistical variability in contrast to *monochromatic waves*, where the properties may be assumed constant. Monochromatic waves may be generated in the laboratory but are rare in nature. "Swell" describes the natural waves that appear most like monochromatic waves in deep water, but swell, too, is fundamentally irregular in nature. We note that the sea state in nature during a storm is always short-crested and irregular. Waves that have travelled far from

EXAMPLE PROBLEM II-1-6

FIND:

Applicable wave theory for waves in (a) and (b). Which of these waves is a long wave?

GIVEN:

(a). d = 15 m, H = 12.2 m, T = 12 sec; (b). d = 150 m, H = 30 m, T = 16 sec.

SOLUTION:

(a) Calculate dimensionless parameters necessary for using Figure II-1-20. These are

$$\frac{d}{gT^2} \approx 0.01$$

$$\frac{H}{gT^2} \approx 0.009$$

$$\frac{H}{d} = 0.8$$

$$\sqrt{gd} \approx 12 \frac{m}{\text{sec}}$$

$$U_R \approx 55$$

From Figure II-1-20, the applicable theory is cnoidal.

(b) In a similar fashion, compute

$$\frac{d}{gT^2} \approx 0.06$$

$$\frac{H}{gT^2} \approx 0.01$$

$$\frac{H}{d} = 0.2$$

$$\sqrt{gd} \approx 40 \frac{m}{\text{sec}}$$

$$U_R \approx 1.5$$

With these values, Figure II-1-20 indicates the applicable theory is Stokes third- or fifth-order. It is noted that the linear theory is also applicable.

Based on the values of Ursell parameter, neither wave (a) or (b) is a true long wave. Wave (a) may be considered a long wave in comparison to wave (b).

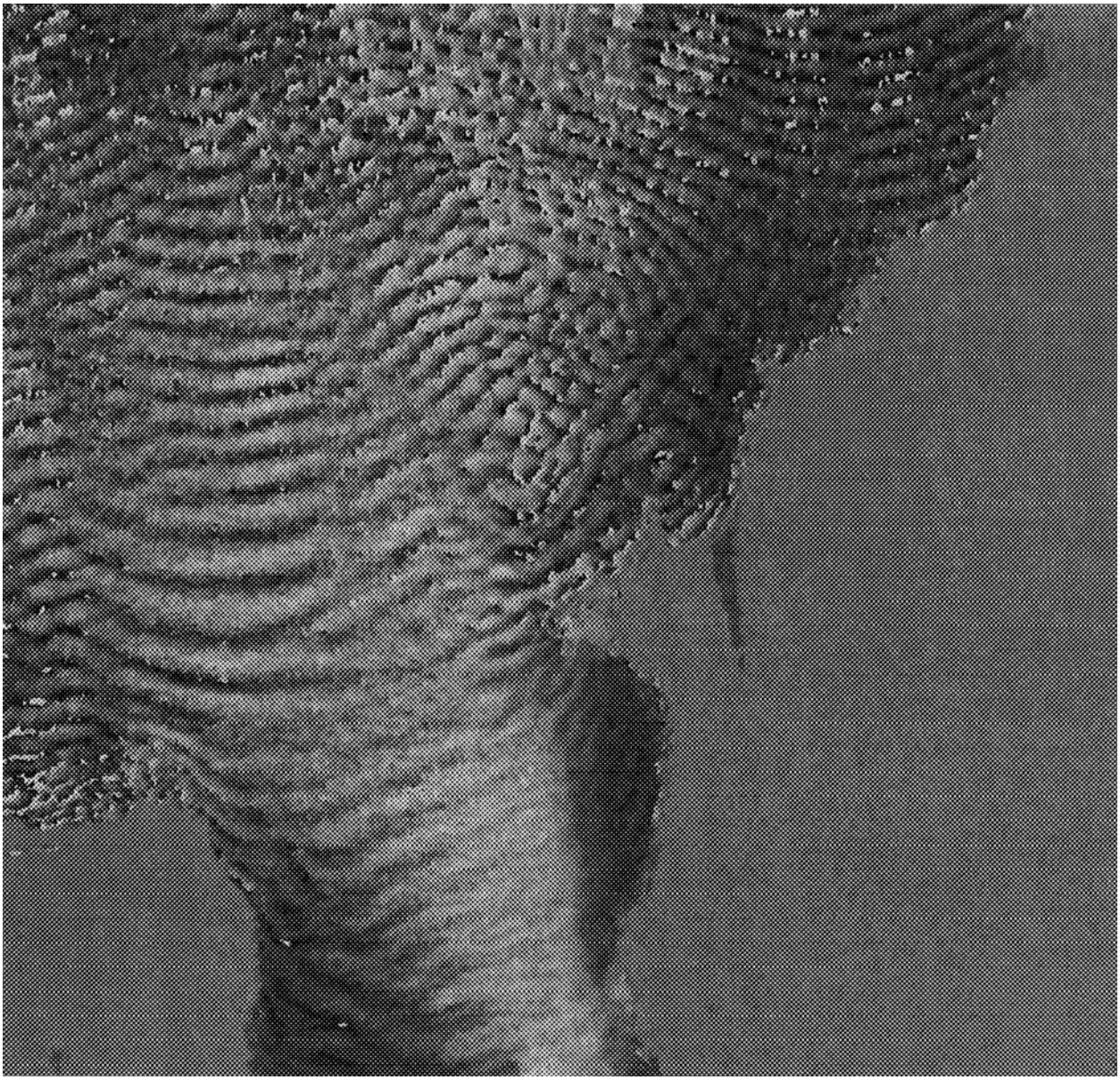

Figure II-1-22. Radar image of the sea surface in the entrance to San Francisco Bay

the region of generation are called *swells*. These waves have a much more limited range of variability, sometimes appearing almost monochromatic and long-crested.

(2) When the wind is blowing and the waves are growing in response, the sea surface tends to be confused: a wide range of heights and periods is observed and the length of individual wave crests may only be a wave length or two in extent (short-crested). Such waves are called wind seas, or often, just sea. Long-period waves that have traveled far from their region of origin tend to be more uniform in height, period, and direction and have long individual crests, often many wave lengths in extent (i.e., long-crested). These are termed swell. A sea state may consist of just sea or just swell or may be a combination of both.

(3) The ocean surface is often a combination of many wave components. These individual components were generated by the wind in different regions of the ocean and have propagated to the point of observation.

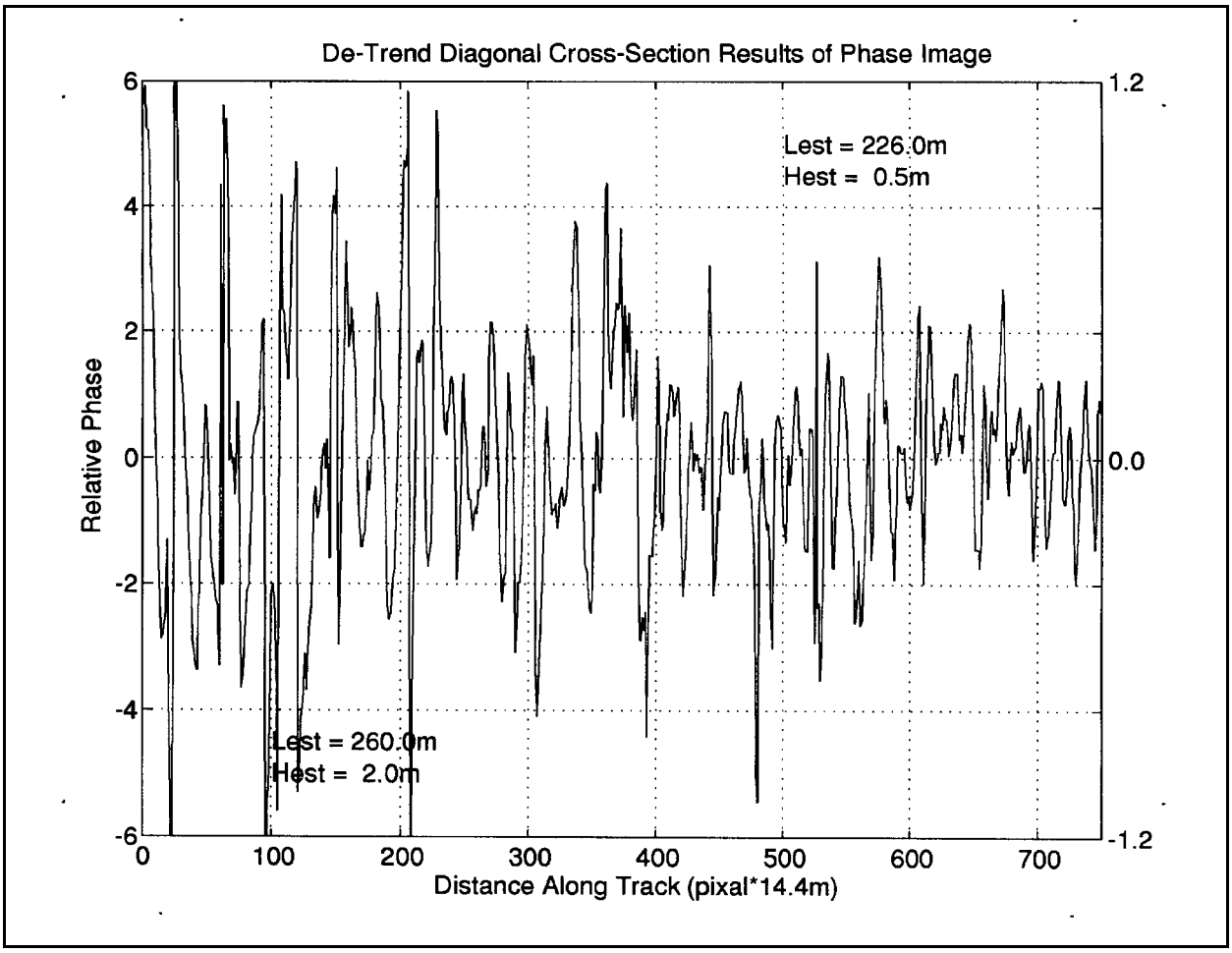

Figure II-1-23. Measured sea surface velocity in the entrance to San Francisco Bay

If a recorder were to measure waves at a fixed location on the ocean, a non-repeating wave profile would be seen and the wave surface record would be rather irregular and random (Figure II-1-23). Although individual waves can be identified, there is significant variability in height and period from wave to wave. Consequently, definitions of wave height, period, and duration must be statistical and simply indicate the severity of wave conditions.

(4) Wave profiles are depicted in Figure II-1-24 for different sea conditions. Figure II-1-25 shows a typical wave surface elevation time series measured for an irregular sea state. Important features of the field-recorded waves and wave parameters to be used in describing irregular waves later in this section are defined in Figures II-1-26 and II-1-27. We note that the sea state in nature during a storm is always short-crested and irregular. Waves that have traveled far from the region of generation are called *swells*. These waves have much more limited range of variability sometimes appearing monochromatic and long-crested.

(5) This part of Part II-1 will develop methods for describing and analyzing natural sea states. The concept of *significant wave height*, which has been found to be a very useful index to characterize the heights of the waves on the sea surface, will be introduced. *Peak period* and *mean wave direction* which characterize the dominant periodicity and direction of the waves, will be defined. However, these parameterizations of the sea surface in some sense only index how big some of the waves are. When using irregular wave heights in engineering, the engineer must always recognize that larger and smaller (also longer and shorter) waves

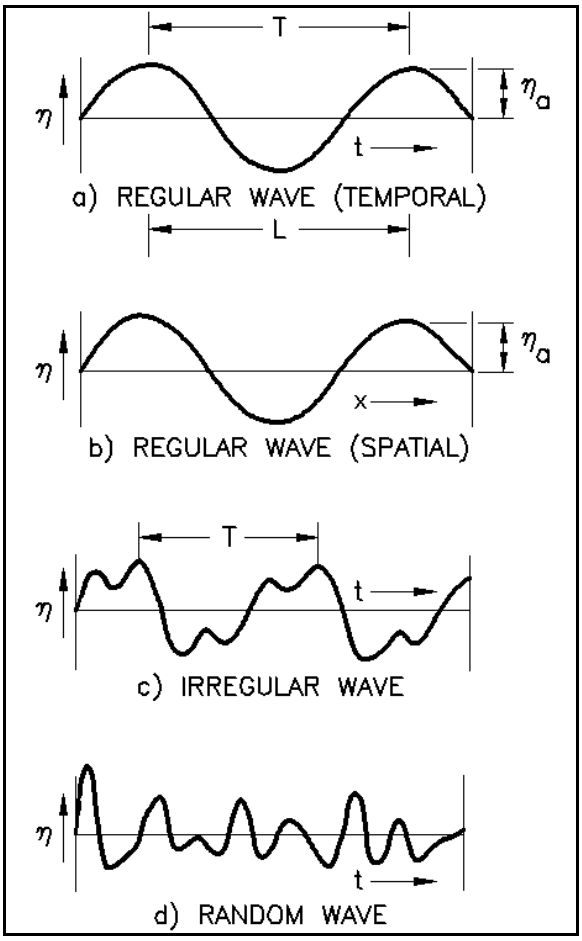

Figure II-1-24. Representations of an ocean wave

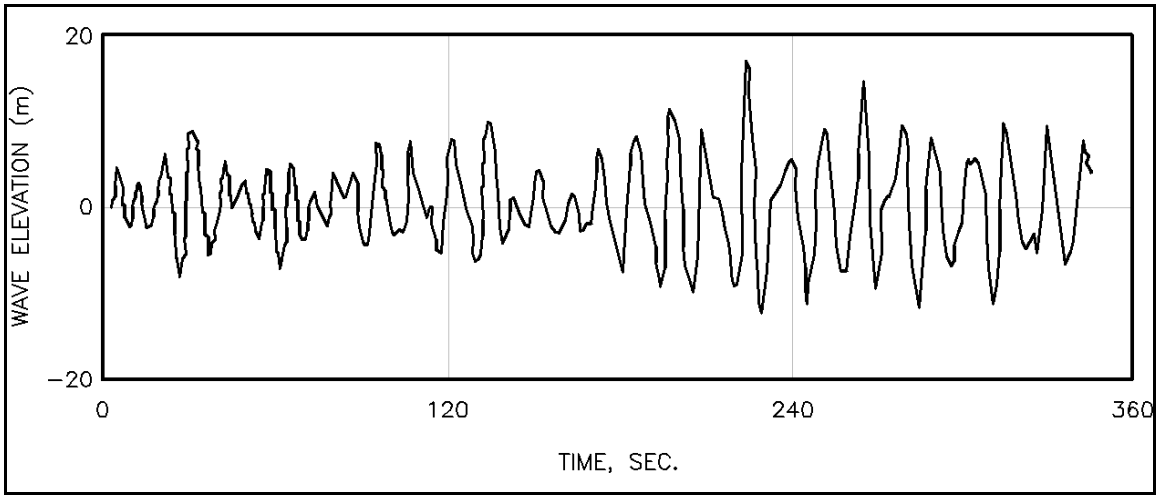

Figure II-1-25. Wave profile of irregular sea state from site measurements

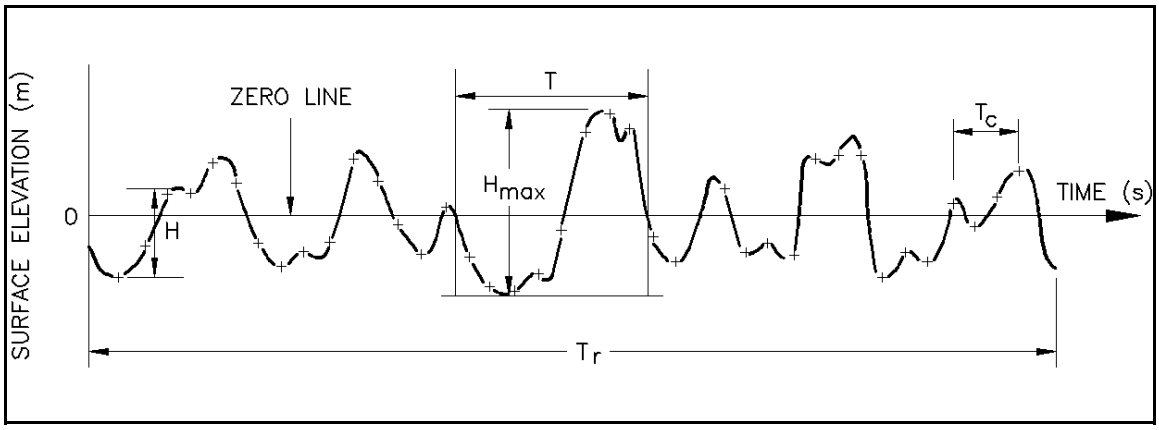

Figure II-1-26. Definition of wave parameters for a random sea state

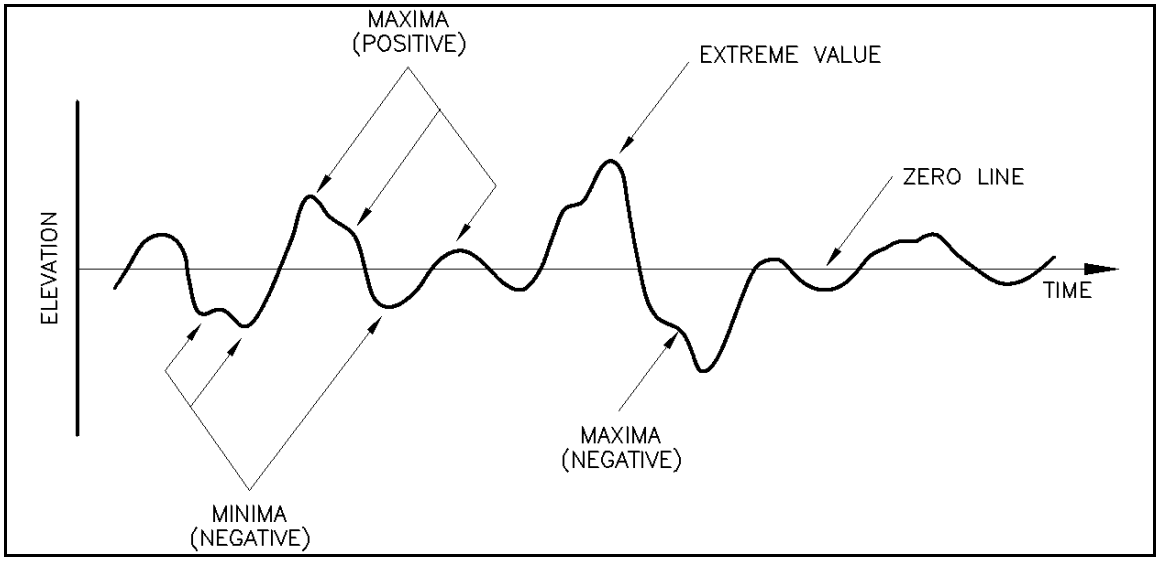

Figure II-1-27. Definition sketch of a random wave process (Ochi 1973)

are present. The monochromatic wave theories described in the first part of this chapter will be seen to have two major uses. One use is to estimate the kinematics and dynamics associated with a wave with the significant wave height, peak period, and direction. The other is when an individual wave has been isolated in a wave record to estimate the velocities, accelerations, forces, etc., associated with that individual wave event. The engineer must recognize that the implication of the statistical nature of irregular waves implies that the kinematics and dynamics likewise require statistical treatment. IAHR (1986) provides a detailed description of parameters and terminology used with irregular waves.

(6) Two approaches exist for treating irregular waves: *spectral methods* and *wave-by-wave (wave train) analysis*. Spectral approaches are based on the Fourier Transform of the sea surface. Indeed this is currently the most mathematically appropriate approach for analyzing a time-dependent, three-dimensional sea surface record. Unfortunately, it is exceedingly complex and at present few measurements are available that could fully tap the potential of this method. However, simplified forms of this approach have been proven to be very useful. The other approach used is wave-by-wave analysis. In this analysis method, a time-history of the sea surface at a point is used, the undulations are identified as waves, and statistics of the record are

developed. This is a very natural introduction to irregular waves and will be presented first before the more complicated spectral approach is presented. The primary drawback to the wave-by-wave analysis is that it cannot tell anything about the direction of the waves. Indeed, what appears to be a single wave at a point may actually be the local superposition of two smaller waves from different directions that happen to be intersecting at that time. Disadvantages of the spectral approach are the fact that it is linear and can distort the representation of nonlinear waves.

b. Wave train (wave-by-wave) analysis.

(1) Introduction.

(a) Wave train analysis requires direct measurements of irregular seas. A typical irregular wave record obtained from a wave-measuring device is shown in Figure II-1-25. The recorded wave traces have to be of finite length with the sea surface sampled at a set interval (typically every second). The time-history of sea surface elevation at a point is a random-appearing signal exhibiting many maxima and minima (Figures II-1-26 and II-1-27). It is necessary to develop a criterion for identifying individual waves in the record.

(b) In a wave-by-wave analysis, undulation in the time-history of the surface must be divided into a series of segments, which will then be considered as individual waves. The height and period of each wave will be measured. Once this is done for every segment of the record, statistical characteristics of the record can be estimated, and the statistics of the record are compiled.

(c) Knowing the statistics of one record can be useful in itself, particularly if the record is important (such as the observation of waves at a site when a structure failed). However, it would be helpful to know whether the statistical characteristics of individual wave records followed any consistent pattern. Statistics of the sea state could be predicted knowing only a little about the wave conditions. It would be very useful if the distribution of wave characteristics in a wave record followed a known statistical distribution. After defining characteristics of individual records, the larger statistical question will be addressed.

(d) In the time-domain analysis of irregular or random seas, wave height and period, wavelength, wave crest, and trough have to be carefully defined for the analysis to be performed. The definitions provided earlier in the regular wave section of this chapter assumed that the crest of a wave is any maximum in the wave record, while the trough can be any minimum. However, these definitions may fail when two crests occur within an intervening trough lying below the mean water line. Also, there is not a unique definition for wave period, since it can be taken as the time interval between either two neighboring wave troughs or two crests. Other more common definitions of wave period are the time interval between successive crossings of the mean water level by the water surface in a downward direction called *zero down-crossing period* or *zero up-crossing period* for the period deduced from successive up-crossings.

(2) Zero-crossing method.

(a) The adopted engineering procedure is the zero-crossing technique, where a wave is defined when the surface elevation crosses the zero-line or the mean water level (MWL) upward and continues until the next crossing point. This is the *zero-upcrossing* method. When a wave is defined by the downward crossing of the zero-line by the surface elevation, the method is the *zero-downcrossing*.

(b) The *zero-crossing wave height* is the difference in water surface elevation of the highest crest and lowest trough between successive zero-crossings. The definition of wave height depends on the choice of trough occurring before or after the crest. Here, a wave will be identified as an event between two successive zero-upcrossings and wave periods and heights are defined accordingly. Note that there can be differences

between the definitions of wave parameters obtained by the zero up- and down-crossing methods for description of irregular sea states.

(c) Both methods usually yield statistically similar mean values of wave parameters. There seems to be some preference for the zero-downcrossing method (IAHR 1986). The downcrossing method may be preferred due to the definition of wave height used in this method (the vertical distance from a wave trough to the following crest). It has been suggested that this definition of wave height may be better suited for extreme waves (IAHR 1986).

(d) Using these definitions of wave parameters for an irregular sea state, it is seen in Figures II-1-26 and II-1-27 that, unlike the regular (monochromatic) sinusoidal waves, the periods and heights of irregular waves are not constant with time, changing from wave to wave. Wave-by-wave analysis determines wave properties by finding average statistical quantities (i.e., heights and periods) of the individual wave components present in the wave record. Wave records must be of sufficient length to contain several hundred waves for the calculated statistics to be reliable.

(e) Wave train analysis is essentially a manual process of identifying the heights and periods of the individual wave components followed by a simple counting of zero-crossings and wave crests in the wave record. The process begins by dissecting the entire record into a series of subsets for which individual wave heights and periods are then noted for every zero down-crossing or up-crossing, depending on the method selected. In the interest of reducing manual effort, it is customary to define wave height as the vertical distance between the highest and lowest points, while wave period is defined as the horizontal distance between two successive zero-crossing points (Figures II-1-26 and II-1-27). In this analysis, all local maxima and minima not crossing the zero-line have to be discarded. From this information, several wave statistical parameters are subsequently calculated. Computer programs are available to do this (IAHR 1986).

(3) Definition of wave parameters.

(a) Determination of wave statistics involves the actual processing of wave information using the principles of statistical theory. A highly desirable goal is to produce some statistical estimates from the analyzed time-series data to describe an irregular sea state in a simple parametric form. For engineering, it is necessary to have a few simple parameters that in some sense tell us how severe the sea state is and a way to estimate or predict what the statistical characteristics of a wave record might be had it been measured and saved. Fortunately, millions of wave records have been observed and a theoretical/empirical basis has evolved to describe the behavior of the statistics of individual records.

(b) For parameterization, there are many short-term candidate parameters which may be used to define statistics of irregular sea states. Two of the most important parameters necessary for adequately quantifying a given sea state are characteristic height H and characteristic period T. Other parameters related to the combined characteristics of H and T, may also be used in the parametric representation of irregular seas.

(c) Characteristic wave height for an irregular sea state may be defined in several ways. These include the *mean height*, the *root-mean-square height*, and the mean height of the highest one-third of all waves known as the *significant height*. Among these, the most commonly used is the significant height, denoted as H_s or $H_{1/3}$. Significant wave height has been found to be very similar to the estimated visual height by an experienced observer (Kinsman 1965). The characteristic period could be the *mean period*, or *average zero-crossing period*, etc.

(d) Other statistical quantities are commonly ascribed to sea states in the related literature and practice. For example, the mean of all the measured wave heights in the entire record analyzed is called the *mean wave height* $\bar{H}$. The largest wave height in the record is the *maximum wave height* H_{max}. The root-mean-square of

all the measured wave heights is the *rms wave height* H_{rms}. The average height of the largest *1/n* of all waves in the record is the $H_{1/n}$ where n = 10, 11, 12, 13,..., 99, 100 are common values. For instance, $H_{1/10}$ is the mean height of the highest one-tenth waves. In coastal projects, engineers are faced with designing for the maximum expected, the highest possible waves, or some other equivalent wave height. From one wave record measured at a point, these heights may be estimated by ordering waves from the largest to the smallest and assigning to them a number from *1* to *N*. The significant wave height $H_{1/3}$ or H_s will be the average of the first (highest) *N/3* waves.

(e) The probability that a wave height is greater (less) than or equal to a design wave height H_d may be found from

$$P(H > H_d) = \frac{m}{N}$$
$$P(H \leq H_d) = 1 - \frac{m}{N} \tag{II-1-114}$$

where *m* is the number of waves higher than H_d. For an individual observed wave record the probability distribution $P(H > H_d)$ can be formulated in tabular form and possibly fitted by some well-known distribution. The root-mean-square wave height H_{rms} may be computed as

$$H_{rms} = \sqrt{\frac{1}{N}\sum_{j=1}^{N} H_j^2} \tag{II-1-115}$$

in which H_j denote the ordered individual wave heights in the record.

(f) Probability distributions discussed in the irregular wave section of the CEM refer to short term wave statistics. This subject concerns the probability that a wave of a given height will occur given that we know the statistics of the sea surface over a 16- to 60-min period. A short-term wave statistics question might be, for example, "If we have measured the waves for 15 min and found that H_s is 2m, what is the chance that a wave of 4 m may occur?" This must be contrasted to long-term wave statistics. To obtain long-term wave statistics, a 15-min record may have been recorded (and statistics of each record computed) every 3 hr for 10 years (about 29,000 records) and the statistics of the set of 29,000 significant wave heights compiled. A long-term wave statistics question might be, "If the mean significant wave height may be 2m with a standard deviation of 0.75m, what is the chance that once in 10 years the significant wave height will exceed 4 m?" These are two entirely different statistical questions and must be treated differently.

(g) A similar approach can be used for the wave period. The mean zero-crossing period is called the *zero-crossing period* T_z. The average wave period between two neighboring wave crests is the wave crest period T_c. Therefore, in the time domain wave record analysis, the average wave period may also be obtained from the total length of *record length* T_r either using T_z or T_c (Tucker 1963). These periods are related to T_r by

$$T_z = \frac{T_r}{N_z}$$
$$T_c = \frac{T_r}{N_c} \tag{II-1-116}$$

where N_z and N_c are the number of zero-upcrossings and crests in the wave record, respectively. We emphasize that in Tucker's method of wave train analysis, crests are defined by zero-crossing. Note also by definition of these periods that $T_c \leq T_z$.

(h) The list of definitions stated above is not all-inclusive, and several other statistical quantities may be obtained from a wave train analysis (Ochi 1973; IAHR 1986). For example, the rms surface elevation η_{rms} (described later in the short-term sea states section) (σ in IAHR list) defines the standard deviation of the surface elevation, and the significant wave height H_s is related to η_{rms} by

$$H_s = 3.8\ \eta_{rms} \approx 4\ \eta_{rms} \tag{II-1-117}$$

(4) Significant wave height.

(a) The *significant wave height* H_s (or $H_{1/3}$) is the most important quantity used describing a sea state and thus, is discussed further here for completeness. The concept of significant wave height was first introduced by Sverdrup and Munk (1947). It may be determined directly from a wave record in a number of ways. The most frequently used approach in wave-by-wave analysis is to rank waves in a wave record and then choose the highest one-third waves. The average of the chosen waves defines the significant wave height as

$$H_s = \frac{1}{\frac{N}{3}} \sum_{i=1}^{N/3} H_i \tag{II-1-118}$$

where N is the number of individual wave heights H_i in a record ranked highest to lowest.

(b) Sverdrup and Munk (1947) defined significant wave height in this fashion because they were attempting to correlate what sailors reported to what was measured. Hence, this is an empirically driven definition. Today, when wave measuring is generally automated, some other parameter might be appropriate, but significant wave height remains in recognition of its historical precedence and because it has a fairly tangible connection to what observers report when they try to reduce the complexity of the sea surface to one number. It is important to recognize that it is a statistical construct based only on the height distribution. Knowing the significant height from a record tells us nothing about period or direction.

(5) Short-term random sea state parameters.

(a) It is well-known that any periodic signal $\eta(t)$ with a zero mean value can be separated into its frequency components using the standard *Fourier analysis*. Periodic wave records may generally be treated as random processes governed by laws of the probability theory. If the wave record is a random signal, the term used is *random waves*. For a great many purposes, ocean wave records may be considered random (Rice 1944-1945, Kinsman 1965, Phillips 1977, Price and Bishop 1974).

(b) The statistical properties of a random signal like the wave surface profile may be obtained from a set of many simultaneous observations called an *ensemble* or set of signals $\{\eta_1(t), \eta_2(t), \eta_3(t),...\}$, but not from a single observation. A single observation even infinitely long may not be sufficient for determining the spatial variability of wave statistics. An ensemble consists of different realizations or measurements of the process $\eta(t)$ at some known locations. To determine wave properties from the process $\eta(t)$, certain assumptions related to its time and spatial variation must be made.

(c) First, it would be necessary to assume that the process described by the wave record (i.e., a sea state), say $\eta(t)$, is *stationary*, which means that the statistical properties of $\eta(t)$ are independent of the origin of time measurement. Since the statistics of stationary processes are time-invariant, there is no drift with time in the statistical behavior of $\eta(t)$. The stationarity requirement is necessary as we shall see later for developing a *probability distribution* for waves, which is the fraction or percentage of time an *event* or *process* (say, the sea state depicted in time series of the wave surface profile) is not exceeded. The probability distribution may be obtained by taking $\eta_1(t_1)$, $\eta_2(t_1)$, $\eta_3(t_1)$,..., as variables, independent of the instant t_1. If in addition, $\eta(t)$ can be measured at different locations and the properties of $\eta(t)$ are invariant or do not depend on location of measurements, the process may then be assumed *homogenous*. In reality, $\eta(t)$ may be assumed stationary and homogenous only for a limited duration at the location data are gathered. Wind waves may be considered approximately stationary for only a few hours (3 hr or less), beyond which their properties are expected to change.

(d) Second, the process $\eta(t)$ is assumed to be *ergodic*, which means that any measured record of the process say $\eta_1(t)$ is typical of all other possible realizations, and therefore, the average of a single record in an ensemble is the same as the average across the ensemble. For an ergodic process, the sample mean from the ensemble approaches the real mean μ, and the sample variance approaches the variance σ of the process (sea state). The ergodicity of $\eta(t)$ implies that the measured realization of $\eta(t)$, say $\eta_1(t_1)$ is typical of all other possible realizations $\eta_2(t_1)$, $\eta_3(t_1)$, ..., all measured at one instant t_1. The concept of ergodicity permits derivation of various useful statistical information from a single record, eliminating the need for multiple recordings at different sites. The assumptions of stationarity and ergodicity are the backbones of developing wave statistics from wave measurements. It is implicitly assumed that such hypotheses exist in reality, and are valid, particularly for the sea state.

(e) To apply these concepts to ocean waves, consider an ensemble of records representing the sea state by $\eta(t)$ over a finite time T. The *mean* or *expected value* of the sea state, denoted by $\bar{\eta}$, or μ_η, or $E[\eta]$, is defined as

$$\mu_\eta = E[\eta(t)] = \frac{1}{\tau} \int_{-\frac{\tau}{2}}^{\frac{\tau}{2}} \eta(t)\, dt \tag{II-1-119}$$

where the symbol E denotes the expected value of $\eta(t)$. Similarly, the mean-square of η corresponds to the second moment of η, denoted by $E[\eta^2]$. The standard deviation σ_η or the root-mean-square value of the process is the square root of this. The *variance* of η, represented by σ_η^2 may be expressed in terms of the variance of the process V as

$$\sigma_\eta^2 = V[\eta(t)] = E[\eta^2] - \mu_\eta^2 \tag{II-1-120}$$

(f) The *standard deviation* σ_η is the square root of the variance, also called the second central moment of $\eta(t)$. The standard deviation characterizes the spread in the values of $\eta(t)$ about its mean.

(g) The *autocorrelation* or *autocovariance function* of the sea state is denoted by R_η, relating the value of η at time t to its value at a later time $t+\tau$. This is defined as

$$R_\eta(t, t+\tau) = E[\eta(t)\ \eta(t+\tau)] \tag{II-1-121}$$

(h) The value of R_η gives an indication of the correlation of the signal with itself for various time lags τ, and so it is a measure of the temporal variation of $\eta(t)$ with time. If the signal is perfectly correlated with itself for zero lag τ, its autocorrelation coefficient, defined as

$$\rho_\eta = \frac{E[\eta(t)\ \eta(t+\tau)]}{E[\eta^2]} = \frac{R_\eta}{E[\eta^2]} \tag{II-1-122}$$

will be equal to 1.

(i) For two different random signals η_1 and η_2, the *cross-correlation coefficient R* may be defined as

$$R = E[\eta_1(t)\ \eta_2(t+\delta t)] = \frac{1}{\tau}\int_{-\frac{\tau}{2}}^{\frac{\tau}{2}} \eta_1(t)\ \eta_2(t+\delta t)\ dt \tag{II-1-123}$$

which measures the degree of correlation between two signals. This concept is useful for example in relating wave velocities and pressures obtained at two separate locations during wave gauge measurements in coastal projects. Note that the process $\eta(t)$ is stationary if μ_η and σ_η are constant for all values of t, and that R is a function only of $\tau = t_2 - t_1$.

(j) Assuming that the water surface elevation $\eta(t)$ is a stationary random process, representing a sea state over the duration of several hours, we will next focus our attention on defining the probabilistic properties of ocean waves. The probabilistic representation of sea state is useful in practice for two reasons. First, it allows the designer to choose wave parameters within a limit that will yield an acceptable level of risk. Second, a probabilistic-based design criterion may result in substantial cost savings by considering uncertainties in the wave estimates. Therefore, an overview of the probability laws and distributions for ocean waves follows.

(6) Probability distributions for a sea state.

(a) As noted earlier, irregular sea states are random signals. For engineers to effectively use irregular waves in design, properties of the individual wave records must follow some probability laws so that wave statistics can readily be obtained analytically. Rice (1944-1945) developed the statistical theory of random signals for electrical noise analysis. Longuet-Higgins (1952) applied this theory to the random water surface elevation of ocean waves to describe their statistics using certain simplified assumptions. Longuet-Higgins found that the parameters of a random wave signal follow known probability laws.

(b) The *probability distribution P(x)* is the fraction of events that a particular event is not exceeded. It can be obtained directly from a plot of the proportion of values less than a particular value versus the particular value of the variable x_0, and is given by

$$P(x) = prob\{x \le x_0\} \tag{II-1-124}$$

(c) The *probability density p(x)* is the fraction of events that a particular event is expected to occur and thus, it represents the rate of change of a distribution and may be obtained by simply differentiating *P(x)* with respect to its argument x.

(d) The two most commonly used probability distributions in the study of random ocean waves are the *Gaussian* (Figure II-1-28) and *Rayleigh* distributions (Figure II-1-29). The Gaussian distribution is particularly suited for describing the short-term probabilities of the sea surface elevation η. Its probability density is given by

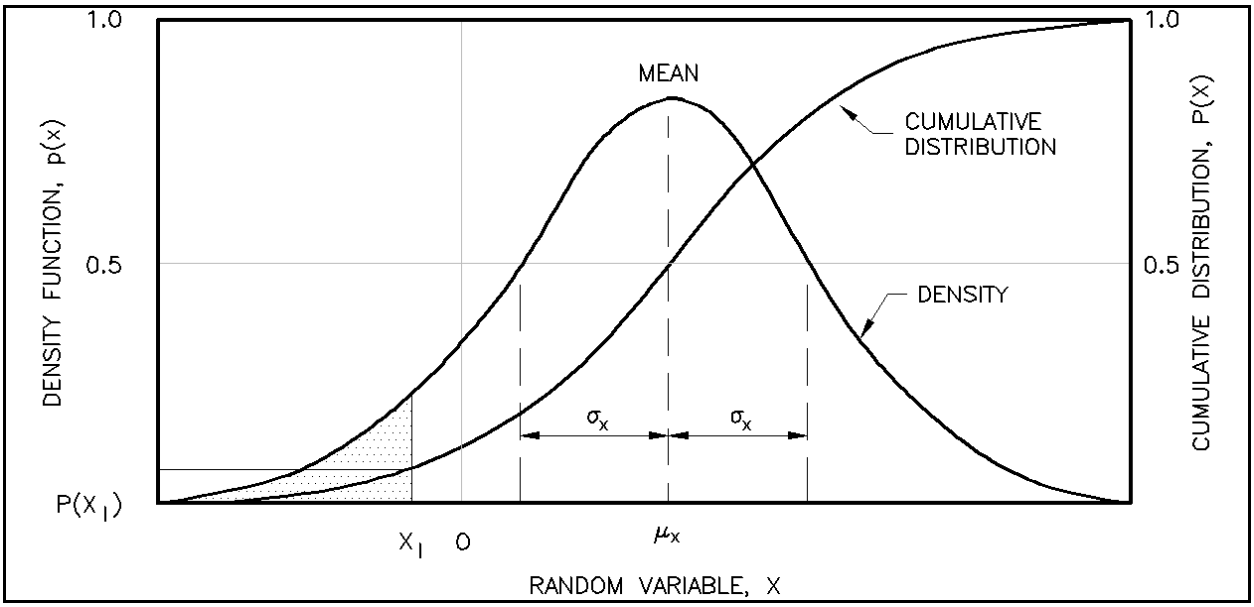

Figure II-1-28. The Gaussian probability density and cumulative probability distribution

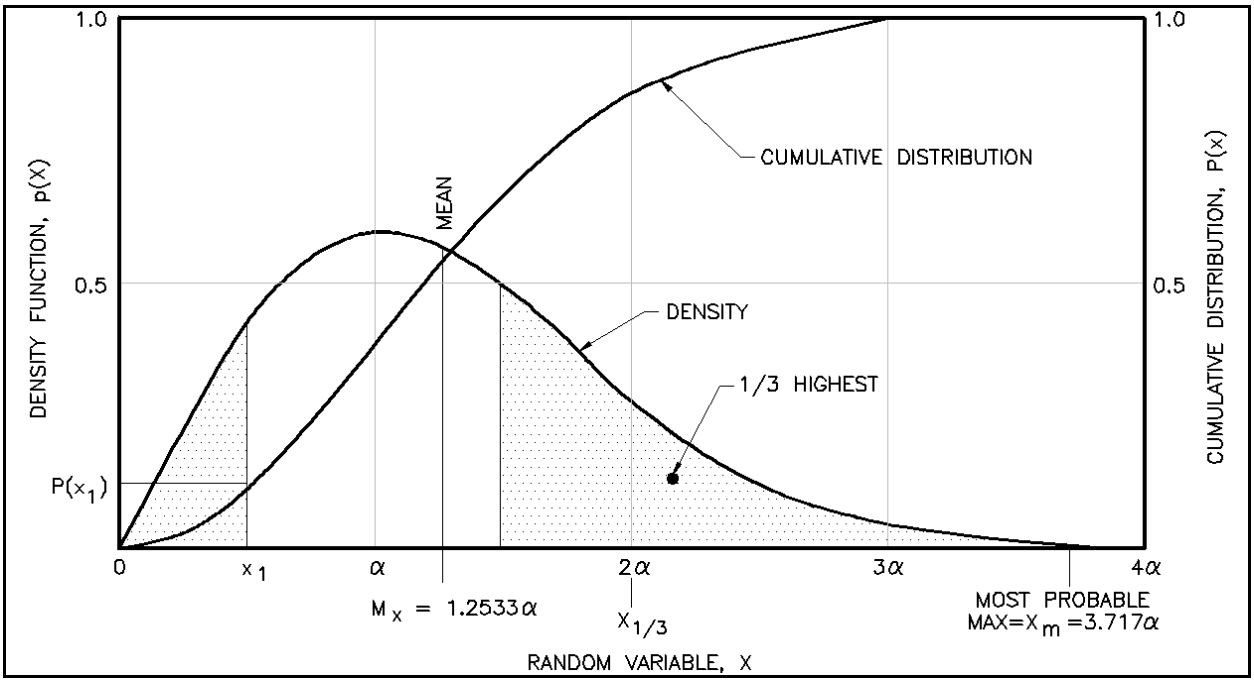

Figure II-1-29. The Rayleigh probability density and cumulative probability distribution (x = α corresponds to the mode)

$$p(x) = \frac{1}{\sigma_x\sqrt{2\pi}} e^{-\left(\frac{(x-\mu_x)^2}{2\sigma_x^2}\right)} \tag{II-1-125}$$

where μ_x is the mean of x and σ_x is the standard deviation. The Gaussian cumulative probability or probability distribution denoted by *P(x)* in Figure II-1-28, is the integral of p(x). A closed form of this integral is not possible. Therefore, Gaussian distribution is often tabulated as the normal distribution with the mean μ_x and standard deviation σ_x in handbooks (e.g., Abramowitz and Stegun (1965)), and is written as

$$p(x) = N(\mu_x,\sigma_x) \qquad P(x) = \Phi\left[\frac{x-\mu_x}{\sigma_x}\right] \tag{II-1-126}$$

For zero mean ($\mu_x = 0$) and unit standard deviation ($\sigma_x = 1$), the Gaussian probability density and distributions reduce to

$$p(x) = \frac{1}{\sqrt{2\pi}} e^{\left(-\frac{x^2}{2}\right)}$$
$$\Phi(x) = \int_0^x p(y)\, dy \tag{II-1-127}$$

where the last integral is the *error function*.

(e) The probability of exceedence *Q(x)* may be expressed in terms of the probability of non-exceedence P(x) as

$$Q\left[x(t)>x_1\right] = 1 - P\left[x(t)<x_1\right] = 1 - \Phi\left[\frac{x-\mu_{x_1}}{\sigma_x}\right] \tag{II-1-128}$$

(f) This is the probability that x will exceed x_1 over the time period t, and is shown as the shaded area in the bottom lower end of Figure II-1-28. The probability of exceedence is an important design parameter in risk-based design.

(g) In engineering practice, we are normally concerned with wave height rather than surface elevation. However, to define wave height distribution, we only need to examine the statistics of the slowly varying envelope of the surface elevation $\eta(t)$. With this approach, Longuet-Higgins (1952) found from statistical theory that both wave amplitudes and heights follow the Rayleigh distribution shown in Figure II-1-29. Note that this distribution can never be negative, it decays asymptotically to zero for large x, but never reaches zero. The probability density function of the Rayleigh distribution and its cumulative probability are given by

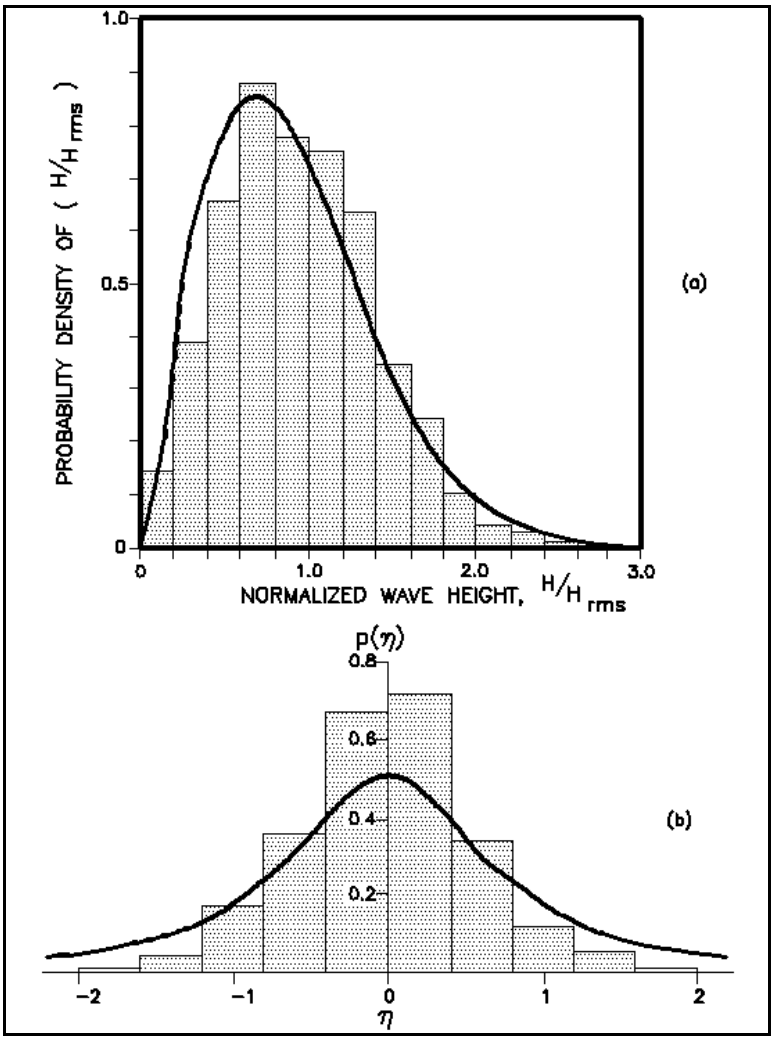

Figure II-1-30. Histograms of the normalized (a) wave heights, and (b) wave periods with theoretical distributions (Chakrabarti 1987)

$$p(x) = \left\{ \frac{\pi x}{2\mu_x^2} \; e^{-\frac{\pi}{4}\left(\frac{x}{\mu_x}\right)^2} \qquad for\ x \geq 0 \right\} \tag{II-1-129}$$

$$P(x) = \left\{ 1 - e^{-\frac{\pi}{4}\left(\frac{x}{\mu_x}\right)^2} \quad for\ x \geq 0 \right\}$$

where μ_x is the mean. These are displayed in Figure II-1-29 in which the density function is offset to the right and has only positive values. The distributions used for wave heights, wave periods, and their joint relations are described next.

(7) Wave height distribution.

(a) The heights of individual waves may be regarded as a stochastic variable represented by a probability distribution function. From an observed wave record, such a function can be obtained from a histogram of wave heights normalized with the mean heights in several wave records measured at a point (Figure II-1-30). Thompson (1977) indicated how well coastal wave records follow the Rayleigh distribution. If wave energy is concentrated in a very narrow range of wave period, the maxima of the wave profile will coincide with the wave crests and the minima with the troughs. This is termed a *narrow-band condition*. Under the narrow-band condition, wave heights are represented by the following Rayleigh distribution (Longuet-Higgins 1952, 1975b, 1983)

$$p(H) = \frac{2H}{H_{rms}^2} \exp\left[-\frac{H^2}{H_{rms}^2}\right]$$

$$P(H) = 1 - \exp\left[-\frac{H^2}{H_{rms}^2}\right] \tag{II-1-130}$$

(b) The significant wave height $H_{1/3}$ is the centroid of the area for $H \geq H_*$ under the density function where $H > H_*$ corresponds to waves in the highest one-third range as shown in Figure II-1-29, that is

$$P(H_*) = 1 - \frac{1}{3} = 1 - e^{\left(-\frac{H_*^2}{H_{rms}^2}\right)} \tag{II-1-131}$$

from which we find $H_* = 1.05 H_{rms}$. Various estimates of wave heights may then be obtained upon integration of the above equation using certain mathematical properties of the Error function (Abramowitz and Stegun 1965). We find

$$\begin{aligned} H_{1/3} &\approx 4.00 \sqrt{m_0} = 1.416\, H_{rms} \\ H_{1/10} &= 1.27\, H_{1/3} = 1.80\, H_{rms} = 5.091 \sqrt{m_0} \\ H_{1/100} &= 1.67\, H_{1/3} = 2.36\, H_{rms} = 6.672 \sqrt{m_0} \\ H_{max} &= 1.86\, H_{1/3} \quad (\textit{for } 1000 \textit{ wave cycles in the record}) \end{aligned} \tag{II-1-132}$$

(c) The *most probable maximum wave height* in a record containing N waves is related to the rms wave height (Longuet-Higgins 1952) by

$$H_{max} = \left[\sqrt{\log N} + \frac{0.2886}{\sqrt{\log N}} - \frac{0.247}{(\log N)^{3/2}}\right] H_{rms} \tag{II-1-133}$$

(d) The value of H_{max} obtained in this manner can be projected to a longer period of time by adjusting the value of N based on the mean zero-upcrossing period (Tucker 1963).

(e) The fact that the statistics of wave height for wave records in general follows a Rayleigh distribution is of great significance in coastal engineering. For instance, an engineer may have information from a hindcast (see Part II-2) that the significant height for a storm is 10 m. Assuming that the Rayleigh distribution describes the wave record, the engineer can estimate that the 10-percent wave will be 12.7 m and that the H_{max} (assuming 1,000 waves in the record) will be 18.6 m. Often measured ocean wave records are analyzed spectrally (see "Spectral Analysis" section later in this chapter) by the instrument package and only condensed information is reported via satellite to a data bank, with no other information retained. The inherent assumption made is that the Rayleigh distribution is adequate.

(f) Theoretical relationships derived from the Rayleigh distribution generally agree well with the values determined directly from the records. The Rayleigh probability distribution density function is compared with a histogram of the measured deepwater wave heights in Figure II-1-30 (Chakrabarti 1987). Clearly the Rayleigh distribution fits this data well, even though the frequency spectra of ocean waves may not always be narrow-banded as assumed in the Rayleigh distribution. Field measurements sometimes deviate from the Rayleigh distribution, and the deviation appears to increase with increasing wave heights, and decrease as the wave spectrum becomes sharply peaked. The effect of bandwidth on wave height distribution has been accounted for theoretically (Tayfun 1983).

(g) Deepwater wave height measurements from different oceans have been found to closely obey a Rayleigh distribution (Tayfun 1983a,b; Forristall 1984; Myrhaug and Kjeldsen 1986). This is not true for shallow-water waves, which are strongly modulated by the bathymetric effects combined with the amplitude nonlinearities. The wave energy spectrum of the shallow-water waves is not narrow-banded and may substantially deviate from the Rayleigh distribution especially for high frequencies. In general, the Rayleigh distribution tends to overpredict the larger wave heights in all depths.

(h) In summary, the Rayleigh distribution is generally adequate, except for near-coastal wave records in which it may overestimate the number of large waves. Investigations of shallow-water wave records from numerous studies indicate that the distribution deviates from the Rayleigh, and other distributions have been shown to fit individual observations better (SPM 1984). The primary cause for the deviation is that the large waves suggested in the Rayleigh distribution break in shallow water. Unfortunately, there is no universally accepted distribution for waves in shallow water. As a result, the Rayleigh is frequently used with the knowledge that the large waves are not likely.

(8) Wave period distribution.

(a) Longuet-Higgins (1962) and Bretschneider (1969) derived the wave period distribution function assuming the wave period squared follows a Rayleigh distribution. This distribution is very similar to the normal distribution with a mean period given by

$$T_{0,1} = \frac{m_0}{m_1} \tag{II-1-134}$$

where the moments are defined in terms of cyclic frequency (i.e., Hertz). The probability density of wave period T is given by (Bretschneider 1969)

$$p(T) = 2.7\frac{T^3}{\bar{T}} \exp\left[-0.675\tau^4\right]$$

$$\tau = \frac{T}{\bar{T}} \tag{II-1-135}$$

(b) A different probability density distribution of the wave period has been derived by Longuet-Higgins (1962). This is given by

$$p(\tau) = \frac{1}{2(1 + \tau^2)^{3/2}}$$

$$\tau = \frac{T - T_{0,1}}{\upsilon T_{0,1}} \quad ; \quad \nu = \frac{m_0 m_2 - m_1^2}{m_1^2} \tag{II-1-136}$$

where ν is the *spectral width parameter* and m_0, m_1, and m_2 are *moments* of the wave spectrum, which will be defined later. This probability density function is symmetric about $\tau = 0$ where it is maximum, and is similar to the normal distribution with a mean equal to $T_{0,1}$. This distribution fits field measurements reasonably well, and is often used in offshore design. In general, probability density for the wave period is narrower than that of wave height, and the spread lies mainly in the range 0.5 to 2.0 times the mean wave period.

(c) Various characteristic wave periods are related. This relationship may be stated in a general way as

$$T_{max} \approx T_{1/3} \approx C\bar{T} \tag{II-1-137}$$

where the coefficient C varies between 1.1 and 1.3.

(9) Joint distribution of wave heights and periods.

(a) If there were no relation between wave height and wave period, then the joint distribution between wave height and wave period can simply be obtained from the individual probability distributions of the height and period by

$$p(H,T) = p(H)\, p(T) \tag{II-1-138}$$

(b) The distribution p(H,T) so obtained is inappropriate for ocean waves, since their heights and periods are correlated. For the joint distribution of wave height-period pairs, Longuet-Higgins (1975b) considered wave heights and periods also representable by a narrow-band spectrum. He derived the joint distribution assuming wave heights and periods are correlated, a more suitable assumption for real sea states.

(c) The probability density function of wave period may be obtained directly from the joint distribution, provided that a measure of the spectrum width is included in the latter. Under this condition, the distribution of wave period is simply the marginal probability density function of the joint distribution of H and T. This is done by integrating $p(H,T)$ for the full range of H from 0 to ∞. Likewise, the distribution for wave heights may be obtained by integrating $p(H,T)$ for the full range of periods. The joint distribution derived by Longuet-Higgins (1975b) was later modified (Longuet-Higgins 1983), and is given by

$$p(H,T) = \frac{\pi f(\nu)}{4}\left(\frac{H_*}{T_*}\right)^2 \exp\left\{-\frac{\pi H_*^2}{4}\left[1 + \frac{1-\frac{\sqrt{1+\nu^2}}{T_*}}{\nu^2}\right]\right\}$$

$$H_* = \frac{H}{\bar{H}} \quad ; \quad T_* = \frac{T}{\bar{T}_z} \quad ; \quad f(\nu) = \frac{2(1+\nu^2)}{\nu + \frac{\nu}{\sqrt{1+\nu^2}}} \tag{II-1-139}$$

with ν as the spectral width parameter. The period $\bar{T}_z$ is the mean zero-upcrossing period and its relation to the mean wave period $\bar{T}$ and mean crest period $\bar{T}_c$ defined in terms of moments of spectrum is as follows:

$$\bar{T}_z = 2\pi\sqrt{\frac{m_0}{m_2}} \quad ;$$

$$\bar{T} = 2\pi\frac{m_0}{m_1} \quad ; \quad \bar{T}_c = 2\pi\sqrt{\frac{m_2}{m_4}} \tag{II-1-140}$$

(d) The *most probable maximum period* associated with any given H_* is

$$T_*^{\max} = \frac{2\sqrt{1+\nu^2}}{1+\sqrt{1+\frac{16\nu^2}{\pi H_*^2}}} \tag{II-1-141}$$

(e) Chakrabarti and Cooley (1977) investigated the applicability of the joint distribution and determined that it fits field data provided the spectrum is narrow-banded and has a single peak. A different theoretical model has been suggested by Cavanie et al. (1978), and it also compares well with the field data.

c. Spectral analysis.

(1) Introduction.

(a) In the period 1950-1960, Rice's (1944-1945) work on signal processing was extended to ocean waves (Kinsman 1965; Phillips 1977). In pinciple, the time-history of surface elevation (such as in Figures II-1-31 and II-1-32) was recognized to be similar to a noise record. By assuming that it is a discrete sample of a continuous process, the principles of Fourier analysis could be extended to describe the record. The power of Fourier representation is such that given a series of time snapshots of measurements of a three-dimensional surface, a full mathematical representation of the surface and its history may be obtained. Unfortunately, this is a lot of information. As an example, the image in Figure II-1-22 of the entrance to San Francisco Bay is one snapshot of the surface current field and represents nearly 1 million sample points. To understand the time variation of the field it would be reasonable to do this every 2 sec or so for an hour. The result is about 1.8 billion sample points that would need to be Fourier transformed. Although, this is computationally feasible such a measurement cannot be made on a routine basis and it is not clear how the information could be condensed into a form for practical engineering. However, the utility of the spectral analysis approach is that it uses a reduced dimensional approach that is powerful and useful. This section will discuss the

underlying approach to using spectral representations in engineering, discuss the basic approach for the simplified spectral approaches, and describe how the spectral information can be used. However, the underlying statistical theory and assumptions will only be touched upon and details of the derivations will only be referenced.

(b) The easiest place to begin is with a nonrigorous discussion of what a spectral analysis of a single-point measurement of the surface can produce and then generalize it to the case of a sea surface. The following sections would then describe of the procedure.

(c) Considering a single-point time-history of surface elevation such as in Figures II-1-25, II-1-31, and II-1-32, spectral analysis proceeds from viewing the record as the variation of the surface from the mean and recognizes that this variation consists of several periodicities. In contrast to the wave-by-wave approach, which seeks to define individual waves, the spectral analysis seeks to describe the distribution of the variance with respect to the frequency of the signal. By convention, the distribution of the variance with frequency is written as *E(f)* or *S(f)* with the underlying assumption that the function is continuous in frequency space. The reason for this assumption is that all observations are discretely sampled in time, and thus, the analysis should produce estimates as discrete frequencies which are then statistically smoothed to estimate a continuum. Although *E(f)* is actually a measurement of variance, it is often called the *one-dimensional* or *frequency energy spectrum* because (assuming linear wave theory) the energy of the wave field may be estimated by multiplying *E(f)* by ρg.

(d) Figures II-1-31 (a regular wave) and II-1-32 (an irregular wave) provide two wave records and their spectrum. One immediate value of the spectral approach is that it tells the engineer what frequencies have significant energy content and thus acts somewhat analogous to the height-period diagram. The primary disadvantage of spectral analysis is that information on individual waves is lost. If a specific record is analyzed, it is possible to retain information about the phases of the record (derived by the analysis), which allows reconstruction of waves. But this is not routinely done.

(e) The surface can be envisioned not as individual waves but as a three-dimensional surface, which represents a displacement from the mean and the variance to be periodic in time and space. The simplest spectral representation is to consider $E(f,\theta)$, which represents how the variance is distributed in frequency f and direction θ (Figure II-1-33). $E(f,\theta)$ is called the 2-D or directional energy spectrum because it can be multiplied by ρg to obtain wave energy. The advantage of this representation is that it tells the engineer about the direction in which the wave energy is moving. A directional spectrum is displayed in Figure II-1-34 with its frequency and direction spectrums.

(f) The power of spectral analysis of waves comes from three major factors. First, the approach is easily implemented on a microchip and packaged with the gauging instrument. Second, the principal successful theories for describing wave generation by the wind and for modelling the evolution of naturalsea states in coastal regions are based on spectral theory. Third, it is currently the only widely used approach for measuring wave direction. A final factor is that Fourier or spectral analysis of wave-like phenomena has an enormous technical literature and statistical basis that can be readily drawn upon.

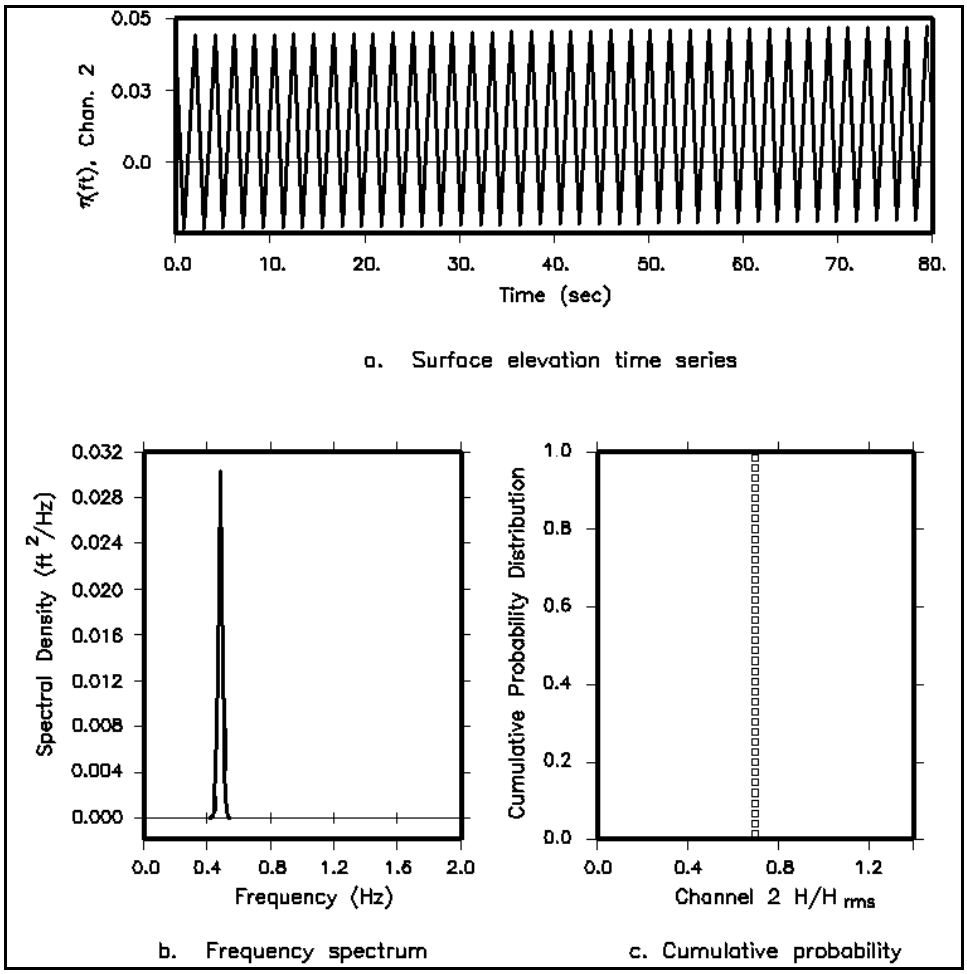

Figure II-1-31. Surface elevation time series of a regular wave and its spectrum (Briggs et al. 1993)

(g) Before proceeding to the details of how a wave spectrum is derived from a record, it is important to touch upon some statistical assumptions that are important in analyzing a wave record spectrally. Many of these assumptions also hold for making a wave-by-wave analysis useful as well. First of all, wave records are finite in length (typically 17-68 min long) and are made up of samples of surface elevation at a discrete sampling interval (typically 0.5-2.0 sec). For the wave records to be of general use, the general characteristics of the record should not be expected to change much if the record was a little shorter or longer, if the sampling was started some fraction of time earlier or later, or if the records were collected a short distance away. In addition, it is desirable that there not be any underlying trend in the data.

(h) If the above assumptions are not reasonably valid, it implies that the underlying process is unstable and may not be characterized by a simple statistical approach. Fortunately, most of the time in ocean and coastal areas, the underlying processes are not changing too fast and these assumptions reasonably hold. In principal the statistical goal is to assume that there is some underlying statistical process for which we have obtained an observation. The observation is processed in such a way that the statistics of the underlying process are obtained.

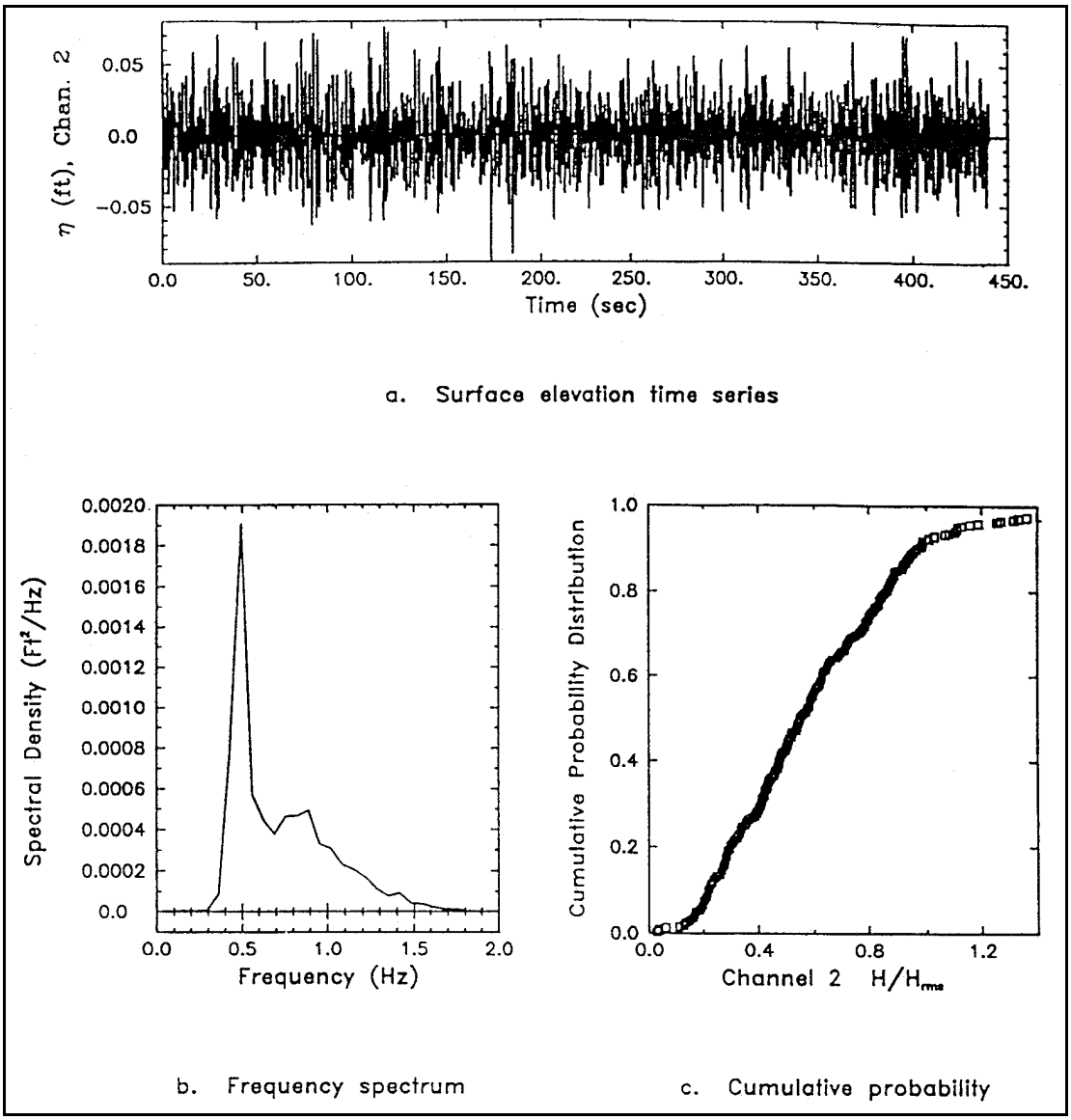

Figure II-1-32. Surface elevation time series of an irregular wave and its spectrum (Briggs et al. 1993)

(2) Description of wave spectral analysis.

(a) Unlike the wave train or wave-by-wave analysis, the spectral analysis method determines the distribution of wave energy and average statistics for each wave frequency by converting time series of the wave record into a wave spectrum. This is essentially a transformation from time-domain to the frequency-domain, and is accomplished most conveniently using a mathematical tool known as the Fast Fourier Transform (FFT) technique (Cooley and Tukey 1965). Here we will treat analysis of the time recording ofthe surface at a point, in order to obtain a frequency spectrum of the record. In a later section, we will describe how to obtain a frequency-directional spectrum.

(b) The *wave energy spectral density E(f)* or simply the *wave spectrum* may be obtained directly from a continuous time series of the surface $\eta(t)$ with the aid of the Fourier analysis. Using a Fourier analysis, the

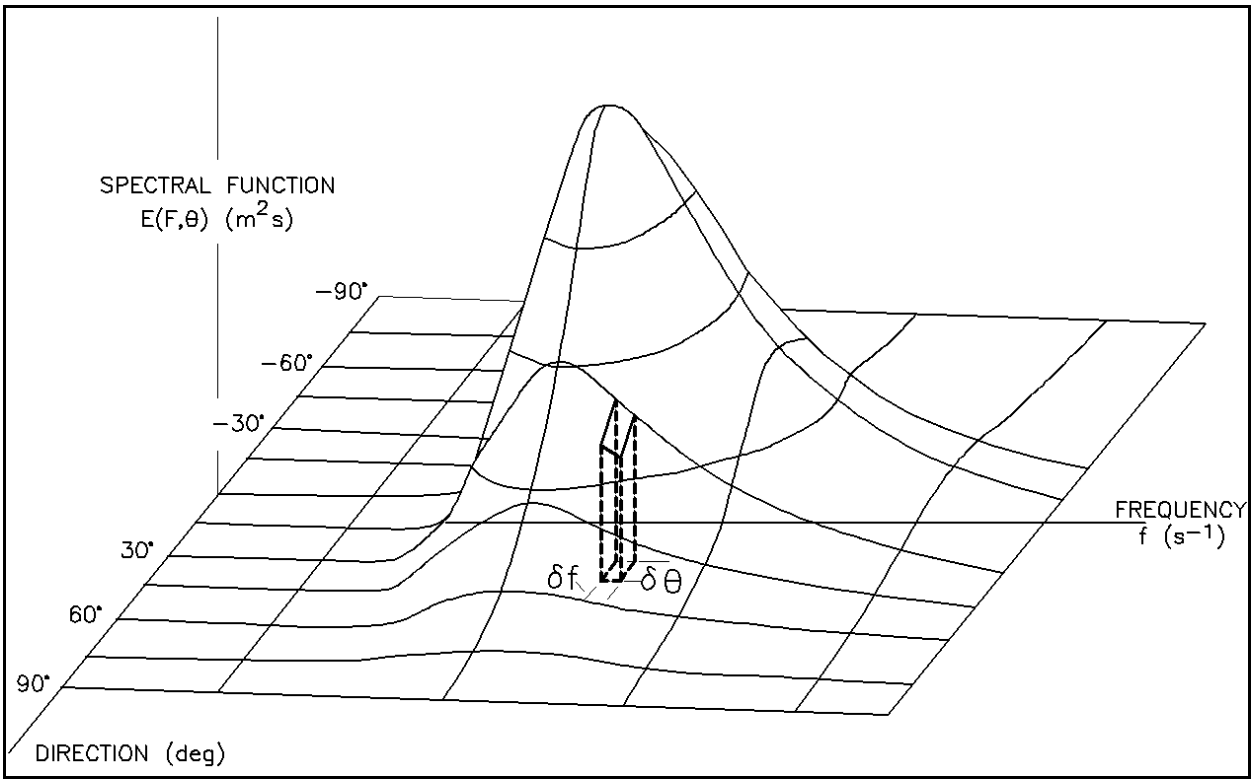

Figure II-1-33. A schematic for a two-dimensional wave spectrum E(f,θ)

wave profile time trace can be written as an infinite sum of sinusoids of amplitude A_n, frequency ω_n, and relative phase ϵ_n, that is

$$\eta(t) = \sum_{n=0}^{\infty} A_n \cos(\omega_n t - \epsilon_n) = \sum_{n=0}^{\infty} a_n \cos n\omega t + b_n \sin n\omega t \quad \text{(II-1-142)}$$

(c) The coefficients a_n and b_n in the above equation may be determined explicitly from the orthogonality properties of circular functions. Note that a_0 is the mean of the record. Because real observations are of finite length, the finite Fourier transform is used and the number of terms in the sum n is a finite value.

(d) The *covariance* of $\eta(t)$ is related to the wave energy spectrum. This is defined in terms of the squares of component amplitudes as

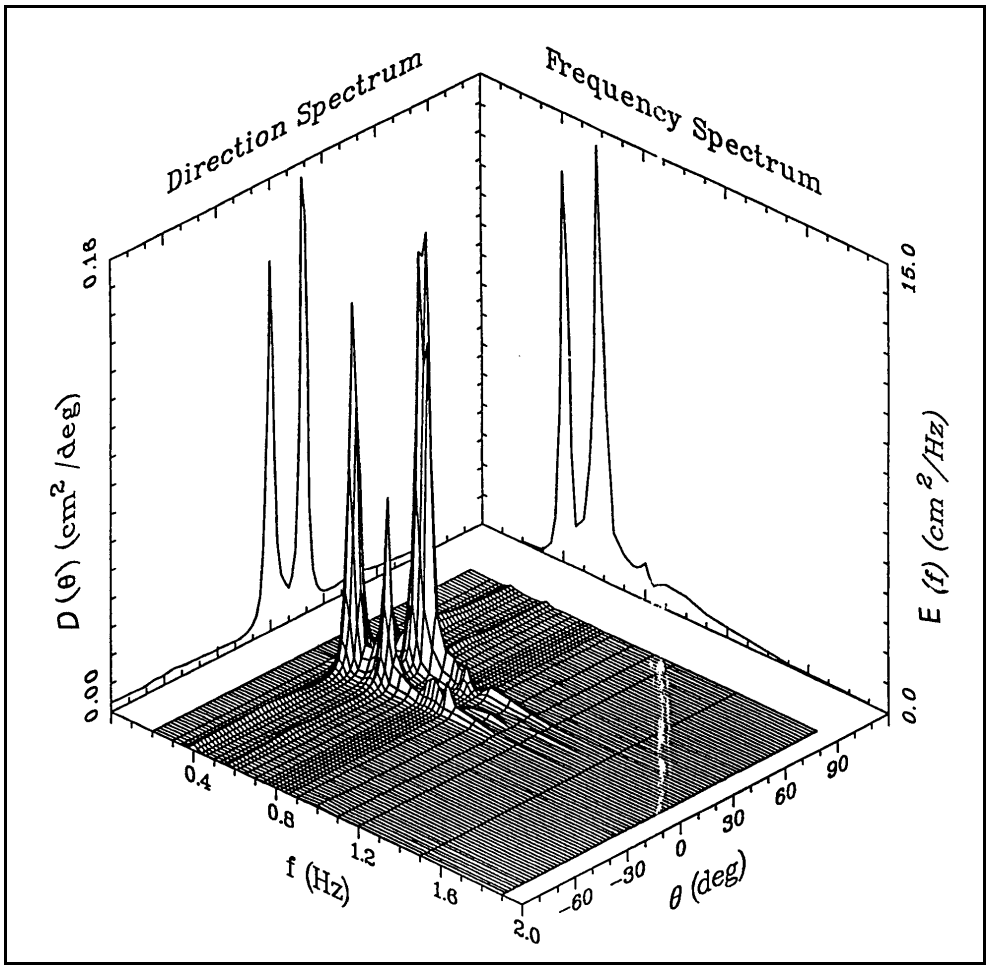

Figure II-1-34. A directional spectrum and its frequency and direction spectrum (Briggs et al 1993)

$$\bar{\eta}^2(t) = \sum_0^\infty A_n^2 \, \Delta f$$

$$A_n^2 = \frac{1}{2}\sqrt{a_n^2 + b_n^2} \qquad \text{(II-1-143)}$$

$$\epsilon_n = \tan^{-1} \frac{b_n}{a_n}$$

(e) By induction, an estimate of the continued energy spectrum of $\eta(t)$ may be obtained by

$$E(f) = \frac{1}{T_r}\left[\sum_{n=0}^{N} \eta(n\Delta t)\; e^{2\pi i f(n\Delta t)}\; \Delta t\right]^2 \qquad \text{(II-1-144)}$$

where T_r is the *record length* and Δt is the *sampling interval*.

(f) There are numerous intricacies involved in the application of these discrete formulas, ranging from the length of time series necessary to digitizing frequency and many others. For unfamiliar users, most computer library systems now have *FFT (Finite Fourier Transform) algorithms* available to perform the above computations. Part VII-3 of the CEM provides a discussion of the methods. Some general guidelines are provided next.

(g) In actual practice, the total data length is divided into M smaller segments with equal number of data points N. By letting N be a power of *2* for computational efficiency, the result then is averaged over the M sections. In an FFT, the variables M, N, and Δt have to be independently selected, though T_r and Δt are fixed for a given record so that the total number of data points can be obtained from these values. Therefore, the only choice that has to be made is the number of sections M. Traditionally, the most common values of N used range from *512* to *2,048*, while the value of M is usually *8* or greater. Since T_r is dependent on N, M, and Δt as $T_r = M N \Delta t$, then higher N and M values in general yield better resolution and high confidence in the estimate of spectra. The larger the N, the more spiky or irregular the spectrum, and the smaller the N, the smoother the spectrum (Cooley and Tukey 1965; Chakrabarti 1987).

(h) To better understand the wave spectrum by the FFT method, consider first the wave surface profile of a single-amplitude and frequency wave given by a sinusoidal function as

$$\eta(t) = a \sin \omega t \tag{II-1-145}$$

where a and ω are the amplitude and frequency of the sine wave. The variance of this wave over the wave period of 2π is

$$\sigma^2 = \overline{[\eta(t)]^2} = \frac{1}{2\pi} \int_0^{2\pi} a^2 \sin^2 2\pi ft \; d(2\pi ft)$$

$$= \frac{a^2}{2} = 2 \int_0^{\infty} E^1(f) \, df = \int_{-\infty}^{\infty} E^2(f) \, df \tag{II-1-146}$$

(i) Thus the quantity $a^2/2$ represents the contribution to the variance σ^2 associated with the component frequency $\omega = 2\pi f$ (Figure II-1-35). The connection between the variance, wave energy, and the wave energy spectrum is now more obvious since these all are proportional to the wave amplitude (or height) squared. For consistency of units, an equality between these quantities requires that the wave spectrum not include the ρg term.

(j) The difference between a *two-sided spectrum* E^2 and a *one-sided spectrum* E^1 as illustrated in Figure II-1-36 is quite important. Note that the two-sided spectrum is symmetric about the origin, covering both negative and positive frequencies to account for all wave energy from -∞ to +∞. But, it is customary in ocean engineering to present the spectrum as a one-sided spectrum. This requires that the spectral density ordinates of E^2 be doubled in value if only the positive frequencies are considered. This is the reason for introducing a factor of two in Equation II-1-146. This definition will be used subsequently throughout Part II-1; thus, it is henceforth understood that $E(f)$ refers to E^1 (Figures II-1-35 and II-1-36).

(k) By an intuitive extension of this simple wave, the variance of a random signal with zero mean may be considered to be made up of contributions with all possible frequencies. For a random signal using the above equations, we find

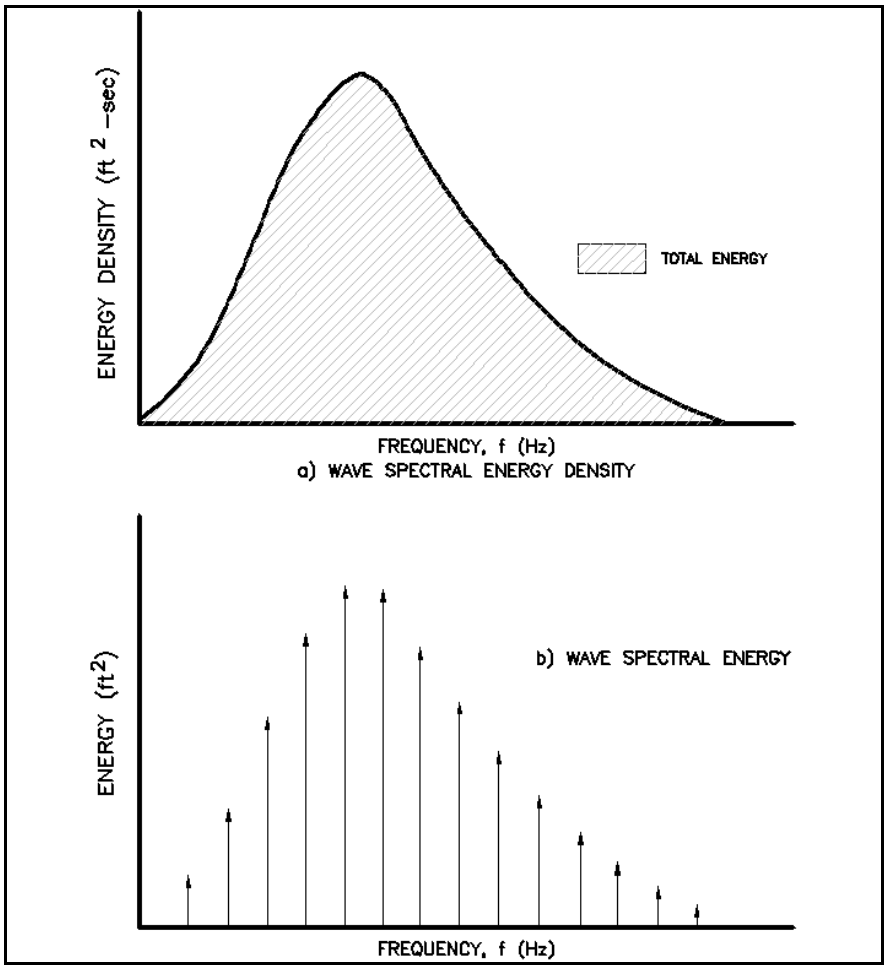

Figure II-1-35. Sketches of wave spectral energy and energy density (Chakrabarti 1987)

$$\sigma_\eta^2 = \sum_{n=1}^{\infty} \frac{a_n^2}{2} = \int_0^{\infty} E(f)\, df = m_0 \tag{II-1-147}$$

where m_0 is the zero-th moment of the spectrum. Physically, m_0 represents the area under the curve of $E(f)$. The area under the spectral density represents the variance of a random signal whether the one-sided or two-sided spectrum is used.

(l) The moments of a spectrum can be obtained by

$$m_i = \int_0^{\infty} f^i\, E(t)\, df \qquad i = 0,1,2,... \tag{II-1-148}$$

(m) We now use the above definition of the variance of a random signal to provide a third definition of the significant wave height. As stated earlier, this gives an estimate of the significant wave height by the wave spectrum. For Rayleigh distributed wave heights, H_s may be approximated (Longuet-Higgins 1952) by

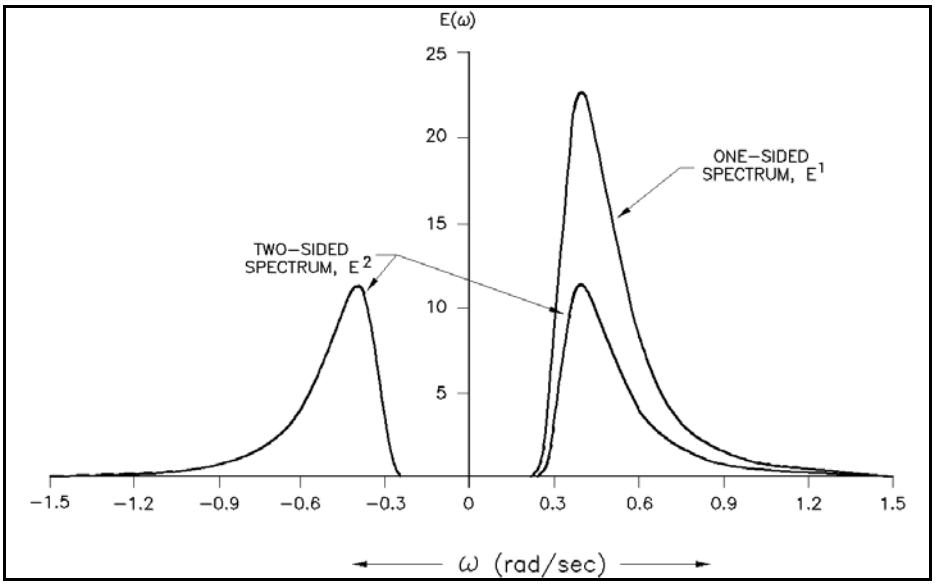

Figure II-1-36. Definition of one- and two-side wave spectrum (Chakrabarti 1987)

$$H_s = 3.8\sqrt{m_0} \approx 4\sqrt{m_0} \tag{II-1-149}$$

(n) Therefore, the zero-th moment m_0, which is the total area under the wave energy density spectrum, defines the significant wave height for a given *E(f)* (Figure II-1-37).

(3) Examples of frequency spectra. The frequency spectrum is normally plotted as energy density on the ordinate versus frequency on the abscissa (Figures II-1-31 through II-1-37). In principal, the form of *E(f)* can be quite variable. However, some generalizations are possible. First of all, during strong wind events, the spectrum tends to have a strong central peak and a fairly predictable shape. For swell that has propagated a long distance from the source of generation, waves tend to have a single sharp peak. Waves in shallow water near breaking tend to have a sharp peak at the peak frequency f_p and have a series of smaller peaks at frequencies $2f_p$, $3f_p$, etc., which are harmonics of the main wave. The presence of harmonics indicates that the wave has the sharp crest and flat trough of highly nonsinusoidal waves often found near breaking. To complicate matters, Thompson (1977) has shown that about two-thirds of U.S. coastal wave records have more than one peak, indicating the presence of multiple wave trains. These wave trains most likely originated from different areas and have different directions of propagation. Moreover, it is possible to have a single-peak spectrum, which consists of two trains of waves of about the same frequency but different directions of propagation. In order to sort these issues out, observations of the directional spectrum are required. Figures II-1-31, II-1-32, and II-1-35 include examples of different frequency spectra providing some indication of their range of variability.

(4) Wave spectrum and its parameters.

(a) Two parameters are frequently used in the probability distribution for waves. These are the s*pectral width* ν and the *spectral bandwidth* ϵ, and are used to determine the narrowness of a wave spectra. These parameters range from 0 to 1, and may be approximated in terms of spectral moments by

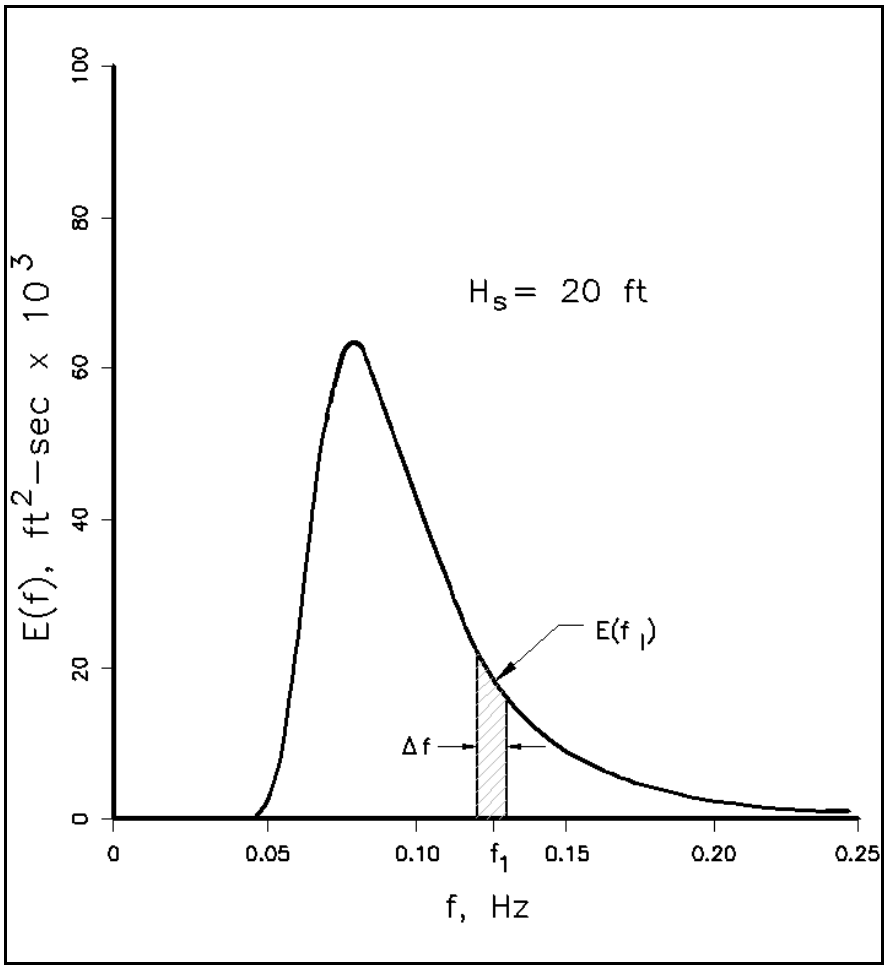

Figure II-1-37. Energy density and frequency relationship (Chakrabarti 1987)

$$\nu = \sqrt{\frac{m_0 m_2}{m_1^2} - 1}$$

$$\epsilon = \sqrt{1 - \frac{m_2^2}{m_0 m_4}} \qquad \text{(II-1-150)}$$

(b) For a narrow-band spectrum, both ν and ϵ must be close to *0* (Figure II-1-38). For example, for the two most common empirical spectra, the *Pierson-Moskowitz (PM)* spectrum (Pierson and Moskowitz 1964) and the *JONSWAP* spectrum (Hasselmann et al. 1973), which are discussed in the next section, ν = 0.425 and 0.389, respectively, with ϵ = 1 for both. Natural ocean waves, therefore, have a broad-banded spectrum.

(c) The values of ϵ obtained from a wave energy spectrum are generally not considered as the sole indication of how broad the spectra are. This is due to the amplification of the noise present in the wave energy spectral density at higher frequencies that enters into the calculation of the higher moments m_2 and m_4 in the above equation for ϵ. Goda (1974) proposed a *spectral peakedness parameter* called Q_p defined as

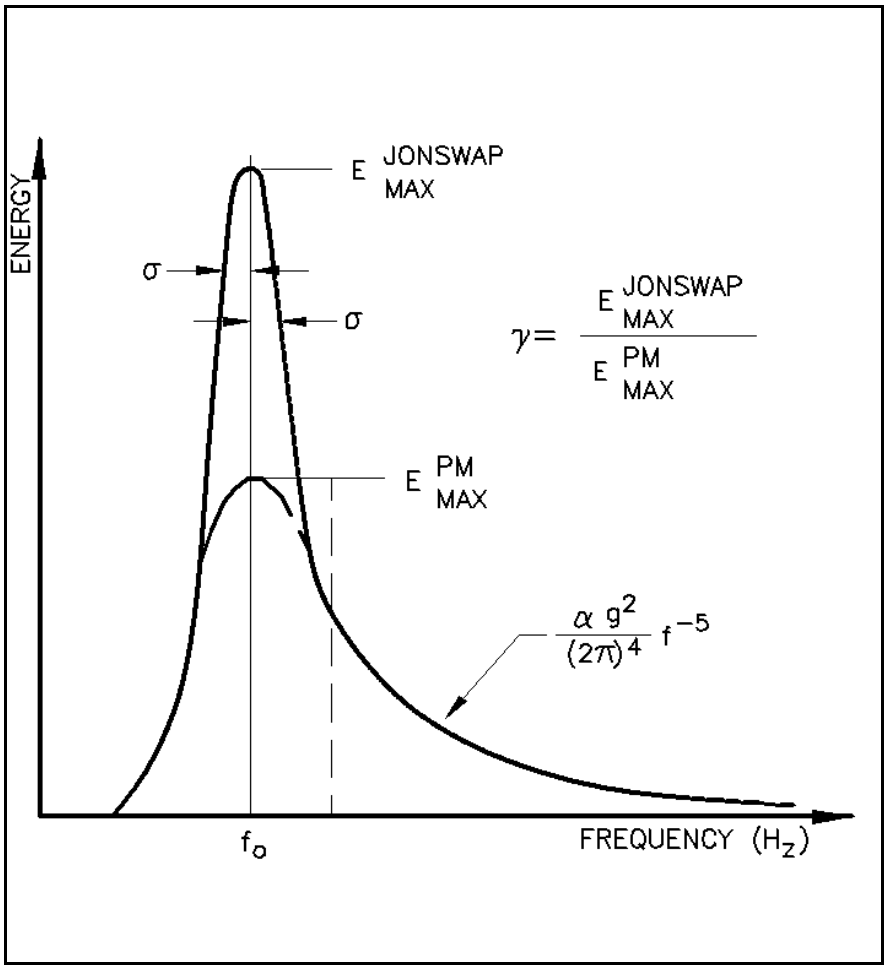

Figure II-1-38. Comparison of the PM and JONSWAP spectra (Chakrabarti 1987)

$$Q_p = \frac{2}{m_0^2} \int_0^\infty f\, E^2(f)\, df \tag{II-1-151}$$

which depends only on the first moment of the energy density spectrum, and is not directly related to ϵ. In general, a small ϵ implies that Q_p is large, and a large ϵ means Q_p is small.

(d) Approximate relations for most common wave parameters by the statistical analysis are

$$H_S = 4.0\sqrt{m_0} \quad ; \quad H_{1/10} = 5.1\sqrt{m_0}$$

$$T_z = \sqrt{\frac{m_0}{m_2}} \quad ; \quad T_c = \sqrt{\frac{m_2}{m_4}} \tag{II-1-152}$$

$$\bar{\eta} = \sqrt{m_0} \quad ; \quad \epsilon = \sqrt{1 - \frac{m_2^2}{m_0 m_4}}$$

(e) In deep and intermediate water depths, the significant wave height obtained by the spectral analysis using the above equation is usually greater than that from the wave train analysis. The zero-crossing period from the spectral method is only an approximation, while the period associated with the largest wave energy known as the *peak period* T_p, can only be obtained via the spectral analysis. In the spectral representation of swell waves, there is a single value of the peak period and wave energy decays at frequencies to either side. The spectra for storm waves is sometimes multi-peaked. One peak (not always the highest) corresponds to the swell occurring at lower frequencies. One and sometimes more peaks are associated with storm waves occurring at comparatively higher frequencies. In a double-peaked spectra for storm waves, the zero-crossing period generally occurs at higher frequencies than the peak period. In a multi-peaked spectrum, the zero-crossing period is not a measure of the frequency where peak energy occurs.

(5) Relationships among $H_{1/3}$, H_s, and H_{m0} in shallow water.

(a) By conception, significant height is the average height of the third-highest waves in a record of time period. By tradition, wave height is defined as the distance from crest to trough. Significant wave height H_s can be estimated from a wave-by-wave analysis in which case it is denoted $H_{1/3}$, but more often is estimated from the variance of the record or the integral of the variance in the spectrum in which case it is denoted H_{m0}. Therefore, H_s in Equation II-1-152 should be replaced with H_{m0} when the latter definition of H_s is implied. While $H_{1/3}$ is a direct measure of H_s, H_{m0} is only an estimate of the significant wave height which under many circumstances is accurate. In general in deep water $H_{1/3}$ and H_{m0} are very close in value and are both considered good estimates of H_s. All modern wave forecast models predict H_{m0} and the standard output of most wave gauge records is H_{m0}. Few routine field gauging programs actually compute and report $H_{1/3}$ and report as H_s with no indication of how it was derived. Where $H_{1/3}$ and H_s are equivalent, this is of little concern.

(b) Thompson and Vincent (1985) investigated how $H_{1/3}$ and H_{m0} vary in very shallow water near breaking. They found that the ratio $H_{1/3}/H_{m0}$ varied systematically across the surf zone, approaching a maximum near breaking. Thompson and Vincent displayed the results in terms of a nomogram (Figure II-1-40). For steep waves, $H_{1/3}/H_{m0}$ increased from 1 to about 1.1, then decreased to less than 1 after breaking. For low steepness waves, the ratio increased from 1 before breaking to as much as 1.3-1.4 at breaking, then decreased afterwards. Thompson and Vincent explained this systematic variation in the following way. As low steepness waves shoal prior to breaking, the wave shape systematically changes from being near sinusoidal to a wave shape that has a very flat trough with a very pronounced crest. Although the shape of the wave is significantly different from the sine wave in shallow water, the variance of the surface elevation is about the same, it is just arranged over the wave length differently from a sine wave. After breaking, the wave is more like a bore, and as a result the $H_{1/3}$ can be smaller (by about 10 percent) than H_{m0}.

(c) The critical importance of this research is in interpreting wave data near the surf zone. It is of fundamental importance for the engineer to understand what estimate of significant height he is using and what estimate is needed. As an example, if the data from a gauge is actually H_{m0} and the waves are near breaking, the proper estimate of H_s is given by $H_{1/3}$. Given the steepness and relative depth, $H_{1/3}$ may be estimated from H_{m0} by Figure II-1-40. Numerically modelled waves near the surf zone are frequently equivalent to H_{m0}. In this case, H_s will be closer to $H_{1/3}$ and the nomogram should be used to estimate H_s.

(6) Parametric spectrum models.

(a) In general, the spectrum of the sea surface does not follow any specific mathematical form. However, under certain wind conditions the spectrum does have a specific shape. A series of empirical expressions have been found which can be fit to the spectrum of the sea surface elevation. These are called *parametric spectrum models*, and are useful for routine engineering applications. A brief description of these follows.

(b) There are many forms of wave energy spectra used in practice, which are based on one or more parameters such as wind speed, significant wave height, wave period, shape factors, etc. Phillips (1958) developed an equation for the equilibrium range of the spectrum for a fully-developed sea in deep water, which became the basis of most subsequent developments. Phillips' equilibrium range is often written in terms of the *angular frequency* ω and is of the form

$$E(\omega) = \alpha g^2 \omega^{-5} \tag{II-1-153}$$

where α is the *Phillips' constant* (= .0081) and g the gravitational acceleration.

(c) One commonly used spectrum in wave hindcasting and forecasting projects is the single-parameter spectrum of *Pierson-Moskowitz PM* (Pierson and Moskowitz 1964). An extension of the PM spectrum is the *JONSWAP* spectrum (Hasselmann et al. 1973, 1976); this is a five-parameter spectrum, although three of these parameters are usually held constant. The relationship between PM and JONSWAP spectra is shown in Figure II-1-38. Other commonly used two-parameter wave spectra forms, including those proposed by Bretschneider (1959), ISSC (1964), Scott (1965), ITTC (1966), Liu (1971), Mitsuyasu (1972), Goda (1985a), and Bouws et al. (1985) are essentially derivatives of the *PM* and *JONSWAP* spectra. A six-parameter wave spectrum has been developed by Ochi and Hubble (1976). The utility of this spectrum is that it is capable of describing multi-peaks in the energy spectrum in a sea state mixed with swell (Figure II-1-39). Only the parametric wave spectra forms most often used in coastal engineering will be briefly discussed here.

(d) The equilibrium form of the *PM* spectrum for fully-developed seas may be expressed in terms of wave frequency f and wind speed U_w as

$$E(f) = \frac{0.0081 g^2}{(2\pi)^4 f^5} \exp\left(-0.74 \left[\frac{2\pi U_w f}{g} \right]^{-4} \right) \tag{II-1-154}$$

where U_w is the wind speed at 19.5 m above mean sea level. The *PM* spectrum describes a *fully-developed sea* with one parameter, the wind speed, and assumes that both the fetch and duration are infinite. This idealization is justified when wind blows over a large area at a constant speed without substantial change in its direction for tens of hours.

(e) The *JONSWAP* spectrum for *fetch-limited seas* was obtained from the Joint North Sea Wave Project - JONSWAP (Hasselmann et al. 1973) and may be expressed as

$$E(f) = \frac{\alpha g^2}{(2\pi)^4 f^5} \exp\left[-1.25 \left(\frac{f}{f_p} \right)^{-4} \right] \gamma^{\exp\left[-\frac{\left(\frac{f}{f_p} - 1 \right)^2}{2\sigma^2} \right]} \tag{II-1-155}$$

$$f_p = 3.5 \left[\frac{g^2 F}{U_{10}^3} \right]^{-0.33} \quad ; \quad \alpha = 0.076 \left[\frac{gF}{U_{10}^2} \right]^{-0.22} \quad ; \quad 1 \le \gamma \le 7$$

$$\sigma = 0.07 \quad for \; f \le f_p \quad and \quad \sigma = 0.09 \quad for \quad f > f_p$$

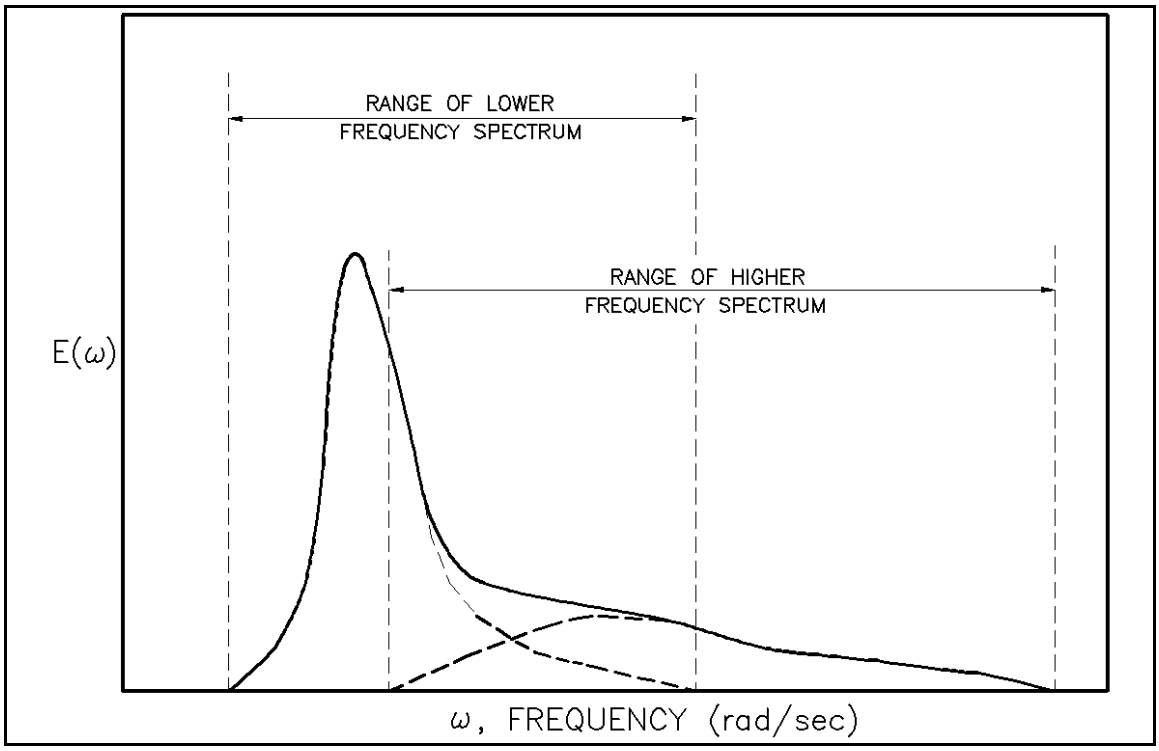

Figure II-1-39. Definition sketch for Ochi-Hubble spectrum (Ochi and Hubble 1976)

(f) In this equation, α is the scaling parameter, γ the peak enhancement factor, f_p the frequency at the spectral peak, U_{10} the wind speed at the elevation 10 m above the sea surface, F the fetch length. Figure II-1-38 qualitatively illustrates the relationship between JONSWAP and PM spectra. The JONSWAP spectrum can also be fitted mathematically to observed spectra by iteratively solving for d, γ, f_m, and σ.

(g) A six-parameter spectrum developed by Ochi and Hubble (1976) is the only wave spectrum which exhibits two peaks (Figure II-1-39), one associated with underlying swell (lower frequency components) and the other with locally generated waves (higher frequency components). It is defined as

$$E(\omega) = \frac{1}{4}\sum_{j=1}^{2} \frac{\left(\frac{4\lambda_j + 1}{4}\omega_{0j}^4\right)^{\lambda_j}}{\Gamma(\lambda_j)} \frac{H_{sj}^2}{\omega^{4\lambda_j+1}} \exp\left[-\frac{4\lambda_j+1}{4}\left(\frac{\omega_{0j}}{\omega}\right)^4\right] \quad \text{(II-1-156)}$$

where H_{s1}, ω_{01}, and λ_1 are the significant wave height, modal frequency, and shape factor for the lower-frequency components while H_{s2}, ω_{02}, and λ_2 correspond to the higher frequency components (Figure II-1-39). The value of λ_1 is usually much higher than λ_2. For the most probable value of ω_{01}, it can be shown that $\lambda_1 = 2.72$, while λ_2 is related to H_s in feet as

$$\lambda_2 = 1.82\, e^{(-0.027H_s)} \quad \text{(II-1-157)}$$

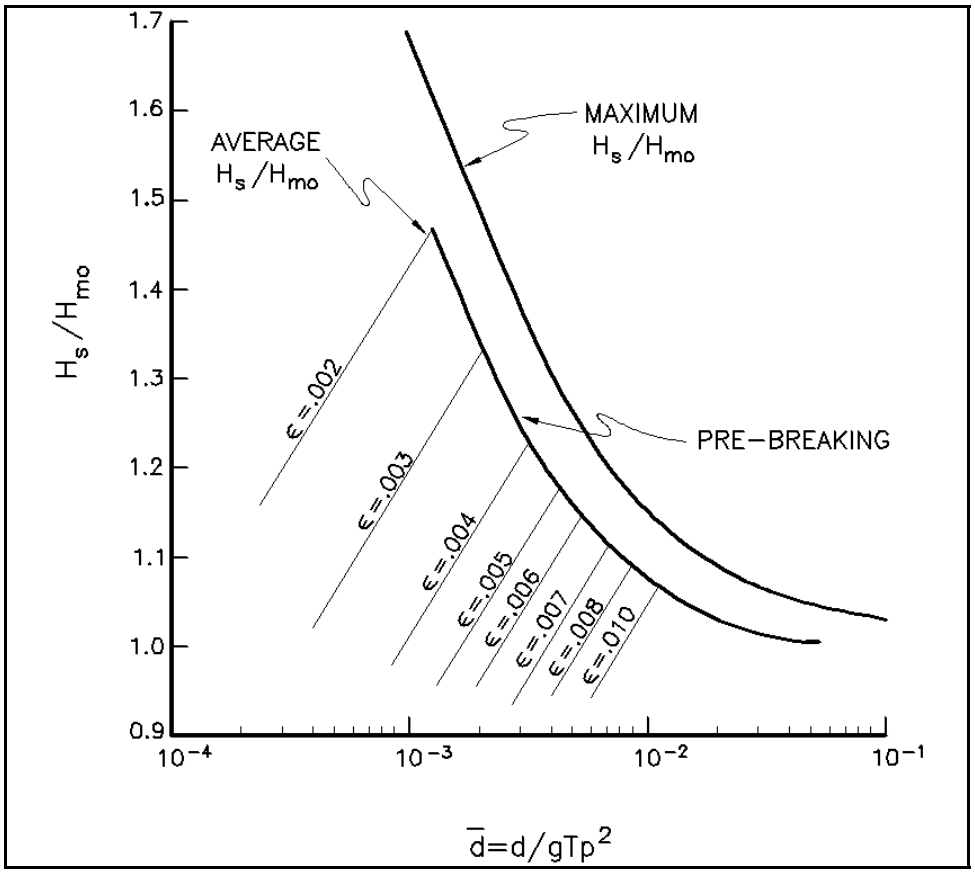

Figure II-1-40. Variation of H_s/H_{mo} as a function of relative depth $\bar{d}$ and significant steepness (Thompson and Vincent 1985)

(h) The parameters λ_j control the shape and the sharpness of the spectral peak of the Ochi-Hubble spectral model if in either spectral component (i.e., sea or swell) the values of H_{sj} and ω_{0j} are held constant. Therefore, λ_1 and λ_2 are called the *spectral shape parameters*. On the assumption of a narrow-bandedness of the entire Ochi-Hubble spectrum, an equivalent significant wave height may be calculated by

$$H_s = \sqrt{H_{s1}^2 + H_{s2}^2} \tag{II-1-158}$$

Note that for $\lambda_1 = 1$ and $\lambda_2 = 0$, the *PM* spectra may be recovered from this equation.

(i) In shallow water, the wave spectrum deviates from the standard spectra forms presented so far, and at frequencies above the peak, the spectrum no longer decays as f^5. Kitaigorodoskii et al. (1975) showed that the equilibrium range is proportional to *-3* power of the wave number, and thus, the form of the spectrum is of f^3 in the high-frequency range. This change is attributed to the effect of water depth on wave spectrum and to the interaction between spectral components. Bouws et al. (1984) proposed a variation to the *JONSWAP* energy spectrum for representing wave spectra in finite-depth water. The spectrum so obtained, the product of *JONSWAP* and the *Kitaigorodoskii depth function* accounting for the influence of the water depth, is called the *TMA spectrum* after the names of three sources of data used in its development (Texel, Marsen, and Arsloe).

(j) Kitaigorodoskii et al. (1975) obtained the form of depth dependence as

$$\Phi(\omega,d) = \frac{\left[k^{-3}\frac{\partial k}{\partial \omega}\right]_{d=finite}}{\left[k^{-3}\frac{\partial k}{\partial \omega}\right]_{d=\infty}} \text{s} \tag{II-1-159}$$

(k) Thus, Φ is a *weighing factor* of the quantity in the bracket, which is determined from the ratio of the quantity evaluated for finite and infinite water depth cases. Using the linear wave theory, the above equation has been approximated by Kitaigorodoskii et. al. (1975) as

$$\Phi(\omega^*,d) \approx \begin{cases} \frac{1}{2}\omega^{*2} & for\ \omega^* \le 1 \\ 1 - \frac{1}{2}(2-\omega^*)^2 & for\ \omega^* > 1 \end{cases} \tag{II-1-160}$$

(l) The *TMA* spectrum was intended for wave hindcasting and forecasting in water of finite depth. This spectrum is a modification of the *JONSWAP* spectrum simply by substituting Kitaigorodoskii's expression for effects of the finite depth equilibrium function. By using the linear wave theory, we find the following complete form of the *TMA* spectrum:

$$S_{TMA}(\omega,d) = S_{JONSWAP}(\omega)\ \Phi(\omega^*,d)$$

$$\Phi(\omega^*,d) = \frac{1}{[f(\omega^*)]^{\frac{1}{2}}}\left[1 + \frac{K}{\sinh K}\right]^{-1} \quad ; \quad \omega^* = \omega\sqrt{\frac{d}{g}} \tag{II-1-161}$$

$$f(\omega^*) = \tanh^{-1}[k(\omega^*)d] \quad ; \quad K = 2\omega^{*2} f(\omega^*)$$

(m) In effect, this substitution transforms the decay or slope of the spectral density function of the *JONSWAP* spectrum in the high-frequency side from ω^{-5} to ω^{-3} type dependence during the shoaling process approximated by linear wave theory. Bouws et. al (1984) present equations for α, γ, and σ. As with the JONSWAP, the equation may be iteratively fit to an observed spectrum and α, γ, f_m , and σ may be estimated.

(n) The *PM*, *JONSWAP*, and *TMA* spectra can be estimated if something about the wind, depth and fetch are known. Furthermore, these spectral equations can be used as target spectra whose parameters can be varied to fit observed spectra which may have been measured. In the first situation, the value of the parameterization is in making an educated guess at what the spectrum may have looked like. The value in the second case is for ease of analytical representation. However, very often today engineering analyses are made on the basis of numerical simulations of a specific event by use of a numerical model (see Part II-2). In this case, the model estimates the spectrum and a parametric form is not required.

(7) Directional spectra.

(a) The wave spectra described so far have been one-dimensional frequency spectra. Wave direction does not appear in these representations, and thus variation of wave energy with wave direction was not considered. However, the sea surface is often composed of many waves coming from different directions. In addition to wave frequency, the mathematical form of the sea state spectrum corresponding to this situation should therefore include the wave direction θ. Each wave frequency may then consist of waves from different directions θ. The wave spectra so obtained are *two-dimensional*, and are denoted by $E(f,\theta)$. Figures II-1-33 and II-1-34 display directional spectra.

(b) Measurement of a directional spectrum typically involves measurement of either the same hydrodynamic parameter (such as surface elevation or pressure) at a series of nearby locations (within one to tens of meters) or different parameters (such as pressure and two components of horizontal velocity) at the same point. These records are then cross-correlated through a cross-spectral analysis and a directional spectrum is estimated. In general, the more parameters or more locations involved, the higher the quality of the directional spectrum obtained. The procedures for converting measurements into estimates of the directional spectrum are outside the scope of this chapter. Part VII-3 of the CEM and Dean and Dalrymple (1991) provide some additional details on this subject.

(c) The major systems routinely employed at the present time for measuring directional spectra include directional buoys, arrays of pressure or velocity gauges, and the p-U-V technique. With directional buoys, pitch-roll-and-heave or heave-and-tilt methods are used. Most directional buoys are emplaced in deeper water. Arrays of pressure gauges or velocity gauges arranged in a variety of shapes (linear, cross, star, pentagon, triangle, rectangle, etc.) are also used, but these are usually restricted to shallower water. The p-U-V technique uses a pressure gauge and a horizontal component current meter almost co-located to measure the wave field. This can be used in shallow or in deeper water if there is something to attach it to near the surface. Other techniques include arrays of surface-piercing wires, triaxial current meters, acoustic doppler current meters, and radars.

(d) A mathematical description of the directional sea `state is feasible by assuming that the sea state can be considered as a superposition of a large number of regular sinusoidal wave components with different frequencies and directions. With this assumption, the representation of a spectrum in frequency and direction becomes a direct extension of the frequency spectrum alone, allowing the use of *FFT* method. It is often convenient to express the wave spectrum $E(F,\theta)$ describing the angular distribution of wave energy at respective frequencies by

$$E(f,\theta) = E(f)\ G(f,\theta) \tag{II-1-162}$$

where the function $G(f,\theta)$ is a dimensionless quantity, and is known as the *directional spreading function*. Other acronyms for $G(f,\theta)$ are the *spreading function*, *angular distribution function*, and the *directional distribution*.

(e) The one-dimensional spectra may be obtained by integrating the associated directional spectra over θ as

$$E(f) = \int_{-\pi}^{\pi} E(f,\theta)\ d\theta \tag{II-1-163}$$

(f) It therefore follows from the above last two equations that $G(f,\theta)$ must satisfy

$$\int_{-\pi}^{\pi} G(f,\theta)\, d\theta = 1 \tag{II-1-164}$$

(g) The functional form of $G(f,\theta)$ has no universal shape and several proposed formulas are available. In the most convenient simplification of $G(f,\theta)$, it is customary to consider G to be independent of frequency f such that we have

$$G(\theta) = \frac{2}{\pi} \cos^2\theta \quad for \quad |\theta| < 90° \tag{II-1-165}$$

(h) This cosine-squared distribution is due to St. Denis and Pierson (1953), and testing with field data shows that it reproduces the directional distribution of wave energy. Longuet-Higgins (1962) found the cosine-power form

$$G(\theta) = C(s) \cos^{2s} \frac{\theta - \bar{\theta}}{2}$$

$$C(s) = \frac{\sqrt{\pi}}{2\pi} \frac{\Gamma(s+1)}{\Gamma\left(s + \frac{1}{2}\right)} \tag{II-1-166}$$

where θ is the principal (central) direction for the spectrum, s is a controlling parameter for the angular distribution that determines the peakedness of the directional spreading, $C(s)$ is a constant satisfying the normalization condition, θ is a counterclockwise measured angle from the principal wave direction, and Γ is the Gamma function.

(i) Mitsuyasu et al. (1975), Goda and Suzuki (1976), and Holthuijsen (1983) have shown that for wind waves, the parameter s varies with wave frequency and is related to the stage of wave development (i.e., wind speed and fetch) by

$$s = \begin{cases} s_{max} \left(\frac{f}{f_p}\right)^{5} & for\ f \le f_p \\ s_{max} \left(\frac{f}{f_p}\right)^{-2.5} & for\ f > f_p \end{cases} \tag{II-1-167}$$

where s_{max} and f_p are defined as

$$s_{max} = 11.5 \left(\frac{2\pi f_p U}{g}\right)^{-2.5}$$

$$\frac{2\pi f_p U}{g} = 18.8 \left(\frac{gF}{U^2}\right)^{-0.33} \tag{II-1-168}$$

(j) In the above equations, U is the wind speed at the 10-m elevation above the sea surface and F is the fetch length. These equations remain to be validated with field data for wind waves. The parameter s for shallow-water waves may also vary spatially during wave transformation. This is due to refraction. A large value greater that 50, may be necessary if dependence of s_{max} on refraction is of concern. For deepwater

applications where wind waves are jointly present with swells in deep water, Goda and Suzuki (1976) proposed the following values for s_{max} : 10 for wind waves, and 25 for swells present with wind waves of relatively large steepness, and 75 for swells with wind waves of small steepness. Under simple wind wave conditions, the spreading function may be approximated by the equations provided. They are typical of deepwater wind seas for which the wind has been constant. If the wind has shifted in direction, if there is significant swell, or if the waves are in shallow water, the directional distribution may be different than the shape functions presented.

(8) Wave groups and groupiness factors.

(a) Measurements of waves usually show a tendency of grouping between waves that is; high waves; often seem to be grouped together. Examination of the sea surface profile records indicates that wave heights are not uniform and they occur in successive groups of higher or lower waves. The interest in wave groups is stimulated by the fact that wave grouping and associated nonlinear effects play an important role in the long-period oscillation of moored vessels (Demirbilek 1988, 1989; Faltinsen and Demirbilek 1989), surf beats, irregular wave runup, resonant interaction between structures (Demirbilek and Halvorsen 1985; Demirbilek, Moe, and Yttervoil 1987;), and other irregular fluctuations of the mean water level nearshore (Goda 1985b; 1987). Unfortunately there is no way to predict grouping.

(b) Wave grouping is an important research topic and there are several ways to quantify wave grouping. These include the smoothed instantaneous wave energy history analysis (Funke and Mansard 1980), the concept of the run of wave heights (Goda 1976), and the Hilbert transform. A short exposition of the wave grouping analysis is provided here.

(c) The length of wave grouping can be described by counting the number of waves exceeding a specified value of the wave height which could be the significant, mean, or other wave height. The succession of high wave heights is called *a run* or *a run length* with an associated wave number j_1. The definition sketch for two wave groups is shown in Figure II-1-41 with the threshold wave height limit set at $H = H_c$. The recurrence interval or repetition length above the threshold value of wave height is called the *total run* denoted by j_2.

(d) The group occurrence for N waves with k number of lags between waves in a sequence in a record may be defined in terms of a correlation coefficient. The correlation coefficient R_H so defined will describe the correlation between wave heights as a function of the mean μ and standard deviation σ and is given by

$$R_H = \frac{1}{\sigma_0} \frac{1}{N-k} \sum_{i=1}^{N-k} (H_i - \mu)(H_{i+k} - \mu)$$

$$\sigma_0 = \frac{1}{N} \sum_{i=1}^{N} (H_i - \mu)^2 \qquad \text{(II-1-169)}$$

(e) Thus, R_H varies with the number of lags k between waves. If the succeeding waves are uncorrelated, then $R_H \rightarrow 0$ as $N \rightarrow \infty$. Real wave data indicate that $R_H(1) \approx 0.20$ to 0.40 while $R_H(k) \approx 0$ for $k > 1$. Furthermore, a positive value of R_H suggests that large waves tend to be succeeded by large waves, and small waves by other small waves.

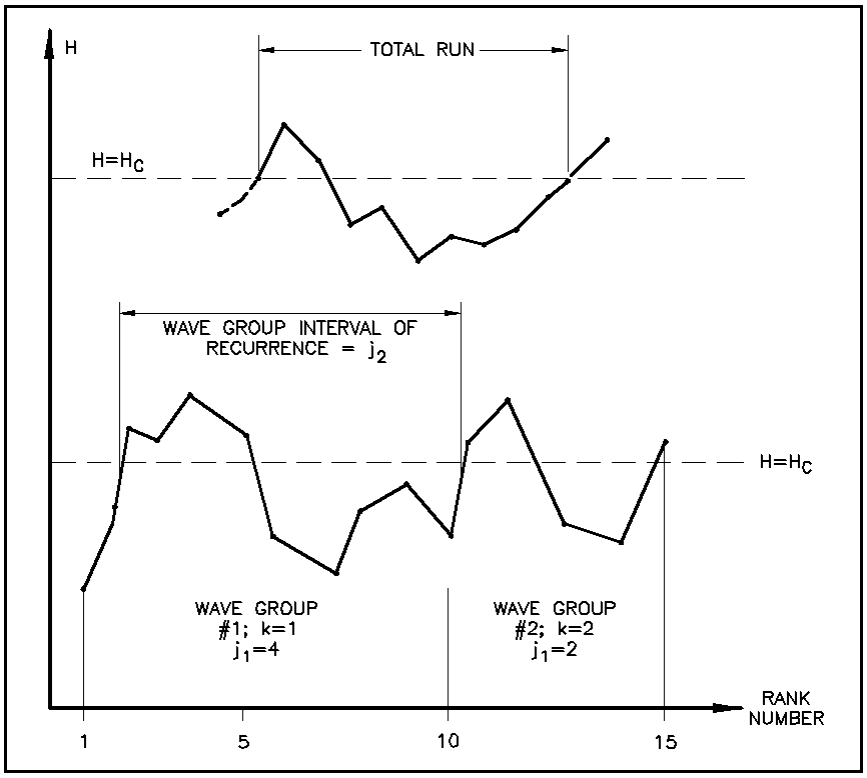

Figure II-1-41. Identification and description of wave groups through ordered statistics (Goda 1976)

(f) Assuming that successive wave heights are uncorrelated, the probability of *a* run length j_1 is (Goda 1976)

$$P(j_1) = p^{(j_1-1)}(1-p) \tag{II-1-170}$$

in which p is the occurrence probability for $H > H_c$. The mean and standard deviation of j_1 are

$$\mu_{j_1} = \frac{1}{q} \quad ; \quad q = 1 - p \quad ; \quad \sigma_{j_1} = \frac{\sqrt{1-q}}{q}$$
$$p = p(H>H_c) = \exp\left[-\frac{1}{8}\eta_c^2\right] \quad ; \quad \eta_c = \frac{H_c}{\sigma_\eta} \tag{II-1-171}$$

(g) The probability of a *total run* with the length j_2 can be derived by mathematical induction as

$$\mu_{j_2} = \frac{1}{p} + \frac{1}{q} \quad ; \quad \sigma_{j_2} = \sqrt{\frac{p}{q^2} + \frac{q}{p^2}} \tag{II-1-172}$$

where it has been assumed that successive wave heights are uncorrelated. Successive wave heights of the real ocean waves are mutually correlated, and the degree of correlation depends on the sharpness of the spectral peak. The effect of spectral bandwidth on wave height distribution has been considered by Kimura (1980), Tayfun (1983a), and Longuet-Higgins (1984). Tayfun has shown that the parameter that best describes the

spectral peakedness is the correlation coefficient of the wave envelope, relating wave height variation between successive wave heights. This coefficient R_{HH} may be calculated as (Tayfun 1983)

$$R_{HH} = \frac{E(\lambda) - (1-\lambda^2)\frac{K(\lambda)}{2} - \frac{\pi}{4}}{1 - \frac{\pi}{4}}$$

$$\lambda(\bar{T}) = \frac{1}{m_0}\sqrt{A^2 + B^2} \qquad \text{(II-1-173)}$$

$$A = \int_0^\infty E(f) \cos 2\pi f \bar{T}\, df \quad ; \quad B = \int_0^\infty E(f) \sin 2\pi f \bar{T}\, df$$

(h) By further assuming that Rayleigh distribution is suitable for the consecutive wave heights, the joint probability density function $p(H_1, H_2)$ for two successive wave heights H_1 and H_2 in the wave group may then be established. See Tayfun (1983) for details.

(i) The correlation coefficient R_{HH} takes a value of about 0.2 for wind waves and 0.6 or greater for swells (Goda 1976), a clear indication that wind waves rarely develop significant grouping of high waves. Su (1984) has shown that the wave group containing the highest wave in a record is often longer than the ordinary groups of high waves, and that the extreme wave usually consists of three high waves with the highest greater than the significant wave height. Wave groups and their characteristics have been investigated by analyzing the successive wave groups (Goda 1976 and Kimura 1980).

(j) Wave grouping and its consequences are of significant concern, but there is little guidance and few practical formulae for use in practical engineering. The engineer needs to be aware of its existence and, for designs that would be sensitive to grouping-related phenomena, attempt to evaluate its importance to the problem of concern. This may involve performing numerical simulations or physical model simulations in which a wide variety of wave conditions are tested and are designed to include those with high levels of groupiness. The procedures for this lie beyond the scope of the CEM.

(9) Random wave simulation.

(a) Given a one-dimensional parametric spectrum model or an actual wave energy density spectrum, it is sometimes necessary to use these quantities to calculate the height, period, and phase angle of a wave at a particular frequency. Such an approach for simulating random waves from a known wave spectra is sometimes termed the *deterministic spectral amplitude method*, since individual wave components in this superposition method are deterministic (Borgman 1967). The method is also called the *random phase method* because the phases of individual components are randomly chosen (Borgman 1969). Random waves simulated by this approach may not satisfy the condition of a Gaussian sea unless $N \rightarrow \infty$ in the limit. In practice, for $200 \leq N \leq 1200$ components, the spectrum can be duplicated accurately.

(b) The wave profile generated by simulation methods is used in a number of engineering applications in spite of requiring a large number of components and considerable computer time. For example, random wave simulation is frequently used during modeling studies in a wave tank for duplicating a required target wave energy density spectrum. Random wave profiles are also extensively used in numerical models for calculating structural loads and responses due to a random sea. The simulation method permits direct prediction of the wave particle kinematics at any location in a specified water depth for given wave height-period pair and random phase angle. The ARMA algorithms (Spanos 1983) and digital simulation methods

(Hudspeth and Chen 1979) are two alternatives for simulating random waves from a given one-dimensional spectrum.

(c) There are two ways for simulating wave surface profiles from known wave spectra; deterministic and non-deterministic spectral amplitude methods. In the deterministic spectral simulation method, the wave height, period, and phase angle associated with a frequency f_1 whose corresponding energy density is $E(f_1)$ may be obtained from

$$\begin{aligned} H(f_1) &= H|_{f_1} = 2\sqrt{2E(f_1)\,\Delta f} \\ T(f_1) &= T|_{f_1} = \frac{1}{f_1} \\ \epsilon(f_1) &= \epsilon|_{f_1} = 2\pi r_N \end{aligned} \tag{II-1-174}$$

where the phase angle ϵ is arbitrary since r_N is a random number between zero and one. The time series of the wave profile at a point x and time t may be computed by (Tucker et al. 1984)

$$\eta(x,t) = \sum_{n=1}^{N} H(n)\cos\left[k(n)x - 2\pi f(n)t + \epsilon(n)\right] \tag{II-1-175}$$

where $k(n) = 2\pi/L(n)$, and $L(n)$ is the wavelength corresponding to the nth frequency $f(n)$; N the total number of frequency bands of width Δf. It is not required to divide the spectrum curve equally, except that doing so greatly facilitates computations. The value of wave height is sensitive to the choice of Δf, but as long as Δf is small, this method produces a satisfactory random wave profile. The use of the equal increments, Δf, requires N to be greater than 50 to assure randomness and duplicating the spectrum accurately.

(d) In the non-deterministic spectral amplitude method, the wave surface profile is represented in terms of two independent Fourier coefficients. These Gaussian distributed random variables a_n and b_n with zero mean and variance of $E(f)\,\Delta f$ are then obtained from

$$\begin{aligned} \eta(x,t) = &\sum_{n=1}^{N} a_n \cos\left[k(n)x - 2\pi f(n)t\right] \\ &+ \sum_{n=1}^{N} b_n \sin\left[k(n)x - 2\pi f(n)t\right] \end{aligned} \tag{II-1-176}$$

(e) In essence, an amplitude and a phase for individual components are replaced by two amplitudes, the coefficients of cosine and sine terms in the wave profile. This random coefficient scheme may yield a realistic representation of a Gaussian sea, provided that N is large for a true random sea. This method differs from the deterministic spectral amplitude approach by ensuring that sea state is Gaussian. Elgar et al. (1985) have considered simultaneous simulation of both narrow and broad-banded spectra using more than 1000 Fourier components, and concluded that both simulation methods yield similar statistics. These approaches may be extended to the two-dimensional case. This is beyond the scope of the CEM.

(10) Kinematics and dynamics of irregular waves. In the above sections of the CEM we have considered definition of irregular wave parameters and development of methods to measure them and use them analytically. Velocities, pressures, accelerations, and forces under irregular waves are estimated analytically in three ways. In the first, an individual wave is measured by either a wave-by-wave analysis or constructed synthetically (such as choosing, H_s, T_z, and a direction) and monochromatic theory is used to estimate the

desired quantities at a given wave phase (Faltinsen and Demirbilek 1989). In the second, pressure, velocity, and acceleration spectra are estimated by applying linear theory to translate the surface elevation spectra to the desired parameter (Dean and Dalrymple 1991). Finally, the random wave simulation technique may be used to synthetically generate a surface time history and corresponding kinematic and dynamic properties (Borgman 1990). Of the three methods, the last may provide the most realistic results, but it is also the most complex approach. These methods lie beyond the CEM and generally require the assistance of a knowledgeable oceanographic engineer.

II-1-4. References and Bibliography

Abramowitz and Stegun 1965
Abramowitz, M. and Stegun, I. A. 1965. *Handbook of Mathematical Functions*, Dover Pub., New York.

Airy 1845
Airy, G. B. 1845. *Tides and Waves*, Encyc. Metrop., Article 192, pp 241-396.

Barthel et al. 1983
Barthel, V. et al. 1983. "Group Bounded Long Waves in Physical Models," *Intl. Jour. Ocean Engr.,* Vol 10, pp 261-294.

Battjes 1970
Battjes, J. A. 1970. "Long-Term Wave Height Distribution at Seven Stations Around the British Isles," Rep. No.A44, Natl. Inst. Ocean., Godalming, U.K.

Battjes 1972
Battjes, J. A. 1972. "Set-Up due to Irregular Waves," *Proceedings of the 13th Coastal Engineering Conference*, American Society of Civil Engineers, pp 1993-2004.

Bendat and Piersol 1971
Bendat, J. S. and Piersol, A. G. 1971. *Random Data: Analysis and Measurement Procedures*, Wiley-Interscience.

Borgman 1963
Borgman, L. E. 1963. "Risk Criteria," *ASCE Jour. Waterw., Port, Coastal and Ocean Engr.,* Vol 89, pp 1-35.

Borgman 1967
Borgman, L. E. 1967. "Spectral Analysis of Ocean Wave Forces on Piling," *ASCE Jour. Waterw., Port, Coastal and Ocean Engr.,* Vol 93, pp 129-156.

Borgman 1969
Borgman, L. E. 1969. "Ocean wave Simulation for Engineering Design," *ASCE Jour. Waterw., Port, Coastal and Ocean Engr.,* Vol 95, pp 557-583.

Borgman 1975
Borgman, L. E. 1975. "Extremal Statistics in Ocean Engineering," *Proc. Civil Engr. in the Oceans,* Vol 1, pp 117-133.

Borgman 1990
Borgman, L. E. 1990. "Irregular Ocean waves: Kinematics and Forces," *The Sea*, B. Le Méhauté and D. M. Hanes, ed., Part A, Vol 9, pp 121-168.

Boussinesq 1871
Boussinesq, J. 1871. "Theorie de L'intumescence Liquide Appelee Onde Solitaire ou de Translation se Propageant dans un Canal Rectangulaire," *Comptes Rendus Acad. Sci. Paris,* Vol 72, pp 755-759.

Bouws, Gunther, Rorenthal, and Vincent 1984
Bouws, E., Gunther, H., Rorenthal, W., and Vincent, C. L. 1984. "Similarity of the Wind Wave Spectrum in Finite Depth Water, Part I-Spectral Form," *Jour. Geophys. Res.,* Vol 89, No. C1, pp 975-986.

Bouws, Gunther, and Vincent 1985
Bouws, E., Gunther, H., and Vincent, C. L. 1985. "Similarity of the wind wave spectrum in finite-depth water, Part I-Spectral form," *J. Geophys. Res.,* Vol 85, No. C3, pp 1524-1530.

Bowen 1969
Bowen, A. J. 1969. "The Generation of Longshore Currents on a Plain Beach," *Jour. Marine Res.,* Vol 27, pp 206-215.

Bretschneider 1959
Bretschneider, C. L. 1959. "Wave Variability and Wave Spectra for Wind-Generated Gravity Waves," U.S. Army Corps of Engrs., Beach Erosion Board, Tech. Memo. No. 118.

Bretschneider 1961
Bretschneider, C. L. 1961. "One-Dimensional Gravity Wave Spectrum," *Ocean Wave Spectra*, Prentice-Hall, Englewood Cliffs, NJ.

Bretschneider 1960
Bretschneider, C. L. 1960. "A Theory for Waves of Finite Height," *Proc. 7th Coastal Engr. Conf.,* Vol 1, pp 146-183.

Bretschneider 1969
Bretschneider, C. L. 1969. "Wave Forecasting," Chapter 11 in *Handbook of Ocean and Underwater Engineering*, J. J. Myers et al., eds., McGraw-Hill Book Co., New York.

Briggs et al. 1993
Briggs, M. J., Thompson, E. F., Green, D. R., and Lillycrop, L. S. 1993. "Laboratory Description of Harbor Idealized Tests," Vol 1, U.S. Army Engineer Waterways Experiment Station, CERC-93-1, Vicksburg, MS.

Byatt-Smith and Longuet-Higgins 1976
Byatt-Smith, J. G. B., and Longuet-Higgins, M. S. 1976. "On the Speed and Profile of Steep Solitary Waves," *Proc. Roy. Soc. London, Series* A, Vol 350, pp 175-189.

Cartwright and Longuet-Higgins 1956
Cartwright, D. E., and Longuet-Higgins, M. S. 1956. "The Statistical Distribution of the Maxima of a Random Function," *Proc. Roy. Soc. London, Series A,* Vol 237, pp 212-232.

Cavanie et al. 1978
Cavanie, A. et al. 1978. "A Statistical Relationship Between Individual Heights and Periods of Storm Waves," *Proc. BOSS'76 Conf.,* Vol 2, pp 354-360.

Chakrabarti 1987
Chakrabarti, S. K. 1987. "Hydrodynamics of Offshore Structures," WIT Press, Southampton, UK.

Chakrabarti and Cooley 1977
Chakrabarti, S. K. and Cooley, R. P. 1977. "Statistical Distribution of Periods and Heights of Ocean Waves," *Jour. Gephys. Res.,* Vol 82, pp 1363-1368.

Challenor and Srokosz 1984
Challenor, P. G., and Srokosz, M. A. 1984. "Extraction of Wave Period from Altimeter Data," *Proc. Workshop on Radar Alti. Data,* Vol 1, pp 121-124.

Chaplin 1980
Chaplin, J. R. 1980. "Developments of Stream-Function Wave Theory," *Coastal Engr.,* Vol 3, pp 179-205.

Chappelear 1961
Chappelear, J. E. 1961. "Direct Numerical Calculation of Wave Properties," *Journal of Geophysical Research*, Vol 66, pp 501-508.

Chappelear 1962
Chappelear, J. E. 1962. "Shallow Water Waves," *Journal of Geophysical Research*, Vol 67, pp 4693-4704.

Cialone et al. 1991
Cialone, M. A., Mark, D. J., Chou, L. W., Leenknecht, D. A., Davis, J. A., Lillycrop. L. S., Jensen, R.E., Thompson, Gravens, M. B., Rosati, J. D., Wise, R. A., Kraus, N. C., and Larson, P. M. 1991. "Coastal Modeling System (CMS) User's Manual." Instruction Report CERC-91-1, U.S. Army Engineer Waterways Experiment Station, Coastal Engineering Research Center, Vicksburg, MS.

Cokelet 1977
Cokelet, E. D. 1977. "Steep Gravity Waves in Water of Arbitrary Uniform Depth," *Phil. Trans. Roy. Soc. London,* Series A, Vol 286, pp 183-230.

Collins 1970
Collins, J. I. 1970. "Probabilities of Breaking Wave Characteristics," *Proceedings of the 12th Coastal Engineering Conference*, American Society of Civil Engineers, pp 399-412.

Collins 1972
Collins, J. I. 1972. "Prediction of Shallow-Water Wave Spectra," *Journal of Geophysical Research*, Vol 77, pp 2693-2707.

Cooley and Tukey 1965
Cooley, J. W. and Tukey, J. W. 1965. "An Algorithm for the Machine Computation of Complex Fourier Series," *Math. Comp.,* Vol 19, pp 297-301.

Crapper 1984
Crapper, G. D. 1984. *Introduction to Water Waves*, John Wiley & Sons, New York.

Dalrymple 1974a
Dalrymple, R. A. 1974. "A Finite Amplitude Wave on a Linear Shear Current," *Journal of Geophysical Research*, Vol 79, pp 4498-4504.

Dalrymple 1974b
Dalrymple, R. A. 1974. "Models for Nonlinear Water Waves in Shear Currents," *Proc. 6th Offshore Tech. Conf.,* Paper No. 2114.

Dalrymple and Dean 1975
Dalrymple, R. A. and Dean R. G. 1975. "Waves of Maximum Height on Uniform Currents," *ASCE Jour. Waterw., Port, coastal and Ocean Engr.,* Vol 101, pp 259-268.

Dalrymple and Solana 1986
Dalrymple, R. A., and Solana, P. 1986. "Nonuniqueness in stream function wave theory, *J. Waterway, Port, Coastal and Ocean Engr., ASCE,* Vol 112, pp 333-337.

De 1955
De, S. C. 1955. "Contribution to the Theory of Stokes Waves," *Proc. Phil. Soc.,* Vol 51, pp 713-736.

Dean 1965
Dean, R. G. 1965. "Stream Function Representation of Nonlinear Ocean Waves," *Journal of Geophysical Research*, Vol 70, pp 4561-4572.

Dean 1968
Dean, R. G. 1968. "Relative Validity of Water Wave Theories," *Proc. Civil Engr. in Ocean, ASCE,* Vol 1, pp1-30.

Dean 1974
Dean, R. G. 1974. *Evaluation and Development of Water Wave Theories for Engineering Applications*, Coastal Engineering Research Center, U.S. Army Engineer Waterways Experiment Station, Special Report No.1.

Dean and Dalrymple 1991
Dean, R. G. and Dalrymple, R. A. 1991. *Water Wave Mechanics for Engineers and Scientists*, World Scientific Pub. Co., Teaneck, NJ.

Demirbilek 1977
Demirbilek, Z. 1977. "Transverse Oscillations of a Circular Cylinder in Uniform Flow," Thesis Rept., Naval Postgraduate School, Monterey, Calif.

Demirbilek 1985
Demirbilek, Z. 1985. "A Computer Program for Wave Kinematics by Fenton's Theory," Proprietary of Conoco Inc., prepared for the Jolliet Project. Also in Conoco's Riser and Mooring Systems Analysis Programs, Houston, TX.

Demirbilek 1988
Demirbilek, Z. 1988. "Forces on Marine Risers in a Coexisting Environment," *J. Waterway, Port, Coastal, and Ocean Engineering,* Vol 114, No. 3, pp 346-362.

Demirbilek 1989
Demirbilek, Z. 1989. *Tension Leg Platform: A State-Of-The-Art Review*, New York, pp 335.

Demirbilek and Halvorsen 1985
Demirbilek, Z. and Halvorsen, T. 1985. "Hydrodynamic Forces on Multitube Production Risers Exposed to Currents and Waves," *Trans. ASME, J. Energy Resources Technology,* Vol 107, No. 2, pp 226-234.

Demirbilek, Moe, and Yttervoll 1987
Demirbilek, Z., Moe, G., and Yttervoll, P. 1987. "Morison's Formula: Relative Velocity versus Independent Flow Fields Formulations for a Case Representing Fluid Damping," *Proc. Intl. Symposium on Offshore Mech. and Arctic Engineering,* Vol II, pp 25-32, Houston, TX.

Eckart 1952
Eckart, C. 1952. "The Propagation of Gravity Waves From Deep to Shallow Water," Natl. Bur. Standards, Circular 521, Washington, DC, pp 165-173.

Elgar et al. 1985
Elgar, S. et al. 1985. "Wave Group Statistics from Numerical Simulation of a Random Sea," *Jour. Applied Ocean Res.,* Vol 7, pp 93-96.

Faltinsen 1990
Faltinsen, O. M. 1990. *Sea Loads on Ships and Offshore Structures*, Cambridge Press, New York, p 328.

Faltinsen and Demirbilek 1989
Faltinsen, O. M., and Demirbilek, Z. 1989. "Hydrodynamics of Tension Leg Platforms - TLP's," *Tension Leg Platform: A State-of-the-art Review*, Z. Demirbilek, ed., ASCE Publ., New York.

Fenton 1972
Fenton, J. D. 1972. "A Ninth-Order Solution for Solitary Waves," *Jour. Fluid Mech.,* Vol 53, pp 257-271.

Fenton 1979
Fenton, J. D. 1979. "A Higher-Order Cnoidal Wave Theory," *Jour. Fluid Mech.,* Vol 94, pp 129-161.

Fenton 1985
Fenton, J. D. 1985. "A Fifth-Order Stokes Theory for Steady Waves," *ASCE Jour. Waterw., Port, Coastal and Ocean Engr.,* Vol 111, pp 216-234.

Fenton 1988
Fenton, J. D. 1988. "The Numerical solution of Steady Water Wave Problem," *Jour. Comp. and Geo.,* Vol 14, pp 357-368.

Fenton and McKee 1990
Fenton, J. D. and McKee, W. D. 1990. "On Calculating the Lengths of Water Waves," *Coastal Engr.,* Vol 14, pp 499-513.

Forristall 1984
Forristall, G. Z. 1984. "The Distribution of Measured and Simulated Wave Heights as a Function of Spectral Shape," *Journal of Geophysical Research*, Vol 89, No. C6, pp 10547-10552.

Funke and Mansard 1980
Funke, E. R. and Mansard, E. P. D. 1980. "On the Synthesis of Realistic Sea State," *Proc. 17th Coastal Engr. Conf.,* Vol 2, pp 2974-2991.

Goda 1974
Goda, Y. 1974. "Estimation of wave Statistics from Spectra Information," *Proc. Intl. Symp. on Ocean Wave Meas. and Anal., ASCE,* Vol 1, pp 320-337.

Goda 1975
Goda, Y. 1975. "Irregular Wave Deformation in the Surf Zone," *Coastal Engineering in Japan*, Vol 18, pp 13-26.

Goda 1976
Goda, Y. 1976. "On Wave Groups," *Proc. BOSS'76,* Vol 1, pp 115-128.

Goda 1978
Goda, Y. 1978. "The Observed Joint Distribution of Periods and Heights of Sea Waves," *Proc. 16th Coastal Engr. Conf.,* Vol 2, pp 227-246.

Goda 1983
Goda, Y. 1983. "A Unified Nonlinearity Parameter of Water Waves," *Rept. Port and Harbor Res. Inst. of Japan,* Vol 22, No. 3, pp 3-30.

Goda 1985a
Goda, Y. 1985a. "Numerical Examination of Several Statistical Parameters of Sea Waves," *Rept. Port and Harbor Res. Inst.,* Vol 24, No. 4, pp 65-102.

Goda 1985b
Goda, Y. 1985b. *Random Seas and Design of Maritime Structures*, Univ. of Tokyo Press, Tokyo, Japan.

Goda 1987
Goda, Y. 1987. "Statistical Variability of Sea State Parameters as a Function of Wave Spectrum," *Proc. IAHR Seminar on Wave Anal. and Gen. in Lab. Basins,* Lausanne, Switzerland.

Goda and Suzuki 1976
Goda, Y. and Suzuki, Y. 1976. "Estimation of Incident and Reflected Waves in Random Wave Experiments," *Proc. 15th Coastal Engr. Conf.,* Vol 1, pp 828-845.

Gumbel 1958
Gumbel, E. J. 1958. *Statistics of Extremes*, Columbia Univ. Press, New York.

Hasselmann et al. 1973
Hasselmann et al. 1973. "Measurements of Wind-Wave Growth and Swell Decay During the Joing North Sea Wave Project (JONSWAP)," *Deutsche Hydrograph*. Zeit., Erganzungsheft Reihe A (8^0), No. 12.

Hasselmann et al. 1976
Hasselmann, K. et al. 1976. "A Parametric Wave Prediction Model," *Jour. Phys. Ocean.,* Vol 6, pp 200-228.

Havelock 1918
Havelock, T. H. 1918. "Periodic Irrotational Waves of Finite Height," *Trans. Royal Soc. of London,* Vol 95 series A, pp 37-51.

Hedges 1981
Hedges, T. S. 1981. "Some Effects of Currents on Wave Spectra," *Proc., 1st Indian Conf. on Ocean Engr.,* Vol 1, pp 30-35.

Hedges 1987
Hedges, T. S. 1987. "Combinations of Waves and Currents: An Introduction," *Proc. Inst. Civil Engrs.,* Vol 82, pp 567-585.

Hoffman and Walden 1977
Hoffman, D., and Walden, D. A. 1977. "Environmental Wave Data for Determining Hull Structural Loadings," SSC-268, Final Tech. rep., Ship Struc. Comm., U.S. Coast Guard, Washington, DC.

Holthuijsen 1983
Holthuijsen, L. H. 1983. "Observation of the Directional Distribution of Ocean-Wave Energy in Fetch-Limited Conditions," *Jour. Phys. Ocean.,* Vol 13, No. 2, pp 191-207.

Horikawa and Kuo 1966
Horikawa, K., and Kuo, C. T. 1966. "A Study of Wave Transformation Inside Surf Zone," *Proc. 10th Coastal Engr. Conf.,* Vol 1, pp 217-233.

Huang et al. 1981
Huang, N. E., et al. 1981. "A Unified Two-Parameter Wave Spectral Model for a General Sea State," *Jour. Fluid Mech.,* Vol 112, pp 203-224.

Huang and Hudspeth 1984
Huang, M-C., and Hudspeth, R. T. 1984. "Stream Function Solutions for Steady Water Waves," *Continental Shelf Res.,* Vol 3, pp 175-190.

Huang and Long 1980
Huang, N. E., and Long, S. R. 1980. "An Experimental Study of the Surface Elevation Probability Distribution and Statistics of Wind-Generated Waves," *Jour. Fluid Mech.,* Vol 101, pp 179-200.

Hudspeth and Chen 1979
Hudspeth, R. T., and Chen, M. C. 1979. "Digital Simulation of Nonlinear Random Waves," *ASCE Jour. Waterw., Port, Coastal and Ocean Engr.,* Vol 105, pp 67-85.

Hughes and Borgman 1987
Hughes, S. A., and Borgman, L. E. 1987. "Beta-Rayleigh Probability Distribution for Shallow Water Wave Heights," *Coastal Hydro.,* R. A. Dalrymple, ed., Vol 1, pp 17-31.

Hunt 1979
Hunt, J. N. 1979. "Direct Solution of Wave Dispersion Equation," *ASCE Jour. Waterw., Port, Coastal and Ocean Engr.,* Vol 105, pp 457-459.

IAHR 1986
IAHR 1986. *List of Sea State Parameters*, Intl. Assoc. Hydr. Res., Suppl. to Bull. No. 52, Brussels.

Ippen 1966
Ippen, A.T., 1966. *Estuary and Coastline Hydrodynamics,* McGraw-Hill Book Company, Inc, New York.

Isaacson 1978
Isaacson, M. de St. Q. 1978. "Mass Transport in Shallow Water Waves," *ASCE Jour. Waterw., Port, Coastal and Ocean Engr.,* Vol 104, No. 2, pp 215-225.

ISSC 1964
ISSC 1964. *Proceedings of the Second International Ship Structures Congress*, Delft, The Netherlands.

ITTC 1966
ITTC 1966. "Recommendations of the 11th International Towing Tank Conference," *Proc. 11th ITTC,* Tokyo, Japan.

Jasper 1956
Jasper, N. H. 1956. "Statistical Distribution Patterns of Ocean Waves and Wave-Induced Ship Stress and Motions with Engineering Applications," *Trans. SNAME,* Vol 64.

Jonsson 1990
Jonsson, I. G. 1990. "Wave-Current Interactions," *The Sea*, B. Le Méhauté and D. M. Hanes, eds., Part A, Vol 9, pp 65-120.

Kadono et al. 1986
Kadono, T., et al. 1986. "An Observation of Nonlinear Coastal Waves," *Proc. 33rd Japanese Coastal Engr. Conf.,* Vol 1, pp 149-153.

Keller 1948
Keller, J. B. 1948. "The Solitary Wave and Periodic Waves in Shallow Water," *Commun. Appl. Math.,* Vol 1, pp 323-339.

Keulegan and Patterson 1940
Keulegan, G. H. and Patterson, G. W. 1940. "Mathematical Theory of Irrotational Translation Waves," *Res. Jour. Natl. Bur. Stand.,* Vol 24, pp 47-101.

Kimura 1980
Kimura, A. 1980. "Statistical Properties of Random Wave Groups," *Proc. 1th Coastal Engr. Conf.,* Vol 2, pp 2955-2973.

Kinsman 1965
Kinsman, B. 1965. *Wind Waves*, Prentice-Hall, Englewood Cliffs, NJ.

Kitaigorodoskii et al. 1975
Kitaigorodoskii, S. A. et al. 1975. "On Phillips' Theory of equilibrium Range in the Spectra of Wind-Generated Gravity Waves," *Jour. Phys. Ocean.,* Vol 5, No. 3, pp 410-420.

Klopman 1990
Klopman, G. 1990. "A note on integral properties of periodic gravity waves int eh case of non-zero mean Eulerian velocity," *J. Fluid Mech,* Vol 211, pp 609-615.

Korteweg and de Vries 1895
Korteweg, D. J. and de Vries, G. 1895. "On the Change of Form of Long Waves Advancing in a Rectangular Canal, and on a New Type of Stationary Waves," *Phil. Mag.,* 5th Series, Vol 39, pp 422-443.

Kuo and Kuo 1974
Kuo, C. T., and Kuo, S. T. 1974. "Effect of Wave Breaking on Statistical Distribution of Wave Heights," *Proceedings of Civil Engineering Oceans*, pp 1211-1231.

Laitone 1960
Laitone, E. V. 1960. "The Second Approximation to Cnoidal and Solitary Waves," *Jour. Fluid Mech.,* Vol 9, pp 430-444.

Laitone 1962
Laitone, E. V. 1962. "Limiting Conditions for Cnoidal and Stokes Waves," *Journal of Geophysical Research*, Vol 67, pp 1555-1564.

Laitone 1965
Laitone, E. V. 1965. "Series Solutions for Shallow Water Waves," *Journal of Geophysical Research*, Vol 70, pp 995-998.

Lamb 1945
Lamb, H. 1945. *Hydrodynamics*, 6th ed., Dover, New York.

Le Méhauté 1976
Le Méhauté, B. 1976. *Introduction to Hydrodynamics and Water Waves*, Springer-Verlag, New York.

Le Méhauté and Webb 1964
Le Méhauté, B., and Webb, L. M. 1964. "Periodic Gravity Waves Over a Gentle Slope at a Third Order of Approximation," *Proc. 10th Coastal Engr. Conf.,* Vol 1, pp 23-40.

Leenknecht, Szuwalski, and Sherlock 1992
Leenknecht, D. A., Szuwalski, A. and Sherlock, A. R. 1992. "Automated Coastal Engineering System, User Guide and Technical Reference, Version 1.07," Coastal Engineering Research Center, U.S. Army Engineer Waterways Experiment Station, Vicksburg, MS 39180.

Liu 1971
Liu, P. C. 1971. "Normalized and Equilibrium Spectra of Wind-Wave in Lake Michigan," *Jour. Phys. Ocean.,* Vol 1 No. 4, pp 249-257.

Liu 1984
Liu, P.-L. F. 1984. "Wave-Current Interactions on a Slowly Varying Topography," *Journal of Geophysical Research*, Vol 88, pp 4421-4426.

Liu and Dalrymple 1978
Liu, P.-L. F., and Dalrymple, R. A. 1978. "Bottom Friction Stresses and Longshore Currents due to Waves with Large Angles of Incidence," *Jour. Marine Res.,* Vol 36, pp 357-375.

Longuet-Higgins 1952
Longuet-Higgins, M.S. 1952. "On the Statistical Distribution of the Wave Heights of Sea Waves," *Jour. Marine Res.,* Vol 11, pp 245-266.

Longuet-Higgins 1953
Longuet-Higgins, M. S. 1953. "Mass Transport in Waves," *Phil. Trans. Roy. Soc. London, Series A,* Vol 245, pp 535-581.

Longuet-Higgins 1957
Longuet-Higgins, M.S. 1957. "Statistical Analysis of a Random, Moving Surface," *Phil Trans. Roy. Soc.* London, Series A, Vol 249, pp 321-387.

Longuet-Higgins 1962
Longuet-Higgins, M.S. 1962. "The Distribution of Intervals Between Zeros of Random Function," *Phil. Trans. Roy. Soc. London,* Series A, Vol 254, pp 557-599.

Longuet-Higgins 1970
Longuet-Higgins, M. S. 1970. "Longshore Currents Generated by Obliquely Incident Sea Waves," *Journal of Geophysical Research*, Vol 75, pp 6778-6789.

Longuet-Higgins 1974
Longuet-Higgins, M. S. 1974. "On the Mass, Momentum, Energy, and Circulation of a Solitary Wave," *Proc. Roy. Soc. London, Series A,* Vol 337, pp 1-13.

Longuet-Higgins 1975a
Longuet-Higgins, M. S. 1975a. "Longshore Currents Generated by Obliquely Incident Sea Waves," *Journal of Geophysical Research*, Vol 75, pp 6778-6789.

Longuet-Higgins 1975b
Longuet-Higgins, M. S. 1975b. "On the Joint Distribution of the Periods and Amplitudes of Sea Waves," *Journal of Geophysical Research*, Vol 80, pp 2688-2694.

Longuet-Higgins 1976
Longuet-Higgins, M. S. 1976. "Recent Developments in the Study of Breaking Waves," *Proc. 15th Coastal Engr. Conf.,* Vol 1, pp 441-460.

Longuet-Higgins 1980
Longuet-Higgins, M. S. 1980. "On the Joint Distribution of Heights of Sea Waves: Some Effects of Nonlinearity and Finite Band Width," *Journal of Geophysical Research*, Vol 85, pp 1519-1523.

Longuet-Higgins 1983
Longuet-Higgins, M. S. 1983. "On the Joint Distribution of Wave Period and Amplitudes in a Random Wave Field," *Proc. Roy. Soc. London, Series A,* Vol 389, pp 241-258.

Longuet-Higgins 1984
Longuet-Higgins, M. S. 1984. "Statistical Properties of Wave Groups in a Random Sea State," *Phil. Trans. Roy. Soc. London, Series A,* Vol 310, pp 219-250.

Longuet-Higgins 1985
Longuet-Higgins, M. S. 1985. "A New Way to Calculate Steep Gravity Waves," *The Ocean Surface*, Y. Toba and H. Mitsuyasu, eds., Univ. of Tokyo Press, pp 1-15.

Longuet-Higgins and Fenton 1974
Longuet-Higgins, M. S., and Fenton, J. D. 1974. "On Mass, Momentum, Energy, and Calculation of a Solitary Wave," *Proc. Roy. Soc. London, Series A,* Vol 340, pp 471-493.

Longuet-Higgins and Fox 1977
Longuet-Higgins, M. S., and Fox, M. J. H. 1977. "Theory of the Almost Highest Wave: the Inner Solution," *Jour. Fluid Mech.,* Vol 80, pp 721-741.

Longuet-Higgins and Stewart 1962
Longuet-Higgins, M. S., and Stewart, R. W. 1962. "Radiation Stress and Mass Transport in Gravity Waves, with Application to 'Surf Beats'," *Journal of Fluid Mechanics*, Vol 13, No. 4, pp 481-504.

Longuet-Higgins and Stewart 1964
Longuet-Higgins, M. S., and Stewart, R. W. 1964. "Radiation Stresses in Water Waves: A Physical Discussion with Applications," *Deep Sea Research*, Vol 11, pp 529-562.

Mei 1991
Mei, C. C. 1991. *The Applied Dynamics of Ocean Surface Waves*, World Scientific Pub. Co., Teaneck, NJ.

Miche 1944
Miche, R. 1944. "Mouvements Ondulatoires des Mers en Profondeur Constante on Decroisante," *Annales des Ponts et Chaussees,* pp 25-78, 131-164, 270-292, 369-406.

Michell 1893
Michell, J. H. 1893. "On the Highest Wave in Water," *Phil. Mag.,* Vol 36, pp 430-435.

Miles 1979
Miles, J. W. 1979. "On the Korteweg de Vries Equation for Gradually Varying Channel," *Jour. Fluid Mech.,* Vol 91, pp 181-190.

Miles 1980
Miles, J. W. 1980. "Solitary Waves," *Annual Rev. Fluid Mech.,* Vol 12, pp 11-43.

Miles 1981
Miles, J. W. 1981. "The Korteweg de Vries Equation: A Historical Essay," *Jour. Fluid Mech.,* Vol 106, pp 131-147.

Milne-Thompson 1976
Milne-Thompson, L. M. 1976. *Theoretical Hydrodynamics*, The MacMillan Press Ltd., London.

Mitsuyasu 1971
Mitsuyasu, H. 1971. "On the Form of Fetch-Limited Wave Spectrum," *Coastal Engr. in Japan,* Vol 14, pp 7-14.

Mitsuyasu 1972
Mitsuyasu, H. 1972. "The One-Dimensional Wave Spectra at Limited Fetch," *Proc. 13th Coastal Engr. Conf.,* Vol 1, pp 289-306.

Mitsuyasu et al. 1975
Mitsuyasu, H. et al. 1975. "Observations of the Directional spectrum of Ocean Waves Using a Cloverleaf Buoy," *Jour. Phys. Ocean.,* Vol 5, pp 750-760.

Morison et al. 1950
Morison, J. R., et al. 1950. "The Forces Exerted by Surface Waves on Piles," *Petroleum Trans. AIME,* Vol 189, pp 149-157.

Munk 1949
Munk, W. H. 1949. "The Solitary Wave Theory and Its Application to Surf Problems," *Annals New York Acad. Sci.,* Vol 51, pp 376-423.

Myrhaug and Kjeldsen 1986
Myrhaug, D. and Kjeldsen, S. P. 1986. "Steepness and Asymmetry of Extreme Waves and the Highest Waves in Deep Water," *Intl. Jour. Ocean Engr.,* Vol 13, pp 549-568.

Nishimura et al. 1977
Nishimura, H., et al. 1977. "Higher Order Solutions of Stokes and Cnoidal Waves," *Jour. Faculty Engr. Univ. of Tokyo,* Series B, Vol 34, pp 267-293.

Ochi 1973
Ochi, M. K. 1973. "On Prediction of Extreme Values," *Jour. Ship Res.,* Vol 1, pp 29-37.

Ochi 1982
Ochi, M. K. 1982. "Stochastic Analysis and Probabilistic Prediction of Random Seas," *Advances in Hydrosci,,* V. T. Chow, ed., Academic Press, Vol 13, pp 217-375.

Ochi and Hubble 1976
Ochi, M. K. and Hubble, E. N. 1976. "Six Parameter Wave Spectra," *Proc. 15th Coastal Engr. Conf.,* Vol 1, pp 301-328.

Ottesen-Hansen 1980
Ottesen-Hansen, N.-E. 1980. "Correct Reproduction of Group-Induced Long Waves," *Proc. 17th Coastal Engr. Conf.,* Vol 1, pp 784-800.

Peregrine 1972
Peregrine, D. H. 1972. "Equations for Water Waves and the Approximation Behind Them," *Waves on Beaches and Resulting Sediment Transport*, R. E. Meyer, ed., Academic Press, pp 95-121.

Peregrine 1976
Peregrine, D. H. 1976. "Interaction of Water Waves and Currents," *Advances in Applied Mechanics*, Academic Press, New York, Vol 16, pp 9-117.

Phillips 1958
Phillips, O. M. 1958. "On the Generation of Waves by Turbulent Wind," *Jour. Fluid Mech.,* Vol 2, pp 417-445.

Phillips 1977
Phillips, O. M. 1977. *The Dynamics of the Upper Ocean*, 2nd ed., Cambridge University Press.

Pierson and Moskowitz 1964
Pierson, W. J., and Moskowitz, L. 1964. "A Proposed Spectral Form for Fully-Developed Wind Sea Based on the Similarity Law of S. A. Kitaigorodoskii," *Journal of Geophysical Research*, Vol 69, pp 5181-5203.

Price and Bishop 1974
Price, W. G., and Bishop, R. E. D. 1974. *Probabilistic Theory of Ship Dynamics*, Chapman and Hall, London.

Rayleigh 1876
Rayleigh, L. 1876. "On Waves," *Phil. Mag.,* Vol 1, pp 257-279.

Rice 1944-1945
Rice, S. O. 1944-1945. "Mathematical Analysis of Random Noise," *Bell System Tech. Jour.,* Vol 23, pp 282-332.; Vol 24, pp 45-156.

Rienecker and Fenton 1981
Rienecker, M. M. and Fenton, J. D. 1981. "A Fourier Representation Method for Steady Water Waves," *Jour. Fluid Mech.,* Vol 104, pp 119-137.

Russel and Osorio 1958
Russel, R. C. H., and Osorio, J. D. C. 1958. "An Experimental Investigation of Drift Profiles in a Closed Channel," *Proc. 6th Coastal Engr. Conf.,* Vol 1, pp 171-193.

Russell 1838
Russell, J. S. 1838. "Report of the Committee on Waves," *Rep. Meet. British Assoc. Adv. Sci 7th,* Liverpool, 1837, John Murray, London, pp 417-496.

Russell 1844
Russell, J. S. 1844. "Report on Waves," *14th Meeting Brit. Assoc. Adv. Sci.,* pp 311-390.

Sakai and Battjes 1980
Sakai, T., and Battjes, J. A. 1980. "Wave Shoaling Calculated from Cokelet's Theory," *Coastal Engr.,* Vol 4, pp 65-84.

Sand 1982
Sand, S. S. 1982. "Long Wave Problems in Laboratory Models," *ASCE Jour. Waterw., Port, Coastal and Ocean Engr.,* Vol 108, pp 492-503.

Sarpkaya and Isaacson 1981
Sarpkaya, T. and Isaacson, M. 1981. *Mechanics of Wave Forces on Offshore Structures*, Van Nostrand Reinhold Co., New York.

Schwartz 1974
Schwartz, L. W. 1974. "Computer Extension and Analytic Continuation of Stokes' Expansion for Gravity Waves," *Jour. Fluid Mech.,* Vol 62, pp 553-578.

Scott 1965
Scott, J. R. 1965. "A Sea Spectrum for Model Tests and Long-Term Ship Prediction," *Jour. Ship Res.,* Vol 9, pp 145-152.

Shore Protection Manual 1984
Shore Protection Manual. 1984. 4th ed., 2 Vol. U.S. Army Engineer Waterways Experiment Station, U.S. Government Printing Office, Washington, DC.

Silvester 1974
Silvester, R. 1974. *Coastal Engineering*, Vols I & II, Elsevier, Amsterdam.

Skjelbreia and Hendrickson 1961
Skjelbreia, L., and Hendrickson, J. 1961. "Fifth Order Gravity Wave Theory," *Proc. 7th Coastal Engr. Conf.,* Vol 1, pp 184-196.

Sobey 1990
Sobey, R. J. 1990. "Wave Theory Predictions of Crest Kinematics," *Water Wave Kinematics*, A. Torum and O. T. Gudmestad, eds., Kluwer Acad. Pub, The Netherlands, pp 215-231.

Sobey et al. 1987
Sobey, R. J., et al. 1987. "Application of Stokes, Cnoidal, and Fourier Wave Theories," *ASCE Jour. Waterw., Port, Coastal and Ocean Engr.,* Vol 113, pp 565-587.

Spanos 1983
Spanos, P. D. 1983. "ARMA Algorithms for Ocean Wave Modeling," *ASME Jour. Energy Resources Tech.,* Vol 105, pp 300-309.

St. Denis and Pierson 1953
St. Denis, M., and Pierson, W. J. 1953. "On the Motion of Ships in Confused Seas," *Trans. SNAME,* Vol 61, pp 280-357.

Stoker 1957
Stoker, J. J. 1957. *Water Waves, The Mathematical Theory with Applications*, Interscience, New York.

Stokes 1846
Stokes, G. G. 1846. "Report on Recent Research in Hydrodynamics," Mathematical and Physical Paper (1880), Vol 1, pp 167-187, Cambridge University Press.

Stokes 1847
Stokes, G. G. 1847. "On the Theory of Oscillatory Waves," *Trans. Camb. Phil. Soc.,* Vol 8, pp 441-455.

Stokes 1880
Stokes, G. G. 1880. *Math. Phys. Papers*, Vol 1, Camb. Univ. Press.

Su 1984
Su, M.-Y. 1984. "Characteristics of Extreme Wave Groups," *Oceans'84 Conf.,* Washington, DC.

Sverdrup and Munk 1947
Sverdrup, H. U., and Munk, W. H. 1947. *Wind, Sea and Swell: Theory of Relations for Forecasting*, U.S. Navy Hydro. Office, Publication No. 601.

Tayfun 1981
Tayfun, A. 1981. "Distribution of Crest-to-Trough Wave height," *ASCE Jour. Waterw., Port, Coastal and Ocean Engr.,* Vol 107, pp 149-158.

Tayfun 1983a
Tayfun, A. 1983a. "Effects of Spectrum Bandwidth on the Distribution of Wave Heights and Periods," *Intl. Jour. Ocean Engr.,* Vol 10, pp 107-118.

Tayfun 1983b
Tayfun, A. 1983b. "Nonlinear Effects on the Distribution of Crest-to-Trough Wave Heights," *Intl. Jour. Ocean Engr.,* Vol 10, pp 97-106.

Tayfun, Dalrymple, and Yang 1976
Tayfun, A., Dalrymple, R. A. and Yang, C. Y. 1976. "Random Wave-Current Interaction in Water of Varying Depth," *Ocean Engr.,* Vol 3, pp 403-420.

Thom 1961
Thom, H. C. S. 1961. "Distribution of Extreme Winds in the United States," *Trans ASCE,* Vol 126, Part II.

Thom 1973
Thom, H. C. S. 1973. "Distribution of Extreme Winds Over Ocean," and "Extreme Wave Height Distribution Over Oceans," *ASCE Jour. Waterw., Port, Coastal and Ocean Engr.,* Vol 99, pp 1-17 and 355-374.

Thompson 1977
Thompson, E. F. 1977. "Wave Climate at Selected Locations Along U.S. Coasts," Technical Report TR 77-1, U. S. Army Engineer Waterways Experiment Station, Vicksburg, MS.

Thompson and Vincent 1985
Thompson, E. F., and Vincent, C. L. 1985. "Significant wave Height for Shallow Water Design," *ASCE Jour. Waterw., Port, Coastal and Ocean Engr.,* Vol 111, pp 828-842.

Thornton and Guza 1983
Thornton, E. B., and Guza, R. T. 1983. "Transformation of Wave Height Distribution," *Journal of Geophysical Research*, Vol 88, No. C10, pp 5925-5938.

Tucker 1963
Tucker, M. J. 1963. "Analysis of Records of Sea Waves," *Proc. Inst. Civil Engrs.,* Vol 26, pp 305-316.

Tucker et al. 1984
Tucker, M. J., et al. 1984. "Numerical Simulation of a Random Sea: A Common Error and Its Effect Upon Wave Group Statistics," *Jour. Applied Ocean Res.,* Vol 6, pp 118-122.

Tung and Huang 1976
Tung, C. C. and Huang, N. E. 1976. "Interaction Between Waves and Currents and Their Influence on Fluid Forces," *Proc. BOSS'76,* Vol 1, pp 129-143.

Ursell 1953
Ursell, F. 1953. "The Long Wave Paradox in the Theory of Gravity Waves," *Proc. Camb. Philos. Soc.,* Vol 49, pp 685-694.

Van Dorn 1965
Van Dorn, W. G. 1965. "Source Mechanism of the Tsunami of March 28, 1964 in Alaska," *Proc. 9th Coastal Engr. Conf., ASCE,* pp 166-190.

Venezian 1980
Venezian, G. 1980. Discussion of "Direct Solution of Wave Dispersion Equation," by J.N. Hunt, *ASCE Jour. Waterw., Port, Coastal and Ocean Engr.,* Vol 106, pp 501-502.

Venezian and Demirbilek 1979
Venezian, G., and Demirbilek, Z. 1979. "Pade Approximants for Water Waves," Texas Engr. and Exp. Station Research Center Notes, College Station, Texas.

Vincent 1984
Vincent, C. L. 1984. "Shallow Water Waves: A Spectral Approach," *Proc. 19th Coastal Engr. Conf.,* Vol 1, pp 370-382.

Vincent 1985
Vincent, C. L. 1985. "Depth-Controlled Wave Height," *ASCE Jour. Waterw., Port, Coastal and Ocean Engr.,* Vol 111, pp 459-475.

Vincent and Hughes 1985
Vincent, C. L. and Hughes, S. A. 1985. "Wind Wave Growth in Shallow Water," *ASCE Jour. Waterw., Port, Coastal and Ocean Engr.,* Vol 111, pp 765-770.

Wang 1985
Wang, W. C. 1985. "Non-Gaussian Characteristics of Waves in Finite Water Depth," Rept. No.85-009, Univ. of Florida, Gainesville, FL.

Wehausen and Laitone 1960
Wehausen, J. V., and Laitone, E. V. 1960. "Surface Waves," *Handbuch der Physik,* S. Flugge, ed., Springer-Verlag, Berlin, Vol IX, pp 446-778.

Whitham 1967
Whitham, G. B. 1967. "Variational Methods and Applications to Water Waves," *Proc. Roy. Soc. London, Series A*, Vol 299, pp 6-25.

Whitham 1974
Whitham, G. B. 1974. *Linear and Nonlinear Waves,* Wiley Interscience, New York.

Wiegel 1954
Wiegel, R. L. 1954. *Gravity Waves, Tables of Functions*, Univ. of Calif., Council on Wave Res., The Engr. Found., Berkeley, CA.

Wiegel 1960
Wiegel, R. L. 1960. "A Presentation of Cnoidal Wave Theory for Practical Application," *Jour. Fluid Mech.,* Vol 7, pp 273-286.

Wiegel 1964
Wiegel, R. L. 1964. *Oceanographical Engineering*, Prentice-Hall, Englewood Cliffs, NJ.

Williams 1981
Williams, J. M. 1981. "Limiting Gravity Waves in Water of Finite Depth," *Phil. Trans. Roy. Soc. London, Series A,* Vol 302, pp 139-188.

Williams 1985
Williams, J. M. 1985. *Tables of Progressive Gravity Waves*, Pitman, Boston.

Wirsching 1986
Wirsching, P. 1986. "Reliability Methods in Mechanical and Structural Design," Lecture Notes on Short Course for Conoco R&D Dept., Ponca City, OK.

Wu and Liu 1984
Wu, C-S., and Liu, P.-L. F. 1984. "Effects of Nonlinear Inertial Forces on Nearshore Currents," *Coastal Engr.,* Vol 8, pp 15-32.

Wu and Thornton 1986
Wu, C-S., and Thornton, E. B. 1986. "Wave Numbers of Linear Progressive Waves," *ASCE Jour. Waterw., Port, Coastal and Ocean Engr.,* Vol 112, pp 536-540.

Yu 1952
Yu, Y.-Y. 1952. "Breaking of Waves by an Opposing Current," *Trans. Amer. Geophys. Union,* Vol 33, No.1, pp 39-41.

II-1-5. Definitions of Symbols

α	Dimensionless scaling parameter used in the JONSWAP spectrum for fetch-limited seas
α	Phillips' constant (= 0.0081) (Equation II-1-153)
α_x , α_z	Fluid particle accelerations [length/time^2]
γ	Peak enhancement factor used in the JONSWAP spectrum for fetch-limited seas
Γ	Gamma function
Δp	Difference in pressure at a point due to the presence of the solitary wave [force/length^2]
Δt	Sampling interval (Equation II-1-144) [time]
ϵ	Dimensionless pertubation expansion parameter
ϵ	Spectral bandwidth used in the probability distribution for waves (Equation II-1-150)
ϵ	Wave steepness (= H/L)
ζ	Vertical displacement of the water particle from its mean position (Equation II-1-27) [length]
η	Displacement of the water surface relative to the SWL [length]
$\eta(t)$	Sea state depicted in time series of the wave profile [length]
$\eta(x,t)$	Time series of the wave profile at a point x and time t (Equation II-1-175) [length]
$\overline{\eta}$	Mean or expected value of the sea state (Equation II-1-119) [length]
$\eta_{envelope}$	Envelope wave form of two or more superimposed wave trains (Equation II-1-48) [length]
η_{rms}	Root-mean-square surface elevation [length]
θ	Angle between the plane across which energy is being transmitted and the direction of wave advance [deg]
θ	Principal (central) direction for the spectrum measured counterclockwise from the principal wave direction [deg]
$\lambda_{1,2}$	Spectral shape parameters controlling the shape and the sharpness of the spectral peak of the Ochi-Hubble spectral model
μ_η	Mean or expected value of the sea state (Equation II-1-119) [length]
ν	Dimensionless Spectral width parameter
ξ	Horizontal displacement of the water particle from its mean position (Equation II-1-26) [length]

ρ	Mass density of water (salt water = 1,025 kg/m^3 or 2.0 slugs/ft^3; fresh water = 1,000kg/m^3 or 1.94 slugs/ft^3) [force-time^2/length^4]
ρ_η	Autocorrelation coefficient (Equation II-1-122)
σ_η	Standard deviation or square root of the variance
Φ	Velocity potential [length^2/time]
Φ	Weighing factor (Equation II-1-159)
Ψ	Stream function
ω	Wave angular or radian frequency (= 2π/T) [time^{-1}]
a	Wave amplitude [length]
A, B	Major- (horizontal) and minor- (vertical) ellipse semi-axis of wave particle motion (Equations II-1-34 and II-1-35) [length]. The lengths of A and B are measures of the horizontal and vertical displacements of the water particles (Figure II-1-4).
B_j	Dimensionless Fourier coefficients (Equation II-1-103)
C	Phase velocity or wave celerity (= $L/T = \omega/k$) [length/time]
$C(s)$	Dimensionless constant satisfying the normalization condition
C_g	Wave group velocity [length/time]
cn	Jacobian elliptic cosine function
d	Water depth [length]
E	Total wave energy in one wavelength per unit crest width [length-force/length^2]
$E(\omega)$	Phillips' equilibrium range of the spectrum for a fully-developed sea in deep water (Equation II-1-153)
$E(f)$	One-dimensional spectrum or frequency energy spectrum or wave energy spectral density (Equation II-1-144)
$\overline{E}$	Total average wave energy per unit surface area or specific energy or energy density (Equation II-1-58) [length-force/length^2]
$\overline{E_k}$	Kinetic energy per unit length of wave crest for a linear wave (Equation II-1-53) [length-force/length^2]
$\overline{E_p}$	Potential energy per unit length of wave crest for a linear wave (Equation II-1-55) [length-force/length^2]
$E[\eta]$	Mean or expected value of the sea state (Equation II-1-119) [length]
F	Fetch length [length]
f_p	Frequency of the spectral peak used in the JONSWAP spectrum for fetch-limited seas [time^{-1}]

g	Gravitational acceleration [length/time^2]
$G(f,\theta)$	Dimensionless directional spreading function
H	Wave height [length]
$\overline{H}$	Mean wave height [length]
$H_{1/3}$	Significant wave height [length]
$H_{1/n}$	The average height of the largest $1/n$ of all waves in a record [length]
H_d	Design wave height [length]
H_j	Ordered individual wave heights in a record (Equation II-1-115) [length]
H_{max}	Maximum wave height [length]
H_{rms}	Root-mean-square of all measured wave heights [length]
H_s	Significant wave height [length]
k	Modulus of the elliptic integrals
k	Number of lags between waves in a sequence in a record (Equation II-1-169)
k	Wave number ($= 2\pi/L = 2\pi/CT$) [length^{-1}]
$K(k)$	Complete elliptic integral of the first kind
K_z	Pressure response factor (Equation II-1-43) [dimensionless]
L	Wave length [length]
M	Dimensionless parameter which is a function of H/d used in calculating water particle velocities for a solitary wave (Equations II-1-92 & II-1-93) (Figure II-1-17).
$m_{0,1,2,4}$	Moments of the wave spectrum
N	Dimensionless correction factor in determination of η from subsurface pressure (Equation II-1-46)
N	Dimensionless parameter which is a function of H/d used in calculating water particle velocities for a solitary wave (Equations II-1-92 & II-1-93) (Figure II-1-17).
N	Number of waves in a record
N_c	Number of crests in the wave record
N_z	Number of zero-upcrossings in the wave record
$_O$	The subscript 0 denotes deepwater conditions
p	Pressure at any distance below the fluid surface [force/length^2]
P	Probability

$p(x)$	Probability density
$P(x)$	Probability distribution function - fraction of events that a particular event is not exceeded (Equation II-1-124)
$\overline{P}$	Wave power or average energy flux per unit wave crest width transmitted across a vertical plane perpendicular to the direction of wave advance (Equation II-1-59) [length-force/time-length]
p_a	Atmospheric pressure [force/length^2]
p'	Total or absolute subsurface pressure -- includes dynamic, static, and atmospheric pressures (Equation II-1-39) [force/length^2]
$Q(x)$	Probability of exceedence (Equation II-1-128)
Q_p	Spectral peakedness parameter proposed by Goda (1974) (Equation II-1-151)
R	Bernoulli constant (Equation II-1-102)
R	Cross-correlation coefficient - measures the degree of correlation between two signals (Equation II-1-123)
R_η	Autocorrelation or autocovariance function of the sea state (Equation II-1-121)
R_H	Correlation coefficient describing the correlation between wave heights as a function of μ and standard deviation σ (Equation II-1-169)
R_{HH}	Correlation coefficient of the wave envelope, relating wave height variation between successive wave heights (Equation II-1-173)
s	Dimensionless controlling parameter for the angular distribution that determines the peakedness of the directional spreading
T	Wave period [time]
$\overline{T}$	Mean wave period [time]
$\overline{T_c}$	Mean crest period [time]
$\overline{T_z}$	Mean zero-upcrossing wave period [time]
T_c	Average wave period between two neighboring wave crests (Equation II-1-116) [time]
T_p	Wave period associated with the largest wave energy [time]
T_r	Sampling record length [time]
T_r	Total wave record length [time]
T_z	Zero-crossing wave period (Equation II-1-116) [time]
T_*^{max}	Most probable maximum wave period (Equation II-1-141) [time]
u	Fluid velocity (water particle velocity) in the x-direction [length/time]

U	Current speed [length/time]
U	Wind speed at the 10-m elevation above the sea surface [length/time]
$\overline{U(z)}$	Mass transport velocity (Equation II-1-69) [length/time]
u_{max}	Maximum fluid velocity in the horizontal direction [length/time]
U_P	Universal parameter for classification of wave theories
U_R	Dimensionless Ursell number (Equation II-1-67)
U_w	Wind speed at 19.5 m above mean sea level (Equation II-1-155) [length/time]
V	Volume of water within the wave above the still-water level per unit crest (Equation II-1-90) [length^3/length of crest]
w	Fluid velocity (water particle velocity) in the z-direction [length/time]
y_c	Vertical distance from seabed to the wave crest (Equation II-1-79) [length]
y_s	Vertical distance from seabed to the water surface (Equation II-1-77) [length]
y_t	Vertical distance from seabed to the wave trough [length]
z	Water depth below the SWL (Figure II-1-1) [length]

II-1-6. Acknowledgments

Authors of Chapter II-1, "Water Wave Mechanics:"

Zeki Demirbilek, Ph.D., Coastal and Hydraulics Laboratory (CHL), Engineer Research and Development Center, Vicksburg, Mississippi.
C. Linwood Vincent, Ph.D., Office of Naval Research, Arlington, Virginia.

Reviewers:

Robert A Dalrymple, Ph.D., Center for Applied Coastal Research, University of Delaware, Newark, Delaware.
Yoshimi Goda, Ph.D., Yokohama National University, Yokohama, Japan (emeritus).
Lee E. Harris, Ph.D., Department of Marine and Environmental Systems, Florida Institute of Technology, Melbourne, Florida.
Bernard LeMéhauté, Ph.D., University of Miami, Miami, Florida, (deceased).
Philip L.-F. Liu, Ph.D., School of Civil and Environmental Engineering, Cornell University, Ithaka, New York.
J. Richard Weggel, Ph.D., Dept. of Civil and Architectural Engineering, Drexel University, Philadelphia, Pennsylvania.
Robert L. Wiegel, University of California at Berkeley, Berkeley, California, (emeritus).

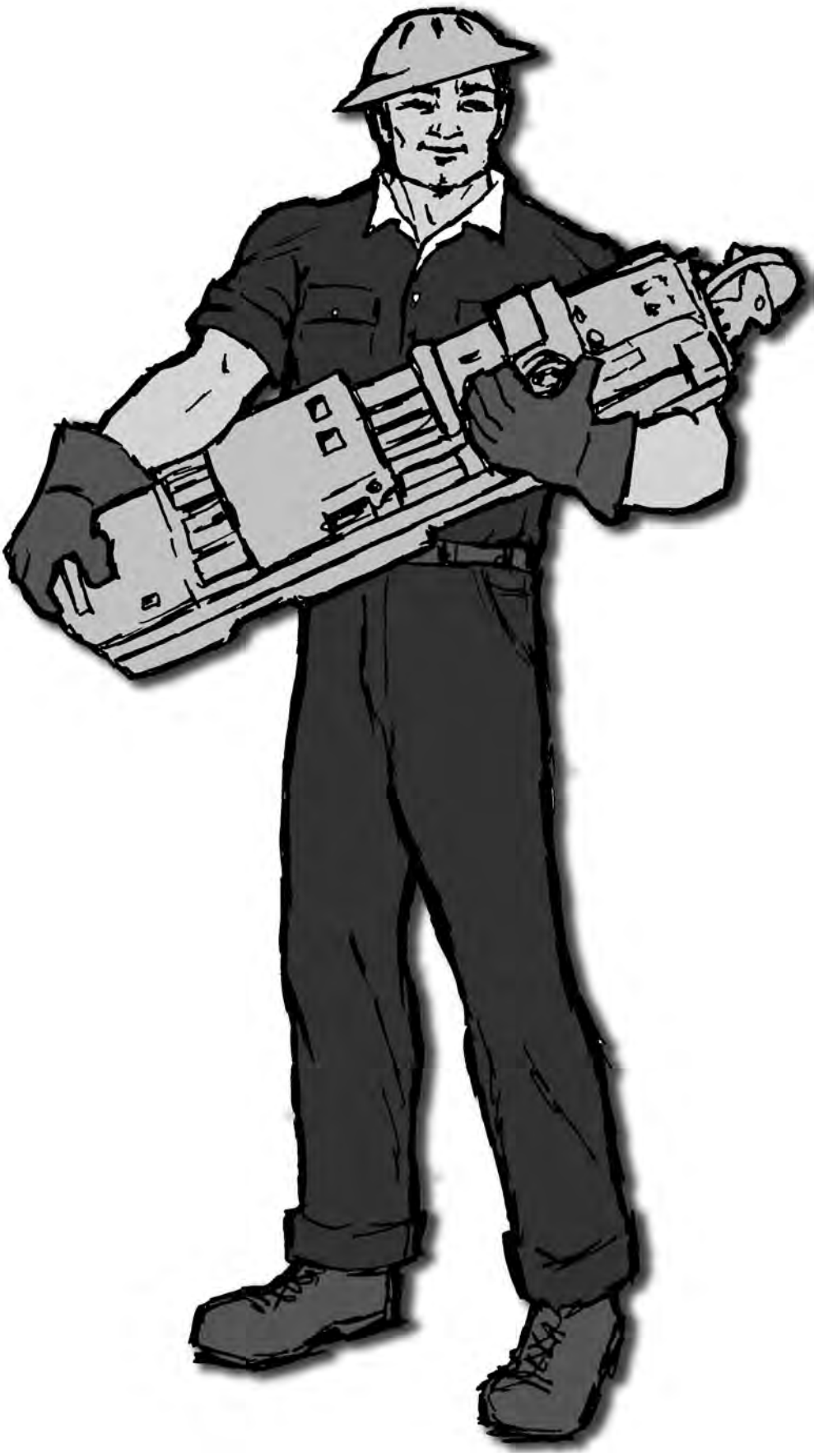

Table of Contents

Page

II-2-1. Meteorology II-2-1
a. Introduction II-2-1
(1) Background II-2-1
(2) Organized scales of motion in the atmosphere II-2-1
(3) Temporal variability of wind speeds II-2-3
b. General structure of winds in the atmosphere II-2-5
c. Winds in coastal and marine areas II-2-7
d. Characteristics of the atmospheric boundary layer II-2-8
e. Characteristics of near-surface winds II-2-9
f. Estimating marine and coastal winds II-2-11
(1) Wind estimates based on near-surface observations II-2-11
(2) Wind estimates based on information from pressure fields and weather maps II-2-15
g. Meteorological systems and characteristic waves II-2-23
h. Winds in hurricanes II-2-27
i. Step-by-step procedure for simplified estimate of winds for wave prediction II-2-34
(1) Introduction II-2-34
(2) Wind measurements II-2-34
(3) Procedure for adjusting observed winds II-2-34
(a) Level II-2-34
(b) Duration II-2-34
(c) Overland or overwater II-2-36
(d) Stability II-2-36
(4) Procedure for adjusting winds from synoptic weather charts II-2-36
(a) Geostrophic wind speed II-2-36
(b) Level and stability II-2-36
(c) Duration II-2-36
(5) Procedure for estimating fetch II-2-36

II-2-2. Wave Hindcasting and Forecasting II-2-37
a. Introduction II-2-37
b. Wave prediction in simple situations II-2-43
(1) Assumptions in simplified wave predictions II-2-44
(a) Deep water II-2-44
(b) Wave growth with fetch II-2-44
(c) Narrow fetches II-2-45
(d) Shallow water II-2-45
(2) Prediction of deepwater waves from nomograms II-2-46
(3) Prediction of shallow-water waves II-2-47
c. Parametric prediction of waves in hurricanes II-2-47

II-2-3. Coastal Wave Climates in the United States II-2-50
a. Introduction II-2-50
b. Atlantic coast II-2-52
c. Gulf of Mexico II-2-56
d. Pacific coast II-2-58
e. Great lakes II-2-58

II-2-4. Additional Example Problem II-2-61

II-2-5. References II-2-63

II-2-6. Definitions of Symbols II-2-70

II-2-7. Acknowledgments II-2-72

List of Tables

Page

Table II-2-1. Ranges of Values for the Various Scales of Organized Atmospheric Motions II-2-2

Table II-2-2. Local Seas Generated by Various Meteorological Phenomena II-2-25

Table II-2-3. Wave Statistics in the Atlantic Ocean II-2-53

Table II-2-4. Wave Statistics in the Gulf of Mexico II-2-57

Table II-2-5. Wave Statistics in the Pacific Ocean II-2-59

Table II-2-6. Wave Statistics in the Great Lakes II-2-60

List of Figures

Page

Figure II-2-1. Ratio of wind speed of any duration U_t to the 1-hr wind speed U_{3600} II-2-4

Figure II-2-2. Duration of the fastest-mile wind speed as a function of wind speed U_f (for open terrain conditions) II-2-5

Figure II-2-3. Equivalent duration for wave generation as a function of fetch and wind speed II-2-6

Figure II-2-4. Wind profile in atmospheric boundary layer II-2-7

Figure II-2-5. Coefficient of drag versus wind speed II-2-11

Figure II-2-6. Ratio of wind speed at any height to the wind speed at the 10-m height as a function of measurement height for selected values of air-sea temperature difference and wind speed: a) ΔT=+3°C; b) ΔT=0°C; c) ΔT=-3°C II-2-12

Figure II-2-7. Ratio R_L of wind speed over water U_W to wind speed over land U_L as a function of wind speed over land U_L (after Resio and Vincent (1977)) II-2-14

Figure II-2-8. Amplification ratio R_T accounting for effects of air-sea temperature difference . . . II-2-15

Figure II-2-9. Surface synoptic chart for 0030Z, 27 October 1950 . . . . . II-2-16

Figure II-2-10. Surface synoptic weather charts for the Halloween storm of 1991 . . . . . II-2-17

Figure II-2-11. Key to plotted weather report II-2-18

Figure II-2-12. Geostrophic (free air) wind scale (after Bretschneider (1952)) II-2-20

Figure II-2-13. Ratio of wind speed at a 10-m level to wind speed at the top of the boundary layer as a function of wind speed at the top of the boundary layer, for selected values of air-sea temperature difference II-2-22

Figure II-2-14. Ratio of U_*/U_g as a function of U_g, for selected values of air-sea temperature difference II-2-22

Figure II-2-15. Common wind direction conventions II-2-23

Figure II-2-16. Climatological variation in Holland's "B" factor (Holland 1980) II-2-30

Figure II-2-17. Relationship of estimated maximum wind speed in a hurricane at 10-m elevation as a function of central pressure and forward speed of storm (based on latitude of 30 deg, R_{max}=30 km, 15- to 30-min averaging period) II-2-32

Figure II-2-18. Definition of four radial angles relative to direction of storm movement II-2-32

Figure II-2-19. Horizontal distribution of wind speed along Radial 1 for a storm with forward velocity V_F of (a) 2.5 m/s; (b) 5 m/s; (c) 7.5 m/s II-2-33

Figure II-2-20. Logic diagram for determining wind speed for use in wave hindcasting and forecasting models II-2-35

Figure II-2-21. Phillips constant versus fetch scaled according to Kitaigorodskii. Small-fetch data are obtained from wind-wave tanks. Capillary-wave data were excluded where possible. (Hasselmann et al. 1973) II-2-42

Figure II-2-22. Definition of JONSWAP parameters for spectral shape II-2-43

Figure II-2-23. Fetch-limited wave heights II-2-46

Figure II-2-24. Fetch-limited wave periods II-2-47

Figure II-2-25. Duration-limited wave heights II-2-48

Figure II-2-26. Duration-limited wave periods II-2-49

Figure II-2-27. Maximum value of H_{mo} in a hurricane as a function of V_{max} and forward velocity of storm (Young 1987) II-2-50

Figure II-2-28. Values of $H_{mo}/H_{mo\ max}$ plotted relative to center of hurricane (0,0). II-2-51

Figure II-2-29. Reference locations for Tables II-2-3 through II-2-6 . . . . . II-2-52

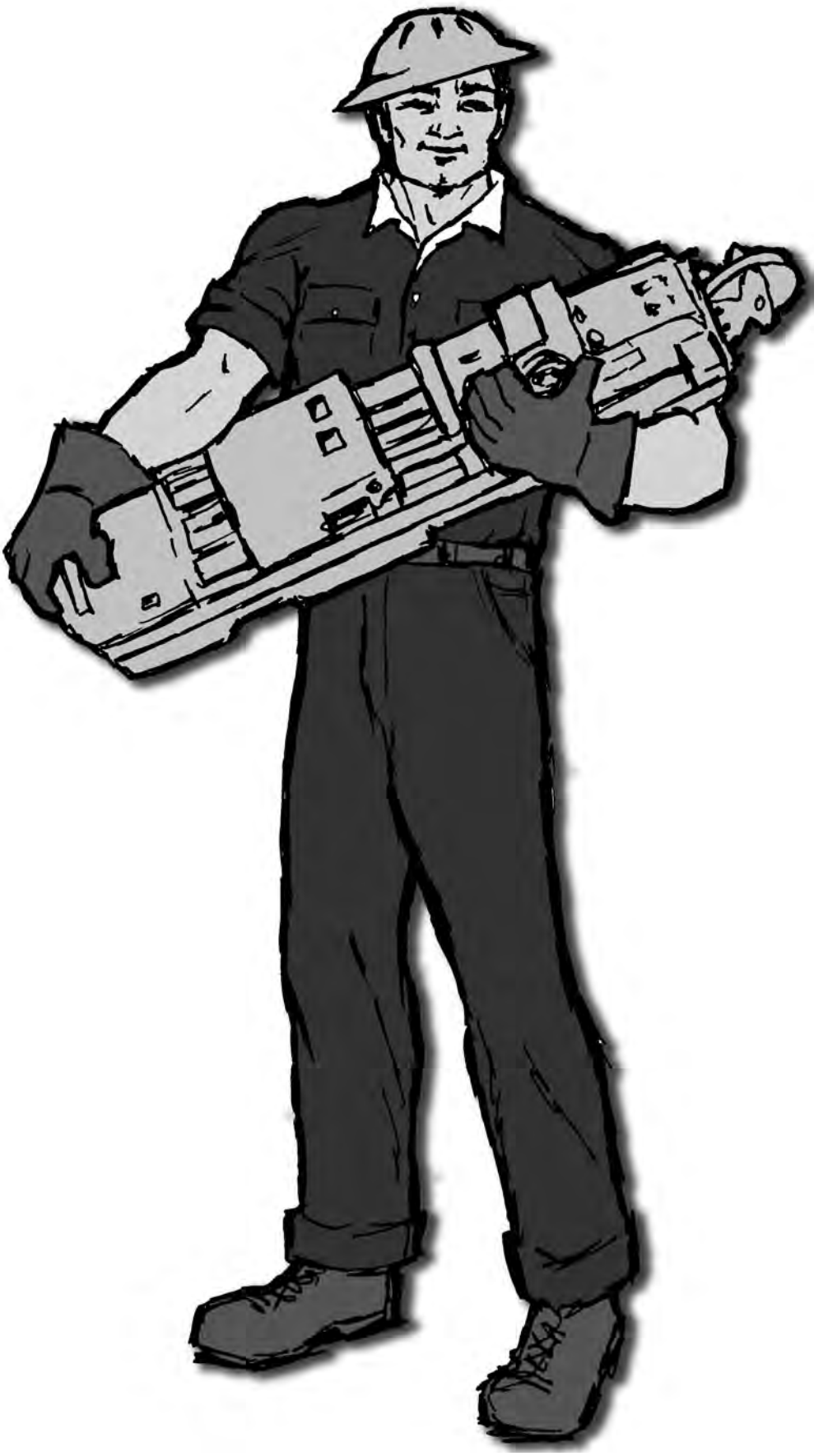

Chapter II-2
Meteorology and Wave Climate

II-2-1. Meteorology

a. Introduction.

(1) Background.

(a) A basic understanding of marine and coastal meteorology is an important component in coastal and offshore design and planning. Perhaps the most important meteorological consideration relates to the dominant role of winds in wave generation. However, many other meteorological processes (e.g., direct wind forces on structures, precipitation, wind-driven coastal currents and surges, the role of winds in dune formation, and atmospheric circulations of pollution and salt) are also important environmental factors to consider in man's interactions with nature in this sometimes fragile, sometimes harsh environment.

(b) The primary driving mechanisms for atmospheric motions are related either directly or indirectly to solar heating and the rotation of the earth. Vertical motions are typically driven by instabilities created by direct surface heating (e.g., air mass thunderstorms and land-sea breeze circulations), by advection of air into a region of different ambient air density, by topographic effects, or by compensatory motions related to mass conservation. Horizontal motions tend to be driven by gradients in near-surface air densities created by differential heating (for example north-south variations in incoming solar radiation, called insolation, and differences in the thermal response of ocean and continental areas), and by compensatory motions related to conservation of mass. The general structure and circulation of the earth's atmosphere is described in many excellent textbooks (Hess 1959)

(c) The rotation of the earth influences all motions in the earth's coordinate system. The net effect of the earth's rotation is to deflect all motion to the right in the Northern Hemisphere and to the left in the Southern Hemisphere. The strength of this deflection (termed Coriolis acceleration) is proportional to the sine of the latitude. Hence Coriolis effects are strongest in polar regions and vanish at the equator. Coriolis effects become significant when the trajectory of an individual fluid/gas particle moves over a distance of the same order as the Rossby radius of deformation, defined as

$$R_o = \frac{c}{f} \tag{II-2-1}$$

where

R_o = Rossby radius of deformation

f = Coriolis parameter defined as $1.458 \times 10^{-4} \sin \phi$, where ϕ is latitude (note f here is in $\sec^{-1}$)

c = characteristic velocity of the particle

For a velocity of 10 m/s at a latitude of 45 deg, R_o is about 100 km. This suggests that scales of motion with this velocity and with particle excursions of about 10 km and greater will begin to be significantly affected by Coriolis at this latitude.

(2) Organized scales of motion in the atmosphere.

(a) Table II-2-1 presents ranges of values for the various scales of organized atmospheric motions. This table should be regarded only as approximate spatial and temporal magnitudes of typical motions characteristic of these scales, and not as any specific limits of these scales. As can be seen in this table, the smallest scale of motion involves the transfer of momentum via molecular-scale interactions. This scale of motion is extremely ineffective for momentum transport within the earth's atmosphere and can usually be neglected at all but the slowest wind speeds and/or extremely small portions of some boundary layers. The next larger scale is that of turbulent momentum transfer. Turbulence is the primary transfer mechanism for momentum passing from the atmosphere into the sea; consequently, it is of extreme importance to most scientists and engineers. The next larger scale is that of organized convective motions. These motions are responsible for individual thunderstorm cells, usually associated with unstable air masses.

Table II-2-1
Ranges of Values for the Various Scales of Organized Atmospheric Motions

Transfer Mechanism	Typical Length Scale, meters	Typical Time Scale, sec
Molecular	10^{-7} - 10^{-2}	10^{-1}
Turbulent	10^{-2} - 10^{3}	10^{1}
Convective	10^{3} - 10^{4}	10^{3}
Meso-scale	10^{4} - 10^{5}	10^{4}
Synoptic-scale	10^{5} - 10^{6}	10^{5}
Large	> 10^{6}	10^{6}

(b) The next larger scale is termed the meso-scale. Meso-scale motions such as land-sea breeze circulations, coastal fronts, and katabatic winds (winds caused by cold air flowing down slopes due to gravitational acceleration) are important components of winds in near-coastal areas. Important organized meso-scale motions also exist in frontal regions of extratropical storms, within the spiral bands of tropical storms, and within tropical cloud clusters. An important distinction between meso-scale motions and smaller-scale motions is the relative importance of Coriolis accelerations. In meso-scale motions, the lengths of trajectories are sufficient to allow Coriolis effects to become important, whereas the trajectory lengths at smaller scales are too small to allow for significant Coriolis effects. Consequently, the first signs of trajectory curvature are found in meso-scale motions. For example, the land-breeze/sea-breeze system in most coastal areas of the United States does not simply blow from sea to land during the day and from land to sea at night. Instead, the wind direction tends to rotate clockwise throughout the day, with the largest rotation rates occurring during the transition periods when one system gives way to the next.

(c) The next larger scale of atmospheric motion is termed the synoptic scale. To many engineers and scientists, the synoptic scale is synonymous with the term storm scale, since the major storms in ocean areas occupy this niche in the hierarchy of scales. Storms that originate outside of tropical areas (extratropical storms) take their energy from horizontal instabilities created by spatial gradients in air density. Storms originating in tropical regions gain their energy from vertical fluxes of sensible and latent heat. Both the extratropical (or frontal) storms and tropical storms form closed or semi-closed trajectory motions around their circulation centers, due to the importance of Coriolis effects at this scale.

(d) The next larger scale of atmospheric motions is termed large scale. This scale of motion is more strongly influenced by thermodynamic factors than by dynamic factors. Persistent surface temperature differentials over large regions of the globe produce motions that can persist for very long time periods. Examples of such phenomena are found in subtropical high pressure systems, which are found in all oceanic areas and in seasonal monsoonal circulations developed in certain regions of the world.

(e) Scales of motion larger than large scale can be termed interannual scale, and beyond that, climatic scale. El Ninõ Southern Oscillation (ENSO) episodes, variations in year-to-year weather, changes in storm

patterns and/or storm intensity, and long-term (secular) climatic variations are all examples of these longer-term scales of motion. The effects of these phenomena on engineering and planning considerations are very poorly understood at present. This is compounded by the fact that there does not even exist any real consensus among atmospheric scientists as to what mechanism or mechanisms control these variations. This may not diminish the importance of climatic variability but certainly detracts from the ability to treat it objectively. As better information is collected over longer time intervals, these scales of motion will be better understood.

(3) Temporal variability of wind speeds.

(a) Winds at any point on the earth represent a superposition of various atmospheric scales of motion, all interacting to produce local weather phenomena. Each scale plays a specific role in the transfer of momentum in the atmosphere. Due to the combination of different scales of motion, winds are rarely, if ever, constant for any prolonged interval of time. Because of this, it is important to recognize the averaging interval (explicit or implicit) of any data used in applications. For example, some winds represent "fastest mile" estimates, some winds represent averages over small, fixed time intervals (typically from 1 to 30 min), and some estimates (such as those derived from synoptic pressure fields) can even represent average winds over intervals of several hours. Design and planning considerations require different averages for different purposes. Individual gusts may contribute to the failure mode of some small structures or of certain structural elements on larger structures. For other structures, 1-min (or even longer) average wind speeds may be more related to critical structural forces.

(b) When dealing with wave generation in water bodies of differing sizes, different averaging intervals may also be appropriate. In small lakes and reservoirs or in riverine areas, a 1- to 5-min wind speed may be all that is required to attain a fetch-limited condition. In this case, the fastest 1- to 5-min wind speed will produce the largest waves, and thus be the appropriate choice for design and planning considerations. In large lakes and oceanic regions, the wave generation process tends to respond to average winds over a 15- to 30-min interval. Consequently, it is important in all applications to be aware of and use the proper averaging interval for all wind information.

(c) Figure II-2-1 shows the estimated ratio of winds of various durations to 1-hr average wind speeds. The proper application of Figure II-2-1 would be in converting extremal estimates of wind speeds from one averaging interval to another. For example, this graph shows that a 100-sec extreme wind speed is expected to be 1.2 times as high as a 1-hr extreme wind speed. This means that the highest average wind speed in 36 samples of 100-sec duration is expected to be 1.2 times higher than the average for all 36 samples added together.

(d) Occasionally, wind measurements are reported as fastest-mile wind speeds. The averaging time is the time required for the wind to travel a distance of 1 mile. The averaging time, which varies with wind speed, can be estimated from Figure II-2-2. Note that two axis are provided, for metric and English units.

(e) Figure II-2-3 shows the estimated time to achieve fetch-limited conditions as a function of wind speed and fetch length, based on the calculations of Resio and Vincent (1982). The proper averaging time for design and planning considerations varies dramatically as a function of these parameters. At first, it might not seem intuitive that the duration required to achieve fetch-limited conditions should be a function of wind speed; however, this comes about naturally due to the nonlinear coupling among waves in a wind-generated wave spectrum. The importance of nonlinear coupling is discussed further in the wave prediction section of this chapter. The examples are intended to illustrate the correct usage of figures and tables. Numerical values given in the solution of the examples were read from figures as approximate values or rounded off from the equations. Users need to use their own estimates and professional judgement when applying figures or equations to their particular engineering conditions or projects.

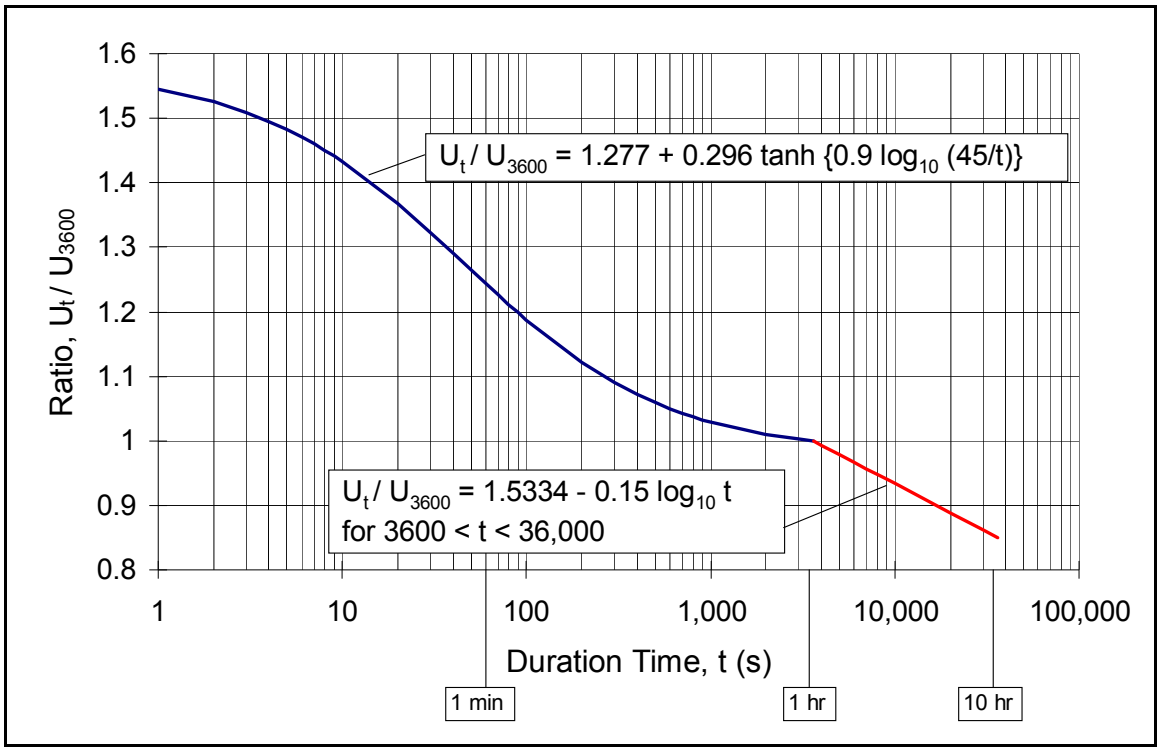

Figure II-2-1. Ratio of wind speed of any duration U_t to the 1-hr wind speed U_{3600}

EXAMPLE PROBLEM II-2-1

FIND:

1-hr average winds for wave prediction

GIVEN:

10-, 50-, and 100-year values of observed winds at a buoy located in the center of a large lake (U_{10} = 20.3 m/s, U_{50} = 24.8 m/s, U_{100} = 28.2 m/s). It is also known that the averaging interval for the buoy winds is 5 min.

SOLUTION:

Using Figure II-2-1, the ratio of the fastest 5-min wind speed to the average 1-hr wind speed is approximately 1.09. Using this as a constant conversion factor, the 10-, 50-, and 100-year, 1-hr wind speeds are estimated as U'_{10}=18.6 m/s, U'_{50}=22.8 m/s, and U'_{100}=25.9 m/s.

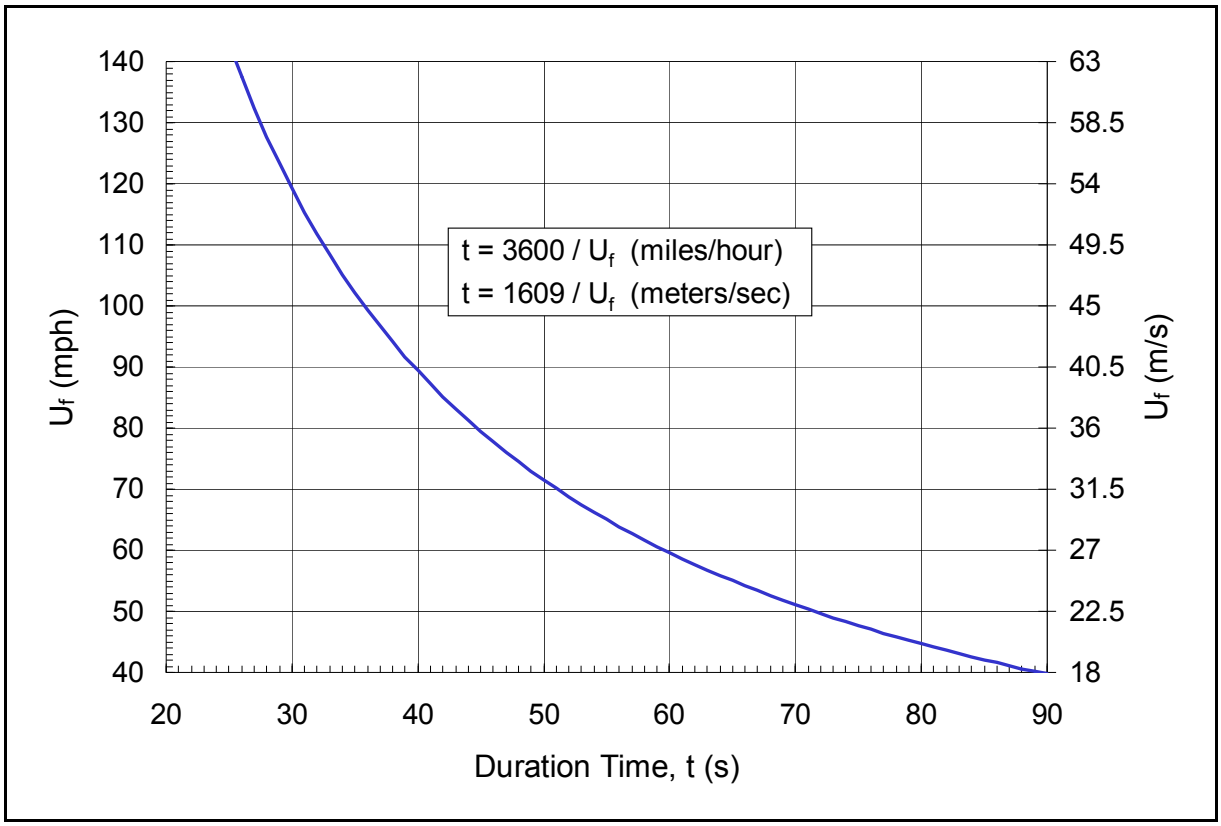

Figure II-2-2. Duration of the fastest-mile wind speed U_t as a function of wind speed (for open terrain conditions)

b. General structure of winds in the atmosphere.

(1) The earth's atmosphere extends to heights in excess of 100 km. Considerable layering in the vertical structure of the atmosphere occurs away from the earth's surface. The layering is primarily due to the absorption of specific bands of radiation in vertically localized regions. Absorbed radiation creates substantial warming in these regions which, in turn, produces inversion layers that inhibit local mixing. Processes essential to coastal engineering occur in the *troposphere*, which extends from the earth's surface up to an average altitude of 11 km. Most of the meteorological information used in estimating surface winds in marine areas falls within the troposphere. The lower portion of the troposphere is called the atmospheric or planetary boundary layer, within which winds are influenced by the presence of the earth's surface. The boundary layer typically reaches up to an altitude of 2 km or less.

(2) Figure II-2-4 shows an idealized relationship for an extended wind profile in a spatially homogeneous marine area (i.e. away from any land). The lowest portion is sometimes termed the constant stress layer, since there is essentially a constant flux of momentum through this layer. In this bottom layer, the time scale of momentum transfer is so short that there is little or no Coriolis effect; hence, the wind direction remains approximately constant. Above this layer is a region that is sometimes termed the Ekman layer. In this region, the influence of Coriolis becomes more pronounced and wind direction can vary significantly with

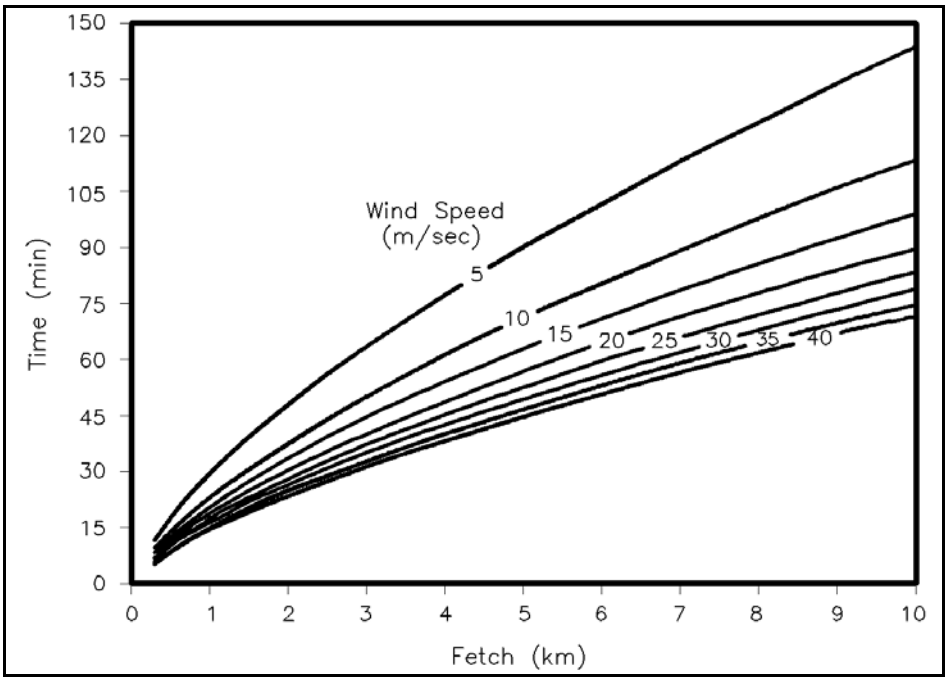

Figure II-2-3. Equivalent duration for wave generation as a function of fetch and wind speed

EXAMPLE PROBLEM II-2-2

FIND:

The appropriate 100-year wind speed for a basin with a fetch length of 10 km.

GIVEN:

A 100-year wind speed of 19.9 m/s, derived from 3-hr synoptic charts.

SOLUTION:

Figure II-2-3 requires knowledge of both wind speed and fetch distance; however, reasonable accuracy is gained by simply using the original wind speed and the appropriate fetch. In this case from Figure II-2-3, the appropriate wind-averaging interval is approximately 90 min. Using information from Figure II-2-1, the ratio of the highest 90-min wind speed to the highest 3-hr wind speed is given by the relationship

$$U_{5400}/U_{10800} = [-0.15 \log_{10}(5400)+1.5334]/[-0.15 \log_{10}(10800)+1.5334] = 0.9735/0.9284 = 1.048$$

Thus, the appropriate wind speed should be 1.048 times 19.9 m/sec, or 20.8 m/sec.

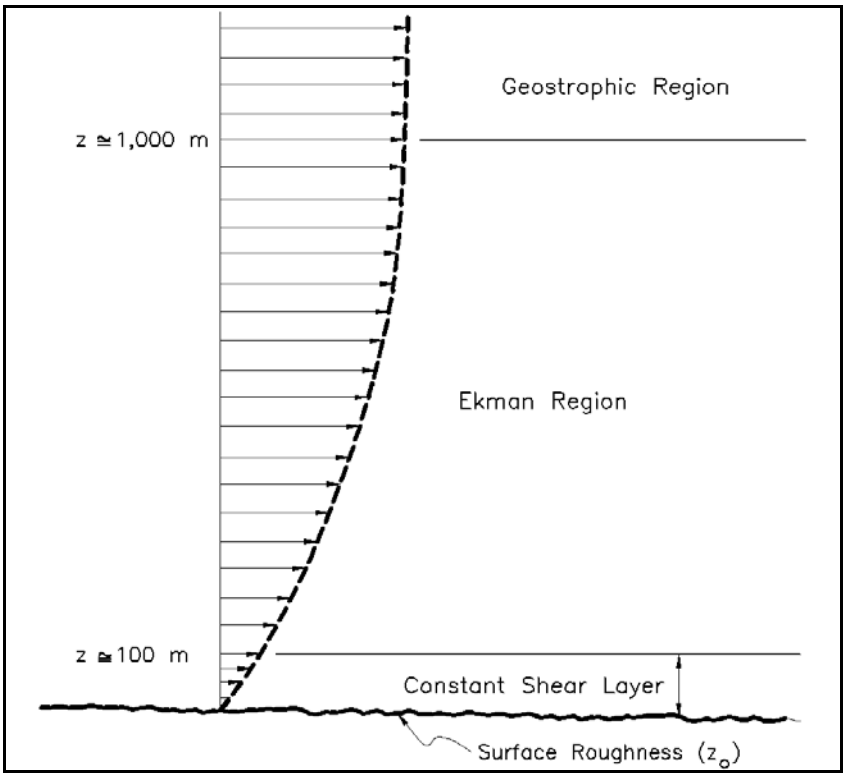

Figure II-2-4. Wind profile in atmospheric boundary layer

height. This results in wind directions at the top of the boundary layer which typically deviate about 10 to 15 deg to the right of near-surface wind directions over water and about 25 to 35 deg to the right of near-surface winds over land. Above the Ekman layer, the so-called geostrophic level is (asymptotically) approached. Winds in this level are assumed to be outside of the influence of the planetary surface; consequently, variations in winds above the Ekman layer are produced by different mechanisms than exist in the atmospheric boundary layer.

(3) Estimates of near-surface winds for wave prediction have historically been based primarily on two methods: direct interpolation/extrapolation/transformation of local near-surface measurements and transformation of surface winds from estimates of winds at the geostrophic level. The former method has mainly been applied to winds in coastal areas or to winds over large lakes. The latter method has been the main tool for estimating winds over large oceanic areas. A third method, termed "kinematic analysis" has received little attention in the engineering literature. All three of these methods will be discussed following a brief treatment of the general characteristics of winds within the atmospheric boundary layer.

c. Winds in coastal and marine areas.

(1) Background.

(a) Winds in marine and coastal areas are influenced by a wide range of factors operating at different space and time scales. Two potentially important local effects in the coastal zone, caused by the presence of land, are orographic effects and the sea breeze effect. Orographic effects are the deflection, channeling, or blocking of air flow by land forms such as mountains, cliffs, and high islands. A rule of thumb for blocking of low-level air flow perpendicular to a land barrier is given by the following:

$$\frac{U}{h_m} \begin{cases} < 0.1 \Rightarrow \textit{blocked} \\ > 0.1 \Rightarrow \textit{no blocking} \end{cases} \qquad \text{(II-2-2)}$$

where

1. U = wind speed

h_m = height of the land barrier (in units consistent with U)

(b) An elevation of only 100 m will cause blocking of wind speeds less than about 10m/s, which includes most onshore winds (Overland 1992). The horizontal scale of these effects is on the order of 50 - 150 km. Another orographic effect called katabatic wind is caused by gravitational flow of cold air off higher ground such as a mountain pass. Since katabatic winds require cold air they are more frequent and strongest in high latitudes. These winds can have a significant impact on local coastal areas and are very site-specific (horizontal scale on the order of 25 km).

(c) Another local process, the sea breeze effect, is air flow caused by the differences in surface temperature and heat flux between land and water. Land temperatures change on a daily cycle while water temperatures remain relatively constant. This results in a sea breeze with a diurnal cycle. The on/offshore extent of the sea breeze is about 10 -20 km with wind speeds less than 10 m/s.

(d) Although understanding of atmospheric flows in complicated areas is still somewhat limited, considerable progress has been made in understanding and quantifying flow characteristics in simple, idealized situations. In particular, synoptic-scale winds in open-water areas (more than 20 km or so from land) are known to follow relatively straightforward relationships within the atmospheric boundary layer. The flow can be considered as a horizontally homogeneous, near-equilibrium boundary layer regime. As described in Tennekes (1973), Wyngaard (1973,1988), and Holt and Raman (1988), present-day boundary layer parameterizations appear to provide a relatively accurate depiction of flows within the homogeneous, near-equilibrium atmospheric boundary layers. Since these boundary-layer parameterizations have a substantial basis in physics, it is recommended that they be used in preference of older, less-verified methods.

d. Characteristics of the atmospheric boundary layer.

(1) Since the 1960's, evidence from field and laboratory studies (Clarke 1970, Businger et al. 1971, Willis and Deardorff 1974, Smith 1988) and from theoretical arguments (Deardorff 1968, Tennekes 1973, Wyngaard 1973, 1988) have supported the existence of a self-similar flow regime within a homogeneous, near-equilibrium boundary layer in the atmosphere. In the absence of buoyancy effects (due to vertical gradients in potential temperature) and if no significant horizontal variations in density (baroclinic effects) exist, the atmospheric boundary layer can be considered as a neutral, barotropic flow. In this case, all flow characteristics can be shown to depend only on the speed of the flow at the upper edge of the boundary layer, roughness of the surface at the bottom of the boundary layer, and local latitude (because of the influence of the earth's rotation on the boundary-layer flow). Significantly for engineers and scientists, this theory predicts that wind speed at a fixed elevation above the surface cannot have a constant ratio of proportionality to wind speed at the top of the boundary layer.

(2) Deardorff (1968), Businger et al. (1971), and Wyngaard (1988) clearly established that flow characteristics within the atmospheric boundary layer are very much influenced by thermal stratification and horizontal density gradients (baroclinic effects). Thus, various relationships can exist between flows at the top of the boundary layer and near-surface flows. This additional level of complication is not negligible in many applications; therefore, stability effects should be included in wind estimates in important applications.

e. Characteristics of near-surface winds.

(1) Winds very close to a marine surface (within the constant-stress layer) generally follow some form of the "law-of-the-wall" for near-boundary flows. At wind speeds above about 5 m/s (at a 10-m reference level), turbulent transfers, rather than molecular processes, dominate air-sea interaction processes. Given a neutrally stable atmosphere, the wind speed close to the surface follows a logarithmic profile of the form

$$U_z = \frac{U_*}{k} \ln\left(\frac{z}{z_0}\right) \tag{II-2-3}$$

where

U_z = wind speed at height z above the surface

U_* = friction velocity

k = von Kármán's constant (approximately equal to 0.4)

z_0 = roughness height of the surface

(2) In this case, the rate of momentum transfer into a water column (of unit surface area) from the atmosphere can be written in the parametric form

$$\begin{aligned} \tau &= \rho_a U_*^2 \\ &= \rho_a C_{Dz} U_z^2 \end{aligned} \tag{II-2-4}$$

where

τ = wind stress

ρ_a = density of air

ρ_w = density of water

C_{Dz} = coefficient of drag for winds measured at level z

(3) The international standard reference height for winds is now taken to be 10 m above the surface. If winds are taken from this level, the z is usually dropped from the subscript notation and the momentum transfer is represented as

$$\tau = \rho_a C_D U^2 \tag{II-2-5}$$

where C_D specifically refers now to a 10-m reference level.

(4) Extensive evidence shows that the coefficient of drag over water depends on wind speed (Garratt 1977, Large and Pond 1981, Smith 1988).

(5) When surfaces (land or water) are significantly warmer or cooler than the overlying air, thermal stability effects tend to modify the logarithmic profile in Equation II-2-3. If the underlying surface is colder

than the air, the atmosphere becomes stably stratified and turbulent transfers are suppressed. If the surface is warmer than the air, the atmosphere becomes unstably stratified and turbulent transfers are enhanced. In this more general case, the form of the near-surface wind profile can be approximated as

$$U_z = \frac{U_*}{k}\left[\ln\left(\frac{z}{z_0}\right) - \phi\left(\frac{z}{L}\right)\right] \tag{II-2-6}$$

where

ϕ = universal similarity function characterizing the effects of thermal stratification

L = parameter with dimensions of length that represent the relative strength of thermal stratification effects (Obukov stability length)

(6) L is positive for stable stratification, negative for unstable stratification, and infinite for neutral stratification. Algebraic forms for ϕ and additional details on the specification of near-surface flow characteristics can be found in Resio and Vincent (1977), Hsu (1988), and the ACES Technical Reference (Leenhnecht, Szuwalski, and Sherlock 1992; Sec. 1-1).

(7) Transfer of momentum into water from the atmosphere can be markedly influenced by stability effects. For example, at the 10-m reference level, Equations II-2-4 through II-2-6 give

$$C_D = \left(\frac{U_*}{U}\right)^2 = \left[\frac{k}{\ln\left(\frac{z}{z_0}\right) - \phi\left(\frac{z}{L}\right)}\right]^2 \tag{II-2-7}$$

(8) The system of equations representing the boundary layer is readily solved via a number of numerical techniques. However, a relationship between z_0 and U_* must also be specified.

(9) Since ϕ is negative for stable conditions and positive for unstable conditions, stratification clearly reduces the coefficient of drag for stable conditions and increases the coefficient of drag for unstable conditions (Figure II-2-5). Consequently, for the same wind speed at a reference level, the momentum transfer rate is lower in a stable atmosphere than in an unstable atmosphere.

(10) Studies by Hsu (1974); Geernaert, Katsaros, and Richter (1986); Huang et al. (1986); Janssen (1989, 1991); and Geernaert (1990) suggest that the coefficient of drag depends not only on wind speed but also on the stage of wave development. The physical mechanism responsible for this appears to be related to the phase speed of the waves in the vicinity of the spectral peak relative to the wind speed. At present, there does not appear to be sufficient information to establish this behavior definitively. Future studies may shed more light on these effects and their importance to marine and coastal winds.

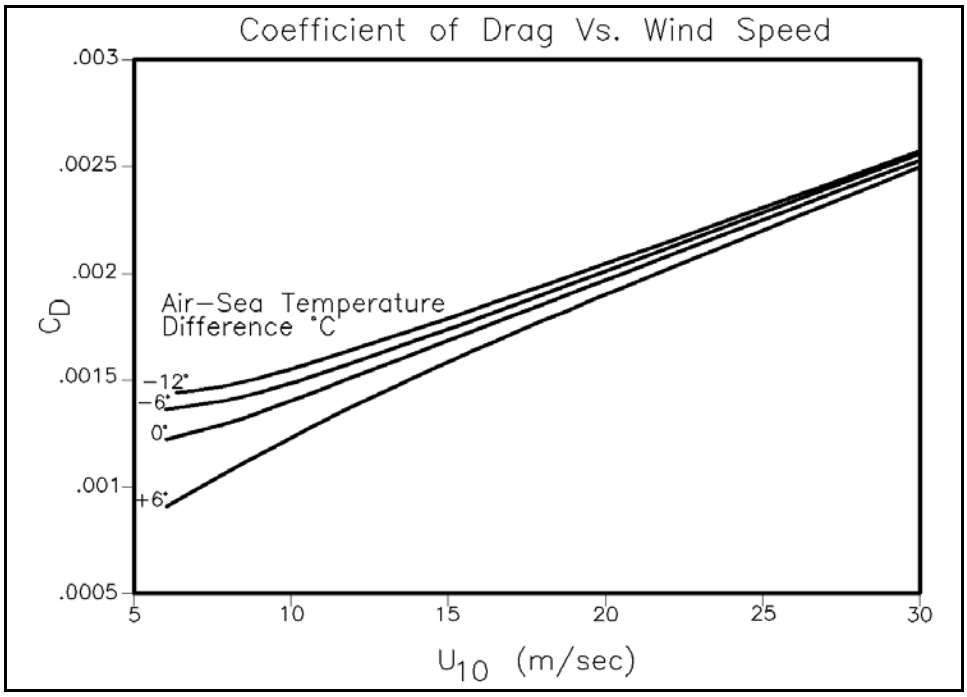

Figure II-2-5. Coefficient of drag versus wind speed

f. Estimating marine and coastal winds.

(1) Wind estimates based on near-surface observations. Three methods are commonly used to estimate surface marine wind fields. The first of these, estimation of winds from nearby measurements, has the appeal of simplicity and has been shown to work well for water bodies up through the size of the Great Lakes. To use this method, it is often necessary to transfer the measurements to different locations (e.g. from overland to overwater) and different elevations. Such complications necessitate consideration of the factors given below.

(a) Elevation correction of wind speed. Often winds taken from observations of opportunity (ships, oil rigs, offshore structures, buoys, aircraft, etc.) do not coincide with the standard 10-m reference level. They must be converted to the 10-m reference level for predicting waves, currents, surges, and other wind-generated phenomena. Failure to do so can produce extremely large errors. For the case of winds taken in near-neutral conditions at a level near the 10-m level (within the elevation range of about 8-12 m), the "1/7" rule can be applied. This simple approximation is given as

$$U_{10} = U_z\left(\frac{10}{z}\right)^{\frac{1}{7}} \tag{II-2-9}$$

where z is measured in meters.

(b) Elevation and stability corrections of wind speed. Figure II-2-6 provides a more comprehensive method to accomplish the above transformation, including both elevation and stability effects. The "1/7" rule is given as a special case. In Figure II-2-6, the ratio of the wind speed at any height to the wind speed

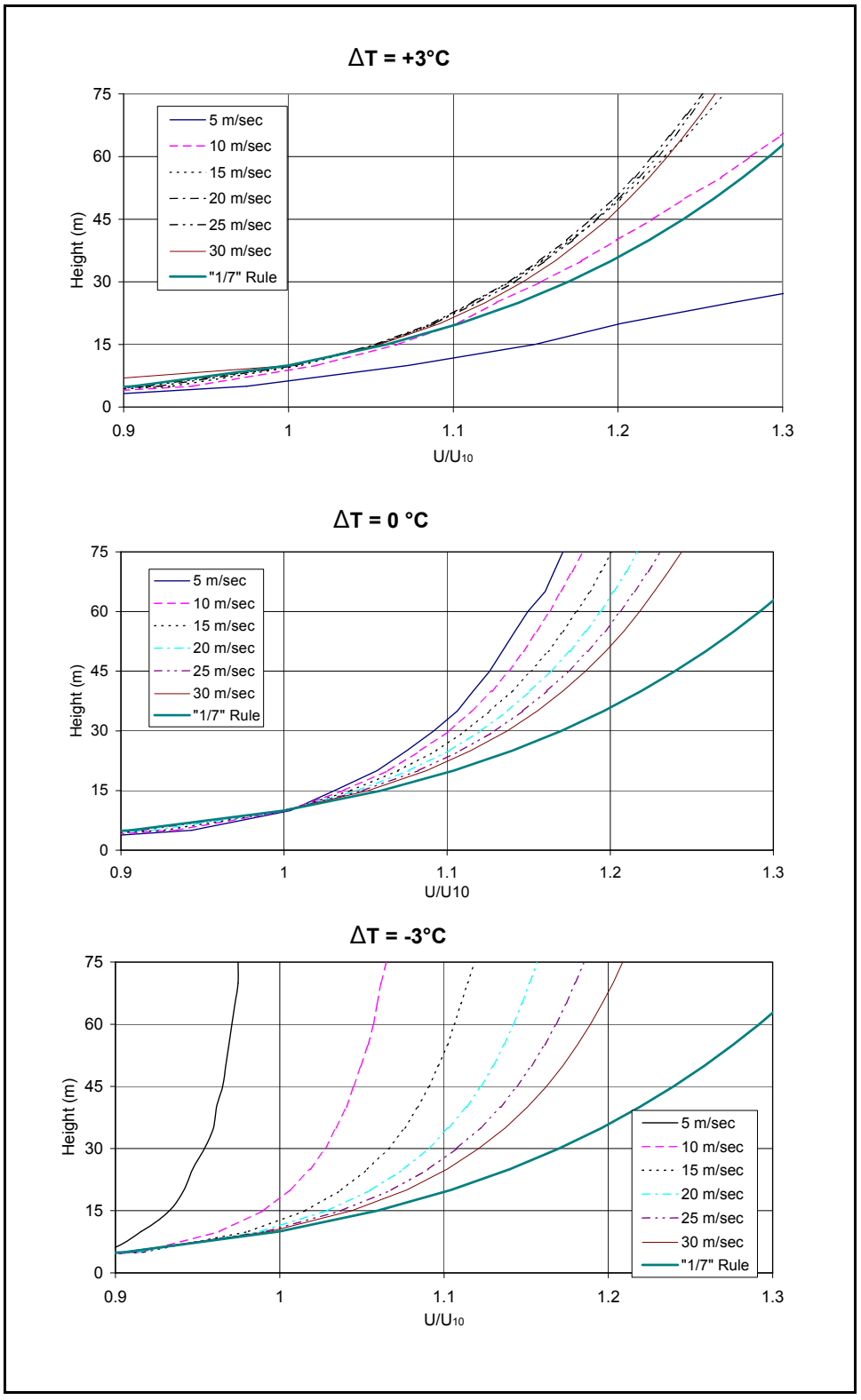

Figure II-2-6. Ratio of wind speed at any height to the wind speed at the 10-m height as a function of measurement height for selected values of air-sea temperature difference and wind speed: a) ΔT=+3°C; b) ΔT=0°C; c) ΔT=-3°C. Plots generated with following conditions: duration of observed and final wind = 3 hrs; latitude = 30° N; fetch = 42 km; wind observation type - over water; fetch conditions - deep open water

at the 10-m height is given as a function of measurement height for selected values of air-sea temperature difference and wind speed. Air-sea temperature difference is defined as

$$\Delta T = T_a - T_s \tag{II-2-9}$$

where

ΔT = air-sea temperature difference, in deg C

T_a = air temperature, in deg C

T_s = water temperature, in deg C

As can be seen in Figure II-2-6, the "1/7" rule should not be used as a general method for transforming wind speeds from one level to another in marine areas. The ACES software package (Leenhnecht, Szuwalski, and Sherlock 1992) contains algorithms, based on planetary boundary layer physics, which compute the values shown in Figure II-2-6; so it is recommended that ACES be used if at all possible for individual situations.

EXAMPLE PROBLEM II-2-3

FIND:
The estimated wind speed at a height of 10 m.

GIVEN:
The wind speed at a height of 25 m is 20 m/s and the air-sea temperature difference is +3°C.

SOLUTION:
From Figure II-2-6 (a), the ratio U/U_{10} is about 1.18 for a 20-m/s wind at a height of 25 m. So the estimated wind speed at a 10-m height U_{10} is equal to U at 25 m (20 m/s) divided by U/U_{10} (1.18), which gives U_{10} = 16.9 m/s.

(c) Simplified estimation of overwater wind speeds from land measurements. Due to the behavior of water roughness as a function of wind speed, the ratio of overwater winds at a fixed level to overland wind speeds at a fixed level is not constant, but varies nonlinearly as a function of wind speed. Figure II-2-7 provides guidance for the form of this variation. **The specific values shown in this figure are from a study of winds in the Great Lakes and care should be taken in applying them to other areas.** Figure II-2-8 indicates the expected variation with air-sea temperature difference (calculated with ACES). Although air-sea temperature difference can significantly affect light and moderate winds, it has only a small impact (5 percent or less) on high wind speeds typical of design. If at all possible, it is advisable to use locally collected data to respecify the exact form of Figures II-2-7 and II-2-8 for a particular project. One concern here would be the use of wind measurements from aboveground elevations that are markedly different from those used in the Resio and Vincent study (9.1 m or 30 ft).

(d) Wind speed variation with fetch. When winds pass over a discontinuity in roughness (e.g., a land-sea interface), an internal boundary layer is generated. The height of such a boundary layer forms a slope in the neighborhood of 1:30 in the downwind direction from the roughness discontinuity. This complication can make it difficult to use winds from certain locations at which winds from some directions fall within the

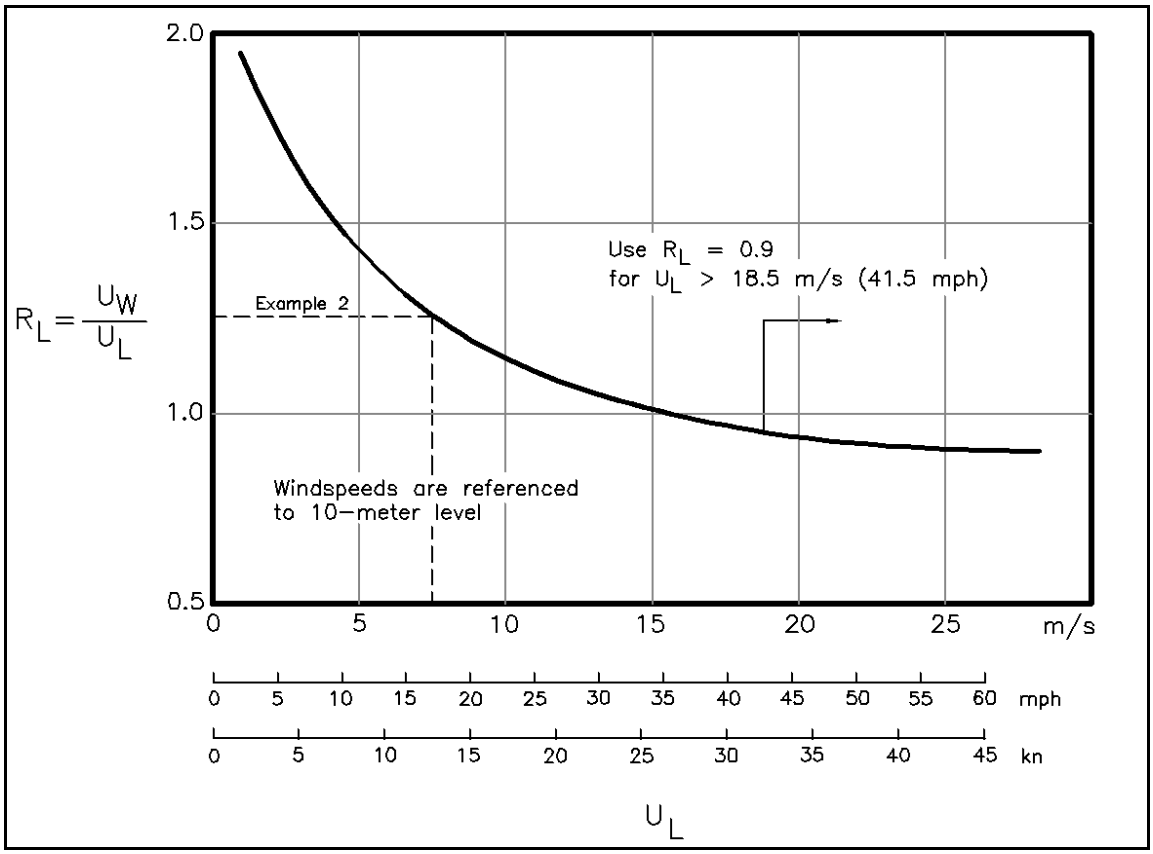

Figure II-2-7. Ratio R_L of windspeed over water U_W to windspeed over land U_L as a function of windspeed over land U_L (after Resio and Vincent (1977))

marine boundary layer and winds from other directions fall within a land boundary layer. In areas such as this, a land-to-sea transform (similar to that shown in Figures II-2-7 and II-2-8) can be used for all angles coming from the land. Depending on the distance to the water and the elevation of the measurement site, winds coming from the direction of open water may or may not still be representative of a marine boundary layer. Guidance for determining the effects of fetch on wind speed modifications can be found in Resio and Vincent (1977) and Smith (1983). These studies indicate that fetch effects wind speeds significantly only at locations within about 16 km (10 miles) of shore.

(e) Wind speed transition from land to water. The net effect of wind speed variation with fetch is to provide a smooth transition from the (generally lower) wind speed over land to the (generally higher) wind speed over water. Thus, wind speeds tend to increase with fetch over the first 10 miles or so after a transition from a land surface. The exact magnitude and characteristics of this transition depend on the roughness characteristics of the terrain and vegetation and on the stability of the air flow. A very simplistic approximation to this wind speed variation for the Resio and Vincent curves used here could be obtained by fitting a logarithmic curve to the asymptotic overland and overwater wind speed values. However, for most design and engineering purposes, it is probably adequate to simply use the long-fetch values with the recognition that they are somewhat conservative. The one situation that should cause some concern would be if overwater wind speed measurements are taken near the upwind end of a fetch. These winds could be considerably lower than wind speeds at the end of the fetch and underconservative values for wave conditions could result from the use of such (uncorrected) winds in a predictive scheme.

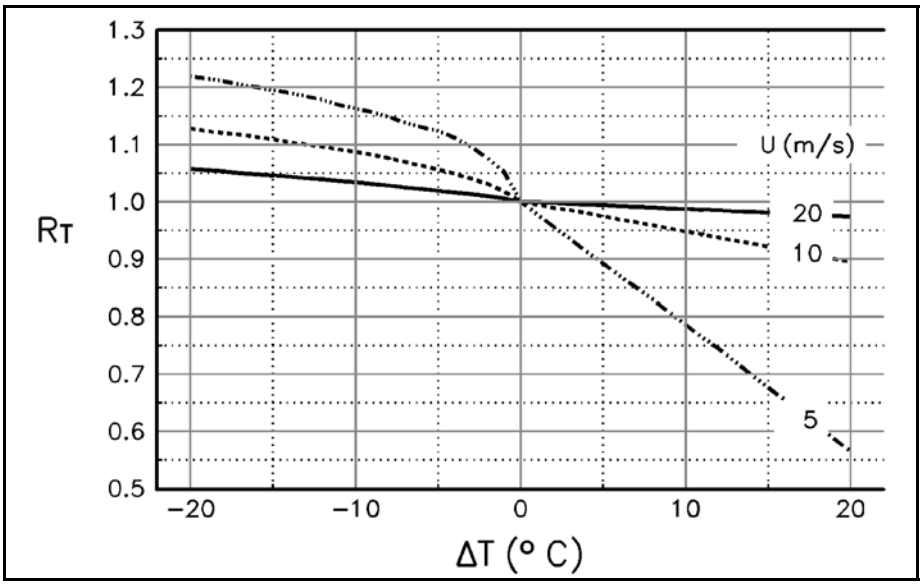

Figure II-2-8. Amplification R_T ratio of W_c (wind speed accounting for effects of air-sea temperature difference) to W_w (wind speed over water without temperature effects)

(f) Empirical relationship. A rough empirical relationship between overwater wind speeds and land measurements is discussed in Part III-4-2-b. This highly simplified relationship is based on several restrictive assumptions including land measurements over flat, open terrain near the coast; and wind direction is within 45 deg of shore-normal. The approach may be helpful where wind measurements are available over both land and sea at a site, but the specific relationship of Equation III-4-12 is not recommended for general hydrodynamic applications.

(2) Wind estimates based on information from pressure fields and weather maps. A primary driving force of synoptic-scale winds above the boundary layer is produced by horizontal pressure gradients. Figure II-2-9 is a simplified surface chart for the north Pacific Ocean. The area labeled L in the right center of the chart and the area labeled H in the lower left corner of the chart are low- and high-pressure areas. The pressures increase moving outward from L (isobars 972, 975, etc.) and decrease moving outward from H (isobars 1026, 1023, etc.). Synoptic-scale winds at latitudes above about 20 deg tend to blow parallel to the isobars, with the magnitude of the wind speed being inversely proportional to the spacing between the isobars. Scattered about the chart are small arrow shafts with a varying number of feathers. The direction of a shaft shows the direction of the wind, with each one-half feather representing a unit of 5 kt (2.5 m/s) in wind speed.

(a) Figure II-2-10 shows a sequence of weather maps with isobars (lines of equal pressure) for the Halloween Storm of 1991. An intense extratropical storm (extratropical cyclone) is located off the coast of Nova Scotia. Other information available on this weather map besides observed wind speeds and directions includes air temperatures, cloud cover, precipitation, and many other parameters that may be of interest. Figure II-2-11 provides a key to decode the information.

(b) Historical pressure charts are available for many oceanic areas back to the end of the 1800's. This is a valuable source of wind information when the pressure fields and available wind observations can be used to create marine wind fields. However, the approach for linking pressure fields to winds can be complex, as discussed in the following paragraphs.

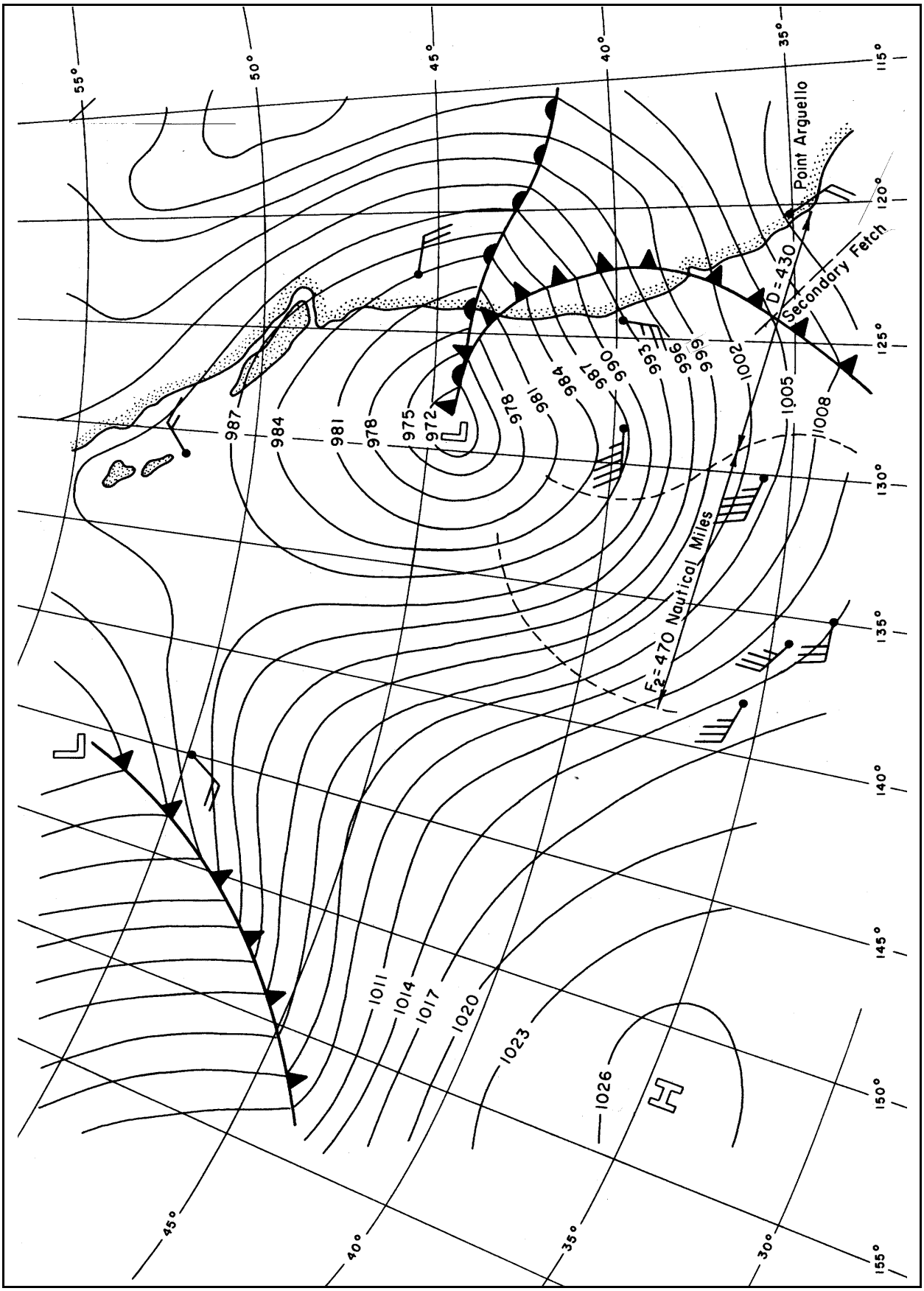

Figure II-2-9. Surface synoptic chart for 0030Z, 27 October 1950

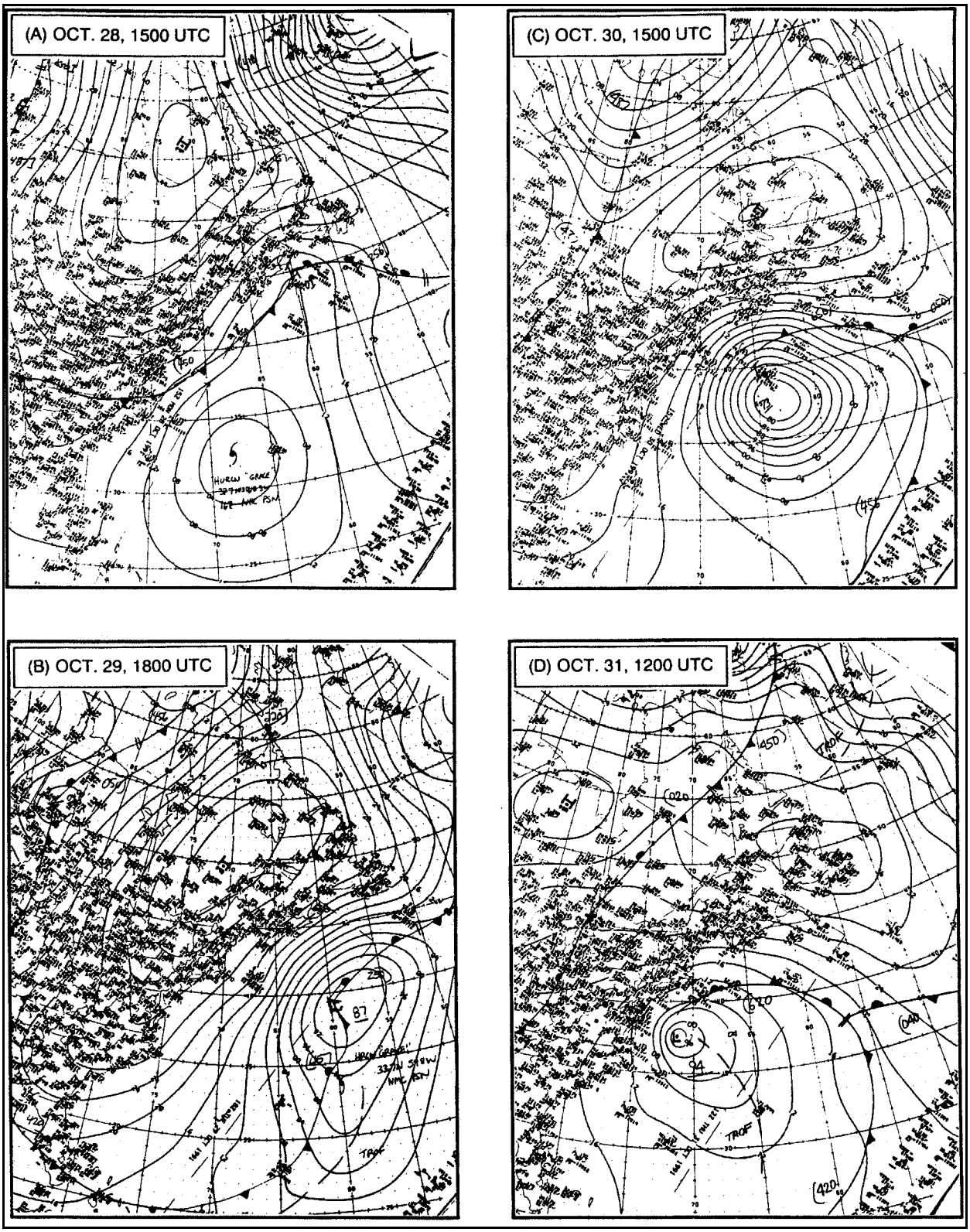

Figure II-2-10. Surface synoptic weather charts for the Halloween storm of 1991

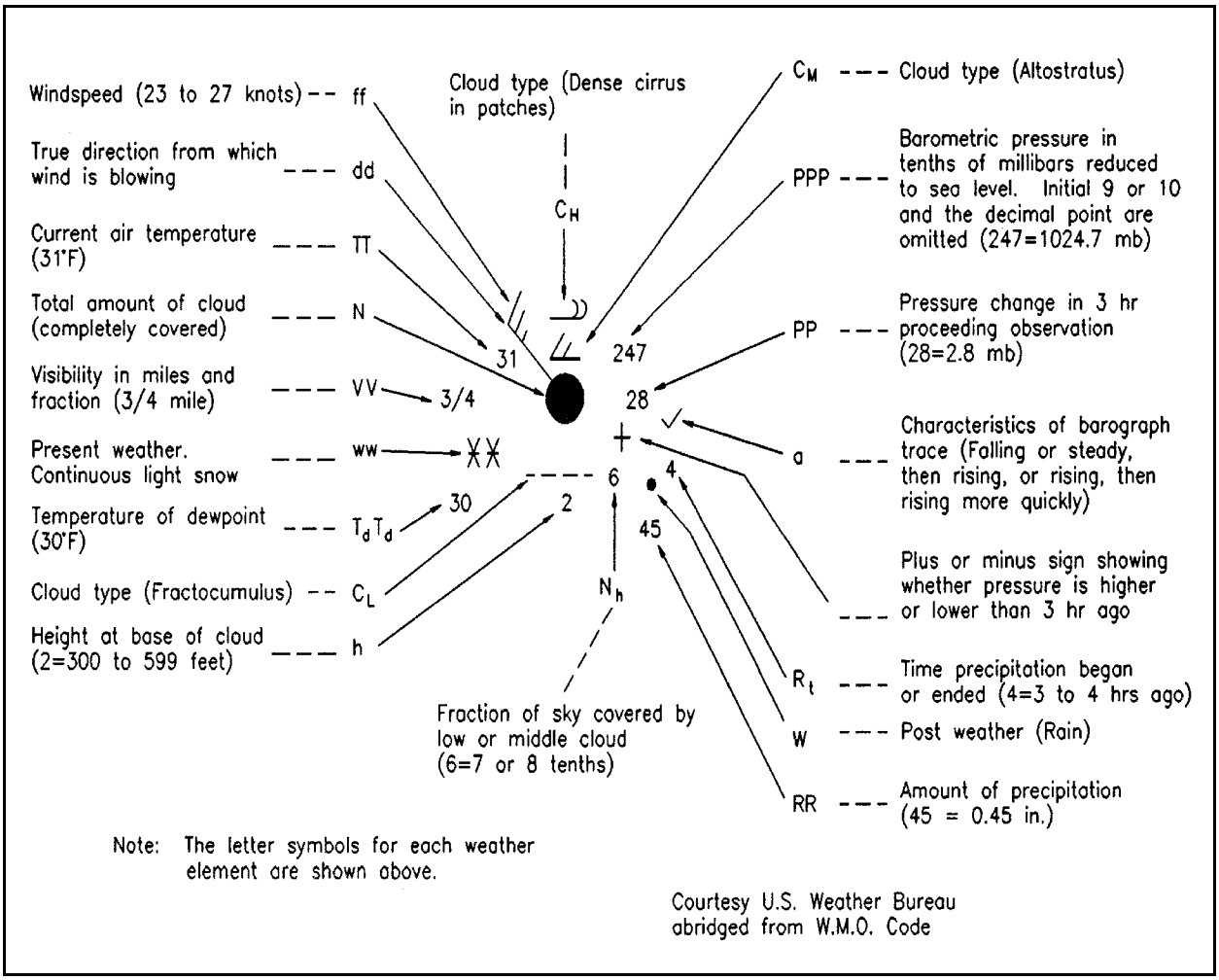

Figure II-2-11. Key to plotted weather report

EXAMPLE PROBLEM II-2-4

FIND:

The estimated overwater wind speed at a site over 10 miles from shore, given that the air-sea temperature difference is near zero ($\Delta T \approx 0$).

GIVEN:

A wind speed of 7.5 m/s at an airport location well inland (at the airport standard of 30 ft above ground elevation).

SOLUTION:

From Figure II-2-7 the ratio of overwater wind to overland wind is about 1.25. In the absence of information to calibrate a local relationship, multiply the 7.5-m/s wind speed by 1.25 to obtain an estimated overwater wind speed of 9.4 m/s. It should be recognized that the 90-percent confidence interval for this estimate is approximately 15 percent. It may be desirable to include this factor of conservatism in some calculations. However, at this short fetch, there is already conservatism due to the lack of consideration of wind speed variations with fetch.

(c) Synoptic-scale winds in nonequatorial regions are usually close to a geostrophic balance, given that the isobars are nearly straight (i.e. the radius of curvature is large). For this balance to be valid, the flow must be steady state or very nearly steady state. Furthermore, frictional effects, advective effects, and horizontal and vertical mixing must all be negligible. In this case, the Navier-Stokes equation for atmospheric motions reduces to the geostrophic balance equation given by

$$U_g = \frac{1}{\rho_a f}\frac{dp}{dn} \tag{II-2-10}$$

where

U_g = geostrophic wind speed (located at the top of the atmospheric boundary layer)

dp/dn = gradient of atmospheric pressure orthogonal to the isobars

Wind direction at the geostrophic level is taken to be parallel to the local isobars. Hence, purely geostrophic winds in a large storm would move around the center of circulation, without converging on or diverging from the center.

(d) Figure II-2-12 may be used for simple estimates of geostrophic wind speed. The distance between isobars on a chart is measured in degrees of latitude (an average spacing over a fetch is ordinarily used), and the latitude position of the fetch is determined. Using the spacing as ordinate and location as abscissa, the plotted, or interpolated, slant line at the intersection of these two values gives the geostrophic wind speed. For example, in Figure II-2-9, a chart with 3-mb isobar spacing, the average isobar spacing (measured normal to the isobars) over fetch F_2 located at 37 deg N. latitude, is 0.70 deg latitude. Scales on the bottom and left side of Figure II-2-12 are used to find a geostrophic wind of 34.5 m/s (67 kt).

(e) If isobars exhibit significant curvature, centrifugal effects can become comparable or larger than Coriolis accelerations. In this situation, a simple geostrophic balance must be replaced by the more general gradient balance. The equation for this motion is

$$U_{gr} = \frac{1}{\rho_a f}\frac{dp}{dn} + \frac{U_{gr}^2}{f r_c} \tag{II-2-11}$$

where

U_{gr} = gradient wind speed

r_c = radius of curvature of the isobars

Winds near the centers of small extratropical storms and most tropical storms can be significantly affected and even at times dominated by centrifugal effects, so the more general gradient wind approximation is usually preferred to the geostrophic approximation. Gradient winds tend to form a small convergent angle (about 5^o to 10^o) relative to the isobars.

(f) An additional complication results when the center of a storm is not stationary. In this case, the steady-state approximation used in both the geostrophic and gradient approximations must be modified to include non-steady-state effects. The additional wind component due to the changing pressure fields is

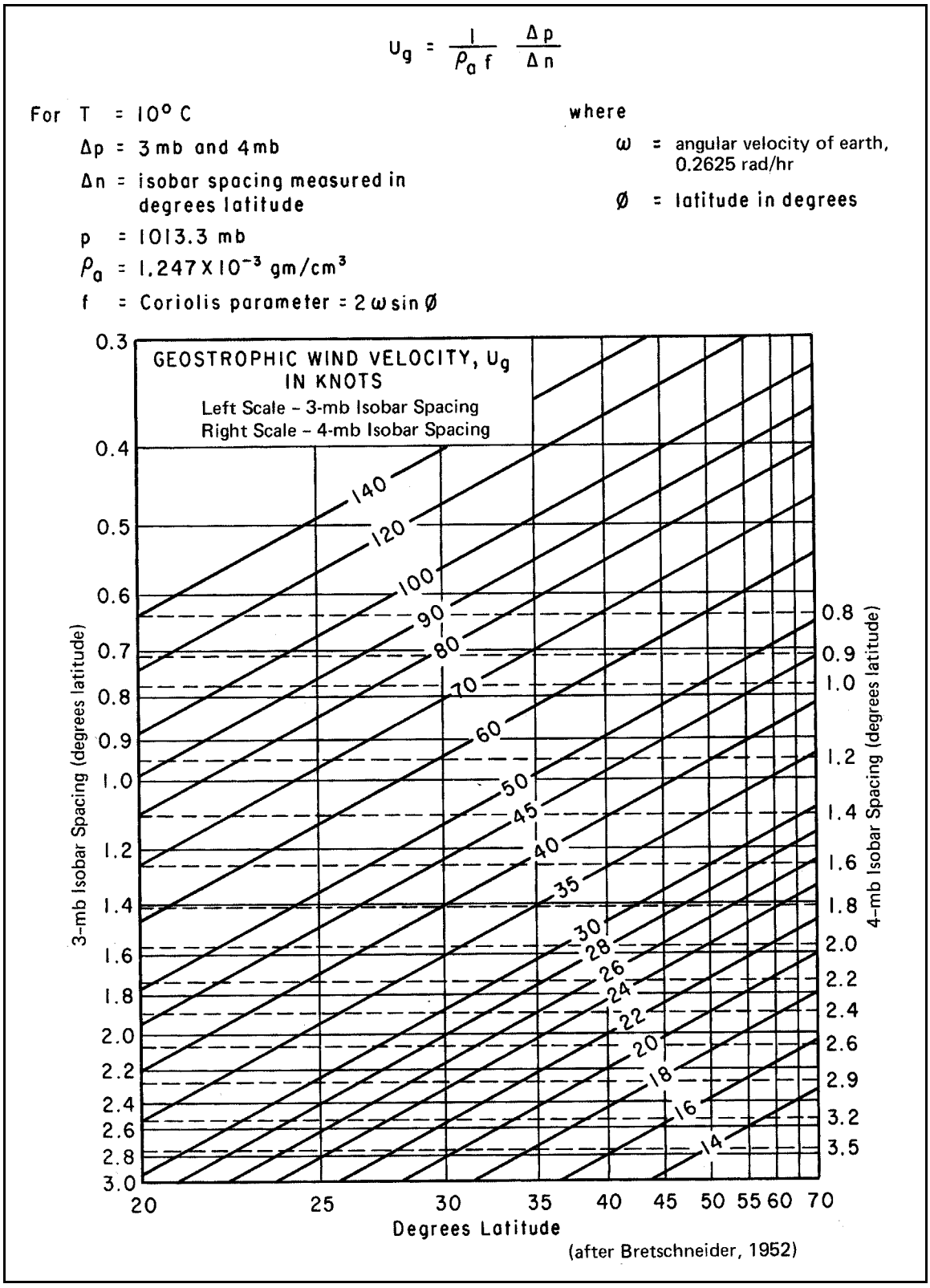

Figure II-2-12. Geostrophic (free air) wind scale (after Bretschneider (1952))

termed the isallobaric wind. In certain situations, the isallobaric wind can attain magnitudes nearly equal to those of geostrophic wind.

(g) Due to the factors discussed above, winds at the geostrophic level can be quite complicated. Therefore, it is recommended that these calculations be performed with numerical computer codes rather than manual methods.

(h) Once the wind vector is estimated at a level above the surface boundary layer, it is necessary to relate this wind estimate to wind conditions at the 10-m reference level. In some past studies, a constant proportionality was assumed between the wind speeds aloft and the 10-m wind speeds. Whereas this might suffice for a narrow range of wind speeds if the atmospheric boundary layer were near neutral and no horizontal temperature gradients existed, it is not a very accurate representation of the actual relationship between surface winds and winds aloft. Use of a single constant of proportionality to convert wind speeds at the top of the boundary layer to 10-m wind speeds is not recommended.

(i) Over land, the height of the atmospheric boundary layer is usually controlled by a low-level inversion layer. This is typically not the case in marine areas where, in general, the height of boundary layer (in non-equatorial regions) is a function of the friction velocity at the surface and the Coriolis parameter, i.e.

$$h \approx \lambda \frac{U_*}{f} \tag{II-2-12}$$

where

λ = dimensionless constant

(j) Researchers have shown that, within the boundary layer, the wind profile depends on latitude (via the Coriolis parameter), surface roughness, geostrophic/gradient wind velocity, and density gradients in the vertical (stability effects) and horizontal (baroclinic effects). Over large water bodies, if the effects of wave development on surface roughness are neglected, the boundary-layer problem can be solved directly from specification of these factors. Figure II-2-13 shows the ratio of the wind at a 10-m level to the wind speed at the top of the boundary layer (denoted by the general term U_g here) as a function of wind speed at the top of the boundary layer, for selected values of air-sea temperature difference. Figure II-2-14 shows the ratio of friction velocity at the water's surface to the wind speed at the upper edge of the boundary layer as a function of these same parameters. It might be noted from Figure II-2-14 that a simple approximation for U_* in neutral stratification as a function of U_g is given by

$$U_* \approx 0.0275\ U_g \tag{II-2-13}$$

This approximation is accurate within 10 percent for the entire range of values shown in Figure II-2-14.

(k) Measured wind directions are generally expressed in terms of azimuth angle from which winds come. This convention is known as a *meteorological coordinate system*. Sometimes (particularly in relation to winds calculated from synoptic information), a mathematical vector coordinate or *Cartesian coordinate system* is used (Figure II-2-15). Conversion from the vector Cartesian to meteorological convention is accomplished by

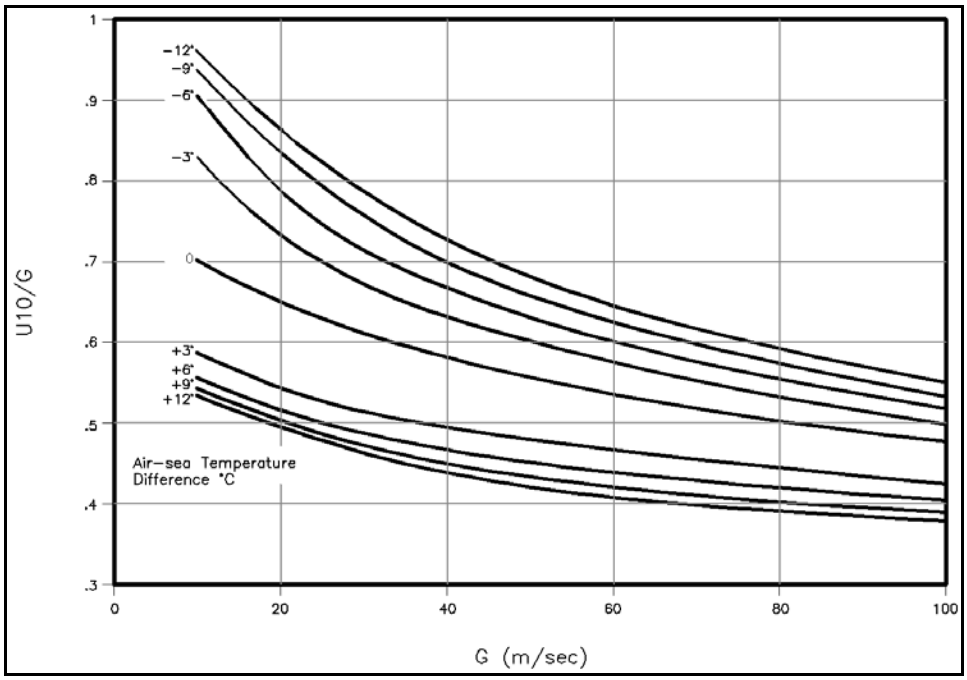

Figure II-2-13. Ratio of wind speed at a 10-m level to wind speed at the top of the boundary layer as a function of wind speed at the top of the boundary layer, for selected values of air-sea temperature difference

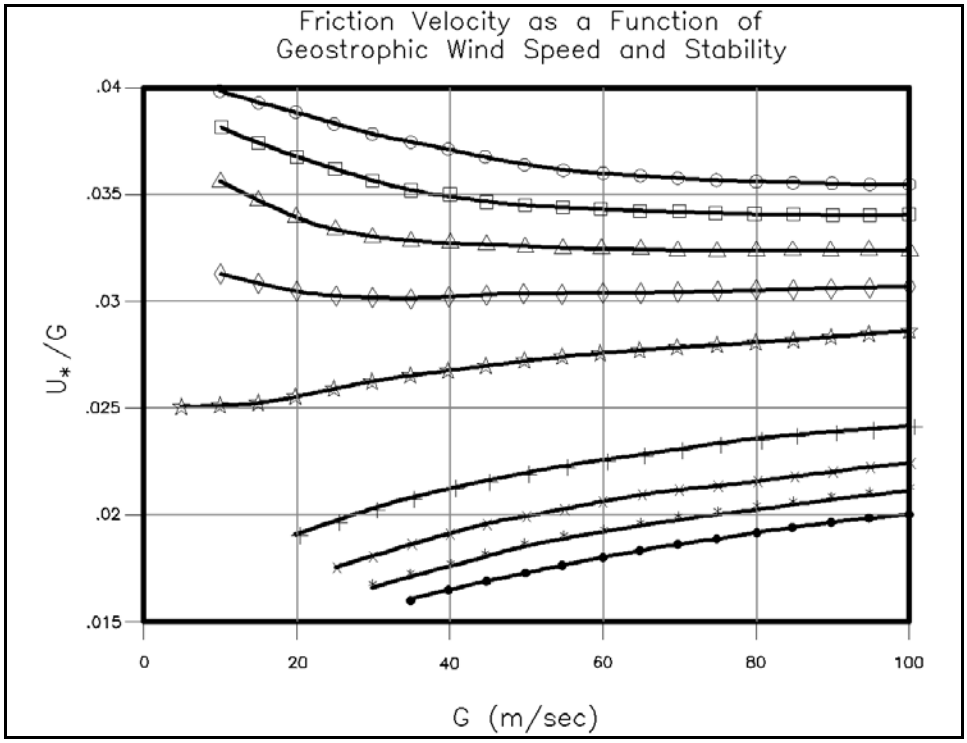

Figure II-2-14. Ratio of U*/Ug as a function of Ug for selected values of air-sea temperature difference

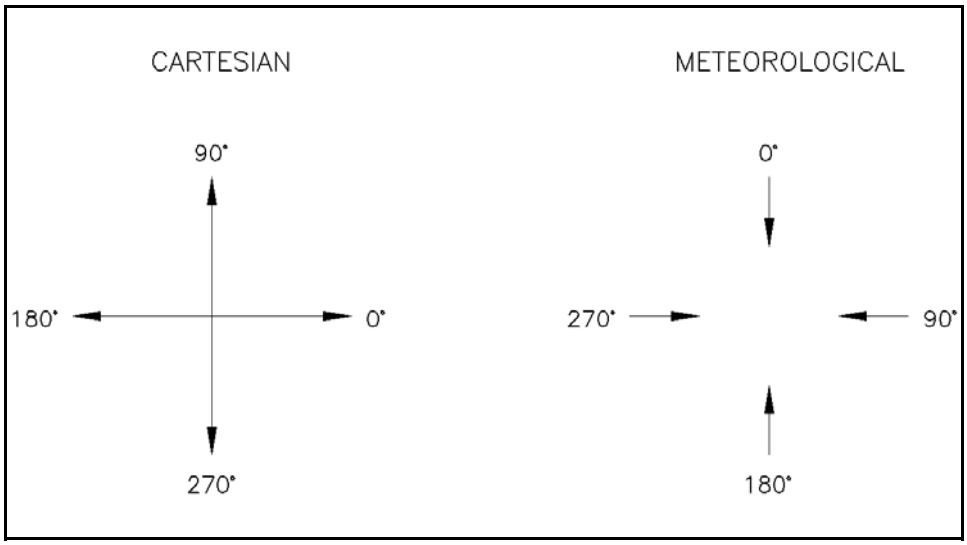

Figure II-2-15. Common wind direction conventions

$$\theta_{met} = 270 - \theta_{vec} \quad \text{(II-2-14)}$$

where

θ_{met} = direction in standard meteorological terms

θ_{vec} = direction in a Cartesian coordinate system with the zero angle wind blowing toward the east

(l) Wind estimates based on kinematic analyses of wind fields. In several careful studies, it has been shown that one method of obtaining very accurate wind fields is through the application of "kinematic analysis" (Cardone 1992). In this technique, a trained meteorological analyst uses available information from weather charts and other sources to construct detailed pressure fields and frontal positions. Using concepts of continuity along with this information, the analyst then constructs streamlines and isotachs over the entire analysis region. Unfortunately, this procedure is very labor-intensive; consequently, most analysts combine kinematic analyses of small subregions within their region with numerical estimates over the entire region. This method is sometimes referred to as a man-machine mix.

g. Meteorological systems and characteristic waves. Many engineers and scientists working in marine areas do not have a firm understanding of wave conditions expected from different wind systems. Such an understanding is helpful not only for improving confidence in design conditions, but also for establishing guidelines for day-to-day operations. Two problems that can arise directly from this lack of experience are (1) specification of design conditions with a major meteorological component missing, and 2) underestimation of the wave generation potential of particular situations. An example of the former situation might be the neglect of extratropical waves in an area believed to be dominated by tropical storms. For example, in the southern part of the Bay of Campeche along the coast of Mexico, one might expect that hurricanes dominate the extreme wave climate. However, outbursts of cold air termed "northers" actually contribute to and even control some of the extreme wave climate in this region. An example of the second situation can be found in decisions to operate a boat or ship in a region where storm waves can endanger life and property. Table II-2-2 assists users of this manual in understanding such problems. Potentially threatening wind and wave conditions from various scales of the meteorological system are categorized.

EXAMPLE PROBLEM II-2-5

FIND:

The 10-m wind speed, the wind direction, and the coefficient of drag.

GIVEN:

A pressure gradient of 5 mb in 100 km, an air-sea temperature difference of -5° C (i.e. the water is warmer than the air, as is typical in autumn months), the latitude of the location of interest (equal to 45° N), and the geographic orientation of the isobars.

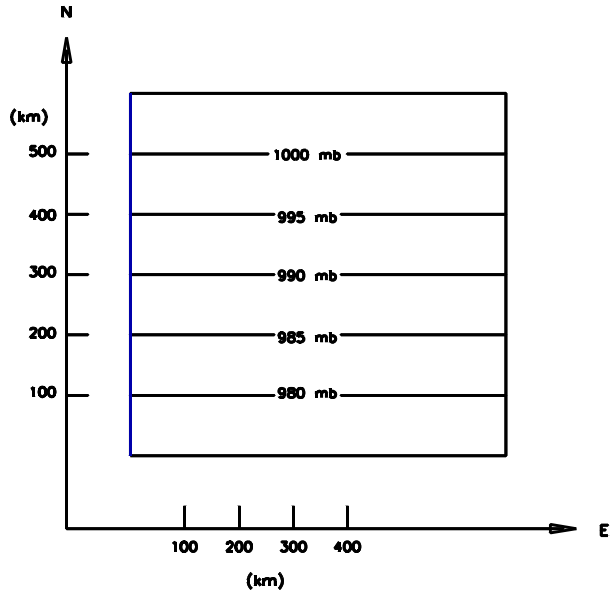

SOLUTION:

Option 1 - From Equation II-2-10, wind speed is calculated (in cgs units) as

$U_g = 1/(1.2\text{x}10^{-3} \text{ x } 1.03\text{x}10^{-4}) \text{ x } (dp/dn)$ (a)

$= 1/1.236\text{x}10^{-7} \text{ x } (5 \text{ x } \underline{1000}\ )/(100 \text{ x } 100000)$ (b)

$= 4045$ cm/sec (c)

$= 40.45$ m/sec

The $1.2\text{x}10^{-3}$ factor in step (a) is air density in g/cm^3.

The underlined 1000 factor in step (b) converts mb to dynes/cm^2. The 100000 factor in step (b) converts km to cm. From U_g and ΔT and Figure II-2-13

$U_{10}/U_g = 0.68$ and $U_{10} = U_g \text{ x } U_{10}/U_g = 40.45 \text{ x } 0.68 = 27.5$ m/s

From Figure II-2-5

$C_D = 0.0024$

Wind Direction: Parallel to isobars, counterclockwise circulation around low, therefore the direction is west

Option 2 - Use Figure II-2-12, though it requires pressure gradient information in a different form than given in this example.

Table II-2-2
Local Seas Generated by Various Meteorological Phenomena

Type of Wind System	Wave Characteristics	Characteristic Height and Period
Individual thunderstorm No significant horizontal rotation. Size, 1-10 km	Very steep waves. Waves can become relatively large if storm speed and group velocity of spectral peak are nearly equal. Can be a threat to some operations in open-ocean, coastal, and inland waters.	H 0.5 - 1.5 m T 1.5 - 3 sec
Supercell thunderstorms Begins to exhibit some rotation. Size, 5-20 km	Very steep waves. Waves can become relatively large if storm speed and group velocity of spectral peak are nearly equal. Can pose a serious threat to some operations in open-ocean, coastal, and inland waters.	H 2 - 3 m T 3 - 6 sec
Sea breeze Thermally driven near-coast winds. Size, 10-100 km	Waves of intermediate steepness. Can modify local wave conditions when superposed on synoptic systems. Can affect some coastal operations.	H 0.5 - 1.5 m T 3 - 5 sec
Coastal fronts Results from juxtaposition of cold air and warm water. Size, 10 km across and 100 km long	Can modify local wave conditions near coasts. Minimal effects on wave conditions due to orientation of winds and fetches.	H 0.5 - 1.0 m T 3 - 4 sec
Lee waves “Spin-off” eddies due to interactions between synoptic winds and coastal topography Size, 10's of km	Generates waves that can deviate significantly in direction from synoptic conditions. Can affect coastal wave climates.	H 0.5 - 1.5 m T 2 - 5 sec
Frontal squall lines Organized lines of thunderstorms moving within a frontal area. Size, 100's of km long and 10 km across	Can create severe hazards to coastal and offshore operations. Can generate extreme wave conditions for inland waters. Waves can become quite large if frontal area becomes stationary or if rate of frontal movement matches wave velocity of spectral peak. Can create significant addition to existing synoptic-scale waves.	H 1 - 5 m T 4 - 7 sec

(Sheet 1 of 3)

Table II-2-2 (Continued)

Mesoscale Convective Complex (MCC) Large, almost circular system of thunderstorms with rotation around a central point (2-3 form in the U.S. per year). Size, 100-400 km in diameter	Important in interior regions of U.S. Can generate extreme waves for short-fetch and intermediate-fetch inland areas.	H fetch-limited T fetch-limited U ≈ 20 m/s
Tropical depression Weakly circulating tropical system with winds under 45 mph.	Squall lines superposed on background winds can produce confused, steep waves.	H 1 - 4 m T 4 - 8 sec
Tropical storm Circulating tropical system with winds over 45 mph and less than 75 mph.	Very steep seas. Highest waves in squall lines.	H 5 - 8 m T 5 - 9 sec
Hurricane Intense circulating storm of tropical origin with wind speeds over 75 mph. Shape is usually roughly circular.	Can produce large wave heights. Directions near storm center are very short-crested and confused. Highest waves are typically found in the right rear quadrant of a storm. Wave conditions are primarily affected by storm intensity, size, and forward speed, and in weaker storms by interactions with other synoptic scale and large-scale features.	Saffir Simpson Hurricane Scale SS H(m) T(sec) 1 4-8 7-11 2 6-10 9-12 3 8-12 11-13 4 10-14 12-15 5 12-17 13-17 (see Table IV-1-4)
Extratropical cyclones Low pressure system formed outside of tropics. Shapes are variable for weak and moderate strength storms, with intense storms tending to be elliptical or circular.	Extreme waves in most open-ocean areas north of 35° are produced by these systems. Large waves tend to lie in region of storm with winds parallel to direction of storm movement. Predominant source of swell for most U.S. east coast and west coast areas.	Weak: H 3-5m T 5-10 sec Moderate: H 5-8m T 9-13 sec Intense: H 8-12m T 12-17sec Extreme: H 13-18m T 15-20sec
Migratory highs Slowly moving high-pressure systems.	Produce moderate storm conditions along U.S. east coast south of 30° latitude when pressure gradients become steep.	H 1 - 4 m T 4 - 10 sec
Stationary highs Permanent systems located in subtropical ocean areas. Southern portions constitute the trade winds.	Produce low swell-like waves due to long fetches. Can interact with synoptic-scale and large-scale weather systems to produce moderately intense wave generation. Very persistent wave regime.	H 1 - 3 m T 5 - 10 sec

(Sheet 2 of 3)

Table II-2-2 (Concluded)

Monsoonal winds Biannual outbursts of air from continental land masses.	Episodic wave generation can generate large wave conditions. Very important in the Indian Ocean, part of the Gulf of Mexico, and some U.S. east coast areas.	H 4 - 7 m T 6 - 11 sec
Long-wave generation	Long waves can be generated by moving pressure/wind anomalies (such as can be associated with fronts and squall lines) and can resonate with long waves if the speed of frontal or squall line motion is approximately $\sqrt{g\,d}$. Examples of this phenomenon have been linked to inundations of piers and beach areas in Lake Michigan and Daytona Beach in recent years.	
Gap winds Wind acceleration due to local topographic funneling.	These winds may be extremely important in generating waves in many U.S. west coast areas not exposed to open-ocean waves.	U ≈ 40 m/s

(Sheet 3 of 3)

h. Winds in hurricanes.

(1) In tropical and in some subtropical areas, organized cloud clusters form in response to perturbations in the regional flow. If a cloud cluster forms in an area sufficiently removed from the Equator, then Coriolis accelerations are not negligible and an organized, closed circulation can form. A tropical system with a developed circulation but with wind speeds less than 17.4 m/s (39 mph) is termed a tropical depression. Given that conditions are favorable for continued development (basically warm surface waters, little or no wind shear, and a high pressure area aloft), this circulation can intensify to the point where sustained wind speeds exceed 17.4 m/s, at which time it is termed a tropical storm. If development continues to the point where the maximum sustained wind speed equals or exceeds 33.5 m/s (75 mph), the storm is termed a hurricane. If such a storm forms west of the international date line, it is called a typhoon. In this section, the generic term hurricane includes hurricanes and typhoons, since the primary distinction between them is their point of origin. Tropical storms will also follow some of the wind models given in this section, but since these storms are weaker, they tend to be more poorly organized.

(2) Although it might be theoretically feasible to model a hurricane with a primitive equation approach (i.e. to solve the coupled dynamic and thermodynamic equations directly), information to drive such a model is generally lacking and the roles of all of the interacting elements within a hurricane are not well-known. Consequently, practical hurricane wind models for most applications are driven by a set of parameters that characterize the size, shape, rate of movement, and intensity of the storm, along with some parametric representation of the large-scale flow in which the hurricane is imbedded. Myers (1954); Collins and Viehmann (1971); Schwerdt, Ho, and Watkins (1979); Holland (1980); and Bretschneider (1990) all describe and justify various parametric approaches to wind-field specification in tropical storms. Cardone, Greenwood, and Greenwood (1992) use a modified form of Chow's (1971) moving vortex model to specify winds with a gridded numerical model. However, since this numerical solution is driven only by a small set of parameters and assumes steady-state conditions, it produces results that are similar in form to those of parametric models (Cooper 1988). Cardone et al. (1994) and Thompson and Cardone (1996) describe a more general model version that can approximate irregularities in the radial wind profile such as the double maxima observed in some hurricanes.

(3) All of the above models have been shown to work relatively well in applications; however, the Holland (1980) model appears to provide a better fit to observed wind fields in early stages of rapidly

developing storms and appears to work as well as other models in mature storms. Consequently, this model will be described in some detail here. In presently available hurricane models, wind fields are assumed to have no memory and thus can be determined by only a small set of parameters at a given instant.

(4) In the Holland model, hurricane pressure profiles are normalized via the relationship

$$\beta = \frac{p - p_c}{p_n - p_c} \tag{II-2-15}$$

where

p = pressure at radius r

r = arbitrary radius

p_c = central pressure in the storm

p_n = ambient pressure at the periphery of the storm

(5) Holland showed that the family of β-curves for a number of storms resembled a family of rectangular hyperbolas and could be represented as

$$r^B \ln(\beta^{-1}) = A$$

or

$$\beta^{-1} = \exp\left(\frac{A}{r^B}\right) \tag{II-2-16}$$

or

$$\beta = \exp\left(\frac{-A}{r^B}\right)$$

A = scaling parameter with units of length

B = dimensionless parameter that controls the peakedness of the wind speed distribution

(6) This leads to a representation for the pressure profile as

$$p = p_c + (p_n - p_c)\exp\left(\frac{-A}{r^B}\right) \tag{II-2-17}$$

which then leads to a gradient wind approximation of the form

$$U_{gr} = \left[\frac{AB(p_n - p_c)\exp\left(\frac{-A}{r^B}\right)}{\rho_a r^B} + \frac{r^2 f^2}{4}\right]^{\frac{1}{2}} - \frac{rf}{2} \tag{II-2-18}$$

where

U_{gr} = gradient approximation to the wind speed

(7) In the intense portion of the storm, Equation II-2-18 reduces to a cyclostrophic approximation given by

$$U_c = \left[\frac{AB(p_n - p_c) \exp\left(\frac{-A}{r^B} \right)}{\rho_a r^B} \right]^{\frac{1}{2}} \quad \text{(II-2-19)}$$

where

U_c = cyclostrophic approximation to the wind speed

which yields explicit forms for the radius to maximum winds as

$$R_{max} = A^{\frac{1}{B}} \quad \text{(II-2-20)}$$

where

R_{max} = distance from the center of the storm circulation to the location of maximum wind speed

(8) The maximum wind speed can then be approximated as

$$U_{max} = \left(\frac{B}{\rho_a e} \right)^{\frac{1}{2}} (p_n - p_c)^{\frac{1}{2}} \quad \text{(II-2-21)}$$

where

U_{max} = maximum velocity in the storm

e = base of natural logarithms, 2.718

(9) Rosendal and Shaw (1982) showed that pressure profiles and wind estimates from the Holland model appeared to fit observed typhoon characteristics in the central North Pacific. If B is equal to 1 in this model, the pressure profile and wind characteristics become similar to results of Myers (1954); Collins and Viehmann (1971); Schwerdt, Ho, and Watkins (1979); and Cardone, Greenwood, and Greenwood (1992). In the case of the Cardone, Greenwood, and Greenwood model, this similarity would exist only for the case of a storm with no significant background pressure gradient.

(10) Holland argues that B=1 is actually the lower limit for B and that, in most storms, the value is likely to be more in the range of 1.5 to 2.5. As shown in Figure II-2-16, this argument is supported by the data from Atkinson and Holliday (1977) and Dvorak (1975) taken from studies of Pacific typhoons. The effect of a higher value of B is to produce a more peaked wind distribution in the Holland model than exists in models with B set to a value of 1. According to Holland (1980), use of a wind field model with B=1 will underestimate winds in many tropical storms. In applications, the choices of A and B can either be based on

the best two-parameter fit to observed pressure profiles or on the combination of an R_{max} value with the data shown in Figure II-2-16. It is worth noting here that the Holland model is similar to several other parametric models, except that it uses two parameters rather than one in describing the shape of the wind profile. This second parameter allows the Holland model to represent a range of peakedness rather than only a single peakedness in applications.

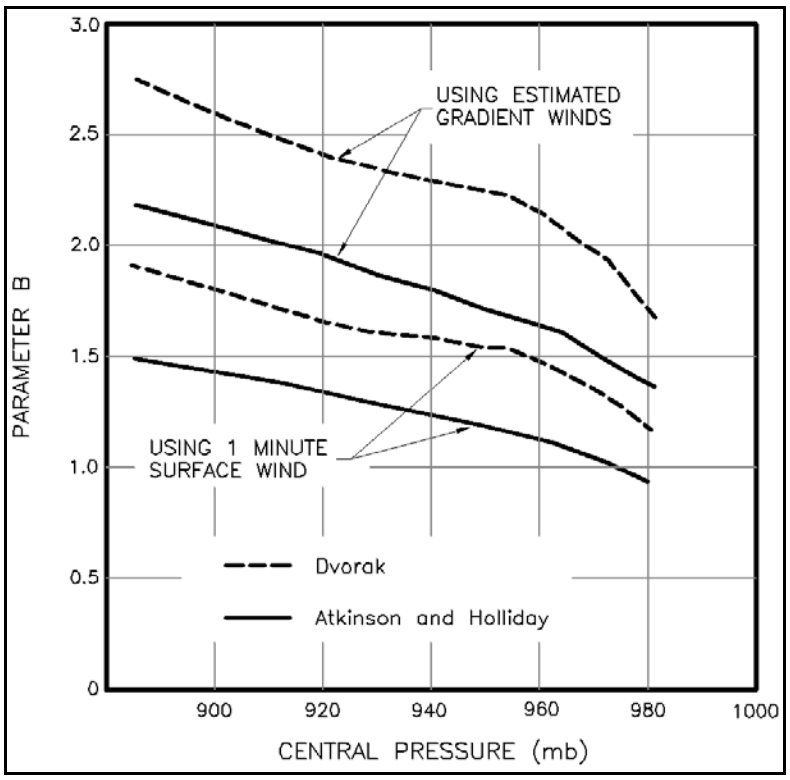

Figure II-2-16. Climatological variation in Holland's "B" factor (Holland 1980)

(11) As a final element in application of the Holland wind model, it is necessary to consider the effects of storm movement on the surface wind field. Since a hurricane moves most of its mass along with it (unlike an extratropical storm), this step is a necessary adjustment to the storm wind field and can create a marked asymmetry in the storm wind field, particularly for the case of weak or moderate storms. Hughes' (1952) composite wind fields from moving hurricanes indicated that the highest wind speeds occurred in the right rear quadrant of the storm. This supports the interpretation that the total wind in a hurricane can be obtained by adding a wind vector for storm motion to the estimated winds for a stationary storm. On the other hand, Chow's (1971) numerical results suggest that winds in the front right and front left quadrants are more likely to contain the maximum wind speeds in a moving hurricane. These contradictory results have made it difficult to treat the effects of storm movement of surface wind fields in a completely satisfactory fashion. Various researchers have either ignored the problem or suggested that, at least in simple parametric models, the effects of storm movement can be adequately approximated by adding a constant vector representative of the forward storm motion to the estimated wind for a stationary storm. In light of the overall lack of definitive information on this topic, the latter approach is considered sufficient.

(12) At this point, it should be stressed that Equations II-2-18, 19, and 21 and superposition of the storm motion vector are only applicable to winds above the surface boundary layer. In order to convert these winds to winds at a 10-m reference level, it is necessary to apply a model of the type described in Part II-2-1-c-(3)-

(b). As shown in that section, it is not advisable to use a constant ratio between winds at the top of the boundary layer and winds at a 10-m level. If a complete wind field is required for a particular application it is recommended to use a planetary-boundary-layer (PBL) model combined with either a moving vortex formulation or a numerical version of a parametric model.

(13) To provide some guidance regarding maximum sustained wind speeds at a 10-m reference level, Figure II-2-17 shows representative curves of maximum sustained wind speed versus central pressure for selected values of forward storm movement. It should be noted that maximum winds at the top of the boundary layer are relatively independent of latitude, since the wind balance equation is dominated by the cyclostrophic term; however, there is a weak dependence on latitude through the boundary-layer scaling, which is latitude-dependent. This dependence and dependence of the maximum wind speed on the radius to maximum wind were both found to be rather small; consequently, only fixed values of latitude and R_{max} have been treated here. From the methods used in deriving these estimates, winds given here can be regarded as typical values for about a 15- to 30-min averaging period. Thus, winds from this model are appropriate for use in wave models and surge models, but must be transformed to shorter averaging times for most structural applications.

(14) Values for wind speeds in Figure II-2-17 may appear low to people who recall reports of maximum wind speeds for many hurricanes in the range of 130-160 mph (about 58-72 m/s). First, it should be recognized that very few good measurements of hurricane wind speed exist today. Where such measurements exist, they give support to the values presented in Figure II-2-17. Second, the values reported as sustained wind speeds often come from airplane measurements, so they tend to be considerably higher than corresponding values at 10 m. Third, winds at airports and other land stations often use only a 1-min averaging time in their wind speed measurements. These winds are subsequently reported as sustained wind speeds. An idea of the magnitude that some of these effects can have on wind estimates may be gained via the following example. The central pressure of Hurricane Camille as it moved onshore at a speed of about 6 m/s in 1969 was about 912 mb. From Figure II-2-17, the 15- to 30-min average wind speed is estimated to be 52.5 m/s. Converting this to a 1-min wind speed in miles per hour yields approximately 150 mph, which is in very reasonable agreement with the measured and estimated winds in this storm. It is important to recognize though that these higher wind speeds are not appropriate for applications in surge and wave models.

(15) Figures II-2-18 and II-2-19 are examples of the output from the hurricane model presented here. Figure II-2-18 shows the four radials. Figure II-2-19 shows wind speed along Radials 1 and 3, as a function of dimensionless distance along the radial (r/R_{max}) for a central pressure p_c of 930 mb and forward speeds of 2.5 m/s, 5.0 m/s, and 7.5 m/s. The inflow angle along these radii (not shown) can be quite variable. The behavior of this angle is a function of several factors and is still the subject of some debate.

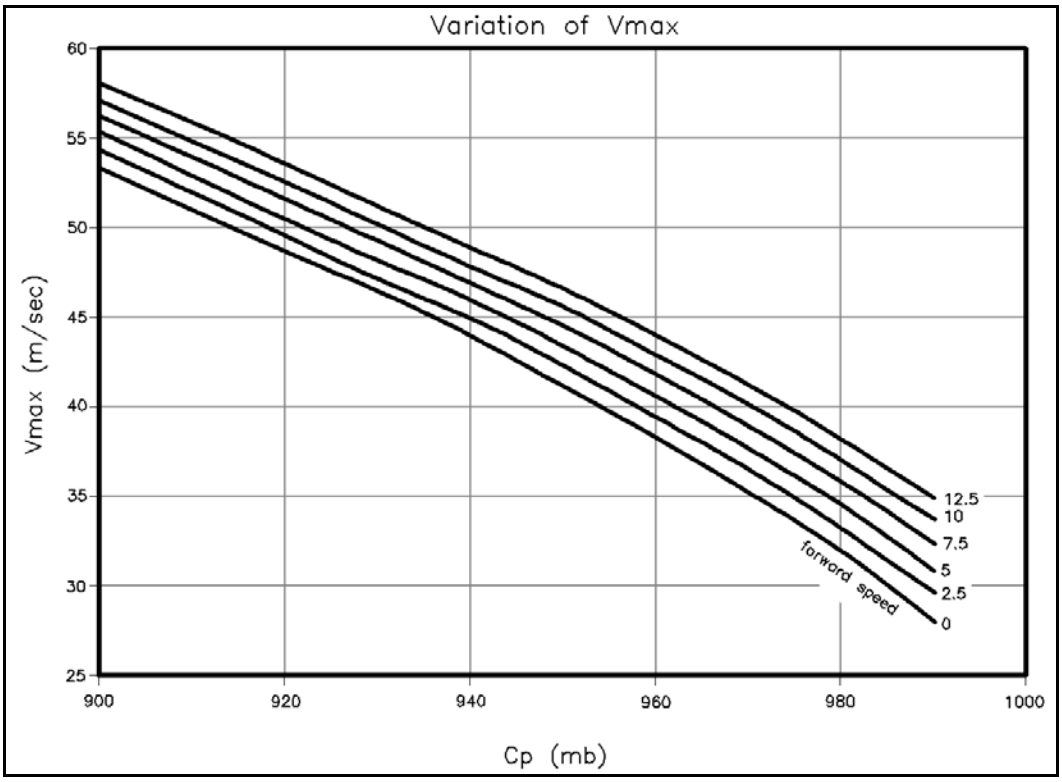

Figure II-2-17. Relationship of estimated maximum wind speed in a hurricane at 10-m elevation as a function of central pressure and forward speed of storm (based on latitude of 30 deg, R_{max}=30 km, 15- to 30-min averaging period)

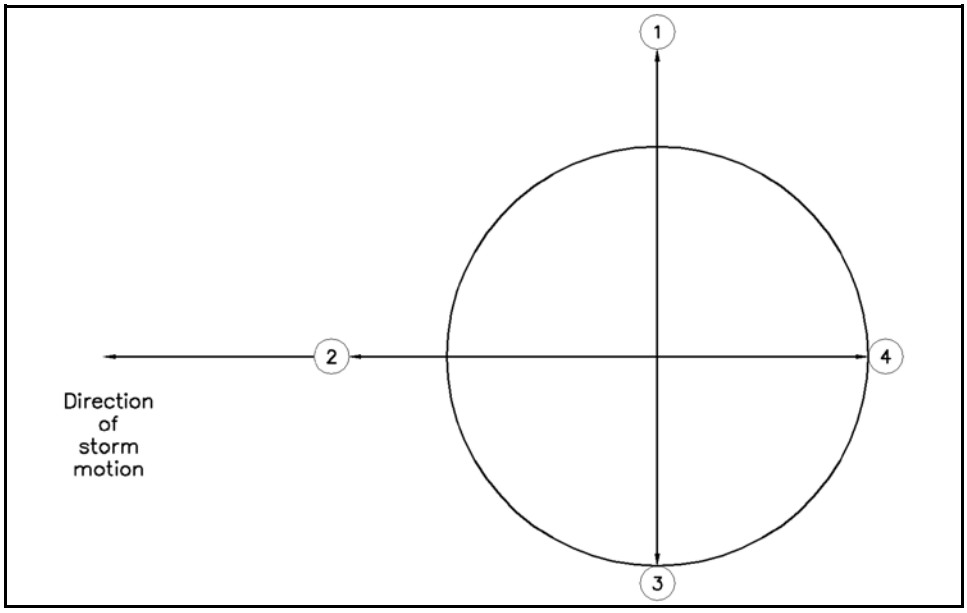

Figure II-2-18. Definition of four radial angles relative to direction of storm movement

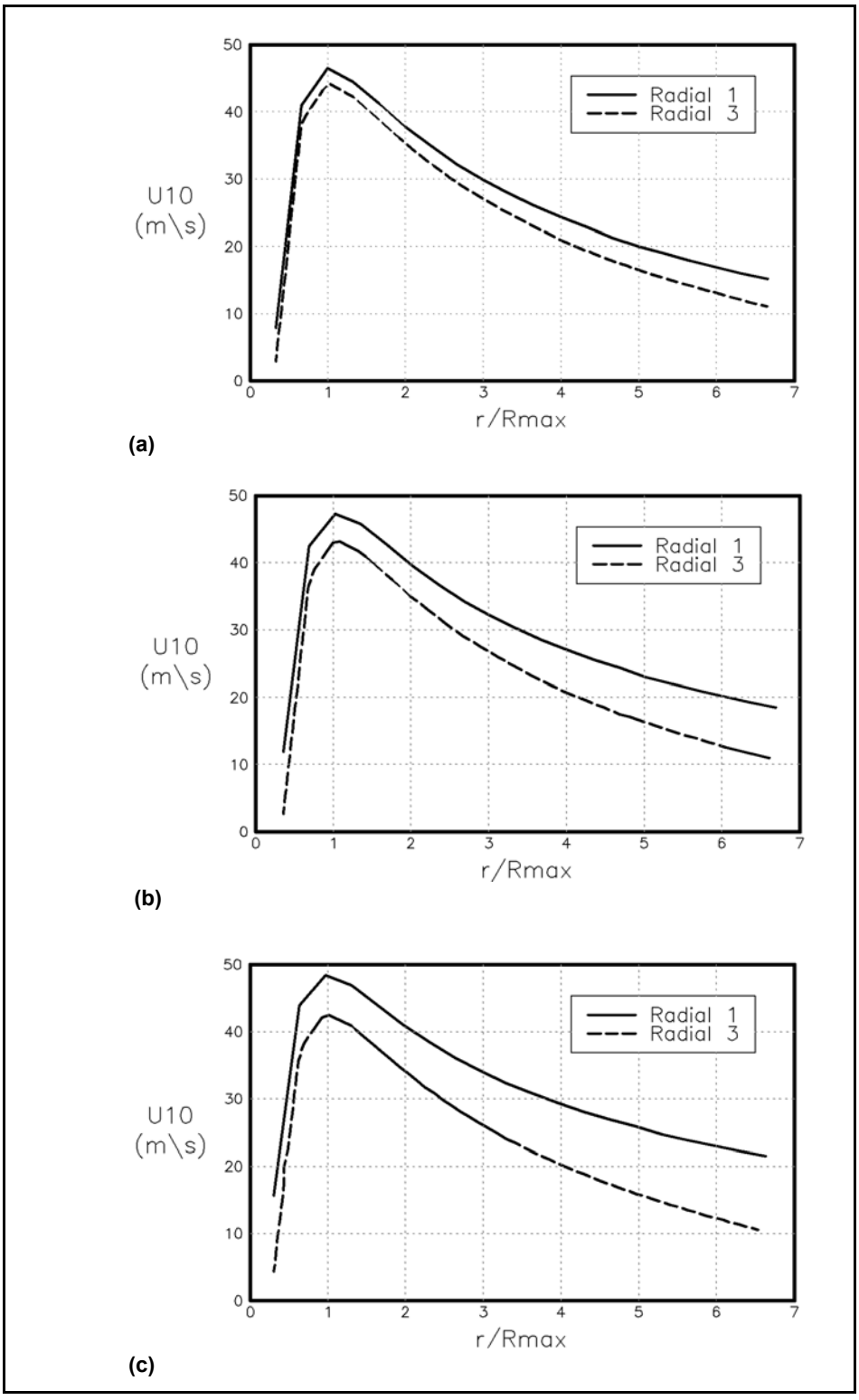

Figure II-2-19. Horizontal distribution of wind speed along Radial 1 for a storm with forward velocity V_F of (a) 2.5 m/s; (b) 5 m/s; (c) 7.5 m/s

EXAMPLE PROBLEM II-2-6

FIND:

The expected maximum sustained wind speed for this storm for surge and/or wave prediction and the maximum 1-min wind speed.

GIVEN:

A hurricane located at a latitude of 28° with a central pressure of 935 mb and a forward velocity of 10 m/s.

SOLUTION:

Using Figure II-2-17, the maximum wind speed in a moving storm with the parameters given here is approximately 47.3 m/s for a 15- to 30-min average at the 10-m level. From Figure II-2-1, the ratio of a 30-min wind (chosen here to give a conservative approximation) to a 1-min wind is approximately 1.23. Multiplying this factor times 47.3 yields a 1-min wind speed of 58.2 m/s (130 mph).

i. Step-by-step procedure for simplified estimate of winds for wave prediction.

(1) Introduction. This section presents simplified, step-by-step methods for estimating winds to be used in wave prediction. The methods include the key assumption that wind fields are well-organized and can be adequately represented as an average wind speed and direction over the entire fetch. Most engineers can conveniently use computer-based wind estimation tools such as ACES, and such tools should be used in preference to the corresponding methods in this section. The simplified methods provide an approximation to the processes described earlier in this chapter. The methods embody graphs presented earlier, some of which were generated with ACES. The simplified methods are particularly useful when quick, low-cost estimates are needed. They are reasonably accurate for simple situations where local effects are small.

(2) Wind measurements. Winds can be estimated using direct measurements or synoptic weather charts. For preliminary design, extreme winds derived from regional records may also be useful (Part II-9-6). Actual wind records from the site of interest are preferred so that local effects such as orographic influences and sea breeze are included. If wind measurements at the site are not available and cannot be collected, measurements at a nearby location or synoptic weather charts may be helpful. Wind speeds must be properly adjusted to avoid introducing bias into wave predictions.

(3) Procedure for adjusting observed winds. When ACES is unavailable, the following procedure can be used to adjust observed winds with some known level, location (over water or land), and averaging time. A logic diagram (Figure II-2-20) outlines the steps in adjusting wind speeds for application in wave growth models.

(a) Level. If the wind speed is observed at any level other than 10 m, it should be adjusted to 10 m using Figure II-2-6 (see Example Problem II-2-3).

(b) Duration. If extreme winds are being considered, wind speed should be adjusted from the averaging time of the observation (fastest mile, 5-min average, 10-min average, etc.) to an averaging time appropriate for wave prediction using Figure II-2-1 (see Example Problem II-2-1). Typically several different averaging times should be considered for wave prediction to ensure that the maximum wave growth scenario has been identified. When the fetch is limited, Figure II-2-3 can be used to estimate the maximum averaging time to

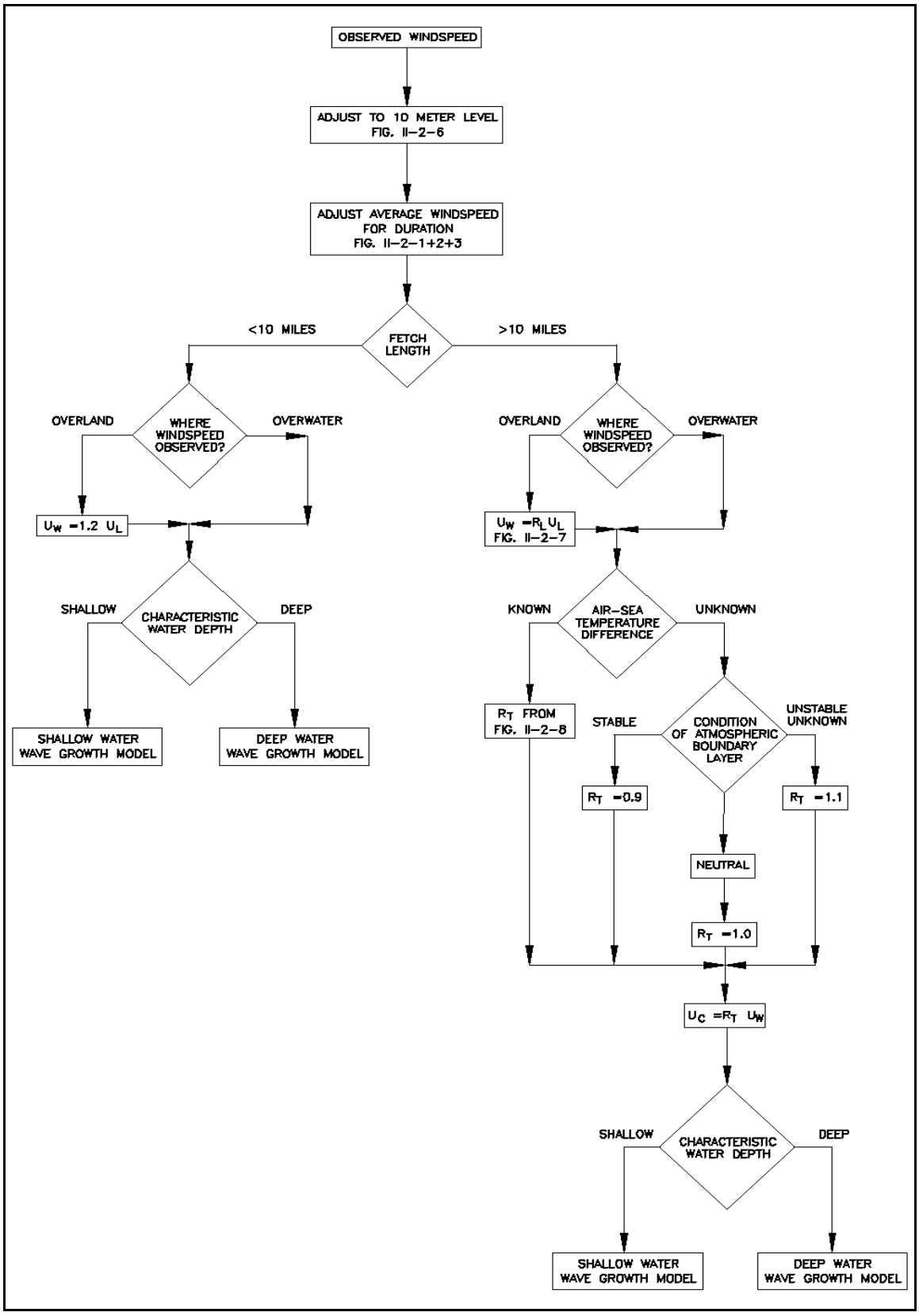

Figure II-2-20. Logic diagram for determining wind speed for use in wave hindcasting and forecasting models

be considered. When the observed wind is given in terms of the fastest mile, Figure II-2-2 can be used to convert to an equivalent averaging time.

(c) Overland or overwater. When the observation was collected overwater (within the marine boundary layer), this adjustment is not needed. When the observation was collected overland and the fetch is long enough for full development of a marine boundary layer (longer than about 16 km or 10 miles), the observed wind speed should be adjusted to an overwater wind speed using Figure II-2-7 (see Example Problem II-2-4). Otherwise (for overland winds and fetches less than 16 km), wave growth occurs in a transitional atmospheric boundary layer, which has not fully adjusted to the overwater regime. In this case, wind speeds observed overland must be increased to better represent overwater wind speeds. A factor of 1.2 is suggested here, but no simple method can accurately represent this complex case. In relation to all of these adjustments, the term overland implies a measurement site that is predominantly characterized as inland. If a measurement site is directly adjacent to the water body, it may, for some wind directions, be equivalent to overwater.

(d) Stability. For fetches longer than 16 km, an adjustment for stability of the boundary layer may also be needed. If the air-sea temperature difference is known, Figure II-2-8 can be used to make the adjustment. When only general knowledge of the condition of the atmospheric boundary layer is available, it should be categorized as stable, neutral, or unstable according to the following:

Stable - when the air is warmer than the water, the water cools air just above it and decreases mixing in the air column ($R_T = 0.9$).
Neutral - when the air and water have the same temperature, the water temperature does not affect mixing in the air column ($R_T = 1.0$).
Unstable - when the air is colder than the water, the water warms the air, causing air near the water surface to rise, increasing mixing in the air column ($R_T = 1.1$).

When the boundary layer condition is unknown, an unstable condition, $R_T = 1.1$, should be assumed.

(4) Procedure for adjusting winds from synoptic weather charts. As discussed earlier, synoptic weather charts are maps depicting isobars at sea level. The free air, or geostrophic, wind speed is estimated from these sea level pressure charts. Adjustments or corrections are then made to the geostrophic wind speed. Pressure chart estimations should be used only for large areas, and the estimated values should be compared with observations, if possible, to verify their accuracy.

(a) Geostrophic wind speed. To estimate geostrophic wind speed, Equation II-2-10 or Figure II-2-12 should be used (see Example Problem II-2-5).

(b) Level and stability. Wind speed at the 10-m level should be estimated from the geostrophic wind speed using Figure II-2-13. The resulting speed should then be adjusted for stability effects as needed using Figure II-2-8.

(c) Duration. Wind duration estimates are also needed. Since synoptic weather charts are prepared only at 6-hr intervals, it may be necessary to use interpolation to determine duration. Linear interpolation is adequate for most cases. Interpolation should not be used if short-duration phenomena, such as frontal passages or thunderstorms, are present.

(5) Procedure for estimating fetch. Fetch is defined as a region in which the wind speed and direction are reasonably constant. Fetch should be defined so that wind direction variations do not exceed 15 deg and wind speed variations do not exceed 2.5 m/s (5 knots) from the mean. A coastline upwind from the point of interest always limits the fetch. An upwind limit to the fetch may also be provided by curvature, or spreading, of the isobars or by a definite shift in wind direction. Frequently the discontinuity at a weather front will limit fetch.

II-2-2. Wave Hindcasting and Forecasting

a. Introduction.

(1) The theory of wave generation has had a long and rich history. Beginning with some of the classic works of Kelvin (1887) and Helmholtz (1888) in the 1800's, many scientists, engineers, and mathematicians have addressed various forms of water wave motions and interactions with the wind. In the early 1900's, the work of Jeffreys (1924, 1925) hypothesized that waves created a "sheltering effect" and hence created a positive feedback mechanism for transfer of momentum into the wave field from the wind. However, it was not until World War II that organized wave predictions began in earnest. During the 1940's, large bodies of wave observations were collated and the bases for empirical wave predictions were formulated. Sverdrup and Munk (1947, 1951) presented the first documented relationships among various wave-generation parameters and resulting wave conditions. Bretschneider (1952) revised these relationships based on additional evidence; methods derived from these exemplary pioneer works are still in active use today.

(2) The basic tenet of the empirical prediction method is that interrelationships among dimensionless wave parameters will be governed by universal laws. Perhaps the most fundamental of these laws is the fetch-growth law. Given a constant wind speed and direction over a fixed fetch, it is expected that waves will reach a stationary fetch-limited state of development. In this situation, wave heights will remain constant (in a statistical sense) through time but will vary along the fetch. If dimensionless wave height is taken as

$$\hat{H} = \frac{gH}{u_*^2} \tag{II-2-22}$$

where

H = characteristic wave height, originally taken as the significant wave height but more recently taken as the energy-based wave height H_{m0}

u_* = friction velocity

and dimensionless fetch is defined as

$$\hat{X} = \frac{gX}{u_*^2} \tag{II-2-23}$$

where

X = straight line distance over which the wind blows

then idealized, fetch-limited wave heights are expected to follow a relationship of the form

$$\hat{H} = \lambda_1 \hat{X}^{m_1} \tag{II-2-24}$$

where

λ_1 = dimensionless coefficient

m_1 = dimensionless exponent

(3) If dimensionless wave frequency (defined simply as one over the spectral peak wave period) defined as

$$\hat{f}_p = \frac{u_* f_p}{g} \tag{II-2-25}$$

where

f_p = frequency of the spectral peak

then a stationary wave field also implies a fixed relationship between wave frequency and fetch of the form

$$\hat{f}_p = \lambda_2 \hat{X}^{m_2} \tag{II-2-26}$$

where

λ_2 and m_2 are more empirical coefficients.

(4) Since u_* scales the effective rate of momentum transfer from the atmosphere into the waves, all empirical coefficients in these wave generation laws are expected to be universal values. Unfortunately, there is still some ambiguity in these values; however, in lieu of any demonstrated improvements over values from the *Shore Protection Manual* (1984), those values for fetch-limited wave growth will be adopted here.

(5) From basic conservation laws and the dispersion relationship, it is anticipated that any law governing the rate of growth of waves along a fetch will also form a unique constraint on the rate of growth of waves through time. If we define dimensionless time as

$$\hat{t} = \frac{g\, t}{u_*} \tag{II-2-27}$$

where

t = time

additional relationships governing the duration-growth of waves will be

$$\hat{H} = \lambda_3 \hat{t}^{m_3} \tag{II-2-28}$$

and

$$\hat{f}_p = \lambda_4 \hat{t}^{m_4} \tag{II-2-29}$$

where

λ_4 and m_4 are more "universal" coefficients to be determined empirically.

(6) The form of Equations II-2-26 and II-2-27 imply that waves will continue to grow as long as fetch and time continue to increase. This concept was observed to be incorrect in the early compendiums of data

(Sverdrup and Munk 1947, Bretschneider 1952), which suggested that a "fully developed" wave height would evolve under the action of the wind. Available data indicated that this fully developed wave height could be represented as

$$H_{\infty} = \frac{\lambda_5 \, u^2}{g} \tag{II-2-30}$$

where

H_{∞} = fully developed wave height

λ_5 =dimensionless coefficient (approximately equal to 0.27)

u = wind speed

Wave heights defined by Equation II-2-30 are usually taken as representing an upper limit to wave growth for any wind speed.

(7) In the 1950's, researchers began to recognize that the wave generation process was best described as a spectral phenomenon (e.g. Pierson, Neumann, and James (1955)). Theoreticians then began to reexamine their ideas on the wave-generation process, with regard to how a turbulent wind field could interact with a random sea surface. Following along these lines, Phillips (1958) and Miles (1957) advanced two theories that formed the cornerstone of the understanding of wave generation physics for many years. Phillips' concept involved the resonant interactions of turbulent pressure fluctuations with waves propagating at the same speed. Miles' concept centered on the mean flux of momentum from a "matched layer" above the wave field into waves travelling at the same speed. Phillips' theory predicted linear wave growth and was believed to control the early stages of wave growth. Miles' theory predicted an exponential growth and was believed to control the major portion of wave growth observed in nature. Direct measurements of the Phillips' resonance mechanism indicated that the measured turbulent fluctuations were too small by about an order of magnitude to explain the observed early growth in waves; however, it was still adopted as a plausible concept. Subsequent field efforts by Snyder and Cox (1966) and Snyder et al. (1981) have supported at least the functional form of Miles' theory for the transfer of energy into the wave field from winds.

(8) From basic concepts of energy conservation and the fact that waves do attain limiting fully developed wave heights, it is obvious that wave generation physics cannot consist of only wind source terms. There must be some physical mechanism or mechanisms that leads to a balance of wave growth and dissipation for the case of fully developed conditions. Phillips (1958) postulated that one such mechanism in waves would be wave breaking. Based on dimensional considerations and the knowledge that wave breaking has a very strong local effect on waves, Phillips argued that energy densities within a spectrum would always have a universal limiting value given by

$$E(f) = \frac{\alpha \, g^2 \, f^{-5}}{(2\pi)^4} \tag{II-2-31}$$

where E(f) is the spectral energy density in units of length squared per hertz and α was understood to be a universal (dimensionless) constant approximately equal to 0.0081. It should be noted here that energy densities in this equation are proportional to f^{-5} (as can be deduced from dimensional arguments) and that they are independent of wind speed. Phillips hypothesized that local wave breaking would be so strong that wind effects could not affect this universal level. In this context, a saturated region of spectral energy densities is assumed to exist in some region from near the spectral peak to frequencies sufficiently high that viscous

effects would begin to be significant. This region of saturated energy densities is termed the equilibrium range of the spectrum.

(9) Kitaigorodskii (1962) extended the similarity arguments of Phillips to distinct regions throughout the entire spectrum where different mechanisms might be of dominant importance. Pierson and Moskowitz (1964) followed the dimensional arguments of Phillips and supplemented these arguments, with relationships derived from measurements at sea. They extended the form of Phillips spectrum to the classical Pierson-Moskowitz spectrum

$$E(f) = \frac{\alpha\, g^2\, f^{-5}}{(2\pi)^4} \exp\left[-0.74\left(\frac{f}{f_u}\right)^{-4}\right] \tag{II-2-32}$$

where

f_u = limiting frequency for a fully developed wave spectrum (assumed to be a function only of wind speed)

(10) Based on these concepts of spectral wave growth due to wind inputs via Miles-Phillips mechanisms and a universal limiting form for spectral densities, first-generation (1G) wave models in the United States were born (Inoue 1967, Bunting 1970). It should be pointed out here that the first model of this type was actually developed in France (Gelci, Cazale, and Vassel 1957); however, that model did not incorporate the limiting Pierson-Moskowitz spectral form as did models in the United States. In these models, it was recognized that waves in nature are not only made up of an infinite (continuous) sum of infinitesimal wave components at different frequencies but that each frequency component is made up of an infinite (continuous) sum of wave components travelling in different directions. Thus, when waves travel outward from a storm, a single "wave train" moving in one direction does not emerge. Instead, directional wave spectra spread out in different directions and disperse due to differing group velocities associated with different frequencies. This behavior cannot be modeled properly in parametric (significant wave height) models and understanding of this behavior formed the basic motivation to model all wave components in a spectrum individually. The term discrete-spectral model has since been employed to describe models that include calculations of each separate (frequency-direction) wave component. The equation governing the energy balance in such models is sometimes termed the radiative transfer equation and can be written as

$$\frac{\partial E(f,\theta,x,y,t)}{\partial t} = -c_{\vec{G}}\, \vec{\nabla} E(f,\theta,x,y,t) + \sum_{k=1}^{K} S(f,\theta,x,y,t)_k \tag{II-2-33}$$

where

$E(f,\theta,x,y,t)$ = spectral energy density as a function of frequency (f), propagation direction (θ), two horizontal spatial coordinates (x and y) and time (t)

$S(f,\theta,x,y,t)_k$ = the k^{th} source term, which exists in the same five dimensions as the energy density

The first term on the right side of this equation represents the effects of wave propagation on the wave field. The second term represents the effects of all processes that add energy to or remove energy from a particular frequency and direction component at a fixed point at a given time.

(11) In the late 1960's evidence of spectral behavior began to emerge which suggested that the equilibrium range in wave spectra did not have a universal value for α. Instead, it was observed that α varied

as a function of nondimensional fetch (Mitsuyasu 1968). This presented a problem to the "first-generation" interpretation of wave generation physics, since it implied that energies within the equilibrium range are not controlled by wave breaking. Fortunately, a theoretical foundation already existed to help explain this discrepancy. This foundation had been established in 1961 in an exceptional theoretical formulation by Klaus Hasselmann in Germany. In this formulation, Hasselmann, using relatively minimal assumptions, showed that waves in nature should interact with each other in such a way as to spread energy throughout a spectrum. This theory of wave-wave interactions predicted that energy near the spectral peak region should be spread to regions on either side of the spectral peak.

(12) Hasselmann et al. (1973) collected an extensive data set in the Joint North Sea Wave Project (JONSWAP). Careful analysis of these data confirmed the earlier findings of Mitsuyasu and revealed a clear relationship between Phillips' α and nondimensional fetch (Figure II-2-21). This finding and certain other spectral phenomena, such as the tendency of wave spectra to be more peaked than the Pierson-Moskowitz spectrum during active generation, could not be explained in terms of "first-generation" concepts; however, they could be explained in terms of a nonlinear interaction among wave components. This pointed out the necessity of incorporating wave-wave interactions into wave prediction models, and led to the development of second-generation (2G) wave models. The modified spectral shape which came out of the JONSWAP experiment has come to bear the name of that experiment; hence we now have the JONSWAP spectrum, which can be written as

$$E(f) = \frac{\alpha g^2}{(2\pi)^4 f^5} \exp\left[-1.25\left(\frac{f}{f_p}\right)^{-4}\right]\gamma^{\exp\left[-\frac{\left(\frac{f}{f_p}-1\right)^2}{2\sigma^2}\right]} \qquad \text{(II-2-34)}$$

where

α = equilibrium coefficient

σ = dimensionless spectral width parameter, with value σ_a for $f<f_p$ and value σ_b for $f \geq f_p$

γ = peakedness parameter

The average values of the σ and γ parameters in the JONSWAP data set were found to be $\gamma = 3.3$, $\sigma_a = 0.07$, and $\sigma_b = 0.09$. Figure II-2-22 compares this spectrum to the Pierson-Moskowitz spectrum.

(13) Early second-generation models (Barnett 1968, Resio 1981) followed an f^{-5} equilibrium-range formulation since prior research had been formulated with that spectral form. Toba (1978) was the first researcher to present data suggesting that the equilibrium range in spectra might be better fit by an f^{-4} dependence. Following his work, Forristall et al. (1978); Kahma (1981); and Donelan, Hamilton, and Hu (1982) all presented evidence from independent field measurements supporting the tendency of equilibrium ranges to follow an f^{-4} dependence. Kitaigorodskii (1983); Resio (1987,1988); and Resio and Perrie (1989) have all presented theoretical analyses showing how this behavior can be explained by the nature of nonlinear fluxes of energy through a spectrum. Subsequently, Resio and Perrie (1989) determined that, although certain spectral growth characteristics were somewhat different between the f^{-4} and f^{-5} formulations,

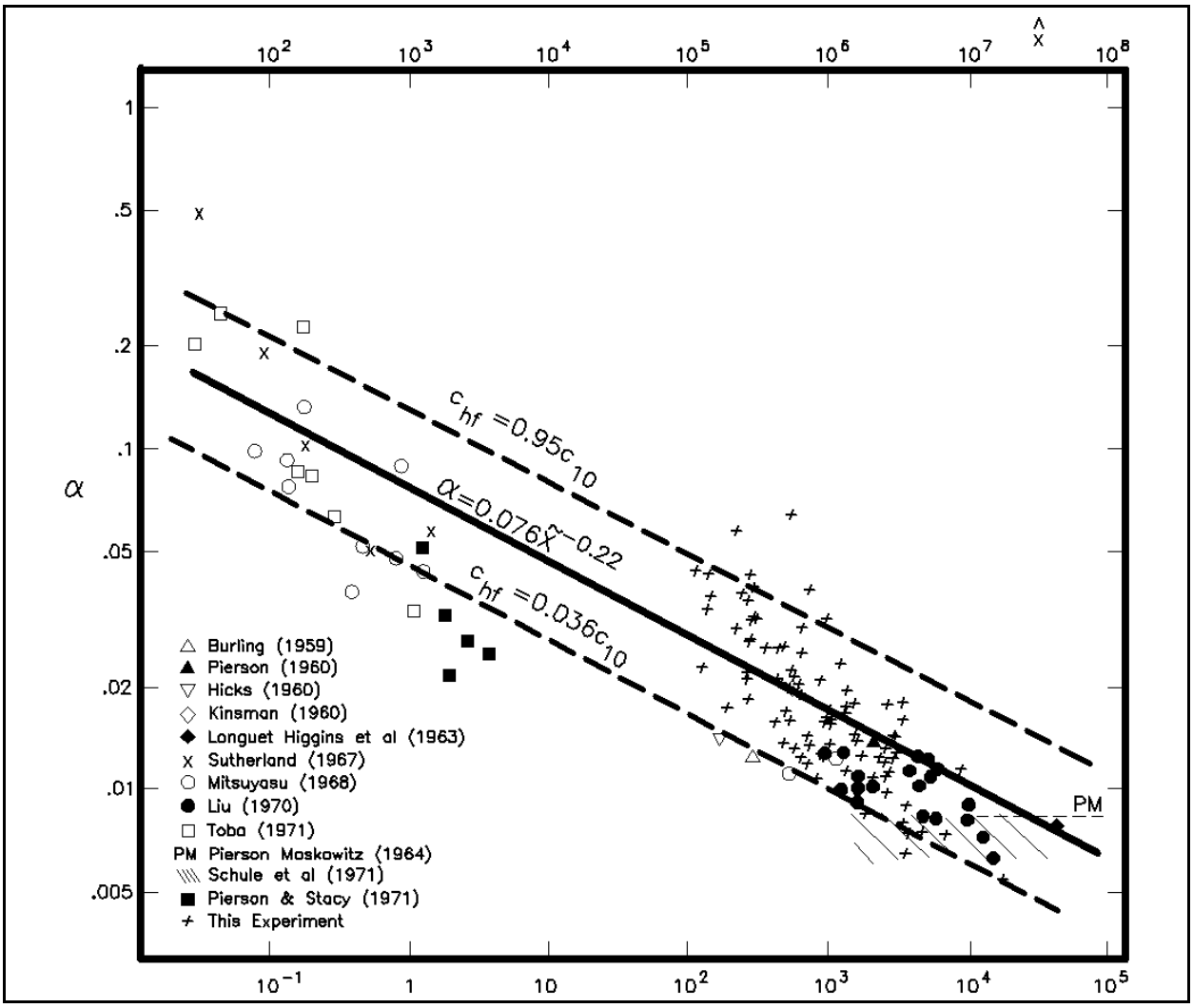

Figure II-2-21. Phillips' constant versus fetch scaled according to Kitaigorodskii. Small-fetch data are obtained from wind-wave tanks. Capillary-wave data were excluded where possible (Hasselmann et al. 1973)

the basic energy-growth equations were quite similar for the two formulations. The f^4 formulation is incorporated into CERC's WAVAD model, used in its hindcast studies.

(14) Since the early 1980's, a new class of wave model has come into existence (Hasselmann et al. 1985). This new class of wave model has been termed a third-generation wave model (3G). The distinction between second-generation and third-generation wave models is the method of solution used in these models. Second-generation wave models combine relatively broad-scale parameterizations of the nonlinear wave-wave interaction source term combined with constraints on the overall spectral shape to simulate wave growth. Third-generation models use a more detailed parameterization of the nonlinear wave-wave interaction source terms and relax most of the constraints on spectral shape in simulating wave growth. Various third-generation models are used around the world today; however, the third-generation model is probably the WAM model.

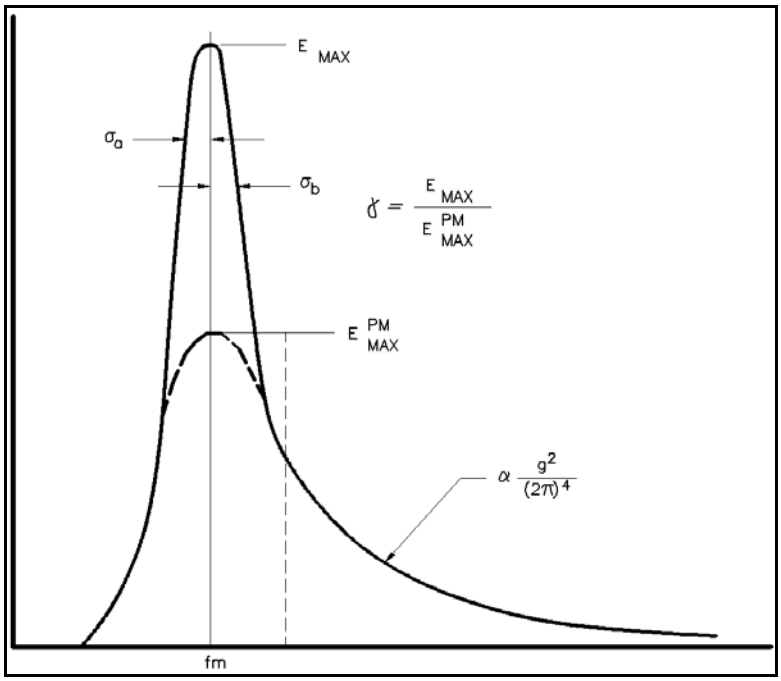

Figure II-2-22. Definition of JONSWAP parameters for spectral shape

(15) Part of the motivation to use third-generation models is related to the hope that future simulations of directional spectra can be made more accurate via the direct solution of the detailed source-term balance. This is expected to be particularly important in complex wave generation scenarios where second-generation models might not be able to handle the general source term balance. However, recent research by Van Vledder and Holthuisen (1993) has demonstrated rather convincingly that the "detailed balance" equations in the WAM (WAMDI Group 1988)model at this time still cannot accurately simulate waves in rapidly turning winds. Hence, there remains much work to be done in this area before the performance of third-generation models can be considered totally satisfactory.

(16) First-generation models that have been modified to allow the Phillips equilibrium coefficient to vary dynamically (Cardone 1992) , second-generation models (Resio 1981; NORSWAM, Hubertz 1992), and third-generation models (Hasselmann et al. 1985) have all been shown to produce very good predictions and hindcasts of wave conditions for a wide range of meteorological situations. These models are recommended in developing wave conditions for design and planning situations having serious economic or safety implications, and should be properly verified with local wave data, wherever feasible. This is not meant to imply that wave models can supplant wave measurements, but rather that in most circumstances, these models should be used instead of parametric models.

b. Wave prediction in simple situations. In some situations it is desirable to estimate wave conditions for preliminary considerations in project designs or even for final design in cases where total project costs are minimal. In the past, nomograms have played an important role in providing such wave information. However, with today's proliferation of user-friendly computer software such as the ACES Program, reliance on nomograms is discouraged. ACES will assist a user in his or her calculations, will facilitate most applications, and will help avoid most potential pitfalls related to misuse of wave prediction schemes. In spite of this warning and advice to use ACES, conventional prediction methods will be discussed here in order to provide such information for appropriate applications.

(1) Assumptions in simplified wave predictions.

(a) Deep water. There are three situations in which simplified wave predictions can provide accurate estimates of wave conditions. The first of these occurs when a wind blows, with essentially constant direction, over a fetch for sufficient time to achieve steady-state, fetch-limited values. The second idealized situation occurs when a wind increases very quickly through time in an area removed from any close boundaries. In this situation, the wave growth can be termed duration-limited. It should be recognized that this condition is rarely met in nature; consequently, this prediction technique should only be used with great caution. Open-ocean winds rarely can be categorized in such a manner to permit a simple duration-growth scenario. The third situation that may be treated via simplified prediction methods is that of a fully developed wave height. Knowledge of the fully developed wave height can provide valuable upper limits for some design considerations; however, open-ocean waves rarely attain a limiting wave height for wind speeds above 50 knots or so. Equation II-2-30 provides an easy means to estimate this limiting wave height.

(b) Wave growth with fetch. In this section, SI units should be used in formulas and figures. Figure II-2-3 shows the time required to accomplish fetch-limited wave development for short fetches. The general equation for this can be derived by combining the JONSWAP growth law for peak frequency, an equation for the fully developed frequency, and the assumption that a local wave field propagates at a group velocity approximately equal to 0.85 times the group velocity of the spectral peak. This factor accounts for both frequency distribution of energy in a JONSWAP spectrum and angular spreading. This yields

$$t_{x,u} = 77.23 \frac{X^{0.67}}{u^{0.34} g^{0.33}} \tag{II-2-35}$$

where

$t_{x,u}$ = time required for waves crossing a fetch of length x under a wind of velocity u to become fetch-limited

Equation II-2-35 can be used to determine whether or not waves in a particular situation can be categorized as fetch-limited.

The equations governing wave growth with fetch are

$$\frac{gH_{m_0}}{u_*^2} = 4.13 \times 10^{-2} * \left(\frac{gX}{u_*^2} \right)^{\frac{1}{2}}$$

and

$$\frac{gT_p}{u_*} = 0.751 \left(\frac{gX}{u_*^2} \right)^{\frac{1}{3}} \tag{II-2-36}$$

$$C_D = \frac{u_*^2}{U_{10}^2}$$

$$C_D = 0.001(1.1 + 0.035\, U_{10})$$

where

X = straight line fetch distance over which the wind blows (units of m)

H_{m0} = energy-based significant wave height (m)

C_D = drag coefficient

U_{10} = wind speed at 10 m elevation (m/sec)

u_* = friction velocity (m/sec)

See Demirbilek, Bratos, and Thompson (1993) for more details.

Fully developed wave conditions in these equations are given by

$$\frac{gH_{m_*}}{u_*^2} = 2.115 \; x \; 10^2$$

and (II-2-37)

$$\frac{gT_p}{u_*} = 2.398 \; x \; 10^2$$

Equations governing wave growth with wind duration can be obtained by converting duration into an equivalent fetch given by

$$\frac{gX}{u_*^2} = 5.23 \times 10^{-3} \left(\frac{gt}{u_*} \right)^{\frac{3}{2}} \quad \text{(II-2-38)}$$

where t in this equation is the wind duration. The fetch estimated from this equation can then be substituted into the fetch-growth equations to obtain duration-limited estimates of wave height and period. An example demonstrating these procedures is provided at the end of this chapter.

(c) Narrow fetches. Early wave prediction nomograms included modifications to predicted wave conditions based on a sort of aspect ratio for a fetch area, based on the ratio of fetch width to fetch length. Subsequent investigations (Resio and Vincent 1979) suggested that wave conditions in fetch areas were actually relatively insensitive to the width of a fetch; consequently, it is recommended here that fetch width not be used to estimate an effective fetch for use in nomograms or the ACES Program. Instead, it is recommended that the straightline fetch be used to define fetch length for applications.

(d) Shallow water. Many studies suggest that water depth acts to modify wave growth. Bottom friction and percolation (Putnam 1949, Putnam and Johnson 1949, Bretschneider and Reid 1953) have been postulated as significant processes that diminish wave heights in shallow water; however, recent studies in shallow water (Jensen 1993) indicate that fetch-limited wave growth in shallow water appears to follow growth laws that are quite close to deepwater wave growth for the same wind speeds, up to a point where an asymptotic depth-dependent wave height is attained. In light of this evidence, it seems prudent to disregard bottom friction effects on wave growth in shallow water. Also, evidence from Bouws et al. (1985) indicates that wave spectra in shallow water do not appear to have a noticeable dependence on variations in bottom

sediments. Consequently, it is recommended that deepwater wave growth formulae be used for all depths, with the constraint that no wave period can grow past a limiting value as shown by Vincent (1985). This limiting wave period is simply approximated by the relationship

$$T_p \approx 9.78\left(\frac{d}{g}\right)^{\frac{1}{2}} \tag{II-2-39}$$

In cases with extreme amounts of material in the water column (for example sediment, vegetation, man-made structures, etc.), it is likely that the dissipation rate of wave energy will become very large. In such cases, Camfield's work (1977) may be used as a guideline for estimating frictional effects on wave growth and dissipation; however, it should be recognized that little experimental evidence exists to confirm the exact values of these dissipation rates.

(2) Prediction of deepwater waves from nomograms. Figures II-2-23 through II-2-26 are wave prediction nomograms under fetch-limited and duration-limited conditions. The curves in these nomograms are based on Equations II-2-30 and II-2-36 through II-2-38 presented previously in this section. The asymptotic upper limits in both cases provide information on the fully developed wave heights as a function of wind speed. The same information can be obtained more expediently via the ACES Program.

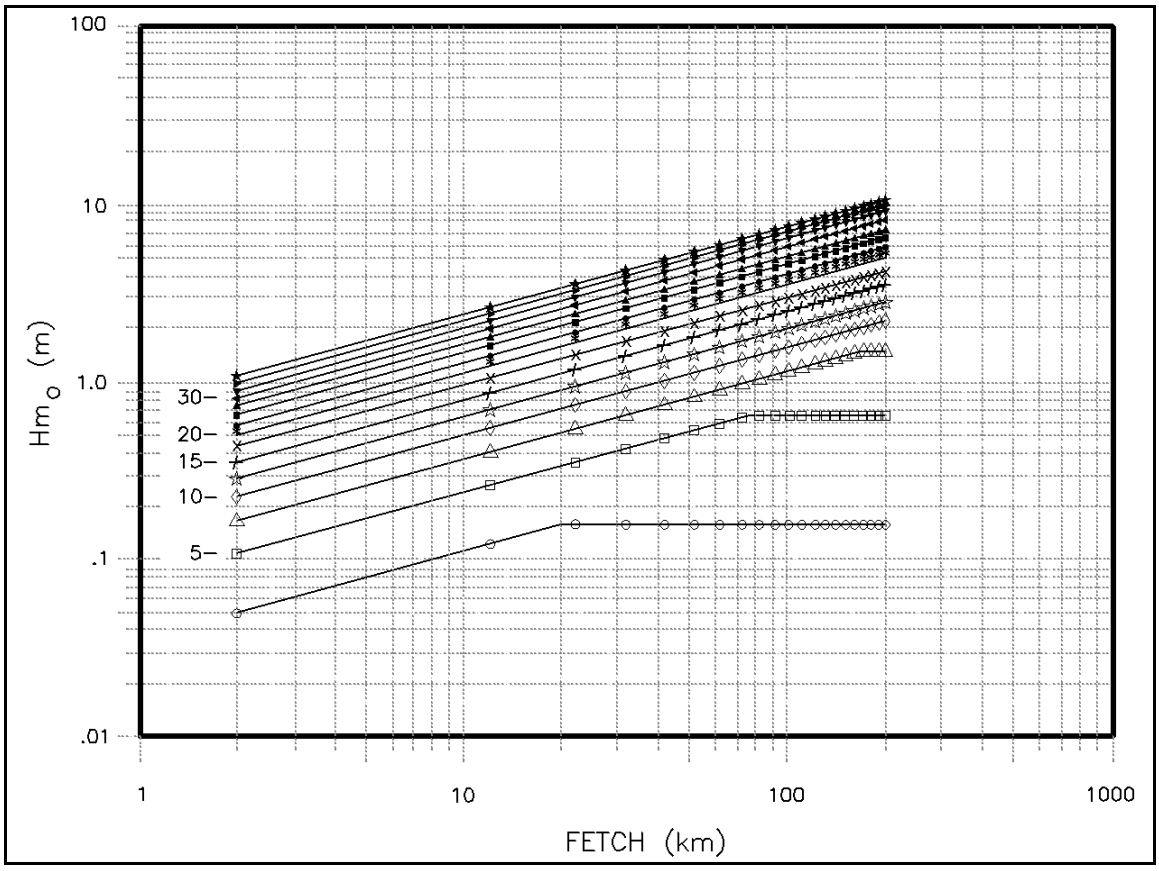

Figure II-2-23. Fetch-limited wave heights

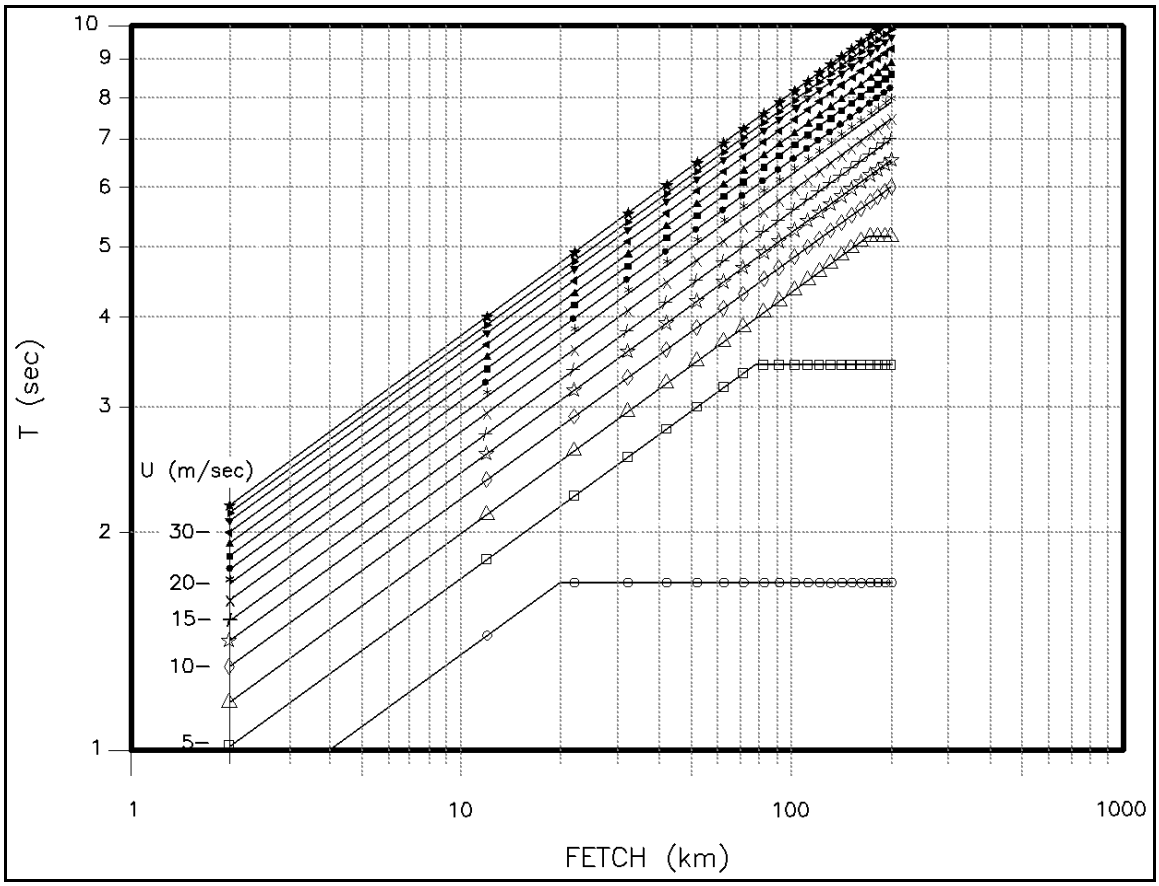

Figure II-2-24. Fetch-limited wave periods (wind speeds are plotted in increments of 2.5 m/s)

(3) Prediction of shallow-water waves. Rather than providing separate nomograms for shallow-water wave generation, the following procedure is recommended for estimating waves in shallow basins:

- Determine the straight-line fetch and over-water wind speed.
- Using the fetch and wind speed from (1), estimate the wave height and period from the deepwater nomograms.
- Compare the predicted peak wave period from (2) to the shallow-water limit given in Equation II-2-39. If that wave period is greater than the limiting value, then reduce the predicted wave period to this value. The wave height may be found by noting the dimensionless fetch associated with the limiting wave period and substituting this fetch for the actual fetch in the wave growth calculation.
- If the predicted wave period is less than the limiting value, then retain the deepwater values from (2).
- If wave height exceeds 0.6 times the depth, wave height should be limited to 0.6 times the depth.

c. Parametric prediction of waves in hurricanes.

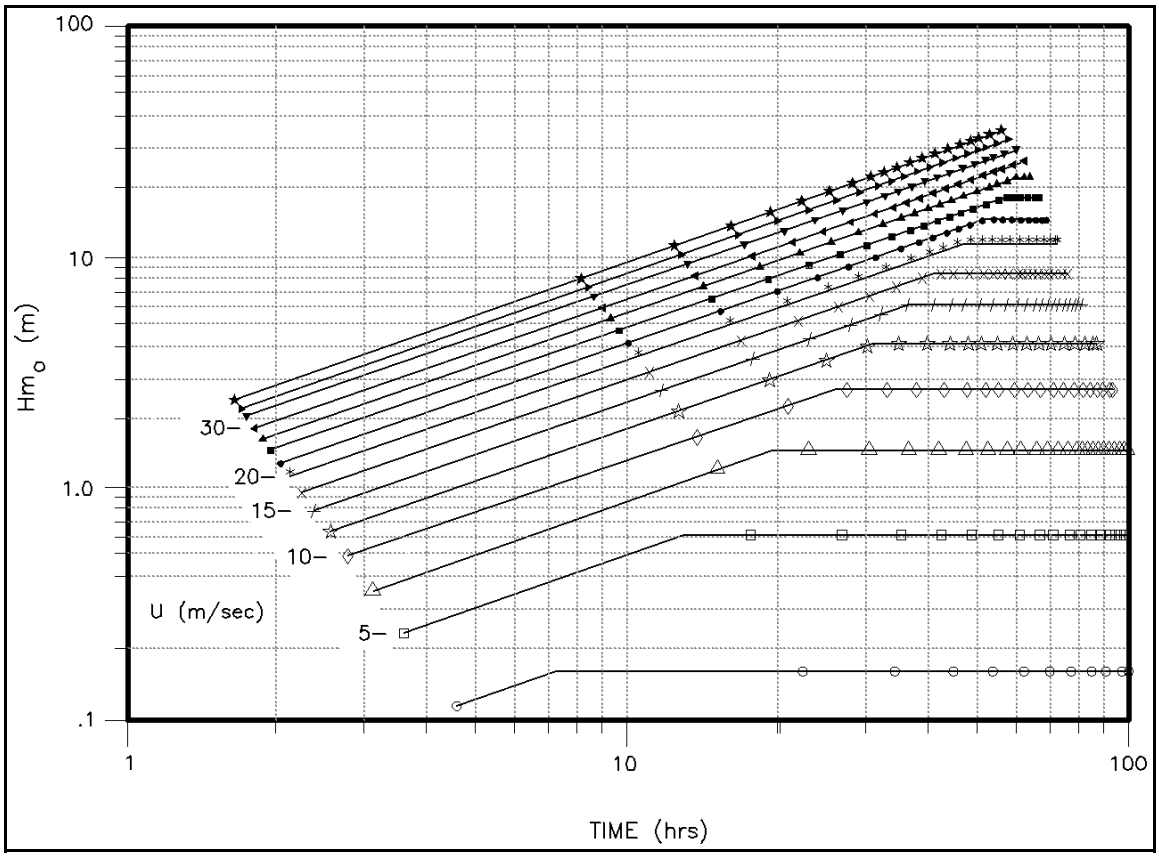

Figure II-2-25. Duration-limited wave heights (wind speeds are plotted in increments of 2.5 m/s)

(1) As shown Table II-2-2, waves from tropical storms, hurricanes, and typhoons represent a dominant threat to coastal and offshore structures and activities in many areas of the world. In this section, the generic term "hurricane" refers to all of these classes of storms. As pointed out previously in this chapter, the only distinction between tropical storms and hurricanes/typhoons is storm intensity (and somewhat the storm's degree of organization). The only distinction between hurricanes and typhoons is the point of origin of the storm.

(2) Spectral models have been shown to provide accurate estimates of hurricane wave conditions, when driven by good wind field information (Ward, Evans, and Pompa 1977; Corson et al. 1982; Cardone 1992; Hubertz 1992). Numerical spectral models can be run on most available PC's today, so there is little motivation not to use such models in any application with significant economic and/or safety implications. However, certain situations remain in which a parametric hurricane wave model may still play an important role in offshore and coastal applications. Therefore, some documentation of parametric models is still included in this manual.

(3) In general, parametric prediction methods tend to work well when applied to phenomena that have little or no dependence on previous states (i.e. systems with little or no memory). A good example of such a physical system is a hurricane wind field. It has been demonstrated (Ward et al. 1977) that hurricane wind fields can be well-represented by a small number of parameters, since winds in a hurricane tend always to remain very close to a dynamic balance with certain driving mechanisms. On the other hand, waves depend not only on the present wind field but also on earlier wind fields, bathymetric effects, pre-existing waves from other wind systems, and in general on the entire wave-generation process over the last to 12 to 24 hr.

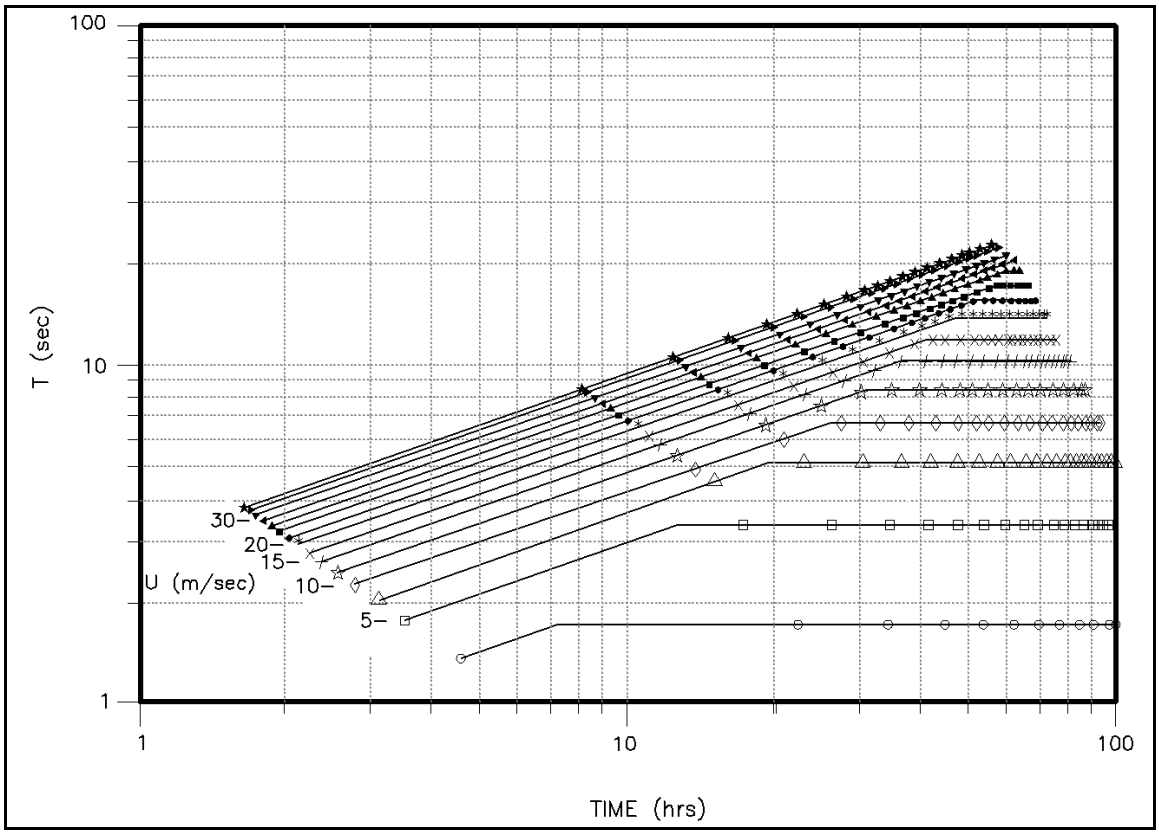

Figure II-2-26. Duration-limited wave periods

Thus, parametric models do not work well for all hurricanes, but do provide accurate results when the following criteria are met for an interval of about 12 to 18 hr prior to the application of a parametric model:

- Hurricane intensity (maximum velocity) is relatively constant.
- Hurricane track is relatively straight.
- Hurricane forward speed is relatively constant.
- Hurricane is not affected by land or bathymetric effects.
- No strong secondary wind and/or wave systems affect conditions in the area of interest.

(4) In certain situations, where there is a lack of detail on the actual characteristics of a hurricane (such as in hurricane forecasts, older historical storms, hurricanes in some regions of the world where meteorological data are sparse), parametric models may provide accuracies equal to those of spectral models, provided that land effects and bathymetric effects are minimal. However, even when these criteria are met, situations where secondary wind and/or wave systems can seriously affect wave conditions in an area should be avoided. Examples of this occur when large-scale pressure gradients (monsoonal or extratropical) significantly affect the shape and/or wind distribution of a hurricane. Winds and waves in such a storm will not be distributed in a manner consistent with the assumptions made in this section.

(5) Young (1987) developed a parametric wave model based on results from simulations with a numerical spectral model. His results show that there is a strong dependence of wave height on the relative values of maximum wind speed and forward storm velocity (Figure II-2-27). These results can be used to estimate the maximum value of H_{m0} in a hurricane. The distribution of wave heights within a hurricane is also affected by the ratio of maximum wind speed to forward storm velocity; however, in an effort to simplify applications here, only one chart is presented (Figure II-2-28). This chart is characteristic of storms with strong winds (maximum wind speed greater than 40 m/sec) and slow-to-moderate forward velocities (V_f less than 12 m/sec).

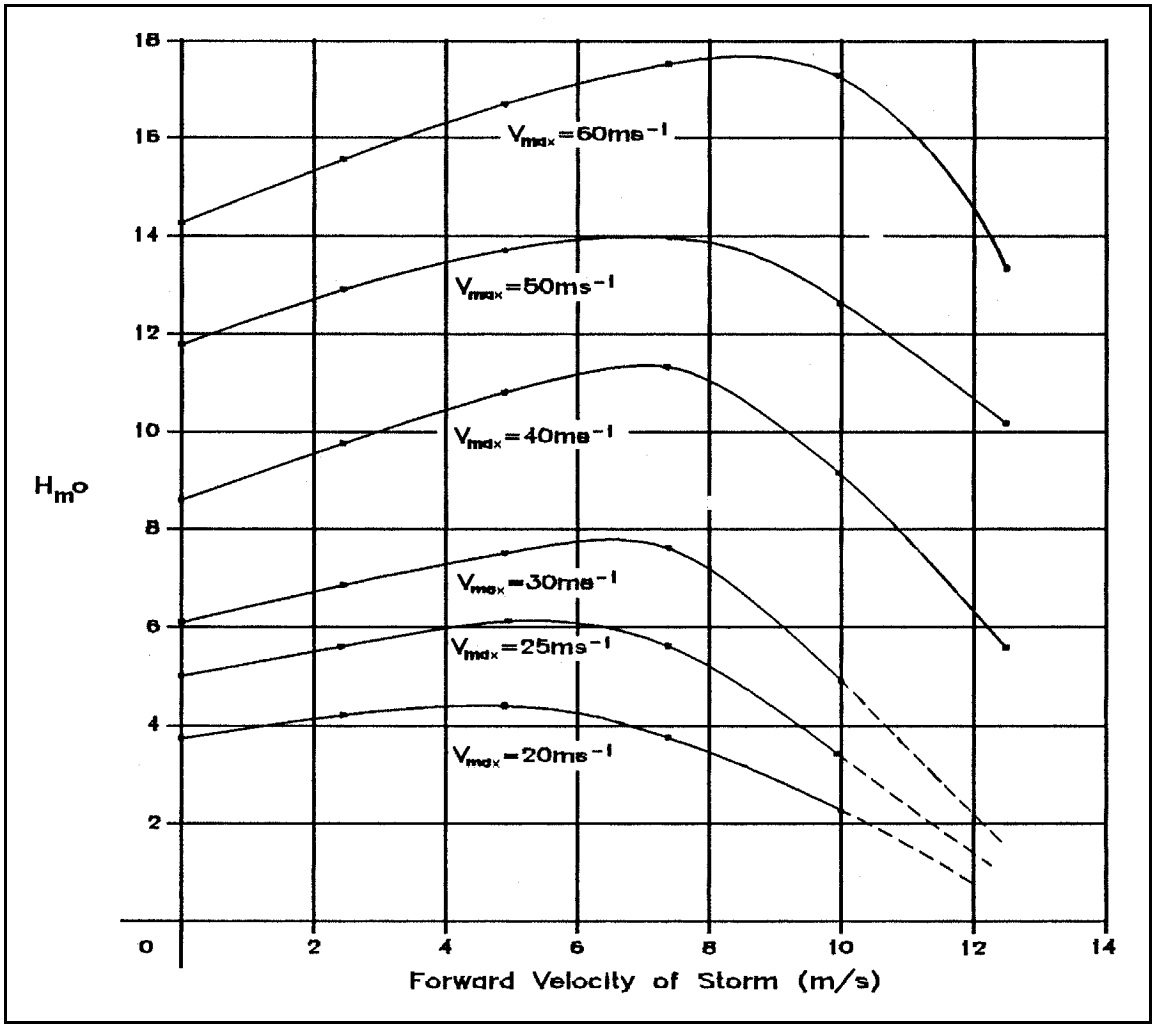

Figure II-2-27. Maximum value of H_{mo} in a hurricane as a function of V_{max} and forward velocity of storm (Young 1987)

II-2-3. Coastal Wave Climates in the United States.

a. Introduction.

(1) Coastal wave climates around U.S. coastlines are extremely varied. Past studies such as that by Thompson (1977) have relied primarily on measured wave conditions in coastal areas to specify nearshore wave climates. However, we now know that coastal wave heights can vary markedly as a function of distance

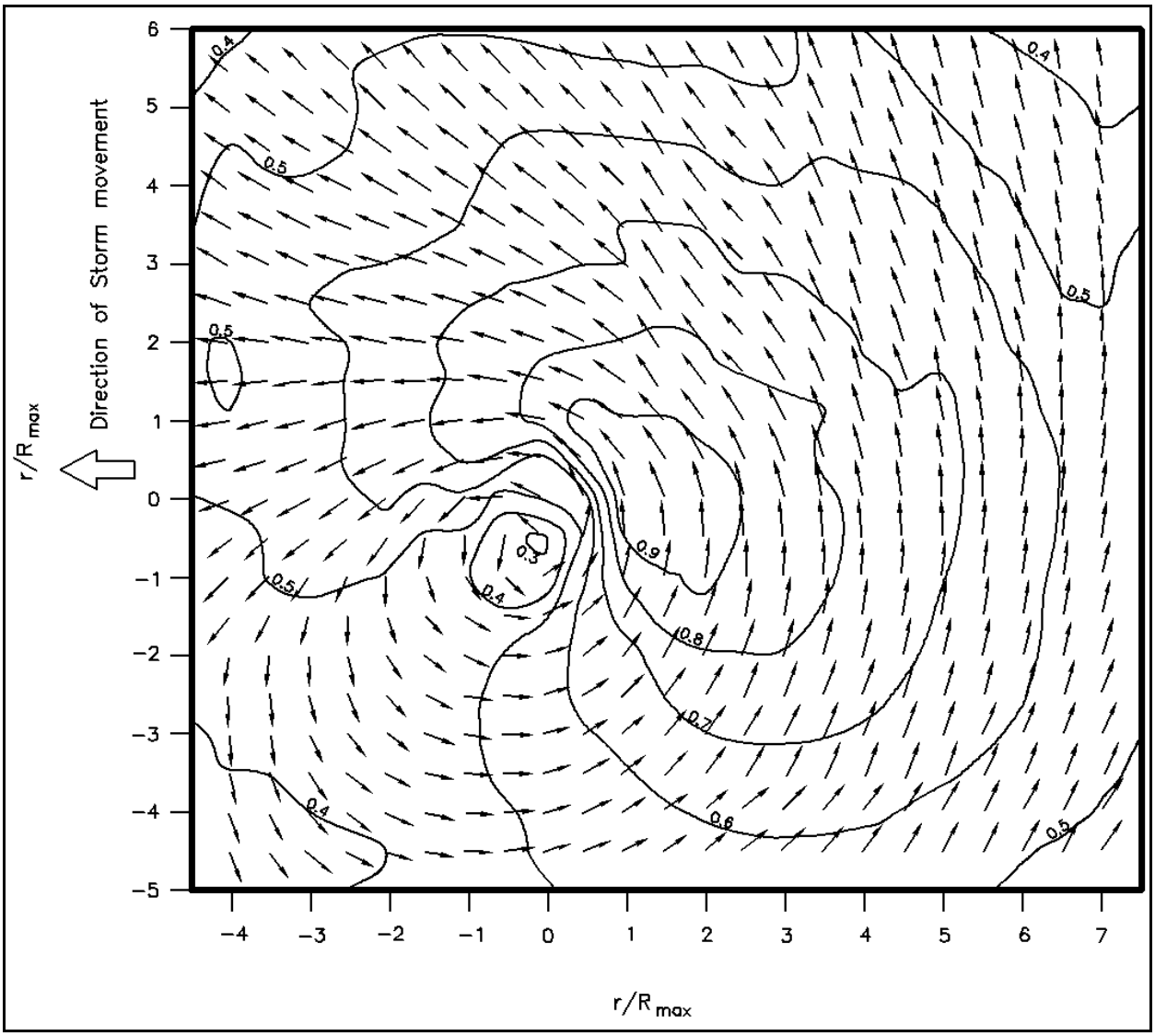

Figure II-2-28. Values of $H_{mo}/H_{mo\ max}$ plotted relative to center of hurricane (0,0)

offshore, degree of coastal sheltering, and various wave transformation factors. This means that measured waves in nearshore areas represent site-specific data. Also, even though measurements in U.S. waters have proliferated, they still do not offer comprehensive coverage. Because of these inherent difficulties in using measurements for a national climatology, hindcast information is used in this section to describe a general coastal wave climate. This is not meant to be interpreted that such models produce information that is as accurate as wave gauges or in any other way superior to wave measurements; but merely that they represent a consistent, comprehensive database for examining regional variations. In the near future, data assimilation methods will combine measurements and hindcasts into a unified database.

(2) In this section, typical wave conditions and storm waves for each of four general coastal areas will be described, along with some of the important meteorological systems that produce these waves. The areas covered here include all coastal areas within the United States, except for Alaska and Hawaii. The wave information presented in Tables II-2-3 through II-2-6 is based on numerical hindcast data provided by CERC's Wave Information Study (WIS). WIS is a multi-year study to develop wave climates for U.S. coastal regions. This information is not yet available for Alaskan and Hawaiian coastal areas; thus, these areas are

omitted in the presentations shown here. It should be noted that this information is very generalized. Waves at a specific site can vary from these estimates due to many site-specific factors, such as: variations in exposure to waves from different directions (primarily related to offshore islands and coastal orientation), bathymetric effects (refraction, shoaling, wave breaking, diffraction, etc.), interactions with currents near inlets or river mouths, and variations in fetches for wave generation.

(3) Figure II-2-29 provides the locations of reference sites along U.S. coastlines that will be used in subsequent parts of this section. A nominal depth of 20 m is assumed for these sites.

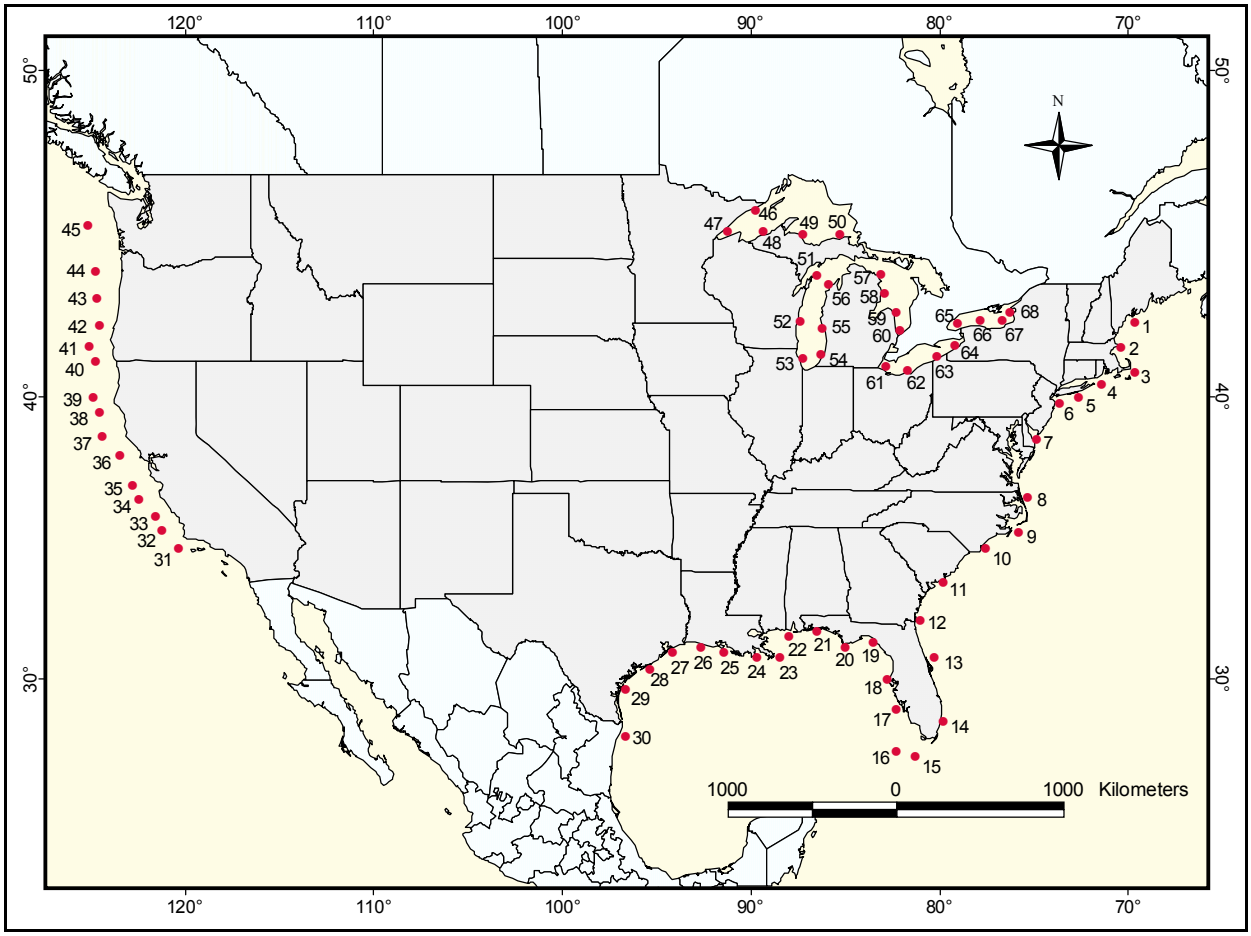

Figure II-2-29. Reference locations for Tables II-2-3 through II-2-6

b. Atlantic coast.

(1) Table II-2-3 provides wave information for the Atlantic coast. Mean wave heights are fairly consistent along the entire Atlantic coast (0.7 to 1.3 m); however, the overall distribution suggests a subtle multi-peak pattern with maxima at Cape Cod (1.3 m) and Cape Hatteras (1.2 m) and possibly a third peak in the vicinity of Cape Canaveral (1.1 m). These peaks are superimposed on a pattern of slight overall decreasing wave heights as one moves from north to south. Mean wave periods exhibit a relatively high degree of consistency along the entire Atlantic coast, varying only between 6.4 and 7.4 sec, except along the extreme southern part of Florida. The modal direction of the waves is taken here as the 22.5-deg direction class with the highest probability and appears to be primarily a function of coastal exposure.

Table II-2-3
Wave Statistics in the Atlantic Ocean

Map ID	WIS Station	Lat (deg)	Long (deg)	Depth (m)	H_s (m)	T_d (sec)	H_d (deg)	H_s90 (m)	T_d90 (sec)	H_d90 (deg)	H_s 5yr (m)	T_d 5yr (sec)	H_d 5yr (deg)
1	au2100	43.50	-69.75	110	1.4	7.5	160	2.6	8.8	165	11.6	13.8	131
2	au2095	42.50	-70.50	55	1.2	7.2	80	2.3	8.2	79	9.5	14.8	80
3	au2090	41.50	-69.75	18	1.5	7.8	118	2.7	9.2	113	8.4	14.0	52
4	au2082	41.00	-71.50	46	1.4	7.2	167	2.5	8.3	169	8.7	12.6	159
5	au2077	40.50	-72.75	37	1.4	7.2	162	2.5	8.1	170	8.2	12.7	147
6	au2072	40.25	-73.75	27	1.2	7.1	132	2.2	7.9	128	7.2	12.8	129
7	au2066	38.75	-75.00	18	1.0	7.2	124	1.9	7.9	126	5.7	12.8	124
8	au2056	36.25	-75.50	27	1.2	8.1	59	2.3	8.8	46	7.7	13.7	70
9	au2049	34.75	-76.00	35	1.3	7.5	139	2.3	8.1	142	8.1	14.0	129
10	au2042	34.00	-77.75	9	1.1	8.1	124	2.0	8.8	124	6.0	15.2	126
11	au2035	32.50	-80.00	9	1.0	7.5	122	1.7	8.2	122	5.1	14.2	132
12	au2028	30.75	-81.25	11	1.1	8.9	94	1.8	9.3	91	5.7	15.7	95
13	au2021	29.00	-80.50	18	1.2	9.4	65	2.1	10.0	61	6.5	15.4	65
14	au2009	26.00	-80.00	220	0.9	7.3	62	1.8	7.6	64	6.1	10.8	44

For location, refer to Figure II-2-29. Statistics computed from time-series hindcast covering 1976 - 1995 period.

EXAMPLE PROBLEM II-2-7

FIND:

The significant wave height at the end of this fetch, assuming that the duration of the wind is sufficient to generate fetch-limited waves (from Figure II-2-3, this is found to be greater than about 1.25 hr).

GIVEN:

A constant wind speed of 15 m/sec over a fetch of 10 km in a basin with a constant depth of 3 m. (Note: as pointed out in the previous section on winds, wind speeds tend to increase with fetch over a fetch of this size, so care should be taken in estimating this wind speed)

SOLUTION:

OPTION 1 - Use ACES

OPTION 2 - From Figure II-2-24 the fetch-limited peak wave period is about 2.7 sec, from Equation II-2-39, the limiting wave period in 3 m is 5.4 sec; therefore, T_p = 2.7 sec and H_{m0} = 1.0 m (deepwater values).

EXAMPLE PROBLEM II-2-8

FIND:

The significant wave height at the end of this fetch.

GIVEN:

A constant wind speed of 25 m/sec over a fetch of 50 km in a basin with a constant depth of 1.6 m.

SOLUTION:

OPTION 1 - Use ACES

OPTION 2 - From Figure II-2-24, the fetch-limited peak wave period is about 5.8 sec, from Equation II-2-39, the limiting wave period in 1.6 m is 4.0 sec; therefore, the waves stopped growing at this limit. This corresponds to a fetch of 20 km at this wind speed; thus, the final values of T_p and H_{m0} are 4.0 sec and 2.1 m (using the 20-km fetch and 25-m/sec wind speed in Figure II-2-23). However, this value exceeds 0.6 times the depth, so the final answer should be 0.8 m. The wave height is limited in this example to be half the water depth. In shallow depths, this is a reasonable approximation.

(2) These results appear consistent with the mean storminess expected in these Atlantic coastal regions. In the northern portion of the Atlantic coast, the primary source of large waves is migratory extratropical cyclones. Between storm intervals in this region, waves come primarily from swell propagating from storms moving away from the coast. Due to this direction of storm movement, the swell from these storms is usually not very large (less than 2 m). As one moves southward past Cape Hatteras, waves from high-pressure systems (both migratory and semipermanent) begin to become dominant in the wave population. Once south of Jacksonville, the wave climate is typically dominated by easterly winds from high pressure systems, with a secondary source of swell from northeasters. Farther south, as one approaches Miami, the Bahamas provide considerable shelter for waves approaching from the east. In coastal areas without significant swell, sea breeze winds can play a significant role in producing coastal waves during afternoon periods. This situation occurs over much of the U.S. east coast during intervals of the year.

(3) The 90th percentile wave heights can be considered as representative of typical large wave conditions. As can be seen here, this wave height varies from 1.9 to 2.4 m along the New England region down to 1.4 to 1.9 m along the Florida coast. As was seen in the distribution of mean wave heights, the overall pattern appears to have maxima at Cape Cod (2.4 m), Cape Hatteras (2.1 m), and Cape Canaveral (1.9 m). The associated periods are very consistent along most of the Atlantic coast (8.5 to 9.9 sec) except for the southern half of Florida, where the periods are somewhat lower (6.2 to 7.7 sec). Directions of the 90th-percentile wave reflect the general coastal orientation.

(4) Extreme waves along the Atlantic coast are often produced by both intense extratropical storms and tropical storms. Table II-2-3 does not provide any information that extends into the return period domain dominated by tropical storms; consequently, this table can be regarded as actually providing information only on extratropical storms. Since this table is not intended to be used directly for any coastal design considerations, information on large-return-period storms is specifically excluded.

(5) The 5-year wave heights presented in Table II-2-3 can be considered as representing typical large storms that might affect short-term projects (beach nourishment, dredging operations, sand bypassing, etc.). Values of the 5-year wave height range from generally greater than 6 m north of Long Island to only 4.2 m in the Florida Keys. Again, north to south decreasing maxima appear in the regions of Cape Cod (6.7 m), Cape Hatteras (5.9 m), and Cape Canaveral (4.9 m). Associated wave periods are generally in the range of 11 to 13 sec, except for the Florida Keys site, where this period is only 9.5 sec.

(6) Various types of extratropical storms have wreaked havoc along different coastal areas. These storms range from “bombs” (small, intense, rapidly developing storms) to large almost-stationary storms (developing typically after a change in the large-scale global circulation). Bombs produce higher wind speeds (sustained winds can exceed 70 knots) but due to fetch and duration considerations, the larger, slower-moving storms produce larger wave heights (a measured H_{m0} greater than 17 m south of Nova Scotia in the Halloween Storm). Other examples of classic storms along the U.S. east coast include the Ash Wednesday Storm of 1962 (affecting mainly the mid-Atlantic region), the Blizzard of 1978 (affecting mainly the northeastern states), and the Storm of March 1993, which affected most of the U.S east coast. This last storm has been called the “Storm of the Century” by some; however, it is by no means the worst storm in terms of waves for most areas along the east coast in this century. In fact, along much of the Atlantic coast, the wind direction was toward offshore; consequently, there was almost no wave action at the coast in many locations. Farther offshore the situation was considerably different and many ships and boats were lost.

(7) Hurricanes can also produce extreme wave conditions along the coast. Particularly at the coast itself where storm surges of 10 ft or more can accompany waves, hurricane waves represent an extreme threat to both life and property. An excellent source of hurricane information is the HURDAT file at the National Climatic Center in Asheville, NC. This file (available on magnetic tape or PC diskette format) contains storm tracks, maximum wind speeds, central pressures, and other parameters of interest for all hurricanes affecting

the United States since 1876. The effects of Hurricanes Hugo in 1988 and Andrew in 1992 have shown the tremendous potential for coastal destruction that can accompany these storm systems in southern reaches of the Atlantic coast. The effects of the Hurricane of 1933 in New England and Hurricane Bob in 1990 show that even farther north, the risk of hurricanes cannot be neglected.

c. Gulf of Mexico.

(1) Table II-2-4 shows the same information for the U.S. Gulf coast as was given in Table II-2-3 for the Atlantic coast. Mean wave heights for this coast are often considered to be considerably lower than those on the Atlantic coast; however, as can be seen in this table, this is not evident in the wave data. In fact, mean wave heights near Brownsville are larger than anywhere on the Atlantic coast. The reason for this is that the mean wind direction in this location is directed toward land, whereas, along the Atlantic coast, the mean wind direction is directed away from land except for areas south of Jacksonville, FL. Mean wave heights generally decrease eastward to the Appalachicola area and then remain fairly constant southward to the Florida Keys.

(2) Many of the larger waves in the Gulf of Mexico are generated by storms that are centered well to the north over land. Thus, large waves can be experienced at offshore sites even when conditions along the coast are quite calm. Typical day-to-day wave conditions in many coastal areas are produced by a combination of relatively small synoptic-scale winds and sea-breeze circulations. As noted in Table II-2-2 in this section, these waves are rarely very large. At times, the Gulf of Mexico comes under the influence of large-scale high pressure systems, with winds blowing from east to west across much of the Gulf. These winds are primarily responsible for the higher wave conditions in the western Gulf. Due to the lack of strong storms centered within the Gulf, there is little or no swell reaching Gulf shorelines, with the notable exception being swell from remote tropical systems. Consequently, except for the extreme western Gulf of Mexico, mean wave periods tend to be somewhat smaller than those along the Atlantic coast (4 to 6 sec).

(3) The 90^{th} percentile wave heights indicate that typical large wave conditions along the coast are only about 50 percent larger than the mean wave heights (compared to about a 100-percent factor for the Atlantic coast). This is consistent with the idea that the Gulf of Mexico is, in fact, a calmer basin than the Atlantic. These wave heights in the Gulf vary from a maximum of 1.5 m near Brownsville to 1.2 m along Florida's west coast. Associated wave periods range from 6 to 8 sec.

(4) Values of the 5-year wave heights in the Gulf of Mexico vary from 3.2 m along the west coast of Florida to 4.6 m near Brownsville. Associated wave periods vary between 9 and 10.5 sec. Some of the higher non-tropical waves in the Gulf of Mexico are generated by wind systems called "Northers." Since these winds blow out of the north, they typically do not create problems at the coast itself, but can produce large waves at offshore sites. Occasionally an extratropical cyclone will develop within the Gulf. One example, the intense storm of 10-13 March, 1993 (the so-called "Storm of the Century"), produced high surges and large waves along extensive portions of Florida's west coast. Damages and loss of life from this storm demonstrated that, although rare, strong extratropical storms can still be a threat to some Gulf coastal areas.

(5) The primary source of extreme waves in the Gulf of Mexico is hurricanes. Hurricanes Betsy (1965), Camille (1969), Carmen (1975), Frederick (1979), Alicia (1985), and Andrew (1992) have clearly shown the devastating potential of these storms in the Gulf of Mexico. Even though shallow-water effects may diminish coastal wave heights from the values listed in Table II-2-2, wave conditions are still sufficient to control design and planning considerations for most coastal and offshore structures/facilities in the Gulf.

Table II-2-4
Wave Statistics in the Gulf of Mexico

Map ID	WIS Station	Lat (deg)	Long (deg)	Depth (m)	H_s (m)	T_d (sec)	H_d (deg)	H_s90 (m)	T_d90 (sec)	H_d90 (deg)	H_s 5yr (m)	T_d 5yr (sec)	H_d 5yr (deg)
15	gu1002	24.25	-81.50	451	0.8	4.4	83	1.5	5.7	77	4.8	9.9	140
16	gu1006	24.50	-82.50	14	0.7	4.3	48	1.4	5.8	37	3.9	9.3	202
17	gu1017	26.50	-82.50	18	0.4	3.9	270	0.9	5.1	303	4.5	10.5	219
18	gu1023	28.00	-83.00	11	0.4	3.9	264	0.8	5.2	274	4.6	12.2	244
19	gu1030	29.75	-83.75	5	0.4	3.8	224	0.8	4.8	252	3.1	10.6	210
20	gu1036	29.50	-85.25	19	0.7	4.2	170	1.3	5.4	113	5.5	11.8	183
21	gu1042	30.25	-86.75	14	0.6	4.2	153	1.1	5.3	149	5.5	11.9	174
22	gu1048	30.00	-88.25	29	0.7	4.4	135	1.3	5.7	135	5.6	10.6	128
23	gu1054	29.00	-88.75	209	0.9	4.9	98	1.8	6.6	89	6.8	11.7	136
24	gu1059	29.00	-90.00	25	0.8	4.7	138	1.5	6.0	138	5.4	11.4	167
25	gu1066	29.25	-91.75	7	0.7	4.6	162	1.3	6.0	164	4.0	11.3	190
26	gu1071	29.50	-93.00	12	0.8	4.7	150	1.4	6.1	153	4.2	11.1	167
27	gu1077	29.25	-94.50	15	0.8	5.1	140	1.5	6.5	142	4.5	11.9	145
28	gu1082	28.50	-95.75	20	0.9	5.4	137	1.5	6.8	143	4.5	11.7	132
29	gu1088	27.50	-97.00	27	0.9	5.8	119	1.5	7.0	123	5.3	11.2	108
30	gu1102	25.25	-97.00	48	1.1	6.0	100	1.7	7.2	102	5.8	9.9	73

For location, refer to Figure II-2-29. Statistics computed from time-series hindcast covering 1976 - 1995 period.

d. Pacific coast.

(1) Table II-2-5 provides information for the Pacific coast that is comparable to that presented in Tables II-3-3 and II-2-4 for the Atlantic and Gulf of Mexico coasts, respectively. The Pacific coast is very different from the east coast in that wave-producing storms within the Pacific Ocean are travelling toward this coast. This means that the west coast typically has a much richer source of swell waves tha do other U.S. coastal areas. As can be seen by comparison to the Atlantic coast results (Table II-2-3), this results in higher wave conditions along the Pacific coast, with mean wave heights ranging from 2.5 m near the Mexican border to 3.2 m near the Canadian border. This difference is also reflected in the mean periods along these coasts, which vary from 9.6 to 12.1 sec. During (Northern Hemisphere) summer months, storm tracks usually move far to the north and storms are less intense. Consequently, swell from mid-latitude storms in the Northern Hemisphere diminish in size and frequency, allowing swell from tropical storms spawned off the west coast of Mexico and from large winter storms in the Southern Hemisphere to become important elements in the summer wave climate.

(2) Typical winter storm tracks move storm centers inland in the region from northern California to the Canadian border. Hence, large waves in these regions frequently come in the form of local seas. South of San Francisco, local storms strike the coast with less frequency; thus, many of the large waves in this area arrive in the form of swell. Many notable exceptions to this general rule of thumb can be found in the late 1970's and 1980's, however. In particular, the storm of January 1989 moved across the California coast in the vicinity of Los Angeles and caused much damage to southern California coastal areas.

(3) The 90^{th} percentile wave heights along the Pacific coast are about twice their Atlantic coast counterparts. In the southern California region, these values are typically in the 3.9- to 4.2-m range. As one moves northward, the 90^{th} percentile wave height increases to a maximum of about 5.4 m along the coast of Washington. Periods associated with these waves tend to be quite long, ranging between 11 and 14 sec.

(4) The 5-year wave heights in the southern California region are comparable to those found along the New England coast on the Atlantic (6.8-6.9 m compared to 6.7 m). However, associated periods are considerably longer (16.8 sec compared to 12-13 sec). As one moves northward, these wave heights increase to levels greater than 10 m along much of the coast north of the California-Oregon border. Periods of these large waves tend to fall in the 14- to 16-sec range.

(5) Although many studies have dismissed the importance of tropical storms to the extreme wave climate along the Pacific coast, at least one tropical storm has moved into the Los Angeles basin during this century, suggesting that this threat is not negligible. Given the curvature of the coast and the water temperatures north of Point Conception, it is unlikely that tropical storms can produce a significant threat at coastal sites north of this point; however, south of this point it is important to include tropical storms in any design and planning considerations.

e. Great Lakes.

(1) Table II-2-6 provides comparable information for the Great Lakes as provided for previous coastal areas in Tables II-2-3 through II-2-5. Wave conditions within the Great Lakes are strongly influenced by fetches aligned with the dominant directions of storm winds. These winds are mainly produced by various extratropical storms moving across the Great Lakes region. Table II-2-6 compares the largest 50-year (return period) wave heights for each lake. Since strong storms are not very frequent in late spring through early autumn, this interval is usually relatively calm along most shorelines. During the period from mid-autumn until ice effects on the lakes reduce the wave generation potential, the largest waves are generated. Again

Table II-2-5
Wave Statistics in the Pacific Ocean

Map ID	WIS Station	Lat (deg)	Long (deg)	Depth (m)	H_s (m)	T_d (sec)	H_d (deg)	H_s90 (m)	T_d90 (sec)	H_d90 (deg)	H_s 5yr (m)	T_d 5yr (sec)	H_d 5yr (deg)
31	p2008	34.01	-120.92	1650	2.7	10.3	293	4.1	12.5	290	7.0	15.4	285
32	p2011	34.82	-121.82	2122	2.8	10.3	294	4.2	12.5	291	7.5	15.7	283
33	p2013	35.41	-122.16	2944	2.8	10.3	292	4.2	12.5	287	7.8	15.8	279
34	p2016	36.22	-123.06	3365	2.9	10.4	295	4.3	12.5	290	7.9	15.1	264
35	p2018	36.82	-123.41	3387	3.0	10.5	294	4.4	12.6	289	8.2	14.8	250
36	p2022	38.04	-124.11	3655	3.1	10.8	292	4.6	12.9	285	8.5	14.6	245
37	p2025	38.85	-125.05	3435	3.2	10.7	287	4.9	12.7	281	9.3	14.3	242
38	p2028	39.87	-125.17	2471	3.2	10.7	286	4.8	12.7	278	9.4	13.8	235
39	p2030	40.49	-125.53	2702	3.2	10.7	284	4.9	12.6	275	9.7	14.0	219
40	p2034	41.93	-125.39	3151	3.2	10.7	274	5.2	12.9	265	10.4	14.1	235
41	p2036	42.55	-125.74	2993	3.3	10.7	271	5.4	12.9	262	10.8	13.6	224
42	p2038	43.37	-125.21	1783	3.3	10.9	271	5.4	13.0	263	10.4	14.1	238
43	p2041	44.41	-125.29	2227	3.0	10.9	271	4.9	13.0	264	9.2	14.0	219
44	p2044	45.45	-125.36	2033	3.0	10.9	266	4.8	12.9	259	9.5	14.3	213
45	p2049	47.14	-125.77	1630	3.2	10.7	257	5.4	12.7	250	10.5	14.4	224

For location, refer to Figure II-2-29. Statistics computed from time-series hindcast covering 1956 - 1975 period.

Table II-2-6
Wave Statistics in the Great Lakes

Map ID	WIS Station	Lat (deg)	Long (deg)	Depth (m)	H_s (m)	T_d (sec)	H_d (deg)	H_s90 (m)	T_d90 (sec)	H_d90 (deg)	H_s 5yr (m)	T_d 5yr (sec)	H_d 5yr (deg)
46	s0004	47.67	-90.07	174	0.8	3.9	255	1.6	5.2	279	7.4	11.1	88
47	s0014	46.95	-91.57	154	0.7	3.6	27	1.3	4.6	325	6.0	10.2	56
48	s0028	46.95	-89.63	101	0.8	4.0	318	1.8	5.7	313	5.9	9.7	17
49	s0046	46.80	-87.50	55	1.0	4.2	2	2.0	5.7	351	7.7	10.2	10
50	s0055	46.80	-85.57	119	1.1	4.6	322	2.2	6.3	328	7.0	10.3	310
51	mu0025	45.27	-86.75	55	0.9	4.4	172	1.7	5.9	164	4.9	8.4	194
52	mu0013	43.55	-87.67	64	0.8	4.3	98	1.6	5.6	109	4.6	8.4	54
53	mu0003	42.10	-87.55	24	0.9	4.1	22	1.6	5.5	23	5.4	9.3	11
54	mu0058	42.22	-86.58	36	1.0	4.5	308	1.8	6.2	302	5.1	8.8	342
55	mu0051	43.23	-86.50	73	1.0	4.4	256	1.9	6.3	259	5.3	8.6	238
56	mu0039	44.95	-86.17	36	0.9	4.4	286	1.8	6.0	291	5.2	9.0	222
57	h0020	45.35	-83.32	30	0.8	4.0	5	1.7	5.3	360	5.8	9.1	83
58	h0015	44.63	-83.12	20	0.9	4.2	83	1.9	5.6	301	6.7	9.4	52
59	h0007	43.90	-82.52	30	0.8	4.2	346	1.7	5.6	335	6.1	9.4	12
60	h0002	43.18	-82.32	14	0.9	4.0	334	1.7	5.2	322	6.8	9.8	356
61 [1]	e0002	41.73	-83.08	9	0.6	3.5	285	1.1	4.4	299	2.4	5.5	14
62	e0009	41.58	-81.90	17	0.9	3.9	280	1.7	5.3	292	4.0	7.6	339
63	e0017	42.15	-80.35	20	1.0	4.3	263	2.0	5.9	272	4.8	8.5	271
64	e0022	42.58	-79.37	30	0.9	4.0	253	1.8	5.5	255	5.2	8.8	252
65 [2]	o0037	43.45	-79.25	128	0.4	3.0	271	0.9	3.9	273	3.5	6.6	236
66	o0040	43.60	-78.05	185	0.4	3.2	262	1.0	4.5	266	4.8	8.2	260
67	o0043	43.60	-76.85	174	0.4	3.3	266	1.0	4.7	266	5.5	9.4	265
68	o0020	43.88	-76.45	24	0.4	3.2	243	0.9	4.2	247	5.1	8.7	243

For location, refer to Figure II-2-29. Statistics computed from time-series hindcast covering 1956 - 1987 period.
[1] Station e0002 is sheltered from the east by islands.
[2] Station o0037 reflects west-to-east weather patterns.

in the spring, after the ice has thawed, large waves (although usually significantly smaller than waves in autumn) can be generated and can affect coastal areas.

(2) One of the issues of critical concern in the Great Lakes is that of mean lake level. These levels have fluctuated considerably through recorded history in response to periods of low and high precipitation in the general geographic area. Critical design criteria for many Great Lakes coastal areas are defined by the superposition of high wave conditions (generated by extratropical storms) on top of high mean lake levels and storm surges.

II-2-4. Additional Example Problem

This problem demonstrates use of assumptions in simplified wave predictions.

EXAMPLE PROBLEM II-2-9

FIND: The significant wave height and spectral peak wave period generated by a mean wind speed of 30 m/s over a fetch of 50 km. (Work the problem in metric units.)

SOLUTION:

Step 1. Check required wind duration. Given that x is the fetch in meters, g is the acceleration due to gravity in meters/second-squared, u_{10} is the wind speed in meters/second, we have

$$t_{x,u} = 77.23\frac{x^{0.67}}{u_{10}^{0.34}g^{0.33}} = 77.23\frac{(50,000)^{0.67}}{30^{0.34}9.82^{0.33}} = 16,087\,\text{sec} = 4.47\text{hrs}$$

If the wind duration is equal to or longer than this than a fetch-limited situation exists.

Step 2. Estimate friction velocity. First, estimate the coefficient of drag as

$$C_d \approx 0.001(1.1 + 0.035u_{10});$$

Then, estimate the friction velocity as

$$u_* = \sqrt{C_d}u_{10} = \sqrt{0.00215} \times 30 = 1.39m/\text{sec}$$

Step 3. Estimate Significant Wave Height. Estimate nondimensional fetch as

$$\hat{x} = \frac{gx}{u_*^2} = 9.82 \times 50,000/(1.39)^2 = 2.54 \times 10^5$$

Estimate nondimensional wave height as

$$\hat{H}_{m0} = \lambda_1 \hat{x}^{m_1};$$
$$\lambda_1 = 0.0413;$$
$$m_1 = \frac{1}{2};$$
$$\hat{H}_{m0} = 0.0413 \times \left(2.54 \times 10^5\right)^{\frac{1}{2}} = 20.8;$$
$$H_{m0} = \hat{H}_{m0} \times \frac{u_*^2}{g} = 20.8 \times \frac{(1.39)^2}{9.82} = 4.1m$$

Step 4. Estimate Spectral Peak Period. Since we already have calculated the nondimensional fetch in Step 3, we can proceed to estimate the nondimensional spectral peak period:

$$\hat{T}_p = \frac{gT_p}{u_*} = \lambda_2 \hat{x}^{m_2}$$
$$\lambda_2 = 0.751$$
$$m_2 = \frac{1}{3}$$
$$\hat{T}_p = 0.751 \times \left(2.54 \times 10^5\right)^{\frac{1}{3}} = 47.5$$
$$T_p = \hat{T}_p \frac{u_*}{g} = \frac{47.5 \times 1.39}{9.82} = 6.7\,\text{sec}$$

II-2-5. References

Atkinson and Holliday 1977
Atkinson, G. D., and Holliday, C. R. 1977. "Tropical Cyclone Minimum Sea Level Pressure/Maximum Sustained Wind Relationship for the Western Northern Pacific," *Mon. Wea. Rev.,* Vol 105, pp 421-427.

Barnett 1968
Barnett, T. P. 1968. "On the Generation, Dissipation, and Prediction of Ocean Wind Waves," *J. Geophys. Res.,* Vol 2, pp 531-534.

Bouws, Gunther, and Vincent 1985
Bouws, E., Gunther, H., and Vincent, C. L. 1985. "Similarity of Wind Wave Spectrum in Finite-Depth Water, Part I: Spectral Form," *J. Geophys. Res.*, Vol 85, No. C3, pp 1524-1530.

Bretschneider 1952
Bretschneider, C. 1952. "Revised Wave Forecasting Relationships," *Proceedings of the 2nd Coastal Engineering Conference*, American Society of Civil Engineers, pp 1-5.

Bretschneider 1990
Bretschneider, C. 1990. "Tropical Cyclones," *Handbook of Coastal and Ocean Engineering,* Vol 1, J. B. Herbich, ed., pp 249-270.

Bretschneider and Reid 1953
Bretschneider, C., and Reid, R. O. 1953. "Change in Wave Height Due to Bottom Friction, Percolation and Refraction," *34th Annual Meeting of American Geophysical Union.*

Bunting 1970
Bunting, D. C. 1970. "Evaluating Forecasts of Ocean-Wave Spectra," *Journal of Geophysical Research*, Vol 75, No. 21, pp 4131-4143.

Businger et al. 1971
Businger, J. A., Wyngaard, J. C., Izumi, Y., and Bradley, E. F. 1971. "Flux-Profile Relationships in the Atmoshperic Surface Layer," *J. Atmos. Sci.,* Vol 25, pp 1021-1025.

Camfield 1977
Camfield, F. E. 1977. "Wind-Wave Propagation Over Flooded, Vegetated Land," Technical Paper No. 77-12, Coastal Engineering Research Center, U.S. Army Engineer Waterways Experiment Station, Vicksburg, MS.

Cardone 1992
Cardone, V. J. 1992. "On the Structure of the Marine Surface Wind Field," *3rd International Workshop of Wave Hindcasting and Forecasting,* Montreal, Quebec, May 19-22, pp 54-66.

Cardone, Cox, Greenwood, and Thompson 1994
Cardone, V. J., Cox, A. T., Greenwood, J. A., and Thompson, E. F. 1994. "Upgrade of the Tropical Cyclone Surface Wind Field Model," Miscellaneous Paper CERC-94-14, U.S. Army Engineer Waterways Experiment Station, Vicksburg, MS.

Cardone, Greenwood, and Greenwood 1992
Cardone, V. J., Greenwood, C. V., and Greenwood, J. A. 1992. "Unified Program for the Specification of Hurricane Boundary Layer Winds over Surfaces of Specified Roughness," Contract Report CERC-92-1, U.S. Army Engineer Waterways Experiment Station, Vicksburg, MS.

Chow 1971
Chow, S. 1971. "A Study of the Wind Field in the Planetary Boundary Layer of a Moving Tropical Cyclone," M. S. thesis, New York University.

Clarke 1970
Clarke, R. H. 1970. "Observational Studies of the Atmospheric Boundary Layer," *Quart. J. Roy. Meteor. Soc,* Vol 96, pp 91-114.

Collins and Viehmann 1971
Collins, J. I., and Viehmann, M. J. 1971. "A Simplified Model for Hurricane Wind Fields," Paper 1346, *Offshore Technology Conference,* Houston, TX.

Cooper 1988
Cooper, C. K. 1988. Parametric Models of Hurricane-Generated Winds, Waves, and Currents in Deep Water," *Proc. Offshore Tech. Conf.*, Paper 5738, Houston, TX.

Corson et al. 1982
Corson, W. D., Resio, D. T., Brooks, R. M., Ebersole, B. A., Jensen, R. E., Ragsdale, D. S., and Tracy, B. A. 1982. "Atlantic Coast Hindcast Phase II, Significant Wave Information," WIS Report 6, U.S. Army Engineer Waterways Experiment Station, Vicksburg, MS.

Deardorff 1968
Deardorff, J. W. 1968. "Dependence of Air-Sea Transfer Coefficients on Bulk Stability," *J. Geophys. Res,* Vol 73, pp 2549-2557.

Demirbilek, Bratos, and Thompson 1993
Demirbilek, Z., Bratos, S. M., and Thompson, E. F. 1993. "Wind Products for Use in Coastal Wave and Surge Models,"Miscellaneous Paper CERC-93-7, U.S. Army Engineer Waterways Experiment Station, Vicksburg, MS.

Donelan, Hamilton, and Hu 1982
Donelan, M. A., Hamilton, J., and Hu, W. H. 1982. "Directions Spectra of Wind-Generated Waves," Unpublished manuscript, Canada Centre for Inland Waters.

Dvorak 1975
Dvorak, V. F. 1975. "Tropical Cyclone Intensity Analysis and Forecasting from Satellite Imagery," *Mon. Wea. Rev.,* Vol 105, pp 369-375.

Forristall, Ward, Cardone, and Borgman, 1978
Forristall, G. Z., Ward, E. G., Cardone, V. J., and Borgman, L. E. 1978. "The Directional Spectra and Kinematics of Surface Gravity Waves in Tropical Storm Delia," *J. Pmys. Oceanogr.,* Vol 8, pp 888-909.

Garratt 1977
Garratt, J. R. 1977. "Review of Drag Coefficients Over Oceans and Continents," *Mon. Wea. Rev.,* Vol 105, pp 915-929.

Geernaert 1990
Geernaert, G. L. 1990. " Bulk Parameterizations for the Wind Stress and Heat Fluxes," *Surface and Fluxes: Theory and Remote Sensing; Vol 1: Current Theory.* G. L. Geernaert and W. J. Plant, ed., Kluwer Academic Publisher, Worwell, MA, pp 91-172.

Geernaert, Katsaros, and Richter 1986
Geernaert, G. L., Katsaros, K. B., and Richter, K. 1986. "Variation of the Drag Coefficient and its Dependence on Sea State," *J. Geophys. Res.,* Vol 91, pp 7667-7679.

Gelci, Cazale, and Vassel 1957
Gelci, R., Cazale, H., and Vassel, J. 1957. "Prevision de la Houle," *La Methode des Densites Spectroangularies, Bull. Infor.,* Comite Central Oceangr. d' Etude Cotes, Vol 9, pp 416-435.

Hasselmann et al. 1973
Hasselmann, K., Barnett, T. P., Bouws, E., Carlson, H., Cartwright, D. E., Enke K., Weing, J. A., Gienapp, H., Hasselmann, D. E., Kruseman, P., Meerburg, A., Muller, P., Olbers, K. J., Richter, K., Sell, W., and Walden, W. H. 1973. "Measurements of Wind-Wave Growth and Swell Decay During the Joint North Sea Wave Project (JONSWAP)," *Deutsche Hydrograph, Zeit., Erganzung-self Reihe,* A 8(12).

Hasselmann, Hasselmann, Allender, and Barnett 1985
Hasselmann, S., Hasselmann, K., Allender, J. H., and Barnett, T. P. 1985. "Computations and Parameterizations of Nonlinear Energy Transfer in a Gravity-wave Spectrum; Part II: Parameterization of Nonlinear Transfer for Application in Wave Models," *J. Phys. Oceanogr.,* Vol 15, pp 1378-1391.

Helmholtz 1888
Helmholtz, H. 1888. "Uber Atmospharische Bewwgungen," *S. Ber. Preuss. Akad. Wiss. Berlin, Mathem.* Physik Kl.

Hess 1959
Hess, S. L. 1959. *Introduction to Theoretical Meteorology.* Holt, New York.

Holland 1980
Holland, G. J. 1980. "An Analytic Model of the Wind and Pressure Profiles in Hurricanes," *Mon. Wea. Rev.,* Vol 108, pp 1212-1218.

Holt and Raman 1988
Holt, T., and Raman, S. 1988. "A Review and Comparative Evaluation of Multilevel Boundary Layer Parameterizations for First-Order and Turbulent Kinetic Energy Closure Schemes," *Rev. Geophys.,* Vol 26, pp 761-780.

Hsu 1974
Hsu, S. A. 1974. "A Dynamic Roughness Equation and its Application to Wind Stress Determination at the Air-Sea Interface," *J. Phys. Oceanogr.,* Vol 4, pp 116-120.

Hsu 1988
Hsu S.A. 1988. *Coastal Meteorology,* Academic Press, New York.

Huang et al 1986
Huang, N. E., Bliven, L. F., Long, S. R., and DeLeonibus, P. S. 1986. "A Study of the Relationship Among Wind Speed, Sea State, and the Drag Coefficient for a Developing Wave Field," *J. Geophys. Res.,* Vol 91, No. C6, pp 7733-7742.

Hughes 1952
Hughes L. A. 1952. "On the Low-Level Wind Structure of Tropical Storms," *J. of Meteorol.,* Vol 9, pp 422-428.

Hubertz 1992
Hubertz, J. M. 1992. "User's Guide to the Wave Information Studies (WIS) Wave Model, Version 2.0," WIS Report 27, U.S. Army Engineer Waterways Experiment Station, Vicksburg, MS.

Hydraulics Research Station 1977
Hydraulics Research Station. 1977. "Numerical Wave Climate Study for the North Sea (NORSWAM)," Report EX 775, Wallingford, England.

Inoue 1967
Inoue, T. 1967. "On the Growth of the Spectrum of a Wind Generated Sea According to a Modified Miles-Phillips Mechanism and Its Application to Wave Forecasting," Geophysical Sciences Laboratory Report No. TR-67-5, Department of Meteorology and Oceanography, New York University.

Janssen 1989
Janssen, P. A. E. M. 1989. "BAR Wave-Induced Stress and the Drag of Air Flow Over Sea Waves," *J. Phys. Oceanogr.,* Vol 19, pp 745-754.

Janssen 1991
Janssen, P. A. E. M. 1991. "Quasi-linear Theory of Wind wave generation Applied to Wave Forecasting," *J. Phys. Oceanogr.,* Vol 21, pp 745-754.

Jeffreys 1924
Jeffreys, H. 1924. "On the Formation of Waves by Wind," *Proc. Roy. Soc. Lond.*, Vol 107, pp 189-206.

Jeffreys 1925
Jeffreys, H. 1925. "On the Formation of Waves by Wind," *Proc. Roy. Soc. Lond*., Ser. A., Vol 110, pp 341-347.

Kahma 1981
Kahma, K. K. 1981. "A Study of the Growth of the Wave Spectrum with Fetch," *Journal of Physical Oceanography*, Vol 11, Nov., pp 1503-15.

Kelvin 1887
Kelvin, Lord, 1887. "On the Waves Produced by a Single Impulse in Water of Any Depth or in a Dispersive Medium," *Mathematical and Physical Papers,* Vol IV, London, Cambridge University Press, 1910, pp 303-306.

Kitaigorodskii 1962
Kitaigorodskii, S. A. 1962. "Application of the Theory of Similarity to the Analysis of Wind Generated Wave Motion as a Stochastic Process," *Bull. Acad. Sci.*, USSR Ser. Geophys., Vol 1, No.1, pp 105-117.

Kitaigorodskii 1983
Kitaigorodskii, S. A. 1983. "On the Theory of the Equilibrium Range in the Spectrum of Wind-Generated Gravity Waves," *J. Phys. Oceanogr.,* Vol 13, pp 816-827.

Large and Pond 1981
Large, W. G., and Pond, S. 1981. "Open Ocean Momentum Flux Measurements in Moderate to Strong Winds," *J. Phys. Oceanogr.,* Vol 11, pp 324-336.

Leenhnecht, Szuwalski, and Sherlock 1992
Leenhnecht, D. A., Szuwalski, A., and Sherlock, A. R. 1992. "Automated Coastal Engineering System Technical Reference, Version 1.07, Coastal Engineering Research Center, Waterways Experiment Station, Vicksburg, MS.

Miles 1957
Miles, J. W. 1957. "On the Generation of Surface Waves by Shear Flows," *Journal of Fluid Mechanics*, Vol 3, pp185-204.

Mitsuyasu 1968
Mitsuyasu, H. 1968. "On the Growth of the Spectrum of Wind-Generated Waves (I).," Reports of the Research Institute of Applied Mechanics, Kyushu University, Fukuoka, Japan, Vol 16, No. 55, pp 459-482.

Myers 1954
Myers, V. A. 1954. "Characteristics of United States Hurricanes Pertinent to Levee Design for Lake Okeechobee, Florida," Hydromet. Rep. No. 32., U.S. Weather Bureau, Washington, DC.

Phillips 1958
Phillips, O. M. 1958. "The Equilibrium Range in the Spectrum of Wind-Generated Waves," *Journal of Fluid Mechanics*, Vol 4, pp 426-434.

Pierson and Moskowitz 1964
Pierson, W. J., and Moskowitz, L. 1964. "A Proposed Spectral Form for Fully Developed Wind Seas Based in the Similarity Theory of S. A. Kitiagorodskii," *J Geophys. Res.,* Vol 9, pp 5181-5190.

Pierson, Neuman, and James 1955
Pierson, W. J., Neuman, G., and James, R. W. 1955. "Observing and Forecasting Oceanwaves by Means of Wave Spectra and Statistics," U.S. Navy Hydrographic Office Pub. No. 60.

Putnam 1949
Putnam, J. A. 1949. "Loss of Wave Energy Due to Percolation in a Permeable Sea Bottom," *Transactions of the American Geophysical Union*, Vol 30, No. 3, pp 349-357.

Putnam and Johnson 1949
Putnam, J. A., and Johnson, J. W. 1949. "The Dissipation of Wave Energy by Bottom Friction," *Transactions of the American Geophysical Union*, Vol 30, No. 1, pp 67-74.

Resio 1981
Resio, D. T. 1981. "The Estimation of a Wind Wave Spectrum in a Discrete Spectral Model," *J. Phys. Oceanogr.,* Vol 11, pp 510-525.

Resio 1987
Resio, D. T. 1987. "Shallow Water Waves; Part I: Theory," *J. Waterway, Port, Coastal and Ocean Eng.,* Vol 113, pp 264-281.

Resio 1988
Resio, D. T. 1988. "Shallow Water Waves; Part II: Data Comparisons," *J. Waterway, Port, Coastal and Ocean Eng.,* Vol 114, pp 50-65.

Resio and Perrie 1989
Resio, D. T., and Perrie, W. 1989. "Implications d and f Equilibrium Range for Wind-Generated Waves," *J. Phys. Oceanogr.,* Vol 19, pp 193-204.

Resio and Vincent 1977
Resio, D. T., and Vincent, C. L. 1977. "Estimation of Winds Over the Great Lakes," *J. Waterways Harbors and Coastal Div.,* American Society of Civil Engineers, Vol 102, pp 263-282.

Resio and Vincent 1979
Resio, D. T., and Vincent, C. L. 1979. "A Comparison of Various Numerical Wave Prediction Techniques," *Proceedings of the 11th Annual Ocean Technology Conference*, Houston, TX, p 2471.

Resio and Vincent 1982
Resio, D. T., and Vincent, C. L. 1982. "A Comparison of Various Numerical Wave Prediction Techniques," *Proc. 11th Annual Offshore Technology Conf.,* Houston, TX, pp 2471-2485.

Rosendal and Shaw 1982
Rosendal, H., and Shaw, S. L. 1982. "Relationship of Maximum Sustained Wind to Minimum Sea Level Pressure in Central North Pacific Tropical Cyclones," NOAA Tech. Memo. NWSTM PR24.

Schwerdt et. al 1979
Schwerdt, R. W., Ho, F. P., and Watkins, R. R. 1979. "Meteorological Criteria for Standard Project Hurricane and Probable Maximum Hurricane Windfields, Gulf and East Coasts of the United States," Tech. Rep. NOAA-TR-NWS-23, National Oceanic and Atmospheric Administration.

Shore Protection Manual 1984
Shore Protection Manual. 1984. 4th ed., 2 Vol, U.S. Army Engineer Waterways Experiment Station, U.S. Government Printing Office, Washington, DC.

Smith 1988
Smith, S. D. 1988. "Coefficients for Sea Surface Wind Stress, Heat Flux, and Wind Profiles as a Function of Wind Speed and Temperature," *J. Geophys. Res.,* Vol 93, pp 467-47.

Snyder and Cox 1966
Snyder, R. L., and Cox, C. S. 1966. "A Field Study of the Wind Generation of Ocean Waves," *J. Mar. Res.,* Vol 24, p 141.

Snyder, Dobson, Elliott, and Long 1981
Snyder, R., Dobson, F. W., Elliott, J. A., and Long, R. B. 1981. "Array Measurements of Atmospheric Pressure Fluctuations Above Surface Gravity Waves," *Journal of Fluid Mechanics*, Vol 102, pp 1-59.

Sverdrup and Munk 1947
Sverdrup, H. U., and Munk, W. H. 1947. "Wind, Sea, and Swell: Theory of Relations for Forecasting." Pub. No. 601, U.S. Navy Hydrographic Office, Washington, DC.

Szabados 1982
Szabados, M. W. 1982. "Intercomparsion of the Offshore Wave Measurements During ARSLOE," *Proceedings OCEANS 82 Conference*, pp 876-881.

Tennekes 1973
Tennekes, H. 1973. "Similarity Laws and Scale Relations in Planetary Boundary Layers," *Workshop on Micrometeorology,* D. A. Haugen, ed., American Meteorology Society, pp 177-216.

Thompson 1977
Thompson, E. F. 1977. "Wave Climate at Selected Locations Along U.S. Coasts," TR 77-1, Coastal Engineering Research Center, U.S. Army Engineer Waterways Experiment Station, Vicksburg, MS.

Thompson and Cardone 1996
Thompson, E. F., and Cardone, V. J. 1996. "Practical Modeling of Hurricane Surface Wind Fields," *Journal of Waterway, Port, Coastal, and Ocean Engineering*, Vol 122, No. 4, pp 195-205.

Toba 1978
Toba, Y. 1978. "Stochastic Form of the Growth of Wind Waves in a Single Parameter Representation with Physical Implications," *Journal of Physical Oceanography*, Vol 8, pp 494-507.

Van Vledder and Holthuijsen 1993
Van Vledder, G. P., and Holthuijsen, L. H. 1993. "The Directional Response of Ocean Waves to Turning Winds," *J. Phys. Oceanogr.,* Vol 23, pp 177-192.

Vincent 1985
Vincent, C. L. 1985. "Depth-Controlled Wave Height," *J. Waterway, Port, Coastal and Ocean Eng.,* Vol 111, No. 3, pp 459-475.

WAMDI Group 1988
WAMDI Group. 1988. "The WAM Model - a Third Generation Wave Prediction Model," *Journal of Physical Oceanography,* Vol 18, 1775-1810.

Ward, Evans, and Pompa, 1977
Ward, E. G., Evans, D. J., and Pompa, J. A. 1977. "Extreme Wave Heights Along the Atlantic Coast of the United States. *Offshore Technology Conference*, OTC 2846, pp 315-324.

Willis and Deardorff 1974
Willis, G. E., and Deardorff, J. W. 1974. "A Laboratory Model of The Unstable Planetary Boundary Layer," *J. Atmos. Sci.,* Vol 31, pp 1297-1307.

Wyngaard 1973
Wyngaard, J. C. 1973. "On Surface-Layer Turbulence," *Workshop on Micrometeorology,* D. A. Haugen, ed., American Meteorology Society, Boston, pp 101-149.

Wyngaard 1988
Wyngaard, J. C. 1988. "Structure of the PBL," *Lectures on Air Pollution Modeling.* A. Venkatram and J. Wyngaard, ed., American Meteorological Society, Boston.

Young 1987
Young, I. R. 1987. "Validation of the Spectral Wave Model ADFA1," *Res. Rep. 17, Dep. Civ. Eng., Augt.* Defense Force Acad., Canberra, Australia.

II-2-6. Definitions of Symbols

α	Equilibrium coefficient
γ	Peak enhancement factor used in the JONSWAP spectrum for fetch-limited seas
ΔT	Air-sea temperature difference [deg °C]
θ_{met}	Measured wind direction in standard meteorological terms (Equation II-2-14) [deg]
θ_{vec}	Measured wind direction in a Cartesian system with the zero angle wind blowing toward the east (Equation II-2-14) [deg]
λ	Dimensionless constant in determining the height of the atmospheric boundary layer (Equation II-2-12)
λ_{1-5}	Dimensionless empirical coefficients used in empirical wave predictions
ρ_a	Mass density of air [force-time^2/length^4]
ρ_w	Mass density of water (salt water = 1,025 kg/m^3 or 2.0 slugs/ft^3; fresh water = 1,000kg/m^3 or 1.94 slugs/ft^3) [force-time^2/length^4]
σ	Dimensionless spectral width parameter
τ	Wind stress [force/length^2]
φ	Dimensionless universal function characterizing the effects of thermal stratification
ω	Angular velocity of the earth (= 0.2625 rad/hr = 7.292x10^{-5} red/sec)
A	Scaling parameter in the Holland wind model [length]
B	Dimensionless parameter that controls the peakedness of the wind speed distribution in the Holland wind model
c	Particle velocity [length/time]
C_D, c_d	Coefficient of drag for winds measured at 10-m [dimensionless]
C_{Dz}	Coefficient of drag for winds measured at level z [dimensionless]
e	Base of natural logarithms (= 2.718)
$E(f)$	Spectral energy density [length/hertz]
f	Coriolis parameter (= 2 $\omega \sin \phi$ = 1.458 x 10^{-4} sin ϕ), where ϕ is geographical latitude [sec^{-1}]. Also, f = frequency [Hz] = $\frac{1}{\text{Period [sec]}}$
f_p	Peak frequency of the spectral peak
f_u	Limiting frequency for a fully developed wave spectrum (Equation II-2-32)
g	Gravitational acceleration [length/time^2]

h	Height of the boundary layer (Equation II-2-12) [length]
$\hat{H}$	Dimensionless wave height (Equation II-2-22)
h_m	Height of the land barrier [length]
H_{m0}	Energy-based significant wave height [length]
H_{stable}	Stable wave height (Equation II-4-14) [length]
H_∞	Fully developed wave height (Equation II-2-30) [length]
k	Dimensionless von Kármán's constant (approximately equal to 0.4). Also, k = wave number [length^{-1}] defined as = $\frac{2\pi}{L}$ where L = wave length [length]
L	Parameter that represents the relative strength of thermal stratification effects [length]
$m_{1\text{-}5}$	Dimensionless empirical exponents used in empirical wave predictions
$_O$	The subscript 0 denotes deepwater conditions
p	Pressure at radius r of a storm [force/length^2]
p_c	Central pressure in the storm [force/length^2]
p_n	Ambient pressure at the periphery of the storm [force/length^2]
r	Arbitrary radius [length]
r_c	Radius of curvature of the isobars [length]
R_L	Ratio of over water windspeed, U_W to over land windspeed, U_L as a function of over land windspeed (Figure II-2-7)
R_{max}	Distance from the center of the storm circulation to the location of maximum wind speed (Equation II-2-20) [length]
R_O	Rossby radius of deformation (Equation II-2-1) [length]
R_T	Amplification ratio (Figure II-2-8), ratio of wind speed accounting for effects of air-sea temperature difference to wind speed over water without temperature effects
t	Duration [time]
T_a	Air temperature [deg C]
T_p	Limiting wave period (Equation II-2-39) [time]
T_s	Water temperature [deg C]
$t_{x,u}$	Time required for waves crossing a fetch (Equation II-2-35) [time]
u	Wind speed [length/time]
U'_t	Estimated wind speed of any duration [length/time]

U_c	Cyclostrophic approximation to the wind speed [length/time]
U_f	Fastest mile wind speed [length/time]
U_g	Geostrophic wind speed (Equation II-2-10) [length/time]
U_{gr}	Gradient wind speed (Equations II-2-11 and II-2-18) [length/time]
U_L	Wind speed over land [length/time]
U_{max}	Maximum velocity in the storm (Equation II-2-21) [length/time]
U_t	Wind speed of any duration [length/time]
U_W	Wind speed over water [length/time]
U_z	Wind speed at height z above the surface (Equation II-2-3) [length/time]
u_*	Wind friction velocity [length/time]
U_*	Wind friction velocity [length/time]
W_C	Wind speed accounting for effects of air-sea temperature difference [length/time]
W_W	Wind speed over water without temperature effects [length/time]
X	Straight line distance over which the wind blows [length]
z_0	Roughness height of the surface [length]

II-2-7. Acknowledgments

Authors of Chapter II-2, "Meteorology and Wave Climate:"

Donald T. Resio, Ph.D., Coastal and Hydraulics Laboratory (CHL), Engineer Research and Development Center, Vicksburg, Mississippi.
Steven M. Bratos, U.S. Army Engineer District, Jacksonville, Jacksonville, Florida.
Edward F. Thompson, Ph.D., CHL.

Reviewers:

Lee E. Harris, Ph.D., Department of Marine and Environmental Systems, Florida Institute of Technology, Melbourne, Florida.
Robert O. Reid, Ph.D., Texas A. & M. University, College Station, Texas (emeritus).
J. Richard Weggel, Ph.D., Dept. of Civil and Architectural Engineering, Drexel University, Philadelphia, Pennsylvania.
Zeki Demirbilek, Ph.D., CHL.
H. Lee Butler, CHL (retired)

Table of Contents

Page

II-3-1. Introduction II-3-1
a. Background II-3-1
b. Practical limitations II-3-1
c. Importance of water level II-3-2
d. Role of gauging II-3-3
e. Physical modeling II-3-3

II-3-2. Principles of Wave Transformation II-3-4
a. Introduction II-3-4
b. Wave transformation equation II-3-4
c. Types of wave transformation II-3-5

II-3-3. Refraction and Shoaling II-3-6
a. Wave rays II-3-6
b. Straight and parallel contours II-3-7
c. Realistic bathymetry II-3-11
d. Problems in ray approach II-3-15
e. Wave diffraction II-3-16
f. Reflection II-3-16
g. Refraction and shoaling of wave spectra II-3-17
h. Alternate formulations II-3-17
(1) Mild slope equation II-3-17
(2) Boussinesq equations II-3-17

II-3-4. Transformation of Irregular Waves II-3-18

II-3-5. Advanced Propagation Methods II-3-19
a. Introduction II-3-19
b. RCPWAVE II-3-20
(1) Introduction II-3-20
(2) Examples of RCPWAVE results II-3-21
(3) Data requirements for RCPWAVE II-3-24
c. REFDIF II-3-24
(1) Introduction II-3-24
(2) Wave breaking II-3-25
(3) Wave damping mechanisms II-3-25
(4) Wave nonlinearity II-3-25
(5) Numerical noise filter II-3-25
(6) Examples of REF/DIF1 results laboratory verification II-3-26
(7) Data requirements for REFDIF II-3-26
d. STWAVE II-3-26

(1) Introduction II-3-26
(2) Examples of STWAVE results II-3-29
(a) Spectral versus monochromatic calculations II-3-29
(b) Effects of coupled source terms II-3-29
(c) Wind effects II-3-29
(3) Data requirements for STWAVE II-3-30
e. Limitations II-3-30

II-3-6. Guidance for Performing Wave Transformation Studies II-3-31
a. Introduction II-3-31
b. Problem formulation II-3-32
c. Site analysis II-3-32
d. Selection of input data site II-3-33
e. Selection of wave transformation method II-3-33
f. Calibration/verification II-3-33
g. Post-processing II-3-34

II-3-7. References II-3-34

II-3-8. Definitions of Symbols II-3-40

II-3-9. Acknowledgments II-3-41

List of Tables

Page

Table II-3-1. Example Problem II-3-1 Refraction and Shoaling Results II-3-14

Table II-3-2. Guidance for Selection of Wave Transformation Methods II-3-33

List of Figures

Page

Figure II-3-1. Waves propagating through shallow water influenced by the underlying bathymetry and currents II-3-2

Figure II-3-2. Amplification of wave height behind a shoal for waves with different spreads of energy in frequency and direction II-3-3

Figure II-3-3. Straight shore with all depth contours evenly spaced and parallel to the shoreline II-3-7

Figure II-3-4. Idealized plots of wave rays II-3-8

Figure II-3-5. Wave-height variation along a wave ray II-3-10

Figure II-3-6. Solution nomogram II-3-12

Figure II-3-7. Highly regular bathymetry but undulatory contours II-3-16

Figure II-3-8. Typical RCPWAVE application, bathymetry II-3-22

Figure II-3-9. Typical RCPWAVE application, wave height II-3-23

Figure II-3-10. Bathymetry input to REF/DIF1 for a simulation of wave propagations at Revere Beach, MA II-3-27

Figure II-3-11. Wave heights calculated by REF/DIF 1 . . . . . II-3-28

Figure II-3-12. Spectral model results compared to laboratory measurements for broad directional spectrum II-3-30

Figure II-3-13. STWAVE results for a 1:30 sloping beach II-3-31

Figure II-3-14. STWAVE results for CHL's Field Research Facility at Duck, NC II-3-32

Chapter II-3
Estimation of Nearshore Waves

II-3-1. Introduction

a. Background.

(1) Coastal engineering considers problems near the shoreline normally in water depths of less than 20 m. Project designs usually require knowledge of the wave field over an area of 1-10 km^2 in which the depth may vary significantly. Additionally, study of shoreline change and beach protection frequently requires analysis of coastal processes over entire littoral cells, which may span 10-100 km in length. Wave data are generally not available at the site or depths required. Often a coastal engineer will find that data have been collected or hindcast at sites offshore in deeper water or nearby in similar water depths. This chapter provides procedures for transforming waves from offshore or nearby locations to nearshore locations needed by the engineer.

(2) Understanding the processes that affect coastal waves is essential to coastal engineering. Waves propagating through shallow water are strongly influenced by the underlying bathymetry and currents (Figure II-3-1). A sloping or undulating bottom, or a bottom characterized by shoals or underwater canyons, can cause large changes in wave height and direction of travel. Shoals can focus waves, in some cases more than doubling wave height behind the shoal. Other bathymetric features can reduce wave heights. The magnitude of these changes is particularly sensitive to wave period and direction and how the wave energy is spread in frequency and direction (Figure II-3-2). In addition, wave interaction with the bottom can cause wave attenuation. The influence of bathymetry on local wave conditions cannot be overstated as a critical factor in coastal engineering design.

(3) Wave height is often the most significant factor influencing a project. Designing with a wave height that is overly conservative can greatly increase the cost of a project and may make it uneconomical. Conversely, underestimating wave height could result in catastrophic failure of a project or significant maintenance costs. Approaches for transforming waves are numerous and differ in complexity and accuracy. Consequently transformation studies require careful analysis. They are but one part of selecting project design criteria, which will be treated in Part II-9.

(4) Wave transformation across irregular bathymetry is complex. Simplifying assumptions admit valid and useful approximations for estimating nearshore waves. After this introduction, a basic principles section provides an overview of the theoretical basis for wave transformation analyses, followed by development of a simple method for refraction and shoaling estimates. Transformation of irregular waves is then discussed. Next, advanced wave transformation models currently used by the Corps of Engineers are discussed. A final section provides guidance on selecting the approach used in calculating wave transformation. This chapter is primarily directed at open coast wave problems excluding structures such as breakwaters or jetties. Analyses involving structures are provided in Part II-7.

b. Practical limitations.

(1) The purpose of this chapter is to provide methods for estimating waves at one site given information at another. The assumption made is that *the wave information used as input to the analysis is characteristic of the waves that would propagate to the site*. In each case, the engineer should assure that there is no limitation of fetch, sheltering of waves, or oddness of bathymetry that would make selection of the input site inappropriate.

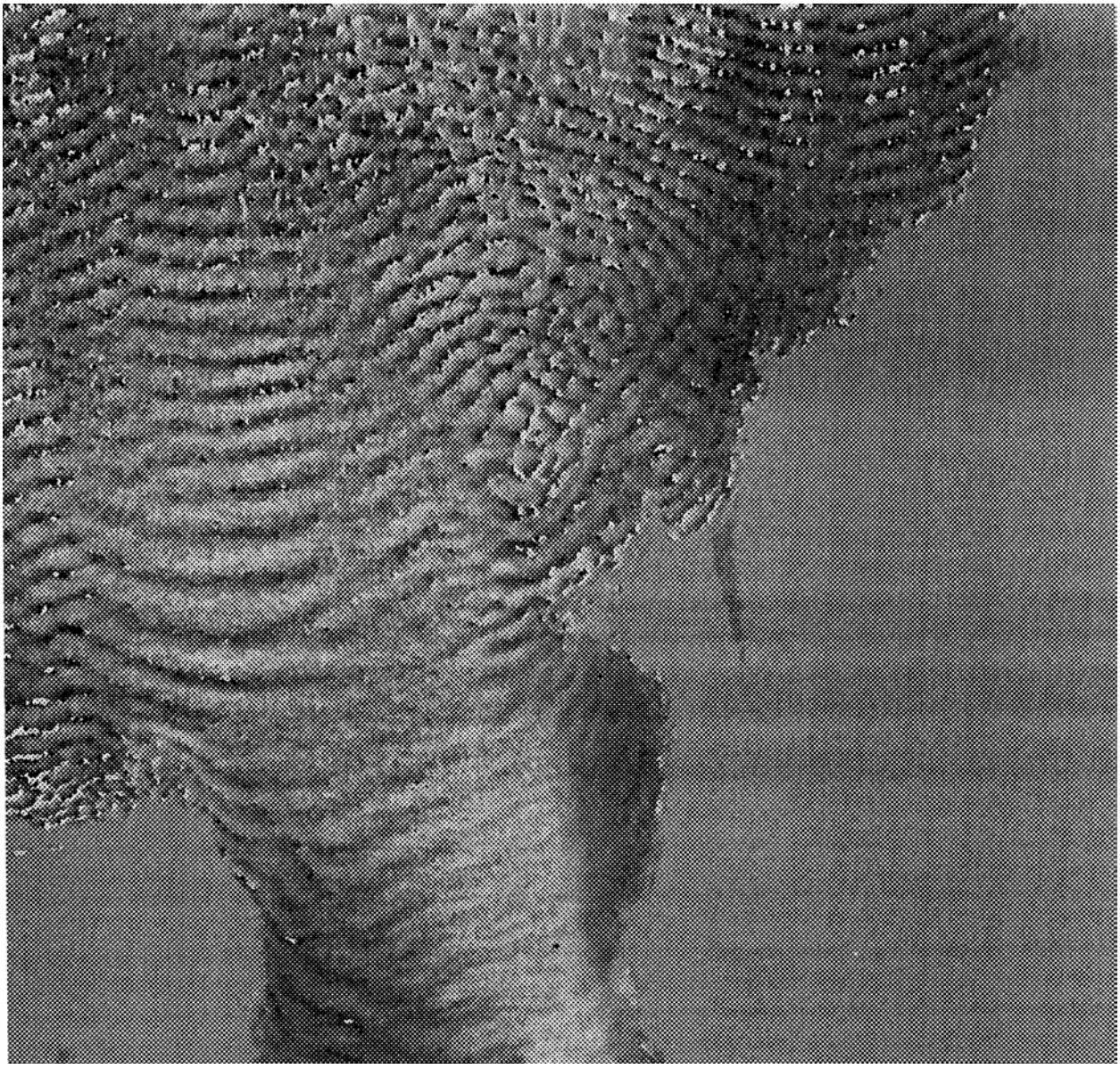

Figure II-3-1. Waves propagating through shallow water influenced by the underlying bathymetry and currents

(2) For most of the open U.S. coastline, Wave Information Study data or data from gauges provide adequate spacing of sites along the coast to give estimates of the wave climate that can be used as input to nearshore transformation studies. In other places or for simulation of a specific event, a special hindcast of the deepwater wave climate may be required to provide input for a transformation analysis.

c. Importance of water level. Near the coast, variable water depths can produce major variations in wave conditions over short distances. The important physical parameter is the depth of the water on which the surface waves are traveling. In nature, water depth is not a constant: it varies with tide stage, hurricane or extratropical storm surge, or for a variety of other reasons (Part II-5). These variations in water level influence wave breaking. *Hence, any study of wave transformation must account for expected water levels for the site and the situation of interest.*

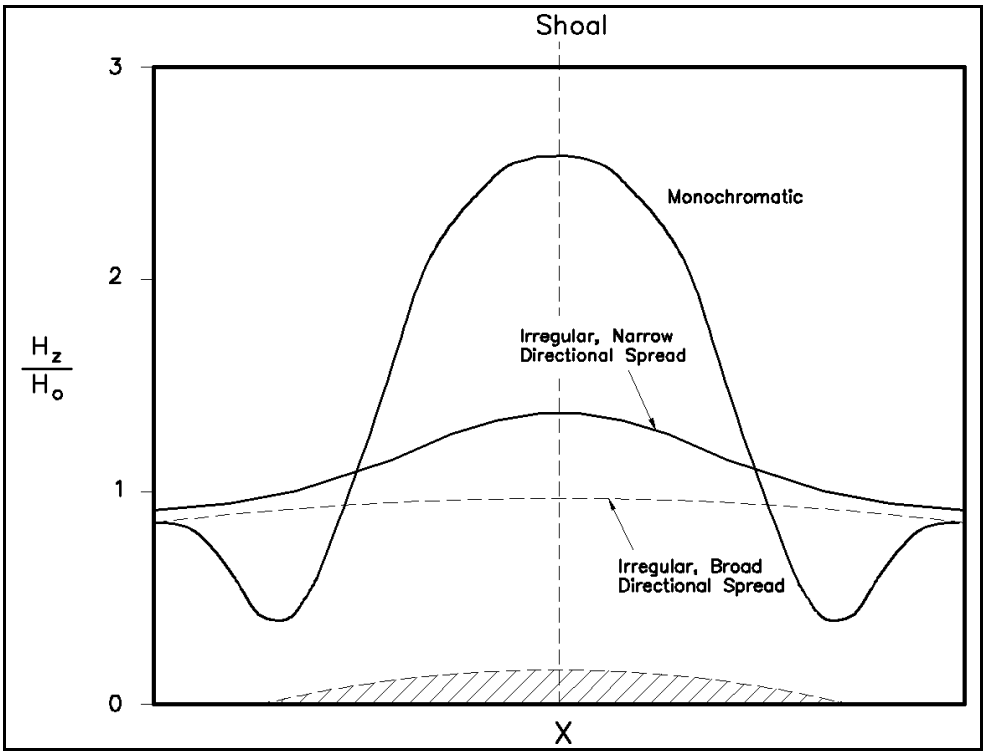

Figure II-3-2. Amplification of wave height behind a shoal for waves with different spreads of energy in frequency and direction

d. Role of gauging. The procedures described here are needed because long-term site-specific data often do not exist. If time and funding are available, a short-term gauging program should be considered. A gauging program can help in two ways:

(1) It may provide a simple statistically based transformation procedure.

(2) It can be used to validate/calibrate a numerical model as a transformation procedure for the project.

Even a few months of gauge data can be a significant complement to any wave-transformation analysis. Short-term gauging is generally not useful in providing, by itself, a design-wave height.

e. Physical modeling. This chapter emphasizes calculation procedures for estimating nearshore waves. However, some sites are so complicated that a physical model of the site may be required to determine the wave conditions. Physical modeling is a well-established procedure for analysis of wave propagation and breaking effects and is particularly useful in analysis of the effects of structures on the wave field. Physical modeling is not useful for evaluating bottom friction or percolation effects or inclusion of wind inputs. Because of scaling limitations and costs, physical models are generally used for small areas (a few square kilometers or less). If strong currents transverse to a wave field are present, such as at a tidal inlet, a physical model may be the only dependable method for estimating the wave field.

II-3-2. Principles of Wave Transformation

a. Introduction.

(1) In this section, the scientific principles governing the transformation of waves from deep water to shallow will be presented in sufficient detail to highlight critical assumptions and simplifications. Unfortunately, the problem is so complex that detailed computations require use of complicated numerical models whose background and implementation are beyond the scope of the Coastal Engineering Manual. This chapter provides the principles of wave transformation, a simplified approach, and an introduction to three numerical models used by the Corps of Engineers.

(2) Processes that can affect a wave as it propagates from deep into shallow water include:

(a) Refraction.

(b) Shoaling.

(c) Diffraction.

(d) Dissipation due to friction.

(e) Dissipation due to percolation.

(f) Breaking.

(g) Additional growth due to the wind.

(h) Wave-current interaction.

(i) Wave-wave interactions

The first three effects are *propagation* effects because they result from convergence or divergence of waves caused by the shape of the bottom topography, which influences the direction of wave travel and causes wave energy to be concentrated or spread out. Diffraction also occurs due to structures that interrupt wave propagation. The second three effects are *sink* mechanisms because they remove energy from the wave field through dissipation. The wind is a *source* mechanism because it represents the addition of wave energy if wind is present. The presence of a large-scale current field can affect wave propagation and dissipation. Wave-wave interactions result from nonlinear coupling of wave components and result in transfer of energy from some waves to others. The procedures presented will stop just seaward of the surf zone, which is treated in Part II-4, "Surf Zone Hydrodynamics."

b. Wave transformation equation.

(1) The general problem of wave transformation will be introduced in terms of the concept of directional wave spectra discussed in Part II-1 and II-2. Adopting the notation of Part II-2, consider a directional spectrum $E(x,y,t,f,\theta)$ where f,θ represents a particular frequency-direction component, x,y represents a location in geographic space, and t represents time. The waves are propagating over a region with varying water depths with no current. Water level will not be time-dependent in the following analyses. Structures are not considered. The general equation used to estimate wave transformation is the radiative transfer equation introduced in Part II-2.

$$\underset{A}{\frac{\partial E(x,y,t,f,\theta)}{\partial t}} + \underset{B}{\nabla \cdot [C_g(x,y,f)\ E(x,y,t,f,\theta)]} = \underset{C}{S_w} + \underset{D}{S_n} + \underset{E}{S_D} + \underset{F}{S_F} + \underset{G}{S_P} \qquad \text{(II-3-1)}$$

(2) Although multidimensional, this equation is fundamentally simple. Term *A* represents the temporal rate of change of the spectrum, term *B* represents the propagation of wave energy, term *C* represents inputs from the wind, term *D* represents the redistribution of wave energy between different wave components that arise from nonlinearities of the waves, term *E* represents dissipation due to breaking, term *F* represents losses due to bottom friction, and term *G* represents losses due to percolation. Many different algebraic forms have been suggested for the various S_i; three references that provide examples are WAMDI (1988), Sobey and Young (1986), and Young (1988). Since they are complicated and cannot be used in manual computations, their algebraic form is not provided here. More detailed discussion of spectral wave mechanics may be found in Leblond and Mysak (1978), Hasselmann (1962, 1963a, 1963b), Hasselmann et al. (1973), Barnett (1968), Phillips (1977), Resio (1981), WAMDI (1988), and in Parts II-1 and II-2.

(3) Surface wave motions produce a velocity field that extends to some depth in the water column. This depth for a deepwater wave is $L/2$ where L is the deepwater wave length. If the water depth is less than $L/2$, the motion extends to the bottom. In cases where the wave motion interacts with the bottom, several physical changes occur as shown in Part II-1: the celerity C and group velocity C_g are changed, as is the wavelength. If the waves are propagating in a region in which the depths are variable (and sufficiently shallow so that the wave interacts with the bottom), the changes in wave speed change the direction of wave travel and change the amplitude of the wave (*refraction and shoaling*). If the patterns of wave propagation lead to strong focusing of waves, wave energy may be radiated away from the convergence by diffraction (Penny and Price 1944; Berkhoff 1972). The interaction of the wave with the bottom produces a boundary layer, which will result in the loss of wave energy to the bed due to bottom friction (Term *F*) resulting from bottom materials and bed forms (Bagnold 1946). If the bed is reasonably porous, the pressure field associated with the passing wave can induce flow into and out of the bed (Bretschneider and Reid 1953), resulting in energy losses due to percolation (Term *G*). If the bed is muddy or visco-elastic other losses may occur (Forristall and Reece 1985). Typically, only one of the bottom loss mechanisms is dominant at one locality although in a large, complicated area a variety of bottom types may exist with differing mechanisms important at different sites along the path of wave travel. However, the bottom-loss terms are often not applied because inadequate information is available on bottom-material composition to allow their proper use.

(4) Wind input, interwave transfers, and breaking follow the principles outlined in Part II-2, though modified due to depth effects. Of the three, wave breaking is most affected by depth. If shoals exist, depth-induced breaking may be significant even though it is outside of the surf zone. Surf zone wave breaking is treated in Part II-4. The effect of sporadic breaking of large waves on shoals or other depth-related features outside the surf zone is not negligible in high sea states. Even in deep water, waves break through whitecapping or oversteepening due to superposition of large waves. The interaction of waves and an underlying current can result in refraction of the waves and wave breaking (Jonsson 1978; Peregrine 1976).

c. Types of wave transformation.

(1) Three classic cases of wave transformation describe most situations found in coastal engineering:

(a) A large storm generates deepwater waves that propagate across shallower water while the waves continue to grow due to wind.

(b) A large storm generates winds in an area remote from the site of interest and as waves cross shallower water with negligible wind, they propagate to the site as swell.

(c) Wind blows over an area of shallow water generating waves that grow so large as to interact with the bottom (no propagation of waves from deeper water into the site).

(2) All cases are important, but the first and third are relatively complex and require a numerical model for reasonable treatment. The second case, swell propagating across a shallow region, is a classic building block that has served as a basis for many coastal engineering studies. Often the swell is approximated by a monochromatic wave, and simple refraction and shoaling methods are used to make nearshore-wave estimates. Since the process of refraction and shoaling is important in coastal engineering, the next section is devoted to deriving some simple approaches to illustrate the need for more complex approaches.

(3) Often it is necessary for engineers to make a steady-state assumption: i.e., wave properties along the outer boundary of the region of interest and other external forcing are assumed not to vary with time. This is appropriate if the rate of variation of the wave field in time is very slow compared to the time required for the waves to pass from the outer boundary to the shore. If this is not the case, then a time-dependent model is required. Cases (a) and (c) would more typically require a time-dependent model. Time-dependent models are not discussed here due to their complexity. Examples are described by Resio (1981), Jensen et al. (1987), WAMDI (1988), Young (1988), SWAMP Group (1985), SWIM Group (1985), and Demirbilek and Webster (1992a,b).

II-3-3. Refraction and Shoaling

In order to understand wave refraction and shoaling, consider the case of a steady-state, monochromatic (and thereby long-crested) wave propagating across a region in which there is a straight shoreline with all depth contours evenly spaced and parallel to the shoreline (Figure II-3-3). In addition, no current is present. If a wave crest initially has some angle of approach to the shore other than 0 deg, part of the wave (point A) will be in shallower water than another part (point B). Because the depth at *A,* h_A, is less than the depth at *B,* h_B, the speed of the wave at A will be slower than that at B because

$$C_A = \frac{g}{\omega} \tanh k h_A < \frac{g}{\omega} \tanh k h_B = C_B \tag{II-3-2}$$

The speed differential along the wave crest causes the crest to turn more parallel to shore. The propagation problem becomes one of plotting the direction of wave approach and calculating its height as the wave propagates from deep to shallow water. For the case of monochromatic waves, wave period remains constant (Part II-1). In the case of an irregular wave train, the transformation process may affect waves at each frequency differently; consequently, the peak period of the wave field may shift.

a. Wave rays.

(1) The wave-propagation problem can often be readily visualized by construction of wave rays. If a point on a wave crest is selected and a wave crest orthogonal is drawn, the path traced out by the orthogonal as the wave crest propagates onshore is called a ray. Hence, a group of wave rays map the path of travel of the wave crest. For simple bathymetry, a group of rays can be constructed by hand to show the wave transformation, although it is a tedious procedure. Graphical computer programs also exist to automate this process (Harrison and Wilson 1964, Dobson 1967, Noda et al. 1974), but to a large degree such approaches have been superseded by the numerical methods discussed in Part II, Section 3-5. Refraction and shoaling analyses typically try to specify the wave height and direction along a ray.

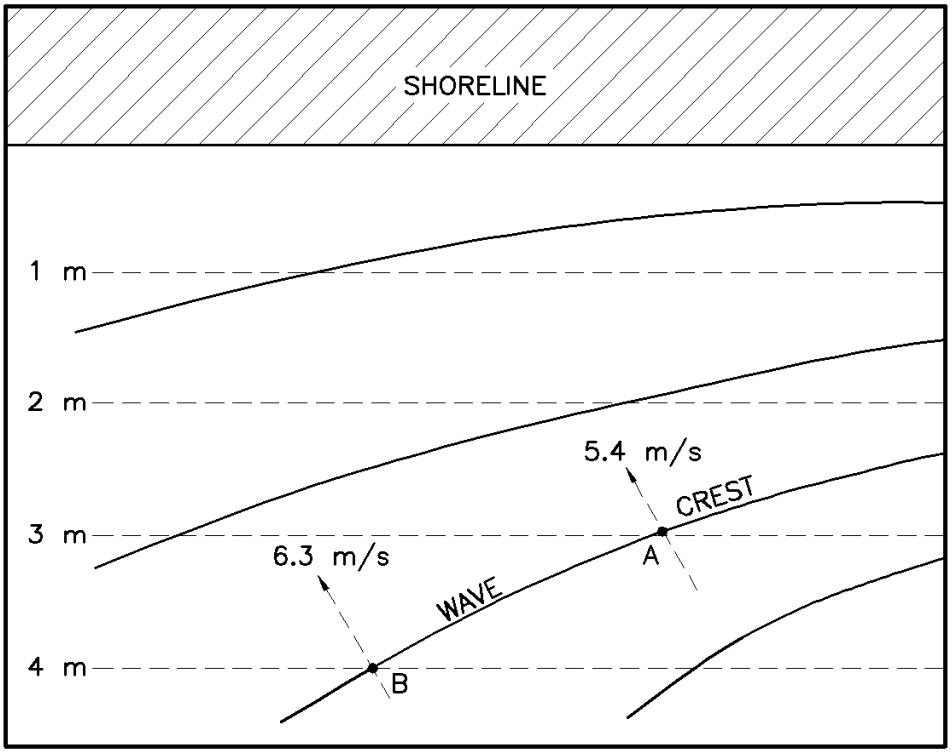

Figure II-3-3. Straight shore with all depth contours evenly spaced and parallel to the shoreline

(2) Figure II-3-4 provides idealized plots of wave rays for several typical types of bathymetry. Simple parallel contours tend to reduce the energy of waves inshore if they approach at an angle. Shoals tend to focus rays onto the shoals and spread energy out to either side. Canyons tend to focus energy to either side and reduce energy over the head of the canyon. The amount of reduction or amplification will depend not only on bathymetry, but on the initial angle of approach and period of the waves. For natural sea states that have energy spread over a range of frequencies and directions, reduction and amplification are also dependent upon the directional spread of energy (Vincent and Briggs 1989).

(3) Refraction and shoaling have been derived and treated widely. The following presentation follows that of Dean and Dalrymple (1991) very closely. Other explanations are provided in Ippen (1966), the *Shore Protection Manual* (1984), and Herbich (1990).

b. Straight and parallel contours.

(1) First, the equation for specifying how wave angle changes along the ray is developed, followed by the equation for wave height. The derivation is only for parallel and straight contours with no currents present. The x-component of the coordinate system will be taken to be orthogonal to the shoreline; the y-coordinate is taken to be shore-parallel. The straight and shore-parallel contours assumption will imply that any derivative in the y-direction is zero because dh/dy is zero.

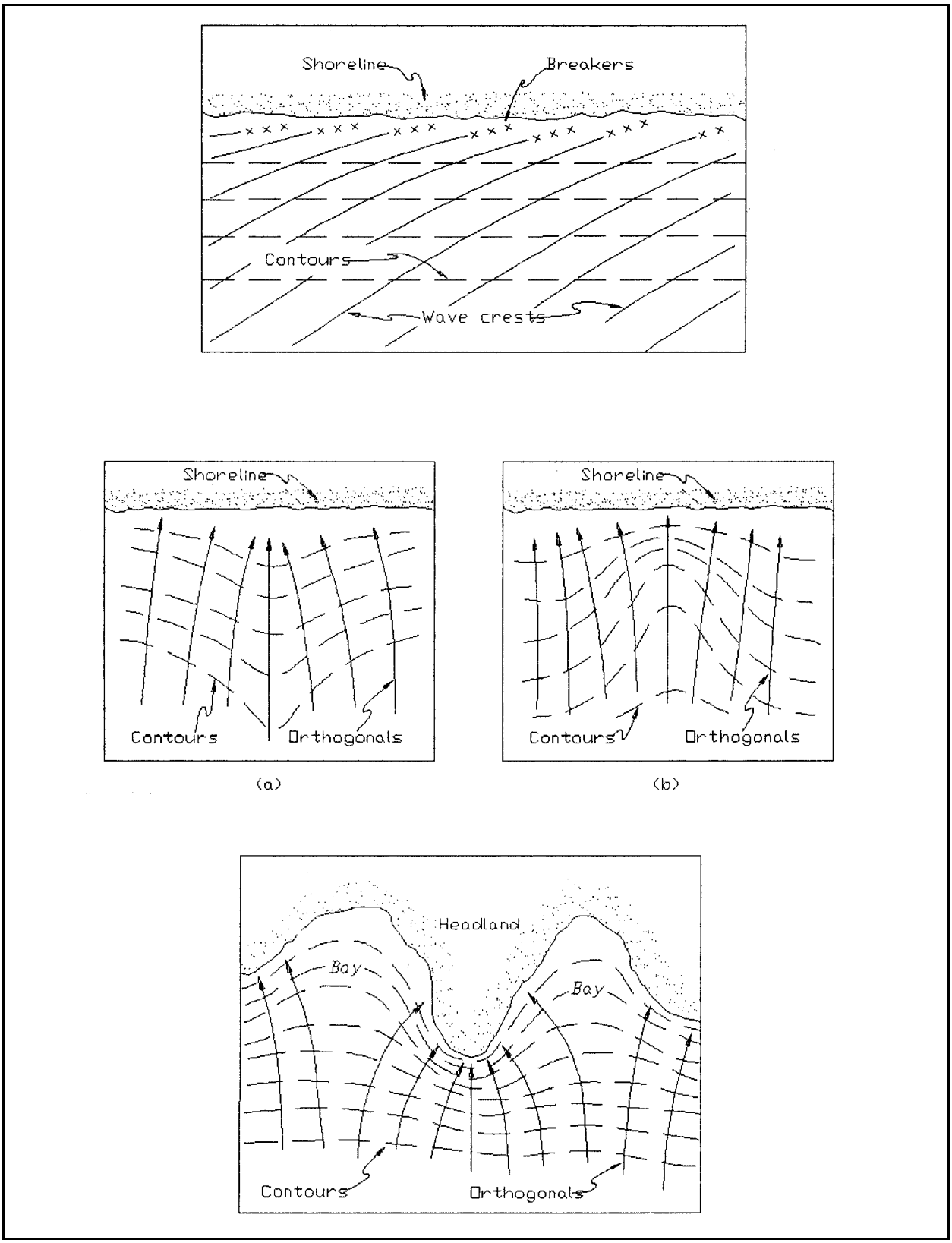

Figure II-3-4. Idealized plots of wave rays

(2) For a monochromatic wave, the wave phase function

$$\Omega\ (x,y,t) = (k\ \cos\theta + k\ \sin\theta - \omega t) \tag{II-3-3}$$

can be used to define the wave number vector $\vec{k}$ by

$$\vec{k} = \nabla\ \Omega \tag{II-3-4}$$

(3) Since $\vec{k}$ is a vector, one can take the curl of $\vec{k}$

$$\nabla \times \vec{k} = 0 \tag{II-3-5}$$

which is zero because $\vec{k}$ by definition is the gradient of a scaler and the curl of a gradient is zero.

(4) Substituting the components of $\vec{k}$, Equation II-3-5 yields

$$\frac{\partial(k\ \sin\theta)}{\partial x} - \frac{\partial(k\ \cos\theta)}{\partial y} = 0 \tag{II-3-6}$$

(5) Since the problem is defined to have straight and parallel contours, derivatives in the y direction are zero and using the dispersion relation linking k and C (and noting that $k = 2\pi/CT$ and wave period is constant) Equation II-3-6 simplifies to

$$\frac{d}{dx}\left(\frac{\sin\theta}{C}\right) = 0 \tag{II-3-7}$$

or

$$\frac{\sin\ \theta}{C} = constant \tag{II-3-8}$$

(6) Let C_0 be the deepwater celerity of the wave. In deep water, sin $(\theta_0)/c_0$ is known if the angle of the wave is known, so Equation II-3-8 yields

$$\frac{\sin\ \theta}{C} = \frac{\sin\ \theta_0}{C_0} \tag{II-3-9}$$

along a ray. This identity is the equivalent of Snell's law in optics. The equation can be readily solved by starting with a point on the wave crest in deep water and incrementally estimating the change in C because of changes in depth. The direction $\ominus$ of wave travel is then estimated plotting the path traced by the ray. The size of increment is selected to provide a smooth estimate of the ray.

(7) The wave-height variation along the ray can be estimated by considering two rays closely spaced together (Figure II-3-5). In deep water, the energy flux (EC_n), which is also EC_g, across the wave crest distance b_0 can be estimated by $(ECn)_0 b_0$. Considering a location a short distance along the ray, the energy flux is $(ECn)_1 b_1$. Since the rays are orthogonal to the wave crest, there should be no transfer of energy across the rays and conservation principles give

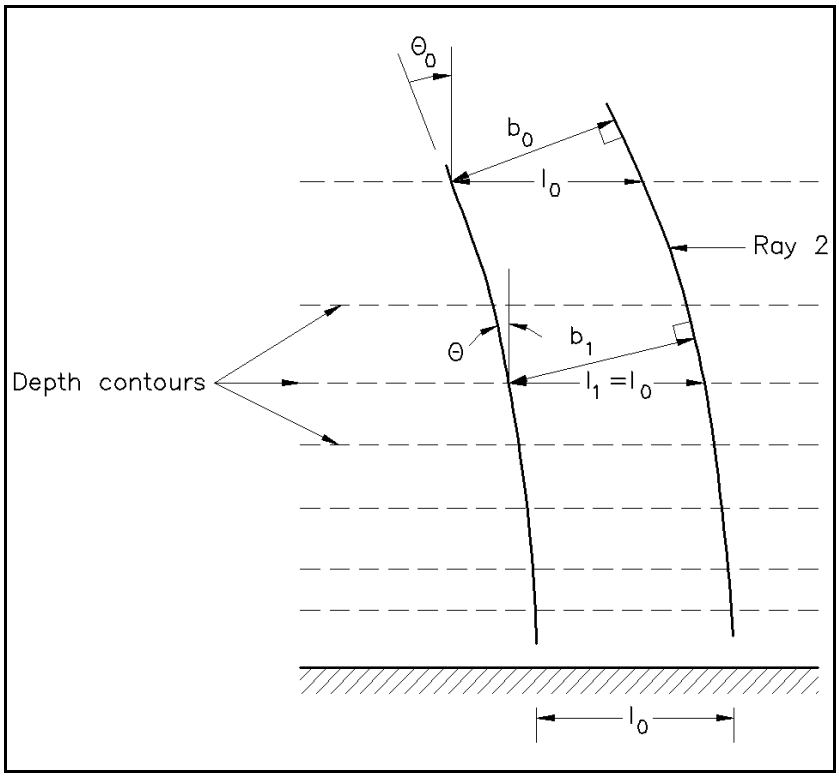

Figure II-3-5. Wave-height variation along a wave ray

$$(ECn)_0 b_0 = (ECn)_1 b_1 \tag{II-3-10}$$

(8) From Part II-1, the height and energy of a monochromatic wave are given by

$$E = \frac{1}{8} \rho g H^2 \tag{II-3-11}$$

and the wave height at location 1 is thus related to the wave height in deep water by

$$H_1 = H_0 \sqrt{\frac{C_{g_0}}{C_{g_1}}} \sqrt{\frac{b_0}{b_1}} \tag{II-3-12}$$

(9) This equation is usually written as

$$H_1 = H_0 K_s K_r \tag{II-3-13}$$

where K_s is called the shoaling coefficient and K_r is the refraction coefficient. From the case of simple, straight, and parallel contours, the value at b_1 can be found from b_0

$$K_r = \left(\frac{b_o}{b_1} \right)^{\frac{1}{2}} = \left(\frac{\cos \theta_0}{\cos \theta_1} \right)^{\frac{1}{2}} = \left(\frac{1 - \sin^2 \theta_0}{1 - \sin^2 \theta_1} \right)^{\frac{1}{4}} \tag{II-3-14}$$

by noting that ray 2 is essentially ray 1 shifted downcoast. For straight and parallel contours, Figure II-3-6 is a solution nomogram. This is automated in the ACES program (Leenknecht, Szuwalski, and Sherlock 1992) and the program NMLONG (Kraus 1991). Figure II-3-6 provides the local wave angle K_R and $K_R K_S$ in terms of initial deepwater wave angle and d/gT^2. Although the bathymetry of most coasts is more complicated than this, these procedures provide a quick way of estimating approximate wave approach angles.

c. Realistic bathymetry.

(1) The previous discussion was for the case of straight and parallel contours. If the topography has variations in the y direction, then the full equation must be used. Dean and Dalrymple (1991) show the derivation in detail for ray theory in this case. Basically, the (x,y) coordinate system is transformed to (s,n) coordinates where s is a coordinate along a ray and n is a coordinate orthogonal to it. Algebraically, the equation for wave angle can be derived in the ray-based coordinate system

$$\frac{\partial \theta}{\partial s} = \frac{1}{k}\frac{\partial k}{\partial n} = -\frac{1}{C}\frac{\partial C}{\partial n} \tag{II-3-15}$$

and the ray path defined by

$$\frac{ds}{dt} = C \tag{II-3-16}$$

$$\frac{dx}{dt} = C \cos\theta \tag{II-3-17}$$

$$\frac{dy}{dt} = C \sin\theta \tag{II-3-18}$$

(2) Equation II-3-15 represents the discussion at the beginning of this section; the rate at which the wave turns depends upon the local gradient in wave speed along the wave crest. Munk and Arthur's computation for the refraction coefficient is more complicated: defining

$$K_r = \left(\frac{1}{\beta}\right)^{\frac{1}{2}} \tag{II-3-19}$$

where $\beta = b/b_0$ then

$$\frac{d^2\beta}{ds^2} + p\,\frac{d\beta}{ds} + q\beta = 0 \tag{II-3-20}$$

with

$$p(s) = -\frac{\cos\theta}{C}\frac{\partial C}{\partial x} - \frac{\sin\theta}{C}\frac{\partial C}{\partial y} \tag{II-3-21}$$

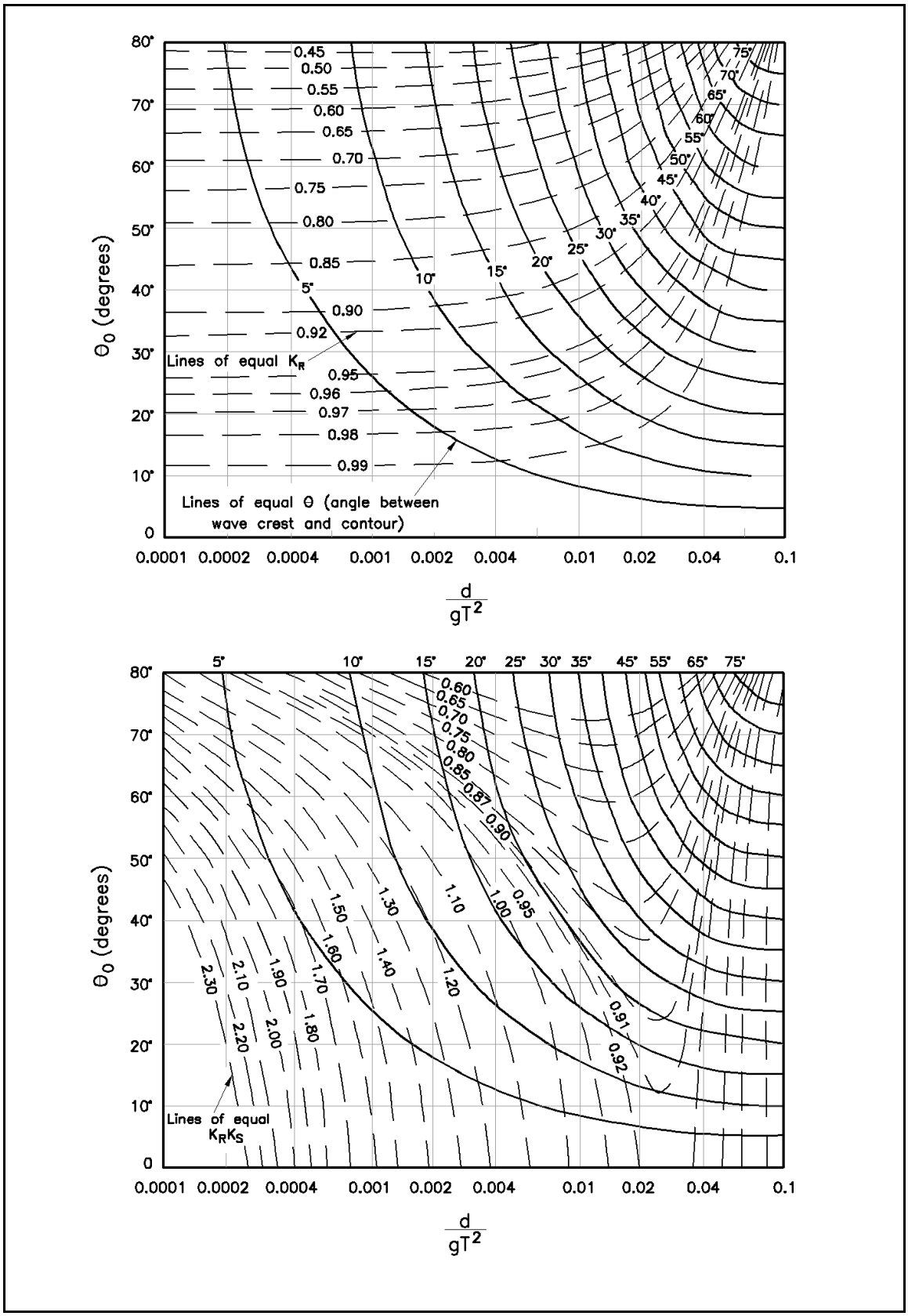

Figure II-3-6. Solution nomogram

EXAMPLE PROBLEM II-3-1

FIND:

Wave height H and angle θ at water depths of 200, 100, 90, 80, 70, 60, 50, 40, 30, 20, 10, 16, 14, 12, 10, 8, 6, and 4 m for deepwater wave angles of 0°, 15°, and 45°.

GIVEN:

A wave 1 m high and 15-sec period in 500 m of water, with a plane, sloping beach.

SOLUTION:

Routine solutions for a plane beach can be obtained using the ACES wave transformation code, by direct calculation, or graphically using Figure II-3-6.

Table II-3-1 provides the results obtained by directly using the ACES code. On a personal computer with a 486-level microprocessor, the results may be obtained in seconds.

For a wave with a depth of 10 m and an initial wave angle of 45 deg, wave height and angle are calculated as follows:

Since the deepwater wave length of a 15-sec wave is

$$L_0 = 1.56\ T^2 = 1.56\ (15)^2 = 351\ m$$

and since 500 m is greater than $L_0/2$, the given initial wave is a deepwater condition. The wave length of the wave in 10 m must be estimated from

$$L = \frac{g\ T^2}{2\ \pi} \tanh\left(\frac{2\ \pi\ d}{L}\right)$$

and is 144 m (see Problem II-1-1).

The shoaling coefficient K_s can be estimated from

$$K_s = \left(\frac{C_{g0}}{C_{gl}}\right)^{\frac{1}{2}}$$

In deep water C_{g0} for a 15-sec wave is

$$\frac{1}{2}\ C_0 = \frac{1}{2}\ (1.56\ T) = \frac{23.4}{2} = 11.7\ \text{m/s}$$

The group velocity is given by

$$C_g = nC = \frac{1}{2}\left(1 + \frac{4\pi d/L}{\sinh\ (4\pi d/L)}\right)\ \frac{gT}{2\pi} \tanh\left(\frac{2\pi d}{L}\right)$$

Substitution of d = 10 m, L = 144 m, T = 15 sec, and g = 9.8 m/sec^2 yields 9.05 m/s.

$$K_s = \left(\frac{11.70}{9.05}\right)^{\frac{1}{2}} = 1.14$$

Solution for K_r involves

$$K_r = \left(\frac{1\ -\ \sin^2\theta_0}{1\ -\ \sin^2\theta_1}\right)^{\frac{1}{4}}$$

(Continued)

Example Problem II-3-1 (Concluded)

In deep water, θ is 45 deg. From Equation II-3-9,

$$\sin\ \theta\ =\ \frac{C_1\ \sin\ \theta_0}{C_0}$$

In deep water C_0 = 1.56T = 23.4 m/s. In 10 m of water, $C_1 = L_1/T$ = 144 m/15$_s$ = 9.60 m/s.

$$\sin\ \theta\ =\ \frac{9.6\ \sin\ (45^0)}{23.4}\ =\ \frac{9.6\ (7.07)}{23.4}\ =\ 0.29$$

$$K_r\ =\ \left(\frac{1\ -\ \sin^2\theta_0}{1\ -\ \sin^2\theta}\right)^{\frac{1}{4}}\ =\ \left(\frac{1\ -\ (0.707)^2}{1\ -\ (0.29)^2}\right)^{\frac{1}{4}}\ =\ \left(\frac{0.50}{0.91}\right)^{\frac{1}{4}}\ =\ 0.86$$

Therefore: $H_i = H_0\ K_s\ K_r$ = 1(1.14) (0.86) = 0.98 m.

The angle of approach is arc sin (sinθ) = 16.8^0. Thus, the l-m, 15-sec wave has changed 2 percent in height by 28.2 deg in angle of approach.

The largest differences caused by refraction and shoaling will be seen at the shallowest depths. From Table II-3-1 at the 4-m depth, the wave height for a 45-deg initial angle is 1.18 m compared to 1.39 m for a wave with initial angle of 0 deg. If the initial angle had been 70 deg, $K_r\ K_s$ would be about 0.8.

Table II-3-1
Example Problem II-3-1 Refraction and Shoaling Results

Depth	θ_o = 0°		θ_o = 15°		θ_o = 45°	
	θ	H	θ	H	θ	H
500	0	1.00	15.0	1.00	45.0	1.00
400	0	1.00	15.0	1.00	45.0	1.00
300	0	1.00	15.0	1.00	45.0	1.00
200	0	1.00	15.0	1.00	45.0	1.00
100	0	0.94	14.3	0.94	42.4	0.92
90	0	0.93	14.0	0.93	41.2	0.91
80	0	0.93	13.7	0.92	30.4	0.89
70	0	0.92	13.2	0.91	38.9	0.88
60	0	0.91	12.7	0.91	37.0	0.86
50	0	0.91	12.0	0.91	34.5	0.85
40	0	0.92	11.1	0.92	31.8	0.84
30	0	0.95	9.9	0.94	28.1	0.85
20	0	1.00	8.4	0.99	23.4	0.88
18	0	1.02	8.0	1.01	22.3	0.89
16	0	1.04	7.8	1.03	21.1	0.91
14	0	1.07	7.1	1.05	19.8	0.92
12	0	1.10	6.6	1.08	18.4	0.95
10	0	1.14	6.1	1.12	16.8	0.98
8	0	1.19	5.5	1.17	15.1	1.02
6	0	1.27	4.8	1.25	13.15	1.08
4	0	1.39	3.9	1.37	10.8	1.18

and

$$q(s) = \frac{\sin^2\theta}{C}\frac{\partial^2 C}{\partial x^2} - 2\frac{\sin\theta\ \cos\theta}{C}\frac{\partial^2 C}{\partial x\,\partial y} + \cos^2\theta\frac{\partial^2 C}{\partial y^2} \quad \text{(II-3-22)}$$

(3) These equations are solved for a set of rays for each wave component of interest (typically combinations of periods and directions). Since this analysis is linear, often a unit wave height is applied for the offshore wave height, which yields a series of refraction and shoaling coefficients at sites of interest. Then the wave transformation for any non-unit initial wave height is obtained by multiplication. This is permissible as long as wave breaking does not occur along a wave ray.

d. Problems in ray approach.

(1) Estimating wave propagation patterns with wave rays is intuitively and visually satisfying, and often very useful. The engineer obtains a good picture of how a wave propagates to a site. However, the procedure has several drawbacks when applied to even mildly irregular bathymetry. One problem is ray convergence/crossing; another is bathymetry inadequacy on ray paths.

(2) An example calculation from Noda et al. (1974) illustrates the basic problem. Bathymetry is highly regular, but has undulatory contours (Figure II-3-7). From the ray pattern, convergence and divergence of adjacent rays are apparent as the waves sweep over the undulations in bathymetry. However, in shallow water near the shore, the rays are sufficiently perturbed by the bathymetry that several converge, with the ray spacing going to zero (in some ray programs the rays actually are computed to cross). Remembering the conservation of wave energy argument used to define the refraction coefficient, the flux across an orthogonal between the rays remains constant. As the spacing between rays approaches zero, the energy flux becomes infinite. Practically, if strong wave convergence occurs, breaking either due to depth constraints (Part II-4) or steepness constraints (Part II-1) naturally limits the wave height. However, situations which generate strong gradients or discontinuities in wave height along a wave crest give rise to ***diffraction*** effects, which can reduce the wave height and keep it below the breaking value.

(3) The second problem with ray theory is the sensitivity of the wave ray calculations. In most locations, the bathymetry is not well-known. Discretizations of the bathymetry can produce sharper local gradients in the computational depth field than may exist locally or, conversely, may reduce local gradients. Most wave ray calculation schemes calculate each wave ray uncoupled from all others. Ray paths are very sensitive to gradients in bathymetry. The smoothing algorithms that are used to numerically compute the required derivatives can alter the ray field significantly. Since the ray calculations are uncoupled, adjacent rays may take radically different paths due to how the bathymetry was discretized or smoothed. Also, if the ray calculations were started at slightly different spatial locations, the resulting patterns may be significantly different for the same reason. *In the cases where ray patterns are unstable with respect to perturbations of initial positions or where adjacent rays show unusual divergences and crossings, the coastal engineer must carefully assess whether the propagation is indeed that unusual (in which case ray theory results may not be accurate) or decide that more careful analysis of the bathymetry and smoothing is needed.*

(4) Wave propagation discussion has centered on the concept of waves traveling from deep water to shallow. At some locations, the bathymetry is such that waves propagating from offshore towards a beach may initially propagate from deeper to shallow water, then propagate across a zone where the water becomes deeper again. In the region where the wave is propagating at an angle to the progressively shallower depths, the process of refraction previously described occurs: the waves turn more shore-normal. Once the depth gradient reverses, the wave turns in the opposite direction (because of the reversed depth gradient, the part

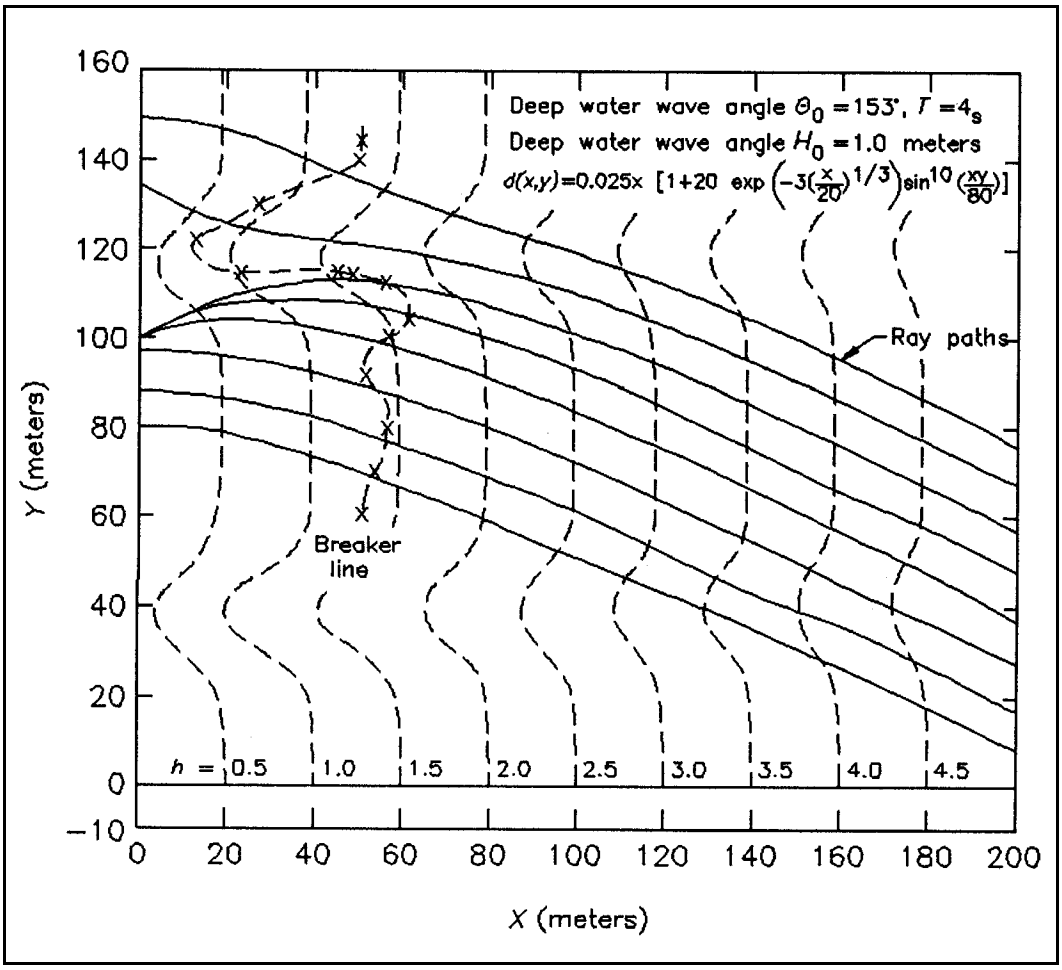

Figure II-3-7. Highly regular bathymetry but undulatory contours

of the wave crest nearer shore is in deeper water than the part of the wave offshore and is hence moving faster). If the combination of wave angle of approach to the bathymetry and wave period is correct, the wave will turn back and go offshore, giving the appearance of a reflected wave. Calculation of wave heights where waves crook or bend backwards is not treated here.

e Wave diffraction. Wave diffraction is a process of wave propagation that can be as important as refraction and shoaling. The classical introduction to diffraction treats a wave propagating past the tip of a breakwater. Since diffraction theory is most often applied to the interaction of waves with harbor structures, derivation of wave diffraction is deferred until Part II-7 (Harbor Hydrodynamics). Any process that produces an abrupt or very large gradient in wave height along a wave crest also produces diffracted waves that tend to move energy away from higher waves to the area of lower waves. So initial wave energy is reduced as diffracted waves are produced. However, if the rate of convergence is too great, the wave may still break.

f. Reflection. Waves that propagate into a solid object such as a breakwater, a seawall, a cliff, or a sloping beach may reflect. In the case of a vertical, hard structure, the fraction of wave energy reflected can be large. For permeable structures or gentle slopes, the reflection will be much less. For nearshore wave propagation problems, reflections are usually ignored because the reflected wave may often be less than 10 percent of the incident wave.

g. Refraction and shoaling of wave spectra. The previous discussion of refraction and shoaling was for a single wave component. However, wave propagation was introduced in Equation II-3-1 through the concept of spectral components. In principle, refraction and shoaling of a wave field in terms of its spectral components simply requires computing the refraction and shoaling coefficient for each frequency-direction (f,θ) component and computing the transformed sum:

$$E(f,\theta) = \sum K_s^2 (f,\theta) \quad K_r^2 (f,\theta) \quad E_o (f,\theta) \quad \Delta f \, \Delta\theta \tag{II-3-23}$$

where $E_o(f,\theta)$ is the offshore directional spectrum. This is possible as long as no breaking or other loss or gain occurs along the propagation path of the individual waves. If it does occur, most advanced spectral models compute the wave transformation locally. In this approach, the area of interest is covered by a discrete series of computation points and the ray path for each (f,θ) component in the spectrum is computed for each grid point only by tracing the ray back to the grid cell boundary defined by adjacent grid points. This approximation, called backward ray tracing, is adequate as long as the wave energy and bathymetry vary smoothly and gently over the domain.

h. Alternate formulations.

(1) Mild slope equation. The refraction and shoaling analyses presented above were based on linear wave theory and a ray approach equivalent to geometrical optics. This works well for simple cases, but once the bathymetry becomes even moderately undulatory, the ray approach runs into difficulty. Berkhoff (1972) formulated a more advanced approach for wave propagation that includes refraction, shoaling, and diffraction simultaneously and can incorporate structures. Berkhoff developed what is termed the mild-slope equation given by

$$\nabla (CC_g\Phi) + \omega^2 \left(\frac{C_g}{C} \right) \Phi = 0 \tag{II-3-24}$$

with

$$\varphi(x,y,z) = \Phi \frac{\cosh k(h+z)}{\cosh kh} \tag{II-3-25}$$

where

$$\nabla = \left(\frac{\partial}{\partial x_i} , \frac{\partial}{\partial y_j} \right) \tag{II-3-26}$$

which provides a solution φ for amplitude and phase of the waves in the horizontal plane. To obtain the equation, Berkhoff assumed that the bottom slope was mild (no abrupt steps, shoals, or trenches). Often slopes of interest violate this assumption, but the models based on the mild-slope equation perform better than the ray approach. Many approaches have been taken to computationally solve this equation. Berkhoff's approach solves the velocity potential of the wave in the horizontal, which can require 5-10 computational grid points per wave length. This is impractical for many cases. Another approach, developed by Radder (1979), is to use a parabolic approximation, which is far more computationally efficient (but subsequently adds more limitations).

(2) Boussinesq equations. Another approach for wave propagation problems close to the coast and in harbors is the use of vertically integrated shallow-water equations in which a Boussinesq (Part II-1) approximation has been made. The numerical models (e.g., Abbott, Peterson, and Skovgaard 1978) resulting from this approach require 10-20 grid points per wave length but have the advantage of being time-dependent

so that the pattern of wave propagation can be directly visualized. Wave crests evolve during the shoaling process to have nonsinusoidal shapes characteristic of shallow-water waves. Currents may be applied directly. Wave breaking, however, is simulated empirically.

II-3-4. Transformation of Irregular Waves

a. The preceding discussion emphasized the refraction and shoaling of monochromatic waves. When this process is applied to an initial significant wave height and period, it is called a *significant wave analysis.* For many conditions where propagation is the dominant factor (as opposed to additional wave growth or bottom dissipation) the significant wave analysis provides a reasonable and generally conservative approximation. The significant wave analysis may be inadequate when wave conditions have spectra characterized by wide directional spreads or broad (frequency) spectral widths or multiple spectral peaks. Cases where the significant wave analysis is adequate primarily involve narrow band swell. This section outlines differences that may be expected between the application of significant wave analyses and application of an irregular wave approach.

b. Rrefraction and shoaling for monochromatic waves may be applied to the individual frequency and direction components of the spectrum of an irregular wave system. Two factors become important: directional spreading and spectral wave mechanics. Directional spreading is important whenever it is present. Spectral wave dynamics are most important in high-energy, high-steepness wave cases, and negligible for low-energy, low-steepness cases.

c. Directional spreading is important for two reasons. First, laboratory tests (Berkhoff, Boij, and Radder 1982; Vincent and Briggs 1989) with unidirectional waves indicate that shoals concentrate wave energy immediately behind the shoal and reduce it on the flanks. The increase behind the shoal can be nearly 250 percent of the initial wave height; the reduction to either side can be about 50 percent. However, laboratory tests with wave spectra having significant directional spread (Vincent and Briggs 1989) show only a 110- to 140-percent increase behind the shoal and only a 10- to 15-percent reduction on the sides. Numerical models incorporating directional spread also replicate this (Panchang et al. 1990). In the case with directional spread, the shoal focusses each frequency-direction component at a different location behind the shoal rather than at one spot as in the unidirectional case. Consequently some of the high- and low-energy regions overlap and cancel each other out. Secondly, if the mean angle of wave approach is not directly onshore, one consequence of directional spreading is that some fraction of the wave energy is heading parallel to shore or offshore. In the case of a wave system with symmetric directional spread (i.e., 50 percent to the left and right of the mean direction), if the mean direction were parallel to a straight shoreline (and the measurement were made in deep water), half of the energy would be moving in directions that could not refract towards shore. So even for angles up to 30 deg offshore-parallel, significant amounts of energy are not propagating shoreward. In a significant wave analysis, all the energy would propagate shoreward. If the shoreline, fetch, or bathymetry is complicated, the fraction of energy that propagates towards shore is more difficult to define.

d. Spectral dynamics arise because waves of different lengths and steepness are propagating through and with other waves. According to Equation II-3-1, these waves can exchange energy between each other (nonlinear transfers) and superposition of waves can lead to dissipation due to breaking. Analysis of thousands of wave records (Bouws et al. 1987; Bouws, Gunther, and Vincent 1985; Miller and Vincent 1990) indicates that higher energy wind sea spectra achieve a characteristic shape that is different from that obtained simply by shoaling. As a result, the energy level for shoaling irregular wave tends to be less than that predicted from linear monochromatic shoaling of the wave components, especially near the surf zone. Smith and Vincent (1992) also indicate that the shoaling and breaking of irregular waves with two spectral peaks can substantially differ from the monochromatic (and even single peak spectral) case. Moreover, the wave spectrum after refraction and shoaling can have a substantially different peak period. Although a satisfactory

explanation of these phenomena is not available, their impact is significant, with differences up to 30-40 percent from the significant wave approach.

e. Treatment of spectral wave mechanics in any detail requires use of a numerical model. However, in using a significant wave approach, it can generally be assumed that:

(1) It may overestimate wave focussing effects.

(2) Careful estimates of the fraction of wave energy heading shoreward should be made for oblique angles cases.

(3) Shoaling calculations may overestimate wave heights in high energy conditions.

f. Shifts in wave period may also occur. As a result, significant wave analysis tends to be conservative; this may be why it has been an acceptable approach for design. However, for cost-sensitive projects, a more complicated approach may be warranted.

g. The following precautions are suggested. In a significant wave analysis, if regions of highly focussed wave energy occur with corresponding lobes of low energy, the regions of low energy should be carefully considered. In the field, natural wave systems generally have significant directional spread, so calculated values in the low energy lobes may significantly underestimate wave heights. In cases where irregular waves are modeled spectrally, typically only the wave height H_s is estimated. In shallow water, larger waves do occur ($H_{1/10}$, etc.) and combinations of individual wave height, period, and bottom depth can result in individual waves or groups of waves significantly larger than H_s (see Part II-2).

II-3-5. Advanced Propagation Methods

a. Introduction.

(1) As indicated in Part II-3-2, as waves propagate, they may continue to grow due to the continued action of the wind or may lose energy due to breaking, bottom friction, or percolation. These effects cannot be realistically incorporated through manual calculations. The preceding discussion indicates that computations involving rays are tedious by hand and subject to many inaccuracies. Advances have been made in computing wave transformation; they were briefly indicated in the preceding sections. Many of these procedures may run efficiently on a personal computer or a work station and do not require a large mainframe or supercomputer. Hence they can be applied readily by most engineers (ACES 1992).

(2) This section describes three computer programs that are available and in use by the Corps of Engineers. Each program is briefly described and a reference indicates where the program can be obtained. Each program is complicated and requires some effort to use properly. A short description is provided here to indicate to the engineer the potentials of these codes. The three have been selected to provide a cross section of the types of technology available. Other computer programs can be obtained and may be as suitable for use as those described here.

(3) Examples of technology available to practicing engineers is provided. **The Corps of Engineers does not endorse the codes discussed or certify their accuracy.** Indeed, the suitability and accuracy of any of these codes depend upon the problem under study and the way in which the code is applied. **With the exception of very simple bathymetry, it is recommended that nearshore wave transformation studies use a numerical code capable of handling the complexities required.** However, the particular numerical approach selected depends upon the problem.

(4) The three models discussed below are all steady-state models. Time-dependent, shallow-water models are available (Jensen et al. 1987; Demirbilek and Webster 1992a, 1992b). They are not discussed here because they require extensive sets of meteorological data and cannot be easily applied. The basic characteristics of the three models discussed are as follows:

(a) (RCPWAVE) RCPWAVE is a steady-state, linear-wave model based on the mild-slope equation and includes wave breaking. It is applicable for open coast areas without structures. It is basically a monochromatic-wave approach.

(b) (REFDIF1) REFDIF is a steady-state model based on the parabolic approximation solution to the mild-slope equation. The model includes wave breaking, wave damping, and some nonlinear effects. Although primarily used as a monochromatic wave model, a spectral version is available. The model can simulate aspects of propagation associated with simple currents and can include structures.

(c) (STWAVE) STWAVE is a steady-state, linear wave model that computes the evolution of the directional spectrum over space (Equation II-3-1). The model includes breaking, bottom friction, percolation, and wind input and solves for the nonlinear transfers of energy within the wave spectrum. It has two modes for handling diffraction of wave energy and the computational domain may include simple structures. The models can handle aspects of propagation associated with simple currents.

(5) The three models are theoretically complicated and computationally demanding. All can be effectively used on a powerful PC-type computer or work station. Each model has considerable strengths and each can be an appropriate choice for wave transformation. However, none can be considered universally applicable and the results from all can be inaccurate if the assumptions made in model development are significantly violated. Users of any of the models must become thoroughly familiar with the model, its assumptions, and limitations.

b. RCPWAVE.

(1) Introduction.

(a) The RCPWAVE model (Ebersole 1985; Ebersole, Cialone, and Prater 1986) was developed in the early 1980's as an engineering tool for calculating the properties of waves as they propagate into shallow water and eventually break. The theoretical basis for the model (linear-wave theory) and the types of information generated by the model (wave height, period, and direction as a function of location) are consistent with current theories and equations used by the engineering community to calculate potential longshore sand-transport rates and shoreline and beach change. The model was designed to operate efficiently for coastal regions that may be tens of kilometers in length, and to overcome deficiencies of previously developed refraction models that could be applied on a regional scale. The wave ray refraction models of Harrison and Wilson (1964), Dobson (1967), Noda et al. (1974), and others "failed" in regions of strong wave convergence and divergence (i.e., highly irregular bathymetry), leaving users with no wave solutions and little guidance for interpreting results in these regions. Berkhoff (1972, 1976) derived an elliptic equation that approximately represented the complete transformation process for linear waves over arbitrary bathymetry, where the bathymetry was only constrained to have mild slopes. Numerical solution of this equation requires discretization of the spatial domain and subsequent computations with grid resolutions that are a fraction of the wave lengths being considered (typically one tenth or smaller). This requirement limits the utility of the approach for large regions of coastline.

(b) RCPWAVE is based on the mild-slope equation. An assumed form for the velocity potential associated with only the forward scattered wave field is used with the mild slope equation to develop two equations, one describing the conservation of wave energy (assuming a constant wave frequency) and the

other defining the magnitude of the wave phase gradient as a function of the wave number and the spatial variability in wave amplitude. The finite difference forms of these two equations and a third equation defining the irrotationality of the wave phase function gradient are solved for the wave height, direction, and phase gradient. A forward-marching (in the direction of wave propagation) solution scheme is used, and solutions are obtained at the center of each rectangular grid cell of the discretized model domain. RCPWAVE differs from the complete solution of the mild-slope equation by neglecting reflections of waves by structures and bathymetry. This allows RCPWAVE to use a grid resolution only sufficient to resolve bathymetric gradients, permitting RCPWAVE to cover larger spatial regions than those usually covered in full solutions to the mild-slope equation.

(c) Wave breaking is also treated in the model. The occurrence of wave breaking is first considered by comparing the computed local wave height with a limiting wave height calculated using the method of Weggel (1972). If the computed wave height exceeds the limiting value, then energy is dissipated according to the breaker decay model of Dally, Dean, and Dalrymple (1984). When the calculated local wave height falls below the stable value proposed by Dally, Dean, and Dalrymple, energy dissipation is again set to zero. The influence of wave height variability on wave phase is neglected in the surf zone. Details of the RCPWAVE model derivation and solution scheme can be found in Ebersole, Cialone and Prater (1986).

(2) Examples of RCPWAVE results.

(a) Figures II-3-8 and II-3-9 show results from a typical application of RCPWAVE. The model domain is the region offshore of Homer Spit, Alaska. The section of coast being considered is approximately 33 km in length. A rectangular grid mesh was constructed within the domain, with grid resolution of approximately 130 m in the on-offshore direction and 250 m in the alongshore direction. Figure II-3-8 shows bathymetric contours in the model domain. The nearshore region is characterized by a fairly broad shelf with depths of 20 m or less, and offshore the depths increase to 200 ft and greater in the lower right-hand corner of the domain. The shallow-water region is characterized by irregular contours, with extensive shoals at locations A and B in Figure II-3-8.

(b) Figure II-3-9 shows the wave height field (shaded contours) throughout the model domain for an incident deepwater wave with the characteristics shown. Note the areas of wave convergence and divergence and the resulting variation in wave height observed along the coast (darker shades indicate convergence and lighter shades indicate divergence). The shoals cause wave convergence, which is evidenced by zones of higher wave height in the lee of the shoals. Wave heights are lower in divergent zones that are created as waves attempt to align their propagation direction to be perpendicular to bathymetric contours and propagate toward the shoals. A plot of wave direction vectors would also indicate zones of wave convergence and divergence. Also note the position of the breaker line (indicated by the seawardmost pattern of dots), as it follows the shallower bathymetric contours. Shoals can cause the focussed incident wave to break at a greater distance from shore than elsewhere in the region. Information that can be obtained using the model includes wave height and direction variability at many locations along the coast under different incident wave conditions, variability of inshore wave conditions with changing water levels, and zones of potentially high and low longshore sand transport.

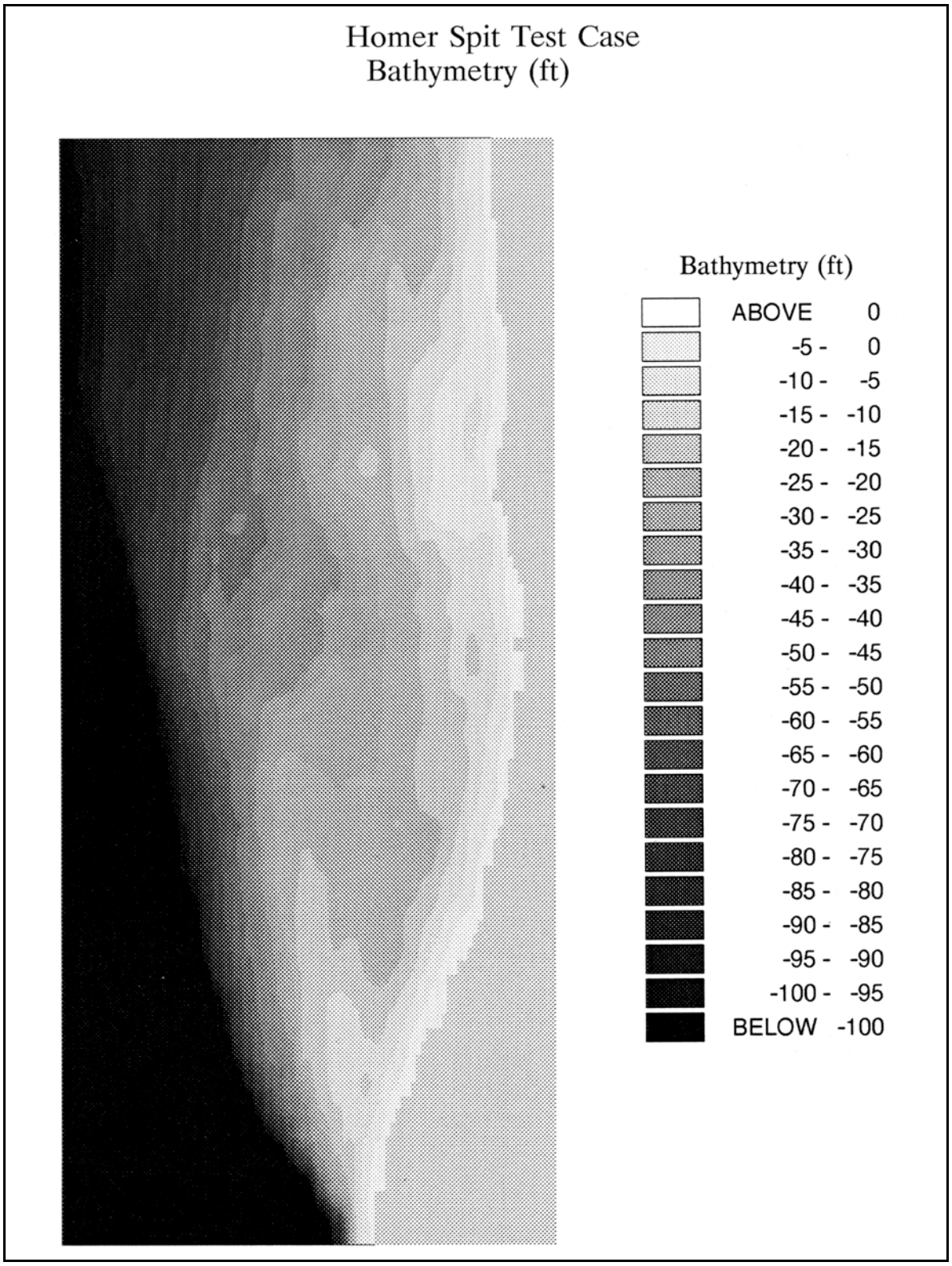

Figure II-3-8. Typical RCPWAVE application, bathymetry

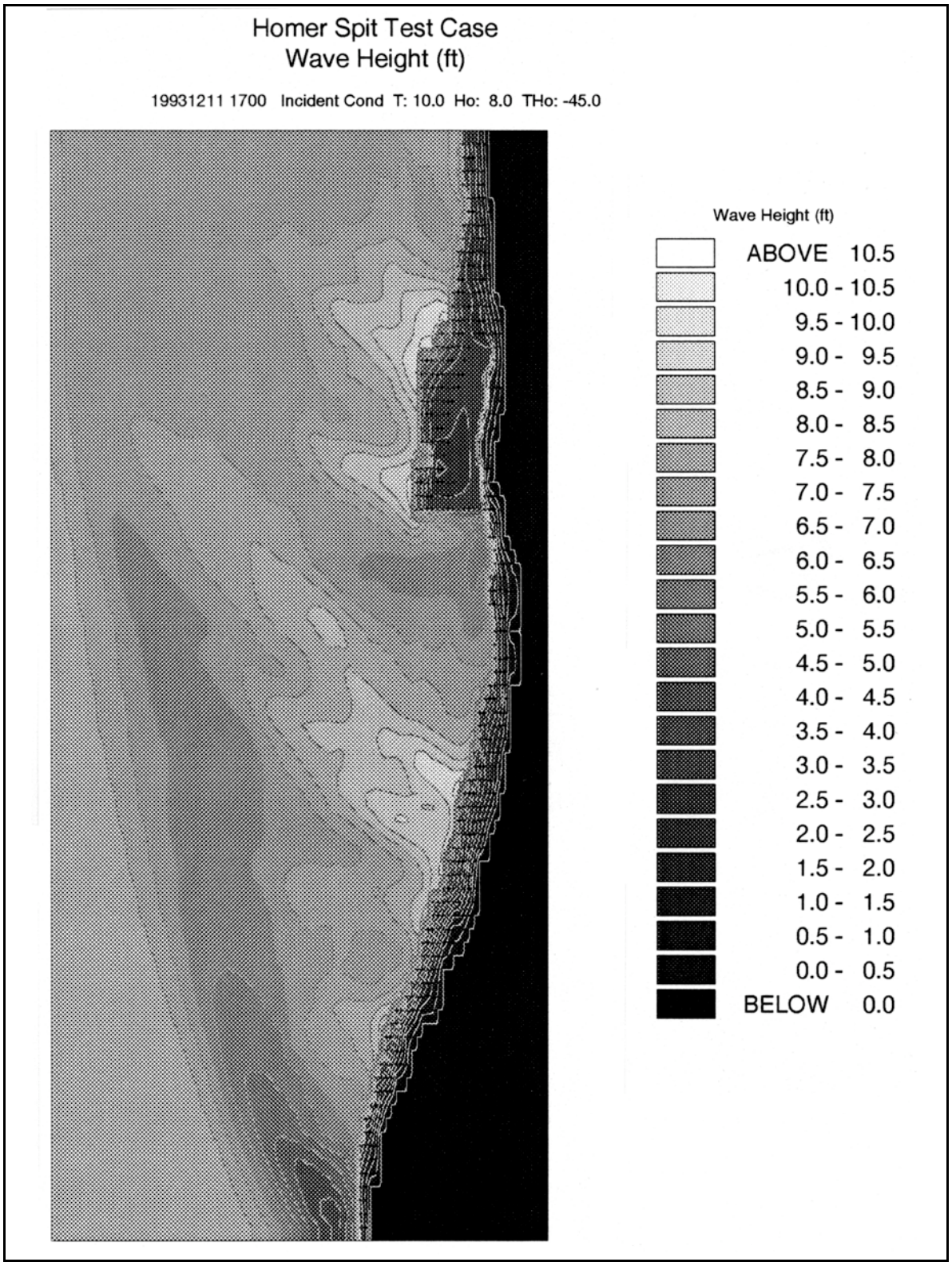

Figure II-3-9. Typical RCPWAVE application, wave height

(3) Data requirements for RCPWAVE.

(a) Primary input to the RCPWAVE model includes the following: parameters describing the domain to be modeled, such as the number of computational grid cells in each direction and the cell dimensions; definition of the water depth at each cell; and definition of the incident wave height, period, and direction along the offshore domain boundary for each wave condition to be simulated. Model output includes wave height, period, and direction at each cell of the computational domain, and an indication of whether or not the wave is calculated to be a broken wave.

(b) Typically the first step in the model application process is to discretize the model domain into a rectangular mesh. The grid mesh that is created can be overlaid on a bathymetric chart, assuming the grid and chart are plotted to the same horizontal scale, and depths at each cell can be digitized for use as model input. A constant correction to the depths, representing a datum change or a specific water level change, can be included in the input data set. An arbitrary number of wave conditions, each defined by a unique combination of height, period and direction, can be simulated. Wave conditions to be simulated are usually defined after a statistical analysis of the wave climate in the region being studied. Bathymetry specification and incident wave conditions comprise the bulk of the effort to create the input data set.

c. REFDIF.

(1) Introduction. The model REF/DIF 1, which has been developed for practical application, is based on the mild-slope, wave-current model equation developed by Kirby (1984), which may be written as

$$\frac{D^2\varphi}{Dt^2} + \nabla \cdot U \frac{D\varphi}{Dt} - \nabla \cdot (CC_g \nabla\varphi) + (\sigma^2 - k^2 CC_g)\,\varphi = 0 \tag{II-3-27}$$

where φ is the velocity potential at the free surface, and where

$$\frac{D}{Dt} = \frac{\partial}{\partial t} + U \cdot \nabla \tag{II-3-28}$$

$$\nabla = \left(\frac{\partial}{\partial x} \;,\; \frac{\partial}{\partial y} \right) \tag{II-3-29}$$

$$U = (U(x,y)\;,\; V(x,y)) = \text{ambient current vector} \tag{II-3-30}$$

$$\sigma = \omega - k \cdot U \tag{II-3-31}$$

$$C = \frac{\sigma}{k} \tag{II-3-32}$$

$$C_g = \frac{\partial\sigma}{\partial k} \tag{II-3-33}$$

$$\sigma^2 = gk \tanh(kh) \tag{II-3-34}$$

Several additional features are included in the model in order to increase its range of application and accuracy.

(2) Wave breaking. The model tests whether the local wave height has exceeded a fixed threshold, which is set at $h/d = 0.78$. For local wave heights exceeding this value, a breaking wave energy flux decay model is started in order to remove energy from the wave train. The model used is described in Dally, Dean, and Dalrymple (1985). The reader is referred to Kirby and Dalrymple (1986a) for further details.

(3) Wave damping mechanisms.

(a) In addition to the strong wave breaking mechanism described above, REF/DIF 1 also provides the user with three selectable bottom damping mechanisms. These are: laminar bottom boundary layer damping, sand-bed percolation damping, and turbulent bottom boundary layer damping.

(b) At present, no laboratory or field data sets clearly point to the need for including bottom damping effects in model simulations. Laboratory experiments usually include too short a propagation distance for damping effects to accumulate significantly. In the field, damping due to bottom effects may be balanced or overshadowed by wave growth resulting from wind-wave interaction, and so one should not be considered in the absence of the other. At present, it is recommended that these user-selectable damping mechanisms not be included in model simulations.

(4) Wave nonlinearity.

(a) Wave nonlinearity has a strong effect on the phase speed of waves and thus can significantly modify both refraction and diffraction effects. For example, waves shoaling on a plane beach refract more slowly than predicted by linear theory, since the increase in wave height with decreasing water depth speeds up the waves, in opposition to the direct, linear-theory effect decreasing depth, which slows them. Diffraction effects are typically enhanced. Phase speed is greater in a high-amplitude, illuminated area than in a low-amplitude, shadowed area; this causes refractive bending of waves into the shadow area, causing an increase in wave height in the shadow zone relative to the predictions of linear theory.

(b) REF/DIF 1, designed to predict the propagation of a monochromatic wave in intermediate water depth, includes the effects of nonlinearity as predicted by third-order Stokes wave theory (Kirby and Dalrymple 1983). Since the model is often used to predict wave-height distributions into the surf zone and up to dry land boundaries, the model must also be corrected to avoid the singularities arising from the invalidity of Stokes theory in shallow water. In order to provide a smooth correction to the model results in the shallow-water limit, Kirby and Dalrymple (1986b) provided an algorithm that gives a smooth patch between Stokes theory and an empirical modification to linear theory developed by Hedges (1976). The approximate theory does not cause any degradation in solution accuracy in comparison to the Stokes theory alone for intermediate depth experiments; see Kirby and Dalrymple (1986b) for relevant documentation.

(5) Numerical noise filter. Higher-order forms of the parabolic approximation have the undesirable effect of allowing high-wave number noise (i.e., noise with rapid lateral variation) to propagate rapidly across the computational grid. This effect has been described in detail by Kirby (1986a), and is usually found in association with the start of surf zones around complicated planforms such as island shores. The resulting noise component may be damped by the application of various types of smoothing filters. The three-point moving average filter described by Kirby (1986a) has been found to be heavy-handed in practical applications, and has been replaced in present versions of the REF/DIF 1 model by a damping filter included in the governing differential equation, whose effect is centered around the lateral wave number, which spread rapidly in the undamped model. A full description of the damping method and a range of tests may be found in Kirby (1993).

(6) Examples of REF/DIF1 results laboratory verification. REF/DIF 1 (and the parabolic approximation model in general) are capable of providing a detailed picture of the water surface in the region of study if the

grid resolution is sufficiently high. This picture includes the geometry of crests and troughs as well as the location of regions of high or low wave height resulting from short-crestedness of the wave field. Since irregular waves in the field usually lead to a fairly smooth spatial variation in wave height estimates (after statistical averaging), a more stringent test of model accuracy is provided by comparison to laboratory tests with monochromatic waves. Parabolic models have been tested against data of this type in a number of studies, including Berkhoff, Booij, and Radder (1982); Tsay and Liu (1982); Kirby and Dalrymple (1984), Panchang et al. (1990), and Demirbilek (1994). The results showed that the higher-order parabolic approximation, together with nonlinear correction to the wave phase speed, can correctly predict the distribution of wave heights and nodal points in the evolving wave field. Figure II-3-10 shows the bathymetry input to REF/DIF1 for a simulation of wave propagations at Revere Beach, MA. Figure II-3-11 shows the wave heights calculated by the models.

(7) Data requirements for REFDIF.

(a) REF/DIF 1 computes a grid-based wave evolution over an arbitrary bathymetry and current field. To run the model, the user must provide, at minimum, an array of depth values h on a grid with regular spacing in x and y. The model always assumes that x is the preferred direction, or the direction in which the computation marches. No provision is made at present for relating the model coordinate system to a global coordinate system. If the user wishes to include the effects of tidal currents in the model study, then arrays of velocity components U and V must also be provided for the same regular grid used to specify h values. This information establishes the geometry for the model run.

(b) The user must also specify the form of the wave train at the offshore boundary. This may be done by specifying a combination of one or more monochromatic waves at the offshore boundary, or the offshore wave field may be specified at the first grid row by means of input data. The user's manual provided in Kirby and Dalrymple (1992) should be consulted for more details about the input data.

(c) The model provides the user with a grid of computed wave heights and directions on the same geometric grid used for input. In addition, the complex amplitude values are provided and may be used to reconstruct plots of the computed wave field, if these are desired and if the grid resolution is fine enough to permit it. For larger-scaled model areas, this last step is often not feasible, as it requires 5 to 6 grid points per modeled wave length in the input bathymetry grid. A version of REF/DIF capable of simulating wave spectra has recently been released.

d. STWAVE.

(1) Introduction.

(a) STWAVE is a steady-state spectral model for predicting wave conditions in coastal areas. It solves the complete radiative transfer equation (Equation II-3-1) including both propagation effects (refraction, shoaling, diffraction, and wave-current interactions) and source-term effects (wave breaking, wind inputs, and nonlinear wave-wave interactions). STWAVE was developed under the premise that waves in nature should be treated as nonlinearly interacting stochastic wave components rather than as deterministic nonlinear waves. This is particularly relevant when dealing with wave transformations over distances of hundreds of thousands of wavelengths (typical of many coastal wave transformation studies). At much shorter distances a deterministic, long-crested approximation can provide an appropriate framework for understanding and interpreting wave behavior. At longer distances, theoretical and empirical evidence

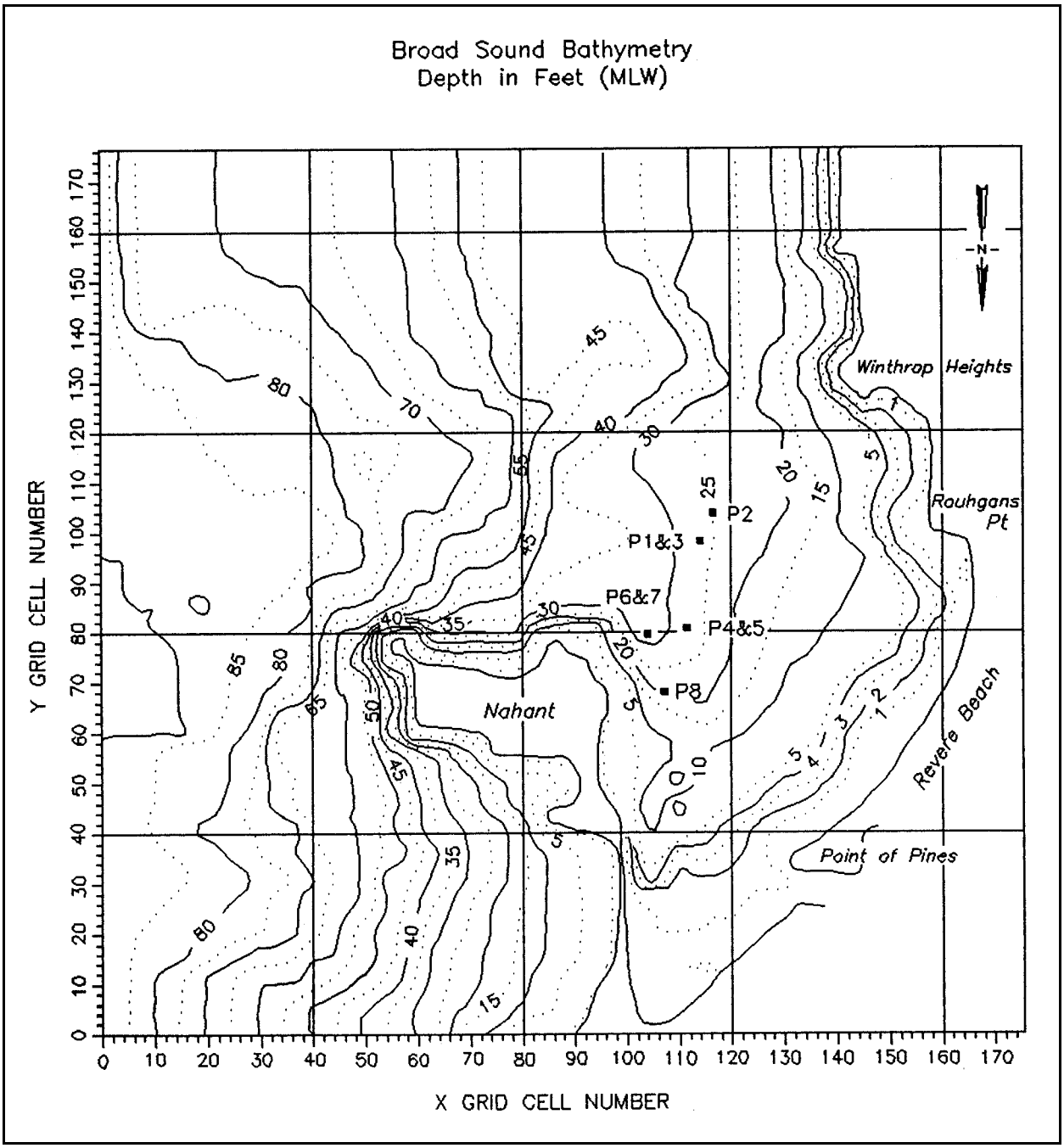

Figure II-3-10. Bathymetry input to REF/DIF1 for a simulation of wave propagations at Revere Beach, MA

strongly supports a stochastic approximation for wave phenomena (West 1981). Over small distances, near discontinuities in a wave field (such as breakwaters), STWAVE can incorporate wave phase information into its solution; otherwise, it uses a random-phase approximation for its diffraction and combined refraction-diffraction (CRD) calculations. Theoretical details of STWAVE can be found in Resio (1993).

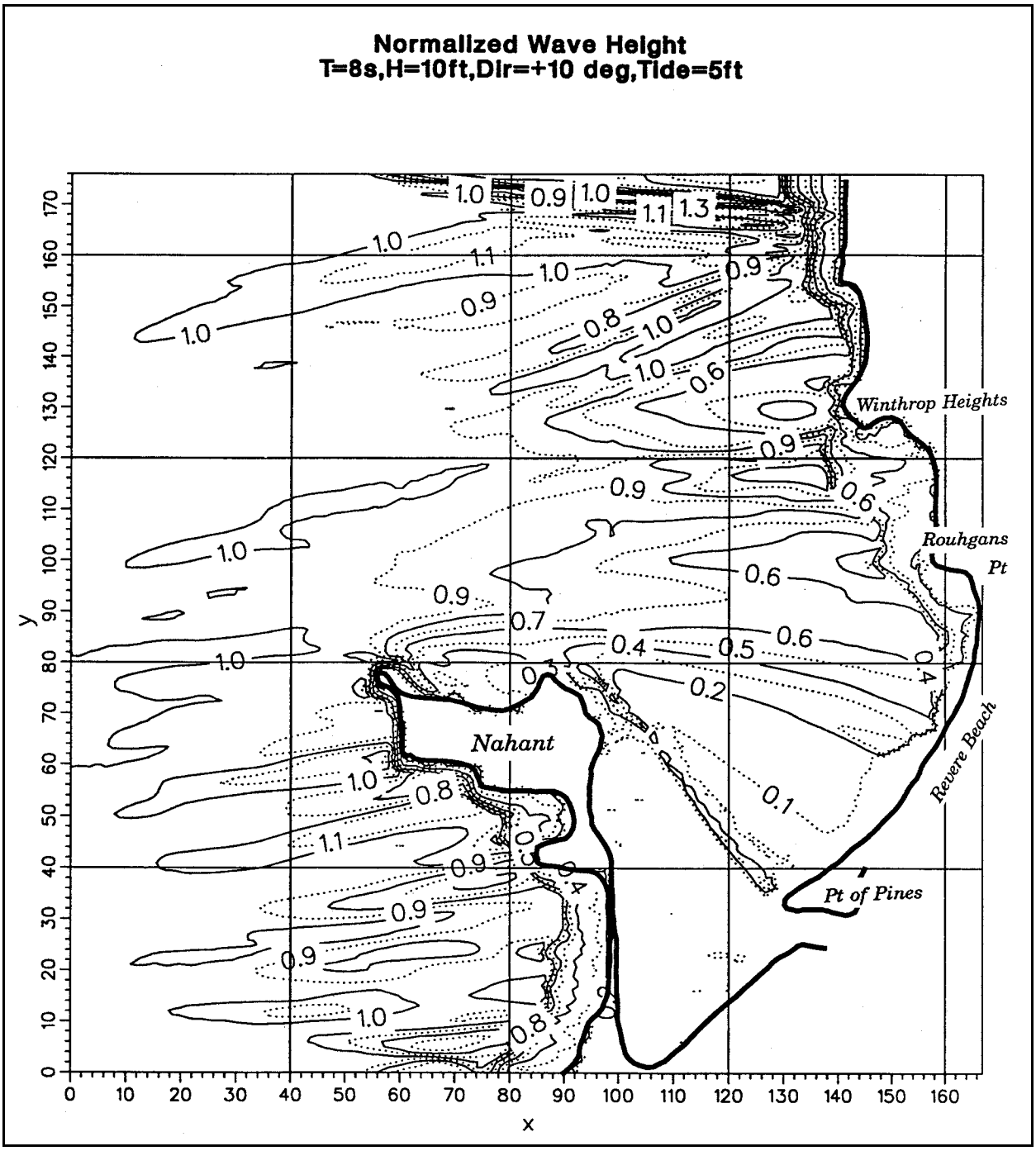

Figure II-3-11. Wave heights calculated by REF/DIF 1

(b) The following two assumptions have been inherent in essentially all previous steady-state models for predicting nearshore wave transformations:

- Predictions based on unidirectional, monochromatic wave theories can provide solutions that are equivalent to the behavior of naturally occurring directional wave spectra.

- Nearshore transformations are dominated by conservative processes (refraction, shoaling, and diffraction) and hence nonconservative effects (energy sinks and sources) can be neglected as a first approximation.

(c) A corollary to the first assumption above is that increased accuracy in deterministic propagation estimates translates into commensurate increases in accuracy in real-world applications. Unfortunately, laboratory studies by Thompson and Vincent (1984) and Vincent and Briggs (1989) have clearly demonstrated that the first assumption is not valid unless the wave field is narrow-banded in both frequency and direction. Thus, for most coastal wave predictions to be accurate, they must solve all wave components and not just a hypothetical "dominant" component. This presents significant problems for wave models that solve only one wave component at a time, since wave energy traveling in one direction can be "scattered" into another direction via diffraction. Hence, diffraction causes wave components in a spectrum to interact and attempts to solve the CRD equation on a component-by-component basis have difficulty properly accounting for this effect. STWAVE overcomes this problem by using a piecewise solution method that simulates the propagation of all wave components simultaneously.

(d) Returning to the second assumption above, field and laboratory data presented in Bouws, Gunther, and Vincent (1985) and Resio (1988) show that nonconservative effects, rather than conservative propagation effects, dominate wave transformations in many coastal areas, particularly during storm conditions. Moreover, the form of many of the source terms affecting shallow-water wave transformations is such that they depend on energy content within the entire wave spectrum. Methods that solve for each component of the spectrum independently cannot provide suitable estimates of coupled source terms. STWAVE is formulated in a manner that permits straightforward solution of these processes.

(2) Examples of STWAVE results. The following comparisons are intended to demonstrate the importance of various terms in coastal wave transformations and the ability of STWAVE to handle these terms.

(a) Spectral versus monochromatic calculations. Figure II-3-12 compares predicted wave heights behind a shoal using STWAVE, for a unidirectional, monochromatic wave and for a JONSWAP spectrum with a spectral peak frequency of 0.1 Hz and a $\cos^4$ angular distribution of energy. Monochromatic calculations from the laboratory study of Vincent and Briggs (1989), while mathematically accurate, do not reasonably represent propagation effects in a wave spectrum with natural frequency and direction energy spreads.

(b) Effects of coupled source terms. Figure II-3-13 compares spectral transformation over 1:30, 1:100, and 1:500 slopes for the same JONSWAP spectrum as above with a mean approach angle to the coast of 30 deg, for the case of no source terms and for the case of wave breaking and nonlinear wave-wave interaction source terms included. This comparison suggests that CRD effects account for only about 5 percent of the total energy variations in coastal waves passing over moderate to shallow slopes. This finding is consistent with those of Resio (1988) and helps to explain why nearshore wave spectra tend strongly toward self-similar forms during local storms (Bouws, Gunther, and Vincent 1985; Resio 1987; Miller and Vincent 1990).

(c) Wind effects. Figure II-3-14 shows the differences in wave transformations with and without a 20-m/sec onshore wind over an offshore profile typical of the U.S. east coast. In this example, waves at the seaward boundary are set to the same JONSWAP spectrum as Examples 1 and 2. These results show a marked difference between the two cases. This difference is consistent with theoretically expected wind input and indicates that, particularly during storm conditions, neglecting wind input can lead to significant misestimations of wave conditions.

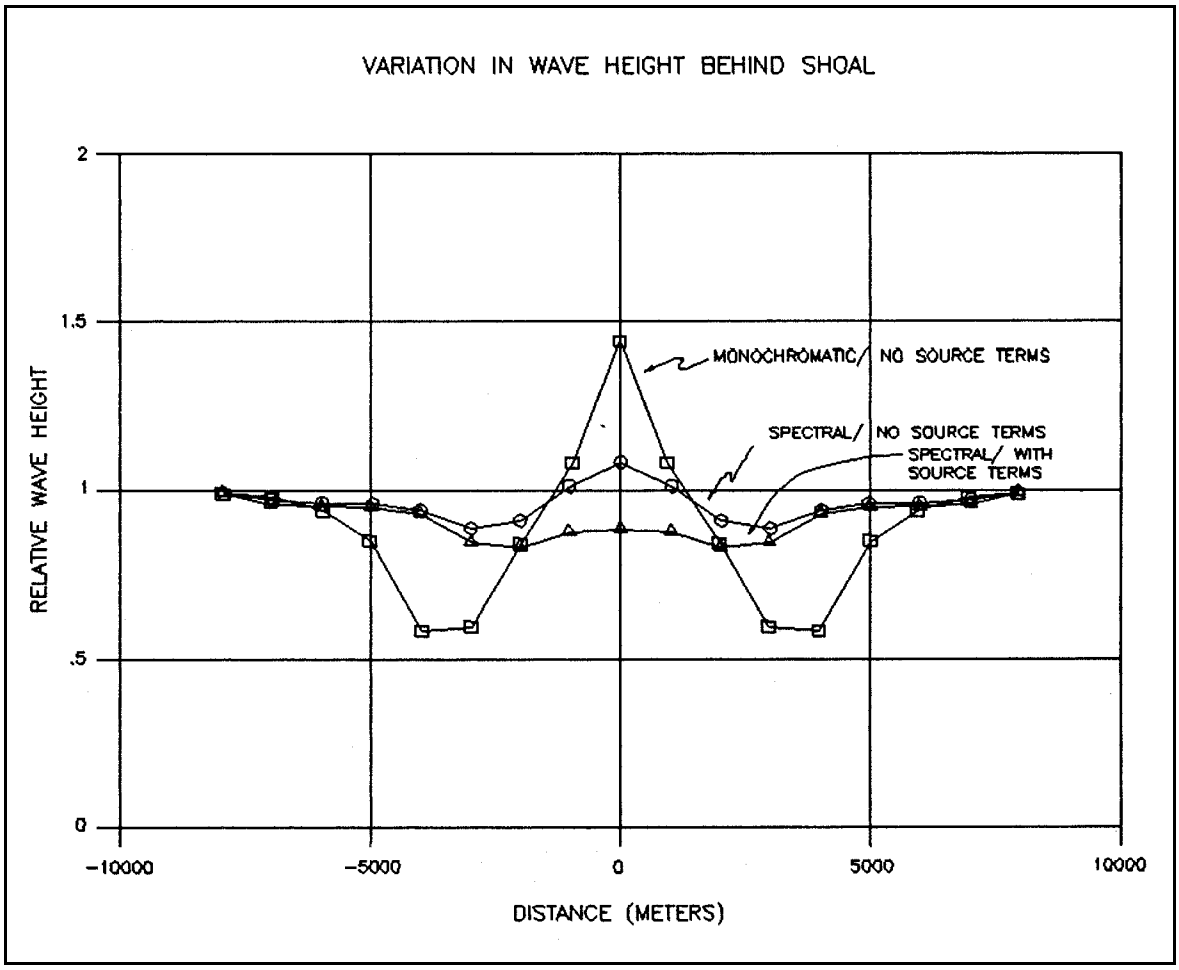

Figure II-3-12. Spectral model results compared to laboratory measurements for broad directional spectrum

(3) Data requirements for STWAVE. In STWAVE, a square grid mesh covers the computational domain. Water depth must be supplied at each node. If currents are included, a current must be supplied at each point. Wave characteristics are computed at each of these grid points. The model requires an input directional spectrum for the outer boundary and information about wind speed and direction and bottom friction coefficients.

e. Limitations.

(1) Each model has natural limitations reflecting its theoretical basis. The references provided discuss these in some detail. If strictly interpreted, each model has a narrow range over which it is valid. Almost all of these models are regularly used to simulate conditions outside a strict interpretation of limits, with the results often effectively accurate. Considerable judgement and experience are required to determine if the simulation is valid.

(2) The following limitations indicate where the model may or may not be useful. RCPWAVE may be inaccurate for waves crossing behind shoals, or in the vicinity of structures. Wave approach directions should not be too oblique relative to the offshore boundary. REF/DIF1 can allow for some structures and islands but again should not use waves with highly oblique wave angles (In both RCPWAVE and REF/DIF1,

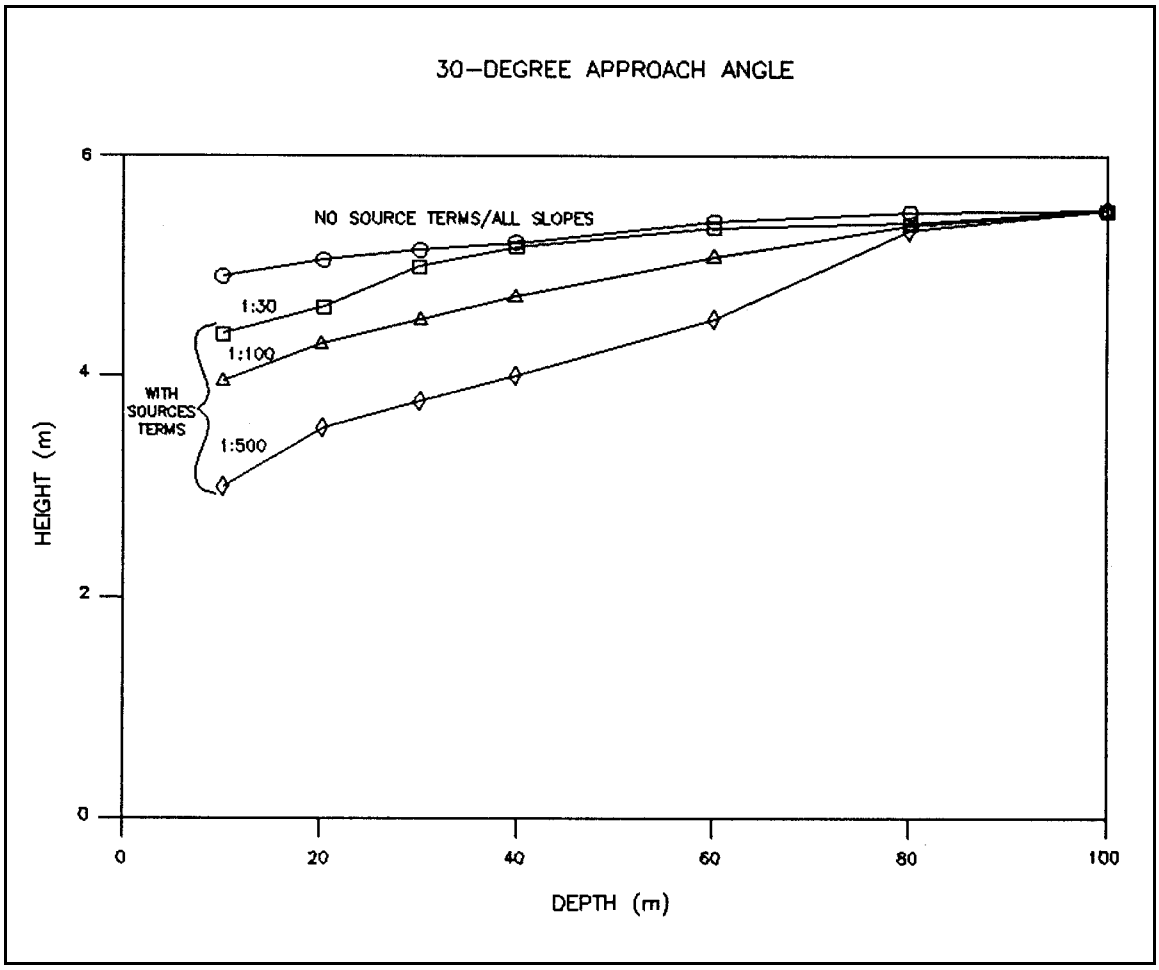

Figure II-3-13. STWAVE results for a 1:30 sloping beach

the oblique angle dilemma often can be resolved by using a different grid). STWAVE may underrepresent wave focussing for very narrow swell.

II-3-6. Guidance for Performing Wave Transformation Studies

a. Introduction.

(1) The preceding parts of this chapter provide the engineer with an understanding and some techniques for taking a wave condition offshore of a project or nearby and transforming it to the site of interest. In practice, an engineer will typically consider a suite of wave conditions perhaps representing different storms, different seasonal characteristics, and different water levels (particularly in shallow water or at the beach if there is a high tide or storm surge to be considered). Selection of the conditions for project design studies is a very important component of any coastal engineering study and Part II-2 and Part II-3 both treat this problem.

(2) Transformation analyses are needed because there is often a lack of site-specific data. In some instances, a cursory transformation analysis may be required to help decide whether an offshore or nearby site is adequate for determining offshore boundary conditions. Typically this may be approached by setting up one of the transformation procedures described and running a small set of wave conditions that might span

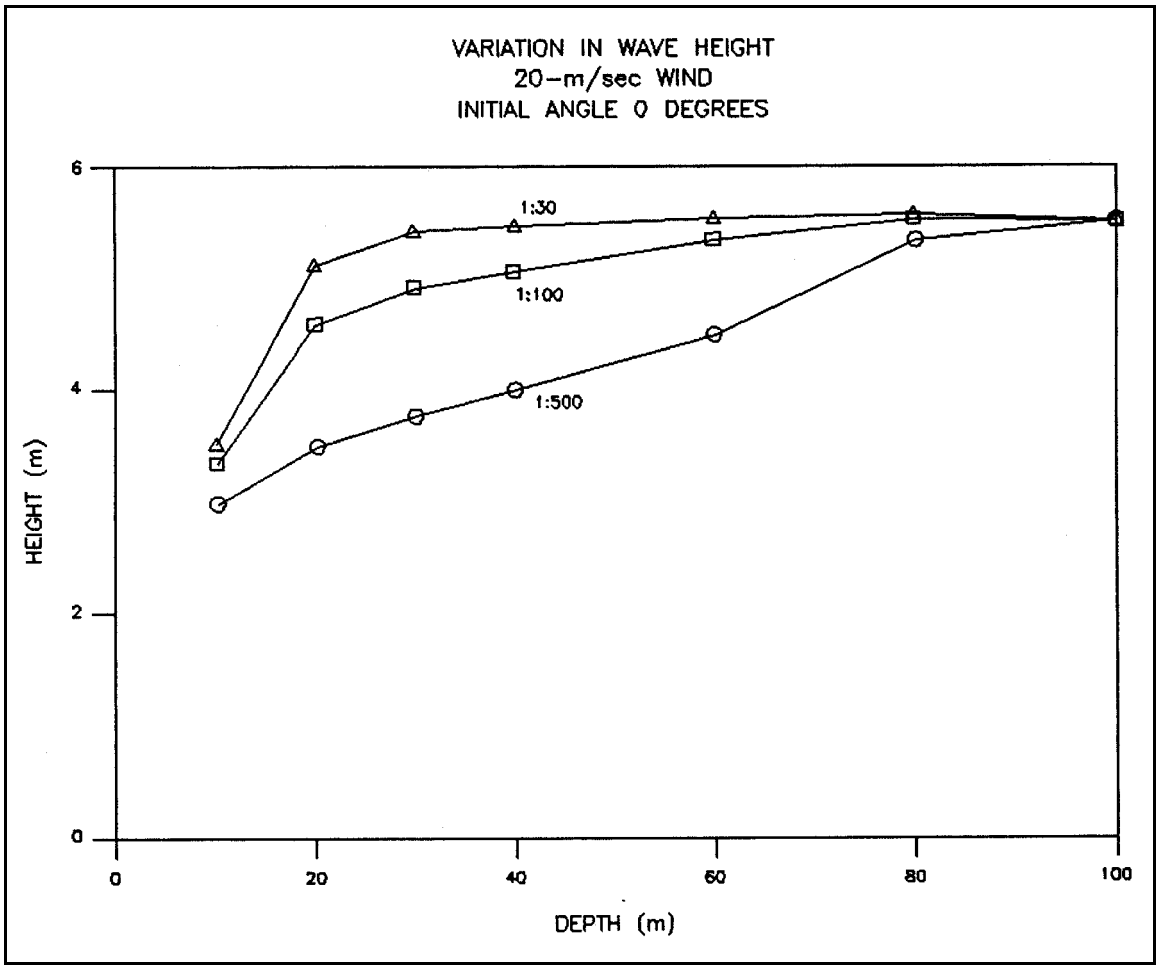

Figure II-3-14. STWAVE results for CHL's Field Research Facility at Duck, NC

the final set to be studied. As an example, waves of a certain period or direction offshore may not propagate to the site, and the engineer can thus ignore such wave conditions in a more detailed study.

(3) Some of the decisions and actions an engineer will need to make in performing a wave transformation analysis follow.

b. Problem formulation. At the initiation of the study, the engineer should clearly understand what wave information must be produced for the site, how it will be used, and the accuracy required. The engineer should gather all pertinent bathymetry data, water level data, and nearby wave data. Aerial photography of the site can be very useful by providing the engineer with indications of wave propagation patterns, areas of offshore breaking, etc., that a transformation procedure should properly simulate. Short-term gauge records can be used in checking the procedure. Again, a short-term gauging program is desirable.

c. Site analysis. The physical characteristics of the site and any ancillary information should be carefully scrutinized so that the engineer can understand how irregular the bathymetry is, the presence of significant currents, shoals, canyons, islands, structures, etc., that would be important in selecting the offshore or nearby site for a source of data input, for selecting the transformation procedure used, and in understanding what problems may arise in the analysis. Usually this type of knowledge is gained through experience, and a consultant may be required to assist someone unexperienced in such analyses. If time permits, one of the

advanced models could be set up and run in an exploratory mode to help the engineer understand possible problems.

d. Selection of input data site. Based on project formulation and site analysis, offshore/nearby sites are evaluated in terms of any feature that would preclude their use (see Part II-3-1d). In particular, the use of nearby sites in similar depths of water must be evaluated in terms of whether waves reaching the site have broken. As an example, if waves at a nearshore site have propagated over a shoal where breaking can occur, there is no way to "unbreak" the waves. So they cannot be used to eliminate offshore wave conditions. In general the offshore data site will need as a minimum information on **wave height, period, and direction.** If adequate data are not available, methods for hindcasting, as described in Part II-2, may be used to simulate the information required. The methods of Parts II-2 and 3 should be used to develop the wave information to be transformed.

e. Selection of wave transformation method. Table II-3-2 provides guidance on the applicability of the various methods described in this chapter. It does not provide guidelines for all cases. With some skill, the models described can be pushed somewhat beyond their inherent limitations (but such results must be carefully scrutinized and used conservatively). In very complicated cases or in cases in which a time-dependent model is required, use of an expert consultant to provide assistance is recommended. In some complicated cases, a physical model may be required.

Table II-3-2
Guidance for Selection of Wave Transformation Methods

Case	Fig.II-3-6 or ACES	NMLONG	RCPWAVE	REFDIF1	STWAVE
Planar topography (no shoals, etc)	yes	yes	yes	yes	yes
Highly Irregular Bathymetry					
Swell, no structures	no	no	yes	yes	yes
Swell, structures	no	no	no	yes	yes
Complicated directional Spectra, but narrow frequency spectra	no	no	no	yes	yes
High winds or broad band frequency spectra	no	no	no	no	yes
Irregular Bathymetry, High resolution Computations Near Structure					
Swell	no	no	no	yes	no

f. Calibration/verification. After the method is set up, it is important to check the calculations with observations if at all possible. If measured wave data are not available, then aerial photographs can be helpful in deciding if the model reproduces observed wave patterns. If no wave data or photographs are available, the method should be applied to a range of heights, periods, and directions and the results should be carefully scrutinized for odd or unstable results. If the calculations are overly sensitive to small variations in input data, a careful decision should be made as to whether the technique should be applied. A physical model may be appropriate in situations with very irregular bathymetry, complicated or multiple structures, reefs, and where currents are important.

g. Post-processing.

(1) Plotted results should be carefully examined for any signs of computational instability. These typically are unreasonable variations in height or direction over short distances.

(2) The techniques provided in this chapter, if used carefully by an experienced engineer, can provide very useful information in a wide range of cases. However, there are some cases where they simply will not work. Anyone who applies these techniques should understand the limitations of the techniques, and be versed in understanding when they have been used inappropriately. The user should be aware that the models can provide realistic-looking answers that unfortunately are just wrong.

II-3-7. References

Abbott, Peterson, and Skovgaard 1978
Abbot, M. B., Peterson, H. M., and Skovgaard, O. 1978. "On the Numerical Modelling of Short Waves in Shallow Water," *Journal Hydraulic Research*, Vol 16, No. 3, pp 173-203.

Bagnold 1946
Bagnold, R. A. 1946. "Motion of Waves in Shallow Water - Interaction Between Waves and Sand Bottoms," *Royal Society of London*, Vol 187, pp 1-18.

Barnett 1968
Barnett, T. P. 1968. "On the Generation, Dissipation, and Prediction of Wind Waves," *Journal of Geophysical Research,* Vol 73, pp 6879-6885.

Berkhoff 1972
Berkhoff, J. C. W. 1972. "Computation of Combined Refraction - Diffraction," *Proceedings, 13th International Conference on Coastal Engineering,* American Society of Civil Engineers, Vol 1, pp 471-490.

Berkhoff 1976
Berkhoff, J. C. W. 1976. "Mathematical Models for Simple Harmonic Linear Water Waves, Wave Diffraction and Refraction," Publication 1963, Delft Hydraulics Laboratory, Delft, The Netherlands, April.

Berkhoff, Booij, and Radder 1982.
Berkhoff, J. C., Booij, N., and Radder, A. C. 1982. "Verification of Numerical Wave Propagation Models for Simple Harmonic Linear Water Waves," *Coastal Engineering,* Vol 6, pp 255-279.

Bouws et al. 1987
Bouws et al. 1987. "Similarity of the Wind Wave Spectrum in Finite Depth Water; Part 2: Statistical Relations Between Shape and Growth Stage," *Deutsche Hydogr. Z.,* Vol 40, pp 1-24.

Bouws, Gunther, and Vincent 1985
Bouws, E, Gunther, H., and Vincent, C. L. 1985. "Similarity of Wind Wave Spectrum in Finite-Depth Water, Part I - Spectral Form," *Journal of Geophysical Research*, Vol 85, No. C3, pp 1524-1530.

Bretschneider and Reid 1953
Bretschneider, C. L., and Reid, R. O. 1953. "Change in Wave Height Due to Bottom Friction, Percolation and Refraction," *34th Annual Meeting of American Geophysical Union.*

Dally, Dean, and Dalrymple 1984
Dally, W. R., Dean, R. G., and Dalrymple, R. A. 1984. "Modeling Wave Transformation in the Surf Zone," Miscellaneous Paper CERC-84-8, U.S. Army Engineer Waterways Experiment Station, Vicksburg, MS.

Dean and Dalrymple 1991
Dean, R. G., and Dalrymple, R. A. 1991. *Water Wave Mechanics for Engineers and Scientists*, World Scientific Pub. Co., Teaneck, NJ.

Demirbilek 1994
Demirbilek, Z. 1994. "Comparison of REFDIF Model and CERC Elliptical Shoal Laboratory Data," Memorandum for Record, dated 18 June 1994, for the Coastal Inlets Research Program, Coastal Engineering Research Center, Vicksburg, MS.

Demirbilek and Webster 1992a
Demirbilek, Z., and Webster, W. C. 1992a. "Application of the Green-Naghdi Theory of Fluid Sheets to Shallow-Water Wave Problems; Report 1: Model Development," Technical Report CERC-92-11, U.S. Army Engineer Waterways Experiment Station, Vicksburg, MS.

Demirbilek and Webster 1992b
Demirbilek, Z., and Webster, W.C. 1992b. "User's Manual and Examples for GNWAVE, Final Report," Technical Report CERC-92-13, U.S. Army Engineer Waterways Experiment Station, Vicksburg, MS.

Dobson 1967
Dobson, R. S. 1967. "Some Applications of a Digital Computer to Hydraulic Engineering Problems," Technical Report No. 80, Department of Civil Engineering, Stanford University, Stanford, CA.

Ebersole 1985
Ebersole, B. A. 1985. "Refraction-Diffraction Model for Linear Water Waves," *Journal of Waterways, Port, Coastal, and Ocean Engineering*, American Society of Civil Engineers, Vol III, No. WW6, pp 939-953.

Ebersole, Cialone, and Prater 1986
Ebersole, B. A., Cialone, M. A., and Prater, M. D. 1986. "RCPWAVE - A Linear Wave Propagation Model for Engineering Use," Technical Report CERC-86-4, U.S. Army Engineer Waterways Experiment Station, Vicksburg, MS.

Forristall and Reece 1985
Forristall, G. Z., and Reece, A. M. 1985. "Measurements of Wave Attenuation Due to a Soft Bottom: The SWAMP Experiment," *Journal of Geophysical Researc*h, Vol 90, No. C2, pp 3367-3380.

Harrison and Wilson 1964
Harrison, W., and Wilson, W. S. 1964. "Development of a Method for Numerical Calculation of Wave Refraction," Technical Memorandum No. 6, Coastal Engineering Research Center, U.S. Army Engineer Waterways Experiment Station, Vicksburg, MS.

Hasselmann 1962
Hasselmann, K. 1962. "On the Non-Linear Energy Transfer In A Gravity-Wave Spectrum - General Theory," *J. Fluid Mech*., Vol 12, pp 481-500.

Hasselmann 1963a
Hasselmann, K. 1963a. "On the Non-Linear Energy Transfer In A Gravity-Wave Spectrum - Part 2," *J. Fluid Mech*., Vol 15, pp 273-281.

Hasselmann 1963b
Hasselmann, K. 1963b. "On the Non-Linear Energy Transfer In A Gravity-Wave Spectrum - Part 3," *J. Fluid Mech*., Vol 15, pp 385 - 398.

Hasselmann et al. 1973
Hasselmann et al. 1973. "Measurements of Wind-Wave Growth and Swell Decay During the Joint North Sea Wave Project (JONSWAP)," *Deutsche Hydrograph. Zeit.,* Erganzungsheft Reihe A (8^0), No. 12.

Hedges 1976
Hedges, T. S. 1976. "An Empirical Modification to Linear Wave Theory," *Proc. Inst. Civ. Engrs*., Vol 61, pp 575-579.

Jensen et al. 1987
Jensen, R. E., et al. 1987. "SHALWV - Hurricane Wave Modeling and Verification; User's Guide to SHALWV: Numerical Model for Simulation of Shallow-Water Wave Growth, Propagation, and Decay," Instruction Report CERC-86-2, No. 2, U.S. Army Engineer Waterways Experiment Station, Coastal Engineering Research Center, Vicksburg, MS.

Jonsson 1978
Jonsson, I. G. 1978. "Combinations of Waves and Currents," *Stability of Tidal Inlets*, Per Bruun, ed., Amsterdam, Elsenir, pp 162-203.

Kirby 1984
Kirby, J. T. 1984. "A Note on Linear Surface Wave-Current Interaction Over Slowly Varying Topography," *Journal of Geophysical Research*, Vol 89, pp 745-747.

Kirby 1986a
Kirby, J. T. 1986a. "Higher-Order Approximations in the Parabolic Equation Method for Water Waves," *Journal of Geophysical Research*, Vol 91, pp 933-952.

Kirby and Dalrymple 1983
Kirby, J. T., and Dalrymple, R. A. 1983. "A Parabolic Equation for the Combined Refraction-Diffraction of Stokes Waves by Mildly Varying Topography," *J. Fluid Mech*., Vol 136, pp 453-466.

Kirby and Dalrymple 1984
Kirby, J. T., and Dalrymple, R. A. 1984. "Verification of a Parabolic Equation for Propagation of Weakly-Nonlinear Waves," *Coastal Engineering*, Vol 8, pp 219-232.

Kirby and Dalrymple 1986a
Kirby, J. T., and Dalrymple, R. A. 1986a. "Modeling Waves in Surfzones and Around Islands," *J. Waterways, Port, Coastal and Ocean Engrg*., Vol 112, pp 78 -93.

Kirby and Dalrymple 1986b
Kirby, J. T., and Dalrymple, R. A. 1986b. "An Approximate Model for Nonlinear Dispersion in Monochromatic Wave Propagation Models," *Coastal Engineering*, Vol 9, pp 545-561.

Kirby and Dalrymple 1992
Kirby, J. T., and Dalrymple, R. A. 1992. "Combined Refraction/Diffraction Model REF/DIF 1, Version 2.4.; Documentation and User's Manual," Research Report CACR-92-04, Center for Applied Coastal Research, University of Delaware.

Kraus 1991
Kraus, N. C. 1991. "NMLONG: Numerical Model for Simulating the Longshore Current," U.S. Army Engineer Waterways Experiment Station, Vicksburg, MS.

Leblond and Mysak 1978
Leblond, P. H., and Mysak, L. A. 1978. "*Waves in the Ocean*," Elsevier Scientific Pub. Co., Amsterdam-Oxford, NY.

Leenknecht, Szuwalski, and Sherlock 1992
Leenknecht, D. A., Szuwalski, A., and Sherlock, A. R. 1992. "Automated Coastal Engineering System; User Guide and Technical Reference, Version 1.07," U.S. Army Engineer Waterways Experiment Station, Vicksburg, MS.

Miller and Vincent 1990
Miller, H. C., and Vincent, C.L. 1990. "FRF Spectrum: TMA with Kitaigoredskii's F^4 Scaling," *Journal of Waterway, Port, Coastal, and Ocean Engineering*, Vol 116, No. 1, pp 57-78.

Noda 1974
Noda, E. K. 1974. "Wave-Induced Nearshore Circulation," *Journal of Geophysical Research*, Vol 79, No. 27, pp 4097-4106.

Noda et al. 1974
Noda, E. K., et al. 1974. "Nearshore Circulations Under Sea Breeze Conditions and Wave-Current Interactions in the Surf Zone," Technical Report No. 4, Tetra Tech, Inc., Pasadena, CA.

Panchang et al. 1990
Panchang, V. G., Pearce, B. R., Wei, G., and Briggs, M. J. 1990. "Numerical Simulation of Irregular Wave Propagation Over Shoal," *J. Waterway, Port, Coastal, and Ocean Engrg.*, Vol 116, pp 324-340.

Penny and Price 1944
Penny, W. G., and Price, A. T. 1944. "Diffraction of Waves by Breakwaters," Directorate of Miscellaneous Weapons Development History No. 20 - Artificial Harbors, Sec 3D.

Peregrine 1976
Peregrine, D. H. 1976. "Interaction of Water Waves and Currents," *Advances in Applied Mechanics*, Academic Press, New York, Vol 16, pp 9-117.

Phillips 1977
Phillips, O. M. 1977. *The Dynamics of The Upper Ocean*, 2nd ed., Cambridge University Press.

Radder 1979
Radder, A. C. 1979. "On the Parabolic Equation Method for Water-Wave Propagation," *Journal of Fluid Mechanics*, Vol 95, Part 1, pp 159-176.

Resio 1981
Resio, D. T. 1981. "The Estimation of Wind-Wave Generation in a Discrete Spectral Model," *Journal of Geophysical Research*, Vol 11, pp 510 - 525.

Resio 1987
Resio, D. T. 1987. "Shallow Water Waves. I - Theory," *J. Waterway, Port, Coastal and Ocean Engr*., American Society of Civil Engineers, Vol 113, pp 264-281.

Resio 1988
Resio, D. T. 1988. "Shallow Water Waves II - Data Comparisons," *J. Waterway, Port, Coastal and Ocean Engr*., Vol 114, pp 50-65.

Resio 1993
Resio, D. T. 1993. "STWAVE: Wave Propagation Simulation Theory, Testing and Application," Department of Oceanography, Ocean Engineering, and Environmental Science, Florida Institute of Technology.

Shore Protection Manual 1984
Shore Protection Manual. 1984. 4th ed., 2 Vol, U. S. Army Engineer Waterways Experiment Station, U.S. Government Printing Office, Washington, DC.

Smith and Vincent 1992
Smith, J. M., and Vincent, C. L. 1992. "Shoaling and Decay of Two Wave Trains on a Beach," *J. Waterways, Port, Coastal and Ocean Engr.,* Vol 118, No. 5, pp 517-533.

Sobey and Young 1986
Sobey, R. J., and Young, I. R. 1986. "Hurricane Wind Waves - A Discrete Spectral Model," *J. Waterway, Port, Coastal and Ocean Engineering*, Vol 112, No. 3, pp 370-389.

SWAMP Group 1985
SWAMP Group. 1985. "*The Sea Wave Modeling Project (SWAMP): Principal Results and Conclusion*," Plenum, New York, p 256.

SWIM Group 1985
SWIM Group. 1985. "A Shallow Water Intercomparison of Three Numerical Prediction Models (SWIM)," *Quarterly Journal of the Royal Meteorological Society*, Vol 111, pp 1087-1112.

Thompson and Vincent 1984
Thompson, E. F., and Vincent, C. L. 1984. "Shallow-Water Wave Height Parameters," *J. Waterway, Port, Coastal and Ocean Engr*., American Society of Civil Engineers, Vol 110, No. 2, pp 293-299.

Tsay and Liu 1982
Tsay, T. K., and Liu, P. L. -F. 1982. "Numerical Solution of Water-Wave Refraction and Diffraction Problems in the Parabolic Approximation," *Journal of Geophysical Research*, Vol 87, pp 7932-7940.

Vincent and Briggs 1989
Vincent, C. L., and Briggs, M. J. 1989. "Refraction-Diffraction of Irregular Waves Over A Mound," *J. Waterway, Port, Coastal and Ocean Engrg*, American Society of Civil Engineers, Vol 115, No. 2, pp 269-284.

WAMDI 1988
WAMDI. 1988. "The WAM Model - A Third Generation Ocean Wave Prediction Model," *Journal of Physical Oceanography*, Vol 18, pp 1775-1810.

Weggel 1972
Weggel, J. R. 1972. "Maximum Breaker Height," *Journal of the Waterways, Harbors, and Coastal Engineering Division*, Vol 98, No. WW4, pp 529-548.

West 1981
West, B. J. 1981. "On the Simpler Aspects of Nonlinear Fluctuating Gravity Wave (Weak Interaction Theory)," *Lecture Notes in Physics 146*, Springer-Verlag, New York.

Young 1988
Young, L. R. 1988. "A Shallow Water Spectral Wave Model," *Journal of Geophysical Research*, Vol 93, No. C5, pp 5113-5129.

II-3-8. Definitions of Symbols

$\vec{k}$	Wave number vector (Equation II-3-4)
θ	Angle between the plane across which energy is being transmitted and the direction of wave advance [deg]
ρ	Mass density of water (salt water = 1,025 kg/m^3 or 2.0 slugs/ft^3; fresh water = 1,000kg/m^3 or 1.94 slugs/ft^3) [force-time^2/length^4]
φ	Velocity potential at the free surface [length^2/time]
ω	Wave angular or radian frequency (= $2\pi/T$) [time^{-1}]
Ω	Wave phase function (Equation II-3-3)
C	Wave celerity [length/time]
C_g	Wave group velocity [length/time]
d	Water depth [length]
E	Total wave energy in one wavelength per unit crest width [length-force/length^2]
$E(x,y,t,f,\theta)$	Directional spectrum where x,y represents a location in geographic space, t represents time, and f,θ represents a particular frequency-direction component
h	Water depth [length]
H	Wave height [length]
k	Wave number (= $2\pi/L = 2\pi/CT$) [length^{-1}]
K_r	Refraction coefficient [dimensionless]
K_s	Shoaling coefficient [dimensionless]
L	Wave length [length]
$-_O$	The subscript 0 denotes deepwater conditions
T	Wave period [time]
U	Ambient current vector (Equation II-3-30) [length/time]
φ	Velocity potential at the free surface [length^2/time]

II-3-9. Acknowledgments

Authors of Chapter II-3, "Estimation of Nearshore Waves:"

C. Linwood Vincent, Ph.D., Office of Naval Research, Arlington, Virginia.
Zeki Demirbilek, Ph.D., Coastal and Hydraulics Laboratory, Engineer Research and Development Center, Vicksburg, Mississippi.
J. Richard Weggel, Ph.D., Dept. of Civil and Architectural Engineering, Drexel University, Philadelphia, Pennsylvania.

Reviewers:

Robert A Dalrymple, Ph.D., Center for Applied Coastal Research, University of Delaware, Newark, Delaware.
Lee E. Harris, Ph.D., Department of Marine and Environmental Systems, Florida Institute of Technology, Melbourne, Florida.
Philip L.-F. Liu, Ph.D., School of Civil and Environmental Engineering, Cornell University, Ithaca, New York.

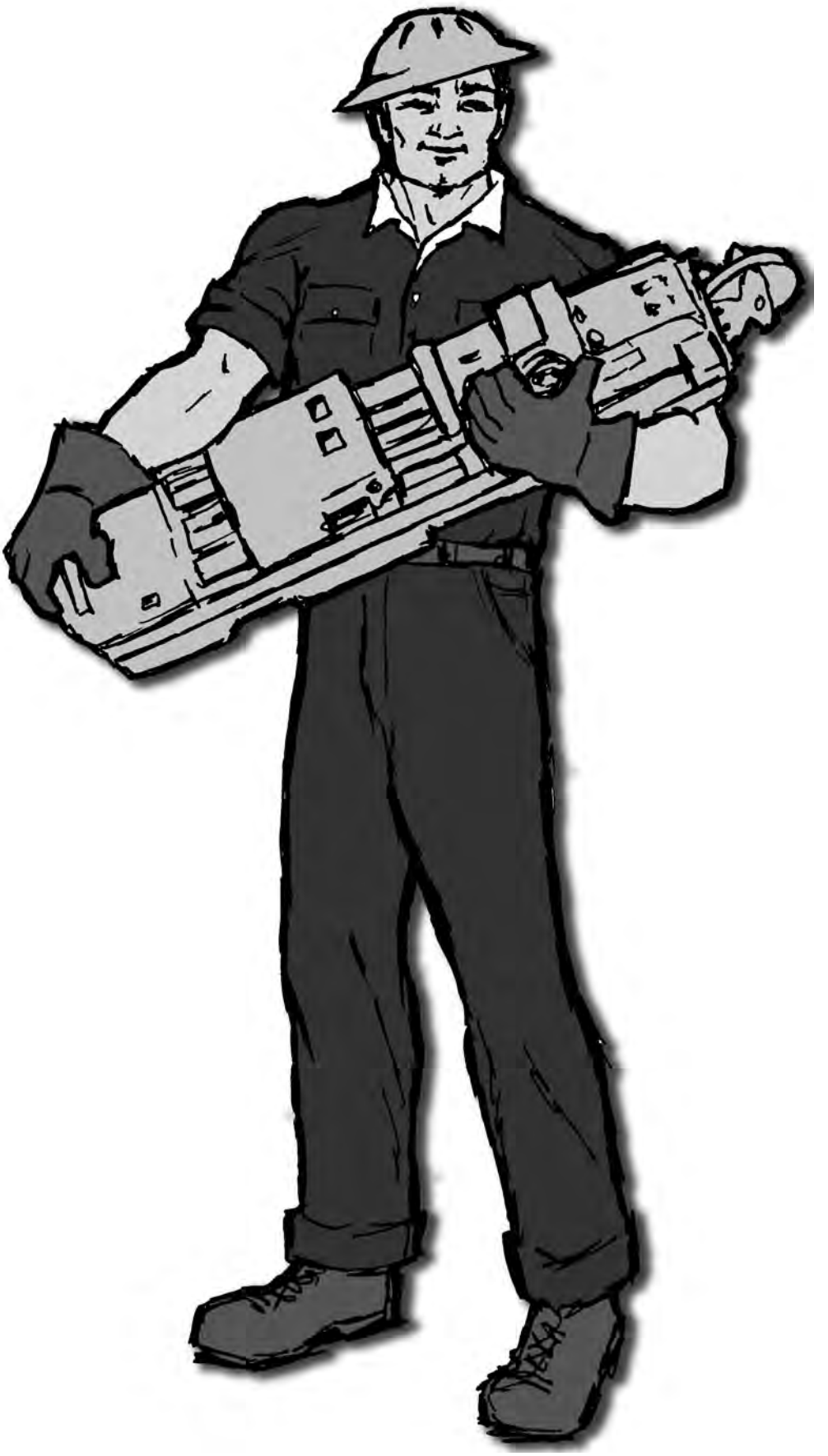

Table of Contents

Page

II-4-1. Introduction II-4-1

II-4-2. Surf Zone Waves II-4-1
a. Incipient wave breaking II-4-1
(1) Breaker type II-4-1
(2) Breaker criteria II-4-3
(3) Regular waves II-4-3
(4) Irregular waves II-4-4
b. Wave transformation in the surf zone II-4-5
(1) Similarity method II-4-5
(2) Energy flux method II-4-6
(3) Irregular waves II-4-8
(4) Waves over reefs II-4-11

II-4-3. Wave Setup II-4-12

II-4-4. Wave Runup on Beaches II-4-14
a. Regular waves II-4-17
b. Irregular waves II-4-18

II-4-5. Infragravity Waves II-4-19

II-4-6. Nearshore Currents II-4-20
a. Introduction II-4-20
b. Longshore current II-4-22
c. Cross-shore current II-4-25
d. Rip currents II-4-26

II-4-7. References II-4-27

II-4-8. Definitions of Symbols II-4-37

II-4-9. Acknowledgments II-4-40

List of Figures

Page

Figure II-4-1. Breaker types II-4-2

Figure II-4-2. Breaker depth index as a function of $H_b/(gT^2)$ (Weggel 1972) II-4-5

Figure II-4-3. Change in wave profile shape from outside the surf zone (a,b) to inside the surf zone (c,d). Measurements from Duck, North Carolina (Ebersole 1987) II-4-7

Figure II-4-4. Transformation of H_{rms} with depth based on the initial wave approach and the Dally, Dean, and Dalrymple (1985) model II-4-9

Figure II-4-5. NMLONG simulation of wave height transformation (Leadbetter Beach, Santa Barbara, California, 3 Feb 1980 (Thornton and Guza 1986)) II-4-10

Figure II-4-6. Shallow-water transformation of wave spectra (solid line - incident, d = 3.0m; dotted line - incident breaking zone, d = 1.7m; dashed line - surf zone, d = 1.4m) II-4-11

Figure II-4-7. Definition sketch for wave setup II-4-13

Figure II-4-8. Irregular wave setup for plane slope of 1/100 . . . . . II-4-15

Figure II-4-9. Irregular wave setup for plane slope of 1/30 . . . . . II-4-15

Figure II-4-10. Example problem II-4-2 . . . . . II-4-16

Figure II-4-11. Definition sketch for wave runup II-4-17

Figure II-4-12. Definition of runup as local maximum in elevation II-4-17

Figure II-4-13. Measured cross-shore and longshore flow velocities II-4-21

Figure II-4-14. Nearshore circulation systems II-4-22

Figure II-4-15. Longshore current profiles (solid line - no lateral mixing; dashed lines - with lateral mixing) II-4-24

Figure II-4-16. Equation II-4-37 compared with field and laboratory data (Komar 1979) II-4-25

Figure II-4-17. NMLONG simulation of longshore current (Leadbetter Beach, Santa Barbara, California, 3 Feb 1989 (Thornton and Guza 1986)) II-4-26

Figure II-4-18. Field measurement of cross-shore flow on a barred profile (Duck, North Carolina, October 1990) II-4-27

Chapter II-4
Surf Zone Hydrodynamics

II-4-1. Introduction

a. Waves approaching the coast increase in steepness as water depth decreases. When the wave steepness reaches a limiting value, the wave breaks, dissipating energy and inducing nearshore currents and an increase in mean water level. Waves break in a water depth approximately equal to the wave height. The *surf zone* is the region extending from the seaward boundary of wave breaking to the limit of wave uprush. Within the surf zone, wave breaking is the dominant hydrodynamic process.

b. The purpose of this chapter is to describe shallow-water wave breaking and associated hydrodynamic processes of wave setup and setdown, wave runup, and nearshore currents. The surf zone is the most dynamic coastal region with sediment transport and bathymetry change driven by breaking waves and nearshore currents. Surf zone wave transformation, water level, and nearshore currents must be calculated to estimate potential storm damage (flooding and wave damage), calculate shoreline evolution and cross-shore beach profile change, and design coastal structures (jetties, groins, seawalls) and beach fills.

II-4-2. Surf Zone Waves

The previous chapter described the transformation of waves from deep to shallow depths (including refraction, shoaling, and diffraction), up to wave breaking. This section covers incipient wave breaking and the transformation of wave height through the surf zone.

a. Incipient wave breaking. As a wave approaches a beach, its length L decreases and its height H may increase, causing the wave steepness H/L to increase. Waves break as they reach a limiting steepness, which is a function of the relative depth d/L and the beach slope $\tan\beta$. Wave breaking parameters, both qualitative and quantitative, are needed in a wide variety of coastal engineering applications.

(1) Breaker type.

(a) *Breaker type* refers to the form of the wave at breaking. Wave breaking may be classified in four types (Galvin 1968): as spilling, plunging, collapsing, and surging (Figure II-4-1). In *spilling breakers*, the wave crest becomes unstable and cascades down the shoreward face of the wave producing a foamy water surface. In *plunging breakers*, the crest curls over the shoreward face of the wave and falls into the base of the wave, resulting in a high splash. In *collapsing breakers* the crest remains unbroken while the lower part of the shoreward face steepens and then falls, producing an irregular turbulent water surface. In *surging breakers*, the crest remains unbroken and the front face of the wave advances up the beach with minor breaking.

(b) Breaker type may be correlated to the surf similarity parameter ξ_o, defined as

$$\xi_o = \tan\beta \left(\frac{H_o}{L_o} \right)^{-\frac{1}{2}} \tag{II-4-1}$$

where the subscript o denotes the deepwater condition (Galvin 1968, Battjes 1974). On a uniformly sloping beach, breaker type is estimated by

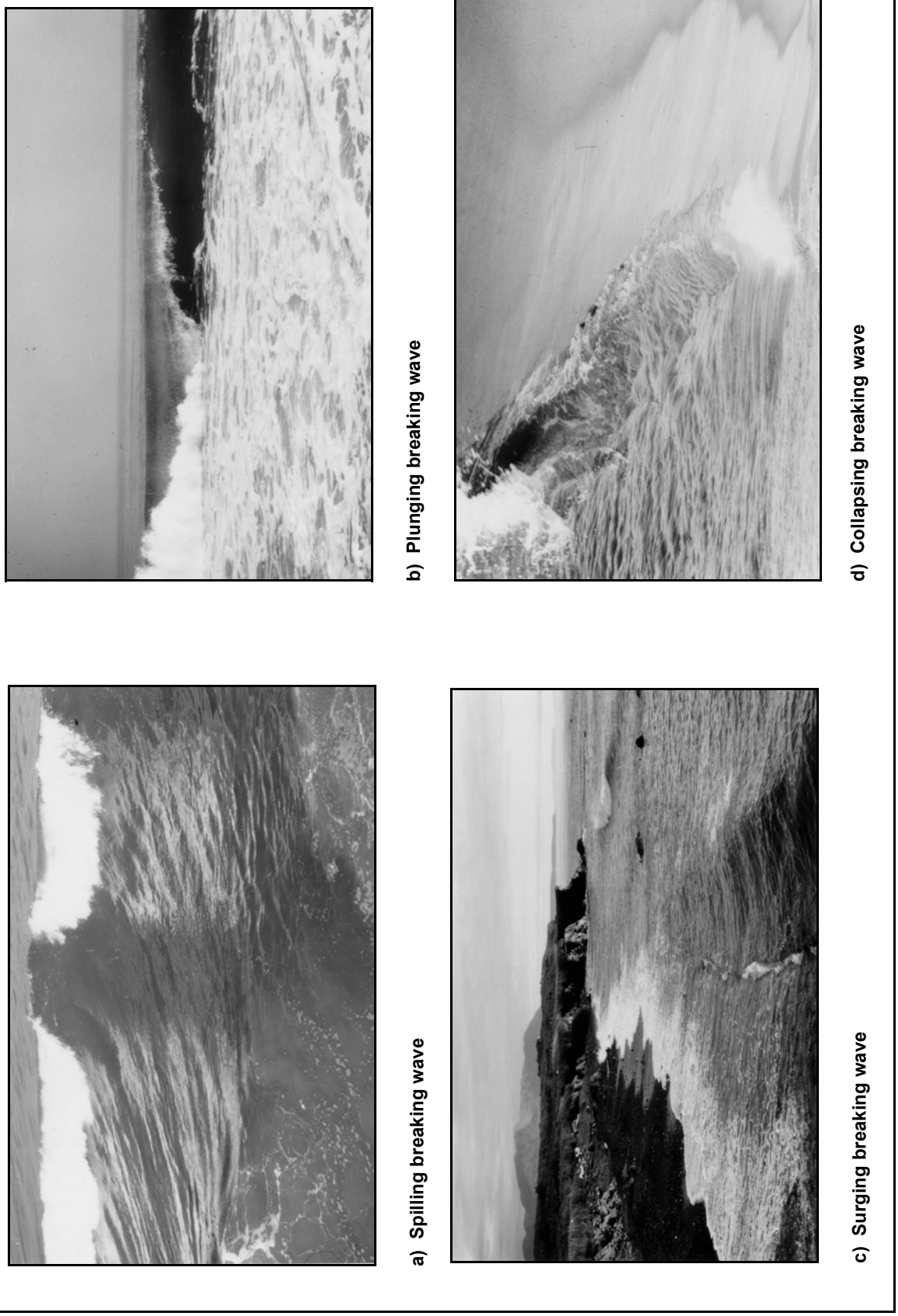

Figure II-4-1. Breaker types

$$\begin{aligned} \text{Surging/collapsing} \quad & \xi_o > 3.3 \\ \text{Plunging} \quad & 0.5 < \xi_o < 3.3 \\ \text{Spilling} \quad & \xi_o < 0.5 \end{aligned} \tag{II-4-2}$$

(c) As expressed in Equation II-4-2, spilling breakers tend to occur for high-steepness waves on gently sloping beaches. Plunging breakers occur on steeper beaches with intermediately steep waves, and surging and collapsing breakers occur for low steepness waves on steep beaches. Extremely low steepness waves may not break, but instead reflect from the beach, forming a standing wave (see Part II-3 for discussion of reflection and Part II-5 for discussion of tsunamis).

(d) Spilling breakers differ little in fluid motion from unbroken waves (Divoky, Le Méhauté, and Lin 1970) and generate less turbulence near the bottom and thus tend to be less effective in suspending sediment than plunging or collapsing breakers. The most intense local fluid motions are produced by a plunging breaker. As it breaks, the crest of the plunging wave acts as a free-falling jet that may scour a trough into the bottom. The transition from one breaker type to another is gradual and without distinct dividing lines. Direction and magnitude of the local wind can affect breaker type. Douglass (1990) showed that onshore winds cause waves to break in deeper depths and spill, whereas offshore winds cause waves to break in shallower depths and plunge.

(2) Breaker criteria. Many studies have been performed to develop relationships to predict the wave height at incipient breaking H_b. The term *breaker index* is used to describe nondimensional breaker height. Two common indices are the *breaker depth* index

$$\gamma_b = \frac{H_b}{d_b} \tag{II-4-3}$$

in which d_b is the depth at breaking, and the *breaker height* index

$$\Omega_b = \frac{H_b}{H_o} \tag{II-4-4}$$

Incipient breaking can be defined several ways (Singamsetti and Wind 1980). The most common definition is the point that wave height is maximum. Other definitions are the point where the front face of the wave becomes vertical (plunging breakers) and the point just prior to appearance of foam on the wave crest (spilling breakers). Commonly used expressions for calculating breaker indices follow.

(3) Regular waves.

(a) Early studies on breaker indices were conducted using solitary waves. McCowan (1891) theoretically determined the breaker depth index as $\gamma_b = 0.78$ for a solitary wave traveling over a horizontal bottom. This value is commonly used in engineering practice as a first estimate of the breaker index. Munk (1949) derived the expression $\Omega_b = 0.3(H_o / L_o)^{-1/3}$ for the breaker height index of a solitary wave. Subsequent studies, based on periodic waves, by Iversen (1952), Goda (1970), Weggel (1972), Singamsetti and Wind (1980), Sunamura (1980), Smith and Kraus (1991), and others have established that the breaker indices depend on beach slope and incident wave steepness.

(b) From laboratory data on monochromatic waves breaking on smooth, plane slopes, Weggel (1972) derived the following expression for the breaker depth index

$$\gamma_b = b - a \frac{H_b}{g T^2} \tag{II-4-5}$$

for $\tan \beta \le 0.1$ and $H_o'/L_o \le 0.06$, where T is wave period, g is gravitational acceleration, and H_o' is equivalent unrefracted deepwater wave height. The parameters a and b are empirically determined functions of beach slope, given by

$$a = 43.8 \left(1 - e^{-19 \tan \beta}\right) \tag{II-4-6}$$

and

$$b = \frac{1.56}{\left(1 + e^{-19.5 \tan \beta}\right)} \tag{II-4-7}$$

(c) The breaking wave height H_b is contained on both sides of Equation II-4-5, so the equation must be solved iteratively. Figure II-4-2 shows how the breaker depth index depends on wave steepness and bottom slope. For low steepness waves, the breaker index (Equation II-4-5) is bounded by the theoretical value of 0.78, as the beach slope approaches zero, and twice the theoretical value (sum of the incident and perfectly reflected component), or 1.56, as the beach slope approaches infinity. For nonuniform beach slopes, the average bottom slope from the break point to a point one wavelength offshore should be used.

(d) Komar and Gaughan (1973) derived a semi-empirical relationship for the breaker height index from linear wave theory

$$\Omega_b = 0.56 \left(\frac{H_o'}{L_o} \right)^{-\frac{1}{5}} \tag{II-4-8}$$

(e) The coefficient 0.56 was determined empirically from laboratory and field data.

(4) Irregular waves. In irregular seas (see Part II-1 for a general discussion of irregular waves), incipient breaking may occur over a wide zone as individual waves of different heights and periods reach their steepness limits. In the *saturated* breaking zone for irregular waves (the zone where essentially all waves are breaking), wave height may be related to the local depth d as

$$H_{rms,b} = 0.42 \, d \tag{II-4-9}$$

for root-mean-square (rms) wave height (Thornton and Guza 1983) or, approximately,

$$H_{mo,b} = 0.6 \, d \tag{II-4-10}$$

for zero-moment wave height (see Part II-1). Some variability in $H_{rms,b}$ and $H_{mo,b}$ with wave steepness and beach slope is expected; however, no definitive study has been performed. The numerical spectral wave transformation model STWAVE (Smith et al. 2001) uses a modified Miche Criterion (Miche 1951).

$$H_{mo,b} = 0.1 \text{ L tan h } kd \tag{II-4-11}$$

to represent both depth- and steepness-induced wave breaking.

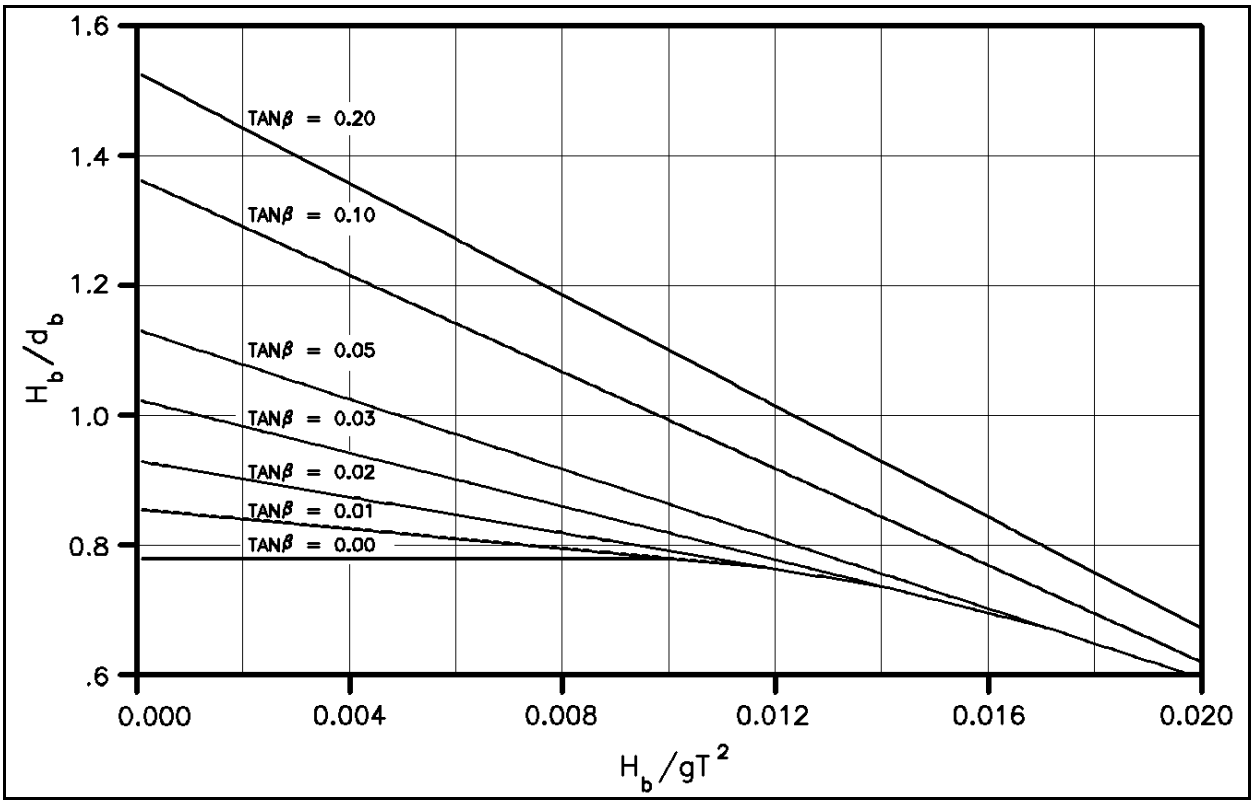

Figure II-4-2. Breaker depth index as a function of $H_b/(gT^2)$ (Weggel 1972)

b. Wave transformation in the surf zone. Following incipient wave breaking, the wave shape changes rapidly to resemble a bore (Svendsen 1984). The wave profile becomes sawtooth in shape with the leading edge of the wave crest becoming nearly vertical (Figure II-4-3). The wave may continue to dissipate energy to the shoreline or, if the water depth again increases as in the case of a barred beach profile, the wave may cease breaking, re-form, and break again on the shore. The transformation of wave height through the surf zone impacts wave setup, runup, nearshore currents, and sediment transport.

(1) Similarity method. The simplest method for predicting wave height through the surf zone, an extension of Equation II-4-3 shoreward of incipient breaking conditions, is to assume a constant height-to-depth ratio from the break point to shore

$$H_b = \gamma_b \, d_b \tag{II-4-12}$$

This method, also referred to as saturated breaking, has been used successfully by Longuet-Higgins and Stewart (1963) to calculate setup, and by Bowen (1969a), Longuet-Higgins (1970a,b), and Thornton (1970) to calculate longshore currents. The similarity method is applicable only for monotonically decreasing water depth through the surf zone and gives best results for a beach slope of approximately 1/30. On steeper slopes, Equation II-4-12 tends to underestimate the wave height. On gentler slopes or barred topography, it tends to overestimate the wave height. Equation II-4-12 is based on the assumption that wave height is zero at the mean shoreline (see Part II-4-3 for discussion of mean versus still-water shoreline). Camfield (1991) shows that a conservative estimate of wave height at the still-water shoreline is 0.20 H_b for $0.01 \leq \tan\beta \leq 0.1$.

EXAMPLE PROBLEM II-4-1

FIND:

Wave height and water depth at incipient breaking.

GIVEN:

A beach with a 1 on 100 slope, deepwater wave height H_o = 2 m, and period T = 10 sec. Assume that a refraction analysis (Part II-3) gives a refraction coefficient K_R = 1.05 at the point where breaking is expected to occur.

SOLUTION:

The equivalent unrefracted deepwater wave height H_o' can be found from the refraction coefficient (see Part II-3, Equation II-3-14)

$$H_o' = K_R H_o = 1.05\ (2.0) = 2.1 \text{ m}$$

and the deepwater wavelength L_o is given by (Part II-1)

$$L_o = g\ T^2/(2\pi) = 9.81\ (10^2)/(2\pi) = 156 \text{ m}$$

Estimate the breaker height from Equation II-4-8

$$\Omega_b = 0.56\ (H_o'/L_o)^{-1/5} = 0.56\ (2.1/156.)^{-1/5} = 1.3$$
$$H_b \text{ (estimated)} = \Omega_b\ H_0' = 2.7 \text{ m}$$

From Equations II-4-6 and II-4-7, determine a and b used in Equation II-4-5, tan β = 1/100

$$a = 43.8(1 - e^{-19\ (1/100)}) = 7.58$$
$$b = 1.56 / (1 + e^{-19.5\ (1/100)}) = 0.86$$

$$\gamma_b = b - a\ H_b / (gT^2) = 0.86 - 7.58\ (2.7)/(9.81\ 10^2) = 0.84$$
$$d_b = H_b / \gamma_b = 2.7/0.84 = 3.2 \text{ m}$$

Breaker height is approximately 2.7 m and breaker depth is 3.2 m. The initial value selected for the refraction coefficient would now be checked to determine if it is correct for the actual breaker location. If necessary, a corrected refraction coefficient should be used to recompute breaker height and depth.

(2) Energy flux method.

(a) A more general method for predicting wave height through the surf zone for a long, straight coast is to solve the steady-state energy balance equation

$$\frac{d(EC_g)}{dx} = -\delta \qquad \text{(II-4-13)}$$

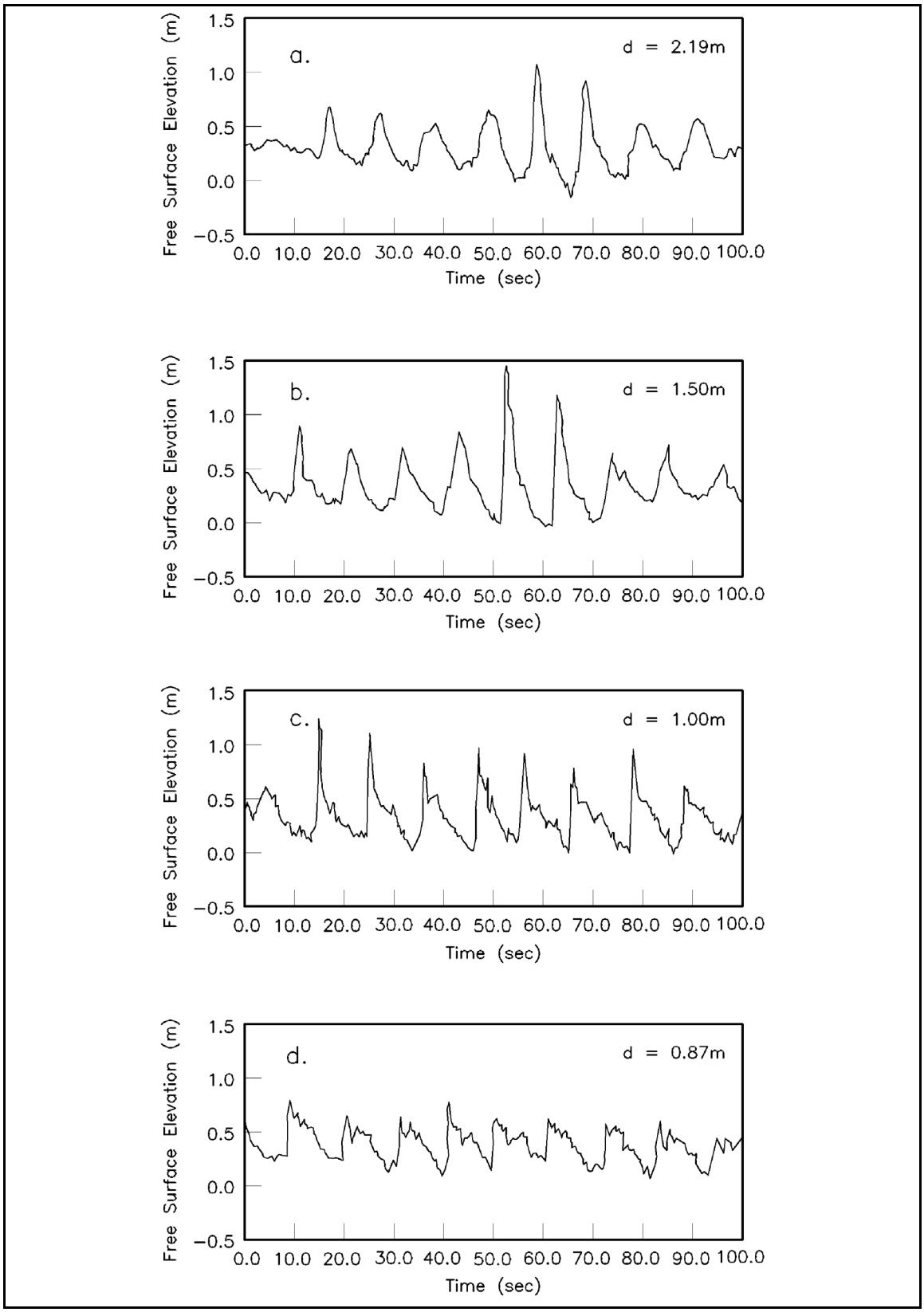

Figure II-4-3. Change in wave profile shape from outside the surf zone (a,b) to inside the surf zone (c,d). Measurements from Duck, NC (Ebersole 1987)

where E is the wave energy per unit surface area, C_g is the wave group speed, and δ is the energy dissipation rate per unit surface area due to wave breaking. The wave energy flux EC_g may be specified from linear or higher order wave theory. Le Méhauté (1962) approximated a breaking wave as a hydraulic jump and substituted the dissipation of a hydraulic jump for δ in Equation II-4-13 (see also Divoky, Le Méhauté, and Lin 1970; Hwang and Divoky 1970; Svendsen, Madsen, and Hansen 1978).

(b) Dally, Dean, and Dalrymple (1985) modeled the dissipation rate as

$$\delta = \frac{\kappa}{d}\left(EC_g - EC_{g,s}\right) \tag{II-4-14}$$

where κ is an empirical decay coefficient, found to have the value 0.15, and $EC_{g,s}$ is the energy flux associated with a *stable* wave height

$$H_{stable} = \Gamma d \tag{II-4-15}$$

(c) The quantity Γ is an empirical coefficient with a value of approximately 0.4. The stable wave height is the height at which a wave stops breaking and re-forms. As indicated, this approach is based on the assumption that energy dissipation is proportional to the difference between local energy flux and stable energy flux. Applying linear, shallow-water theory, the Dally, Dean, and Dalrymple model reduces to

$$\begin{aligned} \frac{d(H^2 d^{\frac{1}{2}})}{dx} &= -\frac{\kappa}{d}\left(H^2 d^{\frac{1}{2}} - \Gamma^2 d^{\frac{5}{2}}\right) \quad \text{for} \quad H > H_{stable} \\ &= 0 \quad \text{for} \quad H < H_{stable} \end{aligned} \tag{II-4-16}$$

This approach has been successful in modeling wave transformation over irregular beach profiles, including bars (e.g., Ebersole (1987), Larson and Kraus (1991), Dally (1992)).

(3) Irregular waves.

(a) Transformation of irregular waves through the surf zone may be analyzed or modeled with either a statistical (individual wave or wave height distribution) or a spectral (parametric spectral shape) approach. Part II-1 gives background on wave statistics, wave height distributions, and parametric spectral shapes.

(b) The most straightforward statistical approach is transformation of individual waves through the surf zone. Individual waves seaward of breaking may be measured directly, randomly chosen from a Rayleigh distribution, or chosen to represent wave height classes in the Rayleigh distribution. Then the individual waves are independently transformed through the surf zone using Equation II-4-13. Wave height distribution can be calculated at any point across the surf zone by recombining individual wave heights into a distribution to calculate wave height statistics (e.g., $H_{1/10}$, $H_{1/3}$, H_{rms}). This method does not make a priori assumptions about wave height distribution in the surf zone. The individual wave method has been applied and verified with field measurements by Dally (1990), Larson and Kraus (1991), and Dally (1992). Figure II-4-4 shows the nearshore transformation of H_{rms} with depth based on the individual wave approach and the Dally, Dean, and Dalrymple (1985) model for deepwater wave steepness (H_{rmso} / L_o) of 0.005 to 0.05 and plane beach slopes of 1/100 and 1/30.

(c) A numerical model called NMLONG (Numerical Model of the LONGshore current) (Larson and Kraus 1991) calculates wave breaking and decay by the individual wave approach applying the Dally, Dean,

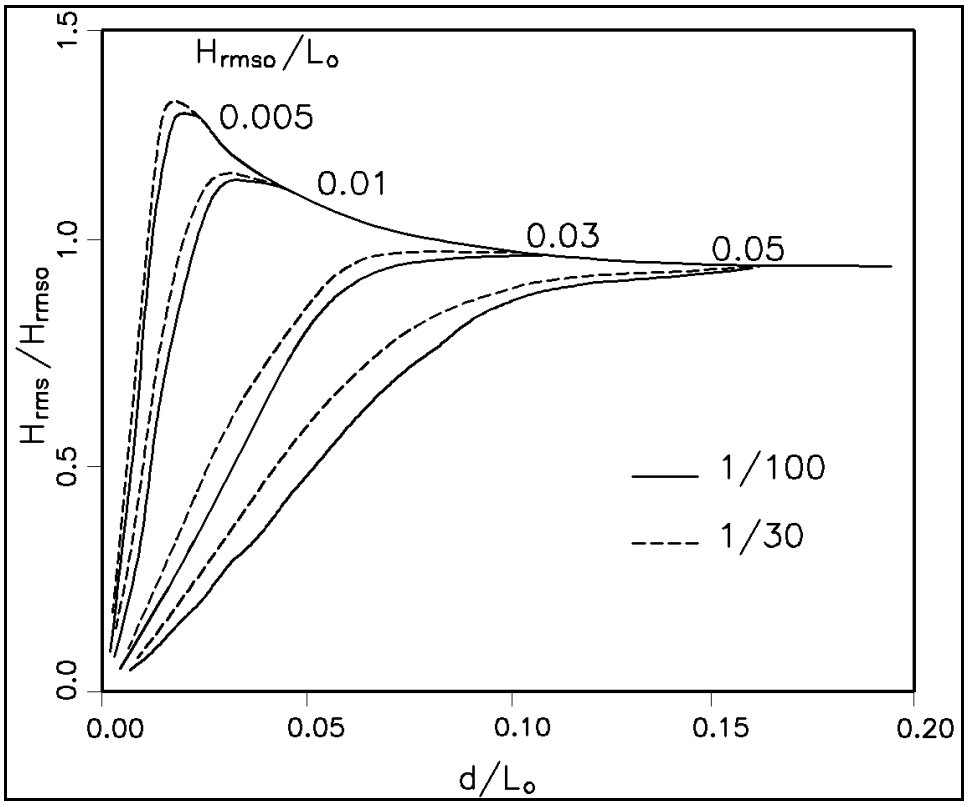

Figure II-4-4. Transformation of H_{rms} with depth based on the individual wave approach and the Dally, Dean, and Dalrymple (1985) model

and Dalrymple (1985) wave decay model (monochromatic or irregular waves). The main assumption underlying the model is uniformity of waves and bathymetry alongshore, but the beach profile can be irregular across the shore (e.g., longshore bars and nonuniform slopes). NMLONG uses a single wave period and direction and applies a Rayleigh distribution wave heights outside the surf zone. The model runs on a personal computer and has a convenient graphical interface. NMLONG calculates both wave transformation and longshore current (which will be discussed in a later section) for arbitrary offshore (input) wave conditions and provides a plot of results. Figure II-4-5 gives an example NMLONG calculation and a comparison of wave breaking field measurements reported by Thornton and Guza (1986).

(d) A second statistical approach is based on assuming a wave height distribution in the surf zone. The Rayleigh distribution is a reliable measure of the wave height distribution in deep water and at finite depths. In the surf zone, depth-induced breaking acts to limit the highest waves in the distribution, contrary to the Rayleigh distribution, which is unbounded. The surf zone wave height distribution has generally been represented as a truncated Rayleigh distribution (e.g., Collins (1970), Battjes (1972), Kuo and Kuo (1974), Goda 1975). Battjes and Janssen (1978) and Thornton and Guza (1983) base the distribution of wave heights at any point in the surf zone on a Rayleigh distribution or a truncated Rayleigh distribution (truncated above a maximum wave height for the given water depth). A percentage of waves in the distribution is designated as broken, and energy dissipation from these broken waves is calculated from Equation II-4-13 through a model of dissipation similar to a periodic bore. Battjes and Janssen (1978) define the energy dissipation as

$$\delta = 0.25 \rho g Q_b f_m (H_{\max})^2 \tag{II-4-17}$$

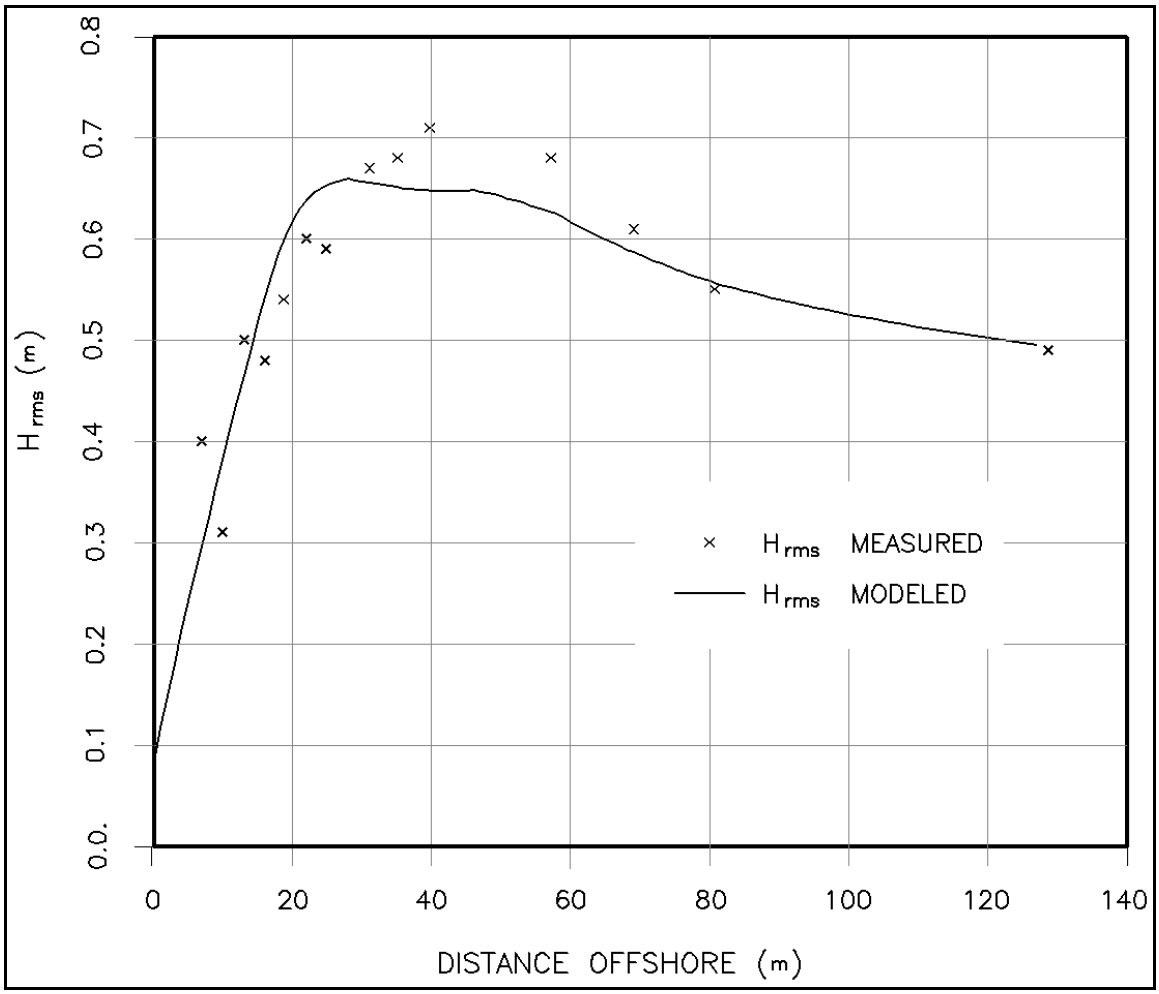

Figure II-4-5. NMLONG simulation of wave height transformation (Leadbetter Beach, Santa Barbara, California, 3 Feb 1980 (Thornton and Guza 1986))

where Q_b is the percentage of waves breaking, f_m is the mean wave frequency, and the maximum wave height is based on the Miche (1951) criterion

$$H_{\max} = 0.14L\tanh(kd) \tag{II-4-18}$$

where k is wave number. Battjes and Janssen base the percentage of waves breaking on a Rayleigh distribution truncated at H_{max}. Baldock et al. (1998) show improved results and reduced computational time by basing Q_b on the full Rayleigh distribution (Smith 2001). Goda (2002) documented that although the wave height distribution in the midsurf zone is narrower than the Rayleigh distribution, in the outer surf zone and near the shoreline the distribution is nearly Rayleigh. This method has been validated with laboratory and field data (e.g., Battjes and Janssen 1978; Thornton and Guza 1983) and implemented in numerical models (e.g., Booij 1999). Specification of the maximum wave height in terms of the Miche criterion (Equation II-4-18) has the advantage of providing reasonable results for steepness-limited breaking (e.g., waves breaking on a current) as well as depth-limited breaking (Smith et al. 1997).

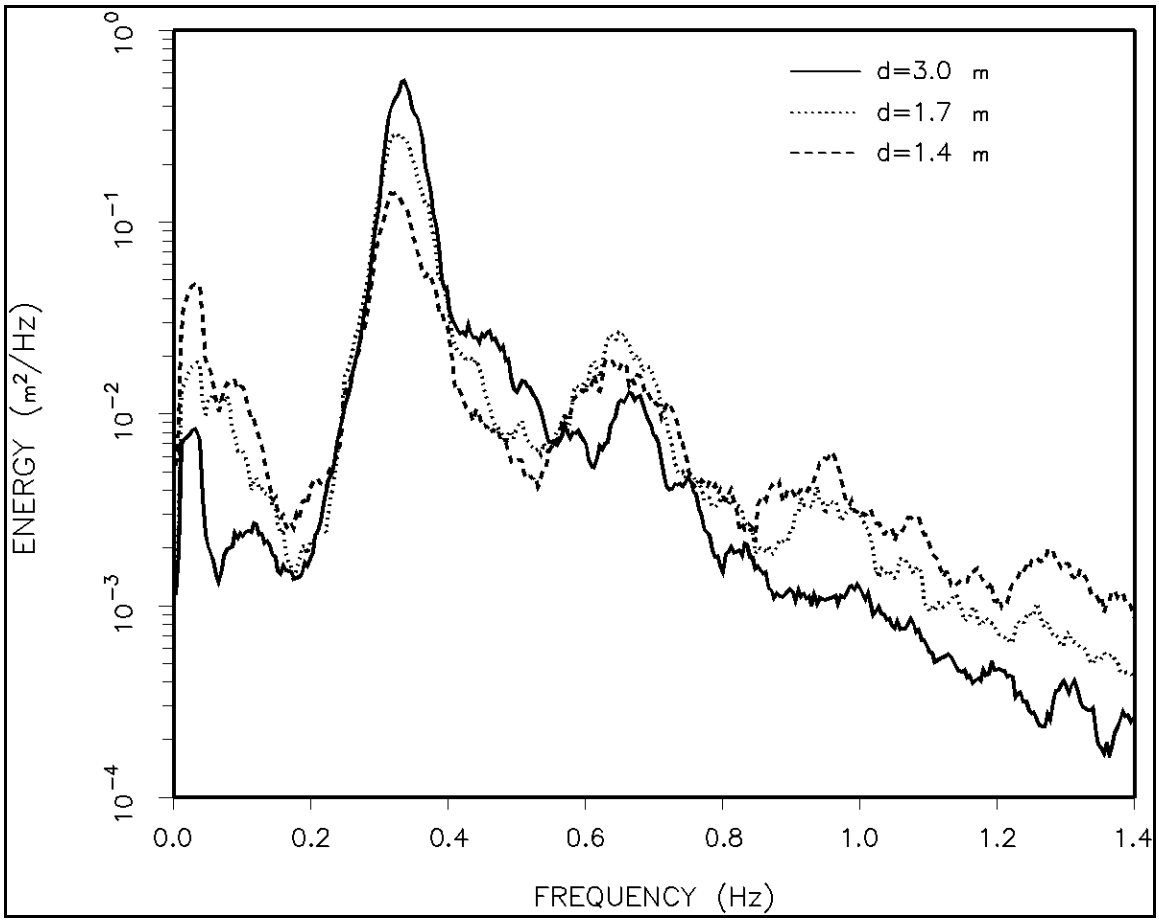

Figure II-4-6. Shallow-water transformation of wave spectra (solid line - incident, d = 3.0m; dotted line - incident breaking zone, d = 1.7m; dashed line - surf zone, d = 1.4m)

(e) In shallow water, the shape of the wave spectrum is influenced by nonlinear transfers of wave energy from the peak frequency to higher frequencies and lower frequencies (Freilich and Guza 1984; Freilich, Guza, and Elgar 1990). Near incipient breaking higher harmonics (energy peaks at integer multiples of the peak frequency) appear in the spectrum as well as a general increase in the energy level above the peak frequency as illustrated in Figure II-4-6. Low-frequency energy peaks (subharmonics) are also generated in the surf (Figure II-4-6, also see Part II-4-5). Figure II-4-6 shows three wave spectra measured in a large wave flume with a sloping sand beach. The solid curve is the incident spectrum (d = 3.0 m), the dotted curve is the spectrum at the zone of incipient breaking (d = 1.7 m), and the dashed curve is within the surf zone (d = 1.4 m). Presently, no formulation is available for the dissipation rate based on spectral parameters for use in Equation II-4-13. Therefore, the energy in the spectrum is often limited using the similarity method. Smith and Vincent (2002) found that in the inner surf zone, wave spectra evolve to a similar, single-peaked shape regardless of the complexity of the shape outside the surf zone (e.g., multipeaked spectra evolve to a single peak). It is postulated that the spectral shape evolves from the strong nonlinear interactions in the surf zone.

(4) Waves over reefs. Many tropical coastal regions are fronted by coral reefs. These reefs offer protection to the coast because waves break on the reefs, so the waves reaching the shore are less energetic. Reefs typically have steep seaward slopes with broad, flat reef tops and a deeper lagoon shoreward of the reef. Transformation of waves across steep reef faces and nearly flat reef tops cannot be modeled by simple wave breaking relationships such as Equation II-4-12. Generally, waves refract and shoal on the steep reef face,

break, and then reform on the reef flat. Irregular transformation models based on Equation II-4-13 give reasonable results for reef applications (Young 1989), even though assumptions of gentle slopes are violated at the reef face. Wave reflection from coral reefs has been shown to be surprisingly low (Young 1989; Hardy and Young 1991). Although the dominant dissipation mechanism is depth-limited wave breaking, inclusion of an additional wave dissipation term in Equation II-4-13 to represent bottom friction on rough coral improves wave estimates. General guidance on reef bottom friction coefficients is not available, site-specific field measurements are recommended to estimate bottom friction coefficients.

(5) Advanced modeling of surf zone waves. Numerical models based on the Boussinesq equations have been extended to the surf zone by empirically implementing breaking. In time-domain Boussinesq models, a surface roller (Schäffer et al. 1993) or a variable eddy viscosity (Nwogu 1996; Kennedy et al. 2000) is used to represent breaking induced mixing and energy dissipation. Incipient breaking for individual waves is initiated based on velocity at the wave crest or slope of the water surface. These models accurately represent the time-varying, nonlinear wave profile (including vertical and horizontal wave asymmetry) and depth-averaged current. Boussinesq models also include the generation of low-frequency waves in the surf zone (surf beat and shear waves) (e.g., Madsen, Sprengen, and Schäffer 1997; Kirby and Chen 2002). Wave runup on beaches and interaction with coastal structures are also included in some models. Although Boussinesq models are computationally intensive, they are now being used for many engineering applications (e.g., Nwogu and Demirbilek 2002). The one-dimensional nonlinear shallow-water equations have also been used to calculate time-domain irregular wave transformation in the surf zone (Kobayashi and Wurjanto 1992). This approach has been successful in predicting the oscillatory and steady fluid motions in the surf and swash zones (Raubenheimer et al. 1994). Reynolds Averaged Navier Stokes (e.g., Lin and Liu 1998) and Large Eddy Simulation (Watanabe and Saeki 1999; Christensen and Deigaard 2001) models have been developed to study the turbulent 3-D flow fields generated by breaking waves. These models can represent obliquely descending eddies generated by breaking waves (Nadaoka, Hino, and Koyano 1989) which increase the turbulent intensity, eddy viscosity, and near-bottom shear stress (Okayasu et al. 2002). Results from these models may help explain the difference in sediment transport patterns under plunging and spilling breakers (Wang, Smith, and Ebersole 2002). These detailed large-scale turbulence models are still research tools requiring large computational resources for short simulations. However, results from the models are providing insights to surf zone turbulent processes that are difficult to measure in the laboratory or field.

II-4-3. Wave Setup

a. *Wave setup* is the superelevation of mean water level caused by wave action (additional changes in water level may include wind setup or tide, see Part II-5). Total water depth is a sum of still-water depth and setup

$$d = h + \overline{\eta} \tag{II-4-19}$$

where

h = still-water depth

$\overline{\eta}$ = mean water surface elevation about still-water level

b. Wave setup balances the gradient in the cross-shore directed radiation stress, i.e., the pressure gradient of the mean sloping water surface balances the gradient of the incoming momentum. Derivation of radiation stress is given in Part II-1.

c. Mean water level is governed by the cross-shore balance of momentum

$$\frac{d\bar{\eta}}{dx} = -\frac{1}{\rho g d}\frac{dS_{xx}}{dx} \tag{II-4-20}$$

where S_{xx} is the cross-shore component of the cross-shore directed radiation stress, for longshore homogeneous waves and bathymetry (see Equations II-4-34 through II-4-36 for general equations). Radiation stress both raises and lowers (*setdown*) the mean water level across shore in the nearshore region (Figure II-4-7).

d. Seaward of the breaker zone, Longuet-Higgins and Stewart (1963) obtained setdown for regular waves from the integration of Equation II-4-20 as

$$\bar{\eta} = -\frac{1}{8}\frac{H^2\,\frac{2\pi}{L}}{\sinh\left(\frac{4\pi}{L}\,d\right)} \tag{II-4-21}$$

assuming linear wave theory, normally incident waves, and $\bar{\eta} = 0$ in deep water. The maximum lowering of the water level, setdown, occurs near the break point $\bar{\eta}_b$.

e. In the surf zone, $\bar{\eta}$ increases between the break point and the shoreline (Figure II-4-7). The gradient, assuming linear theory ($S_{xx} = 3/16\ \rho\ g\ H^2$), is given by

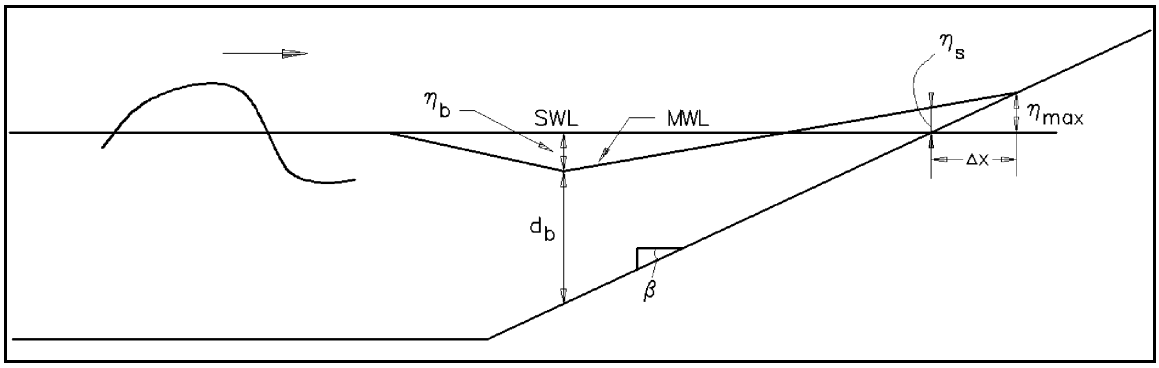

Figure II-4-7. Definition sketch for wave setup

$$\frac{d\bar{\eta}}{dx} = -\frac{3}{16}\frac{1}{h+\bar{\eta}}\frac{d(H^2)}{dx} \tag{II-4-22}$$

where the shallow-water value of $S_{xx} = 3/16\ \rho\ g\ d\ H^2$ has been substituted into Equation II-4-20. The value of $\bar{\eta}$ depends on wave decay through the surf zone. Applying the saturated breaker assumption of linear wave height decay on a plane beach, Equation II-4-22 reduces to

$$\frac{d\bar{\eta}}{dx} = \frac{1}{1+\frac{8}{3\gamma_b^2}}\tan\beta \tag{II-4-23}$$

f. Combining Equations II-4-21 and II-4-23, setup at the still-water shoreline $\bar{\eta}_s$ is given by

$$\bar{\eta}_s = \bar{\eta}_b + \left[\frac{1}{1 + \frac{8}{3\gamma_b^2}}\right] h_b \tag{II-4-24}$$

g. The first term in Equation II-4-24 is setdown at the break point and the second term is setup across the surf zone. The setup increases linearly through the surf zone for a plane beach. For a breaker depth index of 0.8, $\bar{\eta}_s \approx 0.15\, d_b$. Note that, for higher breaking waves, d_b will be greater and thus setup will be greater. Equation II-4-24 gives setup at the still-water shoreline; to calculate maximum setup and position of the mean shoreline, the point of intersection between the setup and beach slope must be found. This can be done by trial and error, or, for a plane beach, estimated as

$$\Delta x = \frac{\bar{\eta}_s}{\tan\beta - \frac{d\bar{\eta}}{dx}}$$

$$\bar{\eta}_{\max} = \bar{\eta}_s + \frac{d\bar{\eta}}{dx}\,\Delta x \tag{II-4-25}$$

where Δx is the shoreward displacement of the shoreline and $\bar{\eta}_{max}$ is the setup at the mean shoreline.

h. Wave setup and the variation of setup with distance on irregular (non-planar) beach profiles can be calculated based on Equations II-4-21 and II-4-22 (e.g., McDougal and Hudspeth 1983, Larson and Kraus 1991). NMLONG calculates mean water level across the nearshore under the assumptions previously discussed.

i. Setup for irregular waves should be calculated from decay of the wave height parameter H_{rms}. Wave setup produced by irregular waves is somewhat different than that produced by regular waves (Equation II-4-22) because long waves with periods of 30 sec to several minutes, called *infragravity waves*, may produce a slowly varying mean water level. See Part II-4-5 for discussion of magnitude and generation of infragravity waves. Figures II-4-8 and II-4-9 show irregular wave setup, nondimensionalized by H_{rmso}, for plane slopes of 1/100 and 1/30, respectively. Setup in these figures is calculated from the decay of H_{rms} given by the irregular wave application of the Dally, Dean, and Dalrymple (1985) wave decay model (see Figure II-4-4). Nondimensional wave setup increases with decreasing deepwater wave steepness. Note that beach slope is predicted to have a relatively small influence on setup for irregular waves.

II-4-4. Wave Runup on Beaches

Runup is the maximum elevation of wave uprush above still-water level (Figure II-4-11). Wave uprush consists of two components: superelevation of the mean water level due to wave action (setup) and fluctuations about that mean (*swash*). Runup, R, is defined in Figure II-4-12 as a local maximum or peak in the instantaneous water elevation, η, at the shoreline. The upper limit of runup is an important parameter for determining the active portion of the beach profile.

At present, theoretical approaches for calculating runup on beaches are not viable for coastal design. Difficulties inherent in runup prediction include nonlinear wave transformation, wave reflection, three-dimensional effects (bathymetry, infragravity waves), porosity, roughness, permeability, and groundwater elevation. Wave runup on structures is discussed in Chapter VI-2.

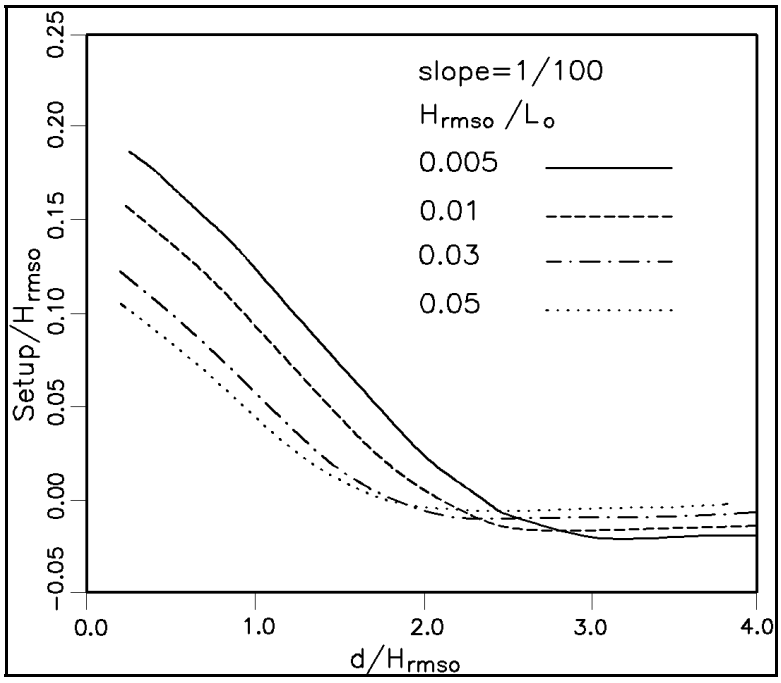

Figure II-4-8. Irregular wave setup for plane slope of 1/100

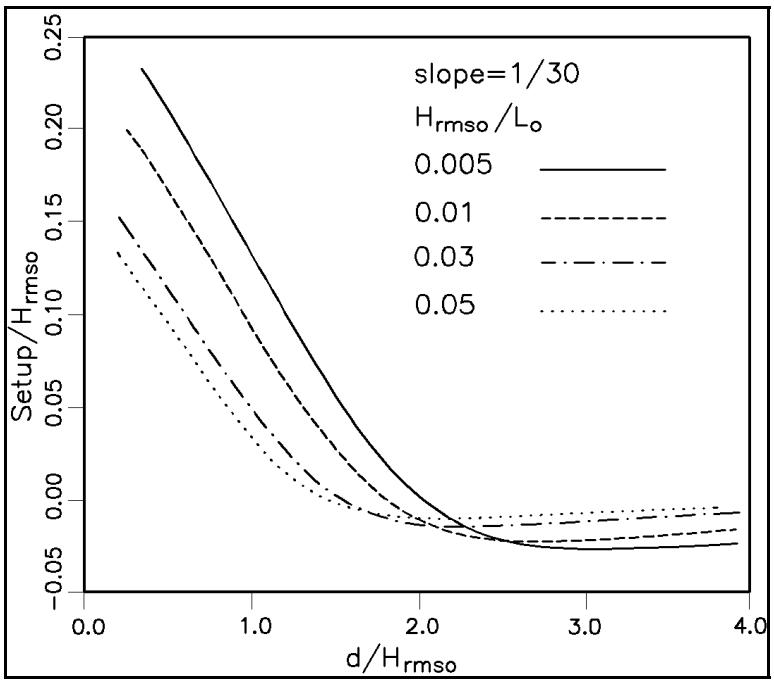

Figure II-4-9. Irregular wave setup for plane slope of 1/30

EXAMPLE PROBLEM II-4-2

FIND:

Setup across the surf zone.

GIVEN:

A plane beach having a 1 on 100 slope, and normally incident waves with deepwater height of 2 m and period of 10 sec (see Example Problem II-4-1).

SOLUTION:

The incipient breaker height and depth were determined in Example Problem II-4-1 as 2.7 m and 3.2 m, respectively. The breaker index is 0.84, based on Equation II-4-5.

Setdown at the breaker point is determined from Equation II-4-21. At breaking, Equation II-4-21 simplifies to $\bar{\eta}_b = -1/16\ \gamma_b^2\ d_b$, (sinh $2\pi d/L \approx 2\pi d/L$, and $H_b = \gamma_b\ d_b$), thus

$$\bar{\eta}_b = -1/16\ (0.84)^2\ (3.2) = -0.14 \text{ m}$$

Setup at the still-water shoreline is determined from Equation II-4-24

$$\bar{\eta}_s = -0.14 + (3.2 + 0.14) + 1/(1 + 8/(3\ (.84)^2)) = 0.56 \text{ m}$$

The gradient in the setup is determined from Equation II-4-23 as

$$d\bar{\eta}/dx = 1/(1 + 8/(3\ (0.84)^2))(1/100) = 0.0021$$

and from Equation II-4-25, $\Delta x = (0.56)/(1/100 - 0.0021) = 70.9$ m, and

$$\bar{\eta}_{max} = 0.56 + 0.0021(64.6) = 0.65 \text{ m}$$

For the simplified case of a plane beach with the assumption of linear wave height decay, the gradient in the setup is constant through the surf zone. Setup may be calculated anywhere in the surf zone from the relation $\bar{\eta} = \bar{\eta}_b + (d\bar{\eta}/dx)(x_b - x)$, where x_b is the surf zone width and $x = 0$ at the shoreline (x is positive offshore).

x, m	h, m	$\bar{\eta}$, m
334	3.3	-0.14
167	1.7	0.21
0	0.0	0.56
-71	-0.7	0.71

Setdown at breaking is - 0.14 m, net setup at the still-water shoreline is 0.56 m, the gradient in the setup is 0.0021 m/m, the mean shoreline is located 71 m shoreward of the still-water shoreline, and maximum setup is 0.71 m (Figure II-4-10).

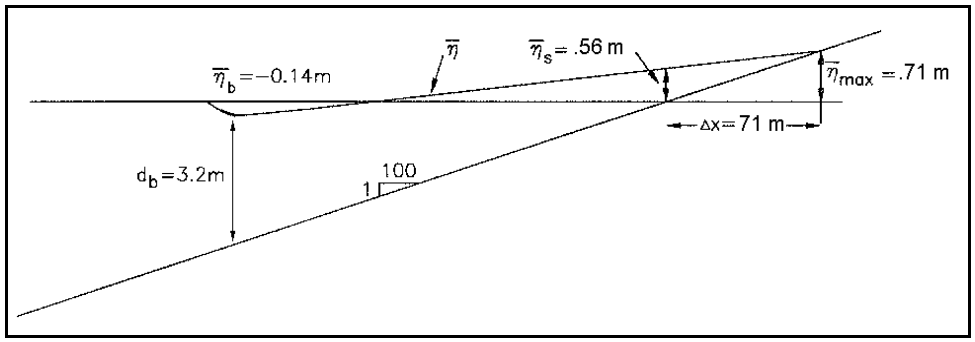

Figure II-4-10. Example problem II-4-2

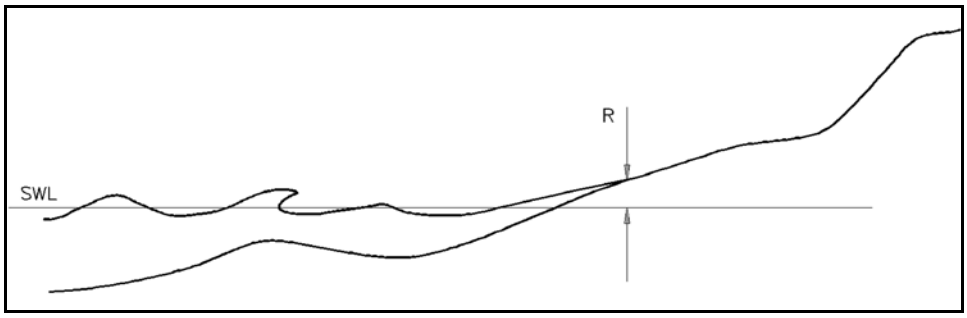

Figure II-4-11. Definition sketch for wave runup

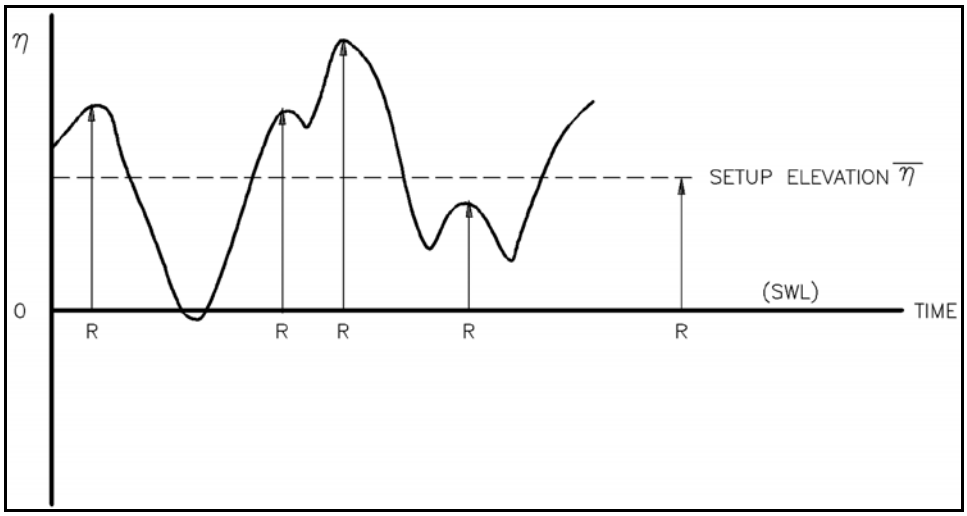

Figure II-4-12. Definition of runup as local maximum in elevation

a. Regular waves.

(1) For breaking waves, Hunt (1959) empirically determined runup as a function of beach slope, incident wave height, and wave steepness based on laboratory data. Hunt's formula, given in nondimensional form (Battjes 1974), is

$$\frac{R}{H_o} = \xi_o \quad for \quad 0.1 < \xi_o < 2.3 \tag{II-4-26}$$

for uniform, smooth, impermeable slopes, where ξ_o is the surf similarity parameter defined in Equation II-4-1. Walton et al. (1989) modified Equation II-4-26 to extend the application to steep slopes by replacing tan β in the surf similarity parameter, which becomes infinite as β approaches $\pi/2$, with sin β. The modified Hunt formula was verified with laboratory data from Saville (1956) and Savage (1958) for slopes of 1/10 to vertical.

(2) The nonbreaking upper limit of runup on a uniform slope is given by

$$\frac{R}{H_o} = (2\pi)^{\frac{1}{2}} \left(\frac{\pi}{2\beta} \right)^{\frac{1}{4}} \tag{II-4-27}$$

based on criteria developed by Miche (1951) and Keller (1961) (Walton et al. 1989).

b. Irregular waves.

(1) Irregular wave runup has also been found to be a function of the surf similarity parameter (Holman and Sallenger 1985, Mase 1989, Nielsen and Hanslow 1991), but differs from regular wave runup due to the interaction between individual runup bores. Uprush may be halted by a large backrush from the previous wave or uprush may be overtaken by a subsequent large bore. The ratio of the number of runup crests to the number of incident waves increases with increased surf similarity parameter (ratios range from 0.2 to 1.0 for ξ_o of 0.15 to 3.0) (Mase 1989, Holman 1986). Thus, low-frequency (infragravity) energy dominates runup for low values of ξ_o. See Section II-4-5 for a discussion of infragravity waves.

(2) Mase (1989) presents predictive equations for irregular runup on plane, impermeable beaches (slopes 1/5 to 1/30) based on laboratory data. Mase's expressions for the maximum runup (R_{max}), the runup exceeded by 2 percent of the runup crests ($R_{2\%}$), the average of the highest 1/10 of the runups ($R_{1/10}$), the average of the highest 1/3 of the runups ($R_{1/3}$), and the mean runup ($\overline{R}$) are given by

$$\frac{R_{\max}}{H_o} = 2.32\ \xi_o^{0.77} \tag{II-4-28}$$

$$\frac{R_{2\%}}{H_o} = 1.86\ \xi_o^{0.71} \tag{II-4-29}$$

$$\frac{R_{1/10}}{H_o} = 1.70\ \xi_o^{0.71} \tag{II-4-30}$$

$$\frac{R_{1/3}}{H_o} = 1.38\ \xi_o^{0.70} \tag{II-4-31}$$

$$\frac{\overline{R}}{H_o} = 0.88\ \xi_o^{0.69} \tag{II-4-32}$$

for $1/30 \le \tan\beta \le 1/5$ and $H_o/L_o \ge 0.007$, where H_o is the significant deepwater wave height and ξ_o is calculated from the deepwater significant wave height and length. The appropriate slope for natural beaches is the slope of the beach face (Holman 1986, Mase 1989). Wave setup is included in Equations II-4-28 through II-4-32. The effects of tide and wind setup must be calculated independently. Walton (1992) extended Mase's (1989) analysis to predict runup statistics for any percent exceedence under the assumption that runup follows the Rayleigh probability distribution.

(3) Field measurements of runup (Holman 1986, Nielsen and Hanslow 1991) are consistently lower than predictions by Equations II-4-28 through II-4-32. Equation II-4-29 overpredicts the best fit to $R_{2\%}$ by a factor of two for Holman's data (with the slope defined as the beach face slope), but is roughly an upper envelope of the data scatter. Differences between laboratory and field results (porosity, permeability, nonuniform slope, wave reformation across bar-trough bathymetry, wave directionality) have not been quantified. Mase (1989) found that wave groupiness (see Part II-1 for a discussion of wave groups) had little impact on runup for gentle slopes.

EXAMPLE PROBLEM II-4-3

FIND:

Maximum and significant runup.

GIVEN:

A plane beach having a 1 on 80 slope, and normally incident waves with deepwater height of 4.0 m and period of 9 sec.

SOLUTION:

Calculation of runup requires determining deepwater wavelength

$$L_o = g\,T^2/(2\pi) = 9.81\,(9^2)/(2\pi) = 126 \text{ m}$$

and, from Equation II-4-1, the surf similarity parameter

$$\xi_o = \tan\beta\,(H_o/L_o)^{-1/2} = (1/80)\,(4.0/126.)^{-1/2} = 0.070$$

Maximum runup is calculated from Equation II-4-28

$$R_{max} = 2.32\,H_o\,\xi_o^{0.77} = 2.32\,(4.0)(0.070)^{0.77} = 1.2 \text{ m}$$

Significant runup is calculated from Equation II-4-31

$$R_{1/3} = 1.38\,H_o\,\xi_o^{0.70} = 1.38\,(4.0)(0.070)^{0.70} = 0.86 \text{ m}$$

Maximum runup is 1.2 m and significant runup is 0.86 m.

II-4-5. Infragravity Waves

a. Long wave motions with periods of 30 sec to several minutes often contribute a substantial portion of the surf zone energy. These motions are termed *infragravity waves*. Swash at wind wave frequencies (period of 1-20 sec) dominates on reflective beaches (steep beach slopes, typically with plunging or surging breakers), and infragravity frequency swash dominates on dissipative beaches (gentle beach slopes, typically with spilling breakers) (see Wright and Short (1984) for description of dissipative versus reflective beach types).

b. Infragravity waves fall into three categories: a) bounded long waves, b) edge waves, and c) leaky waves. Bounded long waves are generated by gradients in radiation stress found in wave groups, causing a lowering of the mean water level under high waves and a raising under low waves (Longuet-Higgins and Stewart 1962). The bounded wave travels at the group speed of the wind waves, hence is bound to the wave group. Edge waves are freely propagating long waves which reflect from the shoreline and are trapped along shore by refraction. Long waves may be progressive or stand along the shore. Edge waves travel alongshore with an antinode at the shoreline, and the amplitude decays exponentially offshore. Leaky waves are also freely propagating long waves or standing waves, but they reflect from the shoreline to deep water and are not trapped by the bathymetry. Proposed generation mechanisms for the freely propagating long waves include time-varying break point of groupy waves (Symonds, Huntley, and Bowen 1982), release of bounded waves through wave breaking (Longuet-Higgins and Stewart 1964), and nonlinear wave-wave interactions (Gallagher 1971).

c. Field studies have clearly identified bounded long waves and edge waves in the nearshore (see discussion by Oltman-Shay and Hathaway (1989)). The relative amount of infragravity energy and incident wind wave energy is a function of the surf similarity parameter (Holman and Sallenger 1985, Holman 1986), with infragravity energy dominating for low values of the surf similarity parameters ($\xi_o < 1.5$). For low values, the energy spectrum at incident frequencies is generally saturated (the spectral energy density is independent of the offshore wave height, due to wave breaking), but at infragravity frequencies, the energy density increases linearly with increasing offshore wave height (Guza and Thornton 1982, Mase 1988). Storm conditions with high steepness waves tend to have low-valued surf similarity parameters, so infragravity waves are prevalent in storms. Velocities and runup heights associated with infragravity waves have strong implications for nearshore sediment transport, beach morphology evolution, structural stability, harbor oscillation, and energy transmission through structures, as well as amplification or damping of infragravity waves by the local morphology or structure configuration. Presently, practical questions of how to predict infragravity waves and design for their effects have not been answered.

II-4-6. Nearshore Currents

a. Introduction.

(1) The current in the surf zone is composed of motions at many scales, forced by several processes. Schematically, the total current u can be expressed as a superposition of these interrelated components

$$u = u_w + u_t + u_a + u_o + u_i \tag{II-4-33}$$

where u_w is the steady current driven by breaking waves, u_t is the tidal current, u_a is the wind-driven current, and u_o and u_i are the oscillatory flows due to wind waves and infragravity waves. Figure II-4-13 shows longshore and cross-shore currents measured in the surf zone at the Field Research Facility in Duck, NC. The mean value of the current in the figure is the steady current driven by breaking waves and wind, the long period oscillation is due to infragravity waves, and the short-period oscillation is the wind-wave orbital motion.

(2) Currents generated by the breaking of obliquely incident wind waves generally dominate in and near the surf zone on open coasts. Strong local winds can also drive significant nearshore currents (Hubertz 1986). Wave- and wind-driven currents are important in the transport and dispersal of sediment and pollutants in the nearshore. These currents also transport sediments mobilized by waves. Tidal currents, which may dominate in bays, estuaries, and coastal inlets, are discussed in Parts II-5 and II-7.

(3) Figure II-4-14 shows typical nearshore current patterns: a) an alongshore system (occurring under oblique wave approach), b) a symmetric cellular system, with longshore currents contributing equally to seaward-flowing rip currents (occurring under shore-normal wave approach), and c) an asymmetric cellular system, with longshore currents contributing unequally to rip currents (Harris 1969). The beach topography is often molded by the current pattern, but the current pattern also responds to the topography.

(4) Nearshore currents are calculated from the equations of momentum (Equations II-4-34 and II-4-35) and continuity (Equation II-4-36):

$$U\frac{\partial U}{\partial x} + V\frac{\partial U}{\partial y} = -g\frac{\partial \bar{\eta}}{\partial x} + F_{bx} + L_x + R_{bx} + R_{sx} \tag{II-4-34}$$

$$U\frac{\partial V}{\partial x} + V\frac{\partial V}{\partial y} = -g\frac{\partial \bar{\eta}}{\partial y} + F_{by} + L_y + R_{by} + R_{sy} \tag{II-4-35}$$

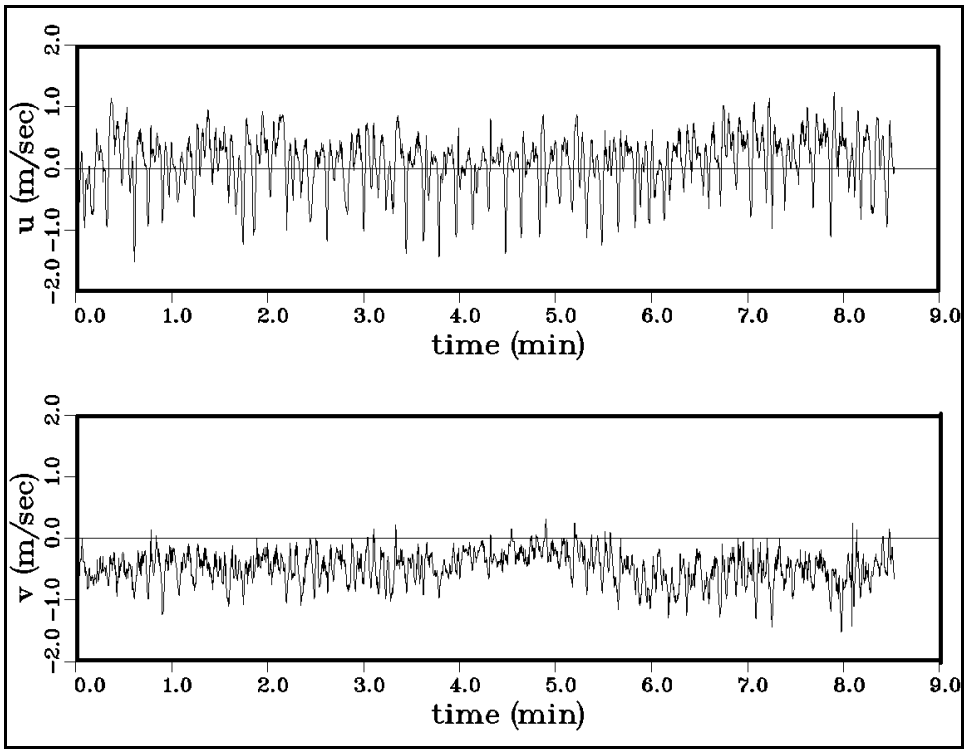

Figure II-4-13. Measured cross-shore and longshore flow velocities

$$\frac{\partial(Ud)}{\partial x} + \frac{\partial(Vd)}{\partial y} = 0 \qquad \text{(II-4-36)}$$

where

U = time- and depth-averaged cross-shore current

V = time- and depth-averaged longshore current

F_{bx} , F_{by} = cross-shore and longshore components of bottom friction

L_x , L_y = cross-shore and longshore components of lateral mixing

R_{bx} , R_{by} = cross-shore and longshore components of wave forcing

R_{sx} , R_{sy} = cross-shore and longshore components of wind forcing

(5) These equations include wave and wind forcing, pressure gradients due to mean water level variations, bottom friction due to waves and currents, and lateral mixing of the current. The primary driving force is the momentum flux of breaking waves (radiation stress), which induces currents in both the longshore and cross-shore directions. Radiation stress is proportional to wave height squared, so the forcing that generates currents is greatest in regions of steep wave height decay gradients. Bottom friction is the resisting force to the currents. Bottom roughness and wave and current velocities determine bottom friction. Lateral mixing is the exchange of momentum caused by turbulent eddies which tend to "spread out" the effect of wave forcing beyond the region of steep gradients in wave decay. Longshore, cross-shore, and rip current components of nearshore circulation are discussed in the following sections.

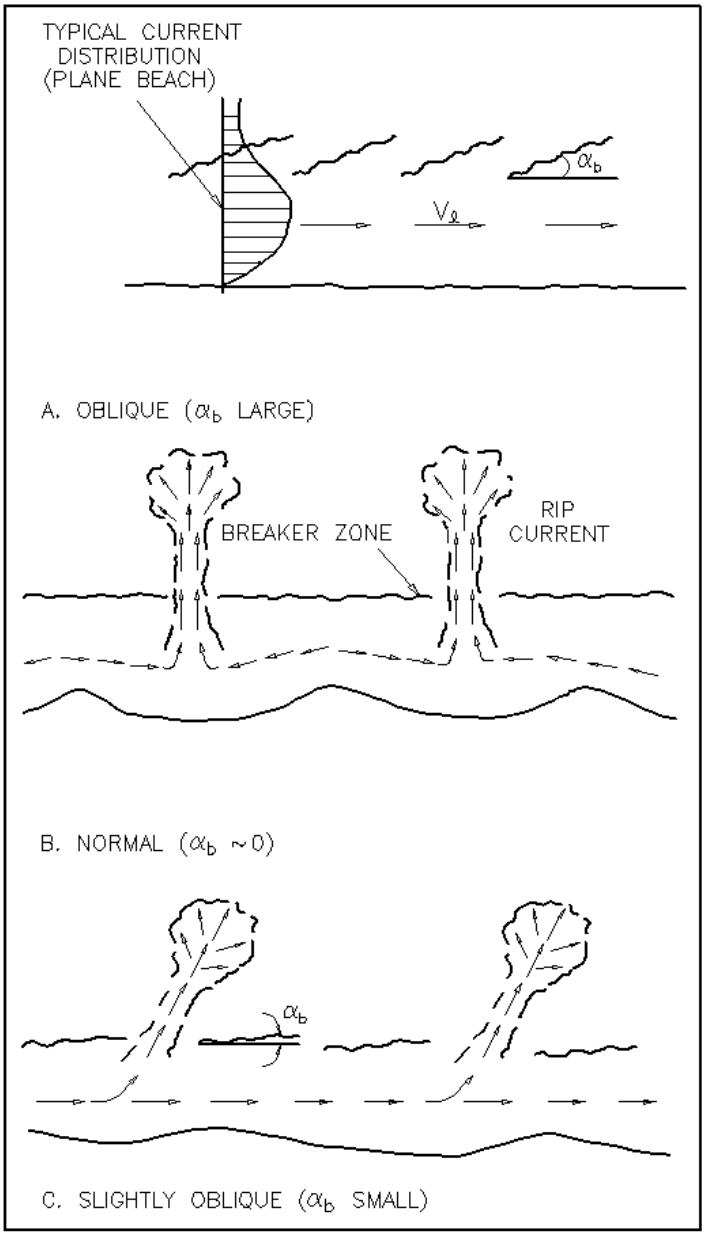

Figure II-4-14. Nearshore circulation systems

b. Longshore current.

(1) Wave- and wind-induced longshore currents flow parallel to the shoreline and are strongest in the surf zone, decaying rapidly seaward of the breakers. These currents are generated by gradients in momentum flux (radiation stress) due to the decay of obliquely incident waves and the longshore component of the wind. Typically, longshore currents have mean values of 0.3 m/sec or less, but values exceeding 1 m/sec can occur in storms. The velocities are relatively constant over depth (Visser 1991).

(2) The concept of radiation stress was first applied to the generation of longshore currents by Bowen (1969a), Longuet-Higgins (1970a,b), and Thornton (1970). These studies were based on the assumptions of longshore homogeneity (Figure II-4-14a) and no wind forcing, reducing Equation II-4-35 to a balance

between the wave forcing, bottom friction, and lateral mixing. The wave driving force for the longshore current is the cross-shore gradient in the radiation stress component S_{xy},

$$R_{by} = -\frac{1}{\rho d}\frac{\partial S_{xy}}{\partial x} \tag{II-4-37}$$

where, using linear wave theory,

$$S_{xy} = \frac{n}{8}\rho g H^2 \cos\alpha \sin\alpha \tag{II-4-38}$$

where n is the ratio of wave group speed and phase speed. The variables determining wave-induced longshore current, as seen in the driving force given in Equations II-4-37 and II-4-38, are the angle between the wave crest and bottom contours, and wave height. Wave height affects not only longshore velocity, but also the total volume rate of flow by determining the width of the surf zone.

(3) A simple analytical solution for the wave-induced longshore current was given by Longuet-Higgins (1970a,b) under the assumptions of longshore homogeneity in bathymetry and wave height, linear wave theory, small breaking wave angle, uniformly sloping beach, no lateral mixing, and saturated wave breaking ($H = \gamma_b d$) through the surf zone. Under these assumptions, the longshore current in the surf zone is given by:

$$V = \frac{5\pi}{16}\frac{\tan\beta^*}{C_f}\gamma_b\sqrt{gd}\sin\alpha\cos\alpha \tag{II-4-39}$$

where

V = longshore current speed

$\tan\beta^*$ = beach slope modified for wave setup = $\tan\beta/(1+(3\gamma_b^2/8))$

C_f = bottom friction coefficient

α = wave crest angle relative to the bottom contours

(4) The modified beach slope $\tan\beta^*$ accounts for the change in water depth produced by wave setup. The bottom friction coefficient C_f has typical values in the range 0.005 to 0.01, but is dependent on bottom roughness. This parameter is often used to calibrate the predictive equation, if measurements are available. The cross-shore distribution of the longshore current given by Equation II-4-39 is triangular in shape with a maximum at the breaker line and zero at the shoreline (Figure II-4-15) and seaward of the breaker line. Inclusion of lateral mixing smooths the current profile as shown by the dotted lines in Figure II-4-15. The parameter V_o in Figure II-4-15 is the maximum current for the case without lateral mixing, and it is used to nondimensionalize the longshore current.

(5) Komar and Inman (1970) obtained an expression for the longshore current at the mid-surf zone V_{mid} based on relationships for evaluating longshore sand transport rates which is given by Komar (1979):

$$V_{mid} = 1.17\sqrt{g\,H_{rms,b}}\sin\alpha_b\cos\alpha_b \tag{II-4-40}$$

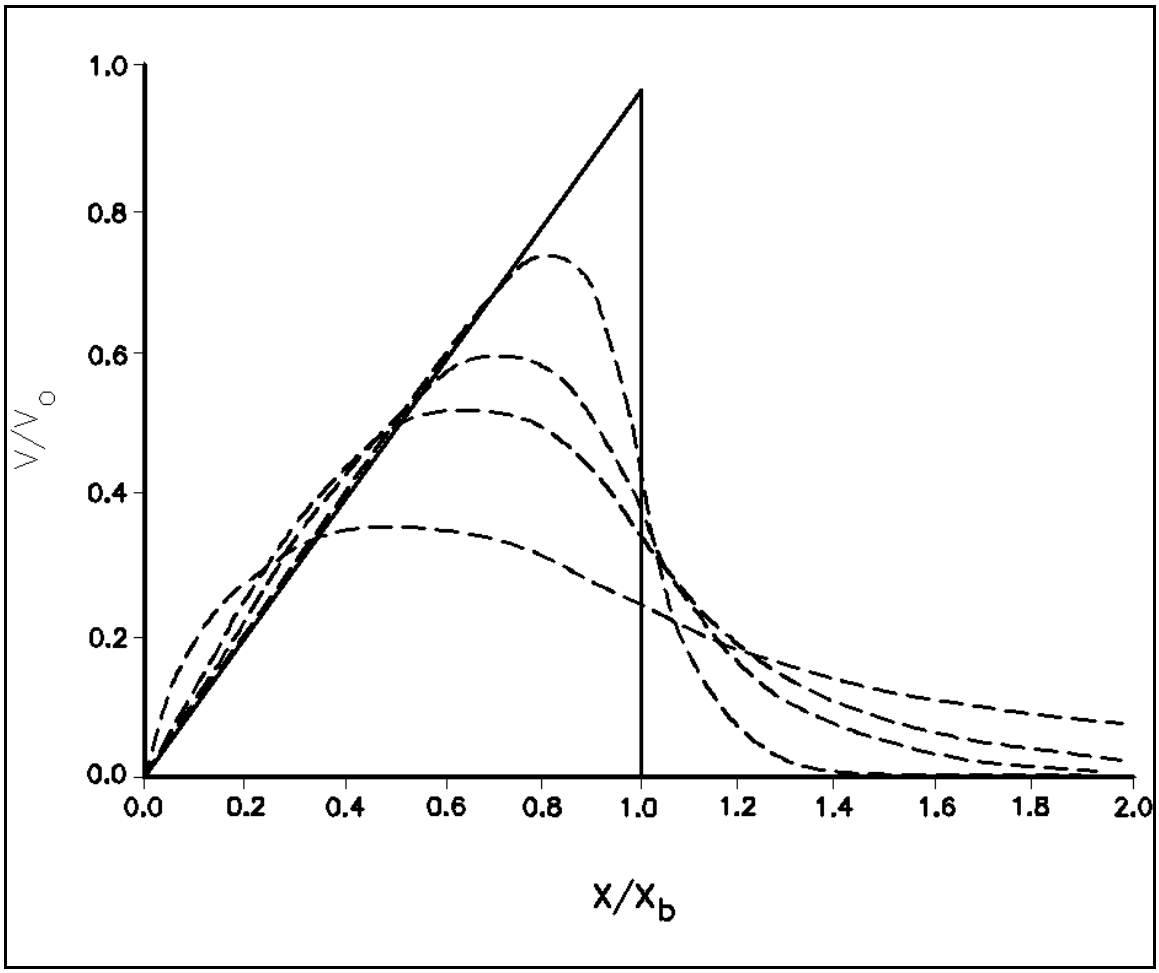

Figure II-4-15. Longshore current profiles (solid line - no lateral mixing; dashed lines - with lateral mixing)

(6) Equation II-4-40 shows good agreement with available longshore current data (Figure II-4-16). Although Equations II-4-39 and II-4-40 are similar in form, Equation II-4-4037 is independent of beach slope, which implies that tan β/C_f is constant in Equation II-4-39. The interdependence of tan β and C_f may result from the direct relationship of both parameters to grain size or an apparent dependence due to beach-slope effects on mixing (which is not included in Equation II-4-39) (Komar 1979, Huntley 1976, Komar and Oltman-Shay 1990).

(7) Longshore current, eliminating many simplifying assumptions used in Equation II-4-39, is solved numerically by the model NMLONG (Larson and Kraus 1991) for longshore-homogenous applications. NMLONG, which was briefly discussed for the simulation of breaking waves, calculates wave and wind-induced longshore current, wave and wind-induced setup, and wave height across the shore. Figure II-4-17 gives an example NMLONG calculation and comparison to field measurements of wave breaking and longshore current reported by Thornton and Guza (1986). The two-dimensional equations (Equations II-4-34 through II-4-36) are solved numerically by Noda (1974), Birkemeier and Dalrymple (1975), Ebersole and Dalrymple (1980), Vemulakonda (1984), and Wind and Vreugdenhil (1986).

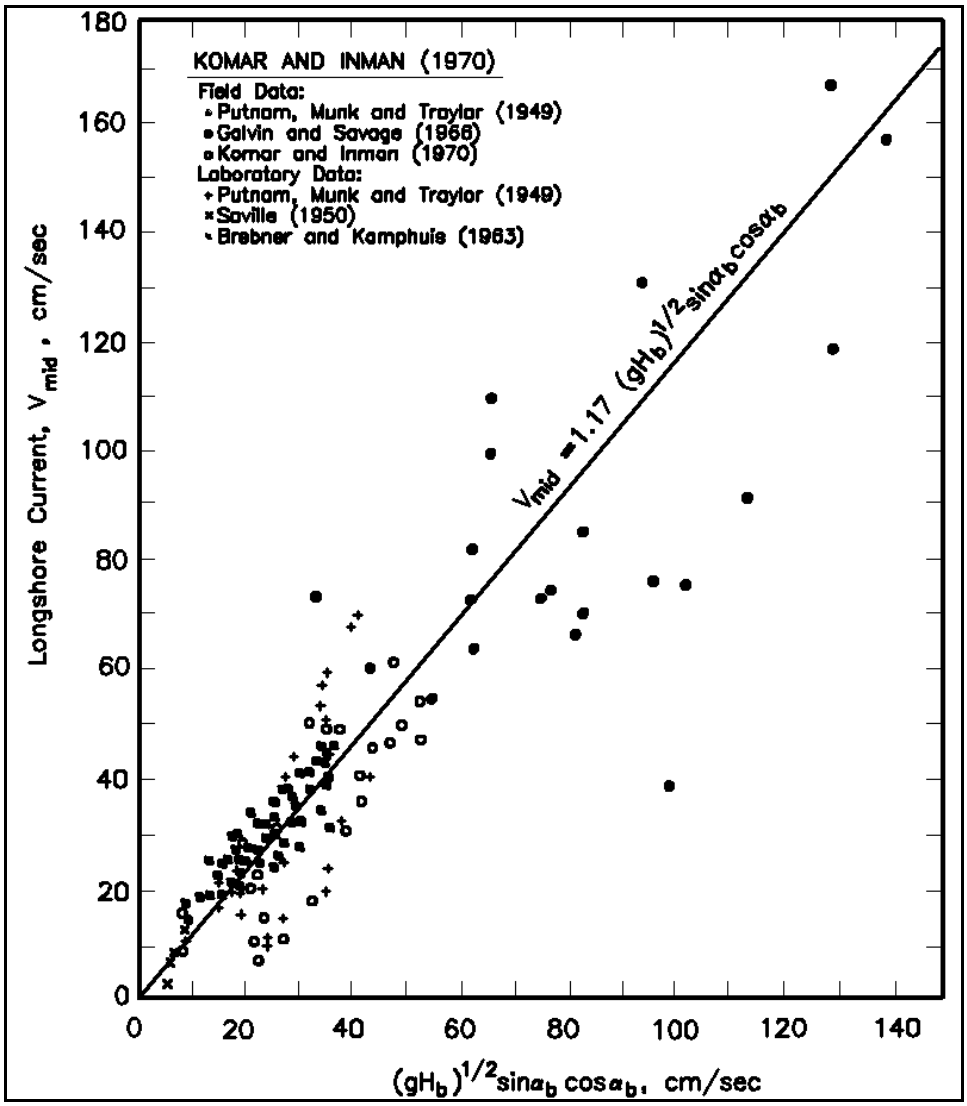

Figure II-4-16. Equation II-4-37 compared with field and laboratory data (Komar 1979)

c. Cross-shore current. Unlike longshore currents, the cross-shore current is not constant over depth. The mass transport carried toward the beach due to waves (see Part II-1) is concentrated between the wave trough and crest elevations. Because there is no net mass flux through the beach, the wave-induced mass transport above the trough is largely balanced by a reverse flow or *undertow* below the trough. Figure II-4-18 shows field measurements of the cross-shore flow below trough level on a barred profile. The undertow current may be relatively strong, generally 8-10 percent of $\sqrt{g\,d}$ near the bottom. The vertical profile of the undertow is determined as a balance between radiation stresses, the pressure gradient from the sloping mean water surface, and vertical mixing. The first quantitative analysis of undertow was given by Dyhr-Nielsen and Sorensen (1970). The undertow profile is solved by Dally and Dean (1984), Hansen and Svendsen (1984), Stive and Wind (1986), and Svendsen, Schäffer, and Hansen (1987).

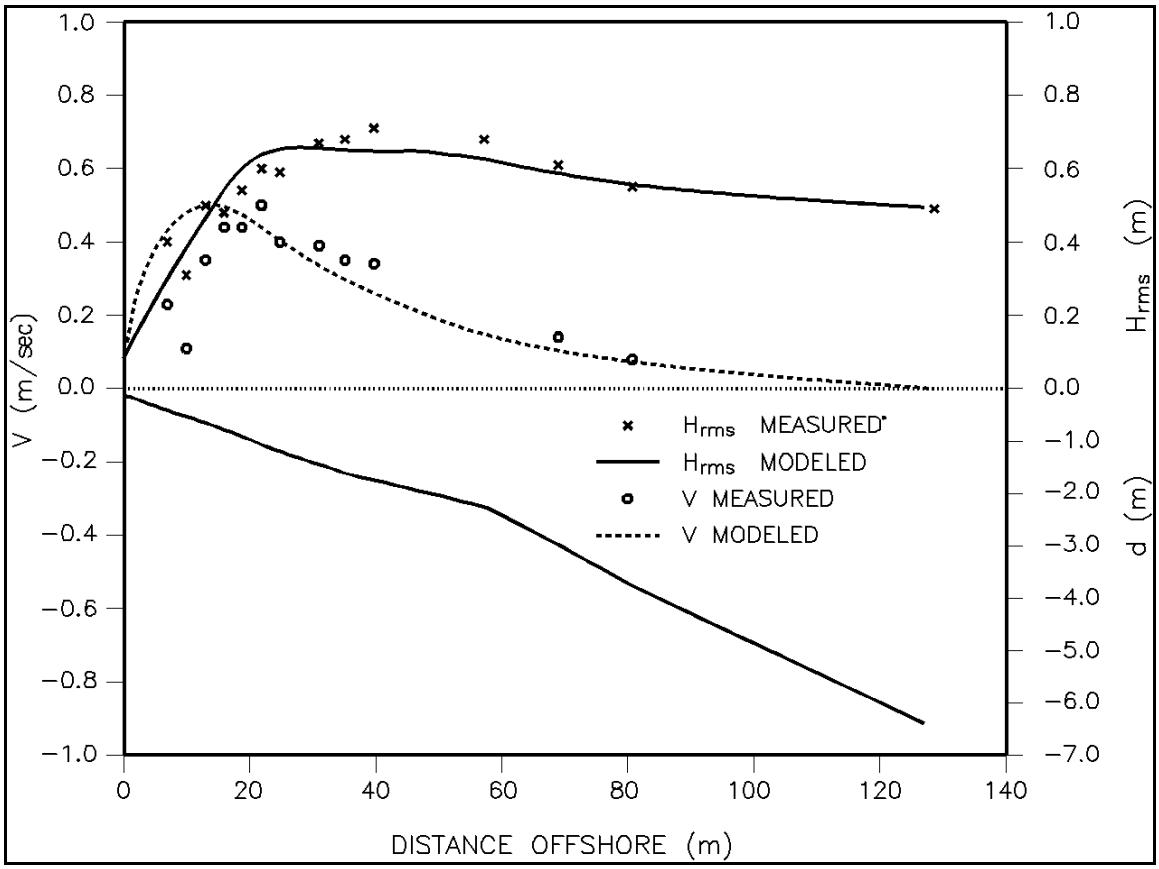

Figure II-4-17. NMLONG simulation of longshore current (Leadbetter Beach, Santa Barbara, California, 3 Feb 1989 (Thornton and Guza 1986))

d. Rip currents.

(1) The previous sections on longshore current, cross-shore current, and wave setup focused on processes that are two-dimensional, with waves, currents, and water levels changing only in the cross-shore and vertical directions, but homogeneous alongshore. *Rip currents*, strong, narrow currents that flow seaward from the surf zone, are features of highly three-dimensional current patterns. Rip currents are fed by longshore-directed surf zone currents, which increase from zero between two neighboring rips, to a maximum just before turning seaward to form a rip current. Rip currents often occur periodically along the beach, forming circulation cells (Figure II-4-14b,c). High offshore-directed flows in rip currents can cause scour of the bottom and be a hazard for swimmers.

(2) Rip currents and cell circulation can be generated by longshore variations in wave setup. Breaking wave height and wave setup are directly related; thus ,a longshore variation in wave height causes a longshore variation in setup. The longshore gradient in setup generates longshore flows from the position of highest waves and setup toward the position of the lowest waves and setup (Bowen 1969b). This effect can be seen in the term $\partial\overline{\eta}/\partial y$ in the longshore momentum equation (Equation II-4-35). The longshore variation in wave setup may be caused by convergence or divergence of waves transforming across bottom topography (Sonu 1972, Noda 1974) or the sheltering effect of headlands, jetties, or detached breakwaters (Gourley 1974, 1976; Sasaki 1975; and Mei and Liu 1977). Edge waves can interact with incident waves to produce a regular variation in the breaker height alongshore, and thus generate regularly spaced rip currents (Bowen 1969b, Bowen and Inman 1969). Interaction of two intersecting wave trains can similarly generate regularly spaced rip currents (Dalrymple 1975).

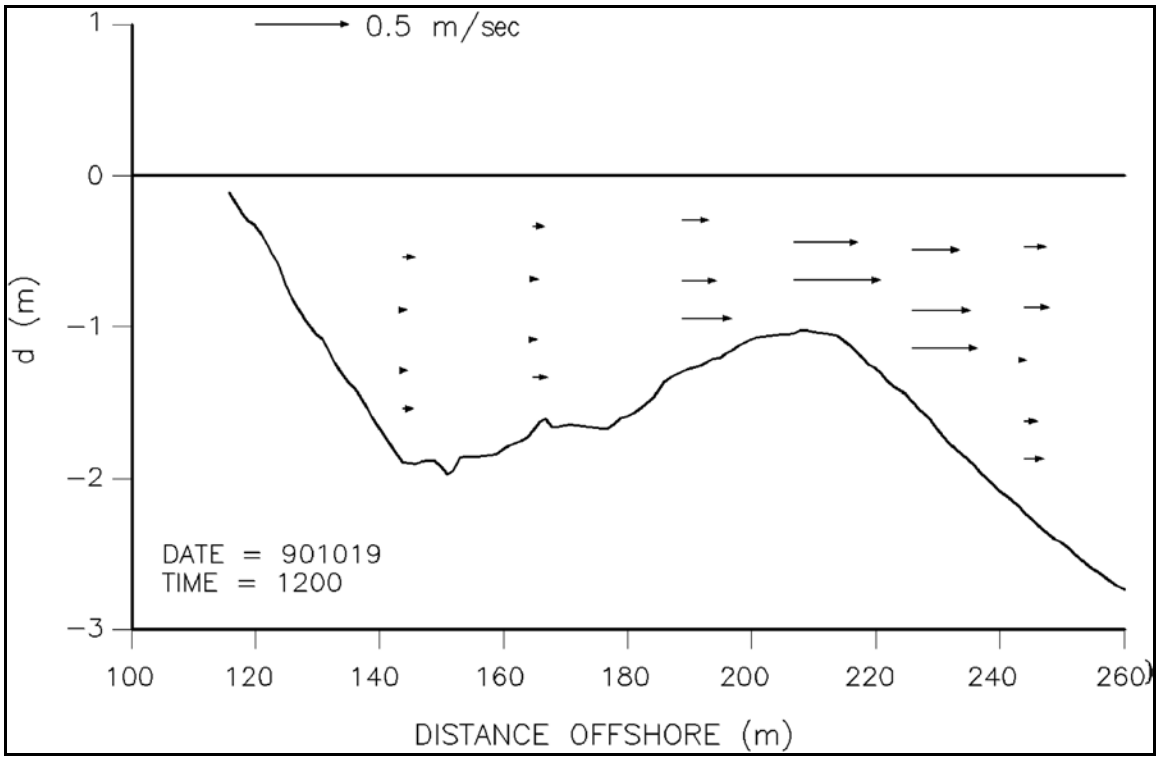

Figure II-4-18. Field measurement of cross-shore flow on a barred profile (Duck, North Carolina, October 1990)

(3) An alternate hypothesis for the generation of cell circulation is hydrodynamic instability (Hino 1974, LeBlond and Tang 1974, Miller and Barcilon 1978). Instability models are based on small, periodic perturbations in the setup and currents, with feedback between the currents and incident waves, to produce regular patterns of nearshore circulation.

(4) Several generation mechanisms for rip currents and cell circulation have been proposed. On a given beach, one or more of these mechanisms may drive the circulation pattern. Circulation patterns are dynamic, changing spatially and temporally. Presently, there is no proven method to predict rip current generation or the spacing between rips.

II-4-7. References

Baldock et al. 1998
Baldock, T. E., Holmes, P., Bunker, S., and Van Weert, P. 1998. "Cross-shore Hydrodynamics within an Unsaturated Surf Zone," *Coastal Engineering*, 34, pp 173-196.

Battjes 1972
Battjes, J. A. 1972. "Set-up Due to Irregular Waves," *Proceedings of the 13th Coastal Engineering Conference*, American Society of Civil Engineers, pp 1993-2004.

Battjes 1974
Battjes, J. A. 1974. "Surf Similarity," *Proceedings of the 14th Coastal Engineering Conference*, American Society of Civil Engineers, pp 466-480.

Battjes and Janssen 1978
Battjes, J. A., and Janssen, J. P. F. M. 1978. "Energy Loss and Setup due to Breaking of Random Waves," *Proceedings of the 16th Coastal Engineering Conference*, American Society of Civil Engineers, pp 569-587.

Birkemeier and Dalrymple 1975
Birkemeier, W. A., and Dalrymple, R. A. 1975. "Nearshore Water Circulation Induced by Wind and Waves," *Proceedings of Modeling '75 Conference*, American Society of Civil Engineers, pp 1062-1081.

Booij, Ris, and Holthuijsen 1999
Booij, N., Ris, R. C., and Holthuijsen, L. H. 1999. "A Third-Generation Wave Model for Coastal Regions 1. Model Description and Validation," *Journal of Geophysical Research*, 104(C4), pp 7649-7666.

Bowen 1969a
Bowen, A. J. 1969a. "The Generation of Longshore Currents on a Plane Beach," *Journal of Marine Research*, Vol 27, No. 1, pp 206-215.

Bowen 1969b
Bowen, A. J. 1969b. "Rip Currents, 1: Theoretical Investigations," *Journal of Geophysical Research*, Vol 74, No. 23, pp 5467-5478.

Bowen and Inman 1969
Bowen, A. J., and Inman, D. L. 1969. "Rip Currents, 2: Laboratory and Field Observation," *Journal of Geophysical Research*, Vol 74, No. 23, pp 5479-5490.

Camfield 1991
Camfield, F. E. 1991. "Wave Forces on Wall," *Journal of Waterway, Port, Coastal, and Ocean Engineering*, Vol 117, No. 1, pp 76-79.

Christensen and Deigaard 2001
Christensen, E. D., and Deigaard, R. 2001. "Large Eddy Simulation of Breaking Waves," *Coastal Engineering*, 42, pp 53-86.

Collins 1970
Collins, J. I. 1970. "Probabilities of Breaking Wave Characteristics," *Proceedings of the 12th Coastal Engineering Conference*, American Society of Civil Engineers, pp 1993-2004.

Dally 1990
Dally, W. R. 1990. "Random Breaking Waves: A Closed-Form Solution for Planar Beaches," *Coastal Engineering*, Vol 14, No. 3, pp 233-263.

Dally 1992
Dally, W. R. 1992. "Random Breaking Waves: Field Verification of a Wave-by-Wave Algorithm for Engineering Application," *Coastal Engineering*, Vol 16, pp 369-397.

Dally and Dean 1984
Dally, W. R., and Dean, R. G. 1984. "Suspended Sediment Transport and Beach Profile Evolution," *Journal of Waterway, Port, Coastal, and Ocean Engineering*, Vol 110, No. 1, pp 15-33.

Dally, Dean, and Dalrymple 1985
Dally, W. R., Dean, R. G., and Dalrymple, R. A. 1985. "Wave Height Variation Across Beaches of Arbitrary Profile," *Journal of Geophysical Research*, Vol 90, No. C6, pp 11917-11927.

Dalrymple 1975
Dalrymple, R. A. 1975. "A Mechanism for Rip Current Generation on an Open Coast," *Journal of Geophysical Research*, Vol 80, No. 24, pp 3485-3487.

Divoky, LeMéhauté, and Lin 1970
Divoky, D., LeMéhauté, B., and Lin, A. 1970. "Breaking Waves on Gentle Slopes," *Journal of Geophysical Research*, Vol 75, No. 9, pp 1681-1692.

Douglass 1990
Douglass, S. L. 1990. "Influence of Wind on Breaking Waves," *Journal of Waterway, Port, Coastal, and Ocean Engineering*, Vol 116, No. 6, pp 651-663.

Dyhr-Nielsen, and Sorensen 1970
Dyhr-Nielsen, M., and Sorensen, T. 1970. "Some Sand Transport Phenomena on Coasts with Bars," *Proceedings of the 12th Coastal Engineering Conference*, American Society of Civil Engineers, pp 1993-2004.

Ebersole 1987
Ebersole, B. A. 1987. "Measurement and Prediction of Wave Height Decay in the Surf Zone," *Proceedings of Coastal Hydrodynamics*, American Society of Civil Engineers, pp 1-16.

Ebersole and Dalrymple 1980
Ebersole, B. A., and Dalrymple, R. A. 1980. "Numerical Modelling of Nearshore Circulation," *Proceedings of the 17th Coastal Engineering Conference*, American Society of Civil Engineers, pp 2710-2725.

Freilich and Guza 1984
Freilich, M. H., and Guza, R. T. 1984. "Nonlinear Effects on Shoaling Surface Gravity Waves," *Philosophical Transactions*, Royal Society of London, A311, pp 1-41.

Freilich, Guza, and Elgar 1990
Freilich, M. H., Guza, R. T., and Elgar, S. L. 1990. "Observations of Nonlinear Effects in Directional Spectra of Shoaling Gravity Waves," *Journal of Geophysical Research*, Vol 95, No. C6, pp 9645-9656.

Gallagher 1971
Gallagher, B. 1971. "Generation of Surf Beat by Non-Linear Wave Interaction," *Journal of Fluid Mechanics*, Vol 49, Part 1, pp 1-20.

Galvin 1968
Galvin, C. J. 1968. "Breaker Type Classification on Three Laboratory Beaches," *Journal of Geophysical Research*, Vol 73, No. 12, pp 3651-3659.

Goda 1970
Goda, Y. 1970. "A Synthesis of Breaker Indices," *Transactions of the Japan Society of Civil Engineers*, Vol 2, Part 2, pp 227-230.

Goda 1975
Goda, Y. 1975. "Irregular Wave Deformation in the Surf Zone," *Coastal Engineering in Japan*, Vol 18, pp 13-26.

Goda 2002
Goda, Y. 2002. "A Fast Numerical Scheme for Unsaturated Random Breaking Waves in 3-D Bathymetry," *Proceedings*, 28th International Conference on Coastal Engineering. *World Scientific*, pp 508-520.

Gourley 1974
Gourley, M. R. 1974. "Wave Set-Up and Wave Generated Currents in the Lee of a Breakwater or Headland," *Proceedings of the 14th Coastal Engineering Conference*, American Society of Civil Engineers, pp 1976-1995.

Gourley 1976
Gourley, M. R. 1976. "Non-Uniform Alongshore Currents," *Proceedings of the 15th Coastal Engineering Conference*, American Society of Civil Engineers, pp 701-720.

Guza and Thornton 1982
Guza, R. T., and Thornton, E. G. 1982. "Swash Oscillations on a Natural Beach," *Journal of Geophysical Research*, Vol 87, No. C1, pp 483-491.

Hansen and Svendsen 1984
Hansen, J. B., and Svendsen, I. A. 1984. "A Theoretical and Experimental Study of Undertow," *Proceedings of the 19th Coastal Engineering Conference*, American Society of Civil Engineers, pp 2246-2262.

Hardy and Young 1991
Hardy, T. A., and Young, I. R. 1991. "Modelling Spectral Wave Transformation on a Coral Reef Flat," *Proceedings of the Australasian Conference on Coastal and Ocean Engineering*, pp 345-350.

Harris 1969
Harris, T. F. W. 1969. "Nearshore Circulations; Field Observation and Experimental Investigations of an Underlying Cause in Wave Tanks," *Proceedings of Symposium on Coastal Engineering*, Stellenbosch, South Africa, 11 pp.

Hino 1974
Hino, M. 1974. "Theory on Formation of Rip-Current and Cuspidal Coast," *Proceedings of the 14th Coastal Engineering Conference*, American Society of Civil Engineers, pp 901-919.

Holman 1986
Holman, R. A. 1986. "Extreme Value Statistics for Wave Run-up on a Natural Beach," *Coastal Engineering*, Vol 9, No. 6, pp 527-544.

Holman and Sallenger 1985
Holman, R. A., and Sallenger, A. H. 1985. "Setup and Swash on a Natural Beach," *Journal of Geophysical Research*, Vol 90, No. C1, pp 945-953.

Hubertz 1986
Hubertz, J. M. 1986. "Observations of Local Wind Effects on Longshore Currents," *Coastal Engineering*, Vol 10, No. 3, pp 275-288.

Hunt 1959
Hunt, I. A. 1959. "Design of Seawalls and Breakwaters," *Journal of the Waterways and Harbors Division*, Vol 85, No. WW3, pp 123-152.

Huntley 1976
Huntley, D. A. 1976. "Long-Period Waves on a Natural Beach," *Journal of Geophysical Research*, Vol 81, No. 36, pp 6441-6449.

Hwang and Divoky 1970
Hwang, L., and Divoky, D. 1970. "Breaking Wave Setup and Decay on Gentle Slope," *Proceedings of the 12th Coastal Engineering Conference*, American Society of Civil Engineers, pp 377-389.

Iversen 1952
Iversen, H. W. 1952. "Waves and Breakers in Shoaling Water," *Proceedings of the 3rd Coastal Engineering Conference*, American Society of Civil Engineers, pp 1-12.

Keller 1961
Keller, J. B. 1961. "Tsunamis -- Water Waves Produced by Earthquakes," *Proceedings of the Tsunami Meetings Associated with the 10th Pacific Science Congress*, International Union of Geodesy and Geophysics, pp 154-166.

Kennedy et al. 2000
Kennedy, A. B., Chen, Q., Kirby, J. T., and Dalrymple, R. A. 2000. "Boussinesq Modeling of Wave Transformation, Breaking and Runup. I: 1D," *Journal of Waterway, Port, Coastal and Ocean Engineering,* Vol 126, pp 39-47.

Kirby and Chen 2002
Kirby, J. T., and Chen, Q. 2002. "Examining the Low Frequency Predictions of a Boussinesq Wave Model," *Proceedings*, 28th International Conference on Coastal Engineering. *World Scientific,* pp 1075-1087.

Kobayashi and Wurjanto 1992
Kobayashi, N., and Wurjanto, A. 1992. "Irregular Wave Setup and Run-Up on Beaches," *Journal of Waterway, Port, Coastal, and Ocean Engineering*, Vol 118, No. 4, pp 368-386.

Komar 1979
Komar, P. D. 1979. "Beach-Slope Dependence of Longshore Currents," *Journal of Waterway, Port, Coastal, and Ocean Division*, Vol 105, No. WW4, pp 460-464.

Komar and Gaughan 1973
Komar, P. D., and Gaughan, M. K. 1973. "Airy Wave Theory and Breaker Height Prediction," *Proceedings of the 13th Coastal Engineering Conference*, American Society of Civil Engineers, pp 405-418.

Komar and Inman 1970
Komar, P. D., and Inman, D. L. 1970. "Longshore Sand Transport on Beaches," *Journal of Geophysical Research*, Vol 75, No. 30, pp 5914-5927.

Komar and Oltman-Shay 1990
Komar, P. D., and Oltman-Shay, J. 1990. "Nearshore Currents," *Handbook of Coastal and Ocean Engineering*, Vol. 2, J. Herbich, ed., Gulf Publishing Co., Houston, TX, pp 651-680.

Kuo and Kuo 1974
Kuo, C. T., and Kuo, S. T. 1974. "Effect of Wave Breaking on Statistical Distribution of Wave Heights," *Proceedings of Civil Engineering Oceans*, pp 1211-1231.

Larson and Kraus 1991
Larson, M., and Kraus, N. C. 1991. "Numerical Model of Longshore Current for Bar and Trough Beaches," *Journal of Waterway, Port, Coastal, and Ocean Engineering*, Vol 117, No. 4, pp 326-347.

Le Méhauté 1962
Le Méhauté, B. 1962. "On the Nonsaturated Breaker Theory and the Wave Run Up," *Proceedings of the 8th Coastal Engineering Conference*, American Society of Civil Engineers, pp 77-92.

LeBlond and Tang 1974
LeBlond, P. H., and Tang, C. L. 1974. "On Energy Coupling Between Waves and Rip Currents," *Journal of Geophysical Research*, Vol 79, No. 6, pp 811-816.

Lin and Liu 1998
Lin, P., and Liu, P. L.-F. 1998. "A Numerical Study of Breaking Waves in the Surf Zone," *Journal of Fluid Mechanics*, Vol 359, pp 239-264.

Longuet-Higgins 1970a
Longuet-Higgins, M. S. 1970a. "Longshore Currents Generated by Obliquely Incident Sea Waves, 1," *Journal of Geophysical Research*, Vol 75, No. 33, pp 6778-6789.

Longuet-Higgins 1970b
Longuet-Higgins, M. S. 1970b. "Longshore Currents Generated by Obliquely Incident Sea Waves, 2," *Journal of Geophysical Research*, Vol 75, No. 33, pp 6790-6801.

Longuet-Higgins and Stewart 1962
Longuet-Higgins, M. S., and Stewart, R. W. 1962. "Radiation Stress and Mass Transport in Gravity Waves, with Application to 'Surf Beats'," *Journal of Fluid Mechanics*, Vol 13, No. 4, pp 481-504.

Longuet-Higgins and Stewart 1963
Longuet-Higgins, M. S., and Stewart, R. W. 1963. "A Note on Wave Setup," *Journal of Marine Research*, Vol 21, No. 1, pp 4-10.

Longuet-Higgins and Stewart 1964
Longuet-Higgins, M. S., and Stewart, R. W. 1964. "Radiation Stresses in Water Waves: A Physical Discussion with Applications," *Deep Sea Research*, Vol 11, pp 529-562.

Madsen, Sørensen, and Schäffer 1997
Madsen, P. A., Sørensen, O. R., and Schäffer, H. A. 1997. "Surf Zone Dynamics Simulated by a Boussinesq Type Model; Part II: Surf Beat and Swash Oscillations for Wave Groups and Irregular Waves," *Coastal Engineering*, Vol 32, pp 289-319.

Mase 1988
Mase, H. 1988. "Spectral Characteristics of Random Wave Runup," *Coastal Engineering*, Vol 12, No. 2, pp 175-189.

Mase 1989
Mase, H. 1989. "Random Wave Runup Height on Gentle Slope," *Journal of Waterway, Port, Coastal, and Ocean Engineering*, Vol 115, No. 5, pp 649-661.

McCowan 1891
McCowan, J. 1891. "On the Solitary Wave," *Philosophical Magazine*, 5th Series, Vol 36, pp 430-437.

McDougal and Hudspeth 1983
McDougal, W. G., and Hudspeth, R. T. 1983. "Wave Setup/Setdown and Longshore Current on Non-Planar Beaches," *Coastal Engineering*, Vol 7, No. 2, pp 103-117.

Mei and Liu 1977
Mei, C. C., and Liu, P. L.-F. 1977. "Effects of Topography on the Circulation in and Near the Surf Zone - Linear Theory," *Journal of Estuary and Coastal Marine Science*, Vol 5, pp 25-37.

Miche 1951
Miche, M. 1951. "Le Pouvoir Réfléchissant des Ouvrages Maritimes Exposés à l'Action de la Houle," *Annals des Ponts et Chaussess*, 121e Annee, pp 285-319 (translated by Lincoln and Chevron, University of California, Berkeley, Wave Research Laboratory, Series 3, Issue 363, June 1954).

Miller and Barcilon 1978
Miller, C., and Barcilon, A. 1978. "Hydrodynamic Instability in the Surf Zone as a Mechanism for the Formation of Horizontal Gyres," *Journal of Geophysical Research*, Vol 83, No. C8, pp 4107-4116.

Munk 1949
Munk, W. H. 1949. "The Solitary Wave Theory and Its Applications to Surf Problems," *Annals of the New York Academy of Sciences*, Vol 51, pp 376-462.

Nadaoka, Hino, and Koyano 1989
Nadaoka, K., Hino, M., Koyano, Y. 1989. "Structure of the Turbulent Flow Field Under Breaking Waves in the Surf Zone," *Journal of Fluid Mechanics*, Vol 204, pp 359-387.

Nielsen and Hanslow 1991
Nielsen, P., and Hanslow, D. J. 1991. "Wave Runup Distributions on Natural Beaches," *Journal of Coastal Research*, Vol 7, No. 4, pp 1139-1152.

Noda 1974
Noda, E. K. 1974. "Wave-Induced Nearshore Circulation," *Journal of Geophysical Research*, Vol 79, No. 27, pp 4097-4106.

Nwogu 1996
Nwogu, O. G. 1996. "Numerical Prediction of Breaking Waves and Currents with a Boussinesq Model," *Proceedings*, 25th International Conference on Coastal Engineering, American Society of Civil Engineers, pp 4807-4820.

Nwogu and Demirbilek 2001
Nwogu, O.G., and Demirbilek, Z. 2001. "BOUSS-2D: A Boussinesq Wave Model for Coastal Regions and Harbors," ERDC/CHL TR-01-25. US Army Engineer Research and Development Center, Vicksburg, MS, 90 p.

Okayasu et al. 2002
Okayasu, A., Katayama, H., Tsuruga, H., and Iwasawa, H. 2002. "A Laboratory Experiment on Velocity Field Near Bottom Due to Obliquely Descending Eddies," *Proceedings*, International Conference on Coastal Engineering. *World Scientific,* pp 521-531.

Oltman-Shay and Hathaway 1989
Oltman-Shay, J., and Hathaway, K. K. 1989. "Infragravity Energy and its Implications in Nearshore Sediment Transport and Sandbar Dynamics," Technical Report CERC-89-8, U.S. Army Engineer Waterways Experiment Station, Coastal Engineering Research Center, Vicksburg, MS.

Raubenheimer et al. 1994
Raubenheimer, B., Guza, R.T., Elgar, S., and Kobayashi, N. 1994. "Swash on a Gently Sloping Beach," *Journal of Geophysical Research*, Vol 100, No. C5, pp 8751-8760.

Sasaki 1975
Sasaki, T. 1975. "Simulation on Shoreline and Nearshore Current," *Proceedings of Civil Engineering in the Oceans, III*, American Society of Civil Engineers, pp 179-196.

Savage 1958
Savage, R. P. 1958. "Wave Run-Up on Roughened and Permeable Slopes," *Journal of the Waterways and Harbors Division*, American Society of Civil Engineers, Vol 84, No. WW3, Paper 1640.

Saville 1956
Saville, T., Jr. 1956. "Wave Runup on Shore Structures," *Journal of the Waterways and Harbors Division*, American Society of Civil Engineers, Vol 82, No. WW2, Paper 925.

Schäffer, Madsen, and Deigaard 1993
Schäffer, H.A., Madsen, P.A., and Deigaard, R. 1993. "A Boussinesq Model for Waves Breaking in Shallow Water," *Coastal Engineering*, Vol 20, pp 185-202.

Singamsetti and Wind 1980
Singamsetti, S. R., and Wind, H. G. 1980. "Characteristics of Breaking and Shoaling Periodic Waves Normally Incident on to Plane Beaches of Constant Slope," Report M1371, Delft Hydraulic Laboratory, Delft, The Netherlands.

Smith and Kraus 1991
Smith, E. R., and Kraus, N. C. 1991. "Laboratory Study of Wave-Breaking Over Bars and Artificial Reefs," *Journal of Waterway, Port, Coastal, and Ocean Engineering*, Vol 117, No. 4, pp 307-325.

Smith, Resio, and Vincent 1997
Smith. J. M., Resio, D. T., and Vincent, C. L. 1997. "Current-Induced Breaking at an Idealized Inlet," *Proceedings,* Coastal Dynamics'97. American Society of Civil Engineers, pp 993-1002.

Smith 2001
Smith, J. M. 2001. "Breaking in a Spectral Wave Model," *Proceedings*, Waves 2001, American Society of Civil Engineers, pp 1022-1031.

Smith, Sherlock, and Resio 2001
Smith, J. M., Sherlock, A. R., and Resio, D. T. 2001. "STWAVE: Steady-State Spectral Wave Model User's Guide for STWAVE Version 3.0," ERDC/CHL SR-01-01, U.S. Army Engineer Research and Development Center, Vicksburg, MS, 80 pp.

Smith and Vincent 2002
Smith, J. M., and Vincent, C. L. 2002. "Application of Spectral Equilibrium Ranges in the Surf Zone," *Proceedings*, 28th International Conference on Coastal Engineering. *World Scientific*, pp 508-520.

Sonu 1972
Sonu, C. J. 1972. "Field Observation of Nearshore Circulation and Meandering Currents," *Journal of Geophysical Research*, Vol 77, No. 18, pp 3232-3247.

Stive and Wind 1986
Stive, M. J. F., and Wind, H. F. 1986. "Cross-shore Mean Flow in the Surf Zone," *Coastal Engineering*, Vol 10, No. 4, pp 325-340.

Sunamura 1980
Sunamura, T. 1980. "A Laboratory Study of Offshore Transport of Sediment and a Model for Eroding Beaches," *Proceedings of the 17th Coastal Engineering Conference*, American Society of Civil Engineers, pp 1051-1070.

Svendsen 1984
Svendsen, I. A. 1984. "Wave Heights and Setup in a Surf Zone," *Coastal Engineering*, Vol 8, No. 4, pp 303-329.

Svendsen, Madsen, and Hansen 1978
Svendsen, I. A., Madsen, P. A., and Hansen, J. B. 1978. "Wave Characteristics in the Surf Zone," *Proceedings of the 16th Coastal Engineering Conference*, American Society of Civil Engineers, pp 520-539.

Svendsen, Schäffer, and Hansen 1987
Svendsen, I. A., Schäffer, H. A., and Hansen, J. B. 1987. "The Interaction Between the Undertow and the Boundary Layer Flow on a Beach," *Journal of Geophysical Research*, Vol 92, No. C11, pp 11845-11856.

Symonds, Huntley, and Bowen 1982
Symonds, G., Huntley, D. A., and Bowen, A. J. 1982. "Two-Dimensional Surf Beat: Long Wave Generation by a Time-Varying Breakpoint," *Journal of Geophysical Research*, Vol 87, No. C1, pp 492-498.

Thornton 1970
Thornton, E. B. 1970. "Variation of Longshore Current Across the Surf Zone," *Proceedings of the 12th Coastal Engineering Conference*, American Society of Civil Engineers, pp 291-308.

Thornton and Guza 1983
Thornton, E. B., and Guza, R. T. 1983. "Transformation of Wave Height Distribution," *Journal of Geophysical Research*, Vol 88, No. C10, pp 5925-5938.

Thornton and Guza 1986
Thornton, E. B., and Guza, R. T. 1986. "Surf Zone Longshore Currents and Random Waves: Field Data and Models," *Journal of Physical Oceanography*, Vol 16, pp 1165-1178.

Vemulakonda 1984
Vemulakonda, S. R. 1984. "Erosion Control of Scour During Construction: Report 7, CURRENT -- a Wave-Induced Current Model," Technical Report HL-80-3, U.S. Army Engineer Waterways Experiment Station, Vicksburg, MS.

Wisser 1991
Visser, P. J. 1991. "Laboratory Measurements of Uniform Longshore Currents," *Coastal Engineering*, Vol 15, No. 5, pp 563-593.

Walton 1992
Walton, T. L., Jr. 1992. "Interim Guidance for Prediction of Wave Run-up on Beaches," *Ocean Engineering*, Vol 19, No. 2, pp 199-207.

Walton et al. 1989
Walton, T. L., Jr., Ahrens, J. P., Truitt, C. L., and Dean, R. G. 1989. "Criteria for Evaluating Coastal Flood-Protection Structures," Technical Report CERC-89-15, U.S. Army Engineer Waterways Experiment Station, Coastal Engineering Research Center, Vicksburg, MS.

Wang, Smith, and Ebersole 2002
Wang, P., Smith, E. R., and Ebersole. B. A. 2002. "Large-Scale Laboratory Measurements of Longshore Sediment Transport Under Spilling and Plunging Breakers," *Journal of Coastal Research*, Vol 18, No. 1, pp 118-135.

Watanabe and Saeki 1999
Watanabe, Y. and Saeki, H. 1999. "Three-Dimensional Large Eddy Simulation of Breaking Waves," *Coastal Engineering in Japan*, Vol 41, pp 281-301.

Weggel 1972
Weggel, J. R. 1972. "Maximum Breaker Height," *Journal of the Waterways, Harbors and Coastal Engineering Division*, Vol 98, No. WW4, pp 529-548.

Wind and Vreugdenhil 1986
Wind, H. G., and Vreugdenhil, C. B. 1986. "Rip-Current Generation Near Structures," *Journal of Fluid Mechanics*, Vol 171, pp 459-476.

Wright and Short 1984
Wright, L. D., and Short, A.D. 1984. "Morphodynamic Variability of Surf Zones and Beaches: A Synthesis," *Marine Geology*, Vol 56, pp 93-118.

Young 1989
Young, I. R. 1989. "Wave Transformation Over Coral Reefs," *Journal of Geophysical Research*, Vol 94, No. C7, pp 9779-9789.

II-4-8. Definitions of Symbols

α	Wave crest angle relative to bottom contours [deg]
β	Beach slope (tan β = length-rise/length-run)
β^*	Beach slope (tan β = length-rise/length-run) modified for wave setup
Γ	Empirical coefficient (= 0.4) (Equation II-4-14)
γ_b	Breaker depth index (Equation II-4-3) [dimensionless]
δ	Energy dissipation rate per unit surface area due to wave breaking
Δx	Shoreward displacement of the shoreline (Equation II-4-22) [length]
$\overline{\eta}$	Mean water surface elevation about the still-water level [length]
$\overline{\eta}_b$	Setdown at the breaker point [length]
$\overline{\eta}_{max}$	Setup at the mean shoreline (Equation II-4-22) [length]
$\overline{\eta}_s$	Setup at the still-water shoreline (Equation II-4-21) [length]
κ	Empirical decay coefficient (= 0.15) [dimensionless]
ξ	Surf similarity parameter (Equation II-4-1)
π	Constant (= 3.14159)
ρ	Mass density of water (salt water = 1,025 kg/m^3 or 2.0 slugs/ft^3; fresh water = 1,000kg/m^3 or 1.94 slugs/ft^3) [force-time^2/length^4]
Ω_b	Breaker height index (Equation II-4-4) [dimensionless]
a, b	Empirically determined dimensionless functions of beach slope (Equations II-4-6 and II-4-7)
C_f	Bottom friction coefficient with typical values in the range 0.005 to 0.01
C_g	Wave group velocity [length/time]
d	Water depth [length]
d_b	Water depth at breaking [length]
E	Wave energy per unit surface area [length-force/length^2]
F_{bx}, F_{by}	Cross-shore and longshore components of bottom friction [length/time^2]
f_m	Mean wave frequency (Equation II-4-17) [time^{-1}]
g	Gravitational acceleration [length/time^2]
h	Water depth [length]
H	Wave height [length]

$H_{1/10}$	Average of the highest 1/10 wave heights [length]
$H_{1/3}$	Significant wave height [length]
H_b	Wave height at incipient breaking [length]
$H_{m0,b}$	Zero-moment wave height at breaking (Equation II-4-10) [length]
H_{max}	Maximum wave height (Equation II-4-17) [length]
H_{rms}	Root-mean-square of all measured wave heights [length]
$H_{rms,b}$	Root-mean-square wave height at breaking (Equation II-4-9) [length]
H'_0	Equivalent unrefracted deepwater wave height [length]
K_r	Refraction coefficient [dimensionless]
L	Wave length [length]
L_x , L_y	Cross-shore and longshore components of lateral mixing [length/time^2]
n	Ratio of wave group speed and phase speed
$-_O$	The subscript 0 denotes deepwater conditions
Q_b	Percentage of waves breaking (Equation II-4-17)
R	Wave runup above the mean water level [length]
$\overline{R}$	Mean runup [length]
$R_{1/10}$	Average of the highest 1/10 of the runups [length]
$R_{1/3}$	Average of the highest 1/3 of the runups [length]
$R_{2\%}$	Runup exceeded by 2 percent of the runup crests [length]
R_{bx} , R_{by}	Cross-shore and longshore components of wave forcing [length/time^2]
R_{max}	Maximum wave runup [length]
R_{sx} , R_{sy}	Cross-shore and longshore components of wind forcing [length/time^2]
S_{xx}	Cross-shore component of the cross-shore directed radiation stress [force/length]
S_{xy}	Radiation stress component [force/length]
T	Wave period [time]
u	Total current in the surf zone (Equation II-4-30) [length/time]
U	Time- and depth-averaged cross-shore current [length/time]
u_a	Wind-driven current [length/time]
u_i	Oscillatory flow due to infragravity waves [length/time]
u_o	Oscillatory flow due to wind waves [length/time]

u_t	Tidal current [length/time]
u_w	Steady current driven by breaking waves [length/time]
V	Longshore current speed (Equation II-4-36) [length/time]
V_0	Maximum current for the case without lateral mixing (Figure II-4-15) [length/time]
V_{mid}	Longshore current at the mid-surf zone (Equation II-4-37) [length/time]

II-4-9. Acknowledgments

Author of Chapter II-4, "Surf Zone Hydrodynamics:"

Jane M. Smith, Ph.D., Coastal and Hydraulics Laboratory, Engineer Research and Development Center (CHL), Vicksburg, Mississippi.

Reviewers:

William R. Dally, Ph.D., Florida Institute of Technology, Melbourne, Florida, (currently private consultant).
Zeki Demirbilek, Ph.D., CHL.
Lee E. Harris, Ph.D., Department of Marine and Environmental Systems, Florida Institute of Technology, Melbourne, Florida.
Todd K. Holland, Ph.D., Naval Research Laboratory, Stennis Space Center, Mississippi.
Robert A. Holman, Ph.D., College of Oceanic & Atmospheric Sciences, Oregon State University, Corvallis, Oregon.
Bradley D. Johnson, CHL
Nicholas C. Kraus, Ph.D., CHL
Okey G. Nwogu, University of Michigan
Joan Pope, CHL.
Edward F. Thompson, Ph.D., CHL
Greg L. Williams, Ph.D., U.S. Army Engineer District, Wilmington, North Carolina.
C. Linwood Vincent, Ph.D., Office of Naval Research, Arlington, Virginia.

Table of Contents

Page

II-5-1. Introduction II-5-1
a. Purpose II-5-1
b. Applicability II-5-1
c. Scope of manual II-5-1

II-5-2. Classification of Water Waves II-5-2
a. Wave classification II-5-2
b. Discussion II-5-5

II-5-3. Astronomical Tides II-5-5
a. Description of tides II-5-5
(1) Introduction II-5-5
(2) Tide-producing forces II-5-6
(3) Spring/neap cycle II-5-8
(4) Diurnal inequality II-5-9
b. Tidal time series analysis II-5-11
(1) Introduction II-5-11
(2) Harmonic constituents II-5-11
(3) Harmonic reconstruction II-5-18
(4) Tidal envelope classification II-5-23
c. Glossary of tide elevation terms II-5-25

II-5-4. Water Surface Elevation Datums II-5-27
a. Introduction II-5-27
b. Tidal-observation-based datums II-5-27
c. 1929 NGVD datum II-5-28
d. Great Lakes datums II-5-32
e. Long-term variations in datums II-5-32
f. Tidal datums II-5-32
g. Changes in lake level datums II-5-37
h. Design considerations II-5-38

II-5-5. Storm Surge II-5-38
a. Storm types II-5-38
(1) Tropical storms II-5-39
(2) Extratropical storms II-5-42
(3) Surge interaction with tidal elevations II-5-43
b. Storm event frequency-of-occurrence relationships II-5-43
(1) Introduction II-5-43
(2) Historical method II-5-46
(3) Synthetic method II-5-47
(4) Empirical simulation technique II-5-47

(a) Introduction II-5-47
(b) EST - tropical storm application II-5-47
(c) EST - extratropical storm application II-5-49

II-5-6. Seiches II-5-51

II-5-7. Numerical Modeling of Long-Wave Hydrodynamics II-5-54
a. Long-wave modeling II-5-54
b. Physical models II-5-54
c. Numerical models II-5-55
(1) Introduction II-5-55
(2) Example - tidal circulation modeling II-5-56
(3) Example - storm surge modeling II-5-57

II-5-8. References II-5-64

II-5-9. Definitions of Symbols II-5-69

II-5-10. Acknowledgments II-5-71

List of Tables

Page

Table II-5-1. Wave Classification (Ippen 1966) II-5-3

Table II-5-2. Hyperbolic Function Asymptotes II-5-4

Table II-5-3. NOS Tidal Constituents and Arguments II-5-16

Table II-5-4. Node Factors for 1970 through 1999 (Schureman 1924) II-5-17

Table II-5-5. Equilibrium Argument for Beginning of Years 2001 through 2010 (Schureman 1924) II-5-19

Table II-5-6. Summary of Harmonic Arguments for Sandy Hook, NJ (1 January 1984 at 0000 hr) II-5-23

Table II-5-7. Datums for Reference Tide Stations (Harris 1981) II-5-29

Table II-5-8. Low Water (chart) Datum for IGLD 1955 and IGLD 1985 . . . . . II-5-35

List of Figures

Page

Figure II-5-1. Long wave geometry (Milne-Thompson 1960) II-5-3

Figure II-5-2. Variation of particle velocity with depth (Ippen 1966) II-5-4

Figure II-5-3. Schematic representation of water particle trajectories (Ippen 1966) II-5-5

Figure II-5-4. Schematic diagram of tidal potential (Dronkers 1964) II-5-7

Figure II-5-5. Tide predictions for Boston, MA (Harris 1981) II-5-9

Figure II-5-6. Spring and neap tides (Shalowitz 1964) II-5-10

Figure II-5-7. The daily inequality (Dronkers 1964) II-5-11

Figure II-5-8. Typical tide curves along the Atlantic and Gulf coasts (*Shore Protection Manual* 1984) II-5-12

Figure II-5-9. Typical tide curves along Pacific coasts of the United States (*Shore Protection Manual* 1984) II-5-13

Figure II-5-10. Tidal phase relationships II-5-18

Figure II-5-11. Phase angle argument relationship II-5-20

Figure II-5-12. NOS harmonic analysis for Sandy Hook, NJ II-5-21

Figure II-5-13. Tide tables for Sandy Hook, NJ (NOAA 1984) II-5-22

Figure II-5-14. Reconstructed tidal envelope for Sandy Hook, NJ II-5-24

Figure II-5-15. Areal extent of tidal types (Harris 1981) II-5-25

Figure II-5-16. Types of tides (*Shore Protection Manual* 1984) II-5-26

Figure II-5-17. Reference and comparative tide stations, Atlantic, Gulf, and Pacific coasts (Harris 1981) II-5-31

Figure II-5-18. Locations of tide stations used in establishing the National Geodetic Vertical Datum (NGVD) of 1929 (Harris 1981 (after Rappleye (1932)) II-5-33

Figure II-5-19. Sample NOS description of tidal bench marks (Harris 1981) II-5-34

Figure II-5-20. Vertical and horizontal relationships for the IGLD 1985 . . . . . II-5-35

Figure II-5-21. Sample NOS tabulation of tide parameters (Harris 1981) II-5-39

Figure II-5-22. Variations in annual MSL (Harris 1981) II-5-40

Figure II-5-23. Schematic diagram of storm parameters (U.S. Army Corps of Engineers 1986) II-5-41

Figure II-5-24. Hurricane Gloria track from 17 September to 2 October 1985 (Jarvinen and Gebert 1986) II-5-44

Figure II-5-25. Hurricane Gloria track offshore of Delaware and New Jersey (Jarvinen and Gebert 1986) II-5-45

Figure II-5-26. Example phasing of storm surge and tide (Jarvinen and Gebert 1986) II-5-46

Figure II-5-27. Stage-frequency relationship - coast of Delaware II-5-50

Figure II-5-28. Sediment transport magnitude-frequency relationship - December 1992 Northeaster II-5-51

Figure II-5-29. Atlantic tropical storm tracks during the period 1886-1980 . . . . . II-5-52

Figure II-5-30. Long wave surface profiles (*Shore Protection Manual* 1984) II-5-53

Figure II-5-31. First, second, and third normal modes of oscillation for Lake Ontario (Rao and Schwab 1976) II-5-54

Figure II-5-32. Computational grid for the New York Bight II-5-58

Figure II-5-33. Model and prototype tidal elevation comparison at the Battery II-5-59

Figure II-5-34. Wind-induced circulation pattern II-5-60

Figure II-5-35. Global limits of ADCIRC computational grid II-5-61

Figure II-5-36. Blow-up of ADCIRC grid along Delaware coast II-5-62

Figure II-5-37. Model-to-prototype tidal comparison at Lewes, DE II-5-63

Figure II-5-38. Model-to-prototype surge comparison at Lewes, DE II-5-64

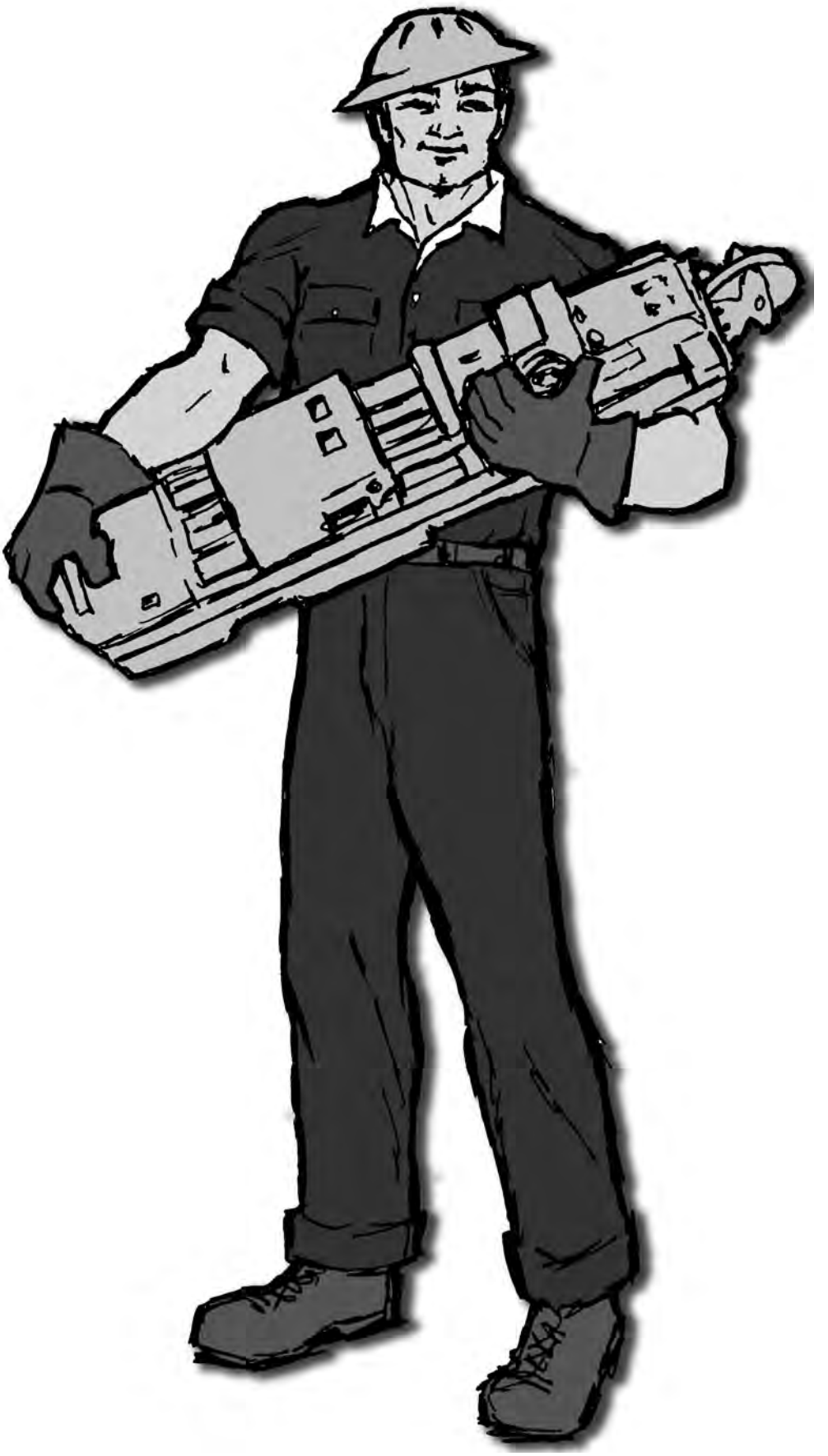

Chapter II-5
Water Levels and Long Waves

II-5-1. Introduction

a. Purpose.

(1) This chapter describes water levels and the various long wave components that contribute to a total water surface elevation. Vertical datums are also described to define some of the more commonly used reference datums.

(2) The following sections provide project engineers with sufficient guidance to develop a preliminary study approach and design procedure to analyze engineering projects that require consideration of water level elevations. References are provided from existing Engineer Manuals that describe generic design-criteria formulae for use in preliminary analyses. Additional references and approaches to problem solving are provided for complex projects that require detailed surface elevation and current input data for design. These data are generally provided by numerical models.

b. Applicability. Information contained in this chapter is directly applicable to any project requiring local water levels or currents as a primary design consideration. Applications include the design of coastal structures intended to provide protection against some pre-defined water surface elevation, specified according to an appropriate economic analysis and evaluation. Determining acceptable design elevations may require developing local stage relationships as opposed to frequency-of-occurrence relationships. This information can be generated through historical records or numerical modeling techniques to simulate the propagation of historical storm events. Additional examples of water surface and current variability include circumstances where tidal circulation patterns and surface elevations change as a result of structural or bathymetric modifications to existing coastal inlets or navigable waterways. These circulation-dominated problems can be addressed using either numerical or physical models.

c. Scope of manual.

(1) Water wave classification is used to describe the behavior of long waves and to distinguish between intermediate waves and short waves (described in Part II-2). This allows the reader to select which chapter of this manual is appropriate for the intended application. If long waves are appropriate, this chapter will provide a means of approximating basic wave characteristics such as celerity, current magnitudes, and surface elevation.

(2) The speed of propagation, surface profile, and vertical velocity distribution of long waves are different from those of short waves described in Part II-2. Because these properties of waves represent important design criteria, it is important to make a distinction between long and short waves. Therefore, Part II-5-2 reviews wave classification criteria and summarizes long wave properties.

(3) Tides are the most common and visible example of long wave propagation. Part II-5-3 summarizes tidal hydrodynamics and describes characteristic tidally induced long wave variability. This section includes a background description of the forces responsible for generating tides, gives examples of the variability of tides, and presents a methodology for harmonic reconstruction of tides.

(4) Many of the concepts described by tidal records are used as a basis for defining tidal datums. Part II-5-4 describes reference elevation datums commonly in use in the United States. Attention is also paid

to the change in coastal datums that may result from sea (or lake) level rise and/or land subsidence or rebound.

(5) Parts II-5-5 through II-5-7 describe nontidal variability in water surfaces. These fluctuations can be storm-generated, as in the case of tropical and extratropical storms; atmospheric- and geometry-related, as in the case of seiches or tidal bores; or be due to responses stemming from earthquake-generated tsunamis or other rapid changes in the environment.

(6) The primary goal of this chapter is to define tidal and storm-generated fluctuations in the water surface and describe the datums to which they are referenced. Seiches will only be briefly discussed and tsunamis are not addressed because a special report on tsumanis has been prepared by the Coastal and Hydraulics Laboratory (CHL) (Camfield 1980). In addition to Camfield, Engineer Manual 1110-2-1414, "Water Levels and Wave Heights for Coastal Engineering Design," addresses the propagation of tsunamis. However, because both seiches and tsunamis are classified as long waves, the numerical modeling techniques discussed in Part II-5-7 are an appropriate means of analysis.

II-5-2. Classification of Water Waves

a. Wave classification.

(1) The long wave descriptions that follow are based on small-amplitude wave theory solutions to the governing equations. This theory places certain criteria on the physical shape of the wave. For example, from Figure II-5-1, the amplitude is assumed small with respect to the depth (i.e., η/h ratio is small, and the surface slope $d\eta/dx$ is assumed small).

(2) Although wave amplitude is assumed small with respect to depth, the manner in which the wave propagates is a function of just how small this ratio is. The propagation of small-amplitude waves in water can now be described as a function of the wave length and the depth of water in which the wave is propagating. In fact, waves can be classified according to a parameter referred to as the "relative depth," defined as the ratio of water depth h to wave length L. When this ratio is less than approximately 1/20, waves can be classified as long waves or "shallow-water waves." Figure II-5-1 shows typical long wave geometry for a wave whose length L is large with respect to the depth of water h.

(3) Astronomical tides represent one important example of long waves. In Chesapeake Bay, for example, the M_2 primary lunar tidal constituent is contained completely within the Bay at a given instant in time, producing a wavelength of approximately 300 km. The mean depth of flow in the Bay is approximately 10 m; therefore, the relative depth is 3.3×10^{-5}. Long waves are not limited to what is normally considered shallow water because the relative depth is a function of wavelength. In fact, most tides are long waves over the entire ocean because their wavelengths are on the order of 1,000 km and depths are on the order of kilometers. Similarly, seismic-forced phenomena such as tsunamis propagate across the Pacific Ocean in depths of up to 20 km but have wavelengths on the order of hundreds of kilometers.

(4) Waves are classified as short waves, also referred to as "deepwater waves," when the relative depth is greater than approximately 1/2. Coastal waves described in Part II-2 are generally of this class. The geometry of short waves implies wave steepness great enough to cause them to break. The class of waves between short (deep) and long (shallow) are referred to as "intermediate waves." Table II-5-1 (Ippen

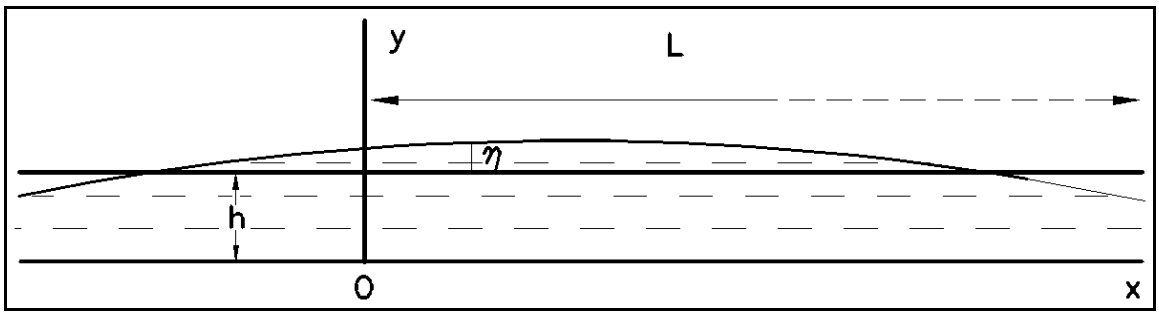

Figure II-5-1. Long wave geometry (Milne-Thompson 1960)

Table II-5-1
Wave Classification (Ippen 1966)

Range of h/L	Range of kh=2πh/L	Types of waves
0 to 1/20	0 to π/10	Long waves (shallow-water wave)
1/20 to 1/2	π/10 to π	Intermediate waves
1/2 to ∞	π to ∞	Short waves (deepwater waves)

1966) summarizes wave classification criteria according to relative depth and the wave parameter *kh* defined below.

(5) Applying the relative depth and wave number parameter to the characteristics of long waves can be seen in the simplification to progressive small-amplitude wave theory solutions. For example, from Part II-1, the wave celerity, wave length, horizontal (x-direction) and vertical velocities can be written as

$$C^2 = \frac{g}{k}\tanh(kh) \tag{II-5-1}$$

$$L = \frac{gT^2}{2\pi}\tanh\,(kh) \tag{II-5-2}$$

$$u = \frac{agk}{\sigma}\,\frac{\cosh\,k(h+z)}{\cosh kh}\,\sin(kx-\sigma t) \tag{II-5-3}$$

$$w = -\frac{agk}{\sigma}\,\frac{\sinh\,k(h+z)}{\cosh kh}\,\cos(kx-\sigma t) \tag{II-5-4}$$

where k is the wave number ($2\pi/L$), σ is the angular frequency ($2\pi/T$ where T is the period of the wave), a is the amplitude of the wave, g the acceleration of gravity, h is the total depth, and z is the depth measured downward from the quiescent fluid surface. A schematic diagram of the variation of velocity as a function of depth is shown in Figure II-5-2.

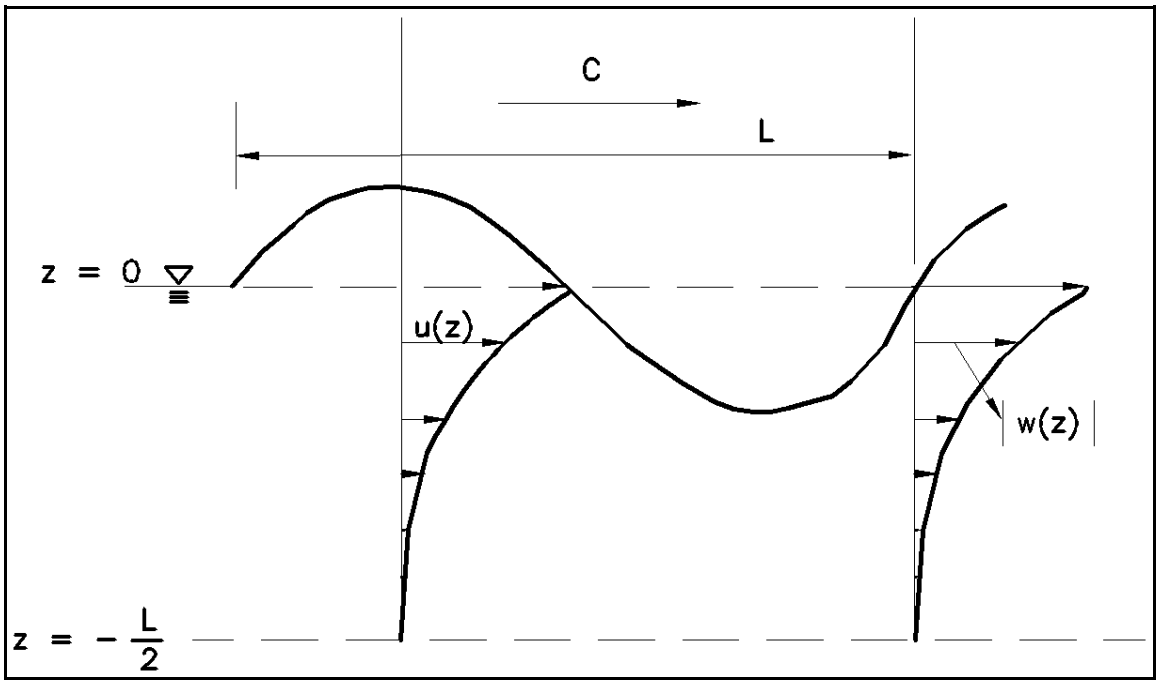

Figure II-5-2. Variation of particle velocity with depth (Ippen 1966)

(6) Certain simplifications to Equations II-5-1 through II-5-4 result from the asymptotic values of the hyperbolic functions. For example, Table II-5-2 (Ippen 1966) presents the hyperbolic functions contained in the long- and short-wave representations, as well as their asymptotes. No simplification results for intermediate waves.

Table II-5-2
Hyperbolic Function Asymptotes

	Asymptotes	
Function	**Long waves**	**Short waves**
sinh kh	kh	$e^{kh}/2$
cosh kh	1	$e^{kh}/2$
tanh kh	kh	1

(7) The resulting long wave simplification for celerities and wave lengths is shown below.

$$C = \sqrt{gh} \tag{II-5-5}$$

$$L = T\sqrt{gh} \tag{II-5-6}$$

(8) Therefore, long waves propagate as the square root of *gh*. This relationship will be shown to be useful in analyzing and interpreting long-wave phase propagation data, because wave celerity is predictable for a given depth.

(9) Additionally, one important difference between long waves and short waves can be seen in the computed orbital velocities. Figure II-5-3 shows water particle trajectories for long, short, and intermediate waves as a function of depth. As can be seen, and computed from Equations II-5-3 and II-5-4, the horizontal velocity of a long wave is maintained throughout the water column, from the surface to the bottom. In the case of short waves, the strength of the horizontal and vertical component decreases with depth to the point that waves do not induce bottom currents. The fact that long waves affect the bottom is important in that bottom sediments can be eroded and transported by tidal and other long-wave currents. For example, tidal flood and ebb currents contribute to the transport of sediments to form ebb and flood shoals. Potential erosion and deposition considerations will be discussed in Part 3 of this manual.

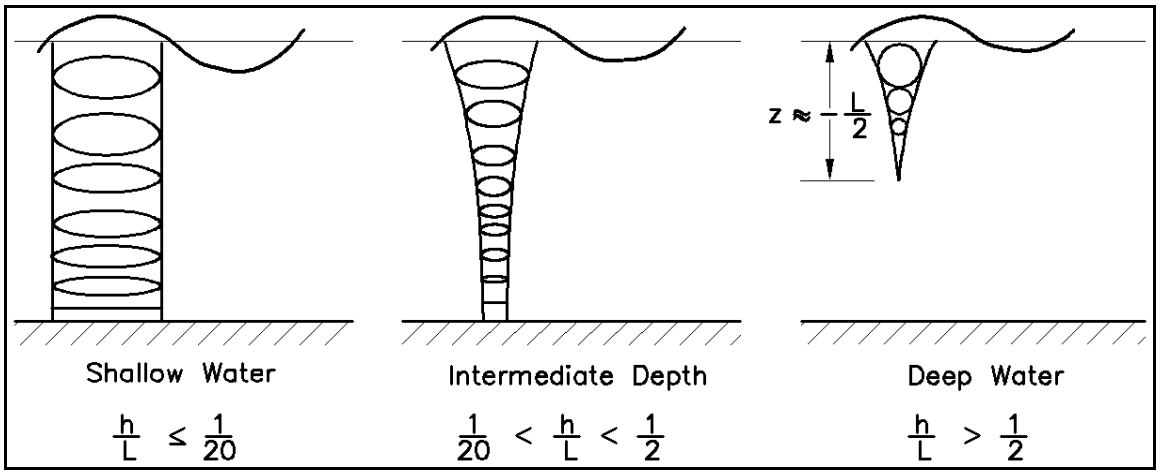

Figure II-5-3. Schematic representation of water particle trajectories (Ippen 1966)

b. Discussion. Short waves impact nearshore water surface elevations by creating the wave setup condition. Details of wave setup and associated setdown are described in Part II-4. Including setup can be critical in developing water surface design criteria, as setup can create an elevated surface on which tide and storm surge propagate. Because the interactions of these components of the water surface are not linear, and because they are of different time scales (Part II-1), they are generally considered separately in the development of total water level design criteria. Methods for computing and combining these effects are given in Part II-3 and 4. The following sections concentrate on tidal and storm surge elevations.

II-5-3. Astronomical Tides

a. Description of tides.

(1) Introduction.

(a) Astronomical tides are observable as the periodic rising and falling of the surface of major water bodies on the earth. Tides are produced in response to the gravitational attraction of the moon, sun, and (to a considerably smaller extent) all other celestial bodies. Because of its relative closeness to the earth, the moon induces the strongest effect on the tides. Tidal currents are produced in response to differences in the water surface elevation.

(b) Tidal height, or the vertical distance between the maximum and successive minimum water surface elevation, is a function of the relative position of the moon and sun with respect to the earth, and varies from location to location. Typically, the dominant tidal cycle is related to the passage of the moon over a fixed

meridian. This occurs an average of 50 min later each succeeding day. This passage of the moon produces approximately two tides per solar day (referred to as semidiurnal), with a maximum tide occurring approximately every 12 hr 25 min. However, differences in the relationship of the moon and sun in conjunction with local conditions can result in tides that exhibit only one tidal cycle per day. These are referred to as diurnal tides. Mixed tides exhibit characteristics of both semidiurnal and diurnal tides. At certain times in the lunar month, two peaks per day are produced, while at other times the tide is diurnal. The distinction is explained in the following paragraphs.

(c) The description of typical tidal variability begins with a brief background description of tide-producing forces, those gravitational forces responsible for tidal motion, and the descriptive tidal envelope that results from those forces. This sub-section will be followed by more qualitative descriptions of how the tidal envelope is influenced by the position of the moon and sun. Once this basic pattern is established, measured tidal elevations can, in part, be shown to be a function of the influence of the continental shelf and the coastal boundary on the propagating tide.

(2) Tide-producing forces.

(a) The law of universal gravitation was first published by Newton in 1686. Newton's law of gravitation states that every particle of matter in the universe attracts every other particle with a force that is directly proportional to the product of the masses of the particles and inversely proportional to the square of the distance between them (Sears and Zemansky 1963). Quantitative aspects of the law of gravitational attraction between two bodies of mass m_1 and m_2 can be written as follows:

$$F_g = f\frac{m_1\, m_2}{r^2} \tag{II-5-7}$$

where F_g is the gravitational force on either particle, r is separation of distance between the centers of mass of the two bodies, and f is the universal constant with a value of 6.67×10^{-8} cm^3/gm sec^2. The gravitational force of the earth on particle m_1 can be determined from Equation II-5-7. Let $F_g = m_1\, g$ where g is the acceleration of gravity (980.6 cm/sec^2) on the surface of the earth, and m_2 equal the mass of the earth E. By substitution, an expression for the gravitational constant can be written in terms of the radius of the earth a and the acceleration of gravity g.

$$f = g\frac{a^2}{E} \tag{II-5-8}$$

(b) Development of the tidal potential follows directly from the above relationship. The following variables are referenced to Figure II-5-4 (although Figure II-5-4 refers to the moon, an analogous figure can be drawn for the sun). Let M and S be the mass of the moon and sun, respectively. r_m and r_s are the distances from the center of the earth O to the center of the moon and sun. Let r_{mx} and r_{sx} be the distances of a point $X(x,y,z)$ located on the surface of the earth to the center of the moon and sun. The following relationships define the tidal potential at some arbitrary point X as a function of the relative position of the moon and sun.

(c) The attractive force potentials per unit mass for the moon and sun can be written as

$$V_M = \frac{fM}{r_{MX}} \quad , \quad V_S = \frac{fS}{r_{SX}} \tag{II-5-9}$$

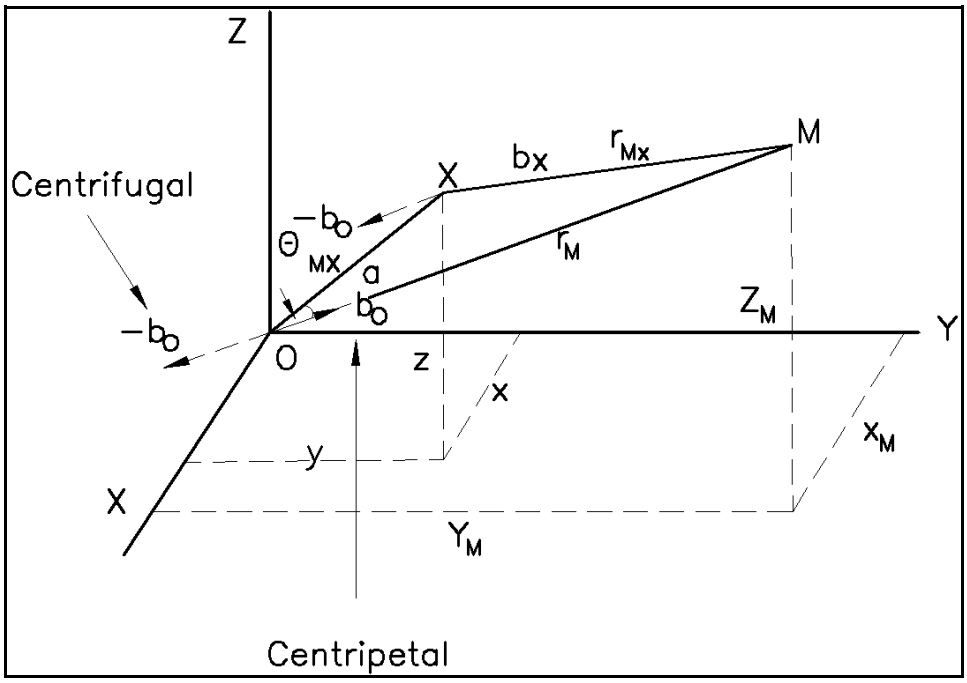

Figure II-5-4. Schematic diagram of tidal potential (Dronkers 1964)

where the separation distance $r_{MX} = [(x_m - x)^2 + (y_m - y)^2 + (z_m - z)^2]^{1/2}$ with an equivalent expression for r_{SX}.

(d) The attractive force of the moon and sun at any point X is defined as

$$\vec{b}_X = \nabla [V_M(X) + V_S(X)] \tag{II-5-10}$$

where ∇ is the vector gradient operator defined as

$$\vec{\nabla} = \left(\frac{\partial}{\partial x} + \frac{\partial}{\partial y} + \frac{\partial}{\partial z}\right) \tag{II-5-11}$$

(e) From Figure II-5-4, the attractive force at the center of the earth (centripetal) b_O is balanced by the centrifugal force $-b_O$ (i.e., equal in magnitude but opposite in direction). Because any point on the earth experiences the same centrifugal force as that at O, the resultant force at any point X will be equal to $b_X - b_O$. This resultant force difference is the tide generating force, the force that causes the oceans to deform in order to balance the sum of external forces. Therefore, the difference between the tidal potential at point O and at point X becomes the tidal potential responsible for the tide-producing forces.

(f) The moon's tide-generating potential can be written as

$$V_M = fM\left[\frac{1}{r_{MX}} - \frac{1}{r_M} - \frac{a \cos\theta_{MX}}{r_M^2}\right] \tag{II-5-12}$$

with the tide potential for the sun written as

$$V_S = fS\left[\frac{1}{r_{SX}} - \frac{1}{r_S} - \frac{a\cos\theta_{SX}}{r_S^2}\right] \tag{II-5-13}$$

where a is the mean radius of the earth. Various geometric relationships are used to write Equations II-5-12 and II-5-13 in the following forms:

$$V_M = fM\left(\frac{a^2}{r_M^3}\right) P_M \tag{II-5-14}$$

$$V_S = fS\left(\frac{a^2}{r_S^3}\right) P_S \tag{II-5-15}$$

where the terms P_M and P_S represent harmonic polynomial expansion terms that collectively describe the relative positions of the earth, moon, and sun. Note that in both cases, the tidal potential term is written as an inverse function of the distance between the earth and the moon or sun. Both Dronkers (1964) and Schureman (1924) present detailed derivations of the terms of Equations II-5-14 and II-5-15. For the purpose of this manual, however, the tidal potential terms shown here are adequate to describe the two most important features of a tidal record, the spring/neap cycle and the diurnal inequality.

(3) Spring/neap cycle.

(a) The semidiurnal rise and fall of tide can be described as nearly sinusoidal in shape, reaching a peak value every 12 hr and 25 min. This period represents one-half of the lunar day. Two tides are generally experienced per lunar day because tides represent a response to the increased gravitational attraction from the (primarily) moon on one side of the earth, balanced by a centrifugal force on the opposite side of the earth. These forces create a “bulge” or outward deflection in the water surface on the two opposing sides of the earth.

(b) The magnitude of tidal deflection is partially a function of the distance between the moon and earth. When the moon is in perigee, i.e., closest to the earth, the tide range is greater than when it is furthest from the earth, in apogee. For example, the potential terms in Equation II-5-14 contain the multiplier $1/r_M$, describing the distance of the moon from the earth. When the moon is closest to the earth, r_M is a minimum value and the tidal potential term is maximum. Conversely, when the moon is in apogee, the potential term is at a minimum value. This difference may be as large as 20 percent.

(c) The maximum water surface deflection of semidiurnal tides changes as the relative position of the moon and sun changes. The amplitude envelope connecting any two successive high tides (and low tides) gradually increases from some minimum height to a maximum value, and then decreases back to a minimum. Periods of maximum amplitude are referred to as spring tides, times of minimum amplitude are neap tides. This envelope of spring to neap occurs twice over a period of approximately 29 days. An example tidal signal for Boston, MA, is shown in Figure II-5-5 (Harris 1981) in which the normalized tidal signal exhibits two amplitude envelopes during the total time series.

(d) Spring tides occur when the sun and moon are in alignment. This occurs at either a new moon, when the sun and moon are on the same side of the earth, or at full moon, when they are on opposite sides of the earth. Neap tides occur at the intermediate points, the moon's first and third quarters. Figure II-5-6 is a schematic representation of these predominant tidal phases. Lunar quarters are indicated in the tidal time

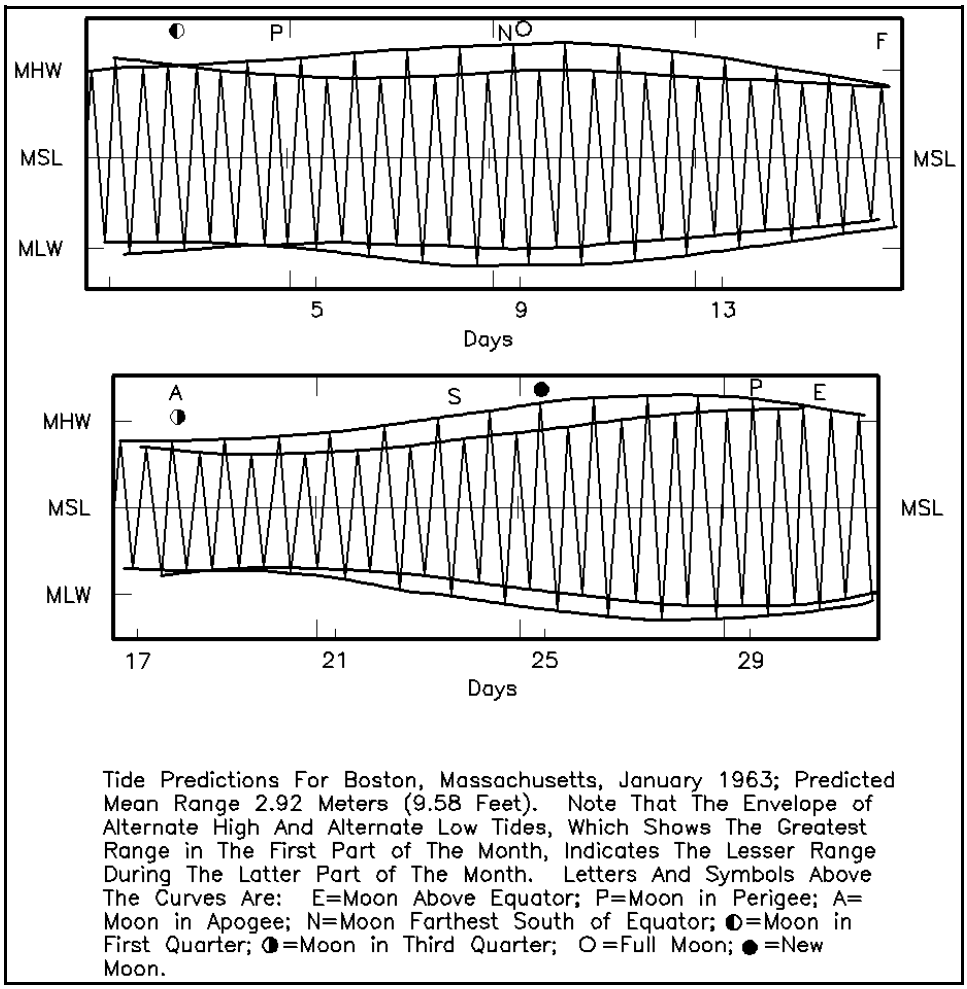

Figure II-5-5. Tide predictions for Boston, MA (Harris 1981)

series shown in Figure II-5-5. Note that in Figure II-5-5, the envelope that connects higher-high tide values for the first spring tide during the first 14.5 days becomes an envelope of the lower-high tide values during the second spring tide.

(4) Diurnal inequality.

(a) In the above example, the envelope of two successive high or low tides defines spring and neap conditions. Alternate tides were used because the ranges of two successive tides at a given location are generally not identical, but exhibit differences in height. Examples are evident in Figure II-5-5. These differences are referred to as the diurnal inequality of the tide and result from the relative position of the sun and moon as well as the specific location of an observer on the earth.

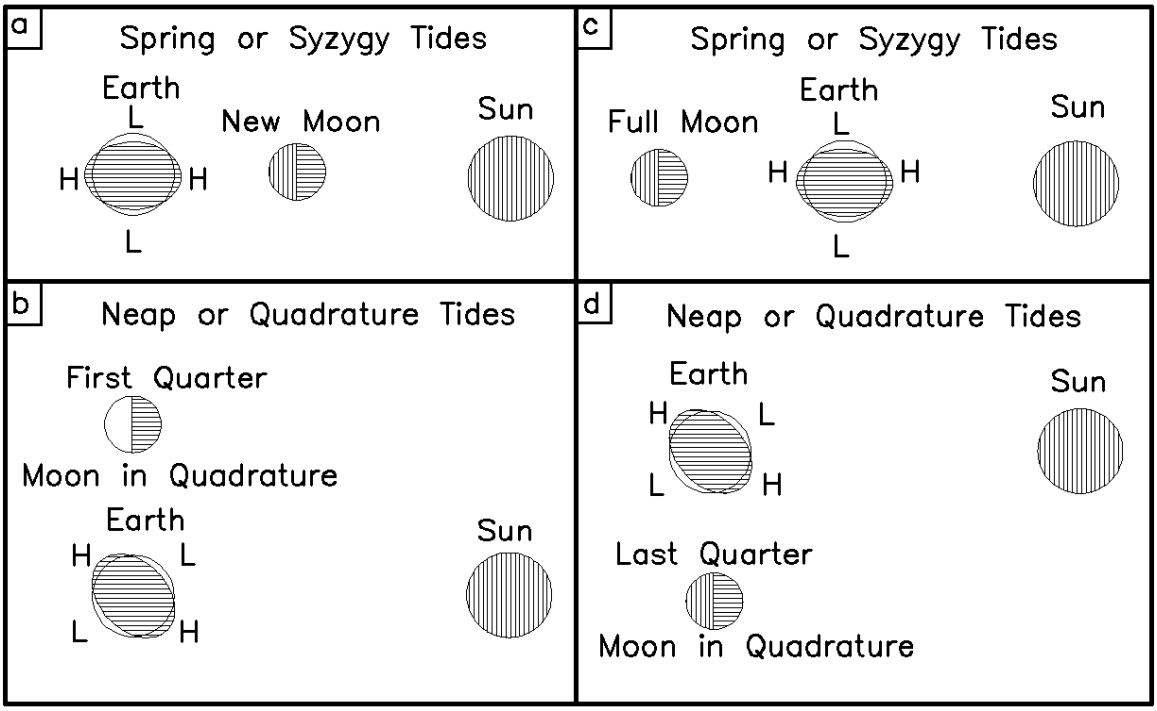

Figure II-5-6. Spring and neap tides (Shalowitz 1964)

(b) Diurnal inequality can be explained as follows. The tidal bulge is centered along a line from the center of the moon or sun to the center of the earth. The tidal bulge at a given sublunar or subsolar (location on the earth nearest the moon or sun) location has an equivalent bulge on the opposite side of the earth, i.e., on a line drawn from the sublunar or subsolar point through the center of the earth on the opposite side of the equator. If the sublunar or subsolar point appears at a given north latitude, the peak of the corresponding tidal bulge on the opposite side of the equator will appear at a corresponding south latitude. Thus, a point on the same north latitude but 180 deg in longitude from the sublunar or subsolar point will show a reduced amplitude.

(c) A schematic example of the daily inequality is presented by Dronkers (1964) for the simple case of an earth-moon system. Referring to Figure II-5-7, the moon is located in the direction M and earth is rotating about the polar axis *P*. The deformed water surface resulting in response to the tide-producing forces is shown in the figure. Four locations (I - IV) are indicated to demonstrate the effect of location on the diurnal inequality. The fluctuating tide can be seen as the deviation in the deformed surface from a line at constant latitude on the undeformed spherical surface corresponding to each location. Location I corresponds to an observer on the equator. In this case, it can be seen that the tidal deformations from static conditions are equal; therefore, there is no diurnal inequality, each high tide is equal. However, at locations II and III, the inequality is evident with the second tide being substantially lower than the first. In the extreme case, location IV exhibits a diurnal tide only due to its location with respect to the deformed water surface.

(d) The combinations of astronomical forcing that define spring and neap cycles and diurnal inequalities is further modified by local bathymetry and shoreline boundary influences. All of these factors combine to produce tidal envelopes that vary from location to location. The result is site-specific tidal signatures, which can be classified as semidiurnal, diurnal, or mixed. Examples of these classes of tides are shown in Figures II-5-8 and II-5-9. Tides along the Atlantic coast are generally semidiurnal with a small diurnal inequality. Typical east coast envelopes for Boston, MA; New York, NY; Hampton Roads, (Hampton), VA;

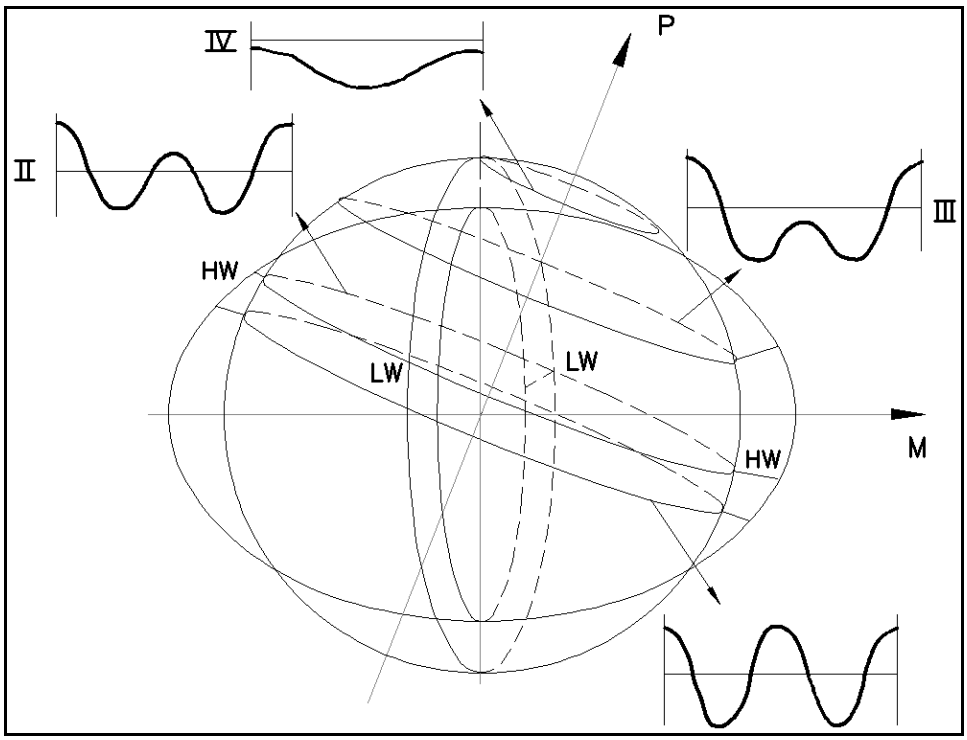

Figure II-5-7. The daily inequality (Dronkers 1964)

and the entrance to the Savannah River at Savannah, GA, are shown in the figure. Each time series exhibits two distinct and nearly equal tides per day. As one moves to Key West, FL, the character of the tide begins to change with a noticeable diurnal inequality. Tides inside the Gulf of Mexico range from semidiurnal at Key West, FL, to diurnal at Pensacola, FL, to mixed at Galveston, TX. Note that the Galveston data progresses from a diurnal tide during the first third of the record to a semidiurnal tide. Tides in the Gulf of Mexico are more complex than open ocean stations because astronomical forcing is modified by geometrically forced nodes and antinodes. These seiche-related phenomena are discussed in Part II-5-6. Pacific coast tides, shown in Figure II-5-9, are generally of larger amplitude than Atlantic and Gulf coast tides and often have a decided diurnal inequality.

b. Tidal time series analysis.

(1) Introduction. The equilibrium theory of tides is a hypothesis that the waters of the earth respond instantaneously to the tide-producing forces of the sun and moon. For example, high water occurs directly beneath the moon and sun, i.e., at the sublunar and subsolar points. This tide is referred to as an equilibrium tide. Part II-5-3 a (1), states that tide-producing forces are written in a polynomial expansion approximation for the exact solution of Equations II-5-12 and II-5-13. These expansion terms involve astronomical arguments describing the location of the sun and moon as well as the location of the observer on the earth. Although several variational forms of the series expansion have been published, the development presented in Schureman (1924) is given below. Alternate forms of expansion are discussed in Dronkers (1964).

(2) Harmonic constituents.

(a) According to equilibrium theory, the theoretical tide can be predicted at any location on the earth as a sum of a number of harmonic terms contained in the polynomial expansion representation of the

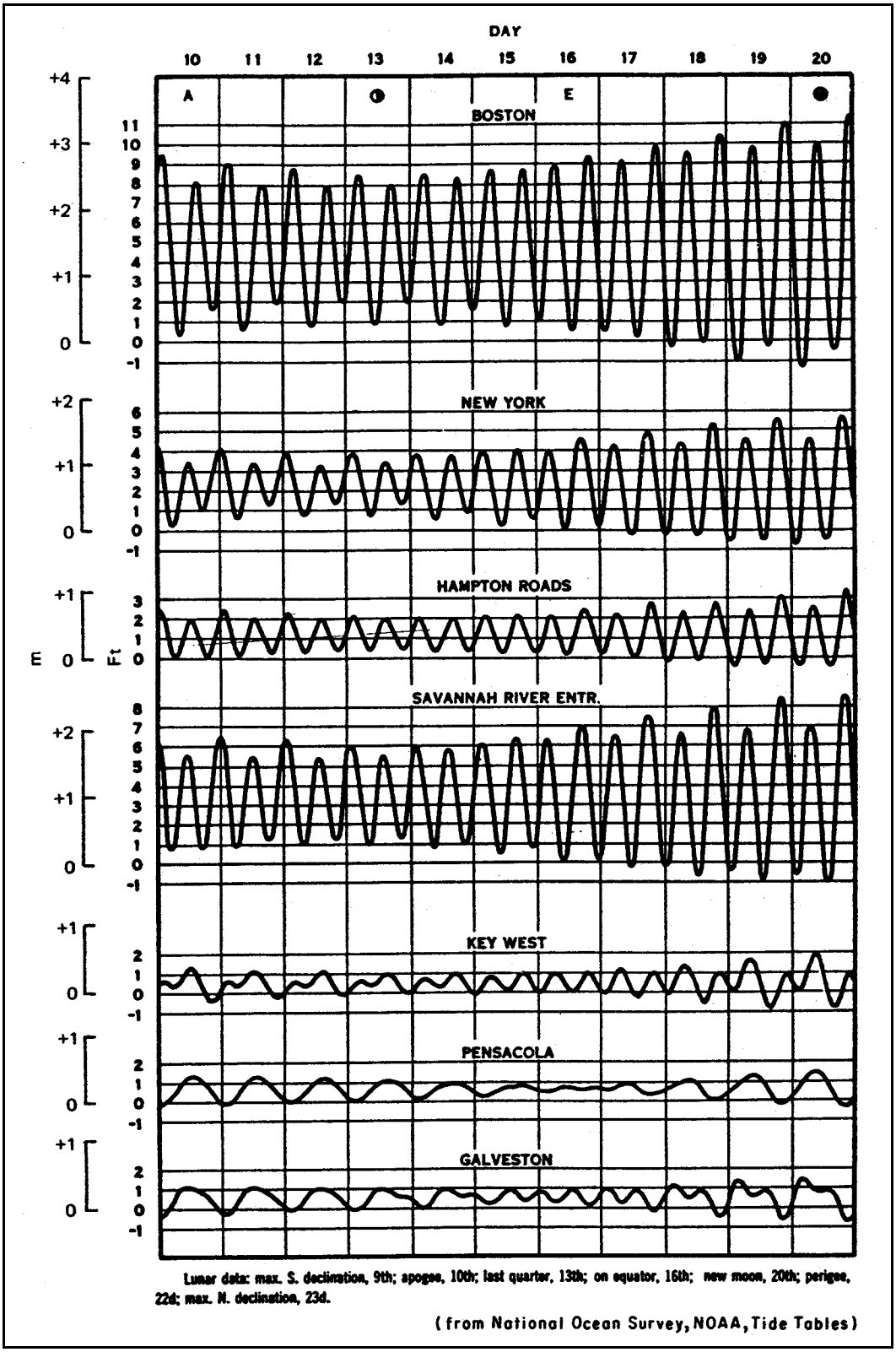

Figure II-5-8. Typical tide curves along the Atlantic and Gulf coasts *(Shore Protection Manual* 1984)

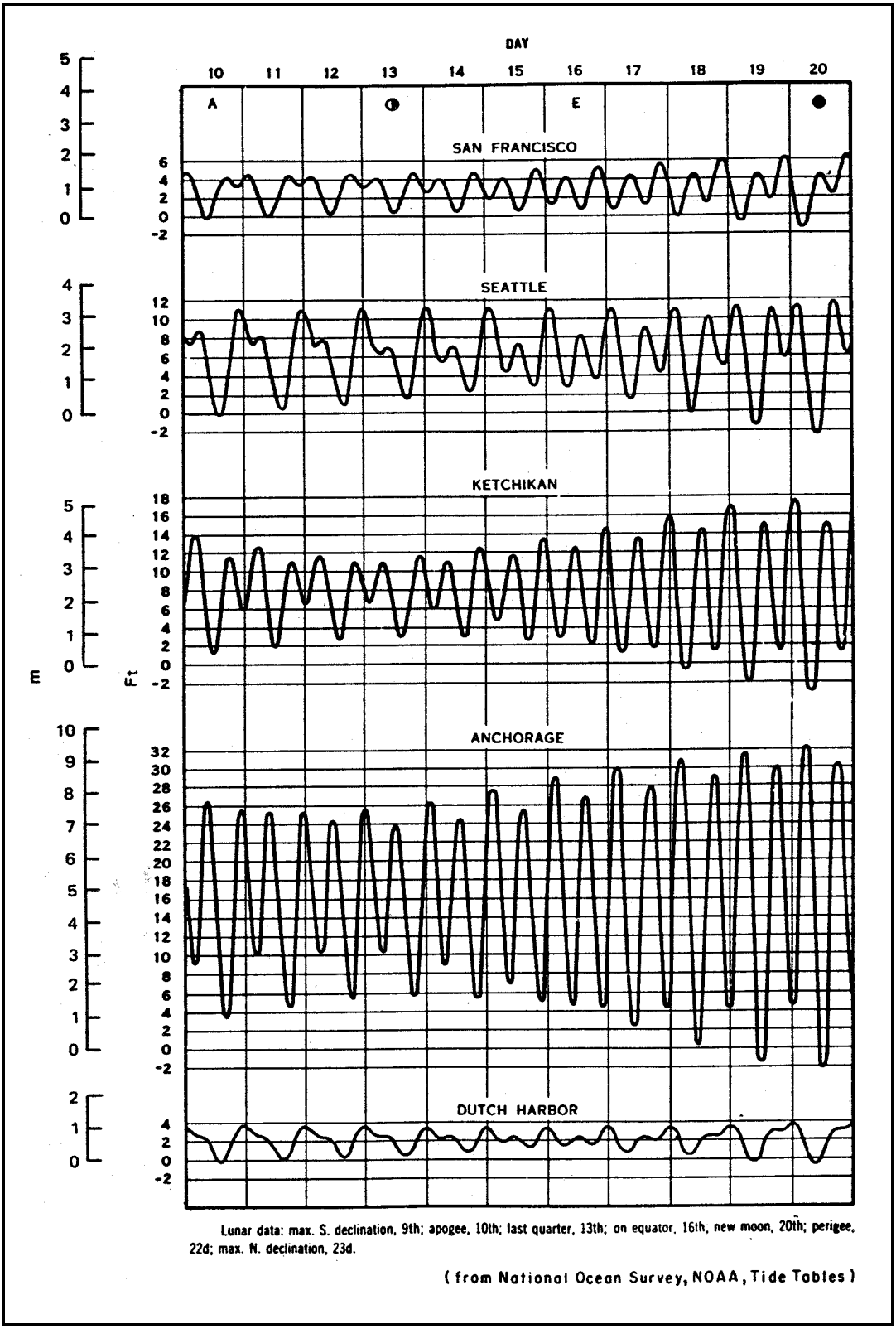

Figure II-5-9. Typical tide curves along Pacific coast of the United States (*Shore Protection Manual* 1984)

tide-producing forces. However, the actual tide does not conform to this theoretical value because of friction and inertia as well as differences in the depth and distribution of land masses of the earth.

(b) Because of the above complexities, it is impossible to exactly predict the tide at any place on the earth based on a purely theoretical approach. However, the tide-producing forces (and their expansion component terms) are harmonic; i.e., they can be expressed as a cosine function whose argument increases linearly with time according to known speed criteria. If the expansion terms of the tide-producing forces are combined according to terms of identical period (speed), then the tide can be represented as a sum of a relatively small number of harmonic constituents. Each set of constituents of common period are in the form of a product of an amplitude coefficient and the cosine of an argument of known period with phase adjustments based on time of observation and location. Observational data at a specific time and location are then used to determine the coefficient multipliers and phase arguments for each constituent, the sum of which are used to reconstruct the tide at that location for any time. This concept represents the basis of the harmonic analysis, i.e., to use observational data to develop site-specific coefficients that can be used to reconstruct a tidal series as a linear sum of individual terms of known speed. The following presentation briefly describes the use of harmonic constants to predict tides.

(c) Tidal height at any location and time can be written as a function of harmonic constituents according the following general relationship

$$H(t) = H_0 + \sum_{n=1}^{N} f_n H_n \cos\left[a_n t + (V_0 + u)_n - \kappa_n\right] \tag{II-5-16}$$

where

$H(t)$ = height of the tide at any time t

H_0 = mean water level above some defined datum such as mean sea level

H_n = mean amplitude of tidal constituent n

f_n = factor for adjusting mean amplitude H_n values for specific times

a_n = speed of constituent n in degrees/unit time

t = time measured from some initial epoch or time, i.e., $t = 0$ at t_0

(V_0+u) = value of the equilibrium argument for constituent n at some location and when $t = 0$

κ_n = epoch of constituent n, i.e., phase shift from tide-producing force to high tide from t_0

(d) In the above formula, tide is represented as the sum of a coefficient multiplied by the cosine of its respective arguments. A finite number of constituents are used in the reconstruction of a tidal signal. Values for the site-specific arguments (H_0, H_n, and κ_n) are computed from observed tidal time series data, usually from a least squares analysis. The National Oceanic and Atmospheric Administration's (NOAA) National Ocean Survey (NOS) generally provides 37 constituents in their published harmonic analyses (generally based on an analysis of a minimum of 1 year of prototype data). The NOS constituents, along with the corresponding period and speed of each, are listed in Table II-5-3. The time-specific arguments (f_n and $V_0 + u$) are determined from formulas or tables as will be discussed below or through application of programs

available through the Automated Coastal Engineering System (ACES) (Leenknecht, Szuwalski, and Sherlock 1992).

(e) Most of the constituents listed in Table II-5-3 are associated with a subscript indicating the approximate number of cycles per solar day (24 hr). Constituents with subscripts of 2 are semidiurnal constituents and produce a tidal contribution of approximately two high tides per day. Diurnal constituents occur approximately once a day and have a subscript of 1. Symbols with no subscript are termed long-period constituents and have periods greater than a day; for example, the Solar Annual constituent Sa has a period of approximately 1 year.

(f) In most harmonic analyses of tidal data in the continental United States, the majority of constituents shown above have amplitude contributions that are negligible with respect to the magnitude of the full tide. For example, in the Gulf of Mexico and east coast of the United States, well over 90 percent of the tidal energy can be represented by the amplitudes of the M_2, S_2, N_2, and K_2 semidiurnal and K_1, O_1, P_1, and Q_1 diurnal constituents. In other locations, many more tidal constituents are needed to adequately represent the tide. For example, over 100 constituents are needed for Anchorage, AK.

(g) Two categories of tidal constituents are necessary to reconstruct a tidal signal:

- Those that represent the elevation of the water surface.
- Those that specify a time and the phase shift associated with that time.

For example, the value for H_n in Equation II-5-16 is the mean constituent amplitude and is a function of both location and variations arising from changes in the latitude of the moon's node. The nodal effect of the moon is reflected by the introduction of the node factor f_n, which modifies each constituent amplitude to correspond to a specific time period. Mid-year values are usually specified for reconstructed time series because node factors vary slowly in time. Mid-year values for each constituent listed in Table II-5-3 are presented in Shureman (1924) for the years 1850 through 1999. An example is shown in Table II-5-4 for the years 1970 through 1999. Equations for computing f_n are given by Schureman.

(h) The second category of arguments specifies the phasing of high water for each constituent with respect to both time and location. These arguments are based on the fact that phases of the constituents of the observed tide do not coincide with the phases of the corresponding constituents of the equilibrium tide. For example, a high tide does not occur directly beneath the moon. There is a lag between the location of the tide-producing force (i.e., location of the moon) and the observed time of high water. This lag, due to frictional and inertial forces acting on the propagating tide, is referred to as the epoch of the constituent and is denoted by κ_n in Equation II-5-16.

(i) The relationship between the constituent arguments and high tide is shown in the schematic Figure II-5-10. In this figure, the cosine curve represents the surface elevation in the y-direction as a function of time or degrees of phase (maximum at 0 and 360 deg). For the M_2 tidal constituent, the cosine curve has a period of 12.42 hr (other constituent periods are indicated in Table II-5-3). Therefore, in Figure II-5-10, the horizontal axis represents either time or phase, both increasing to the right. The value of κ represents the actual phase lag required for the water surface to reach high water (HW) following the passing of the tide-producing force. In the case of the semidiurnal constituents, this force is the crossing of the moon.

Table II-5-3
NOS Tidal Constituents and Arguments

Symbol	Speed, deg/hr	Period, hr	Symbol	Speed, deg/hr	Period, hr
M_2	28.984	12.421	Mm	0.544	661.765
S_2	30.000	12.000	Ssa	0.082	4390.244
N_2	28.439	12.659	Sa	0.041	8780.488
K_1	15.041	23.935	Msf	1.015	354.680
M_4	57.968	6.2103	Mf	1.098	327.869
O_1	13.943	25.819	ρ_1	13.471	26.724
M_6	86.952	4.140	Q_1	13.398	26.870
$(MK)_3$	44.025	8.177	T_2	29.958	12.017
S_4	60.000	6.000	R_2	30.041	11.984
$(MN)_4$	57.423	6.269	$(2Q)_1$	12.854	28.007
ν_2	28.512	12.626	P_1	14.958	24.067
S_6	90.000	4.000	$(2SM)_2$	31.015	11.607
μ_2	27.968	12.872	M_3	43.476	8.280
$(2N)_2$	27.895	12.906	L_2	29.528	12.192
$(OO)_1$	16.139	22.306	$(2MK)_3$	42.927	8.386
λ_2	29.455	12.222	K_2	30.082	11.967
S_1	15.000	24.000	M_8	115.936	3.105
M_1	14.496	24.834	$(MS)_4$	58.984	6.103
J_1	15.585	23.099			

(j) The value κ is approximately constant at every location in the world because it represents the actual lag between the passing of the tide-producing force (i.e., moon) at a specific location and the following high-tide contribution of that force at that same location. It is computed as the sum of the theoretical phase or time lead of the tide-producing force relative to the observer at some fixed time and the measured phase lag ζ from the observer at that fixed time to the following high water. The theoretical location of the tide-producing force is referred to as the equilibrium argument ($V_0 + u$). In Figure II-5-10, the tide-producing force and corresponding equilibrium tide at location *M* are located ($V_0 + u$) degrees ahead of point *T*. Conversely, the equilibrium tide will be located at point *T* if shifted ($V_0 + u$) degrees. The value of ζ represents the phase lag from point *T* to *HW*.

(k) The equilibrium argument ($V_0 + u$) is computed from equations defining the time-varying relationship between the earth, moon, and sun. The value of ζ is computed from observed tidal time series data. As stated, the sum of these two values is approximately constant for any fixed location at any time.

(l) Values of the equilibrium argument for the constituents of Table II-5-3 relative to the passing of the tidal potential force at the Greenwich meridian for each calendar year from 1850 through 2000 are tabulated in Schureman (1924). An example is shown in Table II-5-5 for the years 1990 to 2000. Monthly and daily adjustment tables are also presented. Each of the values is computed according to the respective constituent speeds shown in Table II-5-3. The equilibrium arguments tabulated in Schureman are referenced to the meridian of Greenwich; therefore, the argument ($V_0 + u$) represents the phase difference in degrees between the location of the tidal potential term (moon or sun) and Greenwich relative to some specific time.

Table II-5-4
Node Factors for 1970 through 1999 (Schureman 1924)

Constituent	1970	1971	1972	1973	1974	1975	1976	1977	1978	1979
J_1	1.155	1.132	1.097	1.051	0.995	0.936	0.881	0.842	0.827	0.839
K_1	1.105	1.088	1.063	1.029	0.991	0.951	0.916	0.891	0.882	0.890
K_2	1.289	1.232	1.150	1.055	0.957	0.871	0.804	0.763	0.748	0.760
L_2	0.882	0.668	1.118	1.270	1.014	0.808	0.988	1.179	1.169	0.994
M_1	1.987	2.176	1.503	1.012	1.535	1.777	1.428	0.870	0.874	1.361
M_2[1], N_2, 2N, λ_2, μ_2, ν_2	0.966	0.973	0.983	0.995	1.008	1.020	1.029	1.035	1.038	1.036
M_3	0.950	0.960	0.975	0.993	1.012	1.029	1.044	1.054	1.057	1.054
M_4, MN	0.934	0.948	0.967	0.991	1.016	1.039	1.059	1.072	1.077	1.073
M_6	0.903	0.922	0.951	0.986	1.024	1.060	1.090	1.110	1.118	1.112
M_8	0.873	0.898	0.935	0.981	1.032	1.081	1.122	1.149	1.160	1.151
O_1, Q_1, 2Q, ρ_1	1.170	1.143	1.101	1.047	0.984	0.920	0.863	0.822	0.806	0.819
OO	1.716	1.575	1.380	1.159	0.940	0.750	0.607	0.517	0.485	0.512
MK	1.068	1.059	1.045	1.024	0.998	0.970	0.943	0.923	0.915	0.922
2MK	1.032	1.031	1.028	1.020	1.006	0.989	0.970	0.956	0.950	0.955
Mf	1.417	1.341	1.233	1.102	0.962	0.831	0.723	0.652	0.625	0.647
Mm	0.882	0.906	0.940	0.982	1.025	1.067	1.100	1.123	1.131	1.121
Constituent	**1980**	**1981**	**1982**	**1983**	**1984**	**1985**	**1986**	**1987**	**1988**	**1989**
J_1	0.877	0.930	0.989	1.045	1.093	1.130	1.153	1.164	1.163	1.148
K_1	0.913	0.948	0.987	1.026	1.060	1.086	1.104	1.112	1.111	1.100
K_2	0.799	0.864	0.949	1.045	1.142	1.226	1.285	1.315	1.310	1.270
L_2	0.848	1.001	1.238	1.157	0.745	0.811	1.263	1.244	0.749	0.746
M_1	1.656	1.468	0.974	1.323	2.050	2.032	1.292	1.367	2.142	2.122
M_2[1], N_2, 2N, λ_2, μ_2, ν_2	1.030	1.021	1.009	0.997	0.984	0.974	0.967	0.964	0.964	0.969
M_3	1.045	1.031	1.013	0.994	0.977	0.962	0.951	0.946	0.947	0.954
M_4, MN	1.061	1.042	1.018	0.993	0.969	0.949	0.935	0.928	0.930	0.939
M_6	1.092	1.063	1.027	0.989	0.954	0.924	0.904	0.894	0.896	0.910
M_8	1.125	1.085	1.036	0.986	0.939	0.901	0.874	0.862	0.864	0.881
O_1, Q_1, 2Q, ρ_1	0.858	0.915	0.979	1.041	1.096	1.140	1.168	1.182	1.180	1.161
OO	0.596	0.735	0.921	1.137	1.361	1.560	1.706	1.778	1.766	1.668
MK	0.941	0.967	0.996	1.022	1.043	1.058	1.068	1.072	1.071	1.065
2MK	0.969	0.987	1.005	1.019	1.027	1.031	1.032	1.032	1.032	1.032
Mf	0.715	0.820	0.949	1.088	1.221	1.333	1.412	1.450	1.443	1.392
Mm	1.103	1.070	1.029	0.986	0.944	0.909	0.884	0.872	0.874	0.891
Constituent	**1990**	**1991**	**1992**	**1993**	**1994**	**1995**	**1996**	**1997**	**1998**	**1999**
J_1	1.120	1.080	1.030	0.972	0.914	0.864	0.833	0.829	0.852	0.896
K_1	1.079	1.051	1.015	0.976	0.937	0.905	0.886	0.883	0.897	0.926
K_2	1.203	1.115	1.016	0.922	0.842	0.785	0.754	0.750	0.772	0.821
L_2	1.216	1.248	0.898	0.801	1.077	1.208	1.107	0.921	0.893	1.096
M_1	1.334	1.156	1.778	1.829	1.282	0.800	1.083	1.487	1.560	1.214
M_2[1], N_2, 2N, λ_2, μ_2, ν_2	0.977	0.988	1.000	1.013	1.024	1.032	1.037	1.038	1.034	1.027
M_3	0.966	0.982	1.000	1.019	1.036	1.048	1.056	1.057	1.051	1.040
M_4, MN	0.955	0.976	1.000	1.025	1.048	1.065	1.075	1.076	1.069	1.054
M_6	0.932	0.964	1.000	1.038	1.072	1.099	1.115	1.117	1.105	1.082
M_8	0.911	0.952	1.000	1.051	1.098	1.134	1.156	1.159	1.143	1.111
O_1, Q_1, 2Q, ρ_1	1.128	1.081	1.024	0.960	0.897	0.844	0.812	0.808	0.832	0.879
OO	1.505	1.296	1.072	0.863	0.688	0.565	0.498	0.489	0.538	0.643
MK	1.054	1.038	1.015	0.988	0.959	0.934	0.918	0.916	0.928	0.950
2MK	1.030	1.025	1.015	1.000	0.982	0.964	0.952	0.951	0.959	0.976
Mf	1.303	1.184	1.048	0.910	0.786	0.691	0.636	0.629	0.669	0.752
Mm	0.918	0.956	0.998	1.042	1.081	1.110	1.128	1.130	1.117	1.091

[1] Factor *f* of MS, 28M, and M8f are each equal to factor *f* of M2.

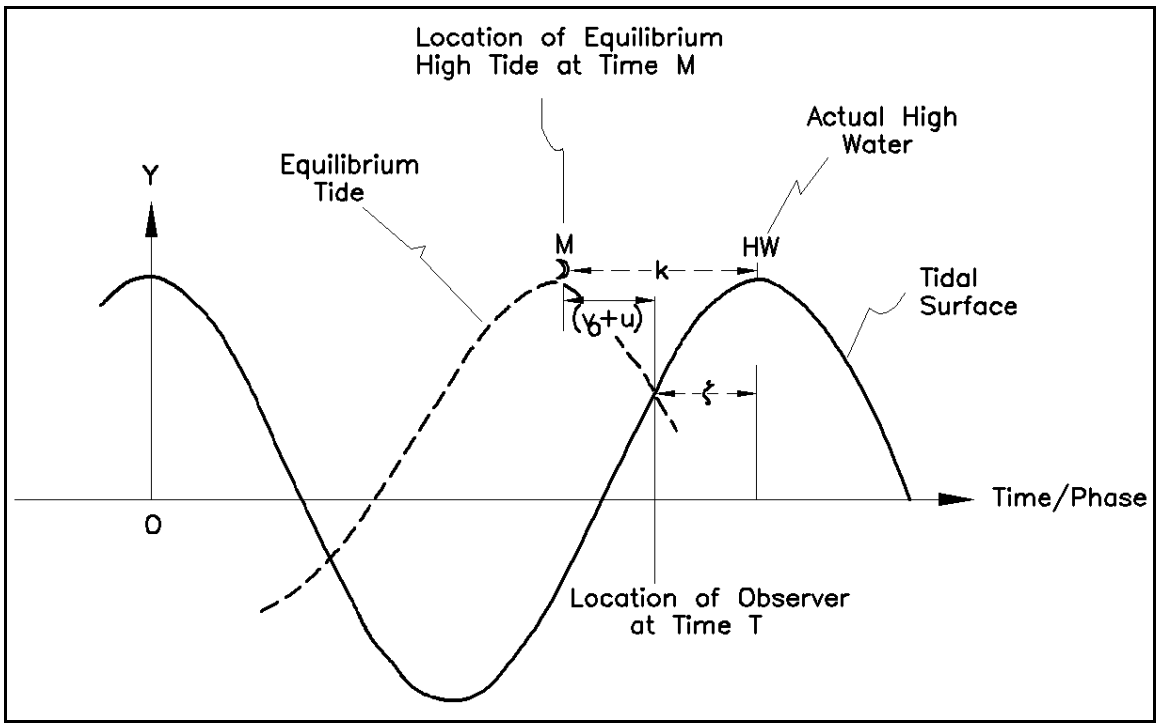

Figure II-5-10. Tidal phase relationships

(m) A tidal simulation computer program is available in ACES (Leenknecht, Szuwalski, and Sherlock 1992) to compute nodal factors and local (or Greenwich) equilibrium argument values for any time period and generate the corresponding water surface time series as a function of input constituent amplitudes. Formulas for computing the equilibrium arguments are found in Shureman (1924), but are too lengthy for this manual.

(3) Harmonic reconstruction.

(a) In order to reconstruct a tidal series for a specific time and location, the various phase arguments of Equation II-5-16 must be defined according to local conditions. Generally, local values of κ_n, H_0, and H_n are available from NOS harmonic analyses. Because the values of the nodal factors f_n are slowly varying, the yearly values determined according to Schureman are sufficiently accurate for the particular time of interest throughout the world. However, local values of $(V_0 + u)_n$ vary with the speed of the constituent and have to be determined for the location and time of interest. This information can be computed from tabulated equilibrium arguments relative to Greenwich such as those presented in Schureman or computed with programs developed for that purpose such as those contained in ACES.

(b) Values of the local equilibrium arguments, i.e., local $(V_0 + u)_n$, represent the instantaneous value of each of the equilibrium tide-producing force constituents (in degrees) with respect to some specific point on the earth; for example, the time-varying location of the moon and sun with respect to some location on the earth. Referring to Figure II-5-11, the horizontal axis represents distance with the point *G* representing Greenwich, England, and *O* representing an observer located at some point west of Greenwich. The location of the moon with respect to Greenwich at longitude 0° at Greenwich time t_0 is indicated by the Greenwich equilibrium argument presented in Shureman, denoted as Greenwich $(V_0 + u)$, for time Greenwich t_0.

Table II-5-5
Equilibrium Argument for Beginning of Years 2001 through 2010

Constituent		2001	2002	2003	2004	2005	2006	2007	2008	2009	2010
J_1		227.9	316.9	47.0	138.0	243.7	335.7	67.8	159.8	265.5	356.5
K_1		1.9	1.8	2.6	4.1	7.1	9.3	11.7	13.9	1 6.8	18.3
K_2		184.0	183.3	184.6	187.6	193.7	198.5	203.5	208.2	214.3	217.1
L_2		269.1	105.4	267.4	94.8	295.2	141.6	297.3	121.4	321.6	165.8
M_1		145.4	52.1	303.7	204.7	139.6	58.2	311.4	210.3	141.0	64.7
M_2		210.8	311.4	52.4	153.5	230.4	331.9	73.4	174.8	251.7	352.9
M_3		316.1	287.1	258.5	230.2	165.7	137.8	110.0	82.2	17.6	349.3
M_4		61.5	262.9	104.7	307.0	100.9	303.8	146.7	349.6	143.5	345.7
M_6		272.3	214.3	157.1	100.5	331.3	275.6	220.1	164.4	35.2	338.6
M_8		123.1	165.7	209.4	254.0	201.7	247.5	293.4	339.2	286.9	331.4
N_2		340.5	353.5	4.7	17.1	352.3	5.0	17.7	30.4	5.6	18.0
2N		110.3	33.5	317.0	240.7	114.1	38.1	322.1	246.1	119.5	43.1
O_1		213.0	313.5	53.0	151.8	224.9	323.0	61.2	159.3	232.4	331.3
OO		322.4	222.3	125.6	31.5	326.3	234.6	143.3	51.6	346.3	251.9
P_1		349.3	349.5	349.8	350.0	349.3	349.5	349.7	350.0	349.2	349.5
Q_1		342.8	354.6	5.3	15.5	346.7	356.1	5.5	15.0	346.3	356.4
2Q		112.6	35.6	317.7	239.0	108.5	29.2	309.9	230.6	100.1	21.5
R_2		177.8	177.5	177.3	177.0	177.7	177.5	177.2	177.0	177.7	177.4
S_1		180.0	180.0	180.0	180.0	180.0	180.0	180.0	180.0	180.0	180.0
$S_{2,4,6}$	0.0	0.0	0.0	0.0	0.0	0.0	0.0	0.0	0.0	0.0	
T_2		2.2	2.5	2.7	3.0	2.3	2.5	2.8	3.0	2.3	2.6
λ_2	307.7	218.9	130.3	42.0	300.8	212.8	124.8	36.7	295.5	207.1	
μ_2		63.6	265.0	106.7	308.6	101.9	304.1	146.3	348.5	141.8	343.7
ν_2		293.8	224.0	154.4	85.0	340.1	271.0	202.0	132.9	28.0	318.6
ρ_1		296.1	226.1	155.0	83.3	334.5	262.2	189.7	117.4	8.6	297.0
MK		212.6	313.2	54.9	157.6	237.5	341.2	85.0	188.7	268.6	11.1
2MK	59.6	261.1	102.1	302.9	93.8	294.4	135.1	335.7	126.6	327.4	
MN		191.3	303.9	57.0	170.6	222.7	336.9	91.1	205.2	257.3	10.9
MS		210.8	311.4	52.4	153.5	230.4	331.9	73.4	174.8	251.7	352.9
2SM	149.2	48.6	307.6	206.5	129.6	28.1	286.6	185.2	108.3	7.1	
Mf		324.7	224.4	126.3	29.8	320.7	225.8	131.0	36.1	326.9	230.3
MSf		147.2	46.4	305.7	204.9	128.5	27.8	287.0	186.3	109.9	9.2
Mm		230.2	318.9	47.7	136.4	238.2	326.9	55.6	144.3	246.1	334.9
Sa		280.7	280.5	280.2	280.0	280.8	280.5	280.3	280.0	280.8	280.5
Ssa		201.4	201.0	200.5	200.0	201.5	201.0	200.5	200.1	201.6	201.1

Methodology based on Schureman 1924. Values computed May 2001.

(c) The location of the moon at Greenwich time t_0 is different for an observer at some point O located at longitude L^o than it is for the observer located at Greenwich. For each constituent, the observer is located pL deg from Greenwich; therefore, the local equilibrium argument must be adjusted by $-pL$ to account for the difference in location between the point of interest (i.e., point O) and Greenwich.

(d) The $-pL$ adjustment provides the necessary equilibrium argument correction for differences in location between some point and Greenwich, i.e., a local equilibrium argument corresponding to an observer at location O. However, the value of the equilibrium argument Greenwich ($V_0 + u$) was specified with respect to Greenwich t_0. Therefore, Greenwich time must be written with respect to local time. Because local time for the observer located west of Greenwich is earlier than local time in Greenwich (t_0), the following adjustment is made to convert local time to Greenwich time.

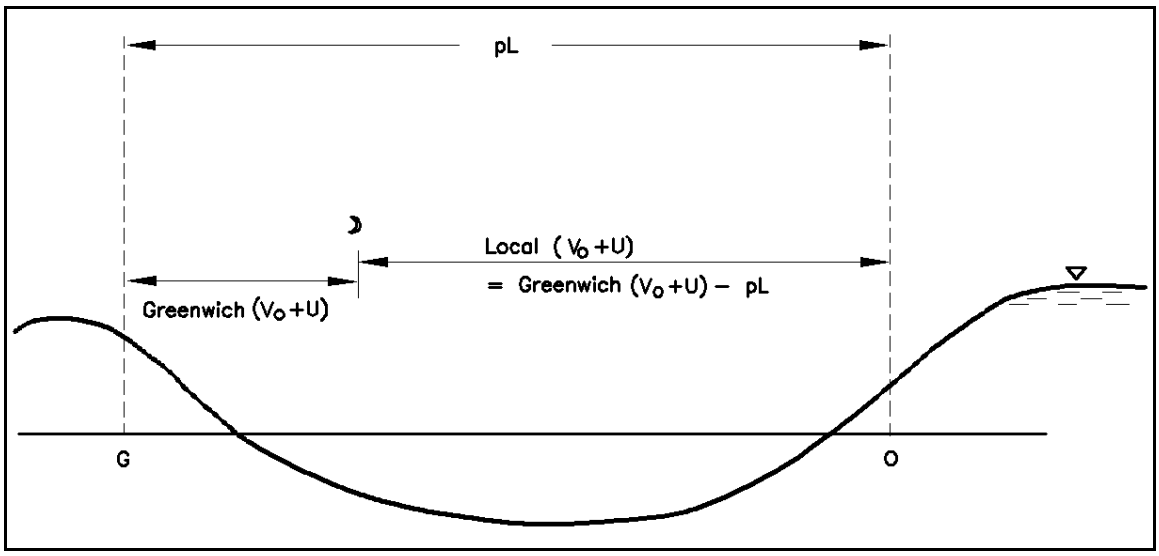

Figure II-5-11. Phase angle argument relationship

$$\text{Greenwich}\,(t_0) = \text{local}\,(t_0) + \frac{S}{15} \tag{II-5-17}$$

where S is the local time meridian (shown on NOS analyses) and the number 15 indicates a time change of 1 hr per 15 deg longitude.

(e) The speed of the time argument ($a_n t$ in Equation II-5-16) in degrees with respect to time is equal to the speed of the constituent a_n multiplied by Equation II-5-17. Therefore, the final relationship between local and Greenwich phase arguments that account for both differences in location ($-pL$) and local time ($aS/15$) can be written as:

$$\text{local}\,(V_0 + u) = \text{Greenwich}\,(V_0 + u) - pL \tag{II-5-18}$$

Therefore, a tide at any arbitrary location is computed as

$$H(t)_{local} = H_0 + \sum_{n=1}^{N} f_n H_n \cos\left[a_n t + \text{Greenwich}\, V_0 + u) - pL + \frac{a_n S}{15} - \kappa_n\right] \tag{II-5-19}$$

(f) A reconstructed tidal time series of a published NOS harmonic analysis is presented for Sandy Hook, NJ. The NOS analysis is shown in Figure II-5-12. As can be seen by the reported amplitudes, the M_2, S_2, N_2, K_1, Sa, O_1, ν_2, and K_2 constituents contain the majority of the tidal energy. These constituents are used to generate a 15-day tidal signal beginning on 1 January 1984 at 0000 hr Eastern Standard Time. Computed values are compared to the high and low tide predictions published in the Tide Tables for 1984 (NOAA 1984) shown in Figure II-5-13. Because all 37 constituents are not used in the reconstruction, the match is not perfect; however, it demonstrates the degree of accuracy that can be achieved by using only major constituents.

FORM C&GS-444
(11-67)

U.S. DEPARTMENT OF COMMERCE
ESSA- COAST AND GEODETIC SURVEY

TIDES ~~CURRENTS~~ STANDARD HARMONIC CONSTANTS FOR PREDICTION

STATION Sandy Hook, N. J.

Lat. 40° 28.1' N.
Long. 74° 0.7' W.
Long. 74° .01 W.

COMPONENT	H AMPLITUDE ft.	H AMPLITUDE m	g EPOCH °	A g'−g °	B 1.04×H ft.	B 1.04×H m	C 360°−g' °	D −g' °
M_2	2.151	219.1	+ 3.1	2.237	+			−222.2
S_2	0.448	246.0	− 2.0	0.466	+			−244.0
N_2	0.473	204.1	+ 5.8	0.492	+			−209.9
K_1	0.319	102.2	− 1.2	0.332	+			−101.0
M_4	0.036	347.4	+ 6.2	0.037	+			−353.6
O_1	0.172	98.4	+ 4.3	0.179	+			−102.7
M_6	0.048	356.4	+ 9.3	0.050	+			− 5.7
$(MK)_3$					+			−
S_4	0.032	61.4	− 4.0	0.033	+			− 57.4
$(MN)_4$					+			−
ν_2	0.109	191.1	+ 5.5	0.113	+			−196.6
S_6					+			−
μ_2	0.073	243.7	+ 8.2	0.076	+			−251.9
$(2N)_2$	0.063	189.1	+ 8.5	0.066	+			−197.6
$(OO)_1$					+			−
λ_2	0.015	231.6	+ 0.7	0.016	+			−232.3
S_1	0.037	56.2	− 1.0	0.038	+			− 55.2
M_1	0.012	100.3	+ 1.5	0.012	+			−101.8
J_1	0.014	104.1	− 3.9	0.015	+			−100.2
Mm					+			−
Ssa	0.067	38.3	− 0.4	0.067	+			− 37.9
Sa	0.254	128.7	− 0.2	0.254	+			−128.5
MSf					+			−
Mf					+			−
ρ_1					+			−
Q_1	0.037	104.5	+ 7.0	0.038	+			−111.5
T_2	0.026	246.0	− 1.8	0.027	+			−244.2
R_2					+			−
$(2Q)_1$					+			−
P_1	0.096	105.7	− 0.8	0.100	+			−104.9
$(2SM)_2$					+			−
M_3	0.032	198.6	+ 4.6	0.033	+			−203.2
L_2	0.089	205.5	+ 0.4	0.093	+			−205.9
$(2MK)_3$					+			−
K_2	0.121	251.9	− 2.4	0.126	+			−248.5
M_8					+			−
$(MS)_4$					+			−

REMARKS

Time meridian 75° W. = +.5 h.
Extreme range ft. / kn.
Dial
Marigram gear
Marigram scale
z_o 2.56 ~~2.37~~ 2.36 ~~8.89~~ ft.
Permanent current kn.
The DATUM is ~~a plane~~ MLLW ~~ft.~~
~~below~~ mean {~~low water springs~~ lowest low water.

First used for 1947 Tables (modified 1966)

Amplitudes of short period constituents increased 4%

New 1960-78 z_o first used in 1985 TT (GMT)

z_o = 2.56
1989 TT *
DATUM = MLLW

Source of constants 3 - 369 day series (1933, 1937, 1940)
Sa & Ssa from 10 years monthly MSL (1933-1942)

Compiled by RAC 2-5-69 (Date) Verified by (Date)

Figure II-5-12. NOS harmonic analysis for Sandy Hook, NJ

SANDY HOOK, N.J., 1984

Times and Heights of High and Low Waters

JANUARY

Day	Time	Height		Day	Time	Height	
	h m	ft	m		h m	ft	m
1 Su	0619	5.1	1.6	16 M	0542	5.0	1.5
	1242	-0.5	-0.2		1213	-0.5	-0.2
	1840	3.9	1.2		1813	4.0	1.2
2 M	0042	-0.4	-0.1	17 Tu	0009	-0.6	-0.2
	0701	5.1	1.6		0632	5.4	1.6
	1328	-0.5	-0.2		1306	-0.8	-0.2
	1924	3.9	1.2		1903	4.3	1.3
3 Tu	0128	-0.3	-0.1	18 W	0105	-0.8	-0.2
	0741	5.0	1.5		0721	5.6	1.7
	1411	-0.5	-0.2		1356	-1.1	-0.3
	2001	3.8	1.2		1951	4.5	1.4
4 W	0213	-0.2	-0.1	19 Th	0158	-0.9	-0.3
	0819	4.9	1.5		0808	5.6	1.7
	1452	-0.5	-0.2		1446	-1.3	-0.4
	2042	3.7	1.1		2043	4.6	1.4
5 Th	0254	-0.1	0.0	20 F	0250	-1.0	-0.3
	0859	4.7	1.4		0859	5.6	1.7
	1531	-0.4	-0.1		1533	-1.3	-0.4
	2124	3.7	1.1		2134	4.7	1.4
6 F	0331	0.1	0.0	21 Sa	0341	-1.0	-0.3
	0939	4.5	1.4		0951	5.4	1.6
	1607	-0.3	-0.1		1619	-1.2	-0.4
	2205	3.6	1.1		2229	4.7	1.4
7 Sa	0408	0.2	0.1	22 Su	0432	-0.8	-0.2
	1019	4.3	1.3		1045	5.1	1.6
	1645	-0.1	0.0		1709	-1.0	-0.3
	2248	3.5	1.1		2322	4.7	1.4
8 Su	0445	0.4	0.1	23 M	0529	-0.6	-0.2
	1100	4.1	1.2		1139	4.7	1.4
	1721	0.0	0.0		1802	-0.8	-0.2
	2330	3.5	1.1				
9 M	0530	0.6	0.2	24 Tu	0018	4.6	1.4
	1141	3.9	1.2		0630	-0.3	-0.1
	1802	0.2	0.1		1234	4.3	1.3
					1856	-0.5	-0.2
10 Tu	0012	3.6	1.1	25 W	0114	4.5	1.4
	0620	0.7	0.2		0735	-0.1	0.0
	1227	3.7	1.1		1330	4.0	1.2
	1849	0.2	0.1		1959	-0.3	-0.1
11 W	0100	3.6	1.1	26 Th	0212	4.5	1.4
	0726	0.7	0.2		0840	0.0	0.0
	1316	3.5	1.1		1432	3.7	1.1
	1943	0.2	0.1		2057	-0.2	-0.1
12 Th	0150	3.8	1.2	27 F	0311	4.4	1.3
	0831	0.6	0.2		0942	0.0	0.0
	1412	3.4	1.0		1535	3.5	1.1
	2039	0.2	0.1		2153	-0.1	0.0
13 F	0248	4.0	1.2	28 Sa	0414	4.5	1.4
	0930	0.4	0.1		1038	-0.1	0.0
	1514	3.4	1.0		1639	3.5	1.1
	2130	0.0	0.0		2245	-0.1	0.0
14 Sa	0350	4.3	1.3	29 Su	0510	4.6	1.4
	1026	0.1	0.0		1131	-0.2	-0.1
	1621	3.5	1.1		1736	3.6	1.1
	2222	-0.2	-0.1		2336	-0.1	0.0
15 Su	0449	4.6	1.4	30 M	0558	4.7	1.4
	1120	-0.2	-0.1		1221	-0.3	-0.1
	1720	3.7	1.1		1822	3.7	1.1
	2316	-0.4	-0.1				
				31 Tu	0027	-0.2	-0.1
					0642	4.8	1.5
					1307	-0.4	-0.1
					1904	3.8	1.2

FEBRUARY

Day	Time	Height		Day	Time	Height	
	h m	ft	m		h m	ft	m
1 W	0112	-0.2	-0.1	16 Th	0050	-0.9	-0.3
	0722	4.8	1.5		0705	5.6	1.7
	1349	-0.4	-0.1		1335	-1.2	-0.4
	1944	3.9	1.2		1935	4.9	1.5
2 Th	0154	-0.2	-0.1	17 F	0145	-1.1	-0.3
	0759	4.8	1.5		0754	5.7	1.7
	1429	-0.5	-0.2		1424	-1.4	-0.4
	2022	3.9	1.2		2024	5.1	1.6
3 F	0235	-0.2	-0.1	18 Sa	0235	-1.2	-0.4
	0838	4.7	1.4		0843	5.6	1.7
	1504	-0.4	-0.1		1510	-1.4	-0.4
	2058	3.9	1.2		2113	5.2	1.6
4 Sa	0312	-0.1	0.0	19 Su	0326	-1.2	-0.4
	0914	4.5	1.4		0932	5.4	1.6
	1539	-0.4	-0.1		1555	-1.3	-0.4
	2135	3.9	1.2		2205	5.2	1.6
5 Su	0347	0.0	0.0	20 M	0416	-1.1	-0.3
	0949	4.3	1.3		1024	5.1	1.6
	1611	-0.2	-0.1		1642	-1.0	-0.3
	2211	3.9	1.2		2256	5.1	1.6
6 M	0419	0.1	0.0	21 Tu	0508	-0.7	-0.2
	1027	4.1	1.2		1116	4.7	1.4
	1642	-0.1	0.0		1730	-0.7	-0.2
	2250	3.9	1.2		2349	4.9	1.5
7 Tu	0456	0.3	0.1	22 W	0604	-0.4	-0.1
	1104	3.9	1.2		1209	4.2	1.3
	1713	0.1	0.0		1824	-0.3	-0.1
	2327	3.9	1.2				
8 W	0535	0.4	0.1	23 Th	0041	4.7	1.4
	1146	3.7	1.1		0705	0.0	0.0
	1750	0.2	0.1		1303	3.8	1.2
					1923	0.0	0.0
9 Th	0010	3.9	1.2	24 F	0138	4.5	1.4
	0630	0.6	0.2		0810	0.2	0.1
	1232	3.5	1.1		1401	3.5	1.1
	1839	0.3	0.1		2027	0.2	0.1
10 F	0100	4.0	1.2	25 Sa	0240	4.3	1.3
	0742	0.6	0.2		0915	0.2	0.1
	1327	3.4	1.0		1509	3.3	1.0
	1941	0.3	0.1		2127	0.3	0.1
11 Sa	0200	4.1	1.2	26 Su	0343	4.2	1.3
	0852	0.4	0.1		1014	0.2	0.1
	1432	3.3	1.0		1617	3.3	1.0
	2051	0.2	0.1		2223	0.3	0.1
12 Su	0306	4.3	1.3	27 M	0446	4.3	1.3
	0956	0.2	0.1		1106	0.1	0.0
	1548	3.4	1.0		1715	3.5	1.1
	2153	0.0	0.0		2315	0.2	0.1
13 M	0417	4.6	1.4	28 Tu	0536	4.5	1.4
	1053	-0.2	-0.1		1156	0.0	0.0
	1657	3.7	1.1		1805	3.8	1.2
	2252	-0.3	-0.1				
14 Tu	0520	5.0	1.5	29 W	0005	0.1	0.0
	1150	-0.5	-0.2		0621	4.6	1.4
	1753	4.1	1.2		1239	-0.2	-0.1
	2352	-0.6	-0.2		1845	4.0	1.2
15 W	0613	5.3	1.6				
	1245	-0.9	-0.3				
	1845	4.5	1.4				

MARCH

Day	Time	Height		Day	Time	Height	
	h m	ft	m		h m	ft	m
1 Th	0052	0.0	0.0	16 F	0035	-0.9	-0.3
	0701	4.7	1.4		0646	5.6	1.7
	1322	-0.3	-0.1		1310	-1.1	-0.3
	1922	4.2	1.3		1915	5.4	1.6
2 F	0134	-0.1	0.0	17 Sa	0129	-1.1	-0.3
	0738	4.7	1.4		0735	5.7	1.7
	1400	-0.4	-0.1		1359	-1.3	-0.4
	1957	4.3	1.3		2002	5.7	1.7
3 Sa	0214	-0.2	-0.1	18 Su	0220	-1.3	-0.4
	0812	4.7	1.4		0822	5.6	1.7
	1436	-0.4	-0.1		1445	-1.3	-0.4
	2031	4.3	1.3		2049	5.7	1.7
4 Su	0250	-0.2	-0.1	19 M	0309	-1.2	-0.4
	0848	4.6	1.4		0910	5.3	1.6
	1507	-0.3	-0.1		1529	-1.1	-0.3
	2104	4.3	1.3		2138	5.6	1.7
5 M	0325	-0.1	0.0	20 Tu	0357	-1.0	-0.3
	0923	4.4	1.3		0958	5.0	1.5
	1539	-0.2	-0.1		1612	-0.8	-0.2
	2136	4.3	1.3		2229	5.4	1.6
6 Tu	0355	0.0	0.0	21 W	0445	-0.7	-0.2
	0955	4.2	1.3		1049	4.5	1.4
	1605	0.0	0.0		1658	-0.4	-0.1
	2211	4.3	1.3		2317	5.1	1.6
7 W	0429	0.1	0.0	22 Th	0538	-0.3	-0.1
	1032	4.0	1.2		1143	4.1	1.2
	1632	0.1	0.0		1749	0.1	0.0
	2248	4.3	1.3				
8 Th	0504	0.3	0.1	23 F	0010	4.8	1.5
	1112	3.8	1.2		0636	0.1	0.0
	1704	0.2	0.1		1236	3.8	1.2
	2330	4.3	1.3		1847	0.4	0.1
9 F	0554	0.5	0.2	24 Sa	0105	4.5	1.4
	1159	3.6	1.1		0740	0.4	0.1
	1749	0.4	0.1		1336	3.5	1.1
					1956	0.7	0.2
10 Sa	0023	4.3	1.3	25 Su	0204	4.2	1.3
	0703	0.6	0.2		0845	0.5	0.2
	1257	3.4	1.0		1440	3.4	1.0
	1857	0.5	0.2		2059	0.8	0.2
11 Su	0125	4.3	1.3	26 M	0308	4.1	1.2
	0821	0.5	0.2		0942	0.4	0.1
	1407	3.4	1.0		1548	3.4	1.0
	2021	0.5	0.2		2158	0.7	0.2
12 M	0235	4.4	1.3	27 Tu	0409	4.1	1.2
	0929	0.2	0.1		1035	0.3	0.1
	1524	3.6	1.1		1646	3.7	1.1
	2135	0.2	0.1		2251	0.5	0.2
13 Tu	0350	4.6	1.4	28 W	0507	4.3	1.3
	1031	-0.1	0.0		1120	0.1	0.0
	1636	4.0	1.2		1736	4.0	1.2
	2238	-0.1	0.0		2343	0.3	0.1
14 W	0459	5.0	1.5	29 Th	0552	4.5	1.4
	1127	-0.5	-0.2		1204	0.0	0.0
	1736	4.5	1.4		1816	4.3	1.3
	2336	-0.5	-0.2				
15 Th	0555	5.3	1.6	30 F	0026	0.1	0.0
	1219	-0.8	-0.2		0632	4.6	1.4
	1827	5.0	1.5		1246	-0.1	0.0
					1853	4.5	1.4
				31 Sa	0109	0.0	0.0
					0712	4.7	1.4
					1325	-0.2	-0.1
					1927	4.7	1.4

Time meridian 75° W. 0000 is midnight. 1200 is noon.
Heights are referred to mean low water which is the chart datum of soundings.

Figure II-5-13. Tide tables for Sandy Hook, NJ (NOAA 1984)

(g) Reconstruction of the tide involves determining the equilibrium arguments, node factors, longitude and time adjustment for each constituent, and using the published values for κ, H_n, and H_0 in the NOS harmonic analysis. Table II-5-6 summarizes all necessary quantities.

Table II-5-6
Harmonic Arguments for Sandy Hook NJ (1 January 1984 at 0000 hr)

Symbol	$G(V_0+u)$	pL	aS/15	κ	f	H
M_2	60.0	148.0	144.92	219.1	0.99	2.151
S_2	0.0	148.0	150.00	246.0	1.00	0.448
N_2	323.4	148.0	142.20	204.1	0.99	0.473
K_1	2.4	74.0	75.20	102.2	1.04	0.319
Sa	279.8	0.0	0.20	128.7	1.00	0.254
O_1	60.8	74.0	69.71	98.4	1.07	0.172
ν_2	148.0	148.0	142.56	191.1	0.99	0.109
K_2	184.2	148.0	150.41	251.9	1.09	0.121

(h) The NOS harmonic analysis indicates that a multiplier of 1.04 should be used for all short-period constituents and that the value of H_0 is 2.36 MSL. Also indicated on the analysis is the time meridian of 75° west longitude for use in computing the time zone compensation term $aS/15$. The 15-day tidal envelope is shown in Figure II-5-14. The open circles shown in the figure represent high- and low-water level predictions extracted from the tide tables in Figure II-5-13. As stated, the comparison is not exact because only eight constituents were used in the reconstruction. The match is, however, adequate for the majority of design applications.

(i) The phase lag κ in Equation II-5-19 is called the local epoch in order to distinguish it from other forms of epochs (see Schureman (1924)). Some harmonic analyses use a modified form of the epoch that automatically accounts for the longitude and time meridian corrections. This modification is designated as κ' and is defined as shown below

$$\kappa' = \kappa + pL - \frac{aS}{15} \tag{II-5-20}$$

(j) This modified form is usually included on NOS harmonic analyses as indicated on Figure II-5-12. Use of this form of epoch in the reconstruction of tides is as shown below

$$H(t)_{local} = H_0 + \sum_{n=1}^{N} f_n H_n \cos\left[a_n t + \text{Greenwich}\,(V_0 + u) - \kappa'_n\right] \tag{II-5-21}$$

(4) Tidal envelope classification.

(a) Semidiurnal, diurnal, and mixed tidal classifications were described in Part II-5-3a. Equation II-5-22 is a more quantitative delineation of tide types.

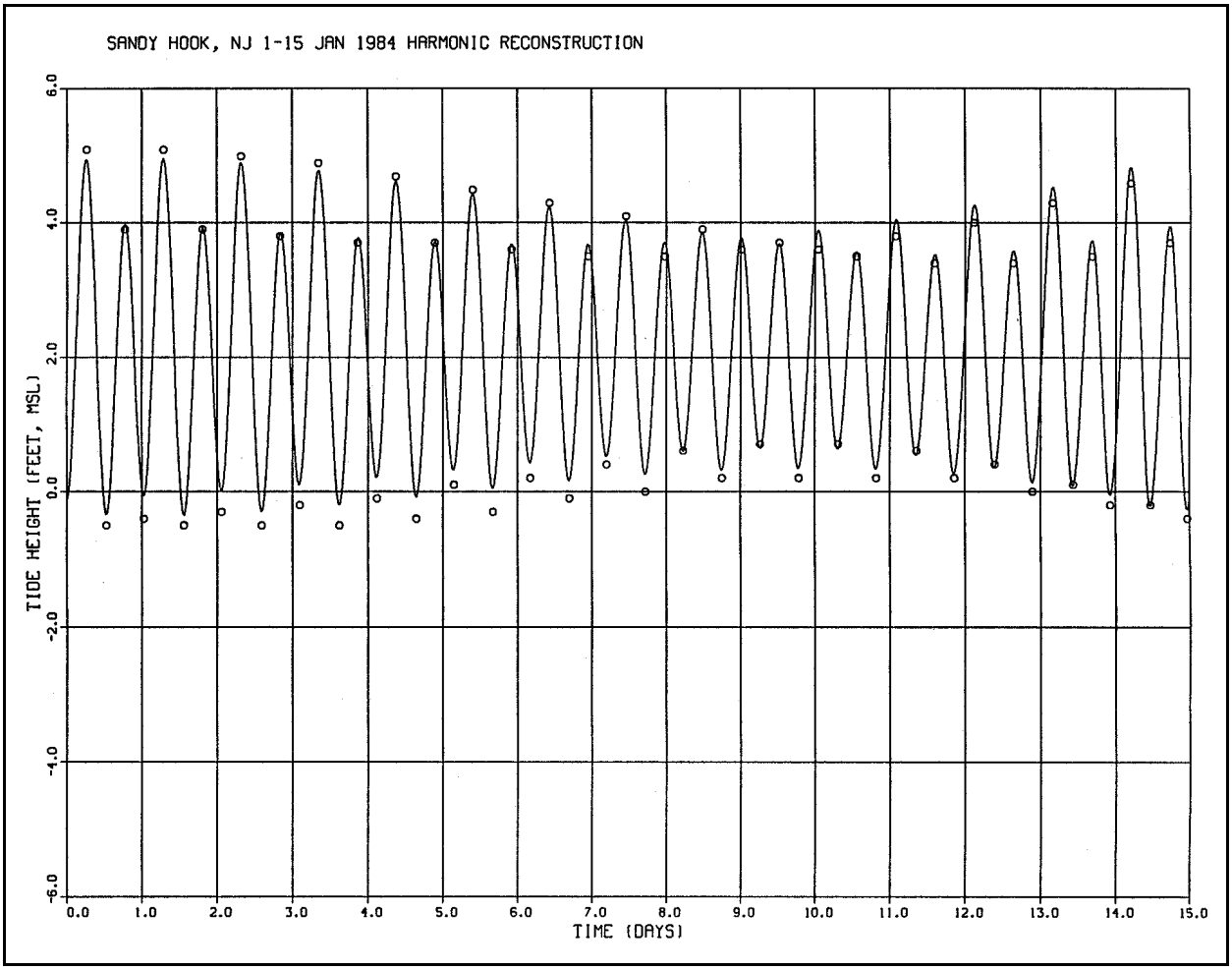

Figure II-5-14. Reconstructed tidal envelope for Sandy Hook, NJ

$$R = \frac{A(K_1) + A(O_1)}{A(M_2) + A(s_2)} \tag{II-5-22}$$

where $A(K_1)$, $A(O_1)$, $A(M_2)$, and $A(S_2)$ represent the amplitudes of the corresponding constituents. A general classification of tides can be separated according to the following criteria:

$R \leq 0.25$	Semidiurnal
$0.25 < R \leq 1.50$	Mixed
$1.50 < R$	Diurnal

(b) The tidal classification for the Sandy Hook, NJ, example can be computed as shown below:

$$R = \frac{A(K_1) + A(O_1)}{A(M_2) + A(s_2)} = \frac{0.319 + 0.172}{2.151 + 0.448} = 0.189 \tag{II-5-23}$$

(c) According to the classification criteria, the tides at Sandy Hook are semidiurnal. In fact, most tides along the northern east coast of the United States are semidiurnal. Tides in the lower east coast and Gulf of Mexico begin to change from semidiurnal, to mixed, to diurnal as shown in Figure II-5-15.

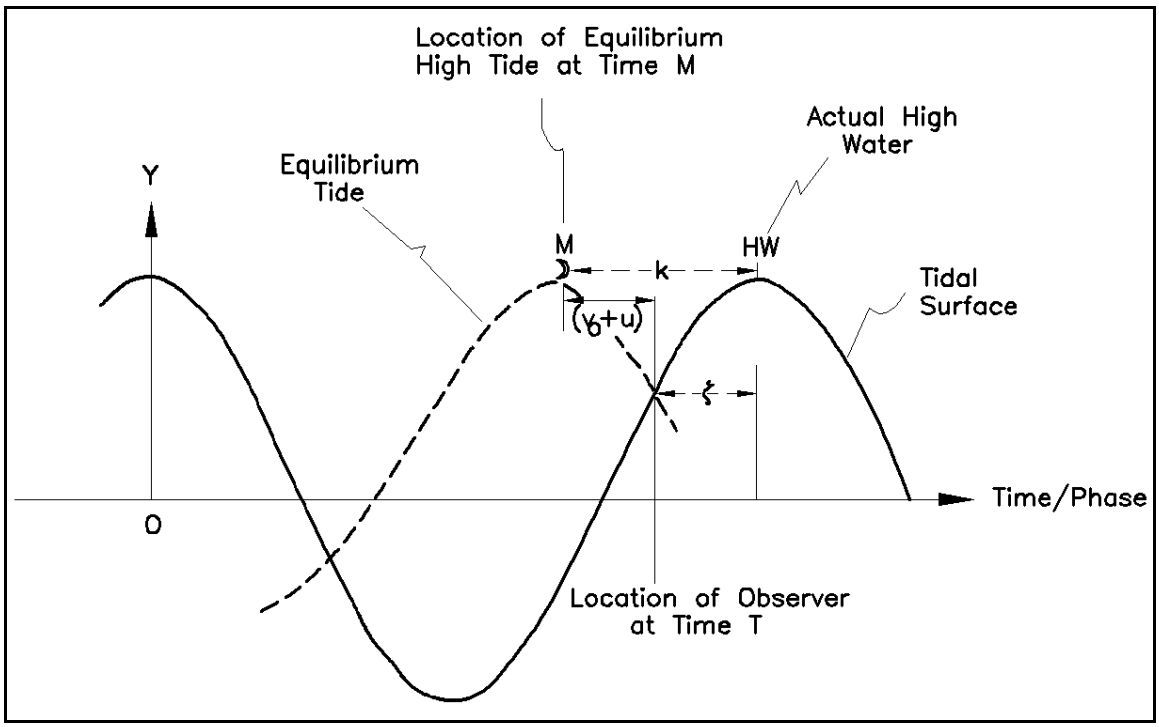

Figure II-5-15. Areal extent of tidal types (Harris 1981)

c. Glossary of tide elevation terms.

(1) The differences in tidal envelopes have given rise to certain terminologies regarding the high and low crests of the tide. The following list of terms, reprinted from the "Glossary of Terms" of the *Shore Protection Manual* (1984), describes specific aspects of typical tidal records. Each term is referenced to Figure II-5-16.

(2) DATUM. A base elevation from which vertical heights or depths are referenced. The reference elevation is locally defined; therefore, a list of commonly used datums is presented in Part II-5-4.

(3) DIURNAL TIDE. A tide with one high water and one low water in a tidal day.

(4) EBB CURRENT. The tidal current away from shore or down a tidal stream; usually associated with the decrease in height of a tide, associated with a falling tide.

(5) EBB TIDE. The period of tide between high water and the succeeding low water: a falling tide.

(6) FLOOD CURRENT. The tidal current toward shore or up a tidal stream, usually associated with the increase in height of the tide associated with a rising tide.

(7) FLOOD TIDE. The period of tide between low water and the succeeding high water; a rising tide.

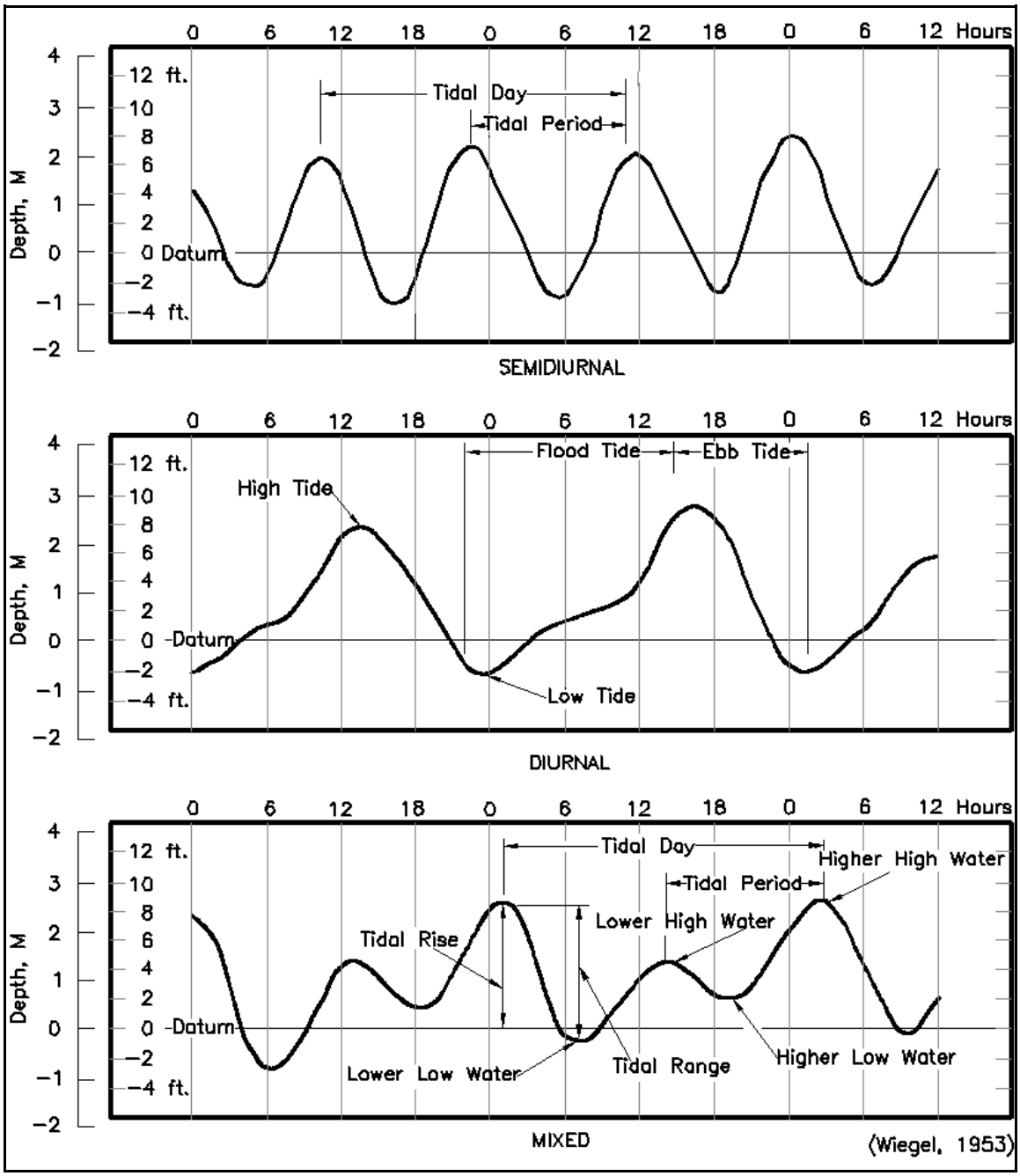

Figure II-5-16. Types of tides (*Shore Protection Manual* 1984)

(8) HIGHER HIGH WATER (HHW). The higher of the two high waters of any tidal day. The single high water occurring daily during periods when the tide is diurnal is considered to be a higher high water.

(9) HIGHER LOW WATER (HLW). The higher of two low waters of any tidal day.

(10) HIGH TIDE, HIGH WATER (HW). The maximum elevation reached by each rising tide.

(11) LOW TIDE, LOW WATER (LW). The minimum elevation reached by each falling tide.

(12) LOWER HIGH WATER (LHW). The lower of the two high waters of any tidal day.

(13) LOWER LOW WATER (LLW). The lower of the two low waters of any tidal day. The single low water occurring daily during periods when the tide is diurnal is considered to be a lower low water.

(14) MIXED TIDE. A tide in which the presence of a diurnal wave is conspicuous due to a large inequality in either the high or low water heights, with two high waters and two low waters usually occurring each tidal day. In strictness, all tides are mixed, but the name is usually applied without definite limits to the tide intermediate to those predominantly semidiurnal and those diurnal.

(15) SEMIDIURNAL TIDE. A tide with two high and two low waters in a tidal day with comparatively little diurnal inequality.

(16) TIDAL DAY. The time of the rotation of the earth with respect to the moon, or the interval between two successive upper transits of the moon over the meridian of a place, approximately 24.84 solar hours (24 hr and 50 min) or 1.035 times per solar day. Also called a lunar day.

(17) TIDAL PERIOD. The interval of time between two consecutive, like phases of the tide.

(18) TIDAL RANGE. The difference in height between consecutive high and low (or higher high and lower low) waters.

(19) TIDAL RISE. The height of the tide as referenced to the datum of a chart.

II-5-4. Water Surface Elevation Datums

a. Introduction. Water level and its change with respect to time have to be measured relative to some specified elevation or datum in order to have a physical significance. In the fields of coastal engineering and oceanography this datum represents a critical design parameter because reported water levels provide an indication of minimum navigational depths or maximum surface elevations at which protective levees or berms are overtopped. It is therefore necessary that coastal datums represent some reference point which is universally understood and meaningful, both onshore and offshore. Ideally, two criteria should be expected of a datum: 1) that it provides local depth of water information, and 2) that it is fixed regardless of location such that elevations at different locations can be compared. These two criteria are not necessarily compatible. The following list of datums represents those commonly in use in the United States.

b. Tidal-observation-based datums.

(1) Tidal-observation-based datums are computed from measured time series of tidal elevations. As such, they vary with geographical location and exposure. Geographic variability of tide records can be seen in Figures II-5-8 and II-5-9. Although datums based on tidal series do indicate site-specific conditions, they

may not be comparable with similar measurements at other geographic locations because of the difficulty of assigning a comparable gauge zero. The most widely accepted of the datums computed from time series are described below.

(2) Mean sea level (MSL) was widely adopted as a primary datum on the assumption that it could be accurately computed from tidal elevation records measured at any well-exposed tide gauge. MSL determinations are based on the arithmetic average of hourly water surface elevations observed over a long period of time. The ideal length of record is approximately 19 years, a period that accounts for the 18- to 19-year long-term cycle in tides and is sufficient to remove most meteorological effects. In order to fix the datum in time for a specific location, a common 19-year period is selected for computing MSL. The specific 19-year cycle was adopted by the National Ocean Survey as the official time segment for use in computing mean values for tidal datums. The 19-year period, called the National Tidal Datum Epoch, is updated approximately every 25 years.

(3) When estimates of MSL are required, but less than 19 years of data are available, computations should be based on an integral number of tidal cycles, for example, an integral number of years or 29-day spring/neap cycles. For gauges where hourly data are not available, or their use is impractical, MSL can be approximated as the tidal datum midway between MHW and MLW. This datum, referred to as Mean Tide Level (MTL), may differ from MSL depending on the local relative importance of the diurnal components of the tide.

(4) Alternate tidal datums are based on low water tidal elevations. These datums provide minimum depth information for navigational needs. Two commonly used low-water datums in the United States are the Mean Low Water (MLW) for the Atlantic Coast and the Mean Lower Low Water (MLLW) for the Pacific coast. The MLLW datum is currently being adopted to several locations along the Atlantic coast. Both datums are defined as the average tidal height at low water or lower low water during the 19-year period. Additional datums, applicable to specific locations or purposes, include Mean High Water (MHW) and Mean Higher High Water (MHHW). These are derived in a manner similar to MLW and MLLW. For areas of primarily semidiurnal tides, the difference between MHW and MLW is called the mean tidal range. The difference between MHHW and MLLW gives a corresponding diurnal range or the great diurnal range of the tide. Both numbers provide an estimate of the magnitude of the local tidal range. An example of the variability of the above datums is given by Harris (1981) and reproduced in Table II-5-7. Reference tide stations used in the preparation of Table II-5-7 are shown in Figure II-5-17.

c. *1929 NGVD datum.*

(1) One difficulty with using any of the observation-based datums described above is that they vary considerably with location, as evidenced in Table II-5-7. Also, because each datum can be computed independently, there is little or no connectivity between datum locations. This lack of a reference elevation for areas near the coast where no tide observations are available and at interior locations where tide observations are difficult to obtain led to the establishment of a national fixed datum. This datum does not account for spatial variability in sea level. The following paragraphs describe the development of the 1929 National Geodetic Vertical Datum (NGVD).

(2) First-order leveling lines established in the mid-1920's provided survey connections between the Atlantic and Pacific coasts. These surveys indicated that sea levels were higher on the Pacific coast than on the Atlantic coast and were also higher in the north than in the south on both coasts. The goal of developing a fixed reference datum was accomplished by defining a geodetic leveling-based datum whose "zero" coincided with local MSL at locations at which both MSL and geodetic leveling elevations were known.

Table II-5-7
Datums for Reference Tide Stations (Harris 1981)

Station	Normalizing Factor[2]	MSL	MTL	NGVD	MLLW	MLW	MHW	MHHW	Extremes of Record: Highest	Extremes of Record: Lowest	Interval for Establishing of Datum
Atlantic and Gulf Coasts											
Eastport, Maine	M	9.2	9.10	9.00	--[3]	0.00	18.20	--[3]	23.1	-4.4	1941-61
Portland, Maine	M	4.5	4.50	4.28		0.00	9.00		13.9	-3.7	1941-59
Boston, Mass.	M	5.2	5.05	4.89		0.30[4]	9.80		14.2	-3.5	1941-59
Newport, R.I.	M	1.6	1.75	1.37		0.00	3.50		13.5	-2.9	1941-59
New London, Conn.	M	1.4	1.30	0.97		0.00	2.60		10.7[5]	-3.4	1941-59
Bridgeport, Conn.	M	3.4	3.35	2.86		0.00	6.70		12.4	-3.5[5]	1967 (1 yr)
Willets Point, N.Y.	M	3.6	3.55	3.02		0.00	7.10		16.7	-4.1	1941-59
New York, N.Y. (The Battery)	M	2.3	2.25	1.81		0.00	4.50		10.2	-4.2	1941-59
Albany, N.Y.	M	2.5	2.5	--[6]		0.00	4.60		--[6]	--[6]	1941-59
Sandy Hook, N.J.	M	2.3	2.30	1.79		0.00	4.60		10.3	-4.4	1941-59
Breakwater Harbor, Del.	M	2.1	2.05	1.69		0.00	4.10		9.5	-3.9	1953-61
Reedy Point, Del.	M	2.8	2.75	2.45		0.00	5.50		10.0[5]	-6.3	1957-61
Philadelphia, Pa.	M	3.2	3.10	2.14		0.00	6.19[7]		10.7	-6.6	1941-59
Baltimore, Md.	M	1.0	0.97	0.57		0.42[8]	1.52		8.3	-4.5	1941-59
Washington, D.C.	M	1.97	1.97	1.43		0.52[9]	3.42		11.9	-4.2	1941-59
Hampton Roads, Va. (Sewells Point)	M	1.3	1.25	1.28		0.00	2.50		8.5	-3.1	1941-59
Wilmington, N.C.	M	1.9	2.10	1.52		0.00	4.20		8.2	-1.7	Jan. 1969 to Nov. 1973
Charleston, S.C.	M	2.7	2.91	2.65		0.31[10]	5.51		10.7	-3.3	1941-59
Savannah River Entrance, Ga. (Ft. Pulaski)	M	3.6	3.45	3.32		0.00	6.90		11.1	-4.4	1941-59
Savannah, Ga.	M	4.0	3.7	--[6]		0.00	7.40		--[6]	--[6]	1941-59
Mayport, Fla.	M	2.3	2.25	2.00		0.00	4.50		7.4	-3.2	1941-59
Miami Harbor Entrance, Fla.	M	1.3	1.25	0.96		0.00	2.50		6.4	-1.6	1941-59
Key West, Fla.	M	0.6	0.65	0.42		0.00	1.30		3.8	-1.6	1941-59
St. Petersburg, Fla.	D	1.2	1.15	0.83		0.00	2.30		5.3	-2.5[5]	1941-59

[1] Except as footnoted, chart datum is MLW for the Atlantic and gulf coasts and MLLW for the Pacific coast.
[2] D = diurnal; M = mean.
[3] MLLW and MHHW were not routinely derived for Atlantic and gulf coast stations for the 1941-59 epoch used for establishing most of the datums.
[4] Boston Low Water Datum (adopted about 1927).
[5] Estimated value.
[6] Data unavailable at the time of compilation.
[7] Datums and the mean range for Philadelphia were revised in July 1979 based on observations for the period 1969-77.
[8] Baltimore Low Water Datum (adopted 1922 by NOS and COE based on observations 1903-1921).
[9] Mean River Level.
[10] Charleston Low Water Datum (used since 1905 by NOS, and by COE in May 1929).
[11] Low Water Datum at the Presidio, Golden Gate, San Francisco, is based on miscellaneous observations before 1907.

(Continued)

Table II-5-7 (Concluded)

Station	Normalizing Factor[2]	MSL	MTL	NGVD	MLLW	MLW	MHW	MHHW	Extremes of Record Highest	Extremes of Record Lowest	Interval for Establishing of Datum
Atlantic and Gulf Coasts (Continued)											
St. Marks River Entrance, Fla.	D	1.8	1.8	--[6]		0.00	2.40		8.0	-3.5	1941-59
Pensacola, Fla.	D	0.6	0.65	0.33		0.00	1.30		8.9	-2.2	1941-59
Mobile, Ala.	D	0.8	0.75	--[6]		0.00	1.50		9.0[5]	-3.0[5]	1941-59
Galveston, Tex. (Ship channel)	D	0.8	0.70	0.70		0.00	1.40		11.4	-5.3	1941-59
San Juan, P.R.	D	0.6	0.55	--[6]		0.00	1.10		2.4	-1.1	Apr. 1962 to Dec. 1963
Pacific Coast											
San Diego, Calif.	D	3.0	2.95	2.79	0.00	0.90	5.00	5.70	8.3	-2.8	1941-59
Los Angeles, Calif. (Outer Harbor)	D	2.8	2.80	2.72	0.00	0.90	4.70	5.40	7.8	-2.6	1941-59
San Francisco, Calif. (Golden Gate)	D	3.0	3.30	3.06	0.20[11]	1.30	5.30	5.90	8.6	-2.5	1941-59
Humboldt Bay, Calif	D	3.4	3.75	--	0.00	1.20	5.70	6.40	9.5[5]	-3.0[5]	1962
Astoria, Oreg. (Tongue Point)[9]	D	4.3	4.35	3.05	0.00	1.10	7.60	8.30	12.1	-2.8	1941-59
Aberdeen, Wash.	D	5.5	5.45	--	0.00	1.50	9.40	10.10	14.9	-2.9	1955, 1956
Port Townsend, Wash.	D	4.8	5.10	--	0.00	2.50	7.70	8.40	12.0[5]	-4.5[5]	1972-74
Seattle, Wash.	D	6.6	6.60	6.25	0.00	2.80	10.40	11.30	14.8	-4.7	1941-59
Ketchikan, Alaska	D	8.0	7.95	--	0.00	1.50	14.40	15.30	21.2	-5.2	1941-59
Juneau, Alaska	D	8.6	8.50	--	0.00	1.60	15.40	16.40	23.2	-5.2	1966-72
Sitka, Alaska	D	5.2	5.30	--	0.00	1.40	9.10	9.90	14.6	-3.8	1941-59
Cordova, Alaska	D	6.6	6.45	--	0.00	1.40	11.50	12.40	16.8	-4.9	1965-74
Seldovia, Alaska	D	9.4	9.35	--	0.00	1.60	17.00	17.80	24.3	-6.2	1971-74
Anchorage, Alaska	D	16.8	15.25	--	0.00	2.20	28.30	29.00	35.5[5]	-6.5[5]	1964-68
Kodiak, Alaska	D	4.3	4.30	--	0.00	1.00	7.60	8.50	13.0[5]	-4.0[5]	1935-36
Dutch Harbor, Alaska	D	2.2	1.30	--	0.00	1.20	3.40	3.70	6.6	-2.7	1935-38
Sweeper Cove, Alaska (Adak Island)	D	2.1	1.85	--	0.00	--	--	3.70	7.0[5]	-3.3	1958-60; 1944, 1949
Massacre Bay, Alaska (Attu Island)	D	1.9	1.65	--	0.00	--	--	3.30	7.0[5]	-3.0[5]	1950, 1952, 1960
Nashagak Bay, Alaska (Clarks Pt)	D	10.3	10.15	--	0.00	2.50	17.80	19.50	24.5	-5.0	1958
St. Michael, Alaska	D	2.0	--	--	--	--	--	--	--	--	--
Honolulu, Hawaii	D	0.8	0.80	--	0.00	0.20	1.40	1.90	3.5	-1.3	1941-59

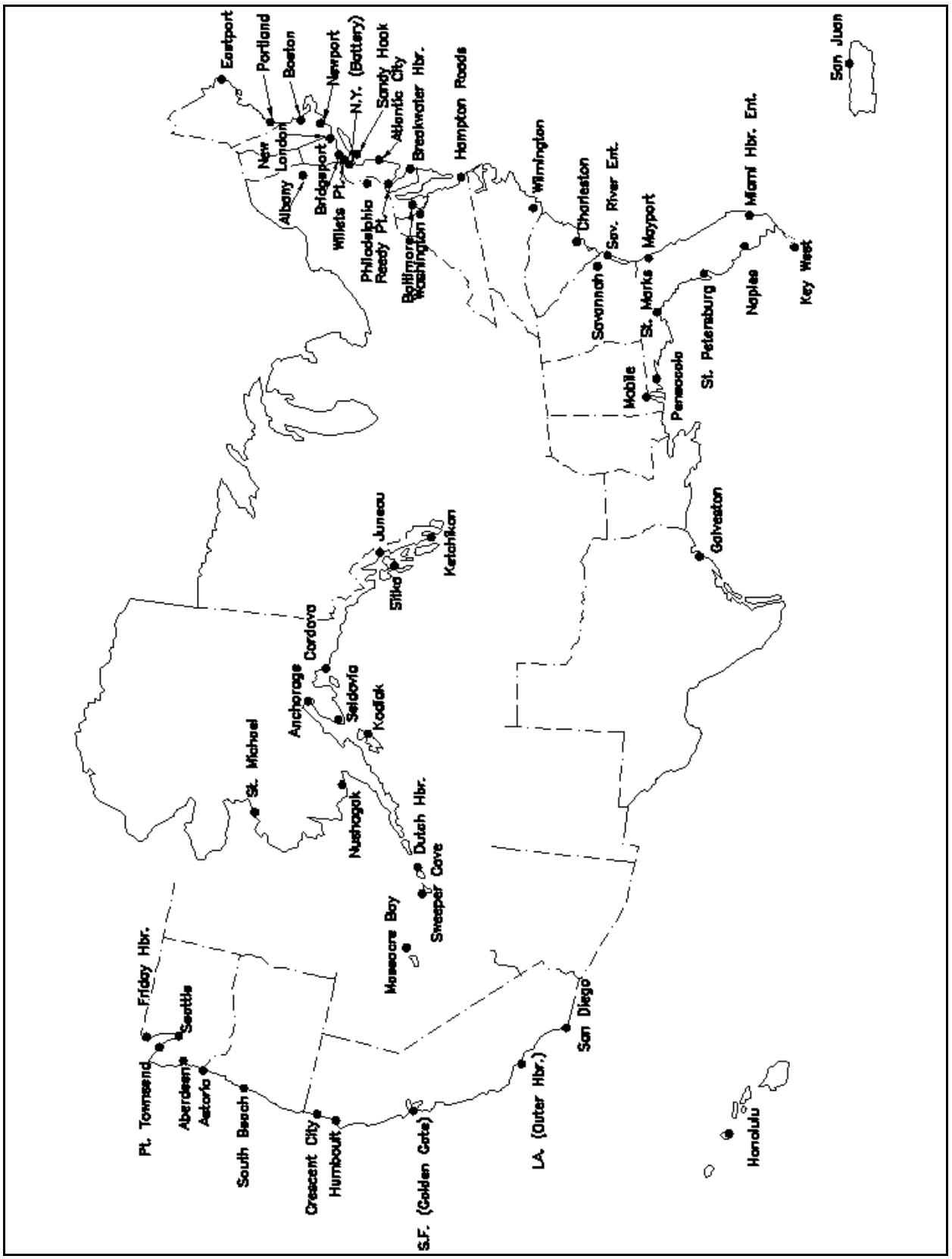

Figure II-5-17. Reference and comparative tide stations, Atlantic, Gulf, and Pacific coasts (Harris 1981)

Thus, a general adjustment was made in 1929 in which it was assumed that the geodetic and local sea levels were equal to zero at 26 selected tide gauges in the United States and Canada (Rappleye 1932). The differences previously computed were treated as errors and were distributed over the network of observation points (Harris 1981). The tide gauge locations used in this computation are shown in Figure II-5-18. The datum, originally called the "Sea Level Datum of 1929," was officially renamed the "National Geodetic Vertical Datum (NGVD) of 1929" in 1963.

(3) Index maps of tidal benchmarks and lists of established references between the 1929 NGVD and the local MSL are available for each coastal state through the NOS. An NOS tidal benchmark sheet is shown in Figure II-5-19. These sheets often describe several benchmarks established in the vicinity of each tidal observation point and describe the relationship between the various datums common to the area. NGVD and tidal benchmarks are discussed more thoroughly in Harris (1981).

(4) The primary distinction between the NGVD and all other tidal datums is that the NGVD is defined as a fixed surface whose elevation does not change with time. Therefore, the procedure adopted to account for recognized changes in relative mean sea level is to compute updated MSL (or other) datum relationships. Relative changes in sea level will be discussed in the following section.

d. Great Lakes datums.

(1) A separate water surface elevation datum was established for the Great Lakes basin and St. Lawrence River. The datum was originally established by an international coordination committee composed of representatives of the U.S. Army Corps of Engineers, the National Oceanic and Atmospheric Administration, and the Department of the Environment, Canada. This first datum was called the International Great Lakes Datum (IGLD) of 1955. The "zero" of the datum was established as the average of all hourly water surface water level readings at Pointe-au-Pere, Quebec, located on the Gulf of St. Lawrence for the period between 1941 and 1956.

(2) First-order leveling lines from Pointe-au-Pere were used to systematically define datums for Lake Ontario, Lake Erie, Lakes Michigan and Huron, and Lake Superior. Lakes Michigan and Huron are assumed to have the same elevation because of the deep and wide connection of both lakes at the Straits of Mackinac. The IGLD of 1955 was replaced by the IGLD of 1985 to reflect certain corrections to the elevations assigned to the various lakes. Elevations of the IGLD of 1955 and IGLD of 1985 are given in Table II-5-8. This revision was implemented in January 1992. The zero reference of the IGLD 1985 has been specified to be Rimouski, Quebec. Revised lake elevations are shown in Figure II-5-20.

e. Long-term variations in datums. Water level observation based datums such as MSL or IGLD vary over time periods much longer than a tidal cycle. These variations can be seasonal or of much longer duration. Long-term changes are often described as a relative change in sea level and necessitate the 25-year interval updating of the 19-year tidal datum period. In the following section, some of the contributing factors to sea level change are discussed. In the final section, factors contributing to long-term elevation changes in the Great Lake are presented.

f. Tidal datums.

(1) The apparent rise in worldwide sea level has been of great concern to the United States, as well as other countries, for several years. Much of this concern stems from the claims of some climatologists and oceanographers that the rise will accelerate in the future due to warming of the atmosphere associated with the "greenhouse effect," a global warming produced by increased levels of carbon dioxide and other gasses in the atmosphere. Because of the potential consequences associated with sea level rise, a Committee on

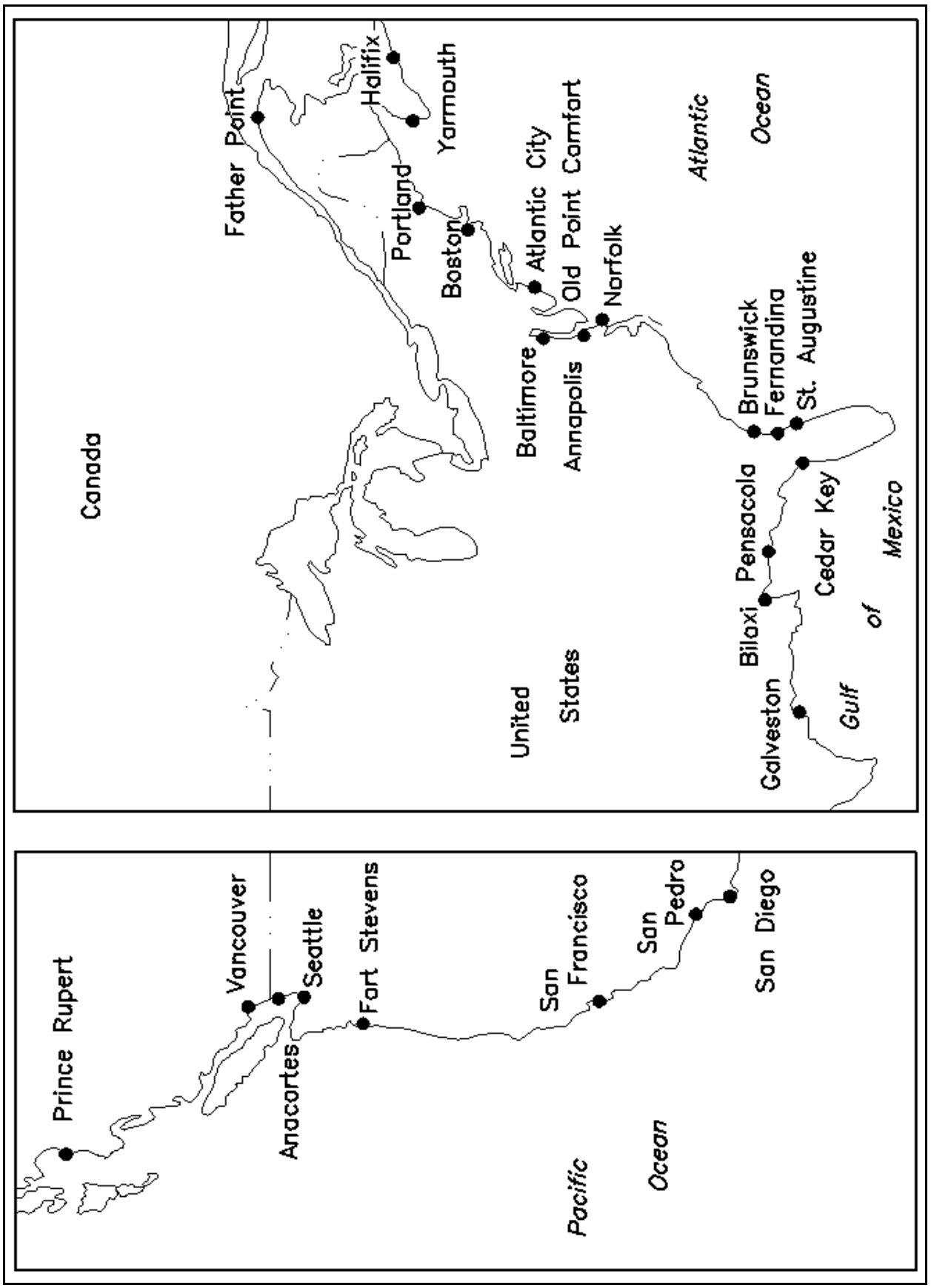

Figure II-5-18. Tide stations used in establishing the National Geodetic Vertical Datum (NGVD) of 1929 (Harris 1981 (after Rappleye (1932))

FLORIDA - I - 74

U.S. DEPARTMENT OF COMMERCE
NATIONAL OCEANIC AND ATMOSPHERIC ADMINISTRATION
NATIONAL OCEAN SURVEY

TIDAL BENCH MARKS

Miami Beach (City Pier)
Lat. 25° 46′.1; Long 80° 07′.9

BENCH MARK 4 (1928) is a standard disk, stamped "NO 4 1928", set vertically in the south face of the south post in the north-south fence line around a large city water tank. It is about 66 feet north of the extended centerline of Commerce Street, 36 feet west of the centerline of Jefferson Avenue, and 1/2 foot above ground level. Elevation: 5.62 feet above mean low water.

BENCH MARK 6 (1931) is a standard Corps of Engineers disk, stamped "BM NO 6," set in top of a 2-inch pipe surrounded at top with a 12-inch by 18-inch manhole frame with a removable cast iron cover, directly in centerline of a blacktop driveway which parallels Government Cut. It is at the U.S. Government Reservation on the north side of Government Cut, about 186 feet east of U.S. Engineers flagpole and 13 1/2 feet west of the center of a road junction. Elevation: 7.13 feet above mean low water.

BENCH MARK 7 (1937) is a standard disk, stamped "7 1937," set in the top of the northwest side of the concrete base to the east post of entrance gate to drive to the Corps of Engineers Office Building. It is about 100 yards south of intersection of Washington Avenue and Biscayne Street, 8 feet east of the extended centerline of the Avenue and 1/2 foot above ground level. Elevation: 5.03 feet above mean low water.

BENCH MARK 9 (1955) is a standard disk, stamped "9 1955," set in top of concrete deck along north edge of City Pier near the east end of Biscayne Street. It is about 122 yards east of the west end of pier, 39 feet northwest of the northeast corner of the ladies rest room and 1/2 foot south of south face of north guardrail. Elevation: 11.29 feet above mean low water.

BENCH MARK 10 (1956) is a standard disk, stamped "NO 10 1956," set on top of the northwest corner of the concrete base of light pole No. 166D6 about 68 yards west of the junction of Biscayne Street and Alton Road. It is near the northwest corner of the South Shore Recreation Park about 62 feet east of the west edge of the bulkhead on the water front and 9 1/2 feet northeast of the east edge of the north entrance to the Recreation Building. Elevation: 5.23 feet above mean low water.

BENCH MARK 11 (1956) is a standard disk, stamped "NO 11 1956," set in top of north corner of a concrete base which supports a 6 inch metal post near the City of Miami Beach Warehouse. It is near the intersection of Alton Road and First Street about 21 1/2 feet southwest of the southwest curb of Alton Road and 9 feet northwest of the northwest corner of the warehouse building. Elevation: 4.92 feet above mean low water.

Mean low water at Miami Beach is based on 19 years of records, 1941-1959. Elevations of other tide planes referred to this datum are as follows:

	Feet
Highest tide (observed)	
September 8, 1965	6.4
Mean high water	2.50
Mean tide level	1.25
NGVD, 1929	0.96
Mean low water	0.00
Lowest tide observed	
(March 24, 1936)	-1.6

Figure II-5-19. Sample NOS description of tidal benchmarks (Harris 1981)

Table II-5-8
Low Water (chart) Datum for IGLD 1955 and IGLD 1985

Low Water Datum in Meters		
Location	**IGLD 55**	**IGLD 85**
Lake Superior	182.9	183.2
Lake Michigan	175.8	176.0
Lake Huron	175.8	176.0
Lake St. Clair	174.2	174.4
Lake Erie	173.3	173.5
Lake Ontario	74.0	74.2
Lake St. Lawrence at Long Sault Dam, Ontario	72.4	72.5
Lake St. Francis at Summerstown, Ontario	46.1	46.2
Lake St. Louis at Pointe Claire, Quebec	20.3	20.4
Montreal Harbour at Jetty Number 1	5.5	5.6

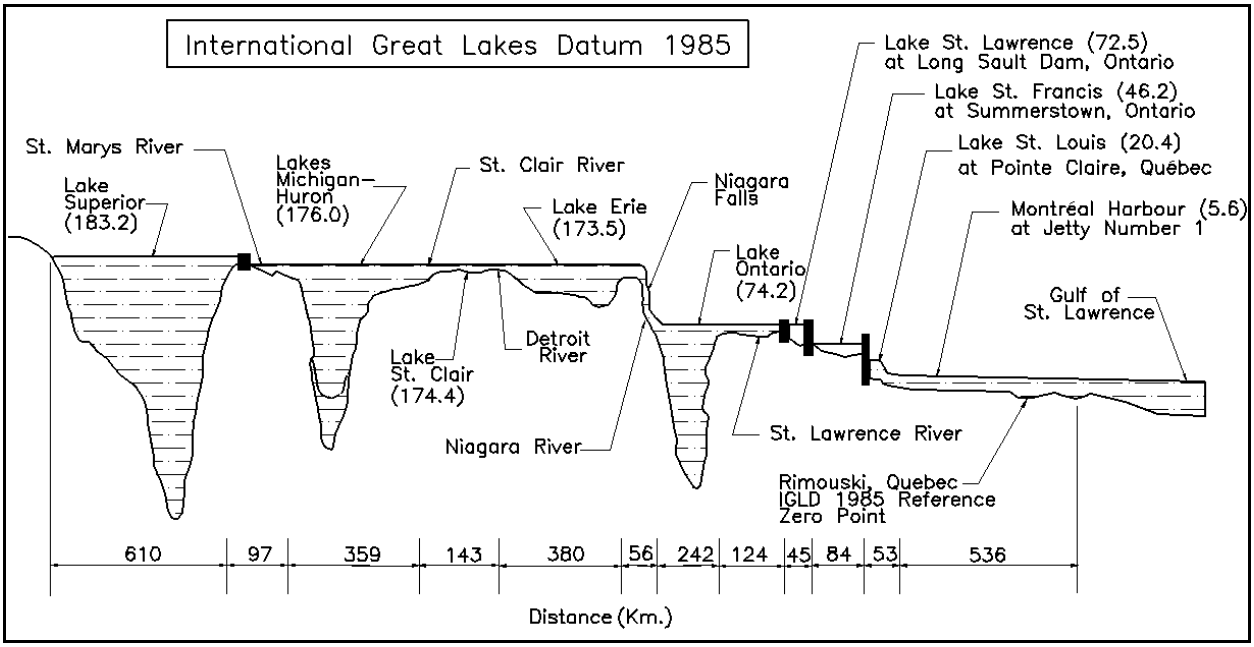

Figure II-5-20. Vertical and horizontal relationships for the IGLD of 1985 (Coordinating Committee on Great Lakes Basic Hydraulic and Hydrologic Data 1992)

Engineering Implications of Changes in Relative Mean Sea Level (CCMSL) was formed to examine existing knowledge concerning sea level change, to document existing relative rise rates, and to provide recommendations concerning their conclusions.

(2) Relative mean sea level change can be defined as the difference between local changes in land elevation and global sea level changes. These changes result from a variety of processes, several of which can occur simultaneously. The following six processes can contribute to long-term relative mean sea level change; however, all processes do not necessarily apply to all geographic locations:

(a) Eustatic rise. Refers to a global change in the oceanic water level. Examples of eustatic rise include melting of land-based glaciers and the expansion of near-surface ocean water due to global ocean warming.

(b) Crustal subsidence or uplift from tectonic uplifting or downwarping of the earth's crust. These changes can result from uplifting or cooling of coastal belts, sediment loading and consolidation, or subsidence due to volcanic eruption loading.

(c) Seismic subsidence. Caused by sudden and irregular incidence of earthquakes.

(d) Auto-subsidence. Due to compaction or consolidation of soft underlying sediments such as mud or peat.

(e) Climatic fluctuations. May also create changes in sea level; for example, surface changes produced by El Niño due to changes in the size and location of high pressure cells.

(3) The above processes have been evaluated with respect to their historical and potential contribution to sea level change on U.S. coasts. The Committee report assesses changes in sea level as well as the affected hydrodynamic processes and the effect on the coastal zone. The report also investigates feasible response strategies that could be used to mitigate the effects of sea level change. Although it is beyond the scope of this chapter to reproduce the contents of the report, conclusions relevant to this chapter are reproduced below.

(a) Relative mean sea level, on statistical average, is rising at the majority of tide gauge stations situated on continental coasts around the world. Relative mean sea level is generally falling near geological plate boundaries and in formerly glaciated areas such as Alaska, Canada, Scandinavia, and Scotland. Relative mean sea level is not rising in limited areas of the continental United States, including portions of the Pacific Coast.

(b) The contrasting signals concerning relative mean sea level behavior in different parts of the United States (and the world in general) are interpreted as due to differing rates of vertical motion of the land surfaces. Subsidence and glacial rebound are significant contributors to vertical land displacements.

(c) Large, short-term (2- to 7-year) fluctuations worldwide are related to meteorological phenomena, notably shifts in the mean jet-stream path and the El Niño-Southern Oscillation mechanisms, which lead to atmospheric pressure anomalies and temperature changes that may cause rise or fall of mean sea level by 15-30 cm over a few years.

(d) Studies of a very small number of tide gauge records dating more than 100 years (the oldest being Amsterdam, started in 1682) show that after removal of the subsidence factor where known, mean sea level has been fluctuating through a range of not more than 40-150 cm (in long-term fluctuations) for at least 300 years.

(e) The geological record over the last 6,000 years or so indicates that there has been a general, long-term rise (with short-term fluctuations) probably not exceeding 200 cm during the last 1,500 years.

(f) Monitoring of relative mean sea level behavior is at present inadequate for measuring the possible global result of future climate warming due to rising greenhouse gases.

(g) The risk of accelerated mean sea level rise is sufficiently established to warrant consideration in the planning and design of coastal facilities. Although there is substantial local variability and statistical uncertainty, average relative sea level over the past century appears to have risen about 30 cm relative to the east coast of the United States and 11 cm along the west coast, excluding Alaska, where glacial rebound has resulted in a lowering of relative sea level. Rates of relative sea level rise along the Gulf Coast are highly variable, ranging from a high of more than 100 cm/century in parts of the Mississippi delta plain to a low of less than 20 cm/century along Florida's west coast.

(h) Accelerated sea level rise would clearly contribute toward a tendency for exacerbated beach erosion. However, in some areas, poor sand management practices or navigational modification at channel entrances has resulted in augmented erosion rates that are clearly much greater than would naturally occur. Thus, for some years into the future, sea level rise may play a secondary role in these areas.

(i) As noted previously, the two response options to sea level rise are stabilization and retreat. Retreat is most appropriate in areas with a low degree of development. Given that a “proper” choice exists for each location, selecting an incorrect response alternative could be unduly expensive.

(j) There does not now appear to be reason for emergency action regarding engineering structures to mitigate the effects of anticipated increases in future eustatic sea level rise. Sea level change during the design service life should be considered along with other factors, but it does not present such essentially new problems as to require new techniques of analysis. The effects of sea level rise can be accommodated during maintenance periods or upon redesign and replacement of most existing structures and facilities. There are very limited geographic areas where current subsidence rates may require near-term action as has been the case in Japan and Terminal Island, California.

(4) The above conclusions represent the state of knowledge on the subject of relative sea level change. For additional information, the reader is referred to the Committee report. It presents a complete and comprehensive investigation of the subject based on known facts and engineering and scientific principles.

(5) For the purposes of this report, the primary conclusion is that, with some regional exceptions, sea level is not rising at a rate to cause undue concern. Results of the report indicate an average sea level rise over the past century of approximately 30 cm/century on the east coast, and 11 cm/century on the west coast, and a range along the Gulf of Mexico coast of less than 20 cm/century along the west coast of Florida to more than 100 cm/century in parts of the Mississippi delta plain. The above summary remarks lead to the conclusion that normal design criteria should be followed in which the design life of a project should consider the possible local relative sea level rise rates shown above.

g. Changes in lake level datums. As with long-term change in the relative mean sea level of the oceans, lake levels also change in time. Although lake levels are subject to the same tectonic types of relative movement, the primary form of change is due to shorter-term phenomena. For example, lake levels are subject to seasonal and annual variations in precipitation and freshwater inflow resulting from regulated reservoirs. These hydrologically related effects produce water surface elevations in the Great Lakes that vary irregularly from one year to the next. The annual cycle consists of water surfaces that consistently fall in elevation to their lowest stage during winter. Falling stages are due to the fact that the majority of precipitation is in the form of snow or rainfall that freezes before becoming spring runoff into streams that empty into the lakes. Lake levels then begin to rise in the spring as the snow and ice melt into runoff. Lake levels generally reach their maximum during the summer. These long-term changes were the basis of the revised IGLD of 1985 described in the previous section.

h. Design considerations.

(1) The datums described above and the reported variability of those datums represent design criteria considerations that directly impact the expected lifetime of a project. If, for example, a coastal project is to be situated in an area of known subsidence, then design elevations need to reflect additional freeboard as a factor-of-safety consideration. For example, if levee systems are to be situated in an area of known subsidence (i.e., the Gulf coast) and a crest elevation level of 20 ft NGVD is considered a minimum level of protection, the subsidence rate should be included in the design calculations to provide adequate protection for the life of the project. For example, if the relative sea level change is 1 cm/year, then the levee will subside by approximately 1 ft in 30 years. This rate of change should be accounted for in the design of projects expected to provide some predetermined level of protection. In this case, the levee should be designed with a 21-ft NGVD crest elevation if it is intended to provide a minimum of 20 ft MSL (present time) protection for 30 years.

(2) If a design project needs to consider the possibility of long-term water level change, then accurate sources of data must be obtained for use in the design evaluation. The NOS continuously summarizes monthly MSL values, the mean and extreme high and low waters of the month, and many other tidal statistics. These records can be obtained from NOS in the form of either photocopies or magnetic media. Figure II-5-21 is a sample of NOS tide and sea level data. If data are available for a specific project location for a long period of time (i.e., 30-50 years), then relative sea level change rates for project design can be estimated. For example, plotted variations in annual sea level for several locations are shown in Figure II-5-22. These data can be used to indicate relative sea level change.

(3) Although relative water surface elevations and datum changes are important over the life of a project, it is usually the short-term changes in water surface elevations that are responsible for project failure (although sudden elevation changes due to tectonic influence can be catastrophic). These short-term changes to elevation are the subject of the following sections.

II-5-5. Storm Surge

a. Storm types. Storms are atmospheric disturbances characterized by low pressures and high winds. A storm surge represents the water surface response to wind-induced surface shear stress and pressure fields. Storm-induced surges can produce short-term increases in water level that rise to an elevation considerably above mean water levels. This is especially true when the storm front coincides with a local high spring tide. There are two types of storms that impact coastal regions. Storms that originate in the tropics are referred to as “tropical storms.” These events primarily impact the east coast and gulf coast
of the United States, the Caribbean Sea, and islands in the Pacific Ocean. Although infrequent, tropical events can also impact the western coast of Mexico and southern coast of California.

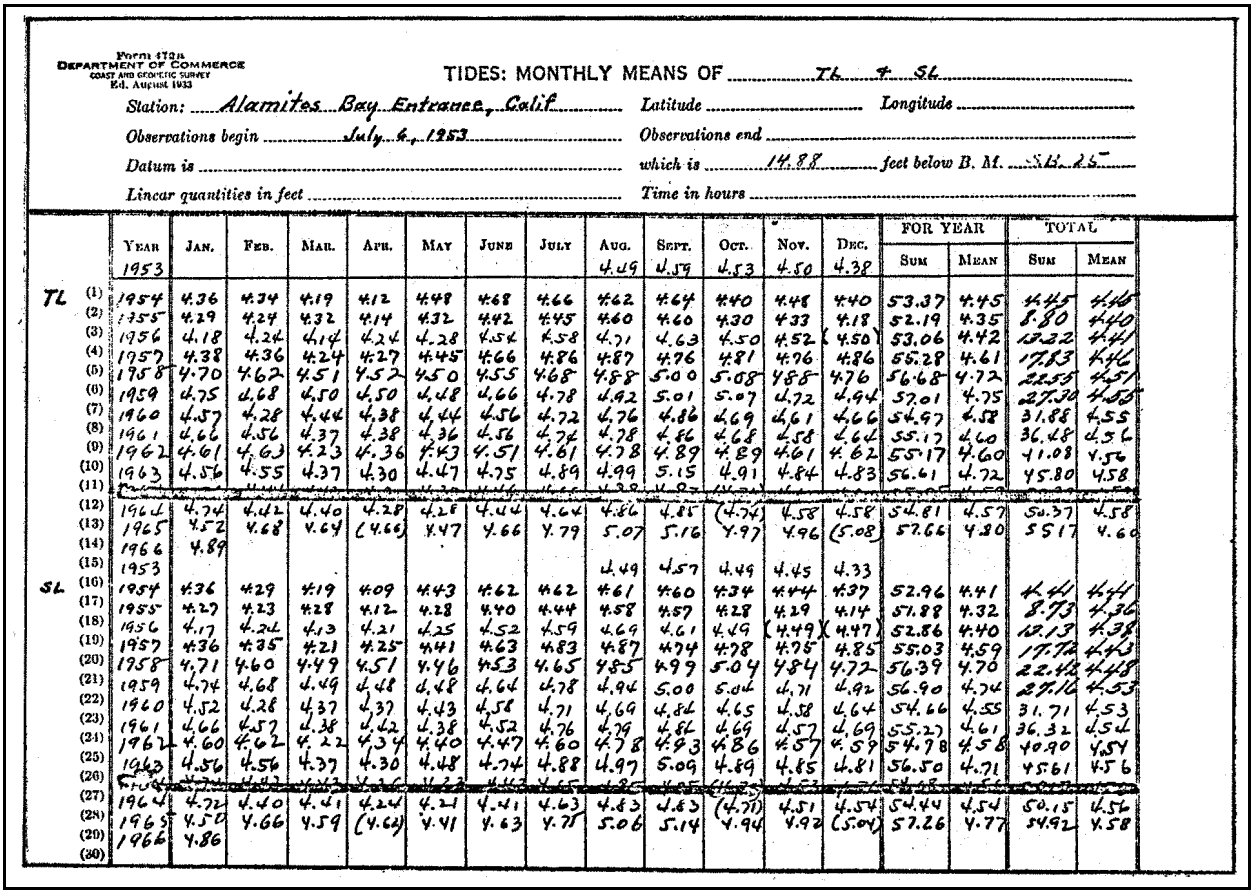

Form 433a
DEPARTMENT OF COMMERCE
COAST AND GEODETIC SURVEY
Ed. August 1933

TIDES: MONTHLY MEANS OF TL & SL

Station: Alamitos Bay Entrance, Calif. Latitude ____ Longitude ____

Observations begin July 4, 1953 Observations end ____

Datum is ____ which is 14.88 feet below B. M. SL 25

Linear quantities in feet ____ Time in hours ____

		Year	Jan.	Feb.	Mar.	Apr.	May	June	July	Aug.	Sept.	Oct.	Nov.	Dec.	For Year Sum	For Year Mean	Total Sum	Total Mean
		1953								4.49	4.59	4.53	4.50	4.38				
TL	(1)	1954	4.36	4.34	4.19	4.12	4.48	4.68	4.66	4.62	4.64	4.40	4.48	4.40	53.37	4.45	4.45	4.45
	(2)	1955	4.29	4.24	4.32	4.14	4.32	4.42	4.45	4.60	4.60	4.30	4.33	4.18	52.19	4.35	8.80	4.40
	(3)	1956	4.18	4.24	4.14	4.24	4.28	4.54	4.58	4.71	4.63	4.50	4.52	4.50	53.06	4.42	13.22	4.41
	(4)	1957	4.38	4.36	4.24	4.27	4.45	4.66	4.86	4.87	4.76	4.81	4.76	4.86	55.28	4.61	17.83	4.46
	(5)	1958	4.70	4.62	4.51	4.52	4.50	4.55	4.68	4.88	5.00	5.08	4.85	4.76	56.68	4.72	22.55	4.51
	(6)	1959	4.75	4.68	4.50	4.50	4.48	4.66	4.78	4.92	5.01	5.07	4.72	4.94	57.01	4.75	27.30	4.55
	(7)	1960	4.57	4.28	4.44	4.38	4.44	4.56	4.72	4.76	4.86	4.69	4.61	4.66	54.97	4.58	31.88	4.55
	(8)	1961	4.66	4.56	4.37	4.38	4.36	4.56	4.74	4.78	4.66	4.68	4.58	4.64	55.17	4.60	36.48	4.56
	(9)	1962	4.61	4.63	4.23	4.36	4.43	4.51	4.61	4.78	4.89	4.89	4.61	4.62	55.17	4.60	41.08	4.56
	(10)	1963	4.56	4.55	4.37	4.30	4.47	4.75	4.89	4.99	5.15	4.91	4.84	4.83	56.61	4.72	45.80	4.58
	(11)																	
	(12)	1964	4.74	4.42	4.40	4.28	4.26	4.44	4.64	4.86	4.85	(4.74)	4.58	4.58	54.81	4.57	50.37	4.58
	(13)	1965	4.52	4.68	4.64	(4.66)	4.47	4.66	4.79	5.07	5.16	4.97	4.96	(5.08)	57.66	4.80	55.17	4.60
	(14)	1966	4.89															
	(15)	1953								4.49	4.57	4.49	4.45	4.33				
SL	(16)	1954	4.36	4.29	4.19	4.09	4.43	4.62	4.62	4.61	4.60	4.34	4.44	4.37	52.96	4.41	4.41	4.41
	(17)	1955	4.27	4.23	4.28	4.12	4.28	4.40	4.44	4.58	4.57	4.28	4.29	4.14	51.88	4.32	8.73	4.36
	(18)	1956	4.17	4.24	4.13	4.21	4.25	4.52	4.59	4.69	4.61	4.49	4.49	4.47	52.86	4.40	13.13	4.38
	(19)	1957	4.36	4.35	4.21	4.25	4.41	4.63	4.83	4.87	4.74	4.78	4.75	4.85	55.03	4.59	17.72	4.43
	(20)	1958	4.71	4.60	4.49	4.51	4.46	4.53	4.65	4.85	4.99	5.04	4.84	4.72	56.39	4.70	22.42	4.48
	(21)	1959	4.74	4.68	4.49	4.48	4.48	4.64	4.78	4.94	5.00	5.04	4.71	4.92	56.90	4.74	27.16	4.53
	(22)	1960	4.52	4.28	4.37	4.37	4.43	4.58	4.71	4.69	4.84	4.65	4.58	4.64	54.66	4.55	31.71	4.53
	(23)	1961	4.66	4.57	4.38	4.42	4.38	4.52	4.76	4.79	4.84	4.69	4.57	4.69	55.27	4.61	36.32	4.54
	(24)	1962	4.60	4.62	4.22	4.34	4.40	4.47	4.60	4.78	4.93	4.86	4.57	4.59	54.78	4.58	40.90	4.54
	(25)	1963	4.56	4.56	4.37	4.30	4.48	4.74	4.88	4.97	5.09	4.89	4.85	4.81	56.50	4.71	45.61	4.56
	(26)																	
	(27)	1964	4.72	4.40	4.41	4.24	4.21	4.41	4.63	4.83	4.83	(4.71)	4.51	4.54	54.44	4.54	50.15	4.56
	(28)	1965	4.50	4.66	4.59	(4.64)	4.41	4.63	4.75	5.06	5.14	4.94	4.92	(5.04)	57.26	4.77	54.92	4.58
	(29)	1966	4.86															
	(30)																	

Figure II-5-21. Sample NOS tabulation of tide parameters (Harris 1981)

Storms that result from the interaction of a warm front and a cold front are called “extratropical storms” and are often referred to as Northeasters. Extratropical events impact the east and west coasts of the United States as well as Alaska and the Great Lakes, but storm-generated surges are most significant along the upper east coast. Characteristics of both storm types and sources of detailed description follow.

(1) Tropical storms.

(a) Tropical storms are classified according to their intensity, the most severe of which is referred to as a hurricane. These storms have maximum sustained winds in excess of 74 mph. Similar storms in the Pacific ocean, west of the International Date Line, are referred to as typhoons. Storms in the Southern Hemisphere are called tropical cyclones. In order to indicate hurricane intensity, and associated potential damage, the NOAA National Hurricane Center has adopted the Saffir/Simpson (Saffir 1977, NOAA 1977) Hurricane Scale. This scale, based partially on maximum wind speeds shown below, ranges from category 1 through the most severe category 5 event. Associated damage, storm surge levels, and evacuation limits are described in the NOAA publication on tropical cyclones (NOAA 1981).

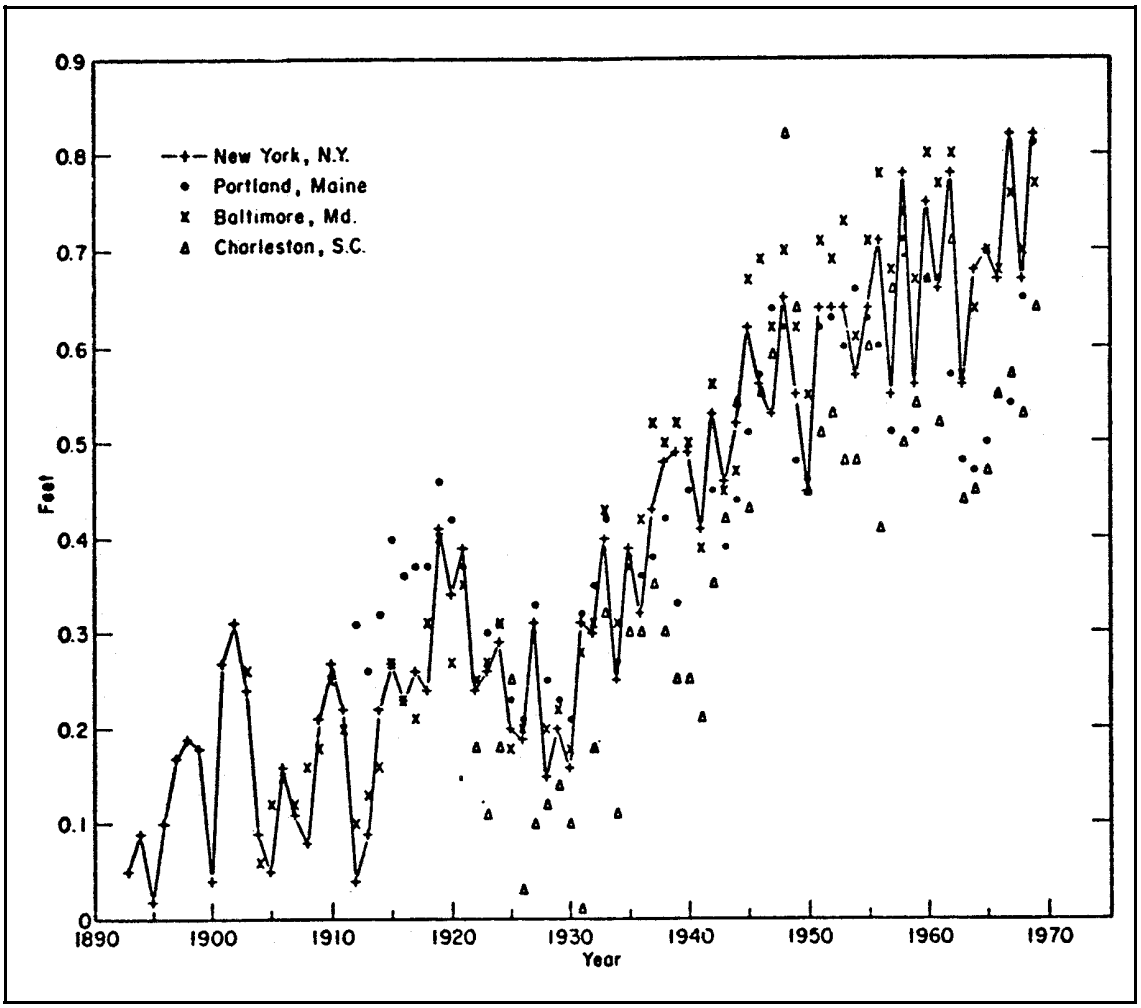

Figure II-5-22. Variations in annual MSL (Harris 1981)

Category 1 - Winds of 74 - 95 mph
Category 2 - Winds of 96 - 110 mph
Category 3 - Winds of 111 - 130 mph
Category 4 - Winds of 131 - 155 mph
Category 5 - Winds over 155 mph

(b) Hurricanes are characterized by circular wind patterns that rotate in a counterclockwise direction in the Northern Hemisphere and clockwise in the Southern Hemisphere. The direction of rotation is a consequence of the Coriolis effect induced by the rotation of the earth (see Part II-1).

(c) Unlike extratropical storm events such as northeasters, tropical storms are well-organized with respect to their wind and pressure patterns. As a result, they can be reasonably well-described by several descriptive parameters listed below and shown on Figure II-5-23. Note that these parameters have been identified as descriptive of average events; precise modeling of some tropical events may require more detailed information.

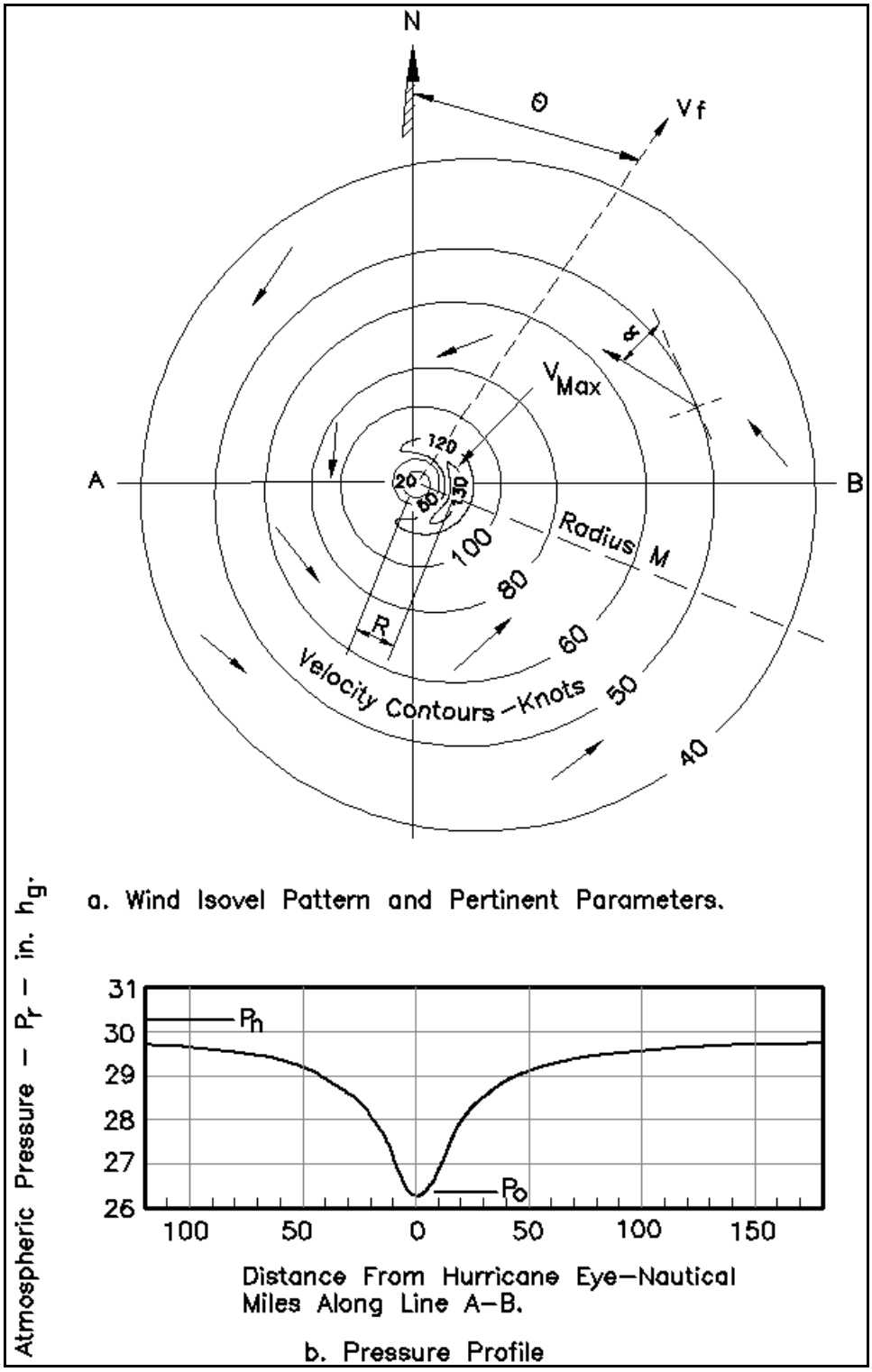

Figure II-5-23. Schematic diagram of storm parameters (U.S. Army Corps of Engineers 1986)

R = radius to maximum wind

V = maximum wind

V_f = forward speed of the eye of the storm

p_0 = central pressure of the eye of the storm

p_n = peripheral or far-field pressure

θ = angle of storm propagation

α = inflow angle

(d) The Corps presently uses two approaches to model tropical storm wind fields. The first is the Standard Project Hurricane (SPH) model. The SPH is defined as a hurricane having a severe combination of storm parameters that will produce a storm with high sustained wind speeds that are reasonably characteristic of the particular location. Guidance on the selection of site-specific storm parameters is given in National Hurricane Research Project Report No. 33 (Graham and Nunn 1959) and NOAA Technical Report NWS 38 (Ho et al. 1987). The SPH model is an empirical model that produces steady-state hypothetical wind and atmospheric pressure fields as a function of the above parameters. The SPH model and its use are thoroughly described in the Coastal Modeling System (CMS) user's manual (Cialone et al. 1991).

(e) The second approach to hurricane modeling is the Planetary Boundary Layer (PBL) model. The PBL model is based on the equations of motion for a vertically integrated boundary layer. The PBL model is currently supported by CHL for all tropical storm surge studies. This selection is due to the fact that the PBL model is based on the equations of motion and boundary layer physics. As such, the model is more flexible in its ability to incorporate a variety of land/sea boundary conditions to represent spatially variable wind and pressure fields that cannot be properly represented by the empirical SPH model.

(f) Input to the PBL model is the time-varying location of the storm and all of the parameters given above, except maximum wind. Maximum winds are computed by the PBL model as a function of the above parameters. The model has provisions to account for spatial asymmetry of parameters as mentioned above. The PBL model is also supported by the CMS and the model, input, and application are described in detail by Cialone et al. (1991).

(2) Extratropical storms.

(a) Unlike hurricanes, which can severely impact local regions (typically less than 50 miles) for less than a day, extratropical storms such as northeasters can impose high winds with accompanying surges over large geographical areas (hundreds of miles) for extended periods of time, i.e., several days or more. Generally, extratropical events have lower wind magnitudes and generate smaller maximum surge elevations than hurricanes. Although lower storm surge elevations are associated with northeasters than with hurricanes, they can cause substantial damage because of their large area of influence and extended period of duration.

(b) An additional design consideration for extratropical events is that they generally occur with a much greater frequency than hurricanes. For example, a hurricane with a peak storm surge elevation of 6 ft at Sandy Hook, NJ, has a return period of 10 years. A northeaster with a 6-ft surge has a return period of approximately 2 years (Gravens, Scheffner, and Hubertz 1989).

(c) Extratropical events cannot be parameterized in the same manner as hurricanes. Therefore, the development of stage-frequency relationships based on the Joint Probability Method (to be discussed in the following section) is not a viable approach for assigning frequency-of-occurrence relationships to extratropical events. As an alternative approach, frequency indexing is now established through application of a new statistical procedure called the empirical simulation technique. This approach will be discussed in the following section.

(d) Because a large number of extratropical storm events have impacted coastal areas of the United States, the 20- to 30-year database of hindcast storms of the Wave Information Study (WIS) is adequate for representing the historical population of storms along the coasts of the United States. Wind fields produced by the storms of this database are input to numerical hydrodynamic long-wave models to produce storm surges as a function of historically hindcast wind fields contained in the WIS database. Because of the frequency of events and large area of impact, this database is considered adequate for determining stage-frequency relationships for design use.

(3) Surge interaction with tidal elevations.

(a) A final consideration on the specification of tropical and extratropical storm surge elevations relates to the time of occurrence. The timing of storm events with respect to the phase of the astronomical tide cannot be overemphasized. When a storm surge coincides with a spring high tide, the resulting total surge can be many times more devastating than the surge alone. For example, a moderate event at low tide can become the storm surge of record at high tide. An example situation is shown for Hurricane Gloria, which moved along the Delaware and New Jersey coasts, making landfall on Long Island, NY, at 1100 EST on 27 September 1985. The total storm track is shown on Figure II-5-24, and a more detailed plot of the track in the vicinity of Long Island is shown on Figure II-5-25 (Jarvinen and Gebert 1986).

(b) The significance of timing between the surge peak and the tide phase can be seen in Figure II-5-26. The observed storm surge at Sandy Hook, NJ, had a peak value of 7.5 ft and occurred near low tide (1.0 ft). As a result, the total measured water level was 8.5 ft, corresponding to just 3.5 ft above normal high tide. If the storm surge had occurred 4.5 hr earlier to coincide with high tide (5.0 ft), the peak surge value would have been 12.5 ft. The differences in levels of damage resulting from an 8.5-ft versus a 12.5-ft surge level can be considerable, and the only difference between the two scenarios is a 4.5-hr difference in time of occurrence. As shown in this example, the phasing of the storm and tide impacts both the design of the structure and the probability analysis of the design.

b. Storm event frequency-of-occurrence relationships.

(1) Introduction.

(a) The majority of coastal structures are designed to provide some specific level of protection to the beach and its surrounding population and supporting structures. This level of protection is generally based on the frequency of occurrence of a storm surge of some specified maximum elevation selected by assessing the risks of structural failure or consequences of overtopping versus the economics of the cost of the design project. Therefore, one important aspect of coastal design criteria is the development of stage-frequency or frequency-of-occurrence relationships for the design area.

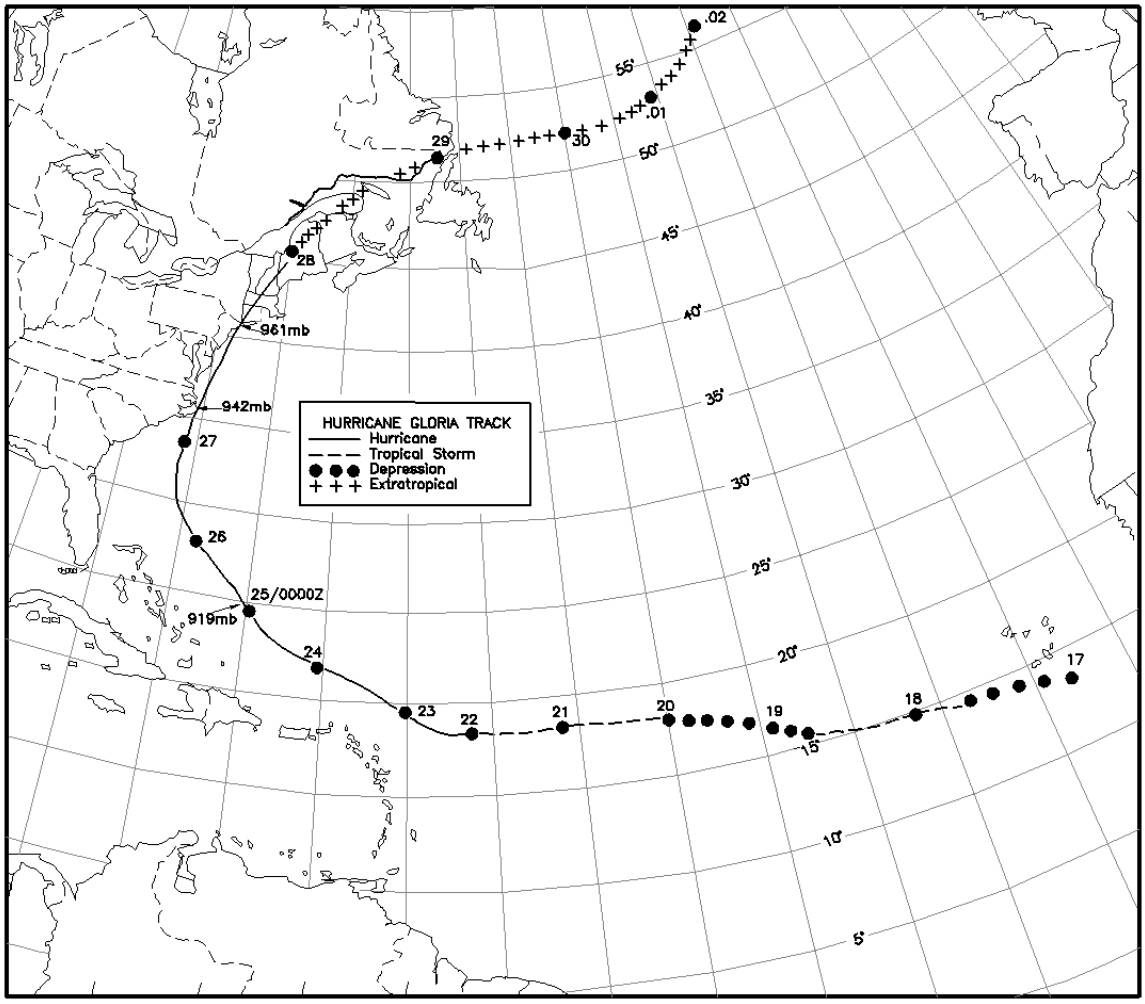

Figure II-5-24. Hurricane Gloria track from 17 September to 2 October 1985 (Jarvinen and Gebert 1986)

(b) Three approaches are commonly used for developing site-specific frequency relationships. These are based on: 1) historical data, 2) synthetic data, and 3) empirical simulation technique (EST) approaches. The historical approach assumes that a database of historical storm events and their respective surge elevations is available for the study area. It is further assumed that the available database provides a representative sample of all possible events for that particular site. Many coastal locations do not have adequate historical data from which frequency-of-occurrence relationships can be developed. Even if a reasonable number of years of data are available, there is no assurance that the data represent a full population of possible storm events. Therefore, it is usually the case that historical data are insufficient for generating a reliable frequency-of-occurrence relationship. For this reason, synthetic or empirically based approaches are generally preferred.

(c) The synthetic approach is based on the construction of a large number of hypothetical storm events based on assumed probability laws dictating the intensity of the storms and their associated frequency relationships. A more recent approach to the developing frequency-of-occurrence relationships is through the statistical approach known as the empirical simulation technique. This approach is a resampling or "bootstrap" scheme in which the probability relationships of a historical database are used to develop frequency relationships.

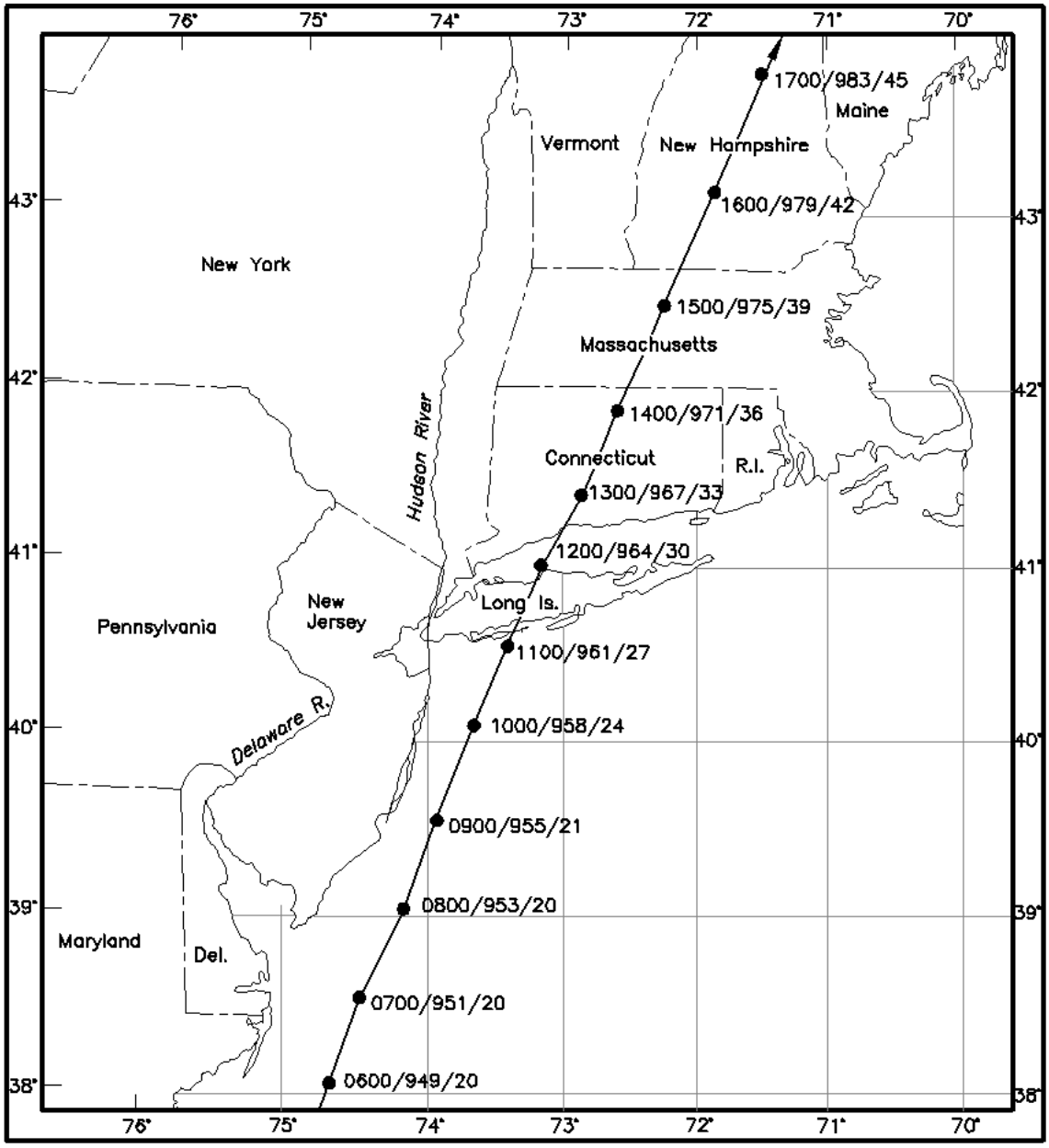

Figure II-5-25. Hurricane Gloria track offshore of Delaware and New Jersey (Jarvinen and Gebert 1986)

(d) CHL recommends the empirical simulation technique and uses this statistically based method for all frequency-related studies. This technique has been adopted because it generates multiple data sets of events from historical data and then generates not only frequency-of-occurrence relationships, but also error bands associated with those determinations. When computer facilities are not available for application of the EST, the other approaches can be successfully used; however, each has limitations which should be considered. All three approaches are briefly discussed in the following paragraphs.

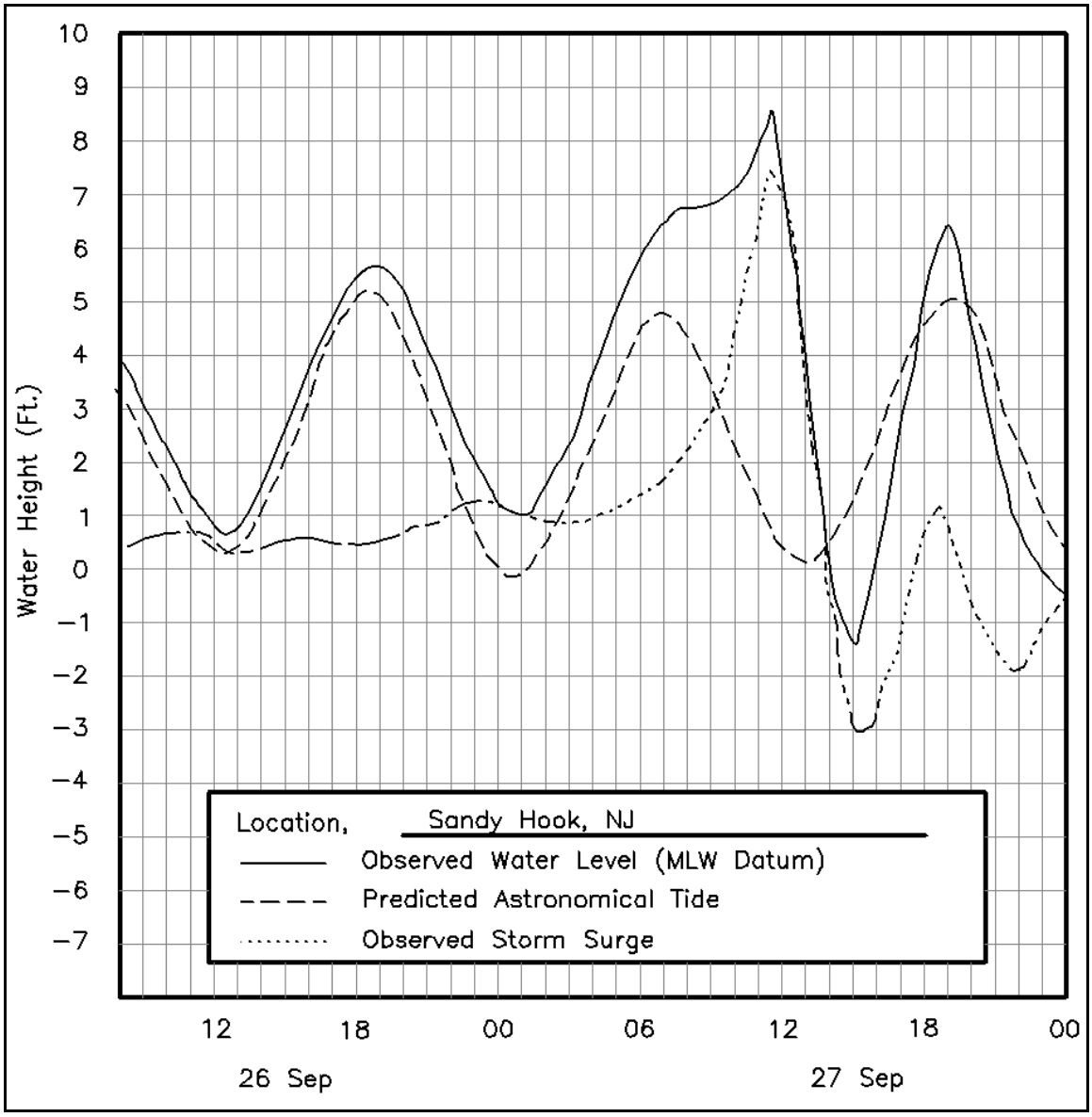

Figure II-5-26. Example phasing of storm surge and tide (Jarvinen and Gebert 1986)

(2) Historical method.

(a) There are two basic approaches to the use of historical data for generating recurrence interval relationships. The first is the graphical method, the second makes use of analytical formulas to describe the behavior of the frequency relationship.

(b) The graphical method involves construction of a cumulative probability density function (or probability distribution function) in which the magnitude of the event is plotted against percent probability of exceedance.

(c) In addition to the graphical approach of developing a pdf, a variety of analytical methods exist for estimating these functions. Selection of a specific form depends on the behavior of the historical data and

the purpose of the study. One function, the Pearson Type III distribution, is presented in detail in many texts on probability and statistics.

(3) Synthetic method.

(a) The synthetic method is based on the assumption that a particular event can be characterized by several descriptive (component) parameters, and that the probability associated with each of those parameters can be used to determine the joint probability of the total event. For example, tropical storm events were described by parameters such as radius to maximum wind, maximum wind, pressure deficit, etc. It is assumed that the frequency of the event can be described by the frequencies associated with each parameter.

(b) The most commonly used form of the synthetic approach is the Joint Probability Method (JPM). The assumption basic to the JPM is that the probability of occurrence of a given storm event can be written as the product of the probabilities corresponding to each storm parameter and that the probabilities for each parameter are independent. For example, a common assumption is that the storm can be described by five storm parameters. If the parameters are statistically independent, then the joint probability density function for the five-dimensional set is the product of the individual probability density functions, i.e.,

$$f = f_D f_R f_\theta f_v f_L \tag{II-5-24}$$

where f_D, f_R, etc., represent the pdf for the central pressure deficit D (far-field pressure p_n less central pressure p_0), radius to maximum R, azimuth of the storm track θ, forward speed V, and closest distance to landfall (with respect to some specified location) of the eye of the storm L. The JPM has been widely used in the past for storm surge analyses. Details are well-documented in USACE (1986) and the reader is referred to that document for a more detailed description.

(4) Empirical simulation technique.

(a) Introduction. Few locations have an adequate historical database of storm events from which to develop reliable stage-frequency relationships. The JPM is subject to error because it is based on simplifying assumptions of parameter independence, and specifying the pdf of each parameter according to parametrically based relationships. The empirical simulation technique (EST) is a statistical resampling scheme that uses historical data to develop joint probability relationships among the various storm parameters. These relationships are based on data derived from actual storm events. There are no simplifying assumptions concerning the pdf's; the interdependence of parameters is computed directly from the respective parameter interdependencies contained in the historic data. In this manner, probabilities are site-specific, do not depend on fixed parametric relationships, and do not assume parameter independence. Thus, the EST is "distribution-free" and nonparametric. There are presently two approaches to applying the EST. The first approach is a multi-parameter simulation approach developed for application to tropical events. The second is a single-parameter approach developed for use in extratropical events. EST applications for tropical and extratropical events are discussed briefly below.

(b) EST - tropical storm application.

(1) The multi-parameter EST Program (Scheffner et al. 1999) utilizes historic data to generate a large number of multi-year simulations of possible future hurricane storm events for a specific location. The approach is based on resampling and interpolation of data contained in a database of events derived from historic events. The ensemble of simulations is consistent with the statistics and correlations of past storm activity at the site, but allows for random deviations in behavior that are likely to occur in the future.

(2) The simulation approach is based on the selection of a set of historic "training storms" extending over the range of storms that actually occurred at the site location. The training events are selected from the data set of historic storms as well as from storms that could occur, such as a historic event with a slightly shifted track. The descriptive storm parameters for each of these events (pressure deficit, radius to maximum wind, maximum wind, forward speed, angle of propagation, and tidal phase) are computed and referred to as input vectors describing each storm event.

(3) These input vectors define the multi-vector space of input parameters associated with each storm event. These parameters are input to the PBL storm model to produce a time-varying spatial distribution of wind and pressure fields subsequently used as input to a numerical hydrodynamic model for computing storm surge hydrographs over the computational domain. (Examples of numerical modeling of storm surge and tidal circulation are presented in Part II-5-7.) The maximum storm surge elevation reached at specified gauge locations is defined as the response vector of the storm at that location.

(4) Other output vectors such as maximum shoreline erosion, maximum dune recession, or maximum wave height can be described. The output vector(s) represents the environmental response to the storm. This response is defined at location *X* and is a direct consequence of the storm via the storm parameter values defined at the point of nearest proximity of the storm eye to point *X*. For the case of stage-frequency analyses, maximum surge is assumed to occur when the eye of the storm is nearest location *X*.

(5) Input to the EST model is the training set database of storm input and response vector(s) for a specific location. An example storm surge analysis for the coast of Delaware (Scheffner, Borgman, and Mark 1993) identified 33 tropical events that impacted the study region during the 104-year period of 1886 through 1989. Of these events, 15 were selected to be representative of the full set. All events were extracted from the NOAA (1981) database of historic storms. These data were used to develop input to the PBL model to generate input data to a hydrodynamic long-wave model. Storm surge hydrographs were computed for each of the 15 storm events. This preliminary analysis generated a set of input and response vectors for 15 storm events for input to the EST.

(6) Each storm surge is computed independent of the local tidal phase. Each event has an equal probability of occurring at high tide, MSL after flood, low tide, or MSL after ebb. Each of the computed surge elevations were linearly combined with the four phases of the tide to generate an expanded training set of 60 events, which included tidal elevation.

(7) A cumulative pdf for the 60 storm events is developed based on the assumption that each of the 60 events has an equal probability of occurrence, and that the number of hurricanes along the coast of Delaware is defined by the number of historical events, i.e., 33 events in 104 years. Each storm is considered a point event in time with each storm occurring independently. The empirical simulation technique utilizes a resampling scheme in which a random number seed from 0.0 to 1.0 is used to select a historic event from the training set. Each selected event is described according to its respective input vectors and the maximum surge elevation response vector.

(8) Input vectors corresponding to the randomly selected event are used to define a new set of input vectors, based on the initial selected storm values but weighted to reflect the value of the "nearest neighbor" parameter contained in a vector space representing parameters corresponding to all events in the 60-storm database. In this manner, a new storm is defined according to a new set of parameters that is similar to those defining the selected event but adjusted to reflect the parameter interrelationships of the full database. Multi-vector interpolation schemes use the new event input parameters to estimate a new response parameter - the peak storm surge at point X.

(9) The EST simulation approach is to perform N-repetitions of M-years of simulation; for example, 100 simulations of a 200-year sequence of storms. Details of the EST are given in Borgman and Scheffner (1991). The number of storms simulated per year is specified according to a Poisson probability law of the form:

$$P[N=n] = \frac{e^{-\lambda T}(\lambda T)^n}{n!} \tag{II-5-25}$$

for $n = 0,1,2,3,....$ Equation II-5-25 defines the probability of having N storm events in T years. The variable λ defines the mean frequency of observed events per time period. For the example shown for the coast of Delaware, the value of λ was chosen to be 0.32 events per year, computed as the ratio of 33 observed events above some selected threshold intensity over a 104-year period.

(10) A 10,000-element array is initialized to the above Poisson distribution. The number corresponding to 0 storms per year from Equation II-5-25 is 0.7234; thus, if a random number selection is less than or equal to 0.7234 on an interval of 0.0 to 1.0, then no hurricanes would occur during that year of simulation. If the random number is between 0.7234 and $0.7234 + P[N=1] = 0.7234 + 0.2343 = 0.9577$, one event is selected. Two events for $0.9577 + 0.0379 = 0.9956$, etc. When one or more storms are indicated for a given year, they are randomly selected from the expanded training set. In this manner, a randomly selected number of storms per year is computed for each year to generate a 200-year simulation.

(11) Each 200-year sequence is rank ordered, a cumulative pdf computed, and a frequency-of-occurrence relationship developed according to the approach described above. However, in the EST, tail functions (Borgman and Scheffner 1991) are used to define probabilities for events larger than the largest the 200-year simulation.

(12) This computation is repeated 100 times, resulting in 100 individual pdfs from which 100 stage-frequency relationships are computed. This family of curves is averaged and the standard deviation computed, resulting in the generation of a stage-frequency relationship containing a measure of variability of data spread about the mean. This variation is well-suited to the development of design criteria requiring the quantification of the element of risk associated with the frequency predictions. A computed stage-frequency relationship for a coastal station in the Delaware study is shown in Figure II-5-27.

(c) EST - extratropical storm application.

(1) Extratropical events cannot be easily parameterized; therefore, the multi-parameter application of the EST is not appropriate for events such as northeasters. An alternate small-parameter application of the EST (Palermo et al. 1998) was used for this class of events. Northeasters have a much greater frequency of occurrence than hurricanes. For example, several northeasters impact large regions of the east coast every year. The existing WIS database of northeasters represents an adequate population of storms from which frequency-of-occurrence relationships can be computed.

(2) The extratropical EST approach is conceptually simpler than the multi-parameter version used for hurricanes because parameters such as tidal phase, wave height, and wave period are specified as input vectors. In this approach, a database of extratropical events is assembled and respective surge elevations computed for each storm in the training set using numerical modeling techniques. If 20-30 years of reliable storm surge elevation data are available for a particular location, the numerical modeling phase may not be necessary. The extratropical analogy to the tropical implementation is that there are fewer input vectors. The database of response vectors is combined with tide, rank ordered, and a pdf is computed.

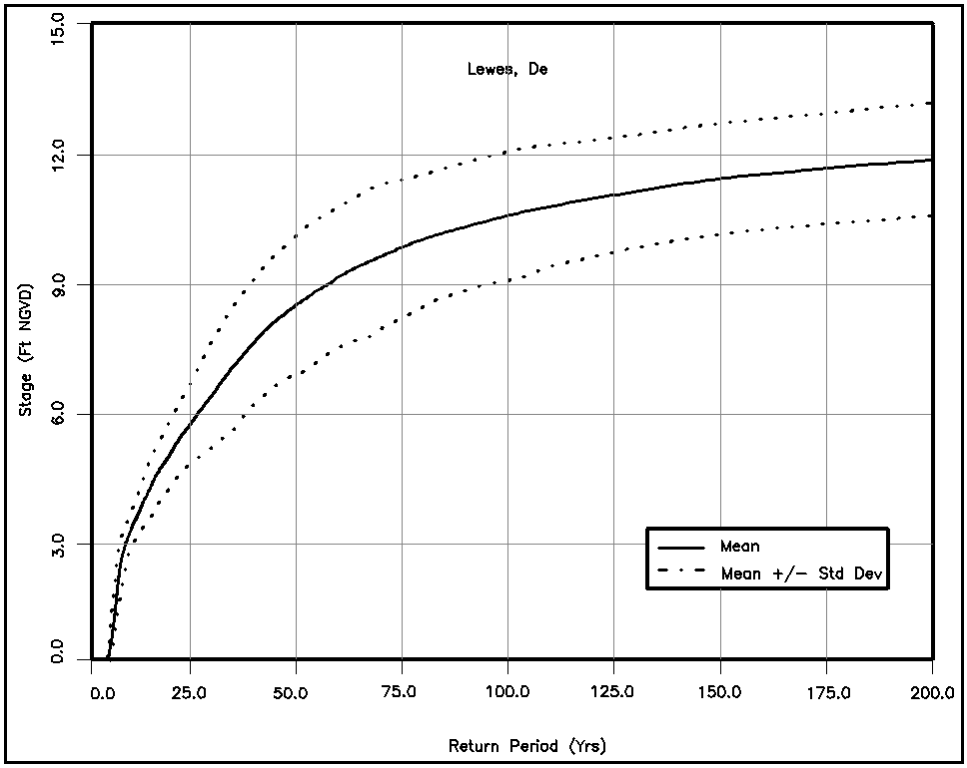

Figure II-5-27. Stage-frequency relationship - coast of Delaware

(3) The extratropical application of the EST can be used to develop recurrence relationships for any parameter if the database of parameters is sufficiently large to define the full population of possible events. A sample application was made to a dredged disposal site located in the New York Bight, on the east coast of the United States. The goal was to determine the recurrence interval of bottom erosion resulting from the 11 December 1992 extratropical storm event. An existing database of severe extratropical storms that impacted the Bight was available with corresponding wave conditions, maximum storm surge elevation, and tidal phase for each storm of the set. These data were used to define a database of peak sediment transport magnitudes, computed as a function of wave height, current (computed from surge elevations), depth, and grain size (Scheffner 1992). These data were input to the EST specifying only one input vector, the peak sediment transport magnitude (QX), to generate 1,000 repetitions of a 500-year simulation. For each 500-year simulation, a transport versus frequency-of-occurrence relationship was computed. As described above, an average curve was computed, which included variability. Results of the analysis are shown in the transport-frequency curve of Figure II-5-28 in which transport is given in $ft^3/sec/ft\text{-}width \times 10^{-4}$.

(4) Historical data on storms in and around the coasts of the United States have been recorded and published in detail since the late 1800's. For example, NOAA publishes an atlas of tropical storms (NOAA 1981) that is continuously updated to reflect recent events. The distribution of east coast tropical events over the period of 1886-1980 is shown in Figure II-5-29, in which the tracks of the 793 Atlantic tropical cyclones reaching at least tropical storm intensity are shown. The Wave Information Study (WIS) of CHL has hindcast data for extratropical storms covering over 30 years.

(5) Recent advances in numerical modeling techniques make it possible to use these very large databases of storm event track, wind, and pressure to simulate storm surges associated with each event. These sources provide data used to develop storm surge versus frequency-of-occurrence relationships.

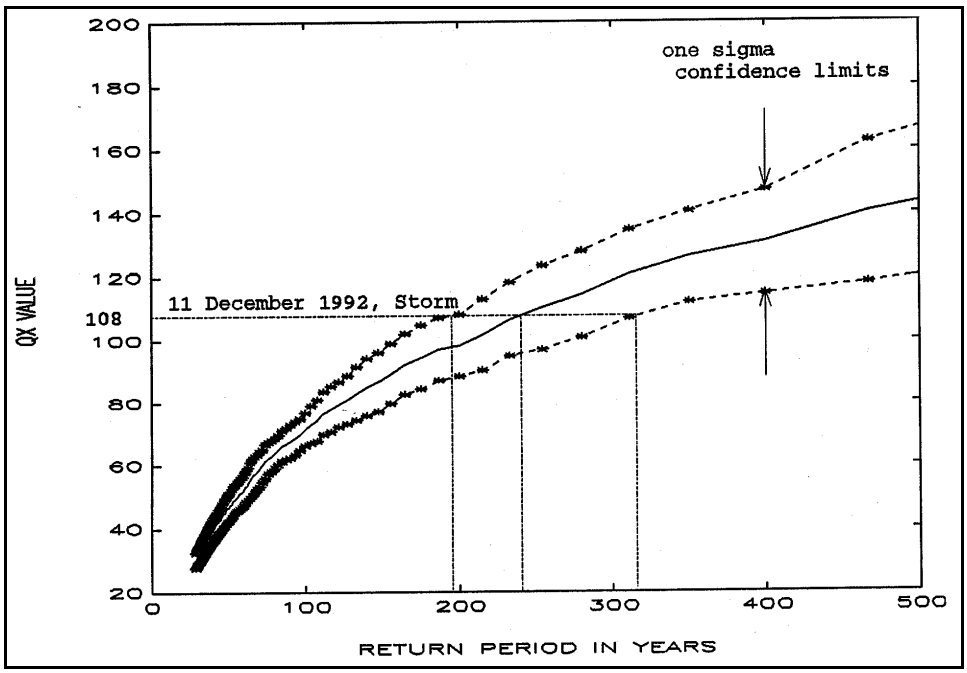

Figure II-5-28. Sediment transport magnitude-frequency relationship - December 1992 northeaster

II-5-6. Seiches

a. Seiches are standing waves or oscillations of the free surface of a body of water in a closed or semiclosed basin. These oscillations are of relatively long period, extending from minutes in harbors and bays to over 10 hr in the Great Lakes. Any external perturbation to the lake or embayment can force an oscillation. In harbors, the forcing can be the result of short waves and wave groups at the harbor entrance. Examples include 30- to 400-sec wave-forced oscillations in the Los Angeles-Long Beach harbor (Seabergh 1985). Dominant long-period seiche conditions on the Great Lakes have resonant modes with periods varying from 2 to 12 hr. These oscillations result primarily from changes in atmospheric pressure and the resultant wind conditions and occur over the entire basin. The frequency of oscillation is a function of the forcing, together with geometry and bathymetry, of the system.

b. In areas of simple geometry, modes of oscillation can be predicted from the shape of the basin. For example, Figure II-5-30 shows surface profiles for various simple geometric configurations.

c. For the one-dimensional case of a closed rectangular basin with vertical walls and uniform depth (Figure II-5-30b), the natural free oscillating period T_n can be written as

$$T_n = \frac{2l_B}{n\sqrt{gh}} \tag{II-5-26}$$

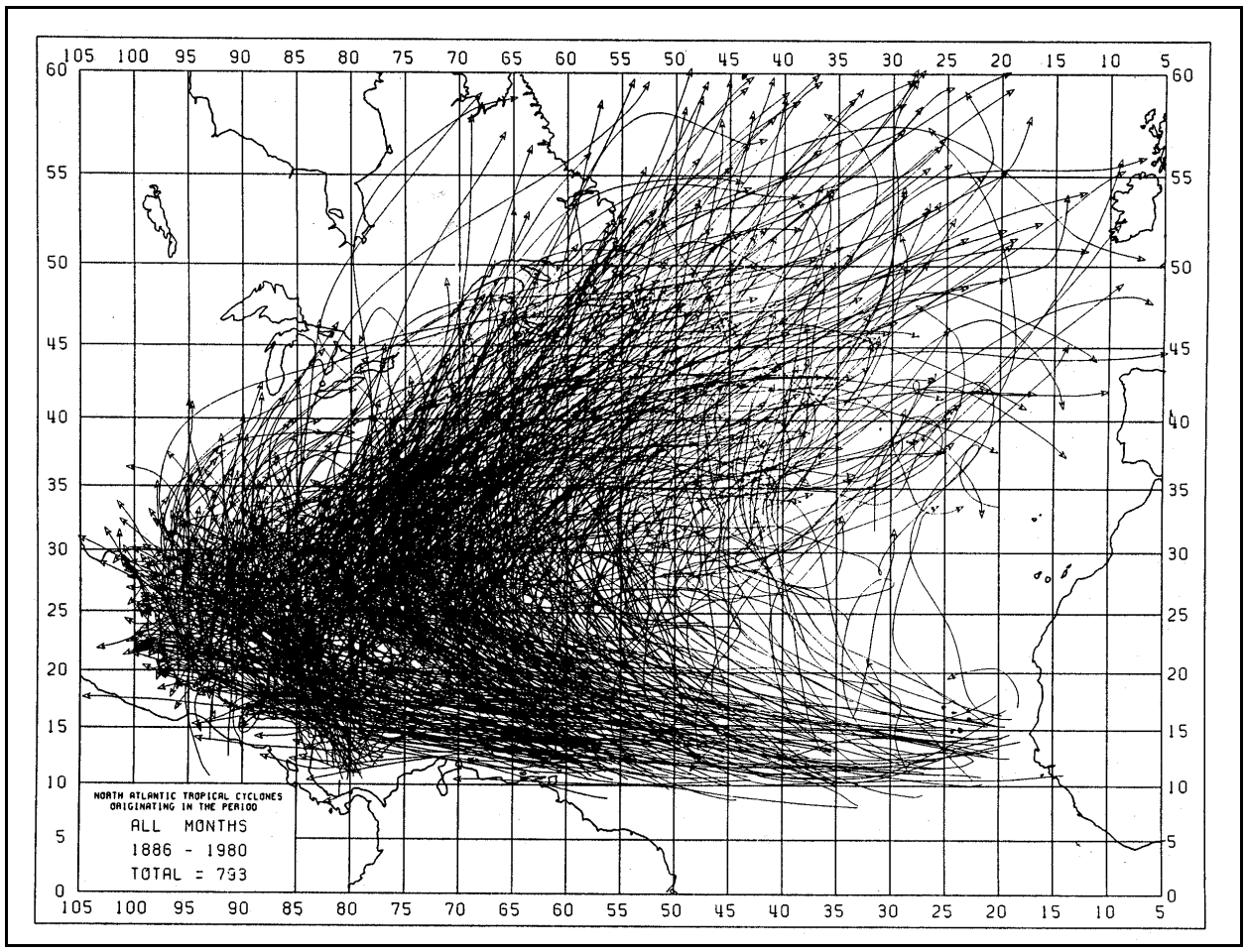

Figure II-5-29. Atlantic tropical storm tracks during the period 1886-1980

where n is the number of nodes along the axis of the basin, h is the water depth, and l_B is the length of the basin. The fundamental and maximum period corresponds to T_n for n = 1. As shown in Figure II-5-30b, nodes (locations of no vertical deflection) are located at interior points and antinodes (locations of maximum deflection) are located on the boundaries of the basin. Longitudinal seiches oscillate from end to end, while transverse seiches oscillate from side to side in the basin.

d. For an open rectangular basin (Figure II-5-30c), the free oscillation period is written as follows:

$$T_n = \frac{4l_B}{(1 + 2n)\sqrt{gh}} \tag{II-5-27}$$

e. The fundamental mode corresponds to n=0. As shown in Figure II-5-30c, the node is located on the opening with an antinode on the opposite end.

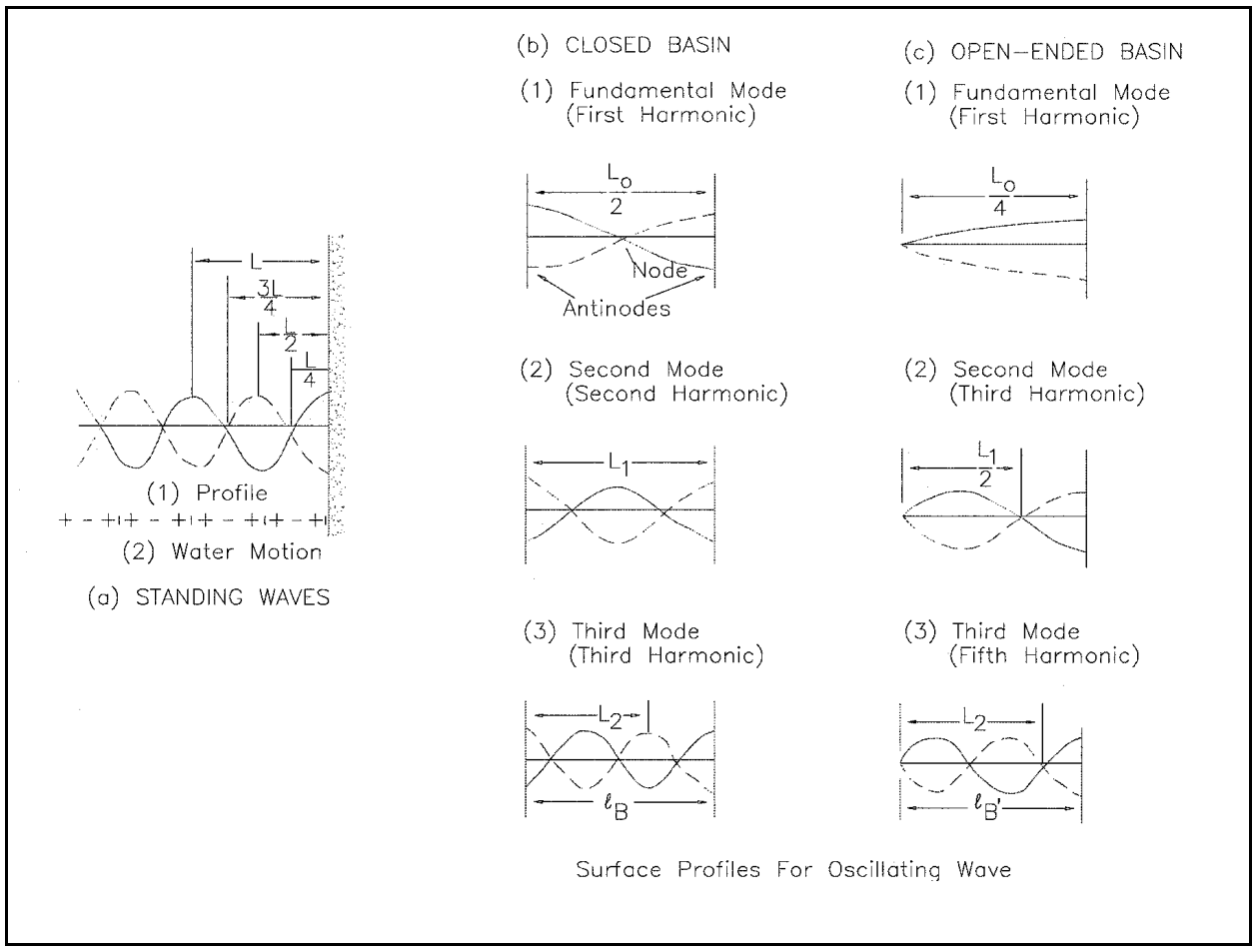

Figure II-5-30. Long wave surface profiles (*Shore Protection Manual* 1984)

f. Methods are available to estimate free oscillations in long narrow lakes of variable width and depth (Defant 1961); however, seiche periods and node/antinode locations are determined most accurately through long-wave modeling. For this class of problem, numerical solutions of the governing equations are necessary. An example is presented in Rao and Schwab (1976), in which a numerical model is used to investigate the normal modes of oscillation in an arbitrary enclosed basin on a rotating earth. Applications are made to Lakes Ontario and Superior. Rao and Schwab describe two distinct types of free oscillations, gravitational modes and rotational modes. Gravitational modes result from undulations of the free surface and are independent of the rotation of the earth. Rotational modes are a function of gravity via the Coriolis parameter. Figure II-5-31 represents the first, second, and third normal modes of oscillation for Lake Ontario. The periods of the computed six lowest modes in Lake Ontario are 5.11, 3.11, 2.13, 1.87, 1.78, and 1.46 hr for modes 1 through 6. The complexity of the nodal points and lines of phase demonstrate that idealized solutions such as those shown in Figure II-5-30 are often not adequate to explain natural phenomena. For applications requiring detailed information on maximum seiche elevations and nodal distributions, numerical models such as those described in the following section are the only viable approach to developing reliable solutions.

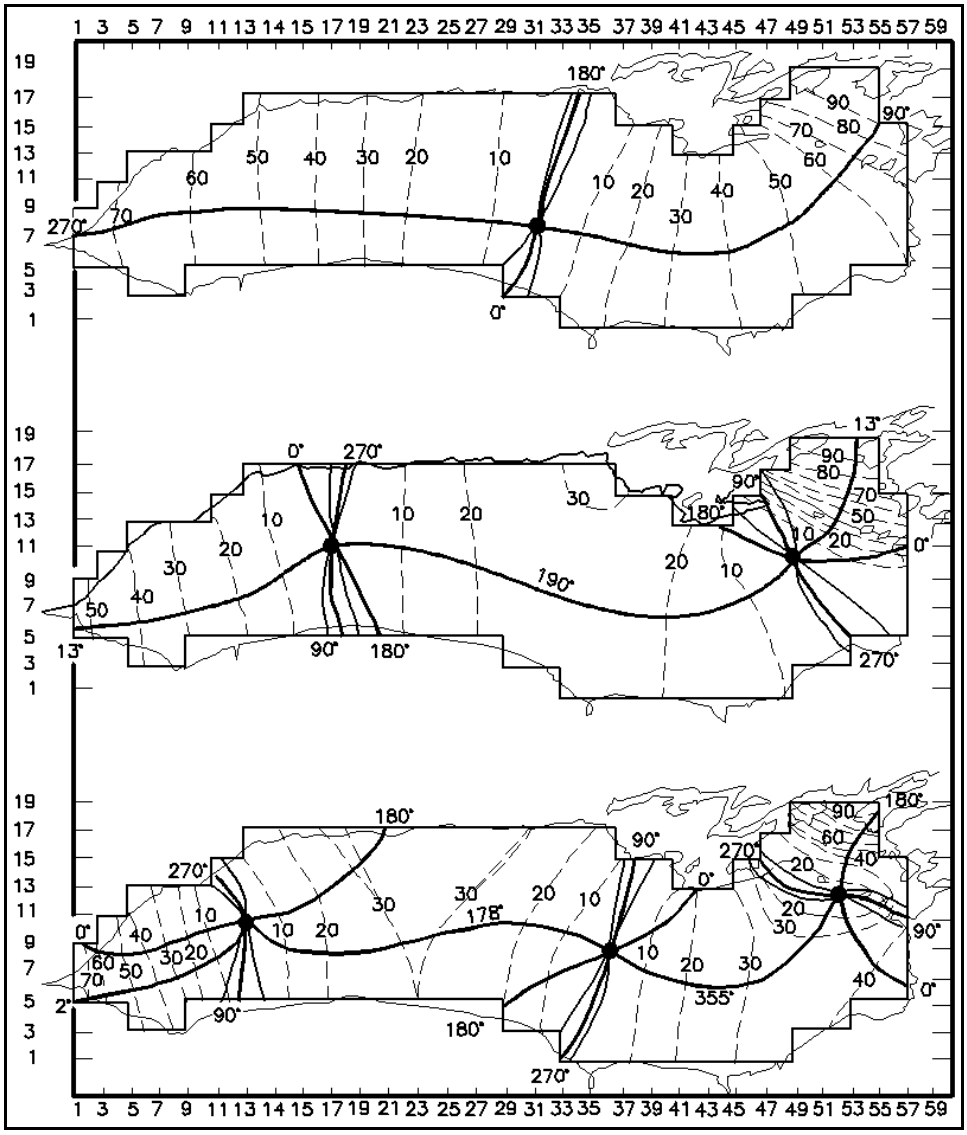

Figure II-5-31. First, second, and third normal modes of oscillation for Lake Ontario (Rao and Schwab 1976)

II-5-7. Numerical Modeling of Long-Wave Hydrodynamics

a. Long wave modeling. Most natural flow systems are extremely complex. They have variable bathymetry and irregular shorelines and are driven by a combination of tidal, wind, and pressure forcing, as well as temperature- and salinity-driven density gradient forcing. If a realistic approximation of flow hydrodynamics is necessary for the formulation of design criteria or testing of design alternatives (for example), numerical long-wave hydrodynamic models should be used. Although these models are generally not easy to apply and require mainframe computers, they provide the most accurate flow field approximation.

b. Physical models. Prior to describing example applications of numerical models, physical models may provide a viable alternative to numerical approaches if the problem of concern is not wind-dominated. For example, if a physical model of a particular estuary exists, and the problem of interest is of tidal origin,

then a physical model may be cost-effective. A substantial amount of literature on physical models and modeling is available. An extremely comprehensive source of information is Hudson et al. (1979).

c. Numerical models.

(1) Introduction.

(a) Numerical hydrodynamic models generally fall into two solution scheme categories, finite difference and finite element. Finite difference models use a rectangular orthogonal grid, although grid transformation schemes permit the mapping of the grid to conform to curvilinear boundaries. Finite element models use a variable-size, either triangular or rectangular, unstructured computational grid. The ability to define elements of variable size gives the finite element method an advantage over finite difference schemes for accurately representing areas of very complex geometry. However, both modeling techniques produce accurate results when applied correctly. Both models are in common use, as is demonstrated in the following two examples of numerical model applications to specific coastal and estuarine applications. These examples are intended to demonstrate the capability and accuracy of numerical models to reproduce natural hydrodynamic systems and generate an appreciation for the difficulty involved with applying them to specific flow-field situations.

(b) In addition to differences in computational schemes, hydrodynamic models are also categorized as 1-, 2-, and 3-dimensional. One-dimensional models provide a cross-sectional average solution to the governing equations. This class of solution is well-suited to pipeline or river flow problems, but not coastal/estuarine problems. Therefore, 1-D models are not addressed in this chapter because their solutions provide little detailed flow-field information that cannot be computed from the formulas given in Part II-1, "Water Wave Mechanics."

(c) Two-dimensional models are generally depth-integrated (depth-averaged); they provide a single velocity vector corresponding to each horizontal cell of a computational domain representing large areas of surface flow. Currents are defined at nodes or on cell faces, depending on the computational scheme used. Two-dimensional models are generally used in situations where the modeled system is well-mixed, i.e., currents are approximately uniform throughout the water column. These models are appropriate for studies in which changes in surface elevation are the primary concern. Typical examples include storm surge or lake seiche studies.

(d) An additional class of two-dimensional models is the laterally averaged model. In this case, instead of depth-averaged governing equations, a width-averaged set of equations is defined. In this form of solution, currents are defined at multiple locations through the water column; however, no horizontal distribution information is given. Laterally averaged models are generally used in conjunction with river flow, reservoir operation, and/or salinity intrusion applications and these models are not described in this manual.

(e) Three-dimensional applications are used when the vertical structure of currents is not uniform and the vertical distribution of currents is an important aspect of the study. Example applications include areas exhibiting flow reversal situations where surface currents and bottom currents flow in opposite directions. Included in this class of problems are cases in which vertical temperature and salinity gradients create density-driven flows. Although these non-tidal flows can be small in comparison to the tidal ebb and flood currents, they can contribute to residual circulation patterns that may affect the transport and dispersion of certain water quality parameters such as dissolved oxygen. An additional example may include channel-deepening effects on salinity intrusion.

(f) Before presenting example applications of models, it is stressed that all models are not equal with respect to computational speed and accuracy. Depending on how the governing equations are written and solved and how and what boundary conditions are defined and used to drive the models, any two finite-element or finite-difference models can produce different results. Therefore, for some applications, one model may produce accurate results while another formulation will be unstable and produce totally unrealistic simulations. For this reason, any application of a numerical model should begin with a calibration and verification procedure in which the model is run to reproduce the hydrodynamic flow field corresponding to a specific time period during which prototype data (i.e., surface elevations and currents) have been collected. Additional data comparisons may include hydrodynamically driven parameters such as temperatures and salinities.

(g) In the calibration phase, model parameters such as the friction factor distribution or depth resolution are adjusted to optimize the comparison of model-generated data to measured prototype data. Comparisons are generally made to surface elevations and velocities, but may include reproduction of temperature and salinity. In the verification procedure, the model is used to simulate an alternate time period containing additional prototype data. Model coefficients are not adjusted in the verification phase. An acceptable calibration and verification demonstrates that the model is capable of simulating the total flow regime over the entire computational domain. This ability is basic and necessary to the use of numerical models to quantify the flow-field response to proposed or existing changes in flow-field boundaries.

(h) If data are available or can be collected, the calibration and verification procedures represent a minimum criterion required of a model before it can be applied to any specific problem. If these two steps are not performed in a satisfactory manner, model results can only be considered qualitative. Situations do exist where prototype data are not available and cannot be obtained within the time and cost limits of the budget. In these cases, models can be used to generate qualitative trends; however, unverified model results should not be the basis for quantitative decision making unless some data are available, even at a minimum level, to demonstrate that the model is producing realistic results. This aspect of modeling may be vital to a particular project because decisions based on unverified model results can be legally challenged and shown to be invalid.

(2) Example - tidal circulation modeling.

(a) The New York Bight project (Scheffner et al. 1993) is an excellent example of tidal circulation modeling. The goal of the study was to develop a hydrodynamic simulation tool that could be used to address questions concerning how certain modifications to the New York Bight may affect the local or global hydrodynamics of the system and how the computed flow fields affected the transport of certain water quality parameters. The model was therefore required to be capable of simulating the flow-field hydrodynamics, temperature, and salinity distribution over a large computational domain.

(b) The model selected for this study was the CH3D (Curvilinear Hydrodynamics in Three (3) Dimensions) (Johnson et al. 1991) model, a three-dimensional, finite difference formulation model with boundary-fitted coordinates. The modeled area represents the region extending offshore from Cape May, NJ, and Nantucket Shoals to beyond the continental shelf, including Long Island Sound, the Hudson and East Rivers, and New York Harbor. Depths vary from less than 10 m to more than 2,000 m. The geographical boundaries are shown in Figure II-5-32a. The computational grid used to represent this area of interest is shown in Figure II-5-32b. The grid contains 76 cells in the alongshore direction and 45 cells in the cross-shore direction. There are 2,641 active computational cells in the horizontal and 10 in the vertical.

(c) The model was preliminarily tested to demonstrate steady-state response to long-term circulation patterns, wind-induced circulation, and Hudson River inflow-induced circulation. Non-steady testing included modeling of the dynamic response to tidal constituents, both to the M_2 semidiurnal tide and to mixed tides. Calibration and verification were performed for the periods of April 1976 and May 1976, respectively.

(d) Model results were compared to MESA project prototype data collected during the period from mid-September 1975 to mid-August 1976. Figure II-5-33 compares model-to-prototype tidal elevations at the Battery. A global circulation pattern of wind-field-induced circulation is shown in Figure II-5-34.

(3) Example - storm surge modeling.

(a) The coast of Delaware study (Mark, Scheffner, and Borgman 1993) provides an excellent example of storm surge modeling over very large computational domains. Goals of the effort were to generate stage-frequency relationships at a variety of locations along the open coast of Delaware and inside Delaware Bay. The study required tidal calibration and verification to demonstrate that the model could successfully reproduce tidal circulation. In addition to tide, the model was verified for storm surge by reproducing the storm surge hydrograph produced by Hurricane Gloria.

(b) Storm track and pressure information for Hurricane Gloria was extracted from the National Hurricane Center's (NOAA 1981) database and used to generate input to the PBL model. The model selected for the hydrodynamic effort was the two-dimensional depth-integrated version of the Three-Dimensional **AD**vanced **CIRC**ulation (ADCIRC) finite-element model (Luettich, Westerink, and Scheffner 1993). This application demonstrates a very large-domain modeling capability (Luettich, Westerink, and Scheffner 1993), developed for the Dredging Research Program (DRP) to compute tidal and storm surge simulations along the open coast.

(c) The DRP computational grid covers the east coast of the United States, Gulf of Mexico, and Caribbean Sea on the landward boundary. The offshore boundary is located in the mid-Atlantic Ocean, extending from Novia Scotia to Venezuela along the 60-deg west longitude line. “Continental-scale” computational domains are used in the model to minimize difficulties in specifying offshore and lateral boundary conditions.

(d) The DRP computational grid was modified to provide increased resolution in Delaware Bay and within several small bays between the entrances of the Chesapeake and Delaware Bays. Figure II-5-35 shows the global limits of the 12,000-node grid. A blow-up of the coast of Delaware and Delaware Bay areas is shown in Figure II-5-36.

(e) The ADCIRC model was verified to several locations at which NOAA tidal constituents were available. An example model-to-prototype (constituent) comparison to Lewes, DE, is shown in Figure II-5-38. Model-to-prototype data for the storm surge produced by Hurricane Gloria are also compared at Lewes, as shown in Figure II-5-39.

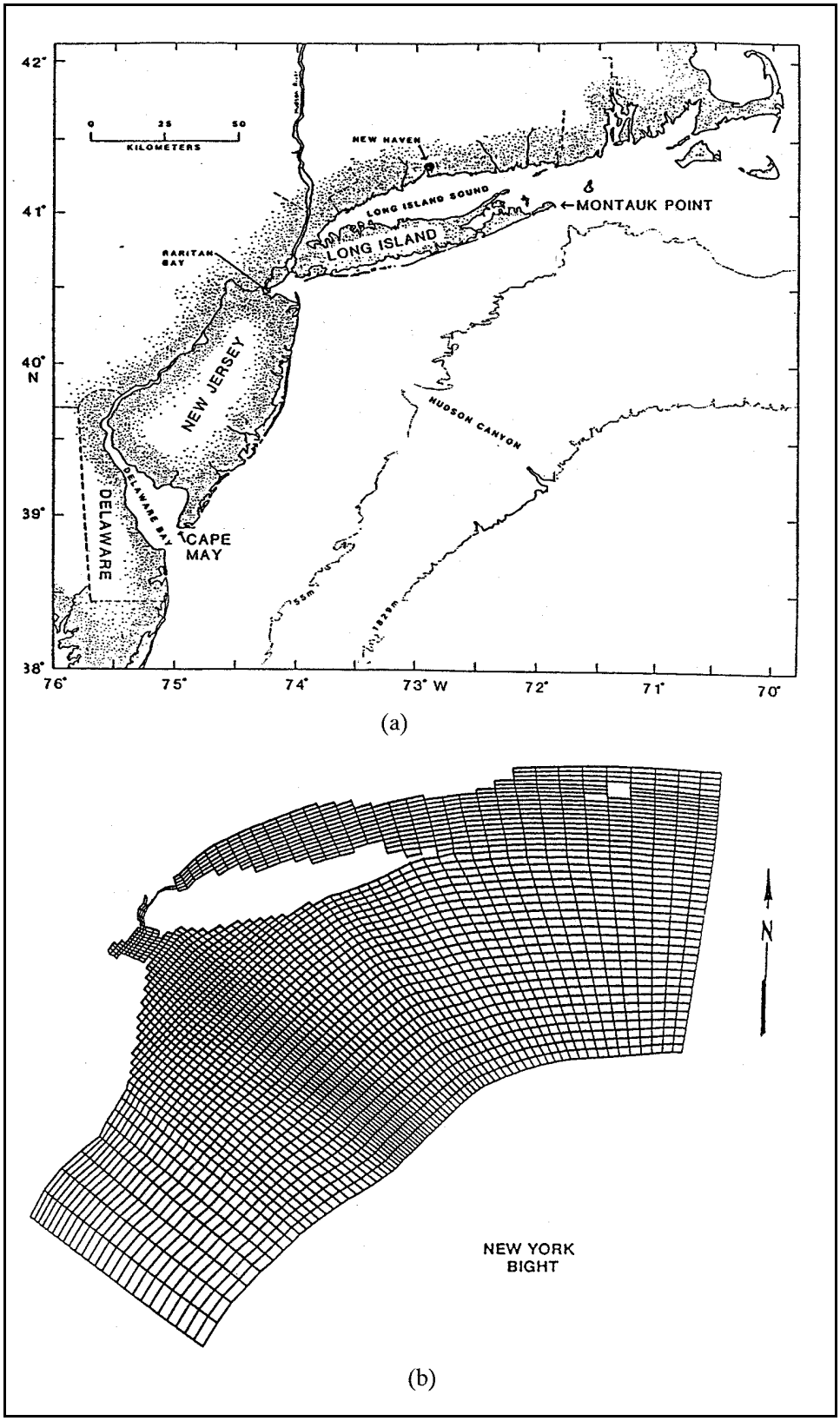

Figure II-5-32. Computational grid for the New York Bight

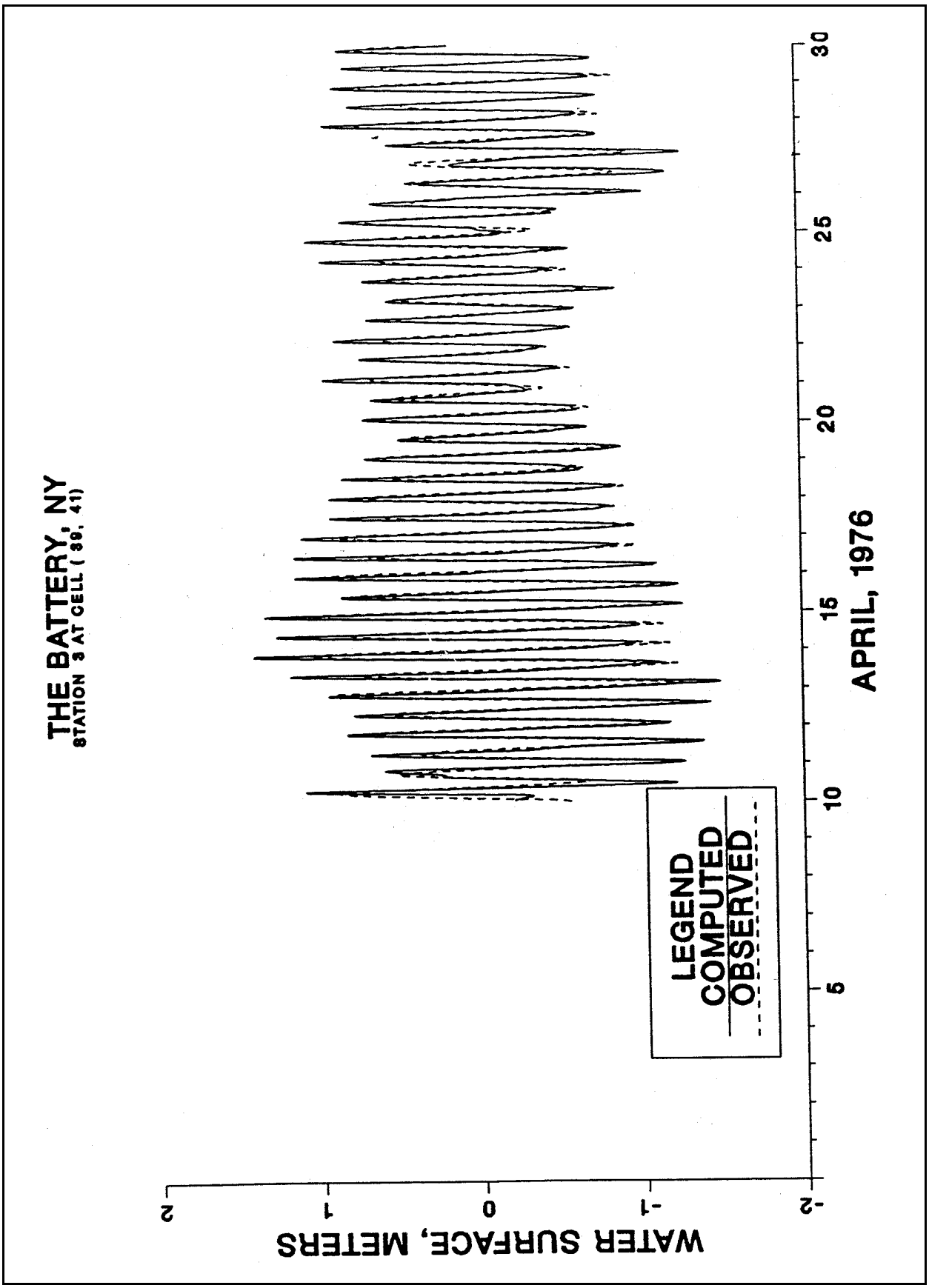

Figure II-5-33. Model and prototype tidal elevation comparison at the Battery

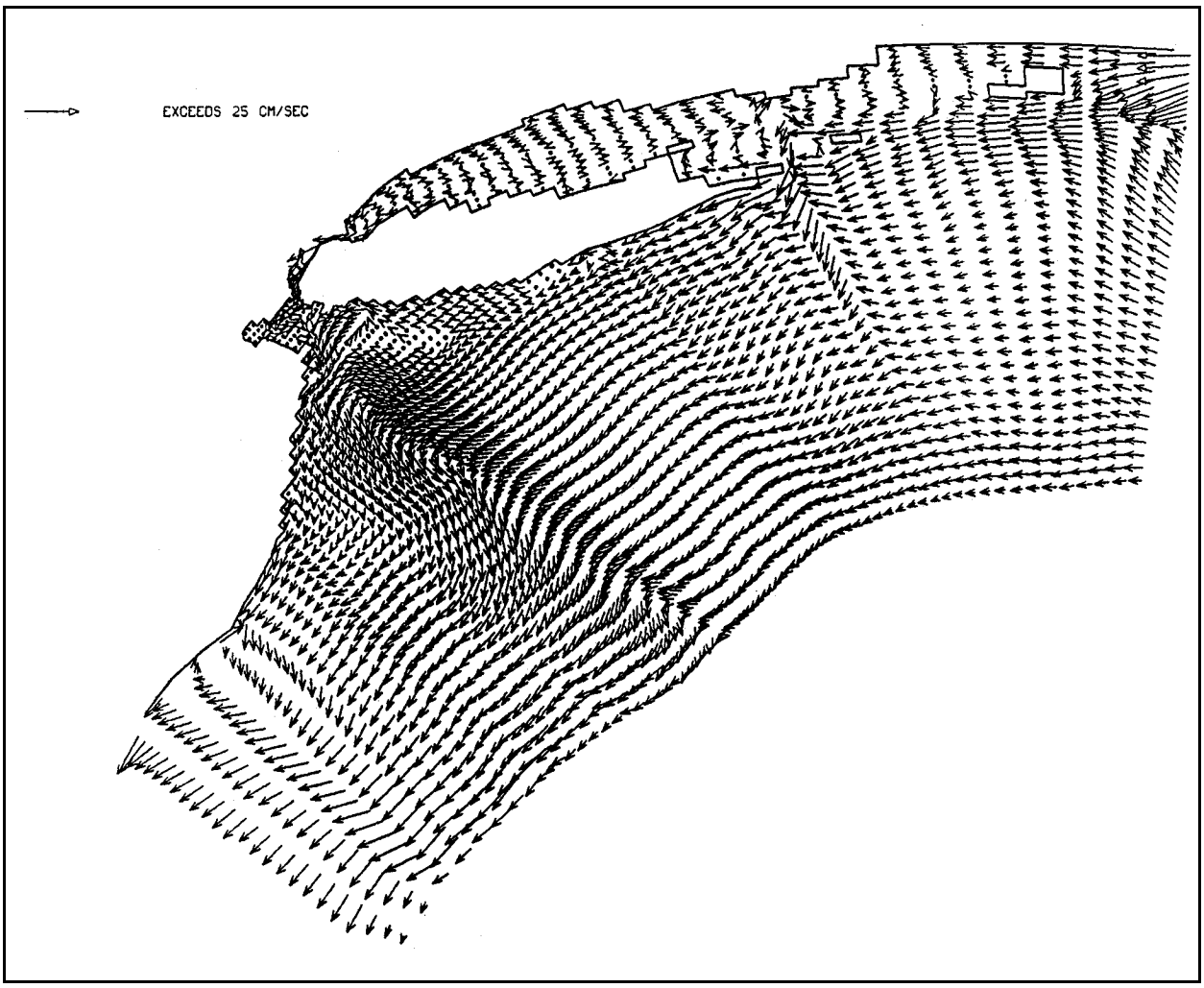

Figure II-5-34. Wind-induced circulation pattern

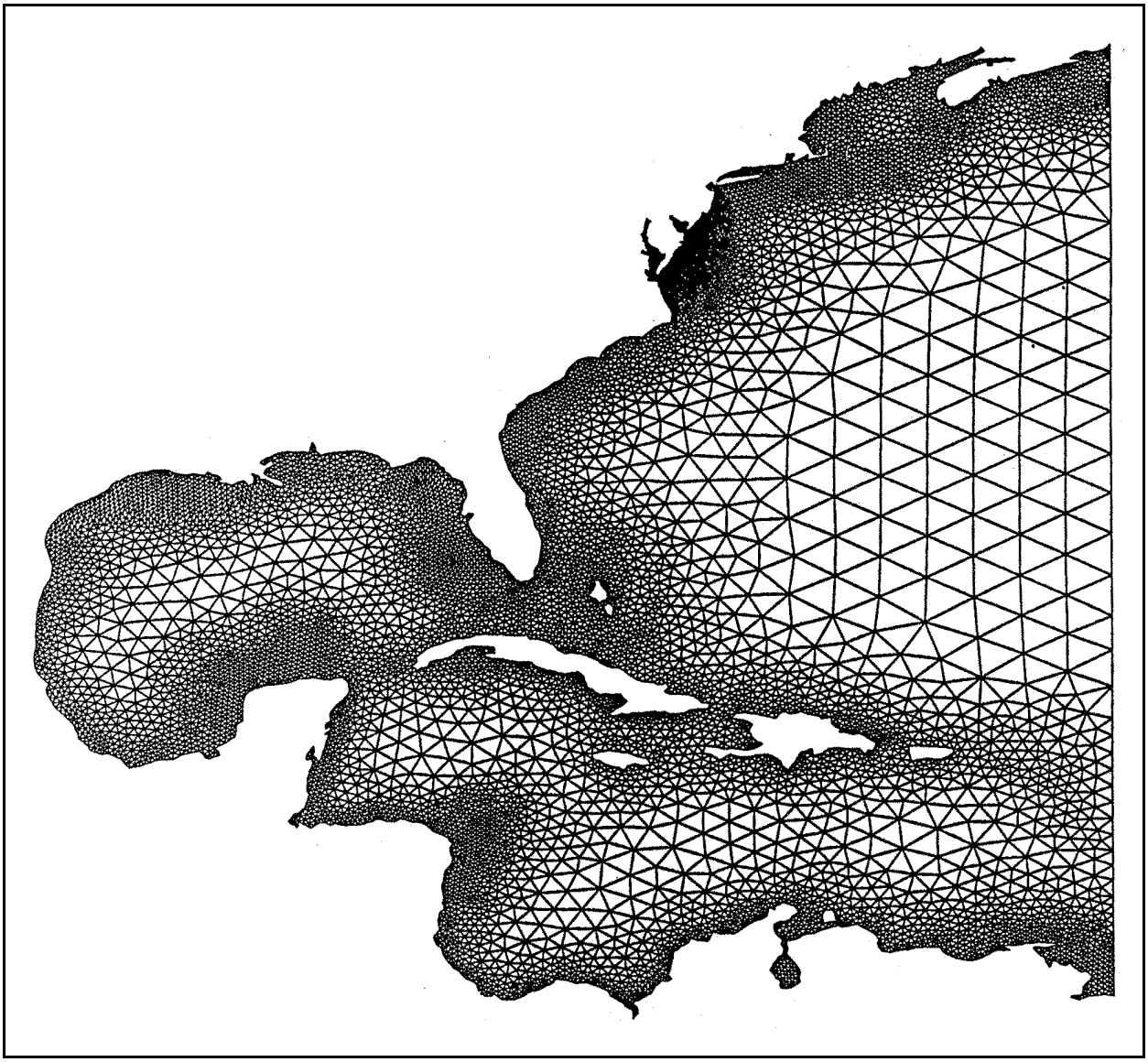

Figure II-5-35. Global limits of ADCIRC computational grid

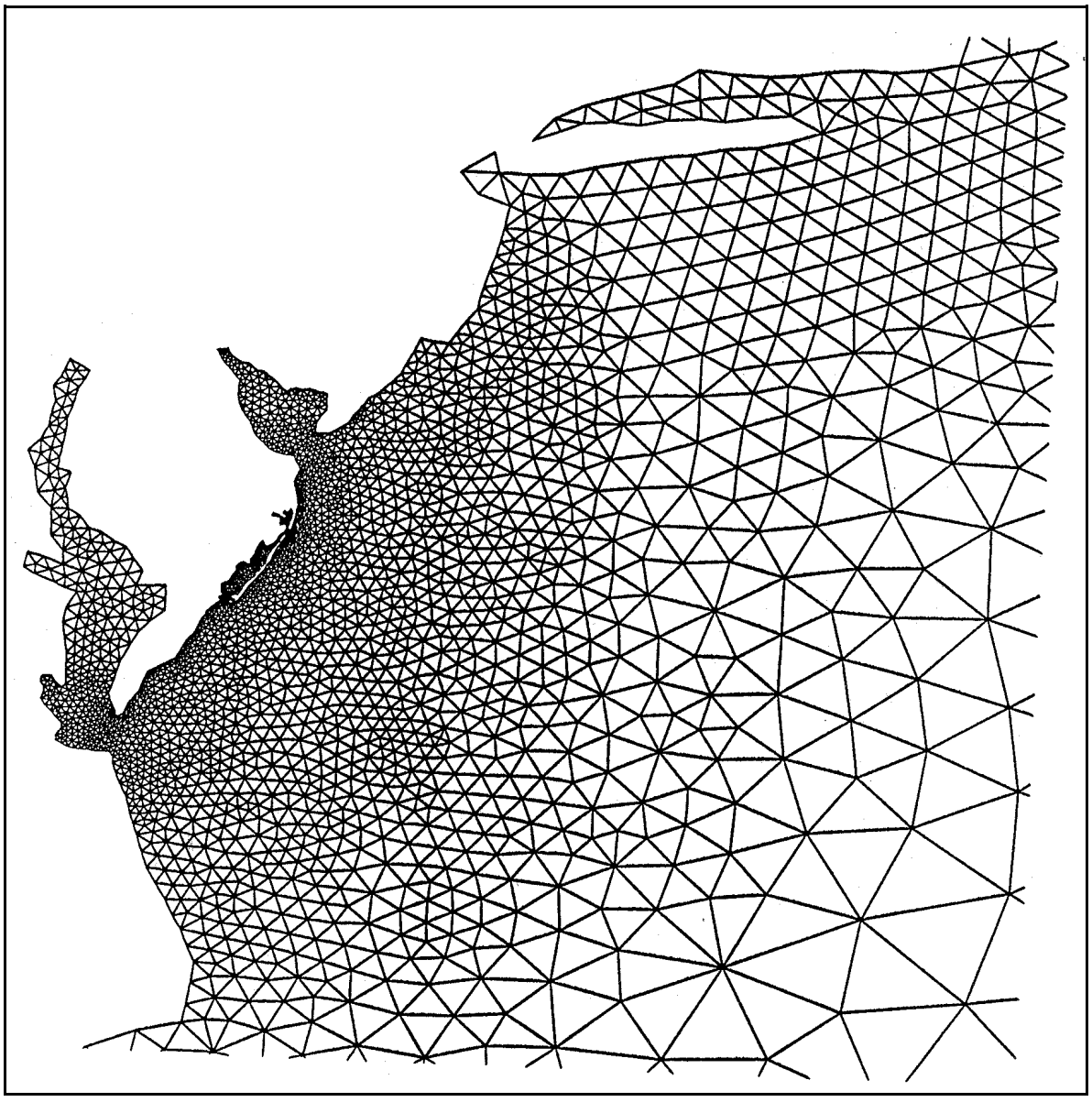

Figure II-5-36. Blow-up of ADCIRC grid along Delaware coast

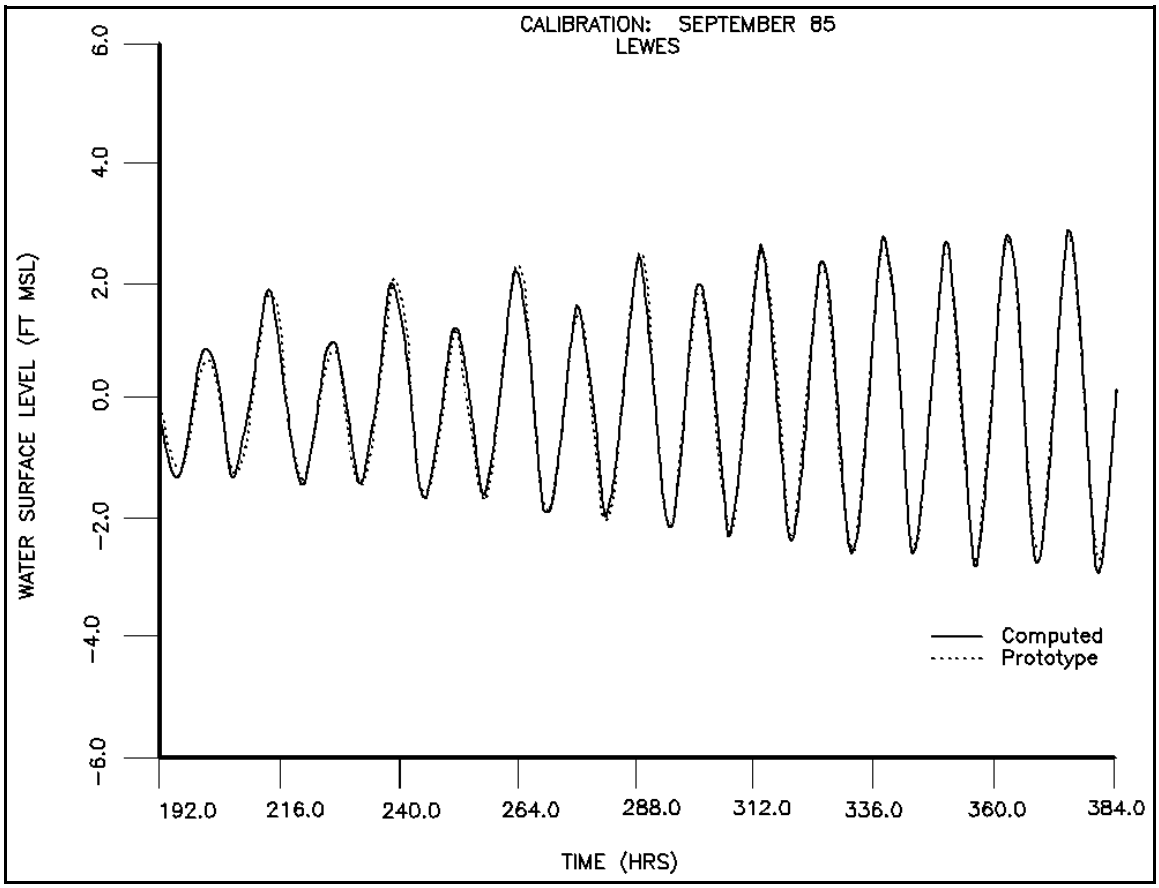

Figure II-5-37. Model-to-prototype tidal comparison at Lewes, DE

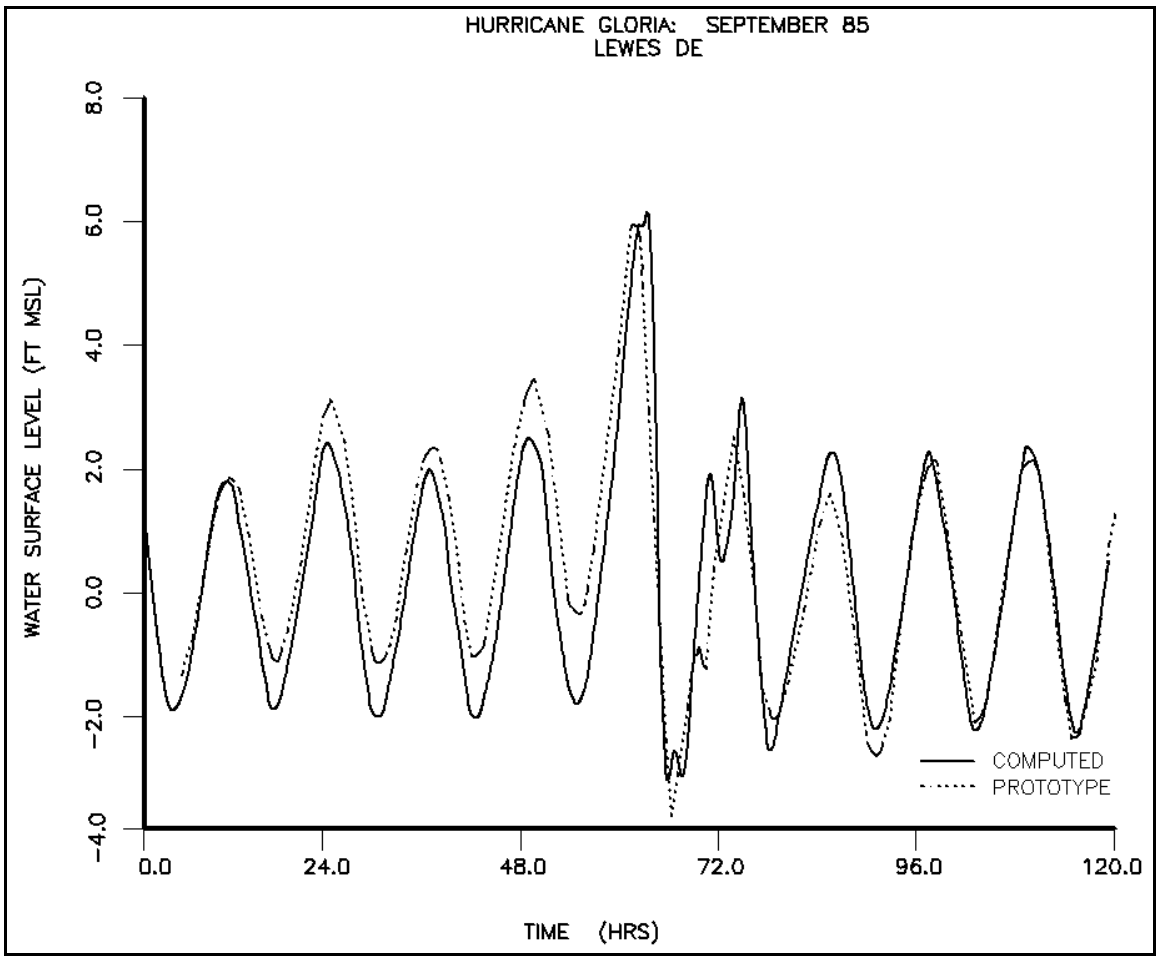

Figure II-5-38. Model-to-prototype surge comparison at Lewes, DE

II-5-8. References

EM 1110-2-1415
Hydrologic Frequency Analysis

Borgman and Resio 1982
Borgman, L. E., and Resio, D. T. 1982. "Extremal Statistics in Wave Climatology," *Topics in Ocean Physics*, A. Osborne and P. M. Rizzoli, ed., Italian Physical Society, Bologna, Italy, pp 439-471.

Borgman and Scheffner 1991
Borgman, L. E., and Scheffner, N. W. 1991. "The Simulation of Time Sequences of Wave Height, Period, and Direction," Technical Report TR-DRP-91-2, U.S. Army Engineer Waterways Experiment Station, Vicksburg, MS.

Camfield 1980
Camfield, F. E. 1980. "Tsunami Engineering," Special Report No. 6, U.S. Army Engineer Waterways Experiment Station, Vicksburg, MS.

CCCMSL 1987
Committee on Engineering Implications of Changes in Relative Mean Sea Level. 1987. "Responding to Changes in Sea Level Engineering Implications," Marine Board, Commission on Engineering and Technical Systems, National Research Council. National Academy Press, Washington, DC, 148 p.

Cialone et al. 1991
Cialone, M. A., Mark, D. J., Chou, L. W., Leenknecht, D. A., Davis, J. A., Lillycrop. L. S., Jensen, R. E., Thompson, E. F., Gravens, M. B., Rosati, J. D., Wise, R. A., Kraus, N. C., and Larson, P. M. 1991. "Coastal Modeling System (CMS) User's Manual," Instruction Report CERC-91-1, U.S. Army Engineer Waterways Experiment Station, Vicksburg, MS.

Coordinating Committee on Great Lakes Basin Hydraulic and Hydrologic Data 1992
Coordinating Committee on Great Lakes Basin Hydraulic and Hydrologic Data. 1992. Brochure on the International Great Lakes Datum 1985, U.S. Government Printing Office, 1992-644-640.

Defant 1961
Defant, A. 1961. *Physical Oceanography*, Vol II, Pergamon Press, New York.

Dronkers 1964
Dronkers, J. J. 1964. "Tidal Computations in Rivers and Coastal Waters," North-Holland Publishing Company - Amsterdam, John Wiley & Sons, Inc., New York.

Graham and Nunn 1959
Graham, H. E., and Nunn, D. E. 1959. "Meteorological Considerations Pertinent to Standard Project Hurricane, Atlantic and Gulf Coasts of the United States," National Hurricane Research Project, Report No. 33, Department of Commerce, Washington, DC.

Gravens, Scheffner, and Hubertz 1989
Gravens, M. B., Scheffner, N. W., and Hubertz, J. M. 1989. "Coastal Processes from Asbury Park to Manasquan, New Jersey," Miscellaneous Paper CERC-89-11, U.S. Army Engineer Waterways Experiment Station, Vicksburg, MS.

Gumbel 1954
Gumbel, E. J. 1954. "Statistical Theory of Extreme Value and Some Practical Application," National Bureau of Standards Applied Math. Series 33, U.S. Gov. Publication, Washington, DC.

Harris 1981
Harris, D. L. 1981. "Tides and Tidal Datums in the United States," Special Report No. 7, U.S. Army Corps of Engineers, Fort Belvoir, VA., U.S. Government Printing Office (GPO Stock No. 008-022-00161-1).

Ho et al. 1987
Ho, F. P., Su, J. C., Hanevich, K. L., Smith, R. J., and Richards, F. P. 1987. "Hurricane Climatology for the Atlantic and Gulf Coasts of the United States," NOAA Technical Report NWS 38.

Hubertz et al. 1993
Hubertz, J. M., Brooks, R. M., Brandon, W. A., and Tracy, B. A. 1993. "Hindcast Wave Information for the U.S. Atlantic Coast," WIS Report 30, U.S. Army Engineer Waterways Experiment Station, Vicksburg, MS.

Hudson et al. 1979
Hudson, R. Y., Herrmann, F. A., Sager, R. A., Whalin, R. W., Keulegan, G. H., Chatham, C. E., and Hales, L. Z. 1979. "Coastal Hydraulic Models," Special Report No. 5, Coastal Engineering Research Center, U.S. Army Engineer Waterways Experiment Station, Vicksburg, MS.

Ippen 1966
Ippen, A. T. 1966. *Estuary and Coastline Hydrodynamics*. McGraw-Hill Book Company, Inc., New York.

Jarvinen and Gebert 1986
Jarvinen, B., and Gebert, J. 1986. "Comparison of Observed Versus Slosh Model Computed Storm Surge Hydrographs along the Delaware and New Jersey Shorelines for Hurricane Gloria, September 1985," NOAA Technical Memorandum NWS NHC 32, National Hurricane Center, Coral Gables, FL.

Johnson et al. 1991
Johnson, B. H., Heath, R. E., Hsieh, H. H., Kim, K. W., and Butler, H. L. 1991. "Development and Verification of a Three-Dimensional Numerical Hydrodynamic, Salinity, and Temperature Model of Chesapeake Bay; Volume I, Main Text and Appendix D," Technical Report HL-91-7, U.S. Army Engineer Waterways Experiment Station, Vicksburg, MS.

Leenknecht, Szuwalski, and Sherlock 1992
Leenknecht, D. A., Szuwalski, A., and Sherlock, A. R. 1992. "Automated Coastal Engineering System User Guide and Technical Reference, Version 1.07," U.S. Army Engineer Waterways Experiment Station, Vicksburg, MS.

Luettich, Westerink, and Scheffner 1993
Luettich, R. A., Westerink, J. J., and Scheffner, N. W. 1993. "ADCIRC: An Advanced Three-Dimensional Circulation Model for Shelves, Coasts and Estuaries; Report 1: Theory and Methodology of ADCIRC-2DDI and ADCIRC-3DL," Technical Report DRP-92-6, U.S. Army Engineer Waterways Experiment Station, Vicksburg, MS.

Mark and Scheffner 1997
Mark, D. J., and Scheffner, N. W. 1997. "Coast of Delaware Hurricane Stage-Frequency Analysis," Miscellaneous Paper CHL-97-1, U.S. Army Engineer Waterways Experiment Station, Vicksburg, MS.

Milne-Thompson 1960
Milne-Thompson, L. M. 1960. *Theoretical Hydrodynamics*. The MacMillan Company, New York.

Morang, Mossa, and Larson 1993
Morang, A., Mossa, J., and Larson, R. J. 1993. "Technologies for Assessing the Geologic and Geomorphic History of Coasts," Technical Report CERC-93-5, U.S. Army Engineer Waterways Experiment Station, Vicksburg, MS.

National Oceanic and Atmospheric Administration 1977
National Oceanic and Atmospheric Administration. 1977. "NOAA Federal Coordinator for Meteorological Services and Supporting Research, 1977: National Hurricane Operations Plan, ΦX 77-2."

National Oceanic and Atmospheric Administration 1981
National Oceanic and Atmospheric Administration. 1981. "Tropical Cyclones of the North Atlantic Ocean 1971-1980," U.S. Government Printing Office, Washington, DC.

National Oceanic and Atmospheric Administration 1984
National Oceanic and Atmospheric Administration. 1984. "Tide Tables 1984 High and Low Water Predictions, East Coast of North and South America, Including Greenland," National Ocean Service, Rockville, MD.

Palermo et al. 1998
Palermo, M. R., Clausner, J. E., Rollings, M. P., Williams, G. L., Myers, T. E., Fredette, T. J., and Randall, R. E. 1998. "Guidance for Subaqueous Dredged Material Capping," Technical Report DOER-1, U.S. Army Engineer Waterways Experiment Station, Vicksburg, MS.

Rao and Schwab 1976
Rao, D. B., and Schwab, D. J. 1976. "Two Dimensional Normal Modes in Arbitrary Enclosed Basins on a Rotating Earth: Application to Lakes Ontario and Superior," *Philosophical Transactions of the Royal Society of London*, Vol 281, pp 63-96.

Rappleye 1932
Rappleye, H. S. 1932. "The 1929 Adjustment of the Level Net," *The Military Engineer*, Vol 24, No. 138, pp 576-578.

Saffir 1977
Saffir, H. S. 1977. "Design and Construction Requirements for Hurricane Resistant Construction," American Society of Civil Engineers, Reprint Number 2830, New York.

Scheffner 1992
Scheffner, N. W. 1992. "A Numerical Simulation Approach to Estimating Disposal Site Stability," 1992 National Conference on Hydraulic Engineering, Baltimore, MD.

Scheffner, Borgman, and Mark 1993
Scheffner, N. W., Borgman, L. E., and Mark, D.J. 1993. "Applications of Large Domain Hydrodynamic Models to Generate Frequency-of-Occurrence Relationships," *3rd International Conference on Estuarine and Coastal Modeling,* Chicago, IL.

Scheffner et al. 1994
Scheffner, N. W., Vemulakonda, S. R., Kim, K. W., Mark, D. J., and Butler, H. L. 1994. "New York Bight Study; Report 1: Hydrodynamic Modeling," Technical Report CERC-94-4, U.S. Army Engineer Waterways Experiment Station, Vicksburg, MS.

Scheffner et al. 1999
Scheffner, N. W., Clausner, J. E., Militello, A., Borgman, L. E., Edge, B. L., and Grace, P. E. 1999. Use and Application of the Empirical Simulation Technique: Users Guide, Technical Report CHL-99-21, U.S. Army Engineer Waterways Experiment Station, Vicksburg, MS.

Seabergh 1985
Seabergh, W. C. 1985. "Los Angeles and Long Beach Harbors Model Study, Deep-Draft Dry Bulk Export Terminal, Alternative No. 6: Resonant Response and Tidal Circulation Studies," Miscellaneous Paper CERC-85-8, U.S. Army Engineer Waterways Experiment Station, Vicksburg, MS.

Sears and Zemansky 1963
Sears, F. W., and Zemansky, M. W. 1963. *University Physics*. Addison-Wesley Publishing Company, Inc., Reading, MA.

Shalowitz 1964
Shalowitz, A. L. 1964. "Shore and Sea Boundaries," Vol 2, Publication 10-1, U.S. Coast and Geodetic Survey, Washington, DC.

Shore Protection Manual 1984
Shore Protection Manual. 1984. 4th ed., 2 Vol, U. S. Army Engineer Waterways Experiment Station, U.S. Government Printing Office, Washington, DC.

Scheffner et al. 1999
Scheffner, N. W., Clausner, J. E., Militello, A., Borgman, L. E., Edge, B. L., and Grace, P. E. 1999. Use and Application of the Empirical Simulation Technique: Users Guide, Technical Report CHL-99-21, U.S. Army Engineer Waterways Experiment Station, Vicksburg, MS.

Schureman 1924
Schureman, P. 1924. "Manual of Harmonic Analysis and Prediction of Tides," Special Publication No. 98, U.S. Department of Commerce, Coast and Geodetic Survey, U.S. Government Printing Office, Washington, DC.

II-5-9. Definitions of Symbols

$\vec{\nabla}$	Vector gradient operator (Equation II-5-11)
α	Inflow angle (tropical storm parameter) [deg]
ζ	Tidal phase lag [deg]
θ	Angle of storm propagation (tropical storm parameter) [deg]
κ_n	Epoch of constituent n, i.e., phase shift from tide-producing force to high tide from t_0 [deg]
κ'	Modified form of the epoch that automatically accounts for the longitude and time meridian corrections (Equation II-5-20) [deg]
λ	Mean frequency of observed events per time period used in the Poisson probability law (Equation II-5-25)
σ	Angular frequency (= $2\pi/T$) [time^{-1}]
a	Wave amplitude [length]
a_n	Speed of tide constituent n [degrees/time]
$\vec{b}_X$	Attractive force of the moon and sun at any point X (Equation II-5-10)
C	Wave celerity [length/time]
f	Universal constant (= 6.67×10^{-8} cm^3/ gm sec^2)
F_g	Gravitational force (Equation II-5-7) [force-length/time^2]
f_n	Factor for adjusting mean tidal amplitude H_n values for specific times
g	Gravitational acceleration [length/time^2]
h	Water depth [length]
$H(t)$	Height of the tide at any time t (Equation II-5-16) [length]
H_0	Mean water level above some defined datum [length]
H_n	Mean amplitude of tidal constituent n [length]
k	Wave number (= $2\pi/L = 2\pi/CT$) [length^{-1}]
L	Wave length [length]
l_B	Length of a basin [length]
M	Mass of the moon
n	Number of nodes along the axis of a basin
N	Number of storm events used in the Poisson probability law (Equation II-5-25)
$-_O$	The subscript 0 denotes deepwater conditions

p_0	Central pressure of the eye of the storm (tropical storm parameter) [force/length^2]
P_M , P_S	Harmonic polynomial expansion terms that collectively describe the relative positions of the earth, moon, and sun (Equations II-5-14 and II-5-15)
p_n	Peripheral or far-field pressure (tropical storm parameter) [force/length^2]
$P[N=n]$	Poisson probability law (Equation II-5-25)
r	Distance between the centers of mass of two bodies (Equation II-5-7) [length]
R	Radius to maximum wind (tropical storm parameter) [length]
R	Tide classification parameter (Equation II-5-22) [dimensionless]
r_m	Distance from the center of the earth to the center of the moon [length]
r_{mx}	Distance of a point located on the surface of the earth to the center of the moon [length]
r_s	Distance from the center of the earth to the center of the sun [length]
r_{sx}	Distance of a point located on the surface of the earth to the center of the sun [length]
S	Local time meridian (Equation II-5-17)
S	Mass of the sun
t	Time measured from some initial epoch or time
T	Number of years used in the Poisson probability law (Equation II-5-25)
T	Wave period [time]
T_n	Natural free oscillating period of a basin (Equation II-5-26) [time]
u	Fluid velocity (water particle velocity) in the x-direction [length/time]
V	Maximum wind (tropical storm parameter) [length/time]
V_f	Forward speed of the eye of the storm (tropical storm parameter) [length/time]
V_M , V_S	Attractive force potentials per unit mass for the moon and sun (Equation II-5-9)
w	Fluid velocity (water particle velocity) in the z-direction [length/time]
z	Water depth below the SWL [length]

II-5-10. Acknowledgments

Author of Chapter II-5, "Water Levels and Long Waves:"

Norman W. Scheffner, Ph.D., Coastal and Hydraulics Laboratory, Engineer Research and Development Center (CHL), Vicksburg, Mississippi (retired).

Reviewers:

Zeki Demirbilek, Ph.D., CHL.
Lee E. Harris, Ph.D., Department of Marine and Environmental Systems, Florida Institute of Technology, Melbourne, Florida.
Edward F. Thompson, Ph.D., CHL.

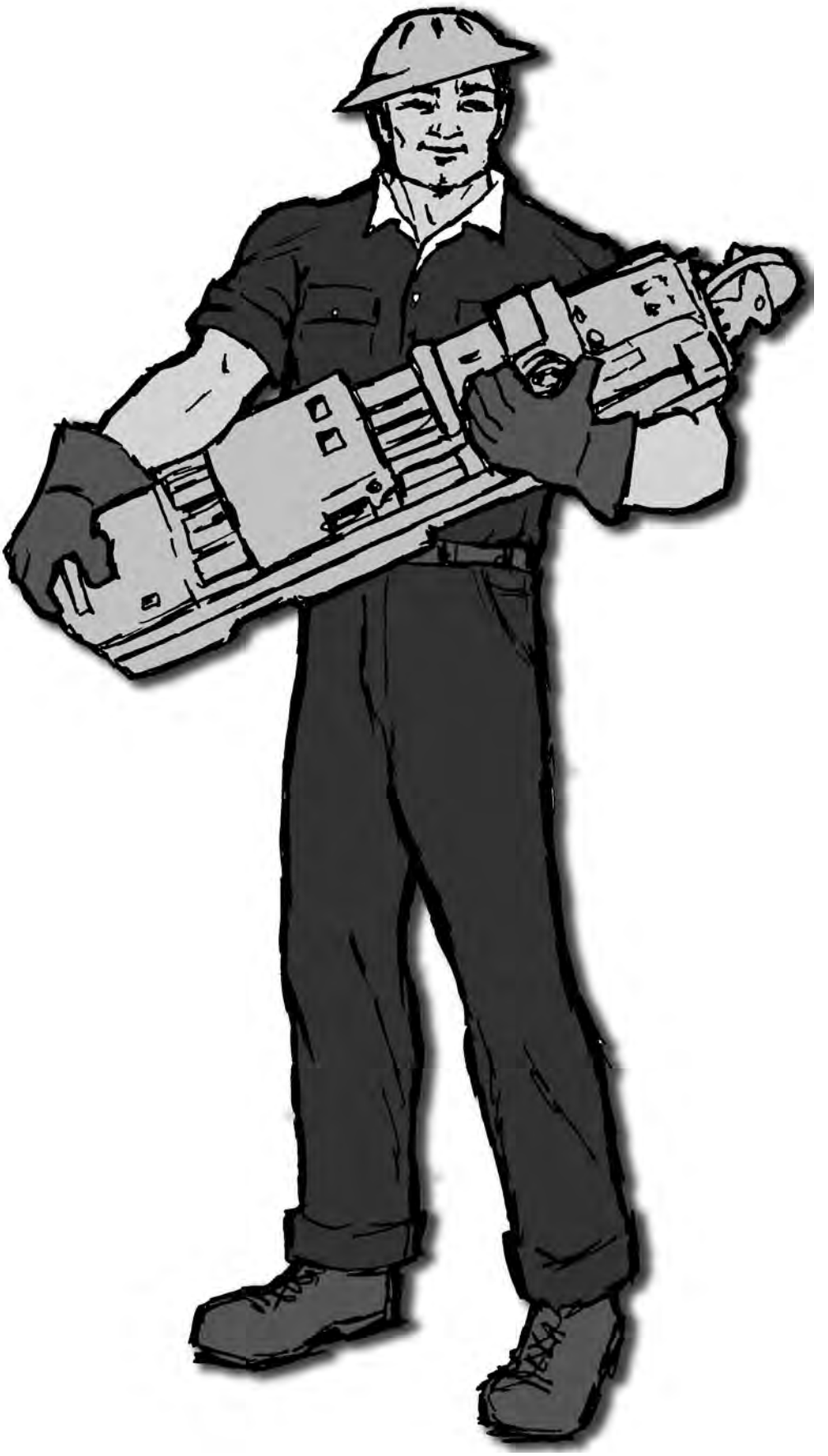

Table of Contents

Page

II-6-1. Introduction to Inlet Hydrodynamic Processes II-6-1
a. Inlet functions II-6-1
b. Inlet characteristics II-6-3
c. Inlet variables II-6-3
d. Inlet flow patterns II-6-4

II-6-2. Inlet Hydrodynamics II-6-5
a. Introduction II-6-5
b. Inlet currents and tidal elevations II-6-7
c. Tidal prism II-6-13
d. Determining important inlet parameters II-6-19
(1) Cross-sectional area II-6-19
(2) Bay area II-6-21
(3) Friction factor II-6-21
(4) Inlet length II-6-22
(5) Hydraulic radius II-6-23
e. Evaluating inlet hydraulics with Keulegan K II-6-26
(1) Introduction II-6-26
(2) Jarrett's classification II-6-26
(a) Class I: Keulegan $K < 0.3$ II-6-26
(b) Class II: Keulegan $K > 0.80$ II-6-26
(c) Class III: $0.3 < K < 0.8$ II-6-26
f. Effect of freshwater inflow II-6-26
g. Bay superelevation II-6-29
h. The inlet as a filter, flow dominance, and net effect on sedimentation processes II-6-32
(1) Introduction II-6-32
(2) Tidal constituents II-6-32
(3) Flow dominance II-6-36
i. Multiple inlets II-6-37
j. Tidal jets II-6-37
k. Tidal dispersion and mixing II-6-39
l. Wave-current interaction II-6-39
(1) Wave-current interaction II-6-40
(2) Current-channel interaction II-6-43
m. Other methods of inlet analysis II-6-43
(1) Automated Coastal Engineering System (ACES) II-6-43
(2) DYNLET1 . . . . . II-6-44
(3) Coastal Modeling System (CMS) II-6-44
(a) WIFM II-6-44
(b) CLHYD II-6-46

(4) Other models II-6-47
(5) Physical models II-6-47

II-6-3. Hydrodynamic and Sediment Interaction at Tidal Inlets II-6-47
a. Introduction II-6-47
b. Tidal prism - channel area relationship II-6-47
c. Inlet stability analysis II-6-49
d. Scour hole problems II-6-53
e. Methods to predict channel shoaling II-6-55
(1) Introduction II-6-55
(2) Procedure II-6-56
(3) Phase I: Daily littoral materials transport volumes II-6-56
(4) Phase II: Channel sedimentation II-6-57
(5) Phase III: Regression analysis II-6-58
(6) Normalized, independent filling index II-6-58
(7) Ebb tidal energy flux II-6-58
(8) Hoerls special function distribution II-6-60
f. Inlet weir jetty hydraulic and sediment interaction II-6-60
(1) Weir location II-6-60
(2) Weir length II-6-60

II-6-4. References II-6-61

II-6-5. Definitions of Symbols II-6-70

II-6-6. Acknowledgments II-6-73

List of Tables

Page

Table II-6-1. Hydraulic Characteristics of Tidal Inlets by Cubature Method II-6-28

Table II-6-2. Semidiurnal and Shallow-Water Tidal Constituents and Harmonic Frequencies II-6-36

Table II-6-3. Tidal Prism-Minimum Channel Cross-sectional Area Relationships II-6-48

Table II-6-4. Inlet Stability Ratings II-6-52

List of Figures

Page

Figure II-6-1. Typical structured and unstructured inlet II-6-2

Figure II-6-2. Typical ebb-tidal delta morphology (Hayes 1980) II-6-4

Figure II-6-3. Channel parameter measurement (Vincent and Corson 1980) II-6-5

Figure II-6-4. Ebb delta area measurement (Vincent and Corson 1980) II-6-6

Figure II-6-5. Minimum width cross-sectional area of channel A_{mw} versus channel length L_{mw} (Vincent and Corson 1980) II-6-7

Figure II-6-6. A_{mw} versus ebb-tidal delta area (AED) (Vincent and Corson 1980) II-6-8

Figure II-6-7. A_{mw} versus maximum channel depth at minimum width section DMX (Vincent and Corson 1980) II-6-10

Figure II-6-8. A_{mw} versus minimum controlling channel depth DCC (Vincent and Corson 1980) II-6-11

Figure II-6-9. Tidal prism-inlet area relationship II-6-12

Figure II-6-10. Schematic diagram of flood and ebb currents outside an inlet (O'Brien 1969) II-6-13

Figure II-6-11. Wave refraction pattern in the vicinity of Merrimack River Estuary entrance just south of the Merrimack Inlet (from Hayes (1971)) II-6-14

Figure II-6-12. Ebb and flood flow patterns from a model study of Masonboro Inlet, North Carolina II-6-15

Figure II-6-13. Tidal current plus wave-generated currents approaching jettied inlet, measured in physical model study II-6-16

Figure II-6-14. Sediment transport gyres associated with both updrift and downdrift portions of the delta at Essex River Inlet, Massachusetts (Note different arrow types to denote wave or tide-generated sediment transportation (Smith 1991)) II-6-17

Figure II-6-15. Inlet bay system II-6-18

Figure II-6-16. Variation of dimensionless parameters with Keulegan's repletion coefficient K II-6-18

Figure II-6-17. Sample tides and currents for an ocean-inlet-bay system that satisfy the Keulegan assumptions (Keulegan 1967) II-6-19

Figure II-6-18. Ratio of bay to sea tidal amplitude versus K_1 and K_2 . . . . . II-6-20

Figure II-6-19. Dimensionless maximum velocity versus K_1 and K_2 . . . . . II-6-20

Figure II-6-20. Bay tidal phase lag versus K_1 and K_2 . . . . . II-6-21

Figure II-6-21. Inlet flow net II-6-22

Figure II-6-22. Inlet impedance (F) versus the ratio of inlet length to inlet hydraulic radius to the 4/3 power ($l/R^{4/3}$) for various inlet width to inlet hydraulic radius ratios, W/R II-6-23

Figure II-6-23. Results from Example Problem II-6-1 . . . . . II-6-25

Figure II-6-24. Examples of hydraulic response of inlet and bay tide phasing and bay tide amplitude for various Keulegan K values II-6-27

Figure II-6-25. $a_{b\,max}/a_o$ versus K for values of Q_r' (river discharge model) II-6-29

Figure II-6-26. $a_{b\,min}/a_o$ versus K for values of Q_r' (river discharge model) II-6-30

Figure II-6-27. $u'_{max\,e}$ versus K for values of Q_r' (river discharge model) II-6-31

Figure II-6-28. $u'_{max\,f}$ versus K for values of Q_r' (river discharge model) II-6-32

Figure II-6-29. ε versus K for values of Q_r' (river discharge model) II-6-33

Figure II-6-30. Ratio of bay superelevation to ocean tide range as a function of the coefficient of repletion K II-6-33

Figure II-6-31. Relation between duration of outflow and bay superelevation II-6-36

Figure II-6-32. Plume expansion II-6-38

Figure II-6-33. Center-line velocity II-6-38

Figure II-6-34. Contours of dimensionless wave height factor R_H given by Equation II-6-29. Waves cannot propagate for values of F and Ω which lie in the forbidden region (boundary line F = FM) II-6-40

Figure II-6-35. Refraction of currents by channel II-6-44

Figure II-6-36. Typical inlet flow nets II-6-45

Figure II-6-37. Typical inlet cross section II-6-45

Figure II-6-38. Sea and bay water elevations at inlet 1 . . . . . II-6-46

Figure II-6-39. Average velocity at minimum cross section II-6-46

Figure II-6-40. Variations in cross-sectional area for Wachapreaque Inlet (Byrne, De Alteris, and Bullock 1974) II-6-47

Figure II-6-41. Tidal prism (P) versus jetty spacing (W) II-6-49

Figure II-6-42. Escoffier (1940) diagram, maximum velocity and equilibrium velocity versus inlet cross-sectional area II-6-51

Figure II-6-43. Another version of Escoffier (1977) diagram, maximum velocity and equilibrium velocity versus Keulegan repletion coefficient K II-6-51

Figure II-6-44. Examples of channel geographic instability II-6-53

Figure II-6-45. Little River Inlet geographical variability II-6-54

Figure II-6-46. Example Problem II-6-4. Plot of P versus A_C from the hydraulic response calculations and the stability equation II-6-55

Figure II-6-47. 1988 and 1989 bathymetry of Moriches Inlet II-6-56

Figure II-6-48. Weir jetty flow patterns II-6-57

Chapter II-6
Hydrodynamics of Tidal Inlets

II-6-1. Introduction to Inlet Hydrodynamic Processes

a. Inlet functions.

(1) Inlets provide both man and nature with a means of access between the ocean and a bay. Commercial and recreational vessels need a navigable channel for safe transit to interior harbors. The flow of currents into and out of a bay through an inlet provides natural flushing to maintain good water quality and reasonable salinity levels. The migration of fish, fish larvae, and other sea life through the inlet conduit is also an important function of an inlet. Successful engineering of inlets requires knowledge of water and sediment movement in and adjacent to the inlet.

(2) Hydrodynamic conditions at tidal inlets can vary from a relatively simple ebb-and-flood tidal system to a very complex one in which tide, wind stress, freshwater influx, and wind waves (4- to 25-s periods) have significant forcing effects on the system. Figure II-6-1 shows a structured and an unstructured inlet with waves breaking on a shallow ebb shoal nearly surrounding the inlet itself. Flow enters the bay (or lagoon) through a constricted entrance, which is a relatively deep notch (usually 4 to 20 m at the deepest point). Entrance occurs after flow has traversed over a shallow shoal region where the flow pattern may be very complex due to the combined interaction of the tidal-generated current, currents due to waves breaking on the shallow shoal areas, wind-stress currents, and currents approaching the inlet due to wave breaking on adjacent beaches. The inlet acts to interrupt longshore current, which either reinforces or interferes with tidal currents, dependent on the time in the tidal cycle. The longshore current also is variable, dependent on wave conditions. Particularly during stormy conditions with strong winds, flow patterns may be highly complex. Also, the complicated two-dimensional flow pattern is further confounded because currents transverse to the coast tend to influence the propagation of waves, in some cases blocking them and causing them to break. The inlet has a complex shoal pattern that would cause odd refraction patterns and breaking regions, even if tidal flows were weak . Final complications are structures such as jetties, which cause wave diffraction patterns and reflections.

(3) In inlets with large open bays and small tidal amplitudes, flows can be dominated by wind stress (Smith 1977). In such cases, ebb conditions can last for days when winds pile up water near the bay side of the inlet, or long floods can occur when winds force bay water away from the inlet. Most inlet bays, however, are small and some are highly vegetated, so wind stress is not a dominant feature, except under storm conditions (this chapter will emphasize tidal components of the system; Part II-5 provides approaches for considering storm surges and seiche). Though not forced by tides, inlets on large lakes may have significant currents due to seiching (Seelig and Sorensen 1977), and may be studied by the methods in this chapter. Although many bays do not receive much fresh water relative to the volume of tidal flow, substantial freshwater input due to river flow can sometimes create vertically stratified flows through a tidal inlet. Typically, however, well-mixed conditions exist for most inlets. Neither the effects of wind on the bay nor stratified flows will be examined in this chapter; however, the gross effect of freshwater flow on inlet hydraulics will be discussed.

This chapter also provides simplified methods for estimating tidal hydraulics. In general, the inlet problem requires complex, complicated analyses, and reference will be made to such techniques.

Ocean City Inlet, Maryland

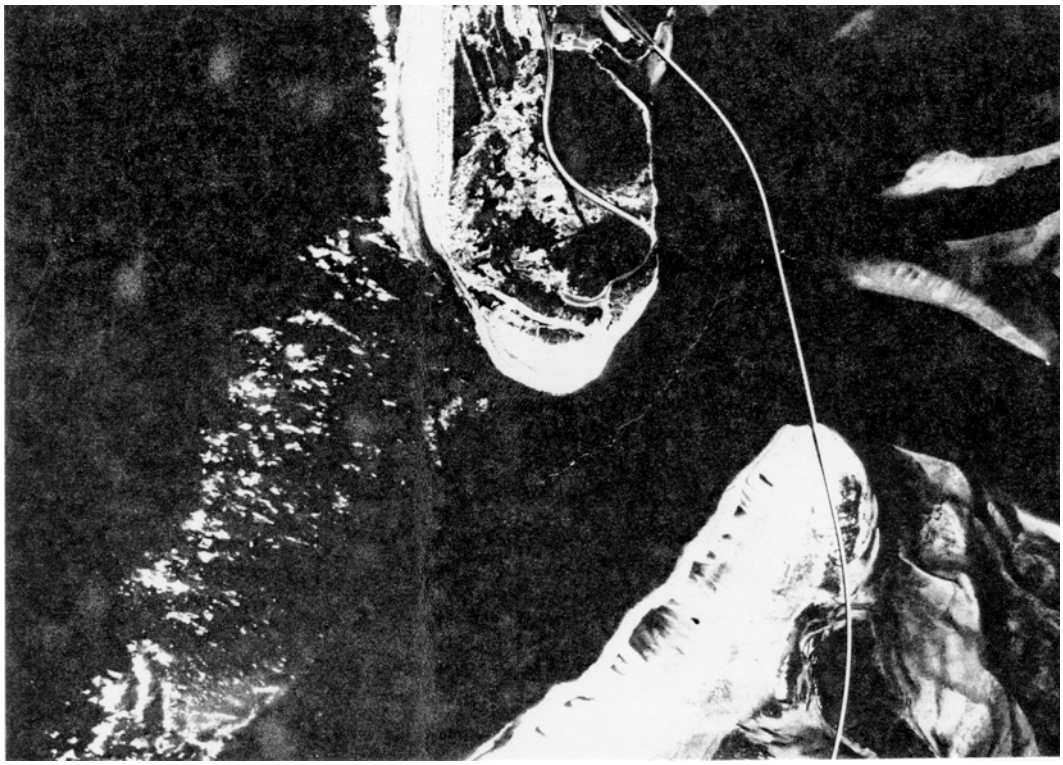

Oregon Inlet, North Carolina

Figure II-6-1. Typical structured and unstructured inlet

b. Inlet characteristics.

(1) Tidal inlets generally have a short, narrow channel passing between two sandy barrier islands (Figure II-6-1) and connect the ocean (or sea) to a bay. Some bays are small enough (on the order of tens of kilometers or less) for the water surface to rise and fall uniformly (co-oscillate) in response to the forcing ocean tide. Larger estuaries sometimes have broader junctions with the sea and may be long enough (hundreds of kilometers) to contain nearly an entire tidal wave length, thus having a variable water level at a given instant of time throughout the bay. Most methods discussed in this chapter apply to inlets that are closer to having a co-oscillating tide, but can be applied to most inlet systems as long as the tidal period is long compared to the time required for a shallow-water wave to propagate from the inlet to the farthest point in the bay, i.e.,

$$T >> \frac{L_b}{\sqrt{gd_b}} \tag{II-6-1}$$

where L_b is the distance to the farthest point, d_b is average bay depth, and T is typically taken as 12.42 hrs × 60 min/hr × 60 sec/min or 44,712 sec (for locations with semidiurnal or twice daily tides) or 89,424 sec for once-daily tides.

(2) The configuration of an individual inlet can vary significantly over time. Often the configuration is highly influenced by geology or peculiarities of the site, rather than a simple equilibrium of sediment and hydrodynamics. Convergence of flows from several directions at either side of the inlet can create strong turbulence that scours the channel deeply through the narrowest part of the inlet, called the inlet gorge, and silts in the channel on the bay and ocean sides. Maximum depths generally in the range of 4-15 m may occur in such channels, whereas seaward channel depths may diminish to 1.5-3 m where the flow has diffused and wave-driven sediment transport is important. Inside the inlet, water may diverge into one or more channels among shoal areas created by the deposition of sand from the ocean beaches. The resulting bathymetry can be a complex pattern of bars, shoals, and channels. Hayes (1980) shows the ocean-side ebb-tidal delta morphology for an unstructured inlet (Figure II-6-2).

c. Inlet variables. Although inlet systems can be quite complex, for the purpose of simple hydraulic analysis, the immediate inlet region can be approximated by key parameters which, although simplified, permit an analytical treatment of its hydraulics and a useful analysis of inlet systems. Analysis by Vincent and Corson (1980, 1981) shows the range of size of a number of inlet parameters based on 67 inlets that had been subjected to little or no human intervention. Figure II-6-3 defines an oceanside channel length L_{mw} (used for their particular study, and not to be confused with channel length defined later), depth at the crest of the outer bar in the channel (DCC), and location of inlet minimum width A_{mw}. Figure II-6-4 defines the area of the ebb tidal delta, AED, bounded by the depth contour of DCC (until it parallels the shoreline), the line joining this location and the shoreline and the line across the inlet minimum width. Cross-sectional area at the minimum inlet width (A_{mw}) is plotted against channel length (L_{mw}) in Figure II-6-5, against ebb tidal delta area (AED) in Figure II-6-6, against maximum channel depth (DMX) measured at minimum width section in Figure II-6-7, and against channel-controlling depth (DCC), the minimum depth across the outer bar, in Figure II-6-8. All parameters vary in log-linear relation to A_{mw} over several orders of magnitude. The 95-percent confidence bands are also plotted. O'Brien's (1931) observed that there is a direct relationship between the inlet's minimum cross-sectional flow area A (this is the minimum area A_c, not necessarily the area at the location of the minimum width), and the tidal prism (P) filling the bay (Figure II-6-9). This relationship will aid in defining the stability of inlet channels. The tidal prism in this case is defined as the volume of water entering through the inlet on a spring tide. Detailed methods to define inlet parameters will be discussed later.

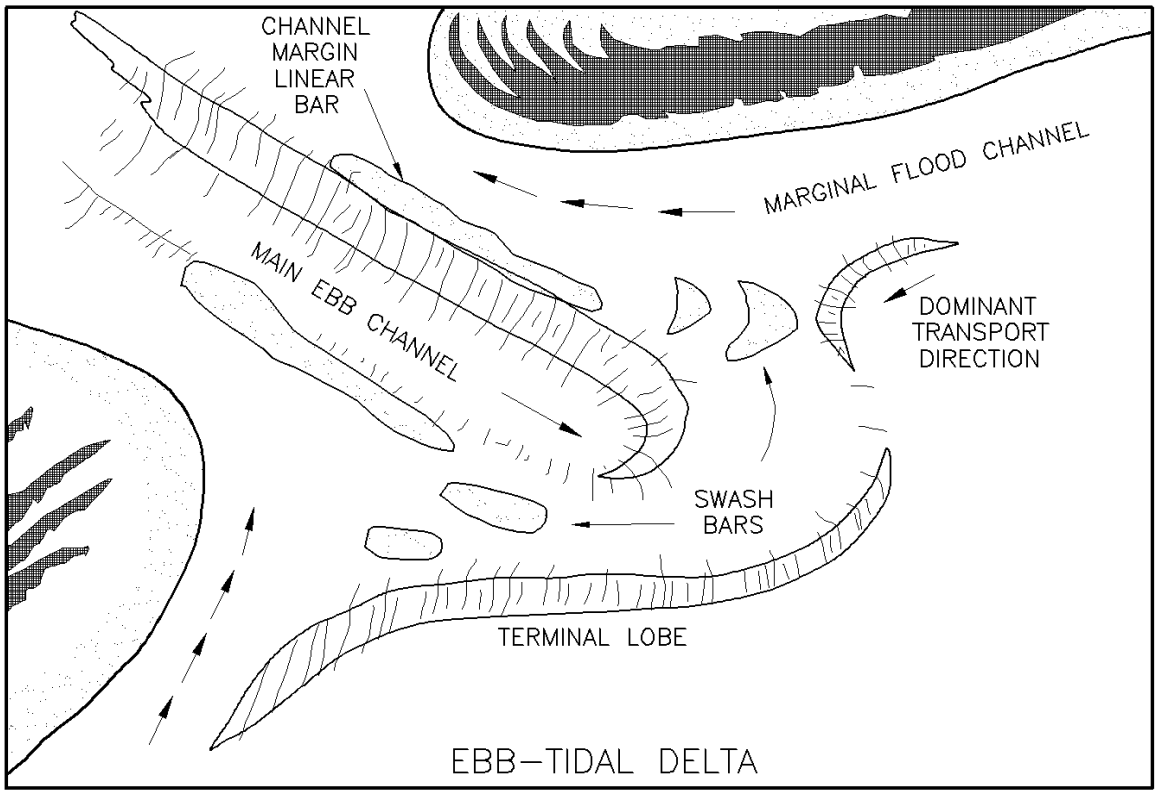

Figure II-6-2. Typical ebb-tidal delta morphology (Hayes 1980)

d. Inlet flow patterns.

(1) An inlet has a "gorge" where flows converge before they expand again on the opposite side. Shoal (shallow) areas that extend bayward and oceanward from the gorge depend on inlet hydraulics, wave conditions, and general geomorphology. All these interact to determine flow patterns in and around the inlet and locations where flow channels occur.

(2) Typical flood and ebb current patterns on the ocean side of a tidal inlet are shown in Figure II-6-10. The important aspect of this general circulation pattern is that currents usually flow toward the inlet near the shoreline (in the flood channels), even on ebb tide. The reason for this seeming paradox is the effect of wave-driven currents, (on the downdrift side of the inlet, breaking waves are turned toward the inlet due to refraction over the outer bar and on breaking, create currents toward the inlet). Further downdrift, currents are directed away from the inlet (an example of this is given in Figure II-6-11) and the effect of the ebb jet convecting or entraining ocean water as it exits the inlet creates an alongshore current at the base of the ebb jet. The “sink” flood flow pattern of the previous flood tide flow's momentum also helps sustain this flow pattern. Figure II-6-12 shows ebb and flood flow patterns from a model study of Masonboro Inlet, North Carolina, for both pre- and post-jetty conditions. Figure II-6-13 shows strength and direction of wave-generated currents plus tidal currents approaching a jetty at an inlet as measured in a physical model study. Figure II-6-14 shows the complexity of sediment flow patterns at an inlet as resolved by a field study at Essex River Inlet, Massachusetts (Smith 1991). Ebb and flood flow patterns are discussed in detail in Part II-6-2, paragraph *j*, *Tidal jets.*

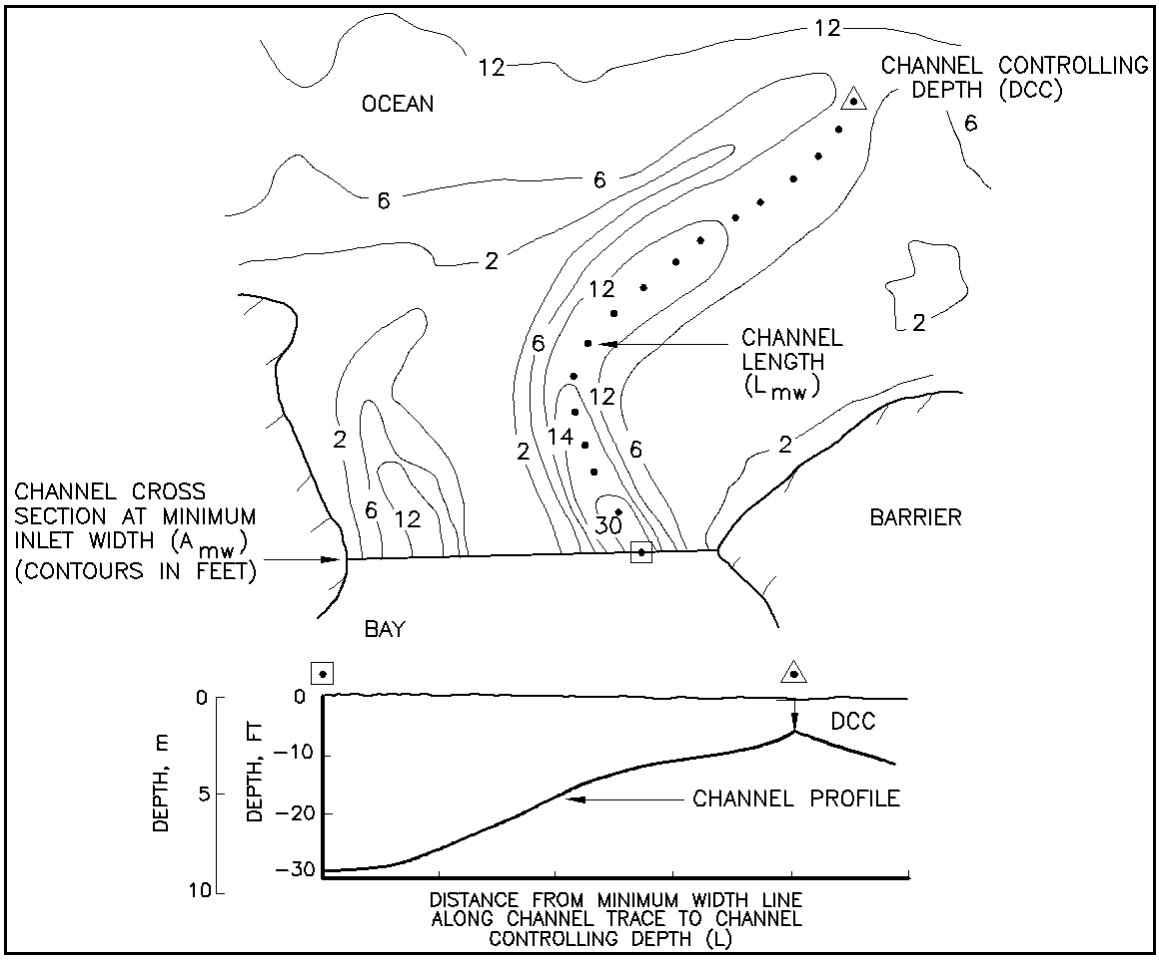

Figure II-6-3. Channel parameter measurement (Vincent and Corson 1980)

II-6-2. Inlet Hydrodynamics

a. Introduction.

(1) Many approaches are available to evaluate inlet hydrodynamics. Analytic expressions, numerical models, and physical models can be used. This section will present some simple analytic techniques to determine average velocities in a channel cross section due to the ocean tide and tidal elevation change in the bay. This section also will aid in understanding inlet response with regard to important parameters such as size of bay or channel area and length. Tidal inlet hydrodynamics are summarized by van de Kreeke (1988) and by Mehta and Joshi (1984).

(2) To characterize the development of inlet currents, COL E. I. Brown (1928) wrote the following:

To trace the characteristics of the flow of the tides through an inlet, assume the case of an inland bay being formed by the prolongation of a sandspit. It is quite evident that in the earlier stages of the growth of the spit the tide will rise and fall in the bay equally and simultaneously with its rise and fall in the surrounding ocean, and that a tidal current will be practically negligible. This state of affairs will continue for a long time, as long as the full and free propagation of the tidal wave is

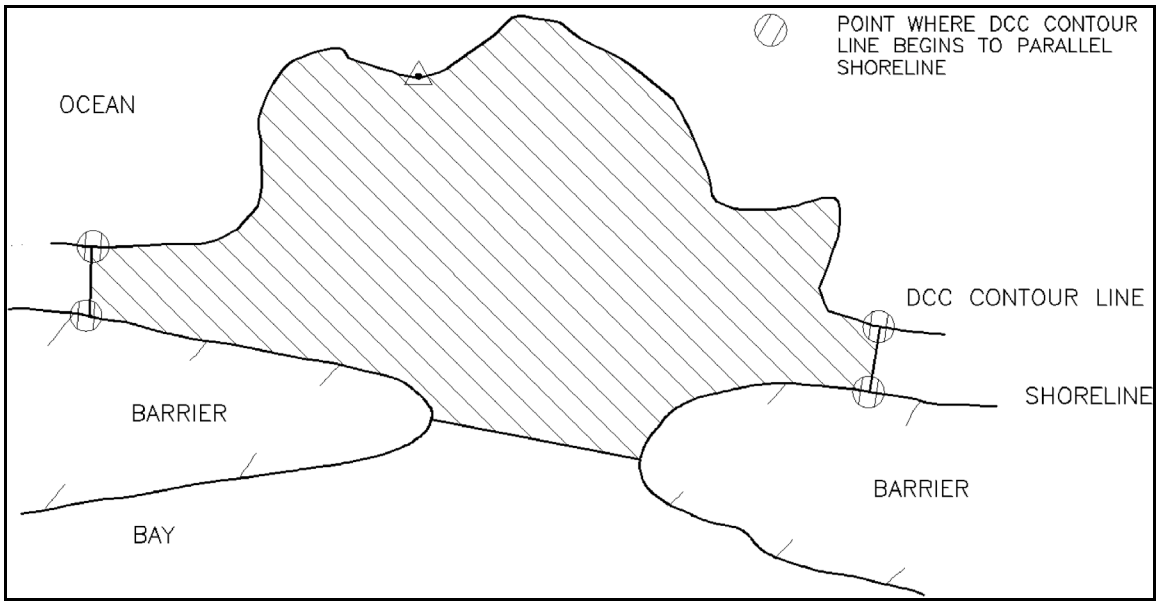

Figure II-6-4. Ebb delta area measurement (Vincent and Corson 1980)

unimpeded by the continually narrowing opening. When it does begin to be so impeded and the entrance acts as a barrier to the incoming tide, a delay in the advance of the tide will be caused, and a difference of head will occur between the water outside the inlet and that inside. This will create a hydraulic current into the bay, in addition to such movement as may be due solely to tidal wave propagation.

It is clear that as long as the inlet is wide and deep in proportion to the area of the bay, hydraulic currents will be small and tidal wave propagation will predominate. Tidal waves in the shallow waters near the shore will be essentially waves of translation, that is, the whole body of water moves with practically the same velocity horizontally. Now, if the size of the inlet becomes very small with respect to the bay area, tidal wave propagation will be negligible, the flow through the inlet will be hydraulic, that is, the water surface through the inlet will have a slope, causing a flow, and it can be considered mathematically in accordance with known hydraulic laws.

(3) With this in mind, early development of inlet hydraulics achieved reasonable results by using simplified approaches of steady-flow hydraulics to understand inlet currents and response of the bay (or lagoon) tide (Brown 1928). Keulegan (1951, 1967) solved the one-dimensional, depth-averaged shallow water wave equation for flow analytically. Others since have formulated a variety of analytical solutions for inlets (including van deKreeke (1967), Mota Oliveira (1970), Shemdin and Forney (1970), King (1974), Mehta and Özsöy (1978), Escoffier and Walton (1979), and DiLorenzo (1988)). Paralleling analytical development, physical models were used for detailed studies of inlet design (see below). More recently, numerical models have provided greater refinements and details using one-, two- and three-dimensional longwave equations of motion (including developments by Harris and Bodine (1977), Butler (1980), and Amein and Kraus (1991)). Some analytical models for inlets will be examined here to provide understanding of the inlet system and because they actually produce usable information with minimal effort. Application of the techniques of this chapter would include use of numerical models (e.g., Automated Coastal Engineering System (ACES); Leenknecht et al. 1992). ACES includes a spatially integrated one-dimensional numerical model. Additional information about ACES and other available models is provided in Part II-6-2, paragraph *m, "Other methods for inlet analysis."*

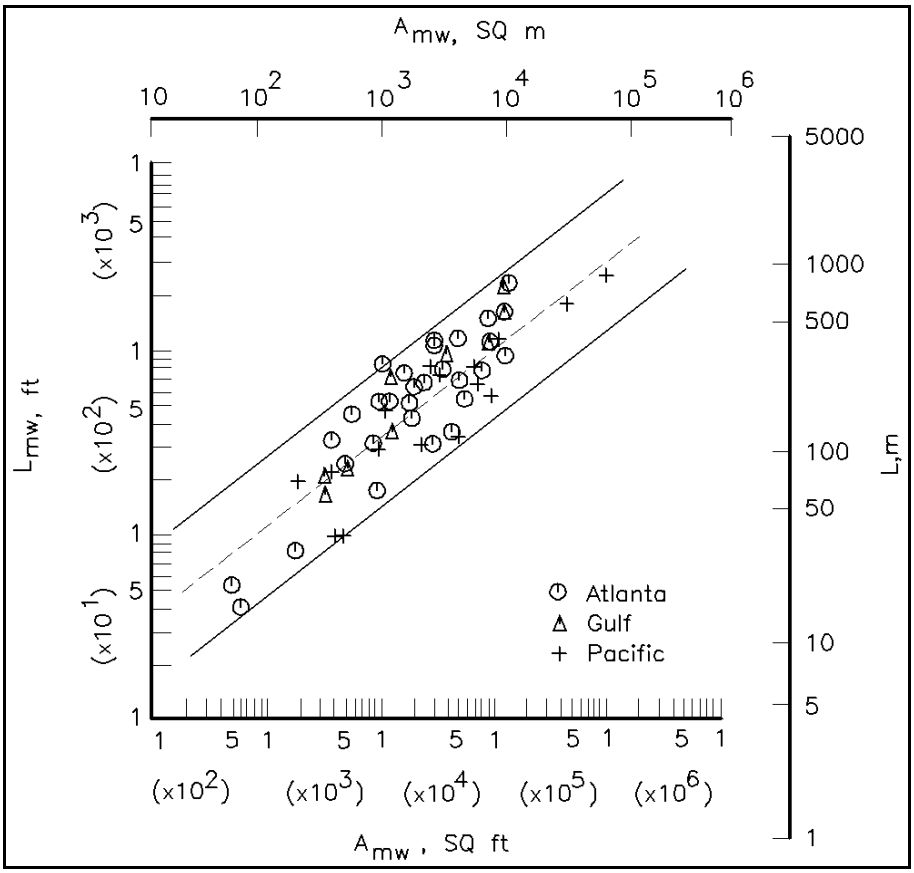

Figure II-6-5. Minimum width cross-sectional area of channel A_{mw} versus channel length L_{mw} (Vincent and Corson 1980)

b. Inlet currents and tidal elevations.

(1) A simple introduction to inlet hydraulics will consider applying the one-dimensional equation of motion and the continuity equation. We want to find the maximum inlet current, the tide range of the bay and the phase lag of the bay tide relative to the tide in the ocean in terms of parameters which can be easily measured or determined, including inlet cross-sectional area, bay surface area, ocean tide amplitude and period, length of channel, and head loss coefficients. The simplified inlet system is shown in Figure II-6-15. Keulegan's assumptions (1967) were as follows:

(a) Walls of the bay are vertical.

(b) There is no inflow from streams.

(c) No density currents are present.

(d) Tidal fluctuations are sinusoidal.

(e) Bay water level rises uniformly.

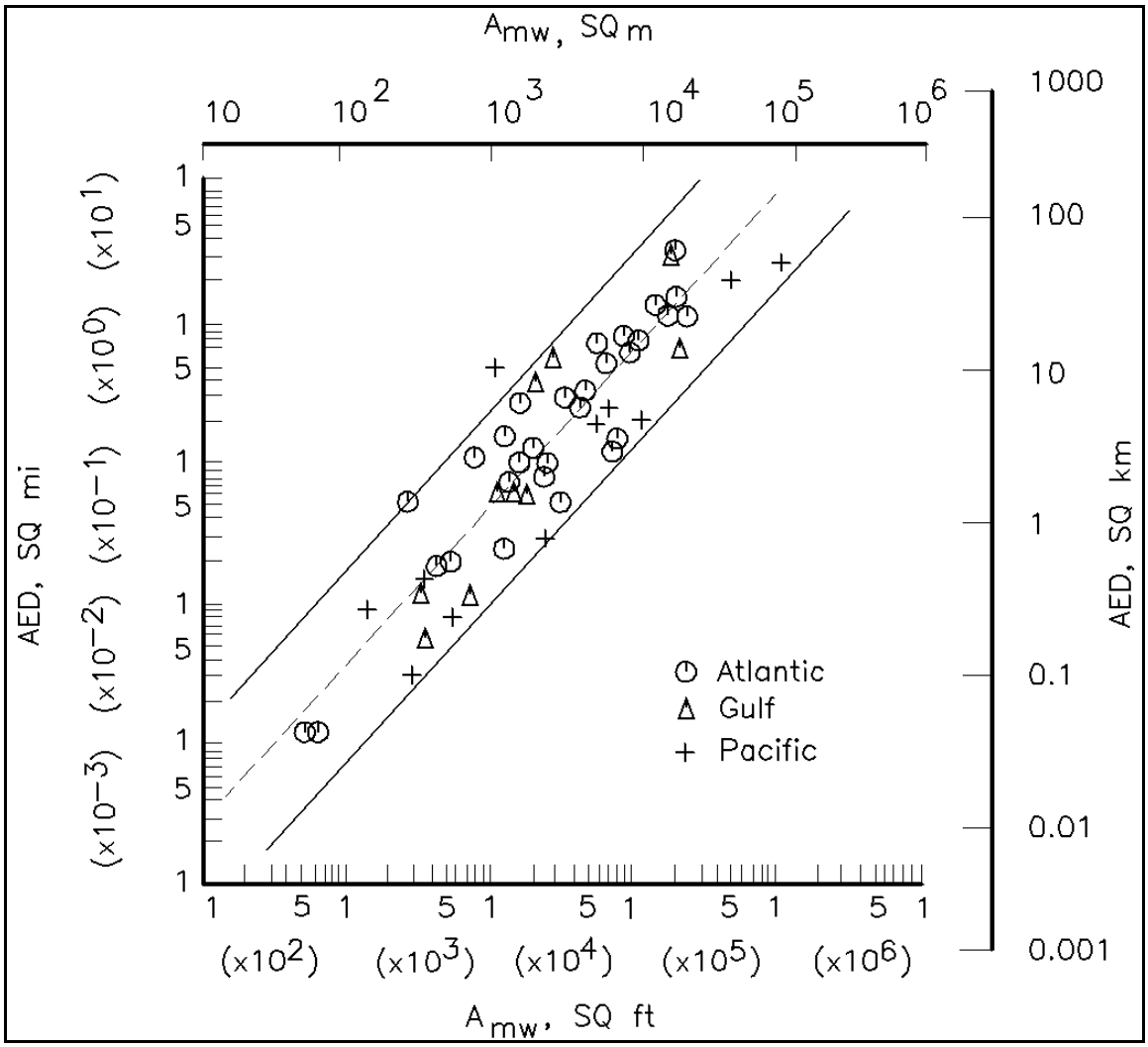

Figure II-6-6. A_{mw} versus ebb-tidal delta area (AED) (Vincent and Corson 1980)

(f) Inlet channel flow area is constant.

(g) Inertia of the mass of the water in the channel is negligible.

(2) Some assumptions may seem stringent (e.g., assumption (e), which essentially assumes a frictionless bay). This could be a problem if the entire bay is composed of very shallow tidal flats with no significant channelization. Also, in assumption (f), a relatively large tidal range compared to channel depth might occur. However, reasonable results can be determined for most cases. For more complex inlet systems, more sophisticated modeling should be performed, as discussed earlier.

(3) The one-dimensional equation of motion for flow in the channel is:

$$\frac{\partial V}{\partial t} + V\frac{\partial V}{\partial x} = -g\frac{\partial h}{\partial x} - \frac{f}{8R}V|V| \qquad \text{(II-6-2)}$$

where

V = average velocity in channel

h = channel water surface elevation

f = Darcy - Weisbach friction term

R = hydraulic radius

g = acceleration due to gravity

(4) Keulegan neglected local acceleration (the first term in Equation II-6-2) and integrated the equation over the length of the inlet. Using the equation of continuity for flow through the inlet into the bay:

$$VA_{avg} = A_b \frac{dh_b}{dt} \tag{II-6-3}$$

where

A_{avg} = average area over the channel length

A_b = surface area of bay

dh_b/dt = change of bay elevation with time

(5) Combining Equations II-6-2 and II-6-3, Keulegan developed a solution for velocity and resulting bay tide which contained the dimensionless parameter K, known as the coefficient of repletion, or filling, which is defined as

$$K = \frac{TA_{avg}}{2\pi A_b} \sqrt{\frac{2g}{a_o \left[k_{en} + k_{ex} + \frac{fL}{4R} \right]}} \tag{II-6-4}$$

where A_{avg}, A_B , g, f, and R are as defined above, and

T = tidal period

a_O = ocean tide amplitude (one-half the ocean tide range)

k_{en} = entrance energy loss coefficient

k_{ex} = exit energy loss coefficient

L = inlet length

R = inlet hydraulic radius (see Equation II-6-18)

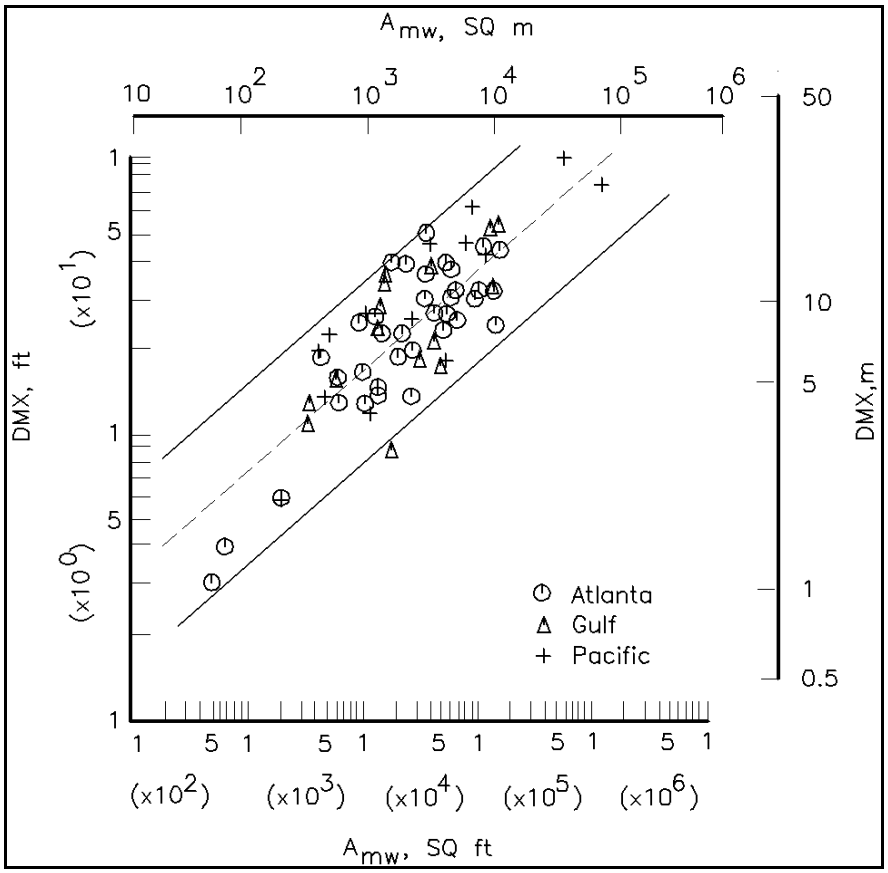

Figure II-6-7. A_{mw} versus maximum channel depth at minimum width section DMX (Vincent and Corson 1980)

(6) Keulegan's assumptions of prismatic channel cross section and vertical bay walls greatly simplify prototype conditions, because natural inlets generally have a complex morphology, making accurate determination of effective hydraulic radius, channel length, cross-sectional area, and bay area difficult. Considerable subjectivity is required to determine these values from bathymetric charts. Some aid is provided later in determining this information. Figure II-6-16 shows the variation of bay tide amplitude (a_b) to that of the ocean (a_o) and the phase lag (ε) for various values of the coefficient of filling K. Figure II-6-17 defines phase lag and provides a sample of output that can be determined from simple analytical models. Approximate values for k_{en}, k_{ex}, and f are given in Example Problem II-6-1. For flow entering an inlet channel, K_{en} is usually taken between 0.005 and 0.25. For natural inlets, which are rounded at the entrance, $K_{en} \simeq 0.05$ or less. For inlets with jetties and flow bending sharply as it enters the inlet channel, $K_{en} = 0.25$ may be appropriate. The exit flow is usually taken near unity, meaning kinetic head is fully lost. If there is significant flow inertia, as in a very channelized bag, K_{ex} may be less than 1.0.

(7) King (1974) solved the same equations but included the effect of inertia (first term of Equation II-6-2). If inertia effect is important, then at times when the tide curves of ocean and bay intersect, there still would be a flow into the bay, e.g., on flood flow there would still be movement of the water mass into the bay, even as the bay elevation dropped below that of the ocean. This would be likely to occur when L is large (channel is long, and therefore a large mass of water moving through the inlet has significant inertia to move against an opposing head difference). Also the possibility exists that the inlet system could have a Helmholtz frequency (or pumping mode, where the basin oscillates uniformly) that is tuned to the forcing

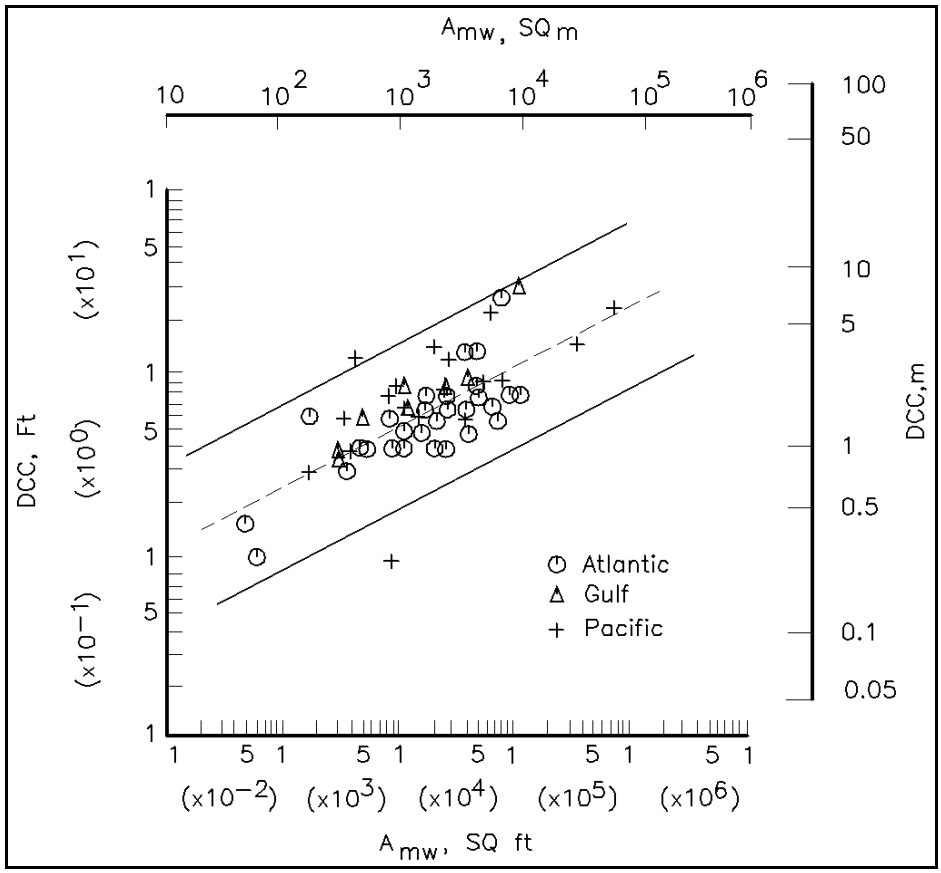

Figure II-6-8. A_{mw} versus minimum controlling channel depth DCC (Vincent and Corson 1980)

ocean tide and amplification of the bay tide could occur. This will be seen in King's solution also (and can be noted in Figure II-6-18 where the bay-ocean tide ratio is greater than one). King defines the dimensionless velocity as:

$$V'_m = \frac{A_{avg} T V_m}{2\pi a_o A_b} \tag{II-6-5}$$

where V_m is the maximum cross-sectionally averaged velocity during a tidal cycle. (To determine V_m, use Equation II-6-5 and refer to Figure II-6-19.) Two parameters are calculated with the variables defined previously.

$$K_1 = \frac{a_o A_b F}{2 L A_{avg}} \tag{II-6-6}$$

$$K_2 = \frac{2\pi}{T}\sqrt{\frac{L A_b}{g A_{avg}}} \tag{II-6-7}$$

where F is defined as

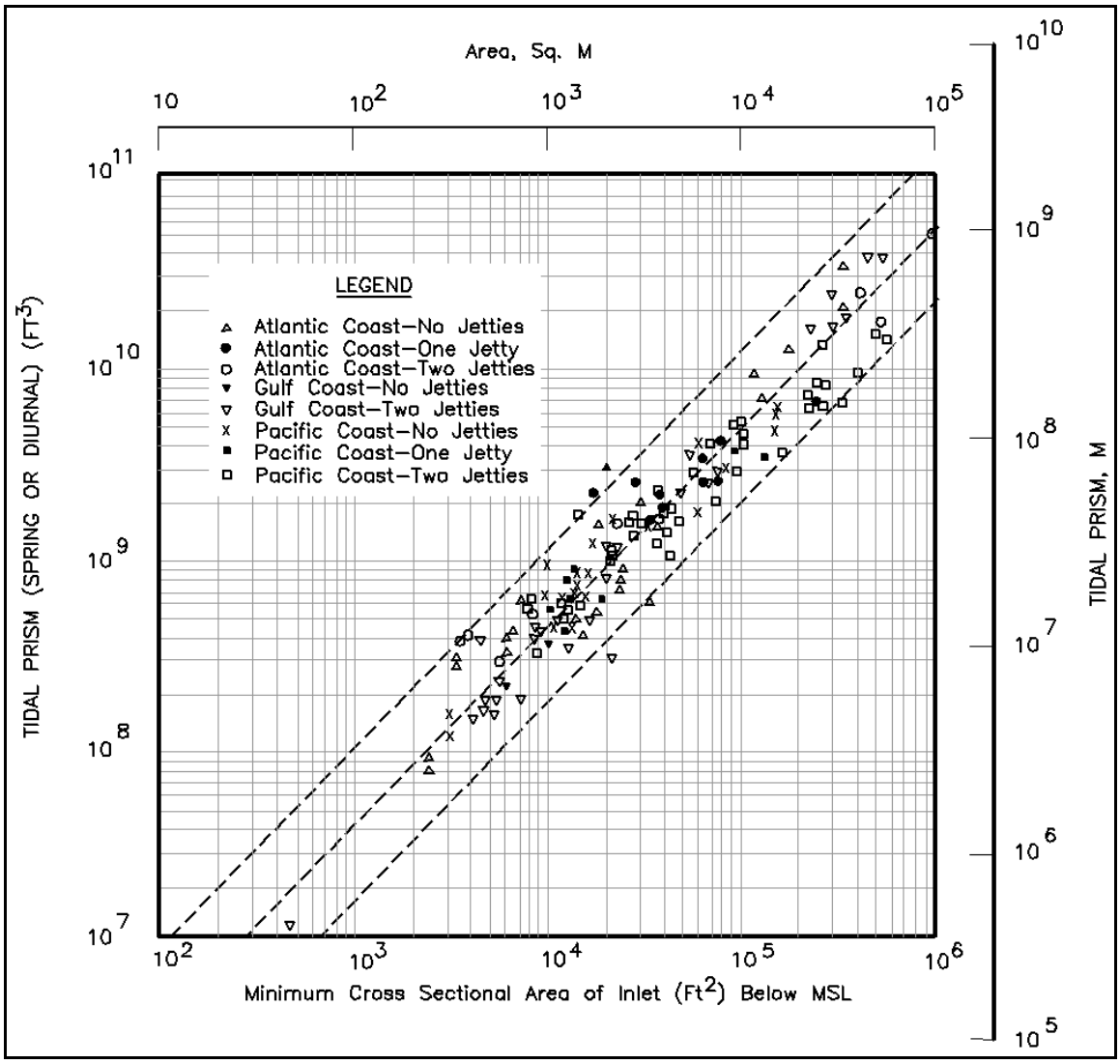

Figure II-6-9. Tidal prism-inlet area relationship

$$F = k_{en} + k_{ex} + \frac{fL}{4R} \tag{II-6-8}$$

(8) Figures II-6-18 through II-6-20 provide a means to determine the bay tide range and phase and velocity in the channel. A sample problem is presented in Part II-6-2, paragraph *d*, where determining important parameters is discussed.

(9) Since channel resistance is nonlinear, channel velocity and bay tide will not be sinusoidal (Keulegan 1967). Other effects such as a relatively large tidal amplitude-to-depth ratio through the channel and nonvertical walls in the channel and bay may be important in causing nonsinusoidal bay tides (Boon and Byrne 1981, Speer and Aubrey 1985, Friedrichs and Aubrey 1988). However, for a first approximation, channel velocity over time is represented as

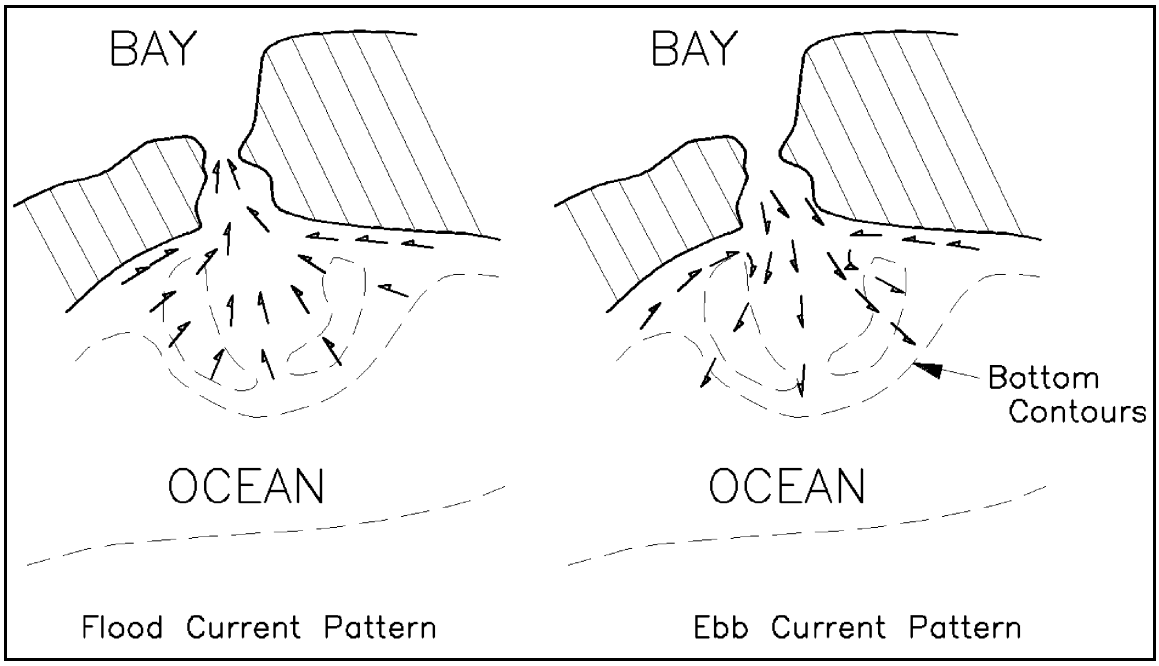

Figure II-6-10. Schematic diagram of flood and ebb currents outside an inlet (O'Brien 1969)

$$V \approx V_m \sin \frac{2\pi t}{T} \tag{II-6-9}$$

and bay tide can be represented as (see Figure II-6-17)

$$h_b \approx a_b \cos\left(\frac{2\pi t}{T} - \varepsilon\right) \tag{II-6-10}$$

where ε is phase lag, a_b is bay tide amplitude (one-half the bay tide range), T is tide period, and t is time of interest during the tide cycle. Also King's K_1 and K_2 are related to the Keulegan repletion coefficient K by

$$K = \frac{1}{K_2}\sqrt{\frac{1}{K_1}} \tag{II-6-11}$$

c. Tidal prism.

(1) The volume of water that enters through the inlet channel during flood flow and then exits during ebb flow is known as the tidal prism. If the hydraulic analysis as described above is used, then tidal prism P can be calculated as

$$P = 2\, a_b\, A_b \tag{II-6-12}$$

(2) Another technique for prism estimation can use observed velocity (or discharge Q) data. Assuming a sinusoidal discharge in the channel and integrating over the flood or ebb portion of the tidal cycle

$$P = \frac{T Q_{\max}}{\pi} \quad \equiv \quad P = \frac{T V_m A_{avg}}{\pi} \tag{II-6-13}$$

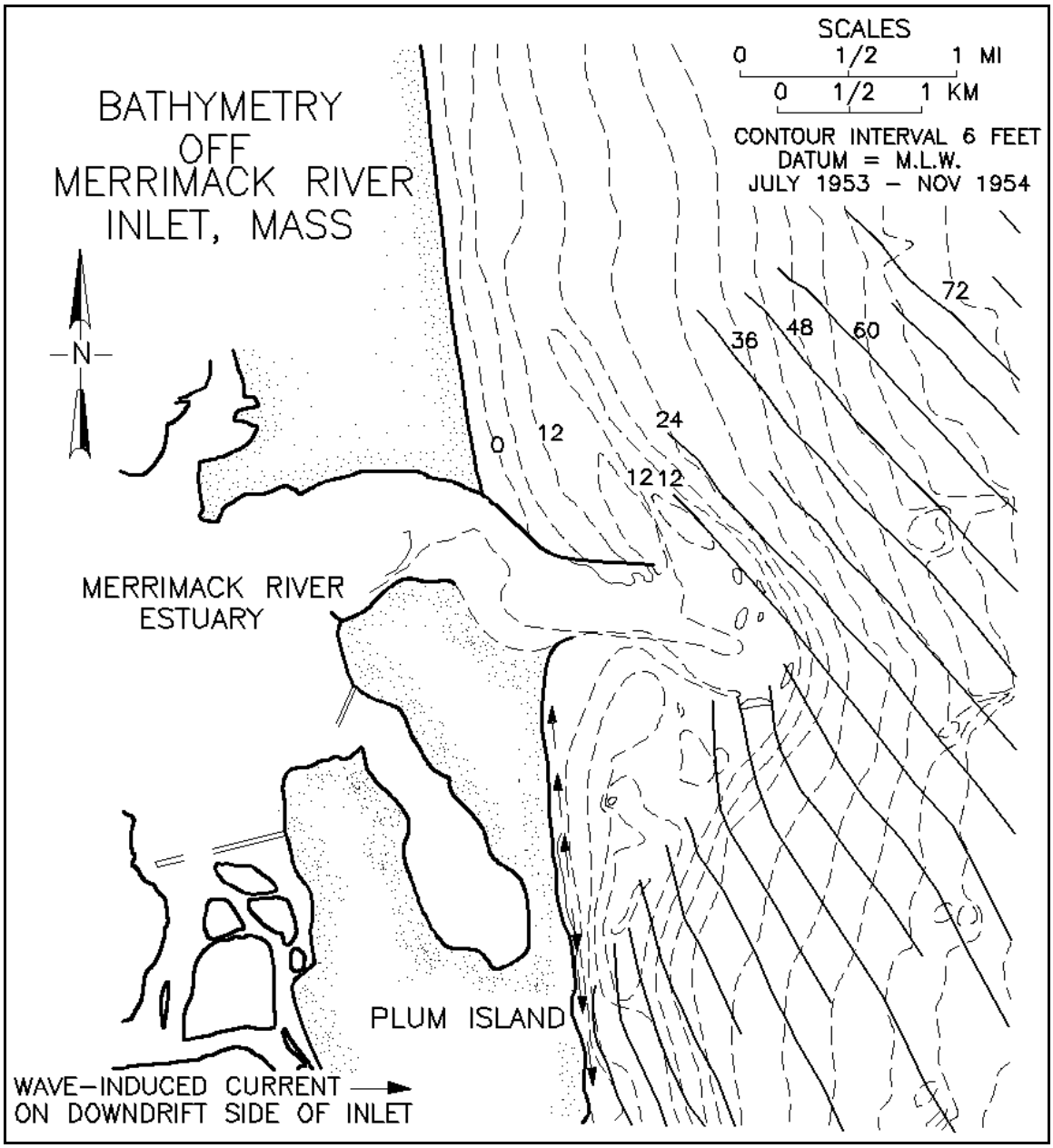

Figure II-6-11. Wave refraction pattern in the vicinity of the Merrimack River Estuary entrance, just south of the Merrimack Inlet (from Hayes (1971))

(3) To account for a non-sinusoidal character of the prototype flow, Keulegan determined

$$P = \frac{T Q_{\max}}{\pi C} \equiv P = \frac{T V_m A_{avg}}{\pi C} \tag{II-6-14}$$

and found C varying between 0.81 and 1.0 for K, the filling coefficient, varying between 0.1 and 100. For practical application, if $0.1 < K < 1.8$, use $C = 0.86$, and for $K > 1.8$, use $C = 1.0$.

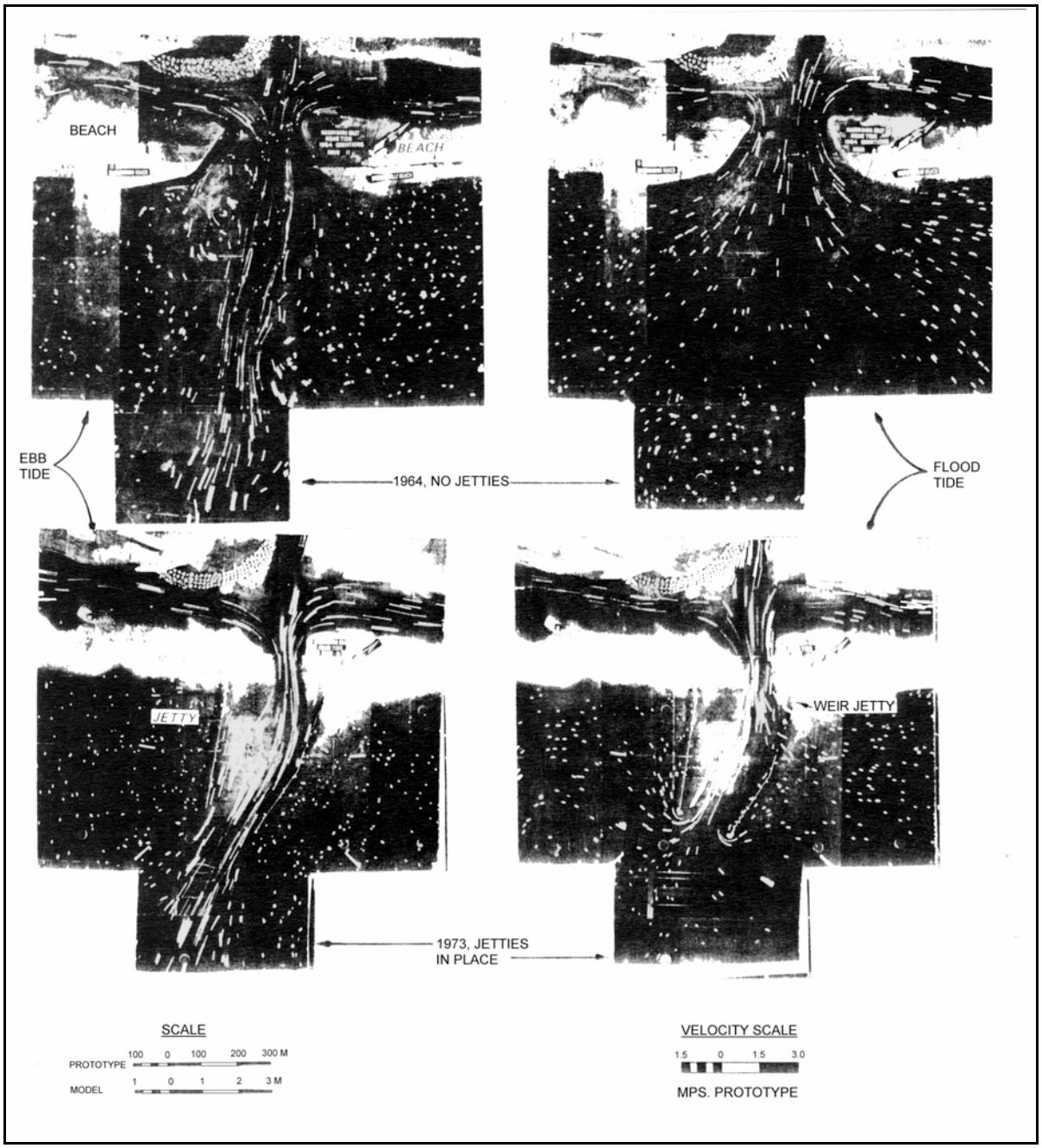

Figure II-6-12. Ebb and flood flow patterns from a model study of Masonboro Inlet, North Carolina (Seabergh 1975)

(4) A more precise method of prism determination includes the cubature method (Jarrett 1976), which takes into account the time required for a tide to propagate through a bay and segments the bay into subareas rather than assuming a uniform rise and fall of the bay tide. Jarrett (1976) also recommends ways to relate point measurements of maximum velocity in the center of the channel (as can be obtained from NOS current tables) to velocities representative of the entire inlet, using

$$\frac{V_{avg}}{V_{meas}} = \left(\frac{R}{D}\right)^{\frac{2}{3}} \tag{II-6-15}$$

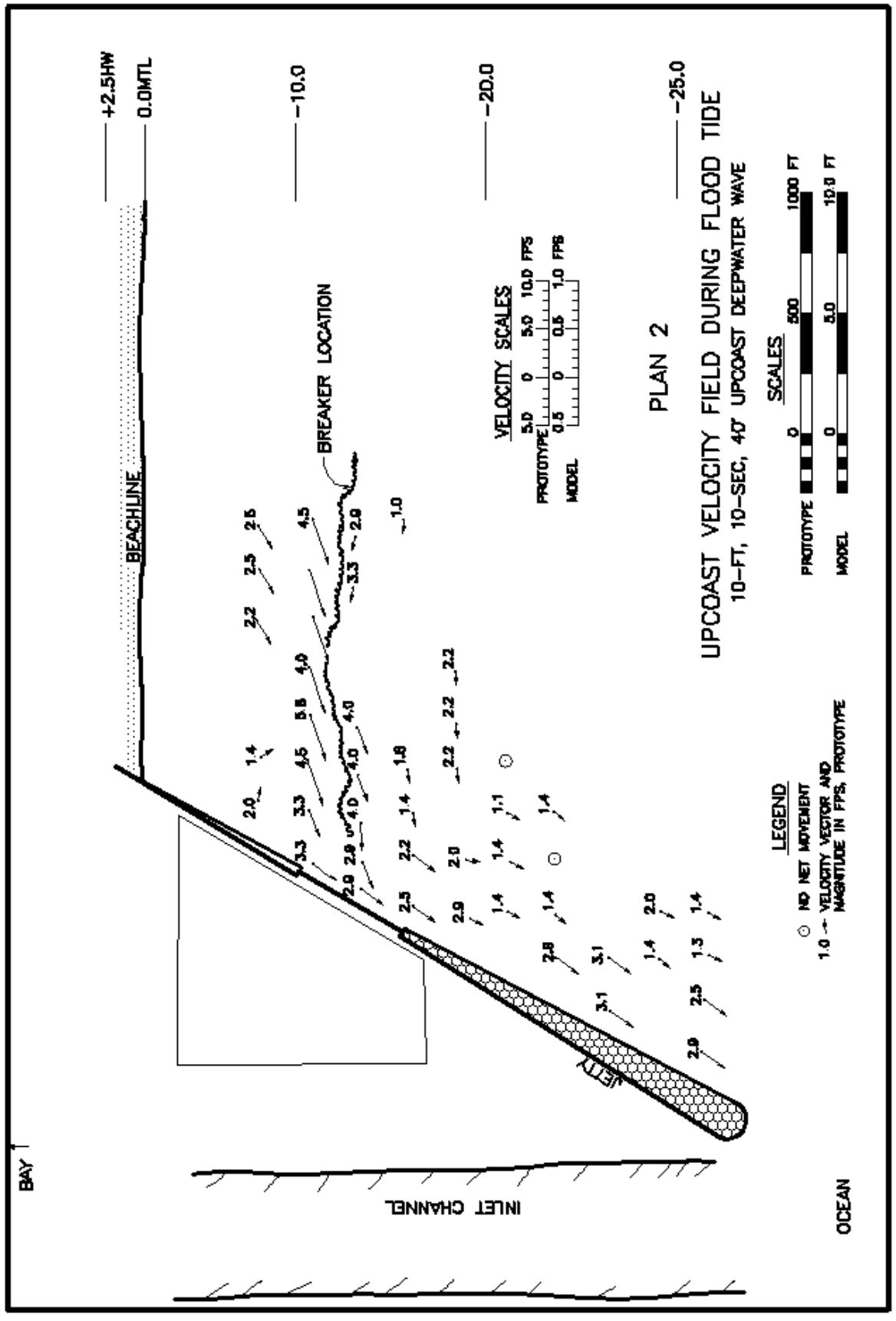

Figure II-6-13. Tidal current plus wave-generated currents approaching jettied inlet, measured in physical model study

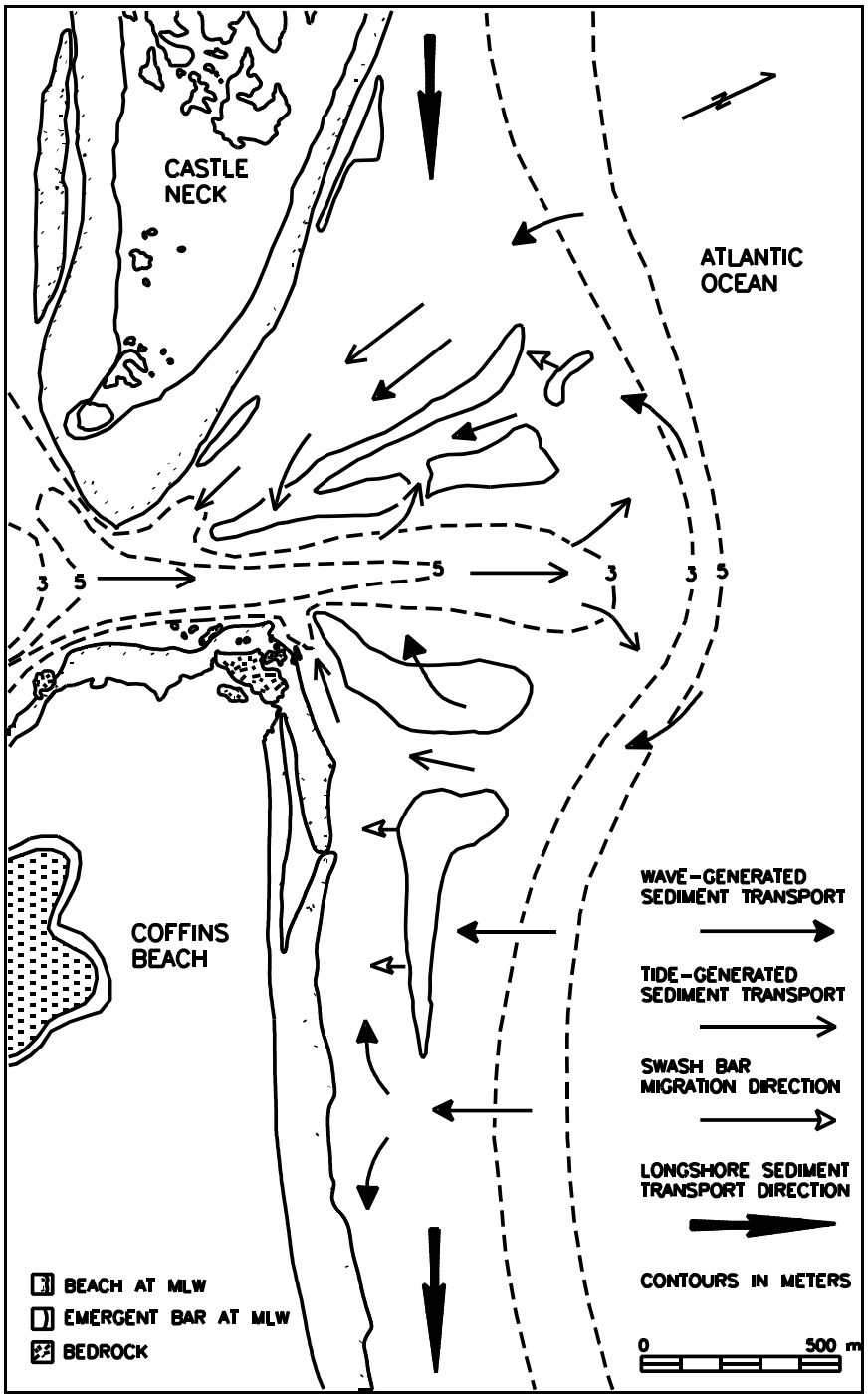

Figure II-6-14. Sediment transport gyres associated with both updrift and downdrift portions of the delta at Essex River Inlet, Massachusetts. (Note different arrow types to denote wave or tide-generated sediment transportation (Smith 1991)

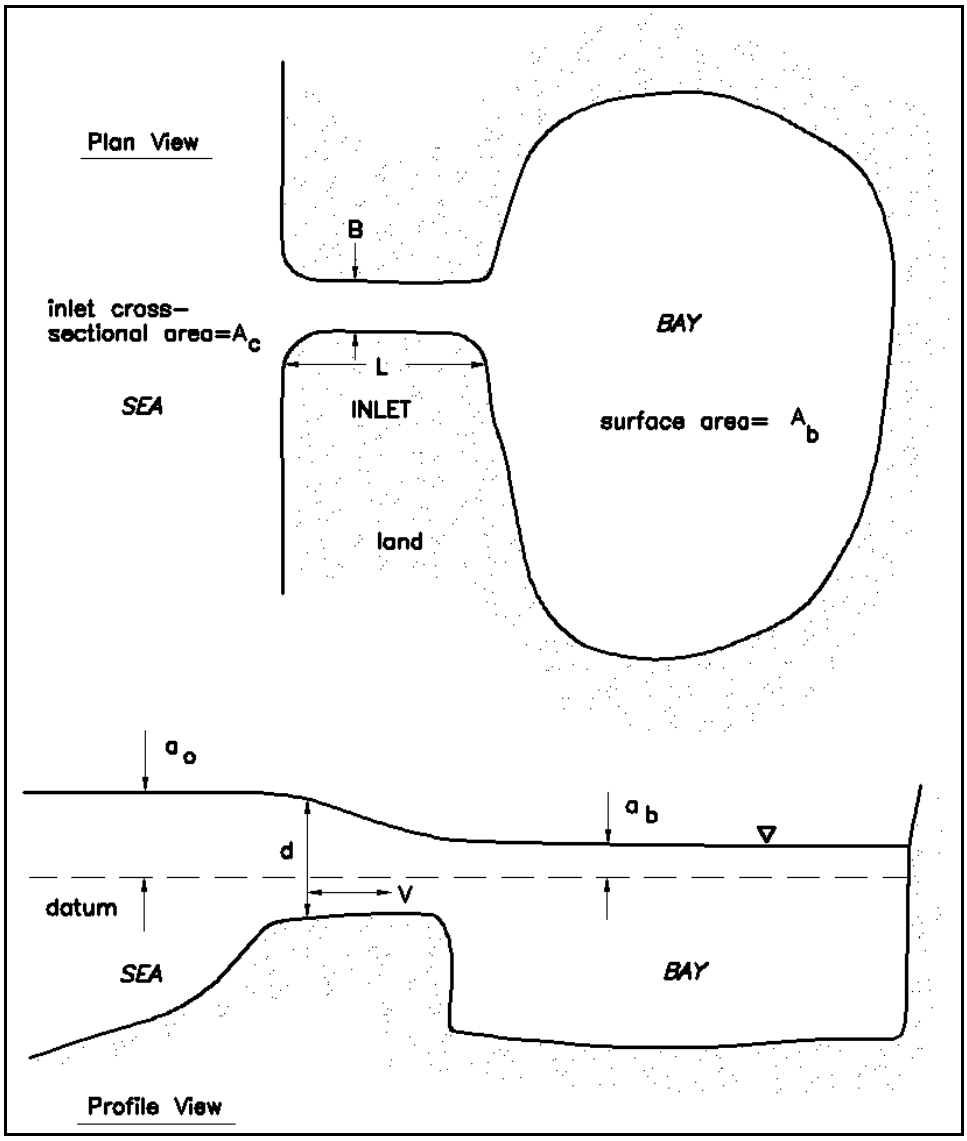

Figure II-6-15. Inlet bay system

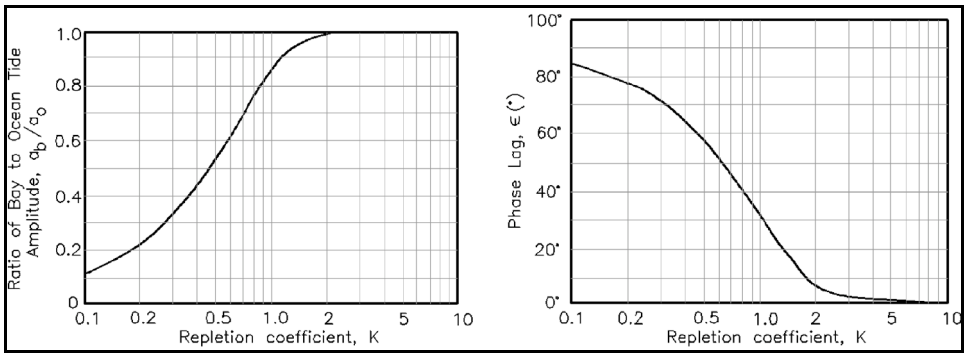

Figure II-6-16. Variation of dimensionless parameters with Keulegan's repletion coefficient, K

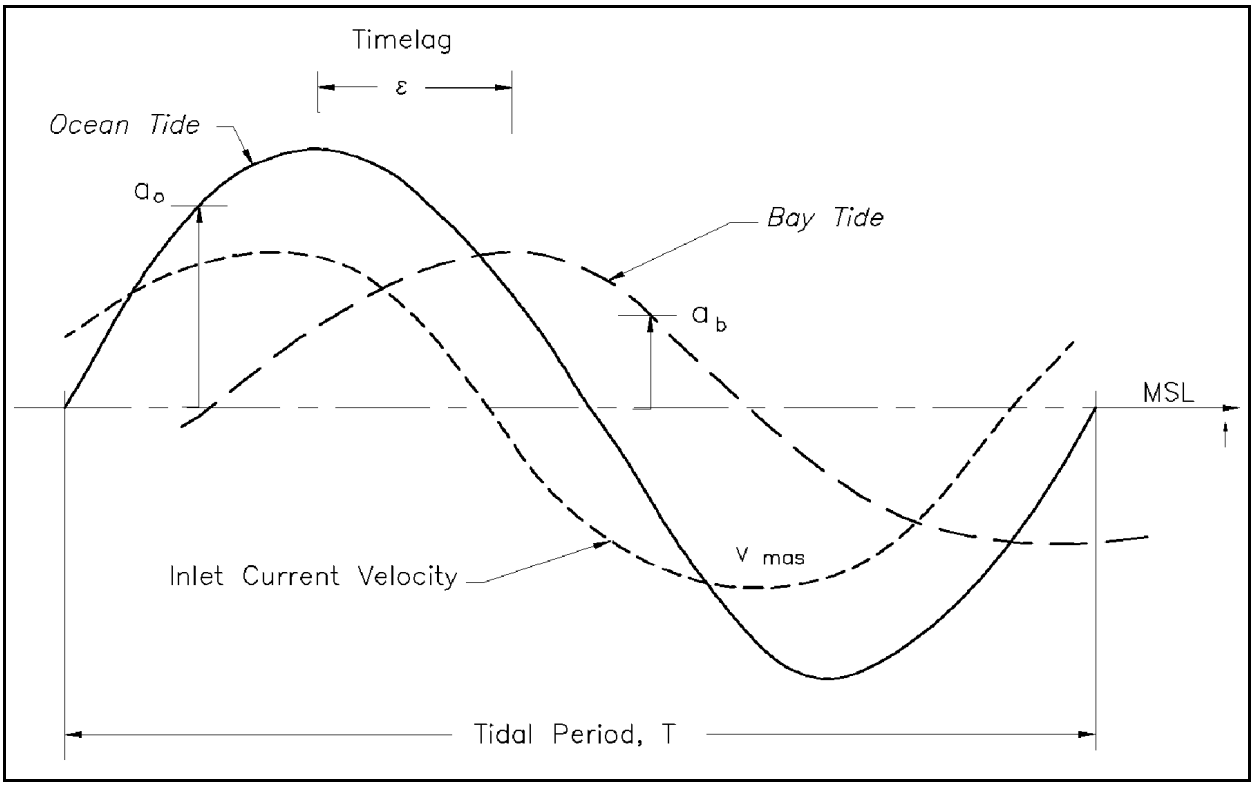

Figure II-6-17. Sample tides and currents for an ocean-inlet-bay system that satisfy the Keulegan assumptions (Keulegan 1967)

where

V_{avg} = maximum velocity averaged over entire cross section

V_{meas} = point measurement of maximum velocity

R = hydraulic radius of entire cross section

D = depth of water at current meter location

The V_{avg} value then can be used in Equation II-6-13.

d. Determining important inlet parameters. Graphs can easily be used to determine inlet hydraulics; however, evaluation of important parameters requires some effort. Mason (1975) determined appropriate techniques for defining cross-sectional area, bay area, inlet (channel) length, hydraulic radius, friction factor and exit and entrance loss coefficients. The following offers guidance in the evaluation of parameters.

(1) Cross-sectional area. Problems in defining location and magnitude of the cross-sectional area result in greatest variability in computed values of the repletion coefficient. To reduce such variability, the cross section should be determined in the following manner:

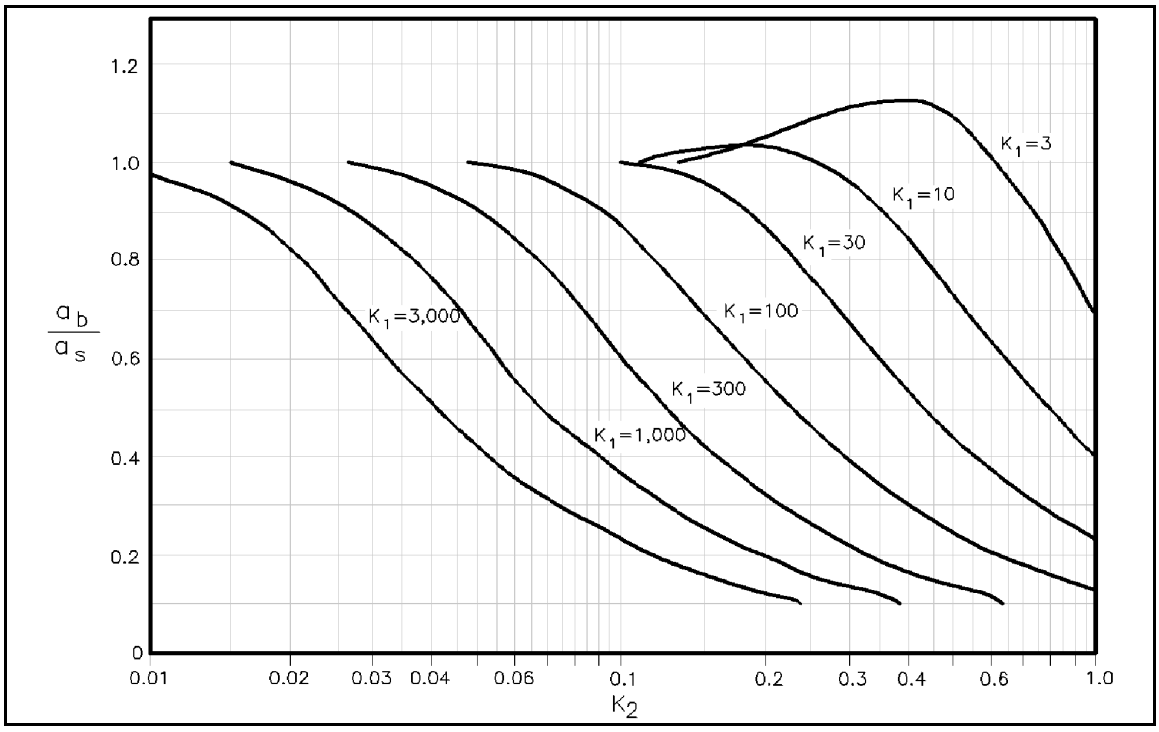

Figure II-6-18. Ratio of bay to sea tidal amplitude versus K_1 and K_2

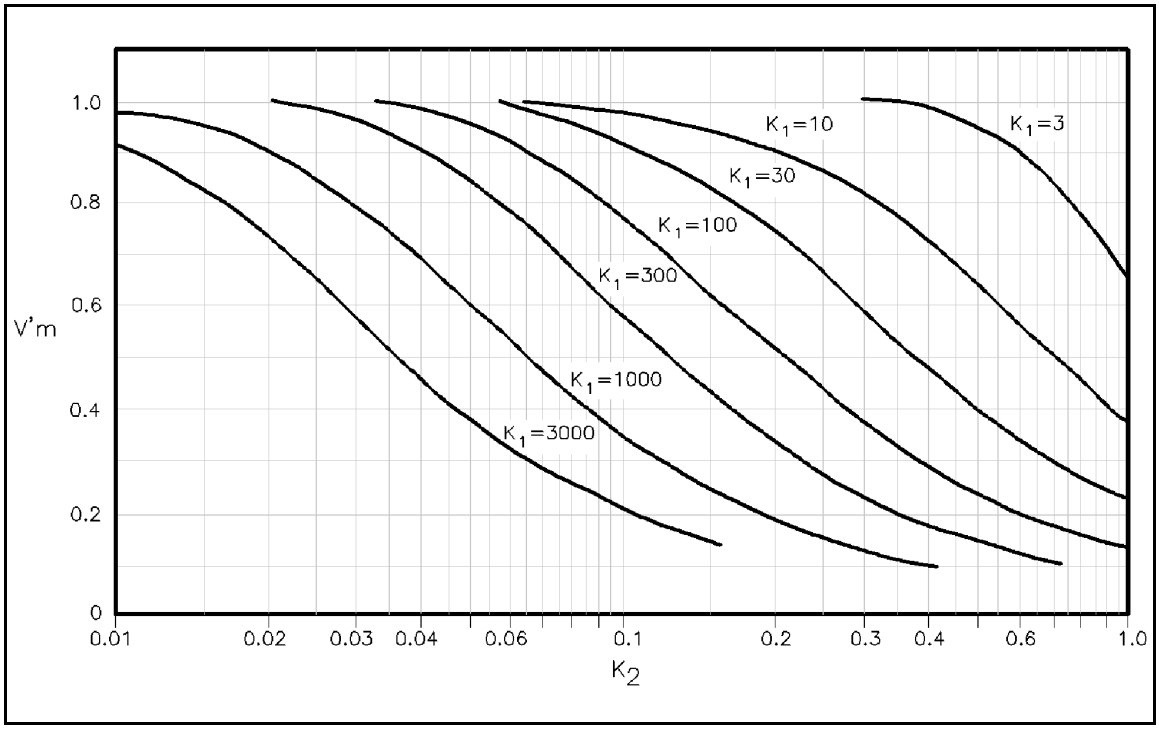

Figure II-6-19. Dimensionless maximum velocity versus K_1 and K_2

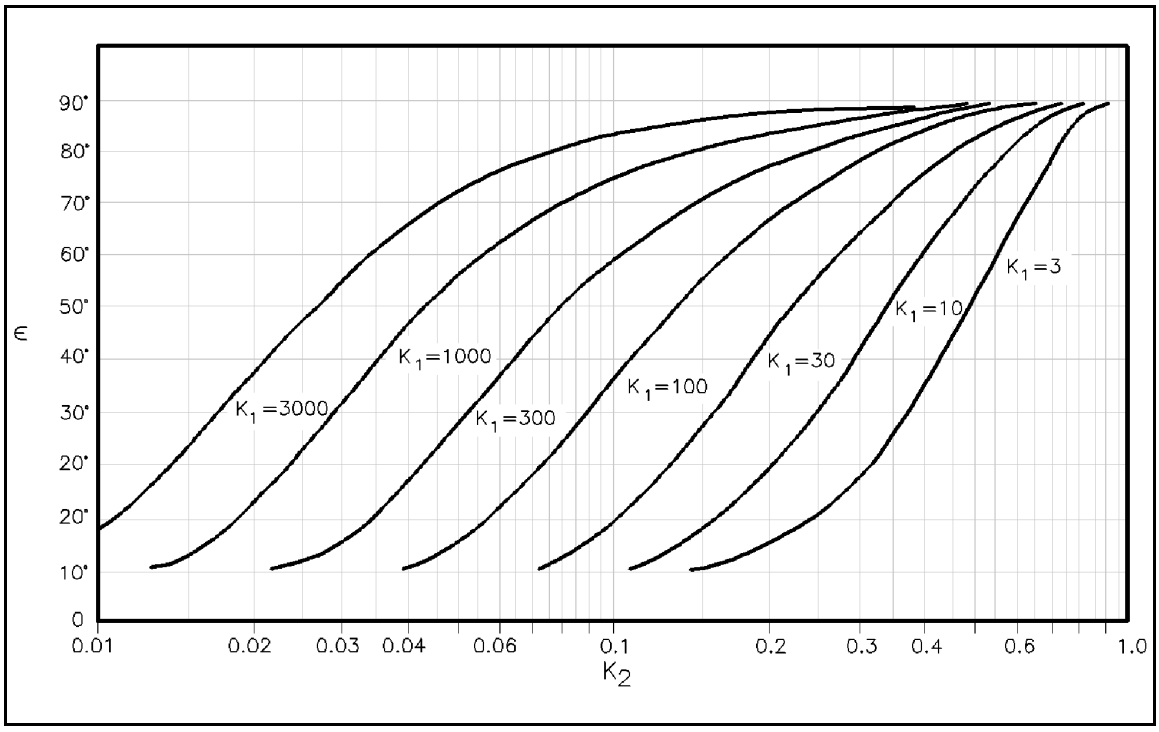

Figure II-6-20. Bay tidal phase lag versus K_1 and K_2

From a detailed bathymetric chart of the inlet, sketch lines that best approximate flood flow lines through the inlet as shown in Figure II-6-21. Establish 10 equally spaced cross-section ranges perpendicular to these flow lines, extending from MSL (mean sea level) on one side of the channel to MSL on the other (i.e. from one side of the inlet to the other). Measure cross-sectional area below MSL of each range and determine average area. Depths on most navigation charts are referenced to mean low or mean lower low water, and a correction factor should be added to these depths to determine the area below MSL.

(2) Bay area. Typically the problem is to define the extent of the inlet's influence throughout the bay. To do this, the following are recommended:

(a) Examine any existing tide records from stations located throughout the bay to define limit of the inlet's influence.

(b) Examine bathymetry of the bay to determine presence of natural sills, narrows, or shoal areas which can preclude significant tidal exchange.

(c) Locate any areas of heavy shoaling at points distant from the inlet, particularly in waterways connecting the bay of interest with more remote bodies of water, and define these sites as the effective bay limits.

(d) The surface area of the bay is usually varying to some degree, but for an initial iteration, the mean water line could be chosen (as well as it can be delineated).

(3) Friction factor.

(a) "f" is a dimensionless parameter that is a function of hydraulic radius R and Manning's roughness coefficient n:

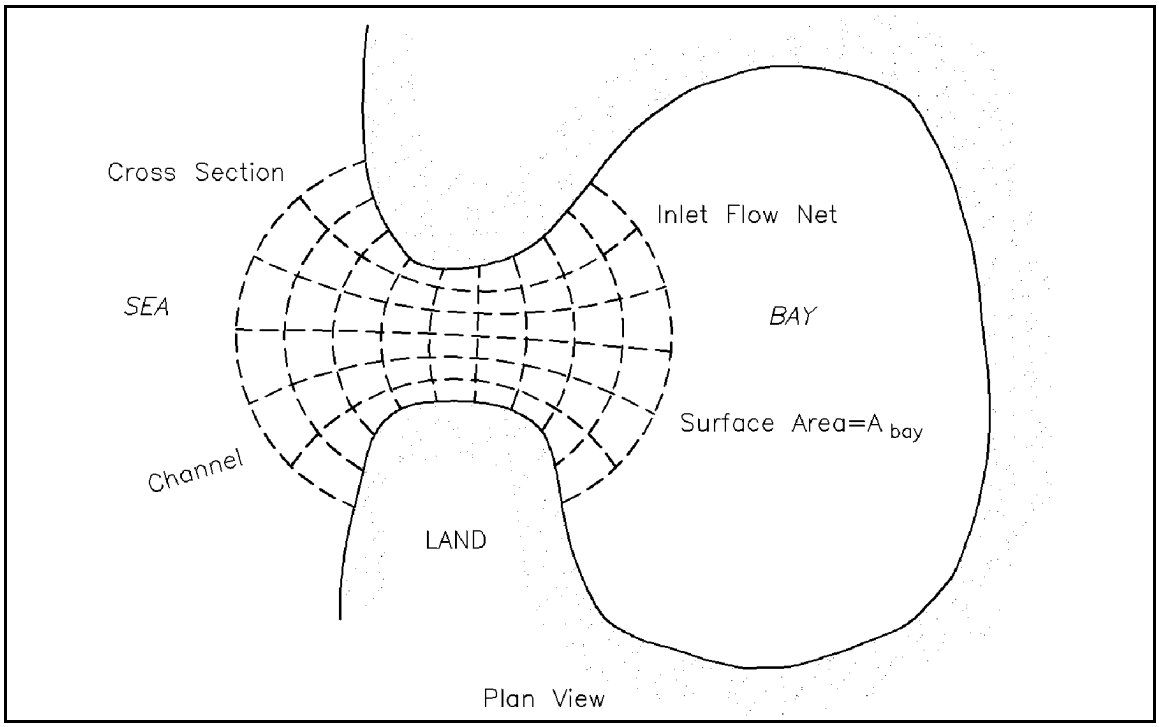

Figure II-6-21. Inlet flow net

$$f = \frac{116 n^2}{R^{1/3}} \tag{II-6-16}$$

(b) It seems reasonable to assume a constant n for an inlet in sand rather than a uniform f value. For open channels in hard-packed smooth sand, Chow (1959) recommends an n value of 0.020 (in English units, or 0.016 in SI). Since inlets often have rippled or duned bottoms, which generally increase frictional resistance, a higher n value might be expected, for instance between 0.025 and 0.030 (English units or 0.021 and 0.025, SI). Using an estimated value of n = 0.0275 (English units or 0.0225 SI), a friction factor defined by $f = 0.088/R^{1/3}$ (English units, R in feet, or $0.059/R^{1/3}$, SI, R in meters) is recommended for use in the equation for K.

Jarrett (1975) examined the friction aspect of Keulagan K (Equation II-6-4) and defined F, inlet impedance, as

$$F = k_{en} + k_{ex} + \frac{fL}{4R} \tag{II-6-17}$$

with k_{en}, k_{ex}, f, and L as defined earlier, and hydraulic radius R measured at the minimum cross section of the inlet. Figure II-6-22 plots inlet impedance against the ratio of inlet length to the 4/3 power of hydraulic radius for four ratios of minimum cross-section inlet width to hydraulic radius. These curves can be used for determining F.

(4) Inlet length. Inlet length is one of the more difficult parameters to define. The following standardized method is recommended to determine inlet length. On a detailed bathymetric chart, beginning in deep water just offshore from the inlet, mark the points of maximum depth moving across the bar, through the inlet, and into the bay. The bayward end point should be seaward of any major division of the inlet

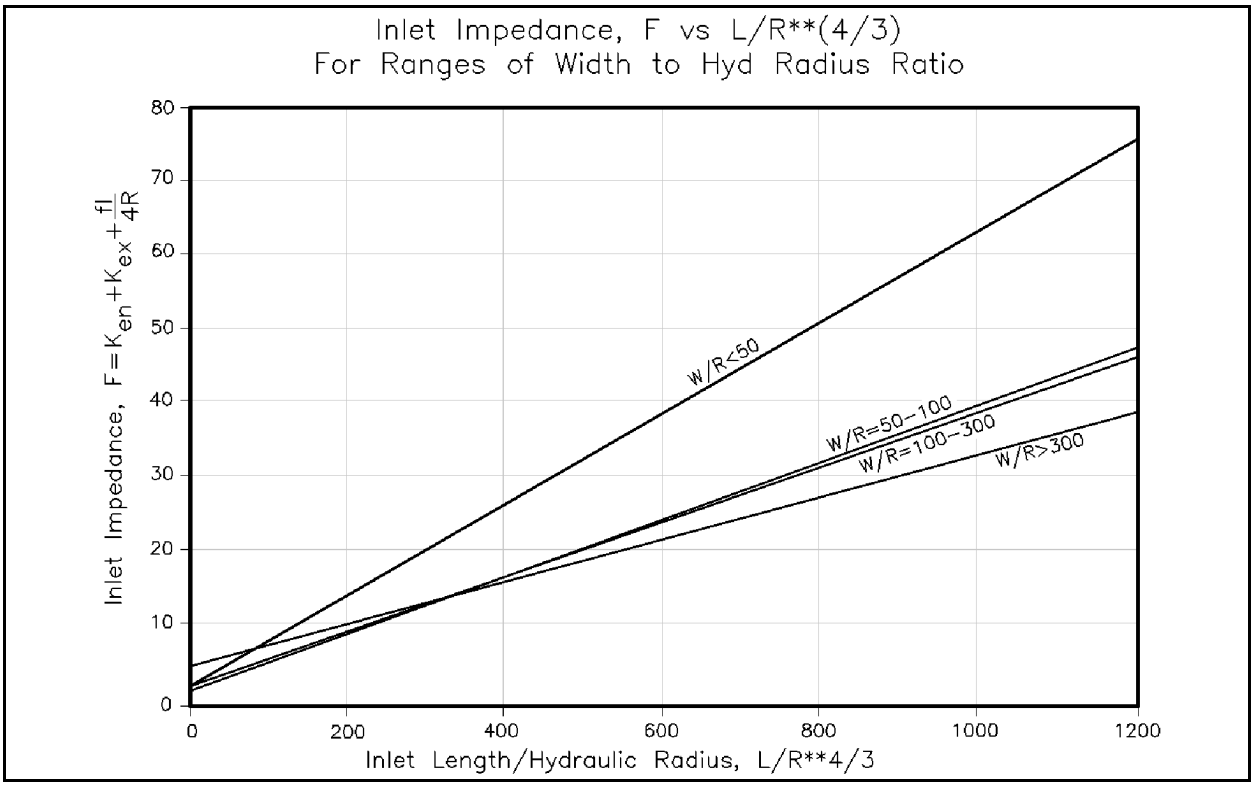

Figure II-6-22. Inlet impedance (*F*) versus the ratio of inlet length to inlet hydraulic radius to the 4/3 power ($l/R^{4/3}$) for various inlet width to inlet hydraulic radius ratios, *W/R*

channel. Connect these points of maximum depth with a series of straight lines to define the thalweg of the channel. Construct a plot of depth versus distance from the oceanward point along the thalweg. Define inlet length as the distance between the depth minimum oceanward of the deepest part of the inlet and the depth minimum bayward of the deepest part. Where the channel does not shoal near either end, the limit of the inlet must be estimated by considering the relationship of the inlet to adjacent beaches, i.e., draw a line perpendicular to the thalweg from MSL on one shoulder of the inlet to MSL on the other, and assume its intersection with the thalweg defines the channel end.

(5) Hydraulic radius. For a given cross-section area, the corresponding value of R should be computed from

$$R = \frac{A_{avg}}{Average\ \ Wetted\ \ Perimeter} \approx \frac{A_{avg}}{Average\ \ Width} \qquad \text{(II-6-18)}$$

These methods are intended to provide a simplified approach to understanding inlet hydraulics in a rapid manner. If possible, field data should be examined to correlate with existing condition calculations, adjustments made to various controlling parameters, and calculations reiterated until reasonable results are achieved. Then calculations may proceed to evaluate design changes. It must be remembered that for extreme events, when wind and wave breaking may be significant factors influencing the hydrodynamics of the inlet system, more sophisticated approaches will be needed. Even a relatively well-behaved inlet is only approximately represented by these approaches, but much insight can be gained by these techniques.

EXAMPLE PROBLEM II-6-1

Find:

If a channel has a depth below MSL of 3.7 m (12.1 ft) and a width of 180 m (590 ft), what are the maximum flow velocity, maximum discharge bay tidal range, and the volume of water flowing into and out of the bay on a tidal cycle (tidal prism) for a tide having the spring range?

Given:

A bay with a surface area of 1.9×10^7 m^2 (2.0×10^8 ft^2) and an average depth of 6.0 m (19.7 ft) is located on the Atlantic coast. The tide is semidiurnal (T = 12.42 hr), with a spring range of 1.30 m (4.3 ft), as given by the National Ocean Survey Tide Tables (U.S. Department of Commerce 1989). An inlet channel, that will be the only entrance to the bay, is to be constructed across the barrier beach that separates the bay from the ocean. The inlet is to provide a navigation passage for small vessels, dilution water to control both salinity and pollution levels, and a channel for fish migration. The channel is to have a design length of 1,100.0 m (3,609 ft) with a pair of vertical sheet-pile jetties that will extend the full length of the channel.

Solution:

Using King's method, assume $k_{en} = 0.1$, $k_{ex} = 1.0$, and $f = 0.03$: $B = 180$ m and $d = 3.7$ m.

$$A_c = Bd = 180\ (3.7) = 666\ \text{m}^2\ (7166\ \text{ft}^2)$$

$$R = \frac{A_c}{(B + 2d)} = \frac{666.}{(180 + 2(3.7))} = 3.55\ \text{m}\ (11.54\ \text{ft})$$

$$F = k_{en} + k_{ex} + \frac{fL}{4R} = 1.0 + 0.1 + \frac{0.03\ (1100)}{4\ (3.55)} = 3.42$$

$$K_1 = \frac{a_o\ A_b\ F}{2\ L\ A_c} = \frac{(1.30/2\ (1.9)\ (10^7)\ 3.42}{2\ (1100)\ (666)} = 28.8$$

$$K_2 = \frac{2\pi}{T}\sqrt{\frac{L\ A_b}{g\ A_c}} = \frac{2\pi}{12.4\ (60\ (60)}\sqrt{\frac{1100\ (1.9)\ 10^7}{9.8\ (666)}} = 0.25$$

From Figures II-6-18, II-6-19, and II-6-20 with the above values of K_1 and K_2

$$\frac{a_b}{a_s} = 0.78$$

$$V_m' = 0.66$$

$$\varepsilon = 53^o$$

(Continued)

Example Problem II-6-1 (Concluded)

Therefore, from Equation II-6-5

$$V_m = \frac{V_m' \, 2\pi \, a_s \, A_b}{A_c \, T}$$

$$V_m = \frac{0.66 \; (2) \; (3.14) \; (0.65) \; (1.9) \; 10^7}{666 \; (12.42) \; (3{,}600)} = 1.72 \text{ m/s} \quad (5.64 \text{ ft/s})$$

$$Q_m = V_m \, A_c = (1.72) \; (666) = 1145 \text{ m}^3\text{/s} \; (40{,}430 \text{ ft}^3\text{/s})$$

Since $a_b/a_s = 0.78$, $a_b = 0.78 \; (0.65) = 0.51$ m (1.67 ft) and the bay tidal range is 0.51 (2) or 1.02 m (3.35 ft).

The tidal prism is

$$2 \; a_b \, A_b = 2 \; (0.51) \; (1.90) \; (10^7) = 1.94 \times (10^7) \text{ m}^3 \qquad (6.27 \times 10^8 \text{ ft}^3)$$

If the average depth of the bay is 6.0 m and the distance to the farthest point in the bay is 6.0 km, the time t_* it will take for the tide wave to propagate to that point is

$$t_* = \frac{L_b}{\sqrt{g d_b}} = \frac{6000}{\sqrt{9.8 \; (6.0)}} = 782 \text{ sec or } 0.22 \text{ hr}$$

Since this time is significantly less than 12.42 hr, the assumption that the bay surface remains horizontal is quite satisfactory.

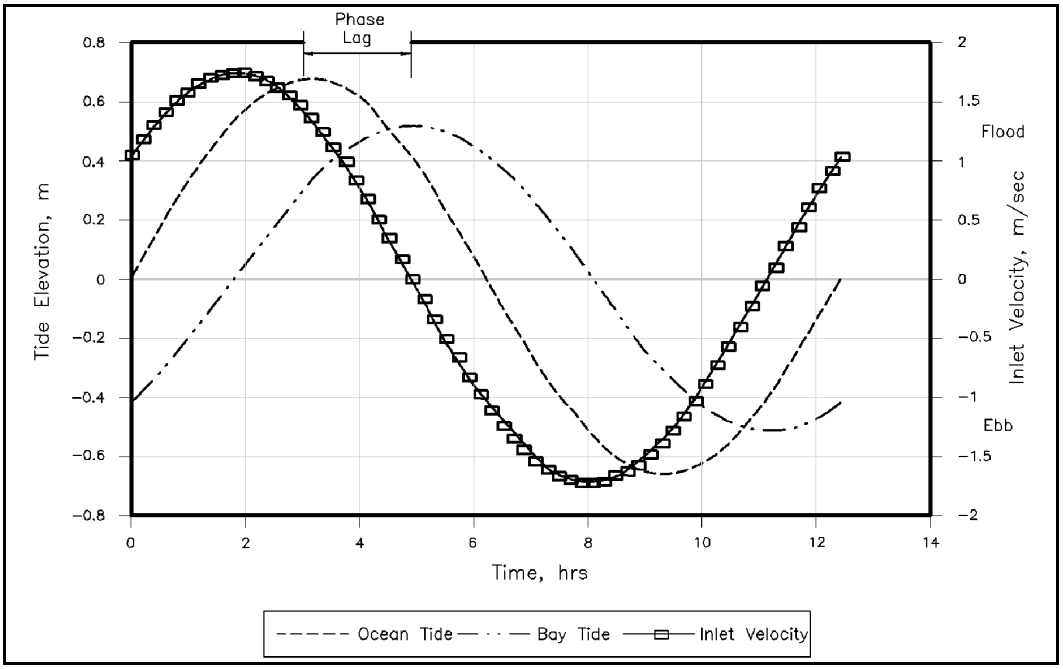

Figure II-6-23. Results from Example Problem II-6-1

e. Evaluating inlet hydraulics with Keulegan K.

(1) Introduction. The Keulegan K value can be used to understand effects of gross geometric variations on inlet hydraulics. Figure II-6-24 shows ocean and bay tide curves and velocity in the channel during a tidal cycle. Three K values are represented. The lower the K or filling coefficient, the lower the tide range in the basin and the greater the phase lag (or time difference between high water (low water) in the ocean and high water (low water) in the bay. Also noted from the velocity curve, maximum current occurs during maximum head difference between ocean and bay tides and as K decreases, maximum ebb and flood currents shift from occurrence at a mid-tide level to tidal elevation extremes. For $K = 0.2$, maximum flood currents occur near high water and maximum ebb currents occur during low water. Therefore for low K inlets, flood flow occurs when depths in the channel and over tidal deltas are greatest (near high water), and flow is more broadly distributed. During ebb flow, depths are shallower (approaching low water) and flow is likely to be more channelized. As K increases, and the bay fills more completely, peak ebb and flood flows tend to occur near the same tide level. These variations can have implications with regard to sediment transport. Mota Oliveira (1970) found that, using an analysis similar to Keulegan but with variable entrance cross-sectional area, when $0.6 < K < 0.8$, the inlet had maximum sediment flushing ability. When $K > 0.8$, there was flood dominance in sediment transport capability, meaning net bayward transport and when $K < 0.6$, there was ebb dominance of sediment transport capability. Also when a variable bay surface area was considered, ebb sediment transport was enhanced to the detriment of flood transport. Part II-6-2, paragraph *h* contains more information on flow dominance.

(2) Jarrett's classification. Jarrett (1975) performed a "hydraulic classification" of inlets based on Keulegan's K after determining tidal characteristics of a large number of U.S. inlets (see Table II-6-1). The classification is as follows:

(a) Class I: Keulegan $K < 0.3$. Phase angle (ε) equal to or greater than 70 deg. For a semidiurnal tide, the phase lag between the ocean tidal extreme and slack water is equal to or greater than 2 hr 25 min. For the most part, bays associated with inlets in this class are open and relatively shallow with only one relatively small inlet (i.e., small ratio A_c/A_b connecting the ocean with the bay. This class also could include relatively long estuaries that are actually long-wave embayments.

(b) Class II: Keulegan $K > 0.80$. Phase angle (ε) equal to or less than 40 deg. For a semidiurnal tide, the phase lag would be equal to or less than 1 hr 25 min. Bays associated with this class are either short or consist of a system of relatively deep channels (Note: by virtue of the long tidal period in the Gulf of Mexico most Gulf Coast inlets fall into this class irrespective of bay shape). The ratio A_c/A_b is relatively large for these inlets.

(c) Class III: $0.3 < K < 0.8$. Phase angle lies between 40 and 70 deg. Characteristics are intermediate to classes I and II. Analysis by Mota Oliveira (1970) indicated that the natural flushing ability of a vertical bank lagoon reaches a maximum for K values of 0.6 to 0.8.

f. Effect of freshwater inflow.

(1) If a significant amount of fresh water is introduced into the bay relative to the tidal prism of the inlet, there will be significant changes in bay tide range and velocity through the inlet. King (1974) included freshwater inflow into a Keulegan type model (which did not include the inertial term in the 1-D equation of motion). He defined a dimensionless variable

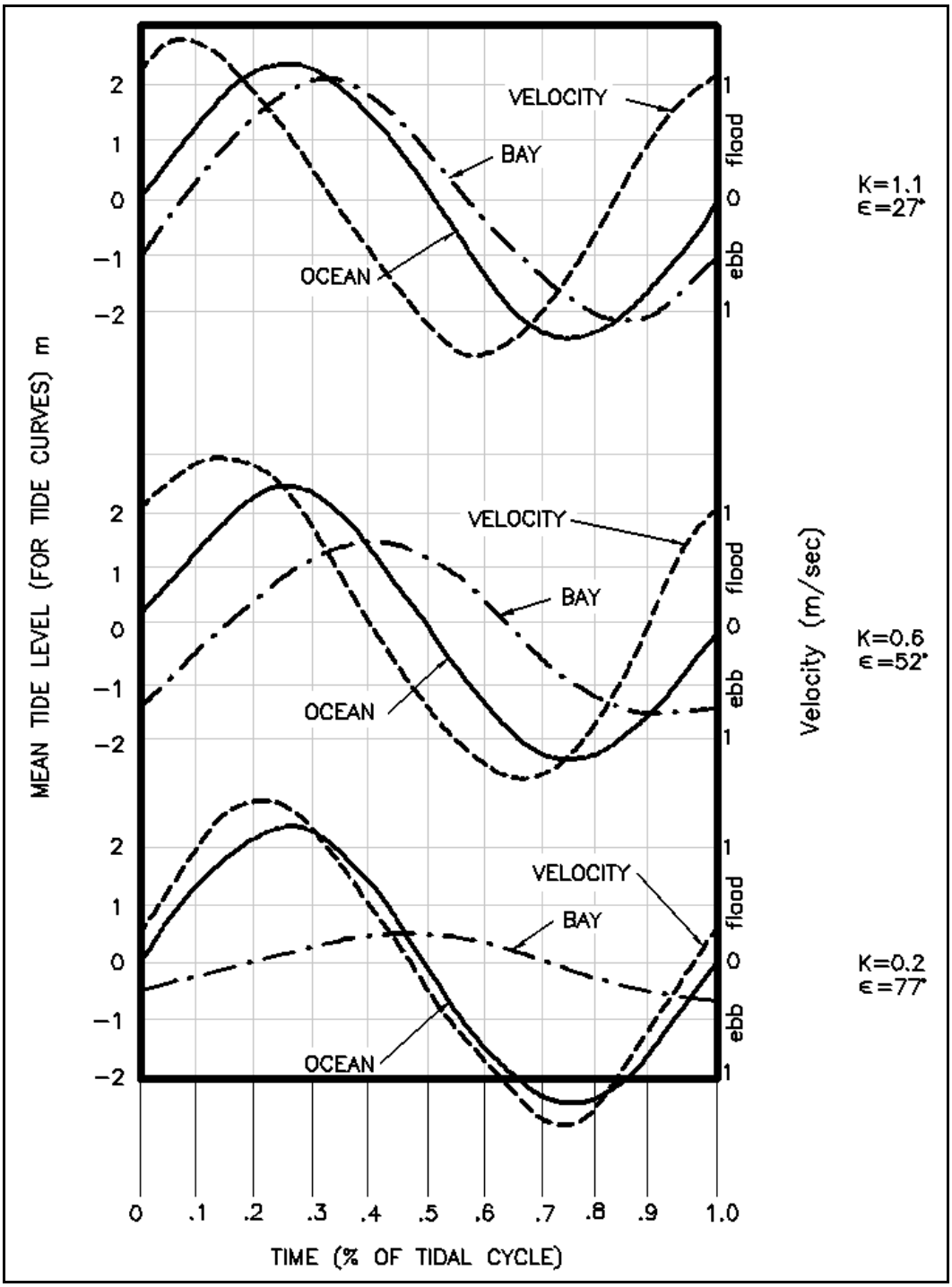

Figure II-6-24. Hydraulic response of inlet and bay tide phasing and bay tide amplitude for various Keulegan *K* values

Table II-6-1
Hydraulic Characteristics of Tidal Inlets by Cubature Method

Inlet	Mean Tidal Prism P, ft^3	Bay Surface Area A_b, ft^2	Avg Phase Range in Bay, $2a_b$	Ocean Tidal Range $2a_o$	a_b/a_o	K	ε deg
Atlantic Coast							
Shinnecock	1.82×10^8	3.65×10^8	0.50	2.90	0.17	0.15	80
Fire Island	1.59×10^9	2.69×10^9	0.59	4.10	0.14	0.14	83
Jones	7.89×10^8	4.48×10^8	1.76	4.50	0.39	0.35	67
East Rockaway	4.03×10^8	1.06×10^8	3.80	4.50	0.84	0.95	33
Rockaway	2.24×10^9	4.64×10^8	4.83	4.70	1.03	--	--
Manasquan	1.40×10^8	4.91×10^7	2.85	4.30	0.66	0.65	49
Barnegat	4.91×10^8	1.34×10^9	0.37	4.20	0.09	0.09	85
Indian River	4.00×10^8	4.20×10^8	1.02	4.10	0.25	0.22	75
Beaufort	4.20×10^9	2.56×10^9	1.64	3.60	0.46	0.41	63
New River	1.59×10^8	5.31×10^8	0.30	3.60	0.08	0.08	86
Winyah Bay	2.47×10^9	9.14×10^8	2.70	4.60	0.59	0.56	54
Port Royal Sd	1.25×10^{10}	2.40×10^9	5.22	6.60	0.78	0.82	40
Calibogue Sd	3.05×10^9	5.28×10^8	5.78	6.60	0.88	1.07	28
Wassaw Sd	3.34×10^9	5.84×10^8	5.72	6.90	0.83	0.95	33
Ossabaw Sd	5.82×10^9	1.17×10^9	4.98	7.20	0.69	0.70	46
Sapelo Sd	6.36×10^9	9.66×10^8	6.59	6.90	0.94	1.30	20
St. Catherines Sd	5.94×10^9	1.04×10^9	5.73	7.10	0.81	0.89	36
Doboy Sd	3.43×10^9	5.19×10^9	6.62	6.80	0.97	1.50	15
Altamaha Sd	2.45×10^9	5.01×10^8	4.90	6.60	0.74	0.75	43
St. Simon Sd	5.52×10^9	8.51×10^8	6.50	6.60	0.98	1.90	0
St. Andrew Sd	8.34×10^9	1.41×10^9	5.92	6.60	0.90	1.12	26
St. Marys	4.11×10^9	7.93×10^8	5.19	5.80	0.89	1.10	27
Nassau Sd	1.87×10^9	4.40×10^8	4.25	5.70	0.75	0.76	43
St. Johns	1.50×10^9	1.22×10^9	1.23	5.20	0.24	0.21	76
Ft. Pierce	5.10×10^8	1.10×10^9	0.46	2.60	0.18	0.16	80
Lake Worth	7.00×10^8	4.00×10^8	1.75	2.60	0.67	0.66	48
Gulf Coast							
Venice Inlet	8.50×10^7	4.43×10^7	1.92	2.60	0.74	0.76	42
Midnight Pass	2.61×10^8	1.29×10^8	2.12	2.60	0.82	0.90	35
Sarasota Bay	2.46×10^9	1.16×10^9	2.12	2.60	0.82	0.90	35
Tampa Bay	1.95×10^{10}	1.01×10^{10}	1.95	2.60	0.75	0.76	43
Pensacola Bay	5.87×10^9	4.65×10^9	1.26	1.30	0.97	1.55	14
Mobile Bay	1.56×10^{10}	1.20×10^{10}	1.30	1.30	1.00	--	0
Galveston	5.94×10^9	8.36×10^9	0.71	2.10	0.33	0.30	70

$$Q_r' = \frac{Q_r T}{2\pi a_o A_b} \tag{II-6-19}$$

with Q_r being the river or freshwater inflow to the bay, and a_0, A_b, and T as defined previously. Figures II-6-25 and II-6-26 give high (or maximum) and low (minimum) dimensionless ratio water levels for values of Q_r' and K (Equation II-6-4). Using Figures II-6-27 and II-6-28, maximum average ebb and flood currents can be found and Figure II-6-29 is used to determine ocean high water to bay high water phase lag.

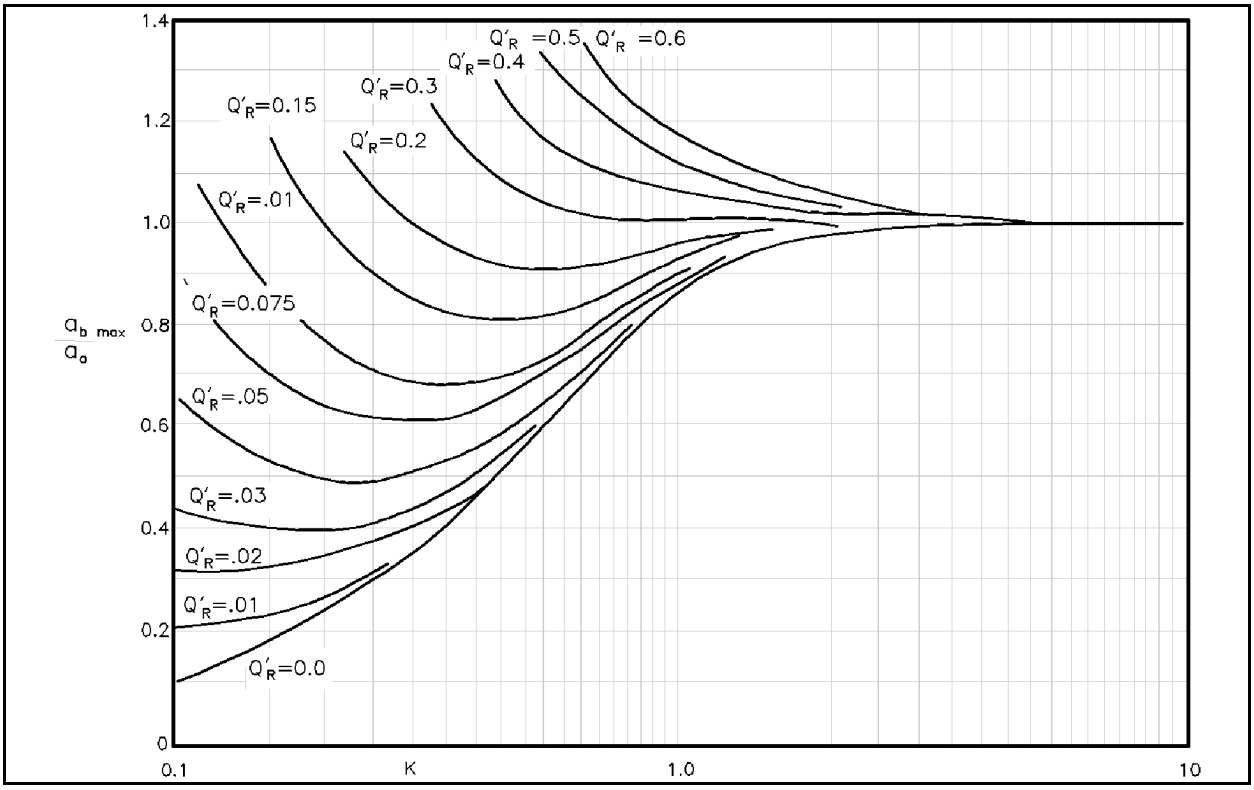

Figure II-6-25. $a_{b\,max}/a_o$ versus K for values of Q_r' (river discharge model)

(2) The above analysis assumes that waters in the inlet are well-mixed at the inlet minimum cross-section, where the salinity variation over a vertical section varies only a small fraction from the local mean salinity. As freshwater influence increases, it approaches a completely stratified flow, i.e., a flow that has a well-defined interface between fresh and saline waters, and in which flow may be simultaneously bidirectional (Wicker 1965). More sophisticated techniques should be used for such cases.

g. Bay superelevation.

(1) A superelevation of the bay means that the average level of the bay is greater than the average elevation of the ocean over a given time period. An obvious cause of this effect is the introduction of fresh water into the bay from local rivers and streams. The effect of long-term (months or years) rise in sea level causing a long-term rise in bay level is not included in this definition of bay superelevation, since both sea and bay are responding simultaneously. The bay may not rise at the same rate as the sea due to possible circulation effects if multiple inlets connect the bay to the ocean.

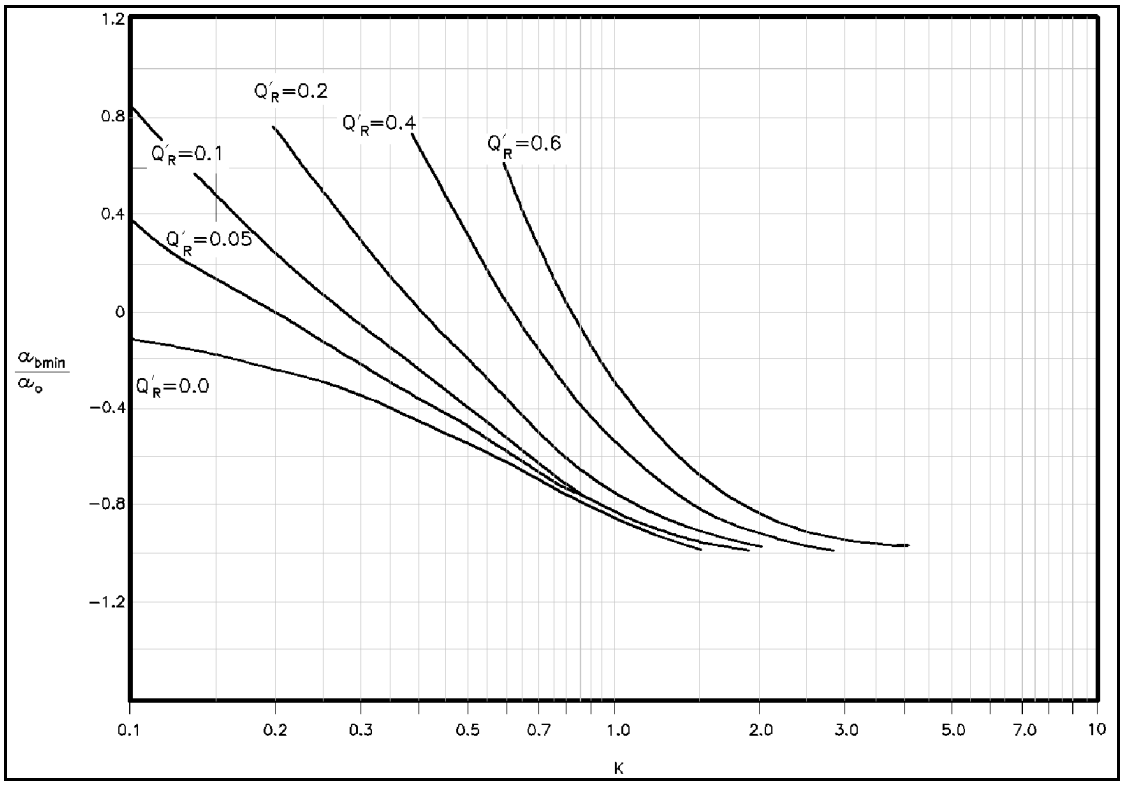

Figure II-6-26. $a_{b\,min}/a_o$ **versus** K **for values of** Q_r' **(river discharge model)**

(2) Laboratory and numerical studies (Mayor-Mora 1973; Mota Oliveira 1970) have indicated that there is an increasing bay superelevation as the coefficient K decreases (Figure II-6-30) and approaches nearly 20 percent of the ocean tide range. This basic cause of setup is due to increased frictional dissipation of ebb flow in comparison to flood flow as K decreases, with peak ebb flows in the channel occurring during lower water levels for inlets with low K values. This increased tractive stress for ebb flow relative to flood flow creates the setup, or increased head, necessary to preserve continuity and drive out the same tidal prism that entered the inlet.

(3) Model studies (Mayor-Mora 1973) show that as K decreases (and superelevation increases) the duration of ebb flow increases relative to flood flow in the inlet channel. Keulegan (1967) determined a relation between inflow duration and bay superelevation (due to any reason) given by

$$\frac{\Delta}{a_o} = \frac{\sin\left(\frac{2\pi t_i}{T}\right)}{1 - \cos\left(\frac{2\pi t_i}{T}\right)} \tag{II-6-20}$$

where

Δ = superelevation

a_o = tidal amplitude in ocean

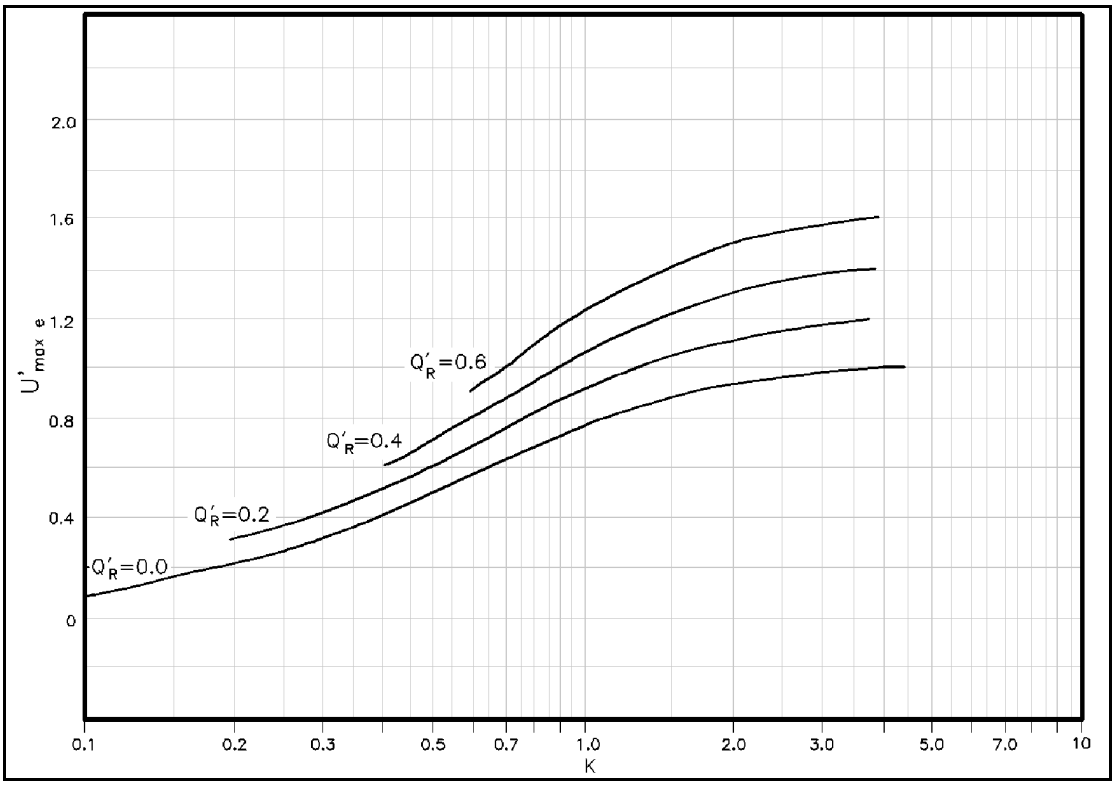

Figure II-6-27. $u'_{max\,e}$ **versus** K **for values of** Q_r' **(river discharge model)**

T = tidal period

t_i = duration of inflow

(4) Figure II-6-31 illustrates this. Mehta (1990) determined that superelevation due to varying entrance channel cross section (by itself only) is

$$\frac{\Delta}{a_o} = 1 - \frac{\left(\frac{a_b}{a_o}\right)^2}{4\left(\frac{d}{a_o}\right)} - \frac{a_o}{mW}\left[\frac{1}{2} - \left(\frac{a_b}{a_o}\right)\cos\varepsilon - \frac{3}{2}\left(\frac{a_b}{a_o}\right)^2 + 4\left(\frac{d}{a_o}\right)^2\right] \tag{II-6-21}$$

where

Δ = superelevation

a_o = sea tide amplitude

a_b = bay tide amplitude

d = mean water depth in channel

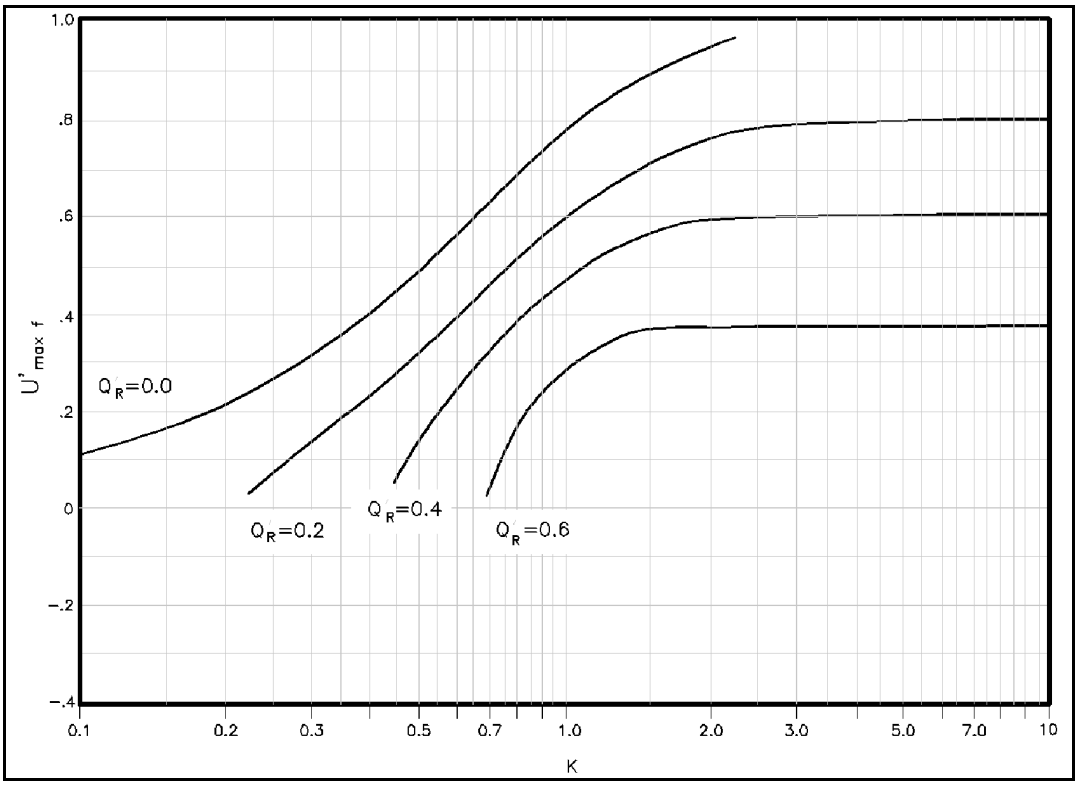

Figure II-6-28. $u'_{max\,f}$ **versus** K **for values of** Q_r' **(river discharge model)**

m = bank slope

W = channel width corresponding to mean water depth in channel

ε = phase lag between sea tide and bay tide

h. The inlet as a filter, flow dominance, and net effect on sedimentation processes.

(1) Introduction. As shown previously, an inlet filters some part of the ocean tide as it translates into the bay, depending on the characteristic inlet parameters defined earlier. Keulegan and King's analytical models, discussed earlier, assumed a sinusoidal ocean tide, and due to the nonlinear friction term (containing u^2), solutions of bay tide response implicitly contained higher-order harmonics (i.e., frequencies higher than that of the basic ocean tide). Other studies have shown that if a variable inlet cross section or variable bay surface area is considered, this will introduce higher-order harmonics. The forcing ocean tide, of course, is composed of many different frequency constituents (Part II-5), so there is interest in using this information to provide more accurate results. Also, investigators have shown that higher harmonics of current velocity (resulting from the forcing tides) are important in relation to sediment transport and its net movement through the inlet (King 1974; Aubrey 1986; DiLorenzo 1988). These effects are important due to the relationship of sediment transport to velocity raised to some power, e.g., V^5 (Costa and Isaacs 1977).

(2) Tidal constituents. Boon (1988) suggests that the seven tidal constituents in Table II-6-2 adequately represent shallow-water tide distortion in inlet-basin systems. Aubrey and Friedrichs (1988) and DiLorenzo (1988) used the amplitude of the ratio of M4 to M2 constituent amplitudes as a measure of nonlinear distortion. Variability in the spring-neap cycle, as well as seasonal mean water level changes, cause characteristic fluctuations in M4/M2.

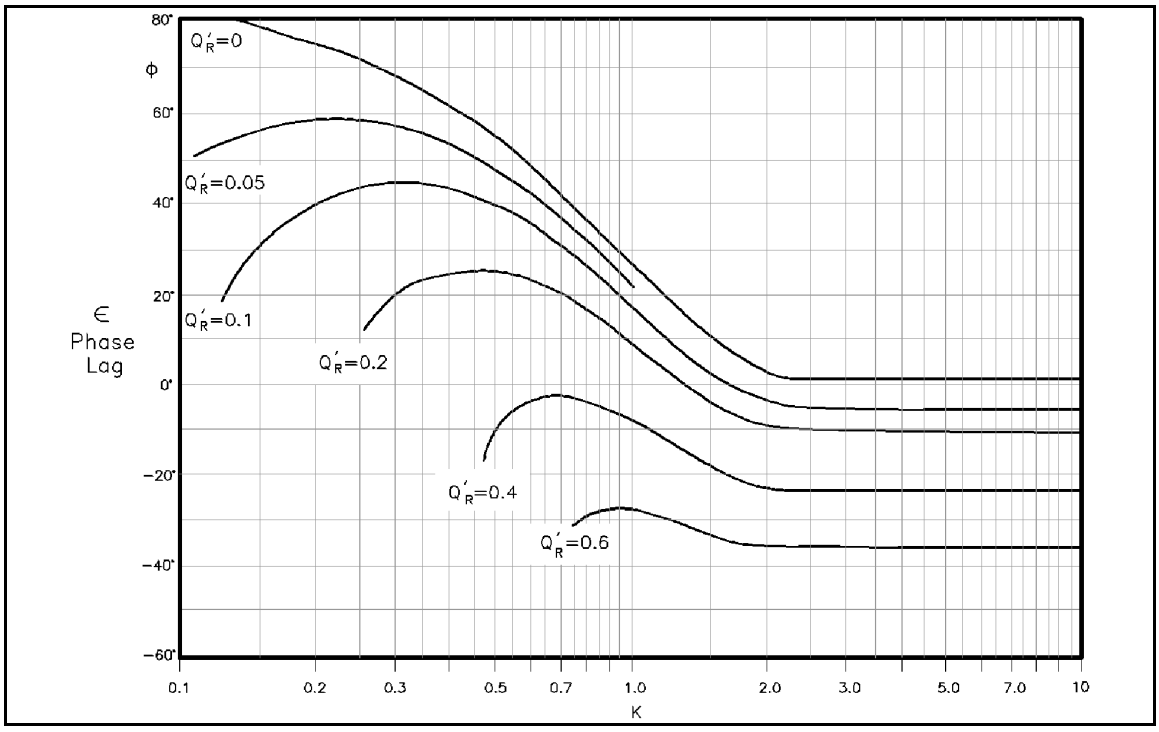

Figure II-6-29. ε versus *K* for values of Q_r' (river discharge model)

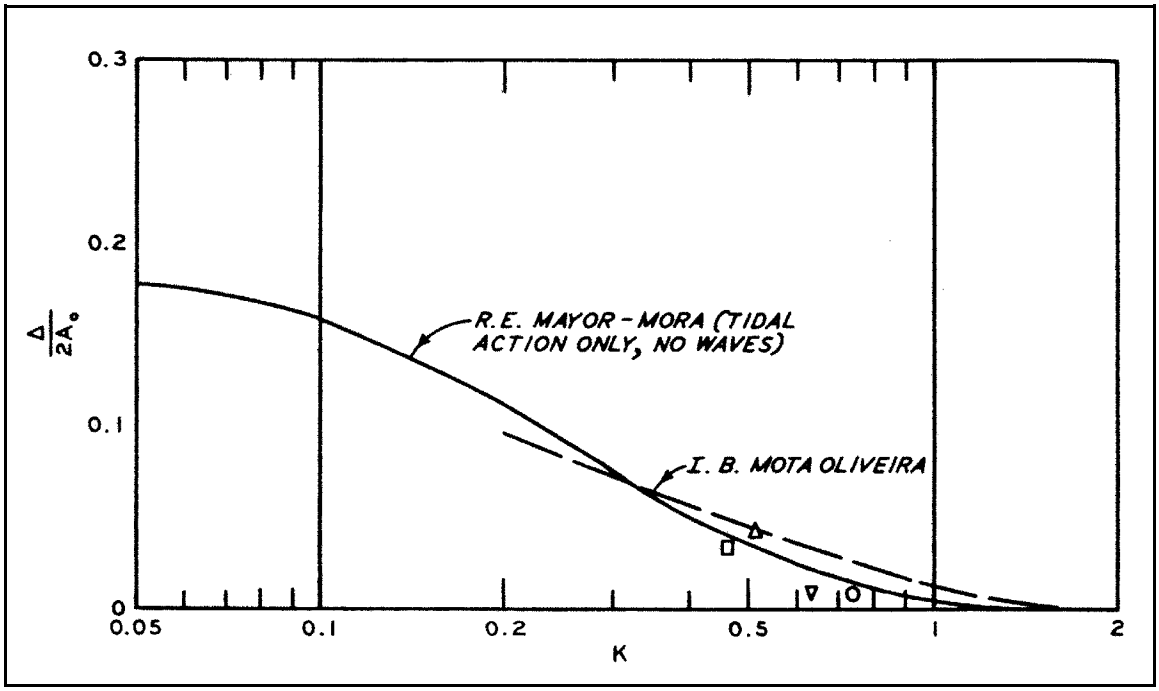

Figure II-6-30. Ratio of bay superelevation to ocean tide range as a function of the coefficient of repletion *K*

EXAMPLE PROBLEM II-6-2

Given:

Using the same inlet system discussed in Example Problem II-6-1, consider the effect of a constant river discharge of 350 m^3/s (12,360 ft^3/s).

Find:

What are the effects of river discharge on high-water and low-water elevations in the bay, bay tide range, and maximum flood and ebb velocities, the maximum flood and ebb discharges, and the bay tide phase lag.

Solution:

Using Equation II-6-19 for dimensionless variable Q_r' with a_o, A_b, and T from Example Problem 1 and Q_r given above

$$Q_r' = \frac{Q_r T}{2\pi a_o A_b}$$

$$Q_r' = \frac{350\ (44712)}{2(3.14)\ (1.30/2)\ (1.90\ x\ 10^7)} = 0.20$$

Using Equation II-6-11, find the Keulegan K, knowing K_1 and K_2, as calculated in Example Problem 1.

$$K = \frac{1}{k_2}\sqrt{\frac{1}{K_1}}$$

$$K = \frac{1}{0.25}\sqrt{\frac{1}{28.8}} = 0.75$$

(or calculate Keulegan K from Equation II-6-4).

With $K = 0.75$ and $Q_r' = 0.20$, bay tidal response is determined from Figure II-6-25

$$\frac{a_{b\ \max}}{a_o} = 0.92 \qquad a_{b\ \max} = 0.92\ (0.65) = 0.60\ \text{m}$$

and from Figure II-6-26

$$\frac{a_{b\ \min}}{a_o} = -0.56 \qquad a_{b\ \min} = -0.56\ (0.65) = -0.36\ \text{m}$$

(Continued)

Example Problem II-6-2 (Concluded)

Bay tide range is 0.96 m and is not symmetric about mean sea level, due to river flow.

Maximum channel velocities are determined from Figure II-6-27 (maximum ebb velocity)

$$U'_{maxe} = 0.80$$

Using Equation II-6-5, and substituting U'_{maxe} for V'_m and U_{maxe} for V_m, and solving for U_{maxe}

$$U_{maxe} = \frac{U'_{maxe}\ 2\pi\ a_o A_b}{A_{avg}\ T} = \frac{0.80\ (2)\ (3.14)\ (0.65)\ (1.90)\ 10^7}{666\ (12.42)\ (3600)} = 2.08\ \text{m/s}$$

From Figure II-6-28 (maximum flood velocity)

$$U'_{maxf} = 0.50$$

and in a manner similar to solving for ebb velocity, flood velocity is determined by

$$U_{maxf} = \frac{U'_{maxf}\ 2\pi\ a_o A_b}{A_{avg}\ T} = \frac{0.50\ (2)\ (3.14)\ (0.65)\ (1.90)\ 10^7}{666\ (12.42)\ (3600)} = 1.30\ \text{m/s}$$

Maximum discharges are determined from

$$Q_{maxe} = U_{maxf}\ A_c = 2.08\ (666) = 1385\ \text{m}^3/\text{s}$$

$$Q_{maxf} = U_{maxf}\ A_c = 1.30\ (666) = 866\ \text{m}^3/\text{s}$$

River flow increases maximum ebb discharge and decreases maximum flood discharge, as one would expect. The values are nearly balanced around the no-river-discharge value of 1,145 m^3/s of Example 1.

Using Figure II-6-29, the value of ε (phase lag of bay tide relative to ocean tide) is determined to be 19 deg, indicating high water occurs earlier than for the non-river-inflow condition of Example 1.

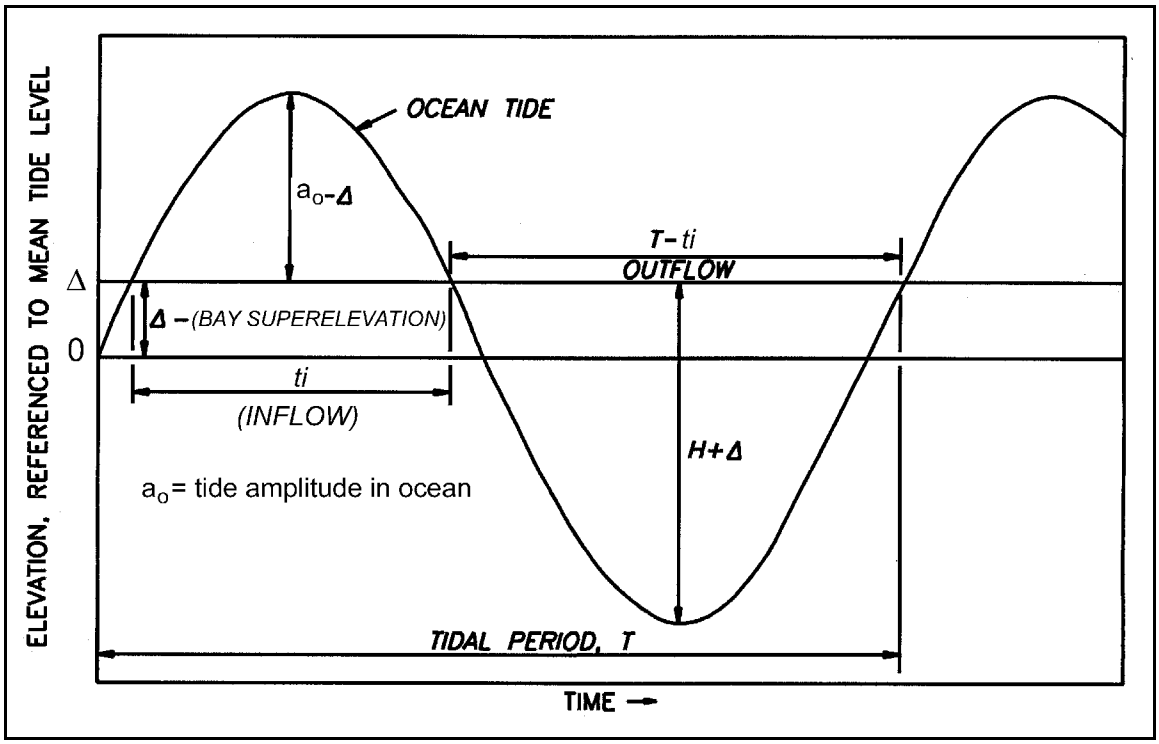

Figure II-6-31. Duration of outflow relative to bay superelevation

Table II-6-2
Semidiurnal and Shallow-Water Tidal Constituents and Harmonic Frequencies

Constituent	Frequency	Degrees/hr	Designation
M_2	a_1	28.9841	Lunar semidiurnal
S_2	a_2	30.0000	Solar semidiurnal
N_2	a_3	28.4397	Lunar elliptic
M_4	$2a_1$	57.9682	Lunar quarter-diurnal
S_4	$2a_2$	60.0000	Solar quarter-diurnal
MS_4	a_1+a_2	58.9841	Compound harmonic
MN_4	a_1+a_3	57.4238	Compound harmonic
MSf	a_2-a_1	1.0159	Lunar long-period

(3) Flow dominance. Entrance area and bay surface area variation impacts flow conditions at the inlet in terms of the continuity equation (Equation II-6-3), which indicates that

$$\frac{dh_b}{dt} \propto \frac{A_{avg}}{A_b} \tag{II-6-22}$$

The rate of change of bay elevation is directly proportional to channel area and inversely proportional to surface area of the bay. If A_{avg} is held constant while A_b increases with the rising tide, then the rate of rise decreases, while the rate of fall increases over time. This means there is a longer rise and faster fall, indicating greater ebb velocity peaks (assuming the same amount of water enters and leaves the bay), which means currents are ebb-dominant when considering only the effect of variable bay area. Similar reasoning

shows that variable entrance area increases the rate of rise of flood tide and decreases the rate fall, causing higher maximum flood velocities than ebb, creating a flood-dominant inlet. These conditions are important to help interpret the movement of sediment through inlets and the locations where shoals form.

i. Multiple inlets.

(1) Often a lagoon is connected to the ocean by more than one inlet. The basic simplified hydraulics can be determined by methods introduced previously or may be numerically modeled for more detailed effects such as residual currents and net circulation (van de Kreeke 1976, 1978). Multiple inlets with a common bay can impact inlet stability if an inlet changes or if an inlet is added (Ward 1982). Changes to a multiple inlet system may be gradual (for example, one inlet gradually lengthens as littoral transport creates shoal regions in the inlet), or change may be rapid (e.g., a hurricane cuts a channel through a barrier beach and begins to rapidly expand in size, capturing a significant portion of the tidal prism from a previously existing inlet connected to the same bay).

(2) For an existing system of multiple inlets, the K values may be added together

$$K_{inlet\ 1} + K_{inlet\ 2} + \ldots\ldots\ldots K_{inlet\ n} = K_{all\ inlets} \tag{II-6-23}$$

to determine the total K for the system, from which the bay tide amplitude and phase lag may be determined (Figures II-6-18 and II-6-20). A total maximum discharge (for the total of all inlets) from the V_{max} determined from Figure II-6-19 is

$$Q_{\max} = \frac{2\pi}{T} a_o A_b V_{\max} \tag{II-6-24}$$

(3) This total maximum discharge then may be apportioned between all inlets

$$Q_{\max} = Q_{1\max} + Q_{2\max} + Q_{3\max} + \ldots\ldots \tag{II-6-25}$$

with the above equation knowing that, for example, for three inlets

$$Q_{1\max} = \frac{Q_{\max}}{1 + \frac{K_2}{K_1} + \frac{K_3}{K_1}} \tag{II-6-26}$$

Q_{2max} and Q_{3max} may be determined by placement of the appropriate K values in the denominator in the same relative positions as in the above equation.

(4) For the case of an inlet connected to a bay that is segmented into separate internal bays connected by narrow openings, reference is made to Dean (1971) and Mota Oliveira (1970).

j. Tidal jets. Some analytical approaches to flow patterns at inlets treat parameters affecting the "plume" of water exiting the inlet (i.e., ebb flow). Joshi (1982) examined the effect of bottom friction, bathymetric changes, and lateral entrainment of water due to turbulent mixing. Generally, as bottom friction increases, the plume becomes wider and water velocity along the center line decreases. As bottom slope increases, the plume contracts. Özsöy (1977) and Özsöy and Ünlüata (1982) developed relationships to determine plume expansion and center-line velocity, as shown in Figures II-6-32 and II-6-33. Example

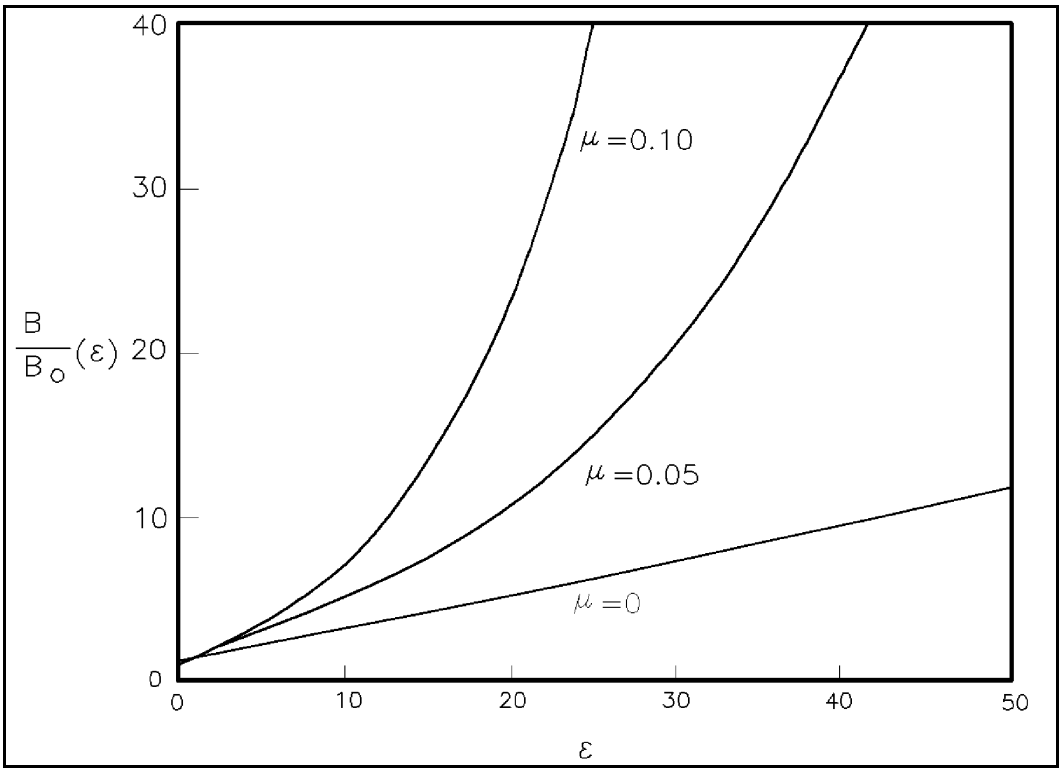

Figure II-6-32. Plume expansion

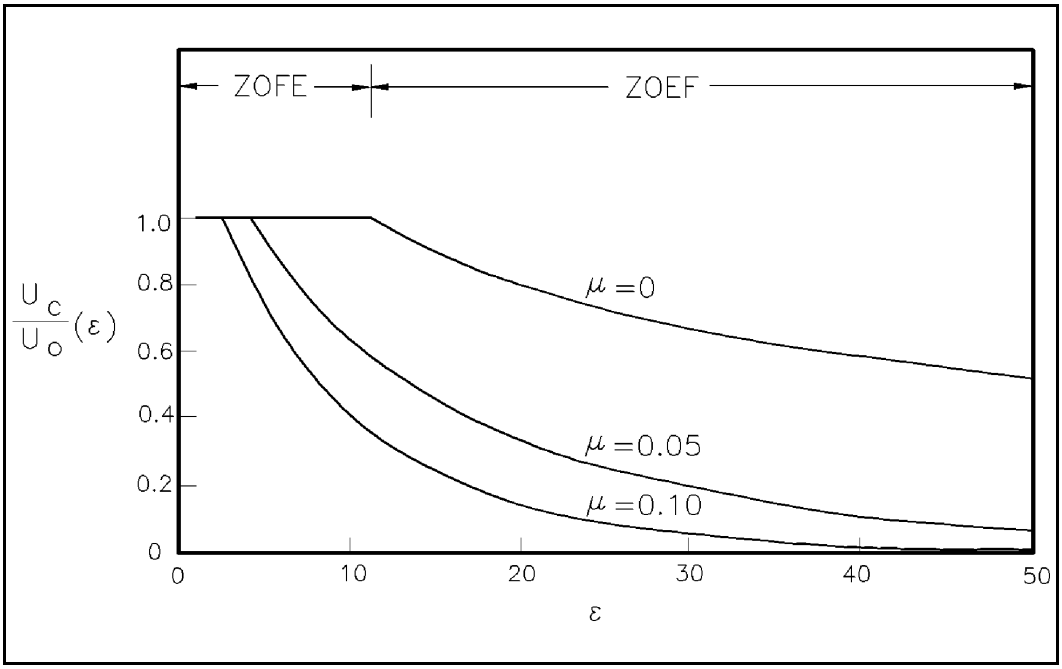

Figure II-6-33. Center-line velocity

Problem II-6-2 shows the effects of a flat bottom with friction. Özsöy and Ünlüata provide additional information for sloping bottoms and the effect of a longshore current approaching perpendicular to the ebb jet, deflecting it downcoast. Joshi and Taylor (1983) examined the alongshore circulation created by tidal jets and predicted that currents toward the inlet along the shoreline (induced by the ebb tidal jet or plume) can range from 0.01 to 0.1 m/s within 10 half-widths (of the minimum inlet width) of the natural inlet entrance. With a jetty in place, the range of induced currents along the shoreline is reduced, finally becoming zero at the junction of the shoreline and jetty. The above work is based on a simplified bathymetry and does not include wave-induced longshore currents, which can be an order of magnitude larger than jet-induced longshore currents. Ismail and Wiegel (1983) found that waves increased the rate of ebb jet spread.

k. Tidal dispersion and mixing.

(1) Flow through inlets can play an important role in the exchange processes and flushing of the bay, both of which impact water quality and bay ecology. Tidal currents, along with wind-driven currents and in some cases density-driven circulation, can drive dispersion processes in the bay where particles of water (or other substances, e.g., pollutants) are scattered or diluted. Tidal dispersion and its role in flushing of bays has been studied by many investigators including Geyer and Signell (1992), Zimmerman (1988), van der Kreeke (1983), Dyer and Taylor (1973), and Sanford, Boicourt, and Rives (1992). There is typically a broad variance in the dispersion coefficient values that can be determined for the processes causing dispersion over a large area. Therefore, analytic techniques to determine flushing of a bay are limited to small basins, and assume complete internal mixing, with detailed numerical simulations required for larger bays. Tidal dispersion is important in regions where flow separations occur; e.g., in regions of abrupt geometric change, with the inlet entrance channel a prime example. The extent of dispersive influence is limited to the tidal excursion in the bay (the distance covered by a particle entering the bay at the start of flood tide until the end of flood tide). For tidal dispersion to influence large spatial scales, spacing between major topographic features must be less than the tidal excursion distance (Geyer and Signell 1992).

(2) For small basins, where it is assumed that waters in the basin are completely mixed at all times, van de Kreeke (1983) defined residence time as the average time for a particle to enter, then leave the basin, with this average based on many particles. For small basins, and with the following relationship met

$$10 > \frac{\langle V \rangle}{\varepsilon P} > 1.5 \tag{II-6-27}$$

where <V> is the average volume of the bay over the tidal cycle, ε is the fraction of new water entering the bay from the sea each tidal cycle, and P is the tidal prism. *A* value of $\varepsilon = 0.5$ is often used when there is no other basis for estimation of this factor. Then residence time can be calculated by

$$\frac{\tau_r}{T} = \frac{\langle V \rangle}{\varepsilon P} \tag{II-6-28}$$

with τ_r residence time and T tidal period. The time to reduce the mass of a substance's concentration by a factor of "e" (2.3) is equal to τ_r and to reduce it a factor of 10 is $2.3\tau_r$.

l. Wave-current interaction. The region where the navigation channel intersects and/or passes through the outer ebb shoal can be a region of intense wave-current interaction. Wave-current interaction can produce difficult navigation and dredge operation conditions. Also, interaction of waves, currents, and local bathymetry/channel typically produces the most severe channel shoaling problems at inlets. These interactions will be discussed in various combinations.

(1) Wave-current interaction.

(a) Horizontal currents can modify surface gravity waves by stretching or shrinking features of a wave train. This distortion can produce a "Doppler Shift" in wave period. Wave orthogonal, crest, and ray directions are modified (see Part II-1 for definitions). Also, a current modifies surface waves by causing an exchange of energy between wave and current. The pressure field accompanying the wave also is modified. Predicting current-modified wave energy, heights, directions, and pressures is typically a complex procedure still under research; however, a graphical method presented by Herchenroder (1981) based on work by Jonsson et al. (1970), can be used to estimate the effect of current on wave height H_A, where this is wave height without current.

Using the equation:

$$H = (R_H)H_A \tag{II-6-29}$$

(b) Figure II-6-34 may be used to determine R_H, the wave height factor, which depends on:

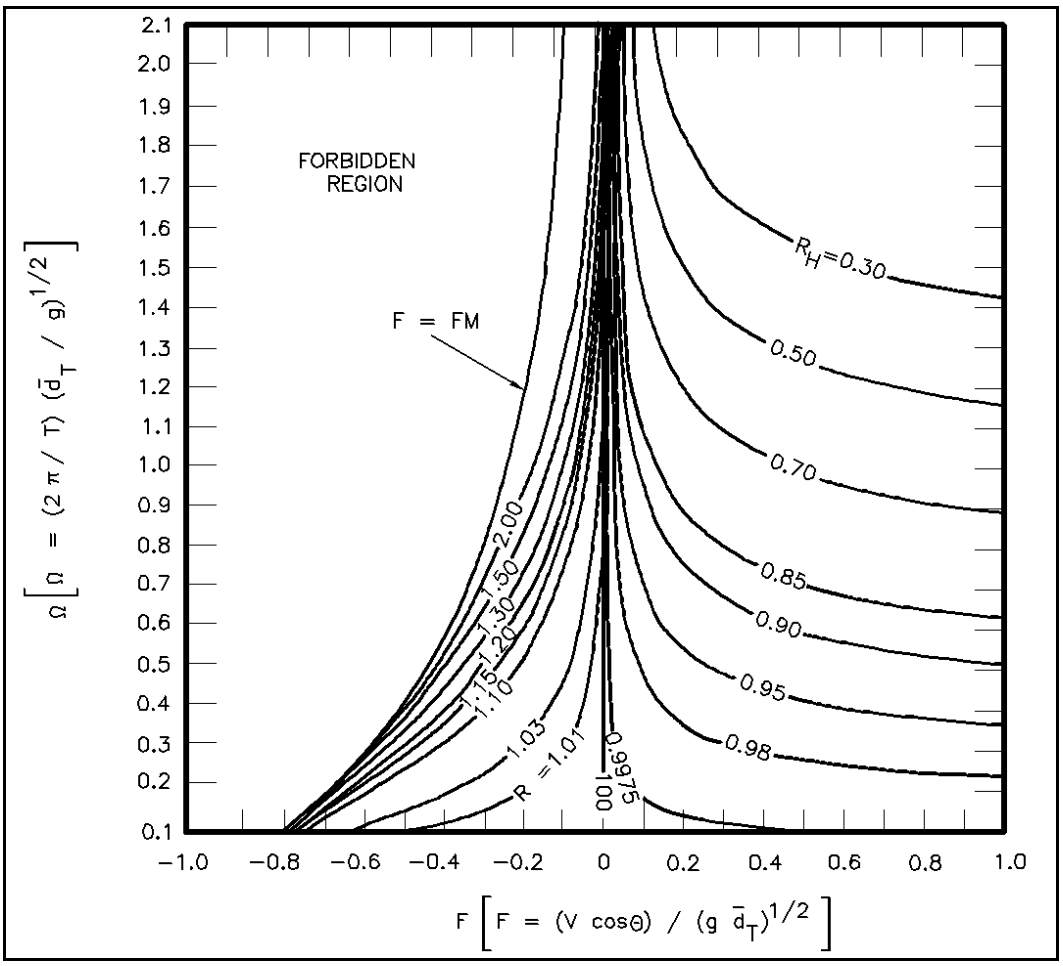

Figure II-6-34. Contours of dimensionless wave height factor R_H given by Equation II-6-29. Waves cannot propagate for values of *F* and Ω lying in the forbidden region (boundary line F = FM)

EXAMPLE PROBLEM II-6-3

FIND:

The width of the ebb jet and its maximum velocity along the centerline 2,000 m seaward from shore.

GIVEN:

The inlet channel width where the ebb jet exits the inlet is 200 m and the channel depth is 8 m. A flat bottom and Mannings n = 0.02 are assumed. The maximum average velocity in the channel is 1.5 m/sec.

SOLUTION:

The friction factor μ (from Özsöy and Ünlüata (1982)) is calculated as

$$\mu = \frac{g b_o n^2}{h_o^{0.75}} = \frac{(9.8)\ (100)\ (0.02)^2}{(8)^{0.75}} = 0.08$$

where b_o = half-width of channel = 200 m / 2 = 100 m and the dimensionless distance offshore parameter is

$$\xi = \frac{x}{b_o}$$

with x, the distance offshore, equal to 2000 m. Calculating these parameters, μ = 0.08 and ξ = 20. Using Figures II-6-32 and II-6-33, and interpolating for μ, the results are

$$\frac{b}{b_o}(\xi) = 18.5 \quad \Rightarrow \quad b = 100\ (18.5) = 1850\ \text{m}$$

and

$$\frac{u_c}{u_o}\ (\xi) = 0.2 \quad \Rightarrow \quad u_c = 0.2\ (1.5) = 0.3\ \text{m/s}$$

Therefore, for a flat bottom, the half-width of the jet expands from 200 m to 1,850 m and the center-line velocity of the jet decreases from 1.5 m/s at the inlet to 0.3 m/s 2,000 m from shore.

EXAMPLE PROBLEM II-6-4

Find:

Determine the wave height in an inlet channel that is 5.0 m (16.4 ft) deep.

Given:

A 5.0-sec, 1.0-m (3.28-ft) wave is entering an inlet having a 1.0 m/s (3.3 ft/s) ebb current. The angle between current and wave orthogonal is 180 deg.

Solution:

$\Omega = (2\pi/T)\ (d_T/g)^{1/2}$

$F = (V \cos \theta)/(g\bar{d}_T)^{1/2}$

T = wave period = 5 s

d_T = time-averaged water depth = 5.0 m

g = 9.8 m/s^2

V = horizontal current speed = 1.0 m/s

θ = angle between horizontal velocity vector and horizontal wave vector = 180^o

Therefore:

$$\Omega = \left(\frac{2\ (3.14)}{5.0}\right)\left(\frac{5}{9.8}\right)^{1/2} = 0.90$$

$$F = \frac{1.0\ (\cos\ 180)}{(9.8 \cdot (5))^{1/2}} = -0.14$$

From Figure II-6-34, R_H = 1.35

Wave height H_A, originally 1 m, is modified by the current to a wave height of:

$$H = (R_H)\ H_A = 1.35\ (1.0) = 1.35 \text{ m}$$

$$F = \frac{V \cos \theta}{\left(g d_T\right)^{\frac{1}{2}}} \tag{II-6-30}$$

and

$$\Omega = \left(\frac{2\pi}{T}\right)\left(\frac{d_T}{g}\right)^{\frac{1}{2}} \tag{II-6-31}$$

where

T = wave period

d_T = channel depth

θ = angle wave orthogonal makes with current

V = velocity in channel

(2) Current-channel interaction. As flow converges on an inlet entrance, the angle at which flow approaches a dredged channel can be important with regard to change in current direction and can ultimately relate to channel shoaling. The direction of current approach will depend on bottom configuration and structure(s) location. Boer (1985) developed a mathematical model to study currents in a dredged channel. He found that a current approaching obliquely to a channel is refracted within the channel and the streamlines contract within the channel causing a velocity increase (Figure II-6-35). This effect becomes relatively small for angles larger than 60° (angle between channel axis and current direction). This effect is largest near the bed and smallest near the surface. Due to continuity, depending on the relative depth of the channel to the surrounding depths, there is a decrease factor because of increased depth in the channel.

m . Other methods of inlet analysis. As mentioned in Part II-6-2, paragraph *a,* follow-up studies using techniques presented in previous sections and numerical and/or physical models, can be conducted after an initial examination of the inlet. Some available tools are discussed below.

(1) Automated Coastal Engineering System (ACES). ACES (Leenknecht et al. 1992) contains an inlet model that operates in the PC environment and estimates inlet velocities, discharges, and bay levels as a function of time. This model is designed for cases where the bay water level fluctuates uniformly. Seaward boundary conditions are specified as water level fluctuations associated with astronomical tides, storm surges, seiches, and tsunamis. Figure II-6-36 shows a flow net and Figure II-6-37 is a typical cross section indicating that the model can handle up to two inlet entrances to a single bay and that the entrance channel(s) can be divided into sub-channels to accommodate change in depth across the inlet. The model will permit up to seven sub-channels and up to sixteen cross sections of the flownet. Figures II-6-38 and II-6-39 show sample output from the program.

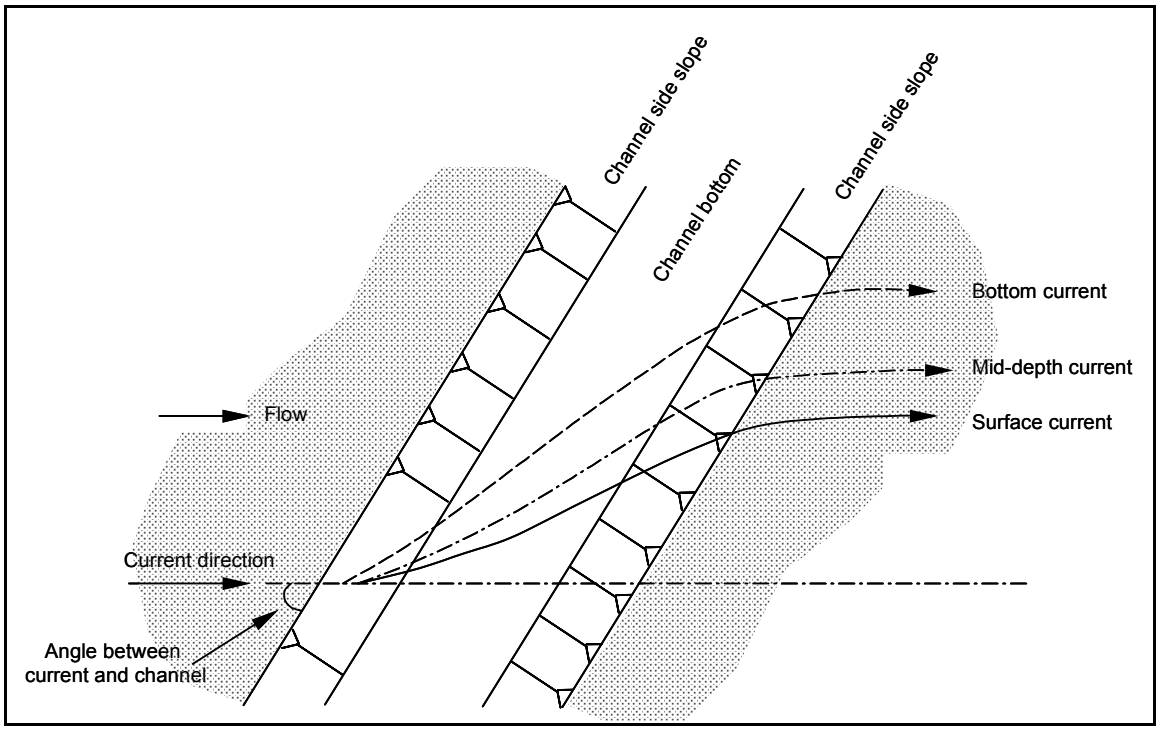

Figure II-6-35. Refraction of currents by channel

(2) DYNLET1. This model (Amein and Kraus 1991) is a one-dimensional PC model that can predict flow conditions in channels with varied geometry, and accepts varying friction factors across an inlet channel. Values of water surface elevation and average velocity are computed at locations across and along inlet channels. The inlet to be modeled may consist of a single channel connecting the sea to the bay, or it may be a system of interconnected channels, with or without bays.

(3) Coastal Modeling System (CMS). The CMS (Cialone et al. 1991) contains two hydrodynamic programs applicable to inlets. This modeling system is a supercomputer-based system of models and supporting software packages. Two models applicable to inlet studies are:

(a) WIFM. This model is a two-dimensional, time-dependent, long-wave model for solving the vertically integrated Navier-Stokes equations in a stretched Cartesian coordinate system. The model simulates shallow-water long-wave hydrodynamics such as tidal circulation, storm surges, and tsunami propagation. WIFM contains many useful features for studying these phenomena such as moving boundaries to simulate flooding/drying of low-lying areas and subgrid flow boundaries to simulate small barrier islands, jetties, dunes, or other structural features. Model output includes vertically integrated water velocities and water surface elevations.

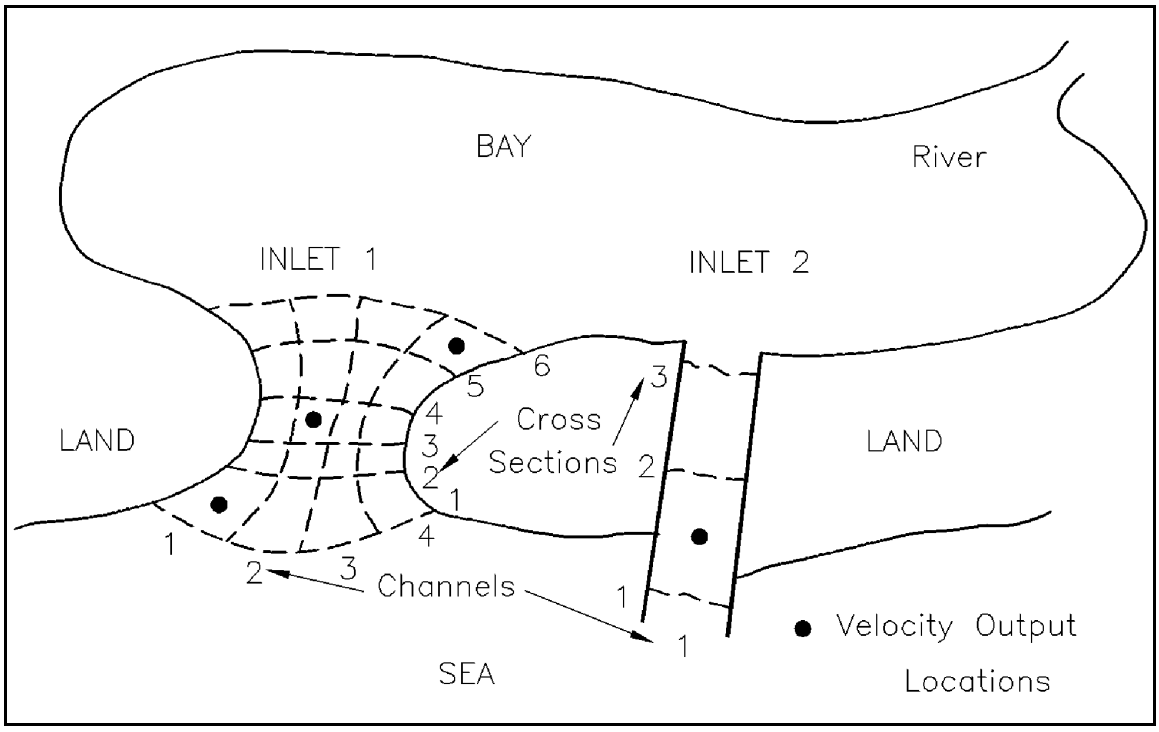

Figure II-6-36. Typical inlet flow nets

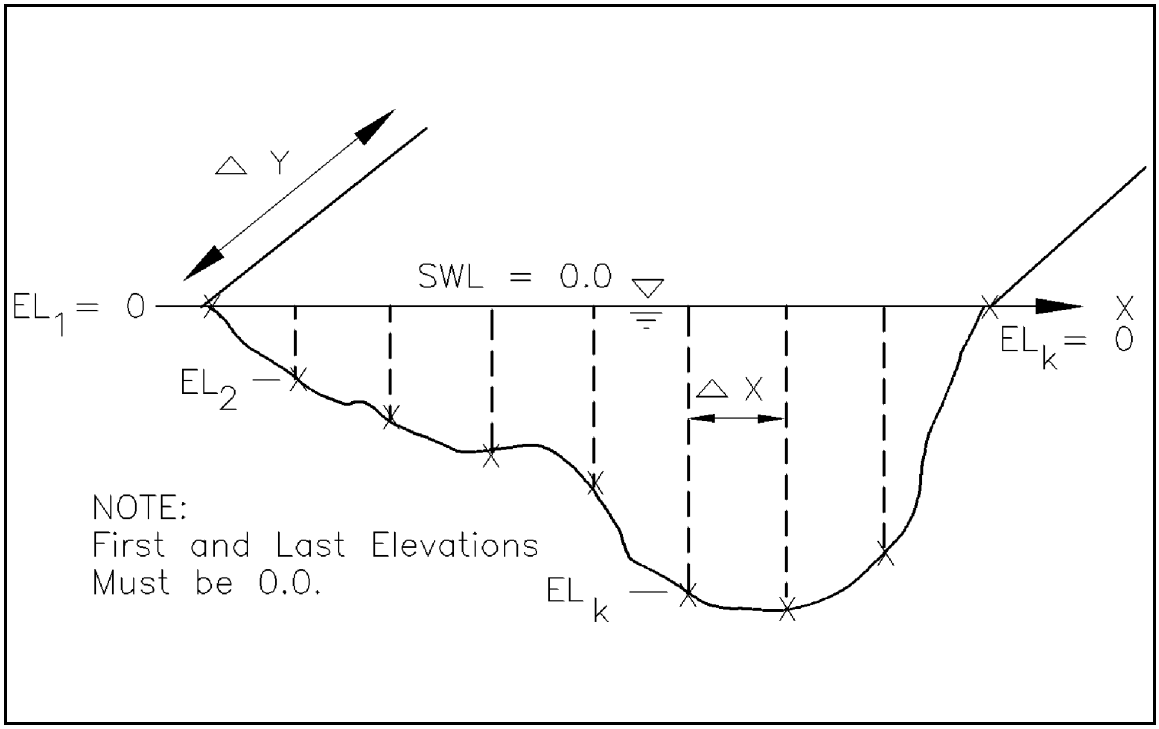

Figure II-6-37. Typical inlet cross section

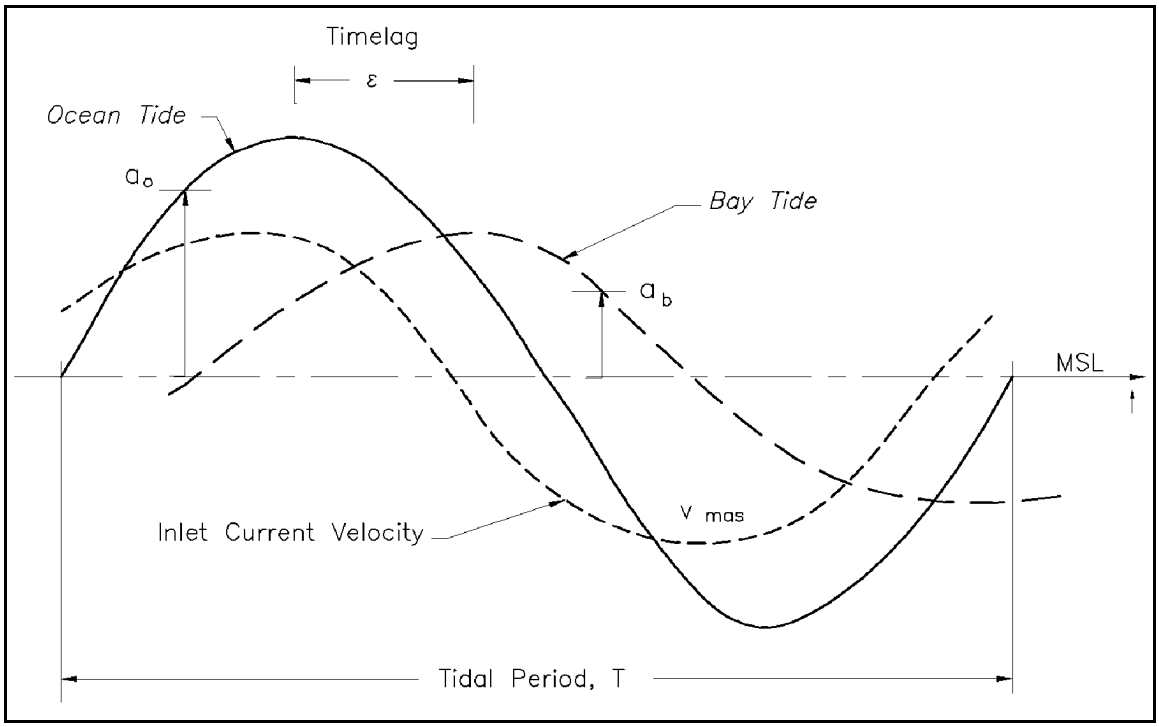

Figure II-6-38. Sea and bay water elevations at inlet 1

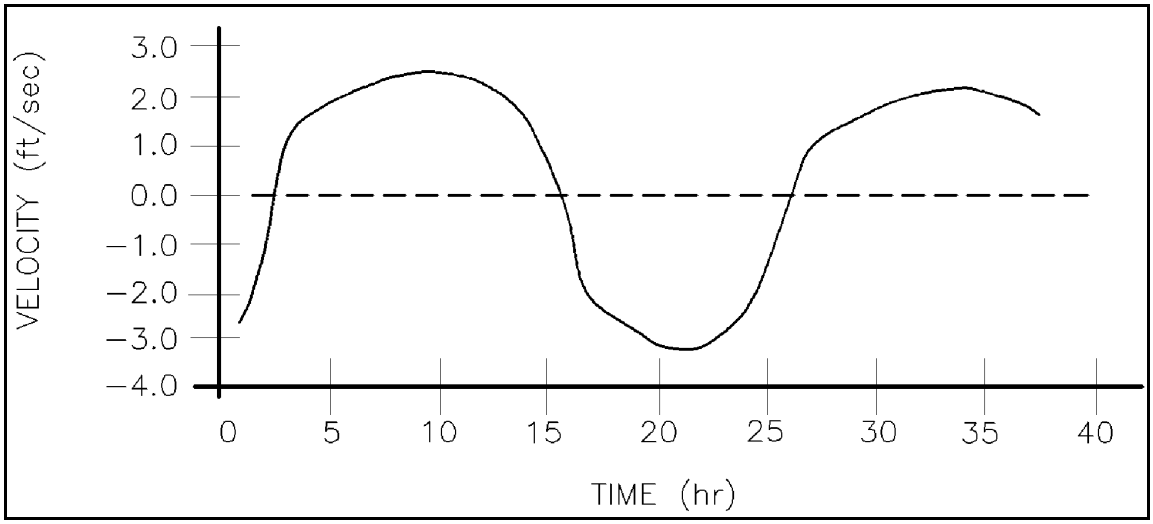

Figure II-6-39. Average velocity at minimum cross section

(b) CLHYD. This model simulates shallow-water, long-wave hydrodynamics such as tidal circulation and storm surge propagation. It can simulate flow fields induced by wind fields, river inflows/outflows, and tidal forcing. CLHYD is similar to WIFM, with the added feature of operating on a boundary-fitted (curvilinear) grid system. However, CLHYD cannot simulate flooding/drying of low-lying areas, as WIFM can. Model output includes vertically integrated water velocities and water surface elevations.

(4) Other models. Other more sophisticated models that require considerable expertise to use already exist or are being developed. The reader is advised to consult current technical literature for details. Part II-5-7, "Numerical Modeling of Long Wave Hydrodynamics," discusses two such sophisticated models, CH3D and ADCIRC.

(5) Physical models. Physical models have also been used for both the hydraulic and sedimentation aspects of inlet studies, but numerical models usually have been used in recent years due to the expense of constructing the large bay system of an inlet and the need to examine processes difficult to reproduce in a physical model, such as storm surge, which would need to include wind effects. However, physical models are appropriate and cost-effective for examining structures and detailed flow patterns in the immediate vicinity of the inlet entrance (sample references include Bottin (1978, 1982), Seabergh (1975), Seabergh and Lane (1977), and Seabergh and McCoy (1982)).

II-6-3. Hydrodynamic and Sediment Interaction at Tidal Inlets

a. Introduction. Waves, currents, and sediment interact at tidal inlets over a large physical area, with varying effects over a tidal cycle (Smith 1991). At the throat or minimum cross-sectional area of the inlet and bayward, tidal currents are the predominant forcing agent interacting with sediments. However, moving seaward and alongshore away from the inlet, the effect of waves increases. Wave energy on the edges of the inlet channel can contribute sediment from adjoining beaches, with the flood tidal currents tending to move bayward to a flood tidal shoal (or middle-ground shoal), or the ebb currents jetting sediment seaward to settle on the ebb shoal. Sediment may again be moved to adjoining beaches by the combination of waves and currents, thus "bypassing" the inlet. The interaction of tidal currents, waves, and wave-generated currents is a complex process.

b. Tidal prism - channel area relationship.

(1) Initial research focused on the relationship to flow through the inlet and the minimum cross-sectional area that could be sustained by that flow. O'Brien (1931, 1969) originally determined a relationship between minimum throat cross-sectional area of an inlet below mean tide level and the tidal prism (i.e., the volume of water entering or exiting the inlet on ebb and flood tide) at spring tide (Figure II-6-40). This relationship was predominantly for Pacific coast inlets, where a mixed tidal pattern is observed and there typically is a strong ebb flow between higher-high water and lower-low water. Jarrett (1976) continued the analysis and performed regression analysis for various coastal areas with different tidal characteristics. A regression equation is given for each of the Atlantic, Pacific, and Gulf coasts. Jarrett also recommended using O'Brien's equation for dual-jettied inlets. The equations, in metric and English units, are given in Table II-6-3.

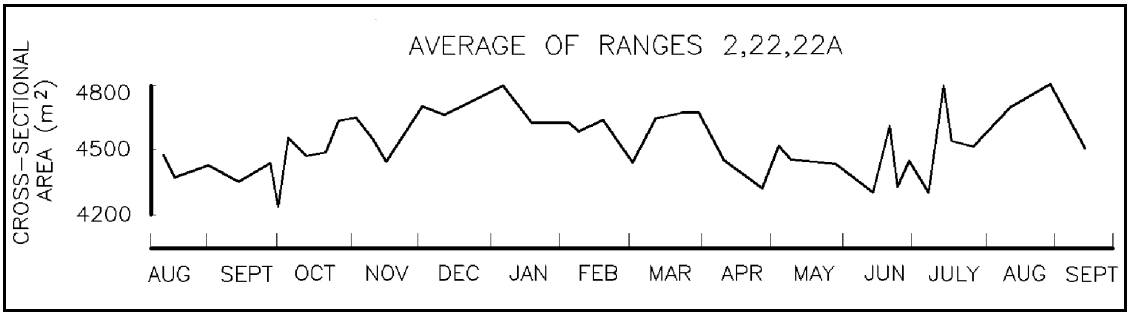

Figure II-6-40. Variations in cross-sectional area for Wachapreaque Inlet (Byrne, De Alteris, and Bullock 1974)

Table II-6-3
Tidal Prism-Minimum Channel Cross-sectional Area Relationships

Location	Metric Units	English Units
Atlantic Coast	$A_c = 3.039 \times 10^{-5} P^{1.05}$	$A_c = 7.75 \times 10^{-6} P^{1.05}$
Gulf Coast	$A_c = 9.311 \times 10^{-4} P^{0.84}$	$A_c = 5.02 \times 10^{-4} P^{0.84}$
Pacific Coast	$A_c = 2.833 \times 10^{-4} P^{0.91}$	$A_c = 1.19 \times 10^{-4} P^{0.91}$
Dual-Jettied Inlets (O'Brien)	$A_c = 7.489 \times 10^{-4} P^{0.86}$	$A_c = 3.76 \times 10^{-4} P^{0.86}$

A_c is the minimum cross-sectional area in square meters (square feet) and P is the tidal prism in cubic meters (cubic feet).

(2) Inlet tidal prisms versus minimum cross-sectional area for Jarrett's data is plotted in Figure II-6-9.

(3) Work by Byrne et al. (1980) indicated that for inlets with minimum cross sections less than 100 m^2 (1,076 ft^2), there was a departure from the relationships developed above. They studied small inlets on the Atlantic Coast in Chesapeake Bay. Their relationship for area and tidal prism is

$$A_c = 9.902 \times 10^{-3} p^{0.61} \text{ (metric units)} \quad \text{(II-6-32)}$$

(4) Jarrett's (1976) work pertains to equilibrium minimum cross-sectional areas at tidal channels from one survey at a given date. Byrne, DeAlteres, and Bullock (1974) have shown that inlet cross section can change on the order of ± 10 percent in very short time periods (see Figure II-6-40). This, of course, is due to the variability in tidal currents and wave energy. A storm may bring a large amount of sediment to an inlet region, since the inlet tends to act as a sink for sediment and the tidal current may require a certain time period to return the minimum cross-sectional area to some quasi-equilibrium state. Brown (1928) notes that for Absecon Inlet, New Jersey, "a single northeaster has been observed to push as much as 100,000 cubic yards of sand in a single day into the channel on the outer bar, by the elongation of the northeast shoal, resulting in a decrease in depth on the centerline of the channel by 6 to 7 feet." Sediment changes such as this will affect the hydraulics of the inlet system, which in turn will remodify channel depth and location of sediment shoaling.

(5) Adding jetty structures to natural inlets modifies the inlet's morphology. Careful engineering design can reduce the amount of induced change. For example, jetties are placed so that the minimum cross-sectional area of the inlet is maintained, leaving the volume of water exchanged over a tidal cycle (i.e., the tidal prism) unchanged from the natural state. During design of inlet training structures, the question of appropriate spacing must be answered so that excessive scour does not occur and cause settling or displacement of the structures. Using O'Brien's formula for jettied inlets, the minimum distance between jetties can be calculated. Figure II-6-41 shows lines of average depth expected for given jetty spacing and tidal prism. The data points plotted on Figure II-6-41 describe actual field conditions for 44 inlets. No attempt was made to analyze or judge whether problems existed at a particular project. For example, a very large tidal prism with very narrow jetty spacing may develop problems of erosion along one of the jetties or very high velocities might exist, producing navigational difficulties. Also, if spacing of the jetties is too wide, the channel thalweg may meander in a sinuous manner, making navigation more difficult and reducing efficiency, so as to increase shoaling and lead to possible closure. If the same minimum area is maintained between the entrance channel's jetties that existed for the natural inlet, the tidal prism will be the same, and tides will flush out the bay behind the inlet as well as they did in the natural state. Actually, a more hydraulically efficient channel usually will exist at a jettied inlet because sediment influx is reduced and there are fewer shoals.

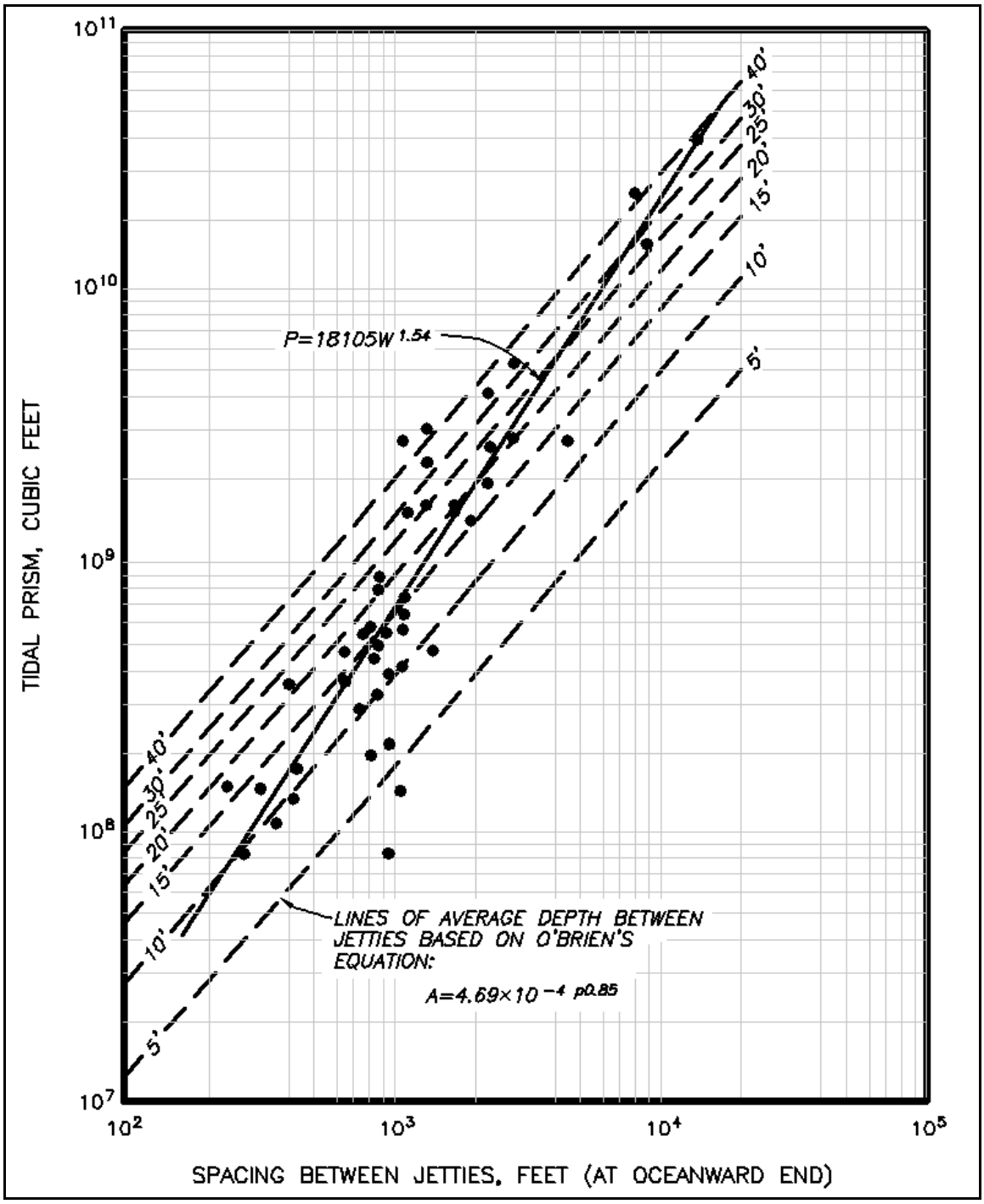

Figure II-6-41. Tidal prism (*P*) versus jetty spacing (*W*)

c. Inlet stability analysis.

(1) Dean (1971) equated the expression for tidal prism, $P = TV_m A_C/\pi$ to O'Brien's (1931) original tidal prism, inlet area relationship ($P = 5 \times 10^4 A_c$) and determined that for a tidal period of 44,640 sec, V_m for the inlet is about 1 m/sec. In other words, 1 m/sec might be interpreted as a level of velocity necessary to maintain an equilibrium flow area. Therefore, as wave action supplies sand to the inlet channel and tends to

reduce the cross-sectional area, the inlet flow will scour out any depositions that reduce the channel cross section below its equilibrium value. This concept was first developed analytically by Escoffier (1940, 1977). He proposed a diagram for inlet stability analysis in which two curves are initially plotted. The first is the velocity versus the inlet's cross-sectional flow area A_c. A single hydraulic stability curve represents changing inlet conditions when ocean tide parameters and bay and inlet plan geometry remain relatively fixed. As area approaches zero, velocity approaches zero due to increasing frictional forces, which are inversely proportional to channel area. As channel area increases, friction forces are reduced but, on the far right side of the curve, velocities decrease as the tidal prism has reached a maximum, and any area increases just decrease velocity as determined by the continuity equation. This curve can be constructed by calculating velocity V_m by varying channel area A_c. V_m can be determined by an analytical or numerical model, remembering that, if using Keulegan or King models, an average maximum velocity is determined. The continuity equation V_{avg} $A = V_m A_c$ must be used to determine maximum velocity at the minimum cross section. The other curve plotted as V_E is a stability criterion curve such as O'Brien and Jarrett's tidal prism versus cross-section area relationship. Escoffier (1940) originally proposed a constant critical velocity (e.g., 1 m/sec, which would plot as a straight horizontal line. If a P versus A_c relationship is used, the appropriate equation (Table II-6-3) can be used to relate V_m to tidal prism. The two curves are shown in Figure II-6-42. The possibilities of intersection of the two curves could possibly intersect at two locations or one location (a tangent), or there could be no intersection at all. In the first case, point b (see Figure II-6-42) is a stable root in that any deviation in area returns movement along the stability curve to its starting point. If channel area increases (move right on curve from point b) velocity will fall and more sediment can fill in the channel to bring it back to "equilibrium." If area decreases, velocity will increase scouring back to the equilibrium point. Point c is an unstable root, where if the area decreases, velocities decrease until the inlet closes. Moving to the right of point c, as velocity increases, area increases until the velocity starts falling and the stable root at point b is reached. If the stability curve falls tangent to or below the stability criterion curve, the inlet will close. Thus, if the inlet area is to the right of the unstable equilibrium point, and a storm occurs that provides a large sediment input to the inlet region, the inlet area could shift to the left of that point, and the inlet would close. van de Kreeke (1992) presents useful commentary on application of Escoffier's analysis where he notes that separation of stable and unstable inlets is not determined by the maximum in the maximum velocity curve (sometimes called the closure curve) of Figure II-6-42, but point c of that curve. Van de Kreeke emphasizes the integral use of O'Brien-type stability correlations with Esscofier's curve, rather than the use of stability equations alone.

(2) Escoffier (1977) presented work similar to the above, except the Keulegan K value was determined for the abscissa of the plot in place of the area. For a given set of parameters for a particular inlet, A_c is varied and K is determined to define the V_m curve. Note: If King's curves are used, K is related to K_1 and K_2 by Equation II-6-11. Figure II-6-43 shows an example diagram. The V_E curve then is determined by selecting an appropriate tidal-prism versus-area relationship and by determining V_{max} for various A values .

(3) A technique by O'Brien and Dean (1972) has also been used to calculate the stability of an inlet affected by deposition. The stability index ß is defined to represent the capacity of an inlet to resist closure under conditions of deposition. It incorporates a buffer storage area available in the inlet cross section, prior to deposition and includes the capability of the inlet to transport excess sand from its throat.

$$\beta = \int_{a_C}^{a_E} (V_{\max} - V_T)^3 \, dA_c \qquad \text{(II-6-33)}$$

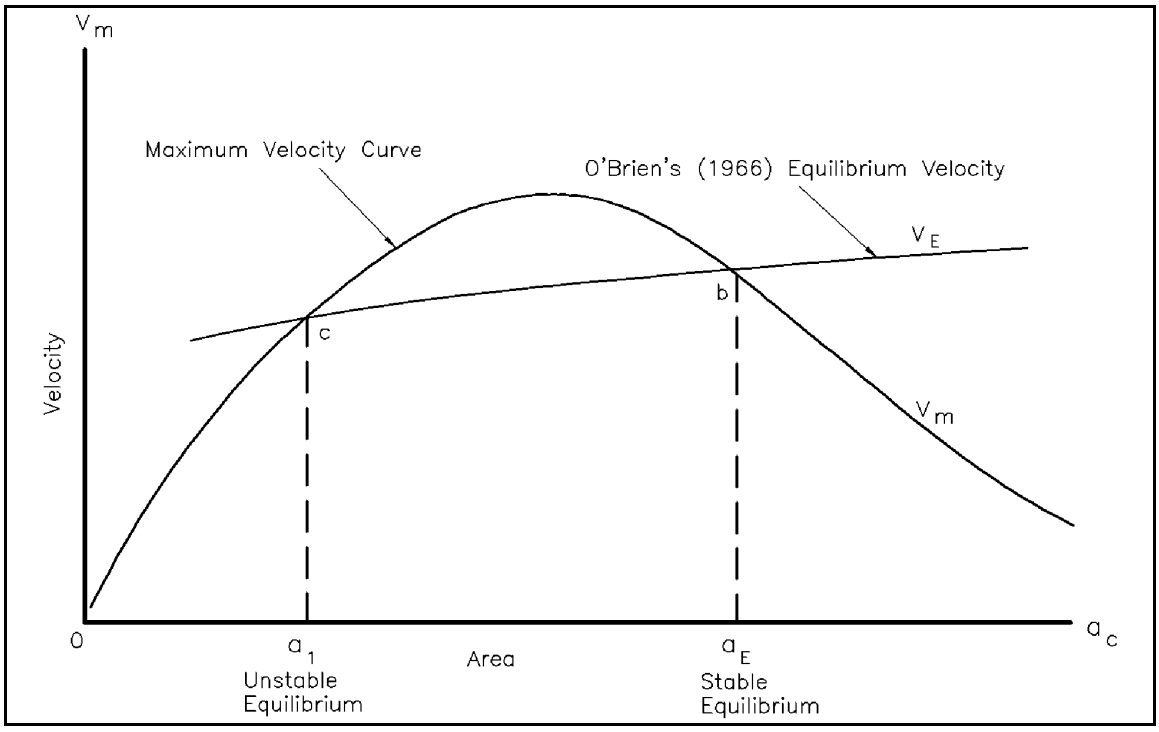

Figure II-6-42. Escoffier (1940) diagram, maximum velocity and equilibrium velocity versus inlet cross-sectional area

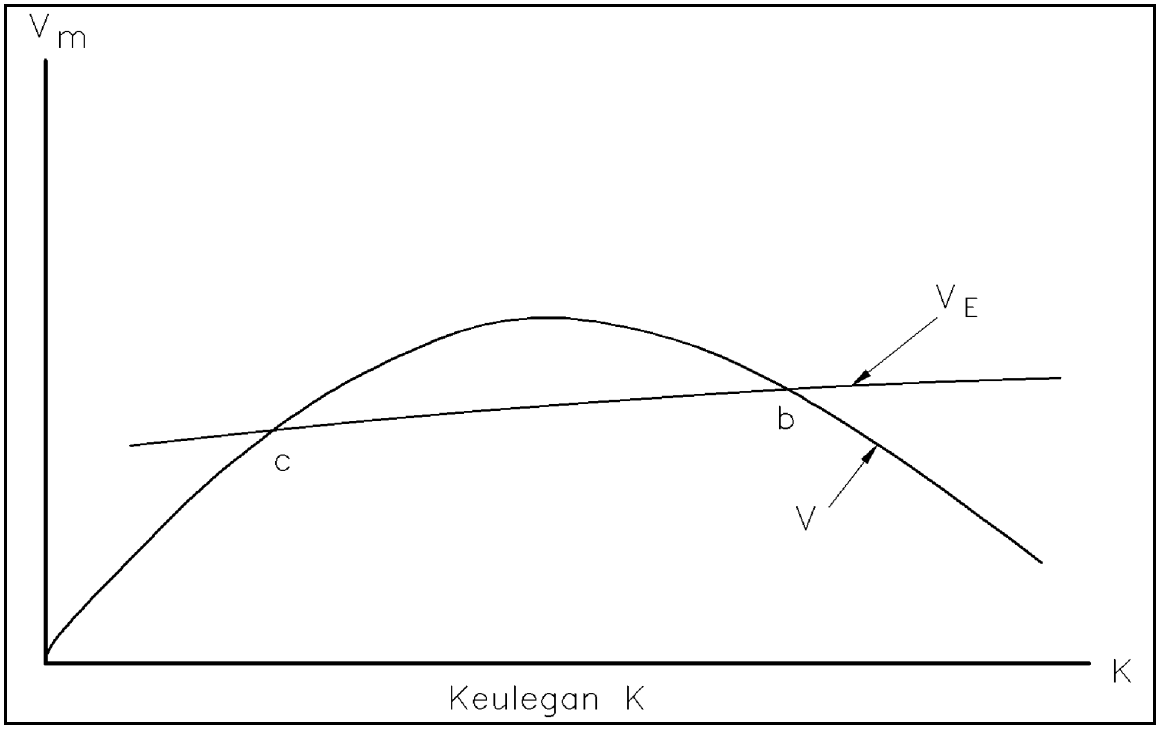

Figure II-6-43. Another version of Escoffier's (1977) diagram, maximum velocity and equilibrium velocity versus Keulegan repletion coefficient *K*

where

β = stability index (units of length^5/time^3)

a_E = equilibrium cross-sectional area of throat

V_{max} = maximum velocity in the throat

V_T = threshold velocity for sand transport

a_c = critical cross-sectional area (as from Figure II-6-42)

(4) Czerniak (1977) applied this technique successfully at Moriches Inlet, New York. Bruun and Gerritsen (1960) and Bruun, Mehta, and Jonsson (1978) developed an overall stability criteria for tidal inlets. They based their relationships on a ratio *P/M,* where *P* is the tidal prism and *M* is the total annual littoral drift (typical values for *M* and their determination are discussed in Part III). The stability of an inlet is rated good, fair, or poor as given in Table II-6-4.

Table II-6-4
Inlet Stability Ratings

$P/M_{tot} \geq 150$	Conditions are relatively good, little bar and good flushing
$100 \leq P/M_{tot} \leq 150$	Conditions become less satisfactory, and offshore bar formation becomes more pronounced
$50 \leq P/M_{tot} \leq 100$	Entrance bar may be rather large, but there is usually a channel through the bar
$20 \leq P/M_{tot} < 50$	All inlets are typical “bar-bypassers”
$P/M_{tot} \leq 20$	Descriptive of cases where the entrances become unstable “overflow channels” rather than permanent inlets

(5) Another aspect of inlet stability was discussed by Vincent, Corson, and Gingench (1991) in which inlet channel geographical location and horizontal topology were studied from aerial photography. They defined four stability indices, including minimum inlet width *W*, channel length *L*, change in geographical position *N*, and orientation variability of inlet channel *E*. Figure II-6-44 shows types of geographic channel instability. Figure II-6-45 shows the Little River Inlet, South Carolina, geographical variability. A stability limit was chosen so as to classify an inlet as stable or unstable. These limits were based on rate of change of width, length, position, and orientation. Records of 51 inlets over various time periods were examined and a change of 100 ft/month was selected as a reasonable arbitrary limit for stability in length and width of *W* and *L*. The 100-ft/month value was also selected as a divider between stable and unstable channel position. Most values examined were below the 100 ft/month rate.

d. Scour hole problems.

(1) Scour hole problems can occur at a variety of inlet locations and much remains to be understood about the mechanisms causing scour. Scour holes form as a result of the interaction of tidal currents, waves, wave-generated currents, sediment and adjacent structures (usually jetties). Scour holes have been observed at the tips of jetties, on the outside of the jetty trunk, and along the inner section of a jetty. Lillycrop and Hughes (1993) review scour problems at Corps projects.

(2) Scour at jetty tips (Figure II-6-47) can be caused by flow separation during flood flow, when turbulent eddies are generated. Ebb currents traversing through this region of scour also might contribute

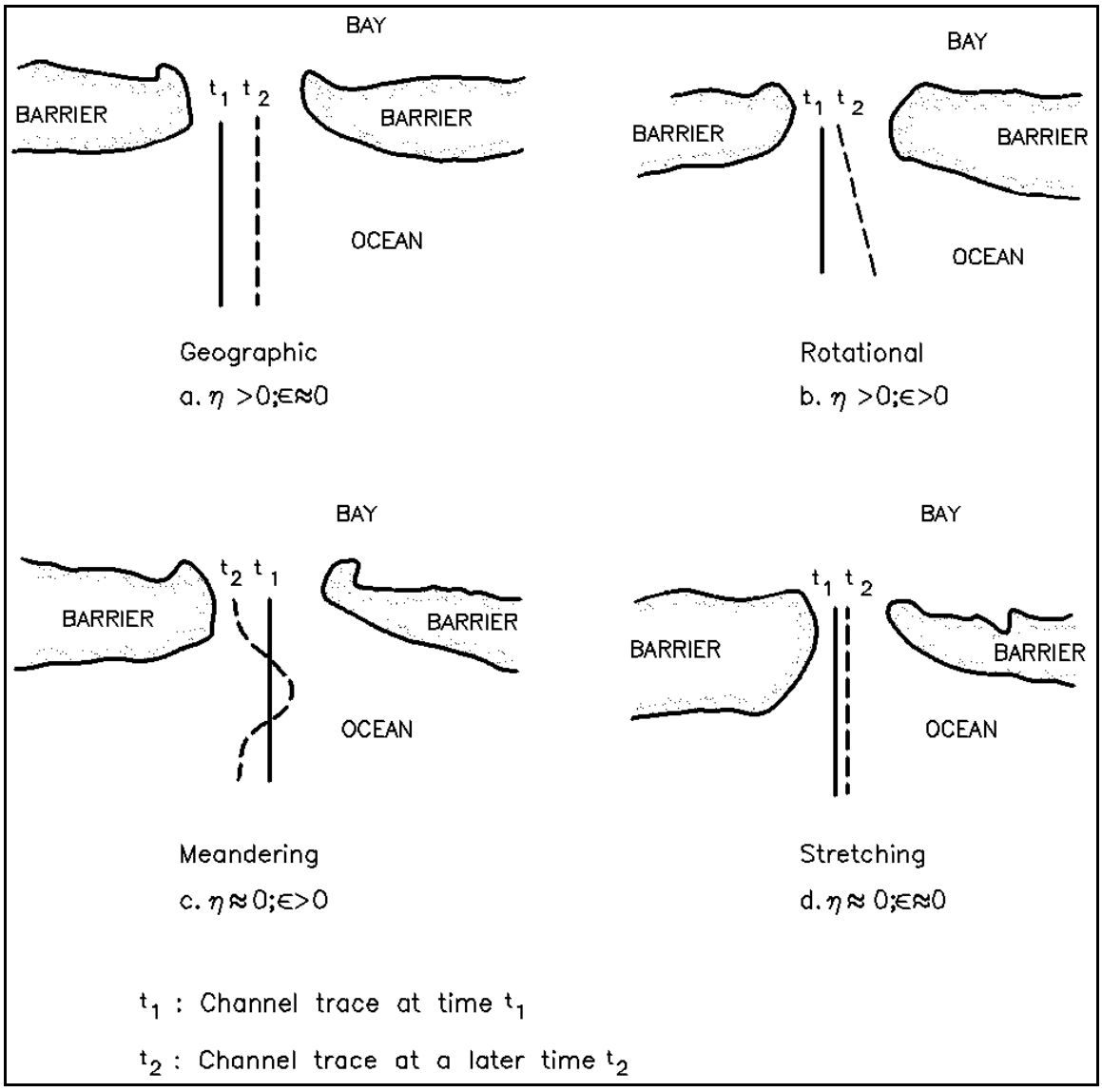

Figure II-6-44. Examples of channel geographic instability

to maintaining a scour hole if channelization in the shoreward portion of the inlet throat directs ebb currents toward the scour hole.

(3) Scour along the inside of jetties can occur as the bathymetry of a newly constructed jetty system adjusts. Little River Inlet (Chasten and Seabergh 1992) had an initial scour hole that was a remnant of the construction process. After the conclusion of construction, scour increased in this area, but as the inlet adjusted, velocities in that scour region decreased.

e. Methods to predict channel shoaling.

(1) Introduction. Entrance channel infill rates can be calculated by a variety of methods (U.S. Army Corps of Engineers 1984). One method is presented to show the parameters involved. A method to determine entrance channel infill rates is called the "Oregon Inlet Method." It is an analytic/empirical approach documented in a U.S. Army Engineer District, Wilmington (1980) report concerning the dredging

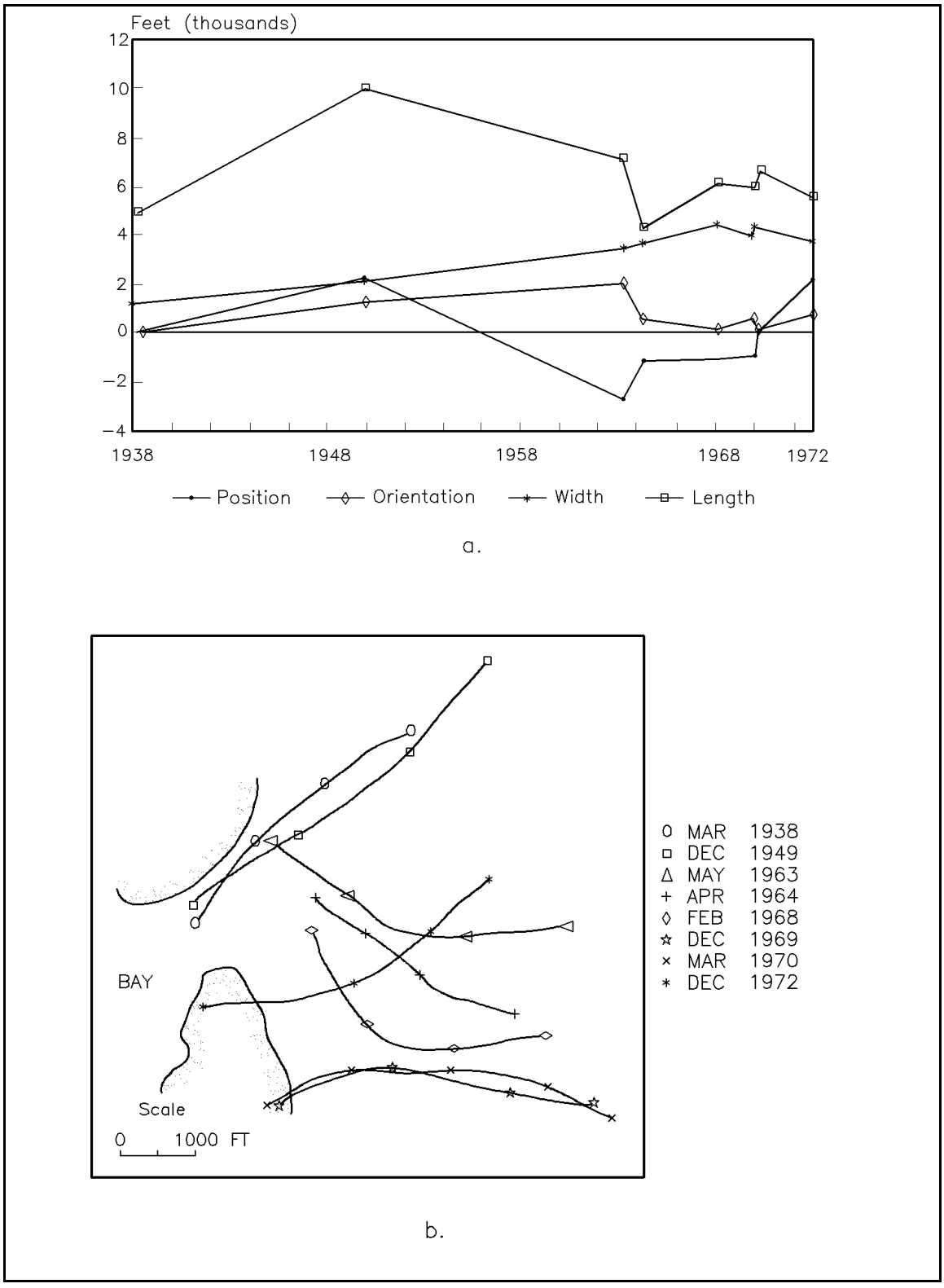

Figure II-6-45. Little River Inlet geographical variability

EXAMPLE PROBLEM II-6-5

FIND:

Using the information provided in Example Problem 1, find the potential stability of the proposed channel cross section. Remember the channel has vertical sheet-pile walls, so its cross section can only change in the vertical.

SOLUTION:

By varying the cross-sectional area of the channel A_C , assuming that the channel width B remains constant and varying the channel depth d and recalculating the tidal prism as described above, the effect of channel area on the bay tidal prism can be evaluated and compared with the appropriate equation from Table II-6-3 (dual jettied inlets, $A_C = 7.489 \times 10^{-4}\ P^{0.86}$). This is done graphically in Figure II-6-46, which shows a plot of P versus A_C from the hydraulic response calculations and from the stability equation. The intersection of the two curves on the right side is the stable solution. It yields a channel cross-sectional area of 1,440 m^2 or a depth of 8 m. This shows that the 180-m by 3.7-m design channel would be unstable, with a strong tendency to erode.

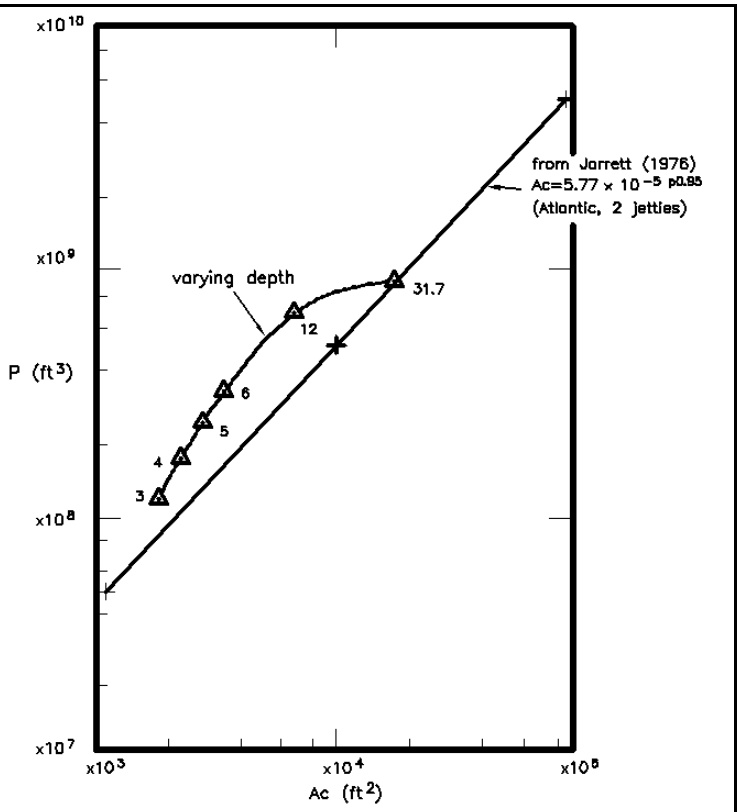

D(ft)	3	4	5	6	8	12	16	25	---	35
K1	345	202	134	97	58	29	18	9		6
K2	.49	.43	.38	.35	.30	.25	.22	.17		.15
V'm	.12	.21	.28	.35	.50	.68	.81	.95		.98
ab/as	.12	.20	.28	.38	.59	.78	.97	1.01		1.00
Vm	4.1	5.4	5.8	6.0	6.5	5.8	5.2	3.9		2.95
P(x10^8)	1.1	1.8	2.5	3.3	5.2	6.8	8.5	8.9		8.8
Ac(ft^2)	1800	2400	3000	3600	4800	7200	9600	15000		21000

Figure II-6-46. Example Problem II-6-4. Plot of *P* versus A_C from the hydraulic response calculations and from the stability equation

Where the hydraulic response curve lies above the stability curve (as in the example) the tidal prism is too large for the inlet channel area and erosion will likely occur until a stable channel develops. If the hydraulic response curve crosses the stability curve twice, the lower point is an unstable equilibrium point from which the channel can either close or scour to the upper stability point. If the hydraulic response curve is substantially below the stability curve at all points, a stable inlet channel is unlikely to develop and the channel should eventually close.

The stable inlet cross-sectional area depends on other factors (e.g., wave climate, monthly tidal range variations, surface runoff) besides the spring or diurnal tidal prism. As a result, the tidal prism-inlet area equations given in Table II-6-3 only serve as an indication of the approximate stable cross-sectional area. The analysis performed in the example demonstrates that the design channel is very likely to erode to a greater depth; however, that depth, which will fluctuate with time, can vary substantially from the indicated depth of 8 m.

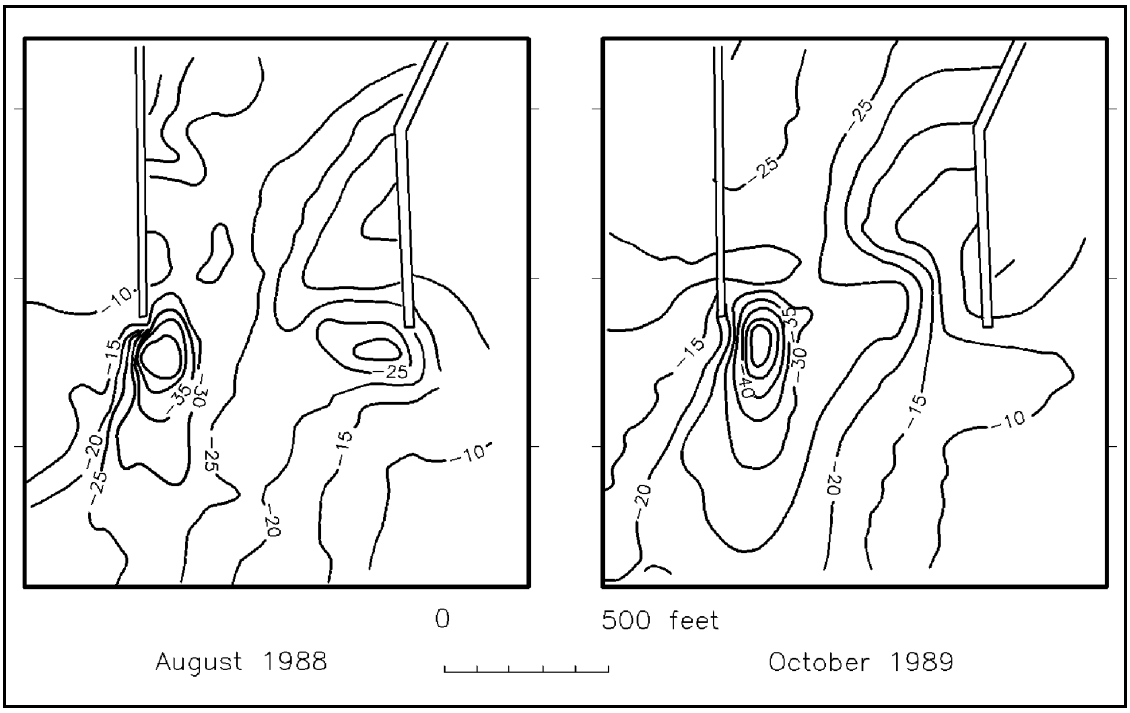

Figure II-6-47. 1988 and 1989 bathymetry of Moriches Inlet

of Oregon Inlet, North Carolina. It is based on the premise that the natural geometry of an inlet's ebb tide delta on the ocean bar results from the integrated effects of tidal currents, wave action, and associated sediment transport and deposition. Of particular importance is the natural elevation of the ocean bar, which represents both the limiting elevation of sediment accumulation resulting from the influx of littoral materials from adjacent shores and the level below which littoral sediments will collect if the ocean bar is dredged to provide a navigation channel. Sediment accumulation should increase with increasing channel depth until it becomes so deep that the channel traps all sediment crossing the inlet.

(2) Procedure. In order to develop a day-by-day simulation of siltation processes and dredging effects, a procedure consisting of three main phases was developed. The phases are (a) daily littoral materials transport volumes, (b) channel sedimentation, and (c) regression analysis.

(3) Phase I: Daily littoral materials transport volumes. It is assumed that the relative magnitude of alongshore sediment transport can be estimated simply on the basis of wave height squared in accordance with the relationship

$$Q_i = Q_g \left(\frac{H_i^2}{\sum_{i=1}^{n} H_i^2} \right) \tag{II-6-34}$$

where

i = number of the day during the year

Q_i = littoral transport occurring on day i [L^3]

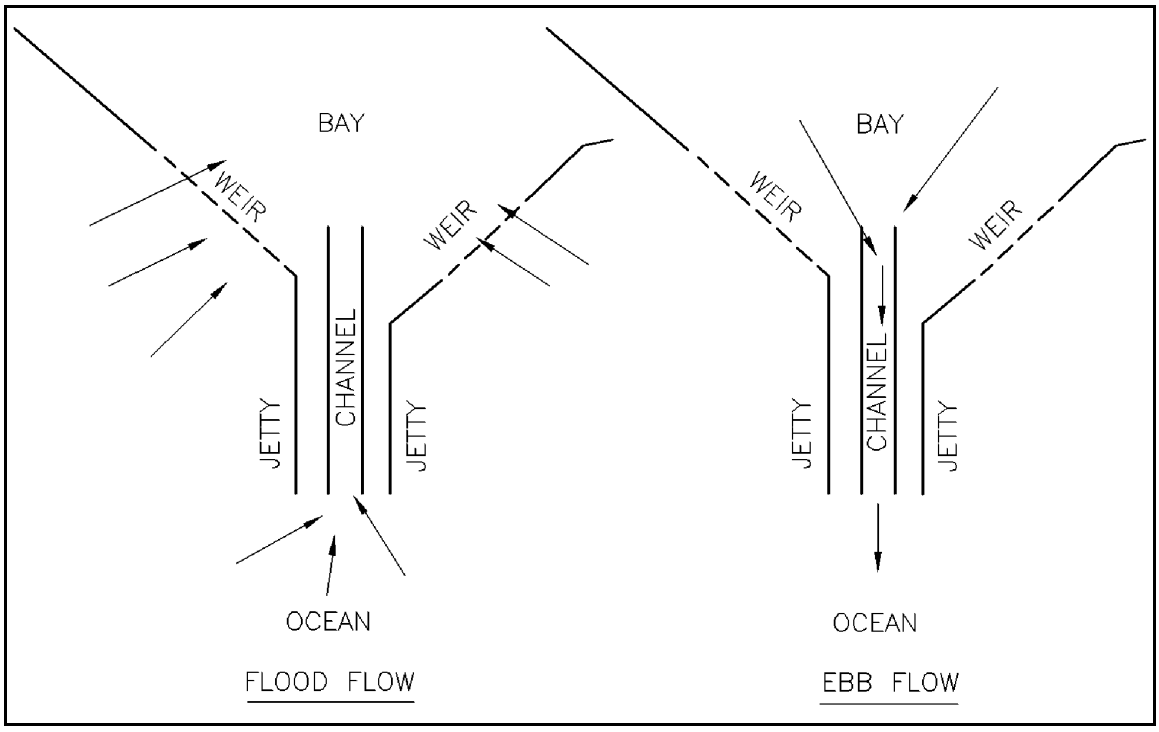

Figure II-6-48. Weir jetty flow patterns

Q_g = total volume of alongshore sediment transport to the inlet each year [L^3]

H_i = average wave height for the i^{th} day of the year [L]

n = total number of days during the year [T]

(4) Phase II: Channel sedimentation. The first portion of the channel sedimentation procedure is

$$Transport\ ratio = \left(\frac{d_1}{d_2}\right)^{\frac{5}{2}} \tag{II-6-35}$$

where the transport ratio equals the ratio of the sediment transport potential in the dredged cut to the sediment transport on the bar before dredging and

d_1 = depth before dredging [L]

d_2 = depth after dredging [L]

On a daily basis, the amount of material that would be retained in the ocean bar channel of the inlet is given by:

$$Daily\ shoal\ volume = CQ_g \left(\frac{H_i^2}{\sum_{i=1}^{n} H_i^2}\right)\left[1 - \left(\frac{d_1}{d_2}\right)^{\frac{5}{2}}\right] \quad [L^3] \tag{II-6-36}$$

in which all terms have been previously defined except for "*C*," which is termed the "potential shoaling factor." As stated previously, the quantity of material entering and depositing in the channel increases with the depth of the cut. However, until sufficient channel depth is attained to intercept all materials moving into the inlet, some material continues to bypass the inlet via the sloping face of the ocean bar below the bottom of the channel cut. Accordingly, *C* is defined as the portion of the total alongshore transport to the inlet entering the domain of the channel. In order to determine *C*, a regression analysis was conducted to correlate the inlet bar siltation with those factors judged to be most influential in the filling and flushing of such channels.

(5) Phase III: Regression analysis. The following three factors were selected as dominant in influencing the magnitude of shoaling at a particular inlet site having a dredge-maintained ocean bar channel. These factors are described as follows:

(a) Ebb tide flow is the primary factor acting to flush intrusive littoral materials from the inlet environment. Its influence in the analysis is represented by the symbol $E_{\Delta T}$, which is the difference between the mean ebb tide flow energy flux across the ocean bar at its natural elevation and the mean ebb tide flow energy flux through the cross section of the excavated ocean bar navigation channel. It is assumed that the tidal discharge is not significantly altered from one condition to the other. A basic concept in the tidal energy flux difference is that the tidal flow velocities directed seaward over the ocean bar at its natural elevation, in combination with wave agitation, are rapid enough to prevent accumulation of sediments above the natural bar depth. If a section of the ocean bar is deepened by a navigation channel, the related average local flow velocity is diminished and sediment deposition is initiated.

(b) Wave energy reaching the littoral zones adjacent to the inlet is the primary factor controlling the quantity of littoral material moving toward the inlet and, as such, determines the shoaling characteristics of an ocean bar navigation channel. In the analysis, the unrefracted wave energy flux per unit width of wave crest offshore of the area of interest, designated E_w, is the basic measure of sediment transport toward the inlet.

(c) The depth of an ocean bar channel determines the degree to which a channel will trap the littoral sediments entering the inlet environment. In the analysis, the amount of channel entrenchment, and hence the measure of sediment entrapment potential, is taken as the ratio D_R of the depth of the channel to the depth at which the seaward slope of the ocean bar meets the sea bottom. Each of these depths is measured from the natural elevation of the ocean bar; therefore, the ratio D_R represents the extent to which the ocean bar's seaward slope has been incised by the channel.

(6) Normalized, independent filling index. The channel sedimentation potential increases or decreases as each of the three factors $E_{\Delta T}$, E_w, and D_R increases or decreases, respectively. The factors were combined as follows to establish a normalized, independent variable F_I (filling index) for the regression analysis.

$$F_I = \frac{(E_{\Delta T} \cdot E_W \cdot D_R)}{10^{14}} \quad \left[\frac{ML^2}{T^2}\right] \tag{II-6-37}$$

The normalized, dependent variable selected for the analysis was the ratio of the volume of channel infill to the computed volume of the total alongshore sediment influx to the inlet multiplied by 100. This percentage value V_R is referred to as the "volume ratio." The regression analysis was based on data from four dredged-maintained inlets within the boundaries of the Wilmington District: Oregon, Beaufort, Masonboro, and Lockwoods Folly Inlets. Information available consisted of: (a) measured tidal discharges or inlet throat cross-sectional areas, which permitted tidal discharge computations by means of tidal prism-inlet area relations, (b) site wave statistics representing one or more years of wave gauge records, (c) detailed

alongshore sediment transport analyses for the shorelines adjacent to each of the inlets, and (d) one or more sets of inlet hydrographic surveys, each set consisting of two surveys taken at different times, thereby allowing measurement of the volume of sediment filling within the navigation channels in the time periods between surveys.

(7) Ebb tidal energy flux. For each inlet selected, the parameter $E_{\Delta T}$, representing the change of ebb tidal energy flux across the ocean bar between natural and channel conditions, was computed and fixed as constant for the given inlet using the following equation:

$$E_{\Delta T} = \frac{4T}{3\pi} q_{\max}^3 \frac{d_2^2 - d_1^2}{d_1^2 d_2^2} \tag{II-6-38}$$

where

T = tidal wave period [T]

q_{max} = maximum instantaneous ebb tide discharge per unit width [L^3/T/L]

d_2 = depth of navigation channel [L]

d_1 = natural depth of ocean bar [L]

The next parameter is E_w, the average daily wave energy flux per unit width of wave crest, offshore of the site of interest. This parameter represents the intensity of sediment transport from the adjacent beaches to the inlet environment. Daily wave energy flux can be expressed as

$$E_W = K \times 10^6 (H_0)^2 T \quad \left[\frac{ML^2}{T^2}\right] \tag{II-6-39}$$

where

K = constant (K = 1.769 slugs/sec in English engineering units or 0.121 Kg/sec) [M/T]

H_o = deepwater wave height equivalent to observed shallow-water wave, if unaffected by refraction and friction [L]

T = wave period [T]

The last parameter is a depth ratio D_R, which is given as

$$D_R = \frac{d_2 - d_1}{d_3 - d_1} \tag{II-6-40}$$

where

d_3 = water depth where seaward tip of ocean bar meets offshore sea bottom [L]

(8) Hoerls special function distribution. Tests of several regression equations and related curves revealed that the best fit of the data from the four inlets was attained by a "Hoerls" special function distribution, given in general form by:

$$V_R = a\ F_I^b\ e^{cF}\ I \tag{II-6-41}$$

where a, b, and c are the best-fit coefficients. The regression equation was solved for filling index F_I values corresponding to various channel depths, which allows for the proper "C" value to be used in the "daily shoal volume" equation developed in Phase II of this method.

f. Inlet weir jetty hydraulic and sediment interaction. The subject of weir jetty design is dealt with in detail by Seabergh (1983) and Weggel (1981), who discuss several hydraulic and sedimentary aspects including flow over the weir and its elevation, location, length, jetty alignment and orientation, as well as the shoreward end of the weir. The function of the weir jetty is to ideally collect the net sediment movement behind the weir section, where it can then be handled in protected waters and bypassed. A sedimentation benefit may occur in that sediment-laden longshore currents are kept away from the channel. Also, the ebb currents may be hydraulically enhanced, as seen in Figure II-6-48, creating ebb dominance of channel currents, which can aid in flushing sediment seaward.

(1) Weir location. With respect to tidal currents within the jetty system, the farther the weir is from the navigation channel, the less likely it is to capture channel ebb currents that are directed seaward. This can depend on the location of the predominant ebb channels and their orientation. Care must be taken in evaluation of ebb flow direction because once the jetty system is constructed, the channel orientation may change due to removal of wave effects and consequent sediment movement, which, for example, may have deflected the ebb channel downcoast.

(2) Weir length. Primary transport over the weir exists at its intersection with the shoreline. If the wave climate is mild, the weir should only be as long as necessary to prevent a chance of closure, something that has not yet been noted to occur in existing weir jetty systems. The length to prevent closure would need to be evaluated based on wave conditions, beach slope, orientation of the structure, etc. (Weggel 1981). If the wave climate is highly variable, the weir should probably extend further oceanward so as to include a large percentage of the breaker zone since heavy transport over the weir will occur at the breaker location for larger wave conditions; otherwise, the sediment will move offshore along the jetty. Another factor influencing weir length will be consideration of the amount of flow that is desired in the system. If a design objective is to obtain high ebb dominance of flow in the navigation channel, then the weir should be longer, if this would not interfere with other constraints, such as placement of a portion of the weir too close to the channel. The complete hydraulic flow situation must be considered to determine whether the additional flow provided by a wider weir will substantially augment ebb flow predominance and provide additional scouring ability in the entrance channel (see Seabergh (1983)).

II-6-4. References

Amein and Kraus 1991
Amein, A., and Kraus, N. C. 1991. "DYNLET1: Dynamic Implicit Numerical Model of One-Dimensional Tidal Flow Thought Inlets," Technical Report CERC-91-10, U.S. Army Engineer Waterways Experiment Station, Vicksburg, MS.

Aubrey 1986
Aubrey, D. G. 1986. Hydrodynamic Controls on Sediment Transport in Well-mixed Bays and Estuaries," J. van de Kreeke, ed., *Physics of Shallow Estuaries and Bays*, Springer-Verlag, New York.

Aubrey and Friedrichs 1988
Aubrey, D. G., and Friedrichs, C. T. 1988. "Seasonal Climatology of Tidal Non-Linearities on a Shallow Estuary," Lecture Notes on Coastal and Estuarine Studies, Vol 29, D. G. Aubrey and L. Weishar, eds., Springer-Verlag, New York.

Boer 1985
Boer, S. 1985. "The Flow Across Trenches at Oblique Angles to the Flow," Report 5490 Delft Hydraulics Laboratory, Delft, The Netherlands.

Boon 1988
Boon, J. D. 1988. "Temporal Varication of Shallow Water Tides in Basin-Inlet Systems," Lecture Notes on Coastal and Estuarine Studies, Vol 29, D. G. Aubrey and L. Weishar, eds., *Hydrodynamics and Sediment Dynamics of Tidal Inlets*, Springer-Verlag, New York.

Boon and Byrne 1981
Boon, J. D., and Byrne, R. J. 1981. "On Basin Hypsometry and the Morphodynamic Response of Coastal Inlet Systems," *Marine Geology*, Vol 40, pp 27-48.

Bottin 1978
Bottin, R. R. 1978. "Design for Harbor Entrance Improvements, Wells Harbor, Maine, Hydraulic Model Investigation," Technical Report H-78-18, U.S. Army Engineer Waterways Experiment Station, Vicksburg, MS.

Bottin 1982
Bottin, R. R. 1982. "Design for the Prevention of Shoaling, Flood Control, and Wave Protection, Rogue River, Oregon, Hydraulic Model Investigation," Technical Report HL-82-18, U.S. Army Engineer Waterways Experiment Station, Vicksburg, MS.

Brown 1928
Brown, E. I. 1928. "Inlets on Sandy Coasts," *Proceedings of the American Society of Civil Engineers*, Vol 54, Part I, pp 505-523.

Bruun 1967
Bruun, P. 1967. "Tidal Inlets Housekeeping," *Journal of the Hydraulic Division*, American Society of Civil Engineers, Vol 93, pp 167-184.

Bruun and Gerritsen 1960
Bruun, P., and Gerritsen, F. 1960. *Stability of Coastal Inlets*, North Holland Publishing Co., Amsterdam, The Netherlands.

Bruun, Mehta, and Jonsson 1978
Bruun, P., Mehta, A. J., and Jonsson, I. G. 1978. *Stability of Tidal Inlets: Theory and Engineering*, Elsevier Scientific Publishing Co., Amsterdam, The Netherlands.

Butler 1980
Butler, H. L. 1980. "Evolution of a Numerical Model for Simulating Long-Period Wave Behavior in Ocean Estuarine Systems," *Estuarine and Wetland Processes: With Emphasis on Modeling; Marine Science,* Vol 11, Plenum Press, New York.

Byrne, DeAlteris, and Bullock 1974
Byrne, R. J., DeAlteris, J. R., and Bullock, P. A. 1974. "Channel Stability in Tidal Inlets: A Case Study," *Proceedings, 14th Coastal Engineering Conference*, American Society of Civil Engineers, New York, pp 1585-1604.

Byrne, Gammisch and Thomas 1980
Byrne, R. J., Gammisch, R. A., and Thomas, G. R. 1980. "Tidal Prism-Inlet Area Relations for Small Tidal Inlets," *Proceedings of the Seventeenth Coastal Engineering Conference*, American Society of Civil Engineers, Sydney, Australia, Vol III, Ch 151, pp 23-28.

Chasten and Seabergh 1992
Chasten, M. A., and Seabergh, W. C. 1992. "Engineering Assessment of Hydrodynamics and Jetty Scour at Little River Inlet North and South Carolina," Miscellaneous Paper CERC-92-10, U.S. Army Engineer Waterways Experiment Station, Vicksburg, MS.

Chow 1959
Chow, V. T. 1959. *The Open-Channel Hydraulics*, McGraw-Hill Book Company, New York.

Cialone et al. 1991
Cialone, M. A., Mark, D. J., Chou, L. W., Leenknecht, D. A., Davis, J. A., Lillycrop. L. S., Jensen, R. E., Thompson, E., Gravens, M. B., Rosati, J. D., Wise, R. A., Kraus, N. C., and Larson, P. M. 1991. "Coastal Modeling System (CMS) User's Manual," Instruction Report CERC-91-1, U.S. Army Engineer Waterways Experiment Station, Vicksburg, MS.

Costa and Isaacs 1977
Costa, S. L., and Isaacs, J. D. 1977. "The Modification of Sand Transport in Tidal Inlet Inlets," *Coastal Sediments 77, Fifth Symposium of the Waterway, Port Coastal and Ocean Division,* American Society of Civil Engineers, Nov 2-4, Charleston, SC.

Czerniak 1977
Czerniak, M. T. 1977. "Inlet Interaction and Stability Theory Verification," *Coastal Sediments 77*, American Society of Civil Engineers, Charleston, SC.

Dean 1971
Dean, R. G. 1971. "Hydraulics of Inlets," COEL/UFL-71/019, Department of Coastal and Oceanographic Engineering, University of Florida, Gainsville.

DiLorenzo 1988
DiLorenzo, J. L. 1988. "The Overtide and Filtering Response of Small Inlet/Bay Systems," Lecture Notes on Coastal and Estuarine Studies, Vol 29, D. G. Aubrey and L. Weishar, eds., Springer-Verlag, New York.

Dyer and Taylor 1973
Dyer, K. R., and Taylor, P. A. 1973. "A Simple Segmented Prism Model of Tidal Mixing in Well-Mixed Estuaries," *Estuarine and Coastal Marine Science*, Vol 1, pp 411-418.

Escoffier 1940
Escoffier, F. F. 1940. "The Stability of Tidal Inlets," *Shore and Beach*, Vol 8, No. 4, pp 114-115.

Escoffier 1977
Escoffier, F. F. 1977. "Hydraulics and Stability of Tidal Inlets," GITI Report 13, U.S. Army Engineer Waterways Experiment Station, Vicksburg, MS.

Escoffier and Walton 1979
Escoffier, F. F., and Walton, T. L. 1979. "Inlet Stability Solutions for Tributary Inflow," *Journal of the Waterway, Port, Coastal and Ocean Division*, American Society of Civil Engineers, Vol 105, No. WW4, Proc. Paper 14964, pp 341-355.

Fischer, List, Koh, Imberger and Brooks 1979
Fischer, H. B., List, E. J., Koh, R. C. Y., Imberger, J., and Brooks, N. H. 1979. *Mixing in Inland and Coastal Waters*, Academic Press, New York.

French 1960
French, J. L. 1960. "Tidal Flow in Entrances," Technical Bulletin No. 3, U.S. Army Engineer Waterways Experiment Station, Committee on Tidal Hydraulics, Vicksburg, MS.

Friedrichs and Aubrey 1988
Friedrichs, C. T., and Aubrey, D. G. 1988. "Non-Linear Tidal Distortion in Shallow Well-Mixed Estuaries: A Synthesis," *Estuarine, Coastal and Shelf Science*, Vol 27, pp 521-545.

Friedrichs, Lynch, and Aubrey 1992
Friedrichs, C. T., Lynch, D. R., and Aubrey, D. G. 1992. "Velocity Asymmetries in Frictionally Dominated Tidal Embayments: Longitudinal and Lateral Variability," *Dynamics and Exchanges in Estuaries and the Coastal Zone, Coastal and Estuarine Studies*, D. Prandle, ed., American Geophysical Union, Washington, DC, Vol 40, pp 277-312.

Galvin 1971
Galvin, C. J., Jr. 1971. "Wave Climate and Coastal Processes," *Water Environments and Human Needs*, A. T. Ippen, ed., M.I.T. Parsons Laboratory for Water Resources and Hydrodynamics, Cambridge, MA, pp 48-78.

Geyer and Signell 1992
Geyer, W. R., and Signell, R. P. 1992. "A Reassessment of the Role of Tidal Dispersion in Estuaries and Bays," *Estuaries*, Vol 15, pp 97-108.

Harris and Bodine 1977
Harris, D. L., and Bodine, B. R. 1977. "Comparison of Numerical and Physical Hydraulic Models, Masonboro Inlet, North Carolina," GITI Report 6, U.S. Army Engineer Waterways Experiment Station, Vicksburg, MS.

Hayes 1971
Hayes, M. O. 1971. "Lecture Notes for Course on Inlet Mechanics and Design (unpublished)," 10-20 May 1971, Ft. Belvoir, VA, Coastal Engineering Research Center.

Hayes 1980
Hayes, M. O. 1980. "General Morphology and Sediment Patterns in Tidal Inlets," *Sedimentary Geology*, Vol 26, pp 139-156.

Herchenroder 1981
Herchenroder, B. E. 1981. "Effects of Currents on Waves," Coastal Engineering Technical Aid No. 81-14, October 1981, U.S. Army Engineer Waterways Experiment Station, Vicksburg, MS.

Ismail and Wiegel 1983
Ismail, N. M., and Wiegel, R. L. 1983. "Opposing Wave Effect on Momentum Jet Spreading Rate," *Journal of the Waterway Port, Coastal and Ocean Division*, American Society of Civil Engineers, Vol 109, No. WW4, pp 465-487.

Jarrett 1975
Jarrett, J. T. 1975. "Analyses of the Hydraulic Characteristics of Tidal Inlets," Unpublished memorandum for record, U.S. Army Engineer Waterways Experiment Station, Vicksburg, MS.

Jarrett 1976
Jarrett, J. T. 1976. "Tidal Prism-Inlet Area Relationships, GITI Report 3, U.S. Army Engineer Waterways Experiment Station, Vicksburg, MS.

Jonsson, Skovgaard, and Wang 1970
Jonsson, I. G., Skovgaard, C., and Wang, J. D. 1970. "Interaction Between Waves and Currents," *Proceedings of the 12th Conference on Coastal Engineering,* American Society of Civil Engineers, Vol 1, pp 489-509.

Joshi 1982
Joshi, P. B. 1982. "Hydromechanics of Tidal Jets," *Journal of the Waterway, Port, Coastal and Ocean Division*, American Society of Civil Engineers, Vol 108, No. WW3, Proc. Paper 17294, pp 239-253.

Joshi and Taylor 1983
Joshi, P. B., and Taylor, R. B. 1983. "Circulation Induced by Tidal Jets," *Journal of the Waterway, Port, Coastal and Ocean Division*, American Society of Civil Engineers, Vol 109, No. WW4.

Keulegan 1951
Keulegan, G. H. 1951. "Third Progress Report on Tidal Flow in Entrances, Water Level Fluctuations of Basins in Communication with Seas," Report No. 1146, National Bureau of Standards, Washington, DC.

Keulegan 1967
Keulegan, G. H. 1967. "Tidal Flow in Entrances Water-Level Fluctuations of Basins in Communications with Seas," Technical Bulletin No. 14, Committee on Tidal Hydraulics, U.S. Army Engineer Waterways Experiment Station, Vicksburg, MS.

King 1974
King, D. B. 1974. "The Dynamics of Inlets and Bays," Technical Report No. 2, Coastal and Oceanographic Engineering Laboratory, University of Florida, Gainesville.

Leenknecht, Szuwalski, and Sherlock 1992
Leenknecht, D. A., Szuwalski, A., and Sherlock, A. R. 1992. "Automated Coastal Engineering System User Guide and Technical Reference, Version 1.07," U.S. Army Engineer Waterways Experiment Station, Vicksburg, MS.

Lillycrop and Hughes 1993
Lillycrop, W. J., and Hughes, S. A. 1993. "Scour Hole Problems Experienced by the Corps of Engineers; Data Presentation and Summary," Miscellaneous Paper CERC-93-2, U.S. Army Engineer Waterways Experiment Station, Vicksburg, MS.

Mason 1975
Mason, C. 1975. "Tidal Inlet Repletion Coefficient Variability," unpublished report, copy available at Coastal and Hydraulics Laboratory, U.S. Army Engineer Waterways Experiment Station, Vicksburg, MS.

Mayor-Mora 1973
Mayor-Mora, R. E. 1973. "Hydraulics of Tidal Inlets on Sandy Coasts," HEL-24-16, Hydraulic Engineering Laboratory, University of California, Berkeley.

Mehta 1990
Mehta, A. J. 1990. "Significance of Bay Superelevation in Measurement of Sea Level Change," *Journal of Coastal Research*, Vol 6, No. 4, pp 801-813.

Mehta and Joshi 1984
Mehta, A. J., and Joshi, P. B. 1984. "Review of Tidal Inlet Hydraulics UFL/COBL - TR/054," Coastal and Oceanographic Engineering Department, University of Florida, Gainsville.

Mehta and Özsöy 1978
Mehta, A. J., and Özsöy, E. 1978. "Inlet Hydraulics," *Stability of Tidal Inlets: Theory and Engineering*, P. Bruun, Elsevier Scientific Publishing Co., Amsterdam, The Netherlands, pp 83-161.

Mota Oliveira 1970
Mota Oliveira, I. B. 1970. "Natural Flushing Ability in Tidal Inlets," *Proceedings of the Twelfth Coastal Engineering Conference*, American Society of Civil Engineers, Washington, DC, Vol 3, Ch. 111, pp 1827-1845.

O'Brien 1931
O'Brien, M. P. 1931. "Estuary Tidal Prisms Related to Entrance Areas," *Civil Engineering*, pp 738-739.

O'Brien 1969
O'Brien, M. P. 1969. "Equilibrium Flow Areas of Inlets on Sandy Coasts," *Journal of the Waterways and Harbors Division*, American Society of Civil Engineers, No. WWI, pp 43-52.

O'Brien and Clark 1974
O'Brien, M. P., and Clark, R. R. 1974. "Hydraulic Constants of Tidal Entrances," *Proceedings of the Fourteenth Coastal Engineering Conference*, American Society of Civil Engineers, Copenhagen, Denmark, Vol 2, Ch. 90, pp 1546-1565.

O'Brien and Dean 1972
O'Brien, M. L., and Dean, R. G. 1972. "Hydraulics and Sedimentary Stability of Coastal Inlets," *Proceedings of the Thirteenth Coastal Engineering Conference,* American Society of Civil Engineers, Vancouver, Canada.

Özsöy 1977
Özsöy, E. 1977. "Flow and Mass Transport in the Vicinity of Tidal Inlets," Technical Report No. TR-036, Coastal and Oceanographic Engineering Laboratory, University of Florida, Gainesville.

Özsöy and Ünlüata 1982
Özsöy, E., and Ünlüata, E. 1982. "Ebb-Tidal Flow Characteristics Near Inlets," *Estuarine, Coastal and Shelf Science*, Vol 14, No. 3, pp 251-263.

Seabergh 1975
Seabergh, W. C. 1975. "Improvement for Masonboro Inlet, North Carolina, Hydraulic Model Investigation, Vols I and II," Technical Report H-76-4, U.S. Army Engineer Waterways Experiment Station, Vicksburg, MS.

Seabergh 1983
Seabergh, W. C. 1983. "Weir Jetty Performance: Hydraulic and Sedimentary Considerations, Hydraulic Model Investigation," Technical Report HL-83-5, U.S. Army Engineer Waterways Experiment Station, Vicksburg, MS.

Seabergh and Lane 1977
Seabergh, W. C., and Lane, E. F. 1977. "Improvements for Little River Inlet, South Carolina, Hydraulic Model Investigation," Technical Report H-77-21, U.S. Army Engineer Waterways Experiment Station, Vicksburg, MS.

Seabergh and McCoy 1982
Seabergh, W. C., and McCoy, J. W. 1982. "Design for Prevention of Shoaling at Little Lake Harbor, Michigan, Hydraulic Model Investigation," Technical Report HL-82-16, U.S. Army Engineer Waterways Experiment Station, Vicksburg, MS.

Seelig and Sorensen 1977
Seelig, W. N., and Sorensen, R. M. 1977. "Hydraulics of Great Lakes Inlets," Technical Paper No. 77-8, U.S. Army Engineer Waterways Experiment Station, Vicksburg, MS.

Shemdin and Forney 1970
Shemdin, O. H., and Forney, R. M. 1970. "Tidal Motion in Bays," *Proceedings of the Twelfth Coastal Engineering Conference*, American Society of Civil Engineers, Washington, DC, Vol 3, Ch. 134, pp 2225-2242.

Smith 1977
Smith, N. P. 1977. "Meteorological and Tidal Exchanges Between Corpus Christi Bay, Texas, and Northwestern Gulf of Mexico," *Estuarine and Coastal Marine Science*, Vol 5, pp 511-520.

Smith 1991
Smith, J. B. 1991. "Morphodynamics and Stratigraphy of Essex River Ebb-Tidal Delta: Massachusetts," Technical Report CERC-91-11, U.S. Army Engineer Waterways Experiment Station, Vicksburg, MS.

Sorensen 1977
Sorensen, R. M. 1977. "Procedures for Preliminary Analysis of Tidal Inlet Hydraulics and Stability," Coastal Engineering Technical Aid 77-8, U.S. Army Engineer Waterways Experiment Station, Vicksburg, MS.

Sorensen 1980
Sorensen, R. M. 1980. "The Corps of Engineer's General Investigation of Tidal Inlets," *Proceedings of the Seventeenth Coastal Engineering Conference*, American Society of Civil Engineers, Sydney, Australia, Vol III, Ch. 154, pp 2565-2580.

Sorensen and Seelig 1976
Sorensen, R. M., and Seelig, W. N. 1976. "Hydraulics of Great Lakes Inlet-Harbor Systems," *Proceedings of the Fifteenth Coastal Engineering Conference*, American Society of Civil Engineers, Honolulu, HI, Vol 2, Ch. 96, pp 1646-1665.

Speer and Aubrey 1985
Speer, P. E., and Aubrey, D. G. 1985. "A Study of Non-Linear Tidal Propagation in Shallow Inlet/Estuarine Systems; Part II: Theory," *Estuarine, Coastal and Shelf Science*, Vol 21, pp 207-224.

Taylor and Dean 1974
Taylor, R. B., and Dean, R. G. 1974. "Exchange Characteristics of Tidal Inlets," *Proceedings of the Fourteenth Coastal Engineering Conference*, American Society of Civil Engineers, Copenhagen, Denmark, Vol 3, Ch. 132, pp 2268-2289.

U. S. Army Corps of Engineers 1984
U.S. Army Corps of Engineers. 1984. "Entrance Channel Infill Rates," Engineer Technical Letter No. 1110-2-293, March 1984, Washington, DC.

U. S. Army Engineer District, Wilmington 1980
U.S. Army Engineer District, Wilmington. 1980. "Manteo (Shallowbag) Bay, North Carolina," General Design Memorandum, Phase II, Appendix 5, Wilmington, NC.

Ünlüata and Özsöy 1977
Ünlüata, U. A., and Özsöy, E. 1977. "Tidal Jet Flows Near Inlets," *Proceedings of the Hydraulics in the Coastal Zone Conference*, American Society of Civil Engineers, Texas A&M University, College Station, TX, pp 90-98.

van de Kreeke 1967
van de Kreeke, J. 1967. "Water Level Fluctuations and Flows in Tidal Inlets," *Journal of the Waterways, Harbors and Coastal Engineering Division*, American Society of Civil Engineers, Vol 93, No. WW4, Proc. Paper 5575, pp 97-106.

van de Kreeke 1976
van de Kreeke, J. 1976. "Increasing the Mean Current in Coastal Channels." *Journal of the Waterways Harbors and Coastal Engineering Division*, American Society of Civil Engineers, Vol 102, No. WW2, pp 222-234.

van de Kreeke 1978
van de Kreeke, J. 1978. "Mass Transport in a Coastal Channel, Marco River, Florida," *Estuarine and Coastal Marine Science,* No. 7, pp 203-214.

van de Kreeke 1983
van de Kreeke, J. 1983. "Residence Time: Application to Small Boat Basins," *Journal of Waterway, Port, Coastal and Ocean Engineering*, American Society of Civil Engineers, Vol 109, pp 416-428.

van de Kreeke 1988
van de Kreeke, J. 1988. "Hydrodynamics of Tidal Inlets," Lecture Notes on Coastal and Estuarine Studies, Vol 29, *Hydrodynamic and Sediment Dynamics of Tidal Inlets,* Springer-Verlag, New York, pp 1-23.

Vincent and Corson 1980
Vincent, C. L., and Corson, W. D. 1980. "The Geometry of Selected US Tidal Inlets," GITI Report 20, U.S. Army Corps of Engineers, Washington, DC.

Vincent and Corson 1981
Vincent, C. L., and Corson, W. D. 1981. "Geometry of Tidal Inlets: Empirical Equations," *Journal of the Waterway, Port, Coastal and Ocean Division*, American Society of Civil Engineers, Vol 107, No. WW1, Proc. Paper 16032, pp 1-9.

Vincent, Corson, and Gingerich 1991
Vincent, C. L., Corson, W. D., and Gingerich, K. J. 1991. "Stability of Selected United States Tidal Inlets," General Investigation of Tidal Inlets (GITI) Report 21, U.S. Army Engineer Waterways Experiment Station, Vicksburg, MS.

Walton and Escoffier 1981
Walton, T. L., and Escoffier, F. F. 1981. "Linearized Solution to Inlet Equation with Inertia," *Journal of the Waterway, Port, Coastal and Ocean Division*, Paper 16414, Vol 105, No. WW4, pp 191-195.

Ward 1982
Ward, G. H., Jr. 1982. "Pass Cavallo, Texas: Case Study of Tidal-Prism Capture, *Journal of the Waterway Port Coastal and Ocean Division*, American Society of Civil Engineers, Vol 108, No. WW4, pp 513-525.

Watson and Behrens 1976
Watson, R. L., and Behrens, E. W. 1976. "Hydraulics and Dynamics of New Corpus Christi Pass, Texas: A Case History, 1973-1975," GITI Report 9, U.S. Army Engineer Waterways Experiment Station, Vicksburg, MS.

Weggel 1981
Weggel, J. R. 1981. "Weir Sand-Bypassing Systems," *Special Report No. 8*, U.S. Army Engineer Waterways Experiment Station, Vicksburg, MS.

Wicker 1965
Wicker, C. F., ed. 1965. "Evaluation of Present State of Knowledge of Factors Affecting Tidal Hydraulics and Related Phenomena," Committee on Tidal Hydraulics, Report No. 3, U.S. Army Corps of Engineers, Washington, DC.

Zimmerman 1988
Zimmerman, J. T. F. 1988. "Estuarine Residence Times," *Hydrodynamics of Estuaries*; *Vol 1: Estuarine Physics,* B. Kjerfve, ed., CRC Press, Boca Raton, FL, pp 75-84.

II-6-5. Definitions of Symbols

β	Stability index of an inlet (Equation II-6-33) [length^5/time^3]
Δ	Bay superelevation (Equations II-6-20 and II-6-21) [length]
ε	Fraction of new water entering the bay from the sea each tidal cycle [dimensionless]
ε	Phase lag between sea tide and bay tide [deg]
θ	Angle wave orthogonal makes with current entering an inlet [deg]
μ	Friction factor
ξ	Dimensionless distance offshore parameter
τ_r	Residence time (Equation II-6-28)
a_0	Ocean tide amplitude (one-half the ocean tide range) [length]
A_{avg}	Average area over a channel length [length^2]
a_b	Bay tide amplitude (one-half the bay tide range) [length]
A_b	Surface area of a bay or basin [length^2]
a_c	Critical cross-sectional area [length^2]
A_c	Channel cross-sectional flow area of an inlet [length^2]
a_E	Equilibrium cross-sectional area of inlet throat [length^2]
A_{mw}	Cross-sectional area of an inlet at the minimum inlet width [length^2]
B	Channel width between jetties [length]
C	Potential shoaling factor (Equation II-6-36)
d	Mean water depth in channel [length]
D	Depth of water at current meter location [length]
d_1, d_2, d_3	Natural depth of ocean bar, depth of navigation channel, and water depth where seaward tip of ocean bar meets offshore sea bottom [length]
d_b	Average bay depth [length]
D_R	Ratio of depth of the channel to the depth at which the seaward slope of the ocean bar meets the sea bottom (Equation II-6-40)
d_T	Channel depth [length]
$E_{\Delta T}$	Difference between the mean ebb tide flow energy flux across the ocean bar at its natural elevation and the mean ebb tide flow energy flux through the cross section of the excavated ocean bar navigation channel (Equation II-6-38)

E_W	Average daily wave energy flux per unit width of wave crest, offshore of the site of interest (Equation II-6-39)
f	Darcy - Weisbach friction term
f	Dimensionless parameter that is a function of the hydraulic radius R and Manning's roughness coefficient n (Equation II-6-16)
F	Inlet impedance (Equation II-6-17) [dimensionless]
F_I	Filling index (Equation II-6-37)
g	Gravitational acceleration [length/time^2]
h	Inlet channel water surface elevation [length]
H_A	Wave height entering inlet [length]
H_i	Average wave height for the i^{th} day of the year [length]
K	Keulegan repletion coefficient [dimensionless]
K	Keulegan's dimensionless coefficient of repletion or filling (Equation II-6-4)
K_1 , K_2	King's inlet friction coefficient (Equation II-6-6) and King's inlet frequency coefficient (Equation II-6-7) [dimensionless]
k_{en} , k_{ex}	Inlet entrance and exit energy loss coefficient [dimensionless]
L	Inlet length [length]
L_b	Distance from a inlet to the farthest pint in the bay [length]
L_{mw}	Oceanside inlet channel length [length]
m	Bank slope [length-rise/length-run]
M	Total annual littoral drift [length^3/year]
n	Manning's roughness coeeficient
n	Total number of days during the year
$-_O$	The subscript 0 denotes deepwater conditions
P	Tidal prism filling the bay (Equation II-6-12) [length^3]
Q	Inlet discharge [length^3/time]
Q_g	Total volume of alongshore sediment transport to the inlet each year [length^3]
Q_i	Littoral transport occurring on day i (Equation II-6-34) [length^3]
q_{max}	Maximum instantaneous ebb tide discharge per unit width [length^3/time-length]
Q_r	River or freshwater inflow to a bay [length^3/time]
$Q_r^{'}$	King's dimensionless variable (Equation II-6-19)

R	Inlet hydraulic radius [length]
R_H	Inlet current wave height factor (Figure II-6-34) [dimensionless]
T	Tidal period [time]
t_i	Duration of inflow [time]
$U_{max\,f}, U_{max\,e}$	Maximum channel flood and ebb velocity [length/time]
$U'_{max\,f}, U'_{max\,e}$	Dimensionless maximum channel flood and ebb velocity
V	Inlet channel velocity [length/time]
$\langle V \rangle$	Average volume of the bay over the tidal cycle [length^3/time]
V_{avg}	Maximum velocity averaged over entire inlet cross section [length/time]
V_m	Maximum cross-sectionally averaged velocity during a tidal cycle [length/time]
V_{max}	Maximum velocity in the inlet throat [length/time]
V_{meas}	Point measurement of maximum velocity [length/time]
V_R	Hoerls special function distribution (Equation II-6-41)
V_T	Threshold velocity for sand transport [length/time]
V'_m	King's dimensionless velocity (Equation II-6-5)
W	Channel width corresponding to mean water depth in channel [length]

II-6-6. Acknowledgments

Author of Chapter II-6, "Hydrodynamics of Tidal Inlets:"

William C. Seabergh, Coastal and Hydraulics Laboratory, Engineer Research and Development Center, Vicksburg, Mississippi.

Reviewers:

Lee E. Harris, Ph.D., Department of Marine and Environmental Systems, Florida Institute of Technology, Melbourne, Florida.
Tom Jarrett, U.S. Army Engineer District, Wilmington, Wilmington, South Carolina (retired).
Ashish J. Metha, Ph.D., Department of Civil and Coastal Engineering, University of Florida, Gainesville, Florida.
John Oliver, U.S. Army Engineer District, Portland, Portland, Oregon, (retired).
C. Linwood Vincent, Ph.D., Office of Naval Research, Arlington, Virginia.

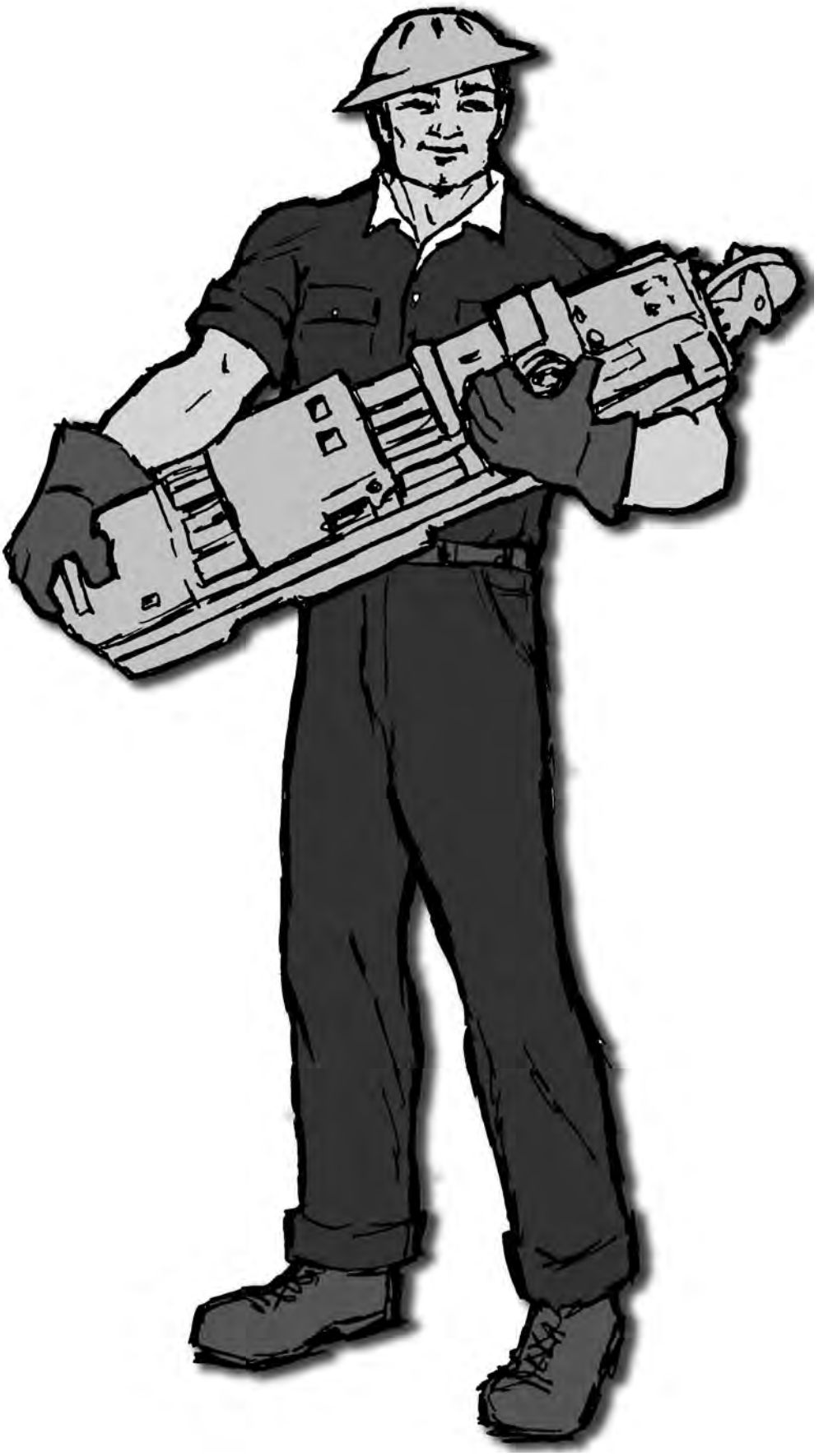

Table of Contents

Page

II-7-1. Introduction II-7-1

II-7-2. Wave Diffraction II-7-3
a. Definition of diffraction II-7-3
b. Diffraction analysis II-7-3
c. Diffraction at a harbor entrance II-7-3
(1) Waves passing a single structure II-7-3
(2) Waves passing through a structure gap II-7-6
d. Irregular wave diffraction II-7-9
e. Combined refraction-diffraction in harbors II-7-12
f. Combined diffraction - reflection in harbors II-7-13

II-7-3. Wave Transmission II-7-19
a. Definition of transmission II-7-19
b. Transmission over/through structures II-7-19
(1) Rubble-mound structures-subaerial II-7-19
(2) Rubble-mound structures-submerged II-7-20
(3) Permeable rubble-mound structures II-7-21
(4) Floating breakwaters II-7-23
(5) Wave barriers II-7-24

II-7-4. Wave Reflection II-7-26
a. Definition of reflection II-7-26
b. Reflection from structures II-7-28
c. Reflection from beaches II-7-29
d. Reflection patterns in harbors II-7-29
e. Reflection problems at harbor entrances II-7-30

II-7-5. Harbor Oscillations II-7-31
a. Introduction II-7-31
b. Mechanical analogy II-7-33
c. Closed basins II-7-34
d. Open basins - general II-7-36
e. Open basins - simple shapes II-7-36
f. Open basins - complex shapes II-7-40
g. Open basins - Helmholtz resonance II-7-44

II-7-6. Flushing/Circulation II-7-48
a. Statement of importance II-7-48
b. Flushing/circulation processes II-7-48
(1) Tidal action II-7-48
(2) Wind effects II-7-49
(3) River discharge II-7-51
c. Predicting of flushing/circulation II-7-51
(1) Numerical models II-7-51
(2) Physical model studies II-7-52
(3) Field studies II-7-53

II-7-7. Vessel Interactions II-7-54
a. Vessel-generated waves II-7-54
b. Vessel motions II-7-57
(1) Response to waves II-7-57
(2) Response to currents II-7-58
(3) Wave-current interaction II-7-58
(4) Vessel sinkage and trim II-7-59
(5) Ship maneuverability in restricted waterways II-7-62
c. Mooring II-7-64
(1) Wave forcing mechanism II-7-64
(2) Mooring configurations II-7-64
(3) Mooring lines II-7-65
(4) Fenders II-7-65
(5) Surge natural period II-7-65
(6) Mooring forces II-7-67

II-7-8. References II-7-73

II-7-9. Definitions of Symbols II-7-87

II-7-10. Acknowledgments II-7-91

II-7-11. Note to Users, Vessel Buoyancy II-7-91

List of Tables

Page

Table II-7-1. Wave Reflection Equation Coefficient Values Structure II-7-28

Table II-7-2. Harbor Oscillation Characteristics II-7-32

Table II-7-3. Flushing Characteristics of Small-Boat Harbors II-7-50

Table II-7-4. Advantages of Physical and Numerical Models II-7-53

Table II-7-5. Selected Vessel-Generated Wave Heights II-7-57

Table II-7-6. Drag Coefficients for Wind Force II-7-70

List of Figures

Page

Figure II-7-1. Harbor siting classifications II-7-2

Figure II-7-2. Wave diffraction, definition of terms II-7-4

Figure II-7-3. Wave diffraction diagram - 60^0 wave angle II-7-5

Figure II-7-4. Wave diffraction through a gap II-7-6

Figure II-7-5. Contours of equal diffraction coefficient gap width = 0.5 wavelength (B/L = 0.5) II-7-7

Figure II-7-6. Wave incidence oblique to breakwater gap II-7-8

Figure II-7-7. Diffraction for a breakwater gap of one wavelength width where ϕ = 0 deg . . . II-7-8

Figure II-7-8. Diffraction for a breakwater gap of one wavelength width where ϕ = 15 deg II-7-9

Figure II-7-9. Diffraction for a breakwater gap of one wavelength width where ϕ = 30 deg II-7-10

Figure II-7-10. Diffraction for a breakwater gap of one wavelength width where ϕ = 45 deg II-7-11

Figure II-7-11. Diffraction for a breakwater gap of one wavelength width where ϕ = 60 deg II-7-12

Figure II-7-12. Diffraction for a breakwater gap of one wavelength width where ϕ = 75 deg II-7-13

Figure II-7-13. Diffraction diagram of a semi-infinite breakwater for directional random waves of normal incidence II-7-14

Figure II-7-14. Diffraction diagrams of a breakwater gap with B/L = 1.0 for directional random waves of normal incidence II-7-15

Figure II-7-15. Diffraction diagrams of a breakwater gap with B/L = 2.0 for directional random waves of normal incidence II-7-16

Figure II-7-16. Diffraction diagrams of a breakwater gap with B/L = 4.0 for directional random waves of normal incidence II-7-17

Figure II-7-17. Diffraction diagrams of a breakwater gap with B/L = 8.0 for directional random waves of normal incidence II-7-18

Figure II-7-18. Schematic breakwater profile and definition of terms II-7-20

Figure II-7-19. Wave transmission for a low-crested breakwater (modified from Van der Meer and Angremond (1992)) II-7-22

Figure II-7-20. Common types of floating breakwaters II-7-24

Figure II-7-21. Wave transmission coefficient for selected floating breakwaters (Giles and Sorensen 1979; Hales 1981) II-7-25

Figure II-7-22. Wave transmission coefficient for vertical wall and vertical thin-wall breakwaters where $0.0157 \leq d_s \quad lgt^2 \leq 0.0793$ II-7-25

Figure II-7-23. Complete and partial reflection II-7-27

Figure II-7-24. Reflected wave crest pattern II-7-30

Figure II-7-25. Reflection of a diffracted wave II-7-31

Figure II-7-26. Surface profiles for oscillating waves (Carr 1953) II-7-33

Figure II-7-27. Behavior of an oscillating system with one degree of freedom II-7-34

Figure II-7-28. Behavior of an oscillating system with one degree of freedom II-7-36

Figure II-7-29. Motions in a standing wave II-7-37

Figure II-7-30. Theoretical response curves of symmetrical, narrow, rectangular harbor (Raichlen 1968) II-7-38

Figure II-7-31. Resonant length and amplification factor of symmetrical rectangular harbor (from Raichlen and Lee (1992); after Ippen and Goda (1963)) II-7-39

Figure II-7-32. Node locations for a dominant mode of oscillation in a square harbor: a) fully open; b) asymmetric, constricted entrance II-7-41

Figure II-7-33. Response curves for rectangular harbor with flat and sloping bottom (Zelt 1986) II-7-42

Figure II-7-34. Resonant response of idealized harbors with different geometry (Zelt 1986) II-7-43

Figure II-7-35. Photograph of physical model, Barbers Point Harbor, HI (Briggs et al. 1994) II-7-44

Figure II-7-36. Numerical model grid for Barbers Point Harbor, HI (Briggs et al. 1994) II-7-45

Figure II-7-37. Amplification factors for five resonant periods, Barbers Point Harbor, HI (Briggs et al. 1994) II-7-46

Figure II-7-38. Phases for five resonant periods, Barbers Point Harbor, HI (Briggs et al. 1994) II-7-47

Figure II-7-39. Exchange coefficients - rectangular harbor, TRP = 0.4 (modified from Falconer (1980)) II-7-50

Figure II-7-40. Wave crest pattern generated at a vessel bow moving over deep water II-7-54

Figure II-7-41. Typical vessel-generated wave record II-7-56

Figure II-7-42. Definition of terms, vessel drawdown II-7-60

Figure II-7-43. Vessel sinkage prediction II-7-61

Figure II-7-44. Pressure fields for moving vessels (vessels moving left to right) II-7-63

Figure II-7-45. Mooring fiber rope elongation curves II-7-67

Chapter II-7
Harbor Hydrodynamics

II-7-1. Introduction

a. A harbor is a sheltered part of a body of water deep enough to provide anchorage for ships or a place of shelter; refuge. The purpose of a harbor is to provide safety for boats and ships at mooring or anchor and to provide a place where upland activities can interface with waterborne activities. Harbors range in complexity from the basic harbor of refuge, consisting of minimal or no upland support and only moderate protective anchorage from storm waves to the most complex, consisting of commercial port facilities, recreational marinas, and fuel docks linked to the sea through extensive navigation channels and protective navigation structures. Key features of all harbors include shelter from both long- and short-period open ocean waves, easy and safe access to the ocean in all types of weather, adequate depth and maneuvering room within the harbor, shelter from storm winds, and minimal navigation channel dredging.

b. Harbors can be classified according to location relative to the shoreline or coast. Figure II-7-1 illustrates six harbor classifications. The inland basin and offshore basin require considerable construction, including protective navigation structures and harbor and channel dredging to provide adequate protection. They are usually constructed where no natural features exist but where a facility is required. Examples of such harbors are Port Canaveral, Florida, Marina del Rey, California (inland basin), and Gulfport, Mississippi.

c. The natural geography can provide partial protection or headlands that can be augmented to construct a protective harbor. This approach may reduce the initial costs of construction. Examples of such harbors are Half Moon Bay Harbor, California; and Barcelona Harbor, New York (bay indentation); Crescent City Harbor, California; and Palm Beach Harbor, Florida (offshore island).

d. In some locations, the land can provide protective harbors requiring minimal modification. Examples include inside estuaries and up rivers such as at Panama City Harbor, Florida; Kings Bay, Georgia, (natural harbor); Port of Portland, Oregon; and New Orleans, Louisiana (river harbor).

e. The U.S. Army Corps of Engineers has constructed hundreds of harbor projects that include protective structures such as breakwaters, jetties, and navigation channels. Projects are classified by depth and range from deep-draft projects with navigation channel depths greater than -45 ft, to intermediate-depth projects with depths between -20 ft and -45 ft, to shallow-draft projects with depths less than -20 ft. Currently, USACE operates and maintains over 25,000 miles of navigation channels in association with hundreds of harbor projects.

f. This chapter covers basic harbor hydrodynamics. Harbor design is covered in Part V. The chapter covers wave diffraction, wave transmission and reflection, harbor oscillations, flushing and circulation, and vessel interactions. These are important elements that must be understood in order to design a safe harbor that is operationally efficient.

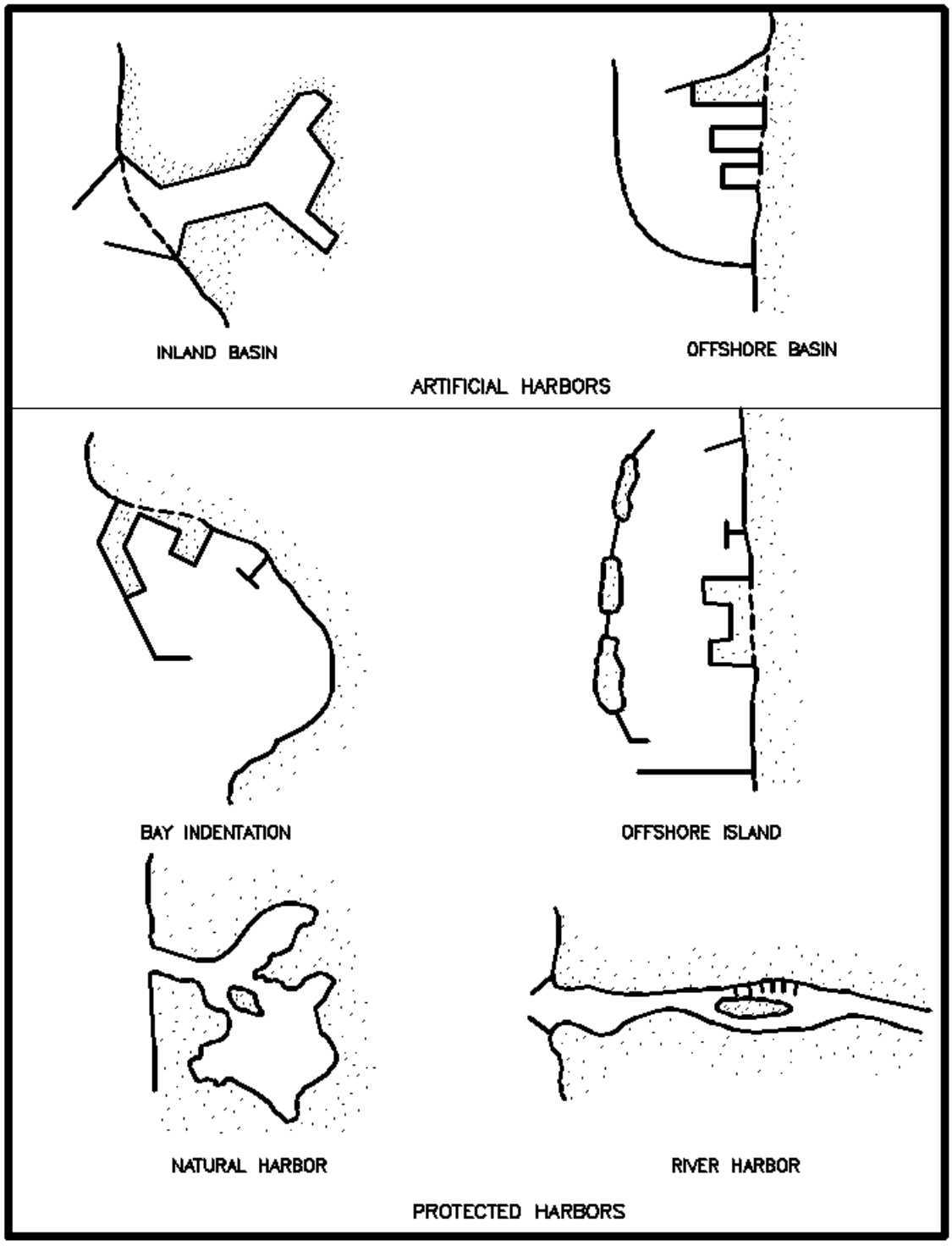

Figure II-7-1. Harbor siting classifications

II-7-2. Wave Diffraction

a. Definition of diffraction.

(1) Consider a long-crested wave that has a variable height along its crest. As this wave propagates forward, there will be a lateral transfer of wave energy along the crest (perpendicular to the direction of wave propagation). The energy transfer will be from points of greater to lesser wave height. This process is known as wave diffraction.

(2) Nearshore wave refraction will cause concentrations of wave energy at points where wave orthogonals converge. Diffraction will lessen this refraction-induced energy concentration by causing wave energy to transfer across the orthogonals away from the region of concentration. Consequently, wave diffraction can have a small effect on the resulting heights of waves that approach harbor entrances.

(3) Diffraction has a particularly significant effect on wave conditions inside a harbor. When waves propagate past the end of a breakwater, diffraction causes the wave crests to spread into the shadow zone in the lee of the breakwater. The wave crest orientations and wave heights in the shadow zone are significantly altered.

b. Diffraction analysis.

(1) Much of the material developed for wave diffraction analysis employs monochromatic waves. Ideally, an analysis should employ the directional spectral conditions. But, for a preliminary design analysis, one or a set of monochromatic wave diffraction analyses is often used to represent the more complex result that occurs when a directional spectrum of waves diffracts at a harbor.

(2) In the material presented below, monochromatic results are presented first. Then, some of the available results for diffraction of irregular waves are presented. These results are based on the superposition of several monochromatic waves having a range of representative frequencies and directions. This type of analysis requires significant effort, but it can be carried out where the situation so requires. Also, physical model tests employing a directional wave spectrum can be used for a harbor diffraction analysis.

c. Diffraction at a harbor entrance. A major concern in the planning and design of coastal harbors is the analysis of wave conditions (height and direction) that occur inside the harbor for selected incident design waves. These waves may shoal and refract after they pass through the harbor entrance; but, the dominant process affecting interior wave conditions is usually wave diffraction. Two generic types of conditions are most commonly encountered: wave diffraction past the tip of a single long breakwater and wave diffraction through a relatively small gap in a breakwater.

(1) Waves passing a single structure.

(a) Figure II-7-2 shows a long-crested monochromatic wave approaching a semi-infinite breakwater in a region where the water depth is constant (i.e. no wave refraction or shoaling). A portion of the wave will hit the breakwater where it will be partially dissipated and partially reflected. The portion of the wave that passes the breakwater tip will diffract into the breakwater lee. The diffracted wave crests will essentially form concentric circular arcs with the wave height decreasing along the crest of each wave. The region where wave heights are affected by diffraction will extend out to the dashed line in Figure II-7-2.

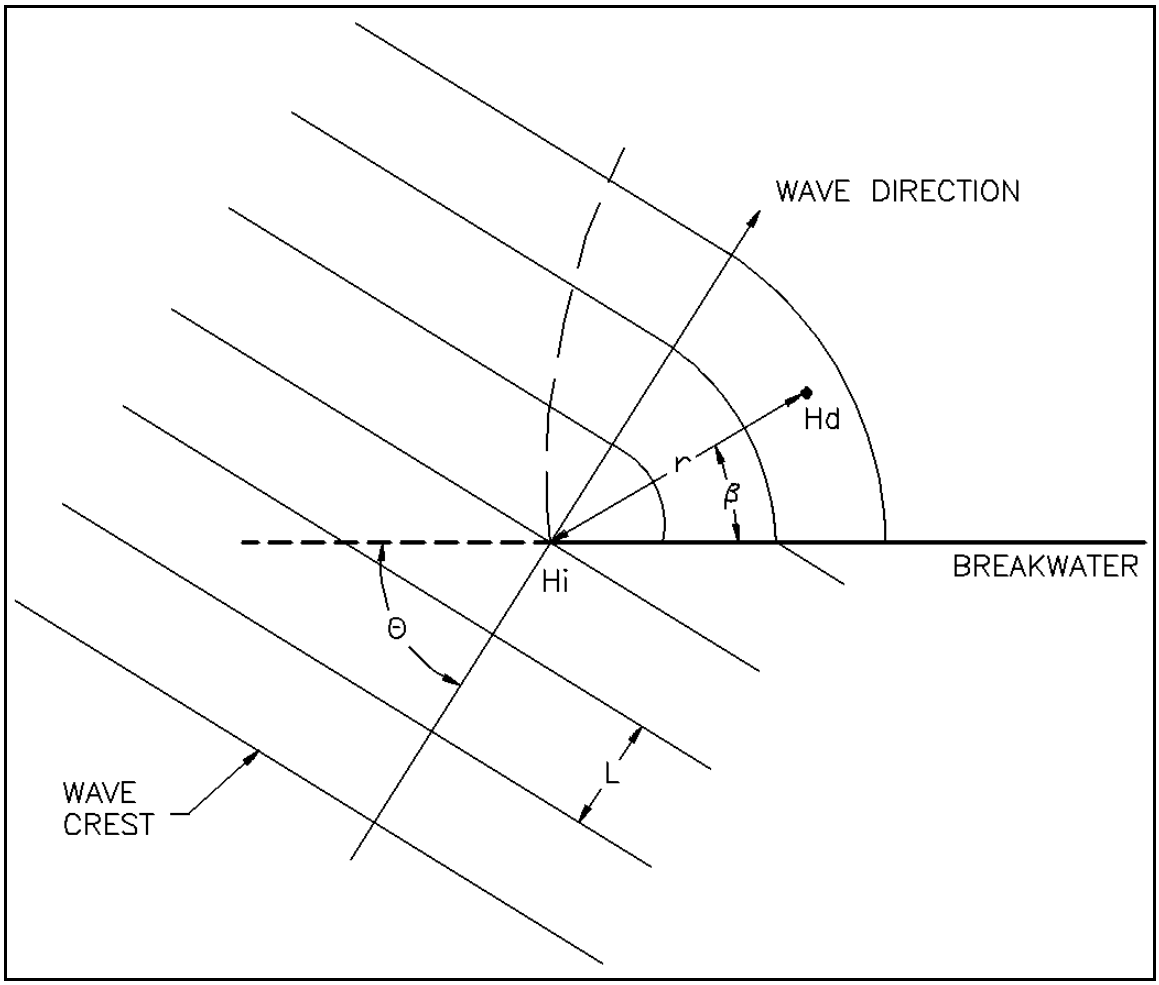

Figure II-7-2. Wave diffraction, definition of terms

(b) The reflected wave crests (not shown in the figure) would also diffract to form concentric wave crests that curl around the breakwater tip into the lee. These waves are typically much lower than the incident waves and are more affected by diffraction when they reach the breakwater lee, so they typically have a very small height in the lee of the breakwater.

(c) A diffraction coefficient $K' = H_d/H_i$ can be defined where H_d is the diffracted wave height at a point in the lee of the breakwater and H_i is the incident wave height at the breakwater tip. If r is the radial distance from the breakwater tip to the point where K' is to be determined and β is the angle between the breakwater and this radial, then $K' = fcn(r/L, \beta, \theta)$ where θ defines the incident wave direction (see Figure II-7-2) and L is the wave length. Consequently, for a given location in the lee of the breakwater, the diffraction coefficient is a function of the incident wave period and direction of approach. So, for a spectrum of incident waves, each frequency component in the wave spectrum would have a different diffraction coefficient at a given location in the breakwater lee.

(d) The general problem depicted in Figure II-7-2 was originally solved by Sommerfeld (1896) for the diffraction of light passing the edge of a semi-infinite screen. Penny and Price (1952) showed that the same solution applies to the diffraction of linear surface waves on water of constant depth that propagate past the end of a semi-infinite thin, vertical-faced, rigid, impermeable barrier. Thus, the diffraction coefficients in the structure lee include the effects of the diffracted incident wave and the much smaller diffracted wave that

reflects completely from the structure. Wiegel (1962) summarizes the Penny and Price (1952) solution and tabulates results of this solution ($K' = fct(r/L, \beta, \theta)$ for selected values of r/L, β and θ. Figure II-7-3 shows Wiegel's (1962) results for an approach angle θ of 60 deg. Plots of approach angles θ varying by 15-deg intervals from 15 to 180 deg can be found in Wiegel (1962) and the *Shore Protection Manual* (1984).

(e) An interesting feature demonstrated by Figure II-7-3 is that for this approach angle, the value of the diffraction coefficient along a line in the lee of the breakwater that extends from the breakwater tip in the direction of the approaching wave is approximately 0.5. This is true not only for the approach angle of 60 deg, but for any approach angle. Note also that for a given location in the lee of a breakwater, a one-dimensional spectrum of waves that comes from the same direction will undergo a greater decrease in height(energy density) for successively higher frequency waves in the spectrum. Increasing frequencies mean shorter wavelengths and consequently larger values of r/L (for given values of β and θ). Thus the diffracted spectrum will have a shift in energy density towards the lower frequency portion of the spectrum.

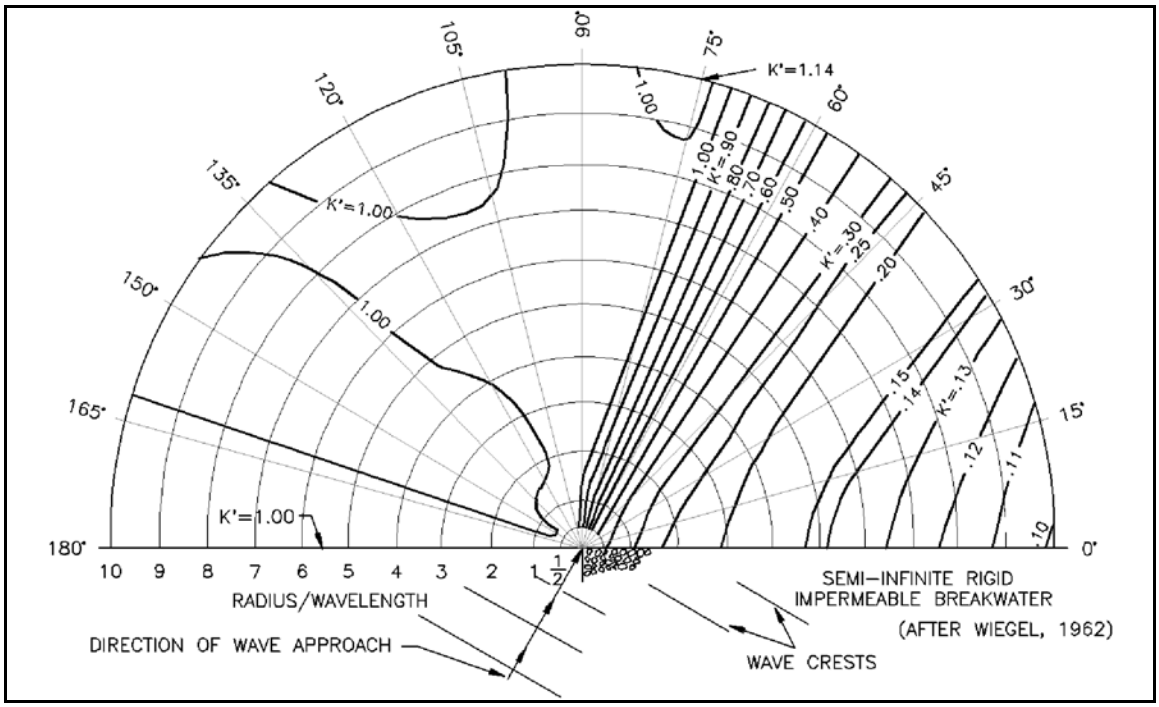

Figure II-7-3. Wave diffraction diagram - 60^0 wave angle

(f) Wave tank measurements of diffracted heights for waves passing a semi-infinite barrier were made by Putnam and Arthur (1948). They considered six approach directions for each of two incident wave periods. Their measurements generally confirm the diffraction theory. But, the diffraction theory assumes small-amplitude waves and Putnam and Arthur (1948) employed relatively small-amplitude waves in their experiments. For steeper waves, finite amplitude effects would cause the results to differ somewhat from the diffraction theory based on small-amplitude waves.

EXAMPLE PROBLEM II-7-1

FIND:

The wave height in the lee of the breakwater at a point specified by β = 30 deg and r = 100 m.

GIVEN:

A train of 6-sec-period 2-m-high waves is approaching a breakwater at an angle θ = 60 deg. The water depth in the lee of the breakwater is 10 m.

SOLUTION:

From the linear wave theory for a period of 6 sec and a water depth of 10 m, the wave length can be calculated to be 48.3 m. Thus, r/L = 100/48.3 = 2.07. From Figure II-7-3 at β = 30 deg and r/L = 2.07, K' = 0.28. This yields a diffracted wave height = (0.28)2 = 0.56 m.

The diffracted wave would be propagating in the direction β = 30 deg and would have a continually diminishing wave height as indicated by Figure II-7-3. If the breakwater has a reflection coefficient that is less than one, the above result would still be reasonable, since the diffracted height of the reflected wave would be very small at the point of interest.

(2) Waves passing through a structure gap.

(a) When waves pass through a gap in a breakwater, diffraction occurs in the lee of the breakwater on both sides of the gap. As the waves propagate further into the harbor, the zone affected by diffraction grows toward the center line of the gap until the two diffraction zones interact (see Figure II-7-4). The wider the gap, the further into the harbor this interaction point occurs. For typical harbor conditions and gap widths greater than about five wavelengths, Johnson (1952) suggests that the diffraction patterns at each side of the gap opening will be independent of each other and Wiegel (1962) may be referenced for diffraction analysis. For smaller gap widths, an analysis employing the gap geometry must be used.

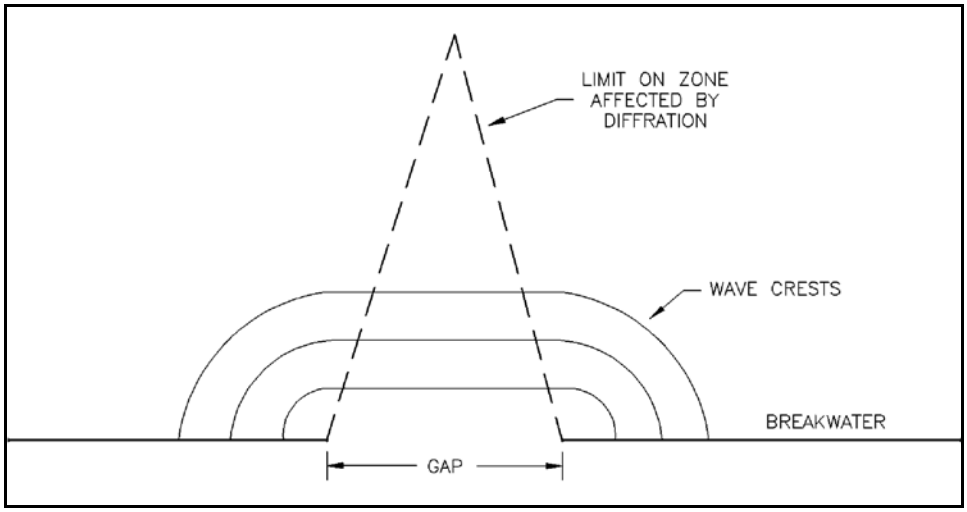

Figure II-7-4. Wave diffraction through a gap

(b) Penny and Price (1952) developed a solution for the diffraction of normally incident waves passing through a structure gap by superimposing the solutions for two mirror image semi-infinite breakwaters. Johnson (1952) employed their solution to develop diagrams that give diffraction coefficients for gap widths (B) that are between one half and five times the incident wavelength. The lateral coordinates (x,y) are again nondimensionalized by dividing by the wavelength. Figure II-7-5 is an example of one of the diagrams Johnson (1952) developed. Only one half of the pattern is shown; the other half would be a mirror image. The reader is referred to Johnson (1952) and the *Shore Protection Manual* (1984) when dealing with gap widths other than 0.5 wavelength.

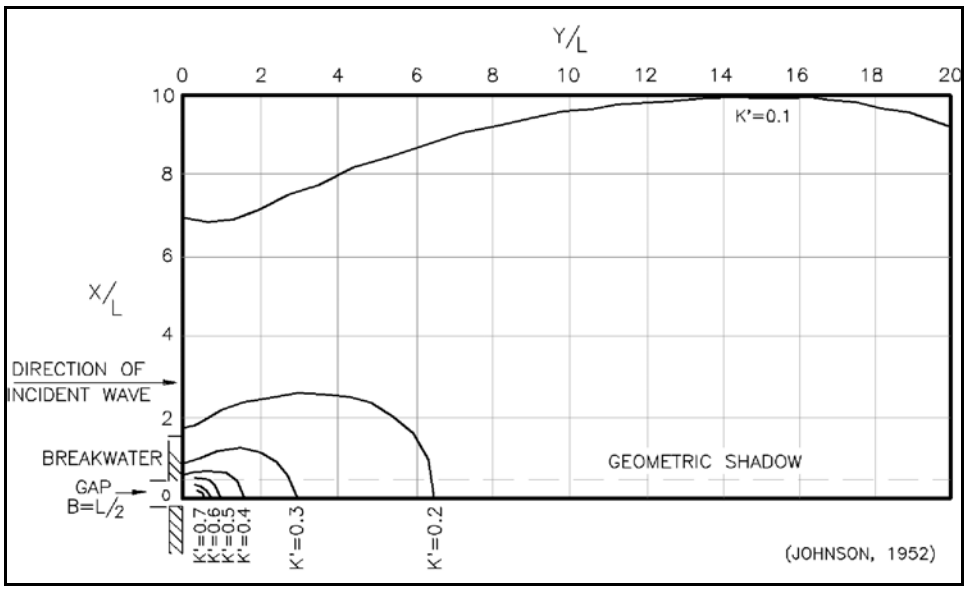

Figure II-7-5. Contours of equal diffraction coefficient gap width = 0.5 wavelength (B/L = 0.5)

(c) It may be necessary to know the wave crest orientation in the diffraction zone. Up to about six wavelengths beyond the gap, it is recommended (*Shore Protection Manual* 1984) that the wave crest position be approximated by two arcs that are centered on the two breakwater tips (as for a semi-infinite breakwater) and that the arcs be connected by a smooth curve that is approximately a circular arc centered on the midpoint of the gap. Beyond eight wavelengths, the crest position may be approximated by a single circular arc centered on the gap midpoint.

(d) The waves approaching a breakwater gap will usually not approach in a direction normal to the gap. Johnson (1952) found that the results presented above for normally incident waves can be used as an approximation for oblique waves by employing an imaginary equivalent gap having an orientation and width B' as defined in Figure II-7-6. Carr and Stelzriede (1952) employed a different analytical approach than that developed by Sommerfeld (1896) and also developed diffraction pattern solutions for barrier gaps that are small compared to the incident wavelength. Johnson (1952) used their approach to develop diffraction coefficient diagrams for a range of wave approach angles and a gap width equal to one wavelength. These are shown in Figures II-7-7 through II-7-12 for approach angles between 0 and 75 deg.

(e) Often, harbor entrance geometries will be different from the semi-infinite and gap geometries presented above. Still, approximate but useful results can be achieved by applying these solutions with some ingenuity in bracketing the encountered entrance geometry and interpolating results.

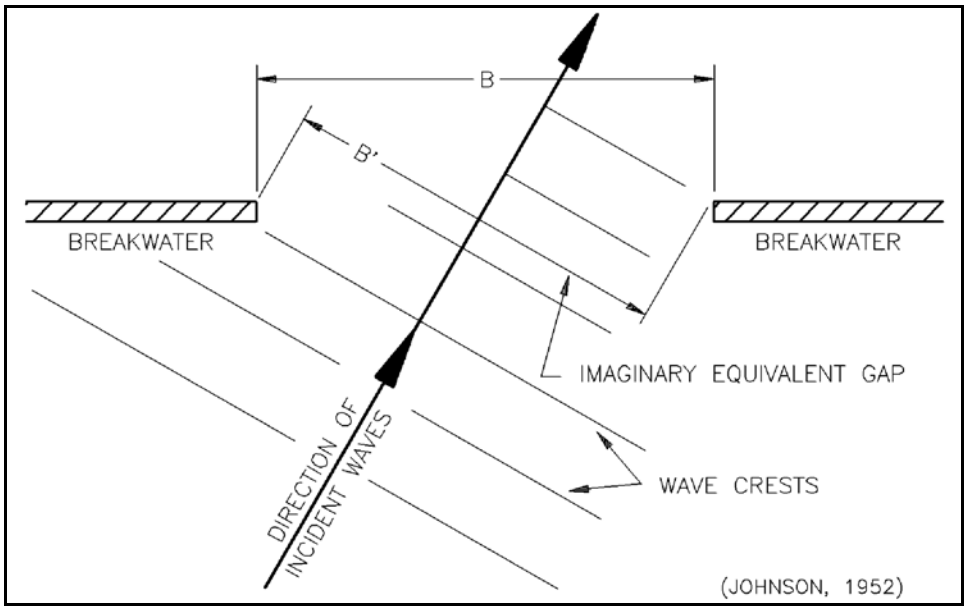

Figure II-7-6. Wave incidence oblique to breakwater gap

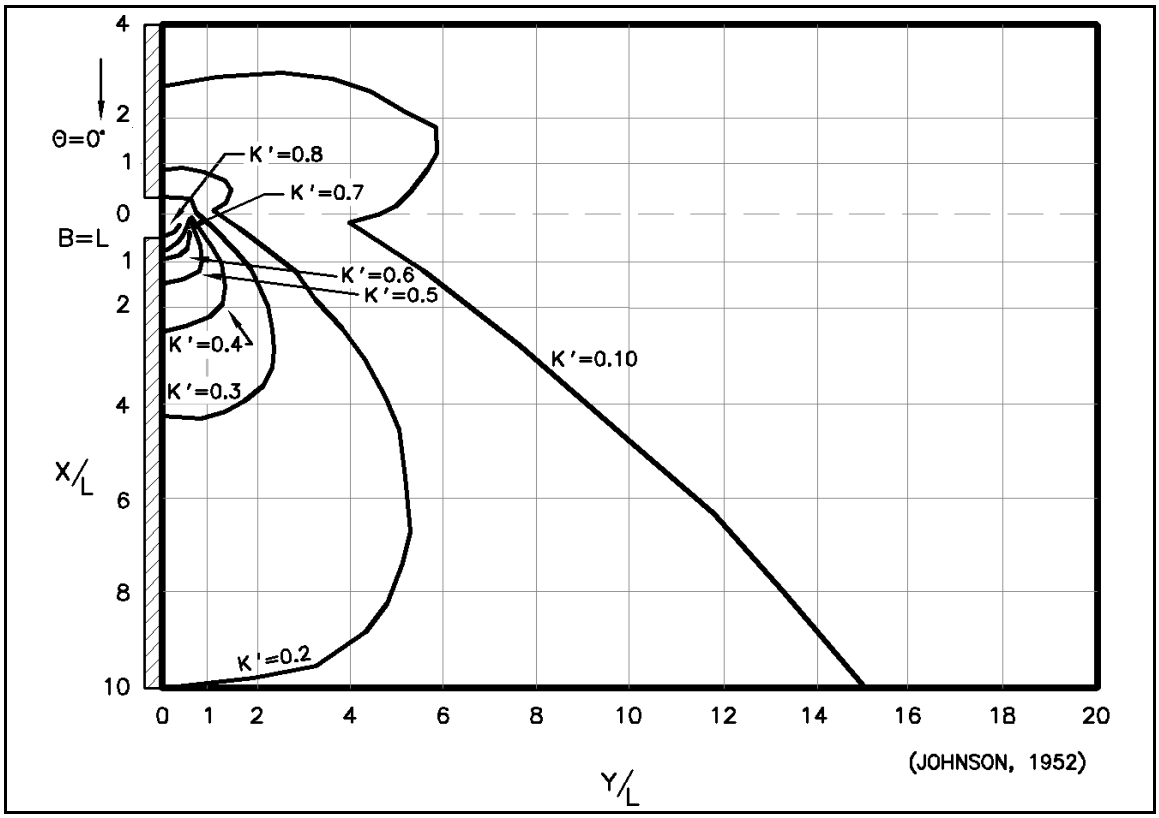

Figure II-7-7. Diffraction for a breakwater gap of one wavelength width where ϕ = 0 deg

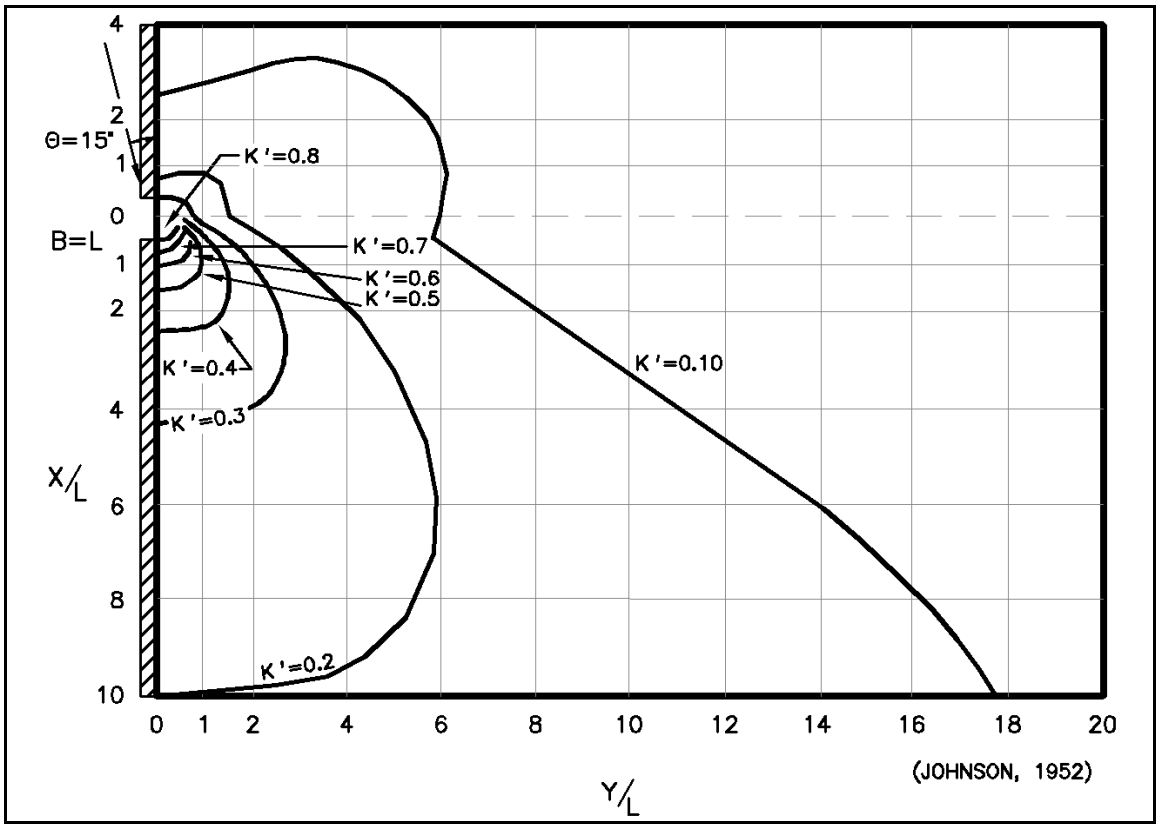

Figure II-7-8. Diffraction for a breakwater gap of one wavelength width where ϕ = 15 deg

(f) Bowers and Welsby (1982) conducted a physical model study of wave diffraction through a gap between two breakwaters whose axes are angled (rather than being collinear, i.e. 180 deg). Breakwater interior angles of 90 deg and 120 deg were employed. As would be expected, angling the breakwaters increased the heights behind the breakwater compared with the results for collinear breakwaters. But the increases were relatively small - up to 15 percent for 120-deg interior angles and up to 20 percent for 90-deg interior angles, when gap widths were in excess of half a wavelength.

(g) Memos (1976, 1980a, 1980b, 1980c) developed an approximate analytical solution for diffraction through a gap formed at the intersection of two breakwaters having axes that are not collinear but intersect at an angle. The point of intersection of the breakwater axes coincides with the tip of one of the breakwaters. Memos' solution can be developed for various angles of wave approach.

d. Irregular wave diffraction.

(1) The preceding discussion of wave diffraction was concerned with monochromatic waves. The effects of wave diffraction on an individual wave depend on the incident wave frequency and direction. Thus, each component of a directional wave spectrum will be affected differently by wave diffraction and have a different K' value at a particular point in the lee of a breakwater.

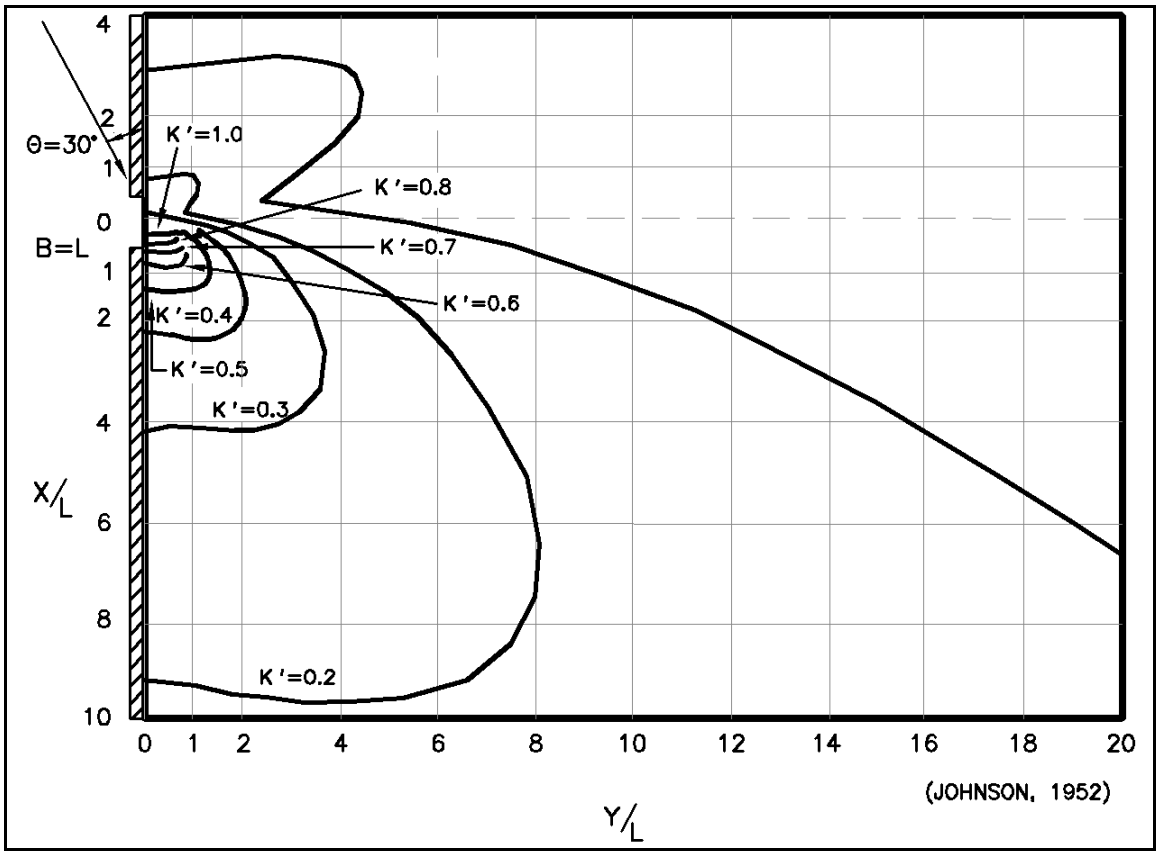

Figure II-7-9. Diffraction for a breakwater gap of one wavelength width where ϕ = 30 deg

(2) To evaluate the effect of diffraction on a directional wave spectrum, Goda, Takayama, and Suzuki (1978) calculated diffraction coefficients for a semi-infinite breakwater and a breakwater gap by breaking the spectrum into number of frequency (10) and direction (20 to 36) components and combining the result at points in the breakwater lee. This produced an effective diffraction coefficient defined by

$$K_e' = \left[\frac{1}{M_o} \int_0^{\infty} \int_{\theta\ \min}^{\theta\ \max} S(f,\theta)\ (K')^2\ d\theta\ df \right]^{\frac{1}{2}} \qquad \text{(II-7-1)}$$

where K' is the diffraction coefficient for each frequency/direction component when acting as a monochromatic wave, M_0 is the zero moment of the spectrum, df and $d\theta$ are the frequency and direction ranges represented by each component of the spectrum, θ_{max} and θ_{min} are the limits of the spectral wave component directions, and $S(f,\theta)$ is the spectral energy density for the individual components. The spectral frequency distribution they employed was similar to most typical storm spectra such as the JONSWAP spectrum. The directional spread of the spectrum was characterized by a directional concentration parameter S_{max}, which equals 10 for widely spread wind waves and 75 for swell with a long decay distance, so the directional spread is quite limited.

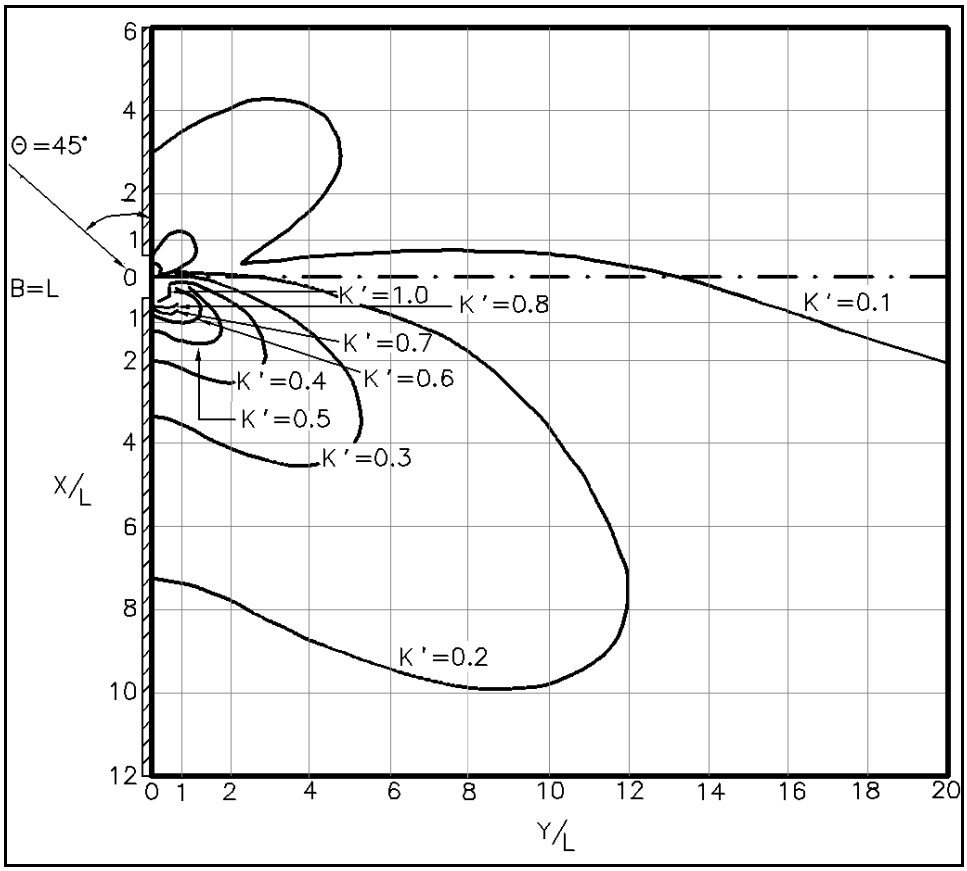

Figure II-7-10. Diffraction for a breakwater gap of one wavelength width where ϕ = 45 deg

(3) The results for waves approaching perpendicular to a semi-infinite breakwater are shown in Figure II-7-13 where the solid lines define values of K'_e and the dashed lines are the ratio of peak spectral period for the diffracted to incident waves. The results for waves approaching normal to a breakwater gap are shown in Figures II-7-14 to II-7-17, where the ratio of gap width to incident wavelength varies from 1 to 8. Note that these diagrams are normalized by dividing by both the gap width and the wavelength, so two different horizontal scales are given for each case. Also, the left-hand side gives the peak period ratio and the right-hand side gives values of K'_e.

(4) The spectral diffraction diagrams for the semi-infinite breakwater show a small change in the peak period ratio as the waves extend into the breakwater lee. (For monochromatic waves the wave period would not change.) The same holds for the breakwater gap. For the semi-infinite breakwater the values of K'_e are generally higher than the equivalent values of K' for monochromatic waves. For a breakwater gap, the spatial variation of K'_e values is smoothed out by the directional spread of the incident waves. That is, there is less variation in K'_e values for the spectral case than in K' for the monochromatic case. For waves approaching a breakwater gap at some oblique angle, the imaginary equivalent gap approach depicted in Figure II-7-6 can be used.

(5) Thus, if the one-dimensional or directional spectrum for the design waves is known at a harbor entrance, Equation II-7-1 can be used with the monochromatic wave diffraction diagrams to more effectively evaluate wave diffraction in the harbor. The spectrum can be broken into a number of direction and/or frequency components, each component can be analyzed as a diffracting monochromatic wave, and the results can be recombined using Equation II-7-1.

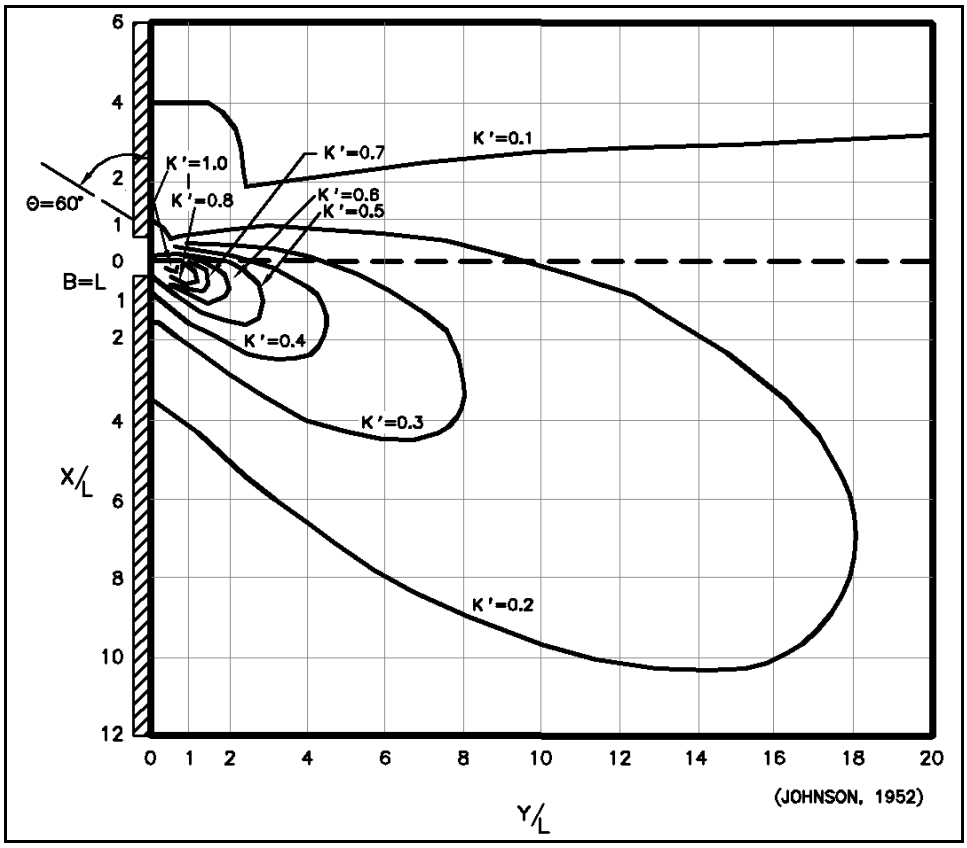

Figure II-7-11. Diffraction for a breakwater gap of one wavelength width where ϕ = 60 deg

e. Combined refraction-diffraction in harbors.

(1) In most harbors, the depth is relatively constant so the diffraction analyses discussed above are adequate to define the resulting wave conditions. However, if the depth changes significantly, then wave amplitudes will change because of shoaling effects. If the harbor bottom contours are not essentially parallel to the diffracting wave crests, then wave amplitudes and crest orientations will be affected by refraction.

(2) Where depth changes in a harbor are sufficient for combined refraction and diffraction effects to be significant, the resulting wave height and direction changes can be investigated by either a numerical or a physical model study. For examples of numerical model studies of combined refraction-diffraction in the lee of a structure, see Liu and Lozano (1979), Lozano and Liu (1980), and Liu (1982). Physical models that investigate the combined effects of refraction and diffraction are routinely conducted (see Hudson et al. 1979). The one major limitation on these models for wind wave conditions is that the model cannot have a distorted scale (i.e., horizontal and vertical scale ratios must be the same). Sometimes, lateral space limitations or the need to maintain an adequate model depth to avoid viscous and surface tension scale effects make a distorted scale model desirable. But such a model cannot effectively investigate combined refraction-diffraction problems.

(3) In many cases, the depth near the entrance to a harbor is relatively constant with the significant depth changes occurring further from the entrance (in the vicinity of the shoreline). Then an approximate (but often adequate) analysis can be carried out using the techniques discussed herein. The diffraction analysis would be carried out from near the harbor entrance to the point inside the harbor where significant

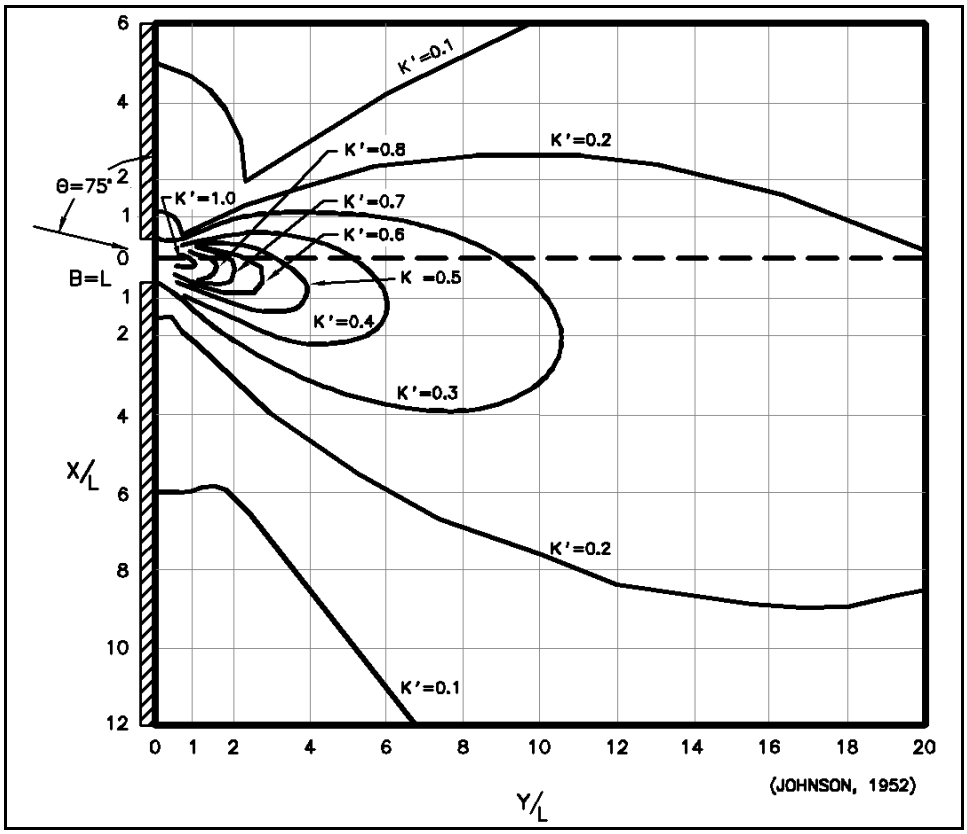

Figure II-7-12. Diffraction for a breakwater gap of one wavelength width where ϕ = 75 deg

depth changes commence. Hopefully, this will be a distance of at least three or four wavelengths from the entrance. This diffraction analysis will define the wave heights and crest orientation at the point where significant shoaling-refraction effects commence. From this point landward, a refraction-shoaling analysis using the procedures described in Part II-3 can be used to carry the wave to the point of breaking or interaction with a land boundary.

f. Combined diffraction - reflection in harbors.

(1) A computer program for dealing with combined diffraction and reflection by a vertical wedge has been developed by Seelig (1979, 1980) and is available in the Automated Coastal Engineering System (ACES) (Leenknecht et al. 1992). This package estimates wave height modifications due to combined diffraction and reflection caused by a structure. It has the ability to simulate a single straight, semi-infinite breakwater, corners of docks, and rocky headlands. Assumptions include monochromatic, linear waves, and constant water depth.

(2) The user has the ability to vary the wedge angle from 0 to 180 deg, where 0 deg would represent the case of a single straight, semi-infinite breakwater and 90 deg, the corner of a dock.

(3) The required input includes incident wave height, wave period, water depth, wave angle, wedge angle, and X and Y coordinates (location of desired calculation). The range of X and Y should be limited to plus or minus 10 wavelengths.

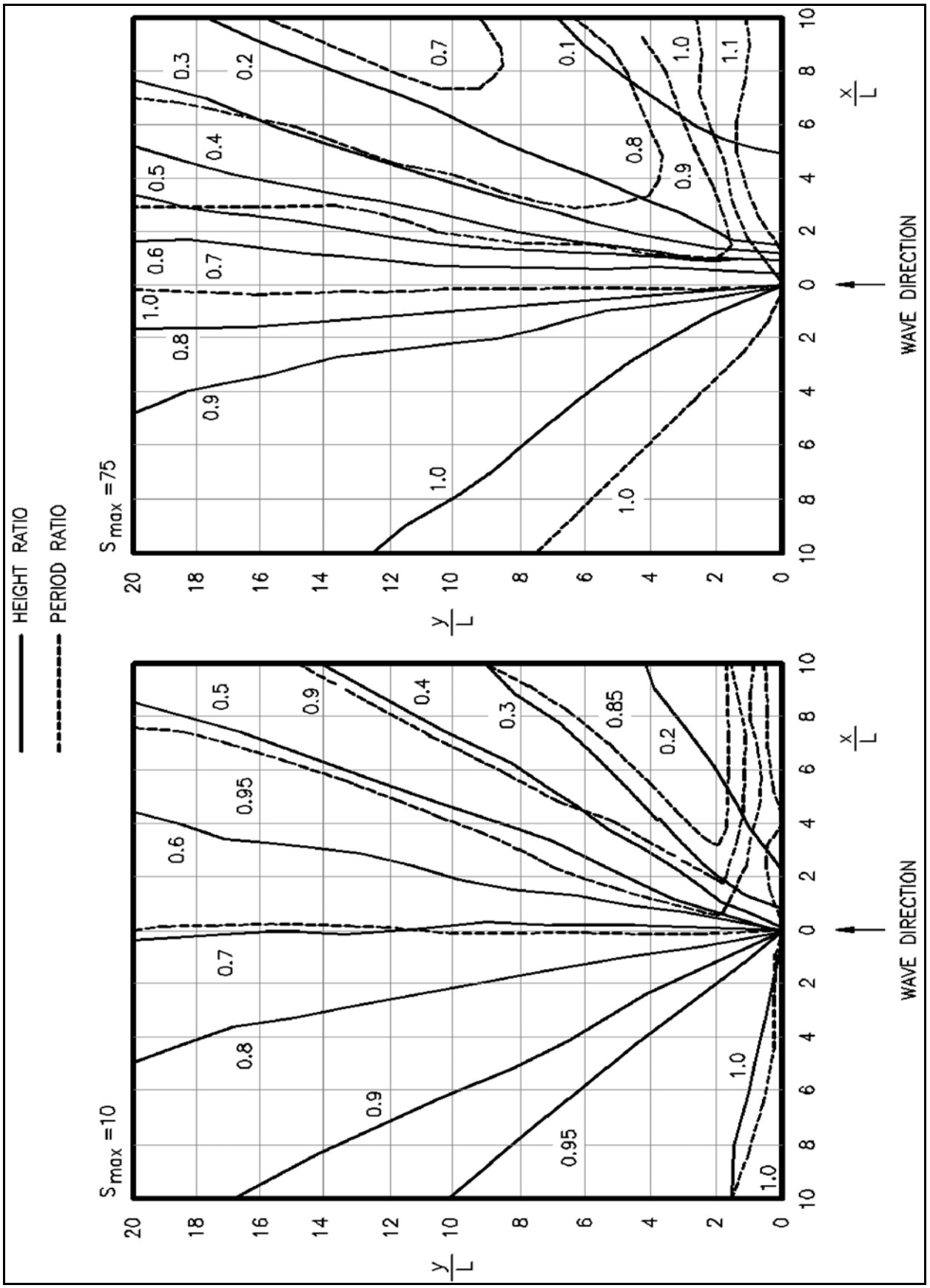

Figure II-7-13. Diffraction diagram of a semi-infinite breakwater for directional random waves of normal incidence (Goda 2000)

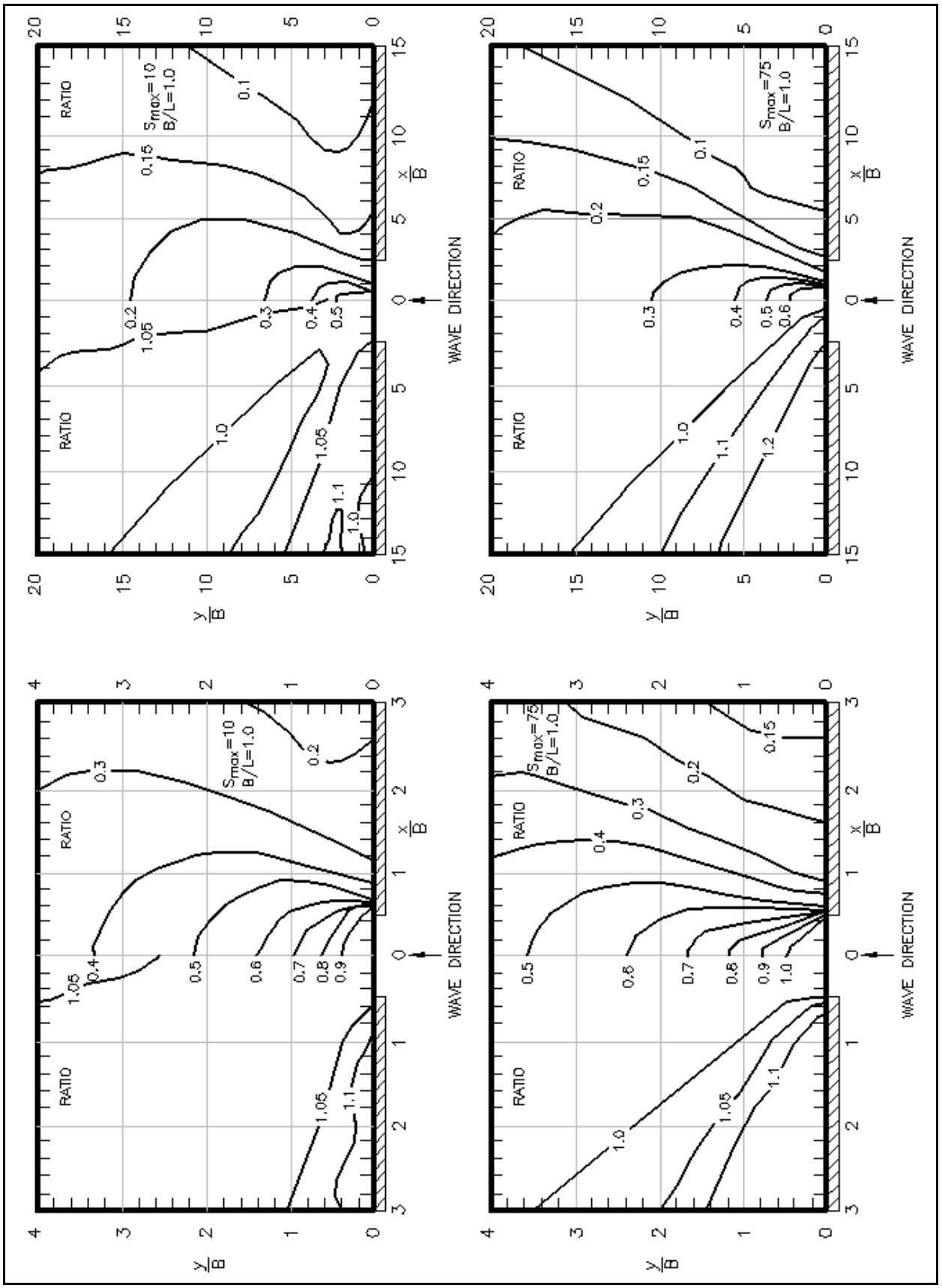

Figure II-7-14. Diffraction diagrams of a breakwater gap with *B/L* = 1.0 for directional random waves of normal incidence (Goda 2000)

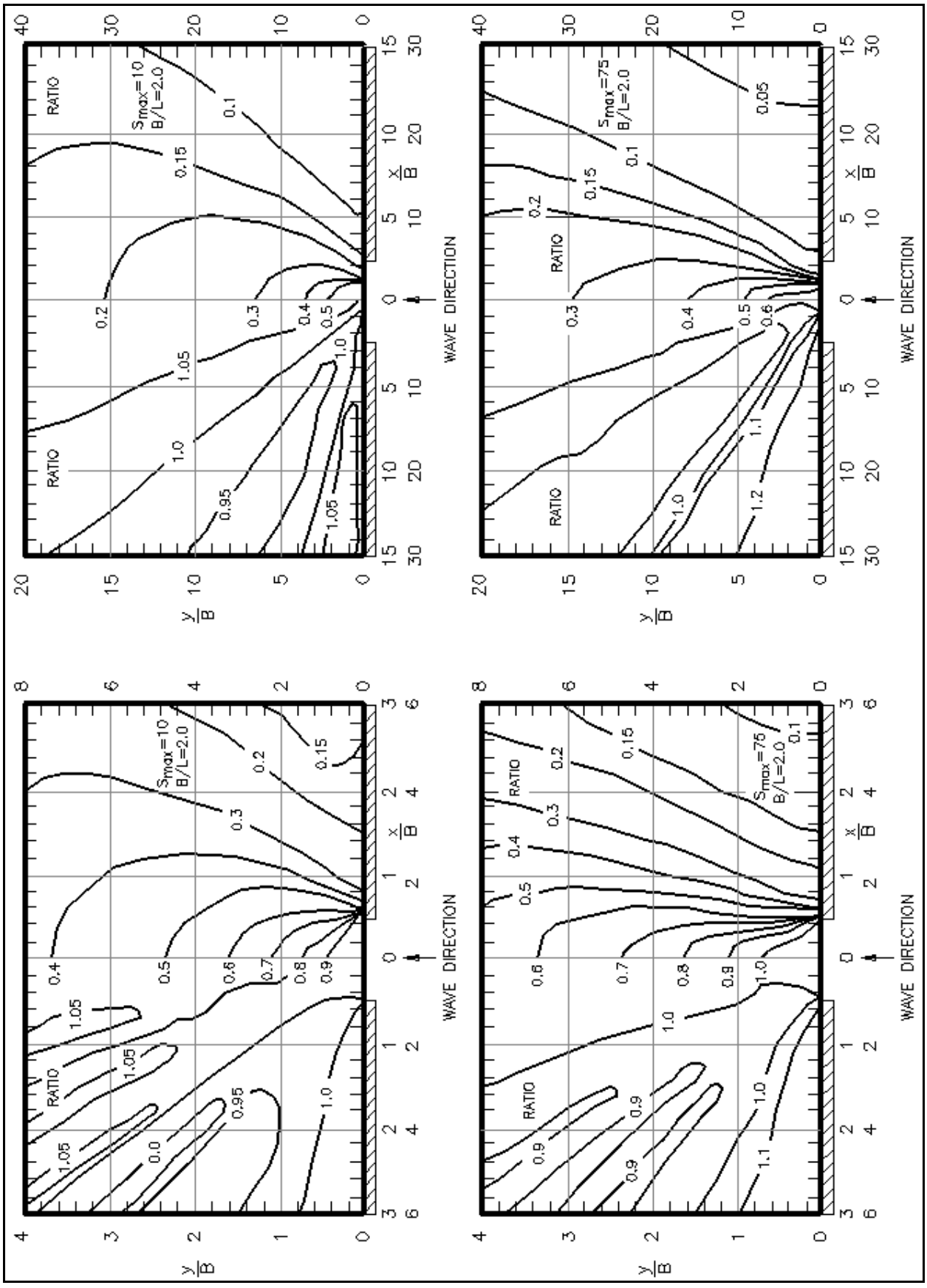

Figure II-7-15. Diffraction diagrams of a breakwater gap with *B/L* = 2.0 for directional random waves of normal incidence (Goda 2000)

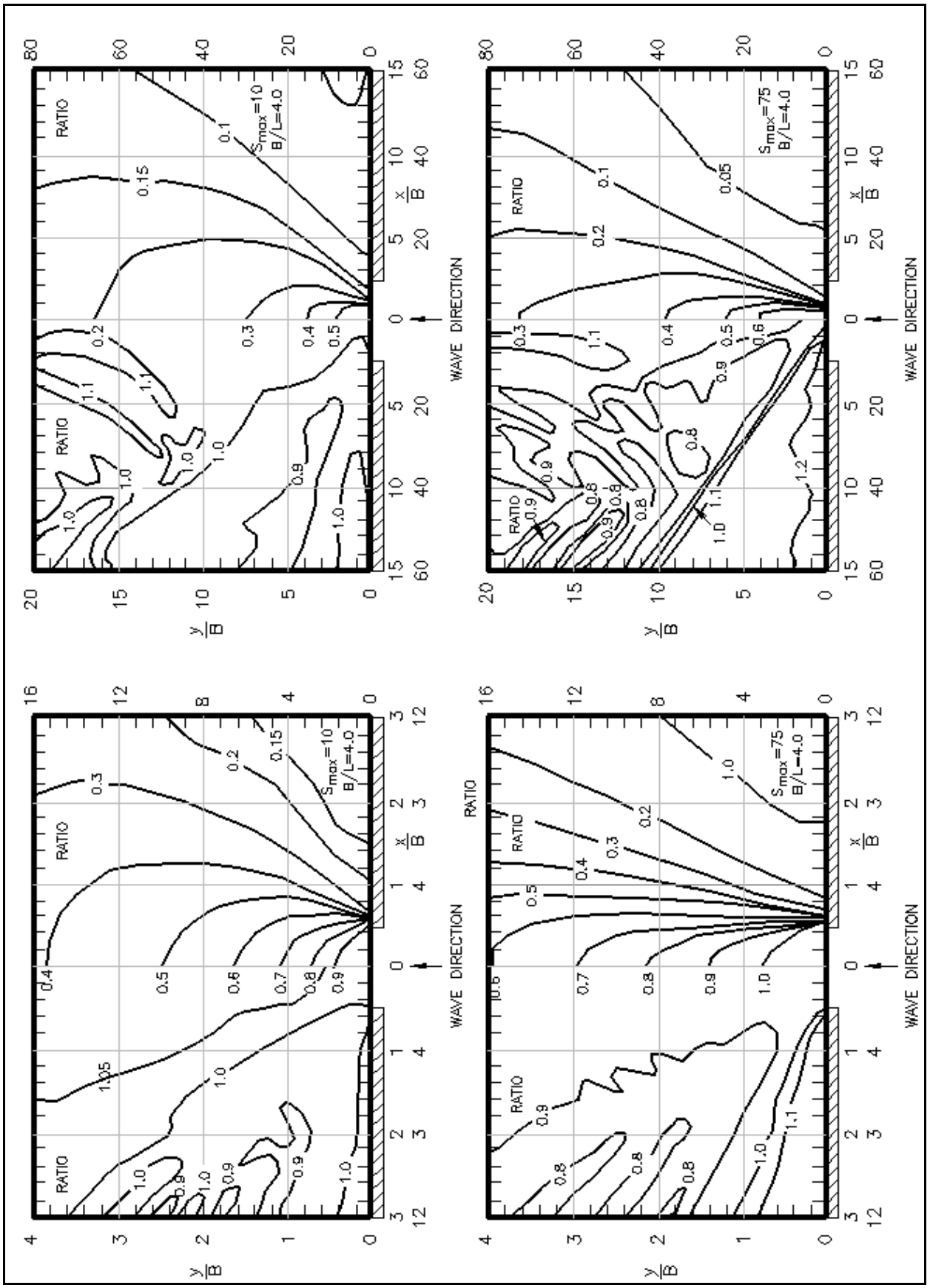

Figure II-7-16. Diffraction diagrams of a breakwater gap with *B/L* = 4.0 for directional random waves of normal incidence (Goda 2000)

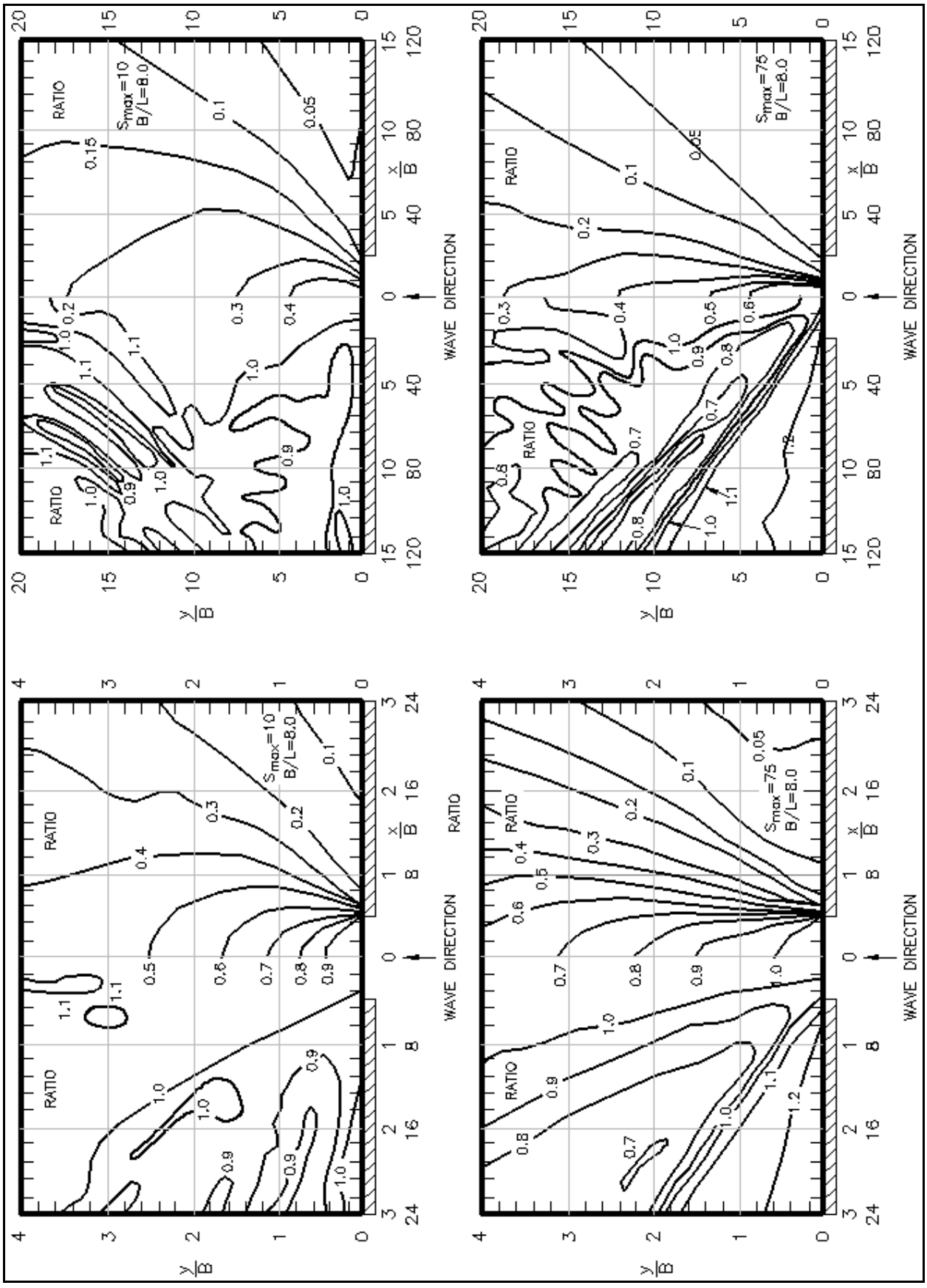

Figure II-7-17. Diffraction diagrams of a breakwater gap with *B/L* = 8.0 for directional random waves of normal incidence (Goda 2000)

(4) The wavelength, ratio of calculated wave height to incident wave height, wave phase, and modified wave height are given as output data. For further information on the ACES system, the reader is referred to Leenknecht et al. (1992).

II-7-3. Wave Transmission

a. Definition of transmission.

(1) When waves interact with a structure, a portion of their energy will be dissipated, a portion will be reflected and, depending on the geometry of the structure, a portion of the energy may be transmitted past the structure. If the crest of the structure is submerged, the wave will simply transmit over the structure. However, if the crest of the structure is above the waterline, the wave may generate a flow of water over the structure which, in turn, regenerates waves in the lee of the structure. Also, if the structure is sufficiently permeable, wave energy may transmit through the structure. When designing structures to protect the interior of a harbor from wave attack, as little wave transmission as possible should be allowed, while optimizing the cost versus performance of the structure.

(2) Transmitted wave height will be less than incident wave height, and wave period will usually not be identical for transmitted and incident waves. Laboratory experiments conducted with monochromatic waves typically show that the transmitted wave has much of its energy at the same frequency as the incident wave, but a portion of the transmitted energy has shifted to the higher harmonic frequencies of the incident wave. For a given incident wave spectrum, there would be a commensurate shift in the transmitted wave spectrum to higher frequencies.

(3) The degree of wave transmission that occurs is commonly defined by a wave transmission coefficient $C_t = H_t/H_i$ where H_t and H_i are the transmitted and incident wave heights, respectively. When employing irregular waves, the transmission coefficient might be defined as the ratio of the transmitted and incident significant wave heights or some other indication of the incident and transmitted wave energy levels.

(4) Most quantitative information on wave transmission past various structure types has necessarily been developed from laboratory wave flume studies. Historically, most of the early studies employed monochromatic waves; but, during the past two decades there has been a significant growth in information based on studies with irregular waves.

b. Transmission over/through structures.

(1) Rubble-mound structures-subaerial.

(a) Figure II-7-18 is a schematic cross section of a typical rubble-mound structure. The freeboard F is equal to the structure crest elevation h minus the water depth at the toe of the structure d_s (i.e., $F = h - d_s$). Also shown is the wave runup above the mean water level R that would occur if the structure crest elevation was sufficient to support the entire runup. When $F < R$, wave overtopping and transmission will occur. The parameter F/R is a strong indicator of the amount of wave transmission that will occur. Procedures for determining wave runup are presented elsewhere in the CEM.

(b) A number of laboratory studies of wave transmission by overtopping of subaerial structures have been conducted (see *Shore Protection Manual* (1984)). The most recent and comprehensive of these studies was conducted by Seelig (1980), who also studied submerged breakwaters.

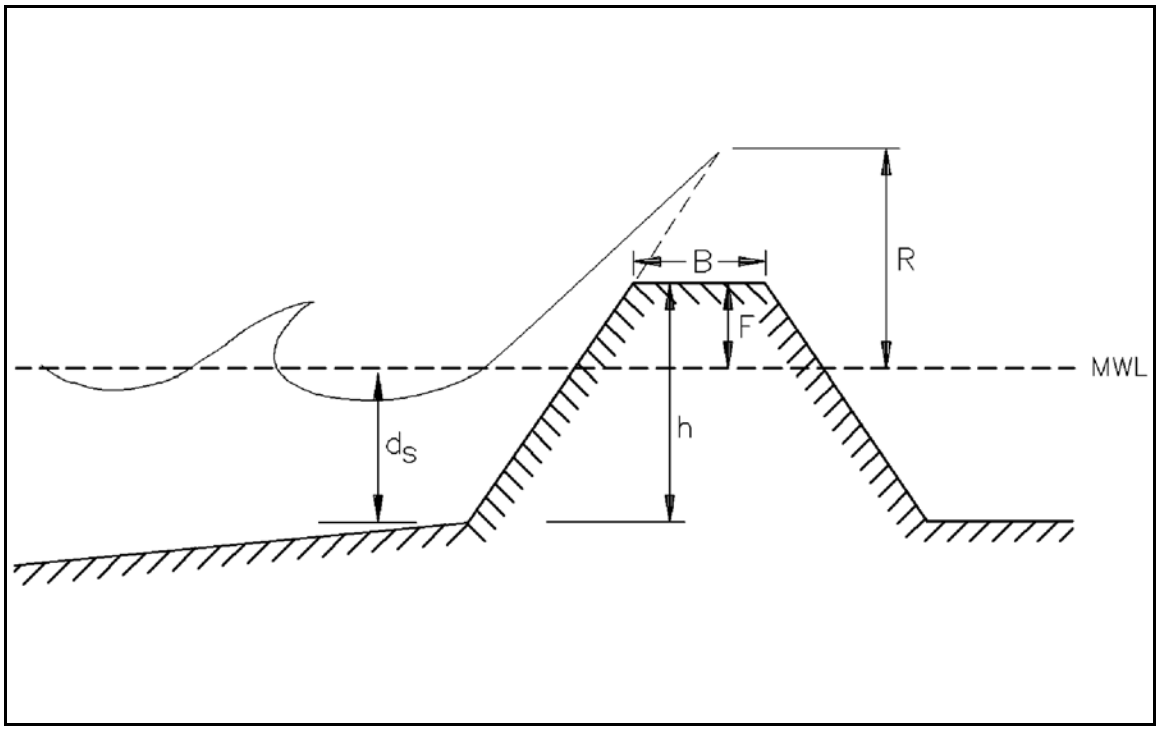

Figure II-7-18. Schematic breakwater profile and definition of terms

(c) Seelig presented a simple formula for estimating the wave transmission coefficient for subaerial stone mound breakwaters, which is valid for both monochromatic and irregular waves:

$$C_t = C\left(1 - \frac{F}{R}\right) \tag{II-7-2}$$

(d) The coefficient C is given by

$$C = 0.51 - \frac{0.11B}{h} \tag{II-7-3}$$

where B is the structure crest width and h is the crest elevation above the bottom (see Figure II-7-18). It is recommended that Equation II-7-2 be applied to the relative depth (d_s/gT^2) range of 0.03 to 0.006 and Equation II-7-3 to the range of B/h between 0 and 3.2, because these are the ranges of experimental data employed to develop the equations.

(e) The report by Seelig (1980) contains laboratory results for 19 different breakwater cross-section geometries. Specific results for one or more of these geometries may closely relate to the prototype structure being analyzed. For irregular waves, the wave transmission coefficients were defined in terms of the incident and transmitted spectral energies.

(2) Rubble-mound structures-submerged.

(a) Rubble-mound structures having their crest at or below the mean water level have seen increasing use recently. Often, they simply consist of a homogeneous wide-graded mass of stone. A functional

advantage for these lower-cost structures is that they may have a relatively high transmission coefficient for everyday lower waves, but as the height of the incident waves increases, the transmission coefficient will generally decrease. For harbor installations, they have been used in tandem with a conventional subareal breakwater placed in their lee - the combined cost of the two structures being less than a single structure with the same operational criteria (Cox and Clark 1992). A number of laboratory experiments on wave transmission past submerged rubble-mound structures have been conducted. Results are summarized in Seelig (1980) and Van der Meer and Angremond (1992).

(b) Van der Meer and Angremond (1992) summarized the available data plus some of their own data to present a comprehensive procedure for predicting wave transmission for low-crested breakwaters. For irregular waves they defined the transmission coefficient as the ratio of incident and transmitted significant wave heights. They correlated C_t with F/H_i where F would have positive values for low subaerial breakwaters and negative values for breakwaters with a submerged crest. Correlations with parameters that also included the incident wave period did not improve results. Figure II-7-19 gives C_t versus F/H_i.

(c) Van der Meer and Angremond (1992) were able to improve the correlations based on experimental data by introducing the median diameter D_{50} of the armor stone used to build the structure. (There is a relationship between D_{50} and the design wave height for a stable structure.) They then correlated C_t with F/D_{50} and secondary factors H_s/gT_p^2, H_i/D_{50}, and B/D_{50}. These relationships are presented in the form of somewhat complex formulas.

(3) Permeable rubble-mound structures.

(a) Wave energy may transmit through a rubble-mound structure, particularly if it is constructed solely of a homogeneous mass of large diameter stone. If the structure contains a number of stone layers including a core of fine stones, the wave transmission will be much less. Also, wave energy transmission through a stone mound structure would be significant for long-period, low waves, but much less for shorter-period waves (e.g. the tide would only be slightly reduced by a rubble-mound structure, but steep, wind-generated waves would have negligible transmission through the structure).

EXAMPLE PROBLEM II-7-2

FIND:

The transmission coefficients and the transmitted wave heights for incident wave heights of 0.5, 1.0, 2.0 and 4.0 m.

GIVEN:

A submerged offshore breakwater situated where the bottom is 4.0 m below the design still-water level. The structure crest elevation is 3.0 m above the bottom.

SOLUTION:

The breakwater freeboard F is 3.0 - 4.0 = -1.0 m. Employing Figure II-7-19 we have:

$H_{i(m)}$	F/H_i	C_t	$H_{t(M)}$
0.5	-2.0	0.82	0.41
1.0	-1.0	0.74	0.74
2.0	-0.5	0.60	1.20
4.0	-0.25	0.52	2.10

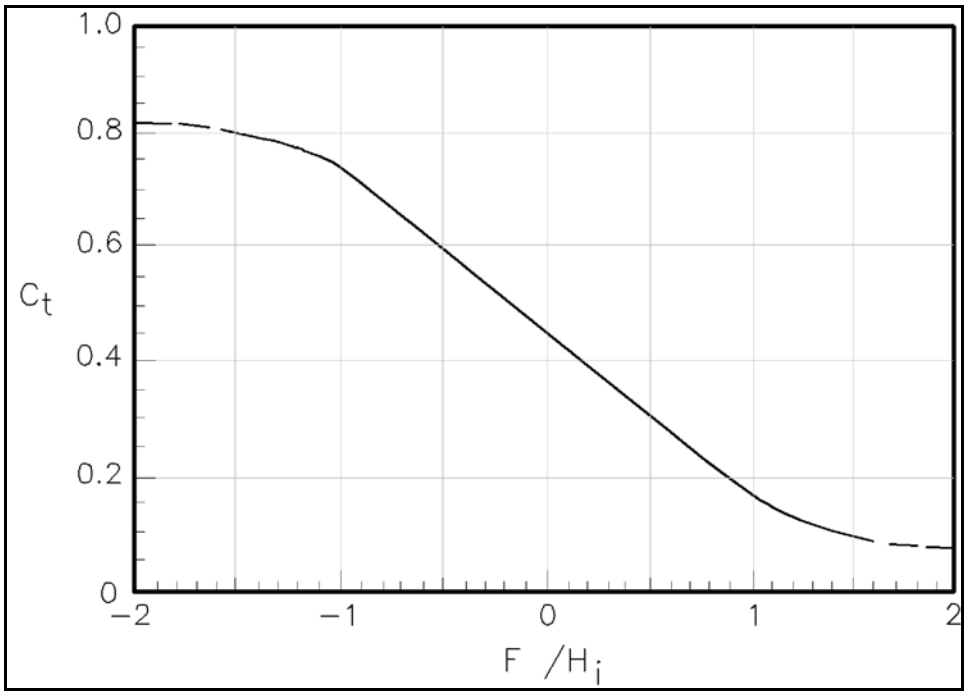

Figure II-7-19. Wave transmission for a low-crested breakwater (modified from Van der Meer and Angremond (1992))

(b) When a porous rubble-mound structure suffers wave transmission caused by wave overtopping and by wave propagation through the structure, the resulting combined transmission coefficient would be

$$C_t = \sqrt{C_{tt}^2 + C_{t0}^2} \tag{II-7-4}$$

where C_{tt} is the coefficient for wave transmission through the structure and C_{t0} is the coefficient for wave transmission by flow over the structure.

(c) Potential scale effects make it difficult to conduct scaled laboratory experiments to measure wave transmission through rubble-mound structures. (Wave motion requires Froude similitude, while flow through porous media requires Reynolds similitude, but the two are incompatible.) Consequently, the best procedure for determining C_{tt} for a rubble-mound structure is a numerical procedure developed by Madsen and White (1976). A computer program for applying this procedure has been developed by Seelig (1979,1980) and is available in the ACES system (Leenknecht et al. 1992).

(d) The procedure developed by Madsen and White (1976) first calculates the amount of wave dissipation caused by wave runup/rundown on the seaward face of the structure. (It is assumed that the wave does not break - a good assumption for longer waves.) Wave reflection from the structure is also determined. The remaining energy propagates into the structure and is partially dissipated by turbulent action. The procedure then determines this rate of turbulent energy dissipation assuming a rectangular homogeneous breakwater cross section that is hydraulically equivalent to the actual layered breakwater. This leads to the transmitted wave height and C_{tt}. Application of this procedure requires a knowledge of the incident wave height and period, the water depth, the breakwater layer geometry, and the stone sizes and porosities for each layer. Seelig (1980) found that this procedure could be applied to irregular waves by using the mean wave height and spectral peak period of the incident waves in the calculation.

EXAMPLE PROBLEM II-7-3

FIND:

The transmission coefficient for incident waves having periods of 2 and 5 sec.

GIVEN:

The catamaran breakwater whose performance is depicted in Figure II-7-21.

SOLUTION:

For a water depth of 7.6 m, using the linear wave theory, wavelengths would be calculated to be 6.24 m (for T = 2 sec) and 34.4 m (for T = 5 sec). For a width W of 6.4 m, this yields W/L = 1.03 and 0.186, respectively. From Figure II-7-21, this yields C_t = 0.2 (extrapolating) for the 2-sec wave and C_t = 0.8 for the 5-sec wave. Thus, this catamaran is quite effective for the 2-sec wave but quite ineffective for the 5-sec wave.

(4) Floating breakwaters.

(a) Moored floating breakwaters have some distinct advantages for harbor installations. They are more adaptable to the water level changes that occur at harbors that are built on reservoirs and in coastal areas having a large tidal range. They are usually more economical than fixed breakwaters for deep-water sites, and they interfere less with water circulation and fish migration. But they also have some significant limitations. Since they are articulating structures, they are prone to damage at connecting points between individual breakwater units and between these units and mooring lines. And, their performance is very dependent on the period of the incident waves. This last factor will establish relatively severe limits on where floating breakwaters can effectively be deployed.

(b) Several different types of floating breakwaters have been proposed. Hales (1981) presents a survey of these various types and their performance. Most of the floating breakwaters in use are of three generic types - prism, catamaran, and scrap tire assembly (see Figure II-7-20). Figure II-7-21 plots the wave transmission coefficients for a typical representative of each of these three types. The transmission coefficient is plotted versus the breakwater's characteristic dimension in the direction of wave propagation W divided by the incident wave length L at the breakwater. The data plotted in Figure II-7-21 are all derived from laboratory experiments. The prism results are for a concrete box having a 4.88-m width (W), a draft of 1.07 m, and a water depth of 7.6 m (Hales 1981). The catamaran (Hales 1981) has two pontoons that are 1.07 m wide with a draft of 1.42 m and a total width (W) of 6.4 m. The water depth was 7.6 m. The tire assembly (Giles and Sorensen 1979) had a width of 12.8 m (W), a nominal draft of one tire diameter, and was tested in water 3.96 m deep. The three breakwaters were all moored fore and aft; other mooring arrangements would somewhat alter the transmission coefficient.

(c) Example Problem II-7-3 demonstrates a major limitation of floating breakwaters. For typical breakwater sizes (i.e., W equals 5 to 10 m) the incident wave period must not exceed 2-3 sec for the breakwater to be very effective. Thus, for typical design wind speeds, the fetch generating the waves to which the structure is exposed cannot be very large. Sorensen (1990) conducted an analysis to determine general wind speed, fetch, and duration guidelines for the three floating breakwaters from Figure II-7-20. He assumed an allowable transmitted wave height of 2 ft (0.61 m). For example, for a wind speed of 60 mph (26.8 m/sec) having a duration of 20-30 min, the fetch must not exceed 2-3 miles (3.2-4.8 km) if the transmitted wave height is to be less than 2 ft.

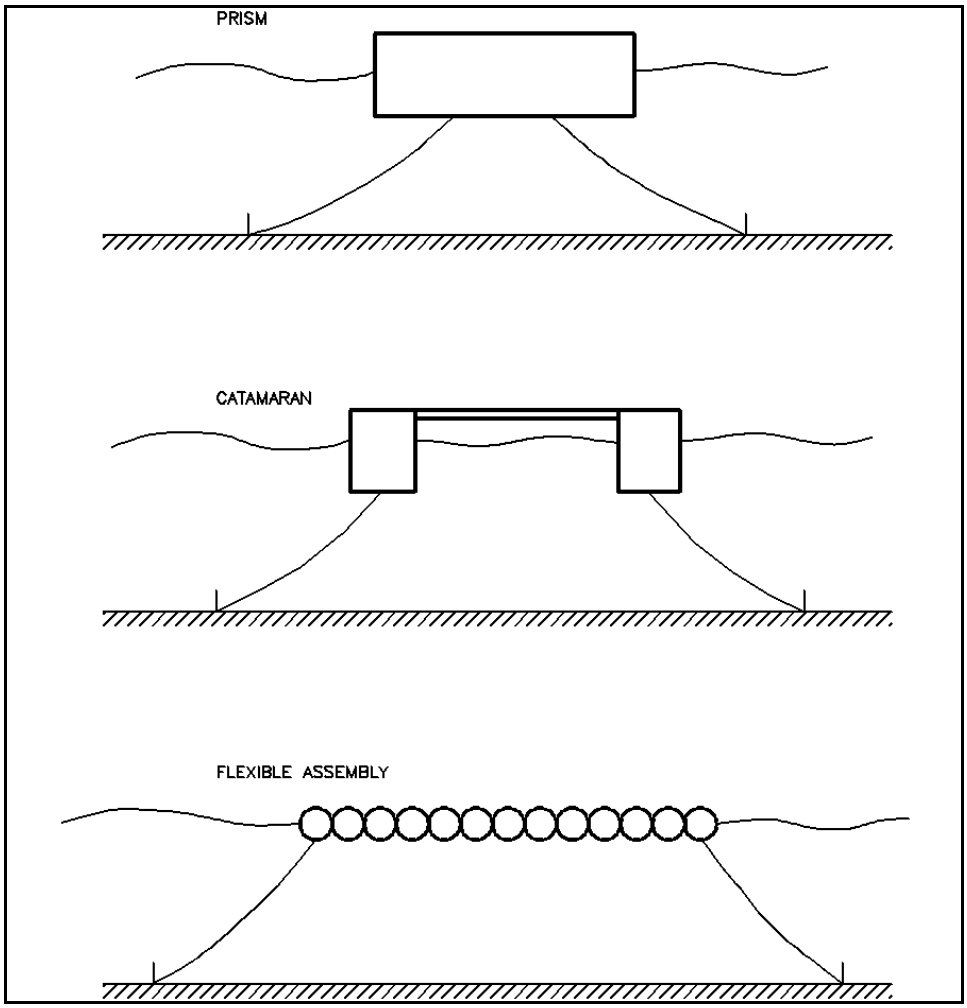

Figure II-7-20. Common types of floating breakwaters

(d) The wave-induced loading on the floating breakwater's mooring/anchor system is also an important design concern. Hales (1981) and Harms et al. (1982) present mooring load data for various types of floating breakwaters. The peak mooring load that develops for a given breakwater geometry and mooring arrangement depends primarily on the incident wave height and increases significantly as the wave height increases; the wave period or length is only of secondary importance in determining the mooring load. If the mooring load cannot be adequately estimated from published information on similar breakwaters, physical model tests may be required to determine these loads for the anticipated design wave conditions.

(5) Wave barriers.

(a) Vertical thin semirigid barriers are used as breakwaters at some harbors, particularly where wave loading is relatively small and wave reflection would not be a problem. For some small-craft harbor installations, the barrier is open at the bottom, which allows water to circulate in and out of the harbor and reduces structure costs (see Gilman and Nottingham (1992) and Lott and Hurtienne (1992). If the incident wave period is relatively short (d/L relatively large), wave action is focused near the surface and wave transmission would be relatively small.

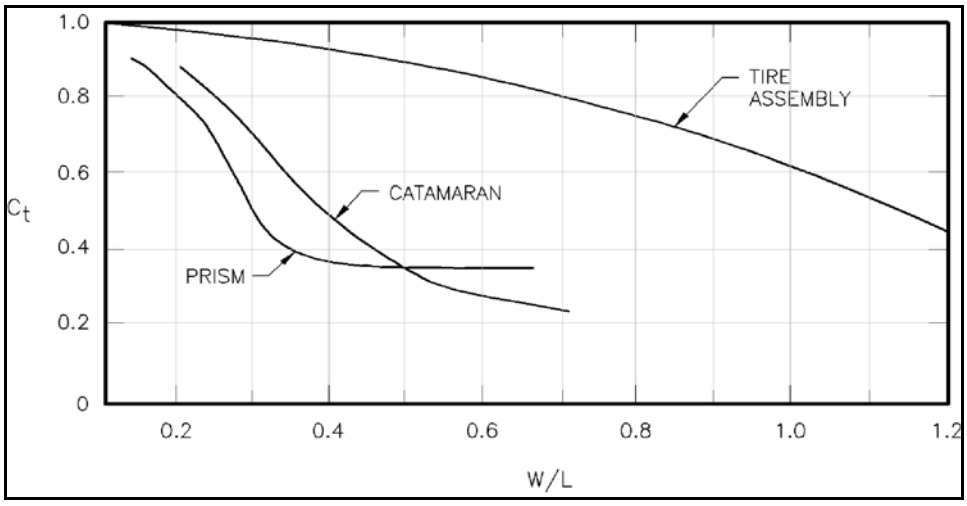

Figure II-7-21. Wave transmission coefficient for selected floating breakwaters (Giles and Sorensen 1979; Hales 1981)

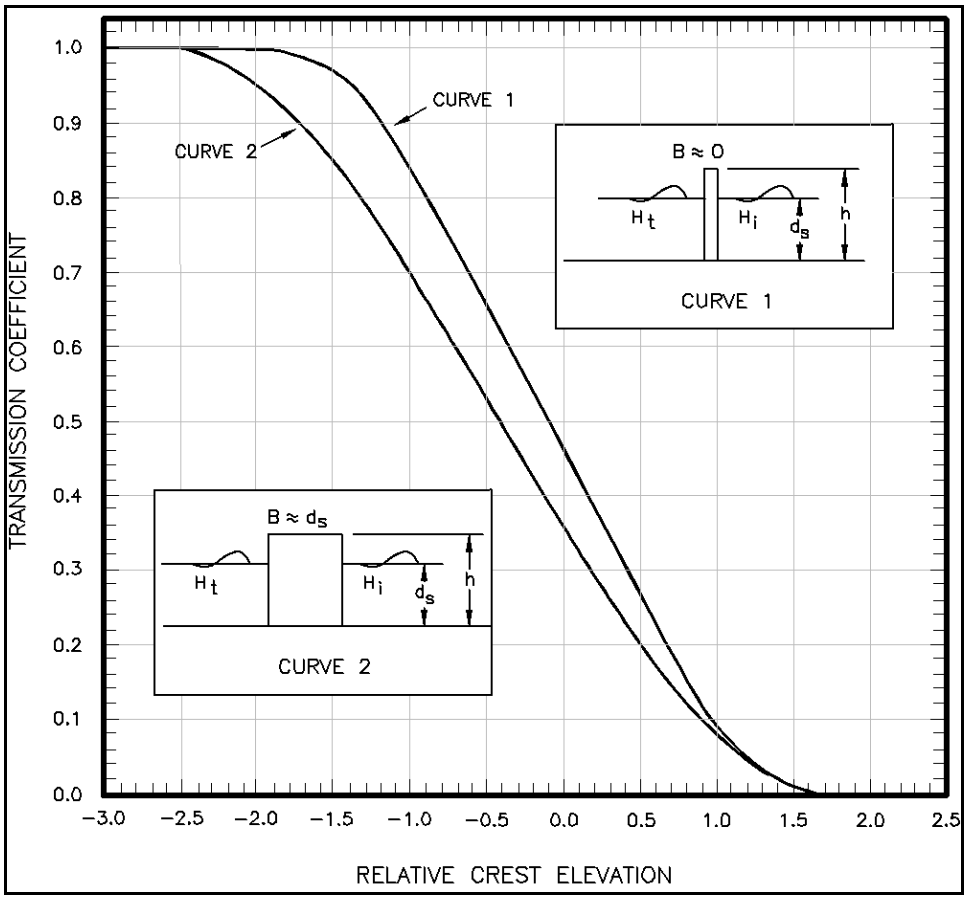

Figure II-7-22. Wave transmission coefficient for vertical wall and vertical thin-wall breakwaters where $0.0157 \le d_s \quad lgt^2 \le 0.0793$ (based on Goda 2000)

(b) Wave transmission coefficients for a thin and a relatively wide vertical barrier that has its crest above or below the water surface were determined from experiments by Goda (1969). The results, which are for monochromatic waves, are shown in Figure II-7-22. Later tests with irregular waves, where the transmission coefficient is defined in terms of the incident and transmitted significant wave heights, showed that Figure II-7-22 can also be used for irregular wave conditions (Goda 2000). As would be expected, a portion of thetransmitted wave energy shifted to higher frequencies so that the transmitted significant wave period was less than the incident significant period.

(c) Wiegel (1960) developed a simple analytical formulation for wave transmission past a thin rigid vertical barrier that does not extend to the bottom. For monochromatic waves and no overtopping, the resulting transmission coefficient is given by

$$C_t = \left[\frac{\frac{2k(d-y)}{\sinh 2kd} + \frac{\sinh 2k(d-y)}{\sinh 2kd}}{1 + \frac{2kd}{\sinh 2kd}} \right]^{\frac{1}{2}} \tag{II-7-5}$$

where d is the water depth, y is the vertical extent of the barrier below the still-water surface, and $k = 2\pi/L$. In developing Equation II-7-5, Wiegel assumed that the portion of the wave power in the water column below the lower edge of the barrier transmits past the barrier. He used the linear wave theory in this analysis and neglected energy dissipation caused by flow separation at the barrier edge. Limited monochromatic wave tests by Wiegel (1960) and irregular wave tests by Gilman and Nottingham (1992) indicate that Equation II-7-5 can be used for preliminary design calculations.

II-7-4. Wave Reflection

a. Definition of reflection.

(1) If there is a change in water depth as a wave propagates forward, a portion of the wave's energy will be reflected. When a wave hits a vertical, impermeable, rigid surface-piercing wall, essentially all of the wave energy will reflect from the wall. On the other hand, when a wave propagates over a small bottom slope, only a very small portion of the energy will be reflected. The degree of wave reflection is defined by the reflection coefficient $C_r = H_r/H_i$ where H_r and H_i are the reflected and incident wave heights, respectively.

(2) Wave energy that enters a harbor must eventually be dissipated. This dissipation primarily occurs at the harbor interior boundaries. Thus, it is necessary to know the reflection coefficients of the interior boundaries to fully define wave conditions inside a harbor. It may also be necessary, because of excessive wave reflection, to decrease the reflection of certain boundary structures in order to keep interior wave agitation at acceptable levels.

(3) The reflection coefficient for a surface-piercing sloped plane will depend on the slope angle, surface roughness, and porosity. It will also depend on the incident wave steepness H_i/L. Consequently, for a given slope roughness and porosity, the wave reflection will depend on a parameter known as the surf similarity number or Iribarren number (Battjes 1974)

$$I_r = \frac{\tan\alpha}{\sqrt{\frac{H_i}{L_o}}} \tag{II-7-6}$$

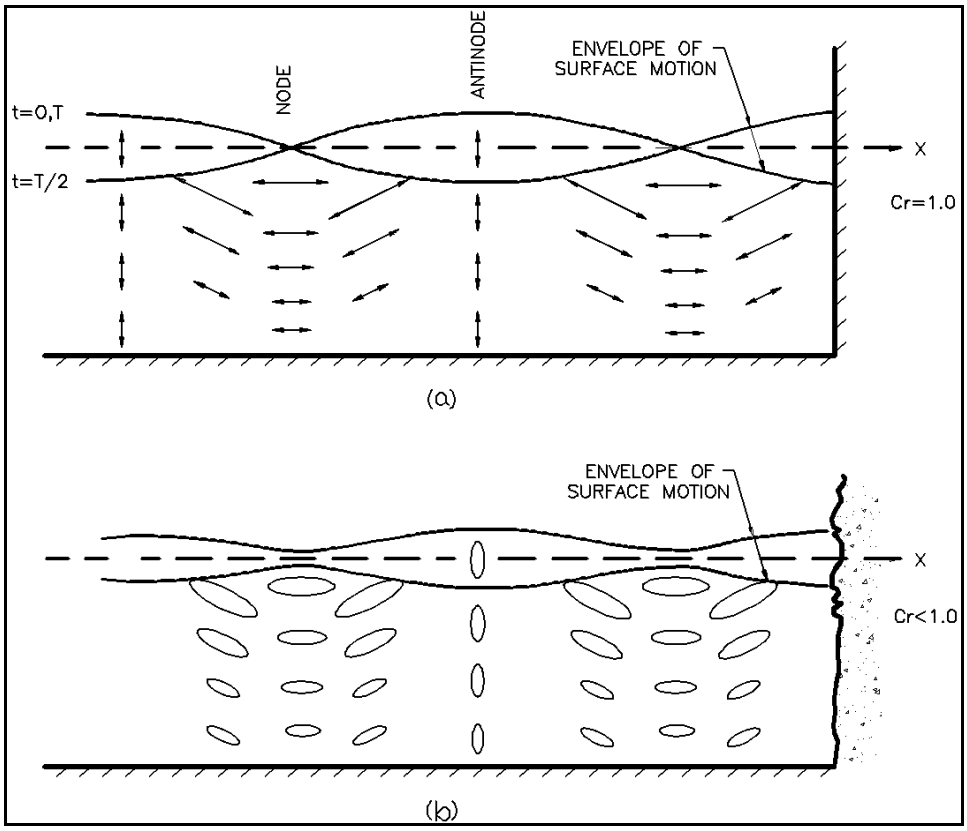

Figure II-7-23. Complete and partial reflection

where α is the angle the slope forms with the horizontal and L_0 is the length of the incident wave in deep water.

(4) Figure II-7-23a is a profile view of the water surface envelope positions for a wave reflecting from a wall that has a reflection coefficient equal to unity (i.e., $H_i = H_r$). The water surface amplitude is given by

$$N = H_i \cos\frac{2\pi x}{L} \cos\frac{2\pi t}{T} \tag{II-7-7}$$

where L and T are the incident and reflected wave length and period respectively, x is the horizontal ordinate and t is the time elapsed. The figure also shows the water particle paths at key points. At nodal points, water particle motions are horizontal and at antinodes, water particle motions are vertical. At $t = 0$, $T/2$, and T, the water is instantaneously still and all of the wave energy is potential energy. At $t = T/4$ and $3T/4$, the water surface is horizontal and all of the energy is kinetic energy.

(5) When the wall reflection coefficient is less than unity, the water surface envelope positions and particle paths are as depicted in Figure II-7-23b. As the reflection coefficient decreases toward zero, the water surface profile and water particle path changes toward the form of a normal progressive wave.

b. Reflection from structures.

(1) Most of the interior boundaries of many harbors are lined with structures such as bulkheads or reveted slopes. Recent laboratory investigations (Seelig and Ahrens 1981; Seelig 1983; Allsop and Hettiarachchi 1988) indicate that the reflection coefficients for most structure forms can be given by the following

$$C_r = \frac{a I_r^2}{b + I_r^2} \tag{II-7-8}$$

where the values of coefficients a and b depend primarily on the structure geometry and to a smaller extent on whether waves are monochromatic or irregular. The Iribarren number employs the structure slope and the wave height at the toe of the structure.

(2) Table II-7-1 presents values for the coefficients a and b collected from the above references.

Table II-7-1
Wave Reflection Equation Coefficient Values Structure

Structure	a	b
Plane slope-monochromatic waves	1.0	5.5
Plane slope-irregular waves	1.1	5.7
Rubble-mound breakwaters[1]	0.6	6.6
Dolos-armored breakwaters - monochromatic waves	0.56	10.0
Tetrapod-armored breakwaters - irregular waves	0.48	9.6

[1]This is an average conservative value. Seelig and Ahrens (1981) recommend a range of values for *a* and *b* that depend on the number of stone layers, the relative water depth (*d*/*L*), and the ratio of incident wave height to breaker height.

EXAMPLE PROBLEM II-7-4

FIND:

The height of the reflected wave.

GIVEN:

A wave in deep water has a height of 1.8 m and a period of 6 sec. It propagates toward shore without refracting or diffracting to reflect from a rubble-mound breakwater located in water 5 m deep. The breakwater front slope is 1:1.75 (29.7 deg).

SOLUTION:

From linear wave theory shoaling calculations (Part II-1) the wave height at the structure would be 1.70 m (this is H_i). From the linear wave theory, the deepwater wave length is $L_0 = 56.2$ m. Then, from Equation II-7-6, the Iribarren number is

$$I_r = \frac{\tan 29.7^o}{\sqrt{1.70/56.2}} = 3.28$$

For the coefficient values $a = 0.6$ and $b = 6.6$ (from Table II-7-1), Equation II-7-8 yields

$$C_r = \frac{0.6\,(3.28)^2}{6.6 + (3.28)^2} = 0.37$$

Thus, the reflected wave height $H_r = C_r H_i = 0.37(1.70) = 0.63$ m.

(3) Note that Equation II-7-8 indicates that C_r approaches the value of a at higher values of the Iribarren number. Thus, the highest reflection coefficients for stone and concrete unit armored structures are around 0.5. As expected, vertical plane slopes (infinite Iribarren number) would have a reflection coefficient near unity. For typical rigid vertical bulkheads, owing to the irregularity of the facing surface, a value of $C_r = 0.9$ might be used.

c. Reflection from beaches.

(1) When the reflecting slope becomes very flat, the incident wave will break on the slope, causing an increase in energy dissipation and commensurate decrease in the reflection coefficient. Thus, beaches are generally very efficient wave absorbers, particularly for shorter period wind-generated waves. An added complexity is that as the incident wave conditions change, the beach profile geometry will change, in turn changing the reflection coefficient somewhat. Laboratory measurements of wave reflection from beaches suffer from scale effects in trying to replicate the prototype beach profile, surface roughness, and porosity. Also, it is harder to select a beach slope angle for the Iribarren number owing to the complexity of beach profiles. Thus, data plots follow the form of Equation II-7-8, but with significant scatter in the data points. Seelig and Ahrens (1981) suggest that $a = 0.5$ and $b = 5.5$ be used for beaches. Since the slope angles are small, the Iribarren number will be relatively small, yielding relatively low reflection coefficients.

(2) An interesting phenomenon (known as Bragg reflections after a similar phenomenon in optics) occurs when the shallow nearshore seabed has uniformly spaced bottom undulations. A resonance develops between the incident surface waves of certain periods and the bottom undulations, causing a reflection of a portion of the incident wave energy (see Davies and Heathershaw (1984), Mei (1985), Kirby (1987)). Resonance and reflection are maximum for that portion of the incident wave spectrum having a wavelength that is twice the length of the bottom undulations. There is an approximately linear increase in the reflection coefficient with the increase in the number of bottom undulations. Reflection also increases if the amplitude of the bottom undulations increases or the water depth over the undulations decreases. For appropriate undulation geometries and water depths, reflection coefficients in excess of 0.5 are possible.

(3) It has been suggested (Mei 1985) that Bragg reflections that develop on a nearshore bar system will set up a standing wave pattern seaward of the bar system which, in turn, causes the bar system to extend in the seaward direction. Theoretical, laboratory, and field studies indicate that it is possible to build a series of shore-parallel submerged bars tuned to the dominant incoming wave periods, that will act as a shore protection device. The feasibility of building these bar systems and their economics need to be studied further.

d. Reflection patterns in harbors.

(1) Figure II-7-24 depicts the plan view of a wave crest approaching and reflecting from a barrier that has a reflection coefficient C_r. The incident wave crest is curved owing to refraction and possibly to diffraction. The actual bottom contours in front of the barrier are as shown. The reflected wave crest pattern can be constructed by:

(a) Constructing imaginary mirror image hydrography on the other side of the barrier.

(b) Constructing the wave crest pattern that would develop as the wave propagates over this imaginary hydrography (this would involve the use of refraction and diffraction analyses as described in previous sections).

(c) Constructing the mirror image of the imaginary wave crest pattern to define the real reflected wave.

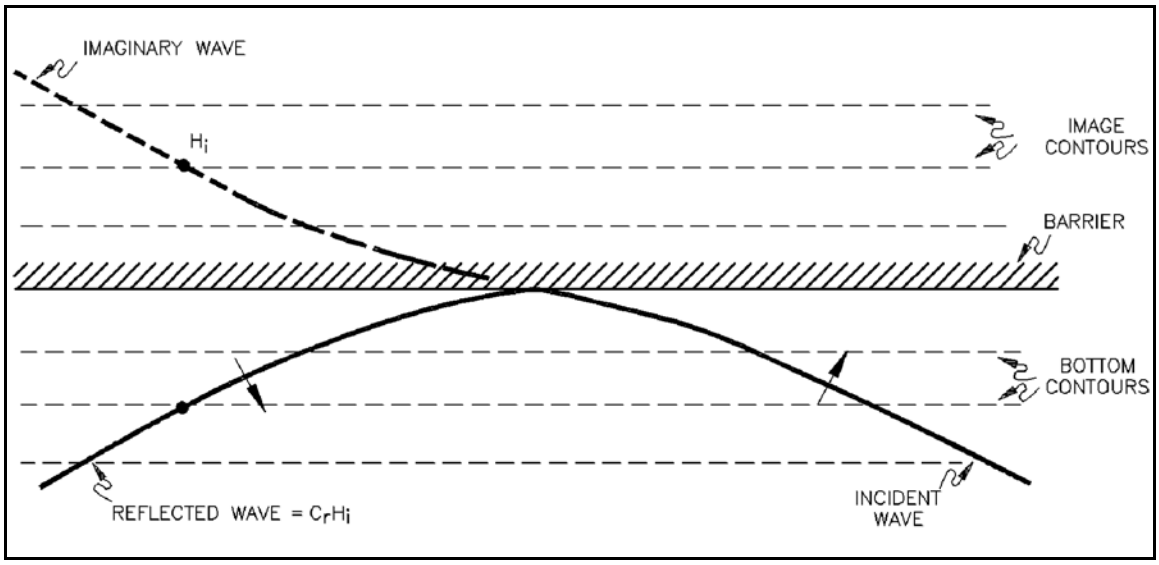

Figure II-7-24. Reflected wave crest pattern

(2) The reflected wave height at any point would be the height at the corresponding point in the imaginary area multiplied by the reflection coefficient at the point on the barrier where that segment of the wave reflected.

(3) Figure II-7-25 shows a wave diffracting in the lee of a breakwater and then reflecting off a wall ($C_r > 0$). The inner end of the reflected wave then hits a beach where it is effectively dissipated; the outer end of the reflected wave diffracts around the breakwater tip and escapes the harbor. The height the reflected wave would have at point A would equal the diffracted height at A' times the reflection coefficient of the wall. By applying the concepts demonstrated in Figures II-7-24 and II-7-25, one can develop the reflection patterns and resulting wave heights for more complex harbor situations (see Carr (1952) and Ippen (1966)).

e. Reflection problems at harbor entrances.

(1) Generally speaking, wave energy that penetrates a harbor entrance should be dissipated as soon as possible, to prevent its subsequent reflection and propagation further into and about the harbor. A number of mechanisms for doing so are discussed in Bruun (1956, 1989). One mechanism is to construct sections of beach, stone mounds or other specially designed wave dissipating structures having low reflection coefficients at appropriate positions just inside the harbor entrance. Another mechanism is to construct resonance chambers at the entrance that are tuned to the dominant frequencies of the incident wave spectrum to set up oscillations that dissipate the penetrating wave energy. Often the general layout of the harbor can be designed to minimize the amount of wave energy that penetrates through the entrance and reflects and rereflects around the harbor.

(2) When significant wave reflection occurs in the vicinity of a harbor entrance (either inside or outside) the incident and reflected waves cross to form a complex “diamond-shaped” wave pattern. Hsu (1990) presents an extensive discussion of the kinematics of the resulting short-crested waves. This form of wave action can cause navigation difficulties and unusual sediment transport and scour patterns (see Silvester and Hsu (1993)).

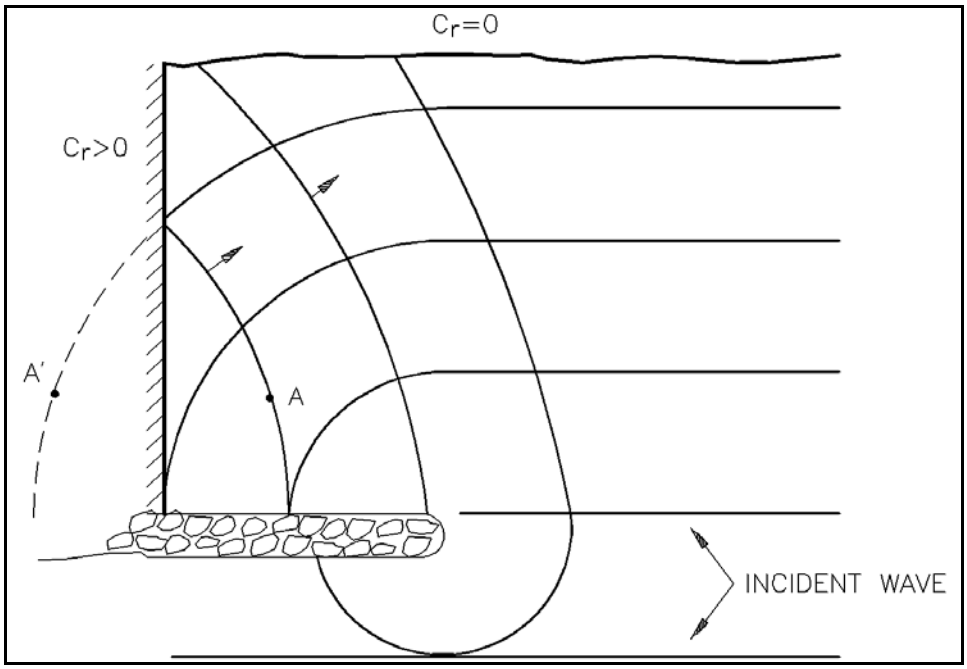

Figure II-7-25. Reflection of a diffracted wave

II-7-5. Harbor Oscillations

a. Introduction.

(1) Harbor oscillations are long-period wave motions that sometimes disrupt harbor activities. The oscillations are standing waves with typical periods between 30 sec and 10 min. Vertical motions are generally small, but horizontal motions can be large. Oscillation characteristics are generally controlled by basin size, shape, and water depth. Oscillations are most damaging when the period coincides with a natural resonant period of the harbor. The phenomenon is also referred to as harbor resonance, surging, seiching, and resonant oscillations.

(2) Harbor oscillations can be a significant problem for inner harbor components and moored vessels within a harbor basin. Resonant periods characteristic of moored vessels often fall into the same range of periods as harbor oscillations. Thus, harbor oscillations can create dangerous mooring conditions including breaking of mooring lines, damage to fender systems, vessel collisions, and delays of loading and unloading operations at port facilities.

(3) Processes and estimation procedures for harbor oscillations are discussed in this section. Discussion of harbor oscillations is generally presented in terms of the characteristics in Table II-7-2.

Table II-7-2
Harbor Oscillation Characteristics

Description	Alternatives	
Basin boundaries	Closed	Open
External forcing	Free	Forced
Dimensionality	2-dimensional	3-dimensional
Basin planform	Simple	Complex

(4) Characteristics are defined as follows:

(a) Closed basin - basin is completely enclosed.

(b) Open basin - basin is semi-enclosed, but open to a larger water body along at least part of one side.

(c) Free oscillations - oscillations that occur without external forcing (although some external forcing was applied earlier to initiate the oscillations).

(d) Forced oscillations - oscillations in response to external forcing.

(e) 2-dimensional - oscillations are independent of one horizontal dimension.

(f) 3-dimensional - oscillations vary in both horizontal dimensions.

(g) Simple - basin planform is a simple geometrical shape, such as a square, rectangle, or circle.

(h) Complex - basin planform is an irregular shape.

(5) A harbor basin generally has several modes of oscillation with corresponding natural resonant frequencies (or periods) and harmonics. Figure II-7-26 illustrates the fundamental, second, and third harmonic modes of oscillation in idealized, perfectly reflecting, closed and open two-dimensional basins.

(6) Following this introduction, the process of resonance is discussed in terms of a more intuitive, but analogous, mechanical system. Closed basins are covered next, mainly in terms of free oscillations and simple shapes. Although they are not closed basins, harbors or parts of harbors can behave much like closed basins under some conditions. The presentation is also applicable to enclosed water bodies such as lakes and reservoirs.

(7) The last parts of the section are devoted to open basins. Open basins are susceptible to oscillations forced across the open boundary. Because of the limited size of harbors, other types of forcing, such as meteorological forcing in the harbor, are generally not considered. Both simple and complex shapes are presented. The final part describes Helmholtz resonance, a very long-period, non-standing wave phenomenon that causes water levels over the entire harbor to oscillate up and down in unison. Practical consequences of harbor oscillation, such as vessel motions, mooring line forces, and fender forces, are not presented in this section. Motions of small boats moored in resonant conditions and possible mitigation measures have been investigated by Raichlen (1968). Comprehensive reviews of harbor oscillations are given by Raichlen and Lee (1992) and Wilson (1972).

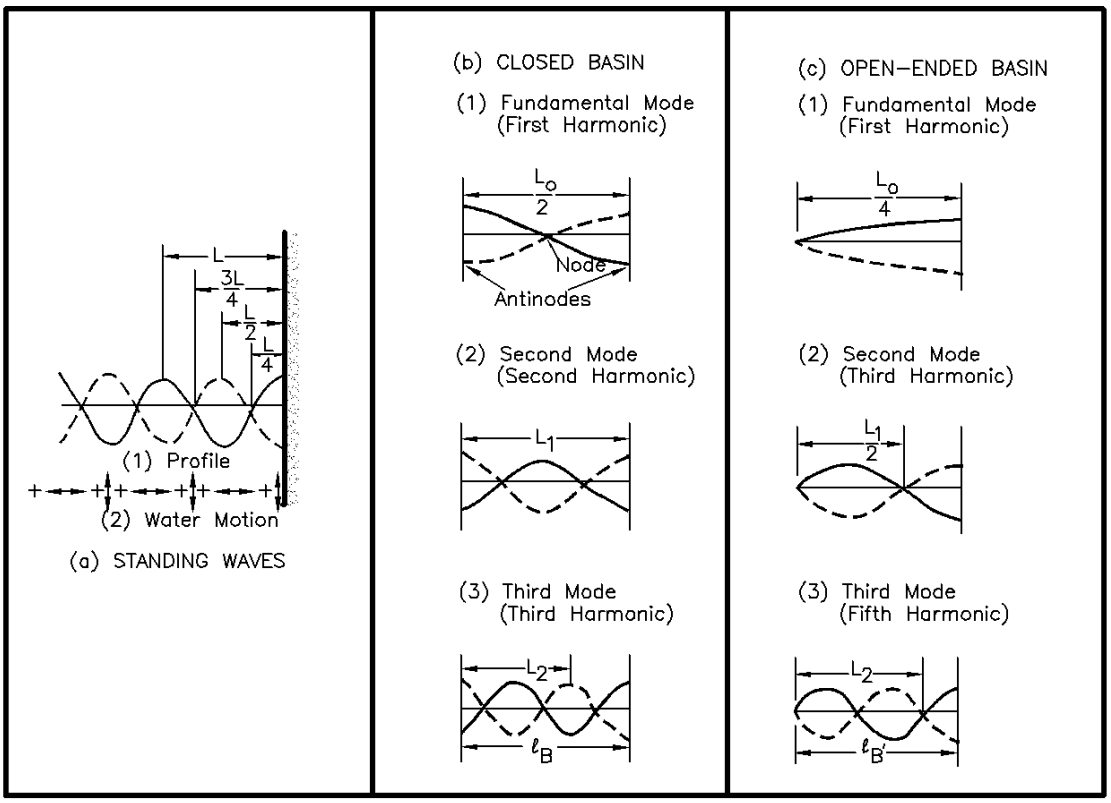

Figure II-7-26. Surface profiles for oscillating waves (Carr 1953)

b. Mechanical analogy.

(1) The basic theory for basin oscillations is similar to that of free and forced oscillations experienced by some mechanical, acoustical, and other fluid systems. Certain systems respond to a disturbance by developing a restoring force that reestablishes equilibrium in the system. A pendulum is a good example of such a system. A free oscillation at the system's natural period or frequency is initiated if the system is carried by inertia beyond the equilibrium condition. If the forces responsible for the initial disturbance are not sustained, free oscillations at the natural frequency will continue, but their amplitude decays exponentially due to friction. The system eventually comes to rest. Forced oscillations can occur at non-natural frequencies if cyclic energy is applied to a system at non-natural frequencies. Continuous excitation at frequencies at or near the natural frequency of a system generally causes an amplified response. The response magnitude depends on the proximity of the excitation to the natural frequency and the frictional characteristics of the system.

(2) The response of a linearly damped, vibrating spring-mass system with one degree of freedom provides a good illustration (Figure II-7-27). Terms are defined as follows: A = amplification factor (ratio of mass displacement to excitation displacement); T = excitation (and response) period; T_n = natural period of the mass-spring system; and ϕ = phase angle by which the mass displacement lags the excitation displacement. The mass responds directly to the excitation if the excitation period is much greater than the natural period of the system; that is, $A = 1$ and $\phi = 0°$ when $T_n/T << 1$. The harbor equivalence to this case is the harbor response to astronomical tides. The mass responds very little and out of phase with the excitation if the excitation period is much shorter than the natural period of the system; that is, $A << 1$ and $\phi \simeq 180°$ when $T_n/T >> 1$. The mass response is amplified and a phase lag develops as the excitation period approaches the natural period of the system. The ratio T_n/T determines the degree of amplification and phase

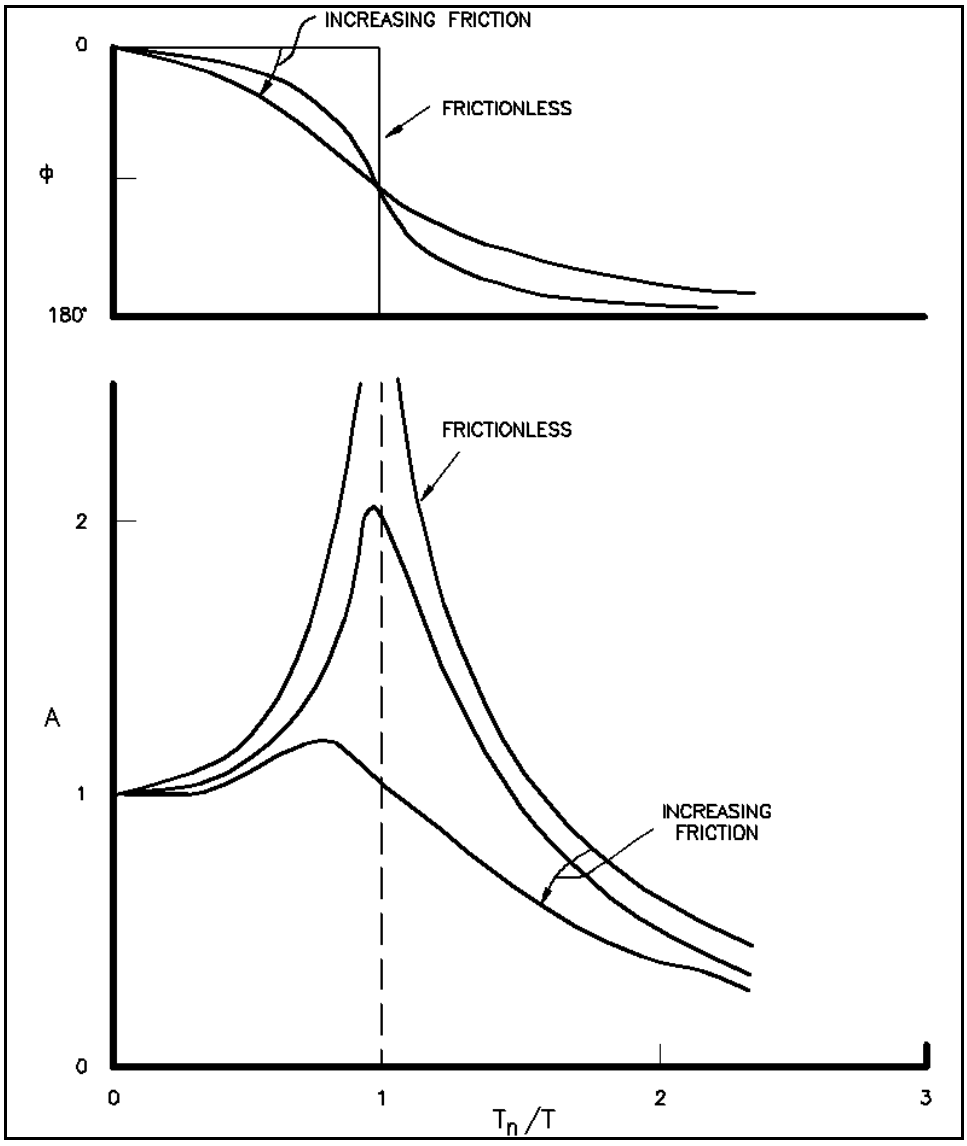

Figure II-7-27. Behavior of an oscillating system with one degree of freedom

lag. The greatest amplification occurs when $T_n/T = 1$ and $\phi = 90$ deg. With a cyclic excitation at period T_n, the amplification factor increases with time until the rate of energy input equals the rate of energy dissipation by friction. When energy input is stopped, the response amplitude decreases exponentially with time as a result of friction. Amplification due to resonance in a mass-spring system and the respective phase relationships are further developed and discussed in Raichlen (1968), Meirovitch (1975), Sorensen (1986), and Wilson (1972).

c. Closed basins.

(1) Enclosed basins can experience oscillations due to a variety of causes. Lake oscillations are usually the result of a sudden change, or a series of intermittent-periodic changes, in atmospheric pressure or wind velocity. Oscillations in canals can be initiated by suddenly adding or subtracting large quantities of water. Harbor oscillations are usually initiated by forcing through the entrance; hence, they deviate from a true closed basin. Local seismic activity can also create oscillations in an enclosed basin.

(2) Basins are generally shallow relative to their length. Hence, basin oscillations involve standing waves in shallow water. The simplest basin geometry is a narrow rectangular basin with vertical sides and uniform depth. The natural free oscillating period for this simple case, assuming water is inviscid and incompressible, is given by

$$T_n = \frac{2\,\ell_B}{n\sqrt{gd}} \qquad \text{Closed basin} \tag{II-7-9}$$

where

T_n = natural free oscillation period

n = number of nodes along the long basin axis (Figure II-7-46)

ℓ_B = basin length along the axis

g = acceleration due to gravity

d = water depth

(3) This equation is often referred to as Merian's formula. The maximum oscillation period T_1 corresponding to the fundamental mode is given by setting $n = 1$ as

$$T_1 = \frac{2\,\ell_B}{\sqrt{gd}} \tag{II-7-10}$$

(4) If the rectangular basin has significant width as well as length (Figure II-7-28), both horizontal dimensions affect the natural period, given by

$$T_{n,m} = \frac{2}{\sqrt{gd}}\left[\left(\frac{n}{\ell_1}\right)^2 + \left(\frac{m}{\ell_2}\right)^2\right]^{\left(-\frac{1}{2}\right)} \qquad \text{Closed basin} \tag{II-7-11}$$

where

$T_{n,m}$ = natural free oscillation period

n,m = number of nodes along the x- and y-axes of basin

ℓ_1, ℓ_2 = basin dimensions along the x- and y-axes

(5) Equation II-7-11 reduces to Equation II-7-9 for the case of a long narrow basin, in which $m = 0$. Further discussion is provided in Raichlen and Lee (1992) and Sorensen (1993). Closed basins of more complex shape require other estimation procedures. Raichlen and Lee (1992) present procedures for a circular basin and approximate solution methods for more arbitrary basin shapes. Defant (1961) outlines a method to determine the possible periods for two-dimensional free oscillations in long narrow lakes of variable width and depth. Locations of nodes and antinodes can also be determined. Usually numerical models are used to properly estimate the response of complex basins.

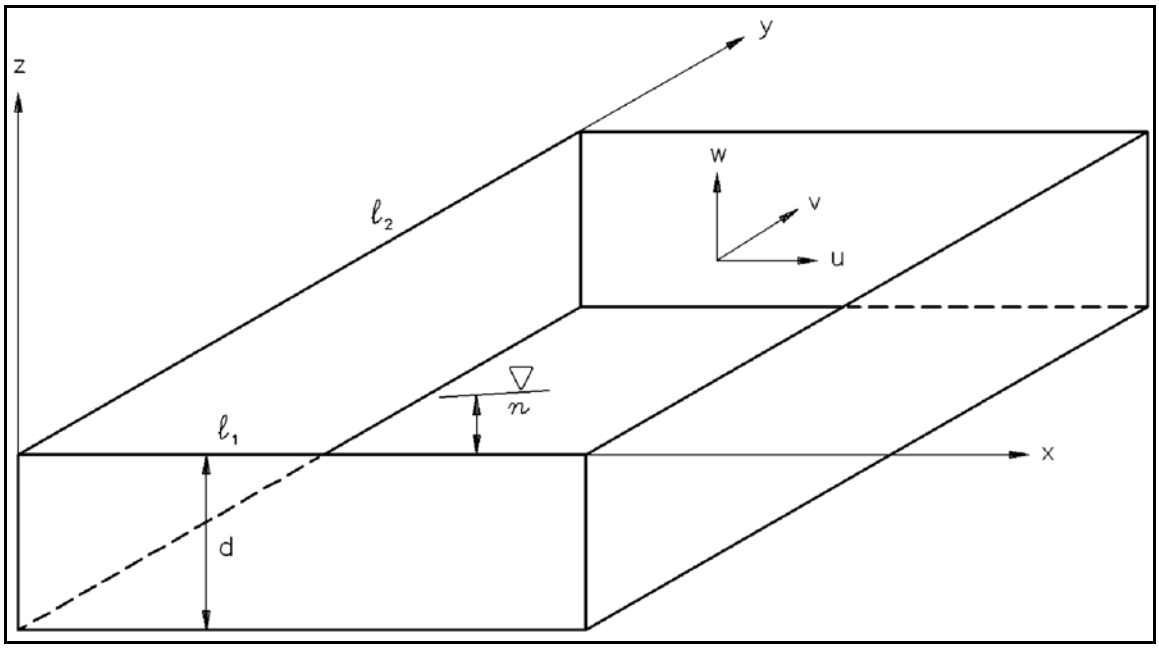

Figure II-7-28. Behavior of an oscillating system with one degree of freedom

(6) Forced oscillations of closed basins can be a concern when the basin is large enough to be affected by moving pressure gradients or strong surface winds, which is generally not true for harbors. Winds can be especially important in large shallow basins, such as Lake Erie. The subject of forced oscillations of closed basins is discussed by Raichlen and Lee (1992).

d. Open basins - general.

(1) Open basins, typically harbors or bays, are most susceptible to oscillations forced across the open boundary. Typical forcing mechanisms include infragravity waves, eddies generated by currents moving past a harbor entrance, and tsunamis (Sorensen 1986). Local seismic activity can also generate oscillations within the basin. Meteorological forces (changes in atmospheric pressure and wind) can initiate oscillations in large bays, but they are not usually a concern over areas the size of a harbor.

(2) The period of a true forced oscillation is the same as the period of the exciting force. However, forced oscillations are usually generated by intermittent external forces, and the period of oscillation is greatly influenced by the basin dimensions and mode of oscillation.

e. Open basins - simple shapes.

(1) In many cases, the geometry of a harbor can be approximated by an idealized, simple shape such as a rectangle or circle. Then the approximate response characteristics can often be determined from guidance based on analytic solutions. Simple harbors are also very helpful for developing an understanding of the general behavior of an open basin.

(2) As with closed basins, the simplest, classical case is a narrow, rectangular basin with uniform depth. The basin has vertical walls on three sides and is fully open at one end. The fundamental mode of resonant oscillation occurs when there is one-quarter of a wave in the basin (Figure II-7-26). The general expression for the free oscillation period in this case is

$$T_n = \frac{4\,\ell_B}{(1 + 2n)\sqrt{gd}} \qquad \text{Open basin} \tag{II-7-12}$$

(3) The number of nodes in the basin n does not include the node at the entrance. The period for the fundamental mode ($n = 0$) is

$$T_0 = \frac{4\,\ell_B}{\sqrt{gd}} \tag{II-7-13}$$

(4) Maximum horizontal velocities and particle excursions in a standing wave occur at the nodes. Thus there is potential for troublesome harbor conditions in the vicinity of nodes. Some additional useful relationships for standing waves are as follows (Figure II-7-29) (see Sorensen (1986) for details)

$$V_{max} = \frac{H}{2}\sqrt{\frac{g}{d}} \tag{II-7-14}$$

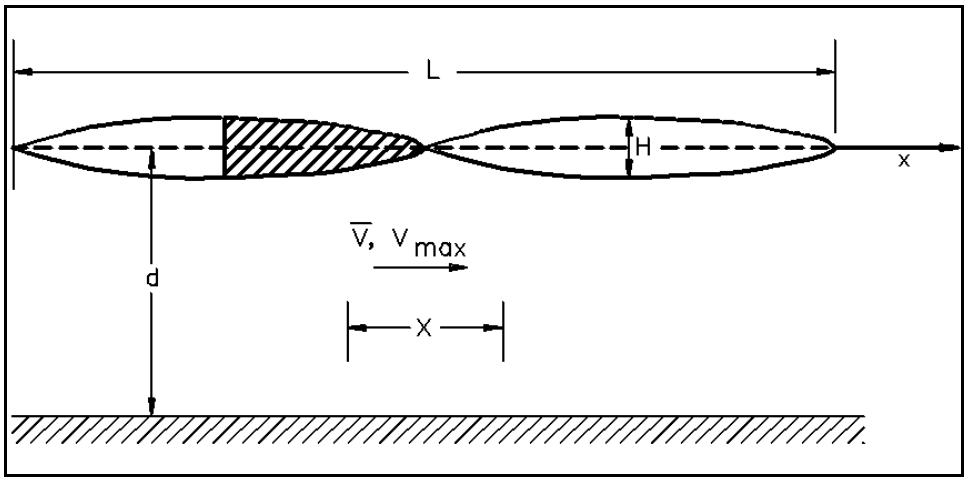

Figure II-7-29. Motions in a standing wave

where

V_{max} = maximum horizontal velocity at a node

H = standing wave height

$$X = \frac{H\,T_n}{2\pi}\sqrt{\frac{g}{d}} \tag{II-7-15}$$

where X = maximum horizontal particle excursion at a node

$$\bar{V} = \frac{H\,L}{\pi\,d\,T_n} \tag{II-7-16}$$

where $\bar{V}$ = average horizontal velocity at a node

(5) For example, when H = 1 ft, T_1 = 200 sec, and d = 30 ft, the maximum horizontal velocity and particle excursion are V_{max} = 0.5 ft/sec and X = 33 ft.

(6) The resonant response of the simple rectangular harbor, presented by Ippen and Goda (1963) in terms of the amplification factor A (assuming no viscous dissipation) and the relative harbor length $k\ell$, where $k = 2\pi/L$, illustrates other important aspects of harbor oscillation. The amplification factor for harbor oscillations is traditionally defined as the ratio of wave height along the back wall of the harbor to standing wave height along a straight coastline (which is twice the incident wave height). The response curve for a long, narrow harbor is given in Figure II-7-30. The left portion of the curve resembles that for the mechanical analogy in Figure II-7-26. Resonant peaks for higher order modes are also shown. The three curves correspond to a fully open harbor and two partially open harbors with different degrees of closure. The $k\ell$ value at resonance decreases as the relative opening width decreases. It is bounded by the value for a closed basin, also shown in the figure. Amplification factors for the inviscid model are upper bounds on those experienced in a real harbor. Because amplification factor decreases at each successive higher order mode, simple analysis methods often focus only on the lowest order modes.

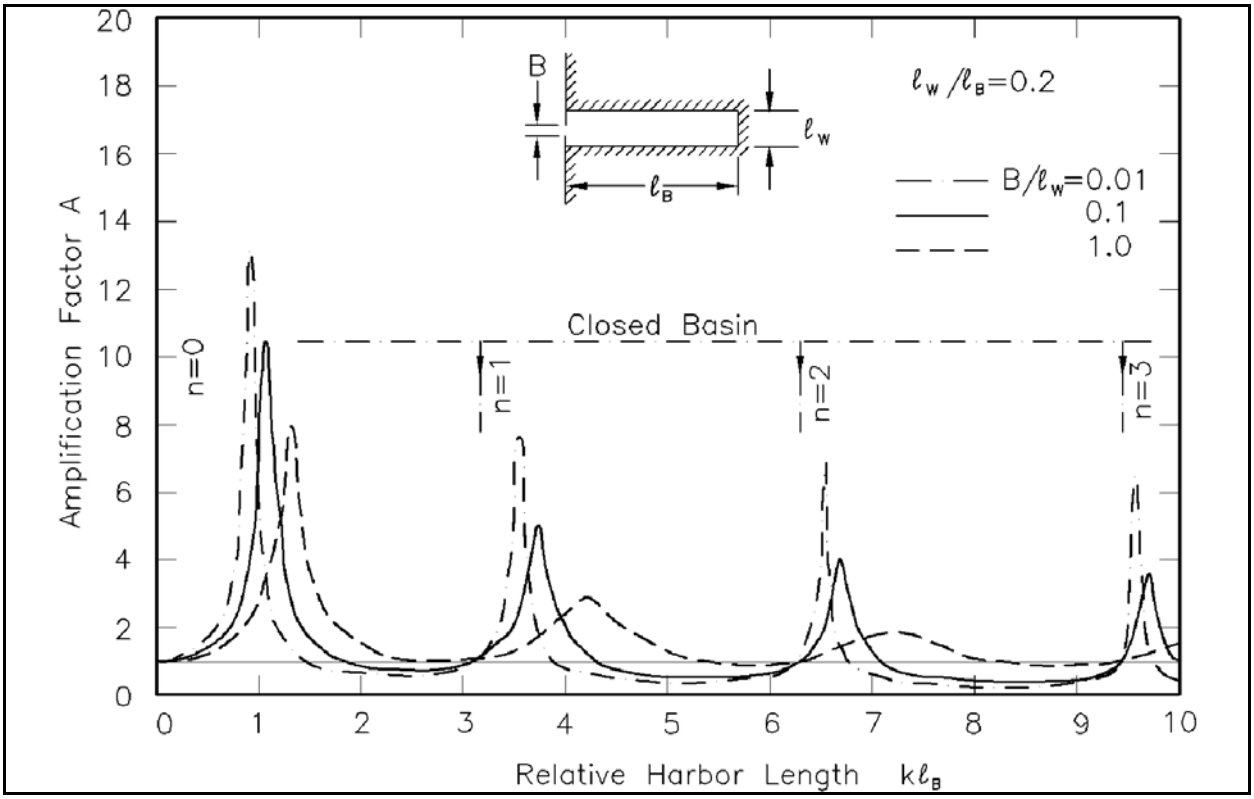

Figure II-7-30. Theoretical response curves of symmetrical, narrow, rectangular harbor (Raichlen (1968); after Ippen and Goda (1963))

(7) Practical guidance for assessing the strength and period of the first two resonant modes in a partially enclosed rectangular harbor with a symmetric entrance is given in Figure II-7-31. A wide range of relative harbor widths (aspect ratios, b/ℓ) and relative entrance widths (d/b) is represented. The $k\ell$ values can be converted to resonant periods by

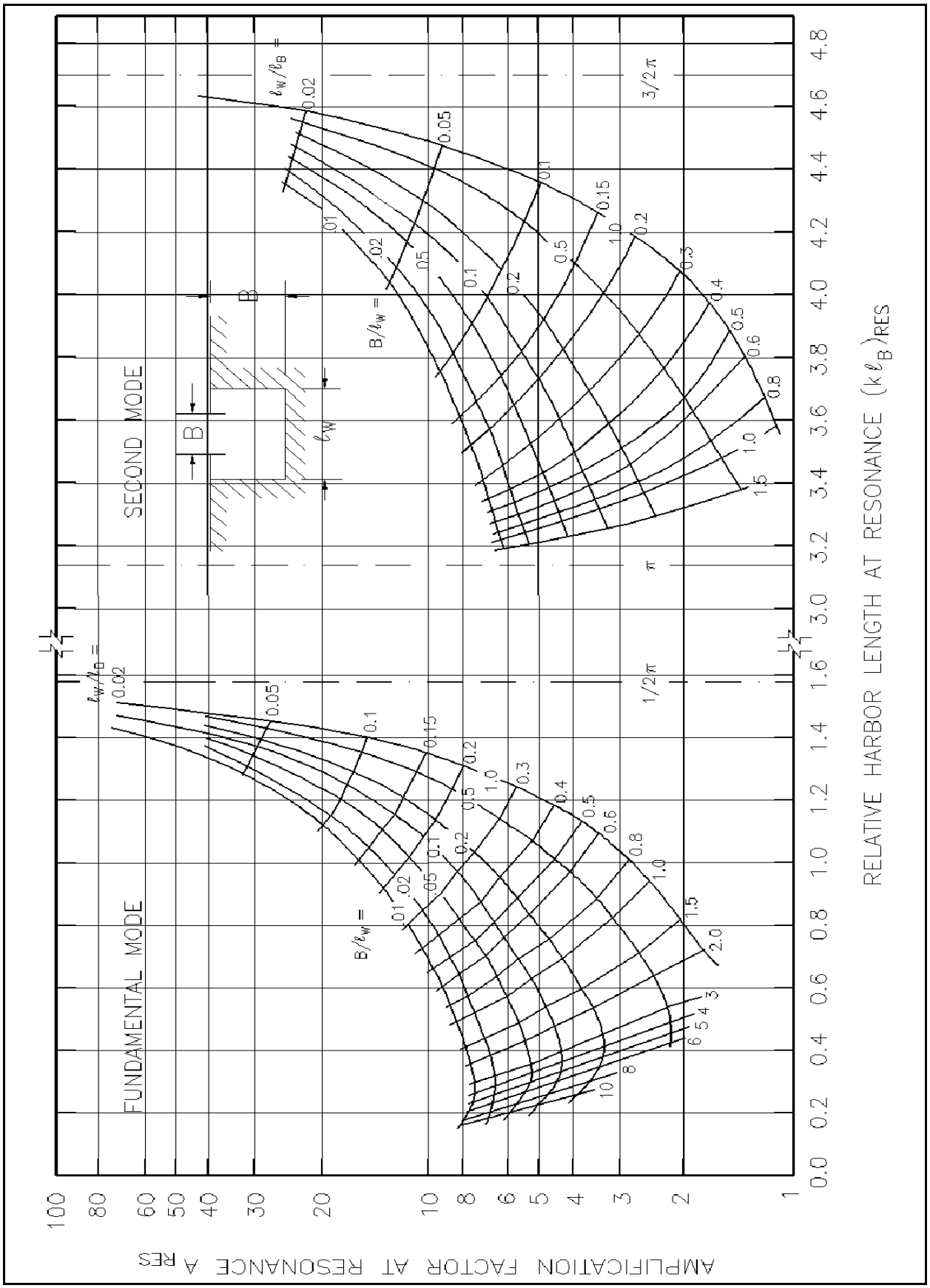

Figure II-7-31. Resonant length and amplification factor of symmetrical rectangular harbor (from Raichlen and Lee (1992); after Ippen and Goda (1963))

$$T = \left(\frac{2\pi \ell}{\sqrt{gd}}\right) \left(\frac{1}{k\ell}\right) \quad \text{(II-7-17)}$$

(8) It is interesting to note that the resonant period increases as the aspect ratio increases, even for the fully open harbor. The change is due to the effect of the confluence of the entrance and the open sea. Resonant periods estimated from Figure II-7-30 generally differ from the simple approximation in Equation II-7-12.

(9) The simple guidance has some important limitations relative to real harbors. Amplification factors are upper bounds, since no frictional losses were modelled. Harbors that are not narrow experience transverse oscillation modes that are not represented in the simple guidance. Harbors with asymmetric entrances experience additional transverse modes of oscillation and possible increases in amplification factor (Ippen and Goda 1963). In addition to introducing new resonant frequencies and modified amplification, transverse oscillations change the locations of nodes, as illustrated in Figure II-7-32 based on numerical model calculations.

(10) Harbor oscillation information is available for some other simple harbor shapes. Circular harbors were investigated by Lee (1969) and reviewed by Raichlen and Lee (1992). Zelt (1986) and Zelt and Raichlen (1990) developed a theory to predict the response of arbitrary shaped harbors with interior sloping boundaries, including runup. The dramatic effect of a sloping rather than flat bottom on the behavior of a rectangular harbor is illustrated in Figure II-7-33. The sloping bottom greatly increases A and greatly reduces $k\ell$ values at resonance. For example, $k\ell$ for the second resonant peak drops from 4.2 for the flat bottom case to 2.6 for the sloping bottom case. The first two resonant modes for six symmetric, fully open configurations are given in Figure II-7-34. The A for the first mode is much more affected by the sloping bottom than by the harbor planform. Details are available in Zelt (1986).

f. Open basins - complex shapes.

(1) Real harbors never precisely match the simple shapes; usually they differ significantly. Complex harbors can be analyzed with physical and numerical models. These modeling tools should be applied even for relatively simple harbor shapes when the study has large economic consequences and accurate results are essential. A combination of physical and numerical modeling is usually preferred for investigating the full range of wave conditions in a harbor (Lillycrop et al. 1993).

(2) Physical models generally represent the shorter-period harbor oscillations more accurately. The harbor and immediately surrounding coastal areas are sculpted in cement in a three-dimensional model basin (Figure II-7-35). Breakwaters and other structures that transmit significant amounts of long-wave energy are properly scaled in the model for size and permeability. Currents can be introduced when needed to represent field conditions. Limitations to physical modeling include cost, no direct simulation of frictional dissipation, and the inherent difficulties in working with long waves in an enclosed basin. Special care is required to properly generate long waves. Once generated, they tend to produce undesirable reflections from basin walls.

(3) Numerical models are most useful for very long-period investigations, initial studies, comparative studies of harbor alternatives, and revisiting harbors documented previously with field and/or physical model data. They are also most useful when unusually large areas and/or very long waves are to be studied. For example, numerical models have been used effectively to select locations for field wave gauges (to avoid nodes) and to identify from many alternatives the few most promising harbor modification plans for fine tuning in physical model tests. Lillycrop et al. (1993) suggested that numerical modeling is preferable to

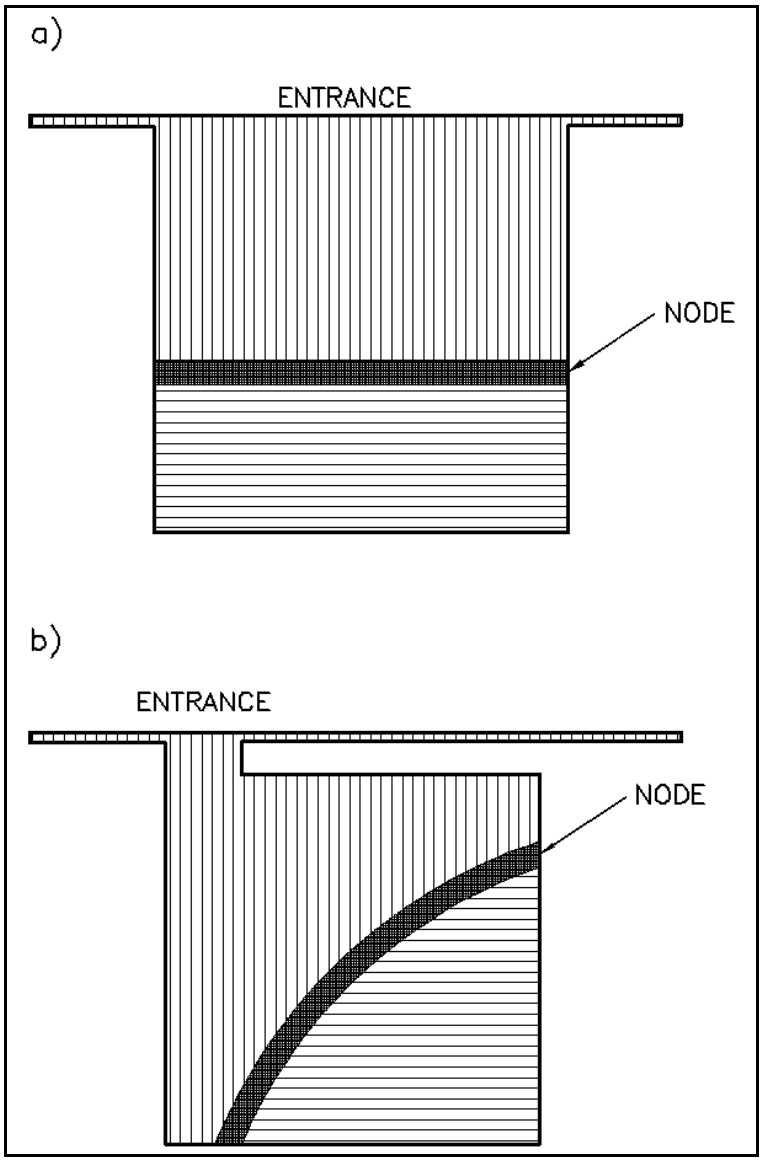

Figure II-7-32. Node locations for a dominant mode of oscillation in a square harbor: a) fully open; b) asymmetric, constricted entrance

physical modeling for periods longer than 400 sec. Both modeling tools can be used effectively for the shorter-period oscillations.

(4) Numerical models can reproduce the geometry and bathymetry of a harbor area reasonably well and estimate harbor response to long waves. Figure II-7-36 is an example numerical model grid. This grid is finer than would normally be required for harbor oscillation studies because it was designed for both wind waves and long waves. Numerical models can be used to generate harbor response curves as in Figure II-7-33 at various points in the harbor. Results for resonance conditions of particular interest can be displayed over the whole harbor to show oscillation patterns. For example, amplification factors and phases calculated with the example grid are presented for five wave periods, corresponding to resonant peaks in the main harbor basin (Figures II-7-37 and II-7-38). Phases are relative to the incident wave. Phase plots are useful because phases in a pure standing wave are constant up to a node and then change 180 deg across the

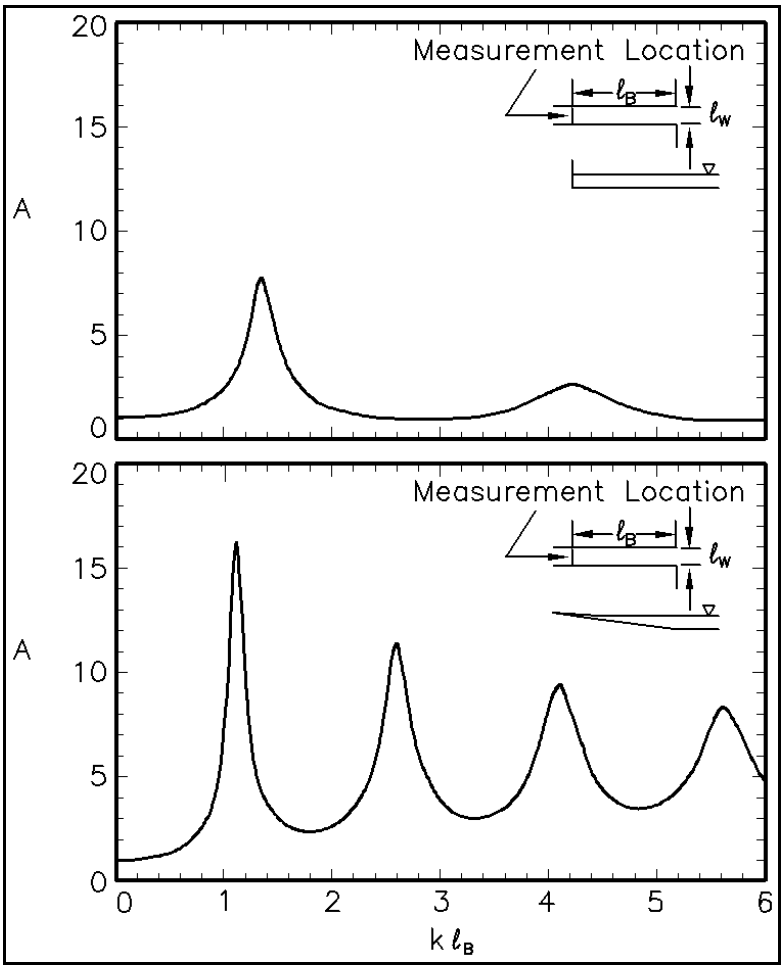

Figure II-7-33. Response curves for rectangular harbor with flat and sloping bottom (Zelt 1986)

node. Thus, phase contour lines cluster together at node locations. Since regions of similar phase, plotted with similar gray shades (or colors on a computer screen), move up and down together, the resonant modes of oscillation can be much more easily visualized. This information about node locations and behavior of resonant modes is quite useful in analyzing harbor oscillations.

(5) Limitations to numerical models relate to approximations in formulating the following items: incident wave conditions, wave evolution during propagation over irregular bathymetry, wave interaction with structures, and harbor boundary features. Numerical model technology is reviewed by Raichlen and Lee (1992) and Abbott and Madsen (1990).

(6) The Corps of Engineers has traditionally used a steady-state, hybrid-element model based on the mild slope equation (Chen 1986; Chen and Houston 1987; Cialone et al. 1991). Variable boundary reflection and bottom friction are included. The seaward boundary is a semicircle outside the harbor entrance. Monochromatic waves are incident along the semicircle boundary. Since the model is linear, results from multiple monochromatic wave runs can be recombined to simulate a spectral response. The model does not account for entrance losses (Thompson, Chen, and Hadley 1993).

	First Resonant Mode		Second Resonant Mode	
Harbor Geometry	$k\ell_B$	A_{RES}	$k\ell_B$	A_{RES}
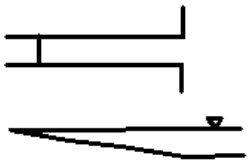	1.089	16.43	2.565	11.45
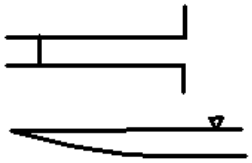	1.229	10.96	3.177	7.61
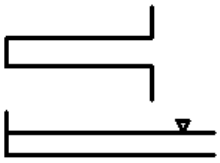	1.315	7.81	4.182	2.68
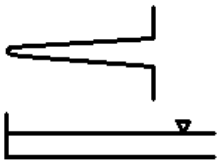	1.696	8.12	4.559	4.32
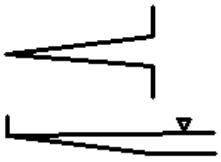	1.757	21.85	3.280	32.18
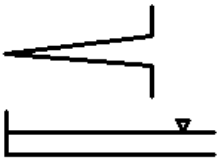	2.050	8.50	4.926	6.19

Figure II-7-34. Resonant response of idealized harbors with different geometry (Zelt 1986)

Figure II-7-35. Photograph of physical model, Barbers Point Harbor, HI (Briggs et al. 1994)

g. Open basins - Helmholtz resonance.

(1) A harbor basin open to the sea through an inlet can resonate in a mode referred to as the Helmholtz or grave mode (Sorensen 1986b). This very long period mode appears to be particularly significant for harbors responding to tsunami energy and for several harbors on the Great Lakes that respond to long-wave energy spectra generated by storms (Miles 1974; Sorensen 1986; Sorensen and Seelig 1976).

(2) Water motion characterizing the Helmholtz mode is like that of a Helmholtz resonator in acoustics. It is analogous to the spring-mass system with one degree of freedom, discussed earlier in this section, where the spring is similar to the basin water surface and the mass represents water in the inlet channel. During Helmholtz resonance, the basin water surface uniformly rises and falls while the inlet channel water oscillates in and out. The period of this mode is greater than the fundamental mode. The resonant period is given by (Carrier et al. 1971).

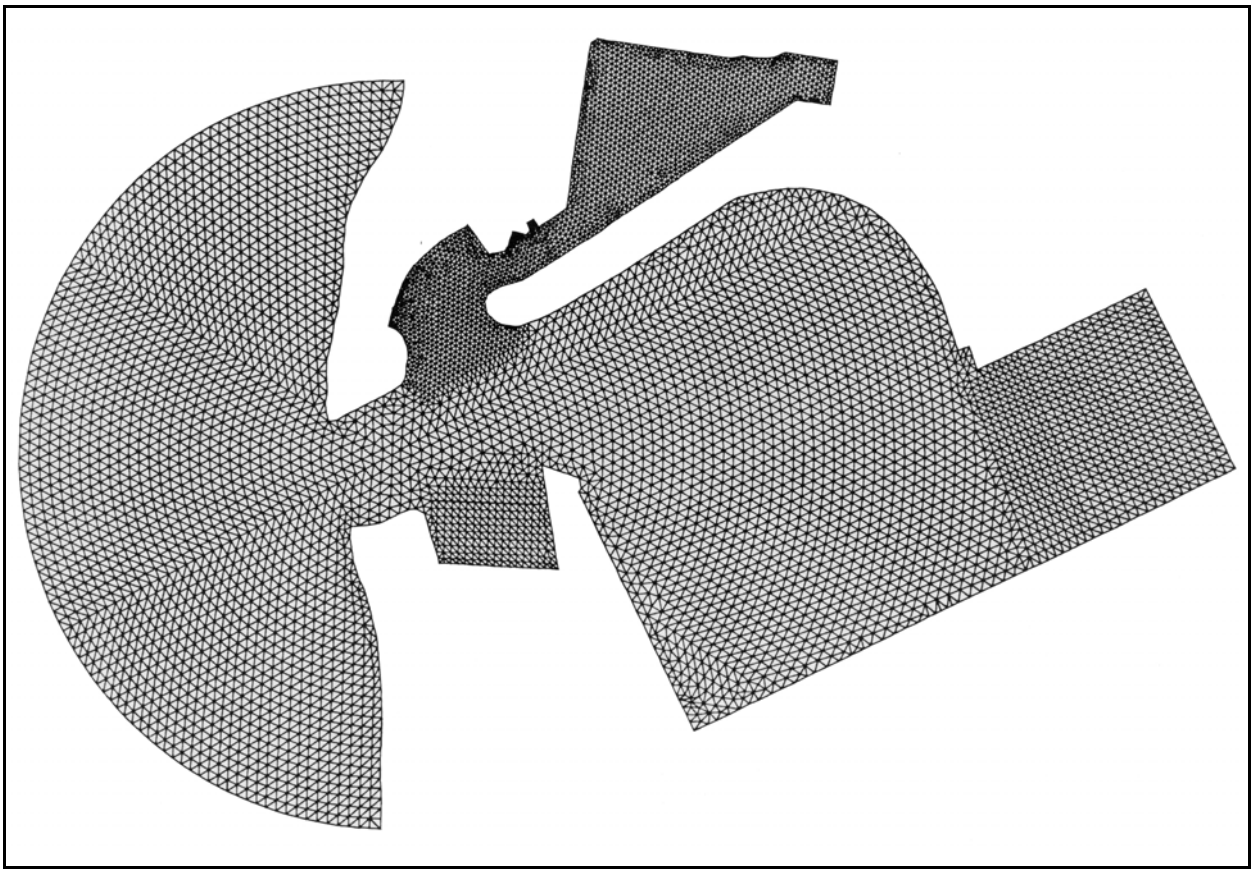

Figure II-7-36. Numerical model grid for Barbers Point Harbor, HI (Briggs et al. 1994)

$$T_H = 2\pi \sqrt{\frac{(\ell_c + \ell'_c)\, A_b}{g A_c}} \tag{II-7-18}$$

where

T_H = resonant period for Helmholtz mode

ℓ_c = channel length

ℓ'_c = additional length to account for mass outside each end of the channel

A_b = basin surface area

A_c = channel cross-sectional area

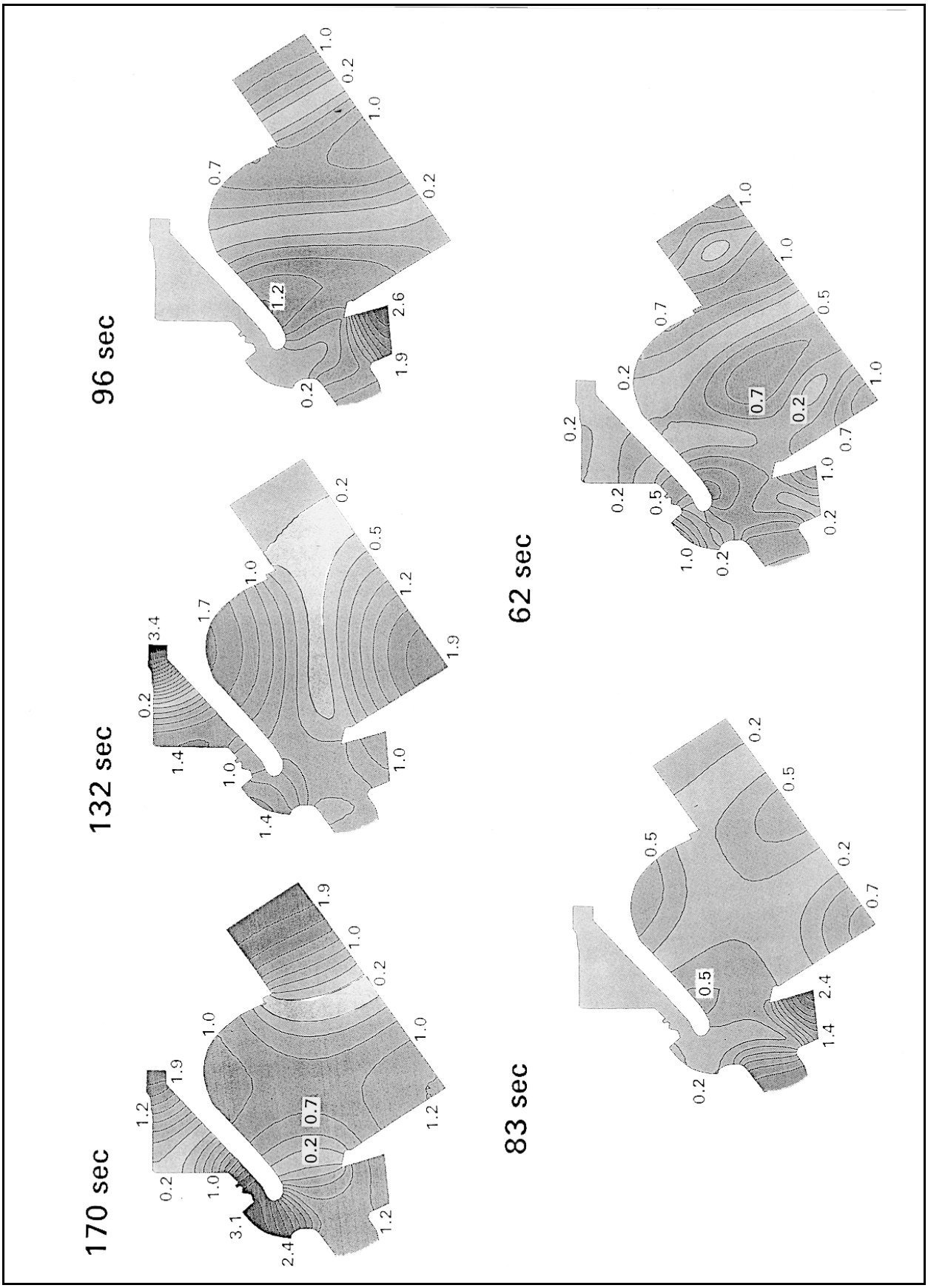

Figure II-7-37. Amplification factors for five resonant periods, Barbers Point Harbor, HI (Briggs et al. 1994)

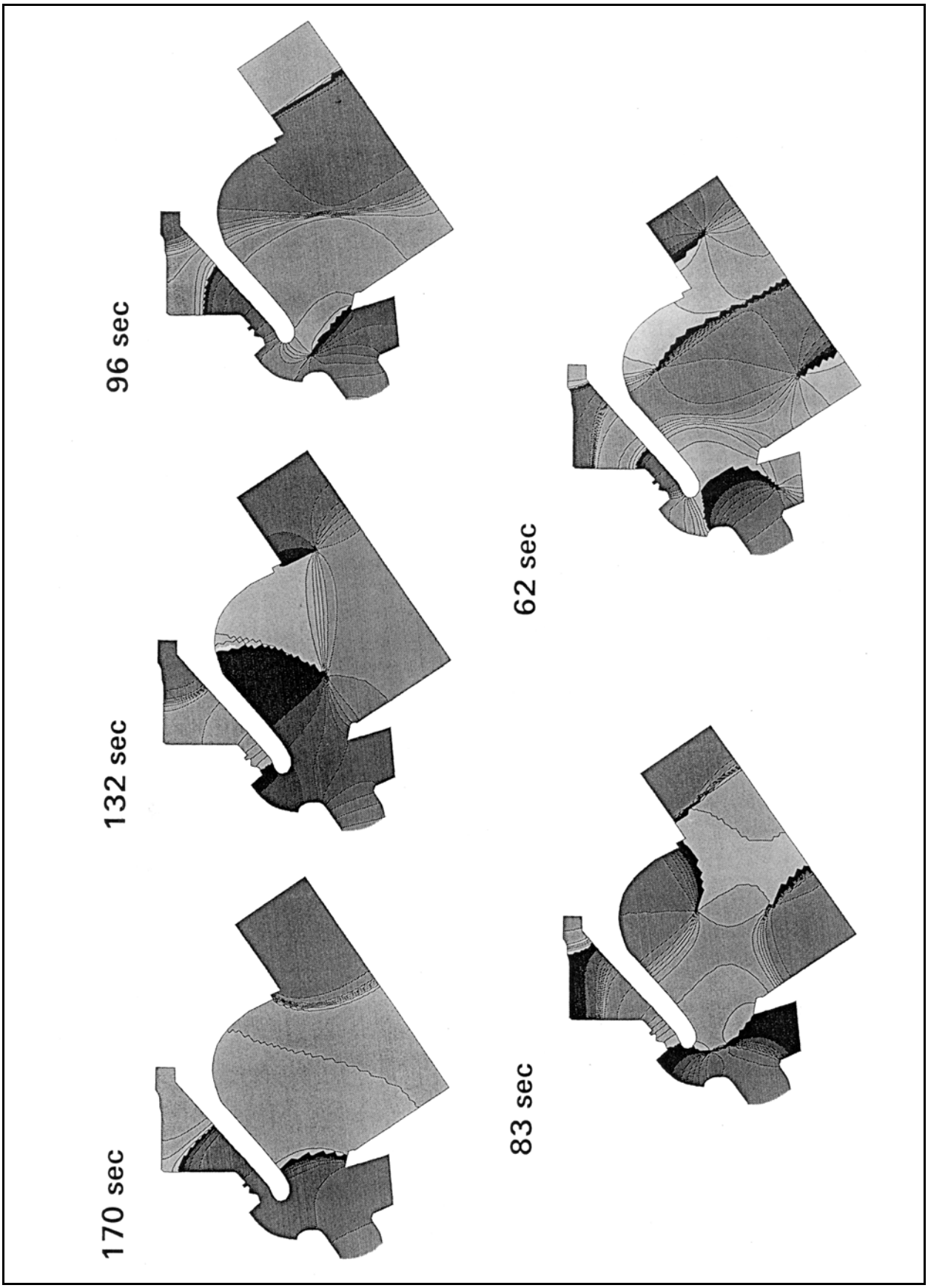

Figure II-7-38. Phases for five resonant periods, Barbers Point Harbor, HI (Briggs et al. 1994)

(3) The added length is given by (Sorensen 1986, adopted from Miles (1948))

$$\ell'_c = \frac{-W}{\pi} \ln\left(\frac{\pi W}{\sqrt{g d_c}\, T_H}\right) \quad \text{(II-7-19)}$$

where

W = channel width

d_c = channel depth

II-7-6. Flushing/Circulation

a. Statement of importance.

(1) An important aspect of harbor design is the water circulation that occurs within the harbor and between the harbor and the surrounding water body. Water exchange with the surrounding water body will produce a flushing action in the harbor. Flushing is important to reduce the level of chemical, biological, and floating solids pollution in the harbor. Typically, a criterion such as the exchange of X percent of the water in the harbor within a certain time period or, alternatively, exchange of Y percent of the water in the harbor each tidal cycle might be set as a design goal.

(2) Circulation patterns within a harbor should eliminate areas of stagnant water where pollution levels will rise and fine sediment deposition may occur. This can occur, for example, in closed-end channels such as pier slips and residential canals. Strong circulation is desired as long as adverse high-velocity currents are not generated.

(3) Natural harbor circulation and flushing should be optimized. This can be accomplished by:

(a) Siting the harbor to make use of ambient currents that will pass the harbor entrance.

(b) Considering water circulation when determining the number, size, and placement of harbor entrances.

(c) Establishing the harbor planform and internal structure locations so that circulation is optimized and potential pollution sources are located in areas of strong water circulation.

(d) Employing (where incident wave action allows) harbor protective structures such as floating breakwaters and vertical barriers with bottom openings that permit flow into and out of the harbor.

(e) Installing culvert pipes through more massive harbor protective structures. This natural flushing can be supplemented by installing pumping systems that bring exterior water into dead areas of the harbor or remove polluted water from these areas.

b. Flushing/circulation processes.

(1) Tidal action.

(a) As the tide rises, ambient water will enter a harbor and mix with the water in the harbor. On the subsequent falling tide, a portion of this ambient/harbor mixture will leave the harbor. The net result is the exchange of some harbor water with water from outside the harbor. The efficiency of this exchange depends primarily on two factors. One factor is the ratio of the volume of water that enters on one tidal cycle (the tidal prism) to the total volume of water in the harbor. This ratio, in turn, will depend on the tide range, the

hydraulic efficiency of the harbor entrance, and the water depths in the harbor. Generally, the larger the value of this ratio, the more exchange that will occur. The other factor is the momentum of the incoming jet of water on the rising tide, and the consequent amount of penetration of this jet and its resulting angular momentum as it establishes a rotating gyre inside the harbor. The strength of this jet is related to the amount of flushing that will occur and the strength of the tidally induced circulation in the harbor.

(b) The most commonly used factor for defining the effectiveness of tidally induced harbor flushing is the average per cycle exchange coefficient E (Nece and Richey 1975) given by

$$E = 1 - \left(\frac{C_i}{C_o} \right)^{\frac{1}{i}} \tag{II-7-20}$$

where C_o is the initial concentration of some substance in the harbor water and C_i is the concentration of this substance after i tidal cycles. E may be defined at a point in the harbor by using concentration values at that point or may be defined for the entire harbor by using spatially average concentration values for the entire harbor. E is the fraction of harbor water removed each tidal cycle. Equation II-7-20 assumes essentially repetitive identical tides and no further addition of the marker substance to the harbor.

(c) As an example of the use of the exchange coefficient, consider Figure II-7-39, which is modified from Falconer (1980) and based on physical and numerical model results. Figure II-7-39 shows the spatial average exchange coefficient for a rectangular harbor having the dimensions L and B shown in the insert. Note where the harbor entrance is located. E has a peak value of about 0.5 when L/B is near unity (i.e. a square harbor). For L/B values outside the range of 0.3 to 3, the flushing of the harbor is much less effective. The tidal prism ratio (TPR), defined as the tidal prism divided by the total harbor volume at high tide, was 0.4 for the results shown in Figure II-7-39.

(d) Another factor used to define the amount of flushing is the "flushing efficiency," defined as the exchange coefficient divided by the tidal prism ratio (i.e. E/TPR) expressed as a percentage (Nece, Falconer, and Tsutumi 1976). Flushing efficiency compares the actual water exchange in one cycle with the volume of exchange that would occur if the incoming tidal prism completely mixed with the harbor water on each cycle. Table II-7-3 shows some results for five small-boat harbors in the state of Washington. These results are based on model tests (Nece, Smith, and Richey 1980).

(e) Note that the exchange coefficients are all around 0.2, which is below the value for the more idealized rectangular harbors (Figure II-7-39). And, for relatively consistent exchange coefficients, the flushing efficiency showed a much greater range of values. For the rectangular harbor in Figure II-7-39 where the TPR is 0.4, the flushing efficiency would vary from 0 up to about 125 percent. The desirable exchange coefficient or flushing efficiency for a given harbor would depend on the level of pollution in the harbor versus the desired harbor water quality. Although higher exchange coefficients and flushing efficiencies generally indicate better harbor flushing by tidal action, there may still be small pockets of stagnant water in a generally well-flushed harbor.

(2) Wind effects.

(a) Wind acting on the water surface will generate a surface current that, in water depths typically found in harbors, will essentially be in the direction of the wind. Owing to Coriolis effects, the current will be a few degrees to the right of the wind in the Northern Hemisphere; e.g., see Neumann and Pierson (1966) or Bowden (1983). If the distance over which the wind blows and the wind duration are sufficient, the surface

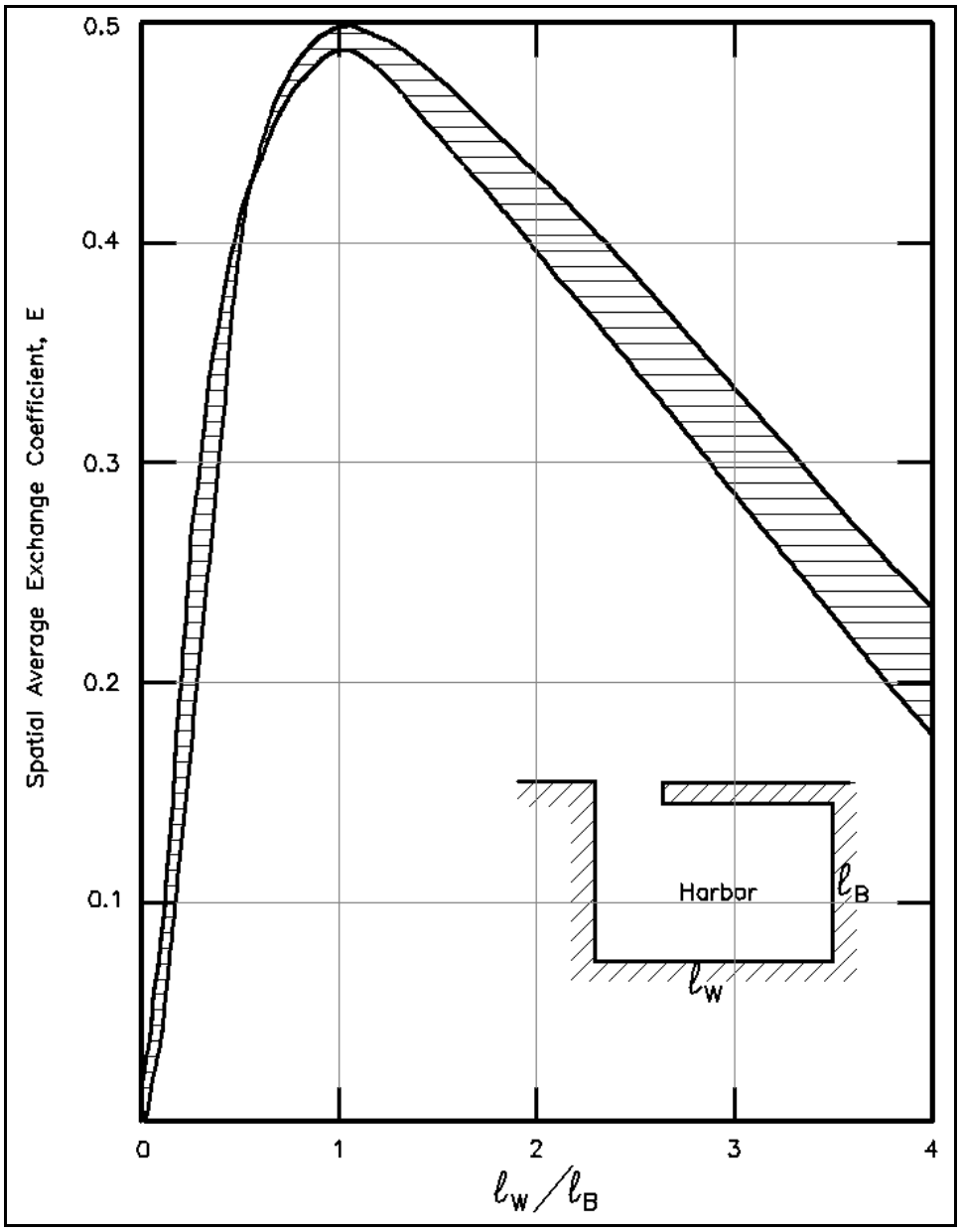

Figure II-7-39. Exchange coefficients - rectangular harbor, TRP = 0.4 (modified from Falconer (1980))

Table II-7-3
Flushing Characteristics of Small-Boat Harbors

Harbor	Tide Range (m)	Exchange Coefficient	Flushing Efficiency (%)
Des Moines	1.07	0.22	123
Edmonds	0.82	0.14	100
Lagoon Point	0.91	0.16	63
Penn Cove	1.22	0.19	75
Lake Crockett	1.83	0.22	78

current will approach a velocity equal to 2 to 3 percent of the wind speed. But, given the lengths of open water found in most harbors, it is likely that the resulting current velocity will be less than this magnitude.

(b) The wind-induced surface current would cause a lateral or bottom return flow to develop, resulting in some circulation in a harbor under sustained winds. The resulting current pattern would be very dependent on the wind direction and the harbor geometry. Some flow in or out of the harbor entrance could develop. Also, the surface current will skim floating materials to the down-wind areas of the harbor. Generally, wind-induced circulation and flushing will be much less effective than circulation and flushing induced by tidal action.

(3) River discharge.

(a) Fresh water may enter a harbor from the land side as surface runoff or as concentrated flow in rivers that enter the harbor. Surface runoff will generally contribute more to the harbor pollution load because of the agricultural or urban pollutants in the water than it will to alleviating pollution by contributing to harbor flushing.

(b) Likewise, the efficacy of river discharge in easing harbor pollution will depend on the quality of the river water. If there are lower chemical and biological pollution loads in the river water than in the harbor, the flushing effect will be positive. But this could be counterbalanced if the river has a suspended silt load that will deposit in the slower moving harbor water. Silt suspension is a particular problem inside sections of the harbor such as pier slips. The silt-laden water may set up a turbidity current that will force bottom water having higher silt concentrations into a dead area, where it then deposits (Lin, Lott, and Mehta 1986). The silt load in a river may be relatively low during periods of normal river flow, but the concentration of suspended sediment may increase by orders of magnitude during storms.

(c) Some harbors are built inland from the coast along river/estuary systems. River flow past the harbor entrance can have conflicting effects. The flow past the entrance can generate a rotary flow system at the entrance that produces some flushing of the harbor. But, if the river silt load is significant, there can be a net deposition of sediment in the harbor near the entrance.

c. Predicting of flushing/circulation. Harbor flushing rates and circulation patterns can be predicted by numerical and physical models and by field studies. Often, some combination of these efforts is the most effective approach. Numerical and physical models benefit from the collection of field data that is usually required to calibrate and verify the models.

(1) Numerical models.

(a) A numerical model of the hydrodynamics of a harbor can be developed by employing finite difference solutions of the equation of mass balance and the two horizontal component momentum equations. With the appropriate boundary conditions at the fixed boundaries of the harbor and the tide as a forcing function at the harbor entrance, one can compute the time-dependent water flow velocities and water surface elevations at selected grid points in the harbor. If so desired, the surface wind stress on the water can also be employed as a forcing function. And river flow into the harbor can be specified at points along the harbor boundary. From the computed time-dependent grid of flow velocities, the resulting circulation patterns in the harbor can be defined.

(b) Commonly, the two-dimensional depth-integrated forms of the equations are used. That is, the horizontal flow velocities are averaged over the water depth and it is assumed that the water column is well mixed so there is no vertical density stratification. Also, it is assumed that vertical flow accelerations are small compared to the acceleration of gravity, so the pressure is hydrostatic and vertical components of flow

velocity may be ignored. This latter limitation would require that there be no abrupt significant depth changes in the harbor. These equations are known as the long-wave equations (see Part II-5). Harris and Bodine (1977) present a derivation of these equations and discuss their formulation for numerical solution.

(c) If the solute advection-diffusion equation is added to the numerical hydrodynamic model, the movement and distribution of pollutants in the harbor can be computed. From this, the harbor exchange coefficients and flushing efficiency can be determined. An interesting application of numerical modeling to investigate harbor circulation, flushing, and variations in dissolved oxygen has been carried out by the Waterways Experiment Station for Los Angeles and Long Beach Harbor in California (Vemulakonda, Chou, and Hall 1991). Typical two-dimensional and a quasi-three-dimensional numerical model investigations studied the impact of deepening channels and constructing landfills in the harbor.

(d) Chiang and Lee (1982), Spaulding (1984), and Falconer (1980, 1984, 1985) provide other examples of applying the long-wave equations to calculate harbor hydrodynamics and adding the solute transport equation to determine the flushing characteristics of harbors.

(e) These numerical models have a number of advantages - they are flexible in that it is easy to adjust input tide and wind conditions as well as harbor bottom and lateral boundary conditions, and they do not have some of the scale/distortion problems found in physical models. But they also have disadvantages - they are a two-dimensional representation of the flow field in the harbor, and since calculations are done for a grid, flow details that are smaller than the grid dimension are not represented. This latter disadvantage makes it difficult to investigate, for example, the eddies generated by flow separation at the harbor entrance or at internal structures. It can be overcome to some extent by decreasing the grid point spacing in key segments of the harbor such as around the harbor entrance (Falconer and Mardapitta-Hadjipandeli 1986).

(f) Numerical models require that a number of empirical coefficients (e.g. surface wind stress and bottom stress, eddy viscosity, and component diffusion coefficients) be defined in order to run the model. Thus, confidence in the model can be significantly increased if field data are available to calibrate the model and verify subsequent model results.

(2) Physical model studies.

(a) Physical model studies have been conducted to investigate flushing and circulation patterns for existing and proposed harbors (Nece and Richey 1972, Schluchter and Slotta 1978, Nece 1985, Nece and Layton 1989) and for basic planform patterns of idealized harbors (Nece, Falconer, and Tsutumi 1976; Jiang and Falconer 1985).

(b) Physical models of harbors are designed to investigate tidal flushing, so they are based on Froude similitude (Hudson et al. 1979). They typically have a distorted scale, with the vertical scale being larger than the horizontal scale. Common model scale ratios that have been used are 1:30 to 1:50 for the vertical scale and 1:300 to 1:500 for the horizontal scale. It is assumed that wind effects are negligible and that the water column has no density stratification. Also, the effects of Coriolis acceleration are not modeled. Most harbors are sufficiently small that Coriolis effects can be neglected.

(c) For models using water and having the typical harbor model/prototype scale ratios, Froude and Reynolds similitude are incompatible. Consequently, model Reynolds numbers are underscaled. Thus, inertial effects are scaled but turbulent diffusion is not scaled. To minimize these effects, some experimenters have installed roughness strips at the model harbor entrance to generate turbulence. Thus, local diffusion-dispersion of solutes is not accurately replicated but advective transport of solutes is replicated. The latter typically dominates. Fine details of the internal flow circulation are not replicated, but gross circulation patterns are.

(d) Circulation patterns are typically measured by photographing the movement of floats. Model exchange coefficients and flushing efficiencies are measured by adding dye to the water at the start of tests and then measuring the decrease of the dye concentration during subsequent tidal cycles. While exchange coefficient values from the model and model circulation patterns do not precisely equate to prototype conditions, these harbor model studies can provide a basis for comparing alternative design features for a proposed harbor or guidance in modifying an existing harbor.

(e) Table II-7-4 lists, for ease of comparison, the relative advantages of physical and numerical models for harbor flushing and circulation studies. The table gives a general comparison, but for a specific application, modelling experts should be consulted before deciding whether to use a numerical or physical model or some combination of both.

Table II-7-4
Advantages of Physical and Numerical Models

Physical Models
Provide good visual demonstration of flow patterns
Some three-dimensional effects can be represented relatively easily
Intricate harbor boundaries can be easily simulated
Numerical Models
Wind stress and Coriolis effects can be simulated
Lower model development and maintenance costs
Easy to store model for future use
Easy to adjust or expand model boundary conditions
Extensive output data can easily be obtained

(3) Field studies.

(a) Limited field studies at an existing harbor may be conducted to obtain sufficient data to calibrate a numerical model of that harbor so the model can be run to investigate a range of other tide and wind conditions. This would provide a detailed look at the flushing and circulation characteristics of the harbor and some insight into possible remedial efforts that may be necessary. Or the model may then be run to evaluate proposed modifications of the harbor.

(b) An alternative is to run more extensive field studies as the sole effort to evaluate conditions at a harbor. This would generally be more costly than the hybrid field-model approach, but it may provide some detail that cannot be achieved from model studies alone.

(c) Also, field studies have been done to support the general development of physical and numerical modelling techniques for the study of harbor flushing and circulation.

(d) Field measurements include those that define the hydrodynamics of a harbor and supplementary measurements to quantify harbor flushing. The former include measurements of tide levels inside and outside the harbor, current velocity measurements at the entrance to quantify flow rates into and out of the harbor, and flow velocity measurements throughout the harbor and/or drogue studies to define circulation patterns in the harbor. If tidal flushing is the primary concern, these measurements would be conducted on days when the wind velocity is low. Otherwise, a directional anemometer would also be used to measure the wind speed and direction.

(e) To determine exchange coefficients throughout the harbor and the harbor's flushing efficiency, the harbor would be uniformly seeded with a harmless detectable solute such as a fluorescent dye and then

sampled periodically at several points in the harbor for a period of several tidal cycles. Initial and subsequent dye concentrations (see Equation II-7-20) can be measured in situ by a standard fluorometer. The dye Rhodamine WT has been used in a number of harbor flushing studies (see Callaway (1981) and Schwartz and Imberger (1988)).

II-7-7. Vessel Interactions

a. Vessel-generated waves.

(1) As a vessel travels across the water surface, a variable pressure distribution develops along the vessel hull. The pressure rises at the bow and stern and drops along the midsection. These pressure gradients, in turn, generate a set of waves that propagate out from the vessel bow and another generally lower set of waves that propagate out from the vessel stern. The heights of the resulting waves depend on the vessel speed, the bow and stern geometry, and the amount of clearance between the vessel hull and channel bottom and sides. The period and direction of the resulting waves depend only on the vessel speed and the water depth. For a detailed discussion of the vessel wave-generating process and the resulting wave characteristics, see Robb (1952), Sorensen (1973a, 1973b), and Newman (1978).

(2) The pattern of wave crests generated at the bow of a vessel that is moving at a constant speed over deep water is depicted in Figure II-7-40. There are symmetrical sets of *diverging* waves that move obliquely out from the vessel's sailing line and a set of *transverse* waves that propagate along the sailing line. The *transverse* and *diverging* waves meet along the cusp locus lines that form an angle of 19°28' with the sailing line. The largest wave heights are found where the *transverse* and *diverging* waves meet. If the speed of the vessel is increased, this wave crest pattern retains the same geometric form, but expands in size as the individual wave lengths (and periods) increase.

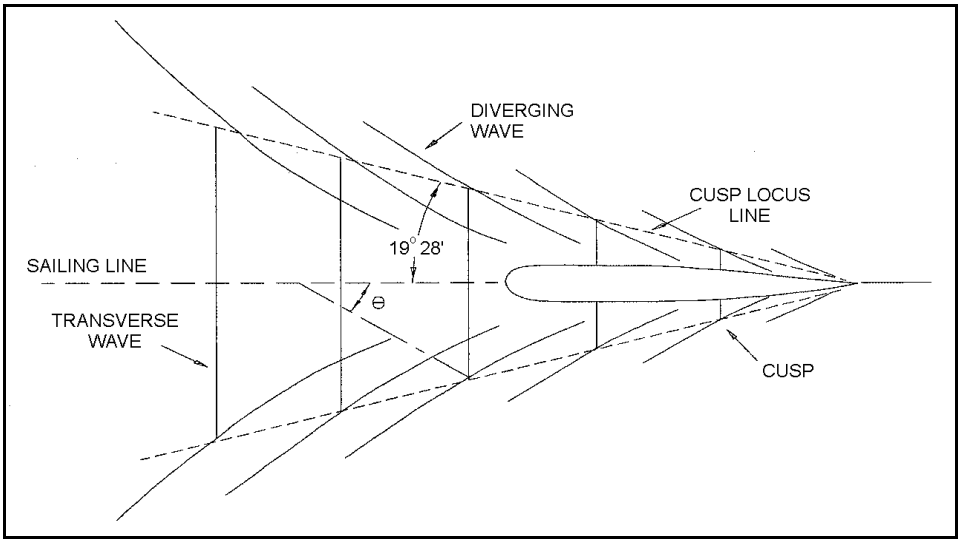

Figure II-7-40. Wave crest pattern generated at a vessel bow moving over deep water

(3) The fixed pattern of wave crests requires that individual wave celerities C be related to the vessel speed V_s by

$$C = V_s \cos\theta \tag{II-7-21}$$

where θ is the angle between the sailing line and the direction of wave propagation (Figure II-7-40). Thus, the *transverse* waves travel at the same speed as the vessel and, in deep water, θ has a value of 35°16' for the *diverging* waves.

(4) At increasing distances from the vessel, diffraction causes the wave crest lengths to continually increase and the resulting wave heights to continually decrease. It can be shown (Havelock 1908) that the wave heights at the cusp points decrease at a rate that is inversely proportional to the cube root of the distance from the vessel's bow (or stern). *Transverse* wave heights at the sailing line decrease at a rate proportional to the square root of the distance aft of the bow (or stern). Consequently, the *diverging* waves become more pronounced with distance from the vessel.

(5) The above discussion applies to deep water, i.e. water depths where the particle motion in the vessel-generated waves does not reach to the bottom. This condition holds for a Froude number less than approximately 0.7, where the Froude number F is defined by

$$F = \frac{V_s}{\sqrt{gd}} \tag{II-7-22}$$

(6) As the Froude number increases from 0.7 to 1.0, wave motion is affected by the water depth and the wave crest pattern changes. The cusp locus line angle increases from 19°28' to 90° at a Froude number of one. The *diverging* wave heights increase more slowly than do the *transverse* wave heights, so the latter become more prominent as the Froude number approaches unity. At a Froude number of one, the *transverse* and *diverging* waves have coalesced and are oriented with their crest perpendicular to the sailing line. Most of the wave energy is concentrated in a single large wave at the bow. Owing to propulsion limits (Schofield 1974), most self-propelled vessels can only operate at maximum Froude numbers of about 0.9. Also, as a vessel's speed increases, if the vessel is sufficiently light (i.e. has a shallow draft), hydrodynamic lift may cause the vessel to plane so that there is no significant increase in the height of generated waves for vessel speeds in excess of the speed when planing commences.

(7) For harbor design purposes, one would like to know the direction, period, and height of the waves generated by a design vessel moving at the design speed. For Froude numbers up to unity, Weggel and Sorensen (1986) show that the direction of wave propagation θ (in degrees) is given by

$$\theta = 35.27\ (1 - e^{12(F-1)}) \tag{II-7-23}$$

(8) Then, from Equation II-7-21, the *diverging* wave celerity can be calculated, and the wave period can be determined from the linear wave theory dispersion equation.

(9) Figure II-7-41 is a typical wave record produced by a moving vessel. Most field and laboratory investigations of vessel-generated waves (Sorensen and Weggel 1984; Weggel and Sorensen 1986) report the maximum wave height (H_m, see Figure II-7-41) as a function of vessel speed and type, water depth, and distance from the sailing line to where the wave measurement was made. Table II-7-5 (from Sorensen (1973b)) tabulates selected H_m values for a range of vessel characteristics and speeds at different distances from the sailing line. These data indicate the range of typical wave heights that might occur for common vessels and show that vessel speed is more important than vessel dimensions in determining the height of the wave generated.

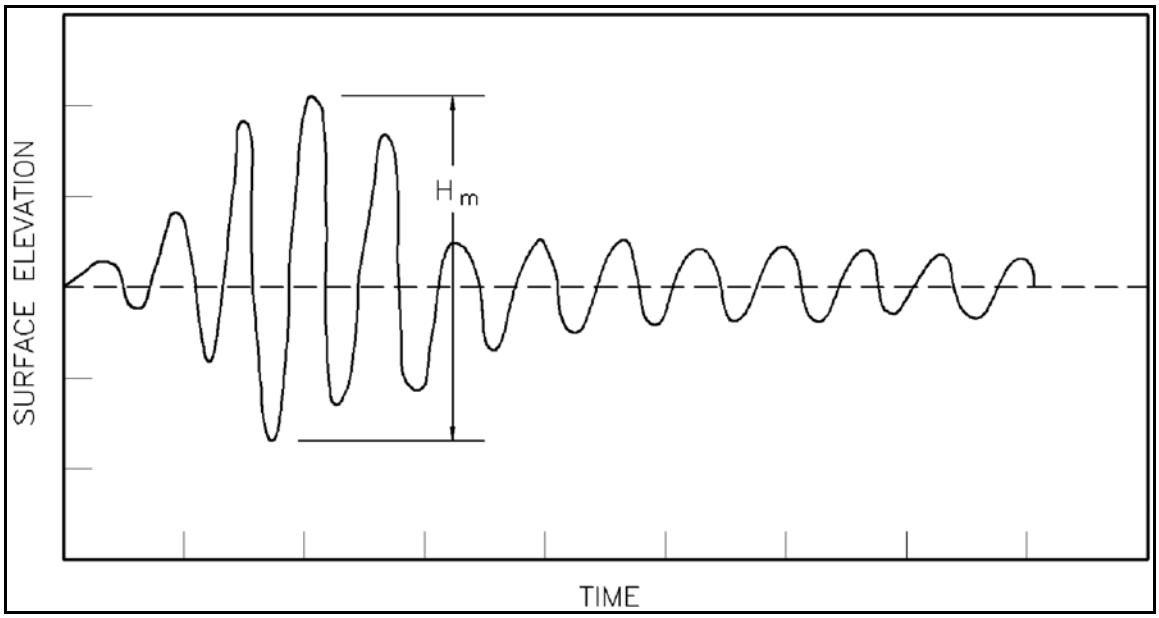

Figure II-7-41. Typical vessel-generated wave record

EXAMPLE PROBLEM II-7-5

FIND:

The period of the *diverging* waves generated by the vessel.

GIVEN:

A vessel is moving at a speed of 10 knots (5.157 m/sec) over water 5 m deep.

SOLUTION:

The vessel Froude number is

$$F = \frac{5.157}{\sqrt{9.81\ (5)}} = 0.73$$

so Equation II-7-23 gives a direction of propagation

$$\theta = 35.27\ [1 - e^{12(0.73-1)}] = 33.88°$$

and Equation II-7-21 gives a wave celerity

$$C = 5.157\ \cos(33.88^{\circ}) = 4.28\ \text{m/s}$$

The linear wave dispersion equation can be written

$$C = \frac{gT}{2\pi} \tanh \frac{2\pi d}{CT}$$

Inserting known values for C, g, and d into the dispersion equation leads to a trial solution for T of 2.8 sec. This is a typical period for vessel-generated waves and demonstrates why floating breakwaters are usually effective in protecting against vessel waves.

(10) A number of quasi-empirical procedures for predicting vessel-generated wave heights have been published (see Sorensen (1986) and Sorensen (1989) for a summary). Most procedures are restricted to a certain class or classes of vessels and specific channel conditions. A comparison (Sorensen 1989) of predicted H_m values for selected vessel speeds and water depths showed significant variation among the results predicted by the various procedures. The best approach for design analyses appears to be to review the published vessel wave measurement data to compare with the vessel, vessel speed, and channel conditions that most closely approach the design condition and select a conservative value of H_m from these data. If this is not possible, then the values in Table II-7-5 can be used as rough estimates for the different types of vessels.

Table II-7-5
Selected Vessel-Generated Wave Heights (Sorensen 1973b)

Vessel	Speed (m/s)	H_m(m) at 30 m	H_m(m) at 150 m
Cabin Cruiser length-7.0 m beam-2.5 m draft-0.5 m	3.1 5.1	0.2 0.4	0.1 0.2
Coast Guard Cutter length-12.2 m beam-3.0 m draft-1.1 m	3.1 5.1 7.2[1]	0.2 0.5 0.7	0.3
Tugboat length-13.7 m beam-4.0 m draft-1.8 m	3.1 5.1	0.2 0.5	0.1 0.3
Air-Sea Rescue Vessel length-19.5 m beam-3.9 m draft-0.9 m	3.1 5.1 7.2[1]	0.1 0.4 0.6	0.2 0.3
Fireboat length-30.5 m beam-8.5 m draft-3.4 m	3.1 5.1 7.2	0.1 0.5 0.9	0.1 0.3 0.8
Tanker length-153.6 m beam-20.1 m draft-8.5 m	7.2 9.3		0.5 1.6

Note: The above data are from tests conducted at water depths ranging from 11.9 to 12.8 m.
[1] Denotes that the vessel was starting to plane.

b. Vessel motions.

(1) Response to waves.

(a) Wave action will excite a floating vessel to oscillate in one or more of six components of motion or degrees of freedom. These are translated in the three coordinate directions (surge, sway, and heave) and rotation around the three principal axes (roll, pitch, and yaw). Which of these motion components is excited and to what extent depends primarily on the direction of wave incidence relative to the primary vessel axes and on the incident wave frequency spectrum compared to the resonant frequencies of the six motion components (Wehausen 1971). If the vessel is moored, the arrangement of the mooring lines and their taughtness will influence the resonant periods and the response amplitudes of the vessel motions. If the vessel is moving, the effective or encounter period of wave agitation is the wave period relative to the ship rather than to a fixed observation point. Wave mass transport will also cause a slow drift of the vessel in the direction of wave propagation.

(b) Small vessels, such as the recreational vessels found in marinas, will commonly respond to shorter wind-wave periods. An analytical study, coupled with some field measurements for seven small boats

(Raichlen 1968), indicated that the periods of free oscillation were less than 10 sec. Larger seagoing deep-draft vessels, depending on the oscillation mode being excited, will respond to the entire range of wind-wave periods. Field measurements by van Wyk (1982) on ships having lengths between 250 and 300 m and beams of about 40 m found maximum roll and pitch responses at encounter periods between 10 and 12 sec. By properly designing the mooring system, the periods and amplitudes of vessel motion can be significantly modified.

(c) The wave-induced lateral and vertical motions of the design vessel will affect the required channel horizontal and depth dimensions, respectively. The problem of wave-induced vessel oscillations has been addressed by analytical/numerical means (Andersen 1979; Madsen, Svendsen, and Michaelsen 1980; Isaacson and Mercer 1982). These efforts usually employ small-amplitude, monochromatic waves and some limitations on vessel geometry and the incident wave directions relative to the vessel.

(d) Some field measurement programs yield valuable design information. Wang and Noble (1982) describe an investigation of vessels entering the Columbia River channel. Pitch, roll, heave, yaw, and horizontal position were measured for selected vessels as they traversed the channel. The data were analyzed statistically to define extreme limits of vessel motion for various wave and other conditions (Noble 1982). van Wyk (1982) reports on a field study of vessel response to wave action at two South African ports. The data were analyzed statistically so extreme motion probabilities could be evaluated. Other field studies of moving large vessels have been reported by Greenstreet (1982) and Zwamborn and Cox (1982). Raichlen (1968) and Northwest Hydraulic Consultants (1980) discuss field measurements of small moored vessels in marinas.

(e) Most of the major coastal engineering labs have also conducted model studies of vessel response to wave motion. Some of these tests are discussed in Mansard and Pratte (1982), Isaacson and Mercer (1982), Zwamborn and Cox (1982), and Briggs et al. (1994).

(2) Response to currents.

(a) There are several possible causes for currents in harbors and in the vicinity of harbor entrances. Wind, wave-induced radiation stress, rivers, and tides can all generate currents in the vicinity of a coastal harbor entrance. Flow from a river that enters a harbor or flows past the entrance to a harbor located in an estuary can generate significant currents. Ebb and flood tide can generate strong reversing currents through a harbor entrance. Tidally induced longshore currents around islands can cause navigation problems at harbor entrances. Long-wave resonant oscillations in harbors can generate noticeable currents at nodal points, which can seriously affect moored vessels and create hazardous navigation conditions if this location is at a place where the flow is constricted.

(b) Currents will directly affect vessel operation, particularly when they act oblique to the sailing line of the vessel. These currents are particularly troublesome when the vessel speed is low and vessel maneuverability is commensurately reduced. The situation is made even more difficult when there are strong winds acting from a different direction than the currents. Physical model studies and numerical simulations of vessel motion have been used to predict vessel paths under various wind and current conditions, particularly as vessels enter a harbor (Bruun 1989, Briggs et al. 1994). Currents can increase vessel sinkage and trim in restricted channels (see next section).

(3) Wave-current interaction.

(a) At harbor entrances, currents can also exert an indirect effect on vessel navigation through their effect on waves. Ebb currents will steepen incoming waves, making the waves more hazardous to the stability of

small vessels in particular. The ebb currents may be of sufficient strength to induce wave breaking and turbulence in the entrance, a condition that is particularly hazardous to vessel operation.

(b) Bruun (1978) summarizes earlier literature and discusses the problem of sediment transport. Mehta and Özsöy (1978) found that the effects of bottom friction are important in the hydrodynamics of two-dimensional turbulent jets because it increases the rate of spreading of the jet, which has a significant effect on incident wave characteristics. Sakai and Saeki (1984) measured the effect of opposing currents on wave height transformation over a 1:30 sloping beach for a range of wave periods and steepness. They found an increase in wave height and decay rate in the presence of the opposing current. Willis (1988) conducted monochromatic wave and ebb current tests in a 1-m-wide rectangular entrance channel cut in a 1:30 sloping beach. Current measurements were averaged over 3 min to obtain a quantitative picture of the mean currents. They experienced major problems with the stability of the current field due to large-scale meandering motions.

(c) Lai, Long, and Huang (1989) conducted flume tests of kinematics of wave-current interactions for strong interactions with waves propagating with and against the current. They found the influence of the waves on the mean current profiles was small, although opposing waves would give a slightly lower current. They observed a drastic change in the spectral shape, especially higher harmonics, following wave breaking in the presence of opposing currents. Their experiments confirmed blockage of waves by a current when the ratio of depth-averaged current velocity to wave celerity without currents approaches -0.25.

(d) Raichlen (1993) conducted a laboratory investigation of waves propagating on an adverse jet to simulate the effect of ebb currents on incoming waves at a tidal inlet. He tested regular waves (depth-to-wavelength ratios from 0.086 to 0.496) for a range of relative channel entrance velocities to wave celerity for locations both upstream (20 channel widths) and downstream (15 channel widths) of the channel entrance. Wave height increased by a factor of 2.5 near the channel entrance in the presence of a current that was only 7 percent of the phase speed, primarily caused by wave refraction. He also found that the wave height decreases significantly as waves propagate up the entrance channel. Refraction and entrainment of the still fluid by the ebb current jet produces a lateral variation in the wave height across the channel width downstream of the entrance.

(e) Briggs and Green (1992) and Briggs and Liu (1993) conducted three-dimensional laboratory experiments of the interaction of regular waves with ebb currents offshore of a tidal entrance channel (6 channel widths) on a 1:30 plane beach. Current velocity to wave celerity ratios ranged from 0.06 to 0.34. Under the influence of ebb currents, waves experienced increases in steepness and corresponding wave height up to a factor of nearly 2 for currents that were 20 to 30 percent of the phase speed. As waves shoal and break, higher harmonics are formed as the wave becomes more nonlinear. Energy is transferred from the fundamental mode due to nonlinear coupling between frequencies. Briggs and Liu found that ebb currents also promote the nonlinear growth of the fundamental frequency, higher harmonics, and subharmonics of the incident wave. This shift in energy can change the response characteristics of vessels in the entrance channel.

(4) Vessel sinkage and trim.

(a) The pressure distribution that develops around the hull of a moving vessel results in an above-average pressure at the bow and stern and a below-average pressure at the midsection of the vessel. The reduced pressure at the midsection dominates and causes a net sinkage of the vessel. The vessel sinkage is also referred to as squat. Since there is usually an imbalance of upward forces between the bow and stern, the vessel will often also trim by the bow (i.e. the vessel bow is lowered relative to the stern) or by the stern.

(b) Sinkage and trim of a vessel in a navigation channel depend on the factors that control the pressure distribution along the vessel hull. Primarily, these are the vessel speed, the ratio of the channel cross section

area to the vessel wetted cross section area (known as the section coefficient), and the ratio of the water depth to the vessel draft. Other factors that might affect sinkage and trim include the vessel hull geometry, the at-rest trim of the vessel, the cross-section geometry of the channel, the sailing line of the vessel relative to the centerline of the channel, vessel acceleration or deceleration, the presence of currents in the channel, and the passing of other vessels in the channel.

(c) A wide variety of analytical, quasi-analytical, and empirical methods for predicting vessel sinkage and a few for predicting vessel trim have been published (Garthune et al. 1948, Constantine 1960, Tuck 1966, Tothill 1967, Sharp and Fenton 1968, Dand and Furgeson 1973, McNown 1976, Beck 1977, Gates and Herbich 1977, Eryuzlu and Hausser 1978, Blauuw and van der Knapp 1983, Ferguson and McGregor 1986). The earliest and most basic approach to predicting vessel sinkage employs the one-dimensional energy and continuity equations. This approach gives generally acceptable results for uniform channels and vessel hull geometries that are not too irregular. The continuity and energy equations are written between a point ahead of the vessel and a point at the vessel midsection. The water surface drawdown is thus calculated and assumed equal to the vessel sinkage. The results for a rectangular channel cross section are presented below; for a trapezoidal channel cross section see Tothill (1967) and for a parabolic channel cross section, see McNown (1976).

(d) Consider a vessel in a channel with the relevant dimensions as defined in Figure II-7-42 where b is the channel width, A_m is the vessel's midsection wetted cross-section area, the undisturbed water depth is d, and the vessel drawdown is Δd. V_s and g are the vessel speed and the acceleration of gravity as defined earlier. The continuity and energy equations in terms of the Froude number F, dimensionless drawdown D, and vessel blockage ratio S are solved by

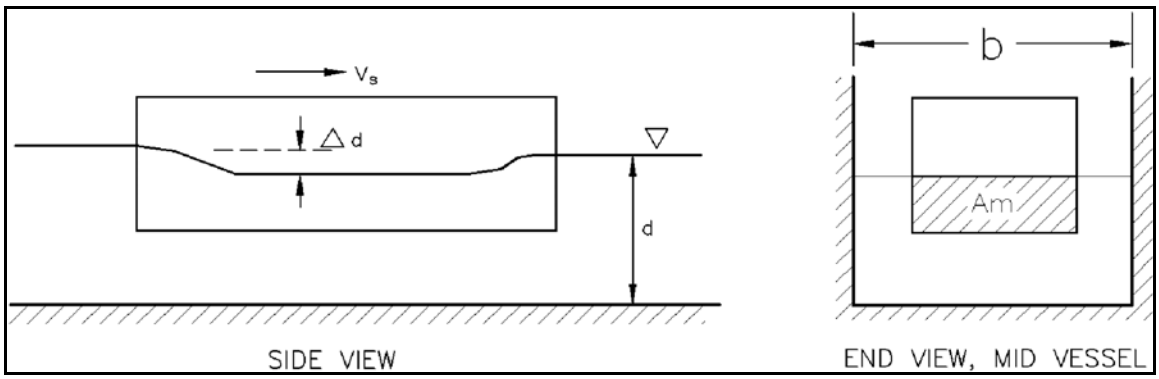

Figure II-7-42. Definition of terms, vessel drawdown

$$F = \sqrt{\frac{2D(1-D-S)^2}{1-(1-D-S)^2}} \tag{II-7-24}$$

where

$$F = \frac{V_S}{\sqrt{gd}} \qquad D = \frac{\Delta d}{d} \qquad S = \frac{A_m}{bd}$$

(e) Figure II-7-43 plots F versus D for selected values of S. Given the channel cross-section dimensions, the water depth, the vessel speed, and the midsection wetted cross-section area of the vessel, D can be determined from the figure. This, in turn, yields the water surface drawdown Δd, which is taken as the vessel sinkage.

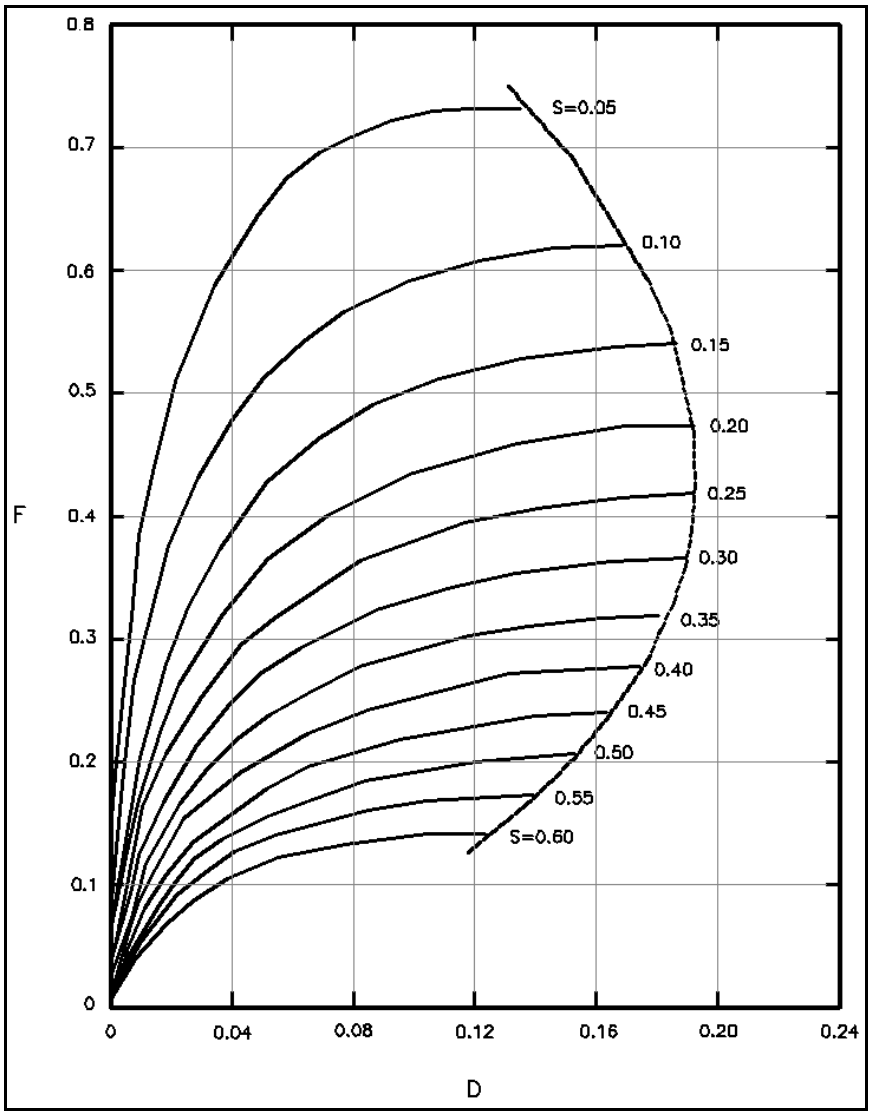

Figure II-7-43. Vessel sinkage prediction

(f) Design of safe channel depths is a function of the loaded draft of the ship, vessel sinkage, minimum underkeel clearance, and effect of pitch and roll in outer channels exposed to wave and current conditions (Herbich 1992).

(g) A self-propelled vessel cannot exceed the critical speed (see Constantine (1960)). However, a vessel can be towed faster than the critical speed, the result being the generation of a bore wave that propagates ahead of the vessel. Before reaching the critical speed, the vessel sinkage increases rapidly. If the initial vessel under-keel clearance is small, the vessel may hit bottom before coming close to the critical speed. Also, near the critical speed, there is a sharp increase in the power required to propel the vessel.

EXAMPLE PROBLEM II-7-6

FIND:

The vessel sinkage and return flow velocity between the vessel hull and the channel bottom and sides.

GIVEN:

A C9 containership has a length of 262 m, a beam of 32 m, and a fully loaded draft of 12 m. The C9 containership with a midsection wetted cross section area of 384 m^2 is moving at a speed of 6 knots (3.09 m/s) in a channel 137 m wide and 15 m deep. This is a typical scenario for deep-draft vessels entering a harbor through a one-way entrance channel.

SOLUTION:

The vessel Froude number is

$$F = \frac{3.09}{\sqrt{9.81\ (15)}} = 0.26$$

and the blockage ratio is

$$S = \frac{384}{137(15)} = 0.19$$

From Figure II-7-43 at the intersection of F = 0.26 and S = 0.19, the dimensionless drawdown is approximately D = 0.02. The vessel sinkage is then given by

$$\Delta d = 15(0.02) = 0.30\ \text{m}$$

The return velocity is calculated from Equation II-7-25 as

$$V_r = 3.09\left[\frac{137(15)}{137(15-0.3)-384} - 1\right] = 0.81\ \text{m/s}$$

Thus, channel depths must include additional clearance to accommodate the vessel drawdown and a substantial return velocity flow can lead to scour along the channel banks.

(h) As a vessel travels in a channel, continuity of flow causes a return flow velocity to develop between the vessel hull and the channel bottom and sides. This return flow velocity V_r can be calculated for a rectangular channel and vessel cross section (as depicted in Figure II-7-42) from

$$V_r = V_s\left[\frac{bd}{b(d - \Delta d) - A_m} - 1\right] \qquad \text{(II-7-25)}$$

(i) Particularly for vessel/channel conditions that produce a large blockage ratio (S) and for high vessel speeds, a substantial return flow velocity can develop. Channel bottom scour and damage to reveted channel sides may result.

(5) Ship maneuverability in restricted waterways.

(a) The pressure distribution along the hull of a vessel will also cause lateral forces and horizontal moments to act on the vessel when it passes another vessel or moves in close proximity to a channel bank or other large structure. These effects affect all sizes of ships, but are particularly dangerous for larger vessels. Figure II-7-44 shows a pressure field for moving vessels, where the plus and minus signs indicate the relative pressures along the side of the hull.

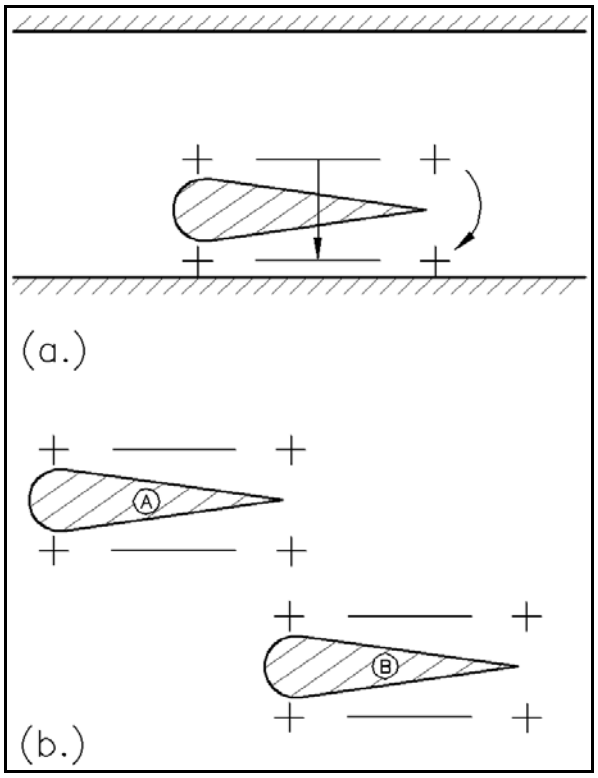

Figure II-7-44. Pressure fields for moving vessels (vessels moving left to right)

(b) Figure II-7-44a shows a vessel sailing close to a channel bank. Owing to the "Bernoulli effect," larger positive and negative pressures occur on the side closest to the channel bank, with the negative pressure dominating to draw the vessel toward the bank and the larger bow pressure than stern pressure causing the bow to rotate (yaw) away from the bank. Lateral force and yawing moment increase as the vessel sails closer to the bank and they are approximately a function of the vessel speed squared. Manipulation of the ship's rudder can correct for these forces, but it is difficult to travel close to a channel bank for any long period of time (Kray 1970).

(c) Figure II-7-44b shows two similar vessels, with vessel A passing vessel B in unrestricted water. For the positions shown, the bow of vessel A and the stern of vessel B would deflect outward because of the positive pressures at both bow and stern. When the ships are even, they would be drawn together because of the negative pressures midships, and their bows would be deflected slightly apart because of the positive pressures at the bows. And as vessel A completes passing vessel B, the stern of B and the bow of A would be deflected outward. Thus, the interacting forces and moments are complex, continually changing while the ships are in the proximity of each other, and dependent on hull sizes and geometries; vessel speeds, directions, and lateral separation; and water depth. Vessel interaction effects are more significant for vessels that have a large cross-section area relative to the channel cross-section area and for higher vessel speeds.

(d) The effects of vessel interaction have been studied for specific conditions by carrying out model studies (e.g. Taylor 1909, Robb 1949, Garthune et al. 1948, Delft Hydraulics Laboratory 1965, Moody 1970, Dand 1976). Some analytical studies that allow calculation of the resulting forces and moments, but not the vessel response, were conducted by Silverstein (1958), Hooft (1973), Tuck and Newman (1974), and Dand (1976).

(e) Vessel interactions with other vessels and with the channel bank must be accounted for in determining required navigation channel widths. For example, guidance given in Engineer Manual (EM) 1110-2-1613, which specifies channel width as a function of the design vessel beam dimension for various channel conditions, includes these effects. The total channel width consists of a maneuvering lane, bank clearance, and ship clearance, if two-way traffic is involved. This specification is based on model studies of large vessels in deep-draft navigation channels and discussions with ship pilots (Garthune et al. 1948).

c. Mooring.

(1) Wave forcing mechanism.

(a) Infragravity waves (wave periods typically between 25 and 300 sec) force long-period oscillations or seiche in harbors. If the natural period of the ship corresponds to a harbor resonance mode and they are moored in the vicinity of the node, excessive ship motion can prevent loading and unloading of the ship for a number of days. In some cases, extensive damage to the ship and pier can result if the mooring lines fail.

(b) Infragravity energy can be divided into bound and free wave energy. Bound or forced infragravity waves are nonlinearly coupled to wave groups, traveling at the group velocity of the wind waves, and phase locked to sea and swell waves. Free infragravity waves radiate to and from deep water after being reflected from the shoreline or are generated by nonlinear interactions and wave breaking of incident wind waves and are refractively trapped in shallow water, propagating in the longshore direction. According to numerous investigators (Herbers et al. 1992; Elgar et al. 1992; Okihiro, Guza, and Seymour 1992), bound and free wave energies increase with increasing swell energy and decreasing water depth. Bound wave contributions are usually more significant when energetic swell conditions exist, but free waves dominate when more moderate conditions prevail.

(2) Mooring configurations.

(a) A vessel moored in a harbor or at some point offshore commonly has one of three types of mooring arrangements:

- A single-point mooring where the vessel is tied to a buoy by a single line from the bow and is thus free to rotate around the buoy (i.e. weathervane) in response to environmental forces.
- A multiple- point mooring where the ship is tied by several fore and aft lines to anchors or buoys.
- A conventional pier anchorage, where the vessel is tied fore and aft to the pier and separated from the pier by a fendering system.

(b) For a deep-draft vessel at a pier, the mooring line system will typically consist of 8 to 12 lines in a symmetrical pattern, half from the bow and half from the stern of the ship. One to two *breast* lines are positioned on both bow and stern. The breast line(s) is perpendicular to the ship and dock and presses the ship against the dock and fenders. Two *head* lines make an angle of 60-70 deg to the *breast* line and go forward from the bow. Two *stern* lines are analogous to the *head* lines, but originate from the stern of the ship. These four lines are on the order of 100 ft long between ship and dock attachment points. Finally, two or four *spring* lines make an angle of 85 deg to the *breast* line and go toward midships. These lines can vary in length from 100 to 200 ft. The *spring* lines, in combination with the *breast* lines, provide the most efficient ship mooring. The deck of the vessel is typically 3 to 8 m above the pier, with the bow being higher than the stern.

(3) Mooring lines.

(a) Mooring lines are made from steel, natural fibers, and synthetic materials. Steel ropes may be made of different strength grades and galvanized for protection against corrosion. Natural fibers include manilla, sisal, and coir. Commonly used synthetic materials are nylon, dacron, polypropylene, Kevlar, and Karastan (Herbich 1992).

(b) Synthetic lines are easy to handle, do not corrode, and have excellent strength-to-weight ratios. Different construction types include stranded, plaited, braided, and parallel yarns. Stranded is the least satisfactory for mooring lines because it tends to unlay under free end conditions. Each has different mechanical properties that make it appropriate for different applications. These include strength, weight, stretch, endurance, and resistance to abrasion and cuts.

(c) Care should be taken not to mix different materials and lengths in mooring arrangements (Oil Companies International Marine Forum (OCIMF) 1978). Elasticity is a measure of a mooring line's ability to stretch under load. It is a function of material, diameter, and length. The ultimate breaking strength has been related to the square of the nominal rope diameter (Wilson 1967). If two lines of different elasticity but similar lengths and orientations are combined at the same point, the stiffer one will assume more of the load. Also, lines of different length will carry different amounts of the total load. Thus, one of the lines may be near breaking while the other one is carrying almost no load.

(4) Fenders. Fenders are like bumpers on cars, designed to protect vessels and piers during berthing and mooring against forces due to winds, waves, and currents. They are designed to absorb impact energy of the vessel through deflection and dissipation. Some respond very fast and violently and others more slowly. The latter are the more desirable because they produce smaller fender forces. Highly elastic, recoiling type fenders should be replaced with the non-recoiling type if possible. Fenders can be continuous or placed in certain areas where vessels land. The mooring system should be designed based on the combined response of mooring lines and fenders to ensure that resonance effects with the environmental forces are minimized. The interested reader should consult Bruun (1989) for additional information on types, materials, characteristics, selection, forces, deformation, and energy absorption of fenders.

(5) Surge natural period.

(a) For moored vessels at a dock or quay, surge is one of the most important parameters to consider. Ranges of allowable movements for different vessels have been given by Bruun (1989).

(b) The motion of a moored ship in surge can be described by the motion of a linear system with a single degree of freedom. Restoring or reaction forces due to the change in position, velocity, and acceleration of the ship from equilibrium are assumed linear. The exciting force is due to the drag force of the water flowing past the ship. The motion of the ship in surge is assumed to be independent of other directions of motion. Damping is assumed to be small for the low-frequency motions of a ship in surge. Solving for the undamped natural period in surge T_s

$$T_n = 2\pi\sqrt{\frac{m_v}{k_{tot}}} \tag{II-7-26}$$

(c) The virtual mass of the ship m_v is the sum of the actual mass or displacement of the ship m and the added mass m_a due to inertial effects of the water entrained with the ship. For a ship in surge, m_a is approximately 15 percent of the actual mass m, which is based on the ship's displacement

$$m_v = m + m_a = 1.15\,\mathrm{m} \tag{II-7-27}$$

(d) A mooring system is composed of many lines, but only those in tension contribute to the stiffness or effective spring constant k_{tot} given by

$$k_{tot} = \sum_n k_n \sin\theta_n \cos\phi_n \tag{II-7-28}$$

where the index n sums over all head, stern, and spring lines in tension during surge motion (breast lines are conservatively assumed to provide no restoring force in surge), θ_n is the angle the line makes in the horizontal plane with the perpendicular to the ship, and ϕ_n is the angle the line makes in the vertical plane between the ship and the dock.

(e) For a taut mooring line in which sag is negligible and deflections are small, the individual stiffness k_n is defined by

$$k_n = \frac{T_n}{\Delta l_n} \tag{II-7-29}$$

where T_n is the axial tension or load and Δl_n is the elongation in the mooring line. The elastic behavior of fiber ropes is difficult to ascertain since it is a function of material, construction, size, load and load history, time, and environmental conditions. Typically, manufacturers supply elongation curves based on experimental data, which show percent elongation ε_n as a function of load as a percent of the breaking strength of the mooring line (Figure II-7-45). A new rope undergoes construction stretch or permanent strain, which occurs when initial loading places the fibers in paths different from their initial construction. Elastic stretch occurs for subsequent loading and is repeatable each time the rope is loaded. Under high loads for a long time, the rope may undergo cold flow of the fibers and eventually break. Thus, previously elongated rope does not stretch as much as new rope and separate elongation curves may be provided. Percent elongation is related to Δl_n by

$$\varepsilon_n = 100\left(\frac{\Delta l_n}{l_n}\right) \tag{II-7-30}$$

where l_n is the length of the mooring line. This formulation assumes that cable dynamics can be neglected, and that the natural frequency of the mooring line in longitudinal and transverse vibration is much higher than the surge frequency of the ship.

(f) Therefore, the natural period of a moored ship in surge is a function of displacement, and number, type, length, size, and tension of the mooring lines. As the ship is off-loaded, displacement of the ship will decrease and this will change the ship response characteristics. Proper ballasting can be used to prevent surge conditions from developing. If this is not possible, other remedies can be sought. The natural period of the moored ship can be adjusted by changing the mooring line configuration or tension. Increased tension will make the moored ship stiffer and will reduce its resonant period of oscillation. A decrease in the mooring line tension will make the moored ship less prone to shorter-period resonant modes. If this is not practical, the number and type of mooring lines can be changed to affect the response of the moored ship.

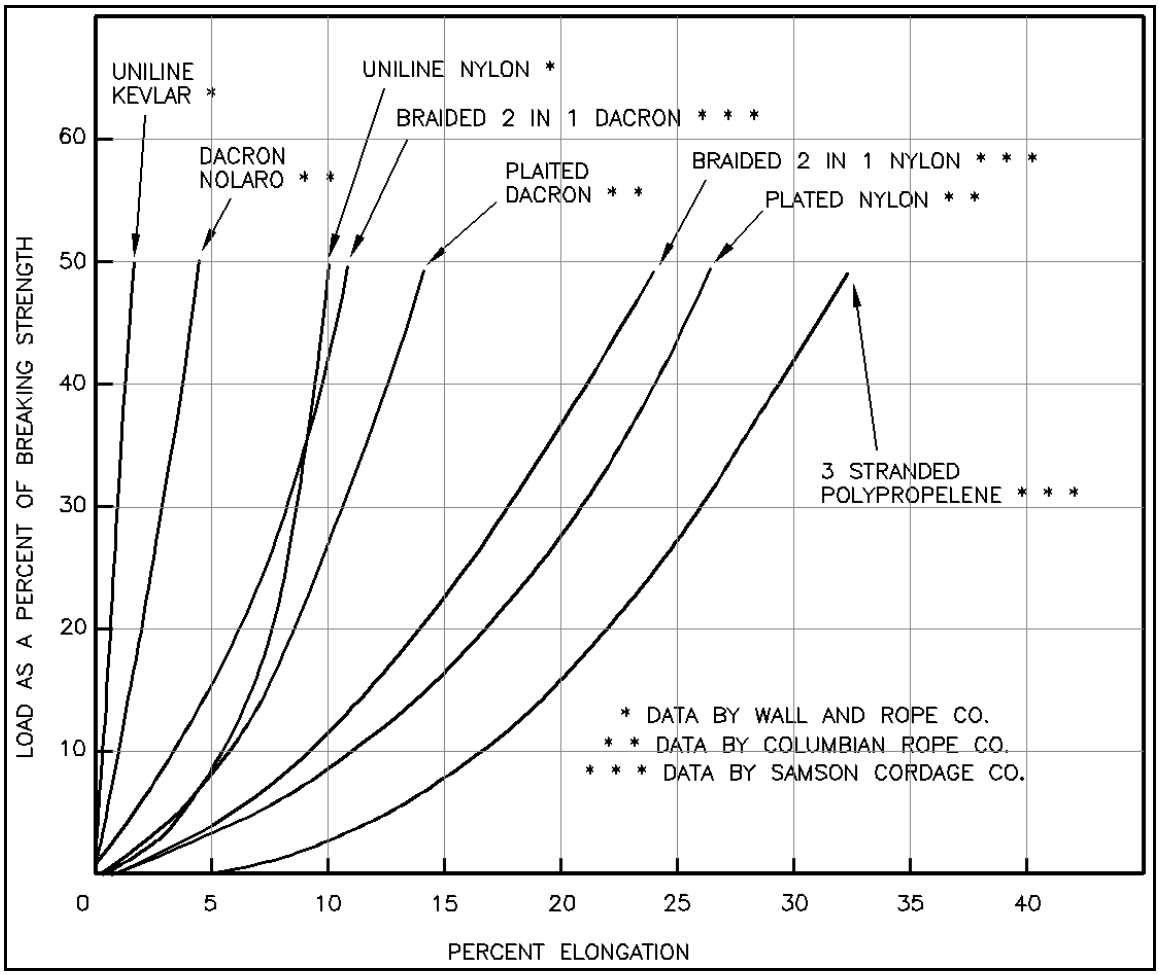

Figure II-7-45. Mooring fiber rope elongation curves

(6) Mooring forces.

(a) Design of any of these systems requires that the primary hydrodynamic loads on the vessel caused by the wind, currents, and waves be determined, usually on a probabilistic basis. Other loads that may be important in certain situations are ice forces and forces induced by passing vessels. The appropriate forces are employed in a dynamic analysis of the mooring system to determine expected loads in the mooring lines and on the fender systems. This analysis can be done by a physical model study or by a computer simulation of the system dynamics equations (see Bruun (1989) and Gaythwaite (1990)). Detailed discussions of the primary vessel mooring forces, those caused by the wind, currents, and waves, can be found in Tsinker (1986), Bruun (1989), and Gaythwaite (1990).

(b) The wind load is determined from the usual drag equation

$$F_w = \frac{1}{2}\rho_a C_D A V_{10}^2 \tag{II-7-31}$$

where F_w is the drag force due to the wind, ρ_a is the air density, C_D is a drag coefficient, A is the projected area of the vessel above the waterline, and V_{10} is the wind speed at the standard elevation of 10 m above the water's surface.

EXAMPLE PROBLEM II-7-7

FIND:

The natural period of the vessel in surge for used mooring lines in good condition.

GIVEN:

A C9 containership is moored at a pier in Barbers Point Harbor, Oahu, Hawaii. Its fully-loaded displacement is 54,978 long tons (55,860,231 kg). Karat Estalon fiber ropes with a 7-1/2-in. circumference (6.3-cm-diam) are used for the two head, two stern, and two spring lines. Head and stern lines are 30.5 m long and make an angle of 70 deg with the perpendicular breast lines. The spring lines are 45.7 m long and form an angle of 85 deg with the breast lines. The tension in these lines is maintained at 20 tons (177,900 N). The deck of the C9 is assumed to be 7 m above the dock at the bow and 4.5 m at the stern.

SOLUTION:

Virtual mass is calculated from Equation II-7-27

$$m_v = 1.15(55{,}860{,}200) = 64{,}239{,}200 \text{ kg}$$

The next step is to calculate the effective spring constant. Karat lines are manufactured by Columbian Rope Company, Guntown, MS, under license from Akzo, Holland. Estalon is a fiber that is a copolymer of polyester and polypropylene. According to manufacturer's literature, the breaking strength for Karat ropes is 526,000 N. The load as a percent of breaking strength is

$$Load = 100\left[\frac{177{,}900}{526{,}000}\right] = 33.8\%$$

From the elongation chart for Karat lines (not shown), the percent elongation is 8.7 percent. The elongation for the head and stern lines is the same and is calculated from Equation II-7-30

$$\Delta l_{Hd} = \Delta l_{St} = \frac{8.7(30.5)}{100} = 2.7 \text{ m}$$

Likewise, the elongation for the spring lines is given by

$$\Delta l_{Sp} = \frac{8.7(45.7)}{100} = 4.0 \text{ m}$$

Example Problem II-7-7 (Continued)

Example Problem II-7-7 (Concluded)

Individual stiffness for the head and stern lines is calculated from Equation II-7-29

$$k_{Hd} = k_{St} = \frac{177{,}900}{2.7} = 65{,}900 \text{ N/m}$$

Similarly, the stiffness for individual spring lines is

$$k_{Sp} = \frac{177{,}900}{4.0} = 44{,}500 \text{ N/m}$$

The vertical angles from the bow, stern, and spring lines are

$$\phi_{Hd} = \arcsin\left[\frac{7.0}{30.5}\right] = 13°$$

$$\phi_{St} = \arcsin\left[\frac{4.5}{30.5}\right] = 8°$$

$$\phi_{Sp} = \arcsin\left[\frac{4.5}{45.7}\right] = 6°$$

When the ship surges forward, the two stern lines and a spring line provide restoring forces. Similarly, when the surge is in reverse, two head lines and a spring line provide the restoring forces. The effective spring constant is calculated both ways and averaged from Equation II-7-28

$$k_{tot} = 2(65{,}900)\ \sin 70°\ \cos 8° + 44{,}500\ \sin 85°\ \cos 6°$$
$$= 122{,}600 + 44{,}100 = 166{,}700 \text{ N/m}$$

$$k_{tot} = 2(65{,}900)\ \sin 70°\ \cos 13° + 44{,}500\ \sin 85°\ \cos 6°$$
$$= 120{,}700 + 44{,}100 = 164{,}800 \text{ N/m}$$

$$k_{tot} = \frac{166{,}700 + 164{,}800}{2} = 165{,}750 \text{ N/m}$$

Finally, the natural period in surge is calculated from Equation II-7-26

$$T_s = 2(3.14)\sqrt{\frac{64{,}239{,}200}{165{,}750}} = 124 \text{ sec}$$

If the rope had been new, the percent elongation would have been higher at 10.7 percent. This would have resulted in a slightly higher surge natural period of approximately 136 sec.

(c) During a storm, it is likely that some water will be entrained in the air. This would significantly increase the air density. Some investigators have argued that the entrained water will also slow down the air so there would be no net increase in wind drag. This issue is still unresolved. Current practice is to neglect entrained water when specifying the air density in the wind drag calculation.

(d) Values for the drag coefficient depend on the vessel geometry and orientation to the wind, and have been determined from wind tunnel tests. C_D values show significant variation, so reference should be made to Benham et al. (1977), Gaythwaite (1990), Isherwood (1973), Naval Facilities Engineering Command (1968), Owens and Palo (1981), and Palo (1983) for information on drag coefficients for a variety of vessels. These references also give some information on projected areas for common types of vessels.
Table II-7-6 lists drag coefficients for wind (Bruun 1989).

Table II-7-6
Drag Coefficients for Wind Force

Wind Direction	C_D		
	Max.	Min.	Mean
Crosswise	1.40	0.80	1.11
Bow	1.04	0.62	0.82
Stern	1.02	0.64	0.77

(e) The wind speed at the standard elevation (10 m) is commonly used because this would be a good reference elevation for most larger vessels. If the center of pressure of the vessel is at a significantly different elevation than 10 m, the 1/7th power velocity profile law may be used to correct the wind velocity. It is defined by

$$V_z = V_{10}\left(\frac{z}{10}\right)^{0.11} \tag{II-7-32}$$

where V_z is the velocity at the desired elevation z. Typically, a 50-year return period wind speed is used or the limiting wind speed for which a vessel might remain moored would be used.

(f) The gustiness of the wind must also be considered; i.e., what duration wind gust is sufficient to envelop the vessel. To account for gustiness, the drag coefficient is often increased by a factor of about 1.4 (Tsinker 1986).

(g) Commonly, current drag forces are determined with less certainty than wind drag forces. Current speeds and directions at the mooring site may be difficult to predict, particularly in a harbor having a complex layout. Currents may be continually shifting if dominated by the tide or river flow. The Reynolds number for currents acting on a vessel is usually in the fully turbulent region, but often close to the transition point where drag coefficients show a wider range of scatter. The vessel draft and resulting bottom clearance can also have a significant impact on the resulting drag force. Gaythwaite (1990) presents several sources for current drag coefficient and vessel projected area information. Seelig, Kreibel, and Headland (1992) have published a recent analysis of new scale-model drag studies and other data collected over the past five decades.

EXAMPLE PROBLEM II-7-8

FIND:

The wind drag for a Beaufort 5 fresh breeze of 20 knots (10.31 m/s) at an angle of 30 deg to the wind. Assume gustiness can be accounted for by applying a factor of 1.20 to the wind speed. Beaufort 5 is usually the limiting wind for port operations of loading and unloading.

GIVEN:

A C9 containership is moored at a pier with an asymmetrical container distribution of 5 high in the bow half of the vessel and none in the aft portion. The useable length of the ship for cargo handling is 246 m. The height above the water is 10.9 m. The containers are 2.7 m tall.

SOLUTION:

The forward and aft areas exposed to the wind are

$$A_{aft} = \frac{246}{2}\ 10.9 = 1{,}340\ \mathrm{m}^2$$

$$A_{forward} = 123\left[10.9 + 5(2.7)\right] = 3{,}000\ \mathrm{m}^2$$

The net effective area is then

$$A_{eff} = \left[1{,}340 + 3{,}000\right] \sin 30° = 2{,}170\ \mathrm{m}^2$$

The wind speed, including a gustiness factor, is

$$V_w = 1.20(10.31) = 12.4\ \mathrm{m/s}$$

Substituting these values into Equation II-7-31, we get

$$F_w = \frac{1}{2}(1.2)(1.0)(2{,}170)(12.4)^2 = 200\ \mathrm{kN}$$

where we have assumed $\rho_a = 1.2$ kg/m^3 at 20 °C and $C_D = 1.0$ as a reasonable value since the mean drag coefficient for bow and transverse winds varies between 0.82 to 1.11.

(h) Longitudinal current loads on ships are taken from procedures by NAVFAC Design Manual DM26.5. The total longitudinal current load $F_{c,tot}$ is composed of form drag $F_{c,form}$, skin friction $F_{c,fric}$, and propeller $F_{c,prop}$ drag components. All three components have similar equations.

$$F_{c,tot} = F_{c,form} + F_{c,fric} + F_{c,prop} \tag{II-7-33}$$

(i) Form drag is due to the flow of water past the vessel's cross-sectional area and is defined as

$$F_{c,form} = -\frac{1}{2}\ \rho_w\ C_{c,form}\ B\ T\ V_c^2\ \cos\theta_c \tag{II-7-34}$$

where ρ_w is the water density, $C_{c,form}$ is the form drag coefficient = 0.1, B is the vessel beam, T is the vessel draft, V_c is the average current speed, and θ_c is the angle of the current relative to the longitudinal axis of the vessel. Skin friction drag is due to the flow of water over the wetted surface area of the vessel and is given by

$$F_{c,fric} = -\frac{1}{2} \rho_w C_{c,fric} S V_c^2 \cos\theta_c \quad \text{(II-7-35)}$$

where $C_{c,fric}$ is the skin friction coefficient and S is the wetter surface area of the vessel. The skin friction coefficient is a function of the Reynolds number R_n

$$C_{c,friction} = \frac{0.075}{(\log_{10} R_n - 2)^2} \quad \text{(II-7-36)}$$

$$R_n = \frac{V_c L_{wl} \cos\theta_c}{\nu} \quad \text{(II-7-37)}$$

where L_{wl} is the waterline length of the vessel and ν is the kinematic viscosity of water. The wetted surface area is defined as

$$S = (1.7 T L_{wl}) + \frac{D}{T\gamma_w} \quad \text{(II-7-38)}$$

where D is the displacement of the vessel in Long Tons (=2240 lb = 1016.0 kg), and γ_w = 1.01 Long Tons / m^3 (LT/m^3).

(j) Finally, the propeller drag is due to the form drag of the propeller with a locked shaft and is given by

$$F_{c,prop} = -\frac{1}{2} \rho_w C_{c,prop} A_p V_c^2 \cos\theta_c \quad \text{(II-7-39)}$$

where $C_{c,prop}$ is the propeller drag coefficient = 1 and A_p is the expanded or developed blade area of the propeller defined as

$$A_p = \frac{L_{wl} B}{0.838 A_r} \quad \text{(II-7-40)}$$

(k) The area ratio A_r is the ratio of the waterline length times the beam to the total projected propeller area. Typical values range between 100 for a destroyer and 270 for a tanker.

(l) Thus, to calculate current loads, the following input parameters are needed: the vessel's beam, draft, waterline length, displacement, and propeller area ratio; and average current speed and direction.

(m) It is difficult to evaluate wave loadings on a moored vessel. Both wind-wave and long-period waves are oscillatory; so there is a complex interaction with the mooring system dynamics. This interaction depends on the incident wave frequencies, the vessel added mass and drag characteristics, and the elastic characteristics of the mooring lines and fender system. The vessel can respond in one or more of the six modes of oscillation (see above). Rather than an analytical treatment of the problem in which actual wave loads are determined, scale model testing is often employed. In the latter, the system response in terms of

mooring line loads, fender loads, and vessel response modes are directly determined for given incident wave spectra. Sarpkaya and Isaacson (1981) and Gaythwaite (1990) discuss this further.

II-7-8. References

EM 1110-2-1613
Hydraulic Design of Deep-Draft Navigation Projects

Abbott and Madsen 1990
Abbott, M. B., and Madsen, P. A. 1990. "Modelling of Wave Agitation in Harbors," *The Sea,* Volume 9, Part B, B. Le Méhauté and D. M. Hanes, ed., John Wiley & Sons, New York.

Allsop and Hettiarachchi 1988
Allsop, N. W. H., and Hettiarachchi, S. S. L. 1988. "Reflections from Coastal Structures," *Proceedings, 21st International Conference on Coastal Engineering*, American Society of Civil Engineers, pp 782-794.

Andersen 1979
Andersen, P. 1979. "Ship Motions and Sea Loads in Restricted Water Depth," *Ocean Engineering*, Vol 6, pp 557-569.

Bailard et al. 1990
Bailard, J. A., DeVries, J., Kirby, J. T., and Guza, R. T. 1990. "Bragg Reflection Breakwater: A New Shore Protection Method?" *Proceedings, 22nd International Conference on Coastal Engineering*, American Society of Civil Engineers, Delft, The Netherlands, pp 1702-1715.

Bailard et al. 1992
Bailard, J. A., DeVries, J. W., and Kirby, J. T. 1992. "Considerations in Using Bragg Reflection from Storm Erosion Protection," *Journal, Waterway, Port, Coastal and Ocean Eng. Division,* American Society of Civil Engineers, Jan/Feb, pp 62-74.

Battjes 1974
Battjes, J. A. 1974. "A Computation of Set-Up, Longshore Currents, Run-Up and Overtopping Due to Wind-Generated Waves," Ph.D. diss., Delft University of Technology, The Netherlands.

Beck 1977
Beck, R. F. 1977. "Forces and Moments on a Ship in a Shallow Channel," *Journal of Ship Research*, June.

Benham et al. 1977
Benham, F. A., et al. 1977. "Wind and Current Shape Coefficients for Very Large Crude Carriers," *Proceedings*, *Offshore Technology Conference,* Paper 2739.

Blaauw and van der Knapp 1983
Blaauw, H. G., and van der Knapp, F. M. C. 1983. "Prediction of Squat of Ships Sailing in Restricted Water," *Proceedings*, *8th International Harbor Conference*, Antwerp, June.

Bowden 1983
Bowden, K. F. 1983. *Physical Oceanography of Coastal Waters*, John Wiley, New York.

Bowers and Welsby 1982
Bowers, E. C., and Welsby, J. 1982. "Experimental Study of Diffraction through a Breakwater Gap," Report IT 229, Hydraulics Research Station, Wallingford, U.K.

Briggs and Green 1992
Briggs, M. J., and Green, D. R. 1992. "Experimental Study of Monochromatic Wave-Ebb Current Interaction," Technical Report CERC-92-9, U.S. Army Engineer Waterways Experiment Station, Vicksburg, MS, p 91.

Briggs and Liu 1993
Briggs, M. J., and Liu, P. L-F. 1993. "Experimental Study of Monochromatic Wave-Ebb Current Interaction," *Proceedings*, *Waves '93 Conference,* American Society of Civil Engineers, New Orleans, LA.

Briggs et al. 1994
Briggs, M. J., Lillycrop, L. S., Harkins, G. S., Thompson, E. F., and Green, D. R. 1994. "Physical and Numerical Model Studies of Barbers Point Harbor, Oahu, Hawaii," Technical Report CERC-94-14, U.S. Army Engineer Waterways Experiment Station, Vicksburg, MS.

Bruun 1956
Bruun, P. 1956. "Destruction of Wave Energy by Vertical Walls," *Journal, Waterways and Harbors Division*, American Society of Civil Engineers, WW1, pp 1-13.

Bruun 1978
Bruun, P. 1978. "Stability of Tidal Inlets, Theory and Engineering," *Developments in Geotechnical Engineering 23*, Elsevier Scientific Publishing, Amsterdam, The Netherlands.

Bruun 1989
Bruun, P. 1989. *Port Engineering*, 4th ed., Vol 1, Gulf Publishing Company, Houston, TX.

Callaway 1981
Callaway, R. J. 1981. "Flushing Study of South Beach Marina, Oregon," *Journal, Waterway, Port, Coastal and Ocean Division*, American Society of Civil Engineers, WW2, pp 47-58.

Carr 1952
Carr, J. H. 1952. "Wave Protection Aspects of Harbor Design," Report E-11, Hydrodynamics Laboratory, California Institute of Technology.

Carr and Stelzriede 1952
Carr, J. H., and Stelzriede, M. E. 1952. "Diffraction of Water Waves by Breakwaters," *Gravity Waves*, Circular 521, National Bureau of Standards, Washington, DC, pp 109-125.

Carrier 1971
Carrier, G. F., Shaw, R. P., and Miyata, M. 1971. "The Response of Narrow-Mouthed Harbors in a Straight Coastline to Periodic Incident Waves," *J. Appl. Mech.,* Vol 38, Series E, Nov 2, 1971.

Chen 1986
Chen, H. S. 1986. "Effects of Bottom Friction and Boundary Absorption on Water Wave Scattering," *Applied Ocean Research*, Vol 8, No. 2, pp 99-104.

Chen and Houston 1987
Chen, H. S., and Houston, J. R. 1987. "Calculation of Water Oscillation in Coastal Harbors; HARBS and HARBD User's Manual," Instruction Report CERC-87-2, U.S. Army Engineer Waterways Experiment Station, Vicksburg, MS.

Chiang and Lee 1982
Chiang, W.-L., and Lee, J.-J. 1982. "Simulation of Large-scale Circulation in Harbors," *Journal, Waterway, Port, Coastal and Ocean Division*, American Society of Civil Engineers, WW1, pp 17-31.

Cialone et al. 1991
Cialone, M. A., Mark, D. J., Chou, L. W., Leenknecht, D. A., Davis, J. A., Lillycrop. L. S., Jensen, R. E., Thompson, Gravens, M. B., Rosati, J. D., Wise, R. A., Kraus, N. C., and Larson, P. M. 1991. "Coastal Modeling System (CMS) User's Manual." Instruction Report CERC-91-1, U.S. Army Engineer Waterways Experiment Station, Vicksburg, MS.

Constantine 1960
Constantine, T. 1960. "On the Movement of Ships in Restricted Waterways," *Journal of Fluid Mechanics*, Vol 9, pp 247-256.

Cox and Clark 1992
Cox, J. C., and Clark, G. R. 1992. "Design Development of a Tandem Breakwater System for Hammond Indiana," *Coastal Structures and Breakwaters*, Institution of Civil Engineers, Thomas Telford, London, pp 111-121.

Dand 1976
Dand, I. W. 1976. "Ship-Ship Interaction in Shallow Water," *11th Symposium on Naval Hydrodynamics*, University College, London, April.

Dand and Furgeson 1973
Dand, I. W., and Furgeson, A. M. 1973. "The Squat of Full Ships in Shallow Water," *Transactions, Royal Institute of Naval Architects*, April.

Davies and Heathershaw 1984
Davies, A. G., and Heathershaw, A. D. 1984. "Surface-Wave Propagation over Sinusoidally Varying Topography," *Journal of Fluid Mechanics*, Vol 144, pp 419-443.

Defant 1961
Defant, A. 1961. *Physical Oceanography*, Vol II, Pergamon Press, New York.

Delft Hydraulics Laboratory 1965
Delft Hydraulics Laboratory. 1965. "Report on Model Tests, North Sea Canal, Part III," Delft, The Netherlands.

Elgar et al. 1992
Elgar, S., Herbers, T. C., Okihiro, M., Oltman-Shay, J., and Guza, R. T. 1992. "Observations of Infragravity Waves," *Journal of Geophysical Research*, Vol 97, No. C10, pp 15573-15577.

Eryuzlu and Hausser 1978
Eryuzlu, N. E., and Hausser, R. 1978. "Experimental Investigation Into Some Aspects of Large Vessel Navigation in Restricted Waterways," *Proceedings, Symposium on Aspects of Navigability*, Delft, The Netherlands.

Falconer 1980
Falconer, R. A. 1980. "Modelling of Planform Influence on Circulation in Harbors," *Proceedings, 17th International Conference on Coastal Engineering*, American Society of Civil Engineers, pp 2726-2744.

Falconer 1984
Falconer, R. A. 1984. "A Mathematical Model Study of the Flushing Characteristics of a Shallow Tidal Bay," *Proceedings, Institution of Civil Engineers*, Vol 77, pp 311-332.

Falconer 1985
Falconer, R. A. 1985. "Application of Numerical Models in the Hydraulic Design of Four U.K. Harbors," *Proceedings, Conference on Numerical and Hydraulic Modelling of Ports and Harbors*, British Hydraulic Research Association, pp 1-11.

Falconer and Mardapitta-Hadjipandeli 1986
Falconer, R. A., and Mardapitta-Hadjipandeli, L. 1986. "Application of a Nested Numerical Model to Idealized Rectangular Harbors," *Proceedings, 20th International Conference on Coastal Engineering*, American Society of Civil Engineers, pp 176-192.

Ferguson and McGregor 1986
Ferguson, A. M., and McGregor, R. C. 1986. "On the Squatting of Ships in Shallow and Restricted Water," *Proceedings, 20th International Conference on Coastal Engineering*, American Society of Civil Engineers.

Garthune et al. 1948
Garthune, R. S., Rosenberg, B., Cafiero, D., and Olson, C.R. 1948. "The Performance of Model Ships in Restricted Channels in Relation to the Design of a Ship Canal," Report 601, U.S. Navy David Taylor Model Basin, Washington, DC.

Gates and Herbich 1977
Gates, E. T., and Herbich, J. B. 1977. "The Squat Phenomenon and Related Effects of Channel Geometry," *Proceedings, Hydraulics in the Coastal Zone Conference*, American Society of Civil Engineers.

Gaythwaite 1990
Gaythwaite, J. W. 1990. *Design of Marine Facilities-For the Berthing, Mooring and Repair of Vessels*, Von Nostrand Reinhold, New York.

Giles and Sorensen 1979
Giles, M. L., and Sorensen, R. M. 1979. "Determination of Mooring Loads and Wave Transmission for a Floating Tire Breakwater," *Proceedings, Coastal Structures '79 Conference*, American Society of Civil Engineers, pp 1069-1085.

Gilman and Nottingham 1992
Gilman, J. F., and Nottingham, D. 1992. "Wave Barriers: An Environmentally Benign Alternative," *Proceedings, Coastal Engineering Practice'92 Conference*, American Society of Civil Engineers, pp 479-486.

Goda 1969

Goda, Y. 1969. "Reanalysis of Laboratory Data on Wave Transmission Over Breakwaters," Port and Harbor Research Institute Report, Vol 8, No. 3, pp 3-18.

Goda 2000
Goda, Y. 2000. *Random Seas and Design of Maritime Structures*, 2nd ed., World Scientific Pub. Co., Teaneck, NJ.

Goda, Takayama, and Suzuki 1978
Goda, Y., Takayama, T., and Suzuki, Y. 1978. "Diffraction Diagrams for Directional Random Waves," *Proceedings, 16th International Conference on Coastal Engineering*, American Society of Civil Engineers, pp 628-650.

Greenstreet 1982
Greenstreet, G. 1982. "Study of Ships Track and Motions at Port Taranaki," *Proceedings, 18th International Conference on Coastal Engineering*, American Society of Civil Engineers, pp 2763-2772.

Hales 1981
Hales, L. Z. 1981. "Floating Breakwaters: State-of-the-Art Literature Review," Technical Report 81-1, U.S. Army Engineer Waterways Experiment Station, Vicksburg, MS.

Harms et al. 1982
Harms, V. W., Westerink, J. J., Sorensen, R. M., and McTamany, J. E. 1982. "Wave Transmission and Mooring Force Characteristics of Pipe-Tire Floating Breakwaters," Technical Paper 82-4, U.S. Army Engineer Waterways Experiment Station, Vicksburg, MS.

Harris and Bodine 1977
Harris, D. L., and Bodine, B. R. 1977. "Comparison of Numerical and Physical Hydraulic Models, Masonboro Inlet, North Carolina," GITI Report 6, General Investigation of Tidal Inlets, U.S. Army Engineer Waterways Experiment Station, Vicksburg, MS.

Havelock 1908
Havelock, T. H. 1908. "The Propagation of Groups of Waves in Dispersive Media, with Application to Waves on Water Produced by a Travelling Disturbance," *Proceedings, Royal Society of London*, Series A.

Herbers et al. 1992
Herbers, T. C., Elgar, S., Guza, R. T., and O'Reilly, W. C. 1992. "Infragravity-Frequency (0.005-0.05 Hz) Motions on the Shelf," *Proceedings of 23rd International Conference on Coastal Engineering (ICCE)*.

Herbich 1992
Herbich, J. B. 1992. "Harbors, Navigational Channels, Estuaries, Environmental Effects," *Handbook of Coastal and Ocean Engineering, Vol 3,* Gulf Publishing Company, Houston, TX, p 1340.

Hooft 1973
Hooft, J. P. 1973. "Maneuvering Large Ships in Shallow Water," *Journal of Navigation*, Vol 26.

Hsu 1990
Hsu, J. R. C. 1990. "Short-Crested Waves," *Handbook of Coastal and Ocean Engineering,Vol 1*, J. B. Herbich, ed., Gulf Publishing Company, Houston, TX.

Hudson et al. 1979

Hudson, R. Y., Herrmann, F. A., Sager, R. A., Whalin, R. W., Keulegan, G. H., Chatham, C. E., and Hales, L. Z. 1979. "Coastal Hydraulic Models," Special Report No. 5, U.S. Army Engineer Waterways Experiment Station, Vicksburg, MS.

Ippen 1966
Ippen, A. T. 1966. "*Estuary and Coastline Hydrodynamics*, McGraw-Hill Book Company, Inc., New York.

Ippen and Goda 1963
Ippen, A. T., and Goda, Y. 1963. "Wave Induced Oscillations in Harbors: The Solution for a Rectangular Harbor Connected to the Open-sea," Report 59, Hydrodynamics Lab., Mass. Inst. Technology, Cambridge, MA.

Isaacson and Mercer 1982
Isaacson, M., and Mercer, A. G. 1982. "The Response of Small Craft to Wave Action," *Proceedings, 18th International Conference on Coastal Engineering*, American Society of Civil Engineers, pp 2723-2742.

Isherwood 1973
Isherwood, R. M. 1973, "Wind Resistance of Merchant Ships," *Transactions, Royal Institute of Naval Architects*, pp 327-338.

Jiang and Falconer 1985
Jiang, J. X., and Falconer, R. A. 1985. "The Influence of Entrance Conditions and Longshore Currents on Tidal Flushing and Circulation in Model Rectangular Harbors," *Proceedings, International Conference on Numerical and Hydraulic Modelling of Ports and Harbors*, British Hydraulic Research Association, pp 65-74.

Johnson 1952
Johnson, J. W. 1952. "Generalized Wave Diffraction Diagrams," *Proceedings, Second Conference on Coastal Engineering*, The Council on Wave Research, Berkeley, CA, pp 6-23.

Kirby 1987
Kirby, J. T. 1987. "A Program for Calculating the Reflectivity of Beach Profiles," Report UFL/COEL-87/004, University of Florida, Gainesville.

Kray 1970
Kray, C. J. 1970. "Supership Effect on Waterway Depth and Alignment," *Journal, Waterways and Harbors Division*, American Society of Civil Engineers.

Lai, Long, and Huang 1989
Lai, R. J., Long, S. R., and Huang, N. E. 1989. "Laboratory Studies of Wave-Current Interaction: Kinematics of the Strong Interaction," *Journal of Geophysical Research*, Vol 94, No. C11, November, pp 16,201-16,214.

Lee 1969
Lee, J. J. 1969. "Wave Induced Oscillations in Harbors of Arbitrary Shape," Report No. KH-R-20, W. M. Keck Lab. of Hydraulics and Water Resources, Calif. Inst. of Technology, Pasadena, CA.

Leenknecht, Szuwalski, and Sherlock 1992
Leenknecht, D. A., Szuwalski, A., and Sherlock, A. R. 1992. "Automated Coastal Engineering System, User Guide and Technical Reference, Version 1.07," U.S. Army Engineer Waterways Experiment Station, Vicksburg, MS.

Lillycrop et al. 1993
Lillycrop, L. S., Briggs, M. J., Harkins, G. S., Boc, S. J., and Okihiro, M. S. 1993. "Barbers Point Harbor, Oahu, HI, Monitoring Study," Technical Report CERC-93-18, U.S. Army Engineer Waterways Experiment Station, Vicksburg, MS.

Lin, Lott, and Mehta 1986
Lin, C.-P., Lott, J. W., and Mehta, A. J. 1986. "Turbidity-Sedimentation in Closed-End Channels," *Proceedings, 20th International Conference on Coastal Engineering*, American Society of Civil Engineers, pp 1336-1350.

Liu 1982
Liu, P. L-F. 1982. "Combined Refraction and Diffraction: Comparison Between Theory and Experiments," *Journal of Geophysical Research*, Vol 87, No. C8, pp 5723-5730.

Liu and Lozano 1979
Liu, P. L-F., and Lozano, C . 1979. "Combined Wave Refraction and Diffraction," *Proceedings, Coastal Structures 79 Conference*, American Society of Civil Engineers, pp 978-997.

Lott and Hurtienne 1992
Lott, J. W., and Hurtienne, A. M. 1992. "Design, Construction and Performance of a Baffled Breakwater," *Proceedings, Coastal Engineering Practice '92 Conference*, American Society of Civil Engineers, pp 487-502.

Lozano and Liu 1980
Lozano, C., and Liu, P.L-F. 1980. "Refraction-Diffraction Model for Linear Surface Waves," *Journal of Fluid Mechanics*, Vol 101, Pt. 4.

Madsen and White 1976
Madsen, O. S., and White, S. M. 1976. "Reflection and Transmission Characteristics of Porous Rubble Mound Breakwaters," Miscellaneous Report 76-5, U.S. Army Engineer Waterways Experiment Station, Vicksburg, MS.

Madsen, Svendsen, and Michaelsen 1980
Madsen, P. A., Svendsen, I. A., and Michaelsen, C. 1980. "Some Recent Results for Wave-Induced Motions of a Ship in Shallow Water," *Proceedings, 17th International Conference on Coastal Engineering*, American Society of Civil Engineers, pp 3043-3062.

Mansard and Pratte 1982
Mansard, E. P. D., and Pratte, B. D. 1982. "Moored Ship Response in Irregular Waves," *Proceedings, 18th International Conference on Coastal Engineering*, American Society of Civil Engineers, pp 2621-2640.

McNown 1976
McNown, J. S. 1976. "Sinkage and Resistance for Ships in Channels," *Journal, Waterways, Harbors and Coastal Engineering Division*, American Society of Civil Engineers.

Mehta and Özsöy 1978
Mehta, A. J., and Özsöy, E. 1978. Chapter 3, "Inlet Hydraulics," *Stability of Tidal Inlets: Theory and Engineering*, P. Bruun, ed., Elseveir Scientific Publishing Co., Amsterdam, The Netherlands, pp 83-161.

Mei 1985
Mei, C. C. 1985. "Resonant Reflection of Surface Water Waves by Periodic Sand Bars," *Journal of Fluid Mechanics*, Vol 152, pp 315-335.

Memos 1976
Memos, C. D. 1976. "Diffraction of Waves Through a Gap Between Two Inclined Breakwaters," Ph.D. diss., University of London.

Memos 1980a
Memos, C. D. 1980a. "An Extended Approach to Wave Scattering Through a Harbor Entrance," *Bulletin, Permanent International Association of Navigation Congresses*, Vol 1, No. 35, pp 20-26.

Memos 1980b
Memos, C. D. 1980b. "Energy Transmission by Surface Waves Through an Opening," *Journal of Fluid Mechanics*, Vol 97, Pt. 3, pp 557-568.

Memos 1980c
Memos, C. D. 1980c. "Water Waves Diffracted by Two Breakwaters," *Journal of Hydraulic Research*, Vol 18, No. 4, pp 343-357.

Meirovitch 1975
Meirovitch, L. 1975. *Elements of Vibration Analysis,* McGraw-Hill, Inc.

Miles 1948
Miles, J. W. 1948. "Coupling of a Cylindrical Tube to a Half Space," *Journal, Acoustic Society of America,* pp 652-664.

Miles 1974
Miles, J. W. 1974. "Harbor Seiching," *Annual Review of Fluid Mechanics,* Vol 6, pp 17-35.

Moody 1970
Moody, C. G. 1970. "Study of the Performance of Large Bulk-Cargo Ships in a Proposed Interoceanic Canal," Report 374-H-01, U.S. Naval Ship Research and Development Center, Carderock, MD.

Naval Facilities Engineering Command 1968
Naval Facilities Engineering Command. 1968. *Harbors and Coastal Facilities*, Design Manual-26, Alexandria, VA.

Nece 1985
Nece, R. E. 1985. "Physical Modeling of Tidal Exchange in Small-Boat Harbors," *Proceedings, International Conference on Numerical and Hydraulic Modelling of Ports and Harbors*, British Hydraulic Research Association, pp 33-41.

Nece and Layton 1989
Nece, R. E., and Layton, J. A. 1989. "Mitigating Marina Environmental Impacts Through Hydraulic Design," *Proceedings, International Conference on Marinas*, Computational Mechanics Institute, pp 435-449.

Nece and Richey 1972
Nece, R.E., and Richey, E.P. 1972. "Flushing Characteristics of Small-Boat Marinas," *Proceedings, 13th International Conference on Coastal Engineering*, American Society of Civil Engineers, pp 2499-2512.

Nece and Richey 1975
Nece, R. E., and Richey, E. P. 1975. "Application of Physical Tidal Models in Harbor and Marina Design," *Proceedings, Symposium on Modelling Techniques*, American Society of Civil Engineers, pp 783-801.

Nece, Falconer, and Tsutumi 1976
Nece, R. E., Falconer, R. A., and Tsutumi, T. 1976. "Planform Influence on Flushing and Circulation in Small Harbors," *Proceedings, 15th International Conference on Coastal Engineering*, American Society of Civil Engineers, pp 3471-3486.

Nece, Smith, and Richey 1980
Nece, R. E., Smith, H. N. and Richey, E. P. 1980. "Tidal Circulation and Flushing in Five Western Washington Marinas," Technical Report 63, Harris Hydraulics Laboratory, University of Washington, Seattle.

Neumann and Pierson 1966
Neumann, G., and Pierson, W. J. 1966. *Principles of Physical Oceanography*, Prentice-Hall, Englewood Cliffs, NJ.

Newman 1978
Newman, J. N. 1978. *Marine Hydrodynamics*, MIT Press, Cambridge, MA.

Noble 1982
Noble, S. 1982. "Ship Motions Related to Deep Draft Channel Design," *Proceedings, 18th International Conference on Coastal Engineering*, American Society of Civil Engineers, pp 2662-2680.

Northwest Hydraulic Consultants 1980
Northwest Hydraulic Consultants. 1980. "Study to Determine Acceptable Wave Climate in Small Craft Harbors," Report to Department of Fisheries and Oceans Government of Canada, Ottawa.

Oil Companies International Marine Forum 1978
Oil Companies International Marine Forum. 1978. "Guidelines and Recommendations for the Safe Mooring of Large Ships at Pier and Sea Island," Witherby and Co. Ltd., London.

Okihiro, Guza, and Seymour 1992
Okihiro, M., Guza, R. T., and Seymour, R. J. 1992. "Bound Infragravity Waves," *Journal of Geophysical Research*, Vol 97, No. C7, pp 11453-11469.

Owens and Palo 1981
Owens, R., and Palo, P. A. 1981. "Wind-Induced Steady Loads on Moored Ships," Technical Memo M-44-81-7, Navy Civil Engineering Laboratory, Pt Hueneme, CA.

Palo 1983

Palo, P. A. 1983. Steady Wind and Current Induced Loads on Moored Vessels," *Proceedings, Offshore Technology Conference*, Paper 4530.

Penny and Price 1952
Penny, W. G., and Price, A. T. 1952. "The Diffraction Theory of Sea Waves by Breakwaters, and the Shelter Afforded by Breakwaters," *Philosophical Transactions*, Royal Society of London, Series A, Vol 244, pp 236-253.

Putnam and Arthur 1948
Putnam, J. A., and Arthur, R.S. 1948. "Diffraction of Water Waves by Breakwaters," *Transactions, American Geophysical Union*, Vol 29, No. 4, pp 481-490.

Raichlen 1968
Raichlen, F. 1968. "The Motions of Small Boats in Standing Waves," *Proceedings, 11th Conference on Coastal Engineering*, American Society of Civil Engineers, pp 1531 -1554.

Raichlen 1993
Raichlen, F. 1993. "Waves Propagating on an Adverse Jet," *Proceedings, Waves '93 Conference*, American Society of Civil Engineers, New Orleans, LA.

Raichlen and Lee 1992
Raichlen, F., and Lee, J.J. 1992. "Oscillation of Bays, Harbors and Lakes," *Handbook of Coastal and Ocean Engineering,* Vol 3, J. B. Herbich, ed., Gulf Publishing Company, Houston, TX.

Robb 1949
Robb, A. M. 1949. "Interaction Between Ships," *Transactions, Institute of Naval Architects*, Vol 91.

Robb 1952
Robb, A. M. 1952. *Theory of Naval Architecture*, Charles Griffen and Co., London.

Sakai and Saeki 1984
Sakai, S., and Saeki, H. 1984. "Effects of Opposing Current on Wave Transformation on a Sloping Bed," *Proc. 19th Conf. on Coastal Engineering*, American Society of Civil Engineers, Vol 1, pp 1132-1148.

Sarpkaya and Isaacson 1981
Sarpkaya, T., and Isaacson, M. 1981. *Mechanics of Wave Forces on Offshore Structures*, Van Nostrand Reinhold Co., New York.

Schluchter and Slotta 1978
Schluchter, S. S., and Slotta, L. 1978. "Flushing Studies of Marinas," *Proceedings, Coastal Zone '78 Conference*, American Society of Civil Engineers, pp 1878-1896.

Schofield 1974
Schofield, R. B. 1974. "Speed of Ships in Restricted Navigation Channels," *Journal, Waterways,Harbors and Coastal Engineering Division*, American Society of Civil Engineers, May.

Schwartz and Imberger 1988
Schwartz, R. A., and Imberger, J. 1988. "Flushing Behavior of a Coastal Marina," *Proceedings, 21st International Conference on Coastal Engineering*, American Society of Civil Engineers, pp 2626-2640.

Seelig 1979
Seelig, W. N. 1979. "Estimation of Wave Transmission Coefficients for Permeable Breakwaters," CETA 79-6, U.S. Army Engineer Waterways Experiment Station, Vicksburg, MS.

Seelig 1980
Seelig, W. N. 1980. "Two-dimensional Tests of Wave Transmission and Reflection Characteristics of Laboratory Breakwaters," Technical Report 80-1, U.S. Army Engineer Waterways Experiment Station, Vicksburg, MS.

Seelig 1983
Seelig, W. N. 1983. "Wave Reflection from Coastal Structures," *Proceedings, Coastal Structures '83*, American Society of Civil Engineers, pp 961-973.

Seelig and Ahrens 1981
Seelig, W. N., and Ahrens, J. P. 1981. "Estimation of Wave Reflection and Energy Dissipation Coefficients for Beaches, Revetments and Breakwaters," Technical Paper 81-1, U.S. Army Engineer Waterways Experiment Station, Vicksburg, MS.

Seelig, Kreibel, and Headland 1992
Seelig, W. N., Kreibel, D., and Headland, J. 1992. "Broadside Current Forces on Moored Ships," *Proceedings, Civil Engineering in the Oceans V Conference*, American Society of Civil Engineers, pp 326-340.

Sharp and Fenton 1968
Sharp, B. B., and Fenton, J. D. 1968. "A Model Investigation of Squat," *The Dock and Harbor Authority*, November.

Shore Protection Manual 1984
Shore Protection Manual. 1984. 4th ed., 2 Vol, U. S. Army Engineer Waterways Experiment Station, U.S. Government Printing Office, Washington, DC.

Silverstein 1958
Silverstein, B. L. 1958. "Linearized Theory of the Interaction of Ships," Institute of Engineering Research, University of California, Berkeley.

Silvester and Hsu 1993
Silvester, R., and Hsu, J.R.C. 1993. *Coastal Stabilization-Innovative Concepts*, Prentice-Hall, Englewood Cliffs, NJ.

Sommerfeld 1896
Sommerfeld, A. 1896. "Mathematische Theorie der Diffraction," *Mathematische Annalen*, Vol 47, pp 317-374.

Sorensen 1973a
Sorensen, R. M. 1973a. "Ship-Generated Waves," *Advances in Hydroscience*, Academic Press, New York, Vol 9, pp 49-83.

Sorensen 1973b
Sorensen, R. M. 1973b. "Water Waves Produced by Ships," *Journal, Waterways,Harbors and Coastal Engineering Division*, American Society of Civil Engineers.

Sorensen 1976
Sorensen, R. M., and Seelig, W. N. 1976. "Hydraulics of Great Lakes Inlet-Harbor Systems," *Proceedings, Fifteenth Conference on Coastal Engineering,* American Society Civil Engineers, Honolulu, p 20.

Sorensen 1986
Sorensen, R. M. 1986. "Bank Protection for Vessel-Generated Waves," Report IHL-117-86, Lehigh University, prepared for U.S. Army Engineer Waterways Experiment Station, Vicksburg, MS.

Sorensen 1989
Sorensen, R. M. 1989. "Port and Channel Bank Protection from Ship Waves," *Proceedings, Ports '89 Conference*, American Society of Civil Engineers.

Sorensen 1990
Sorensen, R. M. 1990. "The Deployment of Floating Breakwaters: Design Guidance," *Proceedings, 12th Coastal Society Conference*, San Antonio, TX.

Sorensen 1993
Sorensen, R. M. 1993. *Basic Wave Mechanics*, John Wiley & Sons, New York.

Sorensen and Weggel 1984
Sorensen, R. M., and Weggel, J. R. 1984. "Development of Ship Wave Design Information," *Proceedings, 19th International Conference on Coastal Engineering*, American Society of Civil Engineers.

Spaulding 1984
Spaulding, M. L. 1984. "A Vertically Averaged Circulation Model Using Boundary-Fitted Coordinates," *Journal of Physical Oceanography*, American Meteorological Society, Vol 14, pp 973-982.

Taylor 1909
Taylor, D. W. 1909. "Some Model Experiments on Suction of Vessels," *Society of Naval Architects and Marine Engineers*, Vol 17.

Thompson, Chen and Hadley 1993
Thompson, E. F., Chen, H. S., and Hadley, L. L. 1993. "Numerical Modeling of Waves in Harbors," *Proceedings, WAVES 93*, American Society of Civil Engineers, New Orleans, LA.

Tothill 1967
Tothill, J. T. 1967. "Ships in Restricted Channels- A Correlation of Model Tests, Field Measurements, and Theory," *Marine Technology*, April.

Tsinker 1986
Tsinker, G. P. 1986. *Floating Ports-Design and Construction Practices*, Gulf Publishing, Houston, TX.

Tuck 1966
Tuck, E. O. 1966. "Shallow-Water Flow Past Slender Bodies," *Journal of Fluid Mechanics*, Vol 26, pp 81-96.

Tuck and Newman 1974
Tuck, E. O., and Newman, J. N. 1974. "Hydrodynamic Interactions Between Ships," *10th Naval Hydrodynamics Symposium*, Massachusetts Institute of Technology, Cambridge.

van Wyk 1982
van Wyk, A. C. 1982. "Wave-induced Ship Motions in Harbor Entrances - A Field Study," *Proceedings, 18th International Conference on Coastal Engineering*, American Society of Civil Engineers, pp 2681-2699.

Van der Meer and Angremond 1992
Van der Meer, J. W., and Angremond, K. 1992. "Wave Transmission at Low-Crested Structures," *Coastal Structures and Breakwaters*, Institution of Civil Engineers, Thomas Telford, London, pp 25-41.

Vemulakonda, Chou, and Hall 1991
Vemulakonda, S. R., Chou, L. W., and Hall, R. W. 1991. "Los Angeles and Long Beach Harbors Additional Plan Testing - Numerical Modeling of Tidal Circulation and Water Quality," Technical Report CERC-91-2, U.S. Army Engineer Waterways Experiment Station, Vicksburg, MS.

Wang and Noble 1982
Wang, S., and Noble, S. 1982. "Columbia River Entrance Channel Ship Motion Study," *Journal, Waterways, Port, Coastal and Ocean Division*, American Society of Civil Engineers, pp 291-305.

Weggel and Sorensen 1986
Weggel, J. R., and Sorensen, R. M. 1986. "Ship Wave Prediction for Port and Channel Design," *Proceedings, Ports '86 Conference*, American Society of Civil Engineers.

Wehausen 1971
Wehausen, J. V. 1971. "The Motion of Floating Bodies," *Annual Review of Fluid Mechanics*, Annual Reviews, Palo Alto, Vol 3, pp 237-268.

Wiegel 1960
Wiegel, R. L. 1960. "Transmission of Waves Past a Rigid Vertical Thin Barrier," *Journal, Waterways and Harbors Division*, American Society of Civil Engineers, pp 1-12.

Wiegel 1962
Wiegel, R. L. 1962. "Diffraction of Waves by Semi-infinite Breakwater," *Journal of the Hydraulics Division*, American Society of Civil Engineers, Vol 88, No. HY1, pp 27-44.

Willis 1988
Willis, D. H. 1988. "Experimental and Theoretical Studies of Wave-Current Systems," Technical Report, Hydraulics Laboratory, National Research Council of Canada, Ottawa, Ontario, Canada.

Wilson 1967
Wilson, B. W. 1967. "Elastic Characteristics of Moorings," *ASCE Journal of the Waterways and Harbors Division*, Vol 93, No. WW4, pp 27-56.

Wilson 1972
Wilson, B. W. 1972. "Seiches," Advances in Hydroscience, Academic Press, New York, Vol 8, pp 1-94.

Zelt 1986
Zelt, J. A. 1986. "Tsunamis: The Response of Harbors with Sloping Boundaries to Long Wave Excitation," Report KH-R-47, W.M. Keck Lab. of Hydraulics and Water Resources, Calif. Inst. of Technology, Pasadena, CA.

Zelt and Raichlen 1990
Zelt, J. A., and Raichlen, F. 1990. "A Lagrangian Model for Wave-Induced Harbor Oscillations," *Journal of Fluid Mechanics*, Vol 213.

Zwamborn and Cox 1982
Zwamborn, J. A., and Cox, P. J. 1982. "Operational Procedures-Richards Bay Harbor," *Proceedings, 18th International Conference on Coastal Engineering*, American Society of Civil Engineers, pp 2700-2722.

II-7-9. Definitions of Symbols

α	Angle a surface-piercing sloped plane forms with the horizontal [deg]
β	Angle between the breakwater and the radial distance from the breakwater tip to the point where the diffraction coefficient (K') is to be determined (Figure II-7-2) [deg]
Δd	Vessel drawdown [length]
Δl_n	Elongation in the mooring line [length]
ϵ_n	Percent elongation in a mooring line
θ	Angle between the sailing line and the direction of wave propagation [deg]
θ_c	Angle of the current relative to the longitudinal axis of the vessel [deg]
θ_n	Angle a mooring line makes in the horizontal plane with the perpendicular to the vessel [deg]
ν	Kinematic viscosity of water [length^2/time]
ρ_a	Mass density of air [force-time^2/length^4]
ρ_w	Mass density of water (salt water = 1,025 kg/m^3 or 2.0 slugs/ft^3; fresh water = 1,000kg/m^3 or 1.94 slugs/ft^3) [force-time^2/length^4]
ϕ	Angle a mooring line makes in the vertical plane between the vessel and the dock [deg]
ϕ	Phase angle by which a mass displacement lags the excitation displacement [deg]
A	Amplification factor (ratio of mass displacement to excitation displacement) [dimensionless]
A	Projected area of a vessel above the waterline [length^2]
A_b	Surface area of a bay or basin [length^2]
A_c	Channel cross-sectional flow area of an inlet [length^2]
A_m	Vessel's midsection wetted cross-sectional area [length^2]
A_p	Expanded or developed blade area of a propeller (Equation II-7-40) [length^2]
A_r	Dimensionless ratio of the waterline length times the beam to the total projected propeller area
b	Channel width [length]
B	Breakwater gap (Figure II-7-6} [length]
B	Structure crest width [length]
B	Vessel beam [length]
B'	Imaginary breakwater gap [length] (Figure II-7-6)

C	Dimensionless coefficient in the Seelig equation (Equation II-7-2) for the wave transmission coefficient (Equation II-7-3)
C	Individual wave celerities created by a moving vessel (Equation II-7-21) [length/time]
$C_{c\,,\,form}$	Form drag coefficient [dimensionless]
$C_{c\,,\,prop}$	Propeller drag coefficient [dimensionless]
$C_{c\,,\,fric}$	Skin friction coefficient [dimensionless]
C_D	Coefficient of drag for winds measured at 10-m [dimensionless]
C_o , C_i	Initial concentration of some substance in the harbor water and concentration of the substance after i tidal cycles (Equation II-7-20)
C_r	Reflection coefficient [dimensionless]
C_t	Wave transmission coefficient [dimensionless]
C_{t0}	Coefficient for wave transmission by flow over the structure [dimensionless]
C_{tt}	Coefficient for wave transmission through the structure [dimensionless]
d	Water depth [length]
D	Dimensionless drawdown
D	Displacement of a vessel [length^3]
D_{50}	Median diameter of armor stone [length]
d_c	Channel depth [length]
d_s	Water depth at the toe of the structure [length]
E	Dimensionless average per cycle exchange coefficient, a factor for defining the effectiveness of tidally induced harbor flushing (Equation II-7-20)
F	Freeboard [length]
F	Froude number
$F_{c,\,form}$	Form drag of a vessel (Equation II-7-34) [force]
$F_{c,\,fric}$	Skin friction of a vessel (Equation II-7-35) [force]
$F_{c,\,prop}$	Vessel propeller drag (Equation II-7-39) [force]
$F_{c,\,tot}$	Total longitudinal current load on a vessel (Equation II-7--33) [force]
F_w	Drag force due to wind (Equation II-7-31) [force]
g	Gravitational acceleration [length/time^2]
h	Structure crest elevation [length]

H	Standing wave height [length]
H_d	Diffracted wave height at a point in the lee of a breakwater [length]
H_i	Incident wave height [length]
H_r	Reflected wave height [length]
H_t	Transmitted wave height [length]
I_r	Surf similarity number or Iribarren number (Equation II-7-6) [dimensionless]
k_n	Individual stiffness of a mooring line (Equation II-7-29) [force/length]
k_{tot}	Effective spring constant (Equation II-7-28) [force/length]
K'	Diffraction coefficient [dimensionless]
K'_e	Effective diffraction coefficient (Equation II-7-1) [dimensionless]
L	Wave length [length]
ℓ_B	Basin length along the axis B [length]
ℓ_c	Channel length [length]
ℓ'_c	Additional length to account for mass outside each end of the channel [length]
l_n	Length of a mooring line [length]
L_{wl}	Waterline length of a vessel [length]
m	Mass of a vessel [force]
M_0	Zero moment of the spectrum
m_a	Mass of a vessel due to inertial effects of the water entrained with the vessel [force]
m_v	Virtual mass of a vessel (Equation II-7-27) [force]
N	Water surface amplitude (Equation II-7-7) [length]
$-_O$	The subscript 0 denotes deepwater conditions
r	Radial distance from the breakwater tip to the point where the diffraction coefficient (K') is to be determined (Figure II-7-2) [length]
R	Wave runup above the mean water level [length]
R_n	Reynolds number
S	Vessel blockage ratio [dimensionless]
S	Wetted surface area of a vessel [length^2]
S_{max}	Directional concentration parameter characterizing the directional spread of the wave spectrum [dimensionless]

T	Excitation (and response) period [time]
T	Vessel draft [length]
T	Wave period [time]
T_H	Resonant period for Helmholtz mode (Equation II-7-18)[time]
T_n	Axial tension or load on a mooring line [force]
$T_{n,m}$	Natural free oscillating period (n, m is the number of nodes along the x- and y-axes of a basin [time]
T_n	Undamped natural period of a vessel (Equation II-7-26) [time]
$\overline{V}$	Average horizontal velocity at a node (Equation II-7-16) [length/time]
V_{10}	Wind speed at the standard elevation of 10 m above the water surface [length/time]
V_c	Average current speed [length/time]
V_{max}	Maximum horizontal velocity at a node [length/time]
V_r	Return flow velocity (Equation II-7-25), velocity that develops between the vessel hull and the channel bottom and sides [length/time]
V_s	Vessel speed [length/time]
V_z	Wind speed at elevation z [length/time]
W	Breakwater's characteristic dimension in the direction of wave propagation [length]
W	Channel width [length]
X	Maximum horizontal particle excursion at a node in a standing wave (Equation II-7-15) [length]
y	Vertical extent of the barrier below the still-water surface [length]

II-7-10. Acknowledgments

Author of Chapter II-7, "Harbor Hydrodynamics:"

Robert Sorensen, Ph.D., Fritz Engineering Laboratory, Lehigh University, Bethlehem, Pennsylvania.
Edward F. Thompson, Ph.D., Coastal and Hydraulics Laboratory (CHL), Engineer Research and Development Center, Vicksburg, Mississippi.

Reviewers:

Zeki Demirbilek, Ph.D., CHL.
Lee E. Harris, Ph.D., Department of Marine and Environmental Systems, Florida Institute of Technology, Melbourne, Florida.
Michael J. Briggs, Ph.D., CHL.
Monica A. Chasten, U.S. Army Engineer District, Philadelphia, Philadelphia, Pennsylvania.
Linda S. Lillycrop, U.S. Army Engineer District, Mobile, Mobile, Alabama.

II-7-11. Note to Users, Vessel Buoyancy

The determination of the buoyancy of and the weight of a floating vessel requires determining the immersed volume at any waterline and multiplying that volume by the specific weight of the water, generally assumed as 64 lb/ft^3. This is nothing but an expression of Archimedes' principle that the weight of any floating body is equal to the weight of the fluid displaced by the body. In naval architecture, the buoyancy is most commonly called the displacement, but although the use of the word displacement suggests volume, the displacement itself is customarily given in tons. The displacement of a vessel is the ratio of the immersed volume divided by the number of cubic feet per ton of water. The immersed volume is generally in cubic feet (ft^3). The vessel displacement is denoted by the symbol Δ, and is in tons. The vessel displacement to any waterline depends on the density or specific weight of water, γ_w. For salt water, γ_w = 64 and the divisor is 2240/64 = 35. For fresh water γ_w = 62.4 and the divisor is 2240/62.4 = 35.85 ~36.0. The volume of displacement is denoted by the symbol ∇, and is customarily in ft^3. Therefore, we have

$$\Delta = \nabla * \frac{\gamma_w lb/ft^3}{2240 lb/ton} = \frac{\nabla}{r}$$

where $r = \dfrac{2240}{\gamma_w}$ and γ_w is in lb/ft^3. For salt water r = 35 and for fresh water r = 36.

In general, the wetted surface area of a vessel whose geometry is approximated by a rectangular solid can be estimated as

$$\nabla = L * B * T * C_B$$

and

$$S = 2 * L * T + \frac{\nabla}{T} = 2 * L * T + L * B * C_B$$

In 1895, Mumford developed a similar expression from the analysis of calculations for a number of ships:

$$s = 1.7 * L * T + \frac{\nabla}{T} = 1.7 * L * T + L * B * C_B$$

Example 1: For a cargo vessel with the values of L = 401 ft, B = 54.83 ft (molded), T = 23.83 ft (molded), C_B = 0.7685 and C_P = 0.7763. We find S =33,150 ft^2.

Example 2: For fast passenger liner with values of L = 513.4 ft, B = 70.54 ft (molded), d = 24.61 (molded), C_B = 0.5751 and C_P = 0.6084. We find S = 42,300 ft^2.

Table of Contents

Page

II-8-1. Overview of Chapter II-8-1
a. Objectives II-8-1
b. Contents II-8-1
c. Relationship to other chapters and parts II-8-1

II-8-2. Identifying Meteorological and Hydrodynamic Processes Impacting Design II-8-1
a. Brief review of processes II-8-1
b. Identifying relevant processes II-8-2
c. Interaction between processes II-8-2

II-8-3. Acquiring Information II-8-2
a. Identifying available information II-8-2
b. Consideration of collecting field measurements II-8-2
c. Numerical and physical modeling possibilities II-8-2

II-8-4. Statistical Methods - Short-term II-8-3
a. Introduction II-8-3
b. Probability distribution functions II-8-3
c. Statistical parameters II-8-4

II-8-5. Statistical Methods - Long-term II-8-4
a. Introduction II-8-4
b. Stochastic time history II-8-6
c. Extremal probability distribution functions II-8-6
d. Empirical simulation technique II-8-6
e. Methods for fitting distributions to data II-8-6
(1) Data selection II-8-6
(2) Estimating parameters in extremal distribution functions II-8-9
(3) Approaches to estimating parameters II-8-10
(4) Outliers II-8-11
(5) Choosing an extremal distribution function II-8-12
(6) Confidence intervals II-8-12
f. Return period and encounter probability II-8-12
g. Extrapolation of data II-8-13

II-8-6. Analysis of Key Meteorological and Hydrodynamic Processes in Design II-8-13
a. Introduction II-8-13
b. Wind II-8-14
(1) Design importance II-8-14
(2) General climate II-8-14
(3) Storms II-8-14
c. Extreme waves II-8-20
(1) Design importance II-8-20
(2) Deep water II-8-20
(3) Intermediate-depth water II-8-25
(4) Shallow water (depth-limited) II-8-25
(5) Extreme individual wave characteristics II-8-26
d. Wave climate II-8-28
(1) Design importance II-8-28
(2) General climate II-8-28
(3) Storms II-8-30
(4) Persistence of high and low wave conditions II-8-31
e. Long waves II-8-31
(1) Tsunamis II-8-31
(2) Seiche II-8-32
(3) Infragravity waves II-8-32
f. Extreme water level II-8-32
(1) Design importance II-8-32
(2) Estimation procedures II-8-32
g. Water level climate II-8-32
(1) Design importance II-8-33
(2) Estimation procedures II-8-33
(3) Long-term changes II-8-33
h. Currents II-8-33
(1) Design importance II-8-33
(a) Nearshore shelf II-8-33
(b) Surf zone II-8-33
(c) Inlets II-8-33
(d) Harbors II-8-33
(2) Estimation procedures II-8-33
i. Design example II-8-34

II-8-7. Interdependence of Processes During Severe Events II-8-57
a. Design importance II-8-57
b. Procedures for estimating realistic design events, probabilities and return periods . . . II-8-57

II-8-8. References II-8-57

II-8-9. Definition of Symbols II-8-61

II-8-10. Acknowledgments II-8-62

List of Tables

Page

Table II-8-1. Definition of Short-Term and Long-Term Statistics II-8-4

Table II-8-2. Parameters in Extremal Distribution Functions II-8-9

Table II-8-3. Percent Chance for H_s Equaling or Exceeding Return Period H_s II-8-13

Table II-8-4. Probability Distribution Functions for Meteorological and Hydrodynamic Processes II-8-14

Table II-8-5. Standard Deviation and Confidence Interval Relationships II-8-16

Table II-8-6. Return Period Adjustment Factor II-8-19

Table II-8-7. Conversion of Extreme Wind Speeds from Fastest-Mile to 1-hr Average II-8-19

Table II-8-8. Averaging Time Adjustments for Extreme Wind Speeds II-8-20

Table II-8-9. Maximum Wind Speed by Month, in m/s II-8-21

Table II-8-10. Wind Speed Statistics II-8-23

Table II-8-11. Wind Speed at 25- and 50-year Return Period II-8-24

Table II-8-12. Tidal Datum Information II-8-35

Table II-8-13. Significant Storm Events II-8-40

Table II-8-14. Tidal Water Levels for Jetty Design II-8-43

Table II-8-15. Calculation of d_{ijetty} for Storm Event 1 . . . . . II-8-44

Table II-8-16. Calculation of d_{jetty} for Storm Event 1 . . . . . II-8-45

Table II-8-17. Calculation of H_{sjetty} for Storm Event 1 . . . . . II-8-46

Table II-8-18. Calculation of Upper Bound H_{sjetty} Based on Maximum Tide Level II-8-49

Table II-8-19. Calculation of Upper Bound H_{sjetty} Based on Maximum During Shoaling II-8-50

Table II-8-20. Design Significant Wave Heights at Jetty Head II-8-51

Table II-8-21. Calculation of H_{stoe} for Storm Event 1 at Jetty Head II-8-52

Table II-8-22. Calculation of Wave Height Modification by Currents II-8-53

List of Figures

Page

Figure II-8-1. Probability distribution functions for short-term statistics II-8-5

Figure II-8-2. Probability distribution functions for long-term statistics II-8-7

Figure II-8-3. Probability distribution functions for long-term statistics II-8-9

Figure II-8-4. Selection of extreme values for a partial duration series II-8-10

Figure II-8-5. Plotting position formulas II-8-11

Figure II-8-6. Example wind rose (Leffler et al. 1990) II-8-15

Figure II-8-7. Extreme fastest-mile wind speeds with 50-year return period across the U.S. at 10-m elevation (ASCE 1993) II-8-17

Figure II-8-8. Milepost map for use with Figure II-8-9; coastal distance intervals marked in nautical miles (1 nautical mile = 1.9 km) II-8-18

Figure II-8-9. Extreme fastest-mile hurricane wind speeds blowing from any direction at 10 m above ground in open terrain near the coastline for various return periods (after National Bureau of Standards (1980)) II-8-19

Figure II-8-10. Example Problem II-8-1 probability distribution of wind speeds II-8-22

Figure II-8-11. Probability distribution of H_s on shallow water II-8-26

Figure II-8-12. Maximum value of H_s in the surf zone (Goda 1985) II-8-27

Figure II-8-13. Water depth at which H_s is maximum in the surf zone (Goda 1985) II-8-28

Figure II-8-14. Crest elevation at the 2-percent probability level of exceedance (Seelig, Ahrens, and Grosskopf 1983) II-8-29

Figure II-8-15. Wave climate summary (Hubertz et al. 1993) II-8-30

Figure II-8-16. Persistence of storm waves II-8-31

Figure II-8-17. Example of short and long-term surf zone current data (Leffler et al. 1990) II-8-34

Figure II-8-18. Jetty plan II-8-35

Figure II-8-19. Probability distribution of astronomical tide levels II-8-36

Figure II-8-20. Probability distribution of storm surge II-8-37

Figure II-8-21. Probability distribution of high tides and combined tide and storm surge II-8-38

Figure II-8-22. Estimation of shoaling coefficient (Goda 1985) II-8-41

Figure II-8-23. Astronomical tide probability referenced to MSL II-8-42

Figure II-8-24. Estimation of wave setup (Goda 1985) II-8-43

Figure II-8-25. Estimation of wave height at the jetty (Goda 1985) II-8-46

Figure II-8-26. Identification of surf zone conditions II-8-47

Figure II-8-27. Return period wave heights, 165 events, jetty head II-8-48

Figure II-8-28. Return period wave heights, H'_0 . . . . . II-8-49

Figure II-8-29. Return period wave heights, 165 events including upper bounds, jetty head II-8-50

Figure II-8-30. Return period wave heights, toe design, jetty head II-8-52

Figure II-8-31. Wave height modification by currents II-8-54

Figure II-8-32. Joint distribution of H_{sjetty} and T_p from 33 storm events, jetty head II-8-55

Figure II-8-33. Example storm event (Leffler et al. 1990) II-8-56

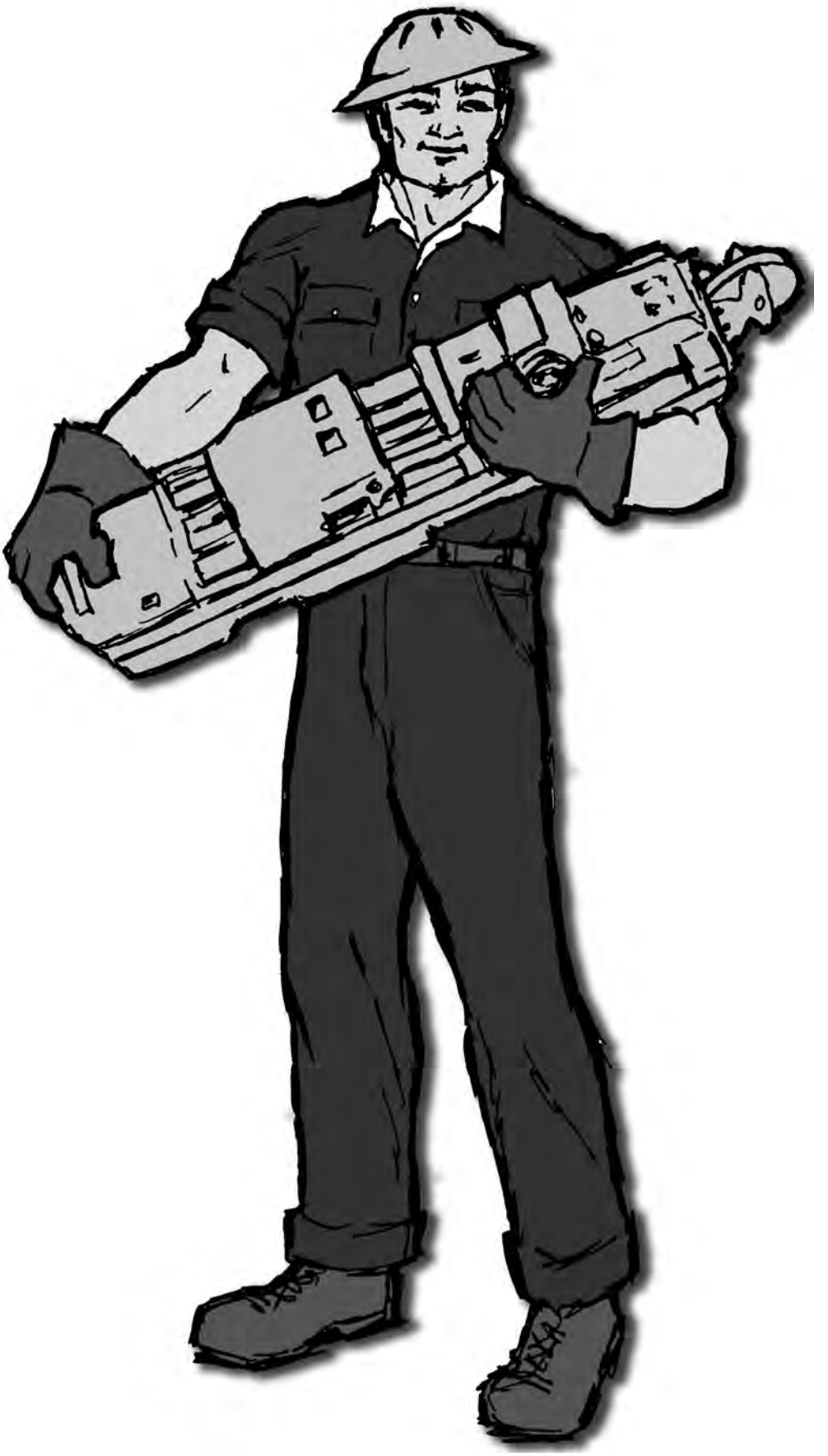

Chapter II-8
Hydrodynamic Analysis and Design Conditions

II-8-1. Overview of Chapter

a. Objectives. Previous chapters in Part II provide detailed descriptions of the various processes involved in coastal hydrodynamics. The purpose of this chapter is to draw together the key aspects of these processes for design.

b. Contents. The following section gives a brief review of hydrodynamic processes covered in earlier chapters and their relative importance to design. Part II-8-3 summarizes approaches to acquiring information needed for design. Statistical methods needed for design analysis of short-term (single sea state) and long-term information are discussed in Part II-8-4 and 8-5. Design aspects of key meteorological and hydrodynamic processes are discussed in detail in Part II-8-6. Two design-related example problems are included. Finally, the interdependence of processes during severe events, which often subjects a project to extreme conditions of multiple processes (for example, extreme winds, waves, and water levels may occur simultaneously in a very severe storm), is discussed in Part II-8-7. References are given in Part II-8-8.

c. Relationship to other chapters and parts.

(1) Earlier chapters in Part II generally present descriptions, statistics, and probability distribution functions for *short-term* hydrodynamic processes. For example, the statistics of individual wave heights in a sea state, a statistical definition of *significant wave height*, and the Rayleigh distribution are given in Part II-1. The short-term variability of hydrodynamic processes can be important in design and results of earlier chapters are briefly summarized in this chapter.

(2) The primary concern for design is long-term variation of processes, particularly extreme occurrences over long time periods. For example, the highest significant wave height to be expected over a 25-year time period (or other long-term time period) is often a critical design parameter. Long-term extremes are the main focus of this chapter. This subject is generally not addressed in earlier chapters, with the notable exception of Part II-5. Long-term water level analysis procedures presented in Part II-5 are referenced and briefly summarized in the general hydrodynamic design framework given in this chapter.

(3) This chapter provides information on the hydrodynamic aspects of design, which are part of the more comprehensive design process and procedures of Parts V and VI. The treatment of hydrodynamics in this chapter is fairly general, whereas Parts V and VI develop more specific hydrodynamic design applications for particular types of projects. This chapter provides necessary background for the material in Parts V and VI. Also, broad design considerations, which encompass more than just the hydrodynamics, are deferred to Part V.

II-8-2. Identifying Meteorological and Hydrodynamic Processes Impacting Design

a. Brief review of processes. The first step in hydrodynamic analysis for design is to identify the meteorological and hydrodynamic processes that are likely to be important for design. The candidate processes, discussed in previous chapters of Part II, are briefly reviewed here with emphasis on design applications. The introduction to Part II-3 also provides perspective on processes.

b. Identifying relevant processes. In any particular design application, some (but not all) of the meteorological and hydrodynamic processes will be relevant for analysis. These processes are identified by

a combination of general understanding of coastal behavior and insight into the design needs of the specific project. Some processes are almost always a concern for certain project types. For example, circulation and flushing are generally evaluated in a harbor project.

c. Interaction between processes. It is important to remember that although meteorological and hydrodynamic processes are often discussed *individually*, they impact a project in *combination*. This combination of processes leads to two strong implications for design:

(1) Processes mutually interact and cannot always be treated as being independent of each other. For example, water level affects waves by influencing shallow-water transformation and breaking.

(2) Extreme occurrences of one process often coincide with strong or extreme occurrences of some other processes. For example, strong winds, large waves, and elevated water levels often occur together during a severe storm.

II-8-3. Acquiring Information

a . Identifying available information. The available meteorological and hydrodynamic information for coastal design is rarely adequate for direct use. Typically all reasonable information sources on relevant processes are identified. Then the information is modified and carefully interpreted in various ways to arrive at the required design conditions. Part II-8 provides a guide to available sources of wind, wave, water level, and current information.

b. Consideration of collecting field measurements. Field measurements can be very helpful at a project site, especially if the information already available is seriously limited in quality and representativeness. Often the needs and scope of coastal projects justify some level of field study. Field measurements must be carefully planned so that the project schedule can accommodate the time and cost required for collecting and analyzing data. Measuring any extreme storm events during the life of a project level study is a matter of chance, but at least some routine storm events are typically recorded. Field measurement options are discussed in Part VII-3. Field measurements have the following potential advantages:

(1) Direct documentation of processes at the project site.

(2) On-site data can be correlated with a better documented, related location (such as a point for which long-term measurements or hindcasts are available).

(3) Onsite data for calibration and validation in model studies.

c. Numerical and physical modeling possibilities. Numerical and physical models offer powerful tools to assist in design analysis. They are used for evaluating existing conditions at a site and various alternative modifications. Both modeling tools are discussed in Part VII. In terms of meteorology and hydrodynamics, numerical models are typically used for:

(1) Extending the length of record.

(2) Hindcasting extreme events not included in the available information.

(3) Synthesizing hypothetical, but possible, extreme events (such as historical hurricanes with modified tracks).

(4) Transferring information from a related, better documented location to the project site.

(5) Providing a more comprehensive assessment of processes over an area than is generally possible with point measurements.

Physical models, properly scaled, often provide a helpful representation of the hydrodynamics of a complex project site, including wave shoaling, wave breaking, wave reflection, and wave-current interaction. They are typically considered for:

(1) Transformation of waves, tides, and/or currents from offshore to a complex project site.

(2) Design forces and overtopping of breakwaters (Part VI).

II-8-4. Statistical Methods - Short-Term

a. Introduction.

(1) Hydrodynamic conditions in a coastal area at any instant in time may be viewed as a *sea state*, that is, a state in which conditions are relatively constant over some short time period. That time period is typically from 1 to 6 hr before the sea transitions to some significantly different state of waves and, in the nearshore area, water level and currents. Since waves are typically the most intensely varying factor outside the nearshore area, the term sea state is often intended to mean waves. Sea states change in response to changing local and offshore winds, tides, and other factors. Thus wave measurement and hindcasting programs often gather wave conditions at 1-hr to 6-hr intervals to adequately sample the range of sea states.

The constancy of a sea state is best defined in statistical terms because components of the sea state, particularly wind waves and swell, have strong variations over time periods of seconds. By contrast, wave theories and many physical model tests performed more than about 10 years ago represent a sea state as a regular wave (e.g., Part II-1). This deterministic representation masks some important aspects of wave behavior.

(2) Most design is based on long-term hydrodynamic statistics representing many years of record. However, statistical variations *within a sea state*, referred to as *short-term* variations, can also be critical for design applications in which damage is a highly sensitive response to individual extreme waves rather than an integrated response to the overall sea state. For example, damage to a pier or platform deck will occur only if a wave crest is high enough to hit it. Damage in this example results from a combination of extremes in *long-term* statistics (extreme combination of H_s and water level) and *short-term* statistics (extreme value of individual wave height). Another example in which both long and short-term statistics are important is the case of waves overtopping a seawall. Only the individual waves that run up over the seawall crest will cause damage behind the wall. Distinctions between short-term and long-term statistics are summarized in Table II-8-1.

b. Probability distribution functions. Short-term statistics are discussed in earlier chapters of Part II. Rayleigh, Gaussian, and normal distribution functions are useful tools. The normal distribution is a normalized version of the Gaussian distribution in which the mean is zero and the standard deviation is one. Characteristics of distribution functions for various short-term statistics are summarized in Figure II-8-1.

Table II-8-1
Definition of Short-Term and Long-Term Statistics

Statistics	Processes Represented	Typical Time Period
Short-Term	Variations within an individual sea state	1 hr
Long-Term	Variations over a long-term collection of sea states	20 yr

c. Statistical parameters. For most design applications, it is sufficient to represent a sea state by a few parameters. A mean value usually suffices for most processes, such as water level, current, wind speed, and direction. Wave parameters require special consideration (see Part II-1). Typically the parameters H_{m0}, T_p, and θ_p are used to represent either the total sea state or each major wave component in the sea state, which may include a locally generated sea and several independent swell components. It is especially important to note in shallow water design applications that the energy-based parameter H_{m0} and the height-based parameter $H_{1/3}$ may differ substantially (see Part II-1). Wave height is often the most critical design parameter and the choice of parameter must be consistent with the particular design application. For example, H_{m0} is appropriate for sediment transport and beach erosion applications, but $H_{1/3}$, H_{10}, or H_1 may be preferred for estimating wave forces on a pier.

II-8-5. Statistical Methods - Long-term

a. Introduction.

(1) Statistical methods for analyzing *long-term* information covering many years are an integral part of most design applications. These methods deal with the various values assumed by selected statistical parameters representing short-term information. Typically the largest parameter values are the primary design concern. For example, the largest value of the statistical parameter H_{m0} to be expected over a 25-year time interval might be needed.

(2) Extreme events are often highly variable in terms of intensity and sequencing. By definition, they are rare. Thus, long-term statistical methods must deal with the problem of using a small, variable sample to estimate parameters that often have a major impact on design. Engineers are continually reminded that events such as the 100-year extreme storm can by chance occur during a much shorter data collection effort. Conversely, a 10-year record may not contain any events that equal or exceed the long-term 10-year extreme. Long-term statistical methods typically address the following two, related problems:

(a) How to extend available information to a longer time period; e.g., how to use 10 years of data to estimate the 25-year extreme.

(b) How to use a small sample of extreme events to get unbiased extreme estimates and some measure of confidence or variability that can be expected in the estimates.

(3) In some applications, the preferred approach is to extend the available information base to longer time periods by generating additional realizations of the process and ensuring that the realizations are statistically consistent with known information. One adaptation of this approach is described in the following section on stochastic time histories.

RAYLEIGH 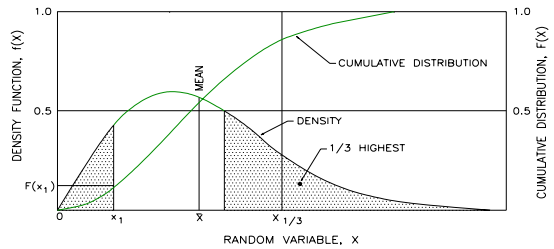 	$f(x) = 2\alpha x e^{(-\alpha x^2)}$ $F(x) = 1 - e^{(-\alpha x^2)}$	$\bar{x} = \frac{0.886}{\sqrt{\alpha}}$ $\sigma_X = \frac{0.463}{\sqrt{\alpha}}$ $coeff.\ of\ var. = 0.52$
GAUSSIAN 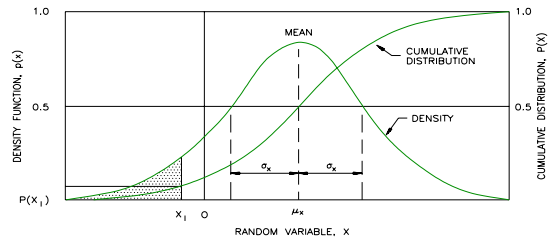 	$f(x) = \frac{1}{\sigma\sqrt{2\pi}}\, e^{-\left[\frac{(x-\mu)^2}{2\sigma^2}\right]}$	$\bar{x} = \mu$ $\sigma_X = \sigma$ $coeff.\ of\ var. = \frac{\sigma}{\mu}$
NORMAL 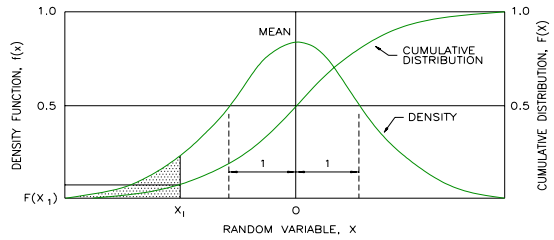 	$f(x) = \frac{1}{\sqrt{2\pi}}\, e^{\left(-\frac{x^2}{2}\right)}$	$\bar{x} = 0$ $\sigma_x = 1$

Figure II-8-1. Probability distribution functions for short-term statistics

b. Stochastic time history.

(1) Applications such as long-term shoreline evolution depend partially on major storm events and partially on a wide variety of day-to-day conditions that also influence sediment movement. Further, the *sequencing* of wave and water level conditions is important in progressive beach erosion and recovery. Thus attention must be focussed on the long-term *time history* of conditions.

(2) A statistical framework is available for using a limited, but multi-year wave information base to define statistical characteristics at the location and then synthesize an unlimited number of additional years of information (Scheffner and Borgman 1992). The synthesized information matches the known information in a statistical sense but includes random variability also present in the process.

c. Extremal probability distribution functions. Many design applications focus only on extreme conditions. Because these conditions are typically difficult to estimate accurately and they often have large economic implications, a number of different probability distribution functions have been used to find a best fit to available data (Figures II-8-2 and II-8-3). The Fisher-Tippett Type I and II (FT-I and FT-II) distributions were derived from statistical theory of extremes, and hence are true extremal distributions. The Weibull distribution with k=2 is equivalent to the Rayleigh distribution. The parameters *A, B,* and k are known as the *scale, location,* and *shape* parameters, respectively (Table II-8-2). Typical values for the shape parameter in coastal engineering applications (e.g. Goda 1988) are given along with the general distribution functions. Expressions for the mean and standard deviation in terms of the distribution function parameters and vice-versa are also included if they can be written in compact form. Of the distributions shown in Figure II-8-3, choosing the Weibull distribution with k=0.75 clearly leads to the highest extremal estimates. Choosing the Weibull distribution with k=2.0 leads to the lowest estimates. The FT-I distribution gives estimates intermediate to the Weibull with k values of 1.0 and 1.4.

d. Empirical simulation technique. The *Empirical Simulation Technique (EST)* offers a powerful tool for estimating extreme responses, especially when multiple input parameters are important and the linkages between inputs and response are complex. This technique makes use of relationships embedded in the input information. There is no requirement for selecting distribution functions or assuming that input parameters are mutually independent. The EST is described in Part II-5-5-b-(3) in relation to storm surge estimation. In addition to providing the traditional stage-frequency relationship, the method gives valuable information on variability about the mean relationship. The information can be used to assess the level of risk associated with surge heights selected for design within the limits of the range of events simulated. The EST can be extended to design applications besides storm surge, such as beach erosion caused by tropical storms (Farrar et al. 1994).

e. Methods for fitting distributions to data. Selecting data for extremal analysis, estimating parameters in the distribution function, and choosing an extremal distribution function must be done carefully. Each of these choices can significantly influence the estimated extreme values, especially those for very rare events.

(1) Data selection.

(a) Data used for extreme analysis should be taken only from significant events in the recorded time history. Further, each data value should be from a different event to ensure statistical independence between values. The events should be representative of the *type* of events (though of lesser intensity) expected to cause the extremes of design concern. It is assumed that the statistics of extreme events are stationary over the period of record and in the future (e.g. no systematic increase in number and severity of extreme storms due to such possible effects as global warming). A full climatological data set (such as observations every 3 hr over 20 years) is not recommended for extreme analysis. Such data sets include multiple data values from each major storm, and one or several very severe storms can dominate the extremes.

Distribution Function	Mathematical Expression	Mean & Standard Deviation	Parameters
Fisher-Tippett I (FT-I) or Gumbel	$F(x) = e^{-e^{-\left(\frac{x-B}{A}\right)}}$	$\bar{x} = B + 0.5772A$ $\sigma = 1.283A$	$A = 0.779\sigma_x$ $B = \bar{x} - 0.4500\ \sigma_x$
Weibull	$F(x) = 1 - e^{-\left(\frac{x-B}{A}\right)^k}$ *general*	$\bar{x} = B + A\ \Gamma\left(1 + \frac{1}{k}\right)$ $\sigma_x = A\sqrt{\Gamma\left(1 + \frac{2}{k}\right) - \Gamma^2\left(1 + \frac{1}{k}\right)}$	
	$k = 0.75$	$\bar{x} = B + 1.191A$ $\sigma_x = 1.611A$	$A = 0.621\sigma_x$ $B = \bar{x} - 0.740\sigma_x$
	$k = 1.0$	$\bar{x} = B + A$ $\sigma_x = A$	$A = \sigma_x$ $B = \bar{x} - \sigma_x$
	$k = 1.4$	$\bar{x} = B + 0.911A$ $\sigma_x = 0.660A$	$A = 1.515\sigma_x$ $B = \bar{x} - 1.380\sigma_x$
	$k = 2.0$	$\bar{x} = B + 0.886A$ $\sigma_x = 0.463A$	$A = 2.160\sigma_x$ $B = \bar{x} - 1.914\sigma_x$
Fisher-Tippett II (FT-II) or Frechet	$F(x) = e^{-\left(\frac{x}{A}\right)^{-k}}$ *general*	$\bar{x} = A\ \Gamma\left(1 - \frac{1}{k}\right)$ $\sigma_x = A\sqrt{\Gamma\left(1 - \frac{2}{k}\right) - \Gamma^2\left(1 - \frac{1}{k}\right)}$	
	$k = 2.5$		
	$k = 3.3$		
	$k = 5.0$		
	$k = 10.0$		

Figure II-8-2. Probability distribution functions for long-term statistics - Part 1 (Continued)

Distribution Function	Mathematical Expression	Mean & Standard Deviation	Parameters
Log-Normal	$f(x) = \frac{1}{Ax\sqrt{\pi}} e^{-\left(\frac{lnx - B}{A}\right)^2}$	$\bar{x} = e^{\left(B + \frac{1}{2}A^2\right)}$ $\sigma_x = \sqrt{e^{(2B + A^2)}(e^{A^2} - 1)}$	
Log Pearson Type III (Kite 1978)	$f(x) = \frac{1}{Ax\Gamma(k)}\left(\frac{lnx - B}{A}\right)^{k-1} e^{-\left(\frac{lnx - B}{A}\right)}$	$ln\bar{x} = B + Ak$ $\sigma_{lnx} = A\sqrt{k}$	k = *skew of ln x corrected for bias* $A = \frac{\sigma_{lnx}}{\sqrt{k}}$ $B = lnx - \sigma_{lnx}\sqrt{k}$
Pearson Type III	$f(x) = \frac{1}{A\Gamma(k)}\left(\frac{x - B}{A}\right)^{k-1} e^{-\left(\frac{x - B}{A}\right)}$	$\bar{x} = B + Ak$ $\sigma_x = A\sqrt{k}$	$k = \left(\frac{2}{G}\right)^2$ G = *skew coefficient* $A = \frac{\sigma_x}{\sqrt{k}}$ $B = \bar{x} - \sigma_x\sqrt{k}$
Binomial (discrete)	$f(x) = \frac{N!}{x!\,(N - x)!} p^x (1 - p)^{N-x}$	$\bar{x} = Np$ $\sigma_x = \sqrt{Np(1 - p)}$	
Poisson (discrete)	$f(x) = \frac{\lambda^x e^{-\lambda}}{x!}$	$\bar{x} = \lambda$ $\sigma_x = \sqrt{\lambda}$	

Figure II-8-2. Probability distribution functions for long-term statistics - Part 2 (concluded)

Table II-8-2
Parameters in Extremal Distribution Functions

Symbol	Name
A	Scale
B	Location
k	Shape

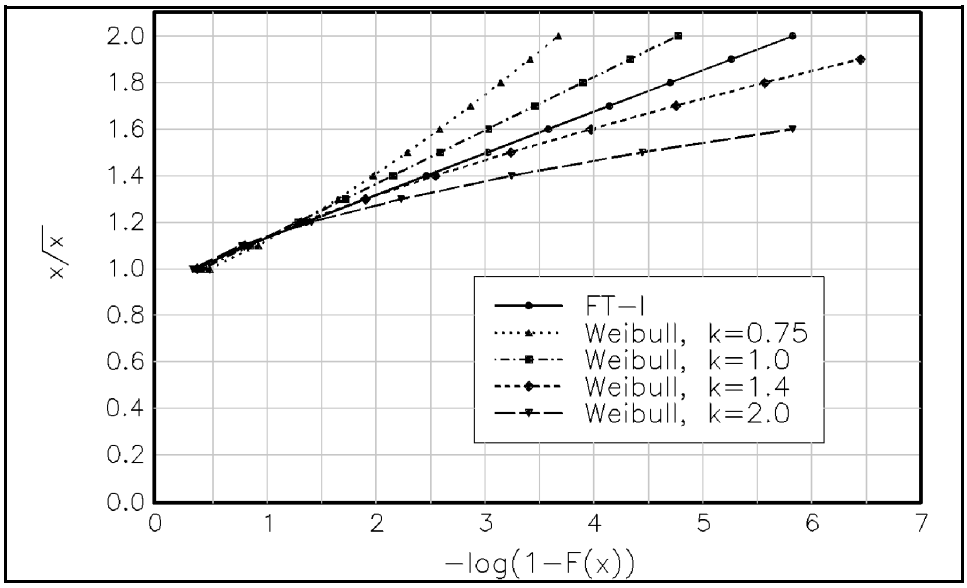

Figure II-8-3. Probability distribution functions for long-term statistics

(b) The preferred approach to data selection is to take the maximum value from each event to create a *partial duration series* of extreme values. Typically, the events are storms, ranging from small, weak events to the most severe storms of record. Small events can be difficult to identify. Further, they are of little interest if an adequate number of bigger storms is available in the record. Often the partial duration series will be *censored* to exclude data values less than some threshold value (Figure II-8-4). Thus the extremal analysis can focus on a smaller series representing truly significant events. The threshold is often chosen so that the number of data values in the series is greater than the number of years of record (generally 1-3 times the number of years of record).

(c) Another accepted approach is to take the maximum value from each year of record to form an *annual maximum series*. A record length on the order of 20 years or more (yielding at least 20 data values) is needed for this approach. In coastal engineering, record lengths are often shorter than this requirement. Another drawback to the annual maximum series arises from the possibility of multiple severe storms occurring in the same year, as in El Ninõ/Southern Oscillation events, which sporadically distort winter storm seasons along the U.S. Pacific Coast (see Part II-2). Only the maximum event in each year is considered. Other storms, which may be bigger than the maximum event in many other years, will be ignored.

(2) Estimating parameters in extremal distribution functions.

(a) Generally an extreme data value series (either partial duration series or annual maximum series) is treated as a sample from a process that follows one of the extremal distribution functions presented in

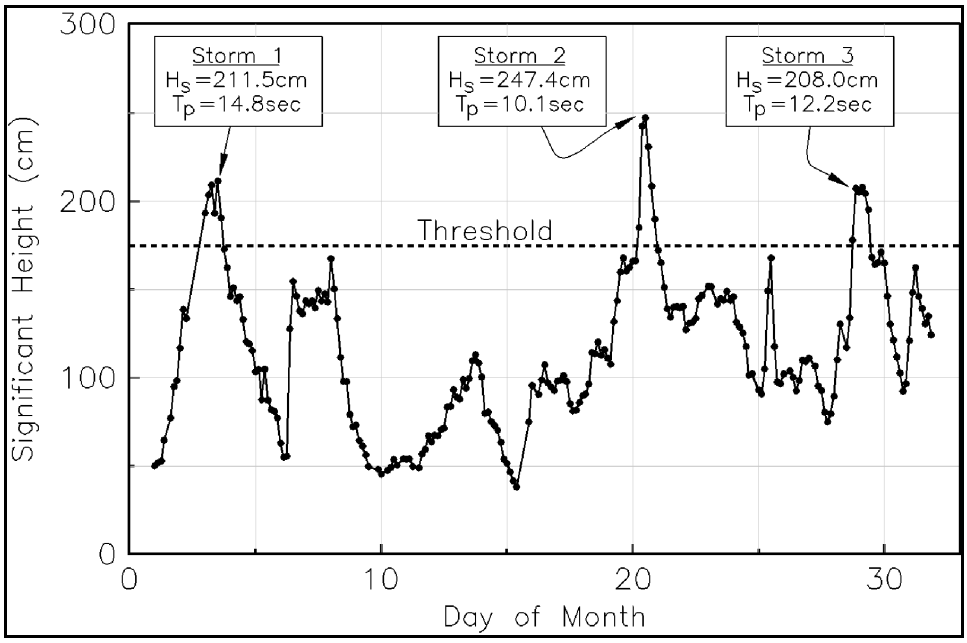

Figure II-8-4. Selection of extreme values for a partial duration series

Part II-8-5-c. There is no strong theoretical reason for preferring one distribution function over another. The single sample cannot be expected to fit the true distribution function exactly, especially for the few largest events. For some processes, such as water levels, one particular distribution function is generally accepted for all applications. For other processes, such as significant wave heights, a best-fitting distribution function is often chosen from among several candidates.

(b) Typically, extreme data values are sorted into descending order. A nonexceedance probability must be assigned to each extreme data value. These *plotting positions* should be chosen so that the distribution function can be accurately estimated. Figure II-8-5 gives the commonly used traditional plotting position formula. The figure also gives formulas developed to remove bias and minimize *rms* errors when fitting to specific distribution functions (Goda 1988, Goda and Kobune 1990).

(3) Approaches to estimating parameters. The following approaches can be used to determine parameters for each candidate distribution function:

(a) Graphical approach. Traditionally, the goodness of fit was determined visually by plotting the data along with candidate distribution functions. By scaling the plotting axes to make a candidate distribution appear as a straight line, the parameters of a visually optimum distribution function can more easily be determined.

(b) Computational approach. An automated computational approach is more objective (though not necessarily more accurate) and often easier to apply than the relatively tedious graphical approach. Three alternatives are the least squares method, the maximum likelihood method, and the method of moments. The least squares method is simplest and, with two-parameter distribution functions, it is often used. It is included in the ACES software package. One caution with this approach is that it is sensitive to even one or two extreme points that deviate greatly from the general trend of the data (*outliers*). The maximum likelihood method has the advantage of being less likely to produce erratic results when the data contain outliers or differ somewhat from the distribution function (Mathiesen et al. 1994). More information on computational approaches is also available from Goda (1988, 1990). Regardless of the method used, it is

Application of Formula	Plotting Position Formula
Traditional (Gumbel 1958)	$\hat{F}_m = 1 - \frac{m}{N + 1}$
Fisher-Tippett I (FT-I) (Gringorten 1963)	$\hat{F}_m = 1 - \frac{m - 0.44}{N + 0.12}$
Weibull Distribution Function (Goda 1988)	$\hat{F}_m = 1 - \frac{m - 0.20 - \frac{0.27}{\sqrt{k}}}{N + 0.20 + \frac{0.23}{\sqrt{k}}}$
Fisher Tippett II (FT-II) or Frechet Distribution Function (Goda and Kobune 1990)	$\hat{F}_m = 1 - \frac{m - 0.11 - \frac{0.52}{k}}{N + 0.12 - \frac{0.11}{k}}$
Log-Normal Distribution Function (Blom 1958)	$\hat{F}_m = 1 - \frac{m - 0.375}{N + 0.25}$

Parameter definitions:
F = probability that the m^{th} highest data value will not be exceeded
m = rank of data value in descending order (m = 1 for largest, etc.)
N = number of events[1]
k = parameter in Weibull distribution function
[1] For censored data, N should represent the total number of events over the time interval considered (not just the number of censored events)

Figure II-8-5. Plotting position formulas

prudent to plot the computed distribution function and data together and ensure that the fit is consistent with good engineering judgement.

(4) Outliers. Outliers are retained in the data, but they should receive special scrutiny, as follows:

(a) Ensure accuracy. Each outlier should be checked to ensure that it is a valid data value, rather than a measurement or modeling error.

(b) Examine each event that produces a high outlier. Typical causes are very severe winter storms or direct impact of an intense hurricane. If extreme events at the site are produced by distinctly different natural processes (different statistical *populations*), it may be preferable to divide the data values into several series, one for each process, and analyze each series separately (e.g. Goda 1988). For example, winter storms and hurricanes should not necessarily be expected to produce extremes that follow the same extremal probability distribution function. Extreme data values can be analyzed as separate populations only if sufficient data values are available in *each* population.

(c) Consider whether an adjustment to the probability assigned to a high outlier data value can be justified. Often a high outlier is due to a storm event and extreme hydrodynamic response which are much more severe than would normally be expected over the length of hydrodynamic record. Meteorological records generally cover a much longer historical time period than hydrodynamic records. By carefully analyzing storm probabilities and longer-term records from nearby sites if available, it may be possible to assign a more realistic (lower) probability to the hydrodynamic outlier. Then a more valid distribution function fit can be obtained.

(5) Choosing an extremal distribution function. When several candidate distribution functions are under consideration, usually one is selected as a best fit to the data. The selection criteria can range from visual inspection of plotted results and simple statistics such as the correlation between data and model (e.g., Leenknecht, Szuwalski, and Sherlock 1992) to more elaborate statistical tests (Mathiesen et al. 1994). An objective approach to selecting a distribution function for significant wave heights is given by Goda and Kobune (1990).

(6) Confidence intervals. Confidence intervals associated with the chosen distribution function should also be estimated, preferably with a computer program (Leenknecht, Szuwalski, and Sherlock 1992; Goda 1988; Goda 1990; Mathiesen et al. 1994). They depend on the distribution function and number of data values. Confidence in computed values can also be influenced by random and systematic errors in the data and physical site characteristics such as long-term variability of water level and climate, possible extreme events not represented in the recorded population, and physical limits on extremes (such as the depth-imposed limit on wave height in shallow water).

f Return period and encounter probability.

(1) Extreme conditions in coastal engineering are often described in terms of *return values* and *return periods*. The *return period* is the average time interval between successive events of the design wave being equalled or exceeded. For example, a 25-year significant wave height is that height that is equalled or exceeded an average of once during a 25-year time period. Return period is expressed as

$$T_r = \frac{t}{1 - P(\hat{H}_s)} \tag{II-8-1}$$

where

T_r = return period, in years

t = time interval associated with each data point, in years

$P(\hat{H}_s)$ = cumulative probability that $H_s \le \hat{H}_s$

$\hat{H}_s$ = design significant wave height

(2) A related concept, *encounter probability*, gives the probability that waves with H_s equal to or greater than $\hat{H}_s$ will occur during the design life or other time period. It is given by

$$P_e = 1 - \left(1 - \frac{t}{T_r}\right)^{\frac{L}{t}} \tag{II-8-2}$$

where

P_e = encounter probability

L = desired time period, in years

(3) Values of P_e expressed in percent for some typical coastal engineering concerns are given in Table II-8-3.

Table II-8-3
Percent Chance for H_s Equaling or Exceeding Return Period H_s

	Desired Time Period (year)					
Return Period	**2**	**5**	**10**	**25**	**50**	**100**
2	75	97	100	100	100	100
5	36	67	89	100	100	100
10	19	41	65	93	99	100
25	8	18	34	64	87	98
50	4	10	18	40	64	87
100	2	5	10	22	39	63

g. Extrapolation of data. The main objective in determining an appropriate extremal distribution function is to get the best possible estimates of extreme conditions at desired return periods. Often the data must be extrapolated to probabilities beyond the record length to match design return periods. Extrapolation beyond 2-3 times the data record length should be avoided if possible. For example, 10 years of data should be used for estimating return values of 20-30 years or less.

II-8-6. Analysis of Key Meteorological and Hydrodynamic Processes in Design

a. Introduction.

(1) Key processes in design are reviewed in this chapter. Applicable chapters of Part II are cited. The design importance of each process is briefly stated. Critical design concerns are discussed, including two design-related examples.

(2) Statistical information about the processes is summarized in Table II-8-4. For each process (as applicable and available), the table includes representative statistical distribution functions and general expressions for parameters of the distribution function.

(3) It is important to bear in mind that the most extreme event of record may not merely be an intensified version of lesser extreme events. Most experienced coastal and ocean engineers and scientists can remember at least one catastrophic event that was distinctly different from typical storm events. Often the catastrophic event arises from an unusual interaction between several major weather features. The “Halloween Storm” that occurred in the northwestern Atlantic Ocean in October 1991 is a good example (U.S. Department of Commerce 1992). Three significant meteorological systems, including a hurricane and an intense winter storm, combined to create very strong winds over an extremely long fetch, which lasted for a period of days. This type of event is difficult to anticipate, but it should be recognized that such things can occur. They may appear as outliers in extreme data distributions.

Table II-8-4
Probability Distribution Functions for Meteorological and Hydrodynamic Processes

Parameter	Representative Distribution Functions
	Short-term Statistics
Surface elevations	Gaussian
Individual wave heights	Rayleigh: $x=H$; $\alpha=1/H_{rms}^2$
Individual wave periods	Rayleigh: $x=T^2$; $\alpha=1/\overline{T}^4$
Wave runup	Rayleigh
	Long-term Statistics
Extreme wind	FT-I
H_s	Weibull: A= standard deviation of H_s; B= minimum value of H_s; k=1
T_p	Weibull: B= minimum value of T_p; A, k estimated from data
Extreme H_s	FT-I; Weibull
Water level	Log-Pearson Type III

b. Wind. Wind is discussed in detail in Part II-2.

(1) Design importance. Wind at a design site may be important for local wave generation, nearshore current generation both inside and outside the surf zone, modification of nearshore breaking waves, nearshore water level, nearshore sediment transport, subaerial sediment transport, intensification of runup, overtopping, and flooding, sail forces on moored and moving boats, and harbor circulation and flushing.

(2) General climate. Winds at a coastal site are determined by some combination of large-scale weather systems, smaller-scale systems, land-sea breeze circulations, land/water roughness differences, and orographic effects. Winds can vary greatly over short distances along a coast. Thus, local measurements *at the project site* are very helpful in establishing the climate. As with waves, 2-3 years of data are generally sufficient for climatological purposes (i.e. annual or monthly mean and standard deviation of wind speed). Even one month of data can be useful, though certainly not ideal, for estimating relationships between the project site and winds at a long-term measurement station within the same region. Often wind climate information is summarized in the form of *wind roses*, which can represent months, seasons, or years (Figure II-8-6).

(3) Storms. Storms are a natural part of the wind climate at a site. They can vary greatly in size and intensity. Frequency of occurrence and intensity of storms are important concerns for functional design. The occurrence of extreme storms is a necessary concern for structural design. The distribution of extreme wind speeds has been modeled with FT-I, FT-II, and Weibull distribution functions (Figure II-8-2). The FT-I distribution function seems to be the preferred choice, especially when the annual extremes do not include rare, unusually powerful events arising from distinctly different meteorology (such as hurricanes) (Simiu and Scanlan 1986).

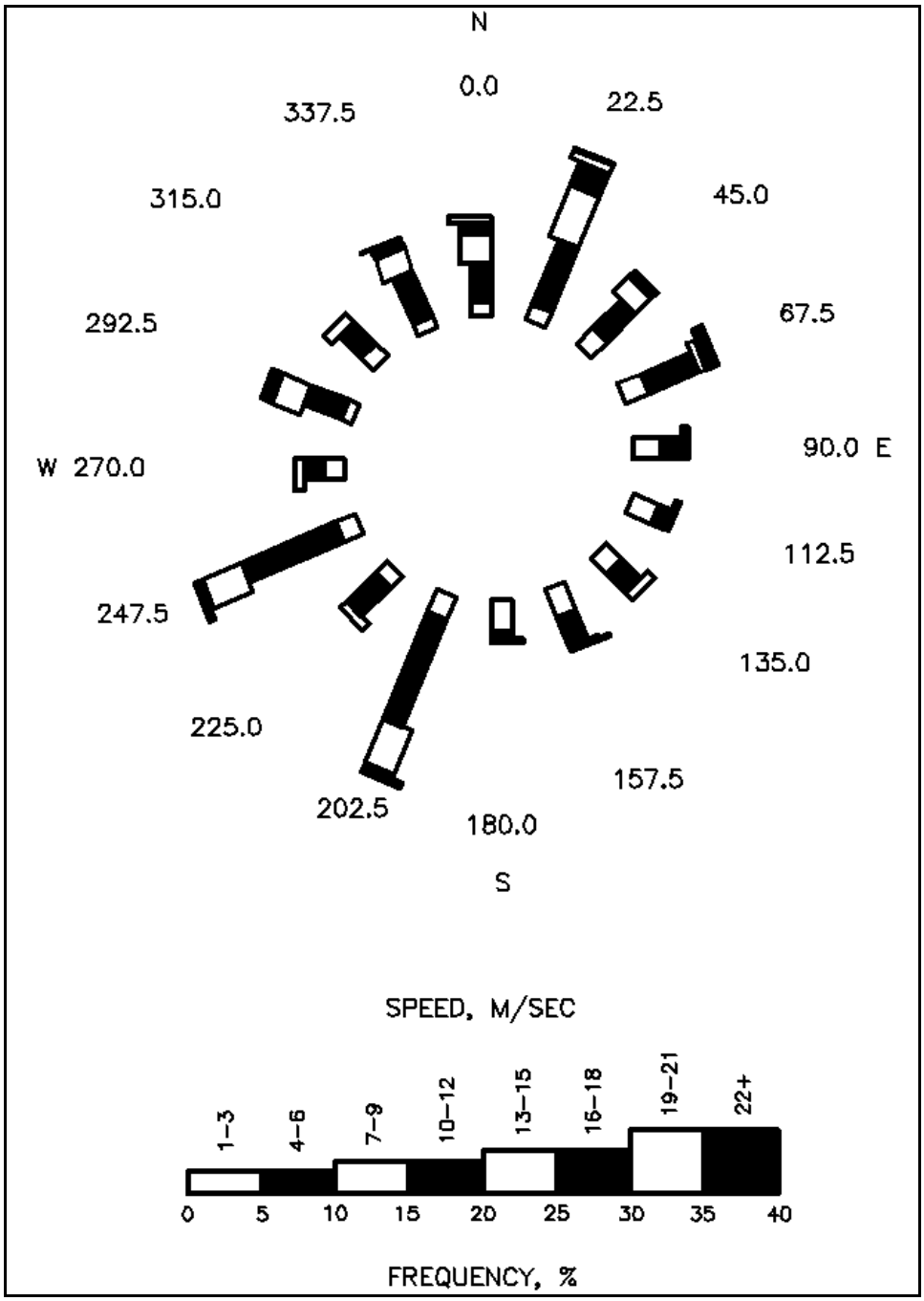

Figure II-8-6. Example wind rose (Leffler et al. 1990)

(a) Extreme wind speeds can conveniently be analyzed with the ACES extremal significant wave height analysis application (using wind speeds in place of wave heights) or with more traditional graphical methods. However, wind records at project sites often cover a very limited time period, and extrapolation to rare events may be difficult. Extreme records from any nearby, long-term wind stations may be transferrable to the project site with due consideration of differences between locations. Also, a simple approach using *monthly* extreme wind speeds may be helpful in conjunction with limited data sets (Simiu and Scanlan 1986). By this approach, based on the assumption that extreme wind speeds follow the FT-I distribution function,

$$U_r = \bar{U}_m + 0.78\ \sigma_m\ [\ \ln\ (12T_r) - 0.577\ ] \quad \text{(II-8-3)}$$

where

U_r = wind speed with r-year return period

$\bar{U}_m$ = mean value of maximum monthly wind speeds

σ_m = standard deviation of maximum monthly wind speeds

and

$$\sigma_{rm} = \sqrt{0.49 + 0.89\ ln\ (12\bar{U}_m) + 0.67\ [ln\ (12\bar{U}_m) - 0.577]^2}\ \ \frac{\sigma_m}{\sqrt{N_m}} \quad \text{(II-8-4)}$$

where

σ_{rm} = standard deviation of the sampling error in estimating U_r

N_m = number of months of data

(b) The parameter σ_{rm} can be related to confidence intervals using Table II-8-5. An integral number of years of data covering at least 3 years (36 months) is needed for this simple approach. Only populations of extreme events that are well-represented in the data can be effectively included in the long-term extreme estimates (e.g., if hurricane events do not appear or are sparsely represented in the data sample, they will not be effectively represented in the extreme estimates).

Table II-8-5
Standard Deviation and Confidence Interval Relationships

Confidence Level, %	Confidence Interval Bounds Around U_r	Probability of Exceeding Upper Bounds, %
80	$\pm 1.28\sigma_{rm}$	10.0
85	$\pm 1.44\sigma_{rm}$	7.5
90	$\pm 1.65\sigma_{rm}$	5.0
95	$\pm 1.96\sigma_{rm}$	2.5
99	$\pm 2.58\sigma_{rm}$	0.5

(c) If data are unavailable, extreme wind speed can be estimated for various return periods with Figures II-8-7 through II-8-9. These figures were developed to estimate maximum wind loads for building design and are expected to be conservative for coastal engineering applications. Figure II-8-7 gives extreme fastest mile wind velocity data with a 50-year return period (annual probability of 0.02 that the wind speed is exceeded). Wind speed information was prepared from data collected at 129 weather stations (Simiu, Changery, and Filliben 1979), representing a 10-m elevation. Data were statistically reduced using extreme value analysis based on Fisher-Tippett Type-I distributions. Wind speed contours of Alaska are based primarily on data collected in open areas (Thom 1968-69). Wind speed contours in the hurricane-prone region, Atlantic and Gulf of Mexico coastlines, are based on Monte Carlo simulations of hurricane storms striking the coastal region (Batts, Russell, and Simiu 1980). Recurrence intervals for 25 and 100 years may be estimated by multiplying wind speed from Figure II-8-7 with the appropriate adjustment factor in Table II-8-6.

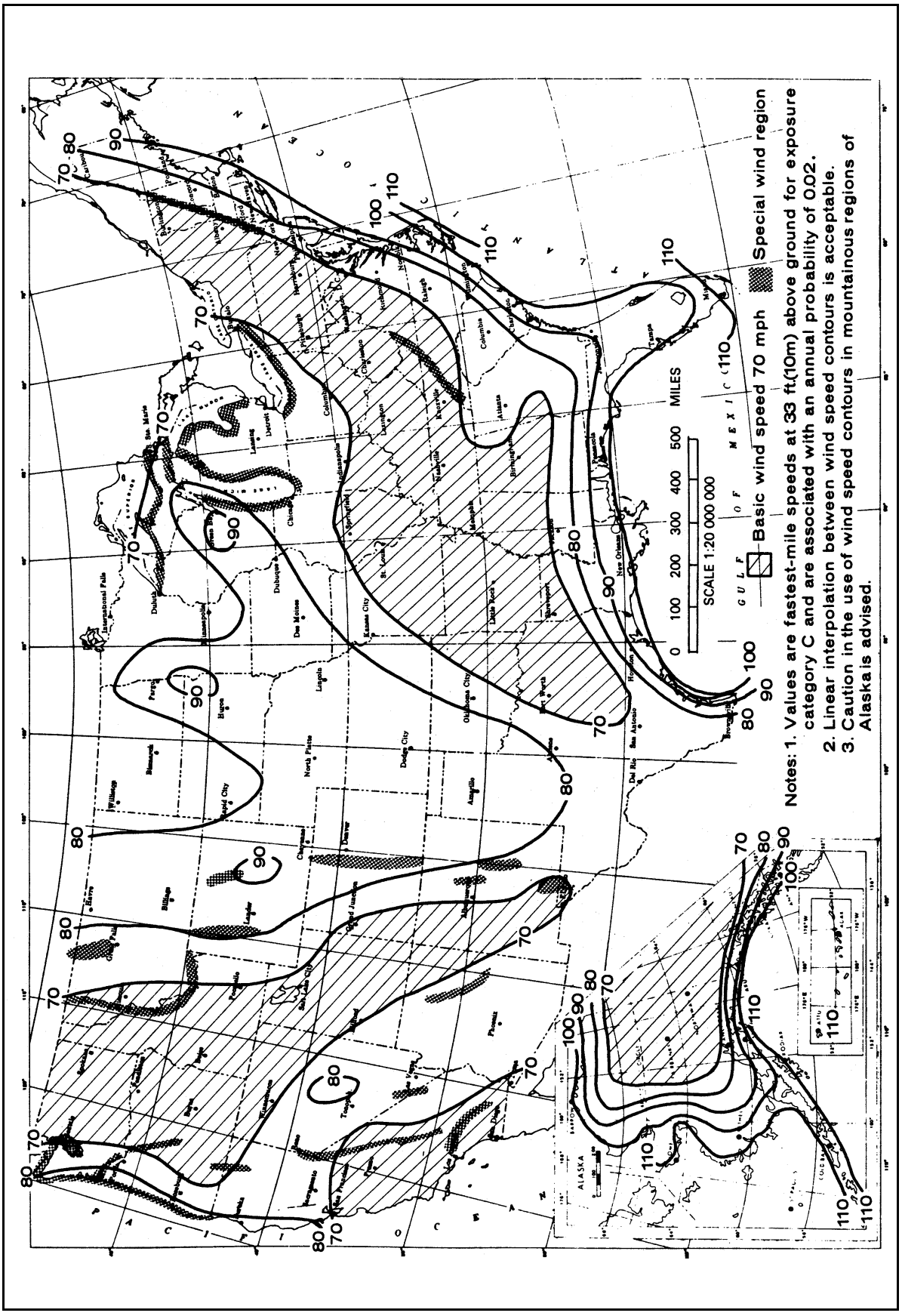

Figure II-8-7. Extreme fastest-mile wind speeds with 50-year return period across the United States at 10-m elevation (ASCE 1993)

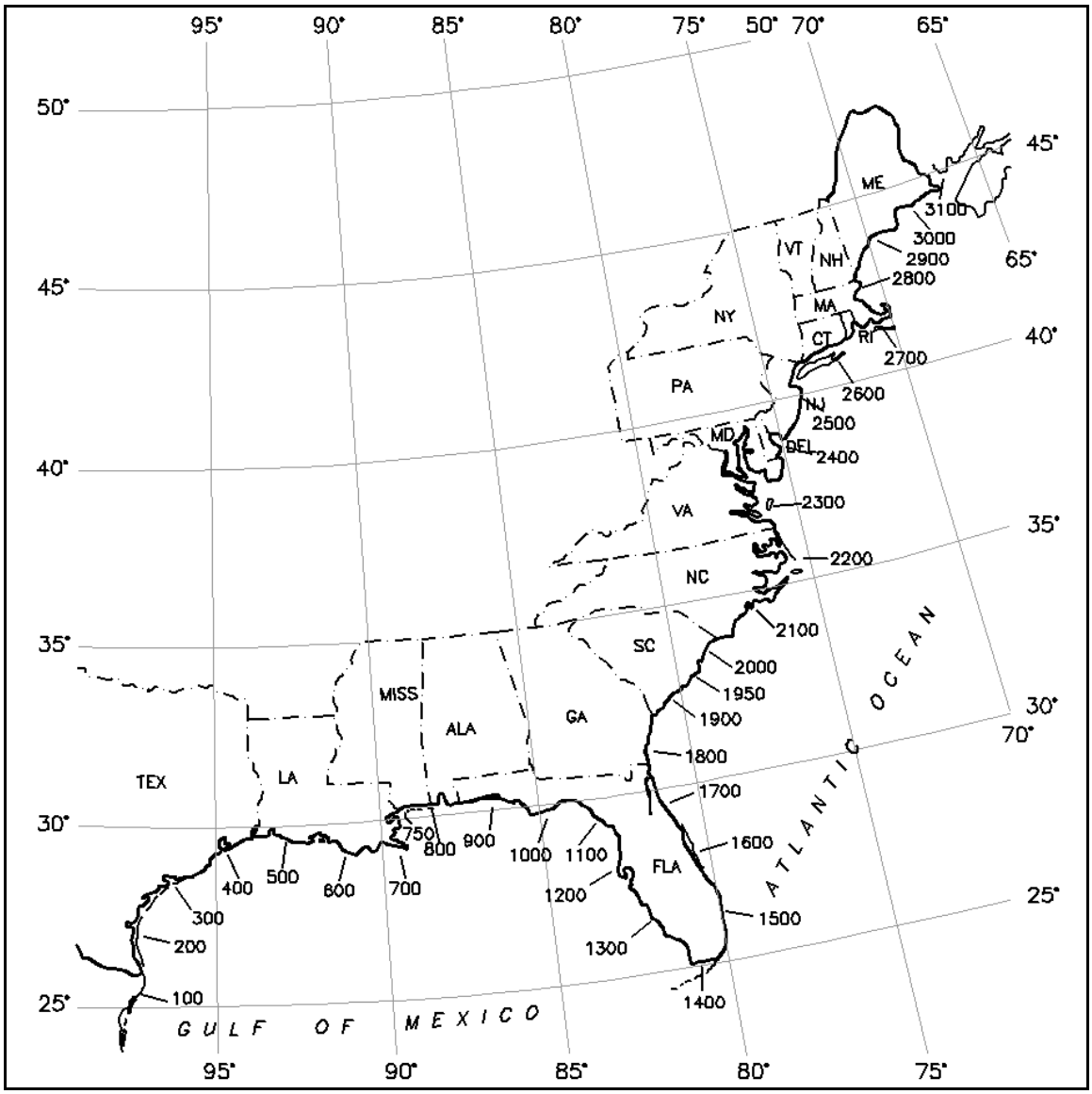

Figure II-8-8. Milepost map for use with Figure II-8-9; coastal distance intervals marked in nautical miles (1 nautical mile = 1.9 km)

(d) The adjustment factor at the hurricane-prone oceanline reflects the difference in probability distributions of hurricane wind speeds and wind speeds in other regions. Hurricane wind effects are assumed to be negligible at distances of more than 100 miles inland from the oceanline. The adjustment factor can be linearly interpolated between the oceanline and 100 miles inland. Some special wind regions are indicated in Figure II-8-7. These regions could have considerably higher wind speeds than indicated in the figure. All mountainous terrain and ocean promontories should be examined for unusual wind conditions. Figures II-8-8 and II-8-9 relate specifically to hurricane winds and are preferable for that application (Batts, Russell, and Simui 1980). It is important to recognize that extreme wind speeds from these figures must be converted from fastest mile to appropriate averaging time. Table II-8-7 provides relationships between fastest mile and 1-hr average wind speeds (also in Figure II-2-2). Averaging time adjustments, including conversion from 1-hr average to other averaging time, can be done using Table II-8-8, Figure II-2-1, or ACES.

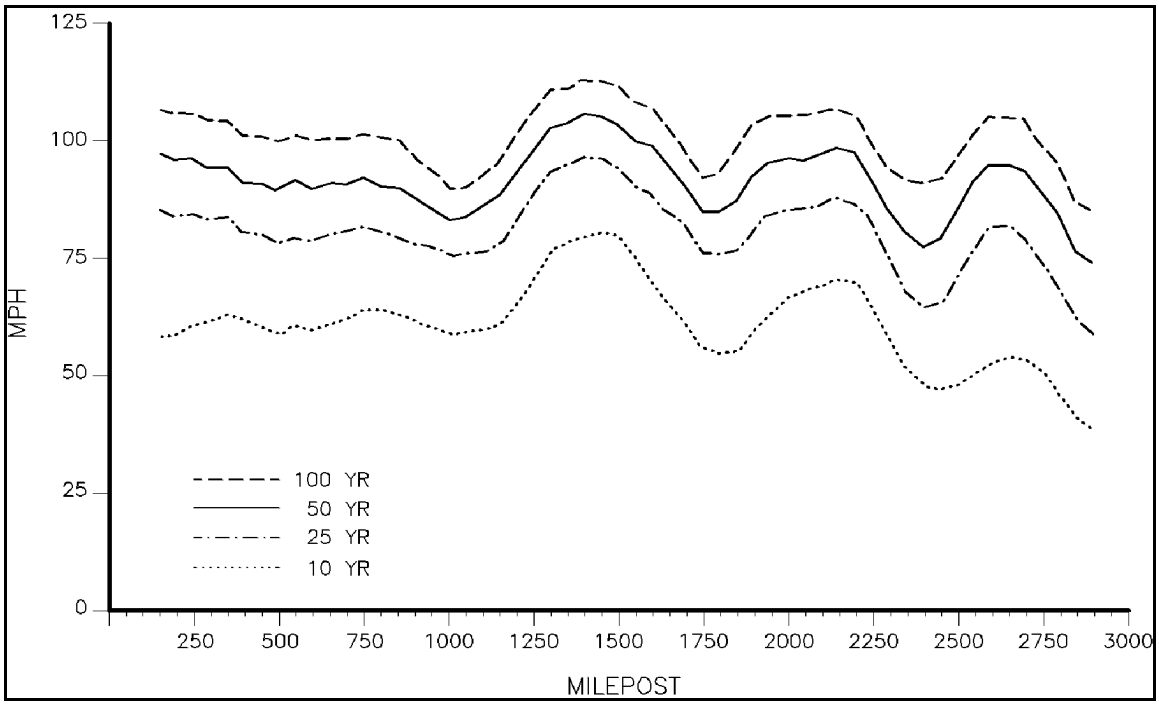

Figure II-8-9. Extreme fastest-mile hurricane wind speeds blowing from any direction at 10 m above ground in open terrain near the coastline for various return periods (after National Bureau of Standards (1980))

Table II-8-6
Return Period Adjustment Factor

	Adjustment Factor	
Return Period, years	**Other Regions**	**Hurricane Region (Gulf & Atlantic)**
25	0.95	1.00
50	1.00	1.05
100	1.07	1.11

Table II-8-7
Conversion of Extreme Wind Speeds from Fastest-Mile to 1-hr Average

Fastest Mile *U*, mph	U_{1hr}, mph	Conversion Factor[1]
50	41.0	0.82
80	62.4	0.78
100	77.0	0.77
120	91.2	0.76
150	111.0	0.74

[1] U_{1hr} = (factor) × (fastest mile *U*)

Table II-8-8
Averaging Time Adjustments for Extreme Wind Speeds[1]

	t_{find}					
t_{given}	1 min	5 min	10 min	1 hr	3 hr	6 hr
1 min	1.00	0.88	0.84	0.80	0.75	0.71
5 min	1.14	1.00	0.96	0.92	0.85	0.81
10 min	1.18	1.04	1.00	0.95	0.88	0.84
1 hr	1.24	1.09	1.05	1.00	0.93	0.88
3 hr	1.34	1.17	1.13	1.08	1.00	0.95
6 hr	1.41	1.23	1.19	1.13	1.05	1.00

[1] $U_{t,find}$ = (factor from table) × $U_{t,given}$

c. Extreme waves. Part II-1 and II-4 discuss some aspects of extreme waves. Further information is provided in this chapter.

(1) Design importance. Extreme wave conditions are almost always a major design concern in coastal engineering projects. Extreme significant wave heights are usually the most critical concern, but wave period, wave direction, and spectral shape (both frequency and direction) can be important as well. Possible secondary wave systems, an integral part of wave climate at exposed ocean sites, are generally not important in conjunction with an extreme event. Energetic extreme waves are usually a key factor causing coastal structure damage, vessel damage, beach erosion, channel sedimentation, and coastal flooding. Extreme waves may be generated by a winter storm, a tropical storm, or some combination of storms (see Part II-8-7).

(2) Deep water.

(a) Extreme values of H_s and associated T_p are usually obtained from measurements or hindcasts. Values of H_s, typically in the form of a partial duration series (see Part II-8-5-e-(1)), can be expected to give a reasonable fit to the FT-I, Weibull, FT-II, or log-normal distribution function (Figure II-8-2), from which design values of H_s can be estimated. FT-I or a form of the Weibull distribution function is generally preferred. Some of the following considerations may also apply:

- If extreme values are generated by more than one population of extreme events (e.g. winter storms and hurricanes) and if sufficient data are available from each population, it may be desirable to fit each population separately.
- If the largest value or several values deviate significantly from the general trend of the data, these outliers should be given special consideration as discussed in Part II-8-5-e-(2).
- Maximum H_s might be limited by sheltering or fetch constraints due to geography or consistent storm characteristics.
- Extreme wave measurements, observations, and hindcasts are often subject to larger errors than would normally be expected. For example, gauges can be affected by large, steep waves, breaking waves, severe winds, and ice accumulation. A floating accelerometer buoy gauge may tilt severely, stretch the mooring lines, or even break loose from the mooring. Wave height estimates may be modified in ways that are difficult to predict. Data loss from gauges, due to equipment damage or loss of power, is more likely during severe storms than during normal conditions.

EXAMPLE PROBLEM II-8-1

FIND:

Wind speed with 25- and 50-year return period (10-min average at 10-m elevation).

GIVEN:

Maximum wind speed by month (10-min average measurement at 10-m elevation) in Table II-8-9.

Table II-8-9
Maximum Wind Speed by Month, in m/s

	Month											
Year	**Jan**	**Feb**	**Mar**	**Apr**	**May**	**Jun**	**Jul**	**Aug**	**Sep**	**Oct**	**Nov**	**Dec**
1969	---	---	20	19	17	11	15	13	15	14	18	18
1970	22	16	18	18	12	14	12	13	11	21	19	22
1971	24	18	24	18	17	16	11	14	16	22	21	20
1972	20	19	18	20	16	15	14	14	20	15	17	23
1973	18	15	18	14	15	13	15	12	19	17	22	20
1974	24	18	23	15	12	17	20	10	11	12	16	22
1975	21	25	22	14	18	12	13	12	12	20	20	22
1976	18	19	22	13	12	13	13	10	11	13	11	13
1977	10	18	19	10	14	13	10	13	12	12	16	23
1978	21	13	11	15	14	10	10	10	10	9	13	15
1979	16	22	15	16	15	11	14	11	14	18	14	18
1980	20	15	23	15	11	11	15	10	11	13	20	21
1981	12	19	15	13	12	14	13	8	12	15	18	20
1982	14	13	7	10	11	10	12	9	11	17	14	21
1983	14	18	17	11	---	---	---	---	---	---	---	---

SOLUTION:

Three options are presented on the following pages.

(Sheet 1 of 4)

Example Problem II-8-1 (Continued)

Option 1: (use ACES; this option is generally preferred)

A series of annual maximum wind speeds is taken from the table of data. The data include 13 complete years (1970-1982) and two partial years (1969 and 1983). Combining January and February from 1982 with the March -December 1969 data gives another full year for analysis. The annual maximum series with 14 values is then:

20, 22, 24, 23, 22, 24, 25, 22, 23, 21, 22, 23, 20, 21 m/s

These values are entered as significant heights into the ACES extremal significant wave height analysis application. Appropriately, ACES provides a warning that a 14-year sample is too short to give a reliable estimate of the 50-year event. The FT-I distribution function is found to provide a good fit (Figure II-8-10). The corresponding 25- and 50-year wind speeds are

U_{25} = 25.5 m/s (10-min average)

U_{50} = 26.3 m/s (10-min average)

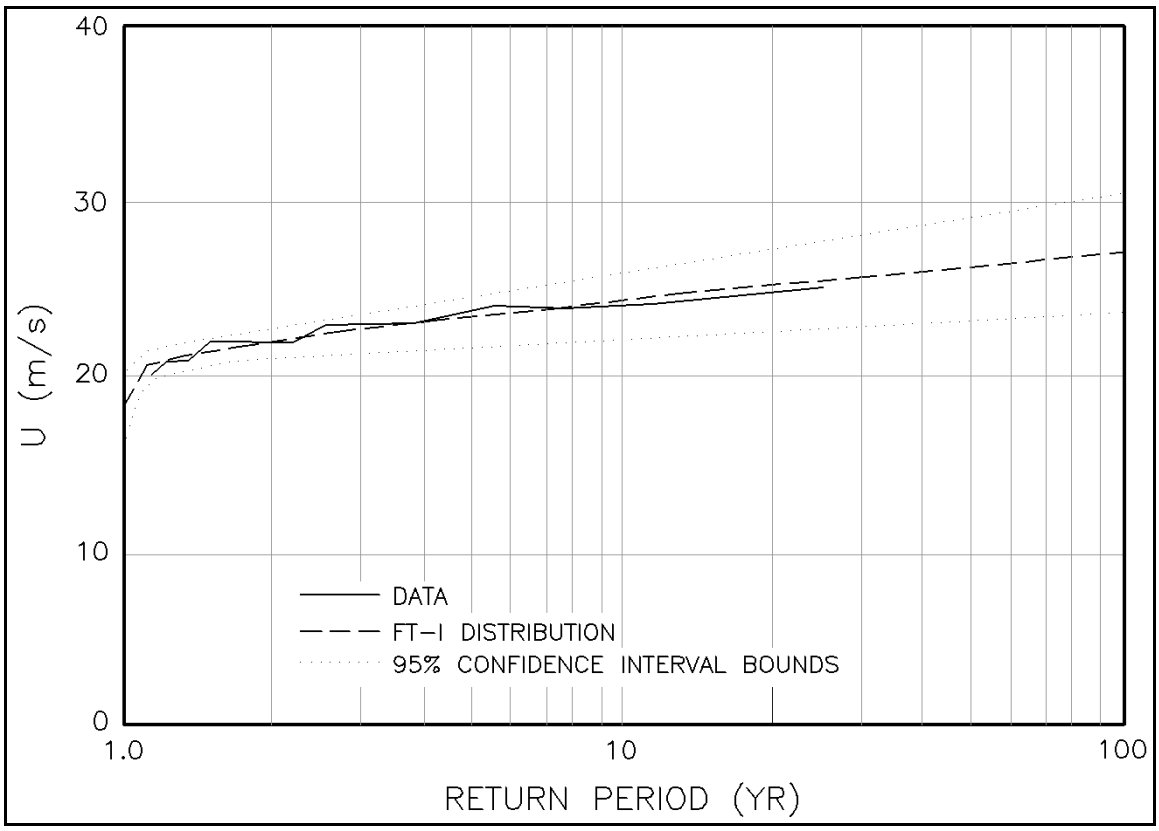

Figure II-8-10. Example Problem II-8-1 probability distribution of wind speeds

(Sheet 2 of 4)

Example Problem II-8-1 (Continued)

Option 2: (use Equation II-8-3)

Equation II-8-3 can be applied to 3 or more complete years of data. Up to 14 years of data are available in this example. Normally, all full years would be used together. For illustration, the following solution treats four 3-year samples from the full record as well as the 14-year sample extending from March 1969 through February 1983. Means and standard deviations of maximum monthly wind speeds are given in Table II-8-10.

Table II-8-10
Wind Speed Statistics

Years	$\bar{U}_m$, m/s	σ_m , m/s
1971-73	17.50	3.32
1974-76	16.08	4.58
1977-79	14.03	3.62
1980-82	14.03	4.02
Mar 69 - Feb 83	15.53	4.06

U_{25} is calculated from Equation II-8-3 for the years 1971-73 as

$$U_{25} = \bar{U}_m + 0.78\,\sigma_m\,[\,ln(12\times25) - 0.577\,]$$
$$= \bar{U}_m + 4.00\,\sigma_m = 17.50 + 4.00\times3.32 = 30.8 \text{ m/s}$$

Similarly, U_{50} is calculated from Equation II-8-3 for the years 1971-73 as

$$U_{50} = \bar{U}_m + 0.78\,\sigma_m\,[\,ln(12\times50) - 0.577\,]$$
$$= \bar{U}_m + 4.54\,\sigma_m = 17.50 + 4.54\times3.32 = 32.6 \text{ m/s}$$

The standard deviation of the sampling error in estimating U_r for the years 1971-73 may be calculated from Equation II-8-4 as

$$\sigma_{rm} = \sqrt{0.49 + 0.89\,ln(12\bar{U}_m) + 0.67\,[ln(12\bar{U}_m) - 0.577]^2}\;\left(\frac{\sigma_m}{\sqrt{36}}\right)$$

$$= \sqrt{0.49 + 0.89\,ln(12\times17.50) + 0.67\,[ln(12\times17.50) - 0.577]^2}\;\left(\frac{3.32}{\sqrt{36}}\right)$$

$$= \sqrt{0.49 + 0.89\times5.347 + 0.67\times[5.347-0.577]^2}\;\left(\frac{3.32}{6}\right) = \sqrt{20.49}\times0.553 = 2.5 \text{ m/s}$$

(Sheet 3 of 4)

Example Problem II-8-1 (Concluded)

These results and those calculated for the other samples are summarized in Table II-8-11.

Table II-8-11
Wind Speed at 25- and 50-year Return Period

Years	U_{25} , m/s	U_{50} , m/s	σ_{rm} , m/s
1971-73	30.8	32.6	2.5
1974-76	34.4	36.9	3.4
1977-79	28.5	30.5	2.6
1980-82	30.1	32.3	2.9
Mar 69 - Feb 83	31.8	34.0	1.4

Option 3: (use Figure II-8-7)

Figure II-8-7 is the least desirable option, since it does not make use of the available measurements at the site. However, it provides a reference to regional behavior against which the data analyses can be interpreted. For this example, the figure indicates that

$$U_{50} \approx 80 \text{ mph} = 35.8 \text{ m/s} \qquad \text{(fastest mile)}$$

From Table II-8-6,

$$U_{25} = 0.95 \times 35.8 = 34.0 \text{ m/s} \qquad \text{(fastest mile)}$$

These wind speeds are converted from fastest mile to 1-hr averages using Table II-8-7:

$$U_{25} = 0.78 \times 34.0 = 26.5 \text{ m/s} \qquad \text{(1-hr average)}$$

$$U_{50} = 0.78 \times 35.8 = 27.9 \text{ m/s} \qquad \text{(1-hr average)}$$

Finally, the 1-hr averages are converted to 10-min averages to be comparable to the results of Options 1 and 2. Using Table II-8-8,

$$U_{25} = 1.05 \times 26.5 = 27.8 \text{ m/s} \qquad \text{(10-min average)}$$

$$U_{50} = 1.05 \times 27.9 = 29.3 \text{ m/s} \qquad \text{(10-min average)}$$

Discussion: Option 1, which is generally preferred, gives the smallest values for U_{25} and U_{50}. Option 3 gives wind speeds about 10 percent higher and Option 2 over 20 percent higher than Option 1. Use of Option 1 with a partial duration series of wind speed maxima, which is recommended in practice rather than the annual maximum series, could be expected to give more realistic estimates.

(Sheet 4 of 4)

- The effect of errors on extreme wave height estimates can be significant. Errors can be expected to increase the width of confidence intervals and induce a systematic, artificial increase in H_s values at return periods of interest (Earle and Baer 1982). Errors can be as important as the finite number of years of record in limiting the reliability of extreme wave height estimates (Le Méhauté and Wang 1984).

(b) Design wave period is a period representative of extreme wave conditions. Along coasts exposed to the ocean, the design T_p is usually an intermediate period between the limits of mild local sea and long swell periods. At locations exposed to large swell, a design T_p representative of long-period swell conditions may be required. At sites sheltered from ocean swell or enclosed water bodies the size of the Great Lakes or smaller, the largest values of T_p can be associated with the largest values of H_s. At many locations, it may be reasonable to estimate design T_p with a scatter plot of peak storm H_s and associated T_p values. A regression line relating H_s and T_p is computed and then used to estimate T_p for any given H_s (e.g., Goda (1990)).

(c) In using a design T_p, it is assumed that this wave period is representative of the irregular or regular wave period needed in follow-on design calculations. Often this assumption is realistic, as high-energy wave events tend to be dominated by a single spectral peak. However, it may be preferable in some applications to consider more than one spectral peak or even a full design spectrum if follow-on calculations can make use of the information.

(d) Design wave direction is estimated based on measurements, hindcasts, and/or knowledge of extreme storm characteristics.

(3) Intermediate-depth water.

(a) When a coastal project is in intermediate water depth (that is, waves are affected by the bottom but depth-induced breaking has not begun), nearshore processes such as refraction and shoaling must be considered to transform from the measurement or hindcast site to the project site (Part II-3). Figure II-3-6 provides the simplest methodology. A more comprehensive approach would be to represent each wave condition as a TMA spectrum with appropriate energy, peak period, and direction, and compute transformation over straight, parallel bottom contours. More typically, a full numerical model representation of bathymetry and wave conditions is used, as discussed in Part II-3.

(b) Values of H_s, T_p, and wave direction in intermediate-depth water can be analyzed for design using the same procedures as for deepwater waves. The H_s and wave direction values are modified from the deep-water values because of nearshore bottom effects. Values of T_p are usually considered to be unchanged from the deepwater values by the transformation process. However, some spectral transformation techniques can predict changes in T_p. These changes are usually quite small.

(4) Shallow water (depth-limited).

(a) Extreme wave heights in coastal engineering applications are often limited by shallow-water depths. Thus, depending on the local water depth and wave climate, the distribution for significant wave heights can be expected to follow one of the appropriate functional forms in Figure II-8-2 up to a significant height of about 0.6 times the water depth (Equation II-4-10) and then increase more slowly beyond that point (Figure II-8-11). The probability at which the curve flattens depends on the local water depth and wave climate. The flattened curve can be expected to continue rising slowly, but in this region increases in significant height depend on other parameters such as wave steepness and water level rather than incident significant height. Water level can be expected to be the main controlling factor. The probability distribution for significant heights in this region may be essentially equivalent to the probability distribution of local water levels.

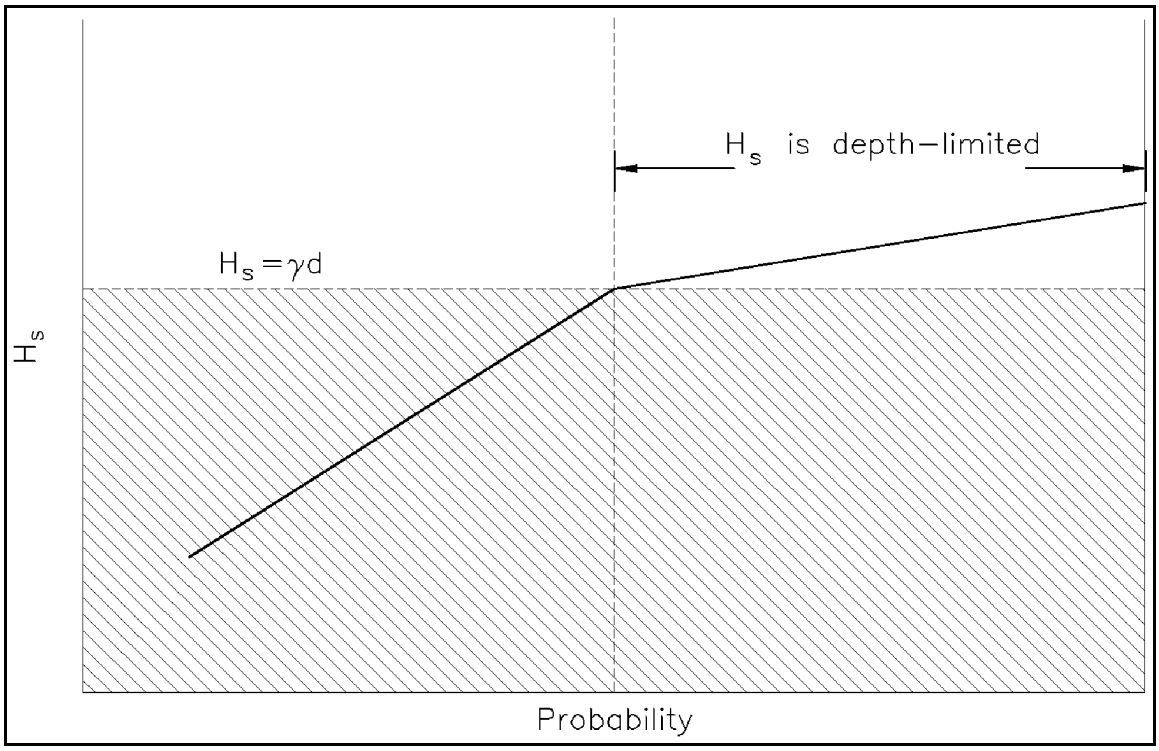

Figure II-8-11. Probability distribution of H_s on shallow water

(b) Often extreme shallow-water waves are estimated with wave information from an offshore source. Extreme waves in shallow water are typically greatly transformed from incident (often deepwater) waves due to a variety of processes discussed in Part II-3 and 4. Consequently, the most extreme incident waves are not necessarily design conditions when transformed to the shallow-water site. A sufficient range of incident wave cases must be analyzed to ensure that the most extreme shallow-water cases are identified.

(c) In shallow water, the competing processes of shoaling (tending to increase wave height) and breaking (decreases wave height in the surf zone) often create a point at which significant height reaches a maximum value in the outer surf zone. That maximum value can be estimated from Figure II-8-12. It should be noted that these values are $H_{1/3}$ rather than the energy-based significant height H_{m0} (Part II-1). The water depth at which the maximum occurs is shown in Figure II-8-13.

(d) Design wave period can be estimated as a representative value for extreme wave conditions, as with waves in deeper water. However, allowances must be made for a range of wave periods accompanying a relatively fixed, depth-limited design H_s. In this case, it may be advisable to consider several design T_p values to adequately represent the range of possibilities impacting design.

(e) Design wave direction is estimated based on measurements, hindcasts, or knowledge of extreme storm characteristics. Due consideration must be given to shallow-water effects on wave direction (Part II-3).

(5) Extreme individual wave characteristics.

(a) Extreme individual waves can have heights on the order of $2H_s$. The Rayleigh distribution function (Part II-1) is usually sufficient for describing individual wave heights in coastal engineering applications, even in extreme (but nondepth-limited) conditions. With the Rayleigh distribution function for individual

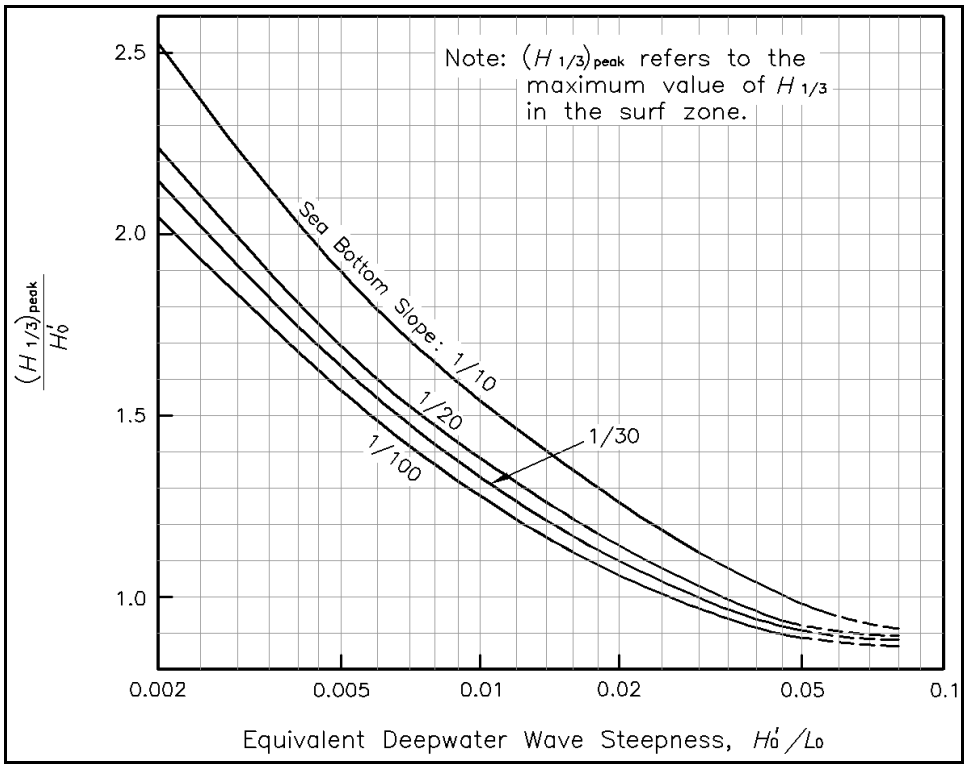

Figure II-8-12. Maximum value of H_s in the surf zone (Goda 1985)

wave heights in a given sea state (a given H_s) and a known joint distribution of H_s and T_p or T_z, an overall probability distribution of individual wave heights can be computed by a straightforward approach (Goda (1990), referring to Battjes (1972)).

(b) Extreme individual wave heights are strongly affected by depth-induced breaking. In the surf zone, the Rayleigh distribution can be expected to overestimate the higher individual wave heights. Practical approximations for extreme individual wave heights in this case are given by the Construction Industry Research and Information Association (CIRIA) (1991) as

$$H_1 = \frac{1.517\ H_{1/3}}{\left(1 + \frac{H_{1/3}}{d}\right)^{\frac{1}{3}}}$$

$$H_{0.1} = \frac{1.859\ H_{1/3}}{\left(1 + \frac{H_{1/3}}{d}\right)^{\frac{1}{2}}} \qquad \text{(II-9-5)}$$

where $H_{1/3}$ and d are the local significant height and water depth.

(c) Extreme wave crest heights are sometimes a design consideration. Coastal field measurements indicate that maximum crest height above the local mean water level can be up to 80 percent of the maximum wave height (Goda 1985). Figure II-8-14, based on a combination of irregular wave tests in the laboratory

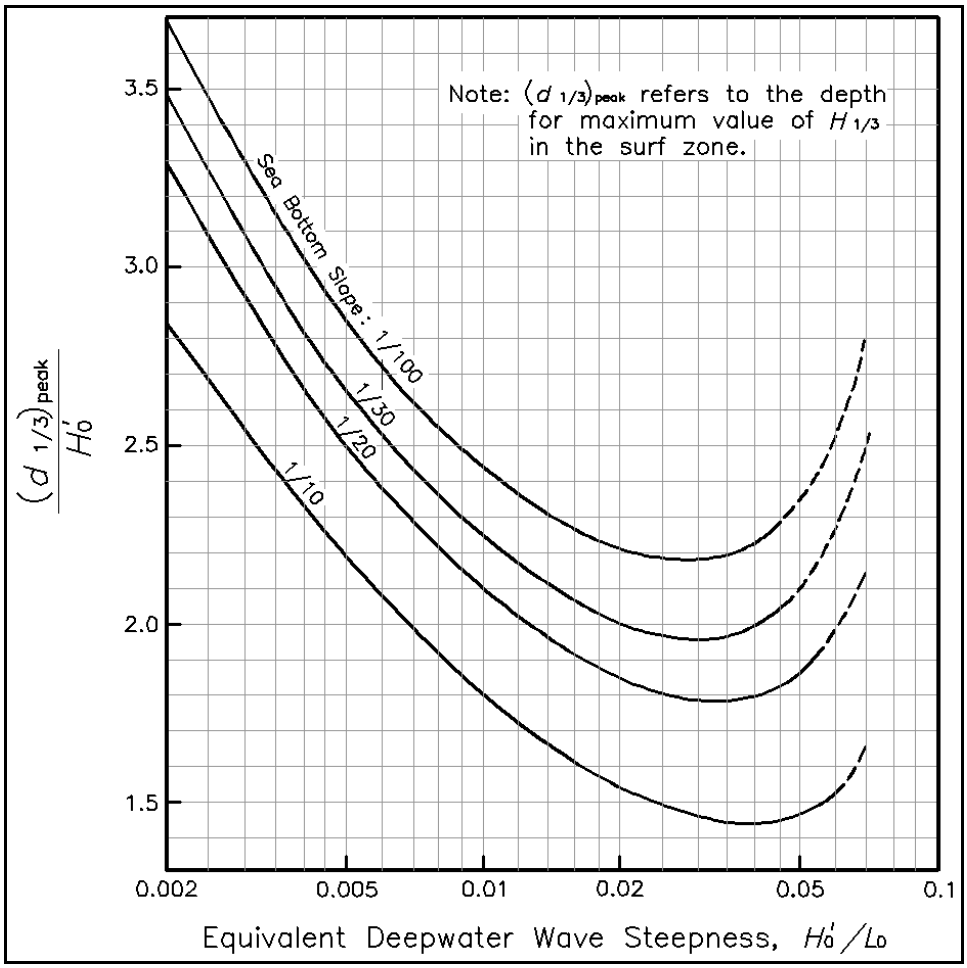

Figure II-8-13. Water depth at which H_s is maximum in the surf zone (Goda 1985)

and stream function wave theory, can be used to estimate (with small conservatism) crest heights at the 2-percent probability level of exceedance.

(d) Grouping of individual high waves can influence functional design (e.g. runup and overtopping of a breakwater or revetment) and structural design. The recommended way to account for this effect is through physical model tests. The tests should ensure that design alternatives that may be prone to damage by wave groups include a realistic sampling of grouping in the incident waves.

d. Wave climate. Wave climate is discussed in Part II-2.

(1) Design importance. Wave climate affects functional performance of a project and operational activities. Its impact includes longshore and cross-shore sediment transport, harbor agitation, navigation, dredging, and surveying.

(2) General climate.

(a) General wave climate is the probabilistic mix of sea states occurring at a site. Key components of a sea state typically include H_s, T_p, and θ_p for each major wave system (such as a sea and one or more swell systems). Sea states along U.S. Atlantic, Pacific, and Gulf of Mexico coasts can be expected to include more

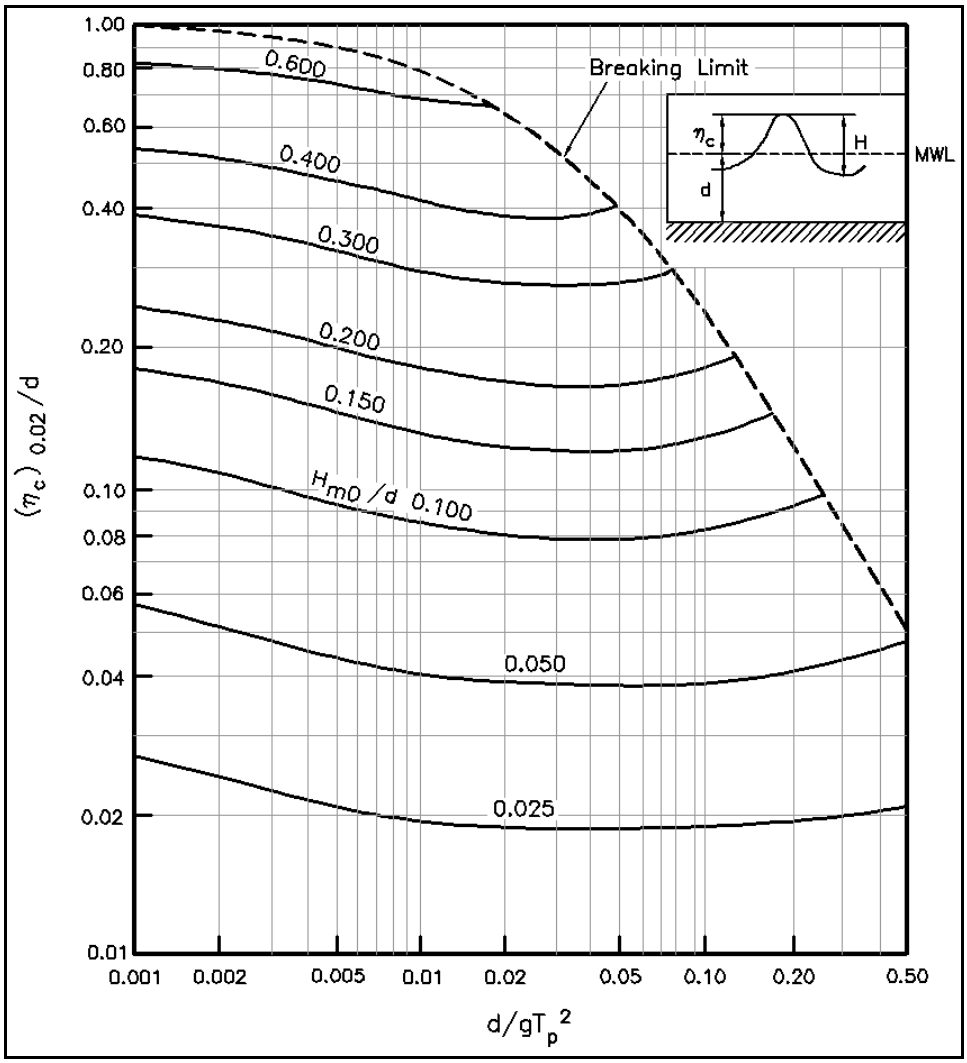

Figure II-8-14. Crest elevation at the 2-percent probability level of exceedance (Seelig, Ahrens, and Grosskopf 1983)

than one major wave system about two-thirds of the time (Thompson 1980). Wave climate can vary greatly between seasons of the year, but variations between years are usually small. At least three full years of data are desirable for a stable estimate of wave climate. Figure II-8-15 is a typical table of wave climate information (from one directional sector) from the Wave Information Studies.

(b) The mean H_s and distribution of H_s are always of interest in describing wave climate. Both Weibull and log-normal distribution functions have been used to represent the distribution of H_s. However, the actual data usually provide a sufficiently stable estimate and the formal distribution functions are unnecessary. Means and distributions of T_p and θ_p are vital for some applications. Joint occurrence probabilities of H_s, T_p, and θ_p give a fairly complete representation of wave climate, which is needed in applications such as nonlinear refraction modeling. When these standard statistical summaries are formed, information about the simultaneous occurrence of more than one wave system is lost.

WIS ATLANTIC REVISION 1956 - 1975
LAT: 36.00 N, LONG: 75.25 W, DEPTH: 37M
OCCURRENCES OF WAVE HEIGHT AND PEAK PERIOD FOR 45-DEG DIRECTION BANDS

STATION: 55 (67.50 - 112.49) 90.0 DEG

Hmo (m) \ Tp (sec)	3.0-4.9	5.0-6.9	7.0-8.9	9.0-10.9	11.0-12.9	13.0-14.9	15.0-16.9	17.0-18.9	19.0-20.9	21.0-LONGER	TOTAL
0.00 - 0.99	381	784	2655	1809	667	267	46	11	4	.	6624
1.00 - 1.99	58	1344	1327	1197	990	347	48	8	1	.	5320
2.00 - 2.99	.	44	429	180	161	67	.	.	.	.	881
3.00 - 3.99	.	.	55	156	54	30	5	.	.	.	300
4.00 - 4.99	.	.	3	64	33	9	5	.	.	.	114
5.00 - 5.99	.	.	.	6	21	4	2	.	.	.	33
6.00 - 6.99	.	.	.	.	6	5	.	1	.	.	12
7.00 - 7.99	.	.	.	.	.	3	2	.	.	.	5
8.00 - 8.99	.	.	.	.	.	7	3	.	.	.	10
9.00-GREATER	.	.	.	.	.	.	.	.	.	.	0
Total	439	2172	4469	3412	1932	739	111	20	5	0	13299

Figure II-8-15. Wave climate summary (Hubertz et al. 1993)

(3) Storms.

(a) Storms are a natural part of the wave climate at a site. On the order of 20-50 storm events can be expected at a site during a year of record. The upper portion of the distribution of H_s is due to storms, either local or distant. Much of the storm wave climate is fairly consistent from year to year. Three years of data usually suffice for a reasonable representation of the storm portion of wave climate (excluding extreme events). Large storm events usually dominate any secondary wave systems present, and the sea state can be well-represented by one H_s, T_p, and θ_p parameter set. Tropical storms are generally a concern only in the extreme portion of wave climate, if at all, since even the more exposed sites are rarely affected by them.

(b) Some areas can experience changes in climate that systematically affect the incidence and intensity of severe storm waves over a time period of months or years. The reasons for climate change are not always easily understood. Short-term climate variation can be related to deviations from characteristic upper air flow patterns or large-scale ocean current patterns that persist over at least one storm season. One documented example is the influence of the El Ninõ-Southern Oscillation climatic anomaly on the occurrence of extreme waves along the California coast (Seymour et al. 1984). Both tropical and winter storms are affected. Long-term systematic climate changes can be generated by factors such as local subsidence and global temperature change. An example of long-term change is the increasing trend in annual mean significant wave height off the southwest tip of England as measured over a 25-year period at Seven Stones Light Vessel (Carter and Draper 1988).

(4) Persistence of high and low wave conditions.

(a) The duration of storm events is another important component of the wave climate. Storm duration in this context is usually defined as the length of time H_s *persists* above some fixed threshold value (Figure II-8-16). Storms with long duration are likely to be more damaging than storms with short duration, in part because they are likely to encompass one or more highs in astronomical tide. Storm duration decreases as threshold increases, but it appears to be fairly independent of storm intensity (Smith 1988). The choice of threshold value is based on the application. Smith (1987) suggested using an H_s value that is exceeded by 6 percent of the observations, which gave mean durations of about 25 hr at U.S. east and west coast hindcast locations. Thus these events can be expected to encompass two high tides along the U.S. east coast and one higher high water along the U.S. west coast.

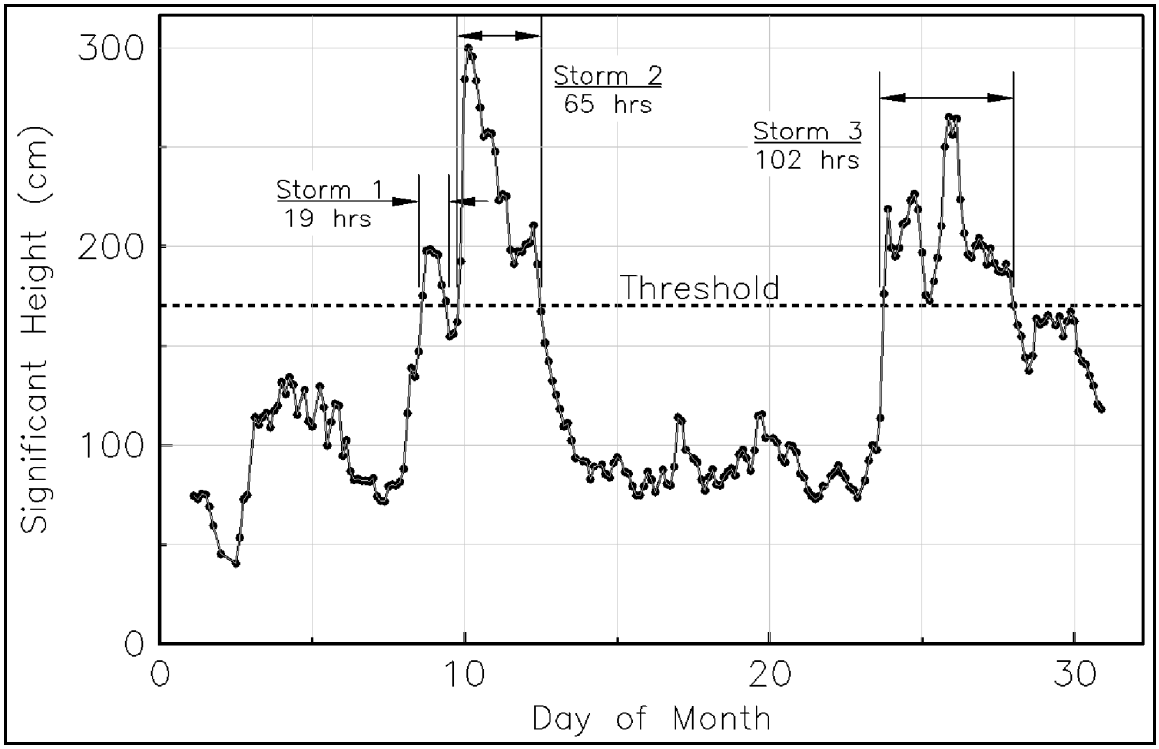

Figure II-8-16. Persistence of storm waves

(b) Persistence of wave conditions *below* a threshold H_s can be an important operational concern, since it provides information on operational windows of low wave activity. It can also be a consideration in functional design of some coastal projects.

e. Long waves. Wave phenomena with periods between those of swell and tides are collectively termed *long waves*. In most coastal engineering applications, they have a limited role in design. Occasionally they can be a major design concern (e.g. harbor oscillations).

(1) Tsunamis. Tsunamis are briefly discussed in Part II-5. They are sufficiently rare and unpredictable that they become a concern for design return periods of about 100 years or longer. Since most coastal engineering works are designed for return periods of 50 years or less, tsunamis can generally be omitted from the design.

(2) Seiche. Seiche is discussed in Part II-7. It can be an important concern in harbor design or modification. Harbors in areas where energetic, long-period swell can occur are especially prone to seiching

problems. In such areas (e.g. the U.S. Pacific coast and Hawaii), seiche should be routinely considered in design.

(3) Infragravity waves. Infragravity waves are discussed in Part II-4-5. They can be an important component of surf zone processes, particularly during storms, and they are a forcing mechanism for harbor oscillations and other seiching phenomena. Methods for estimating infragravity waves and incorporating them into design are relatively immature at present. Infragravity waves can be considered in design by conducting physical model tests with irregular waves if long waves can be sufficiently controlled, a demanding task. They may also be estimated with some confidence from wind wave/swell conditions using theory, numerical modeling, and/or empiricism. For example, Bowers (1992) considered long waves at three coastal sites in intermediate depths typical of harbor entrances. He used theory to estimate a bound long wave H_s and empiricism to estimate a free long wave H_s (including both edge waves and leaky waves described in Part II-4-5). His general expression for free waves is

$$H_s \text{ (free long waves)} = K \frac{H_s^{\alpha} T_p^{\beta}}{d^{\gamma}} \tag{II-9-6}$$

For his three sites, K ranged from 0.0041 to 0.0066 and overall best-fit values for α, β, and γ were 1.11, 1.25, and 0.25, respectively. Bowers observed that bound long waves increasingly dominate free long waves as wind wave/swell H_s increases. For a 10-year return period in the 12-m to 13-m depth, Bowers estimated total long wave H_s values of about 12 percent of the wind wave/swell H_s.

f. Extreme water level. Extreme water levels are discussed in Part II-5.

(1) Design importance. Extreme high water levels cause flooding. They also facilitate wave damage by raising the base level for runup and overtopping, by allowing increased depth-limited wave heights, and by shifting the zone of wave attack further shoreward such that waves can damage dunes and coastal structures. At some locations, extreme high-water levels can lead to pollution and health hazards when sewage treatment ponds or other containment areas are breached.

(2) Estimation procedures. Extreme water levels are caused by some combination of astronomical tides, storm surge (high wind stress, low atmospheric pressure, rainfall/runoff in enclosed or semi-enclosed areas), and wave setup. Probabilities must be estimated as a joint probability of the various combinations that can occur. Procedures for developing storm water level frequency-of-occurrence relationships are reviewed in Part II-5-5.b, including the historical method, synthetic method, and empirical simulation technique (EST). The EST is convenient for development of water level design criteria requiring the quantification of risk and uncertainty associated with the frequency predictions. Traditionally, the distribution of extreme water levels has been fitted to either a Pearson Type III (Engineer Manual (EM) 1110-2-1412) or log-Pearson Type III (U.S. Water Resources Council 1976) distribution function. The EST approach does not require a theoretical distribution function.

g. Water level climate. Water level climate is discussed in Part II-5.

(1) Design importance. The general water level climate at a site impacts navigation channel depths, harbor depths, currents, harbor flushing, and physical and biological processes in the intertidal zone, including marsh areas.

(2) Estimation procedures. The principal component of water level climate at most coastal sites is astronomical tide (Part II-5-3). In areas with little or no tide, particularly very shallow areas, wind,

atmospheric pressure, and rainfall can be the primary components of water level climate (Part II-5-5). In lakes, seasonal fluctuations in water level can be dominant, as in the Great Lakes (Part II-5-4.b.(2)).

(3) Long-term changes. Long-term changes in relative water level can be caused by climatological effects and secular fluctuations (such as melting of the polar ice caps, large-scale isostatic adjustments of the earth's crust, and local subsidence). These long-term changes, which operate on time scales ranging from semiannual to decades, may sufficiently shift the water level datum relative to project features to merit consideration in design.

h. Currents. Surf zone currents are discussed in Part II-4-6. Currents at inlets and harbors are treated in Part II-6 and 7, respectively.

(1) Design importance.

(a) Nearshore shelf. Currents over the continental shelf are important relative to rate and direction of transport of fluids and solids, such as river discharge into the ocean, sewer outfall discharge, movement of sediment from offshore dredge disposal sites, and movement of civic waste material from ocean dump sites. They may also be important for their effect on navigation into harbors, particularly for large vessels subjected to currents moving across the entrance channel. Currents are driven mainly by tides and winds, but temperature and salinity gradients, Coriolis effect, river discharges, and organized current systems (such as the Gulf Stream) can also be important. Currents can vary greatly between the surface and bottom.

(b) Surf zone. Surf zone currents are the driving force transporting sediments in both the longshore and cross-shore directions. As such, they are the key factor in beach erosion and accretion. They may also be important relative to scour and stability of breakwaters and revetments. Surf zone currents are driven by breaking waves and nearshore winds. Currents are very sensitive to wave direction. The magnitude of longshore transport can vary greatly over a time period of days, months, and even from year to year in response to natural variations in wind and wave climate (Figure II-8-17). At many sites, even the dominant direction during a single year (upcoast or downcoast) can deviate from the normal pattern. Thus an adequate sample of years is necessary for stable design estimates. Surf zone currents are discussed in detail in Part II-4-6. Nearshore sediment transport is covered in Part III.

(c) Inlets. Currents through inlets are the primary process affecting exchange of water and sediments between the bay and ocean. They impact water quality, bay ecology, and erosion and shoaling patterns. They can impede navigation by creating steepened, breaking waves when a strong ebb current opposes energetic ocean waves. They may cause scour along jetties and other inlet structures and affect structure stability. Tides, wind, and density differences are typical driving forces. Inlet currents are a necessary consideration in design of projects at inlets.

(d) Harbors. Currents through harbor entrances are generally important in terms of circulation and flushing of the harbor to maintain water quality and, in some cases, to reduce maintenance dredging. They can be driven by tides, winds, and river discharge within the harbor. Additional detail is given in Part II-7-6.

(2) Estimation procedures.

(a) Currents are estimated in terms of time-averaged mean speed and direction and, often, some measure of maximum current speed. For tidal currents, it is helpful to distinguish between ebb and flood tide maxima.

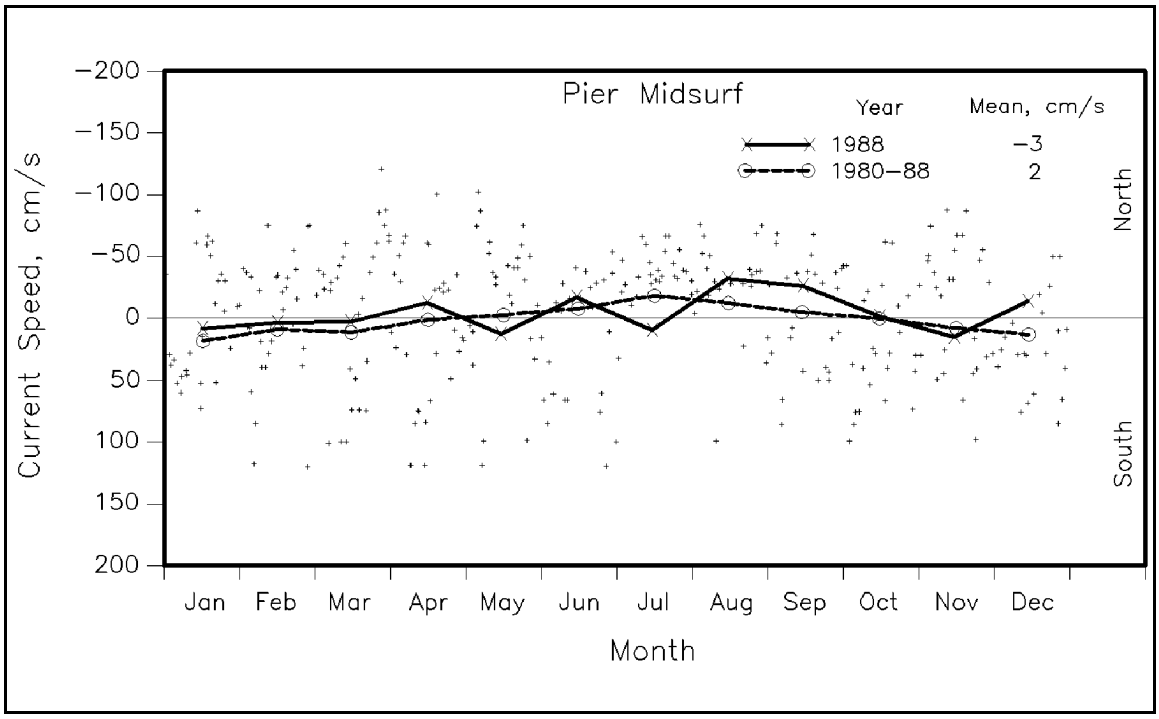

Figure II-8-17. Example of short- and long-term surf zone current data (Leffler et al. 1990)

Currents can vary significantly over short distances, especially around inlets, and some knowledge of the spatial current field can be useful for design.

(b) Currents are best estimated from measurements, numerical modeling, or physical modeling. A combination of both measurement and modeling typically yields the best estimates. Measurements provide boundary conditions and calibration/validation data for the model. The model provides full spatial current fields and a capability for estimating design conditions well beyond any measured events.

(c) More approximate information on currents can be obtained from several sources. Published tidal current tables for use by mariners are available for many U.S. areas important to navigation (Part II-8-7). As with winds, currents at one location can sometimes be transferred to another nearby location, with due consideration of differences between locations. A short measurement record from the desired location can be very helpful in estimating transfer relationships. ACES includes a simplified model for inlet hydraulics. Time-varying inlet currents can be calculated for given time-dependent sea level fluctuation.

i. Design example.

(1) This section contains a detailed example of estimating hydrodynamic parameters for design. Because of the complexities and many variations of design environment possible in coastal engineering (for example, inner surf zone versus outer surf zone versus outside the surf zone), the example is more an illustration than a blueprint for coastal design. Data used in the example are more extensive than would typically be available. When measurements are lacking, the information on water levels and waves must be estimated from some combination of experience, nearby measurements, hindcasts/forecasts, and other physical and numerical modeling. Information must be properly transformed to the project site.

EXAMPLE PROBLEM II-8-2

FIND: Hydrodynamic parameters for design of the north jetty. The intended design life is 25 years.

GIVEN: Two jetties are being designed at a site exposed to energetic waves and currents (Figure II-8-18). The jetties extend from shore to a depth of -10 m MLLW. A representative bottom slope is 1/100. Water level and wave measurements near the site are available at 6-hr intervals over a period of 17 years.

Note: This period of measurement is unusually long for coastal engineering project sites. Typically information on water levels and waves must be generated by numerical modeling to supplement limited measurements. The level of confidence in any calculated results depends highly on the *quality* of available water level and wave information. The level of detail and refinement of calculations should be consistent with the quality of available information and project needs.

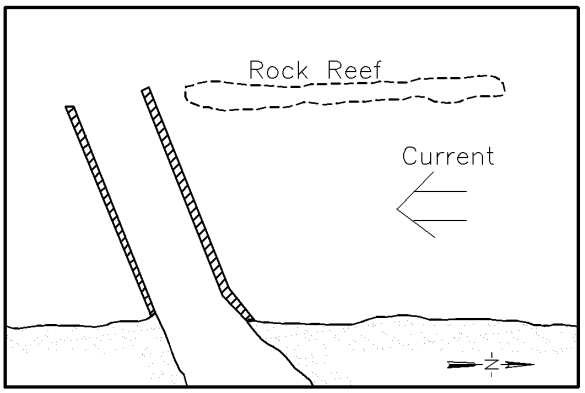

Figure II-8-18. Jetty plan

SOLUTION:

WATER LEVEL:

Assume all storm populations that could affect design are well-represented (both number and intensity of events) in the data.

Note: At sites exposed to tropical storms, the assumption that storms are well-represented in the historical record at the site is often not justified. In such cases, a numerical model study is required to adequately represent the range of possibilities (Part II-5).

Datums. Datum information for the site (obtained from NOS tidal benchmark sheet; see Part II-8) is listed in Table II-8-12.

Table II-8-12
Tidal Datum Information

Datum	Abbreviation	Level (m)
Mean higher high water	MHHW	2.55
Mean high water	MHW	2.34
Mean tide level	MTL	1.38
Mean sea level	MSL	1.36
National Geodetic Vertical Datum	NGVD	1.26
Mean low water	MLW	0.42
Mean lower low water	MLLW	0.00

Example Problem II-9-2 (Sheet 1 of 21)

Example Problem II-8-2 (Continued)

Astronomical tide. A probability distribution of astronomical tide levels (Figure II-8-19) can be obtained from: (1) Harris (1981) for selected tide stations; (2) harmonic reconstruction of a tidal series (Part II-5); or, (3) to a good approximation over all but the more extreme ends, statistical summarization of long-term water level measurements.

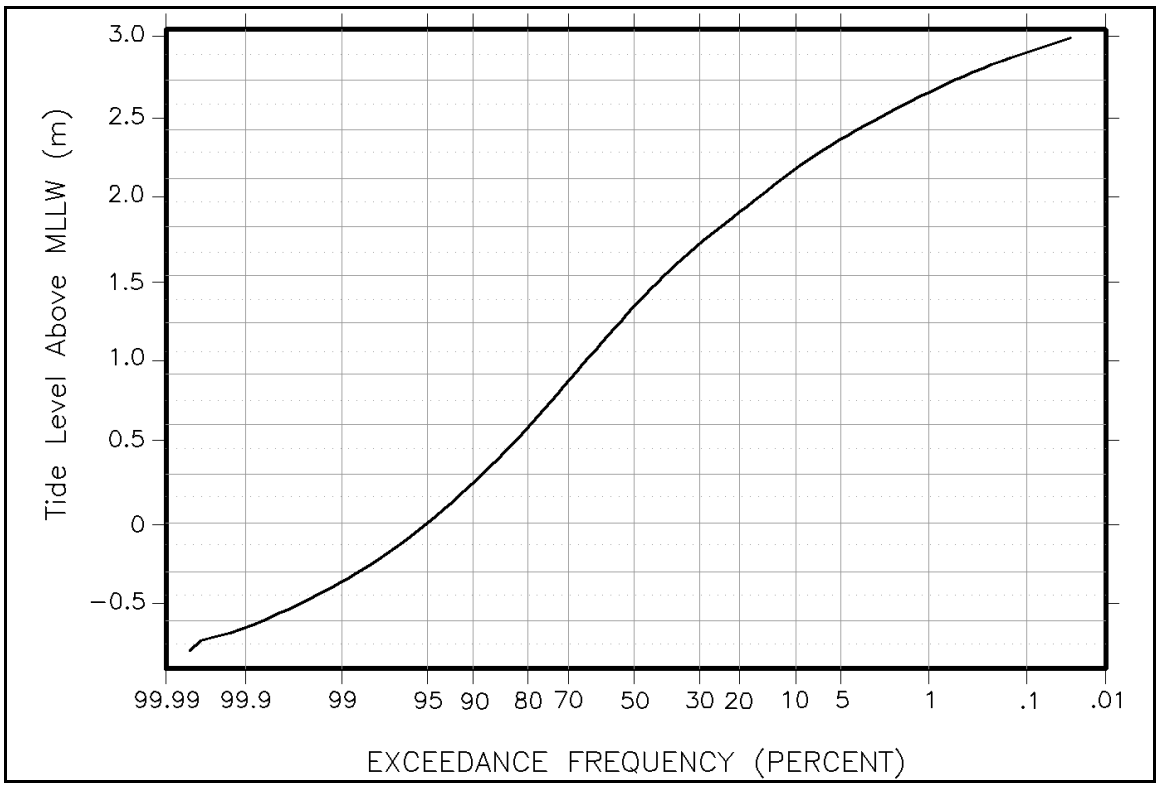

Figure II-8-19. Probability distribution of astronomical tide levels

Storm surge. Storm surge water levels (Figure II-8-20) can be estimated by the following steps:

(1) Develop criteria for identifying storm events, such as events with $H_s \geq 5$ m and separated from each other by 5 or more days.

(2) Identify all cases in the water level measurement record that meet the criteria in (1).

Example Problem II-9-2 (Sheet 2 of 21)

Example Problem II-8-2 (Continued)

(3) For each selected event, subtract the predicted astronomical tide and wave setup from measured water levels. The maximum difference during the event is considered the peak surge. Details of calculating wave setup are omitted here but discussed later in conjunction with wave analysis.

(4) Organize peak surges into a probability distribution. The ACES Extremal Significant Wave Height Analysis (using water levels in place of significant heights) may be a helpful tool for this and the following step.

(5) Fit a probability distribution function to the data to extrapolate to lower probabilities as needed.

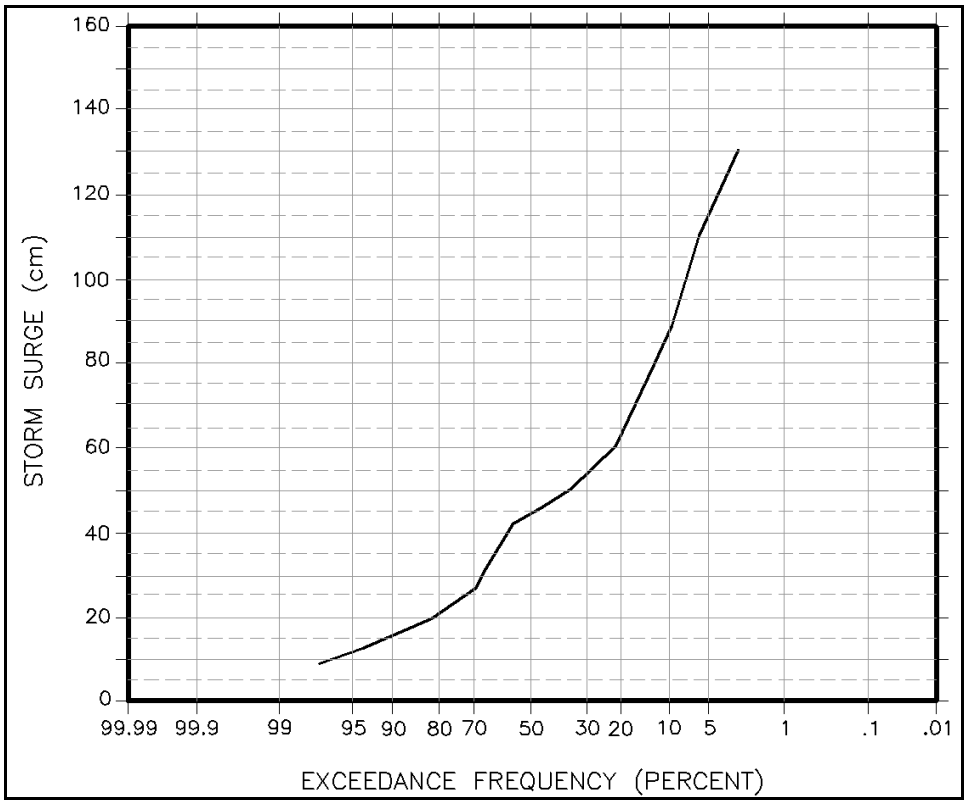

Figure II-8-20. Probability distribution of storm surge

Combined tide and storm surge. A simplified analysis is used here to generate probabilities for combined tide and storm surge. With consideration of general knowledge about the duration of storms, typical storm surge hydrographs, and tidal variations at the site, it is reasonable (but somewhat conservative) to assume that peak water level events can be represented as the measured peak surges coinciding with a high tide.

Example Problem II-9-2 (Sheet 3 of 21)

Example Problem II-8-2 (Continued)

The distribution of high water tide elevations above mean sea level is given by Harris (1981) for a nearby location with similar tidal response (Figure II-8-21). For this example, the traditional *joint probability method* (as described by Harris (1981)) was used to combine high-water tide frequencies with storm surge probability expressed as frequency of occurrence *per year*. Combined tide and storm surge probabilities for design return periods are included in Figure II-8-21.

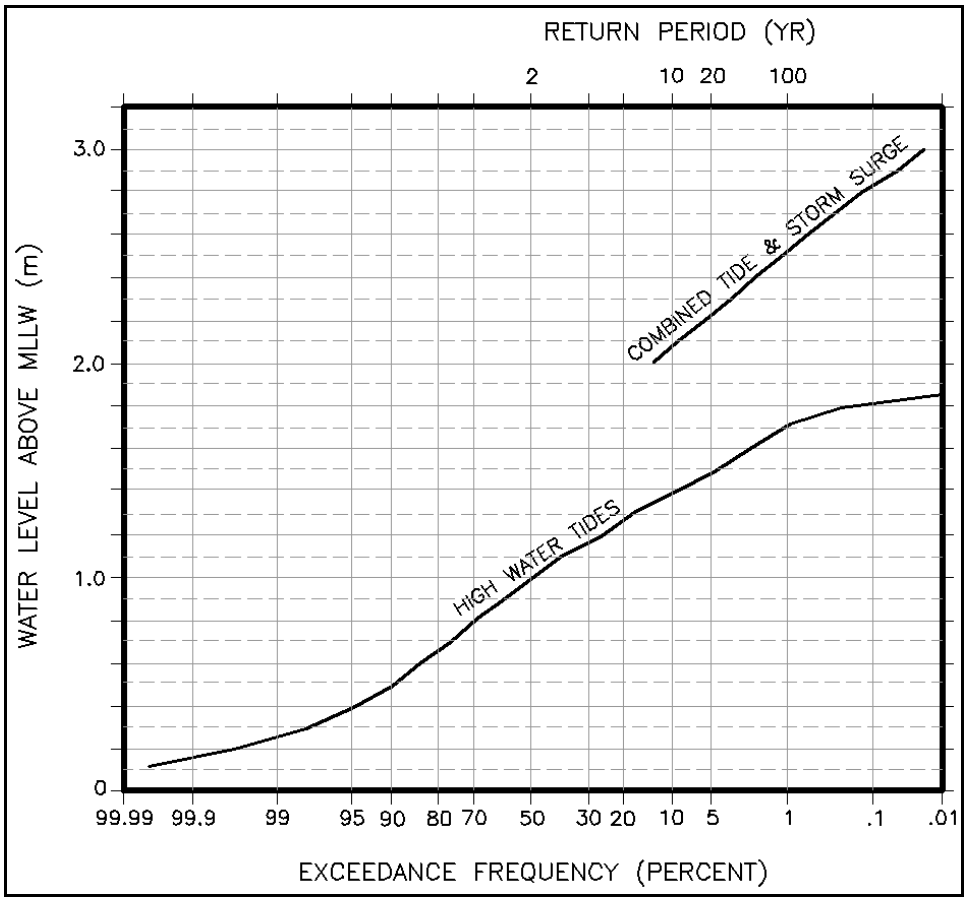

Figure II-8-21. Probability distribution of high tides and combined tide and storm surge

CURRENTS:

The north jetty will deflect a strong longshore current seaward. Therefore strong offshore-directed currents can be expected along the north side of the jetty. Because of the local bathymetry, principally a rocky reef parallel to shore, the current is expected to affect only the area near the jetty head. Local currents can be estimated based on experience at similar sites (if any exist), physical modeling, and, possibly, numerical modeling. For this example, moderate current speed is taken as 1.5 m/s and design current as 3.0 m/s. Tidal currents can also be significant, since the tide range is fairly large. Tidal currents will affect navigation in the entrance, but are not expected to influence jetty structural design.

Example Problem II-9-2 (Sheet 4 of 21)

Example Problem II-8-2 (Continued)

WAVES:

Measurements. Measurements are available over a period of 17 years from a wave gauge located in -15.2-m depth MLLW. Events with H_s>6.1 m were selected for design analysis, a total of 33 cases. The maximum H_s during each event and the corresponding T_p, storm surge, and water depth at the gauge are given in Table II-8-13.

The data record represented in the table is quite long, and it is considered statistically representative of storm events to which the site is exposed. It is used as the basis for design. Measured values of T_p can be taken as representative of both the gauge and jetty locations. Measured values of H_s must be transformed between the gauge location and jetty. Also, the design water level at the jetty must be estimated because it strongly affects calculations of H_s.

Estimation of H_0'. The equivalent deepwater wave height H_0' is calculated as an intermediate step in estimating wave height at the jetty. Refraction between gauge and jetty locations is assumed to be negligible in this example, and values of H_0' estimated from gauge data are also applicable to the jetty location. Steps in estimating H_0' are listed below and calculation results are given in Table II-8-13. The ACES application "Irregular Wave Transformation" (Goda's Method) could be used to assist in these and subsequent calculations. It is advisable to spot-check any ACES calculations with some manual calculations.

(1) Calculate L_0 from known values of T_p , $L_0 = (gT_p^2)/(2\pi) = 1.56gT_p^2$ (L_0 in m).

(2) Calculate d_{gauge}/L_0 .

(3) Calculate H_s/L_0 as an initial estimate of H_0'/L_0 (needed for using the curves in step (4)).

(4) Get shoaling coefficient K_s from Figure II-8-22.

(5) Calculate H_0' from significant height at the gauge H_{sgauge} (Table II-8-13) as

$$H_0' = \frac{H_{sgauge}}{K_s} \qquad \text{(II-9-7)}$$

(6) Calculate H_0'/L_0 to ensure that K_s from step (4) is valid. It may be necessary to repeat steps (4)-(6) to arrive at a final value of H_0'.

Example Problem II-8-2 (Sheet 5 of 21)

Example Problem II-8-2 (Continued)

Table II-8-13
Significant Storm Events

	Measurements				Calculations				
Date	H_s(cm)	T_p(sec)	Surge(cm)	d_{gauge}[1](m)	L_0(m)	d_{gauge}/L_0	K_s	H_0'(cm)	H_0'/L_0
Feb 78	613	13.5	73	17.3	284	0.0609	1.00	613	0.0216
Jan 81	625	17.4	12	15.1	472	0.0320	1.18	530	0.0112
Nov 81	646	13.6	131	17.6	289	0.0609	1.00	646	0.0224
Dec 81	619	15.4	30	14.9	370	0.0403	1.11	558	0.0151
Dec 82	884	15.0	88	17.9	351	0.0510	1.08	819	0.0233
Jan 83	713	16.9	110	16.9	446	0.0379	1.15	620	0.0139
Feb 83	622	15.8	46	17.6	389	0.0452	1.07	581	0.0149
Apr 83	631	15.2	43	17.9	360	0.0497	1.04	607	0.0169
Feb 84	707	15.2	79	17.7	360	0.0492	1.05	673	0.0187
Nov 84	634	14.0	61	16.9	306	0.0552	1.01	628	0.0205
Dec 85	613	17.6	43	16.7	483	0.0346	1.13	542	0.0112
Feb 86	686	17.1	49	18.1	456	0.0397	1.10	624	0.0137
Mar 86	610	16.4	46	18.0	420	0.0429	1.08	565	0.0135
Apr 86	680	15.6	12	16.2	380	0.0426	1.10	618	0.0163
Apr 86	631	14.5	27	16.8	328	0.0512	1.03	613	0.0187
May 86	619	14.5	30	17.0	328	0.0518	1.03	601	0.0183
Sep 86	689	15.4	46	17.5	370	0.0473	1.06	650	0.0176
Nov 86	652	16.9	49	17.1	446	0.0383	1.12	582	0.0130
Jan 87	695	16.0	55	17.5	399	0.0439	1.09	638	0.0160
Feb 87	631	13.0	40	17.3	264	0.0655	0.98	644	0.0244
Apr 87	686	14.6	21	17.2	333	0.0517	1.04	660	0.0198
Sep 87	643	13.8	12	17.5	297	0.0589	1.00	643	0.0217
Nov 87	610	16.7	70	17.1	435	0.0393	1.10	555	0.0128
Dec 87	628	15.4	24	17.6	370	0.0476	1.05	598	0.0162
Mar 88	613	14.8	3	16.9	342	0.0494	1.05	584	0.0171
Apr 88	643	13.0	21	17.2	264	0.0652	0.98	656	0.0248
Nov 88	628	13.2	24	16.6	272	0.0610	1.00	628	0.0231
Jan 90	619	16.9	58	16.2	446	0.0363	1.14	543	0.0122
Nov 91	735	14.0	43	17.4	306	0.0569	1.00	735	0.0240
Dec 91	646	16.7	27	16.7	435	0.0384	1.12	577	0.0133
Jan 92	686	14.6	49	17.3	333	0.0520	1.03	666	0.0200
Sep 92	625	15.8	9	16.9	389	0.0434	1.09	573	0.0147
Jan 94	762	14.1	12	16.9	310	0.0545	1.03	740	0.0239

[1] Water depth at gauge including combined tide and storm surge.

Example Problem II-8-2 (Sheet 6 of 21)

Example Problem II-8-2 (Continued)

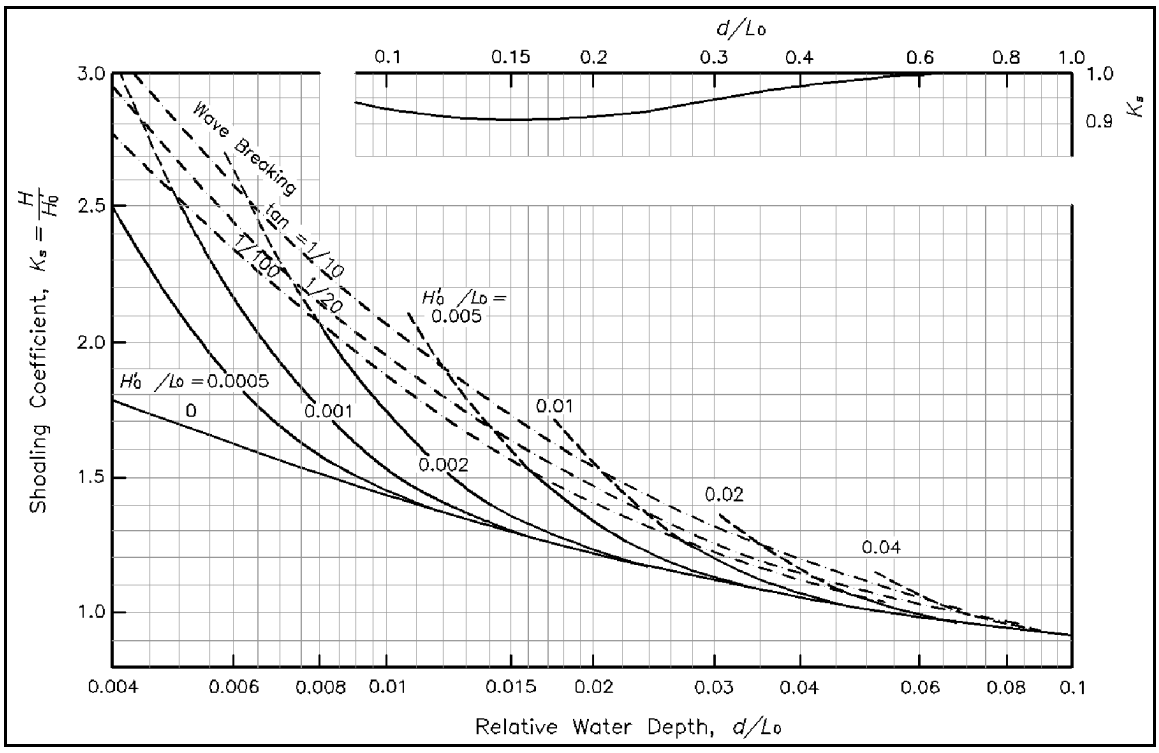

Figure II-8-22. Estimation of shoaling coefficient (Goda 1985)

Combined tide and storm surge for design wave analysis at jetty. For design wave analysis, extreme combinations of tide, storm surge, and waves must be considered. Since extreme storm surge and waves are often highly correlated (both can be produced by intense storms), they should not be treated as independent processes. The relationship between storm surge and waves is embodied in the available measurements to an extreme occurrence of approximately once in 17 years.

For this example problem, combined tide, storm surge, and waves for design analysis are derived by the following approach. Each measured wave and surge event (represented by H_0', T_p, and storm surge height) is coupled with N high tide levels taken from the probability distribution of high tides (see Table B-37b in Harris (1981)). (Figure II-8-23 is a partial extraction of Table B-37b for use in this example). As before, it is assumed that the duration of extreme storm surge events is long enough that peak surge will coincide with a high tide, and high tide level is independent of storm surge level. The N high tide levels are determined by dividing the probability distribution of high tides into N equal probability increments and taking the tide level for the mid-probability of each increment. The number N should be large enough that the combined probability of the highest tide level and the most severe surge/wave event is lower than the design probability.

Example Problem II-8-2 (Sheet 7 of 21)

Example Problem II-8-2 (Continued)

Lower Limit of Class Interval Shown, All Heights are Normalized by Half the Diurnal Range 1.274 m [Extracted from Table B-37b (Harris 1981)]		
High Water		
Lower Limit	Frequency	Cumulative Frequency
1.4547	.0001	.0001
.	.	.
.	.	.
1.1018	.0110	.0989
1.0877	.0105	.1094
.	.	.
.	.	.
0.9183	0.0206	0.2891
0.9043	0.0229	0.3120
.	.	.
.	.	.
0.7771	0.0213	0.4919
0.7630	0.0187	0.5106
.	.	.
.	.	.
0.6218	0.0185	0.6923
0.6077	0.0156	0.7079
.	.	.
.	.	.
0.4101	0.0077	0.8896
0.3960	0.0108	0.9004

Figure II-8-23. Astronomical tide probability referenced to MSL

A value of $N = 5$, corresponding to probability increments of 0.2, was used for this problem. The mid-probabilities are 0.1, 0.3, 0.5, 0.7, and 0.9. High tide levels matching these probabilities, determined from Figure II-8-24, are in Table II-8-14. The probability of the most severe surge/wave event is the reciprocal of the number of possible measurements (at 6-hr intervals or 4 observations per day) during 17 years:

$$\frac{1}{(4/day) \times (365\ days/yr) \times (17\ yr)} = 0.000040$$

Similarly, the probability corresponding to the design life of 25 years is:

$$\frac{1}{(4/day) \times (365\ days/yr) \times (25\ yr)} = 0.000027$$

Example Problem II-8-2 (Sheet 8 of 21)

Example Problem II-8-2 (Continued)

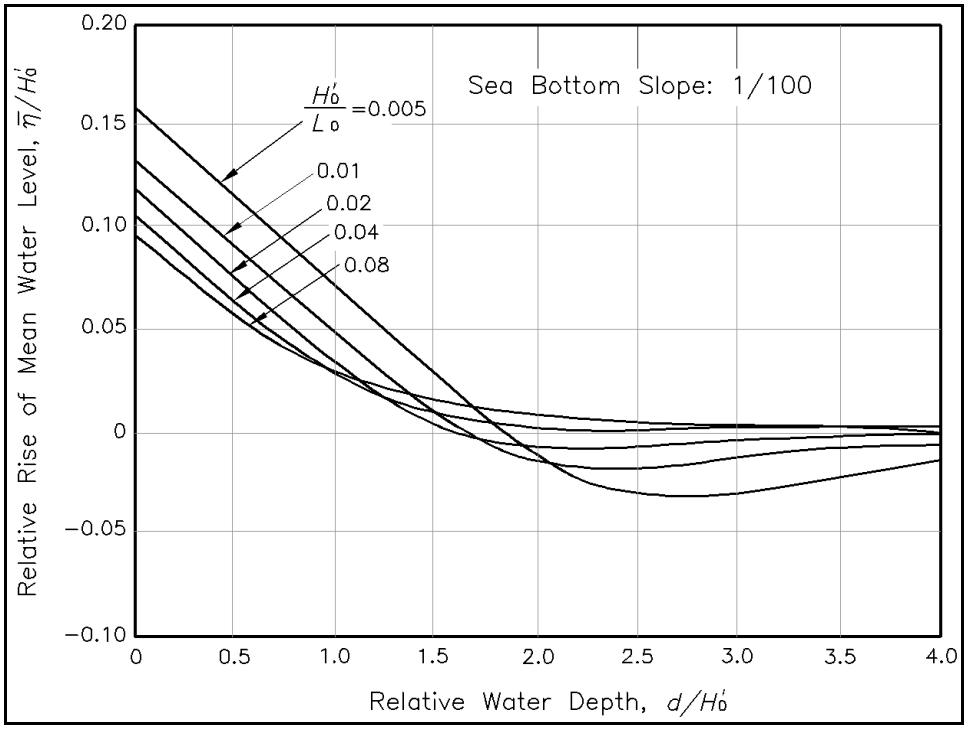

Figure II-8-24. Estimation of wave setup (Goda 1985)

A 1-in-17-year event coupled with a 0.1 probability high tide level corresponds to a combined probability of 0.000040 × 0.1=0.000004. Since this probability is well below the 25-year design probability, the number of tide increments is sufficient for illustration.

The jetty is divided into three design segments with bottom levels of -10 m MLLW (representing the jetty head), -6 m MLLW and -2 m MLLW (representing sections along the jetty trunk). Tidal water levels at the five probability levels (expressed as exceedance frequencies in percent) are summarized in Table II-8-14. Information in Table II-8-12 is used to convert from MSL to MLLW datum.

Table II-8-14
Tidal Water Levels for Jetty Design

	Exceedance Frequency (percent)				
Water Level	**90**	**70**	**50**	**30**	**10**
High tide level, in m MSL	+0.51	+0.78	+0.98	+1.16	+1.40
High tide level, in m MLLW	+1.87	+2.14	+2.34	+2.52	+2.76
Tidal water depth (m)					
Bottom at -10 m MLLW (jetty head)	11.9	12.1	12.3	12.5	12.8
Bottom at -6 m MLLW (jetty trunk)	7.9	8.1	8.3	8.5	8.8
Bottom at -2 m MLLW (jetty trunk)	3.9	4.1	4.3	4.5	4.8

Example Problem II-8-2 (Sheet 9 of 21)

Example Problem II-8-2 (Continued)

The combined effect of tide and storm surge for the first event (excluding wave setup) at the jetty head and nearshore (shallowest) trunk segment are given in Table II-8-15. These initial depth estimates are referenced as $d_{ijettyA}$ for the head and $d_{ijettyC}$ for the nearshore trunk segment. Similarly, combined tide and storm surge levels are computed for each of the 33 storm events at the three jetty design segments.

Table II-8-15
Calculation of d_{ijetty} for Storm Event 1

	Water Level Exceedance Frequency (percent)				
Water Level	**90**	**70**	**50**	**30**	**10**
Storm surge (m)	0.7	0.7	0.7	0.7	0.7
Jetty Head					
Tidal water depth (m)	11.9	12.1	12.3	12.5	12.8
$d_{ijettyA}$ (m)	12.6	12.8	13.0	13.2	13.5
Nearshore Jetty Trunk					
Tidal water depth (m)	3.9	4.1	4.3	4.5	4.8
$d_{ijettyC}$ (m)	4.6	4.8	5.0	5.2	5.5

Inclusion of wave setup. The effect of wave setup on water levels at the jetty can now be considered. Calculation steps are listed below and results for Event 1 at the jetty head and nearshore jetty trunk segment are given in Table II-8-16.

(1) Retrieve H_0'/L_0 from Table II-8-13.

(2) Calculate d_{ijetty}/H_0'.

(3) Estimate ratio of wave setup $\bar{\eta}$ to H_0' from Figure II-8-24.

(4) Calculate $\bar{\eta}$ from ratio in step (3). If $\bar{\eta}$ is less than zero, a value of zero should be used for prudent design.

(5) Calculate a final d_{jetty} as the sum of $\bar{\eta}$ and the previous d_{ijetty}, which included only tide and storm surge. If $\bar{\eta}$ is large, it may be necessary to return to step (1) using d_{jetty} in place of d_{ijetty} and repeat steps (1) through (5).

Example Problem II-8-2 (Sheet 10 of 21)

Example Problem II-8-2 (Continued)

Table II-8-16
Calculation of d_{jetty} for Storm Event 1

	Water Level Exceedance Frequency (percent)				
	90	**70**	**50**	**30**	**10**
H_0'/L_0	0.0216	0.0216	0.0216	0.0216	0.0216
Jetty head					
$d_{ijettyA}$ (m)	12.6	12.8	13.0	13.2	13.5
$d_{ijettyA}/H_0'$	2.06	2.09	2.12	2.15	2.20
$\bar{\eta}/H_0'$	<0	<0	<0	<0	<0
$\bar{\eta}$ (m)	0	0	0	0	0
d_{jettyA} (m)	12.6	12.8	13.0	13.2	13.5
Nearshore jetty trunk					
$d_{ijettyC}$ (m)	4.6	4.8	5.0	5.2	5.5
$d_{ijettyC}/H_0'$	0.75	0.78	0.82	0.85	0.90
$\bar{\eta}/H_0'$	0.053	0.050	0.046	0.043	0.040
$\bar{\eta}$ (m)	0.3	0.3	0.3	0.3	0.2
d_{jettyC} (m)	4.9	5.1	5.3	5.5	5.7

Estimation of $H_{1/3}$ at Jetty. Now significant wave heights at the jetty H_{sjetty} can be estimated. Calculation steps are listed below and results for Event 1 at the jetty head and nearshore trunk segment are given in Table II-8-17.

(1) Calculate d_{jetty}/H_0', where d_{jetty} is the combined tide, storm surge, and wave setup water level at the jetty (Table II-8-16).

(2) Estimate ratio of $H_{1/3}$ at the jetty H_{sjetty} to H_0' from Figure II-8-25.

(3) Calculate H_{sjetty} from ratio in step (2). Note in this example that this is a *breaking* wave. Also note that the higher H_0' values lead to higher $H_{1/3}$ values in the breaker zone, if d and H_0'/L_0 are held constant (because of the gentle slope of the lines in the left portion of Figure II-8-25). Thus the extreme measured H_s values selected for design analysis can be expected to give extreme nearshore wave heights in the surf zone.

After these calculations are completed for all 33 storm events and 5 water levels, there are a total of 33 × 5 = 165 event values of H_{sjetty} at the jetty head and at each of the two trunk sections.

Example Problem II-8-2 (Sheet 11 of 21)

Example Problem II-8-2 (Continued)

Table II-8-17
Calculation of H_{sjetty} for Storm Event 1

	Water Level Exceedance Frequency (percent)				
	90	**70**	**50**	**30**	**10**
Jetty Head					
d_{jettyA}/H_0'	2.06	2.09	2.12	2.15	2.20
$H_{sjettyA}/H_0'$	1.05	1.06	1.07	1.07	1.07
$H_{sjettyA}$ (cm)	644	650	656	656	656
Nearshore Jetty Trunk					
d_{jettyC}/H_0'	0.80	0.83	0.86	0.90	0.93
$H_{sjettyC}/H_0'$	0.57	0.59	0.60	0.62	0.63
$H_{sjettyC}$ (cm)	349	362	368	380	386

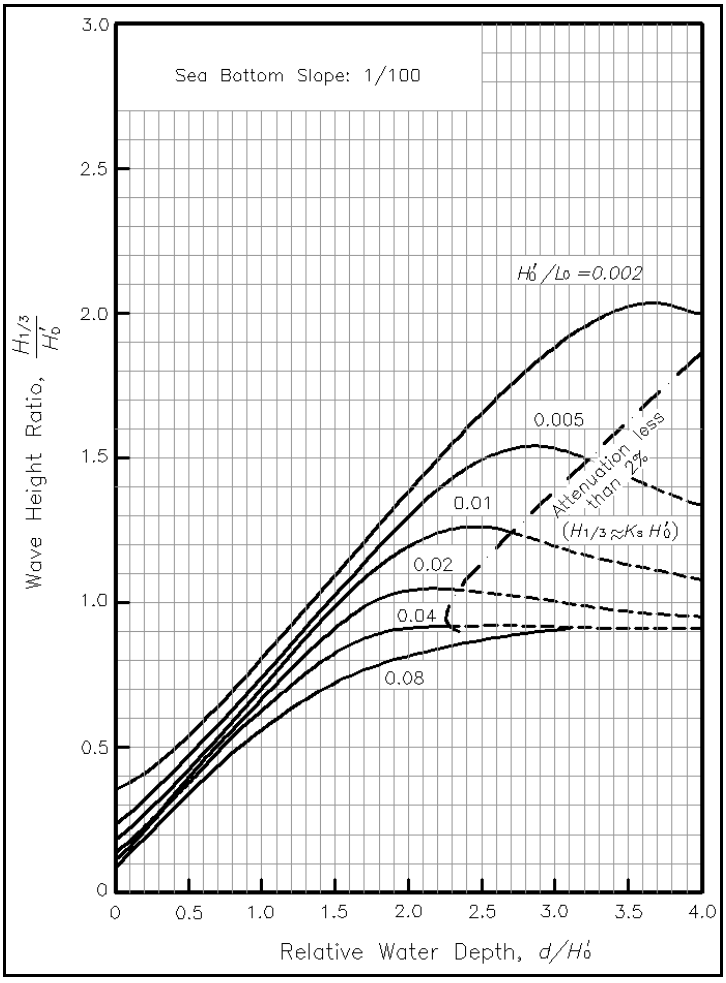

Figure II-8-25. Estimation of wave height at the jetty (Goda 1985)

Example Problem II-8-2 (Sheet 12 of 21)

Example Problem II-8-2 (Continued)

Importance of wave breaking. In estimating design wave conditions, it is important to know whether waves are breaking. Event values of H_0'/L_0 from Table II-8-13 plotted with the curve from Figure II-8-13 with bottom slope of 1/100 show that all values of d_{jetty} at the jetty head are very near or smaller than the depth at which H_{sjetty} reaches a maximum value during shoaling and breaking (Figure II-8-26). Thus, the jetty head can be considered as inside the surf zone and subject to breaking waves for all of the storm events. Since the jetty trunk is in shallower water than the head, it too will be subject to breaking waves for design.

Relationship to H_{m0}. The significant wave height analysis used in this example is based on statistics of crest-to-trough wave heights in a train of irregular waves. This wave height parameter can differ significantly from the energy-based significant wave height parameter H_{m0}, especially for low-steepness waves in shallow water. Some design applications may require H_{m0} instead of H_{sjetty}. If so, the event values of H_{sjetty} may be converted by the procedure described in Part II-1.

Extremal wave height analysis at the jetty. Extremal wave height analysis is presented here only for the jetty head. Similar analyses would be needed for jetty trunk sections, but they are omitted for brevity. Since the design waves are inside the surf zone, water level can be expected to be a key parameter in determining design wave heights. The equivalent deepwater wave steepness H_0'/L_0 and H_0' also influence H_{sjetty}. Design wave estimates should include due consideration of the influence of all three of these parameters: d_{jetty}, H_0'/L_0, and H_0'.

The ACES "Extremal Significant Wave Height Analysis" application was applied to the 165 event values of H_{sjetty} and the FT-I distribution function was selected as a good fit (Figure II-8-27). Confidence intervals of 95 percent were also computed, which is approximately equivalent to ±2 standard deviations.

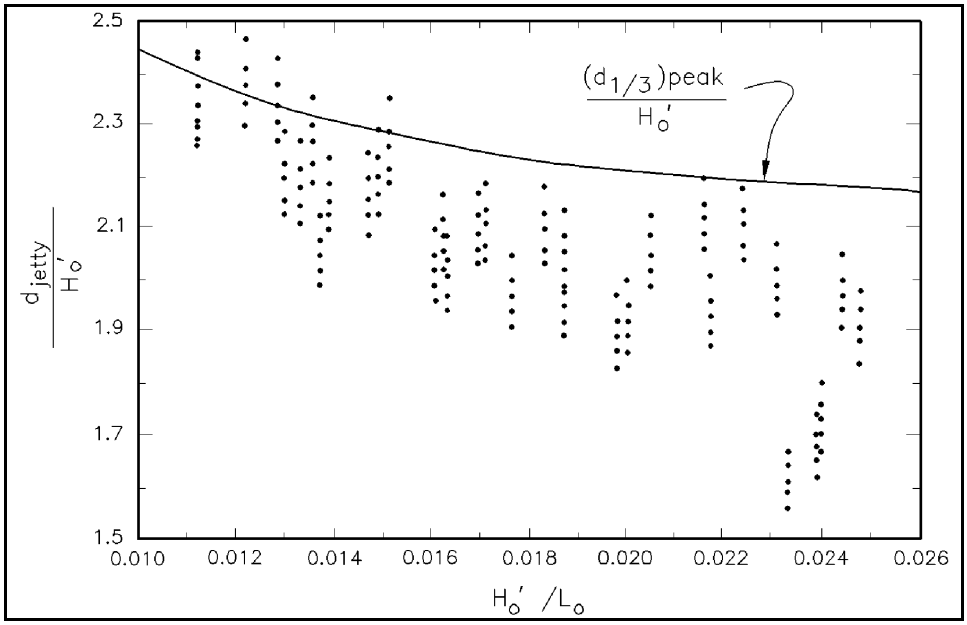

Figure II-8-26. Identification of surf zone conditions

Example Problem II-8-2 (Sheet 13 of 21)

Example Problem II-8-2 (Continued)

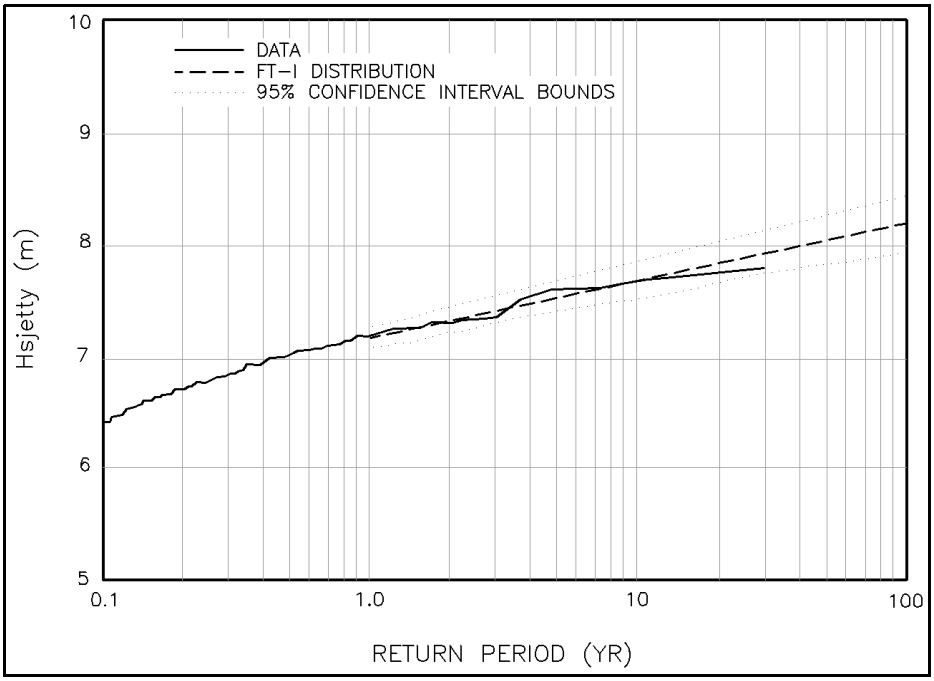

Figure II-8-27. Return period wave heights, 165 events, jetty head

Significant heights in Figure II-8-27 are representative of the extrapolated observed events, but they may have some important limitations. Extreme values of H_{sjetty} are strongly dependent on water depth, and the highest tide level considered in any of the 165 event cases was only at the 10-percent exceedance frequency. (This limit in the tide levels considered was a practical consequence of the manual method being used. If the analysis were done by computer, a much greater range of tide levels could have been included.) For longer return periods, the probability of an event coinciding with a tide level higher than the 10-percent exceedance frequency increases. This concern applies more to the jetty trunk, which is well inside the surf zone for design events, than the jetty head.

It is important in design to be aware of the maximum values of H_{sjetty} which might be encountered. Estimates of the upper bound value of H_{sjetty} were computed by the following two approaches:

(a) Parameters were determined as:

Tide level = maximum from Harris (1981) (Figure II-8-23)
= 1.4547×1.274 m
= +1.85 m MSL
= +1.85+1.36 m MLLW (using Table II-8-12) ≈ +3.2 m MLLW

Storm surge = value estimated from extremal analysis of event storm surges for each T_r (Figure II-8-20)

H_0'/L_0 = 0.01 (lower bound on event values in Table II-8-13)

Example Problem II-8-2 (Sheet 14 of 21)

Example Problem II-8-2 (Continued)

H_0' = value estimated from extremal analysis of H_0' event values (Table II-8-13) for each T_r (Figure II-8-28)

Parameters and calculations of H_{sjetty} are summarized in Table II-8-18.

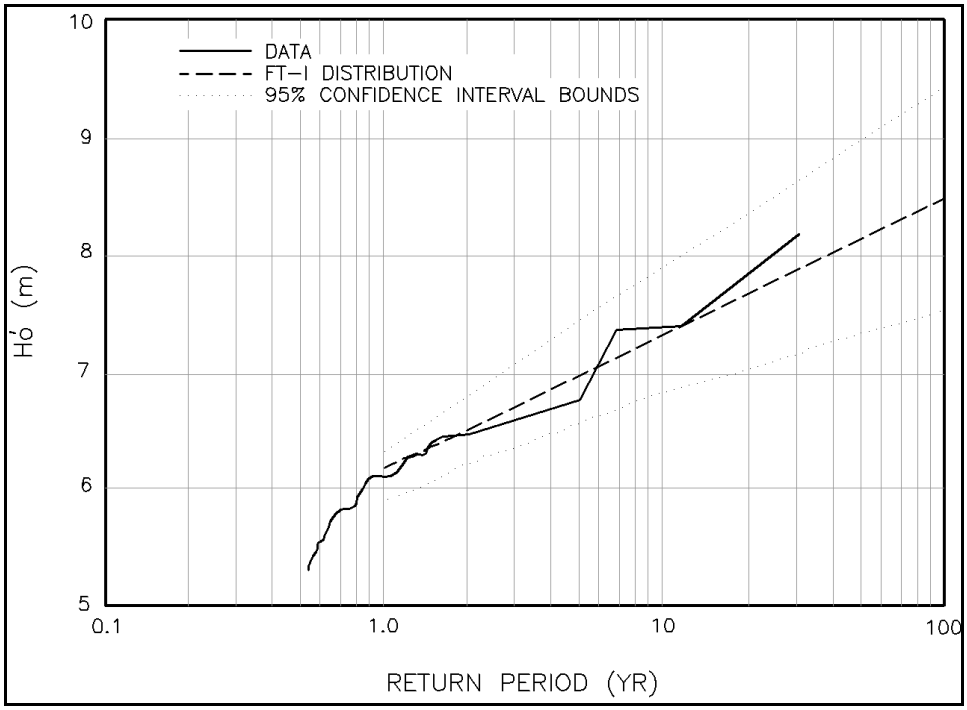

Figure II-8-28. Return period wave heights, H_0'

Table II-8-18
Calculation of Upper Bound H_{sjetty} Based on Maximum Tide Level

T_r (yr)	H_0' (cm)	Storm Surge (m)	Total Water Level [1] (m MLLW)	d_{jetty} (m)	d_{jetty}/H_0'	H_{sjetty}/H_0'	H_{sjetty} (cm)
2	653	0.7	3.9	13.9	2.13	1.24	810
5	702	0.9	4.1	14.1	2.01	1.21	849
10	737	1.0	4.2	14.2	1.93	1.18	870
25	782	1.2	4.4	14.4	1.84	1.14	891
50	816	1.3	4.5	14.5	1.78	1.12	914
100	850	1.4	4.6	14.6	1.72	1.10	935

[1] Combined maximum tide level (+3.2 m) and storm surge

Example Problem II-8-2 (Sheet 15 of 21)

Example Problem II-8-2 (Continued)

(b) As a more conservative check on (a), the peak possible value of H_s during the shoaling/breaking process between deepwater and shore for given values of bottom slope H_0'/L_0 and H_0' was estimated from Figure II-8-12 using the same values of H_0'/L_0 and H_0' as in (a). Results are summarized in Table II-8-19.

Table II-8-19
Calculation of Upper Bound H_{sjetty} Based on Maximum During Shoaling

T_r (yr)	H_0' (cm)	H_{sjetty}/H_0' [1]	H_{sjetty} (cm)
2	653	1.27	829
5	702	1.27	892
10	737	1.27	936
25	782	1.27	993
50	816	1.27	1036
100	850	1.27	1080

[1] From Figure II-8-12 using bottom slope = 1/100 and H_0'/L_0 = 0.01.

Final design wave heights excluding current effects. Upper bound estimates of H_{sjetty} (Tables II-8-18 and II-8-19) are plotted relative to the 165 cases derived from the measured storm events (Figure II-8-29). The return period curve based on the 165 events is taken as the design curve for this example (Table II-8-20).

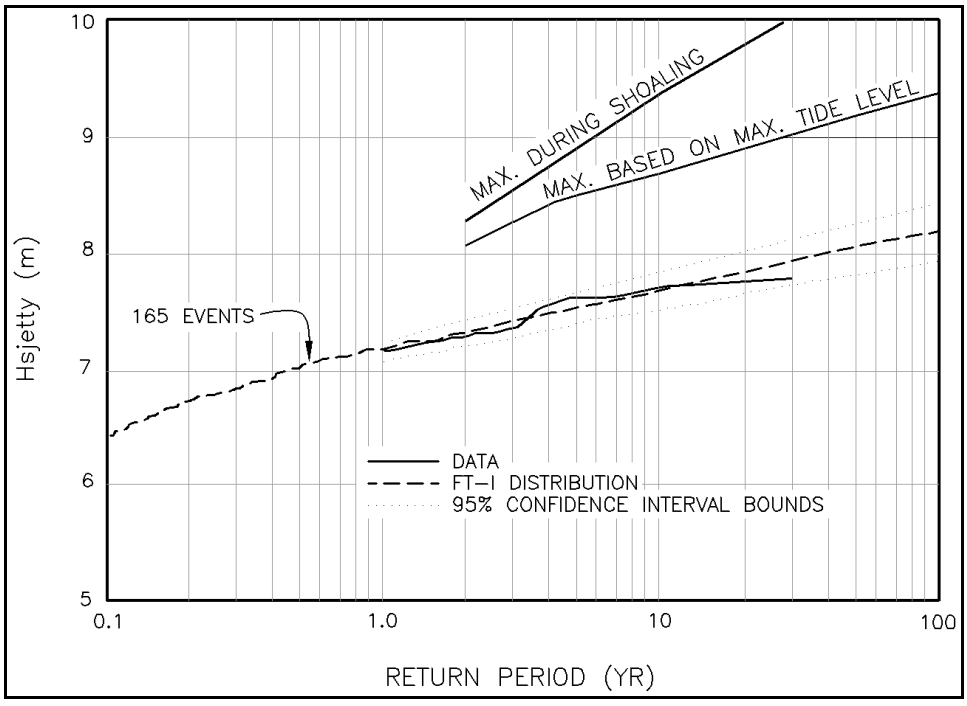

Figure II-8-29. Return period wave heights, 165 events including upper bounds, jetty head

Example Problem II-8-2 (Sheet 16 of 21)

Example Problem II-8-2 (Continued)

Table II-8-20
Design Significant Wave Heights at Jetty Head

T_r (yr)	Jetty Design	Toe Design
	H_{sjetty} (cm)	H_{stoe} (cm)
2	732	612
5	753	622
10	768	628
25	789	637
50	804	644
100	819	650

If a design life longer than 25 years were needed, values of H_{sjetty} approaching the maximum based on maximum tide level might need to be considered. This maximum represents an increase of about 1 m in H_{sjetty} at any selected return period, which would significantly influence jetty design. There is some chance of the maximum occurring even in a 25-year design life. That possibility should be considered if risks are analyzed. Also it should be recognized that the great hydrodynamic energy associated with design events can significantly change nearshore bottom elevations. Storm-induced scour could subject the jetty to increased wave heights, possibly approaching the maximum during shoaling at the jetty head. This effect should also be considered in risk analysis.

Design wave heights - jetty toe. Past physical model studies of some jetty cross sections have shown that waves attacking at water levels of around MLLW are most likely to cause damage to the underwater portion of the structure, including the toe. Similar behavior is assumed in this example. Since this jetty is in a high wave energy environment with fairly large tide range, it is worthwhile to estimate extreme wave heights at MLLW. The lower wave heights (because of reduced depth) can be assessed relative to the lower stability of underwater armor units (due to less precise placement).

Values of H_0' and H_0'/L_0 for each of the observed events (Table II-8-13) are used with a water depth of 10 m (corresponding to MLLW at the jetty head), and bottom slope of 1/100 to estimate a significant wave height for toe design H_{stoe} for each event (illustrated in Table II-8-21 for one event). These 33 values of H_{stoe} were subjected to extremal analysis (Figure II-8-30). The shallow depth greatly limits wave heights, and H_{stoe} values are confined to a very narrow range between 5.8 m and 6.5 m. The Weibull distribution function with k = 2.0, which best simulates the shape of a capped distribution function (Figure II-8-3), provides the best fit. H_{stoe} values for design are summarized in Table II-8-20.

Example Problem II-8-2 (Sheet 17 of 21)

Example Problem II-8-2 (Continued)

Table II-8-21
Calculation of H_{stoe} for Storm Event 1[1] at Jetty Head

d_{jetty} (m)	10.0
d_{jetty}/H_0'	1.63
H_{sjetty}/H_0'	0.95
H_{sjetty} (cm)	582

[1] H_0'=613 cm; H_0'/L_0=0.0216

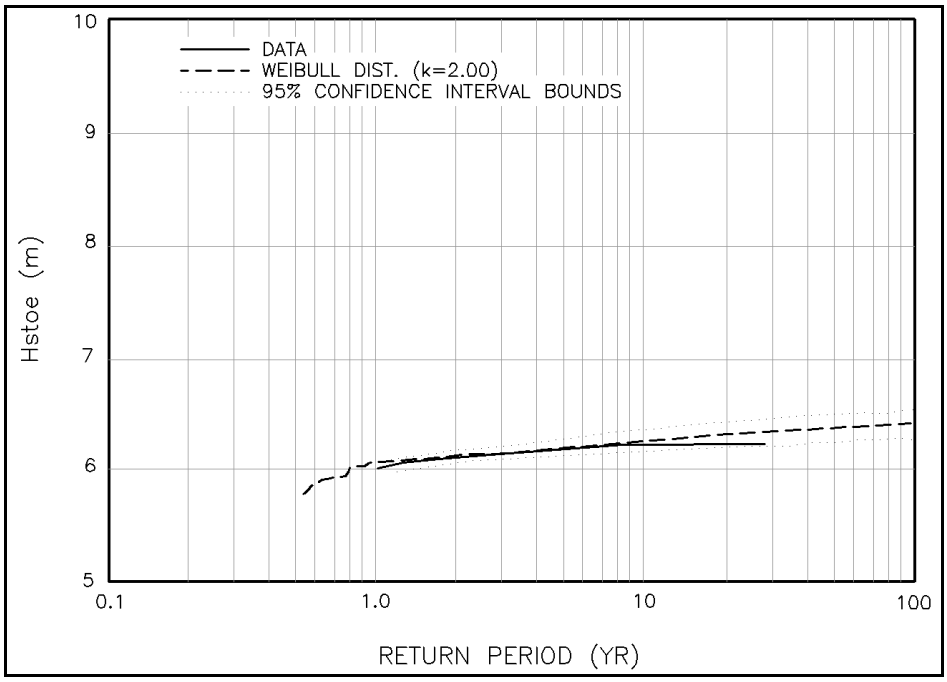

Figure II-8-30. Return period wave heights, toe design, jetty head

Effect of currents on waves. Information on currents around the jetty head is not precise but indicates that strong currents of up to 3 m/s may be experienced during design storms. The currents must be considered in design for two reasons: 1) direct impact on bottom and jetty material stability; and 2) effect on waves. Part II-6-2.l provides a simple method for estimating a factor for wave height modification by currents R_H. The following nondimensional parameters are required:

$$F = \frac{V \cos \theta}{\sqrt{gd}}$$
$$\Omega = \left(\frac{2\pi}{T}\right)\left(\frac{d}{g}\right)^{1/2} \quad \text{(II-8-8)}$$

where V is the current speed and θ is the angle between the current and a wave orthogonal. For this design problem, V= 3 m/s and θ is taken as -180 deg (current directly opposing the waves).

Example Problem II-8-2 (Sheet 18 of 21)

Example Problem II-8-2 (Continued)

Appropriate values for d and T are more subjective. An opposing current amplifies wave height. The amount of amplification increases as Ω increases (Figure II-8-31). A value for T can be determined by considering that any wave period consistent with the observed events is a likely possibility. Thus the smallest reasonable T_p (designated T_{pmin}), giving the largest likely value of Ω can be used. The largest observed equivalent deepwater wave steepness, 0.025 (Table II-8-13), can be used to estimate T_{pmin} as follows:

$$0.025 = \left(\frac{H_0'}{L_0} \right)_{\max} = \frac{2\pi\ H_0'}{g\ T_{pmin}^2} \tag{II-8-9}$$

$$T_{pmin} = \sqrt{\frac{2\pi}{0.025\ g}\ H_0'} = 0.506\ \sqrt{H_0'} \qquad (H_0' \text{ in cm})$$

Return period values of H_0' are given in Tables II-8-18 and II-8-19. For each return period, a maximum depth (d_{jetty} from Table II-8-18) and a minimum depth (10 m, corresponding to MLLW) were used for calculation, as summarized in Table II-8-22. Maximum depth cases relate to jetty design and minimum depth cases to toe design.

Values of R_H ranging from 1.13 to 1.23 indicate that currents could increase wave heights at the jetty head by between 13 percent and 23 percent. A wave height increase of this magnitude has a major impact on design. Since available estimates of current speed are speculative and the methods used to assess their impact are highly simplified (uniform current field, waves coming in opposite direction from current, etc.), a site-specific physical model study would be required in practice to complete the hydrodynamic design.

Table II-8-22
Calculation of Wave Height Modification by Currents

T_r (yr)	H_0' (cm)	T_{pmin} (sec)	Jetty Design				Toe Design (d_{jetty}=10 m)		
			d_{jetty} (m)	F	Ω	R_H	F	Ω	R_H
2	653	12.9	13.9	-0.26	0.58	1.23	-0.30	0.49	1.18
5	702	13.4	14.1	-0.26	0.56	1.19	-0.30	0.47	1.17
10	737	13.7	14.2	-0.25	0.55	1.17	-0.30	0.46	1.16
25	782	14.1	14.4	-0.25	0.54	1.15	-0.30	0.45	1.15
50	816	14.5	14.5	-0.25	0.53	1.14	-0.30	0.44	1.14
100	850	14.8	14.6	-0.25	0.52	1.13	-0.30	0.43	1.13

Example Problem II-8-2 (Sheet 19 of 21)

Example Problem II-8-2 (Continued)

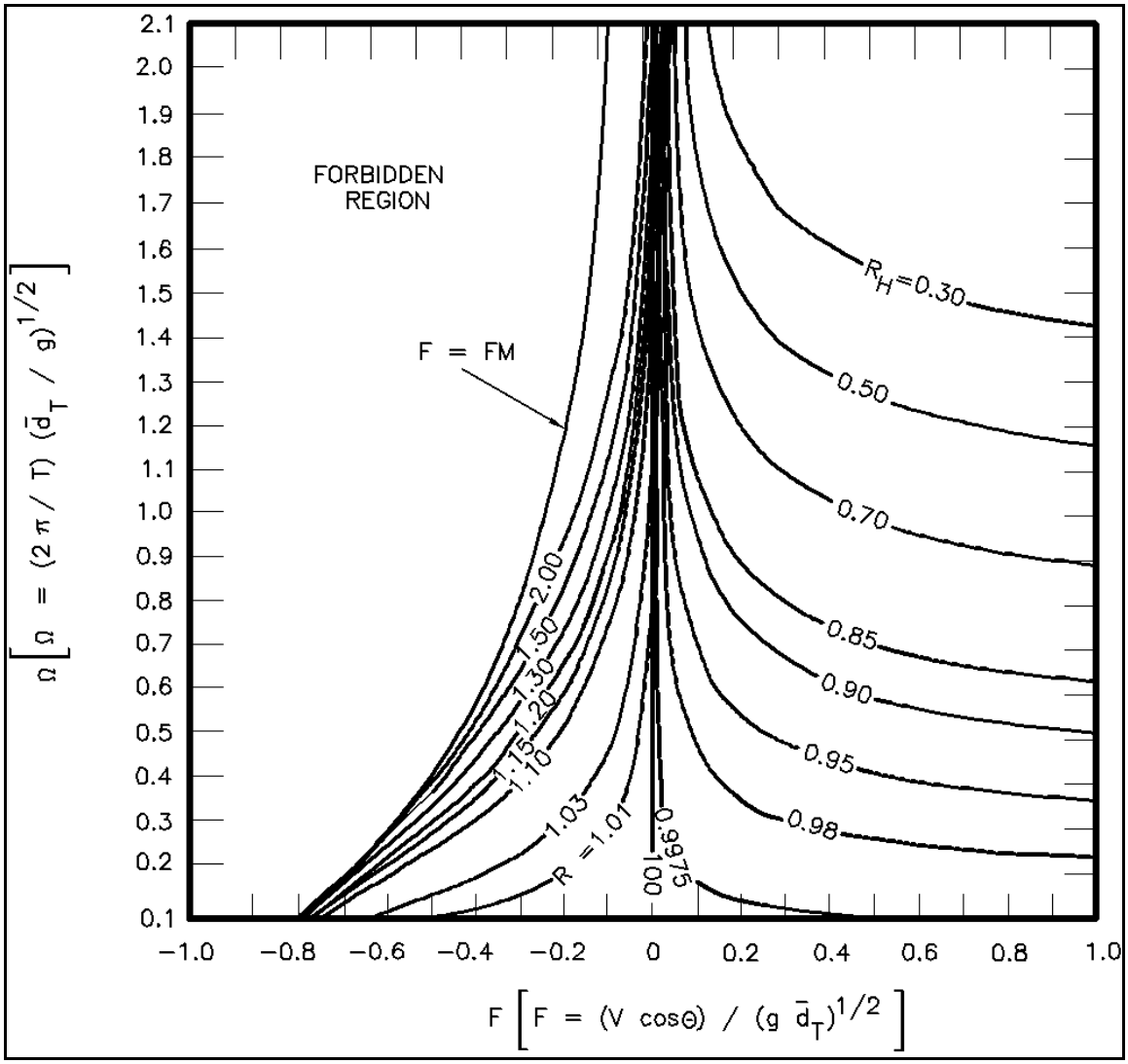

Figure 31. Wave height modification by currents

Example Problem II-8-2 (Sheet 20 of 21)

Example Problem II-8-2 (Concluded)

Design wave period. Design wave periods can be estimated from measured values of T_p (Table II-8-13). A scatter plot of T_p versus H_{sjetty} gives perspective on how wave periods are related to extreme wave heights (Figure II-8-32). Values of H_{sjetty} in the figure are for only the highest of the five tide levels used in conjunction with the 33 storm events. The figure indicates that the design wave period range of 14-18 sec is representative of the higher wave conditions of interest in design.

Confidence intervals. Confidence intervals or uncertainties in hydrodynamic design estimates should always be considered. Confidence intervals associated with statistical aspects of extremal analysis are included in this example. However, there are other sources of uncertainty. For example, the *quality* of available information is an important concern. Wave information may be from accurate, well-maintained gauges, lower quality measurements, hindcasts (which can vary in quality), or observations. Such concerns are not addressed in this example, but they are given some attention in Parts V and VI.

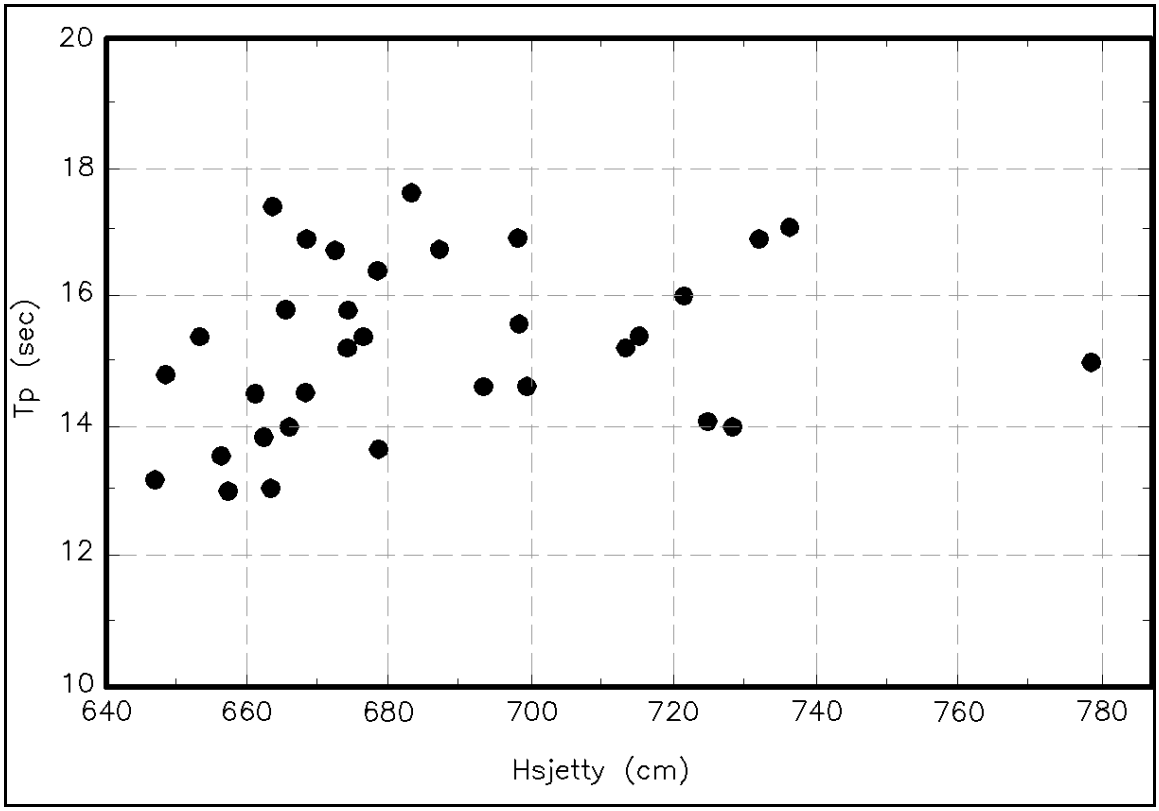

Figure II-8-32. Joint distribution of H_{sjetty} and T_p from 33 storm events, jetty head

Final design conditions. In final design of a jetty or any comparable major coastal engineering project, the complexity of variable bathymetry, breaking waves, currents, interaction between waves, currents, and structures, etc., cannot be adequately represented with the procedures used in this example. Even comprehensive numerical models are limited in their capabilities for reproducing the full design conditions. Standard practice is to construct a three-dimensional physical model and use it to determine the final project design.

Example Problem II-8-2 (Sheet 21 of 21)

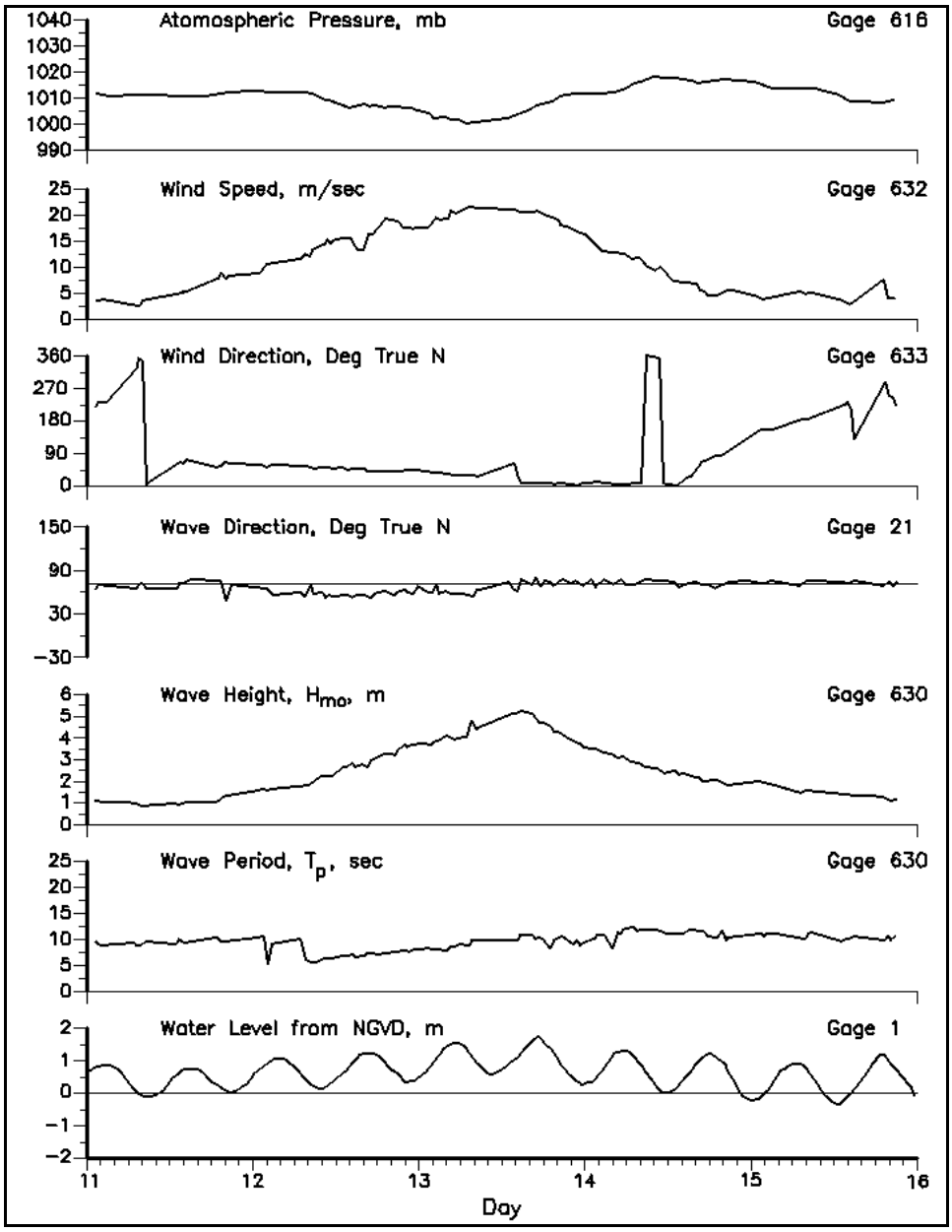

Figure II-8-33. Example storm event (Leffler et al. 1990)

(2) In standard coastal engineering practice, problems such as the one presented here are usually solved with the help of computer programs. However, the example problem solution relies mainly on graphical methods. The graphical approach has two advantages here: 1) it helps convey an intuitive understanding of the solution (one can see in the graphs *how* parameters are interrelated); and 2) it provides a self-contained methodology independent of complex computer programs. Some graphical tools must be introduced in the example because earlier chapters in Part II relating to this problem presuppose the use of computers in practical work. Most graphical tools are taken from Goda (1985).

II-8-7. Interdependence of Processes During Severe Events

a. Design importance.

(1) The interdependence of processes during severe events is a critical consideration for design. For example, an extreme wave event is usually caused by a severe storm which also typically generates extreme occurrences of wind, water level, infragravity waves, and currents (Figure II-8-33). The true probability of occurrence of the combined extremes is higher than would be expected if each of these processes were analyzed separately and treated as independent of each other.

(2) Without knowledge of the interdependence of processes, designs would be based on a chosen nonexceedance probability for each process critical to the design. This design condition tends to be conservatively high, since extremes at the design level of occurrence are unlikely to all occur together.

b. Procedures for estimating realistic design events, probabilities, and return periods. The approach used in Example Problem II-8-2 illustrates one approach by which data may be used to consider both water levels and wave heights in design. Another simplified approach which considers wind, surge level, and H_s is presented in CIRIA/CUR (1991) (pp 223-225). The EST provides a convenient, and more comprehensive, method for taking advantage of historical information to estimate realistic design events. It is often important to consider storm duration in estimating design events.

II-8-8. References

American Society of Civil Engineers 1993
American Society of Civil Engineers. 1993. ASCE Standard, *Minimum Design Loads for Buildings and Other Structures*, ASCE 7-93, a revision of ANSI/ASCE 7-88, American Society of Civil Engineers, New York.

Battjes 1972
Battjes, J. A. 1972. "Long-Term Wave Height Distribution at Seven Stations around the British Isles," *Peutchen Hydr. Zeit,* Band 25, Hefty, pp 179-189.

Batts, Russell, and Simiu 1980
Batts, M. E., Russell, L. R., and Simiu, E. 1980. "Hurricane Wind Speeds in the United States," *J. Struct. Div.*, *American Society of Civil Engineers,* Vol 100, No. STIO, pp 2001-2015.

Blom 1958
Blom, G. 1958. *Statistical Estimates and Transformed Beta-Variables*, Wiley, New York.

Bowers 1992
Bowers, E. C. 1992. "Low Frequency Waves in Intermediate Water Depths," *Proceedings of the 23rd International Conference on Coastal Engineering*, American Society of Civil Engineers, pp 832-845.

Carter and Draper 1988
Carter, D. J. T., and Draper, L. 1988. "Has the North-East Atlantic Become Rougher?" *Nature*, Vol 332, No. 7, p 494.

Construction Industry Research and Information Association (CIRIA)
CIRIA. 1991. "Manual on the Use of Rock in Coastal and Shoreline Engineering," Construction Industry Research and Information Association Special Publication 83, London, UK (also published as: Centre for Civil Engineering Research and Codes Report 154, Gouda, The Netherlands).

Earle and Baer 1982
Earle, M. D., and Baer, L. 1982. "Effects of Uncertainties on Extreme Wave Heights," *Journal of Waterway, Port, Coastal, and Ocean Engineering*, Vol 108, No. WW4, pp 456-478.

Farrar et al. 1994
Farrar, P. D., Borgman, L. E., Glover, L. B., Reinhard, R. D., Pope, J., Swain, A., and Ebersole, B. A. 1994. "Storm Impact Assessment for Beaches at Panama City, Florida," Technical Report CERC-94-11, U.S. Army Engineer Waterways Experiment Station, Vicksburg, MS.

Goda 1985
Goda, Y. 1985. *Random Seas and Design of Maritime Structures*, University of Tokyo Press, Tokyo, Japan.

Goda 1988
Goda, Y. 1988. "On the Methodology of Selecting Design Wave Height," *Proceedings of the 21st International Conference on Coastal Engineering*, American Society of Civil Engineers, pp 899-913.

Goda 1990
Goda, Y. 1990. "Distribution of Sea State Parameters and Data Fitting," *Handbook of Coastal and Ocean Engineering*, Vol 1, Gulf Publishing Co., pp 371-408.

Goda and Kobune 1990
Goda, Y., and Kobune, K. 1990. "Distribution Function Fitting for Storm Wave Data," *Proceedings of the 22nd International Conference on Coastal Engineering*, American Society of Civil Engineers, pp 18-31.

Gringorten 1963
Gringorten, I. I. 1963. "A Plotting Rule for Extreme Probability Paper," *Journal of Geophysical Research*, Vol 68, No. 3, pp 813-814.

Gumbel 1958
Gumbel, E. J. 1958. *Statistics of Extremes*, Columbia University Press, New York.

Harris 1981
Harris, D. L. 1981. "Tides and Tidal Datums in the United States," Special Report No. 7, U.S. Army Corps of Engineers, Fort Belvoir, VA., U.S. Government Printing Office (GPO Stock No. 008-022-00161-1).

Hubertz et al. 1993
Hubertz, J. M., Brooks, R. M., Brandon, W. A., and Tracy, B. A. 1993. "Hindcast Wave Information for the U.S. Atlantic Coast," WIS Report 30, U.S. Army Engineer Waterways Experiment Station, Vicksburg, MS.

Kite 1978
Kite, G. W. 1978. *Frequency and Risk Analysis in Hydrology*, Water Resources Publications, Fort Collins, CO.

Leffler et al. 1990
Leffler, M. W., Hathaway, K. K., Scarborough, B. L., Baron, C. F., and Miller, H. C. 1990. "Annual Data Summary for 1988, CERC Field Research Facility," Technical Report CERC-90-13, U.S. Army Engineer Waterways Experiment Station, Vicksburg, MS.

Le Méhauté and Wang 1984
Le Méhauté, B., and Wang, S. 1984. "Effects of Measurement Error on Long-Term Wave Statistics," *Proceedings of the 19th International Conference on Coastal Engineering*, American Society of Civil Engineers, pp 345-361.

Mathiesen et al. 1994
Mathiesen, M., Goda, Y., Hawkes, P. J., Mansard, E., Martin, M. J., Peltier, E., Thompson, E. F., and Van Vledder, G. 1994. "Recommended Practice for Extreme Eave Analysis," *Journal of Hydraulic Research*, Vol 32, No. 6, pp 803-814.

National Bureau of Standards 1980
National Bureau of Standards. 1980. "Hurricane Wind Speeds in the United States," *Building Science Series 124*, Gaithersburg, MD.

Scheffner and Borgman 1992
Scheffner, N. W., and Borgman, L. E. 1992. "Stochastic Time-Series Representation of Wave Data," *Journal of Waterway, Port, Coastal, and Ocean Engineering*, Vol 118, No. 4, pp 337-351.

Seelig, Ahrens, and Grosskopf 1983
Seelig, W. N., Ahrens, J. P., and Grosskopf, W. G. 1983. "The Elevation and Duration of Wave Crests," Miscellaneous Report 83-1, U.S. Army Engineer Waterways Experiment Station, Vicksburg, MS.

Seymour, Strange, Cayan, and Nathan 1984
Seymour, R. J., Strange, R. R., Cayan, D. R., and Nathan, R. A. 1984. "Influence of El Ninos on California's Wave Climate," *Proceedings of the 19th International Conference on Coastal Engineering*, American Society of Civil Engineers, pp 577-592.

Simiu and Scanlan 1986
Simiu, E., and Scanlan, R. H. 1986. *Wind Effects on Structures, An Introduction to Wind Engineering*, Wiley, New York.

Simiu, Changery, and Filliben 1979
Simiu, E., Changery, M. J., and Filliben, J. J. 1979. "Extreme Windspeeds at 129 Stations in the Contiguous United States," NBS BSS 118, National Bureau of Standards, U.S. Dept. of Commerce, Washington, DC.

Smith 1987
Smith, O. 1987. "Duration of Extreme Wave Conditions," Miscellaneous Paper CERC-87-12, U.S. Army Engineer Waterways Experiment Station, Vicksburg, MS.

Smith 1988
Smith, O. 1988. "Duration of Extreme Wave Conditions," *Journal of Waterway, Port, Coastal, and Ocean Engineering*, Vol 114, No. 1, pp 1-17.

Thom 1968-69
Thom, H.C.S. 1968-69. "New Distribution of Extreme Winds in the United States," *J. Sruct. Div.*, *American Society of Civil Engineers,* Vol 94, No. ST7, pp 1787-1801, July 1968; and Vol 95, No. ST8, pp 1769-1770, Aug. 1969.

Thompson 1980
Thompson, E. F. 1980. "Energy Spectra in Shallow U.S. Coastal Waters," Technical Paper 80-2, U.S. Army Engineer Waterways Experiment Station, Vicksburg, MS.

U.S. Department of Commerce 1992
U.S. Department of Commerce. 1992. "The Halloween Nor'easter of 1991," Natural Disaster Survey Report, National Oceanic and Atmospheric Administration, National Weather Service, Silver Spring, MD.

U.S. Water Resources Council 1976
U.S. Water Resources Council. 1976. "Guidelines for Determining Flood Flow Frequency," Bulletin No. 17 of the Hydrology Committee, Washington, DC.

II-8-9. Definitions of Symbols

σ	Standard deviation
σ_m	Standard deviation of maximum monthly wind speeds [length/time]
σ_{rm}	Standard deviation of the sampling error in estimating U_r (Equation II-8-4) [length/time]
d	Water depth [length]
F	Probability that the mth highest data value will not be exceeded (Figure II-8-5)
$f(x)$	Probability distribution function
G	Skew coefficient in the Pearson Type III distribution function (Figure II-8-2) [dimensionless]
$\hat{H}_s$	Design significant wave height [length]
$H_{1/3}$	Significant wave height [length]
k	Parameter in the Weibull distribution function (Figure II-8-5) [dimensionless]
k	Skew of ln x corrected for bias in the Log Pearson Type III distribution function (Figure II-8-2) [dimensionless]
L	Desired time period used in the encounter probability formula (Equation II-8-2) [years]
m	Rank of data value in descending order (= 1 for largest) in distribution function formulas (Figure II-8-5)
N	Number of events
N_m	Number of months of data used in computing the standard deviation of the sampling error in estimating U_r (Equation II-8-4)
$-_O$	The subscript 0 denotes deepwater conditions
$P(\hat{H}_s)$	Cumulative probability that $H_s \leq \hat{H}_s$
P_e	Encounter probability (Equation II-8-2)
t	Time interval associated with each data point [years]
T_p	Design wave period [time]
T_r	Return period (Equation II-8-1) [years]
$\overline{U}_m$	Mean value of maximum monthly wind speeds [length/time]
U_r	Wind speed with r-year return period (Equation II-8-3) [length/time]

II-8-10. Acknowledgments

Author of Chapter II-8, "Hydrodynamic Analysis and Design Conditions:"

Edward F. Thompson, Ph.D., Coastal and Hydraulics Laboratory, Engineer Research and Development Center, Vicksburg, Mississippi.

Reviewers:

Lee E. Harris, Ph.D., Department of Marine and Environmental Systems, Florida Institute of Technology, Melbourne, Florida.
Thomas Leung, U.S. Army Engineer District, Los Angeles, Los Angeles, California, (deceased).
Heidi P. Moritz, U.S. Army Engineer District, Portland, Portland, Oregon.
Arthur T. Shak, U.S. Army Engineer District, Los Angeles, Los Angeles, California.

DEPARTMENT OF THE ARMY
U.S. Army Corps of Engineers
Washington, DC 20314-1000

EM 1110-2-1100

CECW-EW

Manual
No. 1110-2-1100

30 April 2002

Engineering and Design
COASTAL ENGINEERING MANUAL

1. Purpose. The purpose of the *Coastal Engineering Manual* (CEM) is to provide a comprehensive technical coastal engineering document. It includes the basic principles of coastal processes, methods for computing coastal planning and design parameters, and guidance on how to formulate coastal flood studies, shore protection, and navigation projects.

2. Applicability. This manual applies to all HQUSACE elements and all USACE commands having Civil Works and military design responsibilities.

3. Discussion. The CEM is divided into two major subdivisions: science-based and engineering-based. The science subdivision is further divided into three parts. The first part, "Coastal Hydrodynamics," leads the reader from the fundamental principles of wave theory and ocean wave generation through the process of wave transformation as the wave form approaches and reacts with the shore including water-level variations and currents. The second part, "Coastal Sediment Processes," addresses longshore and cross-shore transport as well as shelf, and wind transport processes. The third part, "Coastal Geology," covers geomorphology, coastal classification, and morphodynamic processes on sandy shores.

The engineering-based subdivision is oriented toward a project-type approach, rather then the individual structure design and is divided into two parts. The first one, "Coastal Planning and Design," provides information on the design process and selection of appropriate type of solution to various coastal problems. The second part, "Design of Coastal Project Elements," provides engineering guidance on materials, fundamentals of design, and reliability.

4. Distribution Statement. Approved for public release, distribution unlimited.

FOR THE COMMANDER:

1 Appendix
Appendix A - Glossary

ROBERT CREAR
Colonel, Corps of Engineers
Chief of Staff

This manual supersedes *Shore Protection Manual,* 1984; EC 1110-2-289, 30 September 1996; EC 1110-2-292, 31 March 1998; EM 1110-2-1004, 30 November 1993; EM 1110-2-1412, 15 April 1986; EM 1110-2-1414, 7 July 1989; EM 1110-2-1502, 20 August 1992; EM 1110-2-1616, 31 January 1991; EM 1110-2-1617, 20 August 1992; EM 1110-2-1618, 28 April 1995; EM 1110-2-2904, 8 August 1986; EM 1110-2-3301, 31 May 1995.

Table of Contents

Page

III-1-1. Introduction III-1-1
a. Bases of sediment classification III-1-1
b. Sediment properties important for coastal engineering III-1-1
(1) Properties important in dredging III-1-2
(2) Properties important in environmental questions III-1-2
(3) Properties important in beach fills III-1-3
(4) Properties important in scour protection III-1-3
(5) Properties important in sediment transport studies III-1-4

III-1-2. Classification of Sediment by Size III-1-4
a. Particle diameter III-1-4
b. Sediment size classifications III-1-5
c. Units of sediment size III-1-9
d. Median and mean grain sizes III-1-9
e. Higher order moments III-1-10
f. Uses of distributions III-1-11
g. Sediment sampling procedures III-1-11
h. Laboratory procedures III-1-14

III-1-3. Compositional Properties III-1-14
a. Minerals III-1-14
b. Density III-1-15
c. Specific weight and specific gravity III-1-16
d. Strength III-1-16
e. Grain shape and abrasion III-1-19

III-1-4. Fall Velocity III-1-21
a. General equation III-1-21
b. Effect of density III-1-24
c. Effect of temperature III-1-24
d. Effect of particle shape III-1-24
e. Other factors III-1-26

III-1-5. Bulk Properties III-1-26
a. Porosity III-1-26
b. Bulk density III-1-27
c. Permeability III-1-27
d. Angle of repose III-1-30
e. Bulk properties of different sediments III-1-31
(1) Clays, silts, and muds III-1-31
(2) Organically bound sediment III-1-31

(3) Sand and gravel III-1-33
(4) Cobbles, boulders, and bedrock III-1-33

III-1-6. References III-1-33

III-1-7. Definition of Symbols III-1-40

III-1-8. Acknowledgments III-1-41

List of Tables

Page

Table III-1-1
Relations Among Three Classifications for Two Types of Sediment III-1-1

Table III-1-2
Sediment Particle Sizes III-1-8

Table III-1-3
Qualitative Sediment Distribution Ranges for Standard Deviation, Skewness, and Kurtosis III-1-11

Table III-1-4
Densities of Common Coastal Sediments III-1-16

Table III-1-5
Average Densities of Rocks Commonly Encountered in Coastal Engineering III-1-16

Table III-1-6
Soil Densities Useful for Coastal Engineering Computations III-1-30

List of Figures

Page

Figure III-1-1. Example of sediment distribution using semilog paper; sample 21c - foreshore at Virginia Beach III-1-6

Figure III-1-2. Example of sediment distribution using log-normal paper III-1-7

Figure III-1-3. Suggested composite sediment sample groups on a typical profile - example from CHL Field Research Facility, Duck, NC III-1-12

Figure III-1-4. Unconfined ultimate strength of three rock types (Hardin 1966) III-1-18

Figure III-1-5. Drag coefficient as a function of Reynolds Number (Vanoni 1975) III-1-22

Figure III-1-6. Fall velocity of quartz spheres in air and water (Vanoni 1975) III-1-25

Chapter III-1
Coastal Sediment Properties

III-1-1. Introduction

a. Bases of sediment classification.

(1) Several properties of sediments are important in coastal engineering. Most of these properties can be placed into one of three groups: the size of the particles making up the sediment, the composition of the sediment, or bulk characteristics of the sediment mass.

(2) In some cases (in clay, for example) there are strong correlations among the three classification groups. A clay particle is, in the compositional sense, a mineral whose molecules are arranged in sheets that feature orderly arrays of silicon, oxygen, aluminum, and other elements (Lambe and Whitman 1969). Clay particles are small and platey. They are small in part because they originate from the chemical modification and disintegration of relatively small pre-existing mineral grains and because the sheet-like minerals are not strong enough to persist in large pieces. The geologist's size classification defines a particle as clay if it is less than 0.0039 mm. Because a clay particle is so small, it has a large surface area compared to its volume. This surface area is chemically active and, especially when wet, the aggregate of clay surfaces produces the cohesive, plastic, and slippery characteristics of its bulk form. Thus, the three classifications each identify the same material when describing "clay."

(3) On the other hand, most grains of beach sand are quartz, a simpler and chemically more inert material than clay minerals. In the geologist's size classification, sand grains are at least 16 times larger and may be more than 500 times larger in diameter than the largest clay particle (4,000 to more than 100 million times larger in volume). At this size, the force of gravity acting on individual sand grains dwarfs the surface forces exerted by those sand grains, so the surface properties of sand are far less important than surface properties of clay particles. Because sand grains do not stick together, a handful of pure dry sand cannot be picked up in one piece like a chunk of clay. Several differences between clay and sand are summarized on Table III-1-1. More inclusive discussions of sediment sizes, compositions, and bulk properties are given later in this chapter.

Table III-1-1
Relations Among Three Classifications for Two Types of Sediment

	Bases of Classification		
Name of Sediment	**Usual Composition**	**Size Range, Wentworth**	**Bulk Properties**
Clay	Clay Minerals (sheets of silicates)	Less than 0.0039 mm	Cohesive Plastic under stress Slippery Impermeable
Sand	Quartz (SiO_2)	Between 0.0625 mm and 2.00 mm	Noncohesive Rigid under stress Gritty Permeable

b. Sediment properties important for coastal engineering. Sediment properties of material existing at the project site, or that might be imported to the site, have important implications for the coastal engineering project. The following sections briefly discuss several examples of ways that sediment properties affect coastal engineering projects and illustrate their importance.

(1) Properties important in dredging.

(a) A hydraulic dredge needs to entrain sediment from the bottom and pump it through a pipe. The entrainment and the pumping are both affected by the properties of the sediment to be dredged. The subject is briefly treated in the following paragraphs, but more details on dredging practice can be obtained from books by Turner (1984) and Huston (1970). Other information is available through the Dredging Research Program of the U.S. Army Corps of Engineers.

(b) Sediment can be classified for entrainment by a hydraulic dredge as fluid, loose, firm, or hard. Fluid muds and loose silt or sand can be entrained relatively easily by dragheads. Firm sand, stiff clay, and organically bound sediment may require a cutterhead dredge to loosen the sediment. Usually, hard material such as rock or coral is not suitable for hydraulic dredging unless the material has previously been well broken.

(c) Sediment can be classified for pumping by a hydraulic dredge as cohesive, noncohesive, or mitigated (Turner 1984). Cohesive sediments get transported through the pipe as lumps and nodules whereas noncohesive sediments disperse as a slurry, which is more easily pumped through the pipe. Mitigated sediments consist mainly of noncohesive sediments with a small amount of clay, which increases the transport efficiency of the pipe.

(d) The diameter of the pipe and the size of the pump limit the size of the material which can be pumped. Usually, oversize material is prevented from entering the pipeline of a suction dredge by a grid placed across the draghead, or the cutterhead reduces material entering the pipeline to adequate size.

(e) Another property of the sediment important in dredging is the degree of its cohesiveness that allows the sediment to stand in near-vertical banks while being dredged. A dredge works more efficiently if the material will maintain such a steep “face” during the dredging process. Muds and loose sands that flow like liquids lack this property.

(f) The above statements apply to those dredging systems that remove material from the bottom through a pipeline by a pump. Such hydraulic dredges are not always the most feasible dredging system to use because of space constraints, navigation requirements, dredging depth, sediment properties, or disposal options. Under some conditions, mechanical dredges, which include a grab bucket operated from a derrick, or a dipper dredge (power shovel) on a barge (Huston 1970), may be more desirable. When mechanical dredges are used, looser sediments are usually dredged with a bucket and harder sediments with a dipper.

(2) Properties important in environmental questions.

(a) Recently, environmental problems associated with the handling and deposition of sediment have received increased attention. These concerns most frequently arise from dredging operations, but can occur anytime sediment is introduced into the marine environment. The usual issues involve the burial of bottom-dwelling organisms, the blockage of light to bottom-dwelling and water-column organisms, and the toxicity of the sediments.

(b) The sediment property of most environmental consequence is size. Turbidity in the water column depends on the fall velocity of the sediment particles, which is a strong function of the grain size. Turbid waters can be carried by currents away from the immediate project site, blocking the light to organisms over a wide area and, as the sediments settle out, blanketing the bottom at a rate faster than the organisms can accommodate. Fine sediments (silts and clays) get greater scrutiny under environmental regulation because they produce greater and longer-lasting turbidity, which will impact larger areas of the seafloor than will

coarser, sand-sized material. The dredging of sand usually encounters less severe environmental objection, provided that there are few fines mixed with it and that the site has no prior toxic chemical history.

(c) Environmental regulation is changing, and many regulatory questions are outside the usual experience of coastal engineers. However, a basic coastal engineering contribution to facilitating the progress of a project through regulatory review is the early collection of relevant sediment samples from the site and obtaining accurate data on their size, composition, and toxicity.

(3) Properties important in beach fills.

(a) Beach fills have two primary functions: to provide temporary protection to upland property, and to increase temporarily the recreational space along the shore. Neither function can be well satisfied with sediment finer than sand. Because the recreational function is inhibited by material coarser than sand, and because fill coarser than sand is frequently less available, the primary beach fill material is usually sand.

(b) The source sediment for a beach fill is known as the borrow material, and the sediment on the beach prior to the fill is known as the native material. The sediment property most important for design is the size distribution of the borrow and native sands. The art of beach fill design consists of calculating the volume of borrow with a given size distribution that will produce a required volume of beach fill.

(c) Ideally, the median size of the borrow sand should not be less than the median size of the native sand, and the spread of the sizes in the borrow size distribution should not exceed the spread of sizes in the native sand. Often it is impossible to meet these ideal conditions because suitable borrow material does not exist in adequate volume at a reasonable cost. Further, on severely eroded beaches, the native sand may be skewed to coarser size ranges because the fines have eroded out, producing unrealistic requirements for borrow sand size distribution.

(d) Beach fill design aims to compensate for the differences between borrow sand and native sand, usually by overfilling with borrow sand and assuming preferential loss of the fine fractions. A favorable feature of beach fill technology is the accidental, partial loss of the fine fraction during the dredging and handling between borrow and beach. There have been cases (mostly anecdotal) where such handling losses have produced sand fill on the beach that is coarser than the borrow sand from which the fill was derived.

(e) The shore protection and the recreational qualities of a beach fill conflict when coarser sediment sizes are used. Usually, a beach provides more protection against erosion when its particles are coarser (also when they are more angular and more easily compacted). However, fill material larger than sand size (about 2.0 mm) will lessen the recreational value of the beach. Also odor and color of beach fill may be objectional to recreational users; but usually, if the grain size of the material is adequate, the objectional odor and color are temporary.

(4) Properties important in scour protection.

(a) Scour, the localized removal of bed material below its natural elevation, usually occurs near (and is usually caused by) marine structures such as jetties, seawalls, bridge pilings, etc. These types of structures can accelerate tidal currents, focus wave energy, and increase turbulence in the water column.

(b) To prevent scour, it is usual to place a layer of less erodible material on the surface of the sediment that is subject to erosion. Such a layer is called a revetment or scour blanket. A typical revetment consists of broken rock, known as riprap, which is essentially a sediment consisting of large rock particles. The sedimentary properties of riprap which are important as scour protection include its size distribution, density of the rock material, and the porosity and permeability of the material as placed. The riprap must be heavy

enough to resist movement under design currents, the porosity and thickness of the riprap must be adequate to dissipate fluid energy before it reaches the underlying material being protected, and the permeability must be adequate to satisfactorily relieve pressure buildup at the seafloor-revetment interface.

(c) For long-term protection, riprap must consist of dense, durable material of blocky shape. Porous carbonate rocks such as coral and some limestones are not satisfactory, and thin slabs of material of any composition (such as shale) are usually more mobile than blocky shapes having the same weight. However, in any situation, economics and available materials may make it advantageous to use materials that depart from the ideal.

(d) It should be recognized that scour protection in coastal engineering differs from scour protection encountered in typical transportation projects both in the magnitude of the forces and in their reversing directions. Though scour protection design for highways is a well-developed art with extensive documentation, the direct transferal of highway riprap experience to coastal problems is usually unsatisfactory.

(5) Properties important in sediment transport studies.

(a) The underlying physics of how water moves sediment is not well understood. This is, perhaps, one reason for the large number of formulas (often conflicting) which have been proposed to predict transport rates. These formulas are usually functions of fluid properties, flow condition properties, and sediment properties. Sediment properties commonly used include: grain size, grain density, fall velocity, angle of repose, and volume concentration. Sediment size distribution and grain shape are also important.

(b) One method used to study sediment transport is to follow the movement of marked (tracer) particles in the nearshore environment. Ideally, tracers should react to coastal processes that move sediment in a manner identical to the native sand, yet provide some signal to the investigator that will distinguish the tracer from the native material. In the last two decades, the most common tracer has been dyed native sand grains. Typically representative samples of sand taken from the site are dyed with a fluorescent dye and then reintroduced to their environment. Care must be taken to ensure that the dying process does not significantly alter the sediment size or density. Transport of these tracers is then monitored by sampling. Because of their dilute distribution, tracers are a very labor-intensive means of studying sediment movement.

(c) Native sand tracers (trace minerals, heavy minerals) have been used to interpret sediment movement, but usually these tracers have a size and density that differ from the majority of grains on the beach. The problem becomes more complicated as beach fills become more common, and inadvertently introduce non-native tracer grains. See Galvin (1987) for a more thorough discussion of this topic.

(d) Recently, a few sensors have become available that can measure the concentration of moving sediment. These sensors are generally quite sensitive to grain size and require calibration using sediments obtained onsite. See, for example, a discussion of an optical backscatter sensor (Downing, Sternberg, and Lister 1981).

III-1-2. Classification of Sediment by Size

a. Particle diameter.

(1) One of the most important characteristics of sediment is the size of the particles. The range of grain sizes of practical interest to coastal engineers is enormous, covering about seven orders of magnitude, from clay particles to large breakwater armor stone blocks. A particle's size is usually defined in terms of its diameter. However, since grains are irregularly shaped, the term diameter can be ambiguous. Diameter is

normally determined by the mesh size of a sieve that will just allow the grain to pass. This is defined as a particle's sieve diameter. When performed in a standard manner, sieving provides repeatable results, although there is some uncertainty about how the size of a sieve opening relates to the physical size of the particle passing through the opening. (See page 58 of Blatt, Middleton, and Murray (1980) for further discussion.)

(2) Another way to define a grain's diameter is by its fall velocity. A grain's sedimentation diameter is the diameter of a sphere having the same density and fall velocity. This definition has the advantage of relating a grain's diameter to its fluid behavior, which is the usual ultimate reason for needing to determine the diameter. However, a settling tube analysis is somewhat less reproducible than a sieve analysis, and testing procedures have not been standardized. Other diameter definitions that have been occasionally used include the nominal diameter, the diameter of a sphere having the same volume as the particle; and the axial diameter, the length of one of the grain's principal axes, or some combination of these axes.

(3) For nearly spherical particles, as many sand grains are (but most shell and shell fragments are not), there is little difference in these definitions. When reporting the results of an analysis, it is always appropriate to define the diameter (or describe the measurement procedure), particularly if the sieve diameter is not being used.

(4) Usually, there is a need to characterize an appropriate diameter for an aggregation of particles, rather than the diameter of a single particle. Even the best-sorted natural sediments have a range of grain sizes. Most sediment samples found in nature have a few relatively large particles covering a wide range of diameters and many small particles within a small range of diameters. That is, most natural sediment samples have a highly skewed distribution, in an absolute sense. However, if size classes are based upon a logarithmic (power of 2) scale and if the contents of each size fraction are considered by weight (not by the number of particles), then most typical sediment samples will have a distribution that is near Gaussian (or normal). When such sediment samples are plotted as a percentage of the total weight of the sample being sieved, the sediment size distribution that results usually approximates a straight line on a log-normal graph. This line is known as the log-normal distribution. Meaningful descriptions of the distributions of this type of data can be made using standard statistical parameters.

(5) Sediment size data normally come from the weight of sediment that accumulates on each sieve in a nest of graduated sieves. This can be plotted on semilog paper as shown in Figure III-1-1 (ENG form 2087) or on log-normal paper as shown in Figure III-1-2.

b. Sediment size classifications.

(1) The division of sediment sizes into classes such as cobbles, sand, silt, etc., is arbitrary, and many schemes have been proposed. However, two classification systems are in general use today by coastal engineers. Both have been adopted from other fields.

(2) The first is the Modified Wentworth Classification, which is generally used in geologic work. Geologists have been particularly active in sediment size research because they have long been interested in interpreting slight differences in size as indicating particular processes or events in the geologic past. A summary of geological work applicable to coastal engineering is found in Chapter 3 of the book by Blatt, Middleton, and Murray (2nd ed., 1980).

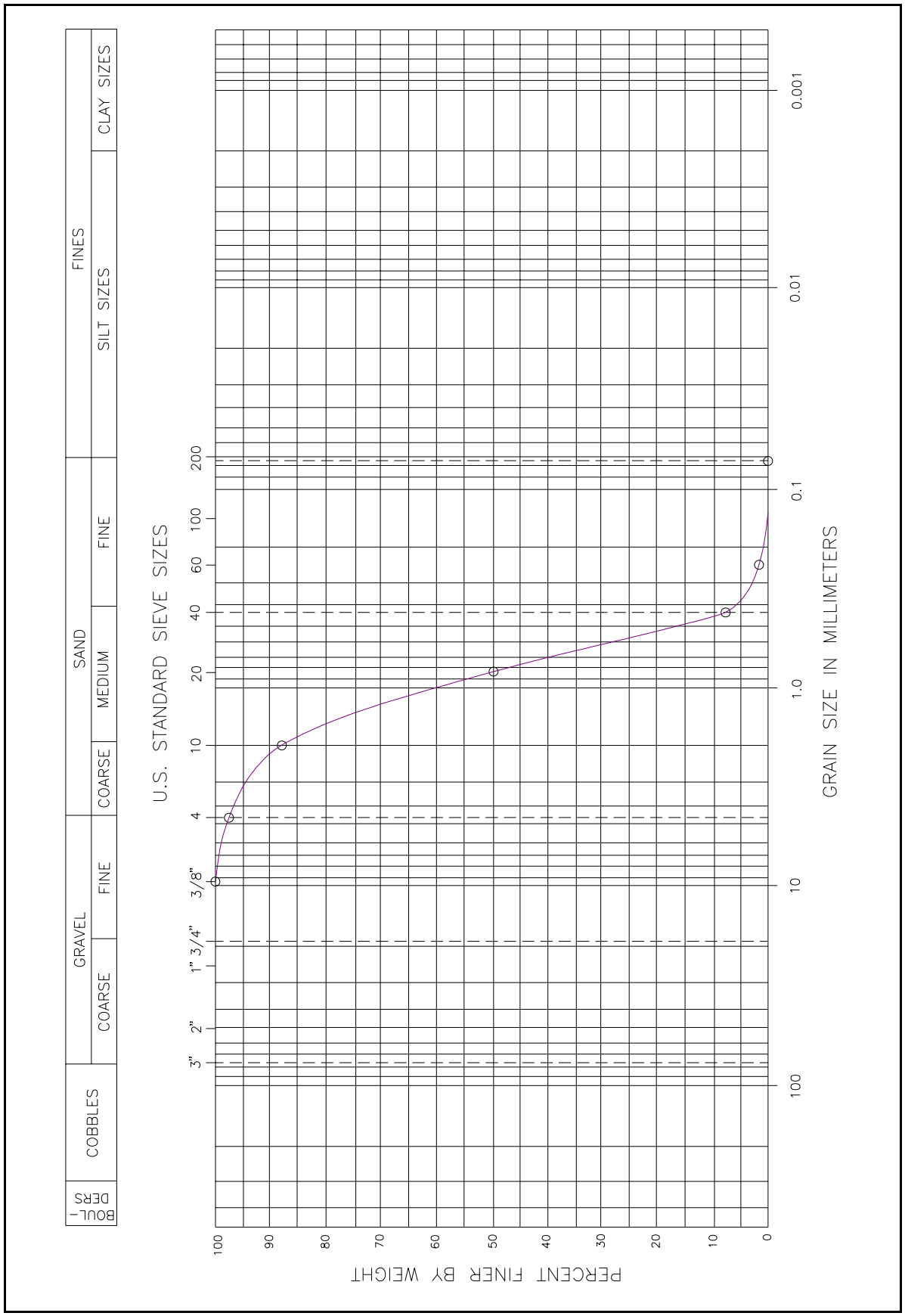

Figure III-1-1. Example of sediment distribution using semilog paper; sample 21c - foreshore at Virginia Beach

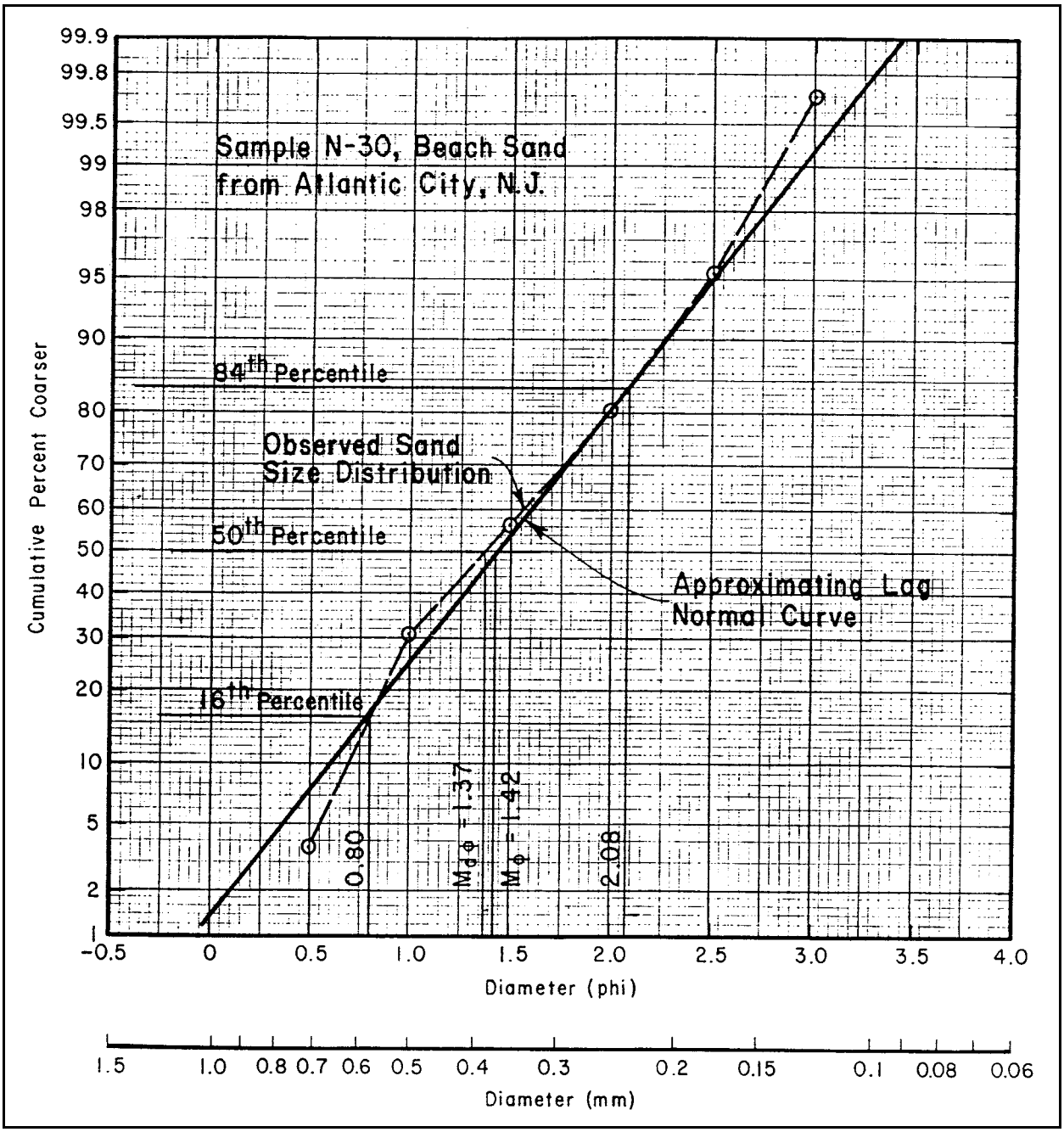

Figure III-1-2. Example of sediment distribution using log-normal paper

(3) The other is the Unified Soils Classification or the ASTM Classification, which various American engineering groups have developed. These groups have been more concerned with standardizing ways to obtain repeatable results in the analyses of sediment. The definitive source for such information is Volume 4.08 of the Standards published by the American Society for Testing and Materials (ASTM). These standards are published annually, with revisions as needed. In what follows, reference to ASTM standards will be to the 1994 edition of Volume 4.08, which deals with soil, as defined by engineers.

(4) These two systems are compared in Table III-1-2. Note that there are differences in the category limits. For example, sand in the engineer's classification is between 0.074 and 4.76 mm, while in the

Table III-1-2
Sediment Particle Sizes

ASTM (Unified) Classification[1]	U.S. Std. Sieve[2]	Size in mm	Phi Size	Wentworth Classification[3]
Boulder		4096.	-12.0	
		1024.	-10.0	Boulder
	12 in. (300 mm)	256.	-8.0	
Cobble		128.	-7.0	Large Cobble
		107.64	-6.75	
		90.51	-6.5	Small Cobble
	3 in. (75 mm)	76.11	-6.25	
		64.00	-6.0	
		53.82	-5.75	
		45.26	-5.5	Very Large Pebble
Coarse Gravel		38.05	-5.25	
		32.00	-5.0	
		26.91	-4.75	
		22.63	-4.5	Large Pebble
	3/4 in. (19 mm)	19.03	-4.25	
		16.00	-4.0	
		13.45	-3.75	
		11.31	-3.5	Medium Pebble
		9.51	-3.25	
Fine Gravel	2.5	8.00	-3.0	
	3	6.73	-2.75	
	3.5	5.66	-2.5	Small Pebble
	4 (4.75 mm)	4.76	-2.25	
	5	4.00	-2.0	
Coarse Sand	6	3.36	-1.75	
	7	2.83	-1.5	Granule
	8	2.38	-1.25	
	10 (2.0 mm)	2.00	-1.0	
	12	1.68	-0.75	
	14	1.41	-0.5	Very Coarse Sand
	16	1.19	-0.25	
	18	1.00	0.0	
Medium Sand	20	0.84	0.25	
	25	0.71	0.5	Coarse Sand
	30	0.59	0.75	
	35	0.50	1.0	
	40 (0.425 mm)	0.420	1.25	
	45	0.354	1.5	Medium Sand
	50	0.297	1.75	
	60	0.250	2.0	
	70	0.210	2.25	
Fine Sand	80	0.177	2.5	Fine Sand
	100	0.149	2.75	
	120	0.125	3.0	
	140	0.105	3.25	
	170	0.088	3.5	Very Fine Sand
	200 (0.075 mm)	0.074	3.75	
	230	0.0625	4.0	
Fine-grained Soil:	270	0.0526	4.25	
	325	0.0442	4.5	Coarse Silt
Clay if PI ≥ 4 and plot of PI vs. LL is on or above "A" line and the presence of organic matter does not influence LL.	400	0.0372	4.75	
		0.0312	5.0	
		0.0156	6.0	Medium Silt
		0.0078	7.0	Fine Silt
		0.0039	8.0	Very Fine Silt
Silt if PI < 4 and plot of PI vs. LL is below "A" line and the presence of organic matter does not influence LL.		0.00195	9.0	Coarse Clay
		0.00098	10.0	Medium Clay
		0.00049	11.0	Fine Clay
(PI = plasticity limit; LL = liquid limit)		0.00024	12.0	
		0.00012	13.0	Colloids
		0.000061	14.0	

[1] ASTM Standard D 2487-92. This is the ASTM version of the Unified Soil Classification System. Both systems are similar (from ASTM (1994)).
[2] Note that British Standard, French, and German DIN mesh sizes and classifications are different.
[3] Wentworth sizes (in mm) cited in Krumbein and Sloss (1963).

geologist's classification, sand is between 0.0625 and 2.0 mm. In describing a sediment, it is necessary to say which classification system is being utilized.

c. Units of sediment size.

(1) Table III-1-2 lists three ways to specify the size of a sediment particle: U.S. Standard sieve numbers, millimeters, and phi units. A sieve number is approximately the number of square openings per inch, measured along a wire in the wire screen cloth (Tyler 1991). Available sieve sizes can be obtained from catalogs on construction materials testing such as Soiltest (1983). The millimeter dimension is the length of the inside of the square opening in the screen cloth. This square side dimension is not necessarily the maximum dimension of the particle which can get through the opening, so these millimeter sizes must be understood as nominal approximations to sediment size. Table III-1-2 shows that the Wentworth scale has divisions that are whole powers of 2 mm. For example, medium sands are those with diameters between 2^{-2} mm and 2^{-1} mm. This property of powers of 2-mm class limits led Krumbein (1936) to propose a phi unit scale based on the definition:

$$\varphi = -\log_2 D \tag{III-1-1a}$$

where D is the grain diameter in millimeters. Phi diameters are indicated by writing φ after the numerical value. That is, a 2.0-φ sand grain has a diameter of 0.25 mm. To convert from phi units to millimeters, the inverse equation is used:

$$D = 2^{-\varphi} \tag{III-1-1b}$$

(2) The benefits of the phi unit include: (a) it has whole numbers at the limits of sediment classes in the Wentworth scale; and (b) it allows comparison of different size distributions because it is dimensionless. Disadvantages of this phi unit are: (a) the unit gets larger as the sediment size gets smaller, which is both counterintuitive and ambiguous; (b) it is difficult to physically interpret size in phi units without considerable experience; and (c) because it is a dimensionless unit, it cannot represent a unit of length in physical expressions such as fall velocity or Reynolds number.

d. Median and mean grain sizes.

(1) All natural sediment samples contain grains having a range of sizes. However, it is frequently necessary to characterize the sample using a single typical grain diameter as a measure of the central tendency of the distribution. The *median grain diameter* M_d is the sample characteristic most often chosen. The definition of M_d is that, by weight, half the particles in the sample will have a larger diameter and half will have a smaller. This quantity is easily obtained graphically, if the sample is sorted by sieving or other method, and the weight of the size fractions are plotted, as seen in Figures III-1-1 and III-1-2.

(2) The median diameter is also written as D_{50}. Other size fractions are similarly indicated. For example, D_{90} is the diameter for which 90 percent of the sediment, by weight, has a smaller diameter. An equivalent definition holds for the median of the phi-size distribution φ_{50} or for any other size fraction in the phi scale.

(3) Another measure of the central tendency of a sediment sample is the *mean grain size*. Several formulas have been proposed to compute this quantity, given a cumulative size distribution plot of the sample (Otto 1939, Inman 1952, Folk and Ward 1957, McCammon 1962). These formulas are averages of 2, 3, 5, or more symmetrically selected percentiles of the phi frequency distribution. Following Folk (1974):

$$M_{\varphi} = \frac{(\varphi_{16} + \varphi_{50} + \varphi_{84})}{3} \quad \text{(III-1-2)}$$

where M_{φ} is the estimated mean grain size of the sample in phi units. This can be converted to a linear diameter using Equation 1-1b. The median and mean grain sizes are usually quite similar for most beach sediments. For example, a study of 465 sand samples from three New Jersey beaches, the mean averaged only 0.01 mm smaller than the median for sands having an average median diameter of 0.30 mm (1.74 phi) (Ramsey and Galvin 1977). If the grain sizes in a sample are log-normally distributed, the two measures are identical. Since the median is easier to determine and the mean does not have a universally accepted definition, the median is normally used in coastal engineering to characterize the central tendency of a sediment sample.

e. Higher order moments.

(1) Additional statistics of the sediment distribution can be used to describe how the sample varies from a log-normal distribution. The *standard deviation* is a measure of the degree to which the sample spreads out around the mean (i.e., its sorting). Following Folk (1974), the *standard deviation* can be approximated by:

$$\sigma_{\varphi} = \frac{(\varphi_{84} - \varphi_{16})}{4} + \frac{(\varphi_{95} - \varphi_{5})}{6} \quad \text{(III-1-3)}$$

where σ_{φ} is the estimated standard deviation of the sample in phi units. For a completely uniform sediment φ_{05}, φ_{16}, φ_{84}, and φ_{95} are all the same, and thus, the standard deviation is zero. There are also qualitative descriptions of the standard deviation. A sediment is described as well-sorted if all particles have sizes that are close to the typical size (small standard deviation). If the particle sizes are distributed evenly over a wide range of sizes, then the sample is said to be well-graded. A well-graded sample is poorly sorted; a well-sorted sample is poorly graded.

(2) The degree by which the distribution departs from symmetry is measured by the *phi coefficient of skewness* α_{φ} defined in Folk (1974) as:

$$\alpha_{\varphi} = \frac{\varphi_{16} + \varphi_{84} - 2(\varphi_{50})}{2(\varphi_{84} - \varphi_{16})} + \frac{\varphi_{5} + \varphi_{95} - 2(\varphi_{50})}{2(\varphi_{95} - \varphi_{5})} \quad \text{(III-1-4)}$$

(3) For a perfectly symmetric distribution, the skewness is zero. A positive skewness indicates there is a tailing out toward the fine sediments, and conversely, a negative value indicates more outliers in the coarser sediments.

(4) The *phi coefficient of kurtosis* β_{φ} is a measure of the peakedness of the distribution; that is, the proportion of the sediment in the middle of the distribution relative to the amount in both tails. Following Folk (1974), it is defined as:

$$\beta_{\varphi} = \frac{\varphi_{95} - \varphi_{5}}{2.44\ (\varphi_{75} - \varphi_{25})} \quad \text{(III-1-5)}$$

Values for the mean and median grain sizes are frequently converted from phi units to linear measures. However, the standard deviation, skewness, and kurtosis should remain in phi units because they have no corresponding dimensional equivalents. If these terms are used in equations, they are used in their dimensionless phi form. Relative relationships are given for ranges of standard deviation, skewness, and kurtosis in Table III-1-3.

Table III-1-3
Qualitative Sediment Distribution Ranges for Standard Deviation, Skewness, and Kurtosis

Standard Deviation	
Phi Range	**Description**
<0.35	Very well sorted
0.35-0.50	Well sorted
0.50-0.71	Moderately well sorted
0.71-1.00	Moderately sorted
1.00-2.00	Poorly sorted
2.00-4.00	Very poorly sorted
>4.00	Extremely poorly sorted
Coefficient of Skewness	
<-0.3	Very coarse-skewed
- 0.3 to - 0.1	Coarse-skewed
- 0.1 to +0.1	Near-symmetrical
+0.1 to +0.3	Fine-skewed
>+0.3	Very fine-skewed
Coefficient of Kurtosis	
<0.65	Very platykurtic (flat)
0.65-0.90	Platykurtic
0.90-1.11	Mesokurtic (normal peakedness)
1.11-1.50	Leptokurtic (peaked)
1.50-3.00	Very leptokurtic
>3.00	Extremely leptokurtic

f. Uses of distributions. The median grain size is the most commonly used sediment size characteristic, and it has wide application in coastal engineering practice. The standard deviation of sediment samples has been used in several ways, including beach-fill design (see Hobson (1977), Ch. 5, Sec. III,3) and sediment permeability (Krumbein and Monk 1942). When a set of samples are taken from a single project site, they will frequently show little or no consistent variation in median diameter. In this case, various higher order moments are usually used to distinguish different depositional environments. There is an extensive literature on the potential application of the measures of size distribution; see, for example, Inman (1957), Folk and Ward (1957), McCammon (1962), Folk (1965, 1966), Griffiths (1967), and Stauble and Hoel (1986).

g. Sediment sampling procedures.

(1) Although a beach can only be composed of the available sediments, grain size distributions change in time and space. In winter, beach distributions are typically coarser and more poorly sorted than in summer. Also, typically, there is more variability in the foreshore and the bar/trough regions than in the dunes and the nearshore.

(2) While a single sample is occasionally sufficient to grossly characterize the sediments at a site, usually a set of samples is obtained. Combining samples from across the beach can reduce the high variability in spacial grain size distributions on beaches (Hobson 1977). Composite samples are created by either physically combining several samples before sieving or by mathematically combining the individual sample

weights. The set of samples obtained can be fairly small if the intent is only to characterize the beach as a whole. However, if the intent is to compare and contrast different portions of the same beach, many more samples are needed. In this case it is usually necessary to develop a sampling scheme prior to fieldwork.

(3) In the cross-shore it is recommended that samples be collected at all major changes in morphology along the profile, such as dune base, mid-berm, mean high water, mid-tide, mean low water, trough, bar crest, and then at 3-m intervals to the depth of closure (Stauble and Hoel 1986). In the longshore direction, sediment sampling should coincide with survey profile lines so that the samples can be spatially located and related to morphology and hydrodynamic zones. Shoreline variability and engineering structures should be considered in choosing sampling locations. A suggested rule of thumb is that a sampling line be spaced every half mile, but engineering judgment is required to define adequate project coverage.

(4) Samples collected along profile sub-environments can be combined into composite groups of similar depositional energy levels as seen in Figure III-1-3. Intertidal and subaerial beach samples have been found to be the most usable composites to characterize the beach and nearshore environment. Stauble and Hoel (1986) found that a composite containing the mean high water, mid-tide, and mean low water gave the best representation of the foreshore beach.

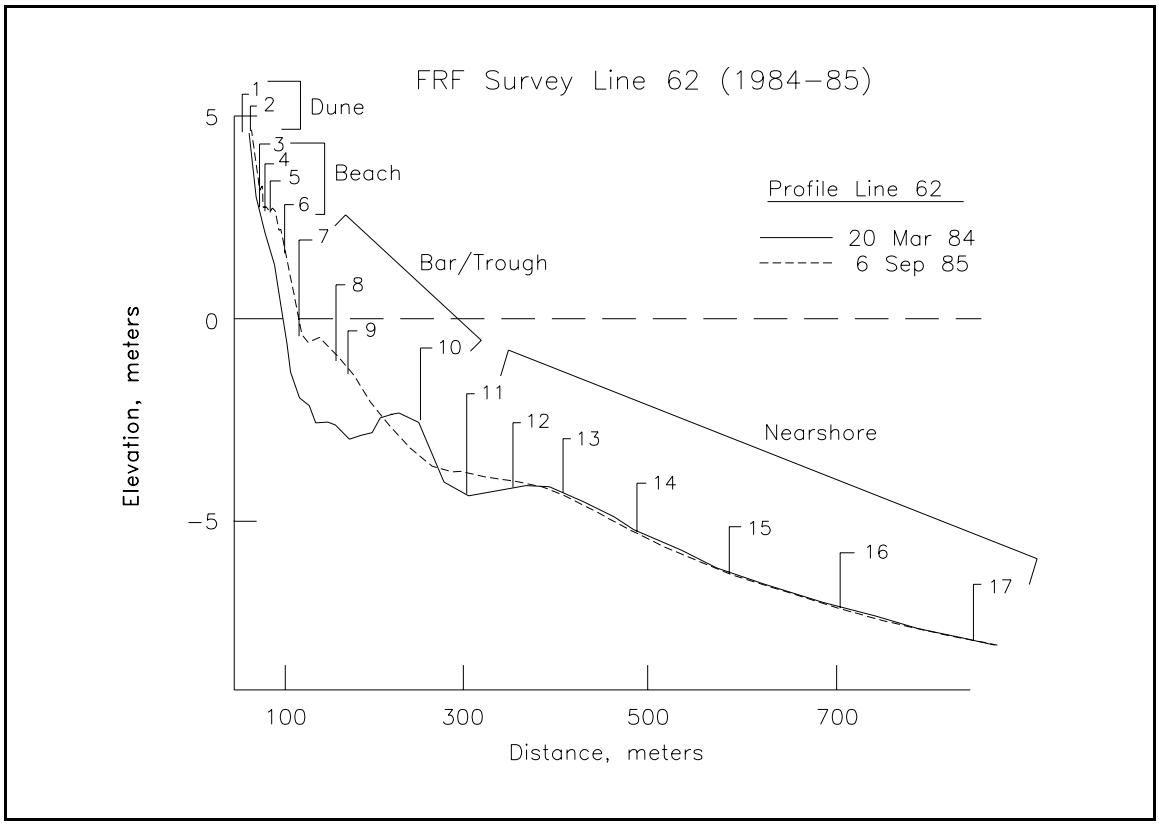

Figure III-1-3. Suggested composite sediment sample groups on a typical profile - example from Field Research Facility, Duck, NC

EXAMPLE PROBLEM III-1-1

FIND:

The statistics of the sediment size distribution shown in Figure III-1-2 and their qualitative descriptions.

GIVEN:

The needed phi values are: $\varphi_{05} = 0.56$, $\varphi_{16} = 0.80$, $\varphi_{25} = 0.93$, $\varphi_{50} = 1.37$, $\varphi_{75} = 1.87$, $\varphi_{84} = 2.08$, and $\varphi_{95} = 2.48$.

SOLUTION:

In phi units, the median grain size is given as:

$$\varphi_{50} = M_{d\varphi} = 1.37\varphi$$

From Equation 1-1b, the median grain size in millimeters is found as:

$$M_d = 2^{-1.37} = 0.39 \text{ mm}$$

From Equation 1-2, the mean grain size is found in phi units as:

$$M_\varphi = (0.80 + 1.37 + 2.08) / 3 = 1.42\varphi$$

From Equation 1-1b, this is converted to millimeters as:

$$D = 2^{-1.42} = 0.37 \text{ mm}$$

From Equation 1-3, the standard deviation is found as:

$$\sigma_\varphi = (2.08 - 0.80)/4 + (2.48 - 0.56)/6.0 = 0.32 + 0.32 = 0.64\ \varphi$$

From Equation 1-4, the coefficient of skewness is found as:

$$\alpha_\varphi = 0.055 + 0.078 = 0.13$$

From Equation 1-5, the coefficient of kurtosis is found as:

$$\beta_\varphi = 1.92 / 2.29 = 0.84$$

Thus, using Tables III-1-2 and III-1-3, the sediment is a medium sand (Wentworth classification), it is moderately well sorted, and the distribution is fine-skewed and platykurtic.

h. Laboratory procedures.

(1) Several techniques are available to analyze the size of beach materials, and each technique is restricted to a range of sediment sizes. Pebbles and coarser material are usually directly measured with calipers. However, this is not practical for sediments smaller than about 8 mm. Coarse sieves can also be used for material up to about 75 mm.

(2) Sand-sized particles (medium gravels through coarse silt) are usually analyzed using sieves. This requires an ordered stack of sieves of square-mesh woven-wire cloth. Each sieve in the stack differs from the adjacent sieves by having a nominal opening less than the opening of the sieve above it and greater than the opening of the sieve below it. A pan is placed below the bottom sieve. The sample is poured into the top sieve, a lid is placed on top, and the stack is placed on a shaker, usually for about 15 min. The different grains fall through the stack of sieves until each reaches a sieve that is too fine for it to pass. Then the amount of sediment in each sieve is weighed. ASTM Standard D422-63 (Reapproved 1990) is the basic standard for particle size analysis of soils, including sieving sedimentary materials of interest to coastal engineers. The application of D422 requires sample preparation described in Standard D421-85 (Reapproved 1993). The wire cloth sieves should meet ASTM Specification E-11.

(3) Sieves are graduated in size of opening according to the U.S. standard series or according to phi sizes. U.S. standard sieve sizes are listed in Table III-1-2, and the most commonly used sieves are shown in Figure III-1-1. Phi sized sieve openings vary by a factor of 1.19 from one sieve size to the next (by the fourth root of 2, or 0.25 phi units); e.g., 0.25, 0.30, 0.35, 0.42, and 0.50 mm.

(4) The range of sieve openings must span the range of sediment sizes to be sieved. Typically, about 6 full-height sieves or 13 half-height sieves plus a bottom pan are used in the analysis of a particular sediment. If 6 sieves are used, each usually varies in size from its adjacent neighbors by a half phi; if 13 sieves are used, each usually varies by a quarter phi. Normally, about 40 grams of sediment is sieved. More is needed if there are large size fractions (see ASTM Standard D2487-94).

(5) Determination of sediment size fractions for silts and clays is usually not necessary. Rather it is normally noted that a certain percentage of the material are fines with diameters smaller than the smallest sieve. When measurements are needed, the pipette method or the hygrometer method is usually used. Both of these methods are based upon determining the amount of time that different size fractions remain in suspension. These are discussed in Vanoni (1975). Coulter counters have also been used occasionally.

III-1-3. Compositional Properties

a. Minerals.

(1) Because of its resistance to physical and chemical changes and its common occurrence in terrestrial rocks, quartz is the mineral most commonly found in littoral materials. On temperate latitude beaches, quartz and feldspar grains commonly account for more than 90 percent of the material (Krumbein and Sloss 1963, p.134), and quartz, on average, accounts for about 70 percent of beach sand. However, it is important to realize that on individual beaches the percentage of quartz grains (or any other mineral) can range from essentially zero to 100 percent. Though feldspars are more common on the surface of the earth as a whole, comprising approximately 50 percent of all crustal rocks to quartz's approximately 12 percent (Ritter 1986), feldspars are more subject to chemical weathering, which converts them to clay minerals, quartz, and solutions. Since quartz is so inert, it accumulates during weathering processes. Thus, feldspars and related silicates are more commonly encountered in coastal sediment close to sources of igneous and metamorphic rocks, especially mountainous and glaciated coasts where streams and ice carry unweathered sediment

immediately to the shore. Quartz sand and clay are more common on shores far from mountains where weathering has had more time to reduce the relative proportions of feldspars and related silicates.

(2) Most carbonate sands owe their formation to organisms (both animal and vegetable) that precipitate calcium carbonate by modifying the very local chemical environment of the organism to favor carbonate deposition. Calcium carbonate may be deposited as calcite or aragonite, but aragonite is unstable and changes with time to either calcite or solutions. Calcite or limestone, the rock made from calcite, may, under some conditions, be altered to dolomite by the partial replacement of the calcium with magnesium. Carbonate sands can contribute up to 100 percent of the beach material, particularly in situations where it is produced in the local marine environment and there are limited terrestrial sediment supplies, such as reef-fringed, tropical island beaches. These sands are generally composed of a combination of shell and shell fragments, oolites, coral fragments, and algal fragments (Halimeda, foraminiferans, etc.). When carbonate shell is mixed with quartz sand, it may be necessary to dissolve out the shell to get a meaningful representation of each size fraction. ASTM Standard 4373 describes how to determine the calcium carbonate content of a beach.

(3) Other minerals that frequently form a small percentage of beach sands are normally referred to as heavy minerals, because their specific gravities are usually greater than 2.87. These minerals are frequently black or reddish and may, in sufficient concentrations, color the entire beach. The most common of these minerals (from Pettijohn (1957)) are andalusite, apatite, augite, biotite, chlorite, diopside, epidote, garnet, hornblende, hypersthene-enstatite, ilmenite, kyanite, leucoxene, magnetite, muscovite, rutile, sphene, staurolite, tourmaline, zircon, and zoisite. Their relative abundance is a function of their distribution in the source rocks of the littoral sediments and the weathering process. Heavy minerals have been occasionally used as natural tracers to identify sediment pathways from the parent rocks (Trask 1952; McMaster 1954; Giles and Pilkey 1965; Judge 1970).

In coastal engineering work, knowledge of the sediment composition is not normally important in its own right, but it is closely related to other important parameters such as sediment density and fall velocity.

b. Density.

(1) *Density* is the mass per unit volume of a material, which, in SI units, is measured in kilograms per cubic meter (kg/m^3). Sediment density is a function of its composition. Minerals commonly encountered in coastal engineering include quartz, feldspar, clay minerals, and carbonates. Densities for these minerals are given in Table III-1-4.

(2) Quartz is composed of the mineral silicon dioxide. Feldspar refers to a closely related group of metal aluminium silicate minerals. The most common clay minerals are illinite, montmorillonite, and kaolinite. Common carbonate minerals include calcite, aragonite, and dolomite. However, carbonate sands are usually not simple, dense solids; but rather the complex products of organisms which produce gaps, pores, and holes within the structure, all of which tend to lower the effective density of carbonate sand grains. Thus, carbonate sands frequently have densities less than quartz.

(3) The density of a sediment sample may be calculated by adding a known weight of dry sediment to a known volume of water. The change in volume is measured; this is the volume of the sediment. The sediment mass (= weight / acceleration of gravity) divided by its volume is the density. A complicating factor is that small pockets of air will stay in the pores and cling to the surfaces of almost all sediments. To obtain an accurate volume reading, this air must be removed by drawing a strong vacuum over the sand-water mixture. ASTM Volume 4.08 gives standards for measuring the density of soils and rocks, respectively (ASTM 1994).

Table III-1-4
Densities of Common Coastal Sediments

Mineral	Density kg/m^3
Quartz	2,648
Feldspar	2,560 - 2,650
Illite	2,660
Montmorillonite	2,608
Kaolinite	2,594
Calcite	2,716
Aragonite	2,931
Dolomite	2,866

Above sand size, sediments encountered in coastal engineering are usually composites of several minerals, that is, rocks. Table III-1-5 lists densities of rocks commonly encountered. These rocks are also used for riprap, which are large sedimentary particles. Lines 5 and 6 of Table III-1-5 deal with carbonate rocks, the dolomites and limestones. Note 3 of Table III-1-5 suggests that typical dolomites are denser, less porous, and geologically older than typical limestones.

Table III-1-5
Average Densities of Rocks Commonly Encountered in Coastal Engineering

Number	Rock Type	Number of Samples	Mass Density, kg/m^3
1	Basalt	323	2,740
2	Dolerite-Diabase	224	2,890
3	Granite	334	2,660
4	Sandstone	107	2,220
5	Dolomite	127	2,770
6	Limestone	182	2,540

Notes:
[1] Basalt and dolerite (or diabase) in lines 1 and 2 are fine-grained dark igneous rock often classed together as trap rock for engineering purposes.
[2] Lines 1, 2, 3, 4 from Table 5 of Johnson and Olhoeft (1984). Lines 5, 6 from Table 4-4 of Daly, Manger, and Clark (1966).
[3] Line 5 is the average of 127 samples from 3 dolomites or dolomitic limestones. Line 6 is the average of 182 samples from 5 limestones. The rocks in line 5 are denser and older than those in line 6. Average porosity of rocks in line 5 $\leq$ 3.0%; in line 6 average porosity is between 3% and 17%. Rocks in line 5 are older than Carboniferous.

c. Specific weight and specific gravity. The specific weight of a material is its density times the acceleration of gravity g. In SI units, the acceleration of gravity is 9.807 m/s^2, and thus, specific weight is measured in kilograms per meter squared per second squared (kg/(m^2 * s^2)). The specific gravity of a material is its density divided by the density of water at 4^0 C, which is 1000.0 kg/m^3. Specific gravity is a dimensionless quantity.

d. Strength.

(1) The material strength of a particle is the maximum stress which the particle can resist without failing, for a given type of loading. The SI unit of stress is the Pascal, and the convenient Pascal multiple is 1 million Pascals, or 1 mega Pascal (MPa). "Strength" in this section is unconfined ultimate strength in compression,

which is equivalent to crushing strength. Tensile strength, which is significantly less than compressive strength, is not discussed here, but tensile strength is usually proportional to compressive strength.

(2) The most commonly encountered material in coastal engineering is the quartz sand grain, which is very strong indeed. A single crystal of quartz has a strength on the order of 2,500 MPa. However, a sandstone, which is a composite of many sand grains, is surprisingly weak (top histogram on Figure III-1-4), being typically less than 100 MPa, or less than 4 percent of the strength of the single crystal. For this reason, sandstone is rarely used in coastal engineering construction.

(3) The difference in strength between quartz crystal and composite sandstone is due to weak intergranular cement and to flaws such as grain boundaries, bedding planes, cleavage, and joints that have a higher probability of being present in larger pieces. The data on Figure III-1-4 are excerpted from the extensive tabulation of Handin (1966), using all samples which were tested at room temperature and zero confining pressure.

(4) For calcium carbonate, strength varies with size in a direction opposite to that of quartz. Single crystals of calcite are weak (~14 MPa, depending on orientation) compared to single crystals of quartz (~2,500 MPa). But limestone rocks, made from interlocking calcium carbonate crystals, are much stronger than single crystals of calcium carbonate, and even somewhat stronger than sandstones, as shown by comparing the top two histograms on Figure III-1-4.

(5) The weaker rocks on the left end of the histograms of Figure III-1-4 are those with macroscopic flaws such as bedding planes, rather than flaws in single grains. The high-strength outliers on the right end of the sandstone and limestone histograms of Figure III-1-4 are special cases. The sandstone outlier is a quartzite, a metamorphosed sandstone recrystallized with silica cement. The limestone outlier is Solnhofen limestone, which is a dense, fine-grained, uniform limestone.

(6) Dolomite is a carbonate rock allied to limestone in which about half of the calcium of calcite has been replaced by magnesium (both the mineral and the rock are called dolomite). On average, dolomite and dolomitic limestones make better riprap than limestone and sandstone, as suggested by comparison of the histograms on Figure III-1-4.

(7) Where available, rocks classified commercially as trap rock (dense basalt, diorite, and related rocks) or granite (including rhyolite and dense gneiss) make even better riprap, with strength typically on the order of 140 to 200 MPa under conditions comparable to those in Figure III-1-4.

(8) A typical specification for rock used as riprap in coastal engineering, extracted from "Low Cost Shore Protection," Report on Section 54, U.S. Army Corps of Engineers (1981, p. 785), is as follows:

> *The stone shall be free of cracks, seams, and other defects that would tend to increase unduly its deterioration from natural causes or breakage in handling or dumping. The stone shall weigh, when dry, not less than 150 pounds per cubic foot.* The inclusion of objectionable quantities of sand, dirt, clay, and rock fines will not be permitted. Selected granite and quartzite, rhyolite, traprock and certain dolomitic limestones generally meet the requirements of these specifications.*

*150 PCF is equivalent to 2,400 kg/m^3.

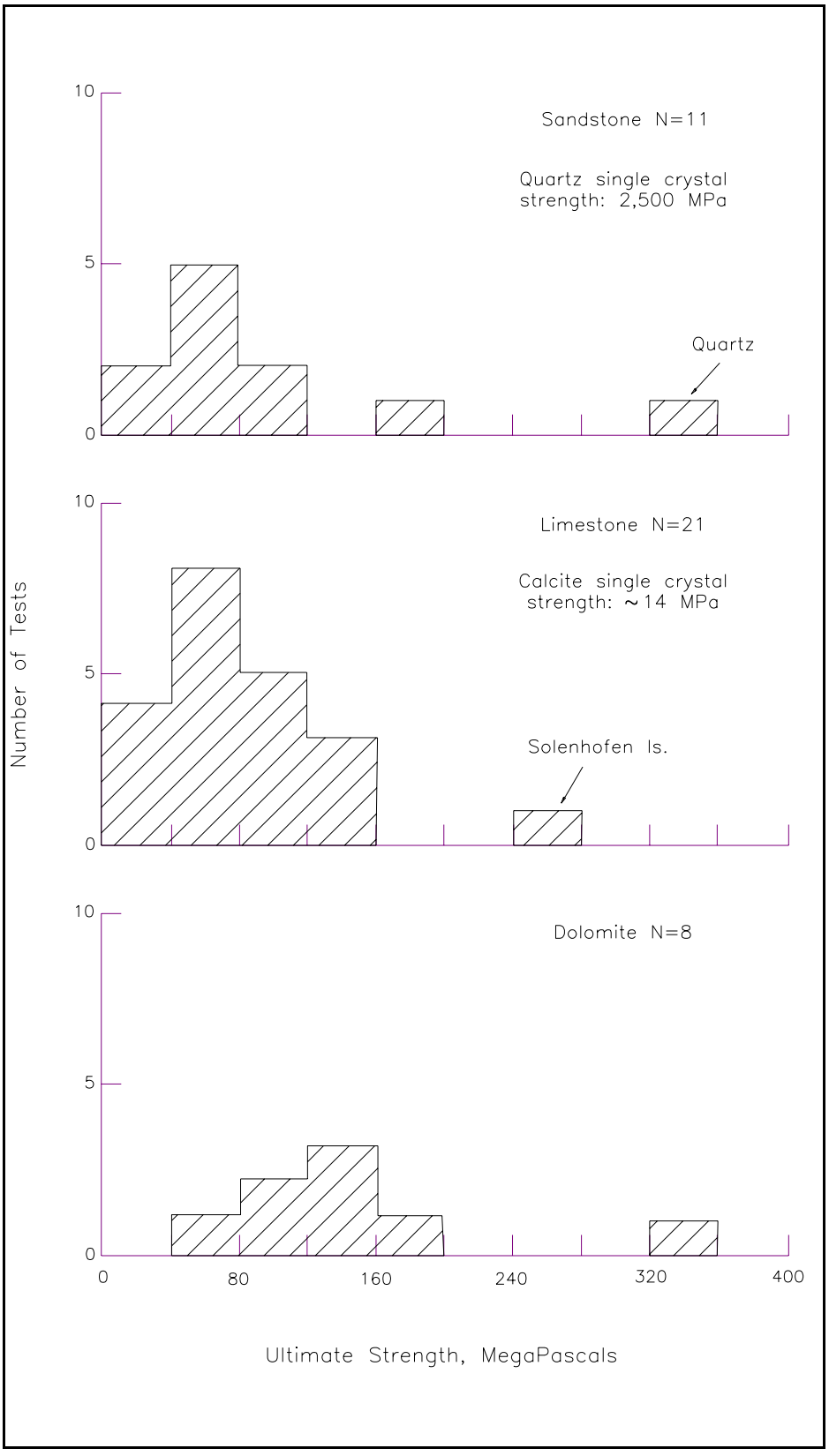

Figure III-1-4. Unconfined ultimate strength of three rock types (after Handin (1966))

EXAMPLE PROBLEM III-1-2

FIND:

The density, specific weight, and specific gravity of a sediment sample.

GIVEN:

18.1 grams of the sample of dry beach sand exactly fills a small container having a volume of 10.0 cm^3 after the filled container is strongly vibrated. When this amount of sand is poured into 50.0 ml of water which is subjected to a strong vacuum, the volume of the sand-water mixture is 56.8 ml.

SOLUTION:

It is important to recognize the difference in the volume of the grains themselves, which is 6.8 cm^3 (= 56.8 - 50) (a milliliter is a cubic centimeter), and the volume of the aggregate (the grains plus the void spaces), which is 10 cm^3.

Density is the sediment mass divided by its volume:

$$\rho_s = 18.1 \text{ gm} / 6.8 \text{ cm}^3 = 2.66 \text{ gm/cm}^3 = 2{,}660 \text{ kg/m}^3$$

If this problem were in English units rather than metric, the sediment weight (in pounds force) would probably be given, rather than the mass. To obtain the mass, the weight would need to be divided by the acceleration of gravity (32.2 ft/sec^2) (mass = weight / g). After dividing by the volume (in ft^3), the density would be obtained in $slugs/ft^3$.

The specific weight of the sand grains themselves is the density times the acceleration of gravity:

$$\text{Sp wt of the grains} = 2.66 \text{ gm/cm}^3 * 980 \text{ cm/sec}^2$$
$$= 2{,}610 \text{ gm/(cm}^2 * \text{sec}^2) = 26{,}100 \text{ kg/(m}^2 * \text{sec}^2)$$

The specific gravity of a material has the same value as its density when measured in gm/cm^3, because the density of water at 4^0 C is 1.00 gm/cm^3:

Specific Gravity = 2.66

e. Grain shape and abrasion.

(1) Grain shape is primarily a function of grain composition, grain size, original shape, and weathering history. The shape of littoral material ranges from nearly spherical (e.g. quartz grains) to nearly disklike (e.g. shell fragments, mica flakes) to concave arcs (e.g. shells). Much of the early work on classifying sediment particle shape divided the problem into three size scales; the sphericity or overall shape of a particle, the roundness or the amount of abrasion of the corners, and the microtexture or the very fine scale roughness. These differences can be illustrated by noting that a dodecahedron has high sphericity but low roundness, while a thin oval has low sphericity but high roundness. A tennis ball has greater micro-texture than a baseball. More recent approaches to the quantification of grain shape have avoided the artificial division of shape into sphericity, roundness, and microtexture by characterizing all the wavelengths of the grain's

irregularities in one procedure using fractal geometry types of analysis. See Ehrlich and Weinberg (1970), and Frisch, Evans, Hudson, and Boon (1987).

(2) Grain shape is important to coastal engineers because it affects several other properties, particularly when the grains are far from spherical, which is the usual assumption. These include fall velocity, sieve analysis, initiation of motion, and also certain bulk properties, such as porosity and angle of repose. One particular area of interest to coastal engineers is in the design of man-made interlocking armor units on breakwaters that have high stability, even when stacked at a high angle of repose. Grain shape has also been used to indicate residence time in the littoral environment. See Krinsley and Doornkamp (1973) and Margolis (1969).

(3) However, most littoral grain shapes are close enough to spheres that a detailed study of their shape is not warranted. Frequently, a qualitative description of roundness is sufficient. This can be done by comparing the grains in a sample to photographs of standardized grains (see Krumbein 1941; Powers 1953; Shepard and Young 1961).

(4) Among the earliest research studies in coastal engineering were investigations of sand grain abrasion, done because of the worry that abrasion of beach sand contributes to beach erosion. These investigations found that abrasion of the typical quartz beach sand is rarely significant. In general, recent information lends further support to the conclusion of Mason (1942) that

> *On sandy beaches the loss of material ascribable to abrasion occurs at rates so low as to be of no practical importance in shore protection problems*.

(5) To achieve the high stress required for quartz to abrade (to fail locally), very large impact forces are needed. These forces are developed by sudden changes in momentum, the product of mass and velocity. Given the small mass of a sand grain, large forces can be achieved only by grains moving at high velocities. But the drag on a sand grain moving in water increases as the square of its velocity, which limits sand grain velocity to a low multiple of its fall velocity. Because fall velocities are only a few centimeters per second, it is extremely difficult to achieve a stress between impacting grains that is anywhere near the strength of quartz. Thus, the rounding of the corners of angular quartz grains in riverine or littoral environments is a very lengthy process. Sands, silts, and clays found in the coastal environment can generally be considered as some of the stable end results of the weathering process of rocks so long as they remain on or near the surface of the earth.

(6) However, abrasion is common in large particles such as boulders and riprap subject to wave action. The mass of a particle increases with the cube of its diameter, so a minimum-size boulder (300 mm on Table III-1-2) compared to a minimum-size coarse sand grain (2 mm) (ASTM classification) will have $(300/2)^3 = 3.375$ million times more mass. If that boulder was a perfect sphere in shape, and this rock sphere rested with a point contact on the plane surface of another rock, then merely the weight of the boulder would crush the point contact of the sphere until the area of contact increased enough to reduce the pressure of the contact to below the crushing strength of the boulder (say 120 MPa, based on Figure III-1-4). The material crushed at this contact is abraded from the boulder. This process of stress concentration at points of contact is considered quantitatively by Galvin and Alexander (1981). If the boulder moves, say, with the rocking motion imparted by the arrival of a wave crest, the slight velocity of the boulder mass provides a momentum which can produce impact forces in excess of crushing strength at points of contact between a boulder and its neighbors, thus abrading the rock.

(7) Because it is probable that a large rock will break along surfaces of weakness, the resulting pieces after breakage will usually be stronger than the rock from which the pieces are broken. Thus, abraded gravel

pieces on a wave-washed shingle beach are apt to have greater strength than the bulk strength of the rock from which the gravel was derived.

III-1-4. Fall Velocity

When a particle falls through water (or air), it accelerates until it reaches its fall or settling velocity. This is the terminal velocity that a particle reaches when the (retarding) drag force on the particle just equals the (downward) gravitational force. This quantity figures prominently in many coastal engineering problems. While simple in concept, its precise calculation is usually not. A particle's fall velocity is a function of its size, shape, and density; as well as the fluid density, and viscosity, and several other parameters.

a. General equation.

(1) For a single sphere falling in an infinite still fluid, the balance between the drag force and the gravitational force is:

$$C_D \frac{\pi D^2}{4} \frac{\rho W_f^2}{2} = \frac{\pi D^3}{6} (\rho_s - \rho) g \tag{III-1-6}$$

or, solving for the velocity:

$$W_f = \left(\frac{4}{3} \frac{gD}{C_D} \left[\frac{\rho_s}{\rho} - 1 \right] \right)^{\frac{1}{2}} \tag{III-1-7}$$

where

W_f = fall velocity

C_D = dimensionless drag coefficient

D = grain diameter

ρ = density of water

ρ_s = density of the sediment

(2) The units of the fall velocity will be the same as the units of $(gD)^{1/2}$. The problem now usually becomes one of determining the appropriate drag coefficient. Figure III-1-5, which is based upon extensive laboratory data of Rouse and many others, shows how the drag coefficient C_D varies as a function of the Reynolds number ($Re = W_f D/\nu$, where ν is the kinematic viscosity) for spherical particles. Re is dimensionless, but W_f, D, and ν must have common units of length and time.

(3) The plot in Figure III-1-5 can be divided into three regions. In the first region, Re is less than about 0.5, and the drag coefficient decreases linearly with Reynolds number. This is the region of small, light grains gently falling at slow velocities. The drag on the grain is dominated by viscous forces, rather than inertia forces, and the fluid flow past the particle is entirely laminar. The intermediate range is from about

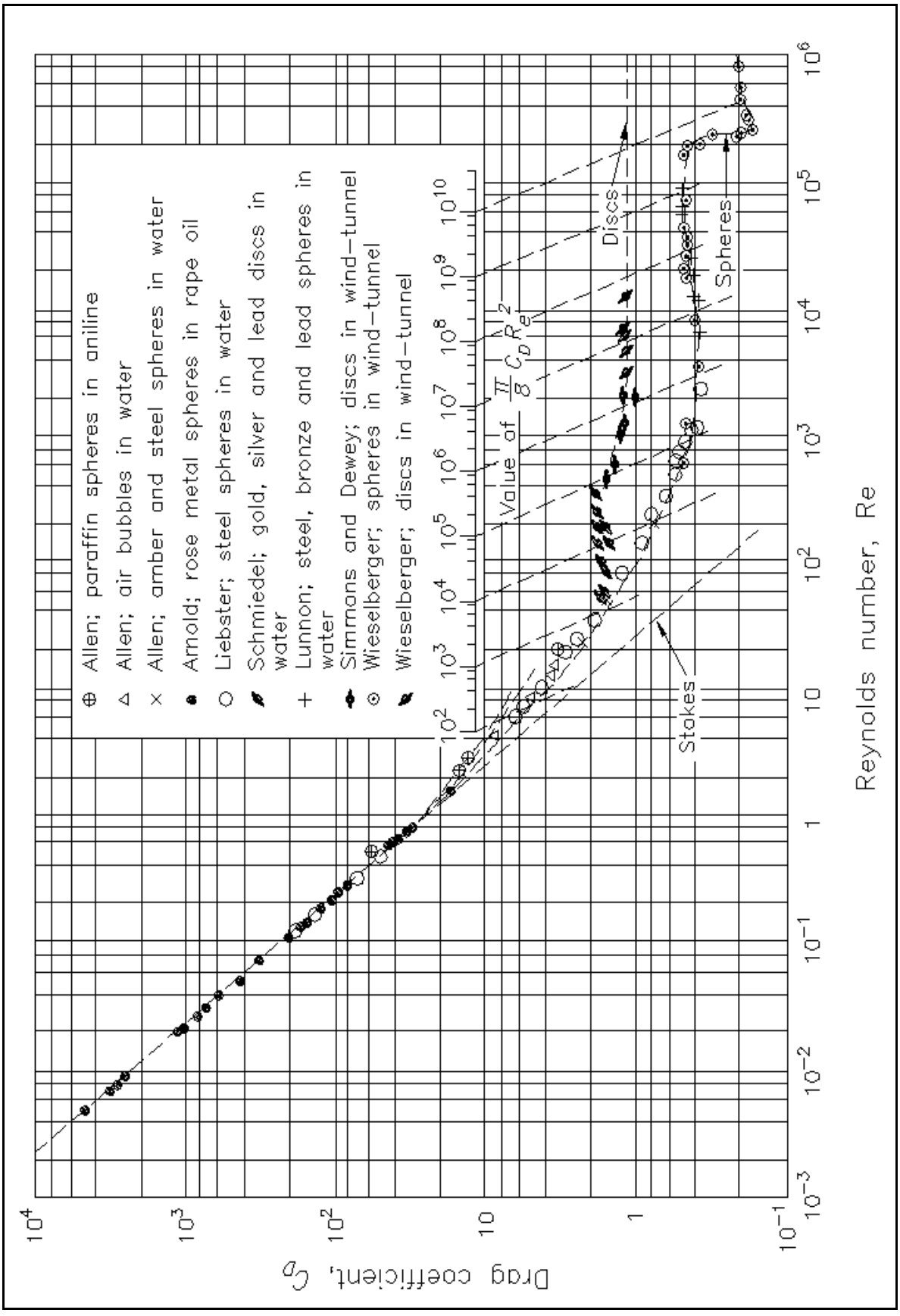

Figure III-1-5. Drag coefficient as a function of Reynolds Number (Vanoni 1975)

Re > 400 to *Re < 200,000*. Here the drag coefficient has the approximately constant value of 0.4 to 0.6. In this range the particles are larger and denser, and the fall velocity is faster. The physical reason for this change in the behavior of C_D is that inertial drag forces have become predominant over the viscous forces, and the wake behind the particle has become turbulent. At about *Re = 200,000* the drag coefficient decreases abruptly. This is the region of very large particles at high fall velocities. Here, not only is the wake turbulent, but the flow in the boundary layer around the particle is turbulent as well.

(4) In the first region, Stokes found the analytical solution for C_D as:

$$C_D = \frac{24}{Re} = \frac{24\ \nu}{W_f\ D} \tag{III-1-8}$$

(5) This line is labeled "Stokes" in Figure III-1-5. Substituting Equation 1-8 into Equation 1-7 gives the fall velocity in this region:

$$W_f = \frac{g\ D^2}{18\ \nu}\left(\frac{\rho_s}{\rho} - 1\right) \tag{III-1-9}$$

(6) Note that in this region the velocity increases as the square of the grain diameter, and is dependent upon the kinematic viscosity.

(7) For the region of *400 < Re < 200,000*, the approximation $C_D \sim 0.5$ is used in Equation 1-7 to obtain:

$$W_f = 1.6\left(g\ D\left[\frac{\rho_s}{\rho} - 1\right]\right)^{\frac{1}{2}} \tag{III-1-10}$$

(8) Here it is seen that the fall velocity varies as the square root of the grain diameter and is independent of the kinematic viscosity.

(9) Similarly, in the region *Re > 200,000*, the approximation $C_D \sim 0.2$ is used in Equation 1-7 to obtain:

$$w_f = 2.6\left(g\ D\left[\frac{\rho_s}{\rho} - 1\right]\right)^{\frac{1}{2}} \tag{III-1-11}$$

(10) There is a large transition region between the first two regimes (between *0.5 < Re < 400*). For quartz spheres falling in water, these Reynolds numbers correspond to grain sizes between about 0.08 mm and 1.9 mm. Unfortunately, this closely corresponds to all sand particles, as seen in Table III-1-2. Thus, for very small particles (silts and clays), the fall velocity is proportional to D^2 and can be calculated from Equation 1-9. For gravel size particles the fall velocity is proportional to $D^{1/2}$ and can be calculated from Equation 1-10. However, for sand, the size of most interest to coastal engineers, no simple formula is available. The fall velocity is in a transition region between a D^2 dependence and a $D^{1/2}$ dependence. In this size range, it is easiest to obtain a fall velocity value from plots such as Figure III-1-6, which show the fall velocity as a function of grain diameter and water temperature for quartz spheres falling in both water and air. The vertical and horizontal axes are grain diameter and fall velocity, in millimeters and centimeters per second, respectively. The short straight lines crossing the curves obliquely are various values of *Re*.

(11) The transition between the second and third regime corresponds to approximately 90-mm quartz spheres (cobbles, as shown on Table III-1-2) falling in water.

(12) Generally for grain sizes outside the range shown in Figure III-1-6 or for spheres with a density other than quartz, or fluids other than air or water, Equation 1-7 can be used with a value of C_D obtained from Figure III-1-5. However, this is an iterative procedure involving repeated calculations of fall velocity and Reynolds number. Instead, Equation 1-7 can be rearranged to yield:

$$\frac{\pi}{8} C_D Re^2 = \frac{\pi D^3 \left(\frac{\rho_s}{\rho} - 1 \right) g}{6 \nu^2} \tag{III-1-12}$$

This quantity, $\pi/8\ C_D\ Re^2$, can be used in Figure III-1-5 to obtain a value of C_D or Re , either of which can then be used to calculate the fall velocity.

b. Effect of density. Equation 1-7 shows that fall velocity depends on $((\rho_s/\rho)-1)^{1/2}$. For quartz sand grains in fresh water, this factor is about 1.28. For quartz grains in ocean water, this factor reduces to about 1.25 because of the slight increase in density of salt water. For quartz grains in very turbid (muddy) water, the factor will decrease somewhat more. If the suspended mud is present in a concentration of 10 percent by mass, $((\rho_s/\rho)-1)^{1/2}$ becomes 1.19. Thus, natural increases in water density encountered in coastal engineering will decrease the fall velocity of quartz by not much more than (1.28 - 1.19) / 1.28 = 0.07, or on the order of 7 percent.

c. Effect of temperature. Temperature has an effect on the density of water; however, this is very small compared to its effect on the coefficient of viscosity. Changes in the fluid viscosity affect the fall velocity for small particles but not for large. (Equation 1-8 contains a viscosity term while Equations 1-9 and 1-10 do not.) Figure III-1-6 has separate lines labeled with temperatures of 0°, 10°, 20°, 30°, and 40 °C, and these lines are reversed for the two fluids. A grain will fall faster in warmer water, but slower in warmer air, compared to its fall velocities at lower temperatures. This difference is the direct result of how viscosity varies with temperature in the two fluids.

d. Effect of particle shape.

(1) Grain shape affects the fall velocity of large particles (those larger than *Re* about 10 or *D* about 0.125 mm in water) but has a negligible effect on small particles. For large grains of a given nominal diameter, the less spherical the particle, the slower the fall velocity. In Figure III-1-5 it is seen that at large Reynolds numbers, discs have higher C_D values, and thus lower fall velocities than spheres.

(2) Mehta, Lee, and Christensen (1980) investigated the fall velocity of natural shells (unbroken bivalve halves). For *Re* in the range of 1,000-5,000, they found that if the shells rocked but did not spin as they fell, C_D values ranged from about 0.7 to 1.0 depending upon a shape factor. The less spherical, the greater the drag. If the shells spun while falling, the drag coefficient increased to the range of 1.0 to 1.5. For large particles that are far from spherical, it is usually best to determine their fall velocity experimentally.

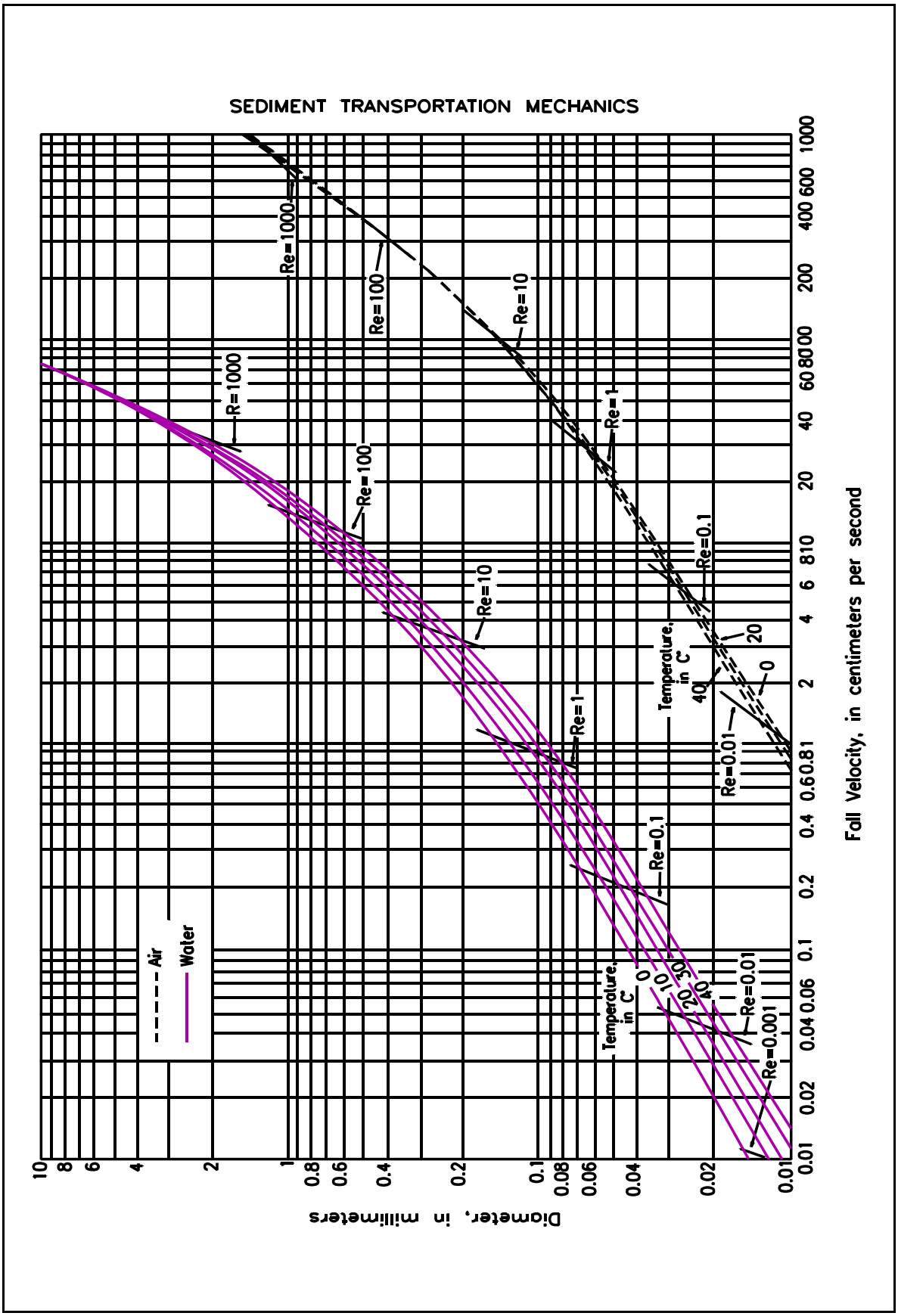

Figure III-1-6. Fall velocity of quartz spheres in air and water (Vanoni 1975)

e. Other factors.

(1) Several other factors affect the fall velocity. A tight clump of grains in an otherwise clear fluid will fall faster than a single grain because the adjacent fluid is partially entrained and thus the drag on each particle decreases. However, if the grains are uniformly distributed in the fluid, each will fall slower because, as each grain falls, replacement fluid must flow upward and this flow impedes the other grains. Likewise, an adjacent wall will decrease the fall velocity. These effects must be considered in the design and calibration of a settling tube used to measure the relationship between grain diameter and fall velocity. Theoretical calculations have shown that an increase in turbulence levels in the fluid should reduce the fall velocity for large particles. However, this has not been shown experimentally. These and other effects are hard to measure and parameterize. However, taken together, they are probably of minor importance and only serve to somewhat decrease the accuracy of fall velocity predictions.

(2) There are no ASTM standards for estimating sand size from fall velocity (see ASTM volume 4.08), and equipment to measure such fall velocity is not usually offered by the construction materials testing industry (Soiltest 1983). However, the fall velocity of grains is an essential parameter in coastal engineering research on sediment transport. Where large grain sizes are of importance and where shell material makes up a large percentage of the sample, fall velocity may be a preferable way to characterize the material as opposed to sieve size.

III-1-5. Bulk Properties

a. Porosity.

(1) Porosity, bulk density, and permeability are related bulk properties that arise from the fact that aggregations of sediments have void spaces around each grain. The *porosity P* is defined as the ratio of pore space, or voids, to the whole volume. It is related to the *volume concentration N*, which is the ratio of the solid volume to the whole volume; and to the *voids ratio e*, which is the ratio of pore space to solid space; by the equation:

$$e = \frac{P}{N} \tag{III-1-13a}$$

$$N = 1 - P = \frac{1}{1 + e} \tag{III-1-13b}$$

(2) Porosity is a function of how tightly the grains are packed together, and thus, is not a constant for a given sediment. As a grain settles to the bed, the greater the effects of gravity relative to the effects of the lateral fluid stresses over the bed, the lower the volume concentration. That is, the grains have less opportunity to roll around and find a position of maximum stability (= most tightly packed position). Thus, grains in the surf zone are typically compacted to near their maximum volume concentration while this is not the case in many quiet estuaries.

(3) In natural sands, volume concentration is essentially independent of grain size within the sand size range. However, the volume concentration is complicated by the irregular shape and nonuniform size of the grains. In general, an increase in nonuniformity of grain sizes increases the volume concentration (decreases the porosity) because small grains can fit into the pore spaces of the large grains. In engineering terms,

porosity decreases as the sand becomes better graded. An increase in the irregularity of the grain shapes tends to decrease the volume concentration. That is, an irregular grain of longest dimension D usually occupies almost as much space as a sphere of the same diameter D.

(4) For uniform spheres the loosest packing arrangement is cubic, yielding $P = 0.476$, while the densest is rhombohedral, yielding $P = 0.260$. Natural sands have porosities in the range $0.25 < P < .0.50$. Blatt, Middleton, and Murray (1980, Chapter 12) and Terzaghi and Peck (1967) showed that for laboratory studies of sands with gaussian size distributions, porosity decreased from 42.4 percent for extremely well-sorted sands to 27.9 percent for very poorly sorted sands, with no clay matrix. Chamberlain (1960) and Dill (1964) measured volume concentration of the fine sand on the beach and around the head of Scripps Canyon in Southern California. When compacted by vibration to its densest packing, the sand had a porosity of 0.40. In situ measurements from the beach yielded $P = 0.42$, while measurements from offshore near the canyon head yielded $P = 0.50$, and some micaceous (very irregular) sands from the canyon yielded $P = 0.62$.

(5) Good porosity data are not often available. The standard assumption in longshore transport computations is that sand has a porosity of 0.40, although there are likely to be significant variations from that figure, as discussed by Galvin (1979).

b. Bulk density. Density was defined in Part III-1-3-b as relating to a particle itself. Bulk density refers to a group of particles. *Dry bulk density* is the mass of an aggregation of grains divided by the volume of the grains (solids) plus the volume of the pore spaces. That is:

$$Dry\ Bulk\ Density = N\ \rho_s \tag{III-1-14}$$

Saturated bulk density is the mass of an aggregation of grains plus the mass of the interstitial water divided by the volume of the sample. That is:

$$Saturated\ Bulk\ Density = (N\ \rho_s) + (P\ \rho) \tag{III-1-15}$$

The dry bulk density is never greater than the grain density, and the saturated bulk density is only greater than the grain density if the interstitial fluid is more dense than the grains (if the grains float). Table III-1-6 lists typical bulk quantities for several sediments that are useful for coastal engineering computations. Table III-1-6 contains three parts: A – typical engineering data; B – saturated densities of naturally occurring surficial soils, along with porosity information; and C – dry densities of synthetic laboratory soils. Comparison of the two columns of data in Part C of Table III-1-6 gives an idea of the consolidation to be expected from settling, and a minimum estimate of the "bulking" of newly placed dry material.

c. Permeability. Permeability is the ability of water to flow through a sediment bed, and is largely a function of the size and shape of the pore spaces. Several aspects of this flow are of interest to coastal engineers. Flow into and out of the bed is one source of energy dissipation for waves traveling in shallow water (see Reid and Kajiura (1957), Packwood and Peregrine (1980)). Permeability is also a major factor in determining the steepness of the foreshore. Sediment is carried shoreward during the wave uprush in the swash zone. The permeability of the swash zone helps control how much of this water returns to the sea on the surface (above the bed) and how much returns through the bed. The surface backrush will transport sediment seaward, decreasing the equilibrium foreshore slope (Savage 1958; McLean and Kirk 1969; Packwood 1983). Just seaward of the breaker zone recent studies have suggested that even small amounts of wave-induced flow into and out of the bed have a major effect on the bottom boundary layer and the resulting sediment transport (Conley and Inman 1992).

EXAMPLE PROBLEM III-1-3

FIND:

Estimate W_f, Re, and C_D for the following particles falling through 20° C fluids.

a) 0.2-mm (=0.02-cm) quartz grain in fresh water
b) 0.2-mm quartz grain in salt water
c) 0.2-mm quartz grain in air
d) 0.001-mm-(=0.0001-cm-) diam kaolinite clay particle (unflocculated) in fresh water
e) 4.5-mm (=0.45-cm) steel BB pellet in air
f) 6-1/2-(=16.5-cm-) diam pine sphere in fresh water

GIVEN:

g = 980 cm/sec^2
ν_{water} = 0.011 cm^2/sec
ν_{air} = 0.15 cm^2/sec
$\rho_{fresh\ water}$ = 1.00 gm/cm^3
$\rho_{salt\ water}$ = 1.03 gm/cm^3
ρ_{air} = 0.0012 gm/cm^3
ρ_{quartz} = 2648 kg/m^3 from Table III-1-4 (=2.648 gm/cm^3)
$\rho_{kaolinite}$ = 2594 kg/m^3 from Table III-1-4 (=2.594 gm/cm^3)
ρ_{steel} = 7800 kg/m^3 (=7.8 gm/cm^3)
ρ_{pine} = 480 kg/m^3 (=0.48 gm/cm^3)

SOLUTION:

For convenience, all calculations will be done in the cgs (centimeters, grams, seconds) system.

a) The fall velocity is read from Figure III-1-6 as 2.3 cm/sec. Re is calculated from its definition as:

$$Re = (2.3 * 0.02)/0.011 = 4.2$$

C_D can be found from Equation III-1-7 when rearranged as:

$$C_D = (4/3) * 980*0.02/(2.3)^2 * ((2.65/1) - 1) = 8.1$$

This agrees reasonably well with Figure III-1-5.

b) From section III-1-4-b, the fall velocity should be decreased from its value in part (a) by the factor 1.25/1.28 = 0.977, thus:

$$W_f = 2.3 * 0.977 = 2.2 \text{ cm/sec}$$

$$Re = (2.2 * 0.02)/0.011 = 4.0$$

$$C_D = 4/3 * 980*0.02/(2.2)^2 * (2.65/1-1) = 8.9$$

(Continued)

Example Problem III-1-3 (Concluded)

c) The fall velocity is read from Figure III-1-6 as 150 cm/sec. *Re* is calculated from its definition as:

$$Re = (150 * 0.02)/0.15 = 20$$

C_D is calculated from 1-7 as:

$$C_D = 4/3 * 980*0.02/(150)^2 * ((2.65/0.0012)-1) = 2.5$$

This agrees reasonably well with Figure III-1-5.

d) Expecting to find Re < 0.5, Equation 1-9 can be used to find W_f.

$$W_f = 980/18\ (0.0001)^2/0.011\ (2.594/1-1) = 7.9 \times 10^{-5} \text{ cm/sec}$$

From its definition:

$$Re = 7.9 \times 10^{-5} * 0.0001 / 0.011 = 7.2 \times 10^{-7}$$

Thus, use of Equation 1-9 is well justified. From Equation 1-8:

$$C_D = 24/7.2 \times 10^{-7} = 3.3 \times 10^{7}$$

e) Estimating that *Re* will be in the range $400 < Re < 200{,}000$, Equation 1-10 can be used to find an estimate of W_f.

$$W_f = 1.6\ (980 * 0.45\ ((7.8/0.0012)-1))^{1/2} = 2{,}700 \text{ cm/sec}$$

$$Re = .45 * 2700 / 0.15 = 8100$$

Thus, use of Equation 1-10 is justified. From Figure III-1-5, it is seen that a C_D value of 0.4 is better than the value of 0.5 used in Equation III-1-10. Iterating using this value in Equation 1-7 yields:

$$W_f = (4/3 * 980 * 0.45/0.4 * (7.8/0.0012-1))^{1/2} = 3{,}100 \text{ cm/sec}$$

$$Re = .45 * 3{,}100 / 0.15 = 9{,}300$$

Alternatively, Equation III-1-12 could have been used to obtain:

$$\pi/8\ C_D\ Re^2 = 3.14*(0.45)^3*(7.8/0.0012-1)*980/(6 * (0.15)^2)=1.3\text{x}10^7$$

Using Figure III-1-5, this yields similar values of 12,000 and 0.4 for *Re* and C_D, respectively.

f) It is important to realize that this particle is lighter than water and its direction of motion will be upward. This is implied in the result by the fall velocity having a negative value. Estimating that *Re* will be in the range $Re > 200{,}000$, Equation 1-11 can be used to find an estimate of W_f.

$$W_f = 2.6\ (980 * 16.5\ ((0.48/1)-1))^{1/2} = -240 \text{ cm/sec}$$

$$Re = 240 * 15.2 / 0.011 = 360{,}000$$

Thus, use of Equation 1-11 is justified. Alternatively, Equation 1-12 could have been used to obtain:

$$\pi/8\ C_D\ Re^2 = 3.14*(16.5)^3*(0.48/1-1)*980/(6 * (0.011)^2)=(-)9.9\text{x}10^9$$

Using Figure III-1-5, this yields similar values of $4\text{x}10^5$ and 0.2 for *Re* and C_D, respectively.

Table III-1-6
Soil Densities Useful for Coastal Engineering Computations

A. Typical Engineering Values (from Terzaghi and Peck (1967), Table 6.3)

Material	Dry Bulk Density, kg/m^3	Saturated Bulk Density, kg/m^3
Uniform Sand		
Loose	1,430	1,890
Dense	1,750	2,090
Mixed Sand		
Loose	1,590	1,990
Dense	1,860	2,160
Clay		
Stiff glacial		2,070
Soft, very organic		1,430

B. Natural Surface Soils (from Daly, Manger, and Clark (1966), Table 4-4)

Material	No. of Samples	Mean Porosity, %	Saturated Bulk Density, kg/m^3	Locality
Sand	12	38.9	1930	Cape May sand spits
Loess	3	61.2	1610	Idaho
Fine Sand	54	46.2	1930	CA seafloor
Very Fine Sand	15	47.7	1920	CA seafloor
Sand-Silt-Clay	3	74.7	1440	CA seafloor

C. Laboratory Soils (from Johnson and Olhoeft (1984), Table 4)

Material	Dry Bulk Density "fluffed" kg/m^3	Dry Bulk Density "tapped", kg/m^3
Gravelly Soil	1,660	1,770
Sandy Soil	1,440	1,560
Dune Sand	1,610	1,760
Loess	990	1,090
Peat	270	320
Muck	800	850

Note: Data for loess in Parts B and C are representative of silty material.

d. Angle of repose.

(1) When a dry sand-size sediment is poured onto a flat surface, it will form a cone-shaped mound. The slope of the surface of the cone (or dune) at the moment of avalanching is called the angle of repose. The angle of repose concept is of interest to coastal engineers for several reasons, including the stability of rubble-mound breakwaters and the modeling of sediment transport.

(2) The angle of repose is a function of grain shape; it increases with increasing grain irregularity. This is easy to see in the extreme case: a pile of jacks (or interlocking breakwater armor units) will stack at a much steeper angle than a pile of ball bearings. Several workers, including Lane (1955), Simons and Albertson (1960), Allen (1970), Cornforth (1973), Statham (1974), and Simons and Senturk (1977) have looked at the variation of the angle of repose in relationship to various sediment characteristics.

(3) Bagnold used the relationship between the shear forces, the normal forces, and the angle of repose to develop his energetics-based sediment transport model. He reasoned that the amount of sediment by weight at the top of a bed that can be supported in an elevated state and then be transported is related to the applied shear stress of the overlying (moving) fluid by the tangent of the angle of repose. Bagnold's concept forms the basis of many of the sediment transport models most frequently used by coastal engineers. For further discussion, see Bagnold (1963), (1966), Bailard and Inman (1979), and Bailard (1981).

e. Bulk properties of different sediments.

(1) Clays, silts, and muds.

(a) Coastal engineers typically encounter clay as a foundation material or as a material to be dredged. The flat topography of coastal plains and the quiet waters of bays and lagoons are often underlain by clay. Some older clays are consolidated and can stand with near-vertical slopes when eroded. For example, the deepest parts of tidal inlets may have steep sides cut into stiff clay. Many eroding coastal flats contain much clay. Revetments laid on these clays, or sheet piles driven into them, need particular attention; such design may require the advice of a geotechnical engineer.

(b) A silt-sized particle is intermediate between sand and clay. Most silt is produced by the gradual chemical weathering of rocks, but some silt is rock flour ground out by glaciers. Sediments consisting mostly of silt are common in deltas, estuaries, and glacial lakes, but are relatively uncommon on beaches where waves drive the dominant processes. Silt remains in suspension far longer than sand grains, so it is easily removed from any shore where wave action is moderate or severe. A mass of pure silt differs from a mass of clay in that, when dry, the silt has very little cohesion and will easily fall apart, whereas clay will cohere like a brick.

(c) Muds are watery mixtures of clay and silt, typically in approximately equal proportions, often with minor amounts of sand and organic material. Muds act more as a viscous fluid than as a cohesive solid. They have coastal engineering importance because muds often accumulate in dredged channels where the upper and lower boundaries of the mud layer can be difficult to determine. Maintenance dredging of channels that accumulate mud requires particular attention, especially a clear definition of the material to be dredged.

(d) Some deposits of mud lie offshore of the coast, where the mud is believed to modify the transmission of water waves. See, for example, Jiang and Zhao (1989); Shen, Isobe, and Watanabe (1994); and deWit, Kranenburg, and Batljes (1994) for introduction to recent work. Such mud deposits have been reported at the mouth of most large Asian rivers, off the Gulf Coast of Louisiana, northeast of the mouth of the Amazon River, and seaward of the Kerala district in India. These mud deposits are believed to oscillate with the passage of water waves above them, absorbing energy from the waves and reducing their height.

(2) Organically bound sediment.

(a) Marsh grasses growing in back bays and other tidal wetlands bind sands, silts, and clays with their root systems to form an organically bound sediment, sometimes called *peat* (typically, organic silt in the engineer's soil classification). These sediments are very compressible; when overlain by a barrier island, field evidence indicates that the compression of organic matter by the weight of the sand results in subsidence of the barrier island. Cores illustrating the vertical sequence of organic sediment overlain by barrier island sands have been shown in many geological studies (e.g., Figures 9 and 15 of Kraft et al. (1979)). Shore erosion can expose the organically bound sediment to ocean waves. Erosion by ocean waves produces pillow- or cobble-shaped fragments of organically bound sediment, often found on barrier island coasts after storms.

EXAMPLE PROBLEM III-1-4

FIND:

The volume concentration, the porosity, the voids ratio, the dry bulk density, and the saturated bulk density of the densely packed aggregate given in example problem III-1-2.

GIVEN:

18.1 grams of dry beach sand exactly fills a small container having a volume of 10.0 cm^3 after the filled container is strongly vibrated. When this amount of sand is poured into 50.0 ml of water that is subjected to a strong vacuum, the volume of the sand-water mixture is 56.8 ml.

SOLUTION:

It is important to recognize the difference in the volume of the grains themselves, 6.8 cm^3 (= 56.8 - 50) (a milliliter is a cubic centimeter), and the volume of the aggregate (the grains plus the void spaces), 10 cm^3.

The volume concentration is the ratio of solid volume to total volume:

$$N = 6.8\ cm^3 / 10.0\ cm^3 = 0.68$$

The porosity is the ratio of void space to total volume, which, from Equation 1-13 is:

$$P = 1 - N = 1 - 0.68 = 0.32$$

The voids ratio is the ratio of pore space to solid space, which, from Equation 1-13 is:

$$e = P/N = 0.32/0.68 = 0.47$$

The dry bulk density from Equation 1-14 is:

$$\text{Dry Bulk Density} = 0.68 * 2{,}660\ kg/m^3 = 1{,}800\ kg/m^3$$

The saturated bulk density from Equation 1-15 is:

$$\text{Saturated Bulk Density} = (0.68*2{,}660) + (0.32*1{,}000)\ kg/m^3 = 2{,}100\ kg/m^3$$

These bulk density values are within the expected range as shown in Table III-1-6A.

(b) Where they are present at coastal engineering projects, such organic sediments must be considered. Pile foundations bearing significant loads must penetrate the organic material. It may be required to remove the compressible sediment before construction.

(3) Sand and gravel.

(a) Ocean beaches of the world consist of sand and some gravel. The typical temperate zone ocean beach is made of quartz sand whose median diameter D_{50} is in the range $0.15 \le D_{50} \le 0.40$ mm. In colder latitudes where geologically recent glacial action has affected sediment supply and the wave climate is more severe, the composition of the beach material becomes more varied and size tends to increase. See, for example, Figure 89 of Davies (1980). In these glacier-affected latitudes, sand grains include silicate and oxide compositions (heavy minerals) as noticeable components along with the quartz, and coarse pebbles (gravel or "shingle") may locally dominate the sediment.

(b) In tropical latitudes, quartz beach sand may give way to calcium carbonate sand produced from shelly organisms, algae, or coral. See, for example, Figure 92 of Davies (1980) derived from earlier work of Hayes. Carbonate sands differ from quartz sand in two important ways: carbonates are chemically more active than quartz, making carbonate grains subject to local cementation or sometimes dissolution, and individual carbonate grains are structurally weaker than single quartz grains so that they may be crushed by traffic and often have sharper edges.

(c) Oolites are a particular variety of carbonate sands locally abundant in the Bahamas and other semi-tropical lands. Oolites are sands whose grains are ellipsoidal in shape, consisting of thin smooth concretionary layers of calcium carbonate. There is a very large literature on this subject, mainly by geologists; section 13.3 of Blatt, Middleton, and Murray (1980) is a good starting point.

(d) Beaches in bays and estuaries often differ from ocean beaches at the same latitudes. Often the beach material along interior shores is coarser and much more limited in volume than along ocean shores, possibly because limited wave action on interior waters has not eroded enough material to produce extensive sand beaches.

(4) Cobbles, boulders, and bedrock. Glaciated lands, tectonically active areas, and hilly or mountainous shorelines often have shores with abundant cobbles, boulders, and bedrock. Such shores result from enhanced supplies of rock produced by glaciers, by stream erosion of mountainous terrain, or by enhanced wave erosion at the downwind end of long fetches.

III-1-6. References

Allen 1970
Allen, J. R. L. 1970. "The Avalanching of Granular Solids on Dune and Similar Slopes," *Journal of Geology*, Vol 78, pp 326-351.

American Society for Testing Materials 1994
American Society for Testing Materials. 1994. Volume 04.08, Soil and Rock (1): D420 – D4914, American Society for Testing and Materials, Philadelphia, PA.

Bagnold 1963
Bagnold, R. A. 1963. "Beach and Nearshore Processes; Part I: Mechanics of Marine Sedimentation," *The Sea: Ideas and Observations*, M. N. Hill, ed., Interscience, New York, Vol 3, pp 507-528.

Bagnold 1966
Bagnold, R. A. 1966. "An Approach to the Sediment Transport Problem from General Physics," U. S. Geological Survey Professional Paper 422-I, U. S. Department of the Interior.

Bailard 1981
Bailard, J. A. 1981. "An Energetics Total Load Sediment Transport Model for a Plane Sloping Beach," *Journal of Geophysical Research*, Vol 86, No. C11, pp 10938-10954.

Bailard and Inman 1979
Bailard, J. A., and Inman, D. L. 1979. "A Reexamination of Bagnold's Granular Fluid Model and Bed Load Transport," *Journal of Geophysical Research*, Vol 84, No. C12, pp 7827-7833.

Blatt, Middleton, and Murray 1980
Blatt, H., Middleton, G., and Murray, R. 1980. *Origin of Sedimentary Rocks*, 2nd ed., Prentice–Hall, Englewood Cliffs, NJ.

Chamberlain 1960
Chamberlain, T. K. 1960. "Mechanics of Mass Sediment Transport in Scripps Submarine Canyon," Ph.D. diss., Scripps Institution of Oceanography, Univ. California, San Diego.

Conley and Inman 1992
Conley, D. C., and Inman, D. L. 1992. "Field Observations of the Fluid-Granular Boundary Layer Under Near-Breaking Waves," *Journal of Geophysical Research*, Vol 97, No. C6, pp 9631-9643.

Cornforth 1973
Cornforth, D. H. 1973. "Prediction of Drained Strength of Sands from Relative Density Measurements," American Society for Testing and Materials, Spec. Tech. Pub. 523, pp 281-303.

Daly, Manger, and Clark 1966
Daly, R. A., Manger, G. E., and Clark, S. P., Jr. 1966. "Density of Rocks," *Handbook of Physical Constants*, S. P. Clark, Jr., ed., revised edition, pp 19-26.

Davies 1980
Davies, J. L. 1980. *Geographical Variation in Coastal Development*, 2nd ed., Longman, London.

deWit, Kranenburg, and Batljes 1994
deWit, P. J., Kranenburg, C., and Batljes, J. A. 1994. "Liquefaction and erosion of mud due to waves and current," *International Conference on Coastal Engineering*, Book of Abstracts, Paper 115, Kobe, pp 278-9.

Dill 1964
Dill, R.F. 1964. "Sedimentation and Erosion in Scripps Submarine Canyon Head," *Papers in Marine Geology*, Shepard Commemorative Volume, R.I. Miller, ed., Macmillian & Co., NY, pp 23-41.

Downing, Sternberg, and Lister 1981
Downing, J. P., Sternberg, R. W., and Lister, C. R. B. 1981. "New Instrumentation for the Investigation of Sediment Suspension Processes in the Shallow Marine Environment," *Marine Geology*, Vol 42, pp 19-34.

Ehrlich and Weinberg 1970
Ehrlich, R., and Weinberg, B. 1970. "An Exact Method for Characterization of Grain Shape," *Journal Sed. Pet*., Vol 40, pp 205-212.

Folk 1965
Folk, R. L. 1965. *Petrology of Sedimentary Rocks*, Hemphill Publishing Company, Austin, TX.

Folk 1966
Folk, R. L. 1966. "A Review of Grain-size Parameters," *Sedimentology*, Vol 6, pp 73-93.

Folk 1974
Folk, R. L. 1974. *Petrology of Sedimentary Rock,* Hemphill Publishing Company, Austin, TX.

Folk and Ward 1957
Folk, R. L. and Ward, W. C. 1957. "Brazos River Bar. A Study in the Significances of Grain Size Parameters," *Journal of Sedimentary Petrology*, Vol 27, pp 3-26.

Frisch, Evans, Hudson, and Boon 1987
Frisch, A. A., Evans, D. A., Hudson, J. P., and Boon, J. 1987. "Shape Discrimination of Sand Samples using the Fractal Dimension," *Proc. Coastal Sediments '87*, American Society of Civil Engineers, New Orleans, Louisiana, May 12-14, pp 138-153.

Galvin 1979
Galvin, C. 1979. "Relation Between Immersed Weight and Volume Rates of Longshore Transport," Technical Paper 79-1, Coastal Engineering Research Center, U.S. Army Engineer Waterways Experiment Station, Vicksburg, MS.

Galvin 1987
Galvin, C. 1987. "Vertical Profile of Littoral Sand Tracers from a Distribution of Waiting Times," *Coastal Sediment '87*, Vol 1, pp 436–451.

Galvin and Alexander 1981
Galvin, C., and Alexander, D. F. 1981. "Armor Unit Abrasion and Dolos Breakage by Wave-Induced Stress Concentrations," American Society of Civil Engineers Preprint 81-172.

Giles and Pilkey 1965
Giles, G. T. and Pilkey, O. H. 1965. "Atlantic Beach and Dune Sediments of the Southern United States," *Journal of Sedimentary Petrology*, Vol 35, No. 4, pp 900-910.

Griffiths 1967
Griffiths, J. C. 1967. *Scientific Method in Analysis of Sediments*, McGraw-Hill, New York.

Handin 1966
Handin, J. 1966. "Strength and Ductility," *Handbook of Physical Constants*, S. P. Clark, Jr., ed., Geological Society of America, Memoir 97, pp 223–289.

Hobson 1977
Hobson, R. D. 1977. "Review of Design Elements for Beach-Fill Evaluation," TP 77-6, Coastal Engineering Research Center, U.S. Army Engineer Waterways Experiment Station, Vicksburg, MS.

Huston 1970
Huston, J. 1970. *Hydraulic Dredging*. Cornell Maritime Press, Cambridge, MD.

Inman 1952
Inman, D. L. 1952. "Measures for Describing the Size Distribution," pp 125-145.

Inman 1957
Inman, D. L. 1957. "Wave Generated Ripples in Nearshore Sands," Technical Memorandum 100, Beach Erosion Board, U.S. Army Corps of Engineers.

Jiang and Zhao 1989
Jiang, L., and Zhao, Z. 1989. "Viscous Damping of Solitary Waves over Fluid-Mud Seabeds," *Journal Waterway, Port, Coastal, and Ocean Engineering*, American Society of Civil Engineers, Vol 115, No. 3, pp 345-362.

Johnson and Olhoeft 1984
Johnson, G. R., and Olhoeft, G. R. 1984. "Density of Rocks and Minerals," *Handbook of Physical Properties of Rocks*, Vol III, R. S. Carmichael, ed., CRC Press, Inc., pp 1-28.

Judge 1970
Judge, C. W. 1970. "Heavy Minerals in Beach and Stream Sediments as Indicators of Shore Processes between Monterey and Los Angeles, California," TM-33, Coastal Engineering Research Center, U.S. Army Engineer Waterways Experiment Station, Vicksburg, MS.

Kraft, Allen, Belknap, John, and Maurmeyer 1979
Kraft, J. C., Allen, E. A., Belknap, D. F., John, D. J., and Maurmeyer, E. M. 1979. "Processes and Morphologic Evolution of an Estuarine and Coastal Barrier System," *Barrier Islands*, S. P. Leatherman, ed., Academic Press, New York, pp 149-183.

Krinsley and Doornkamp 1973
Krinsley, D. H., and Doornkamp, J. C. 1973. "Atlas of Quartz Sand Surface Textures," Cambridge University Press, Cambridge.

Krumbein 1936
Krumbein, W. C. 1936. "Application of Logarithmic Moments to Size Frequency Distribution of Sediments," *Journal of Sedimentary Petrology*, Vol 6, No. 1, pp 35-47.

Krumbein 1941
Krumbein, W. C. 1941. "Measurement and Geological Significance of Shape and Roundness of Sedimentary Particles," *Journal of Sedimentary Petrology*, Vol 11, No. 2, pp 64-72.

Krumbein and Monk 1942
Krumbein, W. C., and Monk, G. D. "Permeability as a Function of the Size Parameters of Unconsolidated Sand, American Institute Mining and Metallurgy Engineering," Technical Publication No. 1492, Petroleum Technology, pp1-11.

Krumbein and Sloss 1963
Krumbein, W. C., and Sloss, L. L. 1963. "Stratigraphy and Sedimentation," Ch. 4, *Properties of Sedimentary Rocks*, W. H. Freeman & Company, pp 93-149.

Lambe and Whitman 1969
Lambe, T. W., and Whitman, R. V. 1969. *Soil Mechanics*, John Wiley, New York.

Lane 1955
Lane, E. W. 1955. "Design of Stable Channels," *Transactions, American Society of Civil Engineers,* Vol 120, pp 1234-1279.

Margolis 1969
Margolis, S. V. 1969. "Electron Microscopy of Chemical Solution and Mechanical Abrasion Features on Quartz Sand Grains," *Sedimentary Geology*, Vol 2, pp 243-256.

Mason 1942
Mason, M. A. 1942. "Abrasion of Beach Sands," TM-2, U.S. Army Corps of Engineers, Beach Erosion Board, Washington, DC.

McCammon 1962
McCammon, R. B. 1962. "Efficiencies of Percentile Measures for Describing the Mean Size and Sorting of Sedimentary Particles," *Journal of Geology*, Vol 70, pp 453-465.

McLean and Kirk 1969
McLean, R. F., and Kirk, R. M. 1969. "Relationship Between Grain Size, Size-sorting, and Foreshore Slope on Mixed Sandy-Shingle Beaches," *N. Z. J. Geol. and Geophys*., Vol 12, pp 128-155.

McMaster 1954
McMaster, R. L. 1954. "Petrography and Genesis of the N.J. Beach Sands," *Geology Series*, Vol 63, New Jersey Department of Conservation & Economic Development.

Mehta, Lee, and Christensen 1980
Mehta, A. J., Lee, J., and Christensen, B. A. 1980. "Fall Velocity of Shells as Coastal Sediment," *Journal of the Hydraulics Division*, *American Society of Civil Engineers,* Vol 106, No. HY 11, pp 1727-1744.

Otto 1939
Otto, G. H. 1939. "A Modified Logarithmic Probability Graph for the Interpretation of Mechanical Analyses of Sediments," *Journal of Sedimentary Petrology*, Vol 9, pp 62-76.

Packwood 1983
Packwood, A. R. 1983. "The Influence of Beach Porosity on Wave Uprush and Backwash," *Coastal Engineering*, Vol 7, pp 29-40.

Packwood and Peregrine 1980
Packwood, A. R., and Peregrine, D. H. 1980. "The Propagation of Solitary Waves and Bores over a Porous Bed," *Coastal Engineering*, Vol 3, pp 221-242.

Pettijohn 1957
Pettijohn, F. J. 1957. *Sedimentary Rocks*, Harper and Brothers, New York, p 117.

Powers 1953
Powers, M. C. 1953. "A New Roundness Scale for Sedimentary Particles," *Journal Sed. Pet*., Vol 23, pp 117-119.

Ramsey and Galvin 1977
Ramsey, M. D., and Galvin, C. 1977. "Size Analyses of Sand Samples from Southern New Jersey Beaches," Miscellaneous Paper 77-3, Coastal Engineering Research Center, U.S. Army Engineer Waterways Experiment Station, Vicksburg, MS.

Reid and Kajiura 1957
Reid, R. O., and Kajiura, K. 1957. "On the Damping of Gravity Waves Over a Permeable Sea Bed," *Trans. Amer. Geophys. Union*, Vol 38, No. 5 (October), pp 662-666.

Ritter 1986
Ritter, D. F. 1986. *Process Geomorphology*, 2nd ed., Wm. C. Brown, Dubuque, IA.

Savage 1958
Savage, R. P. 1958. "Wave Run-Up on Roughened and Permeable Slopes," *Journal of the Waterways and Harbors Division*, *American Society of Civil Engineers,* Vol 84, No. WW3, Paper 1640.

Shen, Isobe, and Watanabe 1994
Shen, D., Isobe, M., and Watanabe, A. 1994. "Mud Transport and Muddy Bottom Deformation Due to Waves," Book of Abstracts, Paper 30, *International Conference on Coastal Engineering*, Kobe, pp 106-107.

Shepard and Young 1961
Shepard, F. P., and Young, R. 1961. "Distinguishing Between Beach and Dune Sands," *Journal Sed. Pet*., Vol 31, No. 2, pp 196-214.

Simons and Albertson 1960
Simons, D. B., and Albertson, M. L. 1960. "Uniform Water Conveyance Channels in Alluvial Material," *Journal Hydraulic Division*, *American Society of Civil Engineers,* Vol 86, No. HY5, pp 33-99.

Simons and Senturk 1977
Simons, D. B., and Senturk, F. 1977. *Sediment Transport Technology*, Water Res. Pub., Fort Collins, CO.

Soiltest 1983
Soiltest. 1983. *Soiltest Catalog*, Evanston, IL.

Statham 1974
Statham, I. 1974. *Ground Water Hydrology*, John Wiley & Sons, New York.

Stauble and Hoel 1986
Stauble, D. K., and Hoel, J. 1986. "Guidelines for Beach Restoration Projects, Part II -Engineering," Report SGR-77, Florida Sea Grant, University of Florida, Gainesville.

Terzaghi and Peck 1967
Terzaghi, K., and Peck, R. B. 1967. *Soil Mechanics in Engineering Practice*, 2nd ed., John Wiley, New York.

Trask 1952
Trask, P. D. 1952. "Source of Beach Sand at Santa Barbara, California, as Indicated by Mineral Grain Studies," Tech. Memo. No. 28, U. S. Army Corps of Engineers, Beach Erosion Board.

Turner 1984
Turner, T. M. 1984. *Fundamentals of Hydraulic Dredging*, Cornell Maritime Press, Centreville, MD.

Tyler 1991
Tyler, W. S. 1991. *Testing Sieves and Their Uses*, Handbook 53, LP9-91.

U. S. Army Corps of Engineers 1981
U. S. Army Corps of Engineers. 1981. *Low-cost Shore Protection*, Final Rept on Shoreline Erosion Control Demonstration Program (Section 54).

Vanoni 1975
Vanoni, V. A. 1975. *Sedimentation Engineering*, American Society of Civil Engineers, Manual No. 54.

III-1-7. Definition of Symbols

α_φ	Phi coefficient of skewness (Equation III-1-4)
β_φ	Phi coefficient of kurtosis (Equation III-1-5)
ν	Kinematic viscosity [length^2/time]
ρ	Mass density of water (salt water = 1,025 kg/m^3 or 2.0 slugs/ft^3; fresh water = 1,000kg/m^3 or 1.94 slugs/ft^3) [force-time^2/length^4]
ρ_s	Mass density of sediment grains [force-time^2/length^4]
σ_φ	Standard deviation of a sediment sample (Equation III-1-3) [phi units]
φ	Sediment grain diameter in phi units ($\varphi = -\log_2 D$, where D is the sediment grain diameter in millimeters)
C_D	Drag coefficient [dimensionless]
D	Sediment grain diameter [length - generally millimeters]
D_x	Sediment grain diameter for which x-percent of the sediment, by weight, has a smaller diameter
e	Voids ratio of a sediment sample - ratio of pore space to solid space (Equation III-1-13a)
g	Gravitational acceleration (32.17 ft/sec^2, 9.807m/sec^2) [length/time^2]
M_d	Median grain diameter - half the particles in the sample will have a larger diameter and half will have a smaller diameter [length]
M_φ	Estimated mean grain size of a sediment sample (Equation (III-1-2) [phi units]
N	Volume concentration of a sediment sample - ratio of the solid volume to the whole volume (Equation III-1-13b)
P	Porosity - ratio of pore space, or voids, to the whole volume
Re	Reynolds number [dimensionless]
W_f	Sediment fall velocity [length/time]

III-1-8. Acknowledgments

Authors of Chapter III-1, "Coastal Sediment Properties:"

David B. King, Ph.D., Coastal and Hydraulics Laboratory (CHL), Engineer Research and Development Center, Vicksburg, Mississippi.
Cyril J. Galvin, Coastal Engineer, Springfield, Virginia.

Reviewers:

Andrew Morang, Ph.D., CHL
Joan Pope, CHL
Todd L. Walton, Ph.D., CHL

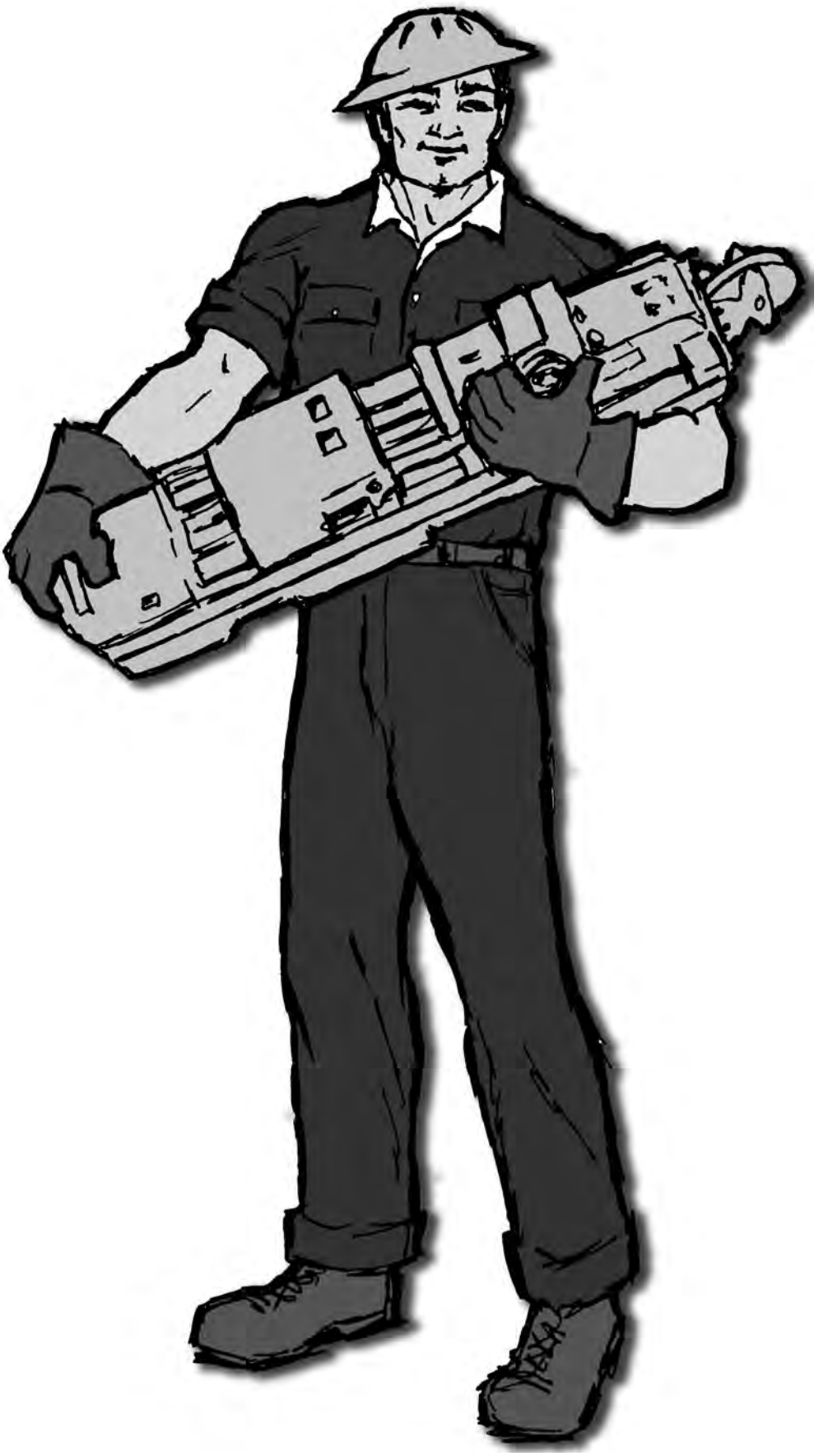

Table of Contents

Page

III-2-1. Introduction III-2-1
a. Overview III-2-1
b. Scope of chapter III-2-1

III-2-2. Longshore Sediment Transport Processes III-2-1
a. Definitions III-2-1
b. Modes of sediment transport III-2-3
c. Field identification of longshore sediment transport III-2-3
(1) Experimental measurement III-2-3
(2) Qualitative indicators of longshore transport magnitude and direction III-2-5
(3) Quantitative indicators of longshore transport magnitude III-2-6
(4) Longshore sediment transport estimations in the United States III-2-7

III-2-3. Predicting Potential Longshore Sediment Transport III-2-7
a. Energy flux method III-2-10
(1) Historical background III-2-10
(2) Description III-2-10
(3) Variation of K with median grain size III-2-13
(4) Variation of K with surf similarity III-2-14
b. Longshore current method III-2-15
c. Using hindcast wave data III-2-21
(1) Wave transformation procedure III-2-21
(2) Wave conditions III-2-22
d. Deviation from potential longshore sediment transport rates III-2-26
(1) Temporal variations and persistence III-2-26
(2) Wave data accuracy III-2-31
(3) Sand supply availability III-2-32
e. Littoral drift roses III-2-33
f. Cross-shore distribution of longshore sediment transport III-2-36
g. Application of longshore sediment transport calculations III-2-43
(1) Littoral budgets III-2-43
(2) Variations in longshore sediment transport along the coast III-2-48
h. Three-dimensionality of shoreline features III-2-49
i. Empirical shoreline models III-2-54
j. Analytical longshore sand transport shoreline change models III-2-56

III-2-4. Numerical Longshore Sand Transport Beach Change Models III-2-78
a. Types of longshore transport models III-2-78
(1) Fully three-dimensional models III-2-78
(2) Schematic three-dimensional models III-2-78
(3) One-line (two-dimensional) models III-2-79
b. Shoreline Change Model GENESIS III-2-80
(1) Overview III-2-80
(2) Input data requirements and model output III-2-81
(3) Capabilities and limitations III-2-81
(4) Example application - Bolsa Chica, California III-2-82

III-2-5. References III-2-90

III-2-6. Definition of Symbols III-2-110

III-2-7. Acknowledgments III-2-111

List of Tables

Page

Table III-2-1
Longshore Transport Rates from U.S. Coasts (SPM 1984) III-2-9

Table III-2-2
Occurrence of Wave Height and Period for Direction Band 112.5° - 157.49°
RAL2 Station 72 . . . . . III-2-22

Table III-2-3
List of Authors Postulating Theories for Cusp Development III-2-51

List of Figures

Page

Figure III-2-1. Impoundment of longshore sediment transport at Indian River Inlet, Delaware III-2-2

Figure III-2-2. Cross-shore distribution of the longshore sand transport rate measured with traps at Duck, North Carolina (Kraus, Gingerich, and Rosati 1989) III-2-5

Figure III-2-3. Estimated annual net longshore transport rates and directions along the east coast of the United States based on data from Johnson (1956, 1957) and Komar (1976) III-2-8

Figure III-2-4. Field data relating I_ℓ and P_ℓ III-2-12

Figure III-2-5. Measured and predicted K coefficients using Bailard's (1984) equation III-2-14

Figure III-2-6. Coefficient K versus median grain size D_{50} (del Valle, Medina, and Losada 1993) III-2-15

Figure III-2-7. Longshore transport definitions III-2-27

Figure III-2-8. Time plot of annual longshore energy flux factor at three east-coast sites (after Douglass (1985)) III-2-28

Figure III-2-9. Time plot of monthly longshore energy flux factor time series for 1956-1975 at three east-coast sites (after Douglass (1985)) III-2-29

Figure III-2-10. Probability plot for monthly average P_{ls} series (Walton and Douglass 1985) III-2-30

Figure III-2-11. Probability plot for weekly average P_{ls} series (Walton and Douglass 1985) III-2-30

Figure III-2-12. Autocorrelation of monthly P_{ls} series (Walton and Douglass 1985) III-2-31

Figure III-2-13. Autocorrelation of weekly average P_{ls} series (Walton and Douglass 1985) III-2-32

Figure III-2-14. Azimuth of normal to shoreline at Ponte Vedra Beach, Florida (Walton 1972) III-2-34

Figure III-2-15. Net and total littoral drift at Ponte Vedra Beach, Florida (Walton 1972) III-2-35

Figure III-2-16. Ideal case of an unstable null point (Walton 1972) III-2-36

Figure III-2-17. Instability-formed capes in Santa Rosa Sound (Walton 1972) III-2-37

Figure III-2-18. Ideal case of a stable null point (Walton 1972) III-2-38

Figure III-2-19. Distribution of tracer density across the surf zone, 20 October 1961 Goleta Point, California, experiment (Ingle 1966) III-2-39

Figure III-2-20. Distribution of mean sediment concentration at 10 cm above the bed, relative to wave breakpoint (Kana 1978) III-2-40

Figure III-2-21. Cross-shore distribution of longshore sediment transport as measured by Bodge and Dean (Bodge 1986, Bodge and Dean 1987a, 1987b) at Duck, North Carolina, and in the laboratory III-2-41

Figure III-2-22. Example III-2-7, predicted cross-shore distribution of longshore sand transport, wave height, and longshore current speed III-2-45

Figure III-2-23. Beach cusps on a sandy beach in Mexico (photograph by Paul Komar) III-2-50

Figure III-2-24. Shoreline fluctuations in plan view at Tokai Beach, Japan III-2-51

Figure III-2-25. Rhythmic shoreline features associated with the presence of crescentic bars welded to the shoreline III-2-52

Figure III-2-26. Cusp rhythmic features in conjunction with rip currents under wave action approaching shoreline obliquely (Sonu 1973) III-2-52

Figure III-2-27. Spiral bay geometry: (a) definition sketch, and (b) coefficients describing parabolic shoreline shape (Silvester and Hsu 1993) III-2-55

Figure III-2-28. Elemental volume on equilibrium beach profile III-2-56

Figure III-2-29. Definition of local breaker angle III-2-57

Figure III-2-30. Structure placed perpendicular to shore III-2-60

Figure III-2-31. Nondimensionalized solution graphs (at different scales) for the condition of no sand transport at the structure location III-2-61

Figure III-2-32. Error function III-2-62

Figure III-2-33. Complementary error function III-2-62

Figure III-2-34. Nondimensional solution curve for plan view of sediment accumulation at a coastal structure after natural bypassing initiated III-2-64

Figure III-2-35. Rectangular beach fill (t=0) III-2-67

Figure III-2-36. Nondimensional solution curves for rectangular initial plan view fill area III-2-67

Figure III-2-37. Proportion of fill $p(t)$ remaining within limits of rectangular plan view fill area III-2-68

Figure III-2-38. Triangular beach fill (t=0) III-2-69

Figure III-2-39. Nondimensional solution curves for triangular initial plan view fill area III-2-71

Figure III-2-40. Long fill project with a gap (t=0) III-2-71

Figure III-2-41. Nondimensional solution curve for long fill with gap in plan view fill area III-2-72

Figure III-2-42. Semi-infinite beach fill (t=0) III-2-72

Figure III-2-43. Nondimensional solution curve for semi-infinite plan view fill area III-2-73

Figure III-2-44. Beach fill placed with groins (t=0) III-2-74

Figure III-2-45. Nondimensional solution curve for plan view of rectangular fill area between coastal structures (w/l = 0.25; tan α_b = 0.1) III-2-74

Figure III-2-46. Width of maintained beach ($x < 0$) as a function of time III-2-75

Figure III-2-47. Bolsa Chica, California, study area (Gravens 1990a) III-2-83

Figure III-2-48. Wave transformation hindcast to RCPWAVE grid (Gravens 1990a) III-2-84

Figure III-2-49. Total littoral drift rose, Anaheim to Santa Ana River (Gravens 1990a) III-2-85

Figure III-2-50. Model calibration results, Bolsa Chica (Gravens 1990a) III-2-86

Figure III-2-51. Model verification results, Bolsa Chica (Gravens 1990a) III-2-87

Figure III-2-52. Sand management alternative with feeder beach (Gravens 1990a) III-2-89

Figure III-2-53. Predicted shoreline change from 1983 shoreline position with sand management alternative and feeder beach (Gravens 1990a) III-2-90

Chapter III-2
Longshore Sediment Transport

III-2-1. Introduction

a. Overview.

(1) The breaking waves and surf in the nearshore combine with various horizontal and vertical patterns of nearshore currents to transport beach sediments. Sometimes this transport results only in a local rearrangement of sand into bars and troughs, or into a series of rhythmic embayments cut into the beach. At other times there are extensive longshore displacements of sediments, possibly moving hundreds of thousands of cubic meters of sand along the coast each year. The objective of this chapter is to examine techniques that have been developed to evaluate the longshore sediment transport rate, which is defined to occur primarily within the surf zone, directed parallel to the coast. This transport is among the most important nearshore processes that control the beach morphology, and determines in large part whether shores erode, accrete, or remain stable. An understanding of longshore sediment transport is essential to sound coastal engineering design practice.

(2) Currents associated with nearshore cell circulation generally act to produce only a local rearrangement of beach sediments. The rip currents of the circulation can be important in the cross-shore transport of sand, but there is minimal net displacement of beach sediments along the coast. More important to the longshore movement of sediments are waves breaking obliquely to the coast and the longshore currents they generate, which may flow along an extended length of beach (Part II-4). The resulting movement of beach sediment along the coast is referred to as littoral transport or longshore sediment transport, whereas the actual volumes of sand involved in the transport are termed the littoral drift. This longshore movement of beach sediments is of particular importance in that the transport can either be interrupted by the construction of jetties and breakwaters (structures which block all or a portion of the longshore sediment transport), or can be captured by inlets and submarine canyons. In the case of a jetty, the result is a buildup of the beach along the updrift side of the structure and an erosion of the beach downdrift of the structure. The impacts pose problems to the adjacent beach communities, as well as threaten the usefulness of the adjacent navigable waterways (channels, harbors, etc.) (Figure III-2-1).

(3) Littoral transport can also result from the currents generated by alongshore gradients in breaking wave height, commonly called diffraction currents (Part II-4). This transport is manifest as a movement of beach sediments toward the structures which create these diffraction currents (such as jetties, long groins, and headlands). The result is transport in the “upwave” direction on the downdrift side of the structure. This, in turn, can create a buildup of sediment on the immediate, downdrift side of the structure or contribute to the creation of a crenulate-shaped shoreline on the downdrift side of a headland.

b. Scope of chapter. This chapter defines terms associated with the longshore transport of littoral material, presents relationships for the longshore sediment transport rate as a function of breaking waves and longshore currents, discusses the dependence of longshore transport relationships on sediment grain size, presents a method for calculating the cross-shore distribution of longshore sand transport, and overviews analytical and numerical models for shoreline changes which include longshore sediment transport relationships.

III-2-2. Longshore Sediment Transport Processes

a. Definitions. On most coasts, waves reach the beach from different quadrants, producing day-to-day and seasonal reversals in transport direction. At a particular beach site, transport may be to the right (looking

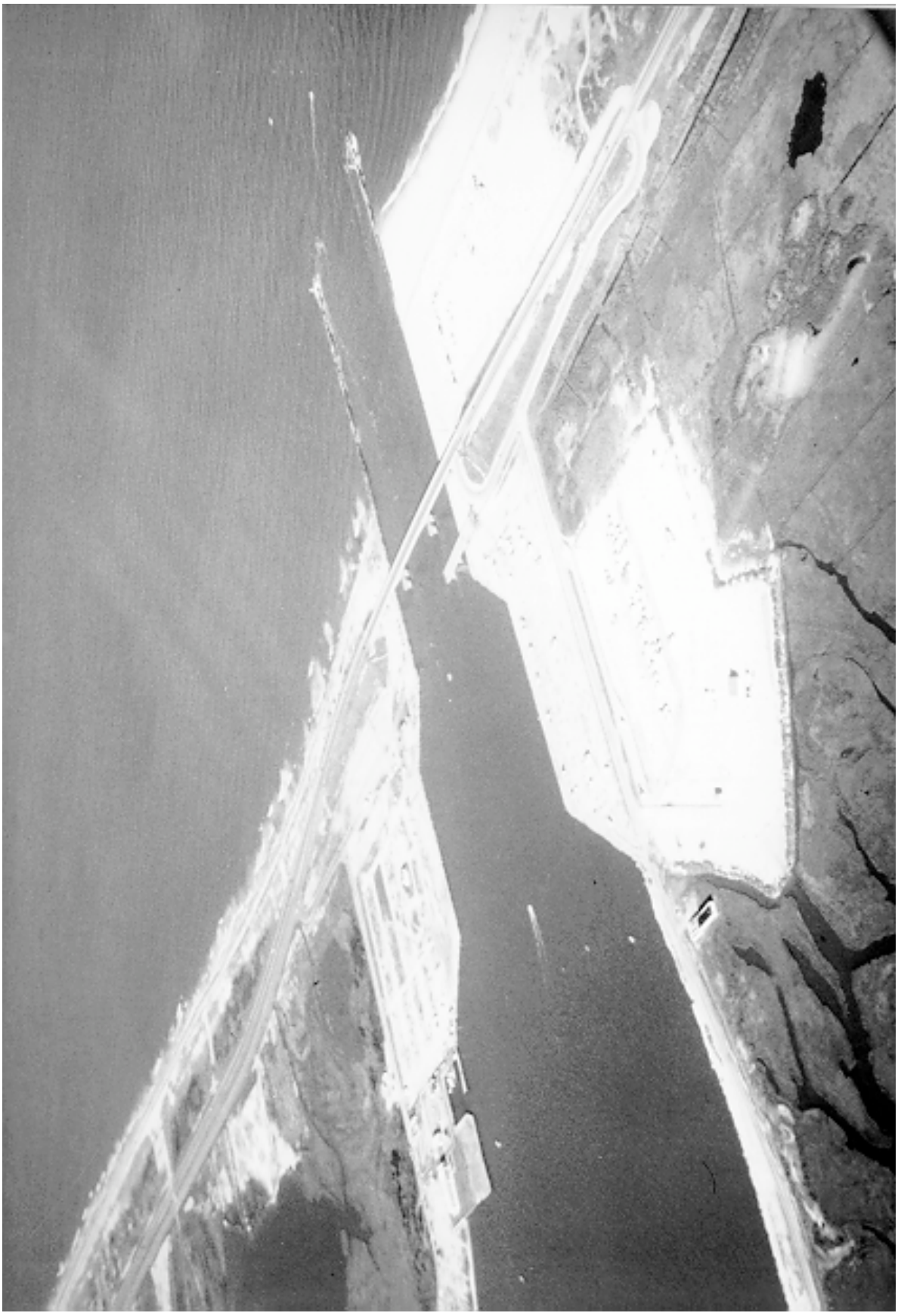

Figure III-2-1. Impoundment of longshore sediment transport at Indian River Inlet, Delaware

seaward) during part of the year and to the left during the remainder of the year. If the left and right transports are denoted respectively $Q_{\ell L}$ and $Q_{\ell R}$, with $Q_{\ell R}$ being assigned a positive quantity and $Q_{\ell L}$ assigned a negative value for transport direction clarification purposes, then the net annual transport is defined as $Q_{\ell NET} = Q_{\ell R} + Q_{\ell L}$. The net longshore sediment transport rate is therefore directed right and positive if $Q_{\ell R} > Q_{\ell L}$, and to the left and negative if $Q_{\ell R} < /Q_{\ell L}/$. The net annual transport can range from essentially zero to a large magnitude, estimated at a million cubic meters of sand per year for some coastal sites. The gross annual longshore transport is defined as $Q_{\ell GROSS} = Q_{\ell R} + / Q_{\ell L} /$, the sum of the temporal magnitudes of littoral transport irrespective of direction. It is possible to have a very large gross longshore transport at a beach site while the net transport is effectively zero. These two contrasting assessments of longshore sediment movements have different engineering applications. For example, the gross longshore transport may be utilized in predicting shoaling rates in navigation channels and uncontrolled inlets, whereas the net longshore transport more often relates to the deposition versus erosion rates of beaches on opposite sides of jetties or breakwaters. (It is noted, however, that the latter may capture the gross transport rate in some cases.)

b. Modes of sediment transport.

(1) A distinction is made between two modes of sediment transport: suspended sediment transport, in which sediment is carried above the bottom by the turbulent eddies of the water, and bed-load sediment transport, in which the grains remain close to the bed and move by rolling and saltating. Although this distinction may be made conceptually, it is difficult to separately measure these two modes of transport on prototype beaches. Considerable uncertainty remains and differences of opinion exist on their relative contributions to the total transport rate.

(2) Because it is more readily measured than the bed-load transport, suspended load transport has been the subject of considerable study. It has been demonstrated that suspension concentrations decrease with height above the bottom (Kraus, Gingerich, and Rosati 1988, 1989). The highest concentrations typically are found in the breaker and swash zones, with lower concentrations at midsurf positions. On reflective beaches, at which a portion of the wave energy is reflected back to sea, individual suspension events are correlated with the incident breaking wave period. In contrast, on dissipative beaches, at which effectively all of the arriving wave energy is dissipated in the nearshore, long-period water motions have been found to account for significant sediment suspension. For dissipative beaches, the suspension concentrations due to long-period (low-frequency) waves have been measured as 3 to 4 times larger than those associated with the short-period high-frequency incident waves (Beach and Sternberg 1987).

c. Field identification of longshore sediment transport. Emphasis is placed herein upon field, or prototype, measurement and identification of littoral transport. Laboratory measurement of longshore sediment transport is generally thought to underestimate prototype transport rates, primarily because of scale effects. Laboratory measurements are also complicated by the need to establish a continuous updrift sediment supply in the model.

(1) Experimental measurement.

(a) Longshore sediment transport relationships are typically based on data measured by surveying impoundments of littoral drift at a jetty, breakwater, spit, or deposition basin; bypassing impounded material (e.g., at an inlet); or measuring short-term sand tracer transport rates. Other techniques focus upon measurement of only the suspended load transport. Longshore sediment transport estimates using impoundment are believed to come closest to yielding total quantities (i.e., the bed load plus suspended load transport), and typically represent longer-term measures (i.e., weeks to years). It is these longer-term, total transport quantities that are of central importance to practical coastal engineering design. Impoundment techniques are discussed below in Part III-2-2.c.(2).

(b) Measurement of sand tracer transport rates involves tagging the natural beach sediment with a coating of fluorescent dye or low-level radioactivity. Tracers are injected into the surf zone, and the beach material is sampled on a grid to determine the subsequent tracer distribution. The longshore displacement of the center of mass of the tracer on the beach between injection and sampling provides a measure of the mean transport distance. The sand advection velocity is obtained by dividing this distance by the elapsed time. The time between tracer injection and sampling is usually an hour to a few hours, so the measurement is basically the instantaneous longshore sand transport under a fixed set of wave conditions. The technique, therefore, provides measurements that are particularly suitable for correlations with causative waves and longshore currents, as in time-dependent numerical models of longshore transport rates and beach change, but is not particularly useful in determining long-term net transport rates or directions. Identification of the appropriate sediment mixing depth also limits the technique's quantitative accuracy. Numerous studies have used sand tracers to determine sand transport rates; examples include Komar and Inman (1970), Knoth and Nummedal (1977), Duane and James (1980), Inman et al. (1980), Kraus et al. (1982), White (1987), and many others. Tracer techniques can also be used in conjunction with geologically distinct materials, such as naturally occurring mineral sediments. These methods, which generally involve larger quantities of material and larger scales of measurement, are potentially more useful for determining longer-term rates and directions and are discussed below.

(c) Measurements of suspended load transport have been the focus of numerous studies. One approach has been to pump water containing suspended sand from the surf zone, a technique which has the advantage that large quantities can be processed, leading to some confidence that the samples are representative of sediment concentrations found in the surf (Watts 1953b; Fairchild 1972, 1977; Coakley and Skafel 1982). These measurements, combined with simultaneous measurements of alongshore current velocity, yield estimates of the longshore sediment transport suspended load. The disadvantages of the approach are that one cannot investigate time variations in sediment concentrations at different phases of wave motions, and the sampling has often been undertaken from piers which may disturb the water and sediment motion. Recent studies of suspended load transport have employed optical and acoustic techniques (Brenninkmeyer 1976; Thornton and Morris 1977; Katoh, Tanaka, and Irie 1984; Downing 1984; Sternberg, Shi, and Downing 1984; Beach and Sternberg 1987; Hanes et al. 1988). These approaches yield continuous measurements of the instantaneous suspended sediment concentrations. Arrays of instruments can be employed to document variations across the surf zone and vertically through the water column.

(d) Another method for measuring suspension concentrations is with traps, usually consisting of a vertical array of sample bins which collect sediment but allow water to pass, and so can be used to examine the vertical distribution of suspended sediments and can be positioned at any location across the surf zone (e.g., Hom-ma, Horikawa, and Kajima 1965; Kana 1977, 1978; Inman et al. 1980; Kraus, Gingerich, and Rosati 1988). Figure III-2-2 shows vertical distributions of the longshore sediment flux (transport rate per unit area) through the water column obtained in a 5-min sampling interval by traps arranged across the surf zone at Duck, North Carolina (Kraus, Gingerich, and Rosati 1989). The steep decrease in transport with elevation above the bed is apparent; such considerations are important in groin and weir design. The sharp decrease in transport at the trap located seaward of the breaker line indicates that the main portion of longshore sediment transport takes place in the surf and swash zones.

(e) The only method presently suitable for distinct measurement of bed load transport is bed-load traps. These are bins which are open-ended or dug into the seabed into which the bed-load transport is to settle. There are questions as to sampling efficiency when used in the nearshore because of the potential for scour (Thornton 1972; Walton, Thomas, and Dickey 1985; Rosati and Kraus 1989).

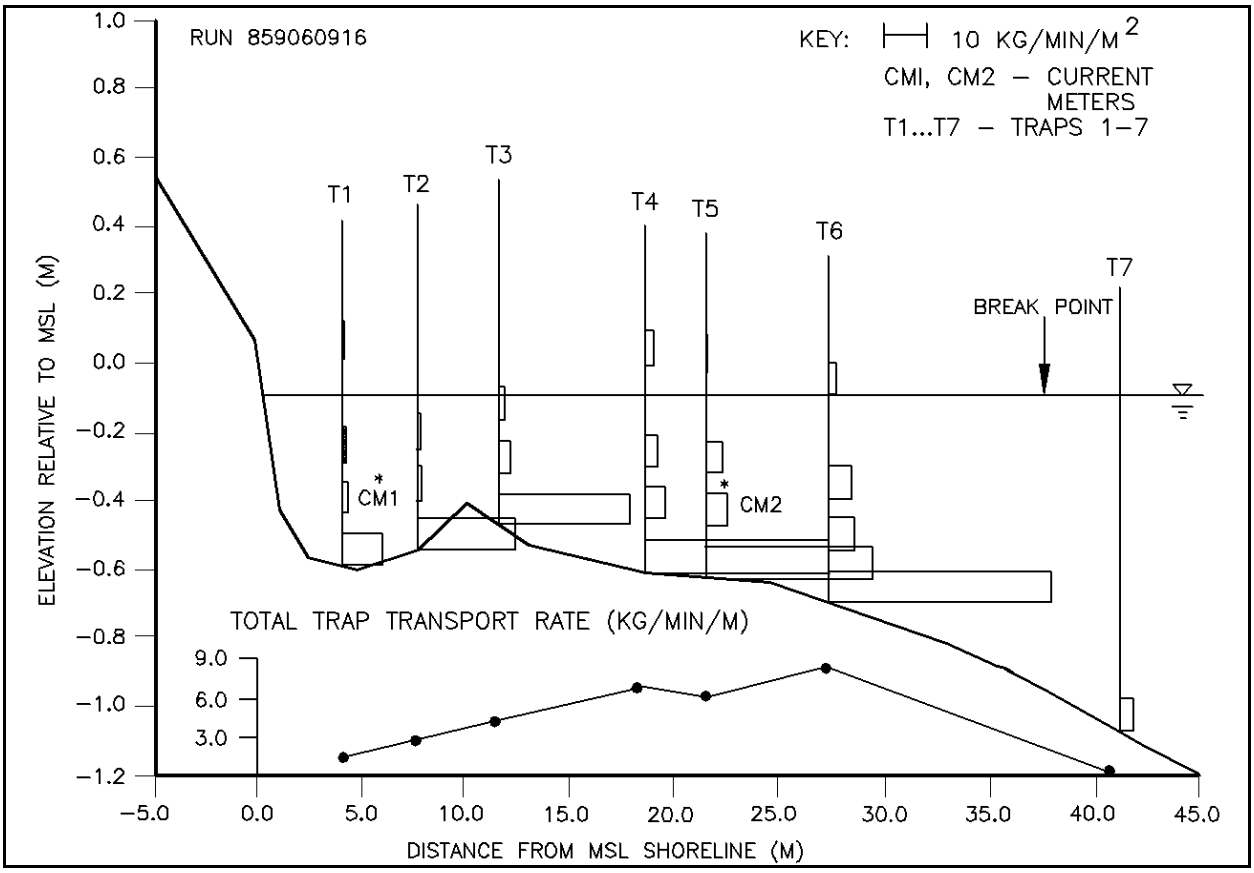

Figure III-2-2. Cross-shore distribution of the longshore sand transport rate measured with traps at Duck, North Carolina (Kraus, Gingerich, and Rosati 1989)

(2) Qualitative indicators of longshore transport magnitude and direction.

(a) The ability to assess directions of longshore sediment transport is central to successful studies of coastal erosion and the design of harbor structures and shore protection projects. It is equally important to evaluate quantities of that transport as a function of wave and current conditions.

(b) Multiple lines of evidence have been used to discern directions of longshore sediment transport. Most of these are related to the net transport; i.e., the long-term resultant of many individual transport events. Blockage by major structures such as jetties can provide the clearest indication of the long-term net transport direction (see Figure III-2-1). Sand entrapment by groins is similar, but generally involves smaller volumes and responds to the shorter-term reversals in transport directions; therefore, groins do not always provide a definitive indication of the net annual transport direction. Other geomorphologic indicators of transport direction include the deflection of streams or tidal inlets by the longshore sand movements, shoreline displacements at headlands similar to that at jetties, the longshore growth of sand spits and barrier islands, and the pattern of upland depositional features such as beach ridges. Grain sizes and composition of the beach sediments have also been used to determine transport direction as well as sources of the sediments. It is often believed that a longshore decrease in the grain size of beach sediment provides an indication of the direction of the net transport. This is sometimes the case, but grain size changes can also be the product of alongcoast variations in wave energy levels and/or sediment sources and sinks that have no relation to sediment transport directions.

(c) Identification of unique minerals within the sand has also been used to deduce transport paths. By using the heavy mineral augite as a tracer of longshore sand movements, Trask (1952, 1955) demonstrated that the sand filling the harbor at Santa Barbara, California, originates more than 160 km up the coast. The augite was derived from volcanic rocks in the Morro Bay area north of Santa Barbara. Likewise, Bowen and Inman (1966) estimated the directions and magnitudes of the net transport along the California coast by studying the progressive dilution of beach sand augite by addition of sand from other sources. In other examples, Meisburger (1989) utilized oolitic carbonate as a natural mineral tracer to deduce transport paths along Florida's east coast. Johnson (1992) noted the net transport paths along parts of the Lake Michigan coastline by examining the movement of gravel placed as beach restoration.

(d) Many of the geomorphic and sedimentological indicators of longshore sediment transport directions are not absolute, and too strong a reliance upon them can lead to misinterpretations. It is best to examine all potential evidence that might relate to transport direction, and consider the relative reliabilities of the indicators.

(3) Quantitative indicators of longshore transport magnitude.

(a) Some of the qualitative indicators of longshore transport discussed above can also be used to estimate the quantities involved in the process. Repeated surveys over a number of years and analyses of aerial photographs of the longshore growth of sand spits have been used to establish approximate rates of sediment transport. For the estimates to be reasonable, it is typically necessary that such surveys span a decade or longer, so the results represent a long-term net sediment transport rate.

(b) The blockage of longshore sediment transport by jetties and breakwaters and the resulting growth and erosion patterns of the adjacent beaches have yielded reasonable evaluations of the net (and sometimes gross) transport rates at many coastal sites. Sand bypassing plants have been constructed at some jetties and breakwaters as a practical measure to reduce the accretion/erosion patterns adjacent to the structures. The first measurements obtained relating sand transport rates to causative wave conditions were collected by Watts (1953a) at Lake Worth Inlet, Florida, using measured quantities of sand pumped past the jetties. The best correlation was obtained using month-long net sand volumes. A number of subsequent studies have similarly employed sand blockage by jetties and breakwaters to obtain data relating transport rates to wave conditions. Caldwell (1956) estimated the longshore sand transport from erosion rates of the beach downdrift of the jetties at Anaheim Bay, California. Bruno and Gable (1976); Bruno, Dean, and Gable (1980); Bruno et al. (1981); and Walton and Bruno (1989) measured transport rates by repeatedly surveying the accumulating blocked sand at Channel Islands Harbor, California; Dean et al. (1982) measured sand accumulations in the spit growing across the breakwater opening at Santa Barbara, California; and Dean et al. (1987) collected data from the weir jetty at Rudee Inlet, Virginia. All of these studies yielded measurements of longshore sediment transport rates that are used in correlations with wave energy flux estimates. Errors are introduced with the use of jetties and breakwaters to measure sediment transport rates, the foremost being the local effects of the structure on waves and currents, and the long-term nature of the determinations. In some cases it takes a month or longer of sand accumulation to have a volume that is large enough to be outside the range of possible survey error, during which time the waves and currents are continuously changing. Therefore, a correlation between a given wave condition and the resulting sediment transport rate due solely to that particular wave condition cannot be obtained; rather, wave parameters occurring during the interval of interest are integrated and then correlated with the total accumulated volume. Nevertheless, rates determined by impoundment and erosion are very valuable as they are closely related to gross quantities involved in the design of projects, such as the amount of sediment required to be bypassed at an inlet.

(c) As discussed above, sand tracer has been used to make short-term estimates of longshore sand transport. Other techniques that have been used to measure sediment movements on beaches include various sand traps, pumps, and optical devices. However, such sampling schemes are also short-term measures and may be related to specific modes of transport, either the bed load or suspended load, rather than yielding total quantities of the long-term littoral sediment transport. Generally, it is the latter quantity which is of importance to engineering design.

(4) Longshore sediment transport estimation in the United States.

(a) Early attempts to estimate the direction and magnitude of net longshore sediment transport along the U.S. coastline centered chiefly upon examination of sand impoundment and bypassing volumes at jetties and breakwaters. Johnson (1956, 1957) compiled data of this type for many shorelines and found net transport rates ranging up to approximately 1 million m^3 (MCM) of sand per year in some locations. Based on Johnson's work, estimated patterns of littoral drift for a portion of the east coast of the United States are shown in Figure III-2-3. Table III-2-1 lists representative net longshore transport rates for selected U.S. coasts (SPM 1984). Transport rate magnitudes are clearly related to the general wave climate as energetic (west coast), intermediate (east coast and parts of the Gulf of Mexico shoreline), and low (Great Lakes and parts of the Gulf of Mexico shoreline).

(b) Since these early estimates of the transport rates, numerous investigations have yielded refined values at specific sites along the U.S. coastlines. These values are not generally archived in a single source, and must therefore be found through a literature search of various site-specific reports and articles. Estimates of both the net and gross transport rates along any particular portion of the coastline may also be developed using hindcast wave data (see Part III-2-2.d.(3) of this chapter below).

III-2-3. Predicting Potential Longshore Sediment Transport

In engineering applications, the longshore sediment transport rate is expressed as the volume transport rate Q_ℓ having units such as cubic meters per day or cubic yards per year. This is the total volume as would be measured by survey of an impoundment at a jetty and includes about 40 percent void space between the particles as well as the 60-percent solid grains. Another representation of the longshore sediment transport rate is an immersed weight transport rate I_ℓ related to the volume transport rate by

$$I_\ell = (\rho_s - \rho)\, g\, (1 - n)\, Q_\ell \tag{III-2-1a}$$

or

$$Q_\ell = \frac{I_\ell}{(\rho_s - \rho)\, g\, (1 - n)} \tag{III-2-1b}$$

where

ρ_s = mass density of the sediment grains

ρ = mass density of water

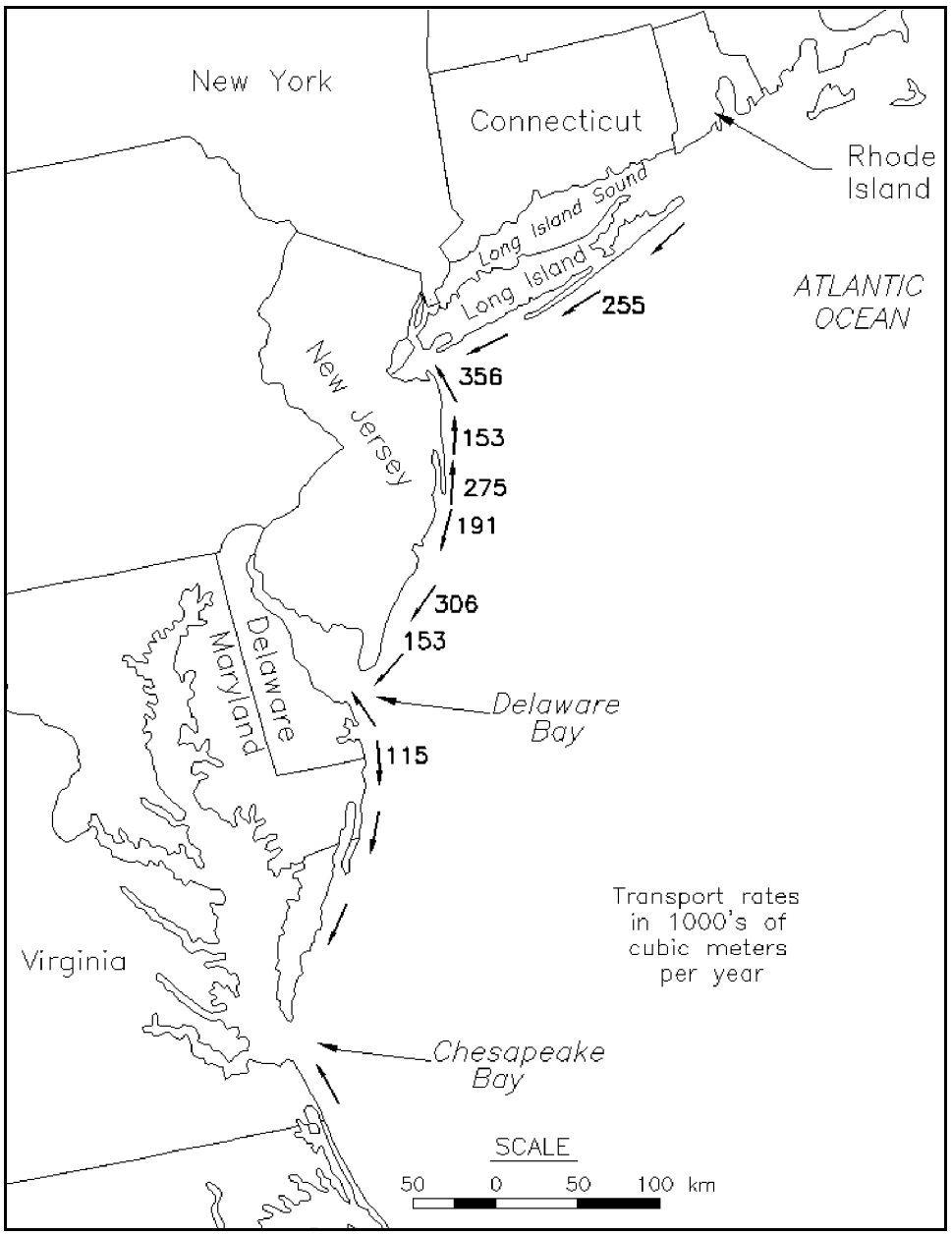

Figure III-2-3. Estimated annual net longshore transport rates and directions along the east coast of the United States based on data from Johnson (1956, 1957) and Komar (1976)

Table III-2-1
Longshore Transport Rates from U.S. Coasts (SPM 1984)[1]

Location	Predominant Direction of Transport	Longshore[2] Transport, cu m/yr	Date of Record	Reference
		Atlantic Coast		
Suffolk County, NY	W	153,000	1946-55	New York District (1955)
Sandy Hook, NJ	N	377,000	1885-1933	New York District (1954)
Sandy Hook, NJ	N	333,000	1933-51	New York District (1954)
Asbury Park, NJ	N	153,000	1922-25	New York District (1954)
Shark River, NJ	N	229,000	1947-53	New York District (1954)
Manasquan, NJ	N	275,000	1930-31	New York District (1954)
Barnegat Inlet, NJ	S	191,000	1939-41	New York District (1954)
Absecon Inlet, NJ	S	306,000	1935-46	New York District (1954)
Ocean City, NJ	S	306,000	1935-46	U.S. Congress (1953a)
Cold Spring Inlet, NJ	S	153,000	---	U.S. Congress (1953b)
Ocean City, MD	S	115,000	1934-36	Baltimore District (1948)
Atlantic Beach, NC	E	22,500	1850-1908	U.S. Congress (1948)
Hillsboro Inlet, FL	S	57,000	1850-1908	U.S. Army (1955b)
Palm Beach, FL	S	115,000 to 175,000	1925-30	BEB (1947)
		Gulf of Mexico		
Pinellas County, FL	S	38,000	1922-50	U.S. Congress (1954a)
Perdido Pass, AL	W	153,000	1934-53	Mobile District (1954)
		Pacific Coast		
Santa Barbara, CA	E	214,000	1932-51	Johnson (1953)
Oxnard Plain Shore, CA	S	765,000	1938-48	U.S. Congress (1953c)
Port Hueneme, CA	S	382,000	---	U.S. Congress (1954b)
Santa Monica, CA	S	206,000	1936-40	U.S. Army (1948b)
El Segundo, CA	S	124,000	1936-40	U.S. Army (1948b)
Redondo Beach, CA	S	23,000	---	U.S. Army (1948b)
Anaheim Bay, CA	E	115,000	1937-48	U.S. Congress (1954c)
Camp Pendleton, CA	S	76,000	1950-52	Los Angeles District (1953)
		Great Lakes		
Milwaukee County, WI	S	6,000	1894-1912	U.S. Congress (1946)
Racine County, WI	S	31,000	1912-49	U.S. Congress (1953d)
Kenosha, WI	S	11,000	1872-1909	U.S. Army (1953b)
IL State Line to Waukegan	S	69,000	---	U.S. Congress (1953e)
Waukegan to Evanston, IL	S	44,000	---	U.S. Congress (1953e)
South of Evanston, IL	S	31,000	---	U.S. Congress (1953e)
		Hawaii		
Waikiki Beach	--	8,000	---	U.S. Congress (1953f)

[1] Method of measurement is by accretion except for Absecon Inlet and Ocean City, NJ, and Anaheim Bay, CA, which were measured by erosion, and Waikiki Beach, HI, which was measured according to suspended load samples.
[2] Transport rates are estimated net transport rates Q_N. In some cases, these approximate the gross transport rates Q_g.

g = acceleration due to gravity

n = in-place sediment porosity ($n \approx 0.4$)

The parameter n is a pore-space factor such that $(1 - n)\, Q_\ell$ is the volume transport of solids alone. One advantage of using I_ℓ is that this immersed weight transport rate incorporates effects of the density of the sediment grains. The factor $(\rho_s - \rho)$ accounts for the buoyancy of the particles in water. The term "potential" sediment transport rate is used, because calculations of the quantity imply that sediment is available in sufficient quantity for transport, and that obstructions (such as groins, jetties, breakwaters, submarine canyons, etc.) do not slow or stop transport of sediment alongshore.

a. Energy flux method.

(1) Historical background. An extensive discussion of the evolution of energy-based longshore transport formulae is presented by Sayao (1982), in his dissertation. The following is a summary of Sayao's discussion, focussing on evolution of the so-called "CERC" formula.

Munch-Peterson, a Danish engineer, first related the rate of littoral sand transport to deepwater wave energy in conjunction with harbor studies on the Danish coast (Munch-Peterson 1938). Because of a lack of wave data, Munch-Peterson used wind data in practical applications, which gave preliminary estimations of the littoral drift direction. In the United States, use of a formula to predict longshore sediment transport based on wave energy was suggested by the Scripps Institute of Oceanography (1947), and applied by the U.S. Army Corps of Engineers, Los Angeles District to the California coast (Eaton 1950). Watts (1953a) and Caldwell (1956) made the earliest documented measurements of longshore sediment transport (at South Lake Worth, Florida, and Anaheim Bay, California, respectively) and related transport rates to wave energy, resulting in modifications to the existing formulae. Savage (1962) summarized the available data from field and laboratory studies and developed an equation which was later adopted by the U.S. Army Corps of Engineers in a 1966 coastal design manual (U.S. Army Corps of Engineers 1966), which became known as the "CERC formula." Inman and Bagnold (1963), based on Bagnold's earlier work on wind-blown sand transport and on sand transport in rivers, suggested use of an immersed weight longshore transport rate, rather than a volumetric rate. An immersed weight sediment transport equation was calibrated by Komar and Inman (1970) based on the available field data including their tracer-based measurements at Silver Strand, California, and El Moreno, Mexico. Based on Komar and Inman's (1970) transport relationship and other available field data, the CERC formula for littoral sand transport was updated from its 1966 version, and has been presented as such in the previous editions of the *Shore Protection Manual* (1977, 1984).

(2) Description.

(a) The potential longshore sediment transport rate, dependent on an available quantity of littoral material, is most commonly correlated with the so-called longshore component of wave energy flux or power,

$$P_\ell = (EC_g)_b \sin\alpha_b \cos\alpha_b \tag{III-2-2}$$

where E_b is the wave energy evaluated at the breaker line,

$$E_b = \frac{\rho g H_b^2}{8} \tag{III-2-3}$$

and C_{gb} is the wave group speed at the breaker line,

$$C_{gb} = \sqrt{g d_b} = \left(g \frac{H_b}{\kappa} \right)^{\frac{1}{2}} \tag{III-2-4}$$

where κ is the breaker index H_b / d_b . The term $(EC_g)_b$ is the "wave energy flux" evaluated at the breaker zone, and α_b is the wave breaker angle relative to the shoreline. The immersed weight transport rate I_ℓ has the same units as P_ℓ (i.e., N/sec or lbf/sec), so that the relationship

$$I_\ell = KP_\ell \tag{III-2-5}$$

is homogeneous, that is, the empirical proportionality coefficient K is dimensionless. This is another advantage in using I_ℓ rather than the Q_ℓ volume transport rate. Equation 2-5 is commonly referred to as the "CERC formula."

(b) Equation 2-5 may be written

$$I_\ell = KP_\ell = K(EC_g)_b \sin\alpha_b \cos\alpha_b \tag{III-2-6a}$$

which, on assuming shallow water breaking, gives

$$I_\ell = K\left(\frac{\rho g H_b^2}{8}\right)\left(\frac{g H_b}{\kappa}\right)^{\frac{1}{2}} \sin\alpha_b \cos\alpha_b \tag{III-2-6b}$$

$$I_\ell = K\left(\frac{\rho g^{3/2}}{8\kappa^{1/2}}\right) H_b^{5/2} \sin\alpha_b \cos\alpha_b \tag{III-2-6c}$$

$$I_\ell = K\left(\frac{\rho g^{\frac{3}{2}}}{16\kappa^{\frac{1}{2}}}\right) H_b^{\frac{5}{2}} \sin(2\alpha_b) \tag{III-2-6d}$$

(c) By using Equation 2-1b, the relationships for I_ℓ can be converted to a volume transport rate:

$$Q_\ell = \frac{K}{(\rho_s - \rho) g (1 - n)} P_\ell \tag{III-2-7a}$$

$$Q_\ell = K\left(\frac{\rho\sqrt{g}}{16\,\kappa^{\frac{1}{2}}\,(\rho_s - \rho)\,(1 - n)}\right) H_b^{\frac{5}{2}} \sin(2\alpha_b) \tag{III-2-7b}$$

(d) Field data relating I_ℓ and P_ℓ are plotted in Figure III-2-4, for which the calculations of the wave power are based on the root-mean-square (rms) wave height at breaking $H_{b\,rms}$. Data presented in Figure III-2-4 include those measured by: (1) sand accumulation at jetties and breakwaters (South Lake Worth Inlet, Florida (Watts 1953a); Anaheim Bay (Caldwell 1956), Santa Barbara (Dean et al. 1987), and Channel Islands (Bruno et al. 1981, Walton and Bruno 1989), California; Rudee Inlet, Virginia (Dean et al. 1987); Cape Thompson, Alaska (Moore and Cole 1960); and Point Sapin, Canada (Kamphuis 1991)); (2) sand tracer at Silver Strand, California (Komar and Inman 1970); El Moreno, Mexico (Komar and Inman 1970); Torrey Pines, California (Inman et al. 1980); and Ajiguara, Japan (Kraus et al. 1982)); and (3) sediment traps at Kewaunee County, Wisconsin (Lee 1975); and Duck, North Carolina (Kana and Ward 1980)). Because of questions in methodologies and trapping efficiencies, probably the data sets most appropriate for engineering application are those based upon category 1 above, sand accumulation (impoundment) at jetties and breakwaters.

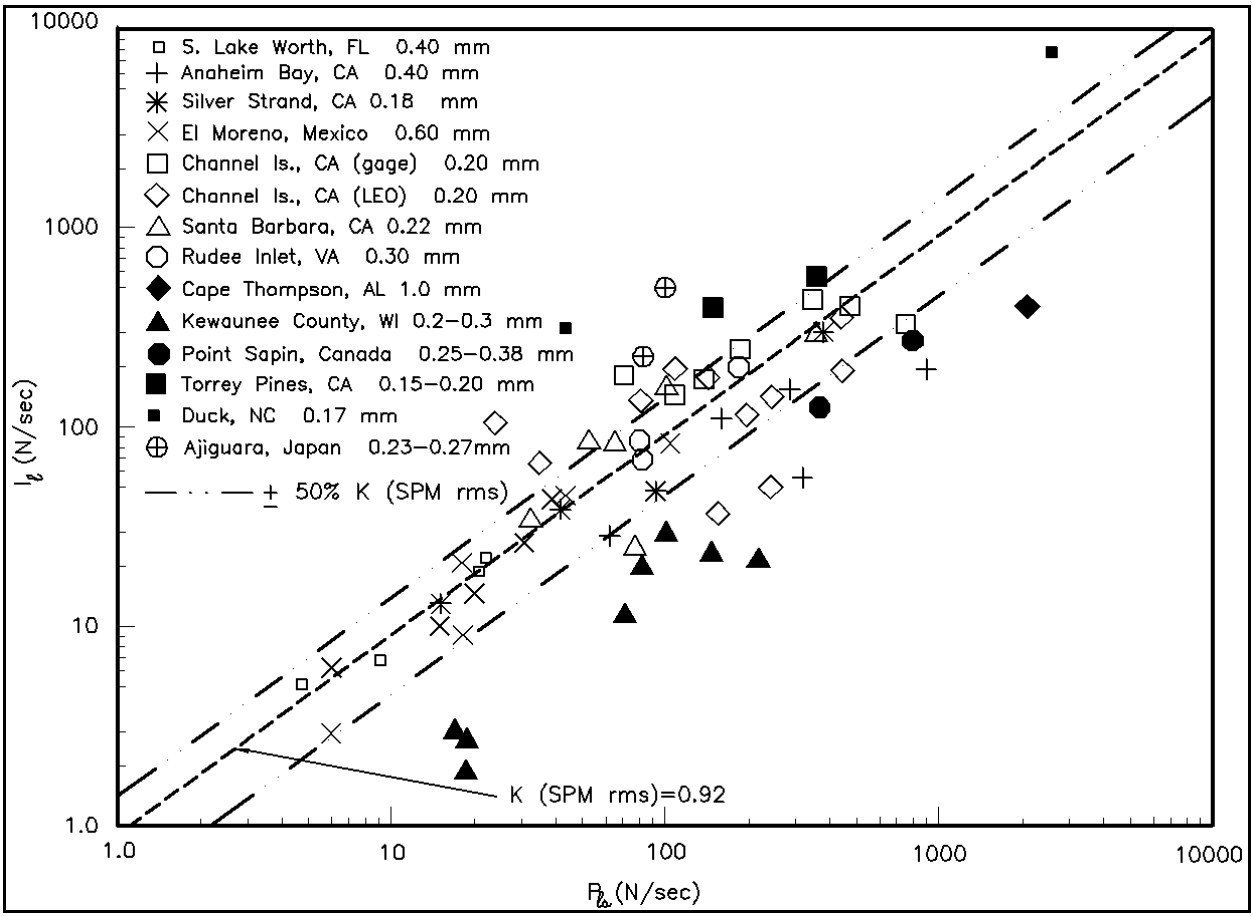

Figure III-2-4. Field data relating I_l and P_l

(e) The K coefficient defined here is based on utilizing the rms breaking wave height $H_{b\,rms}$. The *Shore Protection Manual* (1984) presented a dimensionless coefficient $K_{SPM\,sig}$ = (0.39) based on computations utilizing the significant wave height. The value of this SPM coefficient corresponding to the rms wave height $H_{b\,rms}$ is $K_{SPM\,rms}$ = 0.92, which is indicated in Figure III-2-4 with a dashed line for reference. Judgement is required in applying Equation 2-7. Although the data follow a definite trend, the scatter is obvious, even on the log-log plot. The dash-double-dot lines represent a ±50 percent interval around the SPM reference line ($K_{SPM\,rms}$ = 0.92).

(f) An early design value of the K coefficient was introduced for use with rms breaking wave height by Komar and Inman (1970); $K_{K\&I\,rms}$ = 0.77. This value is commonly seen in many longshore transport rate computations.

(g) Values of the other parameters for use in the sediment transport equations are: ρ_s = 2,650 kg/m^3 (5.14 slugs/ft^3) for quartz-density sand; ρ = 1,025 kg/m^3 (1.99 slug/ft^3) for 33 parts per thousand (ppt) salt water; and ρ = 1,000 kg/m^3 (1.94 slug/ft^3) for fresh water; g = 9.81 m/sec^2 (32.2 ft/sec^2); and n = 0.4. The breaker index (κ) is ≈0.78 for flat beaches and increases to more than 1.0 depending on beach slope (Weggel 1972).

(3) Variation of K with median grain size.

(a) Longshore sand transport data presented in Figure III-2-4 represent beaches with quartz-density grain sizes ranging from ~0.2 mm to 1.0 mm, and wave heights ranging from 0.5 to 2.0 m. Bailard (1981, 1984) developed an energy-based model, which presents K as a function of the breaker angle and the ratio of the orbital velocity magnitude and the sediment fall speed, also based on the rms wave height at breaking. Bailard calibrated the model using eight field and two laboratory data sets, and developed the following equation:

$$K = 0.05 + 2.6 \sin^2 (2\alpha_b) + 0.007 \frac{u_{mb}}{w_f} \tag{III-2-8}$$

where u_{mb} is the maximum oscillatory velocity magnitude, obtained from shallow-water wave theory as

$$u_{mb} = \frac{\kappa}{2} \sqrt{g d_b} \tag{III-2-9}$$

and w_f is the fall speed of the sediment, either calculated using the relationships described in Part III-1, or, if the spherical grain assumption cannot be applied to the material, measured experimentally. Bailard developed his relationship using the following data ranges: $2.5 \le w_f \le 20.5$ cm/sec; $0.2^o \le \alpha_b \le 15^o$; and $33 \le u_{mb} \le 283$ cm/sec. A comparison of observed and predicted K coefficients using Bailard's Equation 2-8 is presented in Figure III-2-5, using the data sets on which Bailard based his calibration. Because Bailard's relationship is based on a limited data set, predicted K coefficients may be highly variable. Bailard's relationship for K is similar to a relationship presented by Walton (1979) and Walton and Chiu (1979), which was compared to limited laboratory data.

(b) Others have proposed empirically based relationships for increasing K with decreasing grain size (or equivalently, fall speed) (Bruno, Dean, and Gable 1980; Dean et al. 1982; Kamphuis et al. 1986; Dean 1987). Komar (1988), after reexamining available field data, suggested that the previous relationships resulted from two data sets with K values based on erroneous or questionable field data. Revising these K values, Komar (1988) concluded that existing data suggests little dependence of the empirical K coefficient on sediment grain sizes, at least for the range of sediments in the data set. Data from shingle beaches, however, indicated a smaller K, but the data were too limited to establish a correlation. Komar stressed that K should depend on sediment grain size, and the absence of such a trend in his analysis must result from the imperfect quality of the data.

(c) Recently, del Valle, Medina, and Losada (1993) have presented an empirically based relationship for the K parameter, adding sediment transport data representing a range in median sediment grain sizes (0.40 mm to 1.5 mm) from the Adra River Delta, Spain to the available database as modified by Komar (1988). Del Valle, Medina, and Losada obtained wave parameters from buoy and visual observations, and sediment transport rates were evaluated from aerial photographs documenting a 30-year period of shoreline evolution for five locations along the delta. Results of their analysis reinforce a decreasing trend in the empirical coefficient K with sediment grain size. Their empirical fit based on the corrections to the database as suggested by Komar (1988) is shown in Figure III-2-6 and given in Equation III-2-10. The empirically based relationship is to be applied with rms breaking wave height,

$$K = 1.4 \, e^{(-2.5 \, D_{50})} \tag{III-2-10}$$

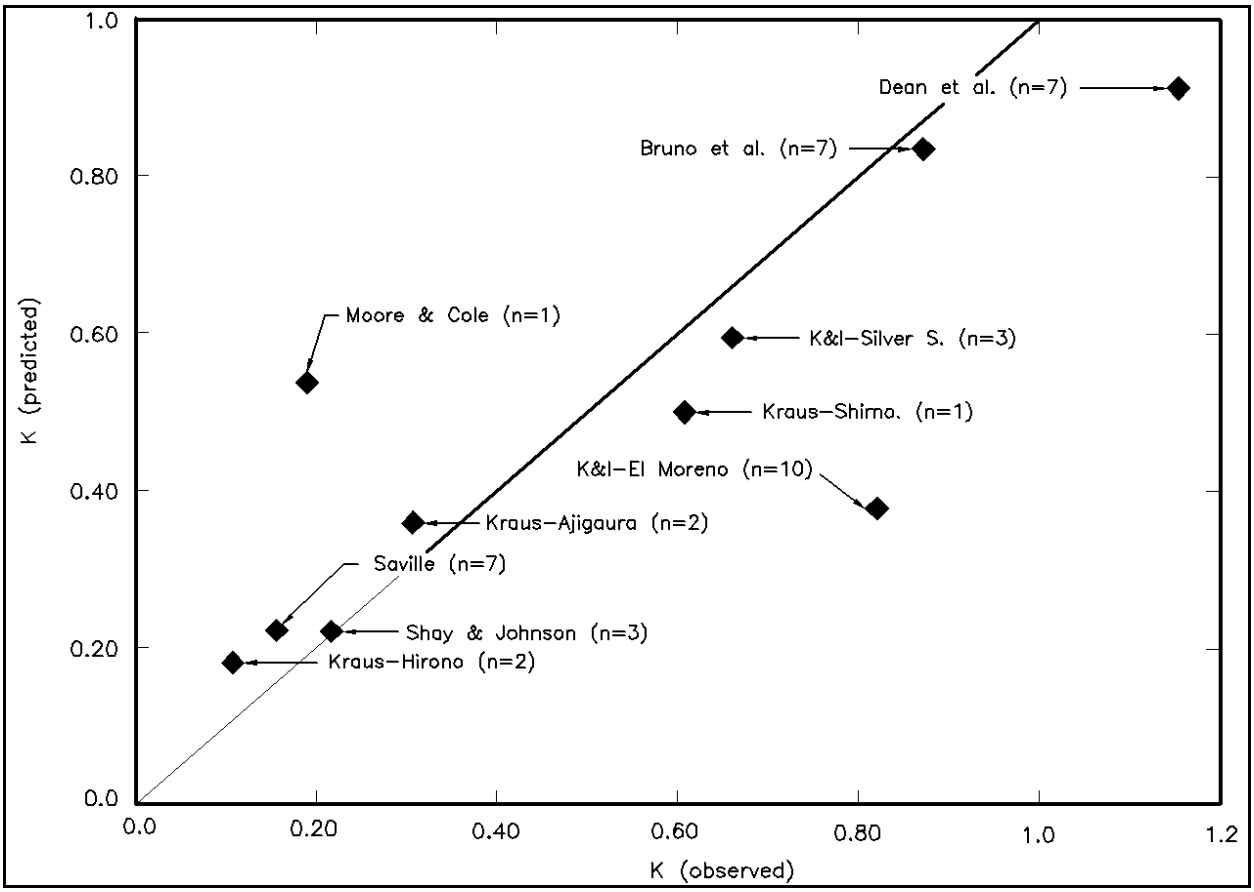

Figure III-2-5. Measured and predicted *K* coefficients using Bailard's (1984) equation

where D_{50} is the median grain size of the beach sediment in millimeters. This relationship is based on limited data and depends strongly on the data from the Adra River Delta.

(d) While it is generally thought that the *K* coefficient should decrease with increasing grain size, the nature of this relationship is not well understood at present. Again, because of the limited data set and inherent variability in measuring longshore sediment transport rates, predicted *K* coefficients may vary considerably from appropriate values for any particular site.

(4) Variation of *K* with surf similarity.

(a) From laboratory data, a relationship between *K* and the surf similarity parameter $\xi_b = m / (H_b/L_o)^{1/2}$ has also been observed (Kamphuis and Readshaw 1978). These data suggest that the value of *K* increases with increasing value of the surf similarity parameter (i.e. as the breaking waves tend from spilling to collapsing condition).

(b) Numerous other relationships for predicting longshore sediment transport rates exist (e.g., Watts (1953a), Kamphuis and Rea shaw (1978), Kraus et al. (1982), Kamphuis et al. (1986), Kamphuis (1991)). A promising empirical relationship based principally upon laboratory results is that developed by Kamphuis (1991) which correlates well with laboratory and field data sets. However, for application to field studies, the use of a physically based relationship based solely on field data, such as the one presented herein (often called the CERC formula) is preferred.

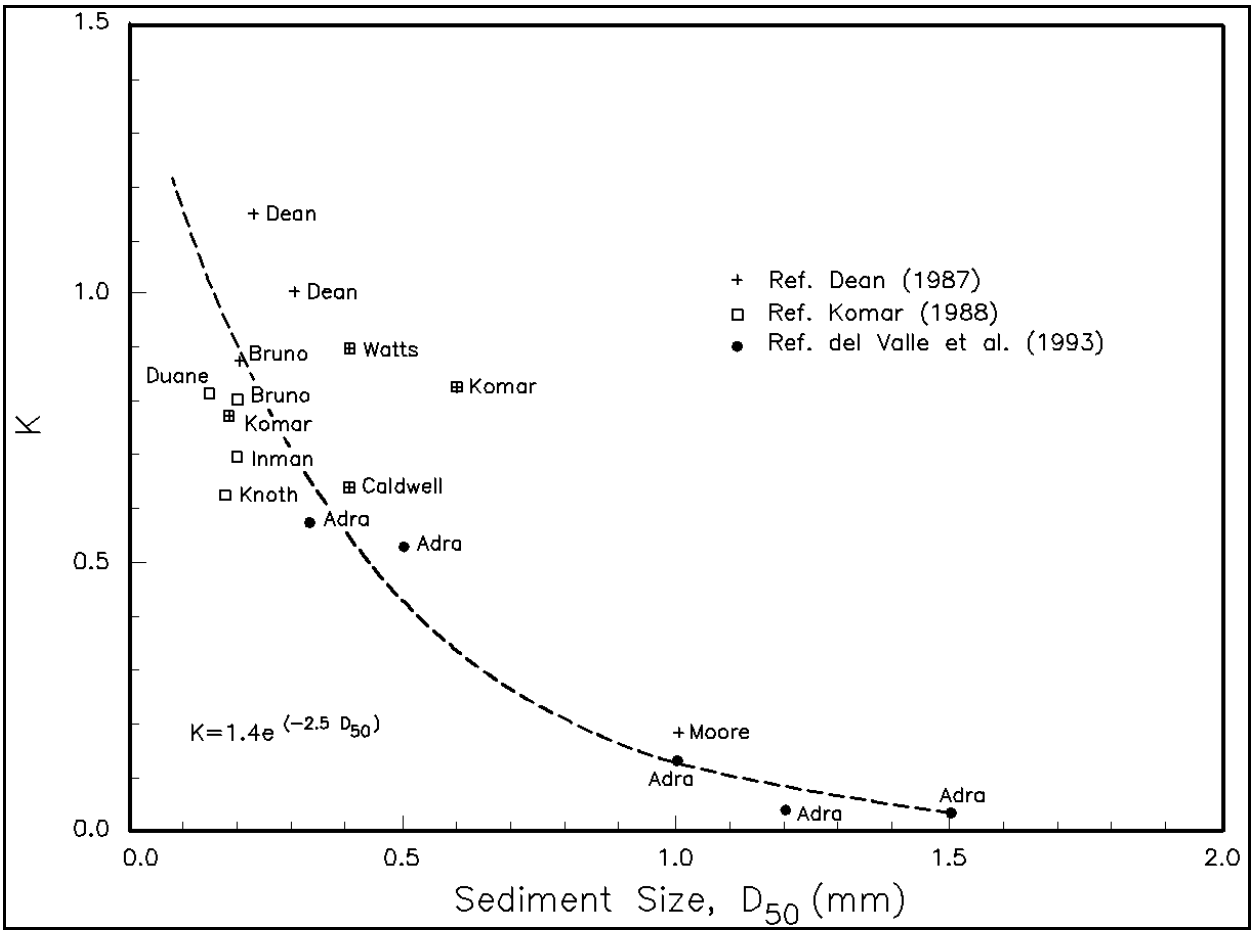

Figure III-2-6. Coefficient *K* versus median grain size D_{50} (del Valle, Medina, and Losada 1993)

(c) Researchers at CHL (unpublished) used sand tracer data from Santa Barbara and Torrey Pines, California, and profile and dredging records from Santa Barbara Harbor, California, to compare 20 longshore sediment transport models. They concluded that the CERC equation performed as well or better than the other models. Of the six models including effects of grain size evaluated (they did not evaluate del Valle, Medina, and Losada's (1993) relationship), they concluded that Bailard's (1984) relationship (given in Equation 2-8) performed the best. However, the data set used for comparison only represented grain sizes in the range 0.15 to 0.25 mm, and therefore was not particularly suited for testing the dependence of longshore sediment transport relationships on grain size outside this limited range.

b. Longshore current method. Early workers such as Grant (1943) stressed that sand transport in the nearshore results from the combined effects of waves and currents; i.e., the waves placing sand in motion and the longshore currents producing a net sand advection. Walton (1980, 1982) proposed a longshore sediment transport calculation method using the breaking-wave-driven longshore current model of Longuet-Higgins (1970) from which the longshore energy flux factor becomes

$$P_\ell = \frac{\rho\, g\, H_b\, W\, V_\ell\, C_f}{\left(\frac{5\pi}{2}\right)\left(\frac{V}{V_o}\right)} \qquad \text{(III-2-11)}$$

EXAMPLE PROBLEM III-2-1

FIND:

Determine the K parameter for use at a site using Bailard's (1984) and del Valle, Medina, and Losada's (1993) relationships, then calculate the potential volumetric longshore transport rate along the beach using each K value.

GIVEN:

Waves having an rms wave height of 2.0 m (6.7 ft) break on a quartz sand beach with median grain size, D_{50} = 1.0 mm at a wave breaking angle $\alpha_b = 4.5^o$. The temperature of the seawater is 20° C and w_f = fall velocity = 13.1 cm/sec. Assume $\kappa = 1.0$ for this problem.

SOLUTION:

w_f = 13.1 cm/sec (0.43 ft/sec), which is within Bailard's data range.

The maximum oscillatory velocity magnitude is calculated from Equation 2-9 as

$$u_{mb} = \frac{\kappa\ (g\ d_b)^{1/2}}{2} = \frac{1\ (9.81\ \times\ 2.0)^{1/2}}{2}$$

u_{mb} = 2.21 m/sec, which is within Bailard's (1984) data range.

Therefore, Equation 2-8 may be used, and the coefficient to apply in the longshore sediment transport equation is,

$$K = 0.05 + 2.6 \sin^2 (2\alpha_b) + 0.007\ u_{mb}/w_f = 0.05 + 2.6 \sin^2 (2(4.5^o)) + 0.007\ (2.21/0.131)$$

$$K = 0.23$$

Applying del Valle, Medina, and Losada's relationship, Equation 2-10,

$$K\ =\ 1.4\ e^{(-2.5\ D_{50})}\ =\ 0.12$$

(Continued)

Example Problem III-2-1 (Concluded)

Using Equation 2-7b with $K = 0.23$,

$$Q_\ell = K \left(\frac{\rho\sqrt{g}}{16\ \kappa^{1/2}\ (\rho_s - \rho)(1 - n)} \right) H_{b\ rms}^{5/2} \sin(2\alpha_b)$$

$$Q_\ell = 0.23\ \frac{(1025)\ (9.81)^{1/2}}{16\ (1)\ (2650 - 1025)\ (1 - 0.4)}\ (2.0)^{5/2}\ \sin\ (2\times 4.5^o)$$

$$Q_\ell = (0.042\ m^3/sec)\ (3600\ sec/hr)\ (24\ hr/day)$$

$Q_\ell = 3.6 \times 10^3\ m^3/day$ ($4.7 \times 10^3\ yd^3/day$) using Bailard's methodology.

Using del Valle, Medina, and Losada's relationship ($K = 0.12$)

$$Q_\ell = 0.12\ \frac{(1025)\ (9.81)^{1/2}}{16\ (2650 - 1025)\ (1 - 0.4)}\ (2.0)^{5/2}\ \sin\ (2\times 4.5^o)$$

$$Q_\ell = (0.021\ m^3/sec)\ (3600\ sec/hr)\ (24\ hr/day)$$

$Q_\ell = 1.9 \times 10^3\ m^3/day$ ($2.5 \times 10^3\ yd^3/day$)

It is noted that the estimates of the transport rate developed from the two relationships for *K*, Equations 2-8 and 2-10, differ by a factor of almost 1.9. This serves to highlight the uncertainty associated with selection of the appropriate *K* coefficient for a given site, and the resulting uncertainty in the prediction of the longshore transport rate's value. The grain size used in this problem is much larger than that typically found on U.S. beaches, and the *K* coefficient found is correspondingly smaller than that recommended in *Shore Protection Manual* (1984).

EXAMPLE PROBLEM III-2-2

FIND:

Calculate the potential immersed-weight and volumetric longshore sand transport rates.

GIVEN:

The same conditions as in Example Problem III-2-1, except assume a median grain size D_{50} corresponding to a K coefficient = 0.60. Assume $\kappa = 1$ for simplicity.

SOLUTION:

With $H_{b\ rms}$ = 2.0 m (6.6 ft), ρ = 1,025 kg/m^3 (1.99 slug/ft^3), ρ_s = 2,650 kg/m^3 (5.14 slug/ft^3), g = 9.8 m/sec^2 (32.2 ft/sec^2) and $\alpha_b = 4.5°$, Equation 2-6d gives

$$I_\ell = K \left(\frac{\rho g^{\frac{3}{2}}}{16\ \kappa^{\frac{1}{2}}} \right) H_{b\ rms}^{\frac{5}{2}} \sin(2\alpha_b)$$

$$0.60\ \frac{(1025)\ (9.81)^{\frac{3}{2}}}{16\ (1)}\ (2.0)^{\frac{5}{2}}\ \sin(2\times 4.5^o) \cong 1050\ N/\text{sec}\ (236\ \text{lbf/sec})$$

This potential immersed-weight transport rate may be converted to a potential volumetric rate by using Equation 2-7b

$$Q_\ell = K \left(\frac{\rho\sqrt{g}}{16\ \kappa^{\frac{1}{2}}\ (\rho_s - \rho)(1 - n)} \right) H_{b\ rms}^{\frac{5}{2}} \sin(2\alpha_b)$$

$$Q_\ell = 0.60\ \frac{(1025)\ (9.81)^{\frac{1}{2}}}{16\ (1)\ (2650 - 1025)\ (1 - 0.4)}\ (2.0)^{\frac{5}{2}}\ \sin(2\times 4.5^o)$$

$$Q_\ell = (0.109\ \text{m}^3/\text{sec})\ (3600\ \text{sec/hr})\ (24\ \text{hr/day})$$

$$Q_\ell = 9.4 \times 10^3\ \text{m}^3/\text{day}\ (12.3 \times 10^3\ \text{yd}^3/\text{day})$$

EXAMPLE PROBLEM III-2-3

FIND:

Calculate the potential volumetric longshore sand transport rate along the beach.

GIVEN:

Spectral analysis of wave measurements at an offshore buoy in deep water yields a wave energy density E_o of 2.1 x 10^3 *N*/m (144 lbf/ft), with a single peak centered at a period T = 9.4 sec. At the measurement site, the waves make an angle of $\alpha_o = 7.5°$ with the trend of the coast, but after undergoing refraction, the waves break on a sandy beach with an angle of $\alpha_b = 3.0°$. Assume that the K coefficient is 0.60.

SOLUTION:

The group speed of the waves in deep water is given in Part II-1 as

$$C_{go} = gT/4\pi = 9.8\ (9.4) / (4\pi) = 7.3 \text{ m/sec } (24.0 \text{ ft/sec})$$

The energy flux per unit shoreline length in deep water is

$$(EC_g)_o \cos\alpha_o = (2.1 \times 10^3)(7.3)\cos(7.5°) = 1.5 \times 10^4 \text{ N/sec } (3.4 \times 10^3 \text{ lbf/sec})$$

The conservation of wave energy flux allows the substitution

$$(EC_g)_b \cos\alpha_b = (EC_g)_o \cos\alpha_o$$

where bottom friction and other energy losses are assumed to be negligible, Equation 2-2 for the longshore component of the energy flux at the shoreline then becomes

$$P_\ell = (EC_g)_b \sin\alpha_b \cos\alpha_b = [(EC_g)_o \cos\alpha_o]\sin\alpha_b = (1.5 \times 10^4) \sin(3.0°)$$

$$P_\ell = 800 \text{ } N/\text{sec } (180 \text{ lbf/sec})$$

Spectra yield wave parameters equivalent to rms conditions, and therefore K = 0.60 may be used in Equation 2-7a to calculate the potential volumetric sand transport rate. This gives

$$Q_\ell = \frac{K}{(\rho_s - \rho)\ g\ (1 - n)}\ P_\ell$$

$$Q_\ell = \frac{0.60}{(2650 - 1025)\ (9.81)\ (1 - 0.4)}\ 800$$

$$Q_\ell = 0.050 \text{ m}^3/\text{sec} \times 3600 \text{ sec/hr} \times 24 \text{ hr/day}$$

$$Q_\ell = 4.3 \times 10^3 \text{ m}^3/\text{day } (5.7 \times 10^3 \text{ yd}^3/\text{day})$$

EXAMPLE PROBLEM III-2-4

FIND:

Calculate the resulting volumetric longshore transport of sand using measured surf zone velocity.

GIVEN:

Breaking waves have an rms height of 1.8 m (5.9 ft) and there is a persistent longshore current in the surf zone with mean velocity 0.25 m/sec (0.82 ft/sec) as measured at approximately the mid-surf position. The width of the surf zone is approximately 75 m (246 ft). Assume the K coefficient was calculated as 0.60.

SOLUTION:

With $H_{b\,rms}$ = 1.8 m (5.9 ft) and V_ℓ = 0.25 m/sec (0.82 ft/sec), Equation 2-12 gives

$$V/V_o = 0.2\,(37.5/75) - 0.714\,(37.5/75)\ln(37.5/75) = 0.35$$

and Equation 2-11 gives

$$P_\ell = [(1025)(9.81)(1.8)(75)(0.25)(0.01)]/[(5\pi/2)(0.35)] = 1234 \text{ N/sec (277 lbf/sec)}$$

From Equation 2-7a,

$$Q_\ell = (0.60)(1234)/[(2650-1025)(9.81)(1-0.4)]$$

$$Q_\ell = 0.077 \text{ m}^3\text{/sec} = 6.7 \times 10^3 \text{ m}^3\text{/day } (8.8 \times 10^3 \text{ yd}^3\text{/day})$$

in which W is the width of the surf zone, V_ℓ is the measured longshore current at a point in the surf zone, C_f is a friction coefficient dependent on Reynolds' number and bottom roughness, and V_o is the theoretical longshore velocity at breaking for the no-lateral-mixing case. A theoretical velocity distribution for a linear beach profile that best fits Longuet-Higgins nondimensionalized data is chosen

$$\left(\frac{V}{V_o}\right) = 0.2\left(\frac{Y}{W}\right) - 0.714\left(\frac{Y}{W}\right)\ln\left(\frac{Y}{W}\right) \qquad \text{(III-2-12)}$$

in which Y equals the distance to the measured current from the shoreline, and V/V_o equals Longuet-Higgins dimensionless longshore current velocity for an assumed mixing coefficient equal to 0.4, which agrees reasonably well with laboratory data. Values of the friction factor C_f in Equation 2-11 were shown by Longuet-Higgins to be approximately 0.01, based on laboratory data. Thornton and Guza (1981) calculated the friction factor using field data measured at Torrey Pines Beach, San Diego, California, and a mean value of the parameter, averaged over four selected days, was 0.01 with a standard deviation of 0.01. Using Equations 2-11 and 2-12 with knowledge of breaking wave height, width of the surf zone, longshore velocity (at some point within the surf zone), distance to the measured longshore velocity, and an assumed friction factor, the longshore sand transport rate may then be calculated. From a practical standpoint, it is often easier

and more accurate to measure the longshore current V_ℓ than it is to determine the breaker angle α_b needed in the P_ℓ formulation. In either method, calculations of longshore sediment transport may be very different than actual values. Formulations for the longshore current distribution across nonplanar, concave-up beach profiles are presented by McDougal and Hudspeth (1983a, 1983b, and 1989) and by Bodge (1988).

c. Using hindcast wave data. Potential longshore sand transport rates can be calculated using Wave Information Study (WIS) hindcast wave estimates (see Part II-2). First, refraction and shoaling of incident linear waves are calculated using Snell's law and the conservation of wave energy flux. The shallow-water wave breaking criterion then defines wave properties at the break point, and potential longshore sand transport rates are calculated by means of the energy flux method.

(1) Wave transformation procedure. To calculate the potential longshore sand transport rate using Equation 2-7b, the breaking wave height and incident angle with respect to the shoreline are required. WIS hindcast estimates, however, are given for intermediate to deepwater depths (Hubertz et al. 1993). Refraction and shoaling transformation of the WIS hindcast wave estimates to breaking conditions are therefore necessary and can be accomplished using linear wave theory for coastlines having reasonably straight and parallel bottom contour lines. Assuming that offshore depth contours are straight and parallel to the trend of the shoreline and neglecting energy dissipation prior to breaking, the wave height and angle at breaking can be computed from the coupled equations

$$H_b = H_1^{\frac{4}{5}} \left[\frac{C_{g1} \cos\alpha_1}{\sqrt{\frac{g}{\kappa}} \cos\alpha_b} \right]^{\frac{2}{5}} \tag{III-2-13}$$

$$\sin\alpha_b = \sqrt{g \frac{H_b}{\kappa}} \frac{\sin\alpha_1}{C_1} \tag{III-2-14}$$

where the subscript "1" refers to offshore (WIS) conditions. Equations 2-13 and 2-14 are derived from energy conservation and Snell's Law. Where it is assumed that wave breaking occurs for shallow-water wave conditions; i.e.,

$$C_b = C_{gb} = \sqrt{g\, d_b} = \sqrt{g \frac{H_b}{\kappa}} \tag{III-2-15}$$

Employing the identity $sin^2\alpha_b = 1 - cos^2\alpha_b$, Equations 2-13 and 2-14 can be combined as

$$H_b = H_1^{\frac{4}{5}} \left(C_{g1} \cos \alpha_1 \right)^{\frac{2}{5}} \left[\frac{g}{\kappa} - \frac{H_b\, g^2 \sin^2(\alpha_1)}{\kappa^2 \; C_1^2} \right]^{-\frac{1}{5}} \tag{III-2-16}$$

and solved iteratively for H_b. The angle α_b can then be found using Equation 2-14. In application of Equations 2-14 and 2-16, the offshore wave angle α_1 should be transformed relative to the shoreline-perpendicular as described below.

(2) Wave conditions.

(a) As discussed in Part II-2, WIS hindcast wave estimates are compiled in intermediate to deepwater depths. The examples presented herein use Revised Atlantic Level 2 (RAL2) WIS data, which are presented in 45-deg wave angle bands. Angles reported for RAL2 WIS Phase III stations α_{WIS} are measured in degrees "from" in a compass sense, for which due north equals zero and other angles are measured clockwise from north. For calculation of longshore sand transport, a right-handed coordinate system is more convenient, in which waves approaching normal to the shoreline are given an angle of 0 deg. Looking seaward, waves approaching from the right are associated with negative angles, and waves approaching from the left are associated with positive angles such that transport directed to the right is given a positive value and transport directed to the left is given a negative value in accord with sign convention discussed earlier. WIS angles may be converted to angles associated with transport calculations α by means of the following relationship:

$$\alpha = \theta_n - WIS\ angle \tag{III-2-17}$$

where θ_n is the azimuth angle of the outward normal to the shoreline. Angles of α over $\pm 90^0$ would be excluded from calculations. The WIS angle is the azimuth angle the waves are coming from.

(b) RAL2 WIS wave data for one particular wave-angle band are summarized in Table III-2-2. The number of occurrences are listed for specific wave height and period bands, with the total number of occurrences listed in the right column (for each wave band) and bottom row (for each period band). The header gives the time period for the data record (1956 - 1975), location of the station in latitude and longitude, water depth, and angle band represented by the tabulated data.

(c) Data given in WIS statistical tables may be used in several ways to calculate the potential longshore sand transport rate. Two examples using the data in Table III-2-2 are given below. In Example III-2-5, the potential longshore sand transport rate is estimated with the average significant wave height for the given

Table III-2-2

Occurrence of Wave Height and Period for Direction Band 112.5° - 157.49° RAL2 Station 72

WIS ATLANTIC REVISION 1956 - 1975

LAT: 40.25 N LONG: 73.75 W, DEPTH = 27 M

OCCURRENCES OF WAVE HEIGHT AND PEAK PERIOD

FOR 45-DEG DIRECTION BAND

STATION 72

(112.50^0 to 157.49^0) mean = 135.0^0

	T_p, seconds								
Hmo(m)	**3.0-4.9**	**5.0-6.9**	**7.0-8.9**	**9.0-10.9**	**11.0-12.9**	**13.0-14.9**	**15.0-16.9**	**17.0-18.9**	**Total**
0.00-0.99	1,022	1,509	6,018	3,261	918	120	10	.	12,858
1.00-1.99	124	1,380	1,437	1,095	610	127	4	.	4,777
2.00-2.99	.	66	440	384	183	60	.	.	1,133
3.00-3.99	.	.	56	140	76	16	.	.	288
4.00-4.99	.	.	.	17	22	6	.	.	45
5.00-5.99	.	.	.	1	2	.	.	.	3
6.00-6.99	.	.	.	.	1	1	.	.	2
7.00-7.99	.	.	.	.	.	.	.	.	0
8.00-8.99	.	.	.	.	.	.	.	.	0
9.00-Greater	.	.	.	.	.	.	.	.	0
Total	1,146	2,955	7,951	4,898	1,812	330	14	0	19,106

EXAMPLE PROBLEM III-2-5

FIND:

Calculate (a) the average (over the directional band) wave height H_{mo} and determine an equivalent significant wave height H_{sig}, (b) wave approach angle in the sediment transport coordinate system, (c) percentage of the total wave data represented by this wave directional angle band, (d) average peak spectral wave period T_p, (e) breaking wave height H_b and angle α_b, and (f) potential longshore sand transport rate.

GIVEN:

Wave statistics presented in Table III-2-2. The water depth at which the wave statistics were developed is 27 m. The azimuth angle (from north) of the outward normal to the beach of interest is approximately 102°. The sediment is quartz-density sand, and K_{sig} = 0.39. Assume κ = 1.0 for simplicity.

SOLUTION:

(a) Weighting the average wave height in each wave height band with the total number of observations in that band, calculate an average wave height, H_{mo} = 0.93 m; that is:

$$H_{mo} = [(0.5)(12858) + (1.5)(4777) + (2.5)(1133) + (3.5)(288) + (4.5)(45) + (5.5)(3) + (6.5)(2)] / 19106 = 0.93 \text{ m}$$

As discussed in Part II-1, H_s and H_{mo} are approximately equal when irregular wave profiles are sinusoidal in shape. However, as depth decreases and waves shoal prior to breaking, they become nonlinear and peaked in shape rather than sinusoidal. According to Part II-1, the two parameters are within 10 percent of each other if the depth (in meters) is greater than or equal to 0.0975 T_p^2. In the example, 27 m is greater than 0.0975 (8.5 sec)^2 = 7.1 m; therefore, the average significant wave H_{sig} may be said to be approximately equal to H_{mo}.

(b) The data in Table III-2-2 represent the angle band that is centered around WIS angle = 135°. However, the shoreline outward normal angle is 102° (from north), which means that the angle associated with transport calculations α = 102° - 135° = -33°.

(c) WIS RAL2 data are presented every 3 hr for a 20-year time period, totalling 58,440 data points for each station (in all wave direction angle bands). The total number of occurrences listed in Table III-2-2 for the 45° direction band centered around 135° equals 19,106, which means that the percentage of the total data represented by this angle band equals 19,106/58,440 x 100 percent = 32.7 percent. Scanning the other data for this station (Hubertz et al. 1993, p. A-288 - A-289), this angle band constitutes the dominant wave direction in terms of number of occurrences for station 72.

(Continued)

Example Problem III-2-5 (Concluded)

(d) A weighting procedure using wave period bands similar to that used for the wave height bands can be used to calculate an average peak spectral wave period T_p = 8.4 sec; that is,

$$T_p = [(4)(1146) + (6)(2955) + (8)(7951) + (10)(4898) + (12)(1812) + (14)(330) + (16)(14)] / 19106 = 8.4$$

(e) Compute the wave celerity C_1 and group celerity C_{g1} for the offshore wave data in water depth d = 27 m and for the wave period T_p = 8.4 sec; and find C_1 = 12.2 m/s and C_{g1} = 7.6 m/s. Use Newton-Raphson iteration (or a similar technique) to solve Equation 2-16 for the breaking wave height H_b using the offshore wave height value H_1 = 0.93 m and angle α_1 = -33°, and find

$$H_b \cong 1.2 \text{ m } (3.9 \text{ ft})$$

The breaking wave angle is then computed from Equation 2-14:

$$\alpha_b = -8.8 \text{ deg}$$

(f) Compute the potential longshore sediment transport rate for K_{sig} = 0.39 using Equation 2-7b:

$$Q = (0.39) [(1025)(9.81)^{0.5} / (16)(2650-1025)(1-0.4)] (1.2)^{5/2} \sin(2(-8.8)) = -0.038 \text{ m}^3/\text{s}$$

Convert the result to annual equivalent transport and multiply by the percent annual occurrence of this event, 32.7%:

$$Q = (-0.038 \text{ m}^3/\text{sec}) (3600 \text{ sec/hr}) (24 \text{ hr/day}) (365.25 \text{ day/yr}) (0.327)$$
$$= -393{,}000 \text{ m}^3/\text{yr } (-514{,}000 \text{ cy/yr}) \text{ (directed to the left).}$$

Note that a similar approach can be utilized to find an answer using the CEDRS database (see Part II, Chapter 8) which provides "percent" occurrences (rather than number of observations) in 22.5° energy bands.

EXAMPLE PROBLEM III-2-6

FIND:

Calculate the potential longshore transport rate using each of the seven wave height bands given in Table III-2-2.

GIVEN:

Data in Table III-2-2, and information in Example III-2-5.

SOLUTION:

For each wave height band in Table III-2-2, the associated weighted average peak wave period T_p is calculated. Using the criteria discussed previously, the wave data are checked to ensure that $H_{sig} \sim H_{mo}$. The percent occurrence for that wave condition is determined by dividing the total number of occurrences in the wave height band in the given 45^0 directional band by the total number of records (58,440) in all directional bands. The results are shown in the table below as the "input" conditions. The breaking conditions may be computed directly by the program WISTRT or by Equations 2-14 and 2-16 in the same manner as described in Example 5, above. The potential longshore sediment transport from the 45^o direction band centered approximately 33^o to the right of shore-normal (looking seaward) was calculated to be -1,014,200 m^3/year (-1,325,500 yd^3/year) (directed to the left) for RAL2 Station 72.

Data for Example Problem III-2-6

	Input Conditions					Program Output		
Wave Condition	H_s (m)	T (sec)	α (deg)	Depth (m)	Percent Occurrence	H_b (m)	α_b (deg)	Q_l (m^3/year)
1	0.5	8.3	-33	27	22.0	0.73	-7.8	-66,500
2	1.5	8.5	-33	27	8.17	1.8	-12.0	-355,000
3	2.5	9.5	-33	27	1.94	2.9	-14.2	-320,000
4	3.5	10.4	-33	27	0.493	4.0	-16.0	-198,800
5	4.5	11.5	-33	27	0.077	5.1	-17.4	-61,200
6	5.5	11.3	-33	27	0.005	6.0	-19.0	-6,500
7	6.5	13.0	-33	27	0.003	7.1	-20.0	-6,200
				Total (directed to the left)				-1,014,200

Note that a similar approach can be utilized to find an answer using the CEDRS database (see Part II, Chapter 8) which provides "percent" occurrences (rather than number of observations) in 22.5° energy bands. Note that engineering judgment must be utilized when assessing actual transport rates. Values of longshore sand transport calculated with Equations 2-14 and 2-16 are based on a limitless supply of sand available for transport, which is often not the case (e.g., if structures are present, geologic features control sand movement, or sediments other than sand are in the transport region). In addition, longshore transport rates calculated using WIS data have been found to be larger than accepted rates (Bodge and Kraus 1991).

For this example calculated using waves offshore of the New Jersey coast, generally-accepted transport rates might be used to adjust the calculated values. Inspection of Figure III-2-3 indicates that net longshore transport rates are between 153,000 and 275,000 cu m/year for this portion of the New Jersey shore. This "calibration" implies that longshore sand transport rates calculated with WIS data and Equations 2-14 and 2-16 might be reduced from 15 to 27 percent of their calculated values to have application for this part of the coastline. Future calculations using WIS data for this portion of the coast could use this calibration for adjustment.

directional band. In Example III-2-6, wave data are more accurately represented by calculating a representative wave period for each of the given wave height bands for the given directional band. Each example requires the transformation of offshore wave data to breaking conditions, and subsequent computation of the associated longshore transport rate. The former can be accomplished using Equations 2-14 and 2-16 or using the program WISTRT (Gravens 1989). Both require knowledge or input of the offshore wave height H_I (WISTRT requires the significant wave height H_{sig}), associated period T, angle relative to the shoreline α, and water depth associated with wave data. The longshore transport rate can then be computed directly by Equation 2-7b. The program WISTRT uses a K value and a breaker wave height-to-depth ratio different than those used here. It also requires the percent occurrence associated with the given wave condition. The ACES program "Longshore Sediment Transport" (Leenknecht, Szuwalski, and Sherlock 1992) also provides a method for calculation of potential longshore sediment transport rates under the action of waves. Again, different constants K and κ are utilized than those presented here. Both WISTRT and the ACES programs use individual wave events as input, rather than an extended time series of wave information. A program for processing the WIS time series to obtain values of sediment transport is presented in Gravens, Kraus, and Hanson (1991).

(d) Note that both Examples III-2-5 and III-2-6 employed the same wave data, but Example III-2-6 computed the transport for discrete wave height bands whereas Example III-2-5 computed the transport for a single, band-averaged wave height. The transport computed in Example III-2-6 is more than double that in Example III-2-5. This difference is due to the nonlinear dependence of the transport equation on breaking wave height. If, for example, wave heights are Rayleigh distributed and the waves are all of uniform period, the transport rate computed using the distribution of wave heights will be about 1.53 times larger than that computed using only the band-averaged wave height.

(e) Bodge and Kraus (1991) and others (e.g., Kraus and Harikai 1983; Gravens, Scheffner, and Hubertz 1989; Gravens 1990a) have observed that use of the CERC formula (with the K_{SPM} coefficient) and WIS hindcast wave data have yielded potential longshore sand transport magnitudes that are two to five times larger than values for the region as estimated from dredging records, bypassing rates, or volumetric change. The longshore sand transport rate determined in Example III-2-6 represents the potential longshore transport rate, which depends on an available supply of littoral material. Consideration of the availability of littoral material; location, type, and condition of coastal structures; and sheltering specific to the project shoreline may contribute to a lower actual longshore transport rate. It is recommended when using hindcast wave data to predict potential longshore sand transport rates that other independent measures or estimates of longshore transport be used to supplement the potential transport estimate.

d. Deviation from potential longshore sediment transport rates.

(1) Temporal variations and persistence.

(a) Longshore sediment transport is a fluctuating quantity which can be depicted as shown in Figure III-2-7 where positive sediment transport is defined as positive in value if toward the right for an observer looking seaward from the beach, and negative in value if sediment transport is toward the left as noted previously and consistent with notation utilized by Walton (1972), Walton and Dean (1973), Dean (1987), and others. In terms of "Q_ℓ," on Figure III-2-7 the net longshore sediment transport rate is the "time average" transport given by

$$Q_{\ell NET} \equiv \overline{Q}_\ell = \frac{1}{T_o} \int_o^{T_o} Q_\ell(t)\, dt \qquad \text{(III-2-18)}$$

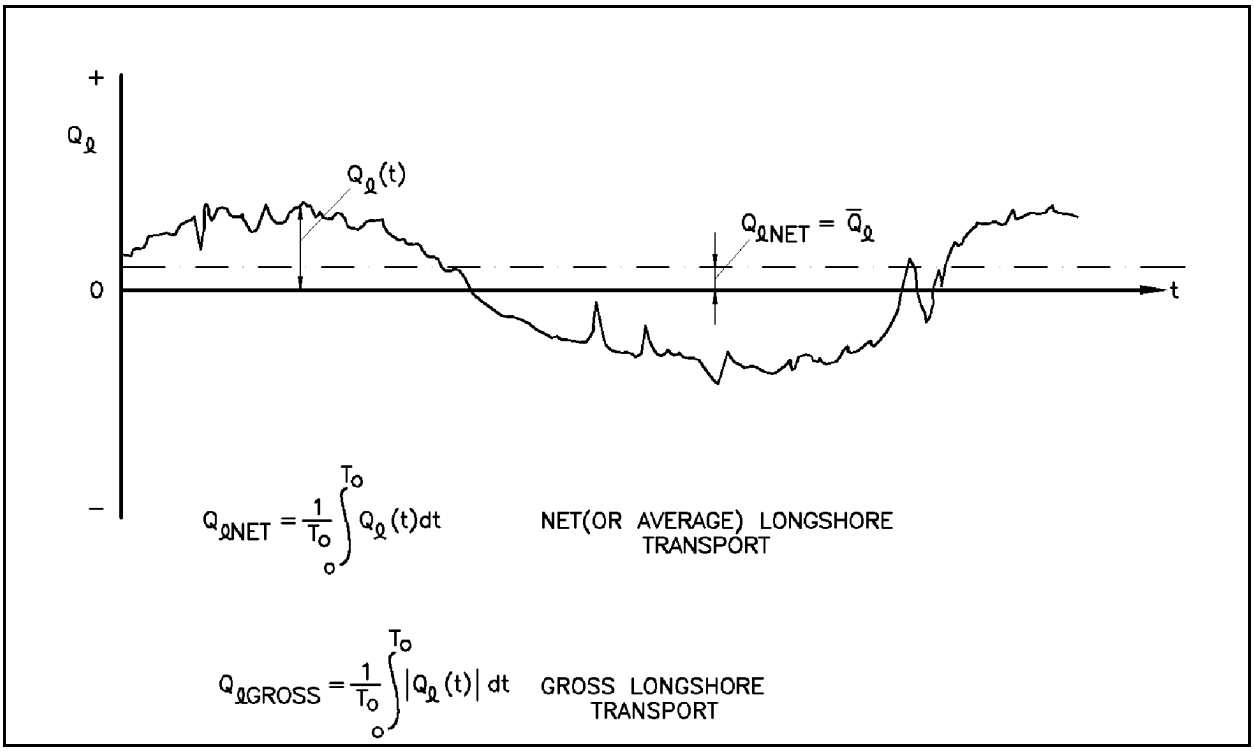

Figure III-2-7. Longshore transport definitions

(b) The gross longshore sediment transport rate is given by

$$Q_{\ell GROSS} = \frac{1}{T_o}\int_o^{T_o} |Q_\ell(t)|\, dt \qquad \text{(III-2-19)}$$

where T_o is the length of record, often taken to be greater than 1 year, and $|Q_\ell|$ is the absolute magnitude of the longshore sediment transport rate. The gross longshore sediment transport rate is always defined positive. When the gross longshore sediment transport rate is multiplied by the time period, the derived quantity represents the total volume of sediment passing through a plane perpendicular to the shoreline regardless of the direction. The net longshore sediment transport rate may be either positive or negative.

(c) Although net and gross longshore sediment transport rates are often the most meaningful quantities for use in engineering design, the variability of the longshore sediment transport on much shorter time intervals is often of critical concern. As an example, if a channel is to be maintained clear of sediment, the pump(s) necessary to dredge the channel would need to be sufficiently large to handle the instantaneous maximum rate of longshore rate of sediment transport (that is projected to reach the channel). Typically, sizing for the maximum instantaneous rate of sediment transport would be economically unfeasible, and therefore some type of temporary sediment storage would be provided to allow for reduced pump sizing. Optimizing of the pump size and the provided sediment storage structures (possibly a groin, a breakwater, or some combination of both) will require knowledge of the fluctuating longshore sediment transport rates.Figure III-2-8 provides an example of the variability of annual rates of (net) longshore energy flux factor (which is proportional to the longshore sediment transport rate as given in Equation 2-2) for three locations on the East Coast of the United States as computed using 20 years of hindcast wave climate.

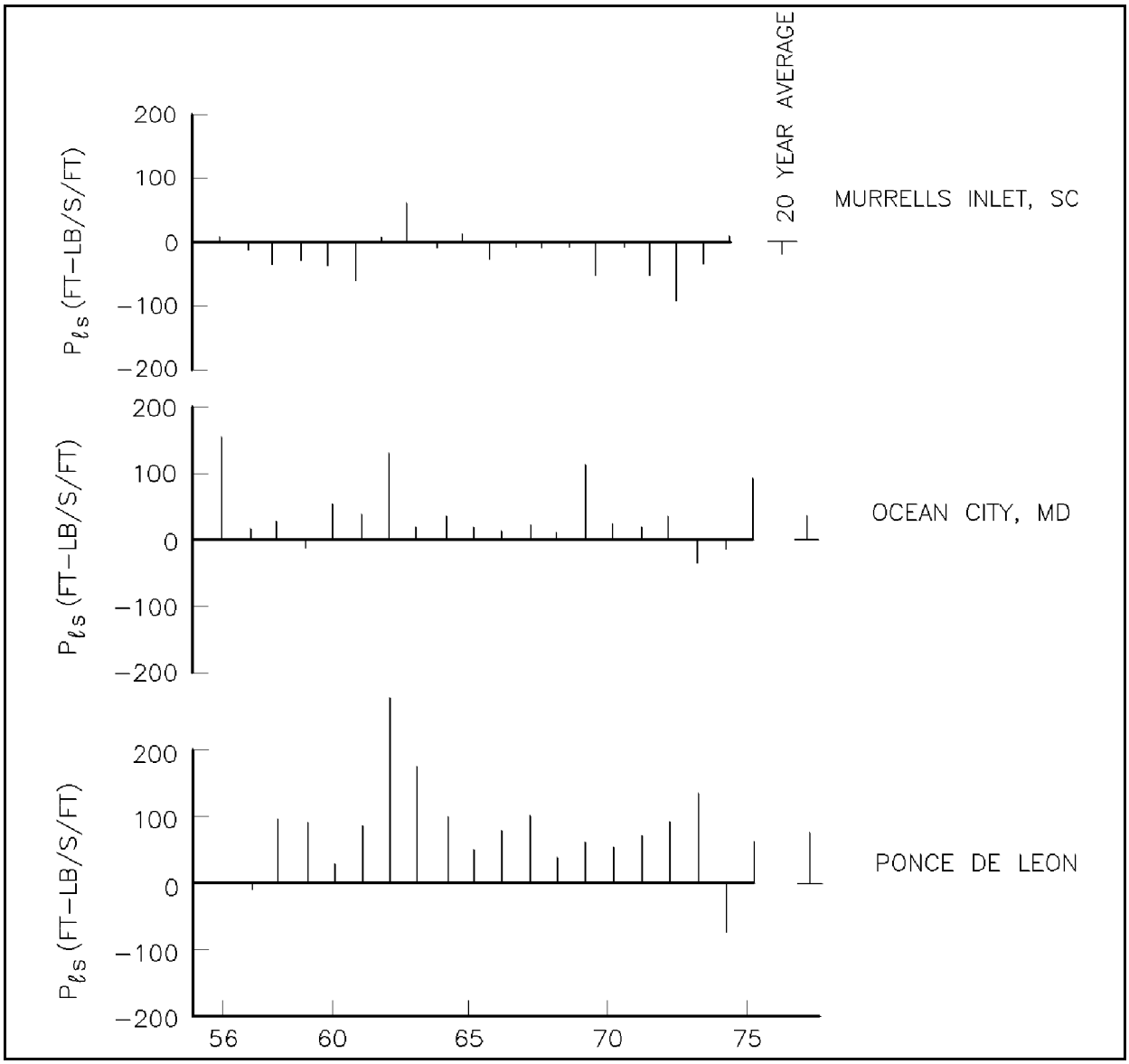

Figure III-2-8. Time plot of annual longshore energy flux factor at three east coast sites (after Douglass (1985))

Figure III-2-9 provides an example of the variability of the monthly (net) longshore energy flux factor for the same three locations. Figures III-2-8 and III-2-9 show that as the averaging period gets shorter, the variability of the sediment transport rate increases due to the fact that integration is a smoothing process and reduces the variance in the data. For design purposes, an assessment of the uncertainty in the sediment transport climate can be addressed via simulation of the sediment transport rates. Walton and Douglass (1985) have provided an approach to such simulation for the case of monthly sand transport rates which, for the locations assessed, appeared to be in reasonable conformance with a normal distribution assumption. Figure III-2-10 from Walton and Douglass (1985) shows the distribution of monthly averages of longshore energy flux factor for a coastal location in South Carolina. The data are reasonably represented by a normal distribution, as shown by the fit of the solid line to the data. Figure III-2-11, also from Walton and Douglass (1985), is for the same location but with weekly averages. In this case, the weekly averages vary considerably from a normal probability distribution.

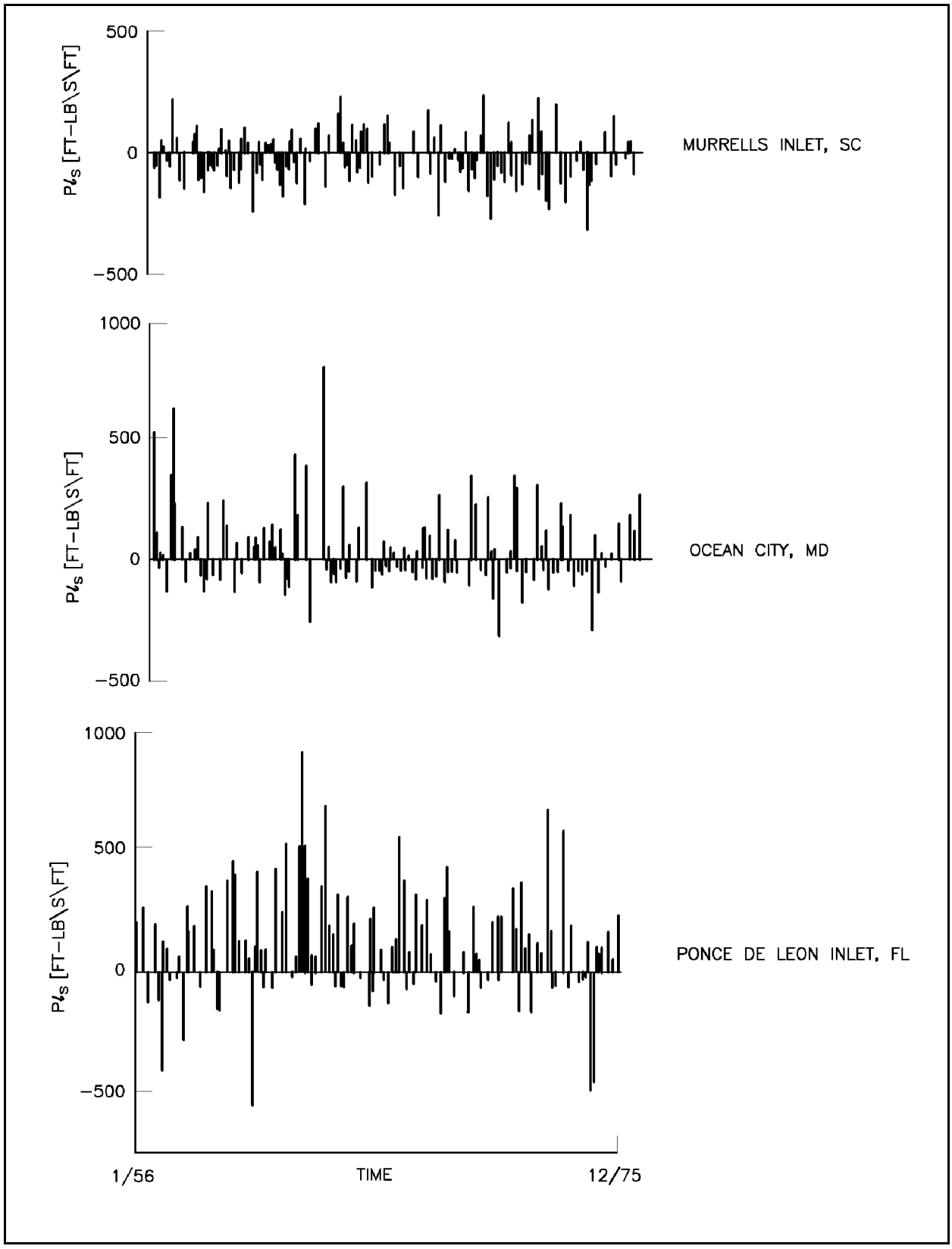

Figure III-2-9. Time plot of monthly longshore energy flux factor time series for 1956-1975 at three east coast sites (after Douglass (1985))

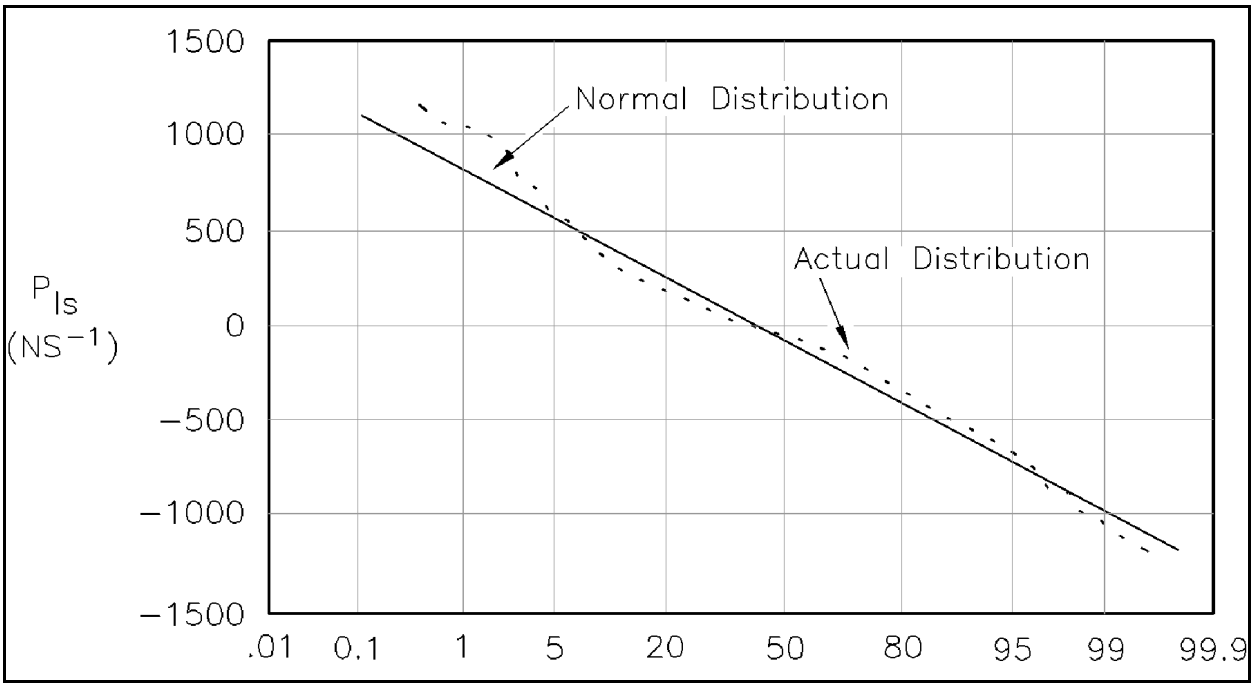

Figure III-2-10. Probability plot for monthly average P_{ls} series (Walton and Douglass 1985)

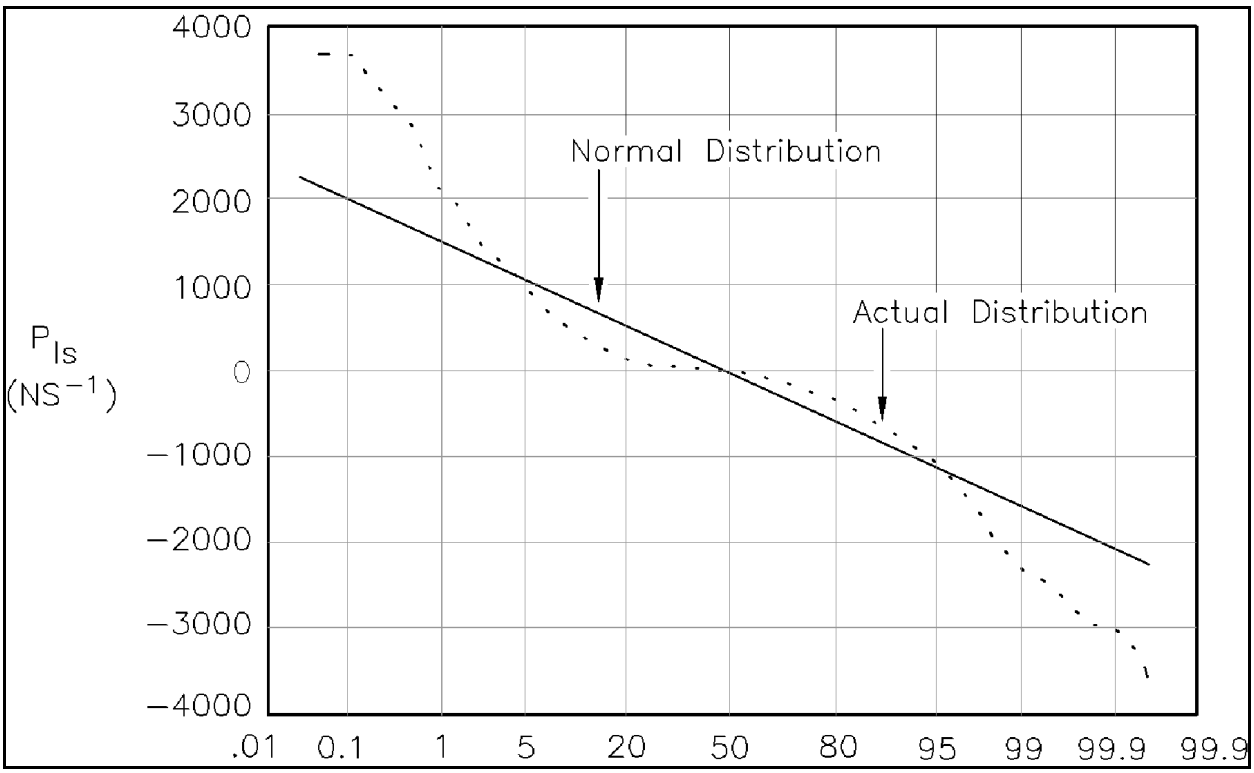

Figure III-2-11. Probability plot for weekly average P_{ls} series (Walton and Douglass 1985)

(d) Weggel and Perlin (1988) demonstrated that unidirectional annual transport variability may be described by a log-normal distribution. Thieke and Harris (1993) described similar results and noted that shorter-term (daily) dominant transports were better described by a Weibull distribution. These results apply only to statistics of transport in a single (positive or negative) direction and bidirectional distributions of transport are necessary to assess the true nature of the transport statistics for proper simulation (Walton 1989).

(e) When assessing various design alternatives, the proper distribution of the sediment transport rate must often be modeled as well as the natural persistence inherent in the data. Persistence is the measure of correlation for data closely spaced in time, i.e., large persistence means high sediment transport rates follow high sediment transport rates and low sediment transport rates follow low sediment transport rates in adjacent timeaveraging intervals. Persistence is typically measured via the autocorrelation coefficient (see, for example, Box and Jenkins (1976)). Autocorrelations for monthly and weekly longshore energy flux factors at the same South Carolina site are shown in Figures III-2-12 and III-2-13 (Walton and Douglass (1985)). Data exceeding the dotted lines suggest that persistence is evident in the data. Nonstationary and non-normal types of data may be simulated via an approach provided in Walton and Borgman (1991).

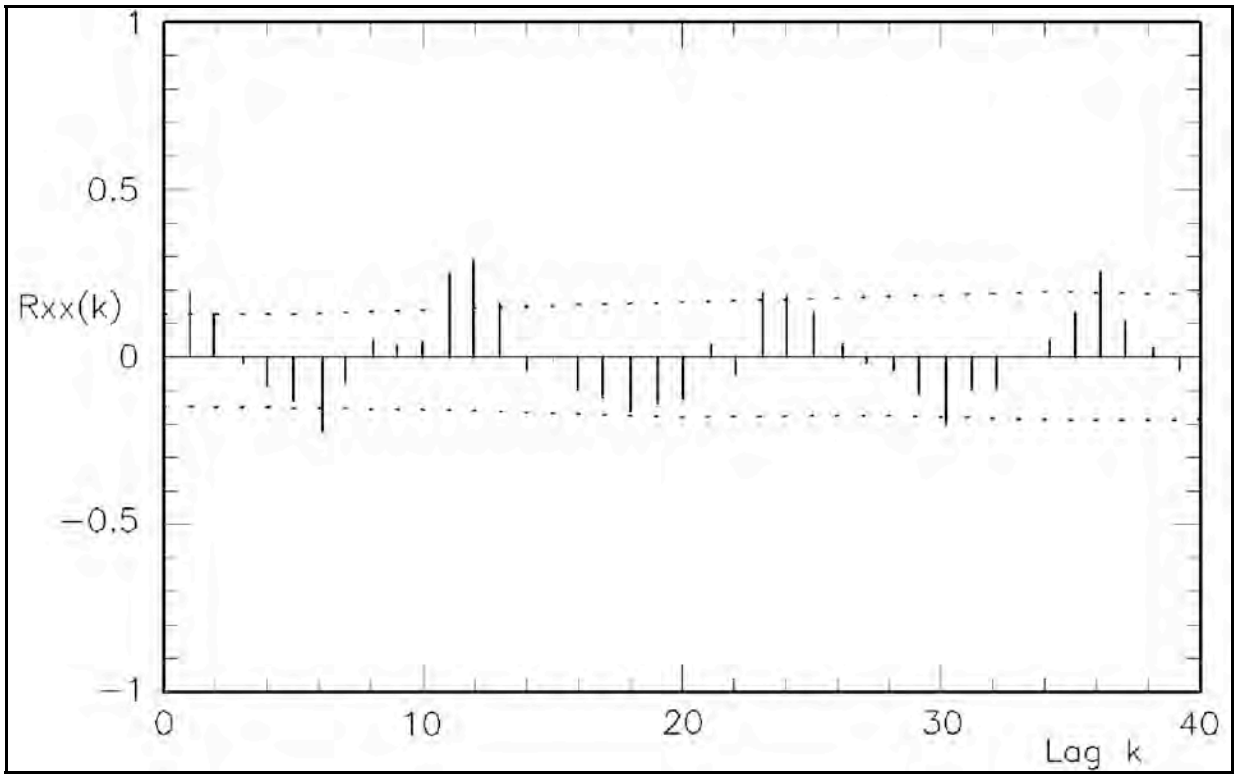

Figure III-2-12. Autocorrelation of monthly P_{ls} series (Walton and Douglass 1985)

(f) The significance of "episodic" transport to annual conditions is not well understood. It is thought that storm-related or other episodic events may cause the bulk of longshore sediment transport observed at some locations in the long term. Douglass (1985) suggested that 70 percent of the gross transport occurred during only 10 percent of the time at many sites via analysis of wave hindcast data.

(2) Wave data accuracy. The accuracy of wave data used to calculate potential transport rates also leads to uncertainty in predictions. Wave measurements and observations have associated uncertainties based on

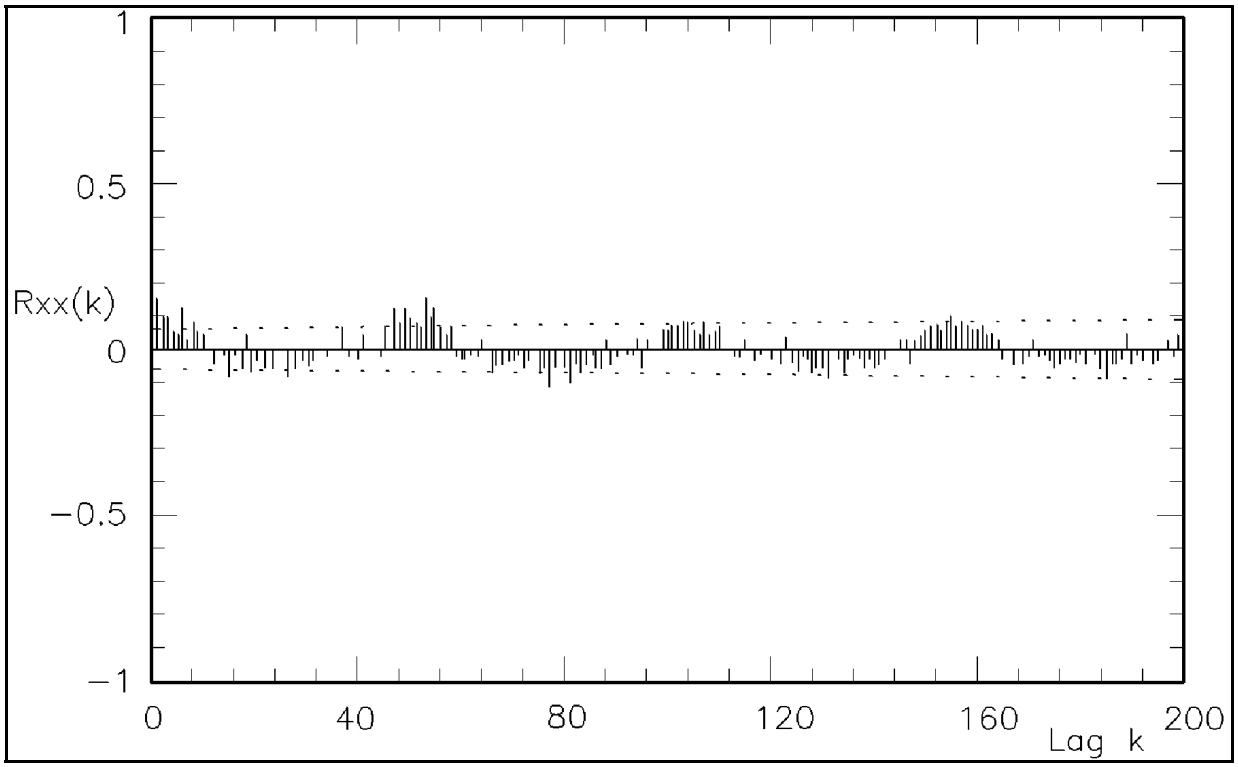

Figure III-2-13. Autocorrelation of weekly average P_{ls} series (Walton and Douglass 1985)

instrumentation accuracy and observer bias. Given that there are breaking wave height and wave angle uncertainty values ΔH_b and $\Delta\alpha_b$, respectively, an associated longshore transport uncertainty ΔQ_ℓ can be calculated. From Equation 2-7b, we see that $Q_\ell \sim H_b^{5/2} \sin 2\alpha_b$. Uncertainty in the longshore transport rate can be estimated by including the uncertainties in breaking wave height and angle:

$$Q_\ell \pm \Delta Q_\ell \sim (H_b \pm \Delta H_b)^{\frac{5}{2}} \; sin2(\alpha_b \pm \Delta\alpha_b) \tag{III-2-20}$$

Assuming that the wave angle at breaking is small, and using the first two terms of a Taylor series expansion of Equation 2-20, the uncertainty in the longshore transport rate is estimated as

$$\Delta Q_\ell \sim \pm Q_\ell \left(\frac{\Delta\alpha_b}{\alpha_b} + \frac{5}{2}\frac{\Delta H_b}{H_b} \right) \tag{III-2-21}$$

Thus, a 15-percent uncertainty in wave height and 15 percent uncertainty in wave angle result in 37.5- and 15-percent uncertainty contributions for height and angle, respectively, totaling a 52.5-percent uncertainty in Q_ℓ.

(3) Sand supply availability. Application of the potential longshore sand transport equations presented herein results in an estimate of transport that implies the availability of an unlimited supply of sand. If sand availability is limited, such as on a rocky or reef coastline, or interrupted such as in the vicinity of groins, jetties, or breakwaters, the actual longshore sand transport rate will be less than the calculated rate.

e. Littoral drift roses.

(1) The littoral drift rose is a potentially useful tool for interpreting littoral drift trends along a section of shoreline where the shoreline curvature is mild and bottom contours are reasonably parallel to the shoreline (Walton 1972, Walton and Dean 1973). The littoral drift rose shows how the littoral drift changes with change in shoreline orientation relative to prevailing wave climatology. The drift rose is constructed using standard prediction techniques for calculating littoral drift given that the shoreline is oriented in a direction $\ominus_n$, where $\ominus_n$ is the azimuth angle of the perpendicular to the shoreline in the seaward direction (see Figure III-2-14 for an example measurement of $\ominus_n$ at Ponte Vedra Beach, FL). The principle behind the littoral drift rose is that a range of shoreline orientations is considered. These orientations correspond to the range that exists at the study site. For each possible shoreline orientation, as described by $\ominus_n$, the total positive and negative littoral drifts along the shoreline are calculated for a given time-averaging interval (i.e., 20 years, annual, monthly, etc.). These calculated drift values are plotted in a polar plot, as shown in Figure III-2-15 for the Ponte Vedra Beach, FL area. From the plots, the littoral transport rate for any given shoreline orientation can be determined by entering the plot with the seaward directed normal of the shoreline orientation "$\ominus_n$" and reading off the total positive, total negative, and net littoral drift values. As the littoral drift for a given wave angle is proportional to sin ($2\alpha_b$), the net drift rose average for a real wave climatology has lobes that cause the magnitude to vary in a similar manner as sin ($2\ominus_n$).

(2) Littoral drift roses so constructed may be utilized in helping to identify tendencies of the shoreline toward stability or instability. As an example, for a long shoreline with variations of shoreline orientation, it is possible that there is a null (also termed nodal) point along the shoreline, which is defined as the location for which the averaged positive and negative littoral transport have the same magnitudes, yielding zero net drift. The littoral drift rose can be utilized in helping to identify this null (nodal) point. On the littoral drift rose, this null (nodal) point is reflected as a crossing of the positive and negative littoral drifts on the total littoral drift rose, or, as the point at which the net drift is zero on a net drift rose. Walton (1972) and Walton and Dean (1976) identified potential null points on barrier islands along the Florida coastline using the littoral drift rose and by integrating the longshore sand transport equation using changes in historical shorelines along with a known boundary condition of sediment accumulation at the end of the islands. Along the East Coast of the United States, there are several well-documented null points, such as just north of the Delaware-Maryland state boundaries and in New Jersey near Barnegat Inlet. At both of these locations the shoreline orientation changes significantly near the sites of the null (nodal) points and the net drift is to the south, south of the null (nodal) points, and to the north, north of the nodal points. Mann and Dalrymple (1986) examined the location of a null point along the Delaware coastline and concluded that there was a significant variation in its annual location, corresponding to the variation in the annual littoral drift rates. Such a shifting should be reflected in littoral drift roses for different averaging periods.

(3) Walton (1972) and Walton and Dean (1973) examined the stability of many shorelines using the littoral drift rose concept. Figure III-2-16 shows an "unstable" littoral drift rose and a barrier island orientation such that the initial island is oriented at the angle of the "unstable" null (nodal) point. Applying this rose to the island in the figure, it can be seen that if a negative perturbation (recession of shoreline due to mining, barrier overwash, etc.) is initiated on the island (away from the ends of the island where the transport scenario would not conform to the assumptions of the calculated littoral drift), the induced transport is away from the null point resulting in an erosional feature growth and potential island breakthrough (hence the term "unstable"). In a similar manner, for the "unstable" littoral drift rose an induced transport response to a positive shoreline perturbation in the same location (perhaps due to dredge spoil placement) would induce further transport of sand toward the perturbation, causing the perturbation to grow (a self-sustaining "positive" feedback mechanism). Walton (1972) has postulated that cuspate features such as shown in Figure III-2-17 (often found in bays, rivers, etc.) may be the result of "unstable" littoral drift roses for those sites due to the wave climatology experienced in long narrow fetch-enclosed locations.

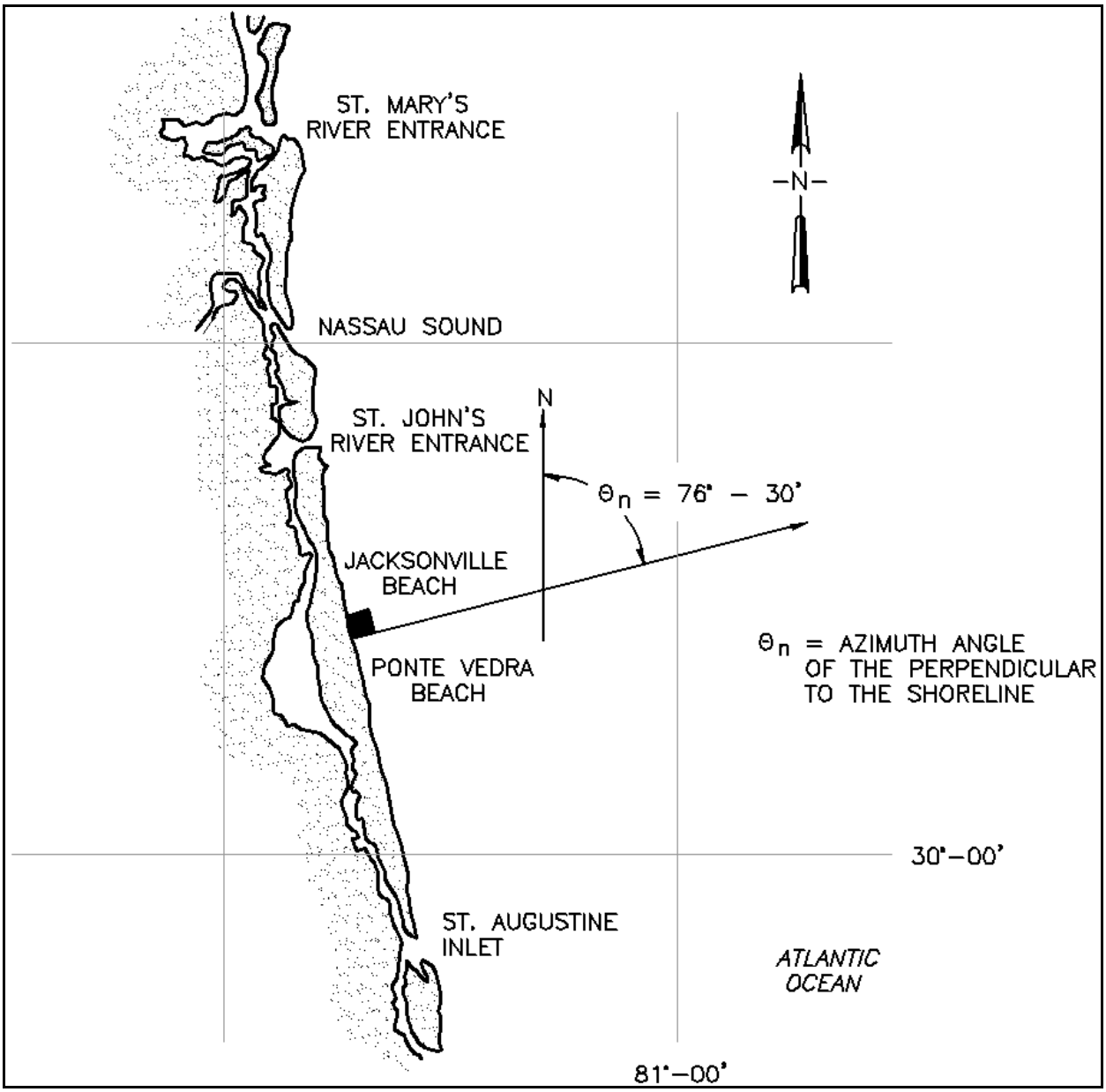

Figure III-2-14. Azimuth of normal to shoreline at Ponte Vedra Beach, Florida (Walton 1972)

(4) Another possibility is that the littoral drift rose along a shoreline is as shown in Figure III-2-18. In this case the null (nodal) point is stable. Perturbations in the shoreline, positive (accretions) or negative (recessions), now result in transport which tends to reduce rather than accentuate the perturbation (a "negative" feedback mechanism). In this case there is not a self-sustaining tendency toward island breaching Walton (1972) noted that the east coast of Florida is characterized by this type of littoral drift rose and, in fact, there are relatively few natural inlets along this coastline and a historical tendency of those inlets that are opened by man to close (unless closure is prevented via coastal structures such as jetties).

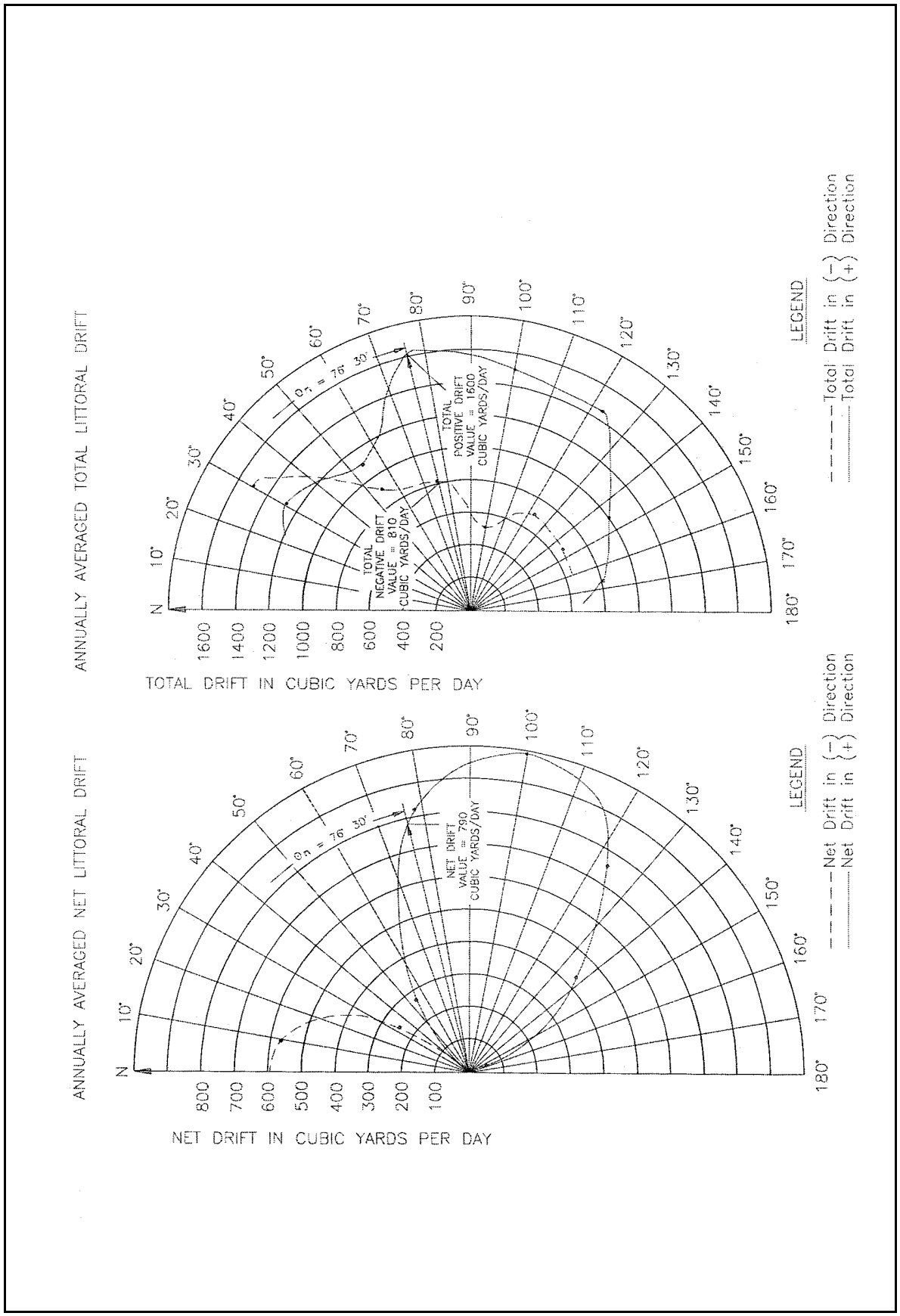

Figure III-2-15. Net and total littoral drift at Ponte Vedra Beach, Florida (Walton 1972)

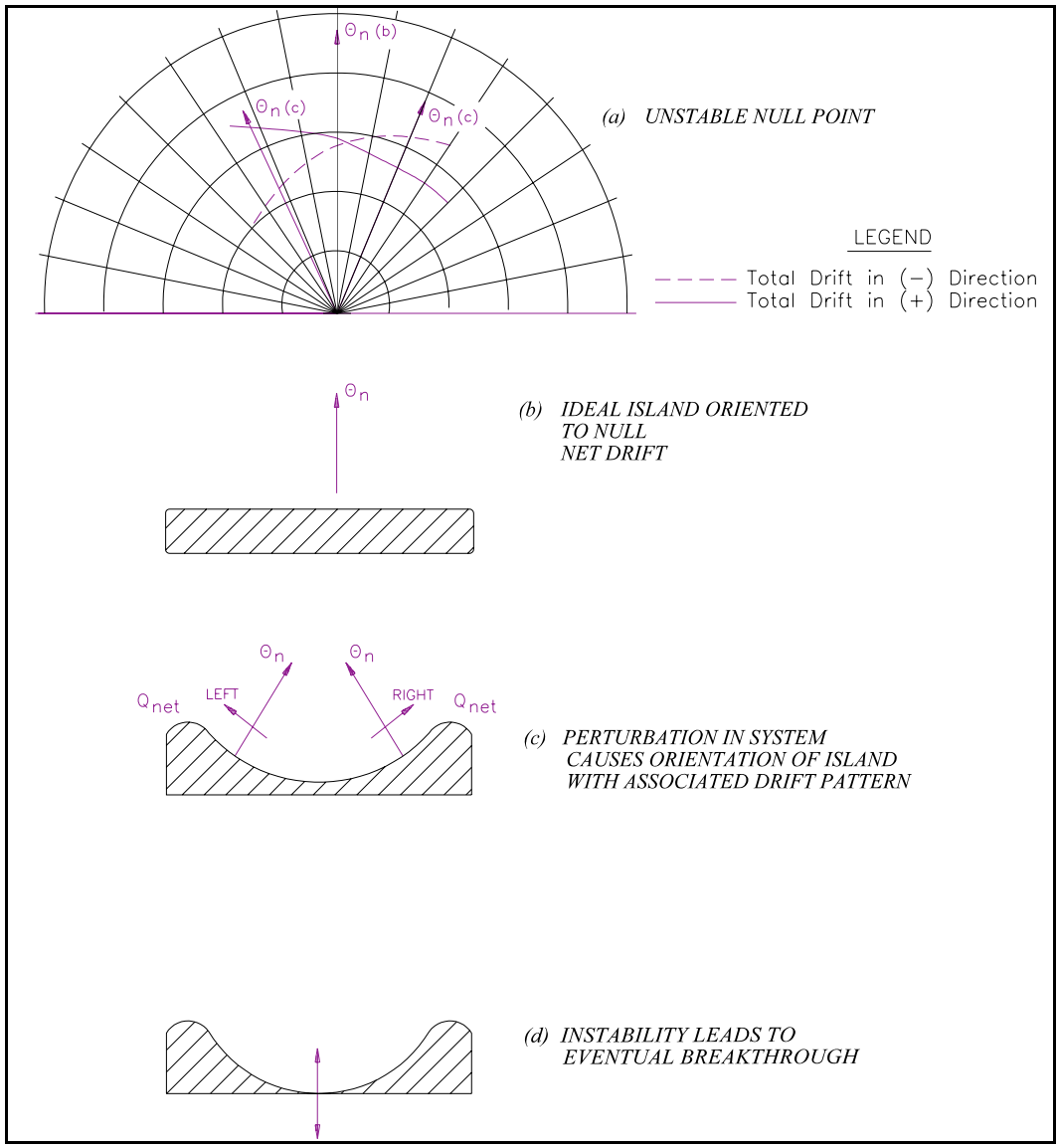

Figure III-2-16. Ideal case of an unstable null point (Walton 1972)

f. Cross-shore distribution of longshore sediment transport.

(1) The relationships given herein yield rates of total longshore sediment transport. Some applications require evaluations of the cross-shore distribution of the transport; e.g., for the effective design of groins, jetties, and sand weirs for weir jetties. In addition, a description of the cross-shore transport distribution is required in many computer simulation models.

(2) Bodge (1986) presents a literature review of the data and models which describe the cross-shore distribution of the longshore sediment transport. The collection of field data regarding this topic is difficult. The earliest approach was to use sand tracers (e.g., Zenkovitch 1960; Ingle 1966; Inman, Komar, and Bowen 1968; Inman, Tait, and Nordstrom 1971; Inman et al. 1980; Kraus et al. 1982, White 1987). As an example, Zenkovitch (1960) determined distributions at a coastal site by averaging a large number of tracer observations and found three maxima for the sand transport: two over longshore bars and a third in the swash

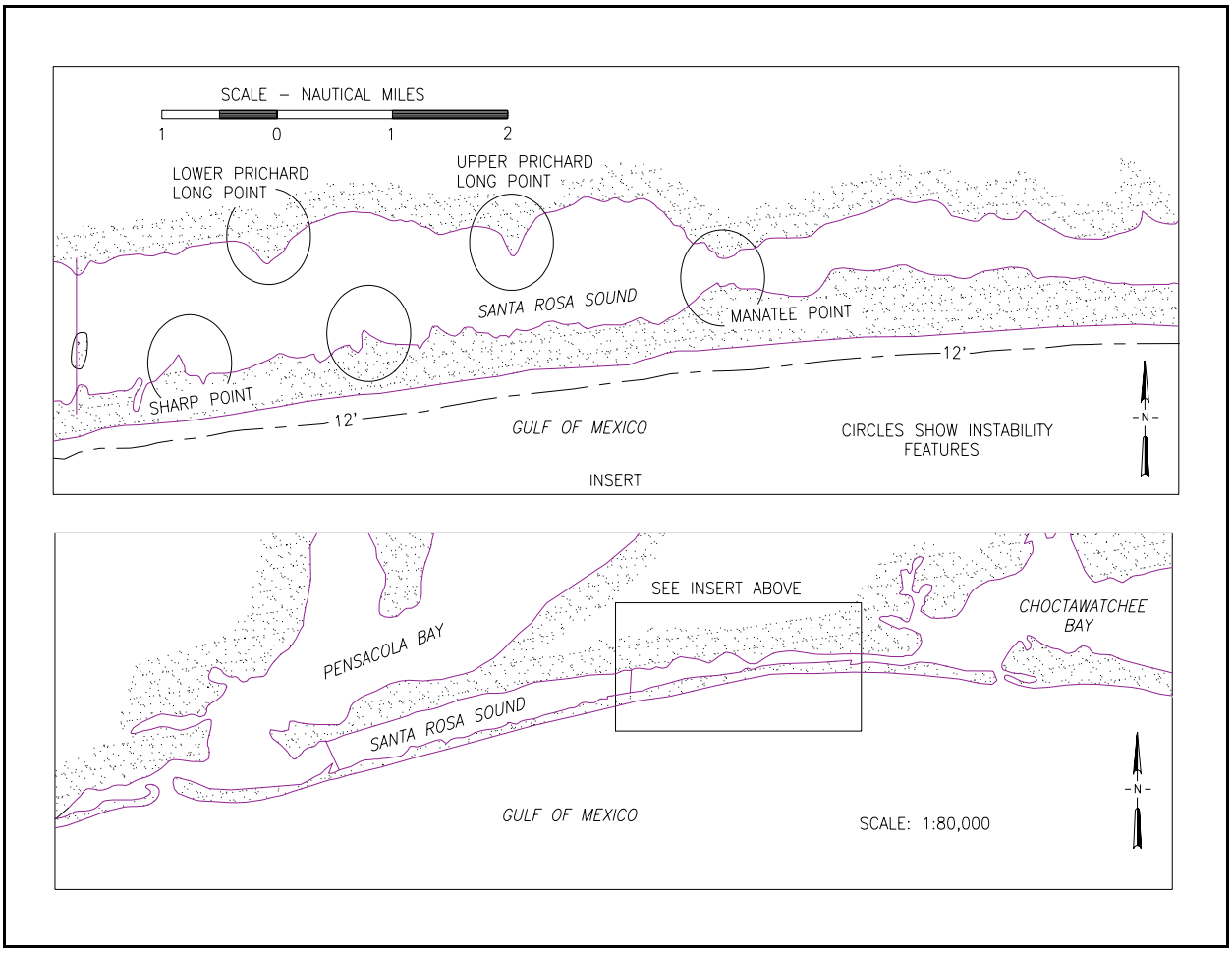

Figure III-2-17. Instability-formed capes in Santa Rosa Sound (Walton 1972)

zone. Ingle (1966) used fluorescent-dyed sediment at five test sites along the California coast to investigate the longshore rate of tracer dispersion, as well as its cross-shore distribution. An example of the cross-shore distribution of tracer density measured at Goleta Point in October 1961 is shown at three measurement intervals for two surf zone cross-sections in Figure III-2-19. Cross-section A represents conditions 46 m (150 ft) downdrift of the release line, and cross-section B is 46 m (150 ft) downdrift of cross-section A. The distributions indicate that the most rapid tracer dispersal took place at the edge of the swash zone, while the greatest tracer transport took place at the breaker zone.

(3) Using sediment traps operated from a Florida pier across the outer portion of the surf zone, Thornton (1972) found that longshore transport was a maximum on the seaward side of the longshore bar where waves were breaking. Sawaragi and Deguchi (1978) placed round sediment traps divided into pie-shaped sections into the beach and found three basic longshore transport distribution profiles: (1) maximum in the swash zone or near the shoreline, (2) maximum at the breaker line, and (3) bimodal with maxima at the shore and breaker lines. From a field study using fluorescent tracers, Kraus et al. (1982) likewise observed similar results in addition to a generally uniform cross-shore distribution. Berek and Dean (1982) inferred longshore transport distribution from measurements of contour rotation in a pocket beach at Santa Barbara, California, and found from their data that the transport was greatest across the inner surf zone. Kraus and Dean (1987) and Kraus, Gingerich, and Rosati (1989) give general examples of vertical and cross-shore distributions of longshore sediment flux measured with portable traps (see Figure III-2-2).

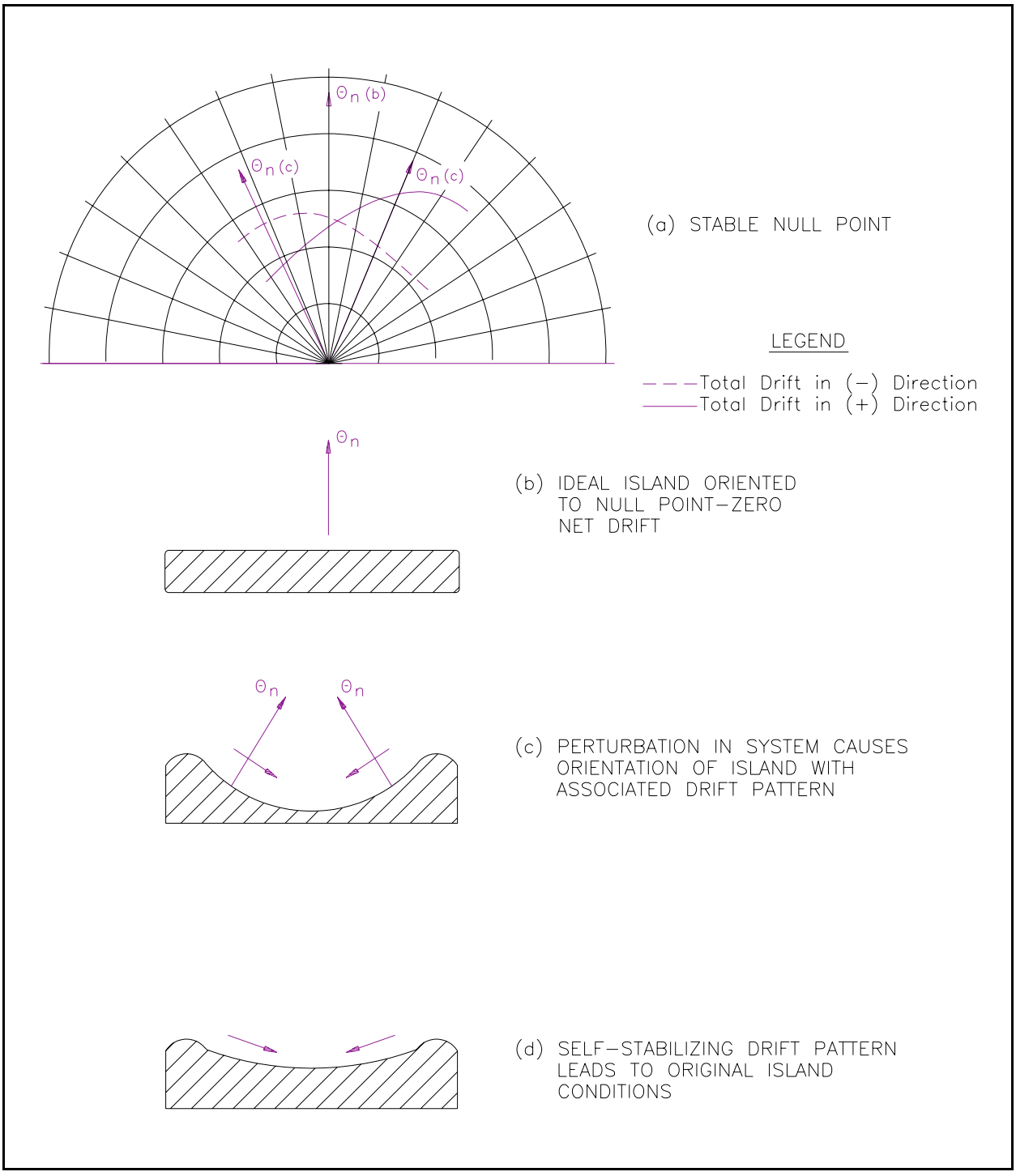

Figure III-2-18. Ideal case of a stable null point (Walton 1972)

(4) Kana (1978) measured the vertical suspended sediment concentration at locations across the surf zone, and longshore current velocity at a mid-surf position. His measurements indicated that, for spilling waves, sediment concentration rapidly increased inside the breakpoint, then remained relatively constant under the bore as it propagated towards the beach. For plunging waves, sediment concentration peaked

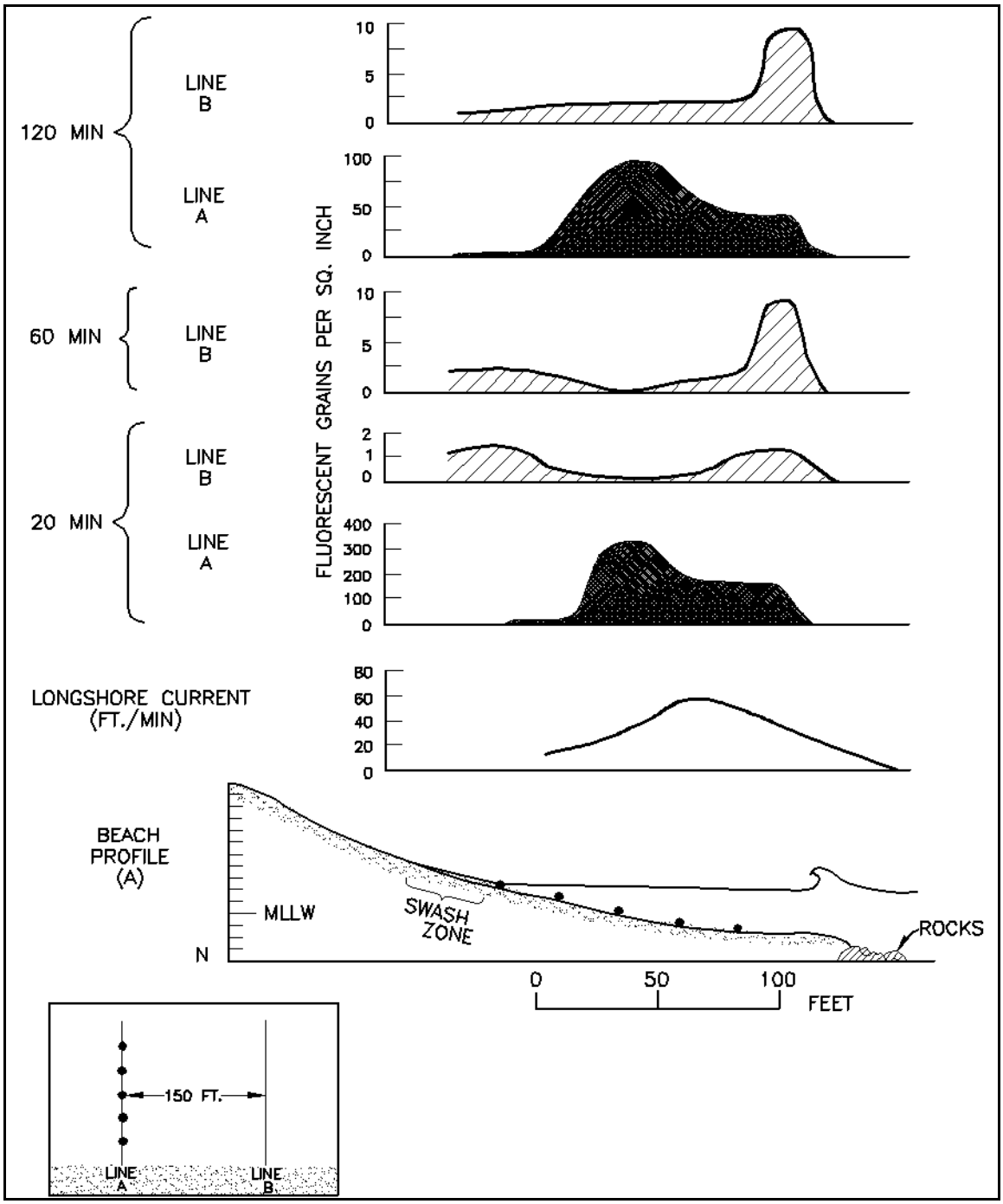

Figure III-2-19. Distribution of tracer density across the surf zone, 20 October 1961 Goleta Point, California, experiment (Ingle 1966)

within a few meters of the breakpoint, then decreased gradually towards shore (see Figure III-2-20). Downing (1984) and Sternberg, Shi, and Downing (1984) likewise measured vertical sediment concentration profiles simultaneously with the longshore current, and found maximum transport at about the mid-surf-zone location. The measurements did not include the inshore portion of the surf zone and did not account for bed-load transport.

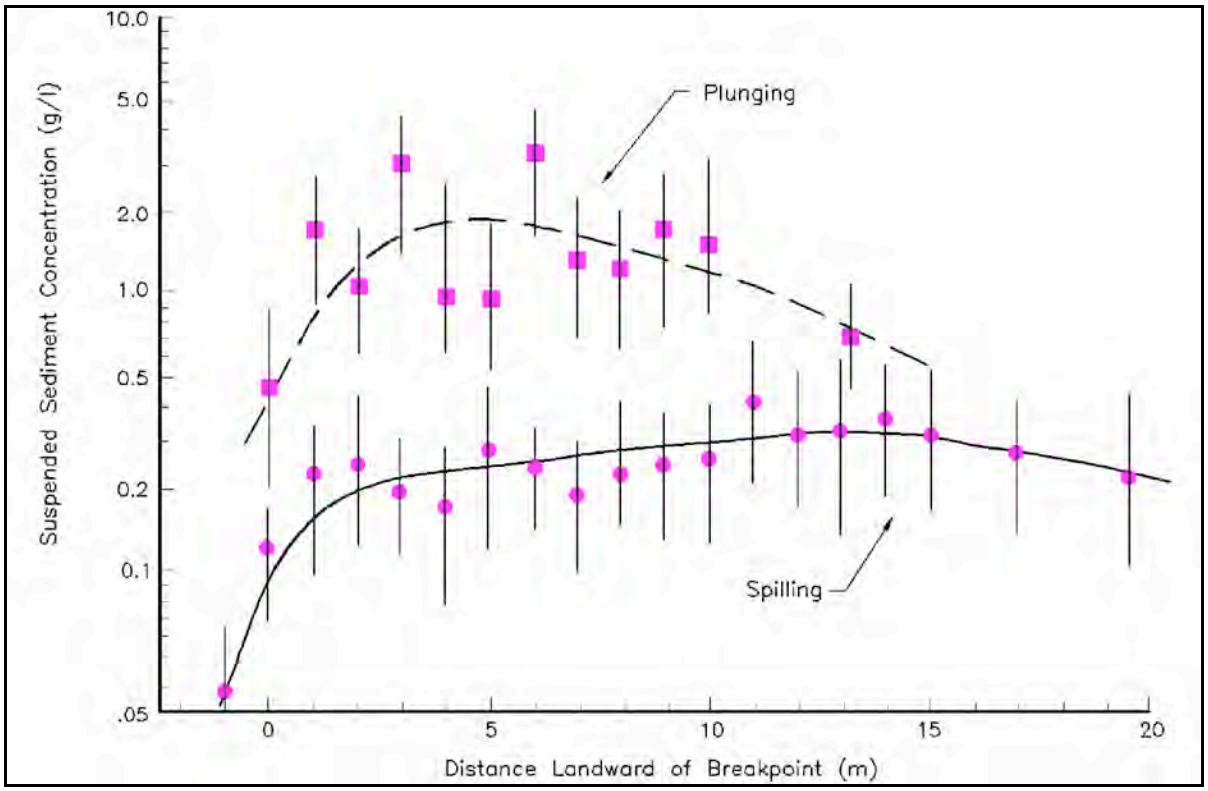

Figure III-2-20. Distribution of mean sediment concentration at 10 cm above the bed, relative to wave breakpoint (Kana 1978)

Bodge and Dean (Bodge 1986; Bodge and Dean 1987a, 1987b) utilized a short-term sediment impoundment scheme in the field and laboratory, consisting of the rapid deployment of a low profile, shore-perpendicular barrier. Beach profile changes in the vicinity of the barrier were determined from repeated surveys over short intervals of time, simultaneously with measurements of surf zone wave heights and currents. Four separate field experiments were undertaken at the CHL Field Research Facility at Duck, North Carolina. Two cross-shore distribution profiles from the field experiments are shown by the light lines in Figures III-2-21a and III-2-21b, indicating the presence of a maxima in the outer surf zone just shoreward of the breaker zone, and a second maxima in the swash zone. Light lines in Figures III-2-21c through III-2-21g show laboratory results for wave types including spilling, plunging, and collapsing. The plunging/spilling laboratory conditions (Figure III-2-21d) were modeled after the surf zone conditions of the field experiment in Figure III-2-21a. The error bars on the light lines indicate the most probable range of the local longshore transport contribution at each location across the surf zone, reflecting uncertainties in the assessed local magnitude of cross-shore transport, updrift limit of impoundment, and/or the degree of groin bypassing. The data suggest that the transport distribution is generally bimodal with peaks at the shoreline and at the mid-outer surf zone. The relative significance of the peaks was seen to shift from the near-breakpoint peak to the near-shoreline peak as the breaking wave condition varied from spilling to collapsing. Longshore transport seaward of the breakpoint represented about 10 to 20 percent of the total. Swash zone transport accounted for at least 5 to 60 percent of the total for spilling to collapsing conditions, respectively.

(5) In general, the field (and laboratory) studies of longshore transport indicate that (1) significant levels of transport may occur at and above the shoreline, (2) about 10 to 30 percent of the total transport occurs seaward of the breaker line, (3) maximum local transport has been noted within the shoreward half of the surf zone as often as within the seaward half, and (4) greater transport is often associated with shallower depths

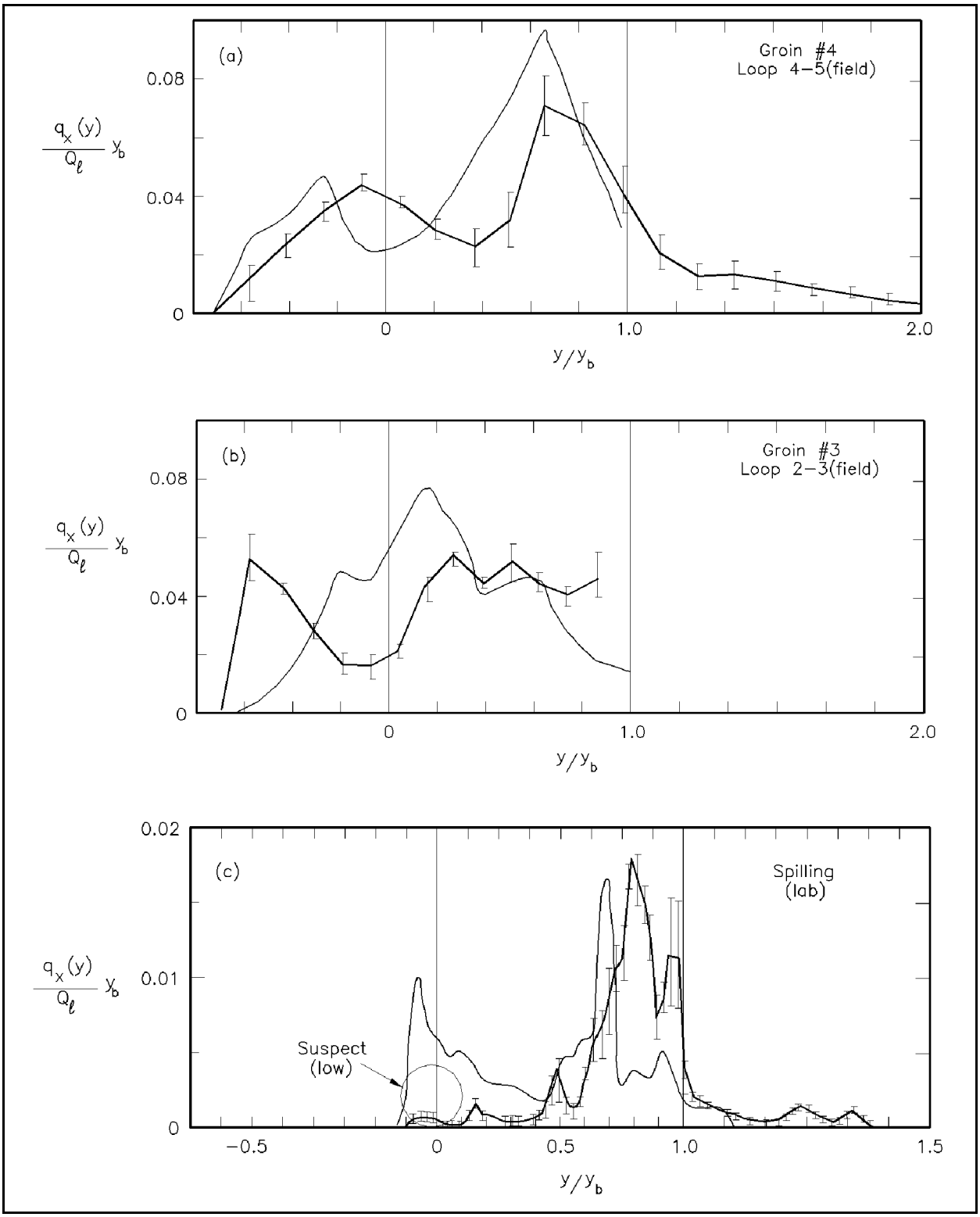

Figure III-2-21. Cross-shore distribution of longshore sediment transport as measured by Bodge and Dean (Bodge 1986, Bodge and Dean 1987a, 1987b) at Duck, North Carolina, and in the laboratory (Continued)

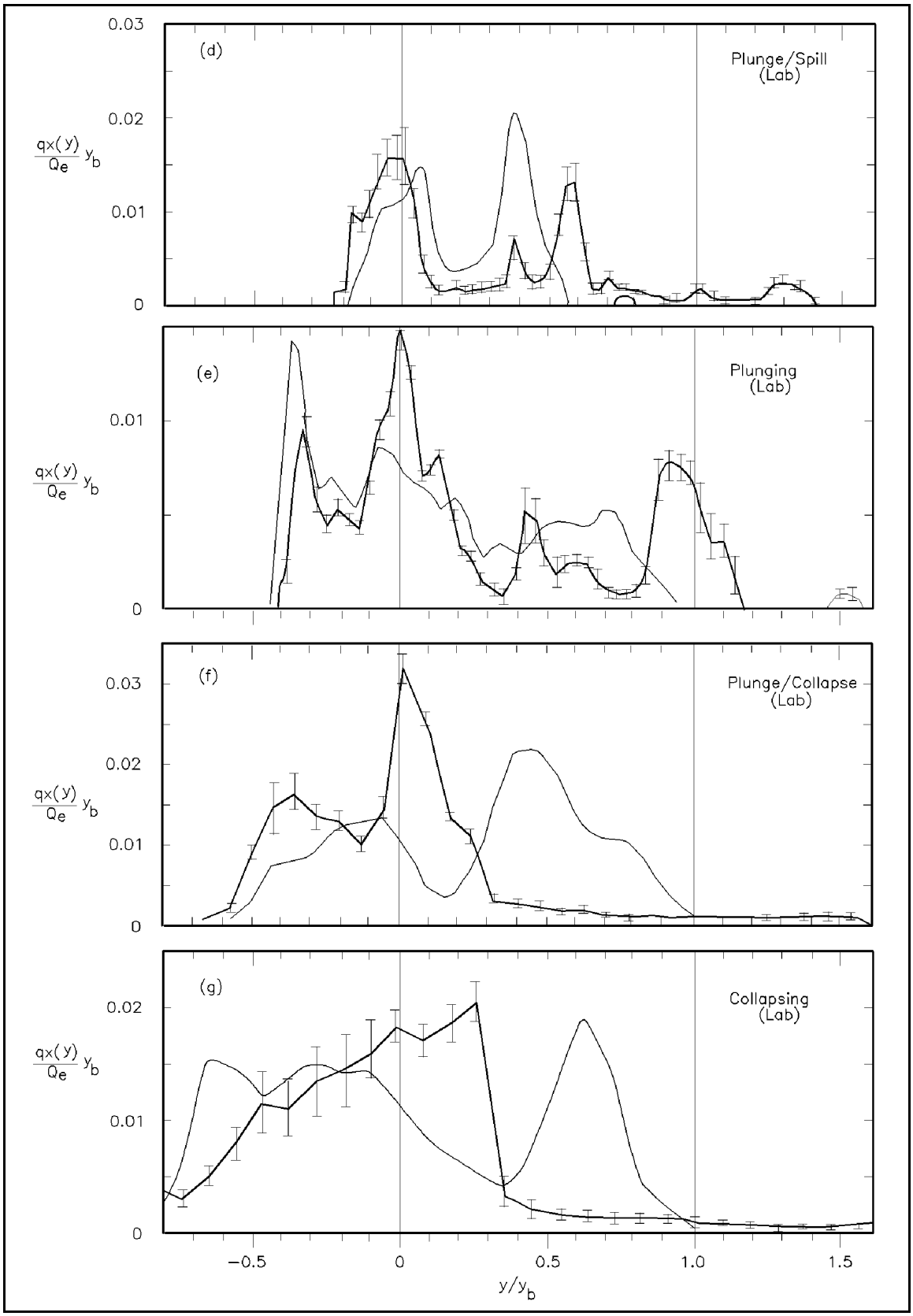

Figure III-2-21. (Concluded)

and breaking waves (i.e., breakpoint bars and the shoreline). Overall, field measurements demonstrate great variability in the shape of the longshore transport distribution profile across shore.

(6) Stresses exerted by waves vary in the cross-shore direction, generally decreasing from the breaker zone to the shoreline, but not necessarily in a uniform manner due to the presence of bars and troughs on the beach profile. The longshore current also has a characteristic profile, and because sand transport is a result of the combined waves and currents, its distribution will be related to their distributions. Theoretical relationships for the cross-shore distribution of longshore sediment transport have been postulated (e.g., Bagnold 1963, Komar 1977, Walton 1979, McDougal and Hudspeth 1981, Bailard and Inman 1981); however, they have not been shown to reproduce field measurements well. Using data from their field and laboratory experiments, Bodge and Dean tested five existing cross-shore distribution relationships, which were concluded to give from fair to poor correlation with measurements. Bodge and Dean based on the work of Bagnold (1963) also proposed a relationship for the cross-shore distribution of longshore sediment transport which assumes that sediment is mobilized in proportion to the local rate of wave energy dissipation per unit volume, and transported alongshore by an ongoing current

$$q_x(y) = k_q \frac{1}{d} \frac{\partial}{\partial x} (E\ C_g)\ V_\ell \tag{III-2-22}$$

where $q_x(y)$ is the local longshore transport per unit width offshore, y represents the cross-shore coordinate, k_q is a dimensional normalizing constant, d is the local water depth in the surf zone (including wave-induced setup), E represents the local wave energy density, C_g is the local wave group celerity, and V_ℓ is the local longshore current speed. Equation 2-22 can be expanded by assuming shallow water conditions, small angles of wave incidence, and assuming a nonlinear value for $C_g = (g(H+d))^{1/2}$

$$q_x(y) = k_q \frac{1}{8} \rho g^{\frac{3}{2}} \frac{H}{\sqrt{H+d}} \left[2\frac{dH}{dy} + \frac{H}{2\ (H+d)} \frac{d}{dy} (H+d) \right] V_\ell \tag{III-2-23}$$

in which H is the local wave height in the surf zone. Equation 2-23 represents conditions landward of the breakpoint; seaward of the breakpoint, $q_x(y) = 0$ under the assumption that no energy dissipation occurs. In application of Bodge and Dean's relationship, the dimensional constant k_q may be determined by integrating the distribution $q_x(y)$ across the surf zone, and equating this quantity to the total longshore sand transport rate Q_ℓ.

(7) The model (solid lines in Figure III-2-21) was compared with field data, and predicted the general trend of the measured transport distribution fairly well for one case (Figure III-2-21a), but shifted the cross-shore distribution slightly shoreward relative to the measured data for the second case (Figure III-2-21b). Comparison of the model with laboratory data indicated that the model generally overpredicted transport in the mid-surf zone (especially for the plunging/collapsing and collapsing cases) and modeled the near-shoreline transport distribution to a more reasonable degree than previous approaches.

g. Application of longshore sediment transport calculations.

(1) Littoral budgets.

(a) A littoral sediment budget reflects an application of the principle of continuity or conservation of mass to coastal sediment. The time rate of change of sediment within a system is dependent upon the rate at which material is brought into a control volume versus the rate at which sediment leaves the same volume. The budget involves assessing the sedimentary contributions and losses and equating these to the net balance of sediment in a coastal compartment. Any process that results in a net increase in sediment in a control

EXAMPLE PROBLEM III-2-7

FIND:

Cross-shore distribution of longshore sediment transport using Equation 2-23.

GIVEN:

Waves in 10-m (32.8-ft) depth have an rms wave height of 2.0 m (6.6 ft), angle of 10 deg to the shoreline, and wave period 8.5 sec. The beach profile is as given below. Assume the wave height to water depth ratio for incipient breaking κ = 1.0, the stable wave height to water depth ratio for wave re-formation $\Gamma_{stb} = 0.40$, the energy flux dissipation rate $\gamma = 0.15$, the lateral mixing coefficient $A_{mix} = 0.30$, and bottom friction coefficient $C_f = 0.01$. The K parameter (for use in longshore transport relationships) was calculated as 0.60.

Beach profile for Example III-2-7

No.	Distance Offshore (m)	Depth (m)
1	100.0	-0.60
2	111.0	0.10
3	132.0	1.00
4	145.0	1.50
5	156.0	1.70
6	169.0	1.90
7	173.0	1.95
8	186.0	1.85
9	190.0	1.80
10	195.0	1.70
11	199.0	1.75
12	207.0	1.81
13	214.0	2.00
14	246.0	3.10
15	340.0	4.00

SOLUTION:

Part II-3 presents relationships for nearshore wave transformation and Part II-4 discusses the cross-shore distribution of nearshore currents. Alternately, the PC-based numerical model NMLONG (see Part II-4 for a complete description) may be used to calculate the cross-shore distribution of total water depth and longshore current speed over an irregular bottom profile (Kraus and Larson 1991), which can be used in application of Equation 2-23. Entering the given data set, with 100 computation points, a cross-shore spacing of 2.0 m (6.6 ft), no wind, and a tidal reference elevation of 0.0, the cross-shore distribution of waves and currents as shown in Figure III-2-22b is obtained. A reduced listing of the NMLONG output, chosen to represent the peaks and minima of the wave height and longshore current distributions, is presented in the first four columns of the following table. The predicted $q_x(y)/k_q$ is shown in the last column and in Figure III-2-22a.

↓↓Example Problem III-2-7 (Sheet 1 of 4)

Example Problem III-2-7 (Continued)

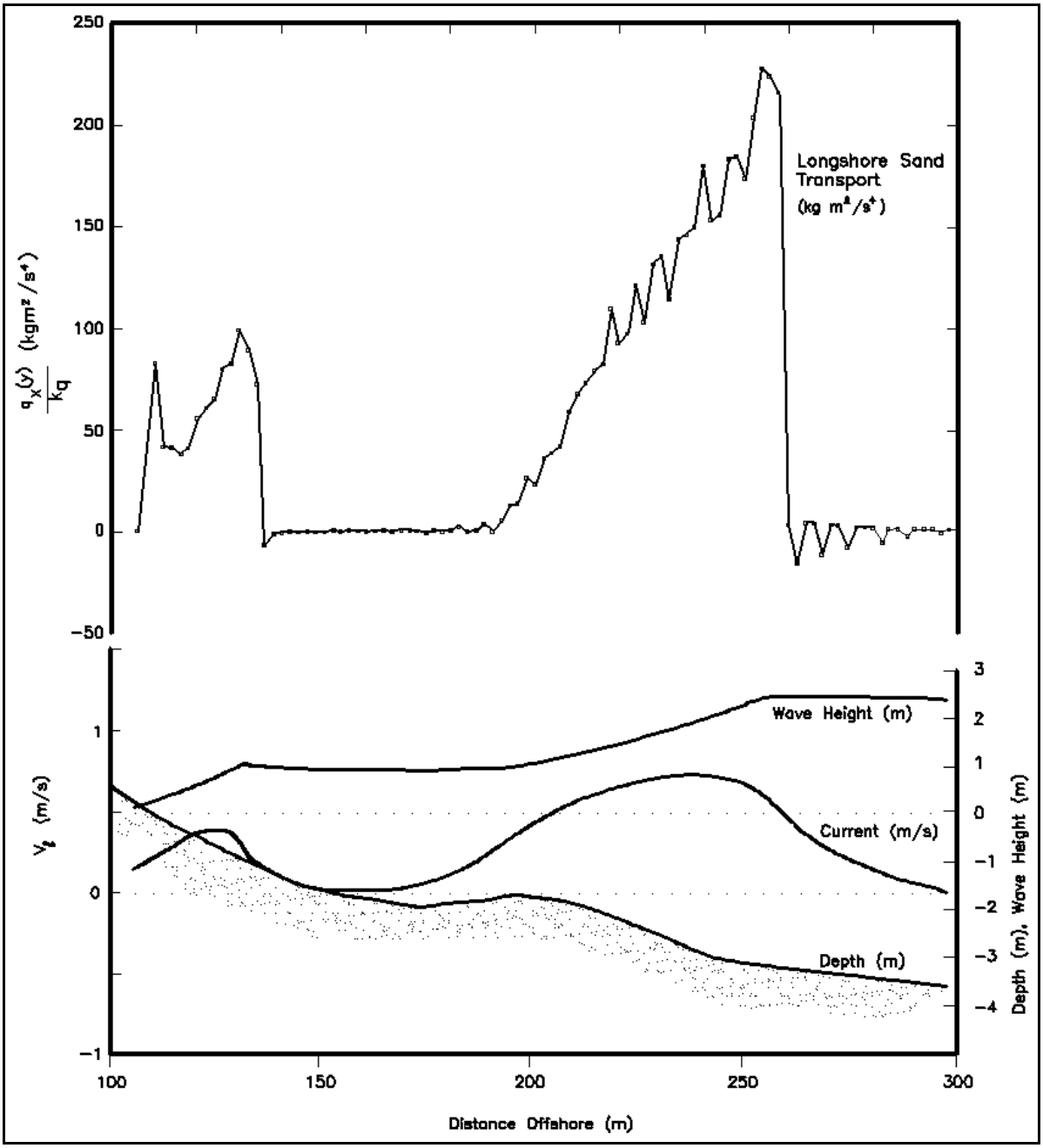

Figure III-2-22. Example III-2-7, predicted cross-shore distribution of longshore sand transport, wave height, and longshore current speed

Example Problem III-2-7 (Sheet 2 of 4)

Example Problem III-2-7 (Continued)

Output from NMLONG and Calculation of Cross-shore Distribution of Longshore Transport for Example Problem III-2-7

Cross-shore Coordinate (m)	Depth d (m)	Wave Height H (m)	Longshore current speed (m/sec)	$q_x(y)/k_q$ (kg m^2/sec^4)
110	0.09	0.20	0.20	83.3
112	-0.04	0.26	0.22	41.6
114	-0.14	0.32	0.25	40.8
126	-0.66	0.67	0.39	80.4
128	-0.74	0.74	0.39	82.9
130	-0.83	0.82	0.39	99.1
132	-0.91	0.90	0.34	89.4
134	-1.00	0.98	0.26	72.0
136	-1.08	0.96	0.20	- 6.9
148	-1.52	0.90	0.05	- 0.6
150	-1.55	0.89	0.04	- 0.7
152	-1.59	0.89	0.03	0.2
160	-1.73	0.87	0.02	- 0.4
162	-1.76	0.87	0.02	0.10
164	-1.79	0.87	0.02	0.10
178	-1.93	0.85	0.07	- 0.4
180	-1.91	0.85	0.08	- 0.3
182	-1.90	0.86	0.10	2.0
204	-1.80	1.10	0.51	37.5
210	-1.84	1.14	0.54	67.0
212	-1.89	1.18	0.56	72.2
238	-2.76	1.77	0.74	149.5
240	-2.83	1.83	0.74	179.7
242	-2.89	1.88	0.74	152.6
256	-3.18	2.34	0.63	223.8
258	-3.20	2.42	0.59	215.2
260	-3.21	2.42	0.53	2.3
278	-3.39	2.39	0.19	1.5
280	-3.41	2.39	0.17	1.4
282	-3.43	2.38	0.15	- 5.2

Example Problem III-2-7 (Sheet 3 of 4)

Example Problem III-2-7 (Concluded)

For some applications, such as weir design, only the percentage of longshore transport in a given region of the surf zone is of interest, and determination of the dimensional normalizing constant k_q may not be necessary. However, k_q may be calculated by integrating $q_x(y)/k_q$ across the surf zone, determined here by calculating the area below the points in Figure III-2-22b

$$\int_{y_s}^{y_b} \frac{q_x\ (y)}{k_q}\ dy\ =\ \frac{1}{k_q} \int_{106}^{260} q_x\ (y)\ dy\ \approx\ \frac{9300}{k_q}\ \ \frac{kg\ m^2}{\sec^4}$$

where y_s is the cross-shore coordinate at the start of the surf zone, (approximately 106 m) and y_b is the cross-shore coordinate at the breaker line (the breaking wave height of 2.42 m occurs at 260 m). Next, the total longshore sand transport rate is calculated. The offshore wave celerity may be calculated using linear wave theory as $C_{g1} = 9.0$ m/sec. Breaking wave angle may be calculated using Snell's Law (Equation 6-13) with input wave conditions ($\alpha_1 = 10^o$, $d_1 = 10$ m) and a depth at breaking = 3.2 m

$$\frac{\sin\ \alpha_1}{C_{g1}}\ =\ \frac{\sin\ \alpha_b}{C_{gb}}$$

$$\frac{\sin\ 10^o}{9.0}\ =\ \frac{\sin\alpha_b}{(9.81\ (3.2))^{\frac{1}{2}}}$$

$$\alpha_b\ =\ 6.2^o$$

The total longshore transport rate may be calculated using Equation 2-7b where $K = 0.60$

$$Q_\ell\ =\ K \left(\frac{\rho\sqrt{g}}{16\ \kappa\ (\rho_s\ -\ \rho)(1\ -\ n)} \right)\ H_{b\ rms}^{\frac{5}{2}}\ \ \sin(2\alpha_b)$$

$$Q_\ell\ =\ 0.60\ \frac{(1025)\ (9.81)^{\frac{1}{2}}}{16\ (1)\ (2650\ -\ 1025)\ (1\ -\ 0.4)}\ (2.42)^{\frac{5}{2}}\ \sin(2(6.2^o))$$

$$Q_\ell = (0.242\ \text{m}^3/\text{sec})\ (3600\ \text{sec/hr})\ (24\ \text{hr/day})$$

$$Q_\ell = 20.9 \times 10^3\ \text{m}^3/\text{day}\ (27.3 \times 10^3\ \text{yd}^3/\text{day})$$

The value of k_q may be calculated

$$\frac{9300}{k_q}\ \ \frac{kg\ m^2}{\sec^4}\ =\ 0.242\ \frac{m^3}{\sec}$$

Therefore, $k_q \sim 38{,}000\ \text{sec}^3/\text{kg}$, and the transport rates in Figure III-2-22b and the table can be converted to values of $q_x(y)$ (units $\text{m}^3/\text{sec/m}$), if desired.

Example Problem III-2-7 (Sheet 4 of 4)

volume is called a *source*. Alternately, any process that results in a net loss of sediment from a control volume is considered a *sink*. Some processes can function as sources and sinks for the same control volume (e.g., longshore sediment transport). The balance of sediment between losses and gains is reflected in localized erosion and deposition. In general, longshore movement of sediment into a coastal compartment, onshore transport of sediment, additions from fluvial transport, and dune/bluff/cliff erosion provide the major sources of sediment. Longshore movement of sediment out of a coastal compartment, offshore transport of sediment, and aeolian transport and washover that increase beach/island elevation produce losses from a control volume. Sediment budgets, including the types and importance of sources and sinks, are discussed in detail in Part IV-5.

(b) The appropriate level of detail for a littoral budget is a function of the intended uses of the littoral budget, and the available resources to complete the project. The essential components of a littoral budget include a site description, background, and examination of previous analyses. Past and present conditions, and the results of other studies, must be examined before initiating a new budget analysis.

(c) The longshore sediment transport rate must be determined next. This requires data on wave conditions over as long a time period as possible. These waves are propagated to and transformed in the surf zone. Appropriate sediment transport equations must be applied, ideally using historical shoreline positions and wave conditions for the same time period to, in effect, "calibrate" the transport equations for the study site. Very often, shoreline change models, which use the sediment transport equations, are applied. Boundary conditions defined at the start of the analysis are changed, so that sensitivity of the budget to these conditions may be evaluated.

(d) The actual sediment budget may then be determined. Usually there are poorly quantified components remaining in the analysis, such as offshore gains and losses. These must be estimated using any available data, engineering judgment, and the requirement that the budget close. Although a significant effort goes into the development of a littoral budget, it must be remembered that it is an estimate and may easily be in error. In addition, the budget is usually calibrated with shoreline positions over a number of years, and therefore indicates long-term average rates of change. It may not be indicative of the changes in any one year.

(2) Variations in longshore sediment transport along the coast.

(a) As described in the next section, noncohesive shorelines are not typically straight. The shoreline orientation and the degree to which waves refract, shoal, and converge or diverge along the shoreline determine variations in the potential transport rate along the coast. These variations are important determinants to shoreline change along the coast. For a nonuniform coastline, the potential longshore sediment transport rate is computed at discrete points along the coastline using values of the local breaking wave height and angle, where the latter is expressed relative to the local shoreline orientation. A ray-tracing or grid-based wave refraction analysis is typically employed to determine these values.

(b) Shoreline change may be related to the computed gradients in transport rate along the coast. For example, areas of convergent transport may correspond to a sediment sink (or deposition). Areas of divergent transport may correspond to a sediment source (or erosion if the area is not a source). As long as there is an unlimited sediment source, a shoreline's response to longshore sediment transport should be dependent on gradients in transport along the coast rather than magnitudes of transport.

h. Three-dimensionality of shoreline features.

(1) The three-dimensionality of noncohesive shoreline shape and its corresponding underwater expression are important to various aspects of engineering design. Dunes are more susceptible to breakthrough where the beach width fronting the dune is narrow due to the diminished protection afforded by the berm. Noncohesive shorelines are typically neither straight nor of smooth curvature. They often have isolated "bumps" or more regularly spaced shoreline features. Migration of such shoreline features can undercut or flank the landward ends of coastal structures such as seawalls or groins. For this reason any regularly spaced (rhythmic) topographic features inherent in the beach/shoreline structure as reflected in its planform shape may be of importance to the engineer for consideration of risk factors in evaluation of projects. Little is known about these features from a quantitative standpoint, although considerable qualitative descriptions of the features are documented.

(2) Typically, shoreline rhythmic features are classified by their planform (longshore) spacing or approximate wavelength if they are of reasonably regular form and hence are often referred to as "sand waves" by many authors. The term "sand wave" in this context should not be confused with underwater sand waves that are ubiquitous in most marine environments. Planform amplitude or height of the shoreline features (defined as cross-shore distance from embayment to cusp point) often is correlated with the wavelength. That is, longer shoreline planform wavelength (or alongshore spacing) suggests larger planform amplitudes (Sonu 1969). Along most shorelines, a spectrum of rhythmic shapes and sizes is present, making the underlying shoreline planform characteristics somewhat confusing. Due to the continuous range of scale in observed shoreline rhythmic features it is impossible to completely separate discussion of the various features by size since the physics governing the various length scales may be similar.

(3) At the small end of the scale of rhythmic shoreline features (and consequently of lesser engineering significance) are "beach cusps." Figure III-2-23 is an example of a beach with developed beach cusps. Russell and McIntire (1965) compile observational statistics on beach cusps from a number of ocean beaches and show cusp planform wavelengths (or longshore spacing) from 6 to 67 m. Numerous authors have postulated theories for the conditions of formation as well as spacing and amplitude of these smaller-scale features.

(4) At present, though, an explanation that would encompass all the numerous small-scale rhythmic features noted along the shoreline is lacking. Extended discussion on these smaller-scale shoreline features can be found in Komar (1976).

(5) As an example of larger-scale rhythmic topography, Figure III-2-24 shows a shoreline from Tokai Beach, Japan (Mogi 1960), in which two predominant wavelength scales of rhythmic sinuous topography dominate over a 3-month period of study. The shorter planform wavelengths in this example are on the order of 250 m while the longer planform wavelengths are on the order of 2.5 km. Although phasing changes are evident, the rhythmic feature length scales appear to have prevailed throughout the different survey periods. Lippmann and Holman (1990) have documented the conditions for rhythmic bars along one section of the North Carolina shoreline (Duck, NC). They found that rhythmic bars were a predominant feature observed in 68 percent of video imaging records and noted that during the strongest wave activity the rhythmic features were destroyed but that the features returned 5-16 days following peak wave events.

(6) Along beaches in Japan, Hom-ma and Sonu (1963) observed that under certain conditions crescentic bars with a regular alongshore spacing would weld to the shoreline with consequent large cusps formed at the attachment points (see Figure III-2-25). Sonu (1973) notes a second type of rhythmic topography in which rhythmic shoreline features are associated with the presence of rip current cell circulation (see Figure III-2-26). Sonu (1973) noted that both types of rhythmic topography could be present independently

Figure III-2-23. Beach cusps on a sandy beach in Mexico (photograph courtesy of Paul Komar)

Table III-2-3
List of Authors Postulating Theories for Cusp Development

Johnson (1910, 1919)	Dalrymple and Lanan (1976)
Dolan and Ferm (1968)	Dubois (1978)
Escher (1937)	Shepard (1973)
Longuet-Higgins and Parkin (1962)	Dolan, Vincent, and Hayden (1974)
Russell and McIntire (1965)	Flemming (1964)
Bagnold (1940)	Krumbein (1944b)
Williams (1973)	Komar (1973)
Kuenen (1948)	Zenkovitch (1964)
Sonu (1972, 1973)	Otvos (1964)
Sonu and Russell (1967)	Sonu, McCloy, and McArthur (1967)
Bowen (1973)	Bowen and Inman (1969)
Guza and Bowen (1981)	Guza and Inman (1975)
Sallanger (1979)	Seymour and Aubrey (1985)
Holman and Bowen (1979, 1982)	Darbyshire (1977)
Darbyshire and Pritchard (1978)	Dean and Maurmeyer (1980)

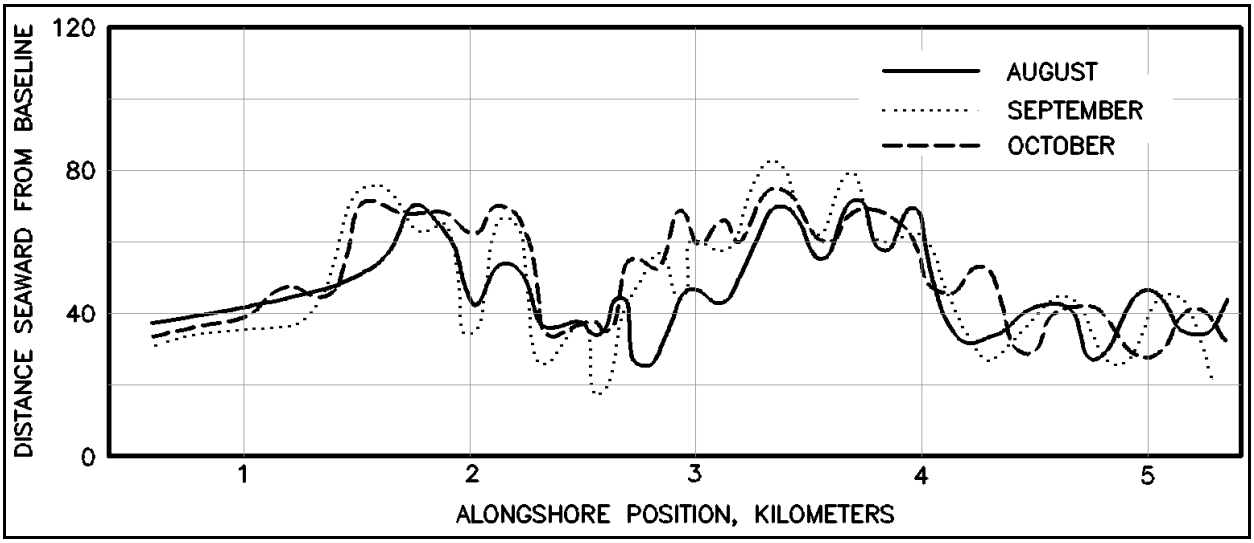

Figure III-2-24. Shoreline fluctuations in plan view at Tokai Beach, Japan (after Mogi (1960))

along a shoreline, and that the crescentic bar type of feature is typically at larger scales than the features associated with rip current cell circulation.

(7) Sonu (1973) details numerous examples of world coastlines with rhythmic shoreline/nearshore features, and notes the ubiquitous nature of these features via their existence on long uninterrupted coastlines as well as embayment shorelines between headlands, in tideless seas as well as coasts with tidal ranges up to 4 m, and on beaches with grain size ranging from sand to gravel. Observations of the planform wavelength (or alongshore spacing) of the features varies markedly, including 100 to 300 m along the east coast of Florida (Bruun and Manohar 1963); 64 to 218 m between transverse bars on the low-energy sheltered coast

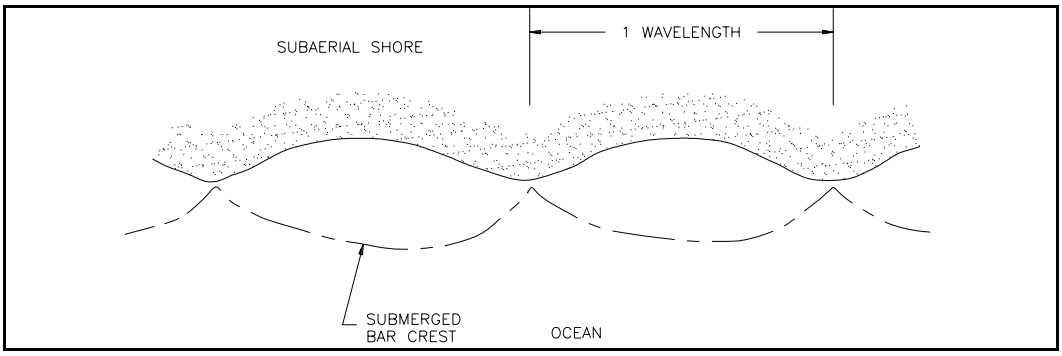

Figure III-2-25. Rhythmic shoreline features associated with the presence of crescentic bars welded to the shoreline

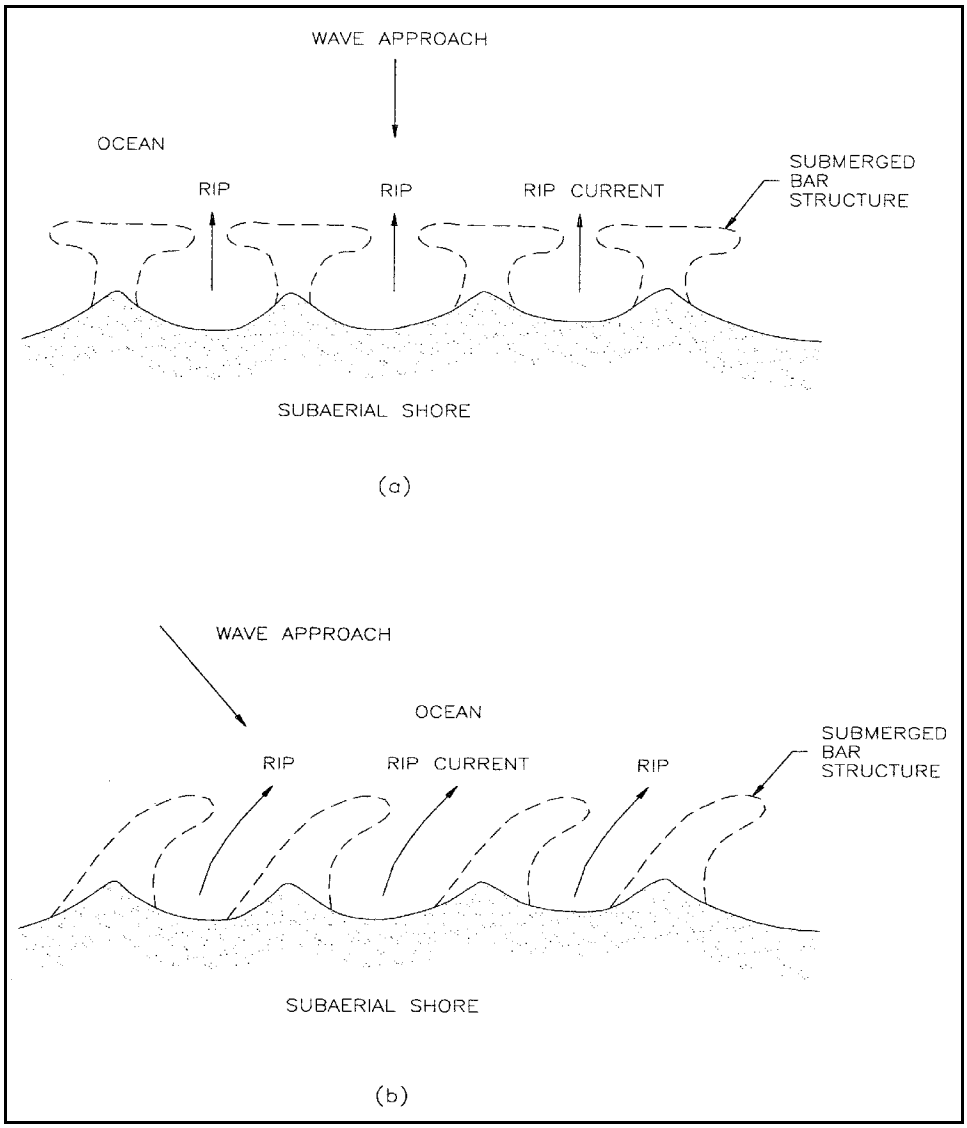

Figure III-2-26. Cusp rhythmic features in conjunction with rip currents under wave action approaching shoreline obliquely (adapted from Sonu (1973))

of St. James Island, Florida (Niedoroda and Tanner 1970); 100 to several thousand meters in the case of the example shown in Figure III-2-25 (Sonu 1973); up to 1,500 m for giant cusps noted along various beaches (Shepard 1952, 1973); and on the order of hundreds of meters along the Atlantic bluff shoreline of Cape Cod, Massachusetts (Aubrey 1980). Sonu and Russell (1967) noted, and later Dolan (1971) measured shoreline rhythmic features along the North Carolina coast with alongshore spacing ranging from 150 to 1,000 m with the predominant spacing about 500 to 600 m. In the same study, Dolan (1971) measure planform amplitudes from 15 to 25 m with large sand waves reaching amplitudes of 40 m. Numerous, well-documented surveys of sand wave/giant cusp rhythmic beach planforms also exist along the Danish and Dutch coasts (van Bendegom 1949, Brunn 1954, Verhagen 1989).

(8) Migration rates of rhythmic features vary widely with some studies reporting short-term fluctuations in position but no net long-term migration. Van Bendegom (1949) documents the monitoring over an 80-year period of large sand waves with amplitudes up to 200 m along the Dutch coast, and discusses the corresponding cycle of beach erosion and accretion as these waves migrate along the coastline with an average speed of 200 m/year. Dolan (1971) noted migration velocities of large sand waves along the North Carolina coast ranging from 100 to 200 m/month during heavy weather seasons. Verhagen (1989) has documented sand waves along the Dutch coast with amplitudes from 25 to 2,500 m and longshore speeds ranging from 45 to 310 m/year. Sonu (1969) has suggested that migration velocities of such shoreline features are inversely proportional to some power of the feature's alongshore spacing (i.e., the larger the feature, the slower the movement).

(9) Edge waves and rip currents are often cited as the main contributing forcing functions to the formation of rhythmic topography at various scales. A discussion of edge wave generation and hypothesized effects on beaches can be found in Guza and Inman (1975), Huntley and Bowen (1973, 1975a, 1975b, 1979), Huntley (1976), Holman and Bowen (1979, 1982), Wright et al. (1979), Guza and Bowen (1981), and Bowen and Inman (1971). A discussion of rip current formation and its effects on beaches can be found in Bowen (1969), Bowen and Inman (1969), Hino (1974), Dalrymple (1975), Dalrymple and Lanan (1976), Dolan (1971), Komar (1971), Komar and Rea (1976), and Komar (1978). Conclusive evidence proving the mechanisms for the formation of the many types of rhythmic topography is lacking.

(10) From an engineering standpoint the importance of rhythmic shoreline features (especially larger ones) and their potential for migration should not be overlooked in planning engineering structures or in analysis of design dune width for storm protection. For example, van Bendegom (1949) documents the structural failure of a groin due to the erosion produced by a large, migrating sand wave along the Dutch coast. Brunn (1954) described migrating sand waves along the Danish North Sea coast with observed planform spacings on the order of 300 to 2,000 m and amplitudes on the order of 60 to 80 m in areas where seasonal beach change was only 20 m/year and long-term shoreline recession only 2 m/year. In this regard, Brunn (1954) also cites a case of a sand wave of 900 m wavelength and 60 m amplitude with a migration speed of 700 m/year, and notes the difficulty of drawing definitive conclusions on average shoreline movements in such areas. Dolan (1971) noted that the regular spacing of dune breaching on Bodie Island, North Carolina, during the Ash Wednesday storm of 7 March 1962 correlated well with the rhythmic topography seen in the shoreline. Dolan (1971) also documented erosion along the Cape Hatteras, North Carolina, shoreline corresponding to embayments of rhythmic topography and suggested that when analyzing beach variability for specific sites, in addition to the seasonal recession-progradation cycle, additional variation (about 20 percent along the Outer Banks) should be considered to account for migration of the rhythmic topographic features.

(11) In practice, aerial photography at a reasonable scale (1 in. = 100 m or larger) or shoreline surveys are necessary to document the existence of rhythmic shoreline features. Sets of such aerial photographs/shoreline surveys with common control points and interspersed over long periods of time should

be useful in detailing both the potential existence and characteristics of such features for consideration in engineering planning.

i. Empirical shoreline models.

(1) In nature, many sections of coastline which are situated in the lee of a natural or artificial headland feature a curved shoreline geometry. Where sections of coastline are situated between two headlands, and particularly when there is a single, dominant wave direction, the shoreline may likewise assume a curved or "scalloped" shape (see Figure III-2-27a). In both cases, the curved portion of the shoreline related to the headland(s) is termed a crenulate or "spiral bay." Because of their geometries, these shorelines are also sometimes termed "parabolic," "zeta-bay," or "log-spiral" shorelines. The shape results from longshore transport processes which move sediment in the downdrift direction along the down-wave section of the shoreline, and from processes associated with wave diffraction which move sediment in the opposite direction in the immediate lee of the up-wave headland.

(2) Krumbein (1944b) and Yasso (1965) were among the first investigators to suggest that many "static" shorelines in the vicinity of rocky or erosion-resistant headlands could be fit to a log-spiral curve. Silvester (1970); Silvester and Ho (1972); Silvester, Tsuchiya, and Shibano (1980); and Hsu and Evans (1989) utilized the concept to develop empirical guidance for maximum coastal indentation between two headlands or coastal structures (such as seawalls or breakwaters) based on one dominant wave direction. Practical application of the approach requires identification of a predominant wave direction and the proper origin of the log-spiral curve. In a more theoretical effort, LeBlond (1972, 1979) derived equations for an equilibrium shoreline shape in the shadow zone of an upcoast headland based upon many simplifying assumptions concerning refraction and diffraction and found the resulting shoreline to be very similar to the log spiral shape. Rea and Komar (1975), Parker and Quigley (1980), and Finkelstein (1982) have also noted the similarity of bay shoreline shapes to log spiral curves. Walton (1977) and Walton and Chiu (1977) demonstrated that the log spiral curve is robust in the sense that most smooth curves found in nature can be fit to a log spiral if fortuitous values of its parameters are chosen. Walton (1977) presents a simplified procedure for evaluating a dynamic progression of static equilibrium shorelines downcoast from headland-type features using the concept of the littoral energy rose.

(3) Using shoreline data from prototype bays considered to be in static equilibrium and from physical models, Hsu, Silvester, and Xia (1987, 1989a, 1989b) presented an alternate expression to approximate the shoreline in the lee of headland-type features:

$$\frac{R}{R_o} = C_o + C_1\left(\frac{\beta}{\theta}\right) + C_2\left(\frac{\beta}{\theta}\right)^2 \qquad \text{(III-2-24)}$$

where the geometric parameters R, R_o, β, and θ are as shown in Figure III-2-27a, and values for the coefficients C_0, C_1, and C_2 are shown in Figure III-2-27b. The distance R_o corresponds to a control line drawn between the ends of the headlands that define a given section of shoreline. In the case of a single, upcoast headland, the distance R_o is the length of a control line drawn from the end of the headland to the nearest point on the downcoast shoreline at which the shoreline is parallel with the predominant wave crest. The distance R, measured from the end of the upcoast headland, defines the location of the shoreline at angles θ measured from the predominant wave crest. The angle β is that between the predominant wave direction and the control line R_o.

(4) The tidal shoreline which Equation 2-24 represents is not clear, but might be interpreted to represent the mean water shoreline. The data upon which Equation 2-24 is based are principally limited to $\beta > 22°$.

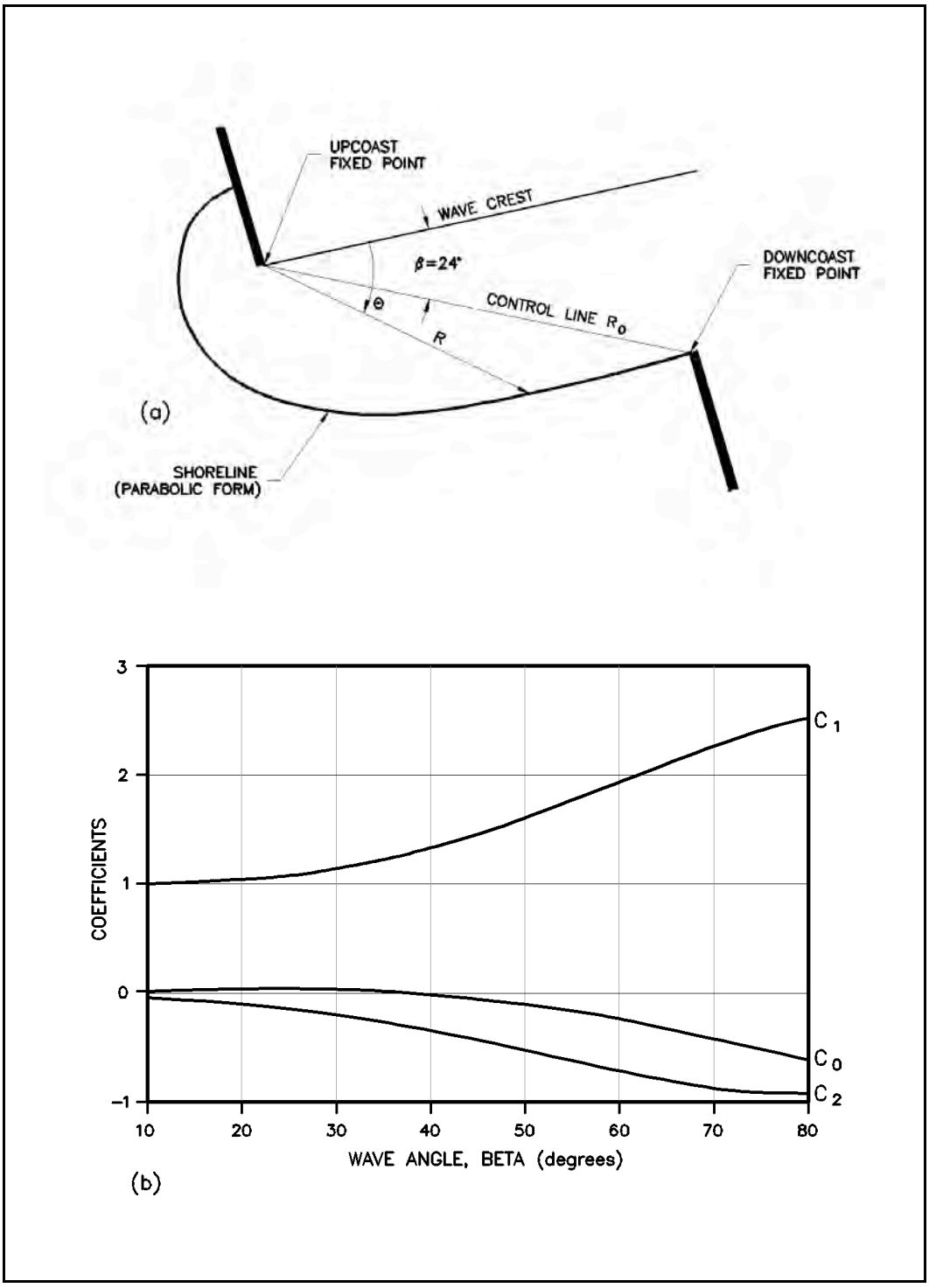

Figure III-2-27. Spiral bay geometry: (a) definition sketch and (b) coefficients describing parabolic shoreline shape (Silvester and Hsu 1993)

Additionally, Equation 2-24 is intended for application for $\beta \leq \theta \leq 180°$, and assumes that a predominant wave direction exists at the site of interest. The latter is often not the case in nature, and so engineering judgement must be utilized in practical application of this method. For $\theta > 180°$, the distance R may be assumed to be constant and equal to the value of R computed at $\theta = 180°$.

(5) Additional empirical guidance on shoreline change at seawalls is provided in Walton and Sensabaugh (1979) where additional localized recession at a seawall under a storm condition (hurricane Eloise along the Florida panhandle), is provided. Similar guidance for other storms and other locations is not available, although McDougal, Sturtevant, and Komar (1987) and Komar and McDougal (1988), have reported similar findings at laboratory scales.

(6) The approach(es) outlined above may be useful for rough, preliminary calculations and estimates of "static" shoreline equilibriums when the assumptions necessary for application of the approaches are fulfilled, where detailed dynamics of the changing shoreline are not sought, and where time and/or budget constraints preclude a more detailed approach. For detailed prediction of shoreline change due to longshore gradients in sand transport or otherwise complicated geometries, a preferred approach would be to utilize a physical model and/or a numerical model, as appropriate to the scale of the study area.

j. Analytical longshore sand transport shoreline change models.

(1) If the angle of the shoreline is small with respect to the x axis and simple relationships describe the waves, analytical solutions for shoreline change may be developed. As an example, utilizing the expression provided in Equation 2-7b for longshore sediment transport along with the assumption that the breaking wave angle α_b is small, the following planform shoreline change equation can be derived utilizing the coordinate system given in Figures III-2-28 and III-2-29:

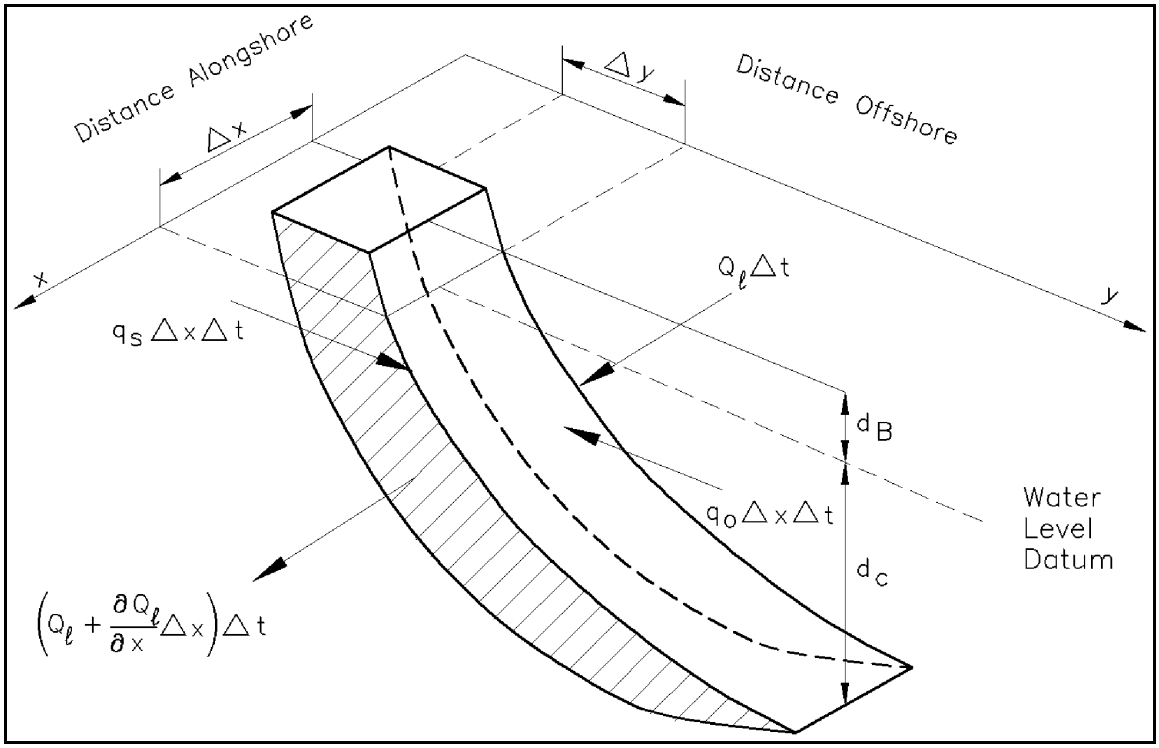

Figure III-2-28. Elemental volume on equilibrium beach profile

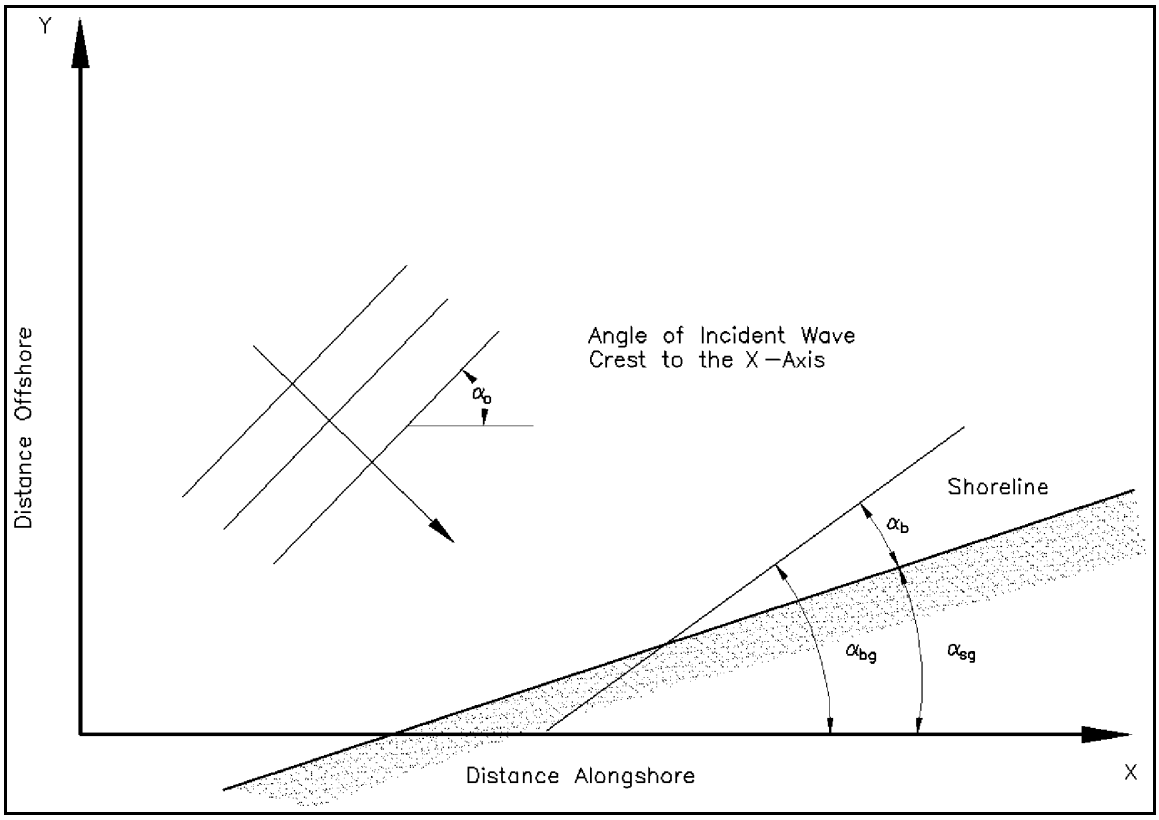

Figure III-2-29. Definition of local breaker angle

$$\varepsilon \frac{\partial^2 y}{\partial x^2} = \frac{\partial y}{\partial t} \tag{III-2-25}$$

where

$$\varepsilon = \frac{K H_b^2 C_{gb}}{8} \left(\frac{\rho}{\rho_s - \rho} \right) \left(\frac{1}{1 - n} \right) \left(\frac{1}{d_B + d_c} \right) \tag{III-2-26}$$

and where d_B = beach berm height above still-water level; d_c = depth of appreciable sand transport as measured from still-water level. Equation 2-25 is a partial differential equation, as it is dependent on both space (variable x) and time (variable t). A number of researchers have employed this equation or slight variations of it to provide analytical solutions to shoreline change under certain assumptions (the boundary conditions and initial conditions of the problem). Pelnard-Considére (1956) first presented an analytical solution to this simplified shoreline change equation for the case of an impermeable groin or jetty impounding the longshore sand transport on the updrift side of the structure under a stationary (constant) wave climate. Pelnard-Considére also verified its applicability with laboratory experiments and derived analytical solutions of the linearized shoreline change equation for two other boundary conditions: shoreline evolution updrift of an impermeable groin (with bypassing) and release of an instantaneous plane source of sand on the beach.

EXAMPLE PROBLEM III-2-8

FIND:

Compute the shoreline geometry of a crenulate bay located between two rock headlands for a shoreline where one dominant wave direction exists.

GIVEN:

The distance between the ends of the headlands is 175 m. The incident wave crests make an angle of 30 deg with a line drawn between the two headlands.

SOLUTION:

From Figure III-2-27b, the values of the coefficients for the wave angle β = 30 deg are approximately $C_0 = 0.05$, $C_1 = 1.14$, and $C_2 = -0.19$. The location of the shoreline may be predicted by plotting the distance R, measured from the end of the upwave headland, at angles θ measured from the line drawn between the headlands. The values R/R_o for various arbitrary angles between the wave angle, 30 deg, and a maximum angle, 180 deg, are computed from Equation 2-24. The corresponding dimensional values of R are then computed by multiplying R/R_o by the distance between the headlands R_o = 175 m. Representative examples are given below:

$$\text{For } \theta = 30 \text{ deg: } R = [\, 0.05 + 1.14(30/30) - 0.19(30/30)^2 \,] \, (\, 175 \text{ m} \,) = 175 \text{ m}$$

$$\text{For } \theta = 75 \text{ deg: } R = [\, 0.05 + 1.14(30/75) - 0.19(30/75)^2 \,] \, (\, 175 \text{ m} \,) = 83 \text{ m}$$

$$\text{For } \theta = 180 \text{ deg: } R = [\, 0.05 + 1.14(30/180) - 0.19(30/180)^2 \,] \, (\, 175 \text{ m} \,) = 41 \text{ m}$$

For $\theta > 180°$, the distance R may be assumed to be constant and equal to the value of R computed at $\theta = 180°$.

(2) Le Méhauté and Brebner (1961) discuss solutions for shoreline change at groins, with and without bypassing of sand, and the effect of sudden dumping of material at a given point. They also present solutions for the decay of an undulating shoreline, and the equilibrium shape of the shoreline between two headlands.

(3) Bakker and Edelman (1965) modified the longshore sand transport rate equation to allow for an analytical treatment without linearization. The sand transport rate is divided into two different cases:

$$Q_\ell = Q_o K_a \tan(\alpha_b) \quad \text{for} \quad 0 \le \tan \alpha_b \le 1.23 \tag{III-2-27a}$$

and

$$Q_\ell = Q_o \frac{K_b}{\tan(\alpha_b)} \quad \text{for} \quad 1.23 < \tan(\alpha_b) \tag{III-2-27b}$$

where K_a and K_b are constants. The growth of river deltas was studied with these equations.

(4) Bakker (1968) extended a one-line shoreline change theory to include the shoreline and an additional offshore depth contour to describe beach planform change. Bakker hypothesized that the two-line theory provides a better description of sand movement downdrift of a long groin since it describes representative changes in the contours seaward of the groin head. Near structures such as groins, offshore contours may have a different shape from the shoreline. The two lines in the model are represented by a system of two differential equations which are coupled through a term describing cross-shore transport. According to Bakker (1968), the cross-shore transport rate depends on the steepness of the beach profile; a steep profile implies offshore sand transport; and a gently sloping profile implies onshore sand transport. Additional complex solutions of cases with groins under very simplistic assumptions are discussed in Bakker, Klein-Breteler, and Roos (1971). Le Méhauté and Soldate (1977) provide an analytical solution of the linearized shoreline change equation for the spread of a rectangular beach fill. Walton (1994) has extended this case to the fill case with tapered ends.

(5) Walton and Chiu (1979) present two derivations of the linearized shoreline change equation. The difference between the two approaches, which both arrive at the same partial differential equation, is that one uses the so-called "CERC Formula" (see Equation 2-5) for describing the longshore sand transport rate by wave action and the other a formula derived by Dean (1973) based on the assumption that the major sand transport occurs as suspended load. Walton and Chiu (1979) also present solutions for beach fill in a triangular shape, a rectangular gap in a beach, and a semi-infinite rectangular fill, and present previous analytical solutions in the literature in a nondimensionalized graphical solution form.

(6) Dean (1984) gives a brief survey of some analytical shoreline change solutions applicable to beach nourishment calculations, especially in the form of characteristic quantities describing loss percentages. One solution describes the shoreline change between two groins initially filled with sand. Larson, Hanson, and Kraus (1987) provide a review of a number of analytical solutions to the one-line model as well as additional solutions where the amplitude of the longshore sand transport rate is a discontinuous function of x, the shoreline coordinate in the longshore direction.

(7) Analytical solutions presented here are in the nondimensionalized form of Walton and Chiu (1979) and easily adaptable to solving simple scenarios. More difficult scenarios are best handled by a numerical model. In arriving at all solutions, it is tacitly assumed that sand is always available for transport unless explicitly restricted by boundary and/or initial conditions.

(8) The first case to be considered is that of a structure trapping sediment. This formulation can be applied to the prediction of the shoreline updrift and downdrift of a littoral barrier extending perpendicular to the initially straight and uniform shoreline. At the barrier, all sediment is assumed to be trapped by the barrier (no bypassing). This boundary condition requires that the shoreline at the structure be parallel to the incoming wave crests. Figure III-2-30 shows the resulting shoreline evolution with increasing time updrift (accretion) and downdrift (erosion). Figures III-2-31a, III-2-31b, and III-2-31c are nondimensionalized solution graphs (at different scales) for the condition of no sand transport at the structure location ($x = 0$),

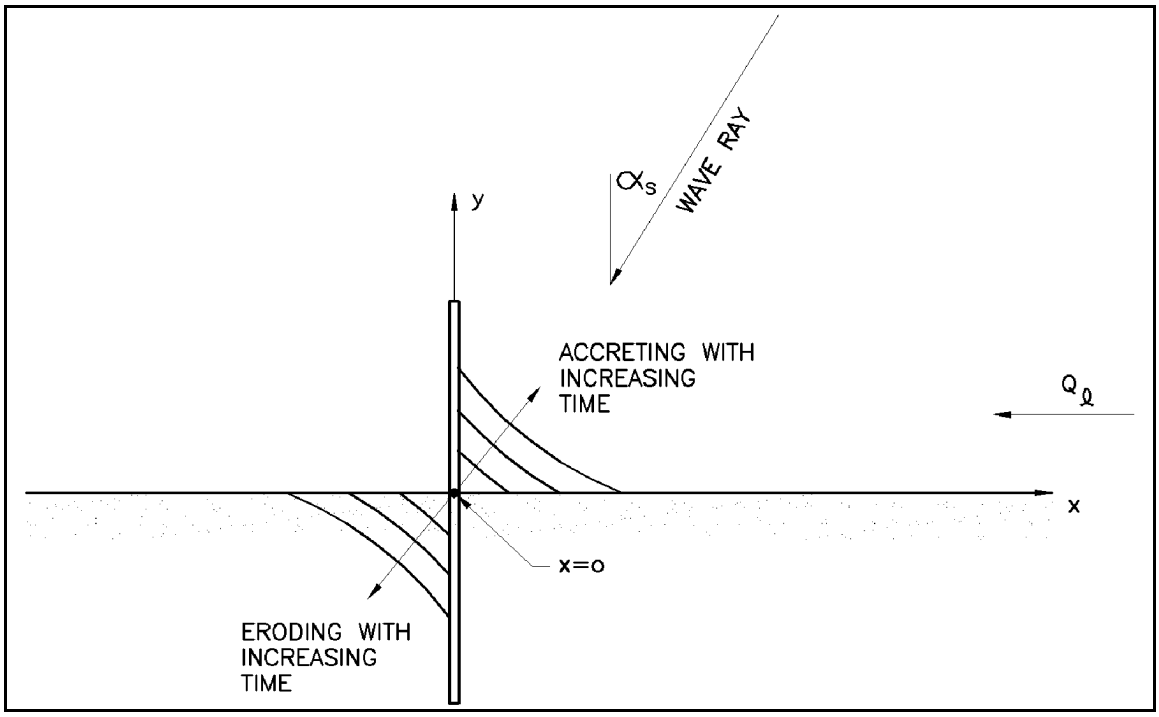

Figure III-2-30. Structure placed perpendicular to shore

with the boundary condition at the structure being tan α_b = dy/dx, and the boundary condition at $x = \infty$ being $y = 0$ for all times. The initial condition for this solution is that $y = 0$ for $t = 0$. This particular solution graph can be utilized to estimate planform shapes on the updrift side of coastal structures where bypassing does not take place.

(9) The dimensionalized solution for these conditions is given by Pelnard-Considére (1956) to be

$$y = 2\sqrt{\varepsilon t}\ \tan(\alpha_b)\left\{\frac{1}{\sqrt{\pi}}\exp\left[-\left(\frac{x}{2\sqrt{\varepsilon t}}\right)^2\right] - \frac{x}{2\sqrt{\varepsilon t}}\,erfc\left(\frac{x}{2\sqrt{\varepsilon t}}\right)\right\},\ \text{for}\ t < t_f \qquad \text{(III-2-28)}$$

where t_f is the time at which the structure fills to its capacity via this solution and where *erfc*( ) is the complementary error function defined as *erfc*( ) = 1 - *erf*( ) where *erf*( ) is the error function and

$$\text{erf}(\ ) = \frac{2}{\sqrt{\pi}}\int_0^{(\ )} e^{-z^2}\,dz$$

Both *erfc*( ) and *erf*( ) are tabulated in various mathematical handbooks. Figures III-2-32 and III-2-33 provide graphs of *erfc*( ) and *erf*( ).

(10) The time required for the structure to fill to capacity $t = t_f$ can be found from the previous solution with ordinate $x = 0$; i.e.,

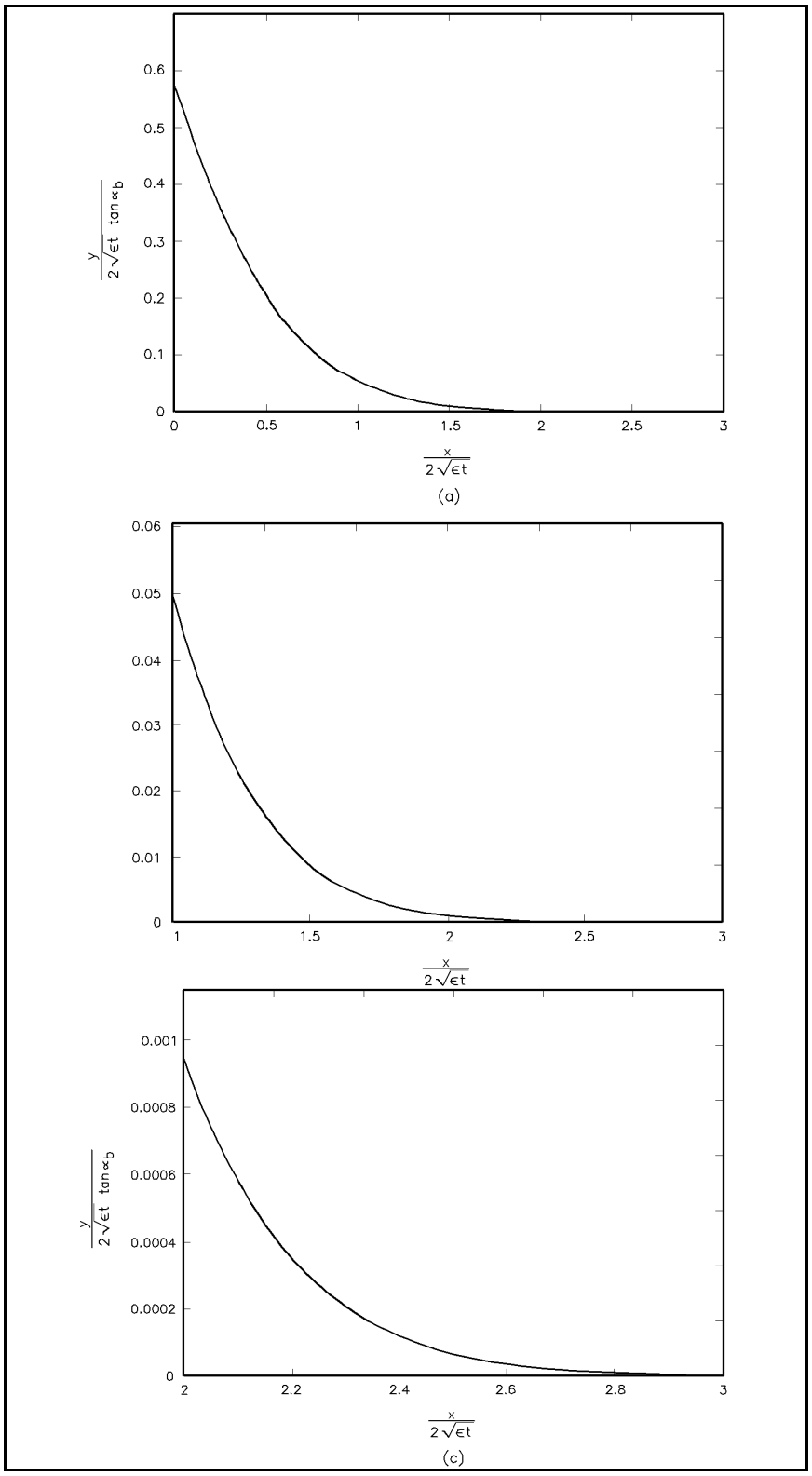

Figure III-2-31. Nondimensionalized solution graphs (at different scales) for the condition of no sand transport at the structure location

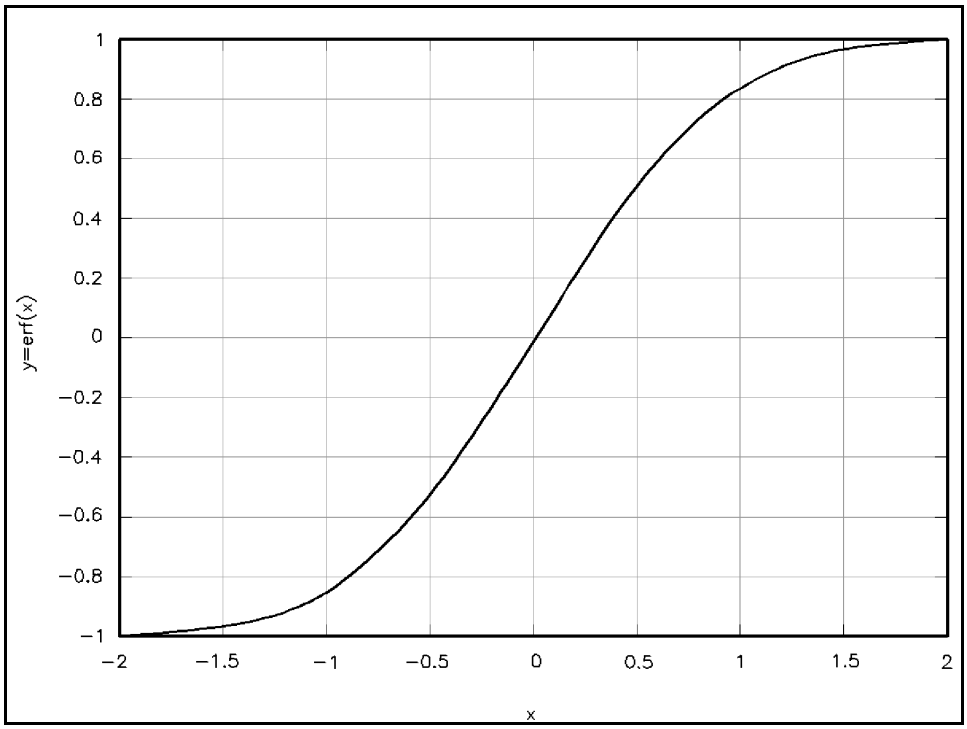

Figure III-2-32. Error function

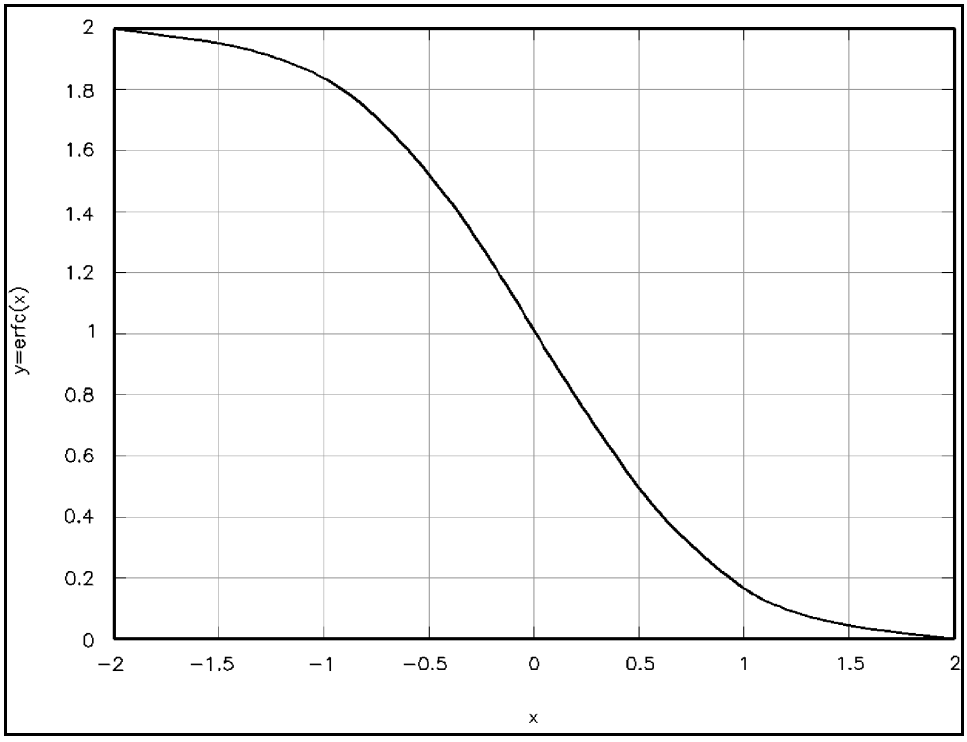

Figure III-2-33. Complementary error function

$$t_f = \frac{Y^2 \pi}{4 \varepsilon \tan^2(\alpha_b)} \quad \text{(III-2-29)}$$

where Y = length of structure.

(11) Pelnard-Considére (1956) also provides a second solution for times after the structure has filled to capacity and bypassing of sediment begins to occur naturally. The boundary conditions for his second solution are that $y = Y$ at $x = 0$ and $y = 0$ at $x = \infty$ for all $t > 0$. The initial conditions are as in the previous solution $y = 0$ at $t = 0$ for $x > 0$. The solution to these specific boundary conditions is as follows:

$$y = Y \, erfc\left(\frac{x}{2\sqrt{\varepsilon \, t_2}}\right) \quad , \; t > t_f \quad \text{(III-2-30)}$$

which can be made dimensionless by dividing the above equation by the length of structure Y. The dimensionless solution is presented graphically in Figures III-2-34a, III-2-34b, and III-2-34c (at different scales). Pelnard-Considére (1956) used a time = t_2 in Equation 2-30 such that areas of shoreline above the x axis would be equal at the time $t = t_f$ when the structure is just filled to capacity (Equation 2-29), i.e., matched solution plan areas. In this manner t_2 was found to be $t_2 = t - 0.38t_f$, where t is the initial solution time at which the structure begins to trap sand. Although the planforms do not match at time $t = t_f$ for the two solutions of Pelnard-Considére, the formulations are still useful for conceptual preliminary design and evolution of projects.

(12) The solution of Pelnard-Considére prior to bypassing (as given by Equation 2-28 and Figure III-2-31) may also be utilized for the situation in which erosion occurs on the sand-starved beach downdrift of an impermeable coastal structure that has no bypassing (natural or man-made). In this specific instance the solution would provide shoreline recession values as opposed to shoreline progradation values. In this scenario the solution should only be utilized far enough downdrift of the structure (i.e., beyond the immediate "shadow" of the structure) such that diffraction and refraction effects due to the structure do not influence the wave field and shoreline geometry.

(13) When applied in this scenario, the solution of Pelnard-Considére suggests that the ultimate downdrift extent of erosion caused by the structure is infinite. In practice, Equations III-2-28 and III-2-29 may be applied to estimate the theoretical downdrift extent of erosion, prior to bypassing, in terms of the structure length Y. That is, the distance downdrift of a structure at which the shoreline recession is less than or equal to some fraction of the structure's length (i.e., y / Y) can be expressed as a multiple of the structure's length (i.e., x / Y). Example III-2-10, below, illustrates this application. It is important to note that this solution is idealized and assumes that the breaking wave angle α_b can be approximated as an average, quasi-steady value. At present, the actual downdrift extent of erosion associated with a structure or other sediment sink is not well understood.

(14) The second case to be considered is that of a rectangular beach fill as shown in Figure III-2-35. Figure III-2-36 is a nondimensionalized solution graph that can be utilized in estimating plan area change for the rectangular beach nourishment fill on an initially straight reach of beach. Fill exists from $-a < x < +a$ and extends Y distance seaward from the original beach. The solution for this specific case is as follows:

$$y = \frac{Y}{2}\left\{ erf\left[\left(\frac{a}{2\sqrt{\varepsilon \, t}}\right)\left(1 - \frac{x}{a}\right)\right] + erf\left[\left(\frac{a}{2\sqrt{\varepsilon \, t}}\right)\left(1 + \frac{x}{a}\right)\right]\right\} \quad \text{(III-2-31)}$$

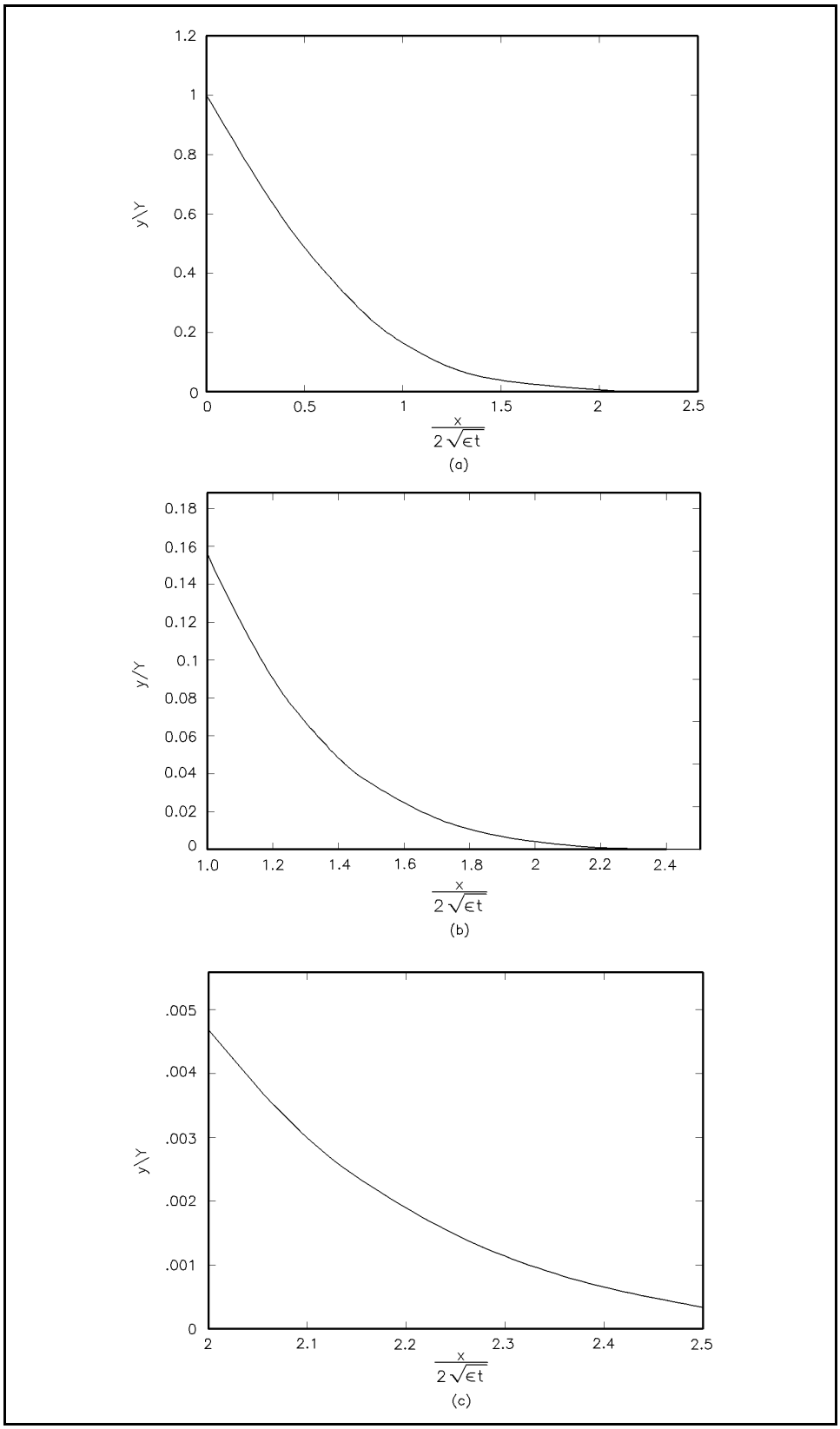

Figure III-2-34. Nondimensional solution curve for plan view of sediment accumulation at a coastal structure after natural bypassing initiated

EXAMPLE PROBLEM III-2-9

FIND:

(a) The time it will take for the structure to fill to half its length, if its length is 600 m.

(b) The distance seaward the shoreline will extend at the structure (y at $x = 0$) after 1 week (t = 604,800 sec) of continuous wave activity, and;

(c) the distance seaward the shoreline will extend at 500 m updrift from the structure (y at x = 500 m) after 1 week (t = 604,800 sec) of continuous wave climate.

GIVEN:

A long terminal groin extending a few surf zone widths at the end of a project reach adjacent to an inlet has been built to prevent sand from being lost from the beach into the inlet shoal system. Waves approach the inlet from the updrift side with a breaking angle $\alpha_b = 5$ deg. Breaking wave height H_b = 2m, and wave period T = 10 sec. The structure is initially expected to block all sediment (i.e., no bypassing). Sediment density to water density ratio $\rho_s/\rho = 2.65$, and porosity $n = 0.4$. Assume $d_B + d_c$ = 6 m, $K = 0.77$, and $K = 1$.

SOLUTION:

Equation 2-26 gives

$$\varepsilon = \frac{0.77\ (2)^2\ \sqrt{9.81 \cdot 2}}{8} \cdot \left(\frac{1}{2.65-1}\right) \cdot \frac{1}{(1-0.4)} \left(\frac{1}{6}\right) = 0.287\ \frac{m^2}{\text{sec}}$$

(a) Express Equation 2-28 for the shoreline location y at the structure $x = 0$:

$$\frac{y}{2\sqrt{\varepsilon\, t}\ \tan(\alpha_b)} = \frac{1}{\sqrt{\pi}} \cong 0.564$$

and solve for y = 1/2 the length of the structure = 300 m, where $\alpha_b = 5$ deg:

$$\frac{300}{2\sqrt{0.287\, t}\ \tan(5^0)} \cong 0.564$$

Solve this expression for time t and find $t = 3.22 \times 10^7$ sec (372 days).

(b) Use the expression for Equation 2-28 at the shoreline $x = 0$, and compute y for t = 1 week:

$$\frac{y}{2\sqrt{0.287\ (604800)}\ \tan(5^0)} = \frac{1}{\sqrt{\pi}}$$

and find y = 41.1 m (at x = 0).

(c) Solve Equation 2-28 for x = 500 m and t = 1 week.

$$\frac{x}{2\sqrt{\varepsilon\, t}} = \frac{500}{2\ \sqrt{0.287\ (604800)}} = 0.60 \quad ; \quad 2\sqrt{\varepsilon\ t}\ \tan(\alpha_b) = 72.9\ \text{m}$$

From Figure III-2-33, *erfc*(0.60) ≃ 0.42, so that Equation 2-28 is solved directly (or by Figure III-2-31) as

$$\frac{y}{2\ \sqrt{\varepsilon\ t}\ \tan(\alpha_b)} \cong \left[\frac{1}{\sqrt{\pi}}\ \exp\ (-0.6^{\,2}) - 0.6\ (0.42)\right] = 0.14$$

and

$$y = (0.14)\ (72.9\ \text{m}) = 10.2\ \text{m}$$

EXAMPLE PROBLEM III-2-10

FIND:

The distance downdrift of a structure at which the shoreline recession is less than or equal to 10 percent of the structure's length before sand begins to naturally bypass the structure.

GIVEN:

A long groin extending a few surf zone widths has been built with no artificial sand fill on either side. The groin's length, measured from the original shoreline, is Y. Assume that the wave activity is continuous with breaking angle $\alpha_b = 5$ deg.

SOLUTION:

The structure becomes filled to capacity at time t_f. Substitution of Equation 2-29 for t_f into Equation 2-28 yields:

$$\frac{y}{Y} = [\exp(-u^2) - \sqrt{\pi}\ u\ erfc(u)]$$

where

$$u = \frac{x}{2\sqrt{\varepsilon\, t_f}} = \frac{x}{Y}\frac{1}{\sqrt{\pi}}\tan(\alpha_b)$$

Determine the value u (graphically or by iteration), for which $y/Y = 0.10$. Find $u \cong 0.96$. Determine the downdrift distance x (relative to the structure's length Y) using this value for u and using $\alpha_b = 5$ deg:

$$\frac{x}{Y} = u\frac{\sqrt{\pi}}{\tan(\alpha_b)} = 0.96\frac{\sqrt{\pi}}{\tan(5^0)} = 19.4$$

That is, the shoreline recession is equal to or less than 10 percent of the structure's length beyond approximately 19.4 structure-lengths downdrift. If, for instance, the structure's length was Y = 200 m, the downdrift location at which the shoreline recession is less than 20 m (at the time the structure is filled to capacity) is (19.4)(200) = 3,880 m downdrift of the structure.

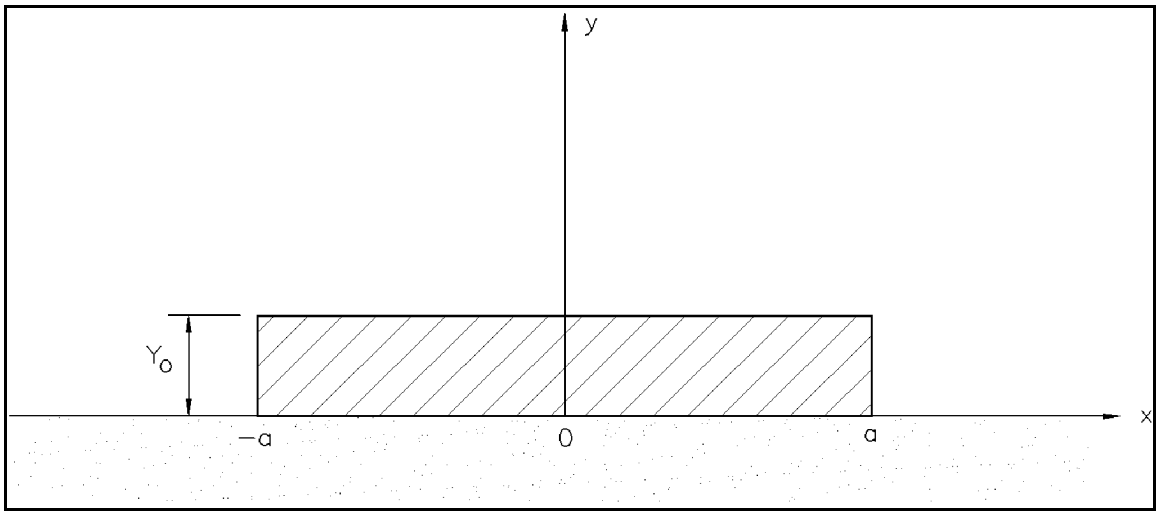

Figure III-2-35. Rectangular beach fill (*t*=0)

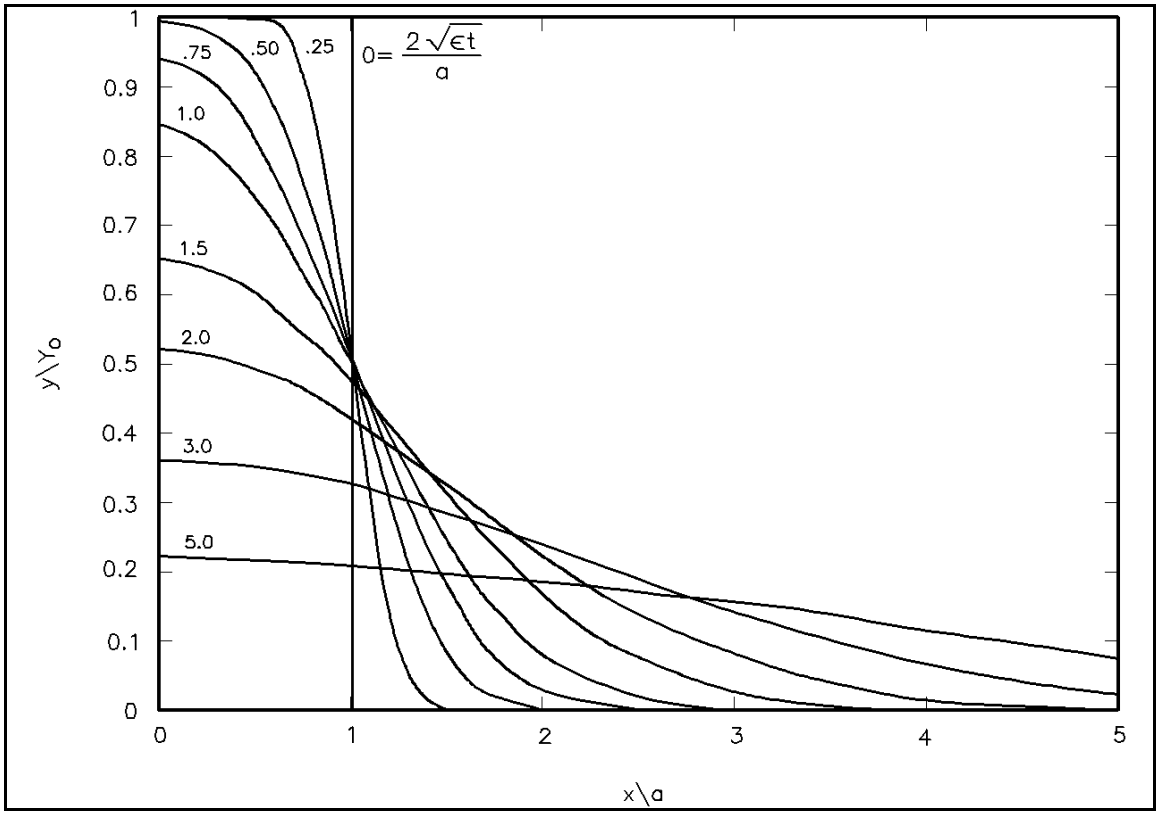

Figure III-2-36. Nondimensional solution curves for rectangular initial plan view fill area

Only the portion of the solution graph for $x \geq 0$ is presented, as the solution is symmetric for values of x less than zero. The situation where tapered sections are included at the ends of the project is presented in Walton (1994).

(15) This equation may be integrated over the project limits to allow estimation of the proportion $p(t)$ of fill left within the project boundaries at a given time after project initiation to give:

$$p(t) = \frac{1}{\sqrt{\pi}} \left(\frac{\sqrt{\varepsilon t}}{a} \right) \left\{ \exp \left(- \left(\frac{a}{\sqrt{\varepsilon t}} \right)^2 \right) - 1 \right\} + erf \left(\frac{a}{\sqrt{\varepsilon t}} \right) \tag{III-2-32}$$

which is plotted in Figure III-2-37 as a function of the inverse of the nondimensionalized beach half length parameter $\frac{a}{2\sqrt{\varepsilon t}}$

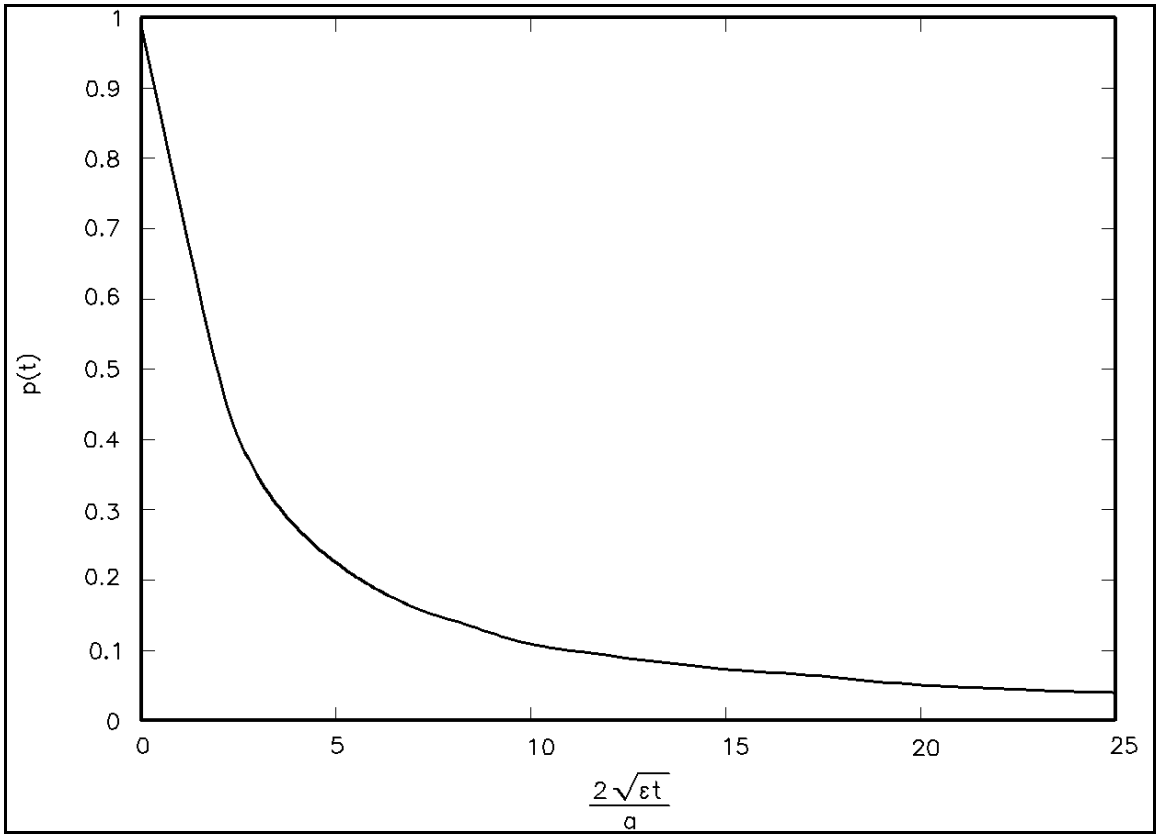

Figure III-2-37. Proportion of fill p(t) remaining within limits of rectangular plan view fill area

(16) A third case to be considered is that of a triangular beach fill as shown in Figure III-2-38. A triangular planform beach nourishment might exist at a location where either a truck dumping of sand occurs or where drag scraping of sand from the offshore occurs. The solution for this specific case (where the original fill has been assumed triangular in shape) is:

$$y = \frac{Y_o}{2} \left\{ (1-X)\ erf\ (U(1-X)) + (1+X)\ erf\ (U\ (1+X)) - 2\ Xerf\ (UX) \right. \\ \left. + \frac{1}{\sqrt{\pi}U} \left(e^{-U^2\ (1+X)^2} + e^{-U^2\ (1-X)^2} - 2e^{-(UX)^2} \right) \right\} \tag{III-2-33}$$

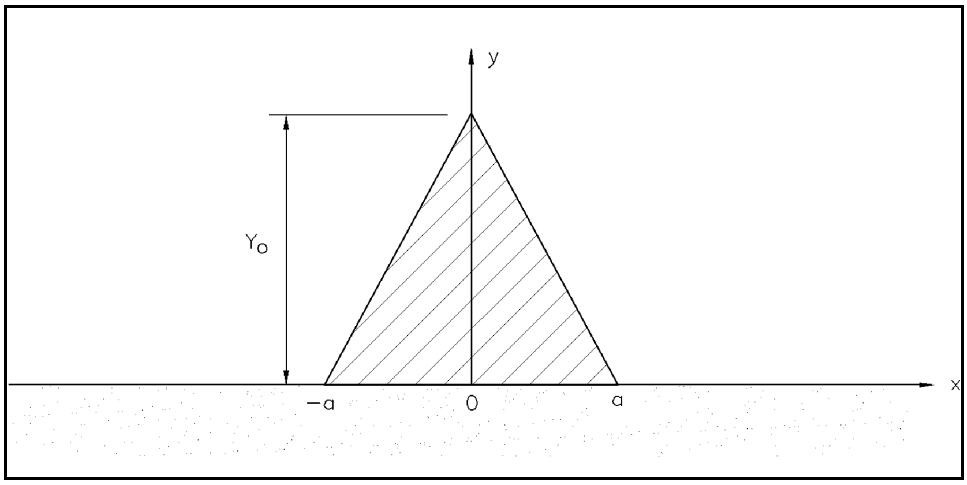

Figure III-2-38. Triangular beach fill (*t*=0)

where

$$X = \frac{x}{a} \qquad and \qquad U = \frac{a}{2\sqrt{\varepsilon t}}$$

(17) Figure III-2-39 is a nondimensionalized solution graph for the case of a triangular planform beach nourishment. Only the portion of the solution graph for $x \geq 0$ is presented, as the solution is symmetric for values of x less than zero.

(18) A fourth case to be considered is that of a long fill project with a gap as shown in Figure III-2-40. For the case in which a beach nourishment has been placed on an existing beach but a gap has been left in the beach nourishment project (such as occurred in a beach nourishment project on Jupiter Island, Florida, in 1974), the following solution would apply:

$$y = \frac{Y}{2}\left\{ erfc\left[\left(\frac{a}{2\sqrt{\varepsilon t}}\right)\left(1 - \frac{x}{a}\right)\right] + erfc\left[\left(\frac{a}{2\sqrt{\varepsilon t}}\right)\left(1 + \frac{x}{a}\right)\right]\right\} \qquad \text{(III-2-34)}$$

The nondimensionalized solution graph for this particular planform of beach nourishment is provided in Figure III-2-41. Only the portion of the solution graph for $x \geq 0$ is presented, as the solution is symmetric for values of x less than 0.

(19) A fifth case to be considered is that of the end of a rectangular fill on a long beach nourishment project as shown in Figure III-2-42. The nondimensional solution graph for the case of a semi-infinite beach fill where the fill is contained within the area $x > 0$ is given in Figure III-2-43. This semi-infinite beach fill case can be utilized to provide the shape of the end of a long beach fill and the extent of the fill as it progresses down the coast with time. The solution for this specific case is

$$y = \frac{Y_o}{2}\left\{1 + erf\left(\frac{x}{2\sqrt{\varepsilon t}}\right)\right\} \qquad \text{(III-2-35)}$$

EXAMPLE PROBLEM III-2-11

FIND:

The width of the beach at the ends of the fill after 3 days and after 12 weeks of design wave action on the beach fill.

GIVEN:

A beach nourishment 5,000 m in length is placed on a reasonably stable shoreline to widen the beach as a protective measure for upland construction during storms. The new beach width is to be 50 m and is to be placed at the same berm elevation as the natural beach $d_B = 3$ m. Depth of appreciable sand transport as estimated from historical profiles in the region is assumed $d_c = 7$ m. A design wave for the area is estimated to be $H_b = 3$ *m*, $T = 12$ sec, $\alpha_b = 10$ deg. The sediment size of the natural beach is the same size as the fill sediment size and ratio of sediment density to water density (i.e., specific gravity) is 2.65. The porosity of beach is $n = 0.4$. The K factor is assumed = 0.77, and κ is assumed = 1.

SOLUTION:

a = 5,000/2 = 2,500 m ; $Y_O = 50$ m

At fill ends x/a = 1.0

From Equation 2-26

$$\varepsilon = \frac{0.77\ (3)^2\ \sqrt{9.81 \cdot 3}}{8} \left(\frac{1}{2.65 - 1}\right) \left(\frac{1}{1 - 0.4}\right) \left(\frac{1}{3 + 7}\right)$$

$$\cong 0.47\ \text{m}^2/\text{s}$$

After 3 days ($t = 259{,}200$ sec)

$$\frac{a}{2\sqrt{\varepsilon t}} = \frac{2{,}500}{2\sqrt{0.47\ (259{,}200)}} = 3.58$$

From Figure III-2-36, for

$$\frac{x}{a} = 1.0 \qquad \frac{y}{Y_o} = 0.56 \quad \text{hence, } y = 0.56\ (50) = 28\ \text{m}$$

After 12 weeks ($t = 7{,}257{,}600$ sec)

$$\frac{a}{2\sqrt{\varepsilon t}} = \frac{2{,}500}{2\sqrt{0.47\ (7{,}257{,}600)}} = 0.68$$

From Figure III-2-36, for

$$\frac{x}{a} = 1.0 \qquad \frac{y}{Y_0} = 0.46 \quad \text{hence, } y = 0.46\ (50) = 23\ \text{m}$$

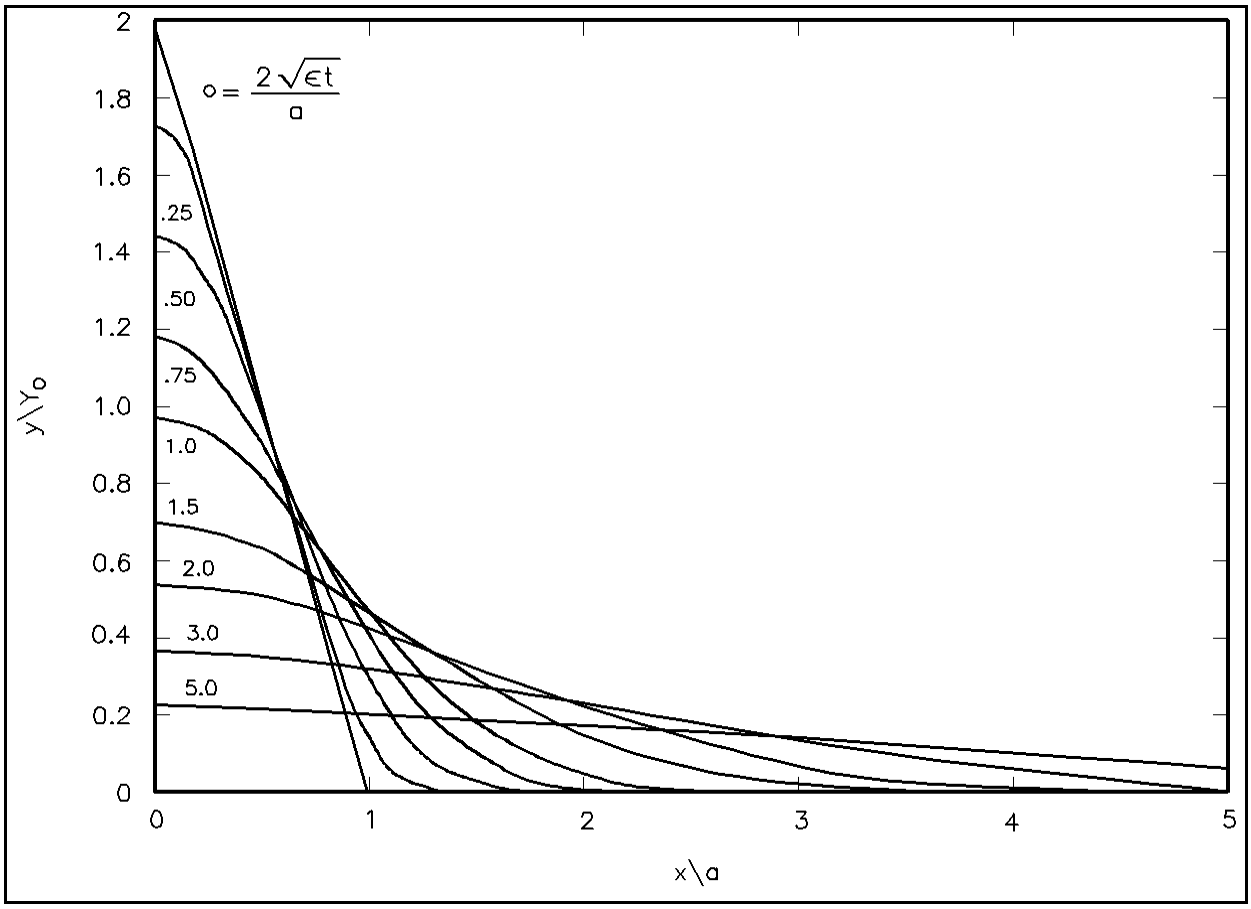

Figure III-2-39. Nondimensional solution curves for triangular initial plan view fill area

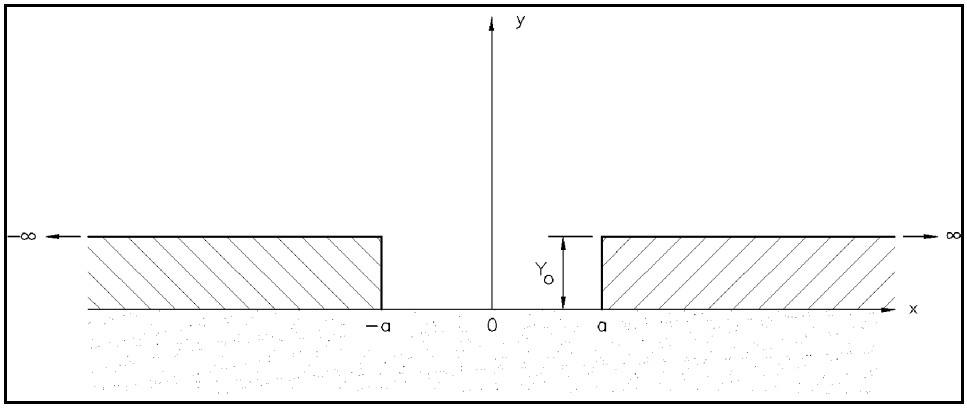

Figure III-2-40. Long fill project with a gap (*t*=0)

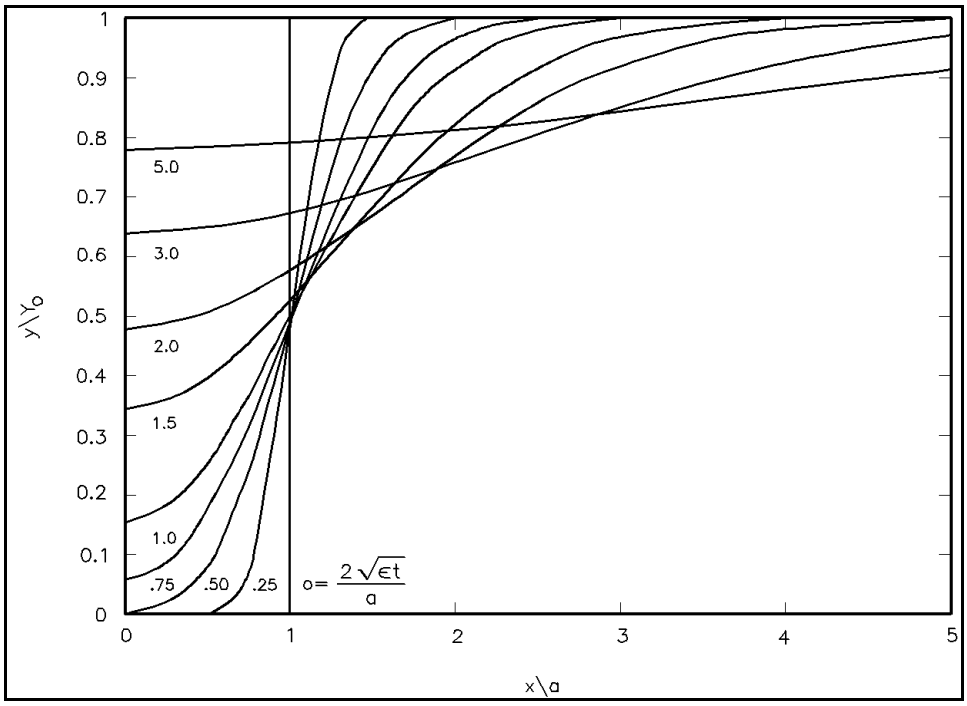

Figure III-2-41. Nondimensional solution curve for long fill with gap in plan view fill area

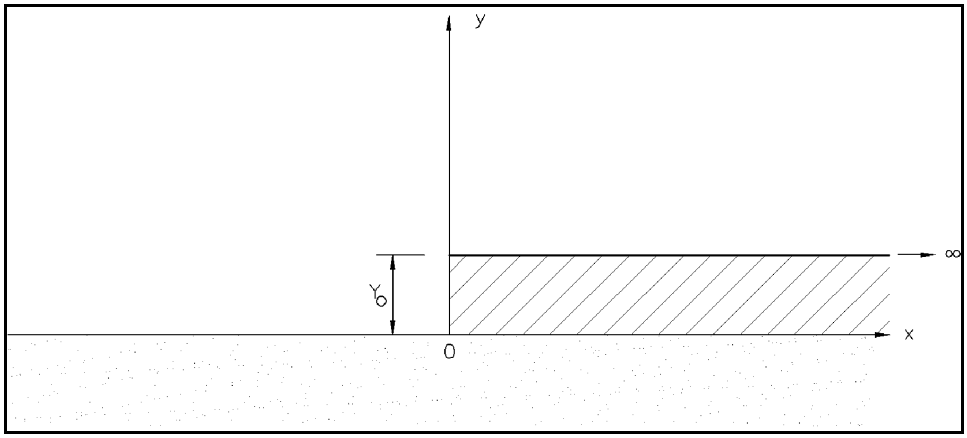

Figure III-2-42. Semi-infinite beach fill (*t*=0)

(20) For the situation in which the fill is in area $x < 0$, the graph can be utilized by flipping the solution presented around the y axis.

(21) A sixth case to be considered is the nourishment fill initially placed in the area ($x > 0$) and maintained at the initial beach width Y within the project area. The solution for the planform beach adjacent to the fill ($x \leq 0$) is given by

$$y = Y_o \left(1 + erf \left(\frac{x}{2\sqrt{\varepsilon t}} \right) \right) \qquad \text{(III-2-36)}$$

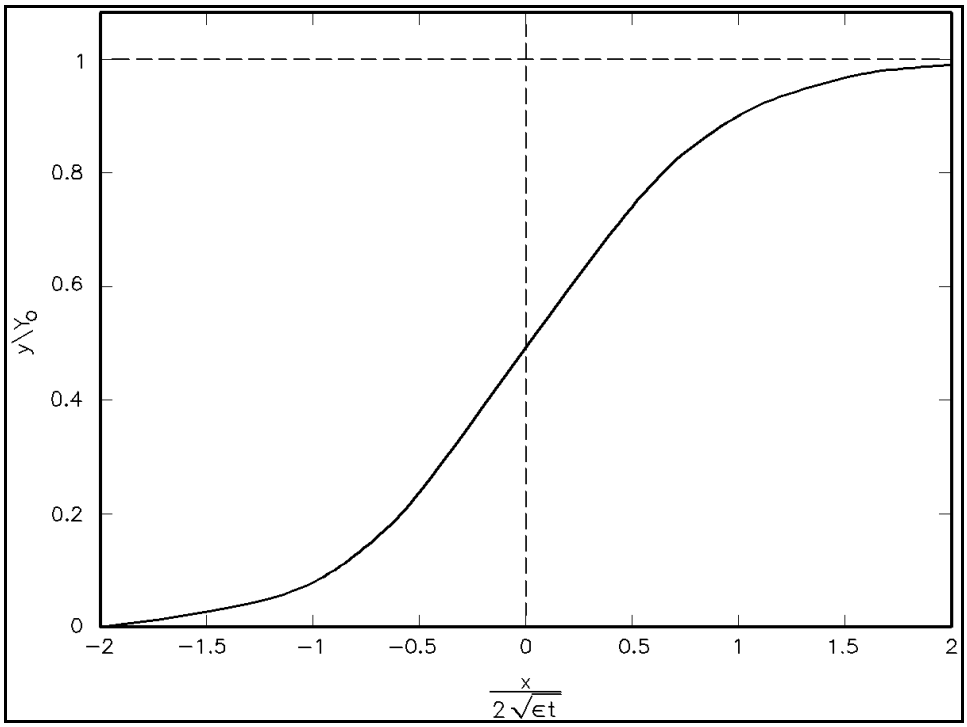

Figure III-2-43. Nondimensional solution curve for semi-infinite plan view fill area

(22) For the analogous case to the above instance where the planform fill is placed in the area ($x < 0$) and maintained at the initial beach width Y in the project area, the solution (for $x \geq 0$) is:

$$y = Y_o \; erfc\left(\frac{x}{2\sqrt{\varepsilon\, t}}\right) \tag{III-2-37}$$

where the nondimensionalized solution graph has the same nondimensionalized solution as provided earlier in Figure III-2-34.

(23) A final case is presented for the situation in which groins and fill are implemented together as in Figure III-2-44. Where the initial fill is placed to the end of the groin, the solution is given by Dean (1984) as:

$$y = w - \ell\left(1 - \frac{x}{\ell}\right) \tan\left(\alpha_b\right) + \frac{2\tan(\alpha_b)}{\ell} \sum_{n=0}^{\infty} \left[\frac{2\ell}{(2n+1)\pi}\right]^2 \exp\left\{-\varepsilon \frac{(2n+1)^2\pi^2 t}{4\ell^2}\right\} \cos\left[\frac{(2n+1)\pi x}{2\ell}\right] \tag{III-2-38}$$

The nondimensionalized shoreline solution graph for this situation is provided in Figure III-2-45 for the parameters W/L = 0.25 and tan (α_b) = 0.1.

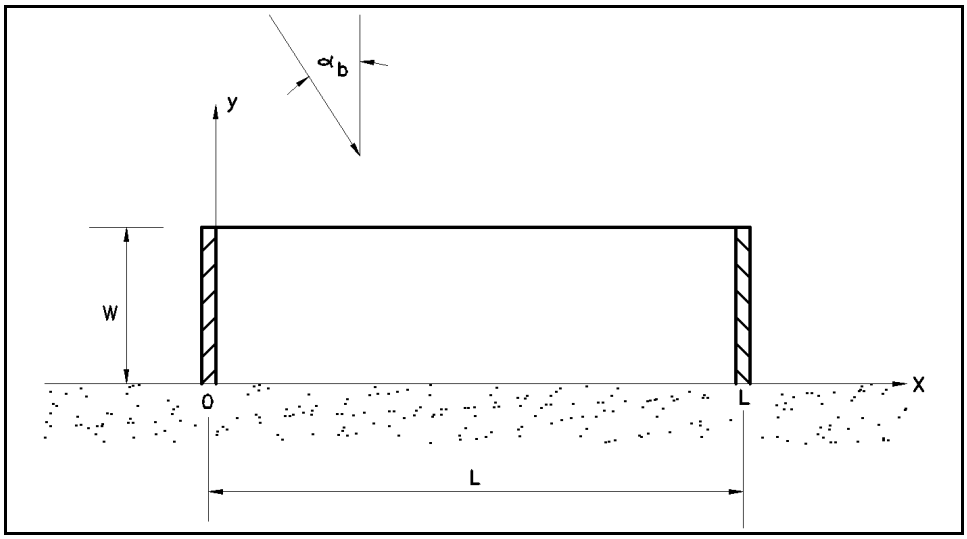

Figure III-2-44. Beach fill placed with groins (*t*=0)

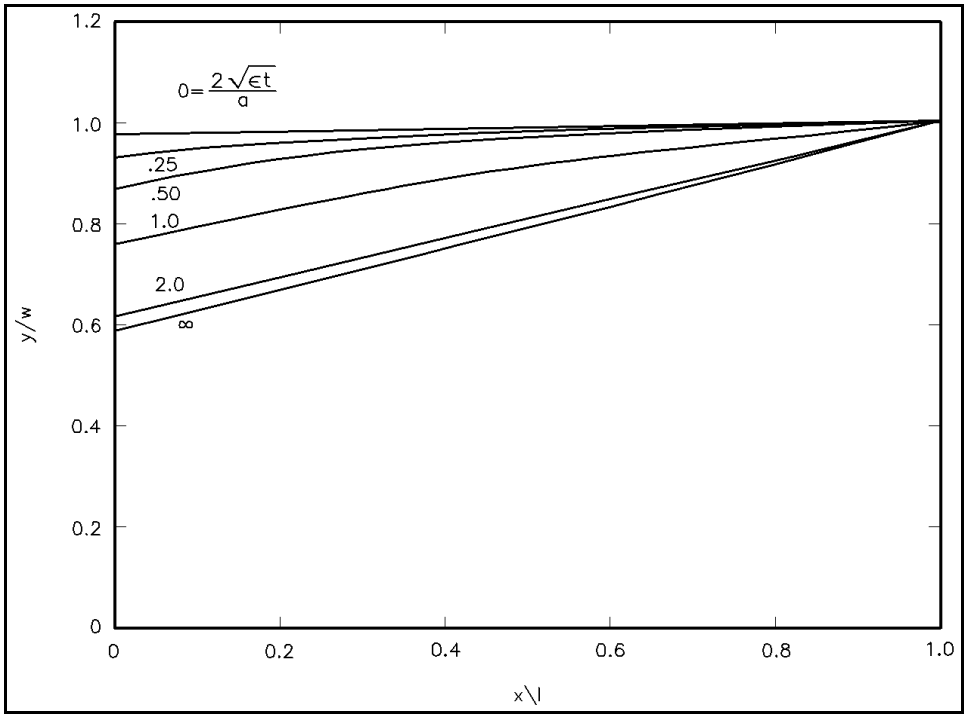

Figure III-2-45. Nondimensional solution curve for plan view of rectangular fill area between coastal structures (*w*/*l* = 0.25; tan α_b = 0.1)

(24) Since Equation 2-24 is linear, the above solutions can be combined to address more complex situations than those presented. As an example, consider the case in which staged construction of a beach nourishment project takes place over a long length of beach and the fill area of the beach is to be confined in the reach $x < 0$ and maintained at its fill width. Equation 2-37 could be utilized for solving this particular example in the case that the entire fill was placed at time $t = 0$. Instead, consider that the fill is placed in

stages with the plan view dimension of the fill as a function of time given in Figure III-2-46. For this particular scenario, the solution (at time *t*) analogous to Equation 2-37 only with the planform beach built in staged increments (as per Figure III-2-46) is:

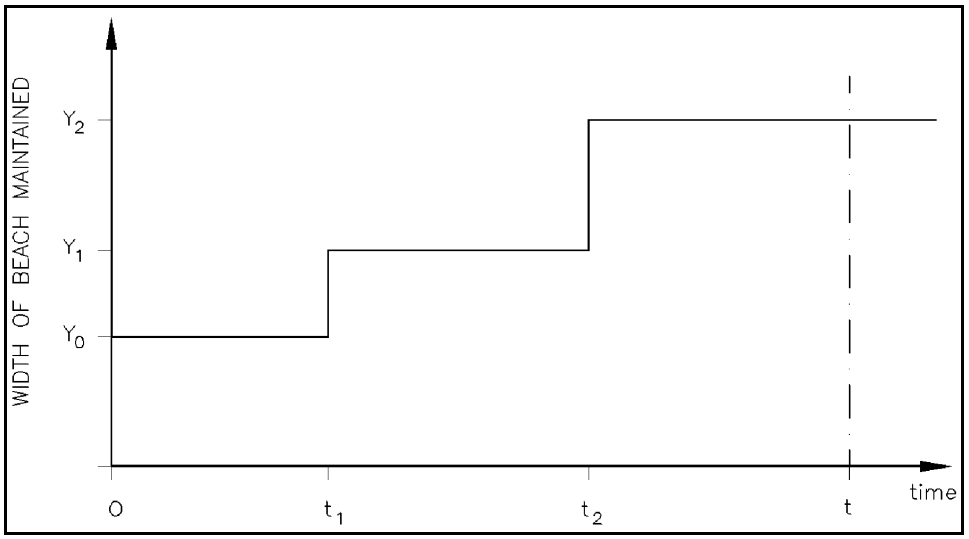

Figure III-2-46. Width of maintained beach ($x < 0$) as a function of time

$$y = Y_o \; erfc\left(\frac{x}{2\sqrt{\varepsilon t}}\right) + \left(Y_1 - Y_o\right) erfc\left(\frac{x}{2\sqrt{\varepsilon (t - t_1)}}\right) + \left(Y_2 - Y_1\right) erfc\left(\frac{x}{2\sqrt{\varepsilon (t - t_2)}}\right) \qquad \text{(III-2-39)}$$

which can be nondimensionalized and solved utilizing the nondimensionalized solution graph provided by the simpler case of Equation 2-37 given in Figure III-2-34.

(25) It should be recognized that the linearized form of shoreline solution will produce a higher rate of shoreline change by overestimating the longshore transport rate because $2\alpha_b > \sin(2\alpha_b)$ in the linearized sand transport solution. Thus, under properly estimated parameters for idealized conditions, a higher rate of attenuation of beach fills will be obtained than is expected to occur in reality, thus providing a conservative answer to project losses.

(26) As a final point, it is noted that when wave angles are very large and the difference between the wave direction and shoreline orientation exceeds 45 deg, the true form of the shoreline diffusivity constant based on the nonlinear $\sin(2\alpha)$ term in the sand transport equation will be negative, which totally changes the characteristics of the shoreline change model equation. In these cases, the shoreline evolves in an unstable manner equivalent to running the previous stable solution forms backwards through time. In other words, a shoreline having a perturbation placed on it (such as a beach fill) would see a growth of the perturbation toward an elongated cuspate feature as time progresses rather than seeing the smoothing out of the perturbation as given in solutions of the preceding paragraphs. This type of shoreline instability may possibly explain certain shoreline features such as cuspate forelands which are ubiquitous on elongated bays where the dominant wave action is along the major axis of the bay and at large angles to the prevailing shoreline trends (Walton 1972).

EXAMPLE PROBLEM III-2-12

FIND:

The level of protection (i.e., width of beach) afforded to a historical lighthouse as a consequence of the nourishment project at the end of 3, 6, 8, 9, and 12 months after initial fill placement. The lighthouse is situated at the shoreline 1 mile (≈ 1,609 m) south of the south end of the proposed beach at the initiation of the project fill.

GIVEN:

A long beach fill is placed along a north-south directed stretch of shoreline along the east coast of the United States (i.e., the azimuth of the offshore direction is 90 deg). The project is to be constructed and maintained continuously to design project width throughout the project fill area. The project will be constructed in two stages; Stage 1 will provide a fill width of 50 m, and Stage 2 (to be placed 3 months after initial placement) will add another 50 m of beach width, making the total finished project width = 100 m. Assume that: H_b = 1 m; T = 10 sec; α_b = 5 deg (from the north) K is assumed = 0.77, and κ = 1.0. Sediment density to water density ratio (i.e., specific gravity) = ρ_s/ρ = 2.65; porosity n = 0.4; $d_B + d_c$ = 6 m. Note that except for breaking wave height H_b, these are the same wave and sediment parameters as given in Example III-2-8.

SOLUTION:

For H_b = 1 m, with other parameters the same as the previous problem;

$$\varepsilon = \frac{0.77\ (1)^2\ \sqrt{9.81 \cdot 1}}{8} \left(\frac{1}{2.65 - 1}\right) \left(\frac{1}{1 - 0.4}\right) \left(\frac{1}{6}\right)$$

$$\cong 0.0508\ \frac{m^2}{sec}$$

At the end of the first 3 months, the solution of Equation 2-37 (graphical solution provided by Figure III-2-34) can be utilized with t = 3 months ≈ 7.78×10^6 sec, and x = 1 mile ≈ 1,609 m:

$$y\ (1\ \text{mile},\ 3\ \text{months}) = 50 \cdot erfc\left(\frac{1{,}609}{2\sqrt{0.0508 \cdot 7.78 \times 10^6}}\right)\ \text{meters}$$

$$\approx 50 \cdot erfc\,(1.28)$$

$$\approx 50\,(0.07) \cong 3.5\ \text{m}$$

(Continued)

Example Problem III-2-12 (Concluded)

For times beyond the 3-month initial fill placement and maintenance, a solution of the form of Equation 2-39 must be utilized. In this particular case, the solution would be of the form (where Y_o = 50 m, Y_1 - Y_o = 50 m, and t_1 = 3 months):

$$y(x, t) = Y_o \cdot erfc\left(\frac{x}{2\sqrt{\varepsilon t}}\right) + (Y_1 - Y_o) \cdot erfc\left(\frac{x}{2\sqrt{\varepsilon(t - t_1)}}\right)$$

which can be reformulated to be:

$$y(x, t) = 50 \cdot erfc\left(\frac{x}{2\sqrt{\varepsilon t}}\right) + 50\ erfc\left(\frac{x}{2\sqrt{\varepsilon t}} \cdot \frac{1}{\sqrt{1 - \frac{t_1}{t}}}\right)$$

$$= term\ 1 \quad + \quad term\ 2$$

The solution is provided in the table below:

(1) t	(2) $\frac{x}{2\sqrt{\varepsilon\ t}}$	(3) (2) $\cdot \left(1 - \frac{t_1}{t}\right)^{-1/2}$	(4) *erfc*((2))	(5) *erfc*((3))	(6) term 1	(7) term 2	(8) y
6 mo. = 15.8 × 10^6 sec.	0.90	0.90 (1.414) = 1.27	0.20	0.07	10.0	3.5	13.5 m
9 mo. = 23.7 × 10^6 sec.	0.73	0.73 (1.225) = 0.89	0.30	0.21	15.0	10.5	25.5 m
12 mo. = 31.6 × 10^6 sec.	0.63	0.63 (1.155) = 0.73	0.37	0.30	18.5	15.0	33.5 m

Note that the solution form assumes that the fill is constantly maintained at its design width. This would probably not be achievable in practice, and solutions would have to be modified in accord with good engineering judgment.

III-2-4. Numerical Longshore Sand Transport Beach Change Models

As opposed to analytical solutions of shoreline change, which simplify the equations used to predict beach evolution, mathematical modeling facilitates generalization of these equations so that input parameters may vary in time and in the longshore, and possibly cross-shore, dimensions. Also, numerical models become necessary where difficult boundary conditions are encountered (say at groins or offshore breakwaters) because of shoreline morphology or wave transformation. Numerical models of beach change perform best when a perturbation is introduced to a system that is in equilibrium. The perturbation to the system might be an introduction or removal of littoral material (e.g., beach fill, sand mining, release of sediment due to a flooded river or landslide) or placement of a hardened structure (e.g., groins, detached breakwaters, seawalls, revetments). Historical trends of beach change and knowledge of the littoral budget are typically used to calibrate and verify the controlling equations, then forecasts may be simulated as a function of various engineering alternatives and/or wave climate scenarios. Therefore, beach response as a function of complex coastal processes may be readily examined in detail with mathematical models. However, the limitations inherent in the controlling equations, and assumptions implied in developing "representative" parameters require that model results be carefully interpreted, ideally within the context of other coastal engineering analyses.

a. Types of longshore transport models

(1) Fully three-dimensional models.

(a) In nature, nearshore beach change due to waves, circulation patterns, and longshore currents varies with time and location; therefore, equations to fully describe effects of these processes on beach evolution must be three-dimensional and time-dependent. Development of these equations is still an area of active research, and fully three-dimensional models are not available for routine engineering design.

(b) The intent of three-dimensional models is to describe bottom elevation changes which may vary in the cross-shore and longshore directions. These models provide insight into wave transformations and circulation for complicated bathymetry and in the vicinity of nearshore structures. However, they are less useful for making long-term shoreline evolution calculations because they are computationally intensive. These models also involve poorly known empirical coefficients such as those related to bottom friction, turbulent mixing, and sediment transport. Integrating the calculated local distributions of sediment transport over the cross-shore and for long time periods may lead to erroneous results because small local inaccuracies will be amplified over a long simulation. Because of their intent to predict local process parameters (e.g., waves, currents, sediment transport), they require a detailed data set for calibration, verification, and sensitivity testing, perhaps from a companion physical model study or field data collection.

(2) Schematic three-dimensional models. Schematic three-dimensional models simplify the controlling equations of fully three-dimensional models by, for example, restricting the shape of the profile or calculating global rather than point transport rates. Bakker (1968) has developed a two-line model which allows the evolution of two contours to be independently simulated. From this model, Perlin and Dean (1983) developed an n-line model that allows an arbitrary number of contour lines to represent the beach profile. Most schematic multi-line models developed to date are restricted to monotomic profile representations. For models that represent the profile by more than one contour, it is necessary to specify a relationship for cross-shore sediment transport. Schematic three-dimensional models have not yet reached the stage of wide application due to their complexity, requirement for considerable computational resources, and need for expertise in operational applications.

(3) One-line (two-dimensional) models.

(a) The Large Scale Sediment Processes Committee at the Nearshore Processes Workshop in St. Petersburg in 1989 concluded that long-term simulations of beach change are more reasonably formulated on the basis of total or bulk transport models such as Equation 2-7. These models have fewer coefficients than three-dimensional models and provide no details of the sediment transport profile. However, they may be calibrated and verified to include the integrated effect of all of the local processes on the total transport.

(b) The shoreline change models developed from bulk transport models are often referred to as one-line models. One-line models assume that the beach profile is a constant shape; thus, the controlling equations may be solved for one contour line only (usually taken as the shoreline). Many shoreline change models have been developed and applied (e.g., Komar 1973a; LeMéhauté and Soldate 1977; Walton, Liu, and Hands 1988; and many others). Documented nonproprietary, one-line models that are also presently available include a model developed at the University of Florida (Dean and Grant 1989, Dean and Yoo 1992, 1994), and the computer model GENESIS (GENEralized model for SImulating Shoreline change) (Hanson 1987; Hanson and Kraus 1989; Gravens, Kraus, and Hanson 1991).

(c) One-line models used to estimate longshore sand transport rates and long-term shoreline changes generally assume that the profile is displaced parallel to itself in the cross-shore direction. The profile may include bars and other features but is assumed to always maintain the same shape. This assumption is best satisfied if the profile is in equilibrium. The one-line model is formulated on the conservation equation of sediment in a control volume or shoreline reach, and a bulk longshore sand transport equation. It is assumed that there is an offshore closure depth d_C at which there are no significant changes in the profile, and the upper end of the active profile is at the berm crest elevation d_B. The constant profile shape moves in the cross-shore direction between these two limits. This implies that sediment transport is uniformly distributed over the active portion of the profile. The incremental volume of sediment in a reach is simply $(d_B + d_C)\Delta x \Delta y$, where Δx is the reach of shoreline segment, and Δy is the cross-shore displacement of the profile. Conservation of sediment volume may be written as

$$\frac{\Delta y}{\Delta t} + \frac{1}{d_B + d_C}\left(\frac{\Delta Q_\ell}{\Delta x} \pm q\right) = 0 \tag{III-2-40}$$

in which Q_ℓ is the longshore transport rate, q is a line source or sink of sediment along the reach, and t is time (Figure III-2-28). As examples, line sources of sediment may be rivers and coastal cliffs, and sinks may be produced by sand mining or dredging.

(d) The longshore transport rate is evaluated using equations similar to Equation 2-7. These require measurement or calculation of the breaking wave angle relative to the beach. The local wave angle relative to the beach is the difference between the wave angle relative to a model baseline and the shoreline angle relative to the model baseline (Figure III-2-29),

$$\alpha_b = \alpha_{bg} - \alpha_{sg} = \alpha_{bg} - \tan^{-1}\left(\frac{dy}{dx}\right) \tag{III-2-41}$$

where x is the distance alongshore, and y is the distance offshore.

(e) If the angle of the shoreline is small with respect to the x axis and simple relationships describe the waves, analytical solutions for shoreline change may be developed, as discussed in the previous section. For

more complex conditions, such as time-varying wave conditions, large shoreline angles, variable longshore wave height (perhaps due to diffraction), multiple structures, etc., numerical models can be used in many instances.

b. Shoreline Change Model GENESIS.

(1) Overview.

(a) The numerical model GENESIS (Hanson 1987; Hanson and Kraus 1989; Gravens, Kraus, and Hanson 1991) is an example of a one-line shoreline change model that is supported for use both on personal computer and mainframe systems (see Cialone et al. (1992)) and has a companion system of support programs (Gravens 1992). GENESIS has been applied to numerous coastal engineering projects, and it calculates shoreline change due to spatial and temporal differences in longshore transport as produced by breaking waves. GENESIS is used in conjunction with grid-based wave transformation models that develop values of breaking wave height and angle for various representative wave periods and approach azimuths along the coast. Shoreline change at grid cells along the coastline is computed in the time domain as a function of these computed values of the breaking wave height and angle.

(b) As discussed by Hanson (1987) and Hanson and Kraus (1989), the empirical predictive formula for the longshore sand transport rate used in GENESIS is

$$Q_{\ell} = H^2_{b\ sig}\ C_{gb} \left(a_1\ sin2\alpha_b - a_2\ \cos\alpha_b \frac{dH_{b\ sig}}{dx} \right) \tag{III-2-42}$$

The nondimensional parameters a_1 and a_2 are given by

$$a_1 = \frac{K_1}{16 \left(\frac{\rho_s}{\rho} - 1 \right) (1 - n)\ (1.416)^{\frac{5}{2}}} \tag{III-2-43}$$

and

$$a_2 = \frac{K_2}{8 \left(\frac{\rho_s}{\rho} - 1 \right) (1 - n)\ m\ (1.416)^{\frac{7}{2}}} \tag{III-2-44}$$

where K_1 and K_2 are empirical coefficients, treated as calibration parameters, and m is the average bottom slope from the shoreline to the depth of active longshore sand transport. The factors involving 1.416 are used to convert the K_1 and K_2 coefficients from use with rms wave height to use with significant wave height (which is the statistical wave height required by GENESIS). That is, Equation 2-43 is presented such that K_1 is equivalent to K_{rms} (as opposed to K_{sig}) in Equation 2-7. Nonetheless, both longshore sand transport coefficients K_1 and K_2 should be viewed as calibration parameters that are to be adjusted to match measured positions of shoreline change (Hanson and Kraus 1989).

(c) The first term in Equation 2-42 corresponds to Equation 2-7, and accounts for longshore sand transport produced by obliquely incident breaking waves. The second term in Equation 2-42 is used to describe the effect of another generating mechanism for longshore sand transport, the longshore gradient in breaking wave height. The contribution arising from the longshore gradient in wave height is usually much

smaller than that from oblique wave incidence in an open-coast situation. However, in the vicinity of structures, where diffraction produces a substantial change in breaking wave height over a considerable length of beach, inclusion of the second term provides an improved modeling result, accounting for diffraction effects.

(d) The boundary conditions at the ends of a study area in a shoreline change modeling project must be specified. There are three common boundary conditions: no sand transport ($Q_\ell = 0$), free sand transport ($dQ_\ell/dx = 0$), and partial sand transport ($Q_\ell \neq 0$). The locations of the study area ends should be selected with these options in mind. Large headlands or jetties which completely block the longshore transport are good choices for model boundaries. At these locations $Q_\ell = 0$. Points where the position of the shoreline has not changed for many years are also good locations for boundaries. At these points, the gradient in longshore transport is small so that a free transport condition can be specified ($dQ_\ell/dx = 0$). At some locations, the longshore transport rate is known and can be used as a boundary condition (i.e., artificial sand bypassing at a jetty). If none of these "good" locations exist, engineering judgment must be used.

(e) In all cases, results should be calibrated and verified using known shoreline positions and wave conditions for the longest period possible. The modeler also attempts to use wave data applicable to the period between the dates of the calibration shorelines. The GENESIS technical reference (Hanson and Kraus 1989) discusses in full the operation of shoreline change numerical simulation models.

(2) Input data requirements and model output.

(a) As discussed by Gravens (1991, 1992), preparation and analysis of the input and output data files occupy a substantial portion, perhaps the majority, of the time spent on a detailed shoreline change modeling project. Gravens (1991, 1992) stresses that the data gathering organization and analysis process cannot be overemphasized because (1) it forms the first necessary level in understanding coastal processes at the project site, and (2) the simulation results must be interpreted within the context of regional and local coastal processes, and the natural variability of the coastal system. Success in modeling shoreline change depends, to a large extent, on preparation and analysis of the input data.

(b) General input information required by GENESIS includes the spatial and temporal ranges of the simulation, structure and beach fill configurations (if any), values of model calibration parameters, and simulated times when output is desired. Initial and measured (if available) shoreline positions as referenced to a baseline established for the simulation are also required. Offshore and nearshore (if available) wave information and associated reference depths are used to calculate longshore sand transport rates. Output information produced by GENESIS includes intermediate and final calculated shoreline positions, and net and gross longshore sand transport rates.

(3) Capabilities and limitations.

(a) GENESIS was designed to predict long-term trends of the beach plan shape in its evolution from one given initial condition. This change is usually caused by a notable perturbation; for example, by beach fill placement, sand mining, sand discharge from a river, construction of a detached breakwater, or jetties constructed at a harbor or inlet. In engineering applications and tests of GENESIS, modeled shoreline reaches have ranged from about 2 to 35 km with a grid resolution of 15 to 90 m, and simulation periods have spanned from approximately 6 months to 20 years, with wave data typically entered at simulated time intervals in the range of 30 min to 6 hr (Gravens, Kraus, and Hanson 1991).

(b) Hanson and Kraus (1989) and Gravens, Kraus, and Hanson (1991) discuss the capabilities and limitations of GENESIS. The model allows an almost arbitrary number and combination of groins, jetties,

detached breakwaters, beach fills, and seawalls, with a primary limitation in this regard being the size and speed of the computer and the maximum number of grid cells that can be accommodated by the program. Compound structures (such as T-shaped, Y-shaped, and spur groins) may be simulated with varying degrees of realism. At least five grid cells are required to reasonably model the shoreline behind and between structures. Sand bypassing around and transmission through groins and jetties may be simulated, as well as diffraction at detached breakwaters, jetties, and groins. Transmission through detached breakwaters may be simulated. GENESIS allows multiple wave trains to be input (such as from independent wave sources), and the wave information may include arbitrary values of wave height, period, and direction. As presented in Equation 2-42, sand transport is calculated due to oblique wave incidence and a longshore gradient in wave height.

(c) GENESIS is not applicable to simulating a randomly fluctuating beach system in which no trend in evolution of the shoreline is evident. In particular, GENESIS is not applicable to calculating shoreline change in the following situations which involve beach change that is not related to coastal structures, boundary conditions, or spatial differences in wave-induced longshore sand transport: beach change inside inlets or in areas dominated by tidal flow; beach change produced by wind-generated currents; storm-induced beach erosion in which cross-shore sediment transport processes are dominant; and scour at structures. GENESIS also does not include wave reflection from structures; cannot reliably simulate tombolo or salient development at a detached breakwater; and there is no direct provision for changing tide level. In addition, the basic assumptions in the development of shoreline change modeling theory apply.

(4) Example application - Bolsa Chica, California.

(a) As discussed by Hanson and Kraus (1989) and Gravens (1990b), GENESIS (either its predecessor, Version 1, or the current Version 2) has been applied at numerous project sites, including locations in Alaska (Chu et al. 1987); California (Gravens 1990a); Louisiana (Hanson, Kraus, and Nakashima 1989; Gravens 1994); New Jersey (Gravens, Scheffner, and Hubertz 1989); New York (Cialone et al. 1994); Florida (by the U.S. Army Engineers District, Jacksonville); and outside the United States (Hanson and Kraus 1986; Kraus 1988). Application of the model to assess a proposed structured inlet system at Bolsa Chica, California, is summarized below (Gravens 1990a) to illustrate model use in coastal project evaluation and refinement.

(b) GENESIS was applied to an approximately 10-mile-long shoreline reach from Anaheim Bay to the Santa Ana River, California (Figure III-2-47) as part of a comprehensive multi-tasked engineering investigation for the California State Lands Commission (SLC). The shoreline change modeling effort was directed towards quantifying the potential long-term impacts of the proposed entrance on adjacent shorelines, and to investigate mitigation of any adverse impacts induced by the entrance. Three major components were involved in the shoreline modeling effort: (1) a preliminary shoreline response study, in which available wave and shoreline data were used to provide preliminary estimates of the introduction of a littoral barrier in the local littoral cell; (2) a comprehensive wave hindcast of locally generated wind sea and North Pacific swell conditions from 1956 to 1975 at 3-hr intervals, and an 18-month hindcast of South Pacific swell; and (3) comprehensive shoreline response modeling using the hindcast wave data to predict response of the project area to various design alternatives. Discussion herein is focussed on this third component, including preparation of input data sets and analysis of model output, as they pertain to application of GENESIS. For a more complete description of the project, the reader is directed to Gravens (1990a).

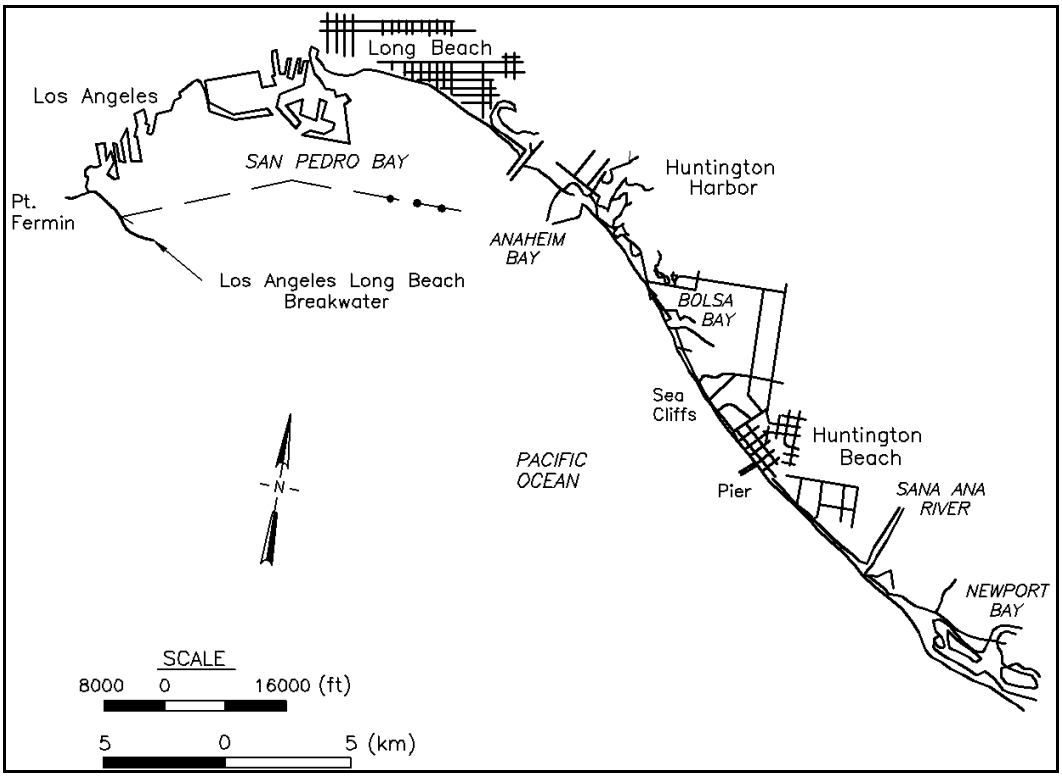

Figure III-2-47. Bolsa Chica, California, study area (Gravens 1990a)

(c) The modeled reach from Anaheim Bay to the Santa Ana River forms a littoral cell, including a complete barrier to littoral transport at Anaheim Bay, and a submarine canyon offshore of Newport Beach (Figure III-2-47). Coastal structures and features of importance within the model reach include the east Anaheim jetty, the sea cliffs at Huntington Beach, the Huntington Beach pier, and the north jetty at the mouth of the Santa Ana River. Each of these features influences the evolution of adjacent shoreline and was represented in the shoreline change model. The sea cliffs at Huntington Beach serve to pin the shoreline between the cliffs and Anaheim Bay to the northwest and the Santa Ana River to the southeast. The Huntington Pier and the east Anaheim Bay jetty modify the local breaking wave pattern and produce a local shoreline signature unique to these structures. Beaches between Anaheim Bay and the Santa Ana River have accreted an average of 1.3 m/year (4.4 ft/year) between 1934 and 1983.

(d) Ten shoreline position data sets dating from 1878 and 1983 were analyzed to determine historical and representative shoreline change trends. As a result of this analysis, the 1963, 1970, and 1983 shorelines were determined to be representative, and were summarized at 61-m (200-ft) intervals for model calibration (1963 to 1970) and verification (1970 to 1983).

(e) For the comprehensive shoreline response study, hindcast wave estimates at stations located near the lateral boundaries of the modeled shoreline reach were transformed from the hindcast stations to the offshore boundary of the GENESIS grid using the linear wave propagation model RCPWAVE (Regional Coastal Processes Wave Model; Ebersole 1985; Ebersole, Cialone, and Prater 1986) (Figure III-2-48). Use of two hindcast stations allowed systematic variations in the incident waves (alongshore wave height and angle) to be accounted for in RCPWAVE and ultimately in GENESIS.

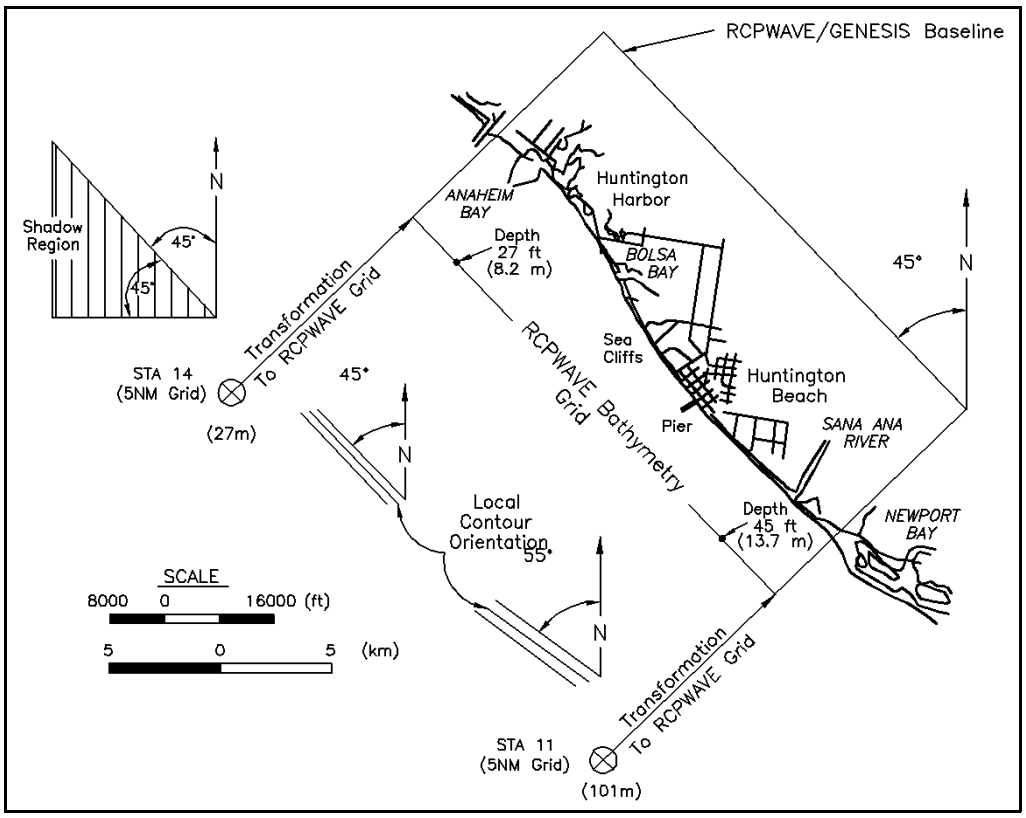

Figure III-2-48. Wave transformation hindcast to RCPWAVE grid (Gravens 1990a)

(f) Potential longshore sand transport rates were calculated using the transformed wave estimates and relationships similar to Equation 2-7 for the various shoreline orientations within the project reach. These potential transport rates are presented in the form of a total littoral drift rose (Walton 1972, Walton and Dean 1973) (Figure III-2-49). The curve with the circular symbols in Figure III-2-49 represents the average downcoast littoral drift for the 20-year Northern Hemisphere hindcast of sea and swell wave conditions. The curves with "x" symbols and "▽" symbols in Figure III-2-49 represent the average upcoast littoral drift for the available 2 years of Southern Hemisphere swell wave estimates. It is interesting to note that there is a reversal in the direction of the average net longshore littoral drift and that this reversal occurs at different shoreline orientations depending on the time series of southern swell wave conditions used in the calculation.

(g) The results of the final model calibration simulation, 1963 to 1970, are presented in Figure III-2-50. In model calibration, the calibration parameters K_1 and K_2 ranged between 0.8 and 0.2; values of these parameters that best estimated gross and net longshore sand transport rates and reproduced observed shoreline change were determined to be $K_1 = 0.45$ and $K_2 = 0.4$. Calibration results lead to three general observations. First, in the Anaheim Bay entrance area (between alongshore coordinates 220 and 260), there are significant differences between the calculated and measured shoreline positions. These differences are due in part to the reflection of waves from the east Anaheim Bay jetty (a process which was not modeled) and to a massive (4 million-cu-yd) renourishment of the Surfside-Sunset feeder beach in 1964. The percentage of fine material contained in the beach fill is unknown; consequently, the initial losses of fill material could not be estimated or accounted for in the model. Model results in this region should be viewed with caution.

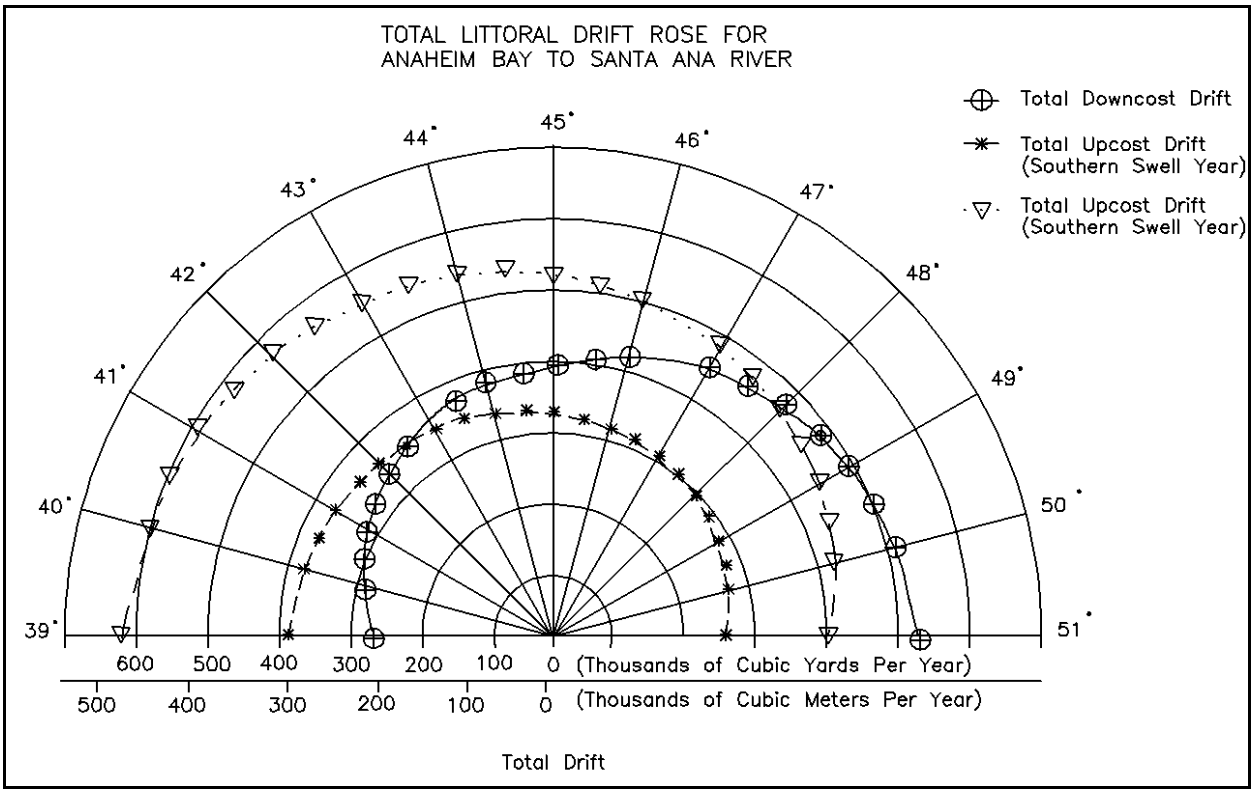

Figure III-2-49. Total littoral drift rose, Anaheim to Santa Ana River (Gravens 1990a)

(h) Secondly, in the vicinity of the Huntington Pier (between alongshore coordinates 80 and 90), it is noted that the predicted shoreline positions do not agree well with the survey. The lack of agreement is due to limitations in the groin boundary condition used to simulate the effects of the pier. The imposed boundary condition at the pier was investigated in detail, and the conclusion was that the boundary condition imposed at the Huntington Pier had no significant effect on the model results northeast of the sea cliffs over the modeling interval.

(i) Finally, in the vicinity of the proposed entrance system (between alongshore coordinates 155 and 220), the predicted and measured shoreline positions are in very good agreement. Model results for this region are considered to have high reliability.

(j) The next step was to verify the model by performing a simulation using the same calibration parameters for a different time period. The verification time period (1970 to 1983) included two beach fill projects at the Surfside-Sunset feeder beach, the first in 1971 (2.3 million cu yd) and the second in 1979 (1.66 million cu yd). The results of the model verification are shown in Figure III-2-51. Although the agreement between the calculated and measured shoreline positions is not as close for the verification as it was for calibration, overall measured change in shoreline position was reproduced and was considered acceptable. The largest discrepancies between measured and predicted shorelines occur adjacent to the Anaheim Bay jetty, where initial losses of fine-grained beach fill to the offshore may have contributed to the differences.

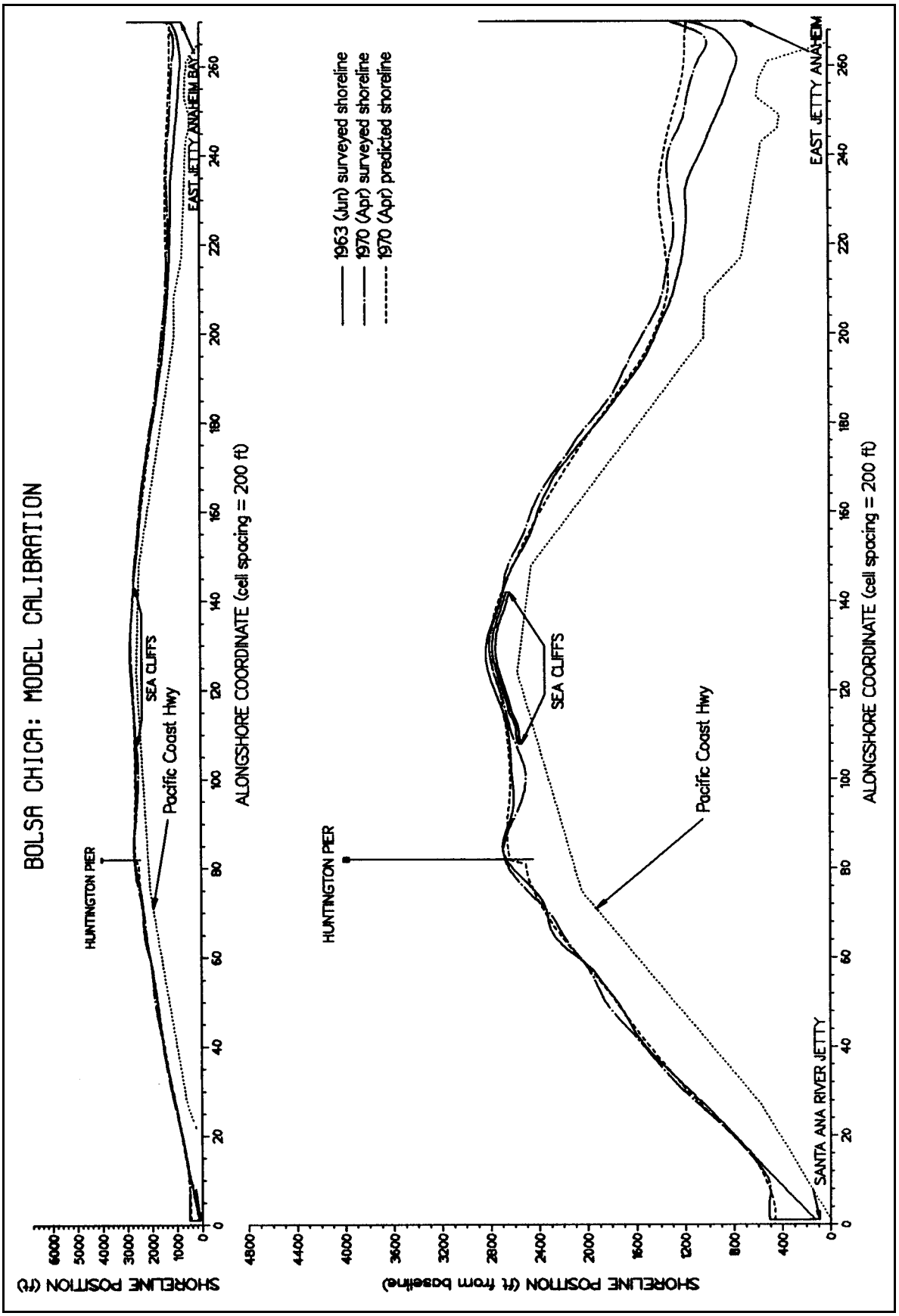

Figure III-2-50. Model calibration results, Bolsa Chica (Gravens 1990a)

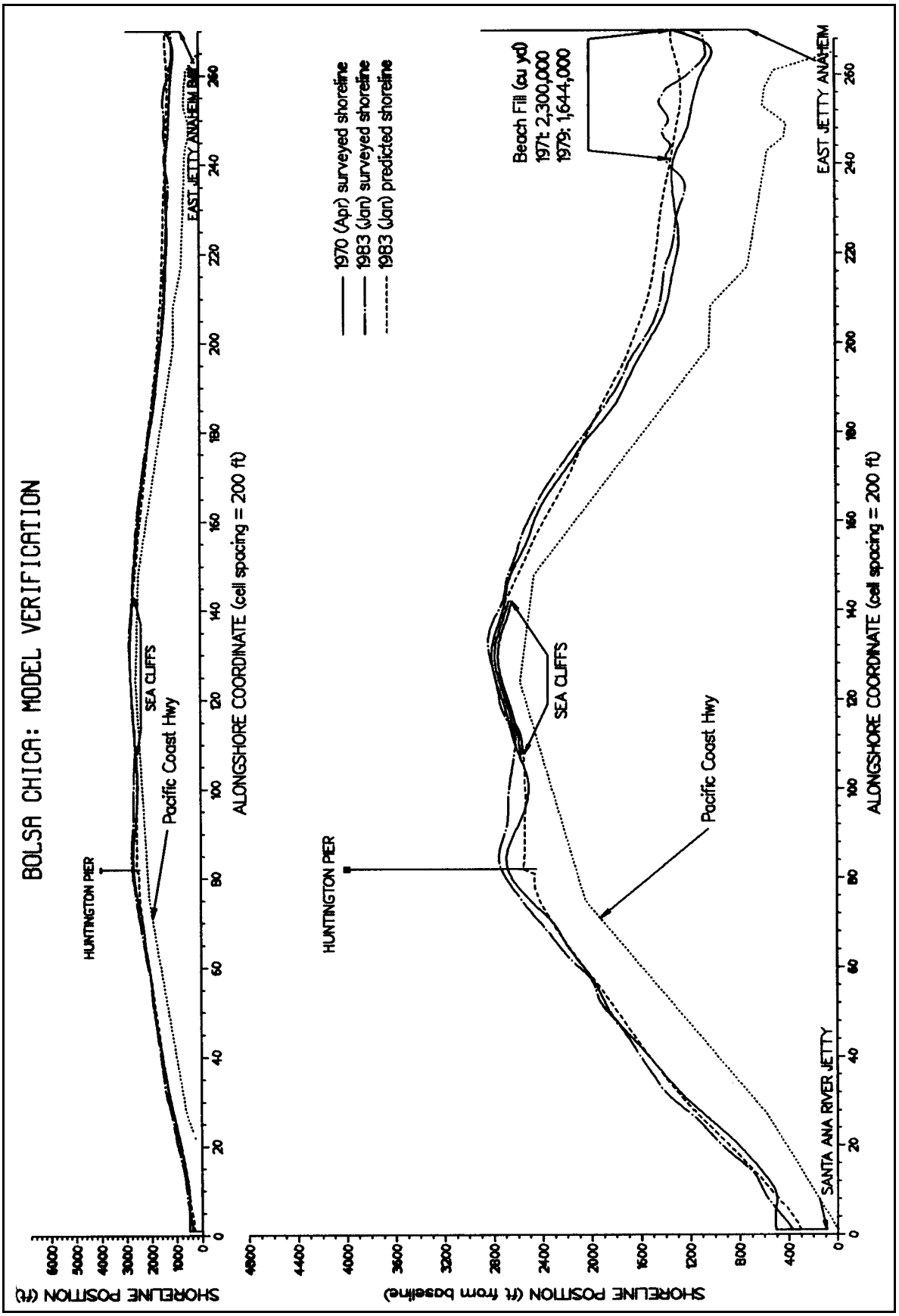

Figure III-2-51. Model verification results, Bolsa Chica (Gravens 1990a)

(k) After model calibration and verification, eight conceptual design alternatives were modeled, and several simulation variations were performed for each alternative. The intent of the simulations was to quantify the shoreline impacts of the proposed Bolsa Chica navigable ocean entrance system. In the simulation of Alternatives 1 and 3, no beach fill was included along the modeled reach. For Alternatives 2, 4, 5, 6, and 8, renourishment of the Surfside-Sunset feeder beach was specified at 1 million cu yd every 5 years. Alternatives 7 and 8 modeled impact mitigation sand management techniques. The 1983 shoreline was used as the initial shoreline, and all model tests were performed for 5- and 10-year simulation (prediction) periods using a randomly selected 10-year time history of Northern Hemisphere sea and swell conditions. The Southern Hemisphere swell component of the incident wave climate was varied from alternating available southern swell wave conditions, low-intensity southern swell, and high-intensity southern swell to predict a range of influence.

(l) Model results and analysis from 24 production simulations are documented by Gravens (1990a); only results from one alternative are presented here for illustrative purposes. Predicted changes in 10-year post-project shoreline position with Alternative 8 are shown in Figure III-2-52. Alternative 8 includes two shore-perpendicular jetties spaced 245 m apart and extending approximately 425 m offshore, a detached breakwater composed of three sections located offshore of the entrance channel, a feeder beach at Surfside-Sunset, and impact mitigation sand management. The impacts of this entrance system with the specified sand management plan as compared to a without-project 10-year projection are shown in Figure III-2-53. This alternative satisfied the criteria established by the SLC for successful impact mitigation. The SLC specified that only sand accumulating within 460 m of the entrance jetties may be used by sand bypassing/backpassing, and that a successful sand management plan would predict more accretive, or equal or less erosive, conditions than would occur without the project in place.

(m) Conclusions from shoreline change modeling of Bolsa Chica Bay were as follows:

- The proposed site of the new entrance system is located in a region of converging longshore sand transport.
- Locating the entrance system approximately 1.6 km up- or downcoast from the proposed site would not significantly change the predicted shoreline response.
- Implementation of a sand management plan would allow for the mitigation of adverse shoreline impacts.
- The Surfside-Sunset feeder beach nourishment program must be continued in order to maintain the shoreline within 3.2 km of the Anaheim Bay entrance. However, the proposed entrance system would neither aggravate nor improve the situation.

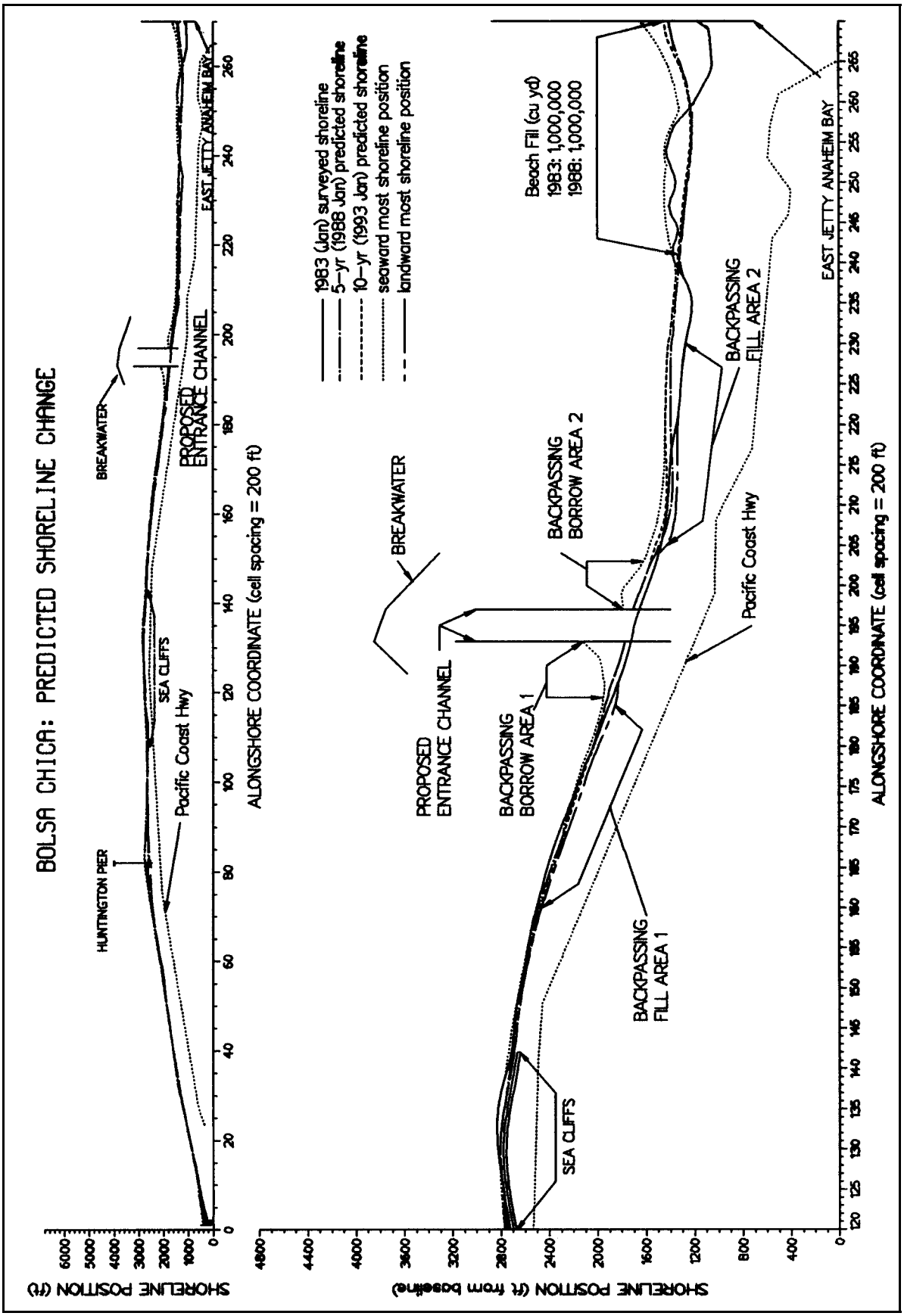

Figure III-2-52. Sand management alternative with feeder beach (Gravens 1990a)

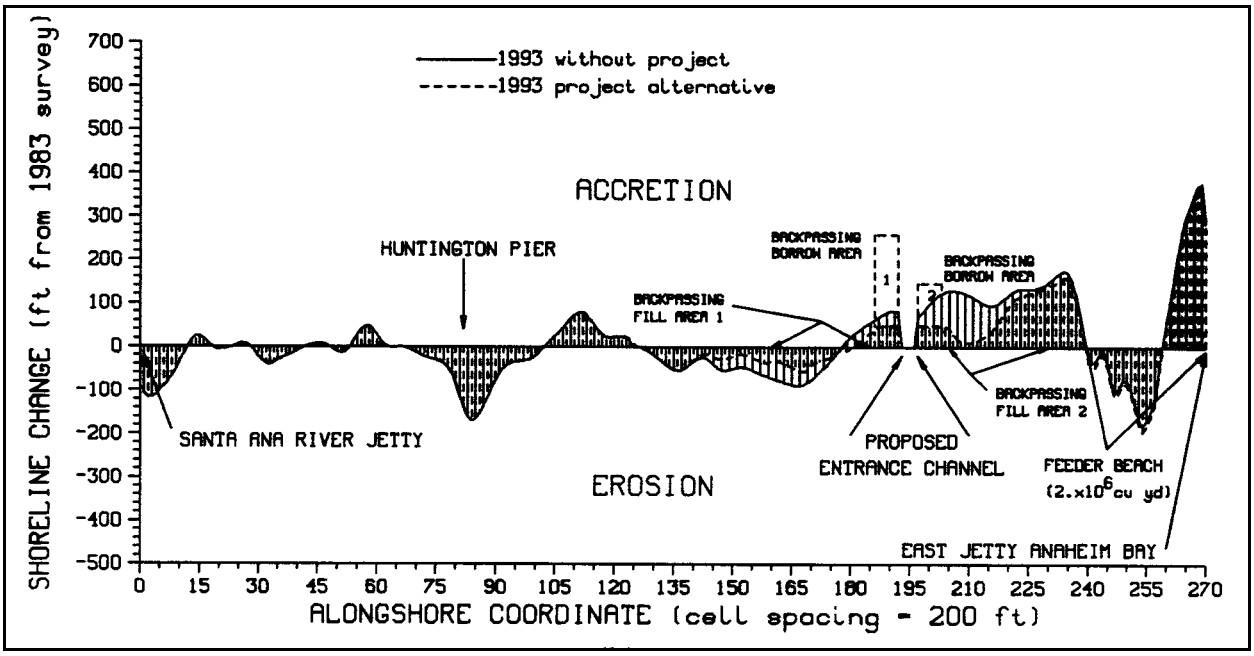

Figure III-2-53. Predicted shoreline change from 1983 shoreline position with sand management alternative and feeder beach (Gravens 1990a)

III-2-3. References

Aubrey 1980
Aubrey, D. G. 1980. "Our Dynamic Coastline," *Oceanus*, Vol 23, No. 4, pp 4-13.

Bagnold 1940
Bagnold, R. A. 1940. "Beach Formation by Waves: Some Model Experiments in a Wave Tank," *Journal Inst. Civil Engineering*, Vol 15, pp 27-52.

Bagnold 1963
Bagnold, R. A. 1963. "Beach and Nearshore Processes; Part I: Mechanics of Marine Sedimentation," *The Sea: Ideas and Observations*, *Vol 3,* M. N. Hill, ed., Interscience, New York, pp 507-528.

Bailard 1981
Bailard, J. A. 1981. "An Energetics Total Load Sediment Transport Model for a Plane Sloping Beach," *Journal of Geophysical Research*, Vol 86, No. C11, pp 10938-10954.

Bailard 1984
Bailard, J. A. 1984. "A Simplified Model for Longshore Sediment Transport," *Proceedings, 19th International Coastal Engineering Conference*, American Society of Civil Engineers, New York, pp 1454-1470.

Bailard and Inman 1981
Bailard, J. A., and Inman, D. L. 1981. "An Energetics Bedload Model for a Plane Sloping Beach: Local Transport," *Journal of Geophysical Research*, Vol 86, pp 2035-2043.

Bakker 1968
Bakker, W. T. 1968. "The Dynamics of a Coast with a Groin System," *Proceedings of the 11th Coastal Engineering Conference*, American Society of Civil Engineers, pp 492-517.

Bakker and Edelman 1965
Bakker, W. T., and Edelman, T. 1965. "The Coastline of River Deltas," *Proceedings of the 9th Coastal Engineering Conference*, American Society of Civil Engineers, pp 199-218.

Bakker, Klein-Breteler, and Roos 1971
Bakker, W. T., Klein-Breteler, E. H. J., and Roos, A. 1971. "The Dynamics of a Coast with a Groin System," *Proceedings of the 12th Coastal Engineering Conference*, American Society of Civil Engineers, pp 1001-1020.

Beach and Sternberg 1987
Beach, R. A., and Sternberg, R. W. 1987. "The Influence of Infragravity Motions on Suspended Sediment Transport in the Inner Surf Zone," *Proceedings of Coastal Sediments '87*, American Society of Civil Engineers, pp 913-928.

Bendat and Piersol 1971
Bendat, J. S., and Piersol, A. G. 1971. *Random Data: Analysis and Measurement Procedures*, Wiley-Interscience, New York.

Berek and Dean 1982
Berek, E. P., and Dean, R. G. 1982. "Field Investigation of Longshore Transport Distribution," *Proceedings, 18th International Conference on Coastal Engineering*, American Society of Civil Engineers, pp 1620-1639.

Bodge 1986
Bodge, K. R. 1986. "Short-Term Impoundment of Longshore Sediment Transport," Ph.D. diss., Department of Coastal and Oceanographic Engineering, University of Florida, Gainesville.

Bodge 1988
Bodge, K. R. 1988. "Longshore Current and Transport Across Non-Singular Equilibrium Beach Profiles," *Proceedings, 21st International Conf. on Coastal Engineering*, American Society of Civil Engineers, pp 1396-1410.

Bodge and Dean 1987a
Bodge, K. R., and Dean, R. G. 1987a. "Short-Term Impoundment of Longshore Transport," *Proceedings of Coastal Sediments '87*, American Society of Civil Engineers, pp 468-483.

Bodge and Dean 1987b
Bodge, K. R., and Dean, R. G. 1987b. "Short-Term Impoundment of Longshore Sediment Transport," Miscellaneous Paper CERC-87-7, U.S. Army Engineer Waterways Experiment Station, Vicksburg, MS.

Bodge and Kraus 1991
Bodge, K. R., and Kraus, N. C. 1991. "Critical Examination of Longshore Transport Rate Magnitude," *Proceedings*, *Coastal Sediments '91*, American Society of Civil Engineers, pp 139-155.

Bowen 1969
Bowen, A. J. 1969. "Rip Currents: 1. Theoretical Investigations," *Journal of Geophysical Research*, Vol 74, pp 5467-78.

Bowen 1973
Bowen, A. J. 1973. "Edge Waves and the Littoral Environment," *Proceedings 13th Conf. on Coast. Eng.*, American Society of Civil Engineers, pp 1313-20.

Bowen and Guza 1978
Bowen, A. J., and Guza, R. T. 1978. "Edge Waves and Surf Beat," *Journal Geophysical Research*, Vol 83, pp 1913-20.

Bowen and Inman 1966
Bowen, A. J., and Inman, D. L. 1966. "Budget of Littoral Sands in the Vicinity of Port Arguello, California," Technical Memorandum No. 19, Coastal Engineering Research Center, U.S. Army Corps Engineer Waterways Experiment Station, Vicksburg, MS.

Bowen and Inman 1969
Bowen, A. J., and Inman, D. L. 1969. "Rip Currents: 2. Laboratory and Field Observations," *Journal of Geophysical Research*, Vol 74, pp 5478-90.

Bowen and Inman 1971
Bowen, A. J., and Inman, D. L. 1971. "Edge Waves and Crescentic Bars," *Journal of Geophysical Research*, Vol 76, No. 76, pp 8662-71.

Box and Jenkins 1976
Box, G. E. P., and Jenkins, G. M. 1976. "Time Series Analysis, Forecasting, and Control," Holden-Day, San Francisco, CA, p 575.

Brenninkmeyer 1976
Brenninkmeyer, B. M. 1976. "In Situ Measurements of Rapidly Fluctuating, High Sediment Concentrations," *Marine Geology*, Vol 20, pp 117-128.

Brunn 1954
Brunn, P. 1954. "Migrating Sand Waves and Sand Humps, with Special Reference to Investigations Carried out on the Danish North Sea Coast," *Proceedings 5th Conf. on Coast. Eng.*, pp 269-95.

Bruno and Gable 1976
Bruno, R. O., and Gable, C. G. 1976. "Longshore Transport at a Total Littoral Barrier," *Proceedings of the 15th International Conference on Coastal Engineering*, American Society of Civil Engineers, pp 1203-1222.

Bruno, Dean and Gable 1980
Bruno, R. O., Dean, R. G., and Gable, C. G. 1980. "Littoral Transport Evaluations at a Detached Breakwater," *Proceedings of the 17th International Conference on Coastal Engineering*, American Society of Civil Engineers, pp 1453-1475.

Bruno, Dean, Gable, and Walton 1981
Bruno, R. O., Dean, R. G., Gable, C. G., and Walton, T. L. 1981. "Longshore Sand Transport Study at Channel Island Harbor, California," Technical Paper No. 81-2, Coastal Engineering Research Center, U.S. Army Engineer Waterways Experiment Station, Vicksburg, MS.

Bruun and Manohar 1963
Bruun, P., and Manohar, M. 1963. "Coastal Protection for Florida," Florida Engineering and Industrial Experiment Station Bulletin No. 113, University of Florida, Gainesville.

Caldwell 1956
Caldwell, J. M. 1956. "Wave Action and Sand Movement Near Anaheim Bay, California," U.S. Army Corps of Engineers, Beach Erosion Board, Technical Memorandum No. 68.

Chu, Gravens, Smith, Gorman and Chen 1987
Chu, Y., Gravens, M. B., Smith, J. M., Gorman, L. T., and Chen, H. S. 1987. "Beach Erosion Control Study, Homer Spit, Alaska," Miscellaneous Paper CERC-87-15, U.S. Army Engineer Waterways Experiment Station, Vicksburg, MS.

Cialone et al. 1992
Cialone, M. A., Mark, D. J., Chou, L. W., Leenknecht, D. A., Davis, J. E., Lillycrop, L. S., and Jensen, R. E. 1992. "Coastal Modeling System (CMS) User's Manual," Instruction Report CERC-91-1, U.S. Army Engineer Waterways Experiment Station, Vicksburg, MS.

Cialone, Neilans, Carson, and Smith (in preparation)
Cialone, M. A., Neilans, P. J., Carson, F. C., and Smith, J. M. "Long-term Shoreline Response Modeling at Westhampton Beach, New York," in preparation, U.S. Army Engineer Waterways Experiment Station, Vicksburg, MS.

Coakley and Skafel 1982
Coakley, J. P., and Skafel, M. G. 1982. "Suspended Sediment Discharge on a Non-Tidal Coast," *Proceedings of the 18th International Conference on Coastal Engineering*, American Society of Civil Engineers, pp 1288-1304.

Dalrymple 1975
Dalrymple, R. A. 1975. "A Mechanism for Rip Current Generation on an Open Coast," *Journal of Geophysical Research*, Vol 80, No. 24, pp 3485-3487.

Dalrymple and Lanan 1976
Dalrymple, R. A., and Lanan, G. A. 1976. "Beach Cusps Formed by Intersecting Waves," *Bull. Geo. Soc. Am.*, Vol 87, pp 57-60.

Darbyshire 1977
Darbyshire, J. 1977. "An Investigation of Beach Cusps in Hells Mouth Bay," *A Voyage of Discovery* (George Deacon 70th Anniversary Volume), M. Angel, ed., Pergamon, Oxford, pp 405-27.

Darbyshire and Pritchard 1978
Darbyshire, J., and Pritchard, E. 1978. *Riv. Ital. Geofisc. Sci. Affi*, Vol 5, pp 73-80.

Dean 1973
Dean, R. G. 1973. "Heuristic Models of Sand Transport in the Surf Zone," *Proceedings, Conference on Engineering Dynamics in the Surf Zone,* Sydney, Australia.

Dean 1984
Dean, R. G. 1984. "Principles of Beach Nourishment," Chapter 11, *CRC Handbook of Coastal Processes and Erosion*, P. D. Komar, ed., CRC Press, Inc., Boca Raton, FL, pp 217-232.

Dean 1987
Dean, R. G. 1987. "Measuring Longshore Transport with Traps," *Nearshore Sediment Transport*, Richard J. Seymour, ed., Plenum Press, New York.

Dean and Grant 1989
Dean, R. G., and Grant, J. 1989. "Development of Methodology for Thirty-Year Shoreline Projection in the Vicinity of Beach Nourishment Projects," University of Florida Report UFP/COEL-89/026, University of Florida, Gainesville.

Dean and Maurmeyer 1980
Dean, R. G., and Maurmeyer, E. M. 1980. "Beach Cusps at Point Reyes and Drakes Bay Beaches, CA," *Proceedings 17th Coastal Engineering Conference*, American Society of Civil Engineers, pp 863-884.

Dean and Yoo 1992
Dean, R. G., and Yoo, C. 1992. "Beach-Nourishment Performance Predictions," *Journal of Waterway, Port, Coastal, and Ocean Engineering*, Vol 118, No. 6, November/December, pp 567-586.

Dean and Yoo 1994
Dean, R. G., and Yoo, C. 1994. "Beach Nourishment in Presence of Seawall," *Journal of Waterway, Port, Coastal, and Ocean Engineering*, Vol 120, No. 3, May/June, pp 302-316.

Dean, Berek, Bodge, and Gable 1987
Dean, R. G., Berek, E. P., Bodge, K. R., and Gable, C. G. 1987. "NSTS Measurements of Total Longshore Transport," *Proceedings of Coastal Sediments '87*, American Society of Civil Engineers, pp 652-667.

Dean, Berek, Gable, and Seymour 1982
Dean, R. G., Berek, E. P., Gable, C. G., and Seymour, R. J. 1982. "Longshore Transport Determined by an Efficient Trap," *Proceedings of the 18th International Conference on Coastal Engineering*, American Society of Civil Engineers, pp 954-968.

del Valle, Medina, and Losada 1993
del Valle, R., Medina, R., and Losada, M. A. 1993. "Dependence of Coefficient *K* on Grain Size," Technical Note No. 3062, *Journal of Waterway, Port, Coastal, and Ocean Engineering*, Vol 119, No. 5, September/ October, pp 568-574.

Dolan 1971
Dolan, R. 1971. "Coastal Landforms: Crescentic and Rhythmic," *Geol. Soc. Am. Bull.*, Vol 82, pp 177-80.

Dolan and Ferm 1968
Dolan, R., and Ferm, J. C. 1968. "Conentric Landforms along the Atlantic Coast of the United States," *Science*, Vol 1959, pp 627-69.

Dolan, Vincent, and Hayden 1974
Dolan, R., Vincent, L., and Hayden, B. 1974. "Crescentic Coastal Landforms," *Zeitschr. fur Geomorph.*, Vol 18, pp 1-12.a.

Douglass 1985
Douglass, S. L. 1985. "Longshore Sand Transport Statistics," M.S. thesis, Mississippi State University, Starkville, MS.

Downing 1984
Downing, J. P. 1984. "Suspended Sand Transport on a Dissipative Beach," *Proceedings of the 19th International Conference on Coastal Engineering*, American Society of Civil Engineers, pp 1765-1781.

Duane and James 1980
Duane, D. B., and James, W. R. 1980. "Littoral Transport in the Surf Zone Elucidated by an Eulerian Sediment Tracer Experiment," *Journal of Sedimentary Petrology*, Vol 50, pp 929-942.

Dubois 1978
Dubois, R. 1978. *Geol. Soc. Am. Bull.*, Vol 89, pp 1133-1139.

Eaton 1950
Eaton, R. O. 1950. "Littoral Processes on Sandy Coasts," *Proceedings, First Coastal Engineering Conference*, Long Beach, California, Council on Wave Research, Chapter 15, pp 140-154.

Ebersole 1985
Ebersole, B. A. 1985. "Refraction-Diffraction Model for Linear Water Waves," *Journal of Waterways, Port, Coastal, and Ocean Engineering*, American Society of Civil Engineers, Vol III (No. WW6) pp 939-953.

Ebersole, Cialone, and Prater 1986
Ebersole, B. A., Cialone, M. A., and Prater, M. D. 1986. "RCPWAVE - A Linear Wave Propagation Model for Engineering Use," Technical Report CERC-86-4, U.S. Army Engineer Waterways Experiment Station, Vicksburg, MS.

Escher 1937
Escher, B. G. 1937. "Experiments on the Formation of Beach Cusps," *Leidse Geologische Mededlingen*, Vol 9, pp 70-104.

Evans 1938
Evans, O. F. 1938. "Classification and Origin of Beach Cusps," *J. Geol.*, Vol 46, pp 615-627.

Fairchild 1972
Fairchild, J. C. 1972. "Longshore Transport of Suspended Sediment," *Proceedings of the 13th International Conference on Coastal Engineering*, American Society of Civil Engineers, pp 1069-1088.

Fairchild 1977
Fairchild, J. C. 1977. "Suspended Sediment in the Littoral Zone at Vetnor, New Jersey, and Nags Head, North Carolina," Technical Paper No. 77-5, U.S. Army Engineer Waterways Experiment Station, Vicksburg, MS.

Finkelstein 1982
Finkelstein, K. 1982. "Morphological Variations and Sediment Transport in Crenulate-Bay Beaches; Kodiak Island, Alaska," *Marine Geology*, Vol 47, pp 261-81.

Flemming 1964
Flemming, N. C. 1964. "Tank Experiments on the Sorting of Beach Material During Cusp Formation," *Journal Sediment. Petrol.*, Vol 34, pp 112-22.

Grant 1943
Grant, U. S. 1943. "Waves as a Transporting Agent," *American Journal of Science*, Vol 241, pp 117-123.

Gravens 1989
Gravens, M. B. 1989. "Estimating Potential Longshore Sand Transport Rates Using WIS Data," CETN-II-19, U.S. Army Engineer Waterways Experiment Station, Vicksburg, MS.

Gravens 1990a
Gravens, M. B. 1990a. "Bolsa Bay, California, Proposed Ocean Entrance System Study; Report 2, Comprehensive Shoreline Response Computer Simulation, Bolsa Bay, California," Miscellaneous Paper CERC-89-17, U.S. Army Engineer Waterways Experiment Station, Vicksburg, MS.

Gravens 1990b
Gravens, M. B. 1990b. "Computer Program: GENESIS Version 2," CETN-II-21, U.S. Army Engineer Waterways Experiment Station, Vicksburg, MS.

Gravens 1991
Gravens, M. B. 1991. "Development of an Input Data Set for Shoreline Change Modeling," *Proceedings, Coastal Sediments '91*, American Society of Civil Engineers, pp 1800-1813.

Gravens 1992
Gravens, M. B. 1992. "User's Guide to the Shoreline Modeling System (SMS)," Instruction Report CERC-92-1, U.S. Army Engineer Waterways Experiment Station, Vicksburg, MS.

Gravens (in preparation)
Gravens, M. B. "Shoreline Change Modeling At Grande Isle, Louisiana," in preparation, U.S. Army Engineer Waterways Experiment Station, Vicksburg, MS.

Gravens, Kraus, and Hanson 1991
Gravens, M. B., Kraus, N. C., and Hanson, H. 1991. "GENESIS: Generalized Model for Simulating Shoreline Change," Instruction Report CERC-89-19, U.S. Army Engineer Waterways Experiment Station, Vicksburg, MS.

Gravens, Scheffner, and Hubertz 1989
Gravens, M. B., Scheffner, N. W., and Hubertz, J. M. 1989. "Coastal Processes form Asbury Park to Manasquan, New Jersey," Miscellaneous Paper CERC-89-11, U.S. Army Engineer Waterways Experiment Station, Vicksburg, MS.

Guza and Bowen 1981
Guza, R. T., and Bowen, A. J. 1981. "On the Amplitude of Beach Cusps," *Journal Geophys Research*, Vol 86, pp 4125-4132.

Guza and Inman 1975
Guza, R. T., and Inman, D. L. 1975. "Edge Waves and Beach Cusps," *Journal Geophysical Research*, Vol 80, No. 21, pp 2997-3012.

Hanes, Vincent, Huntley, and Clarke 1988
Hanes, D. M., Vincent, C. E., Huntley, D. A., and Clarke, T. L. 1988. "Acoustic Measurements of Suspended Sand Concentration in the C^2S^2 Experiment at Stanhope Lane, Prince Edward Island," *Marine Geology*, Vol 81, pp 185-196.

Hanson 1987
Hanson, H. 1987. "GENESIS - A Generalized Shoreline Change Numerical Model for Engineering Use," Report No. 1007, Department of Water Resources Engineering, University of Lund, Lund, Sweden.

Hanson and Kraus 1986
Hanson, H., and Kraus, N. C. 1986. "Forecast of Shoreline Change Behind Multiple Coastal Structures," *Coastal Engineering in Japan*, Vol 29, pp 195-213.

Hanson and Kraus 1989
Hanson, H., and Kraus, N. C. 1989. "GENESIS: Generalized Numerical Modeling System for Simulating Shoreline Change; Report 1, Technical Reference Manual," Technical Report CERC-89-19, U.S. Army Engineer Waterways Experiment Station, Vicksburg, MS.

Hanson, Kraus and Nakashima 1989
Hanson, H., Kraus, N. C., and Nakashima, L. D. 1989. "Shoreline Change Behind Transmissive Detached Breakwaters," *Proceedings, Coastal Zone '89*, American Society of Civil Engineers, pp 568-582.

Hino 1974
Hino, M. 1974. "Theory on Formation of Rip-Current and Cuspidal Coast," *Proceedings of the 14th Coastal Engineering Conference*, American Society of Civil Engineers, pp 901-919.

Holman and Bowen 1979
Holman, R. A., and Bowen, A. J. 1979. "Edge Waves on Complex Beach Profiles," *Journal Geophysical Research*, Vol 84, pp 6339-46.

Holman and Bowen 1982
Holman, R. A., and Bowen, A. J. 1982. "Bars, Bumps, and Holes: Models for the Generation of Complex Beach Topography," *Journal Geophysical Research*, Vol 87, pp 457-468.

Hom-ma and Sonu 1963
Hom-ma, M., and Sonu, C. J. 1963. "Rhythmic Patterns of Longshore Bars Related to Sediment Characteristics," *Proceedings 8th Conf. on Coast. Eng.*, American Society of Civil Engineers, pp 248-78.

Hom-ma, Horikawa and Kajima 1965
Hom-ma, M., Horikawa, K., and Kajima, R. 1965. "A Study of Suspended Sediment Due to Wave Action," *Coastal Engineering in Japan,* Vol 3, pp 101-122.

Hsu and Evans 1989
Hsu, J. R. C., and Evans, C. 1989. "Parabolic Bay Shapes and Applications," *Proceedings, Instn. Civil Engrs.*, Vol 87, pp 557-70.

Hsu, Silvester and Xia 1987
Hsu, J. R. C., Silvester, R., and Xia, Y. M. 1987. "New Characteristics of Equilibrium Shaped Bays," *Proceedings, 8th Aust. Conference on Coastal and Ocean Eng.*, pp 140-44.

Hsu, Silvester and Xia 1989a
Hsu, J. R. C., Silvester, R., and Xia, Y. M. 1989. "Static Equilibrium Bays: New Relationships," *Journal Waterways, Port, Coastal and Ocean Engineering*, American Society of Civil Engineers, Vol 115, No. 3, pp 285-98.

Hsu, Silvester and Xia 1989b
Hsu, J. R. C., Silvester, R., and Xia, Y. M. 1989. "Generalities on Static Equilibrium Bays,"*Journal Coastal Engineering*, Vol 12, pp 353-369.

Hubertz, Brooks, Brandon, and Tracy 1993
Hubertz, J. M., Brooks, R. M., Brandon, W. A., and Tracy, B. A. 1993. "Hindcast Wave Information for the U.S. Atlantic Coast," Wave Information Study Report 30, U.S. Army Engineer Waterways Experiment Station, Vicksburg, MS.

Huntley 1976
Huntley, D. A. 1976. "Long-Period Waves on a Natural Beach," *Journal of Geophysical Research*, Vol 81, No. 36, pp 6441-6449.

Huntley and Bowen 1973
Huntley, D. A., and Bowen, A. J. 1973. "Field Observations of Edge Waves," *Nature*, Vol 243, pp 160-1, Copyright© 1973 Macmillan Journals Ltd.

Huntley and Bowen 1975a
Huntley, D. A., and Bowen, A. J. (1975a). "Comparison of the Hydrodynamics of Steep and Shallow Beaches," *Nearshore Sediment Dynamics and Sedimentation*, J. R. Hails and A. Carr, ed., John Wiley, London, pp 69-109.

Huntley and Bowen 1975b
Huntley, D. A., and Bowen, A. J. (1975b). "Field Observations of Edge Waves and Their Effect on Beach Materials," *Quarterly Journal of the Geological Society (London)*, Vol 131, pp 68-81.

Huntley and Bowen 1979
Huntley, D. A., and Bowen, A. J. 1979. "Beach Cusps and Edge Waves," *Proceedings 16th Conf. Coastal Engineering.*, American Society of Civil Engineers, pp 1378-1393.

Ingle 1966
Ingle, J. C. 1966. "The Movement of Beach Sand; An Analysis using Fluorescent Grains," Department of Geology, University of Southern California, Los Angeles, California, Elsevier Publishing Company, New York.

Inman and Bagnold 1963
Inman, D. L., and Bagnold, R. A. 1963. "Beach and Nearshore Processes; Part II: Littoral Processes," contribution to *The Sea*, Vol 3, M. N. Hille, ed., John Wiley and Sons, pp 529-553.

Inman et al. 1980
Inman, D. L., Zampol, J. A., White, T. E., Hanes, D. M., Waldorf, B. W., and Kastens, K. A. 1980. "Field Measurements of Sand Motion in the Surf Zone," *Proceedings of the 17th International Conference on Coastal Engineering*, American Society of Civil Engineers, pp 1215-1234.

Inman, Komar, and Bowen 1968
Inman, D. L., Komar, P. D., and Bowen. 1968. "Longshore Transport of Sand," *Proceedings of the 11th International Conference on Coastal Engineering*, American Society of Civil Engineers, pp 248-306.

Inman, Tait, and Nordstrom 1971
Inman, D. L., Tait, and Nordstrom, 1971. "Mixing in the Surf Zone," *Journal of Geophysical Research*, Vol 76, pp 3493-3514.

Johnson 1910
Johnson, D. W. 1910. "Beach Cusps," *Geol. Soc. Am. Bull.*, Vol 21, pp 604-24.

Johnson 1919
Johnson, D. W. 1919. *Shore Processes and Shoreline Development*, 1965 facsimile, Hafner, New York.

Johnson 1956
Johnson, J. W. 1956. "Dynamics of Nearshore Sediment Movement," *Bulletin of the American Society of Petroleum Geologists*, Vol 40, pp 2211-2232.

Johnson 1957
Johnson, J. W. 1957. "The Littoral Drift Problem at Shoreline Harbors," *Journal of the Waterways and Harbors Division*, American Society of Civil Engineers, Vol 83, pp 1-37.

Johnson 1992
Johnson, C. N. 1992. "Mitigation of Harbor Caused Shore Erosion with Beach Nourishment, St. Joseph Harbor, MI," *Proceedings, Coastal Engineering Practice '92,* American Society of Civil Engineers, pp 137-153.

Kamphuis 1991
Kamphuis, J. W. 1991. "Alongshore Sediment Transport Rate," *Journal of Waterway, Port, Coastal, and Ocean Engineering*, Vol 117, No. 6, pp 624-640.

Kamphuis and Readshaw 1978
Kamphuis, J. W., and Readshaw, J. S. 1978. "A Model Study of Alongshore Sediment Transport Rate," *Proceedings, 16th International Coastal Engineering Conference*, American Society of Civil Engineers, pp 1656-1674.

Kamphuis and Sayao 1982
Kamphuis, J. W., and Sayao, O. 1982. "Model Tests on Littoral Sand Transport Rate," *Proceedings, 16th International Conference on Coastal Engineering,* American Society of Civil Engineers, pp 1305-1325.

Kamphuis, Davies, Nairn and Sayao 1986
Kamphuis, J. E., Davies, M. H., Nairn, R. B., and Sayao, O. J. 1986. "Calculation of Littoral Sand Transport Rate," *Journal Coastal Engineering Conference*, Vol 10, No. 1, pp 1-21.

Kana 1977
Kana, T. W. 1977. "Suspended Sediment Transport at Price Inlet, S.C.," *Proceedings of Coastal Sediments '77*, American Society of Civil Engineers, pp 366-382.

Kana 1978
Kana, T. W. 1978. "Surf Zone Measurements of Suspended Sediment," *Proceedings of the 16th International Conference on Coastal Engineering*, American Society of Civil Engineers, pp 1725-1743.

Kana and Ward 1980
Kana, T. W., and Ward, L. G. 1980. "Nearshore Suspended Sediment Load During Storms and Post-Storm Conditions," *Proceedings, 17th International Conference on Coastal Engineering*, pp 1158-1171.

Katoh, Tanaka and Irie 1984
Katoh, K., Tanaka, N., and Irie, I. 1984. "Field Observation on Suspended-Load in the Surf Zone," *Proceedings of the 19th International Conference on Coastal Engineering*, American Society of Civil Engineers, pp 1846-1862.

Knoth and Nummedal 1977
Knoth, J. S., and Nummedal, D. 1977. "Longshore Sediment Transport Using Fluorescent Tracer," *Proceedings of Coastal Sediments '77*, American Society of Civil Engineers, pp 383-398.

Komar 1971
Komar, P. D. 1971. "Nearshore Cell Circulation and the Formation of Giant Cusps," *Geol. Soc. Am. Bull.*, Vol 81, pp 2643-50.

Komar 1973a
Komar, P. D. 1973a. "Computer Models of Delta Growth Due to Sediment Input from Waves and Longshore Currents," *Geological Society of America Bulletin*, Vol 84, pp 2217-2226.

Komar 1973b
Komar, P. D. 1973b. "Observations of Beach Cusps at Mono Lake, California," *Geol. Soc. Am. Bull.*, Vol 84, pp 3593-600.

Komar 1976
Komar, P. D. 1976. *Beach Processes and Sedimentation*, Prentice-Hall, Inc., Englewood Cliffs, NJ.

Komar 1977
Komar, P. D. 1977. "Beach Sand Transport: Distribution and Total Drift," *Journal of the Waterway, Port, Coastal and Ocean Engineering Division*, American Society of Civil Engineers, Vol 103, pp 225-239.

Komar 1978
Komar, P. D. 1978. "Wave Conditions on the Oregon Coast During the Winter of 1977-78 and the Resulting Erosion of Nestucca Spit," *Shore and Beach*, Vol 46, pp 3-8.

Komar 1983
Komar, P. D. 1983. "Rhythmic Shoreline Features and their Origins," *Mega-Geomorphology*, R. Garnder and H.G. Scoging, eds., Claredon Press, Oxford, U.K., pp 92-112.

Komar 1988
Komar, P. D. 1988. "Environmental Controls on Littoral Sand Transport," *21st International Coastal Engineering Conference*, American Society of Civil Engineers, pp 1238-1252.

Komar and Inman 1970
Komar, P. D., and Inman, D. L. 1970. "Longshore Sand Transport on Beaches," *Journal of Geophysical Research*, Vol 75, No. 30, pp 5914-5927.

Komar and McDougal 1988
Komar, P.D., and McDougal, W. G. 1988. "Coastal Erosion and Engineering Structures: The Oregon Experience," *Journal Coastal Research*, Vol 4, pp 77-92.

Komar and Rea 1976
Komar, P. D., and Rea, C. C. 1976. "Erosion of Siletz Spit, Oregon," *Shore and Beach*, Vol 44, pp 9-15.

Kraus 1988
Kraus, N. C. 1988. "Part IV: Prediction Models of Shoreline Change," Chapter 6, "Case Studies of Application of the Shoreline Change Model," *Nearshore Dynamics and Coastal Processes: Theory, Measurement, and Predictive Models*, K. Horikawa, ed., University of Tokyo Press, Tokyo, Japan, pp 355-366.

Kraus and Dean 1987
Kraus, N. C., and Dean, J. L. 1987. "Longshore Sand Transport Rate Distributions Measured by Trap," *Proceedings, Coastal Sediments '87*, N. C. Kraus, ed., American Society of Civil Engineers, pp 881-896.

Kraus and Harikai 1983
Kraus, N. C., and Harikai, S. 1983. "Numerical Model of the Shoreline Change at Oarai Beach," *Coastal Engineering*, Vol 7, pp 1-28.

Kraus and Larson 1991
Kraus, N. C., and Larson, M. 1991. "NMLONG: Numerical Model for Simulating the Longshore Current; Report 1: Model Development and Tests," Technical Report DRP-91-1, U.S. Army Engineer Waterways Experiment Station, Vicksburg, MS.

Kraus et al. 1982
Kraus, N. C., Isobe, M., Igarashi, H., Sasaki, T. O., and Horikawa, K. 1982. "Field Experiments on Longshore Sand Transport in the Surf Zone," *Proceedings, 18th International Conference on Coastal Engineering*, American Society of Civil Engineers, pp 969-988.

Kraus, Gingerich, and Rosati 1988
Kraus, N. C., Gingerich, K. J., and Rosati, J. D. 1988. "Toward an Improved Empirical Formula for Longshore Sand Transport," *Proceedings of the 21st International Conference on Coastal Engineering*, American Society of Civil Engineers, pp 1182-1196.

Kraus, Gingerich and Rosati 1989
Kraus, N. C., Gingerich, K. J., and Rosati, J. D. 1989. "DUCK85 Surf Zone Sand Transport Experiment," Technical Report CERC-89-5, U.S. Army Engineer Waterways Experiment Station, Vicksburg, MS.

Krumbein 1944a
Krumbein, W. C. 1944a. "Shore Currents and Sand Movement on a Model Beach," Beach Erosion Board Tech. Memo. No. 7, U.S. Army Engineer Waterways Experiment Station, Vicksburg, MS.

Krumbein 1944b
Krumbein, W. C. 1944b. "Shore Processes and Beach Characteristics," Beach Erosion Board Tech. Memo. No. 37, U.S. Army Engineer Waterways Experiment Station, Vicksburg, MS.

Kuenen 1948
Kuenen, Ph.H. 1948. "The Formation of Beach Cusps," *Journal Geol.*, Vol 56, pp 34-40.

Larson, Hanson and Kraus 1987
Larson, M., Hanson, H., and Kraus, N. C. 1987. "Analytical Solutions of the One-Line Model of Shoreline Change," Technical Report CERC-87-15, U.S. Army Engineer Waterways Experiment Station, Vicksburg, MS.

LeBlond 1972
LeBlond, P. H. 1972. "On the Formation of Spiral beaches," *Proceedings 13th Int. Conf. on Coastal Engineering*, American Society of Civil Engineers, pp 1331-45.

LeBlond 1979
LeBlond, P. H. 1979. "An Explanation of the Logarithmic Spiral Plan Shape of Headland Bay Beaches," *Journal Sedimentary Petrology*, Vol 49, No. 4, pp 1093-1100.

Lee 1975
Lee, K. K. 1975. "Longshore Currents and Sediment Transport in West Shore of Lake Michigan," *Water Resources Research*, Vol 11, pp 1029-1032.

Leenknecht, Szuwalski, and Sherlock 1992
Leenknecht, D. A., Szuwalski, A., and Sherlock, A. R. 1992. "Automated Coastal Engineering System, User Guide and Technical Reference, Version 1.07," U.S. Army Engineer Waterways Experiment Station, Vicksburg, MS.

LeMéhauté and Brebner 1961
LeMéhauté, B., and Brebner, A. 1961. "An Introduction to Coastal Morphology and Littoral Processes," Report No. 14, Civil Engineering Department, Queens University at Kingston, Ontario, Canada.

LeMéhauté and Soldate 1977
LeMéhauté, B., and Soldate, M. 1977. "Mathematical Modeling of Shoreline Evolution," Miscellaneous Report 77-10, U.S. Army Engineer Waterways Experiment Station, Vicksburg, MS.

Lippman and Holman 1990
Lippman, T. C., and Holman, R. A. 1990. "Spatial and Temporal Variability of Sand Bar Morphology," *Journal of Geophysical Research,* Vol 95, No. C7, pp 11575-11590.

Longuet-Higgins 1970
Longuet-Higgins, M. S. 1970. "Longshore Currents Generated by Obliquely Incident Sea Waves, Parts 1 and 2," *Journal of Geophysical Research*, Vol 75, No. 33, November, pp 6778-6801.

Longuet-Higgins and Parkin 1962
Longuet-Higgins, M. S., and Parkin, D. W. 1962. "Sea Waves and Beach Cusps," *Geog. J.*, Vol 128, pp 194-201.

Mann and Dalrymple 1986
Mann, D. W., and Dalrymple, R. A. 1986. "A Quantitative Approach to Delaware's Nodal Point," *Shore and Beach,* Vol 54, No. 2, pp 13-16.

McDougal and Hudspeth 1981
McDougal, W. G., and Hudspeth, R. T. 1981. "Wave Induced Setup/Setdown and Longshore Current; Non-Planar Beaches: Sediment Transport," *Proceedings, Oceans*, IEEE, pp 834-846.

McDougal and Hudspeth 1983a
McDougal, W. G., and Hudspeth, R. T. 1983a. "Wave Setup/Setdown and Longshore Current on Non-Planar Beaches," *Journal Coastal Engineering*, Vol 7, pp 103-117.

McDougal and Hudspeth 1983b
McDougal, W. G., and Hudspeth, R. T. 1983b. "Longshore Sediment Transport on Non-Planar Beaches," *Journal Coastal Engineering,* Vol 7, pp 119-131.

McDougal and Hudspeth 1989
McDougal, W. G., and Hudspeth, R. T. 1989. "Longshore Current and Sediment Transport on Composite Beach Profiles," *Journal Coastal Engineering*, Vol 12, pp 315-338.

McDougal, Sturtevant, and Komar 1987
McDougal, W. G., Sturtevant, M. A., and Komar, P. D. 1987. "Laboratory and Field Investigations of the Impact of Shoreline Stabilization Structures on Adjacent Properties," *Proceedings, Coastal Sediments '87*, American Society of Civil Engineers, pp. 961-73.

Meisburger 1989
Meisburger, E. P. 1989. "Oolites as a Natural Tracer in Beaches of Southeastern Florida," Miscellaneous Paper CERC-89-10, U.S. Army Engineer Waterways Experiment Station, Vicksburg, MS.

Mogi 1960
Mogi, A. 1960. "On the Topographical Change of the Beach at Tokai, Japan," *Japan Geographical Review*, 398-411.

Moore and Cole 1960
Moore, G. W., and Cole, J. Y. 1960. "Coastal Processes in the Vicinity of Cape Thompson, Alaska; Geologic Investigations in Support of Project Chariot in the Vicinity of Cape Thompson, Northwestern Alaska - Preliminary Report," U.S. Geological Survey Trace Elements Investigation Report 753.

Munch-Peterson 1938
Munch-Peterson, J. 1938. "Littoral Drift Formula," *Beach Erosion Board Bulletin,* U.S. Army Engineer Waterways Experiment Station, Vicksburg, MS, Vol 4, No. 4, pp 1-31.

Niedoroda and Tanner 1970
Niedoroda, A. W., and Tanner, W. F. 1970. "Preliminary Study of Transverse Bars," *Mar. Geol.*, Vol 9, pp 41-62.

Otvos 1964
Otvos, E. G. 1964. "Observations of Beach Cusps and Pebble Ridge Formation on the Long Island Sound," *Journal Sediment. Petrol.*, Vol 34, pp 554-60.

Ozhan 1982
Ozhan, E. 1982. "Laboratory Study of Breaker Type Effect on Longshore Sand Transport," *Proceedings, Euromech 156, Mechanics of Sediment Transport,* Istanbul, A. Balkema Publishers.

Parker and Quigley 1980
Parker, G. F., and Quigley, R. M. 1980. "Shoreline Embayment Growth Between Two Headlands at Port Stanley, Ontario," *Proceedings, Canadian Coastal Conference*, pp 380-93.

Pelnard-Considere 1956
Pelnard-Considere, R. 1956. "Essai de theorie de l'Evolution des Forms de Rivages en Plage de Sable et de Galets," *4th Journees de l'Hydralique*, les energies de la Mer, Question III, Repport No. 1, pp 289-298.

Perlin and Dean 1983
Perlin, M., and Dean, R. G. 1983. "A Numerical Model to Simulate Sediment Transport in the Vicinity of Coastal Structures," Miscellaneous Report No. 83-10, Coastal Engineering Research Center, U.S. Army Engineer Waterways Experiment Station, Vicksburg, MS.

Rea and Komar 1975
Rea, C. C., and Komar, P. D. 1975. "Computer Simulation Models of a Hooked Beach Shoreline Configuration," *Journal Sedimentary Petrology*, Vol 45, pp 866-72.

Rosati and Kraus 1989
Rosati, J. D., and Kraus, N. C. 1989. "Development of a Portable Sand Trap for Use in the Nearshore," Technical Report CERC-89-11, U.S. Army Engineer Waterways Experiment Station, Vicksburg, MS.

Russell and McIntire 1965
Russell, R. J., and McIntire, W. G. 1965. "Beach Cusps," *Geol. Soc. Am. Bull.*, Vol 76, pp 307-20.

Sallanger 1979
Sallanger, A. H., Jr. 1979. "Beach Cusp Formation," *Marine Geology*, Vol 29, pp 23-37.

Savage 1962
Savage, R. P. 1962. "Laboratory Determination of Littoral Transport Rates," *Journal of the Waterway, Port, Coastal, and Ocean Division*, American Society of Civil Engineers, No. WW2, pp 69-92.

Sawaragi and Deguchi 1978
Sawaragi, T., and Deguchi, I., 1978. "Distribution of Sand Transport Rate Acros a Surf Zone," *Proceedings, 16th International Conference on Coastal Engineering*, American Society of Civil Engineers, pp 1596-1613.

Sayao 1982
Sayao, O. 1982. "Beach Profiles and Littoral Sand Transport," Ph.D. diss., Department of Civil Engineering, Queen's University, Kingston, Ontario, Canada.

Scripps Institute of Oceanography 1947
Scripps Institute of Oceanography. 1947. "A Statistical Study of Wave Conditions at Five Locations along the California Coast," Wave Report No. 68, University of California, San Diego.

Seymour and Aubrey 1985
Seymour, R. J., and Aubrey, D. G. 1985. *Marine Geology*, Vol 65, pp 289-304.

Shepard 1952
Shepard, F. P. 1952. "Revised Nomenclature for Depositional Ccoastal Features," *Bull. Am. Assoc. Petrol Geol.*, Vol 36, pp 1902-12.

Shepard 1973
Shepard, F. P. 1973. *Submarine Geology,* 3rd ed., Harper & Row, New York.

Shore Protection Manual 1977
Shore Protection Manual. 1977. 3rd ed., 2 Vol, U. S. Army Engineer Waterways Experiment Station, U. S. Government Printing Office, Washington, DC.

Shore Protection Manual 1984
Shore Protection Manual. 1984. 4th ed., 2 Vol, U. S. Army Engineer Waterways Experiment Station, U. S. Government Printing Office, Washington, DC.

Silvester 1970
Silvester, R. 1970. "Development of Crenulate Shaped Bays to Equilibrium," *Journal Waterways and Harbors Div.*, American Society of Civil Engineers, Vol 96(WW2), pp 275-87.

Silvester and Ho 1972
Silvester, R., and Ho, S. K. 1972. "Use of Crenulate-Shaped Bays to Stabilize Coasts," *Proceedings, 13th Int. Conf. on Coastal Engineering*, American Society of Civil Engineers, pp 1347-65.

Silvester and Hsu 1993
Silvester, R., and Hsu, J. R. C. 1993. *Coastal Stabilization: Innovative Concepts*, Prentice Hall, Inc., Englewood Cliffs, NJ.

Silvester, Tsuchiya, and Shibano 1980
Silvester, R., Tsuchiya, T., and Shibano, T. 1980. "Zeta Bays, Pocket Beaches and Headland Control," *Proceedings, 17th Int. Conf. on Coastal Eng.*, American Society of Civil Engineers, pp 1306-19.

Sonu 1969
Sonu, C. J. 1969. "Collective Movement of Sediment in Littoral Environment," *Proceedings 11th Conf. on Coast. Eng.*, American Society of Civil Engineers, pp 373-400.

Sonu 1972
Sonu, C. J. 1972. "Edge Wave and Crescentic Bars," Comments on paper by A. J. Bowen and D. L. Inman, *Journal Geophysical Research*, No. 33, pp 6629-31.

Sonu 1973
Sonu, C. J. 1973. "Three-dimensional Beach Changes," *Journal Geol.*, Vol 81, pp 42-64.

Sonu and Russell 1967
Sonu, C. J., and Russell, R. J. 1967. "Topographic Changes in the Surf Zone Profile," *Proceedings 10th Conf. on Coast Eng.*, American Society of Civil Engineers, pp 502-24.

Sonu and van Beek 1971
Sonu, C. J., and van Beek, J. L. 1971. "Systematic Beach Changes on the Outer Banks, North Carolina," *Journal Geol.* Vol 79, pp 416-25.

Sonu, McCloy, and McArthur 1967
Sonu, C. J., McCloy, J. M., and McArthur, D. S. 1967. "Longshore Currents and Nearshore Topographies," *Proc. 10th Conf. on Coast Eng.*, American Society of Civil Engineers, pp 5255-49.

Sternberg, Shi, and Downing 1984
Sternberg, R. W., Shi, N. C., and Downing, J. P. 1984. "Field Investigation of Suspended Sediment Transport in the Nearshore Zone," *Proceedings of the 19th International Conference on Coastal Engineering*, American Society of Civil Engineers, pp 1782-1798.

Thieke and Harris 1993
Thieke, R. J., and Harris, P. S. 1993. "Application of Longshore Transport Statistics to the Evaluation of Sand Transfer Alternatives at Inlets," *Journal of Coastal Research,* Vol 18, pp 125-145.

Thornton 1972
Thornton, E. B. 1972. "Distribution of Sediment Transport Across the Surf Zone," *Proceedings of the 13th International Conference on Coastal Engineering*, American Society of Civil Engineers, pp 1049-1068.

Thornton and Guza 1981
Thornton, E. B., and Guza, R. T. 1981. "Longshore Currents and Bed Shear Stress," *Proceedings of the Conference on Directional Wave Spectra Applications*, R. L. Weigel, ed., University of California, Berkeley.

Thornton and Morris 1977
Thornton, E. B., and Morris, W. D. 1977. "Suspended Sediments Measured Within the Surf Zone," *Proceedings of Coastal Sediments '77*, American Society of Civil Engineers, pp 655-668.

Trask 1952
Trask, P. D. 1952. "Source of Beach Sand at Santa Barbara, California, as Indicated by Mineral Grain Studies," Beach Erosion Board Tech. Memo. No. 28, U.S. Army Engineer Waterways Experiment Station, Vicksburg, MS.

Trask 1955
Trask, P. D. 1955. "Movement of Sand Around Southern California Promontories," Beach Erosion Board Tech. Memo. No. 76, U.S. Army Engineer Waterways Experiment Station, Vicksburg, MS.

U.S. Army Corps of Engineers 1966
U.S. Army Corps of Engineers. 1966. *Shore Protection, Planning, and Design*, Technical Report No. 4, 3rd ed., Coastal Engineering Research Center, U.S. Army Engineer Waterways Experiment Station, Vicksburg, MS.

van Bendegom 1949
van Bendegom, L. 1949. "Consideration of the Fundamentals of Coastal Protection," Ph.D. diss., Technical University, Delft, The Netherlands [in Dutch].

Verhagen 1989
Verhagen, H. J. 1989. "Sand Waves Along the Dutch Coast," *Coastal Engineering,* Vol 13, pp 129-147.

Vitale 1981
Vitale, P. 1981. "Moveable-Bed Laboratory Experiments Comparing Radiation Stress and Energy Flux Factor as Predictors of Longshore Transport Rate," Miscellaneous Report No. 81-4, U.S. Army Engineer Waterways Experiment Station, Coastal Engineering Research Center, Vicksburg, MS.

Walton 1972
Walton, T. L., Jr. 1972. "Littoral Drift Computations Along the Coast of Florida by Means of Ship Wave Observations," Technical Report No. 15, Coastal and Oceanographic Engineering Laboratory, University of Florida, Gainesville.

Walton 1976
Walton, T. L., Jr. 1976. "Uses of Outer Bars of Inlets as Sources of Beach Nourishment Material," *Shore and Beach,* Vol 44, No. 2.

Walton 1977
Walton, T. L., Jr. 1977. "Equilibrium Shores and Coastal Design," *Proceedings, Coastal Sediments '77*, American Society of Civil Engineers.

Walton 1979
Walton, T. L. 1979. "Littoral Sand Transport on Beaches," Ph.D. diss., University of Florida, Gainesville.

Walton 1980
Walton, T. L. 1980. "Littoral Sand Transport from Longshore Currents," Technical Note, *Journal of the Waterway, Port, Coastal, and Ocean Division*, American Society of Civil Engineers, Vol 106, No. WW4, November, pp 483-487.

Walton 1982
Walton, T. L. 1982. "Hand-held Calculator Algorithms for Coastal Engineering; Second Series," CETA 82-4, Coastal Engineering Research Center, U.S. Army Engineer Waterways Experiment Station, Vicksburg, MS.

Walton 1989
Walton, T. L., Jr. 1989. "Discussion of Sand Bypassing Simulation Using Synthetic Longshore Transport Data," *Journal Waterway, Port, Coastal and Ocean Division*, American Society of Civil Engineers, Vol 115, No. 4, pp 576-557.

Walton 1994
Walton, T. L., Jr. 1994. "Shoreline Solution for Tapered Beach Fill," *Journal Waterway, Port, Coastal and Ocean Engineering*, Vol 120, No. 6, pp 1-5.

Walton and Borgman 1991
Walton, T. L., Jr., and Borgman, L. B. 1991. "Simulation of Nonstationary, Non-Gaussion Water Levels on Great Lakes," *Journal of Waterway, Port, Coastal, and Ocean Engineering*, Vol 116, No. 6, American Society of Civil Engineers, New York.

Walton and Bruno 1989
Walton, T. L., and Bruno, R. O. 1989. "Longshore Transport at a Detached Breakwater, Phase II," *Journal of Coastal Research*, Vol 5, No. 4, pp 679-691.

Walton and Chiu 1977
Walton, T., and Chiu, T. 1977. "Sheltered Shorelines in Florida," *Shore and Beach*, Vol 45, No. 4.

Walton and Chiu 1979
Walton, T., and Chiu, T. 1979. "A Review of Analytical Techniques to Solve the Sand Transport Equation and Some Simplified Solutions," *Proceedings of Coastal Structures '79*, American Society of Civil Engineers, pp 809-837.

Walton and Dean 1973
Walton, T. L., Jr., and Dean, R. G. 1973. "Application of Littoral Drift Roses to Coastal Engineering Problems," *Proceedings, First Australian Conference on Coastal Engineering*, National Committee on Coastal and Ocean Engineering Institution of Engineers, Australia.

Walton and Dean 1976
Walton, T. L., Jr., and Dean, R. G. 1976. "Use of Outer Bars of Inlets as Sources of Beach Nourishment Material," *Shore and Beach*, Vol 44, No. 2.

Walton and Douglass 1985
Walton, T. L., Jr., and Douglass, S. L. 1985. "Stochastic Sand Transport Using ARIMA Modeling," *Proceedings 21st Congress, International Association for Hydraulic Research*, Melbourne, Australia, Vol 4, pp 166-172.

Walton and Sensabaugh 1979
Walton, T. L., and Sensabaugh, W. 1979. "Seawall Design on the Open Coast," Sea Grant Report No. 29, University of Florida, Gainesville.

Walton, Liu and Hands 1988
Walton, T. L., Liu, P. L-F., and Hands, E. B. 1988. "Shoreline at a Jetty Due to Cyclic and Random Waves," *Proceedings, 21st International Conference on Coastal Engineering*, American Society of Civil Engineers, pp 1911-1921.

Walton, Thomas and Dickey 1985
Walton, T. L., Thomas, J. L., and Dickey, M. D. 1985. "Cross-shore Distribution of Sediment Transport at a Weir Jetty," *Australasian Conference on Coastal and Ocean Engineering,* Christchurch, New Zealand, 2-6 December, pp 525-535.

Watts 1953a
Watts, G. M. 1953a. "A Study of Sand Movement at South Lake Worth Inlet, Florida," Beach Erosion Board Tech. Memo. No. 42, U.S. Army Engineer Waterways Experiment Station, Vicksburg, MS.

Watts 1953b
Watts, G. M. 1953b. "Development and Field Test of a Sampler for Suspended Sediment in Wave Action," Beach Erosion Board Tech. Memo. No. 34, U.S. Army Engineer Waterways Experiment Station, Vicksburg, MS.

Weggel 1972
Weggel, J. R. 1972. "Maximum Breaker Height," *Journal of the Waterways, Ports, and Coastal Engineering Division*, Vol 98, ww 4, pp 529-548.

Weggel and Perlin 1988
Weggel, J. R., and Perlin, M. 1988. "Statistical Description of Longshore Transport Environment." *Journal Waterway, Port, Coastal and Ocean Engineering*, American Society of Civil Engineers, Vol 114, No. 2, pp 125-145.

White 1987
White, T. E. 1987. "Nearshore Sand Transport," Ph.D. diss., University of California, San Diego.

Williams 1973
Williams, A. T. 1973. "The Problem of Beach Cusp Development," *Journal Sediment Petrol.*, Vol 43, pp 857-66.

Wright et al. 1979
Wright, L. D., Chappell, J., Thorn, B. G., Bradshaw, M. P., and Cowell, P. 1979. "Morphodynamics of Reflective and Dissipative Beach and Inshore Systems: Southeastern Australia," *Marine Geology*, Vol 32, pp 105-40.

Yasso 1965
Yasso, W. E. 1965. "Plan Geometry of Headland Bay Beaches," *Journal Geology*, Vol 73, pp 702-14.

Zenkovitch 1960
Zenkovitch, V. P. 1960. "Fluorescent Substances as Tracers for Studying the Movement of Sand on the Sea Bed, Experiments Conducted in the U.S.S.R.," *Dock and Harbor Authority*, Vol 40, pp 280-283.

Zenkovitch 1964
Zenkovitch, V. P. 1964. "Cyclic Cuspate Sand Spits and Sediment Transport Efficiency," discussion, *Journal Geol.*, Vol 72, pp 879-80.

III-2-6. Definition of Symbols

α	Wave crest angle relative to bottom contours [deg]
α_b	Wave breaker angle relative to the shoreline [deg]
β	Geometric parameter in the expression to approximate the shoreline in the lee of headland-type features (Equation III-2-24 III-2-24 and Figure III-2-27) [deg]
γ	Energy flux dissipation rate [dimensionless]
Γ_{stb}	Stable wave height to water depth ratio for wave re-formation
ε	Shoreline diffusivity parameter (Equation III-2-26) [length^2/time]
θ	Geometric parameter in the expression to approximate the shoreline in the lee of headland-type features (Equation III-2-24 and Figure III-2-27) [deg]
θ_n	Azimuth angle of the outward normal to the shoreline (Equation III-2-17) [deg]
κ	Breaker index H_b/d_b [dimensionless]
Λ_{mix}	Lateral mixing coefficient [dimensionless]
ξ_b	Surf similarity parameter [dimensionless]
ρ	Mass density of water (salt water = 1,025 kg/m^3 or 2.0 slugs/ft^3; fresh water = 1,000kg/m^3 or 1.94 slugs/ft^3) [force-time^2/length^4]
ρ_s	Mass density of sediment grains (2,650 kg/m^3 or 5.14 slugs/ft^3 for quartz-density sand) [force-time^2/length^4]
a_1, a_2	Dimensionless parameters used in the GENESIS empirical predictive formula for longshore sand transport rate (Equation III-2-42)
C_0, C_1, C_2	Coefficients in expression to approximate the shoreline in the lee of headland-type features (Equation III-2-24)
C_b	Wave group speed at the breaker line [length/time]
C_f	Friction coefficient
C_g	Wave group speed [length/time]
C_{g0}	Wave group speed in deep water [length/time]
C_{gb}	Wave group speed at the breaker line [length/time]
d	Water depth in the surf zone, including wave-induced setup [length]
d_b	Water depth at the breaker line [length]
d_B	Berm crest elevation or beach berm height above still-water [length]
d_c	Depth of appreciable sand transport as measured from still-water level [length]

d_C	Offshore closure depth [length]
E	Total wave energy in one wavelength per unit crest width [length-force/length^2]
E_b	Wave energy at the breaker line per unit crest width [length-force/length]
$erf( )$	Error function
$erfc( )$	Complementary error function
g	Gravitational acceleration (32.17 ft/sec^2, 9.807m/sec^2) [length/time^2]
H	Wave height in the surf zone [length]
H_b	Wave height at breaking [length]
H_{mo}	Average wave height [length]
H_{sig}	Significant wave height [length]
I_ℓ	Immersed weight transport rate [force/sec]
K	Empirical proportionality coefficient [dimensionless]
K_1, K_2	Empirical coefficients, treated as calibration parameters, used in the GENESIS empirical predictive formula for longshore sand transport rate (Equation III-2-42)
$K_{a,b}$	Constants [dimensionless]
k_q	Dimensional normalizing constant [time^3/force]
m	Average bottom slope from the shoreline to the depth of active longshore sand transport [length-rise/length-run]
n	In-place sediment porosity ($\approx$ 0.4) [dimensionless]
$p(t)$	Proportion of fill left within project boundaries at a given time after project initiation (Equation III-2-32)
P_ℓ	Potential longshore sediment transport rate [force/time]
q	Line source or sink of sediment
Q	Potential volumetric longshore transport rate [length^3/time]
$q_x(y)$	Local longshore transport per unit width offshore [length^3/time/length]
$Q_{\ell R}$	Annual longshore transport to the right (looking seaward) [length^3/time]
$Q_{\ell NET}$	Net annual longshore transport [length^3/time]
$Q_{\ell L}$	Annual longshore transport to the left (looking seaward) [length^3/time]
$Q_{\ell GROSS}$	Gross annual longshore transport [length^3/time]
Q_ℓ	Volume longshore transport rate [length^3/time]

R	Geometric parameter in the expression to approximate the shoreline in the lee of headland-type features (Equation III-2-24 and Figure III-2-27) [length]
R_0	Distance between the ends of headlands that define a given section of shoreline (Equation III-2-24 and Figure III-2-27) [length]
T	Wave period [time]
T_0	Length of a wane record [time]
t_f	Time required for structure to fill to capacity (Equation III-2-29)
T_p	Average peak spectral wave period [time]
u_{mb}	Maximum oscillatory velocity magnitude (Equation III-2-9) [length/time]
V_0	Theoretical longshore velocity at breaking point for the no-lateral-mixing case [length/time]
V_ℓ	Longshore current speed [length/time]
W	Width of the surf zone [length]
w_f	Sediment fall velocity [length/time]
y	Distance seaward the shoreline will extend at a structure [length]
Y	Distance to the measured current from the shoreline (Equation III-2-12) [length]
Y	Length of structure (Equation III-2-29) [length]

III-2-7. Acknowledgments

Authors of Chapter III-2, "Longshore Sediment Transport:"

Julie D. Rosati, Coastal and Hydraulics Laboratory (CHL), Engineer Research and Development Center (ERDC), Vicksburg, Mississippi.
Todd L. Walton, Ph.D., CHL
Kevin Bodge, Ph.D., Olsen Associates, Jacksonville, Florida.

Reviewers:

James Bailard, Ph.D., Private consultant
James R. Houston, Ph.D., ERDC
David L. Kriebel, Ph.D., Department of Ocean Engineering, United States Naval Academy, Annapolis, Maryland.
Paul A. Work, Ph.D., School of Civil and Environmental Engineering, Georgia Institute of Technology, Atlanta, Georgia.

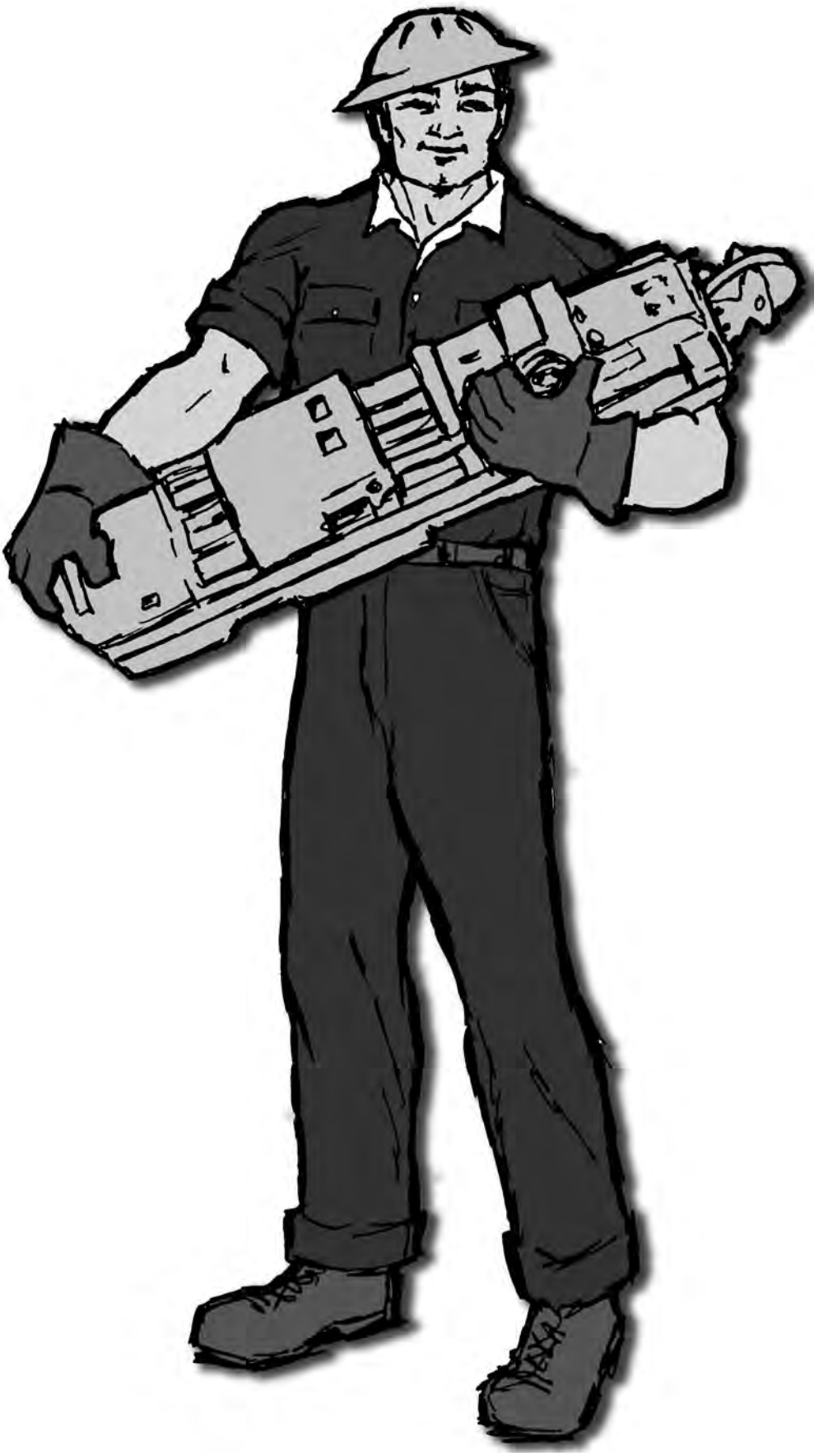

Table of Contents

Page

III-3-1. Introduction III-3-1
a. Overview/purpose III-3-1
b. Scope of chapter III-3-2

III-3-2. General Characteristics of Natural and Altered Profiles III-3-2
a. Forces acting in the nearshore III-3-2
b. Equilibrium beach profile characteristics III-3-9
c. Interaction of structures with cross-shore sediment transport III-3-16
d. Methods of measuring beach profiles III-3-16
(1) Introduction III-3-16
(a) Fathometer III-3-16
(b) CRAB III-3-18
(c) Sea sled III-3-19
(d) Hydrostatic profiler III-3-19
(2) Summary III-3-19

III-3-3. Engineering Aspects of Beach Profiles and Cross-shore Sediment Transport III-3-19
a. Introduction III-3-19
b. Limits of cross-shore sand transport in the onshore and offshore directions III-3-19
c. Quantitative description of equilibrium beach profiles III-3-21
d. Computation of equilibrium beach profiles III-3-25
e. Application of equilibrium profile methods to nourished beaches. III-3-25
f. Quantitative relationships for nourished profiles III-3-26
g. Longshore bar formation and seasonal shoreline changes III-3-32
h. Static models for shoreline response to sea level rise and/or storm effects III-3-43
i. Computational models for dynamic response to storm effects III-3-51
(1) Introduction III-3-51
(2) Numerical and analytical models III-3-51
(3) General description of numerical models III-3-52
(a) Conservation equation III-3-52
(b) Transport relationships III-3-52
(c) Closed loop transport relationships III-3-52
(d) Open loop transport relationships III-3-52
(4) General description of analytical models III-3-54
j. Example application of an analytical model III-3-55
k. Examples of numerical models III-3-59
l. Physical modeling of beach profile response III-3-65

III-3-4. References III-3-69

III-3-5. Definition of Symbols III-3-76

III-3-6. Acknowledgments III-3-79

List of Tables

Page

Table III-3-1
Constructive and Destructive Cross-shore "Forces" in Terms of Induced Bottom Shear Stresses . III-3-11

Table III-3-2
Summary of Field Evaluation of Various Nearshore Survey Systems (Based on Clausner, Birkemeier, and Clark (1986)) III-3-18

Table III-3-3
Summary of Recommended A Values (Units of A Parameter are $m^{1/3}$) III-3-24

List of Figures

Page

Figure III-3-1. Longshore (q_x) and cross-shore (q_y) sediment transport components III-3-1

Figure III-3-2. Problems and processes in which cross-shore sediment transport is relevant III-3-3

Figure III-3-3. Definition sketch III-3-4

Figure III-3-4. Variation with time of the bottom shear stress under a breaking nonlinear wave. H = 0.78 m, h= 1.0 m, T = 8.0 s, and D = 0.2 mm III-3-5

Figure III-3-5. Isolines of nondimensional average bottom shear stress τ_b versus relative depth and wave steepness (Dean 1987a). Note that bottom shear stresses are directed landward. III-3-6

Figure III-3-6. Distribution over depth of the flux of the onshore component of momentum III-3-8

Figure III-3-7. Bottom stresses caused by surface winds III-3-8

Figure III-3-8. Velocity distributions inside and outside the surf zone for no surface wind stress and cases of no overtopping and full overtopping both inside and outside the surf zone III-3-10

Figure III-3-9. Effects of varying wave energy flux (a) on: (b) shoreline position, and (c) foreshore beach slope (dots are shoreline position in (b) and (c), solid curve is trend line in (b), foreshore slope in (c)) (Katoh and Yanagishima 1988) III-3-12

Figure III-3-10. Examples of two offshore bar profiles III-3-13

Figure III-3-11. Variation in shoreline and bar crest positions, Duck, NC (Lee and Birkemeier 1993) III-3-14

Figure III-3-12. Definition of offshore bar characteristics (Keulegan 1945) III-3-15

Figure III-3-13. Nondimensional geometries of natural bars compared with those produced in the laboratory (Keulegan 1948) III-3-15

Figure III-3-14. Profiles extending across the continental shelf for three locations along the East and Gulf coastlines of the United States (Dean 1987a) III-3-17

Figure III-3-15. Comparison of response of natural and seawalled profiles to Hurricane Elena, September, 1985 (Kriebel 1987) III-3-18

Figure III-3-16. Erosional profile evolution, large wave tank results (Vellinga 1983) III-3-21

Figure III-3-17. Variation of sediment scale parameter A with sediment size D and fall velocity w_f (Dean 1987b) III-3-23

Figure III-3-18. Variation of sediment scale parameter $A(D)$ with sediment size D for beach sand sizes III-3-23

Figure III-3-19. Equilibrium beach profiles for sand sizes of 0.3 mm and 0.6 mm $A(D = 0.3\text{ mm}) = 0.12\text{ m}^{1/3}$, $A(D = 0.6\text{ mm}) = 0.20\text{ m}^{1/3}$ III-3-26

Figure III-3-20. Three generic types of nourished profiles (a) intersecting, (b) non-intersecting, and (c) submerged profiles (Dean 1991) III-3-27

Figure III-3-21. Effect of nourishment material scale parameter A_F on width of resulting dry beach. Four examples of decreasing A_F with same added volume per unit beach length (Dean 1991) III-3-28

Figure III-3-22. Effect of increasing volume of sand added on resulting beach profile. $A_F = 0.1\text{ m}^{1/3}$, $A_N = 0.2\text{ m}^{1/3}$, $h_* = 6.0$ m, $B = 1.5$ m (Dean 1991) III-3-29

Figure III-3-23. (1) Volumetric requirement for finite shoreline advancement (Equation 3-23); (2) Volumetric requirement for intersecting profiles (Equation 3-22). Results presented for special case $B' = 0.25$ III-3-31

Figure III-3-24. Variation of nondimensional shoreline advancement $\Delta y/W_*$, with A' and V. Results shown for $h_*/B = 2.0$ ($B'=0.5$) (Dean 1991) III-3-33

Figure III-3-25. Variation of nondimensional shoreline advancement $\Delta y/W_*$, with A' and V. Results shown for $h_*/B = 3.0$ ($B'= 0.333$) (Dean 1991) III-3-34

Figure III-3-26. Variation of nondimensional shoreline advancement $\Delta y/W_*$, with A' and V. Results shown for $h_*/B = 4.0$ ($B'=0.25$) (Dean 1991) III-3-35

Figure III-3-27. Nourishment with coarser sand than native (Intersecting profiles) III-3-37

Figure III-3-28. Example III-3-3. Nourishment with same-sized sand as native (Nonintersecting profiles) III-3-39

Figure III-3-29. Illustration of effect of volume added V and fill sediment scale parameter A_F on additional dry beach width Δy. Example conditions: $B = 1.5\ m, h_* = 6\ m, A_N = 0.1\text{ m}^{1/3}$ III-3-40

Figure III-3-30. Mean monthly shoreline position A and unit volume B at Jupiter, referenced to first survey (Dewall and Richter 1977) III-3-41

Figure III-3-31. Changes in shoreline position and unit volume at Westhampton Beach, New York (Dewall 1979) III-3-42

Figure III-3-32. Components of sand volume balance due to sea level rise and associated profile retreat according to the Bruun Rule III-3-44

Figure III-3-33. The Bruun Rule generalized for the case of a barrier island that maintains its form relative to the adjacent ocean and lagoon (Dean and Maurmeyer 1983) III-3-45

Figure III-3-34. Elements of the Edelman model III-3-46

Figure III-3-35. Profile forms considered by Kriebel and Dean (1993) III-3-48

Figure III-3-36. Two types of grids employed in numerical modelling of cross-shore sediment transport and profile evolution III-3-53

Figure III-3-37. Examples of profile response to idealized sine-squared storm surge: (a) Short-duration hurricane, and (b) Long-duration northeaster (Kriebel and Dean 1993) III-3-56

Figure III-3-38. Maximum relative erosion versus ratio of storm duration to profile time scale T_D/T_S III-3-57

Figure III-3-39. Empirical relationship for determination of erosion time scale T_s III-3-57

Figure III-3-40. Potential and actual shoreline response based on Kriebel and Dean (1993) model III-3-59

Figure III-3-41. Kriebel and Dean erosion model calibration using large-wave tank data of Saville (1957) (from Kriebel (1990)) III-3-61

Figure III-3-42. Comparison of Kriebel and Dean erosion model to measured profiles from northeast storm at Point Pleasant, NJ (from Kriebel (1990)). III-3-61

Figure III-3-43. SBEACH compared to two tests from large-scale wave tanks (Larson and Kraus 1989) III-3-63

Figure III-3-44. SBEACH tested against profile evolution data from Duck, NC (Larson and Kraus 1989) III-3-64

Figure III-3-45. Noda's recommendation for profile modeling (Noda 1972) III-3-66

Figure III-3-46. Profile evolution by small- and large-scale wave tank tests. Based on maintaining the same fall velocity parameter. Length ratio = 1:9.6 (Kriebel, Dally, and Dean 1986) III-3-68

Figure III-3-47. Profile evolution by small- and large-scale wave tank tests. Case of sloping seawall. Based on maintaining the same fall velocity parameter. Length ratio = 1:7.5 (Hughes and Fowler 1990) III-3-69

Chapter III-3
Cross-Shore Sediment Transport Processes

III-3-1. Introduction

a. Overview/purpose.

(1) Sediment transport at a point in the nearshore zone is a vector with both longshore and cross-shore components (see Figure III-3-1). It appears that under a number of coastal engineering scenarios of interest, transport is dominated by either the longshore or cross-shore component and this, in part, has led to a history of separate investigative efforts for each of these two components. The subject of total longshore sediment transport has been studied for approximately five decades. There is still considerable uncertainty regarding certain aspects of this transport component including the effects of grain size, barred topography, and the cross-shore distribution of longshore transport. A focus on cross-shore sediment transport is relatively recent, having commenced approximately one decade ago and uncertainty in prediction capability (including the effects of all variables) may be considerably greater. In some cases the limitations on prediction accuracy of both components may be due as much to a lack of good wave data as to an inadequate understanding of transport processes.

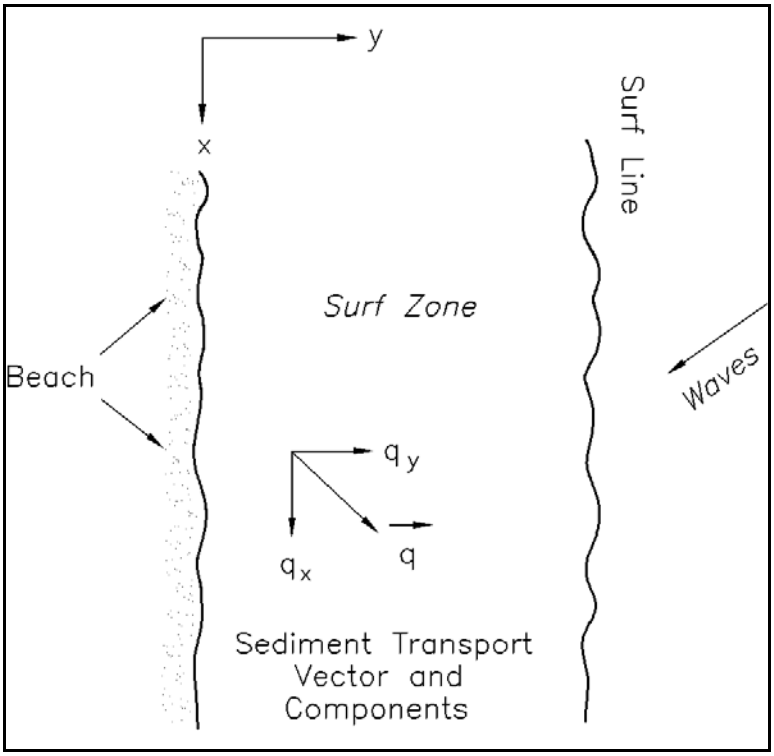

Figure III-3-1. Longshore (q_x) and cross-shore (q_y) sediment transport components

(2) Cross-shore sediment transport encompasses both offshore transport, such as occurs during storms, and onshore transport, which dominates during mild wave activity. Transport in these two directions appears to occur in significantly distinct modes and with markedly disparate time scales; as a result, the difficulties in predictive capabilities differ substantially. Offshore transport is the simpler of the two and tends to occur

with greater rapidity and as a more regular process with transport more or less in phase over the entire active profile. This is fortunate since there is considerably greater engineering relevance and interest in offshore transport due to the potential for damage to structures and loss of land. Onshore sediment transport within the region delineated by the offshore bar often occurs in "wave-like" motions referred to as "ridge-and-runnel" systems in which individual packets of sand move toward, merge onto, and widen the dry beach. A complete understanding of cross-shore sediment transport is complicated by the contributions of both bed and suspended load transport. Partitioning between the two components depends in an unknown way on grain size, local wave energy, and other variables.

(3) Cross-shore sediment transport is relevant to a number of coastal engineering problems, including: (a) beach and dune response to storms, (b) the equilibration of a beach nourishment project that is placed at slopes steeper than equilibrium, (c) so-called "profile nourishment" in which the sand is placed in the nearshore with the expectation that it will move landward nourishing the beach (this involves the more difficult problem of onshore transport), (d) shoreline response to sea level rise, (e) seasonal changes of shoreline positions, which can amount to 30 to 40 m, (f) overwash, the process of landward transport due to overtopping of the normal land mass due to high tides and waves, (g) scour immediately seaward of shore-parallel structures, and (h) the three-dimensional flow of sand around coastal structures in which the steeper and milder slopes on the updrift and downdrift sides of the structure induce seaward and landward components, respectively. These problems are schematized in Figure III-3-2.

b. Scope of chapter.

(1) This chapter consists of two additional sections. The first section describes the general characteristics of equilibrium beach profiles and cross-shore sediment transport. This section commences with a qualitative description of the forces acting within the nearshore zone, the characteristics of an equilibrium beach profile, and a discussion of conditions of equilibrium when the forces are balanced, as well as the ensuing sediment transport when conditions change, causing an imbalance. The general profile characteristics across the continental shelf are reviewed with special emphasis on the more active nearshore zone. Bar morphology and short- and long-term changes of beach profiles due to storms and sea level rise are examined, along with effects of various parameters on the profile characteristics, including wave climate and sediment characteristics. Survey capabilities to quantify the profiles are reviewed.

(2) The second section deals with quantitative aspects of cross-shore sediment transport with special emphasis on engineering applications and the prediction of beach profile change. First, the general shape of the equilibrium beach profile is quantified in terms of sediment grain size and basic wave parameters. Equilibrium profile methods are then used to develop analytical solutions to several problems of interest in beach nourishment design. Similar analytical solutions are developed for the steady-state beach profile response to elevated water levels, including both the long-term response to sea level rise and the short-term response to storm surge. For simplified cases, analytical methods are then presented for estimating the dynamic profile response during storms. For more general applications, numerical modelling approaches are required and these are briefly reviewed.

III-3-2. General Characteristics of Natural and Altered Profiles

a. Forces acting in the nearshore.

(1) There are several identifiable forces that occur within the nearshore active zone that affect sediment motion and beach profile response. The magnitudes of these forces can be markedly different inside and

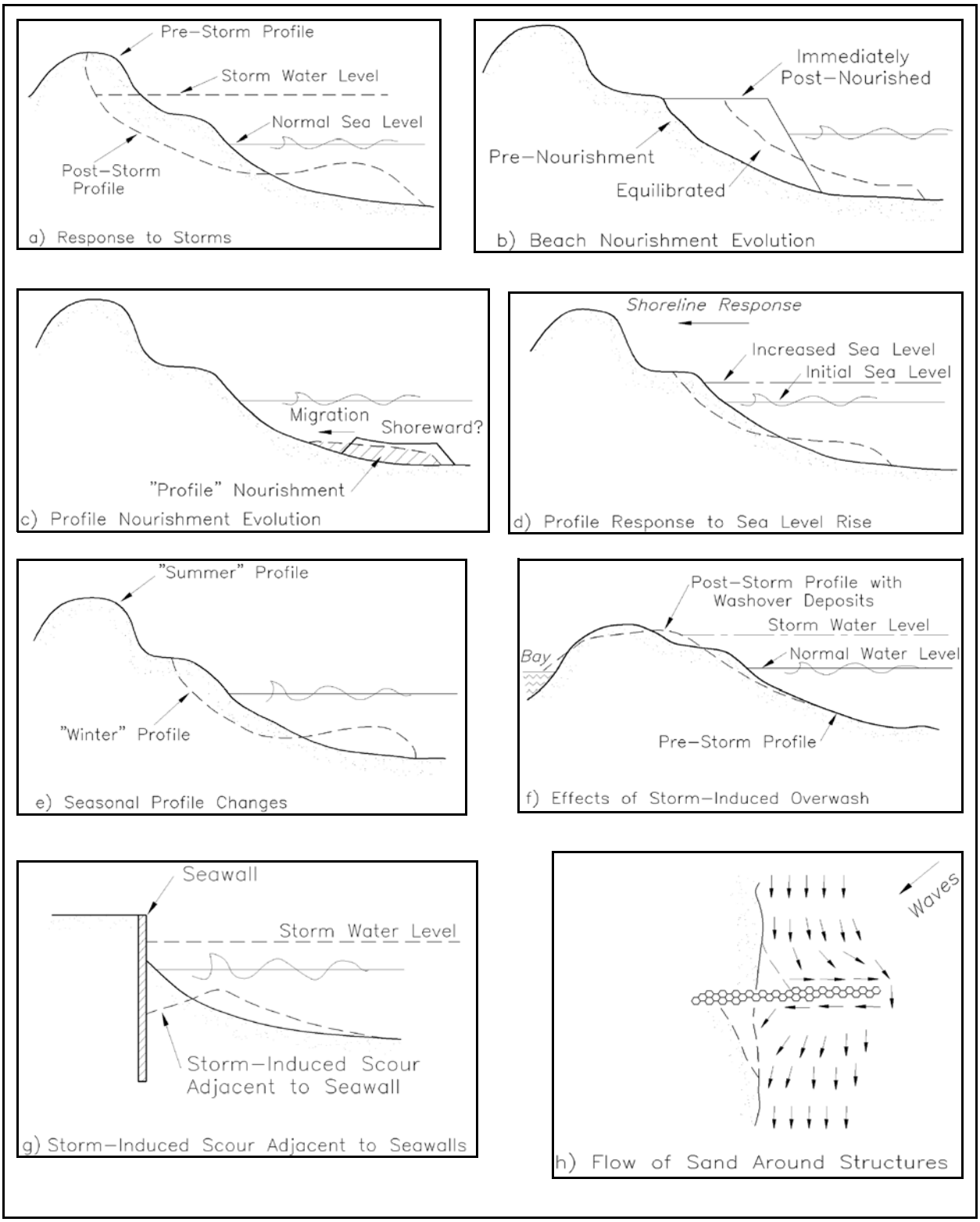

Figure III-3-2. Problems and processes in which cross-shore sediment transport is relevant

outside the surf zone. Under equilibrium conditions, these forces are in balance and although there is motion of the individual sand grains under even low wave activity, the profile remains more or less static. Cross-shore sediment transport occurs when hydrodynamic conditions within the nearshore zone change, thereby modifying one or more of the forces resulting in an imbalance and thus causing transport gradients and profile change. Established terminology is that onshore- and offshore-directed forces are referred to as "constructive" and "destructive," respectively. These two types of forces are briefly reviewed below; however, as will be noted, the term "forces" is used in the generic sense. Moreover it will be evident that some forces could behave as constructive under certain conditions and destructive under others.

(2) As noted, constructive forces are those that tend to cause onshore sediment transport. For classic nonlinear wave theories (Stokes, Cnoidal, Solitary, Stream Function, etc.), the wave crests are higher and of shorter duration than are the troughs. This feature is most pronounced just outside the breaking point and also applies to the water particle velocities. For oscillatory water particle velocities expressed as a sum of phase-locked sinusoids such as for the Stokes or Stream Function wave theories, even though the time mean of the water particle velocity is zero, the average of the bottom shear stress τ_b expressed as

$$\overline{\tau_b} = \rho \frac{f}{8} \overline{|v_b| v_b} \tag{III-3-1}$$

can be shown to be directed onshore. In the above, ρ is the mass density of water, f is the Darcy-Weisbach friction coefficient which, for purposes here is considered constant over a wave period, and v_b is the instantaneous wave-induced water particle velocity at the bottom. A definition sketch is provided in Figure III-3-3. An example of the time-varying shear stress due to a nonlinear (Stream Function) wave is shown in Figure III-3-4. Dean (1987a) has developed the average bottom shear stress based on the Stream Function wave theory and presented the results in the nondimensional form shown in Figure III-3-5.

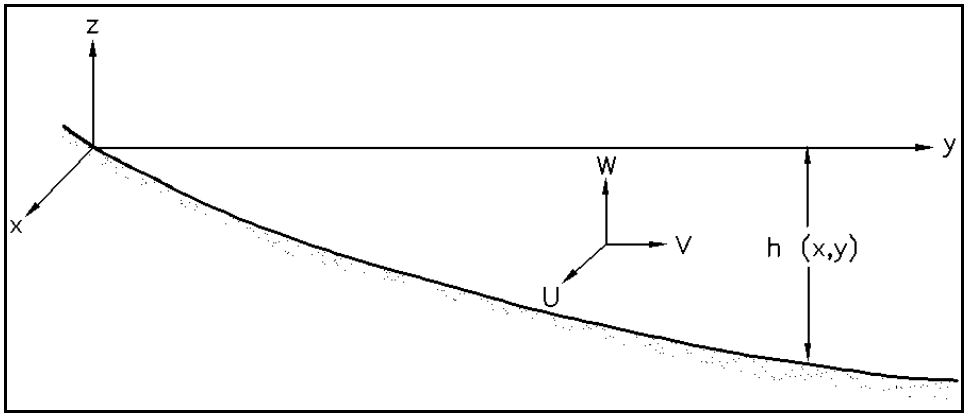

Figure III-3-3. Definition sketch

(3) A second constructive force originates within the bottom boundary layer, causing a net mean velocity in the direction of propagating water waves. This streaming motion was first observed in the laboratory by Bagnold (1940) and has been quantified by Longuet-Higgins (1953) as due to the local transfer of momentum associated with energy losses by friction. For the case of laminar flows, the maximum (over depth) value of this steady velocity v_s is surprisingly independent of the value of the viscosity and is given by

$$v_s = - \frac{3 \sigma k H^2}{16 \sinh^2 kh} \tag{III-3-2}$$

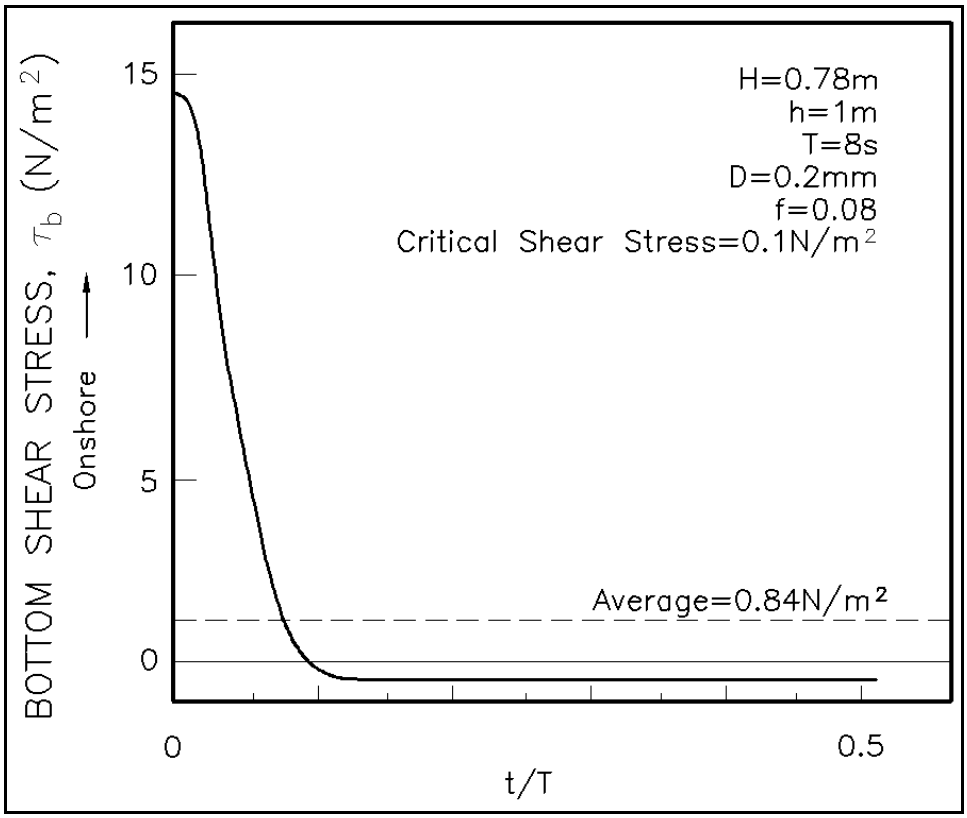

Figure III-3-4. Variation with time of the bottom shear stress under a breaking nonlinear wave. H = 0.78 m, h= 1.0 m, T = 8.0 s, and D = 0.2 mm

which, for the case of shallow water and a wave height proportional to the breaking depth, will be shown to be 1.5 times the average of the return flow due to the mass transport. In Equation 3-2, σ is the wave angular frequency, k is the wave number, and H the wave height. Although the maximum velocity is independent of the viscosity, the bottom shear stress τ_{bs} induced by the streaming velocity is not and is given by

$$\tau_{bs} = - \frac{\rho \epsilon^{\frac{1}{2}} \sigma^{\frac{3}{2}} H^2 k}{8 \sqrt{2} \sinh^2 kh} \qquad \text{(III-3-3)}$$

in which ϵ is the eddy viscosity.

(4) Within the surf zone, cross-shore transport may be predominantly due to sediment in suspension. If the suspension is intermittent, occurring each wave period, the average water particle velocity during the period that the particle is suspended determines the direction of cross-shore transport. Although this cause of sediment transport is not a true force, it does represent a contributing mechanism. Turbulence, although also not a true force, can be effective in mobilizing sediment and dependent on whether the net forces are shoreward or seaward at the time of mobilization, can be constructive or destructive, respectively. Dean (1973) noted that suspended sediment can move either onshore (constructive) or offshore (destructive), depending on how high a sand grain is suspended off the bottom. Under the wave crest, if the sediment particle is suspended a distance above the bottom proportional to the wave height H, and if the particle has a fall velocity w, then the time required for the grain to fall back to the bottom would be proportional to H/w. If this fall time is less than one-half of the wave period, then the particle should experience net onshore

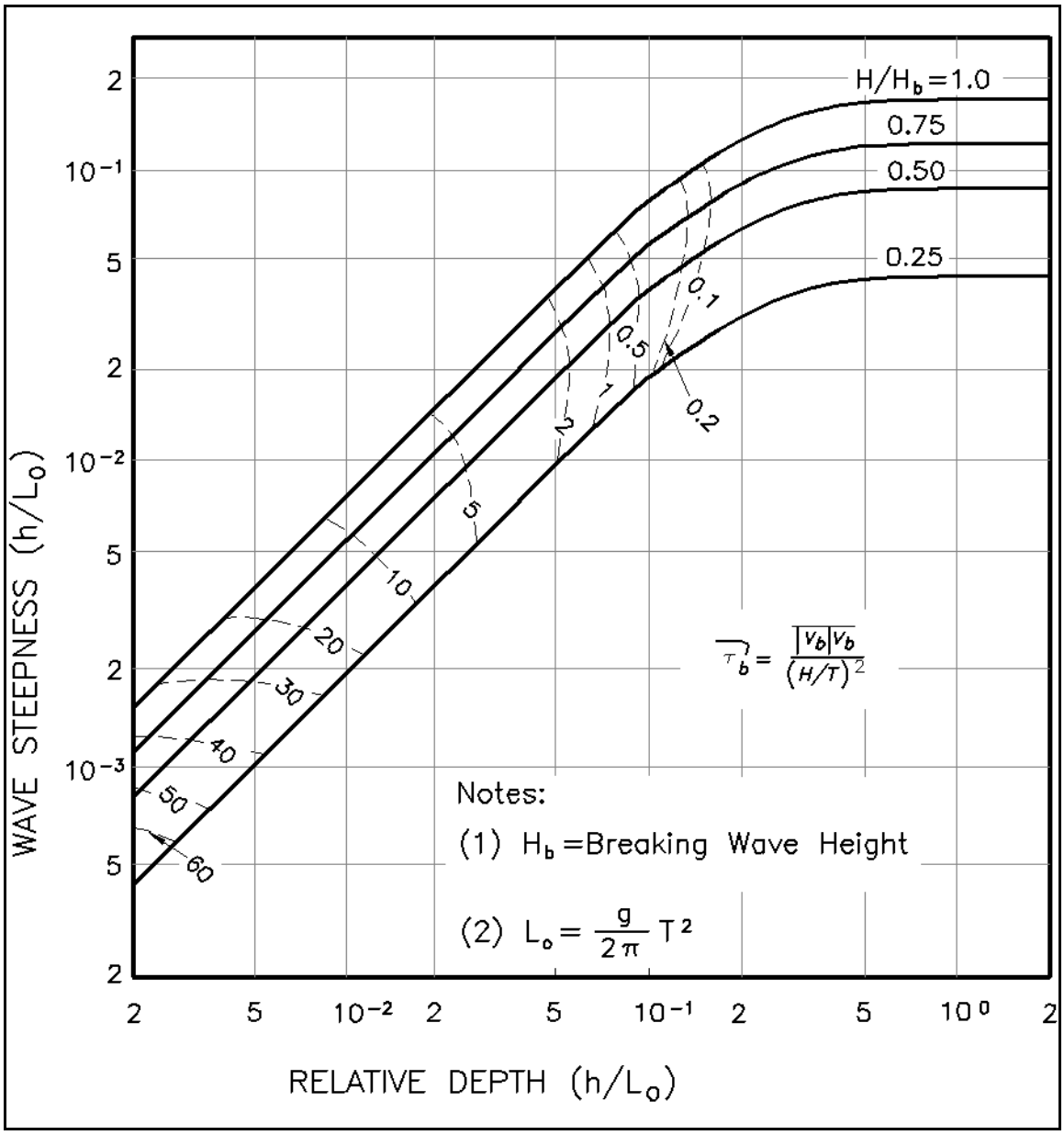

Figure III-3-5. Isolines of nondimensional average bottom shear stress τ_b versus relative depth and wave steepness (Dean 1987a). Note that bottom shear stresses are directed landward

motion, whereas the particle should move offshore if the fall time is greater than one-half the wave period. While such an approach is overly simplistic, and does not include the effects of mean cross-shore currents, it has been shown that net onshore or offshore sediment transport can be correlated to the so-called fall time parameter *H*/*wT,* which will be discussed later in this chapter.

(5) Gravity is the most obvious destructive force, acting downslope and in a generally seaward direction for a monotonic profile. However, for the case of a barred profile, gravity can act in the shoreward direction over portions of the profile. Gravity tends to "smooth" any irregularities that occur in the profile. If gravity were the only force acting, the only possible equilibrium profile would be horizontal and sandy beaches as we know them would not exist. It should be recognized, however, that gravity may also serve as a stabilizing force, since sediment particles cannot be mobilized from the bed unless: (a) upward-directed forces

associated with fluid turbulence can exceed the submerged weight of the sediment, and/or (b) slope-parallel fluid shear forces can exceed the frictional resistance of sediment. Also, as noted, gravity causes suspended sediment to settle out of the water column, with fall velocity w, which may cause suspended sediment to move shoreward if not suspended too high in the water column.

(6) Other destructive forces are generally related to the vertical structure of the cross-shore currents. The undertow, the seaward return flow of wave mass transport, induces a seaward stress on the bottom sediment particles. For linear waves, the time-averaged seaward discharge due to the return flow of shoreward mass transport Q is (Dean and Dalrymple 1991)

$$Q = \frac{E}{\rho C} \tag{III-3-4}$$

where E is the wave energy density and C is the wave celerity. If the return flow due to mass transport were distributed uniformly over the water depth, it can be shown from linear shallow-water wave theory that the mean velocity would be

$$\overline{V} = \frac{\sqrt{g}\, H^2}{8 h^{3/2}} \tag{III-3-5}$$

which, as noted for shallow water, is two-thirds of the maximum streaming velocity. Within the surf zone, the wave height can be considered to be proportional to the local depth, as $H = \kappa h$, so that the mean velocity further simplifies to $0.08\ (gh)^{1/2}$ for $\kappa \approx 0.78$ where $(gh)^{1/2}$ is the wave celerity in shallow water. In storm events where there is overtopping of the barrier island, a portion or all of the potential return flow due to mass transport can be relieved through strong landward flows, thereby eliminating this destructive force and resulting instead in constructive forces.

(7) It is well-known that associated with wave propagation toward shore is a shoreward flux of linear momentum (Longuet-Higgins and Stewart 1964). When waves break, the momentum is transferred to the water column, resulting in a shoreward-directed thrust and thus a wave-induced setup within the surf zone, the gradient of which is proportional to the local bottom slope. This momentum is distributed over depth, as shown in Figure III-3-6. In shallow water, linear water wave theory predicts that one-third of the momentum flux originates between the trough and crest levels and has its centroid at the mean water level. The remaining two-thirds originates between the bottom and the mean water level, is uniformly distributed over this dimension, and thus has its centroid at the mid-depth of the water column. Because of the contribution at the free surface, breaking waves induce an equivalent shear force on the water surface which will be quantified later. This causes a seaward bottom shear stress within the breaking zone. The bottom shear stress is dependent on the rate of energy dissipation. This effective shear force due to momentum transfer must be balanced by the bottom shear stress and the pressure forces due to the slope of the water surface.

(8) Often during major storm events, strong onshore winds will be present in the vicinity of the shoreline. These winds cause a shoreward-directed surface flow and a seaward-directed bottom flow, as shown in Figure III-3-7. Of course, seaward-directed winds would cause shoreward-directed bottom velocities and thus constructive forces. Thus, landward- and seaward-directed winds result in destructive and constructive forces, respectively.

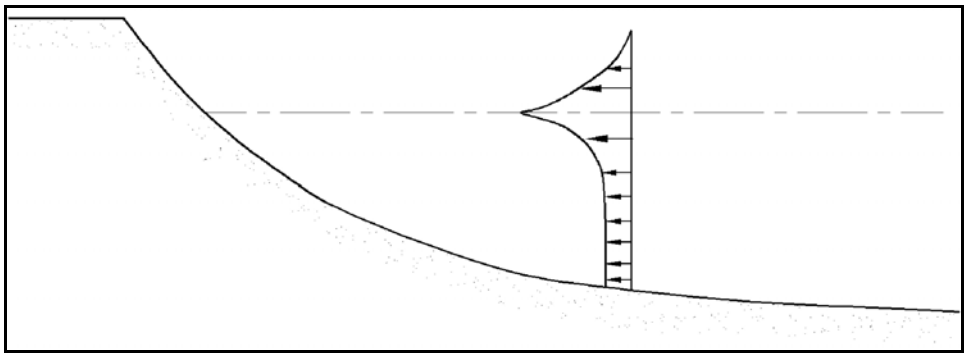

Figure III-3-6. Distribution over depth of the flux of the onshore component of momentum

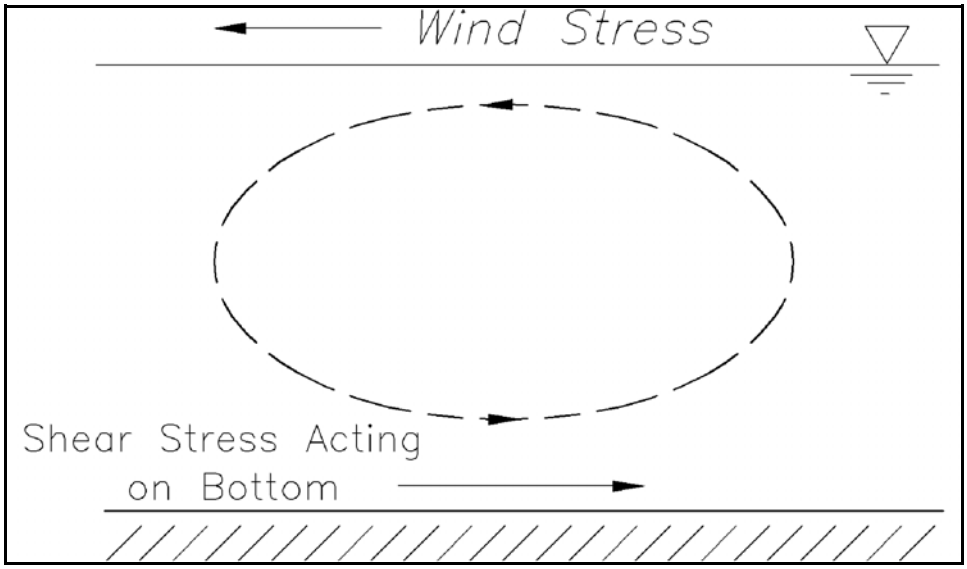

Figure III-3-7. Bottom stresses caused by surface winds

(9) Considering linear wave theory, and a linear shear stress relationship with eddy viscosity ϵ, the distribution of the mean velocity over depth for the case of return of mass transport (no overtopping) and without including the contribution of bottom streaming can be shown to be (Dean and Dalrymple 2000)

$$v(z) = \frac{h}{\rho\epsilon}\left[2\tau_\eta - \frac{\partial E}{\partial y}\right]\left[\frac{3}{8}\left(\frac{z}{h}\right)^2 + \frac{1}{2}\left(\frac{z}{h}\right) + \frac{1}{8}\right] + \frac{3}{2}\frac{Q}{h}\left[1 - \left(\frac{z}{h}\right)^2\right] \quad \text{(III-3-6)}$$

In this expression, the first term is associated with the surface wind stress τ_η. The second term is associated with the vertical gradient of momentum flux and is expressed as a function of the cross-shore gradient in wave energy $\partial E/\partial y$. It is noted that this term is zero outside the breakpoint and contributes only inside the surf zone where energy is dissipated. The third term is associated with the seaward return flow of mass transport, where Q represents the net seaward discharge over the water column as given by Equation 3-4.

(10) For the three effects considered in Equation 3-6, the shear stress associated with the vertical velocity distribution may be computed for any elevation z as

$$\tau = \rho\epsilon\frac{\partial v}{\partial z} \tag{III-3-7}$$

where ϵ is the turbulent eddy viscosity. The resulting seaward-directed shear stress at the bottom ($z = -h$) is then given by

$$\tau_b = \frac{1}{4}\frac{\partial E}{\partial y} - \frac{\tau_\eta}{2} + 3\frac{\epsilon E}{Ch^2} \tag{III-3-8}$$

(11) Velocity distributions and shear stress distributions inside and outside the surf zone based on Equations III-3-6 and III-3-7 are shown in Figure III-3-8 for a condition of no surface wind stress and for cases of no overtopping and full overtopping both inside and outside the breakpoint. Profile conditions assumed for this example are shown in the figure caption and assume an equilibrium beach profile where wave breaking is assumed to occur at a depth of 1 m. For the case with no overtopping, most of the seaward velocity shown in Figure III-3-8 is due to the return flow required to balance the shoreward flows near the surface. This is further illustrated in the cases with overtopping where it is assumed that the shoreward flows overtop the profile so that there is no net return flow due to mass transport.

(12) Table III-3-1 summarizes the mechanisms identified as contributing to constructive and/or destructive forces and, where possible, provides an estimate of their magnitudes. For purposes of these calculations, the following conditions have been considered: an equilibrium beach profile with a grain size of $D = 0.2$ mm, $h = 1$ m, $H = 0.78$ m, $T = 8$ s, $\epsilon = 0.04$ m^2/s, wind speed = 20 m/s. It is seen that of the bottom stresses that can be quantified, those associated with undertow due to mass transport and momentum flux transfer are dominant.

b. Equilibrium beach profile characteristics.

(1) In considerations of cross-shore sediment transport, it is useful to first examine the case of equilibrium in which there is no net cross-shore sediment transport. The competing forces elucidated in the previous section can be fairly substantial, exerting tendencies for both onshore and offshore transport. A change will bring about a disequilibrium that causes cross-shore sediment transport. The concept of an equilibrium beach profile has been criticized, since in nature the forces affecting equilibrium are always changing with the varying tides, waves, currents, and winds. Although this is true, the concept of an equilibrium profile is one of the coastal engineer's most valuable tools in providing a framework to consider disequilibrium and thus cross-shore sediment transport. Also, many useful and powerful conceptual and design relationships are based on profiles of equilibrium.

(2) When applying equilibrium profile concepts to problems requiring an estimate of profile retreat or advance, a related concept of importance is the principle of conservation of sand across the profile. Under conditions where no longshore gradients exist in the longshore transport, onshore-offshore transport causes a redistribution of sand across the profile but does not lead to net gain or loss of sediment. Most engineering methods applied to the prediction of profile change ensure that the total sand volume is conserved in the active profile, so that erosion of the exposed beach face requires a compensating deposition offshore, while deposition on the exposed beach face must be accompanied by erosion of sediment in the surf zone. For cases where longshore gradients in longshore transport do exist, it is then common to assume that the profile

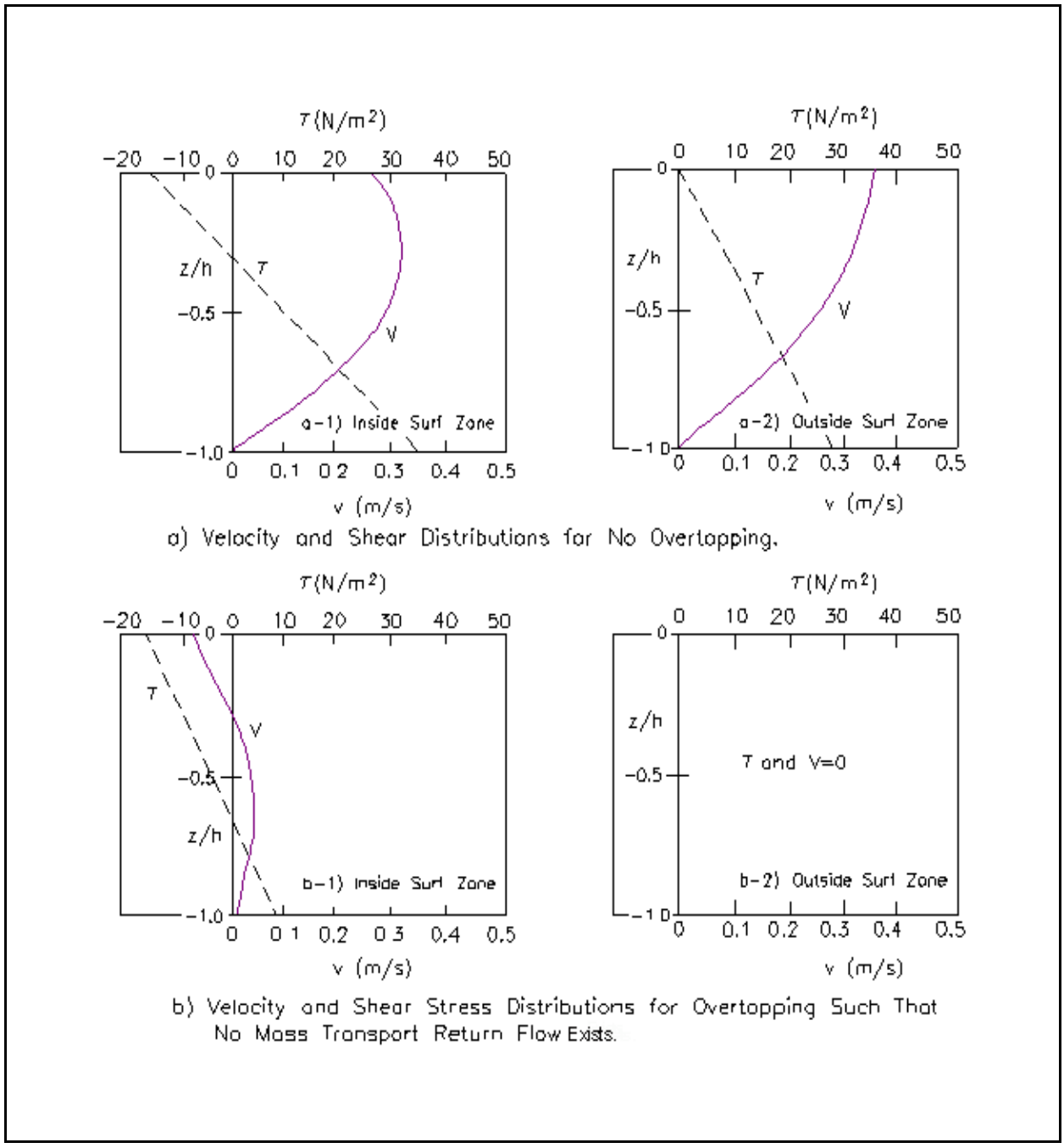

Figure III-3-8. Velocity distributions inside and outside the surf zone for no surface wind stress and cases of no overtopping and full overtopping both inside and outside the surf zone

advances or retreats uniformly at all active elevations while maintaining its shape across the profile. In this way, sediment volume can be added or removed from the profile without changing the shape of the active profile. As a result, most methods for predicting beach profile change treat the longshore and cross-shore components separately so that the final profile form and location are determined by superposition.

Table III-3-1
Constructive and Destructive Cross-shore "Forces" in Terms of Induced Bottom Shear Stresses

Constructive or Destructive	Description of Force	Magnitude of Force (N/m^2)	
		Breaking Waves	Nonbreaking Waves
Constructive	Average Bottom Shear Stress Due to Nonlinear Waves[1]	0.84	0.84
	Streaming Velocities[2]	28.9	28.9
	Overtopping	28.6	28.6
	Gravity[3]	0.046	0.046
Destructive	Undertow Due to Mass Transport	28.6	28.6
	Undertow Due to Momentum Flux Transfer	7.9	0
Constructive or Destructive	Intermittent Suspension	?	?
	Turbulence	Relatively Large	Relatively Small
	Wind Effects[4]	0.95	0.95

Notes:
For the calculations resulting in the values in this table: H = 0.78 m, h = 1.0 m, T = 8 s.
[1] f = 0.08
[2] ϵ = 0.04 m^2/s
[3] Equilibrium profile with D = 0.2 mm
[4] Wind speed = 20 m/s.

(3) Generally observed properties of equilibrium profiles are as follows: (a) they tend to be concave upward, (b) the slopes are milder when composed of finer sediments, (c) the slopes tend to be flatter for steeper waves, and (d) the sediments tend to be sorted with the coarser and finer sediments residing in the shallower and deeper waters, respectively. The effects of changes that induce cross-shore sediment transport can be deduced from these known general characteristics. For example, an increase in water level will cause a disequilibrium, as can be seen by noting that due to the concave upward nature of the profile, the depth at a particular reference distance from the new shoreline is now greater than it was before the increased water level. If the equilibrium profile had been planar, then the increase in water level would not change the depth at a distance from the new shoreline and there would be no disequilibrium. It will be shown that without the introduction of additional sediment into the system, the only way in which the profile can reattain equilibrium is to recede, thus providing sediment to fill the bottom to a depth consistent with the equilibrium profile and the new (elevated) water level.

(4) Since profiles are generally flatter for steeper waves, an increase or decrease in wave steepness will also induce seaward or landward sediment flows, respectively. Naturally, onshore and offshore winds will cause seaward and landward sediment transport, respectively. As an example of the shoreline response to storms, Figure III-3-9 presents results from Katoh and Yanagishima (1988) in which the offshore waves, shoreline position, and beach face slope were measured over a period of approximately 7 months. It is seen that the shoreline retreats abruptly during the higher wave events and advances more gradually during periods of milder wave activity. The beach slope and shoreline changes, of course, correlate with the slope becoming milder during periods of shoreline retreat. The authors also found it of interest that the rate of shoreline advancement during the recovery phase was almost constant at 0.68 m/day.

(5) Many beaches in nature have one or more longshore bars present. At some locations, these bars are seasonal and at some they are more or less permanent. Figure III-3-10a presents a profile from

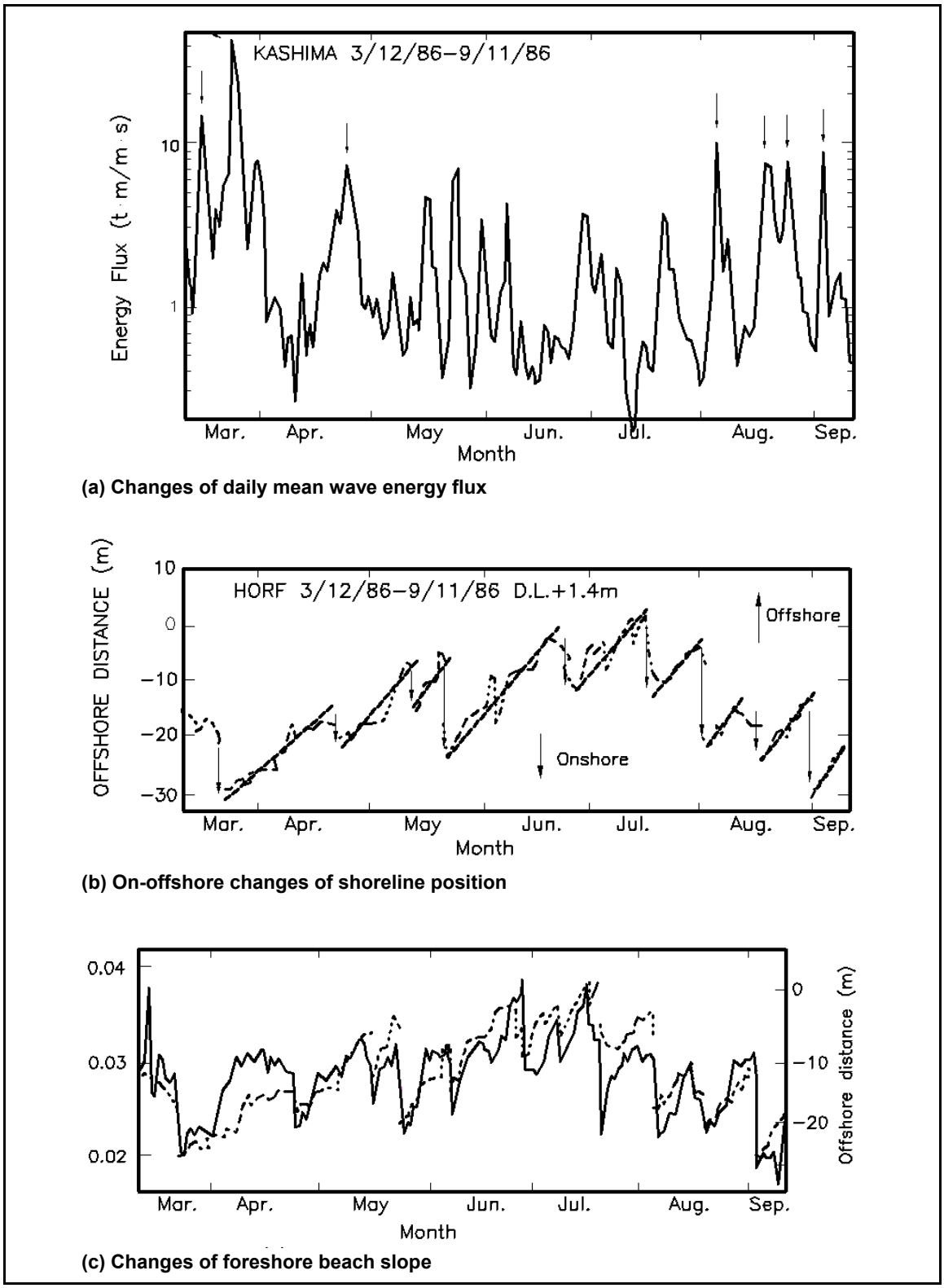

Figure III-3-9. Effects of varying wave energy flux (a) on: (b) shoreline position, and (c) foreshore beach slope (dots are shoreline position in (b) and (c), solid curve is trend line in (b), foreshore slope in (c)) (Katoh and Yanagishima 1988)

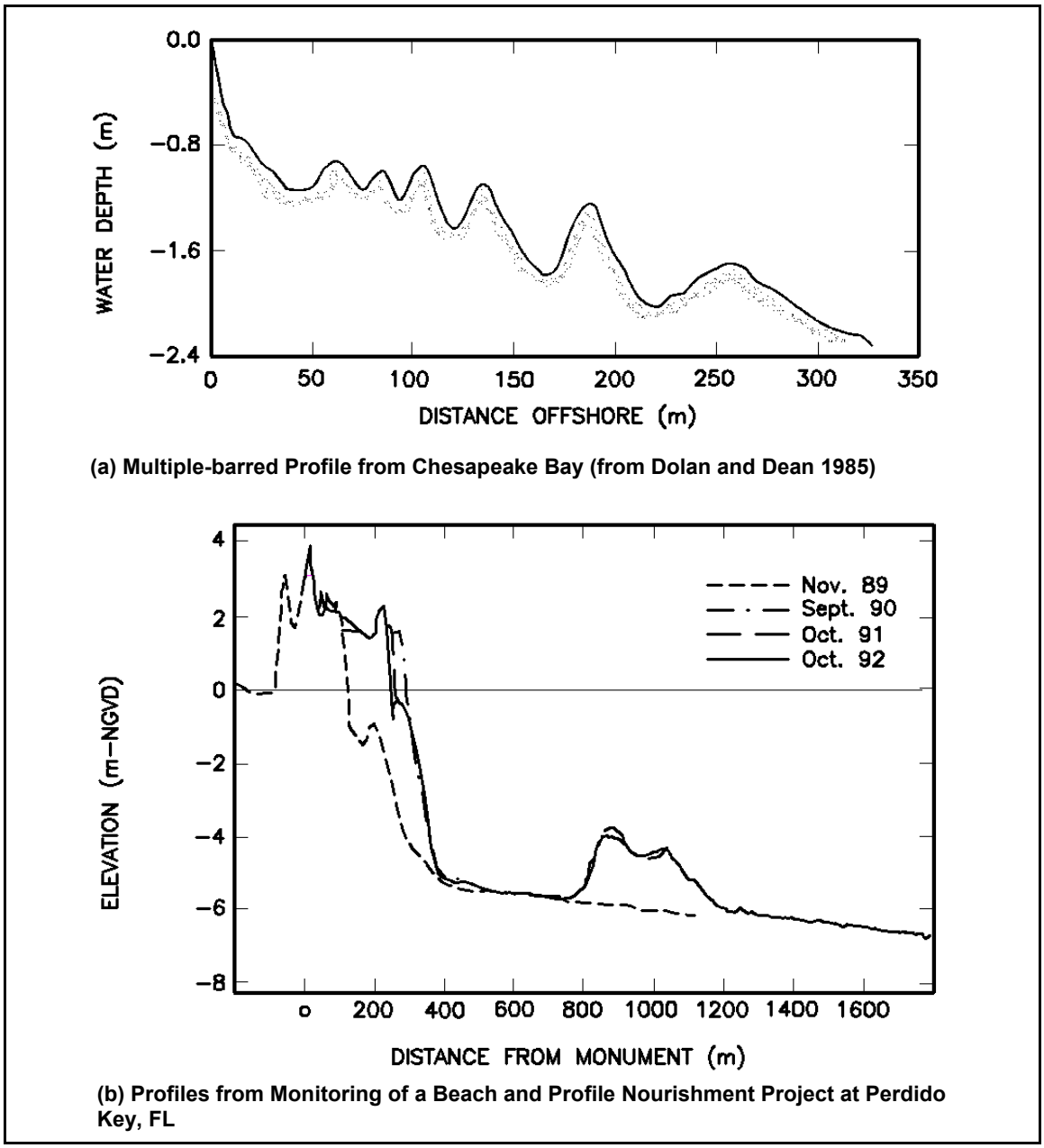

(a) Multiple-barred Profile from Chesapeake Bay (from Dolan and Dean 1985)

(b) Profiles from Monitoring of a Beach and Profile Nourishment Project at Perdido Key, FL

Figure III-3-10. Examples of two offshore bar profiles

Chesapeake Bay in which at least six bars are evident and Figure III-3-10b shows profiles measured in a monitoring program to document the evolution of a beach nourishment project at Perdido Key, FL. This project included both beach nourishment in the form of a large seaward buildup of the berm and foreshore and profile nourishment in the form of a large offshore mound. As seen from Figure III-3-10b, a bar was present before nourishment and gradually re-formed in depths of less than 1 m as the profile equilibrated during the 2-year period shown in Figure III-3-10b.

(6) It will be shown later that the presence of bars depends on wave and sediment conditions and at a particular beach, bars may form or move farther seaward during storms. It appears that the outer bars on some profiles are relict and may have been caused by a past large storm which deposited the sand in water too deep

for fair- weather conditions to return the sand to shore. At some beaches with more than one bar, the inner bar will exhibit more rapid response to changing wave conditions than those farther offshore. Figure III-3-11 presents results from Duck, NC, in which profile surveys were conducted over a period of approximately 11 years. It is seen in this case that both the outer and inner bars undergo significant changes in position whereas the shoreline remains relatively fixed, possibly due to coarser sediment in shallow water and at the shoreline. As an example of the potential rates of change of bar position, Birkemeier (1984) shows examples of offshore migration of the outer bar at Duck, NC, during three successive storms in the fall of 1981 averaging almost 4 m/day while onshore migration of the outer bar following the storm season averaged almost 0.5 m/day.

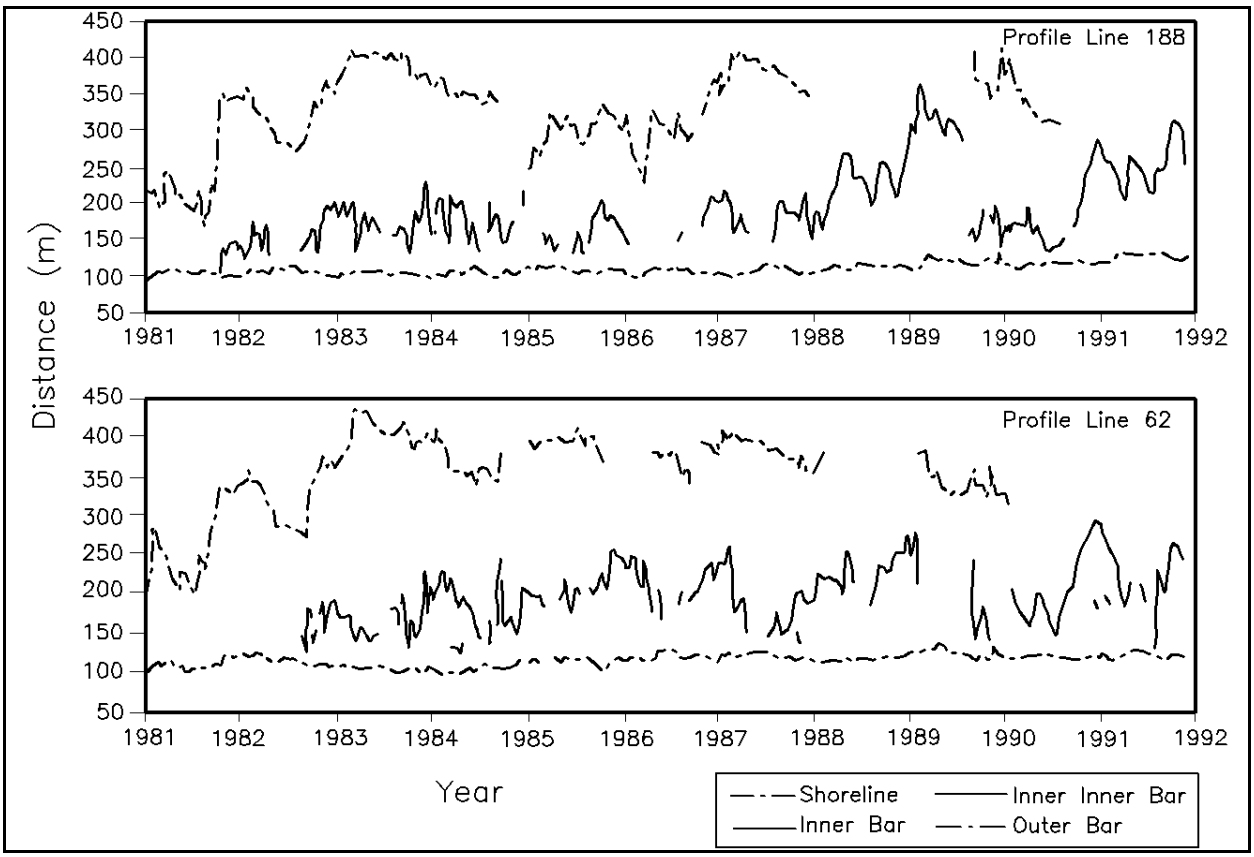

Figure III-3-11. Variation in shoreline and bar crest positions, Duck, NC (Lee and Birkemeier 1993)

(7) Keulegan (1945, 1948) reported on studies which included both laboratory and field data to determine relationships for bar formation. A focus of these studies was the geometric characteristics of the longshore bars. In examining bars from nature, an attempt was made to select sites with small tidal effects. The bar geometry was defined in terms of the depth over the bar crest h_{CR} the depth of the bar trough h_T and the depth to the bar base h_D at the position of the bar crest. These definitions are shown in Figure III-3-12. Keulegan found that the ratio of depths of bar crest to bar base h_{CR}/h_D was approximately 0.58 for both the laboratory and field cases. The ratio of depths of trough to crest h_T/h_{CR} ranged from 1.6 to 1.8. It was also found that bars in nature are considerably broader than those produced in the laboratory. This is probably due to varying wave heights in nature and, to a lesser extent, to varying water levels. Figure III-3-13 compares laboratory and field bar geometries. The field bar is approximately twice as wide as the bar produced in the laboratory.

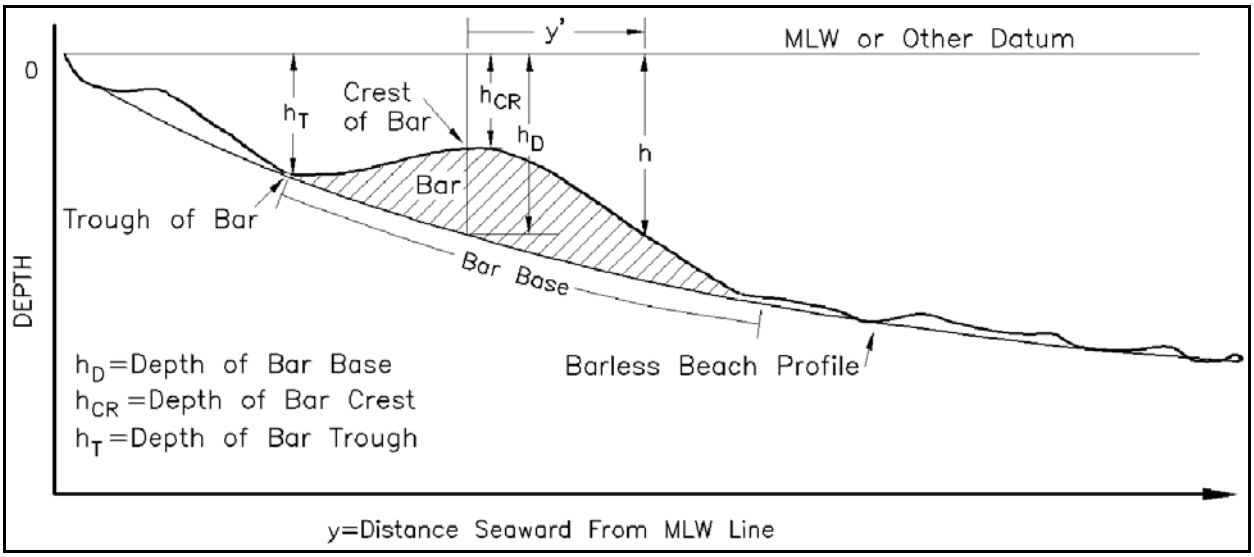

Figure III-3-12. Definition of offshore bar characteristics (Keulegan 1945)

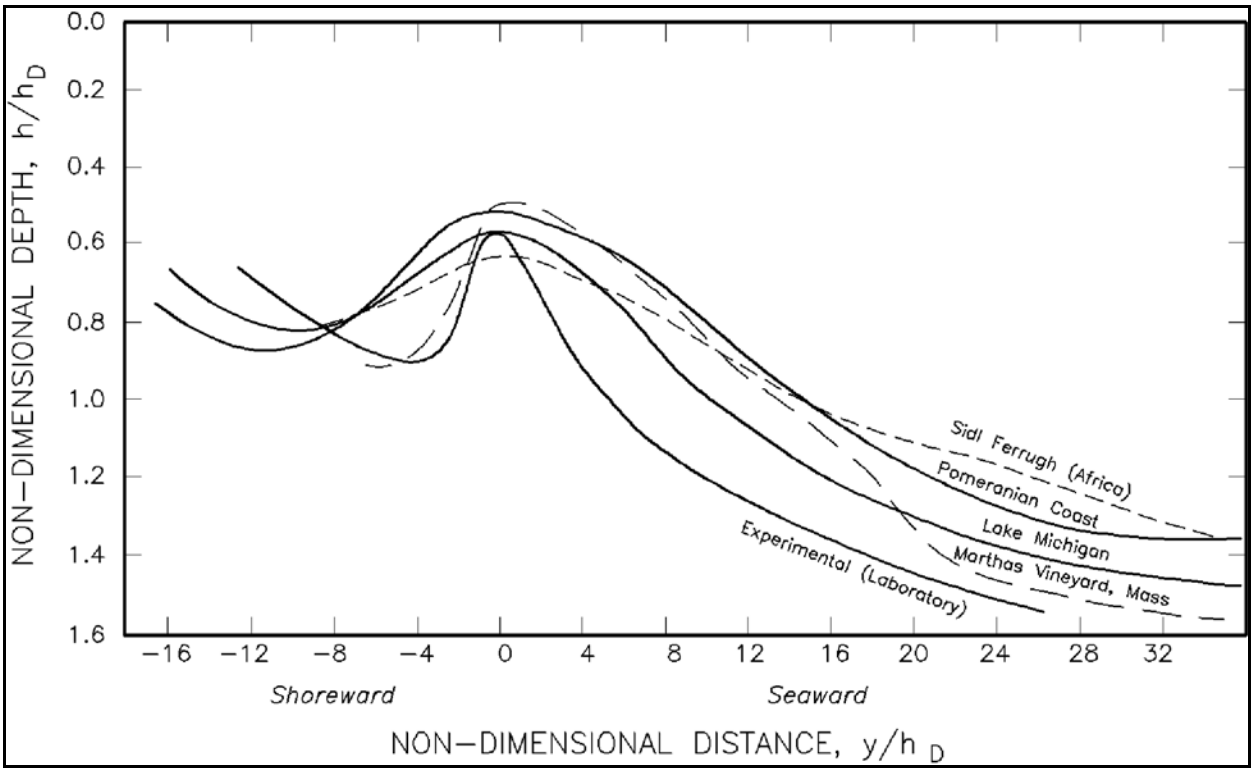

Figure III-3-13. Nondimensional geometries of natural bars compared with those produced in the laboratory (Keulegan 1948)

(8) The shapes of profiles across the continental shelf are less predictable than those within the more active zone of generally greater engineering interest. This may be due to the presence of bottom material different than sand (including rock and peat outcrops), the much greater time constants required for equilibration in these greater depths, the greater role of currents in shaping the profile and the effects of past sea level variations. In general, the slopes seaward of the more active zone are quite small if the bottom is composed of sand or smaller-sized materials. Figure III-3-14 presents three examples of profiles extending off the East and Gulf coasts of Florida. It is seen that at this scale, the profile may be approximated by a nearshore slope that extends to 5 to 18 m and milder seaward slopes, which are on the order of 1/2,000 to 1/10,000.

c. Interaction of structures with cross-shore sediment transport.

The structure that interacts most frequently with cross-shore sediment transport is a shore-parallel structure such as a seawall or revetment. During storm events, a characteristic profile fronting a shore-parallel structure is one with a trough at its base, as shown in Figure III-3-15, from Kriebel (1987) for a profile affected by Hurricane Elena in Pinellas County, Florida, in September 1985. This trough is due to large transport gradients immediately seaward of the structure. Although the hydrodynamic cause of this scour is not well-known, it has been suggested that it is due to a standing wave system with an antinode at the structure. A second, more heuristic explanation is that sand removal is prevented behind the seawall and the transport system removes sand from as near as possible to where removal would normally occur. Barnett and Wang (1988) have reported on a model study to evaluate the interaction of a seawall with the profile and have found that the additional volume represented by the scour trough is approximately 62 percent of what would have been removed landward of the seawall if it had not been present. During mild wave activity, it appears that the profile recovers nearly as it would have if the seawall had not been present. The reader is referred to the comprehensive review by Kraus (1988) for additional information on shore-parallel structures and their effects on the shoreline.

d. Methods of measuring beach profiles.

(1) Introduction. Changes in beach and nearshore profiles are a result of cross-shore and longshore sediment transport. If the longshore gradients in the longshore component can be considered small, it is possible, through the continuity equation, to infer the volumetric cross-shore transport from two successive profile surveys.

(2) Clausner, Birkemeier, and Clark (1986) have carried out a comprehensive field test of four nearshore survey systems, including: (a) the standard fathometer system, (b) the CRAB, which is a self-propelled platform on which a survey prism is mounted, (c) a sea sled, which also carries a prism but is towed by a boat or a cable from shore, and (d) a hydrostatic profiler, which utilizes a cable for towing and an oil-filled tube to sense the elevation difference between the shore and the location of the point being surveyed. Each of these systems is reviewed briefly below and their performance characteristics are described and summarized in Table III-3-2.

(a) Fathometer. This method of measuring nearshore profiles requires knowledge of the water level as a reference datum. To provide a complete description of the active profile, fathometer surveys must be complemented with surveys of the shallow-water and above-water portions of the profile. In the field tests, the fathometer was mounted on a 47-ft vessel and the surveys were conducted under favorable wave conditions, which should result in a lower estimate of the error. Characteristics of this system and results obtained from the field measurements are presented in Table III-3-2.

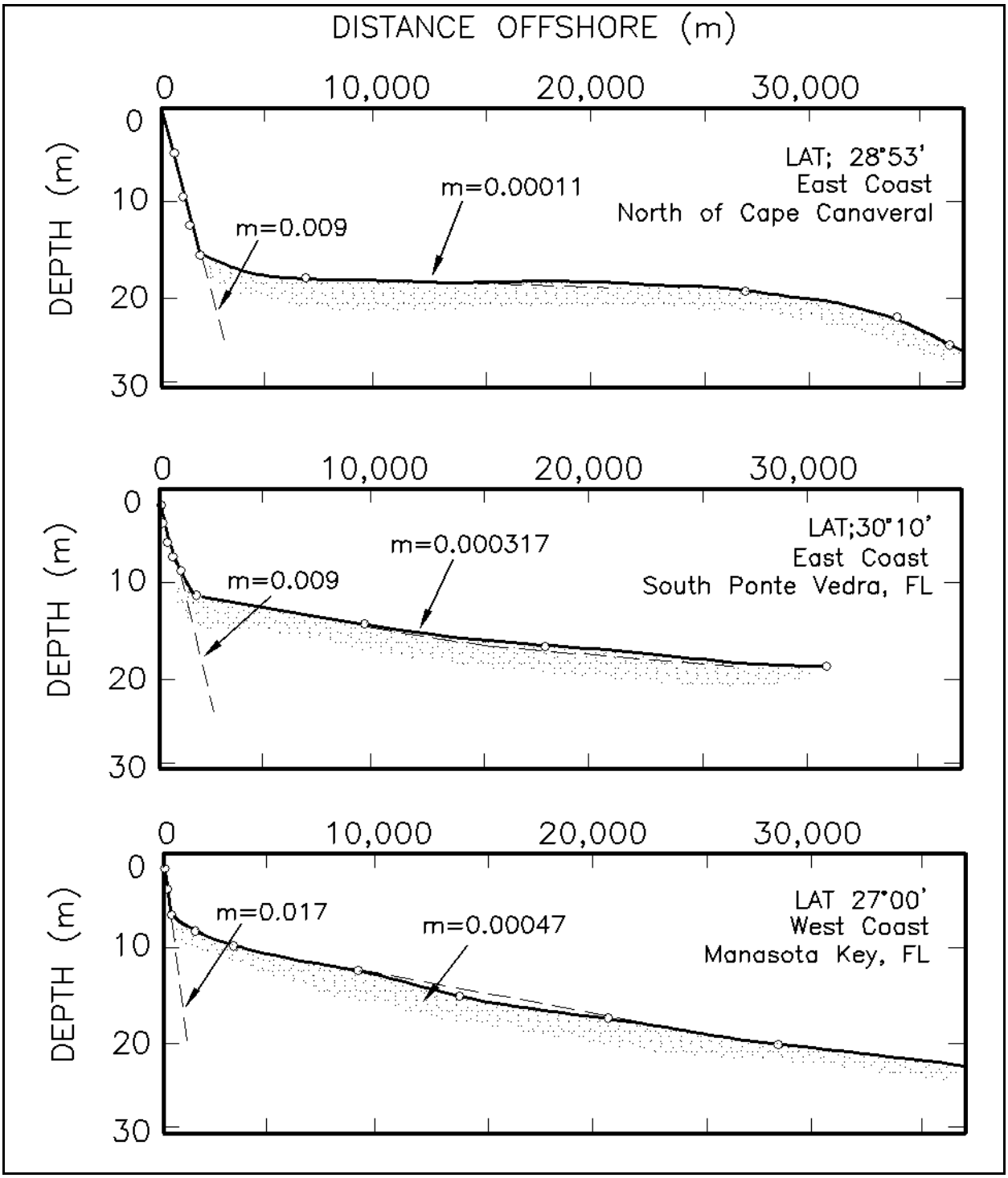

Figure III-3-14. Profiles extending across the continental shelf for three locations along the East and Gulf coastlines of the United States (Dean 1987a)

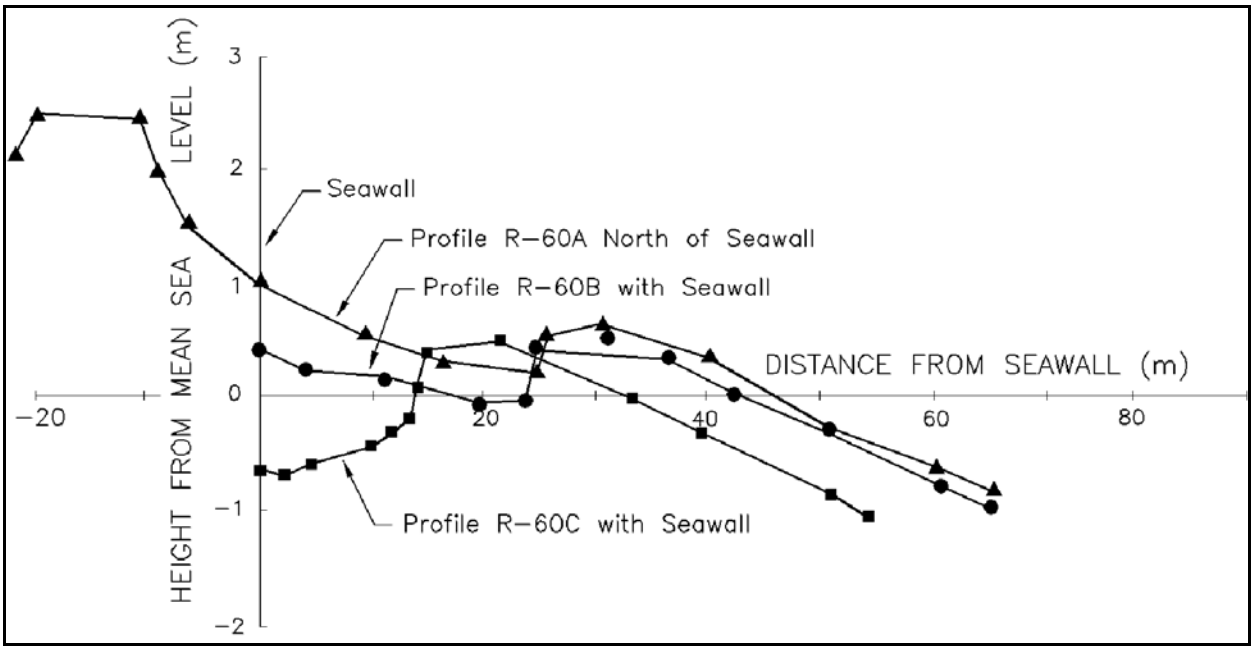

Figure III-3-15. Comparison of response of natural and seawalled profiles to Hurricane Elena, September 1985 (after Kriebel (1987))

Table III-3-2
Summary of Field Evaluation of Various Nearshore Survey Systems (Based on Clausner, Birkemeier, and Clark (1986))

	Operating Requirements		Field Performance Characteristics				
					Vertical Accuracy		Horizontal Accuracy
System	Personnel Required	Wave Heights (m)	Number of Profiles Measured	Profiles per Day	Average Difference From Mean (cm)	Average Vertical Envelope (cm)	Average Distance Off Line (m)
Fathometer	4	< 1	6 (5)[1]	16	9 (6)[1]	31 (20)[1]	1.3
CRAB	2	< 2	5	7	2	5	0.4
Sea Sled	3 - 4	< 1	5	9	1	3	1.6
Hydrostatic Profiler	2 - 3	< 1	4	3	3	7	3.6

[1] Based on the smoothed analog records. All other fathometer data based on digital records.

(b) CRAB. The CRAB (Coastal Research Amphibious Buggy) is a self-propelled vehicle that has a survey prism mounted on it and is used in conjunction with a laser survey system. At the time of the Clausner report (Clausner, Birkemeier, and Clark 1986), it was necessary to stop the CRAB to take a reading. More recently, the system has been upgraded to an automatic self-tracking mode such that the CRAB can be moved continuously and readings taken at predetermined time increments. Since the CRAB avoids the need for a water level datum, the vertical accuracy is inherently superior to that of fathometer measurements.

(c) Sea sled. The sea sled incorporates many of the inherent survey advantages of the CRAB, since dependency on the water level is avoided. The major difference is that the CRAB is self-propelled whereas the sea sled is towed by either a boat or a truck on the shore. Since the sea sled is dependent on some vehicle to transport it through the surf zone and this vehicle is usually a boat, it will be more limited by wave conditions than the CRAB, which can operate in sea states of 2 m.

(d) Hydrostatic profiler. The hydrostatic profiler was developed by Seymour and Boothman (1984) and consists of a long (about 600 m) oil-filled tube extending from the shoreline to a small weighted sled at the measurement location. A pressure sensor at the sled "weighs" the vertical column of oil from the shore to the sled location which can be interpreted as the associated elevation difference. In general, the hydrostatic profiler has not been widely used due to inherent limitations in its performance, related to sensitivity to pressure surges and to longshore currents.

(2) Summary. In summary, referring to Table III-3-2, the CRAB emerges as the overall best system. The sea sled provides slightly better overall vertical accuracy; however, as noted, the CRAB now utilizes an automatic tracking mode, which should reduce possibility of human-induced error. The main disadvantages of the CRAB system are the limited availability of such systems and the difficulties of transporting from one site to another. The reader is referred to the report by Clausner, Birkemeier, and Clark (1986) for additional details of the four systems and the results of the field tests.

III-3-3. Engineering Aspects of Beach Profiles and Cross-shore Sediment Transport

a. Introduction. Previous sections have discussed the natural characteristics of beach profiles in equilibrium, the effects that cause disequilibrium, and the associated profile changes. Also shown in Figure III-3-2 were the numerous possible engineering applications of equilibrium beach profiles. This section presents some of the applications, illustrates these with examples, and investigates approaches to calculation of cross-shore sediment transport and the associated profile changes.

b. Limits of cross-shore sand transport in the onshore and offshore directions.

(1) The long-term and short-term limits of cross-shore sediment transport are important in engineering considerations of profile response. During short-term erosional events, elevated water levels and high waves are usually present and the seaward limit of interest is that to which significant quantities of sand-sized sediments are transported and deposited. It is important to note that sediment particles are in motion to considerably greater depths than those to which significant profile readjustment occurs. This readjustment occurs most rapidly in the shallow portions of the profile and, during erosion, transport and deposition from these areas cause the leading edge of the deposition to advance into deeper water. This is illustrated in Figure III-3-16 from Vellinga (1983), in which it is seen that with progressively increasing time, the evolving profile advances into deeper and deeper water. It is also evident from this figure that the rate of profile evolution is decreasing consistent with an approach to equilibrium. For predicting cross-shore profile change, the depth of limiting motion is not that to which the sediment particles are disturbed but rather these award limit to which the depositional front has advanced. Vellinga recommends that this depth be 0.75 H_s in which H_s is the deepwater significant wave height computed from the breaking wave height using linear water wave theory. In general, the limit of effective transport for short-term (storm) events is commonly taken as the breaking depth h_b based on the significant wave height.

(2) The onshore limit of profile response is also of interest as it represents the maximum elevation and landward limit of sediment transport. During normal erosion/accretion cycles, the upper limit of significant beach profile change coincides with the wave runup limit. Under constructive conditions, as the beach face builds seaward, this upper limit of sediment deposition is usually well-defined in the form of a depositional

beach berm. During erosion conditions, the berm may retreat more or less uniformly. In some cases, the berm may be so high that runup never reaches its crest, in which case an erosion scarp will form above the runup limit. This is also evident in the case of eroding dunes, which are not overtopped by wave runup. In these cases, the slope of the eroding scarp may be quite steep, approaching vertical in some cases. A common assumption is that the eroding scarp will form at more or less the angle of repose of the sediment. Vellinga (1983), based on results shown in Figure III-3-16, suggests adopting a 1:1 slope for this erosion scarp. In other cases, the berm may be significantly overtopped by either the water level (storm surge) or by the wave runup. If overwash occurs, the landward limit may be controlled by the extent to which the individual uprush and overwash events are competent to transport sediment. Often this distance is determined by loss of transporting power due to percolation into the beach or by water impounded by the overwash event itself. In the latter case, the landward depositional front will advance at more or less the angle of repose into the impounded water.

(3) The seaward limit of effective profile fluctuation over long-term (seasonal or multi-year) time scales is a useful engineering concept and is referred to as the "closure depth," denoted by h_c. Based on laboratory and field data, Hallermeier (1978, 1981) developed the first rational approach to the determination of closure depth. He defined two depths, the shallowest of which delineates the limit of intense bed activity and the deepest seaward of which there is expected to be little sand transport due to waves. The shallower of the two appears to be of the greatest engineering relevance and will be discussed here. Based on correlations with the Shields parameter, Hallermeier defined a condition for sediment motion resulting from wave conditions that are relatively rare. Effective significant wave height H_e and effective wave period T_e were based on conditions exceeded only 12 hr per year; i.e., 0.14 percent of the time. The resulting approximate equation for the depth of closure was determined to be

$$h_c = 2.28 H_e - 68.5 \left(\frac{H_e^2}{g T_e^2} \right) \tag{III-3-9}$$

in which H_e can be determined from the annual mean significant wave height $\overline{H}$ and the standard deviation of significant wave height σ_H as

$$H_e = \overline{H} + 5.6 \sigma_H \tag{III-3-10}$$

(4) Based on this relationship, Hallermeier also proposed a form of Equation 3-9 that did not depend on the effective wave period in the form

$$h_c = 2 \overline{H} + 11 \sigma_H \tag{III-3-11}$$

(5) Birkemeier (1985) evaluated Hallermeier's relationship using high-quality field measurements from Duck, NC, and found that the following simplified approximation to the effective depth of closure provided nearly as good a fit to the data

$$h_c = 1.57 H_e \tag{III-3-12}$$

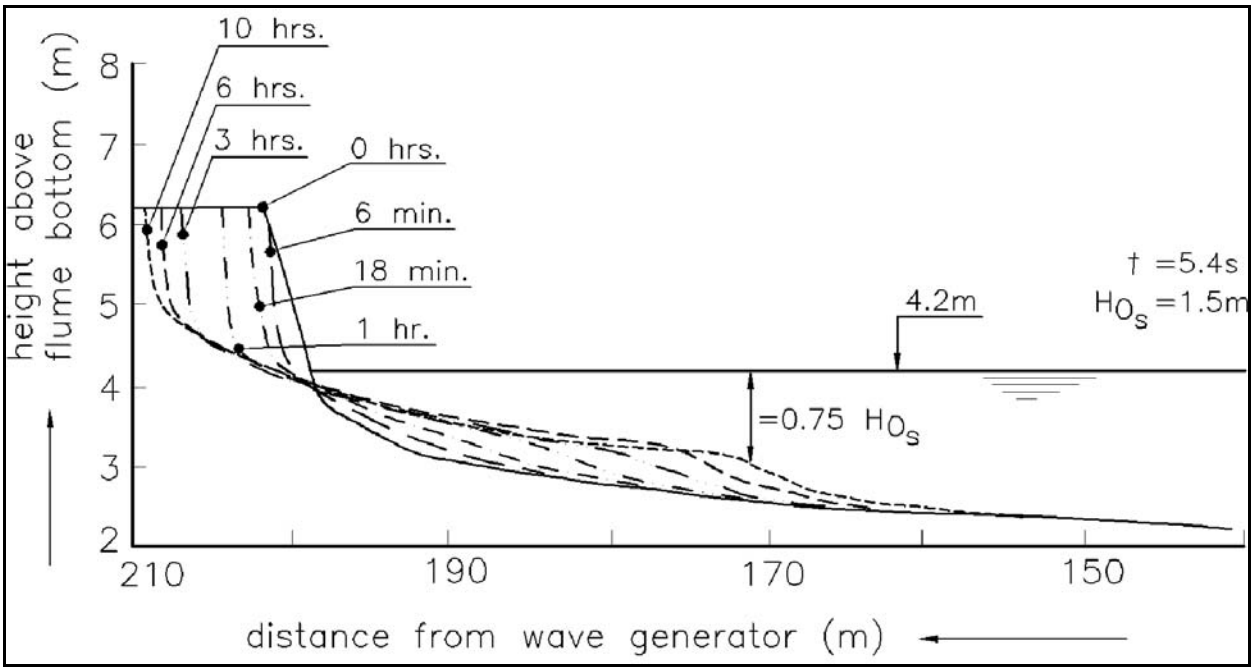

Figure III-3-16. Erosional profile evolution, large wave tank results (Vellinga 1983)

(6) In the applications to follow, it will be assumed that h_c is an appropriate representation of the closure depth for profile equilibration and for significant beach profile change over long time scales. This quantity will be denoted as h_* in most of the examples presented when applied to beach nourishment problems. For short-term profile changes such as those that occur during a storm, the breaking depth h_b will be assumed to delineate the active profile. It should be noted that other approaches to "channel depth" are discussed in the literature (Hands 1983).

c. Quantitative description of equilibrium beach profiles.

(1) Various models have been proposed for representing equilibrium beach profiles (EBP). Some of these models are based on examination of the geometric characteristics of profiles in nature and some attempt to represent in a gross manner the forces active in shaping the profile. One approach that has been utilized is to recognize the presence of the constructive forces and to hypothesize the dominance of various destructive forces. This approach can lead to simple algebraic forms for the profiles for testing against profile data.

(2) Dean (1977) has examined the forms of the EBPs that would result if the dominant destructive forces were one of the following:

(a) Wave energy dissipation per unit water volume.

(b) Wave energy dissipation per unit surface area.

(c) Uniform average longshore shear stress across the surf zone. It was found that for all three of these destructive forces, by using linear wave theory and a simple wave breaking model, the EBP could be represented by the following simple algebraic form

$$h = A y^{n} \tag{III-3-13}$$

in which A, representing a sediment scale parameter, depends on the sediment size D. This form with an exponent n equal to 2/3 had been found earlier by Bruun (1954) based on an examination of beach profiles in Denmark and in Monterey Bay, CA. Dean (1977) found the theoretical value of the exponent n to be 2/3 for the case of wave energy dissipation per unit volume as the dominant force and 0.4 for the other two cases. Comparison of Equation 3-13 with approximately 500 profiles from the east coast and Gulf shorelines of the United States showed that, although there was a reasonably wide spread of the exponents n for the individual profiles, a value of 2/3 provided the best overall fit to the data. As a result, the following expression is recommended for use in describing equilibrium beach profiles

$$h = A y^{\frac{2}{3}} \tag{III-3-14}$$

This allows the appealing interpretation that the wave energy dissipation per unit water volume causes destabilization of the sediment particles through the turbulence associated with the breaking waves. Thus dynamic equilibrium results when the level of destabilizing and constructive forces are balanced.

(3) The sediment scale parameter A and the equilibrium wave energy dissipation per unit volume D_* are related by (Dean 1991)

$$A = \left[\frac{24}{5}\,\frac{D_*}{\rho g\sqrt{g}\,\kappa^2}\right]^{\frac{2}{3}} \tag{III-3-15}$$

(4) Moore (1982) and Dean (1987b) have provided empirical correlations between the sediment scale parameter A as a function of sediment size D and fall velocity w_f as shown in Figure III-3-17. These results are based on a least-squares fit of Equation 3-14 to measured beach profiles. Figure III-3-18 presents an expanded version of the A versus D relationship for grain sizes more typical of beach sands and Table III-3-3 provides a tabulation of A values over the size range D = 0.10 mm to D = 1.09 mm. Although Table III-3-3 provides A values to four decimal places at diameter increments of 0.01 mm, this should not be interpreted as signifying that understanding of EBP justifies this level of quantification. Rather the values are presented for consistency by different users and possibly for use in sensitivity tests.

(5) The equilibrium profile parameter A may also be correlated to sediment fall velocity. In Figure III-3-17, a relationship is suggested between A and w_f that is valid over the entire range of sediment sizes shown. Kriebel, Kraus, and Larson (1991) developed a similar correlation over a range of typical sand grain sizes from D = 0.1 mm to D = 0.4 mm and found the following relationship

$$A = 2.25\left(\frac{w_f^2}{g}\right)^{\frac{1}{3}} \tag{III-3-16}$$

(6) This dependence of A on fall velocity to the two-thirds power has also been suggested by Hughes (1994) based on dimensional analysis.

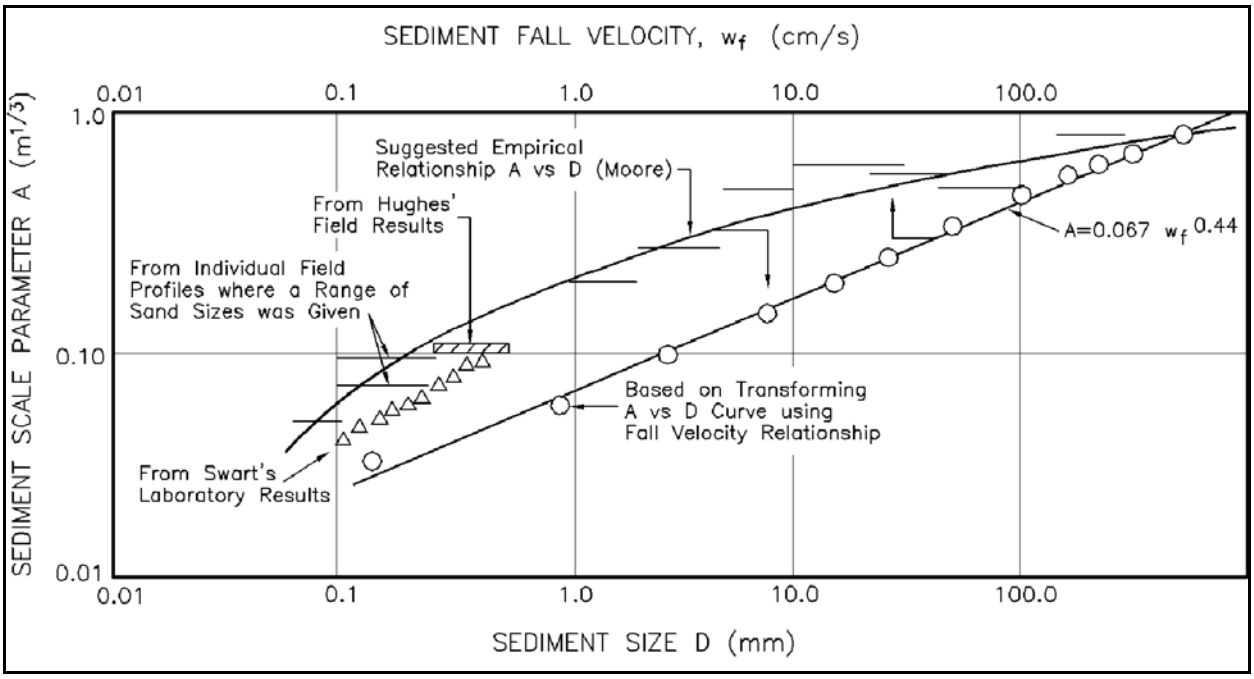

Figure III-3-17. Variation of sediment scale parameter *A* with sediment size *D* and fall velocity w_f (Dean 1987b)

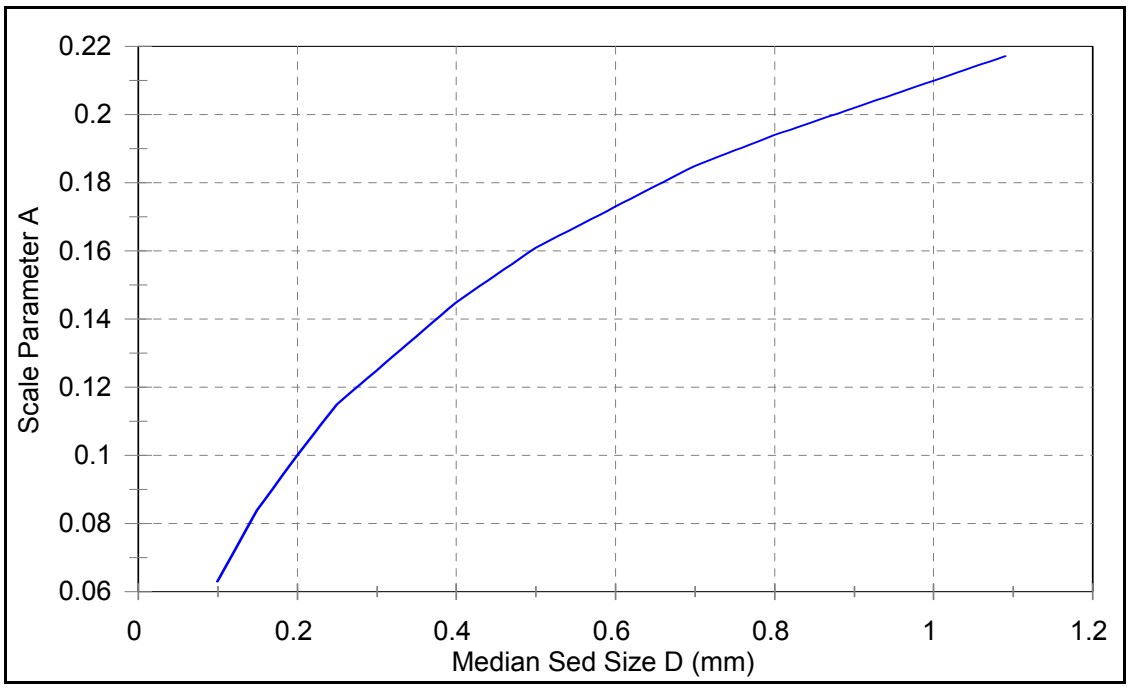

Figure III-3-18. Variation of sediment scale parameter *A*(*D*) with sediment size *D* for beach sand sizes (based on Dean 1978b, values recomputed by Dean, June 2001)

Table III-3-3
Summary of Recommended *A* Values (Units of *A* Parameter are $m^{1/3}$)

D(mm)	0.00	0.01	0.02	0.03	0.04	0.05	0.06	0.07	0.08	0.09
0.1	0.063	0.0672	0.0714	0.0756	0.0798	0.084	0.0872	0.0904	0.0936	0.0968
0.2	0.100	0.103	0.106	0.109	0.112	0.115	0.117	0.119	0.121	0.123
0.3	0.125	0.127	0.129	0.131	0.133	0.135	0.137	0.139	0.141	0.143
0.4	0.145	0.1466	0.1482	0.1498	0.1514	0.153	0.1546	0.1562	0.1578	0.1594
0.5	0.161	0.1622	0.1634	0.1646	0.1658	0.167	0.1682	0.1694	0.1706	0.1718
0.6	0.173	0.1742	0.1754	0.1766	0.1778	0.179	0.1802	0.1814	0.1826	0.1838
0.7	0.185	0.1859	0.1868	0.1877	0.1886	0.1895	0.1904	0.1913	0.1922	0.1931
0.8	0.194	0.1948	0.1956	0.1964	0.1972	0.198	0.1988	0.1996	0.2004	0.2012
0.9	0.202	0.2028	0.2036	0.2044	0.2052	0.206	0.2068	0.2076	0.2084	0.2092
1.0	0.210	0.2108	0.2116	0.2124	0.2132	0.2140	0.2148	0.2156	0.2164	0.2172

Notes:
(1) The *A* values above, some to four places, are not intended to suggest that they are known to that accuracy, but rather are presented for consistency and sensitivity tests of the effects of variation in grain size.
(2) As an example of use of the values in the table, the *A* value for a median sand size of 0.24 mm is: $A = 0.112\ m^{1/3}$. To convert *A* values to $feet^{1/3}$ units, multiply by $(3.28)^{1/3} = 1.49$.

(7) There are two inherent limitations of Equation 3-14. First, the slope of the beach profile at the water line (y=0) is infinite. Second, the beach profile form is monotonic; i.e., it cannot represent bars. It has been shown that the first limitation can be overcome by recognizing gravity as a significant destabilizing force when the profile becomes steep. In this case with the beach face slope denoted as m_o, the form is

$$y = \frac{h}{m_o} + \left(\frac{h}{A}\right)^{\frac{3}{2}} \tag{III-3-17}$$

which, unfortunately, is significantly more cumbersome to apply. Larson (1988) and Larson and Kraus (1989) have shown that an EBP of the form of Equation 3-17 results by replacing the simple breaking wave model leading to Equation 3-14 by the more complex breaking model of Dally et al. (1985). Bodge (1992) and Komar and McDougal (1994) have each proposed slightly different forms of an exponential beach profile. The form proposed by Bodge is

$$h(y) = h_o(1 - e^{-ky}) \tag{III-3-18}$$

in which h_o is the asymptotic depth at a great offshore distance, and k is a decay constant. The form suggested by Komar and McDougal is quite similar with $h_o = m_o/k$ in which m_o is the beach face slope. Bodge fit his profile to the averages of the ten data sets provided by Dean (1977) and found that the majority (about 80 percent) fit the exponential form better than the $Ay^{2/3}$ expression. The exponential forms have two free constants which are determined to provide the best fit and thus should agree better than for the case in which n is constrained to the 2/3 value. Since the exponential profile form requires determination of the two free parameters from the individual profile being represented, it can be applied in a diagnostic manner but not prognostically. In another approach Inman, Elwany, and Jenkins (1993) discuss the fitting of compound beach profile to a number of beaches. The curve-fitting approach requires up to seven free parameters and appears to require subjectivity in parameter choice. This method cannot be applied in a prognostic manner.

d. Computation of equilibrium beach profiles. The most simple application is the calculation of equilibrium beach profiles for various grain sizes, assumed uniform across the profile. This application is illustrated by the following example.

The extension of the equilibrium profile form to cases where the grain size varies across the profile is discussed in Dean (1991).

e. Application of equilibrium profile methods to nourished beaches.

(1) In the design of beach nourishment projects, it is important to estimate the dry beach width after profile equilibration. Most profiles are placed at slopes considerably steeper than equilibrium and the equilibration process, consisting of a redistribution of the fill sand across the active profile out to the depth of closure, occurs over a period of several years. In general, the performance of a beach fill, in terms of the resulting gain in dry beach width relative to the volume of sand placed on the beach, is a function of the compatibility of the fill sand with the native sand. Based on equilibrium beach profile concepts, it should be evident that since profiles composed of coarser sediments assume steeper profiles, beach fills using coarser sand will require less sediment to provide the same equilibrium dry beach width Δy than fills using sediment that is finer than the native sand.

(2) It can be shown that three types of nourished profiles are possible, depending on the volumes added and on whether the nourishment is coarser or finer than that originally present on the beach. These profiles are termed "intersecting," "nonintersecting," and "submerged," respectively, and are shown in Figure III-3-20. It can be shown that an intersecting profile requires the added sand to be coarser than the native sand, although this condition does not guarantee intersecting profiles, since the intersection may be at a depth in excess of the depth of closure. Nonintersecting or submerged profiles always occur if the sediment is of the same diameter or finer than the native sand.

(3) Several more general examples will assist in understanding the significance of the sand and volume characteristics. Denoting the sediment scale parameters for the native and fill sediments as A_N and A_F, respectively, Figure III-3-21 presents the variation in dry beach width for a native sand size of 0.20 mm and various fill diameters ranging from 0.15 mm to 0.40 mm. These results are illustrated for a closure depth h_* of 6 m, a berm height B of 2 m, and a volumetric addition per unit beach length of 340 m^3/m. In the upper panel, the fill sediment is coarser than the native sand and the profiles are intersecting, resulting in an equilibrium additional dry beach width of 92.4 m. In the second panel, the fill sand is of the same size as the native (nonintersecting profiles) and the added beach width is 45.3 m. The third and fourth panels illustrate the effects of further decreases in sediment sizes with an incipient submerged profile in the last panel. These examples have considered the effects only of cross-shore equilibration. In design of beach nourishment projects, the additional effects of more rapid spreading out of the nourishment project due to longshore sediment transport due to fine sediments should also be considered. The next generic example, presented in Figure III-3-22, illustrates the effects of adding greater amounts of sediment that are finer than the native. For small amounts, the profile is totally submerged. However, as greater and greater amounts are added, the landward extremity of the nourished profile advances toward land, and ultimately the profile becomes emergent.

EXAMPLE PROBLEM III-3-1

FIND:

The equilibrium beach profiles.

GIVEN:

Consider grain sizes of 0.3 mm and 0.66 mm.

SOLUTION:

From Figure III-3-18 and/or Table III-3-3, the associated A values are 0.125 $m^{1/3}$ and 0.18 $m^{1/3}$, respectively. Applying Equation 3-14, the two profiles are computed and are presented in Figure III-3-19. The profile composed of the coarser sand is considerably steeper than that for the finer material.

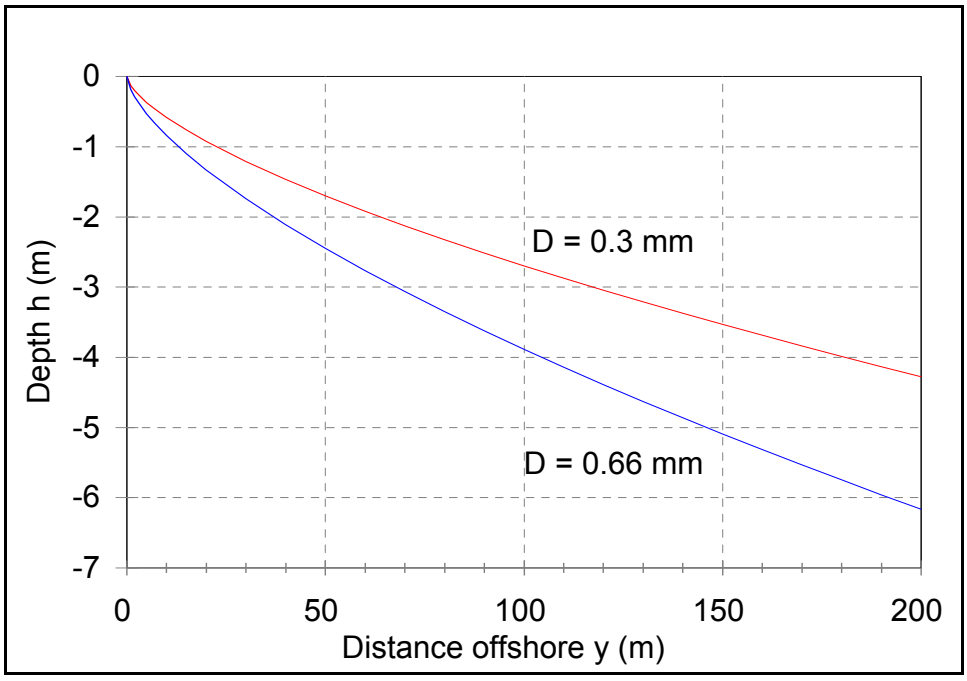

Figure III-3-19. Equilibrium beach profiles for sand sizes of 0.3 mm and 0.66 mm A(D = 0.3 mm) = 0.125 $m^{1/3}$, A(D = 0.66 mm) = 0.18 $m^{1/3}$

f. Quantitative relationships for nourished profiles.

(1) In order to investigate the conditions of profile type occurrence and additional quantitative aspects, it is useful to define the following nondimensional quantities: $A' = A_F/A_N$, $\Delta y' = \Delta y/W_*$, $B' = B/h_*$, and $V' = V/(B\,W_*)$, where the symbol V denotes added volume per unit beach length, B is the berm height, and h_* is the depth to which the nourished profile will equilibrate as shown in Figure III-3-21. In general, this will be considered to be the closure depth. It is important to note that the width W_* is based on the native sediment scale parameter A_N as given by

$$W_* = \left(\frac{h_*}{A_N}\right)^{\frac{3}{2}} \qquad \text{(III-3-19)}$$

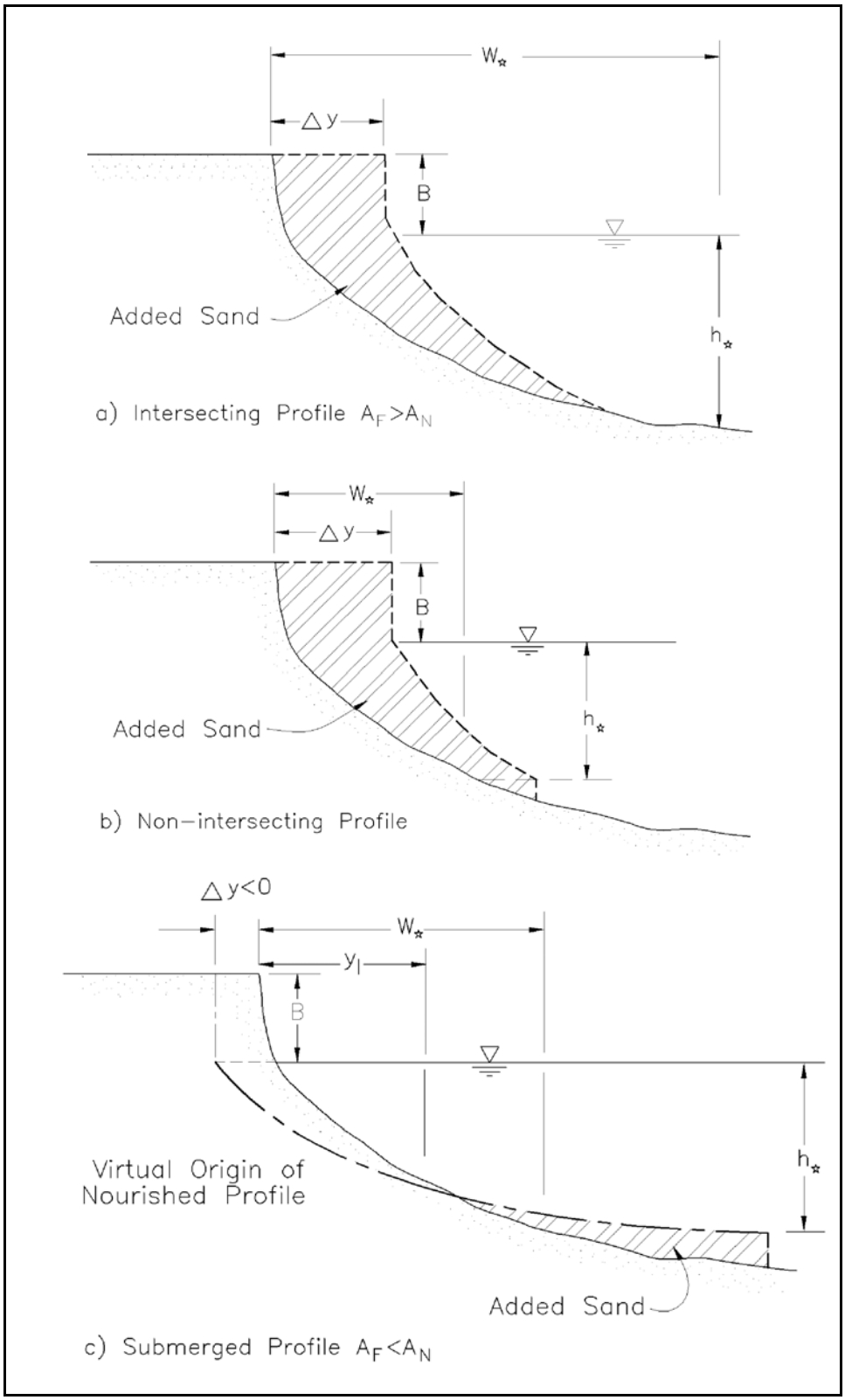

Figure III-3-20. Three generic types of nourished profiles. (a) intersecting, (b) nonintersecting, and (c) submerged profiles (Dean 1991)

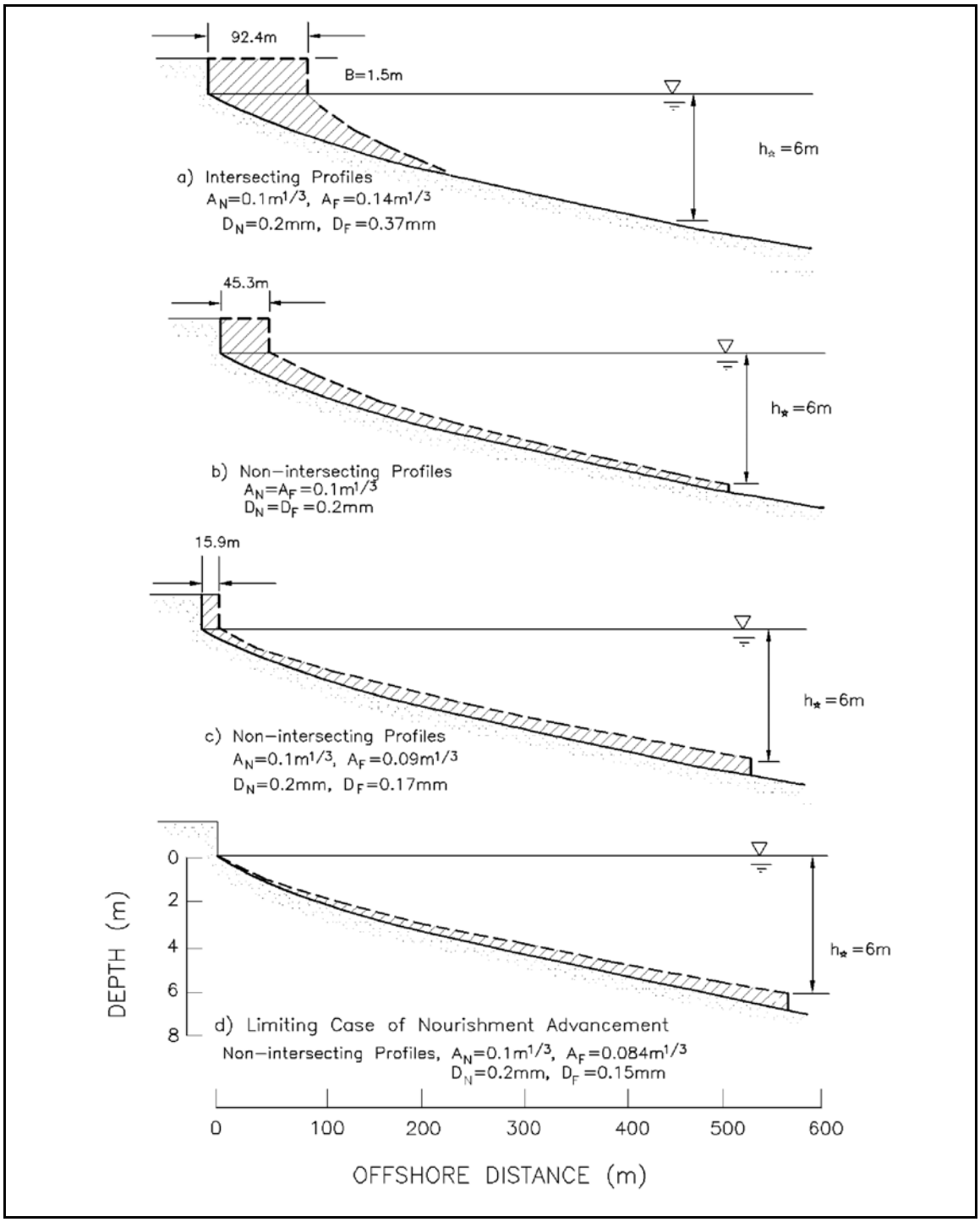

Figure III-3-21. Effect of nourishment material scale parameter A_F on width of resulting dry beach. Four examples of decreasing A_F with same added volume per unit beach length (Dean 1991)

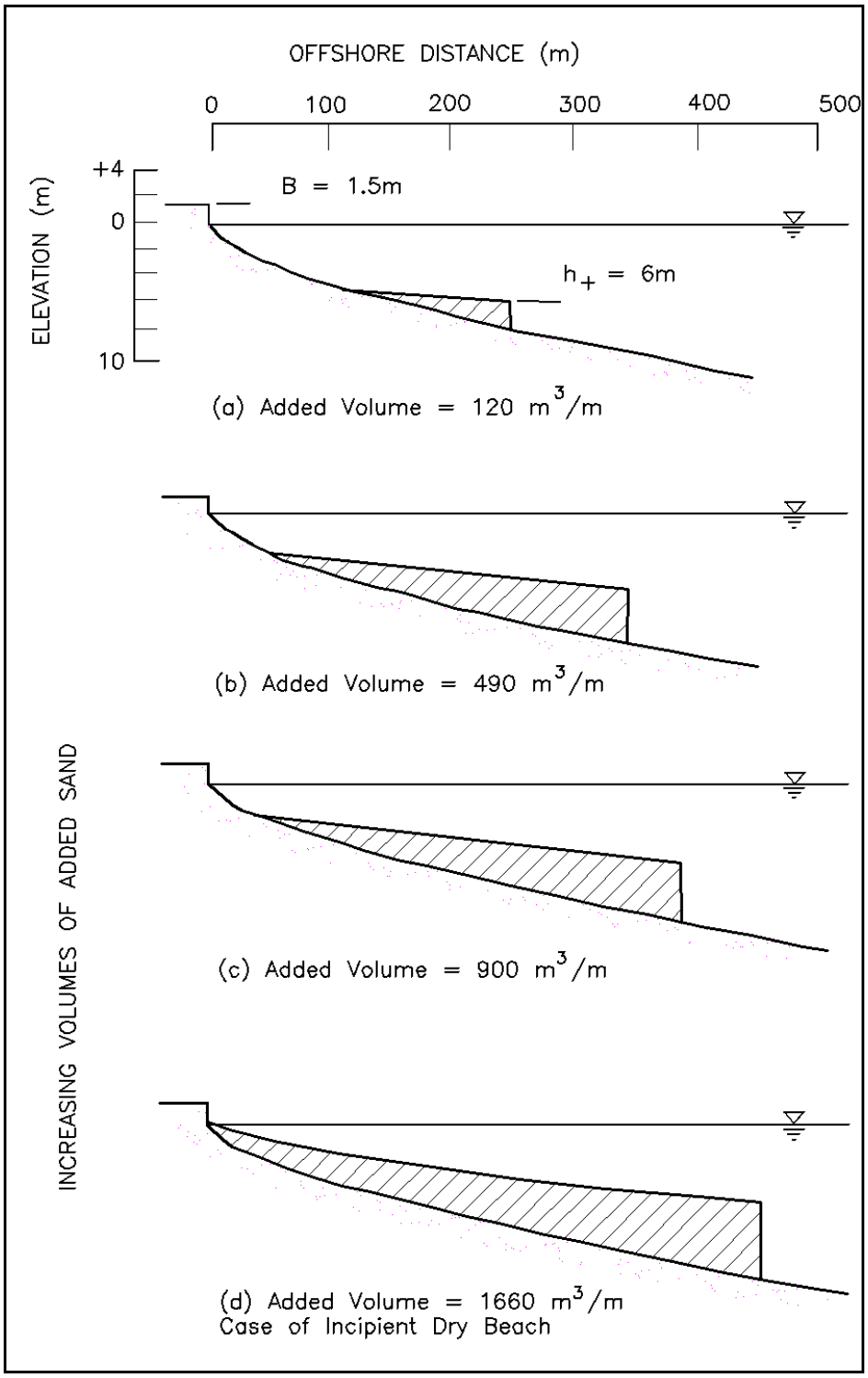

Figure III-3-22. Effect of increasing volume of sand added on resulting beach profile. A_F = 0.1 $m^{1/3}$, A_N = 0.2 $m^{1/3}$, h_* = 6.0 m, B = 1.5 m (Dean 1991)

It is possible to show that the nondimensional equilibrium dry beach width $\Delta y'$ can be presented in terms of three nondimensional quantities

$$\Delta y' = f(B', V', A') \tag{III-3-20}$$

(2) The relationships governing the conditions for intersecting/nonintersecting profiles are

$$\Delta y' + \left(\frac{1}{A'}\right)^{\frac{3}{2}} - 1 \begin{cases} < 0, \text{ intersecting profiles} \\ > 0, \text{ non-intersecting profiles} \end{cases} \tag{III-3-21}$$

given that the fill sediment scale parameter is greater than or equal to the native sediment scale parameter.

The critical volume of sand delineating intersecting and nonintersecting profiles is

$$(V')_{c1} = \left(1 + \frac{3}{5B'}\right)\left[1 - \left(\frac{1}{A'}\right)^{\frac{3}{2}}\right] \tag{III-3-22}$$

which applies only for $A'>1$, since for $A'<1$, the profiles will always be nonintersecting although it should be recognized that nonintersecting profiles can also exist for $A'>1$. If $A'>1$, but $V' > V_{c1}$, then the profile will be nonintersecting. Also of interest is the critical volume of sand V_{c2} that will just yield a finite shoreline displacement for the case of sand that is finer than the native ($A'<1$)

$$(V')_{c2} = \frac{3}{5B'}\left(\frac{1}{A'}\right)^{\frac{3}{2}}\left(\frac{1}{A'} - 1\right) \tag{III-3-23}$$

(3) Figure III-3-23 presents these two critical volumes versus the scale parameter A' for the special case B'=0.25.

(4) For intersecting profiles, the nondimensional volume required to yield an advancement $\Delta y'$ is

$$V_1' = \Delta y' + \frac{3}{5B'}(\Delta y')^{\frac{5}{3}} \frac{1}{\left[1 - \left(\frac{1}{A'}\right)^{\frac{3}{2}}\right]^{\frac{2}{3}}} \tag{III-3-24}$$

This equation would apply for the example in Figure III-3-20a.

(5) For nonintersecting but emergent profiles, the corresponding volume V_2' is

$$V_2' = \Delta y' + \frac{3}{5B'}\left\{\left[\Delta y' + \left(\frac{1}{A'}\right)^{\frac{3}{2}}\right]^{\frac{5}{3}} - \left(\frac{1}{A'}\right)^{\frac{3}{2}}\right\} \tag{III-3-25}$$

This equation would apply for Figure III-3-20b.

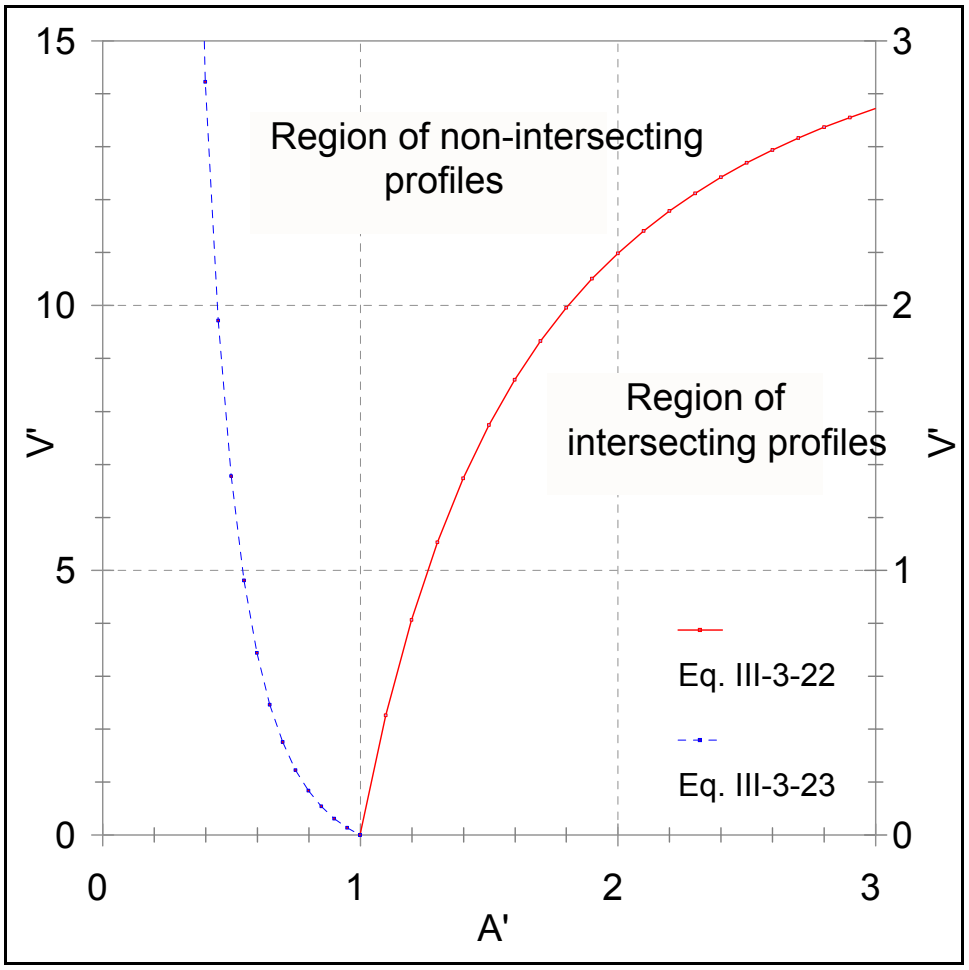

Figure III-3-23. (1) Volumetric requirement for finite shoreline advancement (Equation 3-23); (2) Volumetric requirement for intersecting profiles (Equation 3-22). Results presented for special case B' = 0.25

(6) For submerged profiles, referring to Figure III-3-20c, it can be shown that

$$\frac{\Delta y}{y_I} = 1 - \left(\frac{1}{A'}\right)^{\frac{3}{2}} \tag{III-3-26}$$

where $\Delta y' < 0$, $A' < 1$, and the nondimensional volume of sediment can be expressed as

$$V_4' = \frac{3}{5B'}\left\{\left[\Delta y' + \left(\frac{1}{A'}\right)^{\frac{3}{2}}\right]^{\frac{5}{3}} + \frac{(-\Delta y')^{\frac{5}{3}}}{\left[\left(\frac{1}{A'}\right)^{\frac{3}{2}} - 1\right]^{\frac{2}{3}}} - \left(\frac{1}{A'}\right)^{\frac{3}{2}}\right\} \tag{III-3-27}$$

where $\left(\frac{1}{A'}\right)^{3/2} \geq |\Delta y'|$

This equation would apply for Figure III-3-20c but is of limited value since no beach width would be added.

(7) Equations 3-24 and 3-25 can be displayed in a useful form for calculating the volume required for a particular equilibrium additional dry beach width. However, as is evident from Equation 3-20, there are three independent variables: B', A', and V'. Thus, since only two independent variables can be displayed on a single plot, it is necessary to have a series of plots. Three are presented here, one each for $B' = 0.5$ (Figure III-3-24) $B' = 0.333$ (Figure III-325) and $B' = 0.25$ (Figure III-3-26). The information contained in these plots will be discussed by reference to Figure III-3-24.

(8) The vertical axis is the nondimensional added beach width $\Delta y'$, the horizontal axis is the nondimensional sediment scale parameter A', and the isolines are the nondimensional volumes V'. For a given A' and V', the value of $\Delta y'$ is readily determined. It is seen that $\Delta y'$ increases with increasing V' and A'. The heavy dashed line delineates the regions of intersecting and nonintersecting profiles (Equation 3-23). With decreasing A' and constant V', the value of $\Delta y'$ decreases to the asymptotes for a submerged profile. Several examples will be presented illustrating the application of Figures III-3-24, III-3-25, and III-3-26.

g. Longshore bar formation and seasonal shoreline changes.

(1) Longshore bars were discussed briefly in Part III-3-2. They are elongated mounds more or less parallel to the shoreline and are known to be more prevalent for storm conditions and for finer sediments. Bars may be present as single features or may occur as a series (Figure III-3-10). Additionally, bars can be seasonal or perennial. In most locations where bars are seasonal, their formation is associated with a seaward transport of sediment and a retreat of the shoreline. At a particular location, the amount of seasonal fluctuation depends on the number and intensity of storms during a particular year. Figure III-3-30 shows results of measurements by Dewall and Richter (1977) from Jupiter Island, Florida, where the seasonal fluctuations appear to be on the order of 15 m. Figure III-3-31, from Dewall (1979) shows shoreline and volume changes (above mean sea level) from Westhampton, Long Island, New York, where the seasonal changes may be on the order of 20 to 40 m.

(2) Although the prediction of bar geometry and the associated shoreline changes have not advanced to a reliable stage, parameters have been proposed and correlated successfully with conditions for which bars form. Based on field observations, Dean (1973) hypothesized that sediment was suspended during the crest phase position and that if the fall time were less or greater than one-half the wave period, the net transport would be landward or seaward, respectively, resulting in bar formation in the latter case. This mechanism would be consistent with the wave-breaking cause. Further rationalizing that the suspension height would be proportional to the wave height resulted in identification of the so-called fall velocity parameter H_b/w_fT. Although there is no agreement on the cause of longshore bar formation, it appears to result from wave breaking, with edge waves and other phenomena proposed as possible causes.

(3) Examination of small-scale laboratory data for which the deep water reference wave height H_o values were available led to the following relationship (Dean 1973) for offshore sediment transport leading to bar formation

$$\frac{H_o}{w_f T} \geq 0.85 \tag{III-3-28}$$

(4) Later, Kriebel, Dally, and Dean (1986) examined only prototype and large-scale laboratory data and found a constant of approximately 2.8 rather than 0.85 as in Equation 3-28. Kraus, Larson, and Kriebel (1991) examined only large wave tank data and proposed the following two relationships for bar formation

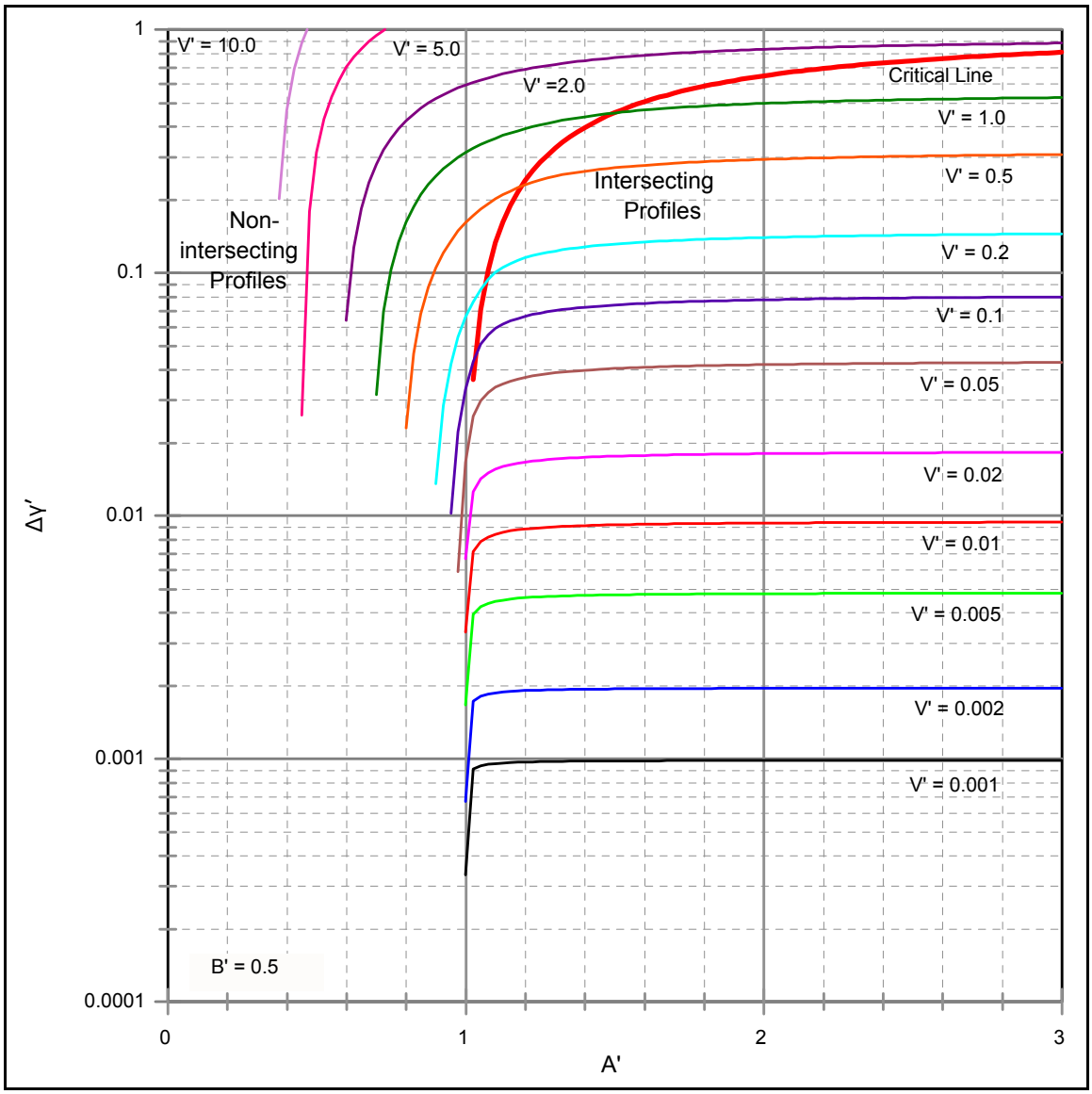

Figure III-3-24. Variation of nondimensional shoreline advancement $\Delta y/W_*$, with A' and V. Results shown for $H_*/B = 2.0$ ($B' = 0.5$) (based on Dean (1991), values recomputed by Dean, May 2001). Intersecting and non-intersecting profiles divided by critical line; definition sketches shown in Figure III-3-20.

$$\frac{H_o}{L_o} \geq 115 \left(\frac{\pi w_f}{gT} \right)^{\frac{3}{2}} \tag{III-3-29}$$

and

$$\frac{H_o}{L_o} \leq 0.0007 \left(\frac{H_o}{w_f T} \right)^3 \tag{III-3-30}$$

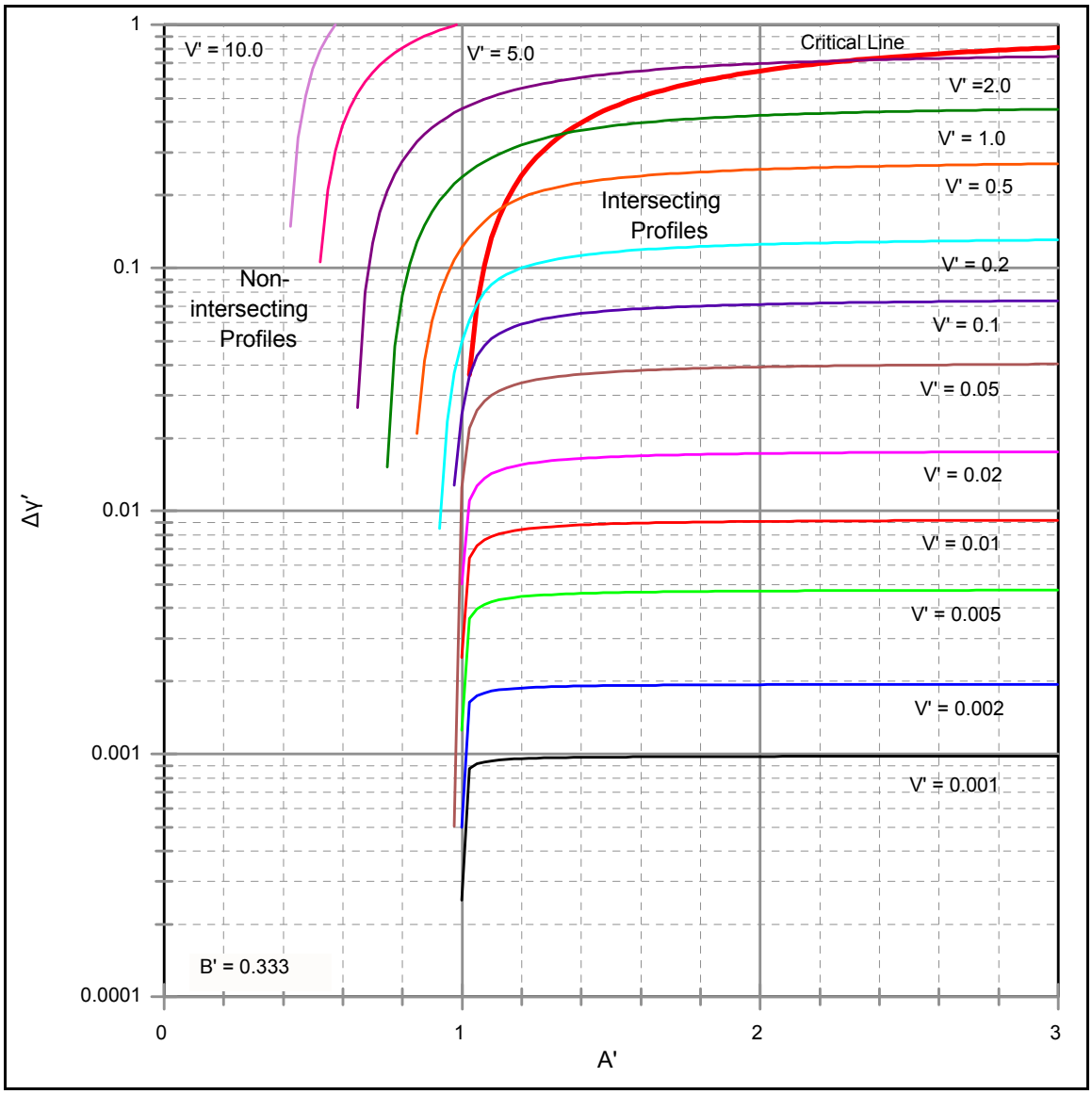

Figure III-3-25. Variation of nondimensional shoreline advancement $\Delta y/W_*$, with A' and V. Results shown for $H_*/B = 3.0$ ($B' = 0.333$) (based on Dean (1991), values recomputed by Dean, May 2001). Intersecting and non-intersecting profiles divided by critical line; definition sketches shown in Figure III-3-20.

in which H_o is the average deepwater wave height. For field data in which the significant deepwater wave height was used, the constant in Equation 3-30 was modified to

$$\frac{H_{o_s}}{L_o} \leq 0.00027 \left(\frac{H_{o_s}}{w_f T} \right)^3 \tag{III-3-31}$$

(5) It is interesting that Equation 3-30 provides a better fit to the laboratory data than a fixed value of the fall velocity parameter; however, for field data, a fixed value of the fall velocity parameter provides a

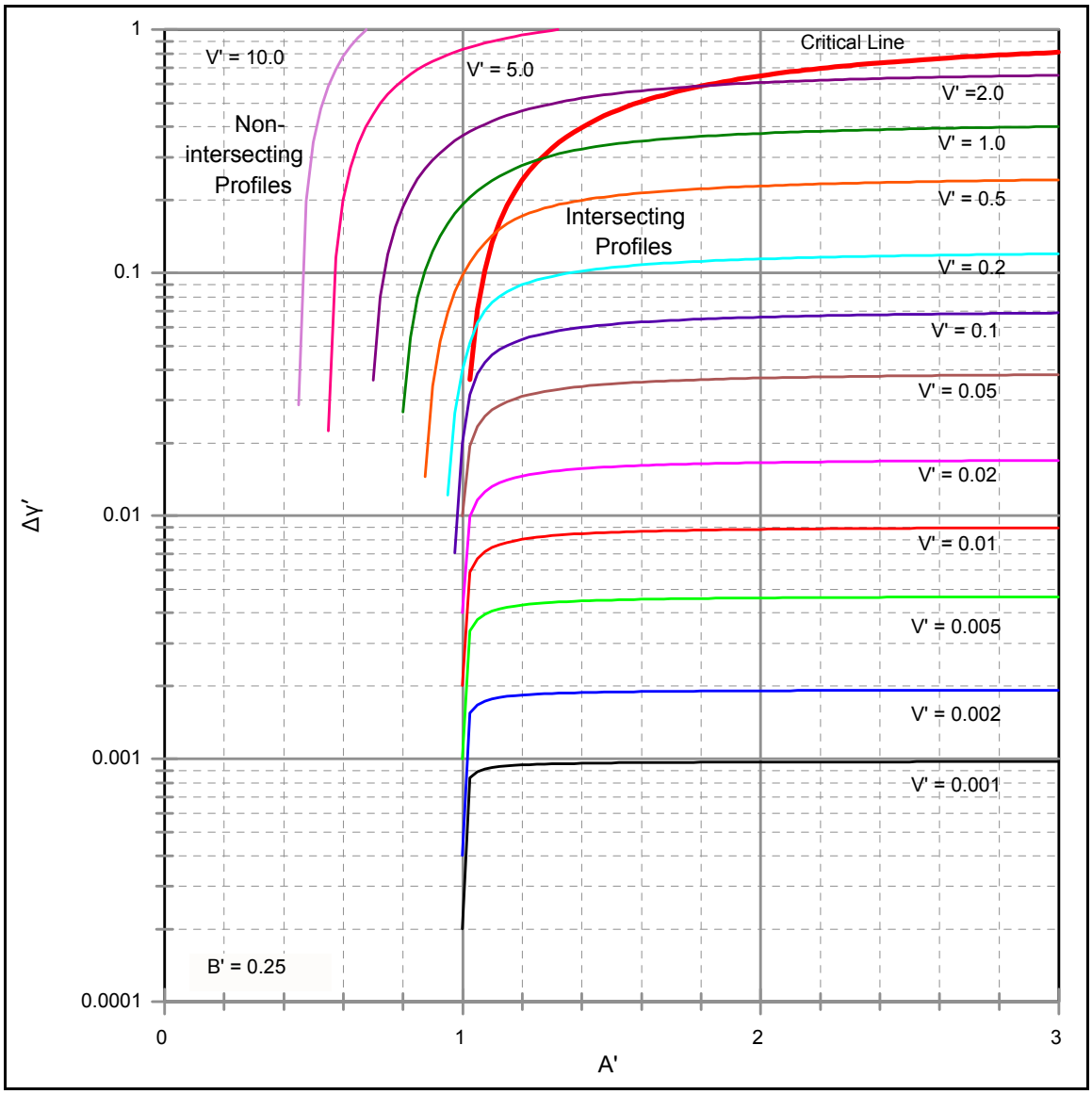

Figure III-3-26. Variation of nondimensional shoreline advancement Δy/W*, with A′ and V. Results shown for H*/B = 4.0 (B′ = 0.25), based on Dean (1991), values recomputed by Dean, May 2001). Intersecting and non-intersecting profiles divided by critical line; definition sketches shown in Figure III-3-20.

better fit than Equation 3-30 (Kraus, Larson, and Kriebel 1991). Dalrymple (1992) has shown that Equations 3-29 and 3-30 can be represented in terms of a single profile parameter P where

$$P = \frac{g H_o^2}{w_f^3 T} \tag{III-3-32}$$

and that the criterion for bar formation is that P exceeds about 10,000.

EXAMPLE PROBLEM III-3-2

FIND:

The equilibrated additional dry beach width Δy due to cross-shore transport.

GIVEN:

$D_N = 0.2$ mm, $D_F = 0.24$ mm, $B = 2$ m, $V = 400$ m^3/m.
$\bar{H} = 1.5$ m, $\sigma_H = 0.64$ m as provided in WES and CEDRS databases discussed in Part II-8.

SOLUTION:

Based on the above, the sediment scale parameters are determined from Figure III-3-18 and/or Table III-3-3 to be: $A_N = 0.1$ m$^{1/3}$, $A_F = 0.11$ m$^{1/3}$. The effective wave height H_e is determined from Equation 3-10 as:

$$H_e = \bar{H} + 5.6\,\sigma_H = 1.5 + (5.6)(0.64) \cong 5.1 \text{ m}$$

The closure depth h_* is determined from Equation 3-12 as:

$$h_* = h_C = 1.57\,H_e = (1.57)\,(5.11) \cong 8 \text{ m}$$

The reference width of effective motion W_* is based on Equation 3-19

$$W_* = \left(\frac{h_*}{A_N}\right)^{\frac{3}{2}} = \left(\frac{8}{0.1}\right)^{\frac{3}{2}} \cong 716 \text{ m}$$

With this information, it is possible to determine the following nondimensional quantities:

$$B' = B/h_* = 2/8 = 0.25, \quad A' = A_F/A_N = 0.11/0.1 = 1.1$$

$$V' = V/(BW_*) = 400/(2)(716) \cong 0.28$$

Since $B' = 0.25$, Figure III-3-26 is applicable and for $A' = 1.1$ and $V' = 0.28$, it is found that $\Delta y' = 0.092$. Thus $\Delta y = (0.092)(716) \cong 65.9$ m. Also, it is seen from Figure III-3-26 that this solution is near the boundary of the intersecting/nonintersecting profiles.The native and nourished profiles are shown in Figure III-3-27. The solution is next carried out with the appropriate equations for comparison with the graphical procedure. Applying Equation 3-22 to determine whether the profiles will be intersecting or nonintersecting

$$(V')_{c1} = \left(1 + \frac{3}{5B'}\right)\left[1 - \left(\frac{1}{A'}\right)^{\frac{3}{2}}\right]$$

$$= \left(1 + \frac{3}{(5)(0.25)}\right)\left[1 - \left(\frac{1}{1.1}\right)^{\frac{3}{2}}\right] \cong 0.45$$

compared with the applied V' of 0.28. Thus since $V' < (V')_{c1}$ the solution is an intersecting profile. Applying Equation 3-24 requires an iterative solution for $\Delta y'$. This equation can be reduced to

$$0.28 = \Delta y' + 9.20(\Delta y')^{5/3}$$

the solution to which yields $\Delta y' = 0.0955$ or $\Delta y = 68.4$ m

(Continued)

Example Problem III-3-2 (Concluded)

Thus, for this example, the graphical solution is reasonable. The calculated intersection distance for the two profiles y_I is determined from

$$h_I = A_N y_I^{\frac{2}{3}} = A_F (y_I - \Delta y)^{\frac{2}{3}}$$

or

$$y_I = \frac{\Delta y \left(\frac{A_F}{A_N}\right)^{\frac{3}{2}}}{\left(\frac{A_F}{A_N}\right)^{\frac{3}{2}} - 1} = \frac{68.4(1.1)^{\frac{3}{2}}}{(1.1)^{\frac{3}{2}} - 1} = 513\,\text{m}$$

and

$$h_I = A_N y_I^{\frac{2}{3}} \cong 6.4\,\text{m}$$

By comparison, the corresponding values from the graphical solution are y_I = 495 m and h_I = 6.25 m. Figure III-3-27 presents the results of the graphical solution.

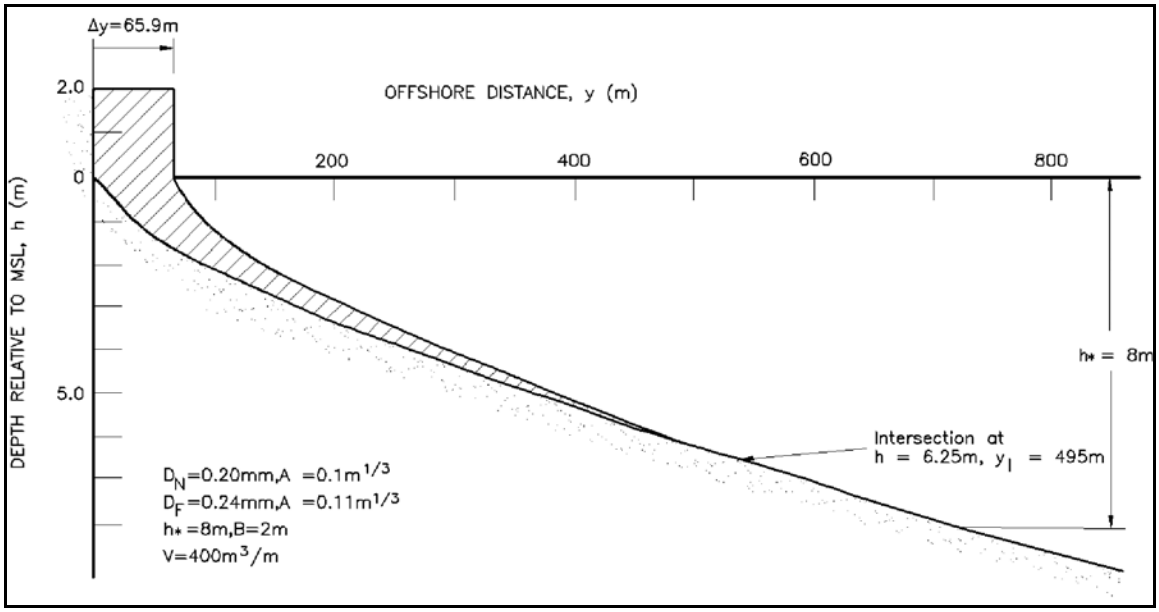

Figure III-3-27. Nourishment with coarser sand than native (intersecting profiles)

EXAMPLE PROBLEM III-3-3

FIND:

V, the volume of sand necessary to achieve the additional dry beach width Δy of 50 m.

GIVEN:

B=2 m, $D_N = D_F$ = 0.25 mm, Δy = 50 m, where $\overline{H}$=*1.5* m, σ_H = 0.4 m.

SOLUTION:

The value of h_* is computed as:

$$h_* = 1.57\,(\overline{H} + 5.6\,\sigma_H) = 1.57\,[1.5 + (5.6)(0.4)] \cong 5.9 \text{ m}$$

For these values, the associated A values are determined from Figure III-3-18 and/or Table III-3-3 to be: $A_N = A_F = 0.115$ m$^{1/3}$. The reference width of active motion W_* is

$$W_* = \left(\frac{h_*}{A_N}\right)^{\frac{3}{2}} \cong 367 \text{ m}$$

and the required nondimensional quantities are:

$$\Delta y/W_* \cong 50/367 \cong 0.136,\ B' = B/h_* \cong 0.34,\ A' = A_F/A_N = 0.115/0.115 = 1.0$$

Since the value of B' lies between the two values represented in Figures III-3-24 and III-3-26, it is necessary to interpolate. The values from these two figures are: $V'(B' = 0.25) = 0.75$, $V'(B' = 0.5) = 0.35$. Interpolating linearly, V' is found to be 0.606 for the desired B' value of 0.34, from which the volume V is determined as $V = V' B W_* = (0.606)\,(2)\,(367) \cong 445$ m^3/m. Since the fill and native sediments are of the same size, it is clear that the two profiles will be nonintersecting and that Equation 3-25 can be used to compute the nondimensional volume directly

$$V' = \Delta y' + \frac{3}{5B'}\left\{\left[\Delta y' + \left(\frac{1}{A'}\right)^{\frac{3}{2}}\right]^{\frac{5}{3}} - \left(\frac{1}{A'}\right)^{\frac{3}{2}}\right\}$$

$$= 0.136 + \frac{3}{(5)(0.34)}\left\{[0.136 + 1]^{\frac{5}{3}} - 1\right\} \cong 0.554$$

(Continued)

Example Problem III-3-3 (Concluded)

which yields a volume of sand, $V = V' B W_* = (0.554)(2)(367) = 407$ m^3/m, which is about 9 percent less than the value determined by interpolating between the values from the two figures. Since in this particular case, the two sand sizes are the same and thus every contour must be displaced by the same amount, an approximate equation for the required volume density is the product of the contour displacement (50 m) and the full depth of active motion: $V = (\Delta y)(h_* + B) = (50)(5.9 + 2) =$ 395 m^3/m. This result differs slightly from the values determined above because a small wedge-shaped sand volume has been neglected near the depth of closure. The native and nourished profiles are plotted in Figure III-3-28.

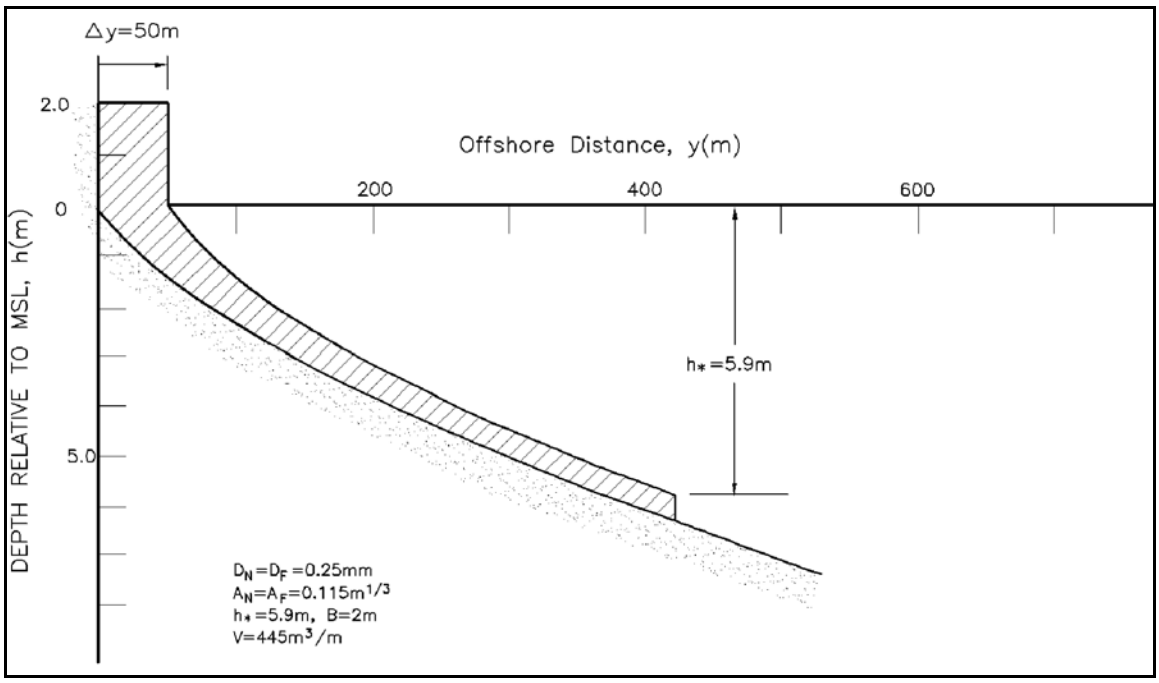

Figure III-3-28. Example III-3-3. Nourishment with same-sized sand as native (nonintersecting profiles)

EXAMPLE PROBLEM III-3-4

FIND:

The variation in equilibrated dry beach width with volume added for three candidate fill sand sizes.

GIVEN:

Three candidate borrow sites with representative sand sizes: D_{F_1} = 0.15 mm, D_{F_2} = 0.2 mm and D_{F_3} = 0.25 mm. The native sand size, D_N = 0.2 mm. The berm height B = 1.5 m and h_* = 6 m.

SOLUTION:

The associated values of the sediment scale parameters are determined from Figure III-3-18 and/or Table III-3-3: A_N = 0.1 m$^{1/3}$, A_{F_1} = 0.084 m$^{1/3}$, A_{F_2} = 0.1 m$^{1/3}$, and A_{F_3} = 0.115 m$^{1/3}$, respectively. The procedures illustrated in Example Problems III-3-2 and III-3-3 produce the results shown in Figure III-3-29. It is seen that there is a nearly linear relationship for the sand that is of the same size as the native in accordance with: $V = (\Delta y)(h_* + B)$. For the fill sand, which is coarser than the native, for volumes less than approximately 450 m^3/m, the increase in dry beach width for each volume added is greater than for the same-sized sand. For this region, the profiles are intersecting. For greater volumes, the profiles are nonintersecting and the slope of the relationship is nearly the same as for A_F/A_N = 1.0. For the sand smaller than the native, the profiles are submerged for the smaller volumes and later become emergent in accordance with Equation 3-23. For larger volumes, the relationship has approximately the same slope as that for sand the same size as the native. The explanation for this is that once the profiles become emergent and nonintersecting, additional volumes of sand added simply displace the profile with all contours moving the same distance over the active depth. Thus the slope in Figure III-3-29 for this situation is nearly independent of the grain size.

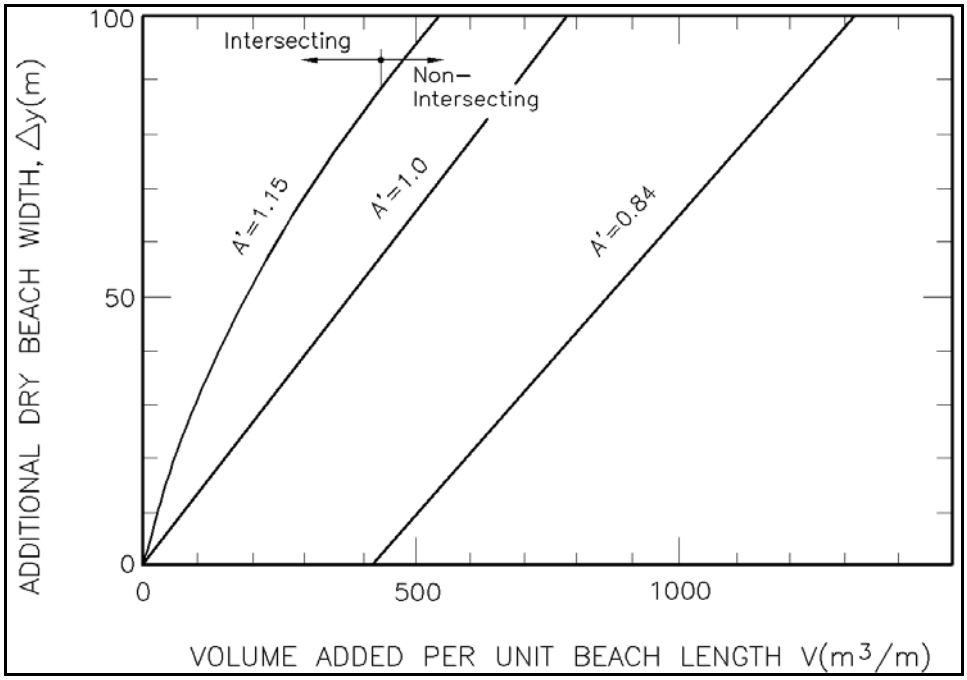

Figure III-2-29. Illustration of effect of volume added *V* and fill sediment scale parameter A_F on additional dry beach width Δy. Example conditions: *B* = 1.5 m, h_* = 6 m, A_N = 0.1 m$^{1/3}$

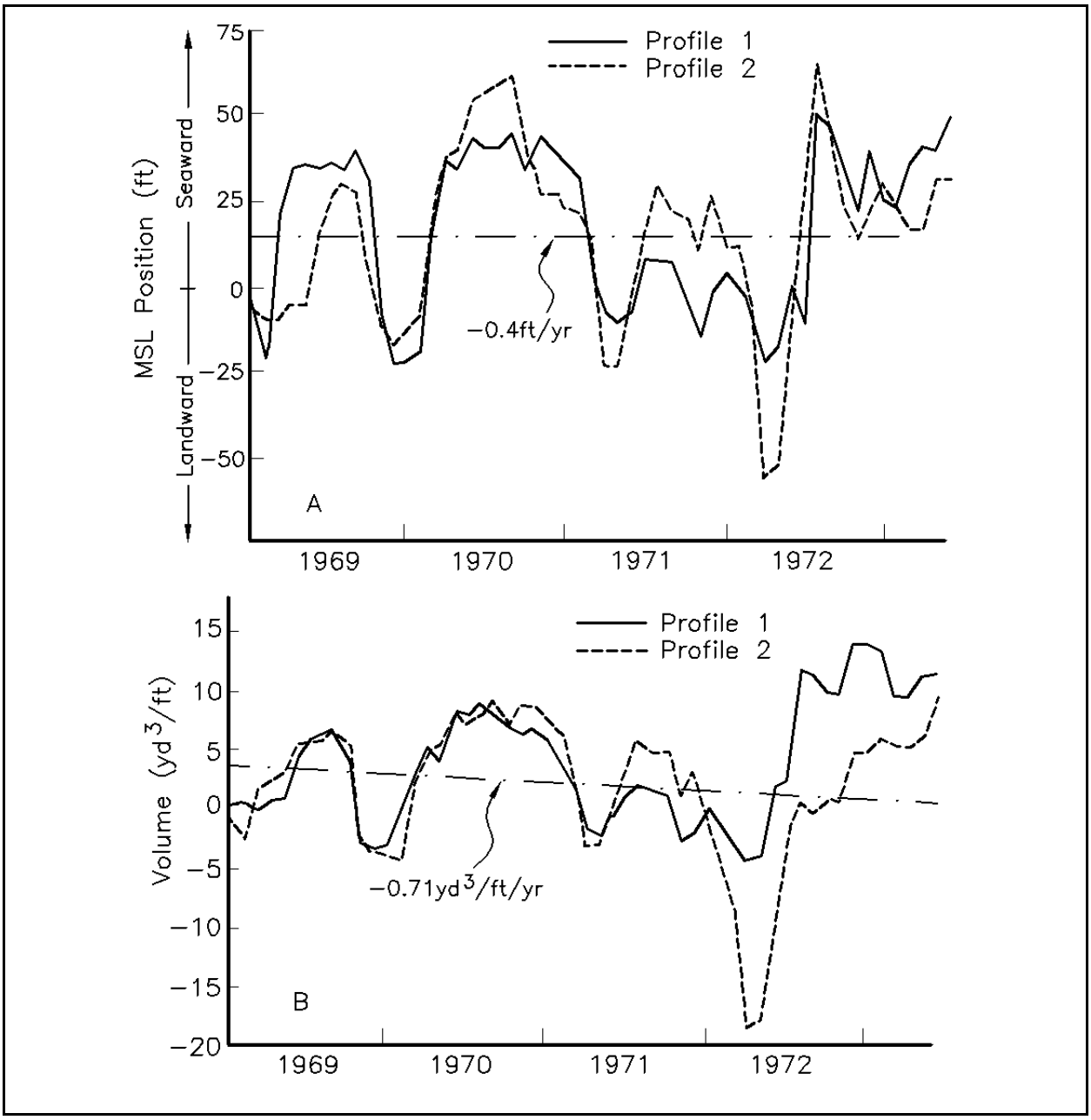

Figure III-3-30. Mean monthly shoreline position (A) and unit volume (B) at Jupiter Island, FL, referenced to first survey (Dewall and Richter 1977)

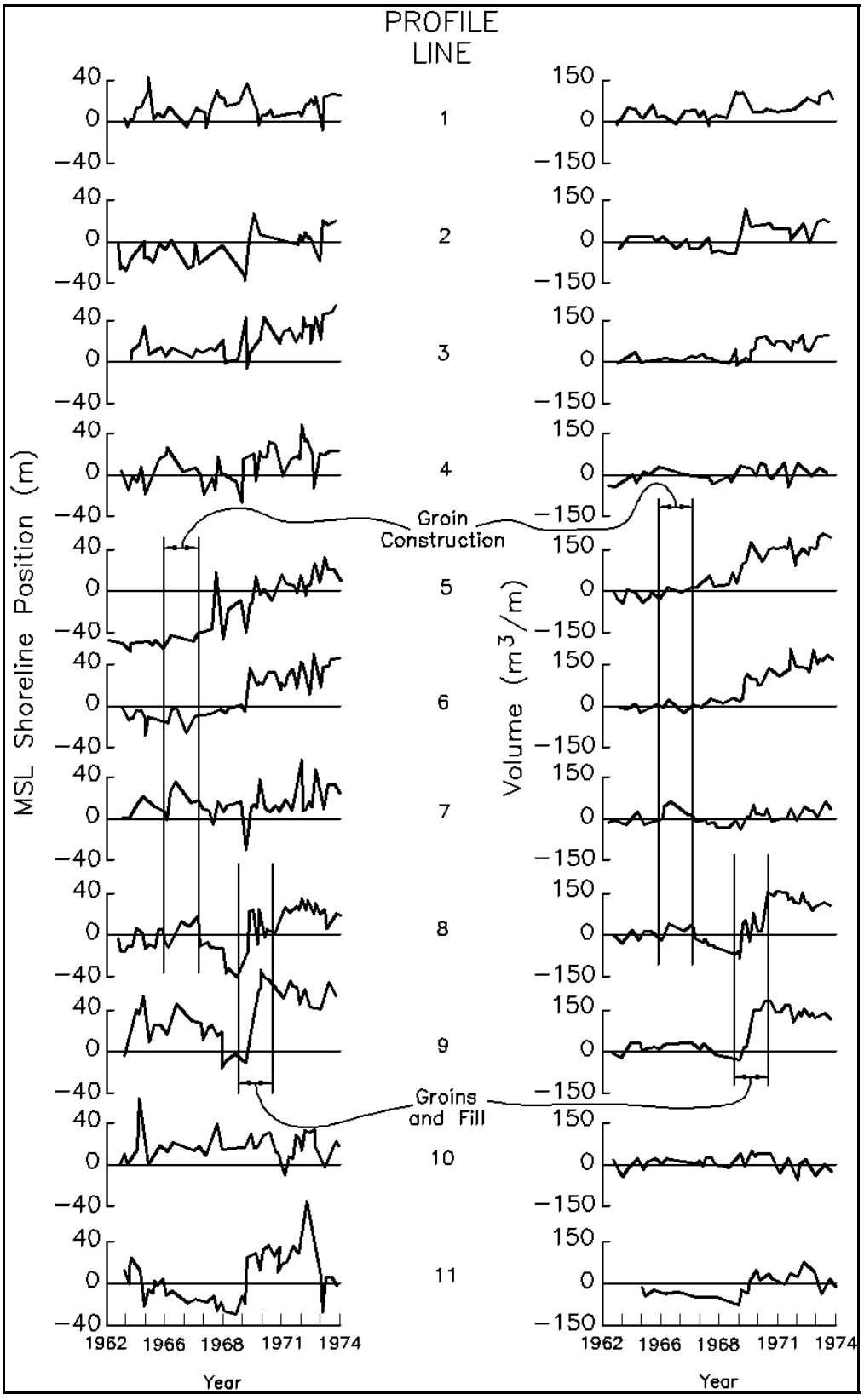

Figure III-3-31. Changes in shoreline position and unit volume at Westhampton Beach, New York (Dewall 1979)

h. Static models for shoreline response to sea level rise and/or storm effects.

(1) As water level and/or wave conditions change, the profile will respond toward a new equilibrium. If the conditions change very slowly, the profile changes will nearly maintain pace with the changed conditions and static models are applicable. However, rapidly changing conditions require dynamic models that account for the time scales of response of the profile. This section presents several useful static models for profile response.

(2) First, consider the long-term profile response to sea level rise. On a worldwide basis, the average sea level has risen approximately 12 cm during the last century. However, the relative sea level changes (difference between absolute sea level rise and vertical land movements) at a particular location can differ substantially from the average, ranging from locations at which the relative sea level (RSL) change is a rise of four times the average (Louisiana (Penland, Suter, and McBride 1987)) and locations where the RSL change is decreasing at a rate of almost 1 m per century (Alaska (Hicks, Debaugh, and Hickman 1983)). Human-induced activities can cause considerable subsidence, primarily from extraction of ground fluids and the consequent reduction of pore pressures (National Research Council 1984), and can be a reason for relative sea level changes higher than average. Uplifting due to tectonic activity is the typical reason for relative sea level changes lower than average. As noted previously, any rise in mean water level on a beach profile that is otherwise in equilibrium must result in a redistribution of sand with erosion of the foreshore and with deposition of sand offshore near the depth of closure to maintain the profile shape relative to the rising water level. In the following discussion, equilibrium profile methods are applied to determine analytical solutions for the shoreline recession, here denoted by the symbol R, which will be more convenient notation than negative values of y.

(3) Bruun (1962) proposed the following relationship for equilibrium shoreline response R_∞ to sea level rise S

$$R_\infty = S \frac{L_*}{h_* + B} \tag{III-3-33}$$

in which L_* and (h_*+B) are the width and vertical extent of the active profile and the subscript "∞" indicates a static response. The basis for this equation is seen in Figure III-3-32 in which the two components of the response are: (1) a retreat of the shoreline R_∞, which produces a sediment "yield" $R_\infty(h_* + B)$, and (2) an increase in elevation of the equilibrium profile by an amount of the sea level rise S, which causes a sediment "demand" equal to SL_*. Equating the demand and the yield results in Equation 3-33, which is known as the "Bruun Rule." It is noted that the Bruun Rule does not depend on the particular profile shape.

(4) The Bruun Rule has been modified to account for several features of natural beaches that were not accounted for in the original development. Bruun (1988), for example, shows that Equation 3-33 may be modified to account for loss or "winnowing" of fine sediment out of the profile or for loss of sediment to deepwater canyons or other "sinks" in the offshore. Similar corrections may be made to account for unbalanced sediment flux into or out of the beach profile due to gradients in the net longshore sediment transport, as shown, for example, by Everts (1985).

(5) Despite these modifications, several aspects of the Bruun Rule have remained problematic. For example, the upper limit of the active profile is not clearly defined in Figure III-3-32 so that it is difficult to establish a realistic profile width L_* in Equation 3-33. Dean and Maurmeyer (1983) later extended Bruun's result to apply to the case of a barrier island in the form

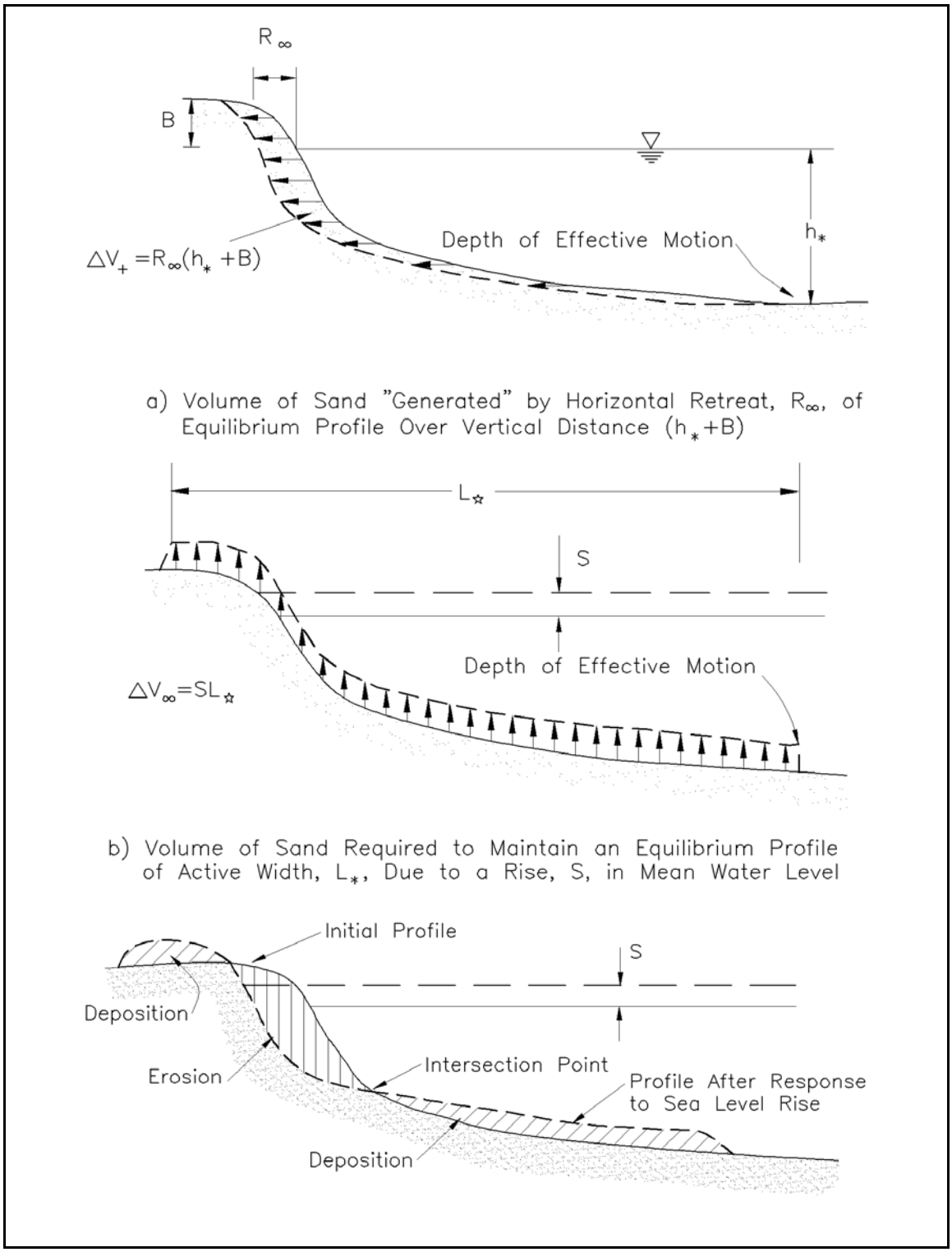

Figure III-3-32. Components of sand volume balance due to sea level rise and associated profile retreat according to the Bruun Rule

$$R_\infty = S \frac{L_* + L_W + L_L}{h_* - h_L} \tag{III-3-34}$$

and the various terms are explained in Figure III-3-33. In general, the shoreline retreat is some 50 to 200 times the sea level rise with the greater factors associated with the milder beach slopes and more energetic wave conditions (i.e., greater h_*). These factors for the case of a barrier island would be considerably greater due to the difference term in the denominator (Equation 3-34). Situations where the region behind the island is deep may explain the geological evidence for some barrier islands which are believed to have "drowned in place" rather than to have migrated landward.

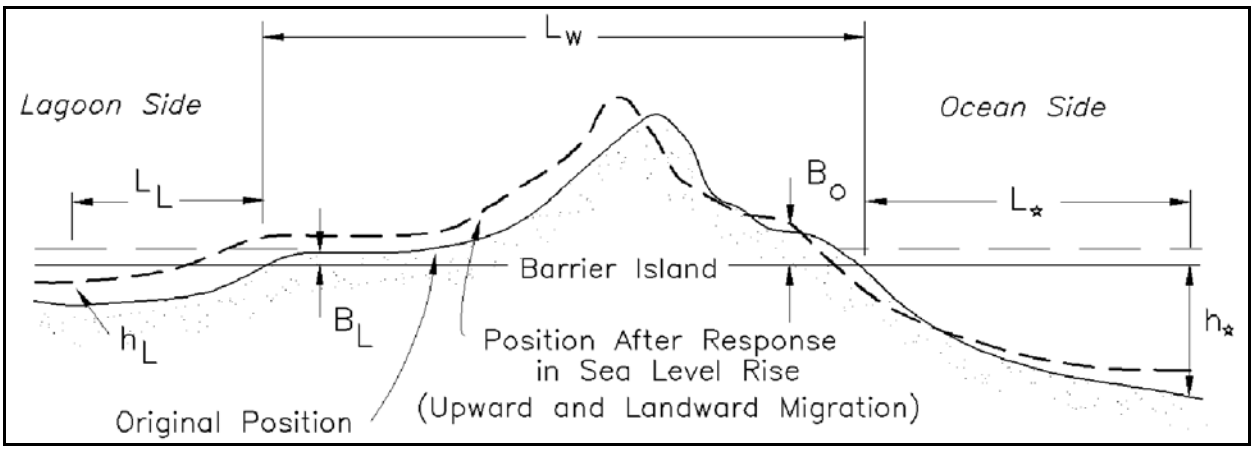

Figure III-3-33. The Bruun Rule generalized for the case of a barrier island that maintains its form relative to the adjacent ocean and lagoon (Dean and Maurmeyer 1983)

(6) The Bruun Rule has been subjected to verifications both in the laboratory and in the field. Hands (1983), evaluated the Bruun Rule in Lake Michigan using 25 beach profiles over a 50-km length of shoreline subjected to a 0.2-m water level rise over a 7-year period from 1969 to 1976. The on- and offshore limits of profile response were determined directly from measured beach profiles. Thus, the depth of closure was identified as the maximum depth of significant profile change observed from beach surveys. Likewise, the upper limit of profile change was selected as the natural vegetation line in the foredunes. With these empirical input parameters, calculated profile retreat over the 7-year period then agreed to within 10 percent of measured values. Over shorter periods of time for example, over a 3-year period, Hands found that the Bruun Rule initially over-estimated the profile response due to the time lag between elevated water levels and the profile response. Storm processes were then identified as being responsible for causing rapid equilibration of the profiles and for causing the profiles to "catch up" or equilibrate relative to the water level.

(7) Edelman (1972) modified the Bruun Rule to make it more appropriate for larger values of increased water levels and for time-varying storm surges. It was assumed that the profile maintained pace with the rising sea level and thus, at each time, the following equation is valid

$$\frac{dR}{dt} = \frac{dS}{dt}\left[\frac{W_b}{h_b + B(t)}\right] \tag{III-3-35}$$

where now $B(t)$ represents the instantaneous total height of the active profile above the current water level. As shown in Figure III-3-34, $B(t)=B_o-S(t)$ where B_o is the original berm height. For application to storm events, Edelman also adopted the breaking depth h_b (and surf zone width W_b) rather than the offshore depth of closure h_* (and corresponding W_*) as would be appropriate for long-term sea level rise. Substituting Equation 3-35 and integrating gives

$$R(t) = W_b \ln\left[\frac{h_b + B_o}{h_b + B_o - S(t)}\right] \tag{III-3-36}$$

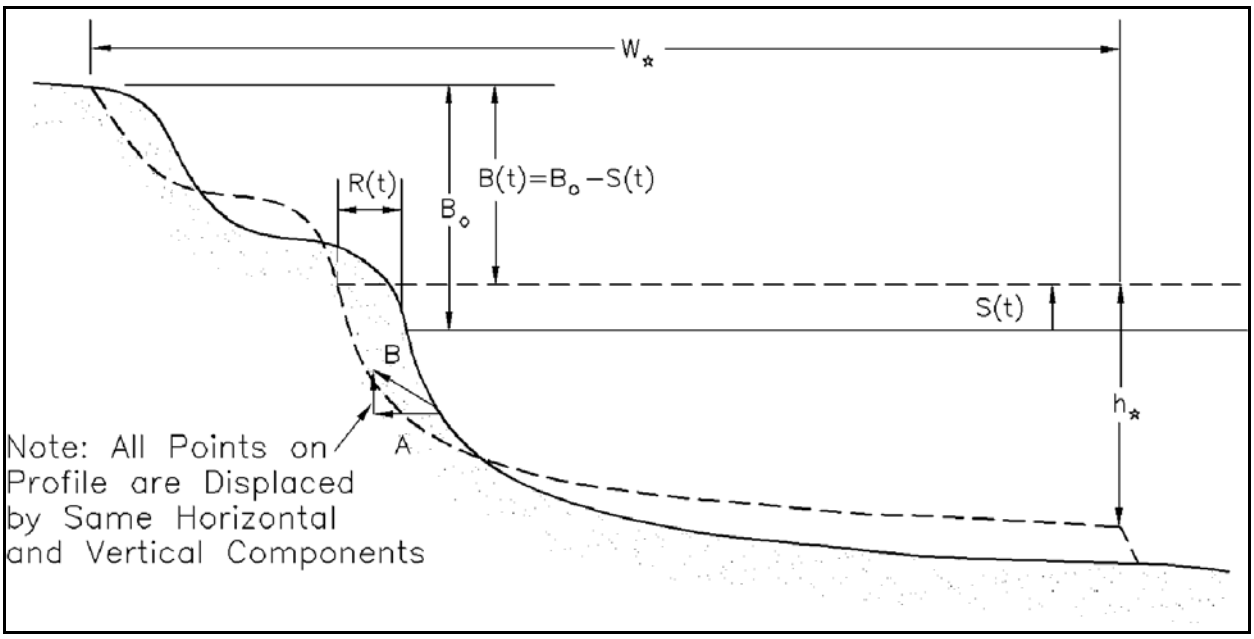

Figure III-3-34. Elements of the Edelman model

(8) Using the small argument approximation for the natural logarithm, it is readily shown that to the first approximation, Edelman's equation is equivalent to the Bruun Rule.

(9) Dean (1991) derived similar solutions for storm-induced berm retreat based on theoretical pre- and post-storm profile forms given by the equilibrium profile in Equation 3-14. Because pre- and post-storm profiles were defined by an analytical form, the equilibrium beach response could be obtained by integrating the areas (volume per unit length) between the initial and final equilibrium profiles and by equating the resulting eroded and deposited areas. Solutions were obtained for both the case of a uniform water level rise and for the case where breaking waves create a distribution of wave setup across the surf zone. One interesting result is the case where water levels are elevated by both a storm surge and by breaking-induced wave setup. For this case, an approximate solution for the steady-state erosion is given as

$$R_\infty = (S + 0.068\,H_b)\frac{W_b}{B + h_b} \tag{III-3-37}$$

where W_b is the width of the surf zone, defined for the equilibrium profile as $W_b=(h_b/A)^{3/2}$. The solution for erosion due to combined storm surge and wave setup is similar in form to the Bruun Rule in Equation 3-33. In this case, wave setup causes a general rise in water level in the surf zone so that it functions much like

storm surge. It is noted, however, that storm surge has a much larger effect than wave setup. For this reason, the other analytical solutions that follow do not include wave setup effects and, instead, assume that beach response is driven primarily by storm surge.

(10) Kriebel and Dean (1993) considered both profiles with a vertical face at the water line as shown in Figure III-3-35a and profiles with a sloping beach face as shown in Figure III-3-35b. They showed that by accounting for the small wedge-shaped sand volume offshore of the breaking depth, somewhat improved expressions could be developed for the potential beach recession due to elevated water levels. The beach profile with a vertical face is a special limiting case of the profile with a sloping beach face, thus only the results for the sloping beach face are given here. As shown by Kriebel and Dean (1993), the general result for equilibrium berm recession due to a storm surge level S is given as

$$R_\infty = S \frac{W_b - \dfrac{h_b}{m_o}}{B + h_b - \dfrac{S}{2}} \tag{III-3-38}$$

where m_o is the slope of the beach profile at the waterline. This slope is joined to the concave equilibrium profile at a depth where the slope of the equilibrium profile is equal to m_o. As a result, the surf zone width can be shown to be equal to

$$W_b = y_o + \left(\frac{h_b}{A}\right)^{\frac{3}{2}} \tag{III-3-39}$$

where y_o is a small offset of the shoreline between the sloping beach face and the imaginary or virtual origin of the equilibrium profile, given by $y_o = (4A^3)/(27m_o^3)$. For most conditions, this offset is negligible and can be neglected when estimating the surf zone width, as will be illustrated in Example Problem III-3-6. For engineering application, it is also of interest to compute the volume of sand eroded between the initial and final profiles per unit length of beach. For the case with a sloping beach face, the volume eroded from the berm above the initial still-water level due to a storm surge level S is given by

$$V_\infty = R_\infty B + \frac{S^2}{2m_o} - \frac{2}{5}\frac{S^{\frac{5}{2}}}{A^{\frac{3}{2}}} \tag{III-3-40}$$

(11) When the beach face slope becomes infinite, the solutions from Equation 3-38 for the vertical beach face depicted in Figure III-3-35a are similar to those obtained by the Bruun Rule in Equation 3-33 or by Dean (1991) in Equation 3-37. The major difference is the term S/2 in the denominator of Equation 3-38, which is the result of considering the small wedge-shaped volume of sand near the breakpoint. For more realistic beach face slopes, the results in Equation 3-38 will yield smaller estimates of the potential berm recession than the Bruun or Dean solutions, since a portion of the rise in water level is accommodated by shifting the shoreline higher on the sloping beach face and less berm retreat is then required. Kriebel and Dean (1993) also provide analytical solutions for cases where the beach profile has a distinct dune on top of the berm.

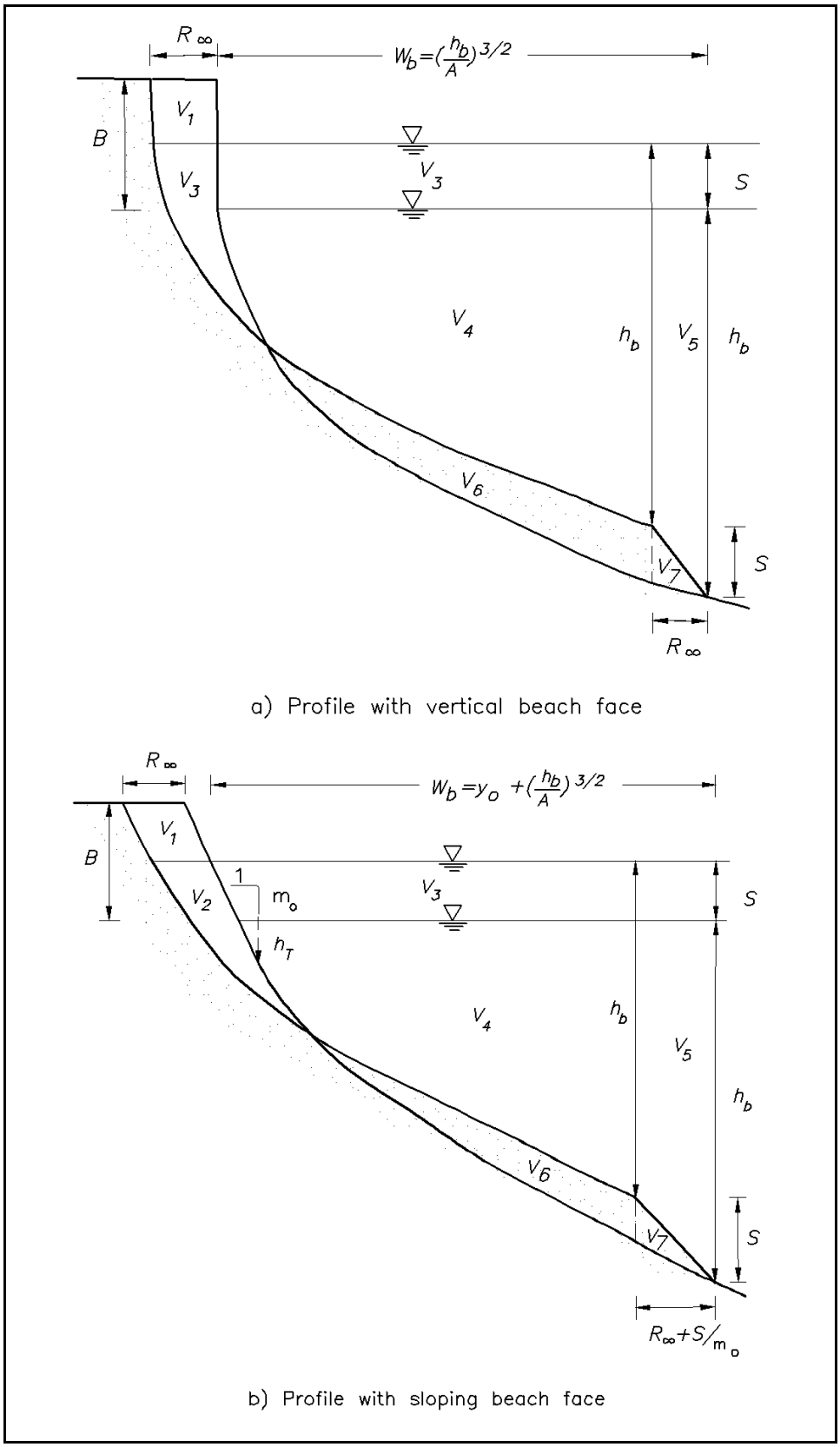

Figure III-3-35. Profile forms considered by Kriebel and Dean (1993)

EXAMPLE PROBLEM III-3-5

FIND:

The rate of shoreline retreat, according to the Bruun Rule, then find the rate at which beach nourishment would be required to maintain the shoreline position.

GIVEN:

$h_* = 6$ m, $B = 2$ m, $D = 0.2$ mm, and a rate of sea level rise of $\frac{dS}{dt} = 0.003$ m/year.

SOLUTION:

The sediment scale parameter is determined from Figure III-3-18 and/or Table III-3-3 as $A = 0.1$ m$^{1/3}$. The width W_* of the active nearshore zone is determined from Equation 3-19 as

$$W_* = \left(\frac{h_*}{A} \right)^{\frac{3}{2}} \cong 465 \text{ m}$$

and from Equation 3-33, assuming the berm stays at a constant elevation, the rate of shoreline retreat is given by

$$\frac{dR_\infty}{dt} = \frac{dS}{dt} \frac{W_*}{h_* + B} \cong 0.17 \text{ m/yr}$$

so that the ratio of shoreline retreat to sea level rise is about 58.

When considering sea level rise and beach nourishment, from Equation 3-42, the rate at which sand must be added to offset the erosion due to sea level rise is

$$\frac{dV}{dt} = W_* \frac{dS}{dt} = (465\text{m})\ (0.003\text{m/year}) \cong 1.4\text{m}^3\text{/m/year}$$

EXAMPLE PROBLEM III-3-6

FIND:

The potential berm retreat, along with the volume of sand eroded from above the mean sea level, for the storm conditions given below.

GIVEN:

Equilibrium beach profile with sand grain size D = 0.25 mm, beach face slope m_o = 0.05, and berm height B = 2 m. Storm conditions with a peak surge level S = 2 m and a breaking depth h_b = 3.0 m.

SOLUTION:

The equilibrium berm retreat may be determined from Equation 3-38, which first requires knowledge of the breaking depth h_b and the surf zone width W_b, which, from Equation 3-39, are given by $W_b = y_o + (h_b/A)^{3/2}$. From Table III-3-3, the so-called A parameter for the equilibrium beach profile is found to be A = 0.115 $m^{1/3}$ based on the grain size of 0.25 mm.

In calculating the surf zone width, the term $(h_b/A)^{3/2}$ is equal to $(3.0m/0.115m^{1/3})^{3/2}$ = 133.2 m while the small shoreline offset is given by $y_o = (4A^3)/(27m_o^3)$ = 1.8 m. The total surf zone width is then W_b = 1.8 m + 133.2 m = 135.0 m. As noted, however, the offset is negligible and could be neglected for simplicity.

From Equation 3-38, the potential berm retreat is now determined as

$$R_\infty = \frac{S\left(W_b - \frac{h_b}{m_o}\right)}{B + h_b - \frac{S}{2}} = \frac{2\left(135.0 - \frac{3.0}{0.05}\right)}{2 + 3.0 - \frac{2}{2}} = 37.5\ \text{m}$$

From Equation 3-40, the potential volume eroded from above the mean sea level datum is given by

$$V_\infty = R_\infty B + \frac{S^2}{2m_o} - \frac{2S^{\frac{5}{2}}}{5A^{\frac{3}{2}}}$$

$$= (37.5)(2) + \frac{(2)^2}{2(0.05)} - \frac{2(2)^{\frac{5}{2}}}{5(0.115)^{\frac{3}{2}}} = 57.0\ \text{m}^3/\text{m}$$

These solutions are known to generally overestimate erosion associated with severe storms. For example, Chiu (1977) compared both the Edelman and Dean methods to erosion measured after Hurricane Eloise on the Florida coast and found that both methods gave erosion estimates that were as much as a factor of 5 higher than observed. The reason for this overprediction is that these methods assume the profile responds instantly to changes in water level while they neglect the transient or time-dependent approach to equilibrium. Such equilibrium solutions are still useful from an engineering perspective since they place a conservative upper bound on the actual beach response.

(12) While these idealized analytical solutions are useful, such computations of the maximum potential response can also be performed numerically for a measured (surveyed) beach and dune profile. In this case,

it may be assumed that the existing profile is in a stable equilibrium configuration, possibly with an offshore bar. The solution for the profile response to a water level rise would then be carried out by shifting the measured profile form upward and landward until a mass balance is achieved between the sand eroded from the berm and dune and the sand deposited offshore near the breakpoint.

(13) The problem of shoreline stabilization through beach nourishment with compatible sands in an era of sea level rise may be treated by combining the two effects. The rate of shoreline retreat is given as

$$\frac{dR_\infty}{dt} = \frac{dS}{dt}\frac{W_*}{h_*+B} - \frac{1}{(h_*+B)}\frac{dV}{dt} \tag{III-3-41}$$

in which dV/dt is the rate at which sand is added per unit length of beach. In order for the shoreline retreat due to sea level rise to be offset by the advancement due to nourishment, ($dR_\infty/dt = 0$)

$$\frac{dV}{dt} = W_*\frac{dS}{dt} \tag{III-3-42}$$

which can be interpreted as adding sufficient sand to just fill the active profile of width W_* at the rate of sea level rise. This result could have been foreseen by referring to Figure III-3-32.

i. Computational models for dynamic response to storm effects.

(1) Introduction. Dynamic computational models are distinguished from the static models discussed earlier by accounting for the transient nature of the profile adjustment. As an illustration, for Example III-3-2, if the initial placement of nourished sand was different (usually steeper) than the equilibrium profile in Figure III-3-27, it is possible to determine from the equation of continuity (conservation of sand) the total cross-shore volumetric transport; however, it is not possible to determine the rate at which the sand was transported to reach equilibrium. The equilibration process could have required 1 year or a decade. In many problems of coastal engineering interest, the rates are extremely important. As examples, it will be shown that a rapidly moving storm may cause only a fraction of its erosion potential due to the relatively long time scales of the sediment transport processes and to the relatively short duration of the more energetic conditions caused by the storm. A second problem in which the time scales are of interest is that of profile equilibration of a beach nourishment project. Although it is accepted that equilibration occurs within 1 to 5 years, and certainly depends on the frequency of energetic storms, the economic value of that portion of added dry beach width associated with disequilibrium during evolution can be substantial.

(2) Numerical and analytical models. More than a dozen numerical models and at least two analytical models have been developed to represent dynamic cross-shore sediment transport processes. These models require a continuity equation and a transport (or dynamic) equation (or equivalent) that governs the rate at which the processes occur. The conservation equation balances the differences between inflows and outflows from a region as predicted by the transport equation. In addition, boundary conditions must be employed at the landward and seaward ends of the active region. These boundary conditions can usually be expressed in terms of a maximum limiting slope such that if the slope is exceeded, adjustment of the profile will occur, a condition sometimes referred to as “avalanching.” The locations of the seaward and landward boundaries are usually taken at the limits of wave breaking and wave runup, respectively. Examples of numerical models for which computer codes are available include those of Kriebel and Dean (1985), Kriebel (1986), Larson (1988), and Larson and Kraus (1989, 1990). Analytical models have been published by Kobayashi (1987), and Kriebel and Dean (1993).

(3) General description of numerical models. In numerical modelling, two representations of the physical domain have been considered as shown in Figure III-3-36. In the first type, shown in

Figure III-3-36a, the cells are finite increments of the distance variable y. Thus the distance is the independent variable and the dependent variable is depth, which varies with time. In the second type shown in Figure III-3-36b, the computational cells are formed by finite increments of the depth h. In this case, the independent variable is h and y varies with time for each h value. There is an inherent advantage of the first type since the presence of bars can be represented with no difficulties. All dynamic models require a continuity equation and a transport (dynamic) equation.

(a) Conservation equation. The conservation equation is very straightforward and for the computational cell type in Figure III-3-36a is given by

$$\frac{\partial h}{\partial t} = \frac{\partial q_y}{\partial y} \tag{III-3-43}$$

in which y and t are the independent variables. If h and t are regarded as the independent variables as in Figure III-3-36b, the conservation equation is

$$\frac{\partial y(h)}{\partial t} = - \frac{\partial q_y}{\partial h} \tag{III-3-44}$$

in which it is noted that for each depth value (h), there is an associated distance value (y).

(b) Transport relationships. Sediment transport relationships fall within the categories of "closed loop," which converge to a target profile and "open loop," which are not a priori constrained to the final (equilibrium) profile. Transport relationships of the "closed loop" type will be reviewed first.

(c) Closed loop transport relationships. One of the first closed loop transport relationships was that proposed by Kriebel and Dean (1985). Recalling that the equilibrium beach profile (EBP) represented by Equation 3-14 is consistent with uniform wave energy dissipation per unit water volume D_*, Kriebel and Dean adopted a simple transport relationship in the form

$$q_y = K'(D - D_*) \tag{III-3-45}$$

such that at equilibrium $D=D_*$, and an equilibrium profile results. The parameter K' is then used to calibrate the model by correlating the sediment transport rate to the excess energy dissipation. The transport relationship above may be modified to be consistent with a profile with beach face slope m_o

$$q_y = K''(D - D_*) + \epsilon \frac{\partial h}{\partial y} \tag{III-3-46}$$

where ϵ is an additional model parameter as suggested by Larson and Kraus (1989). In this expression, the calibration parameter K'' differs from that used in Equation 3-45, since the additional gravitational effects, represented by the slope term, assist in moving sediment offshore.

(d) Open loop transport relationships. These transport relationships depend on the detailed hydrodynamics and attempt to incorporate the actual processes more faithfully than the closed loop variety. Usually both bed load and suspended load transport components are represented based on the hydrodynamic properties averaged over a wave period. Open loop models will not be considered further in this chapter; however, an excellent review of open loop models is given by Roelvink and Broker (1993). In general, these models can be grouped according to the physical processes that are assumed to be dominant for cross-shore

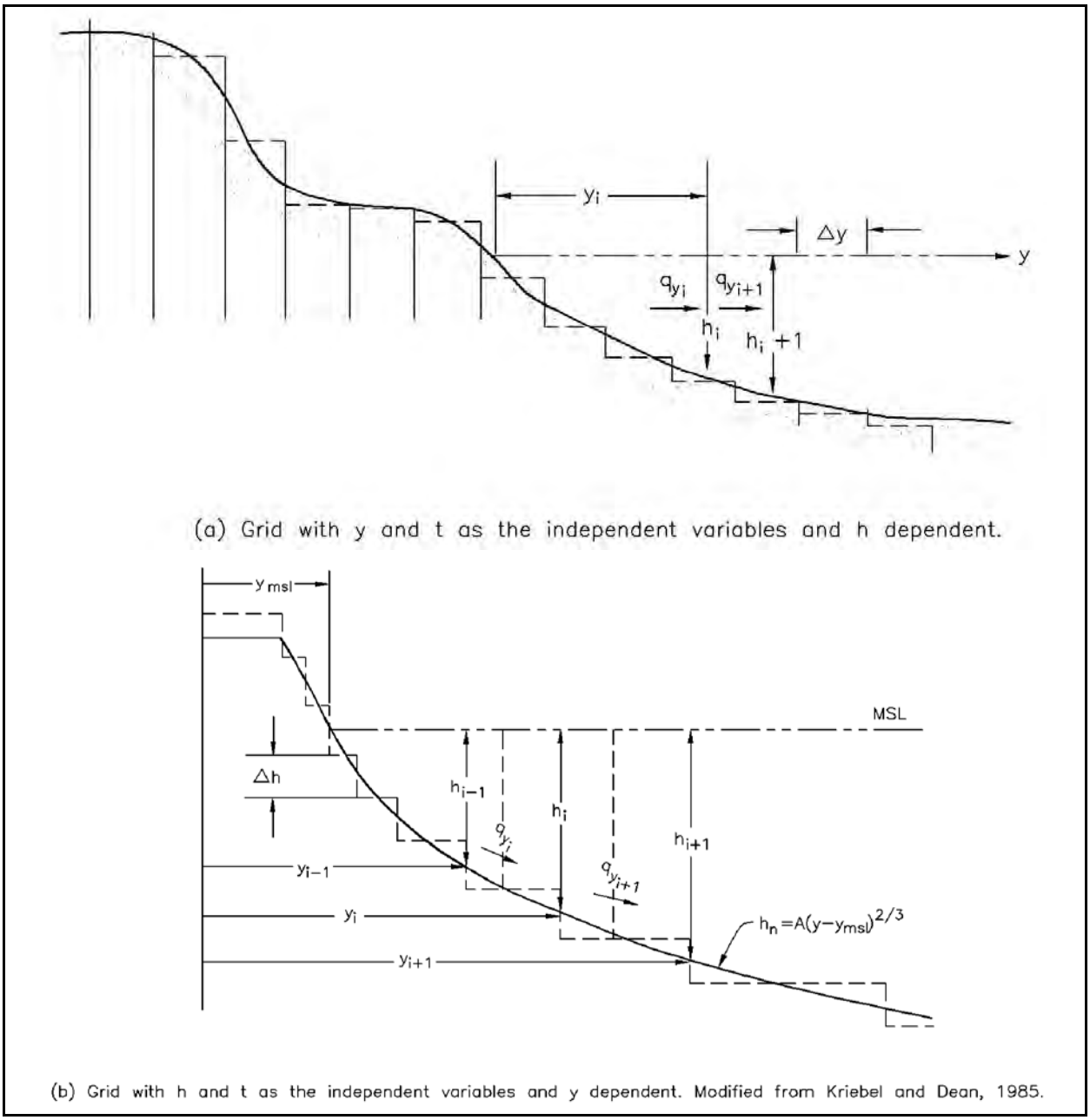

Figure III-3-36. Two types of grids employed in numerical modelling of cross-shore sediment transport and profile evolution

sediment transport. Several models compute transport rates by vertically integrating the distributions of suspended sediment concentration and cross-shore currents. Examples of such models include those of Dally and Dean (1984), Stive and Battjes (1984), and Broker-Hedegaard, Deigaard, and Fredsoe (1991). Other models consider instead that bed shear stress is the dominant forcing mechanism. An example is the model by Watanabe et al. (1980). A third widely used approach has been to compute the combined bed and suspended load transport first, based on the energetics approach proposed by Bagnold (1966). Examples of models based on this approach include those of Roelvink and Stive (1989) and Nairn and Southgate (1993).

(4) General description of analytical models.

(a) The analytical model of profile evolution by Kobayashi (1987) incorporates the conservation and transport relationships (Equations 3-41 and 3-43). The transport equation is linearized such that a diffusion equation results. The landward and seaward receding and advancing limits of the evolving profile are treated as moving boundary conditions. Kobayashi (1987) presents an analytical solution for the case of a constant elevated water level in the form of fairly complex error functions. For more complete water level scenarios, a numerical scheme must be used. As presented, the model does not lend itself readily to engineering applications.

(b) A simpler analytical model for predicting dynamic profile response during storms is the so-called Convolution Method of Kriebel and Dean (1993). This method is based on the observation that beaches tend to respond toward a new equilibrium exponentially over time. For laboratory conditions, where a beach is suddenly subjected to steady wave action, the time-dependent shoreline response $R(t)$ may be approximated by the form

$$R(t) = R_{\infty}\left(1 - e^{-\frac{t}{T_S}}\right) \tag{III-3-47}$$

where R_{∞} is the equilibrium beach response and T_S is the characteristic time-scale of the system. An exponential response of this kind has been observed in wave tank experiments by Swart (1974), Dette and Uliczka (1987), and Larson and Kraus (1989).

(c) A more general result for the dynamic erosion response may be obtained by noting that Equation 3-47 suggests that the rate of profile response is proportional to the difference between the instantaneous profile form and the ultimate equilibrium form. An approximate differential equation governing the profile response to time-dependent variations in water level may be assumed in the form

$$\frac{dR(t)}{dt} = \frac{1}{T_S}\left[R_{\infty} f(t) - R(t)\right] \tag{III-3-48}$$

where $f(t)$ represents a unit-amplitude function of time that describes the storm surge hydrograph, while R_{∞} represents the equilibrium beach response for the peak water level. The general solution to this system may be expressed as a convolution integral as

$$R(t) = \frac{R_{\infty}}{T_S}\int_0^t f(\tau)\; e^{-\frac{(t-\tau)}{T_S}}\; d\tau \tag{III-3-49}$$

(d) As a result, several important characteristics of dynamic beach profile response are evident. First, a beach has a certain "memory," so that the beach response at any one time is dependent on the forcing conditions applied over some preceding time period. As a result, the beach response will *lag* behind the erosion forcing. In addition, because of the exponential response characteristics of the beach system, the beach response will be *damped* so that the actual maximum response will be less than the erosion potential of the system.

j. Example application of an analytical model.

(1) Of the two analytical models, the Kriebel and Dean (1993) analytical model is simpler to apply and thus will be discussed and illustrated by several examples herein.

(2) A useful application of the convolution method is to analyze the erosion associated with an idealized storm surge hydrograph. Consider the case where the storm surge is approximated by the function

$$S(t) = S\sin^2(\sigma t) = S f(t) \tag{III-3-50}$$

with $\sigma = \pi/T_D$ and where T_D is the total storm surge duration. The maximum storm surge level S would be used to determine the maximum potential erosion R_∞ according to Equation 3-38 or one of the other expressions for static profile response developed in the preceding section. As shown by Kriebel and Dean (1993), solution of the convolution integral in Equation 3-49, with the unit-amplitude forcing term $f(t)$ equal to the sine-squared function, gives the following time-dependent erosion response

$$\frac{R(t)}{R_\infty} = \frac{1}{2}\left\{1 - \frac{\beta^2}{1+\beta^2}\exp\left(-\frac{2\sigma t}{\beta}\right) - \frac{1}{1+\beta^2}\left[\cos(2\sigma t) + \beta\sin(2\sigma t)\right]\right\} \tag{III-3-51}$$

where β is the ratio of the erosion time scale to the storm duration, which is given as $\beta = 2\pi T_S/T_D$. The predicted beach response is shown in Figure III-3-37 for two different values of β, corresponding approximately to a short-duration hurricane ($\beta = 10.6$) and to a long-duration northeaster ($\beta = 0.76$). The examples illustrate the role of storm duration in determining the maximum erosion response such that short-duration storms may only achieve a small percentage of their potential equilibrium response.

(3) The magnitude of the beach response from the sine-squared storm surge can be summarized in terms of the expected maximum dynamic erosion relative to the potential static or equilibrium response. This may be shown to be a function of β, as illustrated in Figure III-3-38. In general, short-duration storms fall to the right of this curve such that the predicted maximum erosion may be only 20 to 40 percent of the maximum erosion potential. For long-duration storms, the maximum erosion may be from 40 to 90 percent of the maximum erosion potential. When the storm duration is equal to the erosion time scale, ($\beta = 2\pi$), the dynamic erosion response is only 36 percent of the static response.

(4) The time scale of dynamic profile response T_S has not been as widely considered in coastal engineering as the equilibrium erosion R_∞ and, thus far, the time scale has not been derived analytically. As a result, empirical descriptions of the time scale are required. These have been developed from results of the numerical erosion model of Kriebel (1986, 1990) for various combinations of profile geometry and breaking wave conditions. From these numerical tests, it was found that the time scale was approximately independent of the storm surge level, but varied strongly with sediment size (through the A parameter) and breaking wave height, and varied less significantly as a function of beach profile geometry. Numerical results were analyzed by dimensional analysis to arrive at the following empirical relationship

$$T_S = 320\frac{H_b^{\frac{3}{2}}}{g^{1/2}A^3}\left(1 + \frac{h_b}{B} + \frac{m_o W_b}{h_b}\right)^{-1} \tag{III-3-52}$$

(5) In Figure III-3-39, the numerically generated values of the erosion time scale are plotted as a function of the expression on the right-hand side of the equation (above). In general, beaches composed of

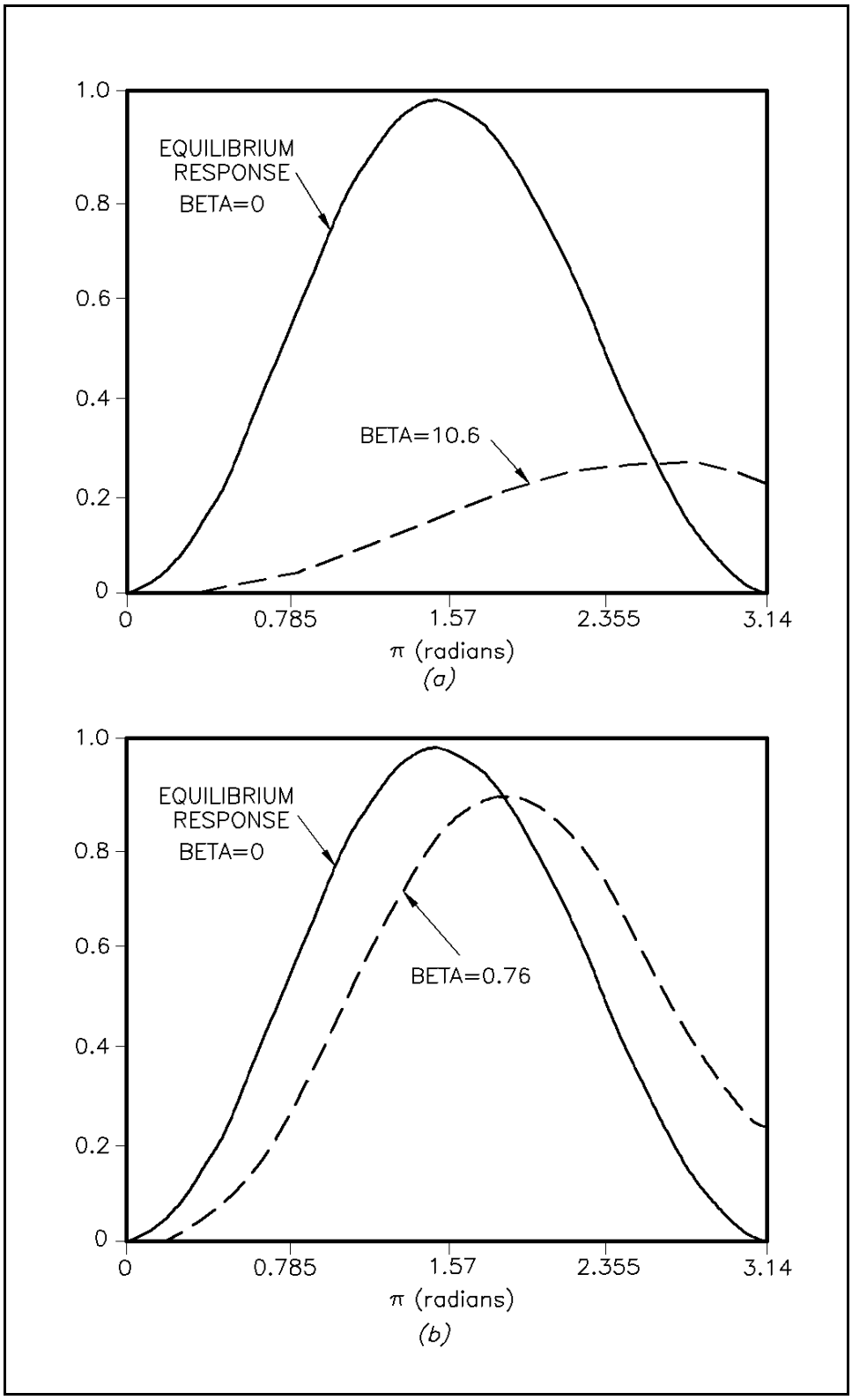

Figure III-3-37. Examples of profile response to idealized sine-squared storm surge: (a) Short-duration hurricane, and (b) Long-duration northeaster (Kriebel and Dean 1993)

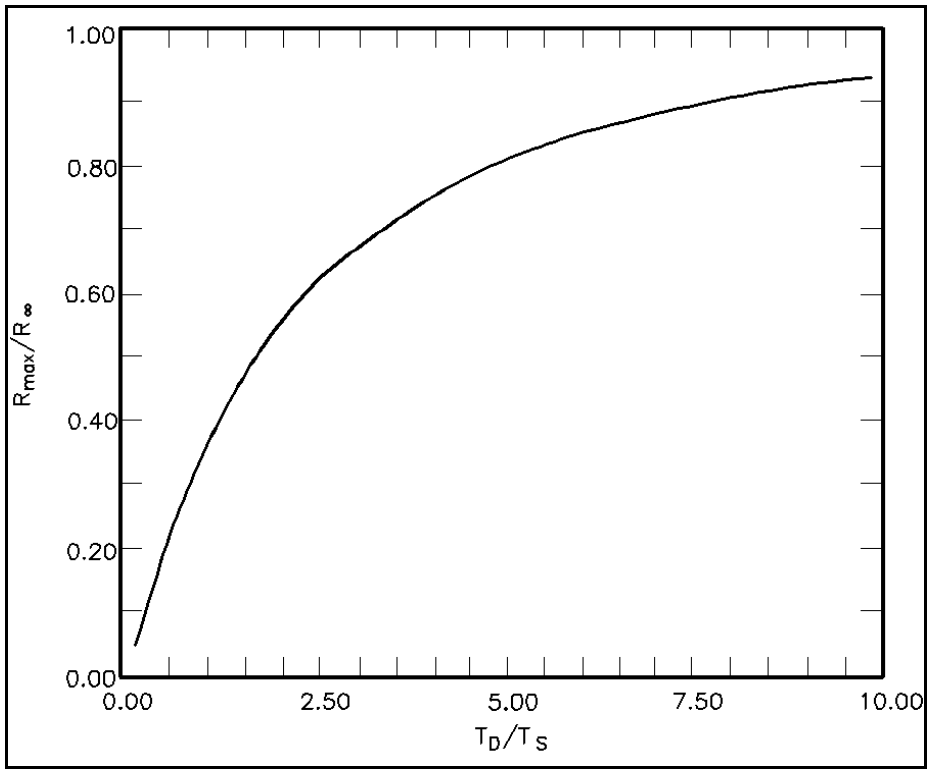

Figure III-3-38. Maximum relative erosion versus ratio of storm duration to profile time scale, T_D/T_S

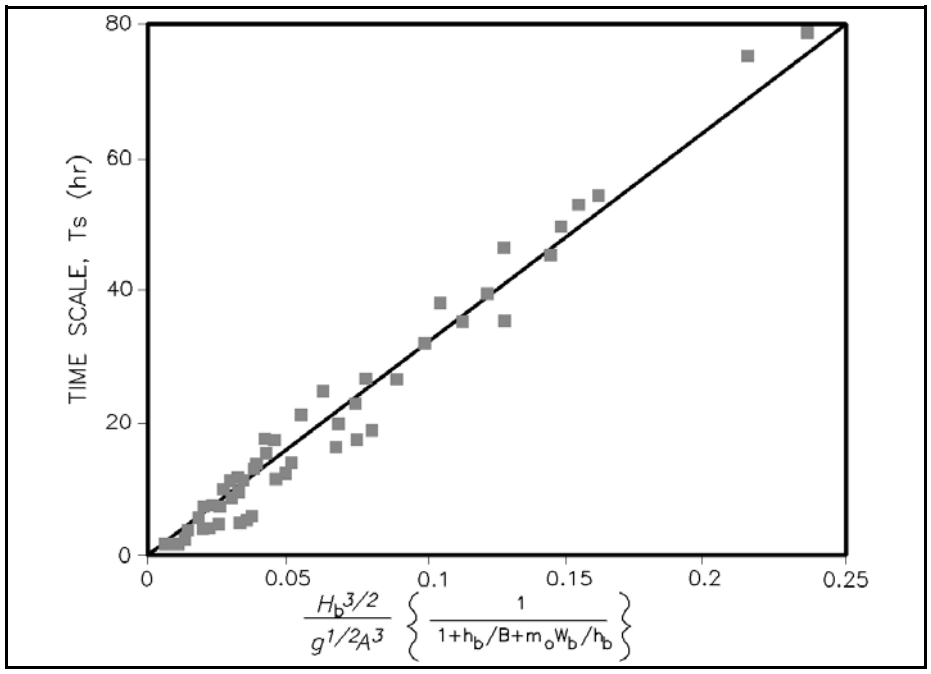

Figure III-3-39. Empirical relationship for determination of erosion time scale, T_s

EXAMPLE PROBLEM III-3-7

FIND:

The shoreline recession, $R(t)$, as a function of time and quantify the maximum erosion, R_{max}.

GIVEN:

H_b = 3 m, h_b = 3.85m, D = 0.2 mm, B = 2 m, m_o = 1:10, T_D = 10 hr, and S_{max} = 1.5 m.

SOLUTION:

As in previous examples, the value of the profile scale parameter is determined from Figure III-3-18 and/or Table III-3-3 as 0.1 $m^{1/3}$. The active width of the surf zone W_b is calculated from Equation 3-19 as

$$W_b = \left(\frac{h_b}{A}\right)^{3/2} = \left(\frac{3.85}{0.1}\right)^{3/2} = 238.9 \text{ m}$$

The equilibrium value of the shoreline response based on the maximum water level S_{max} is determined from Equation 3-38 as

$$R_\infty = \frac{S\left(W_b - \frac{h_b}{m_o}\right)}{B + h_b - \frac{S}{2}}$$

$$= \frac{1.5\left(238.9 - \frac{3.85}{0.1}\right)}{2 + 3.85 - \frac{1.5}{2}} = 58.9 \text{ m}$$

The morphological time scale T_s is determined from Figure III-3-39 by calculating the value of the abscissa in Figure III-3-39 as

$$\frac{H_b^{3/2}}{g^{1/2}A^3}\left(\frac{1}{1 + \frac{h_b}{B} + \frac{m_o W_b}{h_b}}\right)$$

$$\frac{3^{3/2}}{(9.8)^{1/2}(0.1)^3}\left(\frac{1}{1 + \frac{3.85}{2} + \frac{(0.1)(238.9)}{3.85}}\right)$$

$$= 181.8 \text{ sec} \cong 0.053 \text{ hr}$$

(Continued)

Example Problem III-3-7 (Concluded)

The morphological time scale is determined from Figure III-3-39 to be approximately 17.0 hr. The time-varying shoreline recession is determined from Equation 3-49 and is presented in Figure III-3-40. The maximum erosion can be determined from Equation 3-49 or directly from Figure III-3-40 as R_{max}/R_{∞} = 0.236 or R_{max} = 13.9 m.

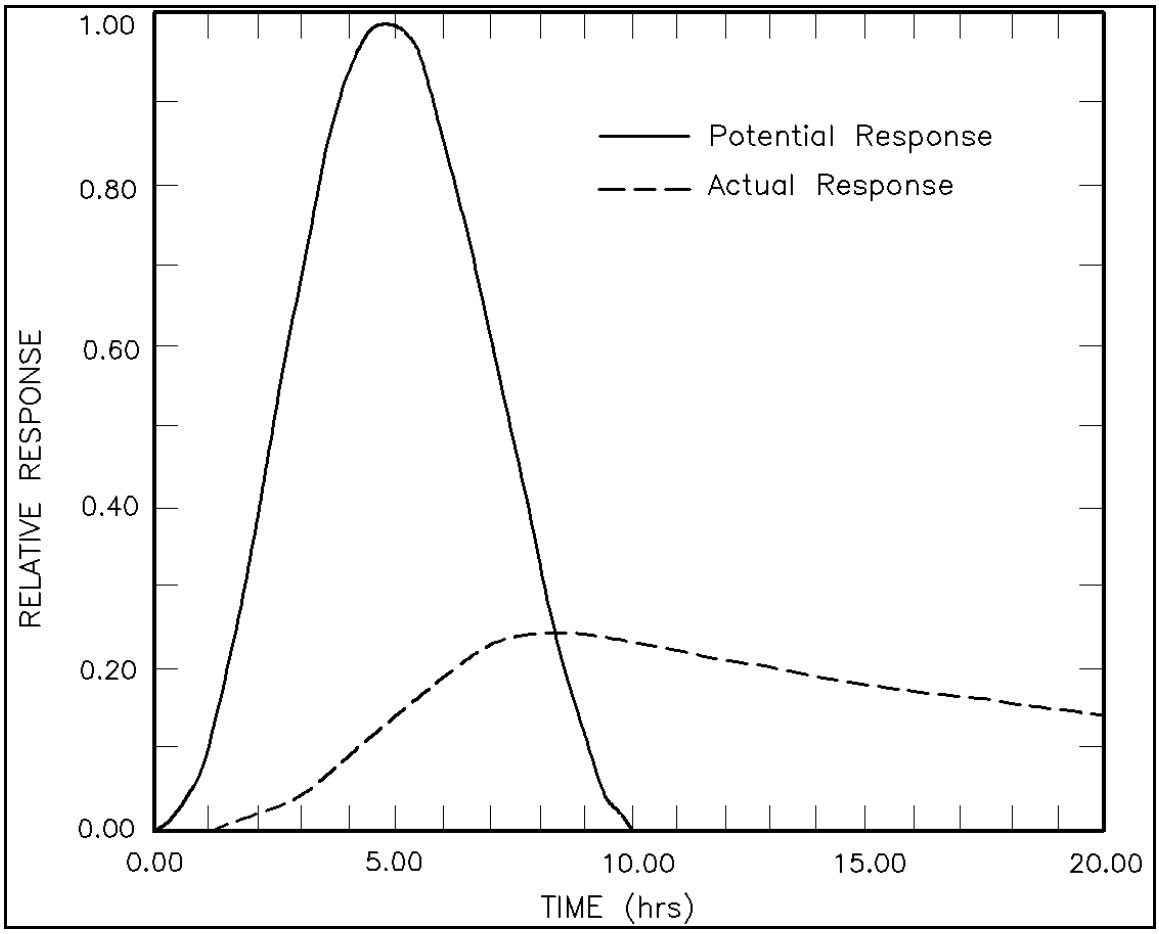

Figure III-3-40. Potential and actual shoreline response based on Kriebel and Dean (1993) model

very fine sand, subjected to very large breaking wave heights, have extremely long time scales such that they will experience only a small percentage of their equilibrium erosion potential during a typical storm.

k. Examples of numerical models.

(1) The numerical model described by Kriebel and Dean (1985) and later Kriebel (1986, 1990), was the first widely used numerical model developed to simulate storm-induced erosion based on equilibrium beach profile concepts. This model assumes that a beach profile will evolve toward an equilibrium form in response

to changing water levels and wave conditions and that the sediment transport rate is proportional to the "disequilibrium" existing between the profile at any instant in time and the equilibrium profile form.

This is quantified in terms of the "excess" energy dissipation per unit volume in the surf zone, as given by Equation 3-45. The energy dissipation per unit volume at any location in the surf zone is given by

$$D_* = \frac{1}{h}\frac{\partial (EC_g)}{\partial y} \approx \frac{5}{16}\rho g^{\frac{3}{2}} \kappa^2 \, h^{\frac{1}{2}} \frac{\partial h}{\partial y} \tag{III-3-53}$$

where the last form is based on the assumption of shallow-water breaking waves. Based on the equilibrium beach profile given by Equation 3-14, the equilibrium energy dissipation per unit volume is given by

$$D_* = \frac{5}{24}\rho g^{\frac{3}{2}} \kappa^2 \, A^{\frac{3}{2}} \tag{III-3-54}$$

where the equilibrium profile parameter A is determined either from the sediment grain size, as suggested in Table III-3-3 or from a best-fit of the equilibrium profile equation $h = Ay^{2/3}$ to the measured beach profile.

(2) The numerical solution for profile response is based on a finite difference solution to the sediment conservation equation given in Equation 3-44. In this case, the profile is gridded in a "stair-step" form as shown in Figure III-3-36(b) so that erosion or accretion (retreat or advance) of each elevation contour is determined by vertical gradients in the sediment transport rate. At each time-step, the local depth h in Equation 3-53 is the depth to the sand bed below the time-varying storm surge. As a result, beach profile change is driven primarily by changes in water level associated with storm surge. Breaking waves are treated very simply by shallow-water, spilling-breaker assumptions and, as a result, have a secondary effect on profile response. In effect, the breakpoint serves to separate the two main computational domains in the model: the offshore region, where the sediment transport rate is assumed to equal zero, and the surf zone, where the transport rate is given by Equation III-3-45.

(3) In this model, an increase in water level due to storm surge allows waves to break closer to shore, thus temporarily decreasing the width of the surf zone and increasing the energy dissipation per unit volume above the equilibrium level. According to Equation III-3-45, this leads to offshore directed sediment transport, the gradients of which cause erosion of the foreshore, deposition near the breakpoint, and an overall widening of the profile toward a new equilibrium form. At each time-step in the finite-difference solution, the profile responds toward equilibrium, but this is rarely, if ever, achieved due to the limited storm durations.

(4) The transport relationship used in the Kriebel and Dean model, given by Equation 3-45, requires calibration of a single empirical parameter K'. Kriebel (1986) first determined this parameter from numerical simulations of both large wave tank tests and hurricane-induced beach profile change as observed in Hurricane Eloise on the Gulf Coast of Florida. Figure III-3-41 shows numerical profile development along with results of large wave tank tests of Saville (1957). This illustrates the time-dependent profile development. It is noted that in the offshore region near the breakpoint, numerical results appear reasonable; however, the model does not simulate bar and trough features. For the Hurricane Eloise data, one profile was calibrated and the calibrated model was then applied to 20 additional profiles. Overall results showed that the model was capable of predicting the volume eroded from the dune to within about 25 to 40 percent, with little bias toward either under- or overestimating the volume eroded. Figure III-3-42 shows numerical model simulation of a long-duration extra-tropical storm from Point Pleasant, New Jersey. In these cases, measured

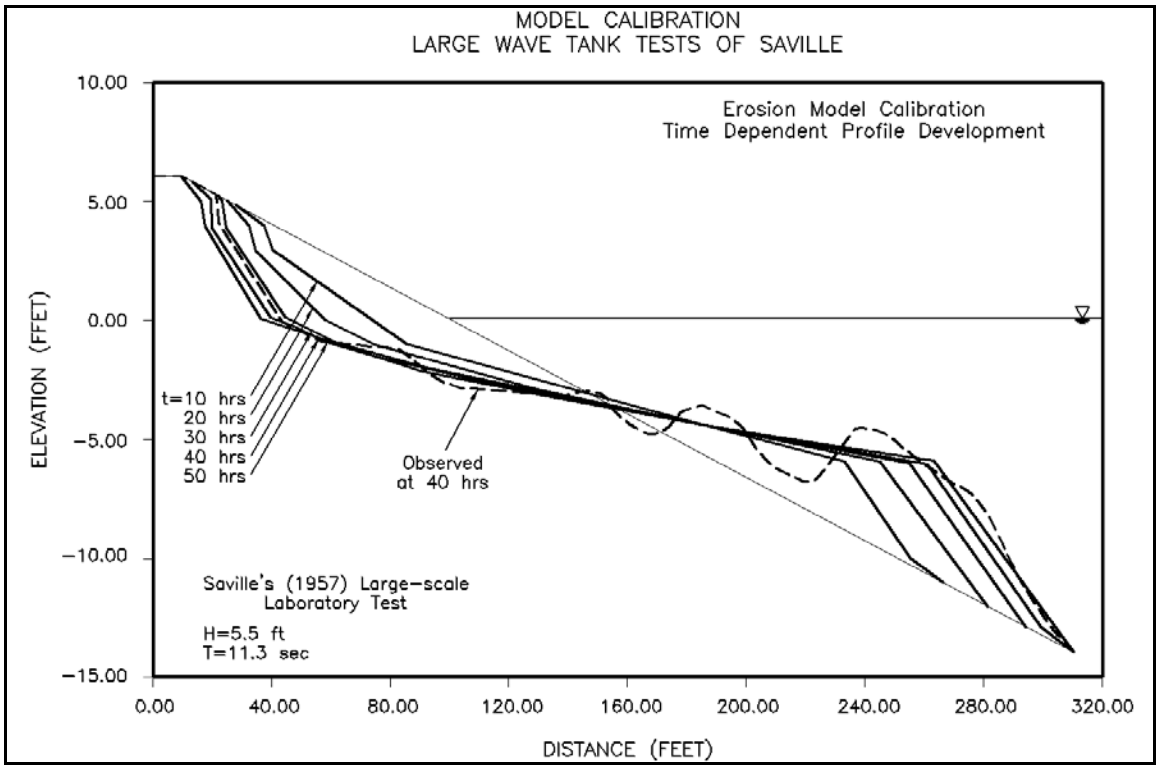

Figure III-3-41. Example of Kriebel and Dean erosion model calibration using large-wave tank data of Saville (1957) (from Kriebel 1990)

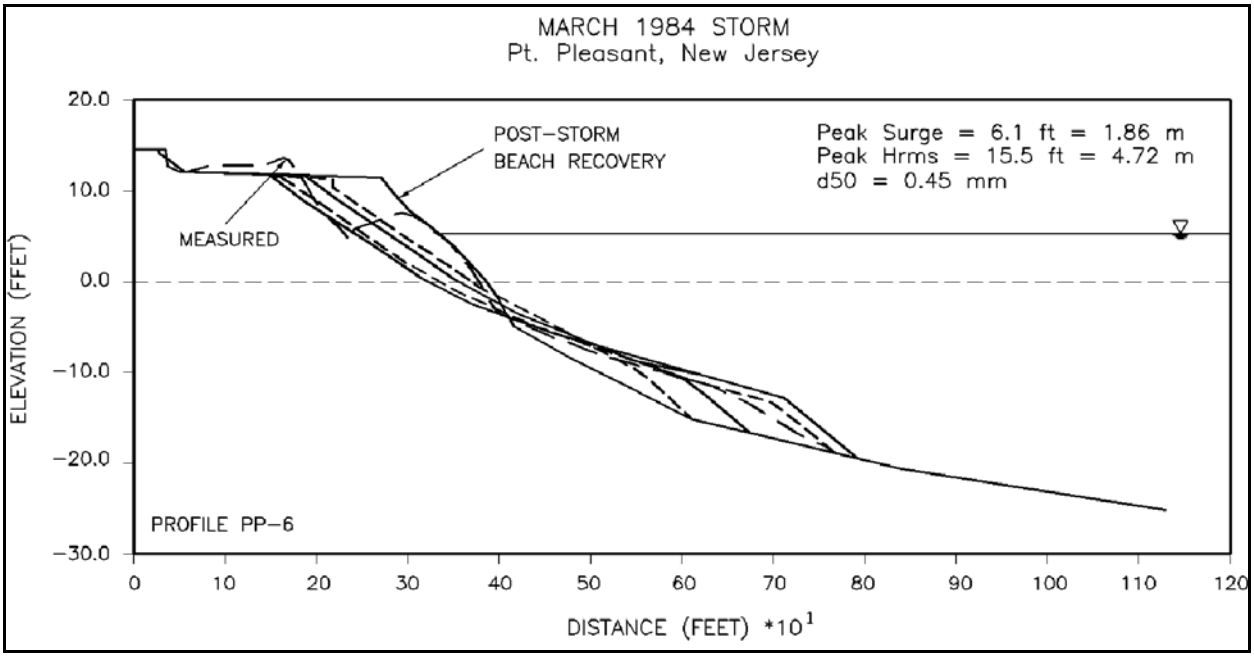

Figure III-3-42. Comparison of Kriebel and Dean erosion model to measured profiles from northeast storm at Point Pleasant, NJ (from Kriebel 1990)

post-storm profiles show evidence of post-storm beach recovery, which is not predicted in the numerical model.

An earlier version of the Kriebel and Dean model is provided in the ACES software package (Leenknecht, Szuwalski, and Sherlock 1992).

(5) The numerical model by Larson (1988) and Larson and Kraus (1989, 1990), SBEACH, is conceptually similar to the model of Kriebel and Dean (1985) but contains a more detailed description of breaking wave transformation and sediment transport across the beach profile, especially near the breakpoint. This model approximates the equation for conservation of sand in Equation 3-43 in finite difference form based on the profile gridding depicted in Figure III-3-36(a). Thus, vertical changes in water depth are determined by horizontal gradients in sediment transport rate. In contrast to the Kriebel and Dean model, this allows simulation of breakpoint bar formation and evolution.

(6) In the Larson and Kraus model, sediment transport rates in the surf zone are generally determined by Equation 3-46 in terms of excess energy dissipation, but with an additional effect of the local bottom slope. Because of this additional term, Equation 3-46 requires calibration through adjustment of two parameters, K'' and ϵ. The breaking wave model employed in the Larson and Kraus model is more sophisticated than that used by Kriebel and Dean, and is based on the breaking wave model of Dally, Dean, and Dalrymple (1985). This breaking wave model introduces gradients in the breaking wave height and energy dissipation that, in turn, lead naturally to gradients in sediment transport that produce bar/trough formations. Because of this improved breaking wave model, beach profile changes can be driven by changes in wave conditions, in addition to changes in water level.

(7) The computational domain used in the Larson and Kraus model is divided into four regions across the beach profile and the exact sediment transport relationship is adjusted somewhat for each of the four regions. In the surf zone, which is the major region for cross-shore sediment transport in the model, transport directions are first determined from the following critical value of wave steepness

$$\frac{H_o}{L_o} > \text{or} < 0.0007\left(\frac{H_o}{w_f T}\right)^3 \tag{III-3-55}$$

which is recognized as Equation 3-30 presented earlier. At each time-step in the solution, if the actual value of wave steepness exceeds the critical value given above, then transport is directed offshore over the entire active profile. Transport is then onshore if wave steepness is smaller than this critical value. Transport magnitudes in the surf zone are then determined by Equation 3-44, although the transport is "turned off" if the wave energy dissipation is below a critical value since this might cause a reversal in transport direction in conflict with the transport direction determined from wave steepness. It is noted, however, that the relationship determining transport direction (Equation 3-53) does not include any of the profile characteristics. In some cases where the profile is very steep, as may occur after beach nourishment, for example, the transport direction utilized in the model may be onshore based on wave and sediment characteristics whereas the actual transport would likely be offshore, even under mild wave conditions, due to the artificially high profile slope.

(8) The Larson and Kraus model has been compared with laboratory and field data as shown in Figures III-3-43 and III-3-44. Figure III-3-43 presents results for the two sets of available large-scale wave tank data. The upper panel shows a comparison from the Saville (1957) data and the comparisons include calculations at various times and the measured profile at 40 hr. The lower panel is for data from the Japan large tank and presents calculations at various times and the measured profile at 30-1/2 hr. The calculations

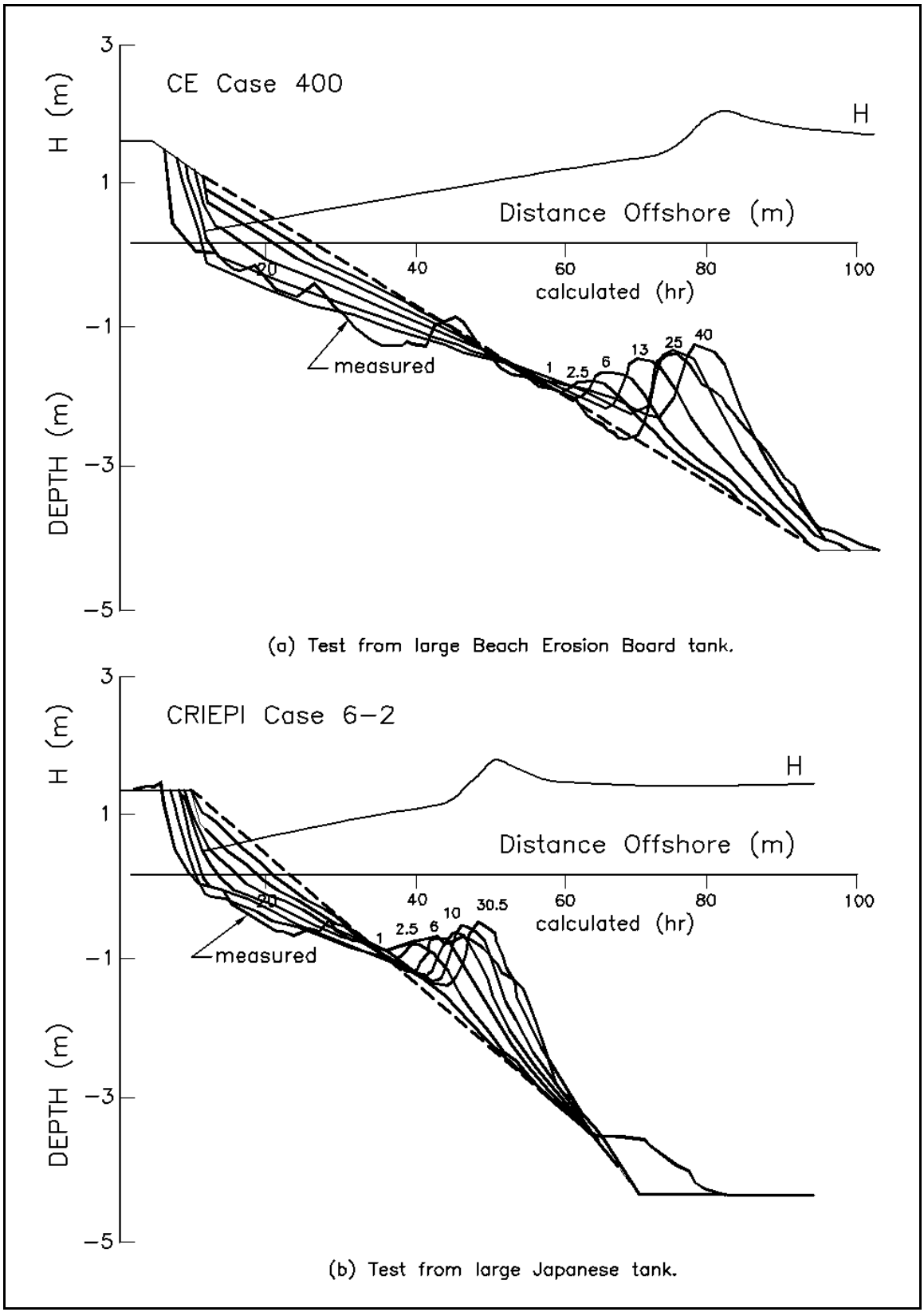

Figure III-3-43. SBEACH compared to two tests from large-scale wave tanks (Larson and Kraus 1989)

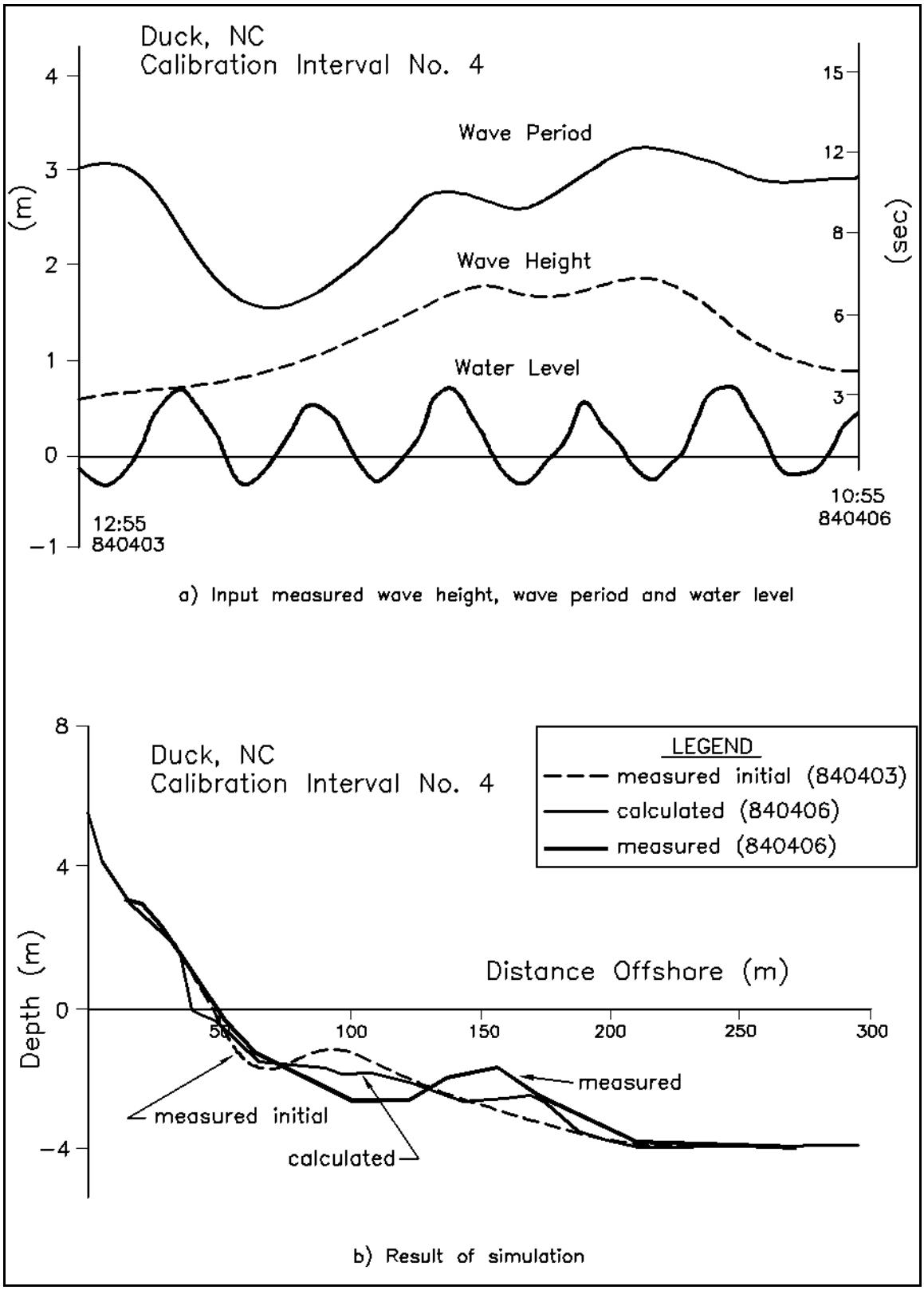

Figure III-3-44. SBEACH tested against profile evolution data from Duck, NC (Larson and Kraus 1989)

are in quite good agreement with the data. The regular waves used in these tests were monochromatic, which tend to favor the well-developed and concentrated bars that are simulated quite well by the numerical model. Figure III-3-44, from Duck, NC, compares the evolution of a profile over a 3-day period in which the wave heights were on the order of 1.5 m. The initial profile included a bar located approximately 40 m from shore. During the period of interest, the bar migrated seaward approximately 65 m. The simulations provide a reasonable qualitative representation of the evolution. The bar becomes more subdued at its initial location, but in contrast to measurements , is still present at the final time. Also, the bar had started to emerge slightly seaward of the measured location. The calculations showed substantially greater erosion at the shoreline than measured. This example demonstrates the extreme difficulty in simulating an actual event in nature. In the SBEACH model, sediment transport rates from Equation 3-46 require calibration through adjustment of two parameters, K' and ϵ.

l. Physical modeling of beach profile response.

(1) Physical modeling of beach profile response is carried out with the model being a scaled version of the prototype. In recent years, physical modelling of profiles has been employed predominantly as a research method to understand transport processes rather than as a means to investigate profile response to a particular scenario of water level and wave conditions. The ratio of quantities in the model to those in the prototype is termed the "scale ratio" and will be designated here by a subscript "*r*." For example, the length and wave period ratios would be L_r and T_r, respectively. In some models, it is appropriate to utilize a distorted model in which the vertical scale ratio is different from that of the horizontal scale. Modelling of cross-shore sediment transport requires the determination of the appropriate scaling relationships for both the waves and sediments. Hughes (1994) presents a complete discussion of scaling laws as applied to predicting cross-shore sediment transport.

(2) Noda (1972) carried out a study of profile modelling and has found that distorted models were appropriate. The horizontal and vertical scale ratios were recommended as

$$D_r \, (S_r)^{1.85} = h_r^{0.55} \tag{III-3-56}$$

$$l_r = h_r^{1.32} \, S^{-0.386} \tag{III-3-57}$$

in which D_r is the grain size ratio, s_r is the submerged specific weight ratio, $s_r = ((\rho_s - \rho)/\rho)_r$ in which ρ_s and ρ are the mass density of sediment and water, respectively, l_r is the horizontal length scale, and h_r is the vertical length ratio. Figure III-3-45 presents Noda's recommended scaling relationships. Usually sand is the common material in both the model and prototype, ρ_s = 2650 kg/m^3, and Equation III-3-56 and III-3-57 become

$$D_r = h_r^{0.55} \tag{III-3-58}$$

and

$$l_r = h_r^{1.32} \tag{III-3-59}$$

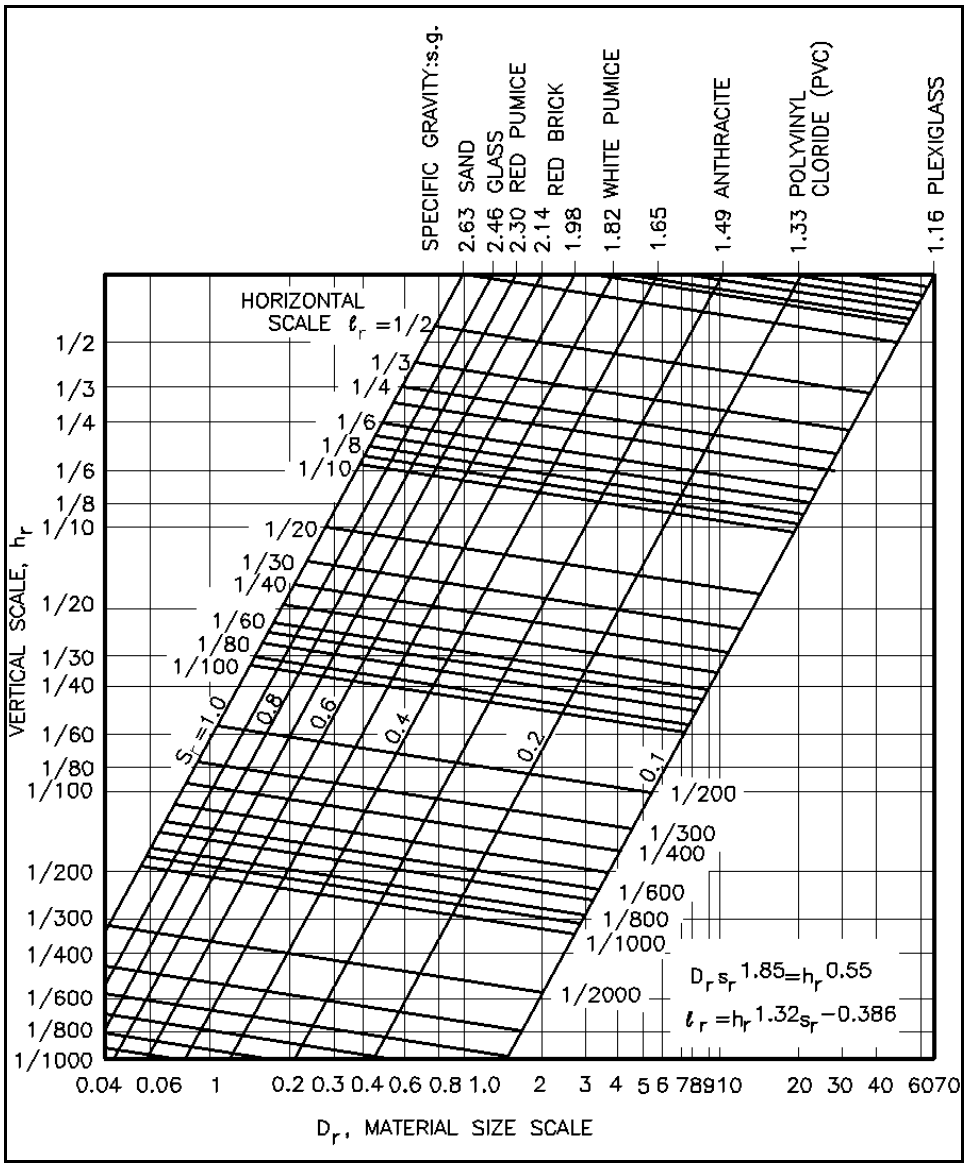

Figure III-3-45. Noda's recommendation for profile modeling (Noda 1972)

(3) Thus, according to Noda's relationships, the diameter would be scaled in accordance with the depth ratio; however, the scaling factor for diameter would be closer to unity than that for the depth ratio and the length ratio would be smaller than the depth ratio. This type of distortion is common for hydraulic models in which it is necessary to represent a large horizontal extent.

(4) Dean (1973) carried out a study of conditions that would lead to bar formation and suggested that the fall time of a sediment particle suspended at the wave crest phase position relative to the wave period would be relevant in modelling applications. This led Dean (1973, 1985) to identify the following combination of parameters which should be maintained the same in model and prototype

$$\frac{H}{w_f T} \tag{III-3-60}$$

(5) This combination of terms will be termed herein as the "Fall Velocity Parameter" (FVP). It was further suggested that an appropriate model for cross-shore sediment transport is one based on undistorted Froude modelling for the wave characteristics and one that maintains the FVP the same in the model and prototype. This simple approach leads to the following requirement for scaling the sediment fall velocity w_f

$$(w_f)_r = \sqrt{L_r} \tag{III-3-61}$$

which is the standard relationship for velocity scaling for a Froude model.

(6) Evaluation of cross-shore modelling according to the FVP has been carried out by Vellinga (1983), Kriebel, Dally, and Dean (1986) and Hughes and Fowler (1990). Each of these studies concluded that the FVP was effective in scaling the erosion process. Figures III-3-46 and III-3-47, from Kriebel, Dally, and Dean (1986) and Hughes and Fowler (1990), compare different scales while maintaining the same FVP in model and prototype. Considering the FVP as valid leads to the following valuable transport relationship for numerical models

$$q_r = L_r^{\frac{3}{2}} \tag{III-3-62}$$

(7) One limitation for scaling by the FVP is that the length ratio L_r and the prototype diameter can result in designated model sediments so small that cohesive forces would be significant. Although there are no strict guidelines for a minimum sediment size, values smaller than approximately 0.08 to 0.09 mm should be avoided.

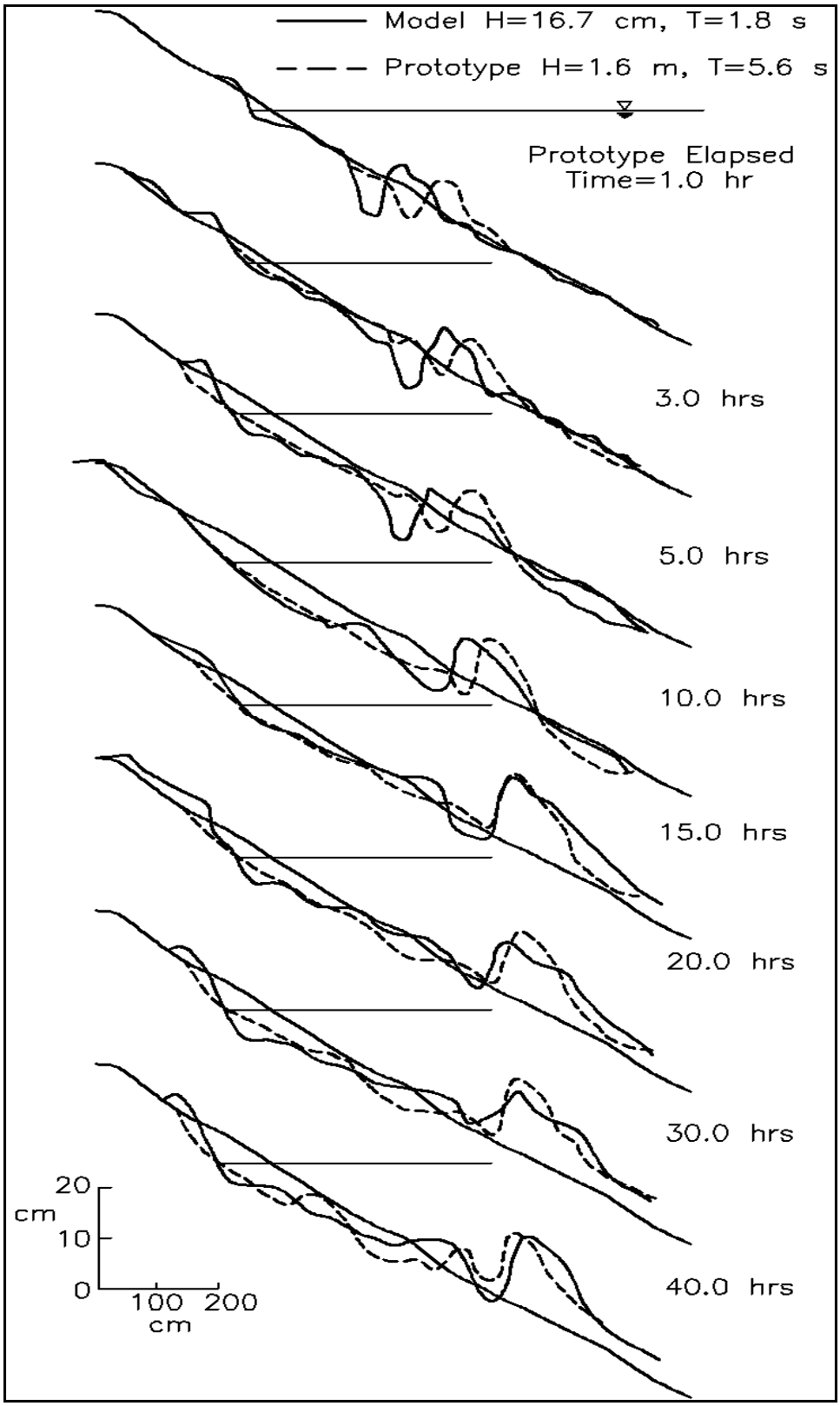

Figure III-3-46. Profile evolution by small- and large-scale wave tank tests. Based on maintaining the same fall velocity parameter. Length ratio = 1:9.6 (Kriebel, Dally, and Dean 1986)

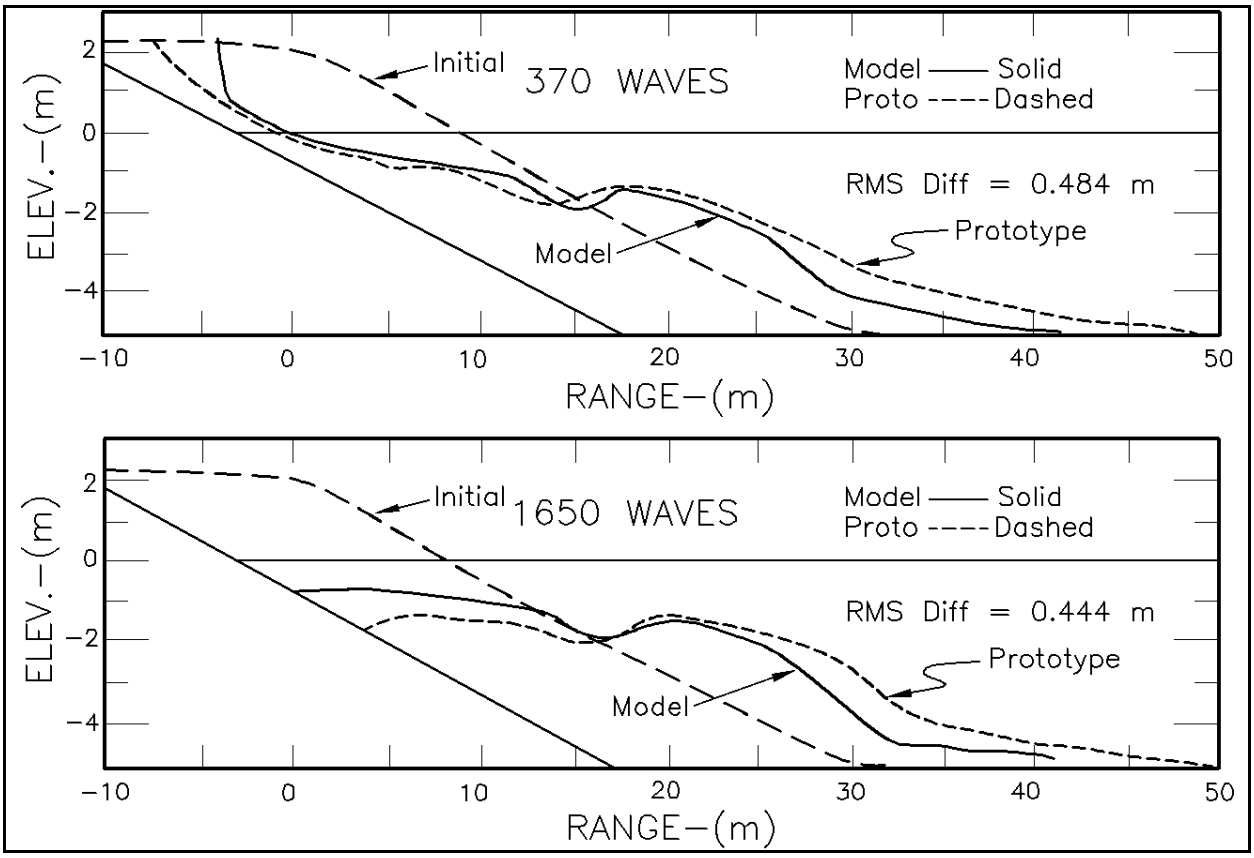

Figure III-3-47. Profile evolution by small- and large-scale wave tank tests. Case of sloping seawall. Based on maintaining the same fall velocity parameter. Length ratio = 1:7.5 (Hughes and Fowler 1990)

III-3-4. References

Bagnold 1940
Bagnold, R. A. 1940. "Beach Formation by Waves: Some Model Experiments in a Wave Tank," *Journal of the Institution of Civil Engineers,* Vol 15, pp 27-52.

Bagnold 1966
Bagnold, R. A. 1966. "An Approach to the Sediment Transport Problem from General Physics," U.S. Geological Survey Professional Paper 422-I, U. S. Dept of Interior.

Bailard 1981
Bailard, J. A. 1981. "An Energetics Total Load Sediment Transport Model for a Plane Sloping Beach," *Journal of Geophysical Research*, Vol 86, No. C11, pp 10938-10954.

Barnett and Wang 1988
Barnett, M., and Wang, H. 1988. "Effects of a Vertical Seawall on Profile Response," American Society of Civil Engineers, *Proceedings of the Twenty-first International Conference on Coastal Engineering,* Chapter 111, pp 1493-1507.

Birkemeier 1984
Birkemeier, W. A. 1984. "Time Scales of Nearshore Profile Change," *Proceedings, 19th International Conference on Coastal Engineering,* Chapter 102, pp 1501-1521.

Birkemeier 1985
Birkemeier, W. A. 1985. "Field Data on Seaward Limit of Profile Change," *Journal of the Waterways, Port Coastal and Ocean Engineering,* American Society of Civil Engineers, Vol 111, No. 3, pp 598-602.

Bodge 1992
Bodge, K. R. 1992. "Representing Equilibrium Beach Profiles with an Exponential Expression," *Journal of Coastal Research,* Vol 8, No. 1, pp 47-55.

Broker-Hedegaard, Deigaard, and Fredsoe 1991
Broker-Hedegaard, I., Deigaard, R., and Fredsoe, J. 1991. "Onshore/Offshore Sediment Transport and Morphological Modelling of Coastal Profiles,"*Proceedings Coastal Sediments '91 Conference*, pp 643-657.

Bruun 1954
Bruun, P. 1954. "Coast Erosion and the Development of Beach Profiles," Beach Erosion Board Technical Memorandum No. 44, U.S. Army Engineer Waterways Experiment Station, Vicksburg, MS.

Bruun 1962
Brunn, P. 1962. "Sea-Level Rise as a Cause of Shore Erosion," *Journal of Waterways and Harbor Division,* American Society of Civil Engineers, Vol 88, pp 117-130.

Bruun 1988
Bruun, P. 1988. "The Bruun Rule of Erosion by Sea Level Rise: A Discussion on Large-Scale Two- and Three-Dimensional Usages," *Journal of Coastal Research*, Vol 4, No. 4, pp 627-648.

Chiu 1977
Chiu, T. Y. 1977. "Beach and Dune Response to Hurricane Eloise of September 1975. *Proceedings of Coastal Sediments '77,* pp 116-134.

Clausner, Birkemeier, and Clark 1986
Clausner, J. E., Birkemeier, W. A., and Clark, G. R. 1986. "Field Comparison of Four Nearshore Survey Systems," Miscellaneous Paper CERC-86-6, U.S. Army Engineer Waterways Experiment Station, Vicksburg, MS.

Dally and Dean 1984
Dally, W. R., and Dean, R. G. 1984. "Suspended Sediment Transport and Beach Profile Evolution," *Journal of Waterway, Port, Coastal, and Ocean Engineering*, Vol 110, No. 1, pp 15-33.

Dally, Dean, and Dalrymple 1985
Dally, W. R., Dean, R. G., and Dalrymple, R. G. 1985. "Wave Height Variation Across Beaches of Arbitrary Profile," *Journal of Geophysical Research*, Vol 90, No. C6, pp 11917-11927.

Dalrymple 1992
Dalrymple, R. A. 1992. "Prediction of Storm/Normal Beach Profiles," *Journal of Waterways, Port, Coastal and Ocean Engineering,* American Society of Civil Engineers, Vol 118, No. 2, pp 193-200.

Dean 1973
Dean, R. G. 1973. "Heuristic Models of Sand Transport in the Surf Zone," *Proceedings, Conference on Engineering Dynamics in the Surf Zone,* Sydney, Australia.

Dean 1977
Dean, R. G. 1977. "Equilibrium Beach Profiles: U.S. Atlantic and Gulf Coasts," Department of Civil Engineering, Ocean Engineering Report No. 12, University of Delaware, Newark, DE.

Dean 1985
Dean, R. G. 1985. "Physical Modelling of Littoral Processes," *Physical Modelling in Coastal Engineering,* R. A. Dalrymple, ed., A. A. Balkema, pp 119-139.

Dean 1987a
Dean, R. G. 1987a. "Additional Sediment Input into the Nearshore Region," *Shore and Beach,* Vol 55, Nos. 3-4, pp 76-81.

Dean 1987b
Dean, R. G. 1987b. "Coastal Sediment Processes: Toward Engineering Solutions," *Coastal Sediments '87,* American Society of Civil Engineers, New Orleans, LA, Vol 1, pp 1-24.

Dean 1991
Dean, R. G. 1991. "Equilibrium Beach Profiles: Characteristics and Applications," *Journal of Coastal Research,* Vol 7, No. 1, pp 53-84.

Dean and Dalrymple 1991
Dean, R. G., and Dalrymple, R. A. 1991. *Water Wave Mechanics for Engineers and Scientists*, World Scientific Pub. Co., Teaneck, NJ.

Dean and Dalrymple 2001
Dean, R. G., and Dalrymple, R. A. 2001. *Coastal Processes with Engineering Applications,* Cambridge University Press, New York.

Dean and Maurmeyer 1983
Dean, R. G., and Maurmeyer, E. M. 1983. "Models for Beach Profile Response," *CRC Handbook on Beach Erosion and Coastal Processes,* P. D. Komar, ed., Chapter 7, pp 151-166.

Dette and Uliczka 1987
Dette, H., and Uliczka, K. 1987. "Prototype Investigation on Time-Dependent Dune Recession and Beach Erosion," *Proceedings Coastal Sediments '87,* New Orleans, pp 1430-1444.

Dewall 1979
Dewall, A. E. 1979. "Beach Changes at Westhampton Beach, New York," MR 79-5, Coastal Engineering Research Center, U.S. Army Engineer Waterways Experiment Station, Vicksburg, MS.

Dewall and Richter 1977
Dewall, A. E., and Richter, J. J. 1977. "Beach and Nearshore Processes in Southeastern Florida," *Coastal Sediments'77,* pp 425-443.

Dolan and Dean 1985
Dolan, T., and Dean, R. G. 1985. "Multiple Longshore Sand Bars in the Upper Chesapeake Bay," *Estuarine Coastal & Shelf Science*, Vol 21, pp 727-743.

Edelman 1972
Edelman, T. 1972. "Dune Erosion During Storm Conditions," *Proceedings of the Thirteenth International Conference on Coastal Engineering,* pp 1305-1312.

Everts 1985
Everts, C. H. 1985. "Sea Level Rise Effects on Shoreline Position," *Journal of Waterway, Port, and Coastal Engineering*, Vol 111, No. 6, pp 985-999.

Hallermeier 1978
Hallermeier, R. J. 1978. "Uses for a Calculated Limit Depth to Beach Erosion," *Proceedings of the 16th International Conference on Coastal Engineering,* American Society of Civil Engineers, Hamburg, pp 1493-1512.

Hallermeier 1981
Hallermeier, R. J. 1981. "A Profile Zonation for Seasonal Sand Beaches from Wave Climate," *Coastal Engineering,* Vol 4, pp 253-277.

Hands 1983
Hands, E. 1983. "Erosion of the Great Lakes Due to Changes in the Water Level," *CRC Handbook of Coastal Processes and Erosion*, P. D. Komar, ed., CRC Press, pp 167-189.

Hicks, Debaugh, and Hickman 1983
Hicks, S. D., Debaugh, H. A., Jr., and Hickman, E. 1983. "Sea Level Variations for the United States, 1955-1980," National Ocean Service, National Oceanic and Atmospheric Administration.

Hughes 1994
Hughes, S. A. 1994. *Physical Models and Laboratory Techniques in Coastal Engineering.* World Scientific, River Edge, NJ.

Hughes and Fowler 1990
Hughes, S. A., and Fowler, J. E. 1990. "Validation of Movable-Bed Modeling Guidance," *Proceedings of the 22nd International Conference on Coastal Engineering,* American Society of Civil Engineers, Chapter 186, pp 2457-2470.

Inman, Elwany, and Jenkkins 1993
Inman, D. L., Elwany, M. H. S., and Jenkkins, S. A. 1993. "Shoreline and Bar-Berm Profiles on Ocean Beaches," *Journal of Geophysical Research*, Vol 98, No. C10, pp 18,181 - 18,199.

Katoh and Yanagishima 1988
Katoh, K., and Yanagishima, S. 1988. "Predictive Model for Daily Changes of Shoreline," *Proceedings of the Twenty-First International Conference on Coastal Engineering,* American Society of Civil Engineers, Hamburg, Chapter 93, pp 1253-1264.

Keulegan 1945
Keulegan, G. H. 1945. "Depths of Offshore Bars," Engineering Notes No. 8, Beach Erosion Board, U.S. Army Engineer Waterways Experiment Station, Vicksburg, MS.

Keulegan 1948
Keulegan, G. H. 1948. "An Experimental Study of Submarine Sand Bars," Technical Report No. 8, Beach Erosion Board, U.S. Army Engineer Waterways Experiment Station, Vicksburg, MS.

Kobayashi 1987
Kobayashi, N. 1987. "Analytical Solutions for Dune Erosion by Storms," *Journal of the Waterway, Coastal and Ocean Engineering,* American Society of Civil Engineers, Vol 113, No. 4, pp 401-418.

Komar and McDougal 1994
Komar, P. D., and McDougal, W. G. 1994. "The Analysis of Exponential Beach Profiles," *Journal of Coastal Research,* Vol 10, pp 59-69.

Kraus 1988
Kraus, N. C. 1988. "The Effects of Seawalls on the Beach: An Extended Literature Review," *Journal of Coastal Research*, Special Issue No. 4, pp 1-28.

Kraus, Larson, and Kriebel 1991
Kraus, N. C., Larson, M., and Kriebel, D. L. 1991. "Evaluation of Beach Erosion and Accretion Predictors," *Proceedings of Conference on Coastal Sediments '91,* American Society of Civil Engineers, pp 572-587.

Kriebel 1986
Kriebel, D. L. 1986. "Verification Study of a Dune Erosion Model," *Shore and Beach,* Vol 54, No. 3, pp 13-20.

Kriebel 1987
Kriebel, D. L. 1987. "Beach Recovery Following Hurricane Elena," *Proceedings of Conference on Coastal Sediments '87,* American Society of Civil Engineers, pp 990-1005.

Kriebel 1990
Kriebel, D. L. 1990. "Advances in Numerical Modeling of Dune Erosion," *22nd Intl. Conf. on Coastal Engineering,* American Society of Civil Engineers, pp 2304-2317.

Kriebel and Dean 1985
Kriebel, D. L., and Dean, R. G. 1985. "Numerical Simulation of Time-Dependent Beach and Dune Erosion," *Coastal Engineering,* Vol 9, pp 221-245.

Kriebel and Dean 1993
Kriebel, D. L., and Dean, R. G. 1993. "Convolution Method for Time-Dependent Beach-Profile Response," *Journal of Waterway, Port, Coastal and Ocean Engineering,* American Society of Civil Engineers, Vol 119, No. 2, pp 204-227.

Kriebel, Dally, and Dean 1986
Kriebel, D. L., Dally, W. R., and Dean, R. G. 1986. "Undistorted Froude Model for Surf Zone Sediment Transport," *Proceedings of the Twentieth International Conference on Coastal Engineering,* American Society of Civil Engineers, pp 1296-1310.

Kriebel, Kraus, and Larson 1991
Kriebel, D. L., Kraus, N. C., and Larson, M. 1991. "Engineering Methods for Predicting Beach Profile Response," *Proceedings of Conference on Coastal Sediments '91,* American Society of Civil Engineers, pp 557-571.

Larson 1988
Larson, M. 1988. "Quantification of Beach Profile Change," *Report No. 1008,* Department of Water Resources and Engineering, University of Lund, Lund, Sweden.

Larson and Kraus 1989
Larson, M., and Kraus, N. C. 1989. "SBEACH: Numerical Model for Simulating Storm-induced Beach Change; Report 1: Empirical Foundation and Model Development," Technical Report CERC-89-9, U.S. Army Engineer Waterways Experiment Station, Vicksburg, MS.

Larson and Kraus 1990
Larson, M., and Kraus, N. C. 1990. "SBEACH: Numerical Model for Simulating Storm-induced Beach Change; Report 2: Numerical Formulation and Model Tests," Technical Report CERC-89-9, U.S. Army Engineer Waterways Experiment Station, Vicksburg, MS.

Lee and Birkemeier 1993
Lee, G. H., and Birkemeier, W. A. 1993. "Beach and Nearshore Survey Data: 1985-1991 CERC Field Research Facility," Technical Report CERC-93-3, U.S. Army Engineer Waterways Experiment Station, Vicksburg, MS.

Leenknecht, Szuwalski, and Sherlock 1992
Leenknecht, D. A., Szuwalski, A., and Sherlock, A. R. 1992. "Automated Coastal Engineering System, User Guide and Technical Reference, Version 1.07," U.S. Army Engineer Waterways Experiment Station, Vicksburg, MS.

Longuet-Higgins 1953
Longuet-Higgins, M. S. 1953. "Mass Transport in Water Waves," *Philosophical Transactions of the Royal Society of London,* Ser A, Vol 245, pp 535-581.

Longuet-Higgins and Stewart 1964
Longuet-Higgins, M. S., and Stewart, R. W. 1964. "Radiation Stresses in Water Waves: A Physical Discussion with Applications," *Deep Sea Research*, Vol 2, pp 529-562.

Moore 1982
Moore, B. D. 1982. "Beach Profile Evolution in Response to Changes to Water Level and Wave Height," M.S. thesis, Department of Civil Engineering, University of Delaware, Newark.

Nairn and Southgate 1993
Nairn, R. B., and Southgate, H. N. 1993. "Deterministic Profile Modelling of Nearshore Processes; Part 2, Sediment Transport and Beach Profile Development," *Coastal Engineering*, Vol 19, pp 57-96.

National Research Council 1984
National Research Council. 1984. "Responding to Changes in Sea Level: Engineering Implications," National Research Council Committee on Engineering Implication of Change in Relative Sea Level.

Noda 1972
Noda, E. K. 1972. "Equilibrium Beach Profile Scale Model Relationships," *Journal of Waterway, Harbors and Coastal Engineering,* American Society of Civil Engineers, Vol 98, No. 4, pp 511-528.

Penland, Suter, and McBride 1987
Penland, S., Suter, J. R., and McBride, R. A. 1987. "Delta Plain Development and Sea Level History in Terrebonne Coastal Region, Louisiana," *Proceedings of Conference on Coastal Sediments '87,* American Society of Civil Engineers, pp 1689-1705.

Roelvink and Broker 1993
Roelvink, J. A., and Broker, I. 1993. "Cross-Shore Profile Models," *Coastal Engineering*, Vol 21, pp 163-191.

Roelvink and Stive 1989
Roelvink, J. A., and Stive, M. J. F. 1989. "Bar Generating Cross-Shore Flow Mechanisms on a Beach," *Journal of Geophysical Research*, Vol 94, No. C4, pp 4785-4800.

Saville 1957
Saville, T. 1957. "Scale Effects in Two-Dimensional Beach Studies," *Transactions of the Seventh General Meeting of the International Association of Hydraulic Research,* Vol 1, pp A3.1 - A3.10.

Seymour and Boothman 1984
Seymour, R. J., and Boothman, D. P. 1984. "A Hydrostatic Profiler for Nearshore Surveying," *Journal of Coastal Engineering,* Vol 8, pp 1-14.

Stive and Battjes 1984
Stive, M. J. F., and Battjes, J. A. 1984. "A Model for Offshore Sediment Transport," *Proceedings 19th Intl. Conf. on Coastal Engineering*, pp 1420-1436.

Swart 1974
Swart, D. H. 1974. "Offshore Sediment Transport and Equilibrium Beach Profiles," Publ. No. 131, Delft Hydraulics Lab, Delft, The Netherlands.

Vellinga 1983
Vellinga, P. 1983. "Predictive Computational Model for Beach and Dune Erosion During Storm Surges," *Proceedings, American Society of Civil Engineers Specialty Conference on Coastal Structures' 83,* pp 806-819.

Watanabe, Riho, and Horikawa 1980
Watanabe, A., Riho, Y., and Horikawa, K. 1980. "Beach Profile and On-Offshore Sediment Transport," *Proceedings 17th International Conference on Coastal Engineering*, pp 1106-1121.

III-3-5. Definition of Symbols

β	Ratio of the erosion time scale to the storm duration [dimensionless]
Δy	Equilibrium dry beach width [length]
$\Delta y'$	Non-dimensional equilibrium dry beach width
ε	Parameter suggested by Larson & Kraus to calibrate a sediment transport model [dimensionless]
ε	Eddy viscosity [length^2/time]
κ	Ratio of wave height to local depth within the surf zone
ν_b	Instantaneous wave-induced water particle velocity at the bottom [length/time]
ν_s	Steady wave-induced water particle velocity [length/time]
ρ	Mass density of water (salt water = 1,025 kg/m^3 or 2.0 slugs/ft^3; fresh water = 1,000kg/m^3 or 1.94 slugs/ft^3) [force-time^2/length^4]
σ	Angular frequency (= $2\pi/T$) [time^{-1}]
σ_H	Standard deviation of significant wave height [length]
$\overline{\tau}_b$	Average bottom shear stress [force/length^2]
$\overline{\tau}_{bs}$	Bottom shear stress [force/length^2]
τ_η	Surface wind stress [force/length^2]
τ_b	Seaward-directed shear stress at the bottom [force/length^2]
A	Sediment scale or equilibrium profile parameter (Table III-3-3) [length$^{1/3}$]
A_F	Nourishment material scale parameter [length$^{1/3}$]
A_N	Native sediment scale parameter [length$^{1/3}$]
A'	Parameter for nourished beach calculations (= A_F / A_N) [dimensionless]
B	Berm height [length]
$B(t)$	Instantaneous total height of the active profile above the current water level [length]
B_0	Original berm height [length]
B'	Parameter for nourished beach calculations [dimensionless]
C	Wave speed [length/time]
D	Sediment grain diameter [length - generally millimeters]
D_*	Excess energy dissipation per unit volume in the surf zone
D_F	Sediment grain diameter of beach fill material [length - generally millimeters]
D_N	Sediment grain diameter of native beach [length] - generally millimeters
D_r	Model to prototype sediment grain size scale ratio

E	Total wave energy in one wavelength per unit crest width [length-force/length]
f	Darcy-Weisbach friction coefficient [dimensionless]
g	Gravitational acceleration (32.17 ft/sec^2, 9.807m/sec^2) [length/time^2]
h	Equilibrium beach profile depth (Equation III-3-13) [length]
h	Water depth [length]
H	Wave height [length]
h_*	Depth to which nourished profile will equilibrate or closure depth [length]
$\overline{H}$	Annual mean significant wave height [length]
h_0	Asymptotic beach profile depth [length]
H_0	Deepwater wave height [length]
h_b	Breaking depth [length]
h_c	Closure depth [length]
h_{CR}	Depth over bar crest [length]
h_D	Depth to the bar base [length]
H_e	Effective significant wave height [length]
h_r	Model to prototype vertical length scale ratio
H_s	Deepwater significant wave height [length]
h_T	Depth over bar trough [length]
k	Decay constant [dimensionless]
k	Wave number (= $2\pi/L = 2\pi/CT$) [length^{-1}]
K'	Parameter used to calibrate the Kriebel & Dean simple transport relationship [dimensionless]
K''	Parameter used to calibrate a sediment transport model [dimensionless]
L_*	Width of active profile [length]
L_0	Deepwater wave length [length]
l_r	Model to prototype horizontal length scale ratio
L_r	Model to prototype length scale ratio
m_0	Beach slope [length-rise/length-run]
n	Empirical exponent used in the equilibrium beach profile equation [dimensionless]
P	Single profile parameter (Equation III-3-32) [dimensionless]
Q	Time-averaged seaward discharge due to the return flow of shoreward mass transport

q_y	Kriebel & Dean simple transport relationship (Equation III-3-45)
R	Shoreline recession [length]
R_{max}	Maximum shoreline recession [length]
R_∞	Equilibrium berm recession due to a storm surge (Equation III-3-38) [length]
S	Storm surge level [length]
S	Sea level rise [length]
s_r	Model to prototype submerged specific weight scale ratio
T	Wave period [time]
T_D	Total storm surge duration [time]
T_e	Effective wave period [time]
T_r	Model to prototype wave period scale ratio
T_S	Time-scale of the equilibrium beach response system (Equation III-3-52) [time]
V	Added volume per unit beach length [length^3 /length]
V_∞	Volume of sand eroded from the berm above the initial still-water level due to a storm surge level S [length^3/length]
V'	Parameter for nourished beach calculations (= $V/(B\ W_*)$) [dimensionless]
V'_{c2}	Critical volume of sand that will just yield a finite shoreline displacement for the case of sand that is finer than the native (Equation III-3-23) [dimensionless]
V'_{cl}	Critical volume of sand delineating intersecting and nonintersecting profiles (Equation III-3-22) [dimensionless]
w	Sediment fall velocity [length/time]
W_*	Width of active nearshore zone (Equation III-3-19) [length]
W_b	Width of the surf zone [length]
w_f	Sediment fall velocity [length/time]
y	Equilibrium beach profile distance offshore (Equation III-3-13) [length]
y	Distance seaward from mean low water [length]
y_0	Offset of the shoreline between the sloping beach face and the imaginary or virtual origin of the equilibrium profile [length]
z	Elevation [length]

III-3-6. Acknowledgments

Authors of Chapter III-3, "Cross-Shore Sediment Transport Processes:"

Robert G. Dean, Ph.D., Coastal & Oceanographic Engineering, University of Florida, Gainesville, Florida.
David L. Kriebel, Ph.D., Department of Ocean Engineering, United States Naval Academy, Annapolis, Maryland.
Todd L. Walton, Ph.D., Coastal and Hydraulics Laboratory, Engineer Research and Development Center, Vicksburg, Mississippi.

Reviewers:
Kevin Bodge, Ph.D., Olsen Associates, Jacksonville, Florida.
James R. Houston, Ph.D., Engineer Research and Development Center, Vicksburg, Mississippi.
Paul A. Work, Ph.D., School of Civil and Environmental Engineering, Georgia Institute of Technology, Atlanta, Georgia.

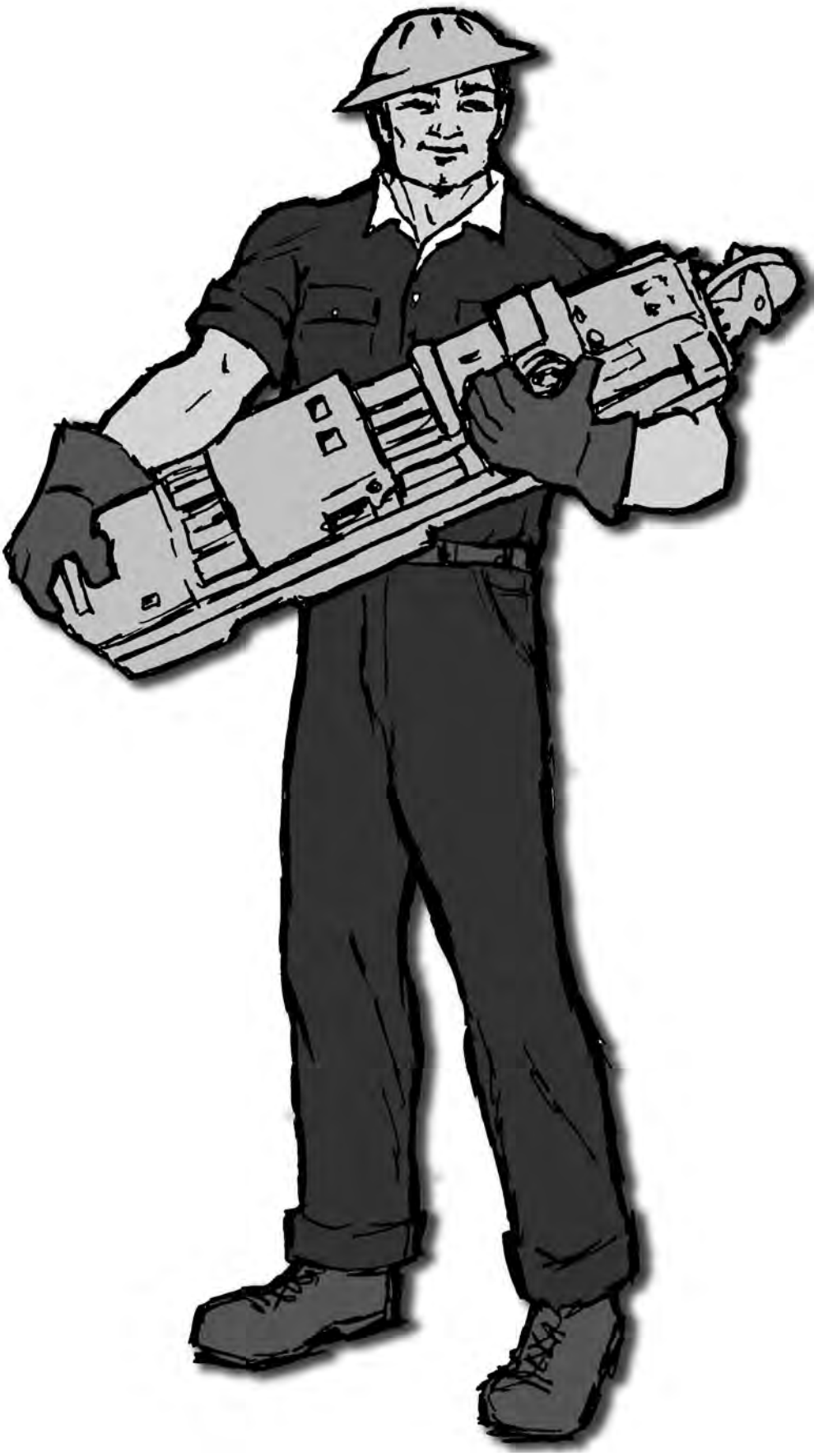

Table of Contents

Page

III-4-1. Introduction III-4-1

III-4-2. Wind Regime of U.S. Coastal Areas III-4-1
a. Introduction III-4-1
b. Sample wind environments III-4-1
c. Wind direction III-4-1
(1) Basic concepts III-4-2
(2) Measurement of wind speed and direction III-4-12
(3) Effects of vegetation, dunes, and buildings III-4-15

III-4-3. Transport Rates III-4-16
a. Processes of sand transport by wind III-4-16
b. Sand transport rate prediction formulas III-4-18
c. Initiation of sand transport III-4-21

III-4-4. Procedures for Calculating Wind-Blown Sand Transport III-4-21

III-4-5. Wind-Blown Sand Transport and Coastal Dunes III-4-39
a. Dunes and dune processes III-4-39
b. Factors affecting dune growth rates III-4-51
c. Dune sediment budget III-4-54
d. Procedure to estimate dune "trapping factor" III-4-55
e. Continuity equation for wind transport of beach sand III-4-59
f. Limited source due to gradation armoring III-4-61

III-4-6. References III-4-72

III-4-7. Definition of Symbols III-4-76

III-4-8. Acknowledgments III-4-77

List of Tables

Page

Table III-4-1
Monthly Mean Wind Speeds Near Westhampton Beach, Long Island, NY - Based on Simultaneous Measurements at C-MAN Station ALSN6 and Offshore Buoy 44025 . . . . . III-4-15

Table III-4-2
Predictive Capability of Sand Transport Equations (Chapman 1990) III-4-19

Table III-4-3
Hourly Wind Data, Westhampton Beach, Long Island, NY III-4-33

Table III-4-4
Hourly Transport Analysis under Dry Conditions, Westhampton Beach, Long Island, NY III-4-34

Table III-4-5
Hourly Transport Analysis Under Wet Conditions, Westhampton Beach, Long Island, NY III-4-38

Table III-4-6
Monthly Sand Transport at Westhampton Beach, Long Island, NY (All Data Considered) (Hsu 1994) III-4-41

Table III-4-7
Monthly Sand Transport at Westhampton Beach, Long Island, NY (Snow Days Excluded) (Hsu 1994) III-4-41

Table III-4-8
Monthly Sand Transport at Westhampton Beach, Long Island, NY (Snow Days and Wet Days Excluded) (Hsu 1994) III-4-41

Table III-4-9
Wind Rose Data, Atlantic City, NJ (Wind Data, 1936 to 1952) III-4-44

Table III-4-10
Wind Rose Data Analysis, Atlantic City, NJ (Anemometer at Standard 10-m Height) III-4-44

Table III-4-11
Wind-Blown Sand Transport Analysis, Wind Rose Data Atlantic City, NJ (Wind Data, 1936 to 1952) III-4-45

Table III-4-12
Estimated Annual Dune Growth at Atlantic City, NJ III-4-50

Table III-4-13
Measured Dune Growth Rates (adapted from SPM 1984) III-4-52

Table III-4-14
Typical Beach and Dune Sand Phi Diameters and Dune Trapping Factors Calculated from Beach and Dune Sand Samples at Various U. S. Beaches III-4-59

Table III-4-15
Size Distribution, Threshold Wind Speeds, and Volumetric Transport Coefficients for Beach Sand Size Intervals, Atlantic City, NJ III-4-63

Table III-4-16
Wind Speeds for Atlantic City Wind Rose Intervals III-4-63

Table III-4-17
Transport Rates for Size Intervals at Atlantic City Wind Rose Speed Intervals III-4-64

Table III-4-18
Wind Transport of Size Intervals for Winds from North Weighted by Fraction of Year Wind was Within Given Speed and Direction Interval III-4-65

Table III-4-19
Summary of Transports for Eight Compass Directions III-4-66

Table III-4-20
Computation of Dune Growth Rate III-4-67

Table III-4-21
Calculated Dune Sand Size Distribution III-4-68

Table III-4-22
Comparison of Calculated Dune Sand Size Distribution and Actual Dune Sand Size Distribution III-4-70

Table III-4-23
Corrected Transport Rates for Size Intervals and Corrected Dune Growth Rate III-4-71

List of Figures

Page

Figure III-4-1. Air masses and fronts over the coastal areas III-4-2

Figure III-4-2. Example wind regime areas (Solid circles denote example wind regime areas. Open circles are nearby buoys used to construct wind roses) III-4-3

Figure III-4-3. Wind roses based on hourly data nearby: (a) Newport, OR, (b) Aransas Pass, TX, (c) Westhampton Beach, Long Island, NY, and (d) New Buffalo, MI III-4-4

Figure III-4-4. Example logarithmic wind profile at Isles Dernieres, LA (adopted from Hsu and Blanchard 1991) III-4-6

Figure III-4-5. Aerodynamic roughness element lengths Z_0 and relationship between shear velocity u_* and wind speed at the 2-m height U_{2m} in coastal environments (adopted from Hsu (1977)) III-4-10

Figure III-4-6. Variation of U_{sea} with U_{land}. (Hsu 1986) III-4-14

Figure III-4-7. Temperature correction factor R_T as a function of air-sea temperature difference (Resio and Vincent 1977) III-4-14

Figure III-4-8. Wind field in the vicinity of a coastal sand dune (q is the local resultant mean velocity and v is the reference velocity in the uniform stream above the dune) (Hsu 1988) III-4-16

Figure III-4-9. Wind-blown sand transport coefficient as a function of mean sand-grain diameter (adopted from Hsu (1977)) III-4-20

Figure III-4-10. Westhampton Beach, Long Island, NY (Hsu 1994) III-4-22

Figure III-4-11. Threshold (critical) wind speed as a function of median sand-grain diameter and the anemometer height at which wind speed is measured III-4-27

Figure III-4-12. Mass transport rate coefficient K^* as a function of median sand-grain diameter and the anemometer height at which wind speed is measured III-4-29

Figure III-4-13. Volume transport rate coefficient K^*_V as a function of median sand-grain diameter and the anemometer height at which wind speed is measured (assumes sediment density = 2.65 gm/cm^3 and porosity = 0.4) III-4-31

Figure III-4-14. Wet sand transport rate coefficient as a function of median sand-grain diameter and the anemometer height at which wind speed is measured III-4-36

Figure III-4-15. Wind-blown sand transport rose at Westhampton Beach, Long Island, NY, for 1989 (Hsu 1994) III-4-40

Figure III-4-16. Wind rose for Atlantic City, NJ (data from 1936 to 1952) III-4-43

Figure III-4-17. Net sand transport at an angle α with the wind direction III-4-47

Figure III-4-18. Shoreline orientation with respect to compass directions at Atlantic City, NJ III-4-48

Figure III-4-19. Sand transport efficiency for winds blowing from dunes toward beach as a function of the angle between wind direction and shoreline III-4-49

Figure III-4-20. Definition of angle ß, between wind and shoreline III-4-49

Figure III-4-21. Schematic views of sorted sand deposits: (a) well-sorted (poorly graded); (b) poorly sorted (well-graded); (c) poorly sorted after fines have been removed by wind erosion III-4-53

Figure III-4-22. Definition of terms, dune sediment budget III-4-54

Figure III-4-23. Dune sand trapping factor T_f III-4-56

Figure III-4-24. Sand conservation equations for a beach showing deflation area, equilibrium area, and deposition area III-4-60

Figure III-4-25. Beach and dune and size gradations for Atlantic City, NJ III-4-62

Figure III-4-26. Actual and calculated dune sand size gradation at Atlantic City, NJ III-4-69

Figure III-4-27. Comparison of actual dune sand size gradation with corrected, calculated gradation III-4-71

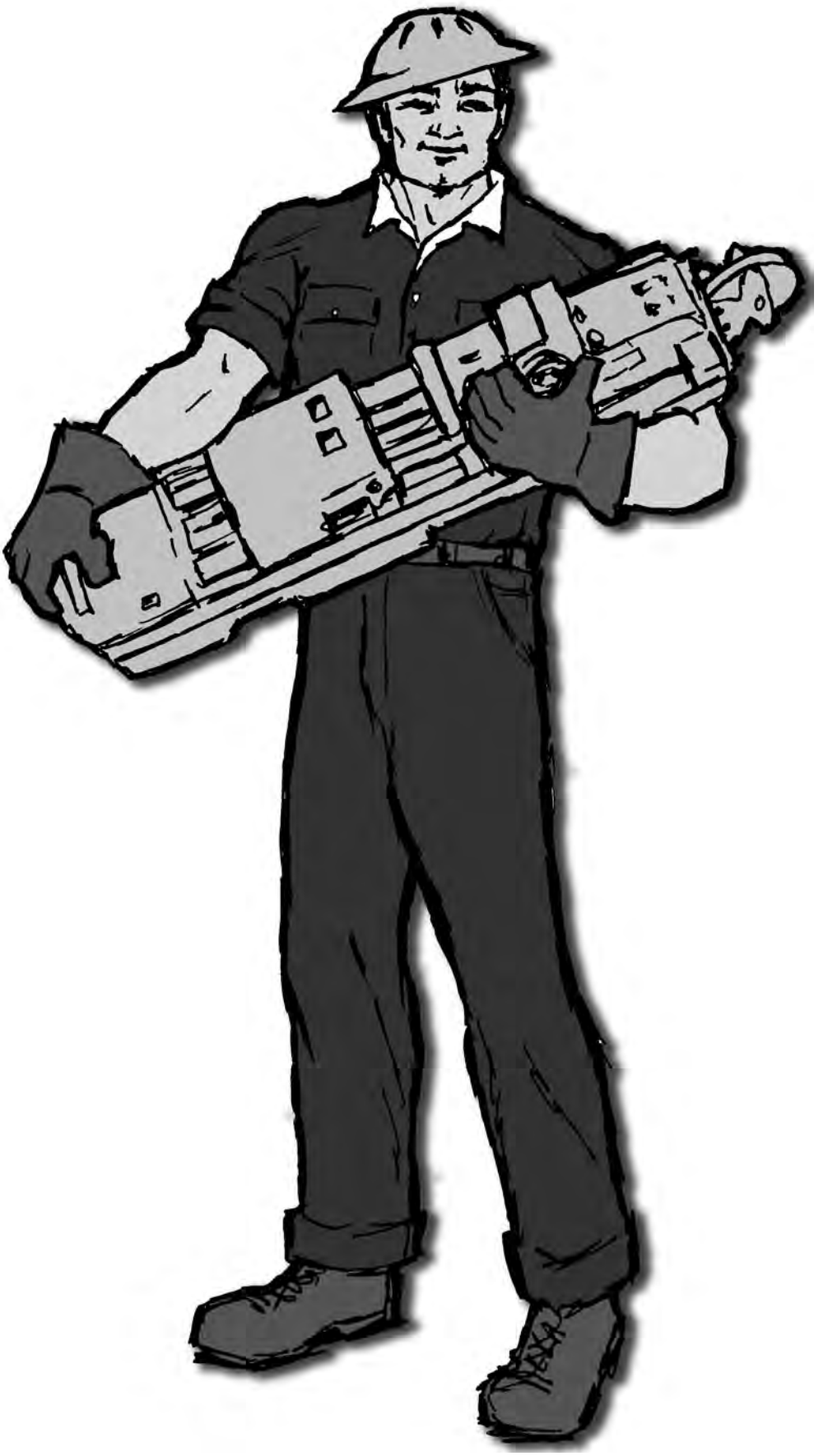

Chapter III-4
Wind-Blown Sediment Transport

III-4-1. Introduction

From an engineering perspective, the transport of sand by wind is often an important component in the coastal sediment budget. Wind transport can lead to the removal of sand or its redistribution within the littoral zone. Onshore winds carry sand from the beach and deposit it in backshore marshes, in developed backshore areas, or in natural or man-made dunes. Offshore winds carry sand from the beach into the sea or lake. In some areas, wind-blown sand is a nuisance and must be controlled. In other areas, the natural growth of protective dunes is limited by the amount of sand transported to them by wind. Wind transport of sand is a continual, natural process that is often significant in bringing about beach changes. It is important to be able to quantitatively predict how much sand will be transported by wind at a given coastal site, the direction in which that sand will be transported, and where it will be deposited. This chapter discusses wind transport prediction in coastal areas by describing the driving force (the wind) and the transport mechanisms. The overall wind regime of U.S. coastal areas, modifications to the wind field brought about by its proximity to the ground (the atmospheric boundary layer), initiation of sediment motion under wind, processes involved in sand transport by wind, and the quantitative prediction of transport rates are described.

III-4-2. Wind Regime of U.S. Coastal Areas

a. Introduction. In the Northern Hemisphere, between the equator and latitude 30° N, winds generally blow from the east (the trade winds), while between 30° N and 60° N, winds blow generally from the west (the prevailing westerlies). From autumn to spring, however, cold fronts frequently pass over the United States. During these events the normal wind regime is different. Ahead of these fronts, winds are generally southerly, while behind the fronts, winds are northerly. Southerly winds ahead of the front transport warmer tropical air northward while behind the front, northerly winds transport cold polar air southward (see Figure III-4-1).

b. Example wind environments. Four coastal areas are considered herein as example wind environments (see Figure III-4-2). The sites are: Newport, OR; Aransas Pass, TX; Westhampton Beach, NY; and New Buffalo, MI on Lake Michigan. The four sites represent a broad range of geographical parameters. Wind roses for each area are given in Figure III-4-3. Since sand transport generally occurs for wind speeds greater than about 5-m/s (approximately 10 knots), the 5 m/s wind speed is used to separate the winds into two regimes.

c. Wind direction. Winds at Newport, OR, have a major north-south component because the Cascade Range immediately behind the shoreline has a north-south orientation and because of the north-south orientation of the shoreline. Occasionally, winds may blow from land toward the sea. In Port Aransas, TX, winds come mostly from the southeast because of the influence of Bermuda high pressure systems. At Westhampton Beach, NY, winds blow mainly from the southwest around through the northwest. At New Buffalo, MI, in the Lake Michigan region, winds blow generally in the north-south direction because of the west-to-east passage of fronts. These wind conditions are in general agreement with the air mass and cold front influences shown in Figure III-4-1.

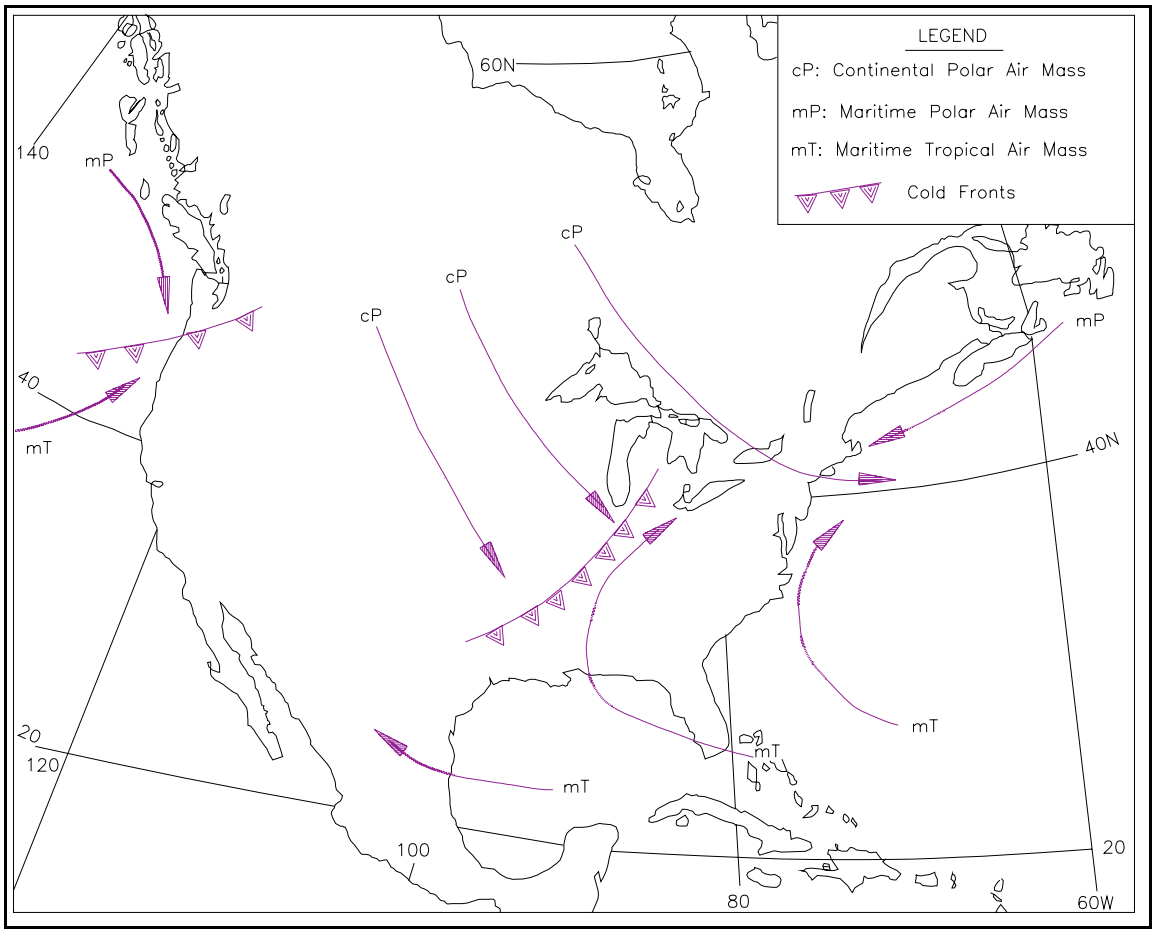

Figure III-4-1. Air masses and fronts over the coastal areas

(1) Basic concepts.

(a) Wind velocity and the vertical gradient of wind speed near the ground are important factors in determining how much sediment will be transported by wind. In addition, sediment characteristics such as size, size distribution, packing, and moisture content play important roles. The vertical gradient of wind speed results in shearing forces within the air and eventually on the ground surface. When vegetation is present, sheer can be transferred into the uppermost soil layers. The steeper the gradient, the greater the shear stress. The velocity gradient is significantly influenced by local topography, vegetation, and land use. These factors contribute to the "roughness" of the ground surface. In the case of wind transport in coastal areas, local perturbations in the wind field may also be important in determining the eventual erosion and deposition patterns of wind-blown sand.

(b) The vertical distribution of wind speed - the velocity profile - generally follows a logarithmic distribution. An important parameter in this representation is the shear velocity defined by

$$u_* = \sqrt{\frac{\tau}{\rho_a}} \qquad \text{(III-4-1)}$$

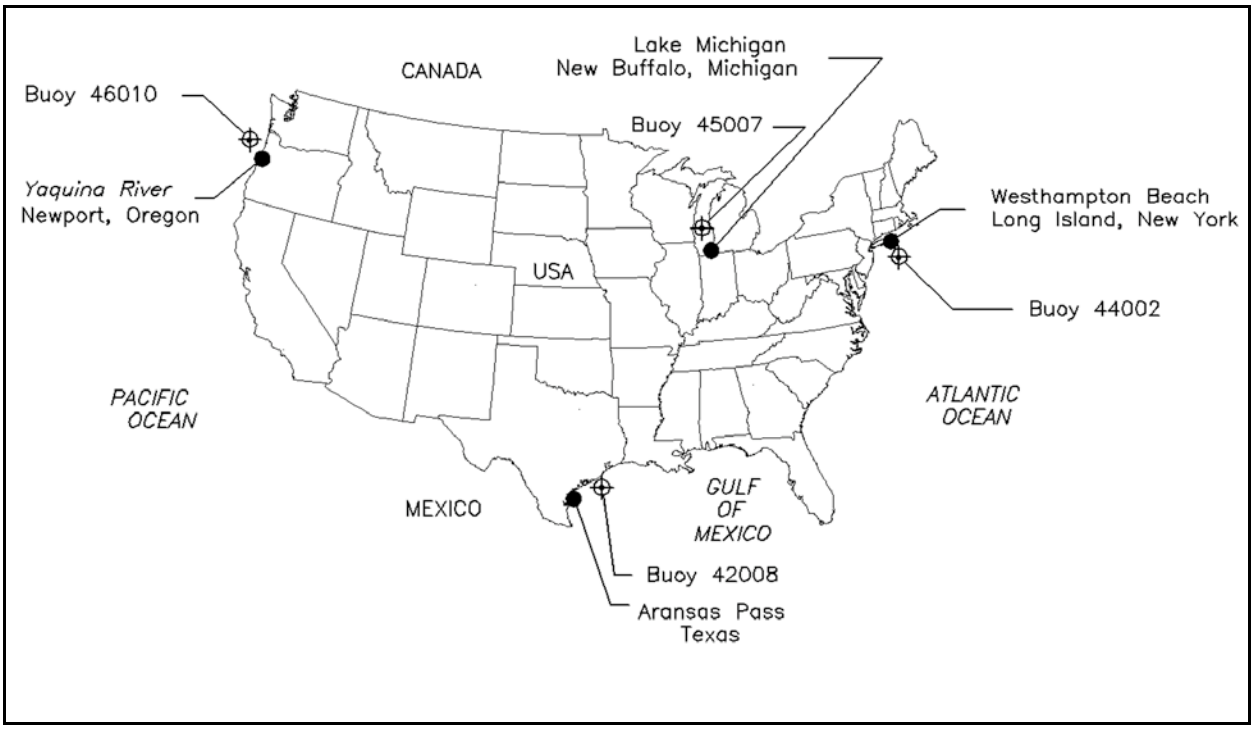

Figure III-4-2. Example wind regime areas (Solid circles denote example wind regime areas. Open circles are nearby buoys used to construct wind roses)

in which u_* = the shear or friction velocity, τ = the boundary shear stress (force per unit surface area), and ρ_a = the density of the air. The logarithmic distribution of wind velocity is given by

$$U_z = \frac{u_*}{\kappa} \ln\left(\frac{Z_o + Z}{Z_o}\right) \tag{III-4-2}$$

in which U_z = the average wind speed as a function of height above ground level, u_* = the shear velocity, Z = the height above ground level, Z_o = the height of a roughness element characterizing the surface over which the wind is blowing, and κ = von Karman's constant (κ = 0.4). Wind speed measurements are usually averaged over a period of several minutes to smooth out fluctuations due to gusts. Averaging time can vary depending on how the measurements are made. If readings are taken from an anemometer dial rather than from a recording, the observer may visually average the speed by observing the needle over a period of several minutes. Wind speeds are occasionally reported as the fastest mile of wind speed where the averaging time is the time it would take the wind to travel the distance of 1 mile; thus, the averaging time for a 60-mph wind would be 1 min; the averaging time for a 30-mph wind would be 2 min, etc.

(c) Since the height of a roughness element Z_o is usually small compared with Z, Equation 4-2 can be approximated by

$$U_z \approx \frac{u_*}{\kappa} \ln\left(\frac{Z}{Z_o}\right) \tag{III-4-3}$$

or

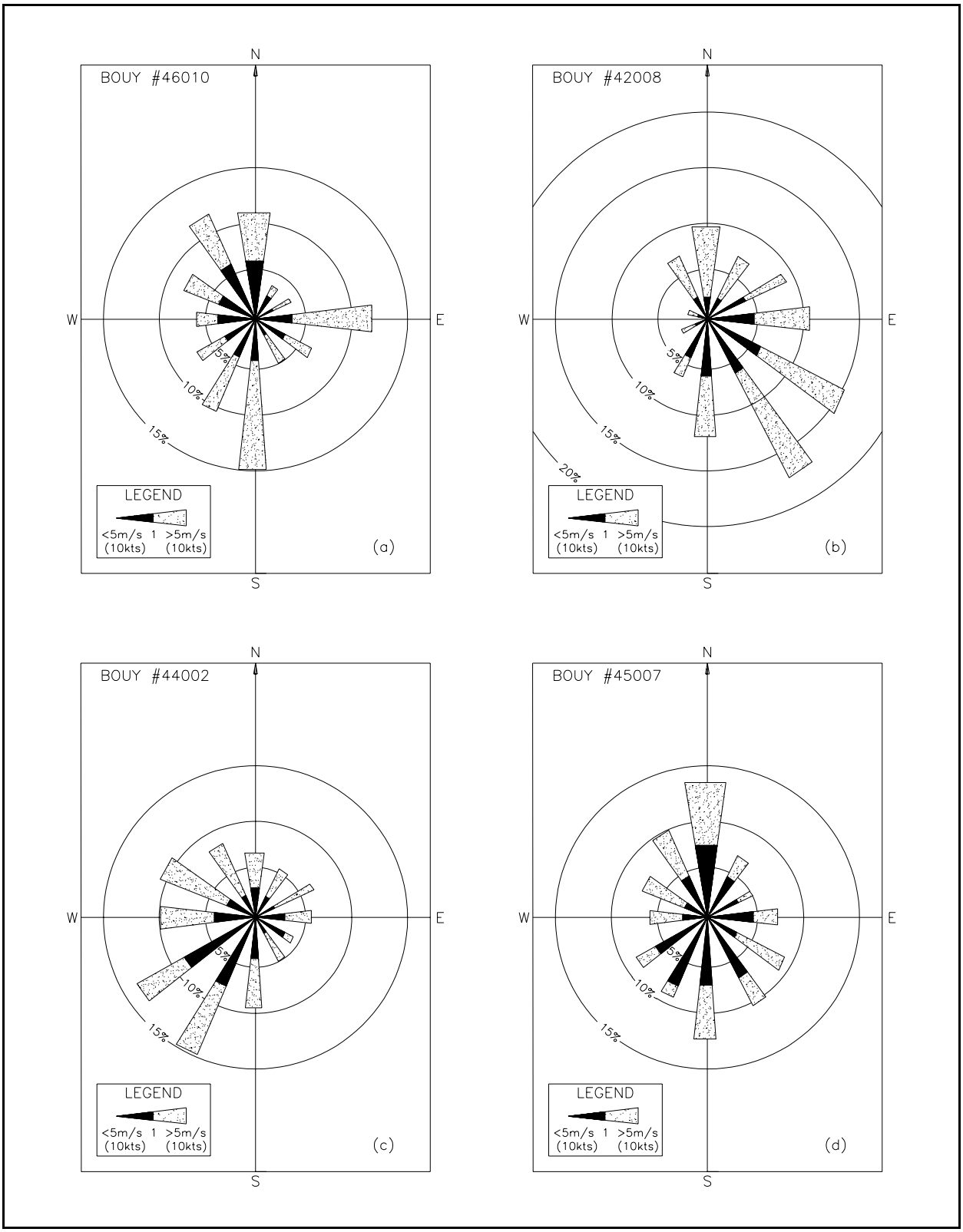

Figure III-4-3. Wind roses based on hourly data nearby: (a) Newport, OR, (b) Aransas Pass, TX, (c) Westhampton Beach, Long Island, NY, and (d) New Buffalo, MI

$$\ln Z = \ln Z_o + \left(\frac{\kappa}{u_*} \right) U_z$$

which is of the form

$$Y = a_o + a_1 X$$

where $Y = \ln Z$ and

$$a_o = \ln Z_o \quad \text{or,} \quad Z_o = e^{a_o}$$

and

$$a_1 = \frac{\kappa}{u_*} \quad \text{or,} \quad u_* = \frac{\kappa}{a_1}$$

(d) A logarithmic velocity distribution as fit by linear regression techniques is given in Figure III-4-4 for Isle Dernieres, LA.

(e) The concept of a drag coefficient is sometimes used in wind transport calculations, where the drag coefficient is defined as

$$C_z = \left(\frac{u_*}{U_z} \right)^2 \tag{III-4-4}$$

in which C_z = the drag coefficient at height Z. Often C_z is considered a constant for a given Z; however, computations by Hsu and Blanchard (1991) for C_{10} showed a variation of from 0.5×10^{-3} to 5.0×10^{-3}, an order of magnitude. In fact, C_z varies with season and wind direction and cannot be considered constant. It is evident that the roughness characteristics of the fetch over which the wind blows depend on wind direction, particularly in coastal regions where onshore and offshore winds experience significantly different fetches. Onshore winds usually experience less friction than offshore winds because of the relative smoothness of the water surface when compared with the rougher land surface. On the other hand, shear stresses on the beach due to onshore winds will be greater than shear stresses due to offshore winds of the same speed.

(f) Because the appropriate height of a roughness element is not known a priori, it must be found by the simultaneous solution of Equation 4-2 applied at two heights above the ground. However, if Z_o is small, and the wind speed is not measured very close to the ground (well outside of the roughness elements), Equation 4-3 can be used to estimate the wind speed distribution without first finding Z_o. Equation 4-3 can be applied at two heights, Z_1 and Z_2 so that

$$\ln Z_1 = \ln Z_o + \left(\frac{\kappa}{u_*} \right) U_{z1} \tag{III-4-5}$$

and

$$\ln Z_2 = \ln Z_o + \left(\frac{\kappa}{u_*} \right) U_{z2} \tag{III-4-6}$$

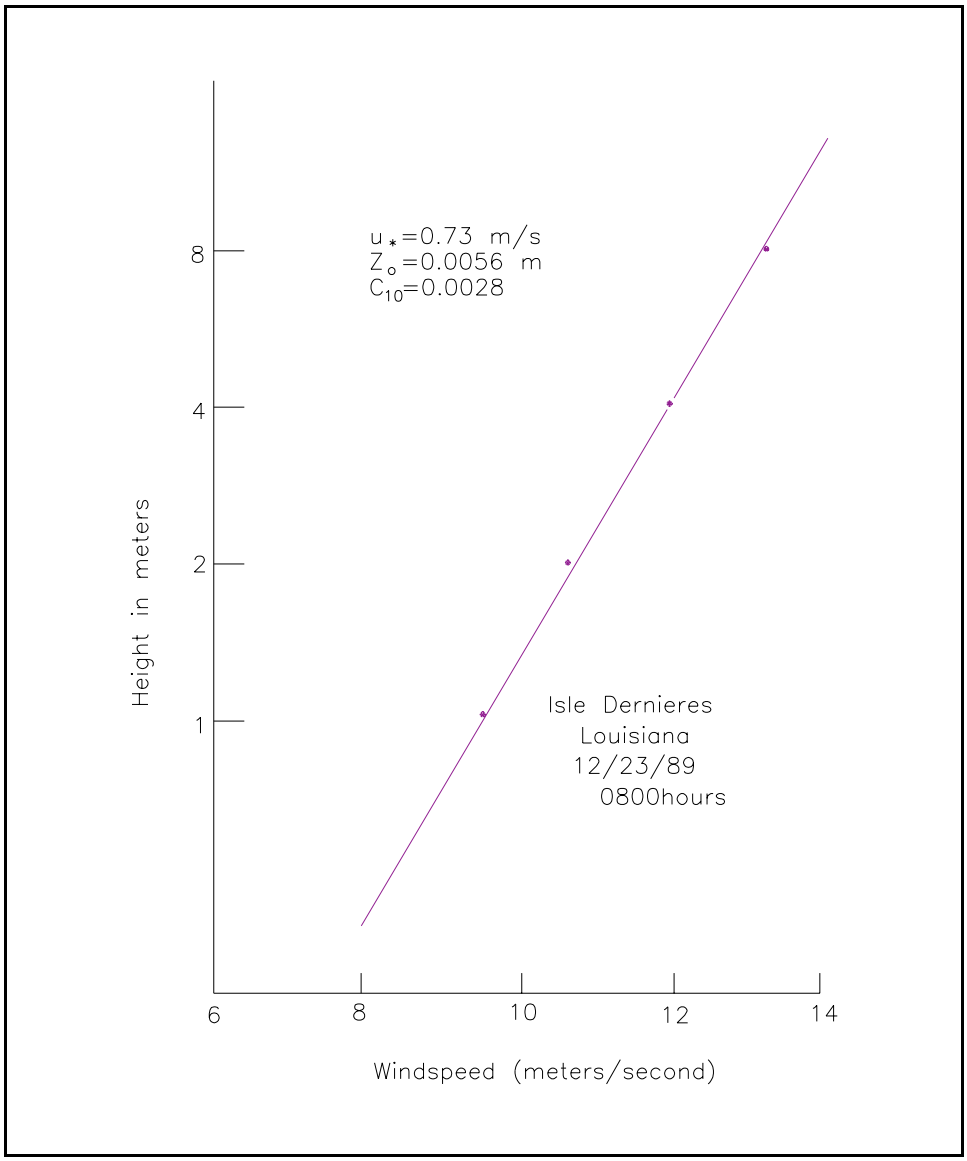

Figure III-4-4. Example logarithmic wind profile at Isles Dernieres, LA (adopted from Hsu and Blanchard (1991))

where Z_1 is below Z_2 so that U_{Z1} is less than U_{Z2}.

(g) Eliminating Z_o from Equations 4-5 and 4-6 gives

$$u_* = \frac{\kappa(U_{z2} - U_{z1})}{\ln\left(\frac{Z_2}{Z_1}\right)} \tag{III-4-7}$$

(h) Consequently, the shear velocity u_* can be determined from Equation 4-7 without first finding Z_o by measuring the wind velocity at two elevations. For wind transport studies, wind velocity sensors used to determine u_* should be spaced vertically as far apart as practical, say a minimum of 3 to 4 m, but preferably more.

EXAMPLE PROBLEM III-4-1

Find:

The shear velocity u_* and the height of a characteristic roughness element Z_o. What is the magnitude of the shear stress acting on the ground surface?

Given:

Wind speed is measured at two elevations above the ground. At 10 m height, the average wind speed is 11.3 m/s; at 4 m, it is 9.36 m/s.

Solution:

The velocity distribution is logarithmic as given by Equation 4-2. Since there are two unknowns, Z_o and u_*, the equation must be solved at the two elevations. Substituting into the equation with $\kappa = 0.4$

$$11.3 = \frac{u_*}{0.4} \ln\left(\frac{10 + Z_o}{Z_o}\right)$$

and

$$9.36 = \frac{u_*}{0.4} \ln\left(\frac{4 + Z_o}{Z_o}\right)$$

Solving for each equation for u_* and equating

$$\frac{9.36\ (0.4)}{\ln\left(\frac{4 + Z_o}{Z_o}\right)} = \frac{11.3\ (0.4)}{\ln\left(\frac{10 + Z_o}{Z_o}\right)}$$

or

$$\ln\left(\frac{10 + Z_o}{Z_o}\right) = 1.207 \ln\left(\frac{4 + Z_o}{Z_o}\right)$$

$$\ln(Z_o + 10) - \ln Z_o = 1.207\left[\ln(Z_o + 4) - \ln Z_o\right]$$

$$\ln(10 + Z_o) = 1.207 \ln(4 + Z_o) - 0.207 \ln Z_o$$

Assuming that Z_o is small with respect to the height at which the wind speeds are measured, a first approximation to Z_o can be obtained,

(Sheet 1 of 3)

Example Problem III-4-1 (Continued)

$$\ln(10) = 1.207 \ln(4) - 0.207 \ln Z_o$$

$$2.303 = 1.673 - 0.207 \ln Z_o$$

$$\ln Z_o = -3.042$$

$$Z_o = 0.0477 \quad \text{m}$$

A second improved approximation can be found by substituting $Z_o = 0.0477$ into,

$$\ln(10 + 0.0477) = 1.207 \ln(4 + 0.0477) - 0.207 \ln Z_o$$

Solving for Z_o

$$Z_o = 0.05 \quad \text{m}$$

Then, substituting back into one of the wind speed equations

$$u_* = \frac{U_z \kappa}{\ln\left(\frac{Z + Z_o}{Z_o}\right)}$$

for the wind speed observation at 10 m

$$u_* = \frac{(11.3)(0.4)}{\ln\left(\frac{10 + 0.05}{0.05}\right)} = 0.852 \text{ m/s}$$

The assumption that Z_o is small with respect to the height at which wind speeds are measured could have been made at the outset by using Equation 4-3. Then

$$U_z = \frac{u_*}{0.4} \ln\left(\frac{Z}{Z_o}\right)$$

and

$$11.3 = \frac{u_*}{0.4} \ln\left(\frac{10}{Z_o}\right)$$

(Sheet 2 of 3)

Example Problem III-4-1 (Concluded)

with

$$9.36 = \frac{u_*}{0.4} \ln\left(\frac{4}{Z_o}\right)$$

or

$$(11.3)(0.4) = u_* \left[\ln(10) - \ln Z_o\right]$$

and

$$(9.36)(0.4) = u_* \left[\ln(4) - \ln Z_o\right]$$

Subtracting

$$0.776 = u_* \ln\left(\frac{10}{4}\right)$$

$$u_* = 0.847 \text{ m/s}$$

On substituting this value for u_* back into one of the above equations and solving for Z_0 gives

$$Z_0 = 0.048 \text{ m}$$

These are the same as the first approximations found above.

The shear stress can be found from Equation 4-1, the definition of u_*

$$u_* = \sqrt{\frac{\tau}{\rho_a}}$$

or

$$\tau = \rho_a u_*^2$$

where $\rho_a = 0.00122$ gm/cm^3 and $u_* = 0.852$ m/sec. Substituting

$$\tau = 0.00122(85.2)^2 = 8.86 \text{ dynes/cm}^2$$

The reader may wish to verify the shear velocity and characteristic roughness element height for the wind speed observation at Isle Dernieres given in Figure III-4-4.

(Sheet 3 of 3)

(i) In most sand transport studies, two-level or multilevel wind velocity measurements are rarely available and the wind speed climatology must be measured at two or more levels to establish u_*. Based on measurements at six beaches, Hsu (1977) established a relationship for u_* in terms of U_{2m}, the wind speed at the 2-m height (see Figure III-4-5). His relationship for the dry beach area is given by

$$u_* = 0.044\, U_{2m} \tag{III-4-8}$$

in which U_{2m} = the average wind speed at the 2-m height. Equations for u_* on tidal flats, dunes, etc. are also given by Hsu (1977) (see Figure III-4-5). Note that the coefficient in this equation depends critically on the height of a roughness element so that Equation 4-8 is valid only for beaches with roughness conditions similar to those for which the equation was developed.

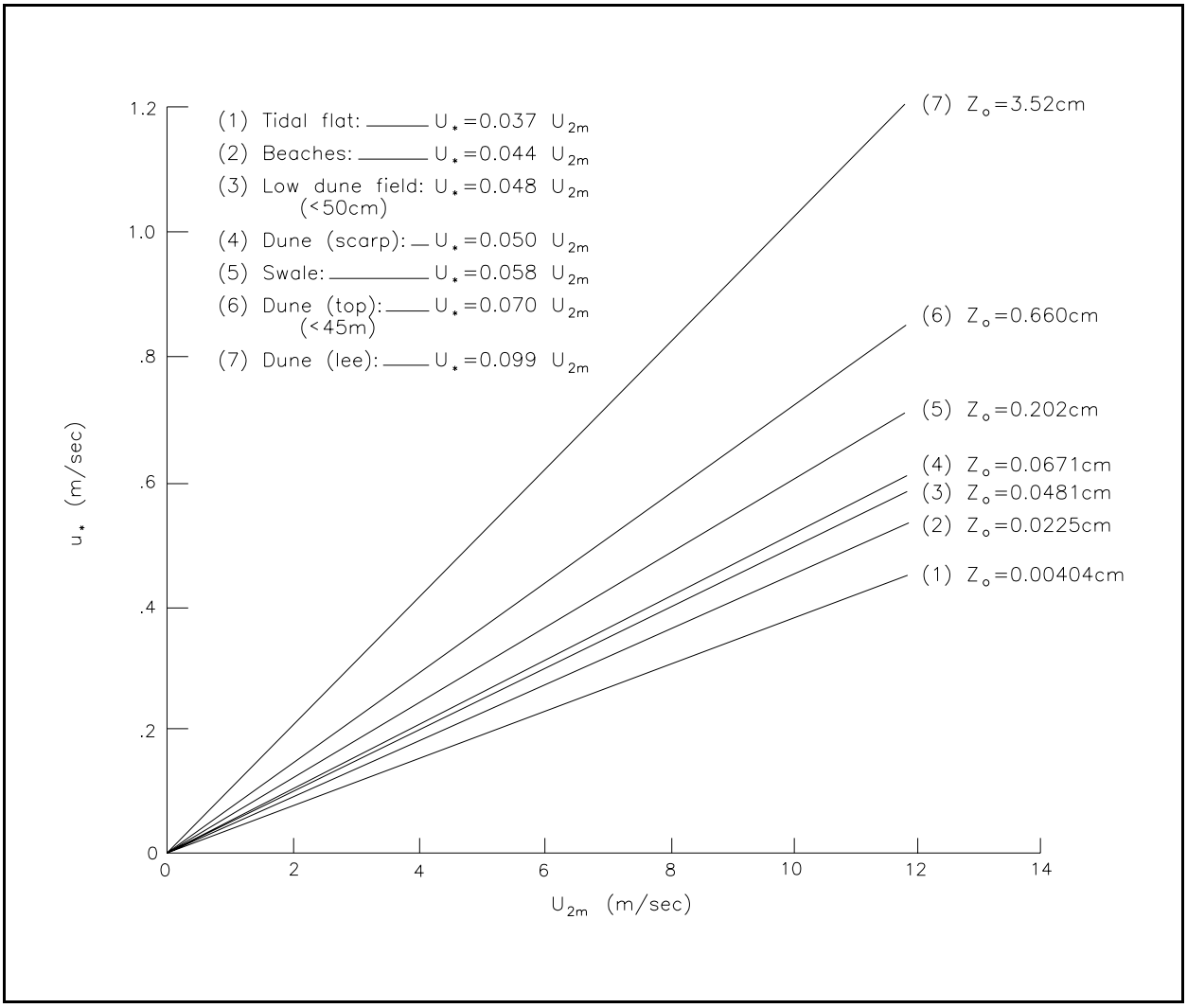

Figure III-4-5. Aerodynamic roughness element lengths Z_0 and relationship between shear velocity u_* and wind speed at the 2-m height U_{2m} in coastal environments (adopted from Hsu (1977))

EXAMPLE PROBLEM III-4-2

Find:

The drag coefficient at the 10-m, 4-m, and 2-m heights using the shear velocity calculated in the preceding problem, then estimate the shear velocity using the wind speed determined for the 2-m height. Compare the shear velocity with the value determined in the preceding example problem.

Given:

The wind speed measurements from the previous example problem.

Solution:

The definition of the drag coefficient is given by Equation 4-4. Thus, for the 10-m height,

$$C_{10m} = \left[\frac{u_*}{U_{10m}}\right]^2$$

$$C_{10m} = \left[\frac{0.852}{11.3}\right]^2 = 0.00568$$

For the 4-m height $C_{4m} = (0.852/9.36)^2 = 0.00829$. The wind speed at the 2-m height must be found from Equation 4-2 (or Equation 4-3 if the roughness element height can be assumed small). Thus,

$$U_{2m} = \frac{(0.852)}{(0.4)} \ln\left(\frac{2 + 0.05}{0.05}\right)$$

$$U_{2m} = 7.91 \quad \text{m/s}$$

and

$$C_{2m} = \left[\frac{0.852}{7.91}\right]^2 = 0.0116$$

Using this wind speed at the 2-m height to estimate the shear velocity u_* in Equation 4-8 gives

$$u_* = 0.044\, U_{2m}$$

$$u_* = 0.044(7.91) = 0.348 \quad \text{m/s}$$

This result is significantly lower than the $u_* = 0.852$ value found from the wind speed distribution because the example wind speed distribution is somewhat unusual for a beach. The characteristic roughness length for the example is larger than what is typically found on beaches. A value of Z_o typical for beaches is 0.000225 m (0.0225 cm); however, based on measurements by Hsu (1977), Z_o can be much larger in the lee of dune areas. See Figure III-4-5 for some typical values of Z_o in various coastal environments.

(2) Measurement of wind speed and direction.

(a) Wind speed is measured with an anemometer. Two types of anemometers are typically used, cup-type or propeller-type anemometers. Wind direction is measured using a vane that indicates the direction *from which* the wind is blowing. When wind speed measurements are made with a cup-type anemometer, a separate vane is needed. Propeller-type anemometers have a built-in vane that keeps the propeller directed into the wind. Wind speed measurements are usually obtained at or corrected to a standard anemometer height of 10 m above ground level, although anemometers may be mounted at other heights. The wind record from an anemometer depends significantly on the physical conditions of the surrounding terrain. The surrounding terrain determines the boundary roughness and thus the rate at which wind speed increases with height above the ground. Consequently, physical conditions characterizing the surrounding fetches determine the wind environment at a site. At coastal sites, the fetch seaward of the beach is over water and is generally characterized by relatively low roughness. The fetch landward of the beach can vary significantly from site to site since it depends on the type of vegetation, terrain, etc.

(b) Differences exist between onshore and offshore wind speeds due to differences in friction conditions over the fetch. The differences are most marked in the observed wind speeds (see Hsu (1988)). Hsu (1986) derived an equation to estimate the difference in overwater and overland wind speeds. The ratio of wind speed overwater to the wind speed overland is given by

$$\frac{U_{sea}}{U_{land}} = \left[\frac{H_{sea}\ C_{D,land}}{H_{land}\ C_{D,sea}}\right]^{\frac{1}{2}} \tag{III-4-9}$$

where

U_{sea} and U_{land} = the wind speed over sea and land, respectively

H_{sea} and H_{land} = the height of the planetary boundary layer over the sea and land

$C_{D,sea}$ and $C_{D,land}$ = the drag coefficients over sea and land

(c) Equation 4-9 should apply for both onshore and offshore winds assuming that the geostrophic wind above the boundary layer does not change appreciably. For a given climatological area, the parameters on the right side of Equation 4-9 are generally known. Holzworth (1972) and SethuRaman and Raynor (1980) found H_{sea} = 620 m, H_{land} = 1014 m, $C_{D,sea}$ 0.0017, and $C_{D,land}$ = 0.0083, leading to U_{sea}/U_{land} = 1.7 for this area. $C_{D,sea}$ and $C_{D,land}$ were measured at the 8-m level.

(d) If the direction between either onshore near-surface winds or offshore near-surface winds is within 45 deg of shore-normal, Equation 4-9 will be valid regardless of whether the wind blows from land to sea or vice versa (Hsu (1988), pp 184-186). Equation 4-9 may, therefore, be applicable to weather systems such as land breezes, sea breezes, hurricanes near landfall, and other synoptic-scale phenomena such as cyclones (low pressure cells), anti-cyclones (high pressure cells), and monsoons. This is not the case for the passage of frontal systems and squall lines, however, since their winds do not usually blow within 45 deg of shore-normal. Typically, winds associated with the passage of fronts and squall lines do not persist for long periods of time.

(e) An empirical relationship between overland wind speed and overwater wind speed can be estimated from measured wind speeds at land and water sites by

$$U_{sea} = A + B\,U_{land} \tag{III-4-10}$$

where A and B are empirical constants.

(f) If the air-water temperature difference is small, say less than 5 °C, and if the aggregate wind estimation error at airports is less than 10 percent (Wieringa 1980), then an estimate is given by Liu, Schwab, and Bennett (1984) as

$$U_{sea} = 1.85 \text{ (m/s)} + 1.2\, U_{land} \tag{III-4-11}$$

where U_{sea} and U_{land} are measured in m/s.

(g) Based on many pairs of measurements of overland and overwater wind speeds, the U_{sea} was correlated with U_{land} for synoptic-scale weather systems (Hsu 1981; Powell 1982). Wind speeds used by Hsu (1981) were less than 18 m/s while Powell's (1982) data included hurricane-force wind speeds obtained during Hurricane Frederic in Alabama in 1979. The correlation between U_{sea} and U_{land} is shown in Figure III-4-6. The best-fit equation by linear regression methods is given by

$$U_{sea} = 1.62 \text{ (m/s)} + 1.17\, U_{land} \tag{III-4-12}$$

(h) Equation 4-11 is also plotted in Figure III-4-6. The difference between Equations 4-11 and 4-12 is not significant even though the correlation on which Equation 4-12 is based did not consider air-sea temperature differences. Equation 4-12 is recommended for use in coastal wind-blown sand transport studies where the air water temperature difference is small ($|Ta - Ts| < 5$ °C).

(i) For air-sea temperature differences exceeding 5 °C, a correction can be applied. A temperature correction applied to wind speed as given by Resio and Vincent (1977) is

$$U'_{10m} = R_T\, U_{10m} \tag{III-4-13}$$

where U'_{10m} is the wind speed corrected for the air-sea temperature difference and R_T is the correction factor applied to the overwater wind speed at the 10-m height. The correction factor R_T is shown in Figure III-4-7 and given by the equation

$$R_T = 1 - 0.06878\, |T_a - T_s|^{0.3811} \quad sign(T_a - T_s) \tag{III-4-14}$$

where T_a = the air temperature in degrees Celsius and T_s = the sea temperature in degrees Celsius.

(j) For wind-blown sand transport studies, wind measurement stations should be close to the study site and preferably on the beach. Land-based wind measurements at airports are generally not useful indicators of nearshore wind conditions and should not be used for coastal sand transport studies. Unfortunately, wind measurements are often not available near coastal study sites and data from nearby Coastal Marine Automated Network (C-MAN) and offshore meteorological buoys must be used. Table III-4-1 compares wind measurements at a C-MAN station (ALSN6), at an offshore buoy 44025, and at Islip Airport on central Long Island. (Wind speeds have been corrected to the standard 10-m elevation using a power-law relation. This correction is discussed below.) Wind speed measurements at Islip Airport are consistently lower than measurements at the coast. On average, $U_{44025}/U_{Islip} = 1.6$, which is consistent with the U_{sea}/U_{land} found earlier for the New York-Massachusetts area (Holzworth 1972, SethuRaman and Raynor 1980). Also, measurements at the offshore buoy are more variable than those at the C-MAN station, making the C-MAN station data preferable in this case.

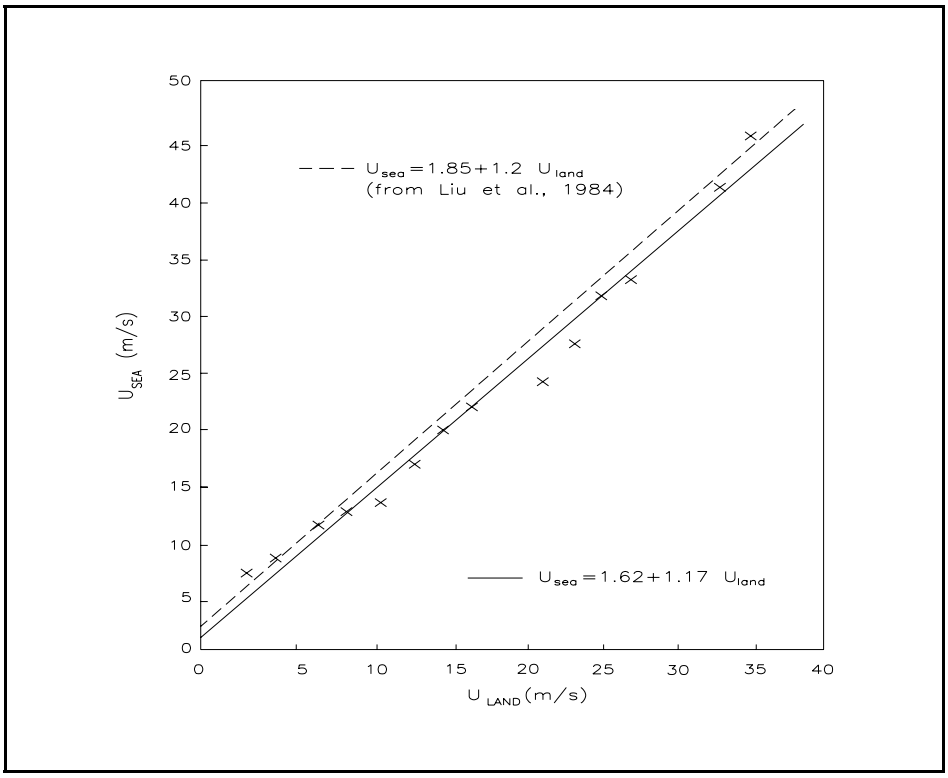

Figure III-4-6. Variation of U_{sea} with U_{land}. (Hsu 1986)

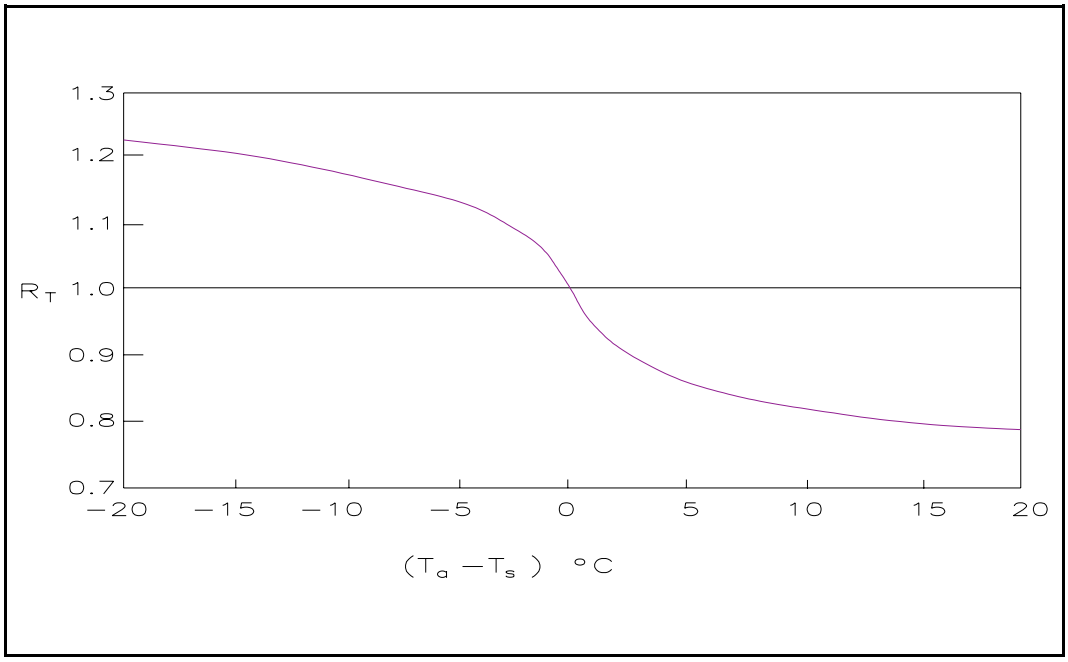

Figure III-4-7. Temperature correction factor R_T as a function of air-sea temperature difference (Resio and Vincent 1977)

Table III-4-1
Monthly Mean Wind Speeds Near Westhampton Beach, Long Island NY - Based on Simultaneous Measurements at C-MAN Station ALSN6 and Offshore Buoy 44025

		Wind Speeds in meters/sec				
YEAR	MONTH	C-MAN ALSN6 @4.9 m	BUOY 44025 @ 4.9 m	C-MAN ALSN6 @ 10 m	BUOY 44025 @ 10 m	ISLIP AIRPORT @ 10 m
1991	May	7.30	4.70	6.20	5.00	2.60
	Jun	6.70	5.40	5.70	5.80	2.90
	Jul	6.00	4.70	5.10	5.00	2.40
	Aug	6.80	5.00	5.80	5.40	2.80
	Sep	6.60	5.80	5.60	6.20	3.80
	Oct	7.60	6.30	6.50	6.70	4.50
1992	Nov	7.70	7.10	6.50	7.60	4.60
	Dec	8.80	7.90	7.50	8.50	4.70
	Jan	8.10	N/A	6.90	N/A	4.70
	Feb	8.70	7.30	7.40	7.80	5.10
	Mar	9.00	7.30	7.70	7.80	5.30
	Apr	7.00	5.40	6.00	5.80	4.50
	May	6.80	5.10	5.80	5.50	4.60
	Jun	7.10	4.80	6.00	5.10	4.70
AVG =		7.44	5.91	6.34	6.32	4.09
STD DEV =		0.91	1.14	0.79	1.22	0.99

(k) Wind speeds are often adjusted to a standard anemometer height by using a power-law relation. The standard anemometer height is usually 10 m above the ground. The power-law adjustment equation is given by

$$U_{ZR} = U_{ZM}\left(\frac{Z_R}{Z_M}\right)^n \tag{III-4-15}$$

in which Z_M = the anemometer height, Z_R = the reference height (usually 10 m), U_{ZM} = the wind speed at the anemometer height, U_{ZR} = the wind speed at the reference height, and n = an empirically determined exponent, ranging from 1/11 to 1/7. The following example details the calculation of this exponent as well as wind speed correction factors for air sea temperature differences.

(3) Effects of vegetation, dunes, and buildings.

(a) Air flow over a flat beach differs from air flow over dunes. There are at least three distinct wind transport zones resulting from the presence of dunes on the backbeach (Hsu 1988). Dunes produce both a stagnation zone on their windward side and a wake zone on their leeward side within which wind patterns are disturbed and no longer exhibit the typical logarithmic distribution with height above the ground. Wind blowing offshore results in a stagnation zone landward of the dune that extends landward approximately two to four times the height of the dune. In this zone, wind speeds are lower than the free stream wind speed (region of underspeed); in fact, near the ground they may even blow in the direction opposite to that of the

free stream. A wake region (cavity) may extend 10 dune heights seaward of the dune. Within the wake cavity, wind speeds are also reduced and may reverse direction near ground level. Over the dune crest, wind speeds are higher than the free stream speed because the streamlines are compressed and the flow is accelerated (region of overspeed) (see Figure III-4-8).

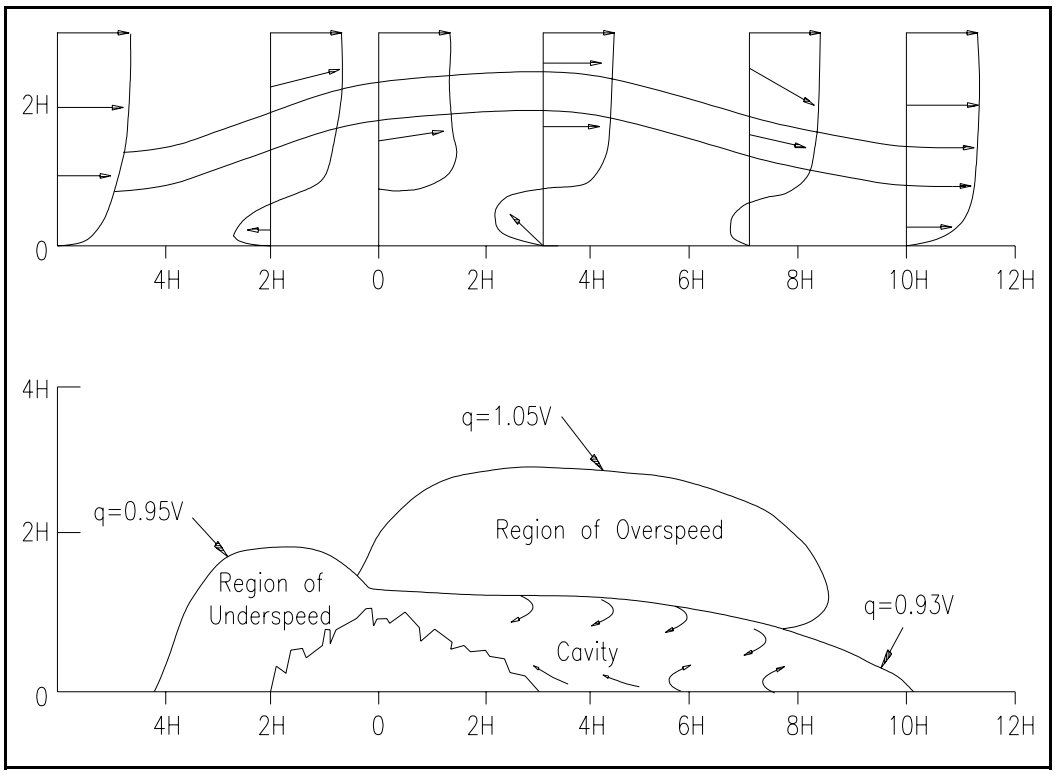

Figure III-4-8. Wind field in the vicinity of a coastal sand dune (*q* is the local resultant mean velocity and *v* is the reference velocity in the uniform stream above the dune) (Hsu 1988)

(b) Buildings and vegetation also locally modify the air flow. Generally, buildings will produce a wake in their lee. Air flow patterns near buildings will be complex, will depend on the specific building geometry, and on the presence of any surrounding buildings. Generalized air flow patterns cannot be established for the numerous building/construction configurations encountered in practice. The effect of vegetation depends on the type of vegetation, its location relative to any dunes, and how far it projects into the near-ground boundary layer. Trees usually have more effect on wind patterns than do shrubs or grasses but, depending on their location, may be less significant than shorter vegetation in affecting sand transport rates and sediment deposition patterns. Most sand transport takes place within a few centimeters of the ground and anything that modifies the air flow in this region will have some effect.

III-4-3. Transport Rates

a. Processes of sand transport by wind.

(1) The processes involved in transporting sand by wind are summarized by Raudkivi (1976). Sand grains move by bouncing along the surface, a process termed saltation, and by surface creep. Sand grains,

EXAMPLE PROBLEM III-4-3

Find:

Determine the overwater wind speed and correct the wind speed due to the air-sea temperature difference. Estimate the exponent in Equation 4-15 using the overwater wind speeds.

Given:

The winds given in Example Problem III-4-1 measured over land on a day when the air temperature is 15 °C and the water temperature is 5 °C.

Solution:

The air-sea temperature difference is (15°-5°) = 10 °C and the correction R_T is given by Equation 4-14

$$R_T = 1 - 0.06878\,|15 - 5|^{0.3811}(+) = 0.8346$$

This correction is applied to the wind speed at the 10-m height. Therefore, from Example Problem III-4-1, U_{10m} = 11.3 m/s and the corrected 10-m wind speed is

$$U_{10m} = 0.8346(11.3) = 9.43 \text{ m/s}$$

Assuming that the height of the roughness elements are Z_o = 0.05 as found in Example Problem III-4-1, the shear velocity can be found from Equation 4-2

$$U_z = \frac{u_*}{\kappa} \ln\left(\frac{Z + Z_o}{Z_o}\right) \qquad 9.43 = \frac{u_*}{0.4} \ln\left(\frac{10 + 0.05}{0.05}\right)$$

$$u_* = 0.7113 \text{ m/s}$$

The wind speed at the 8-m height is then calculated as

$$U_{8m} = \frac{0.7113}{0.4} \ln\left(\frac{8 + 0.05}{0.05}\right) = 9.036 \text{ m/s}$$

Using these two wind speeds to estimate the exponent in Equation 4-15

$$\frac{U_{10m}}{U_{8m}} = \left(\frac{10}{8}\right)^n \qquad \frac{9.43}{9.036} = (1.25)^n$$

$$n = \frac{\ln(1.0436)}{\ln(1.25)} = 0.1913 = \frac{1}{5.23}$$

once dislodged, are carried up into the moving air by turbulence; they acquire energy from the moving air, and they settle through the air column due to their weight and impact on the ground. The saltating grains impact on the ground surface at a flat angle and transmit a portion of their energy to the grains on the ground. Some of the grains on the surface are dislodged and are carried upward into the flow where they continue the process of saltation; others are moved forward on the surface by the horizontal momentum of the impacting, saltating grains. This latter forward movement of sand on the ground surface is termed surface creep. Saltating grains are capable of moving much larger surface grains by surface creep due to their impact. On beaches, saltation is the more important of the two processes.

(2) The presence of sand in the air column near ground level also leads to a reduction in the wind speed near the ground and a modification of the wind speed distribution.

(3) Because saltating sand grains impact the ground surface at a relatively flat angle which ranges from about 10 to 16 deg with the horizontal, there is a tendency for small depressions in the ground surface to lead to the formation of sand ripples. Saltating sand grains have a greater tendency to impact the back face of a small depression because of the flat angle of incidence. This preferential movement on the back face of the depression moves sand up the back face to form a mound or ripple. Once small ripples are established they may grow until they reach a limiting height which is determined by the prevailing wind speed.

(4) On beaches, the most important sand features frequently present are sand dunes. Dunes are much larger than the sand features described above. They are large enough to significantly alter wind patterns and to shelter the area on their leeward side. Once established, dunes cause wind pattern changes which lead to dune growth.

b. Sand transport rate prediction formulas.

(1) Many equations have been proposed to predict sand transport by wind; e.g., see Horikawa (1988) and Sarre (1988). Several example sand transport equations follow:

$$G = 0.036\ U_{5ft}^{3} \qquad \text{(O'Brien and Rindlaub 1936)}$$

in which G = the dry weight transport rate in pounds per foot per day and U_{5ft} = the wind speed at the 5-ft elevation in feet per second ($U_{5ft} > 13.4$ feet per second);

$$q = B_{Bagnold} \frac{\rho_a}{g} \sqrt{\frac{D}{d}}\ u_*^{3} \qquad \text{(Bagnold 1941)}$$

in which q = the mass transport rate in gm/cm-s, $B_{Bagnold}$ = a coefficient, ρ_a = the mass density of the air = 0.001226 gm/cm^3, d = a standard grain size = 0.25 mm, D = grain size in mm, and u_* = the shear velocity in cm/sec;

$$q = Z_{Zingg} \frac{\rho_a}{g} \left[\frac{D}{d}\right]^{\frac{3}{4}}\ u_*^{3} \qquad \text{(Zingg 1953)}$$

in which Z_{Zingg} = a coefficient, and q, D, d, ρ_a, and u_* are as in the previous expression.

(2) Chapman (1990) provides an evaluation of these and several other equations. The predictive capability of the seven equations investigated by Chapman (1990), as gauged by the coefficient of determination, ranged from $r^2 = 0.63$ to $r^2 = 0.87$ (see Table III-4-2).

Table III-4-2
Predictive Capability of Sand Transport Equations (Chapman 1990)

Equation	Value of r^2
Bagnold (1941)	0.63
Horikawa & Shen (1960)	0.84
Hsu (1973)	0.87
Kadib (1964)	0.65
O'Brien & Rindlaub (1936)	0.80
Williams (1964)	0.80
Zingg (1953)	0.78

(3) In Chapman's evaluation, Hsu's (1986) equation, which like Bagnold's (1941) is based on considerations of the turbulent kinetic energy relationship, had an $r^2 = 0.87$. Hsu's equation is given by

$$q = K\left[\frac{u_*}{\sqrt{gD}}\right]^3 \tag{III-4-16}$$

where

q = sand transport rate in gm/cm-s

u_* = shear velocity

g = acceleration of gravity

D = mean sand grain diameter

K = dimensional eolian sand transport coefficient

(4) The term in square brackets in Equation 4-16 is a dimensionless Froude number, which can be computed using any consistent units. The dimensions of K are the same as those of q; in this case, grams per centimeter per second. Values of K as a function of sand grain diameter can be obtained from Figure III-4-9. A regression equation ($r^2 = 0.87$) fitted to both laboratory and field data is given by

$$\ln K = -9.63 + 4.91D \tag{III-4-17a}$$

or

$$K = e^{-9.63 + 4.91D} \tag{III-4-17b}$$

where D is in millimeters and K in grams per centimeter per second, which plots as a straight line on semi-logarithmic graph paper (see Figure III-4-9).

(5) Equations 4-16 and 4-17a can be used to estimate sand transport rates for given wind speeds and mean sand-grain diameters within the range of empirical observations from which the equations were developed. Equation 4-17a is based on the data in Figure III-4-9, which include transport data for mean sand grain diameters up to 1.0 mm; consequently, the equations should not be used to estimate transport on beaches with mean grain diameters greater than about 1.0 mm.

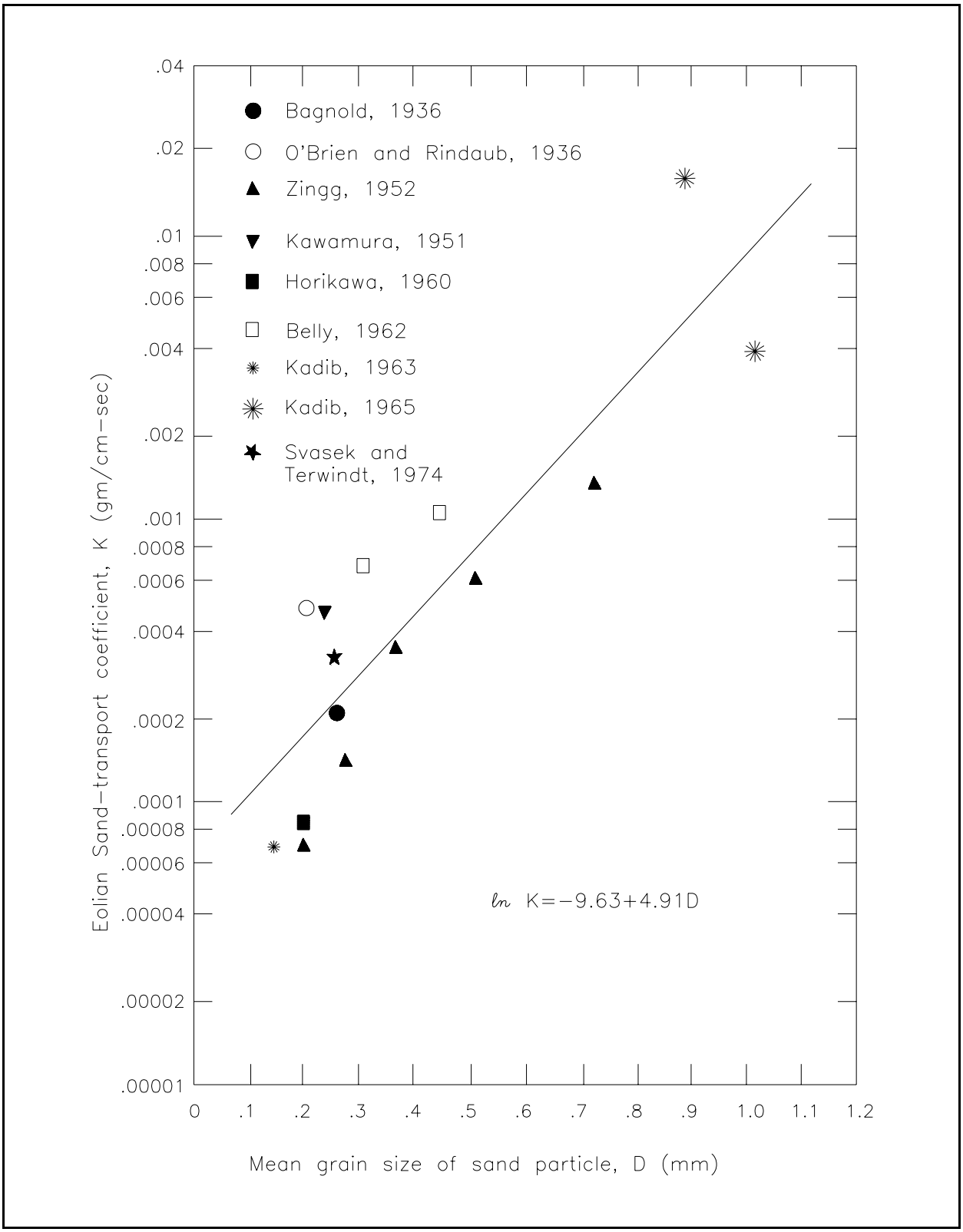

Figure III-4-9. Wind-blown sand transport coefficient as a function of mean sand-grain diameter (adopted from Hsu (1977)

(6) Equation 4-16 can be recast into a dimensionless form, which allows it to be used with any consistent set of units. The revised equation is given by

$$\frac{q}{\nu_a \rho_a} = K' \left[\frac{u_*}{\sqrt{gD}} \right]^3 \tag{III-4-18}$$

in which ν_a = the kinematic viscosity of the air and ρ_a = the mass density of the air. The dimensionless coefficient K' is given by

$$K' = e^{-1.00 + 4.91D} \tag{III-4-19}$$

in which D = *the median grain diameter in millimeters*. Equation 4-18 reduces to Equation 4-16 when $\nu_a = 0.147$ cm^2/sec and $\rho_a = 0.00122$ gm/cm^3 are substituted into it.

c. Initiation of sand transport. Before sand will be transported by wind, the boundary shear stress must be increased above some critical or threshold value. The critical shear stress, in terms of the shear velocity, is given by Bagnold (1941)

$$u_{*t} = A_t \sqrt{\frac{(\rho_s - \rho_a) g D}{\rho_a}} \tag{III-4-20}$$

in which ρ_s = the mass density of the sediment, ρ_a = the mass density of the air, and A_t = a dimensionless constant ($A_t = 0.118$). The effect of soil moisture that increases the critical shear stress is not considered in Equation 4-20.

III-4-4. Procedures for Calculating Wind-Blown Sand Transport

The steps for calculating wind-blown sand transport on beaches follow.

a. Obtain hourly average wind speed and direction data. (Wind data tabulated at intervals less frequent than 1 hr may be used in lieu of hourly data; however, hourly data are preferable.)

b. Obtain daily precipitation data and monthly evaporation records from a nearby National Weather Service (NWS) station. (These data are available in "Climatological Data" summaries published monthly for each state by the National Climatic Data Center (NCDC), Asheville, NC).

c. Obtain the density and median grain size of the beach sand at the study site.

d. Compute the critical shear velocity u_{*t} for the mean grain diameter using Equation 4-20.

e. Compute the critical wind speed at the 2-m height U_{2mt} using Equation 4-8 with the value of u_{*t} computed under Step 4 above. (This is the wind speed measured at the 2-m height that can initiate sand transport.)

f. Shear velocity u_* is relatively independent of height up to a height of about 50 m above ground level; therefore, Equation 4-7 can be used to compute the critical wind speed at any height above the ground using the U_{2mt} and u_{*t}. (For example, let Z_1 = 2 m, $U_{z1} = U_{2mt}$, Z_2 = the height at which the available wind

EXAMPLE PROBLEM III-4-4

Find:

Determine the volume of sand being transported per meter of beach width by the wind if the sand is dry.

Given:

The median sand-grain diameter at Westhampton Beach, Long Island, NY, is 0.26 mm. The wind velocity is measured by an anemometer located 8 m above the beach and found to be 21 m/s (see Figure III-4-10 for site location).

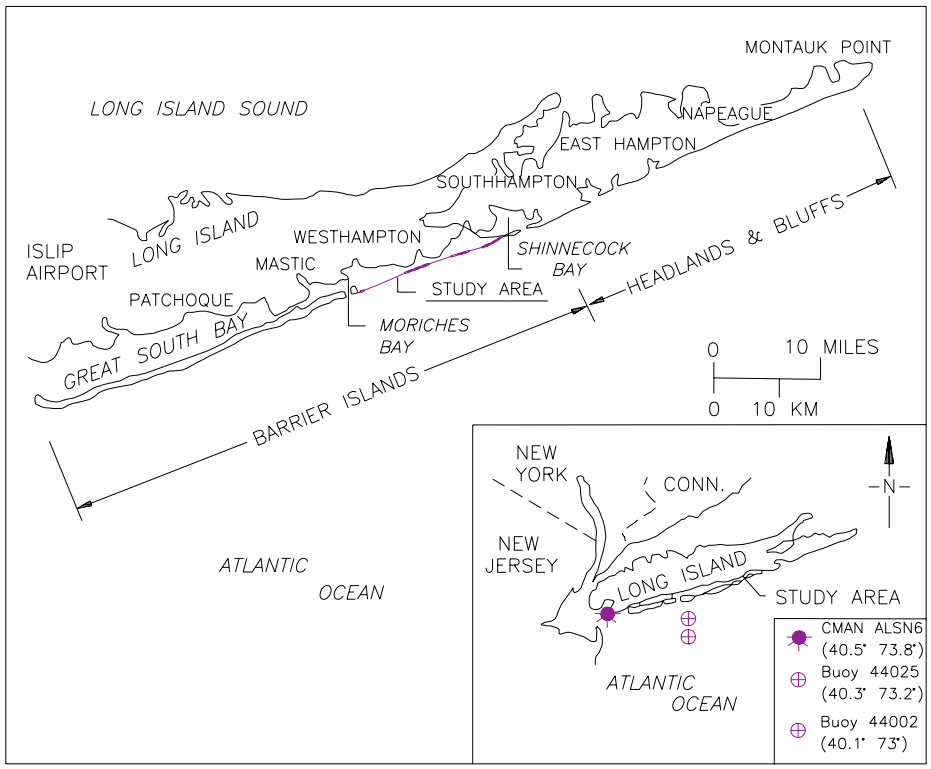

Figure III-4-10. Westhampton Beach, Long Island, NY (Hsu 1994)

Solution:

The first step is to compute the threshold wind speed that will just initiate sand transport. This is obtained from Equation 4-20

$$u_{*t} = A_t \sqrt{\frac{(\rho_s - \rho_a) g D}{\rho_a}}$$

(Sheet 1 of 5)

Example Problem III-4-4 (Continued)

where $A_t = 0.118$, g = acceleration of gravity, D = sand-grain diameter, ρ_a = density of air, and ρ_s = density of the sediment. At 18 °C, $\rho_a = 1.22 \times 10^{-3}$ gm/cm^3; $\rho_s = 2.65$ gm/cm^3, $g = 980$ cm/sec^2, and $D = 0.026$ cm. Note that Equation 4-20 is valid for any consistent set of units. Substituting into the equation

$$u_{*t} = 0.118\sqrt{\frac{(2.65 - 0.00122)(980)(0.026)}{(0.00122)}} = 27.75 \text{ cm/s} \quad (0.2775 \text{ m/s})$$

Next compute the threshold wind speed at the 2-m height. Using Equation 4-8 and the threshold shear velocity determined above

$$u_* = 0.044\, U_{2m}$$

where u_* = the shear velocity and U_{2m} = the wind velocity at the 2-m height. For threshold conditions

$$u_{*t} = 0.044\, U_{2mt}$$

where U_{2mt} is the threshold wind speed at a height of 2 m. Thus

$$U_{2mt} = 630.8 \text{ cm/sec} \quad (6.308 \text{ m/s})$$

This is the wind speed measured at the 2-m height that will initiate sand transport. Only average wind speeds that exceed 630.8 cm/s at the 2-m elevation will transport sand.

Because the wind speed is measured at the 8-m height, the threshold wind speed at that height must be determined. Equation 4-7 is given by

$$u_* = \frac{\kappa\,(U_{Z2} - U_{Z1})}{\ln\,(Z_2/Z_1)}$$

in which u_* is taken equal to u_{*t} since the shear velocity is independent of height above the ground.

Then, letting $U_{Z2} = U_{8mt}$, $U_{Z1} = U_{2mt}$, $Z_2 = 8$ m, $Z_1 = 2$ m, and noting that $u_{2t} = 630.8$ cm/s,

$$27.75 = \frac{0.4\,(U_{8mt} - 630.8)}{\ln(8/2)}$$

Solving for U_{8mt} gives $U_{8mt} = 727.0$ cm/s (7.27 m/s). Consequently, winds speeds that exceed 727.0 cm/s at the 8-m height are capable of transporting sand, while wind speeds less than 727.0 cm/s can be ignored in any wind-blown sediment transport study at this site.

(Sheet 2 of 5)

Example Problem III-4-4 (Continued)

Alternatively, Figure III-4-11a or III-4-11b can be used to find the threshold velocity for wind speed measurements at the 8-m height. The curves on Figures III-4-11a and III-4-11b were calculated using the preceding procedure. Enter the figure with the median sand-grain diameter of 0.26 mm and read from the curve for an anemometer height of 8 m. This gives U_{8mt} = 730 cm/s. (Figure III-4-11b is an enlargement of Figure III-4-11a for median sand sizes up to 0.25 mm.)

The amount of sediment being transported by the 21-m/s wind speed can now be calculated from Equation 4-16 or 4-18.

$$q = K\left[\frac{u_*}{\sqrt{gD}}\right]^3$$

where K = an empirical coefficient given by Equation 4-17a or 4-17b. The term in the square brackets is a dimensionless number having the form of a Froude number. Since this term is dimensionless, variables in any consistent set of units can be used to evaluate it. Equation 4-17b is

$$K = e^{-9.63 + 4.91D} \quad \text{(gm/cm-s)}$$

in which D must be in millimeters. Equation 4-17a yields K in units of gm/cm-s; consequently, when used in Equation 4-16, the resulting mass transport q also will be in units of gm/cm-s. For the example,

$$K = e^{-9.63 + 4.91(0.26)} = e^{-8.354}$$

hence

$$K = e^{-8.354} \quad \text{or} \quad K = 2.355 \times 10^{-4} \text{ gm/cm-s}$$

Then

$$q \text{ (gm/cm-s)} = (2.355 \times 10^{-4})\left[\frac{u_* \text{ (cm/s)}}{\sqrt{(980)(0.026)}}\right]^3$$

in which u_* must be specified in cm/s since g is in centimeters per second squared and D is provided in centimeter units for dimensional consistency. Then

$$q = (1.831 \times 10^{-6})\, u_*^3$$

The shear velocity u_* must now be expressed in terms of the wind speed at the 8-m height. Equation 4-7 is used again, noting that $u_* = 0.044\, U_{2m}$, or $U_{2m} = 22.73\, u_*$

$$u_* = \frac{0.4(U_{8m} - 22.73u_*)}{\ln(8/2)}$$

(Sheet 3 of 5)

Example Problem III-4-4 (Continued)

solving for u_*

$$u_* = 0.0382\, U_{8m}$$

and

$$q = (1.019\ x\ 10^{-10})\, U_{8m}^3$$

in which q is in grams per centimeter-second and U_{8m} is in centimeters per second.

For the given wind speed at the 8-m height, U_{8m} = 2,100 cm/s and

$$q = 0.9433\ \frac{\text{gm}}{\text{cm}-\text{s}}$$

Equation 4-16 can be rewritten simply as

$$q = K^*(D,Z_M)\, U^3{}_{zM}$$

where K^* (D,Z_M) = a coefficient in units of grams-seconds squared per centimeter to the fourth power which depends on the mean grain diameter D and the height at which the wind speed is measured Z_M. Values of K^* can be obtained from Figure III-4-12a or III-4-12b. Entering the figure with a sand-grain diameter of 0.26 mm and reading from the curve for an anemometer height of 8 m, $K^* = 1.01 \times 10^{-10}$ gm-s^2/cm^4, so that

$$q = 1.01 \times 10^{-10}\, U_{8m}^3 \quad \frac{\text{gm}}{\text{cm}-\text{s}}$$

as above (where U_Z must be specified in centimeters per second). Figure III-4-12b is an enlargement of Figure III-4-12a for sand-grain diameters up to 0.25 mm.

Figure III-4-12a indicates that transport rates decrease as the mean grain diameter increases for grain diameters up to about 0.3 mm. For larger grain diameters, transport rates increase with increasing grain diameter. Equation 4-17a, on which Figure III-4-12a is based, was derived empirically for mean grain diameters up to 1.0 mm; consequently, Figure III-4-12a is believed to be valid for grain diameters up to 1.0 mm; however, the relationships should not be used for grain diameters greater than 1.0 mm (i.e., outside the range of data utilized to develop the empirical relationship).

The volumetric sand transport rate can be obtained from the mass transport rate from

$$q_v = \frac{q}{\rho_s(1 - p)}$$

(Sheet 4 of 5)

Example Problem III-4-4 (Concluded)

in which ρ_s = the mass density of the sand and p = the porosity (the fraction of the in situ sand deposit which is pore space). Assuming a typical porosity of 0.4 for the in situ sand and using ρ_s = 2.65 gm/cm^3, the volume rate of dry sand transport per unit width is

$$q_v = \frac{(0.9433)}{(2.65)(1 - 0.4)} \quad \text{or} \quad q_v = 0.5933 \text{ cm}^3/\text{cm-s}$$

Therefore

$$q_v = 5.933 \times 10^{-5} \text{ m}^3/\text{m-s}$$

An equation for the volume sand transport rate can be written

$$q_v = K_v^*(D,Z_M)\, U_{zM}^3$$

in which K_v^* = a coefficient in units of m^2 - sec^2/cm^3 which depends on the mean sand-grain diameter D and the height at which the wind speed is measured Z_M. The coefficient K_v^* can be obtained from Figure III-4-13 which is based on the assumption that the sediment has a mass density of ρ_s = 2.65 gm/cm^2 and an in situ porosity of 0.4. Entering Figure III-4-13 with the grain diameter of 0.26 mm and reading from the curve for an anemometer height of 8 m gives

$$q_v = 6.3 \times 10^{-15} U_{8m}{}^3$$

in which q_v = the volume transport rate in cubic meters per meter-second and U_{8m} is in centimeters per second. Therefore

$$q_v = 6.3 \times 10^{-15}(2{,}100)^3 = 5.83 \times 10^{-5} \text{ m}^3/\text{m-s}$$

which is approximately the same result obtained earlier. Note that the wind speed is specified in centimeters per second and the resulting volume transport is in cubic meters per meter-second.

While the foregoing involves a lot of computation, repeated application of the equations to wind speed and direction data is much simplified, since the equations for the given site reduce to

$$U_{8mt} = 727.0 \text{ cm/s}$$

the threshold wind velocity at the 8-m height, and

$$q = (1.019 \times 10^{-10})\, U_{8m}{}^3 \text{ gm/cm-s}$$

the mass transport rate per unit width where U_{8m} is in centimeters per second. These equations will be used in a subsequent example.

(Sheet 5 of 5)

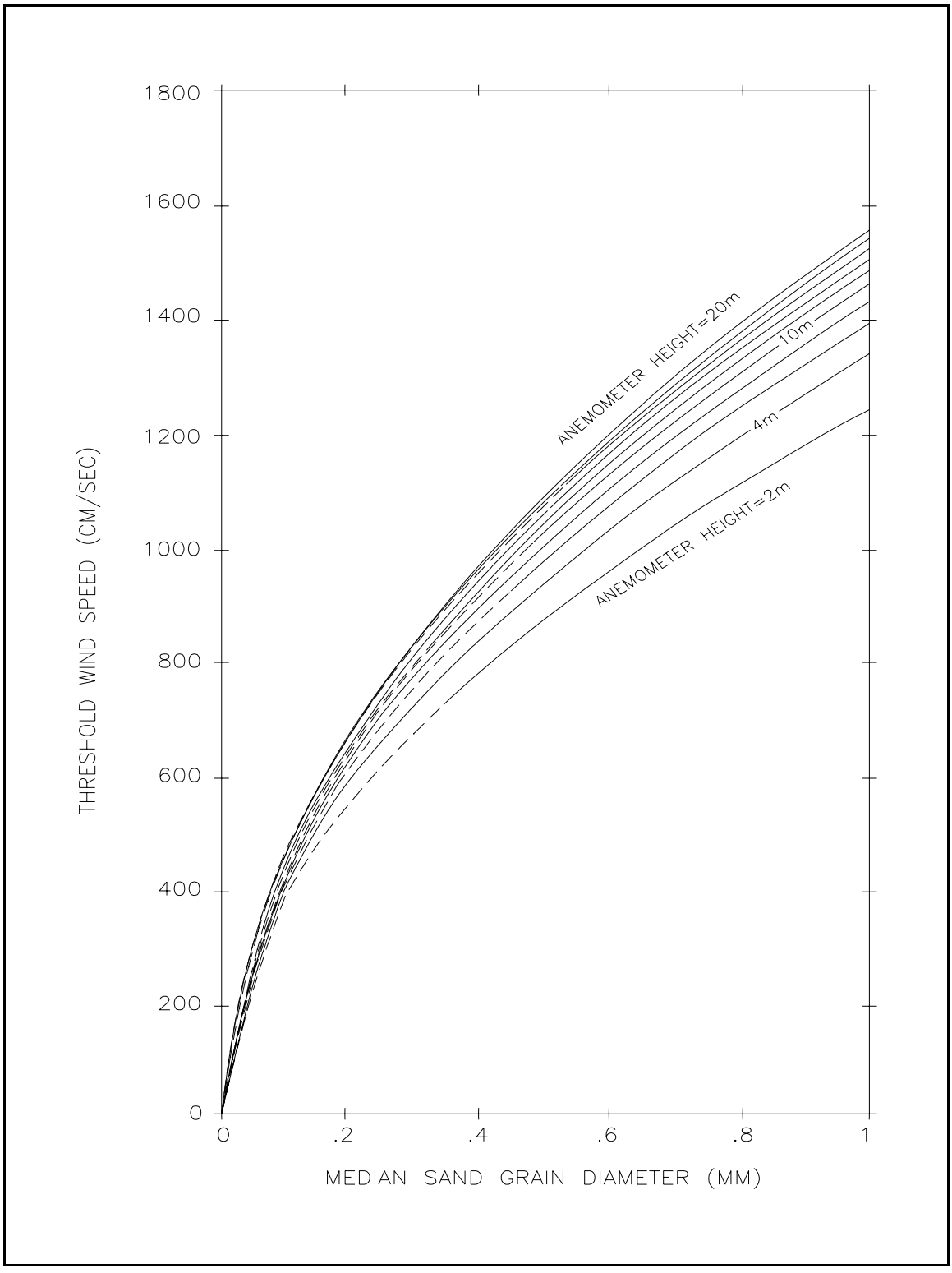

Figure III-4-11a. Threshold (critical) wind speed as a function of median sand-grain diameter and the anemometer height at which wind speed is measured (Continued)

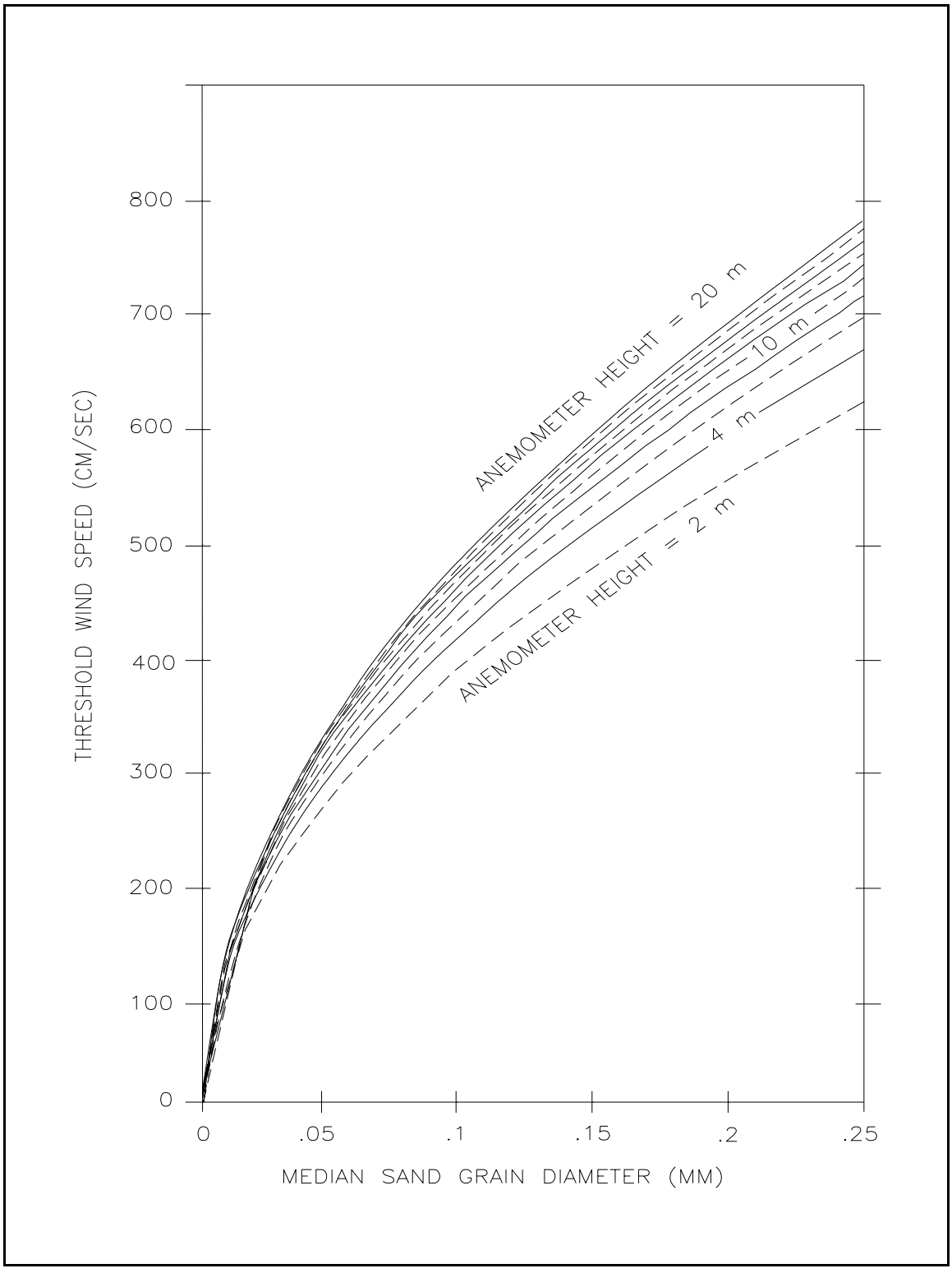

Figure III-4-11b. (Concluded)

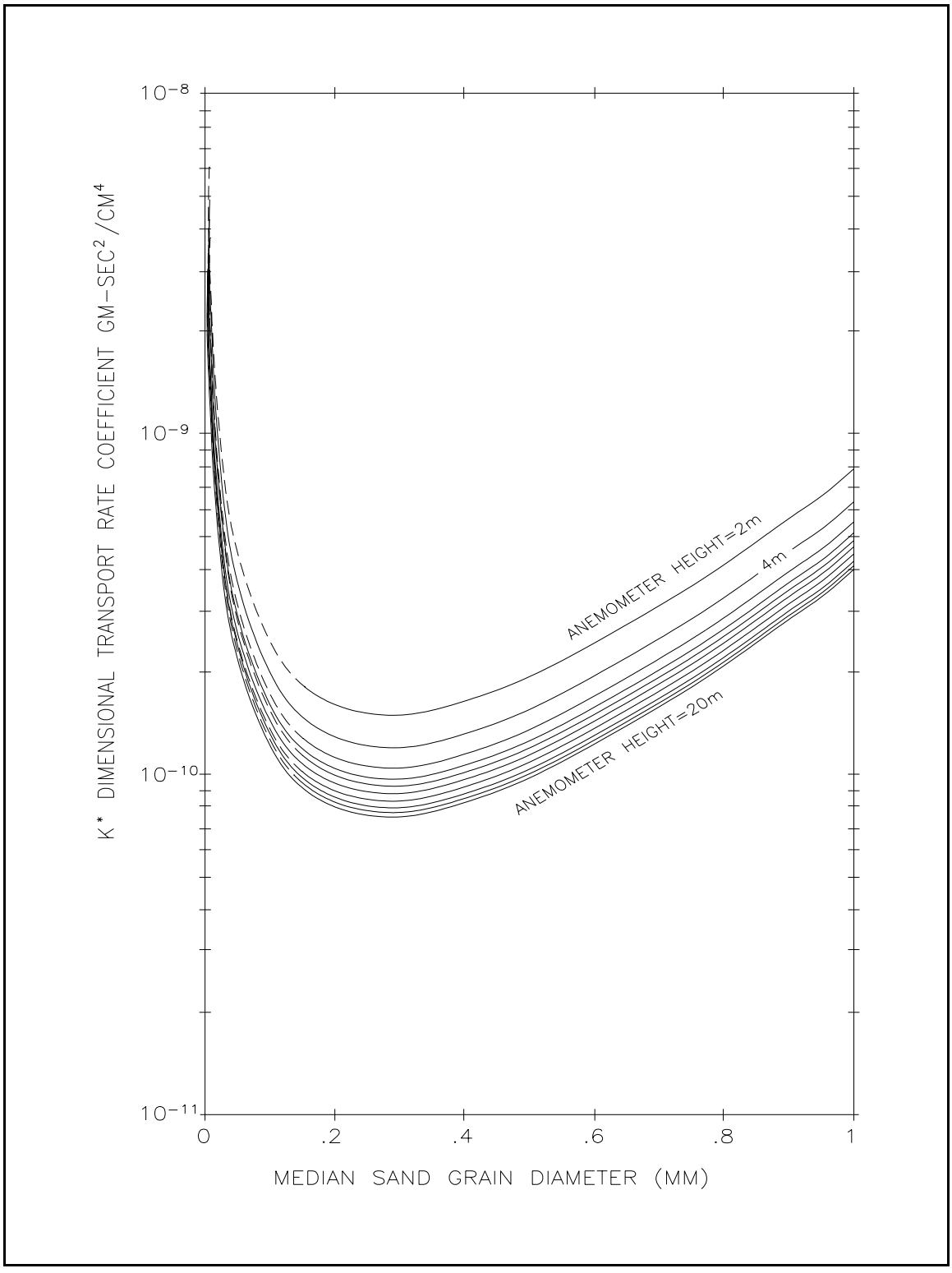

Figure III-4-12a. Mass transport rate coefficient K^* as a function of median sand-grain diameter and the anemometer height at which wind speed is measured (Continued)

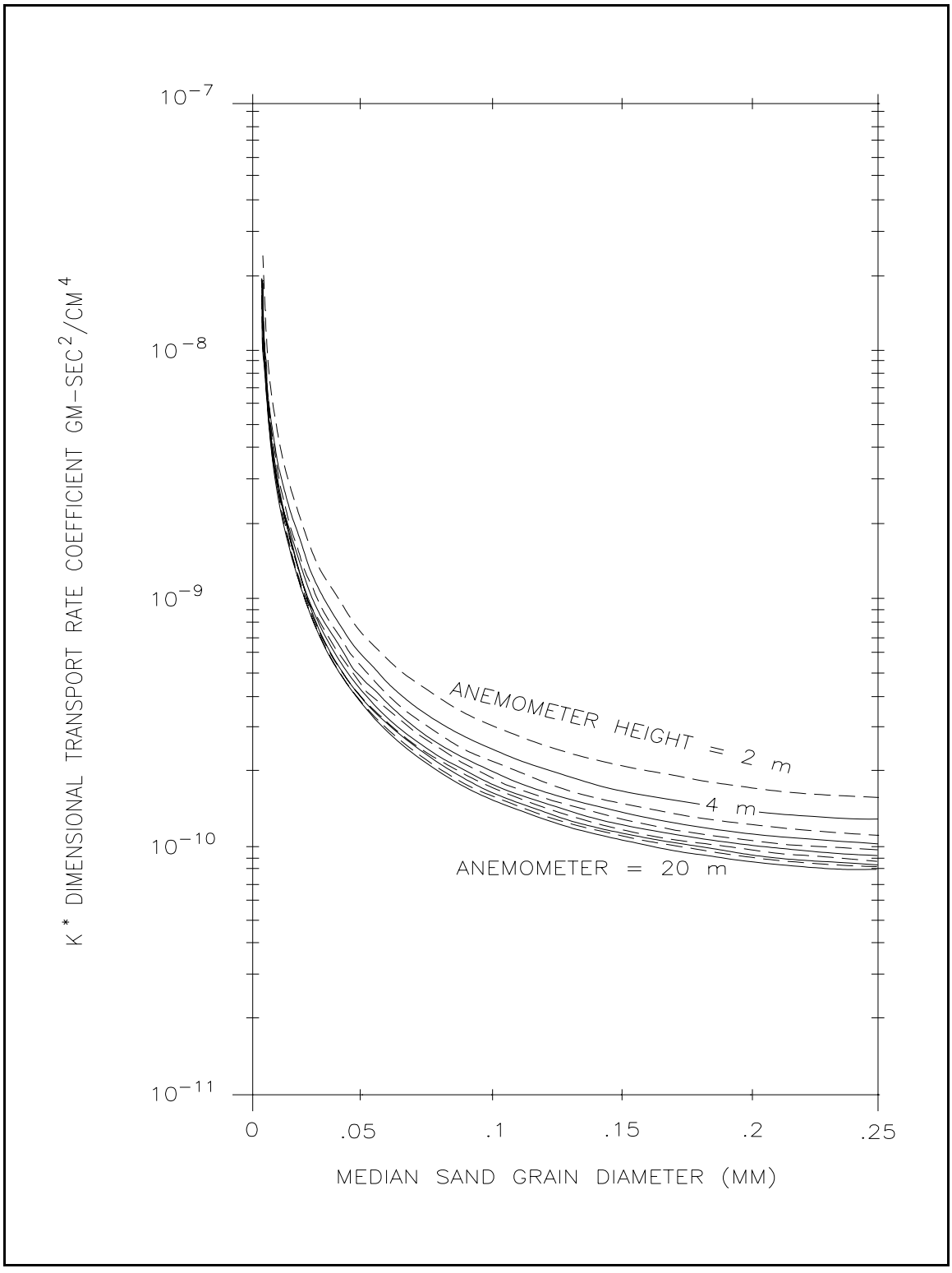

Figure III-4-12b. (Concluded)

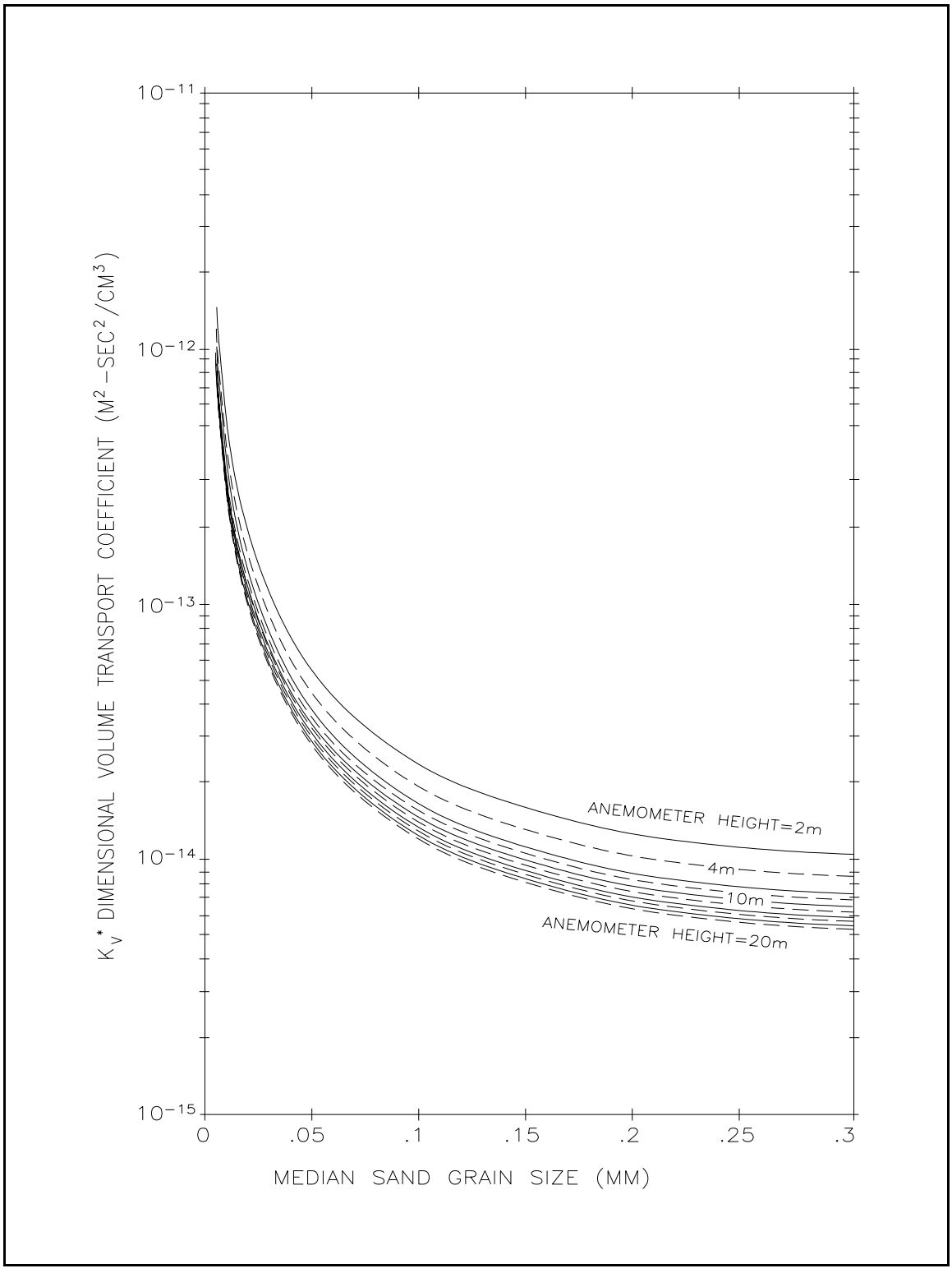

Figure III-4-13. Volume transport rate coefficient K^*_V as a function of median sand-grain diameter and the anemometer height at which wind speed is measured (assumes sediment density = 2.65 gm/cm^3 and porosity = 0.4)

EXAMPLE PROBLEM III-4-5

Find:

The total amount of sand transported by the wind during the given day and the total transported in each of the 16 point compass directions.

Given:

Hourly wind speed and direction data given in Table III-4-3 for Westhampton Beach, Long Island, NY, were measured by an anemometer located 8 m above the ground. The median sand-grain diameter at Westhampton Beach is 0.26 mm.

Solution:

The solution is given in Table III-4-4. The preceding example problem shows that for a sand-grain diameter of 0.26 mm, the threshold wind speed at the 8-m height is 7.27 m/s. Winds less than 7.27 m/s will not transport sand. Columns 1, 2, and 3 in Table III-4-4 are the given data. (Note that wind directions are the direction from which the wind is blowing.) Column 4 is constructed from column 3 and indicates the direction in which the sand will move rather than the direction from which the wind is blowing. The given winds are essentially from the south and will transport sand northward. Column 5 gives the effective winds. Winds less than the threshold value of 7.27 m/sec have been set to zero. Column 6 is computed from column 5 using the equation

$$q = (1.019 \times 10^{-10})\ U_{8m}{}^{3}$$

in which U_{8m} is the wind speed at the 8-m height in centimeters per second; this equation gives q in grams per centimeter-seconds. Column 7 is obtained from column 6 by dividing by the density of the sand, 2.65 gm/cm^3, and the packing factor, (1 - 0.4) = 0.6. The total volume transported during each hour between observations (column 8) is 3,600 s/hr times the average transport rate during each hour. The total sand transport during the day is 0.5994 m^3/m. Transport in each compass direction is given at the bottom of the table.

Table III-4-3
Hourly Wind Data, Westhampton Beach, Long Island, NY

Time (hr)	Wind Speed (m/sec)	Wind Direction (Azimuth)	Transport Direction (Compass)
(1)	(2)	(3)	(4)*
Midnight	12.0	175	N
1	8.0	170	N
2	9.0	175	N
3	11.0	150	NNW
4	9.0	175	N
5	9.0	190	N
6	10.0	170	N
7	9.0	185	N
8	6.0	165	NNW
9	5.0	155	NNW
1	4.0	170	N
1	5.0	195	NNE
Noon	9.0	215	NE
1	14.0	200	NNE
2	12.0	215	NE
3	13.0	190	N
4	11.0	180	N
5	10.0	160	NNW
6	7.0	180	N
7	11.0	170	N
8	16.0	175	N
9	14.0	175	N
10	9.0	175	N
11	9.0	150	NNW
Midnight	7.0	145	NW

* Direction of transport (opposite of wind direction).

Table III-4-4
Hourly Transport Analysis Under Dry Conditions, Westhampton Beach, Long Island, NY

Time (hr) (1)	Speed (cm/sec) (2)	Direction Azimuth (3)	Direction Compass (4)	Effective Winds (cm/sec) (5)	Rate (g/cm-sec) (6)	Rate (m^3/m-sec) (7)	Volume (m^3/m) (8)
1 am	800	170	N	800	0.0522	3.281e-06	0.0258
2	900	175	N	900	0.0743	4.672e-06	0.0143
3	1100	150	NNW	1100	0.1356	8.530e-06	0.0238
4	900	175	N	900	0.0743	4.672e-06	0.0238
5	900	190	N	900	0.0743	4.672e-06	0.0168
6	1000	170	N	1000	0.1019	6.409e-06	0.0199
7	900	185	N	900	0.0743	4.672e-06	0.0199
8	600	165	NNW	0	0	0.000e+00	0
9	500	155	NNW	0	0	0.000e+00	0
10	400	170	N	0	0	0.000e+00	0
11	500	195	NNE	0	0	0.000e+00	0
Noon	900	215	NE	900	0.0743	4.672e-06	0.0084
1 pm	1400	200	NNE	1400	0.2796	1.759e-05	0.0401
2	1200	215	NE	1200	0.1761	1.107e-05	0.0516
3	1300	190	N	1300	0.2239	1.408e-05	0.0453
4	1100	180	N	1100	0.1356	8.530e-06	0.0407
5	1000	160	NNW	1000	0.1019	6.409e-06	0.0269
6	700	180	N	0	0	0.000e+00	0
7	1100	170	N	1100	0.1356	8.530e-06	0.0154
8	1600	175	N	1600	0.4174	2.625e-05	0.0626
9	1400	175	N	1400	0.2796	1.759e-05	0.0789
10	900	175	N	900	0.0743	4.672e-06	0.0401
11	900	150	NNW	900	0.0743	4.672e-06	0.0168
Midnight	700	145	NW	0	0	0.000e+00	0
TOTAL							0.5711
TOTAL NW							0
TOTAL NNW							0.0675
TOTAL N							0.4035
TOTAL NNE							0.0401
TOTAL NE							0.0600

EXAMPLE PROBLEM III-4-6

Find:

If the amount of precipitation on the given day exceeds the amount of evaporation, determine the total amount of sand transported by wind and the amount of transport in each of the 16 compass directions.

Given:

The hourly wind speeds and directions in the preceding example problem (Table III-4-3) for Westhampton Beach, Long Island.

Solution:

Because the amount of precipitation exceeds the amount of evaporation, the sand can be assumed to be wet and the threshold velocity will be greater than the threshold velocity for dry sand. The threshold velocity for wet sand is given by Equation 4-22b

$$u_{*tw} = u_{*t} + 18.75 \quad \text{cm/s}$$

in which u_{*tw} and u_{*t} are in centimeters per second. From the preceding example, $u_{*t} = 27.75$ cm/s. Thus

$$u_{*tw} = 27.75 + 18.75 = 46.5 \quad \text{cm/s}$$

The corresponding wind speed at the 2-m height is

$$u_{*tw} = 0.044\, U_{2mtw}$$

or

$$U_{2mtw} = \frac{46.5}{0.044} = 1057 \quad \text{cm/s}$$

For winds measured at the 8-m height, as before

$$u_* = \frac{\kappa (U_{Z2} - U_{Z1})}{\ln (Z_2/Z_1)}$$

and

$$46.5 = \frac{0.4 (U_{8mtw} - 1057)}{\ln (8/2)} \qquad \text{Therefore} \qquad U_{8mtw} = 1{,}218 \ \text{cm/s}$$

The wind speed measured at the 8-m height must exceed 1,218 cm/s in order to transport sand. Winds less than 1,218 cm/s in the record are not considered in the computations. The wet sand threshold velocity can also be found from Figures III-4-14a or III-4-14b. Entering with a grain diameter of 0.26 mm, read the curve for and anemometer height of 8 m to find the threshold velocity of $U_{8mtw} = 1{,}220$ cm/s. Figure III-4-14b is an enlargement of Figure III-4-14a. Table III-4-5 gives the results of the transport analysis. Wet conditions reduce the total transport from 0.5994 m^3/m to 0.2718 m^3/m.

(Sheet 1 of 4)

Example Problem III-4-6 (Continued)

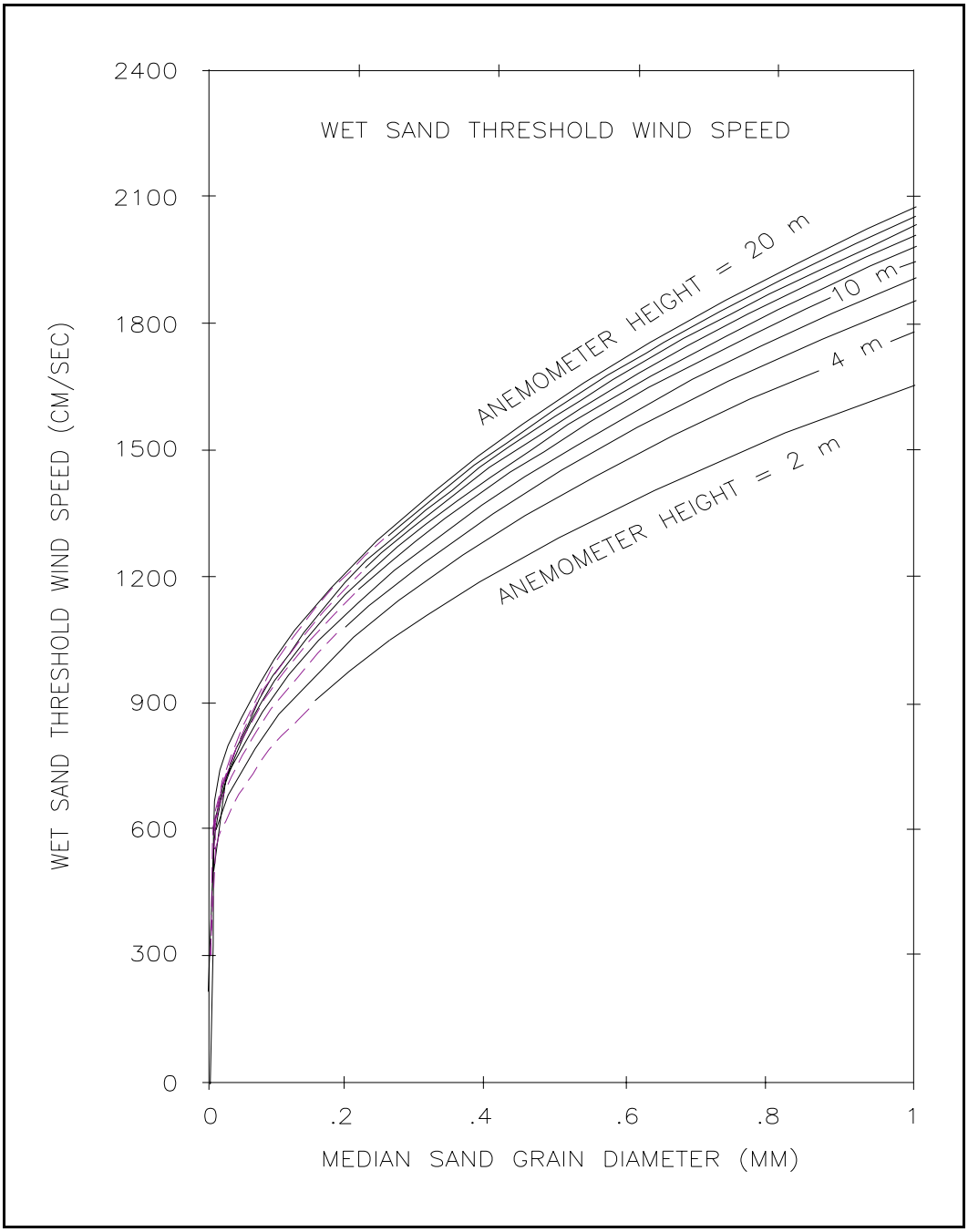

Figure III-4-14. Wet sand transport rate coefficient as a function of median sand grain diameter and the anemometer height at which wind speed is measured (Continued)

(Sheet 2 of 4)

Example Problem III-4-6 (Continued)

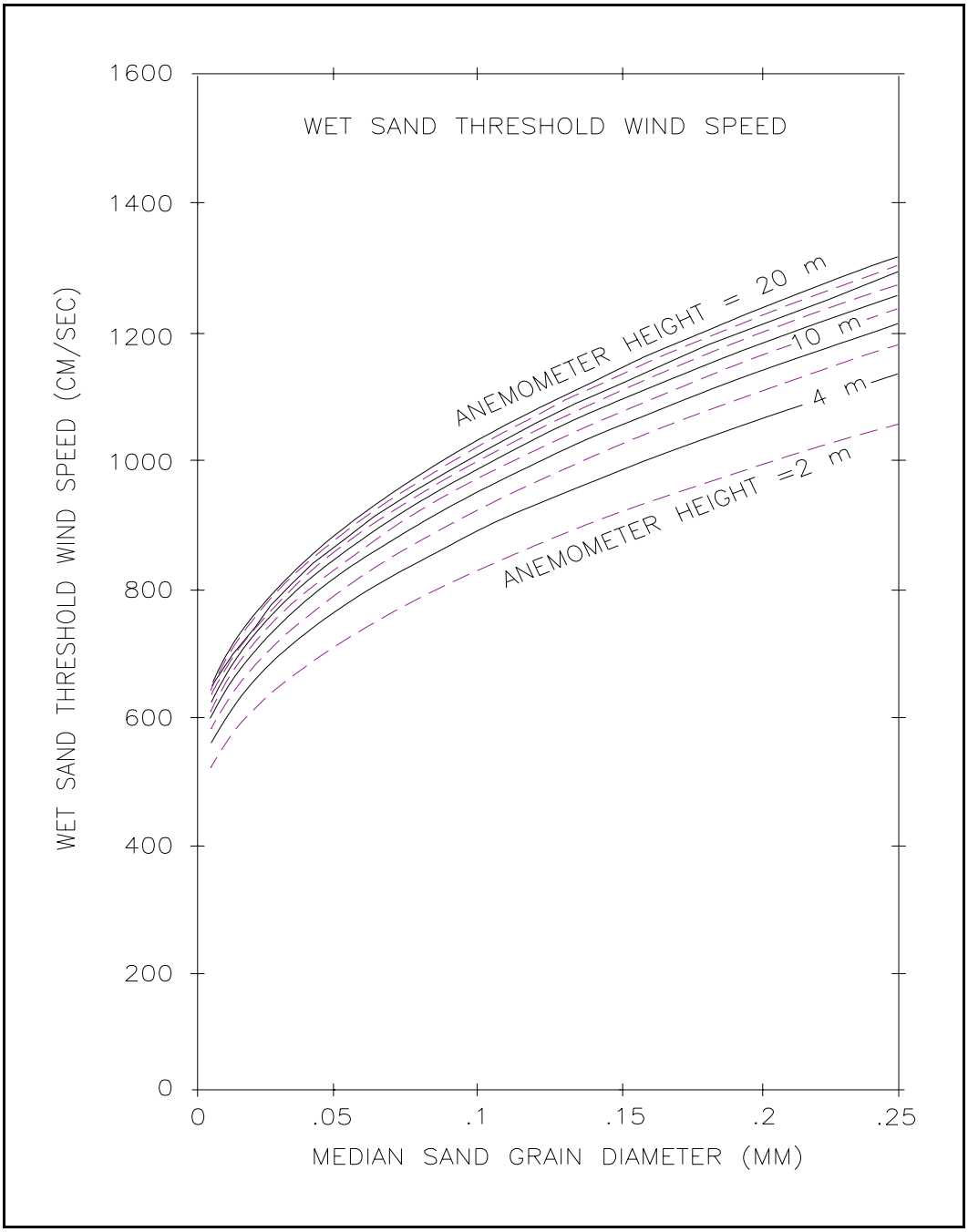

Figure III-4-14. (Concluded)

(Sheet 3 of 4)

Example Problem III-4-6 (Concluded)

Table III-4-5
Hourly Transport Analysis Under Wet Conditions, Westhampton Beach, Long Island, NY.

Time (hr) (1)	Speed (cm/sec) (2)	Direction Azimuth (3)	Direction Compass (4)	Effective Winds (cm/sec) (5)	Rate (g/cm-sec) (6)	Rate (m^3/m-sec) (7)	Volume (m^3/m) (8)
1 am	800	170	N	0	0	0.000e+00	0
2	900	175	N	0	0	0.000e+00	0
3	1100	150	NNW	0	0	0.000e+00	0
4	900	175	N	0	0	0.000e+00	0
5	900	190	N	0	0	0.000e+00	0
6	1000	170	N	0	0	0.000e+00	0
7	900	185	N	0	0	0.000e+00	0
8	600	165	NNW	0	0	0.000e+00	0
9	500	155	NNW	0	0	0.000e+00	0
10	400	170	N	0	0	0.000e+00	0
11	500	195	NNE	0	0	0.000e+00	0
Noon	900	215	NE	0	0	0.000e+00	0
1 pm	1400	200	NNE	1400	0.2796	1.759e-05	0.0317
2	1200	215	NE	0	0	0.000e+00	0
3	1300	190	N	1300	0.2239	1.408e-05	0.0253
4	1100	180	N	0	0	0.000e+00	0
5	1000	160	NNW	0	0	0.000e+00	0
6	700	180	N	0	0	0.000e+00	0
7	1100	170	N	0	0	0.000e+00	0
8	1600	175	N	1600	0.4174	2.625e-05	0.0473
9	1400	175	N	1400	0.2796	1.759e-05	0.0789
10	900	175	N	0	0	0.000e+00	0
11	900	150	NNW	0	0	0.000e+00	0
Midnight	700	145	NW	0	0	0.000e+00	0
TOTAL							0.1832
TOTAL NW							0
TOTAL NNW							0
TOTAL N							0.1515
TOTAL NNE							0.0317
TOTAL NE							0

(Sheet 4 of 4)

measurements were taken, and solve for U_{z2t} = the critical wind velocity at the Z_2 height.) Only wind speeds in excess of the computed U_{z2t} will result in sand transport.

g. If wind speeds exceed the critical value and there was no precipitation on a given day, compute the potential sand transport rate using Equation 4-16 or Equation 4-18.

h. If there was precipitation on a given day, the amount of precipitation should be compared with the amount of evaporation. If evaporation exceeds precipitation, compute the potential sand transport rate using Equation 4-16 or 4-18. (If daily evaporation data are not available, daily evaporation can be estimated by dividing monthly evaporation by the number of days in the month.)

i. If precipitation exceeds evaporation, the critical shear velocity can be computed by

$$u_{*tw} = u_{*t} + 7.5W \quad \text{(III-4-21)}$$

in which W = the fraction water content in the upper 5 mm of the sand (Hotta et al. 1985). Based on measurements in Holland made with a radioactive moisture probe, Svasek and Terwindt (1974) found that W < 0.025 (2.5 percent). Consequently

$$u_{*tw} = u_{*t} + 0.1875 \quad \text{(m/s)} \quad \text{(III-4-22a)}$$

or

$$u_{*tw} = u_{*t} + 18.75 \quad \text{(cm/s)} \quad \text{(III-4-22b)}$$

may be used in the absence of detailed soil moisture data. For days when precipitation exceeds evaporation, u_{*tw} is used as the critical shear velocity rather than u_{*t}. The computations then proceed as above.

j. If precipitation is in the form of snow, there will be no sand transport until the snow cover has melted. In the computations, days with snow and days known to have snow cover are excluded from the record. Data on snow cover are included in "Local Climatological Data" for all major National Weather Service (NWS) stations.

k. The results of a comprehensive study of potential sand transport by wind at Westhampton Beach by Hsu (1994) are shown in the form of a transport rose in Figure III-4-15. The rose gives the direction from which the sand is transported with the most being transported northward or northwestward. Wind data were obtained from C_MAN Station ALSN6 for 1989. The results of the analysis are tabulated in Tables III-4-6 through III-4-8. Table III-4-6 presents the results obtained by not considering snow cover or moisture conditions. The total potential transport for the year is 71.2 m^3/m-yr. The table also shows that most transport at Westhampton Beach occurs during the winter months, with the most transport during November and December. Table III-4-7 corrects for days of snow cover. The total transport is reduced to 64.6 m^3/m-yr. When the data are also corrected for moisture conditions (Table III-4-8), the total transport is further reduced to 53.2 m^3/m-yr, about 75 percent of the uncorrected value of 71.2 m^3/m-yr.

III-4-5. Wind-Blown Sand Transport and Coastal Dunes

a. Dunes and dune processes.

(1) Sand dunes are important coastal features that are created, enlarged, and altered by wind-blown sand. In the absence of dunes, the beach landward of the active shoreface and berm is often characterized by a

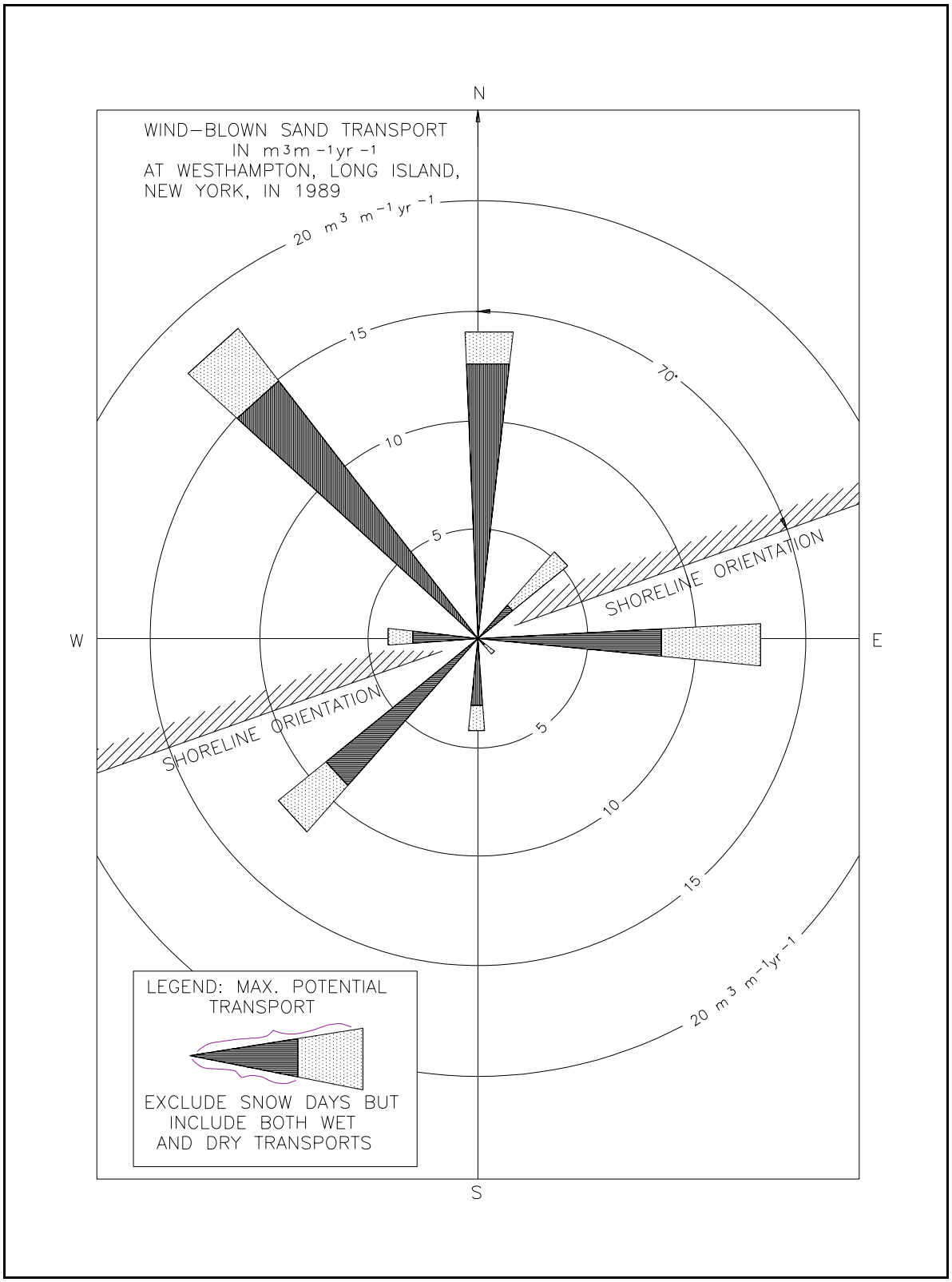

Figure III-4-15. Wind-blown sand transport rose at Westhampton Beach, Long Island, NY, for 1989 (Hsu 1994)

Table III-4-6
Monthly Sand Transport at Westhampton Beach, Long Island, NY (All Data Considered) (Hsu 1994)

Volume, Cubic Meters Per Meter													
Direction	**Jan**	**Feb**	**Mar**	**Apr**	**May**	**Jun**	**Jul**	**Aug**	**Sep**	**Oct**	**Nov**	**Dec**	**Total**
N	2.66	1.06	0.80	0.91	0.33	0.16	0.07	0.09	0.85	0.69	2.88	3.37	13.88
NE	0.14	1.45	1.12	0.38	0.12	0.03	0.15	0.14	0.10	0.24	0.34	0.86	5.07
E	0.92	0.63	3.94	0.13	1.83	0.33	0.23	0.60	1.63	2.41	0.04	0.33	13.01
SE	0.10	0.00	0.16	0.09	0.05	0.01	0.18	0.06	0.14	0.20	0.03	0.00	1.03
S	0.33	0.47	0.08	0.19	0.56	0.09	0.03	0.01	0.52	0.53	1.20	0.30	4.32
SW	0.47	0.95	1.68	2.09	1.54	0.58	0.28	0.12	1.53	0.58	1.67	0.33	11.82
W	0.33	0.30	0.20	0.10	0.24	0.02	0.16	0.08	0.18	0.42	1.85	0.34	4.23
NW	1.65	1.43	0.54	1.04	0.44	0.34	0.01	0.11	0.08	1.17	4.55	6.46	17.82
Total	6.62	6.29	8.53	4.94	5.11	1.55	1.10	1.22	5.03	6.24	12.56	11.99	71.18

Table III-4-7
Monthly Sand Transport at Westhampton Beach, Long Island, NY (Snow Days Excluded) (Hsu 1994)

Volume, Cubic Meters Per Meter													
Direction	**Jan**	**Feb**	**Mar**	**Apr**	**May**	**Jun**	**Jul**	**Aug**	**Sep**	**Oct**	**Nov**	**Dec**	**Total**
N	2.66	0.76	0.78	0.91	0.33	0.16	0.07	0.09	0.85	0.69	2.80	3.12	13.24
NE	0.11	0.28	0.26	0.38	0.12	0.03	0.15	0.14	0.10	0.24	0.00	0.85	2.66
E	0.22	0.60	3.35	0.13	1.83	0.33	0.23	0.60	1.63	2.41	0.04	0.07	11.45
SE	0.10	0.00	0.16	0.09	0.05	0.01	0.18	0.06	0.14	0.20	0.03	0.00	1.03
S	0.33	0.47	0.08	0.19	0.56	0.09	0.03	0.01	0.52	0.53	1.20	0.30	4.32
SW	0.47	0.95	1.68	2.09	1.54	0.58	0.28	0.12	1.53	0.58	1.62	0.33	11.77
W	0.33	0.30	0.20	0.10	0.24	0.02	0.16	0.08	0.18	0.42	1.68	0.16	3.88
NW	1.65	1.18	0.54	1.04	0.44	0.34	0.01	0.11	0.08	1.17	4.27	5.40	16.23
Total	5.90	4.54	7.06	4.94	5.11	1.55	1.10	1.22	5.03	6.24	11.64	10.23	64.58

Table III-4-8
Monthly Sand Transport at Westhampton Beach, Long Island, NY (Snow Days and Wet Days Excluded) (Hsu 1994)

Volume, Cubic Meters Per Meter													
Direction	**Jan**	**Feb**	**Mar**	**Apr**	**May**	**Jun**	**Jul**	**Aug**	**Sep**	**Oct**	**Nov**	**Dec**	**Total**
N	2.54	0.64	0.59	0.73	0.25	0.16	0.07	0.08	0.77	0.69	2.72	3.12	12.36
NE	0.11	0.27	0.19	0.19	0.00	0.03	0.05	0.08	0.08	0.00	0.00	0.85	1.85
E	0.22	0.49	2.89	0.00	1.00	0.02	0.04	0.49	1.00	2.14	0.00	0.07	8.37
SE	0.02	0.00	0.11	0.01	0.01	0.01	0.15	0.06	0.14	0.04	0.00	0.00	0.55
S	0.08	0.31	0.08	0.09	0.33	0.00	0.02	0.01	0.46	0.25	1.15	0.27	3.06
SW	0.44	0.70	1.30	1.86	1.44	0.23	0.28	0.10	1.19	0.32	0.83	0.24	8.93
W	0.23	0.28	0.20	0.09	0.22	0.01	0.06	0.08	0.18	0.30	1.24	0.13	3.03
NW	1.53	1.18	0.52	0.91	0.32	0.30	0.01	0.09	0.08	1.06	3.74	5.26	15.00
Total	5.17	3.87	5.89	3.88	3.56	0.76	0.67	1.00	3.90	4.81	9.69	9.95	53.15

EXAMPLE PROBLEM III-4-7

Find:

Estimate the sand transport in each of the eight compass directions. (Note that the results of this analysis will only be approximate since no information on moisture conditions and/or snow cover is available. Also, the data are daily average wind speeds rather than hourly values.) Ideally, this type of analysis would be performed with several years of hourly wind data; however, a rough estimate can be obtained from wind rose data.

Given:

The wind rose for Atlantic City, NJ, in Figure III-4-16 and the median sand grain diameter of 0.25 mm. The winds have been corrected to offshore conditions and the standard anemometer height of 10 m.

Solution:

Data from the wind rose (Figure III-4-16) are tabulated in Table III-4-9. The transport rates at the wind speed interval boundaries are computed in Table III-4-10. An upper bound of 35 mph was selected to determine the average transport rate over the interval. This upper bound is somewhat arbitrary and was selected only 6 mph above the 29 mph lower bound since it is likely that on those days with average winds exceeding 29 mph, the speed will not exceed 29 mph by much. Column 3 of Table III-4-10 gives the threshold wind speed at the 10-m height for a median sand-grain diameter of 0.25 mm. The transport coefficient in column 4 is from Figure III-4-12b. Column 5 is the transport rate and column 6 is the average transport rate over the interval. (Note that it is important to use average transport rates rather than average wind speeds since transport rate varies with the cube of the wind speed.) For example, the average transport rate over the interval between wind speeds of 29 mph and 35 mph is 0.2944 gm/cm-s. The amounts of sand transported are computed in Table III-4-11.

The threshold velocity of 7.25 m/s is greater than the 6.26 m/s corresponding to the 6.3 m/s (14 mph) interval boundary; therefore, the number of days that the wind speed was between 7.25 m/s and 12.96 m/s (29 mph) was calculated assuming that wind speeds are uniformly distributed over the interval. Adjusted days/year were computed as (12.96 - 7.25)/(12.96 - 6.26) = 0.852 times the total number of days in the 6.3 m/s (14 mph) < U < 13.0 m/s (29 mph) interval. Column 5 is from Table III-4-10. The mass transport (column 6) is column 5 x number of days x number of seconds/day. Column 7 is the volume transport equal to column 6 divided by (0.6) x 2.65 gm/cm^3 and converted to cubic meters per meter. The total amount of sand transported in all directions is 146.1 m^3/m.

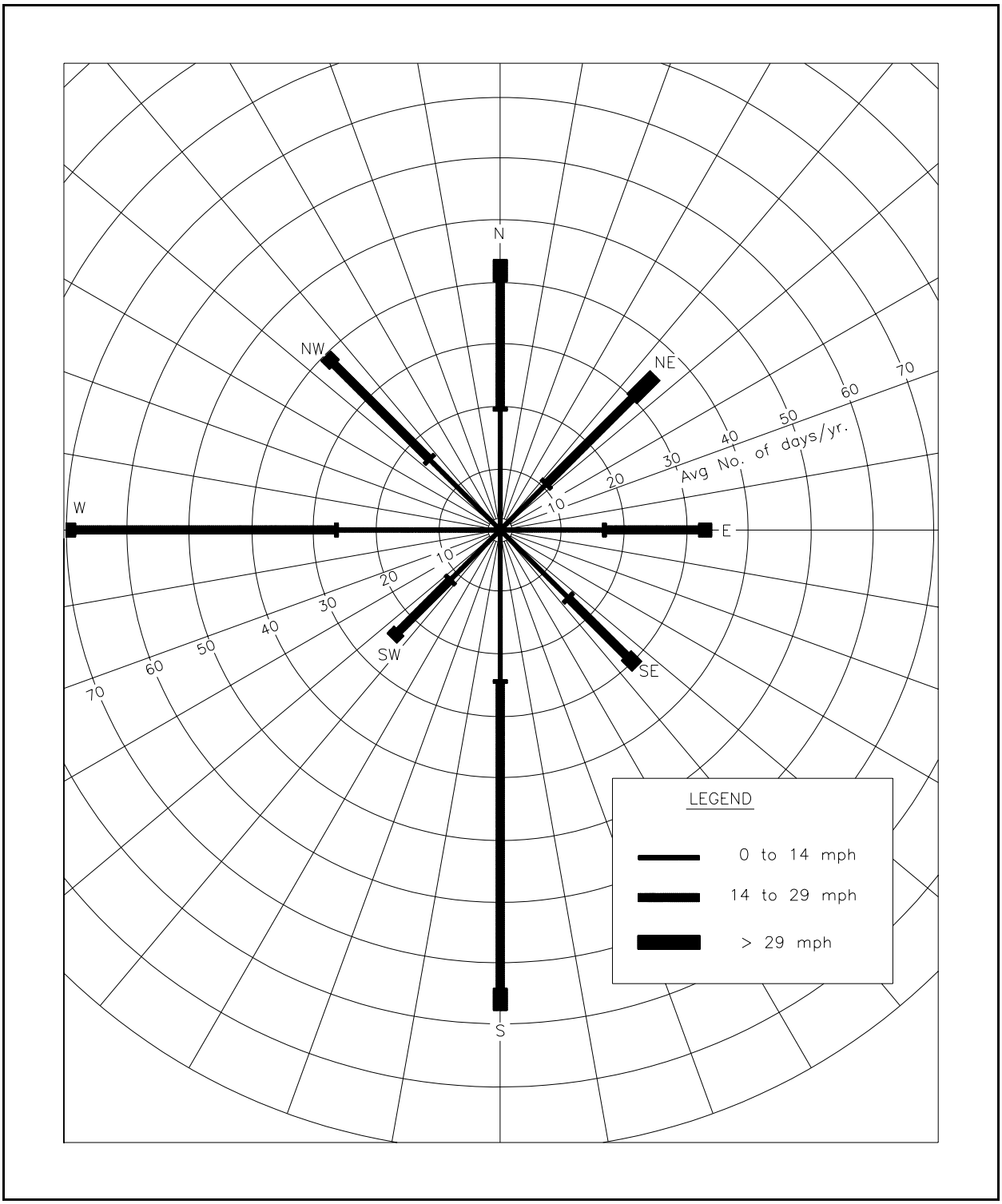

Figure III-4-16. Wind Rose for Atlantic City, NJ (data from 1936 to 1952)

Table III-4-9
Wind Rose Data, Atlantic City, NJ (Wind Data, 1936 to 1952)

Direction	Wind Speed Interval	Days/Year
N	29 mph < U	3
N	14 mph < U < 29 mph	20
N	0 mph < U < 14 mph	20
NE	29 mph < U	5
NE	14 mph < U < 29 mph	19
NE	0 mph < U < 14 mph	11
E	29 mph < U	2
E	14 mph < U < 29 mph	15
E	0 mph < U < 14 mph	17
SE	29 mph < U	2
SE	14 mph < U < 29 mph	13
SE	0 mph < U < 14 mph	16
S	29 mph < U	3
S	14 mph < U < 29 mph	49
S	0 mph < U < 14 mph	25
SW	29 mph < U	1
SW	14 mph < U < 29 mph	23
SW	0 mph < U < 14 mph	12
W	29 mph < U	1
W	14 mph < U < 29 mph	42
W	0 mph < U < 14 mph	27
NW	29 mph < U	1
NW	14 mph < U < 29 mph	21
NW	0 mph < U < 14 mph	17
TOTAL		365

Table III-4-10
Wind Rose Data Analysis, Atlantic City, NJ (Anemometer at Standard 10-m Height)

Wind Speed (mph)	Wind Speed (m/sec)	Threshold Wind Speed * (m/sec)	Transport Coef. * ($gm\text{-}s^2/cm^4$)	Transport Rate (gm/cm-sec)	Average Rate Over Interval (gm/cm-sec)
(1)	(2)	(3)	(4)	(5)	(6)
35	15.64	7.25	9.8000e-11	0.3753	
					0.2944
29	12.96	7.25	9.8000e-11	0.2135	
					0.1254
14	6.26	7.25	9.8000e-11	0.0373 **	
					0 ***
0	0	7.25	9.8000e-11	0	

* Based on median grain size of 0.25 mm
** Calculated for threshold wind speed of 7.25 m/s.
*** Wind speed in interval does not exceed threshold wind speed.

Table III-4-11
Wind Blown Sand Transport Analysis, Wind Rose Data, Atlantic City, NJ (Wind Data, 1936 to 1952)

Wind Direction	Wind Speed Interval	Days/Year	Adjustment Days/Year	Transport Rate (gm/cm-sec)	Mass Transport (gm/cm-yr)	Volume Transport (m^3/m-yr)	Direction in which sand is transported (m^3/m)
(1)	(2)	(3)	(4)	(5)	(6)	(7)	(8)
N	13 m/s < U	3	3	0.2944	76,308	4.80	
N	6.3 m/s < U < 13 m/s	20	17*	0.1254	184,621	11.61	Total S = 16.41
N	0 m/s < U < 6.3 m/s	20	0	0	0	0	
NE	13 m/s < U	5	5	0.2944	127,181	8.00	
NE	6.3 m/s < U < 13 m/s	19	16*	0.1254	175,390	11.03	Total SW = 19.03
NE	0 m/s < U < 6.3 m/s	11	0	0	0	0	
E	13 m/s < U	2	2	0.2944	50,872	3.20	
E	6.3 m/s < U < 13 m/s	15	13*	0.1254	138,466	8.71	Total W = 11.91
E	0 m/s < U < 6.3 m/s	17	0	0	0	0	
SE	13 m/s < U	2	2	0.2944	50,872	3.20	
SE	6.3 m/s < U < 13 m/s	13	11*	0.1254	120,004	7.55	Total NW = 10.75
SE	0 m/s < U < 6.3 m/s	16	0	0	0	0	
S	13 m/s < U	3	3	0.2944	76,308	4.80	
S	6.3 m/s < U < 13 m/s	49	42*	0.1254	452,321	28.45	Total N = 33.25
S	0 m/s < U < 6.3 m/s	25	0	0	0	0	
SW	13 m/s < U	1	1	0.2944	25,436	1.60	
SW	6.3 m/s < U < 13 m/s	23	20*	0.1254	212,314	13.35	Total NE = 14.95
SW	0 m/s < U < 6.3 m/s	12	0	0	0	0	
W	13 m/s < U	1	1	0.2944	25,436	1.60	
W	6.3 m/s < U < 13 m/s	42	36*	0.1254	387,704	24.38	Total E = 25.98
W	0 m/s < U < 6.3 m/s	27	0	0	0	0	
NW	13 m/s < U	1	1	0.2944	25,436	1.60	
NW	6.3 m/s < U < 13 m/s	21	18*	0.1254	193,852	12.19	Total SE = 13.79
NW	0 m/s < U < 6.3 m/s	17	0	0	0	0	
Total		365	190			146.07	

* Number of days when wind speed exceeds the threshold wind speed and some transport occurs. Assumes uniform distribution of wind speeds over the 6.3 m/s < U < 13 m/s interval.

"deflation plain" from which sand is removed and the profile lowered by wind. The presence of vegetation or other obstructions to the wind results in sand being trapped and leads to the creation of sand dunes. Foredunes are the first line of dunes landward of the shoreline. These dunes often result from the natural accumulation of wind-blown sand originating on the beach face; however, they may also be man-made. Whether natural or man-made, they are subject to continued growth, alteration, and movement due to natural wind transport processes. When present and if sufficiently large, foredunes can provide protection from coastal flooding, shoreline erosion, and wave damage. Dunes can also shelter the area landward of them from wind-blown sand by providing an area within which wind-blown sand accumulates. This can be an important function of stabilized dunes, since wind-blown sand is often a nuisance that must be controlled.

(2) A line of dunes can provide protection from flooding due to high-water levels and wave overtopping. Sand stored in dunes is also available as a sacrificial contribution to the increased longshore and offshore sand transport during storms. Dunes, by contributing their volume to the sand in transport, reduce the landward movement of the shoreline during storms. Dunes can also reduce wave damage in developed landward areas by limiting wave heights by causing waves to break as they propagate over the dunes. On undeveloped barrier islands, dunes provide a source of sand for overwash processes. During storms with elevated water levels, waves overtopping the dunes carry sand into the bay or lagoon behind a barrier island. Over a period of time, this natural process results in landward migration of the island.

(3) Dunes can be constructed artificially by: (a) beach nourishment, (b) grading existing sand available on the dry beach, or (c) "beach scraping" - removing sand from below the high-water line during low tide and using it to construct a protective dune. In areas where there is sufficient sand and the beach is wide, dunes can be encouraged to develop by natural accumulation by planting dune grass or other vegetation, or by installing sand fences to trap the landward-blowing sand. The rate at which dunes grow depends on the rate at which sand is transported to the dune from the fronting beach and on the effectiveness of the vegetation, fencing, and/or the dune itself in retaining sand. Because of the effect of the dune on the wind field (see Figure III-4-8) and the absence of a mobile sand supply on the landward side of coastal dunes, there is little transport from the dune to the beach, even during periods when winds blow seaward. Coastal dunes generally grow by trapping and accumulating sand on their seaward side; thus, they grow toward the source of sand - the fronting beach. If more than one line of foredunes is to be developed by natural accumulation, the landward line of dunes must be constructed before the line closest to the shoreline is constructed, otherwise the line closest to the shoreline will trap sand and keep it from reaching the more landward line.

(4) When designing a dune system intended to accumulate sand by natural wind transport processes, the dunes should be set back from the shoreline so that there is sufficient dry beach to provide a source of sand. A distance of 60 m between the toe of the dune and the high-water line has been recommended (*Shore Protection Manual* 1984). This expanse of sand is often not available on many beaches so that lesser distances must be accepted. At the very least, the toe of the foredune should be landward of the normal seasonal fluctuation of the shoreline. Narrow beaches are less effective sand sources and dune growth will be slower. Typical rates of sand accumulation in dunes are about 2.5 to 7.5 m^3/m-yr; however, rates as high as 25 m^3/m-yr have been measured (Woodhouse 1978). Savage (1963) measured accumulations of 4.5 to 6 m^3/m over a period of 7 to 8 months using a single row of sand fencing. Savage and Woodhouse (1968) measured accumulations of 39 m^3/m over a 3-year period in a multiple-fence experiment. This is an average of 13 m^3/m-yr; however, accumulation rates must have been higher than this average rate during portions of the 3-year period.

(5) Dunes that are intended to provide protection against flooding and erosion must be stabilized to prevent their deflation and/or landward migration. Stabilization is also necessary to control the landward movement of wind-blown sand into developed areas. Stabilization can be achieved using vegetation or sand fencing. Guidelines for dune creation and stabilization using vegetation are given by U.S. Army Corps of

EXAMPLE PROBLEM III-4-8

Find:

If the shoreline azimuth at Atlantic City is θ = 50 deg (angle between north and the shoreline), estimate the rate at which sand might accumulate in a dune field behind the beach. (As in the preceding example, this type of analysis ideally should be done with hourly wind data.)

Given:

The transport computations from the preceding Example Problem III-4-7 based on the wind rose at Atlantic City, NJ.

Solution:

The transport rate in a given direction is the transport rate times the cosine of the angle between the wind direction and the given direction. See Figure III-4-17. For Atlantic City, shoreline alignment and compass directions are shown in Figure III-4-18. For example, an easterly wind will transport sand perpendicular to the shoreline $q_{\perp E} = q_E \cos 50°$ where $q_{\perp E}$ is the transport perpendicular to the shoreline into the dunes. For a southeasterly wind, the transport perpendicular to the shoreline is $q_{\perp SE} = q_{SE}$ cos 5 deg. In general,

$$q_{\perp} = q \cos\alpha$$

where α = angle between wind direction and offshore, directed normal to the shoreline.
For the example

$$q_{\perp E} = q_E \cos(50°)$$
$$q_{\perp SE} = q_{SE} \cos(5°)$$
$$q_{\perp S} = q_S \cos(40°)$$
$$q_{\perp SW} = q_{SW} \cos(85°)$$

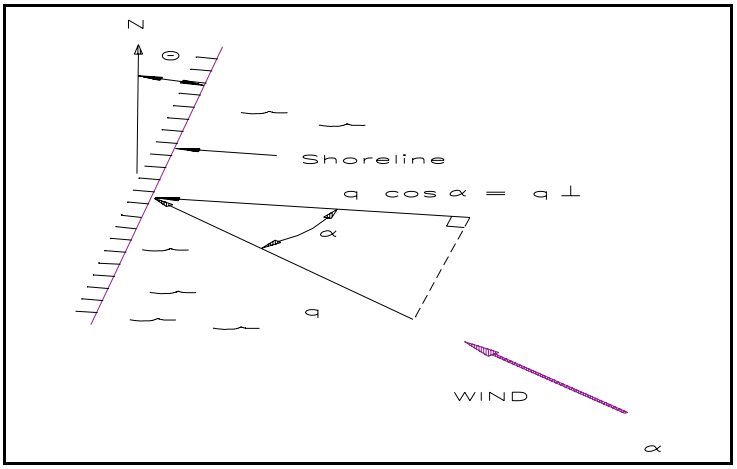

Figure III-4-17. Net sand transport at an angle α with the wind direction

(Sheet 1 of 4)

Example Problem III-4-8 (Continued)

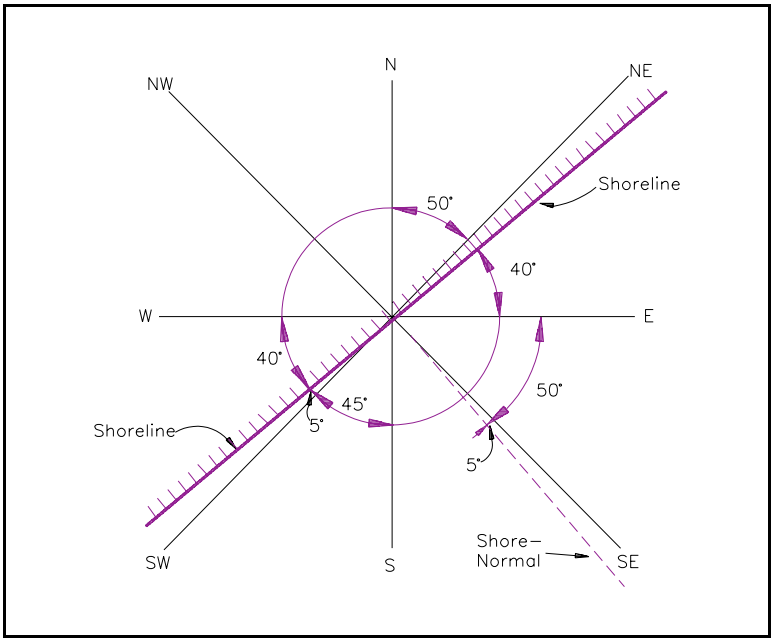

Figure III-4-18. Shoreline orientation with respect to compass directions at Atlantic City, NJ

Winds blowing generally from the dunes or backbeach towards the shoreline are not as efficient in transporting sand as are winds blowing generally onshore. This is because of sheltering provided by the dune itself and stabilization by vegetation on the dune, and because there is often only a limited supply of sand landward of the dunes. This latter condition prevails at Atlantic City, where much of the area landward of the beach is paved or developed. Figure III-4-8 also shows that in the lee of a dune, winds near ground level may be in the direction opposite of the wind direction at a higher elevation. Winds blowing seaward from the dunes are not very efficient in transporting sand from the dunes back onto the beach. Sand transport efficiency, proportional to the square of the cosine of the angle between the wind direction and a vector perpendicular to the shoreline, is assumed. See Figure III-4-19 for the efficiency factor as a function of β, the angle between the shoreline and wind direction. Figure III-4-20 gives the definition of β.

Sand transport rates in the offshore direction, perpendicular to the general orientation of the dune toe, are given by

$$q_{\perp} = q \cos\alpha \cos^2\beta, \qquad 180° < \beta < 360°$$

where β is the angle the wind makes with the shoreline and α is the angle the wind makes with a vector perpendicular to the shoreline. Therefore, $\alpha = \beta - 90°$ and

$$\cos(\alpha) = \cos(\beta - 90°) = -\sin(\beta)$$

(Sheet 2 of 4)

Example Problem III-4-8 (Continued)

Therefore,

$$q_{\perp} = -q \sin\beta \cos^2\beta, \qquad 180° < \beta < 360°$$

The sin β term in the equation corrects the transport from the wind direction to a direction perpendicular to the shore, while the $\cos^2 \beta$ term is the efficiency term introduced to consider the sheltering effects of the dune.

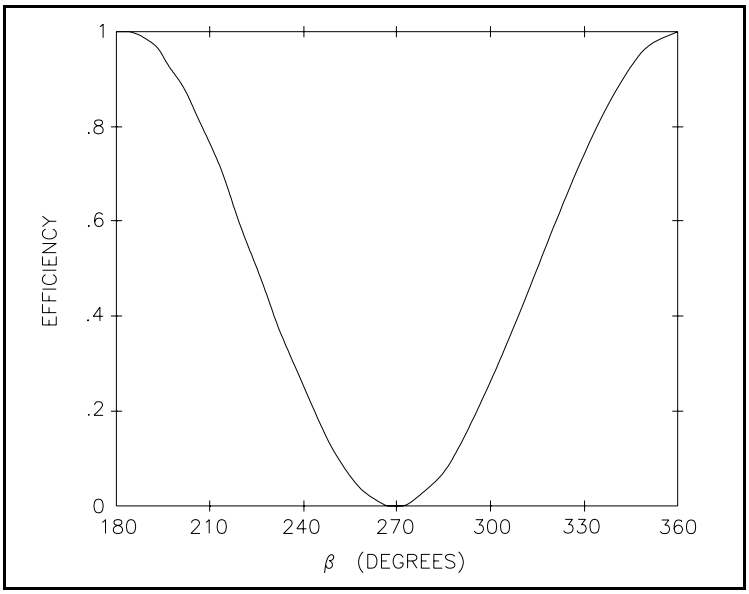

Figure III-4-19. Sand transport efficiency for winds blowing from dunes toward beach as a function of the angle between wind direction and shoreline

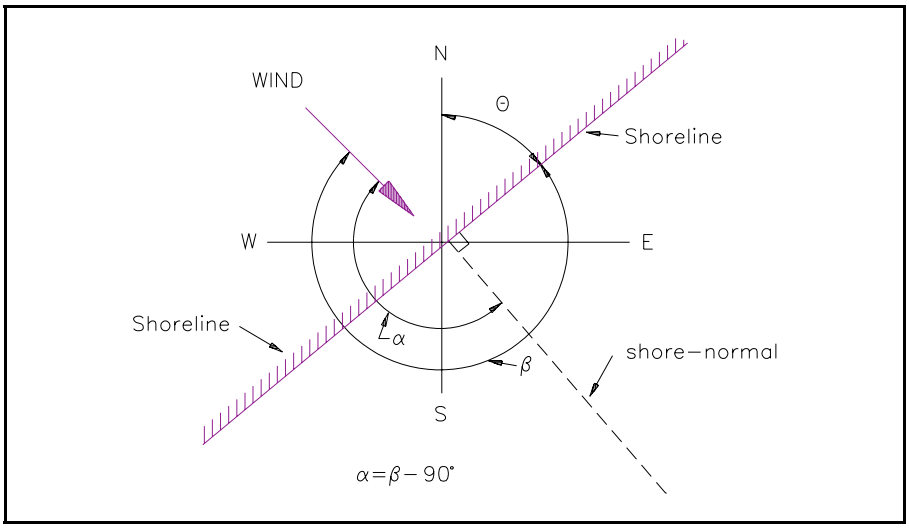

Figure III-4-20. Definition of angle ß, between wind and shoreline

(Sheet 3 of 4)

Example Problem III-4-8 (Concluded)

Results of the analysis are given in Table III-4-12. Columns 1 and 2 are obtained from Table III-4-11. Column 3 is the angle β between the given wind directions and the shoreline azimuth of θ = 50° at Atlantic City. Column 4 is sin(β) and column 5 is the offshore wind transport efficiency, $\cos^2(\beta)$. The efficiency is assumed equal to 1.0 for onshore winds. Column 6, the rate of dune growth due to winds from the given direction, is the product of columns 2, 4, and 5. The estimated total potential dune growth rate is 27.2 m^3/m-yr. This estimate represents a potential growth rate which depends on the sand supply. The analysis does not consider the effects of snow cover and moisture to reduce transport. Woodhouse (1978) reports on a 30-year average dune accumulation rate of 13.7 m^3/m-yr on the Clatsop Plains, Oregon, and suggests that higher accumulation rates probably prevailed in the early years.

Table III-4-12
Estimated Annual Dune Growth at Atlantic City, NJ

Wind Direction	Annual Transport (m^3/m)	Wind Angle (β) (degrees)	COS(α) or SIN(ß)	Efficiency COS^2(ß)	Dune Growth (m^3/m/yr)
(1)	(2)	(3)	(4)	(5)	(6)
N	15.79	310	-0.7660	0.4132	-5.00
NE	18.44	355	-0.0872	0.9924	-1.60
E	11.44	40	0.6428	1.0000[1]	7.35
SE	10.34	85	0.9962	1.0000[1]	10.30
S	31.73	130	0.7660	1.0000[1]	24.31
SW	14.24	175	0.0872	1.0000[1]	1.24
W	24.68	220	-0.6428	0.5868	-9.31
NW	13.14	265	-0.9962	0.0076	-0.10
TOTAL					27.20 m^3/m/yr

[1] Transport efficiency = 1.0 for angles between 0 and 180 deg.

(Sheet 4 of 4)

Engineers (1978) and Woodhouse (1978). The best type of stabilizing vegetation varies with geographical area, location on the dune, exposure of the site, whether the water body is salt or fresh water, etc. Typical plants used for dune stabilization include European beach grass (*Ammophila arenaria*) and, less frequently, American dunegrass (*Elymus mollis*) along the Pacific Northwest and California coasts; American beach grass (*Ammophila breviligulita*) along the mid- and upper-Atlantic and Great Lakes coasts; sea oats (*Uniola paniculata*) along the South Atlantic and gulf coasts, and panic grasses (*Panicum amarum* or *P. amarulum*) along the Atlantic and gulf coasts.

(6) Guidelines for dune creation and stabilization with fencing are given in the *Shore Protection Manual* (1984) and Woodhouse (1978). Typical sand fencing is either wooden-slat fencing of the type used to control snow along highways or geosynthetic fabric fencing. A wooden-slat fence is typically 1.2 m high with 3.8-cm-wide slats wired together to provide about 50 percent porosity. Stabilization by fencing requires periodic inspection of the installation, replacement of damaged or vandalized fencing, and installation of new fencing to continue the stabilization process as the dune grows. The size and shape of a dune can be controlled by stategically installing subsequent lines of fencing to encourage the dune to grow higher or wider. Most fence installations fill within 1 year of construction. Dune growth is most often limited by the available sand supply rather than by the capacity of the fence installation. Dunes created by fencing must also subsequently be planted to stabilize them for when the fencing eventually deteriorates.

(7) Stabilization by vegetation has the advantage that it is capable of growing up through the accumulating dune and of repairing itself if damaged, provided the damage is not too extensive. After planting and for a year or two thereafter, vegetation requires fertilization to establish healthy plants. Traffic through vegetated dunes must also be controlled to prevent damage to plants by excluding any pedestrians and vehicles or by providing dune walk-over structures. Dune areas with barren areas in an otherwise healthy vegetated dune, will be subject to "blowouts," local areas of deflation. Blowouts reduce a dune's capability to protect an area from flooding.

(8) An example of estimating the rate of dune growth follows. Example III-4-8 assumes that all of the sand transported to the dune is trapped by vegetation and/or sand fencing and that the fronting beach is sufficiently wide to supply sand at the potential transport rate for a given wind speed, i.e., dune growth is not limited by sand supply. Subsequent examples consider the effects of armoring and a limited sand supply.

b. Factors affecting dune growth rates.

(1) The dune growth rates presented in the preceding section and Example III-4-8 are "potential" rates, since they consider only the accumulation of sand in the dunes and not any of the processes that remove sand from the dunes. Furthermore, the trapping process is assumed to be nearly perfect, i.e., little sand is removed from the dunes when wind direction reverses and blows offshore and no sand is blown landward of the dunes. In some developed coastal communities, sand is often removed from the area landward of the dunes; hence, the rate of dune growth often underestimates wind-blown sand transport rates or, vice versa, calculated transport rates overestimate the rate of dune growth. Some typical measured dune growth rates are given in Table III-4-13.

(2) On relatively narrow beaches backed by dunes, the dunes are occasionally eroded by waves during storms having elevated water levels. The storms often leave a nearly vertical scarp with the height of the scarp and the amount of erosion depending on the severity of the storm; i.e., the height of the waves and storm surge. Less frequently, during unusual storms, the dune may be completely destroyed. Dunes erode during storms only to be rebuilt during the period between storms with sand transported by winds having an onshore component. The net rate of dune growth, therefore, is only a fraction of what would be predicted if only rates of accumulation are considered and sand losses are ignored. Dune growth rates can be estimated

Table III-4-13
Measured Dune Growth Rates (Field experiments conducted by Coastal Engineering Research Center in 1960s and 1970s)

Site	Padre Island, TX			Padre Island, TX			Ocracoke Island, NC		
Type	Wood fencing (3 fences, 3 lifts)			Wood fencing (4 fences, 3 lifts)			American Beachgrass		
Beach	60 - 90 m			60 - 90 m			180 - 210 m		
Growth Rates	Δt (mos)	ΔV (m^3/m)	Rate (m^3/m-yr)	Δt (mos)	ΔV (m^3/m)	Rate (m^3/m-yr)	Δt (mos)	ΔV (m^3/m)	Rate (m^3/m-yr)
	12	8.5	8.53	12	6.0	6.02	24	12.8	6.40
	12	6.8	6.77	12	10.3	10.28	27	9.8	4.35
	12	10.8	10.79	12	6.5	6.52	29	16.6	6.85
Avg Rate			8.70			7.61			5.86
Site	Core Banks, NC			Padre Island, TX			Core Banks, NC		
Type	American Beachgrass and fence			Sea oats			Sea oats		
Beach	120 - 150 m			60 - 90 m			90 m		
Growth Rates	Δt (mos)	ΔV (m^3/m)	Rate (m^3/m-yr)	Δt (mos)	ΔV (m^3/m)	Rate (m^3/m-yr)	Δt (mos)	ΔV (m^3/m)	Rate (m^3/m-yr)
	32	11.7	4.42	36	29.6	9.87	22	5.0	2.74
	22	11.0	4.98	60	42.6	8.53	14	2.8	2.37
	26	10.8	4.98				19	6.3	3.96
Avg Rate			5.14			9.20			3.02
Site	Clatsop Spit, OR								
Type	European beachgrass								
Beach	180 m								
Growth Rates	Δt (mos)	ΔV (m^3/m)	Rate (m^3/m-yr)						
	360	384	12.79						
Avg Rate			12.79						

by constructing a sediment budget for the dune that balances rates of accumulation against rates of erosion. However, estimating the occurrence and volume of dune erosion is difficult. Estimating how much sand is actually trapped by the dune is also difficult.

(3) The rate at which sand is supplied to a dune depends also on the availability of a sand source upwind of the dunes. A wide beach usually provides an adequate source. However, if the beach is narrow, there may not be a sufficient upwind supply in the sense that the over-sand fetch is insufficient for the transport rate to reach an equilibrium (Nordstrom and Jackson 1992; Gillette et al. 1996). Consequently, calculated transport rates overestimate actual transport rates.

(4) The size gradation of the beach sand also has an influence on transport rates. Sand transport analyses based on a single sand-grain diameter fail to recognize that beach sands are comprised of a gradation of sizes each of which has a different threshold wind speed that initiates motion. Grains finer than the median size are more easily transported and may be moved by lower wind speeds while coarser grains are left behind. Basing transport rates on only the median grain size fails to recognize that finer grains on the surface can be transported even when wind speeds are relatively low. Ideally, each grain size should be considered separately. In addition, as fines are removed from the beach sand surface, the remaining larger size fraction armors the surface, making it difficult to transport additional sand. Figure III-4-21(a) shows a relatively uniform distribution of sand grains where almost all grains have about the same threshold speed. Figure III-4-21(b) shows a well-graded sand prior to wind erosion, while Figure III-4-21(c) shows the same well-graded sand after the fines have been removed leaving behind the coarse fraction on the surface. Higher wind speeds are required to continue the transport process after the fine surficial materials are removed. Alternatively, processes that break up the beach surface to expose additional fine sediments to wind will reestablish the transport of fines. Such processes include pedestrian and vehicular traffic and beach raking.

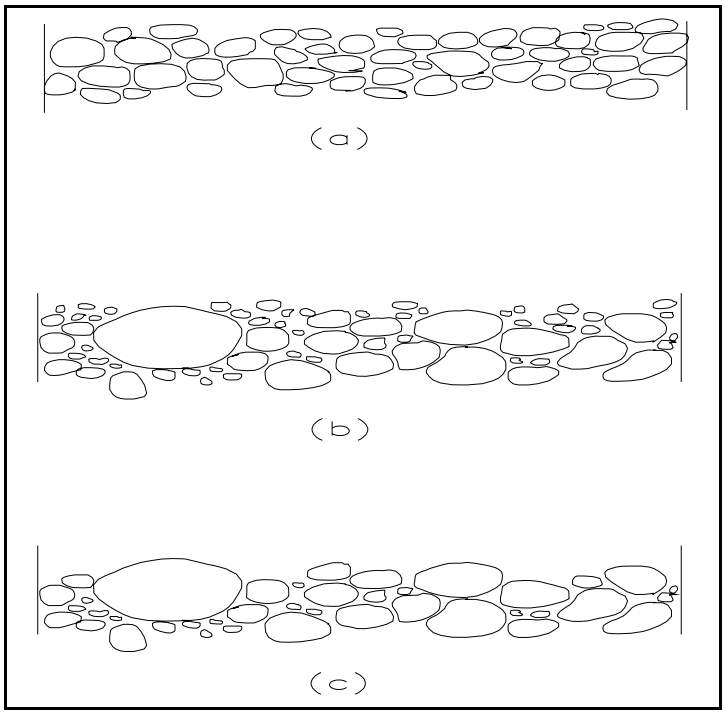

Figure III-4-21. Schematic views of sorted sand deposits: (a) well-sorted (poorly graded); (b) poorly sorted (well-graded); (c) poorly sorted after fines have been removed by wind erosion

(5) The formation of a salt crust on the beach surface by the evaporation of seawater also increases threshold wind speeds and reduces transport (Nickling and Egglestone 1981). Sand below the high tide line is most affected by this process; however, occasional saturation of the beach above the usual high tide level by storm tides will expand the affected beach area inland. Additionally, salt spray carried inland by wind can further expand the affected area. Processes that break up the crust to restore usual threshold wind speeds include pedestrian and vehicular traffic.

c. Dune sediment budget.

(1) Sand gains and losses by a typical dune are illustrated in Figure III-4-22. Sand is transported by onshore winds to the dune where vegetation, sand fencing, or the dune itself alter the wind field and allow the sand to accumulate. If the trapping is incomplete, the same onshore winds may transport sand inland from the dune.

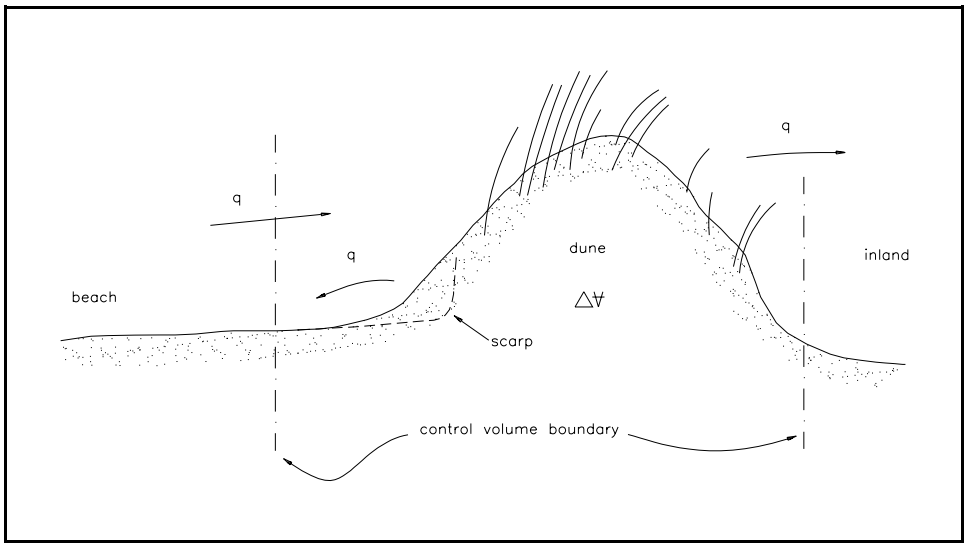

Figure III-4-22. Definition of terms, dune sediment budget

(2) If sand accumulates at the dune's seaward side and erodes from its landward side, the dune will migrate seaward. Occasional high water levels during storms may allow waves to erode the base of the dune to create a scarp. Sand eroded from the dune by waves becomes a part of the littoral transport. Following the storm, onshore winds again rebuild the dune's seaward side. During periods of offshore winds, some sand from the dune will be blown back onto the beach. Similarly, if there is an unstabilized source of sand landward of the dune, it will contribute to building the dune. The sand budget equation for the dune is given by

$$q - q_s - q_i = \rho (1-p) \frac{\Delta \forall}{\Delta t} \tag{III-4-23}$$

in which q = wind-borne sand transport rate (mass per unit time per unit length of beach), q_s = dune erosion by waves (mass per unit time per unit length of beach), q_i = the sand blown inland from the dune, $\Delta\forall$ = the volume change per unit length of beach, ρ = mass density of the sand, p = the porosity of the *in situ* dune sand, and t = time. Note that q and q_i include both sand gains and losses depending on their sign. In fact, q and q_i should each be multiplied by transport efficiency terms, which depend on wind direction and dune conditions such as the presence of vegetation and sand fencing. For example, onshore winds can efficiently transport sand, while offshore winds, which would carry sand out of the dunes, are less efficient if vegetation and fencing are present. The calculations in Example Problem III-4-8 consider only q with a transport efficiency between 0 and 1 depending on the wind direction relative to the axis of the dune. Net dune losses embodied in q_s and q_i are not included. Equation 4-23 might be rewritten

$$\eta\, q - q_s - \eta_i\, q_i = \rho (1 - p) \frac{\Delta \forall}{\Delta t} \tag{III-4-24}$$

in which η = the transport efficiency for winds at the seaward side of the dune and η_i = the transport efficiency for winds at the landward side of the dune. For the calculations in Example Problem III-4-8, η was assumed to be a function of wind direction ($\eta = 1$ for winds with an onshore component and $0 < \eta < 1$ for winds with an offshore component), and η_i was assumed zero (no inland sand losses and no inland sand source). Note that η was assumed to vary as $\cos^2\beta$ with 180 deg $< \beta <$ 360 deg, where β = the angle between the wind and the dune axis (the dunes are usually parallel with the shoreline) so that β = 270 deg represents wind blowing from the back of the dune.

d. Procedure to estimate dune "trapping factor."

(1) Unfortunately, the preceding discussion assumes knowledge of quantities that are most typically unknown and a simple approach must be taken. A "dune trapping factor" can be computed to correct predicted "potential" dune growth rates in order to obtain better estimates of actual rates. The trapping factor T_f is based on the difference between the sand grain size distribution on the dune and the size distribution on the beach in front of the dune. If R_t = a theoretical growth rate based on calculations of sand transport and R_a = the actual growth rate, the relationship is given by

$$R_a = T_f R_t \tag{III-4-25}$$

(2) The value of T_f can be found using the procedure suggested by Krumbein and James (1965) to compare the characteristics of potential beach nourishment sand with native beach sand characteristics. While the Krumbein and James (1965) procedure has been superseded by better methods to estimate beach nourishment overfill ratios, in principle it presents a way to estimate what volume of sand with a given gradation is needed to produce a unit volume of sand having a different gradation. The procedure is based on the assumption that the gradations of the sand on the beach and the sand in the dunes are both log-normally distributed and can be described by their phi-mean μ_φ and phi-standard deviation σ_φ. These parameters can be estimated using the relationships

$$\mu_\varphi = \frac{\varphi_{16} + \varphi_{84}}{2} \tag{III-4-26}$$

and

$$\sigma_\varphi = \frac{\varphi_{16} - \varphi_{84}}{2} \tag{III-4-27}$$

in which φ_{16} = the phi diameter of the 16th percentile (16 percent of the grains are finer) and φ_{84} = the phi diameter of the 84th percentile. The phi diameter is given by

$$\varphi = -\log_2 d_{mm}$$

or equivalently by (III-4-28)

$$\varphi = -3.3219 \log_{10} d_{mm}$$

in which φ = the diameter in phi units and d_{mm} = the grain diameter in millimeters. The phi-mean and phi-standard deviation are calculated for sand taken from the dune, $\mu_{\varphi D}$ and $\sigma_{\varphi D}$, and for sand from the beach in front of the dune, $\mu_{\varphi B}$ and $\sigma_{\varphi B}$, and the following parameters are calculated

$$\frac{\sigma_{\varphi\,D}}{\sigma_{\varphi\,B}} \tag{III-4-29}$$

and

$$\frac{\mu_{\varphi\,D} - \mu_{\varphi\,B}}{\sigma_{\varphi\,B}} \tag{III-4-30}$$

and used with Figure III-4-23 to determine how much beach sand is needed to produce a unit volume of dune sand. Figure III-4-23 is derived from the equation

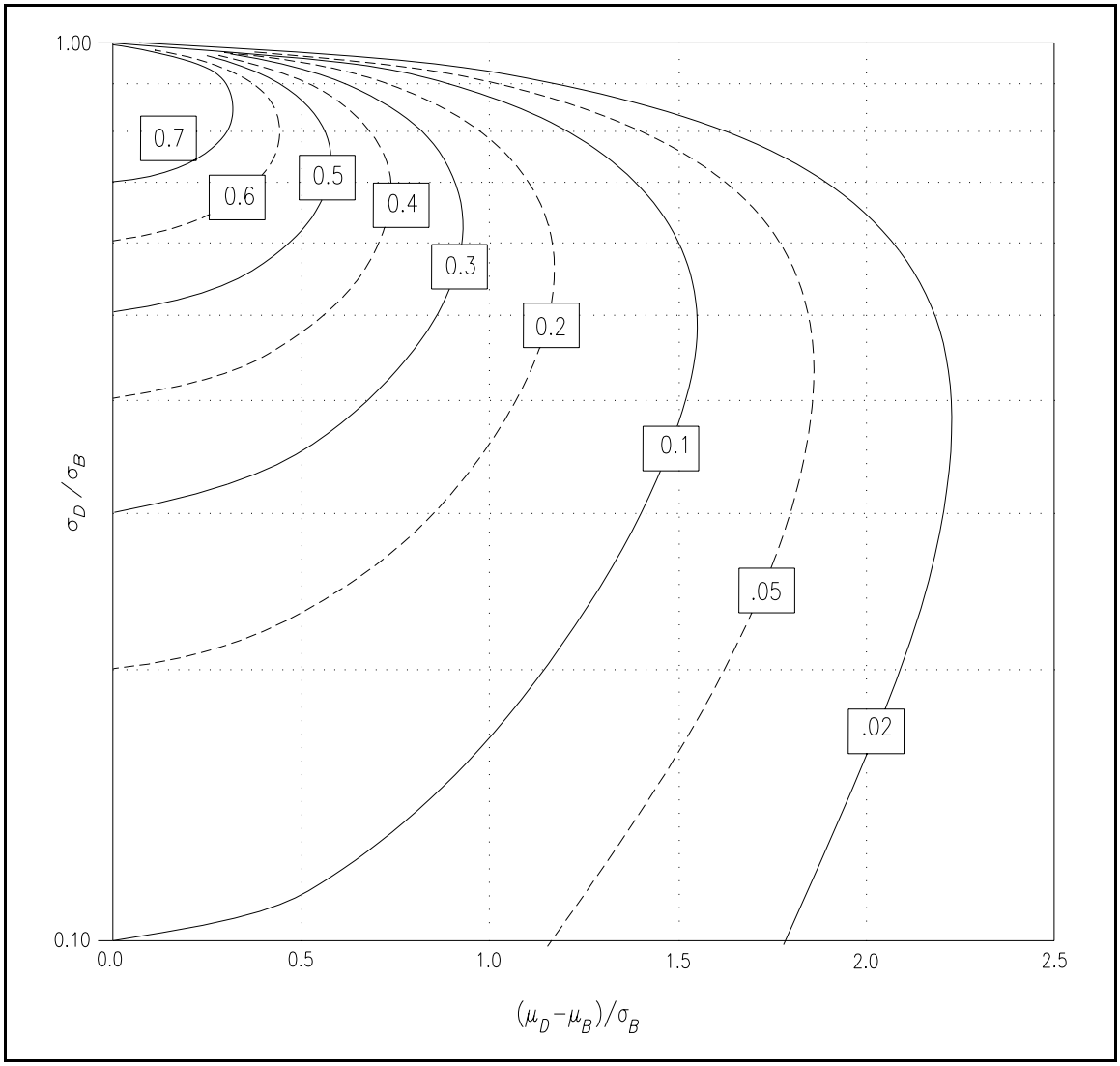

Figure III-4-23. Dune sand trapping factor T_f

EXAMPLE PROBLEM III-4-9

Find:

Determine the dune trapping factor and estimate the rate of dune growth for the sands from the beach and dune in Atlantic City with the size characteristics given below.

Given:

The dune growth rate from Example Problem III-4-8 based on the transport rates of Example Problem III-4-7 and the following data from a sand size analysis of the beach and dune sands at Atlantic City.

Beach sand: $d_{16} = 0.159$ mm $d_{84} = 0.664$ mm

Dune sand: $d_{16} = 0.173$ mm $d_{84} = 0.403$ mm

Solution:

To use the relationships for μ_φ and σ_φ, the phi diameter must be calculated for each of the above percentiles using Equation 4-28.

For the beach sand

$$\varphi = -\log_2 d_{mm}$$

or equivalently

$$\varphi = -3.3219 \log_{10} d_{mm}$$

and, therefore

$$\varphi_{16} = -3.3219 \log_{10} (0.159) = 2.65$$

Similarly

$$\varphi_{84} = 0.59$$

For the dune sand

$$\varphi_{16} = 2.53 \quad \text{and} \quad \varphi_{84} = 1.31$$

From Equation III-4-26 and III-4-27

$$\mu_{\varphi B} = \frac{2.65 + 0.59}{2} = 1.62$$

(Continued)

Example Problem III-4-9 (Concluded)

and

$$\sigma_{\varphi B} = \frac{2.65 - 0.59}{2} = 1.03$$

Similarly, for the dune sand

$$\mu_{\varphi D} = 1.92 \quad \text{and} \quad \sigma_{\varphi D} = 0.61$$

Substituting these values into Equation 4-31 gives

$$T_f = \left(\frac{0.61}{1.03}\right) \exp\left[\frac{(1.92 - 1.62)^2}{2(0.61^2 - 1.03^2)}\right] \cong 0.55$$

The trapping factor T_f can also be found from Figure III-4-23.

Consequently, the transport rate found in example problem III-4-8 should be multiplied by 0.55. The transport rate is therefore

$$R_a = 0.55\ R_t$$

or

$$R_a = 0.55\ (27.2) \cong 15.0\ \frac{\text{m}^3}{\text{m}-\text{yr}}$$

$$T_f = \left(\frac{\sigma_{\varphi D}}{\sigma_{\varphi B}} \right) \exp \left[\frac{(\mu_{\varphi D} - \mu_{\varphi B})^2}{2 (\sigma^2_{\varphi D} - \sigma^2_{\varphi B})} \right] \quad \text{(III-4-31)}$$

which is based on a comparison of the log-normal distributions of dune and beach sands. The procedure is valid only if the dune sand is finer than the beach sand and more narrowly graded (better sorted). This is generally the case since the dune sand is almost always derived from the sand on the beach in front of the dune.

(3) Some example values of the various parameters for typical beach and dune sands along with calculated dune trapping factors are given in Table III-4-14.

Table III-4-14
Typical Beach and Dune Sand Phi Diameters and Dune Trapping Factors Calculated from Beach and Dune Sand Samples at Various U. S. Beaches

Location	φ_{16} (dune)	φ_{84} (dune)	φ_{16} (beach)	φ_{84} (beach)	$\mu_{\varphi B}$	$\mu_{\varphi D}$	$\sigma_{\varphi B}$	$\sigma_{\varphi D}$	T_f
North Street Ocean City, NJ	2.48	1.88	2.61	1.72	2.17	2.18	0.45	0.30	0.67
9th Street Ocean City, NJ	2.59	0.79	2.49	0.19	1.34	1.69	1.15	0.90	0.69
29th Street Ocean City, NJ	2.64	1.98	2.69	1.41	2.05	2.31	0.64	0.33	0.46
36th Street Ocean City, NJ	2.53	1.31	2.65	0.59	1.62	1.92	1.03	0.61	0.55
Cape May, NJ Location 1	1.86	0.60	2.06	0.20	1.13	1.23	0.93	0.63	0.67
Cape May, NJ Location 2	1.62	0.58	1.71	0.39	1.05	1.10	0.66	0.52	0.78
CERC FRF Duck, NC					0.76	1.08	1.00	0.77	0.68
Clearwater Beach, FL	2.87	2.09	2.66	1.41	2.04	2.48	0.63	0.39	0.41

e. Continuity equation for wind transport of beach sand.

(1) The continuity equation for the beach sand transported by an onshore wind is developed in Figure III-4-24.

(2) At the upwind end of the fetch, the ocean and/or saturated sand precludes any wind transport. Further shoreward, the sand is dry and transportable by the prevailing wind; however, the amount in transport has not reached its potential rate predicted by the equations. In this region the wind is deflating the beach. The amount of sand leaving the Δx-long control volume exceeds the amount entering and the difference is comprised of sand eroded from the beach. Downwind along the fetch, the sand transport rate has reached equilibrium and the amount of sand entering the control volume equals the amount leaving. Here the beach is not deflating; rather the amount of sand eroded is balanced by the amount deposited. Further along the fetch, near the base of the dune, the amount of sand entering the control volume is less than the amount removed by the wind, and sand accumulates to build the dune. The change in transport rate is often due to a decrease in local wind speed induced by vegetation, sand fencing, or by the dune itself. Writing a sediment balance for the Δx control volume yields the equation

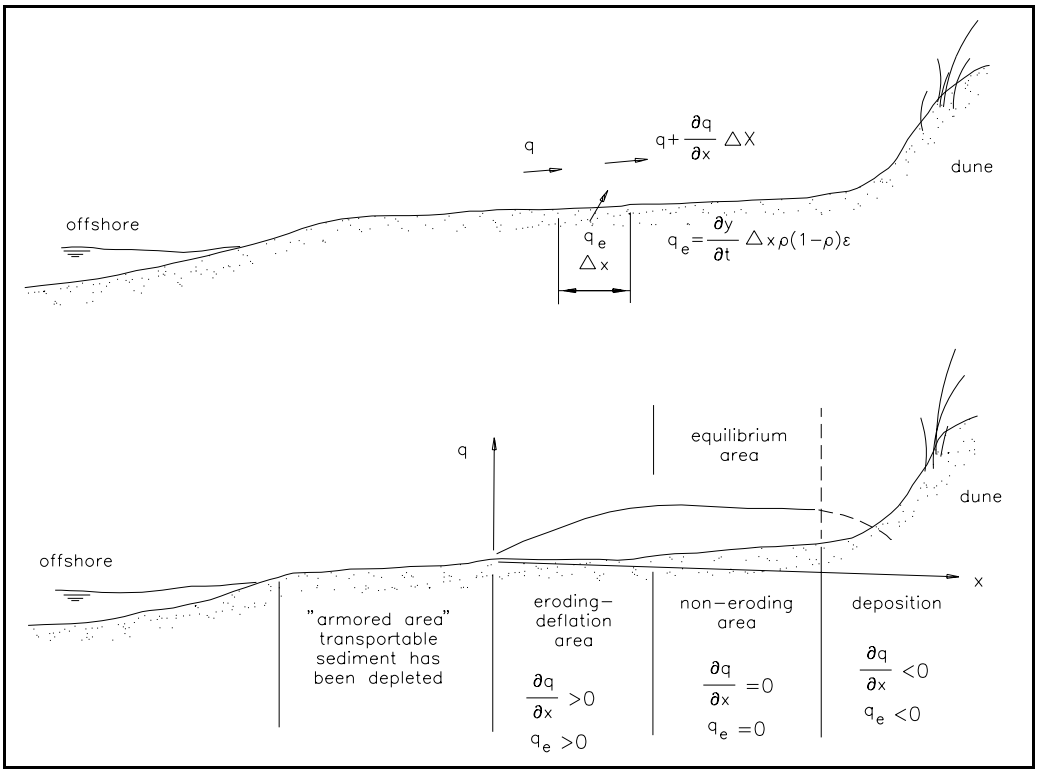

Figure III-4-24. Sand conservation equations for a beach showing deflation area, equilibrium area, and deposition area

$$q + q_e - \left(q + \frac{\partial q}{\partial x} \Delta x \right) = 0 \qquad \text{(III-4-32)}$$

in which q equals the wind-blown transport into the control volume (mass per unit time per unit length perpendicular to the direction of transport), q_e equals the amount contributed to the control volume by erosion from the beach (mass per unit time per unit length), and Δx equals the width of the control volume in the direction of transport. The first two terms are the sand influx to the control volume while the term in brackets is the efflux. Simplifying Equation 4-32 gives

$$\frac{\partial q}{\partial x} = \frac{q_e}{\Delta x} \qquad \text{(III-4-33)}$$

(3) The contribution from the beach q_e can be expressed as a deflation rate times the beach surface area

$$q_e = \frac{\partial y}{\partial t} \Delta x \, \rho (1 - p) \, \varepsilon \qquad \text{(III-4-34)}$$

in which y equals the height of the beach surface above some datum, ρ equals the mass density of the sand, p equals the porosity of the *in-situ* beach sand, and ε equals a dimensionless "erodibility factor" related to the beach sand that is potentially transportable. ε is related to the sand size gradation as well as to any conditions that increase the threshold wind speed such as soil moisture content, salt crust formation, etc. Equation III-4-33 becomes

$$\frac{\partial q}{\partial x} = \frac{\partial y}{\partial t} \rho (1 - p) \varepsilon \quad \text{(III-4-35)}$$

(4) The upwind boundary condition, $q = 0$ at $x = 0$, is applied where the sand is first transportable, i.e., at the shoreline or the point where the sand is no longer wet. Since different size fractions are transported at different rates by a given wind speed, Equation 4-35 must be applied to each range of sizes present on the beach. Unfortunately, the relationship between the size gradation parameters and the amount of surficial, transportable sand is not known. Therefore, it is not possible to establish limit depths of erosion for a given wind speed blowing over sand with a given size distribution.

(5) The amount of sand available for transport at a given wind speed depends on the gradation as well as the mean or median grain size. For a fine, poorly graded sand, once transport is initiated, there is a nearly continuous supply of sizes that can be transported. For a well-graded sand subjected to winds capable of transporting the finer fractions, fine sediments are eventually removed from the surface leaving behind the coarse fraction. See Figure III-4-21. In order to continue the transport process, higher wind speeds must occur or fine sediments must be exposed at the surface again.

f. Limited source due to gradation armoring. Beach sands generally are not uniform in size but have a gradation that is often log-normally distributed. The finer fraction at the beach surface is more easily transported than the coarser fraction. Finer sand in the gradation also has the potential to be transported at a greater rate by lower wind speeds while larger sand is transported at a slower rate, if at all. However, as finer sands are depleted from the surface layer of the beach, the remaining larger particles shelter the underlying fines and armor the beach. Then, at the upwind end of the fetch, transport of fine sand ceases and, unless the wind speed increases to remove and transport the coarser fraction, transport will cease. Further downwind, the fines leaving the control volume balance the fines entering so that transport continues. Consequently, there is a moving, upwind boundary between that portion of beach where the fines have been removed and transport has ceased, and where transport of fines continues. Each size fraction has its own boundary. As fines are removed and the coarser fraction remains behind to armor the surface, the no-transport boundary moves downwind. Note that for sand with a uniform size gradation, this armoring process does not occur while for a well-graded sand it does. Other armoring processes may occur for uniformly graded sands. Figure III-4-24 shows the location of the upwind boundary separating the armored area from the area where transport processes continue.

EXAMPLE PROBLEM III-4-10

Find:

The wind transport rate for each fraction of the sand at Atlantic City having the distribution given in Figure III-4-25. Determine the total transport by summing the transport of all fractions using the beach sand size distribution as a weight function.

Given:

The wind rose data from Atlantic City in Table III-4-9 and the beach and dune sand size distributions in Figure III-4-25.

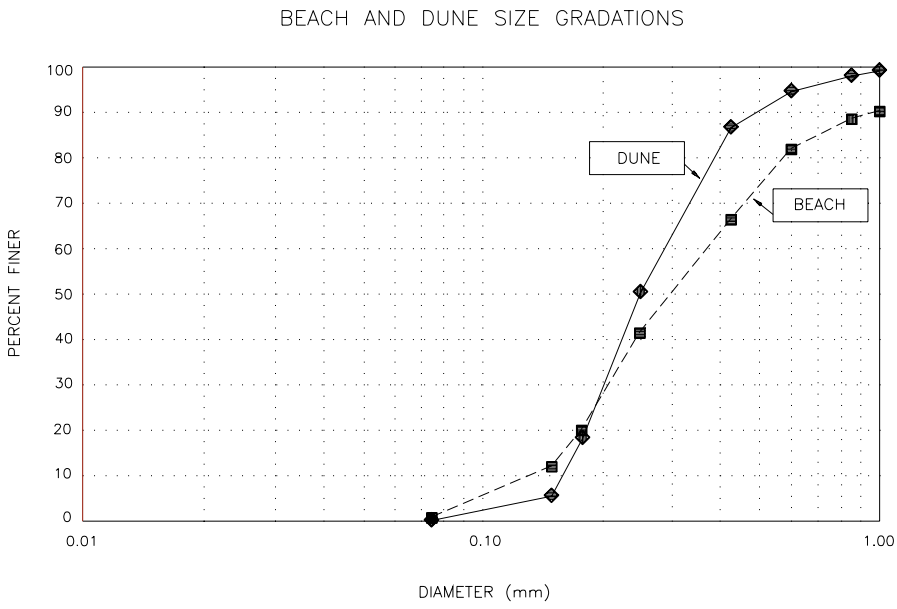

Figure III-4-25. Beach and dune and size gradations for Atlantic City, NJ

Solution:

The first step is to divide the size distribution for the beach sand into discrete increments and to determine the threshold wind speed for the upper limit of each size interval. See Table III-4-15. The volumetric transport coefficient is obtained from Figure III-4-13 entering with the appropriate sand grain diameter and elevation at which the wind speeds are measured (in this example assumed to be 10 m). The wind speeds in both miles per hour (mph) and in centimeters per second at the wind rose interval boundaries are given in Table III-4-16.

(Sheet 1 of 6)

Example Problem III-4-10 (Continued)

Table III-4-15
Size Distribution, Threshold Wind Speeds and Volumetric Transport Coefficients for Beach Sand Size Intervals, Atlantic City, NJ

d (mm)	Fraction Finer	Fraction Within Interval	u_{thresh} (cm/sec)	Volumetric Transport Coefficient K'_v (m^2-sec^2/cm^3)
0.08	0.02	0.020	420	1.80e-14
0.10	0.05	0.030	450	1.50e-14
0.20	0.14	0.090	555	1.00e-14
0.25	0.28	0.140	650	8.00e-15
0.30	1.42	0.140	725	5.90e-15
0.35	0.51	0.090	800	5.35e-15
0.40	0.65	0.140	910	3.36e-15
0.50	0.75	0.100	1020	9.43e-15
0.60	0.83	0.080	1120	1.23e-14
0.70	0.87	0.040	1210	1.57e-14
0.80	0.89	0.015	1310	2.20e-14
0.90	0.90	0.015	1395	3.02e-14

Table III-4-17 gives the potential sand transport at the wind rose interval boundaries for each of the grain size intervals. Column 4 of the table gives the potential transport for each of the size intervals in cubic meters per meter-second. For those cases where the threshold wind speed exceeds the actual wind speed (the coarser fraction), the transport is zero. Column 5 gives the potential transport values in cubic meters per meter-year while column 6 gives the potential transport weighted by the fraction of sand within the given size interval. For example, for a wind speed of 14 mph (626 cm/sec) 77.4 m^3/m-yr of sand with a diameter of 0.2 mm could be transported. However, only 9 percent of the sand is within this size interval so that the weighted transport rate is 0.09(77.4) = 6.96 m^3/m-yr. Note that for a wind speed of 14 mph (626 cm/sec), only sand with a diameter less than about 0.2 mm will be transported. For a wind speed of 29 mph, sand with a diameter less than 0.70 mm is transported.

Table III-4-16
Wind Speeds for Atlantic City Wind Rose Intervals

Wind Speed	
(mph)	(cm/sec)
0	0
14	626
29	1,296
35	1,565

(Sheet 2 of 6)

Example Problem III-4-10 (Continued)

Table III-4-17
Transport Rates for Size Intervals at Atlantic City Wind Rose Speed Intervals

d (mm)	Fraction Within Interval	Wind Speed (cm/sec)	Potential Transport (m^3/m-sec)	Potential Transport (m^3/m-yr)	Transport Weighted by Sand Fraction Within Interval (m^3/m-yr)
0.08	0.020	626	4.413e-6	139.3	2.79
0.10	0.030	626	3.677e-6	116.0	3.48
0.20	0.090	626	2.451e-6	77.4	6.96
0.25	0.140	626	0[1]	0[1]	0[1]
0.30	0.140	626	0	0	0
0.35	0.090	626	0	0	0
0.40	0.140	626	0	0	0
0.50	0.100	626	0	0	0
0.60	0.080	626	0	0	0
0.70	0.040	626	0	0	0
0.80	0.015	626	0	0	0
0.90	0.015	626	0	0	0
0.08	0.020	1296	3.922e-5	1237.7	24.75
0.10	0.030	1296	3.268e-5	1031.4	30.94
0.20	0.090	1296	2.179e-5	687.6	61.88
0.25	0.140	1296	1.743e-5	550.1	77.01
0.30	0.140	1296	1.286e-5	405.7	56.80
0.35	0.090	1296	1.166e-5	367.9	33.11
0.40	0.140	1296	7.321e-6	231.0	32.34
0.50	0.100	1296	2.055e-5	648.4	64.84
0.60	0.080	1296	2.680e-5	845.7	67.66
0.70	0.040	1296	3.421e-5	1079.5	43.18
0.80	0.015	1296	0[1]	0[1]	0[1]
0.90	0.015	1296	0	0	0
0.08	0.020	1565	6.895e-5	2175.8	43.52
0.10	0.030	1565	5.746e-5	1813.2	54.40
0.20	0.090	1565	3.830e-5	1208.8	108.79
0.25	0.140	1565	3.064e-5	967.0	135.38
0.30	0.140	1565	2.260e-5	713.2	99.85
0.35	0.090	1565	2.049e-5	646.7	58.20
0.40	0.140	1565	1.287e-5	406.2	56.86
0.50	0.100	1565	3.612e-5	1139.9	113.99
0.60	0.080	1565	4.711e-5	1486.8	118.94
0.70	0.040	1565	6.014e-5	1897.8	75.91
0.80	0.015	1565	8.427e-5	2659.3	39.89
0.90	0.015	1565	1.157e-4	3650.5	54.76

[1] Threshold wind speed exceeds actual wind speed and there is no transport of coarser sands.

(Sheet 3 of 6)

Example Problem III-4-10 (Continued)

Table III-4-18 is constructed from Table III-4-17 and the wind rose data. Table III-4-18 is only for winds from the north. The values in columns 2, 3, and 4 are the average transport values over the wind speed interval; hence, for example, the first value in column 3 is the average transport over the wind speed interval 14 mph < U < 29 mph, or (2.79 + 24.75)/2 = 13.77 m^3/m-yr. Similarly, the first value in column 4 is the average over the interval 29 mph < U < 35 mph, or (24.75 + 43.52)/2 = 34.14 m^3/m-sec. The values in column 5 are the weighted sums of the values across each row with the number of days that the wind was within the given speed interval used as the weight factor. Hence, the value in the first row is given by (1.395)(20/365) + (13.77)(20/365) + (34.14)(0/365) = 0.831 m^3/m-yr. Consequently, the total amount of sand transported northward is 14.218 m^3/m-yr. Table III-4-18 is for winds from the north only. Similar analyses must be done for the remaining seven compass directions. The results of the analyses for all eight compass directions are summarized in Table III-4-19 where, for example, column 2 is derived from column 5 of Table III-4-18. (Calculations for the remaining compass directions are omitted for brevity.)

Table III-4-18
Wind Transport of Size Intervals for Winds from North Weighted by Fraction of Year Wind was within Given Speed and Direction Interval

(Similar tables must be constructed for the other seven compass directions)

Wind From North

d (mm)	Avg. Transport Over Interval 0<U<14 No. Days = 20	Avg. Transport Over Interval 14<U<29 No. Days = 20	Avg. Transport Over Interval 29<U<35 No. Days = 0	Sum of Transports Weighted by No. of Days (m^3/m-yr)
0.08	1.395	13.77	34.14	0.831
0.10	1.740	17.21	42.67	1.038
0.20	3.480	34.42	85.33	2.077
0.25	0	38.5	106.20	2.110
0.30	0	28.4	78.33	1.556
0.35	0	16.55	45.66	0.907
0.40	0	16.17	44.60	0.886
0.50	0	32.42	89.42	1.776
0.60	0	33.83	93.30	1.854
0.70	0	21.59	59.55	1.183
0.80	0	0	19.95	0
0.90	0	0	27.38	0
			TOTAL N =	14.218

(Sheet 4 of 6)

Example Problem III-4-10 (Continued)

Table III-4-19
Summary of Transports for Eight Compass Directions

d (mm)	Transport (m^2/yr)							
	N	NE	E	SE	S	SW	W	NW
0.08	0.831	1.226	0.818	0.739	2.225	1.007	1.781	0.951
0.10	1.038	1.533	1.022	0.923	2.780	1.259	2.226	1.188
0.20	2.077	3.066	2.044	1.846	5.560	2.517	4.452	2.376
0.25	2.110	3.456	2.164	1.953	6.041	2.717	4.721	2.506
0.30	1.556	2.551	1.596	1.441	4.456	2.004	3.483	1.849
0.35	0.907	1.487	0.930	0.840	2.597	1.168	2.029	1.077
0.40	0.886	1.453	0.909	0.820	2.537	1.141	1.983	1.053
0.50	1.776	2.912	1.822	1.645	5.087	2.288	3.975	2.110
0.60	1.854	3.039	1.902	1.716	5.308	2.387	4.148	2.202
0.70	1.183	1.940	1.214	1.095	3.388	1.524	2.647	1.405
0.80	0	0.273	0.109	0.109	0.164	0.055	0.055	0.055
0.90	0	0.375	0.150	0.150	0.225	0.075	0.075	0.075
TOTAL	14.218	23.314	14.680	13.277	40.307	18.142	31.576	16.847

Dune growth depends on the wind direction relative to the dune axis and the assumptions made regarding the ability of the dune to trap and hold sand. The procedures presented in Example Problem III-4-8 are applied to each individual grain size interval and the values summed to estimate the amount of sand trapped by the dune. Transport in each direction is multiplied by $\sin\beta$, the angle between the dune axis and the direction from which the wind is blowing, and $\cos^2\beta$, the dune trapping efficiency. These values are given at the bottom of Table III-4-20. The values in Table III-4-20 are the net contribution to dune growth by winds from the indicated directions. For example, winds from the north remove sand from the dunes since values in column 2 are negative (the wind is blowing from the dune toward the beach). For this site, most dune growth is due to southerly winds and, to a lesser extent, to southeasterly winds.

(Sheet 5 of 6)

Example Problem III-4-10 (Concluded)

For the example, the total dune growth rate is 38.63 m^3/m-yr. This represents a high rate of growth and most certainly overestimates dune growth at Atlantic City since the example assumes an unlimited supply of sand in all size intervals available for transport. As in Example Problem III-4-9, the calculated dune growth rate can be adjusted by using the trapping efficiency based on a comparison of the beach sand with the dune sand. From the preceding example, T_f = 0.55; hence, the estimated dune growth rate is $R_a = 0.55(38.63) = 21.4$ m^3/m-yr. An alternative procedure to adjust dune growth rates based on comparing the dune sand distribution with the beach sand distribution is given in Example Problem III-4-11, which follows.

Table III-4-20
Computation of Dune Growth Rate

d	Dune Growth (m^2/yr)								
(mm)	N	NE	E	SE	S	SW	W	NW	Total
0.08	-0.263	-0.106	0.526	0.736	1.704	0.088	-0.672	-0.007	2.110
0.10	-0.329	-0.133	0.657	0.919	2.130	0.110	-0.840	-0.009	2.639
0.20	-0.657	-0.265	1.314	1.839	4.260	0.219	-1.679	-0.018	5.277
0.25	-0.668	-0.299	1.391	1.946	4.628	0.237	-1.781	-0.019	5.734
0.30	-0.493	-0.221	1.026	1.435	3.144	0.175	-1.314	-0.014	4.230
0.35	-0.287	-0.129	0.598	0.836	1.989	0.102	-0.766	-0.008	2.465
0.40	-0.280	-0.126	0.584	0.817	1.944	0.100	-0.748	-0.008	2.408
0.50	-0.562	-0.252	1.171	1.638	3.897	0.199	-1.500	-0.016	2.828
0.60	-0.587	-0.263	1.222	1.710	4.066	0.208	-1.565	-0.011	5.038
0.70	-0.374	-0.168	0.780	1.091	2.595	0.133	-0.999	-0.010	3.215
0.80	0	-0.024	0.070	0.109	0.126	0.005	-0.021	-0.000	0.288
0.90	0	-0.032	0.096	0.150	0.172	0.007	-0.028	-0.001	0.396
TOTAL	-4.500	-2.017	9.436	13.226	30.925	1.581	-11.911	-0.127	
$\sin\beta$	-0.7660	-0.0872	0.6428	0.9962	0.7660	0.0872	-0.6428	-0.9962	
$\cos^2\beta$	0.4132	0.9924	1.0000	1.0000	1.0000	1.0000	0.5868	0.0076	

TOTAL DUNE GROWTH RATE = 38.631 m^3/m-yr

(Sheet 6 of 6)

EXAMPLE PROBLEM III-4-11

Find:

The trapping efficiency for natural dune building in Atlantic City and the dune grain size distribution calculated from the results of Example Problem III-4-10 given the measured and calculated grain-size distributions for the dune sand at Atlantic City.

Given:

The dune growth rates based on the individual grain size intervals as calculated in Example Problem III-4-10 and the actual dune sand size distributions given in Figure III-4-25.

Solution:

The calculated amounts of sand trapped in the dune from each size interval are given in Table III-4-21. The values in column 2 of Table III-4-21 are found by summing across the rows in Table III-4-20. Thus, 2.111 m^3/m-yr of sand with a diameter less than 0.08 mm is trapped by the dunes. Similarly, 2.639 m^3/m-yr of sand with a diameter between 0.08 mm and 0.10 mm is trapped. The calculated size distribution of the dune sand is determined by normalizing the values in column 2 by dividing each value in column 2 by the sum of column 2. The resulting values are given in column 3, which represents the fraction of the sand in the dune within the given size interval. For example, 0.0547 or 5.47 percent of the dune sand is finer than d = 0.08 mm and 6.83 percent is between d = 0.10 mm and d = 0.08 mm, etc. Column 4 of Table III-4-21 gives the cumulative distribution.

Table III-4-21
Calculated Dune Sand Size Distribution

d (mm)	Amount Trapped in Dune (m^3/m-yr)	Normalized Amount Trapped in Dune	Cumulative Size Distribution in Dune
0.08	2.111	0.0547	0.0547
0.10	2.639	0.0683	0.1230
0.20	5.277	0.1366	0.2596
0.25	5.732	0.1484	0.4080
0.30	4.230	0.1095	0.5175
0.35	2.465	0.0638	0.5813
0.40	2.408	0.0623	0.6436
0.50	4.828	0.1250	0.7686
0.60	5.038	0.1304	0.8990
0.70	3.215	0.0832	0.9823
0.80	0.288	0.0075	0.9898
0.90	0.396	0.0102	1.0000
TOTAL	38.631	1.0000	

(Sheet 1 of 4)

Example Problem III-4-11 (Continued)

Figure III-4-26 shows the calculated sand size distribution in the dune along with the actual dune size distribution. The actual distribution differs from the calculated distribution because not all of the sand present on the beach is available for transport due to processes like gradation armoring, crust formation, etc. Some fines might be confined between larger grains and once the surficial fines are removed, the remaining fines are not available for transport. Also, the coarser fraction can only be transported by the less frequent high wind speeds.

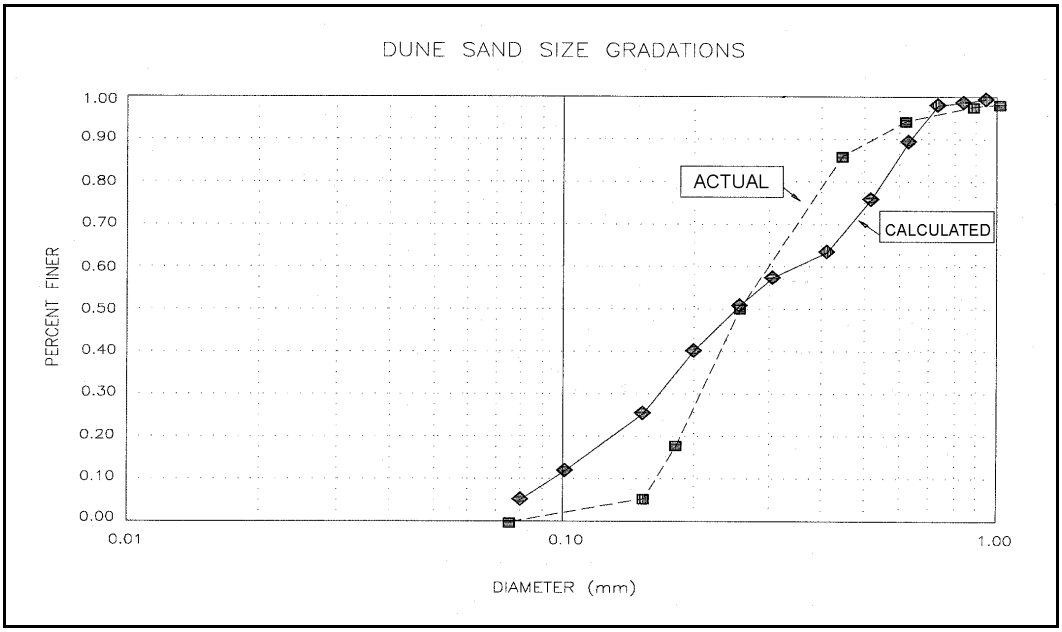

Figure III-4-26. Actual and calculated dune sand size gradation at Atlantic City, NJ

The transport rates calculated for each size interval are potential transport rates. Comparison of the calculated size distribution with the actual distribution allows a correction factor to be calculated for each size fraction. Columns 2 and 3 of Table III-4-22 present the calculated and actual size distributions, respectively. Column 4 is a calculated correction factor equal to the actual interval fraction divided by the calculated interval fraction. For example, the correction factor 0.1818 in the first row equals 0.0100/0.0547, the ratio of column 3 over column 2. Thus column 4 gives the numbers by which calculated values must be multiplied in order to obtain actual values. The amount of sand available for transport in each size interval is limited, so, in order to calculate the amount actually transported in each size interval, the correction factor values in column 4 must be normalized by dividing through by the largest value. (Column 4 would suggest that 300 percent of the amount of sand between 0.35 mm and 0.40 mm is needed to produce the observed distribution. Clearly, no more than 100 percent can be available.) The values in column 5 result. These values can be considered to be transport correction factors for each size interval. They are the values by which the transport rate in each size interval must be multiplied in order to produce the measured dune size distribution.

(Sheet 2 of 4)

Example Problem III-4-11 (Continued)

Table III-4-22
Comparison of Calculated Dune Sand Size Distribution and Actual Dune Sand Size Distribution

d (mm)	Calculated Dune Sand Size Distribution	Actual Dune Sand Size Distribution	Correction = Actual/Calculated	Normalized Correction
0.08	0.0547	0.0100	0.1818	0.0604
0.10	0.0683	0.0470	0.6912	0.2297
0.20	0.1366	0.1355	0.9891	0.3286
0.25	0.1484	0.0908	0.6135	0.2039
0.30	0.1095	0.2250	2.0455	0.6797
0.35	0.0638	0.1334	2.1175	0.7036
0.40	0.0623	0.1896	3.0095	1.0000
0.50	0.1250	0.0832	0.6656	0.2212
0.60	0.1304	0.0397	0.3054	0.1015
0.70	0.0832	0.0125	0.1506	0.0500
0.80	0.0075	0.0125	1.6026	0.5325
0.90	0.0102	0.0100	0.9804	0.3258
TOTAL	1.0000	1.0000		

Table III-4-23 gives the corrected transport rates for each size interval. Column 2 is the calculated amount in each size interval trapped in the dune. (See column 2, Table III-4-21.) Column 3 is the normalized correction factor (see column 5, Table III-4-22) and column 4 is the corrected dune growth rate for sand within the given size fraction. The sum of the values in column 4 gives the corrected dune growth rate. For the given example, the corrected dune growth rate is 12.7 m^3/m-yr. This procedure is similar to the procedure used to derive the trapping factor T_f but by matching the calculated and actual dune size distributions and without assuming that the distributions are log-normal. The value of T_f can be calculated for this example by taking the ratio of the value of the total from column 4 in Table III-4-23 to the total in column 2. This ratio is $T_f = 12.68/38.63 = 0.33$, which can be computed with the value of $T_f = 0.57$ calculated in Example Problem III-4-9.

Figure III-4-27 compares the actual dune size distribution with the calculated distribution after the correction has been applied.

(Sheet 3 of 4)

Example Problem III-4-11 (Concluded)

Table III-4-23
Corrected Transport Rates for Size Intervals and Corrected Dune Growth Rate

d (mm)	Calculated Transport Rates (m^3/m-yr)	Normalized Correction Factor	Corrected Transport Rates (m^3/m-yr)
0.08	2.111	0.0604	0.1275
0.10	2.639	0.2297	0.6062
0.20	5.277	0.3286	1.7340
0.25	5.732	0.2039	1.1688
0.30	4.230	0.6797	2.8751
0.35	2.465	0.7036	1.7344
0.40	2.408	1.0000	2.4080
0.50	4.828	0.2212	1.0680
0.60	5.038	0.1015	0.5114
0.70	3.215	0.0500	0.1608
0.80	0.288	0.5325	0.1534
0.90	0.396	0.3258	0.1290
TOTAL =	38.627		12.6766

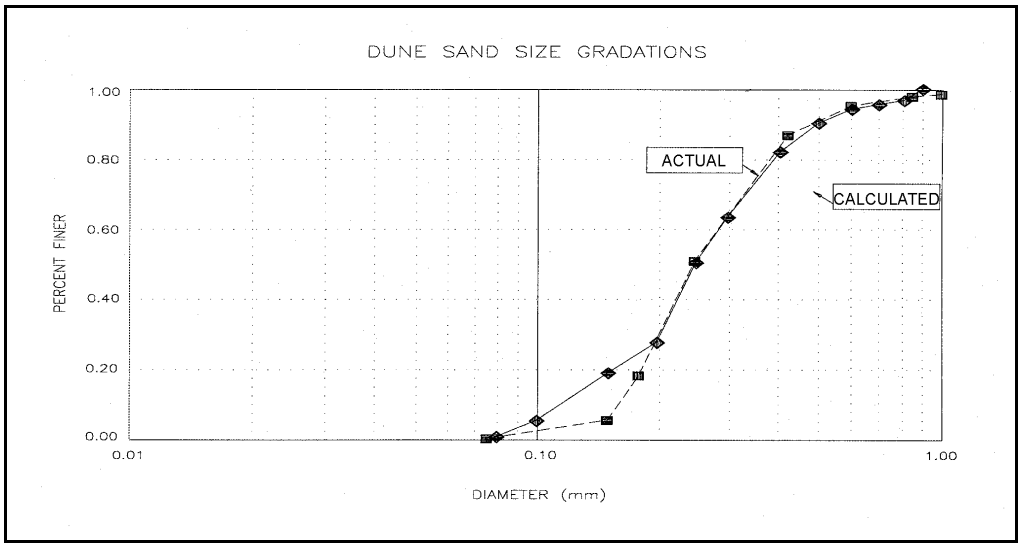

Figure III-4-27. Comparison of actual dune sand size gradation with corrected, calculated gradation

(Sheet 4 of 4)

III-4-6. References

EM 1110-2-5003
Planting Guidelines for Dune Creation and Stabilization

Bagnold 1936
Bagnold, R. A. 1936. "The Movement of Desert Sand," *Proceedings Royal Society of London*, Series A, Vol 157, pp 94-620.

Bagnold 1941
Bagnold, R. A. 1941. *The Physics of Blown Sand and Desert Dunes*, Morrow, New York, (republished in 1954 by Methuen, London).

Belly 1962
Belly, P. Y. 1962. "Sand Movement by Wind," Technical Memorandum, TM-1, Coastal and Hydraulics Laboratory, U.S. Army Engineer Waterways Experiment Station, Vicksburg, MS.

Chapman 1990
Chapman, D. M. 1990. "Aeolian Sand Transport - An Optimized Model," *Earth Surface Processes and Landforms*, Vol 15, pp 751-760.

Gillette, Herbert, Stockton, and Owen 1996
Gillette, D. A., Herbert, G., Stockton, P. H., and Owen, P. R. 1996. " Causes of the Fetch Effect in Wind Erosion," *Earth Surface Processes and Landforms*, Vol 21, pp 641-659.

Holzworth 1972
Holzworth 1972. "Mixing Heights, Wind Speeds, and Potential for Urban Air Pollution Throughout the Contiguous United States," Office of Air Programs, Publication No. AP-101, Environmental Protection Agency, Research Triangle Park, North Carolina.

Horikawa 1988
Horikawa, K. (Editor). 1988. *Nearshore Dynamics and Coastal Processes*, University of Tokyo Press, Tokyo, Japan.

Horikawa and Shen 1960
Horikawa, K., and Shen, H. W. 1960. "Sand Movement by Wind Action - on the Characteristics of Sand Traps," Technical Memorandum 119, Coastal and Hydraulics Laboratory, U.S. Army Engineer Waterways Experiment Station, Vicksburg, MS.

Hotta, Kubota, Katori, and Horikawa 1985
Hotta, S., Kubota, S., Katori, S., and Horikawa, K. 1985. "Sand Transport by Wind on a Wet Sand Surface," *Proceedings, 19th International Conference on Coastal Engineering,* American Society of Civil Engineers, pp 1265-1281.

Hsu 1973
Hsu, S. A. 1973. "Computing Eolian Sand Transport from Shear Velocity Measurements," *Journal of Geology*, Vol 81, pp 739-743.

Hsu 1977
Hsu, S. A. 1977. "Boundary Layer Meteorological Research in the Coastal Zone," *Geoscience and Man*, H. J. Walker, ed., School of Geoscience, Louisiana State University, Baton Rouge, LA, Vol 18, pp 99-111.

Hsu 1981
Hsu, S. A. 1981. "Models for Estimating Offshore Winds from Onshore Meteorological Measurements," *Boundary Layer Meteorology*, Vol 20, pp 341-351.

Hsu 1986
Hsu, S. A. 1986. "Correction of Land-Based Wind Data for Offshore Applications: A Further Evaluation," *Journal of Physical Oceanography*, Vol 16, pp 390-394.

Hsu 1988
Hsu, S. A. 1988. *Coastal Meteorology*, Academic Press, San Diego, CA.

Hsu 1994
Hsu, S. A. 1994. Personal communication, Coastal Studies Institute, Louisiana State University, Baton Rouge, LA.

Hsu and Blanchard 1991
Hsu, S. A., and Blanchard, B. W. 1991. "Shear Velocity and Eolian Sand Transport on a Barrier Island," *Proceedings, Coastal Sediments '91,* American Society of Civil Engineers, New York, Vol 1, pp 220-234.

Kadib 1964
Kadib, A. 1964. "Calculation Procedure for Sand Transport on Natural Beaches," Miscellaneous Paper 2-64, Coastal and Hydraulics Laboratory, U.S. Army Engineer Waterways Experiment Station, Vicksburg, MS.

Kadib 1966
Kadib, A. 1966. "Mechanics of Sand Movement on Coastal Dunes," *Journal of the Waterways and Harbors Division*, American Society of Civil Engineers, WW2, pp 27-44.

Kawamura 1951
Kawamura, R. 1951. "Study on Sand Movement by Wind," Report, Institute of Science and Technology, University of Tokyo. (translation, University of California, Berkeley, Hydraulic Engineering Laboratory Research Report, HEL-2-9, Berkeley, CA, 1964, pp 1-64).

Krumbein and James 1965
Krumbein, W. C., and James, W. R. 1965. "A Lognormal Size Distribution Model for Estimating Stability of Beach Fill Material," TM-16, Coastal and Hydraulics Laboratory, U.S. Army Engineer Waterways Experiment Station, Vicksburg, MS.

Liu, Schwab, and Bennett 1984
Liu, P. C., Schwab, D. J., and Bennett, J. R. 1984. "Comparison of a Two Dimensional Wave Prediction Model with Synoptic Measurements in Lake Michigan," *Journal of Physical Oceanography*, Vol 14, pp 1514-1518.

Nickling and Egglestone 1981
Nickling, W. G., and Egglestone, M. 1981. "The Effects of Soluble Salts on the Threshold Shear Velocity of Fine Sand," *Sedimentology*, Vol 28, pp 505-510.

Nordstrom and Jackson 1992
Nordstrom, K. F., and Jackson, N. L. 1992. "Effect of Source Width and Tidal Elevation Changes on Aeolian Transport on an Estuarine Beach," *Sedimentology*, Vol 39, pp 769-778.

O'Brien and Rindlaub 1936
O'Brien, M. P., and Rindlaub, B. D. 1936. "The Transport of Sand by Wind," *Civil Engineering,* Vol 6, pp 325-327.

Powell 1982
Powell, M. D. 1982. "The Transition of the Hurricane Frederic Boundary-Layer Wind Field from the Open Gulf of Mexico to Landfall," *Monthly Weather Review*, Vol 110, pp 1912-1932.

Raudkivi 1976
Raudkivi, A. J. 1976. *Loose Boundary Hydraulics*, 2nd ed., Pergamon Press, New York.

Resio and Vincent 1977
Resio, D.T., and Vincent, C. L. 1977. "Estimation of Winds Over the Great Lakes," *Journal of the Waterway, Port, Coastal and Ocean Engineering Division*, American Society of Civil Engineers, Vol 103, No. WW2.

Sarre 1988
Sarre, R. D. 1988. "Evaluation of Eolian Transport Equations Using Intertidal Zone Measurements: Saunton Sands, England," *Sedimentology*, Vol 35, pp 671-679.

Savage 1963
Savage, R. P. 1963. "Experimental Study of Dune Building with Sand Fences," *Proceedings, International Conference on Coastal Engineering*, 1963, pp 380-396.

Savage and Woodhouse 1968
Savage, R. P., and Woodhouse, W. W., Jr. 1968. "Creation and Stabilization of Coastal Barrier Dunes," *Proceedings, 11th International Conference on Coastal Engineering*, Vol 1, 1968, pp 671-700.

SethuRaman and Raynor 1980
SethuRaman, S., and Raynor, G. S. 1980. "Comparison of Mean Wind Speeds and Turbulence at a Coastal Site and Offshore Location," *Journal of Applied Meteorology*, Vol 19, pp 15-21.

Shore Protection Manual 1984
Shore Protection Manual. 1984. 4th ed., 2 Vol, U.S. Army Engineer Waterways Experiment Station, U.S. Government Printing Office, Washington, DC.

Svasek and Terwindt 1974
Svasek, J.N., and Terwindt, J. H. J. 1974. "Measurements of Sand Transport by Wind on a Natural Beach," *Sedimentology*, Vol 21, pp 311-322.

Wieringa 1980
Wieringa, J. 1980. "Representativeness of Wind Observation at Airports," Bulletin, American Meteorological Society, Vol 61, pp 962-971

Williams 1964
Williams, G. 1964. "Some Aspects of the Aeolian Saltation Load," *Sedimentology*, Vol 3, pp 257-287.

Woodhouse 1978
Woodhouse, Jr. 1978. "Dune Building and Stabilization with Vegetation," Special Report No. 3, Coastal and Hydraulics Laboratory, U.S. Army Engineer Waterways Experiment Station, Vicksburg, MS.

Zingg 1953
Zingg, A. W. 1953. "Wind Tunnel Studies of the Movement of Sedimentary Material," *Proceedings, 5th Hydraulic Conference*, State University of Iowa, Studies in Engineering, Bulletin, Vol 34, pp 111-135.

III-4-7. Definition of Symbols

$\Delta \forall$	Volume change per unit length of beach [length^3/length]
ε	Erodibility factor related to beach sand that is potentially transportable [dimensionless]
η	Transport efficiency for winds at the seaward side of a dune
η_i	Transport efficiency for winds at the landward side of a dune
κ	von Karman's constant (= 0.4)
μ_φ	Mean of a sediment sample [phi units]
$\mu_{\varphi D \text{ or } B}$	Mean of a sediment sample taken from the dune or beach [phi units]
v_a	Kinematic viscosity of air [length^2/time]
ρ	Mass density of sediment grains [force-time^2/length^4]
ρ_a	Mass density of air [force-time^2/length^4]
σ_φ	Standard deviation of a sediment sample [phi units]
$\sigma_{\varphi D \text{ or } B}$	Standard deviation of a sediment sample taken from the dune or beach [phi units]
τ	Boundary shear stress [force/length^2]
φ	Sediment grain diameter in phi units ($\varphi = -\log_2 d_{mm}$, where d_{mm} is the grain diameter in millimeters)
φ_x	Sediment grain diameter of the x-percentile of a sample (x-percent of the grains are finer) [phi units]
A	Empirical constant (Equation III-4-10) [dimensionless]
A_t	Dimensionless constant (= 0.118) used in calculating the critical shear stress, u_{*_t}, for sand transport by wind (Equation III-4-20)
B	Empirical constant (Equation III-4-10) [dimensionless]
$B_{Bagnold}$	Bagnold coefficient [dimensionless]
$C_{D,land}$	Drag coefficients over land [dimensionless]
$C_{D,sea}$	Drag coefficient over sea [dimensionless]
C_z	Wind drag coefficient at height Z (Equation III-4-4) [dimensionless]
d	Standard grain size (= 0.25mm)
D	Median sediment grain diameter [length - generally millimeters]
D	Mean sediment grain diameter [length - generally millimeters]
d_{mm}	Sediment grain diameter in millimeters

d_x	Sediment grain diameter of the x-percentile of a sample (x-percent of the grains are finer) [length]
e	Base of natural logarithms
g	Gravitational acceleration (32.17 ft/sec^2, 9.807m/sec^2) [length/time^2]
G	Dry weight sand transport rate [force/length/time]
H_{land}	Height of the planetary boundary layer over the land [length]
H_{sea}	Height of the planetary boundary layer over the sea [length]
K	Empirical dimensional eolian sand transport coefficient (Equation III-4-17) [force/length/time]
K'	Eolian sand transport coefficient (Equation III-4-19) [dimensionless]
n	Empirically determined exponent (ranging from 1/11 to 1/17) (Equation III-4-15) [dimensionless]
p	Porosity of the *in situ* dune sand [percent]
q	Wind-borne sand transport rate [mass/time/length]
q_i	Sand blown inland from the dune [mass/time/length]
q_s	Dune erosion by waves [mass/time/length]
q_v	Volumetric sand transport rate [length^3/length/time]
R_a	Actual dune growth rate [length^3/length-time]
R_t	Theoretical dune growth rate [length^3/length-time]
R_T	Temperature correction factor applied to wind speed at the 10-m height (Figure III-4-7) [dimensionless]
t	Time
T_a	Air temperature [degrees Celsius]
T_f	Dune trapping factor [dimensionless]
T_s	Sea temperature [degrees Celsius]
u_*	Wind shear or friction velocity [length/time]
u_{*t}	Critical or threshold velocity for sand transport by wind (Equation III-4-20) [length/time]
u_{*tw}	Critical or threshold velocity for wet sand transport by wind (Equation III-4-20) [length/time]
U_{land}	Wind speed over land [length/time]
U_{sea}	Wind speed over sea [length/time]

U_x	Average wind speed at x-elevation [length/time]
U_z	Average wind velocity as a function of height above ground level [length]
U_{ZM}	Wind speed at the anemometer height [length/time]
U'_{10m}	Wind speed at the 10-meter height corrected for the air-sea temperature difference [length/time]
W	Fraction of water content in the upper 5mm of the sand [percent]
Z	Height at which wind speed is measured [length]
Z_0	Height of a roughness element characterizing the surface over which the wind is blowing [length]
Z_M	Anemometer height [length]
Z_R	Reference height [length]
Z_{Zingg}	Zingg Coefficient [dimensionless]

III-4-8. Acknowledgments

Authors of Chapter III-4, "Wind-Blown Sediment Transport:"

S. A. Hsu, Ph.D., Coastal Studies Institute, School of Geosciences, Louisiana State University, Baton Rouge, Louisiana.
J. Richard Weggel, Ph.D., Dept. of Civil and Architectural Engineering, Drexel University, Philadelphia, Pennsylvania.

Reviewers:

Robert G. Dean, Ph.D., Coastal & Oceanographic Engineering, University of Florida, Gainesville, Florida.
Scott Douglass, Ph.D., Dept. of Civil Engineering, University of South Alabama, Mobile, Alabama.
James R. Houston, Ph.D., Engineer Research and Development Center, Vicksburg, Mississippi.
David B. King, Ph.D., Coastal and Hydraulics Laboratory (CHL), Engineer Research and Development Center, Vicksburg, Mississippi.
Joon Rhee, Ph.D., CHL
Todd L. Walton, Ph.D., CHL

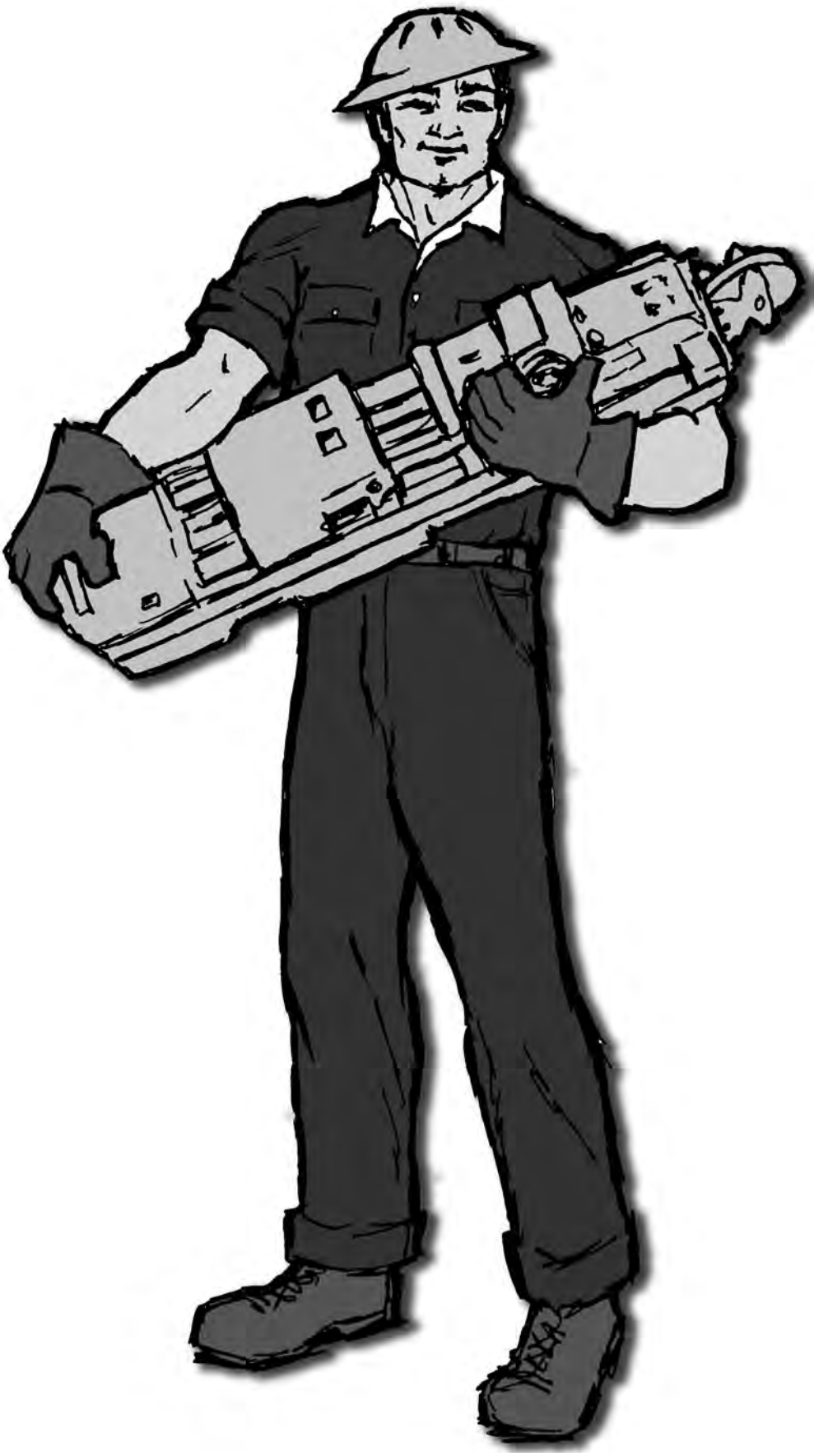

Chapter 5
EROSION, TRANSPORT, AND DEPOSITION OF COHESIVE SEDIMENTS

Table of Contents

Page

III-5-1. Introduction III-5-1

III-5-2. Consolidated and Unconsolidated Shores III-5-2
a. Consolidated shore III-5-2
b. Mud shore III-5-6
(1) Mud flat III-5-6
(2) Coastal wetland III-5-6
(3) Mangrove III-5-8
(4) Mud 'beach' III-5-8

III-5-3. Erosion Processes on Consolidated Shores III-5-8

III-5-4. Physical and Numerical Modeling III-5-10

III-5-5. Geomorphology of Consolidated Shores III-5-11
a. Controlling factors III-5-11
(1) Lag deposits III-5-11
(2) Different stratigraphic units III-5-11
(3) Quantity and mobility of sand cover III-5-13
(4) Local wave and water level conditions III-5-16
b. Profile types III-5-16

III-5-6. Sediment Properties and Measurement Techniques III-5-17
a. Introduction III-5-17
b. Consolidated shore erosion III-5-17
(1) Field sampling and geotechnical analyses III-5-18
(2) Laboratory erodibility experiments III-5-18
(3) Field techniques for assessing surface and subsurface conditions III-5-20
c. Erosion, transport, and deposition of mud III-5-21
(1) Cohesion III-5-21
(2) Critical shear for erosion III-5-21
(3) Erosion rate at twice critical shear III-5-21
(4) Critical shear for deposition III-5-22
(5) Sediment, fluid mud, and water densities III-5-22
(6) Grain size and settling velocity III-5-22
(7) Degree of consolidation III-5-23
(8) Field measurement techniques III-5-23
(9) Laboratory measurement techniques III-5-24
(10) Calibration techniques III-5-26

III-5-7. Erosion Processes III-5-26

a. Shear stress III-5-26
b. Erodibility of consolidated sediments III-5-26
c. Subaqueous erosion of consolidated sediments III-5-30
d. Subaqueous erosion of mud III-5-33
e. Fluid mud III-5-33
f. Subaerial erosion processes III-5-34

III-5-8. Transport Processes III-5-38
a. Advection and dispersion III-5-38
b. Fluid mud III-5-38

III-5-9. Deposition Processes III-5-38
a. Flocculation III-5-38
b. Shear stress III-5-39
c. Krone equation III-5-39
d. Fluid mud III-5-39

III-5-10. Consolidation III-5-39
a. Strength versus consolidation III-5-39
b. Degree of consolidation III-5-40

III-5-11. Wave Propagation III-5-40
a. Roughness and shear III-5-40
b. Fluid mud III-5-40

III-5-12. Numerical Modeling III-5-44
a. Introduction III-5-44
b. Simulating erosion of consolidated sediment III-5-46
c. Simulating erosion and deposition of mud III-5-48

III-5-13. Engineering and Management Implications III-5-48
a. Setbacks and cliff stablilization III-5-48
b. Vegetation III-5-48
c. Interruption to sediment supply and downdrift impacts III-5-49
d. Remedial measures for cohesive shore erosion III-5-49
e. Foundations III-5-50

III-5-14. References III-5-53

III-5-15. Definition of Symbols III-5-60

III-5-16. Acknowledgments III-5-61

List of Tables

Page

Table III-5-1
Cohesive Sediment Density III-5-2

Table III-5-2
Example Problem III-5-1, "Annular Flume Test Results" III-5-41

Table III-5-3
Erodibility Coefficients (from Penner (1993)) III-5-47

List of Figures

Page

Figure III-5-1. Outline of cohesive shore processes III-5-2

Figure III-5-2. Peat exposed on a beach along the Keta shoreline in Ghana, West Africa III-5-4

Figure III-5-3. Pieces of eroded clay (and some rubble) scattered on a beach along the Keta shoreline in Ghana, West Africa III-5-4

Figure III-5-4. Springs flowing over the beach surface along the Keta shoreline in Ghana, West Africa III-5-5

Figure III-5-5. Discolored water from erosion of exposed cohesive sediment along the Keta shoreline in Ghana, West Africa III-5-6

Figure III-5-6. Permanent undulations in the Keta shoreline in Ghana, West Africa III-5-7

Figure III-5-7. Mud flat in Cumberland Basin, Bay of Fundy, showing drainage gullies III-5-7

Figure III-5-8. A mud 'beach' backed with eroding salt marsh at Annapolis Royal, in the Annapolis Basin of the Bay of Fundy. Basalt revetment at top of salt marsh is an attempt to halt the erosion III-5-8

Figure III-5-9. Sand beach disappearing into mangrove on the island of Borneo. Sediment within the mangrove is cohesive mud III-5-9

Figure III-5-10. A convex consolidated cohesive profile with a shelf protected by lag deposits located near Goderich, Ontario, on Lake Huron III-5-12

Figure III-5-11. Plan and cross section of East Point along the Scarborough Bluffs (located east of Toronto on Lake Ontario) showing the influence of the erosion-resistant leaside (or northern) till on the local geomorphology III-5-13

Figure III-5-12. Plan and cross section of the Port Burwell area on the north central shore of Lake Erie showing the influence of a fillet beach and stratigraphy changes on the geomorphology of a cohesive shore III-5-14

Figure III-5-13. Bluff erosion along the Holderness coast of the North Sea. The underlying cohesive profile is exposed at low tide in a trough (referred to as an "Ord") between the upper beach and first bar III-5-15

Figure III-5-14. Close-up of the exposed cohesive profile on the Holderness coast (see Figure III-5-13). A rock-capped pedestal of cohesive sediment, about 10 cm in height, has developed through erosion of the adjacent seabed III-5-15

Figure III-5-15. Distinctions between concave and convex consolidated cohesive profiles III-5-16

Figure III-5-16. Laser doppler velocimeter (LDV) used to determine shear stress exerted on the till bed in a unidirectional flow flume test. This test features sand in the flow acting as an abrasive III-5-19

Figure III-5-17. Prototype direct shear device, the annular flume III-5-25

Figure III-5-18. Clear-water erosion rates from unidirectional flow flume and tunnel tests for various materials III-5-28

Figure III-5-19. Sand in flow erosion rates from unidirectional flow flume and tunnel tests for various materials III-5-29

Figure III-5-20. Bluff retreat and profile downcutting over a 37-year period at Scarborough Bluffs, located east of Toronto on Lake Ontario III-5-32

Figure III-5-21. A rotational bluff failure along the north central shore of Lake Erie III-5-35

Figure III-5-22. Gully erosion of a bluff along the north central shore of Lake Erie III-5-36

Figure III-5-23. An eroding shale bluff along the west Lake Ontario shoreline III-5-36

Figure III-5-24. Shore protection consisting of a wide berm protected by a revetment along the base of the Scarborough Bluffs located east of Toronto on Lake Ontario III-5-37

Figure III-5-25. Plot of erosion rate versus shear for example problem III-5-43

Figure III-5-26. Mud beach processes (after Lee (1995)) III-5-45

Figure III-5-27. A toppled concrete seawall along the Lake Michigan coast of Berrien County. Failure probably resulted from undermining of the underlying glacial till foundation III-5-51

Figure III-5-28. A steel sheet-pile wall and groin field has been ineffective at protecting this section of cohesive shore along the Berrien County shoreline of Lake Michigan III-5-51

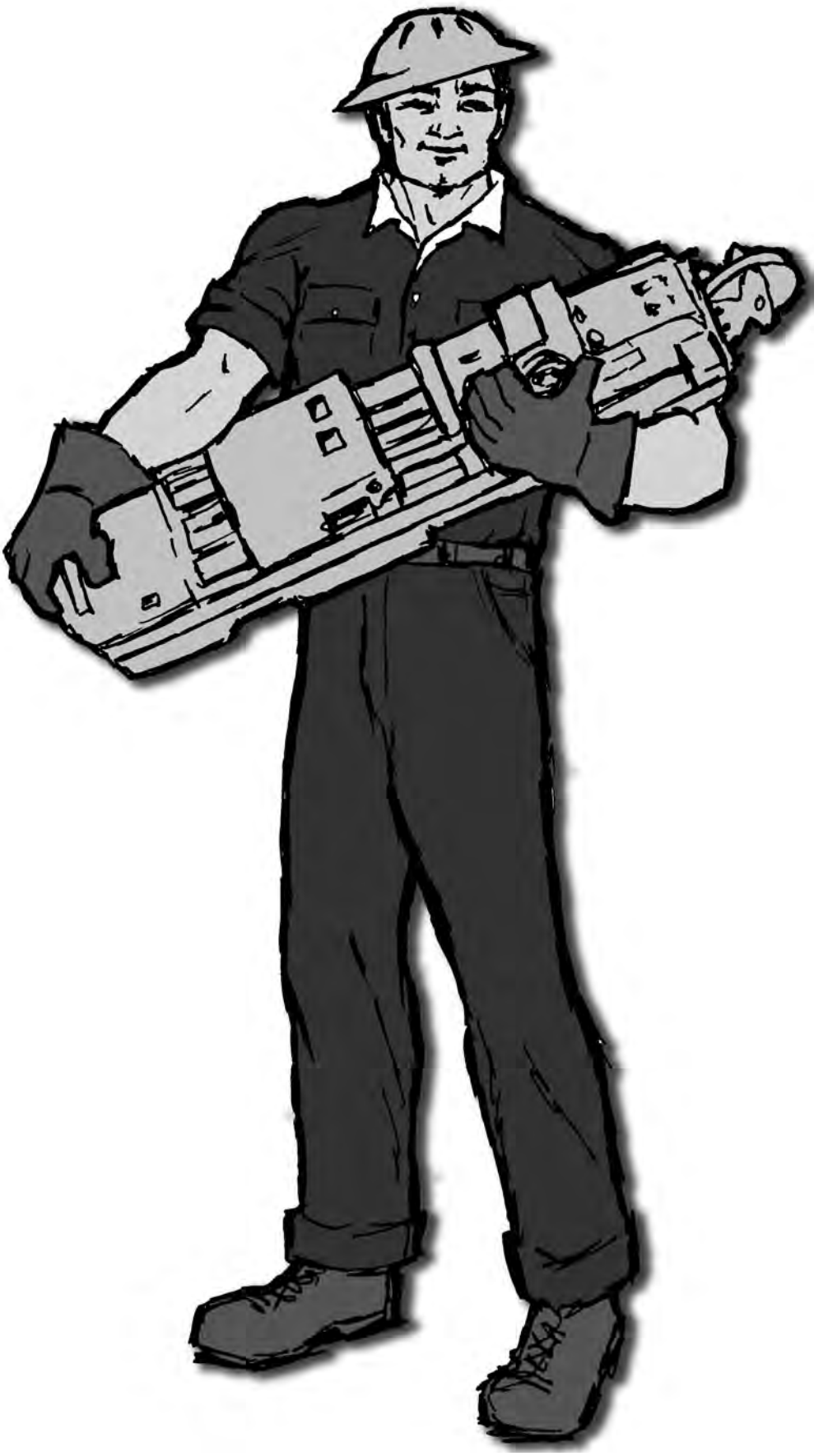

Chapter III-5
Erosion, Transport, and Deposition of Cohesive Sediments

III-5-1. Introduction

a. Cohesive sediments are those in which the attractive forces, predominantly electrochemical, between sediment grains are stronger than the force of gravity drawing each to the bed. Individual grains are small to minimize mass and gravitational attraction, and are generally taken to be in the silt (<70 μ) to clay (<4 μ) range. The strength of the cohesive bond is a function of the grain mineralogy and water chemistry, particularly salinity. Thus, a coarse silt behaves like noncohesive fine sand in fresh water, but is cohesive in an ocean environment. Similarly, a fine sand exhibits cohesion in salt water. In other words, it is easier to define cohesive sediment by behavior than by size.

b. Grain size and shape nevertheless play a significant role in the lack of permeability of cohesive sediment. As grain size decreases, so does the size of the interstitial pore spaces while drainage path length increases. The small pores result in greater resistance to flow, exacerbating the effects of the long drainage path. Clay minerals tend to form flake-shaped platelets, rather than spherical particles. These platelets deposit with the smallest dimension vertical, further reducing pores and increasing vertical drainage paths. For this reason, clay is often used as an impermeable layer in hydraulic earthworks such as dikes and channels.

c. In coastal engineering terms, the principal indicator of cohesive sediment behavior is a critical shear for erosion of bed sediment τ_c, which is significantly greater than the critical shear for deposition τ_s. In other words, once the sediment has been deposited on the bed, the cohesive bond with other bed particles makes it more difficult to remove than particle mass alone would suggest.

d. The processes and states of coastal cohesive sediment listed below are shown schematically in Figure III-5-1 and Table III-5-1.

(1) Consolidated. Stiff or hard cohesive sediment that has had centuries to drain, probably compressed beneath glaciers or other overburden.

(2) Suspension. Individual grains or flocs dispersed in the water column and transported with the water.

(3) Fluid Mud. A static or moving intermediate state between suspension and deposition, analogous to bed-load transport of noncohesive sand, that can move in the direction of flow supported by the bed. Fluid mud is the result of excess pore pressure, built up by hindered settling or wave action. Water cannot escape from the sediment deposit, and builds up the excess interstitial pore pressure necessary to support the weight of sediment above it. The whole mass of sediment and trapped water behaves like a uniform dense viscous fluid, flowing downhill or in the direction of the water flow. Fluid mud layers can often be seen on echo soundings as a false bottom in depressions in the seabed.

(4) Mud. Unconsolidated cohesive sediment that has been recently deposited. ‘Recently’ may be a matter of a few hours to several years.

e. Processes and states in Figure III-5-1 may be skipped. For example: most coastal mud, even fluid mud, is eroded before it has undergone sufficient consolidation to be defined as ‘consolidated’; many cohesive sediments do not form fluid mud, but deposit directly as stationary mud. Differences between mud and consolidated sediments occur during erosion. Transport, deposition, and consolidation are the same for both mud and consolidated cohesive sediments.

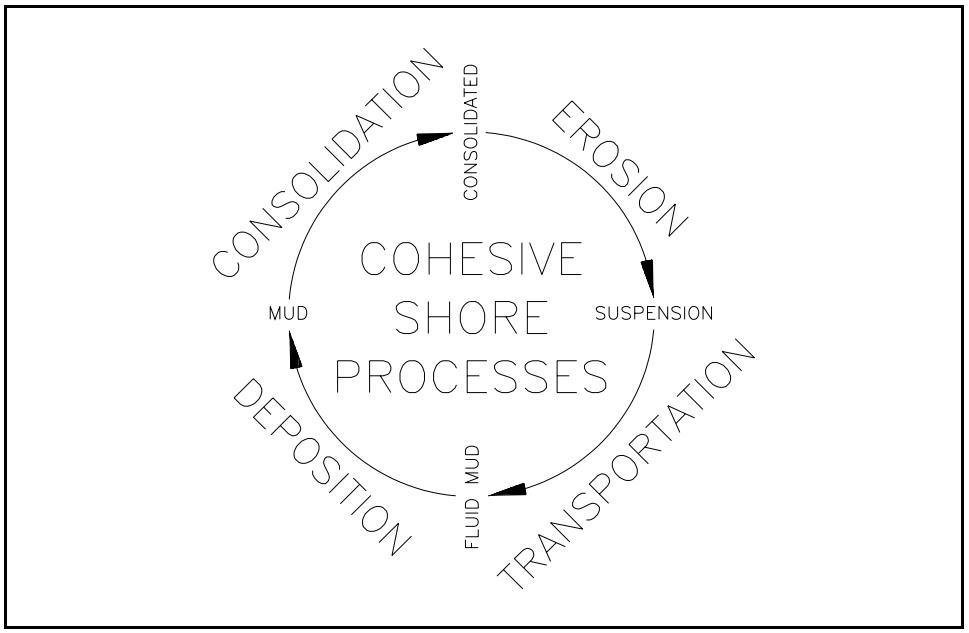

Figure III-5-1. Outline of cohesive shore processes — Any process or state may be bypassed, for example, fluid mud may be eroded without passing through (further) deposition and consolidation

Table III-5-1
Cohesive Sediment Density

	Typical Saturated Bulk Density	
Soil Description	**kg/m^3**	**lb/ft^3**
Suspension	1,020	64
Fluid Mud	1,100	70
Freshly Deposited Mud	1,300	80
Very Soft Consolidated	1,500	90
Soft Consolidated	1,600	100
Medium Consolidated	1,800	110
Stiff Consolidated	1,900	120
Very Stiff Consolidated	2,100	130
Hard Consolidated	2,200	140

III-5-2. Consolidated and Unconsolidated Shores

a. Consolidated shore.

(1) A shore is defined as consolidated cohesive when the erosion process is directly related to the irreversible removal of a cohesive sediment substratum (such as glacial deposits, ancient lagoon peats, tidal flat muds, valley and bay fill muds, lacustrine clays, flood deltas consisting of fine sediments, soft rock or other consolidated or over-consolidated deposits). Even when sand beaches are present, under the sand beach there lies an erodible surface that plays the most important role in determining how these shores erode, and ultimately, how they evolve in the long term. This differs fundamentally from sandy shores where erosion (or deposition) is directly related to the net loss (or gain) of noncohesive sediment from a given surface area.

Erosion on a sandy shore is a potentially reversible process (i.e., due to natural processes), while erosion on a consolidated cohesive shore is irreversible.

(2) Consolidated shores consist of consolidated or partially consolidated cohesive sediments which are usually covered by a thin veneer of sand and gravel, sometimes forming a beach at the shore (Part III-5-3 describes the techniques available for determining the properties of cohesive sediment). In essence, these shores are defined by an insufficient supply of littoral sand and gravel (i.e., noncohesive sediments). Consolidated shorelines may be associated with an eroding bluff or cliff face, or they may consist of a transgressive barrier beach perched over older sediments. The sand veneer often disguises the underlying cohesive substratum, and therefore, at many locations consolidated shores are incorrectly assumed to behave as sandy shores. The veneer thickness is usually in the range of a few centimeters to 2 or 3 m.

(3) Consolidated cohesive shores compose a large part of the Great Lakes, Arctic, Atlantic, Pacific, and U.S. Gulf coasts, a large part of the North Sea coast of England, and sections of the Baltic and Black Seas. Examples along the U.S. Atlantic coast include many of the barrier islands that are perched over older consolidated sediment; Riggs, Cleary, and Snyder (1995) estimate that 50 percent of the North Carolina coast is underlain by older estuarine peats and clays. Other examples along the U.S. east coast include the shores of Chesapeake and Delaware Bays. In many instances, the erosion of the shores associated with the Mississippi Delta and the transgressive barrier islands along the Texas coast is the result of cohesive processes. Cliff erosion along the South California coast and along large parts of the Beaufort Sea coast of Alaska are related to an insufficient supply of littoral sand, the hallmark of consolidated cohesive shores. Many other examples throughout the world, including erodible rocky coasts, are cited by Sunamura (1992). As awareness of the importance of the distinction of this shore type grows, and as sub-bottom investigations become more prevalent, more examples are identified. As Riggs, Cleary, and Snyder (1995) note, in many cases the shore is not just a ‘thick pile of sand.’

(4) Consolidated cohesive shores are often difficult to identify owing to the presence of a sand beach at the shore. The existence of an eroding bluff or cliff at the shore, featuring consolidated or cohesive sediment of some form, is a sure sign of a consolidated shore. However, in many cases, cohesive shores do not feature eroding bluffs. Examples include many of the barriers along the Atlantic and U.S. Gulf coasts.

(5) There are at least six ways of visually identifying the presence of underlying consolidated cohesive sediment, which would distinguish a consolidated cohesive shore from a sandy shore. A series of photos of a transgressive shoreline along the east coast of Ghana in West Africa provide examples of the different types of evidence which may indicate the presence of cohesive sediment under a sand beach. Long-term recession rates along this 7-km section of the Ghanaian coast are in the range of 2 to 8 m/year. The six distinguishing features are:

(a) The most straightforward evidence is the presence of exposed cohesive sediment on the beach. Figure III-5-2 shows a large expanse of peat exposed on the beach in Ghana. Such exposures may be infrequent and result from severe erosion events (where the overlying sand is stripped and carried offshore) or may appear between large alongshore sand waves.

(b) Pieces of clay or peat on the beach. Figure III-5-3 shows some angular clay blocks that have been removed from the seabed and transported towards the shore, along with some pieces of rubble from old buildings that have been destroyed by erosion. In many locations, clay balls can be found along the shoreline. The more rounded clay pieces probably result from transport over a greater distance, i.e., the exposed cohesive sediment may not be located in the immediate vicinity of where the clay balls are found.

Figure III-5-2. Peat exposed on a beach along the Keta shoreline in Ghana, West Africa, May 1996

Figure III-5-3. Pieces of eroded clay (and some rubble) scattered on a beach along the Keta shoreline in Ghana, West Africa, September 1996

(c) Springs or surface runoff across a beach. Figure III-5-4 shows springs near the waterline along the beach in Ghana which result from groundwater flow over the impervious underlying clay and peat sediments. In this case, the groundwater flow gradient is driven by the presence of an enclosed lagoon with water levels higher than mean sea levels on the other side of the washover terrace.

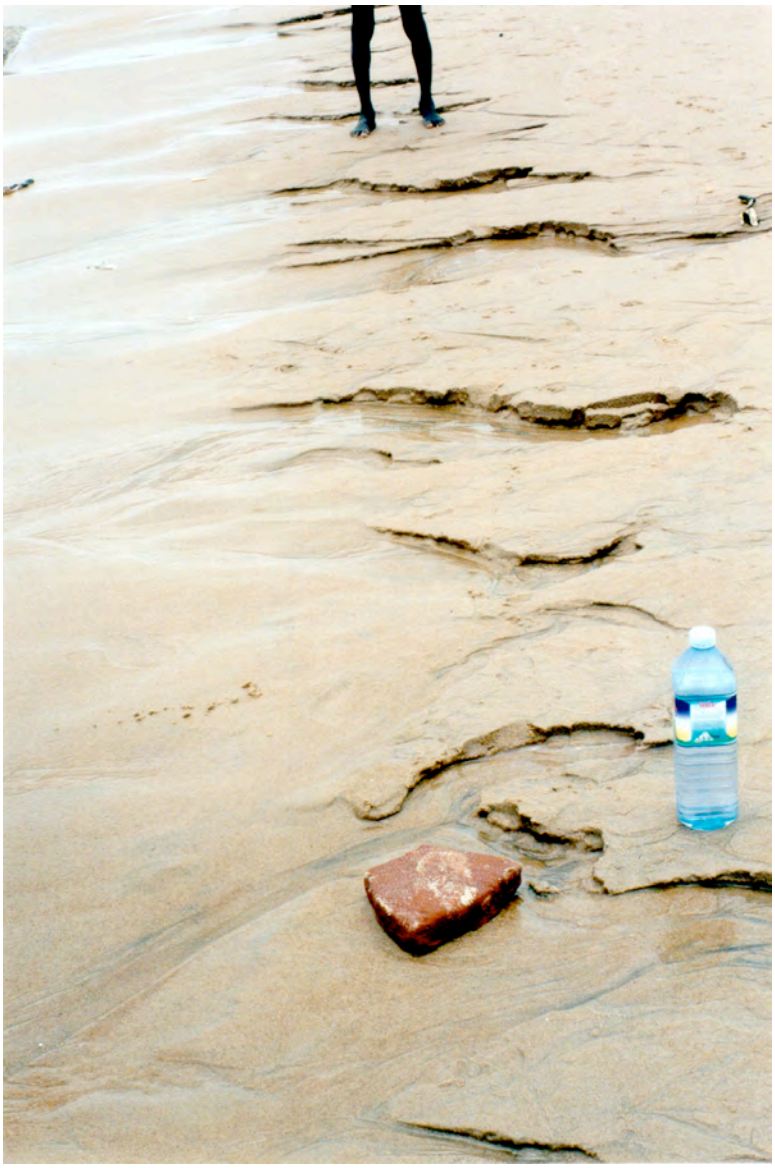

Figure III-5-4. Springs flowing over the beach surface along the Keta shoreline in Ghana, West Africa, September 1996

(d) Discoloration of water in the nearshore zone. Along eroding bluff shorelines, the water takes on the color of the bluff sediment in response to wave attack. Figure III-5-5 shows discoloration of the seawater near the shoreline caused by erosion of underlying lagoon sediments along the Ghana shoreline. At this location, this was the first evidence that easily erodible cohesive sediments existed in the nearshore zone.

(e) Permanent undulations in the shoreline planform may also signify the presence of cohesive or consolidated sediments in the nearshore zone with alongshore variability in erosion resistance. These features are best identified through oblique or overhead aerial photographs. An example along the Ghana

Figure III-5-5. Discolored water from erosion of exposed cohesive sediment along the Keta shoreline in Ghana, West Africa, July 1996

coast is shown in Figure III-5-6. These same undulations could be seen at the same location in several aerial photos taken over a 35-year period. Therefore, these features are distinguished from migrating alongshore sand waves which also occur here. Subsurface investigations at this location have subsequently revealed considerable alongshore variability in the stratigraphy of the underlying sediments, possibly relating to the presence of old channels into the lagoon inshore of the present beach.

(f) Finally, exposed cohesive sediments can often be identified in the troughs between offshore bars through a swimming or diving survey.

(6) At the site in Ghana, subsequent to the initial visual observations of evidence of the presence of underlying cohesive sediments, a series of subsurface investigations was completed to define these conditions. These included augers, boreholes, vibracores and sub-bottom profiling. Use of more detailed subsurface investigations to confirm visual observations and provide more detailed information is discussed in Part III-5-6.

b. Mud shore. Unconsolidated mud coasts are generally the result of more recent deposition of cohesive sediment. Deposition requires quiet or calm hydrodynamic conditions, where large waves are rare. Muddy shore naturally occurs as mud flats and coastal wetlands in protected waters, such as estuaries and other embayments with short fetches.

(1) Mud flat. Generally without vegetation, lying below high water in tidal areas (Figure III-5-7).

(2) Coastal Wetland. Salt marsh in saltwater, stabilized by vegetation, generally above low water in tidal areas, often above mud flats (Figure III-5-8) and mangrove. Marsh vegetation stabilizes the mud bed and provides shelter in which more sediment can deposit.

Figure III-5-6. Permanent undulations in the Keta shoreline in Ghana, West Africa, July 1996

Figure III-5-7. Mud flat in Cumberland Basin, Bay of Fundy, Canada, showing drainage gullies

Figure III-5-8. A mud 'beach' backed with eroding salt marsh at Annapolis Royal, in the Annapolis Bay of the Bay of Fundy. Basalt revetment at top of salt marsh is an attempt to halt the erosion

(3) Mangrove. Tropical coastal wetland where the vegetation, in the form of trees, can withstand relatively severe wave attack (Figure III-5-9). Depth-limited waves will penetrate a mangrove, eroding mud from around the root system in extreme storms, and endangering individual trees. Mangrove can be found between mud flats and salt marsh, and can transmit waves, which erode the adjacent salt marsh behind it.

(4) Mud 'beach.' A sloping mud shore, exposed to wave attack often following the destruction of mangrove or other wetland vegetation (Figure III-5-8). The usual cause of wetland or mangrove destruction is property developers, municipal agencies, and individuals wishing to 'reclaim' the shore. Natural destruction occurs from the seaward edge, through undermining of the root system by waves and currents.

III-5-3. Erosion Processes on Consolidated Shores

a. Erosion processes on cohesive shores are distinctly different from those on sandy shores. There are also differences between consolidated and mud cohesive shores. On consolidated shores, the erosion process is irreversible because, once eroded, the cohesive sediment (e.g., glacial till, glacio-lacustrine deposits, ice bonded sediments, soft rock or other consolidated deposits) cannot be reconstituted in their consolidated form in the energetic coastal environment. Furthermore, since the sand and gravel content is low in these deposits (often less than 20 percent), erosion is not balanced by an equal volume of deposition within the littoral zone. The eroded fine sediments (silt and clay) are winnowed, carried offshore, and deposited in deep water in contrast to the sand fraction, which usually remains in the littoral zone.

Figure III-5-9. Sand beach disappearing into mangrove on the island of Borneo. Sediment within the mangrove is cohesive mud

b. Consolidated cohesive sediment is eroded by at least four mechanisms:

(1) Through abrasion by sand particles moved by waves and low currents.

(2) Through pressure fluctuations associated with turbulence generated at various scales such as wave-breaking-induced turbulence that reaches the lake or seabed and large-scale eddies that may develop in the surf zone.

(3) Through chemical and biological influences.

(4) Through wet/dry and freeze/thaw cycles where exposed to the atmosphere.

c. Sand can also provide a protective cover to the underlying cohesive substratum. However, only when the sand cover is sufficient to protect the cohesive substratum at all times will the shore revert to a sandy classification (i.e., truly a 'thick pile of sand').

d. On consolidated cohesive shores, the rate of lake or seabed downcutting determines the long-term rate at which the bluff or cliff retreats at the shoreline. In other words, while subaerial geotechnical processes may dictate when and where a slope failure will occur, the frequency of failures over the long term is determined by the rate at which the nearshore profile is eroded (i.e. the downcutting rate). Subaqueous and subaerial erosion processes on cohesive shores are discussed in detail in Part III-5-7. In addition, the geomorphology of cohesive shores and the relationship to erosion processes is the topic of Part III-5-5.

III-5-4. Physical and Numerical Modeling

a. Laboratory or physical model experiments have been used in two ways: (1) to improve the understanding of the fundamental principles of cohesive shore erosion processes, and (2) to develop a measure of the erodibility of specific samples of cohesive sediment.

b. In the former category, scale model tests have been performed in wave flumes as described by Sunamura (1975, 1976 and 1992) for erodible rocky coasts similar to consolidated cohesive behavior, by Nairn (1986) for a section of the Lake Erie shoreline using an artificial clay, and by Skafel and Bishop (1994) and Skafel (1995) using intact samples of till removed from the Lake Erie shoreline. The tests described by Skafel and Bishop (1994) included an assessment of the relationship between wave properties (e.g., wave height, orbital velocity, type and fraction of broken waves) and local erosion rate and the relationship between sand cover and erosion rates. Laboratory experiments on erosion and deposition of mud are described in Part III-5-6c(9). The annular flume, used in both the laboratory and the field (e.g., Amos et al. 1992, Krishnappan 1993) may be regarded as a full-scale model of the response of a mud bed to shear.

c. The primary difficulty in the use of physical model experiments of cohesive shores is the scaling of the cohesive material. At present, it is not possible to accurately scale cohesive sediment with respect to its erosion resistance properties. Therefore, model tests must be interpreted qualitatively, or full-scale tests must be conducted using low wave energy conditions. Nevertheless, the noted tests have been extremely valuable in advancing the understanding of cohesive shore erosion processes both inside and outside the surf zone.

d. A technique of assessing the erodibility of intact samples of consolidated cohesive sediment in unidirectional flow conditions has been developed and applied by Kamphuis (1990), and, more recently, for the assessment of cohesive sediment samples removed from the southeast shoreline of Lake Michigan (Parson, Morang, and Nairn 1996). These tests are typically performed for both clear water and sand in flow conditions to elucidate the importance of sand as an abrasive agent. This approach for defining the erodibility of cohesive sediment samples is discussed in more detail in Part III-5-7b.

e. The development and application of numerical models for describing erosion processes on cohesive shores is not far advanced owing to the complexity of the processes involved. Most numerical models may be described as little more than numerical frameworks for interpolating or extrapolating observed behavior of cohesive sediments in water. Essentially, a numerical model of cohesive shore erosion must define the near-bed flow conditions within the surf zone, the movement of any overlying noncohesive sediment cover, as well as the erosion resistance properties of the cohesive sediment (which change with time due to exposure of sediment layers and subaerial drying). Numerical modeling of cohesive shores is summarized in Part III-5-12.

f. The best 3-D numerical mud models (e.g. Le Hir 1994) treat the water column as a continuum: from stationary consolidating bed, through fluid mud, to sediment maintained in suspension by turbulence. There are nevertheless bed sediment ‘modules,’ which use the equations presented in Parts III-5-7, 9, and 10 to calculate erosion and deposition, supplying sediment and new bathymetry to numerical hydrodynamic models that transport the sediment by advection and dispersion (Part III-5-8a).

g. All mud models need to track sediment layering - the composition and state of each sediment layer at each grid point in the model — more a bookkeeping function than numerical modeling.

h. Part III-5-13 provides some detailed guidance on the specific coastal engineering and management issues associated with cohesive shores. The success of engineering and management techniques on cohesive shores is dependent on a recognition of the fundamental differences between sandy and cohesive shore processes. Engineering techniques that may have been successful on the more familiar sandy shores, may be unsuitable or inappropriate along cohesive shores.

III-5-5. Geomorphology of Consolidated Shores

This section provides a review of the geomorphology of cohesive shores and the relationship between the land forms and the erosion processes discussed in the previous sections. The discussion is subdivided under two headings: "Controlling Factors" and "Profile Types." This section focuses on the geomorphology of consolidated cohesive sediment shores. For more detail on erosion processes along rocky coasts, refer to Sunamura (1992).

a. Controlling factors. The primary controlling factors discussed in the following paragraphs influence the geomorphology of cohesive shores:

(1) Lag deposits.

(a) Some consolidated cohesive sediment units have cobbles or boulders within their composition. For example, along the Great Lakes, glacial till may be either fine-grained or stony (i.e., containing gravel and cobbles). During the evolution of stony till shores, the cobbles and boulders that are left behind after the removal of the finer clay, silt, and sand build up to form a protective armor for the underlying till. In these cases, an erosion-resistant nearshore shelf will usually have formed. The depth of the shelf at any location is such that the lag deposit remains immobile, and therefore the depth is determined by the local wave climate and the grain size of the lag deposit. Generally, for the Great Lakes, the depth of this shelf is approximately 2 m below low water datum. Along sea and ocean coasts with large tidal ranges and longer waves, lag deposits may occur at much greater depths (e.g., lag deposits over clay have been found in water depths of 10 m below datum along the North Sea coast of England). The shelf creates what has been referred to as a convex profile, in contrast to the concave profile associated with situations where lags are not present.

(b) The armored shelf acts to dissipate wave energy, and therefore reduce or even prevent bluff erosion. Boyd (1992) gives several examples where a bluff is protected from erosion by a nearshore shelf and notes that the reduced wave energy may also allow a stable beach to exist at the shore, providing additional protection to the bluff toe. Natural headlands along an eroding cohesive shoreline often owe their existence to the presence of a lag-protected nearshore shelf.

(c) An example of a site where a lag deposit has resulted in an erosion-resistant foreshore and a stable shoreline is located near the town of Goderich on the Canadian shore of Lake Huron. A nearshore profile for this site is shown in Figure III-5-10. The cobble-protected shelf has a depth of 1.75 m and is about 200 m wide. The stratigraphy at the site consists of a stony till unit below the average lake level and a fine-grained till unit above the average lake level. At nearby sites where the fine-grained till unit dips below the average lake level to depths of greater than 2 m, and the nearshore shelf is no longer present, the bluff recession rates range from 0.3 m/year to over 1 m/year.

(2) Different stratigraphic units.

(a) Along most cohesive shores, 3-D variations in contact surfaces between stratigraphic units are common. This results from the complex geomorphologic conditions that formed the underlying geology, which, depending on the location, may include some combination of: glacial, lacustrine, estuarine, or fluvial

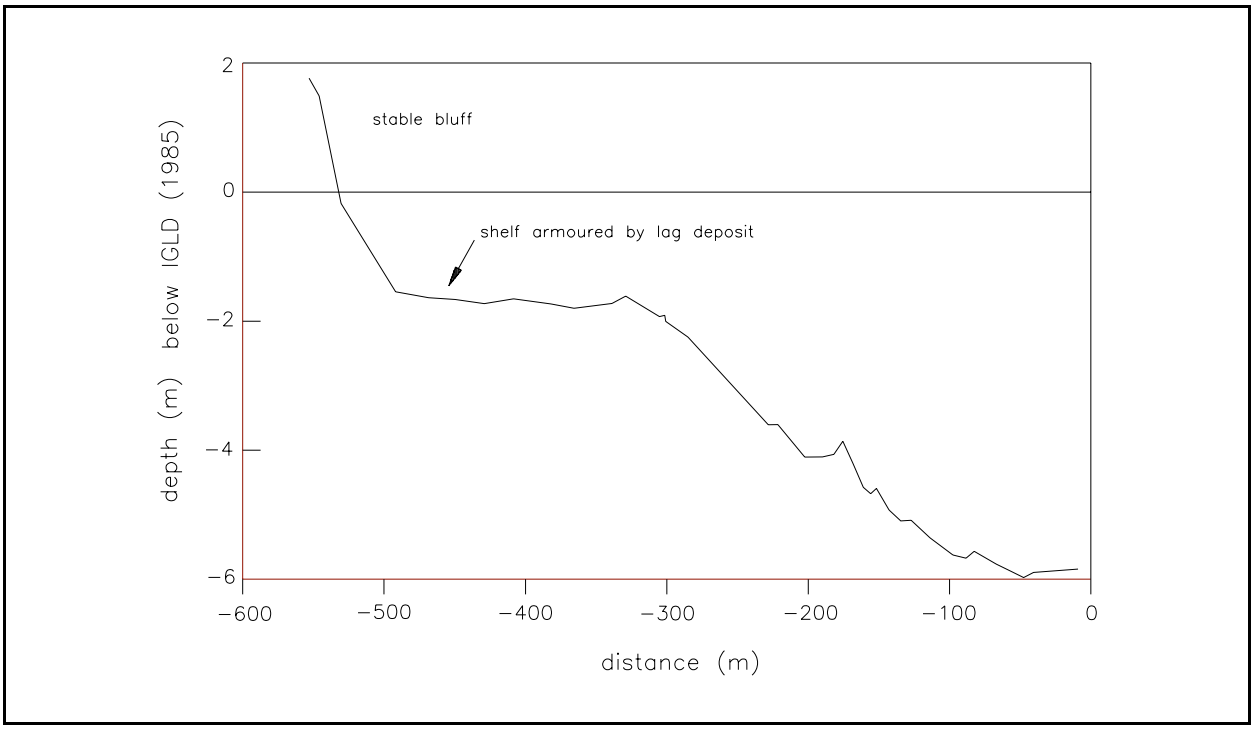

Figure III-5-10. A convex consolidated cohesive profile with a shelf protected by lag deposits located near Goderich, Ontario, on Lake Huron

processes. Therefore, as the shore erodes in time, the recession rates can change, as either more or less erosion resistant, units are encountered further inland. One example of the influence of erosion resistance is East Point located along the Scarborough Bluffs east of Toronto on Lake Ontario. The plan and stratigraphy cross section of this feature are shown in Figure III-5-11. Clearly, East Point is an expression of the more erosion-resistant Leaside (or northern) till unit, which dips below the average lake level at this location. Leaside till is relatively hard and includes boulder pavements (Boyce, Eyles, and Pugin 1995). Along the neighboring shore, the less erosion-resistant Scarborough clay unit exists below the lake level.

(b) Recognition of the variation in erosion resistance of different till units resulted in an unlikely finding during the investigation of the influence of a harbor structure at Port Burwell on downdrift erosion along the north central shore of Lake Erie (Figure III-5-12). A long harbor jetty here intercepts almost all of the sand moving along the shore from west to east, therefore depriving the downdrift shore of sediment. On a sandy shore, this would be a clear case of downdrift erosion due to sediment supply starvation. However, the investigation described by Philpott (1984) revealed that cohesive shores along the north central shore of Lake Erie seldom have (and probably never had) enough sand to halt the downcutting of the underlying till. Updrift of the harbor, the trapping of large quantities of sand eventually halted the nearshore profile downcutting, and the bluff position was stabilized. However, this still did not fully explain why recession rates updrift of the harbor fillet beach were generally lower (about 1 m/year) than those on the downdrift shoreline to the east (in the range of 2 to 4 m/year).

(c) Figure III-5-12 also describes the bluff face stratigraphy at Port Burwell. There is a change in the subaqueous stratigraphic unit at the harbor mouth, where Port Stanley till exists below the lake level on the updrift side and Waterlain till forms the nearshore profile on the downdrift side. Based on a comprehensive investigation, including laboratory testing of the erodibility of the different till units, it was concluded that Waterlain till was less erosion-resistant than the Port Stanley till. It is not coincidental that the change in till

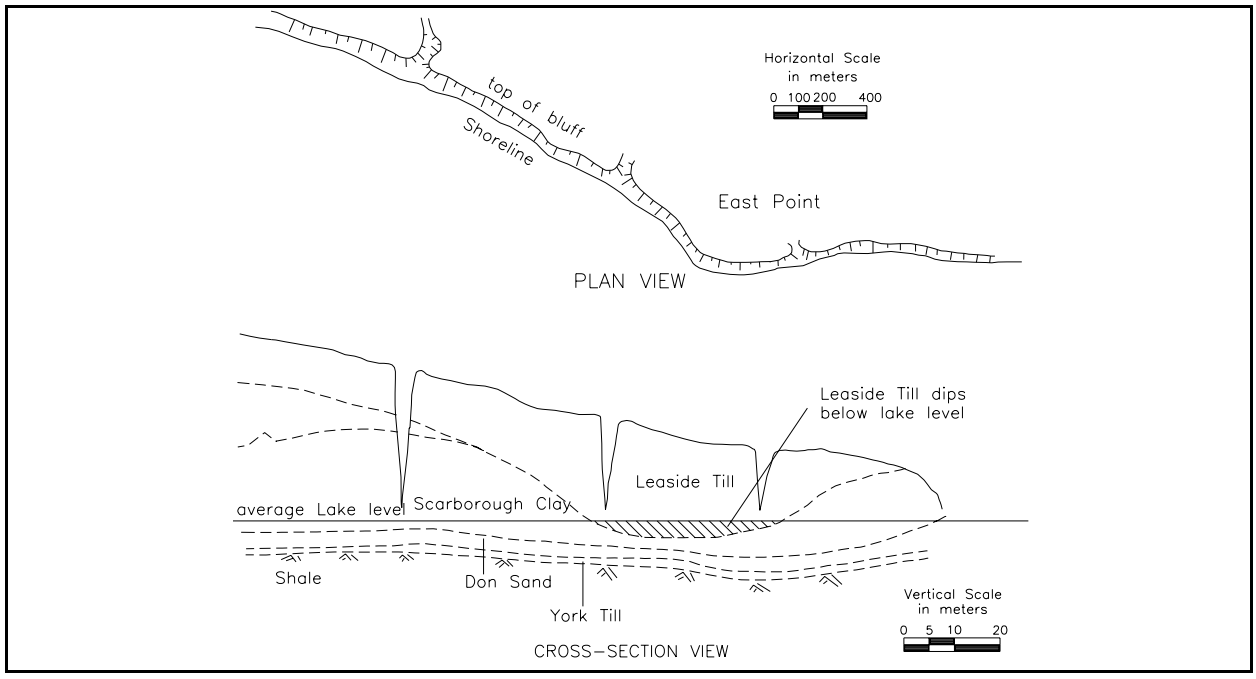

Figure III-5-11. Plan and cross section of East Point along the Scarborough Bluffs (located east of Toronto on Lake Ontario) showing the influence of the erosion-resistant leaside (or northern) till on the local geomorphology

occurred at the harbor mouth, as often creeks or rivers follow the interface between different stratigraphic units.

(d) Riggs, Cleary, and Snyder (1995) provide several examples of both headlands (local areas of slowly retreating or stable shoreline) and local sections of rapidly retreating shoreline, that are a direct result of variability in the erosion resistance of different stratigraphic units that make up the shoreface. They found that headlands result from the presence in the nearshore of more erosion-resistant Pleistocene or older sediments. In contrast, rapidly retreating sections of shore consisted of sand-poor, valley-fill sediment or compact peats and clays deposited in modern estuarine environments.

(3) Quantity and mobility of sand cover.

(a) In natural situations, a protective sand cover can build up over an erodible substrate and protect it from further erosion. Investigations of Great Lakes sites have shown that approximately 200 m^3/m of sand cover (measured from the top of the beach out to the 4-m contour) is required to halt the downcutting process (Nairn 1992). However, even half as much as this quantity can afford at least some protection to the underlying cohesive substratum.

(b) Another important factor is the volatility or mobility of sand cover. If the overlying noncohesive bed forms are rapidly and frequently changing position, the underlying cohesive substratum will be exposed to erosive situations more frequently. Nairn and Parson (1995) have indicated that on the Great Lakes, the shift of bar position in response to changing lake levels has an important influence on the exposure of the underlying till (in the troughs between the bars) to erosion. On an eroding cohesive bluff shore along the North Sea coast of England, Pringle (1985) identified alongshore migrating areas of reduced beach cover and exposed glacial till called 'Ords.' These Ords have an important role in exposing the underlying glacial till to erosion. Figure III-5-13 shows an Ord on the Holderness coast at low tide with glacial till exposed (partly

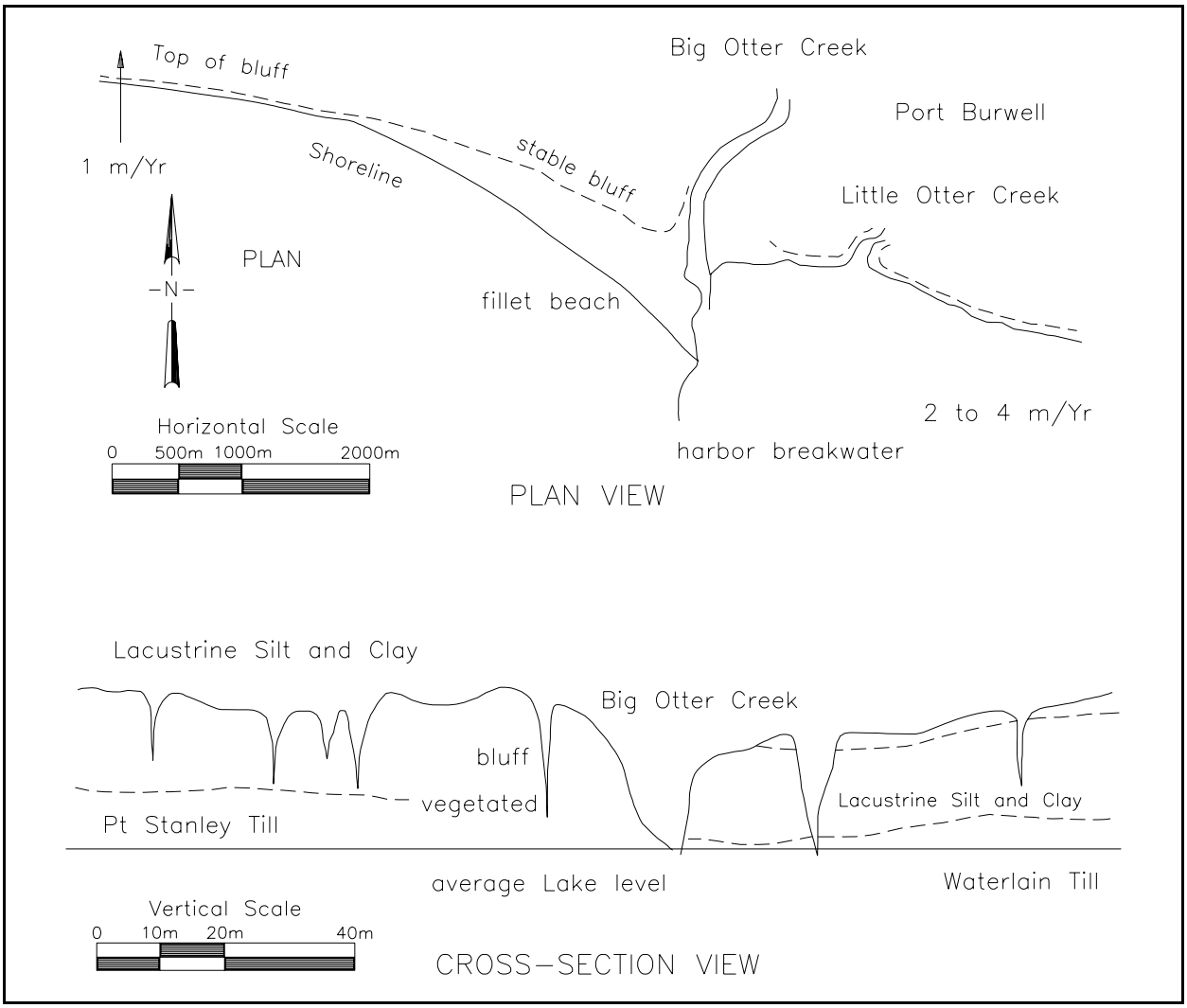

Figure III-5-12. Plan and cross section of the Port Burwell area on the north central shore of Lake Erie showing the influence of a fillet beach and stratigraphy changes on the geomorphology of a cohesive shore

covered with cobbles) between the upper coarse sand beach and a bar consisting of finer sand. The closeup photo of the Ord (Figure III-5-14) shows erosion of the exposed till around a 10-cm-high pedestal protected by a rock cap. Pringle (1985) found that the migration rate for these features was approximately 500 m/year, which is similar to the rate of migration for large sand waves or rhythmic features along Long Island, NY (Thevenot and Kraus 1995). An Ord could be defined as the area between two migrating sand waves. In summary, both cross-shore and alongshore variations in sand cover thickness resulting from migration of bars and sand waves or Ords, respectively, have an important influence on the rate of cohesive sediment erosion in the nearshore zone.

(c) Deposition of large quantities of sand over a cohesive substrate can occur at a change in shoreline orientation where the potential alongshore sediment transport rate rapidly decreases, or at a natural obstruction to alongshore transport, such as at a rock headland. Other instances where sand may eventually build up to protect a profile include sites where the alongshore transport of sediment is intercepted at a harbor jetty. The Port Burwell fillet beach shown in Figure III-5-6, as discussed above, protects the nearshore cohesive substratum and has stopped the bluff recession behind the fillet beach.

Figure III-5-13. Bluff erosion along the Holderness coast of the North Sea. The underlying cohesive profile is exposed at low tide in a trough (referred to as an "Ord") between the upper beach and first bar

Figure III-5-14. Close-up of the exposed cohesive profile on the Holderness coast (Figure III-5-13). A rock-capped pedestal of cohesive sediment, about 10 cm in height, has developed through erosion of the adjacent seabed

(d) Many areas along the Great Lakes shores that once had sufficient sand cover to protect an underlying cohesive substratum from downcutting are now coming under attack as the sediment supply has been reduced through human influences. Reductions to the sediment supply occur through entrapment of sediment at structures which protrude into the lake (including harbor jetties and land reclamation projects that have been created for many purposes, such as power plants, marinas, and docking facilities) as well as through protection of previously eroding sections of shoreline. Shabica and Pranschke (1994) describe one such area north of Chicago on Lake Michigan where the sand cover has decreased from 560 m^3/m in 1975 to 190 m^3/m in 1989. If the depletion of sediment cover continues at this site, the previously very low rates of shoreline recession (less than 0.2 m/year, or 8 in./year) may accelerate.

(4) Local wave and water level conditions. The characteristics of the local wave and water level conditions represent the fourth controlling factor on the geomorphology of consolidated cohesive coasts. Both the intensity and the directionality of the waves can influence the rate of erosion at a particular shore site. Other factors being equal, greater wave energy translates to higher downcutting rates and more rapid shoreline erosion. Directionality of the waves can have a secondary influence on downcutting rates by affecting the mobility of the sand cover over the underlying till. Large swings in wave direction can result in a more dynamic system with respect to the sediment cover. Fluctuations in water level also have an important role in cohesive shore erosion processes as explained by Stewart and Pope (1993) and Fuller (1995). While direct erosion at the bluff toe may be accelerated during high-water conditions, low water leads to acceleration of the nearshore downcutting process (which in turn allows more waves to reach the bluff toe).

b. Profile types. Boyd (1981, 1992) completed an extensive review of nearshore profile shapes for consolidated cohesive shores on the Great Lakes. These essentially fall into two categories: concave profiles and convex profiles. Figure III-5-15 provides a schematic description of these two profile types.

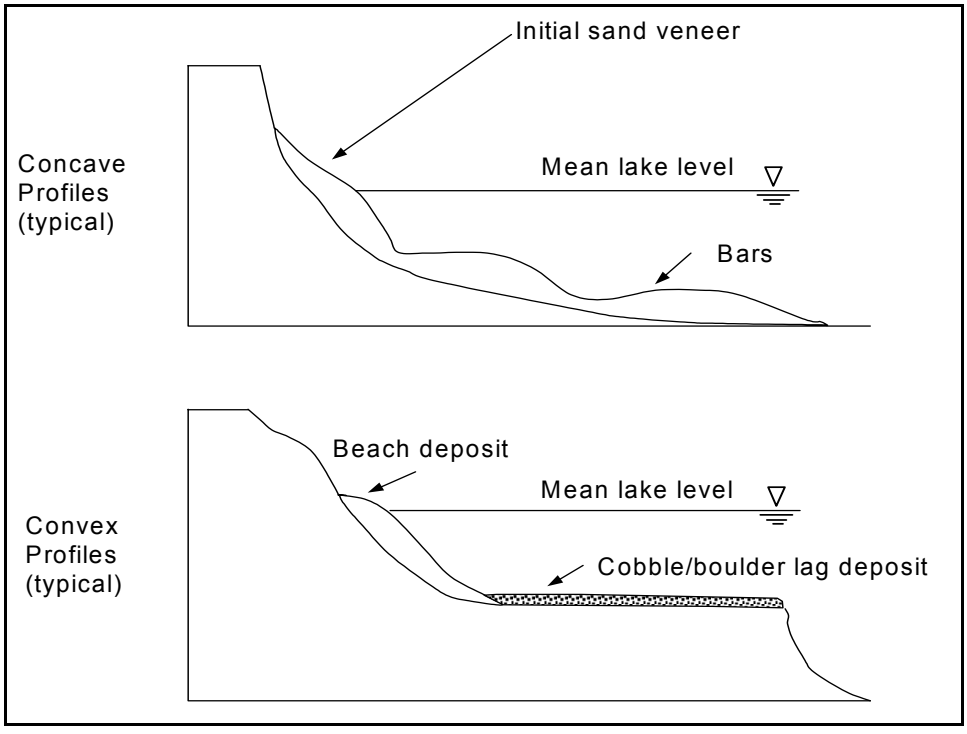

Figure III-5-15. Distinctions between concave and convex consolidated cohesive profiles

(1) Concave profiles. Concave profiles develop in fine-grained sediment with a relatively uniform erosion resistance from the closure point up to the top of the bluff or cliff. These profiles have an exponential form similar to sandy shore profiles described by Dean (1977). Sand cover over these cohesive profiles can range from perhaps as little as 25 to over 200 m^3/m measured between the bluff toe and the 4-m depth contour. The sand cover can be in the form of bars, and, in areas with a sand cover in the high end of the range, a substantial beach at the shore. Stewart and Pope (1993) found that a reduction in the range of water level fluctuations would not reduce the long-term erosion rates for cohesive shores with concave profiles. As explained above, lower water levels result in accelerated lowering of the nearshore profile, which essentially has the same effect as high water levels — allowing waves to reach the bluff toe.

(2) Convex profiles. As noted above, convex profiles develop at locations where potential lag deposits exist within the eroding material. These profiles are characterized by a nearshore shelf, which on the Great Lakes has a depth approximately 2 m below low water datum. At other locations, this depth will be determined by the median grain size of the lag deposit, the wave climate, and the range of water level fluctuations. Long-term erosion rates along these shores are less than rates for concave cohesive shores (having limited sand cover) with the same wave exposure. With the exception of high-water periods, the erosion-resistant nearshore shelf acts to dissipate wave energy before it reaches the shoreline. However, during high water periods, these shorelines are more vulnerable to erosion when waves are able to attack the bluff toe. Therefore, in contrast to cohesive shores with concave profiles, shores with convex profiles would benefit from a reduction in the range of water level fluctuations (Stewart and Pope 1993). Finally, the fish habitat function of cohesive shores with a convex profile shape is much more important owing to the surficial substrate (cobbles and boulders with limited sand cover) and the proximity to a deepwater drop-off at the edge of the shelf.

III-5-6. Sediment Properties and Measurement Techniques

a. Introduction.

(1) In the case of noncohesive sand and gravel, sediment mobility can be estimated just by knowing the grain size and shape, specific gravities of the sediment and water, and the viscosity or temperature of the water (i.e., physical properties). The mobility of cohesive sediment is a more complex phenomenon. Cohesion (particle attraction) is governed by the electrochemistry of the sediment mineral and water; its state of consolidation; and in many cases, by the presence of organisms like diatoms, which can bind the sediment particles together with mucus.

(2) The extent of data requirements will vary depending on the nature of the coastal engineering problem and the nature of the shore. This section presents an overview of the range of possible field and laboratory investigations that can be used to characterize the conditions associated with erosion, transport, deposition, and consolidation on a cohesive shore. This discussion focuses on a characterization of the specific geologic conditions related to the cohesive shore. For the measurement of environmental conditions (e.g., waves and water levels), refer to Part II-3.

b. Consolidated shore erosion. Developing an understanding of consolidated shore erosion requires information on profile shape (beach and nearshore profile techniques are summarized in Part III-3-2), presence or absence of lag deposits, bluff and nearshore stratigraphy, erodibility of the one or more cohesive units in the active nearshore erosion zone (i.e., between high water and the depth of closure), and the sand cover thickness and stability. Available techniques to assess the characteristics listed above are as follows:

(1) Field sampling and geotechnical analyses.

(a) Testing may be performed in situ or in a laboratory on samples extracted from the field. Extraction techniques for seabed or lake bed cohesive sediments include: dredging; coring; box coring; and cutting samples (the latter using a chainsaw with a trenching chain). As noted in Part III-5-6, it is important to retrieve intact samples that, to the extent possible, preserve the natural structure of the cohesive sediment.

(b) None of the available standard geotechnical test procedures provide a direct measure of the erosion resistance of a cohesive sediment in the coastal environment. Nevertheless, the more important characteristics that provide an indirect assessment of erodibility include: grain size analysis (including clay content); liquid and plastic limits; water content; undrained shear strength; bulk density; and consolidation pressure. Techniques for establishing these parameters are presented in the USACE Engineering Manual "Laboratory Soils Testing" (EM 1110-2-1906). Undrained shear strength can be determined in the field using a cone penetrometer or a vane shear apparatus.

(c) Borehole information can be valuable for assessing variations in stratigraphy both above and below the water level.

(2) Laboratory erodibility experiments.

(a) There are no standard and accepted approaches for establishing the erodibility of cohesive sediment in the coastal environment based on geotechnical properties. Therefore, to quantify the relationship between erodibility and shear stress applied under a given flow condition, it is usually necessary to perform laboratory experiments. Experiments may not be required where direct techniques have been applied to determine the erodibility of similar sediment. It is advisable that these experiments be performed with intact, and to the extent possible, undisturbed samples of cohesive sediment in order to preserve the natural structure of the soil.

(b) Four laboratory techniques for assessing erodibility are briefly reviewed in this section. These provide an example of the range of techniques that are available.

(c) Arulanandan, Loganatham, and Krone (1975), and more recently Zeman (1986), describe the use of a rotating cylinder apparatus to assess the erodibility of intact and undisturbed samples of cohesive sediment. This technique is also mentioned for testing the erodibility of mud. In this approach, a long cylindrical sample is mounted inside a larger transparent cell. The cell is then filled with water and rotated. During rotation, the torque transmitted to the inside stationary cylinder is measured to quantify the shear stress applied to the sample. At the end of the test, erosion rates are determined by the loss in mass of the sample. A disadvantage of this approach is the inability to introduce sand to the flow to assess the important influence of sand abrasion.

(d) Another small-scale laboratory technique for testing intact and undisturbed samples is described by Rohan et al. (1986). This procedure is based on an adaptation of the standard pinhole test. Water is circulated through a hole drilled through the axis of a cylindrical sample. The head loss caused by friction in the sample is measured using differential manometers in order to assess the shear stress applied to the soil by the flow. Depending on the size of the hole bored in the sample, it is possible that this technique could be adapted to assess the influence on erosion of sand in the flow.

(e) At a larger scale, intact and undisturbed cohesive sediment samples can be placed in a drop section in the floor of a unidirectional flow flume or tunnel. The sample is then exposed to different flow conditions with and without the presence of sand, and the erosion of the sample surface is surveyed intermittently to determine erosion rates for the different conditions. This technique is also frequently used for mud. Kamphuis (1990) describes the use of a tilting tunnel in which Pitot tubes were used to determine a velocity

profile upstream and downstream of the sample in order to determine the shear stress applied to the sample by the flow. Cornett, Sigouin, and Davies (1994) describe a similar approach using a tilting flume for the analysis of samples extracted from the bed of Lake Michigan near St. Joseph Harbor (Parson, Morang, and Nairn 1996). In this case, a laser doppler velocimeter measured the velocity profile near the bed in order to establish the shear stress applied to the sample by the flow (Figure III-5-16). This figure shows a sand veneer migrating over the till sample in the unidirectional flow flume. In both the Kamphuis (1990) and the Cornett, Sigouin, and Davies (1994) tests, the maximum flows generated were in the range of 3 to 3.5 m/sec (10 to 12 ft/sec). Results from experiments using this technique to estimate erodibility are presented in Part III-5-7b.

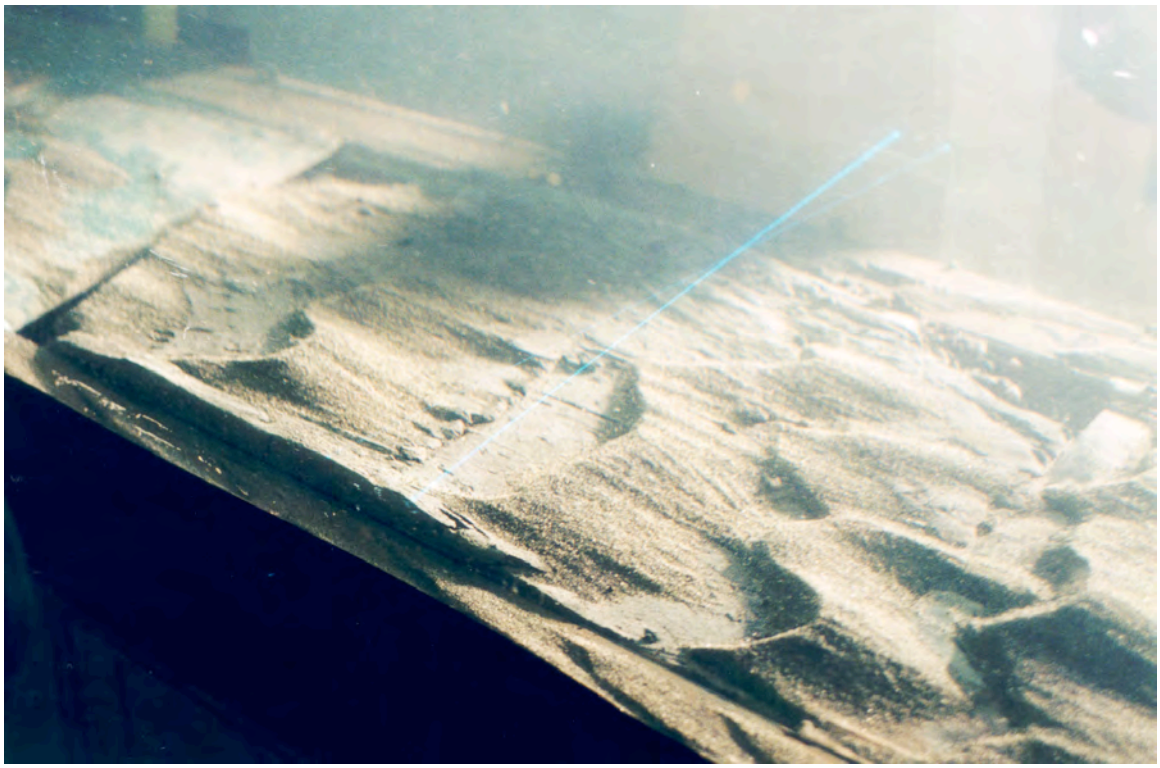

Figure III-5-16. Laser doppler velocimeter (LDV) used to determine shear stress exerted on the till bed in a unidirectional flow flume test. This test features sand in the flow acting as an abrasive

(f) The most realistic approach that can be taken to assess erodibility in a laboratory setting is to create a nearshore profile with intact and undisturbed cohesive sediment samples in a wave flume or basin. This approach was used by Skafel and Bishop (1994) to complete important research into the erosion processes on cohesive shores. Intact samples, measuring 1 m by 0.35 m by 0.45 m, encased in an open-ended steel box were extracted from the top of a bluff on Lake Erie and placed directly in a wave flume. The open-ended steel box was pushed slowly into the till by a 20-ton hydraulic ram and the till at the inner end of the box was cut away using a chainsaw with a trenching chain. The box was then removed with a crane. The till boxes were installed in the flume to create the desired profile shape. In these tests, the effects of sand cover in the form of migrating bars or a patchy veneer were tested. Also, the influence of breaking waves on the erosion of the cohesive sediment was assessed.

(3) Field techniques for assessing surface and subsurface conditions.

(a) One of the most important pieces of information in characterizing a cohesive shore profile is the sand cover thickness across the underlying cohesive profile (i.e., measured from the bluff toe out to a depth of at least 4 m). In addition, where the cohesive profile is exposed, it is also important to determine whether or not a protective lag deposit exists. As with any coastal engineering site investigation, beach and nearshore profiles are essential information. In this section, a variety of techniques for characterizing the surface and subsurface conditions, with particular focus on the sand cover thickness, are presented, ranging from the simplest to the most sophisticated.

(b) The simplest technique of estimating the thickness of the sand cover across the profile involves the following tasks:

- Complete a beach and nearshore profile from the toe of the bluff out to the depth of closure (between the 5- and 10-m water depth).

- Through the use of a steel probe or test pits, attempt to determine the thickness of sand cover near the waterline.

- Estimate the shape of the underlying cohesive profile (as a smooth exponential form) joining points between the toe of the bluff, the position of the till at the waterline (if determinable), and the troughs between the bars on the profile. Typically, the till will be exposed or only thinly covered in the troughs. If repeated profiles are available at a site, these may provide additional information on the position of the underlying till if the position of the troughs between bars shifts between surveys.

(c) In order to complement the simple technique described above, a diving inspection could be completed across the profile. The diver could use an underwater video to document conditions, and a steel probe to estimate sand cover thickness at different locations. Depending on the extent of sand cover, the till may be exposed in some areas. Alternatively, a frame-mounted video camera lowered from a boat or a remotely operated vehicle with video could be used. Video is also valuable in assessing whether or not a lag deposit exists where the cohesive layer is exposed.

(d) In place of a simple steel probe, a jet probe could be used to survey the thickness of the sand cover on the land and underwater. A jet of either water or air can be used to penetrate the sand cover (the latter is only applicable underwater). Shabica and Pranschke (1994) describe the use of a hydraulic probe consisting of an extendible 20 mm diameter pipe through which water is pumped at 2.8 kg/cm^2 (40 psi).

(e) A technique based on electrical resistivity has been used to establish the sand thickness across the subaerial section of beach for sections of the Holderness shoreline. This method is particularly useful at locations with large tidal ranges that allow for significant sections of the profile to be surveyed at low tide.

(f) Ground-penetrating radar was used to survey the thickness of the sand cover for several profiles downdrift of St. Joseph Harbor (Parson, Morang, and Nairn 1996). The limitation of this technique is that it can only be used in a freshwater environment.

(g) Sub-bottom profiling, or high-frequency seismic imaging, is another geophysical technique that is capable of establishing the thickness of sand cover over an underlying cohesive profile. Side-scan sonar is an acoustic technique that provides an image of the seabed or lake bed surficial conditions. While this procedure would not be capable of determining the thickness of sand cover, it could provide useful surficial information such as the extent of exposed gravel and cobble lag deposits. These methods are described in Part IV-5 in greater detail.

c. Erosion, transport, and deposition of mud. In the case of mud, it is useful first to examine the following hydrodynamic sediment properties that will be required by the equations presented later:

(1) Cohesion. The cohesive bond is predominantly electrochemical, increasing with the electrical conductivity of the ambient water and proximity of the particles. Conductivity increases with salinity. The bond between particles may be enhanced, particularly at rest on the bed, by biological 'glues' such as the mucus excreted by diatoms, worm tubes, and feces (Paterson 1994).

(2) Critical shear for erosion.

(a) As water flows over the mud bed, as either steady flow or oscillatory flow under tides and waves, it exerts a shear stress τ on the bed due to viscosity and turbulence (described in greater detail in Part III-6). Not only is shear a real physical stress on the bed sediment, but it also serves as empirical shorthand for the level of turbulence in the flow. Thus, it is a useful parameter in describing suspended load sediment transport; as well as fluid mud (bed load), erosion, and deposition.

(b) At the level of a stationary particle on the bed, shear forces are balanced by the forces of gravity, interparticle friction, and cohesion. Shear is augmented by lift and drag, making the force balance

$$\text{SHEAR} + \text{LIFT} + \text{DRAG} < \text{GRAVITY} + \text{FRICTION} + \text{COHESION}$$

a vector sum, the same as that for noncohesive sand and gravel, but with the addition of cohesion. As flow increases, the left-hand side of this balance increases approximately as the square of velocity, until

$$\text{SHEAR} + \text{LIFT} + \text{DRAG} = \text{GRAVITY} + \text{FRICTION} + \text{COHESION}$$

and the formerly stationary particle leaves the bed and begins to move. The shear stress at which this occurs is known as the *critical shear for erosion* or *erosion threshold* τ_c. τ_c is still shorthand for the entire left-hand side of the balance, not shear alone.

(c) The sediment 'particle' may be an individual grain; but more likely a floc, made up of several grains held together by cohesion. Cohesion plays the major role in the right-hand side of the force balance, and failure (erosion) will occur where cohesion is weakest.

(d) Critical shear τ_c is not a particularly useful concept in fluid mud. At the water/fluid mud interface, the applied shear stress is balanced by a shear strain (flow) of the fluid mud, rather than GRAVITY + FRICTION + COHESION. Also, the fluid mud is essentially a thick, viscous, laminar, boundary layer, protecting the stationary bed from any SHEAR + LIFT + DRAG approaching τ_c. Erosion of fluid mud is better described by densimetric Froude Number entrainment between two fluids (Part III-5-7e).

(3) Erosion rate at twice critical shear. Both the Parthenaides and Krone Equations (Parts III-5-7d and III-5-9c) are 'excess shear' fits to observed erosion and deposition, respectively. For example, the Parthenaides Equation (Part III-5-7d) correlates observed erosion rates with

$$\text{Dimensionless Excess Shear} = (\tau_c - \tau) / \tau_c; \text{ negative } (\tau_c < \tau) \text{ for erosion}$$

The Parthenaides coefficient M_p (in units of kg/m^2/sec) (see Equation III-5-1), is the correlation coefficient between erosion rate and excess shear, when dimensionless excess shear = -1; that is, when $\tau = 2\tau_c$.

(4) Critical shear for deposition.

(a) A critical shear stress for deposition τ_s *Pa* (lbf/ft^2) is not obvious at first glance. In noncohesive sediment, the critical shear for deposition is only slightly less than that for erosion: a noncohesive particle

will come to rest almost as soon as the shear is too small to move it. But the process of deposition of cohesive sediment flocs is quite different; τ_s is generally on the order of one fourth of τ_c.

(b) High shear near the bed breaks up large flocs before they can settle. Then, the resulting smaller flocs and individual particles are resuspended. The critical shear for deposition τ_s is that through which large flocs can pass without being broken up. Note that τ_s is not shorthand for something more; τ_s really is the shear stress in the bottom boundary layer which cannot overcome cohesion in the settling flocs.

(5) Sediment, fluid mud, and water densities.

(a) Important densities and specific gravities:

ρ_w = specific gravity (mass density) of water — 1,000 kg/m^3 (62.4 lb/ft^3) in fresh water, up to 1,030 kg/m^3 (64.3 lb/ft^3) in seawater

ρ_s = specific gravity (mass density) of sediment mineral (no voids): generally 2,000 kg/m^3 (125 lb/ft^3) to 2,700 kg/m^3 (170 lb/ft^3) depending on mineral

(b) Bulk sediment density voids filled with ambient water:

- Of freshly deposited flocs (may be fluid mud if < 1,100 to 1,200 kg/m^3 (70 to 75 lb/ft^3), corresponding to a mass concentration in excess of about 20 kg/m^3 (20 ppt)).
- Of existing bed surface, and layers, e.g., 1,400 kg/m^3 (90 lb/ft^3).
- Of fully consolidated sediment, generally < 2,000 kg/m^3 (125 lb/ft^3).

(6) Grain size and settling velocity.

(a) Settling velocity is a more important hydrodynamic property of cohesive sediment than grain size. Settling velocity is a measure of the sediment's behavior in suspension; grain size only allows us to guess the settling velocity.

(b) The first thing to know about cohesive sediment grain size is that it is *not* a measurable physical constant. True, the size of individual dispersed grains may be inferred from measurements of their settling velocities in distilled (free of dissolved chemicals) water: generally on the order of 10-μ or less. The settling velocity of a 10-μ sphere, 2,500 kg/m^3 (156 lb/ft^3), in water of 20 °C (68 °F) is 0.06 mm/sec (0.002 in./sec).

(c) But cohesive sediment of this size in natural, often salt, water does not stay dispersed for long. Grains stick together when they come close enough for the cohesive forces to overcome the fluid shear and gravity keeping them apart. Aggregations of cohesive sediment grains are called 'flocs.' Flocs are larger than individual grains, of course, but because of water trapped within the floc, they are also less dense than

the pure mineral. Depending on the relationships among floc size, shape, and density, the result is a *floc settling velocity* that may be more or less than that of individual grains. The settling velocity must be determined with the natural sediment in the natural water.

(d) Mud may also be biologically cohesive (Paterson 1994), for example, due to mucus excreted by diatoms. Biological cohesion is even more difficult to predict than electrochemical, providing yet another reason for using natural sediment and natural water in determining floc size and settling velocities.

(7) Degree of consolidation.

(a) The degree of consolidation u is defined as the ratio of the bulk density of the sediment to the bulk density of the 'fully consolidated' sediment, measured under Part III-5-6b(5). Consolidation of cohesive sediment is the compaction of the soil mass accompanied by drainage of the interstitial water, just as with noncohesive sediment. The principal difference is the length and cross-sectional area of the drainage path. In cohesive sediments, the path length is long and the area is small (i.e., low permeability); slowing down drainage and consolidation. Drainage is through the bed surface, into the ambient water, so that a good relative measure of the length of the drainage path P is the depth of burial below the surface. Cross-sectional area of the drainage path must be inferred from measurements of permeability.

(b) Overburden speeds up consolidation but increases the length of the drainage path, especially when the overburden is also cohesive. Nevertheless, consolidation starts at the bottom of a sediment layer and follows the draining water upward, giving even a freshly deposited layer a density gradient, denser at the bottom to less dense at the surface, until the entire layer is fully consolidated. The strength of the sediment represented by the critical shear for erosion τ_c increases with density and consolidation.

(8) Field measurement techniques. Many of the cohesive sediment field and laboratory measurement techniques are the same as those for noncohesive sediment (Part III-1). Nevertheless, some accommodation must be made for mud:

(a) Bed sampling. Much depends on knowledge of the composition and density of surficial sediments, which can be gained from laboratory analysis of surface samples obtained in the field. It is unreasonable to expect that undisturbed mud samples can be collected. In fact, it is difficult to contain most surficial mud in the commonly used Shipek or Ponar grab samplers because the samples leak out. Underwater samples may have to be obtained by divers, and all samples that include entrapped water should be transported in sealed jars and stored at 4 °C (39 °F).

(b) Boreholes and cores. The techniques give information on subsurface sediment layers. Blow counts and cone penetration tests give a relative measure of the strength and density of the layers (but not of the critical shears for erosion and deposition of mud, see below), and cores taken from the layers are as close to undisturbed samples as is possible in cohesive sediment. Boreholes should extend to bedrock or similar hard, impenetrable layers, with cores and cone penetration tests in each major layer.

(c) Suspended sediment sampling. This type of testing is needed to determine composition and quantity of sediment in suspension. Generally, the technique is to pump and filter 4 L of suspension and transport the filter and contents to the laboratory for subsequent analysis. Alternatively, 1 L of suspension may be sealed in jars and transported to the laboratory for filtering and analysis there; this liter may be obtained by pumping or from any of the proprietary suspension samplers. Filters should be no larger than 10 microns. Sampling should be carried out at a minimum of four elevations over the depth, with special attention to the near-bed or fluid mud layer.

(d) Settling tube. Field settling tubes, e.g., the 'Owen Tube' (Eisma, Dyer, and van Leussen 1994) measure the settling velocity of cohesive sediment flocs in 'live' natural water, even in a natural level of turbulence. Typically an undisturbed sample of sediment-water suspension is captured in a horizontal tube. The tube is immediately turned into the vertical position, and the settling velocity of the flocs is determined from density changes that occur in the suspension at various depths in the tube and over various times.

(e) Piezometers. These instruments measure rate of drainage of excess pore pressure from natural muds, and thus permeability and rates of consolidation. Lancelot (Christian, Heffler, and Davis 1993) is a piezometer that first creates excess pore pressure on its insertion in the mud bed, and then measures the rate of decay or drainage.

(f) Optical techniques. These techniques are primarily used as a substitute for suspended sediment sampling. Two basic techniques are used: measuring light transmitted through a known illuminated volume of suspension in a turbidity meter or transmissometer (e.g. Bartz, Zaneveld, and Pak 1978); or measuring light reflected from the suspension by an 'Optical Backscatterance (sic) Sensor' or OBS (e.g. Sternberg, Shi, and Downing 1989). Both require calibration against natural sediment in known concentrations in natural water.

(g) Acoustic techniques. Many novel applications are still under development, mostly in the high-frequency (MHz) range, where for example, suspended sediment concentration and grain size profiles can be measured (e.g. Hay and Sheng 1992). At lower frequencies, echo sounding detects the elevation of the bed and of the surface of fluid mud; and in the side-scan mode, detects bed forms such as ripples and dunes, and their orientation (Hay and Wilson 1994). At still lower (seismic) frequencies, sound penetrates the bed and detects the interfaces between sediment layers of different densities, creating sub-bottom profiles.

(h) Radioactivity techniques. In these techniques, Gamma rays or X-rays are passed through a sediment/water suspension or bed layer (e.g. Sills 1994). The energy passing can be related by calibration to the mass density of the suspension or layer. These techniques are particularly useful in characterizing fluid mud layers, as and where they occur. Radioactivity techniques are also used in laboratory consolidation columns.

(i) Direct shear techniques. There are several field devices that apply a variable shear stress to the surface of a cohesive sediment bed (Gust 1994), and measure the variable rate of erosion (increase in suspended sediment in the water column) and deposition (decrease in suspended sediment in the water column). Results can be used directly in the Parthenaides and Krone equations (Equations 5-1 and 5-4) respectively. The prototype for all such devices is the annular flume, described under Part III-5-6b(9) "Laboratory Measurement Techniques," and sketched in Figure III-5-17. The Sea Carousel described by Amos et al. (1992) is an example of field adaptation of the annular flume.

(j) Correlation with shear strength. Although the critical shear for erosion τ_c would seem to be a function of the shear strength of soft cohesive soil (measured by vane, cone, or penetrometer), the form of that function is not yet known and certainly not linear. Even measuring mechanical surface shear directly on tidal mud flats (Faas et al. 1992) produces mechanical yield stress an order of magnitude larger than the hydrodynamic τ_c.

(9) Laboratory measurement techniques.

(a) Grain size analysis. Standard ASTM D422 laboratory techniques should be applied to determine the physical size of individual grains in bed, core, and suspended sediment samples. Although no ASTM standard has been published, the pipette technique (removing a known volume of suspension from a known

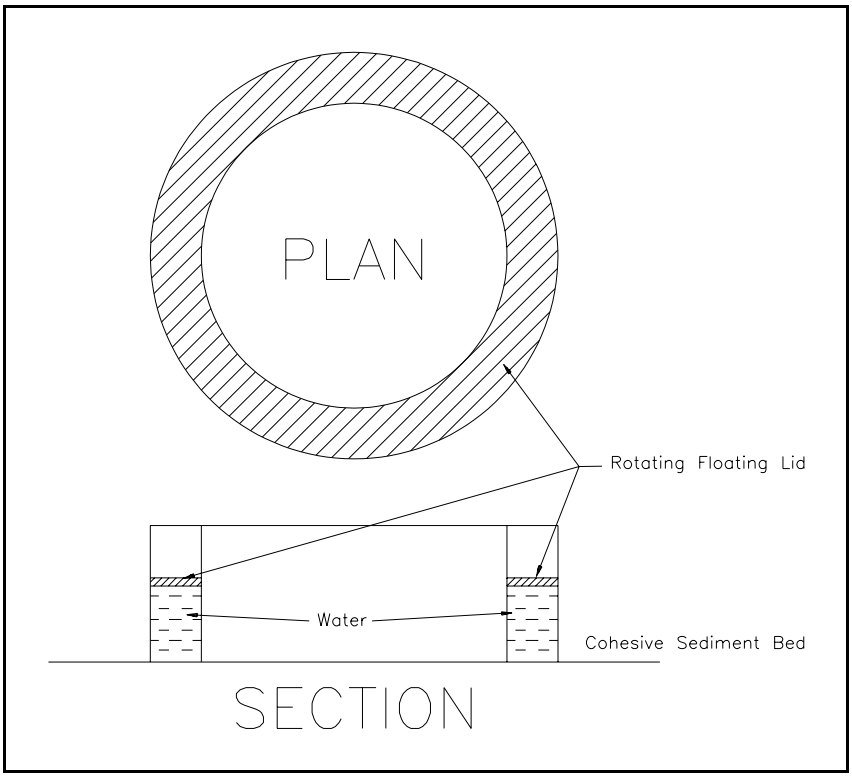

Figure III-5-17. Prototype direct shear device, the annular flume

elevation in the settling column, and filtering or drying to determine sediment concentration), is an alternative to the hydrometer technique. Total dry weight of suspended samples is also required to give field concentration in mg/l (ppm). Both hydrometer and pipette techniques measure settling velocity, and infer grain size from it. The settling column also measures settling velocity in the manner of a large-scale (typically greater than 1 m (40 in.) deep, 0.3 m (12 in.) diameter) hydrometer or pipette test (Gibbs 1972). Sensitive differential pressure transducers record the variations in suspended sediment concentration with depth and time, from which settling velocity distribution in the sample can be computed. Like the consolidation column below, settling columns need to be well-isolated from vibration and temperature changes to prevent artificial flocculation of the settling particles. For clay particules (<4 m), it will be necessary to use a nonstandard particle counter, e.g., Coulter counter. Nonstandard (natural water) hydrometer, pipette, or settling column tests should be used to estimate settling velocity of the flocs and bulk density of deposited sediment.

(b) Consolidation column. A consolidation column is a cylinder containing 2 to 3 m of natural sediment and natural water in a vibration-free environment to ensure natural rates of consolidation (Sills 1994). Variations in pore pressure with time and depth (overburden) are measured with piezometers, and in density, with gamma ray or observed volume. Estimates of permeability (length and diameter of drainage paths, and variation with bulk density) come out of the same measurements, using Equation 5-6, for example.

(c) Direct shear techniques. There are several laboratory devices that apply a variable shear stress to the surface of a cohesive sediment bed and measure the variable rate of erosion (increase in suspended sediment in the water column) and deposition (decrease in suspended sediment in the water column). Results can be used directly in the Parthenaides and Krone Equations of Parts III-5-7d and III-5-9c, respectively. The prototype for all such devices is the annular flume (e.g., Krishnappan 1993), sketched in Figure III-5-17. An annular flume is simply an endless channel in which the shear or velocity of rotation of the lid can be varied

and the changes in the mud bed can be inferred from changes in suspended sediment concentration, measured using one of the techniques described above. The shear force driving the circulation can be measured directly as the force needed to rotate the lid. Laboratory annular flumes generally rotate the flume and the lid in opposite directions, to minimize secondary radial circulation of the water, and to obtain a more uniform distribution of shear on the mud bed. An increase in suspended sediment corresponds to a decrease in the mass of sediment on the bed *m* and a decrease in suspended sediment to an increase in the mass of the bed. It is then possible to extrapolate these measured shear stresses to τ_c and τ_s, at which erosion or deposition ceases; and to interpolate the Parthenaides coefficient M_p and fall velocity *w* (Example Problem III-5-1).

(10) Calibration techniques. Ideally, one should be able to measure all the hydrodynamic properties of a cohesive sediment, and proceed directly to a model of the shore. The model, however, will always need calibration and verification against measurements of erosion and deposition, to fine tune measurements and confirm that the model represents the shore. With some of the hydrodynamic properties unknown, the model can be used to choose between high and low values of the unknown properties, using "design of experiments" techniques (Willis and Crookshank 1994). This still requires intelligent estimates of high and low values of the unknown properties and good field measurements of erosion, deposition, or transport.

III-5-7. Erosion Processes

a. Shear stress.

(1) The formulae for predicting the movement of cohesive sediment predict rates of erosion and deposition, not transport. Try putting a typical cohesive floc size into a noncohesive sediment transport formula (Part III-6) and you will predict virtually infinite transport rates, in which the predicted density of 'sediment in suspension' may exceed its real density on the bed. Noncohesive sediment formulae are generally based on transport limitations: assuming there is a sediment supply to match the transport potential. Cohesive sediment formulae are generally based on supply limitations, and assume the flow can transport all eroded sediment. They define the sediment exchange between the bed and the water column.

(2) The cohesive sediment formulae are also less theoretically based. They form a simple numerical framework for interpolating and extrapolating observed hydrodynamic behavior of cohesive sediment. Generally erosion or deposition is correlated with the excess shear stress.

b. Erodibility of consolidated sediments.

(1) There have been many studies of the erosion resistance of cohesive soils to flowing water. Very few of these investigations have considered the much more complex flow conditions encountered in the coastal zone. Nevertheless, a basic understanding, such as it is, of the complex process of erosion of consolidated cohesive soil provides a basis for assessing the erosion resistance of cohesive soils in the coastal environment.

(2) The erodibility of cohesive soils is controlled by the bonds between cohesive particles. Many tests of remolded cohesive sediments have found that the most important parameters in describing the erodibility of cohesive sediments include consolidation and physio-chemical conditions, both of which influence the degree of bonding between particles. Aside from the difficulty of obtaining intact cohesive samples, the reason for testing remolded and reconsolidated samples is to establish the erodibility of recompacted clays, used as construction materials. Extensive investigations into the relationships between the properties of these 'homogenous' cohesive sediments (e.g., consolidation and other geotechnical parameters), and the physio-chemical properties of the fluid (including temperature, pH, and salt or cation content) have found a direct relationship between these parameters and erodibility (Croad 1981; Arulanandan, Loganatham, and Krone 1975).

(3) More recent investigations of intact consolidated sediment samples have found that the natural structure of the material, including the presence of fissures, fractures, and seams of noncohesive materials such as silt and fine sand, is the most important factor in determining erodibility (Lefebvre, Rohan, and Douville 1985; Hutchinson 1986). The natural structure is uniquely defined by the environmental conditions during the original deposition and subsequent weathering of the sediment (including overconsolidation during glacial periods for some sediments). Conventional geotechnical parameters such as clay content and shear strength do not provide a direct measure of the influence of the natural structure of consolidated sediments as it relates to erodibility. Nevertheless, Kamphuis (1987) suggested that the presence of fissures in samples may be indirectly reflected in the undrained shear strength, consolidation pressure, and clay content.

(4) A technique for assessing the hydraulic erodibility of natural and engineered earth materials including both soil and rock is described by Annandale (1996). This empirical method, which provides a relationship between threshold stream power for erosion and an erodibility index, was developed from field observations of spillway performance downstream of dams. The erodibility index is determined as a scalar product of indices representing the following material properties: (1) mass strength, (2) block/particle size, (3) discontinuity/interparticle bond shear strength, and (4) shape of the material units and their orientation relative to the flow velocity.

(5) For clay materials as for mud, the erodibility index is primarily a function of the shear strength of the soil. Stream power is calculated as the product of near-bed velocity and shear stress. This approach was applied to the scour of weak rock in the presence of waves and currents to investigate scour potential around bridge piers (Anglin et al. 1996).

(6) In summary, in the absence of a reliable and standardized technique for assessing the natural structure of consolidated cohesive sediment, as it relates to erodibility in the coastal environment, more empirical approaches must be followed, such as establishing erodibility coefficients from laboratory tests or field data.

(7) One such example of a direct empirical technique for estimating erodibility is described by Kamphuis (1990) and Parson, Morang, and Nairn (1996). In these tests, intact (undisturbed) samples of consolidated sediment were placed in a drop section of the floor of a high-velocity unidirectional flow flume or tunnel with transparent walls or windows. The shear stress over the samples was determined indirectly by measuring the vertical profile of velocity just above the bed. The average erosion rate was then determined by measuring the volumetric erosion experienced on the surface of a sample within a test period. Rates were determined for velocities in the range of 0.5 to 3 m/sec. Further details on this test procedure are presented in Part III-5-6a. All results determined by using this technique for various types of consolidated sediment (including mudstone, till, and lacustrine clay) are summarized in Figure III-5-18 (from Parson, Morang, and Nairn (1996)). It was found that shear stresses in the range of 0 to 18 Pa resulted in erosion rates in the range of 0 to 8 mm/hr.

(8) In a further extension of this type of testing, Kamphuis (1990) found that the erosion rate increased dramatically when sand was added to the flow. The results of all of the erodibility tests using this technique with sand in flow are presented in Figure III-5-19 (from Parson, Morang, and Nairn (1996)). A comparison of the clear water erosion results of Figure III-5-18 and the sand in flow results of Figure III-5-19, indicates that for the same shear stress and sediment sample, the erosion rate is increased by a factor of 3 to 8 when

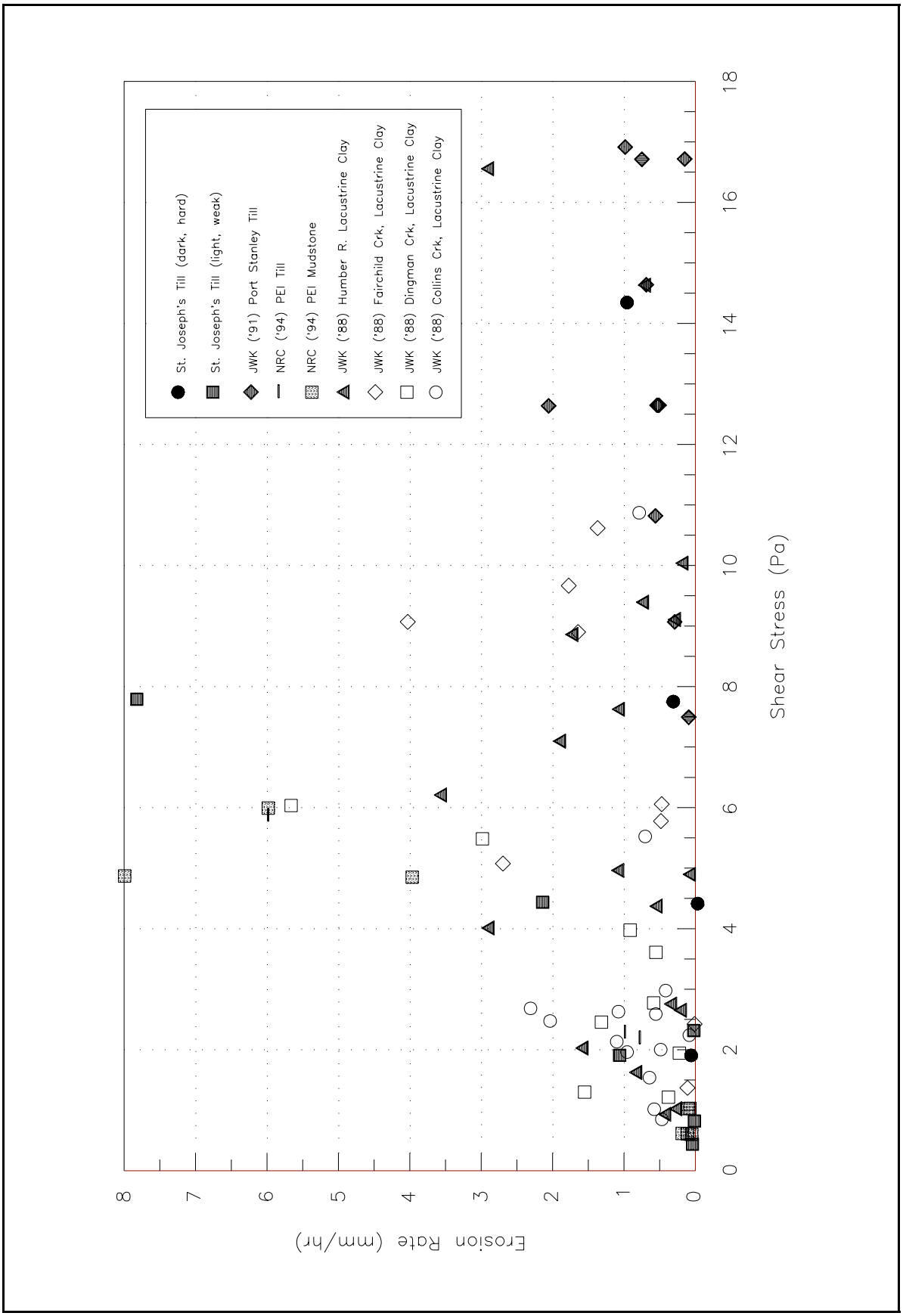

Figure III-5-18. Clear-water erosion rates from unidirectional flow flume and tunnel tests for various materials

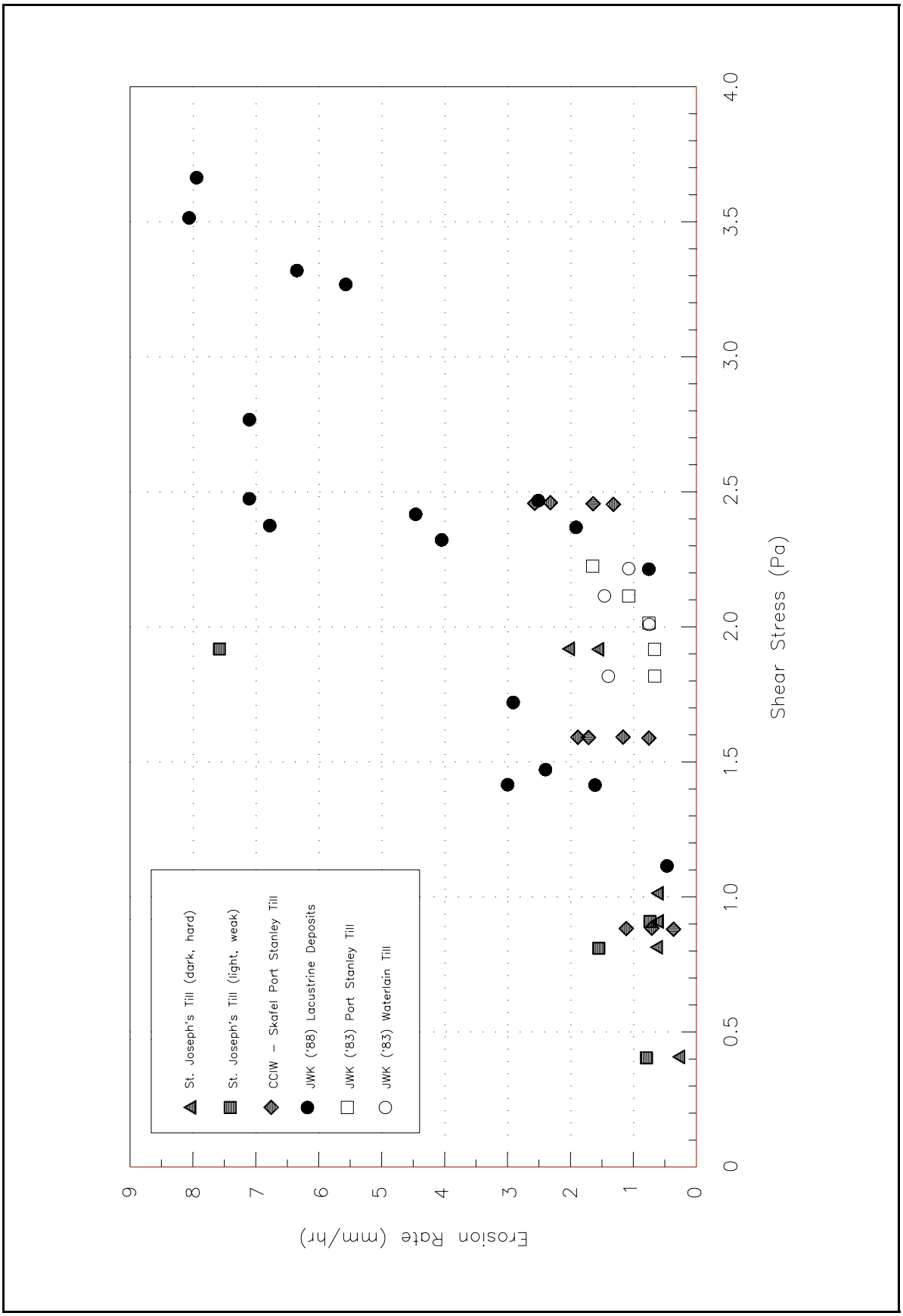

Figure III-5-19. Sand in flow erosion rates from unidirectional flow flume and tunnel tests for various materials

sand is introduced into the flow. It should be noted that the sand-grain size was selected so that sand transport occurred in a saltating (bed load) manner in the tests.

(9) A close review of the results presented in Figure III-5-18 reveals two populations of erosion response. The less erosion-resistant group consists of soft cohesive sediments as well as sediments characterized with a high degree of fracturing and/or the presence of silt seams. In contrast, the more erosion-resistant group consisted of firm, homogenous cohesive sediments. The shear strengths for the material tested ranged from 50 to 200 kPa.

(10) Some of the most recent research into the erodibility of cohesive sediments in the coastal environment has focused on the potential for softening of the exposed surface layer. Davidson-Arnott and Langham (1995) report that at the western end of Lake Ontario, previously overconsolidated till featured shear strengths in the range of 10 to 100 kPa. The softer sediment (10- to 20-kPa shear strength range) was associated with deeper water areas where the till was always exposed (i.e., the noncohesive sediment cover was insignificant) and where the frequency of erosion events was low. In contrast, in shallower areas (depths less than 3 m or 10 ft), the shear strengths were found to be in the range of 30 to 80 kPa. In the shallower depths, the lake bed is exposed to erosion events more frequently and sand cover thicknesses were greater. Using an adapted micro shear vane for a location in a water depth of 3.5 m, they found that the shear strength was lower in the upper 0.1 m of the lake bed and much lower in a 10-mm-thick surface layer. In fresh water, the softening process may be a result of cyclic loading by wave action, whereas in a seawater environment, factors such as salinity and biological activity (such as burrowing organisms) may also be important (Hutchinson 1986).

(11) Finally, an indirect approach to determining the erodibility of consolidated sediment at a specific site is through the use of numerical models to 'back-calculate' the erodibility coefficient through an analysis of environmental conditions (wave action and water levels) and the observed shoreline or lake bed erosion over a given period of time. This approach is discussed in more detail in Part III-5-12.

c. Subaqueous erosion of consolidated sediments.

(1) In this section, the underwater erosion process is described. In the previous section, we explained that the erosion of hard cohesive soils consists of the destruction of bonds between clay particles and the natural structure or framework created through consolidation of the soil matrix. Erosion of consolidated sediment is irreversible. Once the sediment, which often consists of 80 to 90 percent fines, is eroded, it cannot be reconstituted in its consolidated form in the littoral zone. The eroded fines (silt and clay) are winnowed, carried offshore, and deposited in deep water in contrast to the small fraction of sand and gravel, which remains in the littoral zone. Therefore, the erosion of cohesive sediment is fundamentally different from the erosion of noncohesive sediment. In the latter case, for every volume of eroded sand, a large portion of that material will be deposited somewhere in the littoral zone (in some specific instances, onshore or offshore losses of sand from beaches can occur). Therefore, on sandy shores, the process of erosion is reversible.

(2) An extensive study of nearshore profiles on the north central shore of Lake Erie described by Philpott (1984) revealed that the profile shape remained relatively constant over an 80-year interval despite dramatic shore recession. This led Philpott (1984) to conclude that the controlling process in bluff or cliff recession on cohesive shores is not restricted to wave action at the toe (as proposed by Sunamura (1992) for eroding rocky coasts) but by the erosion of the nearshore profile by waves. Boyd (1992) cites many earlier references that also suggest that the nearshore has a controlling influence on shoreline recession. The shoreward shift of the dynamic equilibrium profile implies that erosion or downcutting is proportional to the gradient of the nearshore profile and is, thus, greatest close to shore. Davidson-Arnott (1986) describes field measurements of downcutting for a till profile (through the deployment of micro-erosion meters across a

transect) at a site near Grimsby on Lake Ontario. The results confirm the hypothesis on downcutting, i.e., the rates increase towards the shore in a manner related to the local bed slope, thus allowing for the preservation of the profile shape as it shifts shoreward with time. The downcutting hypothesis has now been confirmed by many other field investigations including 9 years of profile retreat data at Maumee Bay State Park in Ohio (Fuller 1995). Hutchinson (1986) and Sunamura (1992) also note that the rate of lowering or downwasting of the intertidal platform on erodible rocky coasts probably determines the long-term rate of cliff retreat in most instances.

(3) In general, it has also been shown that the underlying cohesive profile, for cases where the properties of the cohesive sediment are uniform along the profile, follows an equilibrium profile shape as defined by Dean (1977). Kamphuis (1990) went on to show that the specific exponential shape of the equilibrium profile at a cohesive shore site was related to the grain size of the overlying noncohesive sediment. In other words, the profile shape could be determined using the grain size of the sand veneer to define the sediment scale parameter A (see Equation 3-15). The shape of the profile can also be influenced by other factors such as variable stratigraphy and the presence of lag deposits as discussed in Part III-5-5. In these cases, a smooth equilibrium profile with an exponential shape will not exist, at least not over the full profile. Riggs, Cleary, and Snyder (1995) note that in most instances along the North Carolina coasts, the complexity of the underlying stratigraphy is such that the profile rarely resembles the equilibrium form found on truly sandy shores.

(4) The downcutting process is illustrated in Figure III-5-20 for a cohesive shore site located east of Toronto along the Scarborough Bluffs. The bluff face has retreated approximately 30 m (100 ft) in a 37-year period. The underlying cohesive profile shape in 1952 is very similar to that in 1989; it has simply shifted shoreward by 30 m. Therefore, the long-term bluff or cliff retreat rate is equivalent to the profile retreat rate. This figure also shows that there can be a significant quantity of sand covering an underlying cohesive profile. The position of the underlying cohesive profile shown in Figure III-5-20 was estimated based on observations that the cohesive sediment is usually exposed or very thinly covered in the troughs between the bars. Also, it is known that the till is exposed at the toe of the bluff (i.e., at the back of the beach).

(5) Figure III-5-20 demonstrates that there is not a cross-shore balance of erosion and deposition. All of the eroded material from the cohesive profile and the bluff is either winnowed offshore (clay and silt fractions) or transported alongshore (sand and gravel fractions).

(6) The profile retreat model for cohesive shores implies that: the amount that the driving forces for erosion exceed the resisting forces is inversely proportional to the water depth. In other words, the most active subaqueous erosion occurs at the shoreline. In general, it may be assumed that the erosion resistance of the cohesive sediment is consistent across the profile (if anything, the sediment may be less erosion-resistant in deeper water due to the increased role of softening). Therefore, the driving force for erosion must increase in the shoreward direction. These observations provide important evidence on the nature of the driving forces for cohesive profile erosion.

(7) Coakley, Rukavina, and Zeman (1986) proposed that outside the surf zone, the downcutting process is driven by shear stresses generated by the orbital motion under waves. Outside the surf zone, this driving force is inversely proportional to water depth. However, considering that wave heights and the related orbital velocity decreases in the surf zone, this mechanism cannot explain the inverse relationship between depth and driving force in this zone. Nairn, Pinchin, and Philpott (1986) proposed that the complex combination of driving forces in the surf zone may be represented by the rate of energy dissipation (described by the rate of wave height decay). Using a model of wave energy dissipation for random waves, it was shown that the rate of energy dissipation was directly proportional to the rate of downcutting in the surf zone. In the surf

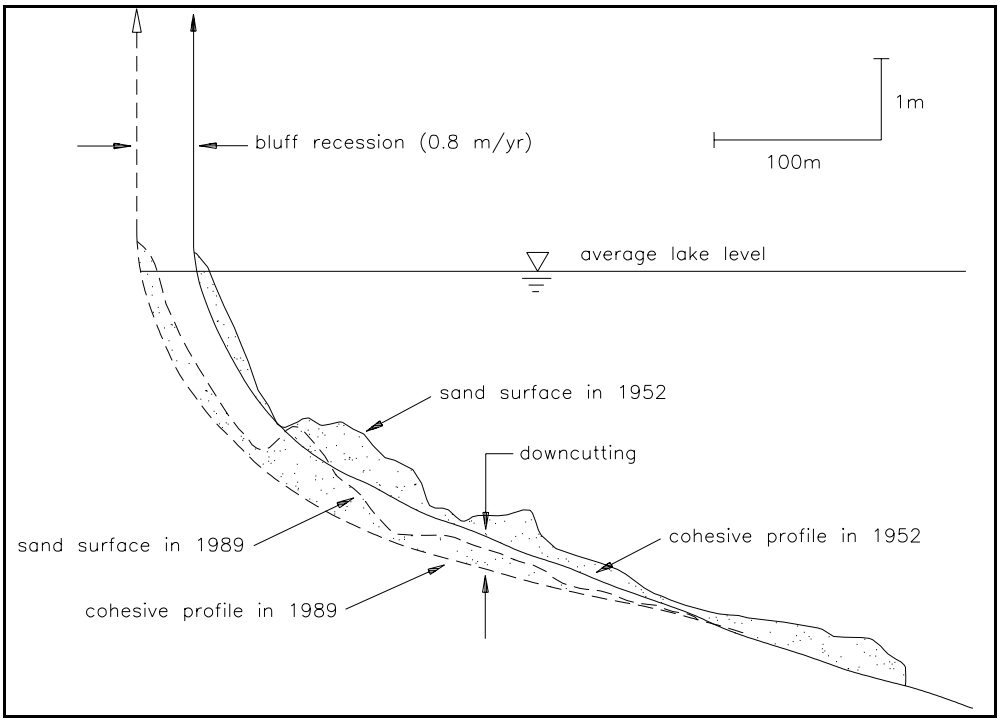

Figure III-5-20. Bluff retreat and profile downcutting over a 37-year period at Scarborough Bluffs, located east of Toronto on Lake Ontario

zone, the rate of energy dissipation provides a good indicator of the possible driving forces such as intensity of flows (e.g., undertow and alongshore currents) as well as the intensity of near-bed turbulence (i.e., plunging breakers, which generate high near-bed turbulence, are associated with rapid wave decay). The erosive nature of plunging breakers (and the associated near-bed turbulence) on cohesive profile erosion was demonstrated through laboratory experiments performed in a wave flume with intact cohesive samples (Skafel 1995).

(8) Sand acts as an abrasive agent in the erosion of consolidated shores. Referring to Figure III-5-20, it is also likely that the presence of alongshore bars can have the opposite effect of protecting the underlying cohesive sediment from exposure and subsequent downcutting. As these bars migrate with changing wave and water level conditions, different areas of the underlying cohesive profile become exposed in the troughs between the bars. The influence of the quantity and mobility of sand cover over a cohesive profile is explored in greater detail in Part III-5-2.

(9) At the boundary between the action of subaqueous and subaerial erosion processes, the bluff or cliff toe can in some instances experience notching. This notching typically occurs in more competent materials such as rock, frozen sediments, and harder cohesive sediments, (i.e., in materials that are capable of withstanding failure when undercut).

(10) In summary, the fundamental principles of consolidated cohesive shore erosion are:

(a) The erosion of consolidated cohesive sediment is irreversible.

(b) The long-term rate of shoreline retreat is directly related to the rate of nearshore downcutting and the associated profile retreat.

(c) The local rate of downcutting is proportional to the gradient of the nearshore slope at any location across the profile.

(d) In addition to acting as an abrasive agent that accelerates consolidated cohesive sediment erosion, sand can also serve to protect an underlying cohesive profile from erosion.

d. Subaqueous erosion of mud. The Parthenaides Equation for mud erosion (Parthenaides 1962, Mehta et al. 1989) is an excess shear equation describing the erosion rate of a cohesive sediment:

$$\frac{dm}{dt} = M_p \frac{(\tau_c - \tau)}{\tau_c} \tag{III-5-1}$$

where

m = mass of sediment on the bed, kg/m^2 (lb/ft^2)

t = time, sec

τ = bed shear, Pa (lbf/ft^2)

τ_c = critical shear for erosion, Pa (psf) (lbf/ft^2)

M_p = 'Parthenaides Coefficient,' erosion rate at twice τ_c, kg/m^2/sec (lb/ft^2/sec)

e. Fluid mud.

(1) This assumes a well-defined interface between bed and water column: sediment on the bed remains at rest; while that in the water column moves with the water. Often, cohesive sediment forms an intermediate layer of fluid mud (denser than water; less dense than the bed; still capable of motion, but slower than the ambient flow). Fluid mud layers are frequently found near the shoreline, where wave activity can 'pump up' excess pore pressures within the fluid mud mass, slowing down drainage and consolidation. Hydrographers generally define fluid mud as having a density of less than 1,100 to 1,200 kg/m^3 (70 to 75 lb/ft^3).

(2) Erosion processes in fluid mud are similar to mixing processes at a salt-wedge interface. A layer of lighter fluid (water with suspended sediment) flowing above the denser fluid mud eventually induces waves in the interface when a critical Richardson Number or densimetric Froude Number is exceeded. Wind-wave activity in the upper layer increases the interfacial waves, diverting energy from the surface waves. As the difference in flow rates increases, the interfacial wave energy increases until breaking occurs, putting some fluid mud back in suspension and entraining clearer water in the fluid mud.

(3) The densimetric Froude Number is defined as:

$$F_r = \sqrt{\frac{(V_w - V_{fm})^2 \rho_{fm}}{g h_{fm} (\rho_{fm} - \rho_w)}} \tag{III-5-2}$$

where

V_w = mean velocity in the water layer, m/sec (fps), above

V_{fm} = mean velocity in the fluid mud layer, m/sec (fps)

ρ_w = density of the water layer, kg/m^3 (lb/ft^3)

ρ_{fm} = density of the fluid mud layer, kg/m^3 (lb/ft^3)

g = acceleration due to gravity, m/sec^2 (ft/sec^2)

h_{fm} = thickness (depth) of fluid mud layer, m (ft)

(4) This reduces to the more familiar Froude Number at the water surface, where the upper layer is air of relatively negligible density and the lower fluid mud layer is the water. It defines the ratio of the velocity differential at the interface (V_w - V_{fm}) to the celerity of a small gravity wave in the interface. When that ratio is unity, the equivalent of a hydraulic jump (breaking wave) may be expected in the interface, with resultant entrainment of fluid mud in the water (erosion of the fluid mud) balanced by entrainment of water in the fluid mud.

(5) At the interface between the fluid mud and the bed, the fluid mud protects the bed from erosion. Shear that develops between the mud and the bed is generally too low to entrain stationary particles. The processes at this interface are entirely deposition, as water drains from the fluid mud.

f. Subaerial erosion processes.

(1) Subaerial erosion processes on cohesive shores do not necessarily have anything to do with the air or wind, although strengthening of mud flats has been noted by Amos et al. (1992) due to evaporation at low water in the macrotidal Bay of Fundy. On consolidated shores, the primary subaerial erosion process is slumping of oversteep bluffs or cliffs.

(2) As stated earlier, the long-term bluff or cliff retreat rate is determined by the rate of profile downcutting. In a review of shoreline erosion data from the Lake Erie shoreline, Kamphuis (1987) points out that cliff height does not exert much influence on the process (in fact, a distinct lack of correlation was noted) because erosional debris from a shore cliff is quickly swept away, winnowed offshore, and deposited in deep water. Exceptions to this generalization include locations where the debris is not easily removed from the toe of the cliff (e.g., in the case of eroded rock cliffs or blocks of frozen sediment along Arctic shores). The primary reason for slope failures along a cohesive shore is the oversteepened nature of the slope owing to the ongoing profile and toe erosion. Nevertheless, even though subaerial processes do not determine the long-term rate of shoreline recession on cohesive shores (i.e., the frequency of slope failures), these processes are critical in determining when and where a failure will occur.

(3) Slope stability is a function of the balance between the downward force of gravity and the strength of the geologic materials in a bluff or cliff. The strength of the geologic materials depends on the cohesion of particles and the presence or absence of groundwater. The stratigraphy of a bluff or cliff can have a significant influence on slope stability. Weak clay layers can provide slip planes for slope failures or serve to confine groundwater flows, which may appear as springs at the bluff face. Where groundwater exits the bluff face, seepage erosion can occur. Also, depending on the sequence of layering, groundwater flows can act to increase pressures within the slope and contribute to instability. This will often occur when seepage pathways at the bluff face are blocked by talus from a slide further up the slope. In some instances, the

combination of surface runoff and seepage can lead to the development of large gullies. Slope failures may be classified as: falls and topples; rotational (i.e., circular) and translational slides; and, spreads and flows. The type of failure is a function of the geologic conditions at the site. There are a variety of methods for assessing slope stability.

(4) Figures III-5-21 to III-5-23 show some examples of eroding bluffs along the Great Lakes. Recent rotational failures are evident in Figure III-5-21 along the north central shore of Lake Erie. The development of a gulley is shown in Figure III-5-22 from another location on the north central shore of Lake Erie. Figure III-5-23 shows an eroding shale bluff along the western Lake Ontario shoreline.

Figure III-5-21. A rotational bluff failure along the north central shore of Lake Erie

(5) In addition to slope stability, surface erosion of the cliff or bluff face can have a secondary influence on the overall erosion of the feature. Surface erosion results from runoff, seepage, rain, and spray from wave action. This would be one of the key processes leading to the erosion of the shale bluff shown in Figure III-5-23.

(6) Edil and Bosscher (1988) present a Great Lakes perspective overview of forces and resistance influencing cohesive shore slope erosion which result in mass movement (including sliding, flow, and creep) and particle movement (including wave, wind, ice, rill and sheet erosion and sapping through seepage flow).

(7) Kuhn and Osborne (1987) investigated the recession of cohesive cliffs on the California coast. The short-term cliff recession is partly related to subaerial processes such as drainage of precipitation and the effects of urbanization at the cliff top. At these locations the cliff base is well protected by a substantial beach deposit which restricts the downcutting of the subaqueous profile. Notably, almost all of the sand at these sites is supplied by nearby rivers and not by cliff recession. This is in contrast to the Great Lakes and barrier islands on the U.S. east coast, where very little sand is supplied by rivers in most areas.

Figure III-5-22. Gully erosion of a bluff along the north central shore of Lake Erie

Figure III-5-23. An eroding shale bluff along the west Lake Ontario shoreline

(8) A cliff stabilization project for the Scarborough Bluffs (east of Toronto on Lake Ontario) is discussed by Parker, Matich, and Denney (1986) (Figure III-5-24). It has been recognized that arresting the foreshore downcutting at the base of the bluffs is not sufficient on its own to control the erosion of an oversteep slope; proper drainage systems must be implemented to prevent gullies from developing and to address the problem of piping through sand and silt lenses. Parker, Matich, and Denney (1986) also note that the toe of the bluff must be surcharged in some locations to prevent large slip failures from occurring. One function of the land base created at the toe of the slope in Figure III-5-24 is to provide sufficient area to construct a surcharge berm. The surcharge provided by extensive shingle beaches along the south coast of England is known to contribute to the stability of cliffs that rise behind the beaches (Fleming and Summers 1986).

Figure III-5-24. Shore protection consisting of a wide berm protected by a revetment along the base of the Scarborough Bluffs located east of Toronto on Lake Ontario

Bioegineering, which consists of promoting the growth of vegetation (e.g., through the placement of mats consisting of bundled twigs to enhance rooting), may also help to stabilize an oversteep slope.

(9) Another extensive review of subaerial processes was made by Hutchinson (1986); other processes that he identified included: freeze/thaw cycles; alternate wetting and drying; and mechanical and hydrodynamic effects of micro-geological features such as erratic cobbles and boring organisms. Hutchinson (1986) provides sample test results indicating that seawater penetrated the pores of glacial tills from the Holderness coast of England (along the North Sea) to depths of at least 0.85 m. He goes on to suggest that an increase in the concentration of NaCl in the pore water from the intrusion of the seawater may increase the net attractive forces between clay particles and increase the degree of aggregation. The degree to which this effect will occur will depend on the clay content and the chemical properties of the cohesive sediment. Hutchinson (1986) concludes that the opposite effect may occur along freshwater shores, where the intrusion of fresh water may dilute the salt or cation content, thus decreasing the net attractive forces between clay particles, and increasing the susceptibility to erosion.

III-5-8. Transport Processes

a. Advection and dispersion.

(1) Cohesive sediments are not transported as bed load, except in the form of fluid mud (see Part III-5-8b below). They almost always are transported in suspension: advected (carried with the ambient water at the flow velocity) and dispersed (moved from areas of high sediment concentration to low by mixing, such as turbulence). Advection and dispersion are described in Part II-6-2.

(2) But sediment, even a floc, is denser than the ambient water and hence settles as it is being advected and dispersed. This results in a downward bias of the vertical dispersion relation

$$S - Cw = -D_z \frac{dC}{dz} \tag{III-5-3}$$

where

S = vertical (upward) dispersion of sediment, kg/m^2/sec (lb/ft^2/sec)

w = settling velocity of floc, m/sec (ft/sec)

D_z = vertical dispersion coefficient, m^2/s (ft^2/sec)

C = suspended sediment concentration, kg/m^3 (lb/ft^3)

z = vertical dimension, m (ft)

b. Fluid mud. Fluid mud, as its name suggests, flows and is a mechanism for transport of cohesive sediment. It flows down slopes by gravity, sometimes referred to as a 'turbidity current,' which is why fluid mud is often found in the bottoms of dredged cuts. Fluid mud is also dragged along by the shear of the water flowing above it. How it flows is determined by its rheology; which in turn, must be measured for each fluid mud combination of sediment and water. Fluid mud may have an apparent yield point, remaining stable until a critical slope or shear is exceeded. More likely, its flow velocity will vary in a nonlinear way with slope or shear, from stiffest at lowest shear to most fluid at highest shear.

III-5-9. Deposition Processes

a. Flocculation.

(1) Cohesive sediments rarely settle as individual grains in nature. Collisions between sediment grains are encouraged by differences in settling velocity, turbulence, Brownian motion, and electrochemical attraction or cohesion.

(2) When cohesive grains collide they tend to stick together, or cohere. To determine settling velocity in the laboratory, cohesive grains can be kept apart in distilled water containing a dispersing agent to neutralize the electrochemical bond.

(3) The process by which individual cohesive particles agglomerate while settling is called *flocculation*; and the resulting large particles with entrapped water, *flocs*. The settling velocity of a floc is a function of its size, shape, and relative density. A floc usually settles faster than its constituent particles; but because of

the entrapped water, its density is less than that of the sediment mineral, and the settling velocity of the floc may actually be slower than that of an individual clay particle. The size and shape of flocs, and their settling velocity, are hydrodynamic sediment properties which must be measured or determined by model calibration as described in Part III-5-3.

b. Shear stress. The principle of excess shear is also used for correlating observed rates of cohesive sediment deposition with flow. But for deposition, 'excess' is the amount by which the shear τ is less than a critical shear for deposition τ_s.

c. Krone Equation. The Krone Equation for mud deposition (Krone 1962, Mehta et al. 1989) is as follows:

$$\frac{dm}{dt} = Cw\frac{(\tau_s - \tau)}{\tau_s} \tag{III-5-4}$$

where

m = mass of sediment on the bed, kg/m^2 (lb/ft^2)

t = time, sec

τ = bed shear, Pa (lbf/ft^2)

τ_s = critical shear for deposition, Pa (lbf/ft^2)

C = suspended sediment concentration above the bed, kg/m^3 (lb/ft^3)

w = settling velocity of sediment floc, m/sec (ft/sec)

Comparison of the Krone and Parthenaides Equations (Part III-5-4d) suggests that the Krone Equation may be less empirical, more theoretical. There is no obvious empirical coefficient to match the Parthenaides coefficient M_p, but the unknown coefficient hidden in the Krone Equation is w, the settling velocity of the flocs.

d. Fluid mud. Deposition takes place at both interfaces: that between water and fluid mud; and also that between fluid mud and the stationary bed. At the water/fluid mud interface, the process can still be predicted by the Krone Equation, except the density of the deposited sediment is less than 1,100 to 1,200 kg/m^3 (70 to 75 lb/ft^3). At the fluid mud/bed interface, the deposition process is one of consolidation: as the fluid mud drains, it consolidates to the point where it is too dense to remain fluid.

III-5-10. Consolidation

a. Strength versus consolidation.

(1) The critical shear for erosion τ_c is a function of the consolidation or density of the bed. Think of the cohesion between sediment particles varying inversely, like the force of gravity, with distance between particles. The closer the particles are to each other, the stronger the cohesive bond and the greater the shear force needed to separate them.

(2) The Migniot Equation expresses the exponential relationship between mud density and critical shear for erosion as:

$$\tau_c = N\rho_s^M \tag{III-5-5}$$

where

ρ_s = bulk density of sediment on the surface of the bed, kg/m^3 (lb/ft^3)

M, N = constants to be determined for the sediment and water.
M is dimensionless and tends to be less than 1; *N* equals 10^{-1} or 10^{-2} in the SI system of units.

b. Degree of consolidation. The Terzaghi consolidation relation, developed for building settlement calculations, also serves to illustrate the consolidation of coastal cohesive sediment.

$$u = 0.964\left(\frac{tC_v}{P^2}\right)^{0.415} \tag{III-5-6}$$

where

u = degree of consolidation, dimensionless ratio

C_v = a consolidation coefficient to be determined, m^2/sec (ft^2/sec) (values on the order of 1 x 10-5 m^2/sec are not uncommon)

P = length of the drainage path, m (ft) (generally depth of burial)

III-5-11. Wave Propagation

a. Roughness and shear.

(1) The predominant nearshore wave transformation associated with muddy beds is wave energy dissipation or attenuation. Refraction, diffraction, and reflection all pretty much obey the rules set out in Part II-3-3, but wave attenuation is generally much greater over mud beaches than over sand and gravel. As more wave energy is absorbed by the mud, less reaches the breaker line.

(2) This energy dissipation can only partially be accounted for through the traditional mechanisms of bed roughness and friction. In fact, a mud bed is usually smoother (less rough) than sand.

b. Fluid mud.

(1) The predominant mechanism of wave attenuation is in the thick, viscous boundary layer of fluid mud (Lee 1995, Lee and Mehta 1994). Part of the wave energy goes to ‘pumping up’ excess pore pressures maintaining the mud in a fluid state. But more is converted to work done in moving the fluid mud against viscous shear.

Example Problem III-5-1

FIND:

Apply the Parthenaides and Krone Equations to the annular flume test results in the table, to determine values of:

M_p = Parthenaides coefficient for this combination of sediment and water

τ_c = Critical shear for erosion at this sediment density

w = Settling velocity of sediment flocs for this combination of sediment and water

τ_s = Critical shear for deposition for this combination of sediment and water

For the purposes of this example, ignore changes in bed elevation and water depth due to erosion and deposition.

GIVEN:

Table III-5-2
Example Problem III-5-1, "Annular Flume Test Results"

Applied Shear (Pa)	Duration (sec)	Starting Concentration (kg/m^3)	End Concentration (kg/m^3)
0	600	0	0
0.2	600	0	0
0.4	600	0	0
0.6	600	0	1
0.8	600	1	3.33
1.0	600	3.33	7
0.8	600	7	7
0.6	600	7	7
0.4	600	7	7
0.2	600	7	1
0	50	1	0

Bulk (dry) density of sediment on the bed = 1,500 kg/m^3

Water density = 1,020 kg/m^3

Area of annular flume bed = 1 m^2

Water depth = 0.2 m

Total water volume, therefore = 0.2 m^3

(Sheet 1 of 3)

Example Problem III-5-1 (Continued)

SOLUTION:

Since the bed area of the annular flume has been carefully chosen to be 1 m^2, the rate of change of total sediment suspension will directly give us the quantity dm_b/dt. Otherwise, we would have had to multiply both sides of both equations by the area of the bed.

Our results are not given as total sediment in suspension, but as concentration in kg/m^3. We need to multiply them by the volume of water in the annular flume, 0.2 m^3, to get total sediment numbers equivalent to dm/dt on the bed.

So, for example, when the applied shear was 0.6 Pa

$$dm/dt = (V \times \Delta C) / (A \times \Delta T) = (0.2\ m^3 \times -1\ kg/m^3) / (1\ m^2 \times 600\ sec)$$
$$= -3.33 \times 10^{-4}\ kg/m^2\text{-sec}$$

Similarly for 0.8 Pa, -7.77×10^{-4} kg/m^2/sec, and for 1.0 Pa, -1.22×10^{-3} kg/m^2-sec.

This concludes the erosion data for the Parthenaides Equation. By plotting erosion rate versus shear (Figure III-5-25), we can extrapolate back to the shear at which the erosion rate is zero, τ_c = 0.45 Pa. From the same plot we can read M_p, the erosion rate at $2\tau_c$ = 0.9 Pa, = 10^{-3} kg/m^2-sec.

In the same way, the deposition results can be used as shear is reduced, with the Krone Equation for

0.2 Pa and C_{avg} = 4.0 kg/m^3, dm/dt = 2×10^{-3} kg/m^2-sec

and for

0.0 Pa and 0.5 kg/m^3, dm/dt = 4×10^{-3} kg/m^2-sec

Note that we can use the mean sediment concentration C_{avg}, since deposition rate is a linear function of concentration. In high concentration, settling velocity also becomes an inverse function of concentration.

The result at 0.0 Pa gives the floc settling velocity directly

$$w = (dm/dt) / (C_{avg} \times \tau_s / \tau_s) = (4 \times 10^{-3}\ kg/m^2\text{-sec}) / (0.5\ kg/m^3) = 8 \times 10^{-3}\ m/sec$$

Substituting this in the Krone Equation at 0.2 Pa, yields

$$\tau_s = (\tau \times C_{avg} \times w) / (C_{avg} \times w - dm/dt)$$
$$= (0.2\ Pa \times 4.0\ kg/m^3 \times 8 \times 10^{-3}\ m/sec) / (4.0\ kg/m^3 \times 8 \times 10^{-3}\ m/sec - 2 \times 10^{-3}\ kg/m^2\text{-sec})$$
$$= 0.21\ Pa$$

A real set of data, whether from field or laboratory annular flume, will be more difficult to work with. Complications to be expected are:

The variation of erosion rate with bed shear will not be linear, but will require some judgment and nonlinear regression to determine τ_c.

(Sheet 2 of 3)

Example Problem III-5-1 (Concluded)

You will never again have the luxury of somebody timing the settlement of the last floc, giving *w* directly. Instead, you will have to solve two or more equations with two or more unknowns, one of which is *w*.

Bed sediment density, and hence τ_c, varies with depth of erosion due to consolidation.

A natural bed will be layered, with discontinuities in consolidation and sedimentology over depth.

Water volume and depth vary with depth of erosion.

Direct measurement of bed shear is often difficult, particularly in the field laboratory where rotation of the lid of the annular flume is resisted by fluid shear, both in the flume and on the upper surface.

The area of the bed in the direct shear device (annular flume in this example) is seldom a convenient 1 m^2 or 1 ft^2.

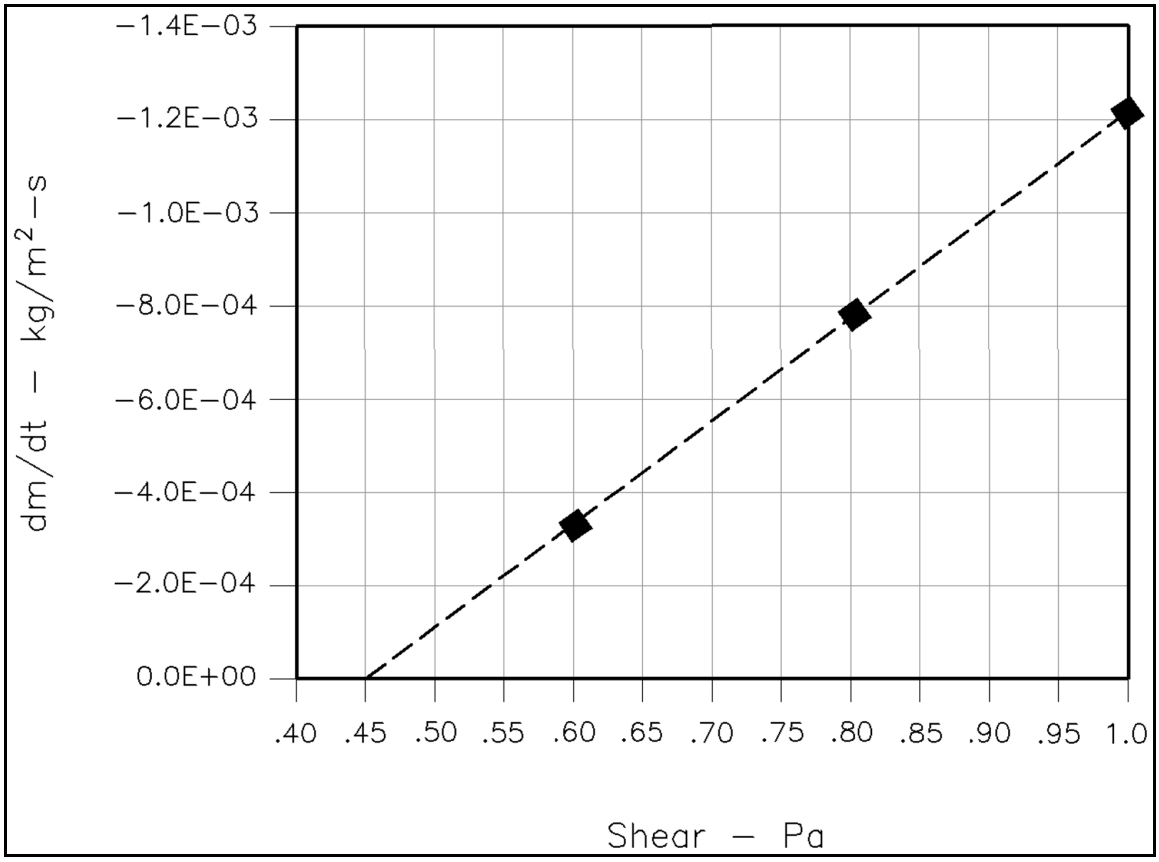

Figure III-5-25. Plot of erosion rate versus shear for example problem

(Sheet 3 of 3)

Figure III-5-26 (Lee 1995) summarizes the interactions between a mud shore and waves:

(a) At low water or under calm seas, the profile formed by the previous wave condition consolidates.

(b) Breaking waves result in mass erosion at the breaker line, with high turbidity in the surf zone; lower turbidity and surface erosion occur seaward of the breaker line, to the point where bed shear is less than the critical shear for erosion.

(c) Turbidity in the surf zone reaches that of fluid mud, flowing generally downhill offshore and collecting in troughs, under the influence of the wave orbital motion within the fluid mud.

(d) Return to (1), consolidation of the new profile under calm seas or at low water.

(3) Lee (1995) and Lee and Mehta (1994) found that wave height decays exponentially across the profile, i.e.

$$H_y = H_0 e^{-k_i y} \tag{III-5-7}$$

where

y = distance along wave ray, m (ft), positive towards shore

H_0 = incident wave height at $y = 0$, m (ft)

H_y = wave height at y, m (ft)

k_i = wave height attenuation coefficient, m^{-1} (ft^{-1})

(4) The wave height attenuation coefficient k_i characterizes the fluidization potential of the mud. It is obviously a function of the rheology of the bed; and also probably of the wave period T and incident wave height H_0. Lee (1995) and Lee and Mehta (1994) believe k_i to be a function of the local wave height, and talk of a spatial mean $\overline{k_i}$ across the profile. In practice, $\overline{k_i}$ is another calibration coefficient, like the Parthenaides coefficient, to be determined by fitting to observations of wave attenuation and profile development. A high $\overline{k_i}$ indicates a thick fluid mud layer, which Lee (1995) and Lee and Mehta (1994) associate with offshore flow on an eroding profile; a low $\overline{k_i}$, with an accreting profile. Lee (1995) quotes values of $\overline{k_i}$ in the range $0.0001 \le k_i \le 0.05$.

III-5-12. Numerical Modeling

a. Introduction.

(1) In this section, the role of numerical modeling is discussed both as an engineering tool and a planning tool. The development of numerical modeling of cohesive shore erosion is not far advanced. Nevertheless, approaches that have been utilized are briefly summarized. Numerical models are generally applied to simulate a future outcome given a known set of input conditions. For cohesive shore applications, there are at least four possibilities where numerical models can provide valuable information as follows:

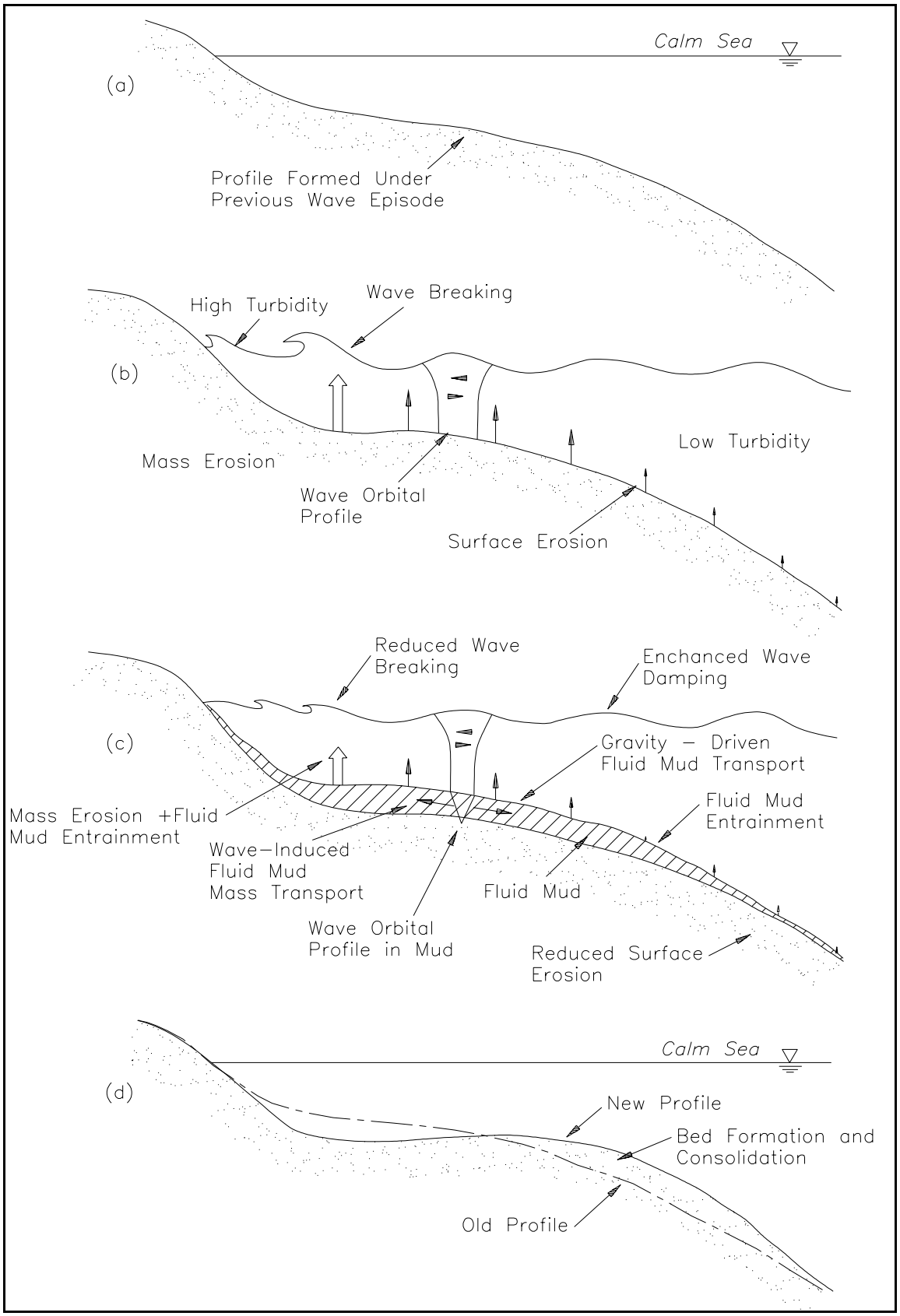

Figure III-5-26. Mud beach processes (after Lee (1995))

(a) To forecast long-term erosion rates (i.e., on the order of 50 years for developing shorelines). 'Developing shorelines' refer to areas where the evolution of a shore profile is at an early stage (e.g., newly created reservoirs). In these cases, the future rate of shoreline recession will probably differ from that experienced in the past owing to the evolving shape of the nearshore profile. Future erosion rates are required to plan setbacks and development around the new water bodies. In addition, the changing nature of the littoral zone (slopes and surficial substrate) may be important to the management of fish habitat.

(b) To forecast long-term erosion rates where either the environmental or the geologic conditions are changing due to natural or human causes. Natural influences that may change include increased storminess, sea level rise, changes to sand supply, or the changing geology encountered as the shoreline erodes. Human influences may include changes to water level fluctuations by water level regulation and reduction in the sand cover over the cohesive profile due to interruptions or reduction in sand supply to the littoral zone.

(c) To forecast the performance and potential impacts of coastal engineering works. For example, downcutting will continue offshore of the toe of a revetment constructed on a cohesive shore, and this outcome must be forecast and addressed in the design of the structure.

(d) Based on known historic recession rates and environmental conditions, numerical models can be applied to 'back-calculate' erodibility coefficients to describe the erosion resistance of a particular type of cohesive sediment. In turn, this can be used to assess future erosion rates at another site with the same sediment type but with different environmental conditions (i.e., the wave and water level climate).

(2) Therefore, there are many situations where numerical modeling would serve as an important tool for coastal engineering and coastal zone planning in cohesive shore environments.

b. Simulating erosion of consolidated sediment.

(1) Two approaches to modeling consolidated cohesive shore erosion are described in this section. Both rely on a significant degree of empiricism.

(2) The first approach is described by Penner (1993) for estimating future bank recession rates on Western Canadian lakes and reservoirs. This procedure consists of using a wave hindcast to determine the amount of wave energy that reaches a bluff face (accounting for losses over the nearshore profile). From this information and a knowledge of an erodibility coefficient, the future rate of shore recession can be determined. The erodibility coefficient relates volumetric erosion to the wave energy that reaches the bluff toe. This coefficient may be determined through back-calculation, or model calibration, for a location with known history of erosion (with the wave climate calculated by a wind-wave hindcast) or it may be estimated based on published values by others who have used this technique in the past (e.g., Penner 1993, Mollard 1986; Kachugin 1970; Newbury and McCullough 1984).

(3) Since this method essentially ignores the role of profile downcutting, it is primarily applicable to profiles that are at an early stage of development (i.e., with a very steep profile and narrow nearshore zone). In these cases, most of the wave energy is dissipated at the bluff face, in contrast to the more developed shoreline profiles on the Great Lakes and ocean coasts where the majority of wave energy is dissipated across the profile.

(4) This method has been applied to estimate the future shoreline position around new reservoirs in order to establish setback and ownership requirements. It has been refined to consider variations in erodibility of the materials encountered through time as the shoreline recedes. A table of erodibility coefficients from Penner (1993) is reproduced in Table III-5-3 below. The empirical coefficients relate wave energy that reaches the bluff toe to the weight of eroded sediment.

(5) Table III-5-3 reveals some interesting comparisons to the previous discussions of erosion processes. The high erodibility coefficient for the case of sand cover over the till confirms the importance of sand as an abrasive agent. For cases with a sand or gravel overlay, the erodibility coefficient is 2-10 times higher than the coefficients for soft and hard till. This compares well with the results of the laboratory experiments where erosion rates were increased by a factor of 3 to 8 with the introduction of sand to the flow for a range of hard and soft consolidated cohesive sediments (Part III-5-4b). Also, the category of a till bluff with a lag-protected nearshore corresponds to the slowly eroding convex profile type discussed above.

Table III-5-3
Erodibility Coefficients (from Penner (1993))

Material Type	Erodibility Coefficient (m^2/tonne)
Till with sand or gravel surficial overlay	0.0004
Soft till	0.0002
Hard till	0.00004
Till with a dense cover of surficial boulders	0.00002
Sandstone, siltstone, or shale covered with till	0.00005 to 0.0002

(6) A second approach to the numerical modeling of cohesive shore erosion is based on the conceptual model proposed by Nairn, Pinekin, and Philpott (1986). This approach relates downcutting to the shear stress generated by orbital velocities under unbroken waves and to the rate of wave energy dissipation for broken waves. The predicted downcutting determines the profile retreat rate which is assumed to determine the bluff or cliff retreat rate above water. A numerical model of coastal processes (Nairn and Southgate 1993) is used to determine the orbital velocity, the rate of wave energy dissipation, and the fraction of broken waves at locations across a nearshore profile. Erodibility coefficients relating downcutting rates to the conditions associated with broken and unbroken waves are determined in one of two ways. First, these coefficients can be back-calculated or calibrated based on a known profile retreat rate and the associated environmental conditions (i.e., the wave and water level conditions corresponding to the period of known profile retreat).

(7) Alternatively, intact cohesive sediment samples can be extracted from the study site and tested in a unidirectional flow flume as discussed in Part III-5-6a. The erodibility coefficients can then be determined based on known coefficients for sediments with a similar laboratory response. However, the latter approach is only valid for locations with similar sand cover conditions. The reason for this is that in long-term applications, the model ignores the presence of sand cover, and therefore the erodibility coefficient also accounts for the mobility and quantity of sand cover.

(8) A more detailed version of the model described in Nairn and Southgate (1993) has been developed to assess short-term erosion on cohesive profiles (i.e., over a period of weeks). This model accounts for the movement of limited quantities of sand over a hard surface. Erosion is activated in the model only where sediment transport occurs over an exposed segment of cohesive sediment. This model has been successfully tested against the laboratory wave flume data of Skafel and Bishop (1994) on cohesive profile erosion (Nairn and Southgate 1993).

(9) The numerical model described in Nairn and Southgate (1993) has been applied to assess the influence on erosion of modifications to the water level regulation on the Great Lakes. Stewart and Pope (1993) determined the potential future long-term (i.e., 50 to 100 years) profile retreat (and the associated shoreline erosion) rates for several different test sites. At each of these sites, the model was calibrated against a known profile retreat rate to determine the erodibility coefficients. These test sites featured a variety of wave exposures and profile types. For a potential lake level regulation scenario with a reduced range of water

level fluctuations (i.e., lower highs and higher lows), the long-term erosion on cohesive shores with convex profiles was found to be reduced, but the long-term erosion on concave profiles was unchanged.

c. Simulating erosion and deposition of mud.

(1) The numerical models described in *a.* above may also be used for erosion of mud shore, given a suitable choice of erodibility coefficient or critical shear for erosion. Nevertheless, these do not handle the other cohesive shore processes (transport, deposition, and consolidation), for which a full hydrodynamic model is required.

(2) Willis and Crookshank (1994) describe a bed sediment 'module' designed to be called as a subroutine to a full 1-, 2-, or 3-D model of wave and current hydrodynamics on the shore. This module applies the equations presented in this chapter to compute the exchange of sediment between the bed and the water column, at each grid point in the model, at each time-step. Because of its 'add-on' nature, it cannot deal with the intermediate state of fluid mud, for which an integrated water-sediment 3-D model is required (e.g. Le Hir 1994).

III-5-13. Engineering and Management Implications

The differences between processes on sandy and cohesive shores are fundamental to successful planning and engineering on cohesive shores. This section provides a discussion of some of the important issues.

a. Setbacks and cliff stablilization.

(1) The two most important issues in the planning and management of cohesive shores relate to implementing setbacks for development and to managing human influences on the sediment supply. Successful coastal management can sometimes avoid the need for costly shore protection structures.

(2) Many jurisdictions along U.S. shorelines impose a setback for new development consisting of some multiple of the average annual recession rate (e.g., 30 to 100 times the average annual recession rate). The purpose of the setback is to avoid the need for shore protection within the life of the new development, recognizing the irreversible and inevitable erosion that occurs along cohesive shores (and some sandy shores as well). However, this procedure may not be fully reliable, for several reasons. Most importantly, the environmental and geologic conditions that determine the recession rate can change through time both naturally (e.g., increased storminess, higher water levels, changes in erodibility as the shore erodes) and through human influences (e.g., by reducing the sand supply to the littoral zone).

b. Vegetation.

(1) Where possible, every effort should be made to replace vegetation (salt marsh, grass, mangrove) whose loss might have triggered or allowed mud shore instability (Part III-5-1b). The root system provides fiber reinforcement to the soil. Above the bed, the body of the vegetation protects the mud from shear due to currents and waves and creates a calm layer close to the bed to encourage deposition and settlement.

(2) Vegetation is required to halt mud erosion, but most vegetation cannot germinate and establish itself on an eroding or unstable shore. Some less natural form of shore protection is needed to create the conditions necessary for the vegetation to establish. This may be as simple as geotextile or willow mats imitating the root system until the natural roots can develop. But (temporary) bunds may be required to protect an area of germinating vegetation, at least until the plants can withstand currents and waves.

(3) Vegetation is also useful on consolidated cohesive shores. Brambles, for example, can help stabilize an eroding bluff or cliff against subaerial erosion while discouraging at least human traffic. However, this type of solution will only be effective in the long term if seabed or lake bed downcutting is halted.

c. Interruption to sediment supply and downdrift impacts.

(1) Another important planning requirement on cohesive shores is the management of sediment budget; specifically, human influences on sand supply. The erosion of cohesive shores results in a contribution of noncohesive sediment to the littoral sediment budget. This contribution consists of the sand and gravel-size fraction of the bluff and nearshore bottom material. There are three human influences that can reduce the sand supply:

(a) The construction of shore protection eliminates the contribution of the noncohesive fraction from the erosion of the bluff (and possibly part of the nearshore) for the protected reach of shore. On an individual-project basis, this reduction in the total supply to the littoral sediment budget may be small. However, the cumulative impact of many shore protection projects along many kilometers may be significant (as explained below).

(b) The construction of harbors, lakefills, or other projects which protrude into the lake result in large quantities of sand being trapped (in fillet beaches) and diverted offshore (once the fillet beaches have reached full capacity). Often, this sand is permanently lost from the active littoral system.

(c) Dredging or sand mining. Dredging is often required at harbor structures where sediment has been diverted offshore and deposited in navigation channels. The sand-sized portion of the dredged sediment is lost from the littoral system if it is placed outside the littoral zone (i.e., offshore, on land, or in a confined disposal facility).

It is also important to note here that sand supply can be reduced or increased through natural changes. For example, as the shore retreats, stratigraphic units containing more or less sand may be exposed to erosion.

(2) The impact of reducing the sand supply depends on the type and characteristics of the downdrift shore. Depending on the quantity of the natural sand cover along the downdrift cohesive shore, the reduction in sand supply may or may not increase the erosion rate. If the sand quantity is high (greater than approximately 150 m^3/m), the erosion rate will be increased. On the other hand, if the sand cover is already low (less than approximately 50 m^3/m), the erosion rate will probably be unaffected. Invariably, at the downdrift end of a reach of eroding consolidated shore, there is an accreting or stable sand beach deposit that receives the noncohesive fraction eroded from the bluffs. The cutoff or reduction in sand supply to this beach may trigger the onset of its erosion.

d. Remedial measures for cohesive shore erosion.

(1) In order to arrest shoreline recession on a consolidated cohesive shore, it is necessary to stop the downcutting across the profile out to a depth where the future rate of downcutting will not adversely affect the coastal protection system. Three examples of how this can be achieved are as follows:

(a) Through beach nourishment (possibly in conjunction with retaining structures such as detached breakwaters) to increase the sand cover volume to a level sufficient to protect the underlying cohesive profile under most conditions (this volume is approximately 200 m^3/m for Great Lakes shorelines).

(b) Through the construction of offshore breakwaters.

(c) Through the construction of revetment with the toe excavated a sufficient distance into the lake bed or seabed. As an alternative to excavating the toe, a toe protection berm could be placed with sufficient thickness and width to accommodate settling through erosion offshore of the toe of the berm. In most cases, this approach will lead to the eventual disappearance of beaches due to ongoing downcutting offshore of the toe of the revetment and the related steepening of the profile to an extent where sand beaches cannot be maintained naturally. Another critical issue affecting the future performance of revetments on consolidated cohesive shores is the flanking erosion of adjacent unprotected shores. The ends of the revetment may have to be periodically extended back to the shore to address flanking.

(2) One key constraint that must be considered in the design of coastal structures on consolidated cohesive shores is that the nearshore profile will continue to erode offshore of the structure. This has two potentially adverse implications for the stability and performance of the structure:

(a) The toe of the structure may be destabilized if it has not been designed to accommodate ongoing downcutting.

(b) With the deepening of the nearshore profile, the structure will be exposed to larger waves in the future. Both of these outcomes should be considered in design.

(3) Figures III-5-27 and III-5-28 demonstrate the consequences of inappropriate shore protection structures along consolidated shores. The cohesive foundations of the gravity seawall in Figure III-5-27 were undermined, causing the wall to topple. Figure III-5-28 shows that the sheet-pile wall and groin system were ineffective at preventing downcutting and arresting bluff retreat.

(4) For design purposes, the rate of foreshore lowering at any point on the profile can be determined using the profile retreat model. The required information is the approximate shape of the underlying cohesive profile and the shoreline retreat rate. Caution should be applied in using this technique since both the profile shape and the retreat rate could change in the future due to: changing stratigraphy in the foreshore, increased storminess, changes in water levels, and changes to the overlying sand cover.

e. Foundations.

(1) The foundation of structures on cohesive coasts should be assessed with respect to the stability of the underlying cohesive sediment. For locations with high bluffs or cliffs, presumably the loading associated with the structure will be much less than that associated with the bluff itself (i.e., prior to erosion).

(2) Protection of the toe of the bluff and the nearshore profile, on its own, may not be sufficient to stabilize an oversteepened bluff face. The bluff or cliff will usually be in an oversteepened condition prior to the implementation of protection (except in the case where a slope failure has recently occurred). One or more of the following three actions could be taken to address this problem:

(a) Allow the slope to naturally stabilize through surface erosion and failures, and to eventually be colonized by natural vegetation.

Figure III-5-27. A toppled concrete seawall along the Lake Michigan coast of Berrien County. Failure probably resulted from undermining of the underlying glacial till foundation, April 1991

Figure III-5-28. A steel sheet-pile wall and groin field has been ineffective at protecting this section of cohesive shore along the Berrien County shore of Lake Michigan, south of the town of St. Joseph, April 1994

Example Problem III-5-2

FIND:

A revetment is being designed to protect an eroding bluff. Find the total downcutting expected over a period of 25 years at the toe of a shore protection structure placed at a water depth of 2 m below low water on a cohesive profile.

Given:

The following information is available:

(1) The long-term bluff retreat rate is 1.0 m/year.

(2) The median grain size of the sand overlying the till is 0.2 mm, 200 μ.

Procedure:

The following steps are taken to develop a solution:

(1) Determine the shape of the underlying cohesive profile. In the absence of direct field information, the cohesive profile shape may be assumed to follow the equilibrium profile for the overlying sand as suggested by Kamphuis (1990) (Part III-5-5a).

(2) Determine the distance offshore to the toe of the revetment (i.e., at the 2-m depth contour) based on the equilibrium profile.

(3) Considering that the bluff retreat rate is equivalent to the profile retreat rate, find the depth of water for the distance determined in step 2 plus 25 m (i.e., 25 years at 1 m/year).

(4) Expected downcutting is the difference between the initial 2-m depth and the depth determined in step 3 above.

Solution:

(1) Using the information provided in Part III-3-3 and Figure III-3-17, the relationship between distance offshore (y) and depth of water (h) for a grain size of 0.2 mm is described by:

$$h = A\, y^{2/3}$$

(2) Therefore, $y = (h/A)^{1.5} = (2/0.1)^{1.5} = 89$ m

The toe of the revetment is located 89 m seaward of the shoreline after construction.

(3) After 25 years, the profile will have shifted inshore by a distance of 25 m. Of course, the erosion inshore of the revetment associated with this shift will be prevented by the presence of the revetment. However, offshore of the toe, the downcutting will continue at the historic rate. Therefore, the new depth at the toe will be the depth associated with a distance of 89 + 25 m from the shoreline (i.e., the distance from shore to the toe of the revetment had the revetment not been constructed). The new depth is calculated as follows:

$$h = A\, y^{0.67} = (0.1)\ 114^{0.67} = 2.39 \text{ m}$$

(Continued)

Example Problem III-5-2 (Concluded)

(4) Therefore, the expected downcutting over a 25-year period at the toe of the revetment in a water depth of 2 m is 0.39 m (i.e., 2.39 - 2.0).

In reality there are factors that may make this either a conservative (high) or nonconservative (low) estimate. If the revetment is located along a shore with steady sand transport, it is possible that the revetment toe may be protected from downcutting most of the time by the presence of a bar at the base of the revetment (this outcome depends very much on the site conditions, including: grain size, profile shape, and wave climate). If this is the case, the 0.39 m of lowering over 25 years may be an overestimate. On the other hand, if the cohesive sediment at the toe of the revetment is not protected by a sandbar, local scour could occur in addition to the erosion associated with profile lowering. Local scour could easily exceed 0.39 m. It is important to note that with the lowering of the offshore profile through the downcutting process, the local scour will increase with time as larger waves are able to reach the revetment. Also, this solution assumed that the nearshore profile was well described by an equilibrium profile shape. This may not be the case if the nearshore stratigraphy consists of geologic units with different erosion resistances.

The lowering at the toe of a shore protection structure built on a cohesive shore should also be considered in the design of the structure. Specifically, armor unit stability and overtopping potential should be estimated for the expected future depths associated with the design life of the structure.

(b) Accelerate the stabilization process by constructing a drainage system and through bioengineering to encourage and promote colonization of the slope by native vegetation.

(c) Control the local groundwater flows to minimize destabilizing factors at the bluff face.

(3) In some cases, the natural stable slope, with its toe at the back of the shore protection, may not be acceptable due to the proximity of development to the top of the bluff or cliff. In these cases, additional measures may be taken to achieve a steeper stable slope either through buttressing at the toe, through the implementation of drainage systems in the slope, or other measures to address the potential causes of slope failures at the site.

(4) What size of seawall can soft mud support? Even an earth dike a couple of meters high can result in an overnight slip circle failure through the 'beach' foundation, and longer-term subsidence will need to be compensated for in the design. Geotechnical considerations are of prime importance in the design of shore protection on soft shores; not just bearing (compressive) strength, but shear strength and consolidation rates as well (Part VI-5). Mud might not be able even to support heavy, land-based construction equipment. On many soft shores, mud has built up over centuries to thicknesses in excess of 30 m (100 ft), so that trenching to firm foundation may be uneconomical.

III-5-14. References

Amos et al. 1992
Amos, C. L., Daborn, G. R., Christian, H. A., Atkinson, A., and Robertson, A. 1992. "In-situ Erosion Measurements on Fine-Grained Sediments from the Bay of Fundy," *Marine Geology*, Vol 108, pp 175-196.

Anglin et al. 1996
Anglin, C. D., Nairn, R. B., Cornett, A., Dunaszegi, L., and Doucette, D. 1996. "Bridge Pier Scour Assessment for the Northumberland Strait Crossing, Canada," *Proceedings of the 25th International Conference on Coastal Engineering*, American Society of Civil Engineers, Orlando, FL.

Annandale 1995
Annandale, G. W. 1995. "Erodibility," *Journal of Hydraulic Research,* IAHR, Vol 33, No. 4, pp 471-494.

Arulanandan, Loganatham, and Krone 1975
Arulanandan, K., Loganathan, P., and Krone, R. B. 1975. "Pore and Eroding Fluid Influences on Surface Erosion of Soil," *Journal of Geotechnical Engineering*, American Society of Civil Engineers, Vol 101(GGT1), pp 51-66.

Bartz, Zaneveld, and Pak 1978
Bartz, R., Zaneveld, J. R. V., and Pak, H. 1978. "A Transmissometer for Profiling and Moored Observations in Water," *Photo-Optical Instrumentation Engineering*, Ocean Optics V, pp 102-108.

Boyce, Eyles, and Pugin 1995
Boyce, J. I., Eyles, N., and Pugin, A. 1995. "Seismic Reflection, Borehole and Outcrop Geometry of Late Wisconsin Tills at a Proposed Landfill Near Toronto, Ontario," *Canadian Journal of Earth Sciences,* Vol 32, pp 1331-1349.

Boyd 1981
Boyd, G. L. 1981. "Canada/Ontario Great Lakes Monitoring Programme Final Report," Department of Fisheries and Oceans Canada, Ocean and Aquatic Sciences Manuscript Report No 12.

Boyd 1992
Boyd, G. L. 1992. "A Descriptive Model of Shoreline Development Showing Nearshore Control of Coastal Landform Change: Late Wisconsinan to Present, Lake Huron, Canada," unpublished Ph.D. diss., Department of Geography, University of Waterloo, Ontario, Canada.

Christian, Heffler, and Davis 1993
Christian, H. A., Heffler, D. E., and Davis, E. E. 1993. "Lancelot — An in-situ Piezometer for Soft Marine Sediments," *Deep-Sea Research*, Vol 40, No. 7, pp 1509-1520.

Christie et al. 1995
Christie, M. C., Dyer, K. R., Fennessy, M. J., and Huntley, D. A. 1995. "Field Measurements of Erosion across a Shallow Water Mudflat," *Proceedings Coastal Dynamics '95*, American Society of Civil Engineers, pp 759-770.

Coakley, Rukavina, and Zeman 1986
Coakley, J. P., Rukavina, N. A., and Zeman, A. J. 1986. "Wave-Induced Subaqueous Erosion of Cohesive Tills: Preliminary Results," *Proceedings of the Symposium on Cohesive Shores*, National Research Council Canada, Associate Committee on Shorelines, pp 120-136.

Cornett, Sigouin, and Davies 1994
Cornett, C., Sigouin, N., and Davies, M. H. 1994. "Erosive Response of Northumberland Strait Till and Sedimentary Rock to Fluid Flow," Technical Report TR-1994-22, Institute for Marine Dynamics, National Research Council Canada.

Croad 1981
Croad, R. N. 1981. "Physics of Erosion of Cohesive Soils," Department of Civil Engineering, University of Auckland, New Zealand, Report 247.

Davidson-Arnott 1986
Davidson-Arnott, R. G. D. 1986. "Rates of Erosion of Till in the Nearshore Zone," *Earth Processes and Landforms,* Vol 11, pp 53-58.

Davidson-Arnott and Langham 1995
Davidson-Arnott, R. G. D., and Langham, D. R. J. 1995. "The Role of Softening in Erosion of a Nearshore Profile on a Cohesive Coast," *Proceedings of the Canadian Coastal Conference*, Canadian Coastal Science and Engineering Association, Vol 1, pp 215-224.

Dean 1977
Dean, R. G. 1977. "Equilibrium Profiles, U.S. Atlantic and Gulf Coasts," University of Delaware, Ocean Engineering Report No 12.

Edil and Bosscher 1988
Edil, T. B., and Bosscher, P. J. 1988. "Lake Shore Erosion Processes and Control," *Proceedings of the 19th Annual Conference of the International Erosion Control Association*, New Orleans, LA.

Eisma, Dyer, and van Leussen 1994
Eisma, D., Dyer, K. R., and van Leussen, W. 1994. "The In-situ Determination of the Settling Velocities of Suspended Fine-grained Sediment — A Review," *Proceedings of INTERCOH '94, 4th Nearshore and Estuarine Cohesive Sediment Transport Conference*, John Wiley & Sons, Paper No. 2.

Faas et al. 1992
Faas, R. W., Christian, H. A., Daborn, G. R., and Brylinsky, M. 1992. "Biological Control of Mass Properties of Surficial Sediments: An Example from Starrs Point Tidal Flat, Minas Basin, Bay of Fundy," *Nearshore and Estuarine Cohesive Sediment Transport*, A. J. Mehta, ed., Coastal and Estuarine Sciences No. 42, American Geophysical Union, pp 360-377.

Fleming and Summers 1986
Fleming, C. A., and Summers, L. 1986. "Artificial Headlands on the Clay Cliff," *Proceedings, Symposium on Cohesive Shores*, National Research Council Canada, Associate Committee on Shorelines, pp 262-276.

Fuller 1995
Fuller, J. A. 1995. "Shore and Lakebed Erosion: Response to Changing Levels of Lake Erie at Maumee Bay State Park, Ohio," Ohio Department of Natural Resources, Division of Geological Survey, Open-File Report 95-662.

Gibbs 1972
Gibbs, R. J. 1972. "The Accuracy of Particle Size Analysis Utilizing Settling Tubes," *Journal of Sedimentary Petrology*, Vol 42, No. 1, March, pp 141-145.

Gust 1994
Gust, G. 1994. "Interfacial Hydrodynamics and Entrainment Functions of Currently Used Erosion Devices," *Proceedings of INTERCOH '94, 4th Nearshore and Estuarine Cohesive Sediment Transport Conference*, John Wiley & Sons, Paper No. 15.

Hay and Sheng 1992
Hay, A. E., and Sheng, J. 1992. "Vertical Profiles of Suspended Sand Concentration and Size from Multifrequency Acoustic Backscatter," *Journal of Geophysical Research*, Vol 97, No. C10, October, pp 15,661-15,677.

Hay and Wilson 1994
Hay, A. E., and Wilson, D. J. 1994. "Rotary Sidescan Images of Nearshore Bedform Evolution During a Storm," *Marine Geology*, Vol 119, pp 57-65.

Hutchinson 1986
Hutchinson, J. 1986. "Behavior of Cohesive Shores," Keynote Paper, *Proceedings Symposium on Cohesive Shores*, National Research Council Canada, Associate Committee on Shorelines, pp 1-44.

Jiang and Mehta 1996
Jiang, F., and Mehta, A. J. 1996. "Mudbanks of the Southwest Coast of India; V: Wave Attenuation," *Journal of Coastal Research*, Vol 12, No. 4, pp 890-897.

Kachugin 1970
Kachugin, E.G. 1970. "Studying the Effect of Water Reservoirs on Slope Processes and their Shores," U.S. Army Cold Regions Research and Engineering Laboratory, Draft Translation 732, p 1980.

Kamphuis 1987
Kamphuis, J. W. 1987. "Recession Rate of Glacial Till Bluffs," *Journal of Waterway, Port, Coastal and Ocean Engineering*, American Society of Civil Engineers, Vol 13, No. 1, pp 60-73.

Kamphuis 1990
Kamphuis, J. W. 1990. "Influence of Sand or Gravel on the Erosion of Cohesive Sediment," *Journal of Hydraulic Research*, Vol 28, No. 1, pp 43-53.

Krishnappan 1993
Krishnappan, B. G. 1993. "Rotating Circular Flume," *Journal of Hydraulic Engineering*, American Society of Civil Engineers, Vol 119, No. 6, pp 758-767.

Krishnappan 1995
Krishnappan, B. G. 1995. "Cohesive Sediment Transport," Preliminary Proceedings of 'Issues and Directions in Hydraulics,' Iowa Institute of Hydraulic Research.

Krone 1962
Krone, R. B. 1962. "Flume Studies of the Transport of Sediment in Estuarial Shoaling Processes," University of California, Hydraulic Engineering Laboratory and Sanitary Engineering Research Laboratory.

Kuhn and Osborne 1987
Kuhn, G. G., and Osborne, R. H. 1987. 'Sea Cliff Erosion in San Diego County, California,' *Proceedings of Coastal Sediments '87*, American Society of Civil Engineers, pp 1839-1853.

Lee 1995
Lee, S.-C. 1995. "Response of Mud Shore Profiles to Waves," unpublished Ph.D. diss., University of Florida, Coastal and Ocean Engineering.

Lee and Mehta 1994
Lee, S.-C., and Mehta, A. J. 1994. "Equilibrium Hypsometry of Fine Grained Shore Profiles," *Proceedings of INTERCOH '94, 4th Nearshore and Estuarine Cohesive Sediment Transport Conference*, John Wiley and Sons, Paper No. 41.

Lefebvre, Rohan, and Douville 1985
Lefebvre, G., Rohan, K., and Douville, S. 1985. "Erosivity of Natural Intact Structured Clays: Evaluation," *Canadian Geotechnical Journal*, Vol 22, No. 4, pp 508-517.

Le Hir 1994
Le Hir, P. 1994. "Fluid and Sediment 'Integrated' Modelling: Application to Fluid Mud Flow in Estuaries," *Proceedings of INTERCOH '94, 4th Nearshore and Estuarine Cohesive Sediment Transport Conference*, John Wiley and Sons, Paper No. 40.

Mehta et al. 1989
Mehta, A. J., Carey, W. P., Hayter, E. J., Heltzel, S. B., Krone, R. B., McAnally, W. H., Jr., Parker, W. R., Schoellhamer, D., and Teeter, A. M. 1989. "Cohesive Sediment Transport: Part 1, Process Description; Part 2, Application," *Journal of Hydraulic Engineering*, American Society of Civil Engineers, August, Vol 115, No. 8, pp 1076-1112.

Mollard 1986
Mollard, J. D. 1986. "Shoreline Erosion and Slumping Studies on Prairie Lakes and Reservoirs," *Proceedings, Symposium on Cohesive Shores*, National Research Council Canada, Associate Committee on Shorelines, pp 277-291.

Nairn 1986
Nairn, R. 1986. "Physical Modeling of Wave Erosion on Cohesive Profiles," *Proceedings from the Symposium on Cohesive Shores,* Associate Committee for Research on Shoreline Erosion and Sedimentation, pp 210-225.

Nairn 1992
Nairn, R. B. 1992. "Designing for Cohesive Shores," *Proceedings Coastal Engineering in Canada*. J. W. Kamphuis, ed., Department of Civil Engineering, Queen's University, Kingston, Canada.

Nairn, Pinchin, and Philpott 1986
Nairn, R. B., Pinchin, B. M., and Philpott, K. L. 1986. "A Cohesive Coast Development Model," *Proceedings, Symposium on Cohesive Shores*, National Research Council Canada, Associate Committee on Shorelines, pp 246-261.

Nairn and Parson 1995
Nairn, R. B., and Parson, L. E. 1995. "Coastal Evolution Downdrift of St. Joseph Harbor on Lake Michigan," *Proceedings of Coastal Dynamics '95*, American Society of Civil Engineers, pp 903-914.

Nairn and Southgate 1993
Nairn, R. B., and Southgate, H. N. 1993. "Deterministic Profile Modelling of Nearshore Processes: Part II, Sediment Transport Processes and Beach Profile Development," *Coastal Engineering*, Vol 19, pp 57-96.

Newbury and McCullough 1984
Newbury, R. W., and McCullough, G. K. 1984. "Shoreline Erosion and Restabilization in the Southern Indian Lake Reservoir," *Canadian Journal of Fisheries and Aquatic Sciences,* Vol 41, pp 558-566.

Parker, Matich, and Denney 1986
Parker, G. F., Matich, M. A. J., and Denney, B. E. 1986. "Stabilization Studies — South Marine Drive Sector, Scarborough Bluffs," *Proceedings, Symposium on Cohesive Shores*, National Research Council Canada, Associate Committee on Shorelines, pp 356-377.

Parson, Morang, and Nairn 1996
Parson, L. E., Morang, A., and Nairn, R. B. 1996. "Geologic Effects on Behavior of Beach Fill and Shoreline Stability for Southeast Lake Michigan," Technical Report CERC-96-10, U.S. Army Engineer Waterways Experiment Station, Vicksburg, MS.

Parthenaides 1962
Parthenaides, E. 1962. "A Study of Erosion and Deposition of Cohesive Soils in Salt Water," unpublished Ph.D. diss., University of California, CITY.

Paterson 1994
Paterson, D. M. 1994. "Biological Mediation of Sediment Erodibility: Ecology and Physical Dynamics," *Proceedings of INTERCOH '94, 4th Nearshore and Estuarine Cohesive Sediment Transport Conference*, John Wiley and Sons, Paper No. 17.

Penner 1993
Penner, L. A. 1993. "Shore Erosion and Slumping on Western Canadian Lakes and Reservoirs — A Methodology for Estimating Future Bank Recession Rates," Environment Canada, Regina, Saskatchewan.

Philpott 1984
Philpott, K. L. 1984. "Comparison of Cohesive Coasts and Beach Coasts," *Proceedings, Coastal Engineering in Canada*, J. W. Kamphuis, ed., Queen's University, Kingston, Ontario.

Pringle 1985
Pringle, A. 1985. "Holderness Coast Erosion and the Significance of Ords," *Earth Surface Processes and Landforms*, Vol 10, pp 107-124.

Riggs, Cleary, and Snyder 1995
Riggs, S. R., Cleary, W. J., and Snyder, S. W. 1995. "Influence of Inherited Geologic Framework on Barrier Shoreface Morphology and Dynamics," *Marine Geology*, Vol 126, No. 1/4, pp 213-234.

Rohan et al. 1986
Rohan, K., Lefebvre, G., Douville, S., and Milette, J. P. 1986. "A New Technique to Evaluate Erosivity of Cohesive Material," *Geotechnical Testing Journal*, Vol 9, No. 2.

Schiereck and Booij 1995
Schiereck, G. J., and Booij, N. 1995. "Wave Transmission in Mangrove Forests," *Proceedings International Conference on Coastal and Port Engineering in Developing Countries (COPEDEC)*, Rio de Janeiro, September, pp 1969-1983.

Shabica and Pranschke 1994
Shabica, C., and Pranschke, F. 1994. "Survey of Littoral Drift Sand Deposits along the Illinois and Indiana Shores of Lake Michigan," *Journal of Great Lakes Research*, Vol 20, No. 1, pp 61-72.

Sills 1994
Sills, G. C. 1994. "Hindered Settling and Consolidation in Cohesive Sediments," *Proceedings of INTERCOH '94*, 4th Nearshore and Estuarine Cohesive Sediment Transport Conference, John Wiley and Sons, Paper No. 10.

Skafel 1995
Skafel, M. G. 1995. "Laboratory Measurement of Nearshore Velocities and Erosion of Cohesive Sediment (Till) Shorelines," *Coastal Engineering*, Vol 24, pp 343-349.

Skafel and Bishop 1994
Skafel, M. G., and Bishop, C. T. 1994. "Flume Experiments on the Erosion of Till Shores by Waves," *Coastal Engineering*, Vol 23, pp 329-348.

Sternberg, Shi, and Downing 1989
Sternberg, R. W., Shi, N. C., and Downing, J. P. 1989. "Suspended Sediment Measurements," *Nearshore Sediment Transport,* R. J. Seymour, ed., Plenum, pp 231-257.

Stewart and Pope 1993
Stewart, C. J., and Pope, J. (1993). "Erosion Processes Task Group Report," Working Committee 2, Land Use and Management. International Joint Commission, Great Lakes Water Level Reference Study.

Sunamura 1975
Sunamura, T. 1975. "A Laboratory Study of Wave-Cut Platform Formation," *Jour. Geology*, Vol 83, pp 389-397.

Sunamura 1976
Sunamura, T. 1976. "Feedback Relationship in Wave Erosion of Laboratory Rocky Coast," *Jour. Geology*, Vol 84, pp 427-37.

Sunamura 1992
Sunamura, T. 1992. *Geomorphology of Rocky Coasts*. John Wiley and Sons, England.

Thevenot and Kraus 1995
Thevenot, M. M., and Kraus, N. C. 1995. "Alongshore Sand Waves at Southampton Beach, New York: Observation and Numerical Simulation of Their Movement," *Marine Geology*, Vol 126, No. 1/4, pp 249-270.

Willis and Crookshank 1994
Willis, D. H., and Crookshank, N. L. 1994. "Modelling Multiphase Sediment Transport in Estuaries," *Proceedings of INTERCOH '94*, 4th Nearshore and Estuarine Cohesive Sediment Transport Conference, John Wiley and Sons, Paper No. 37.

Zeman 1986
Zeman, A. J. 1986. "Erodibility of Lake Erie Undisturbed Tills," *Proceedings, Symposium on Cohesive Shores*, National Research Council Canada, Associate Committee on Shorelines, pp 150-169.

III-5-15. Definition of Symbols

ρ_{fm}	Density of the fluid mud layer [force/length^3]
ρ_s	Mass density of sediment grains [force-time^2/length^4]
ρ_w	Mass density of water (salt water = 1,025 kg/m^3 or 2.0 slugs/ft^3; fresh water = 1,000kg/m^3 or 1.94 slugs/ft^3) [force-time^2/length^4]
τ	Bed shear [force/length^2]
τ_c	Critical shear for erosion or erosion threshold [force/length^2]
τ_s	Critical shear stress for deposition [force/length^2]
C	Suspended sediment concentration [force/length^3]
C_v	Consolidation coefficient [length^2/time]
D_z	Vertical dispersion coefficient [length^2/sec]
F_r	Densimetric Froude number (Equation III-5-2)
g	Gravitational acceleration (32.17 ft/sec^2, 9.807m/sec^2) [length/time^2]
h	Equilibrium beach profile depth (Equation III-3-13) [length]
H_0	Incident wave height [length]
h_{fm}	Thickness of fluid mud layer [length]
H_y	Wave height at location y [length]
$\overline{k_i}$	Spatial mean wave attenuation coefficient [length^{-1}]
k_i	Wave height attenuation coefficient [length^{-1}]
m	Mass of sediment on the bed [force/length^2]
M	Constant in the Mignoit equation (Equation III-5-5) which expresses the exponential relationship between mud density and critical shear for erosion [dimensionless]
M_p	Parthenaides coefficient [force/length^2/time]
N	Constant in the Mignoit equation (Equation III-5-5) which expresses the exponential relationship between mud density and critical shear for erosion [dimensionless]
P	Length of the drainage path [length]
S	Vertical (upward) dispersion of sediment (Equation III-5-3) [force/length^2/time]
t	Time
T	Wave period [time]

u	Degree of consolidation, ratio of bulk density of a sediment to bulk density of a fully consolidated sediment [dimensionless]
V_{fm}	Mean velocity in the fluid mud layer [length/time]
V_w	Mean velocity in the water layer [length/time]
w	Sediment fall velocity [length/time]
y	Distance along wave ray [length]
y	Equilibrium beach profile distance offshore (Equation III-3-13) [length]
z	Vertical dimension [length]

III-5-16. Acknowledgments

Authors of Chapter III-5, "Erosion, Transport, and Deposition of Cohesive Sediments:"

Robert B. Nairn, Ph.D., Baird and Associates, Oakville, Ontario, Canada.
David H. Willis, Ph.D., David H. Willis and Associates Ltd., Ottawa, Ontario, Canada.

Reviewers:

James R. Houston, Ph.D., Engineer Research and Development Center, Vicksburg, Mississippi.
Andrew Morang, Ph.D., Coastal and Hydraulics Laboratory (CHL), Engineer Research and Development Center, Vicksburg, Mississippi.
Todd L. Walton, Ph.D., CHL

Table of Contents

Page

III-6-1. Introduction III-6-1

III-6-2. Combined Wave and Current Bottom Boundary Layer Flow III-6-2
a. Introduction III-6-2
b. Current boundary layer III-6-4
c. Wave boundary layer III-6-9
(1) Introduction III-6-9
(2) Evaluation of the wave friction factor III-6-10
(3) Wave boundary layer thickness III-6-12
(4) The velocity profile III-6-12
(5) Extension to spectral waves III-6-12
(6) Dissipation III-6-17
d. Combined wave-current boundary layers III-6-17
(1) Introduction III-6-17
(2) Combined wave-current velocity profile III-6-18
(3) Combined wave-current bottom shear stress III-6-19
(4) Methodology for the solution of a combined wave-current problem III-6-20

III-6-3. Fluid-Sediment Interaction III-6-27
a. Introduction III-6-27
b. The Shields parameter III-6-28
c. Initiation of motion III-6-29
(1) Introduction III-6-29
(2) Modified Shields diagram III-6-29
(3) Modified Shields criterion III-6-31
d. Bottom roughness and ripple generation III-6-34
(1) The skin friction concept III-6-34
(2) Field data on geometry of wave-generated ripples III-6-35
(3) Prediction of ripple geometry under field conditions III-6-36
e. Moveable bed roughness III-6-36

III-6-4. Bed-load Transport III-6-37
a. Introduction III-6-37
b. Pure waves on sloping bottom III-6-42
c. Combined wave-current flows III-6-42
d. Combined current and bottom slope effect III-6-42
e. Extension to spectral waves III-6-43
f. Extension to sediment mixtures III-6-43

III-6-5. Suspended Load Transport III-6-43
a. Introduction III-6-43
b. Sediment fall velocity III-6-46
c. Reference concentration for suspended sediments III-6-47
(1) Introduction III-6-47
(2) Mean reference concentration III-6-50
(3) Wave reference concentration III-6-50
d. Concentration distribution of suspended sediment III-6-51
(1) Mean concentration distribution III-6-51
(2) Wave-associated concentration distribution III-6-51
e. Suspended load transport III-6-52
(1) Mean suspended load transport III-6-52
(2) Mean wave-associated suspended load transport III-6-53
(3) Computation of total suspended load transport for combined wave-current flows III-6-59
f. Extensions of methodology for the computation of suspended load III-6-59
(1) Extension to spectral waves III-6-59
(2) Extension to sediment mixtures III-6-59

III-6-6. Summary of Computational Procedures III-6-59
a. Problem specification III-6-59
b. Model parameters III-6-60
c. Computational procedures III-6-60

III-6-7. References III-6-63

III-6-8. Definition of Symbols III-6-66

III-6-9. Acknowledgments III-6-67

List of Figures

Page

Figure III-6-1. Turbulent boundary layer structure and mean velocity profile III-6-3

Figure III-6-2. Measured turbulent velocity profile for flow over artificial two-dimensional roughness elements (Mathisen 1993) III-6-6

Figure III-6-3. Wave friction factor diagram (a), and bottom friction phase angle (b) III-6-11

Figure III-6-4. Comparison of present model's prediction of wave orbital velocity within the wave boundary-layer with measurements by Jonsson and Carlson (1976, Test No. 1) III-6-13

Figure III-6-5. Comparison of current profile in the presence of waves predicted by present model III-6-19

Figure III-6-6. Sketch of turbulent flow with logarithmic profile over a granular bed III-6-27

Figure III-6-7. Shields diagram for initiation of motion in steady turbulent flow (from Raudkivi (1976)) III-6-30

Figure III-6-8. Modified Shields diagram (Madsen and Grant 1976) III-6-31

Figure III-6-9. Comparison of Shields curve with data on initiation of motion in oscillatory turbulent flows (Madsen and Grant 1976) III-6-32

Figure III-6-10. Conceptualization of pressure drag τ_b'', skin friction τ_b', total shear stress $\tau_b'+\tau_b''$, for turbulent flow over a rippled bed III-6-34

Figure III-6-11. Nondimensional fall velocity for spherical particles versus the sediment fluid parameter (Madsen and Grant 1976) III-6-47

Figure III-6-12. Definition sketch of coordinates, angles, and bottom slope III-6-61

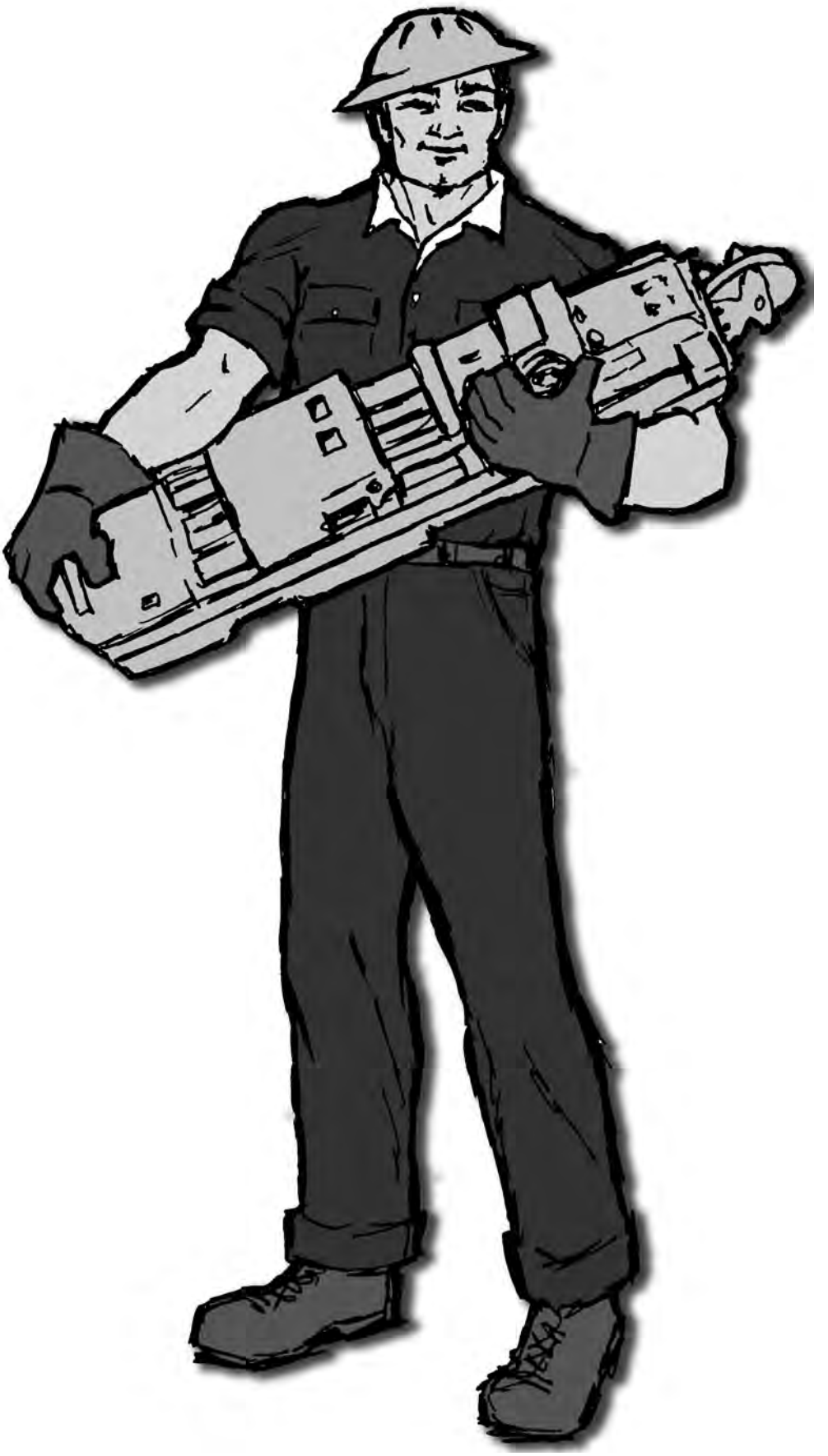

Chapter III-6
Sediment Transport Outside the Surf Zone

III-6-1. Introduction

a. Coastal engineers often regard the seaward boundary of the surf zone as the deepwater limit of significant wave and current effect. From the outer break point shoreward to the beach, waves and their associated currents are recognized as major sources of sediment resuspension and transport. Seaward of this point there is a region from roughly 2 to 3 m depth to approximately 20 to 30 m depth within which the importance of waves and currents on sediment transport processes is not well understood. Sediment transport within this region, usually referred to as the inner shelf, is the central focus of this chapter.

b. During severe coastal storms some material removed from the beach is carried offshore and deposited on the inner shelf in depths at which, under normal wave conditions, it is not resuspended. The fate of this material has, for some time, provided a troublesome set of questions for coastal engineers. Will this sediment be returned to the surf zone and perhaps even the beach or will it be carried further offshore to the deeper waters of the continental shelf? Furthermore, what are the time scales of these sediment motions, regardless of their directionality? Similar questions are relevant for sediment deposited on the inner shelf from human activities e.g., "what is the fate and transport of dredged material from inlets or navigation channels as well as contaminated sediment resulting from discharge of sewage?"). In order to answer these and similar questions related to sedimentary processes in inner shelf waters, it is necessary to establish a quantitative framework for the analysis and prediction of sediment transport processes outside the surf zone.

c. To fully appreciate the complexity of this problem it is necessary to recognize that sediment transport has been extensively studied for decades and yet it is still not possible to predict transport rates with any degree of certainty. A majority of these studies have been carried out in laboratory flumes under highly idealized conditions of steady two-dimensional flow over uniform noncohesive sand. Few studies have addressed the added complications of bed form drag, sediment concentration influence on flow, and cohesive sediment movement. On the inner shelf, as on most of the active seabed, sediment transport is a nonlinear, turbulent, two-phase flow problem complicated by bed forms, bottom material characteristics, current variability, and by the superposition of waves. In addition, transport can be comprised of bed load as well as suspended load, the quantitative separation of which is of considerable complexity.

d. The fundamental approach to predicting sediment transport is to relate the frictional force exerted by the fluid and consequent bed shear stress τ_b to the sediment transport rate q. There are two ways to address prediction of sediment transport. Empirical approaches use measurements of fluid velocity and depth as well as bottom roughness and grain size to determine proportionality relationships over a wide variety of conditions. Theoretical approaches attempt to use turbulent flow dynamics to determine the proportionality values directly. A predictive theory of turbulent flow does not exist and stochastic analysis, though useful, cannot provide an understanding of sediment transport mechanics in turbulent flows. Validating experiments must therefore be used to determine coefficients arising from assumptions incorporated into any theoretical prediction formulations. A major difficulty encountered by either the empirical or theoretical approach is the inability to adequately measure sediment transport rates. Consequently, existing formulations for predicting sediment transport rates show large discrepancies, even when they are applied to the same data (White, Milli, and Crabbe 1975; Heathershaw 1981; Dyer and Soulsby 1988).

e. The purpose of this chapter is to present an approach to the quantitative analysis and prediction of sediment transport outside the surf zone. This approach will incorporate hydrodynamics of wave-current boundary layer flow, fluid-sediment interaction near the bottom, and sediment transport mechanics.

III-6-2. Combined Wave and Current Bottom Boundary Layer Flow

a. Introduction.

(1) In inner shelf waters and over the entire continental shelf during extreme storm events, near-bottom flow will be determined by the nonlinear interaction of waves and slowly varying currents. This superposition of flows of different time scales and hence different boundary layer scales results in the wave bottom boundary layer being nested within the current boundary layer. The high turbulence intensities within the thin wave bottom boundary layer cause the current to experience a higher bottom resistance in the presence of waves than it would if waves were absent. Conversely, the wave bottom boundary layer flow will also be affected by the presence of currents, although far less so than the current is affected by the presence of waves.

(2) A 10-s wave 1 m in height produces a near-bottom orbital velocity exceeding 0.15 m/s in depths less than 30 m. Due to the oscillatory nature of the wave orbital velocity, the bottom boundary layer has only a limited time, approximately half a wave period, to grow. This results in the development of a thin layer, a few centimeters in thickness, immediately above the bottom, called the wave bottom boundary layer, within which the fluid velocity changes from its free stream value to zero at the bottom boundary. The high-velocity shear within the wave bottom boundary layer produces high levels of turbulence intensities and large bottom shear stresses.

(3) In contrast to the wave motion, a current, wind-driven or tidal, will vary over a much longer time scale, on the order of several hours. Hence, even if the current is slowly varying, the current bottom boundary layer will have a far greater vertical scale, on the order of several meters, than the wave bottom boundary layer. Consequently the velocity shear, turbulence intensities, and bottom shear stress will be much lower for a current than for wave motion of comparable velocity.

(4) The simple eddy viscosity model proposed by Grant and Madsen (1986) is adopted throughout most of this chapter in order to obtain simple closed-form, analytical expressions for combined wave-current bottom boundary layer flows and associated sediment transport. A review of alternative models, employing more sophisticated turbulence closure schemes is given in Madsen and Wikramanayake (1991). Alternative wave-current interaction theories applicable to sediment transport are: prescribed mixing length distribution (Bijker 1967), momentum deficit integral (Fredsoe 1984), and turbulent kinetic energy closure (Davies et al. 1988). All four theories are compared in Dyer and Soulsby (1988). A detailed discussion of the eddy viscosity model approach is given in Madsen (1993).

(5) Although limitations of analyses will be pointed out in each section, some major limitations applicable throughout this chapter are stated here. (a) The hydrodynamic environment is limited to *nonbreaking* wave conditions described by *linear wave theory* and near-bottom *unidirectional* steady currents. The former limitation places the applicability of results derived in this chapter well outside the surf zone, whereas the latter precludes the use of formulas presented here for flows exhibiting appreciable turning of the current velocity vector with height above the bottom. (b) Only sediment that can be characterized as *cohesionless* is considered.

(6) Most flows that transport sediment are turbulent boundary layer shear flows and the forces exerted on the sediment bed are governed by the turbulence characteristics. Over a horizontal bottom, these flows are characterized by their large scale of variation in the horizontal plane relative to the scale of variation in the vertical plane. This disparity in length scales makes it possible to neglect vertical acceleration within the boundary layer (Schlichting 1960). Figure III-6-1 shows the turbulent boundary layer structure and mean velocity profile for a two-dimensional horizontal flow in the xz-plane, x being horizontal and z vertical. The turbulent boundary layer is made up of three sublayers; the viscous sublayer, the turbulence generation layer,

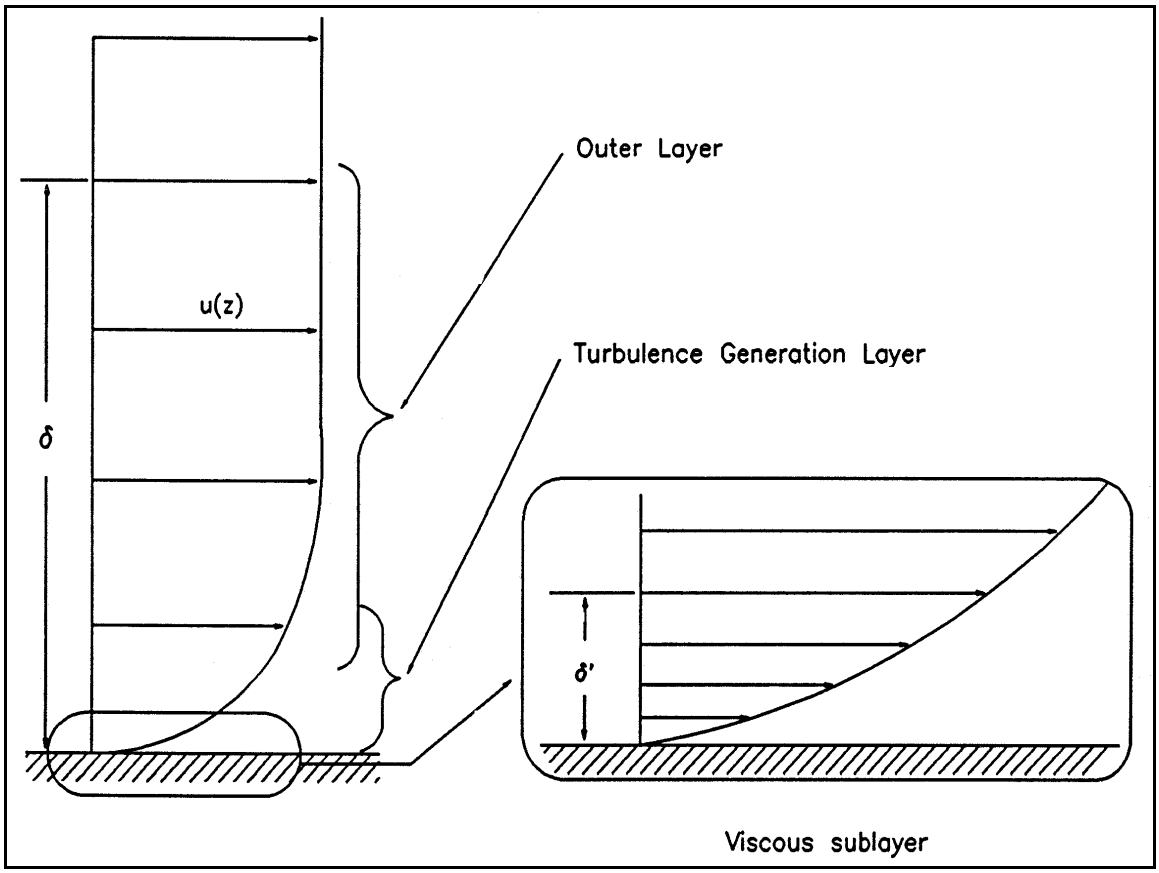

Figure III-6-1. Turbulent boundary layer structure and mean velocity profile

and the outer layer. In the viscous sublayer, turbulent fluctuations in velocity are present, but velocity fluctuations normal to the boundary must tend towards zero as the bottom is approached. Consequently, molecular transport of fluid momentum dominates turbulent transport very near the bottom and the shear stress τ can be modeled approximately by the laminar boundary layer relationship

$$\tau = \rho \nu \frac{\partial u}{\partial z} \tag{III-6-1}$$

where ρ is fluid density, ν the kinematic viscosity of the fluid, and u is horizontal velocity.

(7) The turbulence generation layer is characterized by very energetic small-scale turbulence and high fluid shear. Turbulent eddies produced in this region are carried outward and inward toward the viscous sublayer. If the bottom roughness elements (sediment grains and/or bed forms) have a height greater than the viscous sublayer, the turbulence generation layer extends all the way to the bottom.

(8) The outer layer makes up most of the turbulent boundary layer and is characterized by much larger eddies, which are more efficient at transporting momentum. This high efficiency of momentum transport produces a mean velocity profile that is much gentler than in the turbulence generation layer, Figure III-6-1.

(9) Turbulent boundary layer shear flow models can be simply developed by artificially choosing a constant ν_T (called the eddy viscosity), which is much larger than its laminar (molecular) value and that reflects the size of the eddy structure associated with the turbulent flow. This assumption results in a simple conceptual eddy viscosity model for turbulent shear stress that may be expressed as

$$\tau = \rho \nu_T \frac{\partial u}{\partial z} \tag{III-6-2a}$$

with the turbulent eddy viscosity

$$\nu_T = \kappa u_* z \tag{III-6-2b}$$

where κ is known as von Karman's constant and $u_* = (\tau_b/\rho)^{1/2}$ is called the shear velocity, where τ_b is the shear stress at the bed (z = 0). A complete derivation of this model is given in Madsen (1993).

(10) Experimental determinations have shown relatively little variation of κ, leading to von Karman's "universal" constant assumed to have the value 0.4.

b. Current boundary layer.

(1) Currents on the inner shelf can be considered to flow at a steady velocity compared to the orbital velocity of waves. Defining the shear stress due to currents τ_c, the current velocity profile can be expressed as

$$u_c = \frac{u_{*c}}{\kappa} \ln\frac{z}{z_o} \tag{III-6-3}$$

where $u_{*c} = (\tau_c/\rho)^{1/2}$ denotes the current shear velocity. Equation 6-3 is the classic logarithmic velocity profile expressed in terms of z_o, the value of z at which the logarithmic velocity profile predicts a velocity of zero. For a smooth bottom z_o = z = 0, but for a rough bottom, the actual location of the boundary is not a single value of z. Hence $z = 0$ becomes a somewhat ambiguous definition of the "theoretical" location of the bottom with some portions of the boundary actually located at $z > 0$ and others at $z < 0$. Therefore, application of Equation 6-3 in the immediate vicinity of a solid bottom is purely formal and its prediction of $u_c = 0$ at $z = z_o$ is of no physical significance.

(2) From the extensive experiments by Nikuradse (1933), the value of z_o is obtained as

$$z_0 = \begin{cases} \dfrac{\nu}{9u_*} & \text{for smooth turbulent flow} \\ \dfrac{k_n}{30} & \text{for fully rough turbulent flow} \end{cases} \tag{III-6-4}$$

in which k_n is the equivalent Nikuradse sand grain roughness, so called because Nikuradse in his experiments used smooth pipes with uniform sand grains glued to the walls, and therefore found it natural to specify the wall roughness as the sand grain diameter. Smooth or fully rough turbulent flow are delineated by Madsen (1993).

$$\frac{k_n u_*}{\nu} \geq 3.3 \quad \text{for fully rough turbulent flow}$$
$$\frac{k_n u_*}{\nu} \leq 3.3 \quad \text{for fully smooth turbulent flow} \tag{III-6-5}$$

(3) For turbulent flows over a plane bed consisting of granular material it is natural to take $k_n = D$ = diameter of the grains composing the bed. For flow over a bottom covered by distributed roughness elements (e.g., resembling a rippled bottom), the value $k_n = 30\, z_0$ is referred to as the equivalent Nikuradse sand grain roughness, with z_0 obtained by extrapolation of the logarithmic velocity distribution above the bed, to the value $z = z_0$ where u_c vanishes.

(4) Figure III-6-2 is a semilogarithmic plot of a current velocity profile obtained over a bottom consisting of 1.5-cm-high triangular bars at 10-cm spacing (Mathisen 1993). It is noticed that velocity measurements over crests and midway between crests (troughs) of the roughness elements deviate from the expected straight line within the lower 2.5 to 3 cm and further than ≈10 cm above the bottom. The near-bottom deviations reflect the proximity of the actual bottom roughness elements, which make the velocity a function of location, i.e., the flow is nonuniform immediately above the bottom roughness features. The nonlogarithmic velocity profile far from the boundary is associated with the flow being that of a developing boundary layer flow in a laboratory flume, i.e., the flow above $z \approx 10$ cm is essentially a potential flow unaffected by boundary resistance and wall turbulence.

(5) The well-defined variation of u_c versus log z (Figure III-6-2) can be applied to the case 3 cm < z < 10 cm. By extrapolation to $u_c = 0$, one obtains the value $z = z_0 \approx 0.7$ cm or $k_n = 30\, z_0 \approx 21$ cm, since the flow is rough turbulent. This example clearly illustrates that k_n, the equivalent Nikuradse sand grain roughness, is a function of bottom roughness configuration and does not necessarily reflect the physical scale of the roughness protrusions. Thus, the data shown in Figure III-6-2 were obtained for a physical roughness scale of 1.5 cm, the height of the triangular bars, and result in an equivalent Nikuradse roughness of 21 cm. This large value of k_n is, of course, associated with the much larger flow resistance produced by the triangular bars.

(6) It is often convenient to express the bottom shear stress associated with a boundary layer flow in terms of a current friction factor f_c defined by

$$\tau_c = \frac{1}{2} f_c \rho (u_c\ (z_r))^2 \tag{III-6-6}$$

(7) The somewhat cumbersome notation used in Equation 6-6 is chosen deliberately to emphasize the fact that the value of the current friction factor is a function of the reference level, $z = z_r$, at which the current velocity is specified. From Equation 6-6, the current shear velocity is obtained

$$u_{*c} = \sqrt{\frac{\tau_c}{\rho}} = \sqrt{\frac{f_c}{2}}\ u_c(z_r) \tag{III-6-7}$$

and introducing this expression in Equation 6-3, with $z = z_r$ and $\kappa = 0.4$ leads to an equation for the current friction factor

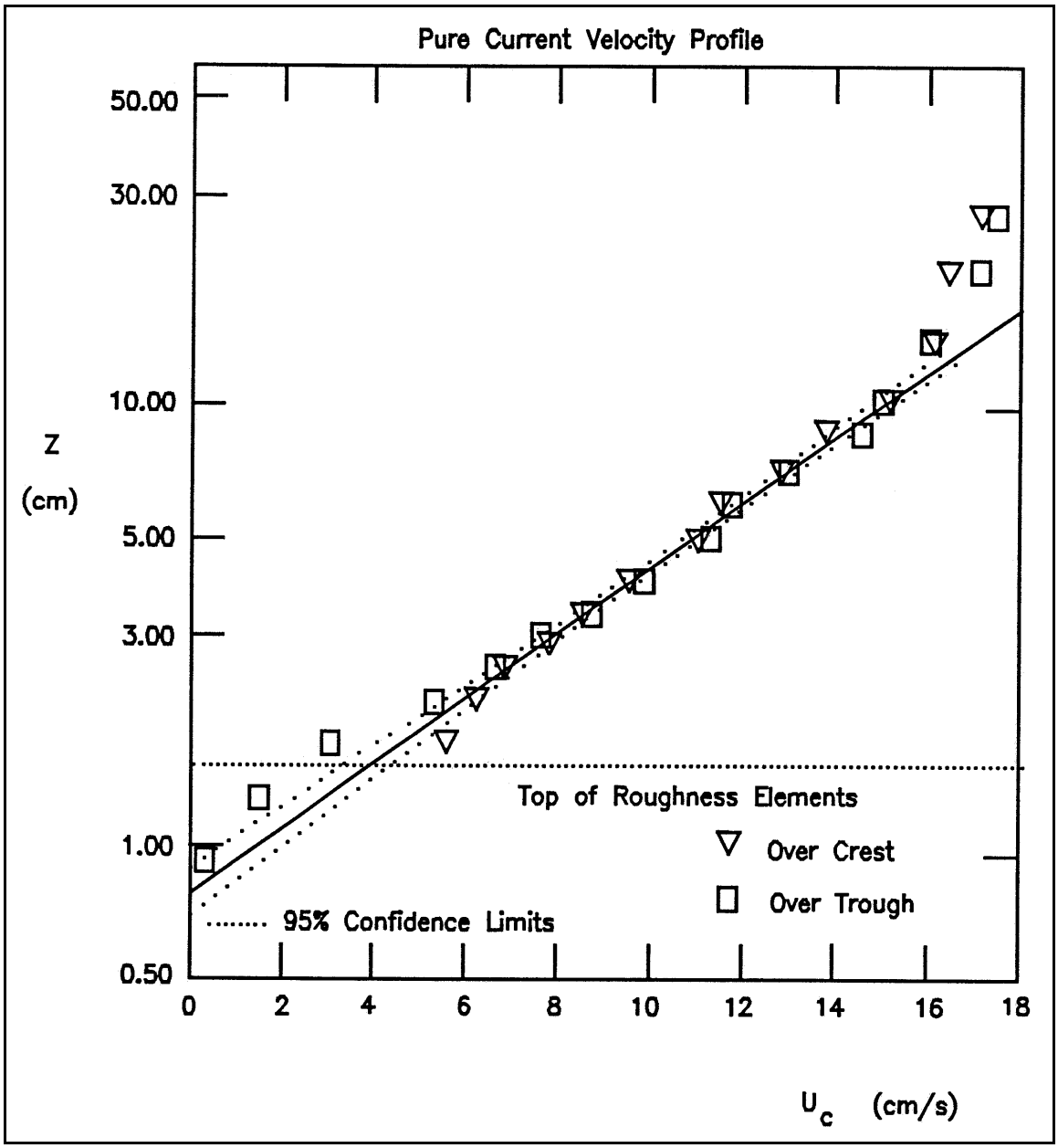

Figure III-6-2. Measured turbulent velocity profile for flow over artificial two-dimensional roughness elements (Mathisen 1993)

$$\frac{1}{4\sqrt{f_c}} \approx \log_{10} \frac{z_r}{z_0} \tag{III-6-8}$$

in terms of the reference elevation and the boundary roughness scale.

(8) For rough turbulent flows $z_0 = k_n/30$ and Equation 6-8 is an explicit equation for f_c in terms of the relative roughness z_r/k_n. For smooth turbulent flows $z_0 = \nu/(9u_{*c})$ and Equation 6-8 leads to an implicit equation for f_c (Madsen 1993)

EXAMPLE PROBLEM III-6-1

FIND:

The current friction factor f_c, the shear velocity u_{*c}, and the bottom shear stress τ_c, for a current over a flat bed.

GIVEN:

The current is specified by its velocity $u_c(z_r) = 0.35$ m/s at $z_r = 1.00$ m. The bottom is flat and consists of uniform sediment of diameter $D = 0.2$ mm. The fluid is seawater ($\rho \approx 1{,}025$ kg/m^3, $\nu \approx 1.0\times10^{-6}$ m^2/s).

PROCEDURE:

1) Start with Equation 6-4 *assuming* rough turbulent flow: $z_0 = k_n/30$.

2) Solve Equation 6-8 for f_c.

3) Obtain u_{*c} from Equation 6-7.

4) Check rough turbulent flow assumption by evaluating $k_n u_{*c}/\nu$ and using Equation 6-5.

5) *If* $k_n u_{*c}/\nu \geq 3.3$, flow *is* rough turbulent. Results (f_c and u_{*c}) obtained in steps 2 and 3 constitute the solution and τ_c is obtained from Equation 6-6 or from the definition $\tau_c = \rho u_{*c}^2$.

6) *If* $k_n u_{*c}/\nu < 3.3$, flow *is smooth turbulent* and the solution is obtained by the following iterative procedure (steps 7 and 8).

7) Obtain $z_0 = \nu/(9u_{*c})$ using u_{*c} from step 3.

8) With z_0 from step 7 return to step 2 to obtain a new f_c, and a new u_{*c} from step 3 and reenter (step 7).

9) When consecutive values of u_{*c} agree to two significant digits, iteration is complete. The last values of f_c and u_{*c} constitute the solution and τ_c is obtained from Equation 6-6 or from the definition $\tau_c = \rho u_{*c}^2$

(Continued)

Example Problem III-6-1 (Concluded)

SOLUTION:

It is first *assumed* that the flow will turn out to be classified as rough turbulent, in which case Equation 6-4 gives

$$z_0 = \frac{k_n}{30} = \frac{D}{30} = 6.67\times10^{-6} \text{ m} = 6.67\times10^{-4} \text{ cm}$$

where $k_n = D$ is chosen, since the bed is flat. With this z_0 value, Equation 6-8 is solved for f_c with $z_r = 1.00$ m, giving

$$f_c = 2.33\times10^{-3}$$

and the corresponding shear velocity is obtained from Equation 6-7 with $u_c(z_r) = 0.35$ m/s

$$u_{*c} = 1.19\times10^{-2} \text{ m/s} = 1.19 \text{ cm/s}$$

But is the flow really rough turbulent as *assumed*? To check this assumption, the boundary Reynolds number is computed using the rough turbulent estimate of u_{*c}

$$\frac{k_n u_{*c}}{\nu} = \frac{D u_{*c}}{\nu} = 2.38 < 3.3$$

From Equation 6-5 it is seen that the flow should be classified as smooth turbulent. (If $k_n u_{*c}/\nu$ had been greater than 3.3, the problem would have been solved.) Therefore, an estimate

$$z_0 = \frac{\nu}{9u_{*c}} \approx 9.3\times10^{-6} \text{ m}$$

is obtained from Equation 6-4 using the rough turbulent u_{*c}. With this value of z_0, Equation 6-8 gives the *current friction factor*

$$f_c = 2.47\times10^{-3}$$

and, from Equation 6-7, the *shear velocity* and the *bottom shear stress*

$$u_{*c} = 1.23\times10^{-2} \text{ m/s} = 1.23 \text{ cm/s and } \tau_c = \rho u_{*c}^2 = 0.155 \text{ N/m}^2 \approx 0.16 \text{ Pa}$$

Since the smooth turbulent u_{*c} obtained here is close to the rough turbulent estimate, returning with it to update $z_0 = \nu/(9u_{*c})$ and repeating the procedure does not change f_c and u_{*c} given above, so they do indeed represent the solution. An alternative solution strategy would be to compute f_c from the implicit Equation 6-9 once it was recognized that the flow was smooth turbulent.

$$\frac{1}{4\sqrt{f_c}} + \log_{10}\frac{1}{4\sqrt{f_c}} = \log_{10}\frac{z_r u_c(z_r)}{\nu} + 0.20 \qquad \text{(III-6-9)}$$

which shows f_c's dependency on a Reynolds number, $\frac{z_r u_c(z_r)}{\nu}$, when the flow is classified as smooth turbulent.

c. Wave boundary layers.

(1) Introduction. Wave boundary layers on the inner shelf are inherently unsteady due to the oscillatory nature of near-bottom wave orbital velocity. However, for typical gravity wave periods on the inner shelf, it is assumed that the boundary layer thickness, here denoted by δ_w, will be sufficiently small so that flow at the outer edge of the boundary layer may be predicted directly from linear wave theory. An extreme complication of the unsteady nature of waves arises in the application of the simple turbulent eddy viscosity model. Specifically, wave turbulent eddy viscosity becomes a time-dependent variable $u_* = (|\tau_b|/\rho)^{1/2} = u_*(t)$. However, the effect of a time-varying eddy viscosity is surprisingly small when compared with results obtained from a simple time-invariant eddy viscosity model in which $u_* = u_{*wm} = (|\tau_{wm}|/\rho)^{1/2}$ is determined from the maximum bottom wave shear stress τ_{wm}, during one wave cycle (Trowbridge and Madsen 1984). Therefore, the eddy viscosity model gives a wave shear stress

$$\tau_w = \rho \nu_t \frac{\partial u_w}{\partial z} = \rho\, \kappa\, u_{*wm}\, z \frac{\partial u_w}{\partial z} \qquad \text{(III-6-10)}$$

where u_w is the wave orbital velocity (Grant and Madsen 1979, 1986). Using Equation 6-10, applying simple linear periodic wave theory to the boundary conditions, and simplifying by taking the limiting form of the solution for the velocity profile gives

$$u_w = \frac{2}{\pi} \sin\varphi\, u_{bm} \ln\frac{z}{z_o} \cos(\omega t + \varphi) \qquad \text{(III-6-11)}$$

in which u_{bm} is the maximum near-bottom wave orbital velocity, ω is $2\pi/T$, and φ, the phase lead of near-bottom wave orbital velocity, is given by

$$\tan\varphi = \frac{\frac{\pi}{2}}{\ln\frac{\kappa u_{*wm}}{z_o \omega} - 1.15} \qquad \text{(III-6-12)}$$

From the near-bottom velocity profile, the bottom shear stress may be obtained from

$$\tau_w = \tau_{\omega m} \cos(\omega t + \varphi) \qquad \text{(III-6-13)}$$

Expressing the maximum bottom shear stress in terms of a *wave friction factor* f_w defined by Jonsson (1966)

$$\tau_{wm} = \frac{1}{2} f_w \rho u_{bm}^2 \qquad \text{(III-6-14)}$$

or equivalently

$$u_{*wm} = \sqrt{\frac{\tau_{wm}}{\rho}} = \sqrt{\frac{f_w}{2}}\, u_{bm} \tag{III-6-15}$$

Using Equations 6-10 to 6-15 and simplifying (Madsen 1993) results in an implicit equation for the wave friction factor

$$\kappa \sqrt{\frac{2}{f_w}} = \sqrt{\left(\ln \frac{\kappa \sqrt{\frac{f_w}{2}}\, u_{bm}}{z_0 \omega} - 1.15 \right)^2 + \left(\frac{\pi}{2} \right)^2} \tag{III-6-16}$$

With $\kappa = 0.4$ and recognizing that

$$A_{bm} = \frac{u_{bm}}{\omega} \tag{III-6-17}$$

is the bottom excursion amplitude predicted by linear wave theory, Equation 6-16 may be approximated by the following implicit wave friction factor relationship (Grant and Madsen 1986)

$$\frac{1}{4\sqrt{f_w}} + \log_{10} \frac{1}{4\sqrt{f_w}} = \log_{10} \frac{A_{bm}}{k_n} - 0.17 + 0.24 \left(4\sqrt{f_w} \right) \tag{III-6-18}$$

for rough turbulent flow when $k_n = 30 z_0$.

For smooth turbulent flow, $30 z_0 = 3.3\nu / u_{*wm}$ replaces k_n in Equation 6-18, which may then be written

$$\frac{1}{4\sqrt{4f_w}} + \log_{10} \frac{1}{4\sqrt{4f_w}} = \log_{10} \sqrt{\frac{\mathrm{RE}}{50}} - 0.17 + 0.06 \left(4\sqrt{4f_w} \right) \tag{III-6-19}$$

in which

$$\mathrm{RE} = \frac{u_{bm} A_{bm}}{\nu} \tag{III-6-20}$$

is a wave Reynolds number. For completeness, the wave friction factor for a *laminar wave boundary layer* is given by (Jonsson 1966)

$$f_w = \frac{2}{\sqrt{\mathrm{RE}}} \tag{III-6-21}$$

(2) Evaluation of the wave friction factor.

(a) From knowledge of the equivalent roughness k_n and wave condition A_{bm} and u_{bm}, three formulas for f_w have been presented. The choice of which f_w to select is quite simply *the largest* of the three values. In this context it is mentioned that the wave friction factors predicted for smooth turbulent and laminar flow,

Equations 6-19 and 6-21, are identical for RE $\approx 3\times10^4$, which may be taken as a reasonable value for the transition from laminar (RE $< 3\times10^4$) to turbulent flow.

(b) The evaluation of wave friction factors from Equations 6-18 and 6-19 can proceed by iteration. The iterative procedure is illustrated for Equation 6-18 by writing it in the following form

$$\frac{1}{x^{(n+1)}} = \left(\log_{10} \frac{A_{bm}}{k_n} - 0.17 \right) - \log_{10} \frac{1}{x^{(n)}} + 0.24 x^{(n)} \qquad \text{(III-6-22)}$$

with the superscript denoting the iteration step $\left(x = 4\sqrt{f_w} \right)$ and iteration started by choosing $x^{(0)} = 0.4$.

(c) It was assumed, in conjunction with the presentation of Equation 6-11 for the orbital velocity profile within the wave boundary layer, that this expression represented an approximation valid only for small values of $z_0\omega/(\kappa u_{*wm}) = (0.12/\sqrt{f_w})(k_n/A_{bm})$, i.e., for relatively large values of A_{bm}/k_n. For this reason and also because the iterative solution of the wave friction factor Equation 6-18 is rather slowly converging for $A_{bm}/k_n < 100$, Figure III-6-3 gives the exact solution for f_w and φ for $A_{bm}/k_n < 100$.

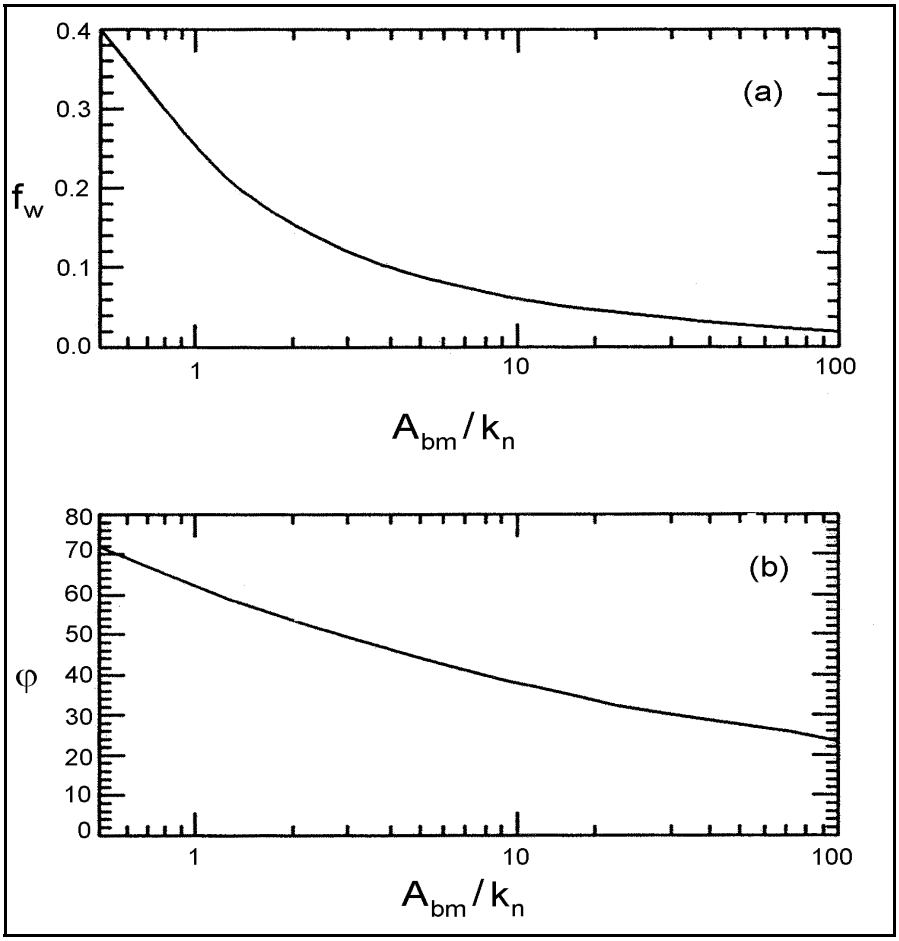

Figure III-6-3. Wave friction factor diagram (a) and bottom friction phase angle (b)

(d) For smooth turbulent boundary layer flows, Equation 6-19 may be arranged in a fashion similar to Equation 6-22, and the iterative solution proceeds as outlined above with $x = 4\sqrt{4f_w}$.

(3) Wave boundary layer thickness. From the logarithmic approximation given by Equation 6-11, which is valid only near the bottom and for large values of $\kappa u_{*wm}/(z_0\omega)$, the location for which $|u_w| = u_{bm}$ is obtained as $z \approx \kappa u_{*wm}/(\pi\omega)$. Although use of Equation 6-11 for the prediction of boundary layer thickness exceeds its validity, the results suggest

$$\delta_w = \frac{\kappa u_{*wm}}{\omega} = \kappa \sqrt{\frac{f_w}{2}}\ A_{bm} \tag{III-6-23}$$

in agreement with conclusions reached based on the complete solution to the boundary layer problem (Grant and Madsen 1986).

(4) The velocity profile.

(a) With the limitation of the validity of the velocity profile given by Equation 6-11 in mind, it is seen from Equation 6-16 that the velocity profile within the wave boundary layer may be expressed in the following extremely simple form, with an upper limit of validity given by the z value for which $|u_w| = u_{bm}$, or approximately $z = \delta_w/\pi$, i.e.,

$$u_w = \frac{\sqrt{\frac{f_w}{2}}\ u_{bm}}{\kappa} \ln \frac{z}{z_0} \cos(\omega t + \varphi) = \frac{u_{*wm}}{\kappa} \ln \frac{z}{z_0} \cos(\omega t + \varphi) \tag{III-6-24}$$

(b) Figure III-6-4 compares the experimentally obtained periodic orbital velocity amplitude within the wave boundary layer (Jonsson and Carlson 1976, Test No. 1) with the prediction afforded by the exact solution obtained from the theory presented here and the approximate solution given by Equation 6-24. Clearly, the approximate velocity profile compares favorably with both the exact and the experimental profiles near the bottom, as it should. Although some differences become apparent further from the boundary, the approximate solution provides an adequate representation of the measured profile, particularly when its intended use for the prediction of sediment transport rates is kept in mind.

(5) Extension to spectral waves.

(a) The preceding analysis of wave bottom boundary layer mechanics was based on the assumption of simple periodic waves. In reality, wind waves are more realistically represented by the superposition of several individual wave components of different frequencies and directions of propagation, i.e., by a directional wave spectrum, rather than by a single periodic component. Madsen, Poon, and Graber (1988) presented a bottom boundary layer model for waves described by their near-bottom wave orbital velocity spectrum. This reference provides the details of an analysis, the basis of which is an assumed time-invariant eddy viscosity similar to the one discussed earlier for a simple periodic wave. The analysis utilizes the near-bottom maximum orbital velocity $u_{bm,i}$ and radian frequency ω_i of the individual i^{th} wave components of the wave spectrum to calculate a single set of representative periodic wave characteristics (see Madsen (1993) for details).

(b) Given the widespread use of the significant wave concept in coastal engineering practice it is important to emphasize that the representative periodic wave characteristics defined by Madsen (1993) are not those of the significant wave, but rather those of a wave with the significant period and the

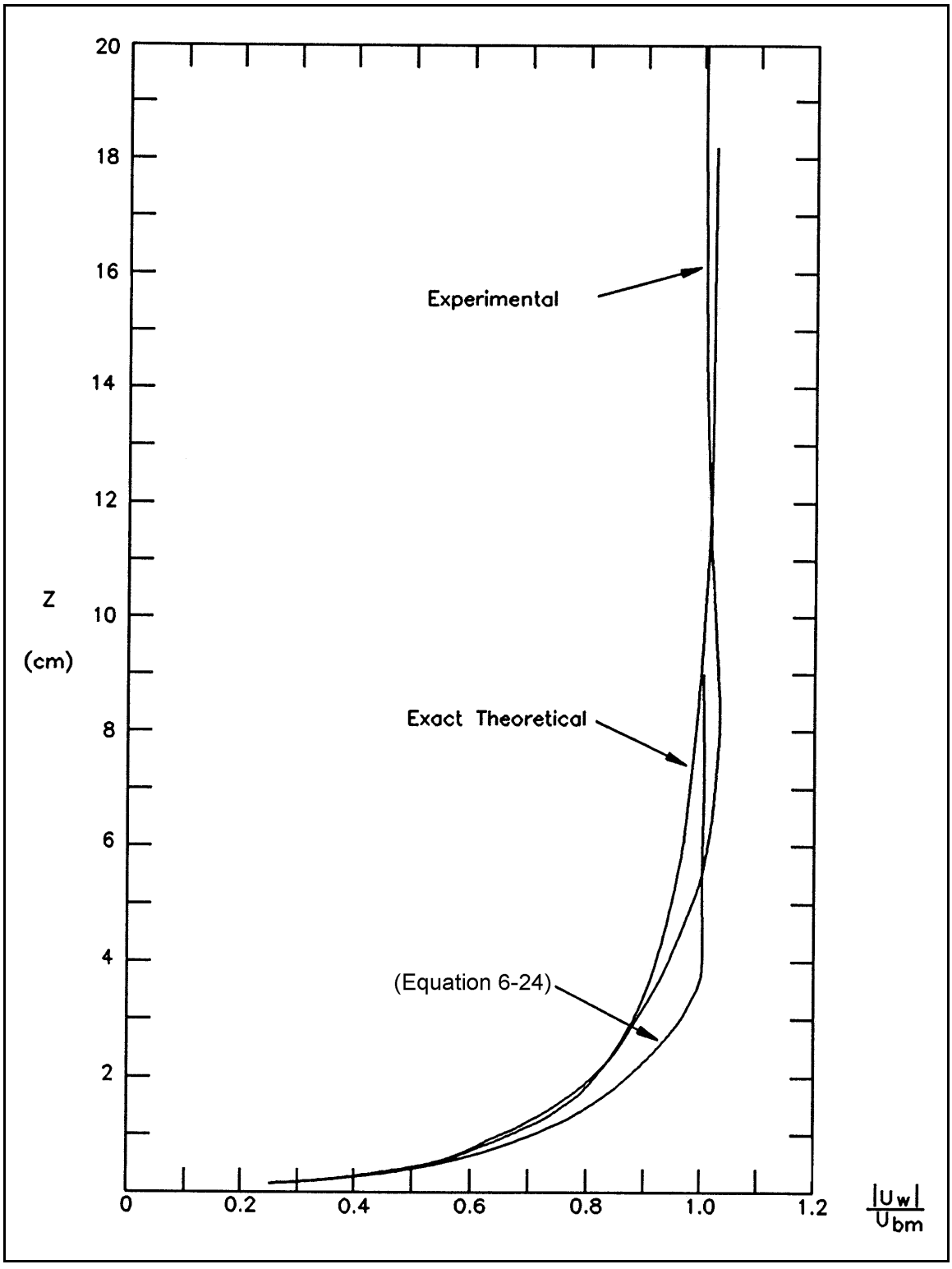

Figure III-6-4. Comparison of present model's prediction of wave orbital velocity within the wave boundary layer with measurements by Jonsson and Carlson (1976, Test No. 1)

EXAMPLE PROBLEM III-6-2

FIND:

The wave friction factor f_w, the maximum shear velocity u_{*wm}, the maximum bottom shear stress τ_{wm}, and the bottom shear stress phase angle φ, for a pure wave motion over a flat bed.

GIVEN:

The wave is specified by its near-bottom maximum orbital velocity u_{bm} = 0.35 m/s and period T = 8.0 s. The bottom is flat and consists of uniform sediment of diameter D = 0.1 mm. The fluid is seawater ($\rho \approx 1{,}025$ kg/m^3, $\nu \approx 1.0\times10^{-6}$ m^2/s).

PROCEDURE:

1) Compute bottom orbital excursion amplitude from linear wave theory: $A_{bm} = (H/2)/\sinh(2\pi h/L) = u_{bm}/\omega$, using $H = H_{rms}$ = root-mean-square wave height = $H_s/\sqrt{2}$, $\omega = 2\pi/T$ with T = significant wave period, and h = water depth. (This step is not needed here, since u_{bm} and T are specified)

2) *Assume* rough turbulent flow and solve Equation 6-18 using the iterative procedure illustrated by Equation 6-22 for f_w.

3) Obtain u_{*wm} from Equation 6-15.

4) Check rough turbulent flow assumption by evaluating $k_n u_{*wm}/\nu$ and using Equation 6-15.

5) *If* $k_n u_{*wm}/\nu \geq 3.3$, flow *is* rough turbulent. Results (f_w and u_{*cw}) obtained in steps 2 and 3 constitute the solution. τ_{wm} is obtained from Equation 6-14 or 6-15 and φ is obtained by solving Equation 6-12 with $z_0 = k_n/30$.

6) *If* $k_n u_{*wm}/\nu < 3.3$ flow *is smooth turbulent* and f_w is obtained by solving Equation 6-19 using the iterative procedure illustrated by Equation 6-22 with A_{bm}/k_n replaced by $\sqrt{RE/50}$ and $x = 4\sqrt{4f_w}$.

7) With f_w from step 6, Equation 6-15 gives u_{*wm} and τ_{wm} is obtained from Equation 6-14 or Equation 6-15.

8) With u_{*wm} from step 7, the value of $z_0 = \nu/(9u_{*wm})$ is obtained from Equation 6-15 for smooth turbulent flow.

9) The phase angle φ is calculated from Equation 6-12 using z_0 from step 8.

(Sheet 1 of 3)

Example Problem III-6-2 (Continued)

SOLUTION:

From the given wave characteristics, it follows that

$$\omega = 2\pi/T = 0.785 \text{ s}^{-1} \; ; \; A_{bm} = u_{bm}/\omega = 0.446 \text{ m} = 44.6 \text{ cm}$$

Assuming the wave boundary layer to be rough turbulent, $k_n = D = 30z_0$, and the wave friction factor is obtained by solving Equation 6-18 using the iterative procedure illustrated by Equation 6-22. For $k_n = D = 0.1$, one obtains

$$\log_{10} \frac{A_{bm}}{k_n} - 0.17 = 3.48$$

and starting with $x^{(0)} = 0.4$, Equation 6-22 gives $x^{(1)} = 0.315$ followed by $x^{(2)} = 0.327$, $x^{(3)} = 0.325$, and finally $x^{(4)} = 0.326 = 4\sqrt{f_w}$. Thus,

$$f_w = (0.326/4)^2 = 6.64 \times 10^{-3}$$

and from Equation 6-15

$$u_{*wm} = \sqrt{\frac{f_w}{2}}\, u_{bm} = 2.02 \times 10^{-2} \text{ m/s} = 2.02 \text{ cm/s}$$

This is the true solution only if the flow is rough turbulent as *assumed*, i.e., only if $k_n u_{*wm}/\nu > 3.3$. Here, $k_n = 0.1$ mm and the u_{*wm} obtained above gives

$$\frac{k_n u_{*wm}}{\nu} = 2.02 < 3.3$$

so the flow is *not rough* but smooth turbulent, i.e., f_w should be obtained from Equation 6-19 and not from Equation 6-18. Equation 6-19 may be rearranged to take the form analogous to Equation 6-22

$$\frac{1}{x^{(n+1)}} = \left(\log_{10} \sqrt{\frac{\text{RE}}{50}} - 0.17 \right) - \log_{10} \frac{1}{x^{(n)}} + 0.06 x^{(n)}$$

(Sheet 2 of 3)

Example Problem III-6-2 (Concluded)

with $x = 4\sqrt{4f_w}$ and

$$\mathrm{RE} = \frac{u_{bm}A_{bm}}{\nu} = 1.56\times10^{5}$$

Therefore

$$\left(\log_{10}\sqrt{\frac{\mathrm{RE}}{50}} - 0.17\right) = 1.58$$

and starting iteration with $x^{(0)} = 0.0$ gives $x^{(1)} = 08.29$, $x^{(2)} = 0.646$, $x^{(3)} = 0.7$,... and finally $x^{(6)} = 0.686 =$

$4\sqrt{4f_w} = 8\sqrt{f_w}$, or the *wave friction factor*

$$f_w = 7.35\times10^{-3}$$

which results in the *maximum shear velocity*

$$u_{*wm} = \sqrt{\frac{f_w}{2}}\,u_{bm} = 2.12\times10^{-2}\ \mathrm{m/s} = 2.12\ \mathrm{cm/s}$$

and a *maximum bottom shear stress*, Equation 6-32,

$$\tau_{wm} = \rho\left(u_{*wm}\right)^2 = 0.461\ \mathrm{N/m^2} = 0.46\ \mathrm{Pa}$$

The *phase angle* φ of the bottom shear stress is obtained from Equation 6-12 with

$$z_0 = \frac{\nu}{9u_{*wm}} = 5.24\times10^{-6}\ \mathrm{m}$$

obtained from Equation 6-4 for smooth turbulent flow

$$\tan\varphi = 0.242 \rightarrow \varphi = 13.6^\circ \approx 14^\circ$$

(Sheet 3 of 3)

root-mean-square wave height. Thus, for surface waves specified in terms of their significant height H_s and period T_s, the near-bottom representative periodic orbital velocity is obtained from a wave with root mean square height $H_{rms} = H_s/\sqrt{2}$, and wave period T = T_s .

(6) Dissipation. Time-averaged rate of energy dissipation in the wave bottom boundary layer is obtained from Kajiura (1968) as

$$D_p = \frac{1}{4} \rho (f_w \cos\varphi) u_{bm}^3 \tag{III-6-25}$$

for periodic waves and can be extended to spectral waves using the representative periodic wave properties as given above (Madsen, Poon, and Graber 1988).

d. Combined wave-current boundary layers.

(1) Introduction.

(a) The simple conceptual model of near-bottom turbulence suggests that the eddy viscosity immediately above the bottom is a function of time whenever the flow is unsteady. In the context of a pure wave motion, it was, however, found that assuming a time-invariant eddy viscosity, based on the maximum shear velocity, resulted in a greatly simplified analysis without sacrificing accuracy appreciably (Trowbridge and Madsen 1984). In the case of combined wave-current bottom boundary layer flows, the eddy viscosity immediately above the bottom is therefore scaled by the maximum combined wave-current shear velocity. Since the vertical extent of wave-associated turbulence is limited by the wave bottom boundary layer thickness, the wave contribution to the turbulent mixing must vanish at some level above which only the current shear velocity contributes to turbulent mixing.

(b) For the general case of combined wave-current flows with the current at an angle φ_{wc} to the direction of wave propagation, the maximum combined bottom shear stress τ_m may be obtained from

$$\begin{aligned} \tau_m &= |\boldsymbol{\tau}_{wm} + \boldsymbol{\tau}_c| \\ &= \sqrt{(\tau_{wm} + \tau_c |\cos \varphi_{wc}|)^2 + (\tau_c \sin \varphi_{wc})^2} \\ &= \tau_{wm} \sqrt{1 + 2\frac{\tau_c}{\tau_{wm}} |\cos \varphi_{wc}| + \left(\frac{\tau_c}{\tau_{wm}}\right)^2} \end{aligned} \tag{III-6-26}$$

(c) Since the boundary layer flow for combined waves and currents at an angle is three-dimensional, one should in principle solve for the horizontal velocity vector's two components. However, when the *x*-direction is chosen as the wave direction, unsteady flow will exist only in this direction. In this case it can be shown that all formulas derived for the pure wave case in Part III-6(2)c are valid also for waves in the presence of a current when u_{*wm} is replaced by u_{*m} obtained from Equation 6-26 with $u_{*m} = (\tau_m/\rho)^{1/2}$. For

example, the velocity profile is given by Equation 6-11 with u_{*wm} replaced by u_{*m}. As mentioned previously, $u_{*wm} \approx u_{*m}$, which shows that the wave motion is only weakly influenced by the presence of a current.

(d) The steady flow is entirely in the direction of the current, i.e., at an angle φ_{wc} to the wave direction. Invoking the "law of the wall," the current velocity is (for $z < \delta_{cw}$ where δ_{cw} is defined in Equation 6-38)

$$u_c = \frac{u_{*c}}{\kappa} \frac{u_{*c}}{u_{*m}} \ln \frac{z}{z_0} \tag{III-6-27}$$

and z_0 is given by Equation 6-4 with u_{*m} replacing u_*.

(e) For $z > \delta_{cw}$ the solution is

$$u_c = \frac{u_{*c}}{\kappa} \ln \frac{z}{z_{0a}} \tag{III-6-28}$$

where z_{0a} denotes an arbitrary constant of integration, referred to as the *apparent bottom roughness*. Matching the two solutions at $z = \delta_{cw}$ and introducing the expression for z_{0a} in Equation 6-28 gives an alternative form of the solution for $z > \delta_{cw}$

$$u_c = \frac{u_{*c}}{\kappa} \left(\ln \frac{z}{\delta_{cw}} + \frac{u_{*c}}{u_{*m}} \ln \frac{\delta_{cw}}{z_0} \right) \tag{III-6-29}$$

(f) These expressions clearly reveal the pronounced effect that waves may have on current velocity profiles. First of all, the velocity gradient inside the wave-current boundary layer is reduced by a factor u_{*c}/u_{*m} relative to its value in absence of waves. This, of course, is a consequence of the increased turbulence intensity within the wave boundary layer arising from the waves. In the extreme case of $u_{*c}/u_{*m} \approx 0$, u_c remains nearly zero throughout the wave boundary layer. Thus, currents in the presence of waves experience an enhanced bottom roughness (i.e., for the same current velocity at a specified level above the bottom the 0current shear velocity and shear stress will increase with wave activity).

(g) Figure III-6-5 compares a current velocity profile in the presence of waves predicted by the present wave-current interaction theory with the measured current profile (Bakker and van Doorn 1978). Two theoretical predictions are shown, one in which δ_{cw} is based on Equation 6-23 with $u_{*wm} = u_{*m}$ and another in which δ_{cw} was increased by a factor of 1.5. From the comparison, it is concluded that the definition of δ_{cw} given by Equation 6-23 may be adopted for the wave-current interaction theory presented here. This wave-current interaction theory may be applied to a wave described by its near-bottom orbital velocity spectrum by using the representative periodic wave with the direction of wave propagation chosen as the peak direction (Madsen 1993).

(2) Combined wave-current velocity profile. Having chosen the x-axis as the direction of wave propagation, the wave orbital velocity profile immediately above the bottom is given by Equation 6-11 where the phase angle φ defined by Equation 6-12 is evaluated with $u_{*wm} = u_{*m}$.

The current velocity vector is given by

$$\boldsymbol{u}_c = u_c(z) \{\cos \varphi_{wc}, \sin \varphi_{wc}\} \tag{III-6-30}$$

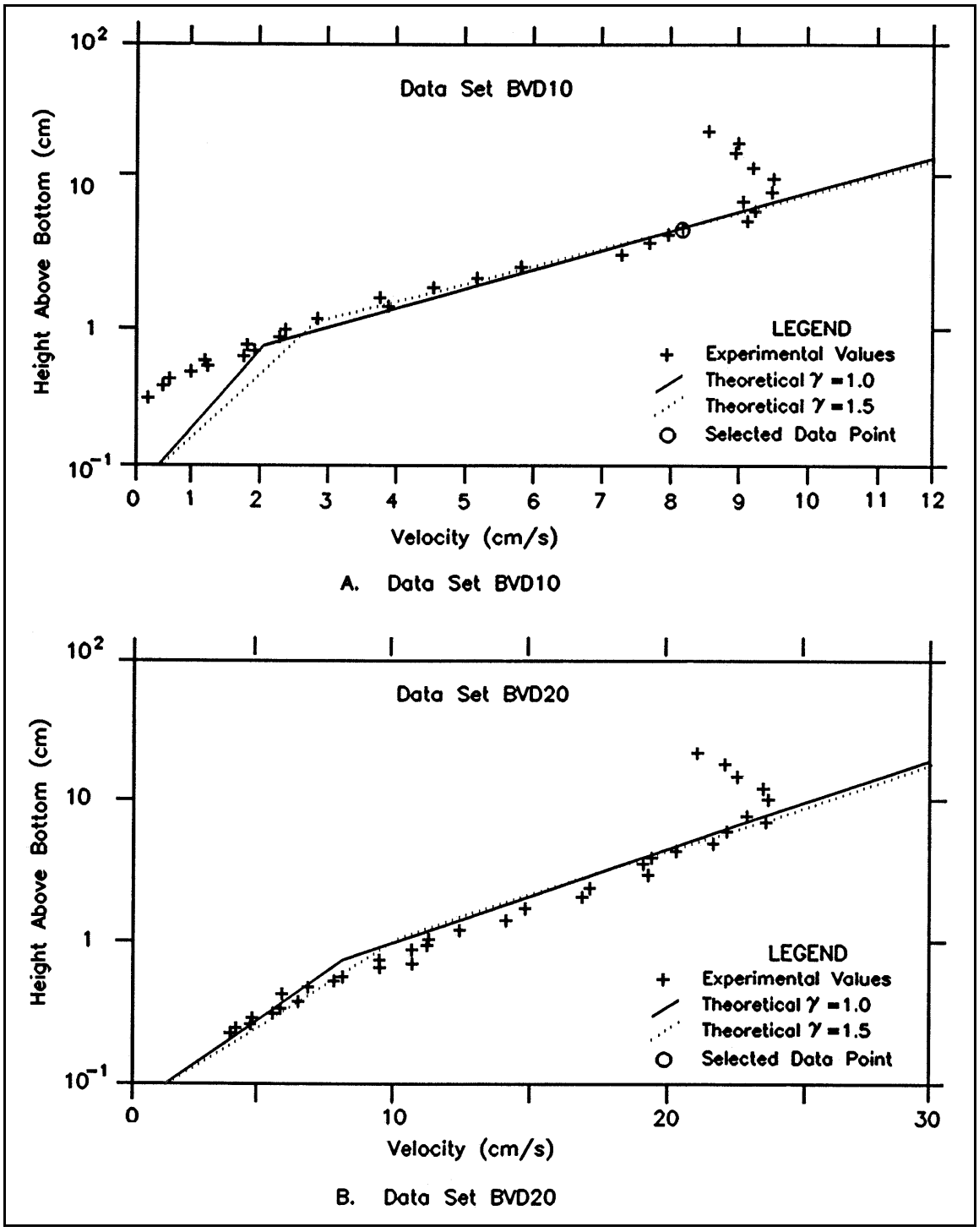

Figure III-6-5. Comparison of current profile in the presence of waves predicted by present model with measured current profile

where $u_c(z)$ is given by Equations 6-27 and 6-29.

(3) Combined wave-current bottom shear stress. Similarly, the time-varying bottom shear stress associated with combined wave-current flows may be obtained from

$$\tau_b(t) = \{\tau_{wm} \cos(\omega t + \varphi) + \tau_c \cos \varphi_{wc}, \tau_c \sin \varphi_{wc}\} \tag{III-6-31}$$

(4) Methodology for the solution of a combined wave-current problem.

(a) For a wave motion specified by u_{bm} and ω ($A_{bm} = u_{bm}/\omega$) and a bottom roughness specified by its equivalent Nikuradse roughness k_n, the pertinent formulas for the solution of a combined wave-current bottom boundary layer flow problem are the relative strengths of currents and waves

$$\mu = \frac{\tau_c}{\tau_{wm}} = \frac{u_{*c}^2}{u_{*wm}^2} \tag{III-6-32}$$

which appears in the factor relating maximum wave and maximum combined bottom shear stresses (Equation 6-26)

$$C_\mu = \sqrt{1 + 2\mu \cos \varphi_{wc} + \mu^2} \tag{III-6-33}$$

and wave friction factor formulas, given by Equations 6-18 and 6-19 for pure waves, become for combined wave-current flows (for derivation see Grant and Madsen (1986))

$$\frac{1}{4\sqrt{\frac{f_{cw}}{C_\mu}}} + \log_{10} \frac{1}{4\sqrt{\frac{f_{cw}}{C_\mu}}} = \log_{10} \frac{C_\mu A_{bm}}{k_n} - 0.17 + 0.24 \left(4\sqrt{\frac{f_{cw}}{C_\mu}} \right) \tag{III-6-34}$$

for rough turbulent flow, i.e., $k_n > 3.3\nu/u_{*m}$, and

$$\frac{1}{4\sqrt{\frac{4f_{cw}}{C_\mu}}} + \log_{10} \frac{1}{4\sqrt{\frac{4f_{cw}}{C_\mu}}} = \log_{10} \sqrt{\frac{C_\mu^2 \, \mathrm{RE}}{50}} - 0.17 + 0.06 \left(4\sqrt{\frac{4f_{cw}}{C_\mu}} \right) \tag{III-6-35}$$

for smooth turbulent flow, i.e., $k_n < 3.3\nu/u_{*m}$.

(b) The solution of Equation 6-34 or Equation 6-35 proceeds in the iterative manner illustrated by Equation 6-22 except $x = 4\sqrt{f_{cw}/C_\mu}$ replaces $x = 4\sqrt{f_w}$. Also, Figure III-6-3 may be used with $C_\mu A_{bm}/k_n$ replacing A_{bm}/k_n as entry, and the value of f_w obtained from the ordinate being interpreted as the value of f_{cw}/C_μ.

(c) The wave friction factor in the presence of currents f_{cw} is defined by

$$\frac{\tau_{wm}}{\rho} = u_{*wm}^2 = \frac{1}{2} f_{cw} u_{bm}^2 \quad \text{(III-6-36)}$$

and when Equation 6-33 is introduced in Equation 6-26, the maximum combined shear stress reads

$$\frac{\tau_m}{\rho} = u_{*m}^2 = C_\mu u_{*wm}^2 \quad \text{(III-6-37)}$$

(d) Finally, the wave boundary layer thickness is given by the modified form of Equation 6-23, i.e.,

$$\delta_{cw} = \frac{\kappa u_{*m}}{\omega} \quad \text{(III-6-38)}$$

(e) Current specified by $\boldsymbol{\tau}_c$, i.e., $\frac{\tau_c}{\rho} = u_{*c}^2$ and φ_{wc} are known.

(f) Starting with $\mu = 0, C_\mu = 1$, the wave friction factor is obtained from Equation 6-34. The values of u_{*wm}^2 and u_{*m}^2 are obtained from Equations 6-36 and 6-37. Rough turbulent flow is checked by calculating $k_n u_{*m}/\nu$. If not greater than 3.3, flow is smooth turbulent and the wave friction factor is recalculated from Equation 6-35, followed by evaluation of u_{*m}^2 and u_{*wm}^2 as before. In most cases, flow is rough turbulent and the check of rough or smooth turbulent flow is only necessary during the first iteration.

(g) With the pure wave estimate of $u_{*wm}^2 = u_{*m}^2$ in hand, one obtains updated values of μ and C_μ from Equations 6-32 and 6-33. The wave friction factor is obtained from the appropriate relationship, Equation 6-34 or Equation 6-35, by solving for f_{cw}/C_μ followed by multiplication with C_μ. Values of u_{*wm}^2 and u_{*m}^2 are obtained from Equations 6-36 and 6-37. Upon return to Equation 6-32 with the latest value of u_{*wm}^2 the procedure may be repeated until f_{cw} remains essentially unchanged from one iteration to the next. As a reasonable convergence criterion, it is recommended to calculate f_{cw} with no more than three significant figures.

(h) The wave-current interaction problem is now solved and, following evaluation of the wave boundary layer thickness δ_{cw} from Equation 6-38, the current velocity profile may be obtained from Equation 6-27 for $z \le \delta_{cw}$ and from Equation 6-29 for $z \ge \delta_{cw}$.

(i) Current specified by $\boldsymbol{u}_c$ at $z = z_r$ (i.e., $u_c(z = z_r)$) and φ_{wc} are known.

(j) Again $\mu = 0$ and $C_\mu = 1$ are used for the first iteration which proceeds as outlined under step e above. For this case, however, the first iteration is carried through determination of δ_{cw} from Equation 6-38. At this point, Equation 6-29, assuming $z_r > \delta_{cw}$, may be regarded as a quadratic equation in the unknown current shear velocity

$$\kappa u_c(z_r) = \ln \frac{z_r}{\delta_{cw}} u_{*c} + \frac{\ln \frac{\delta_{cw}}{z_0}}{u_{*m}} u_{*c}^2 \quad \text{(III-6-39)}$$

with the solution

EXAMPLE PROBLEM III-6-3

FIND:

The current shear velocity and bottom shear stress, u_{*c} and τ_c, the maximum wave shear velocity and bottom shear stress, u_{*wm} and τ_{wm}, as well as the maximum combined shear velocity and bottom shear stress, u_{*m} and τ_m, for a combined wave-current flow over a flat bed.

GIVEN:

The wave is specified by its near-bottom maximum orbital velocity u_{bm} = 0.35 m/s and period T = 8 s. The current is specified by its magnitude $u_c(z_r)$ = 0.35 m/s at z_r = 1.00 m and direction $\varphi_{wc} = 45°$ relative to the direction of wave propagation. The bottom is flat and consists of uniform sediment of diameter D = 0.2 mm. The fluid is seawater (ρ = 1,025 kg/m^3, $\nu \approx 1.0\times10^{-6}$ m^2/s).

PROCEDURE:

1) Compute wave characteristics as in step 1 of Example Problem III-6-2.

2) *Assume* rough turbulent flow and solve the wave-current interaction following the iterative procedure described in subsection III-6(2)d(4)i.

3) Check if flow is rough turbulent by evaluating $k_n u_{*m}/\nu$ with u_{*m} obtained in step 2.

4) *If* $k_n u_{*m}/\nu \geq 3.3$, flow *is* rough turbulent and values of u_{*c}, u_{*wm}, and u_{*m} obtained in step 2 constitute the solution. Bottom shear stresses are obtained from the definition of shear velocities: $\tau = \rho u_*^2$.

5) *If* $k_n u_{*m}/\nu < 3.3$ flow *is smooth turbulent* and the combined wave-current flow is solved as in step 2 except for Equation 6-35 replacing Equation 6-34 when the wave friction factor in the presence of a current is evaluated.

6) With u_{*c}, u_{*wm}, and u_{*m} from step 5, $\tau = \rho u_*^2$ is used to obtain bottom shear stresses.

SOLUTION:

For the given wave parameters, $\omega = 2\pi/T = 0.785$ s^{-1}, $A_{bm} = u_{bm}/\omega = 0.446$ m, and $k_n = D = 2\times10^{-4}$ m since the bottom is flat. Proceeding as outlined in Part III-6(2)d subsection (4)a, starting with $\mu = 0$, Equation 6-33 gives $C_\mu = 1$. *Assuming rough* turbulent flow, Equation 6-34 reduces to the exact form of the pure wave friction factor Equation 6-18 whose solution is obtained iteratively using Equation 6-22 (see Example Problem III-6-2) as

$$f_{cw} = f_w = 7.86\times10^{-3}$$

The maximum shear velocity is given by Equation 6-37, i.e.,

$$u_{*m} = \sqrt{C_\mu}\, u_{*wm} = u_{*wm} = \sqrt{\frac{f_{cw}}{2}}\, u_{bm} = 2.19\times10^{-2} \text{ m/s} = 2.19 \text{ cm/s}$$

(Continued)

Example Problem III-6-3 (Concluded)

since C_μ is currently assumed to be 1. From $k_n u_{*m}/\nu = 4.38$ it follows that the flow indeed is *rough* turbulent *as assumed*. (If $k_n u_{*m}/\nu < 3.3$, one would have to return and compute f_{cw} from Equation 6-35.) It therefore follows from Equation 6-38 that

$$\delta_{cw} = 1.12\times10^{-2} \text{ m} = 1.12 \text{ cm}$$

With these values and $z_0 = k_n/30 = D/30 = 6.67\times10^{-6}$ m, Equation 6-40 is solved to give a first estimate of the current shear velocity

$$u_{*c} = 1.47\times10^{-2} \text{ m/s} = 1.47 \text{ cm/s}$$

Using the first estimates of $u_{*c} = 1.47$ cm/s and $u_{*wm} = 2.19$ cm/s, Equation 6-32 gives

$$\mu = \left(\frac{u_{*c}}{u_{*wm}} \right)^2 = 0.45$$

and with $\varphi_{wc} = 45°$, Equation 6-33 gives $C_\mu = 1.36$.

To solve Equation 6-34 for the wave friction factor in the presence of a current f_{cw}, it is rearranged in a manner identical to Equation 6-22, i.e.,

$$\frac{1}{x^{(n+1)}} = \left(\log_{10} \frac{C_\mu A_{bm}}{k_n} - 0.17 \right) - \log_{10} \frac{1}{x^{(n)}} + 0.24 x^{(n)}$$

with $x = 4\sqrt{f_w/C_\mu}$. Solving iteratively starting with $x^{(0)} = 0.4$ gives $x^{(4)} = 0.342 = 4\sqrt{f_w/C_\mu}$, or

$$f_{cw} = (x/4)^2 C_\mu = 9.94\times10^{-3}$$

The value of the wave shear velocity is now obtained from Equation 6-36

$$u_{*wm} = \sqrt{\frac{f_{cw}}{2}}\, u_{bm} = 2.47\times10^{-2} \text{ m/s} = 2.47 \text{ cm/s} \quad \text{and} \quad \tau_{wm} = \rho u_{*wm}^2 = 0.624 \text{ Pa}$$

followed by

$$u_{*m} = \sqrt{C_\mu}\, u_{*wm} = 2.88\times10^{-2} \text{ m/s} = 2.88 \text{ cm/s} \quad \text{and} \quad \tau_m = \rho u_{*m}^2 = 0.850 \text{ Pa}$$

from Equation 6-37 and

$$\delta_{cw} = \frac{\kappa u_{*m}}{\omega} = 1.47\times10^{-2} \text{ m} = 1.47 \text{ cm}$$

With these values in hand, Equation 6-40 gives a second estimate of the current shear velocity

$$u_{*c} = 1.63\times10^{-2} \text{ m/s} = 1.63 \text{ cm/s} \quad \text{and} \quad \tau_c = \rho u_{*c}^2 = 0.272 \text{ Pa}$$

EXAMPLE PROBLEM III-6-4

FIND:

The current shear velocity u_{*c}, the maximum wave shear velocity u_{*wm}, the maximum combined shear velocity u_{*m}, and the wave boundary layer thickness δ_{cw} for a combined wave-current turbulent boundary layer flow.

GIVEN:

The wave is specified by its near-bottom maximum orbital velocity u_{bm} = 0.35 m/s and period T = 8.0 s. The current is specified by its magnitude u_c = 0.35 m/s at z_r = 1.00 m and direction $\varphi_{wc} = 45°$ relative to the direction of wave propagation. The equivalent Nikuradse roughness of the bottom is k_n = 4.4 cm. The fluid is seawater (ρ = 1,025 kg/m^3, $\nu \approx 10^{-6}$ m^2/s).

PROCEDURE:

Identical to Example Problem III-6-3. However, the iterative solution of the wave friction factor in Equation 6-34 is started with an initial value obtained from Figure III-6-3 to speed up convergence.

SOLUTION:

For the given wave parameters $\omega = 2\pi/T = 0.785$ s^{-1} and $A_{bm} = u_{bm}/\omega = 0.446$ m, the procedure to follow is identical to that used in Example Problem III-6-3, except that here

$$\frac{A_{bm}}{k_n} = \frac{0.446}{0.044} \approx 10$$

is much smaller. Therefore, during the first iteration (with $\mu = 0$ and $C_\mu = 1$) the wave friction factor is obtained from Figure III-6-3

$$f_w = f_{cw} \approx 0.058$$

instead of solving Equation 6-34. The pure wave approximation therefore gives

$$u_{*wm} = u_{*m} = \sqrt{\frac{f_w}{2}}\, u_{bm} = 5.96 \text{ cm/s}$$

and

$$\delta_{cw} = \frac{\kappa u_{*wm}}{\omega} = 3.04 \text{ cm}$$

With these values, the first estimate of the current shear velocity is obtained from Equation 6-40

$$u_{*c} = 2.84 \text{ cm/s}$$

(Continued)

Example Problem III-6-4 (Concluded)

An updated value of μ is then

$$\mu = \left(\frac{u_{*c}}{u_{*wm}} \right)^2 = 0.23$$

and from Equation 6-33

$$C_\mu = 1.17$$

Recognizing that Equation 6-34 is identical to the pure wave friction factor (Equation 6-18) if $C_\mu A_{bm}/k_n$ replaces A_{bm}/k_n and f_{cw}/C_μ replaces f_w, the value of f_{cw}/C_μ may be read off Figure III-6-3 when $C_\mu A_{bm}/k_n = 11.7$ is used as an entry. In this manner

$$f_{cw}/C_\mu \approx 0.053 \rightarrow f_{cw} \approx 0.062$$

is obtained. Clearly, the accuracy of the reading obtained from Figure III-6-3 is not impressive, so the value is regarded only as a rough estimate. From Equation 6-36, Equation 6-37, and Equation 6-38, it follows that

$$u_{*wm} = 6.16 \text{ cm/s}, \; u_{*m} = 6.67 \text{ cm/s}, \; \delta_{cw} = 3.40 \text{ cm}$$

and from Equation 6-40

$$u_{*c} = 2.94 \text{ cm/s}$$

With these values $\mu = (u_{*c}/u_{*wm})^2 = 0.23$, i.e., the iteration is complete.

So the solution is $u_{*c} = 2.94$ cm/s, $\tau_c = \rho u_{*c}^2 = 0.89$ Pa, $u_{*wm} = 6.16$ cm/s, $\tau_{wm} = \rho u_{*wm}^2 = 3.89$ Pa, $u_{*m} = 6.67$ cm/s, $\tau_m = \rho u_{*m}^2 = 4.56$ Pa, and $\delta_{cw} = 3.40$ cm.

EXAMPLE PROBLEM III-6-5

FIND:

The current velocity $u_c(\delta_{cw})$ at $z = \delta_{cw}$, the apparent roughness z_{0a}, and the phase angle of the wave-associated bottom shear stress for a combined wave-current bottom boundary layer flow.

GIVEN:

Wave, current, and bottom roughness are as specified in Example Problem III-6-4.

PROCEDURE:

1) Solve the wave-current interaction problem following the procedure described for Example Problem III-6-4.

2) With u_{*m}, from step 1 δ_{cw} is obtained from Equation 6-38.

3) $u_c\,(z = \delta_{cw})$ is obtained from Equation 6-27 with $z = \delta_{cw}$ obtained in step 2 and $z_0 = k_n/30$ since flow is rough turbulent. If flow had been smooth turbulent, i.e., $k_n u_{*m}/\nu < 3.3$, Equation 6-27 is used with $z_0 = \nu/(9u_{*m})$ as given by Equation 6-5.

4) Equation 6-28 is solved for z_{0a} using u_{*c} from step 1, $z = \delta_{cw}$ from step 2, and $u_c = u_c(z = \delta_{cw})$ from step 3.

5) The phase angle φ is obtained from Equation 6-12 with u_{*wm} replaced by u_{*m} from step 1 and $z_0 = k_n/30$.

SOLUTION:

With u_{*c} = 2.94 cm/s, u_{*m} = 6.67 cm/s, and δ_{cw} = 3.40 cm from Example Problem III-6-4, Equation 6-27 gives (with $z_0 = k_n/30$ = 4.4/30 cm)

$$u_c(\delta_{cw}) = \frac{u_{*c}}{\kappa}\,\frac{u_{*c}}{u_{*m}}\,\ln\frac{\delta_{cw}}{z_0} = 10.2 \text{ cm/s}$$

By matching this with the expression for the current velocity profile outside the boundary layer (Equation 6-28) one obtains

$$u_c(\delta_{cw}) = \frac{u_{*c}}{\kappa}\,\ln\frac{\delta_{cw}}{z_{0a}} \quad \text{and solving for } z_{0a} \text{ gives} \quad z_{0a} = 0.85 \text{ cm/s}$$

The phase of the wave-associated bottom shear stress is obtained from Equation 6-12 with u_{*wm} replaced by u_{*m}, i.e.,

$$\tan\varphi = 0.79 \rightarrow \varphi = 38^\circ$$

$$u_{*c} = u_{*m} \frac{\ln \dfrac{z_r}{\delta_{cw}}}{\ln \dfrac{\delta_{cw}}{z_0}} \left[-\frac{1}{2} + \sqrt{\frac{1}{4} + \kappa \frac{u_c(z_r)}{u_{*m}} \frac{\ln \dfrac{\delta_{cw}}{z_0}}{\left(\ln \dfrac{z_r}{\delta_{cw}} \right)^2}} \right] \tag{III-6-40}$$

(k) Having now obtained an estimate of u_{*_c}, returning to Equation 6-32 with $u_{*_{wm}}$ known from the first iteration, the value of μ is updated. With this updated value of μ, the entire procedure is repeated until a new value of u_{*_c} is obtained. For this iteration, convergence of μ to no more than two significant digits is recommended.

(l) The theoretical predictions shown in Figure III-6-5 were obtained in this manner using the indicated data point to specify the current.

III-6-3. Fluid-Sediment Interaction

a. Introduction.

(1) In Part III-6-2, the purely hydrodynamic problem of turbulent bottom boundary layer flows was treated. There it was found that the fluid-bottom interaction could be represented by a bottom shear stress $\boldsymbol{\tau}_b$, which, for the general case of combined wave-current flows, is given by Equation 6-31. Since the wave component $\tau_{wm}\cos(\omega t + \varphi)$ and the current component τ_c are both associated with logarithmic velocity profiles immediately above the bottom, Equations 6-24 and 6-27, respectively, the combined velocity immediately above the bottom is logarithmic.

(2) For a bottom consisting of a granular material, the physical flow condition in the vicinity of the individual grains is sketched in Figure III-6-6. Recalling that the logarithmic velocity profile in this region is merely an extrapolation from flow conditions obtained further from the boundary, it is evident that the actual resistance experienced by the flow is not a uniformly distributed force per unit horizontal area, but rather a sum of drag forces on individual grains (roughness elements). Thus, in reality

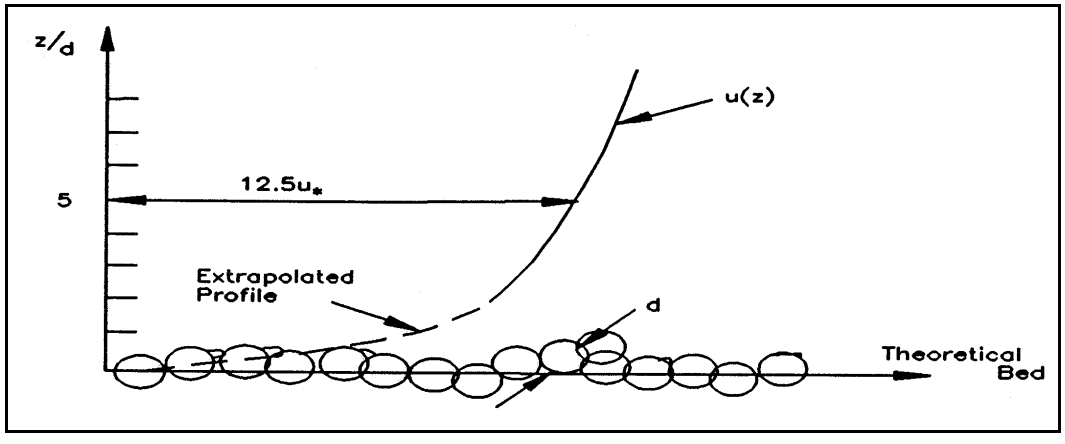

Figure III-6-6. Sketch of turbulent flows with logarithmic profile over granular bed

$$\tau_b = \sum_{\substack{\text{unit} \\ \text{area}}} \bar{F}_{D,\text{grain}}$$

(3) Not until a level somewhat above the individual roughness elements is it reasonable to assume that eddies, forming around individual grains and ejected into the flow, have merged to produce a turbulent shear flow of the type considered in the conceptual model of turbulent shear stresses presented in Part III-6-2.

(4) In addition to the spatial variation of the actual interaction between a turbulent flow and a granular bottom, it should also be kept in mind that a turbulent flow, even for a *steady* current, is inherently *unsteady*. The logarithmic velocity profile represents the time-averaged velocity profile with high-frequency turbulent fluctuations being removed by the averaging process. The drag force on individual grains is therefore not constant but varies with time due to turbulent fluctuations. The drag forces on individual grains are therefore average values as suggested by the overbar notation.

(5) It is evident from the description above that the complex nature of interaction between a flowing fluid and the individual grains on the fluid-sediment interface defies rigorous mathematical treatment unless a hydrodynamic model is employed which resolves the flow structure around individual grains including temporal variation associated with turbulent fluctuations. Since such a detailed hydrodynamic model is not available at present, we are forced to adopt heuristic, physically based conceptual models consistent with the level of our flow description to "derive" quantitative relationships for fluid-sediment interaction, and rely on empirical evidence to determine "constants" that are necessary to render the relationships predictive.

b. The Shields parameter.

(1) From the preceding discussion of the nature of near-bottom turbulent flows, it follows that the bottom shear stress may be taken as an expression for the drag force, i.e., the mobilizing force, acting on individual sediment grains on the bed surface. For a sediment of diameter D there are approximately $1/D^2$ grains per unit area, so

$$\bar{\bar{F}}_{D,grain} \propto \tau_b D^2 \tag{III-6-41}$$

where the double overbar indicates a temporal, as well as a spatial, average.

(2) For a *cohesionless sediment* the individual sediment grains rest and stay on the bottom due to their submerged weight and resist horizontal motion due to the presence of neighboring grains. Thus, for a cohesionless sediment, the stabilizing force is associated with the submerged weight of the individual grains

$$W_{grain} \propto (\rho_s - \rho) g D^3 \tag{III-6-42}$$

where ρ_s denotes the density of the sediment material ($\rho_s \approx 2{,}650$ kg/m^3 for quartz).

(3) The ratio of mobilizing (drag) and stabilizing (submerged weight) forces is of fundamental physical significance in fluid-sediment interaction for *cohesionless sediment*. This ratio is known as the *Shields parameter* (Shields 1936)

$$\psi = \frac{\tau_b}{(\rho_s - \rho) g D} = \frac{\tau_b}{(s - 1) \rho g D} = \frac{u_*^2}{(s - 1) g D} \tag{III-6-43}$$

in which $s = \rho_s/\rho$ is the density of the sediment relative to that of the fluid.

c. Initiation of motion.

(1) Introduction.

(a) For a turbulent flow over a flat bed consisting of cohesionless sediment of diameter D the equivalent Nikuradse sand grain roughness is $k_n = D$. From the discussion of turbulent boundary layer flows it was found that the roughness scale experienced by the flow, z_0 as given by Equation 6-5, depends on whether the flow is characterized as smooth or rough turbulent. The parameter determining the characteristics of the near-bottom flow and hence the mobilizing force acting on individual sediment grains is the *boundary Reynolds number*

$$\mathrm{Re}_* = \frac{u_* k_n}{\nu} = \frac{u_* D}{\nu} \tag{III-6-44}$$

(b) From simple physical considerations it therefore follows that the conditions of neutral stability of a sediment grain on the fluid-sediment interface may be expressed as a *critical value of the Shields parameter*

$$\psi_{cr} = \frac{\tau_{cr}}{(s - 1)\rho g D} = \frac{u_{*cr}^2}{(s - 1) g D} = f(\mathrm{Re}_*) \tag{III-6-45}$$

where $f(\mathrm{Re}_*)$, which is obtained from models or from experimental data, denotes some function of Re_*. Figure III-6-7 shows the traditional Shields diagram given by Equation 6-45 with supporting data obtained from uniform steady flow experiments (Raudkivi 1976). It shows that $\psi_{cr} \approx 0.06$ is approximately constant for $\mathrm{Re}_* > 100$, i.e., for fully rough turbulent flow, whereas the critical Shields parameter increases steadily from a minimum of 0.035 for values of $\mathrm{Re}_* < 10$, i.e., essentially corresponding to smooth turbulent flow conditions.

(c) In establishing the critical condition for initiation of motion, also referred to as threshold or incipient motion condition (expressed formally by Equation 6-45), it is important to keep in mind the nature of fluid-sediment interaction. For values of $\psi > \psi_{cr}$, mobilizing forces exceed stabilizing forces and sediment motion occurs. This does not mean that for $\psi < \psi_{cr}$ by a small amount, sediment does not move at all. For turbulent flow conditions in the vicinity of $\psi \approx \psi_{cr}$, the arrival of particularly strong turbulent eddies from the turbulence generation layer may momentarily increase the drag on one or a few sediment grains and, if the response time of the individual grains is shorter than the duration of this pulse, a few grains may be dislodged (i.e., a movement of the sediment may occur).The empirical curve on a ψ versus Re_* diagram that expresses the critical condition (i.e., the Shields curve or the Shields criterion) should therefore be interpreted as representing a "gray area" around the curve itself. For flow conditions within this gray area, sediment movement may take place but it becomes increasingly sporadic as ψ drops below the curve defining ψ_{cr}.

(2) Modified Shields diagram.

(a) In order to predict the flow condition that will cause sediment motion for a given sediment (i.e., s and D known) the traditional Shields curve given by Equation 6-45 or Figure III-6-7 is somewhat cumbersome to use, since the flow characteristic of interest (u_{*cr}) is involved in both parameters. This problem can be circumvented by recognizing that the Shields curve defines a unique relationship between ψ_{cr} and Re_*. Thus, from the definition of ψ_{cr} (Equation 6-45), one obtains

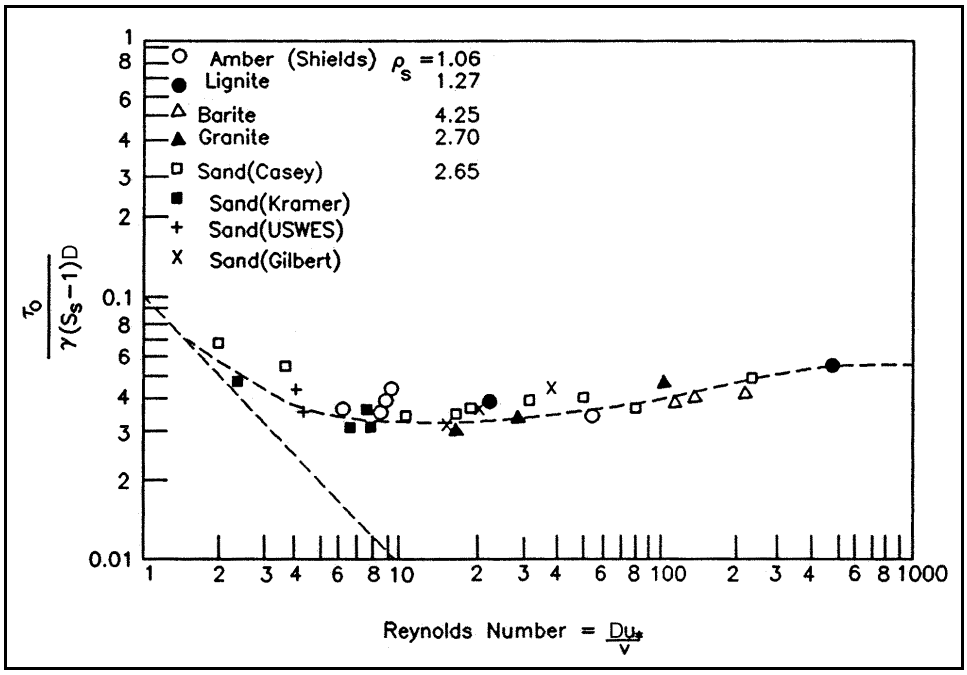

Figure III-6-7. Shields diagram for initiation of motion in steady turbulent flow (from Raudkivi (1967))

$$u_{*cr} = \sqrt{(s - 1) g D}\ \sqrt{\psi_{cr}} \tag{III-6-46}$$

which can be introduced in the definition of Re_* to obtain a parameter (Madsen and Grant 1976)

$$S_* = \frac{D}{4\nu}\sqrt{(s - 1) g D} = \frac{\mathrm{Re}_*}{4\sqrt{\psi_{cr}}} \tag{III-6-47}$$

(b) The factor of 4 appears in the definition of S_* to render the numerical values of S_* comparable with the Re_* values in the traditional Shields diagram. This is done merely for convenience and has no physical significance.

(c) By taking corresponding values of Re_* and ψ_{cr} from the traditional Shields diagram, one can obtain the value of the sediment-fluid parameter S_*, which in turn can be used to replace Re_* in the Shields diagram. In this manner the *modified Shields diagram* (Madsen and Grant 1976) shown in Figure III-6-8 can be constructed.

(d) The modified Shields diagram terminates at the lower end of S_* at a value of 1 which, for quartz sediments in seawater, corresponds to a sediment diameter of $D \approx 0.1$ mm, i.e., a very fine sand. Although cohesion may become important for diameters below 0.1 mm, clean silty sediments, i.e., without too much organic material and/or clay, can be considered cohesionless and therefore governed by a Shields-type initiation of motion criteria. Raudkivi (1976) presents limited experimental data on threshold conditions obtained for low values of Re_* (in the range 0.03 to 1). A best-fit line to the portion of these data obtained for grain-shaped sediments gives the following criterion

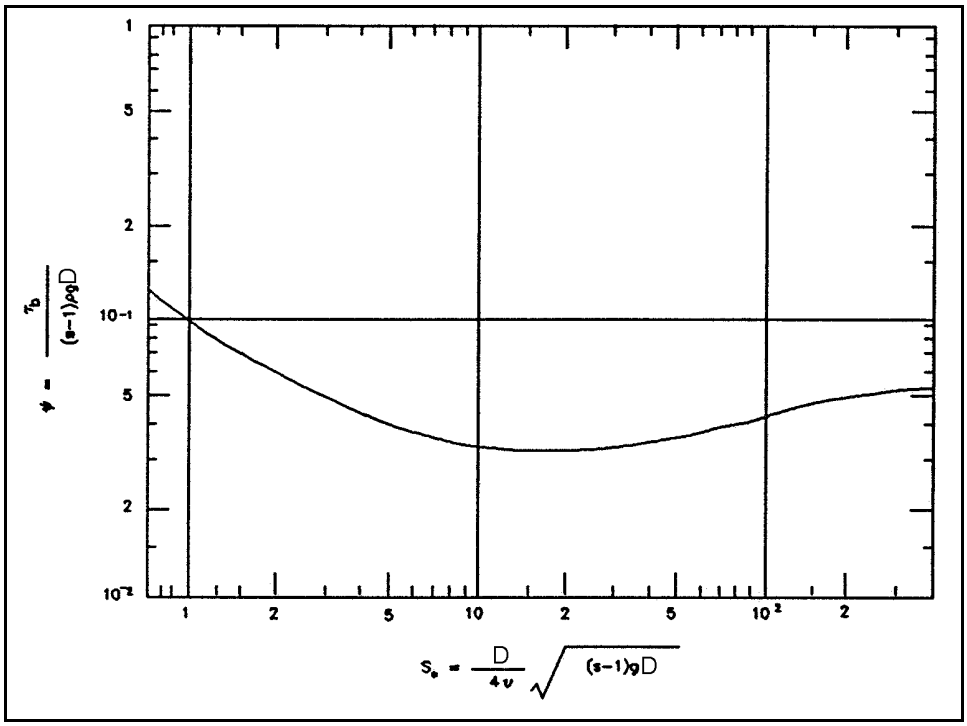

Figure III-6-8. Modified Shields diagram (Madsen and Grant 1976)

$$\psi_{cr} = 0.1 \mathrm{Re}_*^{-1/3} \quad \text{for} \quad \mathrm{Re}_* < 1 \tag{III-6-48}$$

which upon the modification, i.e., using Equation 6-47, may be written as

$$\psi_{cr} = 0.1 S_*^{-2/7} \quad \text{for} \quad S_* < 0.8 \tag{III-6-49}$$

(e) For large values of S_*, the flow corresponding to initiation of motion is fully rough turbulent, $\mathrm{Re}_* > 100$, and the value of $\psi_{cr} \approx 0.06$ may be used for S_* values larger than the range covered in Figure III-6-9.

(3) Modified Shields criterion.

(a) The modified Shields criterion for initiation of motion of a cohesionless sediment shown in Figure III-6-8 was obtained from steady turbulent flow experiments. The fact that this criterion is applicable also for unsteady turbulent boundary layer flows, as demonstrated by the results presented in Figure III-6-9 (Madsen and Grant 1976), is not surprising when the nature of the onset of sediment movement is considered. For flow conditions in the vicinity of $\psi \approx \psi_{cr}$ the sporadic movement of a few grains is, as discussed above, associated with high-frequency turbulent fluctuations in the mobilizing force acting on a grain. Since the near-bottom mean velocity profile is logarithmic for waves as well as for currents, it is physically reasonable to expect the near-bottom turbulence to be similar, i.e., scaled by the instantaneous value of the bottom shear velocity. Provided therefore that the response time of the individual sediment grains is short relative to the time scale of turbulent fluctuations, which are expected to be the same for waves and currents if the shear velocities are the same, initiation of motion will be affected by unsteadiness only if the wave period is on the order of the time scale of the turbulent fluctuations. This not being the case, the effects of unsteadiness

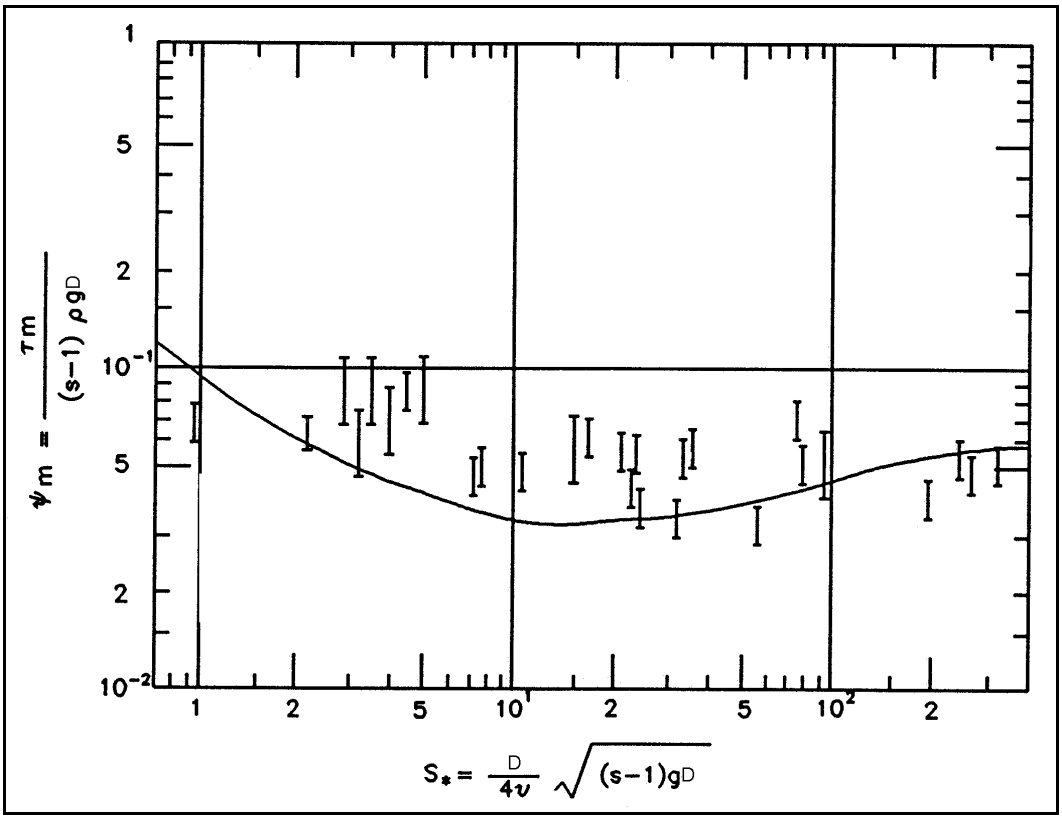

Figure III-6-9. Comparison of Shields curve with data on initiation of motion in oscillatory turbulent flows (after Madsen and Grant ((1976))

of the mean flow are negligible and sediment grains react essentially instantaneously to the applied shear stress, i.e., initiation of motion is obtained from

$$\psi_m = \frac{u_{*m}^2}{(s-1)gD} = \psi_{cr} \tag{III-6-50}$$

in which u_{*m} denotes the maximum shear velocity, i.e., $u_{*m} = u_{*c}$, u_{*wm}, and u_{*m} for pure current, pure wave, and combined wave-current flows, respectively.

(b) The effect of bottom slope on the initiation of motion of sediment grains on the fluid-sediment interface may be accounted for by considering a modification of the simple force balance (Madsen 1991) between fluid drag, gravity, and frictional resistance against movement along a plane bottom inclined at an angle β to horizontal in the direction of flow, where β is taken positive if the bottom is sloping upward in the direction of flow. The resulting force balance suggests that the critical Shields parameter for flow over a sloping bottom may be expressed as

$$\psi_{cr,\beta} = \psi_{cr}\left\{\cos\beta\left(1 + \frac{\tan\beta}{\tan\varphi_s}\right)\right\} \tag{III-6-51}$$

where φ_s is the friction angle for a stationary spherical interfacial grain.

EXAMPLE PROBLEM III-6-6

FIND:

The critical shear velocity u_{*cr} and critical bottom shear stress τ_{cr} for initiation of motion.

GIVEN:

Sediment is quartz sand, ρ_s = 2,650 kg/m^3, of diameter D = 0.2 mm. Fluid is seawater (ρ = 1,025 kg-/m^3, $\nu \approx 1.0\times10^{-6}$ m^2/s).

PROCEDURE:

1) Compute value of the sediment-fluid parameter S_* defined by Equation 6-47.

2) *If* $S_* < 0.8$ obtain ψ_{cr} from Equation 6-49 (be concerned about sediment being cohesive since formula is limited to cohesionless sediments).

3) If $S_* > 300$, $\psi_{cr} \approx 0.06$.

4) If $0.8 < S_* < 300$ obtain ψ_{cr} from Figure III-6-8.

5) Solve Equation 6-45 for u_{*cr} with ψ_{cr} obtained in step 2, 3, or 4.

6) Obtain $\tau_{cr} = z\rho\, u_{*cr}^2$ from definition of shear velocity.

SOLUTION:

The sediment-fluid parameter defined by Equation 6-47 is first computed with $s = \rho_s/\rho = 2.59$ and $g = 9.80$ m/s^2

$$S_* = \frac{D}{4\nu}\sqrt{(s-1)gD} = 2.79$$

With this value of S_* the critical Shields parameter is obtained from Figure III-6-8

$$\psi_{cr} \approx 0.052$$

and using the definition of the Shields parameter given by Equation 6-45

$$u_{*cr} = \sqrt{(s-1)gD\ \psi_{cr}} = 1.27\times10^{-2} \text{ m/s} = 1.27 \text{ cm/s}$$

or $\tau_{cr} = \rho(u_{*cr})^2 = 0.165$ N/m$^2 \approx 0.17$ Pa

If $S_* < 0.8$ had been obtained, Equation 6-49 and *not* Figure III-6-8 should be used to find ψ_{cr}.

d. Bottom roughness and ripple generation. When the flow intensity (expressed in terms of the Shields parameter ψ) exceeds the critical condition for initiation of motion ψ_{cr}, sediment grains will start to move virtually instantaneously (Madsen 1991). However, for ψ exceeding ψ_{cr} by a modest amount (ψ > (1.1 to 1.2)ψ_{cr}), the plane bottom will no longer remain plane. It becomes unstable, deforms, and exhibits bed forms and ripples.

(1) The skin friction concept.

(a) The appearance of bed forms on the sediment-fluid interface changes the appearance of the bottom to the flow above. Rather than giving rise to a flow resistance associated with drag forces on individual sediment grains, i.e., a roughness scaled by the sediment diameter, the flow will separate at the crest of the bed forms and flow resistance will primarily be composed of pressure drag forces on bottom bed forms, i.e., a roughness scaled by the bed form geometry. The appearance of ripples on the bottom changes the physical bottom roughness by orders of magnitude.

(b) Despite the increased bottom roughness associated with a rippled bed, the *drag force acting on individual sediment grains and not the drag force on the bed forms* is responsible for the sediment motion caused by the flow. In the terminology of bottom shear stresses, it is the average shear stress acting on the sediment grains, *the skin friction*, that moves sediment and not the total shear stress comprising skin friction and form drag. The concept of partitioning bottom shear stress into a skin friction and a form drag component, i.e., taking

$$\tau_b = \tau_b^{/} + \tau_b^{//} \tag{III-6-52}$$

in which $\tau_b^{/}$ denotes the skin friction component and $\tau_b^{//}$ the form drag component, illustrated in Figure III-6-10, has received considerable attention in the context of sediment transport mechanics in steady turbulent flows (Raudkivi 1976).

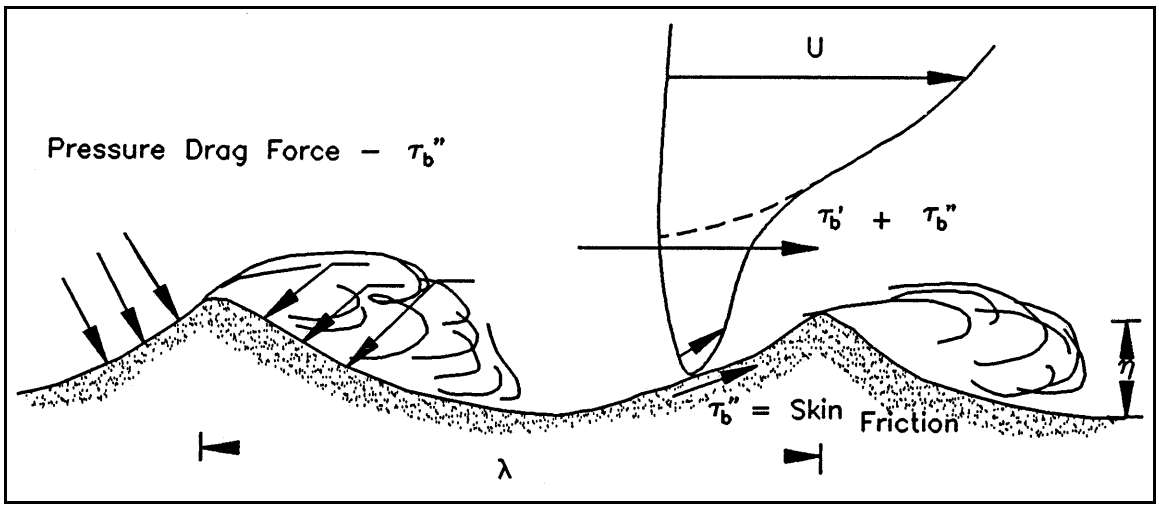

Figure III-6-10. Conceptualization of pressure drag τ_b'', skin friction τ_b', total shear stress $\tau_b'+\tau_b''$, for turbulent flow over a rippled bed

(c) For a pure wave motion, it is assumed that the skin friction bottom shear stress is obtained quite simply (Madsen and Grant 1976) by evaluating the bottom shear stress from the given wave condition, u_{bm} and ω, as if the bottom roughness scale were the sediment grain diameter D. Thus, for a wave motion, the skin friction bottom shear stress is obtained from

$$\tau'_{wm} = \frac{1}{2}\rho f'_w u_{bm}^2 \tag{III-6-53}$$

where f'_w is the wave friction factor obtained from Equation 6-18, Equation 6-19, or Equation 6-21 for a roughness

$$k_n = k'_n = D \tag{III-6-54}$$

Laboratory data on wave-generated ripples as well as ripple geometry for spectral waves is discussed (Madsen 1993) in some detail.

(d) For combined wave-current flows it has been proposed (Glenn and Grant 1987) to evaluate the skin friction bottom shear stress in a similar manner, i.e., using the wave-current interaction model presented in Part III-b(2)d with a roughness specified by Equation 6-54. However, if a combined wave-current boundary layer flow is specified by a current velocity outside the wave boundary layer, i.e., $u_c(z_r)$ with $z_r > \delta_{cw}$, the direct use of this information in the formulas given in Part III-6(2)d with $k_n = k'_n = D$ would lead to an ambiguous determination of the skin friction, since this approach presumes the variation of the current velocity outside the wave boundary layer to be governed by the grain size roughness, which is true only for a flat bed, i.e., in the absence of form drag.

(e) To overcome this problem, the combined wave-current theory presented in Part III-6(2)d is first used with k_n = total equivalent Nikuradse sand grain roughness, accounting for the presence of bed forms, to predict the current velocity at the outer edge of the wave boundary layer, i.e.,

$$u_c(z_r) \quad \text{with} \quad z_r = \delta_{cw} \tag{III-6-55}$$

is obtained from a model considering total bottom shear stresses.

(f) With the current specified by Equation 6-55, the skin friction shear stress is now computed from the general wave-current interaction theory using the grain size roughness $k_n = k'_n = D$. In this manner (Wikramanayake and Madsen 1994a), the ambiguity of the prediction of combined wave-current skin friction shear stresses is avoided.

(2) Field data on geometry of wave-generated ripples.

(a) When field data on ripple geometry are plotted against the skin friction Shields parameter,

$$\psi'_m = \frac{\tau'_{wm}}{(s-1)\rho g D} = \frac{(u'_{*wm})^2}{(s-1)gD} \tag{III-6-56}$$

they exhibit an extensive scatter. By trial and error it was found (Wikramanayake and Madsen 1994a) that the parameter providing the best correlation of field data on ripple geometry was

$$Z = \frac{\psi_m'}{S_*} \tag{III-6-57}$$

in which S_* is the sediment-fluid parameter defined by Equation 6-47.

(b) The equations for the empirical relationships for ripple geometry in the field are (Madsen 1993).

$$\frac{\eta}{A_{bm}} = \begin{cases} 1.8\times10^{-2}\ Z^{-0.5} & 0.0016 < Z < 0.012 \\ 7.0\times10^{-4}\ Z^{-1.23} & 0.012 < Z < 0.18 \end{cases} \tag{III-6-58}$$

and

$$\frac{\eta}{\lambda} = \begin{cases} 1.5\times10^{-1}\ Z^{-0.009} & 0.0016 < Z < 0.012 \\ 1.05\times10^{-2}\ Z^{-0.65} & 0.012 < Z < 0.18 \end{cases} \tag{III-6-59}$$

where A_{bm} is defined by Equation 6-17, η is ripple height, λ is ripple length, and the lowest and highest range of validity indicate the range covered by the experimental data.

(3) Prediction of ripple geometry under field conditions.

(a) From knowledge of the representative periodic wave (recall that this is defined here as the rms wave and not the significant wave) and sediment characteristics, the skin friction shear stress τ_{wm}' is obtained from Equation 6-53.

(b) With τ_{wm}' known, the value of ψ_m' is obtained from Equation 6-56 and if $2\psi_m' > \psi_{cr}$, obtained from the modified Shields curve in Figure III-6-8, sediment motion is assumed to take place and the parameter Z is obtained from Equation 6-57.

With Z known, the empirical relationship given by Equations 6-58 and 6-59 is used to obtain the ripple geometry. If ψ_m' exceeds a value of 0.35 or if $Z > 0.18$, the bed is assumed flat corresponding to sheet flow conditions.

e. Moveable bed roughness.

(1) The determination of moveable bed roughness over naturally rippled beds is limited by the lack of reliable field measurements over a range of wave conditions. The limited amount of available data on wave-generated ripple geometry and the associated rate of energy dissipation in the wave bottom boundary layer above the rippled bed have been analyzed (Wikramanayake and Madsen 1994a). Their analysis results suggest the adoption of the following simple relationship for moveable bed roughness associated with rippled beds

$$k_n = 4\eta \tag{III-6-60}$$

where η is the ripple height. However, the translation of ripple geometry to equivalent roughness, Equation 6-60, is based entirely on laboratory data for periodic waves and is of dubious value for field roughness determinations. Therefore, the following procedure is suggested (Madsen 1993).

(2) For a wave condition specified in terms of the representative periodic wave, the ripple height is obtained from Equation 6-58, and the movable bed roughness k_n is obtained from Equation 6-60.

(3) If ψ_m' suggests no sediment motion, $2\psi_m' < \psi_{cr}$, the movable bed roughness is taken as $k_n = k_n' = D$ unless information on bottom roughness associated with bioturbation of the bottom sediments is available.

(4) If $\psi_m' > \approx 0.35$ or if $Z > 0.18$, the bed is expected to be flat, i.e., corresponding to sheet flow conditions. Recent results from field experiments (Madsen et al. 1993) suggest a value of $k_n = 15D$ to be appropriate for sheet flow conditions. Since the conditions from which this result was obtained correspond to values of $\psi_m' \approx 1$ and since it is physically reasonable to assume the movable bed roughness for sheet flow conditions depends on the intensity of sediment transport over the flat bed, which in turn is related to the magnitude of ψ_m', it is *tentatively proposed* that

$$k_n = 15\psi_m' D \tag{III-6-61}$$

be adopted for sheet flow conditions. This expression agrees in form with an expression proposed for steady flow (Wilson 1989) although the coefficients differ.

III-6-4. Bed-load Transport

a. Introduction.

(1) When flow and sediment characteristics combine to produce a Shields parameter greater than the critical value, sediment is set in motion. One result of this is the generation of bed forms, discussed in Part III-6-3; another is, of course, the initiation of a non-zero transport of sediment.

(2) For values of the Shields parameter slightly above critical or, more specifically, for low transport rates, the predominant mode of sediment transport takes place as individual grains rolling, sliding, and/or jumping (saltating) along the bed. This mode of sediment transport is referred to as *bed load* and, since it takes place in close proximity of the bed, it is dependent on *skin friction*.

(3) Several empirical bed-load transport formulas have been proposed for steady turbulent boundary layer flows (Raudkivi 1976). One of these, the Meyer-Peter and Müller formula (Meyer-Peter and Müller 1948), enjoys particular popularity in the engineering literature. However, since it was originally developed from data obtained for steady flows in rivers and channels of negligible slope, its adoption for unsteady wave or combined wave-current turbulent boundary layer flows over an inclined bed is not straightforward. A conceptual model for bed-load transport of sediment grains rolling or sliding along an inclined bottom has been proposed (Madsen 1993) as a physical interpretation of the purely empirical Meyer-Peter and Müller formula. The resulting formulation is time-averaged and solved under the assumptions that: waves dominate

EXAMPLE PROBLEM III-6-7

FIND:

The height η, length λ, and movable bed roughness k_n, of wave-generated ripples in the field.

GIVEN:

The representative periodic wave motion is specified as in Example Problem III-6-3. Bottom sediment is quartz, ρ_s = 2,650 kg/m^3, of diameter D = 0.2 mm. Fluid is seawater (ρ = 1,025 kg/m^3, $\nu \approx 1.0\times10^{-6}$ m^2/s).

PROCEDURE:

1) Obtain the wave shear velocity u'_{*wm} assuming grain size roughness k'_n = d = median sediment diameter, following the procedure described in Example Problem III-6-2. (Result is denoted here by *prime* to signify *skin friction* shear velocity.)

2) With u'_{*wm} from step 1 compute ψ'_m from Equation 6-56.

3) Evaluate S_* as defined by Equation 6-47.

4) Determine ψ_{cr} following procedure of Example Problem III-6-6.

5) If $\psi'_m < \frac{1}{2}\psi_{cr}$ there will be no sediment motion and no ripples, i.e., $\eta = \lambda = 0$. Bottom roughness *is* the sediment grain diameter ($k_n = k'_n = D$) unless other information is available, e.g., photos showing relict ripples or other roughness features.

6) If $\psi'_m > 0.35$, sheet flow is assumed. The bed is flat, i.e., $\eta = \lambda = 0$, and the movable bed roughness k_n is obtained from Equation 6-61.

7) If $\frac{1}{2}\psi_{cr} < \psi'_m < 0.35$, the parameter Z defined by Equation 6-57 is computed.

8) If Z falls within the range indicated for Equations 6-58 and 6-59, these are used to compute η and λ. The movable bed roughness k_n is obtained from Equation 6-60.

9) If $Z < 0.0016$ and $D < 0.6$ mm, it is *recommended* that η, λ, and k_n be obtained as if $Z = 0.0016$.

10) If $Z > 0.18$ and $D > 0.08$ mm, sheet flow is assumed (i.e., $\eta = \lambda = 0$), and Equation 6-61 is used to obtain k_n.

(Continued)

Example Problem III-6-7 (Concluded)

SOLUTION:

In Example Problem III-6-3, the initial solution for the wave friction factor neglected the presence of a current ($\mu = 0$, $C_\mu = 1$) and gave $f_w = 7.86\times10^{-3}$. Since the wave motion and the bottom roughness ($k_n = k_n' = D = 0.2$ mm) are the same here, the maximum skin friction shear velocity is given by

$$u'_{*wm} = \sqrt{f_w'/2}\; u_{bm} = 2.19\times10^{-2} \text{ m/s} = 2.19 \text{ cm/s}$$

From the definition of the Shields parameter, Equation 6-56, it follows that

$$\psi'_m = \frac{\left(u'_{*wm}\right)^2}{(s-1)gD} = 0.154$$

The sediment being the same as specified in Example Problem III-6-5 where $\psi_{cr} = 0.052$ was obtained, it is seen that the sediment will be moving, since $\psi'_m > \psi_{cr}$. Since $\psi'_m < 0.35$, flat bed (sheet flow) is not predicted and bed forms are therefore expected. The geometry of these bed forms is obtained from the field relationships, Equations 6-58 and 6-59. With the parameter

$$Z = \frac{\psi'_m}{S_*} = 0.055$$

since $S_* = 2.79$ in Example Problem III-6-6, which is within the range $0.012 < Z < 0.18$, one therefore obtains from Equation 6-58

$$\frac{\eta}{A_{bm}} = 7\times10^{-4}\, Z^{-1.23} = 2.47\times10^{-2}$$

or, with $A_{bm} = 44.6$ cm (Example Problem III-6-3)

$$\eta = \frac{\eta}{A_{bm}} A_{bm} = 1.1 \text{ cm}$$

The ripple steepness is obtained from Equation 6-59

$$\frac{\eta}{\lambda} = 1.05\times10^{-2}\, Z^{-0.65} = 6.91\times10^{-2} \rightarrow \lambda = \eta/(\eta/\lambda) = 15.9 \text{ cm} \approx 16 \text{ cm}$$

From Equation 6-60, one obtains the movable bed roughness

$$k_n = 4\eta = 4.4 \text{ cm}$$

EXAMPLE PROBLEM III-6-8

FIND:

The skin friction shear velocities associated with the current $u_{*c}^{/}$, the wave $u_{*wm}^{/}$, and the maximum combined $u_{*m}^{/}$, as well as the phase angle of the wave-associated shear stress φ', for a combined wave-current flow over a movable bed in the field.

GIVEN:

The representative periodic wave is specified by its near-bottom maximum orbital velocity $u_{bm} = u_{br} = 0.35$ m/s and period $T = 8.0$ s. The current is specified by its magnitude $u_c(z_r) = 0.35$ m/s at $z_r = 1.00$ m and direction $\varphi_{wc} = 45°$ relative to the direction of wave propagation. The bed consists of uniform quartz sand, $\rho_s = 2{,}650$ kg/m^3, of diameter $D = 0.2$ mm. The fluid is seawater ($\rho = 1{,}025$ kg/m^3, $\nu \approx 1.0\times10^{-6}$ m^2/s).

PROCEDURE:

1) Considering *only* the wave motion, the movable bed roughness k_n is obtained following the procedure given in Example Problem III-6-7.

2) With k_n from step 1, the combined wave-current problem is solved following the procedure described in Example Problem III-6-4.

3) From the combined wave-current flow solution obtained in step 2, the current velocity $u_c(z = \delta_{cw})$ is computed by the procedure of Example Problem III-6-5.

4) With the current specification $u_c = u_c(\delta_{cr})$ at $z = \delta_{cw}$ from step 3, the wave-current interaction problem is solved for $k_n^{/} = D$ following the procedure described in Example Problem III-6-3.

5) The skin friction phase angle φ' is obtained from Equation 6-12 with $u_{*wm} = u_{*m}^{/}$.

SOLUTION:

The *first step* to follow in determining the skin friction components for a combined wave-current boundary layer flow is to determine the movable bed roughness. Since the presence of a current is neglected in performing this step, this was done in Example Problem III-6-7 for the wave and sediment characteristics considered here and resulted in $k_n = 4.4$ cm.

The *second step* is to determine the current velocity at the edge of the boundary layer, $u_c(\delta_{cw})$ from the wave-current interaction model using the movable bed roughness obtained in step 1. This was done in Example Problems III-6-4 and III-6-5 where the bottom roughness was specified as $k_n = 4.4$ cm, i.e., exactly the movable bed roughness determined in step 1 for the given wave and sediment characteristics.

(Continued)

Example Problem III-6-8 (Concluded)

The *third step* is to determine the shear velocities and stresses associated with the combined wave-current boundary layer flow over a bottom of roughness $k_n = k_n' = D$ = sediment diameter with the current specified as obtained in step 2. From Example Problem III-6-5, the current specification is therefore

$$u_c(z_r) = 10.2 \text{ cm/s} \quad \text{at} \quad z_r = \delta_{cw} = 3.40 \text{ cm}$$

at an angle $\varphi_{wc} = 45$ deg to the direction of wave propagation. With this current specification, $k_n = k_n' = D = 0.2$ mm, and wave characteristics $u_{bm} = 35$ cm/s and $\omega = 2\pi/T = 0.785$ s^{-1} ($A_{bm} = u_{bm}/\omega = 44.6$ cm) solution of the wave-current interaction problem follows Example Problem III-6-3.

For $\mu = 0$ and $C_\mu = 1$, the first iteration is identical to that in Example Problem III-6-3, resulting in $u_{*wm}' = u_{*m}' = 2.19$ cm/s and $\delta_{cw}' = 1.12$ cm. With these values and using the current specifications given above, Equation 6-40 gives

$$u_{*c}' = 0.96 \text{ cm/s}$$

Second iteration is therefore based on $\mu = \left(u_{*c}'/u_{*wm}'\right)^2 = 0.194$ and, from Equation 6-33, $C_\mu = 1.15$. For this value of C_μ solving iteratively for $x = 4\sqrt{f_{cw}/C_\mu}$ in the manner outlined in Example Problem III-6-3 results in $x^{(3)} = 0.349$, or

$$f_{cw}' = 8.73 \times 10^{-3}$$

and therefore

$$u_{*wm}' = 2.31 \text{ cm/s} \; ; \quad u_{*m}' = 2.48 \text{ cm/s} \quad \text{and} \quad \delta_{cw}' = 1.26 \text{ cm}$$

with which Equation 6-40 gives

$$u_{*c}' = 1.01 \text{ cm/s}$$

The next value of $\mu = \left(u_{*w}/u_{*wm}'\right)^2 = 0.191$ is virtually identical to the previous value, so no further iteration is necessary.

The solution is therefore

$$u_{*c}' = 1.01 \text{ cm/s} \; , \quad u_{*wm}' = 2.31 \text{ cm/s} \; , \quad u_{*m}' = 2.48 \text{ cm/s}$$

and the phase angle of the wave-associated skin friction bottom shear stress is obtained from Equation 6-12 with $u_{*wm} = u_{*m}'$ and $z_0 = d/30$

$$\tan \varphi' = 0.25 \rightarrow \varphi' = 13.8° \approx 14°$$

currents $\mu = \tau_c'/\tau_{wm}' << 1$; maximum shear stress is much larger than critical $\mu_{CR} = \tau_{CR}/\tau_{wm}' << 1$; and bottom slope is relatively small

$$\mu_b = \frac{\tan\beta}{\tan\varphi_m} << 1 \tag{III-6-62}$$

where $\beta > 0$ is bottom slope upward relative to direction of flow and φ_m is friction angle (Madsen 1993). Results of this analysis provide the following formulations for the time-averaged bed-load transport $\overline{q_{SB}}$.

b. Pure waves on sloping bottom. For a non-zero bottom slope, i.e., $\mu_b \neq 0$, but still without any current, the time-averaged net bed-load transport is

$$\left(\frac{\bar{q}_{sB}}{\sqrt{(s-1)gD}\,D}\right)_\beta = 8\left(\psi_{wm}'\right)^{\frac{3}{2}}\overline{|\cos\theta|^{\frac{3}{2}}}\{-\mu_b,0\} = 4.5\left(\psi_{wm}'\right)^{\frac{3}{2}}\{-\mu_b,0\} \tag{III-6-63}$$

in the direction of the wave propagation, $+x$, if $-\mu_b > 0$ and opposite the wave direction if $-\mu_b < 0$. Since $\mu_b > 0$ if the wave propagates up a slope, $\beta_w > 0$, and $\mu_b < 0$ if the wave is directed towards deeper water ($\beta_w < 0$), this simply states that the net transport is down-slope as expected.

c. Combined wave-current flows. Since the approximate bed-load transport formula is linear in the small parameters, the net bed-load transport associated with combined wave-current flows can be evaluated by time averaging for $\mu_b = 0$. The resulting net bed-load transport is given by

$$\left(\frac{\bar{q}_{sB}}{\sqrt{(s-1)gD}\,D}\right)_{wc} = 6\left(\psi_c'\right)^{\frac{3}{2}}\frac{u_{*wm}'}{u_{*c}'}\left\{\frac{3}{2}\cos\varphi_{wc},\ \sin\varphi_{wc}\right\} \tag{III-6-64}$$

where ψ_c' denotes the Shields parameter based on the current skin friction shear stress. It should be noted that the direction of sediment transport is *not* in the direction of the current but is obtained from

$$\tan\varphi_{ws} = \frac{2}{3}\tan\varphi_{wc} \tag{III-6-65}$$

This expression shows that φ_{ws}, the direction of the net bed-load transport measured counterclockwise from the x-axis, deviates from the current direction towards the direction of wave orbital velocities.

d. Combined current and bottom slope effect. It is interesting to note that the superposition of a current in the direction of wave propagation, i.e., $\varphi_{wc} = 0$, up a slope may lead to zero net transport. Thus, the sum of transport given by Equations 6-63 and 6-64 is zero if

$$\mu_b = 2\mu \tag{III-6-66}$$

Although the upslope transport here is associated with an assumed current, it is reasonable to anticipate a similar upslope effect associated with nonlinear wave effects, i.e., a larger upslope shear stress under the crest

than the downslope stress under the trough. The balance expressed in Equation 6-66 may therefore be thought of as a simulation of an equilibrium profile condition for inner shelf waters.

e. Extension to spectral waves. To compute the bed load for spectral wave conditions, the procedures outlined in the foregoing sections are followed using the representative periodic wave characteristics defined in Part III 6-2-*b* (4).

f. Extension to sediment mixtures.

(1) For a sediment mixture consisting of several distinct size classes of diameter D_n with the volume fraction of the nth size class being f_n in the bottom sediments, the total bed-load transport of the sediment mixture is given by

$$\bar{q}_{sB} = \sum f_n \bar{q}_{sB,n} \tag{III-6-67}$$

(2) This extension to sediment mixtures follows directly from the conceptual bed-load transport model (Madsen 1993) when it is assumed that the fraction of excess skin friction shear stress carried by moving grains of the nth size class is $f_n\left(\tau_b' - \tau_{cr,n}\right)$.

(3) For each size class, the procedure is therefore exactly as outlined in the preceding section with D replaced by D_n, the diameter of the nth size class. The skin friction bottom shear stress is, however, the same for all size classes and is computed for a single representative grain diameter ($D = D_r = D_{50}$ = the median diameter of the sediment mixture in the bed).

III-6-5. Suspended Load Transport

a. Introduction.

(1) For low transport rates, the predominant mode of transport is sediment grains moving along the bottom, i.e., in the form of bed load. As the flow intensity and, hence, the bed-load transport, is increased individual grains moving along the bottom take off from the bottom with increasing frequency, e.g., due to impact with stationary grains protruding above their neighbors. Thus, as the flow intensity increases, the mode of transport changes from one of rolling and sliding along the bottom to one of jumping along the bottom. For this mode of transport, moving grains are in direct contact with immobile bottom grains only for a fraction of the time they spend in transport, and the basic assumptions behind the conceptual transport model presented in the preceding section are no longer valid.

(2) Sediment transport associated with individual sediment grains making isolated or a series of jumps along the bottom, referred to as saltation, provides a transition from bed-load transport that takes place immediately above the bottom to suspended load transport that takes place in the overlying water column. From this distinction between the bed-load and suspended load transport modes, it follows that suspended load is governed by the turbulence associated with the *total bottom shear stress*, i.e., the shear stress predicted from the movable bed roughness estimate obtained from Part III-6-3, whereas the bed load is governed by the *skin friction shear stress*.

EXAMPLE PROBLEM III-6-9

FIND:

The bed-load transport rate for a combined wave-current flow over a sloping bottom.

GIVEN:

The wave is specified by its maximum near-bottom orbital velocity u_{bm} = 0.35 m/s, period T = 8.0 s, and angle of incidence α = 45 deg. The current is at an angle of φ_{wc} = 45 deg to the wave direction and has a magnitude of $u_c(z_r)$ = 0.35 m/s at z_r = 1.00 m. The bottom has a uniform slope of β = 1 deg and consists of uniform quartz sand ρ_s = 2,650 kg/m^3, with diameter D = 0.2 mm. The fluid is seawater (ρ = 1,025 kg/m^3, $\nu \approx 1.0\times10^{-6}$ m^2/s).

PROCEDURE:

1) The skin friction shear velocities and stresses are computed using the procedure of Example Problem III-6-8.

2) The skin friction Shields parameters, ψ_c' and ψ_{wm}', are obtained from Equation 6-43 with $u_* = u_{*c}'$ and u_{*wm}', respectively, as obtained in step 1.

3) The time-averaged combined wave-current bed-load transport vector is obtained from Equation 6-64 using u_{*c}' and u_{*wm}' from step 1 and ψ_c' from step 2.

4) The bottom slope parameter μ_b is calculated from Equation 6-62, where β is bottom slope in the direction of wave propagation (positive if wave is traveling towards shallower waters) and φ_m = 30 deg.

5) The time-averaged bottom slope bed-load transport vector is obtained from Equation 6-63 with ψ_{wm}' from step 2.

6) The total time-averaged bed-load transport vector is obtained by vector addition of the wave-current and slope bed-load transport vectors obtained in step 3 and step 5, respectively. (The x component denotes the transport in the direction of wave propagation, the y component is transport 90 deg counterclockwise to the direction of wave propagation.)

(Continued)

Example Problem III-6-9 (Concluded)

SOLUTION:

To calculate bed-load transport, one needs to use skin friction shear stresses. The problem specification is here identical to that of Example Problem III-6-8, so the skin friction problem was solved there, i.e., $u'_{*c} = 1.01$ cm/s and $u'_{*wm} = 2.31$ cm/s. The corresponding skin friction Shields parameters are obtained from Equation 6-56 with $s = \rho_s/\rho = 2.59$ and $D = 0.2$ mm

$$\psi'_c = 0.033 \quad \text{and} \quad \psi'_{wm} = 0.17$$

With these values, the bed-load transport associated with the combined wave-current flow is obtained in nondimensional form from Equation 6-64

$$\left(\frac{\bar{q}_{sB}}{\sqrt{(s-1)gD}D} \right)_{wc} = 0.082 \left\{ \frac{3}{2} \cos \varphi_{wc} \, , \quad \sin \varphi_{wc} \right\}$$

or in dimensional form with $\varphi_{wc} = 45$ deg

$$\left(\bar{q}_{sB}\right)_{wc} = \{9.7, 6.5\} \times 10^{-3} \text{ cm}^3/(\text{cm s})$$

To obtain the contribution due to bottom slope, the slope β_w in the direction of wave propagation is needed. Since the bottom slope is $\beta = 1$ deg and the angle of incidence is $\alpha = 45$ deg, the bottom slope in the direction of wave propagation is $\tan \beta_w = \tan \beta \cos \alpha = 0.012$. Equation 6-62 therefore gives, with $\varphi_m = 30$ deg, $\mu_b = \tan \beta_w / \tan \varphi_m = 0.021$. Bed-load transport due to bottom slope is obtained from Equation 6-63 in nondimensional form

$$\left(\frac{\bar{q}_{sB}}{\sqrt{(s-1)gD}D} \right)_{\beta} = 0.32\{-\mu_b, 0\}$$

or in dimensional form

$$\left(\bar{q}_{sB}\right)_{\beta} = \{-7.5, 0\} \times 10^{-4} \text{ cm}^3/(\text{cm s})$$

The total bed-load transport rate is obtained as the sum of the wave-current and bottom slope contributions, i.e.,

$$\bar{q}_{sB} = \left(\bar{q}_{sB}\right)_{wc} + \left(\bar{q}_{sB}\right)_{\beta} \approx \{9.0, 6.5\} \times 10^{-3} \text{ cm}^3/(\text{cm s})$$

with the x component being in the direction of wave propagation and the y component being at 90 deg counterclockwise from the wave direction.

(3) Distribution of suspended sediment in the water column is governed by the fall velocity of the sediment w_f, the sediment diffusion coefficient v_s, and the volume concentration of sediment in suspension c. Assuming the sediment-fluid mixture behaves as a clear fluid, a close analogy can be drawn between the turbulent diffusion of momentum and sediment diffusion such that

$$v_s = v_t = k u_* z \tag{III-6-68}$$

For combined wave-current bottom boundary layer flows, the concentration of suspended sediments c may be resolved into its mean $\bar{c}$ and time-varying wave-associated c_w components.

b. Sediment fall velocity.

(1) In order to solve the equations governing the distribution of suspended sediment concentration in the vertical, it is necessary to obtain the value of the sediment fall velocity w_f.

(2) Assuming a spherical sediment grain, the force balance of submerged weight and fluid drag on a grain falling through an otherwise quiescent fluid gives

$$(\rho_s - \rho)\, g \left(\frac{\pi}{6} D^3 \right) = \frac{1}{2} \rho\, C_D \left(\frac{\pi}{4} D^2 \right) w_f^2 \tag{III-6-69}$$

or

$$\frac{w_f}{\sqrt{(s-1)\, g\, D}} = \sqrt{\frac{4}{3\, C_D}} \tag{III-6-70}$$

(3) The drag coefficient C_D is a function of the Reynolds number $Re_D = D\, w_f / \nu$, which is a function of S_*, the sediment-fluid parameter defined by Equation 6-47.

(4) From the empirical relationship of C_D versus Re_D (Schlichting 1960), C_D is obtained for a specified value of Re_d. With this value of C_D the nondimensional fall velocity is obtained from Equation 6-70, and this value is used with the specified value of Re_D to obtain the corresponding value of S_*. In this manner (Madsen and Grant 1976), the graph of nondimensional fall velocity as a function of the sediment fluid parameter, shown in Figure III-6-11, is obtained.

(5) Extending the graph to values of S_* above the upper limit of Figure III-6-11 is accomplished by using

$$\frac{w_f}{\sqrt{(s-1)\, g\, D}} = 1.82 \quad \text{for} \quad S_* > 300 \tag{III-6-71}$$

(6) For values of S_* below unity, i.e., for quartz grains of $d < 0.1$ mm in seawater, the fall velocity is obtained from Stokes Law, which in the present notation may be written

$$\frac{w_f}{\sqrt{(s-1)\, g\, D}} = \frac{2}{9} S_* \quad \text{for} \quad S_* < 0.8 \tag{III-6-72}$$

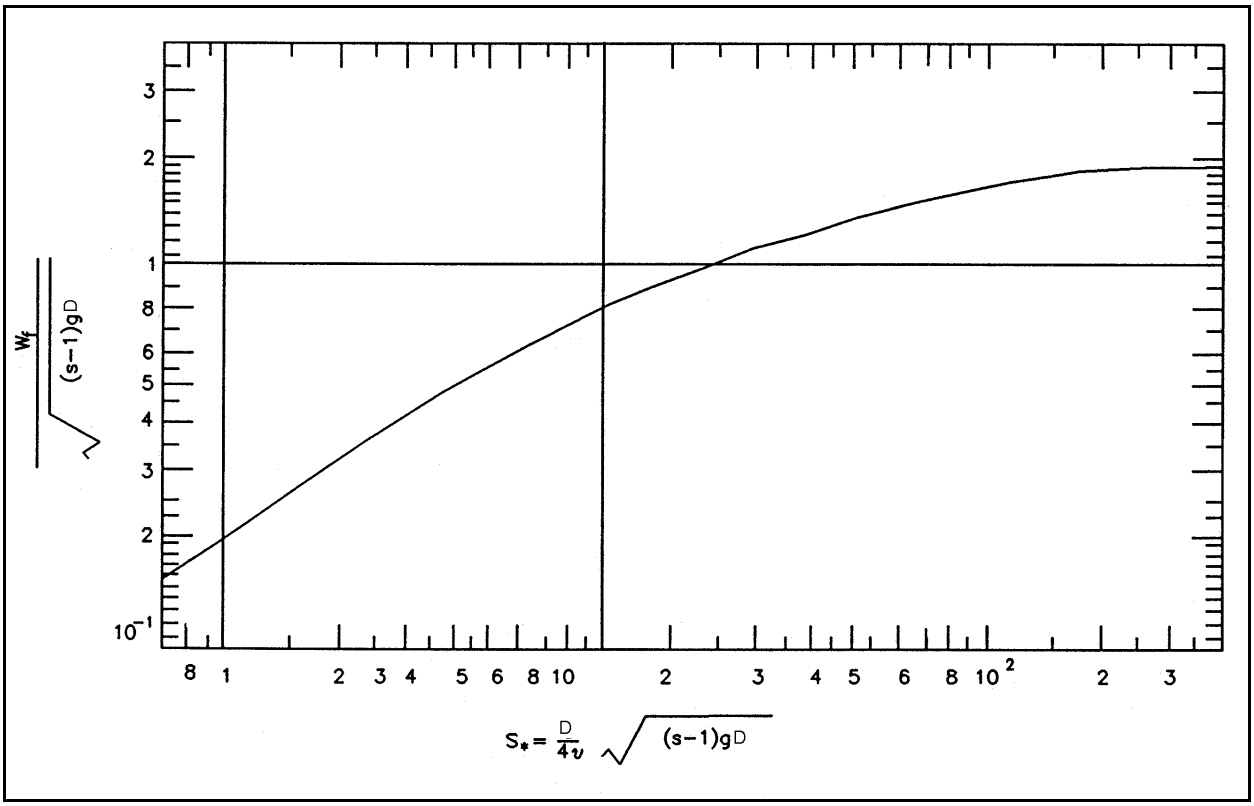

Figure III-6-11. Nondimensional fall velocity for spherical particles versus the sediment fluid parameter (Madsen and Grant 1976)

(7) Although Figure III-6-11 is obtained for sediment assumed to be spherical, it yields reasonably accurate fall velocities for natural cohesionless granular sediments (Dietrich 1982).

c. Reference concentration for suspended sediments.

(1) Introduction.

(a) With the fall velocity determined, all parameters in the equation governing the suspended sediment concentration distribution are in principle known. To solve the equation it is, however, necessary to specify boundary conditions. One boundary condition is simply that no sediment is transported through the water surface or that the suspended sediment concentration vanishes at large distances above the bottom, if the water depth is sufficiently large. Another is the boundary condition that expresses the amount of sediment available for entrainment immediately above the bottom. Whereas the former is universally agreed upon the latter boundary condition is the subject of considerable controversy. It is beyond the scope of this presentation to get into the subtleties of this controversy, so the most commonly accepted form of the bottom boundary condition for suspended sediment concentration, the *specification of a reference concentration*, is adopted here.

(b) The *reference concentration* is given as (Madsen 1993)

$$c_R = \gamma C_b \left(\frac{|\tau_b'(t)|}{\tau_{cr,\beta}} - 1 \right) \tag{III-6-73}$$

EXAMPLE PROBLEM III-6-10

FIND:
Find the sediment fall velocity

GIVEN:
Sediment is quartz sand, ρ_s = 2,650 kg/m^3, of diameter D = 0.2 mm.
Fluid is seawater (ρ = 1,025 kg/m^3, $\upsilon \approx 1.0\times10^{-6}$ m^2/s).

PROCEDURE:
1) The sediment-fluid parameter S_*, defined by Equation 6-47, is calculated.

2) If $S_* > 300$, the sediment fall velocity w_f is obtained from Equation 6-71.

3) If $S_* < 0.8$, the sediment fall velocity w_f is obtained from Equation 6-72.

4) If $0.8 < S_* < 300$, w_f is obtained from Figure III-6-11 using S_* from step 1 as entry.

SOLUTION:
The sediment-fluid parameter is calculated from

$$S_* = \frac{D}{4\nu}\sqrt{(s-1)\,g\,D} = 2.79$$

with $s = \rho_s/\rho = 2.59$.

Figure III-6-11 then gives the nondimensional fall velocity

$$\frac{w_f}{\sqrt{(s-1)\,g\,D}} \approx 0.40$$

and therefore

$$w_f = 2.23 \text{ cm/s}$$

in which γ is the so-called resuspension parameter and C_b is the volume concentration of sediment in the bed, generally taken as 0.65 (Smith and McLean 1977) for a bed consisting of cohesionless sediment.

(c) It is emphasized that the resuspension parameter γ in Equation 6-73 is intimately related to the choice of reference elevation z_r, which explains at least part of the considerable variability of γ values reported in the literature. Similarly, γ values reported in the literature can be used only in conjunction with their particular z_r values. This being said, the numerical values

$$\gamma = \begin{cases} 2\times10^{-3} & \text{for rippled bed} \\ 2\times10^{-4} & \text{for flat bed} \end{cases} \tag{III-6-74}$$

EXAMPLE PROBLEM III-6-11

FIND:

The reference concentration for suspended sediment computations for combined wave-current boundary layer flows.

GIVEN:

Wave, current, sediment, and bottom slope specifications are identical to those of Example Problem III-6-9.

PROCEDURE:

1) Skin friction shear velocities and stresses are computed following the procedure of Example Problem III-6-8.

2) The time-averaged (mean) reference concentration $\bar{c}_R$ is obtained from Equation 6-75 with C_b = 0.65, τ'_{wm}, and τ_{cr} as obtained in step 1, and the appropriate choice of γ from Equation 6-74.

3) The periodic (wave) reference concentration c_{Rw} is obtained from Equation 6-76 using γ and C_b as in step 2 and shear velocities obtained in step 1. The bottom slope in the direction of wave propagation β_w is positive if the wave is traveling up-slope, and φ_m = 30 deg.

SOLUTION:

The reference concentration for suspended load computations depends on skin friction shear velocities, obtained in Example Problem III-6-8 for the same problem specification as here, and may be separated into a mean and a periodic component.

The mean reference concentration is given by Equation 6-75, which may alternatively be written

$$\bar{c}_R = \gamma\ C_b \left\{ \frac{2}{\pi} \left(\frac{u'_{*wm}}{u_{*cr}} \right)^2 - 1 \right\}$$

where u'_{*wm} = 2.31 cm/s (Example Problem III-6-8) and u_{*cr} = 1.27 cm/s (Example Problem III-6-6). The resuspension parameter is given by Equation 6-74. Since the bed is rippled for these problem specifications, cf. Example Problem III-6-7, $\gamma = 2\times10^{-3}$ is chosen here. With C_b = 0.65 the *mean reference concentration* is

$$\bar{c}_R = 1.44\times10^{-3}\ (\mathrm{cm}^3/\mathrm{cm}^3)$$

(Continued)

Example Problem III-6-11 (Concluded)

The periodic reference concentration is given by Equation 6-76. The maximum value may be written

$$c_{Rwm} = \gamma\ C_b \left\{ \frac{4}{\pi} \left(\frac{u'_{*c}}{u_{*cr}} \right)^2 \cos\ \varphi_{wc} - \left(\frac{u'_{*wm}}{u_{*cr}} \right)^2 \frac{\tan\ \beta_w}{\tan\ \varphi_m} \right\}$$

which is evaluated using u'_{*c} = 1.01 cm/s (Example Problem III-6-8), φ_{wc} = 45 deg, and $\tan \beta_w / \tan \varphi_m = \mu_b = 0.021$ (Example Problem III-6-9) to give the *wave-associated maximum reference concentration*

$$c_{Rwm} = 0.65 \times 10^{-3}\ (\mathrm{cm}^3/\mathrm{cm}^3)$$

with a temporal variation $\cos(\omega t + \varphi')$ with φ' = 14 deg (Example Problem III-6-8). Both mean and periodic reference concentrations are specified at

$$z_R = 7D = 0.14\ \mathrm{cm}$$

obtained for and from a model closely resembling the present model, with reference elevation $z_R = 7D$, are adopted here (Wikramanayake and Madsen 1994b). It should, however, be emphasized that there is considerable uncertainty associated with the adoption of these γ values, or any other values for that matter.

(d) To evaluate the general expression for the reference concentration given by Equation 6-73 for combined wave-current flows, the assumption of wave dominance is introduced in the context of evaluation of bed-load transport as previously done in Part III-6-4. Subject to the limitations stated there, the reference concentration is valid for dominant wave conditions ($\tau'_c << \tau'_{wm}$) exceeding critical conditions ($\tau_{cr} << \tau'_{wm}$) over a gently sloping bottom ($\tan\beta_w \ll \tan\varphi_m$).

(2) Mean reference concentration. From the general expression for the reference concentration (Madsen 1993), the time-invariant, mean reference concentration is obtained as

$$\bar{c}_R = \gamma\ C_b \left(\frac{2}{\pi} \frac{\tau'_{wm}}{\tau_{cr}} - 1 \right) \qquad \text{(III-6-75)}$$

and is applied at $z = z_r = 7D$.

(3) Wave reference concentration. The periodic component of the reference concentration (Madsen 1993), the wave reference concentration, is given by

$$c_{Rw} = \gamma\ C_b \left(\frac{4}{\pi}\ \frac{\tau_c^{/}}{\tau_{cr}}\ \cos\ \varphi_{wc} - \frac{\tau_{wm}^{/}}{\tau_{cr}}\ \frac{\tan\ \beta_w}{\tan\ \varphi_m} \right)\ \cos\ \theta = c_{Rwm}\ \cos\ \theta \tag{III-6-76}$$

at $z = z_r = 7D$. In this expression it is recalled that the wave phase is given by

$$\theta = \omega t + \varphi^{/} \tag{III-6-77}$$

where φ' is the phase angle given by Equation 6-14 for skin friction conditions, i.e., with $u_{*wm} = u_{*m}^{/}$.

d. Concentration distribution of suspended sediment. For a combined wave-current flow, the eddy viscosity or eddy diffusivity is given by

$$\nu_s = \begin{cases} \kappa u_{*m} z & z < \delta_{cw} \\ \kappa u_{*c} z & z > \delta_{cw} \end{cases} \tag{III-6-78}$$

with

$$\delta_{cw} = \frac{\kappa u_{*m}}{\omega} \tag{III-6-79}$$

and the shear velocities being those determined from the wave-current interaction model described in Part III-6-2-c using the equivalent Nikruradse roughness corresponding to the movable bed roughness obtained by the procedures outlined in Part III-6(3)e.

(1) Mean concentration distribution. Using the equation governing the distribution of mean concentration (Madsen 1993), and introducing the eddy diffusivity from Equation 6-78 yields

$$\overline{c} = \overline{c}_R \left(\frac{z}{z_r} \right)^{\left(-\frac{w_f}{\kappa u_{*m}} \right)} \qquad \text{for} \quad z < \delta_{cw} \tag{III-6-80}$$

and

$$\overline{c} = \overline{c}_R \left(\frac{\delta_{cw}}{z_r} \right)^{\left(-\frac{w_f}{\kappa u_{*m}} \right)} \left(\frac{z}{\delta_{cw}} \right)^{\left(-\frac{w_f}{\kappa u_{*c}} \right)} \qquad \text{for} \quad z > \delta_{cw} \tag{III-6-81}$$

where $\overline{c}_R$ is given by Equation 6-75, and the mean concentrations are matched at $z = \delta_{cw}$.

(2) Wave-associated concentration distribution. The wave-generated suspended sediment concentration can be approximated as (Madsen 1993)

$$c_w \approx c_{Rwm}\ \cos(\omega\ t + \varphi^{/}) - c_{Rwm}\ \frac{2}{\pi}\ \sin \varphi_s\ \ln \frac{z}{z_r}\ \cos\ (\omega\ t + \varphi^{/} + \varphi_s) \tag{III-6-82}$$

where

$$\tan \varphi_s = \frac{\frac{\pi}{2}}{\ln \frac{\kappa u_{*m}}{z_r \omega} - 1.15} \tag{III-6-83}$$

This is a highly simplified solution for the wave-associated suspended sediment concentration within the wave boundary layer, i.e., for $z < \delta_{cw}$. For a more accurate representation of the wave-associated concentration profile, reference is made to Wikramanayake and Madsen (1994b).

e. Suspended load transport. The suspended load transport is obtained from the product of the velocity vector, and the concentration of suspended sediment followed by integration over depth is denoted by *h*. Time averaging the instantaneous transport rate produces a net transport rate, which is the quantity of interest. Indicating time-averaging by an overbar, the total net suspended load transport rate is obtained from

$$\overline{\boldsymbol{q}}_{sS,T} = \int_{z_r}^{h} \boldsymbol{u}_c \, \overline{c} \, dz + \int_{z_r}^{h} \overline{\boldsymbol{u}_w \, c_w} \, dz \tag{III-6-84}$$

This equation identifies the contribution to the total net suspended load transport as one associated entirely with *mean suspended load transport*

$$\overline{q}_{sS} = \int_{z_r}^{h} u_c \, \overline{c} \, dz \tag{III-6-85}$$

which takes place in the direction of the current ,i.e., at an angle φ_{wc} to the direction of wave propagation, and *mean wave-associated suspended load transport*

$$\overline{q}_{sSw} = \int_{z_r}^{h} \overline{u_w \, c_w} \, dz \tag{III-6-86}$$

which is in the direction of wave propagation when positive.

(1) Mean suspended load transport. The mean suspended load transport, given by Equation 6-85, must be considered for two specific conditions.

(a) When $z_r > z_0$, the current velocity profile is valid for $z \geq z_r$ and the mean suspended load transport is obtained from

$$\overline{q}_{sS} = \frac{u_{*c}}{\kappa} \, \overline{c}_R \left(\frac{\delta_{cw}}{z_r} \right)^{\left(\frac{-w_f}{\kappa u_{*m}} \right)} \delta_{cw} \, (I_1 + I_2) \quad \text{for} \quad z_r > z_0 \tag{III-6-87}$$

where

$$I_1 = \frac{\kappa u_{*c}}{\kappa u_{*m} - w_f}\left\{\ln\frac{\delta_{cw}}{z_0} - \frac{\kappa u_{*m}}{\kappa u_{*m} - w_f} - \left(\frac{z_r}{\delta_{cw}}\right)^{\frac{\kappa u_{*m} - w_f}{\kappa u_{*m}}}\left(\ln\frac{z_r}{z_0} - \frac{\kappa u_{*m}}{\kappa u_{*m} - w_f}\right)\right\} \tag{III-6-88}$$

represents the contribution from inside the wave boundary layer; and

$$I_2 = \frac{\kappa u_{*c}}{\kappa u_{*c} - w_f}\left\{\left(\frac{h}{\delta_{cw}}\right)^{\frac{\kappa u_{*c} - w_f}{\kappa u_{*c}}}\left(\ln\frac{h}{z_{0a}} - \frac{\kappa u_{*c}}{\kappa u_{*c} - w_f}\right) - \left(\ln\frac{\delta_{cw}}{z_{0a}} - \frac{\kappa u_{*c}}{\kappa u_{*c} - w_f}\right)\right\} \tag{III-6-89}$$

expresses the transport above the wave boundary layer.

(b) When $z_r < z_0$, the current velocity profile is not defined for $z_r < z < z_0$. To remedy this physically unrealistic situation, the current velocity profile given by Equation 6-27 is modified to read

$$u_c = \frac{u_{*c}}{\kappa}\,\frac{u_{*c}}{u_{*m}}\,\frac{\ln\frac{\delta_{cw}}{z_0}}{\ln\frac{\delta_{cw}}{z_r}}\,\ln\frac{z}{z_r} \quad \text{for} \quad z < \delta_{cw} \tag{III-6-90}$$

for the purpose of evaluating the transport within the wave boundary layer. The modification retains the matching condition with the outer solution at $z = \delta_{cw}$ and extends the velocity profile down to $z = z_R$.

(c) Introducing Equation 6-90 in the integration leads to

$$\bar{q}_{sS} = \frac{u_{*c}}{\kappa}\,\bar{c}_R\left(\frac{\delta_{cw}}{z_r}\right)^{-\frac{w_f}{\kappa u_{*m}}}\delta_{cw}\,(I_3 + I_2) \quad \text{for} \quad z_r < z_0 \tag{III-6-91}$$

where

$$I_3 = \frac{\ln\frac{\delta_{cw}}{z_0}}{\ln\frac{\delta_{cw}}{z_r}}\,\frac{\kappa u_{*c}}{\kappa u_{*m} - w_f}\left\{\ln\frac{\delta_{cw}}{z_r} - \frac{\kappa u_{*m}}{\kappa u_{*m} - w_f}\left[1 - \left(\frac{z_r}{\delta_{cw}}\right)^{\frac{\kappa u_{*m} - w_f}{\kappa u_{*m}}}\right]\right\} \tag{III-6-92}$$

and I_2 is given by Equation 6-89.

(2) Mean wave-associated suspended load transport. The mean wave-associated suspended load transport is obtained from Equation 6-86. Since u_w and c_w, given by Equations 6-11 and 6-82, respectively, are approximations valid only for $z < \delta_{cw}/\pi$, the integration is extended only to this upper limit. Similar to the computation of the mean suspended load transport, it is necessary here to distinguish between the two cases of $z_0 < z_r$ and $z_r < z_0$. If $z_r > \delta_{cw}/\pi$, wave-associated transport is considered negligibly small.

EXAMPLE PROBLEM III-6-12

FIND:

The mean suspended load transport rate for a combined wave-current boundary layer flow.

GIVEN:

Wave, current, sediment, and bottom slope as given in Example Problem III-6-9. Water depth h = 5.0 m.

PROCEDURE:

1) Movable bed roughness k_n is determined as described in Example Problem III-6-7.

2) Total shear velocities u_{*c}, u_{*wm}, and u_{*m}, and wave boundary layer thickness δ_{cw} are obtained by solving the wave-current interaction following the procedure of Example Problem III-6-4 with k_n from step 1.

3) Apparent bottom roughness z_{0a} and shear stress phase angle φ are obtained as described in Example Problem III-6-5.

4) Skin friction shear velocities u'_{*c}, u'_{*wm}, and u'_{*m}, and phase angle φ′ are obtained as in Example Problem III-6-8.

5) Example Problem III-6-10 is followed to obtain the fall velocity w_f.

6) Mean reference concentration $\overline{c}_R$ is obtained as in Example Problem III-6-11.

7) If $z_r = 7D > z_0 = k_n/30$, the mean suspended sediment transport $\overline{q}_{sS}$ is obtained from Equations 6-87 through 6-89.

8) If $z_r = 7D < z_0 = k_n/30$, the mean suspended sediment transport $\overline{q}_{sS}$ is obtained from Equations 6-91, III-6-92, and 6-89.

9) The mean suspended sediment transport obtained in step 7 or step 8 is in the direction of the current, which in turn is at an angle of φ_{wc} to the direction of wave propagation. In a coordinate system with x in the direction of wave propagation, the mean suspended sediment transport vector is $\overline{\boldsymbol{q}}_{\boldsymbol{sS}} = \overline{q}_{sS}\{\cos\varphi_{wc}, \sin\varphi_{wc}\}$.

(Continued)

Example Problem III-6-12 (Concluded)

SOLUTION:

Since quantities needed for the computation of suspended load transport have been obtained in previous example problems, these are summarized here.

Reference concentration (Example Problem III-6-11): $\bar{c}_R = 1.44\times10^{-3}$ at $z_r = 0.14$

Fall velocity (Example Problem III-6-10): $w_f = 2.23$ cm/s

Shear velocities and *wave boundary layer thickness* based on total movable bed roughness (Example Problem III-6-4): $u_{*c} = 2.94$ cm/s, $u_{*m} = 6.67$ cm/s, and $\delta_{cw} = 3.40$ cm

The *movable bed roughness* and the *apparent bottom roughness* (Example Problems III-6-7 and III-6-5): $z_0 = k_n/30 = 0.15$ cm and $z_{0a} = 0.85$ cm

From the input values summarized above it is seen that $z_r = 0.14$ cm $\approx z_0 = 0.15$ cm. One could therefore choose either Equation 6-87 or Equation 6-91 to obtain the mean suspended load transport. Since $z_r < z_0$, Equation 6-91 is chosen here.

The leading term in Equation 6-91 is computed first

$$\frac{u_{*c}}{\kappa}\,\bar{c}_R\left(\frac{\delta_{cw}}{z_r}\right)^{-\frac{w_f}{\kappa u_{*m}}}\delta_{cw} = 2.5\times10^{-3}\ \text{cm}^3/(\text{cm s})$$

The integral I_3 is evaluated from Equation 6-92

$$I_3 = \frac{3.12}{3.19}\times 2.68\{3.19 - 6.08[1 - 0.59]\} = 1.83$$

and I_2 is obtained from Equation 6-89

$$I_2 = -1.12[0.012(6.38 + 1.12) - (1.39 + 1.12)] = 2.71$$

The mean suspended load transport is therefore obtained from Equation 6-91 as

$$\bar{q}_{sS} = 2.5\times10^{-3}(I_3 + I_2) = 1.1\times10^{-2}\ \text{cm}^3/(\text{cm s})$$

and is in the direction of the current, i.e., at an angle $\varphi_{wc} = 45$ deg to the direction of wave propagation.

(a) For $z_0 < z_r < \delta_{cw}/\pi$, Equations 6-11 and 6-82 may be introduced directly into Equation 6-86 to give

$$\bar{q}_{sSw} = \frac{1}{\pi^2} \sin\varphi \; u_{bm} \, c_{Rwm} \, \delta_{cw} \times \left(\cos(\varphi - \varphi') I_4 - \frac{2}{\pi} \sin\varphi_s \cos(\varphi - \varphi' - \varphi_s) I_5 \right) \quad \text{for} \quad z_0 < z_r \tag{III-6-93}$$

in which

$$I_4 = \ln \frac{\delta_{cw}}{\pi z_0} - 1 - \frac{\pi z_r}{\delta_{cw}} \left(\ln \frac{z_r}{z_0} - 1 \right) \tag{III-6-94}$$

and

$$I_5 = \ln \frac{z_r}{z_0} \left(\ln \frac{\delta_{cw}}{\pi z_r} - 1 + \frac{\pi z_r}{\delta_{cw}} \right) + \left(\ln \frac{\delta_{cw}}{\pi z_r} \right)^2 - 2 \ln \frac{\delta_{cw}}{\pi z_r} + 2 \left(1 - \frac{\pi z_r}{\delta_{cw}} \right) \tag{III-6-95}$$

(b) For $z_r < z_0$ the same modification of the logarithmic velocity profile introduced in the context of mean suspended load transport yields, for $z_r < z_0$

$$\bar{q}_{sSw} = \frac{1}{\pi^2} \sin\varphi \; u_{bm} \; c_{Rwm} \; \delta_{cw} \frac{\ln \frac{\delta_{cw}}{\pi z_0}}{\ln \frac{\delta_{cw}}{\pi z_r}} \times \left(\cos(\varphi - \varphi') I_6 - \frac{2}{\pi} \sin\varphi_s \cos(\varphi - \varphi' - \varphi_s) I_7 \right) \tag{III-6-96}$$

where

$$I_6 = \ln \frac{\delta_{cw}}{\pi z_r} - 1 + \frac{\pi z_r}{\delta_{cw}} \tag{III-6-97}$$

and

$$I_7 = \left(\ln \frac{\delta_{cw}}{\pi z_r} \right)^2 - 2 \ln \frac{\delta_{cw}}{\pi z_r} + 2 \left(1 - \frac{\pi z_r}{\delta_{cw}} \right) \tag{III-6-98}$$

EXAMPLE PROBLEM III-6-13

FIND:

The mean wave-associated suspended load transport rate for a combined wave-current boundary layer flow.

GIVEN:

Same problem specifications as in Example Problem III-6-12.

PROCEDURE:

1) First steps are identical to steps 1 and 2 in Example Problem III-6-12.

2) If $z_r = 7D > \delta_{cw}/\pi$, wave-associated suspended sediment transport is negligibly small.

3) If $z_r = 7D < \delta_{cw}/\pi$, steps 3 through 5 of Example Problem III-6-12 are followed.

4) The wave-associated reference concentration c_{Rw} is obtained as in Example Problem III-6-11.

5) The sediment suspension phase angle φ_s is obtained from Equation 6-83 with $z_r = 7D$.

6) If $z_r = 7D > z_0 = k_n/30$, the mean wave-associated suspended sediment transport $\overline{q}_{sSw}$ is obtained from Equations 6-93 through 6-95.

7) If $z_r = 7D < z_0 = k_n/30$, the mean wave-associated suspended sediment transport $\overline{q}_{sSw}$ is obtained from Equations 6-96 through 6-98.

8) The suspended sediment transport obtained in step 6 or step 7 is in the direction of wave propagation, i.e., $\text{uu}\,\overline{\boldsymbol{q}}_{sSw} = \overline{q}_{sSw}\{1,\ 0\}$ with x in the direction of wave propagation.

(Continued)

Example Problem III-6-13 (Concluded)

SOLUTION:

In addition to the quantities given in Example Problem III-6-12, the computation of the mean wave-associated suspended load transport requires knowledge of *phase angles*

$$\varphi = 38° \quad \text{and} \quad \varphi' = 14°$$

obtained from Example Problems III-6-5 and 8. The sediment suspension phase angle φ_s is obtained from Equation 6-83 with $z_r = 7D = 0.14$ cm

$$\tan \varphi_s = 0.77 \rightarrow \varphi_s = 37.6° \approx 38°$$

and the *maximum wave-associated reference concentration* (Example Problem III-6-11) is

$$c_{Rwm} = 0.65 \times 10^{-3}$$

Since $z_r = 0.14$ cm $< z_0 = 0.15$ cm, the wave-associated mean transport is obtained from Equation 6-96.

The leading term of this equation becomes

$$\frac{1}{\pi^2} \sin \varphi \quad u_{bm} \; c_{Rwm} \; \delta_{cw} \; \frac{\ln \dfrac{\delta_{cw}}{\pi z_0}}{\ln \dfrac{\delta_{cw}}{\pi z_r}} = 5.0 \times 10^{-3} \text{ cm}^3/(\text{cm s})$$

and the integral I_6 is obtained from Equation 6-97

$$I_6 = 2.05 - 1 + 0.13 = 1.18$$

and I_7 is given by Equation 6-98

$$I_7 = 4.18 - 4.09 + 2(1 - 0.13) = 1.83$$

Introducing these quantities in Equation 6-96, the *mean wave-associated suspended load transport* is obtained as

$$\bar{q}_{sSw} = 5.0 \times 10^{-3} \left(1.18 \cos (38° - 14°) - 1.83 \frac{2}{\pi} \sin 38° \cos (38° - 14° - 38°) \right) = 1.9 \times 10^{-3} \text{ cm}^3/(\text{cm s})$$

The direction of this transport is in the direction of wave propagation.

(3) Computation of total suspended load transport for combined wave-current flows.

(a) With the wave and current components of the skin friction bottom shear stress including the phase angle φ' obtained following the procedures given in Part III-6-3-*c*, the mean $\bar{c}_R$ and wave-associated c_{Rwm} reference concentrations are obtained from Equations 6-75 and 6-76, respectively, and the phase angle for the wave-associated concentration φ_s is obtained from Equation 6-83.

(b) From the hydrodynamic wave-current interaction model corresponding to movable bed roughness, u_{*c}, u_{*wm}, u_{*m}, and φ are known and w_f is obtained from Part III-6-5-*a*. Thus, with δ_{cw} given by Equation 6-79, all quantities necessary to evaluate Equations 6-87 and 6-93, for $z_0 < z_r = 7D$, or Equations 6-91 and 6-96, for $z_r = 7D < z_0$, are available.

f. Extensions of methodology for the computation of suspended load.

(1) Extension to spectral waves. For a wave motion described by its near-bottom orbital velocity spectrum, the representative periodic wave characteristics discussed in Part III-6-2-b (4) are used. Once again it is emphasized that this representative wave corresponds to the use of the rms wave height and *not* the significant wave height.

(2) Extension to sediment mixtures. For a sediment mixture, the suspended load transport may be calculated as described above for a single grain size of diameter D.

(a) The skin friction $\tau_b'(t)$ and movable bed roughness k_n are computed using the median grain size $D = D_{50}$.

(b) For each grain size class of diameter D_n, the reference concentration is obtained from the formulas given in Part III-6(5)*c* with τ_{cr}, the critical shear stress, replaced by $\tau_{cr,n}$, the critical shear stress for the nth size class, and C_b, the sediment concentration in the bed, being replaced by $f_n C_b$ where f_n, is the volume fraction in the bed of sediment of diameter D_n. This reference concentration is assumed to be specified at $z = z_r = 7D_{50}$ for all size classes.

(c) For each size class, the suspended load transport is now computed as detailed in Part III-6(5)e using the fall velocity $w_{f,n}$ appropriate for the nth size class.

(d) When suspended load transport has been obtained for each size class, the total suspended load transport for the sediment mixture is obtained by adding the contribution of individual size classes.

III-6-6. Summary of Computational Procedures

a. Problem specification. A properly posed problem requires the following specifications:

(1) *The waves* are specified by near-bottom orbital velocity u_{bm}, radian frequency ω ($A_{bm} = u_{bm}/\omega$), and their angle of incidence α ($|\alpha| < \pi/2$) if waves are traveling towards shallower water). For spectral waves, a representative periodic wave is defined in Part III-6(2)c(5). If the significant wave characteristics H_s and T_s are given, the equivalent periodic wave has a height $H_{rms} = h_s/\sqrt{2}$ and period $T = T_s$.

(2) *The current* is specified by a reference current $u_c(z_r)$ at $z = z_r$ above the bottom and its direction φ_{wc} measured counterclockwise from the direction of wave propagation; or by the average bottom shear stress τ_c and its direction φ_{wc}.

(3) *The fluid* is specified by its density, $\rho \approx 1{,}025$ km/m^3 for seawater, and kinematic viscosity, $\nu \approx 10^{-6}$ m^2/s for seawater.

(4) *The sediment* is specified by its diameter D and density ρ_s ($s = \rho_s/\rho$). The sediment must be characterized as cohesionless.

(5) *The bottom slope* is specified normal to depth contours by $\tan\beta$ ($\beta > 0$). The slope in direction of wave propagation is then $\tan\beta_w = \tan\beta\cos\alpha > 0$ if bottom is sloping upwards in wave direction ($|\alpha| < \pi/2$).

b. Model parameters.

(1) A number of model parameters and constants have been introduced and must be specified to proceed towards a solution

κ = von Karman's constant = 0.4

φ_s = static friction angle of sediment = 50°

φ_m = moving friction angle of sediment = 30°

C_b = volume concentration of sediment in the bed = 0.65

γ = resuspension parameter = 2×10^{-3} for rippled beds, 2×10^{-4} for flat beds (sheet flow)

(2) Figure III-6-12 specifies coordinate, angle, and bottom slope definitions used in this chapter.

c. Computational procedures. The following steps should be followed to obtain the total sediment transport rate at a point:

(1) Movable bottom roughness is determined from the wave and sediment characteristics. The maximum wave skin friction shear stress τ'_{wm} is obtained following the procedures described in Part III-6(2)*c* using $k_n = k_n' = D$. Sediment motion is checked using the modified Shields diagram, Part III-6(3)*c*. If sediment *is not* moving, $k_n = D$ *is* the movable bed roughness. If sediment is found to move, the movable bed roughness k_n is obtained following the procedures outlined in Part III-6(3)*e* using $\tau'_{wm} = \tau'_m$.

(2) With the movable bed roughness k_n known, the wave-current interaction model (Part III-6(2)*d*) is used to obtain total bottom shear stresses, shear velocities, and phase angles so that wave orbital and current velocity profiles may be evaluated.

(3) Using the current at the edge of the wave boundary layer obtained from the movable bed roughness model as the current specification, the wave-current interaction model (Part III-6(2)*d*) is used with $k_n' = D$ to obtain the combined wave-current skin friction shear stress $\tau'_b(t)$.

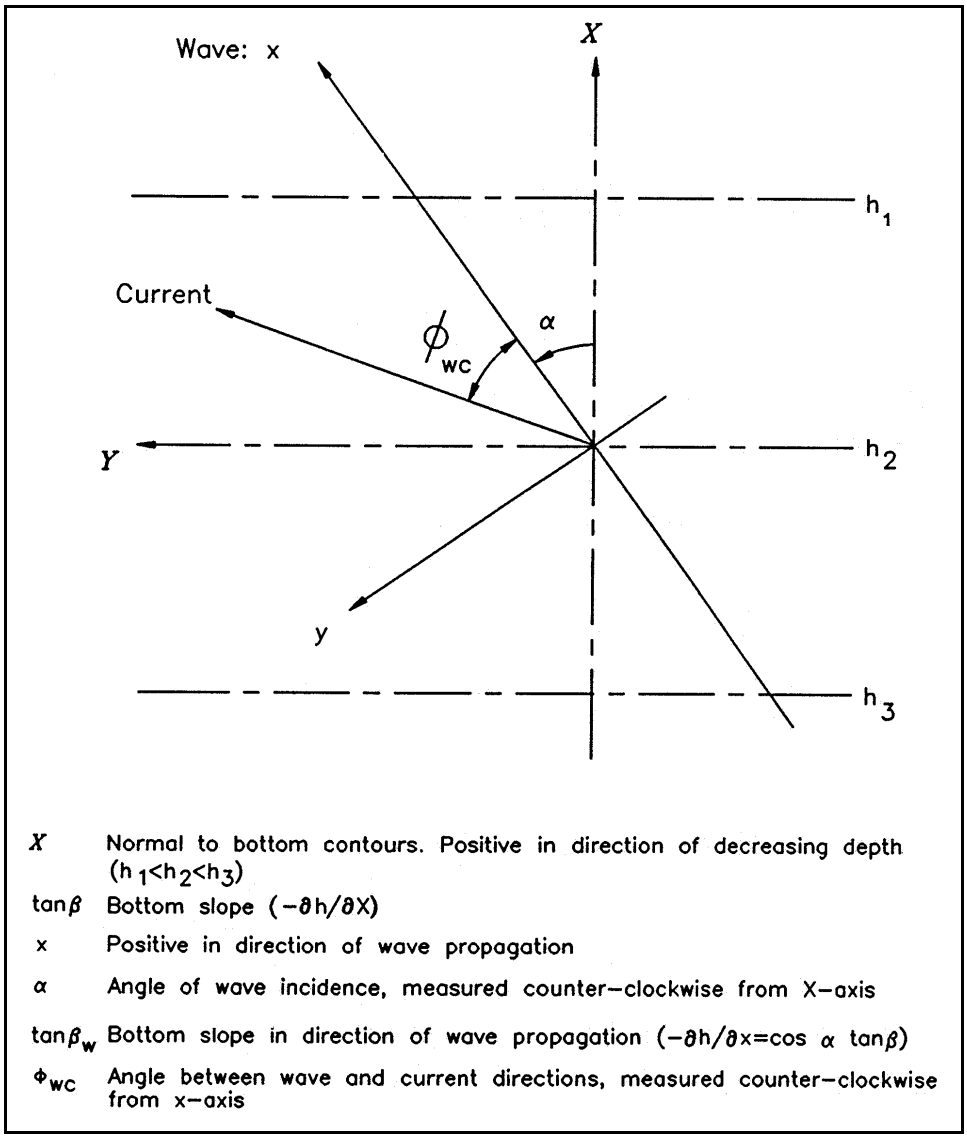

Figure III-6-12. Definition sketch of coordinates, angles, and bottom slope

(4) Bed-load transport can now be computed following the methodology presented in Part III-6(4).

(5) The reference concentration for suspended sediment is next obtained from Part III-6(5)*c*, and the total suspended load transport is obtained by vector addition of the mean and the mean wave-associated contributions that are obtained from Part III-6(5)*e*. The former is in the direction of the current, whereas the latter is in the wave direction.

(6) Adding bed-load and suspended load transport provides a prediction of the total sediment transport rate, expressed as a vector.

EXAMPLE PROBLEM III-6-14

FIND:

The total sediment transport vector for a combined wave-current boundary layer flow.

GIVEN:

All problem specifications are identical to those given in Example Problems III-6-9, 12, and 13.

PROCEDURE:

1) Bed-load sediment transport vector is computed following Example Problem III-6-9.

2) Mean suspended sediment transport vector is obtained following the procedure of Example Problem III-6-12.

3) Mean wave-associated suspended sediment transport vector is obtained from Example Problem III-6-13.

4) Total sediment transport vector is obtained as the vector sum of steps 1, 2, and 3.

SOLUTION:

With x being in the direction of wave propagation and y perpendicular to x, the total sediment transport in the x direction is obtained from Example Problems III-6-9, 12, and 13.

x-component of bed load = 9.0×10^{-3} cm^3/(cm s)
x-component of mean suspended load = $1.1\times10^{-2} \cos \varphi_{wc} = 7.8\times10^{-3}$ cm^3/(cm s)
x-component of mean wave-associated transport = 1.9×10^{-3} cm^3/(cm s)
Total transport in wave direction = $\overline{q}_{sT,x} = 1.9\times10^{-2}$ cm^3/(cm s)

y-component of bed load = 6.5×10^{-3} cm^3/(cm s)
y-component of mean suspended load = $1.1\times10^{-2} \sin \varphi_{wc} = 7.8\times10^{-3}$ cm^3/(cm s)
y-component of mean wave-associated transport = 0 cm^3/(cm s)
Total transport perpendicular to wave direction = $\overline{q}_{sT,y} = 1.4\times10^{-2}$ cm^3/(cm s)

Thus, the magnitude of the total sediment transport vector is

$$|\overline{\boldsymbol{q}}_{sT}| = \sqrt{\overline{q}_{sT,x}^2 + \overline{q}_{sT,y}^2} = 2.4\times10^{-2} \text{ cm}^3/(\text{cm s})$$

directed at an angle $\varphi_{wT} \approx 37°$ to the wave direction.

III-6-7. References

Bakker and van Doorn 1978
Bakker, W. T., and Van Doorn, T. 1978. "Near-Bottom Velocities in Waves with a Current," *Proceedings Sixteenth International Coastal Engineering Conference*, American Society of Civil Engineers, Vol 2, pp 1394–1413.

Bijker 1967
Bijker, E.W. 1967. "Some Considerations about Scales for Coastal Models with Movable Bed," Technical Report, Delft Hydraulics Lab, The Netherlands.

Davies, Soulsby, and King 1988
Davies, A. G., Soulsby, R. L., and King, H. L. 1988. "A Numerical Model of the Combined Wave and Current Bottom Boundary Layer," *Journal of Geophysical Research*, Vol 93, No. C1, pp 491 - 508.

Dietrich 1982
Dietrich, W. E. 1982. "Settling Velocity of Natural Particles," *Water Resources Research*, Vol 18, No. 6, pp 1615–1626.

Dyer and Soulsby 1988
Dyer, K. R., and Soulsby, R.L. 1988. "Sand Transport on the Continental Shelf," *Annual Review of Fluid Mechanics*, Vol 20, pp 295-324.

Fredsoe 1984
Fredsoe, J. 1984. "Sediment Transport in Current and Waves," *Series Paper 35*, Institute of Hydrodynamics and Hydrologic Engineering, Technical University of Denmark, Lyngby.

Glenn and Grant 1987
Glenn, S. M., and Grant, W. D. 1987. "A Suspended Sediment Correction for Combined Wave and Current Flows," *Journal of Geophysical Research*, Vol 92, No. C8, pp 8244–8264.

Grant and Madsen 1979
Grant, W. D., and Madsen, O. S. 1979. "Combined Wave and Current Interaction with a Rough Bottom," *Journal of Geophysical Research*, Vol 85, No. C4, pp 1797–1808.

Grant and Madsen 1982
Grant, W. D., and Madsen, O. S. 1982. "Movable Bed Roughness in Unsteady Oscillatory Flow," *Journal of Geophysical Research*, Vol 87, No. C1, pp 469–481.

Grant and Madsen 1986
Grant, W. D., and Madsen, O. S. 1986. "The Continental Shelf Bottom Boundary Layer," M. Van Dyke, ed., *Annual Review of Fluid Mechanics*, Vol 18, pp 265–305.

Heathershaw 1981
Heathershaw, A.D. 1981. "Comparisons of Measured and Predicted Sediment Transport Rates in Tidal Currents," *Marine Geology*, Vol 42, pp 75-104.

Jonsson 1966
Jonsson, I. G. 1966. "Wave Boundary Layers and Friction Factors," *Proceedings of the Tenth International Coastal Engineering Conference*, American Society of Civil Engineers, Vol 1, pp 127–148.

Jonsson and Carlson 1976
Jonsson, I. G., and Carlsen, N. A. 1976. "Experimental and Theoretical Investigation in an Oscillatory Turbulent Boundary Layer," *Journal of Hydraulic Research*, Vol 14, No. 1, pp 45–60.

Kajiura 1968
Kajiura, K. 1968. "A Model of the Bottom Boundary Layer in Water Waves," *Bulletin of the Earthquake Research Institute*, Disaster Prevention Research Institute, Tokyo University, Vol 46, pp 75–123.

Madsen 1991
Madsen, O. S. 1991. "Mechanics of Cohesionless Sediment Transport in Coastal Waters," *Proceedings, Coastal Sediments '91*, American Society of Civil Engineers, Vol 1, pp 15–27.

Madsen 1992
Madsen, O. S. 1992. "Spectral Wave-Current Bottom Boundary Layer Flows," *Abstracts, Twenty-Third International Coastal Engineering Conference*, American Society of Civil Engineers, pp 197–198.

Madsen 1993
Madsen, O.S. 1993. "Sediment Transport Outside the Surf Zone," unpublished Technical Report, U.S. Army Engineer Waterways Experiment Station, Vicksburg, MS.

Madsen and Grant 1976
Madsen, O. S., and Grant, W. D. 1976. "Quantitative Description of Sediment Transport by Waves," *Proceedings, Fifteenth International Coastal Engineering Conference*, American Society of Civil Engineers, Vol 2, pp 1093–1112.

Madsen and Wikramanayake 1991
Madsen, O. S., and Wikramanayake, P. N. 1991. "Simple Models for Turbulent Wave-Current Bottom Boundary Layer Flow," Contract Report DRP-91-1, U.S. Army Engineer Waterways Experiment Station, Vicksburg, MS.

Madsen et al., in preparation
Madsen, O. S., Wright, L. D., Boon, J. D., and Chisholm, T. A. "Wind Stress, Bottom Roughness and Sediment Suspension on the Inner Shelf during an Extreme Storm Event," in preparation, *Continental Shelf Research*.

Madsen, Poon, and Graber 1988
Madsen, O. S., Poon, Y.-K., and Graber, H. C. 1988. "Spectral Wave Attenuation by Bottom Friction: Theory," *Proceedings, Twenty-First International Coastal Engineering Conference*, American Society of Civil Engineers, Vol 1, pp 492–504.

Mathisen 1993
Mathisen, P.P. 1993. "Bottom Roughness for Wave and Current Boundary Layer Flows over a Rippled bed," Ph.D. diss., Department of Civil and Environmental Engineering, Massachusetts Institute of Technology, Cambridge, MA.

Meyer-Peter and Müller 1948
Meyer-Peter, E., and Müller, R. 1948. "Formulas for Bed-Load Transport," *Report on Second Meeting of International Association for Hydraulic Research*, pp 39–64.

Nikuradse 1933
Nikuradse, J. 1933. "Strömungsgesetze in rauhen Rohren," VDI Forschungsheft No. 361 (English translation NACA Technical Memorandum No. 1292).

Raudkivi 1976
Raudkivi, A. J. 1976. *Loose Boundary Hydraulics* (2nd ed.), Pergamon Press, Oxford, England.

Schlichting 1960
Schlichting, H. 1960. *Boundary Layer Theory* (fourth ed.), McGraw-Hill, New York.

Shields 1936
Shields, A. 1936. "Application of Similarity Principles and Turbulent Research to Bed-Load Movement," (translation of original in German by W. P. Ott and J. C. van Uchelen, California Institute of Technology), *Mitteilungen der Preussischen Versuchsanstalt für Wasserbau und Schiffbau*.

Smith 1977
Smith, J. D. 1977. "Modeling of Sediment Transport on Continental Shelves," *The Sea*, E. D. Goldberg, ed., Wiley Interscience, New York, pp 539–577.

Smith and McLean 1977
Smith, J. D., and McLean, S. R. 1977. "Spatially Averaged Flow Over a Wavy Surface," *Journal of Geophysical Research*, Vol 82, No. 12, pp 1735–1745.

Trowbridge and Madsen 1984
Trowbridge, J. H., and Madsen, O. S. 1984. "Turbulent Wave Boundary Layers," *Journal of Geophysical Research*, Vol 89, No. C5, pp 7989–8007.

White, Milli, and Crabbe 1975
White, W.R., Milli, H., and Crabbe, H.O. 1975. "Sediment Transport Theories: A Review," *Proceedings, Institute of Civil Engineering,* Vol 59, pp 265-292.

Wikramanayake and Madsen 1994a
Wikramanayake, P. N., and Madsen, O. S. 1994a. "Calculation of Movable Bed Friction Factors," Contract Report DRP-94-5, U.S. Army Engineer Waterways Experiment Station, Vicksburg, MS.

Wikramanayake and Madsen 1994b
Wikramanayake, P. N., and Madsen, O. S. 1994b. "Calculation of Suspended Sediment Transport by Combined Wave-Current Flows," Contract Report DRP-94-7, U.S. Army Engineer Waterways Experiment Station, Vicksburg, MS.

Wilson 1989
Wilson, K. C. 1989. "Friction of Wave Induced Sheet Flow," *Coastal Engineering*, Vol 12, pp 371–379.

III-6-8. Definition of Symbols

β	Bottom slope [deg]
β_w	Bottom slope in the direction of wave propagation [deg]
γ	Resuspension parameter [dimensionless]
δ_{cw}	Boundary layer thickness for a combined wave-current turbulent boundary layer [length]
δ_w	Boundary layer thickness [length]
η	Ripple height [length]
κ	von Karman's constant (= 0.4)
λ	Ripple length [length]
μ	Ratio of Shear stress due to currents (τ_c) to Maximum bottom shear stress (τ_{wm})
μ_b	Bottom slope parameter
ν	Kinematic viscosity [length^2/time]
ν_s	Sediment diffusion coefficient
ν_T	Turbulent eddy viscosity [length^2/time]
ρ	Mass density of water (salt water = 1,025 kg/m^3 or 2.0 slugs/ft^3; fresh water = 1,000kg/m^3 or 1.94 slugs/ft^3) [force-time^2/length^4]
ρ_s	Mass density of sediment grains [force-time^2/length^4]
τ_b	Bottom shear stress [force/length^2]
τ_c	Shear stress due to currents [force/length^2]
τ_{cr}	Critical bottom shear stress for initiation of motion [force/length^2]
τ_m	Maximum combined bottom shear stress [force/length^2]
τ_w	Bottom shear stress [force/length^2]
τ_{wm}	Maximum bottom shear stress [force/length^2]
τ'_b	Bottom skin friction shear stress [force/length^2]
τ'_{wm}	Skin friction bottom shear stress for wave motion [force/length^2]
τ''_b	Bottom drag shear stress [force/length^2]
φ	Phase lead of near-bottom wave orbital velocity (bottom shear stress phase angle) [deg]
φ_m	Friction angle [deg]
φ_s	Friction angle for a stationary interfacial sediment grain [deg]

Ψ	Shields parameter (Equation III-6-43) [dimensionless]
Ψ_{cr}	Critical Shields parameter (Equation III-6-45) [dimensionless]
$\Psi_{cr,\beta}$	Critical Shields parameter for flow over a sloping bottom (Equation III-6-51) [dimensionless]
Ψ'_C	Shields parameter based on the current skin friction shear stress [dimensionless]
Ψ'_m	Skin friction Shields parameter [dimensionless]
ω	Wave angular or radian frequency (= $2\pi/T$) [time^{-1}]
A_{bm}	Bottom excursion amplitude predicted by linear wave theory [length]
c	Volume concentration of sediment in suspension [length^3/length^3]
$\overline{c}$	Mean volume concentration of sediment in suspension [length^3/length^3]
$\overline{c}_R$	Mean reference concentration [length^3/length^3]
C_μ	Factor relating maximum wave and maximum combined bottom shear stresses (equation III-6-33)
C_b	Volume concentration of sediment in the bed
c_R	Reference concentration [length^3/length^3]
c_{Rwm}	Wave-associated maximum reference concentration [length^3/length^3]
c_w	Wave-associated volume concentration of sediment in suspension [length^3/length^3]
D	Sediment grain diameter [length - generally millimeters]
D_p	Time-averaged rate of energy dissipation in the wave bottom boundary layer (Equation III-6-25)
f_c	Current friction factor [dimensionless]
f_{cw}	Wave friction factor in the presence of currents [dimensionless]
f_w	Wave friction factor [dimensionless]
f'_w	Wave friction factor [dimensionless]
g	Gravitational acceleration (32.17 ft/sec^2, 9.807m/sec^2) [length/time^2]
h	Water depth [length]
H_{rms}	Root-mean-square wave height [length]
H_s	Significant wave height [length]
k_n	Equivalent Nikuradse sand grain roughness [length]
k_n	Movable bed roughness [length]
q	Sediment transport rate [length^3/time]

$\overline{q_{sB}}$	Total bed-load transport of a sediment mixture [length^3/length-time]
RE	Wave Reynolds number [dimensionless]
Re_*	Boundary Reynolds number [dimensionless]
S_*	Sediment-fluid parameter (Equation III-6-47) [dimensionless]
T	Significant wave period [time]
T_s	Significant wave period [time]
u	Horizontal particle velocity [length/time]
u_*	Shear velocity [length/time]
u_{*c}	Current shear velocity [length/time]
u_{*cr}	Critical shear velocity [length/time]
u_{*m}	Maximum combined shear velocity [length/time]
u_{*wm}	Maximum wave shear velocity [length/time]
u_{bm}	Maximum near-bottom wave orbital velocity [length/time]
u_w	Wave orbital velocity [length/time]
w_f	Sediment fall velocity [length/time]
W_{grain}	Submerged weight of individual sediment grains
z	Elevation from bottom [length]
Z	Parameter providing a correlation of field data on ripple geometry [dimensionless]
z_{0a}	Arbitrary constant of integration (apparent bottom roughness)

III-6-9. Acknowledgments

Authors of Chapter III-6, "Sediment Transport Outside the Surf Zone:"

Ole S. Madsen Ph.D., Dept. of Civil and Environmental Engineering, Massachusetts Institute of Technology, Cambridge, Massachusetts.
William Wood, Ph.D. (Deceased).

Reviewers:

Scott M. Glenn, Ph.D., Institute of Marine and Coastal Sciences, Rutgers University, New Brunswick, New Jersey.
James R. Houston, Ph.D., Engineer Research and Development Center, Vicksburg, Mississippi.
Stephen McLean, Ph.D., Department of Mechanical and Environmental Engineering, University of California, Santa Barbara, Santa Barbara, California.
Todd L. Walton, Ph.D., Coastal and Hydraulics Laboratory, Engineer Research and Development Center (ERDC), Vicksburg, Mississippi.

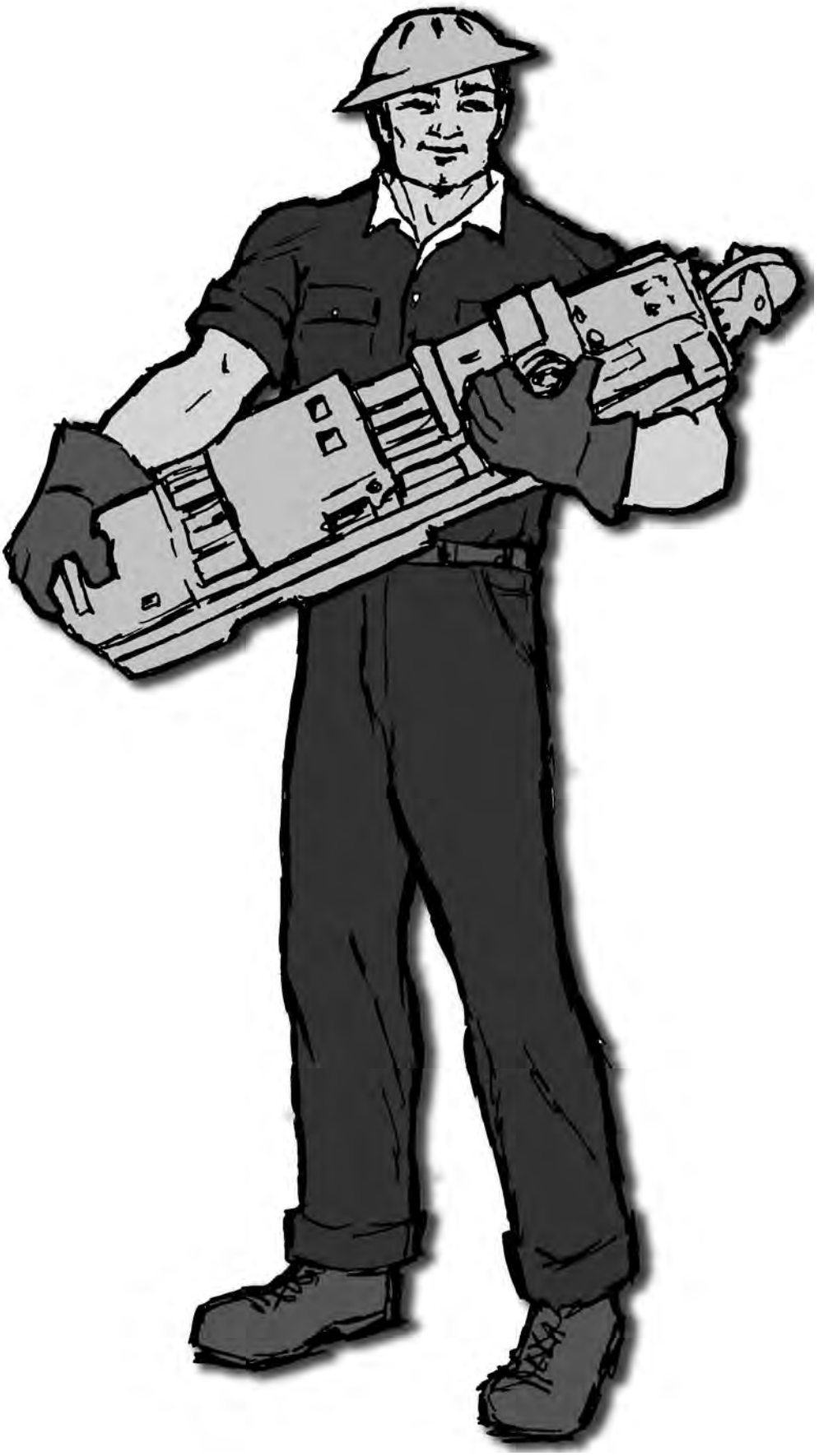

Table of Contents

Page

IV-1-1. Background IV-1-1

IV-1-2. Coastal Zone Definitions and Subdivisions IV-1-2
a. Introduction IV-1-2
b. Coastal zone IV-1-3
c. Coast IV-1-3
d. Shore IV-1-3
e. Shoreface IV-1-3
f. Continental shelf IV-1-3
g. Shoreline definitions IV-1-6

IV-1-3. Geologic Time and Definitions IV-1-7
a. Geologic fossil record IV-1-7
b. Geologic time considerations for coastal engineering IV-1-9

IV-1-4. Water Level Datums and Definitions IV-1-9

IV-1-5. Factors Influencing Coastal Geology IV-1-10
a. Underlying geology and geomorphology IV-1-10
(1) Lithology IV-1-10
(a) Consolidated coasts IV-1-11
(b) Unconsolidated coasts IV-1-11
(2) Tectonics IV-1-11
(3) Volcanic coasts IV-1-11
b. High-frequency dynamic processes IV-1-13
(1) Waves IV-1-13
(2) Tides IV-1-14
(3) Energy-based classification of shorelines IV-1-16
(4) Meteorology IV-1-18
(a) Wind IV-1-18
(b) Direct influence of wind IV-1-18
(c) Indirect effect IV-1-18
(d) Land/sea breeze IV-1-18
(e) Water level setup and setdown IV-1-18
(f) Seiches IV-1-19
(5) Tropical storms IV-1-19
(6) Extratropical storms IV-1-21
c. Biological factors IV-1-24

IV-1-6. Sea Level Changes IV-1-25
a. Background IV-1-25
(1) General IV-1-25
(2) Definitions IV-1-25
(3) Overview of causes of sea level change IV-1-26
b. Short-term causes of sea level change IV-1-27
(1) Seasonal sea level changes IV-1-27
(2) West coast of North America IV-1-27
(3) Rapid land level changes IV-1-27
(4) Ocean temperature IV-1-27
(5) Ocean currents IV-1-29
c. Long-term causes of sea level change IV-1-29
(1) Tectonic instability IV-1-29
(2) Isostacy IV-1-29
(3) Sediment compaction IV-1-29
d. Geologic implications of sea level change IV-1-31
(1) Balance of sediment supply versus sea level change IV-1-31
(2) Historical trends IV-1-32
(3) Specific coastal sites IV-1-33
(a) Sandy (barrier) coasts IV-1-33
(b) Cliff retreat IV-1-33
(c) Marshes and wetlands IV-1-33
e. Engineering and social implications of sea level change IV-1-33
(1) Eustatic sea level rise IV-1-33
(2) Relative sea level (rsl) changes IV-1-34
(3) Engineering response and policy IV-1-36
(4) Impacts of rising sea level on human populations IV-1-36
f. Changes in sea level - summary IV-1-37

IV-1-7. Cultural (Man-Made) Influences on Coastal Geology IV-1-38
a. Introduction IV-1-38
b. Dams/Reservoirs IV-1-38
c. Erosion control and coastal structures IV-1-38
d. Modification of natural protection IV-1-39
(1) Destructive effects IV-1-39
(2) Constructive efforts IV-1-39
e. Beach renourishment (fill) IV-1-39
f. Mining IV-1-39
g. Stream diversion IV-1-39
h. Agriculture IV-1-40
i. Forestry IV-1-40

IV-1-8. References IV-1-40

IV-1-9. Acknowledgments IV-1-49

List of Tables

Page

Table IV-1-1. Definitions of Common Coastal Geomorphic Features IV-1-6

Table IV-1-2. North American Pleistocene Glacial and Interglacial Stages IV-1-10

Table IV-1-3. Damage Estimates and Payouts by Insurance Companies for U.S. Catastrophes . IV-1-20

Table IV-1-4. Saffir-Simpson Damage-Potential Scale IV-1-21

Table IV-1-5. Sea Level Changes Along the Coastal Zone IV-1-28

Table IV-1-6. Major World Cities with Recorded Subsidence IV-1-30

Table IV-1-7. Relative Effects of Sediment Supply Versus Sea Level Change on Shoreline Position IV-1-32

List of Figures

Page

Figure IV-1-1. Temporal and spatial scales of geologic and oceanographic phenomena IV-1-2

Figure IV-1-2. Definition of terms and features describing the coastal zone IV-1-4

Figure IV-1-3. Continental shelf and ocean floor along the trailing-edge of a continent (i.e., representative of the U.S. Atlantic Ocean coast) IV-1-5

Figure IV-1-4. Geologic time scale IV-1-8

Figure IV-1-5. Cross-section views of aspects of geomorphic variability attributable to lithology, structure, and mass movement along semi-consolidated coasts IV-1-12

Figure IV-1-6. Examples of features associated with depositional coastal environments IV-1-13

Figure IV-1-7. Examples of tectonically produced features: (a) stable undeformed block; (b) symmetrical folding resulting from compressional forces; (c) normal faulting resulting from tensional forces; (d) composite volcano composed of alternating layers of pyroclastic material (ash) and lava flows IV-1-14

Figure IV-1-8. Example of a fault coast exhibiting a prominent fault scarp IV-1-15

Figure IV-1-9. Example of a volcanic coast with numerous circular islands IV-1-15

Figure IV-1-10. Energy-based classification of shorelines IV-1-17

Figure IV-1-11. Worldwide tropical storm pathways IV-1-21

Figure IV-1-12. Graphical representation of the Saffir-Simpson Scale, showing the amount of damage that can be expected during different category hurricanes IV-1-22

Figure IV-1-13. Hurricane Opal damage at Navarre Beach, Florida, November 1995, house lifted from foundation and washed into bay IV-1-23

Figure IV-1-14. Hurricane Opal damage at Navarre Beach, Florida, November 1995, sand underneath concrete slab washed away IV-1-23

Figure IV-1-15. Sea level fluctuations during the Pleistocene and Holocene epochs IV-1-26

Figure IV-1-16. Yearly mean sea level changes at Juneau, Alaska, from 1936-1986 . . . . . IV-1-30

Figure IV-1-17. Yearly mean sea level changes at Galveston, Texas, and Eugene Island, Louisiana IV-1-31

Figure IV-1-18. Summary of estimates of local rsl rise along the continental United States in millimeters per year IV-1-35

Figure IV-1-19. Landfilling in Boston, MA, since 1630 has more than doubled the urban area IV-1-35

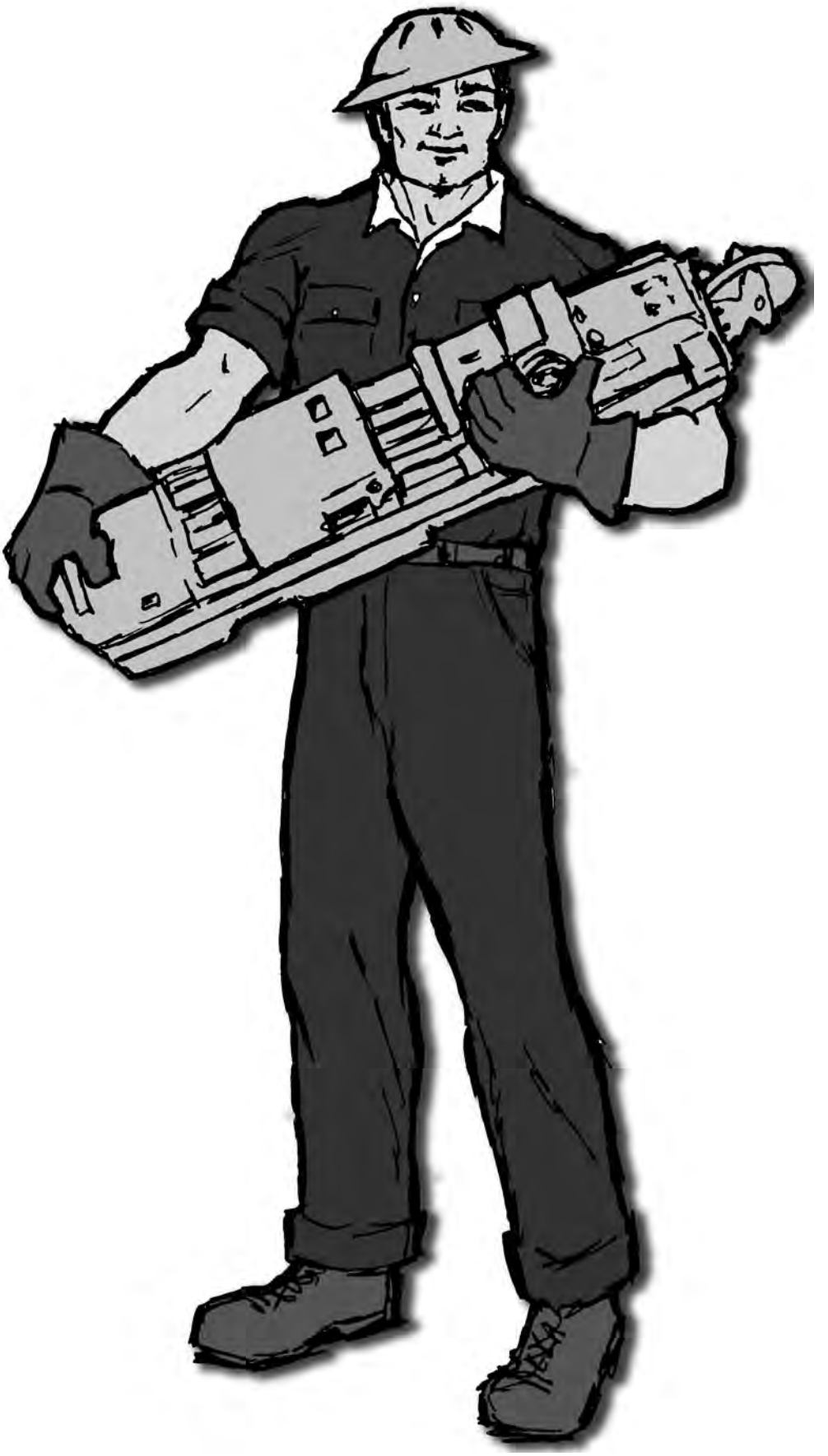

Chapter IV-1
Coastal Terminology and Geologic Environments

IV-1-1. Background

a. Since man has ventured to the sea, he has been fascinated by the endless variety of landforms and biological habitats that occur at the coast. With the exception of high altitude alpine, a full spectrum of environments is found around the world's coastlines. These range from icy arctic shores to rocky faulted coasts to temperate sandy barriers to tropical mangrove thickets, with a myriad of intermediate and mixed forms. This part of the *Coastal Engineering Manual* (CEM) concentrates on the geology of the coastal zone. This broad subject encompasses both the geomorphology (the shape and form) of the landforms and the nature of the ancient strata that underlie or outcrop in the region. The forces that shape, and are shaped by, the coast are part of the overall picture, although here geology merges with the other earth sciences of meteorology and oceanography.

b. This and the two chapters that follow have ambitious goals:

(1) To review overall geological, environmental, and climatological settings of the world's coasts.

(2) To describe particular shore types in detail and provide examples.

(3) To explain how shore types are created by and interact with the forces of waves, currents, and weather (sometimes known as “morphodynamics”).

The emphasis here is on features and landforms that range in size from centimeters to kilometers and are formed or modified over time scales of minutes to millennia (Figure IV-1-1).

c. Another subject of crucial importance to coastal researchers is biology. The biological environment is partly established by the geological setting. Conversely, biology affects coastal geology in many ways:

(1) Coral reefs and mangroves have created large stretches of coastline.

(2) Cliff erosion is accelerated by the chemical solution and mechanical abrasion caused by some organisms.

(3) Lagoons and estuaries slowly fill with the by-products of plants and the sediment they trap, forming wetlands.

These topics are briefly reviewed in this text, but details of the flora and fauna that inhabit the coast are not covered here.

d. Field methods and data analysis procedures applicable to geological field studies at the coast are not reviewed in this part of the CEM. Field methods are constantly evolving and changing as new instruments and technology are developed. Coastal monitoring methods were reviewed in Gorman, Morang, and Larson (1998); Larson, Morang, and Gorman (1997); and Morang, Larson, and Gorman (1997a,b). Readers who plan to conduct field studies should contact surveyors or contractors familiar with the latest technology and should review trade journals that discuss oceanographic, geographic information systems (GIS), remote sensing, and surveying advances.

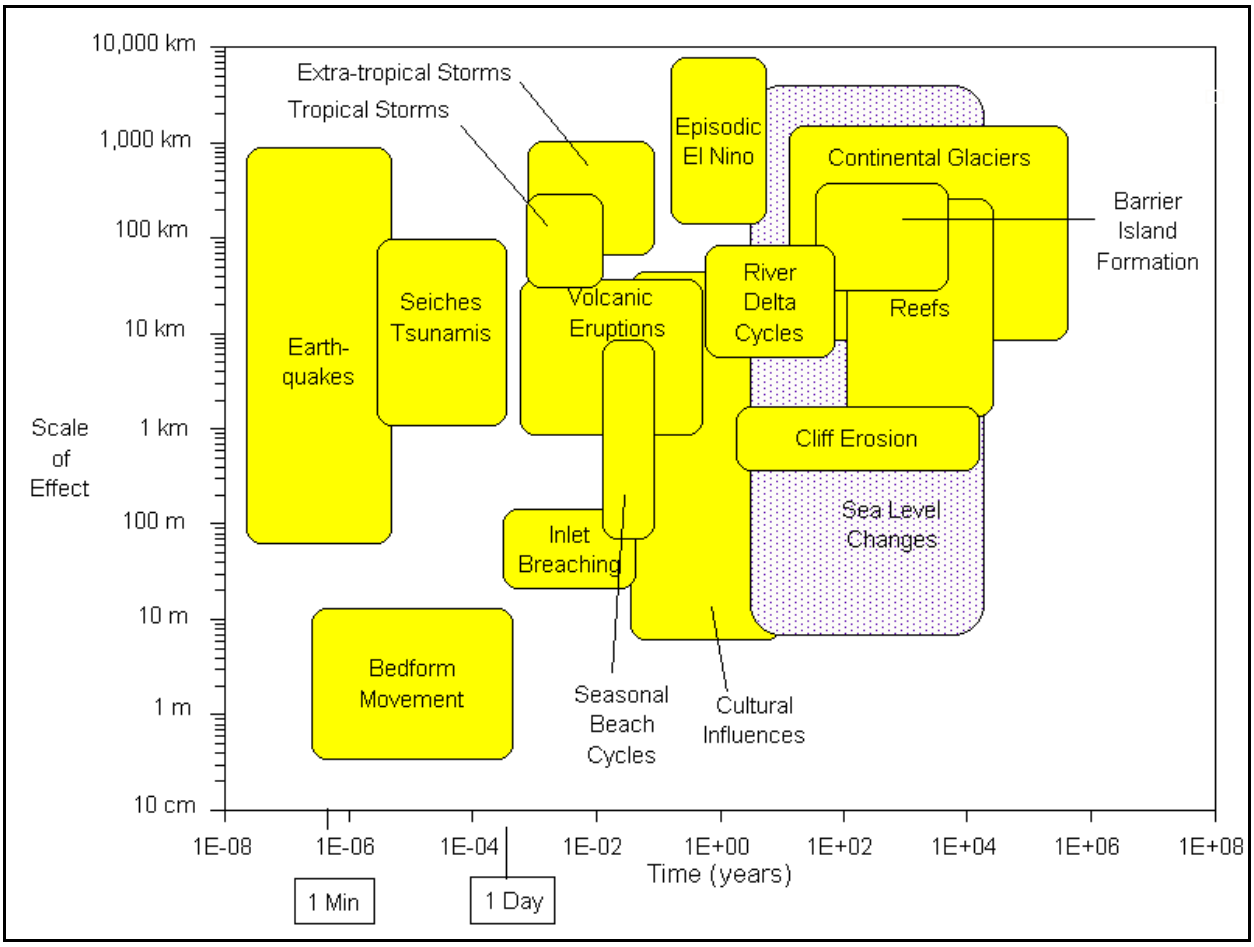

Figure IV-1-1. Temporal and spatial scales of geologic and oceanographic phenomena

IV-1-2. Coastal Zone Definitions and Subdivisions

a. Introduction.

(1) Many coastal zone features and subdivisions are difficult to define because temporal variability or gradational changes between features obscure precise boundaries. In addition, nomenclature is not standardized, and various authors describe the same features using different names. If the same name is used, the intended boundaries may differ greatly. This ambiguity is especially evident in the terminology and zonation of shore and littoral areas. In the absence of a widely accepted standard nomenclature, coastal researchers would do well to accompany reports and publications with diagrams and definitions to ensure that readers will fully understand the authors' use of terms.

(2) The following subparagraphs present coastal zone definitions and subdivisions based largely, but not exclusively, on geological criteria. They do not necessarily coincide with other geological-based zonations or those established by other disciplines. It should be borne in mind that coastal zone geology varies greatly from place to place, and the zonations discussed below do not fit all regions of the world. For example, coral atolls are without a coast, shoreface, or continental shelf in the sense defined here. The Great Lakes and other inland water bodies have coasts and shorefaces but no continental shelves. Thus, while divisions and categories are helpful in describing coastal geology, flexibility and good descriptive text and illustrations are always necessary for adequate description of a given region or study site.

b. Coastal zone. In this manual, *coastal zone* is defined as the transition zone where the land meets water, the region that is directly influenced by marine or lacustrine hydrodynamic processes. The coastal zone extends offshore to the continental shelf break and onshore to the first major change in topography above the reach of major storm waves. Although this discussion excludes upland rivers, river mouth deltas, where morphology and structure are a result of the dynamic interplay of marine and riverine forces, are included. The coastal zone is divided into four subzones (Figures IV-1-2 and IV-1-3):

(1) Coast.

(2) Shore.

(3) Shoreface.

(4) Continental shelf.

c. Coast. The *coast* is a strip of land of indefinite width that extends from the coastline inland as far as the first major change in topography. Cliffs, frontal dunes, or a line of permanent vegetation usually mark this inland boundary. On barrier coasts, the distinctive back-barrier lagoon/marsh/tidal creek complex is considered part of the coast. It is difficult to define the landward limit of the coast on large deltas like the Mississippi, but the area experiencing regular tidal exchange can serve as a practical limit (in this context, New Orleans would be considered "coastal"). The seaward boundary of the coast, the *coastline*, is the maximum reach of storm waves. On shorelines with plunging cliffs, the coast and coastline are one and the same. It is difficult to decide if a seawall constitutes a coast; the inland limit might better be defined at a natural topographic change.

d. Shore. The *shore* extends from the low-water line to the normal landward limit of storm wave effects, i.e., the coastline. Where beaches occur, the shore can be divided into two zones: *backshore* (or berm) and *foreshore* (or beach face). The foreshore extends from the low-water line to the limit of wave uprush at high tide. The backshore is horizontal while the foreshore slopes seaward. This distinctive change in slope, which marks the juncture of the foreshore and backshore, is called the beach or berm crest.

e. Shoreface. The *shoreface* is the seaward-dipping zone that extends from the low-water line offshore to a gradual change to a flatter slope denoting the beginning of the continental shelf. The continental shelf transition is the *toe of the shoreface*. Its location can only be approximately marked due to the gradual slope change. Although the shoreface is a common feature, it is not found in all coastal zones, especially along low-energy coasts or those consisting of consolidated material. The shoreface can be delineated from shore-perpendicular profile surveys or from bathymetric charts (if they contain sufficient soundings in shallow water). The shoreface, especially the upper part, is the zone of most frequent and vigorous sediment transport.

f. Continental shelf. The *continental shelf* is the shallow seafloor that borders most continents (Figure IV-1-3). The shelf floor extends from the toe of the shoreface to the shelf break where the steeply inclined continental slope begins. It has been common practice to subdivide the shelf into inner-, mid-, and outer zones, although there are no regularly occurring geomorphic features on most shelves that suggest a basis for these subdivisions. Although the term *inner shelf* has been widely used, it is seldom qualified beyond arbitrary depth or distance boundaries. Site-specific shelf zonation can be based on project

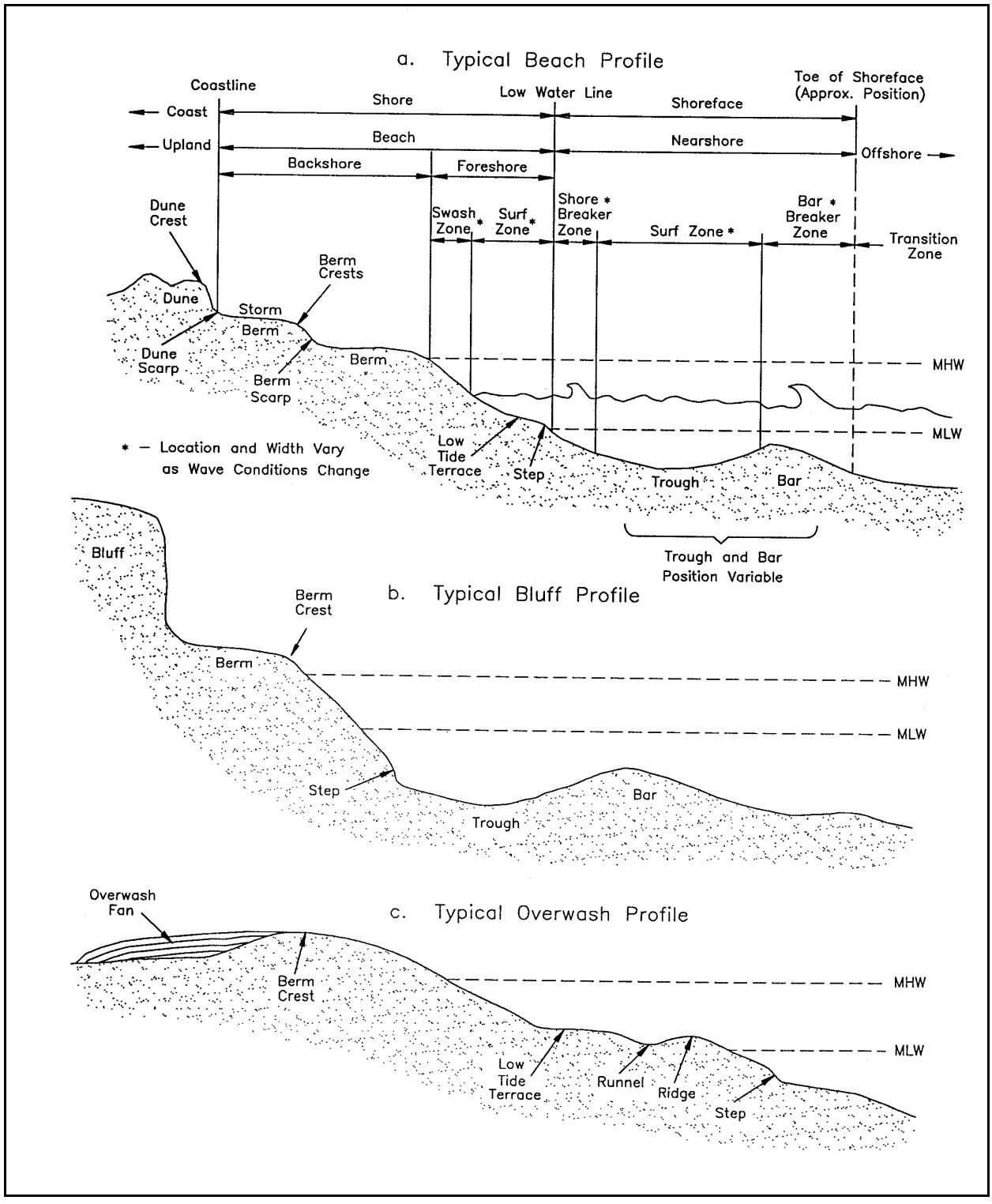

Figure IV-1-2. Definition of terms and features describing the coastal zone

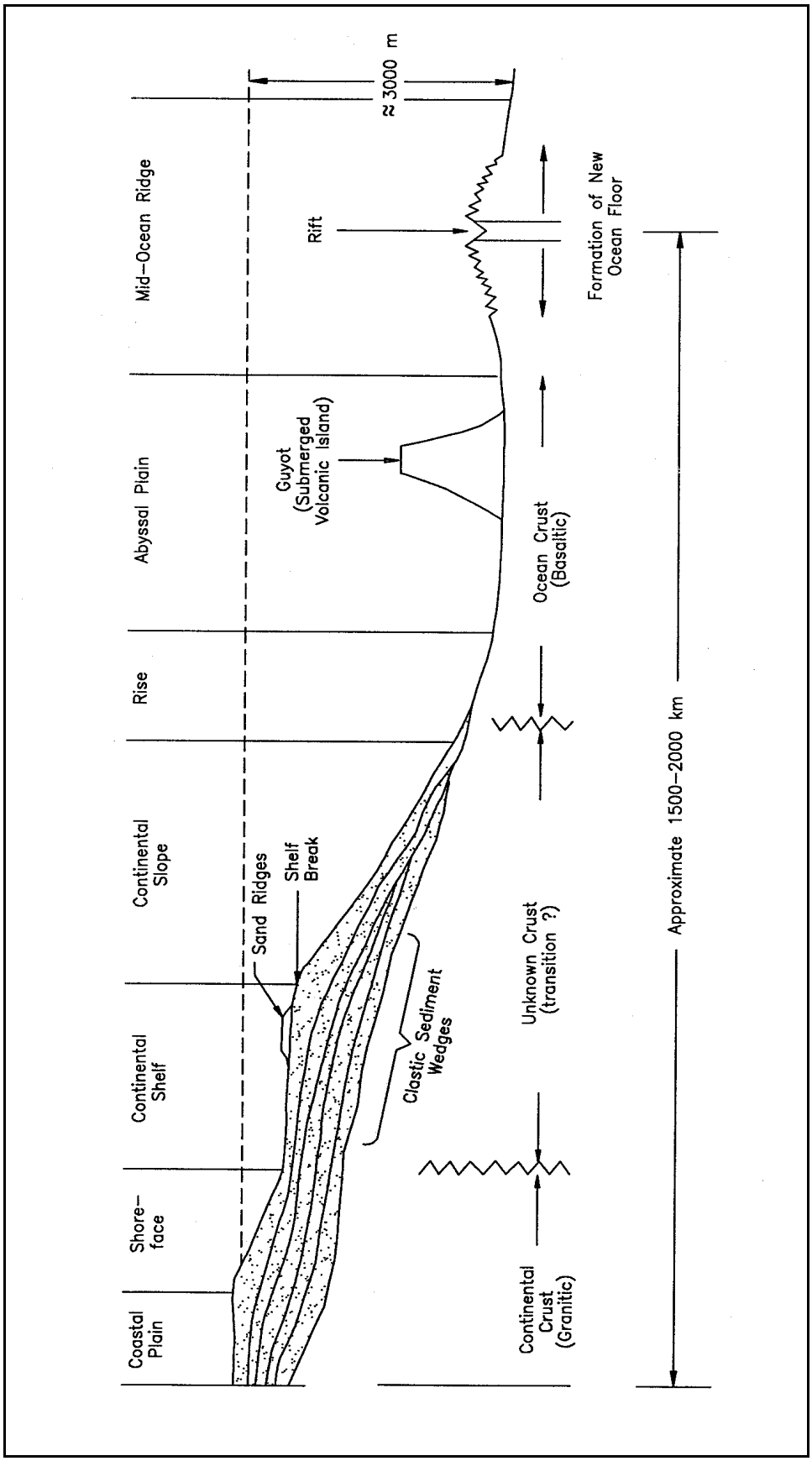

Figure IV-1-3. Continental shelf and ocean floor along the trailing-edge of a continent (i.e., representative of the U.S. Atlantic Ocean coast). Figure not to scale, great vertical exaggeration)

requirements and local geologic conditions. Some coastal areas (e.g., bays and the Great Lakes) do not extend out to a continental shelf.

g. Shoreline definitions. Common coastal geomorphic features are defined in Table IV-1-1 below. These have been adapted from the *National Shoreline Data Standard,* a draft standard prepared by the National Oceanic and Atmospheric Administration (NOAA).

Table IV-1-1
Definitions of Common Coastal Geomorphic Features

Apparent shoreline Line drawn on a map or chart in lieu of a mean high-water line or the mean water level line in areas where either may be obscured by marsh, mangrove, cypress, or other type of marine vegetation. This line represents the intersection of the appropriate datum on the outer limits of vegetation and appears to the navigator as the shoreline (Ellis 1978).

Backshore That part of the beach that is usually dry, being reached only by the highest tides, and by extension, a narrow strip of relatively flat coast bordering the sea (Ellis 1978).

Bank Edge of a cut or fill; the margin of the watercourse; an elevation of the seafloor located on a continental shelf or an island shelf and over which the depth of water is relatively shallow but sufficient for safe surface navigation (reefs or shoals, dangerous to surface navigation may arise above the general depths of a bank) (Ellis 1978).

Beach (or seabeach) Zone of unconsolidated material that extends landward from the low-water line to the place where there are marked changes in material or physiographic form, or to the line of permanent vegetation (usually the effective limit of storm waves). A beach includes foreshore and backshore (Ellis 1978).

Beach berm Nearly horizontal portion of the beach or backshore formed by the deposit of materials by wave action. Some beaches have no berms, others have one or several (Ellis 1978).

Berm Nearly horizontal portion of a beach or backshore having an abrupt fall and formed by wave deposition of material and marking the limit of ordinary high tides (Ellis 1978).

Berm crest Seaward limit of a berm (Ellis 1978).

Bluff A cliff or headland with an almost perpendicular face (International Hydrographic Bureau 1990).

Bottom lands Land below navigable freshwater bodies (Coastal States Organization 1997).

Cliff Land rising abruptly for a considerable distance above the water or surrounding land (Hydrographic Dictionary 1990).

Coast General region of indefinite width that extends from the sea inland to the first major change in terrain features (Ellis 1978).

Coastal zone (legal definition for coastal zone management) The term coastal zone means the coastal waters (including the lands therein and thereunder) and the adjacent shorelands (including the waters therein and thereunder), strongly influenced by each and in proximity to the shorelines of the several coastal states, and includes islands, transitional and inter-tidal areas, salt marshes, wetlands, and beaches. The zone extends, in Great Lakes waters, to the international boundary between the Unites States and Canada and in other areas seaward to the outer limit of the United States territorial sea. The zone extends inland from the shorelines only to the extent necessary to control shorelands, the uses of which have a direct and significant impact on the coastal waters. Excluded from the coastal zone are lands the use of which is by law subject solely to the discretion of or which is held in trust by the Federal Government, its officers, or agents (Hicks 1984).

Coast line (According to Public Law 31) Defined as the line of ordinary low water along that portion of the coast that is in direct contact with the open sea and the line marking the seaward limit of inland waters (Shalowitz 1964).

Coastline Same as shoreline (see coast line) (Hicks 1984).

Dry sand beach Sandy area between the mean high tide line and the vegetation line (Coastal States Organization 1997).

Estuary An embayment of the coast in which fresh river water entering at its head mixes with the relatively saline ocean water. When tidal action is the dominant mixing agent it is usually termed a tidal estuary. Also, the lower reaches and mouth of a river emptying directly into the sea where tidal mixing takes place. The latter is sometimes called a river estuary (Hicks 1984).

Foreshore That part of shore which lies between high and low water mark at ordinary tide (International Hydrographic Bureau 1990).

Freshwaters Waters that do not ebb and flow with the tide. The determinative factor is that the water body does not ebb and flow with the tide, not the salt content of the water (Coastal States Organization 1997).

High-water line A generalized term associated with the tidal plane of high water but not with a specific phase of high water (for example, higher high water, lower high water) (Shalowitz 1964).

High-water mark A line or mark left upon tide flats, beach, or alongshore objects indicating the elevation of the intrusion of high water. The mark may be a line of oil or scum along shore objects, or a more or less continuous deposit of fine shell or debris on the foreshore or berm. This mark is physical evidence of the general height reached by wave runup at recent high waters. It should not be confused with the mean high water line or mean higher high water line (Hicks 1984).

Inshore In beach terminology, the zone of variable width between the shoreface and the seaward limit of the breaker zone (Ellis 1978).

Intertidal zone (technical definition) The zone between the mean higher high water and mean lower low water lines (Hicks 1984).

Island A piece of land completely surrounded by water (International Hydrographic Bureau 1990).

Ledge A shelf -like projection, on the side of a rock or mountain. A rocky formation continuous with and fringing the shore (International Hydrographic Bureau 1990).

Levee Artificial bank confining a stream channel or limiting adjacent areas subject to flooding; an embankment bordering a submarine canyon or channel, usually occurring along the outer edge of a curve (Ellis 1978).

Littoral Pertaining to the shore, especially of the sea; a coastal region. Used extensively with “riparian” (Shalowitz 1964).

Shorelands General term including tidelands and navigable freshwater shores below the ordinary high-water mark (Coastal States Organization 1997).

Shoreline The line of contact between the land and a body of water. On Coast and Geodetic Survey nautical charts and surveys, the shoreline approximates the mean high-water line. In Coast Survey usage, the term is considered synonymous with coastline (Shalowitz 1962).

Submerged lands Lands covered by water at any stage of the tide, as distinguished from tidelands, which are attached to the mainland or an island and cover and uncover with the tide. Tidelands presuppose a high-water line as the upper boundary; submerged lands do not (Shalowitz 1962).

Tidal estuary See estuary (Hicks 1984).

Tidelands The land that is covered and uncovered by the daily rise and fall of the tide. More specifically, it is the zone between the mean high waterline and the mean low waterline along the coast, and is commonly known as the “shore” or “beach.” Referred to in legal decisions as between the ordinary high-water mark and ordinary low-water mark. Tidelands presuppose a high-water line as the upper boundary (Shalowitz 1964).

Tidewaters Waters subject to the rise and fall of the tide. Sometimes used synonymously with tidelands, but tidewaters are better limited to areas always covered with water. The amount of tide is immaterial (Shalowitz 1964).

Upland Land above mean high water mark and subject to private ownership, as distinguished from tidelands, ownership of which is prima facie in the state but also subject to divestment under state statutes (Shalowitz 1964).

Waterline Juncture of land and sea. This line fluctuates, changing with the tide or other fluctuations in the water (Ellis 1978).

Wet sand beach Area between the ordinary high tide and the ordinary low tide lines (Coastal States Organization 1997).

Source: National Oceanic and Atmospheric Administration (NOAA) 1998. National Shoreline Data Standard, Progress Report and Preliminary Draft Standard, NOAA Office of Coast Survey, Silver Spring, MD.

IV-1-3. Geologic Time and Definitions

a. Geologic fossil record. Geologists have subdivided geologic time into *eras, periods,* and *epochs* (Figure IV-1-4). Pioneering geologists of the 1800's based the zonations on the fossil record when they discovered that fossils in various rock formations appeared and disappeared at distinct horizons, thus providing a means of comparing and correlating the relative age of rock bodies from widely separated

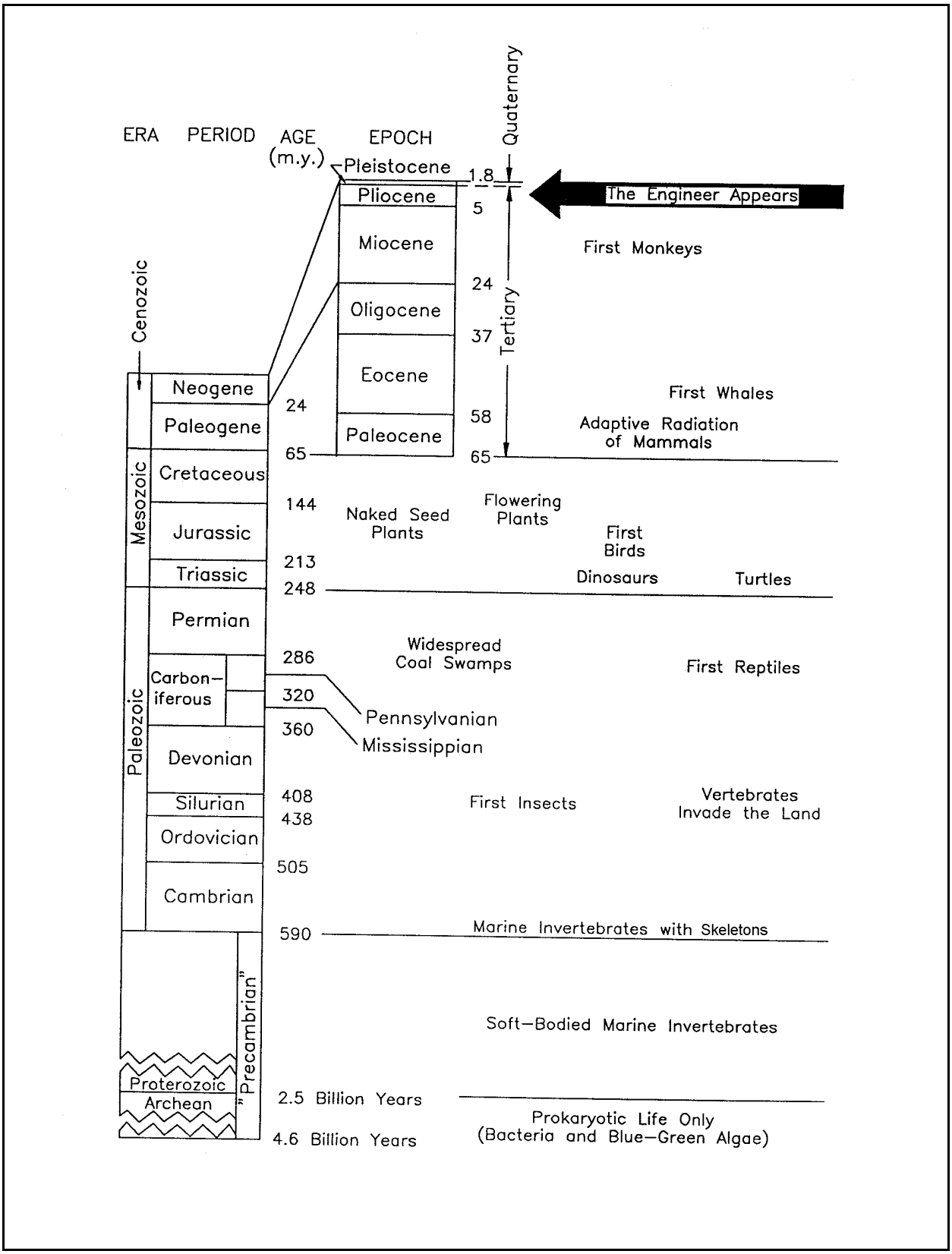

Figure IV-1-4. Geologic time scale. Chronological ages are based on radiometric dating methods (figure adapted from Stanley (1986))

locations. For example, the boundary between the *Mesozoic* ("interval of middle life") and the *Cenozoic* ("interval of modern life") eras is marked by the disappearance of hundreds of species, including the dinosaurs, and the appearance or sudden proliferation of many new species (Stanley 1986). The fossil time scale was relative, meaning that geologists could compare rock units but could not assign absolute ages in years. It was not until the mid-20th century that scientists could measure the absolute age of units by radiometric dating. The geologic times listed in Figure IV-1-4, in millions of years, are best estimates based on radiometric dates.

b. Geologic time considerations for coastal engineering. The epochs of most concern to coastal engineers and geologists are the *Pleistocene* and *Recent* (also commonly known as the *Holocene*), extending back a total of 1.8 million years before present. *Quaternary* is often used to designate the period comprising the Pleistocene and Recent Epochs.

(1) The Pleistocene Epoch was marked by pronounced climatic fluctuations in the Northern Hemisphere - changes that marked the modern Ice Age. The continental glaciers that periodically covered vast areas of the northern continents during this time had profound influence on the surficial geology. Many geomorphic features in North America were shaped or deposited by the ice sheets. Flint's (1971) *Glacial and Quaternary Geology* is an exhaustive study of the effects of Pleistocene ice sheets on North American geology.

(2) The Holocene Transgression started approximately 15,000 to 18,000 years ago with the beginning of global sea level rise. Presumably, a concurrent event was the waning of the continental glaciers possibly caused by a warming climate around the world. Most of the dynamic, morphological features that we associate with the active coastal environment are Holocene in age, but the preexisting geology is often visible, as well. For example, the drumlins of Boston Harbor and the end moraine islands of southern New England (Long Island, Martha's Vineyard, and Block and Nantucket Islands) are deposits left by the Wisconsin stage glaciers (Woodsworth and Wigglesworth 1934), but barrier spits and beaches found along these shores are more recent (Holocene) features.

(3) North American glacial stages.[1] Worldwide climatic fluctuations and multiple glacial and interglacial stages were the overwhelming Quaternary processes that shaped the surficial geomorphology and biological diversity of our world. Major fluctuations in eustatic, or worldwide, sea level accompanied the waxing and waning of the continental glaciers. Oxygen isotope analysis of deep sea sediments suggests that there were as many as nine glacial and ten interglacial events in the last 700,000 years (Kraft and Chrzastowski 1985). North American stages and approximate ages are listed in Table IV-1-2. The most recent glacial stage was the Wisconsin in North America and the Würm in Europe, during which sea level was more than 100 m below present. In northern latitude coasts, the coastal worker will often encounter geologic and geomorphic evidence of the Wisconsin glacial stage. Less evidence remains of the earlier North American stages except raised shore terraces along parts of the U.S. Atlantic and Gulf coasts (e.g., see Winkler (1977); Winkler and Howard (1977)).

IV-1-4. Water Level Datums and Definitions

Critical in evaluating sea level information or in constructing shoreline change maps are the level and type of datum used. Because water levels are not constant over space and time, depths and elevations must be

[1] Stage is a time term for a major subdivision of a glacial epoch, including the glacial and interglacial events (Bates and Jackson 1984).

Table IV-1-2
North American Pleistocene Glacial and Interglacial Stages

Age (approx. years)[1]	Glacial and Interglacial Stages	Age (approx. years)[2]
12,000-Present	Recent (Holocene)	10,000-Present
150,000-12,000	Wisconsin	100,000-10,000
350,000-150,000	Sangamon Interglacial	300,000-100,000
550,000-350,000	Illinoisan	450,000-300,000
900,000-550,000	Yarmouth Interglacial	1,100,000-450,000
1,400,000-900,000	Kansan	1,300,000-1,100,000
1,750,000-1,400,000	Aftonian Interglacial	1,750,000-1,300,000
> 2,000,000-1,750,000	Nebraskan	2,000,000-1,750,000
> 2,000,000(?)	Older glaciations	

[1] Dates based on generalized curve of ocean-water temperatures interpreted from foraminifera in deep sea cores (curve reproduced in Strahler (1981)).
[2] Dates from Young (1975) (original sources not listed).

referenced to established datums. In marine coastal areas, datums are typically based on tide elevation measurements. A glossary of tide elevation terms is presented in Part II-5-3, and water surface elevation datums are discussed in Part II-5-4.

IV-1-5. Factors Influencing Coastal Geology

The coast is probably the most diverse and dynamic environment found anywhere on earth. Many geologic, physical, biologic, and anthropomorphic (human) factors are responsible for shaping the coast and keeping it in constant flux. Ancient geological events created, modified, and molded the rock and sediment that form the foundation of the modern coastal zone. Over time, various physical processes have acted on this preexisting geology, subsequently eroding, shaping, and modifying the landscape. These processes can be divided into two broad classes: active forces, like waves and tides, which occur constantly, and long-term forces and global changes that affect the coast over time scales of years.

a. Underlying geology and geomorphology.[1] The geologic setting of a coastal site controls surficial geomorphology, sediment type and availability, and overall gradient. The geology is modified by physical processes (e.g., waves and climate), biology, and man-made activities, but the overall "look" of the coast is primarily a function of the regional lithology and tectonics. These topics are discussed in the following paragraphs.

(1) Lithology. *Lithology* concerns the general character of rock or sediment deposits. The most critical lithologic parameters responsible for a rock's susceptibility to erosion or dissolution are the mineral composition and the degree of consolidation. Striking contrasts often occur between coasts underlain by consolidated rock and those underlain by unconsolidated material. Marine processes are most effective when acting on uncemented material, which is readily sorted, redistributed, and sculpted into forms that are in a state of dynamic equilibrium with incident energy.

[1] *Geomorphology* is a study of natural topographic features and patterns forming the earth's surface, including both terrestrial and subaqueous environments.

(a) Consolidated coasts. Consolidated rock consists of firm and coherent material. Coastal areas consisting of consolidated rock are typically found in hilly or mountainous terrain. Here, erosional processes are usually dominant. The degree of consolidation greatly influences the ability of a rocky coastline to resist weathering and erosion. Resistance depends on susceptibility to mechanical and chemical weathering, hardness and solubility of constituent minerals and cementation, nature and density of voids, and climatic conditions. Rock type, bedding, jointing, and orientation of the strata greatly influence the geomorphic variability of the shoreline (Figures IV-1-5, IV-2-20, and IV-2-31). For example, large portions of the shorelines of Lakes Superior, Huron, and Ontario are rocky and prominently display the structure of the underlying geology.

- *Mechanical weathering* is the disintegration of rock without alteration of its chemical nature. Examples of mechanical weathering include fluctuations in temperature (causing repetitive thermal expansion and contraction), expansion due to crystallization from salt or ice, wetting and drying, overburden fluctuations, and biological activity.

- *Chemical weathering* is the decomposition of rock material by changes in its chemical composition. This process includes hydration and hydrolysis, oxidation and reduction, solution and carbonation, chelation, and various biochemical reactions.

(b) Unconsolidated coasts. In contrast to consolidated coasts, depositional and erosional processes dominate unconsolidated coasts, which are normally found on low relief coastal plains or river deltas. Commonly, shorelines have been smoothed by erosion of protruding headlands and by the deposition of barrier islands, spits, and bay mouth barriers. Along unconsolidated coasts, large amounts of sediment are usually available, and morphological changes occur rapidly. Waves and currents readily alter relict geomorphic features in this environment. Figure IV-1-6 illustrates features associated with unconsolidated depositional environments. The Atlantic and Gulf of Mexico coasts of the United States are mostly unconsolidated, depositional environments (except select locations like the rocky shores in New England).

(2) Tectonics. Forces within the earth's crust and mantle deform, destroy, and create crustal material. These tectonic activities produce structural features such as faults and folds (anticlines and synclines) (Figure IV-1-7). Tectonic movements produce large-scale uplift and subsidence of land masses. The west coast of the United States is an example of a tectonically dominated coast, in sharp contrast to the east coast, which is mostly depositional. According to Shepard's (1973) coastal classification, a fault coast is characterized by a steep land slope that continues beneath the sea surface. The most prominent feature exhibited by a fault coast is a scarp where normal faulting has recently occurred, dropping a crustal block so that it is completely submerged, leaving a higher block standing above sea level (Figure IV-1-8). Examples of fault-block coasts are found in California. Active faults such as the Inglewood-Rose Canyon structural zone outline the coast between Newport Bay and San Diego, and raised terraces backed by fossil cliffs attest to continuing tectonism (Orme 1985).

(3) Volcanic coasts. The eruption of lava and the growth of volcanoes may result in large masses of new crustal material. Conversely, volcanic explosions or collapses of existing volcanic cones can leave huge voids in the earth's surface known as calderas. When calderas and cones occur in coastal areas, the result is a coastline dominated by circular convex and concave contours (Shepard 1973). Coastlines of this sort are common on volcanic islands such as the Aleutians (Figure IV-1-9). The morphology of volcanic shores is discussed in more detail in Part IV-2.

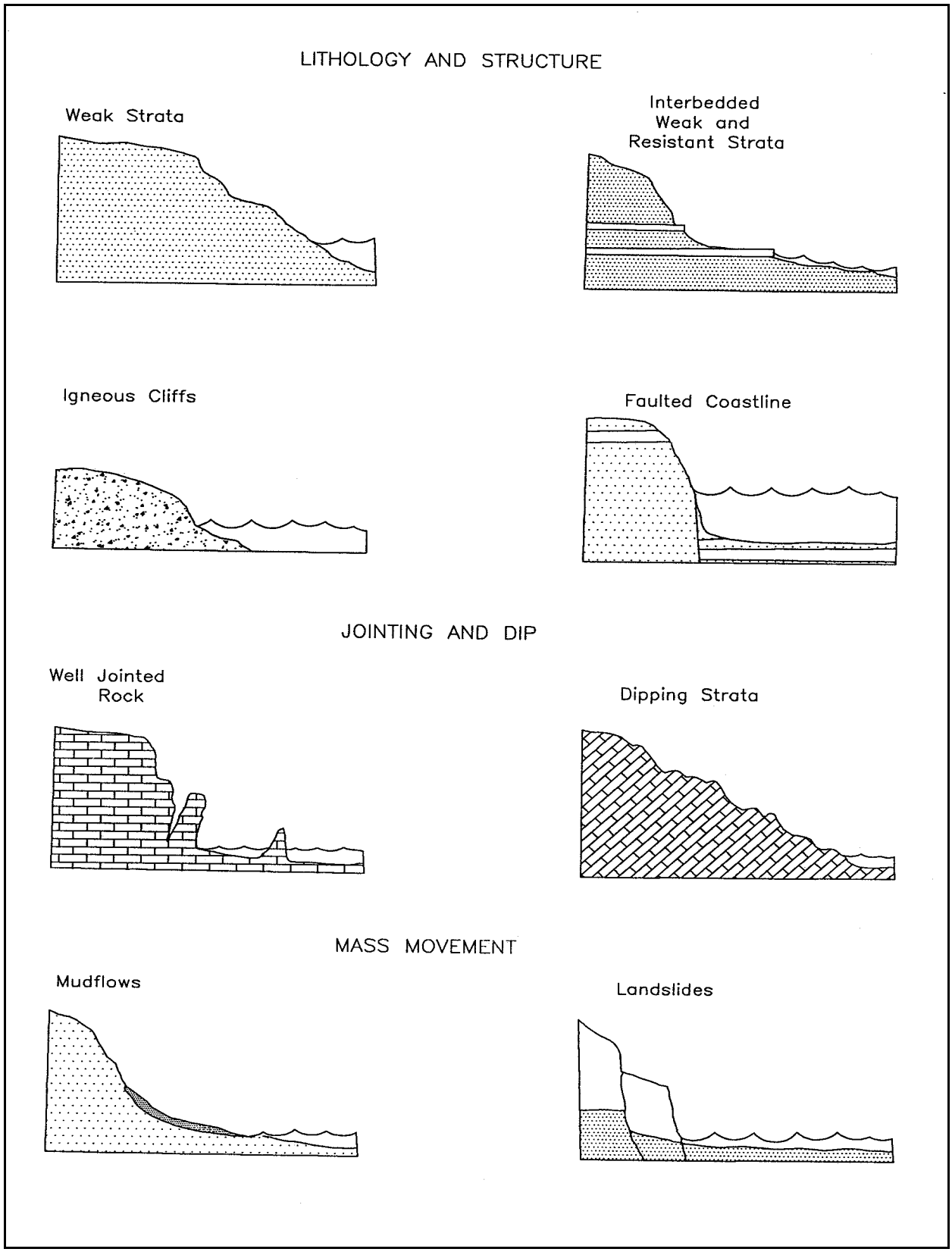

Figure IV-1-5. Cross-section views of aspects of geomorphic variability attributable to lighology, structure, and mass movement along semi-consolidated coasts (from Mossa, Meisberger, and Morang (1992))

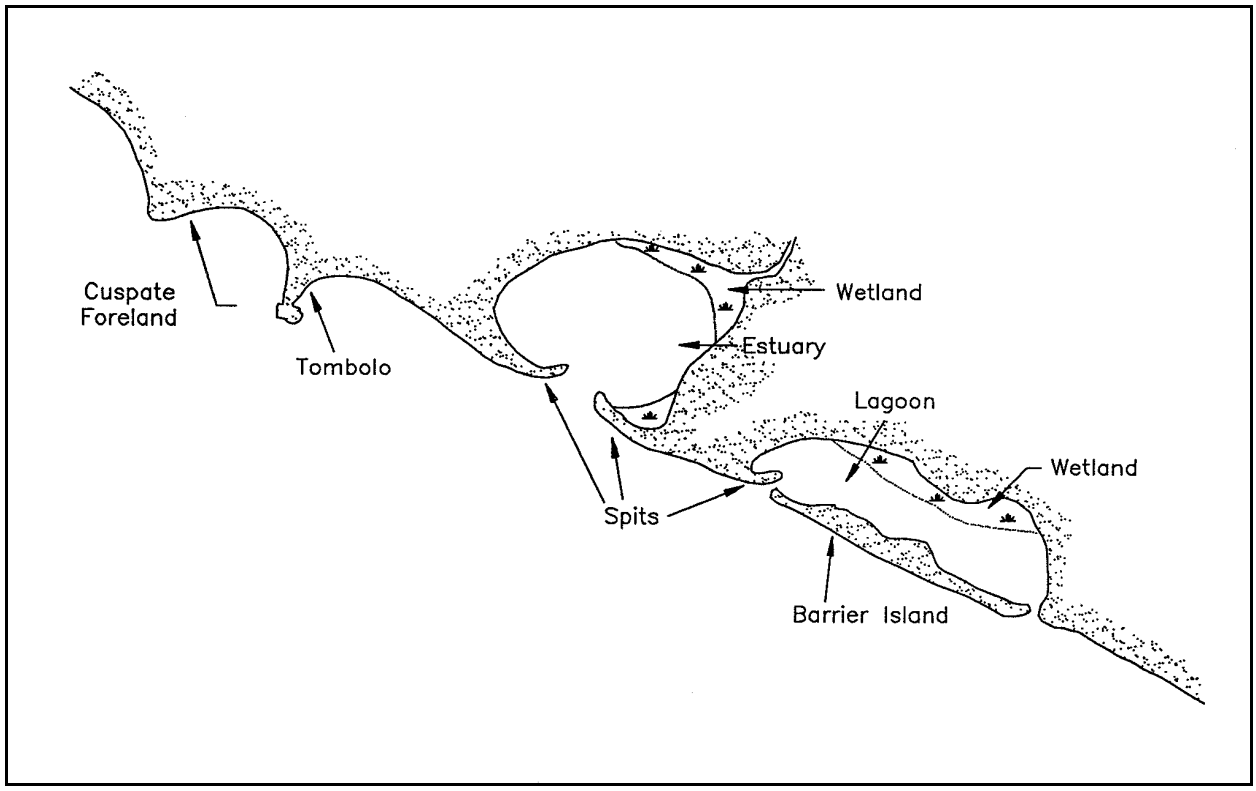

Figure IV-1-6. Examples of features associated with depositional coastal environments. These features consist mostly of unconsolidated sediments (after Komar 1976))

b. High-frequency dynamic processes. The following paragraphs briefly list processes that impart energy to the coastal zone on a continuous or, as with storms, repetitive basis. Any geological or engineering investigation of the coastal zone must consider the sources of energy that cause erosion, move sediment, deposit sediment, and rearrange or shape the preexisting topography. These processes also result in temporary changes in water levels along the coast. Long-term sea level changes are discussed in paragraph IV-1-6.

(1) Waves.

(a) Water waves (sometimes called *gravity waves*) are the dominant force driving littoral processes on open coasts. The following quotes from the *Shore Protection Manual* (1984) underscore the significance of waves in shaping coastal zone geomorphology:

> Waves are the major factor in determining the geometry and composition of beaches and significantly influence the planning and design of harbors, waterways, shore protection measures, coastal structures, and other coastal works. Surface waves generally derive their energy from the winds. A significant amount of this wave energy is finally dissipated in the nearshore region and on the beaches.
>
> Waves provide an important energy source for forming beaches; sorting bottom sediments on the shoreface; transporting bottom materials onshore, offshore, and alongshore; and for causing many of the forces to which coastal structures are subjected. An adequate understanding of the fundamental physical processes in surface wave generation and propagation must precede any attempt to

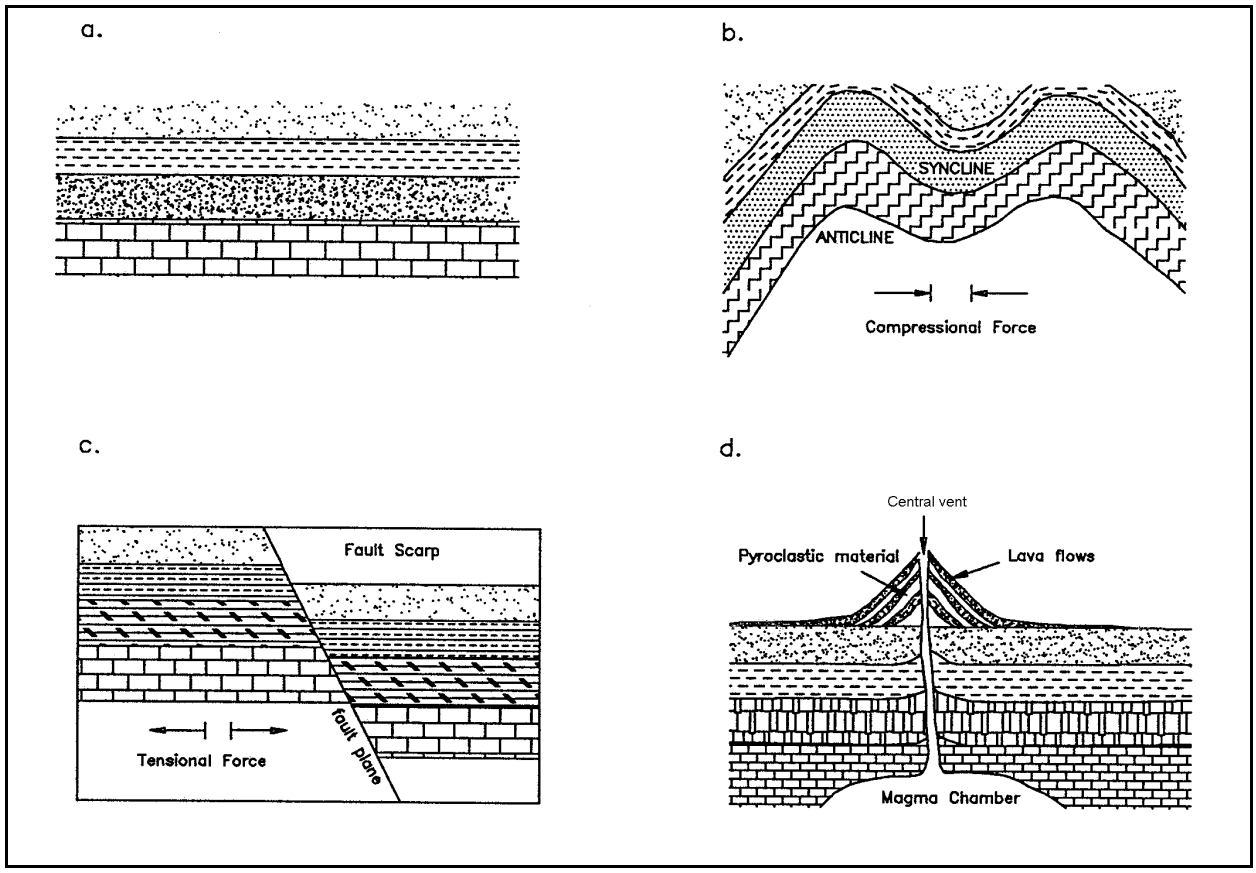

Figure IV-1-7. Examples of tectonically produced features: (a) stable undeformed block; (b) symmetrical folding resulting from compressional forces; (c) normal faulting resulting from tensional forces; (d) composed of alternating layers of pyroclastic material (ash) and lava flows

understand complex water motion in the nearshore areas of large bodies of water. Consequently, an understanding of the mechanics of wave motion is essential in the planning and design of coastal works.

(b) A detailed discussion of water wave mechanics is presented in Parts II-1, II-2, and II-3. Bascom's (1964) *Waves and Beaches* is a general introduction to the subject for the nonspecialist.

(2) Tides.

(a) The most familiar sea level changes are those produced by astronomical tides. *Tides* are a periodic rise and fall of water level caused by the gravitational interaction among the earth, moon, and sun. Because the earth is not covered by a uniform body of water, tidal ranges and periods vary from place to place and are dependent upon the natural period of oscillation for each water basin (Komar 1998). Tidal periods are characterized as diurnal (one high and one low per day), semidiurnal (two highs and two lows per day), and mixed (two highs and two lows with unequal heights) (Figure II-5-16). In the coastal zone, variations in topography, depth, seafloor sediment type, and lateral boundaries also affect the tide. For more background information and theory, refer to Part II-4.

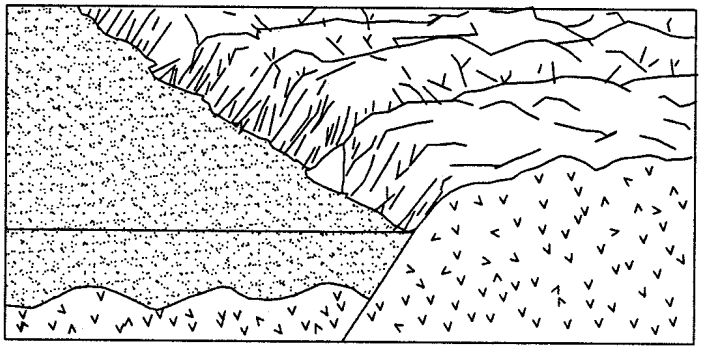

Figure IV-1-8. Example of a fault coast exhibiting a prominent fault scarp

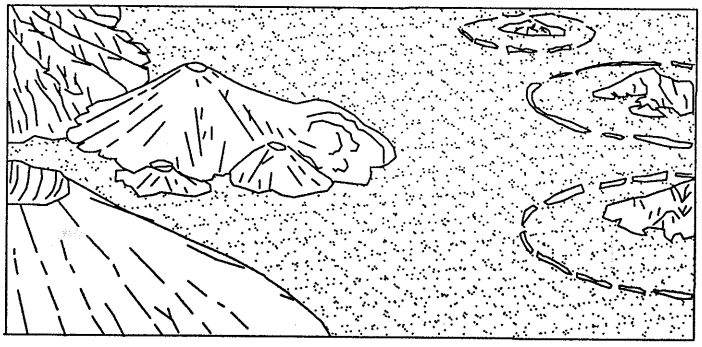

Figure IV-1-9. Example of a volcanic coast with numerous circular islands

(b) The importance of tides to coastal geological processes is threefold. First, the periodic change in water level results in different parts of the foreshore being exposed to wave energy throughout the day. In regions with large tidal ranges, the water may rise and fall 10 m, and the shoreline may move laterally several kilometers between high and low water. This phenomenon is very important biologically because the ecology of tidal flats depends on their being alternately flooded and exposed. The geological significance is that various parts of the intertidal zone are exposed to erosion and deposition.

(c) Second, tidal currents themselves can erode and transport sediment. Generally, tidal currents become stronger near the coast and play an increasingly important role in local circulation (Knauss 1978). Because of the rotating nature of the tidal wave in many locations (especially inland seas and enclosed basins), ebb and flood currents follow different paths. As a result, residual motions can be highly important in terms of transport and sedimentation (Carter 1988). In inlets and estuaries, spatially asymmetric patterns of ebb and flood may cause mass transport of both water and sediment.

(d) Third, tides cause the draining and filling of tidal bays. These bays are found even in low-tide coasts such as the Gulf of Mexico. This process is important because it is related to the cutting and migration of tidal inlets and the formation of flood- and ebb-tidal shoals in barrier coasts. The exchange of seawater in and out of tidal bays is essential to the life cycle of many marine species.

(3) Energy-based classification of shorelines.

(a) Davies (1964) applied an energy-based classification to coastal morphology by subdividing the world's shores according to tide range. Hayes (1979) expanded this classification, defining five tidal categories for coastlines:

- Microtidal, < 1 m.
- Low-mesotidal, 1-2 m.
- High-mesotidal, 2-3.5 m.
- Low-macrotidal, 3.5-5 m.
- Macrotidal, > 5 m.

The Hayes (1979) classification was based primarily on shores with low to moderate wave power and was intended to be applied to trailing edge, depositional coasts.

(b) In the attempt to incorporate wave energy as a significant factor modifying shoreline morphology, five shoreline categories were identified based on the relative influence of tide range versus mean wave height (Figure IV-1-10) (Nummedal and Fischer 1978; Hayes 1979; Davis and Hayes 1984):

- Tide-dominated (high).
- Tide-dominated (low).
- Mixed-energy (tide-dominated).
- Mixed energy (wave-dominated).
- Wave-dominated.

(c) The approximate limit of barrier island development is in the field labeled "mixed energy (tide-dominated)." Notice that these fields cover a range of tide and wave heights. It is the relative effects of these processes that are important, not the absolute values. Also, at the lower end of the energy scales, there is a delicate balance between the forces; where tide-dominated, wave-dominated, or mixed-energy morphologies may develop with very little difference in wave or tide parameters. By extension, tidal inlets have sometimes been classified using this nomenclature.

(d) Continuing research has shown, however, that earlier approaches to classifying the coast on the basis of tidal and wave characteristics have been oversimplified because many other factors can play critical roles in determining shoreline morphology and inlet characteristics (Davis and Hayes 1984; Nummedal and Fischer 1978). Among these factors are:

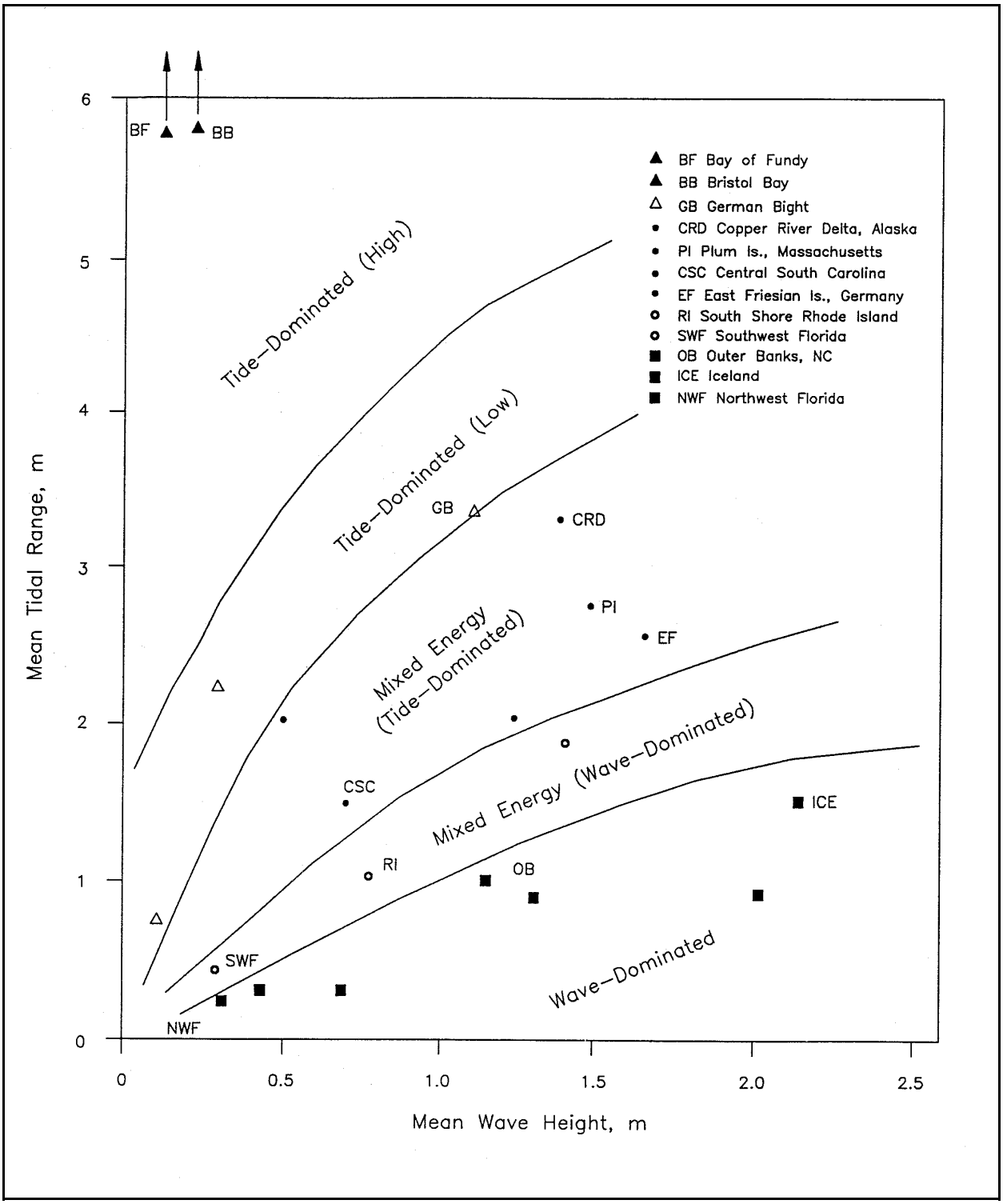

Figure IV-1-10. Energy-based classification of shorelines (from Hayes (1979))

- Physiographic setting and geology.
- Tidal prism.
- Sediment availability.
- Influence of riverine input.
- Bathymetry of the back-barrier bays.
- Meteorology and the influence of storm fronts.

(4) Meteorology. *Meteorology* is the study of the spatial and temporal behavior of atmospheric phenomena. *Climate* characterizes the long-term meteorologic conditions of an area, using averages and various statistics. Factors directly associated with climate such as wind, temperature, precipitation, evaporation, chemical weathering, and seawater properties all affect coastal geology. The shore is also affected by wave patterns that may be due to local winds or may have been generated by storms thousands of kilometers away. Fox and Davis (1976) is an introduction to weather patterns and coastal processes, and Hsu (1988) reviews coastal meteorology fundamentals.

(a) Wind. Wind is caused by pressure gradients, horizontal differences in pressure across an area. Wind patterns range in scale from global, which are generally persistent, to local and short duration, such as thunderstorms.

(b) Direct influence of wind. Wind has a great influence on coastline geomorphology, both directly and indirectly. The direct influence includes wind as an agent of erosion and transportation. It affects the coastal zone by eroding, transporting, and subsequently depositing sediment. Bagnold (1954) found that a proportional relationship exists between wind speed and rate of sand movement. The primary method of sediment transport by wind is through saltation, or the bouncing of sediment grains across a surface. Two coastal geomorphic features that are a direct result of wind are dunes and related blowouts (Pethick 1984). *Dunes* are depositional features whose form and size are a result of sediment type, underlying topography, wind direction, duration, and strength. *Blowouts* form when wind erodes an unvegetated area, thus removing the sand and leaving a depression or trough. These features are discussed in more detail in Parts III-4 and IV-2.

(c) Indirect effect. Wind indirectly affects coastal geomorphology as wind stress upon a water body causes the formation of waves and oceanic circulation.

(d) Land/sea breeze. Diurnal variations in the wind result from differential heating of the ocean and land surfaces. During the day, especially in summer, heating of the land causes the air to expand and rise, thus forming an area of low pressure. The pressure gradient between the water and the land surfaces causes a landward-directed breeze. At night, the ocean cools less rapidly than does the land, thus resulting in air rising over the ocean and subsequently seaward-directed breezes. These breezes are rarely greater than 8 m/sec (18 mph) and therefore do not have a great effect upon coastline geomorphology, although there may be some offshore-onshore transport of sediment on beaches (Komar 1998).

(e) Water level setup and setdown. Onshore winds cause a landward movement of the surface layers of the water and thus a seaward movement of deeper waters. Strong onshore winds, if sustained, may also cause increased water levels or setup. The opposite occurs during offshore winds.

(f) Seiches. *Seiches* are phenomena of standing oscillation that occur in large lakes, estuaries, and small seas in response to sudden changes in barometric pressure, violent storms, and tides. This condition causes the water within the basin to oscillate much like water sloshing in a bowl.

(5) Tropical storms. A *cyclone* is a system of winds that rotates about a center of low atmospheric pressure clockwise in the Southern Hemisphere and anti-clockwise in the Northern Hemisphere (Gove 1986). *Tropical storm* is a general term for a low-pressure, synoptic-scale[1] cyclone that originates in a tropical area. At maturity, tropical cyclones are the most intense and feared storms in the world; winds exceeding 90 m/sec (175 knots or 200 mph) have been measured, accompanied by torrential rain (Huschke 1959). By convention, once winds exceed 33 m/sec (74 mph), tropical storms are known as *hurricanes* in the Atlantic and eastern Pacific, *typhoons* in the western Pacific (Philippines and China Sea), and *cyclones* in the Indian Ocean.

(a) Tropical storms can cause severe beach erosion and destruction of shore-front property because elevated sea level, high wind, and depressed atmospheric pressure can extend over hundreds of kilometers. Tropical storms can produce awesome property damage (Table IV-1-3) and move vast quantities of sediment.

- The great Gulf of Mexico hurricane of 1900 inundated Galveston Island, killing over 6,000 residents (NOAA 1977-estimates range from 8-12,000 dead).

- During the September 1919 hurricane that struck the Florida Keys, 300 lives were lost in Key West, where winds were reported at 50 m/sec (110 mph). The final death toll of over 600, mostly in ships at sea, made this the third deadliest U.S. hurricane on record.

- The Great New England Hurricane that devastated Long Island and southern New England in September of 1938 killed 600 people and eliminated beach-front communities along the southern Rhode Island shore (Minsinger 1988). Survivors reported 15-m (50-ft) breakers sweeping over the Rhode Island barriers (Allen 1976). Shinnecock Inlet was cut through the Long Island barrier (Morang 1999).

- Hurricane Hugo hit the U.S. mainland near Charleston, South Carolina, on September 21, 1989, causing over $4 billion in damage, eroding the barriers, and producing other geologic changes up to 180 km north and 50 km south of Charleston (Davidson, Dean, and Edge 1990; Finkl and Pilkey 1991).

- A cyclone on June 9, 1998, inundated low-lying coastal plains and salt pans in northwest India. Over 14,000 people vanished into the Arabian Sea.

Simpson and Riehl (1981) have examined the effects of hurricanes in the United States. This work and Neumann et al. (1987) list landfall probabilities for the U.S. coastline. Tropical storms from 1871 to 1986 are plotted in Neumann et al. (1987). Tannehill (1956) identified all known Western Hemisphere hurricanes before the 1950's. Worldwide representative tropical storm tracks are shown in Figure IV-1-11 and Atlantic tracks in Figure II-5-29.

(b) The Saffir-Simpson Scale has been used for over 20 years by the U.S. National Weather Service to compare the intensity of tropical cyclones (Table IV-1-4). Cyclones are ranked into five categories based on maximum wind speed and the amount of damage that they cause (Figure IV-1-12), with 5 representing

[1] Synoptic-scale refers to large-scale weather systems as distinguished from local patterns such as thunderstorms.

Table IV-1-3
Damage Estimates and Payouts by Insurance Companies for U.S. Catastrophes

Date	Event (Region of Greatest Influence)	Category	Insured loss (millions)[1]	Total Damage estimate (millions) [2]	Total Damage in 1996 U.S. Dollars (millions)
Aug. 1992	Hurricane Andrew (Florida, Louisiana)[2]	4	$16,500	26,500	30,475
Jan. 1994	Northridge, Cailifornia, earthquake		12,500		
Sep. 1989	Hurricane Hugo (South Carolina)	4	4,195	7,000	8,490
Sep. 1998	Hurricane Georges		2.900	≈ 4,000	
Oct. 1995	Hurricane Opal (Florida, Alabama)	3	2,100	3,000	3,100
March 1993	"Storm of the Century" (24 eastern states)		1,750	6,000	
Aug. 1969	Hurricane Camille (Mississippi, Louisiana)	5	-	1,400	6,100
Oct. 1991	Oakland, California, fire		1,700		
Sep. 1996	Hurricane Fran	3	1,600	3,200	3,200
Sep. 1992	Hurricane Iniki (Hawaiian Islands)	—	1,600	1,800	2,070
Oct. 1989	Loma Prieta, California, earthquake		960		
Dec. 1983	Winter storms, 41 states		880		
April-May 1992	Los Angeles riots		775		
April 1992	Wind, hail, tornadoes, floods (Texas, Oklahoma)		760		
Sep. 1979	Hurricane Frederic (Mississippi, Alabama)	3	753	2,300	4,330
Sep 1964	Hurricane Dora (southeast Florida)	2	250		1,340
Sep 1960	Hurricane Donna (south Florida)	4	300	387	2,100
Sep. 1938	Great New England Hurricane (Long Island, Rhode Island, Connecticut, Massachusetts)	3	400[3]	600	—

Notes:
1. Total damage costs exceed insurance values because municipal structures like roads are not insured. (Source: *The New York Times,* December 28, 1993, citing insurance industry and State of Florida sources; *Daytona Beach News-Journal* web edition, 12 June 1998).
2. Andrew caused vast property damage in south central Florida, when sub-standard structures were torn apart by the hurricane's winds. This proves that hurricanes are not merely coastal hazards, although coastal residents usually are at greatest risk because of the danger from storm surges. (Source: The Deadliest, Costliest, and Most Intense United States Hurricanes of this Century, NOAA Technical Memorandum NWS TPC-1 (www.nhc.noaa.gov/pastcast.html, 23 Dec 1998).
3. Multiplying the 1938 damage value by 10 gives a crude estimate in 1990's Dollars (data source: Minsinger 1988).

storms that cause catastrophic damage to structures. Only two Category 5 storms have hit the United States since record-keeping began: the 1935 Labor Day hurricane that hit the Florida Keys and killed 600 people, and Hurricane Camille, which devastated the Mississippi coast in 1969, killing 256 and causing 1.4 billion in damage (over $6 billion when converted to 1996 values).

(c) During tropical storms and other weather disturbances, water level changes are caused by two factors:

- *Barometric pressure.* Barometric pressure has an inverse relationship to sea level. As atmospheric pressure increases, the sea surface is depressed so that the net pressure on the seafloor remains constant. Inversely, as atmospheric pressure decreases, surface water rises. The magnitude of the "inverse barometer effect" is about 0.01 m for every millibar of difference in pressure, and in areas affected by tropical storms or hurricanes, the potential barometric surge may be as high as 1.5 m (Carter 1988).

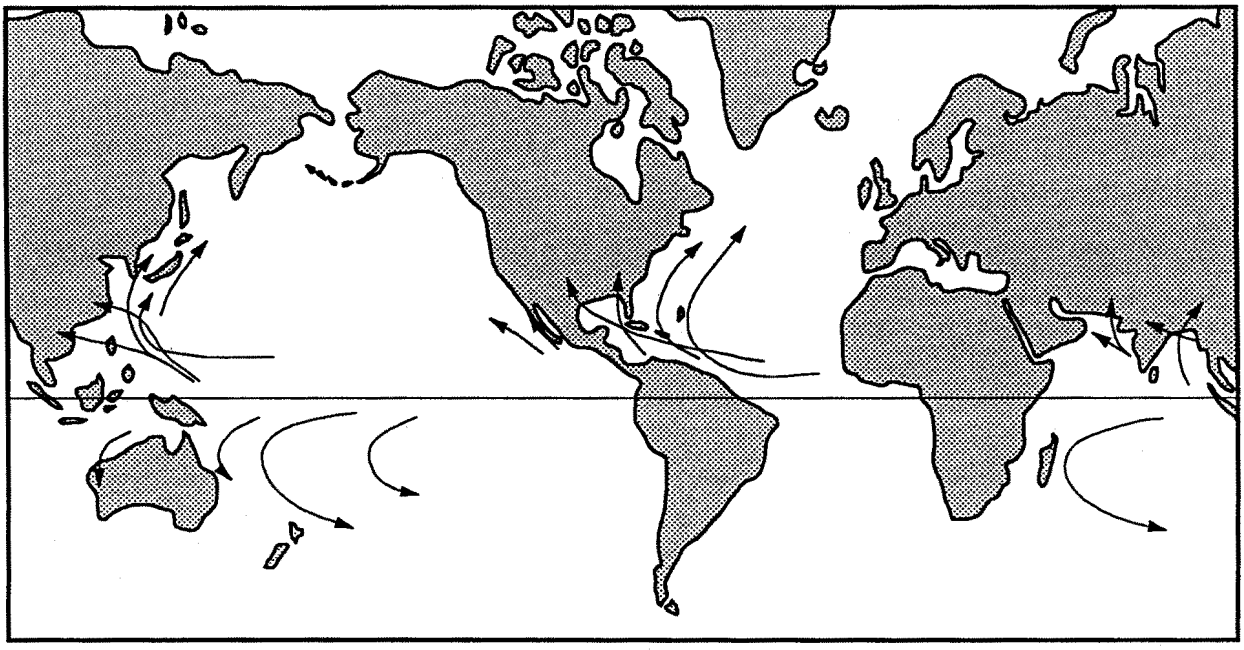

Figure IV-1-11. Worldwide tropical storm pathways (from Cole (1980))

Table IV-1-4
Saffir-Simpson Damage-Potential Scale

Scale Number (category)	Central pressure (millibars)	Wind speed (miles/hr)	Wind speed (m/sec)	Surge (ft)	Surge (m)	Damage
1	≥980	74-95	33-42	4-5	~1.5	Minimal
2	965-979	96-110	43-49	6-8	~2-2.5	Moderate
3	945-964	111-130	50-58	9-12	~2.6-3.9	Extensive
4	920-944	131-155	59-69	13-18	~4-5.5	Extreme
5	<920	>155	>69	>18	>5.5	Catastrophic

(From Hsu (1988); originally from Simpson and Riehl (1981))

- *Storm surges.* In shallow water, winds can pile up water against the shore or drive it offshore. Storm surges, caused by a combination of low barometric pressure and high onshore winds, can raise sea level several meters, flooding coastal property (Figures IV-1-13 and IV-1-14). The Federal Emergency Management Agency (FEMA) determines base flood elevations for the coastal counties of the United States. These elevations include still-water-level flood surges that have a 100-year return interval. In light of rising sea level along most of the United States, it seems prudent that Flood Insurance Rate Maps be periodically adjusted (National Research Council 1987). Besides wind forcing, ocean waves generated by storms can temporarily increase water levels tens of centimeters. Analysis procedures for predicting surge heights are detailed in EM 1110-2-1412.

(6) Extratropical storms. *Extratropical cyclones* (ET's) are cyclones associated with migratory fronts occurring in the middle and high latitudes (Hsu 1988). Although hurricanes are the most destructive storms to pass over the U.S. Atlantic coast, less powerful ET's, more commonly known as winter storms or

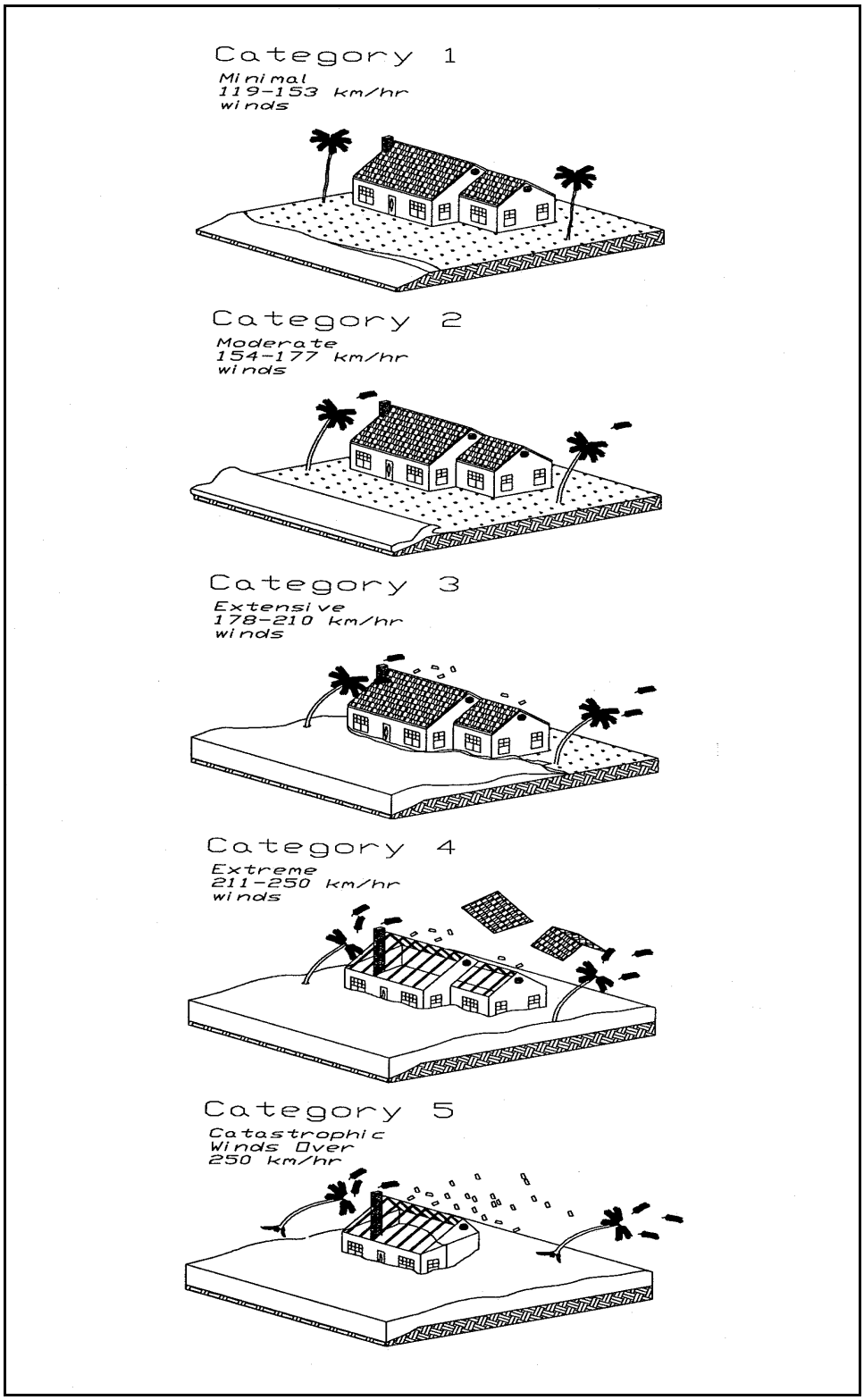

Figure IV-1-12. Graphical representation of the Saffir-Simpson Scale, showing the amount of damage that can be expected during different category hurricanes. Hurricane Andrew, in August 1992, was a Category 5 storm that caused immense damage inland, without a storm surge (Figure modified from Associated Press figure printed in *Vicksburg Post,* 3 Aug 1995)

Figure IV-1-13. Navarre Beach, Florida, November 1995. The house in Santa Rosa Sound was lifted off its foundations and moved back hundreds of meters. Many houses here were built on piles, but during Hurricane Opal, some piles were undermined, while at some properties, waves simply lifted buildings up off their supports. The low area in the foreground is a washover channel

Figure IV-1-14. Hurricane Opal damage at Navarre Beach, Florida, November 1995. The sand underneath the concrete slab washed away, and the unsupported floors collapsed

"northeasters," have also damaged ships, eroded beaches, and taken lives. Northeasters are not as clearly defined as hurricanes and their wind speeds seldom approach hurricane strength. On the other hand, ET's usually cover broader areas than hurricanes and move more slowly; therefore, ET's can generate wave heights that exceed those produced by tropical storms (Dolan and Davis 1992).

(a) Most Atlantic northeasters occur from December through April. Dolan and Davis (1992) have tabulated historic ET's and calculated that the most severe ones are likely to strike the northeast coast in October and January.

(b) The *Halloween Storm* of October 1991 was one of the most destructive northeasters to ever strike the Atlantic coast. The system's lowest pressure dipped to 972 mb on October 30. Sustained winds about 40-60 knots persisted for 48 hr, generating immense seas and storm surges (Dolan and Davis 1992). Another famous northeaster was the *Ash Wednesday Storm* of 1962, which claimed 33 lives and caused great property damage.

(c) In early 1983, southern California was buffeted by the most severe storms in 100 years, which devastated coastal buildings and caused tremendous erosion. During one storm in January 1983, which coincided with a very high tide, the cliffs in San Diego County retreated as much as 5 m (Kuhn and Shepard 1984). Further north, the storm was more intense and cliff retreat of almost 30 m occurred in places. Kuhn and Shepard (1984) speculated that the unusual weather was linked to the eruption of El Chichon Volcano in the Yucatan Peninsula in March 1982. They noted that the 1983 storms in California were the most intense since the storms of 1884, which followed the August 27, 1883, explosion of Krakatoa.

(d) At this time, weather forecasters still have difficulty forecasting the development and severity of ET's. Coastal planners and engineers must anticipate that powerful storms may lash their project areas and need to apply conservative engineering and prudent development practices to limit death and property destruction.

c. Biological factors.

Coastal areas are normally the sites of intense biological activity. This is of enormous geological importance in some areas, while being insignificant and short-lived in others. Biological activity can be constructive; e.g., the growth of massive coral reefs, or it can be destructive, as when boring organisms help undermine sea cliffs. Remains from marine organisms having hard skeletal parts, usually composed of calcium carbonate, contribute to the sediment supply almost everywhere in the coastal environment. These skeletal contributions can be locally important and may even be the dominant source of sediment. Vegetation, such as mangroves and various grasses, plays an important role in trapping and stabilizing sediments. Growth of aquatic plants in wetlands and estuaries is critical in trapping fine-grained sediments, eventually leading to infilling of these basins (if balances between sediment supply and sea level changes remain steady). Kelp, particularly the larger species, can be an important agent of erosion and transportation of coarse detritus such as gravel and cobble. Biological coasts are discussed in greater detail in Part IV-2. Deltaic and estuarine processes, which are greatly influenced by biology, are discussed in Part IV-3.

IV-1-6. Sea Level Changes

a. Background.

(1) General.

(a) Changes in sea level can have profound influence on the geology, natural ecology, and human habitation of coastal areas. A long-term and progressive rise in sea level has been cited as a major cause of erosion and property damage along our coastlines. Predicting and understanding this rise can guide coastal planners in developing rational plans for coastal development and the design, construction, and operation of structures and waterways.

(b) Many geomorphic features on contemporary coasts are the byproducts of the eustatic rise in sea level caused by Holocene climatic warming and melting of continental glaciers. Sea level has fluctuated throughout geologic time as the volume of ocean water has fluctuated, the shape of the ocean basins has changed, and continental masses have broken apart and re-formed.

(c) Sea level changes are the subject of active research in the scientific community and the petroleum industry. The poor worldwide distribution of tide gauges has hampered the study of recent changes (covering the past century) as most gauges were (and still are) distributed along the coasts of industrial nations in the Northern Hemisphere. Readers interested in this fascinating subject are referred to Emery and Aubrey's (1991) excellent book, *Sea Levels, Land Levels, and Tide Gauges.* This volume and Gorman (1991) contain extensive bibliographies. Tabular data and analyses of United States tide stations are printed in Lyles, Hickman, and Debaugh (1988), and worldwide Holocene sea level changes are documented in Pirazzoli (1991). Papers on sea level fluctuations and their effects on coastal evolution are presented in Nummedal, Pilkey, and Howard (1987). Engineering implications are reviewed in National Research Council (1987). Atmospheric carbon dioxide, climate change, and sea level are explored in National Research Council (1983). Houston (1993) discusses the state of uncertainty surrounding predictions on sea level change.

(2) Definitions. Because of the complexity of this topic, it is necessary to introduce the concepts of relative and eustatic sea level:

(a) *Eustatic* sea level change is caused by change in the relative volumes of the world's ocean basins and the total amount of ocean water (Sahagian and Holland 1991). It can be measured by recording the movement in sea surface elevation compared with some universally adopted reference frame. This is a challenging problem because eustatic measurements must be obtained from the use of a reference frame that is sensitive *only* to ocean water and ocean basin volumes. For example, highly tectonic areas (west coasts of North and South America; northern Mediterranean countries) are not suitable for eustatic sea level research because of frequent vertical earth movements (Mariolakos 1990). Tide gauge records from “stable” regions throughout the world have generated estimates of the recent eustatic rise ranging from 15 cm/century (Hicks 1978) to 23 cm/century (Barnett 1984).

(b) A *relative* change in water level is, by definition, a change in the elevation of the sea surface compared with some local land surface. The land, the sea, or both may have moved in *absolute* terms with respect to the earth's geoid. It is exceptionally difficult to detect absolute sea level changes because tide stations are located on land masses that have themselves moved vertically. For example, if both land and sea are rising at the same rate, a gauge will show that relative sea level (rsl) has not changed. Other clues, such as beach ridges or exposed beach terraces, also merely reflect their movement relative to the sea.

(3) Overview of causes of sea level change.

(a) Short-term sea level changes are caused by seasonal and other periodic or semi-periodic oceanographic factors. These include astronomical tides, movements of ocean currents, runoff, melting ice, and regional atmospheric variations. Included in this category are abrupt land level changes that result from volcanic activity or earthquakes. *Short-term* is defined here as an interval during which we can directly see or measure the normal level of the ocean rising or falling (a generation or 25 years). These factors are of particular pertinence to coastal managers and engineers, who are typically concerned with projects expected to last a few decades and who need to anticipate sea level fluctuations in their planning.

(b) Slow, secular sea and land level changes, covering time spans of thousands or millions of years, have been caused by glacioeustatic, tectonic, sedimentologic, climatologic, and oceanographic factors. Sea level was about 100 to 130 m lower during the last glacial epoch (Figure IV-1-15), about 15,000 years before present. Ancient shorelines and deltas can be found at such depths along the edge of the continental shelf (Suter and Berryhill 1985). Changes of this magnitude have been recorded during other geological epochs (Payton 1977).

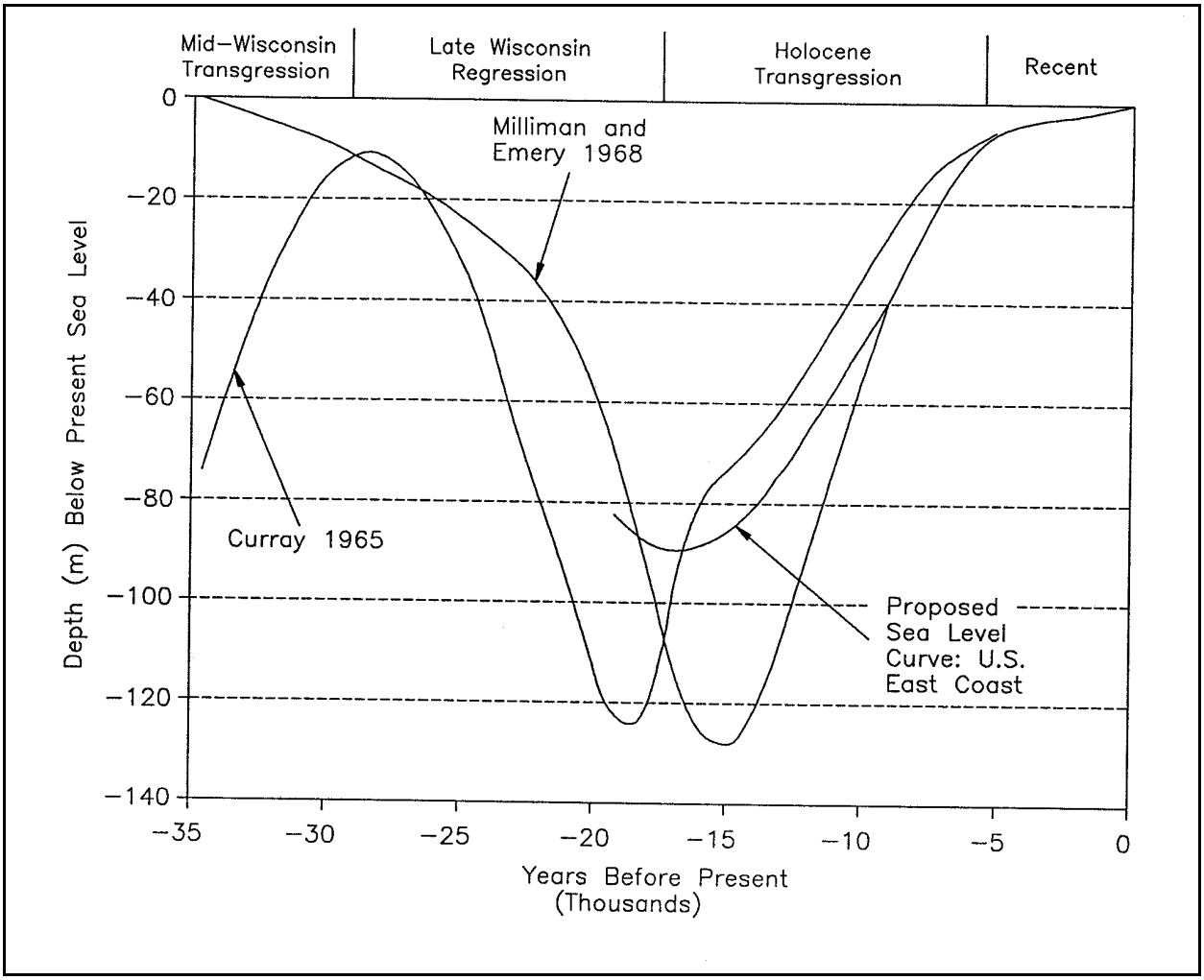

Figure IV-1-15. Sea level fluctuations during the Pleistocene and Holocene epochs (adapted from Nummedal (1983); data from Dillon and Oldale (1978))

(c) Table IV-1-5 lists long-term and short-term factors along with estimates of their effect on sea level. The following paragraphs discuss some factors in greater detail.

b. Short-term causes of sea level change.

(1) Seasonal sea level changes.

(a) The most common of the short-term variations is the seasonal cycle, which in most areas accounts for water level changes of 10 to 30 cm (and in some unusual cases - the Bay of Bengal - as much as 100 cm) (Komar and Enfield 1987). Seasonal effects are most noticeable near river mouths and estuaries. Variations in seasonal river flow may account for up to 21 percent of annual sea level variations in coastal waters (Meade and Emery 1971). Compared to the eustatic rise of sea level, estimated to be up to 20 cm/century, the seasonal factor may be a more important cause of coastal erosion because of its greater year-to-year influence (Komar and Enfield 1987).

(b) Over most of the world, lowest sea level occurs in spring and highest in autumn. Separating the individual factors causing the annual cycle is difficult because most of the driving mechanisms are coherent - occurring in phase with one another. Variations in atmospheric pressure drive most of the annual sea level change (Komar and Enfield 1987).

(2) West coast of North America.

(a) The west coast is subject to extreme and complicated water level variations. Short-term fluctuations are related to oceanographic conditions like the El Niño-Southern Oscillation. This phenomenon occurs periodically when equatorial trade winds in the southern Pacific diminish, causing a seiching effect that travels eastward as a wave of warm water. This raises water levels all along the U.S. west coast. Normally, the effect is only a few centimeters, but during the 1982-83 event, sea level rose 35 cm at Newport, Oregon (Komar 1992). Although these factors do not necessarily cause permanent geologic changes, engineers and coastal planners must consider their potential effects. The most recent El Niño event, during the winter of 1997-98, has been blamed for causing unusual weather in the western United States, including greatly increased rainfall in California and a warm winter in Oregon and Washington. Coastal geological changes caused by the El Niño are difficult to document. It has been argued (especially in the media) that increased rainfall in California caused more mudflows and bluff collapse than normal.

(b) Seasonal winter storms along the Pacific Northwest can combine with astronomical tides to produce elevated water levels over 3.6 m. During the severe storms of 1983, water levels were 60 cm over the predicted level.

(3) Rapid land level changes. Earthquakes are shock waves caused by abrupt movements of blocks of the earth's crust. A notable example occurred during the Great Alaskan Earthquake of 1964, when changes in shoreline elevations ranged from a 10-m uplift to a 2-m downdrop (Hicks 1972; Plafker and Kachadoorian 1966).

(4) Ocean temperature. Changes in the water temperature of upper ocean layers cause changes in water density and volume. As surface water cools, the density of seawater increases, causing a decrease in volume, thus lowering sea level. When temperature increases, the opposite reaction occurs. Variations in water temperature are not simply due to seasonal changes in solar radiation but are primarily caused by changes in offshore wind and current patterns.

Table IV-1-5
Sea Level Changes Along the Coastal Zone

Short-Term (Periodic) Causes	Time scale (P = period)	Vertical Effect[1]
Periodic Sea Level Changes		
Astronomical tides	6-12 hr P	0.2-10+ m
Long-period tides		
Rotational variations (Chandler effect)	14 month P	
Meteorological and Oceanographic Fluctuations		
Atmospheric pressure		
Winds (storm surges)	1-5 days	Up to 5 m
Evaporation and precipitation	Days to weeks	
Ocean surface topography (changes in water density and currents)	Days to weeks	Up to 1 m
El Niño/southern oscillation	6 mo every 5-10 yr	Up to 60 cm
Seasonal Variations		
Seasonal water balance among oceans (Atlantic, Pacific, Indian)		
Seasonal variations in slope of water surface		
River runoff/floods	2 months	1 m
Seasonal water density changes (temperature and salinity)	6 months	0.2 m
Seiches	Minutes-hours	Up to 2 m
Earthquakes		
Tsunamis (generate catastrophic long-period waves)	Hours	Up to 10 m
Abrupt change in land level	Minutes	Up to 10 m

Long-Term Causes	Range of Effect E = Eustatic; L = Local	Vertical Effect[1]
Change in Volume of Ocean Basins		
Plate tectonics and seafloor spreading (plate divergence/convergence) and change in seafloor elevation (mid-ocean volcanism)	E	0.01 mm/yr
Marine sedimentation	E	< 0.01 mm/yr
Change in Mass of Ocean Water		
Melting or accumulation of continental ice	E	10 mm/yr
Release of water from earth's interior	E	
Release or accumulation of continental hydrologic reservoirs	E	
Uplift or Subsidence of Earth's Surface (Isostasy)		
Thermal-isostasy (temperature/density changes in earth's interior)	L	
Glacio-isostasy (loading or unloading of ice)	L	1 cm/yr
Hydro-isostasy (loading or unloading of water)	L	
Volcano-isostasy (magmatic extrusions)	L	
Sediment-isostasy (deposition and erosion of sediments)	L	< 4 mm/yr
Tectonic Uplift/Subsidence		
Vertical and horizontal motions of crust (in response to fault motions)	L	1-3 mm/yr
Sediment Compaction		
Sediment compression into denser matrix	L	
Loss of interstitial fluids (withdrawal of groundwater or oil)	L	$\leq$ 55 mm/yr[1]
Earthquake-induced vibration	L	
Departure from Geoid		
Shifts in hydrosphere, aesthenosphere, core-mantle interface	L	
Shifts in earth's rotation, axis of spin, and precession of equinox	E	
External gravitational changes	E	

[1]Effects on sea level are estimates only. Many processes interact or occur simultaneously, and it is not possible to isolate the precise contribution to sea level of each factor. Estimates are not available for some factors. (Sources: Emery and Aubrey (1991); Gornitz and Lebedeff (1987); Komar and Enfield (1987))
[1] Calculated using Shanghai as an example: 2.7 m subsidence between 1920 and 1970 (Baeteman 1994)

(5) Ocean currents. Because of changes in water density across currents, the ocean surface slopes at right angles to the direction of current flow. The result is an increase in height on the right side of the current (when viewed in the direction of flow) in the Northern Hemisphere and to the left in the Southern Hemisphere. The elevation change across the Gulf Stream, for example, exceeds 1 m (Emery and Aubrey 1991). In addition, major currents in coastal areas can produce upwelling, a process that causes deep colder water to move upward, replacing warmer surface waters. The colder upwelled water is denser, resulting in a regional decrease in sea level.

c. Long-term causes of sea level change.

(1) Tectonic instability. Regional, slow land level changes along the U.S. western continental margin affect relative long-term sea level changes. Parts of the coast are rising and falling at different rates. In Oregon, the northern coast is falling while the southern part is rising relative to concurrent relative sea level (Komar 1992).

(2) Isostacy. *Isostatic adjustment* is the process by which the crust of the Earth attains gravitational equilibrium with respect to superimposed forces (Emery and Aubrey 1991). If a gravitational imbalance occurs, the crust rises or sinks to correct the imbalance.

(a) The most widespread geologically rapid isostatic adjustment is the depression of land masses caused by glaciers and the rebounding caused by deglaciation. In Alaska and Scandinavia, contemporary uplift follows the depression of the crust caused by the Pleistocene ice sheets. Some areas of the Alaska coast (for example, Juneau) are rising over 1 cm/year, based on tide gauge records (Figure IV-1-16) (Lyles, Hickman, and Debaugh 1988).

(b) Isostatic adjustments have also occurred due to changes in sediment load on continental shelves and at deltas. The amount of sediment loading on shelves is not well determined but is probably about 4 mm/year. The effect is only likely to be important at deltas where the sedimentation rate is very high (Emery and Aubrey 1991).

(3) Sediment compaction.

(a) Compaction occurs when poorly packed sediments reorient into a more dense matrix. Compaction can occur because of vertical loading from other sediments, by draining of fluids from the sediment pore space (usually a man-made effect), by desiccation (drying), and by vibration.

(b) Groundwater and hydrocarbon withdrawal is probably the main cause of sediment compaction on a regional scale. Many of the world's great cities are located on coastal plains or on river mouth deltas. Because of the dense population and industrialization, vast quantities of groundwater have been pumped from the subsurface aquifers. The consequence is nearly instantaneous local land subsidence due to sediment compaction, transforming many of these great coastal cities into the sinking cities of the world (Baeteman 1994; see Table IV-1-6). Subsidence exceeding 8 m has been recorded in Long Beach, California, and over 6 m in the Houston-Freeport area (Emery and Aubrey 1991). In Galveston, the annual sea level rise shown on tide records is 0.6 cm/year (Figure IV-1-17) (Lyles, Hickman, and Debaugh 1988). Subsidence at Venice, Italy, caused by groundwater pumping, has been well-publicized because of the threat to architectural and art treasures. Fortunately, subsidence there appears to have been controlled now that alternate sources of water are being tapped for industrial and urban use (Emery and Aubrey 1991).

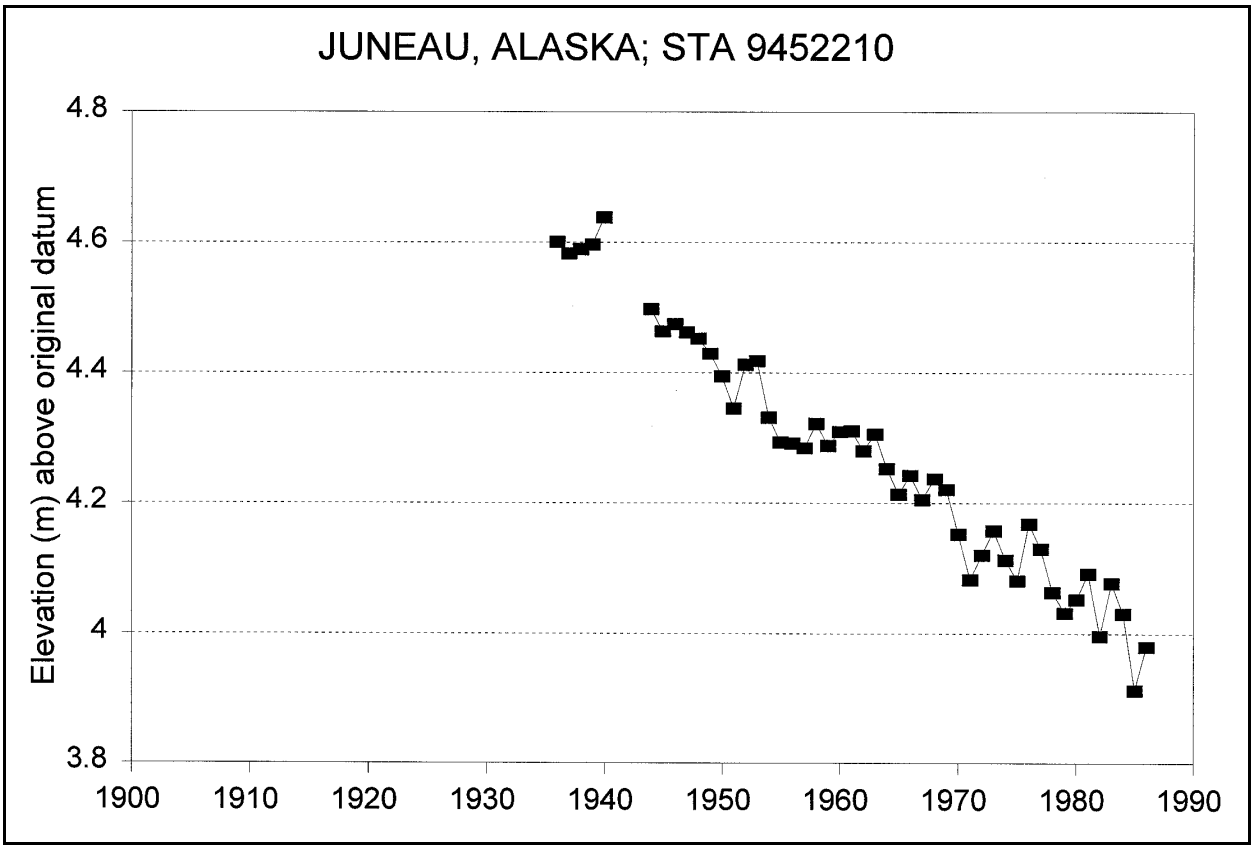

Figure IV-1-16. Yearly mean sea level changes at Juneau, Alaska, from 1936-1986. The fall in sea level shows the effects of isostatic rebound (data from Lyles, Hickman, and Debaugh (1988))

Table IV-1-6
Major World Cities with Recorded Subsidence[1]

City or Region and Country	Subsidence (m)
Tokyo, Japan	4.6
Po Delta, Italy	3.2
Shanghai, China	2.7
Houston, USA	2.7
Tianjin, China	2.5
SW Taiwan	2.4
Taipei, Taiwan	1.9
Bangkok, Thailand	1.6
Ravenna, Italy	1.2
London, England	0.35

[1] Records are not available for many other big cities (e.g., Jakarta, Hanoi, Haiphong, Rangoon, Manila).
From Baeteman (1994)

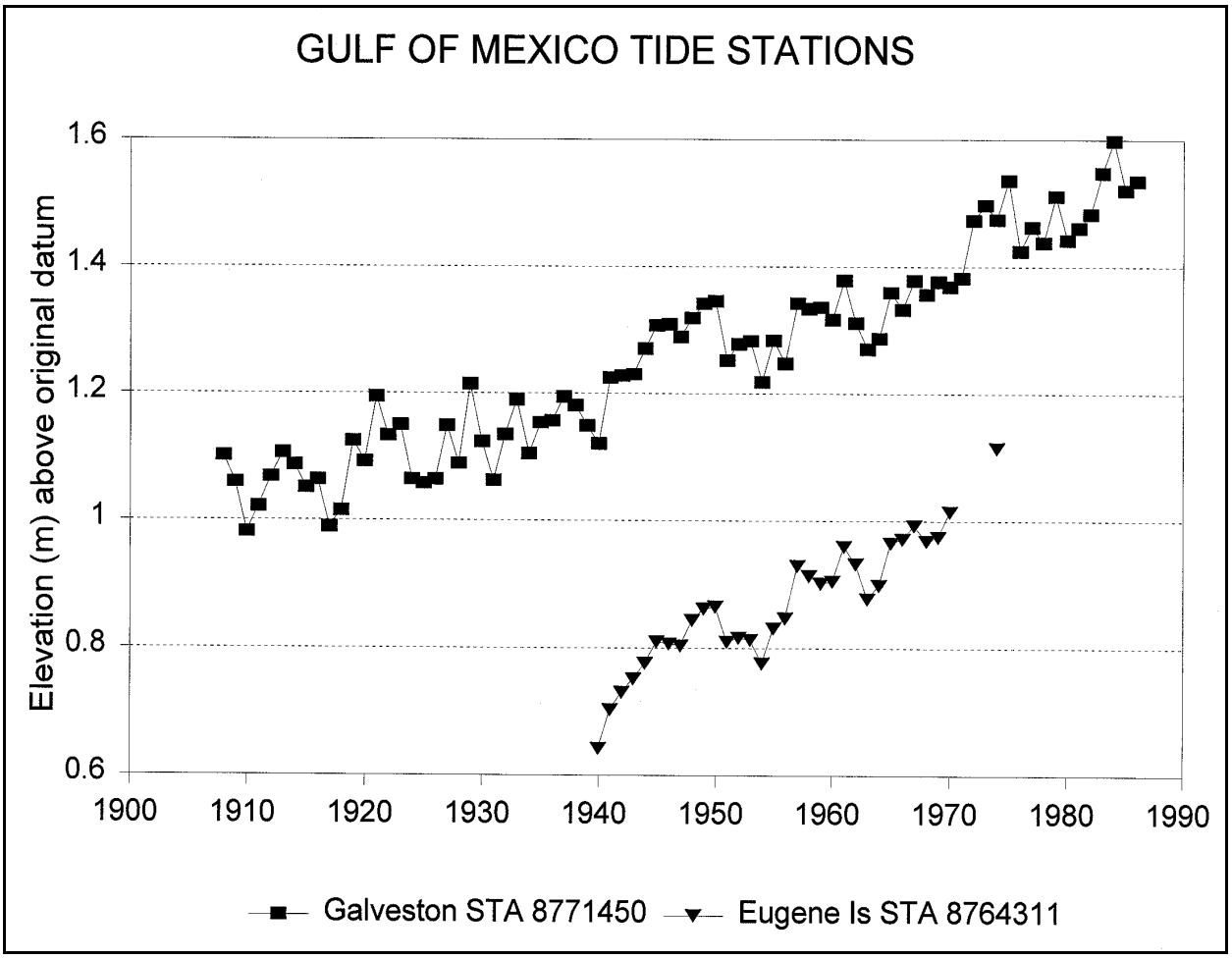

Figure IV-1-17. Yearly mean sea level changes at Galveston, Texas, and Eugene Island, Louisiana. Subsidence of the land around Galveston may be caused by groundwater withdrawal and sediment compaction (data from Lyles, Hickman, and Debaugh (1988))

(c) Significant subsidence occurs in and near deltas, where great volumes of fine-grained sediment accumulate rapidly. Land loss in the Mississippi delta has become a critical issue in recent years because of the loss of wetlands and rapid shoreline retreat. Along with natural compaction of underconsolidated deltaic muds and silts, groundwater and hydrocarbon withdrawal and river diversion might be factors contributing to the subsidence problems in southern Louisiana. Tide gauges at Eugene Island and Bayou Rigaud show that the rate of subsidence has increased since 1960 (Emery and Aubrey 1991). Change in rsl in the Mississippi Delta is about 15 mm/year, while the rate at New Orleans is almost 20 mm/year (data cited in Frihy (1992)).

d. Geologic implications of sea level change.

(1) Balance of sediment supply versus sea level change. Changes in sea level will have different effects on various portions of the world's coastlines, depending on conditions such as sediment type, sediment supply, coastal planform, and regional tectonics. The shoreline position in any one locale responds to the cumulative effects of the various sea level effects (outlined in Table IV-1-7). For simplicity, these factors can be subdivided into two broad categories: sediment supply and relative sea level (rsl) change. Ultimately, shoreline position is a balance between sediment availability and the rate that sea level changes

Table IV-1-7
Relative Effects of Sediment Supply Versus Sea Level Change on Shoreline Position[1]

		Relative Sea Level Change				
		Falling sea level		Stable	Rising sea level	
		Rapid	Slow		Slow	Rapid
Sediment supply	**Rapid net loss**	Neutral	Slow retreat	Medium retreat	Rapid retreat[4]	Extra rapid retreat[2]
	Slow net loss	Slow advance	Neutral	Slow retreat	Medium retreat[6]	Rapid retreat
	Zero net change	Medium advance	Slow advance	Neutral[8]	Slow retreat[9]	Medium retreat
	Low net deposition	Rapid advance	Medium advance[10]	Slow advance[7]	Neutral[3,5]	Slow retreat
	Rapid net deposition	Extra rapid advance	Rapid advance[11]	Medium advance	Slow advance[1]	Neutral

Examples of long-term (years) transgression or regression:

1. Mississippi River Delta - active distributary
2. Mississippi River Delta - abandoned distributary
3. Florida Panhandle between Pensacola and Panama City
4. Sargent Beach, TX
5. Field Research Facility, Duck, NC
6. New Jersey shore
7. Island of Hawaii - volcanic and coral sediment supply
8. Hawaiian Islands without presently active volcanoes
9. South shore of Long Island (sand trapped at inlets is balanced by man-made renourishment and bypassing)
10. Great Lakes during sustained fall in water levels
11. Alaska river mouths

[1] (Table based on a figure in Curray (1964))

(Table IV-1-7). For example, at an abandoned distributary of the Mississippi River delta, rsl is rising rapidly because of compaction of deltaic sediment. Simultaneously, wave action causes rapid erosion. The net result is extra rapid shoreline retreat (the upper right box in Table IV-1-7). The examples in the table are broad generalizations, and some sites may not fit the model because of unique local conditions.

(2) Historical trends. Historical records show the prevalence of shore recession around the United States during the past century (summarized by the National Research Council (1987):

(a) National average (unweighted) erosion rate: 0.4 m/year.

(b) Atlantic Coast: 0.8 m/year (with Virginia barrier islands exhibiting the highest erosion rates).

(c) Gulf Coast: 1.8 m/year (with highest erosion rate in Louisiana, 4.2 m/year).

(d) Pacific coastline: essentially stable (although more than half the shore is hard rock).

Bird (1976) claims that most sandy shorelines around the world have retreated during the past century. However, prograding shores are found where rivers supply excess sediment or where tectonic uplift is in progress.

(3) Specific coastal sites.

(a) Sandy (barrier) coasts. Several models predicting the effects of sea level rise on sandy coasts have been proposed. One commonly cited model is the Bruun rule. The Bruun rule and barrier migration models are discussed in Part IV-2.

(b) Cliff retreat. Cliff retreat is a significant problem in the Great Lakes, along the Pacific coast, and in parts of New England and New York. Increases in water level are likely to accelerate the erosion rate along Great Lakes shores (as shown by Hands (1983) for eastern Lake Michigan). However, along southern California, cliff retreat may be episodic, caused by unusually severe winter storms, groundwater and surface runoff, and, possibly, faulting and earthquakes, factors not particularly influenced by sea level (Kuhn and Shepard 1984). Crystalline cliffs are essentially stable because their response time is so much slower than that of sandy shores. Mechanisms of cliff erosion are discussed in Part IV-2.

(c) Marshes and wetlands. Marshes and mangrove forests fringe or back most of the Gulf and Atlantic coastlines. Marshes have the unique ability to grow upward in response to rising sea level. However, although marshes produce organic sediment, at high rates of rsl rise, additional sediment from outside sources is necessary to allow the marshes to keep pace with the rising sea. Salt marshes are described in Part IV-2-11. Paragraph IV-2-12 describes wetlands, coral and oyster reefs, and mangrove forest coasts. These shores have the natural ability to adjust to changing sea level as long as they are not damaged by man-made factors like urban runoff or major changes in sediment supply.

e. Engineering and social implications of sea level change.

(1) Eustatic sea level rise.

(a) Before engineering and management can be considered, a fundamental question must be asked: Is sea level still rising? During the last decade, the media has “discovered” global warming, and many politicians and members of the public are convinced that greenhouse gases are responsible for rising sea level and the increased frequency of flooding that occurs along the coast during storms. Most scientists accept the findings that the concentrations of greenhouse gasses in the atmosphere have increased greatly in the last century, largely due to industrial and automobile emissions. However, the link between increased gas in the atmosphere and changing sea level is much more difficult to model and verify. Wunsch (1996) has pointed out how difficult it is to separate myth from fact in the politically and emotionally charged issues of climate change and the oceans. The Environmental Protection Agency created a sensation in 1983 when it published a report linking atmospheric carbon dioxide to a predicted sea level rise of between 0.6 and 3.5 m (Hoffman, Keyes, and Titus 1983). Since then, predictions of the eustatic rise have been falling, and some recent evidence suggests that the rate may slow or even that eustatic sea level may drop in the future (Houston 1993).

(b) Possibly more reliable information on Holocene sea level changes can be derived from archaeological sites, wave-cut terraces, or organic material. For example, Stone and Morgan (1993) calculated an average rise of 2.4 mm/year from radiocarbon-dated peat samples from Santa Rosa Island, on the tectonically stable Florida Gulf coast. However, Tanner (1989) states that difficulties arise using all of these methods, and that calculated dates and rates may not be directly comparable.

(c) Based on an exhaustive study of tide records from around the world, Emery and Aubrey (1991) have concluded that it is not possible to assess if a *eustatic* rise is continuing because, while many gauges do record a recent rise in *relative* sea level, an equal number record a fall. Emery and Aubrey state (p. ix):

> In essence, we have concluded that 'noise' in the records produced by tectonic movements and both meteorological and oceanographic factors so obscures any signal of eustatic rise of sea level that the tide gauge records are more useful for learning about plate tectonics than about effects of the greenhouse heating of the atmosphere, glaciers, and ocean water.

They also state (p. 176):

> This conclusion should be no surprise to geologists, but it may be unexpected by those climatologists and laymen who have been biased too strongly by the public's perception of the greenhouse effect on the environment....Most coastal instability can be attributed to tectonism and documented human activities without invoking the spectre of greenhouse-warming climate or collapse of continental ice sheets.

(d) In summary, despite the research and attention devoted to the topic, the evidence about worldwide, eustatic sea level rise is inconclusive. Estimates of the rate of rise range from 0 to 3 mm/year, but some researchers maintain that it is not possible to discover a statistically reliable rate using tide gauge records. In late Holocene time, sea level history was much more complicated than has generally been supposed (Tanner 1989), suggesting that there are many perturbations superimposed on “average” sea level curves. Regardless, the topic is sure to remain highly controversial.

(2) Relative sea level (rsl) changes.

(a) The National Research Council's Committee on Engineering Implications of Changes in Relative Sea Level (National Research Council 1987) examined the evidence on sea level changes. They concluded that rsl, on statistical average, is rising at most tide gauge stations located on continental coasts around the world. In their executive summary, they concluded (p. 123):

> The risk of accelerated mean sea level rise is sufficiently established to warrant consideration in the planning and design of coastal facilities. Although there is substantial local variability and statistical uncertainty, average relative sea level over the past century appears to have risen about 30 cm relative to the East Coast of the United States and 11 cm along the West Coast, excluding Alaska, where glacial rebound has resulted in a lowering of relative sea level. Rates of relative sea level rise along the Gulf coast are highly variable, ranging from a high of more than 100 cm/century in parts of the Mississippi delta plain to a low of less than 20 cm/century along Florida's west coast.

However, they, too, noted the impact of management practices:

> Accelerated sea level rise would clearly contribute toward a tendency for exacerbated beach erosion. However, in some areas, anthropogenic effects, particularly in the form of poor sand management practices at channel entrances, constructed or modified for navigational purposes, have resulted in augmented erosion rates that are clearly much greater than would naturally occur. Thus, for some years into the future, sea level rise may play a secondary role in these areas.

(b) Figure IV-1-18 is a summary of estimates of local rsl changes along the U.S. coast (National Research Council 1987). Users of this map are cautioned that the values are based on tide records only from

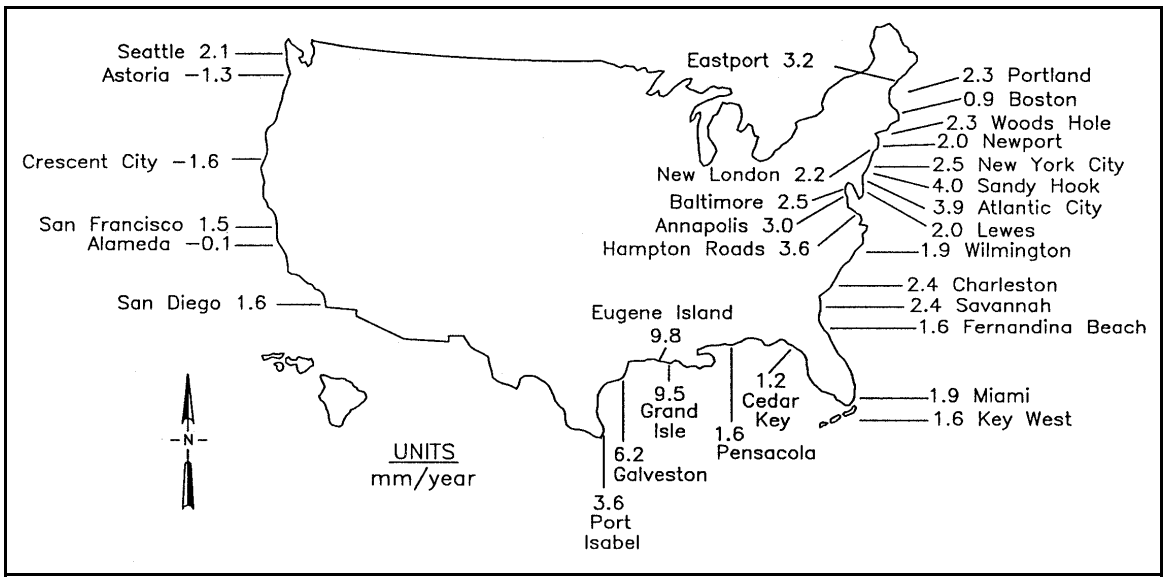

Figure IV-1-18. Summary of estimates of local rsl rise along the continental United States in millimeters per year. Values are based on tide gauge records during the period 1940-1980 (from National Research Council (1987))

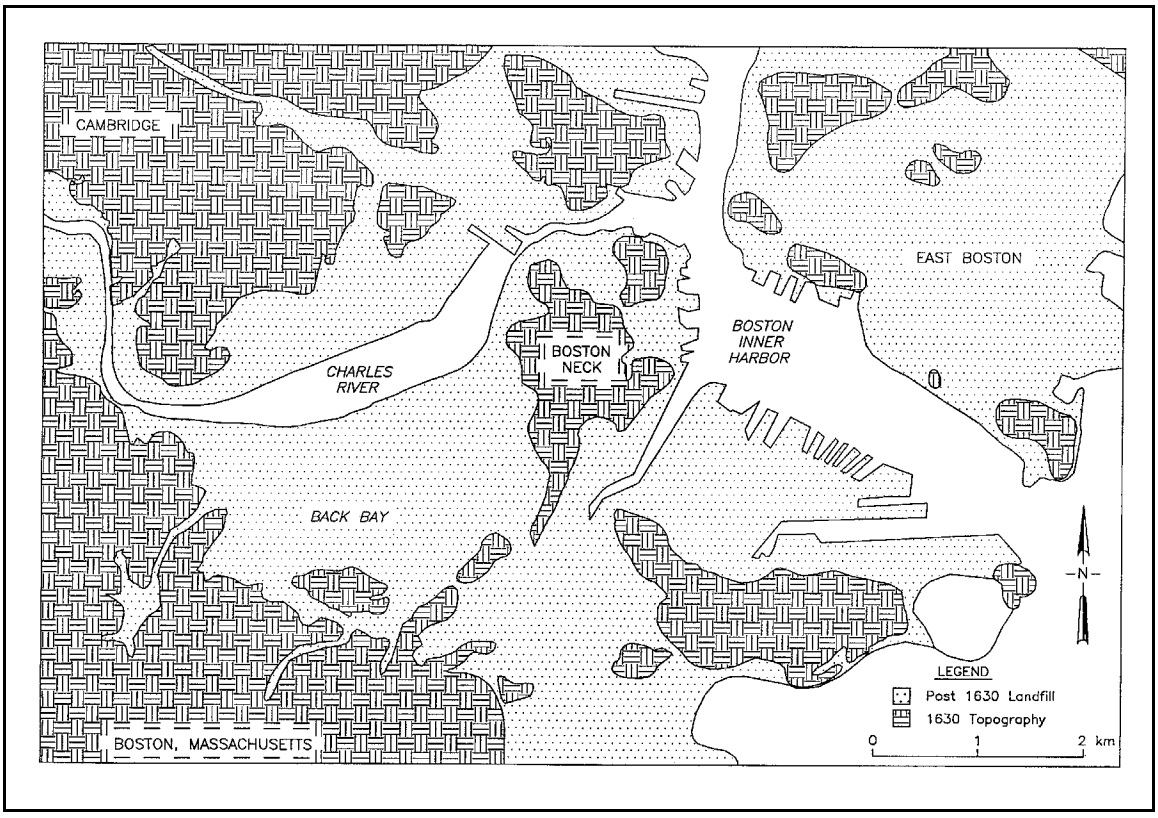

Figure IV-1-19. Landfilling in Boston, MA, since 1630 has more than doubled the urban area (unfortunately, at the expense of destroying what must have been highly productive wetlands) (from Rosen, Brenninkmeyer, and Maybury (1993))

1940-1980 and that much regional variability is evident. The figure provides general information only; for project use, detailed data should be consulted, such as the tide gauge statistics printed in Lyles, Hickman and Debaugh (1988) (examples of three tide stations are plotted in Figures IV-1-16 and IV-1-17) or the statistics available from the NOAA web site.

(3) Engineering response and policy.

(a) Whatever the academic arguments about eustatic sea level, engineers and planners must anticipate that changes in rsl may occur in their project areas and need to incorporate the anticipated changes in their designs and management plans.

(b) Because of the uncertainties surrounding sea level, the U.S. Army Corps of Engineers (USACE) has not endorsed a particular rise (or fall) scenario. Engineer Regulation (ER) 1105-2-100 (28 December 1990) states the official USACE policy on sea level rise. It directs that:

> Feasibility studies should consider which designs are most appropriate for a range of possible future rates of rise. Strategies that would be appropriate for the entire range of uncertainty should receive preference over those that would be optimal for a particular rate of rise but unsuccessful for other possible outcomes.

Potential rsl rise should be considered in every coastal and estuarine (as far inland as the new head of tide) feasibility study that USACE undertakes. Project planning should consider what impact a higher rsl rise would have on designs based on local, historical rates.

(4) Impacts of rising sea level on human populations.

(a) Rising sea level raises the spectre of inundated cities, lost wetlands, and expensive reconstruction of waterways and ports. About 50 percent of the U.S. population lives in coastal counties (1980 census data reported in Emery and Aubrey (1991)), and the number is likely to increase. There has not been a long history of understanding and planning for sea level rise in the United States, but other countries, particularly Holland and China, have coped with the problem for thousands of years (National Research Council 1987). There are three principal ways that people could adapt to rising sea level:

- Retreat and abandonment.
- Armoring by erecting dikes and dams to keep out the sea.
- Construction on landfills and piers.

(b) Among the areas most susceptible to inundation caused by rise in rsl are deltas. Deltas are naturally sinking accumulations of sediment whose subaerial surface is a low-profile, marshy plain. Already, under present conditions, subsidence imposes especially severe hardships on the inhabitants in coastal Bangladesh (10 mm/year) and the Nile Delta (2 mm/year), two of the most densely populated regions on earth (Emery and Aubrey 1991). Even a slow rise in sea level could have devastating effects. How could these areas be protected? Thousands of kilometers of seawalls would be needed to protect a broad area like coastal Bangladesh from the sea and from freshwater rivers. Civil works projects on this scale seem unlikely in developing countries, suggesting that retreat will be the only recourse (National Research Council 1983). Nevertheless, despite the immense cost of large-scale coastal works, the Netherlands has reclaimed from the sea a large acreage of land, which is now used for towns and agriculture.

(c) Retreat can be either a gradual (planned or unplanned) process, or a catastrophic abandonment (National Research Council 1987). The latter has occurred in communities where buildings were not allowed to be rebuilt after they were destroyed or damaged by storms. The State of Texas followed this approach on Galveston Island after Hurricane Alicia in 1983 and the State of Rhode Island for some south shore communities after the Great New England Hurricane of 1938. Construction setback lines represent a form of controlled retreat. Seaward of setback lines, new construction is prohibited. City managers and coastal planners often have difficulty in deciding where setback lines should be located, and their decisions are bitterly contested by property developers who wish to build as close to the beach as possible.

(d) Most of the world's coastal cities are subject to inundation with even a modest rise of sea level. In 1990, of the 15 biggest "megacities" (population > 10 million, such as Tokyo, Shanghai, Buenos Aires, and Calcutta) 12 were in coastal areas (Young and Hale 1998). Unfortunately, 25 to 50 percent of these urban populations live in poverty, a situation that makes coastal management and planning for changing sea level very difficult. Nevertheless, irresistible political pressure will surely develop to defend cities against the rising sea because of the high concentration of valuable real estate and capital assets. Defense will most probably take the form of dikes like the ones that protect large portions of Holland and areas near Tokyo and Osaka, Japan, from flooding. Dikes would be needed to protect low-lying inland cities from rivers whose lower courses would rise at the same rate as the sea. Already, New Orleans (which is below sea level), Rotterdam, and other major cities located near river mouths are kept dry by levees. These levees might have to be raised under the scenario of rising sea level. Storm surge barriers, like the ones at New Bedford, Massachusetts, Providence, Rhode Island, and the Thames, below London, England, might have to be rebuilt to maintain an adequate factor of safety.

(e) Landfilling has historically been a common practice, and many coastal cities are partly built on landfill. Boston's waterfront, including the airport and the Back Bay, is built on 1800's fill (Figure IV-1-19; Whitehill 1968). Large areas around New York City, including parts of Manhattan and Brooklyn, have been filled since the 1600's (Leveson 1980). Venice, one of the world's great architectural treasures, occupies a cluster of low islands in the lagoon of Venice, at the head of the Adriatic Sea. In the early 1700's, Peter the Great built his monumental new capital of Saint Petersburg on pilings and fill in the estuary of the Neva River. Artificial land, which is usually low, is particularly susceptible to rising sea level. Although dikes and levees will probably be the most common means to protect cities threatened by the rising sea, there is a precedent in the United States for raising the level of the land surface where structures already exist: Seattle's downtown was raised about 3 m in the early 1900's to prevent tidal flooding. The elevated streets ran along the second floor of buildings, and the original sidewalks and store fronts remained one floor down at the bottom of open troughs. Eventually, the open sidewalks had to be covered or filled because too many pedestrians and horses were injured in falls.

f. Changes in sea level - summary.

(1) Changes in sea level are caused by numerous physical processes, including tectonic forces that affect land levels and seasonal oceanographic factors that influence water levels on various cycles (Table IV-1-5). Individual contributions of many of these factors are still unknown.

(2) Estimates of the eustatic rise in sea level range from 0 to 3 mm/year. Emery and Aubrey (1991) have strongly concluded that it is not possible to detect a statistically verifiable rate of eustatic sea level rise because of noise in the signals and because of the poor distribution of tide gauges worldwide.

(3) Arguments regarding eustatic sea level changes may be more academic than they are pertinent to specific projects. The rate of *relative* sea level change varies greatly around the United States. Coastal planners need to consult local tide gauge records to evaluate the potential movement of sea level in their project areas.

(4) In many areas, coastal management (mismanagement) practices have the greatest influence on erosion, and sea level changes are a secondary effect (Emery and Aubrey 1991; National Research Council 1987).

(5) USACE does not endorse a particular sea level rise (or fall) scenario. ER 1105-2-100 (28 December 1990) directs that feasibility studies must consider a range of possible future rates of sea level rise. Project planning should use local, historical rates of rsl change.

IV-1-7. Cultural (Man-Made) Influences on Coastal Geology

a. Introduction. Man has modified many of the world's coastlines, either directly, by construction or dredging, or indirectly, as a result of environmental changes that influence sediment supply, runoff, or climate. Human activity has had the most profound effects on the coastal environment in the United States and the other industrial nations, but even shorelines in lesser-developed countries have not been immune to problems wrought by river diversion and loss of wetlands. The most common practices that significantly alter the coastal environment are the construction of coastal works such as jetties and groins and the development of property on and immediately inland of the beach. Historically, many cities have developed on the coast. Although originally most were located in bays or other protected anchorages, many have grown and spread to the open coast. Prominent United States examples include New York, Boston, San Diego, and Los Angeles. Still other communities originally began as resorts on barrier islands and have since grown into full-size cities; examples include Atlantic City, Ocean City, Virginia Beach, and Miami Beach. Land use practices well inland from the coast also often have important effects on coastal sedimentation. These factors are more difficult to detect and analyze because, sometimes, the affecting region is hundreds of kilometers inland. For example, dam construction can greatly reduce the natural supply of sediment brought to the coast by streams and rivers, while deforestation and agricultural runoff may lead to increased sediment load in rivers.

b. Dams/Reservoirs. In many coastal areas, the major source of sediment for the littoral system is from streams and rivers. Dams and reservoirs obstruct the transport of sediment to the littoral system by creating sediment traps. These structures also restrict peak flows, which reduce sediment transport of material that is available downstream of the structures. The net effect is sediment starvation of coastal areas that previously received riverine sediment. If the losses are not offset by new supplies, the results are shrinking beaches and coastal erosion (Schwartz 1982). The most prominent example is the accelerated erosion of the Nile Delta that has occurred since the Aswan Low Dam (1902) and the Aswan High Dam (1964) almost totally blocked the supply of sediment to the coast (Frihy 1992). The Rosetta promontory has been eroding at an average rate of 55 m/year between 1909 and the present. Loss of nutrient-laden silt from the Nile's annual spring floods has also had bad effects on agriculture in the Nile valley and delta and has damaged fisheries in the eastern Mediterranean. Portions of the southern California coast have also suffered this century from loss of fluvially supplied sediment (e.g., Point Arguello, cited by Bowen and Inman (1966)). Increased erosion of the Washington shore near Grays Harbor may be due to the loss of sediment from the Columbia River, which has been massively dammed since the 1930's and 1940's.

c. Erosion control and coastal structures. Coastal structures such as jetties, groins, seawalls, bulkheads, and revetments are probably the most dramatic cause of man-induced coastal erosion (*Shore Protection Manual* 1984). Any coastal structure will have some effect on local sediment dynamics, and in some cases, the effect may extend downdrift for many kilometers.

d. Modification of natural protection.

(1) Destructive effects. The destruction of dunes and beach vegetation, development of backshore areas, and construction on the back sides of barrier islands can increase the occurrence of overwash during storms. In many places, sand supply has diminished because much of the surface area of barriers has been paved and covered with buildings. The result has been backshore erosion and increased barrier island breaching. In most coastal areas of the United States, one need merely visit the local beaches to see examples of gross and callous coastal development where natural protection has been compromised. Carter (1988) reviews examples from the United Kingdom. Serious damage has occurred to biological shores around the world as a result of changes in runoff and sediment supply, increased pollution, and development.

(2) Constructive efforts. Sand dunes are often stabilized using vegetation and sand fences. Dunes afford protection against flooding of low-lying areas. Dunes are also stabilized to prevent sand from blowing over roads and farms. Dunes are discussed in Part IV-2-6.

e. Beach renourishment (fill). An alternative for restoring beaches without constructing groins or other hard structures is to bring sand to the site from offshore by dredges or from inland sources by truck. This is the only coastal management that actually adds sand back into the littoral system (Pope 1997). Although conceptually renourishment seems simple enough, in practice, the planning, design, application, and maintenance of beach renourishment projects are sophisticated engineering and geologic procedures. For design and monitoring information, the reader is referred to Part V-4, Tait (1993), and Stauble and Kraus (1993). *Shore and Beach,* Vol 61, No. 1 (January 1993) is a special issue devoted to the beach renourishment project at Ocean City, Maryland. Stauble et al. (1993) evaluate the Ocean City project in detail. Krumbein (1957) is a classic description of sediment analysis procedures for specifying beach fills. One of the most successful U.S. renourishment projects has been at Miami Beach, Florida (reviewed in Carter (1988)).

f. Mining.

(1) Beach mining can directly reduce the amount of sediment available to the littoral system. In most areas of the United States, beach sand can no longer be exploited for commercial purposes because sand is in short supply, and the health of dunes and biological communities depends vitally on the availability of sand. Strip mining can indirectly affect the coast due to increased erosion, which increases sediment carried to the sea by rivers (unless the sediment is trapped behind dams).

(2) In Britain, an unusual situation developed at Horden, County Durham, where colliery waste was dumped on the shore. The waste material formed a depositional bulge in the shore. As the sediment from Horden moved downcoast, it was sorted, with the less dense coal forming a surface placer on the beach that is commercially valuable (Carter 1988).

g. Stream diversion.

(1) Stream diversion, both natural and man-made, disrupts the natural sediment supply to areas that normally receive fluvial material. With diversion for agriculture or urban use, the results are similar to those produced by dams: sediment that normally would be carried to the coast remains trapped upriver. Its residence time in this artificial storage, decades or centuries, may be short on geological time scales but is long enough to leave a delta exposed to significant erosion.

(2) Natural diversion occurs when a river shifts to a new, shorter channel to the sea, abandoning its less efficient former channel. An example of this process is the gradual occupation of the Atchafalaya watershed by the Mississippi River. If this process were to continue to its natural conclusion, the present Balize ("Birdfoot") delta would be abandoned, causing it to erode at an ever faster rate, while a new delta

would form in Atchafalaya Bay (Coleman 1988). The evolution of the Mississippi River is discussed in Part IV-3-3.

h. Agriculture. Poor farming practices lead to exposure of farmlands and increased erosion rates. Eroded soil is easily carried away by streams and rivers and is ultimately deposited in estuaries and offshore. The consequence of this process is progradation of the depositional areas. If rivers have been dammed, the sediment load is trapped behind the dams in the artificial lakes, and in that case does not get carried to the open sea.

i. Forestry. Deforestation is a critical problem in many developing nations, where mountainsides, stripped of their protective trees, erode rapidly. The soil is carried to the sea, where local coastlines prograde temporarily, but upland areas are left bereft of invaluable topsoil, resulting in human poverty and misery and in the loss of animal habitat. Reckless slash-and-burn practices have destroyed many formerly valuable timber resources in Central America, and some southeast Asian countries have already cut down most of their trees (Pennant-Rea 1994). Fortunately, Malaysia and Indonesia are beginning to curb illegal timber cutting and export, a trend which hopefully will spread to other countries. Unfortunately, the financial turmoil that engulfed Asia in 1998 will probably set back efforts to promote responsible resource management.

IV-1-8. References

EM 1110-2-1412
Storm Surge Analysis and Design Water Level Determinations

Allen 1976
Allen, E. S. 1976. *A Wind to Shake the World,* Little Brown & Co., New York, NY.

Baeteman 1994
Baeteman, C. 1994. "Subsidence in Coastal Lowlands Due to Groundwater Withdrawal: The Geological Approach; Coastal Hazards, Perception, Susceptibility and Mitigation," C. W. Finkl, Jr., ed., *Journal of Coastal Research* Special Issue No. 12, pp 61-75.

Bagnold 1954
Bagnold, R. A. 1954. *The Physics of Blown Sand and Desert Dunes,* 2nd ed., Methuen, London, UK.

Barnett 1984
Barnett, T. P. 1984. "The Estimation of 'Global' Sea Level: A Problem of Uniqueness," *Journal of Geophysical Research,* Vol 89, No C5, pp 7980-7988.

Bascom 1964
Bascom, W. 1964. *Waves and Beaches, the Dynamics of the Ocean Surface,* Doubleday & Co., Garden City, NY.

Bates and Jackson 1984
Bates, R. L., and Jackson, J. A. 1984. *Dictionary of Geologic Terms,* 3rd ed., Anchor Press/Doubleday, Garden City, NY.

Bird 1976
Bird, E. C. F. 1976. "Shoreline Changes During the Past Century," *Proceedings of the 23rd International Geographic Congress, Moscow,* Pergamon, Elmsford, NY.

Bowen and Inman 1966
Bowen, A. J., and Inman, D. L. 1966. "Budget of Littoral Sands in the Vicinity of Point Arguello, California," Technical Memorandum, Coastal Engineering Research Center, U.S. Army Engineer Waterways Experiment Station, Vicksburg, MS.

Carter 1988
Carter, R. W. G. 1988. *Coastal Environments: An Introduction to the Physical, Ecological, and Cultural Systems of Coastlines,* Academic Press, London, UK.

Coastal States Organization 1997
Coastal States Organization. 1997. "Putting the Public Trust Doctrine to Work - the Application of the Public Trust Doctrine to the Management of Lands, Water, and Living Resources of the Coastal States," Washington, DC.

Cole 1980
Cole, F. W. 1980. *Introduction to Meteorology,* John Wiley and Sons, Inc., New York, NY.

Coleman 1988
Coleman, J. M. 1988. "Dynamic Changes and Processes in the Mississippi River Delta," *Bulletin of the Geological Society of America,* Vol 100, pp 999-1015.

Curray 1964
Curray, J. R. 1964. "Transgressions and Regressions," *Papers in Marine Geology: Shepard Commemorative Volume*, R. L. Mills, ed., MacMillan, New York, NY.

Curray 1965
Curray, J. R. 1965. "Late Quaternary History, Continental Shelves of the United States," *The Quaternary of the United States,* H. E. Wright, Jr. and D. G. Frey, eds., Princeton University Press, Princeton, NJ, pp 713-735.

Davidson, Dean, and Edge 1990
Davidson, M. A., Dean, R. G., and Edge, B. L. 1990. *Shore and Beach,* Vol 58, No. 4 (Special issue dedicated to Hurricane Hugo papers).

Davies 1964
Davies, J. L. 1964. "A Morphogenic Approach to World Shorelines," *Zeitschrift für Geomorphology*, Vol 8, pp 27-42.

Davis and Hayes 1984
Davis, R. A., Jr., and Hayes, M. O. 1984. "What is a Wave-Dominated Coast?, Hydrodynamics and Sedimentation in Wave-Dominated Coastal Environments," B. Greenwood and R. A. Davis, Jr., eds., *Marine Geology*, Vol 60, pp 313-329.

Dillon and Oldale 1978
Dillon, W. D., and Oldale, R. N. 1978. "Late Quaternary Sea Level Curve: Reinterpretation Based on Glacio-Eustatic Influence," *Geology,* Vol 6, pp 56-60.

Dolan and Davis 1992
Dolan, R., and Davis, R. E. 1992. "Rating Northeasters," *Mariners Weather Log,* Vol 36, No 1, pp 4-11.

Ellis 1978
Ellis, M. Y. 1978. *Coastal Mapping Handbook.* Department of the Interior, U.S. Geological Survey and U.S. Department of Commerce, National Ocean Service and Office of Coastal Zone Management, U.S. Government Printing Office, Washington, DC.

Emery and Aubrey 1991
Emery, K. O., and Aubrey, D. G. 1991. *Sea Levels, Land Levels, and Tide Gauges,* Springer-Verlag, New York, NY.

Finkl and Pilkey 1991
Finkl, C. W., and Pilkey, O. H. 1991. "Impacts of Hurricane Hugo: September 10-22, 1989," *Journal of Coastal Research,* Special Issue No. 8.

Flint 1971
Flint, R. F. 1971. *Glacial and Quaternary Geology,* John Wiley and Sons, New York, NY.

Fox and Davis 1976
Fox, W. T., and Davis, R. A., Jr. 1976. "Weather Patterns and Coastal Processes," *Beach and Nearshore Sedimentation,* R. A. Davis, Jr., and R. L. Ethington, eds., Society of Economic Paleontologists and Mineralogists Special Publication No. 24, Tulsa, OK.

Frihy 1992
Frihy, O. E. 1992. "Sea-Level Rise and Shoreline Retreat of the Nile Delta Promontories, Egypt," *Natural Hazards,* Vol 5, pp 65-81.

Gorman 1991
Gorman, L. T. 1991. "Annotated Bibliography of Relative Sea Level Change," Technical Report CERC-91-16, U.S. Army Engineer Waterways Experiment Station, Vicksburg, MS.

Gorman, Morang, and Larson 1998
Gorman, L. T., Morang, A., and Larson, R. L. 1998. "Monitoring the Coastal Environment; Part IV: Mapping, Shoreline Change, and Bathymetric Analysis," *Journal of Coastal Research,* Vol 14, No. 1, pp 61-92.

Gornitz and Lebedeff 1987
Gornitz, V., and Lebedeff, S. 1987. "Global Sea-Level Changes During the Past Century," *Sea-Level Fluctuations and Coastal Evolution,* D. Nummedal, O. H. Pilkey, and J. D. Howard, eds., Special Publication No. 41, Society of Economic Paleontologists and Mineralogists, Tulsa, OK, pp 3-16.

Gove 1986
Gove, P. B., ed. 1986. *Webster's Third International Dictionary,* Merriam-Webster, Springfield, MA.

Hands 1983
Hands, E. B. 1983. "The Great Lakes as a Test Model for Profile Response to Sea Level Changes," Chapter 8 in *Handbook of Coastal Processes and Erosion,* P. D. Komar, ed., CRC Press, Inc., Boca Raton, FL. (Reprinted in Miscellaneous Paper CERC-84-14, Coastal Engineering Research Center, U.S. Army Engineer Waterways Experiment Station, Vicksburg, MS.)

Hayes 1979
Hayes, M. O. 1979. "Barrier Island Morphology as a Function of Tidal and Wave Regime," *Barrier Islands from the Gulf of St. Lawrence to the Gulf of Mexico*, S. P. Leatherman, ed., Academic Press, New York, NY, pp 1-29.

Hicks 1972
Hicks, S. D. 1972. "Changes in Tidal Characteristics and Tidal Datum Planes," *The Great Alaska Earthquake of 1964,* Oceanography and Coastal Engineering, National Academy of Sciences, Washington, DC, pp 310-314.

Hicks 1978
Hicks, S. D. 1978. "An Average Geopotential Sea Level Series for the United States," *Journal of Geophysical Research,* Vol 83, No. C3, pp 1377-1379.

Hicks 1984
Hicks, S. D. 1984. *Tide and Current Glossary.* NOAA/National Ocean Service, Rockville, MD.

Hoffman, Keyes, and Titus 1983
Hoffman, J. S., Keyes, D., and Titus, J. G. 1983. "Projecting Future Sea Level Rise; Methodology, Estimates to the Year 2100, and Research Needs," Report 230-09-007, U.S. Environmental Protection Agency, Washington, DC.

Houston 1993
Houston, J. R. 1993. "Responding to Uncertainties in Sea Level Rise," *The State of Art of Beach Nourishment, Proceedings of the 1993 National Conference on Beach Preservation Technology,* The Florida Shore & Beach Preservation Association, Tallahassee, FL, pp 358-372.

Hsu 1988
Hsu, S. A. 1988. *Coastal Meteorology*, Academic Press, Inc., San Diego, CA.

Huschke 1959
Huschke, R. E., ed. 1959. *Glossary of Meteorology,* American Meteorology Society, Boston, MA.

International Hydrographic Bureau 1990
International Hydrographic Bureau. 1990. *Hydrographic Dictionary, Part I.* International Hydrographic Bureau, Monaco.

Knauss 1978
Knauss, J. A. 1978. *Introduction to Physical Oceanography,* Prentice-Hall, Englewood Cliffs, NJ.

Komar 1998
Komar, P. D. 1976. *Beach Processes and Sedimentation,* Prentice-Hall, Englewood Cliffs, NJ.

Komar 1992
Komar, P. D. 1992. "Ocean Processes and Hazards Along the Oregon Coast," *Oregon Geology*, Vol 54, No. 1, pp 3-19.

Komar and Enfield 1987
Komar, P. D., and Enfield, D. B. 1987. "Short-Term Sea-Level Changes on Coastal Erosion," *Sea-Level Fluctuations and Coastal Evolution*, Special Publication No. 41, D. Nummedal, O. H. Pilkey, and J. D. Howard, eds., Society of Economic Paleontologists and Mineralogists, Tulsa, OK, pp 17-28.

Kraft and Chrzastowski 1985
Kraft, J. C., and Chrzastowski, M. J. 1985. "Coastal Stratigraphic Sequences," *Coastal Sedimentary Environments,* Davis, R. A., Jr., ed., Springer-Verlag, New York, NY, pp 625-663.

Krumbein 1957
Krumbein, W. C. 1957. "A Method for Specification of Sand for Beach Fills," Technical Memorandum No. 102, Beach Erosion Board, U.S. Army Engineer Waterways Experiment Station, Vicksburg, MS.

Kuhn and Shepard 1984
Kuhn, G. G., and Shepard, F. P. 1984. *Sea Cliffs, Beaches, and Coastal Valleys of San Diego County; Some Amazing Histories and Some Horrifying Implications,* University of California Press, Berkeley, CA.

Larson, Morang, and Gorman 1997
Larson, R. L., Morang, A., and Gorman, L. T. 1997. "Monitoring the Coastal Environment; Part II: Sediment Sampling and Geotechnical Methods," *Journal of Coastal Research,* Vol 13, No. 2, pp 308-330.

Leveson 1980
Leveson, D. 1980. *Geology and the Urban Environment,* Oxford University Press, New York, NY.

Lyles, Hickman, and Debaugh 1988
Lyles, S. D., Hickman, L. E., Jr., and Debaugh, H. A., Jr. 1988. "Sea Level Variations for the United States, 1855-1986," U.S. Department of Commerce, National Oceanic and Atmospheric Administration, National Ocean Service, Rockville, MD.

Mariolakos 1990
Mariolakos, I. 1990. "The Impact of Neotectonics with Regard to Canals, Pipelines, Dams, Open Reservoirs, etc. in Active Areas: The Case of the Hellenic Arc," *Greenhouse Effect, Sea Level and Drought, Proceedings of the NATO Advanced Research Workshop on Geohydrological Management of Sea Level and Mitigation of Drought (1989),* R. Paepe, R. W. Fairbridge, and S. Jelgersma, eds., Kluwer Academic Publishers, Dordrecht, The Netherlands, pp 427-438.

Meade and Emery 1971
Meade, R. H., and Emery, K. O. 1971. "Sea-Level as Affected by River Runoff, Eastern United States," *Science*, Vol 173, pp 425-428.

Milliman and Emery 1968
Milliman, J. D., and Emery, K. O. 1968. "Sea Levels During the Past 35,000 Years," *Science,* Vol 162, pp 1121-1123.

Minsinger 1988
Minsinger, W. E., ed. 1988. *The 1938 Hurricane, an Historical and Pictorial Summary,* Blue Hill Observatory, East Milton, MA.

Morang, Larson, and Gorman 1997a
Morang, A., Larson, R. L., and Gorman, L. T. 1997a. "Monitoring the Coastal Environment; Part I: Waves and Currents," *Journal of Coastal Research,* Vol 13, No. 1, pp 111-133.

Morang, Larson, and Gorman 1997b
Morang, A., Larson, R. L., and Gorman, L. T. 1997b. "Monitoring the Coastal Environment; Part III: Geophysical and Research Methods," *Journal of Coastal Research,* Vol 13, No. 4, pp 1964-1085.

Morang 1999
Morang, A. 1999. "Coastal Inlets Research Program, Shinnecock Inlet, New York, Site Investigation, Report 1, Morphology and Historical Behavior," Technical Report CHL-98-32, U.S. Army Engineer Waterways Experiment Station, Vicksburg, MS.

Mossa, Meisburger, and Morang 1992
Mossa, J., Meisburger, E. P., and Morang, A. 1992. "Geomorphic Variability in the Coastal Zone," Technical Report CERC-92-4, U.S. Army Engineer Waterways Experiment Station, Vicksburg, MS.

National Research Council 1983
National Research Council, Board on Atmospheric Sciences and Climate. 1983. *Changing Climate, Report of the Carbon Dioxide Assessment Committee,* National Academy Press, Washington, DC.

National Research Council 1987
National Research Council, Committee on Engineering Implications of Changes in Relative Mean Sea Level. 1987. *Responding to Changes in Sea Level,* National Academy Press, Washington, DC.

Neumann, Jarvinen, Pike, and Elms 1987
Neumann, C. J., Jarvinen, B. R., Pike, A. C., and Elms, J. D. 1987. *Tropical Cyclones of the North Atlantic Ocean, 1871-1986,* Third rev., Historical Climatology Series 6-2, National Climatic Data Center, Asheville, NC.

NOAA 1977
National Oceanic and Atmospheric Administration. 1977. "Some Devastating North Atlantic Hurricanes of the 20th Century," Booklet NOAA/PA 77019, U.S. Government Printing Office, Washington, DC.

Nummedal 1983
Nummedal, D. 1983. "Barrier Islands," *CRC Handbook of Coastal Processes and Erosion*, P. D. Komar, ed., CRC Press, Inc., Boca Raton, FL, pp 77-121.

Nummedal and Fischer 1978
Nummedal, D., and Fischer, I. A. 1978. "Process-Response Models for Depositional Shorelines: The German and the Georgia Bights," *Proceedings of the Sixteenth Conference on Coastal Engineering*, American Society of Civil Engineers, New York, NY, pp 1215-1231.

Nummedal, Pilkey, and Howard, eds. 1987
Nummedal, D., Pilkey, O. H., and Howard, J. D., eds. 1987. *Sea-Level Fluctuations and Coastal Evolution,* Special Publication No. 41, Society of Economic Paleontologists and Mineralogists, Tulsa, OK.

Orme 1985
Orme, A. R. 1985. "California," *The World's Coastline,* E. C. Bird, and M. L. Schwartz, eds., Van Nostrand Reinhold, New York, NY, pp 27-36.

Payton 1977
Payton, C. E., ed. 1977. *Seismic Stratigraphy - Applications to Hydrocarbon Exploration,* Memoir 26, American Association of Petroleum Geologists, Tulsa, OK.

Pennant-Rea 1994
Pennant-Rea, R., ed. 1994. "Chainsaw Massacres," *The Economist*, Vol 331, No. 7869, p 39.

Pethick 1984
Pethick, J. 1984. *An Introduction to Coastal Geomorphology,* Edward Arnold Publishers, London, UK.

Pirazzoli 1991
Pirazzoli, P. A. 1991. *World Atlas of Sea-Level Changes*, Elsevier Scientific Publishers, Amsterdam, The Netherlands.

Plafker and Kachadoorian 1966
Plafker, G., and Kachadoorian, R. 1966. "Geologic Effects of the March 1964 Earthquake and Associated Seismic Sea Waves on Kodiak and Nearby Islands, Alaska," Geological Survey Professional Paper 543-D, U.S. Government Printing Office, Washington, DC.

Pope 1997
Pope, J. 1997. "Responding to Coastal Erosion and Flooding Damages," *Journal of Coastal Research,* Vol 13, No. 3, pp 704-710.

Rosen, Brenninkmeyer, and Maybury 1993
Rosen, P. S., Brenninkmeyer, B. M., and Maybury, L. M. 1993. "Holocene Evolution of Boston Inner Harbor, Massachusetts," *Journal of Coastal Research*, Vol 9, No. 2, pp 363-377.

Sahagian and Holland 1991
Sahagian, D. L., and Holland, S. M. 1991. Eustatic Sea-Level Curve Based on a Stable Frame of Reference: Preliminary Results, *Geology*, Vol 19, pp 1208-1212.

Schwartz 1982
Schwartz, M. L., ed. 1982. *The Encyclopedia of Beaches and Coastal Environments,* Encyclopedia of Earth Sciences, Volume XV, Hutchinson Ross Publishing Company, Stroudsburg, PA.

Shalowitz 1962
Shalowitz, A. L. 1962. *Shore and Sea Boundaries, with Special Reference to the Interpretation and Use of Coast and Geodetic Survey Data.* Vol 1, Pub 10-1, U.S. Department of Commerce, Coast and Geodetic Survey, U.S. Government Printing Office, Washington, DC.

Shalowitz 1964
Shalowitz, A. L. 1964. *Shore and Sea Boundaries, with Special Reference to the Interpretation and Use of Coast and Geodetic Survey Data.* Vol 2, Pub 10-1, U.S. Department of Commerce, Coast and Geodetic Survey, U.S. Government Printing Office, Washington, DC.

Shepard 1973
Shepard, F. P. 1973. *Submarine Geology,* 3rd ed., Harper & Row, New York, NY.

Shore Protection Manual 1984
Shore Protection Manual. 1984. 4th ed., 2 Vol, Coastal Engineering Research Center, U.S. Army Engineer Waterways Experiment Station, U.S. Government Printing Office, Washington, DC.

Simpson and Riehl 1981
Simpson, R. H., and Riehl, H. 1981. *The Hurricane and Its Impact,* Louisiana State University Press, Baton Rouge, LA.

Stanley 1986
Stanley, S. M. 1986. *Earth and Life Through Time,* W. H. Freeman, New York, NY.

Stauble and Kraus 1993
Stauble, D. K., and Kraus, N. C. 1993. *Beach Nourishment Engineering and Management Considerations,* Coastlines of the World Series, American Society of Civil Engineers, New York, NY.

Stauble, Garcia, Kraus, Grosskopf, and Bass 1993
Stauble, D. K., Garcia, A. W., Kraus, N. C., Grosskopf, W. G., and Bass, G. P. 1993. "Beach Nourishment Project Response and Design Evaluation, Ocean City, Maryland," Technical Report CERC-93-13, U.S. Army Engineer Waterways Experiment Station, Vicksburg, MS.

Stone and Morgan 1993
Stone, G. W., and Morgan, J. P. 1993. "Implications for a Constant Rate of Relative Sea-Level Rise During the Last Millennium Along the Northern Gulf of Mexico: Santa Rosa Island, Florida," *Shore and Beach,* Vol 61, No. 4, pp 24-27.

Strahler 1981
Strahler, A. N. 1981. *Physical Geology,* Harper & Row, New York, NY.

Suter and Berryhill 1985
Suter, J. R., and Berryhill, H. L., Jr. 1985. "Late Quaternary Shelf-Margin Deltas, Northwest Gulf of Mexico," *Bulletin of the American Association of Petroleum Geologists,* Vol 69, No. 1, pp 77-91.

Tait 1993
Tait, L. S., compiler. 1993. "The State of the Art of Beach Renourishment," *Proceedings of the 6th Annual National Conference on Beach Preservation Technology,* Florida Shore & Beach Preservation Association, Tallahassee, FL.

Tannehill 1956
Tannehill, I. R. 1956. *Hurricanes, Their Nature and History,* 9th Revised ed., Princeton University Press, Princeton, NJ.

Tanner 1989
Tanner, W. F. 1989. "New Light on Mean Sea Level Change," *Coastal Research,* Vol 8, No. 4, pp 12-16.

U.S. Army Corps of Engineers 1995
U.S. Army Corps of Engineers. 1995. "Coastal Geology," Engineer Manual 1110-2-1810, Washington, DC.

Whitehill 1968
Whitehill, W. M. 1968. *Boston, A Topographical History*, 2nd ed. (enlarged), The Belknap Press of Harvard University Press, Cambridge, MA.

Winkler 1977
Winkler, C. D. 1977. "Plio-Pleistocene Paleogeography of the Florida Gulf Coast Interpreted from Relic Shorelines," *Transactions Gulf Coast Association of Geological Societies,* Vol 27, pp 409-420.

Winkler and Howard 1977
Winkler, C. D., and Howard, J. D. 1977. "Correlation of Tectonically Deformed Shorelines on the Southern Atlantic Coastal Plain," *Geology,* Vol 5, pp 123-127.

Woodsworth and Wigglesworth 1934
Woodsworth, J. B., and Wigglesworth, E. 1934. *Geography and Geology of the Region Including Cape Cod, Elizabeth Is., Nantucket, Martha's Vinyard, No Mans Land, and Block Is.,* Memoir 52, Museum of Comparative Zoology, Harvard University, Cambridge, MA.

Wunsch 1996
Wunsch, C. 1996. Doherty Lecture: "The Ocean and Climate - Separating Myth from Fact," *Marine Technical Society Journal,* Vol 30, No. 2, pp 65-68.

Young 1975
Young, K. 1975. *Geology: The Paradox of Earth and Man,* Houghton Mifflin Co., Boston, MA.

Young and Hale 1998
Young, C., and Hale, L. 1998. "Coastal Management: Insurance for the Coastal Zone," *Maritimes*, Vol 40, No. 1, pp 17-19.

IV-1-9. Acknowledgments

Authors of Chapter IV-1, "Coastal Terminology and Geologic Environments:"

Andrew Morang, Ph.D., Coastal and Hydraulics Laboratory (CHL), Engineer Research and Development Center (ERDC), Vicksburg, Mississippi.
Larry E. Parson, U.S. Army Engineer District, Mobile, Mobile, Alabama.

Reviewers:

Stephan A. Chesser, U.S. Army Engineer District, Portland, Portland, Oregon.
Ronald L. Erickson, U.S. Army Engineer District, Detroit, Detroit, Michigan.
James R. Houston, Ph.D., ERDC.
John H. Lockhart, Jr., Headquarters, U.S. Army Corps of Engineers, Washington, DC, (retired).
Edward P. Meisburger, CHL (retired).
Joan Pope, CHL.
John F. C. Sanda, Headquarters, U.S. Army Corps of Engineers, Washington, DC., (retired).
Orson P. Smith, Ph.D., U.S. Army Engineer District, Alaska, Anchorage, Alaska, (retired).

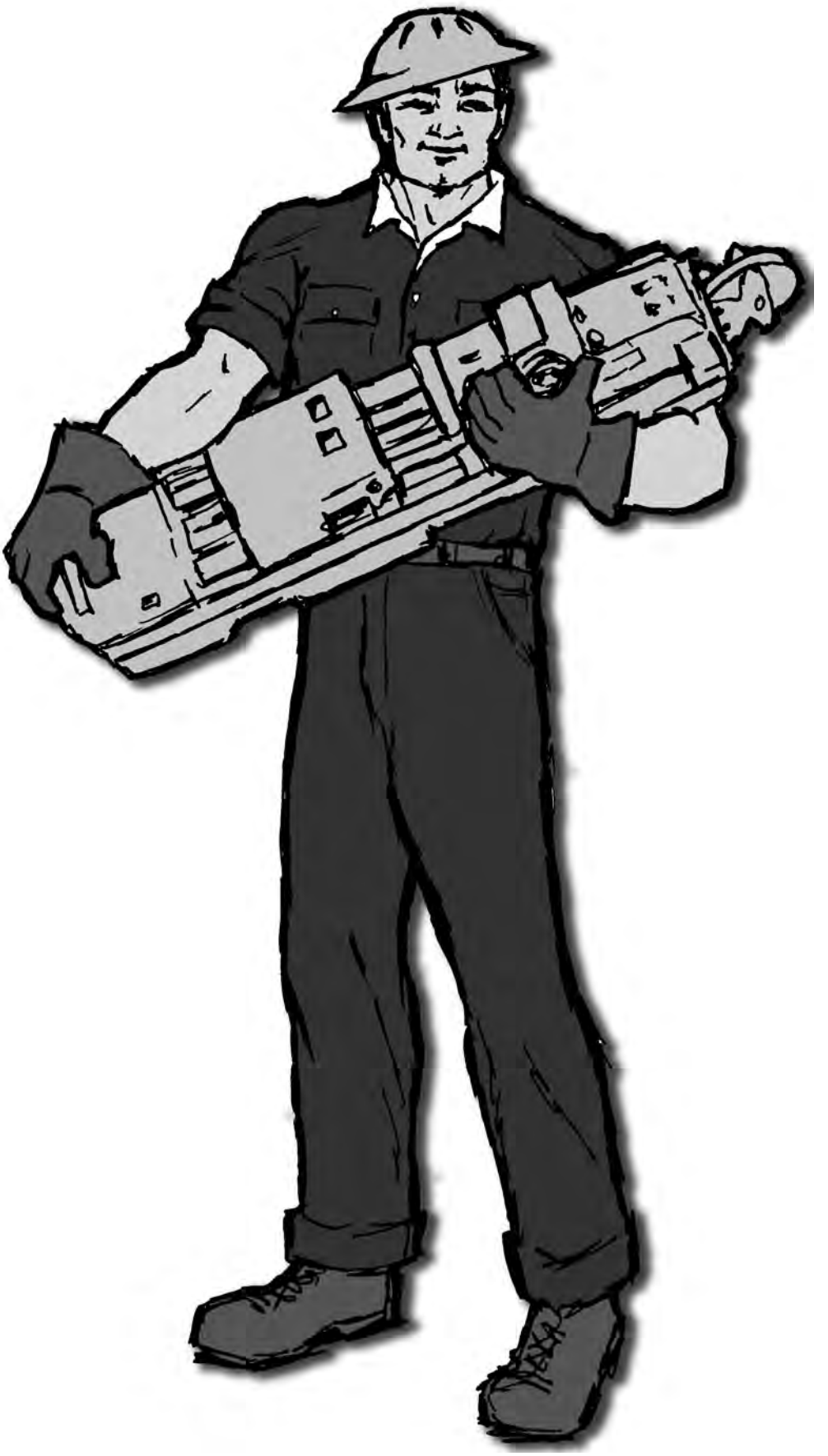

Table of Contents

Page

IV-2-1. Introduction IV-2-1

IV-2-2. Coastal Classification IV-2-1
a. Introduction IV-2-1
b. Early classifications IV-2-1
c. Later classifications IV-2-1
d. Coastal classification of Francis Shepard IV-2-1
e. Classification schemes for specific environments IV-2-3
(1) River systems IV-2-3
(2) Great Lakes of North America IV-2-3

IV-2-3. Drowned River Coasts - Estuaries IV-2-4
a. Introduction IV-2-4
b. Literature IV-2-4
c. Classification IV-2-4
d. Definitions IV-2-4
e. Time relationships and evolution IV-2-4
f. Overall geomorphic characteristics IV-2-7
g. Energy factors and sedimentary structures IV-2-8
(1) Wave-dominated estuaries IV-2-8
(2) Tide-dominated estuaries IV-2-8
(3) Estuarine variability IV-2-8
(a) Wave-to-tide transition IV-2-8
(b) Effects of tide range IV-2-10
(c) Influence of valley shape IV-2-10
(d) Geologic setting IV-2-10
h. Estuarine sediments IV-2-10

IV-2-4. Drowned Glacial Erosion Coasts IV-2-11
a. Introduction IV-2-11
b. Erosion and sediment production IV-2-11
(1) Fjords IV-2-11
(2) Depositional features IV-2-11
c. Variability IV-2-11
d. Atlantic coast IV-2-11
e. Offshore geology IV-2-12

IV-2-5. River Deposition Coasts - Deltas IV-2-12

IV-2-6. Wind Deposition Coasts - Dunes IV-2-12
a. Introduction IV-2-12
b. Origin of dunes IV-2-13
c. Sediment sources IV-2-13
d. Modification and stability IV-2-14
e. Dune vegetation IV-2-16
f. Dune fauna IV-2-17
g. Classification IV-2-17
(1) Foredunes IV-2-17
(2) Parabolic dunes IV-2-17
(3) Barchan dunes IV-2-17
(4) Transverse dune ridges IV-2-17
(5) Longitudinal (seif) dunes IV-2-17
(6) Blowouts IV-2-17
(7) Attached dunes IV-2-17
h. Shoreline protection IV-2-17
i. Dune restoration IV-2-17

IV-2-7. Volcanic Coasts IV-2-20
a. Introduction and definitions IV-2-20
b. General geology IV-2-20
c. Composite volcanoes - coastal Alaska IV-2-21
d. Shield volcanoes - Hawaii IV-2-21
e. Hazards posed by volcanoes IV-2-23
(1) Introduction IV-2-23
(2) Earthquakes and tsunamis IV-2-24
(3) Ash and fluvial sediment IV-2-25
(4) Explosive destruction IV-2-25

IV-2-8. Sea Cliffs - Diastrophic, Erosional, and Volcanic IV-2-26

IV-2-9. Marine Deposition Coasts - Barriers IV-2-32
a. Introduction IV-2-32
b. Distribution of barrier coasts IV-2-36
c. General coastal barrier structure IV-2-36
d. Origin and evolution IV-2-39
(1) Emergence model IV-2-39
(2) Submergence model IV-2-39
(3) Spit detachment model IV-2-39
(4) Combined origin model IV-2-39
e. Barrier response to rising sea level IV-2-39

IV-2-10. Marine Deposition Coasts - Beaches IV-2-45
a. Introduction IV-2-45
b. General definition IV-2-45
c. Major subdivisions IV-2-45
(1) Foreshore IV-2-45
(2) Backshore IV-2-46
(3) Coastline IV-2-47
d. Beach material IV-2-47

(1) Sand beaches IV-2-47
(2) Coarse beaches IV-2-47
(3) Biogenic beaches IV-2-48

IV-2-11. Salt Marshes IV-2-48
a. Distribution of salt marshes IV-2-48
b. Classification of salt marshes IV-2-49
c. Sediment characteristics IV-2-49
(1) Introduction IV-2-49
(2) Marsh plants IV-2-50
(3) Sediment transport and processes IV-2-50
(4) Engineering problems IV-2-51
(a) Sediment deficits IV-2-51
(b) Shoreline erosion IV-2-51
(c) Subsidence IV-2-52
(d) Sea level rise IV-2-52
(e) Saltwater intrusion IV-2-52
(f) Canals IV-2-52
(5) Marsh restoration IV-2-52

IV-2-12. Biological Coasts IV-2-52
a. Introduction IV-2-52
b. High wave-energy coasts IV-2-53
(1) Coral reefs IV-2-53
(2) Worm reefs IV-2-55
(3) Oyster reefs IV-2-55
(4) Rocky coasts IV-2-58
(a) Kelp beds IV-2-58
(b) Kelp biological communities IV-2-58
(c) Rock reefs and shorelines IV-2-58
(5) Sandy coasts IV-2-58
c. Low wave-energy coasts IV-2-59
(1) General IV-2-59
(2) Mangroves IV-2-59
d. Other sources of biogenic sediment in the coastal zone IV-2-60

IV-2-13. Continental Shelf Geology and Topography IV-2-60
a. Introduction IV-2-60
b. Continental shelf sediment studies IV-2-60
c. Continental shelf morphology IV-2-62
d. Examples of specific features - Atlantic seaboard IV-2-63
e. Riverine influence IV-2-63

IV-2-14. References IV-2-65

IV-2-15. Acknowledgments IV-2-77

List of Tables

Page

Table IV-2-1. Classification of Coasts IV-2-2

Table IV-2-2. Worldwide Distribution of Barrier Island Coasts IV-2-36

Table IV-2-3. Barrier Islands and Spits of the United States IV-2-37

Table IV-2-4. Types of Beach Sediment IV-2-47

Table IV-2-5. U.S. Army Corps of Engineers Inner Continental Shelf Sediment and Structure (ICONS) Reports IV-2-62

List of Figures

Page

Figure IV-2-1. (a) Plan view of distribution of energy and physical processes in estuaries; (b) Schematic definition of estuary according to Dalrymple, Zaitlin, and Boyd (1992); (c) Time-averaged sediment transport paths IV-2-5

Figure IV-2-2. Estuary/prograding coast evolution IV-2-6

Figure IV-2-3. Estuary evolution, based on changes in wave or tidal power IV-2-7

Figure IV-2-4. Morphologic models of (a) wave-dominated and (b) tide-dominated estuaries IV-2-9

Figure IV-2-5. Glacial fjord coast: Alaska (Lake George, with Surprise glacier in the background) IV-2-12

Figure IV-2-6. Drowned glacial erosion coast: Maine (Potts Point, South Harpswell, near Brunswick IV-2-13

Figure IV-2-7. Typical glacial depositional structures IV-2-14

Figure IV-2-8. Islands in Boston Harbor, Massachusetts IV-2-15

Figure IV-2-9. Glacial till bluffs just west of Montauk Point, Long Island, New York, facing the Atlantic Ocean IV-2-15

Figure IV-2-10. Partly vegetated coastal sand dunes IV-2-16

Figure IV-2-11. Variety of dune types IV-2-18

Figure IV-2-12. Blowout in dunes IV-2-19

Figure IV-2-13. Huge dune anchored to a rock outcrop in the eastern Sinai Desert IV-2-19

Figure IV-2-14. Alaskan volcanoes along the Aleutian Island arc, marking the boundary between the North American and the Pacific crustal plates IV-2-22

Figure IV-2-15. Southeast coast of Hawaii, near Kalpana IV-2-24

Figure IV-2-16. Laupahoehoe Harbor, Island of Hawaii, Hawaii IV-2-25

Figure IV-2-17. Wave-cut platform exposed by tectonic uplift IV-2-28

Figure IV-2-18. Wave erosion of an indented coastline IV-2-29

Figure IV-2-19. Inundation of a mountainous area by rising sea level or land subsidence IV-2-30

Figure IV-4-20. Pacific Ocean coast of Olympic Peninsula, Washington IV-2-31

Figure IV-2-21. Poorly cemented conglomerate cliffs (near Nauplió, Greece, April 1992) IV-2-32

Figure IV-2-22. Lake Michigan shore south of St. Joseph, Michigan IV-2-33

Figure IV-2-23. Cemented conglomerate with many pits and cavities IV-2-34

Figure IV-2-24. A three-dimensional view of features commonly found in barrier island systems, including the back barrier, overwash fans, and lagoons IV-2-35

Figure IV-2-25. General barrier types: bay, spit, and island IV-2-38

Figure IV-2-26. Emergence model of barrier island formation IV-2-40

Figure IV-2-27. Submergence model of barrier island formation IV-2-41

Figure IV-2-28. Barrier island formation from spit IV-2-42

Figure IV-2-29. Three models of shoreline response to sea level rise IV-2-43

Figure IV-2-30. Westhampton Beach, Long Island, New York IV-2-44

Figure IV-2-31. Ridge and runnel system, low water terrace, Charlestown Beach, Rhode Island IV-2-46

Figure IV-2-32. Shale beach and bluffs, southeast shore of Lake Erie, near Evans, New York IV-2-48

Figure IV-2-33. Typical New England salt marsh, with sinuous channels, estuary of the Sprague River, Maine IV-2-51

Figure IV-2-34. Evolution of a coral island IV-2-56

Figure IV-2-35. Peat horizon exposed on the shoreface, Ditch Plains, Long Island, New York IV-2-61

Figure IV-2-36. Morphology of the Middle Atlantic Bight IV-2-64

Chapter IV-2
Coastal Classification and Morphology

IV-2-1. Introduction

a. Since ancient times, men have gone to sea in a variety of vessels to obtain food and to transport cargo and passengers to distant ports. To navigate safely, sailors needed an intimate knowledge of the appearance of the coast from place to place. By the time that systematic study of coastal geology and geomorphology began, there already existed a large body of observational knowledge about seacoasts in many parts of the world and a well-developed nomenclature to portray coastal landforms. Geologists in the 19th and 20th centuries described coastal landforms, examined their origin and development as a function of geologic character, history, and dynamic processes, and devised classification schemes to organize and refine their observations.

b. The first part of this chapter discusses the coastal classification of Francis Shepard (1973). The second part describes specific coastal environments found around the United States following Shepard's outline.

IV-2-2. Coastal Classification

a. Introduction. By its very nature, the coast is an incredibly complex and diverse environment, one that may defy organization into neat compartments. Nevertheless, the quest for understanding how shorelines formed and how human activities affect these processes has demanded that classification schemes be devised. Most have grouped coastal areas into classes that have similar features because of having developed in similar geological and environmental settings.

b. Early classifications. Many early geologists took a genetic approach to classification and distinguished whether the coast had been primarily affected by rising sea level (submergence), falling sea level (emergence), or both (compound coasts) (Dana 1849; Davis 1896a; Gulliver 1899; Johnson 1919; Suess 1888).

c. Later classifications. The best known of the modern classifications are those of Cotton (1952), Inman and Nordstrom (1971), Shepard (1937), with revisions in 1948, 1971 (with Harold Wanless), 1973, and 1976, and Valentin (1952). Except for Inman and Nordstrom (1971), these classifications emphasized onshore and shoreline morphology but did not include conditions of the offshore bottom. This may be a major omission because the submarine shoreface and the shelf are part of the coastal zone. Surprisingly few attempts have been made to classify the continental shelf. Shepard (1948; 1977) and King (1972) discussed continental shelf types, but their classifications are not detailed and contain only a few broadly defined types.

d. Coastal classification of Francis Shepard. Possibly the most widely used coastal classification scheme is the one introduced by Shepard in 1937 and modified in later years. It divides the world's coasts into primary coasts - formed mostly by non-marine agents - and secondary coasts - shaped primarily by marine processes. Further subdivisions occur according to which specific agent, terrestrial or marine, had the greatest influence on coastal development. The advantage of Shepard's classification is that it is more detailed than others, allowing most of the world's coasts to be incorporated. Although gradational shore types exist, which are difficult to classify, most coasts show only one dominant influence as the cause of their major characteristics (Shepard 1973). Because of its overall usefulness, Shepard's 1973 classification is reproduced in Table IV-2-1. Specific coasts are discussed in detail in this chapter, approximately following the outline of Shepard's table.

Table IV-2-1
Classification of Coasts (Continued)

Excerpt from SUBMARINE GEOLOGY, 3rd ed. by Francis P. Shepard. Copyright 1948, 1963, 1973 by Francis P. Shepard. Reprinted by permission of Harper Collins Publishers.	Paragraph No.
I. *Primary coasts* Configuration due to nonmarine processes.	
A. *Land erosion coasts* Shaped by subaerial erosion and partly drowned by postglacial rise of sea level (with or without crustal sinking) or inundated by melting of an ice mass from a coastal valley.	
1. *Ria coasts (drowned river valleys)* Usually recognized by the relatively shallow water of the estuaries which indent the land. Commonly have V-shaped cross section and a deepening of the axis seaward except where a barrier has built across the estuary mouth.	IV-2-3
2. *Dendritic* Pattern resembling an oak leaf due to river erosion in horizontal beds or homogeneous material.	
3. *Trellis* Due to river erosion in inclined beds of unequal hardness.	
(a) *Drowned glacial erosion coasts* Recognized by being deeply indented with many islands. Charts show deep water (commonly more than 100 m) with a U-shaped cross section of the bays and with much greater depth in the inner bays than near the entrance. Hanging valleys and sides usually parallel and relatively straight, in contrast to the sinuous rias. Almost all glaciated coasts have bays with these characteristics.	IV-2-4
(b) *Fjord coasts* Comparatively narrow inlets cutting through mountainous coasts.	
(c) *Glacial troughs* Broad indentations, like Cabot Strait and the Gulf of St. Lawrence or the Strait of Juan de Fuca.	
4. *Drowned karst topography* Embayments with oval-shaped depressions indicative of drowned sinkholes. This uncommon type occurs locally, as along the west side of Florida north of Tarpon Springs, the east side of the Adriatic, and along the Asturias coast of North Spain.	
B. *Subaerial deposition coasts*	IV-3-3
1. *River deposition coasts* Largely due to deposition by rivers extending the shoreline since the slowing of the postglacial sea level rise.	
2. *Deltaic coasts*	
(a) *Digitate (birdfoot),* the lower Mississippi Delta.	
(b) *Lobate,* western Mississippi Delta, Rhone Delta.	
(c) *Arcuate,* Nile Delta.	
(d) *Cuspate,* Tiber Delta.	
(e) *Partly drowned deltas* with remnant natural levees forming islands.	
3. *Compound delta coasts* Where a series of deltas have built forward a large segment of the coast, for example, the North Slope of Alaska extending east of Point Barrow to the Mackenzie.	
4. *Compound alluvial fan coasts straightened by wave erosion*.	
5. *Glacial deposition coasts*	
(a) *Partially submerged moraines* Usually difficult to recognize without a field study to indicate the glacial origin of the sediments constituting the coastal area. Usually modified by marine erosion and deposition as, for example, Long Island.	
(b) *Partially submerged drumlins* Recognized on topographic maps by the elliptical contours on land and islands with oval shorelines, for example, Boston Harbor and West Ireland (Guilcher 1965).	
(c) *Partially submerged drift features*	IV-2-6
6. *Wind deposition coasts* It is usually difficult to ascertain if a coast has actually been built forward by wind deposition, but many coasts consist of dunes with only a narrow bordering sand beach.	
(a) *Dune prograded coasts* Where the steep lee slope of the dune has transgressed over the beach.	
(b) *Dune coasts* Where dunes are bordered by a beach.	
(c) *Fossil dune coasts* Where consolidated dunes (eolianites) form coastal cliffs.	
7. *Landslide coasts* Recognized by the bulging earth masses at the coast and the landslide topography on land.	
C. *Volcanic coasts*	IV-2-7
1. *Lava-flow coasts* Recognized on charts either by land contours showing cones, by convexities of shoreline, or by conical slopes continuing from land out under the water. Slopes of 10° to 30° common above and below sea level. Found on many oceanic islands.	
2. *Tephra coasts* Where the volcanic products are fragmental. Roughly convex but much more quickly modified by wave erosion than are lava-flow coasts.	
3. *Volcanic collapse or explosion coasts* Recognized in aerial photos and on charts by the concavities in the sides of volcanoes.	
D. *Shaped by diastrophic movements*	
1. *Fault coasts* Recognized on charts by the continuation of relatively straight steep land slopes beneath the sea. Angular breaks at top and bottom of slope.	
(a) *Fault scarp coasts* For example, northeast side of San Clemente Island, California.	
(b) *Fault trough or rift coasts* For example, Gulf of California and Red Sea, both being interpreted as rifts.	
(c) *Overthrust* No examples recognized but probably exist.	

(Continued)

Table IV-2-1 (Concluded)	Paragraph No.
2. *Fold coasts* Difficult to recognize on maps or charts but probably exist.	
3. Sedimentary extrusions	
(a) *Salt domes* Infrequently emerge as oval-shaped islands. Example: in the Persian Gulf.	
(b) *Mud lumps* Small islands due to upthrust of mud in the vicinity of the passes of the Mississippi Delta.	
E. *Ice coasts* Various types of glaciers form extensive coasts, especially in Antarctica.	
II. *Secondary coasts* Shaped primarily by marine agents or by marine organisms. May or may not have been primary coasts before being shaped by the sea.	
A. Wave erosion coasts	IV-2-8
1. *Wave-straightened cliffs* Bordered by a gently inclined seafloor, in contrast to the steep inclines off fault coasts.	
(a) *Cut in homogeneous materials.*	
(b) *Hogback strike coasts* Where hard layers of folded rocks have a strike roughly parallel to the coast so that erosion forms a straight shoreline.	
(c) *Fault-line coasts* Where an old eroded fault brings a hard layer to the surface, allowing wave erosion to remove the soft material from one side, leaving a straight coast.	
(d) *Elevated wave-cut bench coasts* Where the cliff and wave-cut bench have been somewhat elevated by recent diastrophism above the level of present-day wave erosion.	
(e) *Depressed wave-cut bench coasts* Where the wave-cut bench has been somewhat depressed by recent diastrophism so that it is largely below wave action and the wave-cut cliff plunges below sea level.	
2. *Made irregular by wave erosion* Unlike ria coasts in that the embayments do not extend deeply into the land. *Dip coasts* Where alternating hard and soft layers intersect the coast at an angle; cannot always be distinguished from trellis coasts.	
(a) *Heterogeneous formation coasts* Where wave erosion has cut back the weaker zones, leaving great irregularities.	
B. *Marine deposition coasts* Coasts prograded by waves and currents.	
1. Barrier coasts.	
(a) *Barrier beaches* Single ridges.	IV-2-9
(b) *Barrier islands* Multiple ridges, dunes, and overwash flats.	
(c) *Barrier spits* Connected to mainland.	
(d) *Bay barriers* Sand spits that have completely blocked bays.	
(e) *Overwash fans* Lagoonward extension of barriers due to storm surges.	
2. *Cuspate forelands* Large projecting points with cusp shape. Examples include Cape Hatteras and Cape Canaveral.	
3. *Beach plains* Sand plains differing from barriers by having no lagoon inside.	
4. *Mud flats or salt marshes* Formed along deltaic or other low coasts where gradient offshore is too small to allow breaking waves.	IV-2-11
C. *Coasts* built by organisms	IV-2-12
1. *Coral reef coasts* Include reefs built by coral or algae. Common in tropics. Ordinarily, reefs fringing the shore and rampart beaches are found inside piled up by the waves.	
(a) *Fringing reef coasts* Reefs that have built out the coast.	
(b) *Barrier reef coasts* Reefs separated from the coast by a lagoon.	
(c) *Atolls* Coral islands surrounding a lagoon.	
(d) *Elevated reef coasts* Where the reefs form steps or plateaus directly above the coast.	
2. *Serpulid reef coasts* Small stretches of coast may be built out by the cementing of serpulid worm tubes onto the rocks or beaches along the shore. Also found mostly in tropics.	
3. *Oyster reef coasts* Where oyster reefs have built along the shore and the shells have been thrown up by the waves as a rampart.	
4. *Mangrove coasts* Where mangrove plants have rooted in the shallow water of bays, and sediments around their roots have been built up to sea level, thus extending the coast. Also a tropical and subtropical development.	
5. *Marsh grass coasts* In protected areas where salt marsh grass can grow out into the shallow sea and, like the mangroves, collect sediment that extends the land. Most of these coasts could also be classified as mud flats or salt marshes.	

e. Classification schemes for specific environments.

(1) River systems. Coleman and Wright (1971) developed a detailed classification for rivers and deltas.

(2) Great Lakes of North America. The Great Lakes have unique characteristics that set them apart from oceanic coastlines. One of the most comprehensive attempts to include these factors in a classification scheme was developed by Herdendorf (1988). It was applied to the Canadian lakes by Bowes (1989). A

simpler scheme has been used by the International Joint Commission as a basis for studies of shoreline erosion (Stewart and Pope 1992).

IV-2-3. Drowned River Coasts - Estuaries[1]

a. Introduction. An enormous amount of technical literature is devoted to the chemistry and biology of estuaries. In recent years, much research has been devoted to estuarine pollution and the resulting damage to fish and animal habitat. For example, the famous oyster harvesting in Chesapeake Bay has been almost ruined in the last 30 years because of overfishing, urban runoff, and industrial pollution. As a result, the unique way of life of the Chesapeake oystermen, who still use sailing vessels, may be at an end. Possibly because most attention has centered on the biological and commercial aspects of estuaries, our geological understanding of them is still rudimentary (Nichols and Biggs 1985). The estuarine environment can be defined as the complex of lagoon-bay-inlet-tidal flat and marsh that make up 80 to 90 percent of the U.S. Atlantic and Gulf coasts (Emery 1967). Clearly it is vital that we gain a better understanding of their sedimentary characteristics and dynamics.

b. Literature. Only the briefest introduction to estuarine processes and sediments can be presented in this chapter. The purpose of this section is to introduce estuarine classification, regional setting, and geology. The reader is referred to Nichols and Biggs (1985) for an overview of the geology and chemistry of estuaries and for an extensive bibliography. Other general works include Dyer (1979), Nelson (1972), and Russell (1967). Cohesive sediment dynamics are covered in Metha (1986), and the physics of estuaries is covered in van de Kreeke (1986). Research from the 1950's and 1960's is reviewed in Lauff (1967).

c. Classification. Many attempts have been made to define and classify estuaries using geomorphology, hydrography, salinity, sedimentation, and ecosystem parameters (reviewed in Hume and Herdendorf (1988)). A geologically based definition, which accounts for sediment supply pathways, is used in this text.

d. Definitions. Estuaries are confined bodies of water that occupy the drowned valleys of rivers that are not currently building open-coast deltas. The most common definition of an estuary describes it as a body of water where "...seawater is measurably diluted with fresh water derived from land drainage" (Pritchard 1967). Therefore, estuaries would include bodies of water where salinity ranges from 0.1 ‰ (parts per thousand) to about 35 ‰ (Figure IV-2-1). However, this chemical-based definition does not adequately restrict estuaries to the setting of river mouths, and allows, for example, lagoons behind barrier islands to be included. Dalrymple, Zaitlin, and Boyd (1992) felt that the interaction between river and marine processes was an attribute essential to all true estuaries. Therefore, they proposed a new geologically based definition of estuary as:

> ...the seaward portion of a drowned valley system which receives sediment from both fluvial and marine sources and which contains facies influenced by tide, wave, and fluvial processes. The estuary is considered to extend from the landward limit of tidal facies at its head to the seaward limit of coastal facies at its mouth.

These limits are schematically shown in Figure IV-2-1.

e. Time relationships and evolution.

(1) Estuaries, like other coastal systems, are ephemeral. River mouths undergo continuous geological evolution, of which estuaries represent one phase of a continuum (Figure IV-2-2). During a period of high

[1] Material in this section has been condensed from Dalrymple, Zaitlin, and Boyd (1992).

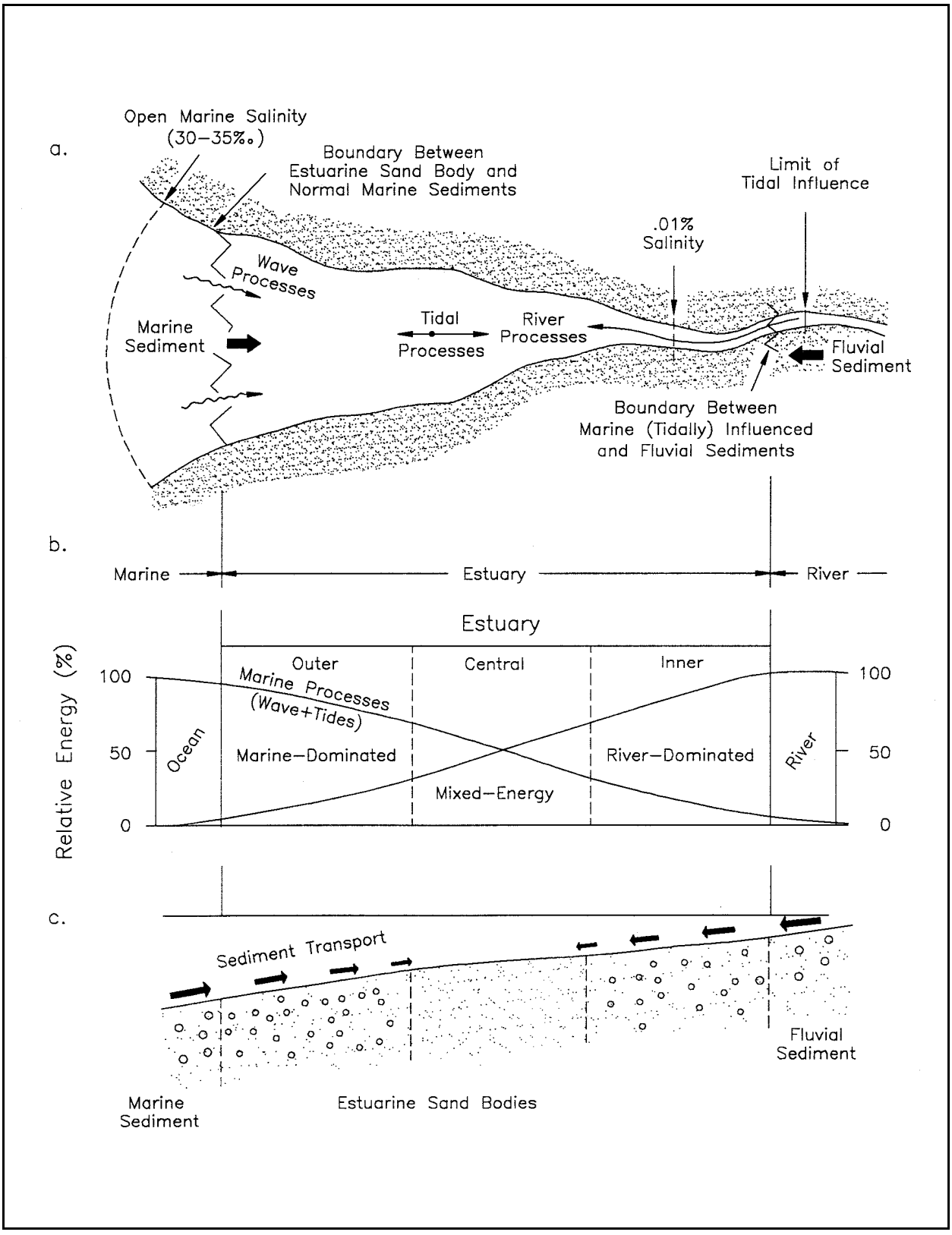

Figure IV-2-1. (a) Plan view of distribution of energy and physical processes in estuaries; (b) Schematic definition of estuary according to Dalyrmple, Zaitlin, and Boyd (1992); (c) Time-averaged sediment transport paths

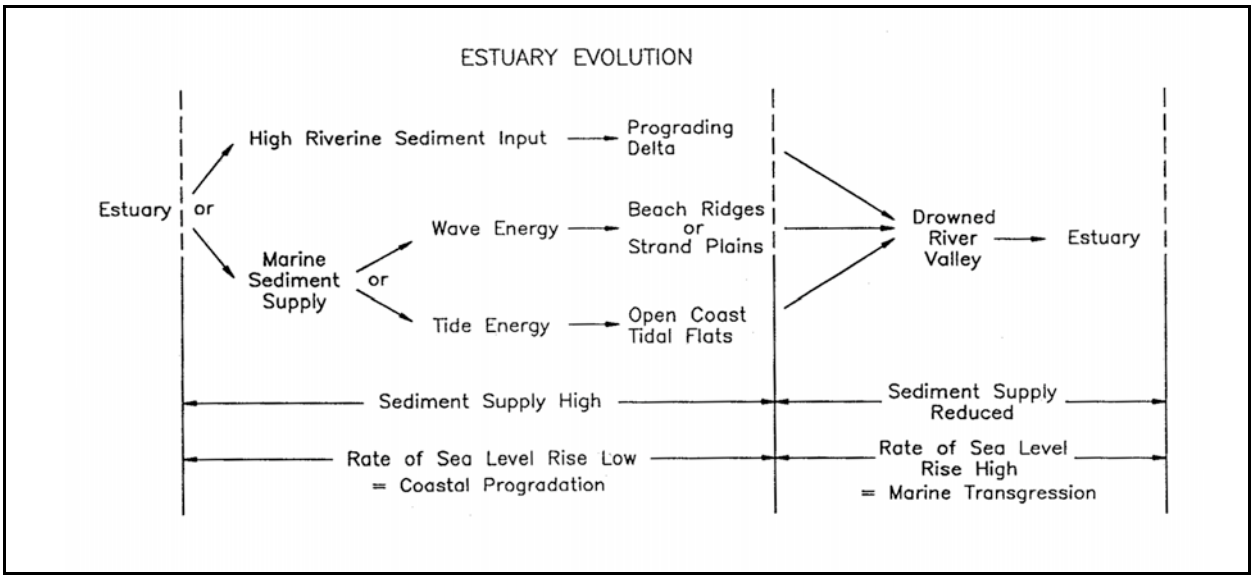

Figure IV-2-2. Estuary/prograding coast evolution. Estuaries are part of a continuum of coastal landforms. With high riverine or marine sediment supply, the shore progrades (left half of figure). Later, if sediment supply is reduced, the river valley is drowned, resulting in an estuary (right half of figure)

sediment supply and low rate of sea level rise, an estuary is gradually filled. Three coastal forms may result, depending on the balance between riverine input and marine sediment supply:

(a) If the sediment is supplied by a river, a delta is formed, which, as it grows, progrades out into the open sea (left side of Figure IV-2-3).

(b) If, instead, most sediment is delivered to the area by marine processes, a straight, prograding coast is formed. This might be in the form of beach ridges or strand plains if wave energy is dominant, or as open-coast tidal flats if tidal energy is dominant.

(c) Later, if sea level rises at a higher rate, then the river valley may be flooded, forming a new estuary (right side of Figure IV-2-3).

(2) Under some conditions, such as when sea level rise and sediment supply are in balance, distinguishing whether a river mouth should be classified as an estuary or as a developing delta may be difficult. Dalrymple, Zaitlin, and Boyd (1992) suggest that the direct transport of bed material may be the most fundamental difference between estuaries and deltas. They state that the presence of tight meanders in the channels suggests that bed-load transport is landward in the region seaward of the meanders and, as a consequence, the system is an estuary. However, if the channels are essentially straight as far as the coast, bed load is seaward throughout the system and it can be defined as a delta.

(3) Fluvial systems are controlled by their erosional base level and the sediment supply. During periods of lowered sea level, rivers incise the lower reaches of their valleys and discharge increasing amounts of sediment out onto the shelf. Deltas accumulate and fluvial channels are cut, dissecting parts of the delta plain (described in greater detail in Part IV-3-3). At the lowest stands of sea level, estuaries almost disappear and are confined to river valleys (Baeteman 1994). When sea level rises again, the valleys are flooded and the estuaries reappear.

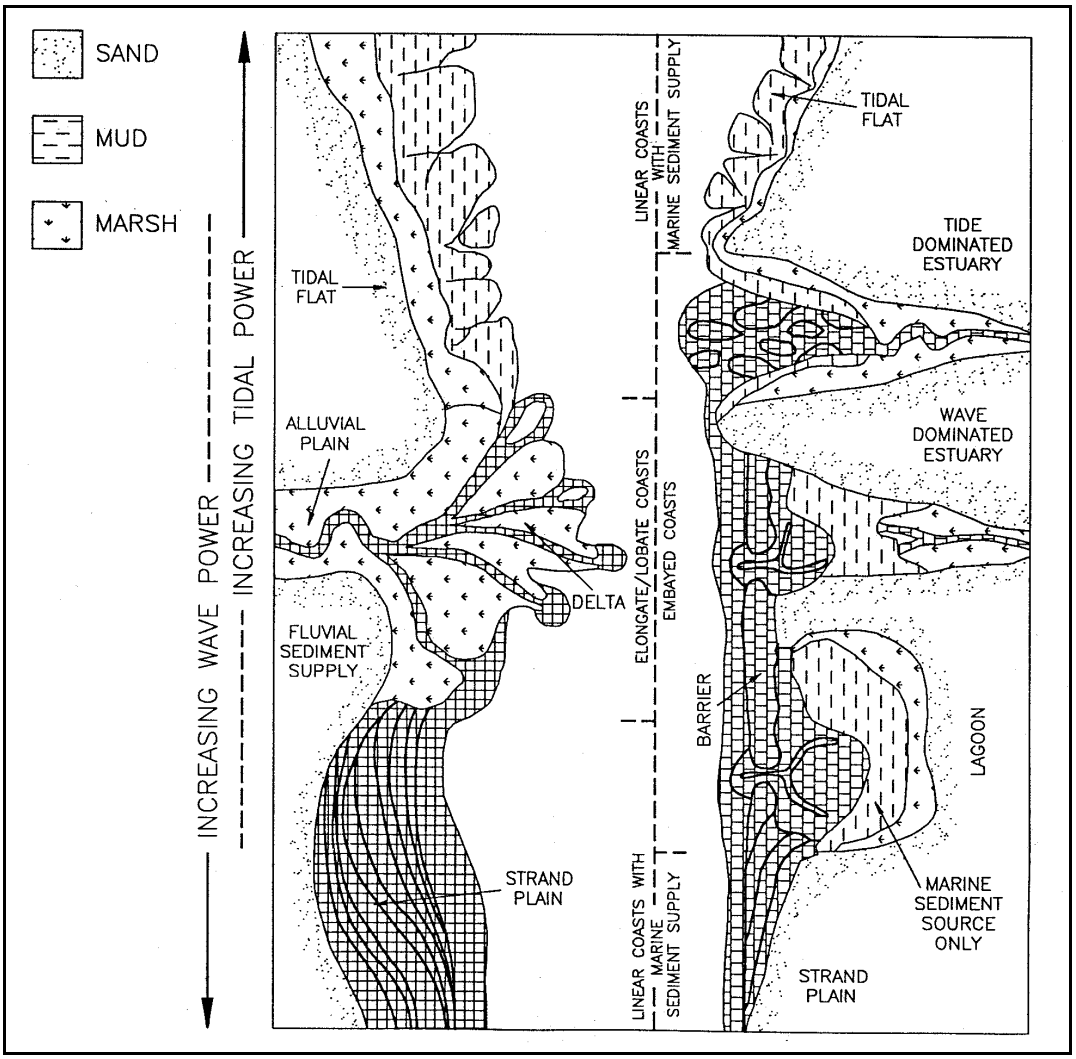

Figure IV-2-3. Estuary evolution, based on changes in wave or tidal power. The left half of the figure shows a prograding coast that results during times of high sediment supply. The right side shows how estuaries develop during reduced sediment supply (also refer to Figure IV-2-2). Adapted from Boyd, Dalrymple, and Zaitlin (1992)

f. Overall geomorphic characteristics. The geologic definition of estuary implies that sediment supply does not keep pace with the local sea level rise; as a result, estuaries become sinks for terrestrial and marine sediment. Sedimentation is the result of the interaction of wave, tide, and riverine forces. All estuaries, regardless of whether they are wave- or tide-dominated, can be divided into three zones (Figure IV-2-1):

(1) The *outer zone* is dominated by marine processes (wave and tidal currents). Because of currents, coarse sediment tends to move up into the mouth of the estuary.

(2) The *central zone* is characterized by relatively low energy, where wave and tidal currents are balanced over the long term by river currents. The central zone is an area of net convergence of sediment and usually contains the finest-grained bed load present in the estuary.

(3) The *inner zone* is river-dominated and extends upriver to the limit of tidal influence. The long-term (averaged over years) bed load transport in this region is seaward.

g. Energy factors and sedimentary structures.

(1) Wave-dominated estuaries.

(a) This type of estuary is characterized by high wave energy compared to tidal influence. Waves cause sediment to move alongshore and onshore into the mouth of the estuary, forming sandbars or subaerial barriers and spits (Figure IV-2-4a). The barrier prevents most of the wave energy from entering the central basin. In areas of low tide range and small tidal prism, tidal currents may not be able to maintain the inlet, and storm breaches tend to close during fair weather, forming enclosed coastal ponds. Sediment type is well-distributed into three zones, based on the variation of total energy: coarse sediment near the mouth, fine in the central basin, and coarse at the estuary head. A marine sand body forms in the high wave energy zone at the mouth. This unit is composed of barrier and inlet facies, and, if there is moderate tide energy, sand deposited in flood-tide deltas (Hayes 1980).

(b) At the head of the estuary, the river deposits sand and gravel, forming a bay-head delta. If there is an open-water lagoon in the central basin, silts and fine-grained organic muds accumulate at the toe of the bay-head delta. This results in the formation of a prodelta similar to the ones found at the base of open-coast deltas (deltaic terms and structures are discussed in Part IV-3). Estuaries that are shallow or have nearly filled may not have an open lagoon. Instead, they may be covered by extensive salt marshes crossed by tidal channels.

(2) Tide-dominated estuaries.

(a) Tide current energy is greater than wave energy at the mouth of tide-dominated estuaries, resulting in the development of elongate sandbars (Figure IV-2-4b). The bars dissipate wave energy, helping protect the inner portions of the estuary. However, in funnel-shaped estuaries, the incoming flood tide is progressively compressed into a decreasing cross-sectional area as it moves up the bay. As a result, the velocity of the tide increases until the effects of the amplification caused by convergence are balanced by frictional dissipation. The velocity-amplification behavior is known as *hypersynchronos* (Nichols and Biggs 1985). Because of friction, the tidal energy decreases beyond a certain distance in the estuary, eventually becoming zero.

(b) As in wave-dominated estuaries, riverine energy also decreases downriver from the river mouth. The zone where tide and river energy are equal is sometimes called a balance point and is the location of minimum total energy. Because the total-energy minimum is typically not as low as the minimum found in wave-dominated estuaries, tide-dominated estuaries do not display as clear a zonation of sediment facies. Sands are found along the tidal channels, while muddy sediments accumulate in the tidal flats and marshes along the sides of the estuary (Figure IV-2-4b). In the central, low-energy zone, the main tidal-fluvial channel consistently displays a sinuous, meandering shape. Here, the channel develops alternate bars at the banks and, sometimes, in mid-channel.

(c) A bay-head delta is usually not present in the river-dominated portion of tidally dominated estuaries. Instead, the river channel merges directly into a single or a series of tidal channels that eventually reach the sea.

(3) Estuarine variability.

(a) Wave-to-tide transition. As tide energy increases relative to wave energy, the barrier system at the mouth of the estuary becomes progressively more dissected by tidal inlets, and elongate sandbars form along

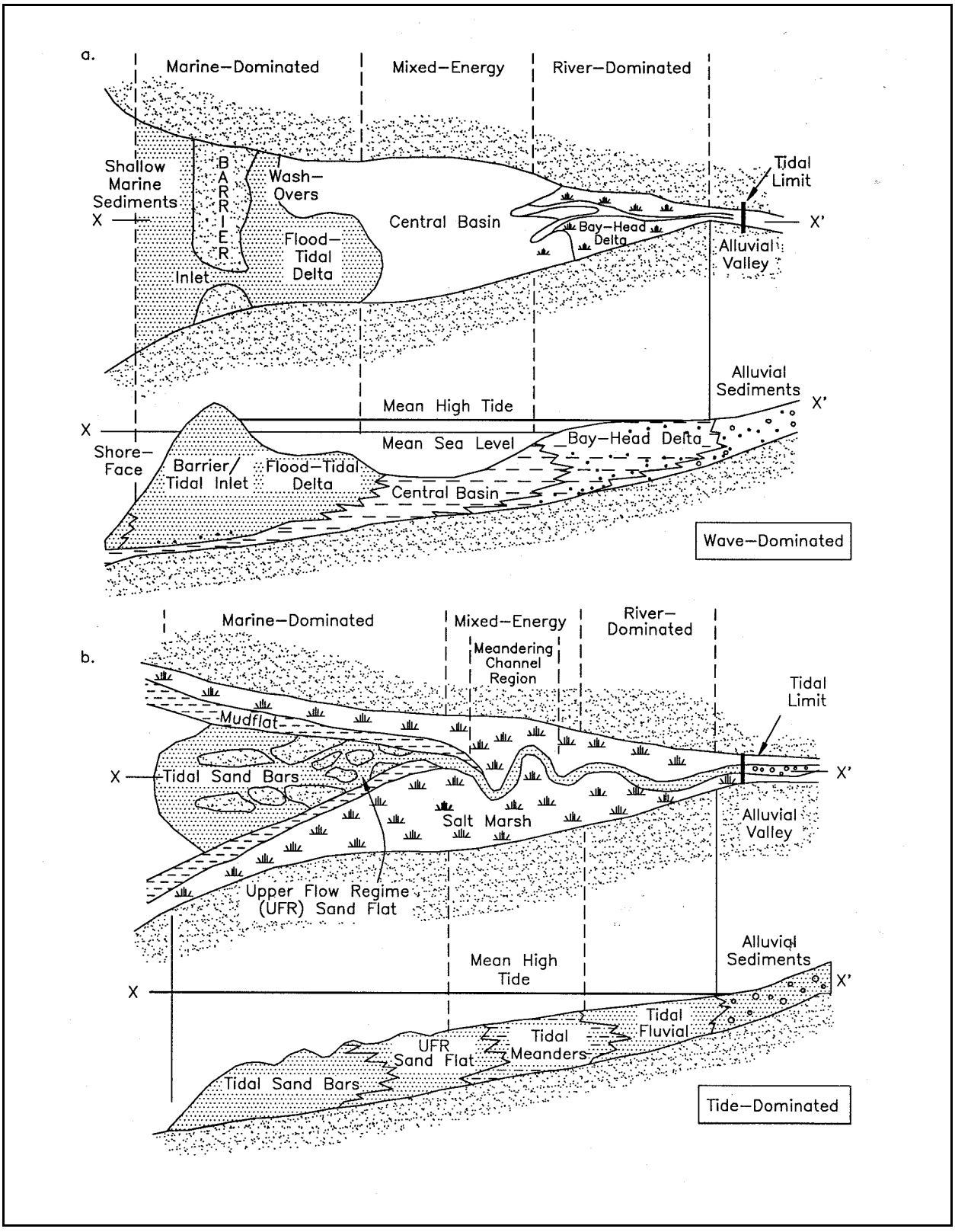

Figure IV-2-4. Morphologic models of (a) wave-dominated and (b) tide-dominated estuaries (adapted from Dalyrmple, Zaitlin, and Boyd (1992)). Wave-dominated estuaries are common along the mid-Atlantic coast of the United States. Tide-dominated estuaries are found in Maine, Massachusetts, and the mid-Atlantic Bight

the margins of the tidal channels. As energy levels increase in the central, mixed-energy part of the estuary, marine sand is transported further up into the estuary, and the muddy central basin is replaced by sandy tidal channels flanked by marshes.

(b) Effects of tide range. The inner end of an estuary has been defined as the limit of detectable tidal influence. Therefore, the gradient of the coastal zone and the tide range have a great influence on the length of estuaries (Dalrymple, Zaitlin, and Boyd 1992). Estuaries become longer as gradient decreases and tide range increases.

(c) Influence of valley shape. The shape of the flooded valley and the pre-existing geology also control the size of the estuary and the nature of sediment deposition. This is particularly evident during the early phases of estuary infilling, before erosion and deposition have modified the inherited geology. For example, tidal-wave amplification is less likely to occur in irregular valleys (Nichols and Biggs 1985). The resulting estuaries are more likely to become wave-dominated. Chesapeake Bay, with its extensive system of tributary valleys, is an example of this type. In contrast, estuaries that initially or later have developed a funnel shape are more likely to be tide-dominated and hypersynchronous (for example, the Gironde Estuary of France.)

(d) Geologic setting. Coastal plain gradient, part of the overall plate tectonic setting, is one factor that determines estuary volume. Sea level rise over a flat coastal plain on a passive margin like the Gulf of Mexico creates long estuaries with large volume. An equivalent rise on a steep, active-margin coast like the U.S. Pacific coast will result in a much smaller estuary volume (Boyd, Dalrymple, and Zaitlin 1992).

h. Estuarine sediments.

(1) Because estuaries occupy drowned river valleys, they function as sinks for enormous volumes of sediment. Estuarine sediments are derived from various sources including rivers, the continental shelf, local erosion, and biological activity. Sedimentation is controlled by tides, river flow, waves, and meteorology. The lower-energy conditions of estuaries, as opposed to those found on open coasts, allow for the deposition of fine-grained silts, muds, clays, and biogenic materials. Estuarine sediments are typically soft and tend to be deposited on smooth surfaces that limit turbulence of the moving water. When allowed to accumulate, these materials consolidate and undergo various chemical and organic changes, eventually forming cohesive sediments.

(2) The shores of estuaries and certain open-water coasts in low-energy environments (e.g., coastal Louisiana, Surinam, Bangladesh, and Indonesia) are characterized as having smooth, low-sloping profiles with turbid water occurring along the shore and extending well offshore (Suhayda 1984). These areas usually exhibit low and vegetated backshores and mud flats that are exposed at low tide. These conditions are also found in Chesapeake and Delaware Bays.

(3) Nichols and Biggs (1985) describe the movement of estuarine sediments as consisting of four processes:

(a) Erosion of bed material.

(b) Transportation.

(c) Deposition on the bed.

(d) Consolidation of deposited sediment.

These processes strongly depend on estuarine flow dynamics and sediment particle properties. The properties most important for cohesive sediments are interparticle bonding and chemical behavior because these parameters make cohesive sediment respond quite differently to hydrodynamic forces than do noncohesive sediments. Due to the cohesive bonding, consolidated materials (clays and silts) require higher forces to mobilize, making them more resistant to erosion. However, once cohesive sediment is eroded, fine-grained clays and silts can be transported at much lower velocity than is required for the initiation of erosion.

IV-2-4. Drowned Glacial Erosion Coasts

a. Introduction. During the Pleistocene epoch, massive continental glaciers, similar to the present Antarctic and Greenland ice caps, covered broad parts of the continents. The glaciers waxed and waned in cycles, probably because of climatic variations, causing vast changes to the morphology of coastal regions in the northern latitudes. As a result, glacially modified features dominate the northern coasts and continental shelves, although in many areas marine processes have reworked the shore and substantially modified the glacial imprint.

b. Erosion and sediment production. Because glacial ice is studded with rock fragments plucked from the underlying rock, a moving glacier performs like a giant rasp that scours the underlying land surfaces. This process, driven by the great size and weight of the ice sheets, caused enormous erosion and modification to thousands of square kilometers during the Pleistocene epoch.

(1) Fjords. The most spectacular erosion forms are drowned glacial valleys known, as *fjords*, that indent the coasts of Alaska, Norway, Chile, Siberia, Greenland, and Canada (Figure IV-2-5). The over-deepened valleys were invaded by the sea as sea level rose during the Holocene epoch. Today, fjords retain the typical U-shaped profile that is also seen in formerly glaciated mountain valleys. Fjords and other drowned glacial erosion features give Maine a spectacular, rugged coastline (Figure IV-2-6).

(2) Depositional features. As a glacier moves, huge amounts of sediment are incorporated into the moving mass. When the ice melts at the glacial front's furthest advance, the sediment load is dropped. Although the major part of the transported material is dumped in the form of a terminal moraine, some sediments are carried further downstream by meltwater streams (Reineck and Singh 1980). The result is a number of distinctive geomorphic features such as drumlins, fjords, moraines, and outwash plains that may appear along the coast or on the submerged continental shelf (Figure IV-2-7). During submergence by the transgressing sea, the features may be modified to such a degree that their glacial origin is lost. This is especially true of outwash, which is easily reworked by marine processes. The original town of Boston was settled on drumlins in the 1600's (Figure IV-1-18), and the islands in Boston Harbor are reworked drumlins (Figure IV-2-8). Nantucket Island, Block Island, and Long Island are partially submerged moraines that have been extensively reworked (Figure IV-2-9).

c. Variability. Glaciated coasts typically display a greater variety of geomorphic forms than are seen in warmer latitudes. The forms include purely glacial, glacio-fluvial, and marine types (Fitzgerald and Rosen 1987). Complexity is added by marine reworking, which can produce barriers, shoals, gravel shores, and steep-cliffed shores. Because of the steep slopes of many glacial coasts, slumping and turbidity flow are major erosive agents. In northern latitudes, the shallow seafloor is gouged by icebergs. In summary, classification of shores in drowned glacial environments can be a major challenge because of the complicated geological history and the large diversity of structures.

d. Atlantic coast. A fundamental division of coastal characteristics occurs along the Atlantic coast of North America due to the presence of glacial moraines. The Wisconsin terminal moraine formed a prominent series of islands (i.e., Long Island, Block Island, Nantucket, and Martha's Vineyard) and offshore banks

Figure IV-2-5. Glacial fjord coast: Alaska (Lake George, with Surprise glacier in the background)

(Georges and Nova Scotian Banks). South of the moraine, the topography is flatter and more regular, except for piedmont streams, which intersect the coastal plain.

e. Offshore geology. Coasts altered by glaciers usually have offshore regions that are highly dissected by relict drainage systems. These sinuous stream channels display highly irregular and varied topography and are composed of sediment types ranging from outwash sand and gravels to till. Note that relict stream channels are also found on continental shelves in temperate climates, for example, off the coast of Texas (Suter and Berryhill 1985). Channels from both temperate and colder environments, and the associated shelf-margin deltas, were formed during late Quaternary lowstands of sea level and are indicators of the position of ancient coastlines.

IV-2-5. River Deposition Coasts - Deltas

Deltas are discussed in Part IV-3. Because energy factors and deltaic structures are intimately linked, morphology and river mouth hydrodynamics are discussed together.

IV-2-6. Wind Deposition Coasts - Dunes

a. Introduction. Sand dunes are common features along sandy coastlines around the world. The only climatic zone lacking extensive coastal dunes is the frozen Arctic and Antarctic (although thin dune sheets on the coast of McMurdo Sound, Antarctica, have been described by Nichols (1968)). Sediment supply is probably the most crucial factor controlling growth of dunes; while there is rarely a lack of wind in most coastal areas, some lack sufficient loose sediment (Carter 1988). Dunes serve multiple valuable purposes:

Figure IV-2-6. Drowned glacial erosion coast: Maine (Potts Point, South Harpswell, near Brunswick, July 1994). Rock headlands and ridges run southwest into the Gulf of Maine

as recreational areas, as habitat for various species of birds, as shore protection, and as temporary sources and sinks of sand in the coastal environment. Although dunes are found along many sandy coasts, they are finite resources and need to be protected and preserved. The seminal work on dunes is Brigadier R.A. Bagnold's *The Physics of Blown Sand and Desert Dunes* (Bagnold 1941). More than 50 years after its publication, this book continues to be cited because of its sound basis on the laws of physics and its readability. Part III-4 of the *Coastal Engineering Manual* reviews the physics of wind-blown sediment transport and presents methods that can be used to estimate transport volumes.

b. Origin of dunes. Many large dune fields are believed to have originated when sea level was lower and sediment supply was greater (Carter 1988). Many are on prograding shorelines, although shoreline advance does not seem to be a requirement for dune formation. In northwest Europe, most of the dunes formed from shelf debris that moved onshore during the late Pleistocene and early Holocene by rising sea level. Dune-building phases have been interrupted by periods of relative stability, marked by the formation of soils. The dunes at Plum Island, Massachusetts, may have formed after 1600 (Goldsmith 1985).

c. Sediment sources. The normally dry backshore of sandy beaches may be the most common source of dune sands. A flat or low-relief area inland of the coastline is needed to accommodate the dunes, and there must be predominant onshore or alongshore winds for at least part of the year. To move sand from the beach to the dunes, wind speed must exceed a threshold velocity for the particular size of sand available. If the sand is damp or if the grains must move up a slope, the velocities required for sediment transport are greatly increased. The foreshore of the beach can also be a source of sand if it dries between tidal cycles. This is especially true in areas where there is only one high tide per day (diurnal), allowing a greater amount of time

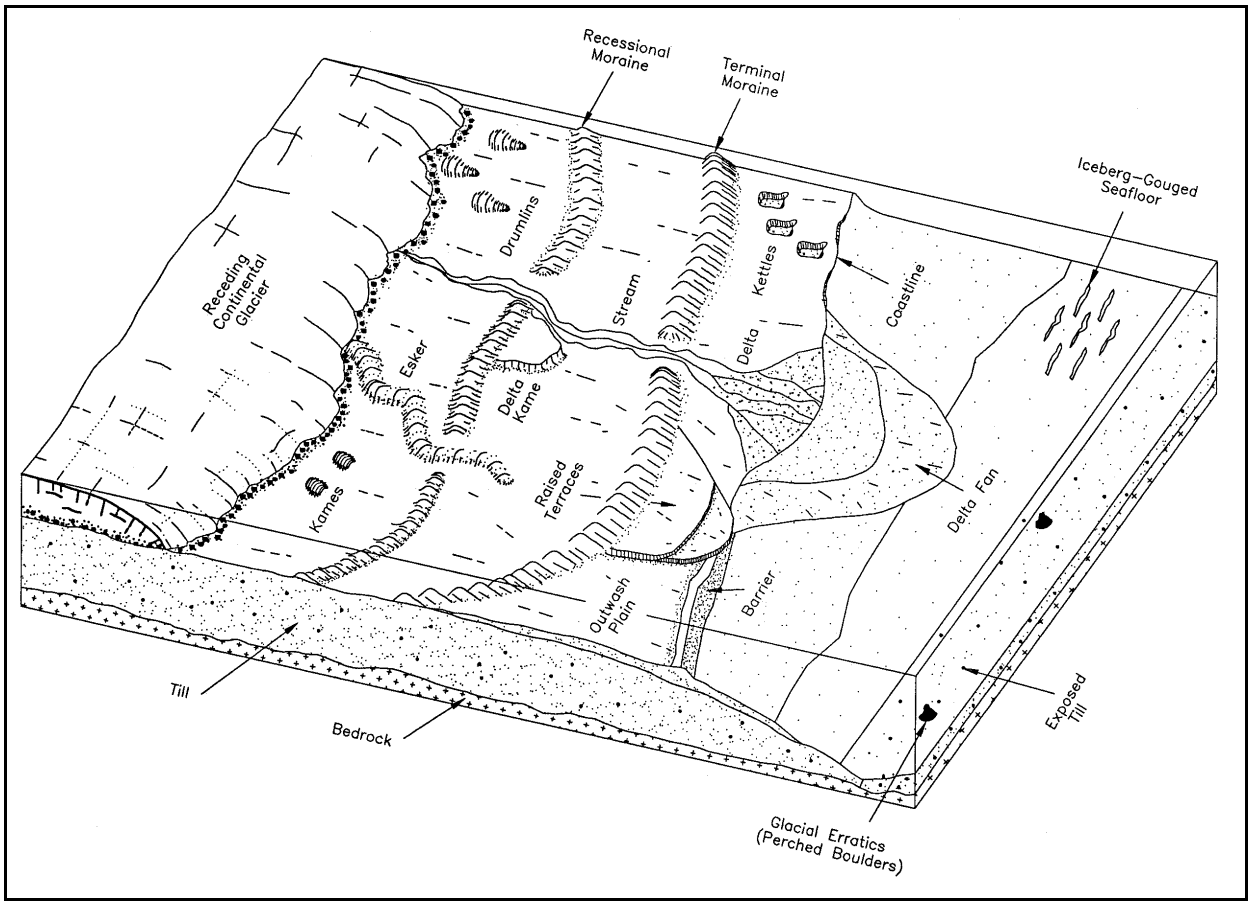

Figure IV-2-7. Typical glacial depositional structures

for the foreshore to dry between inundations. Sand storage in dunes must be estimated as one component of sediment budget calculations (EM 1110-2-1502).

d. Modification and stability. Most dunes show evidence of post-depositional modifications. These include:

(1) Physical changes - slumping, compaction. Sand grains become rounded, frosted, and better sorted.

(2) Chemical alterations - oxidation, leaching, calcification. (The latter can solidify a dune, making it much more resistant to erosion.)

(3) Biological effects - reactivation, humification, soil formation.

The stability of dunes varies greatly, usually depending on vegetation cover. Dunes in arid climates are often not vegetated and are mobile. However, coastal dunes are normally vegetated by plant species adapted to the harsh coastal environment (Figure IV-2-10). Many dune grasses have long roots, rhizomes, and runners that help hold sand in place. In addition, dense vegetation displaces the aerodynamic boundary of the wind velocity profile upwards. This process produces a net downward momentum flux, promoting sediment trapping (Carter 1988).

Figure IV-2-8. Islands in Boston Harbor, Massachusetts (August 1988 - view looking south). These are glacial drumlins that have been extensively reworked by contemporary marine processes. The town of Winthrop (with a tall water tower) is on the drumlin in the center. Deer Island, in the harbor, is attached to Winthrop with a causeway

Figure IV-2-9. Glacial till bluffs just west of Montauk Point, Long Island, New York, facing the Atlantic Ocean (March 1998). As the bluffs erode, the fine material is carried away by waves, leaving a lag of boulders and cobble on the shoreface. In this area, the seafloor offshore is also covered with gravel, cobble, and coarse sand. Sand from the Montauk bluffs is carried by littoral currents to the west, where it nourishes the barrier beaches of Long Island's south shore

Figure IV-2-10. Partly vegetated coastal sand dunes. Rhizomes help hold sand in place and colonize the dune grasses. Eastern Alabama on the Morgan peninsula east of the mouth of Mobile Bay (March 1991). This area was devastated by Hurricane Frederic in 1979 and is slowly recovering. Commercial construction now threatens these dunes

e. Dune vegetation. American beach grass (*Ammophilia breviligulata*) is the most common dune plant in the United States northeast and on the west coast. Along the Gulf coast and the southeast, sea oats (*Uniola paniculata*) is the most abundant species on the dunes. Both plants are remarkably adapted to this environment and are essential to dune stability. They are tolerant of salt spray and occasional inundation by salt water. Growth is stimulated by sand burial, which occurs frequently on the dune. The plant leaves help trap sand on the dune by raising the laminar boundary layer of the wind velocity profile and causing eolian deposition. Regrowth occurs even after rapid deposition of sand up to 1 m thick. Plant growth is by seed and by rhizome extension. Rhizome extension allows rapid plant distribution to help stabilize the surface of the

dune, and allows upward growth of the plant to keep pace with sand deposition. Vehicle and foot traffic that damage the vegetation can greatly diminish dune stability.

f. Dune fauna. Dunes may appear to be harsh and inhospitable environments, but they are hosts to many species of animals. A wide variety of invertebrates are present, including species as large as crabs. Numerous shorebirds and upland birds use the dune zone for foraging and nesting. Other vertebrates, such as rabbit, fox, deer, etc., frequent the dune in search of food.

g. Classification. Dunes can be described or classified on the basis of physical description (external form and internal bedding) or genetic origin (mode of formation). Smith (1954) devised a descriptive classification system that has been widely used. It established the following types (Figure IV-2-11):

(1) Foredunes. Mounds or ridges directly by the beach. Serve as storm buffer.

(2) Parabolic dunes. Arcuate sand ridges with the concave portion facing the beach. Rare; often form downwind of pools or damp areas.

(3) Barchan dunes. Crescent-shaped dunes with the extremities (horns) extending downwind (caused by the horns migrating more rapidly than the central portions). Sometimes show incomplete sand cover moving over a nonerodible pavement.

(4) Transverse dune ridges. Ridges oriented perpendicular or oblique to the dominant winds. Their form is asymmetrical with steep lee and gentle upwind slopes.

(5) Longitudinal (seif) dunes. Dune ridges elongated parallel to the wind direction and symmetrical in profile. Occur in groups over wide areas; feature sinuous crestlines.

(6) Blowouts. Hollows or troughs cut into dunes; may be caused when vehicles or pedestrians damage vegetation (Figure IV-2-12).

(7) Attached dunes. Formations of sand that have accumulated around obstacles such as rocks (Figure IV-2-13).

h. Shoreline protection. In many areas, dunes serve a vital role in protecting inland areas from storm surges and wave attack. As a result, many communities require that buildings be erected behind the dunes or beyond a certain distance (a *setback*) from an established coastline. Unfortunately, the protection is ephemeral because severe storms can overtop and erode the dunes, and changes in sediment supply or local wind patterns (sometimes caused by structures and urban development) can leave them sand-starved. If dunes are cut for roads or for walkways, they become particularly vulnerable to erosion. However, compared with hard structures like seawalls, many communities prefer the protection provided by dunes because of aesthetic considerations.

i. Dune restoration. Historically, sand dunes have suffered from human pressure, and many dune systems have been irreversibly altered by man, both by accident or design. Many coastal areas in Europe, North America, Australia, and South Africa, which had once-stable forested dunes, have been deforested. The early settlers to New England in the 1600's severely damaged the dune vegetation almost immediately upon their arrival by overgrazing and farming. Dune rebuilding and revegetation have had a long history, mostly unsuccessful (Goldsmith 1985). Recent restoration practices have been more effective (Knutson 1976, 1978; Woodhouse 1978). The two main methods for rebuilding or creating coastal dunes are artificial planting and erecting sand fences. Hotta, Kraus, and Horikawa (1991) review sand fence performance.

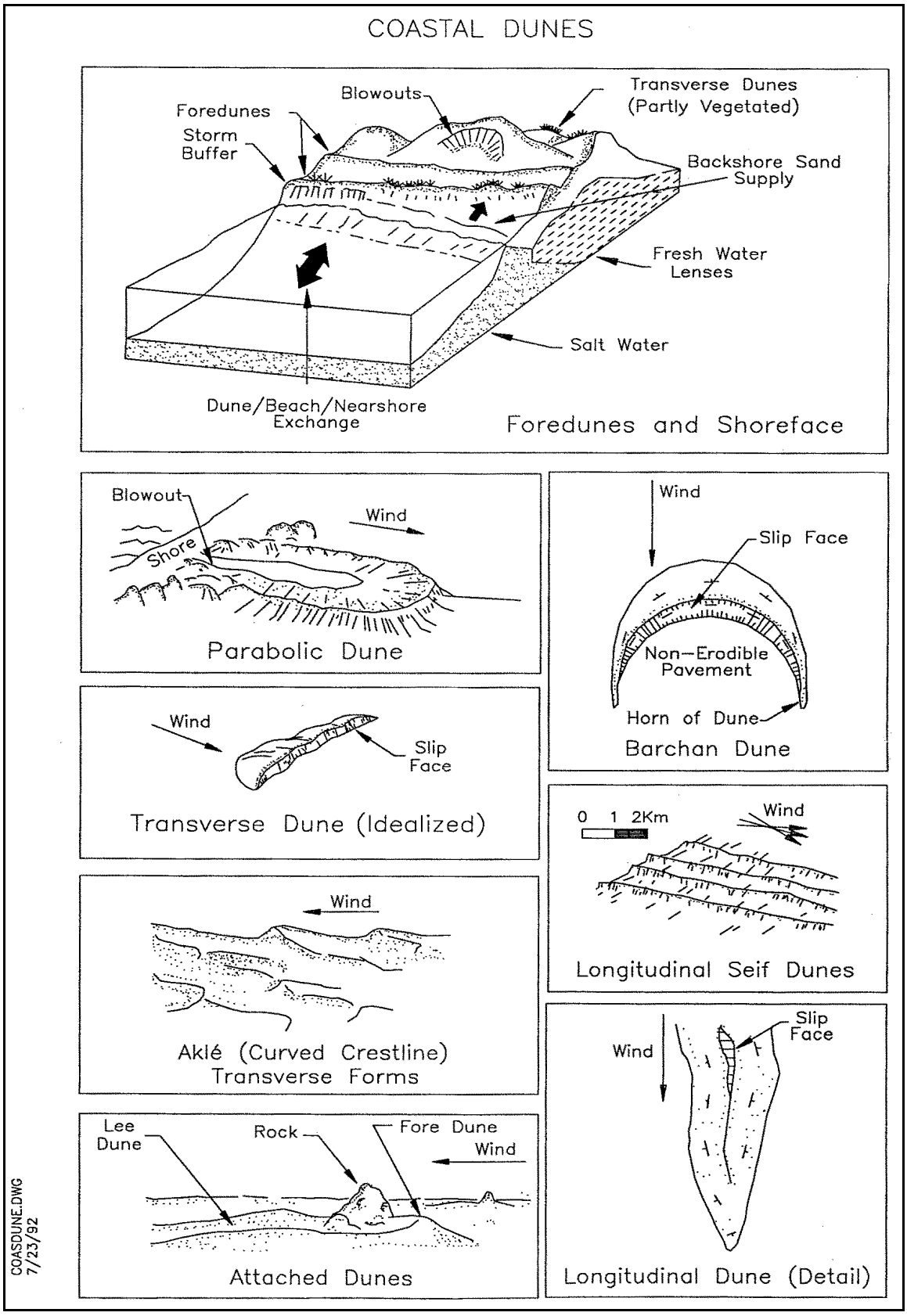

Figure IV-2-11. Variety of dune types (adapted from Carter (1988), Reading (1986), and Flint (1971))

Figure IV-2-12. Blowout in dunes. Eastern Alabama on the Morgan peninsula east of the mouth of Mobile Bay (April 1995)

Figure IV-2-13. Huge dune anchored to a rock outcrop in the eastern Sinai Desert (January 1979). The dune is more than 15 m high. Most of valley floor is hard-packed sand, although there are pockets of loose sand that impede vehicle traffic. As of 1979, many of the bedouins in this area were already using pickup trucks instead of camels

Coastal dune management and conservation practices are reviewed in Carter, Curtis, and Sheehy-Skeffington (1992).

IV-2-7. Volcanic Coasts

a. Introduction and definitions. *Volcanoes* are vents in the earth's surface through which magma and associated gases and ash erupt (Bates and Jackson 1984). Often, conical mountains are formed around the vents as repeated eruptions deposit layer upon layer of rock and ash. Therefore, the definition is extended to include the hill or mountain built up around the opening by the accumulation of rock materials.

(1) The fundamental importance of volcanism to mankind has been clearly documented around the world. The entire west coast of the Unites States is highly active tectonically and most of the continent's volcanoes are within 200 km of the coast. There are more than 260 distinct volcanoes younger than five million years in the Unites States and Canada, most of which are in Alaska and the Hawaiian Islands (Wood and Kienle 1990). Fifty-four have erupted in historic times, and distant memories of others are recounted in Native American legends.

(2) Volcanoes are important to coastal studies for many reasons:

(a) They provide sediment to the littoral environment. Material may reach the coast directly via ash fall-out and lava flows or may be transported by rivers from an inland source (e.g., Mount St. Helens).

(b) Vulcanism affects coastal tectonics (e.g., west coasts of North and South America).

(c) Shoreline geometry is affected by the formation of volcanic islands (Aleutians) and by lava that flows into the sea (Hawaiian Islands).

(d) Shoreline erodability ranges from very erodable for ash and unconsolidated pyroclastic rubble to very resistant for basalt.

(e) Volcanoes can pose a serious threat to coastal communities.

(f) Volcanic debris can choke rivers and harbors.

(3) This section briefly discusses general concepts of volcanism and describes features unique to volcanic shores. Examples from Alaska and the Hawaiian Islands illustrate the differences between composite and shield volcanoes and their associated coastlines. For the general reader, *Exploring our Living Planet*, published by the National Geographic Society (Ballard 1983), is a readable and interesting introduction to plate tectonics, hotspots, and volcanism.

b. General geology. Two classes of volcanoes can be identified, based on the explosiveness of their eruptions and composition of their lava. The ones in the Aleutians and along the west coasts of North and South America are known as *composite* volcanoes and are renowned for their violent eruptions. The paroxysmal explosion of Mount St. Helens on May 18, 1980, which triggered devastating mudflows and floods, killing 64 people, serves as a remarkable example. Composite eruptions produce large amounts of explosive gas and ash and build classic, high-pointed, conic mountains. In contrast, the Hawaiian Islands are *shield* volcanoes: broad, low, basalt masses of enormous volume. Shield eruptions are typically

nonexplosive, and the highly liquid nature of their lava[1] accounts for the wide, low shape of the mountains. Volcanism affects the shore on two levels:

(1) The large-scale geologic setting of the continental margin affects sedimentation and overall coastal geology. Margins subject to active tectonism (and volcanism) are typically steep, with deep water occurring close to shore. Rocks are often young. High mountains close to shore provide a large supply of coarse sediments, and muddy shores are rare. Much sediment may be lost to deep water, particularly if it is funneled down submarine canyons. This is a one-way process, and the sediment is permanently lost to the coastal zone.

(2) Small-scale structures on volcanic shores may differ from those on clastic passive margins. Sediment supply may be frequently renewed from recent eruptions and may range greatly in size. Ash may be quickly destroyed in the sea, while basalt boulders may be tremendously resistant. Hardened shores at the sites of recent lava flows are difficult settings for harbor construction.

c. Composite volcanoes - coastal Alaska. The coastal geology of Alaska is incredibly complex, having been shaped by fault tectonics, volcanism, glaciation, fluvial processes, sea level changes, and annual sea ice. More than 80 volcanoes have been named in the Aleutian arc, which extends for 2,500 km along the southern edge of the Bering Sea and the Alaskan mainland (Wood and Kienle 1990). Over 44 have erupted, some repeatedly, since 1741, when written records began. Aleutian arc volcanism is the result of the active subduction of the Pacific Plate beneath the North America Plate (Figure IV-2-14).

(1) Volcanoes have influenced the Aleutian Arc in two ways. First, they have been constructive agents, creating islands as eruption after eruption has vented rock and ash. In some places, fresh lava or mudflows accompanying eruptions have buried the existing coast, extending the shore seaward. The eruptions of Mts. Katmai and Novarupta in 1912 produced ash layers 3 to 15 m thick. The Katmai River and Soluka Creek carried vast amounts of loose ash to the sea, filling a narrow bay and burying a series of old beach ridges (Shepard and Wanless 1971). Usually, loose mudflow and ash deposits are reworked rapidly by waves, providing sediment for beach development. In addition, for years after an eruption, streams may carry rock and ash to the coast, allowing the coast to locally prograde. The second effect has been destructive, and small islands have been largely destroyed by volcanic explosions. Bogoslof, in the eastern Aleutians, is an example in which both rapid construction and destruction have influenced the island's shape over time (Shepard and Wanless 1971).

(2) Clearly, a history of volcanic instability would be a major consideration for a coastal engineer planning a harbor or project. Most new volcanic islands are uninhabited, but harbors may be needed for refuge, military, or commercial purposes. During World War II, air fields and harbors were built quickly on formerly uninhabited Aleutian Islands. Some islands can supply stone for construction at other locations, requiring loading facilities for boats or barges.

d. Shield volcanoes - Hawaii. Each of the Hawaiian islands is made up of one or more huge shield volcanoes rising from the ocean floor. The islands are at the southern end of a chain of seamounts that extends 3,400 km to the northwest and then turns north and extends another 2,300 km toward Kamchatka as the Emperor Seamounts. More than 100 volcanoes, representing a volume of greater than one million cubic kilometers, make the Hawaiian-Emperor chain the most massive single source of volcanic eruption on earth (Wood and Kienle 1990). The submerged seamounts become successively older away from Hawaii.

---

[1] *Lava* is the term used for molten rock (and gasses within the liquid) that have erupted onto the earth's surface. *Magma* refers to molten rock that is still underground.

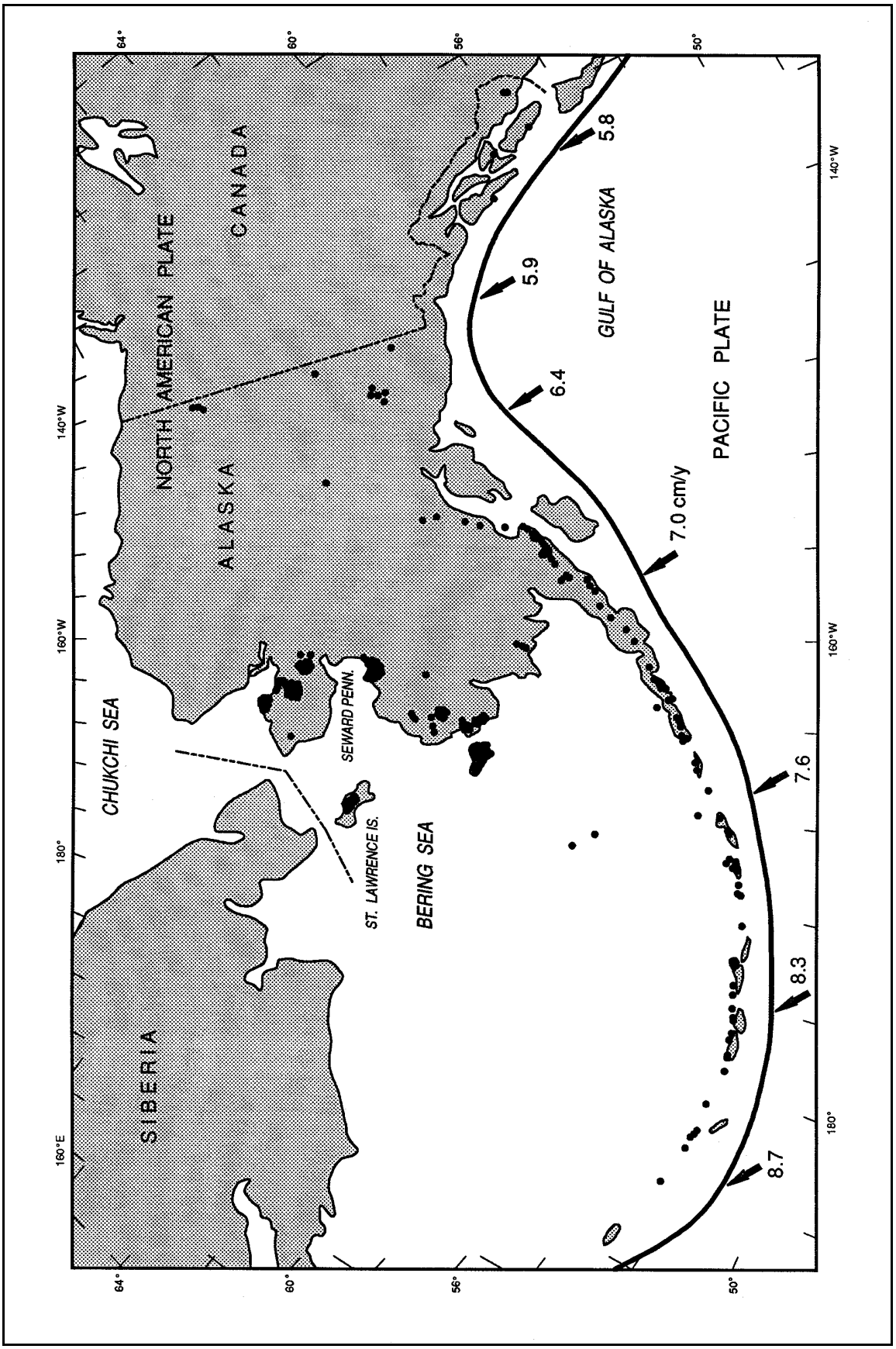

Figure IV-2-14. Alaskan volcanoes along the Aleutian Island arc, marking the boundary between the North American and the Pacific crustal plates. Arrows indicate subduction of the Pacific Plate in cm/year

Meiji Seamount, about to be subducted beneath Kamchatka, is 75-80 million years (my) old, Kilauea is only 0.4 my, while Loihi Seamount, south of the big island of Hawaii, is the newest member of the chain and has not yet emerged from the sea. The islands are found over a semipermanent "hot spot," a site where it is believed that a plume of hot, geochemically primitive material rises convectively through the mantle, interacts with the lithosphere, and vents on the seafloor (Dalrymple, Silver, and Jackson 1973). The Pacific plate is postulated to be moving over the hot spot at a rate of about 13 cm/yr, based on ages of the major vents on Hawaii (Moore and Clague 1992).

(1) Although the coastlines of the Hawaiian Islands are geologically young, wave erosion and the growth of coral reefs have modified most of the shores. Coastal plains have formed around the base of some volcanoes and between others (for example, the intermontaine plateau between Koolau and Waianae on Oahu). The plains are partly alluvial and partly raised reefs (Shepard and Wanless 1971). The greater parts of the Hawaiian coasts are sea cliffs, some as high as 1,000 m on the windward sides of the islands. There are also extensive beaches, the best of which tend to be on the western sides of the islands, protected from waves generated by the northeast trade winds. On southwestern Kauai near Kekaha, there are prograding beach ridges. Surprisingly, most of the beaches are composed not of volcanic debris but primarily of biogenic sediment. The rare volcanic sand beaches are found at the mouths of the larger rivers or along coasts where recent lava flows have killed the coral reefs (Shepard and Wanless 1971). Many beaches are undergoing serious erosion, and finding suitable sources of sand for renourishment has been difficult. This is a critical problem because tourism is a major part of the Hawaiian economy, and the beaches are among the great attractions.

(2) An example from the island of Hawaii helps illustrate the rugged nature of these volcanic shores. Hawaii, at the southeast end of the island chain, has been built up from at least seven independent volcanoes (Moore and Clague 1992). Mauna Loa, a huge dome at the southern end of the island, rises to 4,100 m above the sea (8,500 m above the seafloor). Kilauea, a low dome that rises out of the southeast side of Mauna Loa, has had a remarkable history of eruptions since 1800. Because of the porosity of the lavas, few permanent streams flow down the island, although rainfall on the windward side is heavy. The southeast coast of the island is a barren, rugged rock shore built up from hundreds of Kilauea lava flows (Figure IV-2-15). In Figure IV-2-15, the foreground is cracked, barren basalt, while the plateau in the background supports a cover of grass. The vertical cliffs are about 10 m high and in areas have been notched or undercut by the surf. Small steep pocket beaches consisting of black volcanic sands have developed in some notches. Because of the harsh wave climate and tectonic instability, coastal engineering in the Hawaiian Islands is particularly challenging (Figure IV-2-16).

e. Hazards posed by volcanoes.

(1) Introduction. Coastal projects and communities are subject to four general types of hazards caused by volcanic eruptions:

(a) Explosion-generated tsunamis that can flood coastal areas.

(b) Direct burial by lava or ash (recently experienced in Hawaii, Iceland, and Sicily).

(c) Burial or disruption by mudflows and fluvial sediment from inland eruptions, and changes in stream drainage and coastal sediment-discharge patterns.

(d) Loss of life and destruction from explosions.

Figure IV-2-15. Southeast coast of Hawaii, near Kalpana. Rugged cliffs are built up of many lava flows. Small pocket beaches form between headlands when the cliffs are undermined and loose sediment accumulates

Volcanoes seem a remote hazard to most people, but the danger is imminent and real to those who live in certain parts of the earth, especially along the boundaries of the earth's tectonic plates. Fortunately, fewer than 100 people have been killed by eruptions in Hawaii, where the volcanism is less explosive (Tilling, Heliker, and Wright 1987).

(2) Earthquakes and tsunamis.

(a) *Tsunamis* are waves created by ocean-bottom earthquakes, submarine landslides, and volcanic explosions. These long-period waves can travel across entire oceans at speeds exceeding 800 km/hr, causing extensive damage to coastal areas. The cataclysmic explosion of Krakatau on August 27, 1883, generated waves 30 m high that swept across the Sunda Strait, killing 36,000 coastal villagers on Java and Sumatra. One explosion produced one of the loudest noises in history, which was heard at a distance of 4800 km. The Hawaiian islands are particularly vulnerable to tsunamis caused by disturbances around the Pacific rim. The tsunami of April 1, 1946, generated towering walls of water that swept inland, damaging many coastal structures on the islands. In areas, the water rose to 16 m above the normal sea level. Photographs of the waves and the resulting damage are printed in Shepard and Wanless (1971) (Francis Shepard was living on Oahu at the time and vividly describes how the waves smashed his bungalow, forcing him and his wife to flee for their lives). On July 17, 1998, a wall of water 7 m high hit the northwest coast of Papua, New Guinea without warning, following a 7.0 magnitude earthquake about 30 km off the coast in the Pacific Ocean. Some 6,000 villagers perished in this tragedy.

Figure IV-2-16. Laupahoehoe Harbor, Island of Hawaii, Hawaii. Found on the steep and rugged northeast coast of Hawaii, this harbor provides the only access to the fertile Hamakua coast fishing grounds. This is a hostile environment, as shown by the basalt boulders tossed onto the boat ramp by storm waves

(b) Clearly, there is little that can be done to protect against the random and unpredictable tsunamis. A warning network has been established to notify people around the Pacific of earthquakes and the possibility that destructive waves may follow. Coastal residents are urged to heed these warnings!

(3) Ash and fluvial sediment. When Mount St. Helens exploded on May 18, 1980, 390 m of the top of the mountain was blown off, spewing a cloud of dust and ash high into the stratosphere. From its north flank, an avalanche of hot debris and scalding gasses created immense mudflows, burying the upper 24 km of the North Toutle valley to a depth of 50 m. Lahars, formed from dewatering of the debris avalanche, blocked the shipping channel of the Columbia River. This created an enormous dredging task for the U.S. Army Corps of Engineers, and ultimately much of the dredged material had to be disposed at sea. Dredging related to the explosion continues 18 years after the eruption, as material continues to move downstream from mountain watersheds.

(4) Explosive destruction. Communities close to volcanoes may be destroyed by the explosion and the inhabitants killed by poisonous gasses and superheated steam.

(a) The coastal example frequently cited is the destruction of St. Pierre on Martinique by the violent explosion of Montagne Pelée on May 8, 1902. A glowing cloud overran St. Pierre and spread fan-like over the harbor. Practically instantly, the population of more than 30,000 was smothered with toxic gas and incinerated (Bullard 1962).

(b) The cloud that destroyed St. Pierre consisted of superheated steam filled with even hotter dust particles, traveling more than 160 km/hr. The term *nuée ardente* is now used to describe this type of swiftly flowing, gaseous, dense, incandescent emulsion. It is also used as a synonym for the Peléan type of eruption.

IV-2-8. Sea Cliffs - Diastrophic, Erosional, and Volcanic

a. Sea cliffs are the most spectacular geomorphic features found along the world's coastlines. This section concentrates on bedrock cliffs, with *bedrock* defined as "the solid rock that underlies gravel, soil, or other superficial material" (Bates and Jackson 1984). Bedrock cliffs are found along most of the U.S. and Canadian Pacific coast, in Hawaii, along the Great Lakes shores, and in Maine. South of Maine along the Atlantic coast, cliffs are rare except for some examples in New Hampshire, Massachusetts, and Rhode Island. The eastern end of Long Island, Montauk Point, consists of rapidly eroding till bluffs (Figure IV-2-9). Cliffs constitute portions of the coastlines of Spain, Italy, Greece, Turkey, Iceland, and the South American nations facing the Pacific Ocean. Shorelines with cliffs may be both emergent or submergent. For more information, Trenhaile's (1987) *The Geomorphology of Rock Coasts* presents a comprehensive and global review of cliffs, shore platforms, and erosion and weathering processes.

b. Bedrock cliffs are composed of all three major rock types: igneous, sedimentary, and metamorphic.

(1) ***Intrusive igneous rock***, such as granite, cools and solidifies beneath the earth's surface, while *extrusive igneous rock*, such as basalt, is formed by lava above ground (it may erupt underwater or on land). Usually, igneous rocks are highly resistant; however, two properties affect their susceptibility to weathering and erosion (de Blij and Muller 1993):

(a) *Jointing* is the tendency of rocks to develop parallel sets of fractures without obvious external movement like faulting.

(b) *Exfoliation*, caused by the release of confining pressure, is a type of jointing which occurs in concentric shells around a rock mass.

(2) ***Sedimentary rock*** results from the deposition and lithification (compaction and cementation) of mineral grains derived from other rocks (de Blij and Muller 1993). This category also includes rock created by precipitation (usually limestone).

(a) The particles (clasts) that make up *clastic sedimentary rock* can range in size from windblown dust to waterborne cobbles and boulders. The vast majority of sedimentary rocks are clastic. Common examples include sandstone, composed of lithified sand (usually consisting mostly of quartz), and shale, made from compacted mud (clay minerals). Many cliffs along the south shore of Lake Erie are shale.

(b) *Nonclastic sedimentary rocks* are formed by precipitation of chemical elements from solution in marine and freshwater bodies because of evaporation and other physical and biological processes. The most common nonclastic rock is limestone, composed of calcium carbonate ($CaCO_3$) precipitated from seawater by marine organisms (and sometimes also incorporating marine shell fragments). Many of the Mediterranean cliffs are limestone and are very vulnerable to dissolution.

(3) ***Metamorphic rocks*** are preexisting rocks changed by heat and pressure during burial or by contact with hot rock masses. Common examples include:

(a) *Quartzite*, a very hard, weathering-resistant rock, formed from quartz grains and silica cement.

(b) *Marble*, a fine-grained, usually light-colored rock formed from limestone.

(c) *Slate*, a rock that breaks along parallel planes, metamorphosed from shale.

c. Sea cliffs are formed by three general processes:

(1) Volcanic eruptions and uplift caused by local volcanism (discussed in paragraph IV-2-7).

(2) Diastrophic activity that produces vertical movement of blocks of the crust.

(3) Erosional shorelines - partial drowning of steep slopes in hilly and mountainous terrain and resulting erosion and removal of sediment.

d. Sea cliffs, often found on tectonically active coasts, may be created by two mechanisms. First, if a block of the coast drops, a newly exposed fault plane may be exposed to the sea. The opposite process may occur: a block may be uplifted along a fault plane, exposing a formerly exposed portion of the shoreface to marine erosion. Older cliffs may be raised above sea level and be temporarily protected from further erosion. Earlier shorelines, sometimes tens of meters above the present sea level, are marked by notches or wave-cut platforms (sometimes termed uplifted marine terraces) (Figure IV-2-17). Terraces marking the highstand of eustatic (absolute) sea level have been traced around the world. Deep water is often found immediately offshore of faulted coasts. Cliffs that extend steeply into deep water are known as plunging cliffs.

e. Erosional coasts may be straight or may be irregular, with deeply indented bays. The way the shore reacts to inundation and subsequent marine erosion depends on both the wave climate and the rock type.

(1) Wave-straightened coasts. Cliffs are often found along shores where wave erosion rather than deposition is the dominant coastal process. Exposed bedrock, high relief, steep slopes, and deep water are typical features of erosional shorelines (de Blij and Muller 1993). When islands are present, they are likely to be remnants of the retreating coast rather than sandy accumulations being deposited in shallow water. The sequence of events that create a straightened coast are illustrated in Figure IV-2-18. The original coastline includes headlands and embayments (a). As waves attack the shore, the headlands are eroded, producing steep sea cliffs (b). The waves vigorously attack the portion of the cliff near sea level, where joints, fissures, and softer strata are especially vulnerable. The cliffs are undermined and caves are formed. Pocket beaches may accumulate between headlands from sediment carried by longshore currents. Especially durable pinnacles of rock may survive offshore as stacks or arches. Over time, the coast is straightened as the headlands are eroded back (c).

(a) Beaches. Beaches may form at the base of cliffs if the rubble that has fallen from the cliff face (known as talus) is unconsolidated or friable and breaks down rapidly under wave attack (Figures IV-2-9 and IV-2-15). If the rock debris is durable, it may serve to armor the shore, protecting it from further wave attack except during the most severe storms.

(b) Wave-cut platforms. At the base of cliffs that have been progressively cut back by waves, near-horizontal platforms may form just below sea level. These rocky platforms may be of substantial width, depending on lithology and the time that sea level has been at that height (Figure IV-2-17). The platforms may be clean or may be covered with rubble fallen from the adjacent cliffs.

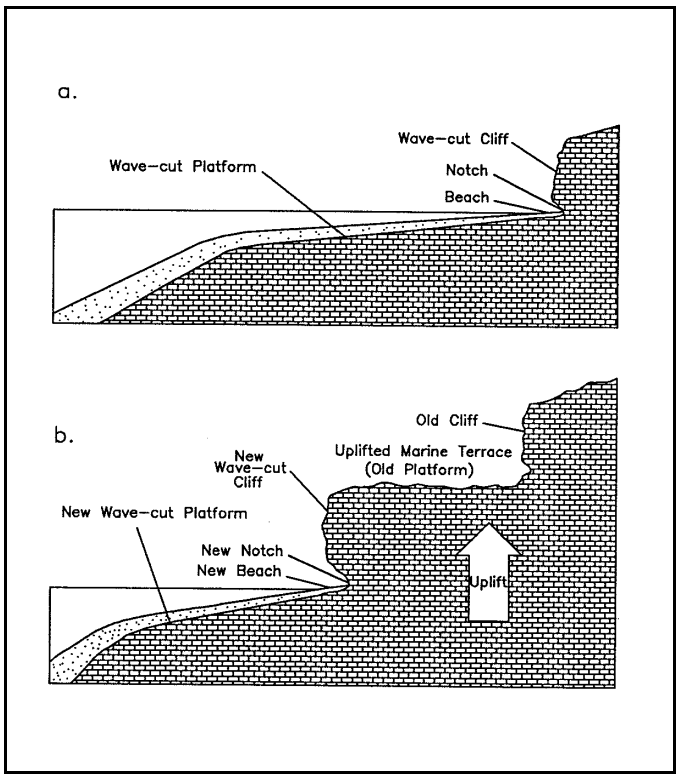

Figure IV-2-17. Wave-cut platform exposed by tectonic uplift. Sediment that accumulated on the platform may temporarily protect the cliff from further erosion

(2) Creation of irregular shorelines. In some mountainous terrains, rising sea level results in deeply incised coastlines. This process is illustrated in Figure IV-2-19. As the sea rises, a river valley is inundated. Once exposed to the sea, the new shoreline is subject to dissolution and biological attack. In southern France, Italy, Greece, and Turkey, thousands of deep embayments are found in the coastal limestone hills. The fact that the wave climate in the Mediterranean is relatively calm (compared with the open oceans) suggests that erosional processes other than wave attack have been instrumental in creating these steep, indented shores. An irregular shore may also be formed when differing rock types outcrop at the coast. Massive rocks, especially igneous and metamorphic ones, withstand erosion better than most sedimentary rocks, which are usually friable and contain bedding planes and fractures. The Pacific coast of Washington off the Olympic Peninsula is irregular because of the complex geology and variety of exposed rock formations (Figure IV-2-20).

e. Marine cliffs are degraded by many physical and biological factors.

(1) Wave attack is most likely the primary mechanism that causes cliffs to erode (Komar 1976). The hydraulic pressure exerted by wave impact reaches values sufficient to fracture the rock. Sand and rock fragments hurled at the cliff by waves grind away at the surface. Komar (1976) states that wave erosion occurs chiefly during storms, but admits that little quantitative research has been conducted. Once a cliff has been undercut at its base, the overlying rock, left unsupported, may collapse and slide down to the shoreline (Figures III-5-21, IV-2-21, and IV-2-22). Temporarily, the talus protects the cliff, but over time the rubble is reduced and carried away, leaving the fresh cliff face exposed to renewed wave attack.

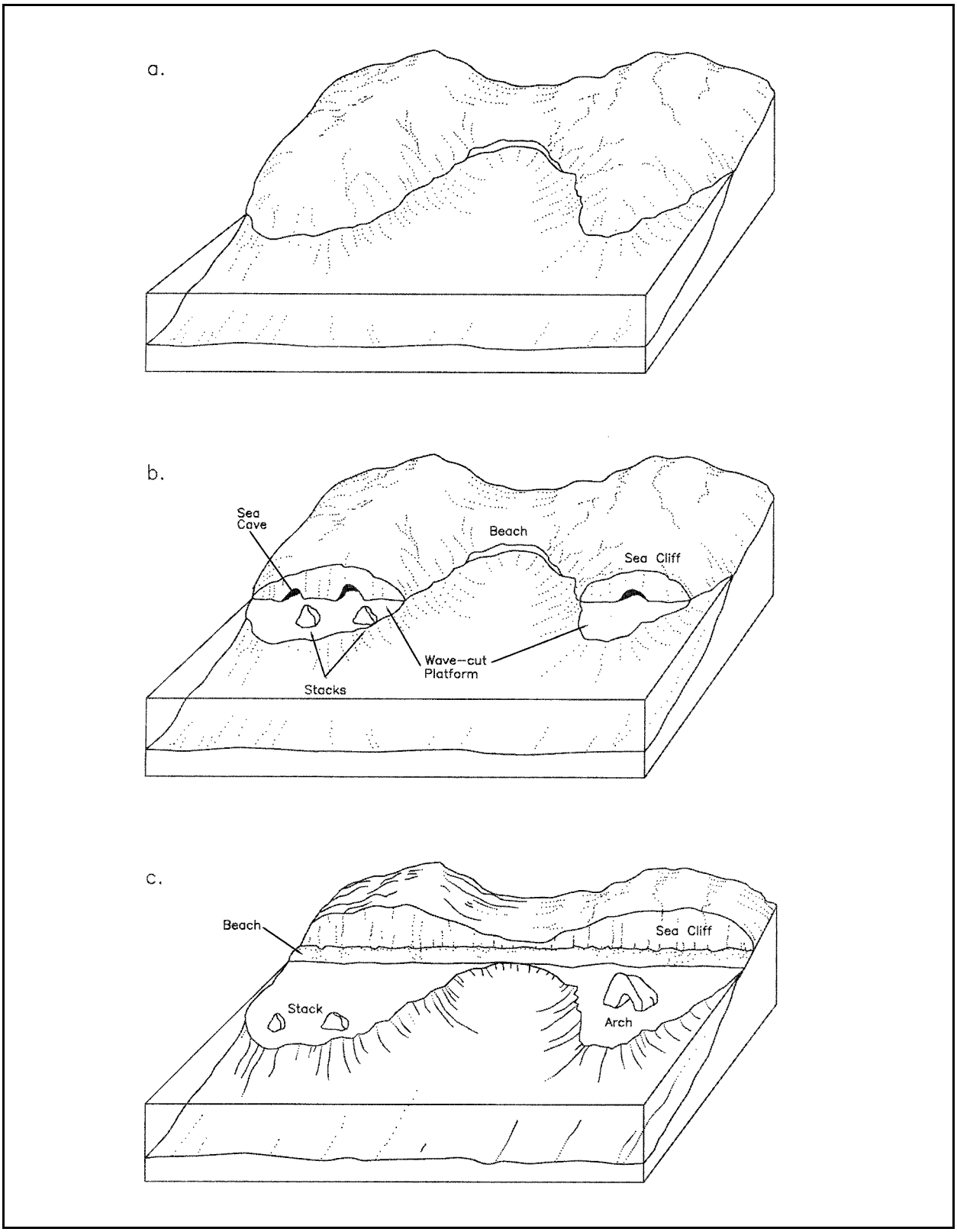

Figure IV-2-18. Wave erosion of an indented coastline produces a straightened, cliff-bound coast. Wave-cut platforms and isolated stacks and arches may remain offshore. Many such features are found along the Washington, Oregon, and California coast (adapted from de Blij and Muller (1993))

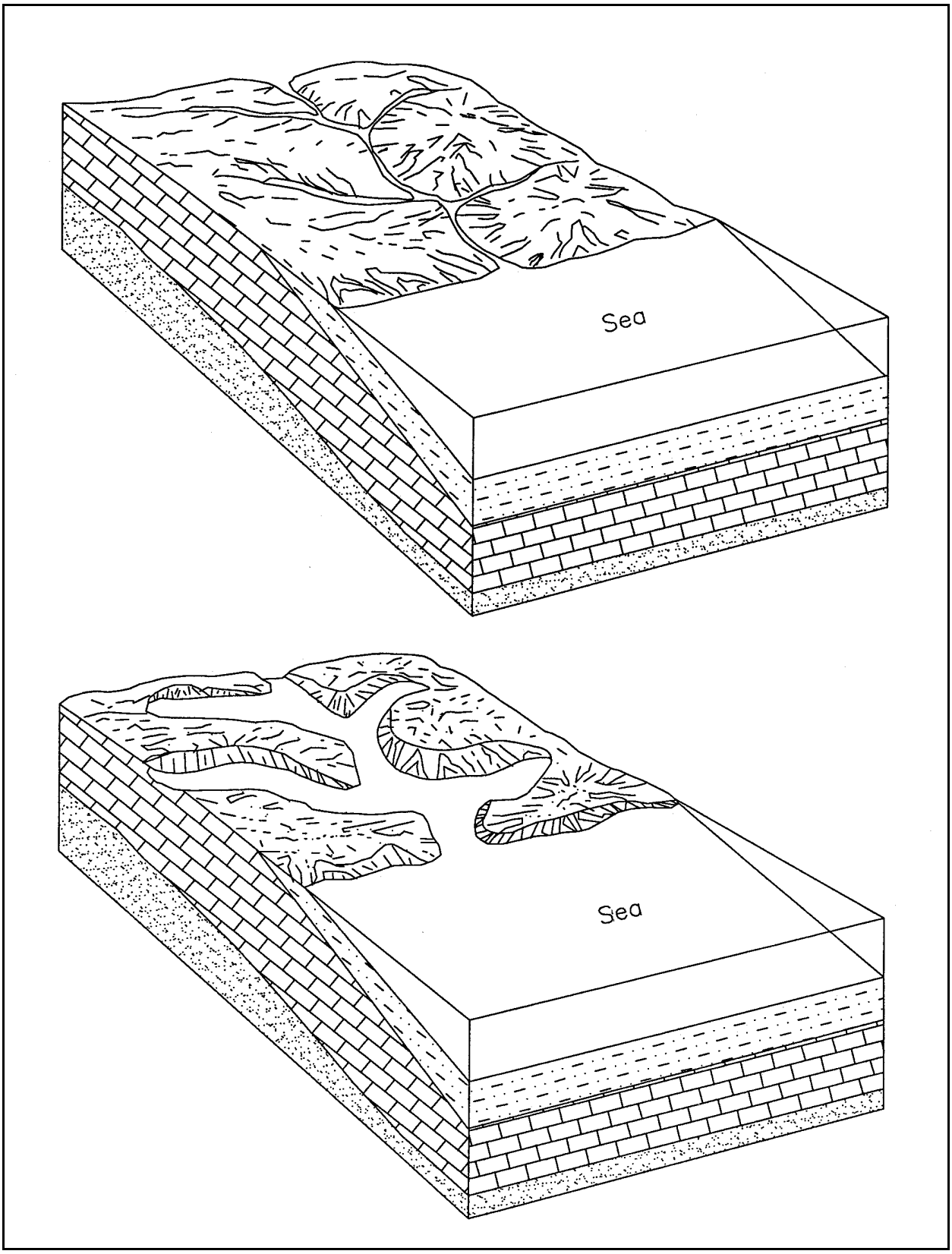

Figure IV-2-19. Inundation of a mountainous area by rising sea level or land subsidence produces a deeply indented shoreline

Figure IV-2-20. Pacific Ocean coast of Olympic Peninsula, Washington, near Jefferson Cove (September 1971). Rugged shore consists of resistant rock headlands with pocket beaches. Much of the beach sediment is cobble and coarse clasts derived from the adjacent cliffs. The beaches are often covered with logs and driftwood

(2) In addition to waves, weathering processes weaken and crumble sea cliffs. Ice wedging in cold climates progressively weakens the rock. Plant roots grow and expand in cracks. Lichens secrete acids that etch the rock surface. Groundwater can lubricate impermeable rock surfaces, upon which large masses of overlying rock can slip. This process is responsible for large slumps in the shale bluffs in Lakes Erie and Ontario (Figure III-5-21).

(3) Mollusks and burrowing animals can weaken otherwise resistant massive rocks. Komar (1976) lists burrowing mollusks such as *Pholadidae* and *Lithophaga*, and periwinkles, worms, barnacles, sponges, and sea urchins as having been observed to erode rock. Boring algae can also weaken rock (Figure IV-2-23).

(4) Under normal circumstances, surface seawater is saturated with calcium carbonate ($CaCO_3$), therefore minimizing dissolution of limestone or $CaCO_3$-cemented sediments. Marine organisms can locally increase the acidity of the water in high-tide rock basins and other protected locations. Small pockets found

Figure IV-2-21. A section of cliff, projecting out from the shore, is likely to collapse soon. To the left, rubble at sea level marks the location of a previous slump. The lower cliffs are poorly cemented conglomerate while the higher, vertical cliffs (above the trees), are limestone (near Nauplió, Greece, April 1992)

at water's edge, often housing periwinkles and other animals, may have been caused by biochemical leaching.

(5) Salt weathering is caused by the pressure exerted by NaCl and other salts in the capillaries of rocks. The weathering is caused by:

(a) Changes of volume induced by hydration.

(b) Expansion of salt crystals caused by temperature changes.

(c) Crystal growth from solution.

The main factor in determining the efficacy of chemical weathering is the amount of water available for chemical reactions and the removal of soluble products. This suggests, but does not necessarily restrict, that the greatest chemical weathering will occur in hot, humid climates (Trenhaile 1987).

IV-2-9. Marine Deposition Coasts - Barriers

a. Introduction.

(1) Barriers are narrow, elongate sand ridges rising slightly above the high tide level and extending generally parallel with the coast, but separated from the mainland by a lagoon or marsh (Bates and Jackson

Figure IV-2-22. Lake Michigan shore south of St. Joseph, Michigan (November 1993). A triangle-shaped wedge of the bluff has recently slumped. The bluffs in this area have suffered rapid retreat, and many homes have been destroyed. At least three factors account for the erosion: (a) offshore downcutting of the till lake bottom; (b) wave attack on the bluffs; (c) ice expansion and lubrication of bedding planes caused by groundwater

1984). The term *barrier* identifies the sand ridges as ones that protect parts of the coast from direct wave attack of the open ocean. In this manual, barrier will refer to the overall structure (sometimes called a barrier complex), which includes the beach, submerged nearshore features, underlying sediments, and the lagoon between the barrier and the mainland (Figure IV-2-24). Inlets and channels can also be considered part of a barrier system.

(2) The term *beach* is sometimes used as a synonym for barrier, but this can lead to confusion because a beach is a geomorphic shore type found throughout the world, even on volcanic or coralline coastlines where barriers are rare. Whereas all barriers include beaches, not all beaches are barriers.

(3) The following sections describe general barrier island morphology, history, and formation, subjects that have fascinated geologists for more than 100 years. The emphasis will be on long-term changes, covering periods of years or centuries. The purpose is to explain factors that lead to barrier migration or evolution. Longshore sediment transport, details on the morphology of sandy shorefaces, and the normal effects of waves and tides will be covered in Part IV-3, "Coastal Morphodynamics." This distinction is arbitrary because, clearly, the day-to-day processes that affect beaches also influence barrier development. In addition, the evolution of barriers during the Holocene Epoch is intimately related to sea level changes (see Part IV-1). These factors underscore the complex interrelationships that exist throughout the coastal zone and the difficulty of separating the constituent elements.

Figure IV-2-23. Cemented conglomerate with many pits and cavities shows evidence of dissolution. The rock mass has been undercut over 1 m (near Nauplió, Greece). Note that the conglomerate is distinctly graded, with fine grains near the bottom and cobble near the top

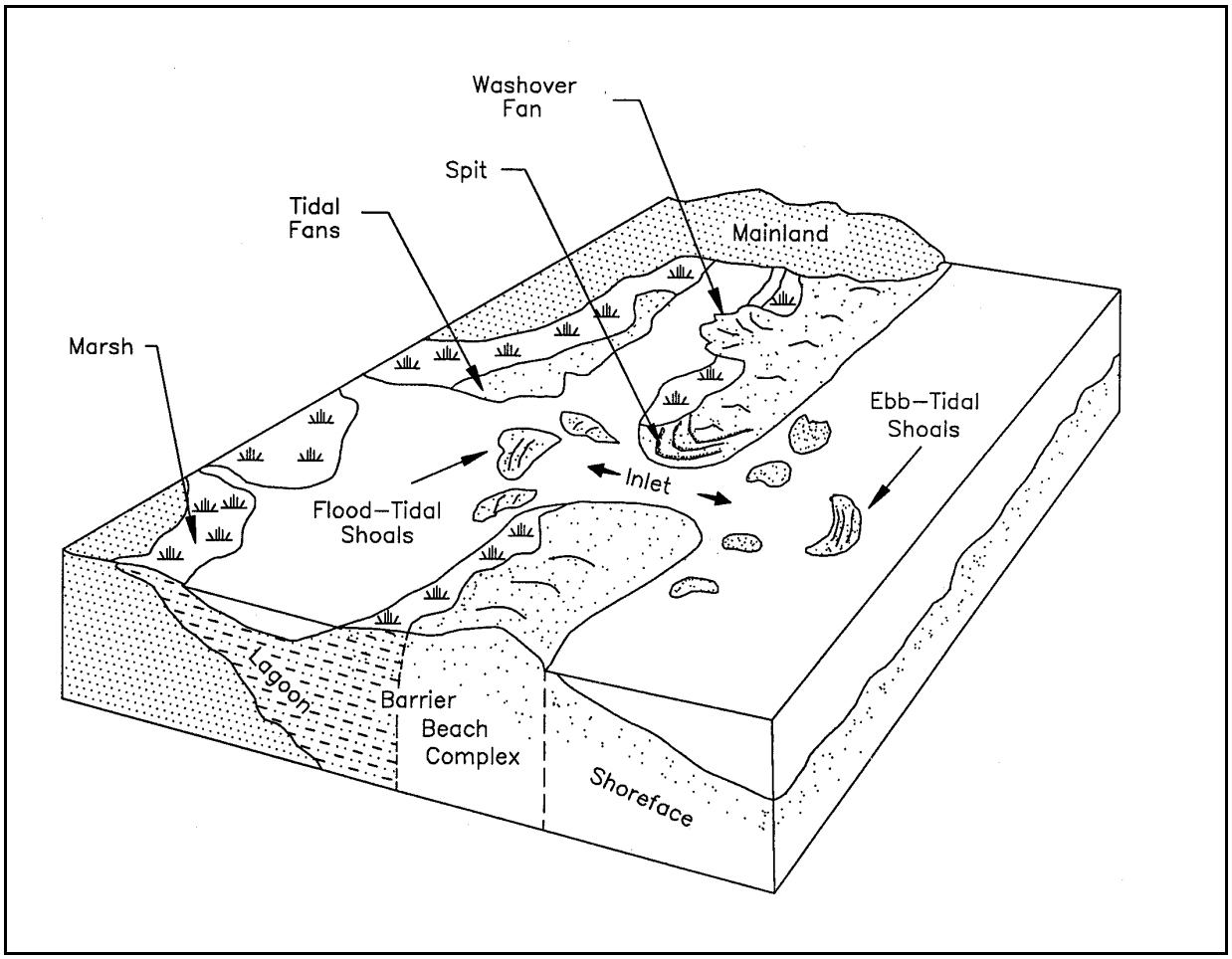

Figure IV-2-24. A three-dimensional view of features commonly found in barrier island systems, including the back barrier, overwash fans, and lagoons. The lagoons often become estuaries, particularly if sediment is supplied by both rivers and inlets

(4) The long-term and widespread interest in barrier islands is largely due to their great economic importance. Ancient buried barriers are important petroleum reservoirs. Contemporary barriers protect lagoons and estuaries, which are the breeding grounds for many marine species and birds. In addition, barrier islands are among the most important recreational and residential regions. In recent years, man's adverse impact on these fragile ecological and geological environments has led to increased need to study their origins and development to improve coastal management and preserve these critical resources for the future.

(5) An enormous literature on barrier islands exists. Nummedal (1983) provides a readable and concise overview. Leatherman's (1979) book is a compilation of papers on U.S. east coast and Gulf of Mexico barriers. Many seminal papers on barrier island evolution have been reprinted in Schwartz (1973). Textbooks by Carter (1988), Davis (1985), King (1972a), and Komar (1976) discuss barriers and include voluminous reference lists. Classic papers on beach processes have been reprinted in Fisher and Dolan (1977).

b. Distribution of barrier coasts. Barrier islands are found around the world (Table IV-2-2). They are most common on the trailing edges of the migrating continental plates (Inman and Nordstrom 1971)[1]. This type of plate boundary is usually non-mountainous, with wide continental shelves and coastal plains. Over 17 percent of the North American coastline is barrier, most of it along the eastern seaboard facing the Atlantic Ocean and the Gulf of Mexico. Table IV-2-3 lists the lengths of barriers and spits in the United States. Of the Atlantic states, Maine and New Hampshire have the fewest barriers because their coasts are largely composed of igneous rock. Massachusetts, with mostly glacial moraines and outwash along the coast, has the surprising total of 184 km of spits and barriers. Of the continental states, Florida has the most barriers and spits, totaling over 1,000 km for both the Atlantic and the Gulf of Mexico. Most of the shorelines facing the Gulf of Mexico consist of barrier islands. A portion of Florida's west coast, where wave energy is low, is mangrove swamp, but the Panhandle is famous for its glistening white barriers.

Table IV-2-2
Worldwide Distribution of Barrier Island Coasts

Continent	Barrier Length (km)	% of World Total Barriers	% of Continent's Coastline that is Barrier
N. America	10,765	33.6	17.6
Europe	2,693	8.4	5.3
S. America	3,302	10.3	12.2
Africa	5,984	18.7	17.9
Australia	2,168	6.8	11.4
Asia	7,126	22.2	13.8
Total	32,038	100.0	

From Cromwell (1971)

Almost the entire shore of Texas consists of long barriers, which continue south into Mexico. Extensive barriers are also found on the Gulf of Alaska north of Bering Strait. Including numerous spits in the Aleutians and the Gulf of Alaska, the state of Alaska has almost 1,300 km of barrier in total, exceeding Florida. The United States total shown in Table IV-2-3 is 4,882 km, about half the North American total computed by Cromwell (1971). For more information, the most extensive survey of United States barriers was documented in the *Report to Congress: Coastal Barrier Resources System* (Coastal Barriers Study Group 1988).

c. General coastal barrier structure. The barrier shore type covers a broad range of sizes and variations. Three general classes of barrier structures can be identified (Figure IV-2-25):

(1) Bay barriers - connected to headlands at both ends and enclosing a bay or wetland.

(2) Spits - attached to a sediment source and growing downdrift. May be converted to a barrier island if a storm cuts an inlet across the spit. May evolve into bay barriers if they attach to another headland and completely enclose a lagoon.

[1] *The trailing edge* of a continent is moving away from an active spreading center. For example, the Atlantic coast of the United States is a trailing edge because new seafloor is being formed along the mid-Atlantic ridge, causing the Atlantic Ocean to grow wider (Figure IV-1-2). The Pacific coast is a *leading edge* because the oceanic plates are being subducted (consumed) at various trenches and are therefore becoming smaller.

Table IV-2-3
Barrier Islands and Spits of the United States

Ocean or Sea	State	Total Length (km)[1]
Atlantic	Maine	11.4
	New Hampshire	2.5
	Massachusetts [2]	184.4
	Rhode Island [3]	17.6
	New York [4]	152.2
	New Jersey	106.0
	Delaware [5]	33.7
	Maryland [5]	49.2
	Virginia [5]	126.0
	North Carolina	380.7
	South Carolina	234.2
	Georgia	159.0
	Florida	533.3
	Atlantic coast total	**1990**
Gulf of Mexico	Florida	478.5
	Alabama	92.7
	Mississippi	59.5
	Louisiana	151.9
	Texas	498.0
	Gulf of Mexico total	**1281**
Pacific - Continental USA	Washington [6]	63.9
	Oregon	91.9
	California	65.4
	Pacific total	**221**
Beaufort, Chukchi, Bering Seas, Gulf of Alaska, Bristol Bay	Alaska total (incl. Aleutians)	**1266**
Lakes Superior, Huron, Michigan, Ontario, Erie	Combined Great Lakes states	**124**
United States total [2,3,4,5,6]		**4882**

Source: Unpublished data generated during the Corps of Engineers' Barrier Island Sediment Study (BISS), 1989.
[1] Length of barriers measured from U.S. Geological Survey topographic maps. Includes barriers and spits enclosing a body of water or marsh, not the total length of beaches in the United States. No data available for Puerto Rico, Virgin Islands, Pacific Trust Territories.
[2] Includes Nantucket and Martha's Vineyard Islands.
[3] Does not include Narragansett Bay.
[4] Atlantic Ocean only; does not include spits in Long Island Sound or Great Peconic Bay.
[5] Does not include Chesapeake Bay.
[6] Includes spits in Strait of Juan de Fuca. Does not include Long Beach Peninsula, enclosing Willapa Bay.

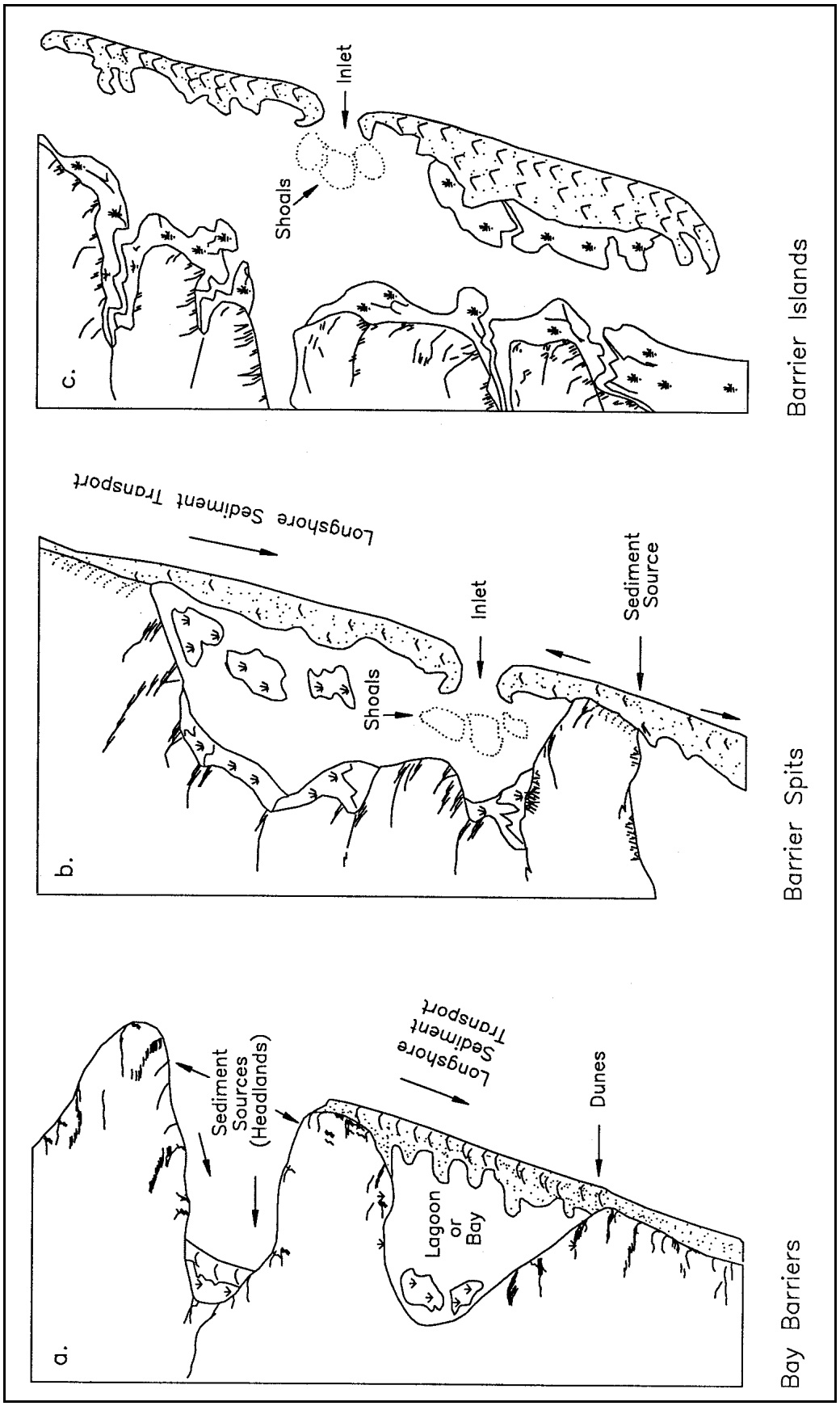

Figure IV-2-25. General barrier types: bay, spit, and island

(3) Barrier islands - linear islands that are not attached to the mainland but that enclose a bay, pond, or marsh/wetland. A series of these islands extending along the coast are defined as a barrier chain.

d. Origin and evolution. The origin of barrier islands has been a topic of debate among geologists for over a century (Schwartz 1973). The differing theories suggest that there are probably several types of barriers, each undergoing its own form of development due to unique physical and geologic factors. Three main theories have evolved, all of which have fierce supporters and critics.

(1) Emergence model. De Beaumont in 1845 was the first naturalist formally to present a theory of barrier island formation. It was supported and modified by the influential Johnson (1919). These researchers theorized that barrier emergence began with the formation of an offshore sand shoal, which consisted of material reworked from the seafloor by waves. Over time, the shoal would accumulate ever more sand and grow vertically, eventually emerging above the sea surface (Figure IV-2-26). Wave swash and wind deposition would continue to contribute sand to the shoal, allowing it to grow larger and larger. Hoyt (1967) objected to this hypothesis because he was unaware of any examples of bars emerging above water and surviving wave action, although the growth of submerged bars was well-recorded. Otvos (1970) reported evidence from the Gulf coast supporting the emergence of submarine shoals (he conveniently noted that subsequent migration of barriers might completely obscure the conditions of formation of the original barrier).

(2) Submergence model. The submergence concept was refined by Hoyt (1967) and has received much support. In this model, the initial physical setting is a mainland beach-and-dune complex with a marsh separating the beach from higher terrain inland. Rising sea level floods the marsh, creating a lagoon that separates the beach from the mainland (Figure IV-2-27). Presumably, usually the sea level rise is part of a worldwide pattern (eustatic), but it may be caused in part by local submergence. Once formed, maintenance of the barrier becomes a balance of sediment supply, rate of submergence, and hydrodynamic factors.

(3) Spit detachment model. The third major model calls for the growth of sandspits due to erosion of headlands and longshore sediment transport (Figure IV-2-28). Periodically, the spit may be breached during storms. The furthest portion of the spit then becomes a detached barrier island, separated by a tidal inlet from the portion that is still attached to the mainland. Gilbert (1885) may have been the first geologist to suggest the spit hypothesis, based on his studies of ancient Lake Bonneville, but the hypothesis lay dormant for many years because of Johnson's (1919) objections. In recent years, it has received renewed support because the cycle of spit growth and breaching can be seen in many locations (for example, at Cape Cod, Massachusetts (Giese 1988)).

(4) Combined origin model. Schwartz (1971) concluded that barrier island formation is most probably a combination of all of the above mechanisms. He felt that only a few examples of barriers could be cited as having been formed by only one method. Most systems were much more complex, as demonstrated by the barriers of southern Louisiana, which were formed by a combination of submergence and spit detachment (Penland and Boyd 1981).

e. Barrier response to rising sea level.

(1) Many of the barriers in the United States, particularly along the Atlantic coast, are eroding, causing serious economic and management challenges. What is responsible for this erosion?

(2) Sea level and sediment availability are probably the major factors that determine barrier evolution (Carter 1988). Three sea level conditions are possible: rising, falling, and stationary. Rising and falling sea

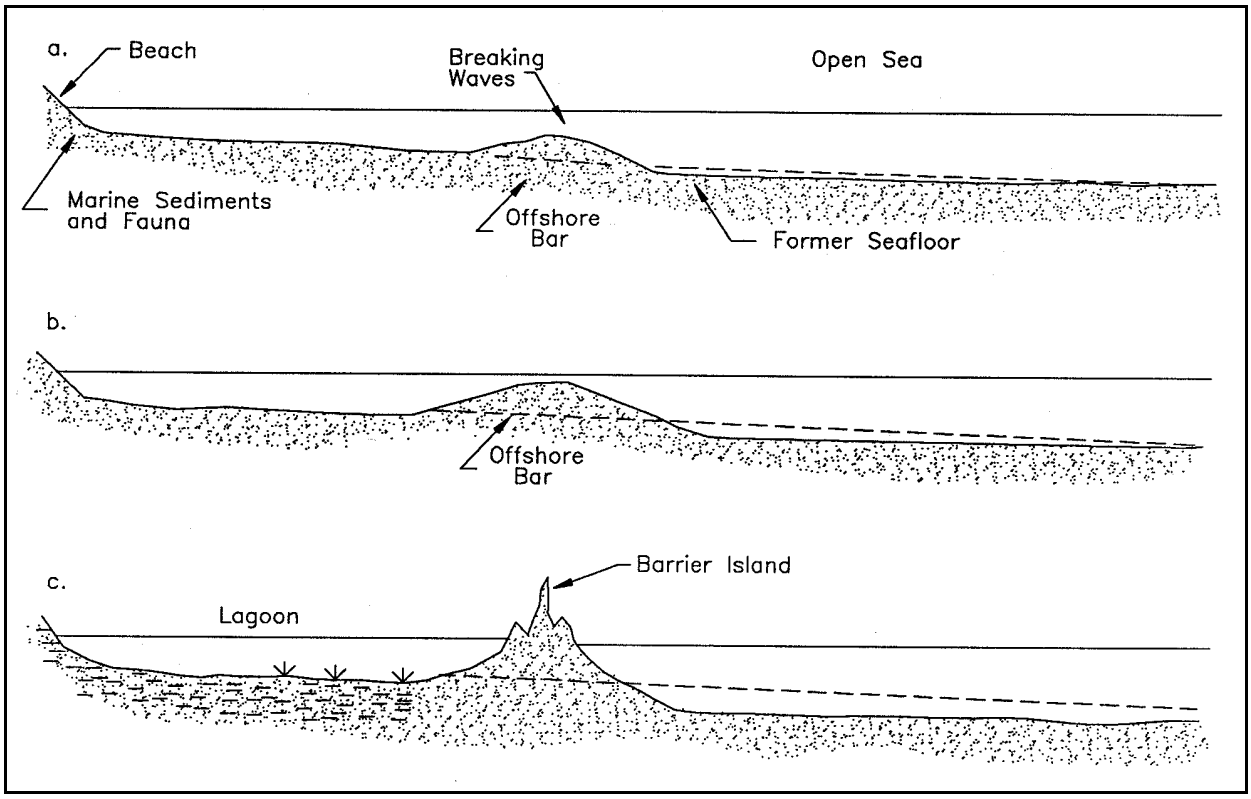

Figure IV-2-26. Emergence model of barrier island formation (modified from Hoyt (1967)), (a) Waves erode the seafloor, forming a sandbar, (b) The bar continues to grow higher and wider, (c) Bar is converted to an island, enclosing a lagoon on the landward side

usually result in great sediment movement as barriers adjust. A stationary stage, however, allows the shore to adjust slowly and achieve equilibrium between sediment supply and dynamic processes. Commonly, if sea level rises and sediment supply is constant, a barrier retreats (*transgression* of the sea). On the other hand, if sea level is rising but a large amount of sediment is supplied locally by rivers or eroding headlands, a particular barrier may be stable or may even aggrade upwards (see Table IV-1-6). However, many other factors can intervene: local geological conditions, biological activity, susceptibility to erosion, the rate of sea level change. Therefore, each location must be evaluated individually.

(3) Given the condition of rising sea level along the eastern United States, what are the mechanisms that cause barrier retreat? Three models of shoreline response to rising sea level have been proposed (Figure IV-2-29). These assume that an equilibrium profile is maintained as the shoreline is displaced landward and upward. In addition, overall sediment budget is balanced and energy input is constant.

(a) The first model, often called the Bruun Rule (Bruun 1962), assumes that sediment eroded from the shoreface is dispersed offshore. As water level rises, waves erode the upper beach, causing the shoreline to recede. Conceptually, this erosion supplies sediment for upward building for the outer part of the profile. The model assumes that the initial profile shape will be reestablished farther inland but at a height above the original position equal to the rise in water level z. Therefore, the retreat of the profile x can be calculated from the following relationship (a modified version of the Bruun Rule):

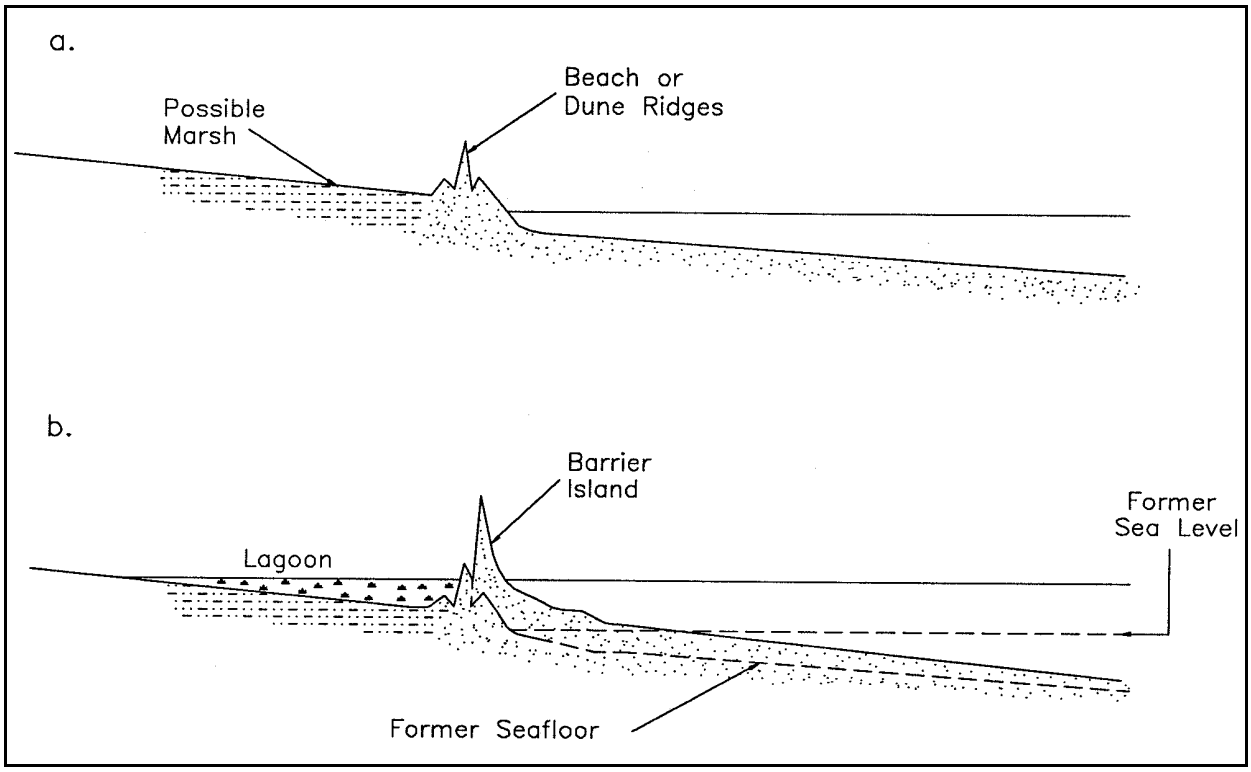

Figure IV-2-27. Submergence model of barrier island formation (modified from Hoyt (1967)), (a) Beach or sand dune ridges form near the shoreline, (b) Rising sea level floods the area landward of the ridge, forming a barrier island and lagoon. Sediment must be available to allow the island to grow vertically as sea level rises

$$x = \frac{zX}{Z} \tag{IV-2-1}$$

where the terms *x, z, X,* and *Z* are shown in Figure IV-2-29a. Attempts to verify the Bruun rule have been ambiguous, and modifications to the model have been proposed (Dolan and Hayden 1983). The most successful studies required long-term data sets, such as the profiles from Lake Michigan examined by Hands (1983). His research showed that the shoreface profile requires a considerable time (years or decades) to adjust to water level changes. It is unclear whether the Bruun Rule would apply if an ample supply of sediment were available during rising sea level. Would the barrier essentially remain in place while sand eroded from the shoreface or newly supplied sand was dispersed offshore to maintain the profile? The Bruun Rule and some of its underlying assumptions are discussed in greater detail in Part IV-3.

(b) Landward migration of a barrier by the rollover model applies to coasts where washover processes are important. As sea level rises, material is progressively stripped from the beach and shoreface and carried over the barrier crest by waves. The sand is deposited in the lagoon or marsh behind the barrier (Figure IV-2-30). Dillon (1970) documented this process along the southern Rhode Island coast. As the barrier moves landward (rolls over itself), lagoonal sediments may eventually be exposed on open shoreface. Evidence of this can be seen in Rhode Island during winter storms, when large pieces of peat are thrown up on the beach. Dingler, Reiss, and Plant (1993) have described a model of beach erosion and overwash deposition on the Isles Dernieres, off southern Louisiana. They attributed a net annual beach retreat of

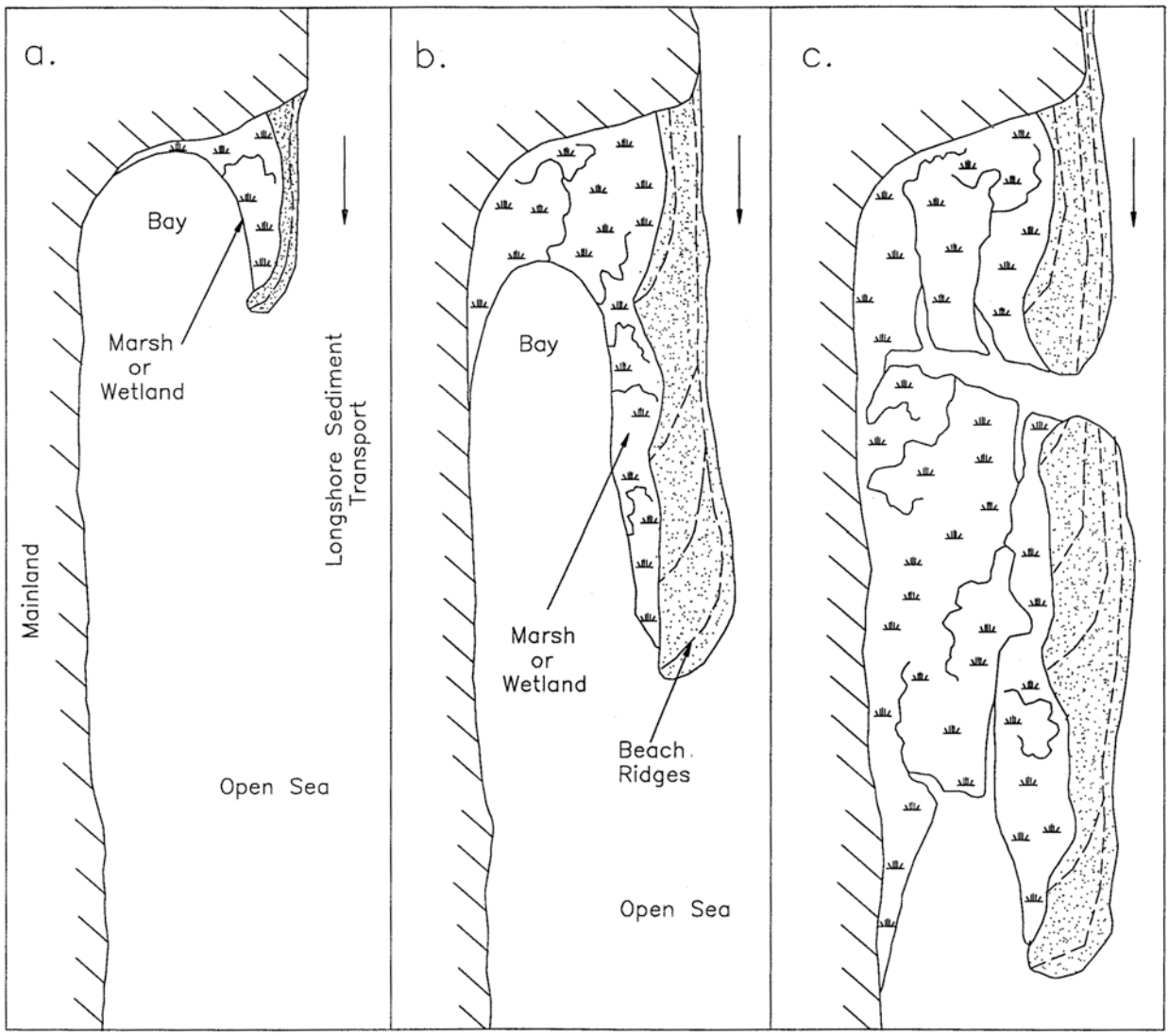

Figure IV-2-28. Barrier island formation from spit (modified from Hoyt (1967)), (a) Spit grows in direction of longshore drift, supplied from a headland, (b) Spit continues to grow downdrift, marsh begins to fill semi-protected bay, (c) Part of spit is breached, converting it to a barrier island

greater than 10 m/yr to winter cold-front-driven storms that removed sediment from the beach face and infrequent hurricanes that shifted a substantial quantity of sediment to the backshore. For the most part, rollover is a one-way process because little of the sand carried over the barrier into the lagoon is returned to the open shoreface.

(c) The barrier overstepping model suggests that a barrier may be drowned, remaining in place as sea level rises above it. Several hypotheses have been proposed to explain how this process might occur:

- If the rate of sea level rise accelerates, the barrier may be unable to respond quickly by means of roll-over or other mechanisms. Carter (1988) cites research that suggests that gravel or boulder barriers are the most likely to be stranded.

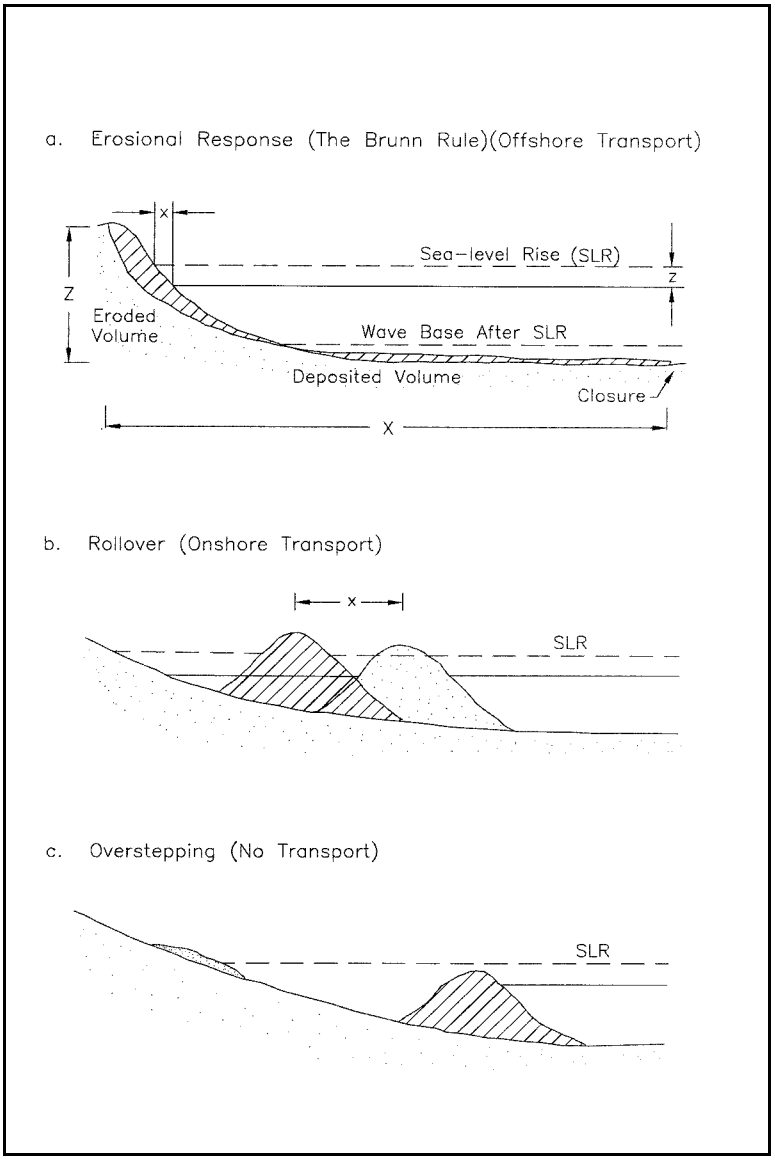

Figure IV-2-29. Three models of shoreline response to sea level rise: (a) Erosional response model/Bruun Rule assumes offshore dispersal of eroded shoreline materials; (b) Island rollover model assumes that barriers migrate landward according to the rate of sea level rise; (c) Overstepping model assumes submergence in place (adapted from Carter (1988))

- A modest influx of sediment may retard barrier migration enough to allow overstepping. If a constant volume of sediment is available, the new material must be distributed over a wider and wider base as sea level rises. The result is that vertical growth per unit time decreases. Eventually, the barrier is overtopped and the surf zone jumps forward to the bay shoreline that was formerly protected.

Figure IV-2-30. Westhampton Beach, Long Island, New York (March 1994 - view looking north towards Moriches Bay). In December 1992, the barrier island breached here during a northeaster, and 60 houses were destroyed. A large overwash fan can be seen in the bay, and to the left are houses that survived the storm. This is an example of the rollover mechanism, when sand from the ocean-facing shoreface is carried over the barrier and deposited in the back bay. The breach was repaired by the Corps of Engineers during 1993 using sand dredged from offshore. This low stretch of the barrier is particularly vulnerable, with several earlier breaches on record. In summer 1998, new homes were again being built here

- A barrier may remain in place because of a dynamic equilibrium that develops between landward and seaward sediment transport. As sea level rises, tidal prism of the lagoon increases, resulting in more efficient ebb transport. During this time, an increasing amount of washover occurs, but the effect is counteracted because sediment is being returned to the exposed shoreface. If little or no new sediment is added to the system, the sea eventually rises above the barrier crest, allowing the surf zone to jump landward to a new location (the formerly protected mainland shore).

- All three of these mechanisms may come into play at various times, depending upon environmental conditions. Sediment supply may be the crucial factor, however. Some stranded barriers, such as the ones in the northeastern Gulf of Mexico, may have maintained vertical growth because of an adequate sediment supply (Otvos 1981).

(4) In all likelihood, barriers respond to all three of the migration models, depending upon timing and local conditions such as sediment supply or preexisting topography (Carter 1988). During the initial stages of sea level rise, the shore erodes and material is dispersed offshore (the Bruun Rule). As the barrier becomes narrower, washover carries more and more sediment to the back lagoon. Eventually, the barrier may become stranded and be drowned. These models have been criticized because they are two-dimensional and do not account for variations in longshore drift. The criticisms are valid because drift is sure to vary greatly as barriers are progressively reshaped or drowned. As a result, pockets of temporarily prograding barriers may remain along a generally retreating coastline.

(5) In summary, several models have been advanced to explain how barrier islands respond to rising sea level. However, because the interactions in the coastal zone are so complex, trying to reduce barrier evolution to a series of simple scenarios is unrealistic. Much more research is needed to define the many factors that contribute to barrier evolution.

IV-2-10. Marine Deposition Coasts - Beaches

a. Introduction. Marine and lacustrine beaches comprise one of the most widely distributed coastal geomorphic forms around the world. Their importance as a buffer zone between land and sea and as a recreational and economic resource has stimulated studies by earth scientists for well over a century. Although much has been learned about how beaches form and how they are modified, the coastal environment is incredibly complex, and each location responds to unique geologic conditions and physical processes. Some of these variable factors include:

(1) Seasonal cycles.

(2) Long-term trends.

(3) Changes in relative sea level.

(4) Variations in sediment supply.

(5) Meteorological cycles.

As a result, it is difficult to characterize beaches and predict future developments without the benefit of long-term studies and observations. The following sections describe the morphology and sediments of beaches and define terms (also see Table IV-1-1). For additional information and extensive bibliographies, the reader is referred to Carter (1988), Davis (1985), Komar (1976, 1983), and Schwartz (1973, 1982).

b. General definition. ***Beach*** is defined as a gently sloping accumulation of unconsolidated sediment at the edge of a sea or other large body of water (including lakes and rivers). The landward limit may be marked by an abrupt change in slope where the beach meets another geomorphic feature such as a cliff or dune. Although this landward boundary has been consistently accepted in the literature, the seaward limit has been more broadly interpreted. Some authors have included the surf zone and the bar and trough topography in their definition because the processes that occur in the surf zone directly affect the exposed portion of the beach. The length of beaches varies greatly. Some stretch for hundreds of kilometers, such as those on the Carolina Outer Banks. Others, called pocket beaches, are restricted by headlands and may be only a few tens of meters long.

c. Major subdivisions. Beaches are part of the littoral zone, the dynamic interface between the ocean and the land. The littoral zone is bounded on one side by the landward limit of the beach and extends tens or hundreds of meters seaward to beyond the zone of wave breaking (EM 1110-2-1502). Beaches can be divided into two major zones: the foreshore and the backshore.

(1) Foreshore.

(a) The foreshore extends from the low-water line to the limit of wave uprush at high water (Figure IV-1-2). The upper portion of the foreshore is a steep slope where the high water uprush occurs. The seaward, lower, portion of the foreshore is sometimes called the *low-water or low-tide terrace.* This terrace often features low, broad ridges separated by shallow troughs, known as ridges and runnels (Figure IV-2-31).

Figure IV-2-31. Ridge and runnel system, low water terrace, Charlestown Beach, Rhode Island. Sea grass debris in the foreground marks the height of the wave runup during the previous high tide. Where should the "shoreline" be defined on this beach?

Because the foreshore is frequently subject to wave swash, it usually has a smoother surface than the backshore. There may be a minor step near the low-water mark, called the *plunge step.* Often, shell or gravel is concentrated at the base of this step, while the sediments to either side are much finer.

(b) The foreshore is sometimes called the *beachface.* However, beachface is also used in a more restricted sense to designate the steepened portion of the upper foreshore where the high-water wave uprush occurs. Therefore, it is recommended that foreshore and beachface not be used synonymously and that beachface be restricted to its upper foreshore definition.

(2) Backshore.

(a) The backshore extends from the limit of high water uprush to the normal landward limit of storm wave effects, usually marked by a foredune, cliff, structure, or seaward extent of permanent vegetation. The backshore is not affected by waves regularly, but only during storms, when high waves and storm surges allow reworking of backshore sediments. Between inundations, the backshore develops a rough surface because of vehicle or animal traffic and the development of wind-blown bed forms. On eroding beaches, the backshore may be missing, and the normal high-water uprush may impinge directly on cliffs or structures.

(b) Alternate terms for backshore are backbeach and berm. "Berm" is a common term because backshore areas are sometimes horizontal and resemble man-made berms. However, many beaches have a sloping backshore that does not resemble a berm, and some have more than one berm, representing the effects of several storms. Thus, berm is not synonymous with backshore, but may be a suitable description for selected areas. The term is sometimes used in beachfill and beach erosion control design.

(3) Coastline (or shoreline). The boundary between the foreshore and backshore, the high water line (hwl), is often defined to be the coastline. This is a practical definition because this land-water interface can be easily recognized in the field and can be approximated on aerial photographs by a change in color or shade of the beach sand (Crowell, Leatherman, and Buckley 1991). In addition, the coastline marked on the topographic sheets ("T-sheets") typically represents this same hwl, allowing a direct comparison between historic maps and aerial photographs. Some researchers have equated the coastline with the low-water line, but this boundary is not always marked by any evident feature or change in sand color. In various studies, one can find shoreline defined by almost any level datum. These inconsistencies make it difficult to compare shoreline maps prepared by different surveyors or agencies. Definition of "shoreline" often is controversial because it affects the legal definition of setback lines and other constraints placed on development in the coastal zone. A more detailed discussion of hwl identification is presented in Anders and Byrnes (1991); Crowell, Leatherman, and Buckley (1991); and Gorman, Morang, and Larson (1998).

d. Beach material.

(1) Sand beaches. On most of the coasts of the United States, the predominant beach material is sand (between 0.0625 and 2.0 mm, as defined by the Wentworth classification). Most sand beaches are composed mostly of quartz, with lesser percentages of feldspars, other minerals, and lithic (rock) fragments. Table IV-2-4 lists beach sediment types and common locations.

Table IV-2-4
Types of Beach Sediment

Type	Typical Locations
Quartz sand	East Coast of U.S. between Rhode Island and North Florida, Gulf Coast between West Florida and Mexico, portions of West Coast of U.S. and Great Lakes
Calcite shell debris	South Florida, Hawaii
Volcanic sand	Hawaii, Aleutians, Iceland
Coral sand	South Florida, Bahamas, Virgin Islands, Pacific Trust Territory
Rock fragments	Maine, Washington, Oregon, California, Great Lakes
Clay balls	Great Lakes, Louisiana

(2) Coarse beaches. Coarse beaches contain large amounts of granule-, pebble-, cobble-, and boulder-sized material (larger than 2.0 in the Wentworth classification). These beaches, found in the northeast, in the Great Lakes, and in mountainous reaches of the Pacific coast, occur under conditions where:

(a) Local streams flow with enough velocity to carry large particles to the shore.

(b) Coarse material underlies the beach (often found in areas influenced by glaciation or on metamorphic coasts).

(c) Coarse material is exposed in cliffs behind the beach (Figure IV-2-9).

The constituent material may be primarily angular rock fragments, especially if the source area, such as a cliff, is nearby (Figure IV-2-32). If the source area is far away, the most common rock types are likely to be quartzite or igneous rock fragments because these hard materials have a relatively long life in the turbulent beach environment. Softer rocks, such as limestone or shale, are reduced more readily to sand-sized particles

Figure IV-2-32. Shale beach and bluffs, southeast shore of Lake Erie, near Evans, New York. Bedding planes in the shale are lubricated by groundwater, and freeze-thaw cycles split the rock along the planes. The rubble on the beach breaks down quickly, leaving a grey sand with plate-shaped grains

by abrasion and breakage during their movement to the coast and by subsequent beach processes. Coarse beaches usually have a steeper foreshore than sand beaches.

(3) Biogenic beaches. In tropical areas, organically produced (biogenic) calcium carbonate in the form of skeletal parts of marine plants and animals can be an important or dominant constituent. The more common particles are derived from mollusks, barnacles, calcareous algae, Bryozoa, echinoids, coral, Foraminifera, and ostacods. The percentage of biogenic material in a beach varies with the rate of organic production and the amount of terrigenous material being contributed to the shore.

IV-2-11. Salt Marshes

Coastal salt marshes are low-lying meadows of herbaceous plants subject to periodic inundations. During the constructional phase of a coastline, a marsh develops when sediment deposition exceeds sediment removal by waves. Three critical conditions are required for marsh formation: abundant sediment supply, low wave energy, and a low surface gradient. Once sediment accumulation reaches a critical height, the mud flats are colonized by halophytic plants that aid in trapping sediment when flooding occurs and add organic material to the substrate.

a. Distribution of salt marshes. Marshes occur in low-energy coastal locations, and the bay side of most barriers is fringed by tidal marsh or tidal flats. Likewise, mainland shorelines adjacent to bays are also typically fringed by marsh. Along the mainland of the United States, three regional marsh types have been recognized: (1) New England marsh; (2) Atlantic and Gulf Coastal Plain marsh; and (3) Pacific coast marsh

(Frey and Basan 1985). As much as 80 to 90 percent of the Atlantic and Gulf coasts have been bordering marsh around lagoons, estuaries, and deltaic environments (Inman and Nordstrom 1971). However, along the West Coast, less than 20 percent of the coastline has marsh because Pacific marshes are usually restricted to protected locations in river mouth lagoons or tectonically controlled bays. Morphologically and sedimentologically, Pacific marshes are similar to Atlantic and Gulf coast types, although they do differ in flora species and in the unequal semidiurnal range of tides.

New England marshes are adapted to high tide ranges, high wave energy, and cold winters. Atlantic Coastal Plain marshes are abundant and almost continuous from New York to northern Florida. The warm weather, low tide range, and low wave energy coastline of both the Atlantic and Gulf coastal areas of southern Florida gives rise to mangrove marshes. The deltaic plain of Louisiana supports a unique type of marsh called "flotant," which is marsh flora sitting atop organic rich ooze. The ooze is a soft substrate that may be several meters thick over harder substrates. The rest of the Gulf Coast has fringing marsh behind its barriers.

b. Classification of salt marshes.

(1) Regional conditions such as temperature, sediment distribution, pH, Eh, and salinity contribute to the zonation of a marsh area. Plant successions, sediment accumulation, and marsh expansion vary but most marshes can be divided into two fundamental zones: low and high. Low marshes are younger, lower topographically, and usually subjected to the adjacent estuarine and marine processes. High marshes are older, occupy a higher topographic position, are more influenced by upland conditions, and are subjected to substantially fewer tidal submersions per year. The boundaries for these zones and their relationship to a given datum may differ from one coast to another. Differences in marsh boundaries might be related to tidal regularity and substrate composition. On the Atlantic coast, the tides are generally regular and near equal in semidiurnal range, whereas those on the Pacific coast are markedly unequal in semidiurnal range. Gulf Coast marshes are subjected to irregular and small-amplitude tides. Consequently, the demarcation of high and low marshes is not well-defined.

(2) Plant structures and animals are significant contributors to sediment accumulation in salt marshes (Howard and Frey 1977). Grasses dampen wind-generated waves. Stems and levees impede current flow, which helps trap suspended sediment (Deery and Howard 1977). The most obvious mechanism of sediment entrapment is the plant root system. Plant roots may extend more than a meter in depth along Georgia stream-side marshes and up to 50 cm in some adjacent habitats (Edwards and Frey 1977).

c. Sediment characteristics.

(1) Introduction.

(a) Salt marshes generally contain finer, better-sorted sediment than other intertidal environments. However, marsh substrates reflect the local and regional sediment sources. Along the Atlantic coast and shelf of the United States, Hathaway (1972) recognized two distinct clay mineral facies. The northern clay-mineral facies, extending from Maine to Chesapeake Bay, is primarily composed of illite, chlorite, and traces of feldspar and hornblende. The southern clay-mineral facies, which extends from Chesapeake to the South, is composed of chiefly kaolinite and montmorillonite.

(b) In New England and along many northern coasts overseas, peat is an important soil component of marsh substrate. Peat forms from the degradation of roots, stems, or leaves of marsh plants, particularly *Spartina* (Kerwin and Pedigo 1971). In contrast, peat is not a significant component of the southern coastal marshes except in Louisiana and Florida (Kolb and van Lopik 1966). The southern marsh substrate generally consists of silt- and clay-size sediment with a large percentage of carbon material. The major sources of organic carbon in most coastal marshes are in-situ plants and animal remains.

(c) Southern marshes can have up to 60 percent silt and up to 55 percent clay. Rapid biological decay and constant flushing prevent the accumulation of thick organic deposits. The exception to this is the "flotant" marshes, which may have over 50 percent organics. In the Unified Soil Classification, the substrate would be considered a fine-grained soil, and the field engineer could anticipate silt, clay, or organic-dominant material with low to high plasticity. Much of the organics present in marshes are incompletely oxidized, which if released into the lagoon/bay by excavation, can profoundly affect the water chemistry.

(2) Marsh plants.

(a) Marsh plants are typically tall, salt-tolerant grasses. About 20 genera of salt marsh plants are found worldwide, with the most important in North America being *Spartina*, *Juncus*, and *Salicornia* (Chapman 1974). Salt marshes are the temperate (and arctic) counterparts of tropical mangrove forests. They generally develop in shallow, low-energy environments where fine-grained sediments are deposited over sandy or till substrates (Figure IV-2-33). As the fine sediments build upward, the marsh plants can take root and become established. The established vegetation increases sediment trapping and leads to more rapid upward and outward building of marsh hummocks, which form the foundation of the marsh. The vegetation also creates lower energy conditions by absorbing wave energy and reducing current velocities, thus allowing accelerated sediment deposition.

(b) Like mangrove forests, many species of invertebrates, fish, birds, and mammals inhabit salt marshes and the adjacent tidal creeks during all or part of their life cycles. Thus, marshes are important to commercial and sport fishermen and hunters. In addition, several marsh species are considered endangered.

(c) Also like mangrove forests, man's main detrimental impact on these marshes has been dredge-and-fill operations for land reclamation and mosquito control. Air and water pollution are also serious problems. Although extensive areas of salt marsh remain on the east and Gulf coasts of North America, significant areas have been lost to development. The situation is much worse on the west coast, where most of the coastal marsh lands have been filled and perhaps permanently destroyed. Efforts to restore degraded coastal marshes have not generally been successful.

(3) Sediment transport and processes.

(a) Typically, most marshes have very slow rates of sediment accumulation, amounting to only a few millimeters per year (Pethick 1984). Natural and man-induced changes can have deleterious effects on marsh growth. For example, building levees or altering the drainage pattern can result in erosion and permanent marsh loss. Not only is suspended sediment important to vertical growth of the marsh, but biologic components, particularly organic detritus suspended in the water column, are critical to marsh health. The exchange of sediment and nutrients is dependent on the exchange between the local bodies of water.

(b) A marsh sediment budget usually includes consideration of the following factors (Davis 1985):

- Riverine sources.
- Offshore or longshore transport.

Figure IV-2-33. Estuary of the Sprague River, Maine (a small river facing the Gulf of Maine west of Popham Beach State Park). This is a typical New England salt marsh, with sinuous channels that alternately flood and drain depending on the stage of the tide. In the past, straight channels were often dug in such marshes to allow more efficient draining to reduce mosquito infestation

- Barrier washover.
- Headlands.
- Eolian transport.
- In situ organic material (i.e., peat, plant detritus, and feces).
- Other terrestrial sources.

(4) Engineering problems. In light of growing concerns to preserve natural coastal marshes and the need to implement the national policy of "no net wetland losses," many agencies are researching ways to manage and implement wetland technology. Studies have identified numerous man-made and natural causes of wetland loss in the coastal zone:

(a) Sediment deficits. Man-made modifications of natural fluvial systems interfere with natural delta-building processes.

(b) Shoreline erosion. Along many marsh shorelines, the rates of retreat have increased because of hurricanes and other storms, engineering activities along the coast, and boating.

(c) Subsidence. Sinking of the land due to natural compaction of estuarine, lagoonal, and deltaic sediments results in large-scale disappearance of wetlands. This effect is exacerbated in some areas (e.g., Galveston Bay) by subsidence caused by groundwater and oil withdrawal.

(d) Sea level rise. Eustatic sea level rise is partially responsible for increased rates of erosion and wetland loss.

(e) Saltwater intrusion. Increased salinities in wetlands harm vegetation, which makes the wetlands more vulnerable to erosion.

(f) Canals. Canals increase saltwater intrusion and disrupt the natural water flow and sediment transport processes.

(5) Marsh restoration. Many agencies, including the U.S. Army Corps of Engineers, are conducting research in the building and restoration of marshes, are developing marsh management techniques, and are developing regulatory guidelines to minimize land loss. Under the Wetlands Research Program sponsored by the USACE, new technology in a multidisciplined approach is being developed. A useful publication is the "Wetlands Research Notebook" (U.S. Army Engineer Waterways Experiment Station 1992), which is a collection of technical notes covering eight field problem areas focusing on wetlands activities in support of USACE civil works projects.

IV-2-12. Biological Coasts

a. Introduction.

(1) On many coasts, such as open wetlands, coral reef, and mangrove forest, biological organisms and processes are of primary importance in shaping the morphology. In contrast, on many other coasts, such as typical sandy beaches, biological activities do not appear to be of major significance when compared to the physical processes at work. Nevertheless, it is important to realize that biological processes are occurring on all shores; all man-made shoreline modifications must address the impact of the modification on the biological community.

(2) The types of organisms that can exist on a coast are ultimately controlled by interrelated physical factors. These include wave climate, temperature, salinity, frequency of storms, light penetration, substrate, tidal range, and the amounts of sediments and nutrients available to the system. Of these, the most important may be wave climate. The amount of wave energy dissipated at a shoreline per unit time ultimately has a dominant influence on whether the substrate is rock, sand, or silt; on the water clarity; on the delivery of nutrients; and, most importantly, on an organism's physical design and lifestyle. The physical forces exerted by a large breaking wave are several orders of magnitude greater than the typical lateral forces affecting organisms in most other environments. For example, mangroves and salt marshes require low wave-energy climates to provide suitable substrate and to keep from being physically destroyed. On the other hand, reef-building corals require reasonably high wave-energy environments to maintain the water clarity, to deliver nutrients, to disperse larvae, to remove sediment, and to limit competition and predation.

(3) Another first-order physical condition controlling biological organisms is temperature. For example, this is the primary factor that restricts mangroves and coral reefs to the tropics. Also, the formation of ice in coastal waters has a major impact on Arctic communities.

(4) Unlike many physical processes on coastlines, biological processes are generally progradational in nature, extending shorelines seaward. Reef-building organisms produce hard substrate and sediments, in addition to sheltering areas behind the reefs. Some mollusks, calcareous algae (*Hallemeda sp.*, etc.), barnacles, echinoids, bryozoa, and worms produce significant amounts of sediment. Under low-energy

conditions in the deep sea and sheltered waters, diatoms and radiolaria produce sediments. Mangroves, salt marsh, and dune vegetation trap and stabilize sediments. The erosional effect of organisms that burrow into sediments or that bore into rocks is usually of lesser importance.

b. High wave-energy coasts. Higher plants have not evolved mechanisms to enable them to physically withstand high wave-energy environments. Thus, simple plants, mainly algaes, form the bases of the food chains for these marine coastal communities.

(1) Coral reefs. Coral reefs are massive calcareous rock structures that are slowly secreted by simple colonial animals that live as a thin layer on the rock surface. The living organisms continually build new structures on top of old, extending the reefs seaward toward deeper water and upward toward the surface. Reef-building corals have algae living within their tissues in a symbiotic relationship. The algae supplies food to the coral and the coral supplies shelter and metabolic wastes as nutrients to the algae. Shallow coral reefs worldwide occupy some 284,300 km^2, about 1.2 percent of the world's continental shelf area (Spalding, Ravilious, and Green 2001). While some corals are found in temperate and Arctic waters, reef-building corals are limited by water temperature to the tropics, mainly between the latitudes of 30 deg north and south. Bermuda, in the North Atlantic, warmed by the Gulf Stream, is the highest latitude location where active coral reefs are presently found. In the United States, coral reefs are found throughout the Florida Keys and the east and west coasts of Florida, in the Hawaiian Islands, the Pacific Trust Territories, Puerto Rico, and the Virgin Islands.

(a) Reef-building corals require clear water. The corals need to be free of sediments in order to trap food particles, and their algae require sufficient light for photosynthesis. While corals can remove a certain amount of sediment from their upper surfaces, heavy siltation will bury and kill them. Light penetration limits the depth of most reef-building corals to the upper 30-50 m, though some corals grow much deeper. The upper limit of reef growth is controlled by the level of low tide. Corals cannot stand more than brief exposures out of the water (for example, during the occasional passage of a deep wave trough).

(b) While coral reefs produce rock structure, they also produce calcareous sediments. Waves and currents pulverize coral skeletons into sand-size particles. However, on many reefs, calcareous algae (Hallemeda sp.) produce a majority of the sediments. The crushed calcareous shells of other animals, such as mollusks, sea urchins, and sand dollars, also provide sediment.

(c) Coral reefs rival tropical rain forests as being among the most complex communities on earth, and rock-producing reef communities are among the most ancient life forms found in the fossil record. Because of their complexity, the dynamics of coral reefs are not yet well understood. At least 100,000 species have been named and described, but the total number inhabiting the world's reefs may exceed one million species. Scientific knowledge of the ecology of reefs has almost entirely accumulated over the last 50 years, since the development of underwater scuba breathing apparatus in the 1940's.

(d) One of the critical ecological issues of our times is the rapid degradation of coral reefs around the world by various natural and human activities. Corals are highly sensitive to increases in temperature, exhibiting a stress response known as coral bleaching. In 1998, a global mass bleaching caused mass mortalities in many areas. Worldwide, however, humans are driving more profound changes to reefs than are natural phenomena. The most widespread impacts are water pollution, dredge and fill operations, over-harvesting of fish and shellfish, and the harvesting of some corals for jewelry. For example, in Indonesia, the world's largest coral nation, 82 percent of the corals are at risk from the illegal practice of dynamite fishing (which is also devastating to fish populations). Even far from the coast, deforestation, urban sprawl, and sloppy agriculture produce vast quantities of sediment and pollution that enter the sea and degrade reefs in the vicinity of river mouths.

(e) Controlled dredging around reefs is possible and is done routinely, causing minimal impact to reef communities. Mechanical damage (from cutter heads, chains, anchors, and pipelines) is often of equal or greater concern than suspended sediment production. Improvements in navigation and positioning have made dredging near reefs more viable. Nevertheless, careful monitoring is mandated in most cases.

(f) Reefs are of major economic importance to the communities along which they are located. For millenia, coastal peoples relied on coral reefs as a source of food. Spurgeon (1992) classifies their economic benefits as:

* Direct extractive uses - fisheries, building material.

* Direct non-extractive uses - tourism.

* Indirect uses - biological support for a variety of other ecosystems.

Reef tourism is now a major global industry. Diving tourism is ubiquitous and now occurs in 91 countries and states (Spalding, Ravilious, and Green 2001). One major benefit of mass tourism is that it had brought to public consiousness the issues of the fragility of reef ecosystems and the need to preserve the world's remaining reefs. Marine protected areas are becoming a critical tool in the preservation of remaining reefs, and some 660 protected areas worldwide incorporate reefs. Tourist income is helping some remote communities police and protect their reefs. The downside of mass tourism is the haphazard growth of infrastructure along the shore. Many vacation communities are built on remote coasts where resources, such as fresh water, are scarce and where trash and sewage effluent are not properly managed.

(g) An additional benefit of reefs is the shelter from waves that they provide to adjacent shores. As an example, the south and southwestern coast of Sri Lanka is battered by waves that travel unhindered across the Indian Ocean. In the past, the coral reefs that surrounded the coast served as buffers against the intense wave energy. But illegal reef breaking and coral mining, combined with negative impacts of tourism and development (sewage, agricultural pollution, physical damage) have greatly reduced the effectiveness of the reef barriers. As a result, much of the Sri Lankan south coast is now experiencing severe erosion (Young and Hale 1998).

(h) Stoddard (1969) has identified four major forms of large-scale coral reef types: fringing reefs, barrier reefs, table reefs, and atolls.

(i) *Fringing reefs* generally consist of three parts: a fore reef, a reef crest, and a back reef. The *fore reef* usually rises steeply from deep water. It may have spur and groove formations of coral ridges interspersed with sand and rubble channels. The *reef crest* usually forms a continuous wall rising to the low tide level. This usually occurs within a few hundred meters from shore. The seaward side of this area, called the *buttress zone*, receives the brunt of the wave action. Between the reef crest (or flat) and the shoreline, the reef usually deepens somewhat in the back reef area. This area typically contains much dead coral as well as rock, rubble, sand, and/or silt. It also contains live coral heads, algae, eel grass, etc. Fringing reefs form as the beginning stages in the evolution of atolls and possibly barrier reefs.

(j) *Barrier reefs* grow on the continental shelf where suitable solid substrate exists to serve as a foundation. Their form is typically a long coral embankment separated from the mainland by a lagoon that may be several kilometers wide. The lagoon is usually flat-floored and may be as much as 16 km wide and 35 to 75 m in depth. Although similar to fringing reefs, barrier reefs are much more massive, the reef crests are much further from shore, and the back reef areas are deeper. Protected shorelines behind barrier reefs are characterized by mangrove swamps and are usually progradational. The seafloor on the seaward side slopes steeply away into deeper water and is covered by coral rubble.

(k) *Table reefs* grow from shallow banks on the seafloor that have been capped with reef-forming organisms. They cover extensive areas but do not form barriers or enclose lagoons.

(l) *Atolls* are ring-shaped reefs that grow around the edges of extinct volcanic islands, enclosing lagoons of open water. The shallow lagoons may contain patch reefs. Atolls are primarily found in isolated groups in the western Pacific Ocean. Small low islands composed of coral sand may form on these reefs. These islands may hold enough of a fresh water lens to support human life, but the islands are quite vulnerable to inundation and to tropical storms. The first theory concerning the development of atolls, the subsidence theory proposed by Charles Darwin in 1842, has been shown to be basically correct (Strahler 1971). Figure IV-2-34 illustrates the evolution of an atoll.

(m) The development of atolls begins with an active volcano rising from the ocean floor and forming a volcanic island. As the volcano ceases activity, a fringing reef forms along the shore. Over geologic time, erosion of the volcanic island and subsidence due to general aging of the ocean basin cause the island to drop below sea level. The actively growing fringing reef keeps pace with the subsidence, building itself upward until a barrier reef and lagoon are formed. As the center of the island becomes submerged, the reef continues its upward growth, forming a lagoon. During the development, the lagoon floor behind the reef accumulates coral rubble and other carbonate sediments, which eventually completely cover the subsiding volcanic island.

(2) Worm reefs. A type of biogenic reef that is not related to coral reefs is that produced by colonies of tubeworms. Serpulid worms and Sabellariid worms are two types known to form significant reef structures by constructing external tubes in which they live. The Serpulids build their tubes from calcareous secretions and the Sabellariids by cementing particles of sand and shell fragments around their bodies. Colonies of these worms are capable of constructing massive structures by cementing their tubular structures together. As new tubes are continually produced over old ones, a reef is formed. These reefs typically originate from a solid rocky bottom, which acts as an anchoring substrate. Worm reefs are most commonly found in sub-tropical and tropical climates (e.g., east coast of Florida). Reefs of this nature can play an important role in coastal stabilization and the prevention of coastal erosion.

(3) Oyster reefs. Oysters flourish under brackish water conditions in lagoons, bays, and estuaries. The oysters cement their shells to a hard stable substrata including other oyster shells. As new individuals set onto older ones, a reef is formed. These reefs can form in temperate as well as tropic waters.

(a) Oysters found around the United States are part of the family *Ostreidae*. The Eastern, or American oyster (*Crassostrea virginica*) is distributed along the entire east coast of North America from the Gulf of St. Lawrence through the Gulf of Mexico to the Yucatan and the West Indies. The other major North American species is *Ostrea lurida*, which ranges along the Pacific coast from Alaska to Baja California (Bahr and Lanier 1981).

(b) Intertidal oyster reefs range in size from isolated scattered clumps a meter high to massive solid mounds of living oysters anchored to a dead shell substrate a kilometer across and 100 m thick (Pettijohn 1975). Reefs are limited to the middle portion of the intertidal zone, with maximum elevation based on a minimum inundation time. The uppermost portion of a reef is level, with individual oysters pointing upwards. At the turn of the century, vast oyster flats were found along the Atlantic coast in estuaries and bays. In South Carolina, the flats covered acres and sometimes square miles (cited in Bahr and Lanier (1981)).

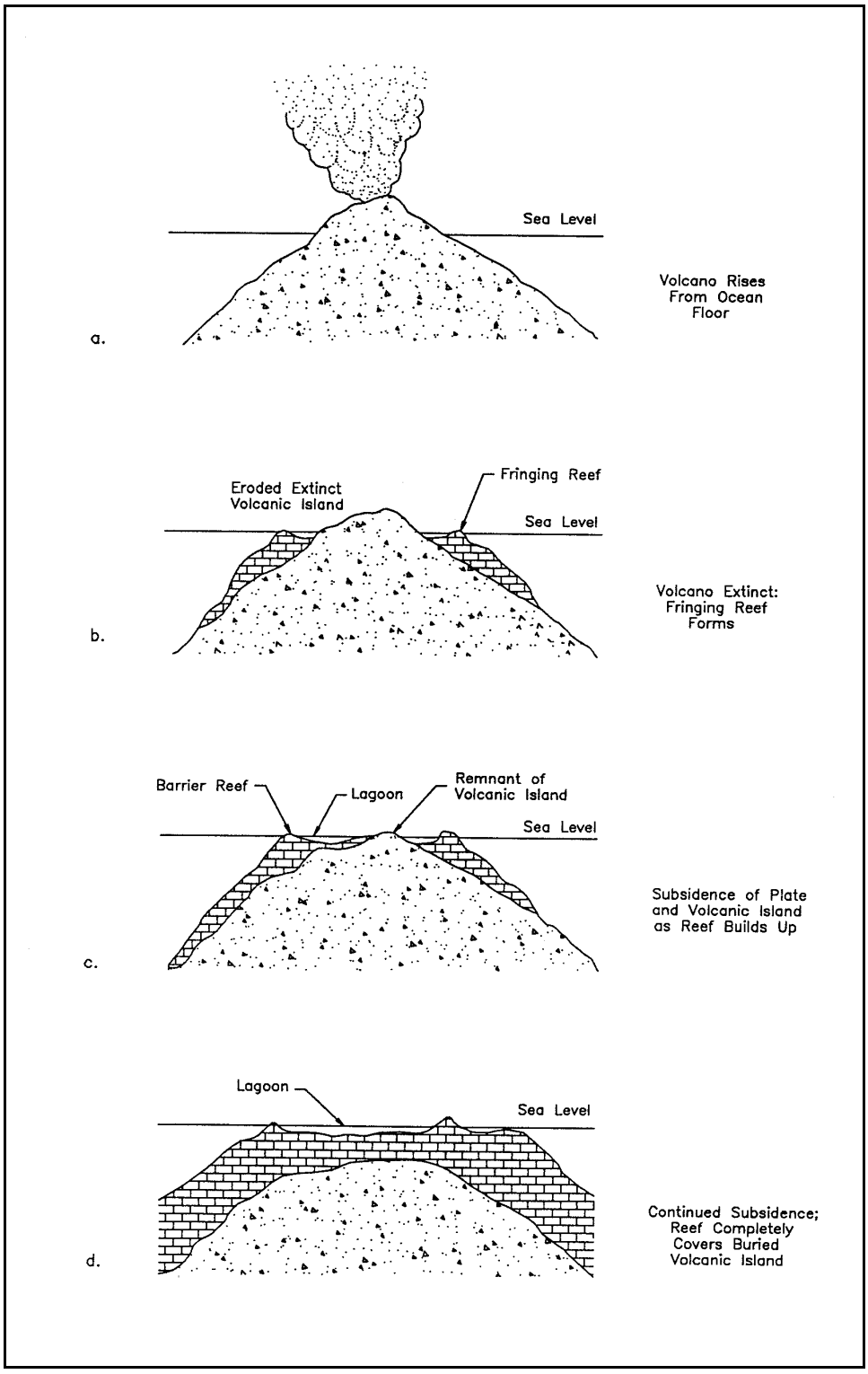

Figure IV-2-34. Evolution of a coral island: (a) Active volcano rising from the seafloor, (b) Extinct volcanic island with fringing reef, (c) Subsiding island; reef builds upward and seaward, forming barrier reef, (d) Continued subsidence causing remnant volcanic island to be completely submerged. Growth continues upward and seaward until remnant volcano is covered (adapted from Press and Siever (1986))

(c) Oyster reefs serve an important biological role in the coastal environment. The reefs are a crucial habitat for numerous species of microfauna and macrofauna. The rough surface of a reef flat provides a huge surface area for habitation by epifauna, especially vital in the marsh-estuarine ecosystem that is often devoid of other hard substrate. The high biological productivity of reef environments underscores one of the reasons why reefs must be protected and preserved.

(d) Oyster reefs play important physical and geological roles in coastal dynamics because they are wave-resistant structures that can biologically adapt to rising sea level. Reefs affect the hydrologic regime of salt marsh estuaries in three ways: by modifying current velocities, by passively changing sedimentation patterns, and by actively augmenting sedimentation by biodeposition. (Biological aggradation increases the size of suspended particles and increases their settling rates.) As reefs grow upward and laterally, modify energy fluxes by damping waves and currents, and increase sedimentation, they ultimately produce major physiographic changes to their basins. These changes can occur on short time scales, on the order of hundreds of years (Bahr and Lanier 1981). During geologic history, massive reefs have accumulated in many areas, some of which became reservoirs for oil and gas.

(e) Although oysters are adapted to a wide range of temperature, turbidity, and salinity conditions, they are highly susceptible to man-made stresses. These stresses on oyster communities can be classified into eight categories (Bahr and Lanier 1981):

- Physical sedimentation, especially from dredging or boat traffic.
- Salinity changes due to freshwater diversion or local hydrologic alterations.
- Eutrophication (oxygen depletion) due to algae growth in water that is over-enriched with organic matter.
- Toxins from industrial and urban runoff.
- Physical impairment of feeding structures by oil.
- Thermal loading, primarily from power plants.
- Overharvesting.
- Loss of wetlands.

There has been a recorded significant decline in the health and extent of living United States east coast oyster reefs since the 1880's, although the data are sometimes conflicting because ground-level surveys are difficult to conduct (Bahr and Lanier 1981). It is easy to account for the declines of reefs near population and industrial centers, but the declines are more difficult to explain in more pristine areas of the coast (e.g. the Georgia coast near Sapelo Island). Population changes may be due, in part, to natural cycles of temperature and salinity or fecundity.

(f) Because oyster reefs are susceptible to fouling and silting, it is important that geologists and engineers consider sediment pathways during the planning phases of coastal construction and dredging projects or stream diversion and other watershed changes. As discussed earlier, dredging near reefs is technically feasible as long as careful technique is observed and environmental conditions are monitored.

(g) In summary, oyster reefs serve critical biological and physical purposes in the estuarine and coastal marsh environment. They enhance biological productivity, provide stable islands of hard substrate in

otherwise unstable soft muddy bottoms, modify hydrodynamic flows and energy fluxes. With respect to shore protection, reefs are a biological wave damper that can accommodate rising sea level as long as they are alive. It is essential that reefs be protected from wanton destruction by pollution and other stresses imposed by human development.

(4) Rocky coasts.

(a) Kelp beds. Kelp forests are formed by various species of algae that attach to hard substrate with a root-like system called a *holdfast*. Some (prominently *Macrosistus sp.*) can grow many tens of meters in length up to the water surface, where their tops float and continue to grow. The plants are quite rubbery and can withstand significant wave action. Kelp beds are found along rocky shorelines having cool clear water. In North America, they occur along much of the Pacific coast and, to a lesser extent, along the North Atlantic coast. Kelp beds are, to some extent, the functional temperate latitude counterpart of coral reefs (Carter 1988).

(b) Kelp biological communities. Kelp beds harbor extensive biological communities that include fish, sea otters, lobster, starfish, mollusks, abalones, and many other invertebrates. In addition, kelp beds absorb wave energy, helping to shelter beaches. Man's main impact has been the commercial harvesting of various portions of this community, including the kelp. In the past, hunting sea otters for their pelts allowed sea urchins to multiply, and the overpopulation of sea urchins grazed and destroyed many beds. Today, the reestablishment of some sea otter populations has led to conflicts with shell fishermen. Water pollution is also a problem in some areas.

(c) Rock reefs and shorelines. Submerged rock reefs provide substantial habitat for organisms. They provide a place of attachment for sessile organisms, and the crevices provide living spaces and havens of refuge for mobile organisms such as fish and lobsters. These structures are a boon to sports fishermen, and many artificial reefs have been built on sandy seafloors out of a wide array of materials. Rocky shorelines have communities of organisms living in the intertidal and subtidal zones. These may or may not be associated with offshore kelp bed or coral reef communities.

(5) Sandy coasts. Much of the biological activity on sandy coasts is confined to algae, various invertebrates, and fish living within the water column. Of these, fish, shrimp, and crabs have the greatest economic importance. In addition, there are infaunal filter feeders, mainly mollusks and sand dollars, that live just beneath the sand surface.

(a) One important and often overlooked biological activity on some sandy beaches is their use as nesting areas by a variety of migratory animals. These include sea turtles, birds, marine mammals, and fish. In North America, many of these species are threatened or endangered, including all five species of sea turtles and some birds such as the piping plover, the snowy plover, and the least tern. For most of these species, their problems are directly related to conflicts with man's recreational use of beaches and the animals' inability to use alternate nesting sites. Fortunately, some states have implemented serious ecological programs to help save these threatened species. For example, Florida has rigorous laws preventing disruption of nesting turtles, and many Florida municipalities have found that maintaining healthy natural biological communities is an excellent way to lure tourists.

(b) Plants occupying sand dunes are characterized by high salt tolerance and long root systems that are capable of extending down to the freshwater table (Goldsmith 1985). Generally, these plants also generate rhizomes that grow parallel to the beach surface. Beach plants grow mainly in the back beach and dune areas beyond the zone of normal wave uprush. The plants trap sand by producing low energy conditions near the ground where the wind velocity is reduced. The plants continue to grow upward to keep pace with the accumulation of sand, although their growth is eventually limited by the inability of the roots to reach

dependable water. The roots also spread and extend downward, producing a thick anchoring system that stabilizes the back beach and dune areas. This stabilization is valuable for the formation of dunes, which provide storm protection for the entire beach. The most common of these plants are typically marram grass, saltwort, American sea grass, and sea oats. With time, mature dunes may accumulate enough organic nutrients to support shrub and forest vegetation. The barrier islands of the U.S. Atlantic coast and the Great Lakes shores support various species of *Pinus*, sometimes almost to the water's edge.

c. Low wave-energy coasts. In locations where the wave climate is sufficiently low, emergent vegetation may grow out into the water. Protection from wave action is typically afforded by local structures, such as headlands, spits, reefs, and barrier islands. Thus, the vegetation is usually confined to the margins of bays, lagoons, and estuaries. However, in some cases, the protection may be more regional in extent. Some of the mangrove forests in the Everglades (south Florida) and some of the salt marshes in northwest Florida and Louisiana grow straight into the open sea. The same is true for freshwater marshes in bays and river mouths in the Great Lakes.

(1) General.

(a) Only a few higher plants possess a physiology that allows them to grow with their roots in soils that are continuously saturated with salt water. These are the mangroves of the tropics and the salt marsh grasses of the higher latitudes. The inability of other plants to compete or survive in this environment allows small groups of species or single species to cover vast tracts of some coastal areas. These communities typically show zonations with different species dominant at slightly different elevations, which correspond to different amounts of tidal flooding. The seaward limit of these plants is controlled by the need for young plants to have their leaves and branches above water. To this end, some mangroves have seedlings that germinate and begin growing before they drop from the parent tree. Upland from these communities, a somewhat larger number of other plants, such as coconuts and dune grasses, are adapted to live in areas near, but not in, seawater.

(b) Understanding and appreciation of the importance of these types of coastal areas are growing. Former attitudes that these areas were mosquito-infested wastelands imminently suitable for dredge- and-fill development are being replaced by an appreciation of their great economic importance as nursery grounds for many species of fish and shellfish, of their ability to remove pollutants, of their ability to protect upland commercial development from storms, of their fragility, and of their beauty.

(2) Mangroves.

(a) *Mangroves* include several species of low trees and shrubs that thrive in the warm, shallow, saltwater environments of the lower latitudes. Worldwide, there are over 20 species of mangroves in at least 7 major families (Waisel 1972). Of these, the red, white, and black mangroves are dominant in south Florida and the Caribbean. They favor conditions of tidal submergence, low coastal relief, saline or brackish water, abundant fine sediment supply, and low wave energy. Mangroves have the ability to form unique intertidal forests that are characterized by dense entangled networks of arched roots that facilitate trapping of fine sediments, thereby promoting accretion and the development of marshlands. The *prop roots* and *pneumatophores* also allow the plants to withstand occasional wave action and allow oxygen to reach the roots in anaerobic soils. The prime example in the United States is the southwest shore of Florida, in the Everglades National Park.

(b) Mangrove coasts are crucial biological habitats to a wide variety of invertebrates, fish, birds, and mammals. In the past, the primary cause of their destruction has been dredge-and-fill operations for the reclamation of land and for mosquito control.

d. Other sources of biogenic sediment in the coastal zone. In areas of high biological activity, organically derived sediments may account for a significant proportion of the sediment composition, especially where terrigenous sediment supplies are low. These biogenic materials, consisting of remains of plants and animals and mineral matter produced by plants and animals, accumulate at beaches, estuaries, and marshlands.

(1) The most familiar types of biogenic sediments are hard calcareous skeletal parts and shell fragments left behind by clams, oysters, mussels, corals, and other organisms that produce calcareous tests. In tropical climates, the sediment commonly consists of coral fragments and calcareous algal remains. Siliceous tests are produced by most diatoms and radiolaria. Sediments predominately containing carbonate or calcareous material are generally referred to as *calcarenites*, while sediments composed predominantly of siliceous matter are referred to as *diatomites* or *radiolarites*, depending upon which organism is most responsible for the sediment (Shepard 1973). In the Great Lakes and some inland U.S. waterways, the zebra mussel has proliferated since the mid-1980's, and now some shorefaces are covered with mussel shell fragments to a depth of over 10 cm. The mussels are a serious economic burden because they choke the inlets of municipal water systems and coolant pipes.

(2) In some areas, wood and other vegetation may be introduced into the sediments in large quantities. This is especially common near large river mouths and estuaries. This organic material may become concentrated in low energy environments such as lakes and salt marshes, eventually producing an earthy, woody composition known as *peat* (Shepard 1973). Peat exposed on the shoreface has been used as an indicator of marine transgression and barrier island retreat (Figure IV-2-35) (Dillon 1970). In Ireland and Scotland, peat is dried and used as a fuel.

IV-2-13. Continental Shelf Geology and Topography

a. Introduction. The geology of the world's continental shelves is of direct significance to coastal engineers and managers in two broad areas. First, the topography of the shelf affects coastal currents and wave climatology. Wave refraction and circulation models must incorporate shelf bathymetry. Bathymetry was incorporated in the wave hindcast models developed by the USACE Wave Information Study (See references in Part II-8). Second, offshore topography and sediment characteristics are of economic importance when offshore sand is mined for beach renourishment or dredged material is disposed offshore.

b. Continental shelf sediment studies.

(1) The Inner Continental Shelf Sediment and Structure (ICONS) study was initiated by the Corps of Engineers in the early 1960's to map the morphology of the shallow shelf and find sand bodies suitable for beach nourishment. This program led to a greater understanding of shelf characteristics pertaining to the supply of sand for beaches, changes in coastal and shelf morphology, longshore sediment transport, inlet migration and stabilization, and led to a better understanding of the Quaternary shelf history. ICONS reports are listed in Table IV-2-5.

Figure IV-2-35. Peat horizon exposed on the shoreface, Ditch Plains, Long Island, New York (March 1998). The peat is in-situ, indicating that lagoonal sediments accumulated here before the barrier beach retreated over the marsh. The peat layer was about 1 m above the ocean water level at the time the photograph was taken. The dune resting on the peat is about 2 m thick

(2) Since the 1970's, the Minerals Management Service (MMS), a bureau of the U.S. Department of the Interior, has been tasked with managing the mineral resources of the Outer Continental Shelf. In conducting its mission, the MMS has sponsored many surveys and studies of mineral resources on the continental shelf. These studies can be accessed via the MMS' Environmental Studies Program Information System (ESPIS) at:

http://mmspub.mms.gov/espis/

(3) For beach renourishment projects, U.S. Army Corps of Engineers Districts typically obtain information on sand resources near the proposed project area from various sources:

(a) In-house studies, typically from vibracoring or rotary borings.

(b) Contracts with marine geophysics/geotechnical surveyors.

(c) The U.S. Geological Survey.

Table IV-2-5
U.S. Army Corps of Engineers Inner Continental Shelf Sediment and Structure (ICONS) Reports

Location	References[1]
Atlantic Coast	
Massachusetts Bay	Meisburger 1976
New York - Long Island Sound	Williams 1981
New York - Long Island shelf	Williams 1976
New York Bight	Williams and Duane 1974
New Jersey - central	Meisburger and Williams 1982
New Jersey - Cape May	Meisburger and Williams 1980
Delaware, Maryland, Virginia	Field 1979
Chesapeake Bay entrance	Meisburger 1972
North Carolina - Cape Fear	Meisburger 1977; Meisburger 1979
Southeastern U.S. shelf	Pilkey and Field 1972
Florida - Cape Canaveral to Georgia	Meisburger and Field 1975
Florida - Cape Canaveral	Field and Duane 1974
Florida - Palm Beach to Cape Kennedy	Meisburger and Duane 1971
Florida - Miami to Palm Beach	Duane and Meisburger 1969
Gulf of Mexico	
Texas - Galveston County	Williams, Prins, and Meisburger 1979
Lake Erie	
Pennsylvania	Williams and Meisburger 1982
Ohio	Williams et al. 1980; Carter et al. 1982
Lake Michigan	
Southeast shore	Meisburger, Williams, and Prins 1979
Sampling tools and methods	
Pneumatic coring device	Fuller and Meisburger 1982
Vibratory samplers	Meisburger and Williams 1981
Data collection methods	Prins 1980

[1] Complete citations are listed in Appendix A

(d) U.S. Army Engineer Research and Development Center, Waterways Experiment Station.

(e) State and local agencies.

New geographic data collected by the Federal Government is documented with Metadata that can be accessed from various computer servers. Unfortunately, there is no consistent method of cataloging historical data or reports. Users who need information on sand resources near the coast must contact the Corps District responsible for that particular area.

c. Continental shelf morphology. Surficial sediment on the continental shelves is largely dependent upon the type of coast (i.e. collision, or leading, versus trailing) and the presence of rivers that supply material to the coast.

(1) Leading edge shelves, such as the Pacific coasts of North and South America, are typically narrow and steep. Submarine canyons, which sometimes cut across the shelves almost to the shore (Shepard 1973), serve as funnels that carry sediment down to the abyssal plain. Normally, very little sand is available offshore.

(2) Trailing edge shelves are, in contrast, usually wide and flat, and the heads of canyons usually are located a considerable distance from shore. Nevertheless, a large amount of sediment is believed to move down these canyons (Emery 1968). Off the United States Atlantic coast, the broad continental shelf contains a vast amount of sand. Unfortunately, much of this sand is not available for beach renourishment because it is either too far from shore or its composition is incompatible with the beaches where it is to be placed (i.e., contains too much rock, shell fragment, mud, or organic material or the grain size is different than the size of the native material where it is to be placed).

d. Examples of specific features - Atlantic seaboard.

(1) The continental shelf of the Middle Atlantic Bight of North America, which is covered by a broad sand sheet, is south of the region directly influenced by Pleistocene glacial scouring and outwash. This sand sheet is divided into broad, flat, plateau-like compartments dissected by shelf valleys that were excavated during the Quaternary lowstands of the sea. Geomorphic features on the shelf include low-stand deltas (cuspate deltas), shoal and cape retreat massifs (bodies of sand that formed during a transgressive period), terraces and scarps, cuestas (asymmetric ridges formed by the outcrop of resistant beds), and sand ridges (Figure IV-2-36) (Swift 1976; Duane et al. 1972).

(2) The larger geomorphic features of the Middle Atlantic Bight are constructional features molded into the Holocene sand sheet and altered in response to storm flows. Off the coasts of Delaware, Maryland, and Virginia, shoreface-connected shoals appear to have formed in response to the interaction of south-trending, shore-parallel, wind-generated currents with wave- and storm-generated bottom currents during winter storms. Storm waves aggrade crests, while fair-weather conditions degrade them. A second shoal area further offshore at the 15-m depth is indicative of a stabilized sea level at that elevation. These shoals may be suitable sources of sand for beach renourishment. However, the often harsh wave conditions off the mid-Atlantic seaboard may limit the economic viability of mining these shoals. The origin and distribution of Atlantic inner shelf sand ridges are discussed in McBride and Moslow (1991).

(3) Linear shoals of the Middle Atlantic Bight tend to trend northeast (mean azimuth of 32 deg) and extend from the shoreline at an angle between 5 and 25 deg. Individual ridges range from 30 to 300 m in length, are about 10 m high, and have side slopes of a few degrees. The shoal regions extend for tens of kilometers. The crests are composed of fine-medium sand, while the ridge flanks and troughs are composed of very fine-fine sand. The mineralogy of shoals reflects that of the adjacent beaches.

e. Riverine influence.

(1) Rivers provide vast amounts of sediment to the coast. The 28 largest rivers of the world, in terms of drainage area (combined size of upland drainage area and subaerial extent of deltas), discharge across trailing-edge and marginal sea coasts (Inman and Nordstrom 1971). Because the larger rivers drain onto trailing edge coasts, these shores tend to have larger amounts of available sediment, which is deposited across a wide continental shelf. The sediment tends to remain on the shelf and is only lost to the abyssal plains when deltas prograde out across the continental rise (e.g., the Mississippi and Nile Deltas) or when submarine canyons are incised across the shelf (e.g., Hudson River sediment funnels down the Hudson Canyon).

(2) The Columbia River, which is the 29th largest river in the world, is the largest one to drain across a collision coast. Until dams were built during the mid-20th century, the Columbia carried a major sediment load, which was deposited on the ebb shoal off its mouth. This shoal provided the sand that formed the Long Beach peninsula and fed the beaches as far north as the Olympic Peninsula. The Columbia appears to be an exception - on most collision coasts, canyons frequently cut across the shelf almost to the shore (Shepard 1973), therefore resulting in the direct loss of sediment from the coastal zone.

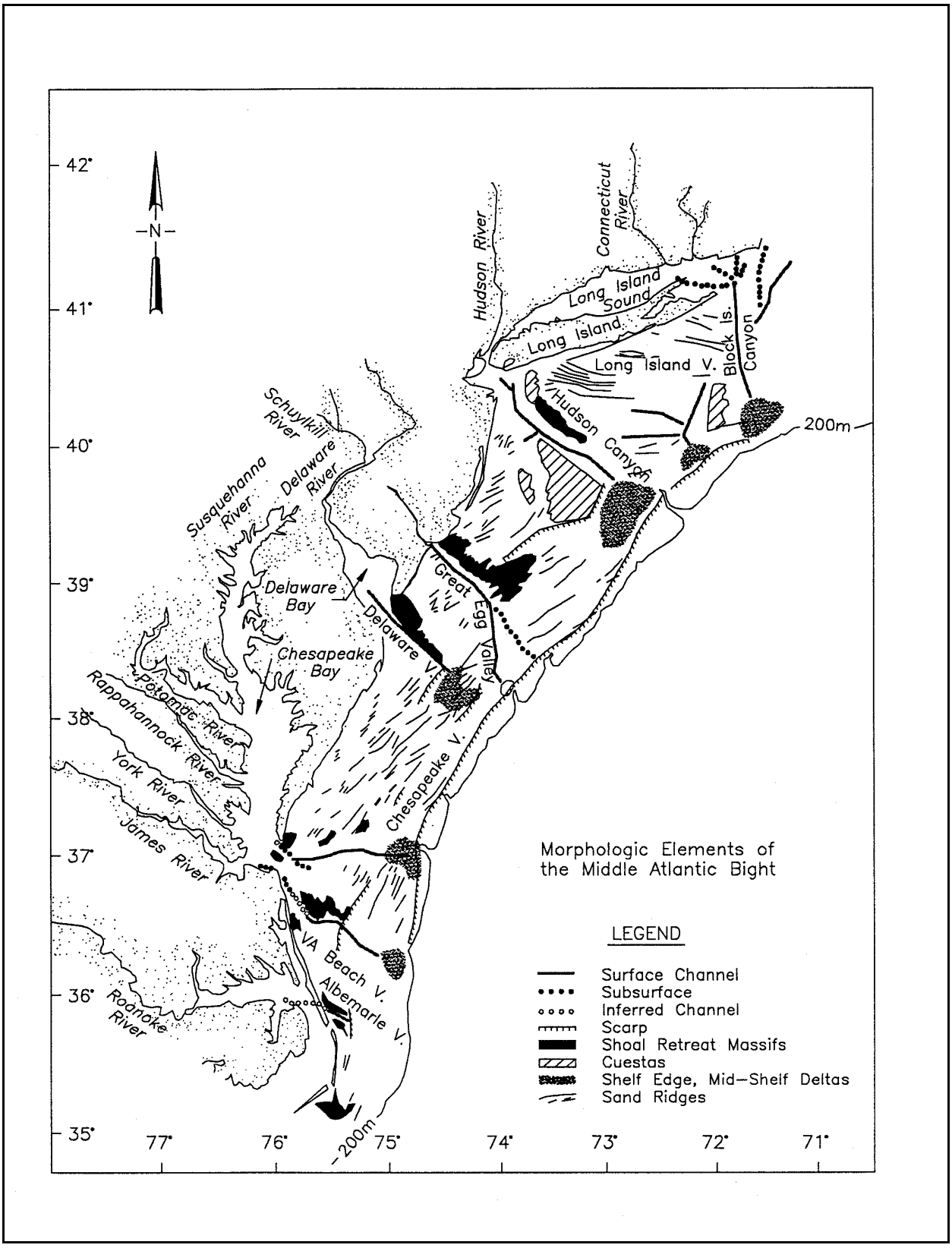

Figure IV-2-36. Morphology of the Middle Atlantic Bight (from Swift (1976)). Sand ridges close to shore may be suitable sources of sand for beach renourishment

IV-2-14. References

EM 1110-2-1502
Coastal Littoral Transport

Anders and Byrnes 1991
Anders, F. J., and Byrnes, M. R. 1991. Accuracy of shoreline change rates as determined from maps and aerial photographs, *Shore and Beach*, Vol 51, No. 1, pp. 17-26.

Baeteman 1994
Baeteman, C. 1994. Subsidence in coastal lowlands due to groundwater withdrawal: the geological approach, "Coastal Hazards, Perception, Susceptibility and Mitigation," Finkl, C. W., Jr., (ed.), *Journal of Coastal Research* Special Issue No. 12, pp 61-75.

Bagnold 1941
Bagnold, R. A. 1941. *The Physics of Windblown Sand and Desert Dunes,* Methuen, London, UK.

Bahr and Lanier 1981
Bahr, L. M., and Lanier, W. P. 1981. "The Ecology of Intertidal Oyster Reefs of the South Atlantic Coast: A Community Profile," Report FWS/OBS-81/15, U.S. Fish and Wildlife Service, Office of Biological Services, Washington, DC.

Ballard 1983
Ballard, R. D. 1983. *Exploring our Living Planet*, National Geographic Society, Washington, DC.

Bates and Jackson 1984
Bates, R. L., and Jackson, J. A. 1984. *Dictionary of Geologic Terms,* 3rd ed., Anchor Press/Doubleday, Garden City, NY.

Bowes 1989
Bowes, M. A. 1989. "Review of the Geomorphic Diversity of the Great Lakes Shore Zone in Canada," Heritage Resources Centre, University of Waterloo, Waterloo, Canada.

Boyd, Dalrymple, and Zaitlin 1992
Boyd, R., Dalrymple, R., and Zaitlin, B. A. 1992. "Classification of Elastic Coastal Depositional Environments," *Sedimentary Geology*, Vol 80, pp 139-150.

Bruun 1962
Bruun, P. M. 1962. "Sea-level Rise as a Cause of Shore Erosion," *Proceedings, Journal of the Waterways and Harbor Division,* American Society of Civil Engineers, Vol 88, No. WW1, pp 117-130.

Bullard 1962
Bullard, F. M. 1962. *Volcanoes in History, in Theory, in Eruption*, University of Texas Press, Austin, TX.

Carter 1988
Carter, R. W. G. 1988. *Coastal Environments: An Introduction to the Physical, Ecological, and Cultural Systems of Coastlines,* Academic Press, London, UK.

Carter, Curtis, and Sheehy-Skeffington 1992
Carter, R. W. G., Curtis, T. G. F., and Sheehy-Skeffington, M. J. 1992. *Coastal Dunes, Geomorphology, Ecology, and Management for Conservation*, A. A. Balkema, Rotterdam, The Netherlands.

Carter, Williams, Fuller, and Meisburger 1982
Carter, C. H., Williams, S. J., Fuller, J. A., and Meisburger, E. P. 1982. "Regional Geology of the Southern Lake Erie (Ohio) Bottom: A Seismic Reflection and Vibracore Study," Miscellaneous Report No 82-15, Coastal Engineering Research Center, U.S. Army Engineer Waterways Experiment Station, Vicksburg, MS.

Chapman 1974
Chapman, V. J. 1974. "Salt Marshes and Salt Deserts of the World," *Ecology of Halophytes*, R. J. Reimold and W. H. Queen, eds., Academic Press, NY, pp 3-19.

Coastal Barriers Study Group 1988
Coastal Barriers Study Group. 1988. Report to Congress: Coastal Barrier Resources System, Recommendations for Additions to or Deletions from the Coastal Barrier Resources System, (in 22 Volumes covering the United States and territories), U.S. Department of the Interior, Washington, DC.

Coleman and Wright 1971
Coleman, J. M., and Wright, L. D. 1971. "Analysis of Major River Systems and Their Deltas: Procedures and Rationale, with Two Examples," Technical Report No. 95, Coastal Studies Institute, Louisiana State University, Baton Rouge, LA.

Cotton 1952
Cotton, C. A. 1952. "Criteria for the Classification of Coasts," Abstract of papers, 17th Congress of International Geographers, Washington, DC, p 15.

Cromwell 1971
Cromwell. 1971. Barrier Coast Distribution: A World-wide Survey," Abstracts, Second Coastal and Shallow Water Research Conference, U.S. Office of Naval Research Geography Program, University Press, University of Southern California, Los Angeles, CA, p 50.

Crowell, Leatherman, and Buckley 1991
Crowell, M., Leatherman, S. P., and Buckley, M. K. 1991. "Historical Shoreline Change: Error Analysis and Mapping Accuracy," *Journal of Coastal Research,* Vol 7, No. 3, pp 839-852.

Dalrymple, Silver, and Jackson 1973
Dalrymple, G. B., Silver, E. I., and Jackson, E. D. 1973. "Origin of the Hawaiian Islands," *American Scientist*, Vol 61, No. 3, pp 294-308.

Dalrymple, Zaitlin, and Boyd 1992
Dalrymple, R. W., Zaitlin, B. A., and Boyd, R. 1992. "Estuarine Facies Models: Conceptual Basis and Stratigraphic Implications," *Journal of Sedimentary Petrology*, Vol 62, No. 6, pp 1130-1146.

Dana 1849
Dana, J. D. 1849. "Geology," *Report of the U.S. Exploring Expedition, 1838-1842*, C. Sherman, Philadelphia, PA.

Davis 1896a
Davis, W. M. 1896a. "Shoreline Topography," reprinted in: *Geographical Essays,* Dover Publications, New York, NY (1954 reprint).

Davis 1985
Davis, R. A., Jr., ed. 1985. *Coastal Sedimentary Environments,* 2nd ed., Springer-Verlag, New York, NY.

de Blij and Muller 1993
de Blij, H. J., and Muller, P. O. 1993. *Physical Geography of the Global Environment*, John Wiley & Sons, New York, NY.

Deery and Howard 1977
Deery, J. R., and Howard, J. D. 1977. "Origin and Character of Washover Fans on the Georgia Coast, USA," *Gulf Coast Association Geologic Society Transactions,* Vol 27, pp 259-271.

Dillon 1970
Dillon, W. P. 1970. "Submergence Effects on a Rhode Island Barrier and Lagoon and Inferences on Migration of Barriers," *Journal of Geology*, Vol 78, pp 94-106.

Dingler, Reiss, and Plant 1993
Dingler, J. R., Reiss, T. E., and Plant, N. G. 1993. "Erosional Patterns of the Isles Dernieres, Louisiana, in Relation to Meteorological Influences," *Journal of Coastal Research*, Vol 9, No. 1, pp 112-125.

Dolan and Hayden 1983
Dolan, R., and Hayden, B. 1983. "Patterns and Prediction of Shoreline Change," *CRC Handbook of Coastal Processes,* P. D. Komar, ed., CRC Press, Boca Raton, FL, pp 123-165.

Duane and Meisburger 1969
Duane, D. B., and Meisburger, E. P. 1969. "Geomorphology and Sediments of the Nearshore Continental Shelf, Miami to Palm Beach, Florida," Technical Memorandum No. 29, Coastal Engineering Research Center, USAE Waterways Experiment Station, Vicksburg, MS.

Duane, Field, Meisburger, Swift, and Williams 1972
Duane, D. B., Field, M. E., Meisburger, E. P., Swift, D. J. P., and Williams, S. J. 1972. "Linear Shoals on the Atlantic Inner Continental Shelf, Florida to Long Island," *Shelf Sediment Transport*, D. J. P. Swift, D. B. Duane, and O. H. Pilkey, eds., Dowd, Hutchinson, and Ross, Stroudsburg, PA.

Dyer 1979
Dyer, K. R., ed. 1979. *Estuarine Hydrography and Sedimentation, a Handbook*, Cambridge University Press, Cambridge, UK.

Edwards and Frey 1977
Edwards, J. M., and Frey, R. W. 1977. "Substrate Characteristics Within a Holocene Salt Marsh, Sapelo Island, Georgia," *Senckenberg. Marit.,* Vol 9, pp 215-259.

Emery 1967
Emery, K. O. 1967. "Estuaries and Lagoons in Relation to Continental Shelves," *Estuaries*, Publication 83, G. H. Lauff, ed., American Association for the Advancement of Science, Washington, DC, pp 9-11.

Emery 1968
Emery, K. O. 1968. "Relict Sediments on Continental Shelves of the World," *American Association of Petroleum Geologists Bulletin*, Vol 52, No. 3, pp 445-464.

Field 1979
Field, M. E. 1979. "Sediments, Shallow Subbottom Structure, and Sand Resources of the Inner Continental Shelf, Central Delmarva Peninsula," Technical Paper No. 79-2, Coastal Engineering Research Center, U.S. Army Engineer Waterways Experiment Station, Vicksburg, MS.

Field and Duane 1974
Field, M. E., and Duane, D. B. 1974. "Geomorphology and Sediments of the Inner Continental Shelf, Cape Canaveral, Florida," Technical Memorandum No. 42, Coastal Engineering Research Center, USAE Waterways Experiment Station, Vicksburg, MS.

Fisher and Dolan 1977
Fisher, J. S., and Dolan, R. 1977. "Beach Processes and Coastal Hydrodynamics," *Benchmark Papers in Geology*, Vol 39, Dowden, Hutchinson & Ross, Stroudsburg, PA.

FitzGerald and Rosen 1987
FitzGerald, D. M., and Rosen, P. S., eds. 1987. *Glaciated Coasts,* Academic Press, San Diego, CA.

Flint 1971
Flint, R. F. 1971. *Glacial and Quaternary Geology,* John Wiley and Sons, New York, NY.

Frey and Basan 1985
Frey, R. W., and Basan, P. B. 1985. Coastal Salt Marshes, *Coastal Sedimentary Environments,* 2nd ed., R. A. Davis, Jr., ed., Springer-Verlag, New York, pp 225-303.

Fuller and Meisburger 1982
Fuller, J. A., and Meisburger, E. P. 1982. "A Lightweight Pneumatic Coring Device: Design and Field Test," Miscellaneous Report No. 82-8, Coastal Engineering Research Center, U.S. Army Engineer Waterways Experiment Station, Vicksburg, MS.

Giese 1988
Giese, G. S. 1988. "Cyclical Behavior of the Tidal Inlet at Nauset Beach, Chatham, Massachusetts," *Hydrodynamics and Sediment Dynamics of Tidal Inlets,* Lecture Notes on Coastal and Estuarine Studies, Vol 29, D. G. Aubrey and L. Weishar, eds., Springer-Verlag, New York, NY, pp 269-283.

Gilbert 1885
Gilbert, G. K. 1885. 5th Annual Report, U.S. Geological Survey, Washington, DC, pp 87-88 (reprinted in Schwartz (1973)).

Goldsmith 1985
Goldsmith, V. 1985. "Coastal Dunes," Coastal Sedimentary Environments, 2nd ed., R. A. Davis, Jr., ed., Springer-Verlag, New York, NY, pp 303-378.

Gorman, Morang, and Larson 1998
Gorman, L. T., Morang, A., and Larson, R. L. 1998. Monitoring the Coastal Environment; Part IV: Mapping, Shoreline Change, and Bathymetric Analysis, *Journal of Coastal Research,* Vol 14, No. 1, pp 61-92.

Guilcher 1965
Guilcher, A. 1965. "Drumlin and Spit Structures in the Kenmare River, Southwest Ireland," *Irish Geography*, Vol 5, No. 2, pp 7-19.

Gulliver 1899
Gulliver, F. P. 1899. "Shoreline Topography," *Proceedings of the American Academy of Arts and Science,* Vol 34, pp 149-258.

Hands 1983
Hands, E. B. 1983. "The Great Lakes as a Test Model for Profile Response to Sea Level Changes," Chapter 8 in *Handbook of Coastal Processes and Erosion,* P. D. Komar, ed., CRC Press, Inc., Boca Raton, FL. (Reprinted in Miscellaneous Paper CERC-84-14, Coastal Engineering Research Center, U.S. Army Engineer Waterways Experiment Station, Vicksburg, MS.)

Hathaway 1972
Hathaway, J. C. 1972. "Regional Clay Mineral Facies in Estuaries and Continental Margin of the United States and East Coast," *Environmental Framework of Coastal Plain Estuaries*, B. W. Nelson, ed., Geologic Society of America Memoir 133, Boulder, CO, pp 293-316.

Hayes 1980
Hayes, M. O. 1980. "General Morphology and Sediment Patterns in Tidal Inlets," *Sedimentary Geology*, Vol 26, pp 139-156.

Herdendorf 1988
Herdendorf, C. E. 1988. "Classification of Geologic Features in Great Lakes Nearshore and Coastal Areas," Committee report prepared for: Protecting Great Lakes Nearshore and Coastal Diversity Project, International Joint Commission, Windsor, Ontario.

Hotta, Kraus, and Horikawa 1991
Hotta, S., Kraus, N. C., and Horikawa, K. 1991. "Functioning of Multi-row Sand Fences in Forming Foredunes," *Proceedings of Coastal Sediments '91,* American Society of Civil Engineers, New York, pp 261-275.

Howard and Frey 1977
Howard, J. D., and Frey, R. W. 1977. "Characteristic Physical and Biogenic Sedimentary Structures in Georgia Estuaries," *American Association of Petroleum Geologist Bulletin,* Vol 57, pp 1169-1184.

Hoyt 1967
Hoyt, J. H. 1967. "Barrier Island Formation," *Bulletin of the Geological Society of America,* Vol 78, pp 1125-1136.

Hume and Herdendorf 1988
Hume, T. M., and Herdendorf, C. E. 1988. "A Geomorphic Classification of Estuaries and Its Application to Coastal Resource Management - a New Zealand Example," *Journal of Ocean and Shoreline Management*, Vol 11, pp 249-274.

Inman and Nordstrom 1971
Inman, D. L., and Nordstrom, C. E. 1971. "On the Tectonic and Morphological Classification of Coasts," *Journal of Geology,* Vol 79, pp 1-21.

Johnson 1919
Johnson, D. 1919. *Shore Processes and Shoreline Development,* John Wiley & Sons, New York, NY.

Kerwin and Pedigo 1971
Kerwin, J. A., and Pedigo, R. A. 1971. "Synecology of a Virginia Salt Marsh," *Chesapeake Science*, Vol 12, pp 125-130.

King 1972
King, C. A. M. 1972. *Beaches and Coasts,* 2nd ed., Edward Arnold, London, UK.

Knutson 1976
Knutson, P. L. 1976. "Summary of CERC Research on Uses of Vegetation for Erosion Control," *Proceedings of Great Lakes Vegetation Workshop*, Great Lakes Basin Commission and USDA Soil Conservation Service, pp 31-36.

Knutson 1978
Knutson, P. L. 1978. "Planting Guidelines for Dune Creation and Stabilization," *Proceedings of Symposium on Technical, Environmental, Socioeconomic and Regulatory Aspects of Coastal Zone Planning and Management,* American Society of Civil Engineers, Vol 2, pp 762-779.

Kolb and van Lopik 1966
Kolb, C. R., and van Lopik, J. R. 1966. "Depositional Environments of the Mississippi River Deltaic Plain-Southeastern Louisiana," In: *Deltas in Their Geologic Framework,* Houston Geological Society, Houston, TX, pp 17-61.

Komar 1976
Komar, P. D. 1976. *Beach Processes and Sedimentation,* Prentice-Hall, Englewood Cliffs, NJ.

Komar 1983
Komar, P. D. 1983. "Computer Models of Shoreline Changes," *CRC Handbook of Coastal Processes and Erosion,* P. D. Komar, ed., CRC Press, Inc., Boca Raton, FL, pp 205-216.

Lauff 1967
Lauff, G. H., ed. 1967. *Estuaries*, American Association for the Advancement of Science, Pub. No. 83, Washington, DC.

Leatherman 1979
Leatherman, S. P., ed. 1979. *Barrier Islands from the Gulf of St. Lawrence to the Gulf of Mexico,* Academic Press, New York, NY.

McBride and Moslow 1991
McBride, R. A., and Moslow, T. F. 1991. "Origin, Evolution, and Distribution of Shoreface Sand Ridges, Atlantic Inner Shelf, U.S.A.," *Marine Geology*, Vol 97, pp 57-85.

Meisburger 1972
Meisburger, E. P. 1972. "Geomorphology and Sediments of the Chesapeake Bay Entrance," Technical Memorandum No. 38, Coastal Engineering Research Center, U.S. Army Engineer Waterways Experiment Station, Vicksburg, MS.

Meisburger 1976
Meisburger, E. P. 1976. "Geomorphology and Sediments of Western Massachusetts Bay," Technical Paper No. 76-3, Coastal Engineering Research Center, U.S. Army Engineer Waterways Experiment Station, Vicksburg, MS.

Meisburger 1977
Meisburger, E. P. 1977. "Sand Resources on the Inner Continental Shelf of the Cape Fear Region," Miscellaneous Report No. 77-11, Coastal Engineering Research Center, U.S. Army Engineer Waterways Experiment Station, Vicksburg, MS.

Meisburger 1979
Meisburger, E. P. 1979. "Reconnaissance Geology of the Inner Continental Shelf, Cape Fear Region, North Carolina," Technical Report No. 79-3, Coastal Engineering Research Center, U.S. Army Engineer Waterways Experiment Station, Vicksburg, MS.

Meisburger and Field 1975
Meisburger, E. P., and Field, M. E. 1975. "Geomorphology, Shallow Structure, and Sediments of the Florida Inner Continental Shelf, Cape Canaveral to Georgia," Technical Memorandum No. 54, Coastal Engineering Research Center, U.S. Army Engineer Waterways Experiment Station, Vicksburg, MS.

Meisburger and Williams 1980
Meisburger, E. P., and Williams, S. J. 1980. "Sand Resources on the Inner Continental Shelf of the Cape May Region, New Jersey," Miscellaneous Report 80-4, Coastal Engineering Research Center, U.S. Army Engineer Waterways Experiment Station, Vicksburg, MS.

Meisburger and Williams 1981
Meisburger, E. P., and Williams, S. J. 1981. "Use of Vibratory Coring Samplers for Sediment Surveys," Coastal Engineering Technical Aid No. 81-9, Coastal Engineering Research Center, U.S. Army Engineer Waterways Experiment Station, Vicksburg, MS.

Meisburger and Williams 1982
Meisburger, E. P., and Williams, S. J. 1982. "Sand Resources on the Inner Continental Shelf Off the Central New Jersey Coast," Miscellaneous Report No. 82-10, Coastal Engineering Research Center, U.S. Army Engineer Waterways Experiment Station, Vicksburg, MS.

Meisburger, Williams, and Prins 1979
Meisburger, E. P., Williams, S. J., and Prins, D. A. 1979. "Sand Resources of Southeastern Lake Michigan," Miscellaneous Report No. 79-3, Coastal Engineering Research Center, U.S. Army Engineer Waterways Experiment Station, Vicksburg, MS.

Metha 1986
Metha, A. J., ed. 1986. *Estuarine Cohesive Sediment Dynamics*, Lecture Notes on Coastal and Estuarine Studies, Vol 14, Springer-Verlag, New York, NY.

Moore and Clague 1992
Moore, J. G., and Clague, D. A. 1992. "Volcano Growth and Evolution of the Island of Hawaii," *Geological Society of America Bulletin*, Vol 104, No. 11, pp 1471-1484.

Nelson 1972
Nelson, B. W., ed. 1972. *Environmental Framework of Coastal Plain Estuaries*, Geological Society of America Memoir 133, Boulder, CO.

Nichols 1968
Nichols, R. L. 1968. "Coastal Geomorphology, McMurdo Sound, Antarctica," *Journal of Glaciology,* Vol 51, pp 694-708.

Nichols and Biggs 1985
Nichols, M. M., and Biggs, R. B. 1985. "Estuaries," *Coastal Sedimentary Environments*, R. A. Davis, Jr., ed., 2nd ed., Springer-Verlag, New York, NY, pp 77-186.

Nummedal 1983
Nummedal, D. 1983. "Barrier Islands," *CRC Handbook of Coastal Processes and Erosion*, P. D. Komar, ed., CRC Press, Inc., Boca Raton, FL, pp 77-121.

Otvos 1970
Otvos, E. G., Jr. 1970. "Development and Migration of Barrier Islands, Northern Gulf of Mexico," *Bulletin of the Geological Society of America,* Vol 81, pp 241-246.

Otvos 1981
Otvos, E. G., Jr. 1981. "Barrier Island Formation Through Nearshore Aggradation - Stratigraphic and Field Evidence," *Marine Geology,* Vol 43, pp 195-243.

Penland and Boyd 1981
Penland, S., and Boyd, R. 1981. "Shoreline Changes on the Louisiana Barrier Coast," *Proceedings of the Oceans '81 Conference,* Boston, Massachusetts, September 16-18, pp 209-219.

Pethick 1984
Pethick, J. 1984. *An Introduction to Coastal Geomorphology,* Edward Arnold Publishers, London, UK.

Pettijohn 1975
Pettijohn, F. J. 1975. *Sedimentary Rocks,* Harper and Row, New York, NY.

Pilkey and Field 1972
Pilkey, O. H., and Field, M. E. 1972. "Onshore Transportation of Continental Shelf Sediment: Atlantic Southeastern United States," *Shelf Sediment Transport,* D. J. Swift, D. B. Duane, and O. H. Pilkey, eds., Dowden, Hutchinson, & Ross, Stroudsburg, PA.

Press and Siever 1986
Press, F., and Siever, R. 1986. *Earth*, 4th. ed., W. H. Freeman and Company, New York, NY.

Prins 1980
Prins, D. A. 1980. "Data Collection Methods for Sand Inventory-Type Surveys," Coastal Engineering Technical Aid No. 80-4, Coastal Engineering Research Center, U.S. Army Engineer Waterways Experiment Station, Vicksburg, MS.

Pritchard 1967
Pritchard, D. W. 1967. "What is an Estuary? Physical Viewpoint," *Estuaries*, Publication 83, G. H. Lauff, ed., American Association for the Advancement of Science, Washington, DC, pp 3-5.

Reading 1986
Reading, H. G., ed. 1986. *Sedimentary Environments and Facies,* 2nd ed., Blackwell Scientific Publications, Oxford, UK.

Reineck and Singh 1980
Reineck, H. E., and Singh, I. B. 1980. *Depositional Sedimentary Environments,* 2nd ed., Springer-Verlag, Berlin, Germany.

Russell 1967
Russell, R. 1967. Origin of estuaries, *Estuaries,* G. H. Lauff, (ed.), American Association for the Advancement of Science, Publication 83, Washington, D.C., pp 93-99.

Schwartz 1971
Schwartz, M. L. 1971. "The Multiple Casualty of Barrier Islands," *Journal of Geology,* Vol 79, pp 91-94.

Schwartz 1973
Schwartz, M. L., ed. 1973. *Barrier Islands,* Dowden, Hutchinson & Ross, Stroudsburg, PA.

Schwartz 1982
Schwartz, M. L., ed. 1982. *The Encyclopedia of Beaches and Coastal Environments,* Encyclopedia of Earth Sciences, Volume XV, Hutchinson Ross Publishing Company, Stroudsburg, PA.

Shepard 1937
Shepard, F. P. 1937. "Revised Classification of Marine Shorelines," *Journal of Geology,* Vol 45, pp 602-624.

Shepard 1948
Shepard, F. P. 1948. *Submarine Geology,* Harper & Row, New York, NY.

Shepard 1973
Shepard, F. P. 1973. *Submarine Geology,* 3rd ed., Harper & Row, New York, NY.

Shepard 1976
Shepard, F. P. 1976. "Coastal Classification and Changing Coastlines," *Geoscience and Man,* Vol 13, pp 53-64.

Shepard 1977
Shepard, F. P. 1977. *Geological Oceanography,* Crane, Russak & Co., New York, NY.

Shepard and Wanless 1971
Shepard, F. P., and Wanless, H. R. 1971. *Our Changing Coastlines*, McGraw-Hill Book Company, New York, NY.

Smith 1954
Smith, H. T. U. 1954. "Coastal Dunes," *Proceedings of the Coastal Geography Conference,* Office of Naval Research, Department of the Navy, Washington, DC, pp 51-56.

Spalding, Ravilious, and Green 2001
Spalding, M. D., Ravilious, C., and Green, E. P. 2001. *World Atlas of Coral Reefs,* The University of California Press, Berkeley, CA.

Spurgeon 1992
Spurgeon, J. P. G. 1992. "The Economic Valuation of Coral Reefs," *Marine Pollution Bulletin*, Vol 24, No. II, pp 529-536.

Stewart and Pope 1992
Stewart, C. J., and Pope, J. 1992. "Erosion Processes Task Group Report," Open file report prepared for the International Joint Commission Water Level Reference Study, International Joint Commission, Canada and U.S.A.

Stoddard 1969
Stoddard, D. R. 1969. "Ecology and Morphology of Recent Coral Reefs," *Biological Reviews*, Vol 44, pp 433-498.

Strahler 1971
Strahler, A. N. 1971. *The Earth Sciences*, 2nd ed., Harper & Row Publishers, New York, NY.

Suess 1888
Suess, E. 1888. *The Faces of the Earth,* Vol 2 (English translation by H. B. Sollas in 1906), Oxford University Press, London, UK (in 5 vols).

Suhayda 1984
Suhayda, J. N. 1984. "Interaction Between Surface Waves and Muddy Bottom Sediments," *Estuarine Cohesive Sediment Dynamics,* Lecture Notes on Coastal and Estuarine Studies, A. J. Mehta, ed., Springer-Verlag, Berlin, pp 401-428.

Suter and Berryhill 1985
Suter, J. R., and Berryhill, H. L., Jr. 1985. "Late Quaternary Shelf-Margin Deltas, Northwest Gulf of Mexico," *Bulletin of the American Association of Petroleum Geologists,* Vol 69, No. 1, pp 77-91.

Swift 1976
Swift, D. J. P. 1976. "Coastal Sedimentation," *Marine Sediment Transport and Environmental Management*, D. J. Stanley and D. J. P. Swift, eds., John Wiley and Sons, New York, NY, pp 255-310.

Tilling, Heliker, and Wright 1987
Tilling, R. I., Heliker, C., and Wright, T. L. 1987. "Eruptions of Hawaiian Volcanoes: Past, Present, and Future," U.S. Geological Survey, Denver, CO.

Trenhaile 1987
Trenhaile, A. S. 1987. *The Geomorphology of Rock Coasts*, Clarendon Press, Oxford, UK.

U.S. Army Engineer Waterways Experiment Station 1992
U.S. Army Engineer Waterways Experiment Station. 1992. "The Wetlands Research Program Notebook," Technical Notes, U.S. Army Engineer Waterways Experiment Station, Vicksburg, MS.

Valentin 1952
Valentin, H. 1952. *Die Kusten der Erde,* Petermanns Geog. Mitt. Erg. 246, Justus Perthes Gotha, Berlin, Germany.

Van de Kreeke 1986
Van de Kreeke, J., ed. 1986. *Physics of Shallow Estuaries and Bays*, Lecture Notes on Coastal and Estuarine Studies, Vol 16, Springer-Verlag, New York, NY.

Waisel 1972
Waisel, Y. 1972. *Biology of Halophytes*, Academic Press, NY.

Williams 1976
Williams, S. J. 1976. "Geomorphology, Shallow Subbottom Structure, and Sediments of the Atlantic Inner Continental Shelf Off Long Island, New York," Technical Paper No. 76-2, Coastal Engineering Research Center, U.S. Army Engineer Waterways Experiment Station, Vicksburg, MS.

Williams 1981
Williams, S. J. 1981. "Sand Resources and Geological Character of Long Island Sound," Technical Paper No. 81-3, Coastal Engineering Research Center, U.S. Army Engineer Waterways Experiment Station, Vicksburg, MS.

Williams and Duane 1974
Williams, S. J., and Duane, D. B. 1974. "Geomorphology and Sediments of the Inner New York Bight Continental Shelf," Technical Memorandum No. 45, Coastal Engineering Research Center, U.S. Army Engineer Waterways Experiment Station, Vicksburg, MS.

Williams and Meisburger 1982
Williams, S. J., and Meisburger, E. P. 1982. "Geological Character and Mineral Resources of South Central Lake Erie," Miscellaneous Report No. 82-9, Coastal Engineering Research Center, U.S. Army Engineer Waterways Experiment Station, Vicksburg, MS.

Williams, Carter, Meisburger, and Fuller 1980
Williams, S. J., Carter, C. H., Meisburger, E. P., and Fuller, J. A. 1980. "Sand Resources of Southern Lake Erie, Conneaut to Toledo, Ohio - a Seismic Reflection and Vibracore Study," Miscellaneous Report No. 80-10, Coastal Engineering Research Center, U.S. Army Engineer Waterways Experiment Station, Vicksburg, MS.

Williams, Prins, and Meisburger 1979
Williams, S. J., Prins, D. A., and Meisburger, E. P. 1979. "Sediment Distribution Sand Resources, and Geologic Character of the Inner Continental Shelf Off Galveston County Texas," Miscellaneous Report No. 79-4, Coastal Engineering Research Center, U.S. Army Engineer Waterways Experiment Station, Vicksburg, MS.

Wood and Kienle 1990
Wood, C. A., and Kienle, J., eds. 1990. *Volcanoes of North America: United States and Canada*, Cambridge University Press, Cambridge, UK.

Woodhouse 1978
Woodhouse, W. W., Jr. 1978. "Dune Building and Stabilization with Vegetation," SR-3, Coastal Engineering Research Center, U.S. Army Engineer Waterways Experiment Station, Vicksburg, MS.

Young and Hale 1998
Young, C., and Hale, L. 1998. "Coastal Management: Insurance for the Coastal Zone," *Maritimes*, Vol 40m, No. 1, pp.17-19.

IV-2-15. Acknowledgments

Authors of Chapter IV-2, "Coastal Classification and Morphology:"

Andrew Morang, Ph.D., Coastal and Hydraulics Laboratory (CHL), Engineer Research and Development Center, Vicksburg, Mississippi.
Laurel T. Gorman, Information Technology Laboratory, Engineer Research and Development Center, Vicksburg, Mississippi.
David B. King, Ph.D., CHL.
Edward Meisburger, CHL (retired).

Reviewers:

Stephan A. Chesser, U.S. Army Engineer District, Portland, Portland, Oregon.
Ronald L. Erickson, U.S. Army Engineer District, Detroit, Detroit, Michigan.
Joan Pope, CHL.
John F. C. Sanda, Headquarters, U.S. Army Corps of Engineers, Washington, DC., (retired).
Orson P. Smith, Ph.D., U.S. Army Engineer District, Alaska, Anchorage, Alaska, (retired).

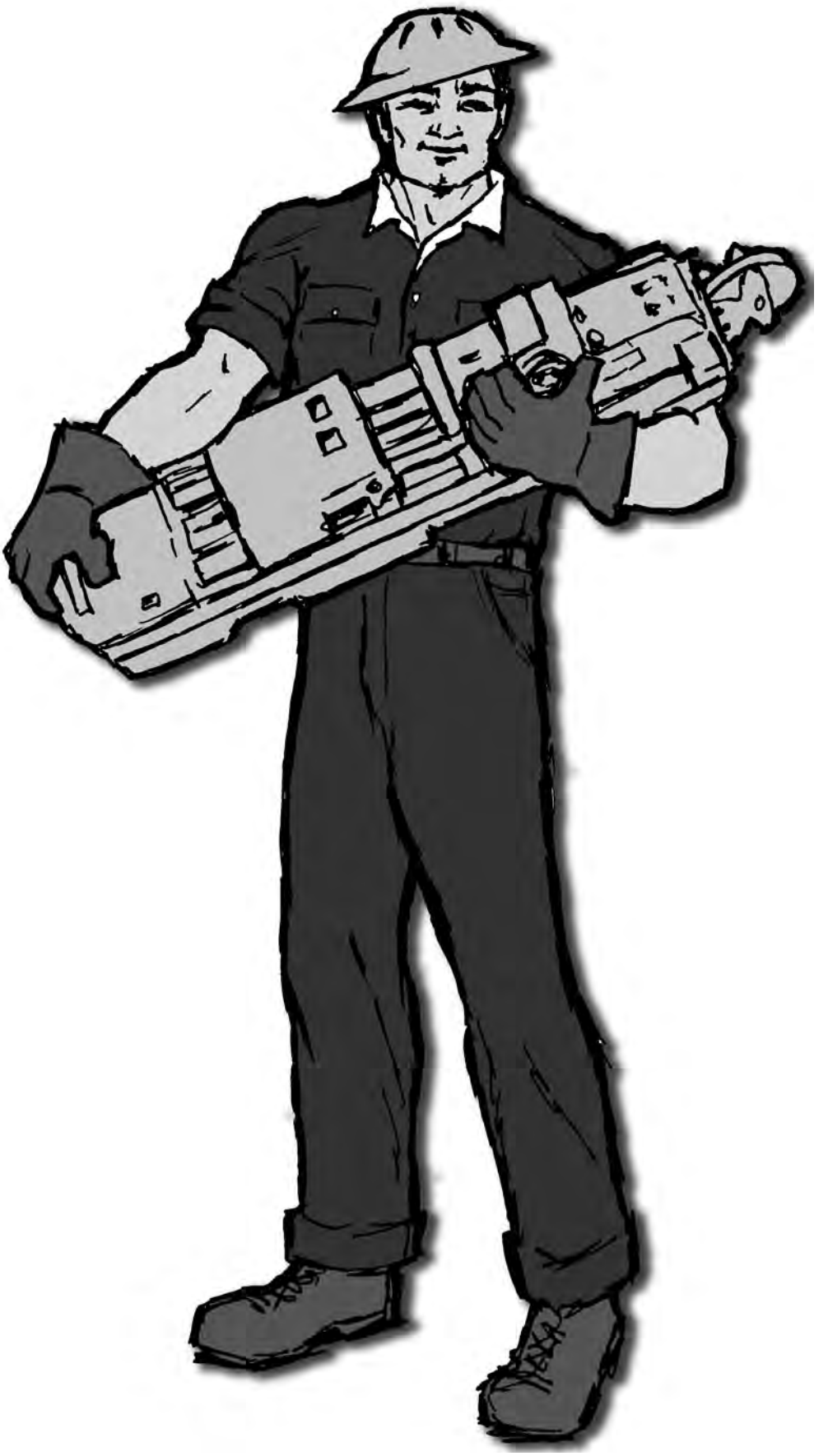

Table of Contents

Page

IV-3-1. Introduction IV-3-1

IV-3-2. Introduction to Bed Forms IV-3-1
a. Introduction IV-3-1
b. Environments IV-3-1
c. Classification IV-3-2
d. Ripples IV-3-2
e. Dunes IV-3-2
f. Plane beds IV-3-2
g. Antidunes IV-3-2
h. Velocity - grain size relationships IV-3-4

IV-3-3. Deltaic Processes IV-3-4
a. Introduction IV-3-4
b. General delta classification IV-3-8
c. Delta-forming processes IV-3-8
(1) Force balance IV-3-8
(2) River-dominant deltas IV-3-9
(3) Wave-dominant deltas IV-3-11
(4) Tide-dominant deltas IV-3-13
(5) Intermediate forms IV-3-13
d. Deltaic components and sediments IV-3-13
e. River mouth flow and sediment deposition IV-3-16
f. Mississippi Delta - Holocene history, dynamic changes IV-3-22
(1) General IV-3-22
(2) Deposition time scales IV-3-22
(3) Holocene history IV-3-23
(4) Modern delta IV-3-23
g. Sea level rise and deltas IV-3-23

IV-3-4. Coastal Inlets IV-3-24
a. Introduction IV-3-24
b. Technical literature IV-3-25
c. Classification of inlets and geographic distribution IV-3-25
d. Hydrodynamic processes in inlets IV-3-26
e. Geomorphology of tidal inlets IV-3-26
(1) Ebb-tidal deltas (shoals) IV-3-26
(2) Flood-tidal deltas (shoals) IV-3-30
(3) Bed forms IV-3-32
f. Inlet stability and migration IV-3-32
(1) Background IV-3-32
(2) Inlet migration and spit breaching IV-3-33

(3) Ebb-tidal delta breaching IV-3-35
(4) Stable inlet processes IV-3-35
(5) Extension of bypassing models to other environments IV-3-36
g. Inlet response to jetty construction and other engineering activities IV-3-36
(1) Introduction IV-3-36
(2) Technical literature IV-3-36
h. Case study of inlet formation and growth: Shinnecock Inlet, Long Island, New York IV-3-38
(1) Background and inlet breaching (1938) IV-3-38
(2) Semi-stabilized inlet (1947) IV-3-38
(3) Stabilized inlet (1966) IV-3-39
(4) Ebb shoal growth IV-3-40

IV-3-5. Morphodynamics and Shoreface Processes of Clastic Sediment Shores . . IV-3-40
a. Overview IV-3-40
(1) Introduction IV-3-40
(2) Literature IV-3-40
(3) Significance of clastic coasts IV-3-42
(4) Range of coastal environments IV-3-44
b. Tide range and overall beach morphology IV-3-44
c. High tidal range (> 2 m) beach morphodynamics IV-3-46
(1) Review IV-3-46
(2) Macrotidal beach groups IV-3-46
(a) GROUP 1 - High wave, planar, uniform slope IV-3-46
(b) GROUP 2 - Moderate wave, multi-bar IV-3-46
(c) GROUP 3 - Low wave beach and tidal flat IV-3-48
(3) Spatial and temporal variations IV-3-49
(4) Summary IV-3-49
d. Morphodynamics of micro- and low-mesotidal coasts IV-3-49
e. Processes responsible for shoreface sediment movement IV-3-56
f. Sea level change and the Bruun rule IV-3-58
(1) General coastal response to changing sea level IV-3-58
(2) Storm response IV-3-59
(3) Bruun Rule beach response model IV-3-59
(4) Use of models to predict shoreline recession IV-3-63
(5) Recommendations IV-3-63
g. Equilibrium profiles on sandy coasts IV-3-63
(1) General characteristics and assumptions IV-3-63
(2) Shape IV-3-64
(3) Discussion of assumptions IV-3-64
(a) Assumption 1 . . . . . IV-3-64
(b) Assumption 2 . . . . . IV-3-64
(c) Assumption 3 . . . . . IV-3-65
(d) Assumption 4 . . . . . IV-3-65
(4) General comments IV-3-66
h. Depth of closure IV-3-66
(1) Background IV-3-66
(2) Energy factors IV-3-67
(3) Time considerations IV-3-67
(4) Predictive methods IV-3-67
(5) Empirical determination IV-3-68

i. Longshore sediment movement IV-3-70
j. Summary IV-3-70

IV-3-6. References IV-3-72

IV-3-7. Definition of Symbols IV-3-84

IV-3-8. Acknowledgments IV-3-86

List of Tables

Page

Table IV-3-1. Modes of Fluid Motion Affecting Clastic Shorelines IV-3-50

List of Figures

Page

Figure IV-3-1. Sediment ripples IV-3-3

Figure IV-3-2. Ripples in a runnel, exposed during low tide, Bon Secour Wildlife Refuge, near Gulf Shores, Alabama IV-3-4

Figure IV-3-3. Two-dimensional and three-dimensional dunes (Reineck and Singh (1980)) . . . IV-3-5

Figure IV-3-4. Ebb shoal, East Pass, Florida IV-3-6

Figure IV-3-5. Flood shoal, East Pass, Florida IV-3-7

Figure IV-3-6. Plot of mean flow velocity against mean grain size, based on laboratory studies, showing stability phases of subaqueous bed forms IV-3-8

Figure IV-3-7. Classification of deltas IV-3-9

Figure IV-3-8. Isopach map for river-dominant deltas IV-3-10

Figure IV-3-9. Mississippi River Delta, Landsat 2 image (date unknown) IV-3-11

Figure IV-3-10. Fraser River Delta, British Columbia (NASA ERTS, 12 Aug 1973) IV-3-12

Figure IV-3-11. Mouth of the Essex River, Massachusetts IV-3-14

Figure IV-3-12. Basic physiographic units common to all deltas IV-3-15

Figure IV-3-13. Structures and types of sediment instabilities on the Mississippi Delta IV-3-16

Figure IV-3-14. Plan view of depositional Model A, inertia-dominated effluent IV-3-17

Figure IV-3-15. Depositional model type B, friction-dominated effluent IV-3-19

Figure IV-3-16. River mouth bar crest features, depositional model type C, buoyant effluent IV-3-20

Figure IV-3-17. Shifting sites of deltaic sedimentation of the Mississippi River IV-3-24

Figure IV-3-18. Definition diagram of a tidal inlet with well-developed flood and ebb deltas IV-3-27

Figure IV-3-19. Four different shapes of ebb-tidal deltas, modified by the relative effects of longshore versus tidal currents IV-3-28

Figure IV-3-20. Ocean City Inlet, Maryland, September 1933 . . . . . IV-3-30

Figure IV-3-21. Ocean City Inlet, Maryland, 11 September 1995 . . . . . IV-3-31

Figure IV-3-22. East Pass, Florida, stratified flow during flood tide IV-3-33

Figure IV-3-23. Three models of inlet behavior and sediment bypassing for mixed-energy coasts IV-3-34

Figure IV-3-24. Spit breaching and inlet migration at East Pass, Florida IV-3-37

Figure IV-3-25. Shinnecock Bay, Long Island, New York 30 June 1938 . . . . . IV-3-39

Figure IV-3-26. Shinnecock Inlet, Long Island, New York, 24 September 1938 . . . . . IV-3-40

Figure IV-3-27. Shinnecock Inlet, New York, 29 November 1938 . . . . . IV-3-41

Figure IV-3-28. Shinnecock Inlet, New York, 1 April 1947 . . . . . IV-3-42

Figure IV-3-29. Shinnecock Inlet, New York, 24 October 1996 . . . . . IV-3-43

Figure IV-3-30. Ebb-shoal volume changes, Shinnecock Inlet, New York IV-3-44

Figure IV-3-31. Summary of factors controlling morphodynamics along a range of coastal environments IV-3-45

Figure IV-3-32. Micro- to macrotidal beach and tidal flat systems IV-3-47

Figure IV-3-33. Tarskavaig, Isle of Skye, Scotland, August 1983 . . . . . IV-3-48

Figure IV-3-34. Plan and profile views of six major beach stages IV-3-51

Figure IV-3-35. Example of a dissipative beach: Southern California near San Diego IV-3-53

Figure IV-3-36. Example of a reflective sand beach: Newport Beach, California IV-3-54

Figure IV-3-37. Example of a reflective cobble beach: Aldeburgh, Suffolk (facing the North Sea) IV-3-55

Figure IV-3-38. Gravel cusps at St. Joseph, Michigan IV-3-56

Figure IV-3-39. Ridge and runnel north of St. Joseph, Michigan IV-3-57

Figure IV-3-40. (a) Shoreline response to rising sea level (SL) depicted by the Bruun Rule. (b) Simplified nomenclature used by Hands (1983) IV-3-60

Figure IV-3-41. Profile adjustment in two stages, first vertical, then horizontal, demonstrating the basis for the Bruun Rule IV-3-62

Figure IV-3-42. Profile surveys and standard deviation of seafloor elevation at 74th Street, Ocean City, Maryland IV-3-69

Figure IV-3-43. Profile surveys and standard deviation of lake floor elevation at St. Joseph, Michigan, on the east shore of Lake Michigan IV-3-70

Figure IV-3-44. Variation in closure depth along the south shore of Long Island, New York . . IV-3-71

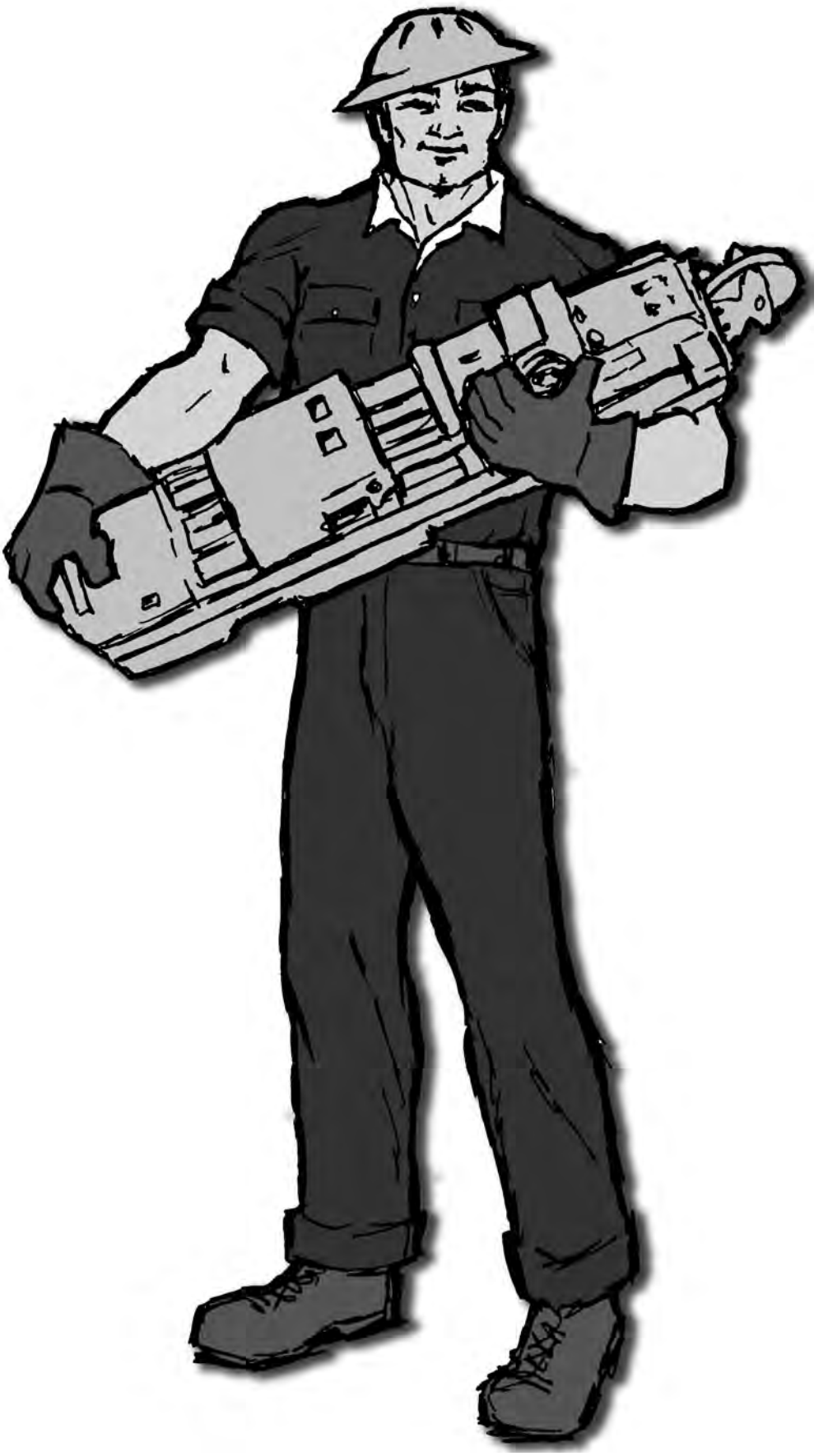

Chapter IV-3
Coastal Morphodynamics

IV-3-1. Introduction

a. This chapter discusses the morphodynamics of three coastal environments: deltas, inlets, and sandy shores. The divisions are somewhat arbitrary because, in many circumstances, the environments are found together in limited areas. For example, within a major river delta like the Mississippi, there are sandy beaches, bays where cohesive sediments accumulate, and inlets which funnel water in and out of the bays. Coastal features and environments are also not constant over time. For example, as we discussed in Part IV-2, estuaries, deltas, and beach ridge shores are elements of a landform continuum that extends over time. Which particular environment or shore type is found at any one time depends on sea level rise, sediment supply, wave and tide energy, underlying geology, climate, rainfall, runoff, and biological productivity.

b. Based on the fact that physical conditions along the coast are constantly changing, it can be argued that there is no such thing as an "equilibrium" state for any coastal form. This is true not only for shoreface profiles but also for deltas, which continue to shift over time in response to varying wave and meteorologic conditions. In addition, man continues to profoundly influence the coastal environment throughout the world, changing natural patterns of runoff and littoral sediment supply and constantly rebuilding and modifying engineering works. This is true even along undeveloped coastlines because of environmental damage such as deforestation, which causes drastic erosion and increased sediment load in rivers. The reader is urged to remember that coastal landforms are the result of the interactions of a myriad of physical processes, man-made influences, global tectonics, local underlying geology, and biology.

c. Cohesive shores, another one of the primary geologic terrains found around the world, have been discussed in Part III-5, "Erosion, Transport, and Deposition of Cohesive Shores."

IV-3-2. Introduction to Bed Forms

a. Introduction. When sediment is moved by flowing water, the individual grains are usually organized into morphological elements called *bed forms.* These occur in a baffling variety of shapes and scales. Some bed forms are stable only between certain values of flow strength. Often, small bed forms (ripples) are found superimposed on larger forms (dunes), suggesting that the flow field may vary dramatically over time. Bed forms may move in the same direction as the current flow, may move against the current (antidunes), or may not move at all except under specific circumstances. The study of bed form shape and size is of great value because it can assist in making quantitative estimates of the strength of currents in modern and ancient sediments (Harms 1969, Jopling 1966). Bed form orientations are indicators of flow pathways. This introduction to a complex subject is by necessity greatly condensed. For details on interpretation of surface structures and sediment laminae, readers are referred to textbooks on sedimentology such as Allen (1968, 1984, 1985); Komar (1998); Leeder (1982); Lewis (1984); Middleton (1965); Middleton and Southard (1984); and Reineck and Singh (1980).

b. Environments. In nature, bed forms are found in three environments with greatly differing characteristics:

(1) Rivers - unidirectional and channelized; large variety of grain sizes.

(2) Sandy coasts and bays - semi-channelized, unsteady, reversing (tidal) flows.

(3) Continental shelves - deep, unchannelized; dominated by geostrophic flows, storms, tidal currents, wave-generated currents.

c. Classification. Because of the diverse natural settings and the differing disciplines of researchers who have studied sedimentology, the classification and nomenclature of bed forms have been confusing and contradictory. The following classification scheme, proposed by the Society for Sedimentary Geology (SEPM) Bed forms and Bedding Structures Research Group in 1987 (Ashley 1990) is suitable for all subaqueous bed forms:

(1) Ripples. These are small bed forms with crest-to-crest spacing less than about 0.6 m and height less than about 0.03 m. It is generally agreed that ripples occur as assemblages of individuals similar in shape and scale. On the basis of crestline trace, Allen (1968) distinguished five basic patterns of ripples: straight, sinuous, catenary, linguoid, and lunate (Figure IV-3-1). The straight and sinuous forms may be symmetrical in cross section if subject to primarily oscillatory motion (waves) or may be asymmetrical if influenced by unidirectional flow (rivers or tidal currents). Ripples form a population distinct from larger-scale dunes, although the two forms share a similar geometry (Figure IV-3-2). The division between the two populations is caused by the interaction of ripple morphology and bed, and possibly shear stress. At low shear stresses, ripples are formed. As shear stress increases above a certain threshold, a "jump" in behavior occurs, resulting in the appearance of the larger dunes (Allen 1968).

(2) Dunes. Dunes are flow-transverse bed forms with spacings from under 1 m to over 1,000 m that develop on a sediment bed under unidirectional currents. These large bed forms are ubiquitous in sandy environments where water depths are greater than about 1 m, sand size coarser than 0.15 mm (very fine sand), and current velocities are greater than about 0.4 m/sec. In nature, these flow-transverse forms exist as a continuum of sizes without natural breaks or groupings (Ashley 1990). For this reason, "dune" replaces terms such as megaripple or sand wave, which were defined on the basis of arbitrary or perceived size distributions. Unfortunately, the term "sand wave" is still used in the literature, often with only the vaguest indication of what size feature is being described. For descriptive purposes, dunes can be subdivided as small (0.6- to 5-m wavelength), medium (5-10 m), large (10-100 m), and very large (> 100 m). In addition, the variation in pattern across the flow must be specified. If the flow pattern is relatively unchanged perpendicular to its overall direction and there are no eddies or vortices, the resulting bed form will be straight-crested and can be termed two-dimensional (Figures IV-3-3a and IV-3-4). If the flow structure varies significantly across the predominant direction and vortices capable of scouring the bed are present, a three-dimensional bed form is produced (Figure IV-3-5).

(3) Plane beds. A plane bed is a horizontal bed without elevations or depressions larger than the maximum size of the exposed sediment. The resistance to flow is small, resulting from grain roughness, which is a function of grain size. Plane beds occur under two hydraulic conditions:

(a) The transition zone between the region of no movement and the initiation of dunes (Figure IV-3-6).

(b) The transition zone between ripples and antidunes, at mean flow velocities between about 1 and 2 m/sec (Figure IV-3-6).

(4) Antidunes. Antidunes are bed forms that are in phase with water-surface gravity waves. Height and wavelength of these bedforms depend on the scale of the system and characteristics of the fluid and bed material (Reineck and Singh 1980). Trains of antidunes gradually build up from a plane bed as water velocity increases. As the antidunes increase in size, the water surface changes from planar to wave-like. The water waves may grow until they are unstable and break. As the sediment antidunes grow, they may

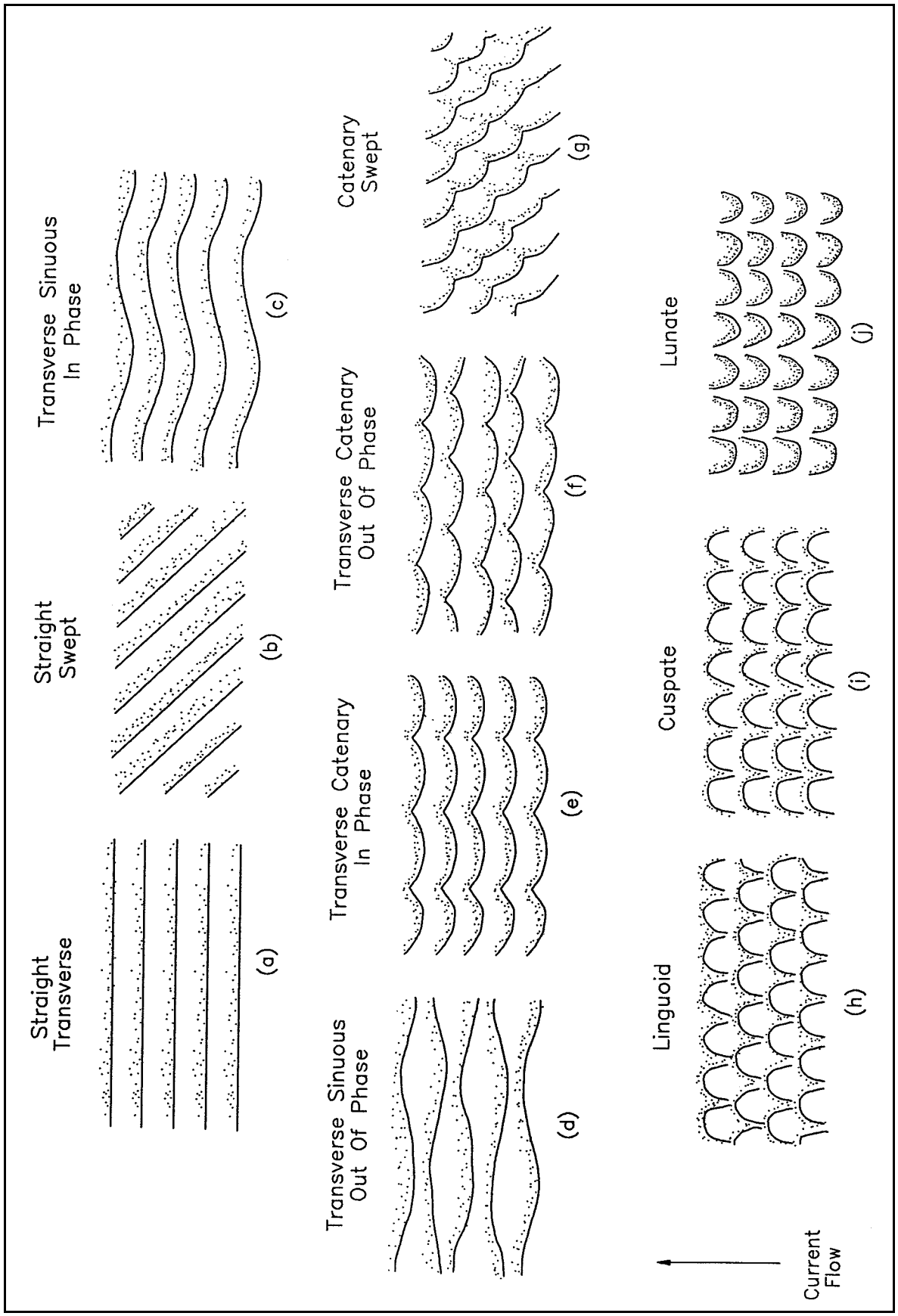

Figure IV-3-1. Sediment ripples. Water flow is from bottom to top, and lee sides and spurs are stippled (modified from Allen (1968))

Figure IV-3-2. Ripples in a runnel, now exposed during low tide. Flow was from upper left to lower right. Complicated pattern is best classified as transverse sinuous out of phase (type d) in Figure IV-3-1. Photographed at Bon Secour Wildlife Refuge, near Gulf Shores, Alabama

migrate upstream or downstream, or may remain stationary (the name "antidune" is based on early observations of upstream migration).

d. Velocity - grain size relationships. Figure IV-3-6 (from Ashley (1990)) illustrates the zones where ripples, dunes, planar beds, and antidunes are found. The figure summarizes laboratory studies conducted by various researchers. These experiments support the common belief that large flow-transverse bed forms (dunes) are a distinct entity separate from smaller current ripples. This plot is very similar to Figure 11.4 in Graf's (1984) hydraulics text, although Graf uses different axis units.

IV-3-3. Deltaic Processes[1]

a. Introduction. River deltas, which are found throughout the world, result from the interaction of fluvial and marine (or lacustrine) forces. According to Wright (1985), "deltas are defined more broadly as coastal accumulations, both subaqueous and subaerial, of river-derived sediments adjacent to, or in close proximity to, the source stream, including the deposits that have been secondarily molded by waves, currents, or tides." The processes that control delta development vary greatly in intensity around the world. As a result, delta-plain landforms span the spectrum of coastal features and include:

[1] Material in this section adapted from Wright (1985).

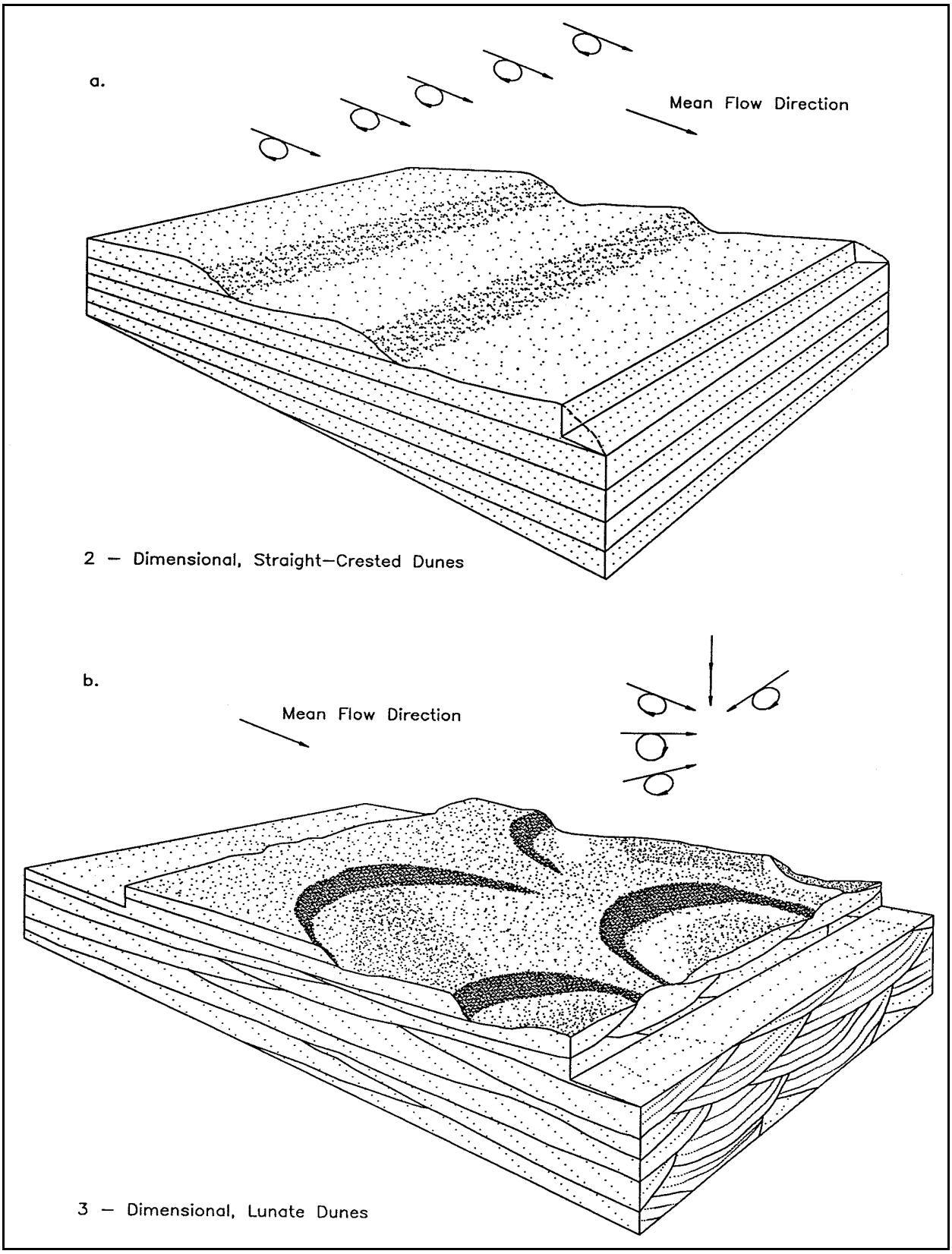

Figure IV-3-3. Two-dimensional and three-dimensional dunes. Vortices and flow patterns are shown by arrows above dunes. Adapted from Reineck and Singh (1980)

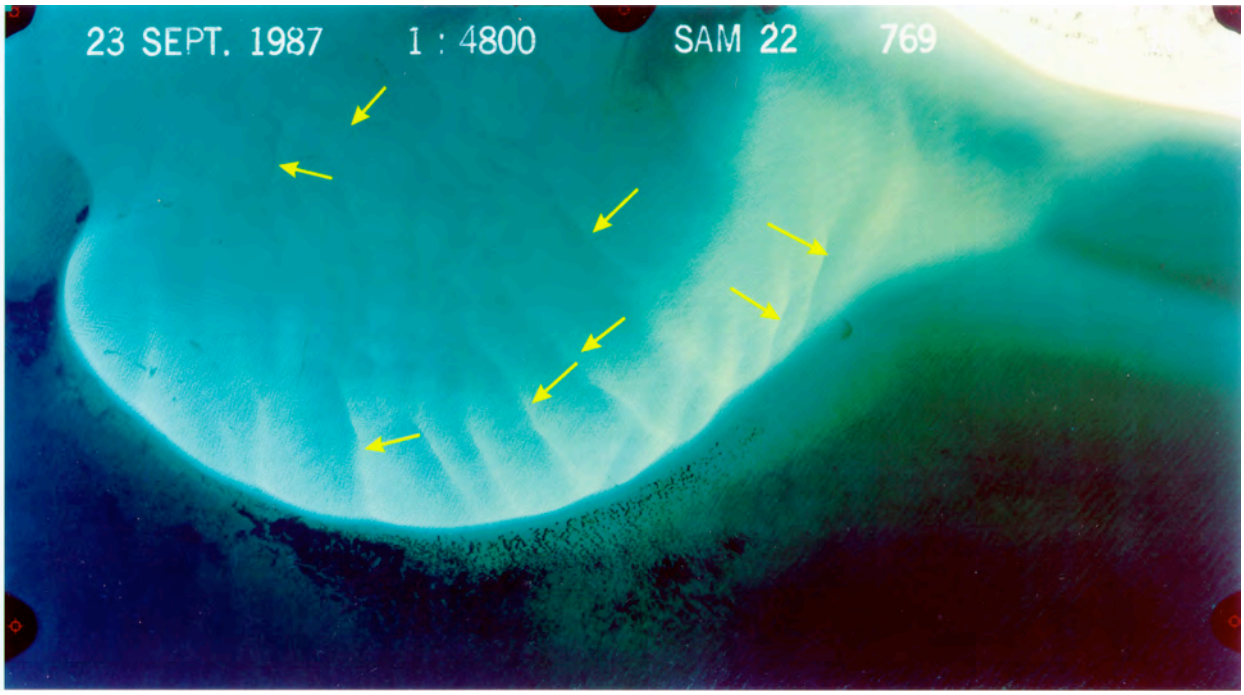

Figure IV-3-4. Ebb shoal, East Pass, Florida (23 Sep 1987). The clear water reveals two-dimensional dunes on the ebb shield. Water depth at the edge of the shoal is 3-4 m. North is to the top of the image. Distance from left to right is about 1 km (photograph of USAED, Mobile)

(1) Distributary channels.

(2) River-mouth bars.

(3) Interdistributary bays.

(4) Tidal flats.

(5) Tidal ridges.

(6) Beaches.

(7) Beach ridges.

(8) Dunes and dune fields.

(9) Swamps and marshes.

Despite the pronounced variety of worldwide environments where deltas are found, all actively-forming deltas have at least one common attribute: a river supplies clastic sediments to the coast and inner shelf more rapidly than marine processes can remove these materials. Whether a river is sufficiently large to transport enough sediment to overcome erosive marine processes depends upon the climate, geology, and nature of the drainage basin, and, most important, the overall size of the basin. The following paragraphs discuss delta classification, riverine flow, sediment deposition, and geomorphic structures associated with deltas.

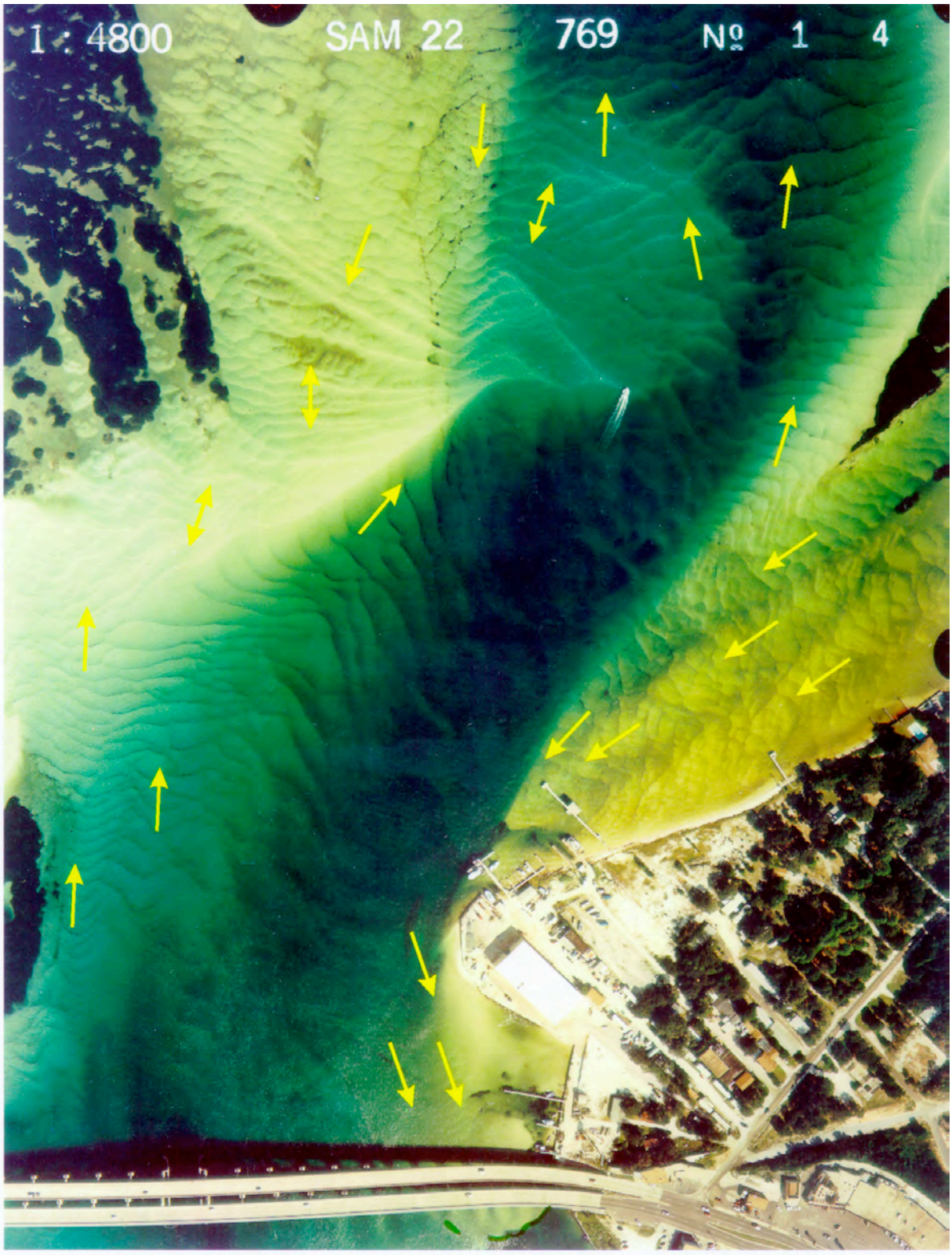

Figure IV-3-5. Flood shoal, East Pass, Florida (23 Sep 1987). North is to the top. The Gulf of Mexico is about 1 km south of the Hwy 98 bridge at the bottom of the image. Dunes in the main channel are flood-oriented (toward the top of the image), while bed forms in the marginal channels are ebb-oriented (Photograph courtesy of USAED, Mobile)

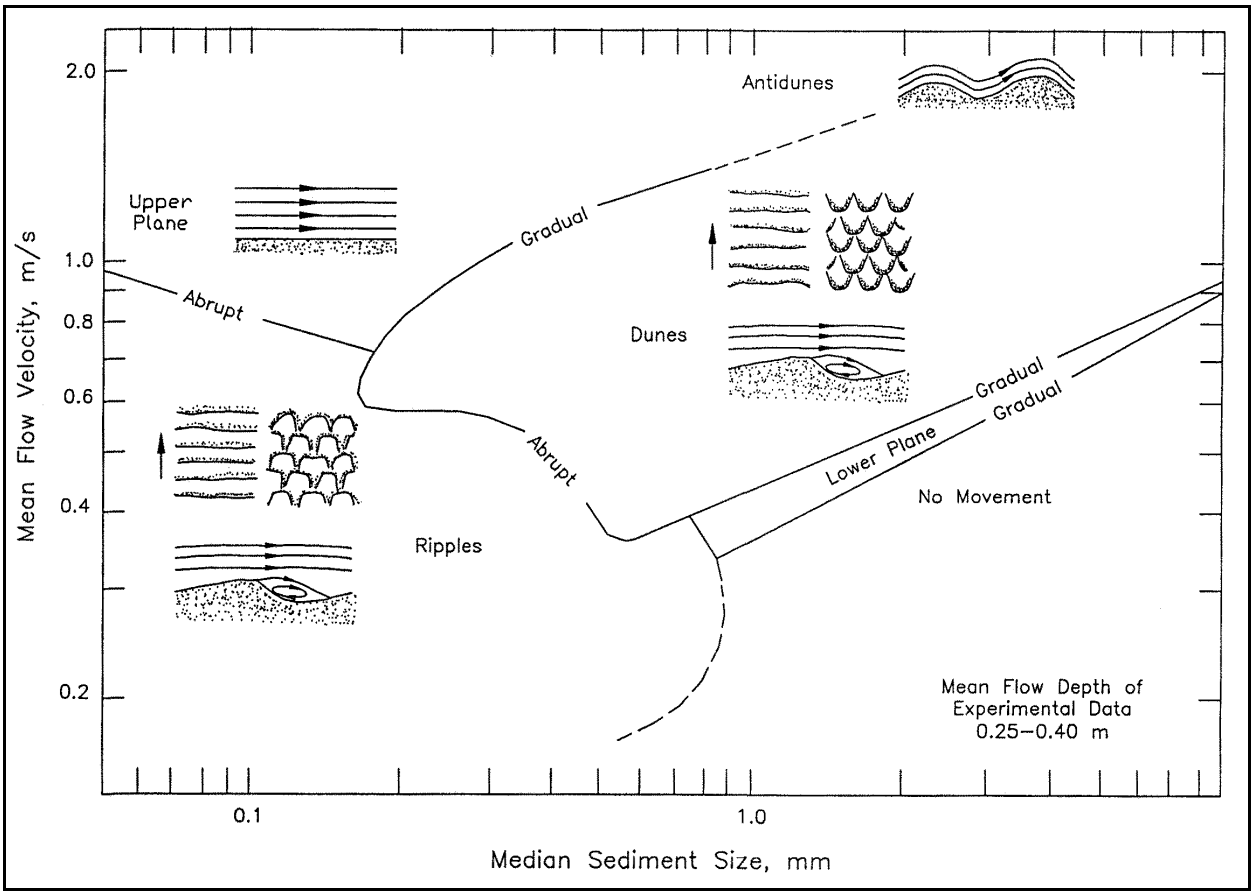

Figure IV-3-6. Plot of mean flow velocity against mean grain size, based on laboratory studies, showing stability phases of subaqueous bed forms (modified from Ashley (1990)). Original data from various sources, standardized to 10° C water temperature (original data points not shown)

b. General delta classification. Coleman and Wright (1975) identified six broad classes of deltas using an energy criteria. These models have been plotted on Figure IV-3-7 according to the relative importance of river, wave, and tide processes. However, Wright (1985) acknowledged that because each delta has unique and distinct features, no classification scheme can adequately encompass the wide variety of environments and structures found at deltas around the world.

c. Delta-forming processes.

(1) Force balance. Every delta is the result of a balance of forces that interact in the vicinity of the river mouth. A river carries sediment to the coast and deposits it beyond the mouth. Tidal currents and waves rework the newly deposited sediments, affecting the shape and form of the resulting structure. The long-term evolution of a delta plain becomes a function of the rate of riverine sediment input and the rate and pattern of sediment reworking, transport, and deposition by marine processes after the initial deposition. On a large scale, gross deltaic shape is also influenced by receiving basin geometry, regional tectonic stability, rates of subsidence caused by compaction of newly deposited sediment, and rate of sea level rise.

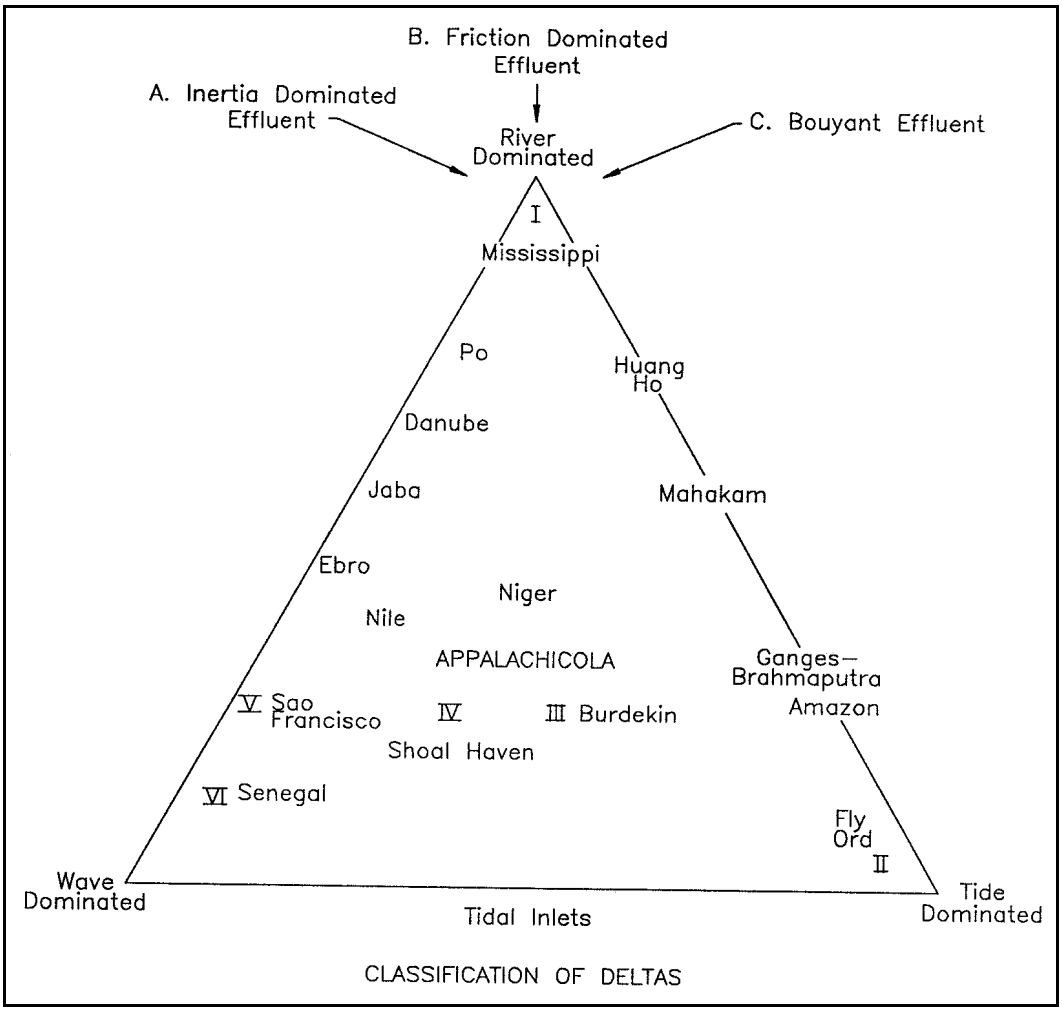

Figure IV-3-7. Classification of deltas

(2) River-dominant deltas.

(a) River-dominant deltas are found where rivers carry so much sediment to the coast that the deposition rate overwhelms the rate of reworking and removal due to local marine forces. In regions where wave energy is very low, even low-sediment-load rivers can form substantial deltas.

(b) When a river is completely dominant over marine forces, the delta shape develops as a pattern of prograding, branching distributary channels (resembling fingers branching from a hand). Interdistributary features include open bays and marshes. A generalized isopach map for this type of delta (Type I in Coleman and Wright's (1975) classification) is shown in Figure IV-3-8. A prime example is the Mississippi River, which not only transports an enormous amount of sediment, but also empties into the low wave-energy, low tide-range Gulf of Mexico (Figure IV-3-9). The Fraser River, which flows into the sheltered Strait of Georgia, is another example (Figure IV-3-10). The Mississippi is discussed in more detail later.

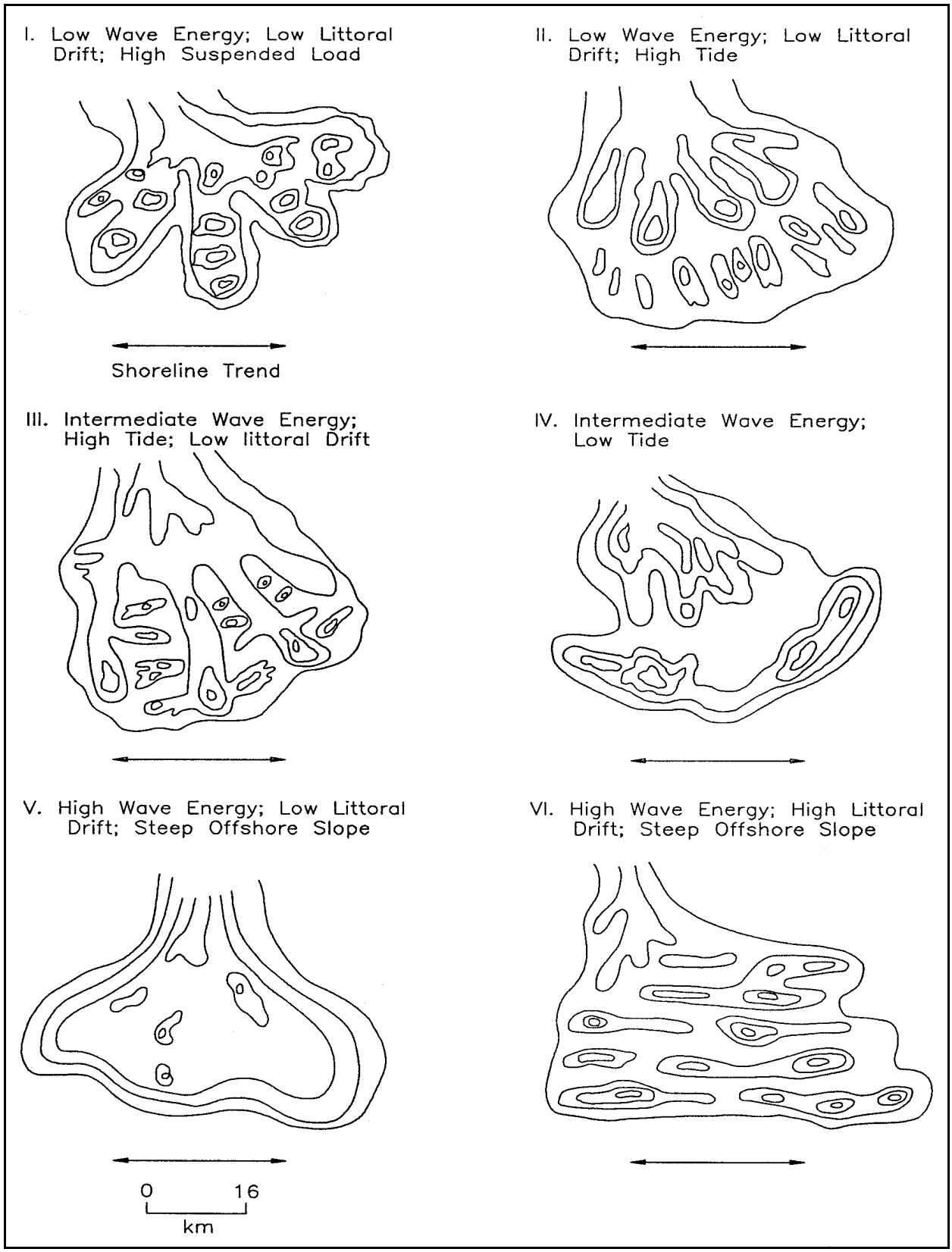

Figure IV-3-8. Isopach map for river-dominant deltas

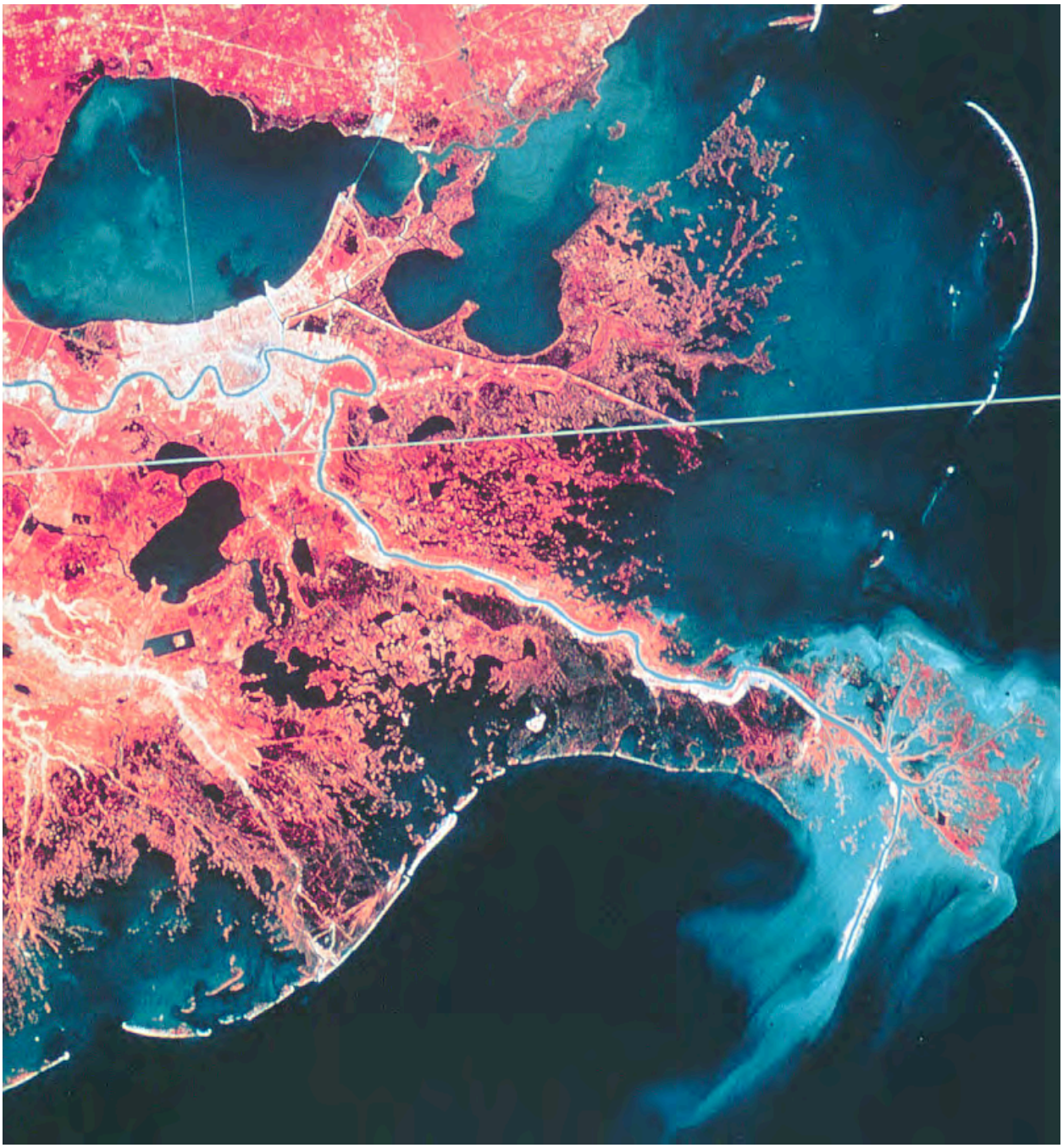

Figure IV-3-9. Mississippi River Delta. The river, which flows into the Gulf of Mexico, has several outlets that are dredged by the Corps of Engineers almost continuously. The city of New Orleans is at the upper left of the image immediately south of Lake Pontchartrain. Landsat 2 image (date unknown)

(3) Wave-dominant deltas.

(a) At wave-dominant deltas, waves sort and redistribute sediments delivered to the coast by rivers and remold them into shoreline features such as beaches, barriers, and spits. The morphology of the resulting delta reflects the balance between sediment supply and the rate of wave reworking and redistribution. Wright and Coleman (1972, 1973) found that deltas in regions of the highest nearshore wave energy flux developed

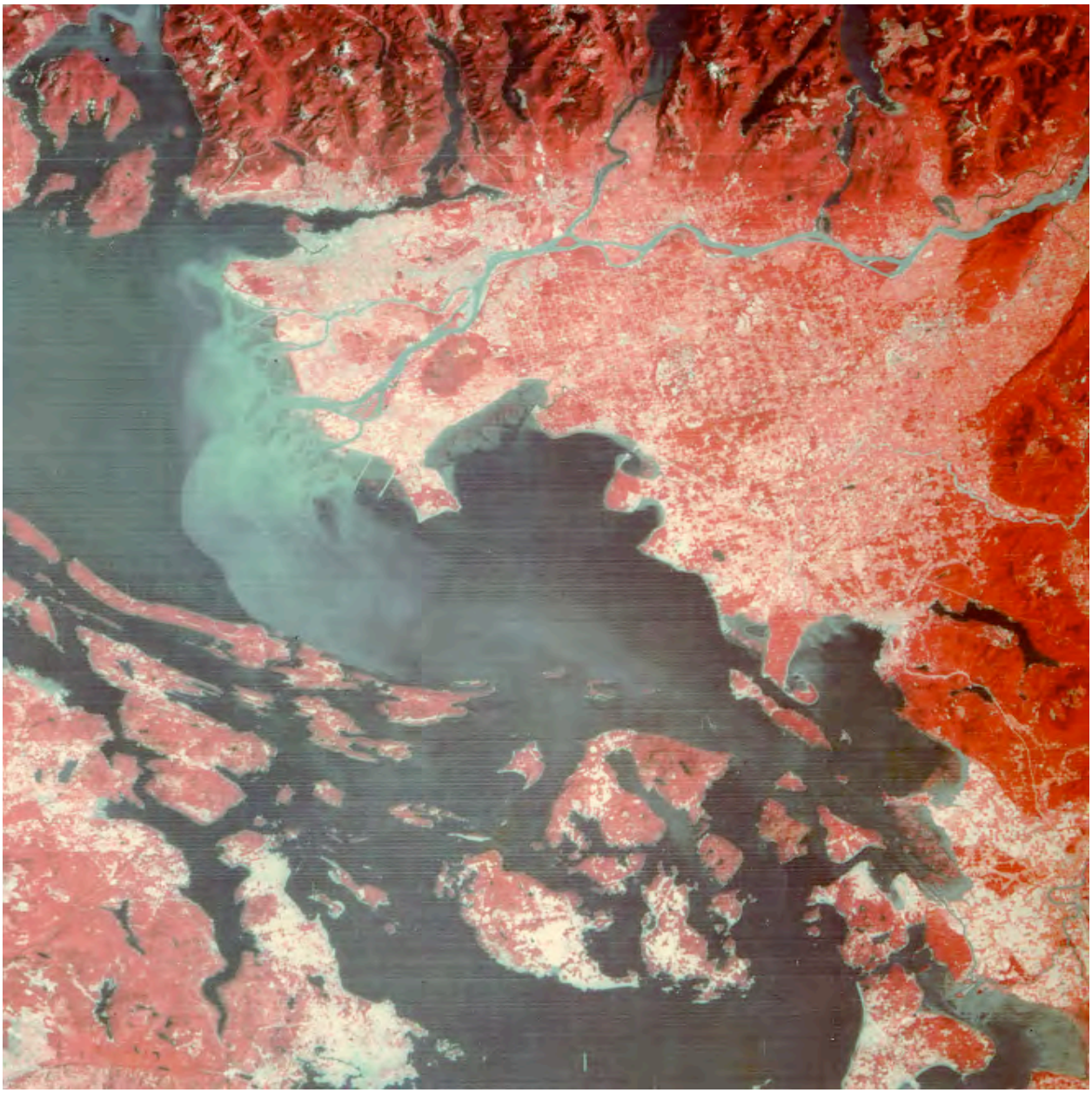

Figure IV-3-10. Fraser River Delta, British Columbia. The river flows into the sheltered Strait of Georgia past the city of Vancouver. The strait has high tidal currents, as shown by the plume of turbid water flowing to the southeast. This delta is also Class I, riverine-dominated (NASA ERTS, 12 Aug 1973)

the straightest shorelines and best-developed interdistributary beaches and beach-ridge complexes (Figure IV-2-3).

(b) Of 16 deltas compared by Wright and Coleman (1972, 1973), the Mississippi was the most river-dominated while the Senegal in west Africa was the other extreme, the most wave-dominated. A model of the Senegal (Type VI in Figure IV-3-8) shows that abundant beach ridges are parallel to the prevailing shoreline trend and that the shore is relatively straight as a result of high wave energy and a strong unidirectional littoral drift.

(c) An intermediate delta form is represented by the delta of the Rio São Francisco del Norte in Brazil (Type V in Figure IV-3-8). Distributary-mouth-bar deposits are restricted to the immediate vicinity of the river mouth and are quickly remolded by waves. Persistent wave energy redistributes the riverine sediment to form extensive sand sheets. The exposed delta plain consists primarily of beach ridges and aeolian dunes.

(4) Tide-dominant deltas.

Three important processes characterize tide-dominated deltas:

(a) At the river mouths, mixing obliterates vertical density stratification, eliminating the effects of buoyancy.

(b) For part of the year, tidal currents may be responsible for a greater fraction of the sediment-transporting energy than the river. As a result, sediment transport in and near the river mouth is bidirectional over a tidal cycle.

(c) The location of the land-sea interface and the zone of marine-riverine interactions is greatly extended both vertically and horizontally. Examples of deltas that are strongly influenced by tides include the Ord (Australia), Shatt-al-Arab (Iraq), Amazon (Brazil), Ganges-Brahmaputra (Bangladesh), and the Yangtze (China). Characteristic features of river mouths in macrotidal environments are bell-shaped, sand-filled channels and linear tidal sand ridges. The crests of the ridges, which have relief of 10-20 m, may be exposed at low tide. The ridges replace the distributary-mouth bars found at other deltas and become the dominant sediment-accumulation form. As the delta progrades over time, the ridges grow until they are permanently exposed, forming large, straight tidal channels (Type II in Figure IV-3-8). An example of a macrotidal delta is the Ord of Western Australia and the Essex River Delta in Massachusetts (Figure IV-3-11).

(5) Intermediate forms.

(a) As stated above, the morphology of most deltas is a result of a combination of riverine, tidal, and wave forces. One example of an intermediate form is the Burdekin Delta of Australia (Type II in Figure IV-3-8). High waves redistribute sands parallel to the coastline trend and remold them into beach ridges and barriers. Within the river mouths, tidal currents produce sand-filled river channels and tidal creeks. This type of delta displays a broad range of characteristics, depending upon the relative strength of waves versus tides. In addition, features may vary seasonally if runoff and wave climate change. Other examples include the Irrawaddy (Burma), Mekong (Vietnam), and Red (Vietnam) Deltas (Wright 1985).

(b) The fourth model of delta geometry is characterized by offshore bay-mouth barriers that shelter lagoons, bays, or estuaries into which low-energy deltas prograde (Type IV, Figure IV-3-8). Examples include the Appalachicola (Florida Panhandle), Sagavanirktok (Alaska), and Shoalhaven (southeastern Australia) Deltas (Wright 1985). In contrast to the river-dominant models, the major accumulation of prodelta mud occurs landward of the main sand body (the barrier), and at the same elevation, within the protected bay. Although suspended fines reach the open sea, wave action prevents mud accumulation as a distinct unit over the open shelf.

d. Deltaic components and sediments.

(1) Generally, all deltas consist of four physiographic zones: an alluvial valley, upper deltaic plain, lower deltaic plain, and subaqueous deltaic plain (Figure IV-3-12). The deposition that occurs adjacent to and between the distributory channels accounts for most of the subaerial delta. In the case of the Mississippi

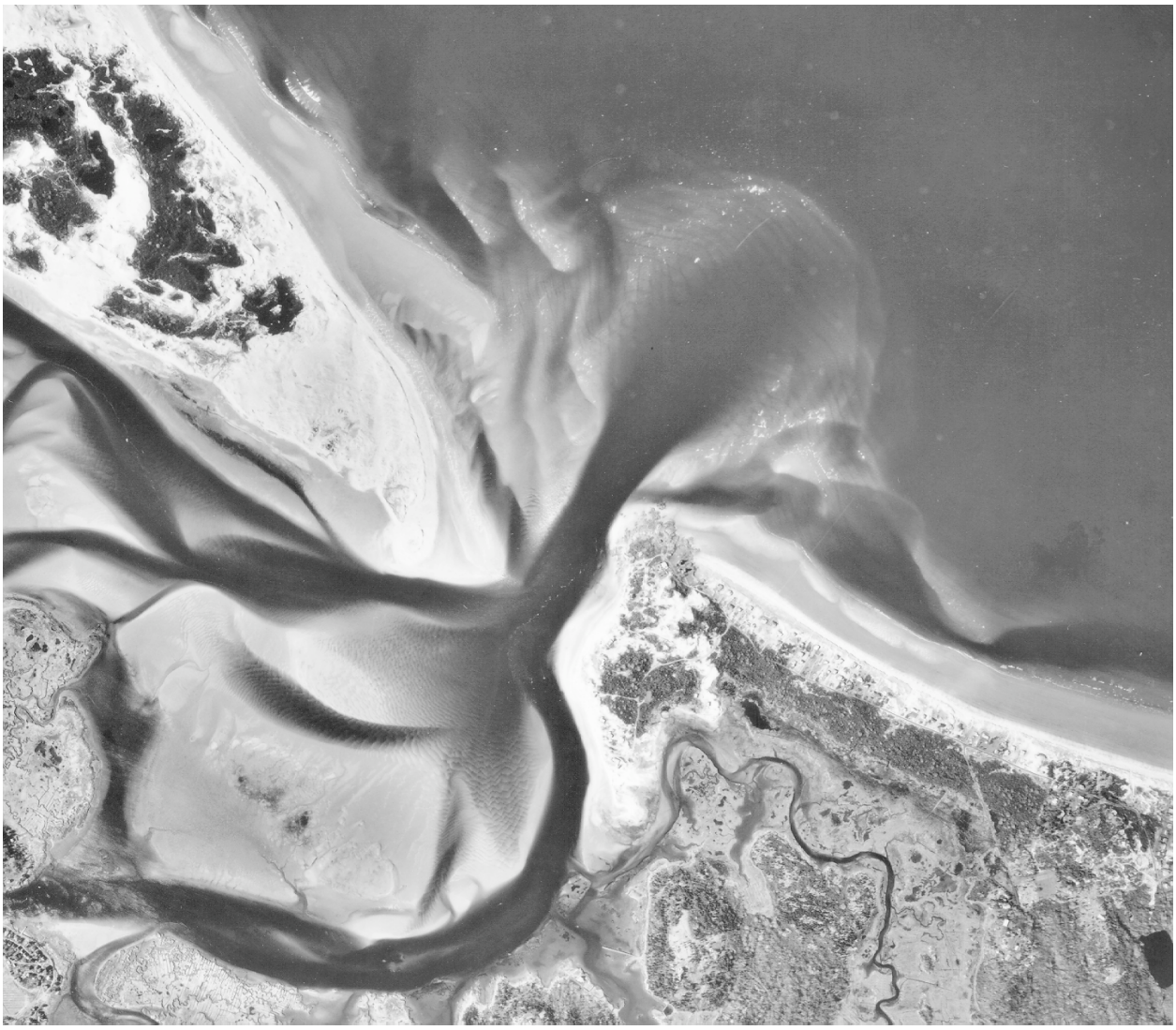

Figure IV-3-11. Mouth of the Essex River, Massachusetts (23 April 1978). This delta is Class II, high tide and low wave energy, or possibly Class III, intermediate wave and high tide. This river mouth is anchored on the south by rock outcrops. Formerly, there may have been more open water in the back bays, and the morphology would have resembled an inlet in a barrier spit

delta, significant sand accumulates in the interdistributory region when breaks in the levees occur, allowing river water to temporarily escape from the main channel. These accumulations are called *crevasse splays*.

(2) The subaqueous plain is the foundation over which the modern delta progrades (as long as the river occupies the existing course and continues to supply sufficient sediment). The subaqueous plain is characterized by a seaward-fining of sediments, with sand being deposited near the river mouths and clays settling further offshore. The seawardmost unit of the plain is the prodelta. It overlies the sediments of the inner continental shelf and consists of a blanket of clays deposited from suspension. The prodelta of the Mississippi ranges from 20 to 50 m thick and extends seaward to water depths of 70 m. The Mississippi's prodelta contains pods of distributory mouth bar sands and their associated cross bedding, flow structures, and shallow-water fauna. These pods may be slump blocks carried down to the prodelta by submarine landslides (Prior and Coleman 1979). Slumping and mudflow are mechanisms that transport large masses of sediment down to the edge of the continental slope and possibly beyond. These mass movements are a

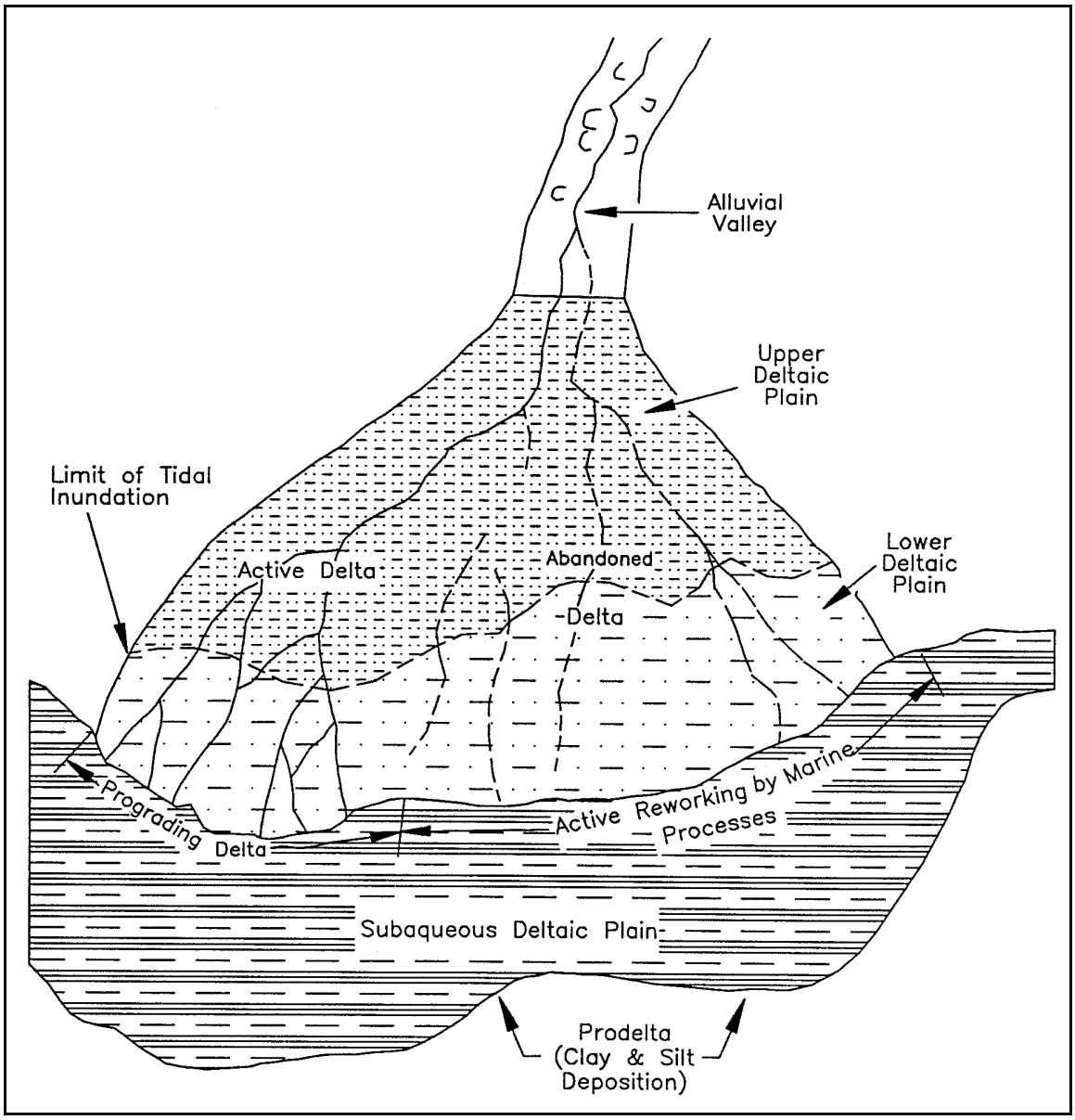

Figure IV-3-12. Basic physiographic units common to all deltas (from Wright (1985))

serious hazard to oil drilling and production platforms. Mud diapirs, growth faults, mud/gas vents, pressure ridges, and mudflow gullies are other evidence of sediment instability on the Mississippi Delta (Figure IV-3-13). Additional details of this interesting subject are covered in Coleman (1988), Coleman and Garrison (1977), Henkel (1970), and Prior and Coleman (1980).

(3) Above the delta front, there is a tremendous variability of sediment types. A combination of shallow marine processes, riverine influence, and brackish-water faunal activity causes the interdistributory bays to display an extreme range of lithologic and textural types. On deltas in high tide regions, the interdistributory bay deposits are replaced by tidal and intertidal flats. West of the Mississippi Delta is an extensive chenier plain. Cheniers are long sets of sand beach ridges, located on mudflats.

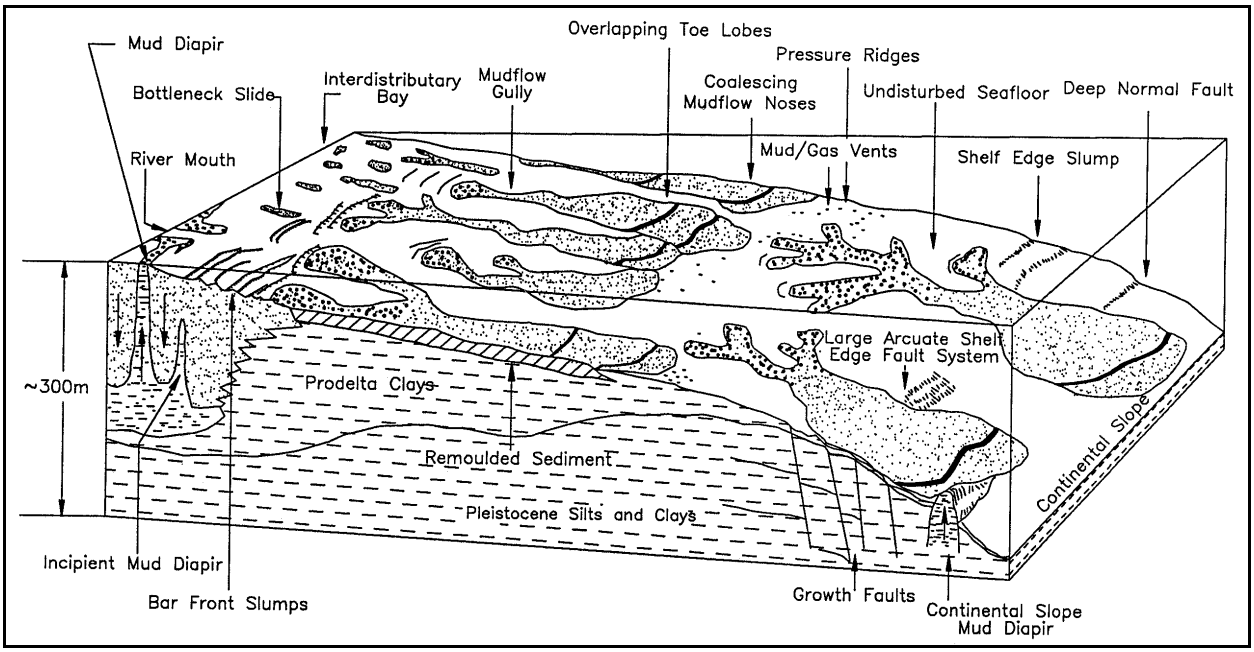

Figure IV-3-13. Structures and types of sediment instabilities on the Mississippi Delta (from Coleman (1988))

e. River mouth flow and sediment deposition.

(1) River mouth geometry and river mouth bars are influenced by, and in turn influence, effluent dynamics. This subject needs to be examined in detail because the principles are pertinent to both river mouths and tidal inlets. Diffusion of the river's effluent and the subsequent sediment dispersion depend on the relative strengths of three main factors:

(a) Inertia of the issuing water and associated turbulent diffusion.

(b) Friction between the effluent and the seabed immediately seaward of the mouth.

(c) Buoyancy resulting from density contrasts between river flow and ambient sea or lake water.

Based on these forces, three sub-classes of deltaic deposition have been identified for river-dominated deltas (Figure IV-3-7). Two of these are well illustrated by depositional features found on the Mississippi Delta.

(2) Depositional model type A - inertia-dominated effluent.

(a) When outflow velocities are high, depths immediately seaward of the mouth tend to be large, density contrasts between the outflow and ambient water are low, and inertial forces dominate. As a result, the effluent spreads and diffuses as a turbulent jet (Figure IV-3-14a). As the jet expands, its momentum decreases, causing a reduction of its sediment carrying capacity. Sediments are deposited in a radial pattern, with the coarser bed load dropping just beyond the point where the effluent expansion is initiated. The result is basinward-dipping foreset beds.

(b) This ideal model is probably unstable under most natural conditions. As the river continues to discharge sediment into the receiving basin, shoaling eventually occurs in the region immediately beyond the mouth (Figure IV-3-14b). For this reason, under typical natural conditions, basin depths in the zone of the

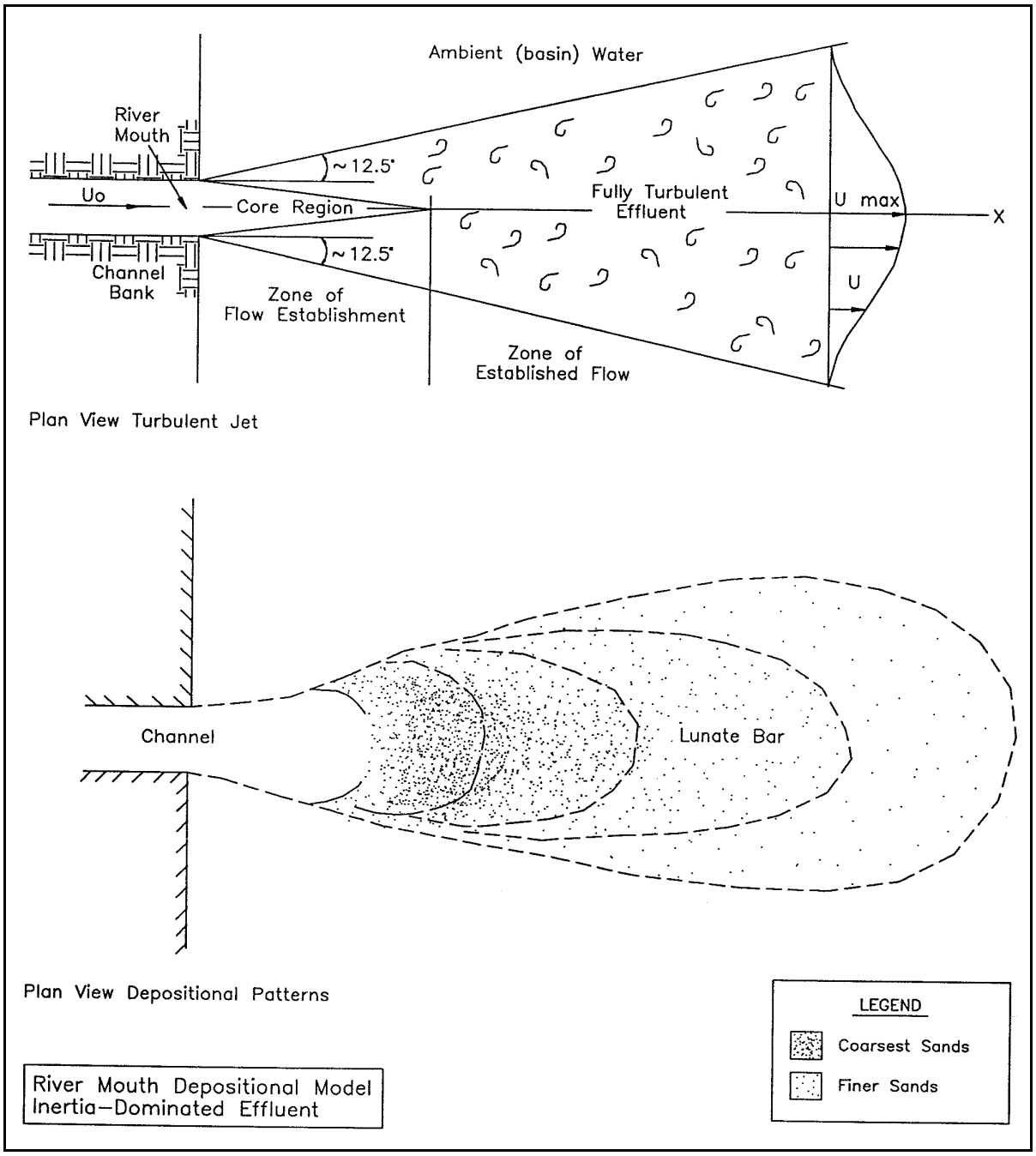

Figure IV-3-14. Plan view of depositional Model A, inertia-dominated effluent (adapted from Wright (1985)) (Continued)

jet's diffusion are unlikely to be deeper than the outlet depth. Effluent expansion and diffusion become restricted horizontally as a plane jet. More important, friction becomes a major factor in causing rapid deceleration of the jet. Model 'A' eventually changes into friction-dominated Model 'B'.

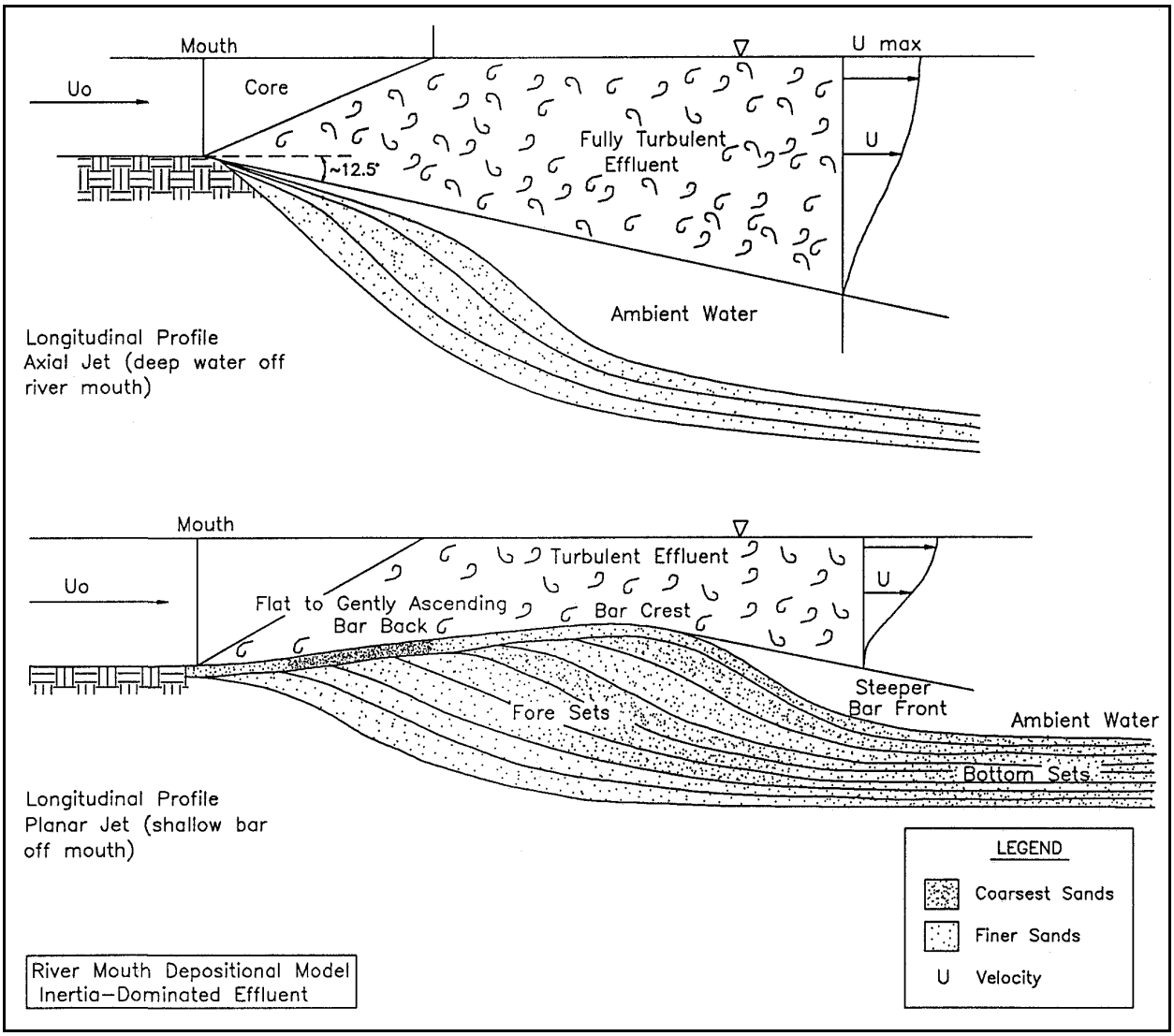

Figure IV-3-14. (Concluded)

(3) Depositional model type B - friction-dominated effluent.

(a) When homopycnal,[1] friction-dominated outflow issues over a shallow basin, a distinct pattern of bars and subaqueous levees is formed (Figure IV-3-15). Initially, the rapid expansion of the jet produces a broad, arcuate radial bar. As deposition continues, natural subaqueous levees form beneath the lateral boundaries of the expanding jet where the velocity decreases most rapidly. These levees constrict the jet from expanding further. As the central portion of the bar grows upward, channels form along the lines of greatest turbulence, which tend to follow the subaqueous levees. The result is the formation of a bifurcating channel that has a triangular middle-ground shoal separating the diverging channel arms. The flow tends to be concentrated into the divergent channels and to be tranquil over the middle ground under normal conditions.

[1] River water and ambient water have the same density (for example, a stream entering a freshwater lake).

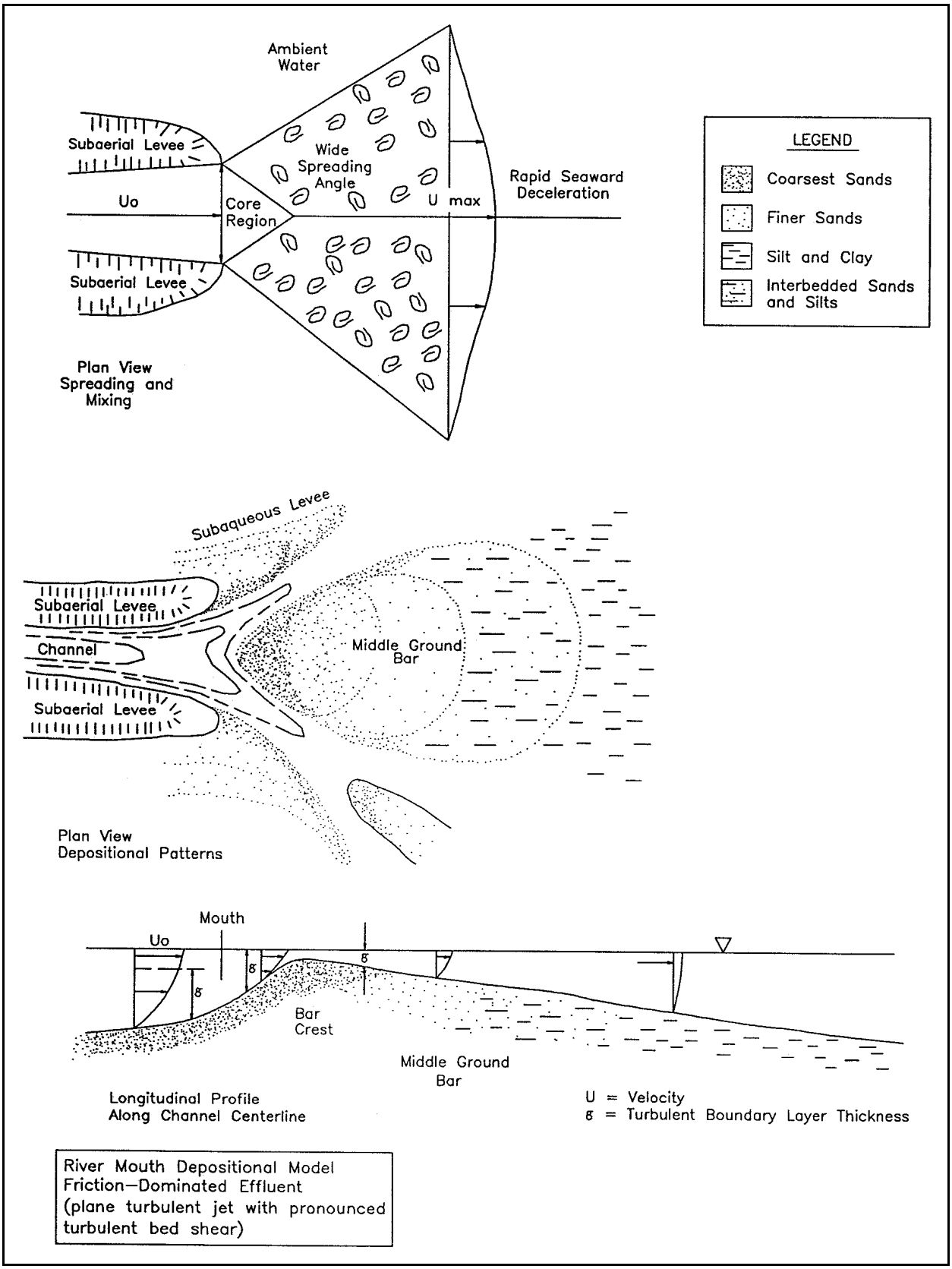

Figure IV-3-15. Depositional model type B, friction-dominated effluent (adapted from Wright (1985))

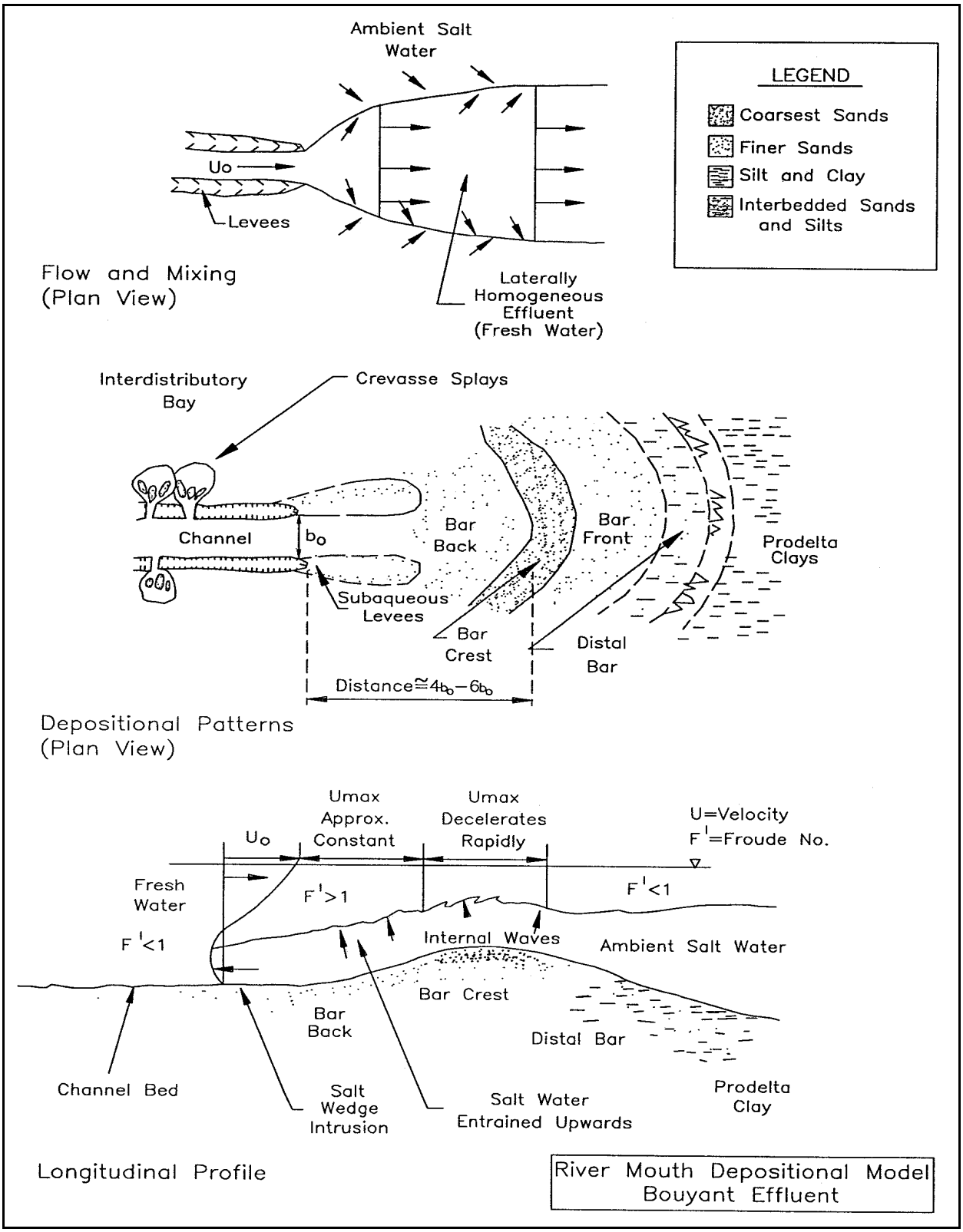

Figure IV-3-16. River mouth bar crest features, depositional model type C, buoyant effluent (adapted from Wright (1985)) (Continued)

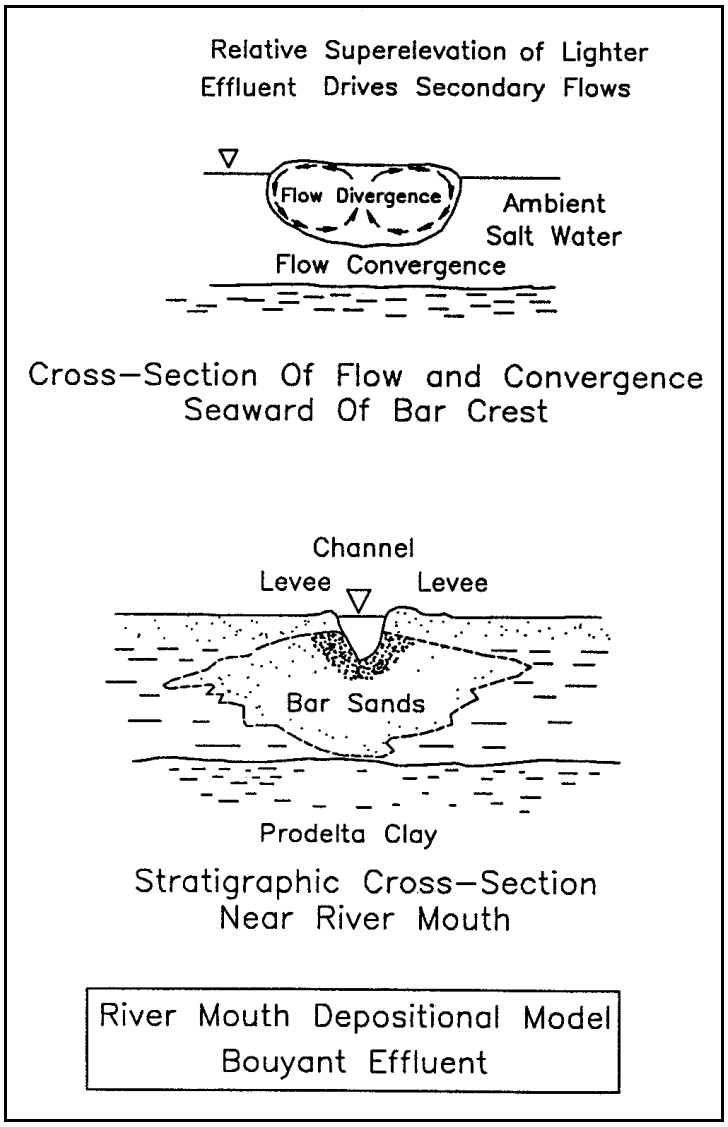

Figure IV-3-16. (Concluded)

(b) This type of bar pattern is most common where nonstratified outflow enters a shallow basin. Examples of this pattern (known as *crevasse splays* or *overbank splays*) are found at crevasses along the Mississippi River levees. These secondary channels run perpendicular to the main Mississippi channels and allow river water to debouch into the broad, shallow interdistributory bays. This process forms the major subaerial land (marsh) of the lower Mississippi delta (Coleman 1988).

(4) Depositional model type C - buoyant effluent.

(a) Stratification often occurs when fresh water flows out into a saline basin. When the salt wedge is well developed, the effluent is effectively isolated from the effects of bottom friction. Buoyancy suppresses mixing and the effluent spreads over a broad area, thinning progressively away from the river mouth (Figure IV-3-16). Deceleration of the velocity of the effluent is caused by the upward entrainment of seawater across the density interface.

(b) The density interface between the freshwater plume and the salt wedge is often irregular due to internal waves (Figure IV-3-16a). The extent that the effluent behaves as a turbulent or buoyant jet depends largely on the Froude number *F'*:

$$F' = \frac{U^2}{\gamma g h'} \tag{IV-3-1}$$

where

U = mean outflow velocity of upper layer (in case of stratified flow)

g = acceleration of gravity

h' = depth of density interface

$$\gamma = 1 - (\rho_f/\rho_s) \tag{IV-3-2}$$

where

ρ_f = density of fresh water

ρ_s = density of salt water

As *F'* increases, inertial forces dominate, accompanied by an increase in turbulent diffusion. As *F'* decreases, turbulence decreases and buoyancy becomes more important. Turbulence is suppressed when *F'* is less than 1.0 and generally increases as *F'* increases beyond 1.0 (Wright 1985).

(c) The typical depositional patterns associated with buoyant effluent are well represented by the mouths of the Mississippi River (Wright and Coleman 1975). Weak convergence near the base of the effluent inhibits lateral dispersal of sand, resulting in narrow bar deposits that prograde seaward as laterally restricted "bar-finger sands" (Figure IV-3-16b). The same processes presumably prevent the subaqueous levees from diverging, causing narrow, deep distributory channels. Because the active channels scour into the underlying distributory-mouth bar sands as they prograde, accumulations of channel sands are usually limited. Once the channels are abandoned, they tend to fill with silts and clays. It is believed that the back bar and bar crest grow mostly from bed-load transport during flood stages. The subaqueous levees, however, appear to grow year-round because of the near-bottom convergence that takes place during low and normal river stages.

f. Mississippi Delta - Holocene history, dynamic changes.

(1) General. The Mississippi River, which drains a basin covering 41 percent of the continental United States (3,344,000 sq km), has deposited an enormous mound of unconsolidated sediment in the Gulf of Mexico. The river has been active since at least late Jurassic times and has dominated deposition in the northern Gulf of Mexico. Many studies have been conducted on the Mississippi Delta, leading to much of our knowledge of deltaic sedimentation and structure. The ongoing research is a consequence of the river's critical importance to commerce and extensive petroleum exploration and production in the northern Gulf of Mexico during the last 50 years.

(2) Deposition time scales. The Mississippi Delta consists of overlapping deltaic lobes. Each lobe covers 30,000 sq km and has an average thickness of about 35 m. The lobes represent the major sites of the river's deposition. The process of switching from an existing lobe to a new outlet takes about 1500 years

(Coleman 1988). Within a single lobe, deposition in the bays occurs from overbank flows, crevasse splays, and biological production. The bay fills, which cover areas of 250 sq km and have a thickness of only 15 m, accumulate in only about 150 years. Overbank splays, which cover areas of 2 sq km and are 3 m thick, occur during major floods when the natural levees are breached. The mouths of the Mississippi River have prograded seawards at remarkable rates. The distributory channels can form sand bodies that are 17 km long, 8 km wide, and over 80 m thick in only 200 years (Coleman 1988).

(3) Holocene history. During the last low sea level stand, 18,000 years ago, the Mississippi River entrenched its valley, numerous channels were scoured across the continental shelf, and deltas were formed near the shelf edge (Suter and Berryhill 1985). As sea level rose, the site of deposition moved upstream to the alluvial valley. By about 9,000 years before present, the river began to form its modern delta. In more recent times, the shifting deltas of the Mississippi have built a delta plain covering a total area of 28,500 sq km. The delta switching, which has occurred at high frequency, combined with a rapidly subsiding basin, has resulted in vertically stacked cyclic sequences. Because of rapid deposition and switching, in a short time the stacked cyclic deltaic sequences have attained thicknesses of thousands of meters and covered an area greater than 150,000 sq km (Coleman 1988). Figure IV-3-17 outlines six major lobes during the last 7,500 years.

(4) Modern delta. The modern delta, the Balize or Birdfoot, began to prograde about 800 to 1,000 years ago. Its rate of progradation has diminished recently and the river is presently seeking a new site of deposition. Within the last 100 years, a new distributory, the Atchafalaya, has begun to divert an increasing amount of the river's flow. Without river control structures, the new channel would by now have captured all of the Mississippi River's flow, leading to rapid erosion of the Balize Delta. (It is likely that there would be a commensurate deterioration of the economy of New Orleans if it lost its river.) Even with river control projects, the Atchafalaya is actively building a delta in Atchafalaya Bay (lobe 6 in Figure IV-3-17).

g. Sea level rise and deltas.

(1) Deltas experience rapid local relative sea level rise because of the natural compaction of deltaic sediments from dewatering and consolidation. Deltas are extremely vulnerable to storms because the subaerial surfaces are flat and only slightly above the local mean sea level. Only a slight rise in sea level can extend the zone subject to storm surges and waves further inland. As stated earlier, delta evolution is a balance between the accumulation of fluvially supplied sediment and the reworking, erosion, and transport of deltaic sediment by marine processes (Wright 1985). Even a river like the Mississippi, which has a high sediment load and drains into a low wave-energy basin, is prograding only in the vicinity of the present distributory channels, the area defined as the active delta (Figures IV-3-9 and IV-3-12).

(2) Deltas are highly fertile agriculturally because of the steady supply of nutrient-laden soil. As a result, some of the world's greatest population densities - over 200 inhabitants per square kilometer - are found on deltas (*The Times Atlas of the World* 1980):

(a) Nile Delta, Egypt.

(b) Chang Jiang (Yangtze), China.

(c) Mekong, Vietnam.

(d) Ganga (Ganges), Bangladesh.

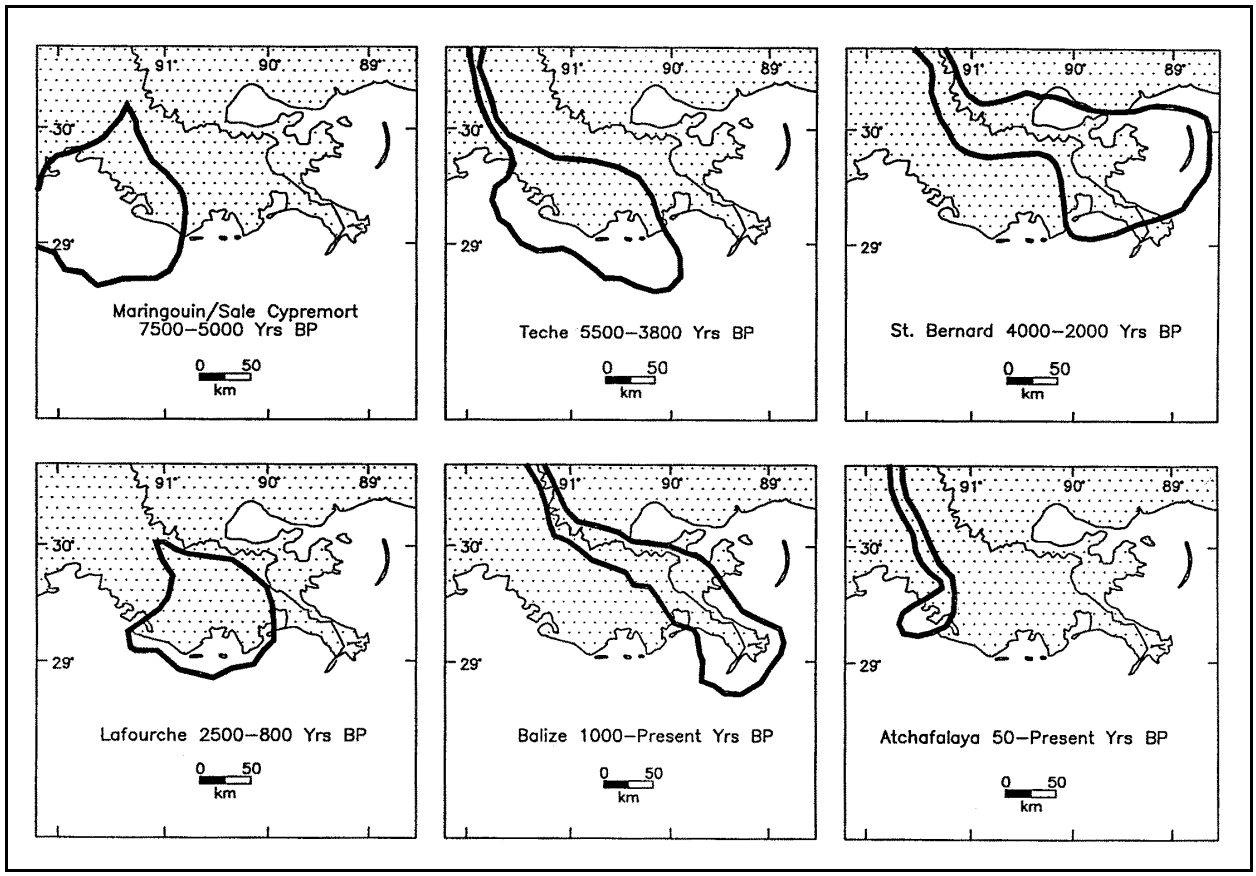

Figure IV-3-17. Shifting sites of deltaic sedimentation of the Mississippi River (from Coleman (1988))

These populations are very vulnerable to delta land loss caused by rising sea level and by changes in sediment supply due to natural movements of river channels or by upland man-made water control projects.

(3) Inhabitants of deltas are also in danger of short-term changes in sea level caused by storms. Tropical storms can be devastating: the Bay of Bengal cyclone of November 12, 1970, drowned over 200,000 persons in what is now Bangladesh (Carter 1988). Hopefully, public education, improving communications, better roads, and early warning systems will be able to prevent another disaster of this magnitude. Coastal management in western Europe, the United States, and Japan is oriented towards the orderly evacuation of populations in low-lying areas and has greatly reduced storm-related deaths. In contrast to the Bay of Bengal disaster, Hurricane Camille (August 17-20, 1969), caused only 236 deaths in Louisiana, Mississippi, Alabama, and Florida.

IV-3-4. Coastal Inlets

a. Introduction.

(1) Coastal inlets play an important role in nearshore processes around the world. *Inlets* are the openings in coastal barriers through which water, sediments, nutrients, planktonic organisms, and pollutants are exchanged between the open sea and the protected embayments behind the barriers. In the United States, the classical image of an inlet is of an opening in one of the Atlantic or Gulf of Mexico barrier islands, but inlets are certainly not restricted to barrier environments or to shores with tides. On the West Coast and in the Great

Lakes, many river mouths are considered to be inlets, while in the Gulf of Mexico, the wide openings between the barriers, locally known as passes, are also inlets. Inlets can be cut through unconsolidated shoals or emergent barriers as well as through clay, rock, or organic reefs (Price 1968). There is no simple, restrictive definition of inlet; based on the geologic literature and on regional terminology, almost any opening in the coast, ranging from a few meters to several kilometers wide, can be called an inlet. Inlets are important economically to many coastal nations because harbors are often located in the back bays, requiring that the inlets be maintained for commercial navigation. At many inlets, the greatest maintenance cost is incurred by repetitive dredging of the navigation channel. Because inlets are hydrodynamically very complex, predictions of shoaling and sedimentation have often been unsatisfactory. A better understanding of inlet sedimentation patterns and their relationship to tidal and other hydraulic processes can hopefully contribute to better management and engineering design.

(2) Tidal inlets are analogous to river mouths in that sediment transport and deposition patterns in both cases reflect the interaction of outflow inertia and associated turbulence, bottom friction, buoyancy caused by density stratification, and the energy regime of the receiving body of water (Wright and Sonu 1975). However, two major differences usually distinguish lagoonal inlets from river mouths, sometimes known as fluvial or riverine inlets (Oertel 1982).

(a) Lagoonal tidal inlets experience diurnal or semidiurnal flow reversals.

(b) Lagoonal inlets have two opposite-facing mouths, one seaward and the other lagoonward. The sedimentary structures which form at the two openings differ because of differing energy, water density, and geometric factors.

(3) The term *lagoon* refers to the coastal pond or embayment that is connected to the open sea by a tidal inlet. The *throat* of the inlet is the zone of smallest cross section, which, accordingly, has the highest flow velocities. The *gorge* is the deepest part of an inlet and may extend seaward and landward of the throat (Oertel 1988). *Shoal* and *delta* are often used interchangeably to describe the ebb-tidal sand body located at the seaward mouth of an inlet.

b. Technical literature. Pioneering research on the stability of inlets was performed by Francis Escoffier (1940, 1977). O'Brien (1931, 1976) derived general empirical relationships between tidal inlet dimension and tidal prism. Keulegan (1967) developed algorithms to relate tidal prism to inlet cross section. Bruun (1966) examined inlets and littoral drift, and Bruun and Gerritsen (1959, 1961) studied bypassing and the stability of inlets. Hubbard, Oertel, and Nummedal (1979) described the influence of waves and tidal currents on tidal inlets in the Carolinas and Georgia. Hundreds of other works are referenced in the USACE *General Investigation of Tidal Inlets* (GITI) reports (Barwis 1976), in special volumes like *Hydrodynamics and Sediment Dynamics of Tidal Inlets* (Aubrey and Weishar 1988), in textbooks on coastal environments (Carter 1988; Cronin 1975; Komar 1998), and in review papers (Boothroyd 1985; FitzGerald 1988). Older papers on engineering aspects of inlets are cited in Castañer (1971). There are also numerous foreign works on tidal inlets: Carter (1988) cites references from the British Isles; Sha (1990) from the Netherlands; Nummedal and Penland (1981) and FitzGerald, Penland, and Nummedal (1984) from the North Sea coast of Germany; and Hume and Herdendorf (1988, 1992) from New Zealand. More references are listed in Parts II-6 and V-6.

c. Classification of inlets and geographic distribution.

(1) Tidal inlets are found around the world in a broad range of sizes and shapes. Because of their diversity, it has been difficult to develop a suitable classification scheme. One approach has been to use an energy-based criteria, in which inlets are ranked according to the wave energy and tidal range of the environment in which they are located (Figure IV-1-10).

(2) Regional geological setting can be a limiting factor restricting barrier and, in turn, inlet development. Most inlets are on trailing-edge coasts with wide coastal plains and shallow continental shelves (e.g., the Atlantic and Gulf of Mexico shores of the United States). High relief, leading-edge coastlines have little room for sediment to accumulate either above or below sea level. Sediment tends to collect in pockets between headlands, few lagoons are formed, and inlets are usually restricted to river mouths. The Pacific coast of North America, in addition to being steep, is subject to high wave energy and has far fewer inlets than the Atlantic.

(3) Underlying geology may also control inlet location and stability. Price and Parker (1979) reported that certain areas along the Texas coast were always characterized by inlets, although the passes tended to migrate back and forth along a limited stretch of the shore. The positions of these permanent inlets were tectonically controlled, but the openings were maintained by tidal harmonics and hydraulics. If storm inlets across barriers were not located at the established stable pass areas, the inlets usually closed quickly. Some inlets in New England are anchored by bedrock outcrops and therefore cannot move freely (for example, the Essex River mouth, Figure IV-3-11).

d. Hydrodynamic processes in inlets. See Part II-6.

e. Geomorphology of tidal inlets. Tidal inlets are characterized by large sand bodies that are deposited and shaped by tidal currents and waves. The *ebb-tide shoal* (or delta) is a sand mass that accumulates seaward of the mouth of the inlet. It is formed by ebb tidal currents and is modified by wave action. The *flood-tide shoal* is an accumulation of sand at the landward opening of an inlet that is mainly shaped by flood currents (Figure IV-3-18). Depending on the size and depth of the bay, a flood shoal may extend into open water or may merge into a complex of meandering tributary channels, point bars, and muddy estuarine sediments.

(1) Ebb-tidal deltas (shoals).

(a) A simplified morphological model of a natural (unjettied) ebb-tidal delta is shown in Figure IV-3-18. The delta is formed from a combination of sand eroded from the gorge of the inlet and sand supplied by longshore currents. This model includes several components:

- A main *ebb channel*, scoured by the ebb jets.
- *Linear* bars that flank the main channel, the result of wave and tidal current interaction.
- A *terminal lobe*, located at the seaward (distal) end of the ebb channel. This is the zone where the ebb jet velocity drops, resulting in sediment deposition.
- *Swash platforms*, which are sand sheets located between the main ebb channel and the adjacent barrier islands.
- *Swash bars* that form and migrate across the swash platforms because of currents (the swash) generated by breaking waves.
- *Marginal flood channels*, which often flank both updrift and downdrift barriers.

Inlets with jetties often display these components, although the marginal flood channels are usually missing.

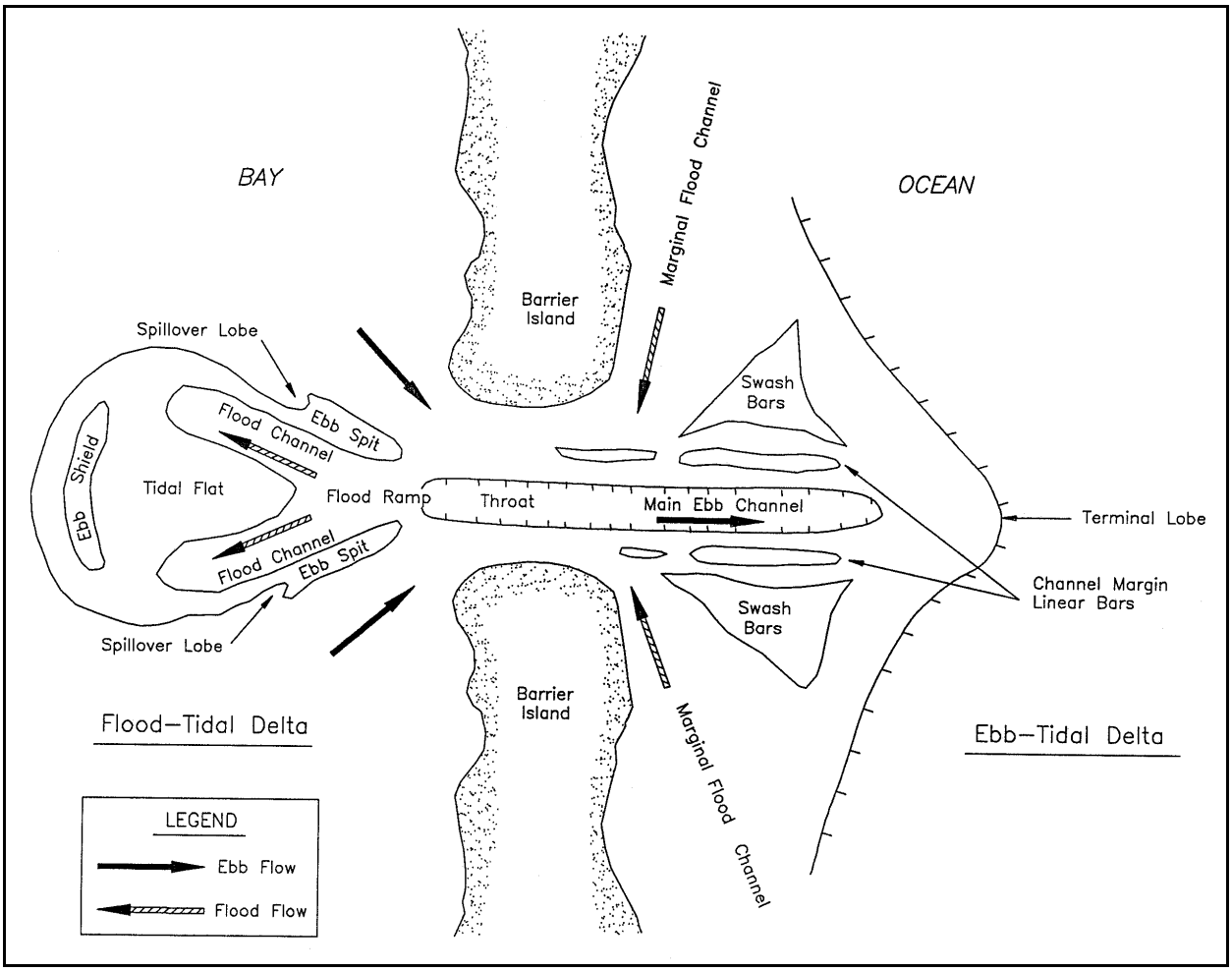

Figure IV-3-18. Definition diagram of a tidal inlet with well-developed flood and ebb deltas (from Boothroyd (1985) and other sources)

(b) For the Georgia coast, Oertel (1988) described simple models of ebb-delta shape and orientation which depended on the balance of currents (Figure IV-3-19). With modifications, these models could apply to most inlets. When longshore currents were approximately balanced and flood currents exceeded ebb, a squat, symmetrical delta developed (Figure IV-3-19a) (example: Panama City, Florida). If the prevailing longshore currents exceeded the other components, the delta developed a distinct northerly or southerly orientation (Figures IV-3-19b and 19c). Note that some of the Georgia ebb deltas change their orientation seasonally, trending north for part of the year and south for the rest. Finally, when inlet currents exceeded the forces of longshore currents, the delta was narrower and extended further out to sea (Figure IV-3-19d) (example: Brunswick, Georgia).

(c) Based on studies of the German and Georgia bights, Nummedal and Fischer (1978) concluded that three factors were critical in determining the geometry of the inlet entrance and the associated sand shoals:

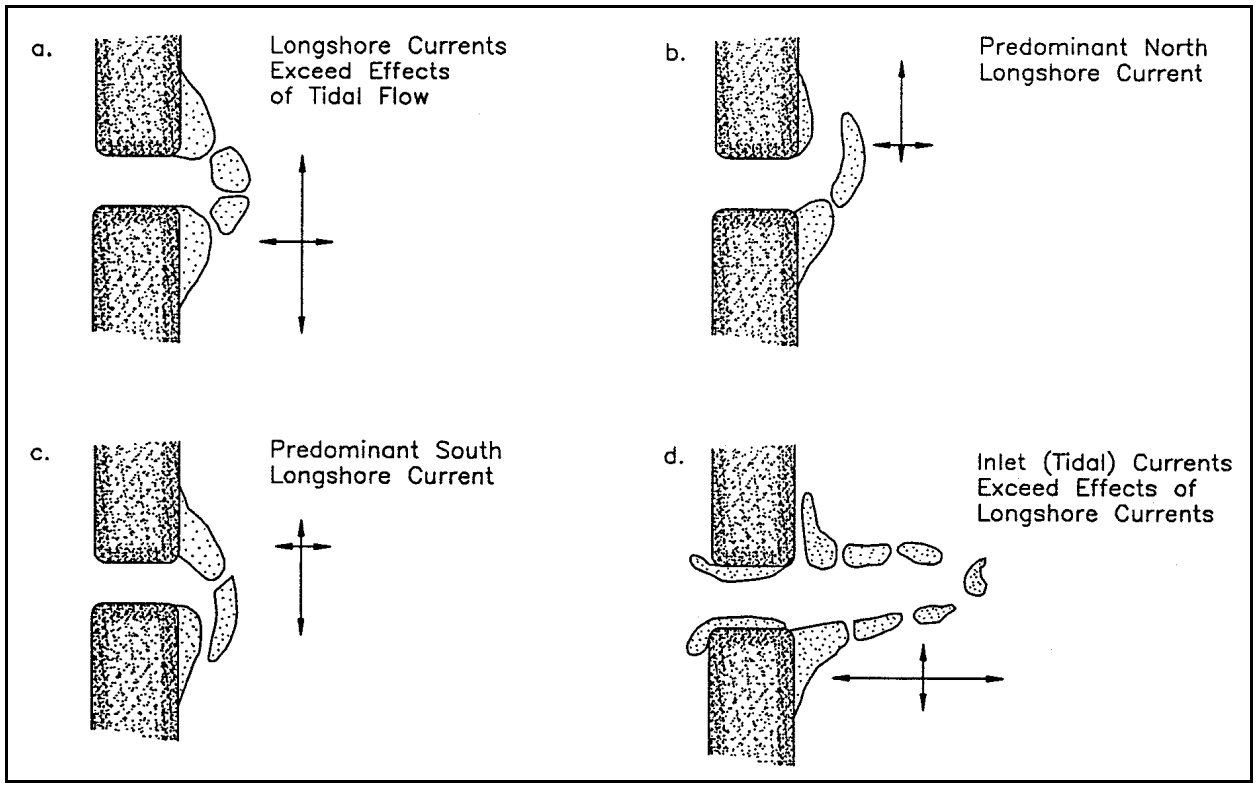

Figure IV-3-19. Four different shapes of ebb-tidal deltas, modified by the relative effects of longshore versus tidal currents (from Oertel (1988))

- Tide range.
- Nearshore wave energy.
- Bathymetry of the back-barrier bay.

For the German and Georgia bights, the latter factor controls velocity asymmetry through the inlet gorge, resulting in greater seaward-directed sediment transport through the inlet than landward transport. This factor has aided the development of large ebb shoals along these coasts, even though the German coast is subject to high wave energy. Back bay area and geometry are likely crucial factors that need to be incorporated in a comprehensive inlet classification scheme.

(d) Net sediment movement. At Price Inlet, South Carolina (FitzGerald and Nummedal 1983) and North Inlet, South Carolina (Nummedal and Humphries 1978), because of peak ebb currents, the resulting seaward-directed sediment transport far exceeded the sediment moved landward during flood. However, ebb velocity dominance does not necessarily mean that net sediment movement is also seaward. At Sebastian Inlet, on Florida's east coast, Stauble et al. (1988) found that net sediment movement was landward although the tidal hydraulics displayed higher ebb currents. The authors concluded that sediment carried into the inlet with the flood tide was deposited on the large, and growing, flood shoal. During ebb tide, current velocities over the flood shoal were too low to remobilize as much sediment as had been deposited on the shoal by the flood tide. The threshold for sediment transport was not reached until the flow was in the relatively narrow throat. In this case, the flood shoal had become a sink for sediment carried into the inlet. Stauble et al. (1988) hypothesized that this pattern of net landward sediment movement, despite ebb hydraulic dominance, may occur at other inlets in microtidal shores that open into large lagoons.

(e) The ebb-tidal deltas along mixed-energy coasts (e.g., East and West Friesian Islands of Germany, South Carolina, Georgia, Virginia, and Massachusetts) are huge reservoirs of sand. FitzGerald (1988) states that the amount of sand in these deltas is comparable in volume to that of the adjacent barrier islands. Therefore, on mixed-energy coasts, minor changes in volume of an ebb delta can drastically affect the supply of sand to the adjacent beaches. In comparison, on wave-dominated barrier coasts (e.g., Maryland, Outer Banks of North Carolina, northern New Jersey, Egypt's Nile Delta), ebb-tidal deltas are more rare and therefore represent a much smaller percentage of the overall coastal sand budget. As a result, volumetric changes in the ebb deltas have primarily local effects along the nearby beaches.

(f) Using data from tidal inlets throughout the United States, Walton and Adams (1976) showed that there is a direct correspondence between an inlet's tidal prism and the size of the ebb-tidal delta, with some variability caused by changes in wave energy. This research underscores how important it is that coastal managers thoroughly evaluate whether proposed structures might change the tidal prism, thereby changing the volume of the ebb-tide shoal and, in turn, affecting the sediment budget of nearby beaches.

(g) Ocean City, Maryland, is offered as an example of the effect of inlet formation on the adjacent coastline: the Ocean City Inlet was formed when Assateague Island was breached by the hurricane of 23 August 1933. The ebb-tide shoal has grown steadily since 1933 and now contains more than 6×10^6 m^3 of sand, located a mean distance of 1,200 m offshore. Since 1933, the growth of the ebb delta combined with trapping of sand updrift of the north jetty have starved the downdrift (southern) beaches, causing the shoreline along the northern few kilometers of Assateague Island to retreat at a rate of 11 m/year (data cited in FitzGerald (1988)) (Figures IV-3-20 and IV-3-21).

(h) In contrast to Ocean City, the decrease in inlet tidal prisms along the East Friesian Islands has been beneficial to the barrier coast. Between 1650 and 1960, the area of the bays behind the island chain decreased by 80 percent, mostly due to reclamation of tidal flats and marshlands (FitzGerald, Penland, and Nummedal 1984). The reduction in area of the bays reduced tidal prisms, which led to smaller inlets, smaller ebb-tidal shoals, and longer barrier islands. Because of the reduced ebb discharge, less sediment was transported seaward. Waves moved ebb-tidal sands onshore, increasing the sediment supply to the barrier beaches.

(i) In many respects, ebb-tide deltas found at tidal inlets are similar to deltas formed at river mouths. The comparison is particularly applicable at rivers where the flow temporarily reverses during the flood stage of the tide. The main difference between the two settings is that river deltas grow over time, fed by fluvially supplied sediment. In contrast, at many tidal inlets, only limited sediment is supplied from the back bay, and the ebb deltas are largely composed of sand provided by longshore drift or reworked from the adjacent beaches. Under some circumstances, inlets and river mouths are in effect the same coastal form. During times of low river flow, the mouth assumes the characteristics of a tidal inlet with reversing tidal currents dominating sedimentation. During high river discharge, currents are unidirectional and fluvial sediment is deposited seaward of the mouth, where it can help feed the growth of a delta. Over time, a tidal inlet that connects a pond to the sea can be converted to a river mouth. This occurs when the back bay fills with fluvial sediment and organic matter. Eventually, rivers that formerly drained into the lagoon flow through channels to the inlet and discharge directly into the sea (for example, see the photograph of the Essex River Delta, Figure IV-3-11).

Figure IV-3-20. Ocean City Inlet, Maryland, September 1933. Ocean City is on Fenwick Island in the top center of the image, the Atlantic Ocean is to the right, and Assateague Island is on the bottom. This photograph was taken only one month after a hurricane breached the barrier island. Note waves breaking at the edge of a small ebb shoal. (Photograph from Beach Erosion Board archives)

(2) Flood-tidal deltas (shoals).

(a) A model of a typical flood-tide shoal is shown in Figure IV-3-18. Flood shoals with many of these features have been described in meso- and micro-tidal environments around the world (Germany (Nummedal and Penland 1981); Florida's east coast (Stauble et al. 1988); Florida's Gulf of Mexico coast (Wright, Sonu, and Kielhorn 1972); and New England (Boothroyd 1985)). The major components are:

Figure IV-3-21. Ocean City Inlet, Maryland, 11 September 1995. Before the 1933 hurricane breached the barrier island, Assateague and Fenwick Islands were joined and had a straight shoreline. The former shoreline ran approximately along the seaward-most road (Photograph provided by USAE District, Baltimore)

- The *flood ramp*, which is a seaward-dipping sand surface dominated by flood-tidal currents. Sediment movement occurs in the form of sand waves (dunes), which migrate up the ramp.

- *Flood channels*, subtidal continuations of the flood ramp.

- The *ebb shield*, the high, landward margin of the tidal delta that helps divert ebb-tide currents around the shoal.

- *Ebb spits*, high areas mainly formed by ebb currents with some interaction with flood currents.

- *Spillover lobes*, linguoid, bar-like features formed by ebb-tidal current flow over low areas of the ebb shield.

(b) Although this model was originally derived from studies in mesotidal, mixed-energy conditions, it is also applicable to more wave-dominated, microtidal inlets (Boothroyd 1985). However, flood-tide shoals apparently are not formed in macrotidal shores.

(c) The high, central portion of a flood-tidal delta often extends some distance into an estuary or bay. This is the oldest portion of the delta and is usually vegetated by marsh plants. The marsh cap extends up to the elevation of the mean high water. The marsh expands aerially by growing out over the adjacent tidal flat. The highest, marsh-covered part of a flood shoal, or sometimes the entire shoal, is often identified on navigation charts as a "middle ground."

(3) Bed forms.

(a) Inlets contain a broad range of bed forms, from ripples due to oscillatory waves to dunes and antidunes caused by tidal currents. Water mass stratification can influence inlet flow and, therefore, bed form orientation. When a lagoon contains brackish water, salt wedge dynamics can occur, where the incoming flood flows under less dense bay water. Mixing between the two waters occurs along a horizontal density interface. During ebb tide, a buoyant planar jet forms at the seaward opening of the inlet similar to the effluent from rivers.

(b) Wright, Sonu, and Kielhorn (1972) described how density stratification affected flow at the Gulf of Mexico and Choctawhatchee Bay openings of East Pass, Florida. During flood tide, drogues and dye showed that the incoming salty Gulf of Mexico water met the brackish bay water at a sharp density front and then dove underneath (Figure IV-3-22). The drogues indicated that the sea water intruded at least 100 m beyond the front into Choctawhatchee Bay. This was the reason that bed forms within the channels displayed a flood orientation over time. This flood orientation can be seen in aerial photographs (Figure IV-3-5).

f. Inlet stability and migration.[1]

(1) Background. Inlets migrate along the coast - or remain fixed in one location - because of complex interactions between tidal prism, wave energy, and sediment supply. Some researchers consider the littoral system to be the principal sediment source that influences the stability of inlets (Oertel 1988). Not all of the sediment in littoral transport is trapped at the mouths of inlets; at many locations, a large proportion may be bypassed by a variety of mechanisms. Inlet sediment bypassing is defined as "the transport of sand from the updrift side of the tidal inlet to the downdrift shoreline" (FitzGerald 1988). Bruun and Gerritsen (1959) described three mechanisms by which sand moves past tidal inlets:

- Wave-induced transport along the outer edge of the ebb delta (the terminal lobe).
- The transport of sand in channels by tidal currents.
- The migration of tidal channels and sandbars.

They noted that at many inlets, bypassing occurred through a combination of these mechanisms. As an extension of this earlier work, FitzGerald, Hubbard, and Nummedal (1978) proposed three models to explain inlet sediment bypassing along mixed-energy coasts. The models are illustrated in Figure IV-3-23 and are discussed below.

[1] Material in this section has been adapted from FitzGerald (1988).

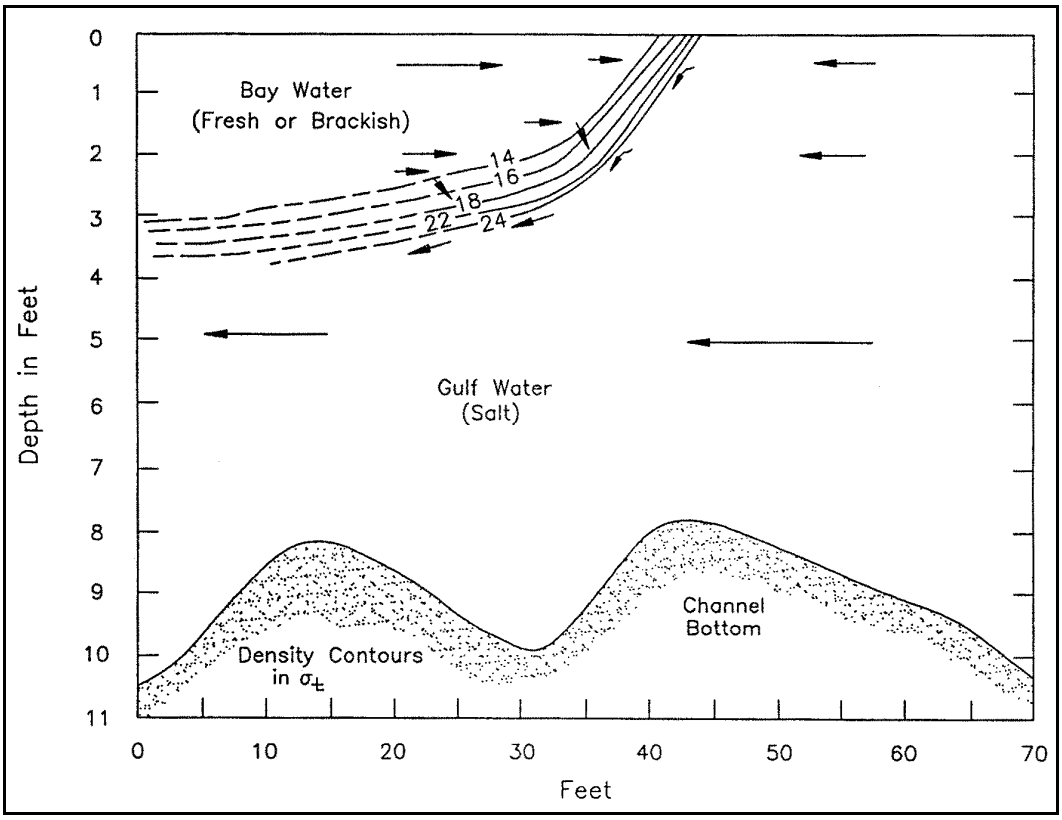

Figure IV-3-22. At the bay opening of East Pass, Florida, stratified flow occurs during flood tide in Choctawhatchee Bay as a wedge of sea water dives underneath the lower density bay water (after Wright, Sonu, and Kielhorn (1972)). A similar phenomenon often occurs in estuaries

(2) Inlet migration and spit breaching.

(a) The first model describes the tendency of many inlets to migrate downdrift and then abruptly shift their course by breaching a barrier spit. The migration occurs because sediment supplied by the longshore current causes the updrift barrier to grow (spit accretion). The growth occurs in the form of low, curved beach ridges, which weld to the end of the spit, often forming a bulbous-tipped spit known as a "drumstick." The ridges are often separated by low, marshy swales. As the inlet becomes narrower, the opposite (downdrift) shore erodes because tidal currents attempt to maintain an opening.

(b) In environments where the back bay is largely filled with marshes or where the barrier is close to the mainland, migration of the inlet causes an elongation of the tidal channel. Over time, the tidal flow between bay and ocean becomes more and more inefficient. Under these conditions, if a storm breaches the updrift barrier, the newly opened channel is a more direct and efficient pathway for tidal exchange. This new, shorter channel is likely to remain open while the older, longer route gradually closes. The breaching is most likely to occur across an area where the barrier has eroded or where some of the inner-ridge swales have remained low. The end result of spit accretion and breaching is the transfer of large quantities of sediment from one side of the inlet to the other. An example of this process is Kiawah River Inlet, South Carolina, whose migration between 1661 and 1978 was documented by FitzGerald, Hubbard, and Nummedal (1978). After a spit is breached and the old inlet closes, the former channel often becomes an elongated pond that parallels the coast.

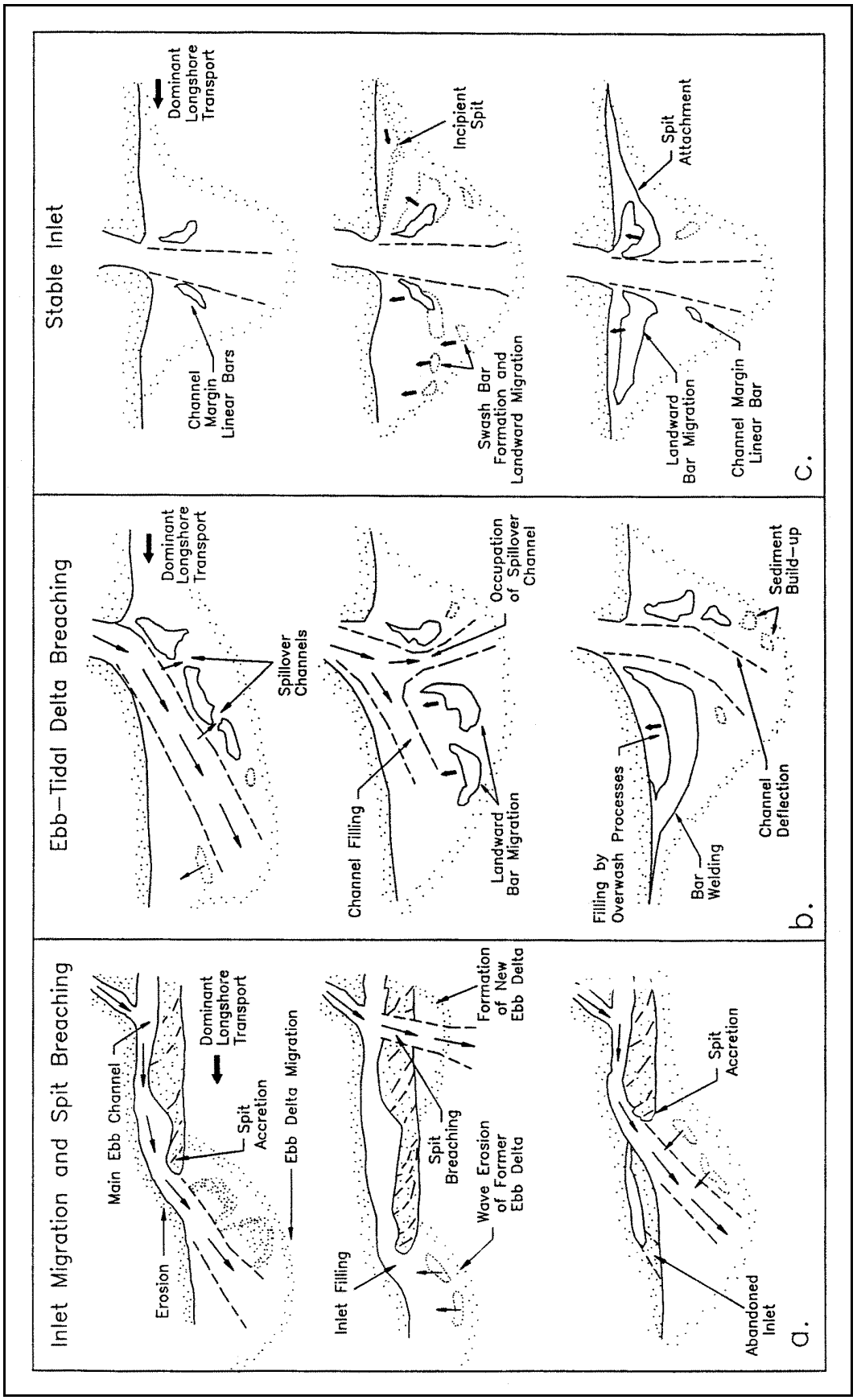

Figure IV-3-23. Three models of inlet behavior and sediment bypassing for mixed-energy coasts (from FitzGerald (1988))

(c) Several notes apply to the inlet migration model: First, not all inlets migrate. As discussed earlier, some inlets on microtidal shores are ephemeral, remaining open only a short time after a hurricane forces a breach through the barrier. If the normal tidal prism is small, these inlets are soon blocked by littoral drift. Short-lived inlets were documented along the Texas coast by Price and Parker (1979). The composition of the banks of the channel and the underlying geology are also critical factors. If an inlet abuts resistant sediment or bedrock, migration is restricted (for example, Hillsboro Inlet, on the Atlantic coast of Florida, is anchored by rock reefs). The gorge of deep inlets may be cut into resistant sediment, which also will restrict migration.

(d) Second, some inlets migrate updrift, against the direction of the predominate drift. Three mechanisms may account for updrift migration (Aubrey and Speer 1984):

- Attachment of swash bars to the inlet's downdrift shoreline.
- Breaching of the spit updrift of an inlet.
- Cutbank erosion of an inlet's updrift shoreline caused by back-bay tidal channels that approach the inlet throat obliquely.

(3) Ebb-tidal delta breaching.

(a) At some inlets, the position of the throat is stable, but the main ebb channel migrates over the ebb delta (Figure IV-3-23b). This pattern is sometimes seen at inlets that are naturally anchored by rock or have been stabilized by jetties. Sediment supplied by longshore drift accumulates on the updrift side of the ebb-tidal delta, which results in a deflection of the main ebb channel. The ebb channel continues to deflect until, in some cases, it flows parallel to the downdrift shore. This usually causes serious beach erosion. In this orientation, the channel is hydraulically inefficient, and the flow is likely to divert to a more direct seaward route through a spillover channel. Diversion of the flow can occur gradually over a period of months or can occur abruptly during a major storm. Eventually, most of the tidal exchange flows through the new channel, and the abandoned old channel fills with sand.

(b) Ebb delta breaching results in the bypassing of large amounts of sand because swash bars, which had formerly been updrift of the channel, become downdrift after the inlet occupies one of the spillover channels. Under the influence of waves, the swash bars migrate landward. The bars fill the abandoned channel and eventually weld to the downdrift beach.

(4) Stable inlet processes.

(a) These inlets have a stable throat position and a main ebb channel that does not migrate (Figure IV-3-23c). Sand bypassing occurs by means of large bar complexes that form on the ebb delta, migrate landward, and weld to the downdrift shoreline. The bar complexes are composed of swash bars that stack and merge as they migrate onshore. Swash bars are wave-built accumulations of sand that form on the ebb delta from sand that has been transported seaward in the main ebb channel. The swash bars move landward because of the dominance of landward flow across the swash platform. The reason for landward dominance of flow is that waves shoal and break over the terminal lobe (or bar) that forms along the seaward edge of the ebb delta. The bore from the breaking waves augments flood tidal currents but retards ebb currents.

(b) The amount of bypassing that actually occurs around a stable inlet depends upon the geometry of the ebb-tidal shoal, wave approach angle, and wave refraction around the shoal. Three sediment pathways can be identified:

- Some (or possibly much) of the longshore drift accumulates on the updrift side of the shoal in the form of a bar that projects out from the shore (Figure IV-3-23c). As the incipient spit grows, it merges with growing bar complexes near the ebb channel. Flood currents move some of the sand from the complexes into the ebb channel. Then, during ebb tide, currents flush the sand out of the channel onto the delta (both the updrift and downdrift sides), where it is available to feed the growth of new swash bars.

- Depending on the angle of wave approach, longshore currents flow around the ebb shoal from the updrift to the downdrift side. Some of the drift is able to move past the ebb channel, where it either continues moving along the coast or accumulates on the downdrift side of the ebb shoal. The sediment probably moves as large bed forms (Figure IV-3-4).

- Wave refraction around some ebb shoals causes a local reversal of longshore current direction along the downdrift shore. During this time, presumably, little sediment is able to escape the confines of the ebb-tidal shoal.

(5) Extension of bypassing models to other environments. The inlet migration models described above were originally based on moderate- to high-energy shores. However, research along the Florida Panhandle suggests that the models may be applicable to much lower energy environments than the original authors had anticipated. For example, between 1870 and 1990, the behavior of East Pass inlet, located in the low-wave-energy Florida Panhandle, followed all three models at various times (Figure IV-3-24; Morang (1992b)). It would be valuable to conduct inlet studies around the world to further refine the models and evaluate their applicability to different shores.

g. Inlet response to jetty construction and other engineering activities.

(1) Introduction. Typically, jetties are built to stabilize a migrating inlet, to protect a navigation channel from waves, or to reduce the amount of dredging required to maintain a specified channel depth. However, jetties can profoundly affect bypassing and other processes at inlets. Some of these effects can be predicted during the design phase of a project. Unfortunately, unanticipated geological conditions often arise, which lead to problems such as increased shoaling or changes in the tidal prism. Several classes of man-made activities affect inlets:

(a) Jetties stabilize inlets and prevent them from migrating.

(b) Jetties can block littoral drift.

(c) Walls or revetments can change the cross section of an inlet.

(d) Dredging can enlarge the cross section of a gorge.

(e) Dam construction and freshwater diversion reduce fluvial input.

(f) Weir sections (low portions of a jetty) allow sediment to pass into an inlet, where it can accumulate in a deposition basin and be bypassed.

(g) Landfilling and development in estuaries and bays can reduce tidal prism.

(2) Technical literature. Many reports have documented the effects of jetties on littoral sediment transport. Early works are cited in Barwis (1976). Dean (1988) discussed the response of modified Florida inlets,

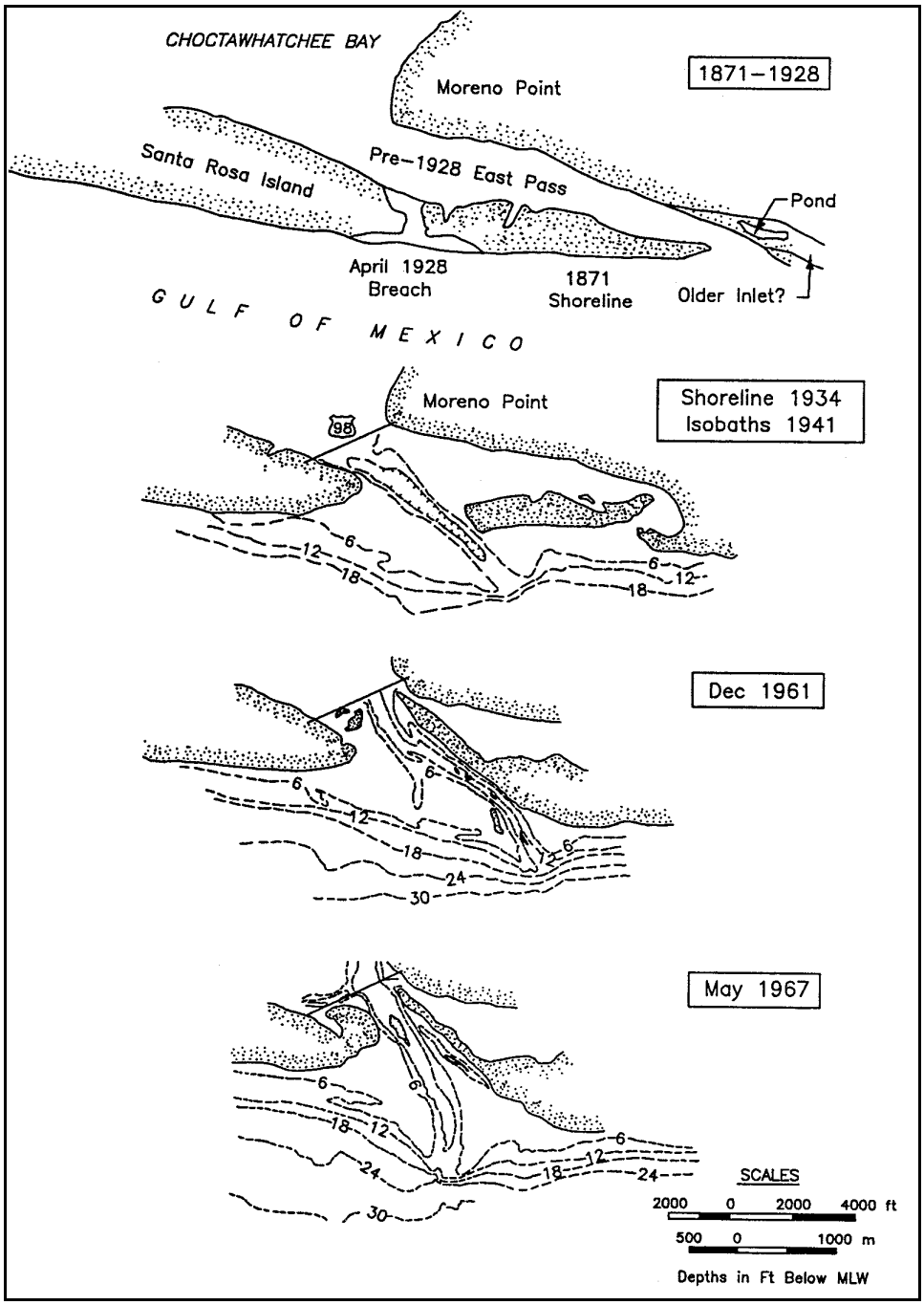

Figure IV-3-24. Spit breaching and inlet migration at East Pass, Florida (from Morang (1992a))

and many other case studies are reviewed in Aubrey and Weishar (1988). Examples of monitoring studies that assess the effects of jetties include:

(a) Shinnecock Inlet, Long Island, New York (Morang, 1999; Pratt and Stauble 2001; Williams, Morang, and Lillycrop 1998)

(b) Ocean City Inlet, Maryland (Bass et al. 1994).

(c) Little River Inlet, North and South Carolina (Chasten 1992, Chasten and Seabergh 1992).

(d) Murrells Inlet, South Carolina (Douglass 1987).

(e) Manasquan Inlet, New Jersey (Bruno, Yavary, and Herrington (1998).

(f) St. Marys Entrance, Florida and Georgia (Kraus, Gorman, and Pope 1994, 1995).

(g) East Pass, Florida (Morang 1992a).

(h) Port Mansfield Channel, Texas (Kieslich 1977).

(3) Weirs and other structures and their effects on sediment movement in and around inlets are discussed in Part V-6.

h. Case study of inlet formation and growth: Shinnecock Inlet, Long Island, New York.[1]

(1) Background and inlet breaching (1938).

(a) Shinnecock Inlet is located on the south shore of Long Island, 136 km east of New York Harbor. It is the easternmost of six inlets that cut the south shore barrier islands and allow boat passage between the Atlantic Ocean and the coastal bays. The present inlet was breached during the Great New England Hurricane of 21 September 1938. Inlets had periodically existed in this area before, but immediately before the 1938 hurricane, the barrier was intact and there was a paved road along the beach (Nersesian and Bocamazo 1992) (Figure IV-3-25).

(b) The first aerial photographs of the new inlet were taken by the U.S. Army Air Corps three days after the hurricane (Figure IV-3-26). The seas had calmed, but the large number of overwash deposits attest to the violence of the storm. All the open breaches in this area trended left of perpendicular to the shoreline trend. Drift was to the east (opposite to the normal prevailing direction) because spits had grown from west-to-east across the mouths of the new openings. Two months after the hurricane (29 November 1938) an oval ebb-tide delta had already formed in the Atlantic Ocean, and there was a small shoal in Shinnecock Bay, showing the initial development of a flood shoal (Figure IV-3-27).

(c) There are no eye-witness accounts of exactly how this inlet was cut. One possibility is that storm waves from the ocean cut across the barrier. The overwash fans to the left and right of the inlet support this option. The other possibility is that Shinnecock Bay elevated due to rainwater and runoff. This is supported by a water level of 2.2 (7.2 ft) above mlw estimated at the south end of the Shinnecock canal, across Shinnecock Bay from the barrier island (U.S. Army Corps of Engineers 1958)). At a low or narrow place in the barrier, a torrent of bay water might have burst through the dunes and run out to sea, scouring a channel that later widened and became the inlet shown in the photograph. This latter hypothesis seems most likely because, only two months after the storm, a prominent ebb shoal already existed, while there was only minimal deposition in Shinnecock Bay. The ebb shoal likely consisted of sand eroded from the barrier.

(2) Semi-stabilized inlet (1947). After 1938, the inlet migrated steadily to the west. In 1939-40, Suffolk County erected timber pile bulkhead and short groins on the west side of the channel to prevent westward migration (Nersesian and Bocamazo 1992). However, a 1947 photograph shows that the inlet had moved

[1] Condensed from Morang (1999).

Figure IV-3-25. Shinnecock Bay, Long Island, New York, 30 June 1938. Photograph taken before the Great New England Hurricane of 21 September cut the barrier island in several locations. The present Shinnecock Inlet was cut where a channel crosses from the bay to the road. The channel may be a remnant of an artificial cut that was dug by the Shinnecock and Peconic Canal Company in 1896. Shoal areas in the bay near the barrier attest to former inlets that had been open long enough to form flood shoals. North is to the top, the water body in the center of the image is Shinnecock Bay, and the Atlantic Ocean is on the bottom. The image is part of a mosaic prepared by the Beach Erosion Board

east, leaving the bulkhead behind a sand beach (Figure IV-3-28). A spit extended out to sea from the west shore, suggesting that longshore transport, at least temporarily, had been to the east (possibly a local reversal). Some small shoals existed in the mouth of the inlet, but sediment transport was largely directed into the bay after 1938. The ebb shoal was a flat oval that hugged the shore. The shoreline in this area trends about 65° (approx NE-SW). The 1947 channel extended out to sea at about 120°, more eastward than perpendicular to the shore. In the following years, the inlet rotated clockwise, until by 1951, the channel was pushing up against the bulkhead and the flood shoal deposition was occurring east of its earlier location.

(3) Stabilized inlet (1996). East and west jetties were built in 1952-54 by Suffolk County and the State of New York and rebuilt in 1992-93 by the Corps of Engineers. A photograph from 24 October 1996 (Figure IV-3-29) shows that the channel inlet was aligned north-south, about 40° clockwise from the orientation in 1947. The jetties were 240 m (800 ft) apart. The updrift beach had advanced almost to the tip of the east jetty. During the 1970's and 1980's, the bay shoreline east of the inlet eroded about 500 ft (150 m) due to scour from the east ebb channel. To the west, the shore has suffered chronic erosion, requiring frequent emergency repair by the highway department to prevent the road from being breached. The ebb shoal (only partially shown in this photograph) is an unsymmetric oval that attaches to the downdrift beach about 1,200 m west of the west jetty.

Figure IV-3-26. Shinnecock Inlet, Long Island, New York, 24 September 1938. Taken three days after Great New England Hurricane breached the barrier, this image shows the new Shinnecock Inlet and many overwash fans along the adjacent shore. Immediately after the storm, all the inlets along this stretch of the coast trended left of the shore-perpendicular. (Photograph mosaic from Beach Erosion Board archives)

(4) Ebb shoal growth. The ebb shoal at Shinnecock Inlet has continued to grow in volume since the inlet was formed. Figure IV-3-30 shows that in 1998, the shoal contained about 6,000,000 m^3 (8,000,000 yd^3) of sand. It appears that the shoal is still growing, but the latest three surveys were spaced only 1 year apart (1996, 1997, and 1998), so another survey will be needed in several years to verify this conclusion. However, present evidence indicates that the shoal is a sediment sink, although some of the littoral drift is probably bypassing.

IV-4-5. Morphodynamics and Shoreface Processes of Clastic Sediment Shores

a. Overview.

(1) Introduction. This section discusses morphodynamics - the interaction of physical processes and geomorphic response - of clastic sediment shores. The topic covers beach features larger than a meter (e.g., cusps and bars) on time scales of minutes to months. Details on grain-to-grain interactions, the initiation of sediment motion, and high frequency processes are not included. A principle guiding this section is that the overall shape of beaches and the morphology of the shoreface are largely a result of oscillatory (gravity) waves, although tide range, sediment supply, and overall geological setting impose limits. We introduce basic relationships and formulas, but the text is essentially descriptive. Waves are discussed in detail in Part II of the *Coastal Engineering Manual*, while sediment properties are covered in Part III-1.

(2) Literature. Beaches and sediment movement along the shore have been subjects of popular and scientific interest for over a century. A few of the many textbooks that cover these topics include Carter (1988), Davis (1985), Davis and Ethington (1976), Greenwood and Davis (1984), Komar (1998), and Zenkovich (1967). Small-amplitude (Airy) and higher-order wave mechanics are covered in EM 1110-2-1502; more detailed treatments are in Kinsman (1965), Horikawa (1988), and Le Méhauté (1976). Interpreting and applying wave and water level data are covered in EM 1110-2-1414.

Figure IV-3-27. Shinnecock Inlet, New York, 29 November 1938, photographed only 2 months after the barrier island was breached during the Great New England Hurricane of 21 September 1938. North is to the top of the image. The body of water to the top is Shinnecock Bay, and the Atlantic Ocean is on the bottom. The inlet already displays an oval ebb-tidal shoal. A small shoal in Shinnecock Bay indicated development of a flood shoal. Washover fans, remnants of the storm, can be seen on both sides of the inlet. (Photograph from Beach Erosion Board archives)

Figure IV-3-28. Shinnecock Inlet, New York, 1 April 1947. The inlet was much wider than in 1938, and a large flood shoal had accumulated. Some small shoals existed in the mouth of the inlet, but sediment transport had been largely directed into the bay since 1938. (Photograph from Beach Erosion Board archives)

(3) Significance of clastic coasts. It is important to examine and understand how clastic shores respond to changes in wave climate, sediment supply, and engineering activities for economic and management reasons:

(a) Many people throughout the world live on or near beaches. Beaches are popular recreation areas and of vital economic importance to many states (Houston 1995, 1996a, 1996b).

Figure IV-3-29. Shinnecock Inlet, New York, 24 October 1996. The inlet has been stabilized with stone jetties 800 ft apart. The beach east of the inlet has advanced to the end of the east jetty. To the west, the shore has suffered chronic erosion, requiring frequent emergency repair by the highway department to prevent the road from being breached. The ebb shoal (only partially shown in this photograph) is an unsymmetric oval that attaches to the downdrift beach about 1,200 m west of the west jetty (Photograph courtesy of USAED, New York)

(b) Beaches are critical buffer zones protecting wetlands and coastal plains from wave attack.

(c) Beaches are habitat or nesting ground for many animal species, some of which are endangered (e.g., turtles).

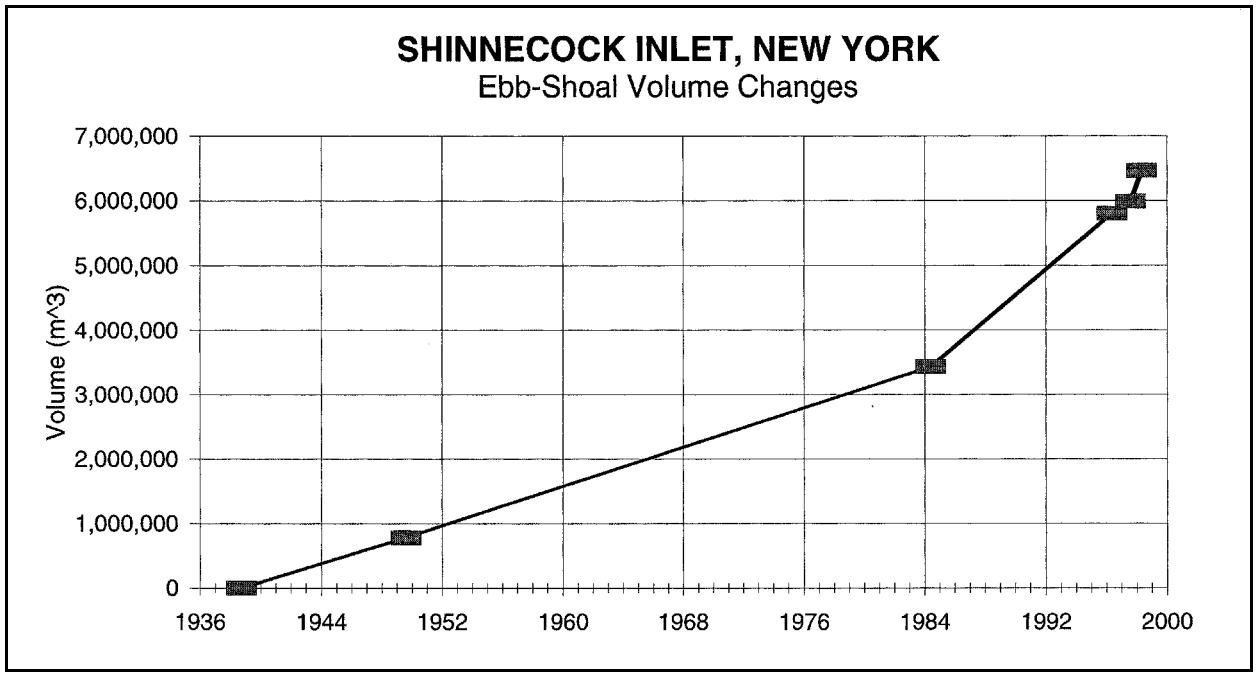

Figure IV-3-30. Ebb-shoal volume changes, Shinnecock Inlet, New York. Volumes were based on subtracting the 1933 U.S. Coast and Geodetic Survey data (pre-inlet) from more recent surveys: 1949, 1985, 1996, 1997, and 1998. The ebb shoal is still growing, indicating that it is a sediment trap, although some of the littoral drift probably bypasses. Hydrographic data courtesy of U.S. Army Engineer District, New York

(d) Much engineering effort and large amounts of funding are expended on planning and conducting beach renourishment.

(e) Sediment supply and, therefore, beach stability, are often adversely affected by the construction of navigation and shore-protection structures.

(f) Sand is a valuable and increasingly rare mineral resource in most of the coastal United States.

(4) Range of coastal environments. Around the world, coasts vary greatly in steepness, sediment composition, and morphology. The most dynamic shores may well be those composed of unconsolidated clastic sediment because they change their form and state rapidly. Clastic coasts are part of a geologic continuum that extends from consolidated (rocky) to loose clastic to cohesive material (Figure IV-3-31). Waves are the primary mechanisms that shape the morphology and move sediment, but geological setting imposes overall constraints by controlling sediment supply and underlying rock or sediment type. For example, waves have little effect on rocky cliffs; erosion does occur over years, but the response time is so long that many rocky shores can be treated as being geologically controlled. At the other end of the continuum, cohesive shores respond very differently to wave action because of the electrochemical nature of the sediment (see Part III-5).

b. Tide range and overall beach morphology.

Most studies of beach morphology and processes have concentrated on microtidal (< 1 m) or low-mesotidal coasts (1-2 m). To date, many details concerning the processes that shape high-meso- and macrotidal beaches (tide range > 2 m) are still unknown. Based on a review of the literature, Short (1991) concluded that

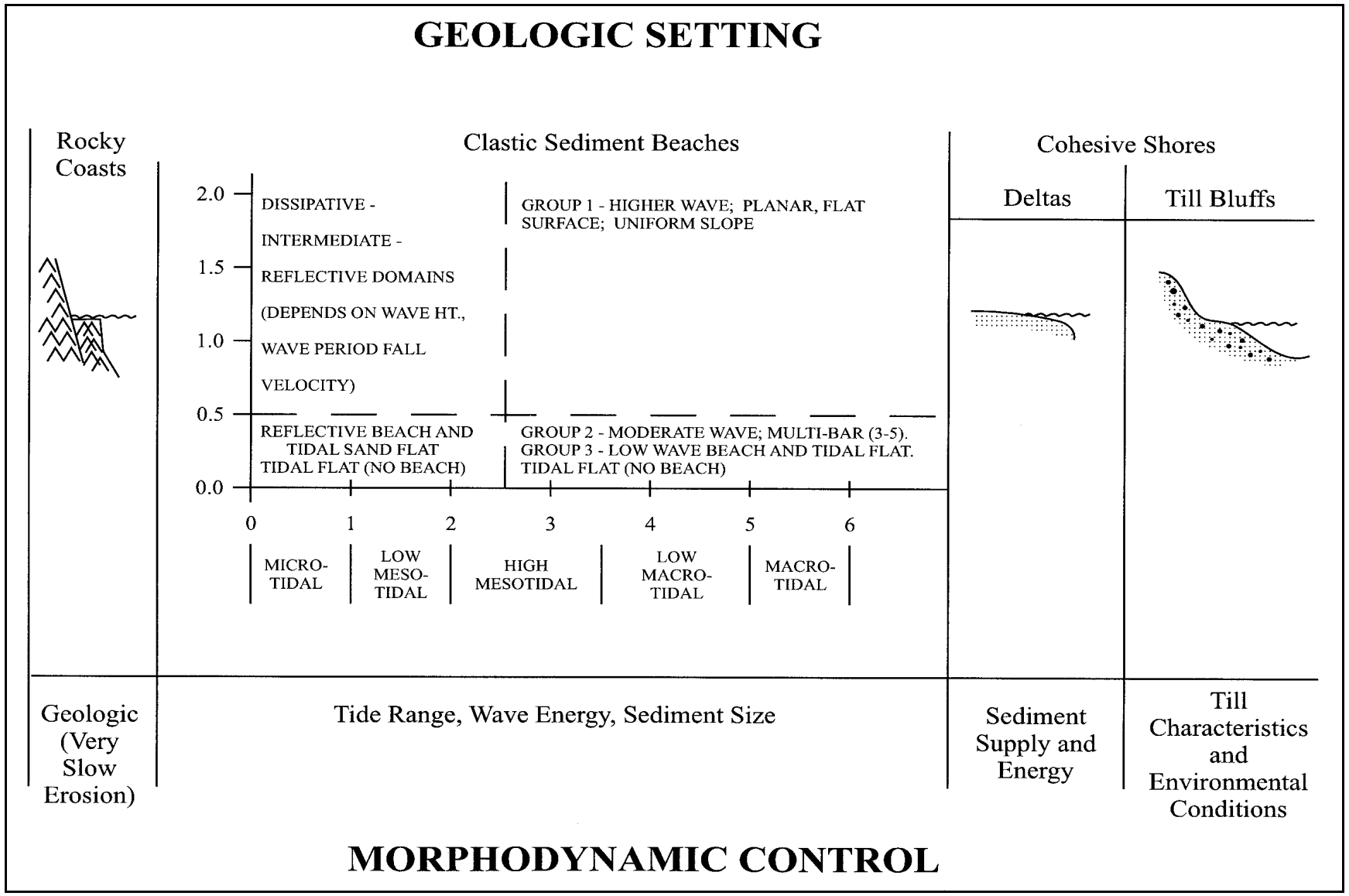

Figure IV-3-31. Summary of factors controlling morphodynamics along a range of coastal environments. Clastic shore processes are detailed in Figure IV-3-26 and discussed in the text

wave-dominated beaches where tide range is greater than about 2 m behave differently than their lower-tide counterparts. Short underscored that high-tide beaches are also molded by wave and sediment interactions. The difference is the increasing impact of tidal range on wave dynamics, shoreface morphodynamics, and shoreline mobility. Short developed a tentative grouping of various beach types (Figure IV-3-32). Discussion of the various shoreface morphologies follows.

c. High tidal range (> 2 m) beach morphodynamics.

(1) Review. Based on a review of research on macrotidal beaches, Short (1991) summarized several points regarding their morphology:

(a) They are widespread globally, occurring in both sea and swell environments.

(b) Incident waves dominate the intertidal zone.

(c) Low-frequency (infragravity) standing waves may be present and may be responsible for multiple bars.

(d) The intertidal zone can be segregated into a coarser, steeper, wave-dominated high tide zone, an intermediate zone of finer sediment and decreasing gradient, and a low-gradient, low-tide zone. The highest zone is dominated by breaking waves, the lower two by shoaling waves.

(e) The cellular rip circulation and rhythmic topography that are so characteristic of microtidal beaches have not been reported for beaches with tide range greater than 3 m.

(2) Macrotidal beach groups. Using published studies and field data from Australia, Short (1991) divided macrotidal beaches into three groups based on gradient, topography, and relative sea-swell energy:

(a) GROUP 1 - High wave, planar, uniform slope. Beaches exposed to persistently high waves ($H_b > 0.5$ m) display a planar, flat, uniform surface. Shorefaces are steep, ranging from 1 to 3 deg, and have a flat surface without ripples, bed forms, or bars. The upper high tide beach is often relatively steep and cuspid and contains the coarsest sediment of the system. On both sand and gravel beaches, the high tide, upper foreshore zone is exposed to the highest waves. Plunging and surging breakers produce asymmetric swash flows, which maintain the coarse sediment and steep gradient. Further seaward, wave shoaling becomes a more important factor than wave breaking because waves are attenuated at low tide (due to shallower water and greater friction). Tidal currents also increase in dominance seaward. Wright (1981) found that tidal currents left no bed forms visible at low tide but were an important factor in longshore sediment transport.

(b) GROUP 2 - Moderate wave, multi-bar. Multi-bar, macrotidal beaches are formed in fetch-limited environments with high tide range and abundant fine sand (King 1972b). The common characteristic of these beaches is a relatively uniform 0.5- to 0.6-deg intertidal gradient and the occurrence of multiple bars (two to five sets) between msl and mlw (Short 1991). Bar amplitude is usually below 1 m and spacing ranges from 50 to 150 m, with spacing increasing offshore. Field observations indicate that the bars are formed by a wave mechanism, particularly during low wave, post-storm conditions. The bars appear to build up onsite rather than migrate into position. These multi-bar beaches probably cause dissipative conditions during most wave regimes, possibly resulting in the development of infragravity standing waves. This would account for the spacing of the bars; however, this hypothesis has not been tested with rigorous field measurements (Short 1991).

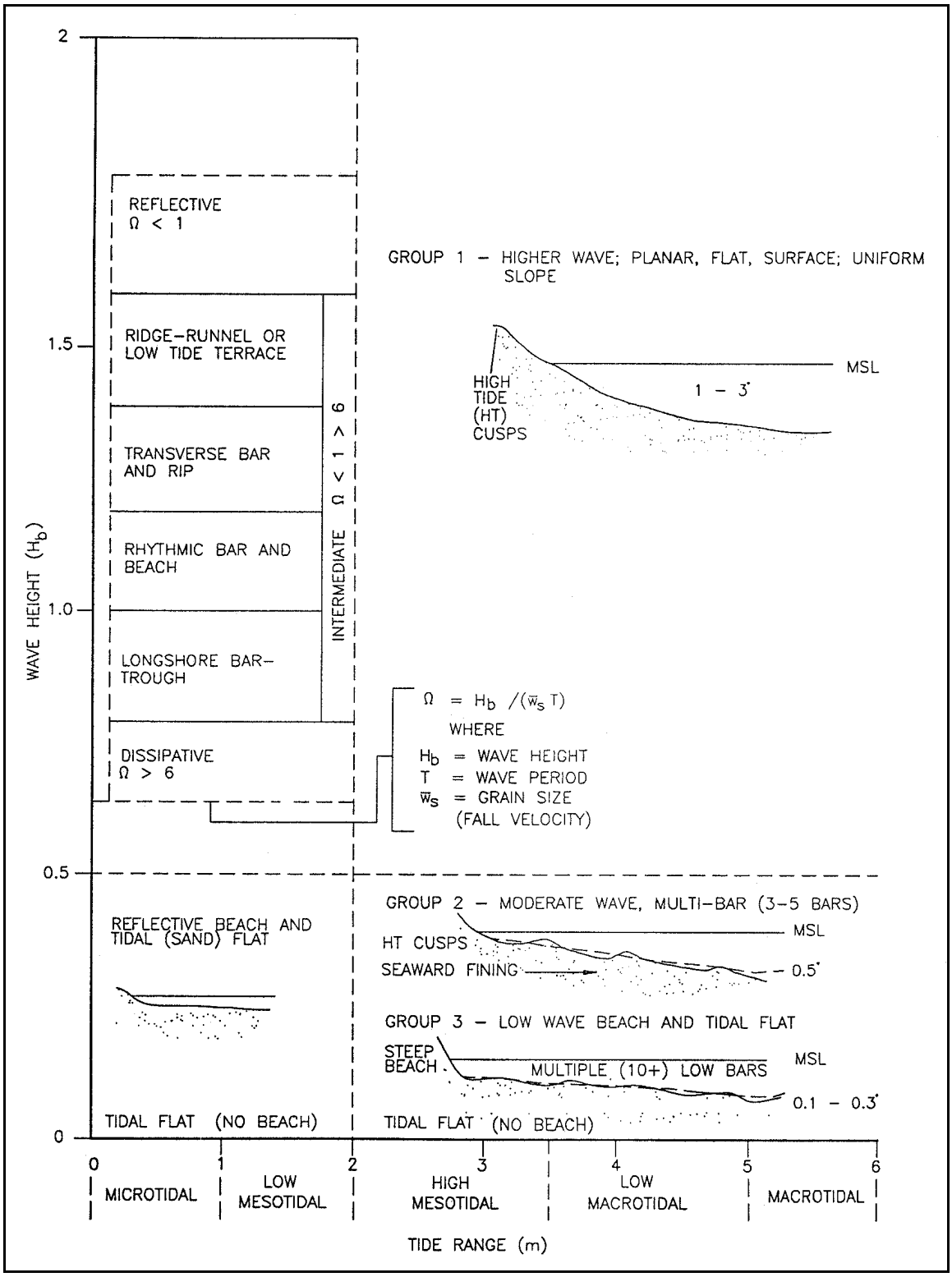

Figure IV-3-32. Micro- to macrotidal beach and tidal flat systems (adapted from Short (1991)). Dimensionless parameter Ω discussed in the text

(c) GROUP 3 - Low wave beach and tidal flat. As wave energy decreases, macrotidal beaches eventually grade into tide-dominated tidal flats. Between the two regimes, there is a transition stage that contains elements of both morphologies. These beach-tidal flat systems are usually characterized by a steep, coarse-grained reflective beach (no cusps usually present) which grades abruptly at some depth below msl into a fine-grained, very low gradient (0.1 deg), rippled tidal flat (Figure IV-3-33). The tidal flat may be uniform or may contain low, multiple bars. Beach-tidal flat shores are found in low-energy environments that are only infrequently exposed to wave attack, but the energy must be sufficient to produce the morphologic zonation.

Figure IV-3-33. View west from Tarskavaig, Isle of Skye, Scotland, August 1983. Photograph taken at low tide. At this macrotidal beach, facing the Sea of the Hebrides, the upper shoreface consists of coarse cobble, while the low foreshore is low gradient and almost featureless

(3) Spatial and temporal variations. Beaches on macro-tidal coasts vary morphologically as important environmental parameters change. Short (1991) cites one setting where the shoreface varies from high-energy, uniform steep beach (Group 1) to beach-tidal flat (Group 3) within 2 km. He suggests that the changes in morphology are due to variations in wave energy: as energy changes alongshore, important thresholds are crossed which result in different ratios of wave versus tide domination. In addition, there may be temporal variations throughout the lunar cycle. As tide range varies during the month, the transitions where one morphologic group merges into another may migrate cyclically along the coast. More field studies are needed to document this phenomenon.

(4) Summary. On tideless beaches, morphology is determined by waves and sediment character. On microtidal beaches, waves still dominate the morphodynamics, but tide exerts a greater influence. As tide range increases beyond 2-3 m, the shape of beaches becomes a function of waves coupled with tides. On the higher tide coasts, as water depth changes rapidly throughout the day, the shoreline and zone of wave breaking move horizontally across the foreshore and tidal currents move considerable sediment.

d. Morphodynamics of micro- and low-mesotidal coasts.

(1) Morphodynamic variability of microtidal beaches and surf zones. Based on field experiments in Australia, Wright and Short (1984) have presented a model of shoreface morphology as a function of wave parameters and sediment grain size. This model is a subset of Figure IV-3-31 that occupies the zone where tide range is between 0 and 2 m and H_b (breaker height) is greater than about 0.5 m.

(a) Wright and Short (1984) determined that the morphodynamic state of sandy beaches could be classified on the basis of assemblages of depositional forms and the signatures of associated hydrodynamic processes. They identified two end members of the morphodynamic continuum:

- Fully dissipative.
- Highly reflective.

Between the extremes were four intermediate states, each of which possessed both reflective and dissipative elements (Figure IV-3-32).

(b) The most apparent differences between the beach states are morphological, but distinct process signatures, representing the relative velocities of different modes of fluid motion, accompany the characteristic morphology. As stated by Wright and Short (1984):

> Although wind-generated waves are the main source of the energy which drives beach changes, the complex processes, which operate in natural surf zones and involve various combinations of dissipation and reflection, can lead to the transfer of incident wave energy to other modes of fluid motion, some of which may become dominant over the waves themselves.

(c) Wright and Short grouped fluid motion into four categories (Table IV-3-1):

- Oscillatory flows.
- Oscillatory or quasi-oscillatory flows.
- Net circulations.
- Non-wave-generated currents.

Table IV-3-1
Modes of Fluid Motion Affecting Clastic Shorelines

Modes	Notes	Frequencies of flows	Examples
Oscillatory	Corresponds directly to incident waves	Frequency band of deep-water incident waves	Sediment-agitating oscillations
Oscillatory or quasi-oscillatory	Shore-normal oriented standing and edge waves	Wide range of frequencies	Trapped edge waves, "leaky" mode standing waves
Net circulations	Generated by wave energy dissipation	Minutes to days	Longshore currents, rip currents, rip feeder currents
Non-wave-generated currents	Generated by tides and wind shear	Minutes to hours (?)	Tidal currents

(Based on Wright and Short (1984))

(d) From repeated observations and surveys of beaches, Wright and Short (1984) concluded that beach state is clearly a function of breaker height and period and sediment size. Over time, a given beach tends to exhibit a *modal* or most frequent recurrent state, which depends on environmental conditions. Variations in shoreline position and profile are associated with temporal variations of beach state around the modal state. Wright and Short found that a dimensionless parameter Ω could be used to describe the modal state of the beach:

$$\Omega = \frac{H_b}{\overline{w_s} T} \tag{IV-3-3}$$

where H_b is breaker height, $\overline{w_s}$ is sediment fall velocity, and T is wave period. For the following values of Ω (Figure IV-3-32):

- Ω about 1: defines the reflective/intermediate threshold
- $1 < \Omega < 6$: intermediate beaches
- $\Omega \cong 6$: marks the threshold between intermediate and dissipative conditions

(e) Beaches take time to adjust their state, and a change of Ω across a threshold boundary does not immediately result in a transformation from reflective to intermediate or from intermediate to dissipative. On the Pacific coasts of Australia and the United States, storms can cause a shift of beach state from reflective or intermediate to dissipative in a few days because the energy is high. The return to reflective conditions under low energy may require weeks or months or longer (the sequence of beach recovery is illustrated in stages *a* through *f* in Figure IV-3-34). In environments where the dominant variation in wave energy occurs on an annual cycle (e.g., high storm waves in winter and low swell in summer), the full range from a dissipative winter profile to a reflective summer profile may be expected.

(f) Wright and Short (1984) concluded that large temporal variations in Ω are accompanied by large changes in state. However, when the variations in Ω take place in the domains of $\Omega < 1$ or $\Omega > 6$, no corresponding changes in *state* result. Intermediate beaches, where Ω is between 1 and 6, are spatially and temporally the most dynamic. They can undergo rapid changes as wave height fluctuates, causing reversals in onshore/offshore and alongshore sediment transport.

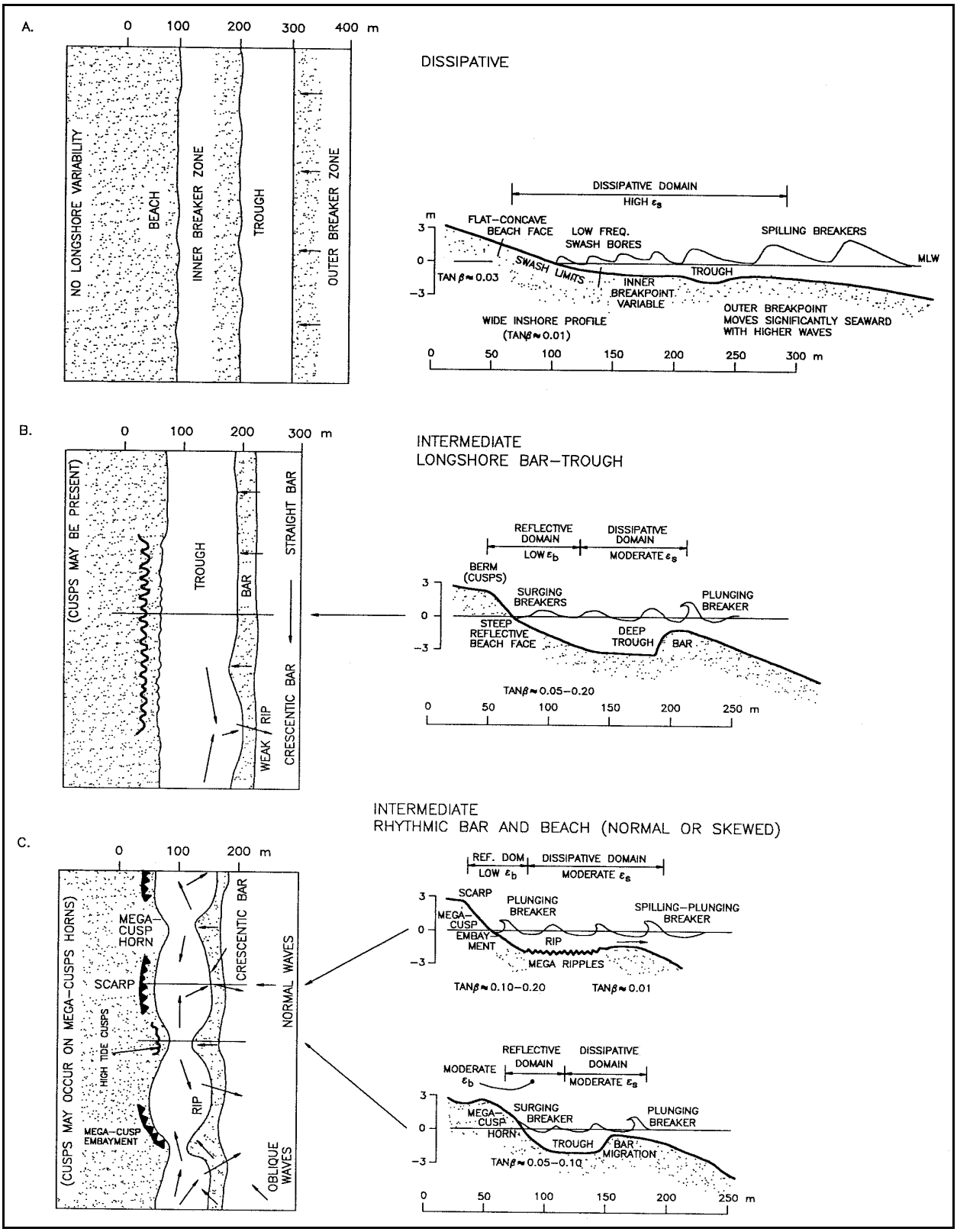

Figure IV-3-34. Plan and profile views of six major beach stages (adapted from Wright and Short (1984)). Surf-scaling parameter ε is discussed in the text; β represents beach gradient. Dimensions are based on Australian beaches, but morphologic configurations are applicable to other coastlines (Continued)

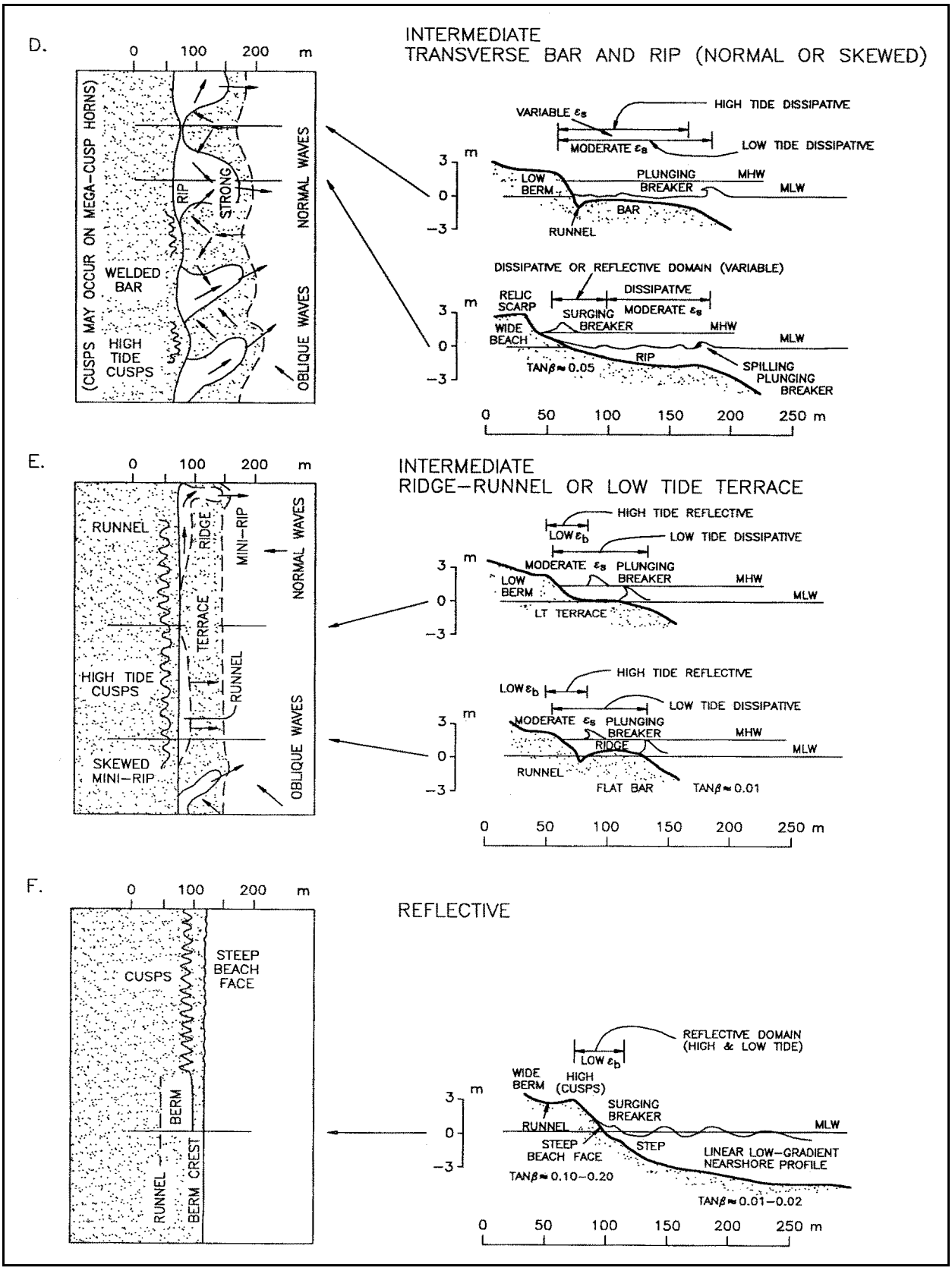

Figure IV-3-34. (Concluded)

(g) The parameter Ω depends critically upon $\overline{w_s}$, the sediment fall velocity. It is unclear how the relationships described above apply to shorefaces where the grain size varies widely or where there is a distinct bimodal distribution. For example, many Great Lakes beaches contain material ranging in size from silt and clay to cobble several centimeters in diameter. During storms, not only do wave height and period change, but fine-grain sediment is preferentially removed from the shoreface; therefore, the effective $\overline{w_s}$ may change greatly within a few hours. Further research is needed to understand how Great Lakes beaches change modally and temporally.

(2) Highly dissipative stage (Figure IV-3-34a). The dissipative end of the continuum is analogous to the "storm" or "winter beach" profile described by Bascom (1964) for shores that vary seasonally. The characteristic feature of these beaches is that waves break by spilling and dissipating progressively as they cross a wide surf zone, finally becoming very small at the upper portion of the foreshore (Figure IV-3-35) (Wright and Short 1984). A dissipative surf zone is broad and shallow and may contain two or three sets of bars upon which breakers spill. Longshore beach variability is minimal.

Figure IV-3-35. Example of a dissipative beach: Southern California near San Diego

(3) Highly reflective stage (Figure IV-3-34f). On a fully reflective beach, breakers impinge directly on the shore without breaking on offshore bars (Figures IV-3-36 and 37). As breakers collapse, the wave uprush surges up a steep foreshore. At the bottom of the steep, usually linear beach is a pronounced step composed of coarser material. Seaward of the step, the slope of the bed decreases appreciably. Rhythmic beach cusps are often present in the swash zone. The fully reflective stage is analogous to the fully accreted "summer profile."

(4) Surf-scaling parameter. Morphodynamically, the two end members of the beach state model can be distinguished on the basis of the surf-scaling parameter (Guza and Inman 1975):

Figure IV-3-36. Example of a reflective sand beach: Newport Beach, California, April 1993

$$\varepsilon = \frac{a_b \omega^2}{g \tan^2 \beta} \tag{IV-3-4}$$

where

a_b = breaker amplitude

ω = incident wave radian energy ($2\pi/T$ where T = period)

g = acceleration of gravity

β = the gradient of the beach and surf zone

Strong reflection occurs when $\varepsilon \leq 2.0\text{-}2.5$; this situation defines the highly reflective extreme. When $\varepsilon > 2.5$, waves begin to plunge, dissipating energy. Finally, when $\varepsilon > 20$, spilling breakers occur, the surf zone widens, and turbulent dissipation of wave energy increases with increasing ε.

(5) Intermediate beach stages. These exhibit the most complex morphologies and process signatures.

(a) Longshore bar-trough state (Figure IV-3-34b). This beach form can develop from an antecedent dissipative profile during an accretionary period. Bar-trough relief is higher and the shoreface is much steeper than on the dissipative profile. Initial wave breaking occurs over the bar. However, in contrast to

Figure IV-3-37. Example of a reflective cobble beach: Aldeburgh, Suffolk (facing the North Sea), August 1983. Note the steep berm and the lack of sand-sized sediment. In the background is part of the town of Aldeburgh, which has lost many buildings and churches since the Middle Ages due to erosion

the dissipative beach, the broken waves do not continue to decay after passing over the steep inner face of the bar, but re-form in the deep trough. Low-steepness waves surge up the foreshore; steeper waves collapse or plunge at the base of the foreshore, followed by a violent surge up the subaerial beach (Wright and Short 1984). Runup is relatively high and cusps often occur in the swash zone.

(b) Rhymthic bar and beach (Figure IV-3-34c). Characteristics are similar to the longshore bar-trough state (described above). The distinguishing features of the rhymthic bar and beach state are the regular longshore undulations of the crescentic bar and of the subaerial beach (Figures III-2-23 (ocean) and IV-3-38 (lake)). A weak rip current circulation is often present, with the rips flowing across the narrow portions of the bar. Wright and Short (1984) state that incident waves dominate circulation throughout the surf zone, but subharmonic and infragravity oscillations become important in some regions.

(c) Transverse-bar and rip state (Figure IV-3-34d). This morphology commonly develops in accretionary sequences when the horns of crescentic bars weld to the beach. This results in dissipative transverse bars (sometimes called “mega-cusps”) that alternate with reflective, deeper embayments. The dominant dynamic process of this beach state is extremely strong rip circulation, with the seaward-flowing rip currents concentrated in the embayments.

(d) Ridge and runnel/low tide terrace state (Figures IV-3-34e, IV-2-31 (ocean), and IV-3-39 (lake)). This beach state is characterized by a flat accumulation of sand at or just below the low tide level, backed by a steeper foreshore. The beach is typically dissipative at low tide and reflective at high tide.

Figure IV-3-38. Gravel cusps at St. Joseph, Michigan, November 1993. This is an example of a rhythmic bar and beach on a freshwater coast without tides but subject to irregular seiching

e. Processes responsible for shoreface sediment movement.

(1) Despite intense study for over a century, the subject of sand movement on the shoreface is still poorly understood. Sand is moved by a combination of processes including the following (Pilkey 1993, Wright et al. 1991):

(a) Wave orbital interactions with bottom sediments and with wave-induced longshore currents.

(b) Wind-induced longshore currents.

(c) Turbidity currents.

(d) Rip currents.

(e) Tidal currents.

(f) Storm surge ebb currents.

(g) Gravity-driven currents.

(h) Wind-induced upwelling and downwelling.

(i) Wave-induced upwelling and downwelling.

Figure IV-3-39. Ridge and runnel north of St. Joseph, Michigan, November 1993. This example shows that these features can be found on lake shores that do not have regular tides

(j) Gravity-induced downslope transport.

(2) Additional complications are imposed by constantly changing shoreface conditions, as follows:

(a) The relative contributions made by the different transport mechanisms vary over time.

(b) Because of differing regional geological configuration and energy climate, the frequencies of occurrence of the different mechanisms vary with location.

(c) Oscillatory flows normally occur at many frequencies and are superimposed on mean flows and other oscillatory flows of long period.

(3) Middle Atlantic Bight experiments of Wright et al. (1991).

(a) Wright et al. (1991) measured suspended sediment movement, wave heights, and mean current flows at Duck, North Carolina, in 1985 and 1987 and at Sandbridge, Virginia, in 1988 using instrumented tripods. During their study, which included both fair weather and moderate energy conditions, onshore mean flows (interpreted to be related to tides), were dominant over incident waves in generating sediment fluxes. In contrast, during a storm, bottom conditions were strongly dominated by offshore-directed, wind-induced mean flows. Wright et al. attributed this offshore-directed flow to a rise of 0.6 m in mean water level (during this particular storm) and a resultant strong seaward-directed downwelling flow.

(b) Wright et al. (1991) examined the mechanisms responsible for onshore and offshore sediment fluxes across the shoreface. They related two factors explicitly to incoming incident waves:

- Sediment diffusion arising from gradients in wave energy dissipation.
- Sediment advection caused by wave orbital asymmetries.

They found that four other processes may also play important roles in moving sediment:

- Interactions between groupy incident waves and forced long waves.
- Wind-induced upwelling and downwelling currents.
- Wave-current interactions.
- Turbidity currents.

Overall, Wright et al. found that incoming incident waves were of primary importance in bed agitation, while tide- and wind-induced currents were of primary importance in moving sediment. The incoming wave orbital energy was responsible for mobilizing the sand, but the unidirectional currents determined where the sand was going. Surprisingly, cross-shore sediment fluxes generated by mean flows were dominant or equal to sediment fluxes generated by incident waves in all cases and at all times.

(c) Based on the field measurements, Wright et al. (1991) concluded that "near-bottom mean flows play primary roles in transporting sand across isobaths on the upper shoreface" (p. 49). It is possible that this dominance of mean flows is a feature that distinguished the Middle Atlantic Bight from other shorefaces. The oscillatory (wave) constituents may be proportionately much more important along coasts subject to persistent, high-energy swell, such as the U.S. west coast. Wright et al. also concluded that the directions, rates, and causes of cross-shore sediment flux varied temporally in ways that were only partly predictable with present theory.

f. Sea level change and the Bruun rule.

(1) General coastal response to changing sea level.[1] Many barrier islands around the United States have accreted vertically during the Holocene rise in global sea level, suggesting that in these areas the supply of sediment was sufficient to allow the beaches to keep pace with the rise of the sea. It is not clear how beaches respond to short-term variations in sea level. Examples of shorter processes include multi-year changes in Great Lakes water levels and multi-month sea level rises associated with the El Niño-Southern Oscillation in the Pacific.

[1] Part IV-1 reviewed sea level change and outlined some of the associated coastal effects and management issues. Table IV-1-7 outlined how shoreline advance or retreat at any particular location is a balance between sediment supply and the rate of sea level change. In this section, sea level change is meant in a general sense to be caused by a combination of factors, including eustatic (global) changes and local effects due to vertical movements of the coastal land.

(2) Storm response.

(a) Based on his pioneering research of southern California beaches in the 1940's, Shepard (1950) developed the classic model that there is an onshore-offshore exchange of sediment over winter-summer cycles. Studies since then have shown that this model applies mostly to beaches on swell-dominated coasts where the wave climate changes seasonally (particularly Pacific Ocean coasts) (Carter 1988). Many beaches do *not* show an obvious seasonal cycle. Instead, they erode during storms throughout the year and rebuild during subsequent fair weather periods. Some coasts, like New Jersey, have a seasonal signature, but storms cause such great perturbations that it can take repetitive surveys over many years to extract the seasonal signature.

(b) In some locations, such as the Gulf Coast, infrequent and irregular hurricanes may be the most important dynamic events affecting beaches. Following one of these storms, beach and dune rebuilding may take years (Figure IV-2-10 shows a portion of the Florida/Alabama shore that was damaged by Hurricane Frederic in 1979 and is slowly recovering). Recently, the popular belief that hurricanes are the most important morphodynamic events causing Gulf Coast beach erosion is being reevaluated with the benefit of new field data. Scientists have learned that, cumulatively, winter cold fronts produce significant annual barrier island retreat. Dingler, Reiss, and Plant (1993) monitored Louisiana's Isles Dernieres and found that Hurricane Gilbert (September 1988) produced substantial beach retreat initially, but it actually reduced the average erosion rate by modifying the slope of the shoreface from that produced by cold-front-generated storms. The different responses were related to the scale of the storms. Cold fronts, which individually were small storms, eroded the entire beach to the same degree. Most sand and mud was deposited offshore and only a small percentage of eroded sand was deposited on the backshore because the fronts usually did not raise the sea enough to cause overtopping. Hurricane Gilbert, in contrast, raised sea level substantially such that the primary erosion occurred on the upper beach, and much of the sand was deposited behind the island via overwash processes. Over a 5-year period, the overall effect of this hurricane on the Isles Dernieres was to retard the retreat rate of the island by about 50 percent over that produced by cold fronts alone.

(3) Bruun Rule beach response model.

(a) One of the best-known shoreface response models was proposed by Bruun in 1962 (rederived in Bruun (1988)). Bruun's concept was that beaches adjust to the dominant wave conditions at the site. He reasoned that beaches had to respond in some manner because clearly they had adjusted and evolved historically as sea level had changed. Beaches had not disappeared, they had moved. How was this translation accomplished? Earlier studies of summer/winter beach morphology provided clues that beaches responded even to seasonal changes in wave climate. The basic assumption behind Bruun's model is that with a rise in sea level, the equilibrium profile of the beach and the shallow offshore moves upward and landward. Bruun made several assumptions in his two-dimensional analysis:

- The upper beach erodes because of a landward translation of the profile.
- Sediment eroded from the upper beach is deposited immediately offshore; the eroded and deposited volumes are equal (i.e., longshore transport is not a factor).
- The rise in the seafloor offshore is equal to the rise in sea level. Thus, offshore, the water depth stays constant.

(b) The Bruun Rule can be expressed as (Figure IV-3-40a):

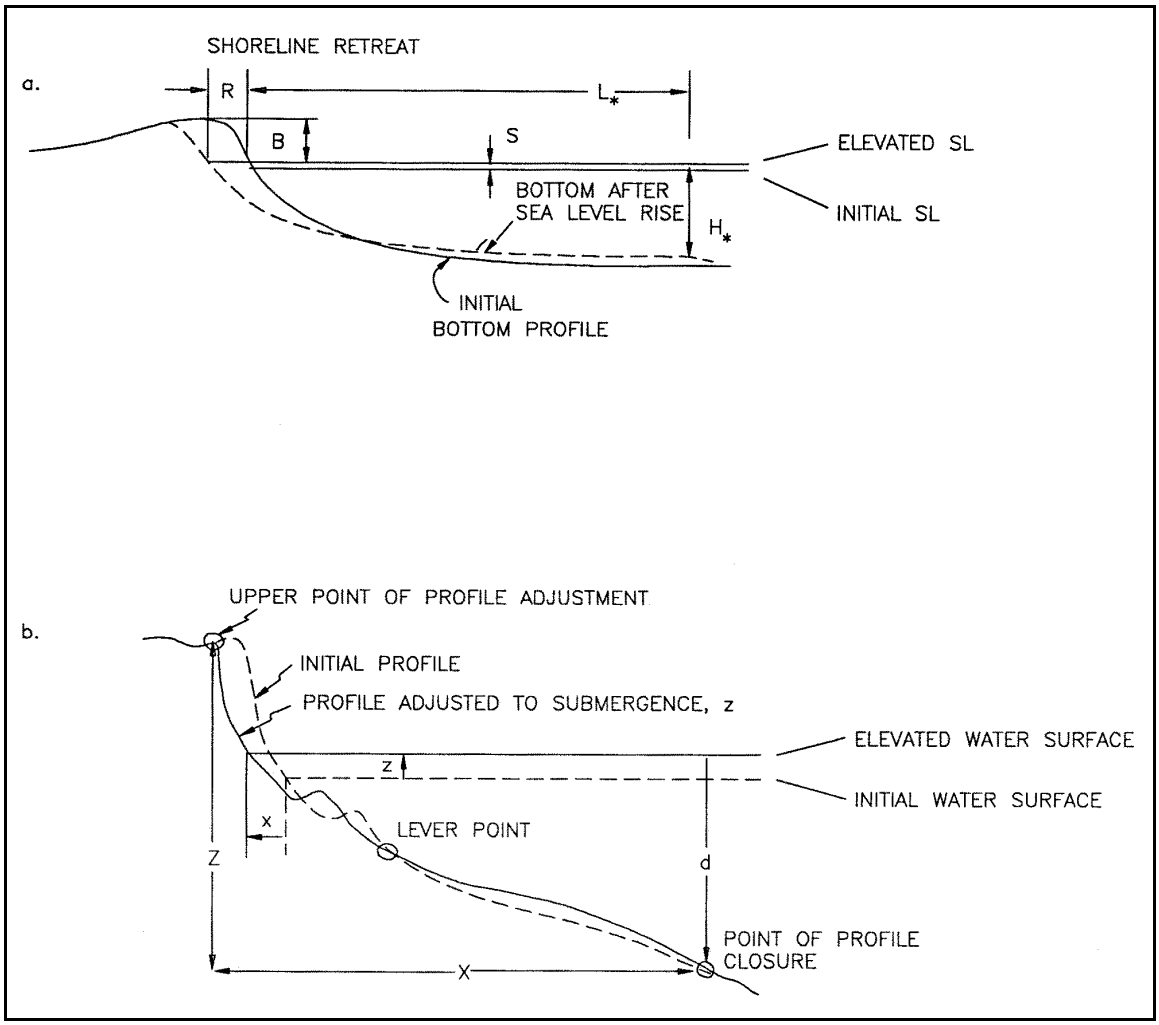

Figure IV-3-40. (a) Shoreline response to rising sea level (SL) depicted by the Bruun Rule. (b) Simplified nomenclature used by Hands (1983). The sandbar shows that the model is valid for complicated profile shapes

$$R = \frac{L_*}{B + H_*} S \tag{IV-3-5}$$

where

R = shoreline retreat

S = increase in sea level

L_* = cross-shore distance to the water depth H_*

B = berm height of the eroded area

Hands (1983) restated the Bruun Rule in simplified form:

$$x = \frac{zX}{Z} \qquad \text{(IV-3-6)}$$

where z is the change in water level. The ultimate retreat of the profile x can be calculated from the dimensions of the responding profile, X and Z, as shown in Figure IV-3-40b. Other expressions for the Bruun Rule are presented in Part III-3-h.

(c) Despite the continued interest in Bruun's concept, there has been only limited use of this method for predictive purposes. Hands (1983) listed several possible reasons for the reluctance to apply this approach:

- Skepticism as to the adequacy of an equilibrium model for explaining short-term dynamic changes.
- Difficulties in measuring sediment lost from the active zone (alongshore, offshore to deep water, and onshore via overwash).
- Problems in establishing a realistic closure depth below which water level changes have no measurable effect on the elevation or slope of the seafloor.
- The perplexity caused by a discontinuity in the profile at the closure depth which appeared in the original and in most subsequent diagrams illustrating the concept.

An additional, and unavoidable, limitation of this sediment budget approach is that it does not address the question of *when* the predicted shore response will occur (Hands 1983). It merely reveals the horizontal distance the shoreline must *ultimately* move to reestablish the equilibrium profile at its new elevation under the assumptions stated in Bruun's Rule.

(d) Hands (1983) demonstrated the geometric validity of the Bruun Rule in a series of figures which show the translation of the profile upward and landward (the figures are two-dimensional; volumes must be based on unit lengths of the shoreline):

- Figure IV-3-41a: The equilibrium profile at the initial water level.
- Figure IV-3-41b: The first translation moves the active profile up an amount z and reestablishes equilibrium depths below the now elevated water level. Hands defines the *active profile* as the zone between the closure depth and the upper point of profile adjustment. The volume of sediment required to maintain the equilibrium water depth is proportional to X (width of the active zone) times z (change in water level).
- Figure IV-3-41c: The required volume of sediment is provided by the second translation, which is a recession (horizontal movement) of the profile by an amount x. The amount of sediment is proportional to x times Z, where Z is the vertical extent of the active profile from the closure depth to the average elevation of the highest erosion on the backshore.
- Figure IV-3-41d: Equating the volume required by the vertical translation and the volume provided by the horizontal translation yields Equation 3-6. In reality, both translations occur simultaneously, causing the closure point to migrate upslope as the water level rises.

(e) One of the strengths of the Bruun concept is that the equations are valid regardless of the shape of the profile, for example, if bars are present (Figure IV-3-40b). It is important that an offshore distance and depth of closure be chosen that incorporate the entire zone where active sediment transport occurs. Thereby,

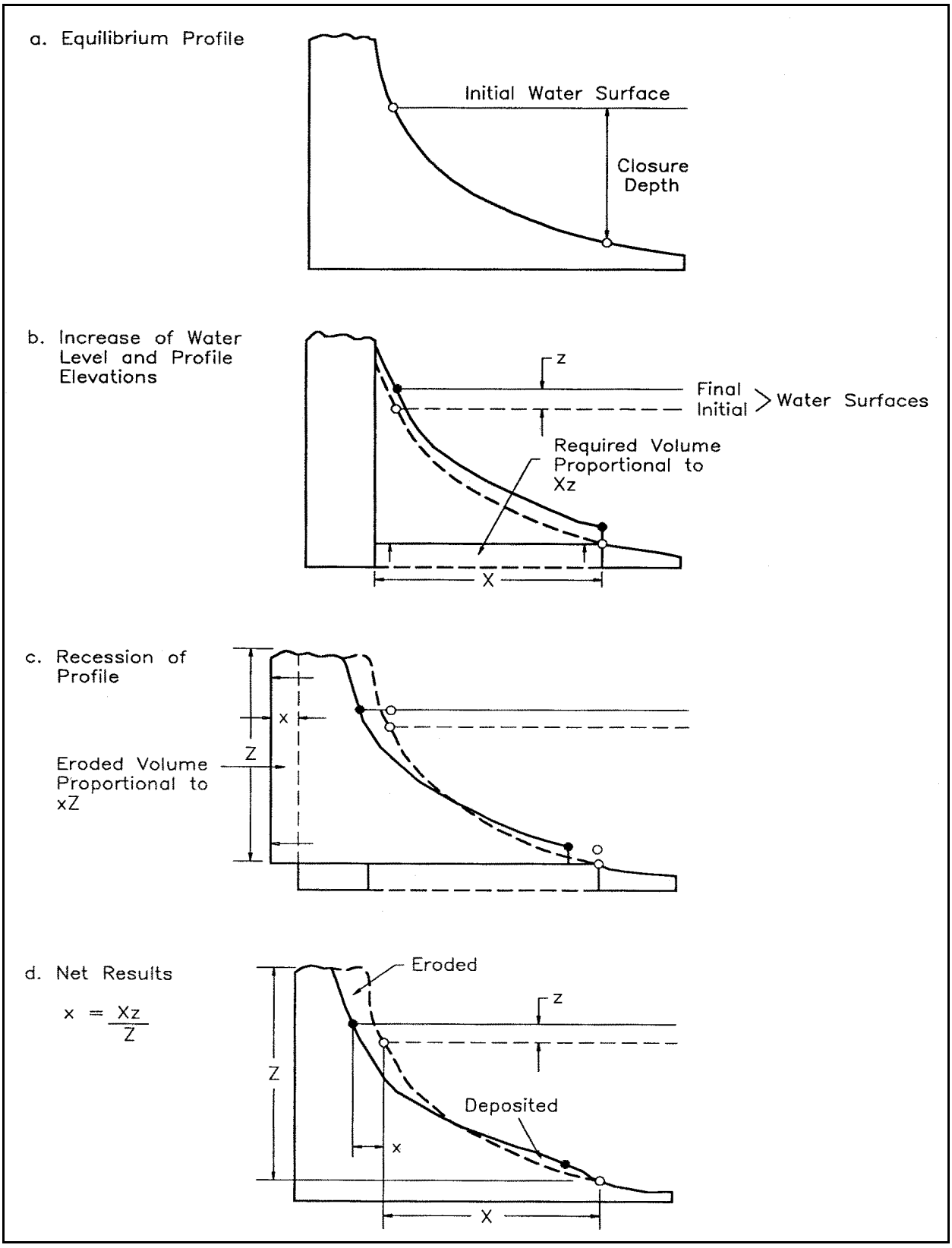

Figure IV-3-41. Profile adjustment in two stages, first vertical, then horizontal, demonstrating the basis for the Bruun Rule (Equation 3-6) (from Hands (1983)). Details discussed in the text

sediment is conserved in spite of the complex processes of local erosion versus deposition as bars migrate (Komar et al. 1991). Another strength is that it is a simple relationship, a geometric conclusion based only on water level. Despite its simplicity and numerous assumptions, it works remarkably well in many settings. Even with its shortcomings, it can be used to predict how beaches can respond to changes in sea level.

(4) Use of models to predict shoreline recession. Although field studies have confirmed the assumptions made by Bruun and others concerning translations of the shoreface, there has been no convincing demonstration that the models can predict shoreline recession rates. Komar et al. (1991) cite several reasons for the inability to use the models as predictive tools:

(a) Existence of a considerable time lag of the beach response following a sustained water level rise (as shown by Hands (1983) for Lake Michigan).

(b) Uncertainty in the selection of the parameters used in the equations (in particular, closure depth).

(c) Local complexities of sediment budget considerations in the sand budget.

(5) Recommendations. More field and laboratory studies are needed to better evaluate the response of beaches to rising (and falling) sea level. For example, it would be valuable to reoccupy the profile lines monitored by Hands (1976, 1979, 1980) in Lake Michigan in the 1970's to determine how the shores have responded to the high water of the mid-1980's and to the subsequent drop in the early 1990's. In addition, conceptual advances need to be incorporated in the theoretical models. How sediment has moved onshore in some locations following sea level rise also needs to be evaluated, because there is evidence that in some areas beach sand compositions reflect offshore rather than onshore sources (Komar et al. 1991).

g. Equilibrium profiles on sandy coasts.

(1) General characteristics and assumptions. The existence of an equilibrium shoreface profile (sometimes called equilibrium *beach* profile) is a basic assumption of many conceptual and numerical coastal models. Dean (1990) listed characteristic features of profiles:

(a) Profiles tend to be concave upwards.

(b) Fine sand is associated with mild slopes and coarse sand with steep slopes.

(c) The beach (above the surf zone) is approximately planar.

(d) Steep waves result in milder inshore slopes and a tendency for bar formation.

The main assumption underlying the concept of the shoreface equilibrium profile is that the seafloor is in equilibrium with *average* wave conditions. Presumably, the term *equilibrium* is meant to indicate a situation in which water level, waves, temperature, etc., are held constant for a sufficient time such that the beach profile arrives at a final, stable shape (Larson and Kraus 1989a). Larson (1991) described the profile as: "A beach of specific grain size, if exposed to constant forcing conditions, normally assumed to be short-period breaking waves, will develop a profile shape that displays no net change in time." This concept ignores the fact that, in addition to wave action, many other processes affect sediment transport. These simplifications, however, may represent the real strength of the concept because it has proven to be a useful way to characterize the shape of the shoreface in many locations around the world.

(2) Shape. Based on studies of beaches in many environments, Bruun (1954) and Dean (1976, 1977) have shown that many ocean beach profiles exhibit a concave shape such that the depth varies as the two-thirds power of distance offshore along the submerged portions:

$$h = Ay^{2/3} \tag{IV-3-7}$$

where

h = water depth (m) at distance y (m) from the shoreline

A = a scale parameter that depends mainly on sediment characteristics

This surprisingly simple expression asserts, in effect, that beach profile shape can be calculated from sediment characteristics (particle size or fall velocity) alone. Moore (1982) graphically related the parameter A, sometimes called the *profile shape parameter,* to the median grain size d_{50}. Hanson and Kraus (1989) approximated Moore's curve by a series of lines grouped as a function of the median nearshore grain size d_{50} (in mm):

$$\begin{aligned} A &= 0.41(d_{50})^{0.94} \quad , \quad d_{50} < 0.4 \\ A &= 0.23(d_{50})^{0.32} \quad , \quad 0.4 \le d_{50} < 10.0 \\ A &= 0.23(d_{50})^{0.28} \quad , \quad 10.0 \le d_{50} < 40.0 \\ A &= 0.46(d_{50})^{0.11} \quad , \quad 40.0 \le d_{50} \end{aligned} \tag{IV-3-8}$$

Note that A has unit dependence ($m^{1/3}$). Equation 3-8 is for SI (metric) values only. Different equations must be used for English units.

Table III-3-3 is a summary of recommended A values, and a more detailed discussion of methods to compute equilibrium profiles is provided in Part III-3.

(3) Discussion of assumptions. Pilkey et al. (1993), in a detailed examination of the concept of the equilibrium shoreface profile, contended that several assumptions must hold true for the concept to be valid:

(a) *Assumption 1: All sediment movement is driven by incoming wave orbitals acting on a sandy shoreface.*

This assumption is incorrect because research by Wright et al. (1991) showed that sediment movement on the shoreface is an exceedingly complex phenomenon, driven by a wide range of wave, tidal, and gravity currents. Even in locations where the wave orbitals are responsible for mobilizing the sand, bottom currents frequently determine where the sand will go.

(b) *Assumption 2: Existence of closure depth and no net cross-shore (i.e., shore-normal) transport of sediment to and from the shoreface.*

Pilkey et al. (1993) state that this assumption is also invalid because considerable field evidence has shown that large volumes of sand may frequently move beyond the closure depth. Such movement can occur during

both fair weather and storm periods, although offshore-directed storm flows are most likely the prime transport agent. Pilkey et al. cite studies in the Gulf of Mexico that measured offshore bottom currents of up to 200 cm/sec and sediment transport to the edge of the continental shelf. The amount of sediment moved offshore was large, but it was spread over such a large area that the change in sea bed elevation could not be detected by standard profiling methods.[1] Wright, Xu, and Madsen (1994) measured significant across-shelf benthic transport on the inner shelf of the Middle Atlantic Bight during the Halloween storm of 1991.

(c) *Assumption 3: There exists a sand-rich shoreface; the underlying and offshore geology must not play a part in determining the shape of the profile.*

Possibly the most important of the assumptions implicit in the equilibrium profile concept is that the entire profile is sand-rich, without excessive areas of hard bottom or mud within the active profile. Clearly these conditions do not apply in many parts of the world. Coasts that have limited sand supplies, such as much of the U.S. Atlantic margin, are significantly influenced by the geologic framework occurring underneath and in front of the shoreface. Many of the east coast barriers are perched on a platform of ancient sediment. Depending upon the physical state, this underlying platform can act as a subaqueous headland or hardground that dictates the shape of the shoreface profile and controls beach dynamics and the composition of the sediment. Niederoda, Swift, and Hopkins (1985) believed that the seaward-thinning and fining veneer of modern shoreface sediments is ephemeral and is easily removed from the shoreface during major storms. During storms, Holocene and Pleistocene strata cropping out on the shoreface provide the immediate source of the bulk of barrier sands. Swift (1976) used the term *shoreface bypassing* to describe the process of older units supplying sediment to the shoreface of barrier islands. Pilkey et al. (1993) contend that:

> ...a detailed survey of the world's shorefaces would show that the sand rich shoreface required by the equilibrium profile model is an exception rather than the rule. Instead, most shorefaces are underlain by older, consolidated or semi-consolidated units covered by only a relatively thin veneer of modern shoreface sands. These older units are a primary control on the shape of the shoreface profile. The profile shape is not determined by simple wave interaction with the relatively thin sand cover. Rather, the shape of the shoreface in these sediment poor areas is determined by a complex interaction between underlying geology, modern sand cover, and highly variable (and often highly diffracted and refracted) incoming wave climate. (p. 271)

(d) *Assumption 4: If a shoreface is, in fact, sand-rich, the smoothed profile described by the equilibrium profile equation (ignoring bars and troughs) must provide a useful approximation of the real shoreface shape.*

In addressing this assumption, Pilkey et al. (1993) cited studies conducted on the Gold Coast, in Queensland, Australia. The Gold Coast shoreface is sand-rich to well beyond a depth of 30 m. Without being directly influenced by underlying geology, the shoreface is highly dynamic. As a consequence, the Gold Coast shoreface shape cannot be described by one equilibrium profile; rather, it is best described by an ever-changing regime profile. Pilkey et al. concluded:

> The local shoreface profile shapes are entirely controlled by relative wave energy "thresholds"; for the sediment properties have not changed at all. Thus principal changes to the shoreface profiles of the Gold Coast are driven by wave power history with some modification by currents, and not by sediment size, or its parameter *A*, as defined within the equilibrium profile concept. (p. 272).

---

[1] This latter statement underscores how important it is to develop improved methods to detect and measure sediment movement in deep water.

(4) General comments.

(a) The idea of a profile only adjusting to waves is fundamentally wrong as shown by Wright et al. (1991) and others. However, although the physical basis for the equilibrium profile concept is weak, critics of this approach have not proven that it always results in highly erroneous answers.

(b) Before the use of the equilibrium profile, coastal engineers had no way to predict beach change other than using crude approximations (e.g., sand loss of 1 cu yd/ft of beach retreat). The approximations were inadequate. Surveys from around the world have shown that shoreface profiles display a characteristic shape that differs with locality but is relatively stable for a particular place (i.e., Duck, North Carolina). With many caveats (which are usually stated, then ignored), a profile can be reasonably represented by the equilibrium equation. The fit between the profile and the real seafloor on a daily, seasonal, and storm variation basis may not be perfect, but the differences may not matter in the long term.

(c) One critical problem for coastal engineers is to predict what a sequence of waves (storm) will do to a locality when little is known about the particular shape of the pre-storm beach. For this reason, numerical models like SBEACH (Larson and Kraus 1989a), despite their reliance on the equilibrium profile concept, are still useful. The models allow a researcher to explore storm impact on a location using a general approximation of the beach. The method is very crude - however, the resulting numbers are of the right order of magnitude when compared with field data from many locations.

(d) Answers from the present models are not exact, and researchers still have much to learn about the weakness of the models and about physical processes responsible for the changes. Nevertheless, the models do work and they do provide numbers that are of the correct magnitudes when run by careful operators. Users of shoreface models must be aware of the limitations of the models and of special conditions that may exist at their project sites. In particular, profile-based numerical models are likely to be inadequate in locations where processes other than wave-orbital transport predominate.

h . Depth of closure.

(1) Background.

(a) *Depth of closure* is a concept that is often misinterpreted and misused. For engineering practice, depth of closure is commonly defined as the minimum water depth at which no measurable or significant change in bottom depth occurs (Stauble et al. 1993). The word *significant* in this definition is important because it leaves considerable room for interpretation. “Closure” has erroneously been interpreted to mean the depth at which no sediment moves on- or offshore, although numerous field studies have verified that much sediment moves in deep water (Wright et al. 1991). Another complication is introduced by the fact that it is impossible to define a single depth of closure for a project site because “closure” moves depending on waves and other hydrodynamic forces. Therefore, it is invalid to assume that “closure” is a single fixed depth at a project site or a stretch of coastline.

(b) Closure depth is used in a number of applications such as the placement of mounds of dredged material, beach fill, placement of ocean outfalls, and the calculation of sediment budgets.

(2) Energy factors. As discussed above, the primary assumption behind the concept of the shoreface equilibrium profile is that sediment movement and the resultant changes in bottom elevation are a function of wave properties and sediment grain size. Therefore, the active portion of the shoreface varies in width throughout the year depending on wave conditions. In effect, “closure” is a time-dependent quantity that may be predicted based on wave climatology or may be interpreted statistically using profile surveys.

(3) Time considerations. The energy-dependent nature of the active portion of the shoreface requires us to consider return period. The closure depth that accommodates the 100-year storm will be much deeper than one that merely needs to include the 10-year storm. Therefore, a closure depth must be chosen in light of a project's engineering requirements and design life. For example, if a berm is to be built in deep water where it will be immune from wave resuspension, what is the minimum depth at which it should be placed? This is an important question because of the high costs of transporting material and disposing of it at sea. It would be tempting to use a safe criterion such as the 100- or 500-year storm, but excessive costs may force the project engineer to consider a shallower site that may be stable only for shorter return period events.

(4) Predictive methods.

(a) Hallermeier (1977, 1978, 1981a, 1981b, 1981c), using laboratory tests and limited field data, introduced equations to predict the limits of extreme wave-related sediment movement. He calculated two limits, d_ℓ and d_i, that included a buffer region on the shoreface called the shoal zone. Landward of d_ℓ, significant alongshore transport and intense onshore-offshore sediment transport occur (the littoral zone). Within the shoal zone, expected waves have neither a strong nor a negligible effect on the sandy bed during a typical annual cycle of wave action. Seaward of d_i, only insignificant onshore-offshore transport by waves occurs. The deeper limit was based on the median nearshore storm wave height (and the associated wave period). The boundary between the shoal zone and the littoral zone (d_ℓ) as defined represents the annual depth of closure. Hallermeier (1978) suggested an analytical approximation, using linear wave theory for shoaling waves, to predict an *annual* value of d_ℓ:

$$d_\ell = 2.28H_e - 68.5\left(\frac{H_e^2}{gT_e^2}\right) \tag{IV-3-9}$$

where

d_ℓ = annual depth of closure below mean low water

H_e = non-breaking significant wave height that is exceeded 12 hr per year (0.137 % of the time)

T_e = associated wave period

g = acceleration due to gravity

According to Equation 3-9, d_ℓ is primarily dependent on wave height with an adjustment for wave steepness. Hallermeier (1978) proposed using the 12-hr exceeded wave height, which allowed sufficient duration for "moderate adjustment towards profile equilibrium." Equation 3-9 is based on quartz sand with a submerged density of $\gamma' = 1.6$ and a median diameter between 0.16 and 0.42 mm, which typifies conditions in the nearshore for many beaches. If the grain size is larger than 0.42 mm, Equation 3-9 may not be appropriate. Because d_ℓ was derived from linear wave theory for shoaling waves, d_ℓ must be seaward of the influence of intense wave-induced nearshore circulation. However, because of various factors, Hallermeier (1978) "proposed that the calculated d_ℓ be used as a minimum estimate of profile close-out depth with respect to low(er) tide level." Because tidal or wind-induced currents may increase wave-induced near-bed flow velocities, Hallermeier suggested using mean low water (mlw) as a reference water level to obtain a conservative depth of closure. Note that Hallermeier's equations critically depend on the quality of wave data at a site. The reader is cautioned that Hallermeier's equations can be expressed in various forms depending on the assumptions made, the datums used as reference levels, and available wave data. The reader is referred

to his original papers for clarification and for details of his assumptions. The equations may not be applicable at sites where currents are more important at moving sand than wave-induced flows.

(b) At the Lake Michigan sites that Hands (1983) surveyed, the closure depth was equal to about twice the height of the 5-year return period wave height (H_5):

$$Z \simeq 2H_5 \tag{IV-3-10}$$

In the absence of strong empirical evidence as to the correct closure depth, this relationship is recommended as a rule of thumb to estimate the 5-year profile response under Great Lakes conditions. The return period of the wave height should approximate the design life of interest. For example, the 20-year closure depth would be estimated by doubling the 20-year return period wave height ($Z \simeq 2H_{20}$).

(5) Empirical determination.

(a) When cross-shore surveys covering several years are available for a project site, closure is best determined by plotting and analyzing the profiles. The closure depth computed in this manner reflects the influence of storms as well as of calmer conditions. Kraus and Harikai (1983) evaluated the depth of closure as the minimum depth where the standard deviation in depth change decreased markedly to a near-constant value. Using this procedure, they interpreted the landward region where the standard deviation increased to be the active profile where the seafloor was influenced by gravity waves and storm-driven water level changes. The offshore region of smaller and nearly constant standard deviation was primarily influenced by lower frequency sediment-transporting processes such as shelf and oceanic currents (Stauble et al. 1993). It must be noted that the smaller standard deviation values fall within the limit of measurement accuracy. This suggests that it is not possible to specify a closure depth unambiguously because of operational limits of offshore profiling hardware and procedures.

(b) An example of how closure was determined empirically at Ocean City, Maryland, is shown in Figure IV-3-42 (from Stauble et al. (1993)). A clear reduction in standard deviation occurs at a depth of about 5.5 - 6 m. Above the ~5.5 m depth, the profile exhibits large variability, indicating active wave erosion, deposition, and littoral transport. Deeper (and seaward) of this zone, the lower and relatively constant deviation of about 7 - 10 cm is within the measurement error of the sled surveys. Nevertheless, despite the inability to precisely measure seafloor changes in this offshore region, it is apparent that less energetic erosion and sedimentation take place here than in water shallower than ~5.5 m. This does not mean that there is no sediment transport in deep water, just that the sled surveys are unable to measure it. For the 5.6 km of shore surveyed at Ocean City, the depth of closure ranged between 5.5 and 7.5 m. Scatter plots indicated that the average closure depth was 6 m.

(c) Presumably, conducting surveys over a longer time span at Ocean City would reveal seafloor changes deeper than ~6 m, depending on storms that passed the region. However, Stauble et al. (1993) noted that the "Halloween Storm" of October 29 to November 2, 1991 generated waves of peak period (T_p) 19.7 sec, extraordinarily long compared to normal conditions along the central Atlantic coast. Therefore, the profiles may already reflect the effects of an unusually severe storm.

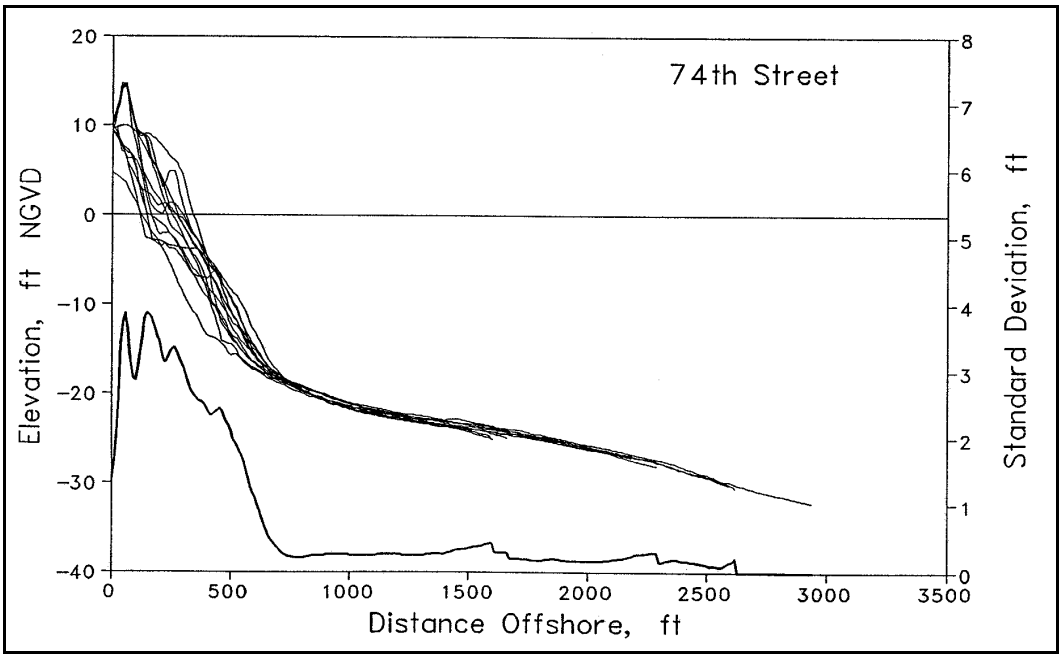

Figure IV-3-42. Profile surveys and standard deviation of seafloor elevation at 74th Street, Ocean City, Maryland (from Stauble et al. (1993)). Surveys conducted from 1988 to 1992. Large changes above the datum were caused by beach fill placement and storm erosion. Figure discussed in the text

(d) Figure IV-3-43 is an example of profiles from St. Joseph, Michigan, on the east shore of Lake Michigan. Along Line 14, dramatic bar movement occurs as far as 760 m offshore to a depth of 7.6 m with respect to International Great Lakes Datum (IGLD) 1985. This is where an abrupt decrease in standard deviation of lake floor elevation occurs and can be interpreted as closure depth. In September 1992, the mean water surface was 0.51 m above IGLD 85. Therefore, closure was around 7.9 - 8.2 m below *water* level.

(e) In the Great Lakes, water levels fluctuate over multi-year cycles. This raises some fundamental difficulties in calculating closure based on profile surveys. Presumably, during a period of high lake level, the zone of active sand movement would be higher on the shoreface than during a time of low lake level (this assumes similar wave conditions). Therefore, the depth where superimposed profiles converge should reflect the *deepest* limit of active shoreface sand movement. This would be a conservative value, but *only with respect to the hydrologic conditions that occurred during the survey program*. Presumably, if lake level dropped further at a later date, sediment movement might occur deeper on the shoreface. This suggests that closure on the lakes should be chosen to reflect the *lowest* likely water level that is expected to occur during the life of a project. (Note that this consideration does not arise on ocean coasts because year-to-year changes in relative sea level are minor, well within the error bounds of sled surveys. Sea level does change throughout the year because of thermal expansion, freshwater runoff, and other factors as discussed in Part IV-1, but the multi-year mean is essentially stable.) In summary, determining closure depth in the Great Lakes is problematic because of changing water levels, and more research is needed to develop procedures that accommodate these non-periodic lake level fluctuations.

(f) The variation of closure depth at approximately 100 profile lines along the south shore of Long Island is plotted in Figure IV-3-44. Generally the depth increases towards the east, with Rockaway Beach averaging 5.0 m below NGVD and the Montauk zone averaging 7.6 m. These values were based on

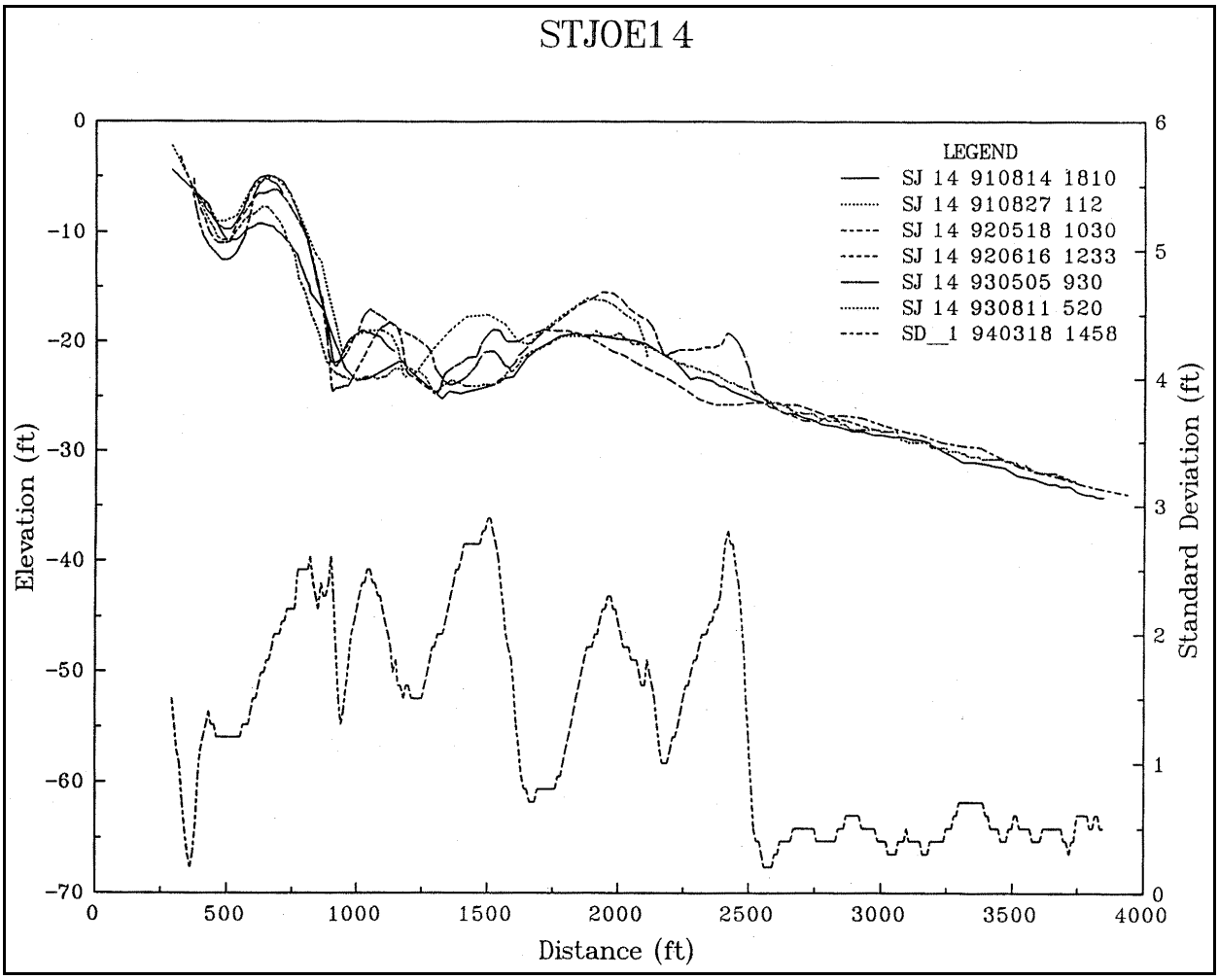

Figure IV-3-43. Profile surveys and standard deviation of lake floor elevation at St. Joseph, Michigan, on the east shore of Lake Michigan. Profiles are referenced to International Great Lakes Datum (IGLD) 1985. Surveys conducted between 1991 and 1994 (Nairn et al. 1997). Figure discussed in the text

surveys in 1995 and 1996 (Morang 1998). The depth increase toward the east is expected because wave energy is greater there than at the west end of Long Island.

i. Longshore sediment movement.

The reader is referred to Part III-2 and to *Coastal Sediment Transport* (EM 1110-2-1502) for a detailed treatment of longshore transport.

j. Summary.

(1) A model of shoreface morphodynamics for micro- and low-mesotidal sandy coasts has been developed by Wright and Short (1984). The six stages of the model (Figure IV-3-34) illustrate the response of sandy beaches to various wave conditions.

(2) Sediment movement on the shoreface is a very complicated phenomenon. It is a result of numerous hydrodynamic processes, among which are: (a) wave orbital interactions with bottom sediments and with

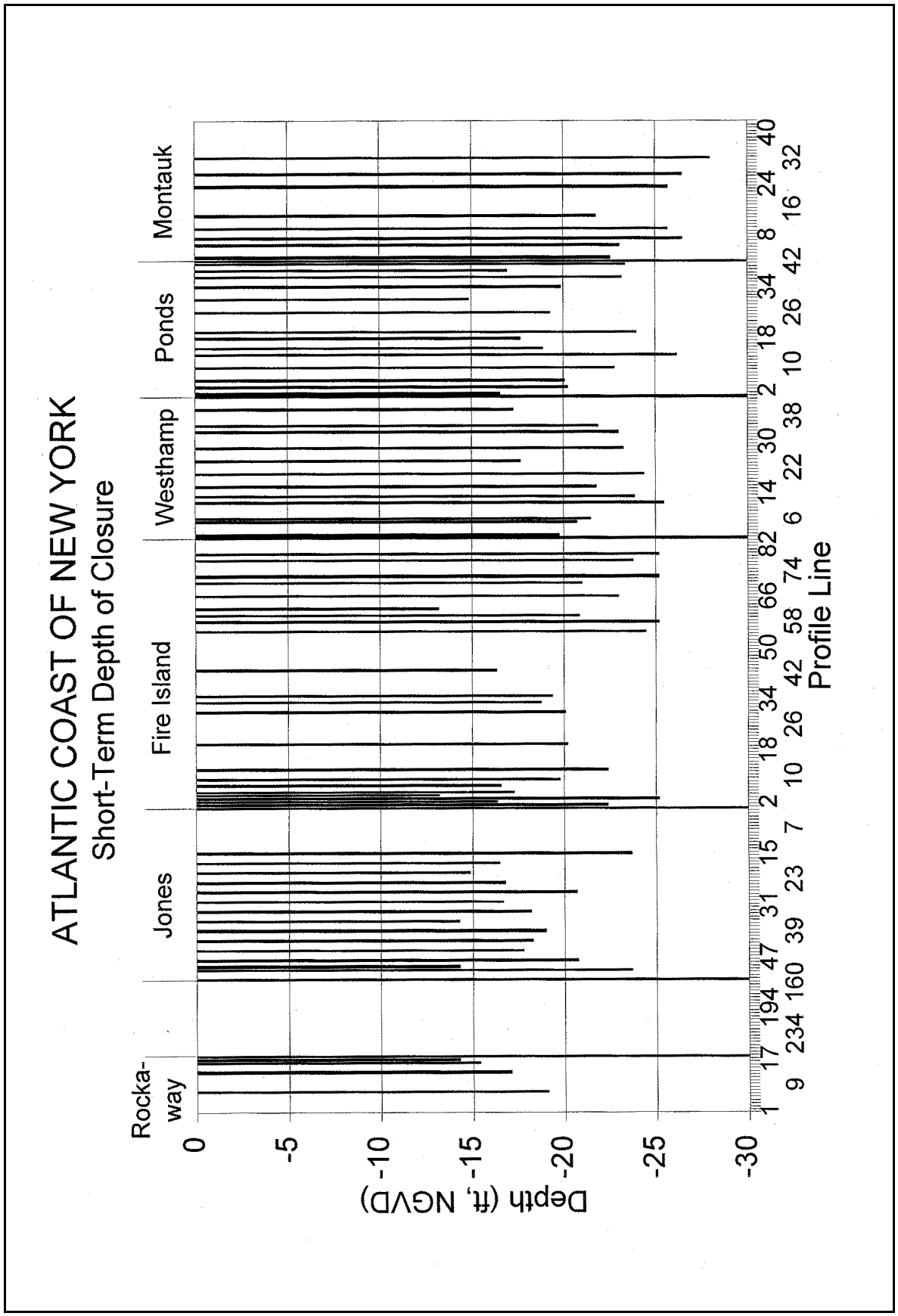

Figure IV-3-44. Variation in short-term closure depth along the south shore of Long Island, New York, computed for four survey dates in 1995 and 1996

wave-induced longshore currents; (b) wind-induced longshore currents; (c) rip currents; (d) tidal currents; (e) storm surge ebb currents; (f) gravity-driven currents; (g) wind-induced upwelling and downwelling; (h) wave-induced upwelling and downwelling; and (i) gravity-induced downslope transport.

(3) The Bruun Rule (Equation 3-5 or 3-6) is a model of shoreface response to rising sea level. Despite the model's simplicity, it helps explain how barriers have accommodated rising sea level by translating upward and landward. A limitation is that the model does not address *when* the predicted shore response will occur (Hands 1983). It merely reveals the horizontal distance the shoreline must *ultimately* move to reestablish the equilibrium profile at its new elevation under the stated assumptions.

(4) The concept of the equilibrium shoreface profile applies to sandy coasts primarily shaped by wave action. It can be expressed by a simple equation (Equation 3-7) which depends only on sediment characteristics. Although the physical basis for the equilibrium profile concept is weak, it is a powerful tool because models based on the concept produce resulting numbers that are of the right order of magnitude when compared with field data from many locations.

(5) *Closure* is a concept that is often misinterpreted and misused. For engineering practice, depth of closure is commonly defined as the minimum water depth at which no measurable or significant change in bottom depth occurs (Stauble et al. 1993). Closure can be computed by two methods: (a) analytical approximations such as those developed by Hallermeier (1978), which are based on wave statistics at a project site (Equation 3-10); or (b) empirical methods based on cross-shore survey profile data. When profiles are superimposed, a minimum value for closure can be interpreted as the depth where the standard deviation in depth change decreases markedly to a near-constant value. Both methods have weaknesses. Hallermeier's analytical equations depend on the quality of wave data. Empirical determinations depend on the availability of several years of profile data at a site. Determining closure in the Great Lakes is problematic because lake levels fluctuate due to changing hydrographic conditions.

IV-3-6. References

EM 1110-2-1502
Coastal Littoral Transport

Allen 1968
Allen, J. R. L. 1968. *Current Ripples: Their Relation to Patterns of Water and sediment Movement,* North Holland, Amsterdam, Netherlands.

Allen 1984
Allen, J. R. L. 1984. "Sedimentary Structures, Their Character and Physical Basis," *Developments in Sedimentology*, Vol 30, Elsevier, New York, NY.

Allen 1985
Allen, J. R. L. 1985. *Principles of Physical Sedimentology,* George Allen and Unwin, London, UK.

Ashley 1990
Ashley, G. M. 1990. "Classification of Large-Scale Subaqueous Bedforms: A New Look at an Old Problem," *Journal of Sedimentary Petrology*, Vol 60, pp 363-396.

Aubrey and Speer 1984
Aubrey, D. G., and Speer, P. E. 1984. "Updrift Migration of Tidal Inlets," *Journal of Geology*, Vol 92, pp 531-546.

Aubrey and Weishar 1988
Aubrey, D. G., and Weishar, L., eds. 1988. *Hydrodynamics and Sediment and Dynamics of Tidal Inlets,* Lecture Notes on Coastal and Estuarine Studies, Vol 29, Springer-Verlag, New York, NY.

Baeteman 1994
Baeteman, C. 1994. Subsidence in coastal lowlands due to groundwater withdrawal: The geological approach, "Coastal Hazards, Perception, Susceptibility and Mitigation," C. W., Finkl, Jr., ed., *Journal of Coastal Research* Special Issue No. 12, pp 61-75.

Barwis 1976
Barwis, J. H. 1976. "Annotated Bibliography on the Geologic, Hydraulic, and Engineering Aspects of Tidal Inlets," General Investigation of Tidal Inlets Report 4, U.S. Army Engineer Waterways Experiment Station, Vicksburg, MS.

Bascom 1964
Bascom, W. 1964. *Waves and Beaches, the Dynamics of the Ocean Surface,* Doubleday & Co., Garden City, NY.

Bass, Fulford, Underwood, and Parson 1994
Bass, G. P., Fulford, E. T., Underwood, S. G., and Parson, L. E. 1994. "Rehabilitation of the South Jetty, Ocean City, Maryland," Technical Report CERC 94-6, U.S. Army Engineer Waterways Experiment Station, Vicksburg, MS.

Boothroyd 1985
Boothroyd, J. C. 1985. "Tidal Inlets and Tidal Deltas," *Coastal Sedimentary Environments*, 2nd ed., R. A. Davis, ed., Springer-Verlag, New York, NY, pp 445-532.

Bruno, Yavary, and Herrington 1998
Bruno, M. S., Yavary, M., and Herrington, T. O. 1998. "The influence of a stabilized inlet on adjacent shorelines: Manasquan, New Jersey," *Shore & Beach,* Vol. 66, No. 2, pp 19-25.

Bruun 1954
Bruun, P. 1954. "Coast Erosion and the Development of Beach Profiles," Technical Memorandum No. 44, Beach Erosion Board, U.S. Army Engineer Waterways Experiment Station, Vicksburg, MS.

Bruun 1966
Bruun, P. 1966. *Tidal Inlets and Littoral Drift,* Universitets-forlaget, Norway (in English).

Bruun 1988
Bruun, P. 1988. "The Bruun Rule of Erosion by Sea-Level Rise: A Discussion of Large-Scale Two- and Three-Dimensional Usages," *Journal of Coastal Research,* Vol 4, pp 627-648.

Bruun and Gerritsen 1959
Bruun, P., and Gerritsen, F. 1959. "Natural By-passing of Sand at Coastal Inlets," *Journal of Waterways and Harbors Division,* American Society of Civil Engineers, New York, pp 75-107.

Bruun and Gerritsen 1961
Bruun, P., and Gerritsen, F. 1961. Stability of Coastal Inlets," *Proceedings of the Seventh Conference on Coastal Engineering,* August 1960, The Hague, Netherlands, J. W. Johnson, ed., Council on Wave Research, University of California, Berkeley, CA, pp 386-417.

Carter 1988
Carter, R. W. G. 1988. *Coastal Environments: An Introduction to the Physical, Ecological, and Cultural Systems of Coastlines,* Academic Press, London, UK.

Castañer 1971
Castañer, P. F. 1971. "Selected Bibliography on the Engineering Characteristics of Coastal Inlets," Report HEL 24-7, Hydraulic Engineering Laboratory, University of California, Berkeley, CA.

Chapman 1974
Chapman, V. J. 1974. "Salt Marshes and Salt Deserts of the World," *Ecology of Halophytes*, R. J. Reimold and W. H. Queen, eds., Academic Press, New York, pp 3-19.

Chasten 1992
Chasten, M. A. 1992. "Coastal Response to a Dual Jetty System at Little River Inlet, North and South Carolina," Miscellaneous Paper CERC-92-2, U.S. Army Engineer Waterways Experiment Station, Vicksburg, MS.

Chasten and Seabergh 1992
Chasten, M. A., and Seabergh, W. C. 1992. "Engineering Assessment of Hydrodynamics and Jetty Scour at Little River Inlet, North and South Carolina," Miscellaneous Paper CERC-92-10, U.S. Army Engineer Waterways Experiment Station, Vicksburg, MS.

Coastal Barriers Study Group 1988
Coastal Barriers Study Group. 1988. Report to Congress: Coastal Barrier Resources System, Recommendations for Additions to or Deletions from the Coastal Barrier Resources System, (in 22 Volumes covering the United States and territories), U.S. Department of the Interior, Washington, DC.

Coleman 1988
Coleman, J. M. 1988. "Dynamic Changes and Processes in the Mississippi River Delta," *Bulletin of the Geological Society of America,* Vol 100, pp 999-1015.

Coleman and Garrison 1977
Coleman, J. M., and Garrison, L. E. 1977. "Geological Aspects of Marine Slope Instability, Northwestern Gulf of Mexico," *Marine Geotechnology,* Vol 2, pp 9-44.

Coleman and Wright 1975
Coleman, J. M., and Wright, L. D. 1975. "Modern River Deltas: Variability of Process and Sand Bodies," *Deltas, Models for Exploration,* M. L. Broussard, ed., Houston Geological Society, Houston, TX, pp 99-149.

Cronin 1975
Cronin, L. E., ed. 1975. *Estuarine Research*, Academic Press, New York (2 volumes).

Davis 1985
Davis, R. A., Jr., ed. 1985. *Coastal Sedimentary Environments,* 2nd ed., Springer-Verlag, New York.

Davis and Ethington 1976
Davis, R. A., Jr., and Ethington, R. L. 1976. *Beach and Nearshore Sedimentation*, Society of Economic Paleontologists and Mineralogists (SEPM) Special Publication No. 24, Tulsa, OK.

Dean 1976
Dean, R. G. 1976. "Beach Erosion: Causes, Processes, and Remedial Measures," *CRC Reviews in Environmental Control*, CRC Press Inc., Boca Raton, FL, Vol 6, Issue 3, pp 259-296.

Dean 1977
Dean, R. G. 1977. "Equilibrium Beach Profiles - U.S. Atlantic and Gulf Coasts," Ocean Engineering Report No. 12, University of Delaware, Newark, pp 1-45.

Dean 1987
Dean, R. G. 1987. "Coastal Sediment Processes: Toward Engineering Solutions," *Proceedings of Coastal Sediments '87*, American Society of Civil Engineers, New York, pp 1-24.

Dean 1988
Dean, R. G. 1988. "Sediment Interaction at Modified Coastal Inlets: Processes and Policies," *Hydrodynamics and Sediment Dynamics of Tidal Inlets*, Lecture Notes on Coastal and Estuarine Studies, D. G. Aubrey and L. Weishar, eds., Vol 29, Springer-Verlag, New York, pp 412-439.

Dean 1990
Dean, R. G. 1990. "Equilibrium Beach Profiles: Characteristics and Applications," Report UFL/COEL-90/001, Coastal & Oceanographic Engineering Department, University of Florida, Gainesville, FL.

Dingler, Reiss, and Plant 1993
Dingler, J. R., Reiss, T. E., and Plant, N. G. 1993. "Erosional Patterns of the Isles Dernieres, Louisiana, in Relation to Meteorological Influences," *Journal of Coastal Research*, Vol 9, No. 1, pp 112-125.

Douglass 1987
Douglass, S. L. 1987. "Coastal Response to Navigation Structures at Murrells Inlet, South Carolina," Technical Report CERC-87-2, U.S. Army Engineer Waterways Experiment Station, Vicksburg, MS.

Escoffier 1940
Escoffier, F. F. 1940. "The Stability of Tidal Inlets," *Shore and Beach*, Vol 8, pp 114-115.

Escoffier 1977
Escoffier, F. F. 1977. "Hydraulics and Stability of Tidal Inlets," General Investigation of Tidal Inlets Report 13, U.S. Army Engineer Waterways Experiment Station, Vicksburg, MS.

FitzGerald 1988
FitzGerald, D. M. 1988. "Shoreline Erosional-Depositional Processes Associated with Tidal Inlets," *Hydrodynamics and Sediment Dynamics of Tidal Inlets*, Lecture Notes on Coastal and Estuarine Studies, D. G. Aubrey and L. Weishar, eds., Vol 29, Springer-Verlag, New York, pp 186-225.

FitzGerald and Nummedal 1983
FitzGerald, D. M., and Nummedal, D. 1983. "Response Characteristics of an Ebb-Dominated Tidal Inlet Channel," *Journal of Sedimentary Petrology*, Vol 53, No. 3, pp 833-845.

FitzGerald, Hubbard, and Nummedal 1978
FitzGerald, D. M., Hubbard, D. K., and Nummedal, D. 1978. "Shoreline Changes Associated with Tidal Inlets along the South Carolina Coast," *Proceedings Coastal Zone '78*, American Society of Civil Engineers, New York, pp 1973-1994.

FitzGerald, Penland, and Nummedal 1984
FitzGerald, D. M., Penland, S., and Nummedal, D. 1984. "Control of Barrier Island Shape by Inlet Sediment Bypassing: Ease Friesian Islands, West Germany," *Marine Geology*, Vol 60, pp 355-376.

Gorman, Morang, and Larson 1998
Gorman, L., Morang, A., and Larson, R. 1998. "Monitoring the Coastal Environment; Part IV: Mapping, Shoreline Changes, and Bathymetric Analysis," *Journal of Coastal Research* 14(1), 61-92.

Graf 1984
Graf, W. H. 1984. *Hydraulics of Sediment Transport,* Water Resources Publications, Littleton, CO.

Greenwood and Davis 1984
Greenwood, B., and Davis, R. A., Jr. 1984. *Hydrodynamics and Sedimentation in Wave-Dominated Coastal Environments*, Developments in Sedimentology 39, Elsevier, Amsterdam, the Netherlands (reprinted from *Marine Geology,* Vol 60, Nos. 1-4).

Guza and Inman 1975
Guza, R. T., and Inman, D. L. 1975. "Edge Waves and Beach Cusps," *Journal of Geophysical Research*, Vol 80, pp 2997-3012.

Hallermeier 1977
Hallermeier, R. J. 1977. "Calculating a Yearly Depth Limit to the Active Beach Profile," Technical Paper TP 77-9, Coastal Engineering Research Center, U.S. Army Engineer Waterways Experiment Station, Vicksburg, MS.

Hallermeier 1978
Hallermeier R. J. 1978. "Uses for a Calculated Limit Depth to Beach Erosion," *Proceedings of the 16th Coastal Engineering Conference,* American Society of Civil Engineers, New York, pp 1493-1512.

Hallermeier 1981a
Hallermeier, R. J. 1981a. "A Profile Zonation for Seasonal Sand Beaches from Wave Climate," *Coastal Engineering*, Vol 4, No. 3, pp 253-277.

Hallermeier 1981b
Hallermeier, R. J. 1981b. "Terminal Settling Velocity of Commonly Occurring Sand Grains," *Sedimentology*, Vol 28, No. 6, pp 859-865.

Hallermeier 1981c
Hallermeier, R. J. 1981c. "Seaward Limit of Significant Sand Transport by Waves: An Annual Zonation for Seasonal Profiles," Coastal Engineering Technical Aide CETA 81-2, Coastal Engineering Research Center, U.S. Army Engineer Waterways Experiment Station, Vicksburg, MS.

Hands 1976
Hands, E. B. 1976. "Observations of Barred Coastal Profiles Under the Influence of Rising Water Levels, Eastern Lake Michigan, 1967-71," Technical Report 76-1, Coastal Engineering Research Center, U.S. Army Engineer Waterways Experiment Station, Vicksburg, MS.

Hands 1979
Hands, E. B. 1979. "Changes in Rates of Shore Retreat, Lake Michigan 1967-76," Technical Paper No. 79-4, U.S. Army Engineer Waterways Experiment Station, Coastal Engineering Research Center, Vicksburg, MS.

Hands 1980
Hands, E. B. 1980. "Prediction of Shore Retreat and Nearshore Profile Adjustments to Rising Water Levels on the Great Lakes," Technical Paper No. 80-7, U.S. Army Engineer Waterways Experiment Station, Coastal Engineering Research Center, Vicksburg, MS.

Hands 1983
Hands, E. B. 1983. "The Great Lakes as a Test Model for Profile Response to Sea Level Changes," Chapter 8 in *Handbook of Coastal Processes and Erosion,* P. D. Komar, ed., CRC Press, Inc., Boca Raton, FL. (Reprinted in Miscellaneous Paper CERC-84-14, Coastal Engineering Research Center, U.S. Army Engineer Waterways Experiment Station, Vicksburg, MS.)

Hanson and Kraus 1989
Hanson, H., and Kraus, N. C. 1989. "GENESIS: Generalized Model for Simulating Shoreline Change; Report 1, Technical Reference, Technical Report CERC-89-19, U.S. Army Engineer Waterways Experiment Station, Vicksburg, MS.

Harms 1969
Harms, J. C. 1969. "Hydraulic Significance of Some Sand Ripples," *Bulletin of the Geological Society of America,* Vol 80, pp 363-396.

Henkel 1970
Henkel, D. J. 1970. "The Role of Waves in Causing Submarine Landslides," *Geotechnique,* Vol 20, pp 75-80.

Horikawa 1988
Horikawa, K., ed. 1988. *Nearshore Dynamics and Coastal Processes: Theory, Measurement and Predictive Models,* University of Tokyo Press, Tokyo, Japan.

Houston 1995
Houston, J. R. 1995. Beach Nourishment, *Shore and Beach,* Journal of the American Shore and Beach Preservation Association, Vol. 63, No. 1.

Houston 1996a
Houston, J. R. 1996a. The Economic Value of Beaches, *Proceedings, 1996 National Conference on Beach Preservation Technology*, St. Petersburg, Florida, Jan 24-26, 1996, pp. 271-280.

Houston 1996b
Houston, J. R. 1996b. International Tourism & U.S. Beaches, *Shore and Beach*, Journal of the American Shore and Beach Preservation Association, Vol. 64, No. 2, pp. 3-4.

Hubbard, Oertel, and Nummedal 1979

Hubbard, D. K., Oertel, G., and Nummedal, D. 1979. "The Role of Waves and Tidal Currents in the Development of Tidal-Inlet Sedimentary Structures and Sand Body Geometry: Examples from North Carolina, South Carolina, and Georgia," *Journal of Sedimentary Petrology*, Vol 49, No. 4, pp 1073-1092.

Hume and Herdendorf 1988
Hume, T. M., and Herdendorf, C. E. 1988. "A Geomorphic Classification of Estuaries and Its Application to Coastal Resource Management - a New Zealand Example," *Journal of Ocean and Shoreline Management*, Vol 11, pp 249-274.

Jopling 1966
Jopling, A. V. 1966. "Some Principles and Techniques Used in Reconstructing the Hydraulic Parameters of a Paleoflow Regime," *Journal of Sedimentary Petrology,* Vol 36, pp 5-49.

Keulegan 1967
Keulegan, G. H. 1967. "Tidal Flow in Entrances: Water-level Fluctuations of Basins in Communication with Seas," Technical Bulletin 14, Committee on Tidal Hydraulics, U.S. Army Corps of Engineers, Washington, DC.

Kieslich 1977
Kieslich, J. M. 1977. "A Case History of Port Mansfield Channel, Texas," General Investigation of Tidal Inlets Report 12, U.S. Army Engineer Waterways Experiment Station, Vicksburg, MS.

King 1972
King, C. A. M. 1972. Beacher and Coasts, 2nd ed., Edward Arnold, London, UK.

Kinsman 1965
Kinsman, B. 1965. *Wind Waves,* Prentice-Hall, Englewood Cliffs, NJ.

Komar 1998
Komar, P. D. 1998. *Beach Processes and Sedimentation,* 2nd ed., Prentice-Hall, Upper Saddle River, NJ.

Komar et al. 1991
Komar, P. D., et al. (Scientific Committee on Ocean Research (SCOR) Working Group 89.) 1991. "The Response of Beaches to Sea-Level Changes: A Review of Predictive Models," *Journal of Coastal Research*, Vol 7, No. 3, pp 895-921.

Kraus and Harikai 1983
Kraus, N. C., and Harikai, S. 1983. "Numerical Model of the Shoreline Change at Oarai Beach," *Coastal Engineering*, Vol 7, No. 1, pp 1-28.

Kraus, Gorman, and Pope (eds.) 1994)
Kraus, N. C., Gorman, L. T., and Pope, J. (eds.) 1994. "Kings Bay Coastal and Estuarine Physical Monitoring and Evaluation Program: Coastal Studies, Volume I, Main Text and Appendix A," Technical Report CERC 94-9, U.S. Army Engineer Waterways Experiment Station, Coastal Engineering Research Center, Vicksburg, MS.

Kraus, Gorman, and Pope (eds.) 1995
Kraus, N. C., Gorman, L. T., and Pope, J. (eds.) 1995. "Kings Bay Coastal and Estuarine Physical Monitoring and Evaluation Program: Coastal Studies, Volume II, Appendices B-G," Technical Report CERC 94-9, U.S. Army Engineer Waterways Experiment Station, Coastal Engineering Research Center, Vicksburg, MS.

Larson 1991
Larson, M. 1991. "Equilibrium Profile of a Beach with Varying Grain Size," *Coastal Sediments '91,* American Society of Civil Engineers, New York, NY, pp 905-919.

Larson and Kraus 1989a
Larson, M., and Kraus, N. C. 1989a. "SBEACH: Numerical Model for Simulating Storm-Induced Beach Change; Report 1, Empirical Foundation and Model Development." Technical Report CERC-89-9, U.S. Army Engineer Waterways Experiment Station, Vicksburg, MS.

Leeder 1982
Leeder, M. R. 1982. *Sedimentology: Process and Product,* George Allen and Unwin, London, UK.

Le Méhauté 1976
Le Méhauté, B. 1976. *An Introduction to Hydrodynamics and Water Waves,* Springer-Verlag, New York, NY.

Lewis 1984
Lewis, D. W. 1984. *Practical Sedimentology,* Hutchinson Ross, Stroudsburg, PA.

Middleton 1965
Middleton, G. V., Compiler. 1965. *Primary Sedimentary Structures and Their Hydrodynamic Interpretation*, Society of Economic Paleontologists and Mineralogists Special Publication No. 12, Tulsa, OK.

Middleton and Southard 1984
Middleton, G. V., and Southard, J. B. 1984. "Mechanics of Sediment Transport," Society for Sedimentary Geology (SEPM), Short Course No. 3, Tulsa, OK.

Moore 1982
Moore, B. D. 1982. "Beach Profile Evolution in Response to Changes in Water Level and Wave Height," M. S. thesis, University of Delaware, Newark, DE.

Morang 1992a
Morang, A. 1992a. "A Study of Geologic and Hydraulic Processes at East Pass, Destin, Florida," (in two volumes), Technical Report CERC-92-5, U.S. Army Engineer Waterways Experiment Station, Vicksburg, MS.

Morang 1992b
Morang, A. 1992b. "Inlet Migration and Geologic Processes at East Pass, Florida," *Journal of Coastal Research*, Vol 8, No. 2, pp 457-481.

Morang 1998
Morang, A. 1998. "Atlantic Coast of New York Monitoring Project; Report 1, Analysis of Beach Profiles, 1995-1996, Report prepared for U.S. Army Engineer District, New York, U.S. Army Engineer Waterways Experiment Station, Vicksburg, MS.

Morang 1999
Morang, A. 1999. Coastal Inlets Research Program, Shinnecock Inlet, New York, Site Investigation, Report 1, Morphology and Historical Behavior, Technical Report CHL-98-32, U.S. Army Engineer Waterways Experiment Station, Vicksburg, MS.

Nairn, Zuzek, Morang, and Parson 1997
Nairn, R. B., Zuzek, P., Morang, A., and Parson, L. 1997. "Effectiveness of Beach Nourishment on Cohesive Shores, St. Joseph, Lake Michigan," Technical Report CHL-97-15, U.S. Army Engineer Waterways Experiment Station, Vicksburg, MS.

Nersesian and Bocamazo 1992
Nersesian, G. K., and Bocamazo, L. M. 1992. Design and construction of Shinnecock Inlet, New York. *Coastal Engineering Practice '92,* American Society of Civil Engineers, New York, pp. 554-570.

Niedoroda, Swift, and Hopkins 1985
Niedoroda, A. W., Swift, D. J. P., and Hopkins, T. S. 1985. "The Shoreface," *Coastal Sedimentary Environments,* R. A. Davis, Jr., ed., 2nd ed., Springer-Verlag, New York.

Nummedal and Fischer 1978
Nummedal, D., and Fischer, I. A. 1978. "Process-Response Models for Depositional Shorelines: The German and the Georgia Bights," *Proceedings of the Sixteenth Conference on Coastal Engineering*, American Society of Civil Engineers, New York, pp 1215-1231.

Nummedal and Humphries 1978
Nummedal, D., and Humphries, S. M. 1978. "Hydraulics and Dynamics of North Inlet, South Carolina, 1975-76," General Investigation of Tidal Inlets Report 16, U.S. Army Engineer Waterways Experiment Station, Vicksburg, MS.

Nummedal and Penland 1981
Nummedal, D., and Penland, S. 1981. "Sediment Dispersal in Norderneyer Seegat, West Germany," *Holocene Marine Sedimentation in the North Sea Basin*, S. D. Nio, R. T. E. Schuttenhelm, and C. E. van Weering, eds., International Association of Sedimentologists Special Publication No. 5, pp 187-210.

O'Brien 1931
O'Brien, M. P. 1931. "Estuary Tidal Prisms Related to Entrance Areas," *Civil Engineering*, Vol 1, pp 738-739.

O'Brien 1976
O'Brien, M. P. 1976. "Notes on Tidal Inlets on Sandy Shores," General Investigation of Tidal Inlets Report 5, U.S. Army Engineer Waterways Experiment Station, Vicksburg, MS.

Oertel 1982
Oertel, G. F. 1982. "Inlets, Marine-Lagoonal and Marine Fluvial," *The Encyclopedia of Beaches and Coastal Environments*, M. L. Schwartz, ed., Hutchinson Ross Publishing Company, Straudsburg, PA, p 489.

Oertel 1988
Oertel, G. F. 1988. "Processes of Sediment Exchange Between Tidal Inlets, Ebb Deltas, and Barrier Islands," *Hydrodynamics and Sediment Dynamics of Tidal Inlets*, Lecture Notes on Coastal and Estuarine Studies, Vol 29, D. G. Aubrey and L. Weishar, eds., Springer-Verlag, New York, pp 297-318.

Pilkey 1993
Pilkey, O. H. 1993. "Can We Predict the Behavior of Sand: In a Time and Volume Framework of Use to Humankind?" *Journal of Coastal Research*, Vol 9, No. 1, pp iii-iv.

Pilkey, Young, Riggs, Smith, Wu, and Pilkey 1993
Pilkey, O. H., Young, R. S., Riggs, S. R., Smith, A. W. S., Wu, H., and Pilkey, W. D. 1993. "The Concept of Shoreface Profile of Equilibrium: A Critical Review," *Journal of Coastal Research*, Vol 9, No. 1, pp 225-278.

Pratt and Stauble 2001
Pratt, T., and Stauble, D. 2001. Coastal Inlets Research Program, Shinnecock Inlet, New York, Site Investigation, Report 3, Selected Field Data Report for 1997, 1998, and 1998 Velocity and Sediment Surveys. Technical Report CHL-98-32, U.S. Army Corps of Engineers, Engineer Research and Development Center, Vicksburg, MS.

Price 1968
Price, W. A. 1968. "Tidal Inlets," *The Encyclopedia of Geomorphology*, Encyclopedia of Earth Sciences Series, Vol III, R. W. Fairbridge, ed., Reinhold Book Corp., NY, pp 1152-1155.

Price and Parker 1979
Price, W. A., and Parker, R. H. 1979. "Origins of Permanent Inlets Separating Barrier Islands and Influence of Drowned Valleys on Tidal Records Along the Gulf Coast of Texas," *Transactions Gulf Coast Association of Geological Societies*, Vol 29, pp 371-385.

Prior and Coleman 1979
Prior, D. B., and Coleman, J. M. 1979. "Submarine Landslides - Geometry and Nomenclature," *Zeitschrift fu̇r Geomorphology,* Vol 23, No. 4, pp 415-426.

Prior and Coleman 1980
Prior, D. B., and Coleman, J. M. 1980. "Sonograph Mosaics of Submarine Slope Instabilities, Mississippi River Delta," *Marine Geology,* Vol 36, pp 227-239.

Reineck and Singh 1980
Reineck, H. E., and Singh, I. B. 1980. *Depositional Sedimentary Environments,* 2nd ed., Springer-Verlag, Berlin, Germany.

Resio and Hands 1994
Resio, D. T., and Hands, E. B. 1994. "Understanding and Interpreting Seabed Drifter (SBD) Data," Technical Report DRP-94-1, U.S. Army Engineer Waterways Experiment Station, Vicksburg, MS.

Russell 1967
Russell, R. 1967. "Origin of estuaries," *Estuaries,* G. H. Lauff, ed., American Association for the Advancement of Science, Publication 83, Washington, DC., 93-99.

Sha 1990
Sha, L. P. 1990. *Sedimentological Studies of the Ebb-tidal Deltas Along the West Frisian Islands, the Netherlands*, Geologica Ultraiectina No. 64, Instituut voor Aardwetenschappen der Rijks-universiteit te Utrecht, Ultrecht, The Netherlands (in English).

Shepard 1950
Shepard, F. P. 1950. "Longshore Bars and Longshore Troughs." Technical Memorandum 41, Beach Erosion Board, U.S. Army Corps of Engineers, Washington, DC.

Short 1991
Short, A. D. 1991. "Macro-meso Tidal Beach Morphodynamics - An Overview," *Journal of Coastal Research*, Vol 7, No. 2, pp 417-436.

Stauble, Da Costa, Monroe, and Bhogal 1988
Stauble, D. K., Da Costa, S. L., Monroe, K. L., and Bhogal, V. K. 1988. "Inlet Flood Tidal Delta Development Through Sediment Transport Processes," *Hydrodynamics and Sediment Dynamics of Tidal Inlets*, Lecture Notes on Coastal and Estuarine Studies, D. G. Aubry and L. Weishar, eds., Vol 29, Springer-Verlag, New York, NY, pp 319-347.

Stauble, Garcia, Kraus, Grosskopf, and Bass 1993
Stauble, D. K., Garcia, A. W., Kraus, N. C., Grosskopf, W. G., and Bass, G. P. 1993. "Beach Nourishment Project Response and Design Evaluation, Ocean City, Maryland," Technical Report CERC-93-13, U.S. Army Engineer Waterways Experiment Station, Vicksburg, MS.

Suter and Berryhill 1985
Suter, J. R., and Berryhill, H. L., Jr. 1985. "Late Quaternary Shelf-Margin Deltas, Northwest Gulf of Mexico," *Bulletin of the American Association of Petroleum Geologists,* Vol 69, No. 1, pp 77-91.

Swift 1976
Swift, D. J. P. 1976. "Coastal Sedimentation," *Marine Sediment Transport and Environmental Management*, D. J. Stanley and D. J. P. Swift, eds., John Wiley and Sons, New York, NY, pp 255-310.

***The Times Atlas of the World* 1980**
The Times Atlas of the World. 1980. Comprehensive edition, Times Books, New York.

U.S. Army Corps of Engineers 1958
U.S. Army Corps of Engineers. 1958. Moriches and Shinnecock Inlets, Long Island, New York, "Survey Report, U.S. Army Engineer District, New York (original report dated September 1957, revised 11 July 1958).

Walton and Adams 1976
Walton, T. L., Jr., and Adams, W. D. 1976. "Capacity of Inlet Outer Bars to Store Sand," *Proceedings of the Fifteenth Coastal Engineering Conference*, July 11-17, Honolulu, HI, American Society of Civil Engineers, New York, pp 1919-1937.

Williams, Morang, and Lillycrop 1998
Williams, G. L., Morang, A., and Lillycrop, L. 1998. "Shinnecock Inlet, New York, Site Investigation; Report 2, Evaluation of Sand Bypass Options," Technical Report CHL-98-3, U.S. Army Engineer Waterways Experiment Station, Vicksburg, MS.

Wright 1981
Wright, L. D. 1981. "Nearshore Tidal Currents and Sand Transport in a Macrotidal Environment," *Geomarine Letters*, Vol 1, pp 173-179.

Wright 1985
Wright, L. D. 1985. "River Deltas," *Coastal Sedimentary Environments,* 2nd ed., R. A. Davis, ed., Springer-Verlag, New York, pp 1-76.

Wright and Coleman 1972
Wright, L. D., and Coleman, J. M. 1972. "River Delta Morphology: Wave Climate and the Role of the Subaqueous Profile," *Science*, Vol 176, pp 282-284.

Wright and Coleman 1973
Wright, L. D., and Coleman, J. M. 1973. "Variations in Morphology of Major River Deltas as Functions of Ocean Wave and River Discharge Regimes," *American Association of Petroleum Geologists Bulletin*, Vol 57, No. 2, pp 370-398.

Wright and Coleman 1975
Wright, L. D., and Coleman, J. M. 1975. "Mississippi River Mouth Processes: Effluent Dynamics and Morphologic Development," *Journal of Geology,* Vol 82, pp 751-778.

Wright and Short 1984
Wright, L. D., and Short, A. D. 1984. "Morphodynamic Variability of Surf Zones and Beaches: A Synthesis," *Marine Geology*, Vol 56, pp 93-118.

Wright and Sonu 1975
Wright, L. D., and Sonu, C. J. 1975. "Processes of Sediment Transport and Tidal Delta Development in a Stratified Tidal Inlet," *Estuarine Research*, Vol 2, L. E. Cronin, ed., Academic Press, New York, pp 63-76.

Wright, Boon, Kim, and List 1991
Wright, L. D., Boon, J. D., Kim, S. C., and List, J. H. 1991. "Modes of Cross-Shore Sediment Transport on the Shoreface of the Middle Atlantic Bight," *Marine Geology*, Vol 96, pp 19-51.

Wright, Sonu, and Kielhorn 1972
Wright, L. D., Sonu, C. J., and Kielhorn, W. V. 1972. "Water-Mass Stratification and Bed Form Characteristics in East Pass, Destin, Florida," *Marine Geology*, Vol 12, pp 43-58.

Wright, Xu, and Madsen 1994
Wright, L. D., Xu, J. P., and Madsen, O. S. 1994. "Across-shelf Benthic Transports on the Inner Shelf of the Middle Atlantic Bight During the 'Halloween Storm' of 1991," *Marine Geology*, Vol 118, No. 1/2, pp 61-77.

Young and Hale 1998
Young, C., and Hale, L. 1998. Coastal Management: Insurance for the Coastal Zone, *Maritimes*, Vol 40m, No. 1, pp. 17-19.

Zenkovich 1967
Zenkovich, V. P. 1967. "Submarine Sandbars and Related Formations," *Processes of Coastal Development*, J. A. Steers, ed., Oliver and Boyd, Ltd., New York, pp 219-236.

IV-3-7. Definition of Symbols

β	Gradient of the beach and surf zone
ε	Surf-scaling parameter (Equation IV-3-4) [dimensionless]
ρ_f	Mass density of fresh water (= 1,000kg/m^3 or 1.94 slugs/ft^3) [force-time^2/length^4]
ρ_s	Mass density of salt water (= 1,025 kg/m^3 or 2.0 slugs/ft^3) [force-time^2/length^4]
ω	Wave angular or radian frequency (= $2\pi/T$) [time^{-1}]
Ω	Modal state of the beach (Equation IV-3-3) [dimensionless]
A	Sediment scale or equilibrium profile parameter or profile shape parameter (Table III-3-3) [length$^{1/3}$]
a_b	Breaker amplitude [length]
B	Berm height of the eroded area [length]
d_ℓ	Annual depth of closure below mean low water (Equation IV-3-9) [length]
F'	Froude number
g	Gravitational acceleration (32.17 ft/sec^2, 9.807m/sec^2) [length/time^2]
h	Equilibrium beach profile depth (Equation IV-3-7) [length]
H_*	Water depth [length]
H_b	Wave height at breaking [length]
H_e	Non-breaking significant wave height that is exceeded 12 hr per year [length]
H_x	Wave height of the x-year return period [time]
h'	Depth of density interface [length]
L_*	Cross-shore distance to the water depth H_* [length]
R	Shoreline retreat (Equation IV-3-5) [length]
S	Increase in sea level [length]
T	Wave period [time]
T_e	Wave period associated with H_e [time]
U	Mean outflow velocity of upper layer (in case of stratified flow) [length/time]
$\overline{w_s}$	Sediment fall velocity [length/time]
x	Retreat of the profile, Bruun Rule (Equation IV-3-6) [length]
X	Horizontal distance of responding profile {Equation IV-3-6 and Figure IV-3-40) [length]

y	Equilibrium beach profile distance offshore (Equation IV-3-7) [length]
z	Change in water level [length]
Z	Closure depth (Equation IV-3-10) [length]
Z	Vertical distance of responding profile {Equation IV-3-6 and Figure IV-3-40) [length]

IV-3-8. Acknowledgments

Authors of Chapter IV-3, "Coastal Morphodynamics:"

Andrew Morang, Ph.D., Coastal and Hydraulics Laboratory (CHL), Engineer Research and Development Center, Vicksburg, Mississippi.
Larry E. Parson, U.S. Army Engineer District, Mobile, Mobile, Alabama.

Reviewers:

Joan Pope, CHL
William E. Birkemeier, CHL
Stephan A. Chesser, U.S. Army Engineer District, Portland, Portland, Oregon.
Ronald L. Erickson, U.S. Army Engineer District, Detroit, Detroit, Michigan.
Edward B. Hands, CHL (retired).
Edward Meisburger, CHL (retired).
Joan Pope, CHL
John F. C. Sanda, Headquarters, U.S. Army Corps of Engineers, Washington, DC., (retired).
Orson P. Smith, Ph.D., U.S. Army Engineer District, Alaska, Anchorage, Alaska, (retired).

DEPARTMENT OF THE ARMY
U.S. Army Corps of Engineers
Washington, DC 20314-1000

EM 1110-2-1100

CECW-EW

Manual
No. 1110-2-1100

30 April 2002

Engineering and Design
COASTAL ENGINEERING MANUAL

1. Purpose. The purpose of the *Coastal Engineering Manual* (CEM) is to provide a comprehensive technical coastal engineering document. It includes the basic principles of coastal processes, methods for computing coastal planning and design parameters, and guidance on how to formulate coastal flood studies, shore protection, and navigation projects.

2. Applicability. This manual applies to all HQUSACE elements and all USACE commands having Civil Works and military design responsibilities.

3. Discussion. The CEM is divided into two major subdivisions: science-based and engineering-based. The science subdivision is further divided into three parts. The first part, "Coastal Hydrodynamics," leads the reader from the fundamental principles of wave theory and ocean wave generation through the process of wave transformation as the wave form approaches and reacts with the shore including water-level variations and currents. The second part, "Coastal Sediment Processes," addresses longshore and cross-shore transport as well as shelf, and wind transport processes. The third part, "Coastal Geology," covers geomorphology, coastal classification, and morphodynamic processes on sandy shores.

The engineering-based subdivision is oriented toward a project-type approach, rather then the individual structure design and is divided into two parts. The first one, "Coastal Planning and Design," provides information on the design process and selection of appropriate type of solution to various coastal problems. The second part, "Design of Coastal Project Elements," provides engineering guidance on materials, fundamentals of design, and reliability.

4. Distribution Statement. Approved for public release, distribution unlimited.

FOR THE COMMANDER:

1 Appendix
Appendix A - Glossary

ROBERT CREAR
Colonel, Corps of Engineers
Chief of Staff

This manual supersedes *Shore Protection Manual,* 1984; EC 1110-2-289, 30 September 1996; EC 1110-2-292, 31 March 1998; EM 1110-2-1004, 30 November 1993; EM 1110-2-1412, 15 April 1986; EM 1110-2-1414, 7 July 1989; EM 1110-2-1502, 20 August 1992; EM 1110-2-1616, 31 January 1991; EM 1110-2-1617, 20 August 1992; EM 1110-2-1618, 28 April 1995; EM 1110-2-2904, 8 August 1986; EM 1110-2-3301, 31 May 1995.

DEPARTMENT OF THE ARMY
U.S. Army Corps of Engineers
Washington, DC 20314-1000

EM 1110-2-1100
(Part V)

CECW-EH

Manual
No. 1110-2-1100

31 July 2003

Engineering and Design
COASTAL ENGINEERING MANUAL

1. Purpose. The purpose of the *Coastal Engineering Manual* (CEM) is to provide a comprehensive technical coastal engineering document. It includes the basic principles of coastal processes, methods for computing coastal planning and design parameters, and guidance on how to formulate coastal flood studies, shore protection, and navigation projects.

2. Applicability. This manual applies to all HQUSACE elements and all USACE commands having Civil Works and military design responsibilities.

3. Discussion. The CEM is divided into six parts in two major subdivisions: science-based and engineering-based. The first four parts of the CEM and an appendix were issued in 30 April 2002 and subsequently updated by change dated 31 July 2003. These included:

Part I, "Introduction"
Part II, "Coastal Hydrodynamics"
Part III, "Coastal Sediment Processes"
Part IV, "Coastal Geology"
Appendix A, "Glossary"

The engineering-based subdivision is oriented toward a project-type approach and is divided into two parts. Part V, "Coastal Project Planning and Design," is included in this transmittal. The text and figures provide information on the design process and selection of appropriate types of solution to various coastal problems. Part VI, "Design of Coastal Project Elements," which provides engineering guidance on materials, fundamentals of design, and reliability, is in preparation.

4. Distribution Statement. Approved for public release, distribution unlimited.

FOR THE COMMANDER:

Barbara A. Caspell

for MICHAEL J. WALSH
Colonel, Corps of Engineers
Chief of Staff

For Geotechnical, Marine or Airport Design and Construction Books, Your Ship Has Come In

Books include classics such as:

- Coastal Engineering Manual (5 volumes)
- NAVFAC DM 7.01—Soil Mechanics, the Classic Reference
- Laboratory Soils Testing
- Bearing Capacity and Settlement
- Mooring Systems: Design, Inspection and Maintenance

...and many more! New titles being added monthly. Competitive prices—always available!

Visit http://www.pz27.net for more information

Table of Contents

Page

V-1-1. Background V-1-1
a. Introduction V-1-1
(1) Purpose V-1-1
(2) Applicability V-1-1
b. The planning process V-1-1
c. Six major planning steps V-1-3
(1) Specify problems and opportunities V-1-3
(2) Inventory and forecast conditions if no action is taken V-1-3
(3) Formulate alternative plans V-1-4
(4) Evaluate effects V-1-4
(5) Compare alternative plans V-1-5
(6) Select a plan V-1-5
d. Planning coordination requirements V-1-5
e. Criteria development V-1-6
f. The design process V-1-6
(1) Final design V-1-6
(2) Plans and specifications V-1-6
g. Construction and monitoring V-1-6
(1) Construction V-1-7
(2) Post-construction inspection and monitoring V-1-7
h. Generic design chart V-1-7

V-1-2. Design Criteria V-1-11

V-1-3. Risk Analysis and Project Optimization V-1-12
a. Introduction V-1-12
b. Traditional vs. risk-based analysis V-1-12
c. Reasons for risk-based analysis V-1-13
(1) Introduction V-1-13
(a) Coastal forcing is probabilistic V-1-13
(b) Coastal engineering embodies major uncertainties V-1-13
(c) Damage and functional performance change incrementally V-1-13
(d) Benefits and risks not fully represented in deterministic terms V-1-13
(e) Uncertain effects on adjacent areas V-1-13
(2) Professional judgement V-1-14
d. Considerations for including risk-based analysis in project design V-1-14
(1) Objectives V-1-14
(2) Key variables V-1-14
(3) Professional judgement V-1-14
(4) Resistance and functional performance vary with time V-1-14

(5) Construction season and mobilization concerns V-1-14
(6) Environmental, aesthetic, social, and political concerns V-1-14
e. Frequency-based vs. life cycle approach V-1-14
f. Typical project elements V-1-15
(1) Site characterization V-1-15
(2) *Without-plan* alternative V-1-15
(3) Formulate, evaluate, and compare alternative plans V-1-15

V-1-4. References V-1-16

V-1-5. Acknowledgments V-1-17

List of Figures

Page

Figure V-1-1. Thought process in the planning and design of a coastal project, Part 1 . . . . . V-1-8

Figure V-1-2. Thought process in the planning and design of a coastal project, Part 2 . . . . . V-1-9

Figure V-1-3. Thought process in the planning and design of a coastal project, Part 3 . . . . . V-1-10

List of Tables

Page

Table V-1-1. Major Coordination Requirements V-1-5

Table V-1-2. Reasons for Risk-Based Analysis of Coastal Projects V-1-13

Chapter V-1
Planning and Design Process

V-1-1. Background

a. Introduction.

(1) Purpose. This chapter provides a comprehensive description of definitions and procedures needed in the planning and design process for coastal projects. The goal of the following sections is to provide the planner/designer with sufficient engineering guidance to accomplish the level of detail necessary to produce an acceptable finished product.

(2) Applicability. Although the information on procedures presented here is directly applicable to the reconnaissance and feasibility studies of the U.S. Army Corps of Engineers (USACE), it is also applicable to all other planning and design efforts because the process is generic. The process of developing a coastal project must be iterative to ensure that the final product is optimum from both the technical and economic viewpoints and will be acceptable to the various levels of decision makers and all project partners.

b. The planning process.

(a) The solution to coastal engineering problems begins with understanding the roles of the engineer as a planner and designer. These roles may be, and often are, embodied in the same person doing sequential tasks. This chapter presents the planning and design processes, the umbrella under which the project evolves from conception through functional detailed technical design phases. Examples of detailed technical designs are found in Part VI of this manual. Although the procedures and examples are those of the USACE, the principles apply to whomever is doing the planning and designing and follow a logical engineering process regardless of project type, scale, geographic siting, or sponsor.

(b) The planning process begins with the questions “What is the problem?” and “What exactly is the project trying to accomplish?” As trite as this sounds, these are the most important and the most difficult questions to answer. To achieve a successful coastal project plan and design requires that the engineer must have a completely open mind, one without preconceived notions of the ultimate form of the project or a specific solution to advocate. An example of a pitfall of the planning process is to answer the second question with “To design a breakwater” without first clearly stating the problem. Is the problem one of navigation difficulties in the vicinity of a harbor, or potential damage to buildings near the shorefront, or water quality problems in a bay? These are symptoms of a problem, but they do not define the problem.

(c) An interdisciplinary team approach is recommended in planning coastal projects to ensure the involvement of physical, natural, and social sciences personnel. The disciplines of the coastal project planners should be appropriate to the problems and opportunities identified in the planning process, and range from coastal, geotechnical, structural, and hydraulic engineers through meteorologists, oceanographers, biologists, and geologists, to economists, urban planners, and transportation specialists. Not all disciplines are needed on all studies, but the team leader needs to be cognizant of the possible need for such talents during the project development.

(d) Interested and affected agencies, groups, coast-sharing partners, and individuals (collectively termed the public) should be provided opportunities to participate with USACE throughout the planning, design, construction, and operation of a Federal project. The purpose of public involvement is to ensure that the project is responsive to the needs and concerns of the public. The objectives of public involvement are to

provide the public with information about proposed Federal activities; to make the public's desires, needs, and concerns known to the decision makers; and to consult with the public and consider the public's views before a decision is reached.

(e) In responding to the question of *problem definition*, the more detailed the engineer can make the statement, the more likely a solution can be found which will satisfy all the numerous stakeholders. A stakeholder is defined as anyone who will be affected by a problem and its potential solution, including a segment of the public. This includes the planner, designer, constructor, manager, all probable sponsors, riparian owners, project users, the political, legal, financial, and environmental entities with interests, and of course the populations that pay the taxes to support the enterprise.

(f) USACE has two levels of planning: one that looks at the problem in a relatively cursory way for a *reconnaissance* level study, and the other for a detailed study of all the factors, conditions, and alternatives for a *feasibility* level study. These terms are equivalent to conceptual design and final design as used in private practice. In the reconnaissance study, the objective is to determine if there is a Federal interest; that is, to determine if the Federal Government should invest in the solution to the problem. Responses are needed to three questions to make this determination: (a) is there a technically doable solution, (b) is it economically and politically feasible, and (c) is it environmentally sound? These are often difficult to answer, but keeping in mind all the stakeholders and the detailed problem definition, the coastal planner can proceed.

(g) Under present laws and regulations (as of the publication date of this manual), a reconnaissance level study is funded entirely by the Federal Government. To be "in the Federal interest," at least one technically adequate solution to the problem must be identified, a cost-sharing sponsor who will pay for one half of the feasibility study costs must be identified, and the economics of the potential solution must be such that the National Economic Development (NED) benefits are larger than the costs. More details of the planning process are found in ER 1105-2-100.

(h) Since reconnaissance and feasibility studies differ in their level of detail, the following discussion concentrates on feasibility requirements. The requirements of a feasibility study differ from those of a reconnaissance study in degree, not kind. A diagram is presented later in this chapter to assist the engineer planner/designer in going through all the steps needed for successful solution of a coastal engineering problem.

(i) In the case where a coastal project is planned and designed by other than USACE, Federal and state permits are usually required before construction can begin. (Requirements for USACE projects are discussed later in the chapter.) The USACE must ascertain that the proposed project would not harm the environment or adjacent property owners, that it would not interfere with navigation, and that water quality would not be impaired. Federal, state, and possibly local permits are required for construction in, across, under, or on the banks of navigable waters of the United States. Federal permits are coordinated by the applicant through the USACE District offices. Permit authorities are Section 10 of the River and Harbor Act of 1899 and Section 404 of the Clean Water Act of 1977, as amended.

Section 10 of the 1899 act requires permits for structures and dredging in navigable waters, which are those coastal waters subject to tidal action and inland waters used for interstate or foreign commerce. In tidal areas, this includes all land below the mean high-water line.

Section 404 of the Clean Water Act mandates a Federal permit for discharges of dredged or fill material in waters of the United States, which include tributaries and wetlands adjacent to navigable waters, and extends to headwaters of streams with flows greater that 0.142 m^3/sec (5 ft^3/sec). Wetlands are defined as "those areas inundated or saturated by surface or groundwater at a frequency and duration sufficient to support, and that under normal conditions do support, a prevalence of

vegetation typically adapted for life in saturated soil conditions. Wetlands generally include swamps, marshes, bogs, and similar areas."

More detailed requirements for the permit process are found in Chapter 33 of the Code of Federal Regulations, paragraphs 320-330 (33 CFR 320-330).

(j) Still, the first question to be answered is: Exactly what is the problem? The more detailed the response, the easier it becomes to be sure all the important factors are considered. A more precise answer to the question posed earlier in this section might be: "The waves and currents in a harbor berthing area are of such magnitude that 30,000-ton tankers find it unsafe to berth there approximately 50 percent of the time." A statement of what the project is trying to accomplish might be "to provide safe berthing for 30,000-ton tankers at least 90 percent of the time." If this is an exact statement of the problem, then investigation is necessary to determine that the engineering, economic, and environmental conditions and constraints can all be resolved satisfactorily.

c. Six major planning steps. The planning process consists of six major steps:

(1) Specify problems and opportunities.

(2) Inventory and forecast conditions if no action is taken.

(3) Formulate alternative plans.

(4) Evaluate effects.

(5) Compare alternative plans.

(6) Select a plan.

The following paragraphs describe these steps in more detail.

(1) Specify problems and opportunities.

(a) The identification of a problem usually begins with a unit of local Government requesting, through its local congressional representative, that USACE investigate and solve a problem. The Senator or Representative then introduces a resolution, which when passed by the Senate or House of Representatives, authorizes USACE to study the problem. The problem and opportunity statements are framed in terms of Federal objectives as well as identifying state and local objectives. The statements are fashioned to ensure that a wide range of alternative solutions can be considered with identifiable levels of achievement.

(b) In the case of a small project, the Secretary of the Army, acting through the Chief of Engineers, may plan, design, and construct certain water resource improvements without specific congressional authorization. This authority is found in the six legislative authorities collectively called the Continuing Authorities Program. The per-project limit on Federal expenditures under the CAP is currently $2,000,000 for a small beach erosion control project (Section 103 of Public Law (PL) 87-874, as amended) and $4,000,000 for a small navigation project (Section 107 of PL 86-645, as amended). A complete discussion of the six legislative authorities, including that for the mitigation of shoreline erosion damage caused by Federal navigation works (Section 111 of PL 90-483, as amended), is found in ER 1105-2-100 Chapter 3.

(2) Inventory and forecast conditions if no action is taken. The next step is to identify the initial site characteristics. These include not only the physical dimension of the site and environs, but also the

biological, cultural, social, safety, political, economic, endangered species, and other environmental aspects such as auditory, olfactory, visual, etc. The complete description of these elements will help to define the positions of the various stakeholders and how they might influence the success of any proposal. If these concerns can be accommodated early on, and the parties made to feel a part of the process, then any compromises that might be called for later are easier to obtain. All alternative schemes are measured against the *without-project plan* (the conditions that would prevail in the future if no plan is constructed), in order to quantify the benefits that would accrue from the various alternative plans examined. This is an important step in the planning process since it is the foundation for evaluating potentials for alleviating the problems and realizing the opportunities. It sets a consistent base upon which alternative plans are formulated, from which all benefits are measured, against which all impacts are assessed, and from which plans are compared and selected.

(3) Formulate alternative plans. Alternative plans are formulated in a systematic manner during both the reconnaissance and feasibility studies to ensure that all reasonable alternative solutions are identified early in the planning process and are refined in subsequent iterations. Alternatives are not merely slight variations; for example, breakwater lengths of 200, 300, or 400 m, but significant ones, such as a breakwater construction, a saltwater barrier, or a harbor realignment. As the process is under way, additional alternatives may be introduced as the need or opportunity presents itself. A plan that reasonably maximizes the net NED benefits and is consistent with protecting the nation's environment, is identified as the NED Plan in the feasibility report. Other plans that reduce net NED benefits in order to further address other Federal, state, local, or international concerns should also be formulated. Each alternative plan is formulated considering the four criteria described in the Water Resources Council's Principles and Guidelines: completeness, efficiency, effectiveness, and acceptability (ER 1105-2-100). The period of analysis must be the same for each alternative plan and appropriate mitigation of adverse effects is an integral part of each alternative plan. It is usual for an economic life of 50 years to be selected for analysis. This does not imply that a coastal structure, such as a breakwater, would only last 50 years, but that analysis of benefits and costs is limited to that period. Alternative plans may include significant nonstructural components or may be completely nonstructural. It should be noted that this step usually involves many iterations in the development of the alternatives, and may also require a restatement of the problem if it is found that the functional needs are not completely met.

(4) Evaluate effects. The evaluation of effects is a comparison of the *with-* and *without-plan* conditions for each alternative plan. Differences between each with- and without-plan condition are measured or assessed, and the differences are appraised or weighted. Four accounts are established to facilitate the evaluation and display the effects of the alternative plans: NED, EQ, RED, and OSE.

NED: The *National Economic Development* account displays changes in the economic value of the national output of goods and services. A comprehensive treatment of analysis required for determining the economic benefits of coastal projects is found in U.S. Army Corps of Engineers (1991).

EQ: The *environmental quality* account displays the nonmonetary effects on ecological, cultural, and aesthetic resources.

RED: The *regional economic development* account registers the changes in regional economic activity. Regional effects are evaluated using nationally consistent projections of income, employment, output, and population.

OSE: The *other social effects* account registers plan effects from perspectives that are relevant to the planning process, but are not reflected in the other three accounts.

Display of the NED account is required. Since technical data concerning benefits and costs in the NED account are expressed in monetary units, the NED account already contains a weighting of the effects; therefore, appraisals are applicable only to the EQ, RED, and OSE account evaluations. Planners must also identify areas of risk and uncertainty in these analyses and describe them clearly so that decisions can be made with knowledge of the degree of reliability of the estimated benefits and costs, and of the effectiveness of the alternative plans (see Section V-1-3).

(5) Compare alternative plans. Plan comparison focuses on the differences among the alternative plans as determined in the preceding step. Both monetary and nonmonetary effects are compared. Again, if the functional requirements of a project are not met, it is time to go back and iterate the formulation step.

(6) Select a plan. After consideration of the various alternative plans, their effects, and public comments, the *NED Plan* is selected as the one to recommend for implementation, unless a justified exception is granted by the Assistant Secretary of the Army for Civil Works (ASA(CW)). The USACE feasibility report, along with expressions of related views by the ASA(CW) and the Office of Management and Budget, is then sent to Congress with a recommendation for authorization for construction.

d. Planning coordination requirements.

(1) Table V-1-1 lists some of the laws enacted to ensure that environmental effects of projects are fully taken into account in the planning process. These laws are briefly described below.

Table V-1-1
Major Coordination Requirements

National Environmental Policy Act, 1970, 33USC234.4
Fish and Wildlife Coordination Act, 1958, 16USC460-1(12) et seq
Coastal Zone Management Act, 1972, 16USC1451 et seq
Clean Water Act, 1977, 33USC1344 et seq
National Historic Preservation Act, 1966, 16USC470a et seq
Coastal Barrier Resources Act, 1982, 16USC3501

(2) The National Environmental Policy Act (NEPA) of 1970, as amended, ensures that all proposed Federal actions take full cognizance of the environmental effects of those actions. This act defines the NEPA process by which an environmental impact statement (EIS) [or an environmental impact assessment (EIA) for a lesser impact activity that does not require a statement] is prepared. (An EIA is sometimes prepared to determine whether an EIS is required.) The EIS is given wide circulation and the public comment and the Federal agency's response are incorporated in the USACE report of its proposed activity. It is through this process that any unforeseen impacts are uncovered and mitigation measures are proposed.

(3) The Fish and Wildlife Coordination Act of 1958, as amended, ensures that fish and wildlife conservation receives equal consideration with other project purposes and is coordinated with other features of any coastal development project. USACE consults with the Regional Director, U.S. Fish and Wildlife Service (FWS), the Regional Director, National Marine Fisheries Service (NMFS), and the head of the state agency responsible for fish and wildlife for the state in which the proposed work is to be performed. Funds are transferred to the FWS and NMFS to accomplish the investigations, and a Fish and Wildlife Report is made part of the USACE report.

(4) The Coastal Zone Management Act of 1972, as amended, ensures that all Federal activities are consistent with an approved coastal zone management plan for that state. If the Secretary of Commerce has approved a state's plan (all but five coastal states have approved plans), then USACE must receive state certification that its proposed activity is consistent with the state's plan.

(5) The Federal Water Pollution Control Act was enacted to regulate the discharge of pollutants. Subsequently the Clean Water Acts, as amended, required water quality certification by the Environmental Protection Agency or a designated state agency to ensure that the USACE-proposed project does not degrade the state's water quality, particularly through any dredge and fill activities.

(6) The National Historic Preservation Act of 1966, as amended, provides for the consideration of the effects of a proposed project on the cultural resources (including archeological and Indian religious and cultural sites) of the area. Studies are coordinated with the National Park Service, the Advisory Council on Historic Preservation, and the appropriate State Historic Preservation Officer.

(7) The Coastal Barrier Resources Act of 1982, as amended, requires that no Federal funds (with some exceptions) are expended in any undeveloped region designated as a unit of the coastal barrier resource system (CBRS). Most notable for coastal projects, a major exception is for beach nourishment since it mimics the natural processes; hard structures in conjunction with beach nourishment are prohibited on areas identified in this Act. Also, maintenance dredging in waters within the CBRS unit is allowed, but new work dredging is not; using sand for beach nourishment that comes from a borrow area within a CBRS unit is not generally permitted. Coordination with the Regional Director, FWS is required for all cases involving the CBRS.

e. Criteria development. The criteria needed to be established are those that must be used to determine at each step of the process whether the objectives of that step are met. This is quite site-specific, and as will be seen in the section describing the generic design chart, the questions are answered either "*yes*, it meets the objective" (go on to the next step) or "*no*, it does not meet the objective" (go back and either refine the question or pick another alternative.) The importance of adequately posing the problem in the first place is readily seen in this approach. The advantage of this method of defining the criteria is that as long as all the questions are answered, the result will be the optimum project that meets the originally stated problem.

f. The design process.

(1) Final design. To produce a final design, it is necessary to continue the iterative process begun in the planning of the project. The project is said to be at final design status when all of the objectives are met, and all the stakeholders are satisfied that an optimum design has been reached. If there are any unanswered questions, then the final design has not been reached, and another iteration is necessary. It is current USACE practice to include the final recommended design in the feasibility report, and if approved for construction, no further design work is needed. The engineer can proceed directly to plans and specifications when the project is approved for construction and funds for construction are appropriated.

(2) Plans and specifications. The documents required for a contract for construction to be awarded include the *plans and specifications* for the job. These incorporate any restrictions or other constraints on the contractor, and spell out the accuracy and tolerances appropriate to the job. The procedures for plans and specifications for construction of USACE projects are found in ER 1110-2-1200, and no further discussion is warranted here.

g. Construction and monitoring.

Although construction and monitoring are not part of the planning and design process, they must be considered before the design process is complete.

(1) Construction. In order to have a successful project, the work to be accomplished must be capable of construction, i.e., have bidability, constructibility, and operability (see ER 415-1-11). If no equipment is available that can do the work prescribed (for example, a crane capable of lifting breakwater armor units into place), then the project is not constructible. If sand for a beach nourishment job is found to be outside the limits of available dredging equipment capability, then the job is not constructible. Guidance for construction management of USACE projects is found in EP 415-1-260, and no further discussion is warranted here.

(2) Post-construction inspection and monitoring. Monitoring is an essential element of a USACE project. The degree of monitoring depends on how the data are to be used. There are two basic types of monitoring: for conformance of construction to the design and for evaluation of performance of the project. The second type is often neglected, although ER 1110-2-1407 and ER 1105-2-100 clearly specify that a monitoring plan and an operation and maintenance plan are to be prepared as part of every project for which USACE has a continuing responsibility. This is especially important in beach nourishment projects to determine when a renourishment is needed. Also, data on project performance are needed for the continuing improvement and refinement of prediction models for coastal projects.

h. Generic design chart.

(1) Figures V-1-1 through V-1-3 show the thought processes that occur in the planning and design of a coastal project. The thought processes to successfully engineer a solution to a problem are basically the same as for the solution of any problem, but for the ease of presenting appropriate examples, will be limited here to the discussion of coastal engineering problems. The diagram is quite comprehensive and represents the steps followed by all engineers in developing successful solutions to coastal problems. It can be modified, however, to fit the needs of the planner and designer.

(2) Figure V-1-1 is generic in the sense that navigation, shore protection, coastal flooding, storm damage reduction, environmental enhancement, or any other set of problems can be treated by following the steps outlined in the diagram. As discussed earlier in this chapter, the project begins with a need, from which an accurate statement of the problem is derived. Figure V-1-1 illustrates the path (or paths) typically followed in developing a coastal project, from initiation to cost completion phases, including the reevaluation and feedback loops. There are ten major segments of the process, with several blocks in each segment. They are designated by the letters in circles, and are keyed to the following list:

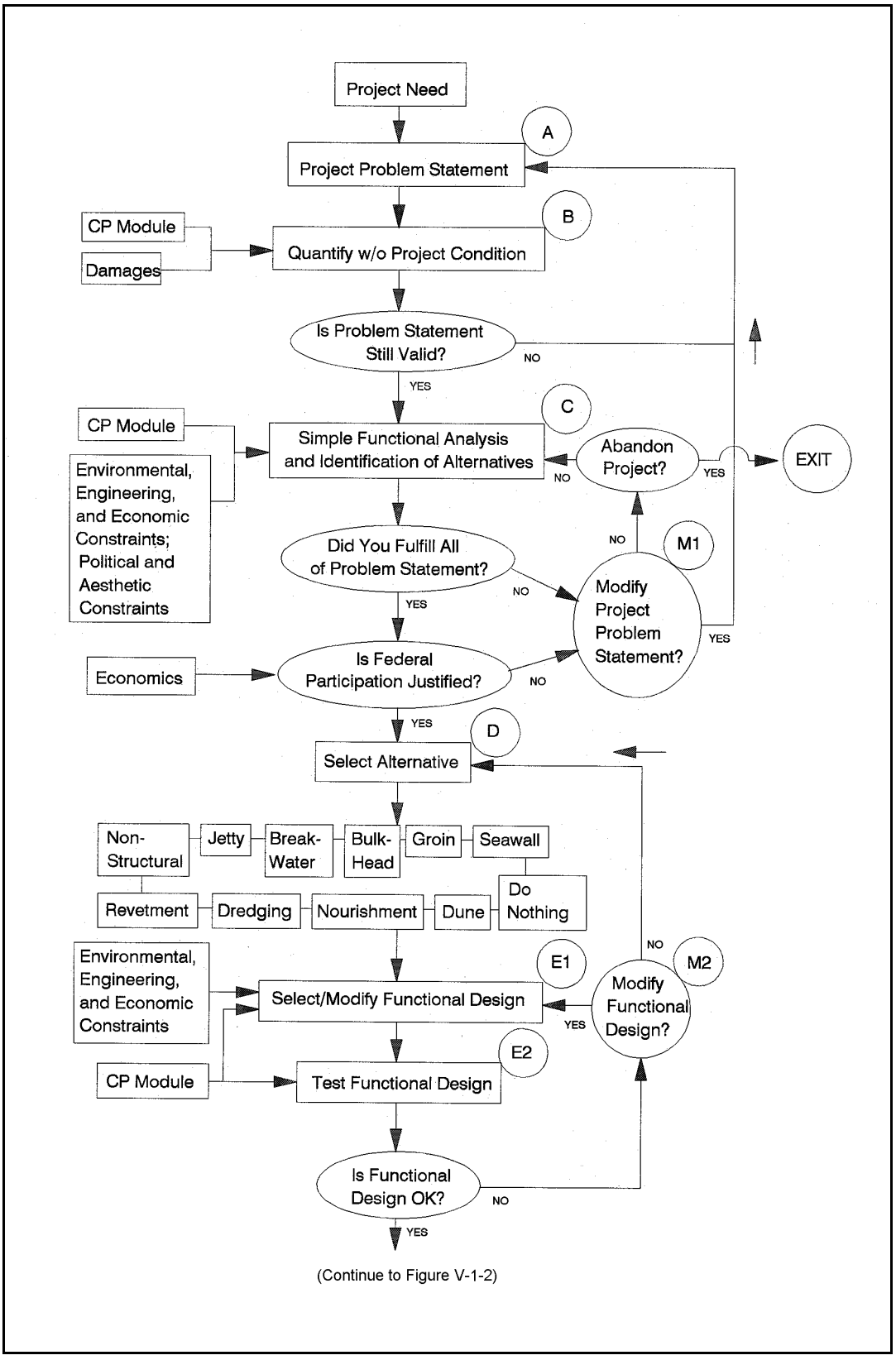

Figure V-1-1. Thought process in the planning and design of a coastal project, Part 1

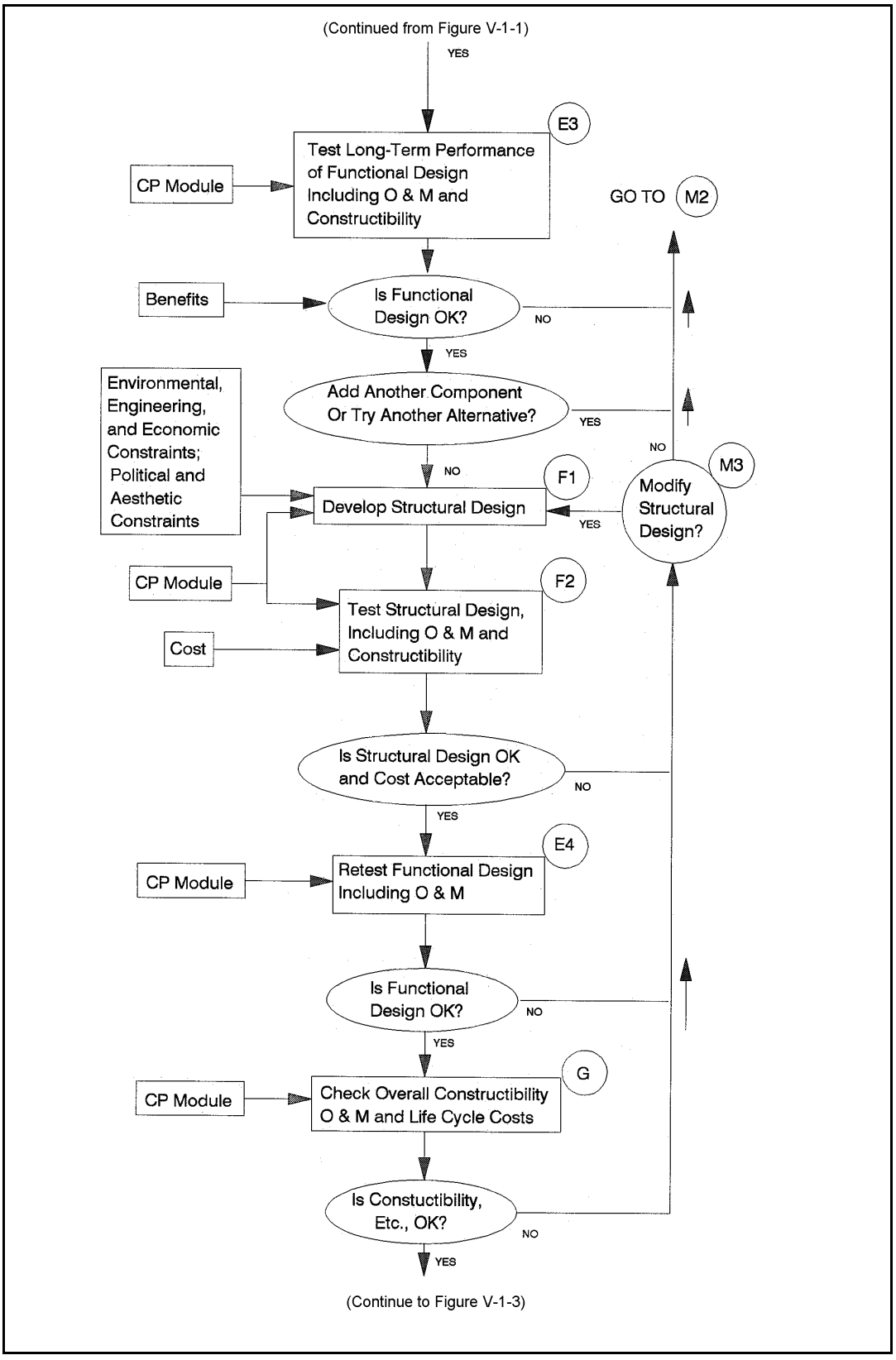

Figure V-1-2. Thought process in the planning and design of a coastal project, Part 2

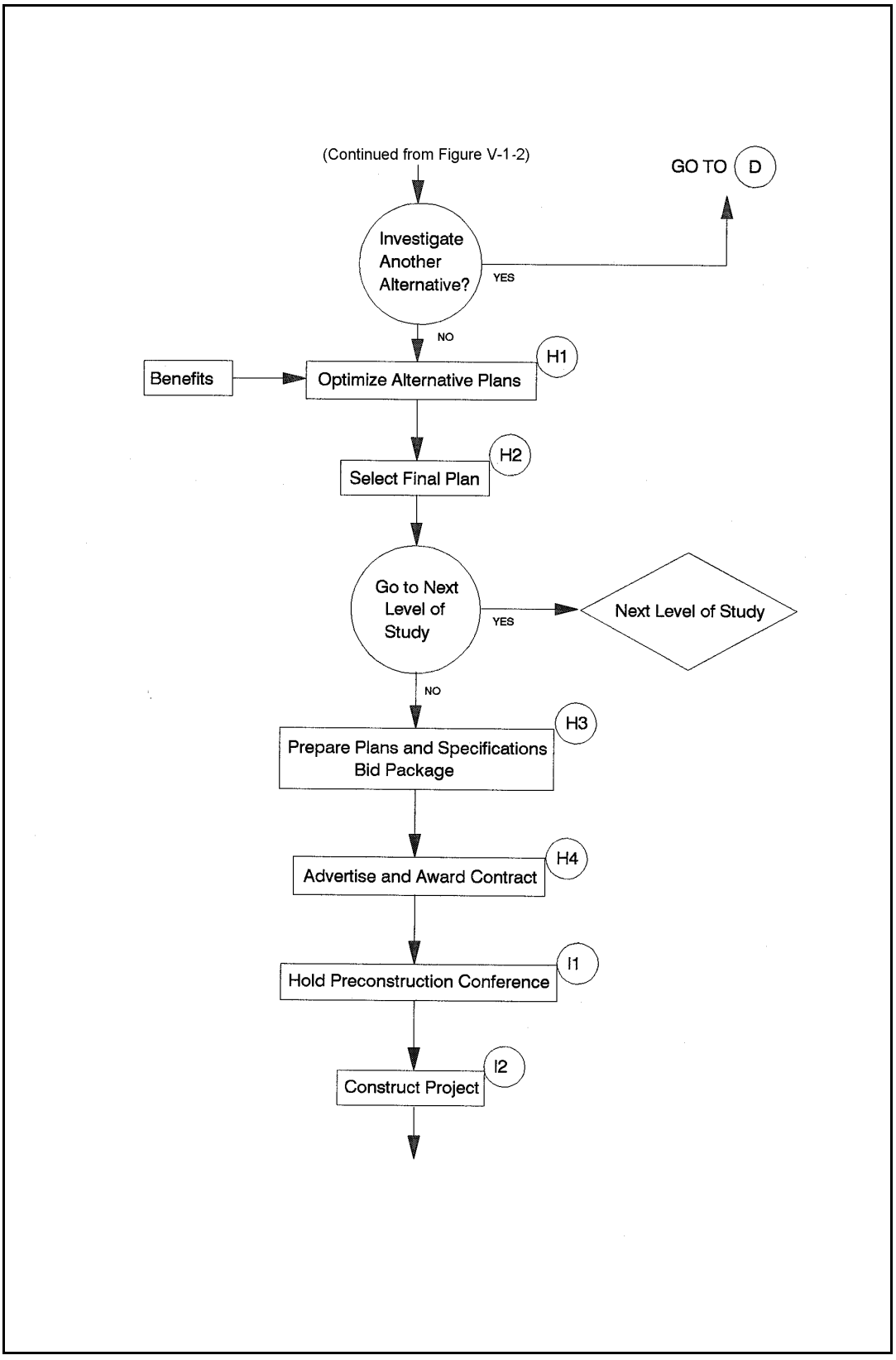

Figure V-1-3. Thought process in the planning and design of a coastal project, Part 3

(a) Clearly define project problem statement, including the project objective.

(b) Quantify existing and most likely future conditions (without project).

(c) Identify and analyze alternatives.

(d) Select alternative.

(e) Develop and test functional design.

(f) Develop and test structural design.

(g) Check for constructibility, operation and maintenance, and life-cycle costs.

(h) Select final plan, and prepare plans and specifications.

(i) Construct project.

(j) Monitor and evaluate project performance.

There are also several key segments concerning decisions about modifying various phases of the project; they are designated by the letter M.

(3) The term "functional design" refers to the effectiveness of a project at its intended function, such as the effectiveness of a breakwater at providing tranquil waters inside a harbor. "Structural design" refers to the ability of a structure to exist in the climate in which it is placed, such as the ability to withstand the effects of extreme storms without affecting its functional requirements. The term "constructibility" refers to the means, methods, and materials involved in successful project construction.

(4) In the diagram, the notation "CP Module" designates a generic concept of a Coastal Processes Module, a repository of physical data and analysis tools relevant to the coastal problem. The module includes information on wind, waves, currents, water levels, bathymetry, geomorphology, stratigraphy, sediment characteristics, sediment transport, ice processes, etc. The output from this module is needed at many points in the process. At the present time, portions of a module exist as limited databases and tools; however, a complete, integrated module, similar to the generic model, is under development, but is yet a long way from completion.

V-1-2. Design Criteria

a. Design criteria are the minimum parameters of design that are followed to ensure that the project function and structure (if any) meet the needs of a customer. A design is based on a number of design criteria that include: forcing function criteria, configuration criteria, materials criteria, geotechnical criteria, construction criteria, maintenance criteria, and economics criteria. These criteria are partly interrelated and partly independent of each other. Materials may depend on configuration, construction (including availability of equipment and manpower), and maintenance criteria. Construction may depend on configuration and materials (including availability). Maintenance depends on materials and construction.

b. Forcing function criteria must always be seen in relation to configuration, materials, and geotechnical criteria. For example, the "design storm" is an obsolete concept. Short- and long-term wave statistics are needed, and the hydrodynamics of wave interaction with its surroundings must be known in detail. The parameters of wave height, wave period, storm duration, and surge water level are quasi-independent

components of a storm whose effects on a design need to be understood to adequately examine the alternatives. The frequency of occurrence (or the return period) of an event (such as a storm) is a primary component of the wave criteria. These concepts are fully discussed in Part II of this manual.

c. Criteria that need to be considered in all coastal projects are: safety, accessibility (as defined by the American Disability Act), and environmental effects. All other effects are highly site-specific, and in addition to those cited above, include project area use, materials corrosion, ice, structural unit stability, subsurface foundations, and susceptibility to seismic events (i.e., earthquakes or tsunamis).

d. In every case, the criteria must be measured against the function to be satisfied by the proposed coastal project. If the alternative does not adequately address the need, then the function is not fully satisfied, and either the problem must be restated or another alternative must be investigated. As discussed in earlier sections of this chapter, the iterative process of planning and design requires the above-cited criteria be used to evaluate each step in the process. Design criteria relative to specific project types are discussed in the remaining chapters of Part V.

V-1-3. Risk Analysis and Project Optimization

a. Introduction.

(1) The approach for analyzing coastal projects is undergoing some fundamental changes, shifting from the traditional deterministic basis to a probabilistic, risk-based methodology. The changes strongly impact both planning and engineering phases of project formulation and design. Concepts of risk analysis and probabilistic optimization of project design are presented in this section. The remaining chapters in Part V include further information on the subject in relation to specific project types. As of this writing, risk-based analysis is a rapidly emerging tool, and significant advances can be expected during the next few years.

(2) The changes in analysis approach, which can be expected to be distilled into a new standard for coastal practice, are driven by several progressive developments. First, general understanding of probabilistic coastal processes continues to advance, particularly due to advances in field measurement, physical modeling, and numerical modeling. Second, standard computing capabilities are increasing rapidly, facilitating lengthy probabilistic calculations which would have been impractical in the past. Third, engineers, cognizant of limitations in the traditional approach, are often eager to implement better procedures, provided that they are well-founded and clearly improve the analysis. Finally, the public is becoming more aware and concerned about coastal project performance, and expects realistic project analyses. In the United States, public involvement in coastal projects is further intensified by legislation which increases the proportion of costs borne by the client (typically state or local Government) in Federal projects.

b. Traditional vs. Risk-based analysis.

(1) Traditional analysis treats a coastal project in deterministic terms. The forces of nature are often represented as a design significant wave height, period, and direction, a design water level, etc. Coastal response is described as *the* response if no project is implemented, *the* response if one plan is implemented, *the* response if another plan is implemented, etc., without much formal recognition of the wide variation in possible responses.

(2) In contrast to traditional analysis, some significant developments in probabilistic treatment of coastal projects have appeared during the 1990's. Most relate to coastal structure design (Construction Industry Research and Information Association/CUR 1991, International Conference on Coastal Engineering (ICCE) 1992). Within USACE, water resource planning guidance has moved from a deterministic to a risk-based

approach, which incorporates considerations of risk and uncertainty. Similar concepts are now being adapted to USACE coastal engineering studies.

c. Reasons for risk-based analysis.

(1) Introduction. There are a number of reasons why coastal projects in the broader sense, not just structural design, may be effectively analyzed from a risk-based point of view (Table V-1-2).

Table V-1-2
Reasons for Risk-Based Analysis of Coastal Projects

(1) Forcing is probabilistic.
(2) Major uncertainties in behavior.
(3) Damage & functional performance change incrementally.
(4) Benefits and risks not fully represented in deterministic terms.
(5) Uncertain effects on adjacent areas.

(a) Coastal forcing is probabilistic. Wave characteristics vary greatly over both short-term (individual waves) and long-term (from one sea state to another). Similar considerations arise with winds, water levels, infragravity waves, and currents.

(b) Coastal engineering embodies major uncertainties. Knowledge of both the forcing processes and coastal response usually involves major uncertainties. Deterministic representations mask the uncertainties and can be misleading.

(c) Damage and functional performance change incrementally. Coastal projects rarely progress from the design condition to total failure during a single storm event. Damage usually occurs incrementally. For example, damage to a rubble-mound breakwater (when it occurs) typically begins during an unusually severe storm and progresses during subsequent severe storms until repairs are done. Similarly, beach fills erode incrementally in response to storms over a period of years. Coastal projects often continue to provide some measure of functional benefit even in a damaged state. A damaged breakwater continues to provide some protection from incident waves; a partially eroded beach fill continues to reduce coastal flooding risks.

(d) Benefits and risks not fully represented in deterministic terms. Because of the above factors, positive impacts and risks of coastal projects cannot be fully represented in deterministic terms. Some projects provide benefits beyond the design configuration, which are generally ignored in traditional practice. For example, a nearshore berm which is overbuilt to allow for progressive deterioration provides increased coastal protection during its early life. Another example is an overdredged entrance channel giving increased vessel access depths until it shoals to the design depth.

(e) Uncertain effects on adjacent areas. In addition to the uncertainties associated directly with coastal projects, the projects can introduce significant possibilities for changing adjacent areas. While projects are designed with the intent of minimizing adverse impacts on adjacent areas, it is important to recognize that uncertainties and risks can increase beyond the without-project condition. In effect, a project can transfer risk from one area or party to another. When the risks of *all* major aspects of a project are represented as best they can be determined, better-informed final decisions can be made.

(2) Professional judgement. Experienced coastal engineers are well aware of the concerns in Table V-1-2. Even with deterministic methods, they can be expected to produce project plans that include a large measure of professional judgement to ensure a technically successful project. However, the ultimate fate of a project can depend upon higher level decision makers who must weigh technical concerns against economic, environmental, aesthetic, social, and political concerns. By quantifying risks, the coastal engineer can better pass his or her experience and judgement on to other decision makers, who may not have coastal expertise.

d. Considerations for including risk-based analysis in project design

(1) Objectives. The main objectives of adopting a risk-based analysis approach rather than a traditional approach are to explicitly identify uncertainties, provide improved information for assessing tradeoffs between risks and cost, and improve decision-making for project optimization.

(2) Key variables. Although a large number of variables affect any coastal project, a small subset can usually be identified as *key variables*; that is, variables that strongly relate to project performance. The key variables will embody the main forcing mechanisms, project sizing, and project response. For example, some of the key variables for a beach nourishment project might be significant wave height (forcing), beach fill width (project size), and erosion width (response).

(3) Professional judgement. Coastal engineering requires an unusually large measure of professional judgement because of the number and complexity of processes and responses involved. Analytical and modeling tools help to represent the variability affecting coastal projects, but the judgement of an experienced engineer is a vital ingredient in risk assessment and project optimization.

(4) Resistance and functional performance vary with time. Both the resistance to damage and functional performance often vary significantly over a coastal project's design life. For example, the resistance (or structural strength) of a rubble-mound breakwater may decrease in time due to deterioration of stone such as loss of angular corners, cracking, and breaking. Resistance may also decrease due to displacement of stone and exposure of underlayers to wave attack, which would also decrease protection provided by the breakwater (functional performance). For a beach nourishment project, loss of material to storms decreases the resistance of the beach to future storms. The effectiveness of the beach as a deterrent to coastal flooding is also decreased (functional performance). In some cases, resistance *increases* with time, as in the progressive growth of protective vegetation on coastal dunes and natural cementation of beach sediments rich in calcium carbonate.

(5) Construction season and mobilization concerns. Often maintenance of coastal projects requires major mobilization efforts and is confined to a *construction season* dictated by climate and environmental factors. Therefore the risk during the *interval between construction seasons* rather than during a single storm becomes a key concern. During an unusually stormy winter (such as the winter of 1987-88 in southern California), this risk can be significantly greater than that for individual storms.

(6) Environmental, aesthetic, social, and political concerns. The role of environmental, aesthetic, social, and political factors in the ultimate planning and design of a coastal project is often at least as important as the technical engineering factors. An optimized final design includes appropriate consideration of these factors and their associated risks and uncertainty.

e. Frequency-based vs. life cycle approach.

(1) Risk-based analysis of coastal projects can be done by either of two fundamentally different approaches. The *frequency-based approach* deals with frequency-of-occurrence relationships among the key variables. By combining key forcing variables with various occurrence frequencies, information about the

frequency-of-occurrence of key project responses can be developed. For example, a traditional stage- (water level)-versus frequency curve and a stage-damage curve can be combined to generate a damage-versus-frequency curve. This approach can be applied as an add-on to traditional planning and design procedures.

(2) The *life cycle approach* deals with multiple realizations of possible evolution of the project with *time* during the span of its design life. The suite of life cycle realizations is constructed with consideration of the probabilities of key variables. For example, the realistic time variation of key forcing and response variables during a 50-year life cycle can be generated for 1,000 different possible life cycles. Probabilities and risks associated with the project are then compiled by analyzing project performance over the 1,000 life cycles.

(3) The life cycle approach appears better suited to most coastal engineering applications. Variation with time is an essential ingredient in most coastal projects, and it is directly incorporated into the life cycle approach. Time variation of resistance and functional performance, constraints imposed by construction season and mobilization, even some economic, environmental, and political factors, can be conveniently and flexibly introduced into the life cycle approach. This approach leads to a unified analysis of technical performance and many economic factors which are critical to project success. In addition to its technical and economic strengths, the life cycle approach is more easily understood by nontechnical parties involved with a project. This type of approach is evident in the Empirical Simulation Technique (Chapter II-5).

(4) The life cycle approach adapted to shore protection projects is particularly instructive (U.S. Army Corps of Engineers 1997). The life cycle embodies sequences of storms (including provisions for multiple storms of varying intensity during each year of the life cycle), erosion and post-storm recovery during each event, partial and complete property damage during each event (depending on water level, waves, extent of storm erosion, and type of building construction), cumulative property damage due to a succession of storms, optional repair or rebuilding after a suitable time lag (with conformance to any stricter building codes in effect), and periodic renourishment of the beach when needed and feasible during the life cycle. Typically, a key result from this analysis is the renourishment required during each life cycle, which can be converted to an economic present-worth dollar value. The expected cost and economic risks associated with maintaining the beach can then be realistically assessed by combining information from many different life cycle simulations.

f. Typical project elements. Risk-based analysis can be integrated into the six major planning steps (Section V-1-1b(2). Typical project elements which are especially well-suited to risk-based analysis include the following.

(1) Site characterization. Significant uncertainty can arise in documenting past and present behavior at a site. The uncertainty can be estimated based on data quality and quantity, methodologies used, observed variability, etc. (Chapter V-3).

(2) *Without-plan* alternative. Evaluation of what would happen in the future if no Federal project were built involves speculation about the natural processes and human interventions that would affect the site during the proposed project life. The impact of the *without-plan* alternative is conveniently described in probabilistic terms.

(3) Formulate, evaluate, and compare alternative plans. Risk-based analysis can be a powerful tool for formulating and comparing alternative plans. It enables decision makers to intercompare not only the expected level of performance, but also the probabilities of enhanced or reduced performance levels, which can differ greatly among alternatives. Typically, alternatives involve hard structures (such as walls, revetments, breakwaters, and jetties) and/or soft structures (such as beach nourishment projects, coastal dunes, and nearshore berms). Risk-based analysis of hard structures is discussed in Part VI. Soft structures (Chapter V-4) involve calculated risks about the movement of sediment through time and the need for future

maintenance. Uncertainties arise in forcing processes, sequencing of storms, initial state of nearshore profile when storms occur, and evolution and recovery of storm profiles (especially three-dimensional aspects). The life cycle approach to risk analysis has been shown to be a powerful tool in this type of application.

V-1-4. References

ER 415-1-11
Biddability, Constructibility, and Operability

ER 1105-2-100
Planning Guidance Notebook.

ER 1110-2-1407
Hydraulic Design for Coastal Shore Protection Projects.

ER 1110-2-1200
Plans and Specifications for Civil Works Projects.

EP 415-1-260
Resident Engineer Management Guide.

CIRIA/CUR 1991
CIRIA/CUR 1991. "Manual on the Use of Rock in Coastal and Shoreline Engineering," *CIRIA Special Publication 83*, Construction Industry Research and Information Association, London, UK: and CUR Report 154, Centre for Civil Engineering Research and Codes, Venice, Italy.

ICCE 1992
ICCE 1992. "Design and Reliability of Coastal Structures," *Proceedings of a short course attached to the 23rd International Conference on Coastal Engineering*, Venice, Italy.

Thompson, Wutkowski, and Scheffner 1996
Thompson, E. F., Wutkowski, and M., Scheffner, N. W. 1996. "Risk-Based Analysis of Coastal Projects," *Proceedings of the 25th International Conference on Coastal Engineering*, Orlando, FL.

U.S. Army Corps of Engineers 1991
U.S. Army Corps of Engineers. 1991. "National Economic Development Procedures Manual - Coastal Storm Damage and Erosion," Report 91-R-6, Institute for Water Resources, Fort Belvoir, VA.

V-1-5. Acknowledgments

Authors of Chapter V-1, "Planning and Design Process:"

John G. Housley, Headquarters, U.S. Army Corps of Engineers, Washington, DC, (retired).
Edward F. Thompson, Ph.D., Coastal and Hydraulics Laboratory (CHL), U.S. Army Engineer Research and Development Center, Vicksburg, Mississippi.

Reviewers:

James E. Clausner, CHL
Jeffrey A. Melby, Ph.D., CHL
Norman W. Scheffner, Ph.D., CHL (retired)
H. Lee Butler, CHL (retired)

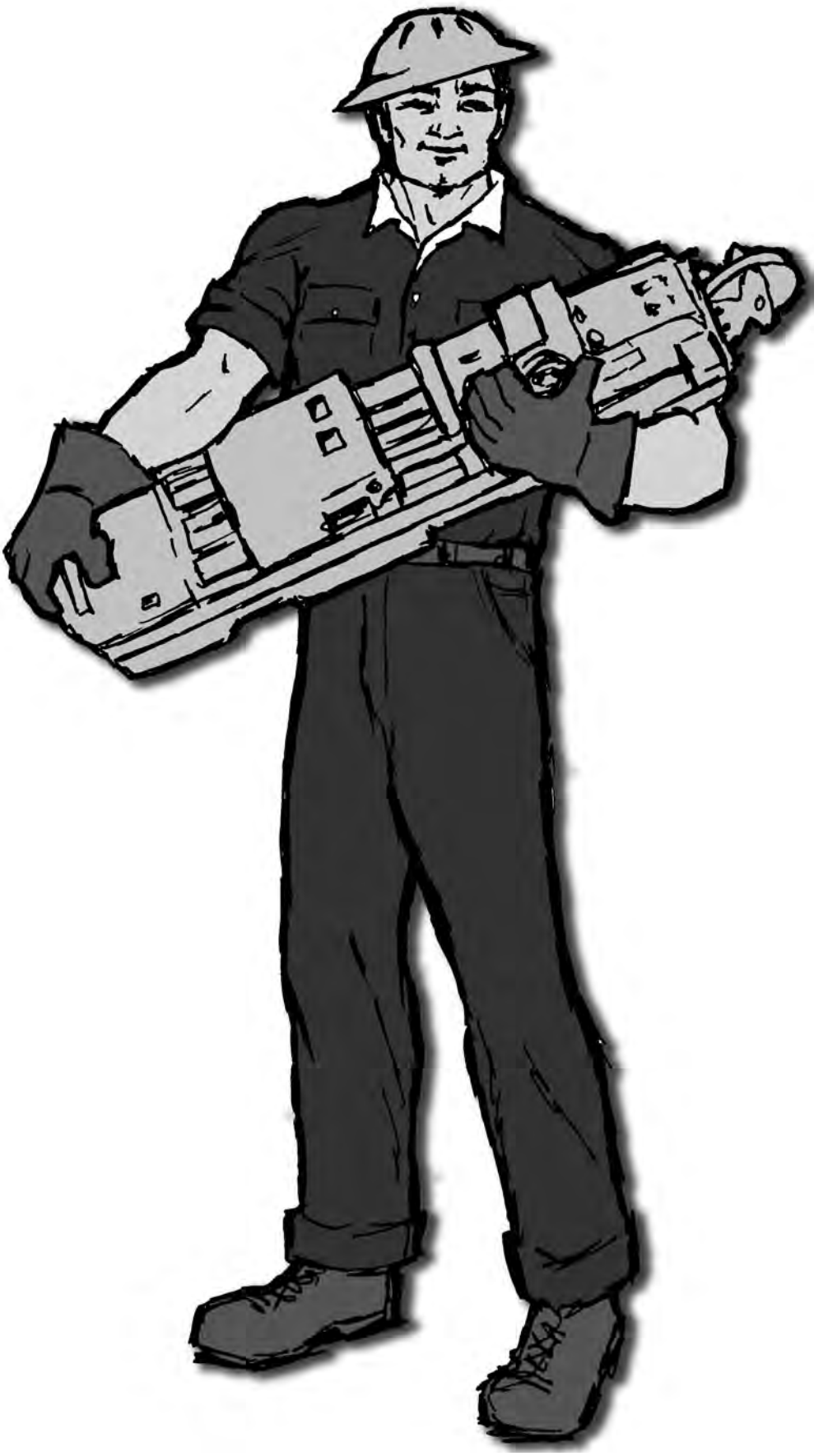

Table of Contents

Page

V-2-1. Introduction V-2-1

V-2-2. Defining Project Area and Boundary Conditions V-2-2

V-2-3. Storm Characteristics/Meteorology V-2-3
a. Storm types V-2-3
b. Storm characteristics V-2-5
c. Hypothetical hurricanes V-2-5

V-2-4. Hydrodynamic Processes (Design Sea State, Water Levels, Currents) V-2-6
a. Design condition V-2-6
b. Design wave height and period V-2-6
c. Design water level V-2-7

V-2-5. Seasonal Variability V-2-7

V-2-6. Topography and Bathymetry (Map Data) V-2-10
a. Data needs V-2-10
b. Available sources V-2-10
c. Reliability V-2-12

V-2-7. Geomorphology/Geometry and Sediment Characteristics V-2-12
a. Types of coasts/principal features V-2-12
b. Sources and sinks V-2-14
c. Prevailing sediment characteristics V-2-16
d. Sediment layering V-2-18

V-2-8. Littoral Drift and Sediment Transport Patterns V-2-18
a. Longshore movement V-2-18
b. Cross-shore movement V-2-18
c. Seasonal reversals V-2-19
d. Long-term reversals V-2-20
e. Slug motion V-2-20
f. Hot spots V-2-20

V-2-9. Shoreline Change Trends V-2-21
a. Evidence of cyclic processes V-2-21
b. Eustatic sea level changes V-2-21
c. Subsidence V-2-21

V-2-10. Land/Shore Use V-2-21

V-2-11. Potential for Project Impacts V-2-22
a. Effects on natural tidal flushing V-2-22
b. Up/downdrift effects and need for bypassing V-2-22
c. Changes in wave climate V-2-23
d. Impact on benthic organisms V-2-23
e. Changes in natural habitat V-2-24

V-2-12. Environmental Considerations V-2-24
a. Surveying the project area V-2-24
b. Mitigation measures V-2-25
c. Water quality V-2-26
d. Disposal of materials V-2-26

V-2-13. Regional Considerations V-2-26
a. Regulations V-2-26
b. Seismic V-2-27
c. Tsunami V-2-27
d. Ice V-2-28

V-2-14. Foundation/Geotechnical Requirements V-2-29

V-2-15. Availability of Materials (Sand/Stone Resources) V-2-29
a. Sand V-2-29
b. Stone V-2-30

V-2-16. Accessibility V-2-32

V-2-17. Monitoring V-2-34

V-2-18. Data Needs and Sources V-2-35

V-2-19. References V-2-38

V-2-20. Acknowledgments V-2-44

List of Figures

Page

Figure V-2-1. Isobaric pattern of a typical extratropical low in the Great Lakes Region (Resio and Vincent 1976) V-2-4

Figure V-2-2. Example of directional wave gauge data for Lanai, Hawaiian Islands (EM 1110-2-1810) V-2-8

Figure V-2-3. Water levels of Lake Erie during storm of December 2, 1985 (NOAA 1985) V-2-9

Figure V-2-4. The 1836 shoreline at Presque Isle, Pennsylvania V-2-11

Figure V-2-5. Example of resistant rock-bound coast of Maine (Bass Harbor Head Light, Maine, south of Acadia National Park) V-2-13

Figure V-2-6. Beach near entrance to North Sand Pond, Lake Ontario, NY. This is a relict dune environment at the eastern end of Lake Ontario V-2-14

Figure V-2-7. Coast at Orick, CA. This is a pocket beach between resistant headlands V-2-15

Figure V-2-8. Shore at Chimney Bluffs State Park, Lake Ontario, NY. Chimneys consist of glacial till more weather resistant than surrounding material V-2-15

Figure V-2-9. Cobble Beach along Lake Ontario, Oswego, NY. Origin of cobble is bluff and glacial drumlin erosion V-2-16

Figure V-2-10. Black Sand Beach, Kalapana, HI. Sand is of volcanic origin V-2-17

Figure V-2-11. Structures threatened by erosion, Lake Ontario, Crescent Beach, NY V-2-27

Figure V-2-12. Cracked dolomitic limestone - Cleveland East Breakwater, Ohio, 1989 (stone is dolomitic limestone) V-2-32

Figure V-2-13. Cracked stone - Cleveland East Breakwater, Ohio, 1990. Note continuing degradation compared to 1989 (stone is dolomitic limestone) V-2-33

List of Tables

Page

Table V-2-1. Some Example USACE Reports and General Design Memorandums (GDMs) Containing Comprehensive Site Characteristics V-2-2

Table V-2-2. Extreme Pressure and Wind Data of Hurricanes Recorded along the Alabama Coast between 1892 and 1969 (U.S. Army Engineer District, Mobile 1978) V-2-5

Table V-2-3. Quarry Inspection Checklist V-2-31

Table V-2-4. Coastal Project Monitoring Matrix V-2-36

Table V-2-5. Data Needs and Sources V-2-37

Chapter V-2
Site Characterization

V-2-1. Introduction

a. Many coastal failures can be traced back to inadequate site characterization analyses. Site characterization involves identifying distinguishing qualities and features of a region that have a direct and indirect impact on the conception, design, economics, aesthetics, construction, and maintenance of a coastal project. The coastal environment varies spatially and temporally and therefore a design that is functionally, economically, and environmentally appropriate at one location may be inappropriate at another. Physical, biological, and cultural attributes need to be delineated so that an acceptable project is adopted and potential effects of the project are determined.

b. Waves bring an enormous amount of energy to the coast that is dissipated through wave breaking, generation of currents, water level changes, movement of sediment, turbulence, and heat. Incident waves vary spatially and temporally, with their properties changing with movement over the bottom. The beach is composed of sediment particles of various types, sizes, and shapes which move along and across the shore. The beach and backshore exhibit different textural properties that vary alongshore, across-shore, and with time. The coastal region supports a diverse biological community of aquatic, terrestrial, and avian organisms. It also must continue to enhance the quality of human existence by providing commercial and recreational benefits. In light of the profound diversity of the coastal zone, it is imperative that the coastal designer have a full understanding of potential impacts of engineering activities on the regional environment.

c. This chapter enumerates important physical and engineering factors that should be identified. Readers are directed to other pertinent sections of this manual for specific details on monitoring the coastal environment and for information on the physics of coastal processes. Not all factors described in this chapter pertain to all coasts. For example, ice and volcanic hazards are not applicable to a Gulf Coast project design. However, most factors should be included in all other site characterizations.

d. General Design Memorandums (GDMs) and monitoring reports (Table V-2-1) prepared by U.S. Army Corps of Engineer (USACE) Districts may be consulted for examples of site characterization studies. The Alaska Coastal Design Manual (U.S. Army Corps of Engineers 1994) also summarizes important site characterization features.

e. In summary, it is important when characterizing a site to:

(1) Include **all components** of the system.

(2) Recognize the extreme **temporal variability** in most physical and biological processes.

(3) Be cognizant of the **spatial variability** of processes, climate, land forms, underlying geology, biological habitat, and cultural resources. Process measurements made at one site may not be valid at another site only a short distance away.

f. In conclusion, the designer must think globally and engineer locally.

Table V-2-1
Some Example USACE Reports and General Design Memorandums (GDMs) Containing Comprehensive Site Characteristics

State	Author	Date	Title
Atlantic Coast			
Virginia	USAED, Norfolk	1984	Beach Erosion Control and Hurricane Protection, Virginia Beach, Virginia, Main Report Phase 1 GDM and Supplemental EIS
Virginia	USAED, Norfolk	1989	Beach Erosion Control and Hurricane Protection, Virginia Beach, Virginia, Phase II GDM
N Carolina	USAED, Wilmington	1973	Beach Erosion Control and Hurricane Protection, Brunswick County, NC, Yaupon Beach and Long Beach Segments, Phase I GDM
Florida	USAED, Jacksonville	1985	Beach Erosion Control Project, Pinellas County, Florida, Long Key Beach Nourishment and Breakwater Feature Design Memorandum
Florida	USAED, Jacksonville	1989	Sand Bypass System Canaveral Harbor, Florida, GDM
Gulf of Mexico			
Alabama	USAED, Mobile	1978	Beach Erosion Control and Hurricane Protection, Mobile County, Alabama (Including Dauphin Island), Feasibility Report
Great Lakes			
Pennsylvania	USAED, Buffalo	1980	Cooperative Beach Erosion Control Project at Presque Isle Peninsula, Erie, Pennsylvania, Phase I GDM
Ohio	USAED, Buffalo	1975	Cooperative Beach Erosion Control Project at Lakeview Park, Lorain, Ohio, Phase II GDM
New York	USAED, Buffalo	1976	Cattaraugus Harbor, New York, Phase II GDM Detailed Design (in three volumes)
Pacific Coast			
Washington	USAED, Seattle	1989	Navigation Improvement Project at Grays Harbor, Washington, GDM

V-2-2. Defining Project Area and Boundary Conditions

a. The total project area encompasses not only the physical limits of the project but also the area in which the project has an effect upon littoral processes. The physical limits of a proposed project usually are predetermined by the local sponsor for the area of interest. Often this is defined by property limits (municipal park, business district, navigation inlet, etc.) and legislative authority. Project boundaries are sometimes defined by the limits of available historic data - particularly bathymetric data. Economic analysis of the project may lead to modification of these limits if a project along the entire reach cannot be economically justified, or is not technically feasible or environmentally acceptable.

b. It is imperative that a project designer be cognizant of potential impacts of the project on the adjoining coast. Mitigation due to disruption of littoral movement is often necessary. Legal requirements for replacement of sediment loss using bypassing or introduction of an equivalent quantity downdrift vary with locality. For example, the state of Florida (1987) requires:

(1) *All construction and maintenance dredging of beach-quality sand should be placed on the downdrift beaches: or, if placed elsewhere, an equivalent quality and quantity of sand from an alternate location should be placed on the downdrift beaches.*

(2) *On an average annual basis, a quantity of sand should be placed on the downdrift beaches equal to the natural net annual longshore sediment transport.*

The lack of legal requirements does not absolve the project designer of responsibility to mitigate project impacts.

c. In order to establish the potential physical impact of the project, a sediment budget for the entire littoral cell in which the project will reside must be determined. A sediment budget quantifies the amount of sediment moving within a littoral cell. A littoral cell is a self-contained reach of coast with its own sand sources and losses or sinks. Updrift and downdrift boundaries (the location at which most, if not all, sediment enters or leaves the cell) may be formed by natural barriers such as a headland or prominent protruding structures. In developing a sediment budget, information on the sources and characteristics of materials, modes and direction of transport in the littoral zone, rates of sediment supply, and transport and loss is required. Complete understanding of the boundaries, significance of individual sources, littoral drift direction and volumes, and sinks is crucial to estimating the effect of any engineering intervention in the littoral system and helps define the project area. Part III presents a complete description of sediment transport processes.

d. Development of the sediment budget will assist in establishing the amount of mitigation required. If no mitigative measures are enacted, the more difficult question will be to determine how erosion, due to loss of sediment, is distributed downdrift as a function of time. To answer this question, the three parameters that need to be identified are (a) length of the adversely affected shore; (b) cross-sectional retreat of the erosion cut; and (c) rate of expansion of erosion, and its distribution downdrift as a function of time (Bruun 1995). It has been observed that a littoral drift barrier has a short- and long-distance influence on the downdrift shoreline as briefly discussed in Section V-2-8. The reader is directed to Bruun (1995) for a discussion on examples of downdrift shoreline impacts and the short- and long-distance influence of a littoral barrier.

V-2-3. Storm Characteristics/Meteorology

a. Storm types.

(1) A storm is an atmospheric disturbance characterized by high winds that may or may not be accompanied by precipitation. Two distinctions are made in classifying storms: a storm originating in the tropics (5 to 350 deg in both hemispheres) is a tropical storm, a storm resulting from a cold or warm front in the middle and high latitudes (30 to 60 deg) is an extratropical storm (Silvester and Hsu 1993). Both storms can generate large waves and produce abnormal rises in water level in shallow water near the edge of water bodies.

(2) A hurricane is a severe tropical storm with maximum sustained wind speeds of 120 km/hour (75 mph or 65 knots). These low pressure centers are known by different names geographically: hurricanes on the east coast of the Americas, typhoons in the western Pacific, monsoons in the Indian Ocean, and tropical cyclones in Australia (Silvester and Hsu 1993). Hurricanes, unlike less severe tropical storms, generally are well-organized and have a circular wind pattern with winds revolving around a center or eye. The eye is an area of low atmospheric pressure and light winds. The Coriolis force causes the radial inflow to rotate counterclockwise in the Northern Hemisphere and clockwise in the Southern Hemisphere. Atmospheric pressure and wind speed increase rapidly with distance outward from the eye to a zone of maximum wind speed, which may range from 7 to 110 km (4 to 70 statute miles) from the center. From the zone of maximum

wind to the periphery of the hurricane, pressure continues to increase; however, wind speed decreases. Atmospheric pressure within the eye is the best single index for estimating surge potential of a hurricane. This index is called the Central Pressure Index (CPI). Central pressures of 950-960 mb (28.0 - 28.3 in.) are common. Hurricane Ida in the Philippines in 1958 had an extremely low pressure of 877 mb (25.9 in.) (Eagleman 1983). Generally, for hurricanes of fixed size, the lower the CPI, the higher the wind speeds.

(3) Unlike tropical storms, which generally occur in summer, extratropical storms generally occur in winter. These depressions in the middle latitudes consist of warm and cold air fronts which rotate about a low pressure center. Winds are not as intense as hurricanes since their horizontal scale is greater with a lesser pressure gradient. However, extratropical storms tend to have a longer duration and their destruction effects may be felt over large areas. Extratropical storms that occur along the northern part of the east coast of the United States, when accompanied by strong winds blowing from the northeast quadrant, are called nor'easters. Nearly all destructive nor'easters have occurred between November and April. Extratropical storms produce the dominant large wave conditions in the Great Lakes and generally occur between mid-October and April. The size of a typical storm of this type is shown in Figure V-2-1 (Resio and Vincent 1976).

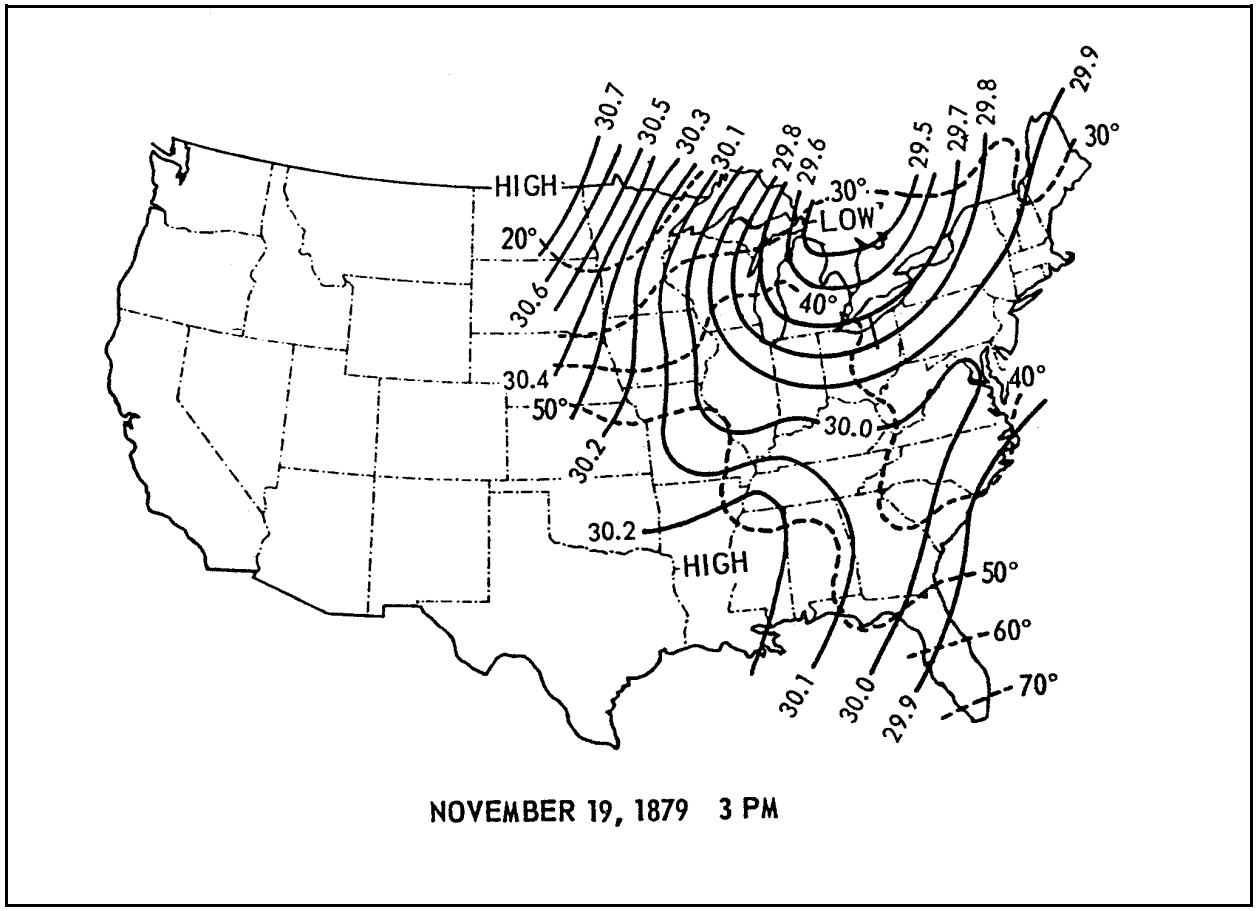

Figure V-2-1. Isobaric pattern of a typical extratropical low in the Great Lakes Region (Resio and Vincent 1976)

b. Storm characteristics. Depending upon availability of observed hurricane data for the open ocean coast, the design analysis for coastal structures may not be based on measured water levels and waves. A statistical approach has evolved that takes into account the expected probability of occurrence of a hurricane with a specific CPI at any particular coastal location. Statistical evaluations of hurricane parameters, based on detailed analysis of many hurricanes, have been compiled for coastal zones along the Atlantic and U.S. Gulf coasts. Parameters that need to be evaluated are radius of the maximum wind, minimum central pressure of the hurricane, forward speed of the hurricane while approaching or crossing the coast, and maximum sustained wind speed at 10 m (33 ft) above the mean water level. Table V-2-2 presents extreme pressure and wind data for hurricanes recorded along the Alabama coast between 1892 and 1969 (U.S. Army Engineer District, Mobile 1978).

Table V-2-2
Extreme Pressure and Wind Data of Hurricanes Recorded along the Alabama Coast between 1892 and 1969 (U.S. Army Engineer District, Mobile 1978).

Date Hurricane Crossed Coast	Approx. no. miles and direction center passed Mobile	Lowest barometric pressure (in.)	Location of pressure measurement	Maximum wind velocity and direction (mph)	Location of wind measurement
2 Oct 1893	50 W	29.16	Mobile	80 SE	Mobile
15 Aug 1901	70 W	29.32	Mobile	61	Mobile
27 Sept 1906	20 SW	28.84	Mobile	94	Ft. Morgan
20 Sept 1909	150 SW	29.62	Mobile	52	Ft. Morgan
14 Sept 1912	20 W	29.37	Mobile	60 SE	Mobile
29 Sept 1915	100 W	29.45	Mobile	60 SE	Mobile
5 July 1916	20 W	28.38	Ft. Morgan	107 E	Mobile
18 Oct 1916	60 E	29.22	Mobile	128 E	Mobile
28 Sept 1917	100 SE	29.17	Mobile	96 NNE	Mobile
20 Sept 1926	30 S	28.20	Perdido Beach	94 N	Mobile
1 Sept 1932	25 SSW	29.03	Bayou La Batre	57 E	Mobile
19 Sept 1947	110 SW	29.54	Mobile	53 E	Mobile
4 Sept 1948	90 W	29.55	Ft. Morgan	42 S	Mobile
30 Aug 1950	20 E	28.92	Ft. Morgan	75	Ft. Morgan
24 Sept 1956	80 S	29.49	Mobile	58	Mobile
15 Sept 1960	80 W	29.48	Mobile	74	Dauphin Is.
3 Oct 1964	230 W	29.39	Alabama Port	80 NNW	Alabama Port
17 Aug 1969	90 WSW	29.44	Mobile	74	Mobile

c. Hypothetical hurricanes. The National Weather Service and the U.S. Army Corps of Engineers have jointly established specific storm characteristics developed from statistical consideration. Since parameters characterizing these storms were statistically derived, they are known as hypothetical storms. Parameters for such storms are assumed constant during the entire surge generation period. The Standard Project Hurricane is defined as a hypothetical hurricane that is intended to represent the most severe combination of hurricane parameters that is reasonably characteristic of a region excluding rare combinations. The Probable Maximum Hurricane is defined as a hypothetical hurricane having that combination of characteristics which will make the most severe storm that is reasonably possible in the region involved if the hurricane should approach the

point under study along a critical path and at an optimum rate of movement. The reader is directed to Part II, Chapter 2 for further discussions on meteorological systems and waves.

V-2-4. Hydrodynamic Processes (Design Sea State, Water Levels, Currents)

a. Design condition.

(1) In selection of design water levels and waves for a project, critical conditions must be considered. These represent critical threshold combinations of tide level, surge (or setup) level, wave conditions and local runoff, which, if surpassed, would endanger the project and/or make the project nonfunctional during their occurrence. It should be recognized that water levels have a direct impact on wave conditions in shallow water. Conversely, waves can have some impact on the water level through wave-induced setup.

(2) In selection of the design condition for the project, it is important to consider the intended structural integrity, and functional performance. Structural integrity relates to the structure's ability to withstand effects of extreme storms without sustaining significant damage. Structural integrity criteria determine the structure's life-cycle costs to the extent that a certain level of investment is necessary to prevent damages from an extreme event. Functional performance determines the incremental economic benefits of a project since it defines the structure's level of effectiveness. For example, the crest height of a shore dike to prevent flooding should be optimized for different storm frequencies with consideration of interior ponding elevations (and damages) in comparison to costs of different structure heights. In performing analyses, one must be aware of the risk and uncertainty inherent in the design process. See U.S. Army Corps of Engineers (1992) for a discussion on risk and uncertainty analysis in water resources planning.

b. Design wave height and period.

(1) Most coastal projects require an estimate of characteristics (height, period, direction and frequency of occurrence) of wind-generated gravity waves at the project site. In the Pacific basin, tsunamis also may need to be considered. Wave characteristics are determined outside the surf zone and then transferred to the project site by considering refraction, diffraction, reflection, shoaling, and breaking effects. Part II, Chapter 3 discusses methods to estimate nearshore waves with guidance for performing wave transformation studies.

(2) Wave data sets are available as summaries of visual observations, wave hindcasts and wave gauge statistics. Shipboard observations generally represent deepwater wave conditions over large areas. For coastal areas of the United States, summaries have been published in Department of the Navy (1976). The USACE's Wave Information Study (WIS) has developed wave hindcasts along U.S. coasts, the Great Lakes, and some international locations. These hindcasts generally consist of wave height, period, and direction time series and summary statistics. WIS data are available on the World Wide Web (WWW) at:
http://chl.erdc.usace.army.mil/CHL.aspx?p=s&a=DATA;1
or at:
http://frf.usace.army.mil/wis/

(3) Wave data can be measured by various forms of floating and bottom-mounted wave gauges. If available for a project site, actual measured data are preferred to hindcasts because these data are obtained by physical measurement. While the amount of wave gauge data may be spatially and temporally limited, they can be used to confirm hindcasts. If the physical measurements include significant storms (Figure V-2-2), this data can confirm hypothetical design storm size and effects. Wave gauge data collected by the Coastal and Hydraulics Laboratory (CHL) can be accessed at:
http://sandbar.wes.army.mil/public_html/pmab2web/htdocs/dataport.html

Wave data, extremal analyses, climatic summaries, buoy data, and aerial photographs, arranged geographically, can be found at the CHL web page:
http://chl.erdc.usace.army.mil/chl.aspx?p=s&a=Data;0
Wave data from the west coast is available from the Coastal Field Data Information Program:
http://cdip.ucsd.edu/
Buoy wave data and meteorological observations can be found at the National Data Buoy Center's web page:
http://www.ndbc.noaa.gov/

c. Design water level.

(1) Storm surge at the shoreline due to a rise in water level above the still-water level is of more interest to the design engineer. Peak surge is generally used to establish design water levels at a site. The highest water levels that occur along the Gulf Coast, the east coast of the United States from Cape Cod to south Florida, and the Hawaiian Islands are generally the result of tropical storms. At most other U.S. locations, high water levels result from extratropical storms. The state of Alaska has experienced peak storm surges over 4 m (13 ft) high. (State of Alaska 1994). Storm surge interaction with tidal elevations is discussed in Chapter II-5, along with methods to determine storm event frequency-of-occurrence relationships.

(2) While large inland water bodies such as the Great Lakes experience negligible tidal fluctuations, they encounter fluctuating water levels due to variations in the hydrologic cycle coupled with storm surges (wind setup) resulting from extratropical storms. Significant water level setup is possible on large shallow inland water bodies, such as Lake Okeechobee, Florida, and Lake Erie of the Great Lakes. Peak water level relationships have been determined for various locations along the Great Lakes coast (U.S. Army Engineer District, Detroit 1993a). Figure V-2-3 presents a lake elevation hydrograph for the December 2, 1985 event on Lake Erie (National Oceanic and Atmospheric Administration (NOAA) 1985).

(3) A complete discussion on tides, surges, and seiches is presented in Chapter II-5. This chapter should be reviewed to determine the type of data required for the study being performed. NOAA is the most comprehensive source of global tide predictions in tables of time and heights of high and low tides, tidal current tables for U.S. coasts, tidal current charts for selected harbors, and other summaries of tidal predictions for selected areas. They may be contacted at:

NOAA National Ocean Service
Tidal Datums and Information Section
6001 Executive Boulevard
Rockville, MD 20852

NOAA'S WWW site lists availability of tide data, charts, and other material.

V-2-5. Seasonal Variability

Recognizing seasonal variability of waves and currents along the coast is important to appropriately interpret historic data and predict a project's response. This variability has effects on littoral transport quantities and direction, and gross profile shape. Alternate erosion and accretion may be seasonal on some beaches; winter storm waves erode the beach and summer swell waves rebuild it. Just as insufficient data can lead to erroneous conclusions, information obtained only during a particular season can lead to similar results. Most ocean coasts experience periods during which storm or swell waves dominate, although both can occur simultaneously. As mentioned in Section V-2-3.a, tropical and extratropical storms occur only during a portion of the year. The WIS wave hindcast (Section V-2-4.b) is a source of storm and swell wave conditions along the U.S. coasts and Great Lakes.

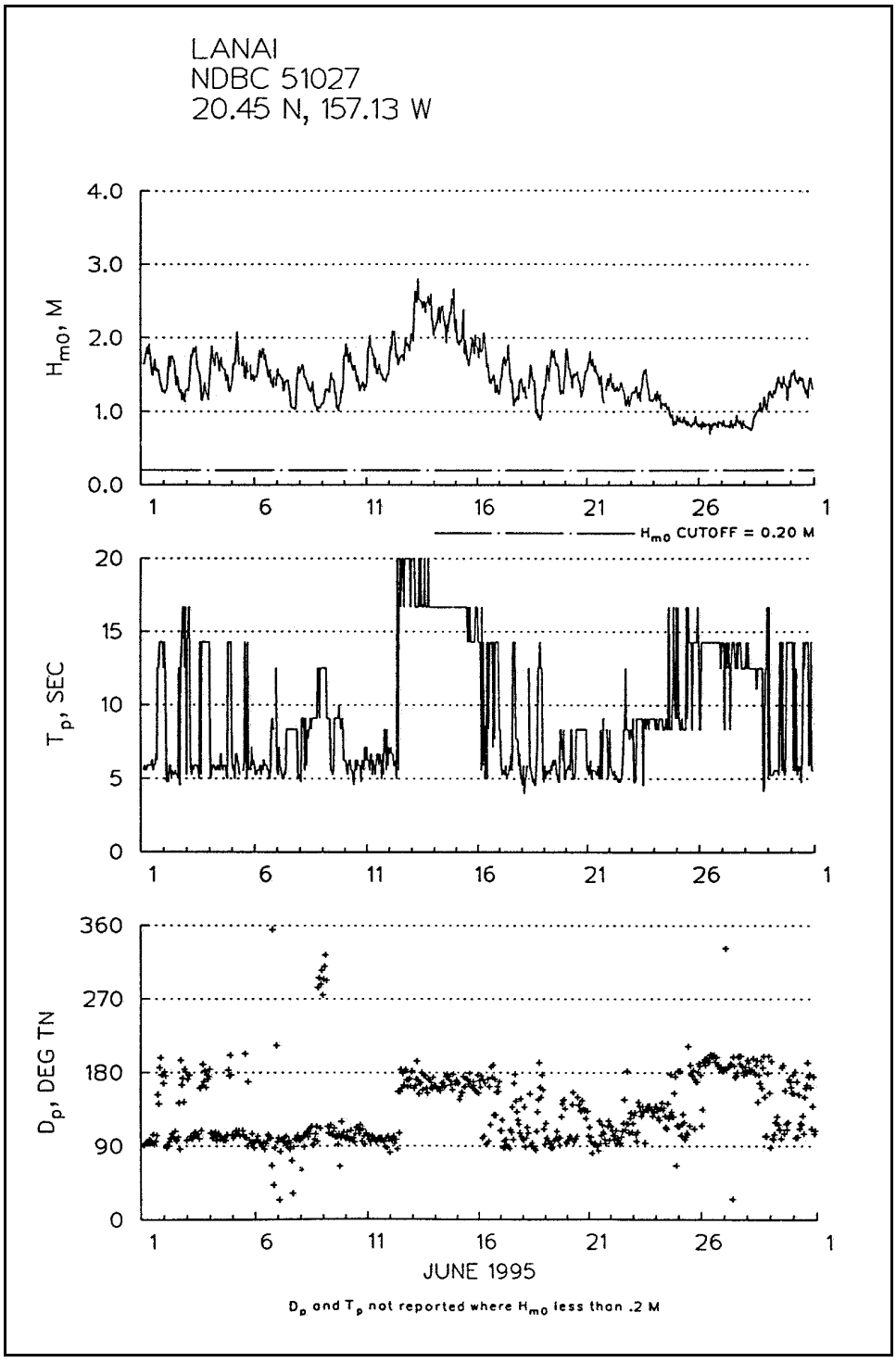

Figure V-2-2. Example of directional wave gauge data for Lanai, Hawaiian Islands (EM 1110-2-1810)

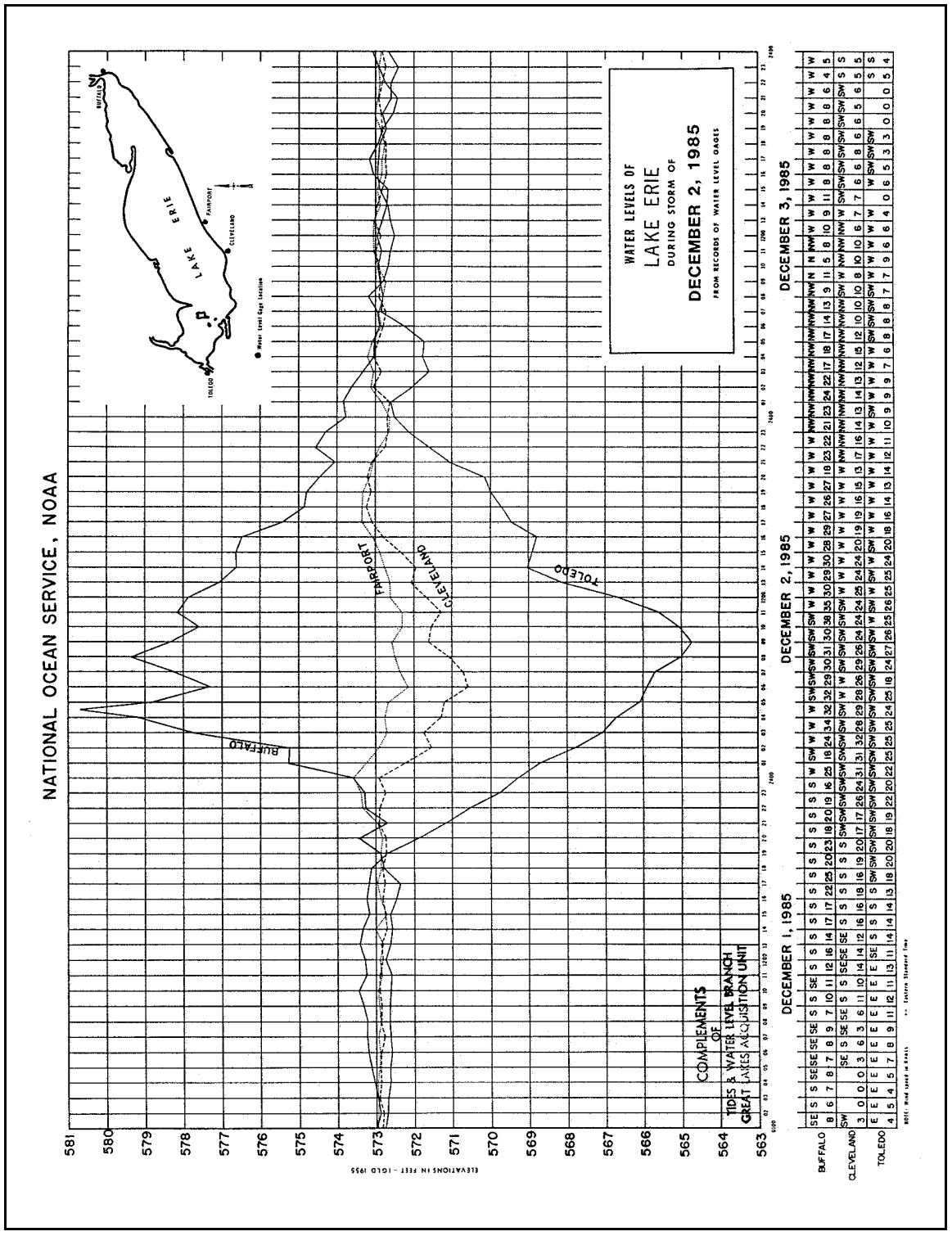

Figure V-2-3. Water levels of Lake Erie during storm of December 2, 1985 (NOAA 1985)

V-2-6. Topography and Bathymetry (Map Data)

a. Data needs.

(1) The amount of data needed for each project varies with the scope and type of project. Maps of the study area should include the updrift coastal zone which may affect the project and the downdrift area that will be affected by the project. Cadastral, topographic, and bathymetric information obtained from different sources should be combined into one or a series of maps. Computer Aided Drafting and Design (CADD) or Geographic Information System (GIS) programs facilitate the consolidation of map information. The advantage of a CADD or GIS drawing is that different types of information can be placed on different levels, allowing the user to access different layers for presentations, and 2- and 3-D illustrations are possible. Calculation of linear, areal, and volumetric change between elevations and distances (profiles) is possible.

(2) Recent surveys will be required to provide data in sufficient detail for cut/fill computations, sediment budgets, shoreline change, existing features, and property boundaries. Comparison with historic data will serve to illustrate shoreline and profile change and development. A review of historic maps and photographs is mandatory to fully understand the nature and processes at work, evolutionary trends, and natural ranges of variability. As windows to the past, they can present information which was at one time common knowledge, but has been lost with the passing of generations. Figure V-2-4 presents a portion of the 1836 shoreline map for Presque Isle, Pennsylvania. The location and extent of the breach along the neck (which afterward healed) give a glimpse of the shoreline position from another era. Most historic information, at least in the United States, only spans a century or less.

(3) Cadastral information relates to the showing or recording of property boundaries, subdivision lines, buildings, utilities, and related data. Topographic data presents the relief of land and the position of natural and man-made features. Often, topographic surveys with a contour interval of 0.3 m (1.0 ft) are required. Hydrographic surveys present the subsurface relief of water bodies and their shoreline position. Hydrographic survey techniques have been experiencing a renaissance. While the use of a lead line or other direct measure surveying procedures are still common, most hydrographic surveys are presently conducted using acoustical echo sounders. Other means such as the Scanning Hydrographic Operational Airborne Lidar Survey (SHOALS), a helicopter-mounted hydrographic surveying system for bathymetric measurement, are being introduced. SHOALS uses Light Detection and Ranging (LIDAR), a technology that uses a laser transmitter and receiver for water surface and water bottom detection. Because SHOALS is airborne, data can be obtained over ten times faster than shipboard echo soundings.

b. Available sources. Existing map data for the United States may be obtained from the following sources:

Cadastral: City, county, and state real estate records.
Topographic: State Department of Transportation, United States Geological Survey (USGS) and the U.S. Army Corps of Engineers (USACE).
Hydrographic: NOAA and USACE.

USACE District offices prepare annual reports on their activities. Review of these historic documents presents a narrative summary of coastal activities at U.S. Government installations. Maps also may be attached to these reports. The reader is referred to Part II, Chapter 8.

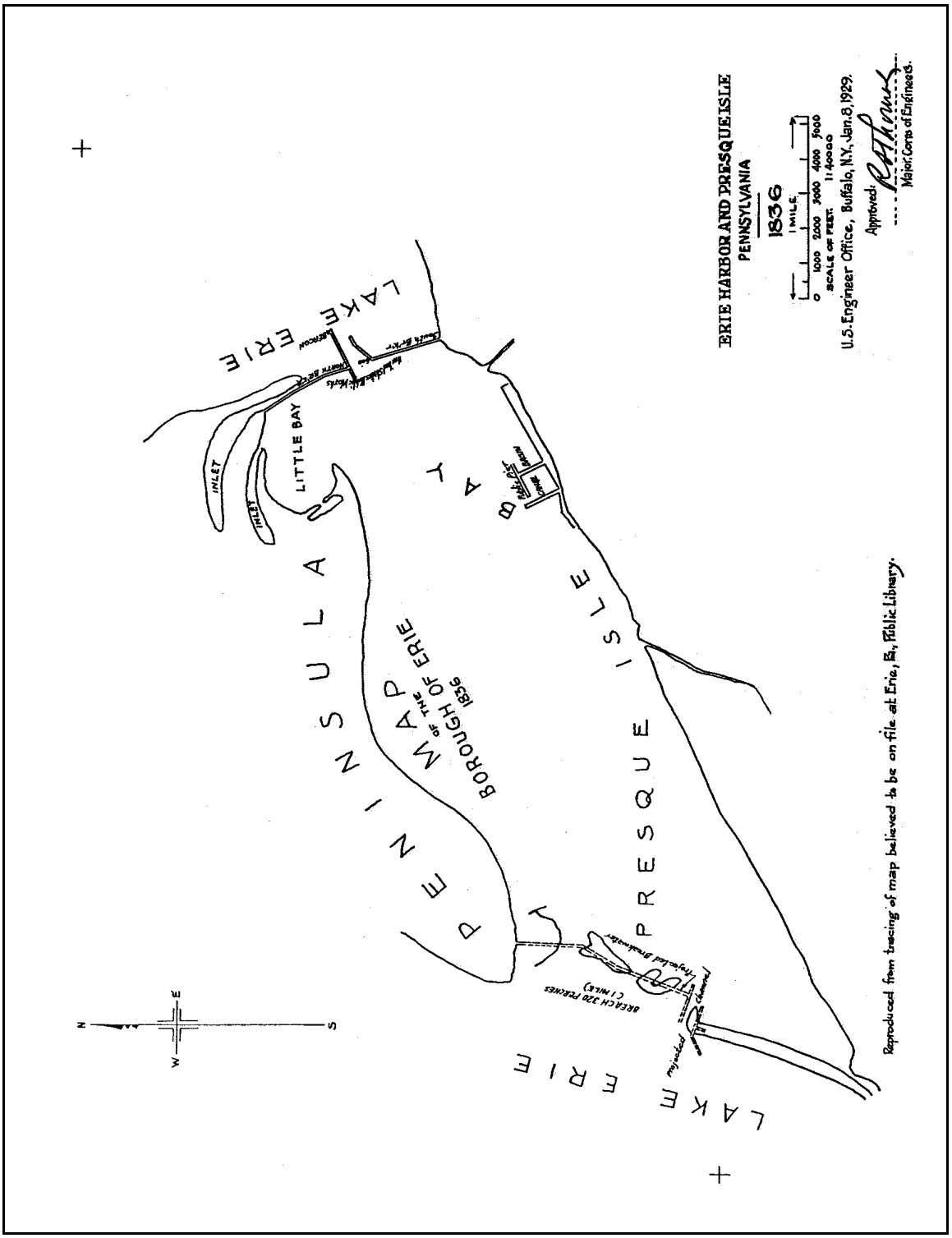

Figure V-2-4. The 1836 shoreline at Presque Isle, Pennsylvania

c. Reliability.

(1) All maps should have a north arrow (or south arrow in the Southern Hemisphere), a scale, and reference to the horizontal and vertical datum planes used. When using a historic map, one should be aware that magnetic north varies with time and one must align the map using true north. A map with a bar scale indicating the actual length is preferred. Be wary of maps that only report the scale, such as 1 cm = 1 km, unless the map is the original. The scale may be different if it is a copy, either due to slight paper shrinkage or reduction or enlargement when the copy was made. Also be aware that the datum plane can change with time or that a different datum plane may have been used. The datum used for topographic surveys may be different than that used for hydrographic work. Also, individual localities, such as cities, may have their own datum planes (Part II, Chapter 5 discusses datums). When comparing historic maps, at least two points of reference will be necessary in order to align the maps.

(2) The accuracy of hydrographic data is affected by four types of error: sounding, spacing, closure, and error due to temporal fluctuations in the lake or sea bottom. These errors may be more significant (greater) for nearshore profiles than for beach or topographic surveys since land surveys are not affected by the latter error and measurement techniques are more precise for topographic work. The presence of errors suggests a need for caution in interpreting differences obtained from two surveys of the same profile. In other words, be sure that different profiles truly represent differences in the sea bottom and do not merely reflect survey or plotting errors. Since the nearshore seafloor can change rapidly in response to changing wave conditions, differences between successive surveys may reflect bottom differences caused by storms and seasonal wave climate changes. These fluctuations may actually be greater than long-term trends. Reviewing available historic bathymetric charts will assist in interpreting long-term trends as short-term changes are often larger than net changes.

V-2-7. Geomorphology/Geometry and Sediment Characteristics

a. The coast is a diverse and dynamic environment. Many geologic, biological, and natural and human-made physical factors are responsible for shaping the coast and keeping it in a constant state of flux. Ancient geological events created, modified, and molded the rock and sediment bodies that form the foundation of the modern coastal zone. Over time, various physical processes have acted on this preexisting geology, subsequently eroding, shaping, and modifying the landscape.

b. Lithology deals with the general characteristics of rock and sediment deposits and is an important factor in shaping the present coast. The most crucial lithologic parameters responsible for a rock's susceptibility to erosion or dissolution are the mineral composition and degree of consolidation. Marine processes are most effective when acting on uncemented material, which is readily sorted, redistributed, and sculpted into forms that are in a state of dynamic equilibrium with incident energy. Part IV describes coastal geomorphology/sediment characteristics.

a. Types of coasts/principal features.

(1) Upon initiation of a study in a coastal area, the investigator needs to be aware of the type of coast being examined. Coasts may generally be classified as consolidated, unconsolidated, tectonic, or volcanic. Consolidated rock consists of firm and coherent material with coasts of this type typically found in hilly or mountainous terrain such as that in Maine (Figure V-2-5). In contrast, depositional and erosional processes dominate unconsolidated coasts, which are normally found on low relief coastal plains or river deltas. The Atlantic and Gulf of Mexico coasts of the United States are mostly unconsolidated depositional environments (except locations like the rocky New England shores). Figure V-2-6 is a photo of an unconsolidated coast.

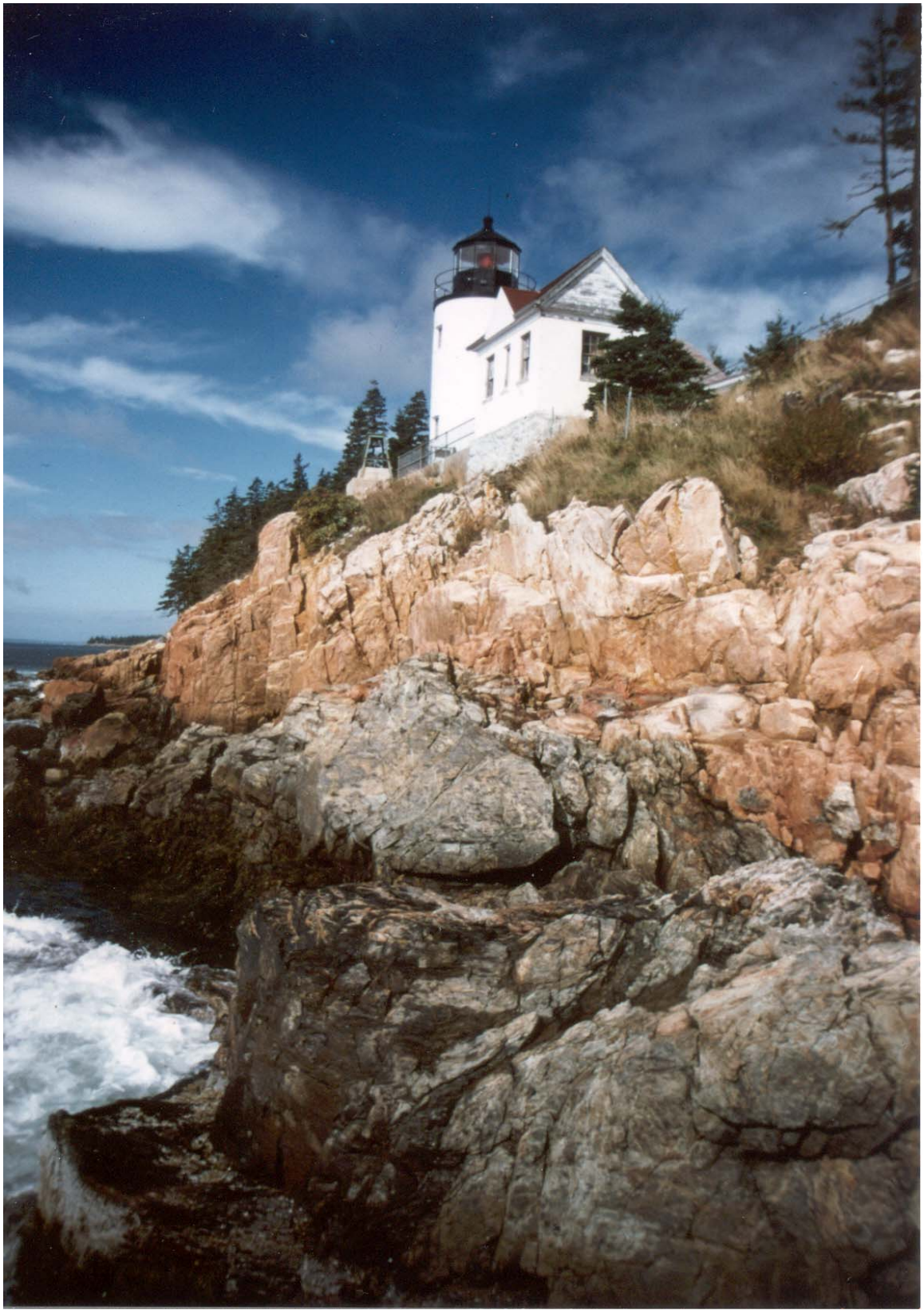

Figure V-2-5. Example of resistant rock-bound coast of Maine (Bass harbor Head Light, Maine, south of Acadia National Park)

Figure V-2-6. Beach near entrance to North Sand Pond, Lake Ontario, NY. This is a relict dune environment at the eastern end of Lake Ontario

Forces within the earth's crust and mantle deform, destroy, and create crustal material. These tectonic activities produce large-scale uplift and subsidence of land masses. The west coast of the United States is an example of a tectonically dominated coast. Sea stacks are prevalent along the U.S. Pacific coast. Sea stacks are steep-sided rocky projections above sea level near the coast. They are formed by wave cutting back on the two sides of a promontory. With the aid of weathering and further cutting behind it, it is left as an island. Sea stacks may be located onshore (Figure V-2-7) or further offshore, are of varied sizes and locally affect the wave patterns near them. The Great Lakes were created by glacial action, and physical characteristics of the shorelands are very diverse. They vary from high bluffs of consolidated or unconsolidated (Figure V-2-8) material to low bluffs and plains, dunes and wetlands. The eruption of lava and the growth of volcanoes may result in large masses of new crustal material, such as in the Hawaiian Islands.

(2) Principal coastal features which have been formed by local processes give indications of the types of coast under investigation. For example, the presence of a barrier island is indicative of a coast consisting primarily of unconsolidated sediments. In contrast, the most prominent feature exhibited by a fault coast is a scarp where normal faulting has recently occurred, dropping a crustal block so that it is completely submerged and leaving a higher block standing above sea level.

b. Sources and sinks. Recognition of the many sources (gains) and sinks (losses) in the coastal zone is important during development of the sediment budget for the region. In general, sand supply from rivers, cliff/bluff erosion, onshore transport from the shelf, biogenic sources (such as reefs), and alongshore sediment transport into the area constitute the major natural sources. Beach nourishment represents a human-induced gain to the budget. Natural losses can include sediment blowing inland to form dunes, offshore transport to deeper water, losses down submarine canyons, and the longshore transport that carries littoral

Figure V-2-7. Coast at Orick, CA. This is a pocket beach between resistant headlands

Figure V-2-8. Shore at Chimney Bluffs State Park, Lake Ontario, NY. Chimneys consist of glacial till more weather resistant than surrounding material

sediments out of the study area. Sand mining or direct removal (e.g., channel dredging with disposal outside of the littoral system) is a human-induced deficit to the budget.

c. Prevailing sediment characteristics.

(1) The geology of the coast and the source of littoral materials ultimately determine the prevalent shape of the shore and the composition of the beach at a specific locality. Littoral materials are classified by size, composition, shape, and other properties such as color. Littoral materials are classified by grain size in clay, silt, sand, gravel, cobble, and boulder. Several size classifications exist, with the Unified Soil Classification being the primary classification used by engineers and the Wentworth by geologists. Part III, Chapter 1 discusses sediment properties and classification.

(2) Littoral material is composed of materials specific to that region. While beach material is most commonly composed of quartz or feldspar particles, it also can be volcanic debris, as in the Hawaiian and Aleutian Islands, shell and coral, organics (peat), silts and clays. Littoral sands, gravel, and cobbles are usually rounded (Figure V-2-9), while departures from this shape are attributed to contributions from shell fragments and sedimentary rock such as shale. These departures from a spherical shape affect sediment motion initiation.

Figure V-2-9. Cobble Beach along Lake Ontario, Oswego, NY. Origin of cobble is bluff and glacial drumlin erosion

Sediment color may be used to trace the source of littoral material. It also is an indication of the relative density of the material. "Light minerals" such as quartz and feldspar, which have specific gravities ranging from 2.65 to 2.76 are generally tan, cream, or transparent. The famous white sands of the Florida panhandle are a very clean, uniformly sized quartz. "Heavy minerals," such as hornblende, garnet, and magnetite, which have specific gravities ranging from 3.0 to 5.2, are dark (black, red, dark green, etc.) in color. Littoral sediments of volcanic islands are dark, often green and black (Figure V-2-10).

Figure V-2-10. Black Sand Beach, Kalapana, HI. Sand is of volcanic origin

d. Sediment layering. It is important to recognize that variation in beach material may occur with depth. Classification of the surficial material only may lead to erroneous interpretations of coastal activity. Underlying the beach material can be layers of cohesive material, peat or rock. These will have significant effects on beach profile response to storm activity and foundation conditions for proposed structures. An understanding of the geology of the area will indicate whether layering (stratigraphic variability) can be expected.

V-2-8. Littoral Drift and Sediment Transport Patterns

Littoral transport is the movement of material in the littoral zone by waves and currents. This includes movement parallel (longshore) and perpendicular (cross-shore). The littoral zone extends from the shoreline to just beyond the seawardmost breakers.

a. Longshore movement. Wave-generated currents tend to dominate water movements in the nearshore zone and are important in the movement of sediments. Wave-induced currents are superimposed on the wave-induced oscillatory motion of the water. When waves break with their crests at an angle to the shoreline, a current is generated parallel to the shore that is largely confined to the nearshore between the breakers and the shoreline. The volume rate of material transport along the shore is sensitive to the breaker angle and height. The longshore gradient in breaking wave height is also a generating mechanism for longshore sand transport. This contribution is usually much smaller than that from oblique wave incidence in an open coast situation. However, in the vicinity of structures, where diffraction produces substantial change in breaking wave height, its inclusion improves transport rate prediction (Hanson and Kraus 1989). Longshore sediment processes are discussed in Part III, Chapter 2.

b. Cross-shore movement.

(1) Wave breaking generates turbulent motion and provides the necessary mechanism for suspending sediment. Sediment transport in a direction perpendicular to the beach is known as cross-shore movement. The equilibrium profile is a profile of constant shape which is approached if exposed to fixed wave and water level conditions. Waters (1939) proved that the existence of an equilibrium profile was a valid concept under laboratory conditions. The concept of the equilibrium profile is discussed in Part IV.

(2) As a beach profile approaches an equilibrium shape, the net cross-shore transport rate decreases to approach zero at all points along the profile (Larson and Kraus 1989). The division of the profile into different transport regions has allowed empirically based relationships for the net transport rate to be formulated. The four transport zones across the profile are defined as:

Zone I: From the seaward depth of effective sand transport to the break point (prebreaking zone).

Zone II: From the break point to the plunge point (breaker transition zone).

Zone III: From the plunge point to the point of wave reformation or to the swash zone (broken wave zone).

Zone IV: From the shoreward boundary of the surf zone to the shoreward limit of runup (swash zone).

(3) The net transport rate in zones of broken waves, where the most active transport occurs, shows good correlation with the wave energy dissipation per unit water volume. The net transport rate in the prebreaking zone decreases exponentially with distance offshore. In the foreshore zone, the net transport rate shows an approximately linear behavior decreasing in the shoreward direction. The reader is referred to

Chapter III-3 for a discussion on cross-shore transport. Larson and Kraus (1989) present an excellent literature summary of the chronological investigations on profile change and the development of cross-shore transport modelling. Dean (1991) summarizes equilibrium profile responses for differing coastal conditions. Houston (1996) applies equilibrium profile responses to beach fill design. The reader is referred to Part III, Chapter 4.

c. Seasonal reversals.

(1) Section V-2-5 discussed the seasonal variability of storms and waves. This variability results in two distinct classes of waves, storm waves and swell waves, which have completely different effects on the beach profile. In general, storm waves remove the beach berm to place it along the offshore portion of the profile while swell waves replace it back onshore (Silvester and Hsu 1993). This occurs primarily along the oceanic coasts and to a reduced degree along inland seas. Recognition of this variability is important in interpreting existing beach change and during the establishment of a monitoring program for a beach.

(2) The following synopsis of this action is presented eloquently in Sylvester and Hsu (1993). In describing the action of swell waves on the beach profile,

> *The broken wave swashes up the beach face with its water percolating through it, so long as there is adequate time between each wave. ...this water soaks down to the water table some distance below the face, eventually to be returned back to the sea. The downrush, when a trough arrives, is smaller than the uprush due to this percolation and therefore cannot carry much of the sediment load back down the beach face. Also, the hydraulic jump associated with this flow reversal is small. The result is that swell waves, with several seconds between each crest, will leave material on the face and hence the beach accretes.*

(3) In contrast to swell waves, storm waves are steeper. Silvester and Hsu (1993) wrote,

> *Now consider what happens to this swell profile when storm waves arrive. These are very steep and contain much water above the mean sea surface. They comprise waves of many periods, or constitute a wide spectrum, with heights appropriate to each. A crest arrives almost every second instead of every few seconds and hence large volumes of water are thrown over the beach face, which is quickly saturated.* By this action, *the water table has become almost coincident with the face itself. The downrush now nearly equals the uprush so that much sand is dragged down the face into the hydraulic jump, which is increased in size. This is one mechanism by which the berm is eroded and its contents placed into suspension.*
>
> *Another factor, of equal if not greater importance, is the flow of the excess ground water returning to the sea. At the waterline, where the hydraulic jump is also located, it is moving vertically, thus causing liquefaction or a "quicksand" effect (Longuet-Higgins 1983). This aids suspension so helping to undermine the toe of the beach, which progressively retreats landward...*

(4) The above briefly described the effect on the profile type (accretion/erosion) and hence a net onshore or offshore cross-shore transport due to the presence of swell or storm waves, respectively. It also is important to recognize during development of the sediment budget that the net direction of the storm and swell waves may be different, resulting in a reversal of longshore drift with season. This can have a significant effect upon the location of accretionary/erosional zones adjacent to the project. The project design needs to tolerate a range of expected conditions. One must be able to change bypassing operations during a year to accommodate these seasonal reversals.

d. Long-term reversals. Recognition of changes in the sediment budget over the long term (years to decades) is important when evaluating historic changes or predicting potential changes due to a proposed project. Modifications of the sediment gains or losses through natural causes or human intervention can shift an accretionary shore to an erosional shore. For example, the construction of large harbor structures or the stabilization of an inlet along the coast have affected the amount of sediment reaching downdrift beaches. Without sediment bypassing around the harbor, downdrift beaches may erode severely. Cyclic climatic changes such as the El Ninõ can cause reversals for many months. Knowledge of these type of activities is necessary to properly interpret profile change.

e. Slug motion.

(1) Sediment movement along the shore rarely occurs at a temporally and spatially constant rate. The presence of large beach protuberances termed "sand slugs" or "longshore sandwaves" is a phenomenon that has been reported at numerous beaches around the world. Along Long Point on the Lake Erie shore, these features have been observed with alongshore lengths of 500 to 2,500 m (1,640 - 8,200 ft) and maximum widths of 50 to 90 m (164 - 295 ft) which migrate alongshore in the direction of net drift at 150 to 300 m/year (492 - 984 ft/year) (Stewart and Davidson-Arnott 1988; Davidson-Arnott and Stewart 1987). Similarly along the Dutch coast, they have been measured with an amplitude of 30 to 500 m (98 - 1,640 ft), a celerity of 50 to 200 m/year (164 - 656 ft/year), and a period of 50 to 150 years (Verhagen 1989).

(2) Bakker (1968) presents a mathematical theory on sandwaves and an application on the Dutch Wadden Isle of Vlieland. Stewart and Davidson-Arnott (1988) describe their formation by the onshore movement and welding of inner nearshore bars during nonstorm periods on areas of local sediment abundance. In addition, growth and downdrift extension and widening of the protuberance in the direction of net sediment transport results from attachment of an inner bar to the slug and infilling of the trough-runnel downdrift of the protuberance. The presence of sand waves results in a spatial pattern of erosion and accretion, with erosion occurring primarily in the embayments between the slugs and accretion occurring opposite the wide beach of the sand wave.

(3) The presence of this type of phenomenon can dwarf the effects of a relatively smaller shore project. At Presque Isle Peninsula, Pennsylvania, three prototype segmented offshore breakwaters were built in 1978. The intent was to study the effect of offshore distance, breakwater length, and gap width upon the shoreline. The movement of a sand wave through the project area a few years later totally covered the breakwaters. They began to emerge more than a decade later. Verhagen (1989) concluded that along the southern part of Holland, groin construction did not change linear long-term coastal erosion and did not change the cyclic behavior of the shore. He concluded that construction of groins on this coast did not have any effect at all.

f. Hot spots. Often at a beach nourishment project, there will be one or more areas that erode more rapidly than others. These areas are termed erosional hot spots. The location may correlate with areas which had previously experienced high erosion. Hot spots at new locations may be due to wave refraction and possibly wave focusing in response to bathymetric change from placed material (National Research Council 1995). Another cause may be a bottom composition change which affects the rate of movement. In any event, erosional hot spots may require renourishment earlier than the rest of the project. This unexpected work will place an additional financial strain on the project. Placement of a greater quantity of sand in hot spot areas may extend the time between renourishment.

V-2-9. Shoreline Change Trends

a. Evidence of cyclic processes.

(1) The presence of cyclic processes due to water levels and waves is observed in coastal features such as tidal inlets and seasonal bars. Inlets are the openings in coastal barriers through which water, sediments, nutrients, planktonic organisms and pollutants are exchanged between the open sea and the protected embayments behind the barriers. Inlets are not restricted to barrier environments or to shores with tides; on the west coast of the United States and in the Great Lakes, many river mouths are considered to be inlets, and in the Gulf of Mexico, the wide openings between the barriers, locally known as passes, are also inlets. Tidal inlets are analogous to river mouths but differ as they experience diurnal or semidiurnal flow reversals and they have two opposite-facing mouths (seaward/lakeward and lagoonward). Tidal inlets are characterized by large sand bodies that are deposited and shaped by tidal currents and waves. The ebb-tide shoal is a sand deposit that accumulates sea/lakeward of the inlet mouth. It is formed by ebb tidal currents and is modified by wave action. The flood-tide shoal is a sediment deposit at the landward opening that is mainly shaped by flood currents. Depending upon the size of the bay (lagoon), the flood shoal may extend into open water or may merge into a complex of meandering tributary channels, point bars, and muddy estuarine sediments.

(2) As indicated in Section V-2-8, seasonal variability of storms and waves results in seasonal reversals in cross-shore drift. The effect of the change from a swell-dominated to storm-dominated profile is clearly seen in the presence of seasonal bars. Storm waves remove the beach berm and place the material offshore as a bar. Swell waves attempt to reverse this action. Interpretation of long-term trends must account for these short-term changes.

b. Eustatic sea level changes. A worldwide change in sea level, referred to as eustatic sea level change, is caused by change in the relative volumes of the world's ocean basins and the total amount of ocean water (Sahagian and Holland 1991). The rise results in a slow, long-term recession of the shoreline, partly due to direct flooding and partly as a result of profile adjustment to the higher water level. Estimates of recent eustatic rise range from 15 cm/century (Hicks 1978) to 23 cm/century (Barnett 1984), although some researchers, after exhaustive studies of worldwide tide records, have not seen conclusive evidence of a continuing eustatic rise (Emery and Aubrey 1991). This topic is reviewed in greater detail in Part IV.

c. Subsidence. Subsidence is the sinking of land due to natural compaction of estuarine, lagoonal, and deltaic sediments resulting in large-scale disappearance of wetlands. This effect has been exacerbated in some areas by human intervention with groundwater and oil withdrawal. Significant subsidence occurs in and near deltas where large areas of fine-grain sediment accumulate. Land loss in the Mississippi delta has become an important issue because of loss of wetlands and rapid shoreline retreat. Along with the natural compaction of the deltaic sediments, groundwater and hydrocarbon withdrawal may have contributed to subsidence problems in southern Louisiana. The change in relative sea level in the Mississippi delta is about 15 mm/year, while the rate at New Orleans is almost 29 mm/year (data cited in Frihy (1992)).

V-2-10. Land/Shore Use

a. The present use of the shore and the area landward of the coast needs to be documented. The areal extent of information to be collected must be determined on a site-by-site basis. An understanding of the sediment budget will assist in defining limits. Information should be gathered not only for engineering purposes but also for environmental and economic documentation. For a project planned in the coastal zone, this information will assist in assessing environmental and economic effects of the project.

b. Information collected on structures will include the type, ownership (residential, commercial, public, and other), density, location, and value. The elevation-versus-damage relation may be required if there is a flooding problem. The distance of structures from the top of bluffs or high-water elevation may be needed for regulatory purposes (setbacks) or expected potential damage at the present recession rate. If a shoreline erosion protection project is proposed, infrastructure data will be needed to estimate damage reduction (project benefits) due to a lower recession rate. Structures which influence sediment supply or surface/groundwater drainage patterns may also be important.

c. In addition to the structure inventory, property boundaries have to be located. Identification of all lands, easements, and rights of way will be needed when assessing the required easements for construction limits and access to the site, as well as for future maintenance. The affected infrastructure (roads, utilities, etc.) also must be identified.

V-2-11. Potential for Project Impacts

a. Effects on natural tidal flushing.

(1) Dredging a channel through a tidal inlet usually results in increased shoaling. Channel dredging also can have a significant effect on adjacent shorelines, although the effect may be difficult to assess. A complete understanding of natural processes prior to dredging is required to discern the change due to dredging. Disposal of dredged material offshore may result in permanent removal from the littoral system if the depth is sufficient to prevent return to the nearshore littoral environment. Although the limiting depth for which material offshore will return to the beach is generally unknown, it is dependent on variables such as sediment size and wave climate. A few tests have suggested that material placed in water depths greater than 6 m (20 ft) in the ocean and about 2 m (6 ft) in the Great Lakes will not readily return to the nearshore littoral system (Harris 1954, Schwartz and Musialowski 1980).

(2) Jetties or breakwaters often are built to stabilize inlets. These structures serve to stop the entry of littoral drift into the channel, function as training walls for tidal currents, stabilize the position of the navigation channel, may increase tidal current velocities which flushes sediment from the channel, and reduce shoaling in the channel. Despite their positive engineering effects, jetties often form a barrier to longshore sediment movement. Where there is no predominant direction of longshore transport, jetties may stabilize nearby shores, but this effect is limited only to the sand impounded at the structures. At most sites the amount of sand available to downdrift shores is reduced, at least until a new equilibrium shore is formed at the jetties. Where longshore transport predominates in one direction, an accretionary fillet will occur on the updrift side of the channel and erosion will occur on the downdrift side. Again, bypassing or nourishment will be required to mitigate this imbalance.

(3) The increase in channel velocities also increases the potential for scour along the structure toe. This effect can be exacerbated by the presence of waves. This potential effect must be considered during project design.

b. Up/downdrift effects and need for bypassing.

(1) Construction of a coastal project that protrudes from the shore or is located nearshore and modifies the local wave climate may result in a change in sediment accretionary and erosional patterns. This perturbation of longshore drift movement will result in an accretionary zone immediately updrift or within the wave shadow of the structure and an erosion zone downdrift of the structure. The effect of the structure may be mitigated by prefilling the fillet (at a protruding structure) or salient (behind a shore-parallel structure). This preventative action may not be adequate. If the structure protrudes sufficiently to trap and deflect most of the littoral drift to deep water, bypassing of material may be required.

(2) Prediction of erosion downdrift of a barrier is challenging. Bruun (1995) presents a discussion, series of examples, and a good reference list on this problem. He notes that downdrift erosion may in some cases be composed of short (local) as well as long-distance effects which move downdrift at various rates. The presence of a 'zero-area' or location of a temporary reduction of erosion a short distance from the barrier does not necessarily indicate the extreme limit of leeside erosion. While the short distance effect is a geomorphological feature, the long-distance effect is due to a sediment deficit. Determination of the maximum recession and length of shore affected by downdrift erosion is further complicated by the presence of natural erosionary processes.

(3) Mitigation of shoreline damage due to the presence of an existing structure requires knowledge of recession rates (sediment budget) before and after its construction. The difference in sediment gain/loss downdrift of the structure is the minimum information required to mitigate effects of the structure. This value is used if bypassing of material is not practical or is politically infeasible (updrift owners enjoy the newly created or enlarged beach) and new material instead is introduced to the system.

c. Changes in wave climate.

(1) Construction of a protruding or an offshore shore-parallel structure will modify the local wave and current climate near the structure. A protruding structure, such as a groin or jetty, may cause development of a rip current along the updrift face. An offshore breakwater will reduce wave activity in the lee since wave energy behind the structure occurs from a combination of diffracted waves from the ends and transmission over/through the structure. This usually will result in deposition of littoral material in the breakwater shadow. Modification of the wave pattern may limit surfing but can enhance other recreational activities such as swimming.

(2) Reflection of incident waves from a natural or man-made structure also will affect local wave climate. The amount of wave reflection, expressed as the reflection coefficient (reflected wave height/incident wave height), is dependent upon the structure's surface roughness, structure height in relation to the wave runup (freeboard), structure slope and incident wave angle (especially as the wave direction approaches the structure orientation). Smooth, vertical, and high (no overtopping) structures (such as sheet-pile walls) reflect most incident wave energy. The resulting increase in wave height near the structure can induce additional scour at the structure toe, increase local transport rate, and result in unacceptable wave conditions within a harbor.

d. Impact on benthic organisms.

(1) Construction of shore protection measures usually produces short-term physical disturbances which directly affect biological communities and may result in long-term impacts. Coastal structures alter bottom habitats by physical eradication and in some cases scour or deposition. However, certain hard structures may create a highly productive, artificial reef-type habitat. Beach nourishment will cover nonmotile organisms.

(2) Species comprising marine bottom communities on most high-energy coastal beaches are adapted to periodic changes related to natural erosion and accretion cycles and storms. Burial of offshore benthic animals by nourishment material has a greater potential for adverse impacts than those in the intertidal and upper beach zone (Nagvi and Pullen 1982). Survival of vegetation and animals will depend upon the deposition depth, rate of deposition, length of burial time, season, particle size distribution and other habitat requirements.

(3) A biological survey of organisms living in and using the proposed project area must be completed before a project is initiated. This must include threatened and endangered species. This inventory and knowledge of habitat requirements will assist in defining potential impacts of the proposed project.

(4) Certain species are very sensitive to placement of beach nourishment. Moderate disturbance of a mature oyster reef can destroy it. Covering of mangrove prop roots can kill the entire plant (Odum, McIvor, and Smith 1982). Hard corals are more sensitive than soft corals to covering with fine sediments. Excessive sedimentation for a nourishment project which buries a reef results in permanent destruction or replacement by soft bottom habitat and community. Nourishment can affect sea turtles directly by burying their nests or by disturbing nest locating and digging during the spring and summer nesting season. Elimination of these adverse effects may be possible by timing of placement (to be discussed in Section V-2-12).

e. Changes in natural habitat. Construction of a project in the coastal zone can cause short- and long-term changes in the natural habitat. Placement or dragging dredge anchors and pipelines can damage environmentally sensitive habitats such as coral reefs, seagrass beds, and dunes. Short-term changes to the grain size and shape of the beach will occur depending on characteristics of the native and borrow material. Waves and currents will winnow and suspend finer sediments and deposit them in deeper water offshore. Eventually, the sediment size distribution will become comparable to the beach sediments prior to nourishment. An increase in compaction of the beach can result from beach nourishment. Burrowing animals such as crabs and sea turtles can have difficulty digging in compacted beaches. As with sediment sorting, the compaction increase will be temporary until the beach is softened by wave action, particularly storms. Construction of a hard structure can result in a permanent change locally by removal of bottom habitat. However, a rubble-mound structure may provide a different (reef-type) habitat. Scraping of the new beach fill face during its initial adjustment can also have an adverse effect on species such as sea turtles and crabs that transit the beach surface for nest building and reproduction.

V-2-12. Environmental Considerations

Selection of the best environmental and engineering solution to a coastal problem requires a thorough understanding of the complexity and diversity of the coastal zone. A clear definition and cause of the problem as well as a comprehensive review of potential solutions is required. In the previous sections, some potential impacts to be expected by a project were discussed. In this section, the principal environmental factors that should be considered in design and construction and techniques to attain environmental quality objectives are discussed briefly. The reader is directed to EM 1110-2-1204 for more detailed information.

a. Surveying the project area.

(1) An understanding of existing environmental conditions is vital to ensuring that the status quo is maintained or enhanced. An environmental survey of the project area is required in order to establish a baseline condition. As in any sampling program, the most critical aspect of data collection is identifying the proper parameters to sample and measure. The quality of information obtained will be dependent upon collecting representative samples, use of appropriate sampling techniques, protecting samples until they are analyzed, accuracy and precision of analysis, and correct interpretation of results.

(2) The purpose of collecting samples is to acquire adequate representation of the project area's characteristics. This requires that samples be taken in locations typical of ambient conditions found at the project site. The number and frequency of samples will need to be assessed. Sampling equipment should be selected based on reliability, efficiency, and the habitat to be sampled. In order to maintain the integrity of the results, preservation of samples is imperative. Preservation is intended to retard biological action and hydrolysis/oxidation of chemical constituents, and to reduce volatility of constituents.

(3) Habitat-based evaluation procedures are developed to document the quality and quantity of habitat. These procedures can be used to compare the relative value of different areas at the same time (baseline studies) or the relative value of one area with time (impact assessment). Two habitat assessment techniques available are the Habitat Evaluation Procedure (HEP) and the Benthic Resources Assessment Technique (BRAT).

(4) HEP has been computerized for use in habitat inventory, planning, management, impact assessment, and mitigation studies (U.S. Fish and Wildlife Service 1980). The method is comprised of a basic accounting procedure that computes quantitative information for each species evaluated. The inventory can pertain to all stages of a species, to a specific life stage, or to groups of species. An HEP analysis includes: scoping, development and use of Habitat Suitability Index models, baseline assessment, impact assessment, mitigation, and decision on course of action.

(5) BRAT procedures use benthic characterization information to produce semiquantitative estimates of potential trophic value of soft-bottom habitats. BRAT estimates the amount of benthos that is both vulnerable and available to target fish species that occur at a site. The utility of BRAT lies in the ability to provide meaningful information relevant to value decisions. While it does not provide an assessment of overall habitat status, it can be viewed as an in-depth assessment of a single habitat variable, that of trophic support. As such, it may contribute semiquantitative input to habitat-based assessments such as HEP.

b. Mitigation measures.

(1) During the design of a project, care must be taken to preserve and protect environmental resources, including important ecological, aesthetic and cultural values. Specific U.S. Army Corps of Engineer mitigation policy for fish and wildlife and historic and archaeological resources is included in Chapter 7 of Engineer Regulation (ER) 1105-2-100. Mitigation consists of avoiding, minimizing, rectifying, reducing, or compensating for impacts. The first elements often can be accomplished through their consideration during project design. The amount of compensation required for significant losses to important resources is quantified through documentation of the amount of actual/predicted losses. Justification must be based on significance of resource losses due to a project compared to costs necessary to carry out mitigation.

(2) Some examples of mitigative measures for the aforementioned mitigative elements are as follows:

(a) Avoid: Adjust the time of construction activities to avoid periods of fish migration, spawning, shorebird or turtle nesting; preserve a public access point.

(b) Minimize: Disturb an immature reef instead of a mature one; use rough-surface facing materials on a structure.

(c) Rectify: Replace a berm; restore flow to former wetland.

(d) Reduce: Control erosion (sedimentation control plan); place restrictions on equipment and movement of construction and maintenance personnel.

(e) Compensate: Use dredged material to increase beach habitat, create offshore islands, increase or develop new wetlands; construct an artificial reef.

c. Water quality. Water quality impacts consist of changes to the water column's characteristics which may have short- and long-term consequences. Construction processes often are responsible for short-term increases in local turbidity levels, releases of toxicants or biostimulants from fill materials, introduction of petroleum products and/or the reduction of dissolved oxygen levels. These impacts can be minimized by construction practices, fill material selection, and in some instances, construction scheduling. These impacts are temporary unless long-term changes in hydrodynamics have occurred. It is these long-term repercussions which must be identified during the design process. The size and type of structural alternatives will result in a range of potential impacts. For example, the design of a jetty or offshore breakwater will greatly influence its impact on circulation and flushing, which affect water quality.

d. Disposal of materials. Physical and chemical testing of the proposed material to be dredged is required in order to assess the appropriate disposal method. Local regulations also may dictate the manner in which material is to be disposed: open-water, upland or in a confined disposal facility. For material that is placed in open water, it may be necessary to predict long-term fate of the disposal mound. This assessment will entail determining whether the material is dispersive or nondispersive. If material is dispersive, rate of erosion and fate of the material should be computed from models or field studies.

V-2-13. Regional Considerations

a. Regulations.

(1) Construction of a shore erosion or navigation project in the coastal zone is governed by national and local regulations. Research of governing laws is an essential part of the planning process in order to determine potential limitations for constructing in the coastal zone. These stipulations may include physical structure limitations such as size, setback requirements, the need for buffer zones, restriction on hard structures (North Carolina, Massachusetts, and Maine), and ability to rebuild after sustaining damage; and environmental limitations such as season when construction can occur and required mitigation (i.e., bypassing, wetland creation, etc). These laws are the result of lessons learned from constructing along the coast (Figure V-2-11).

(2) The Coastal Barrier Resources Act (Public Law 97-348 1982) is an example of a national regulation affecting coastal regions of the United States. The purpose of the Act is to minimize loss of human life; wasteful expenditure of Federal revenues; and damage to fish, wildlife, and other natural resources associated with the coastal barriers of the United States by restricting future Federal expenditures and financial assistance which have the effect of encouraging development of coastal barriers. The Act established the Coastal Barrier Resources System, which identified undeveloped coastal barriers on a series of maps. A coastal barrier is a depositional geologic feature (such as a bay barrier, tombolo, barrier spit, or barrier island) which consists of unconsolidated sedimentary materials, is subject to wave, tidal, and wind energies and which protects landward aquatic habitats including adjacent wetlands, marshes, estuaries, inlets, and nearshore waters. It is considered undeveloped if it contains less than one structure per 0.02 km^2 (5 acres) that is "roofed and walled" and covers at least 18.6 m^2 (200 ft^2).

(3) Article 34 of the New York State Environmental Conservation Law (State of New York 1988) is an example of a state law that regulates the need for coastal erosion management permits and controls activities within defined structural hazard areas and natural protective feature areas. Maps of structural hazard areas are available for the entire state coastline which define a zone in which no new non-movable structures or non-movable major additions to existing structures can be built without formal approval. New public utilities must be located landward of the shore structures that they serve. Within natural protective feature areas, development is generally prohibited, only clean sand or gravel of an equivalent or slightly larger grain size may be deposited nearshore, and a permit is required for any new construction, modification, or restoration

Figure V-2-11. Structures threatened by erosion, Lake Ontario, Crescent Beach, NY

of coastal structures. Many other states and communities have similar regulations and set-back limits, which limit construction activities within a specified distance from the shore or bluff edge.

b. Seismic. Forces within the earth's crust and mantle deform, destroy, and create crustal blocks. These tectonic activities produce physical features such as faults and folds. Tectonic movements produce large-scale uplift and subsidence of land masses. The frequency and magnitude of seismic forces on foundations of marine structures is essential information along tectonically dominated coasts such as the west coast of North America. Rigid structures (e.g. piers and seawalls) and flexible structures (e.g. rubble-mound breakwaters and revetments) should be evaluated for seismic response, according to the same general practices used for building design (U.S. Army Corps of Engineers 1994).

c. Tsunami.

(1) Tsunamis, or seismic sea waves, are long-period waves generated by displacements of the seafloor by submarine earthquakes, volcanic eruptions, landslides and submarine slumps, and explosions. The term tsunami is derived from two Japanese words: "tsu," for harbor and "nami," meaning wave. The underwater disturbance results in uplifting the water surface over a large area, which forms a train of waves with periods exceeding 1 hr, in contrast to normally occurring wind-generated water waves which have periods less than 1 min. In the open ocean, amplitude of tsunamis is usually less than 1 m (3.3 ft) and hence may go unnoticed to passing ships. However, the wave height increases greatly as the shore is approached, resulting in potentially catastrophic flooding and damage. Tsunamis generated by volcanic activity or landslides result in the wave energy spreading along the wave crests and affect mainly the areas near their source. Those generated by tectonic uplifting may travel across an ocean basin, causing great destruction far from their source (Camfield 1980).

(2) Tsunamis can be generated in any large water body, including inland seas and large lakes. However, the majority of seismic activity that usually generates tsunamis occurs along the boundaries of the Pacific Ocean, and some strong activity is concentrated in the Caribbean and Mediterranean Seas. While earthquakes affect the eastern United States, these usually occur inland. The only major recorded tsunami along the east coast of North America was the one which devastated the Burin Peninsula along Placentia Bay, Newfoundland, in November 1929. The tsunami was enhanced by an exceptionally high tide and high storm waves.

(3) Because of the frequency and magnitude of tsunamis in the Pacific Ocean, a warning system has been developed. Although tsunamis travel at speeds as great as 800 km/hour (500 mph), transoceanic distances are sufficiently large to allow several hours warning prior to arrival of a distantly generated tsunami. The Tsunami Warning System (TWS) was founded in 1946 following the Aleutian tsunami of 1 April of that year that caused major damage and many casualties in the Hawaiian Islands. The TWS is a cooperative effort among Pacific Ocean nations with seismograph and tide data collected and communicated to the Pacific Tsunami Warning Center in Hawaii, which disseminates the appropriate warning.

(4) Tsunami flood elevation - frequency information is developed using historic data and numerical models. Unfortunately, good data are available for only a limited number of tsunamis. Cox and Pararas-Carayannis (1969) and Pararas-Carayannis (1969) present a catalog of tsunamis for Alaska and the Hawaiian Islands. Where data are available, the probability of tsunami flood elevations can be determined by the same methods used for the riverine environment. If insufficient information is available, a synthetic record of tsunami activity must be generated. The geophysical and tectonic setting of the area is used to synthesize a record of tsunamigenic, tectonic deformations on the seafloor. A numeric model is used to simulate the tsunamis resulting from each deformation. The resulting data are combined with tide information to produce the combined tsunami and tide elevation - frequency relationship. Houston (1979) presents a description of tsunami modeling, elevation prediction, and structural damage. Houston (1980) and Crawford (1987) present examples of tsunami elevation predictions for the southern California coast and coast of Alaska from Kodiak Island to Ketchikan, respectively.

d. Ice.

(1) An understanding of ice properties and the effect of ice on the shore and marine structures is important in the Great Lakes, in coastal estuaries experiencing significant freshwater inflow which may transport ice, and along the northern ocean coasts. Ocean coasts may be subject to sea ice or pans and floes of freshwater ice originating from river discharges. Northern lakes, such as the Great Lakes, experience significant accumulations of ice during the winter. Sea ice, also known as saline or brackish ice, freezes and is most dense at -1.7 °C (29 °F), in contrast to freshwater ice at 0 °C (32 °F).

(2) A freshwater lake freezes in two stages defined by the water temperature. Cooler water at the surface generates a circulation pattern by sinking to the bottom, exposing warmer water, which successively cools. When the lake reaches a uniform 4 °C (39 °F), that is, the lake becomes isothermal, the lake is termed to have "turned over." As the surface water cools further, it becomes less dense than the water below it until it freezes. At this point, an ice sheet grows laterally (primary ice). In turbulent water, the primary ice cover will consist of a congealed frazil sheet and ball ice. When formed in rivers, upon reaching the outlet, severe ice jams may form which can completely fill the outlet cross section. The ice cover thickens (secondary ice) with continuing freezing temperatures, which may be at a rate of 1 in. per day (Wortley 1984). While the primary ice's axis of symmetry, called the c-axis or optic axis, is oriented perpendicular to the free surface, the secondary ice's c-axis is oriented horizontally. The formation of snow ice on the surface, which is randomly oriented, insulates the underlying ice, resulting in a reduction in growth rate of the secondary ice. Ice thicknesses in the Great Lakes generally are about 0.6 m (2 ft) to 0.9 m (3 ft). However, along the shore and near coastal structures, ice can build up considerably thicker due to ridge formation and spray. Ice ridges

or hummocks 3 to 5 times higher than the flat ice thickness are common and are not only confined to along the shore. Ice ridges ranging from 3 m (10 ft) to 4.5 m (15 ft) above the normal ice surface and extending 18 m (60 ft) below have been observed on Lake Erie. The time that ice clears at spring breakup is dependent upon heat gain from the atmosphere, local snow and ice conditions, and wind and water currents (Wortley 1984).

(3) Shoreline recession is not only caused by wave action, but also by downslope movement of material due to gravity (mass wasting). Exposure of permafrost lenses to seawater along the Arctic Alaskan coasts results in melting of these lenses. The resultant loss in strength may cause catastrophic failure of the bluff above it (U.S. Army Corps of Engineers 1994). In other areas, shore ice may protect the bluff from wave action. However, during the spring thaw, the saturated bluff will experience reduced cohesive strength, making it more vulnerable to mass wasting. This can be exacerbated by the presence of springs emerging along the bluff face, especially if the bluffs have been undercut by wave action.

(4) In addition to recognizing the effect of ice on shore processes and the functionality of a proposed project, calculation of ice loads may be required. The effect of ice on coastal projects is summarized in Chapter VI-3-5, with guidance on calculating ice loads in Chapter VI-6-6.b.

V-2-14. Foundation/Geotechnical Requirements

a. Every proposed coastal structure, nourishment project, or dredging operation requires knowledge of the underlying sea, lake, or river bottom materials. A geotechnical site investigation is required to assess the nature and extent of all sediments and their respective properties. The level of detail of the investigation is predicated on the study phase: reconnaissance, feasibility or detailed design, and the scope of the project. For example, only surface sediment data may be required for a beach fill, whereas a major coastal structure may require additional information on subsurface conditions. These investigations will entail researching available information from previous studies/projects in the area and obtaining new data.

b. The investigations seek to identify the elevation, thickness, and the physical, hydraulic, and mechanical properties of the soil, depth to bedrock and its properties, and groundwater level. Knowledge of the general soil group (clay, sand, etc.) allows one to assess the general characteristics of the soil. However, each soil group includes materials with a great variety of properties, and without a proper assessment, serious consequences can result (structural failure, inability to dredge the channel, etc.). Chapter VI-3-1 and Eckert and Callender (1987) present discussions on foundation/geotechnical requirements. Terzaghi and Peck (1967) also discuss the minimum requirements for adequate soil description and present a table of data required for soil identification.

V-2-15. Availability of Materials (Sand/Stone Resources)

The specification of materials for a proposed project requires the identification of the type, location, quantity, and quality of material available. Sand is the primary choice for beach nourishment projects, although gravel and cobble may be considered in certain situations. Rock is a popular construction material for coastal structures because of the range of sizes, durability, and availability.

a. Sand.

(1) Beach nourishment projects rely on the introduction of additional sand to the littoral zone to reduce a supply imbalance. Beach sand is generally a natural material preferably derived from a borrow area close to the project area. Location of a suitable borrow area requires geotechnical investigations of sediment size, type, and quantity in addition to environmental, hazard, and regulatory restrictions. Additional processing of sand (e.g., from an offshore site, the dredge may be fitted with additional screens) may be

necessary to obtain the desired product. Since sand may not be available in unlimited amounts, other alternatives may need to be considered. Manufactured sand (rock crushed to suitable gradation) was used at Maumee Bay State Park, OH, and crushed and tumbled recycled glass was deposited at Moonlight Beach, Encinitas, CA, for an emergency repair (Finkl 1996). At Fisher Island, FL, oolithic aragonite sand imported from the Bahamas was placed due to the local scarcity and environmental sensitivity of upland and offshore sand sources, the developer's interest in creating a unique and attractive beachfront, and the relatively modest size of the beach fill required (Bodge 1992). The political and engineering issues of placing this sand on other Florida beaches is discussed in Higgins (1995) and Beachler (1995), respectively.

(2) The identification of undesirable materials in the beach sand also may be required. For example, calcareous materials in the source materials have been found to react with available water sources (precipitation, groundwater, etc.) to precipitate fine-grained carbonate cement in pore spaces of the previously unconsolidated sand (Stransky and Greene 1989). This results in undesirable cementation of the beach nourishment material. This action leads to the formation of steep beach scarps, which are susceptible to undercutting and collapse, and inhibit the access of beachgoers to the shore.

b. Stone.

(1) Coastal structures may use a large quantity of stone of various sizes. The location, quantity, cost, suitability, and quality of the stone are important aspects, which must be investigated. A firm or agency that regularly requires large quantities of stone should maintain records on quarries within its geographic area of business. The change from using cut rectangular stone to rubble-mound shot stone for the armor layer in coastal structures in the past decades has resulted in savings in time and cost. However, the importance of stone quality has only been recently recognized. Appropriate quarry inspections and quality control by an experienced geologist or inspector are essential.

(2) Stone should be durable, sound, and free from detrimental cracks (both natural and quarry-induced), seams, and other defects that tend to increase deterioration from natural causes or which cause breakage during handling and placing (EM 1110-2-2302). The stone should also be resistant to localized weathering and disintegration from environmental effects. Inspection records of potential stone suppliers are important to help ensure these conditions are met and to determine the location, sizes, and types of stone available. Table V-2-3 lists data needed to perform a quarry inspection.

(3) During annual inspection of an existing project, the presence of stone cracking should be observed, as this will affect the maintenance schedule and structural integrity. Noting characteristics, location, and number of cracks will assist in assessing whether the stone will continue to deteriorate and at what rate. Cracks are generally classified as multiple penetrating/throughgoing (MP/T) cracks and mirror image cracks (MIC). MP/T cracks are commonly blast-induced fractures and characteristically form radial fractures, which run diagonal to the shot face. They are highly destructive to the stone's integrity and longevity. These sharp penetrating cracks are often initially minute and will not enlarge until exposed to the elements. Elimination/reduction of this type of fracturing is accomplished by proper shot design at the quarry. Mirror image cracks occur when a fracture splits the stone in half and the halves split repeatedly. These cracks generally do not form until the stone has been placed in the project. MRC are generally jagged and the result of the weathering of geologic beds and/or stress relief. Reasons for MIC (Marcus 1996) are:

Table V-2-3
Quarry Inspection Checklist

Item	Comment
SOURCE INVESTIGATION	
General	Purpose of inspection, date of inspection, personnel attending.
Location	Source name, address, contacts, geographic coordinates, descriptive directions of source location.
Production/Transportation	Materials produced, complete description of lift/face development, plant equipment used for production operations, transportation modes, operating season, additional materials, sources interested in producing, summary assessment.
Geology	Stratigraphy, lithology, structure, groundwater, summary assessment. Photographs are extremely useful in documenting the geology.
Blasting Operations	Blast design (description, blast design factors, blast design relationships, analysis), blasting effects (description, fragmentation, development of radial fracturing, transverse fracturing, cratering, back break and throw), summary assessment.
Material Sampling	Number, size, location within quarry samples where taken, photographs of samples.
Summary Assessment	Summary assessment of source, quarry personnel, and quality control.
LABORATORY INVESTIGATIONS / TESTING	
General	Purpose of testing (quality, durability).
Testing Program	Petrographic examination, abrasion resistance, accelerated weathering tests (wet-dry, freeze-thaw), resistance to salt crystallization.
Testing by Others	Report/evaluate laboratory testing by others.
Summary Assessment	From laboratory testing, make assessment of suitability of material for the use intended.
SERVICE RECORD INVESTIGATIONS	
General	This investigation documents the condition of stone used on other projects. Note changes in personnel and operations which may affect evaluation of service records.
Case Histories	Project name, location, description, material types, material sources (quarry , lift, etc.), exposure conditions, dates of placement, evaluations.
Summary Assessment	Assessment of how well the stone is holding up and if deteriorating, the cause should be determined.
SOURCE EVALUATION	
General	Indicate whether quarry is now a listed source for particular material.
Source Summary Assessment	List areas/lifts within quarry which are suitable for particular products.
Conclusions of Investigating Geologist	List evaluations of the geologist performing past/present investigations.
Review/Determination of Geologist	The investigating geologist makes an overall determination of the quarry, quality control, and suitability of the stone for the intended use.

(a) Differences in thermal expansion behavior of the component crystalline minerals (unavoidable).

(b) Freeze-thaw expansion and contraction of interstitial pore water (avoidable by stone curing and eliminating winter quarrying in northern locations).

(c) Wet-dry expansion and contraction of interstitial clays and clay mineral (mostly avoidable).

(d) Stress relief (slow-term stress release).

(4) The reader is directed to Marcus (1996), EM 1110-2-2302, and Construction Industry Research and Information Association (1991). Figures V-5-12 and V-2-13 are photographs of the progressive deterioration (after 3 to 4 years and after a maximum of 5 years, respectively) of 80- to 178-kN (9- to 20-ton) armor stone (dolomite) in the lacustrine environment (Lake Erie).

Figure V-2-12. Cracked dolomitic limestone - Cleveland East breakwater, Ohio, 1989 (stone is dolomitic limestone)

V-2-16. Accessibility

a. Access to the project area is required before, during, and after construction. The total project area encompasses not only the geographic limit of the actual project footprint but also extends a certain distance away due to impacts to the littoral zone. Access requirements before, during, and after construction may be very different. Prior to construction, temporary rights of entry may only be required to survey the site. Complete lands, easements, and rights of way will be required during construction. After project completion, rights of entry may only be necessary for project monitoring and inspection, but similar requirements obtained during construction may be needed for project maintenance.

Figure V-2-13. Cracked stone - - Cleveland East breakwater, Ohio, 1990. Note continuing degradation compared to 1989 (stone is dolomitic limestone)

b. Access to the site may be by land, water, or both, and may be over public or privately owned land. Individual topographic and hydrographic conditions will dictate whether the project may be constructed by water-based and/or land-based equipment. The designer will need to assess the anticipated means of construction and acquire the necessary real estate for access. Locations with difficult access can significantly increase the cost of a project. In these instances, a change in the project design or scope may be warranted.

c. The access should be designed to allow the safe and efficient movement of equipment, materials, and personnel. Access and haul roads should be of sufficient width and grade to safely accommodate large construction vehicles. Grades should be as flat as practical with the maximum allowable grade of 10 percent (EM 385-1-1). A traffic control plan must be developed. All marine work must be accomplished with certified and inspected plant and equipment. Mooring lines and cables must be clearly marked and the vessels must follow all navigation rules applicable to the waters on which the vessels will be operated. Plans to remove and secure plant and evacuate personnel to safe haven during hurricanes, storms, or floods must be considered. Safety and health requirements concerning activities and operations are discussed in EM 385-1-1.

d. Easement requirements may be temporary or permanent. Easements at a project site generally consist of temporary and permanent road easements, temporary work area easements, and permanent easements. A road easement grants possession of the land for location, construction, operation, maintenance, alteration and replacement of a road and appurtenances; together with the right to trim, cut, fell and remove therefrom all trees, underbrush, obstructions and other vegetation, structures, or obstacles within the limits of the right-of-way. A temporary work area easement grants the possession of the land as a work area which includes the right to move, store, and remove equipment and supplies, erect and remove temporary structures on the land and to perform any other work necessary and incident to the construction of the project. It may also include the right to trim, cut, fell, and remove all trees, underbrush, obstructions and other

vegetation, structures, or obstacles within the limits of the right-of-way. A permanent easement is a perpetual and assignable right and easement to construct, maintain, repair, operate, patrol, and replace the project, including all appurtenances. In addition to providing the rights of entry and access to the site, it will be necessary to provide and maintain adequate utilities and install and maintain necessary connections. All necessary arrangements with local Government officials or owners must be made for use of public and private roads to the site. Recognition that other construction projects may be occurring simultaneously is essential to minimize interference and work disruptions.

e. In granting access to the site, certain restrictions and requirements will need to be identified to control environmental pollution and damage. An environmental protection plan must be created which identifies methods and procedures for environmental protection, necessary permits for waste disposal, plan of restoration upon project completion, environmental monitoring plans, traffic control plan, surface and groundwater protection methods, list of fish and wildlife which require special attention, and spill response plan. The protection of environmental resources may encompass a wide range of activities, such as:

(1) Protection of land resources and landscape.

(2) Reduction of exposure on unprotected erodible soils.

(3) Temporary protection of disturbed areas.

(4) Erosion and sedimentation control devices.

(5) Control of ground vibration.

(6) Disposal of waste materials and removal of debris.

(7) Preservation of historical, archaeological, and cultural resources.

(8) Protection of water resources.

(9) Protection of fish and wildlife resources.

(10) Protection of air resources.

(11) Protection from sound intrusions.

f. The above list summarizes of types of protection to be considered prior to granting access to the site for the construction of a project. The list is not all-inclusive and needs to be tailored to the particular project site. Certain restrictions may apply only during certain times of the year, certain days, or certain times of day.

V-2-17. Monitoring

a. Collecting data (monitoring) of coastal projects will assist in proper design of a project, and improve design procedures, construction methods, operations, and maintenance. Comparison with historic information will aid in understanding processes and changes at the site of interest. Monitoring may be classified by its purpose; operational or research monitoring (Weggel 1995). *Operational monitoring* is done to obtain data for the design, operation, and maintenance of a project. *Research monitoring* is performed to assess the performance of a project in comparison with its predicted performance or to assist in broadening the understanding of physical processes.

b. In general, there are three types of monitoring: physical processes, biological, and economic (Weggel 1995). Physical process monitoring consists of gathering data on the physical mechanisms, forces, and littoral zone responses that are characteristic of the project. Biological monitoring entails accumulating data on living organisms that may be affected by the project. Economic monitoring involves collecting information on the monetary impact of the project.

c. Data collection needs to be accomplished before, during, and after construction. Data collected prior to project construction establishes the baseline data. Data may need to be updated during the design phase. Some data such as hydrographic surveys need to be updated during the plans and specifications phase in order to have the most current information available prior to bidding the project. Information may be required such as check surveys or environmental monitoring of threatened or endangered species during project construction. Post-construction monitoring may be operational or research-oriented.

d. The success of a monitoring program depends upon creation of an extensive and implementable plan. In developing the plan, the processes and data which most affect the project should be identified. The relative importance of each element will have to be assigned with only the most pertinent selected based upon cost limitations. To be effective, monitoring should occur when changes are likely to happen and at sufficient intervals to properly assess changes. Timing of the monitoring should account for seasonal changes in order to allow differentiation from a project-induced change. Monitoring frequency also should be variable, with more data being gathered immediately after the project is in place. As project effects diminish, frequency can be reduced. It is important to recognize that the most effective monitoring plan is one that is fluid; that is, the type, amount, and frequency of data are adjusted as collected data are analyzed. Data that were important initially may be superseded by other information needs which are more critical because it is impossible to anticipate all project effects. A partial list of measurable physical properties is presented in Table V-2-4. For further information on project monitoring, the reader is directed to Weggel (1995), Morang, Larson, and Gorman (1997a, 1997b), Larson, Morang, and Gorman (1997), Gorman, Morang, and Larson (1998), and EM 1110-2-1810.

V-2-18. Data Needs and Sources

a. The intent of this chapter has been to introduce the many factors that a coastal manager or engineer should consider, measure, or collect at the beginning of a new coastal project. At the initiation of a project, it is imperative that one fully understand the problem. While this may seem obvious, one cannot assume that the request for a solution to a coastal "problem" is valid or accurately stated. Those soliciting a solution may not perceive the problem objectively due to political/personal motivations, may have an inaccurate understanding of physical processes, or may have inadvertently been the cause of the problem. It should be considered mandatory to meet with those involved and to visit the site in order to gain an appreciation of the scope of the problem and to observe the scale and relationships of the various physical/geologic features.

b. Having gained an understanding of the problem, necessary data should be listed. Table V-2-5 presents a list of data needs and sources. The problem to be confronted may entail not only balancing existing data and the need to gather more with available monetary resources, but also what to do when the project needs to be built with minimal data. The latter situation will require a more imaginative approach to assess the basic governing processes of the region. Narrative and verbal sources of information will be very helpful. These may include newspaper reports, diaries, local historians, fishermen, marina operators, harbor masters, and local residents. Long-time residents who are especially familiar with the area may give a description of

Table V-2-4
Coastal Project Monitoring Matrix

MEASURABLE PROPERTIES	Project Type			
	BEACHES/SHORES **(Dunes, groins, breakwaters, sand bypass systems, submerged sills, borrow areas)**	***JETTIES*** **(Disposal areas, levees, closure stations, seawalls, revetments, bulkheads)**	***BREAKWATERS*** **(Piers, wharves, moles, berths, docks)**	***DREDGING*** **(Inlets, channels, marinas, outfalls)**
Beach profiles	■	■	■	
Bathymetry	■	■	■	■
Waves	■	■	■	■
Tide height	■	■	■	■
Tidal currents		■		■
Tidal prism		■		
Surge	■	■	■	■
Longshore currents	■	■		
Sediment size	■	■		■
Winds	■	■	■	■
Temperatures	■	■	■	■
Salinity		■		■
Ice coverage	■	■		
Structural surveys	■	■	■	

Note: Shaded block indicates property to be monitored. Nonshaded block indicates property usually not monitored except in unusual circumstances.

historical positions of the shore, past structures which have since deteriorated, and major storms. It is imperative that the gathered information be cross-checked with other sources to assess its validity, recognizing that proclamations with numerical statements made without actual measurements should be treated with skepticism. For example, statements such as, "The waves were 12 m (40 ft) high" or "I always had a beach at least 61 m (200 ft) wide in front of my house" should be treated with suspicion. The statement needs to be substantiated or modified by further questioning and through consideration of when the event occurred. While visual wave height measurements are generally difficult to make due to the lack of other physical objects offshore, the resulting runup may give a clue. A verbal account of a large storm(s) will narrow the time frame to search through old newspapers. The type, quantity and time of year various fish are caught will give clues to the aquatic diversity. Old town maps and property deeds will be indications of the historic shoreline/bluff position. Diaries of deceased lighthouse keepers and ship captains may give accounts of the conditions (direction and duration) and date of storms.

c. In addition to verbal and written narrations, a geologic interpretation of the present condition will assist in assessing the past or future trends. Abandoned beach lines, sea stacks, and old shore structures/foundations will suggest the position of past shorelines. Old piers and jetties may indicate the alongshore direction of the migration of an inlet. Stratigraphic information may suggest a change in depositional/erosional patterns. For instance, peat and organic deposits may indicate the presence of a barrier island in the past. The size, amount, and distribution of shoals can give clues to inlet processes. Sedimentological trends such as a change in size of offshore material may explain the presence of headlands or variations in erosion rates. The presence of a fillet at a man-made or natural protruding structure/feature will indicate the littoral transport direction and mean incident wave direction. The shape of the shoreline between headlands also will give an indication of the average incident wave direction.

Table V-2-5
Data Needs and Sources

Data Needed	Best Source(s)	Alternate Sources
Site map/real estate (Needed to locate structures, land features, utilities, roads and property boundaries.)	Recent survey	Town maps USGS quad maps Atlases Local utility companies Digitize aerial photographs Sketch of site with proposed structures located by existing features
Site topography & bathymetry (Land and underwater contours needed to transform waves to site, determine dredge and beach fill quantities, structure lengths.)	Recent USACE high-density acoustic surveys, land surveys, or SHOALS hydrographic LIDAR surveys	NOAA charts USGS quad maps Contractor surveys Emery method Visual estimation of elevations and slopes
Directional wave statistics (height, period & direction) (Needed for estimation of incident wave for structure design, time series for sediment transport evaluation, shoreline response and beach fill design, channel design (vessel effects))	Directional wave gauge deployed near site	Deepwater wave gauge with waves refracted to coast WIS hindcast Wave hindcast using wind statistics Wave hindcast using design wind
Water level • **Tidal** • **Storm setup** (Needed for incident wave computations, flood evaluations, structure toe depths)	NOAA water level gauge near site	Interpolation between gauges to site Peak stage gauge Highwater marks Numerical models
Currents • **Tidal** • **Longshore** (Needed for sediment transport evaluations, dredge disposal fate, scour potential)	Directional current meter	Nondirectional current meter Measurements using drogues/floats Seabed drifters Numerical models
Sediment characteristics • **Littoral zone (a)** • **Subsurface (b)** (Needed for sediment transport analysis, beach fill evaluation, structure foundation design)	Extensive surface samples (a) Extensive boring program (b)	Geophysical subsurface investigations (a&b) Subsurface probe to refusal (b) Regional geologic maps (b) Visual comparison of littoral sediments using sediment card (a) Interpolation between known information (a&b)
Historic shoreline positions (Needed for evaluations of natural shoreline change, effects of human activity, erosion rates, regulatory setbacks)	USACE project maps Shoreline studies from universities and state studies	Digitize from aerial photographs Historic NOAA charts Extrapolate from topographic surveys Historic town property maps and deeds Estimate from ruined structures and verbal/written accounts
Sediment budget (Needed for determination of natural sediment movement; existing and potential effects of human activity: beach fill amounts, channel dredging estimates, bypassing quantities around structures)	Direct measurement using sediment traps in conjunction with estimation from quantity of trapped material at protruding features and sediment supply from bluff & shore erosion	Numerical estimates using longshore drift equations and period of record wave hindcast Budgets in engineering reports, published literature

(Continued)

Table V-2-5 (Concluded)

Data Needed	Best Source(s)	Alternate Sources
Environmental data (Needed for evaluation of natural and existing environment, and the potential effects of human activity on flora, fauna, and water quality)	Habitat evaluation procedures	Benthic resource assessment techniques U.S. Fish and Wildlife Service, USACE and State agency reports University studies National & local environmental agencies (Audubon Soc., Sierra Club, Nature Conservancy, etc.) Sportsman's Clubs
Historic bathymetry (Needed for evaluation of shoal growth, project effect on shore, and inlet migration)	USACE condition surveys NOAA charts in digital form from National Geophysical Data Center	Historic U.S. Coast and Geodetic Survey charts Contractor surveys
Sand/stone resources • **Availability (a)** • **Quality (b)** (Needed for confirmation of size, location, and quantity of sand or stone material for project as available product can dictate design. Use of inferior quality product will result in service life reduction and possibly failure)	USACE inventories of quarries/sand deposits (a) Service records (b)	State inventories of quarries/sand deposits (a) Geotechnical search for sand deposits (a) Laboratory testing (b)

V-2-19. References

EM 385-1-1
Safety and Health Requirements

EM 1110-2-1204
Environmental Engineering for Coastal Shore Protection

EM 1110-2-1810
Coastal Geology

EM 1110-2-2302
Construction with Large Stone

ER 1105-2-100
Planning Guidance Notebook

Barnett 1984
Barnett, T. P. 1984. "The Estimation of 'Global' Sea Level: A Problem of Uniqueness," *Journal of Geophysical Research*, Vol 89, No. C5, pp 7980-7988.

Beachler 1995
Beachler, K. E. 1995. "Bahamian Aragonite: Can it be used on Florida Beaches? Engineering Issues," *Proceedings of the 1995 National Conference on Beach Preservation Technology*, Florida Shore and Beach Preservation Association, Tallahassee, FL.

Bodge 1992
Bodge, K. R. 1992. "Beach Nourishment with Aragonite and Tuned Structures," *Coastal Engineering Practice '92*, ASCE, New York, NY.

Bruun 1995
Bruun, P. 1995. "The Development of Downdrift Erosion," *Journal of Coastal Research*, Vol 11, No. 4, pp 1242-1257.

Camfield 1980
Camfield, F. E. 1980. "Tsunami Engineering," Special Report No. 6, Coastal Engineering Research Center, U.S. Army Engineer Waterways Experiment Station, Vicksburg, MS.

CIRIA 1991
CIRIA. 1991. "Manual on the Use of Rock in Coastal and Shoreline Engineering," Construction Industry Research and Information Association Special Publication 83, (Also published as Centre for Civil Engineering Research and Codes Report 154), Gouda, The Netherlands, London, U.K.

Cox and Pararas-Carayannis 1969
Cox, D. C., and Pararas-Carayannis, G. 1969. Catalog of Tsunamis in Alaska, U.S. Department of Commerce, Environmental Services Administration, Coast and Geodetic Survey.

Crawford 1987
Crawford, P. L. 1987. "Tsunami Predictions for the Coast of Alaska, Kodiak Island to Ketchikan," Technical Report CERC-87-7, U.S. Army Engineer Waterways Experiment Station, Coastal Engineering Research Center, Vicksburg, MS.

Davidson-Arnott and Stewart 1987
Davidson-Arnott, R. G. D., and Stewart, C. J. 1987. "The Effects of Longshore Sand Waves on Dune Erosion and Accretion, Long Point, Ontario," *Proceedings, Canadian Coastal Conference*, Quebec City, National Research Council, Ottawa, pp. 131-144.

Dean 1991
Dean, R. G. 1991. "Equilibrium Beach Profiles: Characteristics and Applications," *Journal of Coastal Research,* Vol 7, No. 1, pp 53-84.

Department of the Navy 1976
U.S. Naval Weather Service Command. 1976. Summary of Synoptic Meteorological Observations, prepared by the National Climatic Data Center, Asheville, NC.

Eagleman 1983
Eagle, J. R. 1983. *Severe and Unusual Weather*, VanNostrand Reinhold Company, New York, NY.

Eckert and Callender 1987
Eckert, J., and Callender, G. 1987. "Geotechnical Engineering in the Coastal Zone," Instruction Report CERC-87-1, U.S. Army Engineer Waterways Experiment Station, Vicksburg, MS.

Emery and Aubrey 1991
Emery, K. O., and Aubrey, D. G. 1991. *Sea Levels, Land Levels and Tide Gauges*, Springer-Verlag, New York, NY.

Finkl 1996
Finkl, C. W. 1996. "Beach Fill from Recycled Glass: A New Technology for Mitigation of Localized 'Hot Spots' in Florida," Department of Geology, Florida Atlantic University, Boca Raton, FL.

Frihy 1992
Frihy, O. E. 1992. "Sea-Level Rise and Shoreline Retreat of the Nile Delta Promontories, Egypt," *Natural Hazards*, Vol 5, pp 65-81.

Gorman, Morang, and Larson 1998
Gorman, L. T., Morang, A., and Larson, R. L. 1998. "Monitoring the Coastal Environment; Part IV: Mapping, Shoreline Change, and Bathymetric Analysis," *Journal of Coastal Research,* Vol 14, No. 1, pp 61-92.

Hanson and Kraus 1989
Hanson, H., and Kraus, N. C. 1989. "GENESIS: Generalized Numerical Modeling System for Simulating Shoreline Change; Report 1, Technical Reference Manual," Technical Report CERC-89-19, U.S. Army Engineer Waterways Experiment Station, Vicksburg, MS.

Harris 1954
Harris, R. L. 1954. "Restudy of Test - Shore Nourishment by Offshore Deposition of Sand, Long Branch, New Jersey," TM-62, U.S. Army Corps of Engineers, Beach Erosion Board, Washington, DC.

Hicks 1978
Hicks, S. D. 1978. "An Average Geopotential Sea Level Series for the United States," *Journal of Geophysical Research*, Vol 83, No. C3, pp 1377-1379.

Higgins 1995
Higgins, S. H. 1995. "Bahamian Aragonite: Can it be used on Florida's Beaches? Political Issues," *Proceedings of the 1995 National Conference on Beach Preservation Technology, Florida Shore and Beach Preservation Association,* Tallahassee, FL.

Houston 1979
Houston, J. R. 1979. "State-of-the-Art for Assessing Earthquake Hazards in the United States: Tsunamis, Seiches, and Landslide-Induced Water Waves," Report 15, Miscellaneous Paper S-73-1, U.S. Army Engineer Waterways Experiment Station, Vicksburg, MS.

Houston 1980
Houston, J. R. 1980. "Type 19 Flood Insurance Study: Tsunami Predictions for Southern California," Technical Report HL-80-18, U.S. Army Engineer Waterways Experiment Station, Vicksburg, MS.

Houston 1996
Houston, J. R. 1996. "Simplified Dean's Method for Beach-Fill Design," *Journal of Waterway, Port, Coastal, and Ocean Engineering*, Vol 122, No. 3, pp. 143-146.

Larson and Kraus 1989
Larson, M., and Kraus, N. C. 1989. "SBEACH: Numerical Model for Simulating Storm-induced Beach Change; Report 1: Empirical Foundation and Model Development," Technical Report CERC-89-9, U.S. Army Engineer Waterways Experiment Station, Vicksburg, MS.

Larson, Morang, and Gorman 1997
Larson, R. L., Morang, A., and Gorman, L. T. 1997. "Monitoring the Coastal Environment; Part II: Sediment Sampling and Geotechnical Methods," *Journal of Coastal Research,* Vol 13, No. 2, pp 308-330.

Longuet-Higgins 1983
Longuet-Higgins, M. S. 1983. "Wave Set-up, Percolation and Underflow in the Surf Zone. *Proc. Roy. Soc.*, Ser A 390: pp 283-291.

Marcus 1996
Marcus, D. W. 1996. "Problems and Improvements of Armor Stone Quality for Coastal Structures," *Ohio River Division Laboratory Accelerated Weathering Workshop*, Cincinnati, OH.

Morang, Larson, and Gorman 1997a
Morang, A., Larson, R. L., and Gorman, L. T. 1997a. "Monitoring the Coastal Environment; Part I: Waves and Currents," *Journal of Coastal Research,* Vol 13, No. 1, pp 111-133.

Morang, Larson, and Gorman 1997b
Morang, A., Larson, R. L., and Gorman, L. T. 1997b. "Monitoring the Coastal Environment; Part III: Geophysical and Research Methods," *Journal of Coastal Research,* Vol 13, No. 4, pp 1964-1085.

Naqvi and Pullen 1982
Naqvi, S. M., and Pullen, E. J. 1982. "Effects of Beach Nourishment and Borrowing on Marine Organisms," Miscellaneous Report 82-14, Coastal Engineering Research Center, U.S. Army Engineer Waterways Experiment Station, Vicksburg, MS.

National Oceanic and Atmospheric Administration 1985
National Oceanic and Atmospheric Administration. 1985. "Chart of Water Levels of Lake Erie During Storm of December 2, 1985," Tides and Water Level Branch, Great Lakes Acquisition Unit.

National Research Council 1995
National Research Council. 1995. *Beach Nourishment and Protection*, National Academy Press, Washington, DC.

Odum, McIvor, and Smith 1982
Odum, W. E., McIvor, C. C., and Smith, T. J. III. 1982. "The Ecology of the Mangroves of South Florida: A Community Profile," FWS/OBS-81/24, U.S. Fish and Wildlife Service, Office of Biological Services, Washington, DC.

Pararas-Carayannis 1969
Pararas-Carayannis, G. 1969. "Catalog of Tsunamis in the Hawaiian Islands," Report WDCA-T 69-2, ESSA - Coast and Geodetic Survey, Boulder, CO.

Public Law 97-348 1982
Coastal Barrier Resources Act of 1982, (16 U.S.C. 3501 Public Law 97-348).

Resio and Vincent 1976
Resio, D. T., and Vincent, C. L. 1976. "Design Wave Information for the Great Lakes, Lake Erie, Report 1," Technical Report H-76-1, U.S. Army Engineer Waterways Experiment Station, Vicksburg, MS.

Sahagian and Holland 1991
Sahagian, D. L., and Holland, S. M. 1991. Eustatic Sea-Level Curve Based on a Stable Frame of Reference: Preliminary Results, *Geology*, Vol 19, pp 1208-1212.

Schwartz and Musialowski 1980
Schwartz, R. K., and Musialowski, F. R. 1980. "Transport of Dredged Sediment Placed in the Nearshore Zone - Currituck Sand-Bypass Study (Phase I)," Technical Paper No. 80-1, Coastal Engineering Research Center, U.S. Army Engineer Waterways Experiment Station, Vicksburg, MS.

Silvester and Hsu 1993
Silvester, R., and Hsu, J. R. C. 1993. *Coastal Stabilization: Innovative Concepts*, Prentice Hall, Inc., Englewood Cliffs, NJ.

State of Alaska 1994
State of Alaska. 1994. "Alaska Coastal Design Manual," Department of Transportation and Public Facilities.

State of Florida 1987
State of Florida. 1987. Section 161.142, Declaration of Public Policy Relating to Improved Navigation Inlets (as referenced in Bruun (1995)).

State of New York 1988
Coastal Erosion Management Regulations Statutory Authority: Environmental Conservation Law Article 34, 6 NYCRR Part 505, State of New York Department of Environmental Conservation, Albany, NY.

Stewart and Davidson-Arnott 1988
Stewart, C. J., and Davidson-Arnott, R. G. D. 1988. "Morphology, Formation and Migration of Longshore Sand Waves; Long Point, Lake Erie, Canada," *Marine Geology* 81, pp 63-77.

Stransky and Green 1989
Stransky, T. E., and Green, B. H. 1989. "Presque Isle Peninsula: A Case Study in Beach Cementation," *Bulletin of the Association of Engineering Geologists*, Vol. XXVI, No. 3, pp. 352-332.

Terzaghi and Peck 1967
Terzaghi, K., and Peck, R. B. 1967. *Soil Mechanics in Engineering Practice*, 2nd ed., John Wiley, New York.

U.S. Army Corps of Engineers 1992
Institute for Water Resources, U.S. Army Corps of Engineers. 1992. "Guidelines for Risk and Uncertainty Analysis in Water Resources Planning," Volumes 1 and 2, IWR Reports 92-R-1 and 92-R-2, Washington, DC.

U.S. Army Corps of Engineers 1994
U.S. Army Engineer Waterways Experiment Station and U.S. Army Engineer District, Anchorage. 1994. "Alaska Coastal Design Manual," prepared for the Alaska Department of Transportation and Public Facilities.

U.S. Army Engineer District, Detroit 1993
U.S. Army Engineer District, Detroit. 1993. "Design Water Level Determination on the Great Lakes," Detroit, MI.

U.S. Army Engineer District, Mobile 1978
U.S. Army Engineer District, Mobile. 1978. "Beach Erosion Control and Hurricane Protection for Mobile County Alabama (Including Dauphin Island)," Feasibility Report.

U.S. Fish and Wildlife Service 1980
U.S. Fish and Wildlife Service. 1980. "Habitat Evaluation Procedures (HEP)," U.S. Fish and Wildlife Service, Ecological Services Manual 102.

Verhagen 1989
Verhagen, H. J. 1989. "Sand Waves Along the Dutch Coast," *Coastal Engineering*, 13, pp 129-147, Elsevier Science Publishers, B. V., Amsterdam.

Waters 1939
Waters, C. H. 1939. "Equilibrium Slopes of Sea Beaches," unpublished M.S. thesis, University of California, Berkeley.

Weggel 1995
Weggel, J. R. 1995. "A Primer on Monitoring Beach Nourishment Projects," *Shore and Beach*, Vol 63, No. 3, Berkeley, CA.

Wortley 1984
Wortley, C. A. 1984. "Great Lakes Small-Craft Harbor and Structure Design for Ice Conditions: An Engineering Manual," University of Wisconsin Sea Grant Institute, WIS-SG-84-426, Madison, WI.

V-2-20. Acknowledgments

Authors of Chapter V-2, "Site Characterization:"

Michael C. Mohr, U.S. Army Engineer District, Buffalo, Buffalo, New York.

Reviewers:

Andrew Morang, Ph.D., Coastal and Hydraulics Laboratory (CHL), U.S. Army Engineer Research and Development Center (ERDC), Vicksburg, Mississippi.
Joan Pope, ERDC
H. Lee Butler, CHL (retired)

Table of Contents

Page

V-3-1. Introduction V-3-1
a. Major concerns for shore protection V-3-1
(1) Storm damage reduction V-3-1
(a) Coastal floodings V-3-1
(b) Wave damage V-3-1
(2) Coastal erosion mitigation V-3-1
(3) Ecosystem restoration V-3-3
b. Alternatives for shore protection V-3-3
(1) Overview V-3-3
(2) Armoring V-3-3
(3) Shoreline stabilization V-3-7
(4) Beach nourishment V-3-7
(5) Adaptation and retreat V-3-7
(6) Combinations and new technologies V-3-7
(7) Do nothing V-3-7
c. Design constraints V-3-7
(1) Scientific and engineering understanding of nature V-3-8
(a) New *Coastal Engineering Manual* V-3-8
(b) CP Module V-3-8
(c) EST methodology V-3-8
(2) Economics V-3-9
(a) Cost V-3-9
(b) Benefits V-3-10
(c) Benefit/cost ratios V-3-12
(d) Sea level rise V-3-12
(3) Environmental V-3-12
(a) Types of environmental concerns V-3-12
(b) Impact on natural sediment transport system V-3-13
(c) Mitigation V-3-13
(4) Institutional, political, legal V-3-14
(a) Institutional (policies and guidelines) V-3-14
(b) Political (social well-being) V-3-15
(c) Legal (laws) V-3-16
(5) Aesthetics V-3-18

V-3-2. Coastal Armoring Structures V-3-19
a. Types V-3-19
(1) Seawalls and dikes V-3-19
(2) Bulkheads V-3-19
(3) Revetments V-3-24
(4) Combinations and other types V-3-25
b. Functional design V-3-25

c. Interaction with adjacent beaches V-3-28
(1) Background V-3-28
(2) Literature review V-3-29
(a) Common concerns V-3-29
(b) Definitions V-3-32
(c) Frontal impacts V-3-32
(d) Impacts on laterally adjacent beach V-3-33
(3) Active volume in the cross-shore profile V-3-34
(4) Sand rights and mitigation V-3-34

V-3-3. Beach Stabilization Structures V-3-35
a. Naturally stable shorelines V-3-35
b. Minimum dry beach width V-3-35
c. Headland breakwaters V-3-37
(1) Background and definitions V-3-37
(2) Physical processes V-3-37
(3) Functional design V-3-37
(a) Parabolic bay shape V-3-39
(b) Minimum width for storm protection V-3-39
(4) Applications on Chesapeake Bay V-3-41
d. Nearshore breakwaters V-3-43
(1) Background and definitions V-3-43
(2) Physical processes V-3-45
(a) Normal morphological responses V-3-45
(b) Storm processes and response V-3-48
(3) Functional design V-3-48
(a) Salients or tombolos V-3-50
(b) Planform configuration V-3-55
(c) Other design factors V-3-56
(d) Minimum dry beach width, Y_{min} V-3-57
(4) Nontraditional designs V-3-57
e. Groins V-3-59
(1) Background and definitions V-3-59
(2) Literature review V-3-67
(3) Physical processes V-3-69
(a) Normal morphological response V-3-69
(b) Storm response V-3-69
(4) Functional design V-3-70
(a) Insight from numerical models V-3-70
(b) Groin profile V-3-72
(c) Permeability V-3-72
(d) Terminal groins V-3-73
(e) Groins system transitions V-3-74
(f) Order of construction V-3-74
(5) Nontraditional configurations V-3-74
(6) Basic rules for functional design of groins V-3-76
f. Reefs, sills, and wetlands V-3-78
(1) Background and definitions V-3-78
(2) Reefs V-3-78
(a) Natural types V-3-78

(b) Wave attenuation V-3-79
(c) Artificial reefs V-3-79
(3) Sills V-3-79
(a) Perched beach V-3-79
(b) Wetlands protection V-3-79
(4) Wetlands V-3-80

V-3-4. Nonstructural Alternatives V-3-80
a. Introduction V-3-80
b. Adaptation V-3-80
(1) Zoning and building codes V-3-80
(2) Setback limits V-3-82
c. Retreat V-3-82
(1) Cape Shoalwater, Washington V-3-82
(2) Baytown, Texas V-3-82
(3) Special cases V-3-84
(a) Brighton Beach Hotel, Coney Island, NY V-3-84
(b) Cape Hatteras Lighthouse, NC V-3-84
(4) Impact of sea level rise V-3-86

V-3-5. Combinations and New Technologies V-3-86
a. Combinations V-3-87
(1) Structural combinations V-3-87
(a) Beach stabilization structures and beach nourishment V-3-87
(b) Seawalls, revetments, and beach nourishment V-3-87
(c) Beach nourishment and rebuilt dune with buried seawall/revetment V-3-87
(2) Nonstructural and structural combinations V-3-87
b. New technologies V-3-87
(1) Introduction V-3-87
(2) Pre-cast, concrete units V-3-88
(3) Geotextile filled bags V-3-90
(4) Beach drains V-3-90
(5) Innovative technology demonstration program V-3-90

V-3-6. Do-Nothing V-3-92
a. Introduction V-3-92
b. Appropriate response V-3-92
c. After the flood V-3-92
d. Government programs available V-3-92
e. National coastal hazard mitigation plan V-3-93

V-3-7. References V-3-93

V-3-8. Definition of Symbols V-3-109

V-3-9. Acknowledgments V-3-110

List of Figures

Figure V-3-1. Oosterschelde storm surge barrier (courtesy Rijkswaterstaat, The Netherlands) V-3-2

Figure V-3-2. Alternatives for shore protection V-3-6

Figure V-3-3. Shift from hard (armored walls, groins, etc.) to soft (beach nourishment) alternatives by the Corps of Engineers (from Hillyer 1996) V-3-9

Figure V-3-4. Different types of seawalls and dikes (from Pilarczyk 1990) V-3-20

Figure V-3-5. Galveston, Texas seawall V-3-21

Figure V-3-6. Virginia Beach seawall/boardwalk V-3-23

Figure V-3-7. Typical bulkhead types V-3-24

Figure V-3-8. Summary of revetment alternatives V-3-26

Figure V-3-9. Time scales for shoreline movements V-3-29

Figure V-3-10. Naturally stable shorelines with beach width dependent on stormwave energy V-3-36

Figure V-3-11. Natural and artificially stable shorelines with minimum dry beach width V-3-38

Figure V-3-12. Definition sketch of artificial headland system and beach planform (from EM 1110-2-1617) V-3-39

Figure V-3-13. Definition sketch of parabolic model for planform shape V-3-40

Figure V-3-14. Definition sketch, headland breakwaters V-3-41

Figure V-3-15. Headland breakwater projects on the James River estuary, Chesapeake Bay (from Hardaway and Gunn 1999) V-3-42

Figure V-3-16. Headland breakwater project on the Chesapeake Bay (from Hardaway and Gunn 1999) V-3-44

Figure V-3-17. Types of shoreline changes associated with single and multiple breakwater (from EM 1110-2-1617) V-3-45

Figure V-3-18. Santa Monica, CA breakwater and salient. Littoral drift from bottom to top (circa 1967) (from Chasten et al. 1993) V-3-46

Figure V-3-19. Breakwater construction and salients, Presque Isle, Pennsylvania (from Mohr 1994) V-3-47

Figure V-3-20. Definition schematic for nearshore breakwaters V-3-48

Figure V-3-21. Definitions of key variables for nearshore breakwater V-3-51

Figure V-3-22. Dimensionless plot of nearshore breakwater projects For Y/d_s versus L_s/L_g (from Pope and Dean 1986) V-3-55

Figure V-3-23. General shoreline adjustment for direction of net longshore transport V-3-60

Figure V-3-24. Rubble-mound groin, Westhampton Beach, New York V-3-62

Figure V-3-25. Timber sheet-pile groin, NASA Space Flight Center, Wallops Island, Virginia . . . V-3-63

Figure V-3-26. Timber-steel sheet-pile groin, New Jersey V-3-64

Figure V-3-27. Prestressed-concrete sheet-pile groin, Dohney Beach State Park, California V-3-65

Figure V-3-28. Cellular-steel sheet-pile groin, Presque Isle, Pennsylvania V-3-66

Figure V-3-29. Definition sketch of key variables in the functioning of groins V-3-71

Figure V-3-30. Westhampton Beach, New York, groin field and renourished beach V-3-73

Figure V-3-31. Typical groin profile with sloping section V-3-74

Figure V-3-32. Transition from groin field to natural beach V-3-75

Figure V-3-33. Possible planform shapes for groins V-3-75

Figure V-3-34. Innovation is groin design to enhance sediment through-passing and smooth the shoreline variation in the groin field V-3-77

Figure V-3-35. Sills and breakwaters V-3-81

Figure V-3-36. Rebuilt dune with buried seawall V-3-88

List of Tables

Table V-3-1. Classes of Management and Engineering Response for Shore Protection (Pope 1997) V-3-3

Table V-3-2. Alternatives for Coastal Hazard Mitigation V-3-4

Table V-3-3. Assessment of Commonly Expressed Concerns Related to Coastal Armoring (Dean 1987) V-3-31

Table V-3-4. Summary of U.S. Breakwater Projects (from Chasten et al. 1993) V-3-49

Table V-3-5. Empirical Relationships for Nearshore Breakwater Design (from Chasten et al. 1993) V-3-52

Table V-3-6. Conditions for Shoreline Response Behind Nearshore Breakwaters (from Chasten et al. 1993) V-3-54

Table V-3-7. Main Parameter Governing Beach Response and Bypassing at Groins (from Kraus et al. 1994) V-3-67

Table V-3-8. Functional Properties Attributed to Groins and their Critical Evaluation (Kraus et al. 1994) V-3-68

Table V-3-9. Process-Based Factors Controlling Groins V-3-72

Table V-3-10. Types of Groins-Section Views V-3-75

Table V-3-11. Cape Hatteras, North Carolina, Shore Protection History V-3-85

Chapter V-3
Shore Protection Projects

V-3-1. Introduction

The main purpose of this chapter is to summarize alternatives and their functional design for shore protection. Coastal defense and stabilization works are used to retain or rebuild natural systems (cliffs, dunes, wetlands, and beaches) or to protect man's artifacts (buildings, infrastructure, etc.) landward of the shoreline. A secondary purpose is to review the many constraints that will influence the final design.

a. Major concerns for shore protection

(1) Storm damage reduction. Coastal storms generally cause damage by two mechanisms.

(a) Coastal floodings. On the Atlantic Ocean and Gulf of Mexico coasts, tropical storms (hurricanes) produce elevated water levels, (storm surge) that inundate and damage coastal property. Extra tropical storms (northeasters) along the eastern seaboard and other coasts also create high water and flood damage. Damage from coastal flooding is arguably greater than that due to high winds on the world's coasts.

- Following the devastating flood in 1953, the Dutch people began the Delta Project to raise the dikes and construct barriers (dams) across the estuarine openings to the North Sea. The last component was the Oosterschelde (Eastern Scheldt) storm surge barrier as displayed in an aerial view in Figure V-3-1a and a photograph of the movable gates in Figure V-3-1b. It is one of the largest coastal engineering projects ever completed in the world and a major engineering achievement.

- Inland flooding also disrupts traffic, business, medical services, and normal life to produce secondary, economic and social impacts.

(b) Wave damage. Elevated water levels also bring higher wave energy inland to damage upland development. Damage is a nonlinear function of wave height. On the West Coast, the elevated ocean surface of El Nino events coupled with high storm waves causes damage to marinas, piers, and coastal infrastructure.

(2) Coastal erosion mitigation. The second major concern is coastal erosion. Storms create short-term erosional events. Natural recovery after the storm and seasonal fluctuations may not be in balance to produce long-term erosion. Shore protection projects moderate the long-term average erosion rate of shoreline change from natural or manmade causes. Reduced erosion means a wider sediment buffer zone between the land and the sea. And consequently, erosion mitigation translates into storm damage reduction from flooding and wave attack. How natural shorelines remain stable and mitigate upland damage is explicitly reviewed in Part V-3-3-a. Use of the terms flood control and erosion control are discouraged. Complete control of coastal flooding and erosion is a myth that gives a false sense of security to the client, the general public, and the media. Man cannot control nature. There is always the chance for a more powerful storm than the level of shore protection provided within the design constraints. A reduction in potential levels of flooding and erosion, i.e., mitigation means storm damage reduction benefits and the need for a risk-based, design philosophy, as discussed herein.

a. Aerial view

b. Moveable gates

Figure V-3-1. Oosterschelde storm surge barrier (courtesy Rijkswaterstaat, The Netherlands)

(3) Ecosystem restoration. A new area of concern is the restoration of lost environmental resources such as wetlands, reefs, nesting areas, etc. In 1990, the U.S. Army Corps of Engineers was directed to also consider ecosystem restoration where a Federal project has contributed to ecosystem degradation. For this chapter, Corps civil works project objectives and special design constraints (economic, environmental, institutional, etc.) have been omitted. They have all been brought together in Part V-7. Where appropriate, differences between the Corps' design approach and a general design approach are discussed here.

b. Alternatives for shore protection.

(1) Overview. Figure V-3-2 (adapted from Gilbert and Vellinga 1990) schematically displays five alternative ways to mitigate the damage of coastal storms, namely, accommodation, protection, beach nourishment, retreat and of course, the do-nothing alternative. Civilization's artifacts at the coast are here represented by the lighthouse at a fixed reference line. Storm surge and storm erosion reduce the distance between the reference line and the sea. Sea level rise and historic, coastal erosion also reduce the distance, but at slower time scales. Beach nourishment accomplishes the same objective as the retreat option (i.e., increase the distance to the sea).

(a) Pope (1997) has a similar classification system summarized in Table V-3-1.

Table V-3-1 Classes of Management and Engineering Response for Shore Protection (Pope 1997)

Type	Common Phrase
1) Armoring	Draw the line
2) Moderation	Slow down the erosion rate
3) Restoration	Fill up the beach
4) Abstention	Do nothing
5) Adaptation	Live with it

(b) The protection category in Figure V-3-2 is divided into armoring (seawalls, bulkheads, etc.) for flooding and moderation (groins, breakwaters, etc.) for erosion mitigation and shoreline stabilization. Beach nourishment or restoration is sometimes called the soft alternative to the armored or hard alternative for shore protection. Figure V-3-3 displays the shift from hard to soft, beach nourishment projects over the past 50 years by the Corps of Engineers (from Hillyer 1996).

(c) For design, consider the following six types of alternatives, namely: armoring, beach stabilization (moderation) structures, beach nourishment, adaptation and retreat, combinations (and new technologies) and the with-no-project (abstention) alternative. Table V-3-2 summarizes these alternatives for coastal hazard mitigation including the sections where full discussions are presented.

(2) Armoring. Seawalls, bulkheads, and protective revetments for cliffs and dikes are the traditional types of armored shorelines. The cost of armoring is justified when flooding and wave damage in low areas threaten substantial human investment. On historic, eroding coasts, it must be expected that erosion will continue to diminish the width of the buffer strip between armored shoreline and the sea. If a recreational beach is present, periodic beach nourishment must be anticipated. Part V-3-2 gives functional design details

Table V-3-2
Alternatives for Coastal Hazard Mitigation

Approach	**Changes to the Natural, Physical System**							
Class	**Armoring Structures**			**Shoreline Stabilization Structures and Facilities**				
Type	**Seawall**	**Bulkhead**	**Dike/Revetment**	**Breakwaters**	**Groins**	**Sills**	**Vegetation**	**Groundwater Drainage**
Geometry (configurations) or location	• Vertical • Curved • Gravity	• Crib • Stepped/Terraced • Cantilevered • Tie-Backed	• Sloped	• Headland • Detached • Single • System • Submerged (reef-type)	• Normal • Angled • Single • System (field) • Notched • Permeable • Adjustable • Shaped (T or L)	• Shoreline • Submerged • Perched beach • Intertidal		• Beachdrain • Bluff dewatering • Interior drainage
Materials of construction	• Concrete • Rock	• Sheet-pile - steel - timber -concrete - aluminum	• Earth • Rock revetment • Geotextiles (bags) • Gabions	• Rock • Precast concrete units • Sheet-pile types - steel - concrete - timber - etc. • Geotextiles bags			• wetland • Submerged Aquatic Vegetation • Mangrove	• System of pipes and pumps with sumps
Discussion in found sections	**Part V-3-2**			**Part V-3-3**				
	V-3-2-a(1)	V-3-2-a(2)	V-3-2-a(1)	V-3-3-c V-3-3-d	V-3-3-e	V-3-3-f		V-3-5-b

(Continued)

Table V-3-2 (Concluded)

Changes to the Natural Physical System (continued)		**Changes to Man's System**			**Changes in Both**		**No Change**
Beach Restoration		**Adaptation and Accomodation**			**Combinations**		**Do Nothing**
Beach Nourishment	**Sand Passing**	**Flood Proofing**	**Zoning**	**Retreat**	**Structural and Restoration**	**Structural and Restoration and Adaptation**	
• Subaerial • Dune • Feeder • Profile • Underwater berms	• Bypassing • Bankpassing	• Elevated structures • Raise grade • Sandbags • Flow diversion	• Setbacks • Land use restrictions • Public lands (Institutional)	• Individuals • Communities • Infrastructure • Move structures	• Any combination of 1, 2, or 3 alternatives	• Any combination of all alternatives except retreat	Let nature take its course
• Borrow sites - offshore - land • Dredged material • Artificially made (crushed rock)	• Littoral traps • Smooth out hot-spots • Downdrift material returned updrift	• Single-family homes on timber piles					
Part V-4		V-3-4 V-3-4-b		V-3-4-c	V-3-5		V-3-6

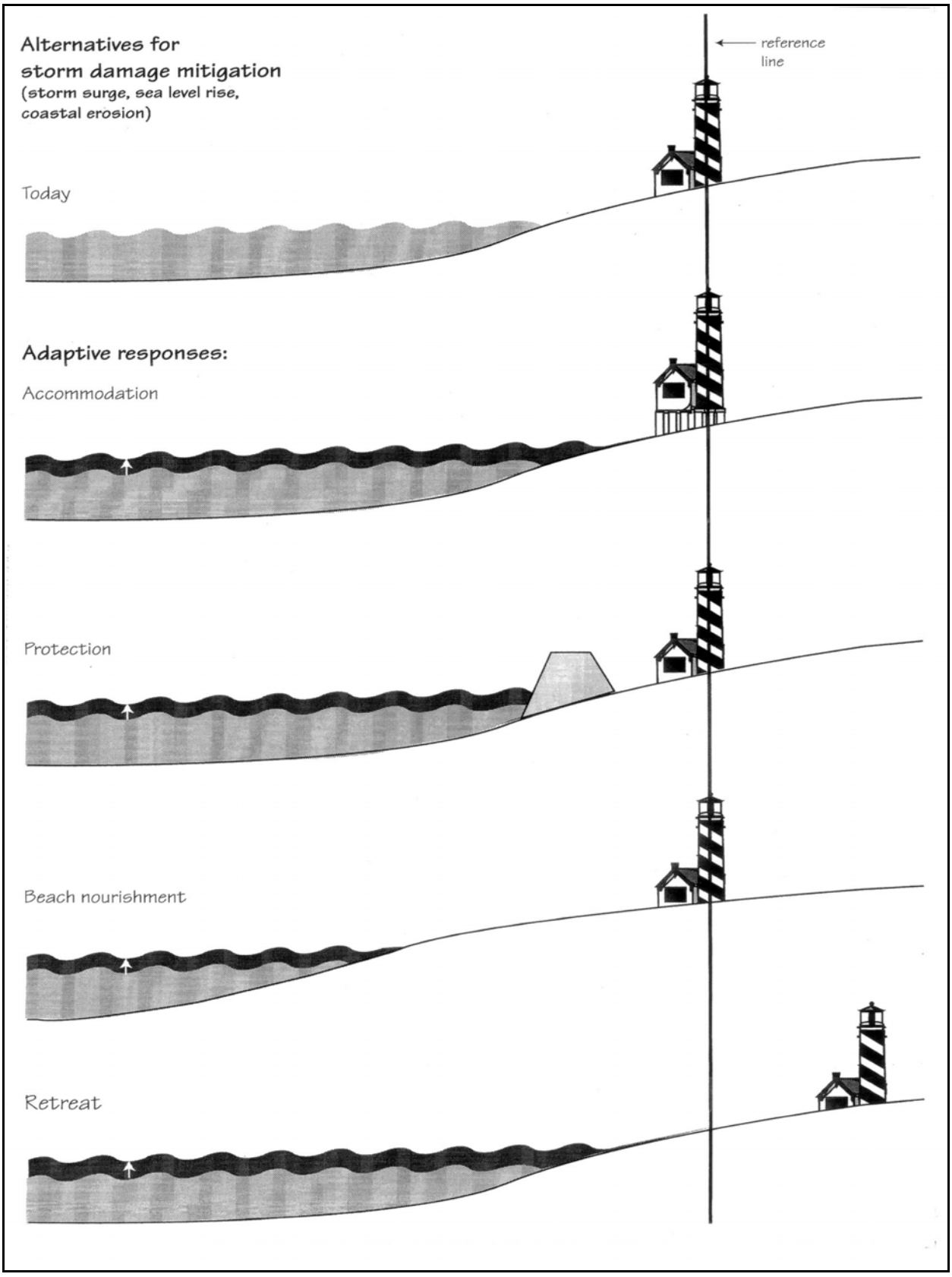

Figure V-3-2. Alternatives for shore protection

and summarizes knowledge on the interaction of armored shorelines and adjacent beaches. See also Engineer Manual 1110-2-1614, "Design of Coastal Revetments, Seawalls, and Bulkheads."

(3) Shoreline stabilization. Headland and nearshore breakwaters, groins, sills and reefs, and wetlands all moderate the coastal sediment transport processes to reduce the local erosion rate. These structures should be considered where chronic erosion is a problem due to the diminished sediment supply. They are often combined with beach nourishment to reduce downdrift impacts. Their purpose is to slow the loss of placed sand, not to trap sand from the littoral system and create more problems elsewhere. In many locations, their improper functional design, or construction without adding extra material, has produced adverse environmental impacts by starving the supply of sand to downdrift beaches. Their proper design is one of the great challenges of coastal engineering, and functional design aspects are found in Part V-3-3.

(4) Beach nourishment. Loose sediment material can be placed on the subaerial beach, as underwater mounds, across the subaqueous profile, or as dunes to rebuild the dunes. The soft alternative solution for shore protection is now the common alternative selected for a variety of reasons (constraints). Because of its importance, a separate chapter, Part V-4 contains all the details for design.

(5) Adaptation and retreat. Elevating structures, flood proofing, zoning restrictions, storm warning and evacuation planning are some of the types of coastal adaptation methods. Further details are in Part V-3-4-b. Retreat is permanent evacuation or abandonment of coastal infrastructure, and for communities subject to high erosion rates and flooding damages, this is always a possible alternative. Total costs and constraints of this alternative must include the environmental impact on the new site to where "retreat" takes place. In contrast to the engineering, decision-making process to determine the best alternative considering all the design constraints for each site, some advocate retreat as the only solution. Further discussion is in section Part V-3-4-c.

(6) Combinations and new technologies. In many locations, elevated structures combined with some type of armoring or shoreline stabilization structure together with beach nourishment are employed for shore protection. Nontraditional technologies (e.g., beach drains, geotextile bags, artificial breakwater structures, wetlands, etc.) are also being investigated in field experiments. Part V-3-5 gives more details.

(7) Do nothing. Finally, the option to allow continued erosion and storm damage with the expected, annual costs for this choice should be determined. The without project condition provides the basis for measuring the effectiveness to reduce the expected damages of each proposed alternative. Further details for estimating damage costs are in Part V-3-1-c. Part V-3-6 presents more general information on this option. See also Part VI-2-1 for more details regarding various subtypes of the armoring, shoreline stabilization, and beach nourishment alternatives. Each alternative must be considered under a wide variety of design constraints.

c. Design constraints.

One good definition of engineering is "design under constraint." Engineering is creating and designing what can be, but it is constrained by our understanding of nature, by economics (costs), by concerns of environmental impact, by institutional, social, legal issues and possibly by aesthetics. Listed are the five design constraint categories which are discussed further in the following paragraphs.

Design Constraints
Scientific and Engineering Understanding of Nature
Economics
Environmental
Institutional, Political (Social), Legal
Aesthetics

We also limit the discussion here to the general practice of coastal engineering. Part V-8 is completely devoted to special, U.S. Federal government planning requirements and design constraints.

(1) Scientific and engineering understanding of nature. The coastal setting is dynamic and influenced by land, water, and air interactions and processes. It is a regime of extremes, surprises, and constant motion as the coast responds to changing conditions.

(a) The *Coastal Engineering Manual* (CEM) demonstrates continued improvement in understanding and ability to analytically and numerically model nature. For example, Part III-3 discusses analytical methods to estimate sandy beach shoreline recession rates during storm events that will be useful later in this chapter. Part III of the CEM also introduces many new, dynamic, numerical models that simulate coastal hydrodynamics and sediment transport processes.

(b) CP Module. In V-1, the idea of a Coastal Processes Module, (CP Module) was defined as a repository of physical data and analysis tools relevant to the coastal problem. Wind, waves, currents, water levels, bathymetry, geomorphology, stratigraphy, sediment characteristics, sediment transport processes, etc. and the analysis tools (mainly numerical models) make up the CP Module that is employed many times in the design process (see Figure V-1-1, 2 and 3). However, a fully dynamic, three-dimensional, numerical model of water levels, waves and sediment transport to simulate bathymetric and shoreline change is still under development. It remains a long way from routine application for the functional design of coastal structures. An example would be the simulation of natural, sediment movement behind and through nearshore breakwaters for both normal conditions and storm events. The inability to accurately predict the short-and long-term impacts of coastal structures on the nearshore physical environment remains a design constraint in coastal engineering. Part of the difficulty is the stochastic variability of the natural environment.

(c) Empirical Simulation Technique (EST) methodology. Numerical models are deterministic tools that produce one solution for each set of boundary conditions. The EST procedure is the numerical, computer simulation of multiple, life-cycle sequences of systems such as storm events and their corresponding environmental impacts (Scheffner et al. 1997; 1999). Multiple life-cycle simulations are then used to compute frequency-of-occurrence relationships, mean value frequencies and standard error estimates of deviation about the mean. Using the EST procedure for a specific project generates risk-based frequency information that relates the effectiveness and cost of the project to the level of protection provided.

- A user's guide for application of the EST with examples is found in Scheffner et al. (1999). One example describes calculations of the frequency-of-occurrence relationship for storm-induced, horizontal recession of beaches and dunes in Brenard County, Florida. Previous references to the EST procedure are found in Part II-5 and II-8. See also Part V-1 for discussion.

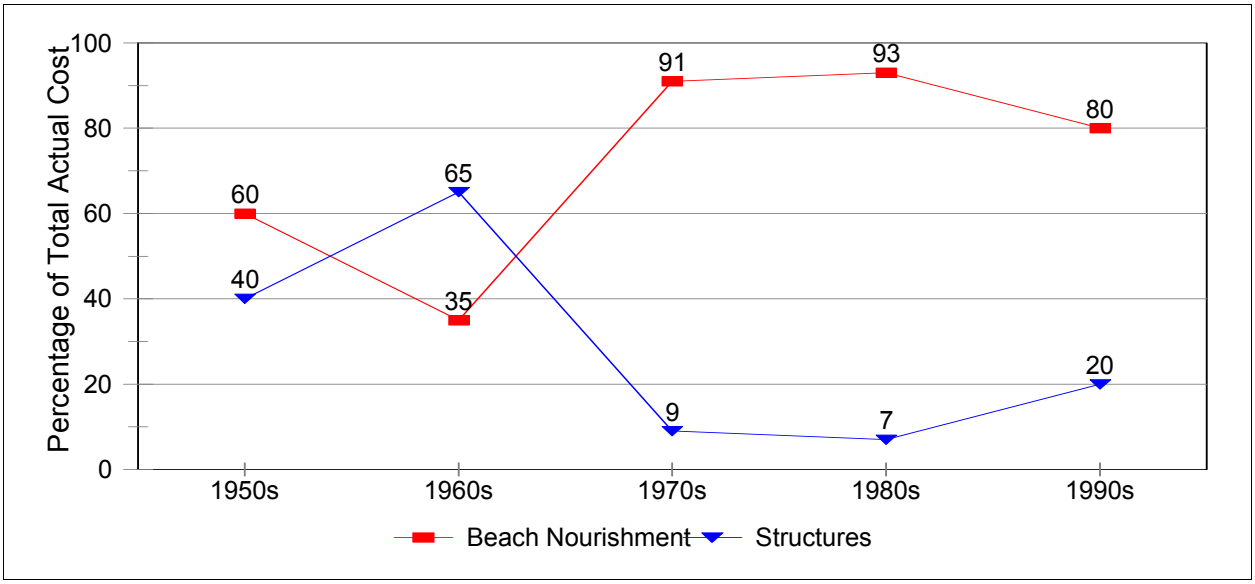

Figure V-3-3. Shift from hard (armored walls, groins, etc.) to soft (beach nourishment) alternatives by the Corps of Engineers (from Hillyer 1996)

- The Corps has specified the EST methodology as a requirement for the risk-based analysis in all shore protection studies (ER 1105-2-101; Thompson et al. 1996). The probabilistic design (functional, structural) of coastal structures remains a constraint, but recent advances such as the EST methodology are helping to produce designs that provide a realistic level of storm protection.

(2) Economics. A key constraint for each shore protection alternative is life-cycle cost. In general, the level of storm protection and, hence, costs (high, medium, low) can only be justified when the corresponding value of property and infrastructure to be protected (benefits) are comparable (high, medium, low). Costs are not subjected to any other constraints. Benefits, however, can be restricted and limited to only those that are perceived to benefit the funding authority. For example, see Part V-8 for the restriction on allowable benefits for Federal government-sponsored projects designed by the Corps.

(a) Cost. It is important to have a clear definition of all terms when discussing costs. Moreover, nothing lasts forever. Advocates for permanent, low cost, or retreat solutions for shore protection fail to understand the following and how they are applied in the professional practice of coastal engineering design economics.

- Costs: The monetary value required for a project. Without additional qualifying words, the word alone is confusing and subject to misinterpretation.

- Initial costs: The total expense for all initial construction and design costs of a project. The year of construction should be noted so that inflationary cost aspects can be estimated in the future. Distinction should be made between estimates and actual contract costs.

- Maintenance costs: The estimated annual expenses required to maintain both the functional and structural integrity of the alternatives which are altered by storm damage and natural processes. Both deterministic estimates and risk-based calculation methods can be employed. (see Part VI-7 for an example of the probabilistic method for rubble-mound breakwaters)

- Alteration/removal costs: The estimated expenses required to alter the design or completely remove the structure if there are significant, downdrift impacts. Evidence from postproject monitoring and decision criteria mechanisms are required for implementation. This cost has been ignored for most projects and could be included in the category of maintenance costs.

- Total, life-cycle cost The combined initial, maintenance and alteration/removal costs required over the design life of the project. Annual maintenance costs are usually converted to their present worth so that they can be directly combined with the initial construction costs. The present worth (value) is determined by multiplying the annual maintenance expense by the present worth factor, PWF. The PWF is a function of the design life and the interest (discount) rate. (See any standard engineering economics text).

- Design life: An estimate of the number of years of useful life of the structure/ alternative. Usually 25 to 50 years is employed for well-designed projects. Design life selection includes structural life of materials (structural integrity), functional life (usefulness), technical life (technologically up-to-date), and aesthetics. Design life is employed for the economic analysis of the present worth of annual maintenance cost for the total, life-cycle cost comparison of all alternatives. It does not mean the length of time the project will last in the field.

- Interest rate: The second variable required to calculate the present worth of the annual maintenance costs. Often, the rate employed is related to the current, bank loan rate for construction projects. It can also be set by government policy as discussed in Part V-8 for the Federal government.

- Damage: When energy levels in storms exceed the design levels, both structural damage and some loss in functional performance may occur. Repair is possible. Damage is an expected aspect of risk-based coastal design.

- Failure: When storms below the design level cause loss of structural integrity and/or functional performance. The design has failed and a redesign is needed before repair or reconstruction. Use of the word “failure” for loss of structural integrity or performance should be avoided until it can be proven that a design failure took place under specified storm conditions.

- Balanced design: The most economical balance between the initial construction costs and maintenance (damage repair) costs so that the total cost is a minimum. Initial costs increase as the level of protection for more powerful (but rarer) storms increases, but maintenance costs decrease because damage is less frequent. The classical U-shaped, total cost curves result. (See Part VI-7 for an example with rubble-mound breakwater design)

(b) Benefits. Storm damage reduction and coastal erosion mitigation are the two major benefits of shore protection. These two along with ecosystems restoration are the only benefits allowed by the Federal government for Corps projects as discussed further in Part V-8.

- Many other benefits exist. As seen in Figure V-3-3, since the 1960s, beach nourishment has been the selected alternative for shore protection. Substantial recreation and tourism benefits have resulted for local, state, and Federal governments. Waterfront property is generally of greater value and generates higher property taxes. Innumerable secondary (ripple effect) benefits result from the coastal, beach-related travel and tourism industry. The economic value of beaches has been well documented (Houston 1995a; 1995b).

- A good example is Miami Beach, Florida, which was renourished in 1979 by a joint Corps of Engineers - City/County government project costing $52 million. The capitalized annual cost is about $4 million and the project has lasted more than 20 years without the need to renourish the beach. Attendance at the beach increased from 8 million in 1978 to 21 million in 1983 (Houston 1995a). More than 2 million foreign visitors spend over $2 billion annually at Miami Beach (Cobb 1992). The Miami Beach experience is roughly $700 return in foreign exchange for every $1 invested in beach nourishment (Houston 1995a; 1995b; 1996).

- Beach nourishment can also enhance the natural environment. Widened beaches reduce the potential for new, tidal inlet formation during storms at narrow reaches of barrier islands. The economic losses to the protected bay environment (property, recreation, farming, fishing, infrastructure, etc.) can be estimated and added to the storm damage and other benefits for the impacted barrier island. In general, however, environmental benefits of the enhanced, flora and fauna habitat are difficult to quantify monetarily.

- All benefits are site specific. Here, we briefly outline the methodology commonly employed to determine storm damage reduction benefits. A key factor, as illustrated in Figure V-3-2 is distance between the reference baseline and the sea. Steps in the methodology are:

  - Make a structure inventory (residential, commercial, public). Employ aerial, orthodigital mapping and Geographic Information System (GIS) technology where possible and adapt new technologies.

  - Obtain software to calculate the depreciated replacement cost of the structures and content value.

  - Obtain the water level, storm frequency-of-occurrence data for the site, and accompanying wave and shoreline erosion data. The EST methodology previously discussed should be employed, whenever possible.

  - Obtain and run storm damage calculation models. Long-term erosion is included to estimated damages under changing future conditions. The key variables are water level and position of each structure in relation to the shoreline. Some models only treat property structure damage and others land and infrastructure (roads, etc.) damage.

  - Apply the models for both the without project conditions and for the alternatives and subalternatives design considered for shore protection.

- The result is the average, annual damages prevented (benefits) of each alternative. Differences for each alternative to prevent or reduce storm damage are quantified by this approach. Complete details can be found in Part V-8 where names and references for some of the software and models presently employed by the Corps are presented. In general, the state of art for these damage calculation models is less well advanced than for other areas of coastal engineering design.

(c) Benefit/cost ratios. A useful indicator of economic performance of each alternative is the benefit to cost ratio (BCR). As previously noted, the total, life-cycle costs do not depend on the other constraints, therefore remain constant. However, the benefits included in the ratio can be limited by the funding authority. Consequently, the BCR calculated can be significantly different depending upon whether all the potential benefits or only limited benefits are considered. Because the Federal government limits the benefits allowable to only storm damage reduction benefits, the total or true BCR is always greater than that specified for Corps projects. In effect, two BCR's exist.

- Federal government, $(BCR)_F$

$$(BCR)_F = \frac{\text{Storm damage reduction benefits}}{\text{Total, life-cycle cost}} \quad \text{(V-3-1)}$$

- Total, true $(BCR)_T$

$$(BCR)_T = \frac{\text{Total benefits}}{\text{Total, life-cycle cost}} \quad \text{(V-3-2)}$$

- Further details regarding the $(BCR)_F$ for Federal-sponsored projects and other methods to measure economic performance are discussed in Part V-8. The total $(BCR)_T$ is never calculated for Corps projects. Consequently, the local sponsors, general public, and media may not understand nor appreciate the true value of shore protection projects to their community. These institutional, political (social), and legal constraints are discussed further in the following paragraphs.

(d) Sea level rise. A detailed summary of present day knowledge of mean sea level change of the world's oceans is given in Part IV-1-6. Over the last 100 years, average, relative sea level rise has been 30 cm (3 mm/year) on the East Coast and 11 cm (1.1 mm/year) along the West Coast (excluding Alaska). The Gulf of Mexico coast is highly variable ranging from 100 cm (10 mm/year) in the Mississippi Delta plain to 20 cm (2 mm/year) along Florida's west coast (National Research Council 1987). Substantial local variability exists. The question remains as to whether these average rates will increase (substantially), stay constant, or decrease in the future. Three things remain clear, however. The existing rates of mean sea level rise at specific sites have not been a severe economic constraint for the shore protection alternatives selected. At many locations, anthropogenic effects (e.g., jettied tidal inlets) causing downdrift, beach erosion are clearly much larger than those occurring due to sea level rise. And finally, long-term, relative changes in sea level can be incorporated into storm surge analysis and the economic design of coastal structures.

(3) Environmental. A third major constraint of shore protection works is their impact on the environment. The Eastern Scheldt, storm-surge barrier shown in Figure V-3-1 was the focus of much discussion in the early 1970s. Environmental scientists favored raising the dikes around the periphery to maintain the saltwater ecology of the tidal estuary. Agricultural and water boards favored a solid dam across the mouth that would create an inland, freshwater lake. A compromise was reached: a storm-surge barrier with movable gates which stay open under normal conditions but are closed at very high storm-surge events. The final design, construction methods and equipment required much research and challenged the ingenuity and technical process of Dutch coastal engineers. In the final analysis, the environmental constraint, to maintain the saltwater ecology, dictated the final design. The additional engineering and construction cost proved to not be the deciding factor.

(a) Types of environmental concerns. As in the preceding example, modification of upland habitat such as land use, resting areas for turtles and shore birds, wetlands, flora and fauna beneficial to the ecosystem, threatened and endangered species, etc. can take place. The aquatic habitat can also be important, for example, water quality, aquatic species, benthic organisms, hazardous, toxic and radiological sediment in

borrow areas, increased turbidity during dredging operations and wave climate alterations by sand volume removal in borrow sites, etc.

- These potentially negative impacts must first be identified. Detailed surveys and sampling investigations are conducted to catalog the species and habitats in the project area under existing conditions. Use should be made of previous studies and summary information. The U.S. Fish and Wildlife Service (F&WS) prepares a planning aid report for large Corps projects that detail existing fish and wildlife resources and their habitats. This report also identifies threatened and endangered species and critical fish and wildlife habitats. The National Marine Fisheries Services (NMFS), state and local resource agencies, and local universities may also provide valuable information.

- The offshore, sand borrow site is the greatest environmental concern for beach nourishment projects. New, benthic sampling and collection efforts are often needed to catalog existing species and habitat. Of concern are species capable of rapid recolonization, commercially important species, or protected species. These surveys provide data on abundance and diversity together with a complete list of all species present. This knowledge can be critical in borrow site selection and hence overall cost of the project.

- In most cases, an Environmental Assessment (EA) report is sufficient to demonstrate the minor environmental impact of shore protection projects. Rarely is a full, Environmental Impact Statement (EIS) needed which is time consuming and can be expensive. Corps project needs for an EIS are discussed in Part V-8.

(b) Impact on natural sediment transport system. The negative, downdrift impact on the local and regional sediment budget can be a key environmental constraint. These concerns are addressed in detail in Part V-3 for armored (Part V-3-2) and shoreline stabilization (Part V-3-3) structures and in Part V-5 for jetties at navigation inlets. A beach nourishment project has many positive, environmental impacts by bringing new material to sand starved beaches and expanding the beach habitat. Studies in turtle nesting areas have proven that renourished beaches increase the number of turtle nests (Broadwell 1991; Nelson et al. 1987).

(c) Mitigation. Procedures, or measures which avoid, minimize and/or compensate for negative impacts are defined as mitigation. Threatened and endangered species such as the piping plover, least tern, sea turtles, and whales required special consideration during the planning and construction stages of shore protection projects. Avoidance of negative impacts is achieved by scheduling construction activities at times when the species do not normally inhabit the project area. Piping plovers and least terns are most vulnerable during the nesting/fledging period from early spring to late summer. Disturbances on the beach cause the nest to be abandoned before the eggs hatch.

- Avoidance for sea turtles and whales is not practical for the southern section of the Atlantic coast because these species inhabit the area for most of the year. Minimization of negative impacts is achieved in various ways including monitoring to document contact; using deflectors on the dragarms and collection boxes on hopper dredges; and conducting turtle relocation projects. These techniques are approved by the National Marine Fisheries Service.

- Mitigation by compensation is employed when resource loss is unavoidable. The most common example is new wetlands construction to compensate for the wetlands area lost due to project construction. Some states require more new area constructed than lost and permit wetland banks that are used to pay for planned, future wetlands loss. New and rebuilt dunes are replanted with grasses to compensate for any plants lost during construction. Mitigation by compensation methods are normally carried out and completed during project construction.

- Ecosystem restoration projects result from habitat lost due to a previous activity such as construction of jetties at a tidal inlet and the long-term, downdrift erosion of the beach. Restoration and protection of unique species habitat could also be the objective. Normally, beach nourishment projects can be designed to meet these project objectives. Methods to quantify these environmental benefits are discussed in Part V-8 as applied by the Corps.

(4) Institutional, political, legal. A fourth area that has a formidable influence on the design process are the institutional, political (social), and legal requirements for all projects.

(a) Institutional (policies and guidelines). The Federal objective of water and related land resources project planning is to contribute to the national economic development (NED) consistent with protecting the nation's environment. Applicable executive orders and other Federal government policies and guidelines as planning requirements are discussed fully in Part V-8. The Corps is responsible for shore protection designs of the Federal government. The Corps District Office engineers with the possible aid of the Coastal Hydraulics Laboratory (CHL), Engineer Research and Development Center (ERDC), do most of the design work. Some design work is performed by the private, civil engineering consulting firms. No general guidelines exist as to when and how the private sector, coastal engineering community participates in the design process for the Federal government.

- Other Federal agencies are responsible for some aspects and alternatives for shore protection. A National Flood Insurance Program (NFIP) was established in 1968 to help reduce the Federal share of costs in connection with flood losses. The NFIP is operated by the Federal Insurance Administration, a division of the Federal Emergency Management Administration (FEMA). An essential component for implementing the NFIP is the Flood Insurance Rate Map (FIRM) which delineates special flood hazard areas and insurance risk zones. These maps are prepared by FEMA's mitigation division. Places subject to flooding at the annual, one percent exceedance probability level are designated as special flood hazard areas. The associated recurrence interval is the so-called, 100-year flood. Use of the 100-year flood designation is discouraged. Many people believe that a 100-year flood happens only once every 100 years. Some areas have experienced flooding at this probability level in consecutive years. The FEMA flood hazard zone maps include special V-zones for both flooding and significant wave energy to cause structural damage. Construction standards (where applicable) and flood insurance rates are usually higher for structures located in V-zones.

- Zoning laws and improved building standards are then implemented by coastal communities based on the FIRM and designated hazard-prone areas. One common standard is the requirement that all, first-floor living quarters of new construction be set at least one foot above the mapped elevation of the one percent chance flood.

- Since 1982, all NFIP policies are actuarial, i.e., the flood insurance policy's annual rates fully reflect the buildings risk of flooding. No taxpayer subsides are required. Presently, about 23 percent of structures vulnerable to flooding damages are covered by the NFIP. And, only 3 percent of these NFIP policies are in coastal communities. These coastal communities generate more premium income that they have received in loss claims (Houston 1999).

•Beaches serving as flood protection works are eligible for disaster relief from FEMA provided the relief is assigned public beach facility status. To qualify, it must have a period renourishment program for long-term maintenance. The local government project sponsor must restore the beach to its normal design shape (template) and pay for the cost of replacing sand eroded prior to the storm. Since natural beach rebuilding begins after the storm, it is not clear what time frame is employed to define the storm erosion volume.

- Several states have established construction setback lines to reduce damage in areas subject to coastal erosion and shoreline retreat. The setback line position is often calculated as some multiple of the annual erosion rate or a specified distance from a contour location in a particular year. In Florida, the line location is based on many factors, namely long-term erosional trends, short-term storm effects, rare water levels at the one percent chance, annual exceedance level, wave uprush, dune line position, wind forces and existing development. In Delaware, 1979 aerial photography has been employed and the restriction line set 30.48 m (100 ft) landward of specified contour elevations, dune toes, or edge of the existing boardwalk structure. These development restrictions affect the without-project calculation of storm damage benefits discussed in Part V-3-1. If homes and structures are not able to be repaired or replaced after a storm by FEMA or state policies, than this will change the without-project estimate of benefits. See also Part III-5-13 for a discussion of setback lines for cohesive shorelines.

(b) Political (social well-being). Specific national policies and laws change as administrations and public interests change. A diverse and broad range of coastal system users with varying economic, social, and environmental expectations and goals exist. Although there have been shifts in the national policy for shore protection by the Administrative Branch of the Federal government, the legislative branch controls the authorization and funding of all Corps projects. Congress has continued to approve and fund the beach nourishment alternative. Shore protection in the U.S. remains political, fragmented, and controversial for a variety of reasons that are further elaborated in Part V-8. National plans for beach management and shore protection do not exist.

- Each project must consider many social aspects.
  - Local, regional and state plans for the coastal zones
  - Public health, safety, and social well-being, including possible loss of life
  - Community cohesion
  - Availability of public facilities and services
  - Potential adverse effects on property values and the tax base
  - Displacement of people, business, and livelihood
  - Disruption of normal and anticipated community and regional growth
  - Sufficient parking and public transport
  - Sufficient dune crossovers

- Public access and safety during construction
- Access for people with disabilities
- Interruption of recreation

- Cultural resources must also be considered.

- Coastal project construction has the potential to severely impact important cultural resources. Project activities such as offshore sand borrowing can damage or destroy important historical sites related to the region's maritime history. Shipwrecks, native American Indian, and prehistoric sites are typically of interest. Investigations by archaeologists to identify cultural resources in the project area provide data necessary to evaluate site significance and potential project impact. Close coordination with the state Historic Preservation Office is necessary for compliance with the National Historic Preservation Act of 1966.

- The politics surrounding shoreline erosion and measures for mitigation provide a wealth of fascinating reading material. For example, the Westhampton groin field on the south shore of Long Island, New York (U.S. Army Engineer District, New York, 1958: Heikoff 1976; Kassner and Black 1983; Nersesian, Kraus, Carson 1992; Spencer and Terchunian 1997; Terchunian 1988) is a classic example of a political decision that significantly altered the original design. The groin field was built in two stages, with 11 units constructed in 1964/65 and four more in 1970/71. It was a Corps project authorized by Congress in 1960. The project area extended from Fire Island Inlet east to Montauk Point and called for beach fill and groins as needed starting at the west end since the natural, net drift of sand was from east to west. A winter storm in 1962 breached the weakened barrier island at Westhampton. Local interests including the Suffolk County government lobbied for and eventually convinced the Corps to construct the groins in reverse sequence, from east to west. In addition, the groins were not filled with sand when constructed and construction was stopped in the middle of the project for political reasons. The result was a massive sand trap along Westhampton that starved the downdrift (westerly) beaches. The interruption of natural sand transport by Shinnecock and Moriches Inlet and the Westhampton Groin Field has accelerated erosion on Fire Island at the west end of the system (Kana 1999). A lawsuit by Fire Island property owners has resulted against the Corps (see Spencer and Terchunian 1997 for more details and reference). The legal constraint has long been a factor in coastal, shore protection design.

(c) Legal (laws). Congress, through passage of the biannual Water Resources Development Acts (WRDA), authorizes studies and funds construction of Corps projects. Sections of this law also include special investigations and establish cost-sharing formulas between the Federal government, state and local interests. For example, in the 1998 WRDA, the cost-sharing law was changed to 50 percent Federal and 50 percent from local/state interest.[1] As a result, some states have passed laws and statues to provide an annual source of funding for the increased cost of participation in Federally-authorized projects.

- The Coastal Barrier Resources Act (CBRA) was passed in 1982 to minimize loss of life, damage to fish, wildlife and natural resources, and wasteful expenditures of Federal revenues on Atlantic Ocean and Gulf of Mexico barrier beaches. The goal is to restrict all Federal government expenditures and assistance that aid development on the coastal barriers. For example, the CBRA relies on the National Flood Insurance Program to discourage building by prohibiting sale of Federal flood insurance in areas covered by the act. The CBRA does permit Federal funding for shoreline

[1] Previously, the formula was 65 percent Federal, 35 percent state/local.

stabilization by nonstructural projects that mimic, enhance, or restore natural stabilization systems, i.e., beach nourishment projects. Federal expenditures are also allowed for the study, management, protection, and enhancement of fish and wildlife resources and habitats.

- The CBRA is one of many Federal laws designed primarily to protect environmental and cultural resources. A partial list includes the following:
  - Archeological Resources Protection Act
  - Clean Air Act
  - Clean Water Act
  - Coastal Barrier Resources Act
  - Coastal Zone Management Act
  - Disabilities Act
  - Endangered Species Act
  - Estuary Protection Act
  - Federal Water Project Recreation Act
  - Fish and Wildlife Coordination Act
  - Land and Water Conservation Act
  - Marine Protection, Research Sanctuaries Act
  - National Historic Preservation Act
  - National Environmental Policy Act
  - Rivers and Harbors Act
  - Watershed Protection and Flood Prevention Act
  - Wild and Scenic River Act
- All shore protection projects must apply for and receive a permit from the USACE prior to construction. This permit is pursuant to Section 10 of Rivers and Harbors Act (1899) and Section 404 of the Clean Water Act (1977). The permit process considers and evaluates many factors, including effects on conservation, economics, aesthetics, general environmental concern, wetlands, cultural values, fish and wildlife resources, flood hazards, flood plain usage, land use, navigation, shore erosion and accretion, recreation, water supply and conservation, water quality, energy needs, safety, food and fiber production, mineral needs, and welfare of people and society. Some states have a Joint Permit Application for local boards, state agencies and the Corps of Engineers permit. This method saves considerable expense and time in that only one permit

application is required to meet the needs of all three levels of government review of the proposed project.

- Some states (North Carolina, Maine) have passed laws banning the use of armored structures (seawalls, bulkheads, revetments) and shore protection on their ocean coasts. South Carolina only bans armored structures and other coastal states are considering similar laws. Florida and California have adopted sand mitigation policies and procedures to permit seawall construction but require the annual placement of sand to compensate for that trapped behind the structure. Further details on seawall and beach interactions are summarized in Part V-3-2.

- Laws for property boundaries at the land-water interface are complex and vary from state to state. A 26-article series entitled "The Law of the Sea in a Clamshell" explaining the applicability and diversity of laws pertaining to the shore has been published by the American Shore and Beach Preservation Association in the magazine *Shore and Beach* (Graber 1980). Clear and legally defendable knowledge of property ownership must be an early step in the design process for coastal protection works.

(5) Aesthetics. A final and especially challenging area in design pertains to the sense of beauty and accepted notions of good taste. Many people feel that natural shorelines (e.g., wide, sandy beaches, rocky cliffs, or vegetated marshes and trees, etc.) are more aesthetically pleasing than ones artificially manipulated for shore protection. An uninterrupted, uncluttered, and natural view of the sea is desirable for most people. Therefore, when possible, an aesthetically balanced and consistent appearance, replicating natural systems is preferred.

(a) The "do nothing" alternative may result in a destructive wake of debris from flooding and wave damage that is visually disturbing for days or weeks following a storm. Some alternatives (e.g., geotextile bags filled with sand) will not survive medium level storm events and leave a debris-strewn beach.

(b) Aesthetics played a major role in selection of the final design for the new, hurricane protection, seawall/boardwalk at Virginia Beach, Virginia. The initial design by the Corps was a massive, curved, concrete seawall patterned after the one in Galveston, Texas. The City of Virginia Beach is a popular tourist, recreation beach and the promenade (boardwalk) features a key aspect of the design. The city rejected this initial design for aesthetic and tourist-economy reasons. First floor hotel guests and restaurant patrons would not be able to see the ocean on the south end. Their view was blocked by the crest elevation of the proposed seawall. The revised design lowered the seawall elevation, modified the structural design, added interior stormwater drainage to accommodate additional overtopping, and widened the nourished beach in front to mitigate storm energy. An artist's perspective and aerial photo are found in Part V-3-2a (Figure V-3-6). The constraints that dictated the final design were aesthetics and the need to accommodate the beach-driven, tourist industry.

(c) Engineering is not applied science. Our limited understanding of nature is one constraint, but it is far from the only one, seldom the hardest one, and almost never the limiting constraint for coastal engineering design.

V-3-2. Coastal Armoring Structures

a. Types.

(1) Seawalls and dikes. The primary purpose of a seawall (and dike) is to prevent inland flooding from major storm events accompanied by large, powerful waves. The key functional element in design is the crest elevation to minimize the overtopping from storm surge and wave runup. A seawall is typically a massive, concrete structure with its weight providing stability against sliding forces and overturning moments. Dikes are typically earth structures (dams) that keep elevated water levels from flooding interior lowlands.

- Various types of seawalls and dikes are depicted in Figure V-3-4. When vertical, they are labeled nonenergy absorbing, whereas if with a sloping surface or rubble mound, they absorb some energy (Pilarczyk 1990). The front face may also be curved or stepped to deflect wave runup. Typical damage modes for seawalls include: toe scour leading to undermining; overtopping and flanking; rotational slide along a slip-surface below and shoreward of the seawall; and corrosion of any steel reinforcement. Vrijling (1990) discusses 14 damage/failure mechanisms for dikes including "stability of the protective revetment." Part VI presents details for functional design.

- Construction of the massive, concrete seawall to protect Galveston, Texas, against overflows from the sea began in 1902, in the aftermath of the major hurricane of September 1900. Over 6,000 (16 percent) of the citizens lost their lives. An original construction photo (top) and chronology of seawall and embankment (dike) cross-section development (bottom) are shown in Figure V-3-5 (from Davis 1961). Major features are the wood piles, a sheet-pile cut-off wall, riprap toe protection, and the curved face to deflect wave runup. Modification and extension occurred in 1909, 1915, 1926, and the last extension to the west completed in 1963. In the almost 100 years of existence, many lives and millions of dollars of property damage have been saved by this project (Davis 1961).

- The City of Virginia Beach has opted for a low-crest elevation, sheet-pile, concrete cap seawall that also serves as a new boardwalk. Figure V-3-6 displays an artist's perspective (top) with cross section and an aerial photo (bottom) of a recently (1998) completed section. Construction of the newly designed, interior drainage system with pumping stations for an ocean outfall and a widened sandy beach will complete the project in 2002.

- Part VI-2 also discusses many other typical cross sections and layouts of seawalls and sea dikes.

(2) Bulkheads. These are vertical retaining walls to hold or prevent soil from sliding seaward. Their main purpose is to reduce land erosion and loss to the sea, not to mitigate coastal flooding and wave damage. For eroding bluffs and cliffs, they increase stability by protecting the toe from undercutting. Bulkheads are either cantilevered or anchored sheet piles or gravity structures such as rock-filled timber cribs and gabions. Cantilever bulkheads derive their support from ground penetration; therefore, the effective embedment length must be sufficient to prevent overturning. Toe scour results in a loss of embedment length and could threaten the stability of such structures. Anchored bulkheads are similar to cantilevered bulkheads except they gain additional support from anchors embedded on the landward side or from structural piles placed at a batter on the seaward side. For anchored bulkheads, corrosion protection at the connectors is particularly important to prevent failures. Gravity structures eliminate the expense of pile driving and can often be used where subsurface conditions support their weight or bedrock is too close to the surface to allow pile driving. They require strong foundation soils to adequately support their weight, and they normally do not sufficiently penetrate the soil to develop reliable passive resisting forces on the offshore side. Therefore, they depend primarily on shearing resistance along the base of the structure to support the applied loads. Gravity bulkheads also cannot prevent rotational slides in materials where the failure surface passes beneath the structure. Typical bulkheads are shown in Figure V-3-7.

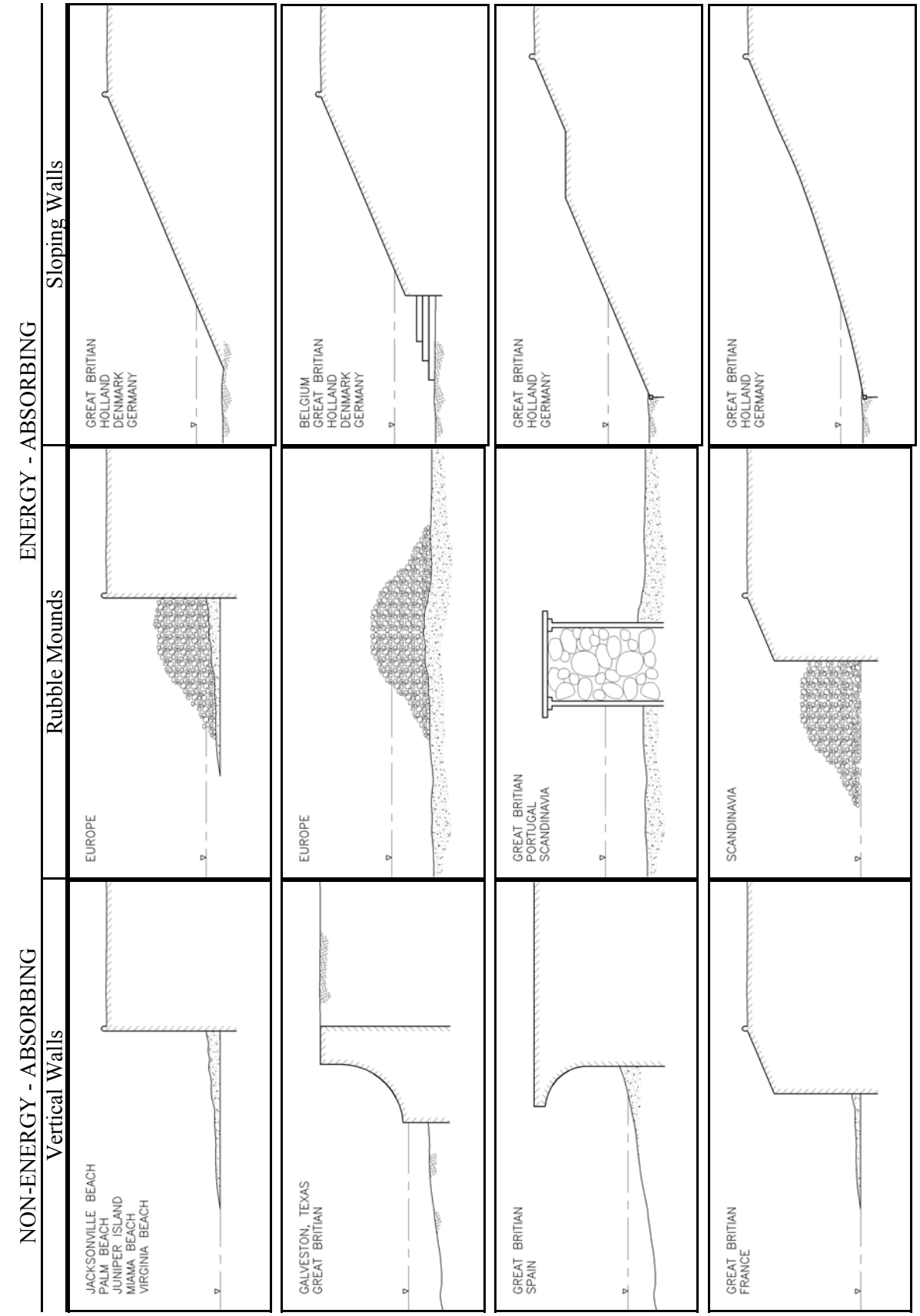

Figure V-3-4. Different types of seawalls and dikes (from Pilarczyk 1990)

a. Photograph of original construction (from USAED, Galveston)

Figure V-3-5. Galveston, Texas, seawall (Continued)

(a) The primary purpose of bulkheads is to hold land or fill in place and prevent shore side losses. A secondary purpose is to protect the land from wave attack. The strength of a bulkhead to protect against wave attack is provided almost solely by the fill, and if this material is lost, the bulkhead has no practical mechanism to adequately protect against waves. Therefore, two critical elements of a good bulkhead design that prevent or limit loss of backfill are: return walls at the alongshore ends of the structure to prevent high water from washing material away from behind the structure; and geotextiles to allow water but not fines to flow through the structure. Drainage of water through, behind, or laterally away from the structure is important to relieve pore pressure from excessive rainfall or overtopping. Drainage can be provided by drilling weep holes in the structure face to allow water to seep out.

(b) Steel and timber sheetpiling are the most commonly used bulkhead material. Steel sheet piles are individual sheets which can be interlocked and driven into hard, dense soils. The interlocking nature of individual steel sheet piles helps to limit erosion losses of backfill through the bulkhead. However, good design practice also includes installation of a geotextile or gravel filter between the bulkhead and the backfill to further prevent sediment losses. Filters are particularly important for timber bulkheads because they lack an interlocking mechanism, though overlapping timber sheets in a two-to-three layer technique can often limit the pathways for sediment to travel. An often encountered difficulty in installing geotextiles is depth of placement. For sheet piles that are driven, placing the geotextiles the full depth of the structure is practically impossible through the structure below the depth of the filter cloth. The loss of the backfill at a timber bulkhead from water (rain and/or wave overtopping) seeping and carrying sand through the bulkhead below the depth of the filter or below the depth of the timber piles is a common damage mechanism.

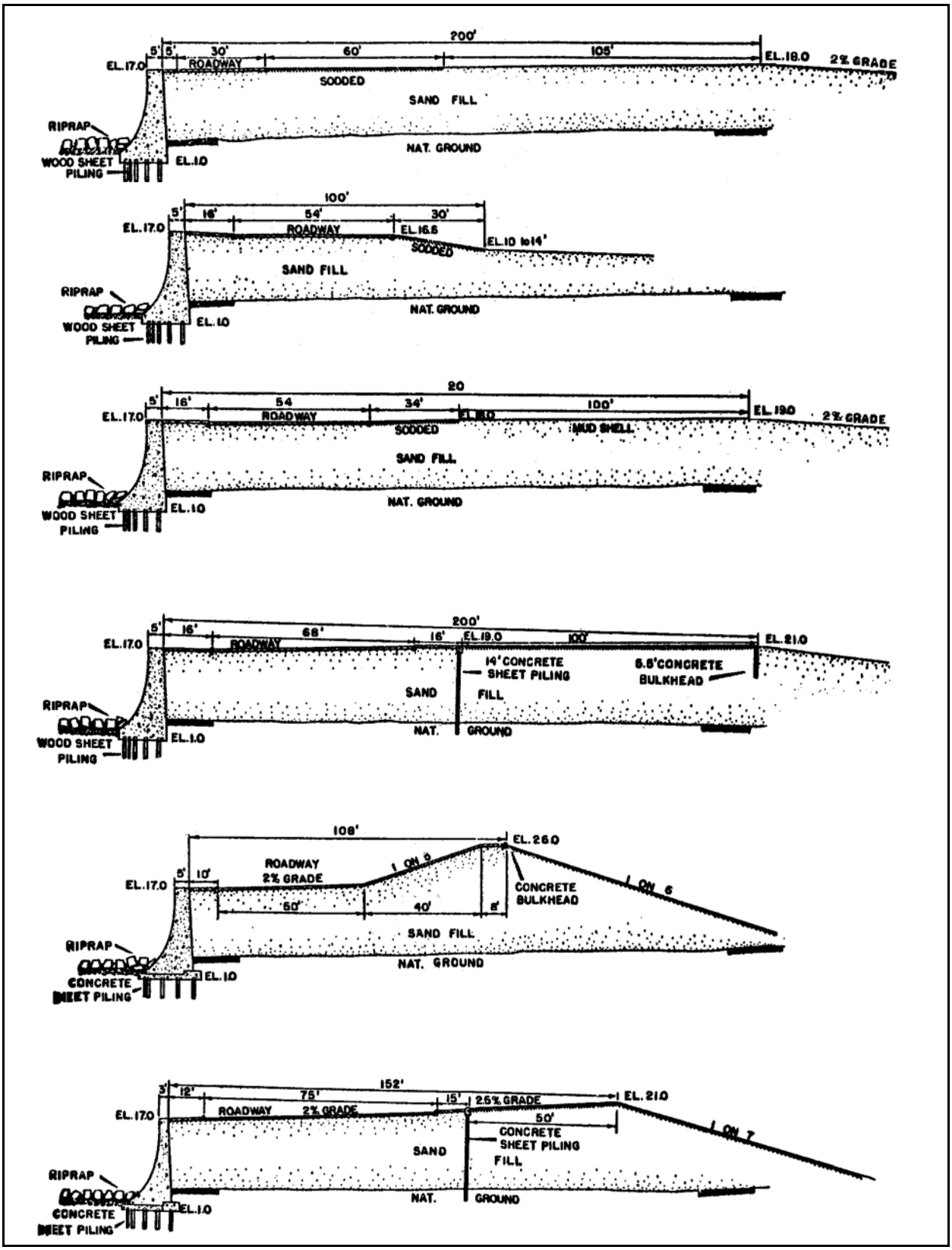

b. Chronology of development (from Weigel 1991)

Figure V-3-5. (Concluded)

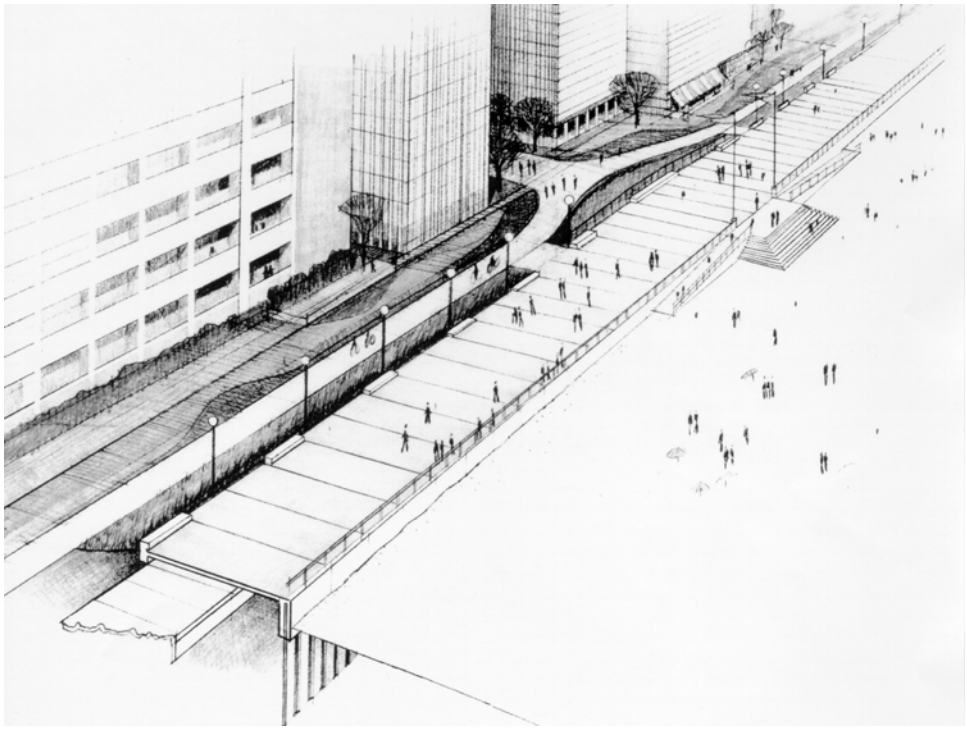

a. Artist's perspective

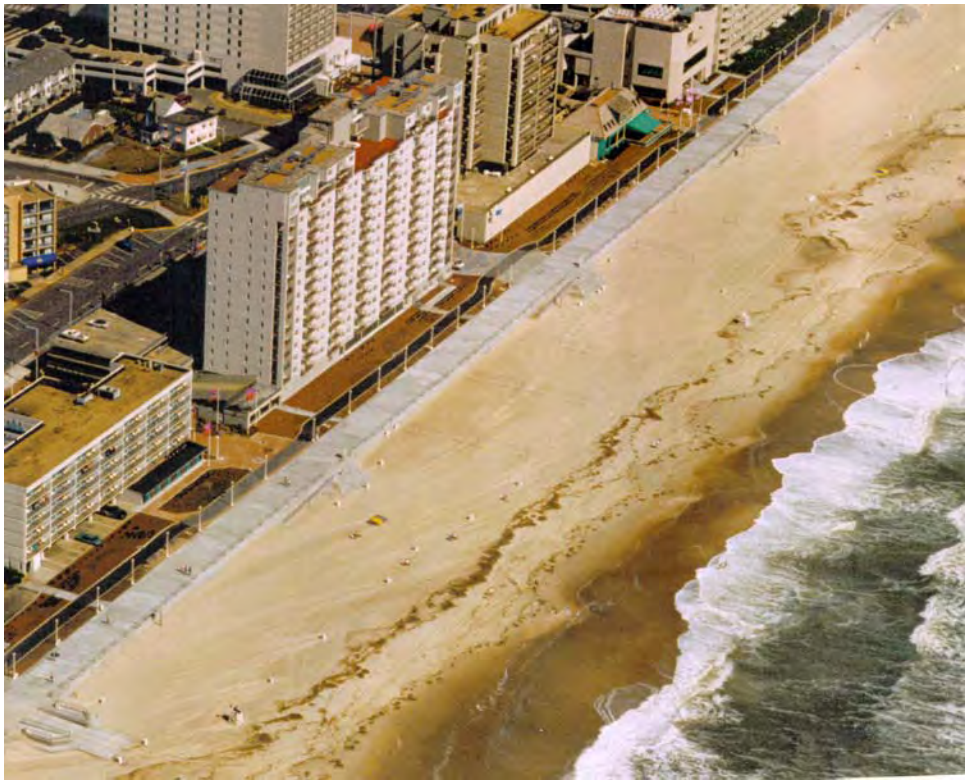

b. Aerial photo

Figure V-3-6. Virginia Beach seawall/boardwalk, 1997 (courtesy City of Virginia Beach, VA)

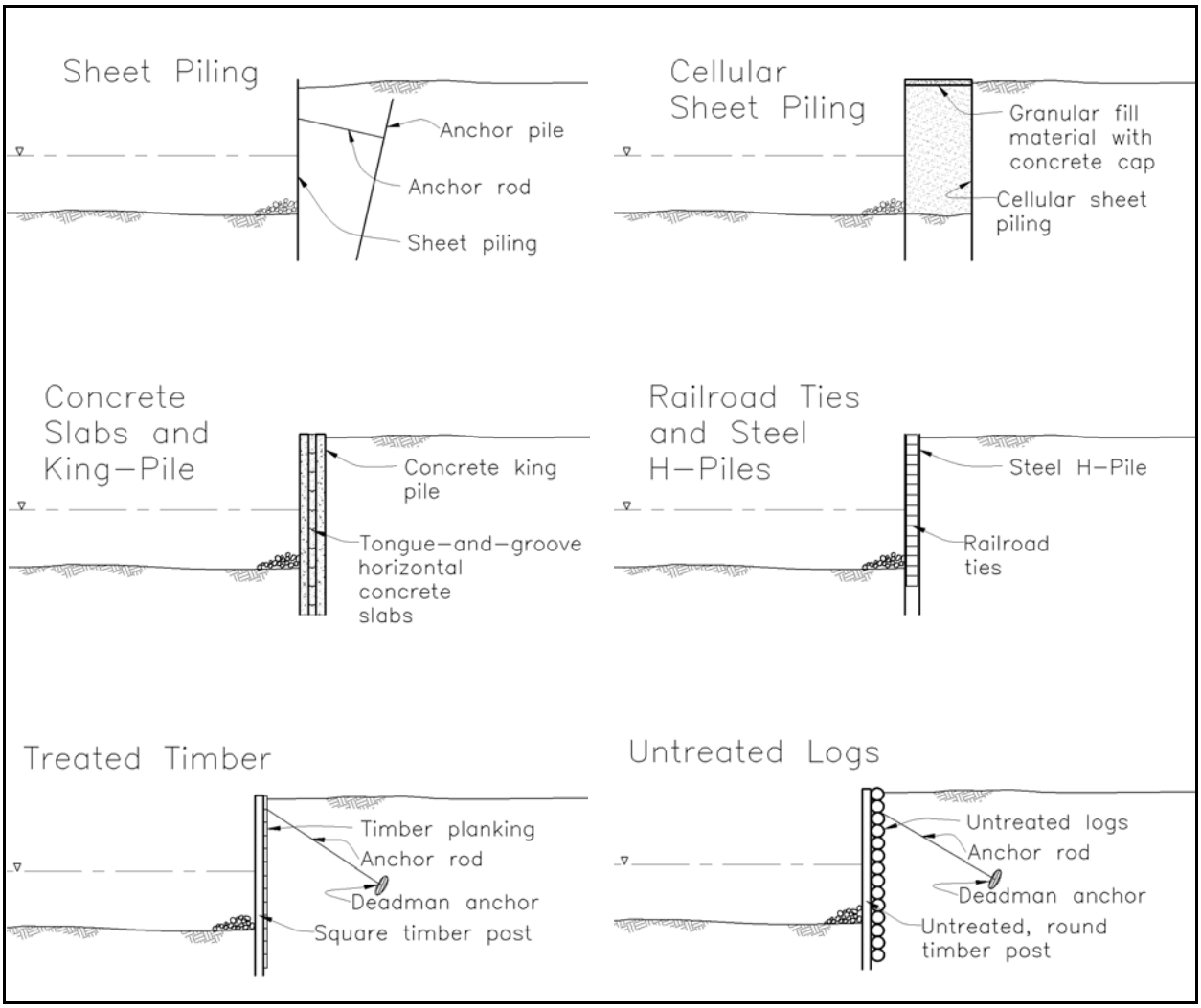

Figure V-3-7. Typical bulkhead types

(3) Revetments. Revetments are a cover or facing of erosion resistant material placed directly on an existing slope, embankment or dike to protect the area from waves and strong currents. Three major features are a stable armor layer, a filter cloth or underlayer, and toe protection. The filter and underlayer support the armor, yet allow for passage of water through the structure. Toe protection prevents undercutting and provides support for all the layer materials previously mentioned. If the toe fails, the entire revetment can unravel.

(a) Figure V-3-8 summarizes a wide range of designs and materials employed for a revetment. Armoring may be either flexible (normal) or rigid. Riprap and quarrystone designs can tolerate some movement and shifting or settling of their underlying foundation, yet remain functional. Rigid, concrete or asphalt slabs-on-grade are generally unable to accommodate any settling.

(b) Typical failure modes for revetment include:

- Armor layer damage and interior exposure.
- Overtopping and loss of foundation material.

- Toe failure and unraveling.
- Excess groundwater pressure and piping failure through the armor layer.
- Rotational sliding along the slip-circle surface
- Flanking of the end sections.

(c) Armor layer stability is discussed in detail in Part VI-5-3-a; toe stability and protection in VI-5-3-d, and filter layer design in VI-5-3-b. Shore protection by revetments can be for all levels of wave energy. For low wave energy environments in bays and rivers, relatively inexpensive and readily available stone sizes makes revetments a common choice for erosion protection by individual property owners. Vegetation and marsh grasses seaward of the revetment also diminish some wave energy to protect the revetment.

(4) Combinations and other types. Protective revetments on dikes are an example of combination coastal armoring structures. Earthen dikes, with stone revetments have been constructed to protect Texas City, Texas, and along the Lake Erie shoreline by the USACE. Due to the nature of the earthen structure, design and specifications should be evaluated by geotechnical engineers (see EM 1110-2-1913, "Design and Construction of Levees"). In the Netherlands, the sea side is heavily armored to protect the dike against the North Sea. On the land side, grazing sheep are used to continually compact the earth.

(a) As previously discussed, a storm surge barrier (see Figure V-3-1) across the opening to the sea provides alternative means of armoring for shore protection. The most notable hurricane barrier in the United States is located at New Bedford Harbor, Massachusetts. The tide (or flood) gate remains open for navigation, then closes to prevent flooding of inland areas during storms.

(b) When insufficient space or earthen dike materials are available, rigid, vertical flood walls may be constructed. Design guidance is available in EM 1110-2-2502, "Retaining and Flood Walls." Crossing the wall requires flood gates that roll, swing, or slide to close the opening EM 1110-2-2705, "Structural Design of Closure Structures for Local Flood Protection Projects." Special, interior drainage facilities may also be needed including pumping stations (EM 1110-2-3102, "General Principles of Pumping Station Design and Layout."). Grade raising, i.e., increasing ground elevation by filling with stable material is also possible. The entire city of Galveston, Texas, was elevated about 4 m to match the seawall crest elevation. (see Figure V-3-5). Sandy material was dredged from nearby Galveston Bay and pumped hydraulically to fill the island. Wiegel (1991) presents a complete history of the Galveston, Texas seawall.

b. Functional design.

(1) The functional design of coastal armoring structures involves calculations of wave runup, wave overtopping, wave transmission, and reflection. These technical factors together with economic, environmental, political (social), and aesthetic constraints all combine to determine the crest elevation of the structure.

(2) Wave runup and overtopping depend on many factors. Part VI-5-2 presents all the details. Empirically determined coefficients, formulas, tables, etc. have mainly come from laboratory scale experiments with irregular waves in large wave tanks. Independent variables include wave characteristics, water depths, slopes, roughness, degree of permeability or impermeable, wave angle, berm or continuous slope, freeboard, etc. Tables VI-6-18, 19, and 20 in Part VI-6 present partial safety factors for runup on rock-armored slopes, hollowed cubes, and dolosse armor units, respectfully.

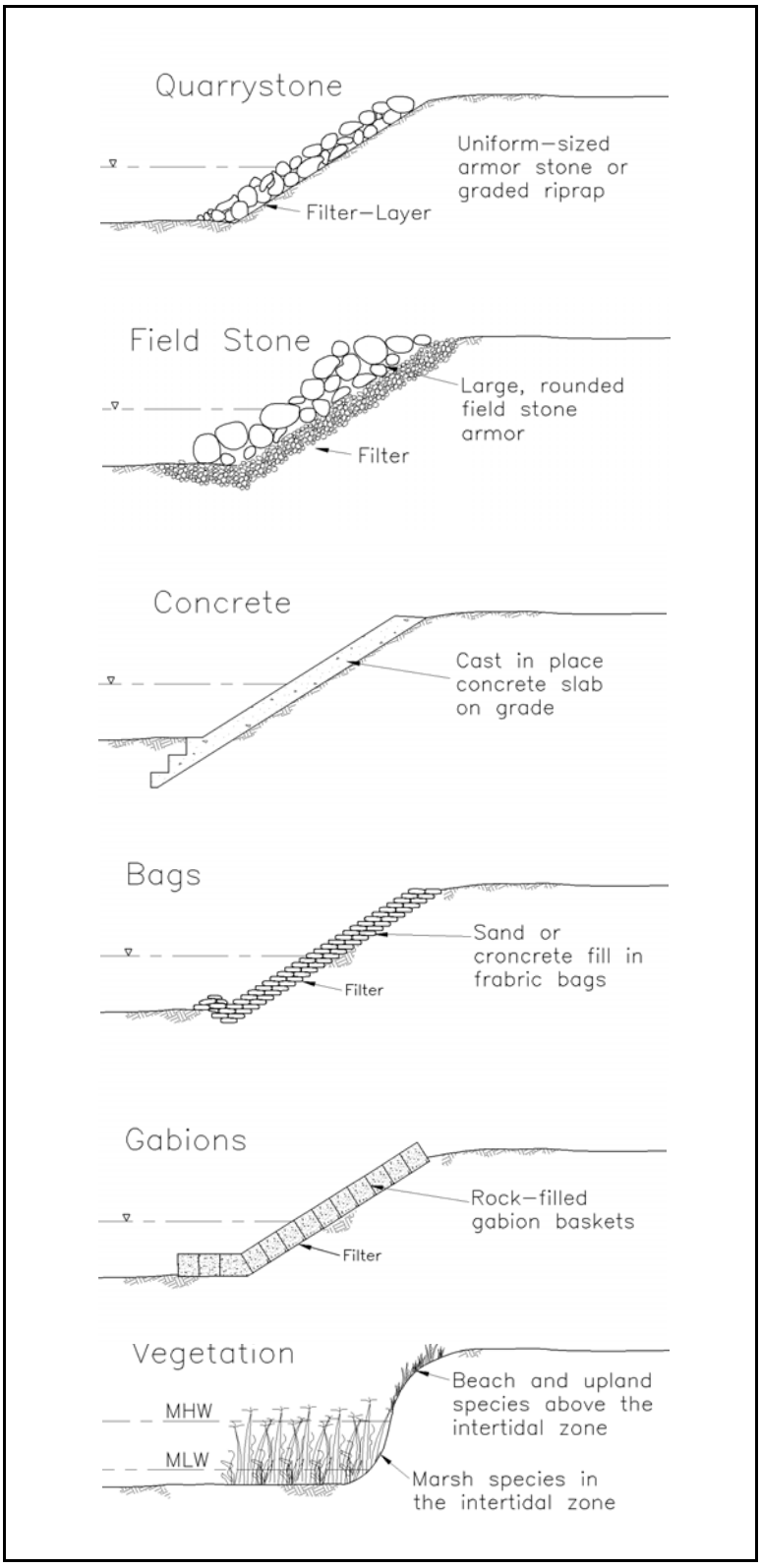

Figure V-3-8. Summary of revetment alternatives (continued)

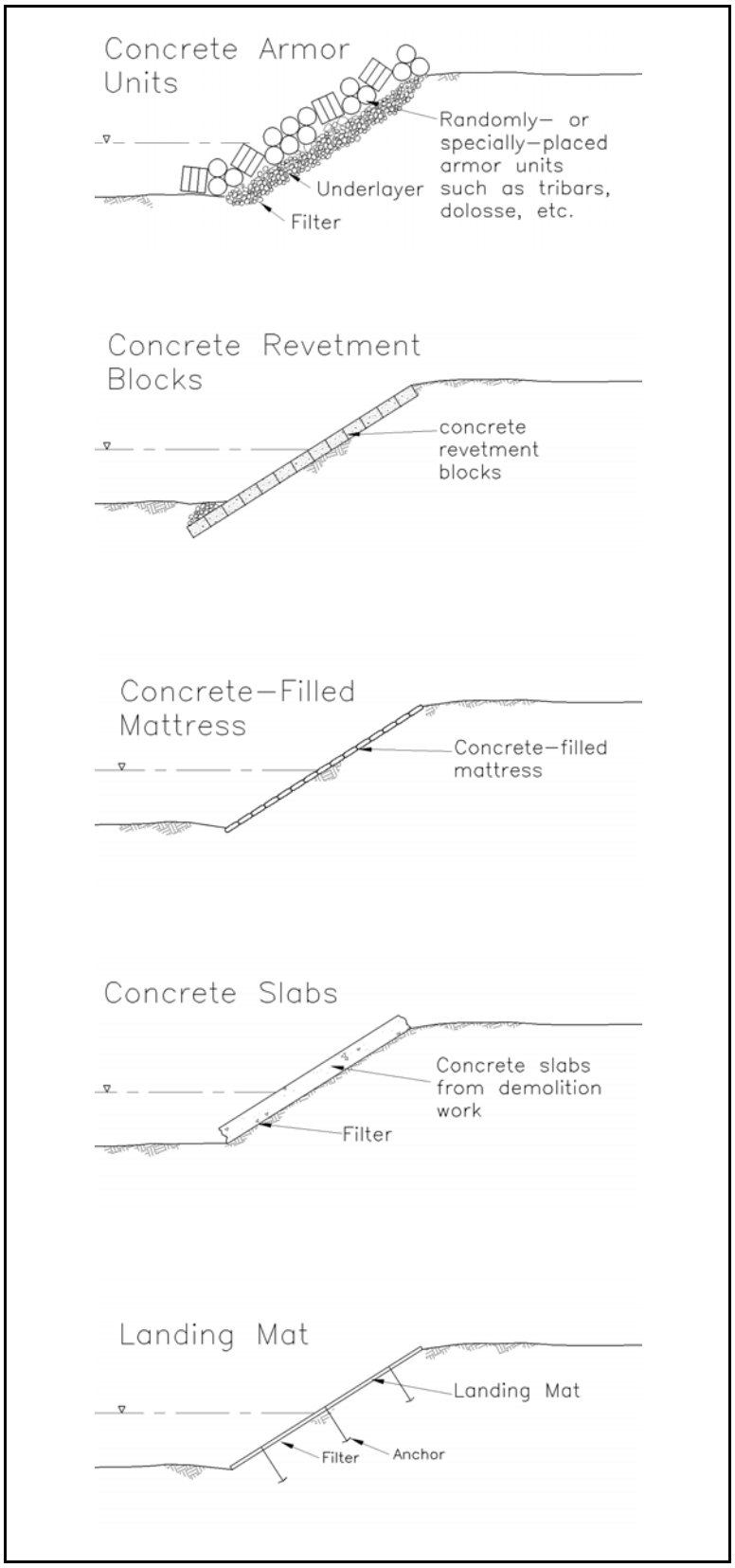

Figure V-3-8. (Concluded)

(3) Wave reflection and transmission through and over sloping structures and beneath vertical wave screens is also found in Part VI-5-2.

c. Interaction with adjacent beaches.

There is a common perception that "… seawalls increase erosion and destroy the beach." The limited available evidence is examined in this section. The term seawall herein means any type of coastal armoring that hardens the shoreline to a fixed position, hence, also applies to bulkheads and revetments.

(1) Background. Concern with how seawalls interact with adjacent beaches can be traced to events in the 1960s and coastal geology studies on the origins and movements of barrier islands (Hoyt 1967). Barrier islands are one of the 11 types of land/water interfaces on earth (Shepard 1976). Barrier beach systems make up about 35 percent of the United States coast stretching from Maine to Texas. They protect the bays and estuaries that lie behind them from direct wave attack, but are dynamic systems with sand volumes that depend on changing ocean conditions, sand supplies, and control boundaries that define the volume.

(a) As depicted schematically in Figure V-3-9a (adapted from Dolan and Lins 1987), barrier islands are commonly perceived to migrate landward with constant volume as sea level rise continues. Storm surge with high waves produce sand overwash into the back bay. The barrier is said to roll over itself, shoreline movement is termed recession, and no volume change means no coastal erosion. Some scientific evidence disputes the rollover model. Leatherman (1988) used shoreline position data to show that tidal inlet formation processes dominate and move far greater sediment quantities over the long term. The migration model also requires the moving sand volume to overlay continuous, basal peat layer from the muds and plants in the lagoon. Stratigraphic evidence contradicts this important aspect along the East Coast of the United States (Oertel et al. 1992). Using the Bruun (1962) rule, a 1-2 mm/year rise in sea level translates to about 0.05-0.2m/year shoreline retreat rate. These are relatively small changes in shoreline position and herein labeled as those at geologic time scales. See Part IV-2-9 for a full discussion of marine depositional coasts and barriers.

(b) When man enters the picture by constructing a road on the shore, he establishes a fixed reference line. The shoreline position relative to the road decreases in time as depicted in Figure V-3-9b. Once development has been permitted, continued erosion may threaten man's artifacts (roads, buildings, bridges, etc.) and some type of shore protection may be undertaken such as seawall construction. These structures are not intended to protect the beach, but areas landward from the beach. Armoring provides a nonmoving reference point on the beach to make the existing, historic erosion more noticeable. Few argue that the road alone is "…destroying the beach", but this same logic is applied by some when a revetment or seawall is present on an eroding shoreline and the dry beach width is reduced each year in front of the hardened shoreline (Pilkey and Wright 1988). Eventually, the ocean will reach the seawall (and road) and the dry beach will be gone.

(c) As also depicted in Figure V-3-9b, a seawall traps sediment behind the structure, reduces overwash and fixes the shoreline position. Continued erosional stress over time acts to deepen the water depth at the structure that is of concern for structural design. The trapped sediment formerly in the dune, bluff or cliff) is removed from that available to contribute to subaqueous bar building during storms. This trapped material is also prevented from contributing to the longshore sediment transport processes along the coast and may alter the sediment budget. The volume trapped relative to that naturally active in the cross-shore profile will be discussed further in the following paragraphs.

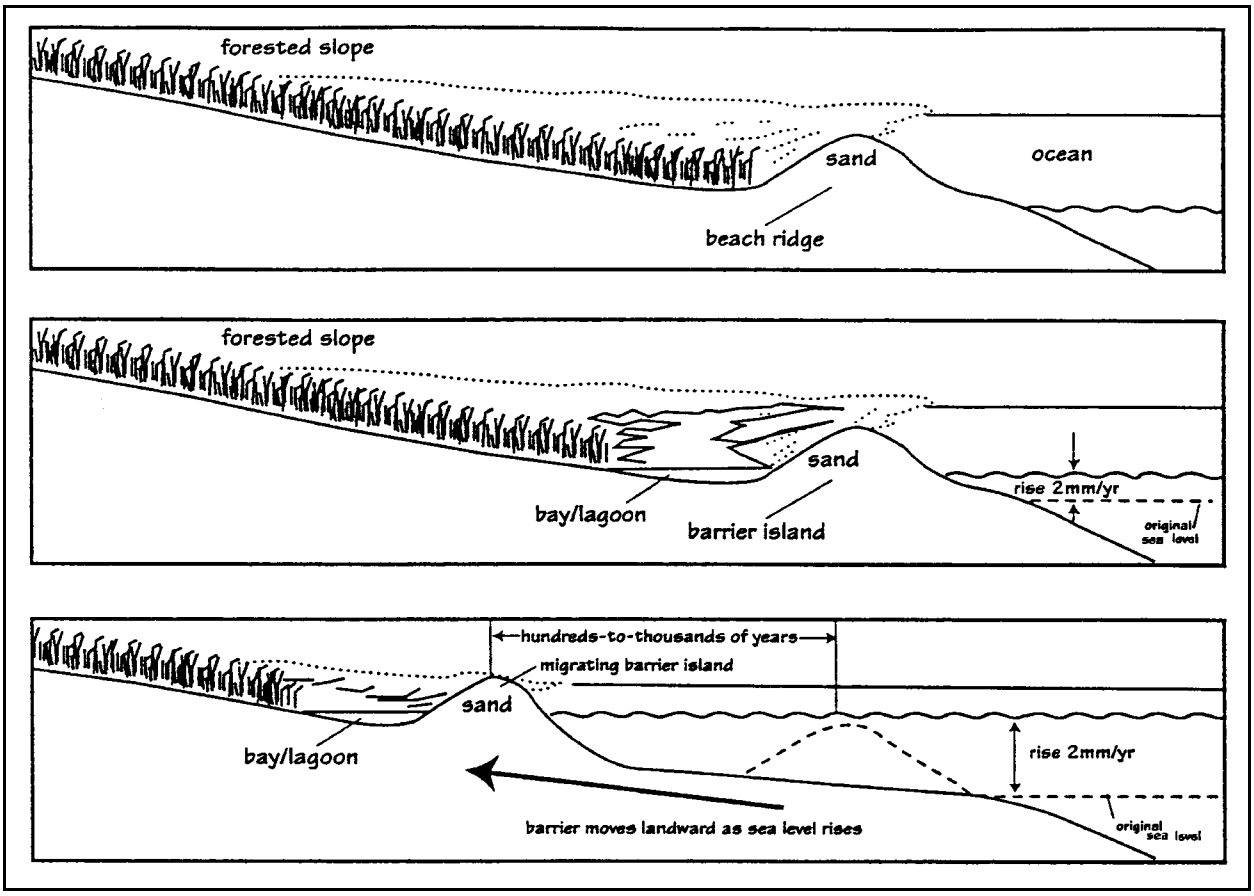

a. Barrier island migration at geologic time scales

Figure V-3-9. Time scales for shoreline movements (Continued)

(d) Natural erosion processes (wave-induced, sediment imbalances) plus anthropogenic induced erosion produce larger erosion rates than sea level rise (Komar et al. 1991). These are herein labeled as those at engineering time scales. The degree to which coastal armoring affects the adjacent beach has been the focus of some research effort.

(2) Literature review.

(a) Common concerns. Dean (1987) critically examined nine commonly expressed concerns about seawalls and adjacent beaches as summarized in Table V-3-3. Use was made of conservation of sediment mass, laboratory and field data, and the theory of sediment transport. Conclusions from this analysis were (numbers coincide with Table V-3-4) as follows:

Concerns Probably False (or Unknown)

- profile steepening (6)
- delayed beach recovery after storms (5)
- increased longshore transport (8)

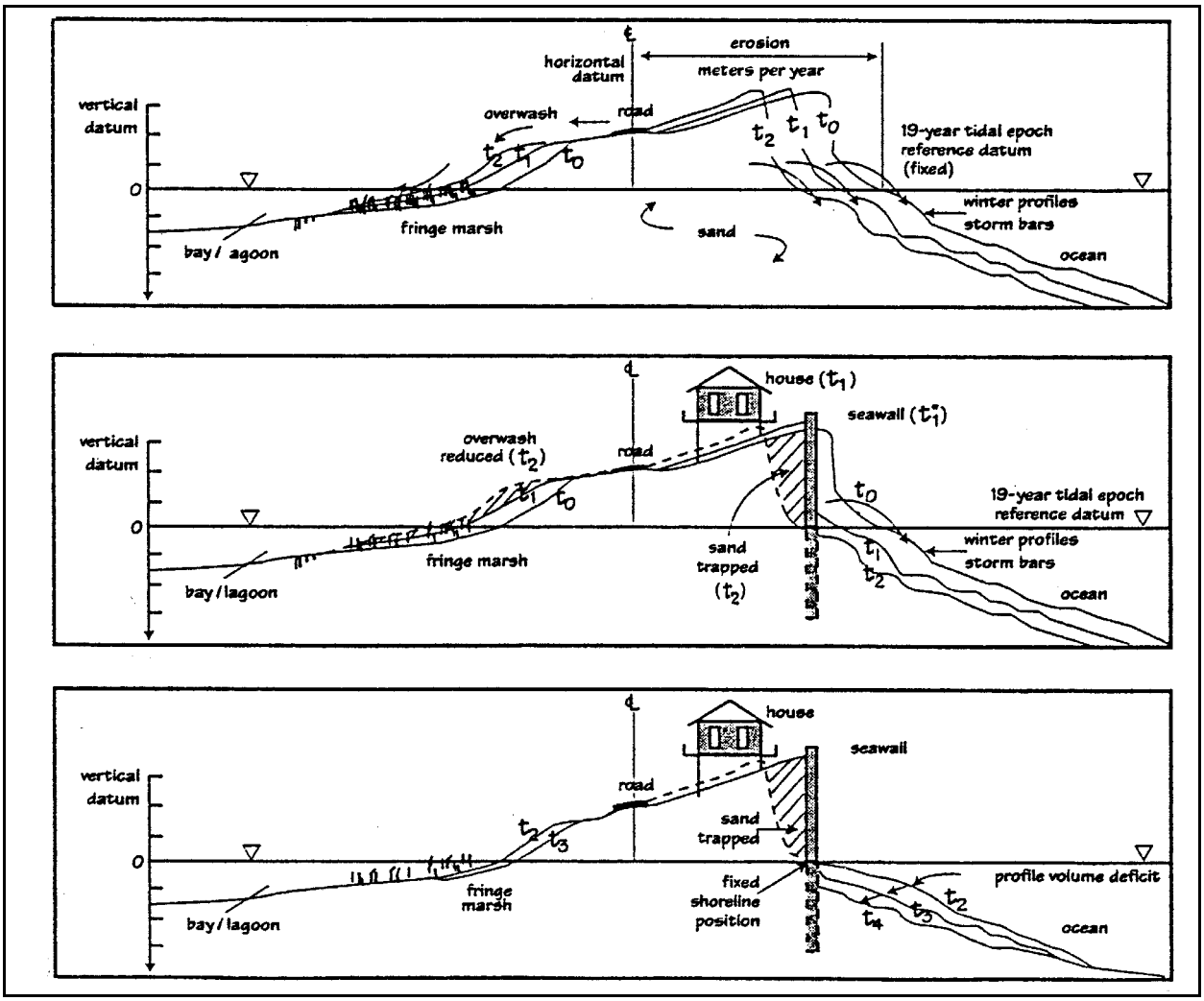

b. Coastal erosion at engineering time scales

Figure V-3-9. (Concluded)

- sand transport far offshore (9)
- increase in long-term, average erosion rate (3)

Concerns Probably True

- frontal effects (toe, scour, depth increase) (1)
- end-wall effects (flanking) (1)
- blockage of littoral drift when projecting into surf zone (groin effect) (4)
- beach width fronting armor likely to diminish (2)

Table V-3-3
Assessment of Commonly Expressed Concerns Related to Coastal Armoring (Dean 1987)

No.	Concern		Assessment
1	Coastal armoring placed in an area of existing erosional stress causes increased erosional stress on the beaches adjacent to the armoring.	True	By preventing the upland from eroding, the beaches adjacent to the armoring share a greater portion of the same total erosional stress.
2	Coastal armoring placed in an area of existing erosional stress will cause the beaches fronting the armoring to diminish.	True	Coastal armoring is designed to protect the upland, but does not prevent erosion of the beach profile waterward of the armoring. Thus, an eroding beach will continue to erode. If the armoring had not been placed, the width of the beach would have remained approximately the same, but with increasing time, would have been located progressively landward (see 2b).
2a	Beaches on eroding coastlines will diminish in front of fixed dune positions.	True	An eroding beach continues to erode relative to a fixed dune position. The width of the beach must diminish if the shoreline is eroding (Figure 1).
2b	Natural beaches on retreating barriers maintain the same beach width.	True	Relative to a retreating duneline, a shoreline eroding at the same rate results in a stable beach width.
3	Coastal armoring causes an acceleration of beach erosion seaward of the armoring.	Probably False	No known data or physical arguments support this concern.
4	An isolated coastal armoring can accelerate downdrift erosion.	True	If an isolated structure is armored on an eroding beach, the structure will eventually protude into the active beach zone and will act to some degree as a groin, interrupting longshore sediment transport and thereby causing downdrift erosion.
5	Coastal armoring results in a greatly delayed poststorm recovery.	Probably False	No known data or physical arguments support this concern.
6	Coastal armoring causes the beach profile to steepen dramatically.	Probably False	No known data or physical arguments support this concern.
6a	Coastal armoring destroys foreshore bar and trough features.	Probably False	No known data or physical arguments support this concern.
7	Coastal armoring placed well-back from a stable beach is detrimental to the beach and serves no useful purpose.	False	In order to have any substantial effects to the beaches, the armoring must be acted upon by the waves and beaches. Moreover, armoring set well-back from the normally active shore zone can provide “insurance” for upland structures against severe storms.
8	Seawalls increase the longshore sediment transport.	Unknown	No known data exists, physical arguments can support or discredit this concern. Needs research.
9	Seawalls cause sand transport a far distance offshore.	Probably False	No known data or physical arguments support this concern.
10	Other		

Kraus (1988) reviewed over 100 references (laboratory, field, theory, and conceptual studies) to make a thorough examination of the literature. This review and seven companion papers are presented in Kraus and Pilkey (eds. 1988). An updated literature review is found in Kraus and McDougal (1996) who examined 40 additional papers. In general, these extensive literature reviews agreed with Dean (1987) regarding which concerns were probably false and which many are true. The interested reader should consult these references for all the details.

(b) Definitions. The natural, background shoreline erosion rate, P_N and the rate *after* human activities P_A can define a coastal erosion ratio, R_P

$$R_p(x,t) = \frac{P_A}{P_N} \tag{V-3-3}$$

where the subscript R_p means shoreline position is used to define R. If profile data are available, then actual, coastal erosion volume could be employed to find a volume ratio, R_V as

$$R_v(x,t) = \frac{V_A}{V_N} \tag{V-3-4}$$

- where V_N is the natural erosion (volume loss) rate and V_A is the volume loss rate after construction of roads, seawalls, etc. at a given location. Clearly, if R_v (or R_p) is proven greater than unity under similar climatological conditions, then we may conclude that armoring has increased the natural, historical conditions at the site. The level of impact (if any) on the frontal and laterally adjacent beaches (1 percent, 5 percent, 10 percent, 50 percent, etc.) needs quantification. Pilkey and Wright (1988) use the terms passive and active erosion of the beach to distinguish between the perceived versus real natural and manmade causes, respectively.

- The volume of sediment trapped behind a seawall depends upon its position on the beach, crest elevation and length. Weggel (1988) defined six types of seawalls depending on their location on the beach and water depth at the toe. At one extreme (type 1) the wall is located landward of the limit of storm wave runup to have zero impact. At the other extreme (type 6) walls are located seaward of the normal breaker line. Types 2-5 lie in between and are said to have increasing effects on coastal sediment processes as the type number increases. Storm surges can create all six type conditions during a single storm event. Coastal erosion may also gradually alter the types.

- Dean (1987) postulated that the sediment trapped behind the wall resulted in an excess erosional stress to produce toe scour and excess erosion on unprotected adjacent property.

(c) Frontal impacts. Beach profile change, toe scour during storms and nearshore bar differences have been attributed to seawalls. Conventional wisdom has been that these impacts were due to wave reflection. Kraus and McDougal (1996) studied the field results by Griggs et al. (1997); laboratory work by Barnett and Wang (1998) and Moody and Madsen (1995) and their own research in the SUPERTANK (large scale) seawall tests (McDougal, Kraus, and Ajiwibowo 1996) to conclude that reflection is not a significant factor in profile change or toe scour. In the field, toe scour is more dependent on local, sediment transport gradients and the return of overtopping water (through permeable revetments or beneath walls) than a result of direct, cross-section wave action. Their conclusions also negate the common perception that sloping and permeable

surfaces produce less effects than vertical, impermeable walls. Scour and scour protection is covered in detail in Part VI-5-6.

(d) Impacts on laterally adjacent beach. Perhaps the key environmental concern is how a seawall affects a neighbor beach with no armoring. Does the wall create end-of-wall or flanking effects, i.e., R (x,t) greater than unity? Two studies are often cited to demonstrate flanking effects. Walton and Sensabaugh (1979) provide posthurricane Eloise field observations (14 data points) of additional bluff (contour) recession adjacent to seawalls in Florida. McDougal, Sturtevant, and Komar (1987) and Komar and McDougal (1988) present small scale, equilibrium beach, laboratory measurements (nine data points) for 7-14-cm waves at 1.1-sec periods normal to a median grain-size, sandy beach. The 23 data points are then combined to demonstrate the excess flanking erosion. The extent and length of the excess erosion is related to seawall length and is explained in terms of the seawall denying sand to the littoral system (e.g., Dean 1987).

- However, other mechanisms may be responsible. If the seawall extends seaward, it may act like a groin to cause downdrift impacts. Tait and Griggs (1991) measured an area of lowered beach profile extending 150 m downcoast at Site No. 4 in California. They proved that the upcoast end of the wall produced sand impoundment or a groin effect. Toue and Wang (1990) conducted laboratory experiments with waves attacking walled and nonwalled beaches at angles and concluded that downdrift impacts were a groin effect.

- Plant (1990) and Plant and Griggs (1992) observed rip currents at interior sections and at the ends of armored sections. These rip currents were attributed to wave overtopping, return flows and elevated, beach water tables during storms. McDougal, Sturtevant, and Komar (1987) also observed rip currents in their model tests previously described and from field evidence in Oregon. They concluded that this mechanism may be more responsible for end-of-wall, flanking effects than the sand trapping theory of Dean (1987).

- Griggs et al. (1997) discuss eight full years of field monitoring including the intense winter storm of January 1995. This storm did not produce end scour on the control beach at Site No. 4. They concluded from a comparison of summer and winter beach profiles at beaches with seawalls and on adjacent, control beaches, that no significant long-term effects were revealed.

- Basco et al. (1997) summarize the results of 15 years of profile survey data with 8-9 years taken before seawall construction at Sandbridge, Virginia, on the Atlantic Ocean. The shoreline has been eroding on average 2m/year (Everts, Battley, and Gibson 1983) long before wall construction began. One part of the study used five years of monthly and poststorm profile data at 28 locations (62 percent walled; 38 percent nonwalled) of the 7,670 m study reach. They concluded that the volume erosion rate was not higher in front of seawalls. However, seasonal variability of sand volume was slightly greater in front of the walled locations. Winter waves drag more sand offshore in front of walls, but summer swell waves pile more sand up against walls in beach rebuilding. Walled sections recovered about the same time as nonwalled beaches for both seasonal transitions (winter to summer) and following erosional storm events. These results were for a weighted average of total sand volume (subaerial) in front of the walled section and seaward of a partition for the nonwalled beach sections.

- At individual profile locations adjacent to walls, using the full 15 years of data, R_v values varied considerably. The evidence for any long-term, end-of-wall effects were considered inclusive for Sandbridge beach. There was never evidence of flanking effects after storms on adjacent beaches (Basco et al. 1997). This study continues. In general, Basco et al. (1997) have confirmed all the conclusions of Dean (1987), Kraus (1988) and Kraus and McDougal (1996) except the end-wall, flanking effect.

- Natural beaches coexist in front of the rocky cliffs and naturally-hardened shorelines at many locations throughout the world. A major, comprehensive research effort is needed to quantify the effect of sand trapping on frontal and downdrift beaches.

(3) Active volume in the cross-shore profile. Successive cross-shore surveys of the beach profile to closure depth reveal spatial variations in vertical elevation at each location. In the absence of lateral transport, the eroded sections balance the accreted areas, i.e., sediment volume is conserved. The active sediment volume is defined as one-half of the total volume change between two successive surveys. The 12-year, biweekly nearshore bathymetric data set surveyed at the Corps of Engineers Field Research Facility, Duck, North Carolina, has been analyzed to quantify the total active sand volume, its spatial variation across the profile, and its relation to long-term, fair-weather, and storm periods (Ozger 2000). An empirical relationship between storm wave power and active sand volume has been developed for the Duck site. Prestorm morphology and duration of storm surge are possible factors for the scatter in the power versus active sand volume relationship. The maximum value of active sand volume was $140 m^3/m$ (350 cu yd/ft). Different tidal conditions, wave climate and hard bottoms (or reefs) limit the cross-shore movement of sediment. Determinations of the naturally active, sand volume should be made for other sites. Basco and Ozger (2001) summarize the above results and discuss various applications in coastal engineering. The seawall trap ratio, WTR can be defined as:

$$\text{WTR} = \frac{\text{Wall Trap Volume}}{\text{Active Sediment Volume}} \tag{V-3-5}$$

to quantify the relative impact of the sand volume removed from the system. Dean (1987) failed to consider the WTR. Weggel (1988) qualitatively addresses the importance of the numerator increasing with type number but also did not consider the significance of the denominator. The spatial distribution of the WTR is also important relative to wall location. At locations with seawalls where the WTR is small, annual mitigation may be economic.

(4) Sand rights and mitigation. A few states have adopted sand mitigation polices and procedures to permit seawall construction and maintain a healthy beach. The idea is to annually replace the beach materials trapped behind the structure with a volume calculated by some formula. The methodology in Florida has both on offshore and longshore transport components which require knowledge of the annual erosion rate and net, longshore transport rate, respectively (Terchunain 1988). Sarb and Ewing (1996) present formulas for cliff and bluff erosion impacted by seawall construction in California. These formulas attempt to deterministically estimate the wall trap volume (numerator) but do not consider the active sediment volume (denominator) in Equation V-3-5. The relative volume trapped is unknown. Field research efforts to date have yet to confirm the trapping theory of Dean (1987). The reason may be that the trapped volume is only a small percentage of the total, active sand volume in the profile. The WTR is near zero so that downdrift impacts are minimal and lost in the data scatter. See also Part III-5-13 for discussion of measures to manage human influence on sediment supply. Who owns the sediments on eroding shorelines, the local property owners or downdrift interests, is a legal question facing society. The subject of sand rights (Magoon 2000) is an extremely complicated issue that may require settlement by the nation's courts.

V-3-3. Beach Stabilization Structures

a. Naturally stable shorelines. Part IV-2 classifies coasts and their morphology. Marine depositional coasts with barriers and beaches are one of the most widely distributed geomorphic forms around the world. (Part IV-2-9, 10). They form a flexible buffer zone between land and sea. The subaerial beach has two major zones. The foreshore extends from the low-water line to the limit of wave uprush at high water. At this point, the backshore extends to the normal landward limit of storm wave effects. This landward limit is usually marked by a foredune, cliff, structure, or seaward extent of permanent vegetation. The backshore is only affected during storms when surges and high waves transport backshore sediments. This exposed, subaerial beach definition is accepted by the general public. Some authors include the surf zone and bars out to closure depth, i.e., the subaqueous part of the beach, because both parts, subaerial and subaqueous, exchange sediment. Beaches may stretch for hundreds of kilometers or others, called pocket beaches, are restricted by headlands and are only tens of meters in length. Figure IV-3-31 schematically summarizes factors controlling morphodynamics along a range of coastal environments extending from rocky, to noncohesive sediments to cohesive shorelines.

(1) Many beaches are naturally stable. In general, wide beaches are exposed to more severe wave conditions at that location, but the relationship between beach width (or section volume) and storm energy for naturally stable shorelines has yet to be determined. Figure V-3-10a displays a stable, pocket beach on Bruny Island, Tasmania, Australia, where beach width increases along the more exposed section of coast (from Silvester and Hsu 1993). The protected reach behind the headland is much narrower than that receiving a direct attack by large waves during storms. The dark area is vegetation and landward limit of the backshore, subject to normal storm wave effects. If this photo were taken at high tide, a minimum beach width for a stable shoreline could be determined.

(2) This concept of a minimum beach width (or volume) is schematically illustrated in Figure V-3-10b. The volume of sediment present protects the uplands (foredune, cliff, structure, or vegetation) from damage under normal or average storm conditions. The landward boundary of the backshore is a reference baseline for shore protection. On eroding beaches, the backshore may be missing, and the high-water uprush may impinge directly on cliffs or structures. Both natural and anthropogenic agents may cause the erosion. But a minimum, beach width is still necessary for natural shore protection at the eroding site.

b. Minimum dry beach width. Professor Richard Silvester in an article on the stabilization of sedimentary coastlines (Silvester 1960) wrote:

> "…to allow for storm-cycles and the short-term reversals of drift, a sufficient width of beach should be allowed as working capital on which the sea can operate. Once the coast has been stabilized, by preventing the net movement of sediment, no long-term erosion need be anticipated and the 'active' beach width can be minimized." (p. 469)

(1) As illustrated in Figure V-3-11a,b, for both naturally open beaches and pocket beaches between headlands, the minimum, dry beach width, Y_{min} is defined as the horizontal distance between the mean highwater (mhw) shoreline and the landward boundary or base (reference) line. The mhw shoreline is employed because it is the common, land/water boundary shoreline on maps; it is more readily identified from aerial photos; and it is a more conservative, minimum width (and volume) for shore protection. It is the minimum, dry beach width required to protect the foredune, cliff, structure, or vegetation behind the baseline from normal storm conditions. The beach does the work, and it's resilience and recovery are critical for long-term shore protection.

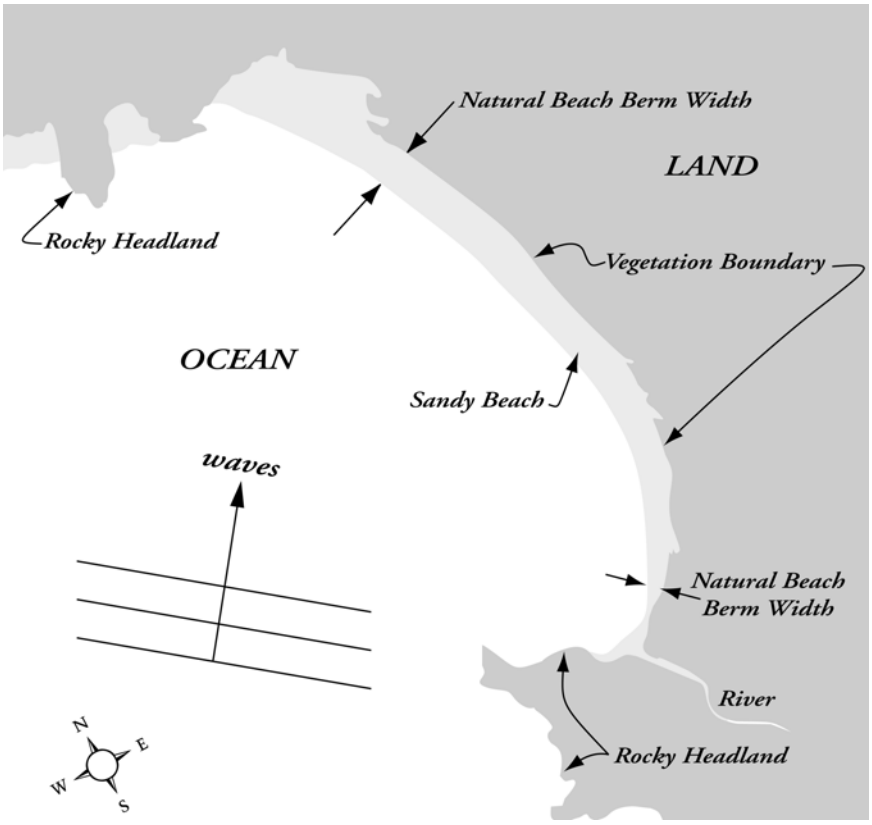

a. Aerial view (schematic from photograph) of Cloudy Bay, Bruny Island, Tasmania, Australia, showing greater natural beach berm width along the more exposed section of coast (adapted from cover photograph and Figure 3-21 in Silvester and Hsu (1993))

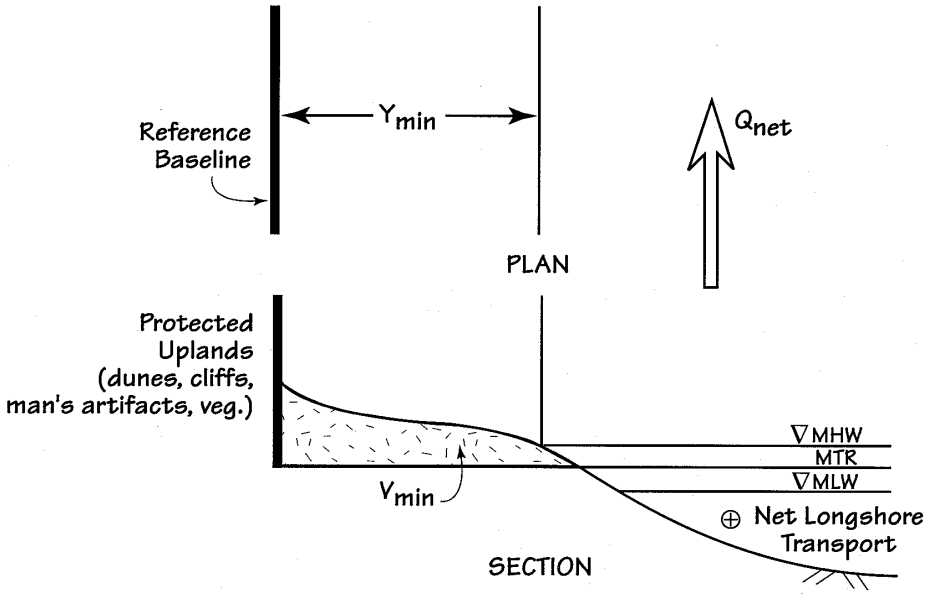

b. Schematic of minimum dry beach width, Y_{min}

Figure V-3-10. Naturally stable shorelines with beach width dependent on stormwave energy (from Silvester and Hsu 1993)

(2) Normal storm wave conditions are expected once every two years or maybe every year. More intense, less frequent storms will reach the foredune, cliffs, structure or vegetation line. Beach stabilization structures can provide upland protection beyond the baseline for these rarer storm events. At a minimum, these structures should be designed to provide the minimum, dry beach width for shore protection.

(3) Figure V-3-11c,d,e depict the three most common beach erosion mitigation structures, namely headland breakwaters, nearshore breakwaters, and a groin field. And, each schematic displays the minimum, dry beach width, Y_{min} that is required for design. In each case, it is located in the gap area with greatest wave energy. The EST methodology discussed in V-3-1-c can be applied to determine the probability distribution of dry beach widths including the minimum for normal storm conditions. Functional design of these structures based on empirical knowledge is presented in the next sections. Two key factors are the minimum dry beach width (or volume) and the natural, sediment transport processes at the site. Explicit acknowledgment of Y_{min} as design criteria is often missing in coastal engineering design.

c. Headland breakwaters.

(1) Background and definitions. Natural sandy beaches between rocky headlands have been called a variety of names in the literature, related to the curved shape of the bay found at many coasts around the world. Silvester and Hsu (1993) summarize the literature. See also Part III-2-3-i. for a list of references. Because of their geometry, they have been called spiral beaches, crenulate-shaped bays, log-spiral and parabolic-shaped shorelines, headland bay beaches and pocket beaches. Half-Moon Bay in California is a good example as first discussed by Krumbein (1944) and shown as Figure 4.3 in Silvester and Hsu (1993). Many researchers have studied the dynamic processes of this geomorphic feature, but Silvester (1960) was the first to examine their static equilibrium and propose the creation of artificial headland breakwaters as a shore protection structure. Figure V-3-12 presents a sketch of an artificial headland system and beach planform (from EM 1110-2-1617, "Coastal Groins and Nearshore Breakwaters."). Normal wave conditions with a predominant swell direction produce a maximum indentation between two fixed points (breakwater structures) and a fully equilibrated, planform shape. Thus man can mimic nature by building the headland breakwaters and letting nature sculpture the beach with a limiting indentation and shoreline that is stable.

(2) Physical processes. Waves from one persistent, dominant direction, β, diffract around the upcoast headland and refract into the bay. Waves will break at angles to the shoreline causing sediment transport and shoreline shape adjustment (nonequilibrium shape) until a full equilibrium shape is reached. At this stage, waves break simultaneously around the entire periphery, no longshore currents and no littoral drifts occur within the embayment. The tangent section, adjacent to the downdrift headland is exactly parallel to the normal wave crest direction from offshore. Such a bay is said to be in static equilibrium (i.e., it is stable until there is a shift in the dominant wave direction). Minimal amounts of additional sediments enter or leave past the headland boundaries. Bidirectional, dominant, wave impact (swells and storms) and sediment bypassing the headlands are two reasons for littoral drift to continue around the bay. These bays are said to be in dynamic equilibrium and can be predicted within certain tolerances. Only the static equilibrium shapes can be related to wave input. The ability to calculate the static equilibrium shape and maximum indentation are needed for the functional design of headland breakwaters.

(3) Functional design. Early investigators employed a log-spiral curve to fit the planform shape (Yasso 1964; Silvester 1970). In practice it is difficult to apply because the center of the log-spiral does not match the point at which diffraction begins to take place.

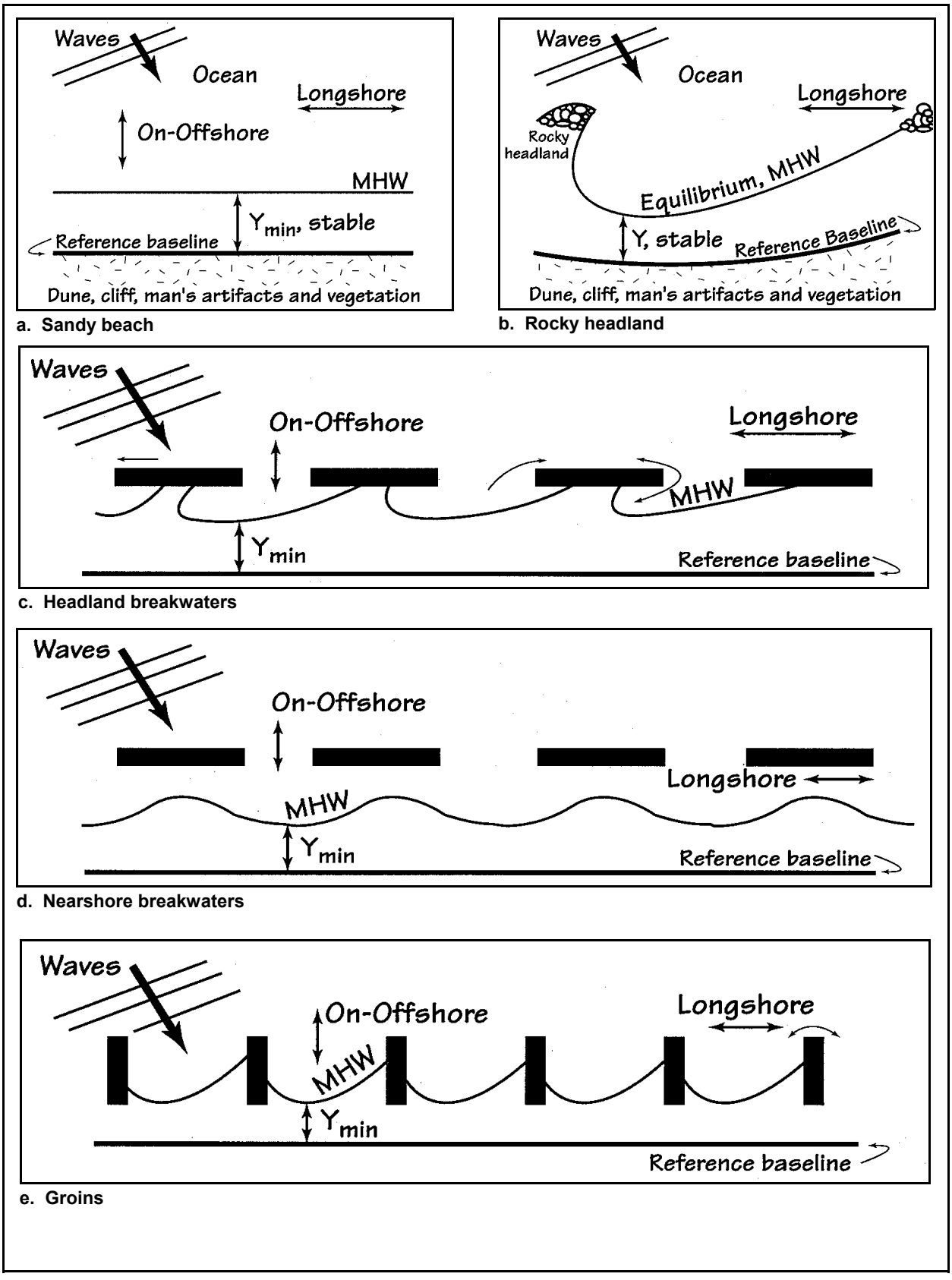

Figure V-3-11. Natural and artificial stable shorelines with minimum dry beach width, Y_{min}

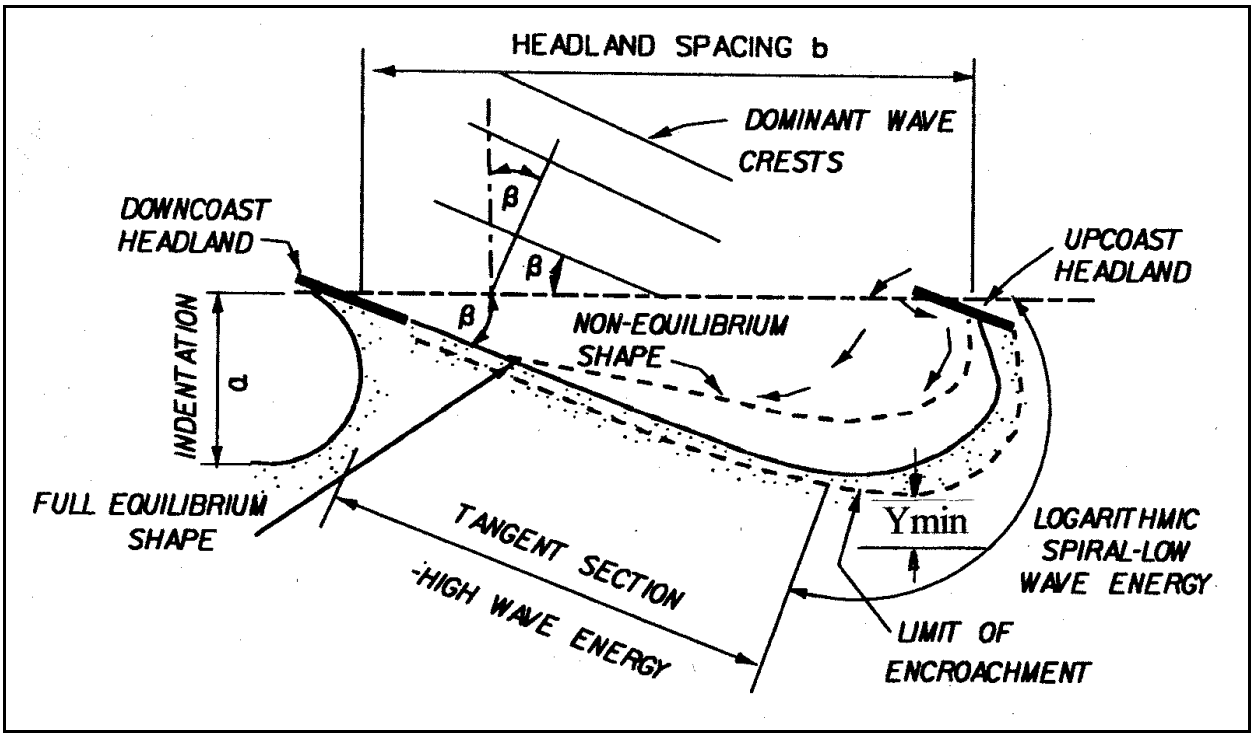

Figure V-3-12. Definition sketch of artificial headland system and beach planform (from EM 1110-2-1617)

(a) Parabolic bay shape. A new empirical approach that uses shoreline data from bays in static equilibrium and physical models has been developed by Hsu, Silvester, and Xia (1987, 1989). It is called a parabolic model because the data has been used to fit a second order polynomial. Figure V-3-13 presents a definition sketch of the four key geometric variables, R, R_o, β and θ, that form the parabolic model. The model center now exactly matches the initial diffraction point. Part III-2-3-i presents complete details including definitions of R, R_o, β and θ; the parabolic model equation (2-24); the three coefficients C_o,C_1, C_2 related to wave angle β in Figure III-2-27 and limitations of the data. An Example Problem III-2-8 is also presented to illustrate an application of the model which assumes one predominant wave direction exists at the site of interest. Many more examples and discussion is found in Silverster and Hsu 1993.

(b) Minimum width for storm protection. As illustrated in Figure V-3-12, storm waves may be from a different direction to cut back the beach and form a new limit of encroachment planform shape. A more detailed definition sketch in perspective and cross section is presented in Figure V-3-14 (adopted from Hardaway, Thomas, and Li 1991). Two nearshore breakwaters together with beach nourishment form the headland breakwater design for shore protection. The following terms are defined:

L_s Length of breakwater structure

L_g Gap distance between adjacent breakwaters

d_s Depth (average) at breakwater below mean water level

e Erosion of shoreline (mhw) from design storm

Y_o Distance of breakwater from original shoreline

Y_g Maximum indentation under normal wave conditions

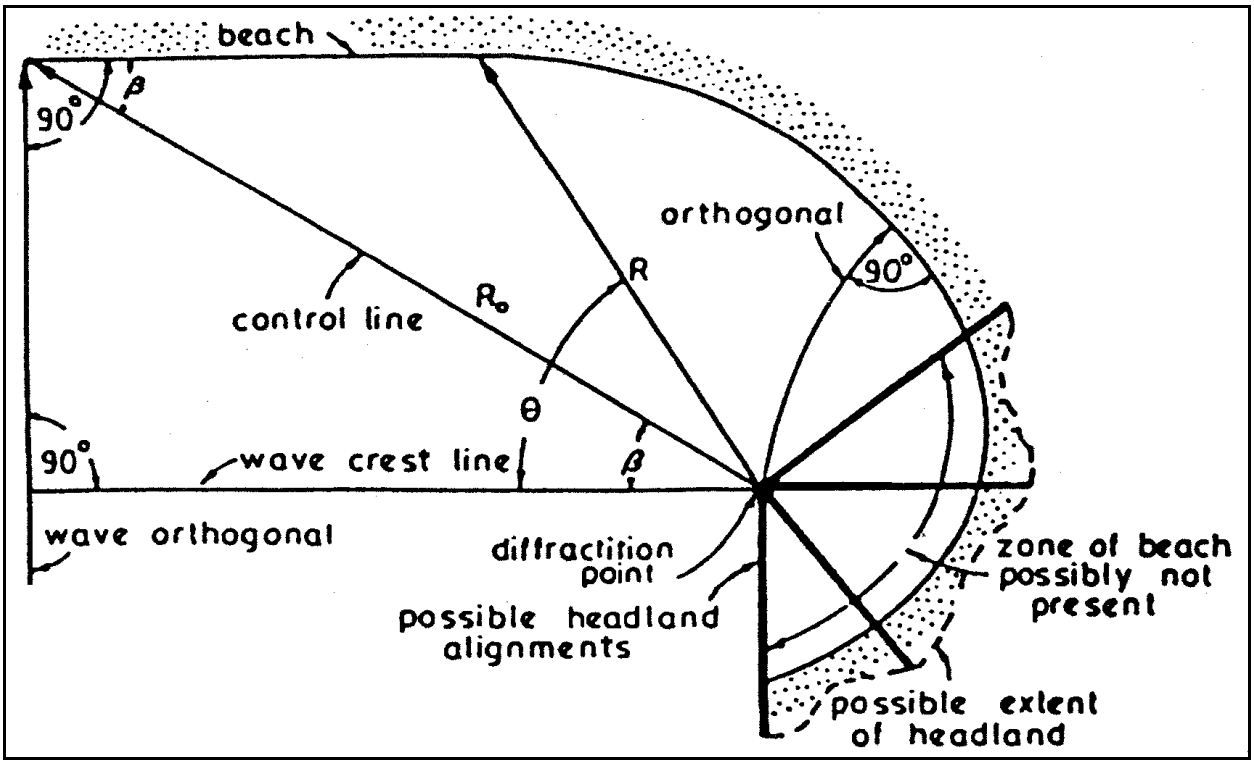

Figure V-3-13. Definition sketch of parabolic model for planform shape

Y Distance of breakwater from nourished shoreline

Y_{min} Minimum distance from base (reference) line to mhw shoreline after design storm event

B Minimum beach width at mhw after nourishment

W Width of design beach nourishment

Z_s Backshore elevation at baseline

F_B Breakwater freeboard, mhw to crest

Q_{net} Net longshore sediment transport rate

Q_{gross} Gross longshore sediment transport rate

$Q_{offshore}$ Offshore sediment transport rate for design storm

The planform shape and maximum indentation, Y_g can be estimated by the parabolic shape model previously discussed above. A hyperbolic tangent shape was developed by Moreno and Kraus (1999), which may be more convenient to apply than the parabolic shape.

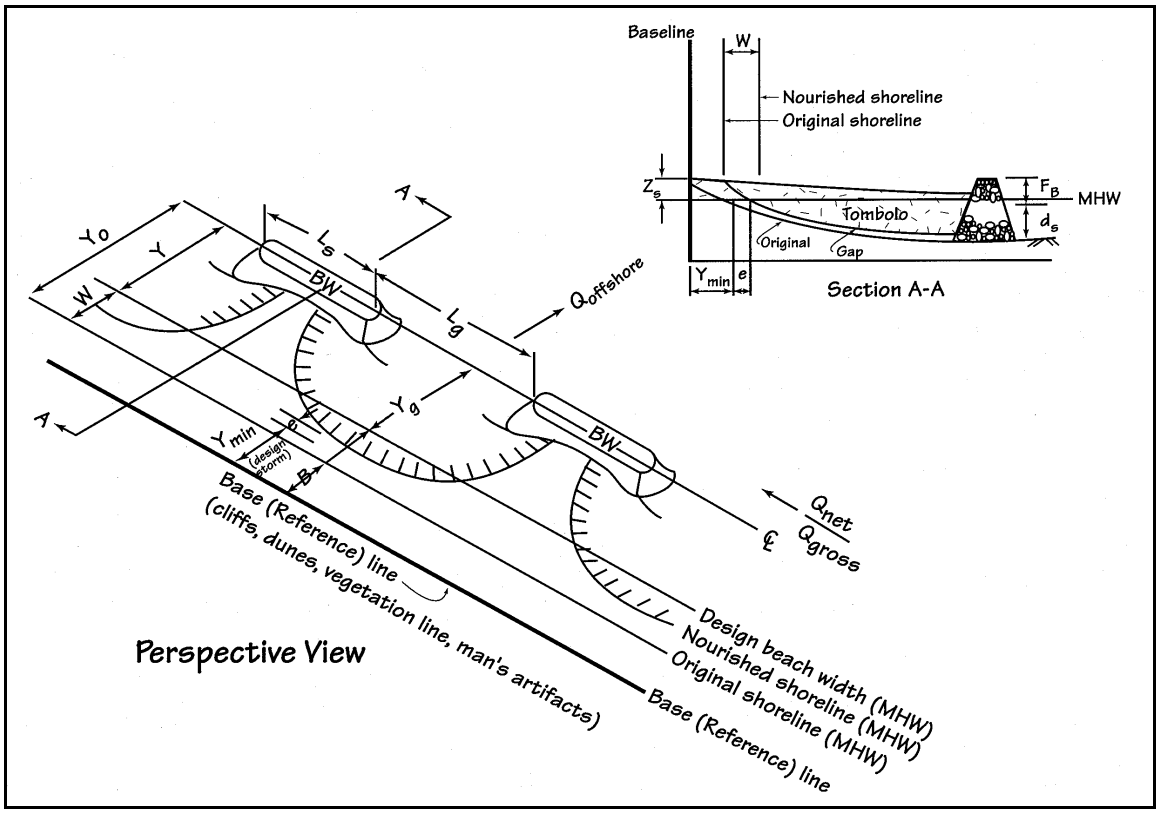

Figure V-3-14. Definition sketch, headland breakwaters

(4) Applications on Chesapeake Bay. Headland breakwater systems have been built along the shoreline of the Chesapeake Bay for shore protection and to maintain recreational beaches. Since 1985, 60 breakwaters at 19 sites have been designed, constructed, monitored and analyzed to learn about their functional performance (Hardaway, Thomas, and Li 1991; Hardaway, Gunn, and Reynolds 1995; Hardaway and Gunn 1991, 1995, 1998, 1999). The design method employs a three-step procedure that accounts for bimodal annual wave climates (annual and storm wave direction) a numerical wave transformation model for near-shore wave refraction and shoaling, and the beach planform shape model for static equilibrium (Silverster and Hsu 1993). System design also includes upland runoff, bank geology, shoreline morphology, sedimentation, and aesthetics. Potential impacts to adjacent shorelines must also be considered and minimized.

Figure V-3-15a displays before and after photos for the Van Dyke project on the James River. The dark area along the shore is vegetation after the new bank was graded to provide sand for beach nourishment as part of the construction. Figure V-3-15b displays 12 nearshore breakwaters at the Luter project site (James River) one year after construction. Note the use of Y-shaped breakwaters to refine the shape of the planform beach. Moving the breakwater ends further offshore changes the diffraction point to provide the desired planform beach shape. Short breakwaters at both ends pin the downdrift beach. Experience since 1991 indicates that on the Chesapeake Bay, the ratio of Y_g/L_g is about 1.7 for stable, equilibrium-shaped beaches. As illustrated in Figure V-3-16, at the Murphy project site (Potomac River) the present shore is still eroding and will require several years to reach the predicted embayment shoreline shape. Hardaway, Thomas, and Li 1991 present minimum design parameters for medium wave energy shorelines (average fetch 1-5 nautical

a. Van Dyke Project

b. Luter Project

Figure V-3-15. Headland breakwater projects on the James River estuary, Chesapeake Bay (from Hardaway and Gunn 1999)

miles) that include guidelines for distance B (Figure V-3-14) related to storm surge and wave conditions. Much more research is needed to relate Y_{min} to design storm conditions for the functional design of headland breakwater systems. The next section discusses analytical methods to estimate Y_{min} during storm conditions.

d. Nearshore breakwaters.

(1) Background and definitions. Nearshore breakwaters are detached, generally shore-parallel structures that reduce the amount of wave energy reaching a protected area. They are similar to natural bars, reefs or nearshore islands that dissipate wave energy. The reduction in wave energy slows the littoral drift, produces sediment deposition and a shoreline bulge or salient feature in the sheltered area behind the breakwater. Some longshore sediment transport may continue along the coast behind the nearshore breakwater.

(a) Figure V-3-17 displays a salient behind a single breakwater and a multiple breakwater system with both salient and a tombolo when the shoreline is attached to the breakwater. The tombolo may occur naturally or be forced during construction to produce a headland breakwater as discussed in the previous section. The tombolo blocks normal, longshore sediment transport behind the structure. Daily tidal variations may expose a tombolo at low tide while only a salient feature is visible at high tide as occurs at the Winthrop Beach, Massachusetts, nearshore breakwaters constructed in 1935 (Dally and Pope 1986). Figure V-3-18 displays the single 610 m long, rubble-mound breakwater at Santa Monica, California, and salient feature (circa 1967). Periodic dredging is needed to prevent tombolo formation. The multiple, nearshore breakwater system at Presque Isle, Pennsylvania, is shown in Figure V-3-19 (Fall 1992). Fifty-five breakwaters were built in 1989-1992 to protect 8.3 km (13.8 miles) of Lake Erie shoreline (Mohr 1994).

(b) In general, the primary objectives of a nearshore breakwater system are to:

- Increase the fill life (longevity) of a beach-fill project.
- Provide protection to upland areas from storm damage.
- Provide a wide beach for recreation.
- Create or stabilize wetland areas.

(c) In addition, adverse effects on downdrift beaches should be minimized by consideration of the impact on longshore sediment transport.

(d) Numerous variations of breakwater types exist. Here, the focus is on detached, offshore breakwaters not connected to shore by any type of sand-holding structure. They may be low-crested to permit increased wave transmission and lower construction costs. They also may be reef-type breakwaters constructed of homogeneous stone size as opposed to the traditional, multilayer, cross-section design. Headland breakwaters (natural or constructed tombolos) are discussed (Part V-3-3). Another type of shore-parallel, offshore structure is called the submerged sill or perched beach and is discussed in (Part V-3-3). Additional

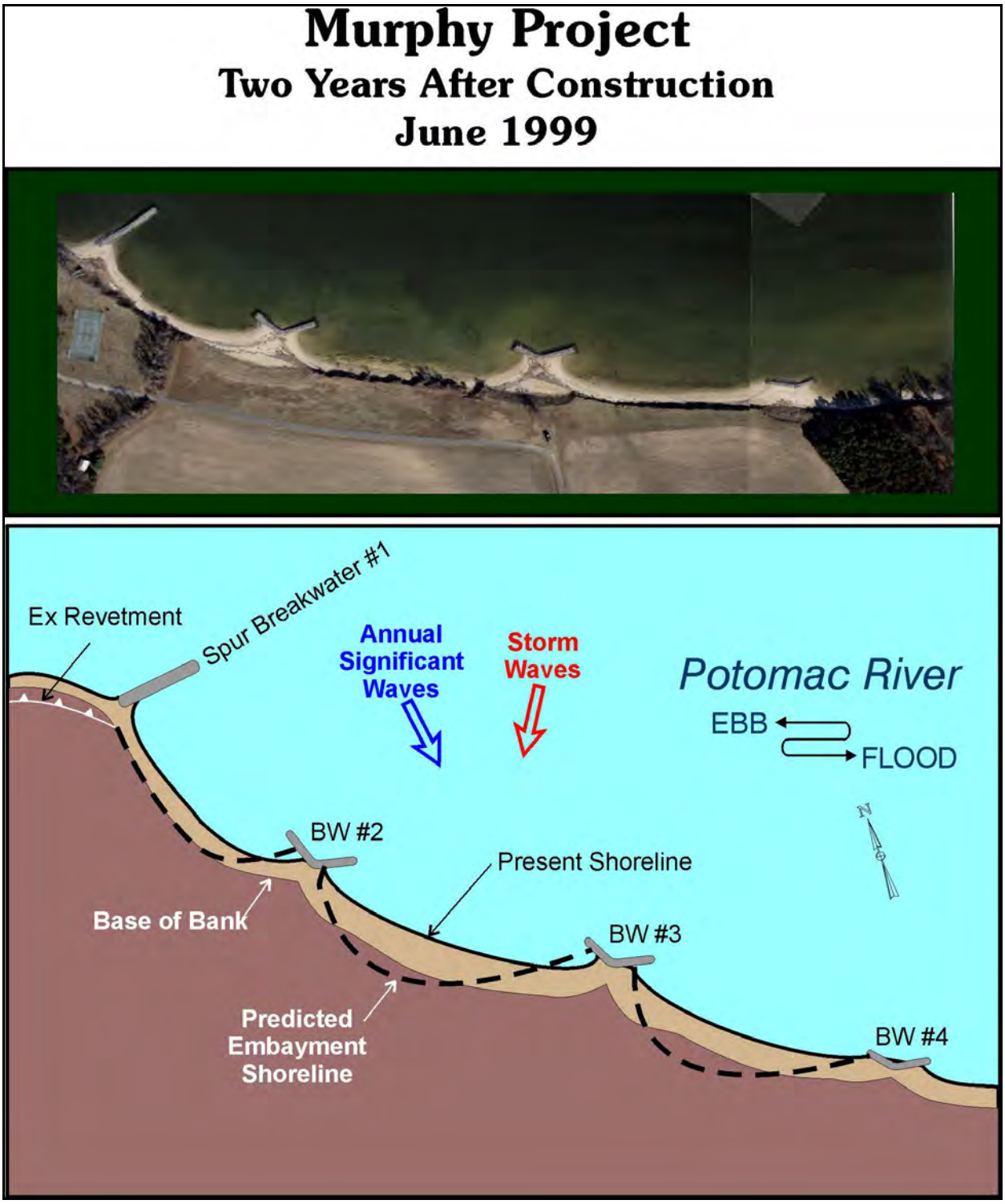

Figure V-3-16. Headland breakwater project on the Chesapeake Bay (from Hardaway and Gunn 1999)

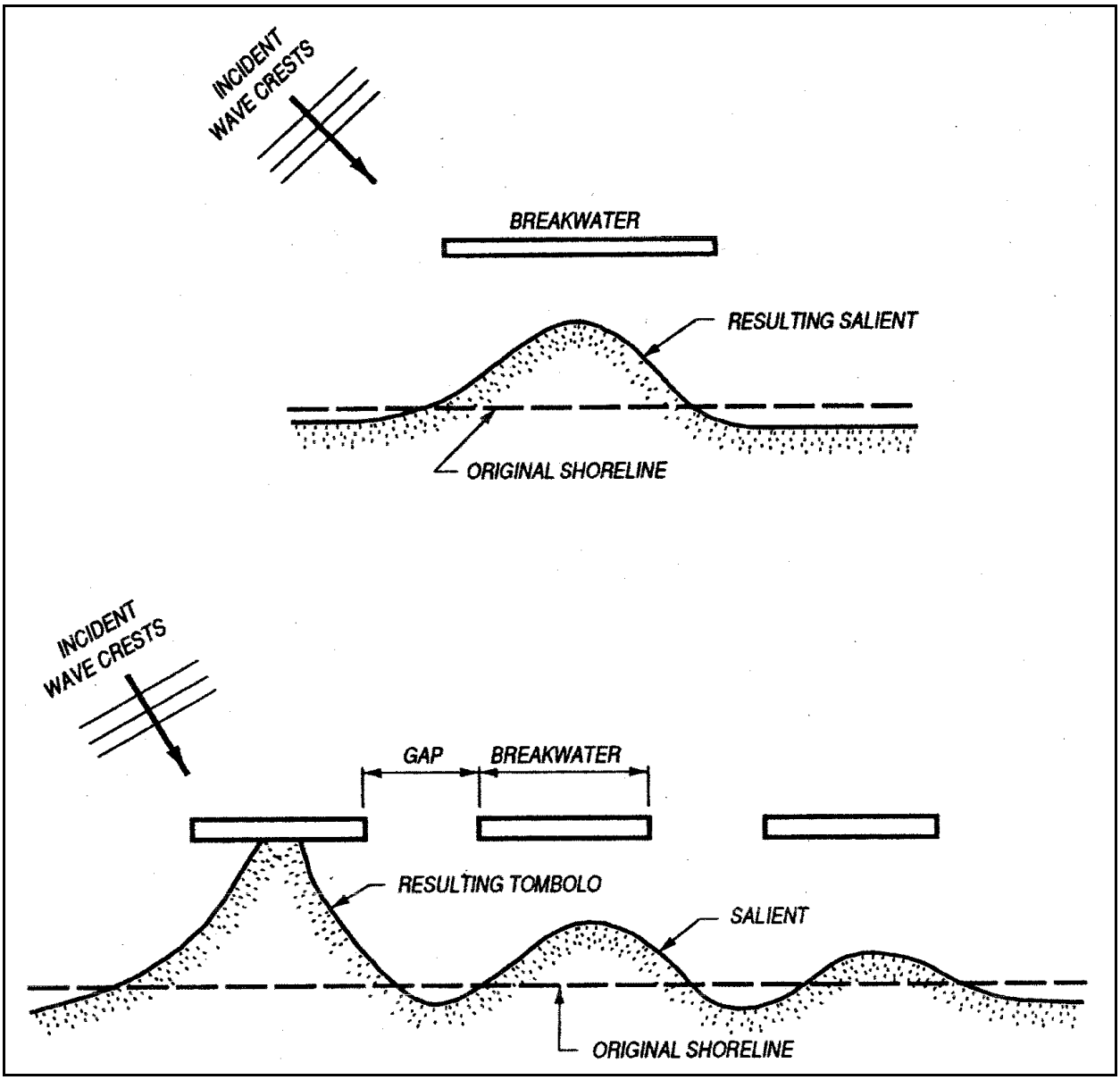

Figure V-3-17. Types of shoreline changes associated with single and multiple breakwater (from EM 1110-2-1617)

information and references on other breakwater classifications can be found in Lesnik (1979), Fulford (1985), Dally and Pope (1986), EM 1110-2-1617 and Chasten et al. (1993).

(2) Physical processes.

(a) Normal morphological responses. Waves breaking at an angle to the shore produce time-averaged, longshore (littoral) currents and longshore sediment transport. Consider the left breakwater in Figure V-3-20 with wave energy in the plus direction. Physical processes at macro-level scales in the vicinity of the breakwater for normal wave and water level conditions are as follows. The breakwater shelters the coast immediately behind the structure and adjacent areas (diffraction) from the incoming waves. Breaking wave heights are smaller in the sheltered areas. The exposed, gap areas have larger breaking wave heights. The

a. Salient with eroded downdrift (longshore drift is from bottom to top)

b. Deteriorated breakwater allowing wave transmission

Figure V-3-18. Santa Monica, California, breakwater and salient (circa 1967). Littoral drift from bottom to top (from Chasten et al. 1993)

Figure V-3-19. Breakwater construction and salients; two views of Presque Isle, Pennsylvania (from Mohr 1994)

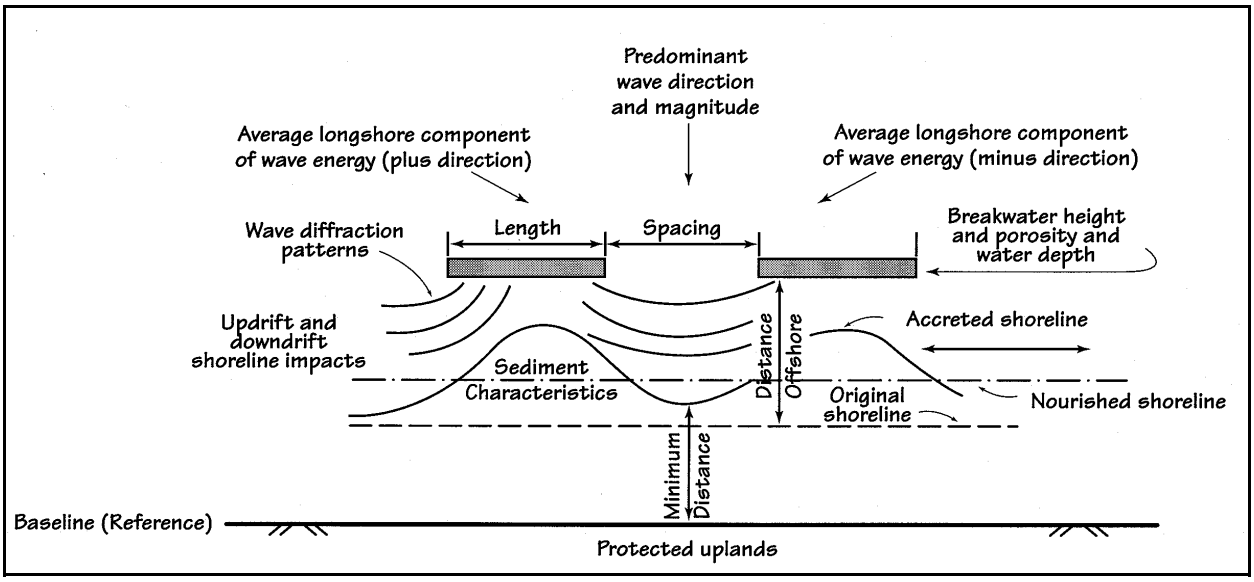

Figure V-3-20. Definition schematic for nearshore breakwaters

wave induced, mean water level change (setup) in the exposed, gap areas is larger than in the sheltered areas. Longshore variability in the wave setup produces gradients in the mean water surface. Water flows from the elevated levels in the gap area towards the lower, sheltered area to accelerate the longshore current flowing towards the sheltered area behind the structure from the left side. These gradients also change the direction of the current which is driven away from the breakwater in the region immediately downdrift of the breakwater (right side). These two current systems (littoral current and setup current) merge behind the structure to give rise to complex circulation patterns. The acceleration of the littoral current updrift causes initial erosion of the beach on the updrift side. The same occurs in the area immediately downdrift. These currents carry the eroded material towards the sheltered area, where it deposits. These mechanisms cause the patterns of deposition behind and erosion on either side that is observed in nature (see Figure V-3-20). The above physical description had been confirmed by a two-dimensional, numerical (horizontal plane) joint processes (waves, currents, sediment transport) morphological modeling system (Zyserman et al. 1998).

(b) Storm processes and response. Protection afforded by the breakwater will limit erosion of the salient during significant storms. The exposed gap area will be eroded with sediment dragged offshore during storms. Breakwater height, length, wave transmission characteristics and distance from shore contribute to its effectiveness to provide a minimum dry beach width, as discussed further in the following paragraphs.

(3) Functional design. Prototype experience for the functional design of nearshore breakwaters in the United States is generally limited to sediment-starved shores with fetch-limited wave climates on the Great Lakes, Chesapeake Bay, and Gulf of Mexico shores (Pope and Dean 1986). Table V-3-4 is a summary of U.S. projects up to 1993 (Chasten et al. 1993). Nearshore breakwaters for shore protection have also been used extensively for shore protection in Japan and Israel (Toyoshima 1982) and in Denmark, Singapore and Spain (Rosati 1990). Detailed summaries of the literature, previous projects, and design guidance are provided in a number of references (Lesnick 1979; Dally and Pope 1986; Pope and Dean 1986; Kraft and Herbich 1989; Pope 1989; Rosati 1990; Rosati and Truitt 1990; EM 1110-2-1617; and Chasten et al. 1993). One key aspect of all these efforts has been to determine under what conditions salients or tombolos will naturally form behind the breakwater.

Table V-3-4
Summary of U.S. Breakwater Projects (from Chasten et al. 1993)

Coast	Project	Location	Date of Construction	Number of Segments	Project Length	Segment Length	Gap Length	Distance Offshore Preproject	Water Depth	Fill Placed	Beach[1] Responses	Constructed By	Maintained By
Atlantic	Winthrop Beach (low tide)	Massachusetts	1935	5	625 m	91 m	30 m	Unknown	3.0 m (mlw)	No	1	State of Mass.	
Atlantic	Winthrop Beach (high tide)	Massachusetts	1935	1		100	30	305	3.0 (mhw)	No	3	State of Mass.	
Atlantic (Potomac River)	Colonial Beach (Central Beach)	Virginia	1982	4	427	61	46	64	1.2	Yes	2	USACE	
Atlantic (Potomac River)	Colonial Beach (Castlewood Park)	Virginia	1982	3	335	61, 93	26, 40	46	1.2	Yes	1	USACE	
Chesapeake Bay	Elm's Beach (wetland)	Maryland	1985	3	335	47	53	44	0.6-0.9	Yes	1	State of Maryland	
Chesapeake Bay	Elk Neck State Park (wetland)	Maryland	1989	4	107	15	15		0.6-0.9	No	2-4	USACE	USACE
Chesapeake Bay	Terrapin Beach (wetland)	Maryland	1989	4		23	15, 31, 23	38.1	0.6-0.9	Yes	5	USACE	USACE
Chesapeake Bay	Eastern Neck (wetland)	Maryland	1992-1993	26	1676	31	23		0.3-0.6	Yes		U.S. Fish and Wildlife Service, USACE	U.S. Fish and Wildlife Service
Chesapeake Bay	Bay Ridge	Maryland	1990-1991	11	686	31	31	42.7		Yes	4	Private	Private
Gulf of Mexico	Redington Shores	Florida	1985-1986	1	100	100	0	104		Yes	1	USACE	USACE
Gulf of Mexico	Holly Beach	Louisiana	1985	6	555	46, 51, 50	93, 89	78, 61	2.5	No	4	State of Louisiana	State of Louisiana
Gulf of Mexico	Holly Beach	Louisiana	1991-1993	76		46, 53	91, 84	122, 183	1.4, 1.6	Yes	3	State of Louisiana	State of Louisiana
Gulf of Mexico	Grand Isle	Louisiana		4	84	70	21	107	2	No	3	City of Grand Isle	City of Grand Isle
Lake Erie	Lakeview Park	Ohio	1977	3	403	76	49	152	3.7	Yes	4	USACE	City of Lorain
Lake Erie	Presque Isle	Pennsylvania	1978	3	440	38	61, 91	60	0.9-1.2	Yes	2	USACE	USACE
Lake Erie	Presque Isle	Pennsylvania	1989-1992	55	8300	45	107	76-107	1.5-2.4 (lwd)	Yes	3-4	USACE	USACE
Lake Erie	Lakeshore Park	Ohio	1982	3	244	38	61	120	2.1	Yes	5	USACE	City of Ashtabula
Lake Erie	East Harbor	Ohio	1983	4	550	45	90, 105, 120	170	2.3	No	5	State of Ohio	State of Ohio
Lake Erie	Meumee Bay (headland)	Ohio	1990	5	823	61	76		1.3	Yes	1	USACE	State of Ohio
Lake Erie	Sims Park (headland)	Ohio	1992	3	975	38	49		2.5	Yes	1	USACE	City of Euclid
Pacific	Venice	California	1905	1	180	180	0	370		No	5	Private	
Pacific	Haleiwa Beach	Hawaii	1965	1	49	49	0	90	2.1 (msl)	Yes	3	USACE/State of HI	USACE
Pacific	Sand Island	Hawaii	1991	3	110	21	23					USACE	USACE

[1] Beach response is coded as follows: 1-permanent tombolos, 2-periodic tombolos, 3-well developed salients, 4-subdued salients, 5-no sinuosity.

(a) Salients or tombolos. A salient is the preferred shoreline response for a detached breakwater system designed for the Corps as stated in EM 1110-2-1617 and in Chasten et al. (1993). This is to allow longshore sediment transport to continue to move through the project area to downdrift beaches. Salients are likely to predominate when the breakwaters are sufficiently far from shore, short relative to incident wavelength, and relatively transmissible (low crested or large gaps with low sediment input). Wave action and longshore currents tend to keep the salient from connecting to the structure.

- Sand will more likely accumulate in the structure lee and form a tombolo when the breakwater is close to shore, is long relative to incident wavelength, and is relatively impermeable (high crest and small gaps and with large sediment input). A tombolo-detached breakwater functions like a tee-shaped groin by blocking longshore transport and promoting sediment movements offshore in rip currents through the gaps. Although some longshore transport can occur seaward of the breakwater, the interruption in the littoral system may starve downdrift beaches of their normal sediment supply, causing erosion. Variable wave energy regimes may produce periodic tombolos to temporarily store and then release sediment to the downdrift region.

- Salient formation provides a recreational swimming environment and limits access for maintenance and to the public. Tombolo formation provides a recreational beach environment and allows direct access to the structure for maintenance, but public access may not be desirable.

- Figure V-3-21 presents a definition sketch for the variables that have been employed to develop empirical relationships for detached, breakwater design by many research efforts listed in Table V-3-5 dating back to the 1960s. For salient or tombolo formation, the key variables are:

Y Distance of breakwater from nourished shoreline

L_s Length of breakwater structure

L_g Gap distance between adjacent breakwater segments

d_s Depth (average) at breakwater structure below mean water level

Three dimensionless ratios, Y/d_s, L_s/L_g and L_s/Y have emerged to separate salient and tombolo response.

- As qualitatively discussed, when the breakwater is long and/or located close to shore, conditions favor tombolo formation. As shown in Table V-3-6, "Conditions for the Formation of Tombolos," many references say $L_s/Y > 1$-2 for tombolo formation (except Gourlay 1981). Dally and Pope (1986) recommend

$$\frac{L_s}{Y} = 1.5 \text{ to } 2 \qquad \text{single breakwater} \tag{V-3-6}$$

$$\frac{L_s}{Y} = 1.5 \qquad L \le L_g \le L_s \text{ segmented breakwater} \tag{V-3-7}$$

where L is the wavelength at the structure.

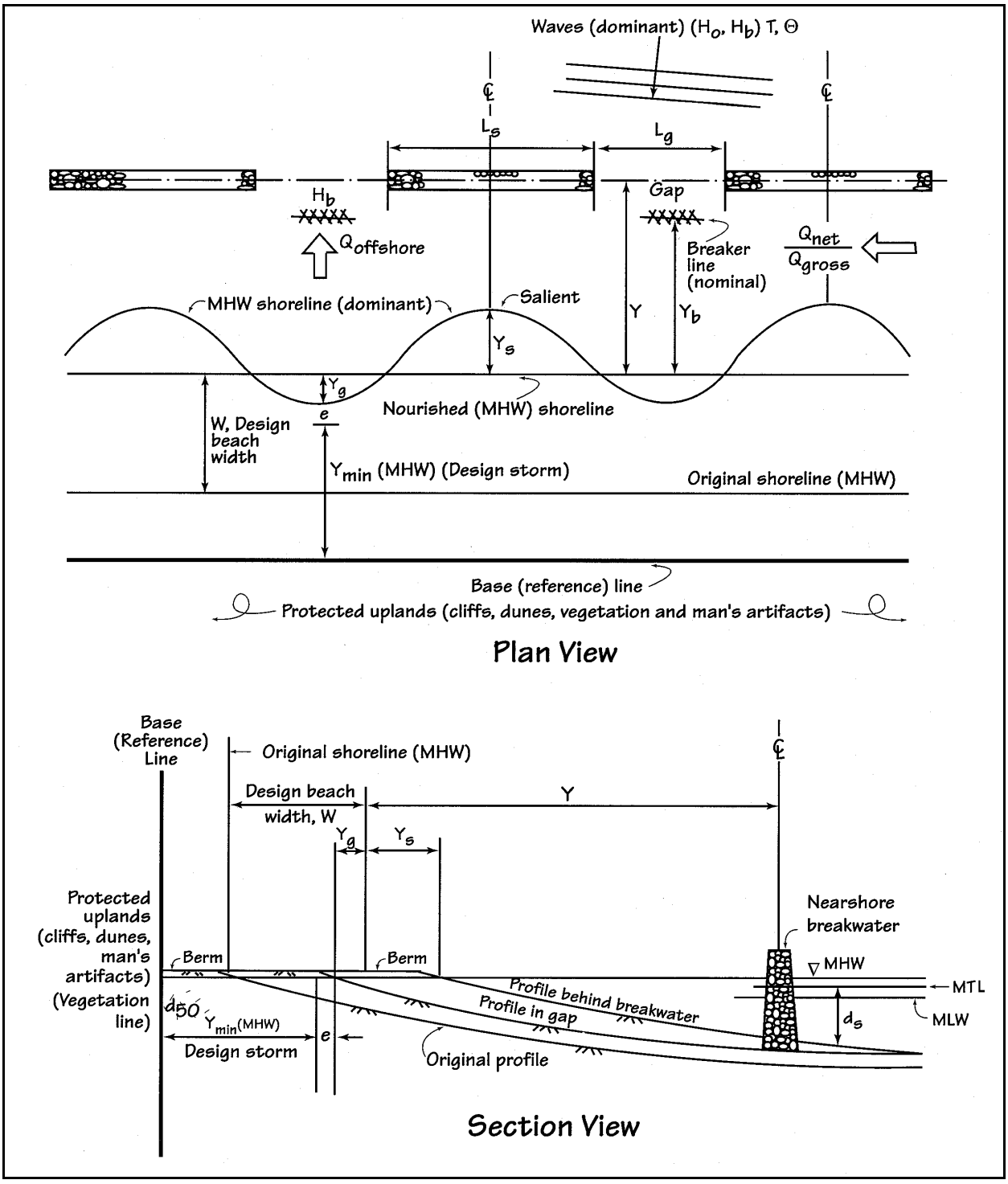

Figure V-3-21. Definitions of key variables for nearshore breakwater

Table V-3-5
Empirical Relationships for Nearshore Breakwater Design

Inman and Frautschy (1966)	Predicts accretion condition; based on beach response at Venice in Santa Monica, CA
Toyoshima (1972, 1974)	Recommends design guidance based on prototype performance of 86 breakwater systems along the Japanese coast
Noble (1978)	Predicts coastal impact of structures in terms of offshore distance and length; based on California prototype breakwaters
Walker, Clark, and Pope (1980)	Discusses method used to design the Lakeview Park, Lorain, OH, segmented system for salient formation; develops the Diffraction Energy Method based on diffraction coefficient isolines for representative waves from predominant directions
Gourlay (1981)	Predicts beach response; based on physical model and field observations
Nir (1982)	Predicts accretion condition; based on performance of 12 Israeli breakwaters
Rosen and Vadja (1982)	Graphically presents relationships to predict equilbrium salient and tombolo size; based on physical model/prototype data
Hallermeier (1983)	Develops relationships for depth limit of sediment transport and prevention of tombolo formation; based on field/laboratory data
Noda (1984)	Evaluates physical parameters controlling development of tombolos/salients; especially due to on-offshore transport; based on laboratory experiments
Shore Protection Manual (1984)	Presents limits of tombolo formation from structure length and distance offshore; based on the pattern of diffracting wave crests in the lee of a breakwater
Dally and Pope (1986)	Recommends limits of structure-distance ratio based on type of shoreline advance desired and length of beach to be protected
Harris and Herbich (1986)	Presents relationship for average quantity of sand deposited in lee and gap areas; based on laboratory tests
Japanese Ministry of Construction (1986); Rosati and Truitt (1990)	Develops step-by-step iterative procedure, providing specific guidelines towards final design; tends to result in tombolo formation; based on Japanese breakwaters
Pope and Dean (1986)	Presents bounds of beach response based on prototype performance; response given as a function of segment length-to-gap ratio and effective distance offshore-to-depth at structure ratio; provides beach response index classification
Seiji, Uda, and Tanaka (1987)	Predicts gap erosion; based on performance of 1,500 Japanese breakwaters
Sonu and Warwar (1987)	Presents relationship for tombolo growth at the Santa Monica, CA breakwater
Suh and Dalrymple (1987)	Gives relationship for salient length given structure length and surf zone location; based on lab tests and prototype data
Berenguer and Enriquez (1988)	Presents various relationships for pocket beaches including gap erosion and maximum stable surface area (i.e., beach fill); based on projects along the Spanish coast
Ahrens and Cox (1990)	Uses Pope and Dean (1986) to develop a relationship for expected morphological response as function of segment-to-gap ratio

(from Chasten et al. 1993)

- Conversely, short breakwaters at greater distance from shore favor salient formation. The "Conditions for the Formation of Salients" in Table V-3-6 presents a wide range of conditions with generally, $L_s/Y < 1$. Dally and Pope (1986) recommend for salient formation

$$\frac{L_s}{Y} = 0.5 \text{ to } 0.67 \tag{V-3-8}$$

for both single and segmented breakwaters. However, for very long distances, to insure that tombolos do not form, the recommended ratio for a segmented system (Dally and Pope 1986) is

$$\frac{L_s}{Y} = 0.125 \text{ (long systems)} \tag{V-3-9}$$

- Permeable structure systems (partly submerged, large gaps) also allow sufficient wave energy to minimize the chance for tombolo formation: As shown in Table V-3-6, "Conditions for Minimal Shoreline Response," the references cited generally recommend $L_s/Y < (0.125 – 0.33)$ to produce a minimal shoreline response. Ahrens and Cox (1990) defined a beach response index, I_s

$$I_s = \exp (1.72 - 0.41\ L_s/Y) \tag{V-3-10}$$

where the five types of beach response (Pope and Dean 1986) give I_s value as:

Permanent tombolo formation, $I_s=1$

Periodic tombolos, $I_s=2$

Well-developed salients, $I_s=3$

Subdued salients, $I_s=4$

No sinuosity, $I_s=5$

- These results are preliminary and require verification.

- The ratio L_s/L_g is also important for salient or tombolo formation. Large gaps will let more wave energy reach the shore to promote salient formation. And, this will coincide with smaller L_s/L_g ratios. A dimensionless plot of U.S. segmented, nearshore breakwater projects by Pope and Dean (1986) using L_s/L_g is shown in Figure V-3-22 and verifies this trend. The vertical axis is Y/d_s and is the distance offshore relative to the local, mean water depth at the breakwater. The water depth is important for it is related to the nominal, surf zone width at breaking Y_b. The dimensionless ratio Y/Y_b is a measure of breaker location relative to the width of the surf zone. For a given L_s/L_g, larger Y/d_s values (or Y/Y_b) mean the breakwater is located further offshore (beyond the normal surf zone width) to foster salient formation. Obviously, breakwaters located far offshore will have less effection the shoreline.

Table V-3-6
Conditions for Shoreline Response Behind Nearshore Breakwaters (from Chasten et al. 1993)

Condition	Comments	Reference
Conditions for the Formation of Tombolos		
$L_s/Y > 2.0$		*Shore Protection Manual* (1984)
$L_s/Y > 2.0$	Double tombolo	Gourlay (1981)
$L_s/Y > 0.67$ to 1.0	Tombolo (shallow water)	Gourlay (1981)
$L_s/Y > 2.5$	Periodic tombolo	Ahrens and Cox (1990)
$L_s/Y > 1.5$ to 2.0	Tombolo	Dally and Pope (1986)
$L_s/Y > 1.5$	Tombolo (multiple breakwaters)	Dally and Pope (1986)
$L_s/Y > 1.0$	Tombolo (single breakwaters)	Suh and Dalrymple (1987)
$L_s/Y > 2\ b/L_s$	Tombolo (multiple breakwaters)	Suh and Dalrymple (1987)
Conditions for the Formation of Salients		
$L_s/Y < 1.0$	No tombolo	*Shore Protection Manual* (1984)
$L_s/Y < 0.4$ to 0.5	Salient	Gourlay (1981)
$L_s/Y = 0.5$ to 0.67	Salient	Dally and Pope (1986)
$L_s/Y < 1.0$	No tombolo (single breakwater)	Suh and Dalrymple (1987)
$L_s/Y < 2\ b/L_s$	No tombolo (multiple breakwater)	Suh and Dalrymple (1987)
$L_s/Y < 1.5$	Well-developed salient	Ahrens and Cox (1990)
$L_s/Y < 0.8$ to 1.5	Subdued salient	Ahrens and Cox (1990)
Conditions for Minimal Shoreline Response		
$L_s/Y \leq 0.17$ to 0.33	No response	Inman and Frautschy (1966)
$L_s/Y \leq 0.27$	No sinuosity	Ahrens and Cox (1990)
$L_s/Y \leq 0.5$	No deposition	Nir (1982)
$L_s/Y \leq 0.125$	Uniform protection	Dally and Pope (1986)
$L_s/Y \leq 0.17$	Minimal impact	Noble (1978)

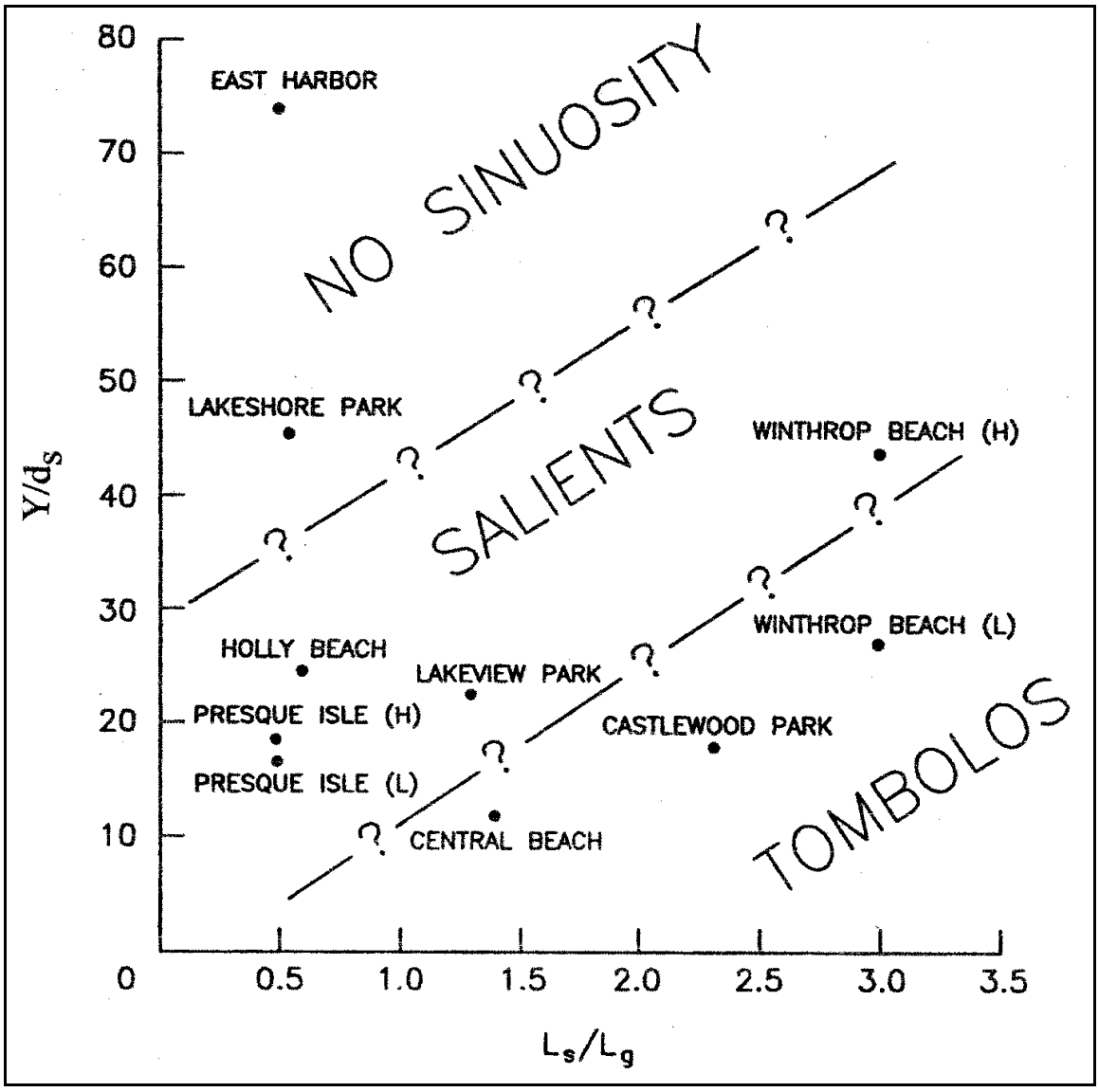

Figure V-3-22. Dimensionless plot of nearshore breakwater projects For Y/d_s versus L_s/L_g (from Pope and Dean 1986)

- Zyserman et al. (1998) used the Y/Y_b ratio in their numerical model, process-oriented studies of nearshore breakwaters. The distance Y_b was taken as Y_{80}, meaning the distance from shore where 80 percent of the undisturbed littoral transport takes place and, hence, a measure of the width of the surf zone. Their research using a numerical model confirmed the empirical formulas of Dally and Pope (1986) for tombolo and salient formation previously summarized.

(b) Planform configuration. Some research has provided insight into other variables that quantify the planform shape of the shoreline as shown in Figure V-3-21. The length of the salient, Y_s increased as the L_s/Y ratio increased, as expected. Suh and Dalrymple (1987) developed an exponential expression involving $L_g Y L_s^2$, where L_g is the gap length for prediction of Y_s, by combining movable-bed laboratory results and prototype data. Rosati (1990) evaluated the relation and found it over-predicted Y_s for the majority of

prototype data. Seiji, Uda, and Tanaka (1987) gave conditions on the L_g/Y ratio for no, possible, and certain erosion, Y_g opposite the gap. The magnitude of Y_g was not determined, but gap erosion occurred for L_g/Y greater than 0.8. Hallermeier (1981) gave an equation for the water depth to locate nearshore breakwaters when tombolo formation was to be avoided. The relation requires knowledge of wave height and period statistics at the 12 hr per year exceedance level. Rosati (1990) also evaluated Hallermeier's relation with the limited, available field data. The correlation was said to be good for seven of the nine data points tested. These relationships to quantify $Y_{s,}$ Y_g and d_s can be found in Chasten et al. (1993).

- Walker, Clark, and Pope (1981) discuss a procedure to apply diffraction analysis to determine the approximate shoreline configuration behind a breakwater. Their studies indicate that if the isolines of the $K' = 0.3$ diffraction coefficients are constructed from each end of the breakwater for a range of incident wave directions (monochromatic waves) and they intersect seaward of the postproject shoreline, a tombolo will not form. This corresponds to $L_g/Y \geq 2$, where Y is after placement of the beach fill, as part of the project shown in Figure V-3-21. Waves coming around each end of the breakwater meet each other before the undiffracted, incident wave (outside the breakwater's shadow) reach the shoreline. The postproject shoreline is estimated as a smoothed crest pattern for all diffracted crests and a balance in the sediment volume.

- The Japanese Ministry of Construction presented a step-by-step interactive procedure for nearshore breakwater design (Japanese Ministry of Construction 1986). Rosati (1990) and Rosati and Truitt (1990) found that 60 percent of the designs produced tombolos and therefore the JMC method was more suitable for headland breakwater design. All are for nonpermeable, high-crested, nearshore breakwaters.

(c) Other design factors. The crest elevation and crest width, permeability, slope of front face, and type of construction are additional design factors that influence functional performance. No general guidelines presently exist.

- Generally, low crests allow more energy to penetrate into the lee of the breakwater to prevent tombolo formation or remove a tombolo by storm waves. Wide crests on low breakwaters can promote breaking to diminish wave energy penetration and encourage tombolo formation. Permeable structures can allow significant amounts of energy to propagate through them to prevent tombolo formation. Types of construction including nontraditional, patented devices are discussed in Part V-3-5.

- Waves in the lee of the breakwater are determined by three processes: diffraction around the ends, wave transmission by overtopping and wave transmission through the structure. For diffraction around single and multiple breakwaters with gaps, see Part II-7-2 for irregular waves and the *Shore Protection Manual* (1984) for many cases with monochromatic waves. Wave transmission due to overtopping and through the structure by permeability is discussed in Part VI-5-2. Wave reflection is covered in Part VI-5-2. The Automated Coastal Engineering Systems (ACES) (Leenknecht, Szuawalski, and Sherlock 1992) provides an application to determine wave transmission coefficients and transmitted wave heights for permeable breakwaters with crest elevation at or above the still-water level.

- Breakwater impact on littoral currents and creation of wave setup gradients to produce setup currents was previously discussed. If the crest elevation is low enough to permit wave overtopping, the mass carried over the structure causes a net seaward return flow of water through the gaps. Seelig and Walton (1980) present a method for estimating the strength of the seaward flowing currents. The effect of the combined littoral and setup currents on the longshore sediment transport to produce salient features with adjacent erosional areas was also previously discussed (physical processes).

- The primary function of nearshore breakwaters is to reduce the offshore sand transport during storms. Hence, these structures help retain sand on nourished beaches for longer intervals. However, overtopping can result in a net seaward flow of water and sand through the gaps between breakwater segments during storm events. The breakwater can also reduce the onshore sediment movement during normal, swell wave conditions that naturally rebuild the beach. The structure blocks the return of sediment to the beach. Following breakwater construction, a new equilibrium between onshore and offshore transport will be established.

(d) Minimum dry beach width, Y_{min}. Figure V-3-21 schematically displays the mhw shoreline for normal wave conditions. During storms, some gap erosion, *e* will occur to impact the minimum, dry beach width, Y_{min} required for shore protection.

- A conservative estimate of the gap erosion, *e*, can be made using analytical models for the dynamic response of natural beach profiles to storm effects (e.g., Kobayashi 1987; Kriebel and Dean 1993). Part III-3-3 gives a general description of these methods and also example applications of the Kriebel and Dean (1993) analytical model. The theory is for open coastal beaches so that wave diffraction in the gap area and wave overtopping to increase the return flows through the gap region are not considered, but tend to offset each other. See Example Problem V-3-1.

- Dynamic, numerical, cross-shore sediment transport models (e.g., SBEACH, Larson and Kraus 1989) could also be applied in the gap area to estimate the erosion potential, e (see Part III-3-3). These two-dimensional (vertical) models also do not consider wave diffraction and return flows in the gap area. These results would be a worst case scenario and the actual erosion can be expected to be significantly less. A general, three-dimensional, wave, current, and sediment transport model is clearly needed in this area.

- Hughes (1994) presents a complete discussion of scaling laws as applied to predicting cross-shore sediment transport in physical, hydraulic models.

(4) Nontraditional designs. Most nearshore breakwaters built in the United States and foreign countries for shore protection have been rubble-mound type structures. Availability of materials and construction equipment have made construction costs relatively inexpensive.

- Several patented, nontraditional devices have been tested in the United States. These have been precast concrete units or sand-filled geotextile tubes and bags. If constructed to the same dimensions as rubble-mound structures, they may produce similar functional performance. Their success (or failure) has been a function of structural stability of the units during storm conditions and their durability over an economic life. Their functional success (or failure) has also been dependent on maintaining the design crest elevation for wave energy reduction. Proper attention to foundation design to minimize settlement must be given for precast, concrete units.

- Some nontraditional designs reduce the bottom footprint to minimize impacts on benthic organisms. And, the costs for removal and/or adjustments to reduce downdrift impacts on adjacent shorelines can be significantly less than for traditional, rubble-mound designs. The need to reduce impact on the environment is increasing the necessity for further research and comprehensive field testing programs for nontraditional designs. (See Part V-3-5 for further details.)

EXAMPLE PROBLEM V-3-1

FIND: Functional design of a nearshore breakwater system coupled with beach nourishment for shore protection, but maintain recreational beach.

GIVEN: A sandy beach shoreline, 685 m in length with historic erosion rate of 0.6-0.9 m/year that threatens a 2.4-7.3-m bank, with road and sewer line parallel to the shoreline along the top of the bank. For an annual probability of exceedance of 2 percent (50-year recurrence interval design storm) the storm surge level is 1.83 m (mlw) and corresponding wave characteristics are H_s=2.2 m, T_p=9.7 sec at the -9.0 m (mwl) depth contour. The design, still water, storm depth is 3.05 m at this location and includes a 0.3 m, astronomical tide. Net sediment transport (sand, d_{50} = 0.6 mm) is 3,750 to 7,500 m^3/year to the north. The existing beach berm is at +0.76 m (mlw) elevation.

Solution:

1. To maintain the longshore transport rate, the desired planform is subdued to well-developed salients. From a table of possible L_s and Y values, the ratio 0.75 is selected giving a breakwater length, L_s=30m and the offshore distance, Y=40 m. This gives the beach response index, I_s=4.1, hence, subdued salients are expected.

2. For shore protection, waves entering the breakwater gaps and diffracting behind the structures will reach the shoreline. Sufficient beach width (Y_{min}) and berm height (Z_s) are required to dissipate this wave energy prior to reaching the toe of the banks. Analysis of nearshore, wave diffraction diagrams indicate that the 50-year design wave height of 2.2 m will be reduced to about 0.9 m at a distance of about 14 m from the bank toe when the breakwater gap is about 30 m. This gap width, L_g=30 m is considered a practical minimum width for this project. For shallow-water wave breaking, (γ_b=0.78, II-4-3), this wave will break in about 1.16 m depth of water. For a design storm surge of 1.83 m (mlw) and existing beach berm elevation of 0.76 m (mlw), these waves will break directly on the bank toe and cause significant erosion. The existing beach width and height are not sufficient to dissipate the storm wave energy at the 50-year frequency level. Two options exist. One is to further decrease the wave energy propagating through the gaps by using smaller gap widths, and resulting longer lengths of breakwater segments. The second option is to add beach fill to the shoreline area and this option is selected to provide the desired protection for the bank area.

3. A beach-fill plan was considered that would increase the beach width to 10 m from the toe of the bank and raise the berm elevation to + 1.8 m (mlw) at a 1:8 construction slope. Wave heights are now reduced to less than 30 cm near the bank toe for the 50-year storm event. The beach fill would be expected to evolve (see Part V-4) to a stable planform with salients behind each breakwater and embayments opposite each gap. The mhw shoreline would recede about 4.5-6 m opposite the gaps as estimated from analysis of diffraction patterns. The beach shape would also evolve to a more natural and milder slope to match those in the area (1:10 to 1:15).

(Continued)

EXAMPLE PROBLEM V-3-1 (Concluded)

4. Protection of the bank toe depends on the performance of the beach berm during storm events. A worst case scenario can be evaluated first by considering the adjusted beach slope and shoreline area with storm wave conditions prior to reduction by the nearshore breakwaters. Using the analytical model of Kriebel and Dean (1993) or a numerical, storm erosion model (e.g., SBEACH, Larson and Kraus 1989) gives the results (for the worst-case, 50-year storm event scenario) that the storm berm would remain with a width of 1.5-3 m. The actual erosion would be expected to be significantly less due to reduction in the storm wave energy as a result of wave diffraction through the gaps. The gap width, L_g=30 m was selected for design.

5. Wave energy is also transmitted over the top of nearshore breakwaters during elevated water level, storm surge events. A wave transmission model (see Part VI-5-2) capable of predicting wave energy over and through submerged, reef-type breakwaters was used for analysis with crest heights of + 1.2 m, +1.5 m and 1.8 m above mlw datum. During the 50-year design storm, wave heights immediately behind the breakwaters are reduced about 60 percent, 54 percent, and 46 percent, respectively for these three breakwater crest elevations. These transmitted waves then propagate shoreward and are further dissipated by the beach salients. With the proposed beach fill in place, a breakwater crest elevation of +1.2 m (mlw) is selected to limit the transmitted, design wave height to about 1.2 m. This is the same, diffracted, design wave height opposite the gaps and is dissipated by the storm berm.

Note: Further details of this example problem are found in Appendix A of Chasten et al. 1993 and was developed by Mr. Ed Fulford of Andrews Miller and Assoc., Inc., Cambridge, Maryland. It is taken from a real project on the Chesapeake Bay for the community of Bay Ridge near Annapolis, Maryland. Construction was completed in July 1991 and postconstruction monitoring commenced soon after and at a November 1991 survey. As of 2000, the project has performed as expected with subdued salients forming behind each breakwater resulting in the overall stability of the shoreline. Numerous, significant storms occurred and the project prevented erosion of the bank area to protect the roadway and sewer pipeline. The project has been well-received by the residents of the community as a result of the stability of the shoreline and the enhancement of the recreational beach area.

e. Groins.

(1) Background and definitions. Groins are the oldest and most common shore-connected, beach stabilization structure. They are probably the most misused and improperly designed of all coastal structures. They are usually perpendicular or nearly at right angles to the shoreline and relatively short when compared to navigation jetties at tidal inlets. As illustrated schematically in Figure V-3-23, for single and multiple groins (groin field) the shoreline adjusts to the presence of the obstruction in longshore sediment transport. Over the course of some time interval, accretion causes a positive increase in beach width updrift of the groin. Conservation of sand mass therefore produces erosion and a decrease in beach width on the downdrift side of the groin. The planform pattern of shoreline adjustment over 1 year is a good indicator of the direction of the annual net longshore transport of sediment at that location.

(a) Groins are constructed to maintain a minimum, dry beach width for storm damage reduction (Figure V-3-11) or to control the amount of sand moving alongshore. Previously stated purposes such as trapping littoral drift are discouraged for this implies removal of sand from the system. Modern coastal

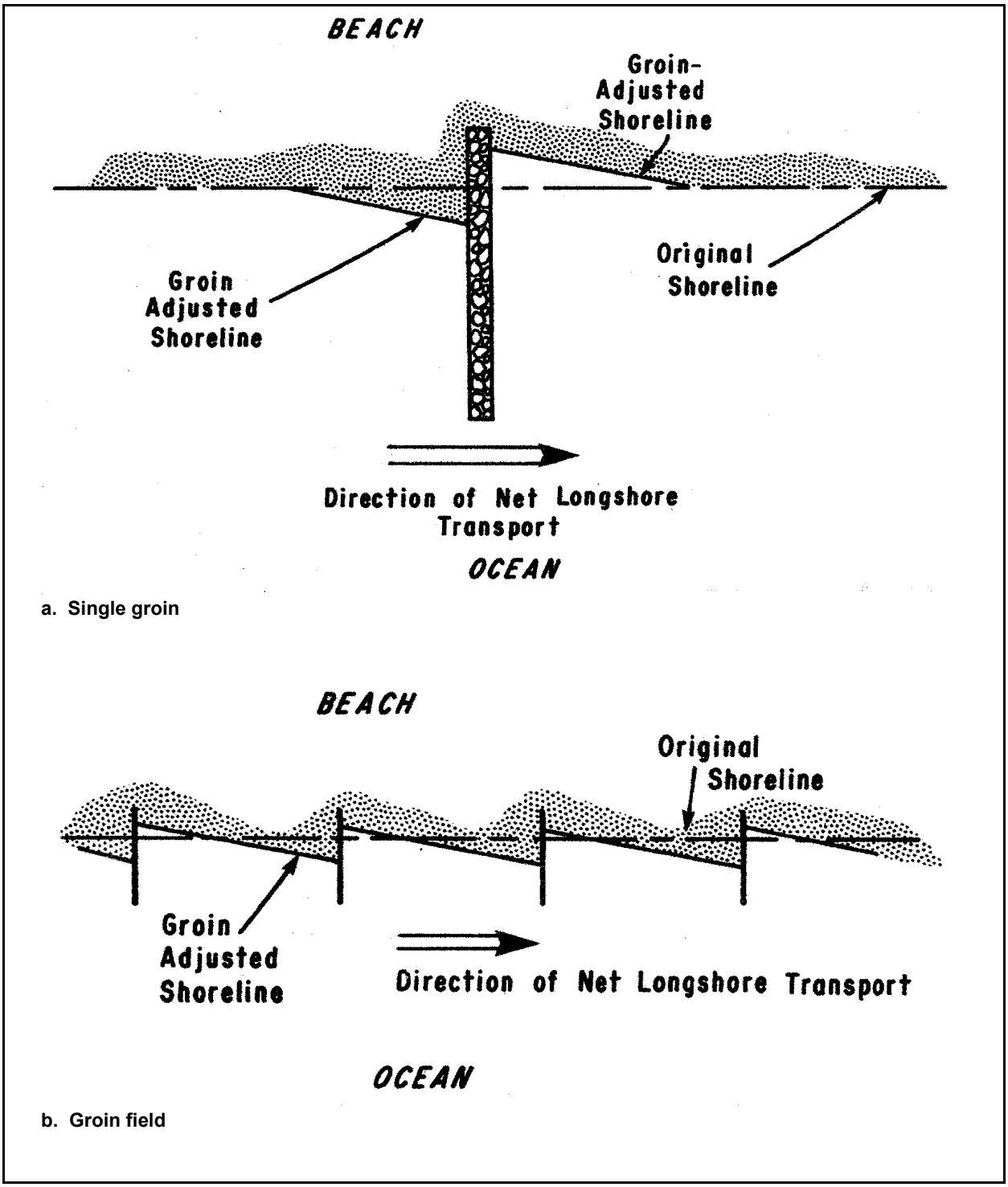

Figure V-3-23. General shoreline adjustment for direction of net longshore transport

engineering practice is to combine beach nourishment with groin construction to permit sand to immediately begin to bypass the groin field. At the end of the sediment cell, terminal groins may be used to anchor the beach and limit the movement of sand into a navigational channel or onto an ebb-tidal shoal at tidal inlets.

(b) Figure V-3-24 shows a photo, profile and cross section of a rubble-mound groin at Westhampton Beach, New York. Sheet-pile construction with timber (Figure V-3-25) timber-steel (Figure V-3-26) prestressed-concrete (Figure V-3-27) or cellular-steel (filled) sheets (Figure V-3-28) have also been constructed in the United States.

(c) Kraus, Hanson, and Blomgren 1994 cite the following situations when the groin field alternative for shore protection and sand management should be considered.

- At divergent, nodal points for littoral drift.
- In the diffraction, shadow some of a harbor breakwater, or jetty.
- On the downdrift side of a harbor breakwater or jetty.
- At the updrift side of an inlet entrance where intruding sand is to be managed
- To reduce the loss of beach fill, but provide material to downdrift beaches in a controlled manner.
- Along the banks at inlets, where tidal currents alongshore are strong.
- Along an entire littoral cell (spit, barrier island, submarine canyon) where sand is lost without return in an engineering time frame.

(d) Groins may not function well and should not be considered under the following conditions (Kraus, Hanson, and Blomgren 1994):

- Where a large tidal range permits too much bypassing at low tide and overpassing at high tide.
- Where cross-shore sediment transport is dominant
- When constructed too long or impermeable, causing sand to be jetted seaward
- When strong rip currents are created to cause potentially dangerous swimming conditions

(e) Coastal zone management policy in many countries and the United States presently discourages the use of groins for shore protection. Many examples of poorly designed and improperly sited groins caused by lack of understanding of their functional design, or failure to implement the correct construction sequence, or failure to fill up the groin compartments with sand during construction, or improper cross-sectional shape are responsible for these restrictions. However, when properly designed, constructed and combined with beach nourishment, groins can function effectively under certain conditions, particularly for increasing the fill life (longevity) of renourished beaches.

(f) Groins are now being reevaluated as sand-retention structures (Kraus, Hanson, and Blomgren 1994; Kraus and Bocamazo 2000) by now asking the question “how much sand can be allowed to pass,” while still maintaining a minimum width of beach at the groin for some level of shore protection.

Westhampton Beach, Long Island, New York, 18 Jan 1980 (courtesy USAED, New York)

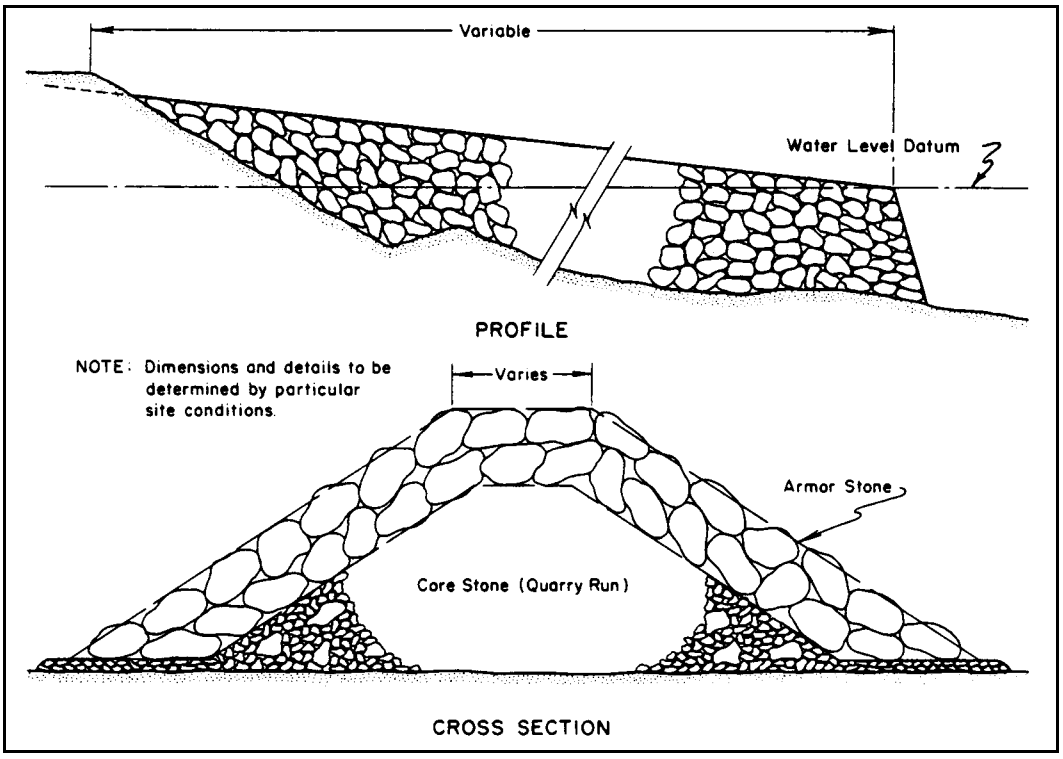

Figure V-3-24. Rubble-mound groin, Westhampton Beach, New York

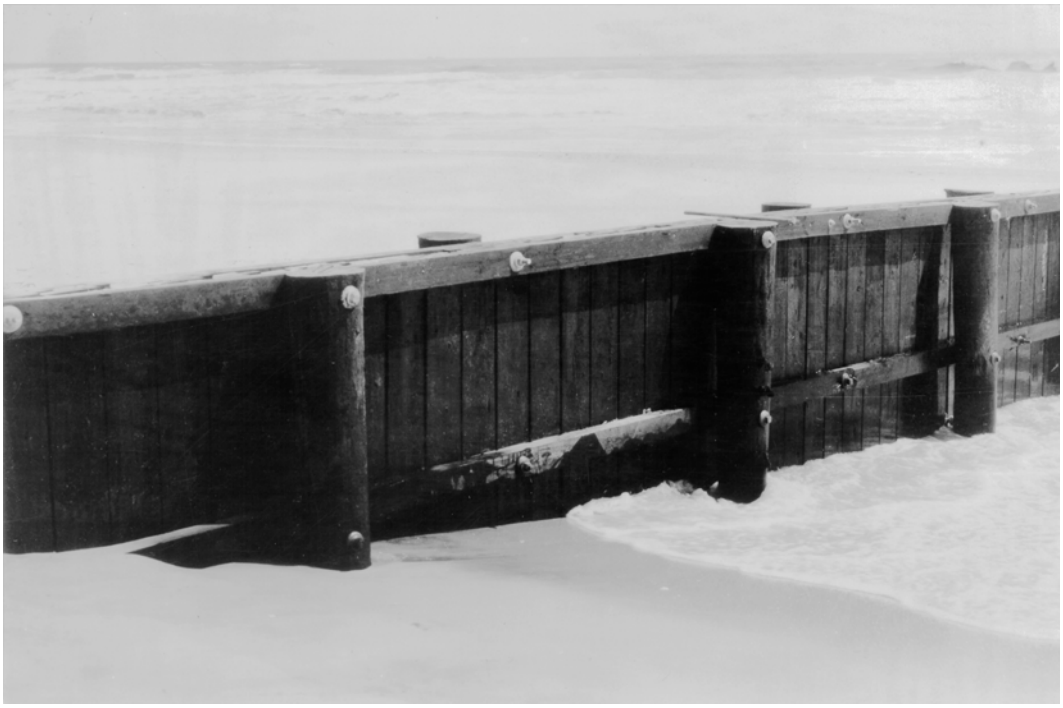

Wallops Island, Virginia (1964)

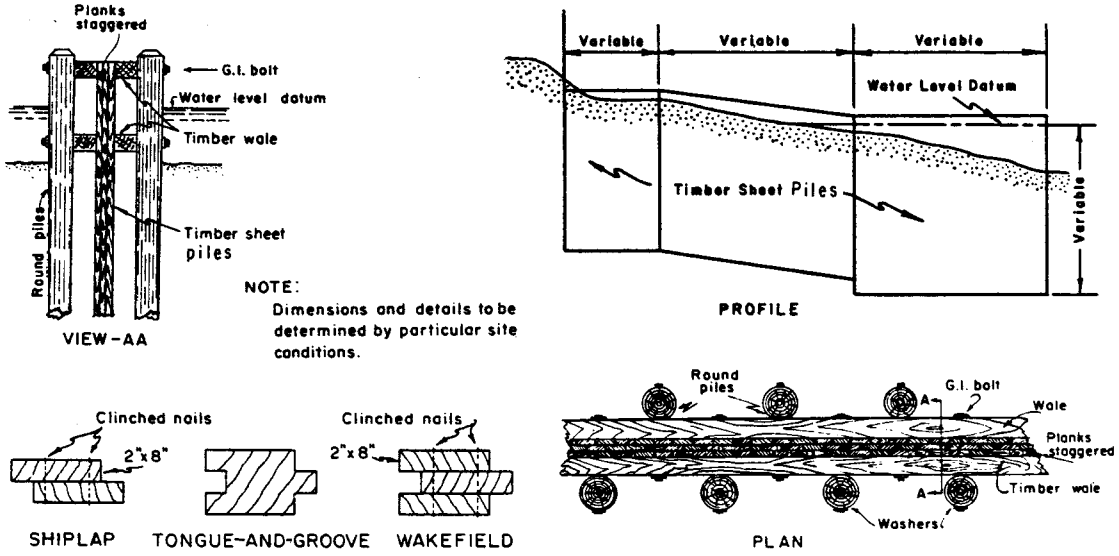

Figure V-3-25. Timber sheet-pile groin, NASA Space Flight Center, Wallops Island, Virginia

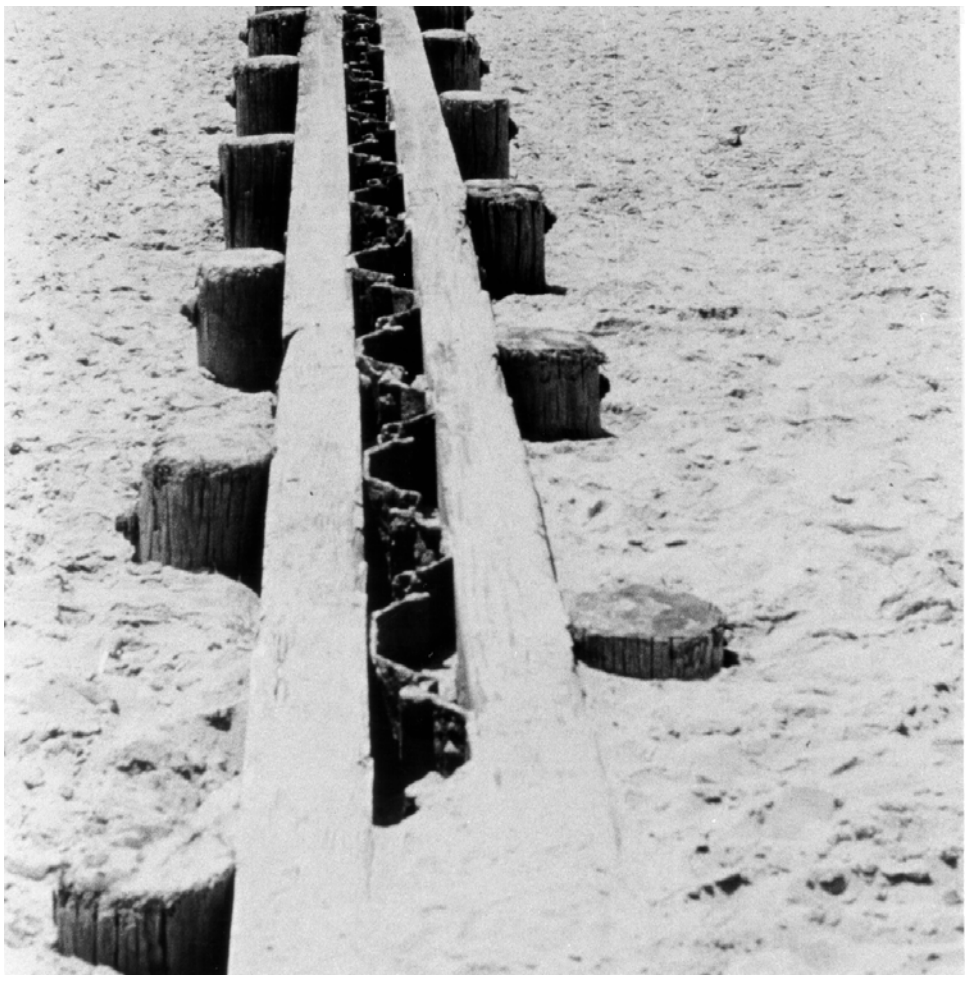

New Jersey (September 1962)

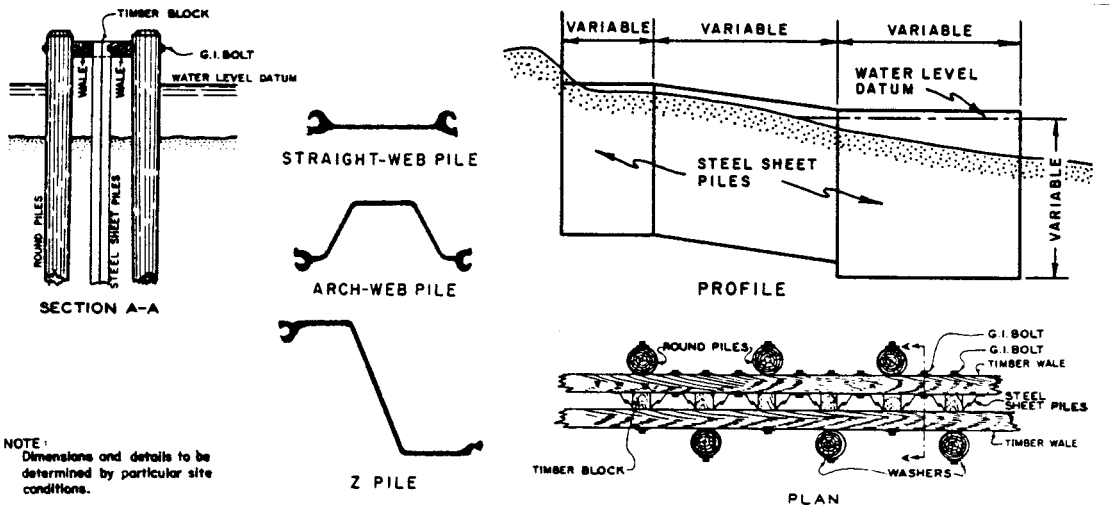

Figure V-3-26. Timber-steel sheet-pile groin, New Jersey

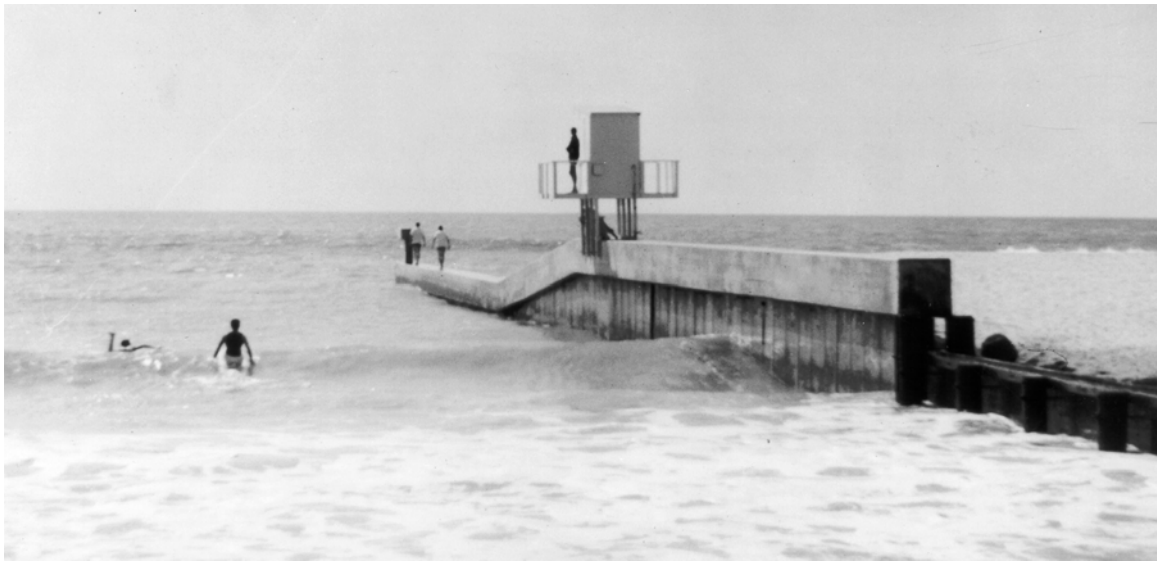

Doheny Beach State Park, California (October 1965)

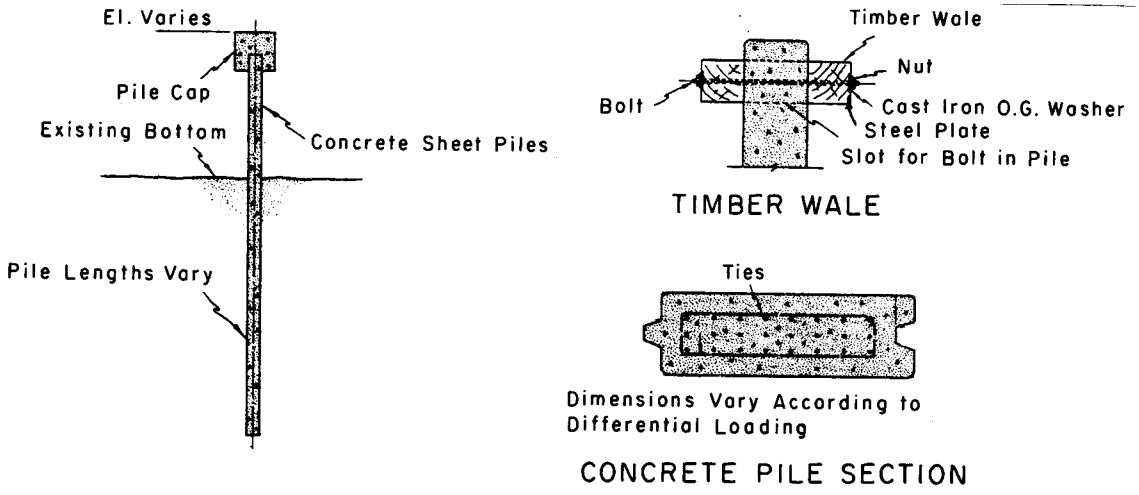

Figure V-3-27. Prestressed-concrete sheet-pile groin, Dohney Beach State Park, California

Presque Isle, Pennsylvania (October 1965)

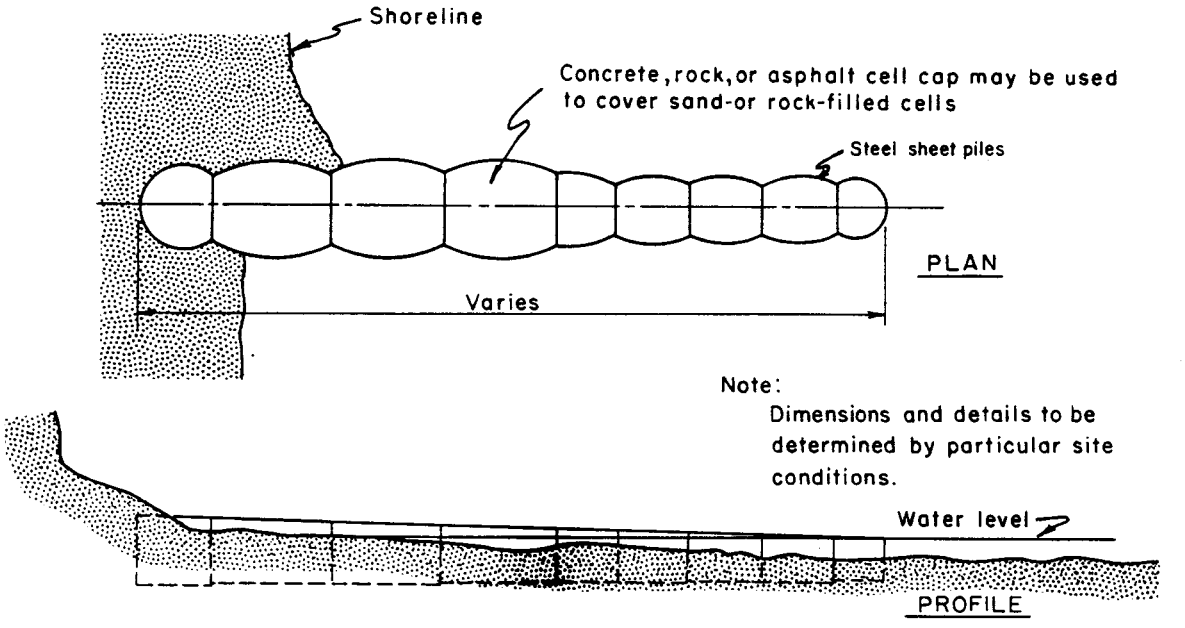

Figure V-3-28. Cellular-steel sheet-pile groin, Presque Isle, Pennsylvania

(2) Literature review. Although groins have been around a long time and many references exist, most only provide a few rules of thumb. No systematic methods for functional design under a wide range of structural shapes, waves, and sediment transport conditions presently exist. Reviews for the functional design of groins can be found in Bruun (1952); Bakker (1968); Balsillie and Berg (1972); Balsillie and Bruno (1972); Nayak (1976) (unpublished); Tomlinson (1980); Fleming (1990); and EM 1110-2-1617. All these reviews restate the same beliefs but fail to reference the sources that verify the concepts and conclusions from theory, model studies (laboratory or numerical), or field experiments. As stated by Kraus, Hanson, and Blomgren (1994)

> "…the literature (on groins) may appear to assign validity to certain concepts and conclusions by weight of repetition (but) not by independent confirmation." (p. 1329).

(a) Laboratory investigations suffered from severe scale distortions in sediment transport to cast serious doubt and questions on their results.

(b) A fresh approach is needed that begins with a summary of over 20 parameters that govern beach response to groins as listed in Table V-3-7 (from Kraus, Hanson, and Blomgren 1994). They are grouped into three main categories (structure, beach, and hydrodynamic conditions), but the large number of variables make analysis difficult. Missing from this table is the minimum, design beach width for shore protection. Groin geometry and possible sediment size for the beach fill can be controlled in the design.

Table V-3-7
Main Parameters Governing Beach Response and Bypassing at Groins (from Kraus, Hanson, and Blomgren 1994)

Groin(s)	Beach and Sediment	Waves, Wind, and a Tide
Length	Depth at tip of groin	Wave height and variability
Elevation	Depth of closure	Wave period and variability
Porosity	Sediment availability	Wave angle and variability
Configuration (straight, T, L, etc.)	Median grain size and variability	Tidal range
Orientation to the shoreline	Sediment density	Wind speed and variability
Spacing between groins	--	Wind direction and variability
Tapering	--	Wind duration and variability

Note: Two integrated parameters governing groin functioning are the ratio of net to gross longshore sand transport, and the presence, location, and number of longshore bars.

(c) From the previously listed review papers, other references and their own experience, Kraus, Hanson, and Blomgren 1994 listed 13 functional properties attributed to groins and present a critical evaluation of each as shown in Table V-3-8. The first five are well accepted properties that have led to the general rule of the thumb to make the groin spacing to length ratio about two to four. However, this rule omits any consideration of the cross-sectional shape of the groin. The length controls water depth at the end and, hence, the amount of sediment by-passing around the tip. But the cross-sectional elevation in the swash zone controls over-passing, the length and elevation on the beach berm control shore-passing, and the structural materials control through-passing as takes place in rubble-mound and permeable groins. Tidal range, predominant wave characteristics (height, period, direction), net and gross longshore sediment transport and grain size are key hydrodynamic and sediment parameters. All these factors together produce the optimum spacing and planform configuration of the shoreline within each compartment for average climate conditions.

Table V-3-8
Functional Properties Attributed to Groins and their Critical Evaluation (from Kraus, Hanson, and Blomgren 1994)

Property	Comment
1. Wave angle and wave height are leading parameters (longshore transport).	Accepted. For fixed groin length, these parameters determine bypassing and the net and gross longshore transport rates.
2. Groin length is a leading parameter for single groins. (Length controls depth at tip of groin.)	Accepted, with groin length defined relative to surfzone width.
3. Groin length to spacing ratio is a leading parameter for groin fields.	Accepted. See previous item.
4. Groins should be permeable.	Accepted. Permeable groins allow water and sand to move alongshore, and reduce rip current formation and cell circulation.
5. Groins function best on beaches with a pre-dominant longshore transport direction.	Accepted. Groins act as rectifiers of transport. As the ratio of gross to net transport increases, the retention functioning decreases.
6. The updrift shoreline at a groin seldom reaches the seaward end of the groin. (This observation was not found in the literature review and appears to be original to the present paper.)	Accepted. Because of sand bypassing, groin permeability, and reversals in transport, the updrift shoreline cannot reach the end of a groin by longshore transport processes alone. On-shore transport is required for the shoreline to reach a groin tip, for a groin to be buried, or for a groin compartment to fill naturally.
7. Groin fields should be filled (and/or feeder beaches emplaced on the downdrift side).	Accepted. Filling promotes bypassing and mitigates downdrift erosion.
8. Groin fields should be tapered if located adjacent to an unprotected beach.	Accepted. Tapering decreases the impoundment and acts as a transition from regions of erosion to regions of stability.
9. Groin fields should be built from the downdrift to updrift direction.	Accepted, but with the caution that the construction schedule should be coordinated with expected changes in seasonal drift direction.
10. Groins cause impoundment to the farthest point of the updrift beach and erosion to the farthest point of the downdrift beach.	Accepted. Filling a groin field does not guarantee 100% sand bypassing. Sand will be impounded along the entire updrift reach, causing erosion downdrift of the groin(s).
11. Groins erode the offshore profile.	Questionable and doubtful. No clear physical mechanism has been proposed.
12. Groins erode the beach by rip current jetting of sand far offshore.	Questionable. Short groins cannot jet material far offshore, and permeable groins reduce the rip current effect. However, long impermeable jetties might produce large rips and jet material beyond the average surfzone width.
13. For beaches with a large predominant wave direction, groins should be oriented perpendicular to the breaking wave crests.	Tentatively accepted. Oblique orientation may reduce rip current generation.

(d) Kraus, Hanson, and Blomgren 1994 also discovered that the updrift shoreline rarely reached the seaward end of the groin (Table V-3-8, No. 6). On-shore sediment transport processes appear to be necessary for a groin to be filled naturally so that the shoreline reaches the tip, or the tip is buried. Longshore sand transport direction reversals, sand bypassing under water at the end, and groin permeability all normally keep the updrift shoreline well landward of the end of the groin.

(e) Properties No. 7, 8, and 9 in Table V-3-8 have long been accepted standard conditions for groin field design and construction. Even so, as noted in No. 10, filling a groin field does not guarantee that 100 percent of the original longshore transport will continue as sand bypassing. The entire, filled, groin field system will impound sand updrift to cause some erosion downdrift of the system.

(f) Properties No. 11 and 12 are often stated reasons by opponents of groins but are questionable because they cannot be supported by physical mechanisms nor principles of conservation of sand. No. 13 will be considered under innovations discussed in the following paragraphs.

(g) A critical review of the literature also shows that little, if any, previous discussion exists on how to judge success (or failure) of a groin design. As discussed further, success should be judged on two factors: to maintain a minimum, dry beach width for specified storm conditions for protection beyond a reference baseline; and to bypass an average, annual amount of sediment to minimize downdrift impacts.

(3) Physical processes.

(a) Normal morphological response. How do groins work? Waves breaking alongshore at an angle create a time-averaged, longshore current and longshore sediment transport. The cross-shore distribution of longshore sediment transport is discussed in Part III-2 (see Equation III-2-23 and Example Problem III-2-7). A key variable is the surf zone width for the theory cited (Bodge and Dean 1987) which assumes sediment mobilized in proportion to the local rate of wave energy dissipation and transported alongshore by the local, wave-induced current. The groin simply blocks a part of this normal transport of sand alongshore and causes it to accumulate in a fillet on the groin's updrift side (the side from which the sediment is coming). This accumulation reorients the shoreline and reduces the angle between the shoreline and the prevailing incident wave direction. The reorientation reduces the local rate of longshore sand transport to produce accumulation and/or redistribution of sand updrift of the groin. The amount of sand transported past the groin is greatly reduced (or eliminated) to significantly impact the downdrift area. The ratio of groin length to some statistical measure of surf zone width (or water depth at the groin tip) is a key factor in sand bypassing, as discussed further in the following paragraphs. Wave diffraction causes reduced wave energy in the lee of the groin relative to the midcompartment, mean water-level setup gradients, and setup induced currents behind the groin. These contribute to complex, current circulation patterns that move sediment alongshore and offshore along the leeside of the groin (Dean 1978). The strength of these internal current patterns depends on groin planform geometry, but also on groin cross-sectional elevation and permeability across the surf zone. Waves diffract around the groin tip, propagate over the submerged section and reflect off the body of the groin. These interactions vary with water depth changes during the tidal cycle. Consequently, sediment can also move over the top of submerged groins (over-passing), through the permeable, groin structure (through-passing) and behind the end of the structure (shore-passing). Impermeable, high crested groins created internal and external current patterns that are far different than permeable, submerged structures. Fleming (1990) discusses the results of physical model studies with current and sediment movements for both high and low groin cross sections. Complex flow patterns were produced, and it was stated that strong local currents may cause a net loss of sediment from the compartment by offshore movement during storm events.

(b) Storm response. Groins offer little or no reduction in wave energy to shore-normal waves during storms. Consequently, cross-shore sediment transport processes as discussed in Part III-3-3 for natural beaches are similar for groin field compartments. And, for near normal wave incidence, the groin system can

create strong local current and rip currents which add to the offshore movement of beach material during storms.

(4) Functional design.

(a) Insight from numerical models.

- Some numerical models of shoreline change include groin field effects (e.g., GENESIS, Hanson and Kraus 1989, see Part III-2-4 for details) Boundary conditions for groins in these models give insight into how they must function (Gravens and Kraus 1989). They are as follows:

  - As the groin length increases, its impact on the shoreline regarding time evolution and equilibrium planform must increase.

  - Increasing groin permeability should decrease the impact of the structure on the shoreline. Different groin permeabilities must produce different equilibrium planforms.

  - A permeability of 100 percent should give longshore transport rates and shoreline evolution identical to that modeled with no structures.

- Groin bypassing around the seaward end is calculated at each time step in the GENESIS model. Key variables are the water depth at the tip and the breaking wave height. In GENESIS, the depth of active longshore sediment transport is taken at 1.6 times the significant breaking wave height (from Hallermeier 1981). Groin length relative to surf zone width could also be employed to calculate the bypassing factor.

- A permeability factor representing groin elevation, groin porosity and tidal range must also be estimated in the model. These three variables represent over-passing, through-passing and shore-passing respectively as sketched in Figure V-3-29. The permeability factor is assigned and must approach unity to satisfy the third criterion previously described.

- A third key factor is the ratio of net transport rate, Q_n to the gross rate, Q_g (Bodge 1992). When the Q_n/ Q_g ratio is zero, a perfectly balanced transport (no net) exists to produce symmetrical fillets on both sides of a single groin. The opposite extreme is $Q_n/Q_g=1$ meaning unidirectional transport. A single fillet on one side results.

- These key factors controlling groin functioning are summarized in Table V-3-9 (Kraus and Bocamazo 2000) with symbols shown in Figure V-3-29.

- These three process factors incorporate many of the 20 or more fundamental variables. The geometry ratio of spacing, X_g to length Y_g is also the controlling factor for groin systems, as found in the literature. Note from Figure V-3-29 that Y_g represents a mean groin length measured from the average, nourished beach shoreline. Using Y_{gu} (updrift) gives a larger ratio or using Y_{gd} (downdrift) produces a smaller ratio that may account for some variability. The *Shore Protection Manual* (1984) says $X_g/ Y_g=2$-3 for the proper functioning of shore-normal groins.

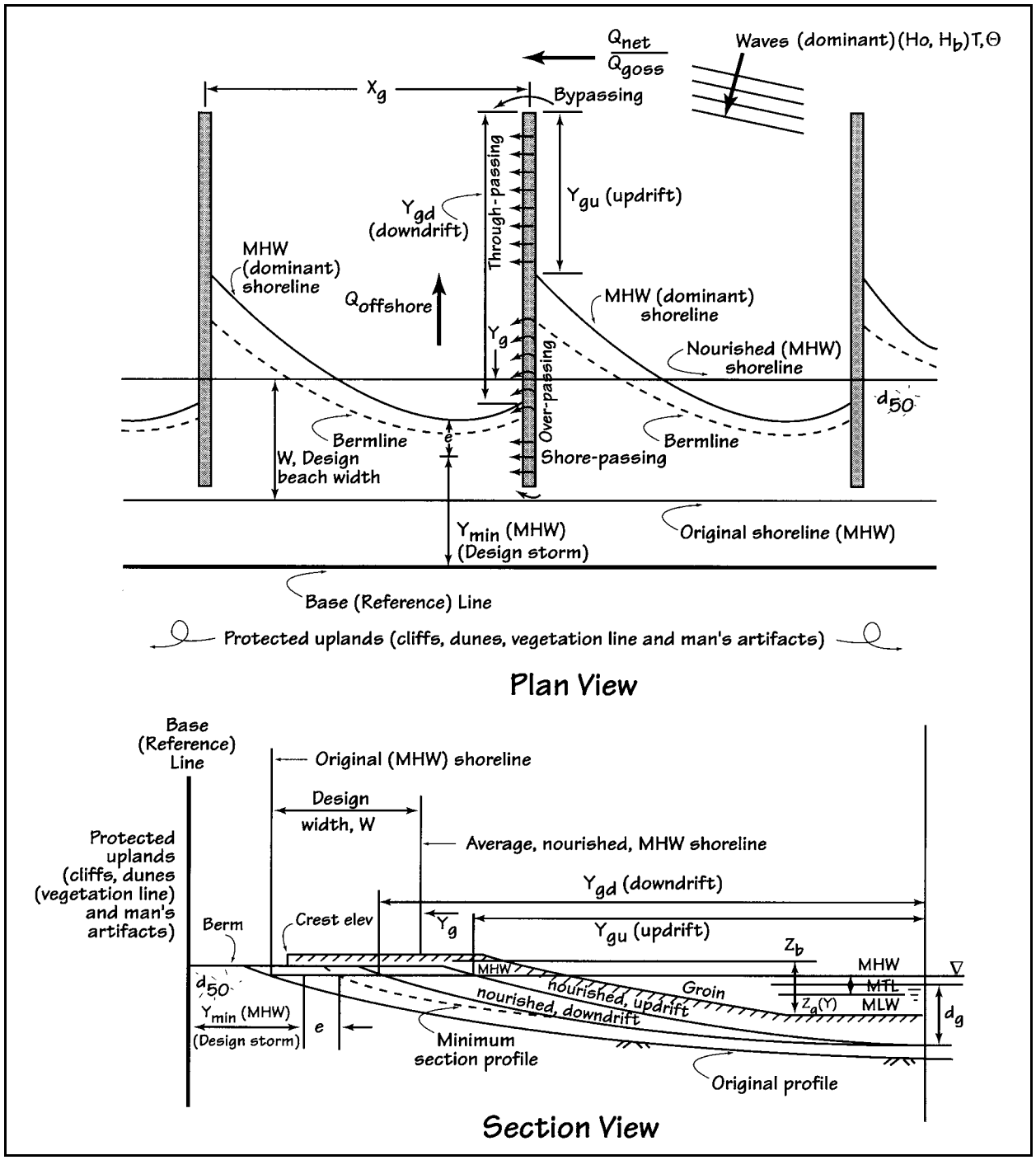

Figure V-3-29. Definition sketch of key variables in the functioning of groins

Table V-3-9
Process-Based Factors Controlling Groins

	Process	Parameter	Description
1	Bypassing	D_g/H_b	depth at groin tip/breaking wave height
2	Permeability		
	• Over-passing	$Z_g(y)$	groin elevation across profile, tidal range
	• Through-passing	P(y)	grain permeability across shore
	• Shore-passing	Z_b/R	berm elevation/runup elevation
3	Longshore Transport	Q_n/Q_g	net rate/gross rate

- Kraus, Hanson, and Blomgren (1994) exercised the GENESIS model for a single groin and studied the bypassing formulation. Rapid filling was followed by a gradual buildup over time that meant an increased amount of material must bypass the groin as the shoreline grows out towards the tip. Filling to capacity was only possible for $Q_n/Q_g=1$ for the unidirectional case. As $Q_g>Q_n$, growth of the shoreline seaward decreased. These tests mean groins seldom fill to capacity by longshore transport processes alone. Cross-shore sediment transport processes must be added to understand how beach elevation and width can build beyond that capable of representation on one-line, shoreline change models. Simulations with multiple-groins and the Westhampton Beach, New York, groin field are also discussed in this paper. An aerial view looking east of the Westhampton Beach, New York, groin field with beach nourishment in 1998 is shown in Figure V-3-30.

- Realistic distributions of longshore current and sediment transport across the surf zone, beach profile shapes with bars and troughs, and other sediment transport mechanisms (wind, tide) are further complicating factors that have yet to be addressed in numerical models.

(b) Groin profile. A typical groin profile with inshore (berm) section, sloping middle section, and horizontal seaward section is shown in Figure V-3-31. In general the landward end is set at the elevation of the natural, existing beach berm, the sloping section is set at the slope of the beach face in the swash zone and the outer, seaward section at a lower elevation such as mean low water (mlw) or lower. The landward and sloping sections function as a beach template for sand to accumulate on the updrift side. The groin profile is shaped to approximately match the postproject beach profile, after nourishment is complete. The seaward end (depth) and seaward elevation are set to the planned bypassing and overpassing in the surf zone. A lower seaward section permits longshore currents to carry sediment over the structure and reduces wave reflections from the groin. A significant amount of sand is transported on the beach face in the swash zone (Weggel and Vitale 1985) and therefore overpassing also takes place in the sloped section when the groin has been filled in this area. Prevention of flanking is the main concern to locate the shoreward end. As seen in Figure V-3-29, calculations of the storm erosion distance, e, together with maximum shoreline recession are needed to establish this position. Seaward limit of the shore section is set relative to the desire, nourished beach width, W, or even further seaward to help retain the nourished beach. Seaward limit of the outer section is the groin length, Y_g, and depends on the amount of longshore sediment transport to be bypassed, as discussed.

(c) Permeability. In general, sheet-pile groins of all types are impermeable whereas rubble-mound groins permit some material to wash through the structure. Some rubble-mound design contain impermeable cores and/or are treated with sealant materials to ensure sand tightness (see EM 1110-2-1617). There are no quantitative guidelines for determining the permeability of sand for a given groin geometry of the rubble-mound type. Some patented, precast concrete groin systems are permeable, as will be discussed later.

Figure V-3-30. Westhampton Beach, New York, groin field and renourished beach, 1998 (courtesy USAED, New York)

(d) Terminal groins. Groins on the updrift side of inlets can benefit nearby beach nourishment projects by controlling (or gating) the amount entering (lost) to the inlet. These terminal structures also benefit navigation projects by reducing the sediment rates within the inlet. They normally are impermeable and high and long to prevent sand from being carried through, over, or around them. Eventually, they will fill and sand bypassing around the end will be maintained. It should be noted that terminal groins are short compared with the length of navigation jetties constructed to reduce wave heights for ships entering the inlet. Consequently, the scale of interruption of normal, longshore sediment transport processes for ebb-and flood- tidal shoals are far different for navigation jetties. Terminal groins fill quickly and do not have major impacts on ebb-tidal shoals and normal, inlet, sand-passing processes. A successful terminal groin is that located on the southern bank of Oregon Inlet, North Carolina. Design and monitoring details are found in Overton et al. (1992); Dennis and Miller (1993); Miller, Dennis, and Wutkowski (1996); and Joyner,

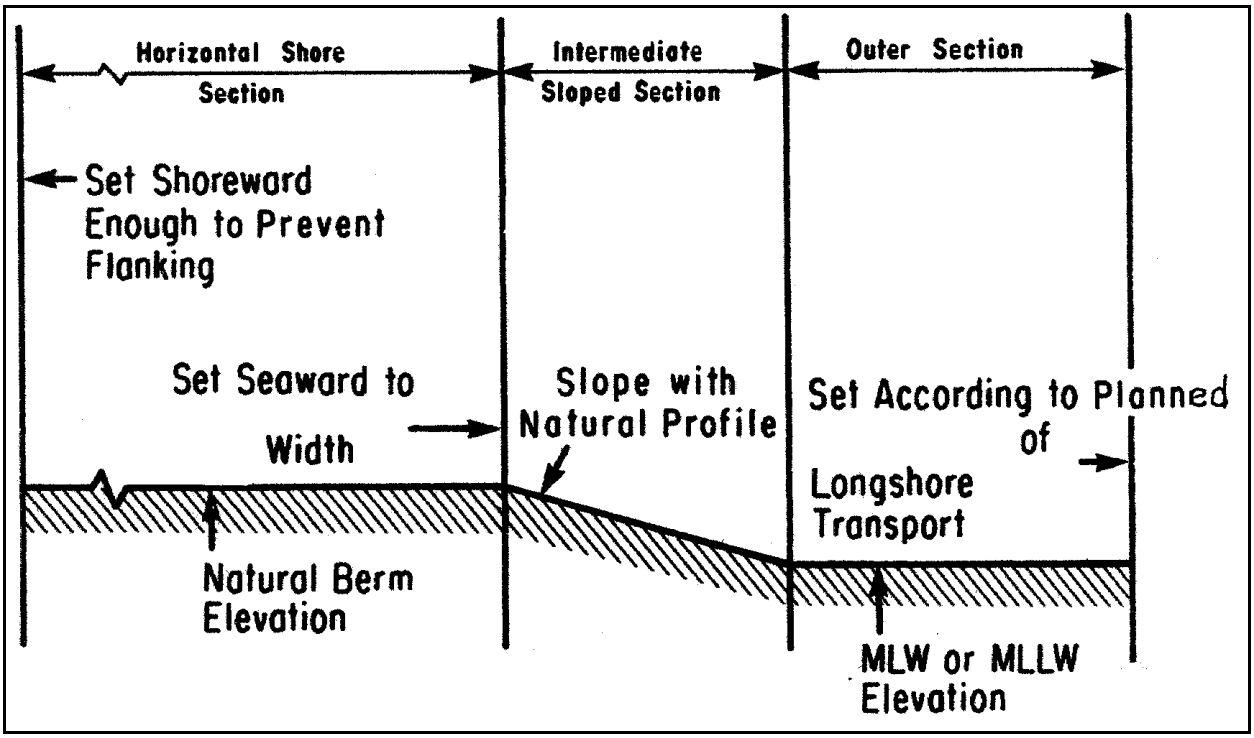

Figure V-3-31. Typical groin profile with sloping section

Overton, and Fisher (1998). See also Dean (1993; 1996) for detailed analysis of terminal structures at the ends of littoral systems.

(e) Groins system transitions. A transition reach is required from a groin field to the adjacent, natural beach. Groin lengths are gradually shortened to allow more bypassing. Generally, groin lengths are decreased along a line converging to the shoreline from the last full-length groin, making an angle of about 6 deg with the natural shoreline as depicted in Figure V-3-32 (Bruun 1952). The spacing is also reduced to maintain the same X_g/Y_g ratio (2-3) used in the design.

(f) Order of construction. The sequence in which a groin field is constructed is a practical design consideration and may not be straightforward. To minimize downdrift impacts, beach nourishment and groin construction should be concurrent. Construction of the first groin should be at the downdrift end of the project, preferably the terminal groin adjacent to an inlet. Net drift will combine with the artificial beach nourishment to fill and stabilize the first compartment. The second groin is then constructed and the process repeated. Gradually working updrift, the groin field construction is completed. This process together with tapering the ends will help to minimize the impact to adjacent, downdrift beaches. This method may increase costs, but it also may result in a more practical guide to spacing of the groins than originally designed.

(5) Nontraditional configurations. Most groins are straight structures, perpendicular to the shoreline. Figure V-3-33 illustrates other possible planform shapes. T-shaped groins are similar to nearshore breakwaters when the tee end is above the mean water level. Inclined groins may reduce rip currents along the updrift side when inclined in the direction of net sediment transport. All shapes shown have been constructed and provide some degree of shoreline stabilization. Sectional variations are also possible as listed in Table V-3-10.

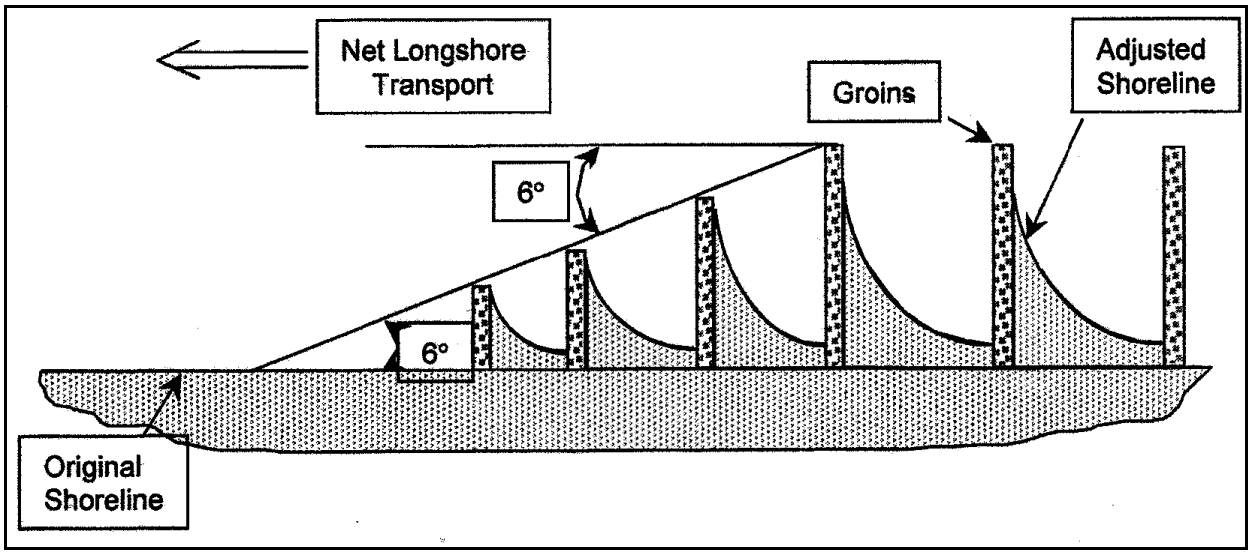

Figure V-3-32. Transition from groin field to natural beach

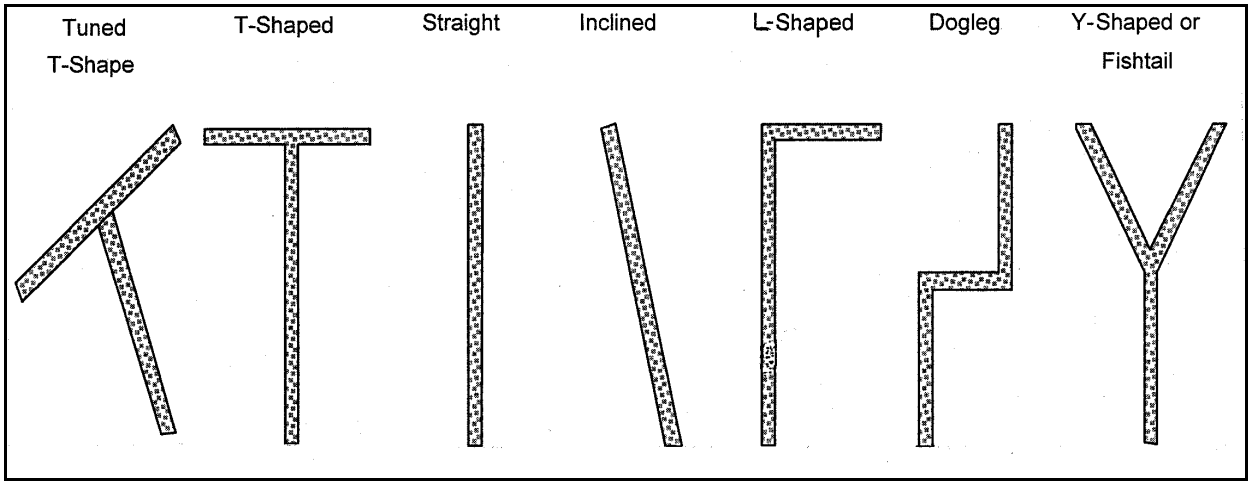

Figure V-3-33. Possible planform shapes for groins

Table V-3-10
Types of Groins-Section Views

Concepts	Comments
Flat (Horizontal)	old
Sloped	common
Notched	(swash zone, new)
Concrete-pile (permeable)	(innovative, patented)
Adjustable	(elevation, length)
Rectifying	(transport-direction sensitive)
Tuned	(elevation, T-head)
Temporary	(geotextiles, sand)
Spur	

(a) Notched groins have recently undergone laboratory and field testing by the USACE (Kraus 2000). Trial notched groins have been implemented by the U.S. Army Engineer District, New York, and the U.S. Army Engineer District, Philadelphia, along the south shore of New Jersey. The purpose of notching is to bypass beach fill and littoral sediment so that the fillet and erosive response of the shoreline are smoothed out, i.e., to straighten the shoreline adjacent to the groin. The goal is shoreline readjustment to approach a smooth, continuous shoreline through a groin field. The efficiency of notching was defined as the amount of sediment that passes the groin system, but that remains on the subaerial beach. Tentative conclusions based on both the laboratory and field experiments are: notches in the swash zone are most efficient; notches in the surf zone are less efficient and can have strong longshore currents, and be hazardous to swimmers; surf zone notches may move sediment further from shore; notching a groin in the swash zone may not be successful depending on how and at what rate sediment typically moves alongshore on the subject beach.

(b) Spur groins are short, stub groins constructed at right angles to navigation jetties and the end groins of groin fields to redirect currents and sediment transports. Sorensen (1990) describes a spur jetty constructed as an emergency measure on the leeward side of two curved jetties to prevent a breach at the landward end. Anderson, Hardaway, and Gunn (1983) document eleven locations in the Chesapeake Bay where short, shore parallel groins are attached to the terminal groin near the beach. Over 12 years of beach response at one site reveals that the spur groins cause diffraction and refraction effects to prevent the detachment of the terminal groin at its landward end.

(c) Another way to smooth the shoreline is to make the groin more permeable as illustrated in Figure V-3-34. A patented, concrete pile, permeable groin field has existed on Cayman Kai, Caribbean Sea, for over 10 years and has survived many hurricanes (from Kraus and Bocamazo 2000). Environmental restrictions against hardened shorelines in North Carolina has resulted in a groin field constructed from geotextile materials filled with sand on Bald Head Island, North Carolina (Denison 1998). In theory, these structures will provide sand for shore protection if they are damaged or fail in major storm events. Other revisited or fresh concepts for groin designs listed in Table V-3-9 have only been proposed conceptually and have yet to be field tested. These new and innovative approaches to groin design benefit from experience and modern understanding of coastal sediment processes.

(6) Basic rules for functional design of groins. Ten modern rules for groins design can be summarized as follows:

- Rule 1 If cross-shore sediment transport processes are dominant, consider nearshore breakwater systems first.

- Rule 2 Conservation of mass for transport of sediment alongshore and cross-shore means groins neither create nor destroy sediment.

- Rule 3 To avoid erosion of adjacent beaches, always include a beach fill in the design

- Rule 4 Agree on the minimum, dry beach width, $Y_{min.}$ for upland protection during storm events as a measured to judge success.

a. Aerial photo

b. Cross-section model

Figure V-3-34. Patented concrete pile permeable groins Cayman Kai, Caribbean Sea (surviving for 10 years, including hurricanes). Innovation is groin design to enhance sediment through-passing and smooth the shoreline variation in the groin field (from Kraus and Bocamazo 2000)

- Rule 5 Begin with X_g/Y_g=2-3 where X_g is the longshore spacing and Y_g is the effective length of the groin from its seaward tip to the design shoreline for beach fill at time of construction.

- Rule 6 Use a modern, numerical simulation model (e.g., GENESIS) to estimate shoreline change around single groins and groin fields.

- Rule 7 Use a cross-shore, sediment transport model (e.g., SBEACH) to estimate the minimum, dry beach width, Y_{min} during storm events.

- Rule 8 Bypassing, structure permeability and the balance between net and gross longshore transport rates are the three key factors in the functional design. Use the model simulation to iterate a final design to meet the Y_{min} criterion.

- Rule 9 Consider tapered ends, alternate planforms and cross sections to minimize impacts on adjacent beaches.

- Rule 10 Establish a field monitoring effort to determine if the project is successful and adjacent beach impacts.

- Rule 11 Establish a "trigger" mechanism for decisions to provide modification (or removal) if adjacent beach impacts are found nonacceptable.

f. Reefs, sills and wetlands.

(1) Background and definitions. Additional types of shore protection alternatives for both high and low wave energy coasts function by reducing the wave energy striking the shoreline. Reefs are platforms of biotic organisms built up to a strict elevation in relation to low tide. Natural reefs require high wave energy to survive. Wetlands are coastal salt or freshwater marshes that are low-lying meadows of herbaceous plants subject to periodic, water level inundations. Wetlands are fragile and only survive in low wave energy environments. See IV-2-11 and IV-2-12 for further details on wetland and reef-type coastlines, respectively. The word "sill" has evolved to take on two separate identities in coastal engineering. Both meanings imply wave attenuation in the lee of the structure. A submerged, continuous, nearshore dike to hold sand moving offshore from a nourished beach is one definition and also labeled a perched beach. Free-standing, low-profile, continuous shoreline structures to permit establishment of a marsh fringe in the lee of the structure are also called sills.

(2) Reefs.

(a) Natural types. Coral reefs are massive calcareous rock structures that slowly grow upward by secretions from simple animals living on the rock surface. They exist throughout the Florida Keys, on both Florida coasts, the Hawaiian Islands, and the U.S. Island territories and serve significantly lower the mean wave energy striking the adjacent shore. Fringing reefs border a coast, barrier reefs lie offshore enclosing a lagoon, and atolls encircle a lagoon. Under favorable growth conditions, coral reefs build upward to form wide, broad platforms that are exposed at low tide. Thus they cause waves to break and to continue breaking across the reef.

- Oyster reefs can exist in much colder, brackish water conditions of lagoons, bays and estuaries. They are found along both coasts and in the Gulf of Mexico. They are wave-resistant structures that can biologically adapt to rising sea levels. Their maximum elevation is related to the minimum time of inundation in the middle range of the intertidal zone.

- A third type of natural reef is produced by colonies of tube worms called a worm reef. The east coast of Florida has some of this type.

- With respect to natural shore protection, reefs are a biological wave damper that can accommodate rising sea levels as long as they are alive. Protection of reefs is essential.

(b) Wave attenuation. Wave transformation processes across broad, flat coral reefs include shoaling, refraction, reflection, and energy dissipation by both bottom friction and wave breaking. Wave energy is also transferred to both higher and lower frequencies in the wave spectrum as the spectral shape flattens (Hardy and Young 1991). Wave setup variations along reefs can occur due to gradients in wave breaking characteristics to produce longshore currents. For engineering purposes, depth-limited wave breaking is the dominant transformation process. A methodology to estimate random wave energy transformation across reefs is presented in USACE (1993). It is based on the breaking wave model of Dally, Dean, and Dalrymple (1985) extended to random waves following Kraus and Larson (1991). Comparison of the numerical model results with field experiments of rms, wave height attenuation on the Great Barrier Reef in Australia (Young 1989) showed good agreement with the measurements. The breaker model without bottom friction is available in the PC-based computer program NMLONG (Kraus and Larson 1991; USACE 1993).

(c) Artificial reefs. The functional design of artificial reef systems for shore protection; increasing the fill life of renourished beaches, and to enhance recreational surfing is a relatively new area of coastal engineering. No general design rules exist. Numerical and physical models have recently been employed for site specific designs in California and Australia of artificial reefs for surfing. These models aid in both wave breaker-type design (Pattiaratchi and Bancroft 2000) and to insure that the structure will not create downdrift erosion. (Turner et al. 2000).

(3) Sills.

(a) Perched beach. A beach or fillet of sand retained above the otherwise normal profile level by a submerged dike (sill) has only been used twice in the United States (National Research Council 1995). Ferrante, Franco, and Boer (1992) describe a successful, 3,000-m-long perched beach project on the coast at Lido di Ostica about 35 km from Rome, Italy, on the Tyrrhenian Sea. The rubble-mound sill was located about 150 m from shore with crest -1.5 below msl datum in -5.0 water depth. An additional 1.000-m stretch with sill closer to shore in shallower water performed better to hold a wider beach. A feasibility study of the perched beach concept in the Netherlands was reported by Ruig and Roelse (1992). Model studies and calculations of life-cycle costs demonstrated that this alternative was roughly as expensive as repeated beach nourishments with no sill construction over a 30-40-year period. Construction at the site selected, Cadzand, Tien Honderd Polder, Zeeland, The Netherlands, has yet to be implemented.

(b) Wetlands protection. In low wave-energy environments, natural, wide, fringe marshes can provide sufficient erosion protection for upland areas, as discussed later. However, for many reasons, the fringe marsh itself may be eroding and require protection, enhancement and/or to be re-established. Sills are typically low, small, continuous rock structures placed at mean low water with some sand fill in the lee to provide a substrate for marsh growth (Hardaway and Byrne 1999). Figure V-3-35b displays a curved, stone sill connecting headland breakwaters with sand fill and marsh planting on the Choptank River, Chesapeake Bay (from Hardaway and Byrne 1999). After 5 years, the sill is practically invisible as shown in Figure V-3-35c. Sills can thus be used in higher wave energy regimes to establish intertidal marsh grasses that aid in the shore protection. Periodic marsh replanting and maintenance may be required under higher wave energy conditions. Advantages and disadvantages of a wide variety of erosion mitigation structures and materials to protect wetlands can be found in the Wetlands Engineering Handbook (Olin et al. 2000).

(4) Wetlands. The final alternative in this section on shoreline stabilization structures are fringe marshes or wetlands. Part IV-2-11 considers their values, distribution classification sediment characteristics, and causes for loss of wetlands in the coastal zone. However, little is known about their importance for shoreline erosion mitigation.

(a) Tidal creeks with fetch exposures less than 0.5 nautical miles and low wave-energy environments can naturally sustain a sufficiently wide marsh fringe. Also, they generally have little or no problem with upland bank erosion because the established marsh fringe absorbs most of the wave energy before it can impact the upland area (Hardaway and Byrne 1999). On the Chesapeake Bay, Hardaway and Anderson (1980) found that low, upland banks erode almost twice as fast as marsh shorelines with similar fetch exposures and nearshore depths.

(b) Some recent field and laboratory research has focused on wave attenuation by wetland vegetation (Kobayashi, Raichle, and Asano 1993; Wallace and Cox 1997; Tschirky, Turke, and Hall 2000). Wave heights are typically reduced by 50 percent and the peak spectral period also drops as the spectrum becomes more broad banded with higher frequency components. No significant design guidance on allowable wave heights or currents for wetlands presently exists. The Wetlands Engineering Handbook (Olin, Fischenich, and Palermo 2000) provides a wealth of valuable information for the restoration and creation of wetlands.

V-3-4. Nonstructural Alternatives

a. Introduction.

Nonstructural alternatives are management strategies for coastal hazard mitigation that are not armoring (Part V-3-2) nor beach stabilization structures (Part V-3-3), nor beach nourishment (Part V-4). Society has developed ways to adapt by setting requirements for the elevation of buildings, providing insurance and planning for continual erosion with setback limits for new construction. The final nonstructural alternative is to retreat by relocation, abandonment, or demolition.

- Three Federal government agencies (the USACE, Federal Emergency Management Administration (FEMA), National Oceanographic and Atmospheric Administration (NOAA)) with different missions, planning methods, and requirements for benefits determination employ or promote the use of nonstructural methods. This section briefly summarizes the role of each and presents some examples of the retreat alternative. Full details of the Federal government's planning requirements and design constraints for all three agencies involved are presented in Part V-8.

- Coastal hazard mitigation is addressed in a piecemeal manner by multiple agencies within states, at the county, city and community level, and by businesses and individuals operating and living at the water front. Property ownership (Federal, state, municipal, community, and individual) and the value of scarce waterfront property strongly motivates all parties to protect their valuable investments. Part V-8 presents details of how each Federal agency (CORPS, FEMA, and NOAA) interacts with each level of responsible group, but details of approaches by these parties are beyond the scope of this chapter.

b. Adaptation.

(1) Zoning and building codes. Any structural or nonstructural change in the design, construction or alteration of a building to reduce damage caused by flooding and flood related factors (storm surges, waves, and erosion) is considered a flood proofing alternative by FEMA. The mechanism to require change in old construction practices is the National Flood Insurance Program (NFIP) administered by FEMA using Flood

a. Stone sill with marsh planting on Chester River, Kent County, MD

b. Stone sill connecting breakwaters with sand fill and marsh implantation on Choptank River, Talbot County, MD

c. Breakwater and sill project after 5 years

Figure V-3-35. Sills and breakwaters (from Hardaway and Bryne 1999)

Insurance Rate Maps (FIRM's) prepared by FEMA. A storm surge elevation at the one percent exceedance level (100-year recurrence interval) plus waves is employed to determine risk and insurance rates for individual properties located on the flood maps. Insurance rates are much lower for structures elevated above the 100-year flood level and is a requirement for all new construction in the coastal, high-hazard zone (including waves). In effect, these regulations become floodplain zoning laws applicable to individual property owners and have resulted in a reduction in Federal government expenditures for insurance claims and disaster assistance benefits (National Research Council 1990).

(2) Setback limits. A second way to adapt is to limit construction close to the shoreline. The NOAA has identified land-use planning and construction siting as the most effective means to reduce coastal storm hazards, particularly on eroding coasts. Here, the mechanism to require change in old construction practices is the Coastal Zone Management Act (CZMA) of 1972. Through the CZMA, the NOAA provides funds to individual states to help solve their own coastal hazard problems. As a result, many states have developed coastal construction setback lines and zones that include historic erosion rates at each site. The methods, definitions, widths, etc., vary from state to state as summarized in Part V-8. A key element is the historic, average erosion rate at each site. Presently, FEMA does not include delineation of erosion zones and erosion hazards on its flood maps. Methods to incorporate both coastal erosion (National Research Council 1990) and beach nourishment (National Research Council 1995) in the national, flood insurance program have been proposed but have yet to be formally adopted. Clearly, coastal erosion increases the risk and beach nourishment reduces the risk of coastal flood and wave damage.

c. Retreat.

Retreat is the final adaptation option. Relocation here also considers abandonment and demolition. To some, retreat is the only option. But practically, all constraints (economic, environmental, social, legal, etc.) must be evaluated for this alternative as well as for all others as previously discussed. This approach may be employed by the Corps as the Federal government agency designated by Congress to protect the nation's shores from the chronic effects of erosion and coastal flooding. Two examples illustrate the USACE's approach and focus on why the retreat alternative was selected.

(1) Cape Shoalwater, Washington. The northern shoreline of the inlet to Willapa Bay, Washington, has been receding at an average rate of 30 to 40 m/year for over 100 years (Terich and Levenseller 1986). Erosion of this area (Cape Shoalwater) has been faster and has lasted longer than any other site on the U.S. Pacific Ocean coast (Komar 1998). Natural, northern migration and progressive deepening of the channel inlet are the two main factors responsible for erosion of the cape. A few homes have been lost, a lighthouse destroyed, the main road moved inland and a historic, pioneer cemetery relocated in this rural area.

(a) In the 1960s and 1970s, the USACE studied the construction of a jetty to stabilize the inlet location and reduce the erosion of the cape. They concluded that a structural solution was not economically feasible to the Federal government. The USACE recommended that if Federal government funds were available at this site, they should be used to purchase land threatened by future erosion. However, no Federal project for relocation could be justified based on the relative benefits and costs to the Federal government.

(b) The rural area (low benefits) and extremely high erosion rate (high costs) were responsible for this outcome, as may have been expected. At other sites, this result is not as obvious.

(2) Baytown, Texas. The northern, upper end of Galveston Bay on the Gulf of Mexico includes Burnett, Crystal, and Scott Bays and low-lying areas that are part of Baytown, Texas, about 24 km east of Houston. Flooding occurs routinely from minor storms and is compounded by subsidence of the ground surface. Withdrawal of oil and gas and groundwater for the metropolitan area of Houston produced 2.5 m (9 ft) of subsidence between 1915 and 1975 (U.S. Army Engineer District, Galveston, 1975).

(a) Both structural (earth levee, concrete floodwall) and nonstructural (permanent relocation and evacuation) alternatives were studied in the early 1970s by the USACE to mitigate the flooding problem. The feasibility study report to Congress (U.S. Army Engineer District, Galveston, 1975) recommended the retreat alternative. Congress authorized this project under the Water Resources Development Act (WRDA 1978).

(b) The final project report (U.S. Army Engineer District, Galveston, 1979) called for the Federal government to purchase approximately 303.51 ha (750 acres), 448 homes and relocate 1,550 people within the 50-year floodplain. Total project costs were $32.131 million (1979 dollars) with the local sponsors' share to be 20 percent or $7.826 million. Annual project benefits were estimated to be $3.530 million and included:

- Reductions for insurable flood damages.
- Reductions for utility service costs.
- Reductions of temporary, emergency evacuation, public health and public relief costs.
- Value of land under new uses.

(c) Other benefits (constant anxiety from flood hazards, depressed property values, health hazards, inconvenience of repetitive, temporary evacuations, and damages to real property and personal possessions) cannot be included as net gain benefits to the national economy. Total, annual costs were $2.678 million giving a benefit to cost (B/C) ratio of 1.3 to the Federal government for the retreat alternative. In contrast, the structural alternative, B/C ratios were 0.1 - 0.3 (USAED, Galveston, 1979).

(d) In 1978, the environment assessment report to the EPA was approved. Plans called for converting the land into a natural area, with possible development of nature areas, bird sanctuaries, green belts, wildlife areas, nature walks, and other uses consistent with the high flood potential. Besides the local sponsor (City of Baytown) paying 20 percent of the final cost, they were also responsible for management of the vacated area.

(e) Unfortunately, the project floundered on local disagreement over the value of the land to be purchased and was never funded. Estimates of project costs rose from $16.980 million in 1975 to $39.131 million in 1979 (less than 5 years). People in the community who did not live in the floodplain were being asked to help buy out those who did. The community was divided over what the property was worth. Some believed their neighbors would be paid far too much for relocation. In July 1979, a bond election was held to provide the local funding for the project and it failed by a 60/40 percent margin (Pendergrass and Pendergrass 1990).

(f) In 1980, Congress was ready to authorize funding, but the local, 20 percent cost share could not be provided. The local residents decided to stay and the Corps placed the project in its inactive category. In the final analysis, the Corps' requirement for cost sharing ($7,589 per residence in 1975 and rising to $17,469 per residence in 1979) prevented an economically viable and environmentally sound project from being implemented. Because the B/C ratio was 1.3, the annual benefits to the Federal government exceeded the 20 percent, local cost share amount. In other words, the Federal government could have paid for the entire project and still realized net economic benefits to the Federal government. This result also does not consider NFIP payments then and over the last 20 years. Partial protection by the NFIP also contributed to the local residents' decisions to stay.

(g) In summary, a nonstructural solution for part of the community of Baytown, Texas, proved difficult to implement because the entire community would not share in the local cost requirement. In contrast, a flood dike and revetment to protect the Texas City – La Marque area on the lower Galveston bay has been

constructed. Here, the perception that all the affected community was "protected" made the local sponsor share obtainable (Pendergrass & Pendergrass 1990).

(3) Special cases.

(a) Brighton Beach Hotel, Coney Island, New York. Komar (1998) shows etchings of the 1888 relocation of a large, beachfront hotel on Coney Island, New York. Twenty-four railway tracks were laid to span the entire hotel width, and the wooden pile-supported hotel was lifted onto freight cars on each track. Six locomotives pulled the hotel inland 150 m. No details on costs were provided for this private project which required property ownership and grading of the inland site. Its economic viability also depended on the availability of railway equipment in that era over 100 years ago. Full details are in Scientific American (1888).

(b) Cape Hatteras Lighthouse, North Carolina. Very recently, relocation of the Cape Hatteras Lighthouse has been completed by the National Park Service (NPS), U.S. Department of Commerce (see, e.g., Civil Engineering 1999). The lighthouse is on the east coast of Hatteras Island about 4.02 km (2.5 miles) north of the tip of Cape Hatteras and 64.37 km (40 miles) south of the Oregon Inlet (Figure I-2-6). It is located within Cape Hatteras National Seashore Park, administered by the NPS. The original lighthouse built at this site in 1803 was replaced in 1870 by the present structure, which is the tallest (61 m) and perhaps best-known brick lighthouse in the United States. When built in 1870, it was approximately 490 m from the shoreline. By 1935, this distance diminished to about 30 m due to landward migration of this cape feature. The mhw, average recession rate between 1852 - 1980 (128 years) has been 5.9 m/year and 3.9 m/year for the 1870 - 1980 (110 years) period (Everts, Battley, and Gibson 1983). In 1996, partly due to a wide variety of piecemeal, temporary and emergency measures (see Table V-3-11), the lighthouse stood about 50 - 90 m from the Atlantic Ocean (U.S. Army Engineer District, Wilmington, 1996) depending on the season and tidal conditions. The existing, steel, sheet-pile groin field was actually designed and constructed by the Navy to protect its installation to the north in 1970. The lighthouse, a national historic landmark, remained in operation, and the NPS decided in 1980 that a long-term solution of the erosion problem was needed.

- A 1982 conference of experts from many disciplines (engineering, geology, economy, and historic preservation) together with a 1985 study by the Wilmington District convinced the NPS to employ a structural solution. A seawall/revetment structure was selected. Also a factor in this decision was scientific and engineering opinion that the lighthouse could not be moved without suffering serious structural damage. Congress approved $5.3 million and construction was to begin during the summer of 1986.

- A Move the Lighthouse Committee Report (private) convinced the NPS to seek the advice of the National Academy of Sciences. Their final report (National Research Council 1988) recommended the retreat alternative and in December 1989, the NPS reversed its decision and announced its approval of the relocation alternative. The next 10 years were filled with further controversy and debate due to lack of congressional funding for the relocation; public sentiment in North Carolina against the move (Save the Lighthouse Committee, private), and other ad hoc committee reports with updated studies. During the period, other structural engineers and large-scale relocation experts became convinced that the lighthouse could be moved without damage.

Table V-3-11
Cape Hatteras, North Carolina, Shore Protection History

Year	Action Taken
1930s	Civilian Conservation Corps builds sand dune system along Hatteras Island
1966	Beach Nourishment – 239,000 m^3 (312,000 cu yd) of sand placed along Buxton Motel area north of lighthouse
1967	Sandbags placed along 340 m of shoreline to protect former Navy Facility north of lighthouse
1970	Navy constructs three concrete & steel groins
1971	Beach Nourishment – 150,000 m^3 (200,000 cu yd) of sand placed along Buxton Motel area north of lighthouse
1973	Beach Nourishment – 960,000 m^3 (1,250,000 cu yd) of sand placed along Buxton Motel area north of lighthouse
1974	Repairs made to northern & southern Navy groins
1980	Emergency Repairs – 50 m landward extension of south groin
1981	Riprap and sandbags placed beyond landward extension of south groin
1982	Additional 50 m landward extension of south groin. Seven hundred sandbags placed around the base of the lighthouse
1983	Riprap scour apron placed along landward end of south groin
1992	Additional sandbags placed around base of lighthouse
1994	Additional sandbags placed around base of lighthouse
1995	Rehabilitation of landward end of south groin with 56 m of steel sheetpiling

- Also contributing to the controversy was a NPS committee study in 1992 to make recommendations for *interim* measures, as required, to ensure that the lighthouse remain protected, until the retreat solution could be implemented. An intermediate measure (15 - 25-year design life) was selected to add a fourth groin south of the existing groin field. The NPS employed the Wilmington District to make this design (USAED, Wilmington, 1996). Opponents to the move cited the costs for the fourth groin alternative ($3.5 million) in the USACE study when objecting to the retreat alternative costs (estimated as $12 million). A complete economic analysis using a 100-year design life to determine life-cycle costs of a groin field with terminal groin versus the retreat alternative has never been made by the USACE.

- The National Academy of Sciences study and report (National Research Council 1988) reveals the following NPS policies that dictated the choice of the retreat alternative.

  - Historic preservation is more important than a do nothing or “let nature take its course” policy.

  - The NPS does not have to follow a benefit/cost analysis procedure with benefits exceeding costs regarding the choice of alternative for shore protection.

  - The NPS policy for coastal shorelines is to not interfere with natural, coastal processes. This policy eliminated all structural options as discussed in Chapter 5 of the NRC 1988 report and made their analysis superficial and irrelevant. The retreat option was the only alternative given consideration.

- The NPS strategy was to use the Cape Hatteras Lighthouse relocations as an example and model of "enlightenment" (page numbers refer to NRC 1988)

  - "an exemplary response ... to the generic problem of shoreline erosion" (p. 72)
    "attract much media attention ... to educate a large national audience on the nature of coastal barriers" (p. 72)
    "use national parks as models of wise management of natural and cultural resources" (p. 71)
    "act as a signal to the country of the problems confronting the coast" (p. 39) and
    "illuminate approaches to solving the problems of living with a rising sea" (p. 39).

- The Cape Hatteras Lighthouse was moved successfully inland about 488 m (1,600 ft) from the mhw shoreline in 1999. Recognizing the engineering and construction skills required to complete the move safely, the project received the Outstanding Civil Engineering Achievement Award from the American Society of Civil Engineers in 2000.

- In the final analysis, the NPS policy against any structural interference with natural, coastal processes was the deciding factor. The decision to relocate was taken in 1989 at a time when the possible, accelerated rise in sea level was also of major concern.

(4) Impact of sea level rise. A detailed summary of present-day knowledge of sea level rise rates is presented in Part IV-1-6. Substantial variability exists when including local subsidence as previously discussed for Baytown, Texas. A National Academy of Sciences report on engineering implications (National Research Council 1987) concluded that whether to defend or to retreat depended on several factors, but mainly the future sea level rise rate and the cost of retreat which varies by site. The NRC recommended that all options should be kept open to enable the most appropriate response to be selected. Retreat is most appropriate in areas of low development. Given that a proper choice exists for each location, selecting an incorrect response alternative could be unduly expensive (National Research Council 1987).

V-3-5. Combinations and New Technologies

Pope (1997) lists the following common types of coastal erosion and flooding problems:

- Long-term, chronic land loss associated with the erosion of cohesive sediments, reduced supply of sandy sediments, and/or subsidence.

- Localized erosion impacts caused by a navigation project jetties or other coastal construction works.

- Lands and facilities impacted by storm-induced erosion.

- Flooding by a storm surge with associated wave attack damages.

- Loss of environmental resources (i.e., wetlands, oyster reefs, nesting areas, etc.).

- Need for more land.

In many cases, combinations of these problems exist that require a combination of structural measures together with nonstructural alternatives to be implemented within a comprehensive, coastal region, management plan for hazard reduction.

a. Combinations.

(1) Structural combinations.

(a) Beach stabilization structures and beach nourishment. Groins and detached breakwaters combined with beach fills are discussed in Part V-3-3e. The combination mitigates downdrift impacts and/or increases the fill life of the renourished beach. Together, their life-cycle costs and environmental impact may be less than if selectively implemented. Construction of the beach stabilization structures without fill is likely to damage adjacent beaches.

(b) Seawalls, revetments, and beach nourishment. The original design of the new seawall for hurricane protection at Virginia Beach was to be a curved, concrete-type structure as at Galveston, Texas (Figure V-3-5). To accommodate a lowered seawall crest for aesthetic reasons (see Part V-3-1-c-(5)and Figure V-3-6) a wide beach nourishment project was added to the design to reduce flooding and wave damage (USAED, Norfolk, 1994). Together with improved interior drainage and pumping equipment, this combined design provides the same hurricane flooding and wave damage protection as the original seawall design.

(c) Beach nourishment and rebuilt dune with buried seawall/revetment. The soft alternative (beach and dune with buried rock seawall/revetment) was determined to be both environmental and economically advantageous when compared against an armored revetment for storm protection against the 1 percent change storm event at Dam Neck, Virginia, on the Atlantic Ocean (Basco 1998). The final design cross section is shown in Figure V-3-36a and includes a buried rock seawall/revetment beneath the dune. In the event of a major storm causing severe dune erosion, the buried seawall will prevent storm damage if a second major storm occurs in the same season. Figure V-3-36b shows a photograph of dune construction with the buried, rock seawall (Basco 2000a). A similar approach was incorporated at Ocean City, Maryland, where a steel, sheet-pile bulkhead was incorporated as a buried backup feature in the design.

(2) Nonstructural and structural combinations.

At many locations, elevated structures combined with some type of armoring or shoreline stabilization together with beach nourishment are employed in combination for coastal hazard mitigation. Presently, 32 of 35 coastal states and territories have some type of setback requirements for new construction and existing structures found uninhabitable after a storm (Heinz Center 2000). These nonstructural, adaptive measures and structural alternatives are often combined to address the wide range of coastal problems previously cited. An example is the barrier island of Grand Isle, Louisiana, where beach nourishment, rebuilt dunes, a groin field and nearshore breakwaters are used for a community where the first floor of most residences are constructed above the 1 percent chance flood level (with waves) and the public lands on the rapidly eroding east end are restricted from any development (Pope 1997).

b. New technologies.

(1) Introduction.

Many nontraditional ways to armor, stabilize, or restore the beach including the use of patented, precast concrete units, geotextile-filled bags, and beach dewatering systems have been tried in the field. Their success depends on their stability during storm events and durability over the economic, design life. Their initial cost and cost for removal if environmental impacts warrant can be less than traditional methods, at some sites. These new technologies often involve nontraditional materials or shapes but are employed in a traditional manner, e.g., nearshore breakwaters. See Pope (1997) for more details.

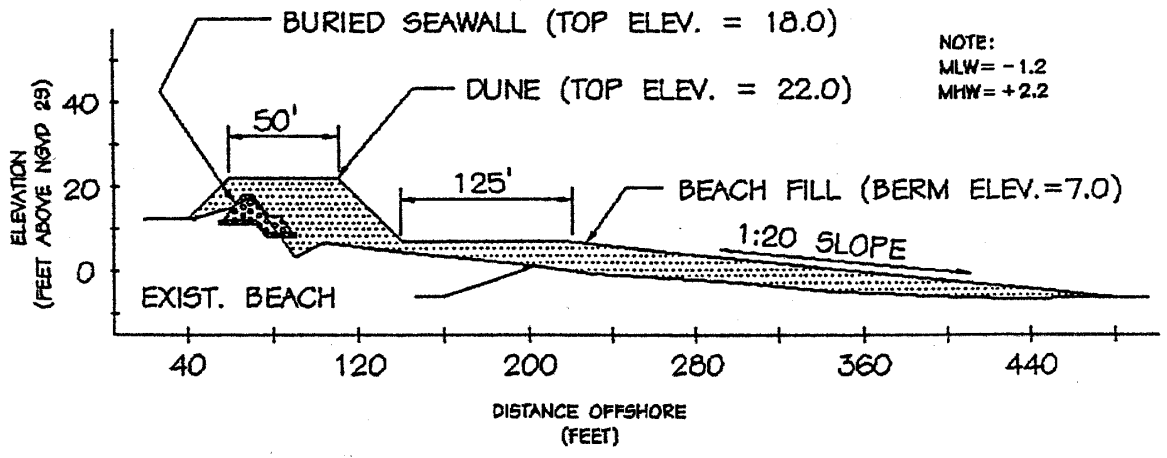

a. Cross section

b. Photo during construction, Dam Neck, Virginia (from Basco 2000)

Figure V-3-36. Rebuilt dune with buried seawall (Basco 2000a)

(2) Precast, concrete units. Patented, modular, precast concrete units that can be interconnected to form one or more, nearshore breakwaters have been tested in Florida, Georgia, and New Jersey.

(a) In late 1989, two nearshore breakwater sections were installed at Sea Isle City, New Jersey, on the Atlantic Ocean. Each unit is 1.7 m long, 4.9 m wide and 2.1 m high and placed on a geotextile fabric. Each unit weighs about 12 metric tonnes and has 1.1 - 1.2 m freeboard at mean sea level (tidal range of 1.2 m). The two breakwaters were about 50 m in length with a 34-m gap and placed 37 m offshore (msl) in about 0.9-m water depth. This position was determined by the developer of the unit called the “Beachsaver” system

(Breakwaters International, Inc., Flemington, New Jersey). Independent monitoring over 18 months revealed significant structure settlement with the maximum over 1.2 m and average about 0.6 m (Sorensen & Weggel 1992). Most settlement occurred the first two months after installation. A large scour hole was found landward of one section and the sand trapping volume in two salients was only about 300 m^3, before settlement (Sorensen & Weggel 1992).

(b) The Town of Palm Beach, Florida, in the early 1990s, experimented with another design labeled the "Prefabricated Erosion Protection" or P.E.P. reef system by its developer, American Coastal Engineering, Inc., West Palm Beach, Florida. Each unit is 3.7 m long, 4.6 m wide, 1.8 m high and is placed on a cloth filter fabric. Each unit weights about 22 metric tonnes with crest elevation below msl to act as a thin-crested, submerged, reef-type breakwater. One long breakwater/reef system, 1,270 m in length, placed 76 m offshore (msl) in 2.9 m National Geodetic Vertical Datum (NGVD) water depth consisting of 330 interlocking units was constructed. The submergence was 1.1 m at msl. Monitoring by the University of Florida's, Department of Coastal and Oceanographical Engineering included nearshore profiles and wave gauges landward and seaward of the structure (Dean and Chen 1996). About 17 percent of the units settled 0.8 m with the remainder settling 0.5 m. Wave transmission coefficients ranged from 0.65 for normal conditions (tide range 1.0 m) to 0.85 for storm conditions. A detailed analysis of the leeward project area revealed that wave overtopping, wave setup, pounding, excess longshore currents and sediment transport (both directions) resulted in an increased erosion trend relative to that present before construction (Dean and Chen 1996; Martin and Smith 1997). The conclusion, that the reef breakwater provided little benefit, resulted in its removal. The units have since been salvaged and used to construct a groin field with beach nourishment at the site (Erickson 1998).

(c) These negative results at West Palm Beach, Florida, resulted in a staggered and gapped, planform configuration being the modified plan for the next P.E.P. reef installation at Vero Beach, Florida, in the late 1990s. Monitoring is being conducted by the USACE (Stauble and Smith 1999) with the latest results reported by Wooduff and Dean (2000). Analysis of nearshore profiles over 25 months (August 1996 - June 1999) when compared with historic volume change (1972 - 1986) revealed that erosion has increased landward of the reef. And, background erosion decreased north but remained the same south in control areas outside the reef area (Stauble and Smith 1999).

(d) The Beachsaver breakwater unit and P.E.P. reef unit shapes are similar, namely triangular with flatter slope on the seaward side than on the landward end. The have been called pyramid-shaped. Both have a thin crest width. In contrast, a vertical, cylindrical shape (circular, concrete pipe) combined with a concrete base forms the Hollow Core Reef System (HCR) as patented by Hollow Core Reef Enterprises, Inc., Newport News, Virginia. Each unit is typically 3.6 m long at its base and 1.7 m wide, but the height varies (pipe length) and is specifically designed for intertidal regions with 1-3-m tidal range. Since 1996, a 116-m-long, nearshore breakwater consisting of 46 units, 2.6 m in height has been installed at Sea Island, Georgia, on the Atlantic Ocean (tide range 1.8 - 2.7 m). Each unit weighs about 22 metric tonnes. Freeboard above msl is unknown. The foundation is timber cross-members to form a subbase and initial settlement was measured at less than 0.5 m. The units have been stable since construction and remain in place after several hurricanes along the south Georgia coast.

(e) In summary, crest width, planform configuration, siting and foundation design appear to be the weakest aspect as revealed by field monitoring of precast, concrete, modules for breakwaters and submerged reefs.

(3) Geotextile filled bags.

(a) Geotextile materials or filter fabrics have a long history for foundation mats beneath rubble-mound structures (See Part VI-5-3); and, they have been used as silt curtains to contain dredged materials in the water column. They have also been formed into bags and long, sausage-shaped cylinders (called Longard Tubes) and filled with sand. They have been deployed as revetments for dune protection, as nearshore breakwaters, and as groins. In the 1980s and 1990s, there has been significant improvement in the quality and durability of geotextile fabrics, making them suitable for a variety of coastal applications.

(b) The design life of a geotextile filled bag depends on many factors. It is generally less than properly designed rock structures serving the same function. However, if found to cause negative impacts to adjacent shorelines, the bags can be cut open and removed with the filled sand remaining on the beach. It is for this reason that a soft groin field was permitted by the North Carolina Coastal Resource Commission (CRC) together with a beach nourishment project for South Beach on the western end of Bald Head Island, North Carolina (Denison 1998). The North Carolina CRC prohibits hardened structures on its ocean coast. Fourteen 2.75-m diameter and 100-m-long geotextile bags filled with sand were constructed to grade out to - 1.2 to - 1.5-m (mlw) depths at 120-m spacing to form the groin field. The beach was also prefilled with 496,960.7 cu m (650,000 cu yd) of sand to + 1.8 m (NGVD) berm elevation and 25 - 30-m berm width over 3.65 km. Two hurricanes in 1996 removed about 76,455.49 cu m (100,000 cu yd) from the beach, but caused no damage to the groin tubes (Denison 1998). The long-term survivability of this system has yet to be determined.

(4) Beach drains.

(a) Beach face dewatering by lowering the groundwater table along the coastline began in Denmark in the early 1980s, by accident. After installation of a filtered, seawater system for a seaside aquarium, it was discovered that the sandy beach width increased where the beach parallel, longitudinal pipe intake was buried beneath the surface (Lenz 1994). Patents were obtained by the Danish Geotechnical Institute (DGI) in many countries including the United States where the system is called Stabeach by the licensee, Coastal Stabilization, Inc., Rockaway, NJ.

(b) Lowering the groundwater table is accomplished by draining water from buried, almost horizontal, filter pipes running parallel to the coastline. The pipes are connected to a collector sump and pumping station further inland. Gravity drains the groundwater beneath the beach and through the pipes to the sump and then the water is pumped from the sump. The sand-filtered seawater can be returned to the sea or used for other purposes.

(c) Lenz (1994) describes laboratory experiments (no reference) and field tests at Stuart, Florida, and Englewood Beach, Florida. The patent belongs to Hans Vesterby, DGI, Denmark. Vesterby (1994) reviews the theory and design elements and describes field tests at three sites on the west coast of Denmark in the North Sea.

(d) Long-term, independent field monitoring is needed to learn more about the functional performance of dewatering systems. The system by itself does not produce new sand, so that its greatest contribution may be in increasing the fill life of renourished beaches.

(5) Innovative technology demonstration program.

(a) Many other ideas and devices have been deployed and/or proposed including beach cones (Davis and Law 1994); ultra-low profile, geotextiles injected with concrete (Janis and Holmberg 1994) and fishnets, stabilizers and artificial seaweed (Stephen 1994) for erosion mitigation. Most do not satisfactorily address

nor answer the questions listed by Pope (1997). Alternative technologies for beach preservation was the theme for the 7th National Beach Technology Conference (Tait 1994, ed.).

(b) Section 227 of the Water Resources Development Act of 1996 authorized a National Shoreline Erosion Control Development and Demonstration (NSECDD) program. Emphasis is on "... the development and demonstration of innovative technologies" to advance the state of the art in coastal shoreline protection. Funding the 6-year effort began in fiscal year 2000. A minimum of seven projects on the Atlantic, Pacific, Gulf of Mexico, and the Great Lakes is mandated by this legislation. Pope (1997) discusses many issues surrounding the application of nontraditional and innovative technologies. The ability to perform their promised function, survive for a predictable life, impact on the environment, and total costs (initial and long-term maintenance) must be carefully examined. Pope (1997) then raises many questions that should be addressed, when considering innovative, alternative, shore protection approaches including:

- Is it heavy enough, particularly considering storm waves?
- Will it be properly anchored so that it doesn't fall apart?
- If the structure does fail, could the loose components become an environmental or public safety hazard?
- Will the installation be tolerant of erosion or scour effects around its base?
- Will the material from which it is being constructed last?
- What are the design criteria in terms of events for longevity?
- How will it perform and will it do what we want it to do?
- If it does perform as promised, could there be adverse impacts to adjacent areas?
- How much will constructing the nontraditional or innovative system cost compared to more traditional methods?
- What will it cost to maintain and can it be repaired when damaged?
- What is its effective (functional and economic) life?
- What will it cost to remove the system, if necessary?

(c) All of these questions and more will be addressed for the nontraditional and innovative technologies deployed in the National Demonstration Program. The search for new and innovative approaches has primarily been driven by the shift from hard to soft alternatives for shore protection (Figure V-3-3) and the need to reduce long-term costs of beach nourishment projects by increasing the time interval between renourishment events. As an example, precast, concrete modules, serving as nearshore breakwaters could replace conventional, rubble-mound breakwaters at some locations, and serve the same function of increasing the fill life of the renourished beach. If properly sited (see Part V-3-3) and set on a proper foundation, these units are attractive to permitting agencies because they have a smaller footprint on the bottom and can be adjusted or removed easily, if downdrift impacts are detected, by monitoring. Nontraditional and innovative technologies are subject to all the same design constraints previously discussed (Part V-3-1) plus the extra need to overcome previous shortcomings and prove that they work. The National Demonstration Program will greatly aid in this effort.

V-3-6. Do-Nothing

a. Introduction.

One final alternative that must always be evaluated is the do-nothing or no-project case. The risk of flooding and wave damage continues or increases if historic erosion is also present at the site. When this response is appropriate, what happens to the area, and what government programs are available to help are briefly discussed in the following paragraphs. Further details of the Federal government's response are found in Part V-8.

b. Appropriate response.

Whenever all structural and nonstructural alternatives considered are too costly, then no economically viable solution exists. If the life-cycle costs for protection or relocation exceed the value of the investment, then do-nothing is the appropriate response. This standard for economic feasibility is adopted automatically in Federal project studies of the Corps. If the benefit to cost ratio exceeds unity but social and environmental constraints govern, then the no-action alternative plan can become the Federally recommended plan. When the natural, coastal sediment transport processes (erosion and accretion) are the most important aspect (character, attractiveness, aesthetics, etc.) of the system, then do-nothing may also be the appropriate response. Many examples exist of highly dynamic barrier island systems that are best left alone. An example is the National Park Service policy. The exception for Cape Hatteras was the historic importance of the lighthouse as previously discussed. Individuals may also explicitly decide to take no action (flood proofing or retreat). The homeowner is willing to take the risk when the potential rental income from the property is high. If the house is eventually damaged or destroyed, it would still be covered by the NFIP, if a policy is in effect for the residence. The problem is when this no-action policy is taken, no NFIP policy exists, flooding damage takes place, and the Federal government declares the damaged region eligible for emergency financial assistance.

c. After the flood.

What happens when the do nothing alternative is selected by economics policy decisions? It is clear that the flood and wave damage potential remains, and the risk increases where erosion exists. It is almost certain that the area impacted will decline economically. Social and economic stresses will continue. Examples include: social stresses from apprehension and helplessness; economic stresses of depressed property values; personal property losses continue; cost and inconvenience of restoration after repetitive flooding continues; reduced recreational opportunities for citizens; reduced tourism benefits; reduced employment opportunities for tourism; property values decrease and related property taxes diminish. The no-action alternative may perpetuate a more costly Federal commitment than would be realized otherwise, because other Federal assistance programs exist (see Part V-8 for further details).

d. Government programs available.

When the no action plan remains, the Federal government relies on three methods to mitigate coastal damages and the possibility of loss of human life. As previously discussed (Part V-3-4), the NFIP provides compensation for flooding and wave damages, but it does not protect property from flooding. The NFIP also only encourages adaptation measures; but they are not mandatory, except for new construction where local authorities have adopted flood zoning ordinances. The Federal government also participates in measures for emergency, evacuation route planning. As discussed in Part V-8, because many coastal communities lack sufficient bridge and highway capacities, emergency evacuation is not a dependable means of hazard mitigation. The third program is Emergency Assistance from FEMA when the President declares the region eligible for this financial package after a major, coastal storm event.

e. National coastal hazard mitigation plan.

The need for a national plan of shore protection and coastal hazard mitigation is addressed in Part V-8.

V-3-7. References

EM 1110-2-1614
"Design of Coastal Revetments, Seawalls, and Bulkheads."

EM 1110-2-1617
"Coastal Groins and Nearshore Breakwaters."

EM 1110-2-1913
"Design and Construction of Levees."

EM 1110-2-2502
"Retaining and Flood Walls."

EM 1110-2-2705
"Structural Design of Closure Structures for Local Flood Protection Projects."

EM 1110-2-3102
"General Principles of Pumping Station Design and Layout."

ER 1105-2-101
"Planning Risk-Based Analysis for Evaluation of Hydrology/Hydraulics, Geotechnical Stability, and Economics in Flood Damage Reduction Studies."

Anderson, Hardaway, and Gunn 1983
Anderson, G. L., Hardaway, C. S., and Gunn, J. R. 1983. "Beach Response to Spurs and Groins," *Proceedings, Coastal Structures '83,* American Society of Civil Engineers, NY, pp 727-739.

Ahrens and Cox 1990
Ahrens, J. P., and Cox, J. 1990. "Design and Performance of Reef Breakwaters," *Journal of Coastal Research*," Vol 6, No.1 pp 61-75

Bakker 1968
Bakker, W. T. 1968. "The Dynamics of a Coast with a Groyne System," *Proceedings, 11th International Coastal Engineering Conference*, ASCE, NY, pp 492-517.

Barnett and Wang 1998
Barnett, M. R., and Wang, H. 1998. "Effects of a Vertical Seawall on Profile Response," *Proceedings, 21st International Conference on Coastal Engineering*, ASCE, NY, pp 1493-1507.

Basco 1998
Basco, D. R. 1998. "The Economic Analysis of 'Soft' Versus 'Hard' Solutions for Shore Protection: An Example," *Proceedings, 26th International Conference on Coastal Engineering*, ASCE, NY, pp 1449-1460.

Basco 2000a
Basco, D. R. 2000a. "Beach Monitoring Results and Management Plan FCTCLANT, Dam Neck, Virginia Beach, VA," Final Report, Beach Consultants, Inc, Norfolk, VA.

Basco 2000b
Basco, D. R. 2000b. "Seawalls, Bulkheads and Revetments," *Coastal Engineering: Beyond It's Golden Anniversary*, Japan Press, Tokyo, Japan.

Basco and Ozger 2001
Basco, D. R., and Ozger, S. S. 2001. "Toward Quantification of the Active Sand Volume in the Surf Zone," Abstract, 28th International Conference on Coastal Engineering, (Cardiff), American Society of Civil Engineers, NY.

Basco et al. 1997
Basco, D. R., Bellomo, D. A., Hazelton, J. M., and Jones, B. N. 1997. "The Influence of Seawalls on Subaerial Beach Volumes With Receding Shorelines," *Coastal Engineering*, Vol 30, pp 203-233.

Balsillie and Berg 1972
Balsillie, J. H., and Berg, D. W. 1972. "State of Groin Design and Effectiveness," *Proceedings, 13th International Conference on Coastal Engineering*, ASCE, NY, pp 1367-1383.

Balsillie and Bruno 1972
Balsillie, J. H., and Bruno, R. O. 1972. "Groynes: An Annotated Bibliography," Miscellaneous Paper 1-72, U.S. Army Corps of Engineers, Coastal Engineering Research Center, Springfield, VA.

Berenguer and Enriquez 1988
Berenguer, J., and Enriquez, J. 1988. "Design of Pocket Beaches: The Spanish Case." *Proceedings, 21st International Conference on Coastal Engineering.* Malaga, Spain, pp 1411-25.

Bernd-Cohen and Gordon 1998
Bernd-Cohen, T., and Gordon, M. 1998. "State Coastal Program Effectiveness in Protecting Beaches, Dunes, Bluffs and Rocky Shores: A National Overview," *Final Report*, NOAA, National Ocean Service, Washington DC.

Bodge 1992
Bodge, K. R. 1992. "Gross Transport Effects at Inlets," *Proceedings, 6th National Conference on Beach Preservation Technology*, Florida Shore and Beach Preservation Assoc., Tallahassee, FL, pp 112-127.

Bodge and Dean 1987
Bodge, K. R., and Dean, R. G. 1987. "Short-Term Impoundment of Longshore Transport," *Proceedings Coastal Sediments* '87, ASCE, NY, pp 468-483.

Broadwell 1991
Broadwell, A. L. 1991. "Effects of Beach Renourishment on the Survivial of Loggerhead Sea Turtle," M.S. thesis, Florida Atlantic University, Boca Raton, FL.

Bruun 1952
Bruun, P. 1952. "Measures Against Erosion at Groins and Jetties," *Proceedings, 3rd International Conference on Coastal Engineering*, ASCE, NY.

Bruun 1962
Bruun, P. 1962. "Sea Level Rise as a Cause of Shore Erosion," *Journal, Waterways and Harbors Division*, ASCE, Vol 88, pp 117-130.

Chasten et al. 1993
Chasten, M. A., Rosati, J. D., McCormick, J. W., and Randall, R. E. 1993. "Engineering Design Guidance for Detached Breakwaters as Shoreline Stabilization Structure," Technical Report CERC-93-19, U.S. Army Engineer Waterways Experiment Station, Vicksburg, MS.

Civil Engineering 1999
Civil Engineering. 1999. "Back from the Brink," *Civil Engineering*, ASCE, NY, October, pp 52-57.

Cobb 1992
Cobb, Charles E., Jr. 1992. "Miami," *National Geographic*, Vol 181, No.1, pp 86-113.

Dally, Dean and Dalrymple 1985
Dally, W. R., Dean, R. G., and Dalrymple, R. A. 1985. "Wave Height Variation Across Beaches of Arbitrary Profile," *Journal of Geophysical Research,* Vol 90, No. C6, pp 11917-11927.

Dally and Pope 1986
Dally, W. R., and Pope, J. 1986. "Detached Breakwaters for Shore Protection," Technical Report CERC-86-1, U.S. Army Engineer Waterways Experiment Station, Vicksburg, MS.

Davis 1961
Davis, A. B. 1961. "Galveston's Bulwark Against The Sea: History of the Galveston Seawall," Technical Report, U.S. Army Engineer District, Galveston, Galveston, TX.

Davis and Law 1994
Davis, E. W., and Law, V. J. 1994. "Field Studies of Beach Cones as Coastal Erosion Control/Reversal Devices," *Proceedings, 7th National Conference on Beach Presentation Technology,* Florida Shore and Beach Preservation Assoc. Tallahassee, FL.

Dean 1978
Dean, R. G. 1978. "Coastal Structures and their Interaction with the Shoreline." *Application of Stochastic Processes in Sediment Transport*. H. W. Shen and H. Kikkaua, eds., Water Resources Publications, Littleton, CO, pp 18-1 to 18-46.

Dean 1987
Dean, R. G. 1987. "Coastal Armormy: Effects, Principles, and Mitigation," *Proceedings, 20th International Conference on Coastal Engineering,* ASCE, NY, pp 1843-1857.

Dean 1993
Dean, R. G. 1993. "Terminal Structures at the End of Littoral Systems," *Journal of Coastal Research*, Special Issue No. 18, pp 195-210.

Dean 1996
Dean, R. G. 1996. "Interaction of Littoral Barriers and Adjacent Beaches: Effects on Profile Shape and Shoreline Change," *Journal of Coastal Research*, Vol 23, pp 103-112.

Dean and Chen 1996
Dean, R. G., and Chen, R. 1996. "Performance of the Midtown Palm Beach PEP Reef Installation," Final Report, Department of Coastal and Oceanographic Engineering, University of Florida, Gaineville, FL.

Denison 1998
Denison, P. S. 1998. "Beach Nourishment/Groin Field Construction Project: Bald Head Island, North Carolina," *Shore and Beach*, Vol 66, No. 1, pp 2-9.

Dennis and Miller 1993
Dennis, W. A., and Miller, H. C. 1993. "Shoreline Response: Oregon Inlet Terminal Groin Construction," *Proceedings, International Coastal Engineering Symposium,* Hitton Head, SC, Vol I, pp 324-332.

Dolan and Lins 1987
Dolan R., and Lins, H. 1987. "Beaches and Barrier Islands," *Scientific American*, Vol 255, No. 7, pp 68-77.

Erickson 1998
Erickson, K. 1998. "Conversion of the P.E.P. Reef Breakwater to a Groin Field for West Palm Beach, FL," *Proceedings, Eighth Beach Technology Conference*, ASBPA, Tallahassee, FL.

Everts, Battley, and Gibson 1983
Everts, C. H., Battley, J. P., Jr., and Gibson, P. N. 1983. "Shoreline Movements: Cape Henry, Virginia to Cape Hatteras, North Carolina, 1849-1980," Technical Report CERC-83-1, U.S. Army Engineer Waterways Experiment Station, Vicksburg, MS.

Ferrante, Franco, and Boer 1992
Ferrante, A., Franco, L., and Boer, S. 1992. "Modeling and Monitoring of a Perched Beach at Lido di Ostia (Rome)," *Proceedings, 23rd International Conference on Coastal Engineering,* Vol 3, ASCE, NY, pp 3305-3318.

Fleming 1990
Fleming, C. A. 1990. "Guide on the Users of Groynes in Coastal Engineering," Report 119, Construction Industry Research and Information Assoc. (CIRIA), London, England.

Fulford 1985
Fulford, E. T. 1985. "Reef Type Breakwaters for Shoreline Stabilization," *Proceedings, Coastal Zone 85*, ASCE, NY.

Gilbert and Vellinga 1990
Gilbert, J., and Vellinga, P. 1990. "Strategies for Adaption to Sea Level Rise," Report of the Coastal Zone Management Subgroup, Intergovernmental Panel on Climate Change, World Meteorological Organization and U.N. Environmental Programme, The Netherlands.

Gourlay 1981
Gourlay, M. R. 1981. "Beach Processes in the Vicinity of Offshore Breakwaters," *Proceedings, 5th Australian Conference on Coastal and Ocean Engineering*, pp 129-134.

Graber 1980
Graber, P. H. F. 1980. "The Law of The Coast in a Clamshell, Part I: Overview of an Interdisciplinary Approach," *Shore and Beach*, Vol 48, No.4, pp 14-20.

Gravens and Kraus 1989
Gravens, M. B., and Kraus, N. C. 1989. "Representation of Groins in Numerical Models of Shoreline Response," *Proceedings, 23rd International Conference on Coastal Engineering*, ASCE, NY, pp 515-522.

Griggs et al. 1997
Griggs, G. B., Tait, J. F., Moore, L. J., Scott, K., Corona, W., and Pembrook, D. 1997. "Interaction of Seawalls and Beaches: Eight Years of Field Monitoring, Monterey Bay, California," Technical Report, CHL-97-1, U.S. Army Engineer Waterways Experiment Station, Vicksburg, MS.

Hall, Tschirky, and Turcke 1998
Hall, K. R., Tschirky, P., and Turcke, D. J. 1998. "Coastal Wetland Stability and Shore Protection," *Journal of Coastal Research*, Special Issue No.26, pp 96-101.

Hallermeier 1981
Hallermeier, R. J. 1981. "A Profile Zonation for Seasonal Sand Beaches from Wave Climate," *Coastal Engineering*, Vol 4, pp 253-277.

Hallermeier 1983
Hallermeier, R. J. 1983. "Sand Transport Limits in Coastal Structure Design." *Proceedings, Coastal Structures '83*. March 9-11, Arlington**,** VA, American Society of Civil Engineers, pp 703-16.

Hanson and Kraus 1989
Hanson, H., and Kraus, N. C. 1989. "GENESIS: Generalized Model for Stimulating Shoreline Change," Technical Report, CERC-89-19, U.S. Army Engineer Waterways Experiment Station, Vicksburg, MS.

Hardaway and Anderson 1980
Hardaway, C. S., and Anderson, G. L. 1980. "Shoreline Erosion in Virginia," *Sea Grant Program*, Virginia Institute of Marine Science, Gloucester Point, VA.

Hardaway and Byrne 1999
Hardaway, C. C., and Byrne, R. J. 1999. "Shoreline Management in Chesapeake Bay," *Virginia Sea Grant Publ.* VSG-99-11, Virginia Institute of Marine Science, Gloucester Point, VA.

Hardaway, Thomas, and Li 1991
Hardaway, C. S., Thomas, G. R., and Li, J. -H. 1991. "Chesapeake Bay Shoreline Study: Headland Breakwaters and Pocket Beaches for Shoreline Erosion Control," Final Report No.313, Virginia Institute of Marine Science, Gloucester Point, VA.

Hardaway and Gunn 1991
Hardaway, C. S., and Gunn, J. R. 1991. "Headland Breakwaters in the Chesapeake Bay," *Proceedings, Coastal Zone'91*, ASCE, NY, pp 1267-1281.

Hardaway and Gunn 1995
Hardaway, C. S., and Gunn, J. R. 1995. "Headland Breakwater Performance in Chesapeake Bay," *Proceeding 1995 National Conference on Beach Preservation Technology*, Florida Shore and Beach Preservation Assoc., Tallahassee, FL, pp 365-383.

Hardaway and Gunn 1998
Hardaway, C. S., and Gunn, J. R. 1998. "Chesapeake Bay: Design, Installation and Early Performance of Four New Headland Breakwater Composite Systems," *Proceedings 1998 National Conference on Beach Preservation Technology*, Florida Shore and Beach Preservation Assoc., Tallahassee, FL.

Hardaway and Gunn 1999
Hardaway, C. S., and Gunn, J. R. 1999. "Chesapeake Bay: Design and Early Performance of Four Headland Breakwater Systems," *Proceedings, Coastal Sediments 99*, ASCE, NY, pp 828-843.

Hardaway, Gunn, and Reynolds 1995
Hardaway, C. S., Jr., Gunn, J. R., and Reynolds, R. N. 1995. "Headland Breakwater Performance in Chesapeake Bay," *Proceedings, 1995 National Conference on Beach Preservation Technology, St. Petersburg, FL.*

Hardy and Young 1991
Hardy, T. A., and Young, I. R. 1991. "Modeling Spectral Wave Transformation on a Coral Reef Flat," *Proceedings, Australasian Conference on Coastal and Ocean Engineering*," pp 345-350.

Harris and Herbich 1986
Harris, M. M., and Herbich, J. B. 1986. "Effects of Breakwater Spacing on Sand Entrapment," *Journal of Hydraulic Research* Vol 24, No. 5, pp 347-57.

Heikoff 1976
Heikoff, J. M. 1976. *Politics of Shore Erosion-Westhampton Beach, NY*. Ann Arbor Press, Ann Arbor, MI.

Heinz Center 2000
Heinz Center. 2000. "Evaluation of Erosion Hazards," The H. John Heinz III Center for Science, Economics and the Environment, Washington, DC, pp 203.

Hillyer 1996
Hillyer, T. M. N. 1996. "An Analysis of United States Army Corps of Engineers Shore Protection Program," Final Report, IWR 96-PS-1, Institute of Water Resources, U.S. Army Corps of Engineers, Alexandria, VA.

Houston 1995a
Houston, J. R. 1995. "Beach Nourishment," Coastal Forum, *Shore and Beach*, Vol 64, No.1, pp 21-24.

Houston 1995b
Houston, J. R. 1995. "The Economic Value of Beaches," *The CERCular*, Vol CERC-95-4, U.S. Army Engineer Waterways Experiment Station, Vicksburg, MS.

Houston 1996
Houston, J. R. 1996. "International Tourism and U.S. Beaches," *Shore and Beach*, Vol 165 No. 2 pp 3-4.

Houston 1999
Houston, J. R. 1999. "The Myth of the Subsidized Beach Resident," *Shore and Beach*, Vol 67, No. 2&3, pp 2-3.

Hoyt 1967
Hoyt, J. H. 1967. "Barrier Island Formation," *Geological Society America Bulletin*, Vol 78, pp 1125-1136.

Hsu, Silvester, and Xia 1987
Hsu, J. R. C., Silvester, R., and Xia, Y. M. 1989. "Static Equilibrium Bays: New Relationships," *Journal Waterways, Port, Coastal and Ocean Engineering*, ASCE, Vol 115 (No.3), pp 285-298.

Hsu, Silvester and Xia 1989
Hsu, J. R. C., Silvester, R., and Xia, Y. M. 1989. "Applications of Headland Control," *Journal Waterway, Port, Coastal and Ocean Engineering*, Vol 115, No. 3, ASCE, NY, pp 299-310.

Hughes 1994
Hughes, S. A. 1994. *Physical Models and Laboratory Techniques in Coastal Engineering*. World Scientific Publishing Co., Singapore.

Inman and Frautschy 1966
"Littoral Processes and the Development of Shorelines." *Proceedings, Coastal Engineering.* Santa Barbara, CA, pp 511-36.

Janis and Holmberg 1994
Janis, W. A., and Holmberg, D. L. 1994. "The Accretion Technology System," *Proceedings, 7th National Conference on Beach Preservation Technology*, Florida Shore and Beach Preservation Assoc., Tallahassee, FL.

Japanese Ministry of Construction 1986
Japanese Ministry of Construction. 1986. "Handbook of Offshore Breakwater Design," River Bureau of the Ministry of Construction, Japanese Government (Translated to English) U.S. Army Engineer Waterways Experiment Station, Vicksburg, MS.

Joyner, Overton, and Fisher 1998
Joyner, B. P., Overton, M. F., and Fisher, J. S. 1998. "Analysis of Morphology of Oregon Inlet, NC, Since Construction of a Terminal Groin," *Proceedings*, 26th *International Conference on Coastal Engineering,* ASCE, NY.

Kana 1999
Kana, T. W. 1999. "Long Island's South Shore Beaches: A Century of Dynamic Sediment Management," *Proceedings, Coastal Sediments '99*, ASCE, NY, pp 1584-1596.

Kassner and Black 1983
Kassner, J., and Black, J. A. 1983. "Inlets and Barrier Beach Dynamics: A Case Study of Shinnecock Inlet, NY," *Shore and Beach*, Vol 51, No.2, pp 22-26.

Kobayashi 1987
Kobayasi, N. 1987. "Analytical Solutions for Dune Erosion By Storms," *Journal of the Waterway Coastal and Ocean Engineering Division*, ASCE, Vol 113, No. 4, pp 401-418.

Kobayashi, Raichle and Asano 1993
Kobayashi, N., Raichle, A. W., and Asano, T. 1993. "Wave Attenvation by Vegetation," *Journal of Waterway, Port, Coastal and Ocean Engineering*, ASCE Vol 199, No. 4, pp 30-48.

Komar 1998
Komar, P. D. 1998. *Beach Processes and Sedimentation*. Second Edition. Prentice Hall, N.J.

Komar et al. 1991
Komar, P. D., Lanfredi, N., Baba, M., Dean, R. G., Dyer, K., Healy, T. Ibe, A. C., Terwindt, J. H. J., Thom, B. G. 1991. "The Response of Beaches to Sea-Level Changes: A Review of Predictive Models," *Journal of Coastal Research*, Vol 7, pp 895-921.

Kraft and Herbich 1989.
Kraft, K., and Herbich, J. B. 1989. "Literature Review and Evaluation of Offshore Detached Breakwaters," Report No. COE-297, Texas A&M University, Ocean Engineering Program, College Station, TX.

Kraus 1988
Kraus, N. C. 1988. "The Effects of Seawalls on the Beach: An Extended Literature Review," *Journal of Coastal Research*, Special Issue No.4, pp 1-29.

Kraus 2000
Kraus, N. C. 2000. "Coastal Forum-Groin Notching," *Shore and Beach*, Vol 68, No. 2, pp 18.

Kraus and Bocamazo 2000
Kraus, N. C., and Bocamazo, L. M. 2000. "State of Understanding of Groin Functioning and Recent Promising Innovations," *Proceedings, 3rd Annual Conference*, Northeast Shore and Beach Preservation Assoc.,

Kraus, Hanson, and Blomgren 1994
Kraus, N. C., Hanson, H., and Blomgren, S. H. 1994. "Modern Functional Design of Groin System," *Proceedings, 24th International Conference on Coastal Engineering*, ASCE, NY, pp 1327-1342.

Kraus and Larson 1991.
Kraus, N. C., and Larson, M. 1991. "NMLONG: Numerical Model for Simulating the Longshore Current," Technical Report DRP-91-1, U.S. Army Engineer Waterways Experiment Station, Vicksburg, MS.

Komar and McDougal 1988
Komar, P. D., and McDougal, W. G. 1998. "Coastal Erosion and Engineering Structures: The Oregon Experience," *Journal of Coastal Research*, Special Issue No.4, pp 79-94.

Kraus and McDougal 1996
Kraus, N. C., and McDougal, W. G. 1996. "The Effects of Seawalls on The Beach: Part I, An Updated Literature Review," *Journal of Coastal Research*, Vol 12, pp 691-701.

Kraus and Pilkey (eds.) 1988
Kraus, N. C., and Pilkey, O. H., (eds.) 1988. "Seawalls and Beaches," *Journal of Coastal Research,* Special Issue No. 4, Gainesville, FL.

Kriebel and Dean 1993
Kriebel, D. L., and Dean, R. G. 1993. "Convolution Method for Time-Dependent Beach-Profile Response," *Journal of Waterway, Port, Coastal and Ocean Engineering*, ASCE, Vol 119, No. 2, pp 204-227.

Krumbein 1944
Krumbein, W. C. 1944. "Shore Processes and Beach Characteristics," Technical Memorandum No.3, Beach Erosion Board, U.S. Army Corps of Engineers, Washington, D.C.

Larson and Kraus 1989
Larson, M., and Kraus, N. C. 1989. "SBEACH: Numerical Model for Simulating Storm-Induced BeachChange; Report 4, Empirical Foundation and Model Development," Technical Report CERC-89-9, U.S. Army Engineer Waterways Experiment Station, Vicksburg, MS.

Leatherman 1988
Leatherman, S. P. 1988. *Barrier Island Handbook*. Coastal Publication Series, University of Maryland, College Park, MD.

Leenknecht Szuawalski, and Sherlock 1992
Leenknecht, D. A., Szuwalski, A., and Sherlock, A. R. 1992. "Automated Coastal Engineering System (ACES) User Guide and Technical Reference, Version 1.07," U.S. Army Engineer Waterways Experiment Station, Vicskburg, MS.

Lenz 1994
Lenz, R. G. 1994. "Beachface Drainage-A Tool for Coastal Stabilization," *Proceedings, 7th National Conference on Beach Preservation Technology*, Florida Shore and Beach Preservation Assoc., Tallahassee, FL.

Lesnick 1979
Lesnick, J. R. 1979. "An Annotated Bibliography on Detached Breakwaters and Artificial Headlands," Miscellaneous Report 79-1, Coastal Engineering Research Center, U.S. Army Engineer Waterways Experiment Station, Vicksburg, MS.

Magoon 2000
Magoon, O. 2000. "Sand Rights," *Proceedings, 3rd Annual Conference*, Northeast Shore and Beach Preservation Association, Voorhees, NJ.

Martin and Smith 1997
Martin, T. R., and Smith, J. B. 1997. "Analysis of the Performance of the Prefabricated Erosion Prevention (PEP) Reef System, Town of Palm Beach, Florida," Coastal Engineering Technical Note, CETN-II-36, U.S. Army Engineer Waterways Experiment Station, Vicksburg, MS.

McDougal, Kraus and Ajiwibowo 1996
McDougal, W. G., Kraus, N. C., and Ajiwibowo, H. 1996. "The Effects of Seawalls on the Beach: Part II, Numerical Modeling of SUPERTANK Seawall Tests," *Coastal Sediments '87*, ASCE, NY, pp 961-973.

McDougal, Sturtevant and Komar 1987
McDougal, W. G., Sturtevant, M. A., and Komar, P. D. 1987. "Laboratory and Field Investigations of Shoreline Stabilization Structures on Adjacent Property," *Coastal Sediments '87*, ASCE, NY, pp 961-973.

Miller, Dennis, and Wutkowski 1996
Miller, H. C., Dennis, W. A., and Wutkowski, M. J. 1996. "A Unique Look at Oregon Inlet, NC, USA," *Proceedings*, *25th International Conference on Coastal Engineering,* ASCE, NY, pp 4517-4529.

Mohr 1994
Mohr, M. C. 1994. "Presque Isle Shoreline Erosion Control Project," *Shore and Beach*, Vol 62, No. 2, pp 23-28.

Moody and Madsen 1995
Moody, P. M., and Madsen, O. S. 1995. "Laboratory Study of the Effect of Seawalls on Beach Erosion," Technical Report, MITSG 95-3, Massachusetts Institute of Technology, Cambridge, MA.

Moreno and Kraus 1999
Moreno, L. J., and Kraus, N. C. 1999. "Equilibrium Shape of Headland-Bay Beaches for Engineering Design," Proceedings, *Coastal Sediments '99*, ASCE, NY, pp 860-875.

National Research Council 1987
National Research Council. 1987. "Responding to Changes in Sea Level: Engineering Implications," Final Report, Committee on Engineering Implications of Changes in Relative Mean Sea Level, National Academy Press, Washington, DC.

National Research Council 1988
National Research Council. 1988. "Saving Cape Hatteras Lighthouse from the Sea," Final Report, Committee on Options for Preserving Cape Hatteras Lighthouse, National Academy Press, Washington, DC.

National Research Council 1990
National Research Council. 1990. "Managing Coastal Erosion," Final Report, Committee on Coastal Erosion Zone Management Water Science and Technology Board, National Academy Press, Washington, DC.

National Research Council 1995
National Research Council. 1995. "Beach Nourishment and Protection, Final Report, Committee on Beach Nourishment and Protection, Marine Board," National Academy Press, Washington, DC.

Nayak 1976
Nayak, U. B. 1976. "On the Functional Design and Effectiveness of Groins in Coastal Protection," Ph.D. diss., University of Hawaii, Honolulu, HI.

Nelson et al. 1987
Nelson, D. A., Mauck, K. A., and Fletemeyer, J. 1987. "Physical Effects of Beach Nourishment on Sea Turtle Nesting, Delray Beach, Florida," Technical Report, TR-87-15, U.S. Army Engineer Waterways Experiment Station, Vicksburg, MS.

Nersesian, Kraus, and Carson 1992
Nersesian, G. K., Kraus, N. C., and Carson, F. C. 1992. "Functioning of Groins at Westhampton Beach Long Island, New York," *Proceedings, 23rd International Conference on Coastal Engineering*, ASCE, NY, pp 3357-3370.

Nir 1982
Nir, Y. 1982. "Offshore Artificial Structures and Their Influence on the Israel and Sinai Mediterranean Beaches." *Proceedings, 18th International Conference on Coastal Engineering.* American Society of Civil Engineers, pp 1837-56.

Noble 1978
Noble, R. M. 1978. "Coastal Structures' Effects on Shorelines." *Proceedings, 17th International Conference on Coastal Engineering.* Sydney, Australia, American Society of Civil Engineers, pp 2069-85.

Noda 1984
Noda, H. 1984. "Depositional Effects of Offshore Breakwater Due to Onshore-Offshore Sediment Movement." *Proceedings, 19th International Conference on Coastal Engineering*. American Society of Civil Engineers, Houston, TX, pp 2009-25.

Oertel et al. 1992
Oertel, G. F., Kraft, J. C., Kearney, M. S., and Woo, H. J. 1992. "A Rational Theory for Barrier-Lagoon Development," *Society for Sedimentary Geology*, Special Publication No.48, pp 77-87.

Olin, Fischenich, Palermo 2000
Olin, T. J., Fischenich, J. C. and Palermo, M. R. 2000. "Wetlands Engineering Handbook," Technical Report, WRP-RE-21, U.S. Army Engineer Research and Development Center, Vicksburg, MS.

Overton et al. 1992
Overton, M. F., Fiser, J. S., Dennis, W. A., and Miller, H. C. 1992. "Shoreline Change At Oregon Inlet," *Proceedings*, *23rd International Conference on Coastal Engineering,* ASCE, NY, pp 2332-2343.

Ozger 2000
Ozger, S. S. 2000. "Towards Quantification of Active Sand Volume in the Nearshore Profile," M.S. thesis, Civil Engineering Department, Old Dominion University, Norfolk, VA.

Pattiaratchi and Bancroft 2000
Pattiaratchi, C., and Bancroft, S. 2000. "Design Studies and Performance Monitoring of an Artificial Surfing Reef: Cable Station, Western Australia," *Abstracts, 27th International Conference on Coastal Engineering*, ASCE, NY, Paper No. 123.

Pendergrass and Pendergrass 1990
Pendergrass, B. B., and Pendergrass, L. F. 1990. "In the Era of Limits: A Galveston District History Update 1976-1986," U.S. Army Engineer District, Galveston, Galveston, TX.

Pilarczyk 1990
Pilarczyk, K. W., ed. 1990. *Coastal Protection*. A.A. Balkema, Rotterdam, The Netherlands.

Pilkey and Wright 1988
Pilkey, O. H., and Wright, H. L. 1988. "Seawalls Versus Beaches," *Journal of Coastal Research*, Special Issue No.4, pp 41-67.

Plant 1990
Plant, N. 1990. "The Effects of Seawalls on Beach Morphology and Dynamic Processes," unpublished M.S. thesis, University of California, Santa Cruz, CA.

Plant and Griggs 1992
Plant, N., and Griggs, G. D. 1992. "Interactions Between Nearshore Processes and Beach Morphology Near a Seawall," *Journal of Coastal Research*, Vol 8, No. 9, pp 183-200.

Pope 1989
Pope, J. 1989. "Role of Breakwaters in Beach Erosion Control," *Proceedings, Beach Preservation Technology '89*, Florida Shore and Beach Preservation Association, Tallahassee, FL, pp 167-176.

Pope 1997
Pope, J. 1997. "Responding to Coastal Erosion and Flooding Damages," *Journal of Coastal Research* Vol 13, No. 3, pp 704-710.

Pope and Dean 1986
Pope, J., and Dean, J. L. 1986. "Development of Design Criteria for Segmented Breakwaters," *Proceedings, 20th International Conference Coastal Engineering*, ASCE, NY, pp 2144-2158.

Rosati 1990
Rosati, J. D. 1990. "Functional Design of Breakwaters for Shore Protection: Empirical Methods," Technical Report, CERC-90-15, U.S. Army Engineer Waterways Experiment Station, Vicksburg, MS.

Rosati and Truitt 1990
Rosati, J. D., and Truitt, C. L. 1990. "Am Alternative Design Approach for Detached Breakwater Projects," Miscellaneous Paper, CERC-90-7, U.S. Army Engineer Waterways Experiment Station, Vicksburg, MS.

Rosen and Vadja 1982
Rosen, D. S., and Vadja, M. 1982. "Sedimentological Influence of Detached Breakwater." *Proceedings, 18th International Conference on Coastal Engineering*. American Society of Civil Engineers, pp 1930-1949.

Ruig and Roelse 1992
Ruig, J. H. M., and Roelse, P. 1992. "A Feasibilty Study of a Perched Beach Concept in the Netherlands," *Proceedings, 23rd International Conference on Coastal Engineering*, ASCE, NY, pp 2581-2598.

Sarb and Ewing 1996
Sarb, S., and Ewing, L. 1996. "Mitigation for Impacts of Seawalls on Sand Supply, Coastal Development Permit Condition and Findings of Support With Methodology and Graphics," Internal Memorandum, California Coastal Commission.

Scheffner et al. 1997
Scheffner, N. W., Borgman, L. E., Clasusner, J. E., Edge, B. L., Grace, P. J., Militello, A., and Wise, R. A. 1997. "Users Guide to the Use and Application of the Empirical Simulation Technique," Technical Report CHL-97-00, U.S. Army Engineer Waterways Experiment Station, Vicksburg, MS.

Scheffner et al. 1999
Scheffner, N. W., Clausner, J. E., Militello, A.,Borgman, L. E., Edge, B. L., and Grace, P. J. 1999. "Use and Application of the Empirical Simulation Technique: User's Guide," Technical Report CHL-99-21, Engineer Research and Development Center, Corps of Engineers, Vicksburg, MS.

Scientific American 1888
Scientific American. 1888. "Relocation of Brighton Beach Hotel on Coney Island, NY," *Scientific American* Vol VIII, No.15, p 230.

Seelig and Walton 1980
Seelig, W. N., and Walton, T. L. 1980. "Estimation of Flow through Offshore Breakwater Gaps Generated By Wave Overtopping," *Coastal Engineering Technical Aid* (CETA) 80-8, Coastal Engineering Research Center, Fort Belvoir, VA.

Seiji, Uda, and Tanaka 1987
Seiji, M., Uda, T., and Tanaka, S. 1987. "Statistical Study on the Effect and Stability of Detached Breakwaters," *Coastal Engineering in Japan*, Vol 30, No. 9, pp 131-141.

Shepard 1976
Shepard, F. P. 1976. "Coastal Classification and Changing Coastlines," *Geoscience and Man*, Vol 14, pp 53-64.

Shore Protection Manual 1984
Shore Protection Manual. 1984. 4th Edition Vol. 1 & 2, U.S. Army Engineer Waterways Experiment Station, U.S. Government Printing Office, Washington, DC.

Silvester 1960
Silvester, R. 1960. "Stabilization of Sedimentary Coastlines," *Nature*, Vol 188, Paper 4744, pp 467-469.

Silvester 1970
Silvester, R. 1970. "Development of Crenulate-Shaped Bays to Equilibrium," *Journal Waterways and Harbors Division*, ASCE, Vol 96 (WWZ) pp 275-287.

Silvester and Hsu 1993
Silvester, R., and Hsu, J. R. C. 1993. *Coastal Stabilization: Innovative Concepts*. PRT Prentice-Hall, Englewood Cliffs, NJ.

Sonu and Warwar 1987
Sonu, C. J., and Warwar, J. F. 1987. "Evolution of Sediment Budgets in the Lee of a Detached Breakwater." *Proceedings, Coastal Sediments '87.* American Society of Civil Engineers, New Orleans, LA, pp 1361-68.

Sorensen 1990
Sorensen, T. 1990. "Review of Coastal Engineering Works at the Pengkalan Datu Seaworks," Final Report Danish Hydraulic Institute, Horsholm, Denmark.

Sorensen and Weggel 1992
Sorensen, R. M., and Weggel, J. R. 1992. "Field Monitoring of a Modular Detached Breakwater System," *Proceedings, Coastal Engineering Practice 1992*, ASCE, New York, pp 189-203.

Spencer and Terchunian 1997
Spencer, R., and Terchunian, A.V. 1997. "The Sand Thieves of Long Island's South Shore," *Shore and Beach*, Vol 65, No.3, pp 4-12.

Stauble and Smith 1999
Stauble, D. K., and Smith, J. B. 1999. "Performance of the PEP Reef Submerged Breakwater Project, Vero Beach, Florida," Twenty-Five Months Report, Coastal Engineering Research Center, U.S. Army Engineer and Research Development Center, Vicksburg, MS.

Stephen 1994
Stephen, M. F. 1994. "Assessment of Alternative Erosion Control Technology in Southwest Florida: A Saga of Fishnets, Stabilizers and Seaweed," *Proceedings, 7th National Conference on Beach Preservation Technology*, Florida Shore and Beach Preservation Assoc., Tallahassee, FL.

Suh and Dalrymple 1987
Suh, K., and Dalrymple, R. A. 1987. "Offshore Breakwaters in Laboratory and Field," *Journal, Waterway, Port, Coastal, and Ocean Engineering*, ASCE, Vol 113, No. 2, pp 105-121.

Tait 1994
Tait, L. S. ed. 1994. "Alternative Technologies in Beach Preservation," *Proceedings, 7th National Conference on Beach Preservation Technology*, Florida Shore and Beach Preservation Assoc., Tallahassee, FL.

Tait and Griggs 1991
Tait, J. F., and Griggs, G. B. 1991. "Beach Response to the Presence of a Seawall: A Comparison of Field Observations," *Shore and Beach*, Vol 58, No.2, pp 11-28.

Terchunian 1988
Terchunian, A. V. 1988. "Permitting Coastal Armoring Structures: Can Seawalls and Beaches Coexist?," Special issue No.4, *Journal of Coastal Research*, pp 65-75.

Terich and Levenseller 1986
Tercih, T., and Levenseller, T. 1986. "The Severe Erosion of Cape Shoalwater, Washington," *Journal of Coastal Research*, Vol 2, pp 465-477.

Thompson et al. 1996
Thompson, E. F., Wutkowski, M., and Scheffner, N. W. 1996. "Risk-Based Analysis of Coastal Projects," *Proceedings, 25th International Conference on Coastal Engineering*, ASCE, NY, pp 4440-4450.

Tomlinson 1980
Tomlinson, J. H. 1980. "Groynes in Coastal Engineering: A Literature Survey and Summary of Recommended Practice," Report No. IT 199, Hydraulics Research Station, Wallingford, England.

Toue and Wang 1990
Tove, T., and, Wnag, H. 1990. "Three Dimensional Effects of Seawall on The Adjacent Beach," *Proceedings, 22nd International Conference on Coastal Engineering*, ASCE, NY, pp 2785-2795.

Toyoshima 1972
Toyoshima, O. 1972. *Coastal Engineering for Practicing Engineers-Beach Erosion.* Morikita Publishing Co., Tokyo, Japan, pp 227-317. (English translation of Chapter 8, "Offshore Breakwaters," available through the Coastal Engineering Research Center, U.S. Army Engineer Waterways Experiment Station, Vicksburg, MS.)

Toyoshima 1974
Toyoshima, O. 1974. "Design of a Detached Breakwater System." *Proceedings, 14th International Conference on Coastal Engineering.* American Society of Civil Engineers, Copenhagen, Denmark, pp 1419-31.

Toyoshima 1982
Toyoshima, O. 1982. "Variation of Foreshore Due to Detached Breakwaters," *Proceedings, 18th International Conference on Coastal Engineering*, ASCE, NY, pp 1873-1892.

Tschirky, Turke, and Hall 2000
Tschirky, P., Turke, D., and Hall, K. 2000. "Wave Attenuation by Emergent Wetland Vegetation," Abstracts, *27th International Conference on Coastal Engineering*, ASCE, NY, paper no. 224.

Turner et al. 2000
Turner, I., Leyden, V., Symonds, G., McGrath, J., Jackson, A., Jancar, T., Aarninkhorf, S., and Elshoff, I. 2000. "Comparison of Observed and Predicted Coastline Changes at the Gold Coast Artificial (Surfing) Reef," *Abstracts, 27th International Conference on Coastal Engineering*, ASCE, NY, Paper No. 125.

U.S. Army Corps of Engineers 1993
U.S. Army Corps of Engineers. 1993. "Wave Attenuation Over Reefs," Coastal Engineering Technical Note, CETNI-56, U.S. Army Engineer, Waterways Experiment Station, Vicksburg, MS.

U.S. Army Engineer District, Galveston 1975
U.S. Army Engineer District, Galveston. 1975. Burnett, Crystal, and Scott Bays and Vicinity, Baytown, Texas," Feasibility Report, Galveston, TX.

U.S. Army Engineer District, Galveston 1979
U.S. Army Engineer District, Galveston. 1979. "Baytown, Texas," Phase I, Phase II, Design Memorandum, Galveston, TX.

U.S. Army Engineer District, New York 1958
U.S. Army Engineer District, New York. 1958. "Atlantic Coast of Long Island, NY, Fire Island Inlet to Montauk Pout: Beach Erosion Control and Interim Hurricane Protection Study," Survey Report, New York.

U.S. Army Engineer District, Norfolk 1994
U.S. Army Engineer District, Norfolk. 1994. "Hurricane Protection Project for Virginia Beach, VA," *General Design Memorandum*-Revised, Norfolk, VA.

U.S. Army Engineer District, Wilmington 1996
U.S. Army Engineer District, Wilmington. 1996. "Cape Hatteras Lighthouse, North Carolina Fourth Groin Alternative," *Design Report and Environment Assessment*, Wilmington District Office, Wilmington, NC.

Vesterby 1994
Vesterby, H. 1994. "Beach Face Dewatering-The European Experience," *Proceedings, 7th National Conference on Beach Preservation Technology*, Florida Shore and Beach Preservation Assoc., Tallahassee, FL.

Vrijling 1990
Vrijling, J. K. 1990. "Probabilistic Design of Flood Defenses," *Coastal Protection*. K. W. Pilarczyk, ed., A.A. Balkema, Rotterdam, The Netherlands, pp 39-97.

Wallace and Cox 1997
Wallace, S., and Cox, R. 1997. "Seagrass and Wave Hydrodynamics," *Proceedings of Combined Australian Coastal Engineering and Ports Conference*, Christchurch, NZ, Vol I, pp 69-73.

Walker, Clark, Pope 1980
Walker, J. R., Clark, D., and Pope, J. 1980. "A Detached Breakwater System for Shore Protection." *Proceedings, 17th International Conference on Coastal Engineering.* American Society of Civil Engineers, Sydney, Australia, pp 1968-87.

Walker, Clark, Pope 1981
Walker, J. R., Clark, D., and Pope, J. 1981. "A Detached Breakwater System for Beach Protection," *Proceedings, 17th International Conference on Coastal Engineering*, ASCE, NY, pp 1968-1987.

Walton and Sensabaugh 1979
Walton, T. L., and Sensabaugh, W. 1979. "Seawall Design on the Open Coast," Florida Sea Grant College Rept. No.29, University of Florida, Gainesville, FL.

Weggel 1988
Weggel, R. 1988. "Seawalls: The Need for Research, Dimensional Consideration and a Suggested Classification," Special Issue No.4, *Journal of Coastal Research*, pp 29-40.

Weggel and Vitale 1985
Weggel, J. R., and Vitale, P. 1985. "Sand Transport Over Weir Jetties and Low Groins," *Physical Modeling in Coastal Engineering*. A.A. Balkema, Boston, MA.

Weigel 1991
Weigel, R. L. 1991. "Protection of Galveston, Texas From Overflows by Gulf Storms: Grade Raising, Seawall and Embankment," *Shore and Beach*, Vol 59, No. 7, pp 4-10.

Woodruff and Dean 2000
Woodruff, P. E., and Dean, R. G. 2000 "Innovative Erosion Control Technology in Florida," *Book of Abstracts 27th International Conference on Coastal Engineering*, Vol 2, ASCE, NY.

WRDA 1996
WRDA. 1996. "National Shoreline Erosion Control Development and Demonstration Program," Section 227 Water Resources Development Act (WRDA) of 1996, *Congressional Record*, Washington, DC.

Yasso 1964
Yasso, W. E. 1964. "Plan Geometry of Headland-Bay Beaches," Final Report, Department of Geology, Columbia University, New York.

Young 1989
Young, I. R. 1989. "Wave Transformation Over Coral Reefs," *Journal of Geophysical Research*, Vol 94, No C7, pp 9779-9789.

Zyserman et al. 1998
Zyserman, J. A., Broker, I., Johnson, H. K., Mangor, K., and Jorgensen, K. 1998. "On The Design of Shore-Parallel Breakwaters," *Proceedings, 26th International Conference Coastal Engineering*, ASCE, NY, pp 1693-1705.

V-3-8. Definition of Symbols

γ_b	Breaker depth index (Equation II-4-3) [dimensionless]
B	Minimum beach width at mhw after nourishment [length]
d_{50}	Size of the 50th percentile of the sediment sample [length]
d_S	Average depth at breakwater below mean water level [length]
e	Erosion of shoreline (mhw) from design storm [length]
F_B	Breakwater freeboard, mhw to crest [length]
I_S	Beach response factor (Equation V-3-10) [dimensionless]
L_g	Gap distance between adjacent breakwaters [length]
L_S	Length of breakwater structure [length]
P_A	Erosion rate after human activities [length^3/time]
P_N	Natural background erosion rate [length^3/time]
Q_{gross}	Gross longshore sediment transport rate [length^3/time]
Q_{net}	Net longshore sediment transport rate [length^3/time]
$Q_{offshore}$	Offshore sediment transport rate for design storm [length^3/time]
R_p	Coastal erosion ratio [dimensionless]
R_v	Coastal erosion volume ratio [dimensionless]
V_A	Volume loss rate after construction of roads, seawalls, etc. [length^3/time]
V_N	Natural erosion volume loss rate [length^3/time]
W	Width of design beach nourishment [length]
WTR	Seawall trap ratio [dimensionless]
X_g	Longshore groin spacing [length]
Y	Distance of breakwater from nourished shoreline [length]
Y_g	Maximum indentation under normal wave conditions [length]
Y_g	Effective groin length measured from its seaward tip to the design shoreline for beach fill at the time of construction [length]
Y_{min}	Minimum dry beach width [length]
Y_{min}	Minimum distance from base (reference) line to mhw shoreline after design storm event [length]
Y_o	Distance of breakwater from original shoreline [length]
Z_S	Backshore elevation at baseline [length]

V-3-9. Acknowledgments

Author of Chapter V-3, "Shore Protection Projects:"

David R. Basco, Ph.D., Department of Civil Engineering, Old Dominion University, Norfolk, Virginia.

Reviewers:

Andrew Morang, Ph.D., Coastal and Hydraulics Laboratory (CHL), U.S. Army Engineer Research and Development Center (ERDC), Vicksburg, Mississippi.
Joan Pope, CHL

Table of Contents

Page

V-4-1. Engineering Aspects of Beach-Fill Design V-4-1
a. Project objectives V-4-1
b. Project features V-4-1
(1) Beach berm V-4-1
(2) Dune V-4-3
(3) Nearshore berm V-4-4
(4) Feeder beach V-4-5
(5) Structures in conjunction with beach nourishment V-4-5
c. Define regional setting and site history V-4-5
(1) Site location within littoral cell V-4-6
(2) Pathways of sediment movement V-4-7
(3) Beach topography V-4-8
(4) Sediment characteristics V-4-8
(5) Wave and water level climate V-4-9
(6) Existing structures and infrastructure V-4-9
(7) Prior engineering activities V-4-10
d. Reach delineation V-4-10
e. Evaluate sediment sources V-4-11
(1) Borrow source types V-4-11
(2) Borrow site exploration V-4-15
(3) Borrow site characterization V-4-19
f. Beach-fill cross-section design V-4-28
(1) Berm elevation V-4-28
(2) Berm width V-4-29
(3) Dune dimensions V-4-32
(4) Design profile shape V-4-32
(5) Optimization of design profile V-4-35
(6) Cross-sectional fill volume requirements V-4-38
g. Evaluating project longevity V-4-46
(1) Periodic renourishment V-4-47
(2) Advance nourishment V-4-49
(3) Fill parameters affecting lateral spreading V-4-49
(4) Shoreline change modeling to estimate advance fill and renourishment requirements V-4-55
(5) Anticipating hot spots V-4-61
h. Fill transitions V-4-66
i. Beach-fill stabilization measures V-4-71
(1) Structures V-4-71
(2) Evaluation and optimization of stabilization structures V-4-74
(3) Dune stabilization V-4-75

j. Construction issues V-4-78
(1) Removal, transfer, and placement of borrow material V-4-78
(2) Construction template V-4-80
(3) Postconstruction profile adjustment V-4-82
k. Plans and specifications V-4-84
(1) Schedules V-4-84
(2) Specifications V-4-85
l. Project monitoring and data analysis V-4-90
(1) Monitoring objectives V-4-90
(2) Physical monitoring components V-4-90
(3) Borrow area monitoring V-4-94
(4) Biological monitoring V-4-95
(5) Structure monitoring V-4-96
m. Operations and maintenance V-4-96
(1) Purpose V-4-96
(2) Scope of the O&M manual V-4-96
(3) Introduction V-4-96
(4) Operations and maintenance V-4-98
(5) Periodic nourishment V-4-99
(6) Responsibilities V-4-101

V-4-2. References V-4-101

V-4-3. Definition of Symbols V-4-108

V-4-4. Acknowledgments V-4-109

List of Figures

Page

Figure V-4-1. Schematic diagram of storm wave attack on a beach, dune, and upland structures V-4-2

Figure V-4-2. Schematic illustration of preproject, postconstruction, and design profile V-4-4

Figure V-4-3. Use of groin structures to enhance beach nourishment projects V-4-6

Figure V-4-4. Cape-associated inner continental shelf shoals off Cape Canaveral, Florida V-4-13

Figure V-4-5. Reconnaissance zigzag line plot from the north Florida coast V-4-17

Figure V-4-6. Grid lines covering a detailed survey area off Fort Pierce, Florida V-4-18

Figure V-4-7. Isopach map of a borrow area used at Ocean City, Maryland V-4-22

Figure V-4-8. Comparison of composite grain size analysis between the native beach and the borrow material used at Ocean City, Maryland V-4-23

Figure V-4-9. Isolines of the adjusted overfill ratio (R_A) for values of ϕ mean difference and ϕ sorting ratio V-4-26

Figure V-4-10. Seasonal variation of a beach berm V-4-29

Figure V-4-11. Berm elevation determined from beach profiles measured at various alongshore stations V-4-30

Figure V-4-12. Example of storm-induced beach erosion as a function of berm width V-4-31

Figure V-4-13. Example of storm-induced beach erosion as a function of dune crest elevation V-4-33

Figure V-4-14. Beach-fill design profile shape determined by profile translation V-4-34

Figure V-4-15. Design profile in front of a seawall V-4-34

Figure V-4-16. Theoretical equilibrium profile shapes for different sand grain sizes V-4-36

Figure V-4-17. Design profiles for different fill sand sizes V-4-36

Figure V-4-18. Combined tropical and extratropical erosion-frequency curve V-4-39

Figure V-4-19. Three basic types of nourishment profiles V-4-44

Figure V-4-20. Advanced fill and renourishment volumes: (a) no background erosion and (b) 0.5 m/year background erosion V-4-57

Figure V-4-21. Cumulative beach nourishment volume: (a) no background erosion and (b) 0.5 m/year background erosion V-4-58

Figure V-4-22. Calculated 50-year shoreline position: (a) no background erosion and (b) 0.5 m/year background erosion V-4-60

Figure V-4-23. Causes of hot spot formation at a convex shoreline feature V-4-63

Figure V-4-24. Project shorelines, nearshore bathymetry, wave modeling domain, and position of offshore wave information V-4-64

Figure V-4-25. Variations in potential longshore sand transport rates caused by offshore shoals at Ocean City, MD V-4-65

Figure V-4-26. Planform adjustment of a beach fill project designed to "wrap around" existing coastal structures V-4-65

Figure V-4-27. Effect of fill transitions: (a) 400-m fill transition and (b) 2,000-m fill transition V-4-68

Figure V-4-28. Effect of fill transitions: (a) 6-km long project, and (b) 22-km long project V-4-69

Figure V-4-29. Groin field at Long Beach Island, New York V-4-70

Figure V-4-30. Terminal groin, Oregon Inlet, North Carolina V-4-72

Figure V-4-31. Sand accumulation by a series of four single fence lifts, Outer Banks, North Carolina V-4-76

Figure V-4-32. Sand accumulation by a series of three double fence lifts, Outer Banks, North Carolina V-4-77

Figure V-4-33. Definition of beach profiles for nourishment projects V-4-81

Figure V-4-34. Sample operations and maintenance manual outline V-4-97

List of Tables

Table V-4-1. Physical Data Collection Schedule for Beach-Fill Monitoring V-4-91

Table V-4-2. Borrow Area Bathymetry and Sediment Sampling Scheme V-4-95

Chapter V-4
Beach Fill Design

V-4-1. Engineering Aspects of Beach-Fill Design

a. Project objectives.

(1) The primary function of a Federal beach nourishment project is to provide improved protection to upland structures and infrastructure from the effects of storms. Figure V-4-1 shows how storms damage upland property. The top panel shows the beach under normal wave and water level conditions. The letters mhw and mlw denote the mean high and low water lines, respectively, which represent the normal range of tidally-induced water level fluctuations. The elevation of the natural beach berm is above the normal high tide elevation. Under nonstorm conditions, breaking waves are confined to the seaward face of the berm. The berm and dune act as a protective buffer between upland structures and the water and waves. Sites with little or no sand buffer are candidates for shore protection projects. The middle panel shows the beach during a storm. The water level is elevated above the normal range. This exposes higher beach elevations to the action of breaking waves, which erode the berm and transport the sand offshore and along the beach. Sand moved offshore during the storm continues to aid in dissipating wave energy; it often forms a shore-parallel bar system. In this panel, a scarp forms on the seaward face of the dune, but the dune remains relatively intact and protects the structures behind it. Had there been no dune, or a much narrower berm, the structure may have been damaged as shown in the bottom panel. The lower panel shows a more severe condition, in which even higher water levels and wave action have completely eroded the dune. Some of the dune material is transported offshore. Some is transported onshore and deposited as a result of wave runup and overwash processes. The exposed structure is subject to damage by undermining, flooding, and by waves breaking directly on it.

(2) A beach nourishment project typically involves constructing a wider beach and/or more substantial dune to reduce storm damage relative to the level of damage that would have resulted without the project. The level of storm protection provided by a nourishment project is not an absolute measure due to the uncertainties in the frequency of high intensity storms. There is always some chance, or risk, that a storm will cause property damage even with the project in place. The level of protection, reduced in the aftermath of a major storm, will remain compromised if proper poststorm maintenance is not performed. The level of protection will also be compromised if scheduled periodic renourishment, which is usually a key element of the design, is not performed when needed.

(3) The wider beach created through construction of a nourishment project also provides recreational benefits. Enhanced recreational opportunity can also be a project objective.

b. Project features. Beach nourishment projects typically involve construction of one or several of the following features: berm, dune, feeder beach, nearshore berm, dune stabilization (i.e., sand fences or vegetation), or structural stabilization (i.e., groins). There are also several aspects of a beach nourishment project that specifically address the future integrity of the dune/berm. These include: periodic renourishment, advance nourishment, and emergency maintenance. These project features are discussed in more detail in the following paragraphs.

(1) Beach berm.

(a) The beach berm is the primary feature of most beach nourishment projects. Most beaches have a natural berm or berms. The lowest berm closest to the water is formed by the uprush of wave action during the ordinary range of water-level fluctuations. Sometimes, several berms will be noticeable at slightly higher

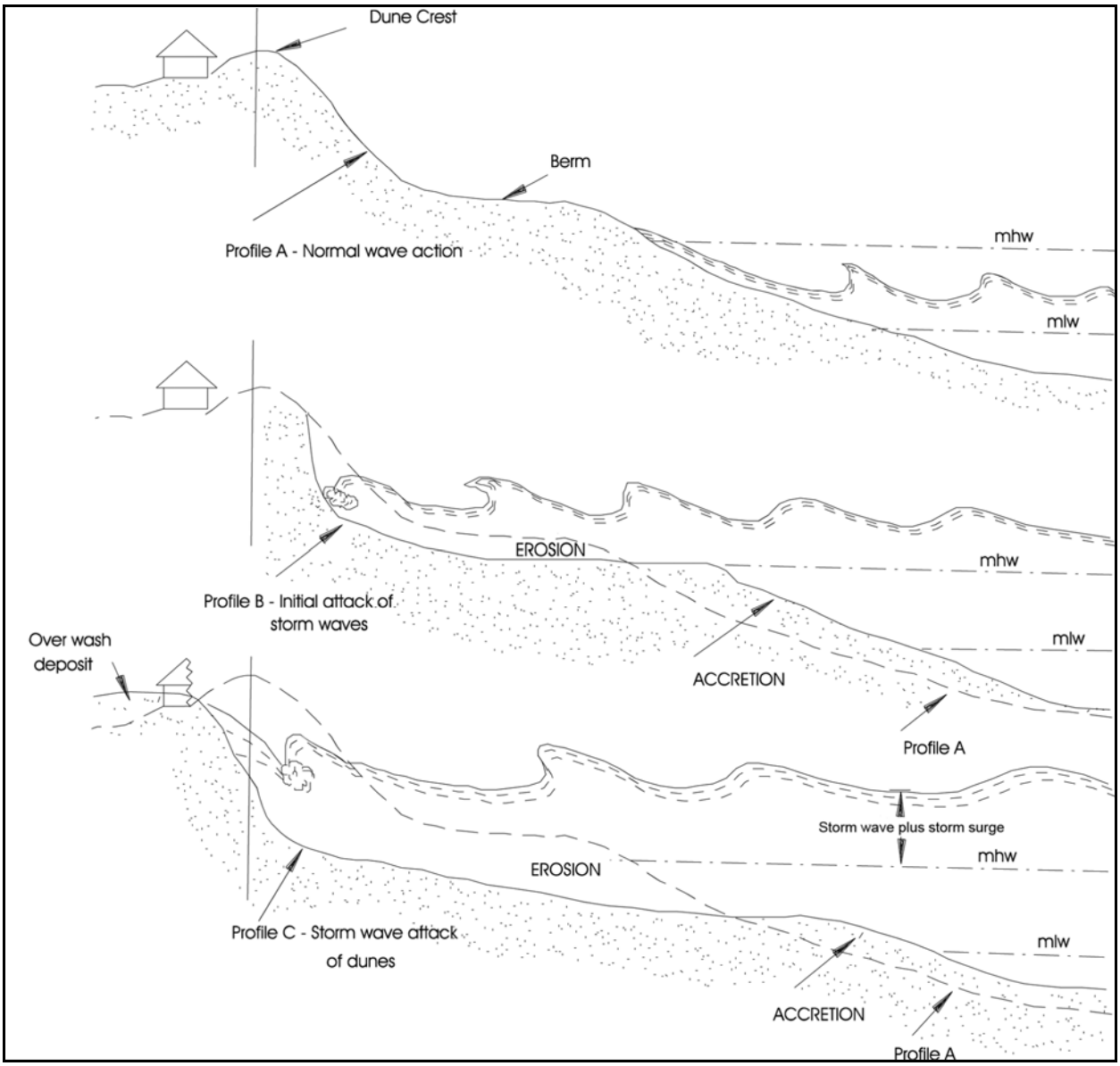

Figure V-4-1. Schematic diagram of storm wave attack on a beach, dune, and upland structures

elevations on the beach. These were formed during previous storms and are either remnant scarps left behind as a result of erosion of the lower berm or as a result of deposits left from wave uprush during higher-than-normal water levels associated with storms. Beaches that are in a severely eroded condition might have little or no berm at high tide.

(b) A nourishment project usually involves widening the beach (i.e., translating it seaward) to create a wider sand buffer for dissipating storm wave energy. The amount of additional width is determined based on the desired level of storm protection, the persistent long-term erosional trends that characterize the project area, and the target renourishment interval. The design berm width is determined through an iterative process that evaluates economic benefits as a function of width. The elevation of the constructed berm is usually set at the same elevation as the natural berm, or slightly higher. If the berm is constructed at an elevation lower than the natural berm crest, a ridge will form along the seaward edge of the fill. Wave uprush during higher water will overtop the ridge, causing temporary undesirable ponding on the beach until the berm elevation

increases naturally. If the berm is constructed to an elevation that is much higher than the natural berm crest, an undesirable persistent scarp may form along the shoreline.

(c) For practical and economic reasons, during the construction of the beach berm, the total fill volume required to advance the berm to the desired width is placed on the visible portion of the beach. This construction method, sometimes referred to as the "over-building" method, enables the economic use of standard earth-moving equipment for the distribution of the fill and minimizes relocation of the discharge point. The method also enables effective verification that the sectional fill volume (design fill volume per unit length of shoreline) has been placed on the beach by the contractor using standard land-based survey techniques. The result of this construction technique is a beach berm that is initially considerably wider than the target design width. Postconstruction berm widths are often two to three times wider than the target design width. Design specifications required a 30-m (100-ft) design berm width in the northern New Jersey beach nourishment project while postconstruction surveys indicated constructed berm widths of 60 to 90 m (200 to 300 ft) and along some survey lines berm widths approaching 120 m (400 ft) were measured. While recognized by project designers, lay persons are often unaware that the initial overbuilt berm is a temporary condition. Consequently, they incorrectly judge the project as a failure when the beach berm adjusts dramatically landward immediately after construction, especially during the first storm season. For this reason, it is important that public outreach programs include easy-to-understand information concerning the expected remolding of the fill material after initial construction. Figure V-4-2 provides a schematic illustration of the preproject beach profile, the post-construction over-built beach berm, and the expected design berm after cross-shore equilibration.

(2) Dune.

(a) Sand dunes are an important protective feature. Naturally occurring dune ridges along the coast prevent storm tides, wave runup, and overtopping from directly damaging oceanfront structures and flooding interior areas. Dune features of beach nourishment projects are intended to function in the same way. A beach nourishment project may involve either reinforcing an existing natural dune by adding elevation and/or cross-sectional area, or constructing a dune where none existed beforehand. Dunes also provide a small reservoir of sand for nourishing the beach during severe storms. However, after the storm, maintenance is required to rebuild the dune because natural dune rebuilding occurs at a much slower rate than natural berm rebuilding.

(b) During hurricanes and very severe northeasters, substantial sections of dune can disappear. This is caused by offshore transport of dune material into the surf zone and by beach and dune sediments being swept landward by wave uprush and overtopping. In the case of overtopped barrier islands, flooding from ocean-side storm surges and waves and/or return flow of water from flooded bays can erode enough sand to cut shallow channels, or breaches, through the island. Occasionally, the channels will evolve into new inlets. Areas most prone to breaching are those where the barrier island is narrow and the dunes are lowest or nonexistent. The crest elevations of natural dunes often varies considerably, and nature tends to erode the low spots first. Dunes and berms built as part of a nourishment project can reduce the potential for barrier island breaching because a relatively uniform dune elevation eliminates the low spots where breaches are most likely to form.

(c) Dune growth can be promoted and the dune structure can be made more resistant to erosion if suitable vegetation can be grown on the dunes for an adequate length of time to establish an extensive root system. It generally takes 2 to 5 years for beach grass to establish a healthy root system, and up to 10 years before the maximum resistance to erosion and breaching is obtained. An active grass fertilization and

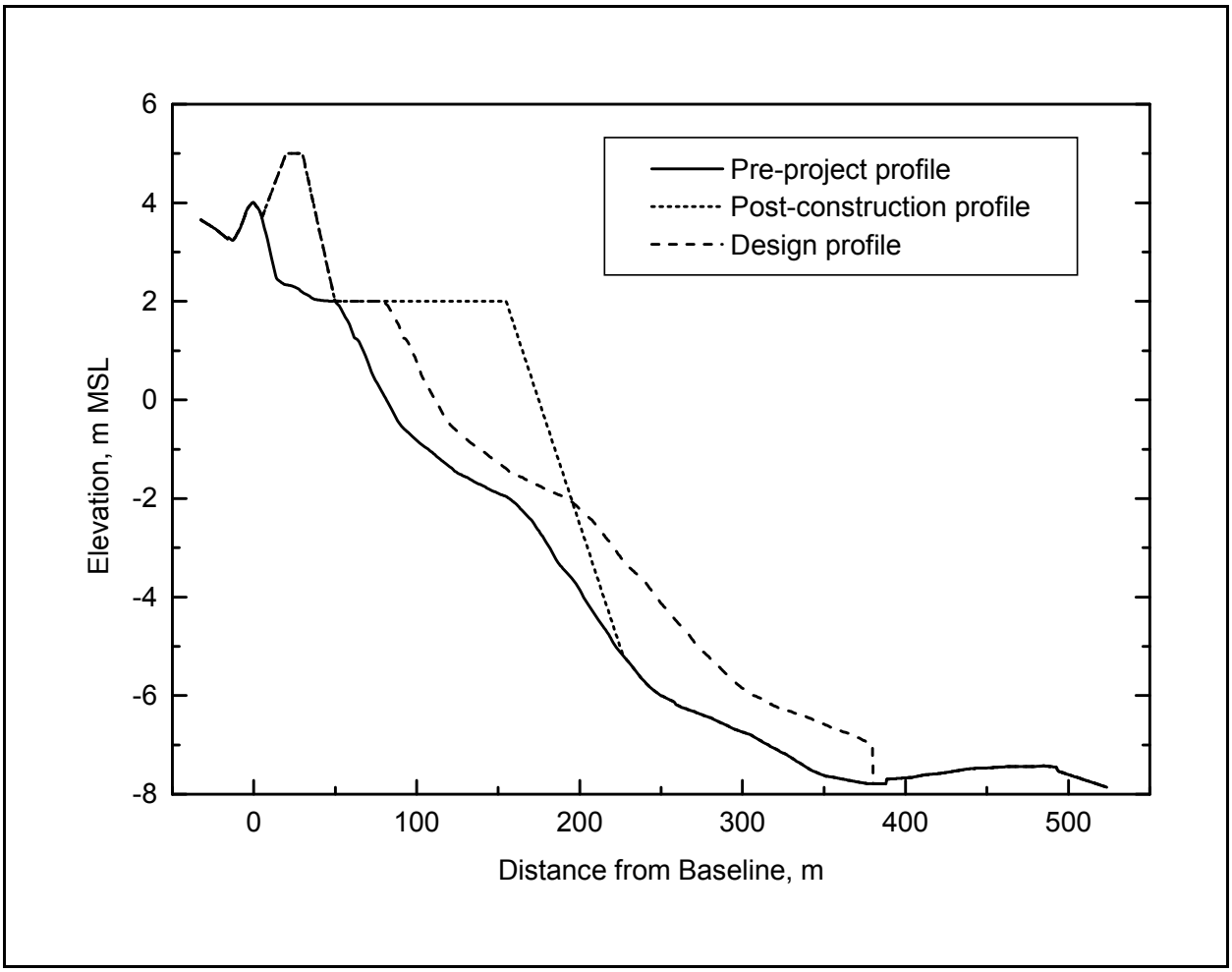

Figure V-4-2. Schematic illustration of pre-project, post-construction and design profile

maintenance program can greatly enhance the survival and effectiveness of beach grass. Part V-4-1-i provides more detailed information on dune stabilization.

(d) Preliminary estimates of dune height, width, and side slope for a beach nourishment project can be made based on characteristics of natural dunes in the vicinity of the project. To be most effective, the crest height of the dune should be above the limit of wave runup for the types of storms for which protection is sought, and the beach berm in front of the dune must be of sufficient width to withstand the erosion associated with these types of storms. If the berm in front of the dune is too narrow, the dune can quickly erode, even for relatively frequent storms, and the benefits of the higher dune elevations will be lost. The design dune height and width (along with the width of the berm) are usually selected based on results of an iterative process in which the benefits are compared with the cost of each configuration. Part V-4-1-f provides more detail on the dune/berm design process. Sometimes other factors such as real estate acquisition issues or aesthetics are factored into the selection of dune crest elevation and width.

(3) Nearshore berm. Beach-fill projects are usually constructed via direct placement of sand on the beach. Sometimes, in an effort to reduce cost, or because of limits in available dredge equipment, or in response to concerns with direct placement of fill material on the beach, material is placed offshore in an underwater berm (i.e., bar). Nearshore berm creation is intended to simulate storm bar formation by creating an artificial shore-parallel bar to dissipate storm wave energy before impacting the beach. If the berm is

placed shallower than the depth of closure (see Part III-3-3-b), it is expected that with time, the material will move onshore, eventually becoming part of the beach berm and beach face system. The material placed in the nearshore berm, however, does not provide direct shore protection to the upland, and prototype experience with the practice has met with mixed results and uncertain net benefit.

(4) Feeder beach. Beach-fill projects usually involve placement of a berm along a finite length of shoreline. Sometimes, beach nourishment projects include the creation of a feeder beach, in which fill material is introduced at the updrift end of the area intended to receive the fill. Then, longshore transport distributes the fill to the rest of the project area. Feeder beaches work best in areas that serve as a source of littoral material for downdrift beaches, in areas that are presently experiencing a deficit in the supply of littoral material and have unusually high loss rates, and in areas where the net longshore transport direction is predictable and the net transport rate is "strong" (i.e., longshore sand transport in one direction greatly exceeds the transport in the other direction). Candidate sites for feeder beaches include areas immediately downdrift from inlets or other manmade structures that form a littoral barrier or in areas that have been identified as erosional "hot spots." As the feeder material spreads under the influence of waves, the orientation of the feeder beach shoreline approaches that of the adjacent beach, resulting in longshore transport out of the feeder area equal to the transport along the adjacent area. Eventually, the shoreline orientation in the feeder beach area will return to its original configuration. Protection provided by feeder beaches will not have the same degree of alongshore uniformity as that provided by placing fill in a prescribed manner throughout the project area.

(5) Structures in conjunction with beach nourishment. Structures can enhance the performance of a beach nourishment project. Figure V-4-3 shows several such examples. When the project is relatively short in length, or significantly affected by an inlet, it may be desirable to limit alongshore losses through the use of a terminal structure or structures (Figures V-4-3a and V-4-3b show examples). Another use of structures is to place them in the interior of the nourishment project, with the intent of increasing project longevity (Figure V-4-3c) by reducing the longshore sand transport rate and minimizing end losses. Structures can also be used locally within a project to maintain the desired level of protection. For example, structures may be used to compartmentalize and stabilize a beach in anticipation of, or in response to, an area of unusually high volume losses (i.e., presence of a hotspot). Whenever structures are used, their potential updrift and downdrift impacts should be assessed. It is important to note that structures do not create sand, they only control its movement. If structures are built without adding beach fill, then sand may accumulate at one location at the expense of erosion at another area. As a general rule, compartments between structures, and the beach immediately updrift and/or downdrift of the structures, should be filled with sand to minimize adverse effects on adjacent beaches. Potential adverse effects of a groin field can be minimized by tapering the lengths of groins at the end of the groin field (see Figure V-4-3c), and adding sand on the downdrift side of the project. Part V-4-1-i provides additional information about the functional design of structures used in conjunction with beach fill projects. Part VI presents information on the structural design aspects of coastal structures.

c. Define regional setting and site history. To maximize a beach nourishment project's effectiveness, it is important to understand the project's physical setting. The term "setting" encompasses local- and regional-scale coastal processes, the geology, and infrastructure that characterize the site and surrounding area. Part V-3 provides a general discussion of site characterization for all coastal projects. The following sections focus on those aspects that are most pertinent to engineering design of beach nourishment projects. A beach fill project can be a significant perturbation to the coastal system, and project performance is directly related to its interaction with its surroundings. The following are a few questions regarding project setting that should be answered at the beginning of the design process: In what type of littoral system, or littoral cell, will the project be constructed?

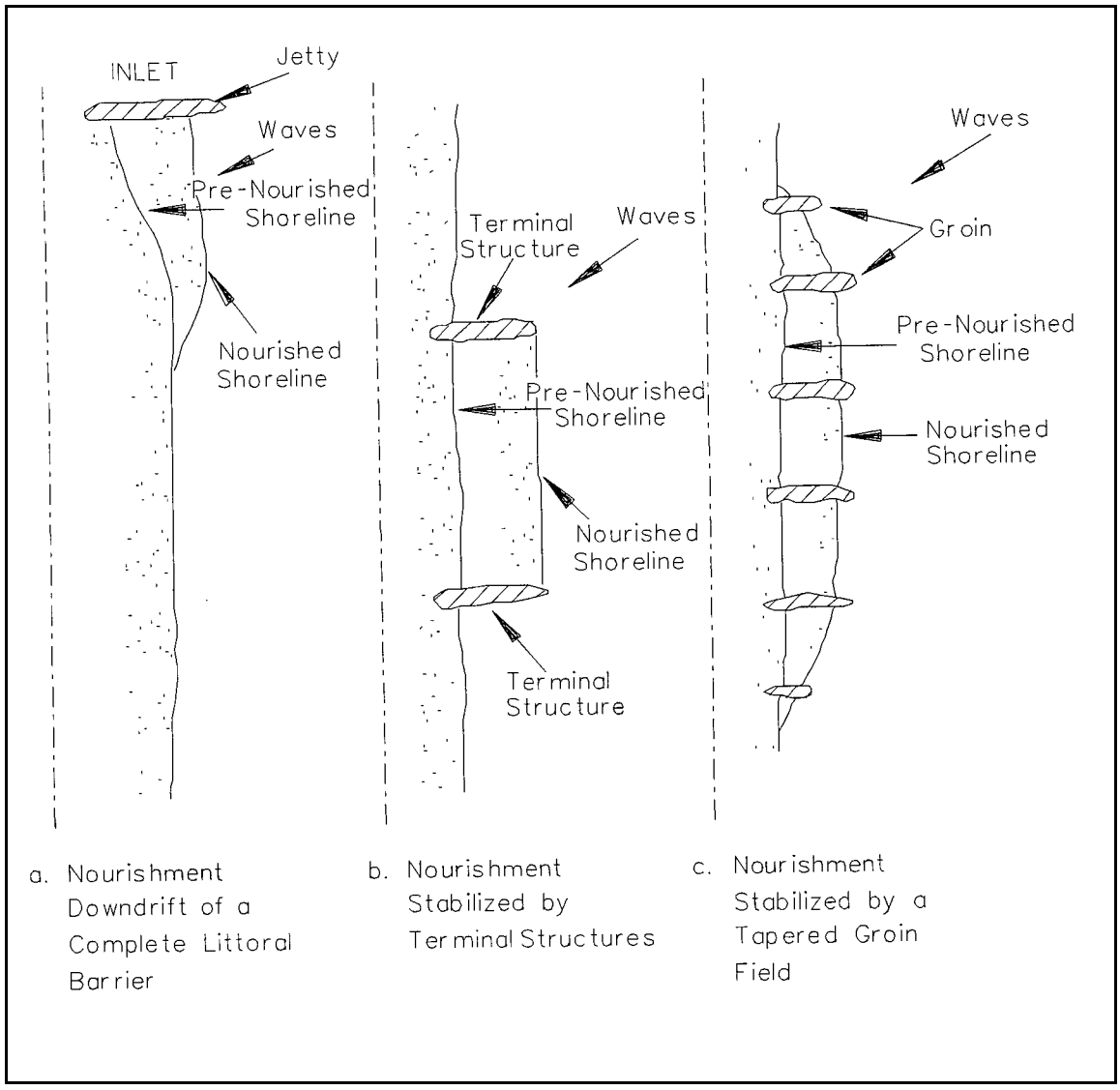

Figure V-4-3. Use of groin structures to enhance beach nourishment projects

What is the extent of the littoral cell, and where within the cell will the project reside? What are the important coastal processes that characterize the littoral cell and the project site? The answers to these questions will influence how a project is designed, how it performs, and what if any impacts it may have on adjacent beaches.

(1) Site location within littoral cell. The location of the project within a littoral cell has great influence on all aspects of a beach nourishment project, from understanding the underlying coastal processes at work, to determining the design concept that might be most effective, to the choice of methods and tools used in the design process. For example, will the project be constructed well within the interior of a littoral cell, miles from the inlets that serve as boundaries of the cell, or will it be built immediately downdrift of an inlet stabilization structure, or along the throat of an unstructured inlet? Sand transport by tidal currents, wave refraction over complex bathymetry, and wave-current interaction may not be important design issues in the former case whereas these processes may be critical in designing an effective project in the latter. In the former case, the project may experience beach recovery following a storm, where much of the sand moved offshore into a storm bar, migrates back onto the shore face with little net loss of sand. In the latter case, sand

moved offshore can be swept into tidal channels, carried away by currents into the inlet's shoals, and not return to the beach face. This will result in a significant permanent loss of sand. Different design concepts may be utilized in each of these two cases. In the former case, beach fill alone may meet the design requirements. In the latter, structures such as T-groins, may be needed to improve beach-fill retention. Different design methods may be utilized in each case. The former case may lend itself to simple analytical design tools, whereas the latter case may require more sophisticated physical or numerical modeling to aid in the design.

(2) Pathways of sediment movement.

(a) Because beach nourishment projects involve placing additional sand into the littoral system, project design is greatly aided by knowing how sand presently moves within the project domain and the littoral cell that is the setting for the project. Specifically, the following pieces of information are valuable: knowledge of the quantities of sand that presently enter and leave the littoral cell, where the sand enters and leaves, and what quantity moves through the project site. The more information known about the movement of sand the better, although this "picture" can be difficult to develop, especially for project sites with sparse data. Estimates of these quantities are often developed through formulation of a sand budget for the littoral cell and project domain. Parts IV and VI discuss development of a sediment budget. The following are types of questions regarding pathways and quantities of sand movement that might be important to the design of the project. If a project is to be constructed within a littoral cell flanked by inlets, are the inlets bypassing sand into the cell? If so, how much is bypassed? Are structures present that might be blocking (partially or completely) the flux of sand into the site from adjacent beaches? Is the project site located on a convex stretch of the barrier island that may be undergoing persistent erosion, or is the site in an area that experiences intermittent periods of erosion and accretion? Is the project to be located in a pocket beach flanked by headlands, and are those headlands blocking longshore sand transport? Are there sources of sand within the littoral cell, such as a river or lagoon, that might periodically discharge sediments to the beach system, or bluffs behind the beach that might serve as a sediment source? Are there sinks within the littoral cell, such as offshore canyons, impoundment fillets updrift of coastal structures, or loss of sand into an adjacent inlet and its shoal system? The closer to inlets, the greater the chance that tidal currents will have an important role in defining sediment pathways. It is important to gain an understanding of the littoral processes at work in the region, including the magnitude and direction of longshore sand transport (net and gross transport rates), sand sources and sinks, and the effects of existing coastal structures on the movement of sand. Parts III-2 and III-3 address the subject of longshore and cross-shore sediment transport processes, respectively, in greater detail.

(b) Historical and current charts, maps, and aerial photographs provide valuable information about the regional setting for a project. They can be valuable data sets for characterizing littoral processes at a project site, and aid in developing a sand budget. A persistent signature of impoundment at coastal structures over several years provides evidence of predominant wave direction and net longshore sand transport direction. Formation and evolution of spits, or migration paths of submerged relic ebb tidal shoals, can provide the same information. Noticeable changes in shoreline orientation and curvature, or persistent changes in bathymetric contour orientation may indicate gradients in longshore sand transport rates or a change in net transport direction. Shoreline positions that are accurately digitized from properly rectified aerial photos and/or charts provide information for identifying current and past erosional and accretional areas, and for calculating shoreline change rates. Calculated change rates can be used to estimate changes in sand volumes along different portions of the beach. Nautical charts and bathymetric surveys show the presence of canyons and proximity of the canyons to the shore, tidal channels, shoals, other morphologic features, and changes in these features through time. Controlled bathymetric surveys (relative to common horizontal and vertical datums) can be analyzed to determine volume changes for use in formulating a sand budget.

(3) Beach topography.

(a) The shape of the beach, above and below water, sheds light on the coastal processes that are at work at the project site. Beach shape also is an important factor in determining the quantity of beach nourishment material needed. The existing beach profile shape seaward of the natural berm crest can be a good indicator of the expected postnourishment beach shape, provided the sand to be placed has similar grain size characteristics as the native beach and there are no coastal structures or other features that are controlling the shape of the beach. One situation where the present profile shape may not be a good indicator of the postconstruction shape would be a beach that is heavily seawalled or reveted, with little to no dry beach in front of the structure at high tide. In this instance, the present beach shape might be unnatural (overly steep) due to the loss of a sand supply at the shoreline (i.e., the beach profile is very much starved of sand). Proximity to a tidal channel or a coastal structure may also produce an "unnatural" beach profile shape, compared to the shape that might exist for the same sediment characteristics but located away from the inlet or coastal structure. Also, if the material to be placed has grain size characteristics that are much different than the native beach, then the present beach profile shape may not be a good indicator of the shape following nourishment. Use of sand finer than the native sand will produce a beach with gentler slopes; use of coarser material will result in a beach with steeper slopes.

(b) Dunes are also an important aspect of project setting. Dune elevation, continuity of the dune "line," position of the dunes relative to the shoreline, and volume of sand in the dune above the natural berm crest elevation are important factors in determining the existing level of protection to property and infrastructure. Well-established vegetated dunes are usually a sign of a healthy beach system. A scarped dune, evidence of regular overwash, or no dune at all indicate an area vulnerable to storm damage. Beach profile surveys, or fully 3-D bathymetric and topographic surveys acquired by lidar systems such as systems such as SHOALS, can effectively characterize the beach/dune system as well as submerged morphologic features. Analysis of well-controlled beach profiles (relative to consistent horizontal and vertical datums) can provide volume change information for use in developing a sand budget, selecting design profiles for the nourishment project, and estimating the required amount of nourishment material.

(4) Sediment characteristics.

(a) Information about the grain size characteristics of the native beach material can shed light on the coastal processes at work. Systematic variations in median grain diameter along the beach, or evidence of natural tracers in the sand, may suggest the direction of net longshore transport. Grain size characteristics are a critical design parameter. Most often, sand with grain size characteristics similar to those of the native beach is sought as beach-fill. This is done to maximize compatibility with the existing beach system. Indirectly, selecting compatible material also maximizes the accuracy of predictions of future project performance, which is often based on past observations of the native beach response. Occasionally, fills are designed using material with different size properties because of limitations on sand availability and the cost to transport it to the project site. Sometimes the choice of a nourishment material with different characteristics is made to satisfy a particular design objective, such as use of coarser-grained fill material to improve resistance to erosion.

(b) Grain size characteristics are quantified based on a sieve analyses of samples which are collected throughout the project domain. Those samples acquired on the profile between the berm crest (or mean high water line) and a water depth corresponding to the position of the typical storm bar should be used to characterize native beach sand for the purpose of assessing the compatibility of sand from potential borrow sources. Compatibility of borrow and native beach material is primarily based on grain size characteristics, and to a lesser extent on color. Part V-4-1-e discusses sediment characterization and compatibility of fill in more detail.

(5) Wave and water level climate.

(a) The wave and water level conditions at the project site represent the major forces that shape the beach, and determine both the longer-term lateral spreading of material comprising the beach nourishment project and the short-term response of the project to storms. Exposure of the project site to wave energy from various directions determines the predominant longshore sand transport rate and direction. Offshore islands or coastal structures, peninsulas, or adjacent land masses may partially or completely shelter the project site from certain waves. The presence of these features modifies the energy, frequency, and directional characteristics of the incident waves that approach the site from deeper water. The presence of submerged offshore shoals, reef outcroppings, shore-attached shoals, or depressions (in general, any irregular bathymetry), also can have a significant persistent influence on local wave transformation and the longshore sand transport regime created by the incident breaking waves. It is important to assess the degree in which the wave climate varies from one end of the project to the other. Persistent variations in wave conditions of 5 to 10 percent can create significant local differences in project performance.

(b) There are several time scales of importance with regard to wave climate. The design life of a beach nourishment project is usually tens of years. Periodic renourishment is typically done every 3 to 5 years. There is evidence of cyclical patterns in weather (e.g., El Niño) that vary on the order of years, which would tend to produce wave climate patterns having similar multiple-year cycles. Annual changes in weather, and annual variations in the frequency and intensity of storm activity create a longshore sand transport regime that can vary considerably from year to year. Definition of the wave climate at these different time scales helps in assessing long-term beach nourishment project performance, potential variation in performance from one renourishment cycle to the next, and from year to year.

(c) Wave and water level conditions that accompany extratropical and tropical storms are also an important aspect of project setting and project design. The time scale of these events is on the order of days. Since most beach nourishment projects are justified based on storm protection benefits, it is important to quantify the frequency and severity of storms that can impact the project site during its design life. Lower-intensity storms typically erode the beach berm. More severe storms, particularly those with higher water levels, can inundate the berm and focus direct wave attack on dunes and exposed upland property. The most important storm parameter influencing beach and dune erosion is maximum water level, followed by wave energy and storm duration.

(d) Hindcast wave and water level information, or data measured nearby, can be used to characterize the wave and water level climate near the project site at the time scales of importance. Sometimes wave information is available in deep water, and other methods must be used to "transform" the information to the project site (e.g., to transform deepwater wave information past islands or very irregular bathymetry). Part II-2 discusses methods for developing wave climate information, including wave hindcasting. Part II-3 discusses techniques for estimating nearshore waves, including wave transformation methods. Part II-5 discusses methods for estimating water levels due to storms.

(6) Existing structures and infrastructure.

(a) How threatened are commercial and private structures, and infrastructure such as roads and utilities, by storm waves and water levels? Formulation of a beach nourishment project often involves compiling an inventory and description of the location of existing infrastructure and commercial and private properties to assess their vulnerability. The properties are valued to aid in quantifying the benefits that accrue from construction of a beach nourishment project. Are there structures that protrude beyond the predominant shoreline position? If so, it may be difficult and not cost-effective to provide a lasting beach having the design width in front of those structures. Attempting to do so may result in a persistent apparent erosional "hot-spot" in these locations. Aerial photos provide a good source of information for describing the

characteristics of infrastructure and property, and the positions of structures relative to the present shoreline. Historical surveys or charts are useful in determining the degree to which existing infrastructure encroaches upon, or is seaward of, the historical beach location. Ground inspections and photos also can be used to characterize the condition and value of structures.

(b) The presence of existing coastal structures, and their characteristics, are also important parameters. What measures are already in place to provide protection to structures (e.g., seawalls and revetments), and what is the condition and effectiveness of those structures? Structures that alter or block the alongshore movement of sand, such as groins, detached breakwaters, or artificial headlands influence the pathways of sand movement at the site. Crest elevation, composition, and condition of groins, revetments, and seawalls determine the structures' functional effectiveness. The "signature" of impoundment adjacent to groins, or lack thereof, can be an indicator of groin functionality. Aerial and ground photos can be used to characterize the condition and effectiveness of existing coastal structures. Engineering drawings that show the subsurface characteristics of the structures, including any toe protection, in concert with present beach profile surveys, can be used to characterize the vulnerability of revetments and seawalls to damage caused by recession of the beach during storms.

(7) Prior engineering activities.

(a) Usually, areas being considered for a beach nourishment project have experienced problematic erosion for some time. Often, there is a record of previous studies and perhaps a record of past engineering activities at the site. This information can shed light on what may or may not work in the future, and why; and aid in designing a nourishment project. For example, records of past beach-fill activities can provide information about expected fill longevity and net longshore transport rates. Historical records documenting impoundment at groins can provide information about net longshore sand transport rates. Dredging and placement records are vital information in the development of a sand budget. The record of past engineering activities may also help explain a particular beach response that has been observed. Compiling a complete chronology and record of past engineering activities can prove to be a very valuable design aid.

(b) This section briefly highlighted some of the more important aspects of project setting and site characterization and history, and how they relate to design of beach nourishment projects. Subsequent sections provide more detailed information about how these factors enter into the design process.

d. Reach delineation.

(1) In addition to the setting for a beach nourishment project and its design features, an equally important design issue is delineation of sections of coast along which a project is to be constructed. Project economics is often a controlling factor in the process of reach delineation. The values of property and infrastructure assets fronting the beach and benefits gained by providing storm-damage reduction enter in assigning bounds of a project reach or subreaches. Project boundaries may be determined by limits of political jurisdiction such as municipal or state boundaries, or may coincide with physical features such as inlets or headlands. Environmental considerations and local preferences may also influence project boundaries.

(2) From an engineering perspective, reach delineation should be evaluated based on physical processes controlling project response. For example, location and characteristics of project terminal boundaries may be evaluated on the basis of fill retention within project bounds and project impacts on adjacent shorelines. Where reaches terminate along the open coast, fill transitions may be used to reduce the rate of spreading losses from project bounds. Transitions may be placed either within or outside project bounds based on design objectives and/or constraints. A more detailed discussion of beach fill transitions is provided in Part V-4-1-h. In cases where reaches terminate at shore-normal structures (e.g., groins and jetties), effects of interrupting littoral drift on downdrift beaches should be assessed. Whether boundaries occur at structures

or on the open coast, project reaches should be of sufficient length to minimize the effect of end losses on the central portion of the project. Part V-4-1-g discusses design parameters and environmental processes that affect project longevity. Economic analyses may identify several discontinuous subreaches within the project main reach (e.g., where areas of development are separated by areas of undeveloped coast). In such cases, a project may function more effectively by designing a single reach spanning both developed and undeveloped sections to avoid multiple areas of end losses.

(3) Beach-fill projects have often employed a uniform design template, with constant berm width and dune elevation, along the entire project. Under most circumstances, however, improved performance can be achieved by modifying the design template along specific subreaches where longshore nonuniformity exists in the without-project condition. For example, consider an existing condition where a particular shore-fronting structure is positioned closer to the shoreline than adjacent structures. A design calling for a uniform width of beach in front of all structures along the entire project reach will produce a planform perturbation at the protruding structure, and will lead to an ongoing problem of accelerated recession in front of the structure. In this case, a viable alternative may be to design a narrower berm in the area of the protrusion with additional storm damage protection provided by higher dunes or protective structures such as seawalls. Other cases where nonuniform design templates may be appropriate include presence of erosional hot spots, changes in shoreline orientation, or nonuniform placement of shore protection structures along the project reach. In design, a practical goal is to distribute the sand fill volume alongshore so as to yield a more or less uniform shoreline location after initial equilibration of the placed fill. Care must be taken in using a variable design template to avoid compromising project performance. For example, dunes placed in front of a developed subreach to prevent overtopping and flooding may not be functional if lower dunes or no dunes are placed on adjacent subreaches of undeveloped shore. In this case, storms could erode and overtop the adjacent low dunes and flank the high dunes, resulting in flooding of the developed area.

e. Evaluate sediment sources.

(1) Borrow source types. Borrow sources for beach fill can be divided into four general categories: terrestrial, backbarrier, offshore, and navigation channels. Each category has favorable and unfavorable aspects; however, selection of an optimum borrow source depends more on individual site characteristics relative to project requirements than type of source. The single most important borrow material characteristic is the sediment grain size.

(a) Terrestrial sources. Terrestrial sources of beach-fill material can be found in many coastal areas. Ancient fluvial and marine terrace and channel deposits, and certain glacial features such as eskers and outwash plains often contain usable material. Because of their potential economic value, information on sand and gravel deposits is often collected by state geological surveys. With this information, field investigations can focus on a few likely sources, thus eliminating need for more general exploration. In some places, commercial sand and gravel mining operations may provide suitable material for direct purchase. In their absence, it would be necessary to locate a suitable deposit and set up a borrow operation specifically for the project. Use of terrestrial borrow sites usually involves lower costs for mobilization-demobilization operations and plant rental, and less weather-related downtime than the use of a submerged borrow source. However, the production capacity of terrestrial borrow operations is comparatively low, and haul distances may be long. Thus, costs per unit volume of placed material may exceed those from alternate submerged sites. In general, terrestrial borrow sources are most advantageous for projects where exploration and mobilization-demobilization costs, relative to the cost of fill, are a large part of overall expense of the operation. Unfavorable aspects of terrestrial borrow sources are typically related to adverse secondary impacts caused by mining and overland transport. Compared to hydraulic placement, mechanical (dump truck) placement of fill additionally results in practical limits in fill volume, and fill placement is mostly limited to the dry and intertidal beach. Consequently, more rapid equilibration and recession of the placed fill is experienced.

(b) Backbarrier sources. Sediment deposits in the backbarrier marsh, tidal creek, bay, estuary, and lagoon environments behind barrier islands and spits have been used in the past for beach fill. They are an attractive source because they are protected from ocean waves and are often close enough to the project beach to allow direct transfer of the material by pipeline. This eliminates the need for separate transport and transfer operations. However, most backbarrier sediments are too fine-grained to use as beach fill. In addition, many backbarrier areas are highly important elements in the coastal ecosystem and are sensitive to disturbance and alteration by dredging. Material in backbarrier sediments coarse enough for beach fill is generally confined to overwash deposits and flood tidal shoals associated with active or relic inlets. Overwash deposits occur on the landward margin of the barrier where storm waves have carried beach and dune sediments across the island or spit. Flood tidal shoals occur inshore of tidal inlets and consist of sediment transported by tidal currents flowing in and out of the inlet. These sediments are usually derived from littoral drift from adjacent beaches. Overwash deposits and relict flood tidal shoals may be ecologically important because they may provide suitable substrate for marsh growth. In addition, on retreating barriers, they may comprise a reserve of sand that will be recycled into the active beach deposits as retreat progresses. Flood tidal shoals at an active inlet may be suitable for borrow sites because the material removed is likely to be replaced by ongoing inlet processes. However, dredging material from active flood tidal shoals can adversely alter both the hydraulic conditions in the inlet and wave action on adjacent shores. A study of the hydraulic effects should be made prior to dredging flood-tidal shoals.

(c) Harbors, navigation channels, and waterways. Creation of harbors, navigation channels, and waterways, and deepening or maintenance dredging of existing navigation projects often requires the excavation and disposal of large volumes of sediment. In some cases, where the dredged sediment is of suitable quality, it can be used as fill on nearby beaches rather than placing it in offshore, upland, or contained disposal sites. Operations of this type are economically attractive because dual benefits are realized at considerably less cost than if both operations were carried out separately.

- Maintenance dredging of projects in low energy environments such as estuaries or protected bays is least likely to produce suitable beach-fill material. In such areas, the dredged material often consists of clay, silt, and very fine sand. However, when dredging new harbors, channels or waterways, or deepening existing channels in low energy areas, the dredge may cut into previously undisturbed material of suitable characteristics.

- Dredged material from higher energy areas, such as rivers above tidewater and open coast inlet shoals, is often more acceptable for beach fill. On barrier coasts, inlets trap beach sediment that has been carried to the inlet by littoral drift. Therefore, material dredged from inlets is typically similar to the native material on the project beach. However, sediment compatibility tests should be performed to determine its suitability for use as beach fill.

(d) Offshore sources. Investigations of potential offshore sources of beach-fill material under the Coastal Engineering Research Center's (CERC's), Inner Continental Shelf Sediments Study (ICONS), by the USACE Districts and others (i.e., Bodge and Rosen (1988)), indicate that large deposits of suitable material often occur in offshore deposits. Data from the Atlantic coast show that the most common suitable sources are in ebb tidal shoals off inlets, and in linear and cape-associated shoals on the inner continental shelf, such as those shown in Figure V-4-4. Potential sources on the inner shelf have also been identified in submerged glaciofluvial features, relic stream channels, and featureless sheet-type deposits.

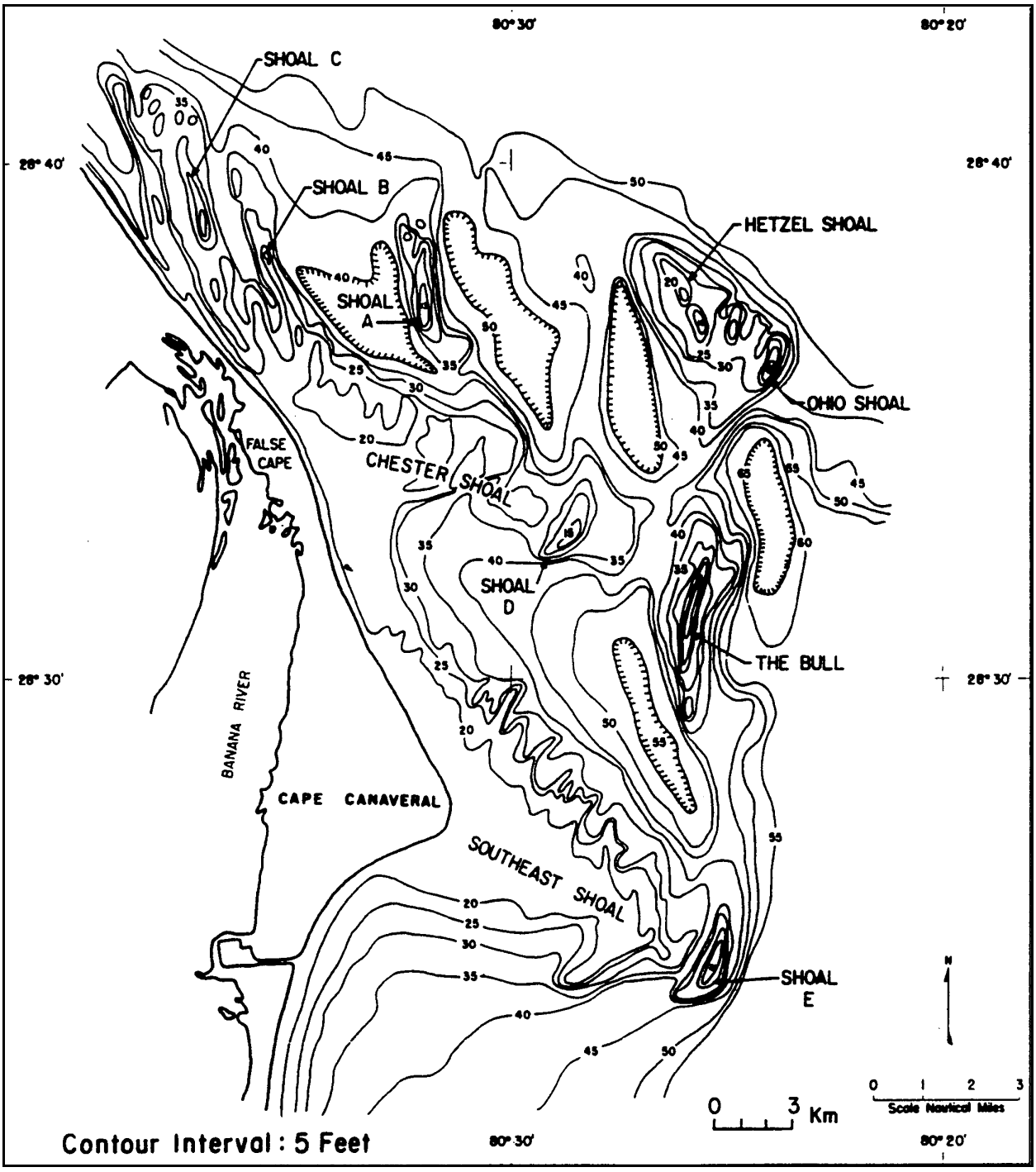

Figure V-4-4. Cape-associated inner continental shelf shoals off Cape Canaveral, Florida (Field and Duane 1974)

- Offshore deposits can be excavated by dredges designed to operate in the open sea. When borrow material is obtained by dredges, it is typically either pumped directly to the beach via pipelines or, in the case of self-propelled hopper dredges with pumpout capability, transported to the shore and pumped onto the beach. Hopper dredges are typically more cost-effective for borrow areas located more than a few kilometers from the project site. These dredges practically require a borrow area

with at least one long dimension that allows the hopper vessel to transit the site; i.e., on the order of at least 1.5 km (5,000 ft). In some cases, the dredged material is taken to a rehandle site and offloaded, then transferred to the beach by hydraulic pipeline or truck haul.

- An alternate placement method is to dump material in a nearshore berm as close as possible to the project beach, in water depths shallower than the depth of closure, where it will possibly be moved ashore by wave action. Experiments in offshore dumping near New River Inlet, NC, in 1.82 to 3.65-m- (6- to 12-ft) depth, resulted in a general onshore and lateral migration of fill material (Schwartz and Musialowski 1980). Placing material in water this shallow requires special equipment such as split hull barges, dredges, or other equipment to cast the material shoreward.

- Offshore borrow sources have several favorable features. Suitable deposits can often be located close to the project area. Offshore deposits, particularly linear and cape-associated shoals usually contain large volumes of sediment with uniform characteristics and little or no silt or clay. Large dredges with high production rates can be used. Environmental effects can be kept at acceptable levels with proper planning.

- An unfavorable aspect of offshore borrow operations is the necessity of operating under open sea conditions. Restrictions on the placement of fill material on beaches during the sea turtle nesting season often requires dredging during the winter, when wave energy is highest. In more protected places, such as backbarrier or otherwise sheltered sources, less seaworthy dredging plant can be used. Dredges capable of working in open sea conditions generally have higher rental and operating costs, although this may be offset by greater production capacity.

- Evaluation of offshore sources should also consider the possible effect of dredging a borrow area on littoral processes along and adjacent to the project area. This analysis should include the use of a numerical wave transformation model and the calculation of longshore sand transport rates and transport rate gradients. Nearshore transformation of a project area's principal incident wave conditions over the pre- and postdredging bathymetry should be simulated. The incipient breaking wave conditions and littoral transport potential alongshore, leeward of the borrow area, should be compared between conditions. The proposed limits or geometry of the borrow area may require alteration to avoid unintended concentrations of wave energy, or alongshore transport gradients, produced by the excavated topography. Additionally, borrow areas near the shoreline or inlet shoals may result in accelerated transport of sediment from the beach to the dredged borrow area. In general, where practicable, borrow areas should be sited in water depths greater than the estimated depth of closure (a rough rule of thumb would be twice as deep).

- In some cases, the original relief maybe restored by natural processes over time. This is more likely to occur in active features such as inlet shoals than in relic features, or on ones that are active only during intense storms. Because the depth of closure is well inshore of offshore relic sand borrow sites, these borrow pits usually fill in with fine-grained material that is not suitable for beach fill.

(e) Environmental factors. In general, environmental effects of borrow operations can be made acceptable by careful site selection, and choice of equipment, technique and scheduling of operations. Restoration of flora and fauna often takes place in a short time after operations (Stauble and Nelson 1984). Alterations in physical features (the pit left behind after excavation) may, in some circumstances, be restored by natural processes.

- One effect of borrow operations is direct mortality of organisms due to the operation itself, and destruction or modification of the natural habitat. Direct mortality of motile fauna, such as fish, is usually not great because they move to other areas during the borrow operation. Sessile flora and fauna cannot vacate the area; mortality of these organisms is therefore higher. However, they usually are replaced by the reproduction of survivors or stocks in unaffected peripheral areas (Nelson 1985; Johnson and Nelson 1985).

- Another consideration is the destruction or modification of the habitat needed for survival of native species. A common alteration is the exposure of a substrate that differs from the natural substrate as a result of excavating overlying material. Many marine benthic, and some pelagic, organisms are adapted to specific substrate conditions. Even though larvae of the native species reach the affected area, they may not survive.

- In comparing borrow sites, it is necessary to consider whether or not natural substrate will be modified by the planned operation. This depends on the thickness of the surficial layer and the depth of excavation needed to produce sufficient fill. In many instances, where the layer of suitable fill material is thin, an increase in the areal extent of the borrow area will allow excavation of sufficient material without altering substrate conditions. While this alternative increases direct mortality, it will preserve favorable conditions for repopulation of native organisms.

- In subaqueous areas, detrimental effects on native organisms, both within and near the borrow site, may occur due to suspending silt and clay size material in the water column as a result of the dredging operation. Deposits containing more than a small amount (generally taken as less than 10 percent by volume) of silt and clay are thus less desirable sources of fill from an environmental standpoint. In addition, the fine fraction will be unstable in the beach environment.

(f) Utilization of bypassing/backpassing material. Consideration should be given to bypassing sand across tidal inlets from accreted areas at updrift jetties and from ebb and flood deltas at inlets. Likewise, back-passing of sand from a terminal downdrift jetty to an updrift beach-fill project should be evaluated as a possible cost-effective sand recycling measure. Different types of sand transfer systems are discussed in Richardson (1977). The effect of these measures on adjacent beaches must be evaluated.

(2) Borrow site exploration. A field exploration program to locate and characterize potential borrow sources is usually necessary for offshore and backbarrier environments. For a detailed discussion of procedures, see Prins (1980) and Meisburger (1990). In terrestrial areas, information on deposits is usually available from state geological surveys. There may be existing commercial sand and gravel mining operations. For existing navigation projects, or planned improvements, information on the dimensions and characteristics of material to be dredged is usually available. Field exploration programs involve four phases: a preliminary office study, general field exploration, detailed survey of the site, and characterization of potential sites. The geographical area covered by these investigations is limited by the distance from the project site that is within an economically feasible range for transportation of fill material. Borrow sources within a few miles of the site should be considered initially. Sources farther away should be considered only if no suitable sources are within this range.

(a) Office study. The first phase of the exploration program is an office study of maps, charts, aerial photographs, and literature sources concerning the survey area (Morang, Mossa, and Larson 1993). A study of these materials provides general information on the geomorphology and geology of the area, and helps to identify features that might contain potential fill material. The office study also involves laying out a plan for the next phase, general field exploration of potential sources. Such a plan would include specification of an exploratory field data collection program and definition of the equipment needed to execute the program.

- The most important equipment used for general field exploration and detailed site surveys are: seismic reflection equipment, vibracore apparatus, navigation positioning system, and vessels. Grab samples of surface sediments and side-scan sonar records are also valuable components of the general exploration phase, and can usually be conducted for a relatively small additional cost. Prins (1980) provides a detailed list of equipment and equipment capabilities recommended for use in general field exploration operations. Seismic reflection equipment should provide the highest resolution possible, consistent with achieving a subbottom penetration of at least 15 m (50 ft). High powered seismic reflection systems used for many deep penetration studies are not suitable because of their relatively poor resolution of closely spaced reflectors. Obtaining sediment cores using vibratory coring equipment is more economical than standard soil boring methods, which require more expensive support equipment. Vibratory coring equipment having 3-, 6-, and 12-m (10-, 20-, and 40-ft) penetration capability is available. A 6-m coring device is necessary; a 12-m capability is desirable. Navigation control should be established using an electronic navigation positioning system having an accuracy of about 3 m (10 ft) at the maximum range anticipated for survey and coring operations. Global Positioning Satellites (GPS) technology provides this type of accurate positioning.

- An important task of an office study is to lay out trackline plots, similar to those shown in Figure V-4-5, that are to be followed by the survey vessel in collecting seismic reflection data during the general reconnaissance phase. A grid pattern as illustrated in Figure V-4-6, having lines approximately (0.8 km (0.5 miles) apart, should be employed for areas that are judged to be the most viable either because they are located near the project site or give promise of containing deposits of usable fill material (Meisburger 1990). Zigzag lines are used to cover areas between grids. The detail of coverage is determined by trackline spacing. More complex or promising areas may call for closer spacing.

- Core sites can be tentatively selected during the office study. However, final locations should be determined based on analysis of the seismic reflection records.

(b) General field exploration. During the general field exploration program, data are collected throughout the survey area to locate and obtain information on potential borrow sources and shallow subbottom stratigraphy. This phase involves collection of a comprehensive set of seismic reflection profiles to identify sediment bodies, and a small number of cores to identify and test potential borrow sources.

- The initial part of the general exploration phase is the collection of echosounder and seismic reflection records along predetermined tracklines. The basic survey procedure is for the survey vessel to proceed along each trackline, collecting data while its position is being monitored by an electronic positioning system with fixes recorded at a minimum of 2-min intervals. Fixes are keyed to the records by means of an event marker and identified by a serial fix number. Because seismic reflection records tend to deteriorate in quality with increasing boat speed, the survey vessel's speed should be slow enough to avoid significant reduction in record quality. In general, a suitable boat speed is likely to be less than 4 or 5 knots. The records should be continuously monitored as they become available. Changes in trackline patterns, if considered desirable, can be made as work progresses.

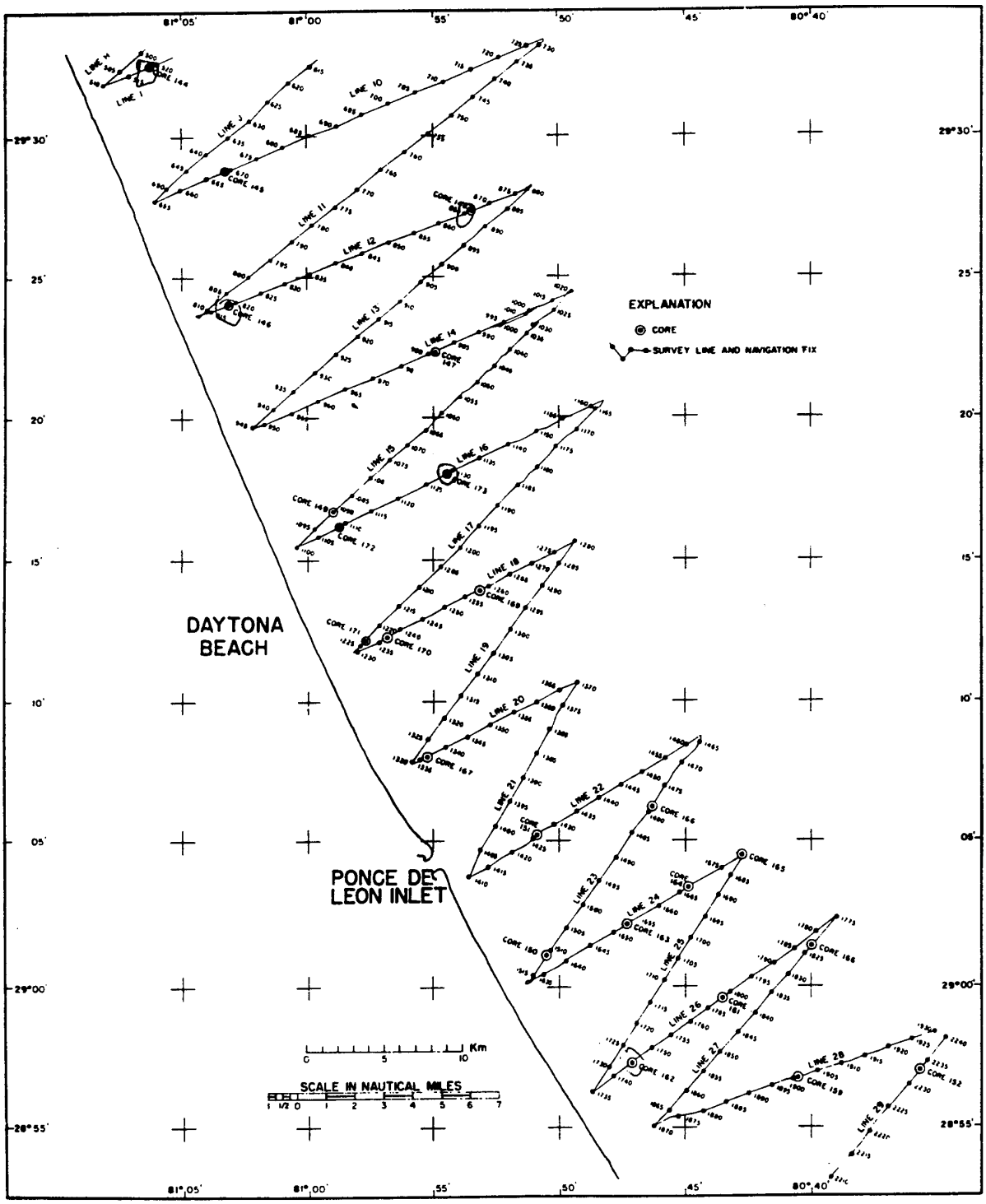

Figure V-4-5. Reconnaissance zigzag line plot from the north Florida coast (from Meisburger and Field 1975)

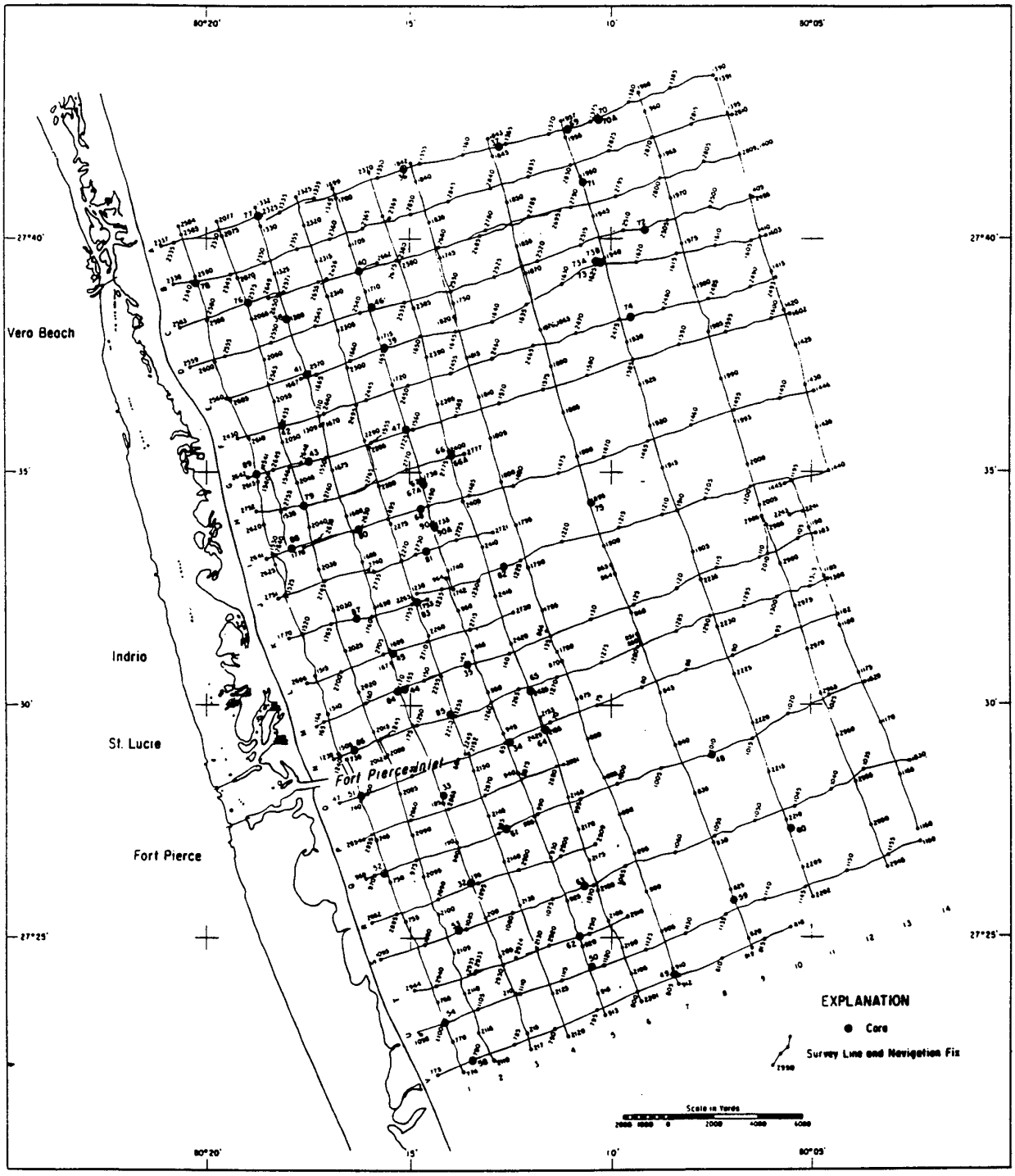

Figure V-4-6. Grid lines covering a detailed survey area off Fort Pierce, Florida (from Meisburger and Duane 1971)

- Sediment core sites are usually selected after the seismic reflection survey, to allow time for preliminary analysis of the records to determine the most prudent and informative core locations.

- Cores should be examined as they are taken. Inspection of cores is often hampered by the presence of silt and by scratching of the acrylic core liners. However, the top and bottom sediments can be directly viewed before the core is capped. As work progresses, changes can be made in core locations.

(c) Detailed site survey. The third phase of borrow site exploration and investigation consists of a detailed investigation of potential sites, which are selected on the basis of data collected during the general exploration survey. If sufficient seismic reflection data were collected at potential sites during the general exploration phase, the detailed site study may only require the collection of additional, more densely-spaced, cores. Since few large sand bodies have uniform size characteristics, it is important to obtain a sufficient number of cores and borings to accurately reflect the variations in size characteristics throughout the deposit. The number of cores and spacing between cores should be determined based on a review of survey and seismic data as well as other geological studies of the area. These values will vary throughout a borrow site, and from one borrow site to another. But in most cases, collection of cores at less than 300-m (1000-ft) nominal spacing is recommended for purposes of ultimately defining the borrow site(s) to be used in construction. It is important to have adequate data for reliably defining the borrow site. Additional seismic reflection data, if needed, should be collected at this time.

- Sometimes the general and detailed field surveys are made in succeeding years so that ample time is available to study results of the seismic reflection survey before coring is undertaken. However, it is possible to complete the operation entirely in one season. This can be done by mobilizing both geophysical and coring equipment early in the most favorable season, and allowing sufficient lag time between the seismic work and the bulk of the coring work for thorough data analyses and selection of core sites.

- Additional data collection is typically required to fully examine the selected borrow area or areas. These additional data include: magnetometer survey to detect cultural resources of historical significance (shipwrecks, etc.) and obstructions to dredging; archaeological-diver survey to investigate magnetic anomalies; sidescan sonar survey to detect obstructions, hard-bottom, or other environmental resources; detailed bathymetric survey suitable for preparation of construction drawings; and benthic or other biologic surveys, if required, to assess the existing biotic resource.

(3) Borrow site characterization. Any beach erosion or shore protection study in which beach fill is considered should include examination of all potential borrow sources and a comparative evaluation of their suitability. The characteristics of potential borrow sources that are most important in evaluating suitability are: location, accessibility, site morphology, stratigraphy, volume of material available, sediment characteristics, geological history, environmental factors, and economic factors.

(a) Location. The distance that the material must be transported and the feasible means of transport have a large influence on project costs and may be decisive in selecting the most suitable source. Location is also important in terms of the surroundings. Use of terrestrial sources located in developed areas may have a direct impact on the population by creating undesirable noise, traffic congestion, and spillage. Offshore sources may involve questions of jurisdiction and be situated in areas where the dredging and transport activities impede or endanger navigation.

(b) Accessibility. In order to be usable, a borrow source must be accessible or made accessible for the equipment needed to excavate and transport the material. Access to terrestrial deposits may involve road construction or improvement of existing routes. Onsite reconnaissance is the best method of determining the adequacy of access and any necessary improvements. A cost estimate of work needed to create accessibility should be prepared and included in the economic analysis.

- In evaluating subaqueous deposits, one of the principal factors is water depth. To be accessible, the deposit must lie in the depth range between the maximum depth to which the dredge can excavate material, and the minimum depth to keep the dredge afloat when laden with fuel and/or sediment. Subaqueous borrow sites should be located sufficiently far offshore and in deeper water so that excavation does not induce adverse shoreline impacts by altering to the incident wave climate.

- Another aspect of accessibility is the presence of incompatible overburden above the usable sediments. The composition, areal extent, and thickness of any overburden should be determined and considered in the economic analysis (i.e., the cost to remove and dispose of it).

(c) Site morphology. Information on borrow site morphology is valuable in defining and evaluating site characteristics. In many cases, the source deposit has surface morphological features that can be used to delineate boundaries and to assist in interpolating between seismic and coring data points. In addition, site morphology may provide indications of the origin and history of the deposit. Subsurface deposits such as filled stream channels are more difficult to delineate because the only sources of data are seismic reflection records, cores, and borings.

- Description of borrow site morphology should contain information on dimensions, relief, configuration, and boundaries, and be illustrated by large-scale maps or charts. Information for compiling the reports can usually be found in hydrographic survey data available from the National Ocean Survey (NOS), National Oceanic and Atmospheric Administration (NOAA), for submerged deposits, and in published U.S. Geological Survey (USGS) topographic maps for terrestrial sources. Fathometer records, which should be made concurrently with the seismic reflection profiles, are valuable for supplementing and updating other sources.

- In cases where the existing information is inadequate, a special detailed bathymetric survey of the site should be made before the main field collection effort is undertaken.

(d) Site stratigraphy. The stratigraphic relationships within and peripheral to the site deposits should be developed from the existing sources and the seismic and coring records to define: limits of the deposit; thickness of usable material; thickness of any overburden; sedimentary structures, and sediment characteristics of each definable bed. The detail and reliability of the stratigraphic analysis depends on the complexity of the deposit, the number of outcrops, number of cores or borings available, and the degree to which stratigraphic features are revealed by seismic reflection profiles.

- In terrestrial areas, outcrops of potentially useful materials may or may not be present. In many cases, such deposits have no topographic expression and must be defined solely on the basis of borings. Seismic refraction surveys in such situations are valuable in defining the areas between data points. Seismic refraction techniques for subsurface exploration are covered in detail in Engineer Manual 1110-1-1802, "Geophysical Exploration for Engineering and Environmental Investigations."

- In submerged areas, site characteristics must be determined by a combination of bathymetric survey, seismic reflection profiling, and sediment coring. It is important, in both seismic reflection and refraction surveys, to collect enough cores or boring samples to identify and correlate the reflectors

with reliable data on sediment properties, and to show significant boundaries that may not have been recorded by the seismic systems.

(e) Volume available. Most beach-fill projects require thousands or millions of cubic meters of suitable fill material. The volume in each potential source must be calculated to determine if a sufficient amount is available to construct and maintain the project for its entire economic life (including initial construction, all subsequent renourishment, and emergency maintenance). In order to do this, it is necessary to delineate the lateral extent and thickness of the deposit. Boundaries may be defined by physical criteria or, in large deposits, arbitrarily set to encompass ample material for the projected fill operation. The thickness of the usable material can be determined from an analysis of site stratigraphy.

- If deposits have a uniform thickness throughout, the available volume can be calculated by multiplying their areas by their thicknesses. Many deposits such as shoals and filled stream channels have more complex shapes, including sloping boundaries and variable thickness. To determine the volume of these deposits, an isopach map of the deposit must be created. An isopach map is a contour map showing the thickness of a deposit between two physical or arbitrary boundaries. Figure V-4-7 shows an isopach map of a borrow area used at Ocean City, Maryland. In this case, the upper boundary of the deposit is defined by the surface of the shoal and can be delineated by bathymetric data. The lower boundary was fixed at a level seismic reflection horizon passing beneath the shoal. Contours, at 1.52-m (5-ft) intervals, were drawn for all the shoal area above the base reflector. Measurements from this type of map can be used to calculate the volume. Commercially available Geographical Information System (GIS) software with Digital Terrain Modeling (DTM) capabilities is now routinely used to generate isopach maps and calculate available sediment volumes.

- Computation of the source's available volume must account for practical limitations of excavation. Particularly for hydraulic dredging (excepting small suction dredge systems), sediment deposits less than about 1-m (3-ft) thickness are impractical to specify. Buffers must be delineated between suitable and nonsuitable sediments, which cannot be included in the source's available volume. These buffers vary with the site and the nature of the sediment strata, but they typically have a minimum thickness of 0.3 m (1 ft) to 0.6 m (2 ft) in subaqueous sources. Buffer areas around sensitive environmental or cultural resources, or around known obstructions, must also be excluded. The size of these radial buffers depends upon the resource or obstruction to be avoided, but a typical radius is 45 to 90 m (150 to 300 ft). Computation of the source's volume must also be limited to those areas or strata in which the sediment is known to be beach-compatible.

(f) Sediment composition. The physical properties of a sediment sample that are most important for determination of suitability for fill on a project beach are composition and grain size distribution. The desirable physical properties of beach-fill material are mechanical strength, resistance to abrasion, and chemical stability.

- In most places, sand-sized sediment is predominantly composed of quartz particles with lesser amounts of other minerals such as feldspar. Quartz has good mechanical strength, resistance to abrasion, and chemical stability. In some deposits, particularly those of marine origin, there is a large and sometimes dominant amount of calcium carbonate that is in most cases of organic origin (biogenic). Calcium carbonate is more susceptible than quartz to breakage, abrasion, and chemical dissolution; but, if it is not highly porous or hollow, it will make serviceable beach fill.

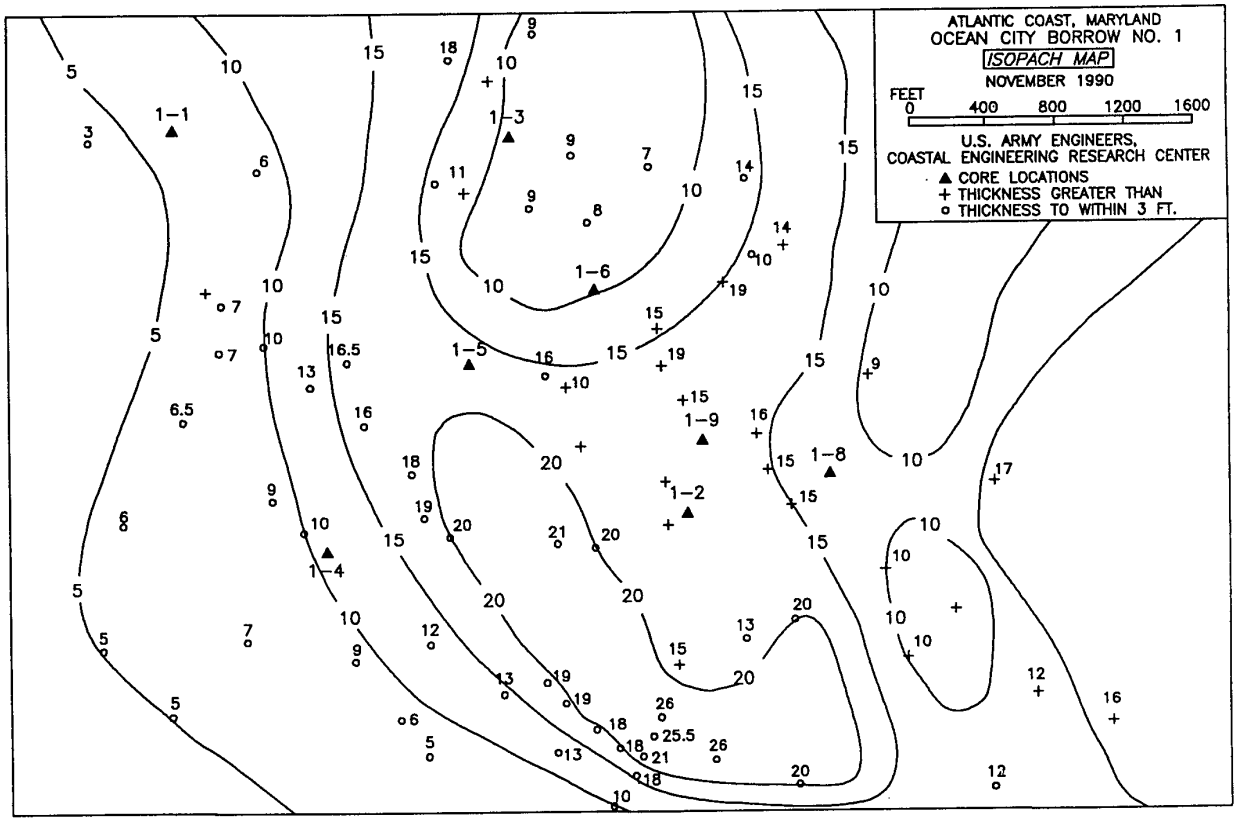

Figure V-4-7. Isopach map of a borrow area used at Ocean City, Maryland

- Sediment composition can be determined by examining representative samples under a binocular microscope. Samples should be prepared by thorough washing to remove fines and clean the surface of the particles. If the material is not well sorted, it should be subdivided into sieve fractions for analysis. A subdivision into the Wentworth classes (see Part III-1) for sand-sized and coarser material is convenient for this purpose. The percentage of carbonate in the material can be estimated by dissolving the carbonate fraction in multiple baths of hydrochloric acid with a subsequent sodium hydroxide wash.

(g) Sediment size characteristics. Generally, suitable material will have grain sizes predominantly in the fine to very coarse sand size range. The presence of very fine sand, silt, and clay in small amounts (generally less that 10 percent) is acceptable, but sources having a substantial amount of fines should be avoided if other more suitable sources are available. When using a borrow area with higher silt or clay content, a large amount of material must be handled to obtain the usable portion, thereby increasing costs. Also, the creation of turbidity during excavation and placement on the beach is environmentally undesirable. However, in the future, as sand resources become more scarce, sand separation may prove to be economically justified depending on the volume of material required and the relative silt and clay content of the borrow site. Borrow material presently discounted because of a comparatively high percentage of fines may become economically viable sand sources in the future.

- One of the main considerations in selecting a borrow source is the similarity between the grain size distributions of the borrow material and the native beach, i.e., the borrow material's compatibility with the native material. To make this comparison, it is necessary to determine, for both native beach and each potential borrow source, a composite grain size distribution representative of overall textural properties. The method used to determine grain size characteristics for both the fill and

borrow sites should be the same. Beach and borrow material should be analyzed with standard sieves as described in Part III-1.

- Native beach composite sediment statistics should be computed based on sieve analyses of samples collected along cross-shore transects through the most active portion of the beach profile (see Part III-1 for information concerning sediment composite statistics). The most active portion is located between the crest of the natural berm (immediately landward of the mean high waterline) and the depth corresponding to the position of the typical storm bar. The composite statistics should be developed for a number of cross-shore transects throughout the project domain. Grain size statistics calculated from such a sampling scheme will account for most of the natural variability on the profile. If cross-shore composites exhibit a wide range of median grain size and sorting values, an alongshore composite should be calculated for the entire project domain to reduce the variability.

- Borrow area composite statistics should be determined using grain size distributions computed for samples taken from several cores within the potential borrow site. For general uniform cores, samples should be collected from the top, middle, and bottom of useable sand within the core. The composite characteristics of the borrow material should be weighted based on the estimated volume of each type of material present in the deposit.

- Figure V-4-8 shows a comparison between the native beach and borrow material used for nourishment at Ocean City, Maryland. The shaded area represents common characteristics between the native beach and fill material.

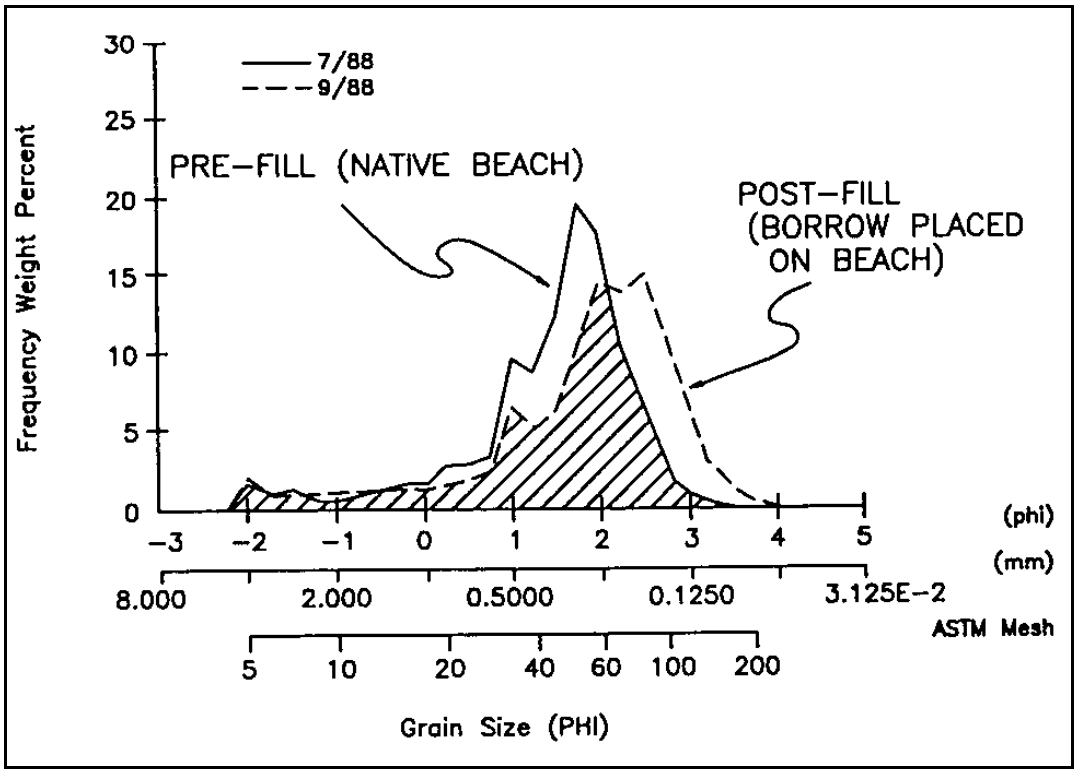

Figure V-4-8. Comparison of composite grain size analysis between the native beach and the borrow material used at Ocean City, Maryland

(h) Sediment suitability. The grain-size distribution of the borrow material will affect the cross-shore shape of the nourished beach profile, the rate at which fill material is eroded from the project, and how the beach will respond to storms. Typically, borrow material will not exactly match the native beach (except perhaps in some bypassing projects). An analysis is required to assess the compatibility of the borrow material with the native beach, from a functional perspective. A comparative analysis of sand suitability is also required to economically evaluate alternative borrow areas for a given project.

- Early research into compatibility of borrow area material by Krumbein (1957), Krumbein and James (1965), James (1974, 1975), and Dean (1974) addressed this issue by various comparative analysis techniques that utilize the sand-size distributions of the natural beach in the fill area and the borrow material in the candidate borrow sites. These approaches develop a factor, or parameter, indicating how much fill material is required in light of the different sediment characteristics between the borrow and native beach materials. They assume that borrow material placed on the beach will undergo sorting as a result of the coastal processes; and given enough time, will approach the native grain-size distribution. The portion of borrow material that does not match the native sediment grain-size distribution is assumed to be lost to the offshore. James (1975) developed this concept into a method to calculate an overfill factor, R_A, and a renourishment factor, R_J. Conceptually, the overfill factor is the volume of borrow material required to produce a stable unit of usable fill material with the same grain size characteristics as the native beach sand. The renourishment factor addresses the higher alongshore transportability of the finer grain sizes in the borrow sands and provides an estimate of renourishment needs. Use of the renourishment factor is no longer recommended in beach-fill design calculations; however, details concerning the renourishment factor and it's calculation may be obtained from the *Shore Protection Manual* (1984).

- Recent research and beach nourishment experiences have questioned the continued use of these grain-size-based factors, R_A and R_J, to estimate beach-fill performance (Dean 2000). Present guidance recommends that design be based on equilibrium beach profile concepts, an assessment of storm-induced erosion, and an assessment of wave-driven longshore transport losses; and that these methods be used to replace or complement the overfill and renourishment factor approaches (National Research Council (NRC) 1995). In practice, these recommended methods treat sediment characteristics using a single grain size parameter, the median grain diameter. They do not consider natural variations in grain size that occur on natural and nourished beaches. However, they have the advantage of incorporating more of the physics of coastal processes into the design, much more so than use of the overfill and renourishment factors. The overfill factor attempts to consider the distribution of grain sizes. Therefore, it does provide an additional piece of information on the amount of borrow material that might be needed to construct a beach nourishment project in more difficult design cases where the grain size characteristics of the borrow material differ significantly from those of the native beach material, especially the case where the borrow sediments are finer than the native sediments. The overfill factor is discussed in more detail in the next section.

- As a general recommendation, a nourishment project should use fill material with a composite median grain diameter equal to that of the native beach material, and with an overfill factor within the range of 1.00 to 1.05. This is the optimal level of sediment compatibility. However, obtaining this level of compatibility is not always possible due to limitations in available borrow sites. Both the overfill factor and equilibrium beach profile concepts indicate that sediment compatibility is sensitive to the native composite median grain diameter. As such, the compatibility range varies depending on the characteristics of the native beach material, with coarse material being less sensitive to small variations between the native and borrow sediments than fine material. As a rule of thumb, for native beach material with a composite median grain diameter exceeding 0.2 mm, borrow material with a composite median diameter within plus or minus 0.02 mm of the native median grain diameter is considered compatible. For native beach material with composite median diameter between 0.15

and 0.2 mm, borrow material can be considered compatible if its composite median diameter is within plus or minus 0.01 mm of the native diameter. For native beach material with a composite median diameter less than 0.15 mm, use of material at least as coarse as the native beach is recommended. Even though material is deemed compatible based on these rules, the designer should factor grain-size differences into estimates of required fill volume through use of equilibrium beach profile methods, or the overfill factor, or both. Methods for computing beach- fill volumes are discussed in Part V-4-1-f. These guidelines are based on composite median diameters established for the entire project and borrow site. Typically, composites for individual profiles, or subsections of the borrow site, will have variations in median diameter which may exceed the compatibility ranges previously discussed.

- Materials that are not compatible according to these guidelines may still be suitable. Borrow material that is coarser than the native material will produce a beach which is at least as stable as a fill comprised of native material. Fills with coarser material provide improved resistance to storm-induced erosion. A lesser volume of coarser fill will be required to create a beach of a given width, compared to the volume of native beach sand that would be needed. If the median diameter of the borrow material exceeds the median diameter of the native material by more than 0.02 mm, a noticeably steeper beach may form. A steeper beach may become a design issue, along with the different texture of the coarser fill. Use of material finer than the native material should be avoided, if possible, but such material still may be suitable. A much greater volume of material will be required to form a beach of a given width, compared to the volume of native sand that would be required. Use of finer sand will produce a beach with flatter slopes, which could be a design issue too. For example, it may be problematic to construct a more gentle beach adjacent to an existing groin or jetty that is intended to block the longshore movement of sand. Sand transport around the structure and into a navigation channel may increase.

(i) Overfill factor. The overfill factor, R_A, is determined by comparing mean sediment diameter and sorting values of the native beach and borrow sediments (in phi,ϕ, units). The phi, ϕ, scale of sediment diameter is defined and discussed in Part III-1, and Equations III-1-1a and III-1-1b enable conversion between sediment grain size diameter in millimeters and the ϕ scale and vice versa. The overfill factor is computed using the following relationships between the borrow and native beach material:

$$\frac{\sigma_{\phi b}}{\sigma_{\phi n}} = \frac{\left[\frac{(\phi_{84}-\phi_{16})}{4} + \frac{(\phi_{95}-\phi_{5})}{6}\right]_b}{\left[\frac{(\phi_{84}-\phi_{16})}{4} + \frac{(\phi_{95}-\phi_{5})}{6}\right]_n} \tag{V-4-3}$$

and

$$\frac{M_{\phi b} - M_{\phi n}}{\sigma_{\phi n}} = \frac{\left[\frac{(\phi_{16}+\phi_{50}+\phi_{84})}{3}\right]_b - \left[\frac{(\phi_{16}+\phi_{50}+\phi_{84})}{3}\right]_n}{\left[\frac{(\phi_{84}-\phi_{16})}{4} + \frac{(\phi_{95}-\phi_{5})}{6}\right]_n} \tag{V-4-4}$$

where:

$\sigma_{\phi b}$ = standard deviation or measure of sorting for borrow material (Equation III-1-3)

$\sigma_{\phi n}$ = standard deviation or measure of sorting for native material (Equation III-1-3)

$M_{\phi n}$ = mean sediment diameter for native material (Equation III-1-2)

$M_{\phi b}$ = mean sediment diameter for borrow material (Equation III-1-2)

- Values obtained using the relationships in Equations V-4-3 and V-4-4 are then plotted on the graph presented in Figure V-4-9. The value of R_A can be obtained by interpolating between the values represented by the isolines. Values of the overfill factor greater than 1.0 indicate that more than one unit of borrow material will be needed to produce one unit of fill material. Example V-4-1 illustrates computation of the overfill factor.

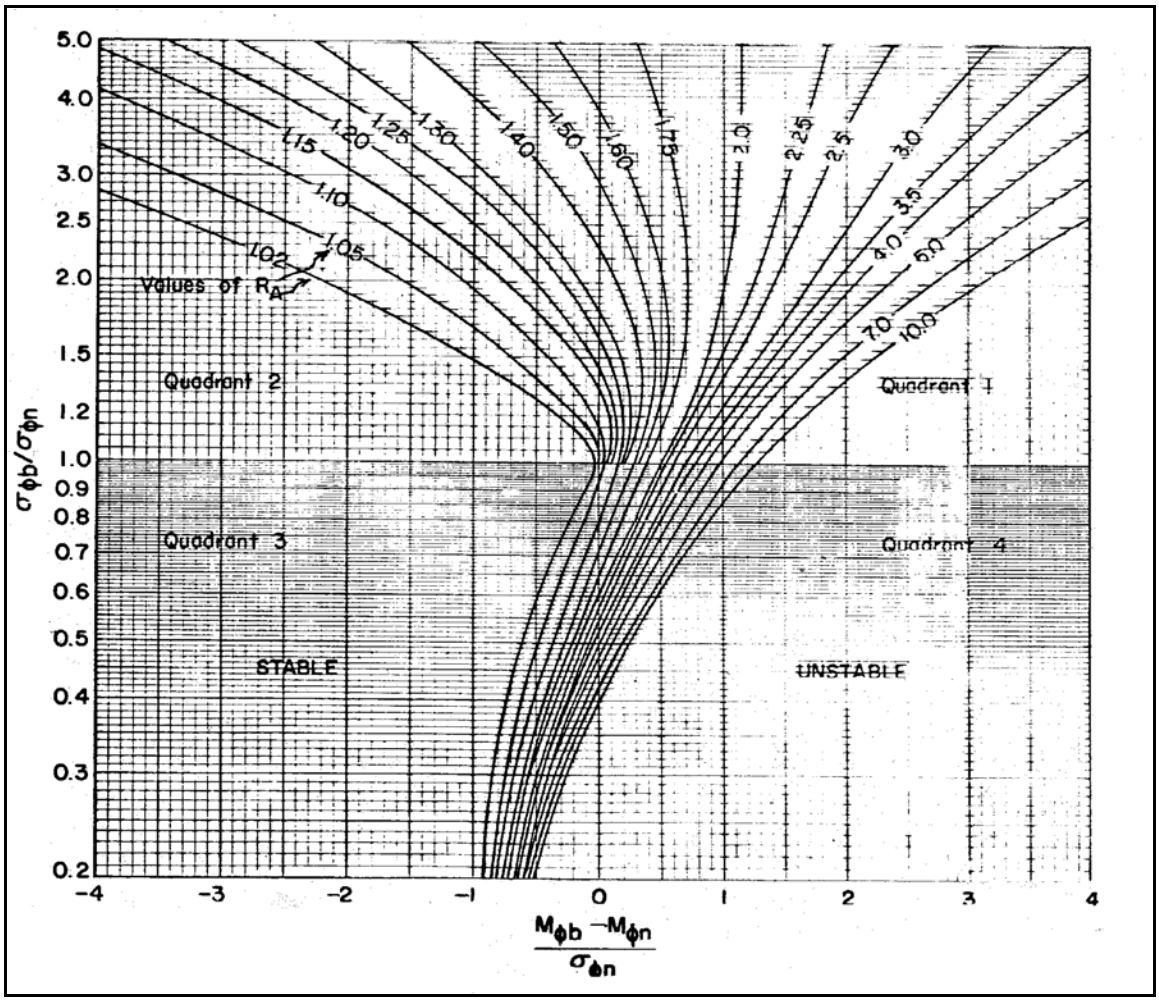

Figure V-4-9. Isolines of the adjusted overfill ratio (R_A) for values of ϕ mean difference and ϕ sorting ratio (*Shore Protection Manual* 1984)

EXAMPLE PROBLEM V-4-1

FIND:

The overfill factor, R_A.

GIVEN:

The native and borrow area phi values are:

native beach: ϕ_{05}=0.95, ϕ_{16}=1.31, ϕ_{50}=1.91, ϕ_{84}=2.66, ϕ_{95}=2.90
borrow area: ϕ_{05}=1.42, ϕ_{16}=1.63, ϕ_{50}=2.49, ϕ_{84}=3.08, ϕ_{95}=3.55

The median grain diameter for native and borrow material is 0.27 and 0.18 mm, respectively.

SOLUTION:

The mean sediment diameter in phi units is given in Part III-1 as

$$M_\phi = (\phi_{16} + \phi_{50} + \phi_{84}) / 3 \qquad \text{(III-1-2)}$$

$M_{\phi n} = (1.31 + 1.91 + 2.66) / 3 = 1.96$
$M_{\phi b} = (1.63 + 2.49 + 3.08) / 3 = 2.40$

The standard deviation in phi units is given in Part III-1 as

$$\sigma_\phi = (\phi_{84} - \phi_{16}) / 4 + (\phi_{95} - \phi_{05}) / 6 \qquad \text{(III-1-3)}$$

$\sigma_{\phi n} = (2.66 - 1.31) / 4 + (2.90 - 0.95) / 6 = 0.66$
$\sigma_{\phi b} = (3.08 - 1.63) / 4 + (3.55 - 1.42) / 6 = 0.72$

The sorting ratio from Equation V-4-3 is

$\sigma_{\phi b} / \sigma_{\phi n} = 0.72 / 0.66 = 1.09$

The phi mean differences ratio from Equation V-4-4 is

$(M_{\phi b} - M_{\phi n}) / \sigma_{\phi n} = (2.40 - 1.96) / 0.66 = 0.67$

Entering Figure V-4-9 with x = 0.67 and y = 1.09 results in an overfill ratio (R_A) equal to 2.5. The finer borrow material may be suitable for use, but it is quite incompatible with the native beach sand. The value of the overfill ratio suggests that 2.5 units of borrow material will be required to create 1.0 unit of stable native beach material.

- The overfill method previously described is the Krumbein-James technique (Krumbein and James 1965). Dean (1974) presents an alternative method for computing the overfill factor, not shown, which generally yields less conservative (lower) estimates of the overfill factor.

f. Beach-fill cross-section design. The design of Federal beach-fill projects is based on the optimization of net annual benefits defined as the difference between average annual costs and average annual benefits. This optimization procedure produces a plan known as the National Economic Development (NED) plan. The NED plan considers the storm damage reduction potential of various beach fill design alternatives and the averaged annual cost. Primary design parameters of each alternative include the physical dimensions of the cross-sectional design profile and the volume of sand required to obtain the design profile. Beach-fill design alternatives typically include combinations of beach berms of varying width and dunes of varying height (see Part V-4-1-b for a description of the characteristics and functions of beach berms and dunes). Design berms are characterized by berm crest elevation and berm width. Dune design dimensions include crest elevation, crest width, and side slopes.

(1) Berm elevation. The elevation of the design berm should generally correspond to the natural berm crest elevation. If the design berm is lower than the natural one, a ridge will form along the crest, which, when overtopped by high water will produce flooding and ponding on the berm. A design berm higher than the natural berm will produce a beach face slope steeper than the natural beach and may result in formation of scarps that interfere with sea turtle nesting and recreational beach use. Many healthy, natural beaches exhibit a gentle downward slope from the toe of the dune to the seaward limit of the berm. Therefore, a gentle berm slope can be specified as an element of the design profile. The berm slope is most appropriately estimated from profiles that represent a nearby, healthy beach. Or the slope can be estimated to fall in the range from 1:100 to 1:150. Adding a gentle slope to the berm also helps prevent overtopping and ponding.

(a) The natural berm elevation can be determined by examining beach profile surveys of existing and historical conditions at the project site. Because beach berms form naturally under low-energy waves, they are typically most well-developed in form at the end of the summer season. Seasonal profile surveys can be used to examine temporal changes in berm shape and to identify well developed berm features from which to estimate the natural berm height. When survey data indicate alongshore variations in the natural berm height, a representative berm height may be determined either by visual inspection of plots showing the alongshore variations or by computing an average profile shape. The Beach Morphology Analysis Package (BMAP) provides automated calculation and visualization tools for performing such analyses. Sommerfeld et al. (1994) provide an overview of the capabilities and a user's guide for operation of the BMAP software.

(b) Figure V-4-10 shows an example of seasonal variation in berm shape measured over two consecutive years at a given profile station. The fall surveys show that the beach berm is widest following the calmer summer waves, whereas the spring surveys show the berm to be in a more eroded condition following winter waves. Based on visual inspection of Figure V-4-10, a natural berm height for this profile can be approximated by the horizontal dotted line, corresponding to an elevation of 3.6 m. Figure V-4-10 shows that it would be difficult to identify the natural berm height based solely on the first spring survey, and illustrates the advantage of using multiple surveys for profile characterization.

(c) Figure V-4-11a shows beach profiles measured during a single fall survey at five different profile stations along the beach. The berm is seen to vary alongshore in height and width. To determine a representative berm height, the beach profiles are horizontally aligned on the seaward face of the dune to superimpose the berm profiles at the base of the dune, as shown in Figure V-4-11b. An average profile is computed by averaging the elevations of the aligned profiles at 1-m increments in distance offshore. Figure V-4-11c shows the average profile, from which a representative berm elevation of 3.5 m is obtained by inspecting the horizontal portion of the profile between the offshore distances of 75 and 100 m.

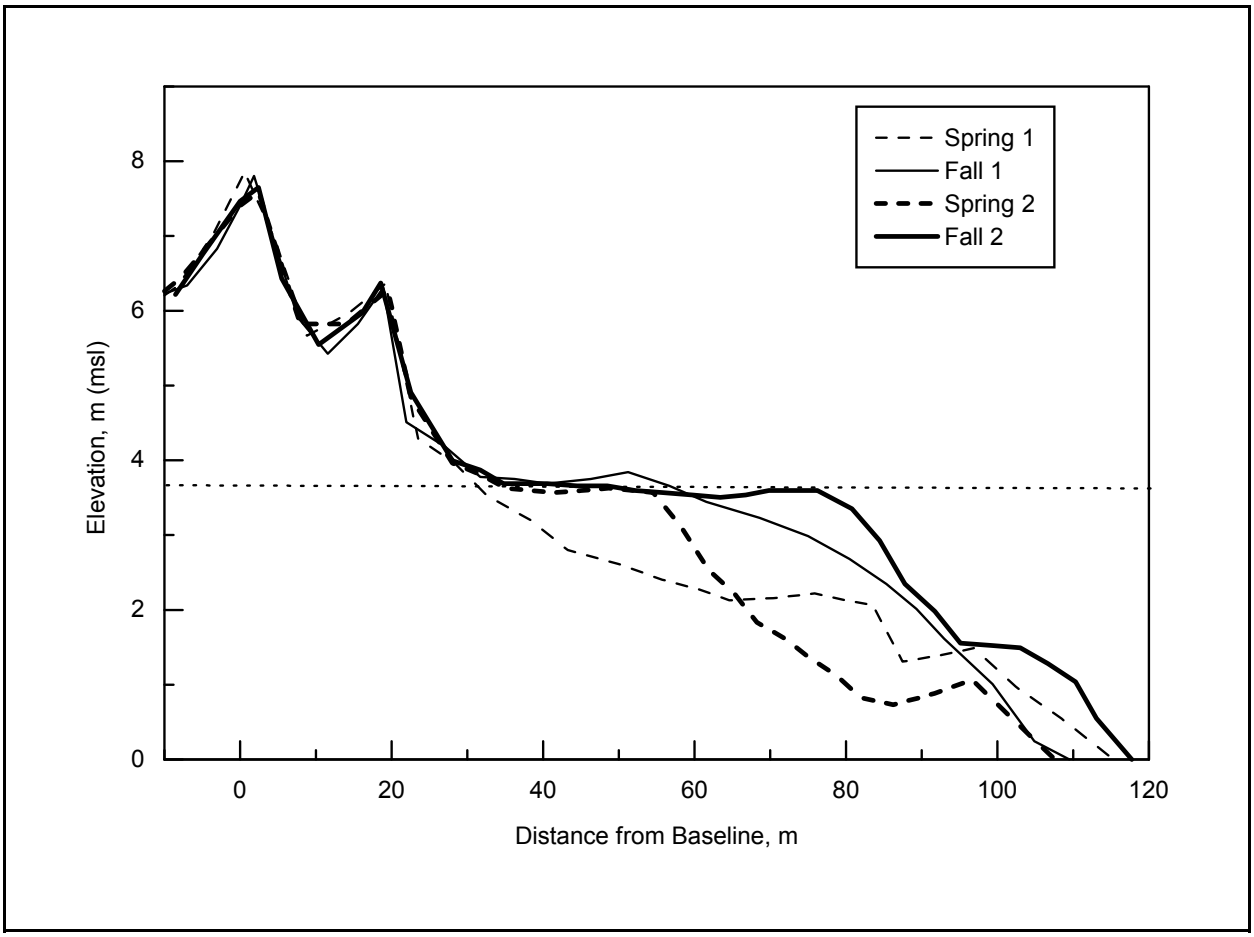

Figure V-4-10. Seasonal variation of a beach berm

(d) In cases where no dry beach exists at the project site, or where the existing beach has a deficit of sand due to substantial reduction or elimination of a critical sediment source, such as in front of a seawall or downdrift of a shore-perpendicular structure, the natural berm elevation should be estimated using profile data from adjacent beaches which are healthier in terms of sand availability but are exposed to similar waves and water levels. Priority should be given to identifying a natural berm elevation using beach measurements from the project site or a similar site. As a last resort, when no suitable beach profile data are available to determine a natural berm height, the limit of wave runup under average (nonstorm) wave and tide conditions at the site can be estimated to establish a design berm height (see Part II-4-4 for calculation of wave runup on beaches).

(2) Berm width.

(a) Selection of the design berm width depends on the purpose of the project and is often constrained by factors such as project economics, environmental issues, or local sponsor preferences. For Federal beach nourishment projects, the berm width is determined through a process of optimization based on storm damage reduction. The design beach width is optimized by computing costs and benefits of various design alternatives and selecting the alternative that maximizes net benefits (USACE 1991). Numerical models of beach profile change such as Storm-Induced BEAch CHange (Larson and Kraus 1989) provide a means of evaluating beach response as a function of berm width. Figure V-4-12 illustrates how berm width influences the landward extent of erosion during a storm. Figure V-4-12a shows four beach profiles with identical dune

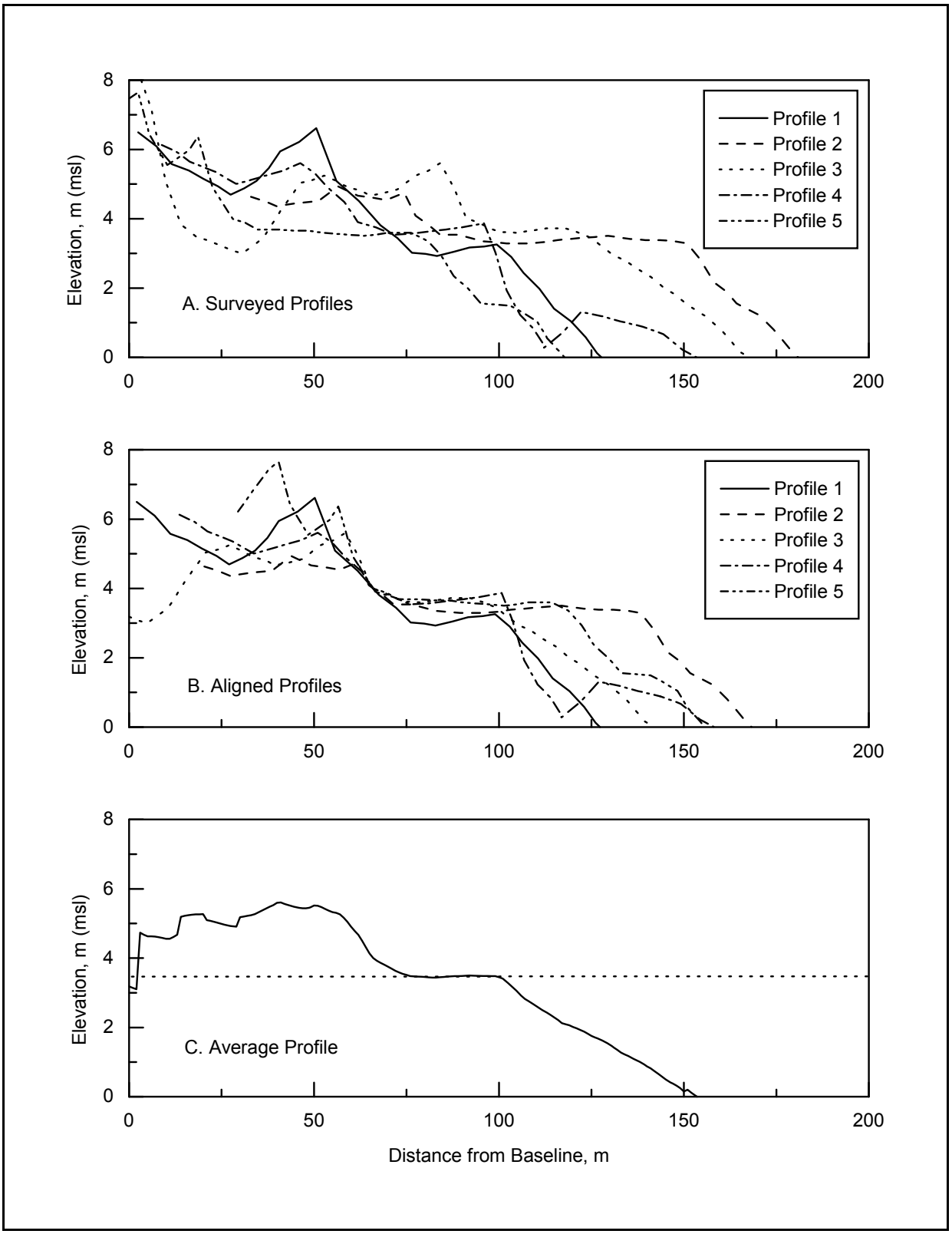

Figure V-4-11. Berm elevation determined from beach profiles measured at various alongshore stations

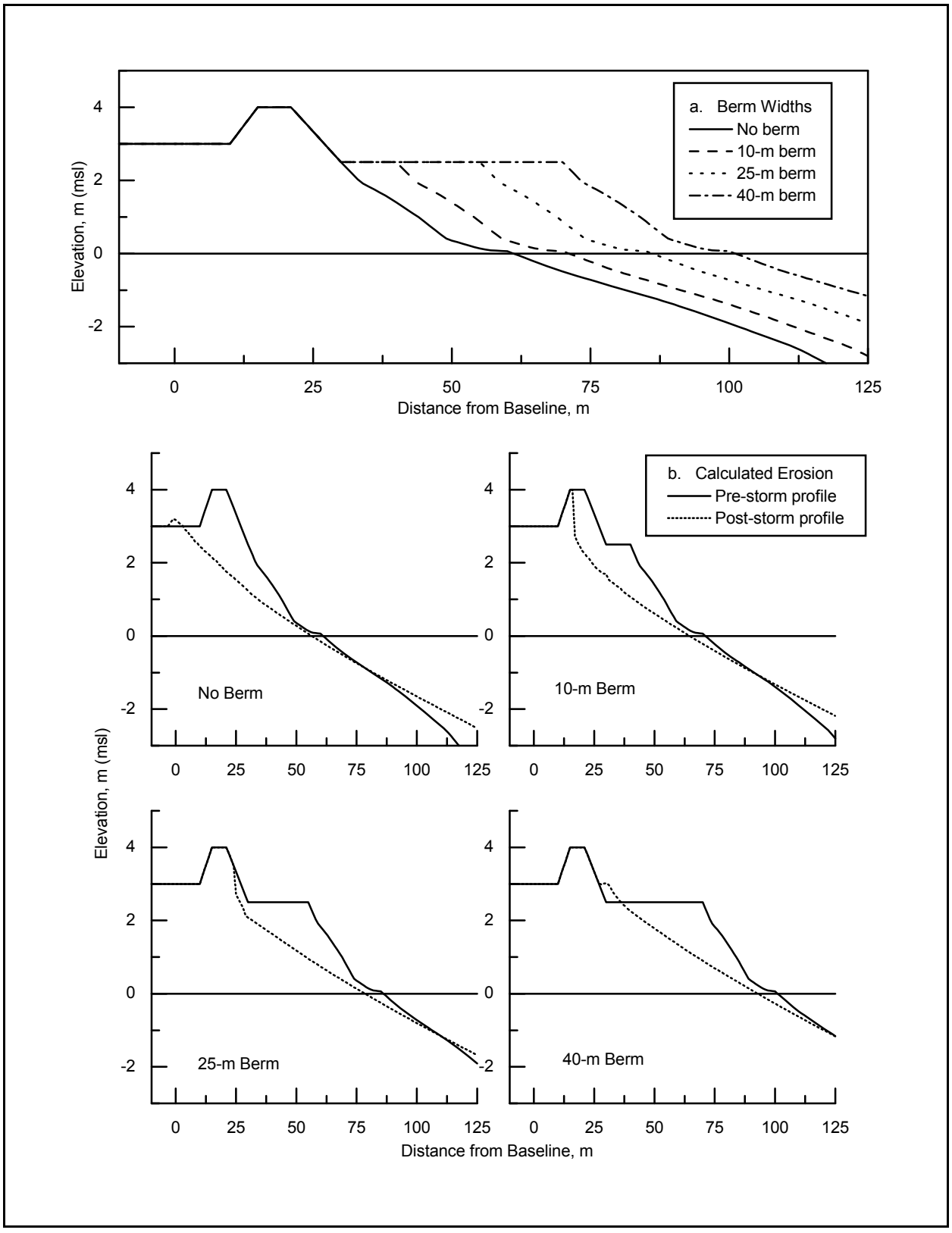

Figure V-4-12. Example of storm-induced beach erosion as a function of berm width

cross sections and varying berm widths. The SBEACH model was used to simulate profile change, and each profile was subjected to a constant wave height of 3 m, wave period of 10 sec, and water level of 1.5 m msl over a duration of 24 hr. Figure V-4-12b shows the calculated results for each profile. The profile with no berm experienced complete erosion and overtopping of the dune. Most of the dune was eroded on the 10-m berm profile, whereas the 25-m berm profile experienced only minor dune erosion. The 40-m berm provided full protection against erosion of the dune and backbeach, and some sand was pushed up against the base of the dune due to overwash across the wide berm. In this example, a shorefront property located immediately landward of the dune would experience varying degrees of damage and/or vulnerability to future storm erosion and flooding as a function of the beach berm width.

(b) Factors other than storm erosion that influence beach width include the rate and variability of long-term shoreline recession, planform spreading losses, and presence of erosional hot spots. These factors typically do not enter in the optimization of the design berm width for storm damage reduction projects, but should be accounted for in optimization of the advanced fill section and renourishment interval as discussed in Part V-4-1-g.

(c) Storm berms may be used in conjunction with a natural berm to provide added protection against damage during storms. Storm berms are constructed at an elevation higher than the natural berm and are set back, landward, from the crest of the natural berm. Storm berms are built to reduce the chance for wave action and erosion from reaching the dune during higher water levels associated with a specified degree of storm intensity (usually, the type of storm that can be expected once every few years). The crest elevation of a storm berm should be set based on the water level and runup elevation associated with the type of storm(s) against which protection is sought. If a storm berm is included in the design, the width of the storm berm can be optimized to maximize net benefits. The seaward extent of the storm berm should also consider the possibility for undesirable, persistent scarp formation.

(3) Dune dimensions.

(a) Dunes protect upland property against wave attack, erosion, and flooding during extreme storm events which overtop or severely erode the beach berm. Design parameters of a dune include the crest elevation, crest width, and side slopes. The design dune crest elevation is typically determined through economic optimization. The dune crest width may also be optimized but is typically fixed at a selected width for all design alternatives. In selecting dune crest width and side slopes, constructibility constraints and angle of repose of the fill material grain size should be considered. A typical dune design may have dimensions on the order of 5-m crest elevation above msl, 10-m dune crest width and one on five side slopes. Planting beach grasses on the constructed dune helps to maintain and build dune volume over time by trapping wind-blown sand.

(b) To illustrate the influence of dune height on storm-induced beach profile change, the no-berm profile shown in Figure V-4-12 was modified to increase the dune elevation from 4 to 4.5 m while maintaining the same crest width and side slopes. The original and modified dune configuration are shown in Figure V-4-13a. The increase in dune height translates to an added volume of 10 cu m/m for this profile. Figure V-4-13b shows profile erosion modeled by SBEACH for the same storm conditions used in the previous berm erosion example. The calculated results in Figure V-4-13b indicate the added dune height prevented dune overtopping and back-beach erosion for these particular wave and water level conditions.

(4) Design profile shape. The shape of the design profile is needed to compute cross-sectional fill volume requirements and as input to storm-induced erosion modeling that is done to optimize berm and dune dimensions. In order to obtain the design dune and berm template on the beach, sufficient sand must be placed to nourish the entire profile out to the depth of closure (see Figure V-4-14 and Part III-3-3-b for details

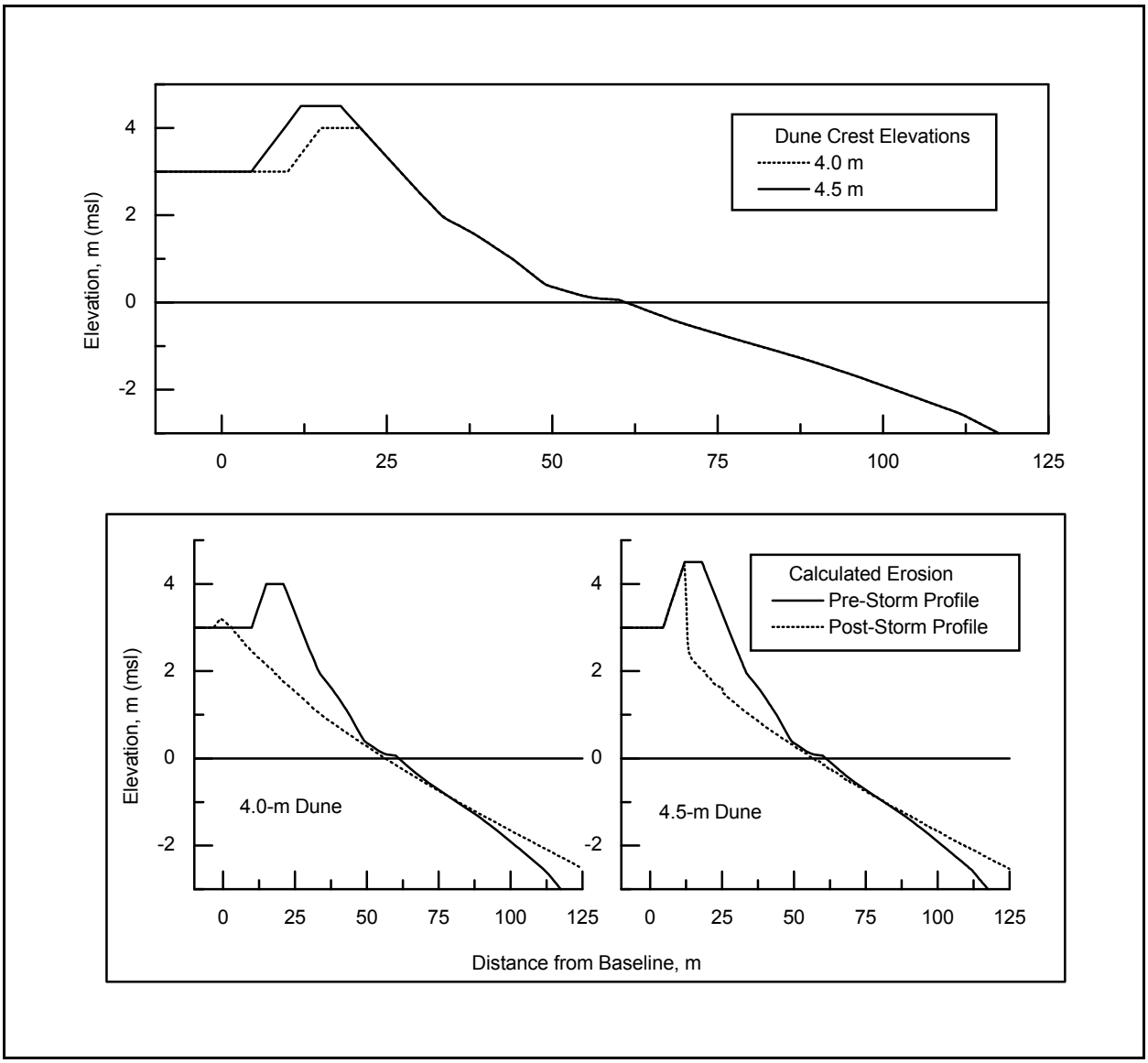

Figure V-4-13. Example of storm-induced beach erosion as a function of dune crest elevation

on depth of closure). Whereas dune and berm dimensions are determined through optimization, the shape of the design profile below the beach berm is a function of the local morphology and grain size of the fill. Local beach morphology often includes a nearshore bar system, which may be absent in erosion-stressed preproject beaches. In such cases, a berm also might be absent from the profile, or may be unnaturally low in elevation; or the preproject profile may reflect an overly steep beach face. A key aspect of defining the design profile shape is to recognize whether or not the preproject beach reflects an unnatural, sediment-starved condition, in which the preproject shape is different from that which will evolve once the fill is placed. For example, a severely eroded beach may lack the commonly observed nearshore bar system, but the bar system will likely form under sediment-rich conditions that follow nourishment. Consequently, the sectional fill volume should include an estimate of bar volume. In these situations, design profile shape can be defined by examining nearby beaches that are healthier in terms of available sediment supply (from the upland beach and from longshore sources). Profile data from adjacent beaches within the project domain, or data from a nearby site that is exposed to similar wave and

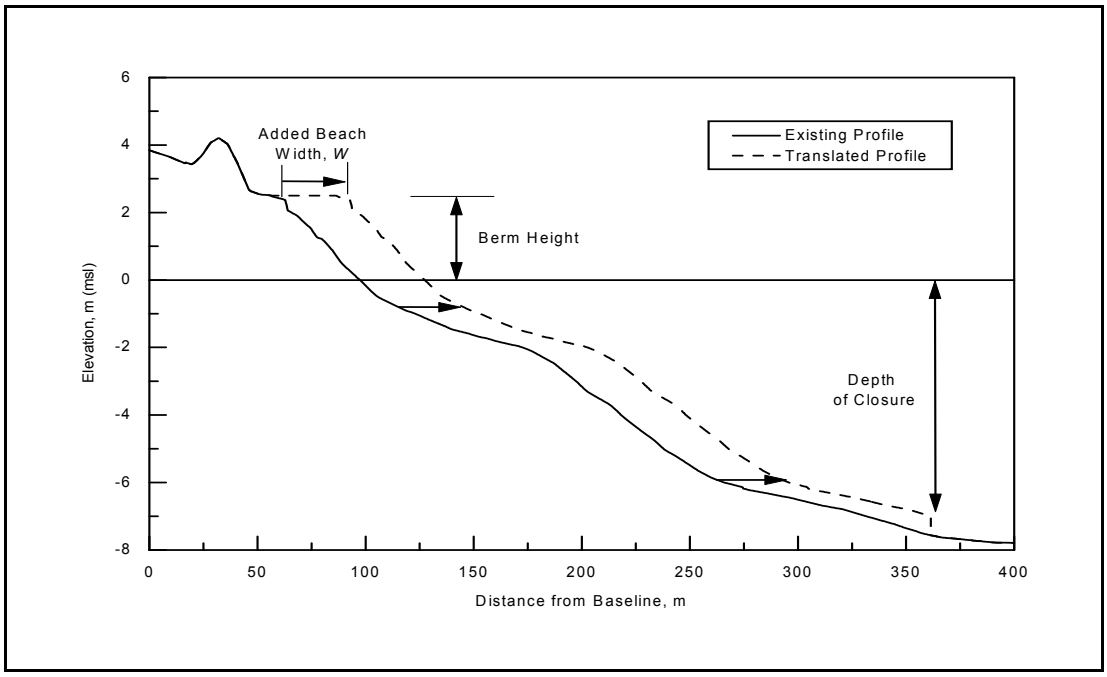

Figure V-4-14. Beach-fill design profile shape determined by profile translation

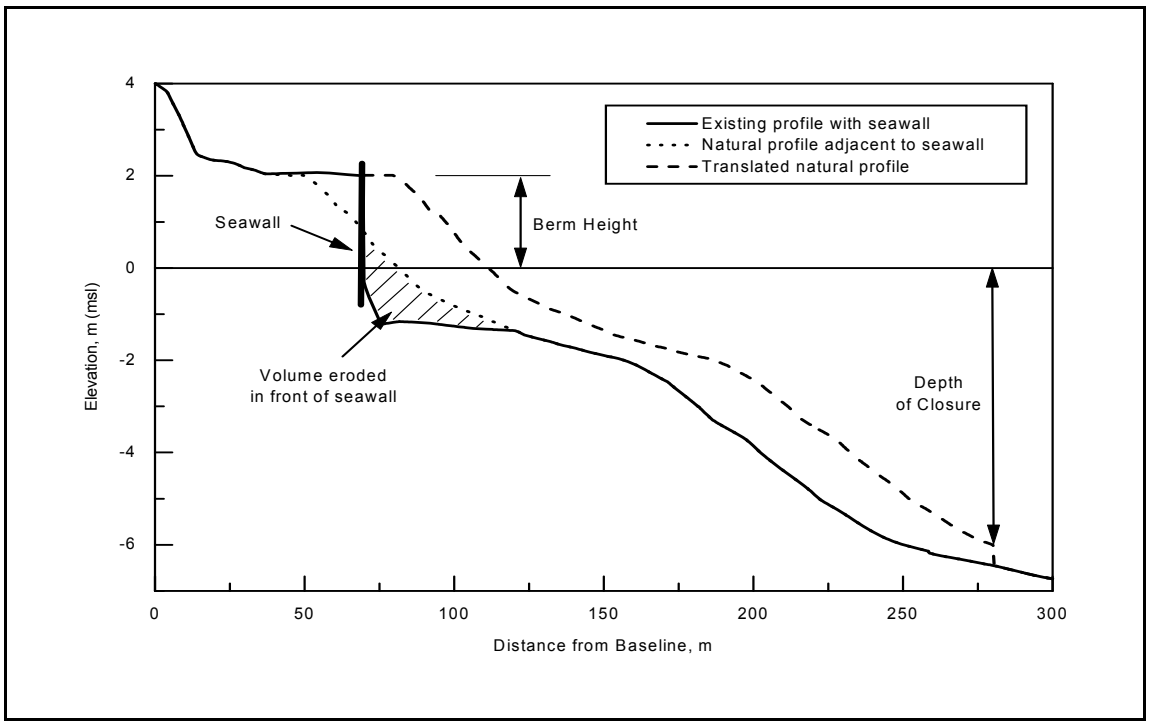

Figure V-4-15. Design profile in front of a seawall

tide conditions and has similar grain size characteristics, can be used to estimate the healthy beach profile shape for reaches where in situ profiles might be misleading. Figure V-4-15 shows an eroded profile in front of an exposed seawall. Translating the existing profile would incorrectly estimate the shape of the nourished beach and would result in an underestimate of the volume required to obtain the design beach width in front of the seawall. In Figure V-4-15, the design profile is determined by translating the natural (healthy) profile shape seaward to obtain the design berm width in front of the seawall. Grain-size differences between the native beach and the fill material also must be considered in defining the design profile shape. If the median grain size of the fill is the same as that of the native beach, the design profile shape should be obtained by translating an average profile shape that represents locally healthy (sediment-rich) beach conditions. For example, given the same composite median grain sizes, the design profile for a beach with 30 m of added berm width is determined by translating the existing profile 30 m seaward between the elevation of the berm crest and the depth of closure, as shown in Figure V-4-14. When applying the profile translation method, the existing beach shape should be determined based on an average of multiple surveys to account for seasonal and/or alongshore variability in profile shape and to avoid including anomalous profile features in the design profile shape.

(a) When fill material is finer or coarser than the native sediment, the design beach profile shape should be estimated based on equilibrium profile concepts (see Part III-3-3-c for details on equilibrium beach profiles). According to equilibrium profile theory, coarser sand will produce a steeper design profile whereas finer sand will produce a profile with a gentler slope as illustrated in Figure V-4-16. Dean (1991) provides additional discussion of equilibrium beach profile concepts and their application. To estimate the design profile shape using equilibrium profile concepts, the average profile shape that represents locally healthy (sediment-rich) beach conditions should first be translated seaward a distance equal to the added berm width (see Figure V-4-14 and Figure V-4-15). To account for the difference in profile shape due to different composite sand sizes, the profile is translated an additional distance as a function of depth between the still-water level and depth of closure, based on differences in the theoretical equilibrium profile shapes as shown in Figure V-4-17. The added distance of translation W_{add} as a function of depth y is given by

$$W_{add}(y) = y^{3/2}\left[\left(\frac{1}{A_F}\right)^{3/2} - \left(\frac{1}{A_N}\right)^{3/2}\right] \tag{V-4-5}$$

where A_N is the A parameter for native sand and A_F is the A parameter for fill sand (see Table III-3-3 for values of the A parameter for different sand sizes). In Equation V-4-5, when the fill material is finer than the native sand, W_{add} is positive, which produces a design profile that is gentler in slope than the native profile. Conversely, for fill that is coarser than the native beach, W_{add} is negative which produces a steeper design profile. If the representative sediment-rich beach profile includes a bar, some smoothing in the bar region may be necessary. The BMAP software provides automated methods for estimating the design profile shape for different native and fill sand sizes based on Equation V-4-5, and for the same sand sizes using the uniform profile translation technique.

(5) Optimization of design profile. Optimization of the design profile involves selecting a range of design alternatives with different dune and berm dimensions, and evaluating the design alternatives together with the existing condition to determine the alternative that provides maximum net economic benefits. Storm-induced beach erosion modeling is the primary engineering analysis performed as part of the optimization process. Model simulations of profile response to a suite of historical or characteristic storms are performed for each alternative to assess erosion, flooding, and wave attack damages to shorefront property and infrastructure.

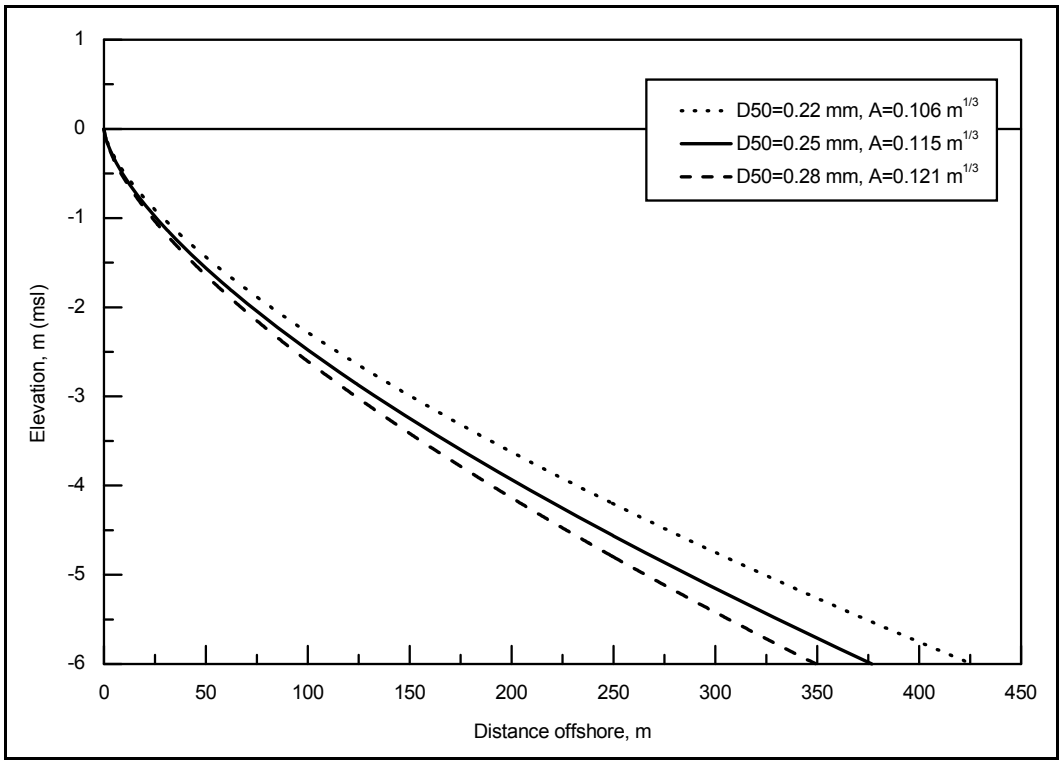

Figure V-4-16. Theoretical equilibrium profile shapes for different sand grain sizes

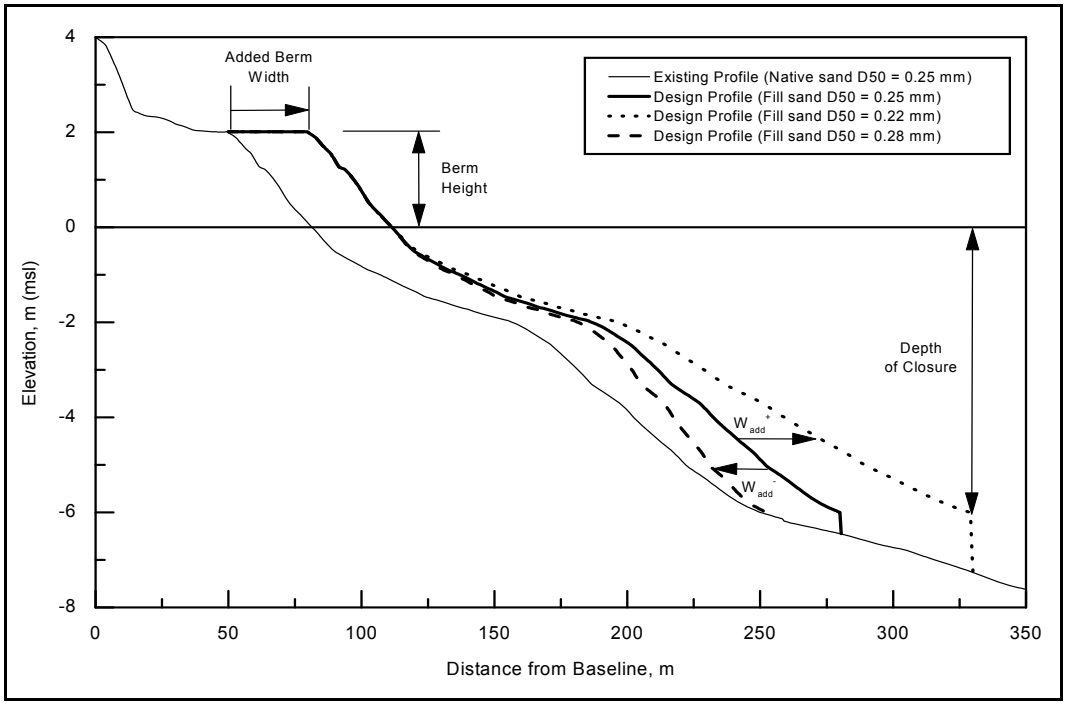

Figure V-4-17. Design profiles for different fill sand sizes

(a) Without-project condition.

- The existing or without-project condition is included in the optimization process to determine baseline damages. Morphologic features of the existing beach, such as dune height, berm width, and offshore profile shape, typically vary along the project study domain. To accurately estimate storm erosion response for the existing condition, a set of representative morphologic reaches should be developed to describe variations in profile shape along the project domain. The BMAP software can be used to define morphologic reaches by analyzing profiles, grouping similar profiles, and calculating an average representative profile for each reach.

- Profile characteristics that should be considered when developing morphologic reaches include dune height and width, berm width, nearshore and offshore profile slopes, sand grain size, presence of seawalls or other structures, and proximity to inlets. As part of the economic analysis to evaluate damages and benefits, the project domain is divided into a series of economic reaches based on value of property and infrastructure (see Part V-4-1-d). Boundaries of economic domains should also be considered in morphologic reach delineation to ensure that storm erosion modeling is consistent with the economic analysis.

(b) Storm selection.

- Evaluation of potential storm damages requires selection of a set of storms representative of future events that may impact the project area. The set of storms should reflect a range of intensities and frequencies of events consistent with the historical record. In developing the storm set, tropical and extratropical events should be treated distinctly because of differences in storm characteristics and frequencies of occurrence.

- One approach to storm selection has been to develop a set of storms characterized by peak surge return period ranging from frequent events (5-year return period or less) to extremely rare events (100-year return period). Peak surges for selected return periods are obtained from available stage-frequency information, and representative storm surge hydrographs are developed using assumed hydrograph shapes and durations. Differences in hydrograph shape between tropical and extratropical storms should be considered; tropical storms typically have much shorter durations. The storm surge hydrographs are combined with corresponding wave height and wave period time histories to fully describe the storms. Using this approach, the frequency of modeled responses are assumed to correspond to return periods of the input storm surges (e.g., a 50-year storm surge produces a 50-year erosion response). This assumption simplifies the analysis but is not strictly accurate because, in addition to peak storm surge, other factors influence the magnitude of erosion (storm duration, hydrograph shape, and wave characteristics). Inconsistencies may arise with this approach related to characterizing the storm based on peak surge alone. For example, a 20-year storm (where frequency is defined solely on maximum surge) may produce more erosion than a 50-year storm, if the 20-year storm has higher waves or a longer duration.

- An alternate and preferred approach is to develop a “training set” of storms by selecting events from historical records and/or hindcasts. A sufficiently long historical period is identified, such as 20 years for extratropical storms or 100 years for tropical storms. All historical events within the period exceeding a selected threshold are included in the training set. For example, all events which have a peak surge exceeding 0.3 m may be considered significant from a storm erosion standpoint and included in the training set. No return periods are assigned to storms in the training set a priori. Each storm is modeled for the existing condition and each project alternative to calculate corresponding erosion responses. Using the training set of storms and modeled responses, life cycle analyses are performed by employing the Empirical Simulation Technique (EST) to generate

frequency-of-occurrence relationships, whereby return periods are associated with storm responses rather than storm input. Scheffner and Borgman (1999) provide detailed guidance in applying the EST to coastal studies. Advantages of this approach are that it involves no arbitrary assignment of recurrence relationships and it utilizes historical rather than representative or hypothetical events to determine frequency-of-occurrence relationships. Part II discusses methods for estimated storm waves and water levels.

- Because water level is a primary factor controlling beach erosion, tide variations should be considered when developing the input storm set. Tide variations can be accounted for by combining storm surges with different tidal phases and ranges. For example, peak storm surges may be aligned with high tide, low tide, midtide preceding high tide, and midtide preceding low tide to generate four different but equally probable events derived from each base storm. Variations in tide ranges (neap, spring, and average) may also be considered in developing a full set of storms.

(c) Storm erosion modeling.

- Upon selection of design alternatives, characterization of the without-project condition, and selection of the storm set, storm-induced beach erosion modeling is performed to calculate parameters required for assessing economic damages based on beach erosion, flooding, and wave attack. The SBEACH model computes relevant storm response parameters such as recession distance, maximum water level and wave height at the shoreline, and wave runup. Required input to the model includes beach profiles describing the design alternatives and without-project condition, time-histories of storm water level, wave height and wave period, median sand grain size, and calibration parameters.
- Detailed examples and guidance for applying the SBEACH model to predict storm erosion are provided in the SBEACH technical report series (Larson and Kraus 1989; Larson, Kraus, and Byrnes 1990; Rosati et al. 1993; Wise, Smith, and Larson 1996; and Larson and Kraus 1998).

(d) Storm damage recurrence relationships and risk analysis. Modeled erosion responses are expressed in terms of frequency of occurrence for input to economic damage models. Typically, tropical and extra-tropical erosion responses are joined to generate a combined frequency curve spanning the recurrence intervals of interest. Risk and uncertainty of storm damage parameters can be addressed by developing mean-value frequency-of-occurrence curves together with confidence bands that indicate the variability or uncertainty associated with the calculated storm responses.

- The EST and supporting analysis tools can be used to calculate mean-value frequency curves and confidence bands. Figure V-4-18 shows an example of frequency-of-occurence relationships generated by the EST technique. The solid line represents the mean or expected value of beach recession as a function of return period, and the dashed lines show the 90 percent confidence band, indicating that 90 percent of variability in beach recession for a given return period falls within these limits.

(6) Cross-sectional fill volume requirements.

(a) A key quantity in beach-fill design is the volume of sand required to produce the desired beach cross-section. The design profile is determined using methods presented in Part V-4-1-f-(4) and results from the optimization process outlined in Part V-4-1-f-(5). The berm width is then increased to reflect the amount of advance nourishment needed to maintain the design profile prior to the first renourishment. The modified design profile shape, which includes advance nourishment, is then estimated

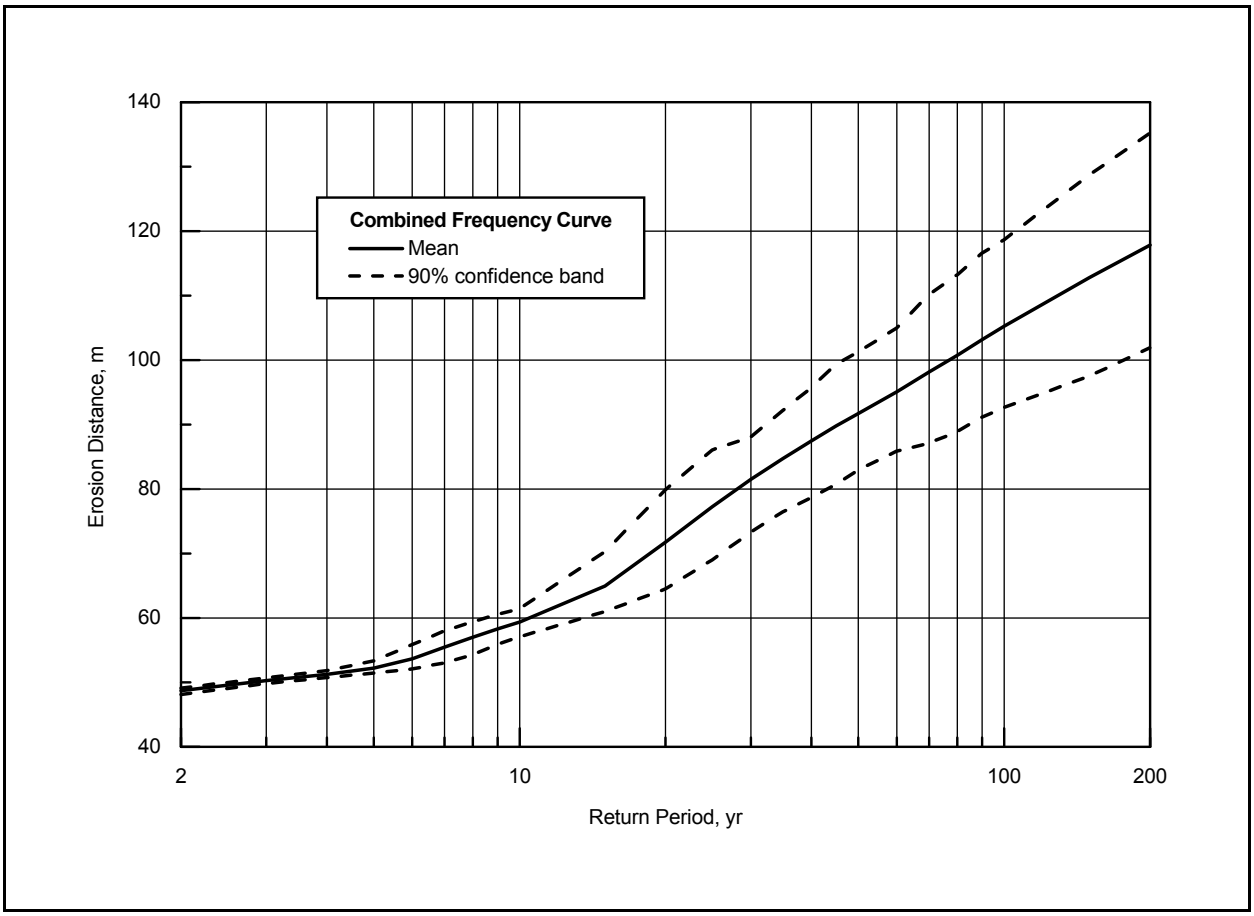

Figure V-4-18. Combined tropical and extratropical erosion-frequency curve

by translating the design profile at elevations between the design berm elevation and the depth of closure (see Figure V-4-14) by an amount equal to the advance nourishment berm width. The sectional fill volume required for initial construction (volume per unit length of shoreline) is calculated as the difference in cross-sectional area between the preproject profile and the modified design profile shape. Example V-4-2 illustrates calculation of sectional fill volume for a case where the preproject profile is in a severely eroded, unnatural, condition.

(b) Advance nourishment beach width, and design berm width, might not have uniform values from reach to reach within the project domain. Variations in the desired level of protection, assessment of long-term fill evolution and renourishment requirements, and consideration of the potential for hot spot formation, will most likely lead to alongshore differences in desired beach width. Therefore, the required sectional fill volume also will vary by reach. Volume calculations for the entire project domain are made by summing results on a reach-by-reach basis, where the volume requirement in a particular reach is calculated as the product of the cross-sectional volume requirement and the length of shoreline in that reach.

(c) For the case of a healthy (sediment-rich), preproject beach profile and a fill material that has a median grain size equal to that of the native beach sand, the volume V per unit length of shoreline required to produce a beach width W can be estimated by

$$V = W\left(B+D_C\right) \tag{V-4-6}$$

EXAMPLE PROBLEM V-4-2

FIND:

Volume per unit length of shoreline required to widen the dry beach by 30 m (at the msl datum), includes both the design berm and advance nourishment. Plot the existing profile and the final design profile.

GIVEN:

Preproject beach profile is not representative of healthy (sediment-rich) conditions.

Existing condition beach profile (Example Figure A).

Representative design beach profile reflecting healthy (sediment-rich) conditions (Example Figure B).

Berm height of 1.5 m and depth of closure of 5.5 m.

Native and fill sand median grain size are the same.

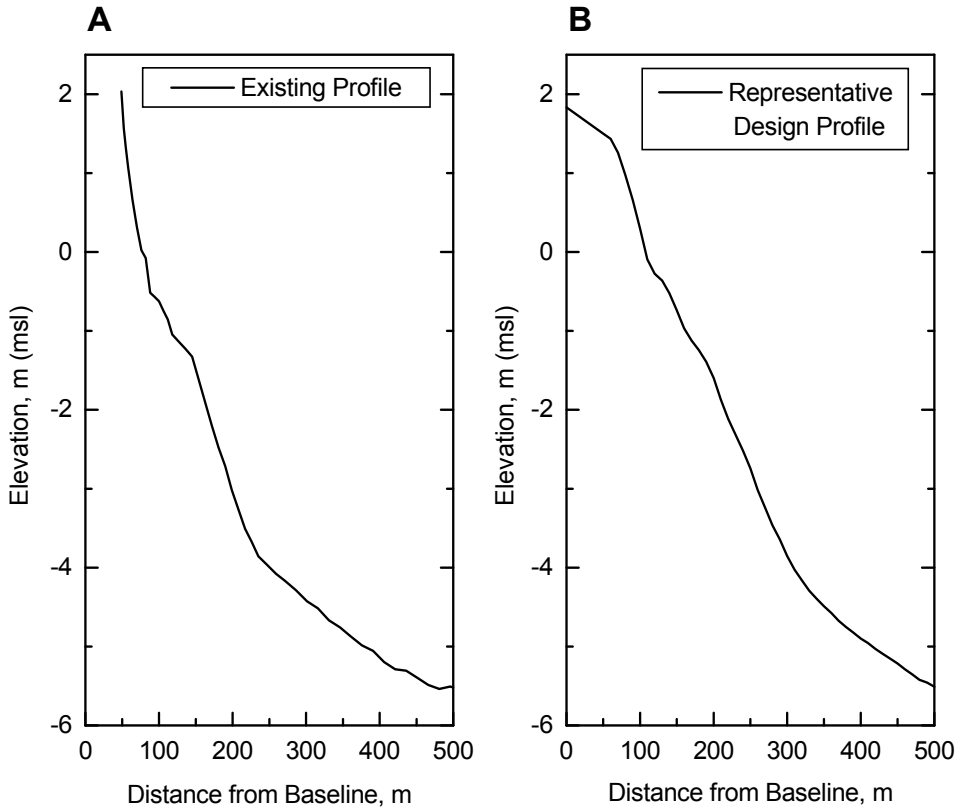

(Continued)

EXAMPLE PROBLEM V-4-2 (Continued)

SOLUTION:

Step 1; Compute sediment deficit volume in existing profile.

Align existing and representative design profile at MSL datum. Compute volume difference between existing and representative design profiles. This volume represents the sediment deficit between the existing condition and the healthy or sediment-rich condition expected to occur after nourishment. The elevation at which the existing and design profiles are aligned will influence the magnitude of the computed profile sediment deficit. In the present example the MSL datum is selected because here beach width is defined relative to this datum. The sediment deficit in the pre-project profile can vary significantly along the project reach. The computed pre-project sediment deficit in the beach profile is 100 m^3/m in this example and is illustrated in Example Figure C. The data manipulations and calculations discussed in this example are automated within the BMAP software (Sommerfeld et al. 1994).

C

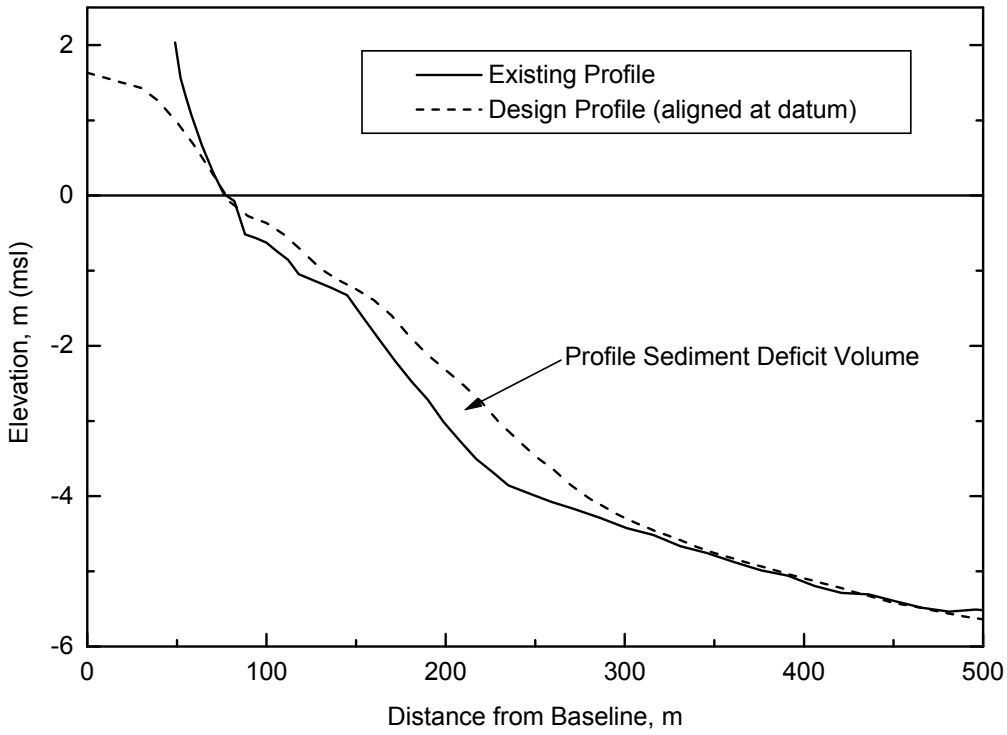

(Continued)

EXAMPLE PROBLEM V-4-2 (Concluded))

Step 2; Compute required sectional fill volume.

Translate the aligned design profile (from Step 1) 30 m seaward to obtain the final design profile. Compute volume difference between the existing and final design profile between the 1.5-m berm elevation and the 5.5-m depth of closure. This volume represents the total sectional fill volume required to advance the dry beach 30 meters seaward at the msl datum. The total sectional fill volume can vary significantly from reach to reach. In the present example, the total sectional fill volume is 298 m^3/m and is illustrated in Example Figure D. Approximately one-third of the total sectional volume was required to offset the sediment deficit associated with the over-steepened erosion-stressed condition of the existing profile.

D

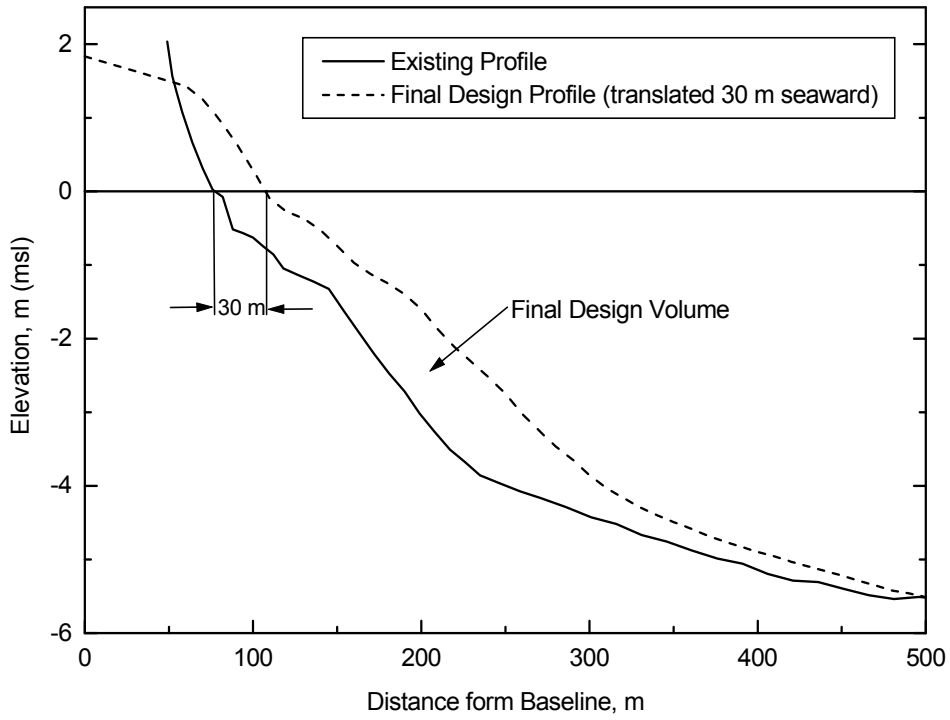

where

B = the design berm elevation

D_C = the depth of closure

Equation V-4-6 is derived by computing the area of the parallelogram formed by translating the existing profile a distance W as shown in Figure V-4-14. Example V-4-3 illustrates this calculation.

EXAMPLE PROBLEM V-4-3

FIND:

Sectional fill volume (fill volume per unit length of shoreline) required to widen the dry beach by 30 m.

GIVEN:

Preproject beach profiles are representative of healthy (sediment-rich) conditions.
Berm height of 2.5 m and depth of closure of 6 m.
Fill material (composite median diameter) same as native beach sand.

SOLUTION:

Equation V-4-6 gives

$$V = 30(2.5 + 6) = 255\ m^3/m$$

(d) Sectional volume computations in situations when the fill and native sediments differ should be made by considering differences between the existing profile and the design profile shape as outlined in Part V-4-1-f-(4) and illustrated in Figure V-4-17. The BMAP software provides capabilities for calculating sectional fill volume in cases where native and fill sediments differ in median grain size.

(e) Equilibrium profile concepts also can be used directly to make preliminary estimates of required fill volume, when the native and fill sediments have differing composite median grain sizes. While not recommended for final fill volume computations, these methods provide valuable insight regarding the implications of using fill material with different grain size characteristics. Dean (1991) defines three basic types of nourished profiles. Figure V-4-19 shows an intersecting profile, where the profile after nourishment intersects the native profile at a depth shallower than the depth of closure; a nonintersecting profile, where the nourished profile does not intersect the native profile before closure depth; and a submerged profile, where after equilibrium there is no dry beach. A submerged profile is a special case of a nonintersecting profile which occurs when insufficient volume is placed to fully develop the underwater equilibrium profile. Dean (1991) shows that whether a profile is intersecting or nonintersecting is determined by the following inequality:

$$W\left(\frac{A_N}{D_C}\right)^{3/2} + \left(\frac{A_N}{A_F}\right)^{3/2} \begin{cases} < 1, & \text{Intersecting profile} \\ > 1, & \text{Nonintersecting profile} \end{cases} \qquad \text{(V-4-7)}$$

- For fill material different from the native beach sand, cross-sectional volume requirements should be estimated with consideration given to the differences in profile slope given by equilibrium profile concepts. Based on theoretical equilibrium beach profile shapes, where A_N and A_F are the A parameters for native and fill sands, respectively (see Table III-3-3 for values of the A parameter for different sand sizes), fill sand that is finer than the native material will always produce a nonintersecting profile according to Equation V-4-7. Fill sand that is coarser than native sand may

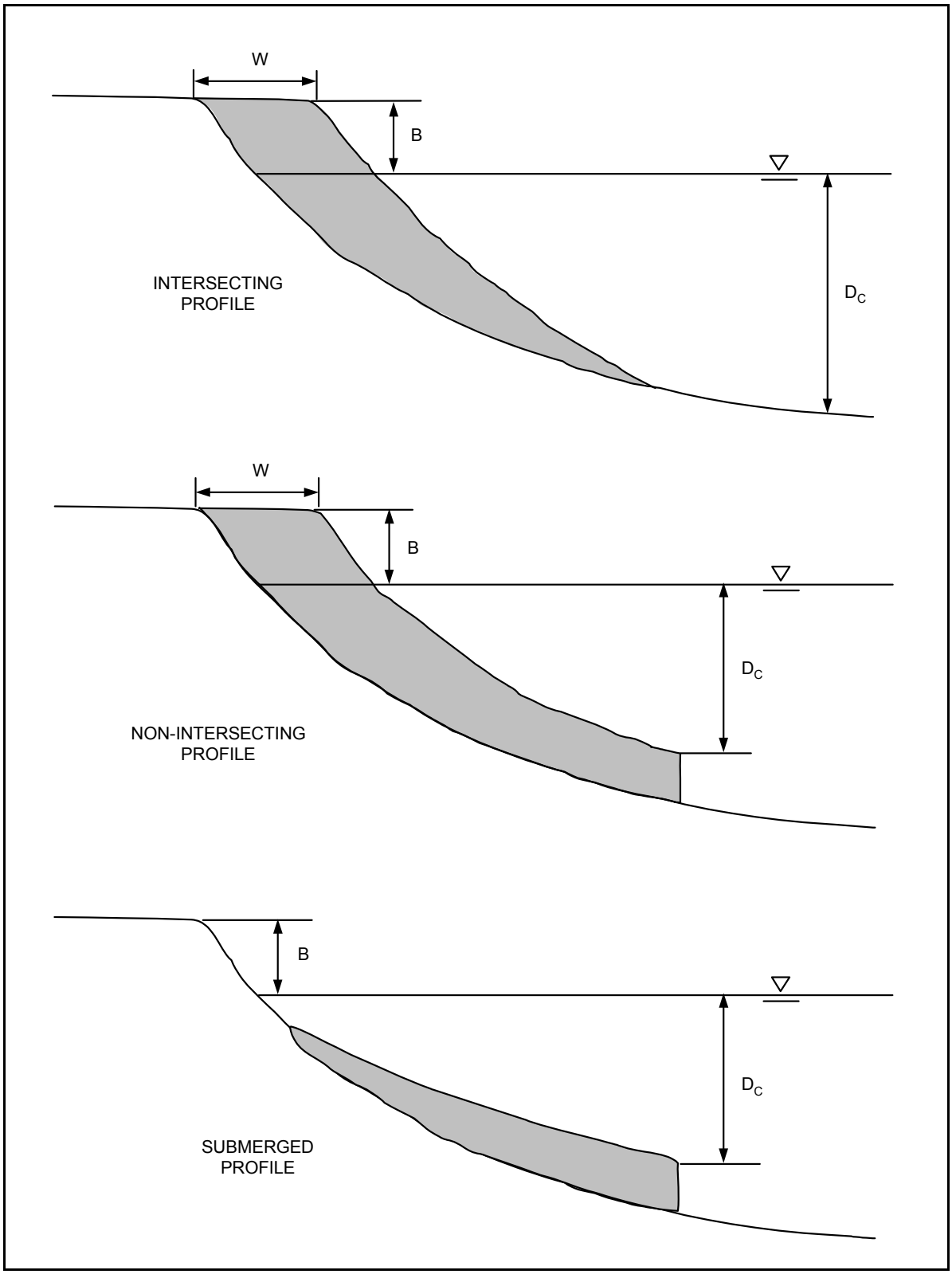

Figure V-4-19. Three basic types of nourishment profiles (adapted from Dean 1991)

produce either an intersecting or a nonintersecting profile. For a nonintersecting profile, the volume of sand per unit length of shoreline that must be placed before there is any dry beach after equilibrium is estimated as

$$V = \frac{3}{5}\left(\frac{D_C}{A_F}\right)^{5/2}\left(A_N - A_F\right) \tag{V-4-8}$$

- If the volume placed is less than that given by Equation V-4-8, a submerged profile is produced after equilibration. Example V-4-4 illustrates volume calculations using Equation V-4-8.

- For nonintersecting profiles with a dry beach after equilibrium (i.e., volume placed is equal to or exceeds that in Equation V-4-8) the volume per unit length of beach required to produce a dry beach of width W may be estimated as

$$V = WB + \frac{3}{5}\left(\frac{D_C}{A_F}\right)^{5/2}\left(A_N\left[1 + W\left(\frac{A_F}{D_C}\right)^{3/2}\right]^{5/3} - A_F\right) \tag{V-4-9}$$

Example V-4-5 illustrates volume calculations using Equation V-4-9.

For intersecting profiles, the volume per unit length of beach required to advance the beach a distance W after equilibriation can be estimated by

$$V = WB + \frac{\frac{3}{5}W^{5/3}A_N A_F}{\left(A_F^{3/2} - A_N^{3/2}\right)^{2/3}} \tag{V-4-10}$$

- It is noted that the depth of closure does not enter Equation V-4-10, because by definition, the nourished profile intersects the native profile landward of the depth of closure (see Figure V-4-19). Example V-4-6 illustrates volume calculations using Equation V-4-10.

- Equilibrium profile methods do not account for a sediment deficit in the preproject beach profile, which is common along erosion-stressed shorelines where beach nourishment projects are typically considered. The methods also only account for volume below the berm elevation. Volume contained in the dune must be added to the estimate. These methods are recommended for quick calculations, and to compliment calculations based on differences between preproject profile shapes and design profiles. They are not recommended for use in computing final sectional fill volume estimates.

- A third method for computing sectional fill volume when fill and native sediments have different grain size characteristics is to translate the healthy, sediment-rich, design profile as shown in Figures V-4-14 and 15, calculate the volume using Equation V-4-6 , and then apply the overfill factor to the volume determined from profile translation (see Part V-4-1-e-(3i) and Example V-4-1). The overfill factor would also be applied to any advance renourishment volume. Dune volume must be

EXAMPLE PROBLEM V-4-4

FIND:

Sectional fill volume that must be placed before any dry beach width is added after equilibrium. Disregard any volume necessary to makeup for a preproject sediment deficit in the beach profile.

GIVEN:

Berm height of 2.5 m and depth of closure of 6 m. Native sand median grain size of 0.26 mm and fill sand median grain size of 0.19 mm.

SOLUTION:

Values of the A parameter for native and fill sand are read from Table III-3-3.

$A_N = 0.117\ m^{1/3}$, $A_F = 0.097\ m^{1/3}$

Profile is nonintersecting because $A_F < A_N$, therefore Equation V-4-8 is applicable.

Equation V-4-8 gives

$$V = \frac{3}{5} \cdot \left(\frac{6}{0.097} \right)^{5/2} \cdot (0.117 - 0.097) = 361\ m^3/m$$

This illustrates that when filling with sand finer than the native beach material, a significant amount of sand must be placed before any dry beach width is produced after equilibrium. Note that the sectional fill volume is 140 percent of the sectional fill volume computed in Example V-4-3, and the present example will produce no additional dry beach width whereas 30 m of additional dry beach width is obtained in Example V-4-3.

added. The overfill method can compliment calculations made using the other methods, but it is not recommended for final fill volume computations.

g. Evaluating project longevity

The longevity of a beach nourishment project is primarily determined by the degree to which the placed sand volume addresses any preproject profile volume deficit, and the rate at which fill material is transported out of the project domain in the alongshore direction, i.e, lateral spreading losses. Wave-driven longshore sand transport processes are the major cause of lateral spreading. Projects tend to be built in erosional areas where waves act to move sand out of the project domain, in a long-term, net sense. In addition to the wave climate and its interaction with the local morphology, there is another important aspect of lateral spreading. The project itself creates a perturbation in shoreline and beach orientation, particularly where the fill transitions into the adjacent beaches. At these transitions, local wave transformation patterns and consequently the longshore sand transport regime are altered, which can lead to high rates of fill loss from the ends of the project (often called end losses). Coastal structures that exist within the project domain, or are built as part of the project, also can impede alongshore sand movement and influence the rate of sand loss. Grain size characteristics of the fill material may be a factor in determining beach-fill longevity. Part III discusses dependency of longshore sand transport on grain size. However, in practice, the role of grain size is not usually considered in evaluating lateral spreading losses.

EXAMPLE PROBLEM V-4-5

FIND:

Volume per unit length of shoreline required to widen the dry beach by 30 m. Disregard any volume necessary to makeup for a preproject sediment deficit in the beach profile.

GIVEN:

Berm height of 2.5 m and depth of closure of 6 m. Native sand median grain size of 0.27 mm and fill sand median grain size of 0.18 mm.

SOLUTION:

Values of the A parameter for native and fill sand are read from Table III-3-3.

$A_N = 0.119\ \text{m}^{1/3}$, $A_F = 0.094\ \text{m}^{1/3}$

Profile is nonintersecting because $A_F < A_N$, therefore Equation V-4-9 is applicable.

Equation V-4-9 gives

$$V = 30 \cdot 2.5 + \frac{3}{5} \cdot \left(\frac{6}{0.094} \right)^{5/2} \cdot \left(0.119 \cdot \left[1 + 30 \cdot \left(\frac{0.094}{6} \right)^{3/2} \right]^{5/3} - 0.094 \right) = 796\ \text{m}^3/\text{m}$$

By comparing with Example V-4-3, it is seen that using the finer material specified in this example requires 3.1 times the volume required using compatible material to generate the same equilibrium beach width. This example illustrates that much higher fill volumes are required when using finer-than-native sand to obtain a given beach width, which is consistent with sand compatibility calculations performed using the overfill ratio (see Example V-4-1).

Although alongshore spreading of fill material represents a loss to the project area, this material is in most cases transported to adjacent beaches. Nearby beaches, particularly those downdrift of the project, realize protective benefits from the neighboring project. Over the life of a beach nourishment project, adjacent beach benefits can be quite significant. If the project is built adjacent to an inlet with navigation channels, the impact of the nourishment project on channel operation and maintenance should be assessed.

(1) Periodic renourishment. Beginning immediately after construction, fill material will be lost from the project due to lateral spreading. Periodic renourishment will be required to maintain the desired beach cross section. It should be recognized by the designer that year-to-year loss rates can deviate from the long-term average erosion rates. In addition to end effects at transitions, losses are significantly influenced by the occurrence of major storms. Annual losses will likely vary from year to year because of the dependency on storm activity. Therefore, while an average renourishment interval and quantity can be estimated, the actual

EXAMPLE PROBLEM V-4-6

FIND:

Volume per unit length of shoreline required to widen the dry beach by 30 m. Disregard any volume necessary to makeup for a preproject sediment deficit in the beach profile.

GIVEN:

Berm height of 2.5 m and depth of closure of 6 m. Native sand median grain size of 0.27 mm and fill sand median grain size of 0.36 mm.

SOLUTION:

Values of the A parameter for native and fill sand are read from Table III-3-3.

$A_N = 0.119\ m^{1/3}$, $A_F = 0.137\ m^{1/3}$

Determine whether profile is intersecting or nonintersecting.

Equation V-4-7 gives

$$30 \cdot \left(\frac{0.119}{6}\right)^{3/2} + \left(\frac{0.119}{0.137}\right)^{3/2} = 0.893 < 1$$

therefore, the profile is intersecting and Equation V-4-10 is applicable.

Equation V-4-10 gives

$$V = 30 \cdot 2.5 + \frac{\frac{3}{5} \cdot 30^{5/3} \cdot 0.119 \cdot 0.137}{\left(0.137^{3/2} - 0.119^{3/2}\right)^{2/3}} = 137\ m^3/m$$

By comparing with Example V-4-3, it is seen that using the coarser fill material specified in this example requires approximately 45 percent less volume than that required using compatible material, to generate the same equilibrium beach width.

required interval/quantity will vary depending on the climatic conditions that occur. Ideally, the need for renourishment will be determined by monitoring performance of the fill. Some level of renourishment, or maintenance such as redistribution of sand within the project domain, is needed when the project design cross section is no longer in place. In this situation, the desired level of protection is compromised. However, the schedule for periodic renourishment may be more fixed, in the sense that budgeting for it may have been set at the outset of the project. If renourishment is needed before the scheduled time, it can be handled as an emergency maintenance action (see Part V-4-1-m). Should permanent changes to the periodic renourishment cycle (volume and/or frequency) be necessary, a reformulation of the project may be needed. Having an adequate project monitoring plan in place is very important. Monitoring data are particularly valuable if the project does not perform as designed. The data can be analyzed to evaluate the nature of the conditions that prompted the need for unexpected renourishment and assess their frequency of occurrence. Analysis of the

monitoring data also can shed light on a design deficiency. Monitoring and analysis of data are discussed in more detail in Part V-4-1-l.

(2) Advance nourishment. Advanced nourishment is the volume of sand that is placed for "sacrificial" purposes during initial construction to maintain the design fill section during the initial renourishment interval (i.e., the time from project completion to the first scheduled renourishment). The magnitude of the advance nourishment should be determined based on results from work done to assess lateral spreading losses and volumetric losses due to long-term shoreline recession, i.e., the historic or background erosion rate. The postproject shoreline erosion rate will be greater than the preproject historic or background erosion rate in those cases where the preproject beach featured a sediment deficit or was otherwise sediment starved. For example, project reaches that feature an armored shoreline may historically exhibit little or no erosion, but can exhibit significant background erosion when replenished with sand fill. Advanced nourishment quantities are included in the initial total construction volume.

(3) Fill parameters affecting lateral spreading. Both simple and detailed methods are available for estimating the rate of alongshore spreading, and identifying renourishment requirements (both volume and interval). Simple methods treat the incident wave climate in a more approximate manner, through use of a representative wave height and neglecting wave direction. They consider the background erosion rate as an input parameter, and they assume the erosion rate is uniform over the project domain. Simple methods are generally most applicable to cases that do not involve coastal structures. On the other hand, detailed methods treat the effects of coastal structures and wave climate more rigorously. They address the issue of alongshore variation in wave conditions that produce the background erosion rates, as well as alongshore variations in erosion rates within the project bounds. Detailed methods treat the directionality of the wave climate. Dominant wave directions become important for projects constructed in the vicinity of engineered structures, littoral barriers, or sediment sinks, such as inlets. Detailed methods consider the actual planform layout of the shoreline and structures, whereas simple methods represent them in an idealized manner. In this section, analytical solutions to the one-line theory of shoreline evolution are examined to reveal the importance of the following beach nourishment design parameters on lateral spreading losses: length of the nourishment project, incident wave climate, and ambient background erosion. The analytical approach is extremely useful in preliminary design and to gain an understanding of the relative importance of these parameters. Detailed methods are also presented later, which rely on the use of numerical models to evaluate project longevity.

(a) Effect of fill length.

- In this section, the effect of beach-fill length (the alongshore extent of the fill) on project longevity will be examined. The influence of length is best illustrated by considering the most simple case of an initially rectangular beach fill constructed on a long straight beach with no background erosion. This situation was first introduced in Part III-2 of this manual where the linearized equation of longshore sediment transport was combined with the equation of continuity to develop the one-line theory of shoreline evolution (see Equations III-2-25 and III-2-26). A number of analytical solutions to this equation were presented. In this section, Equations III-2-31 and III-2-32 will be examined further to extract additional information pertinent to beach nourishment design. Upon close examination of Equation III-2-31 it is seen that the important parameter is

$$\frac{a}{2\sqrt{\varepsilon t}} \tag{V-4-11}$$

where a is one-half the length of the rectangular project, ϵ is the "shoreline diffusivity" parameter defined in Equation III-2-26, and t is time. Here it is seen that if the quantity in Equation V-4-11 is the same for two

different projects their planform evolution would be the same. However, if two projects were exposed to the same wave climate but had different alongshore lengths, then the project with the greatest length would be predicted to last longer (with all other factors being the same). In fact, according to Equation III-2-32 the longevity of a project varies as the square of its length. If more than 50 percent of the placed beach-fill volume remains within the placement area ($0.5<p(t)<1.0$), Equation III-2-32 can be approximated using the following relationship (with an accuracy of ±15 percent).

$$p(t) = 1 - \frac{\sqrt{\varepsilon t}}{a\sqrt{\pi}} \tag{V-4-12}$$

- Example Problem V-4-7 illustrates the importance of project length on project longevity. In this example, a fill with twice the length will last four times as long. The effect of project length on fill longevity is critical for short fills. It is also important in long fills which may be built in stages. For example, construction may be limited to a particular season to avoid turtle nesting season or the tourist season. Therefore it may take 2 or 3 years to complete the work. Projects built in stages will temporarily perform as short fills until the other portions of the project are completed. Actual loss rates from the constructed subreaches will likely exceed losses predicted for the completed as designed project. Any short-term accelerated losses due to construction of the project in stages should be factored into the advance nourishment quantity.

(b) Effect of wave environment.

- The rate of alongshore spreading losses is also a function of the incident wave climate. In Equation III-2-26 it is seen that the shoreline diffusivity term (ϵ) varies inversely with the breaking wave height raised to the 5/2 power. Dean and Yoo (1992) present a method for calculating a representative wave height and period based on assumptions of Rayleigh-distributed wave height, shallow-water linear-wave theory, simplified and linearized wave refraction and shoaling relations, and a constant proportionality between breaking wave height and corresponding water depth. Use of an effective wave height is recommended in the calculation of the shoreline diffusivity term (ϵ). Dean and Yoo (1992) defined the effective wave as one that produces the same spreading of the beach nourishment material as the actual time-varying wave conditions (expressed as pairs of height and period). They provided the following equation to calculate the effective wave height, H_{eff},

$$H_{eff} = \left(\frac{\frac{1}{N}\sum_{n=1}^{N} (K_s H_s^n)^{2.4} \frac{\left(C_{go}^n\right)^{1.2}}{C_*^n}}{\frac{1}{N}\sum_{n=1}^{N} \frac{\left(C_{go}^n\right)^{1.2}}{C_*^n}} \right)^{\frac{1}{2.4}} \tag{V-4-13}$$

where K_s is the proportionality factor between significant deepwater wave height and effective deepwater wave height and is equal to 0.735 (Dean and Yoo 1992), H^n_s is the significant wave height of the n^{th} record in the time series of N wave records, C^n_{go} is the deepwater wave group speed of the n^{th} record, and C^n_* is the wave celerity at breaking of the n^{th} record. The effective wave period T_{eff} is defined as the period corresponding to the expression in the denominator.

EXAMPLE PROBLEM V-4-7

FIND:

The "half-life" of the specified beach fills (time at which 50 percent of the beach-fill material remains within the placement area).

GIVEN:

Both projects have a rectangular planform and differ only in alongshore length. Beach fill A has an alongshore length of 3 km, whereas beach fill B has an alongshore length of 6 km. Both projects are subjected to the same wave environment.

Assume:

$K = 0.77$	$\rho_s/\rho = 2.65$
$H_b = 0.95$ m	$n = 0.4$
$C_{gb} = (g\ h_b)^{1/2}$	$d_b = 2.5$ m
$h_b = H_b/0.78$	$d_c = 6.0$ m
$g = 9.81$ m/s^2	

SOLUTION:

Equation III-2-26 gives

$$\epsilon = \frac{0.77(0.95)^{2.5}\sqrt{9.81/0.78}}{8} \cdot \frac{1}{(2.65-1)} \cdot \frac{1}{(1-0.4)} \cdot \frac{1}{(2.5+6.0)} = 0.03568\ \frac{m^2}{sec}$$

Solving Equation V-4-12 for t and p(t) = 0.5 gives

$$t_{50\%} = \frac{a^2 \pi}{4 \epsilon}$$

Half-life of beach fill A

$$t_{50\%} = \frac{(1500)^2 (3.14)}{(4)(0.03568)} = 49.526 X 10^6 \text{ sec} \cong 1.57 \text{ years}$$

Half-life of beach fill B

$$t_{50\%} = \frac{(3000)^2 (3.14)}{(4)(0.03568)} = 198.102 X 10^6 \text{ sec} \cong 6.28 \text{ years}$$

- Example Problem V-4-8 illustrates the relative importance of the breaking wave height on the expected longevity of a beach-fill project, with all other factors being equal. In this example, a 19 percent increase in breaking wave height resulted in a 35 percent decrease in the project's half-life, which is a measure of fill longevity.

- Differences in longevity are even more pronounced if greater differences in breaking wave height are considered. For example, if the average summer breaking wave height at the project site is 0.6 m, and the average winter breaking wave height is 1.2 m, one would expect that loss rates to be much higher in the winter compared to those in the summer (because of the diffusivity parameter dependence on breaking wave height raised to the 2.5 power). Many beach-fill projects are built during the winter season. The strong dependence of longevity on wave environment helps explain the high rates of lateral spreading loss that can occur during the winter season.

(c) Effect of background shoreline recession.

- The effect of project length and the incident wave environment have been shown to have a significant influence on expected project longevity. The analysis presented to this point has not considered losses due to ambient coastal processes, such as a gradient in the longshore sand transport rate, which tends to produce background erosion at the project site. Equation V-4-12 can be modified to include the effect of a uniform background shoreline recession rate, E , as follows:

$$p(t) = 1 - \left(\frac{\sqrt{\epsilon t}}{a\sqrt{\pi}} + \frac{Et}{\Delta y_o} \right) \qquad 0.5 < p(t) < 1.0 \tag{V-4-14}$$

- Solving Equation V-4-14 for time t yields an expression that predicts the time required for a fraction (1-p) of the material placed to be lost from the project area (or equivalently the time at which a fraction p of the material placed remains in the project area). This expression is provided as

$$t_p = \frac{-m - \sqrt{m^2 - 4ln}}{2l} \qquad for\ \sqrt{\epsilon t}/a < 1.0 \tag{V-4-15}$$

in which

$$l = \left(\frac{E}{\Delta y_o} \right)^2$$

$$m = \frac{2E(p-1)}{\Delta y_o} - \frac{\epsilon}{\pi a^2}$$

and

$$n = (1-p)^2$$

EXAMPLE PROBLEM V-4-8

FIND:

The "half-life" of the specified beach fills (time at which 50 percent of the beach-fill material remains within the placement area).

GIVEN:

Both projects have a rectangular planform with an alongshore length of 6 km. The effective breaking wave height at beach fill A is 0.80 m whereas the effective breaking wave height at beach fill B is 0.95 m.

$K = 0.77$	$\rho_s/\rho = 2.65$	$C_{gb} = (g\ h_b)^{1/2}$	$n = 0.4$
$h_b = H_b/0.78$	$g = 9.81\ m/s^2$	$d_b = 2.5\ m$	$d_c = 6.0\ m$

SOLUTION:

Equation III-2-26 gives: (for beach fill A)

$$\epsilon = \frac{0.77(0.80)^{2.5}\sqrt{9.81/0.78}}{8} \cdot \frac{1}{(2.65-1)} \cdot \frac{1}{(1-0.4)} \cdot \frac{1}{(2.5+6.0)} = 0.02322\ \frac{m^2}{sec}$$

(for beach fill B)

$\epsilon = 0.03568\ m^2/sec$ (see EXAMPLE PROBLEM V-4-7)

Solving Equation V-4-12 for t and p(t) = 0.5 gives

$$t_{50\%} = \frac{a^2 \pi}{4 \epsilon}$$

Half-life of beach fill A

$$t_{50\%} = \frac{(3000)^2 (3.14)}{(4)(0.02322)} = 304.420 \text{X} 10^6\ sec \cong 9.65\ years$$

Half-life of beach fill B

$$t_{50\%} = \frac{(3000)^2 (3.14)}{(4)(0.03568)} = 198.102 \text{X} 10^6\ sec \cong 6.28\ years$$

where Δy_o is the initial dry beach width (after cross-shore equilibration), E is the historical shoreline recession rate and a is the beach-fill half length. Example Problem V-4-9 illustrates the effect of background erosion rate. Comparison of results from this example with results from Example V-4-7 show that the specified background erosion rate decreased the half-life of the fill by about 20 percent. Note that the historical shoreline erosion rate E, may underestimate the postnourishment erosion rate if the preproject beach is armored or otherwise features a deficit in sand volume or sand supply.

EXAMPLE PROBLEM V-4-9

FIND:

The approximate time required for 50 percent of the placed beach fill volume to be lost from the placement area due to alongshore spreading and a background shoreline recession rate of 0.5 m/year.

GIVEN:

Assume the planform of the beach fill is initially rectangular with an alongshore length of 6 km and an estimated offshore width of 50 m (after equilibration).

Assume:	$K = 0.77$	$h_b = H_b/0.78$	$n = 0.4$
	$H_b = 0.95$ m	$g = 9.81$ m/s^2	$d_b = 1.5$ m
	$C_{gb} = (g\ h_b)^{1/2}$	$\rho_s/\rho = 2.65$	$d_c = 6.0$ m

SOLUTION:

Equation III-2-26 gives $\epsilon = 0.03568$ m^2/sec (see EXAMPLE PROBLEM V-4-7)
Equation V-4-15 gives

$$l = \left(\frac{E}{\Delta y_o}\right)^2 = \left(\frac{0.5}{50}\right)^2 = 0.0001 \text{ years}^{-2}$$

$$m = \frac{2E(p-1)}{\Delta y_o} - \frac{\epsilon}{\pi a^2} = \frac{(2)(0.5)(.5-1)}{50} - \frac{0.03568}{(3.14)(3000)^2}(31.536 \text{X} 10^6) = -0.04980 \text{ years}^{-1}$$

$$n = (1-p) = (1-.5)^2 = 0.2500$$

and

$$t_{50\%} = \frac{-m - \sqrt{m^2 - 4ln}}{2l} = \frac{0.04980 - \sqrt{(0.04980)^2 - (4)(0.0001)(0.2500)}}{(2)(0.0001)} \cong 5.07 \text{ years}$$

(4) Shoreline change modeling to estimate advance fill and renourishment requirements. In detailed design, one-line numerical models of shoreline evolution such as the GENEralized model for SImulating Shoreline Change model (Hanson 1987; Hanson and Kraus 1989) are typically used to provide more realistic estimates of project longevity and renourishment requirements than may be possible using the analytical approach discussed previously. Numerical shoreline change models provide the designer with an objective tool for evaluating a variety of potential project design alternatives, which may involve coastal structures in addition to beach fill. The use of numerical models of shoreline evolution for the design, optimization, and comparative evaluation of competing project alternatives has many advantages over the use of the analytical approach. For example, the GENESIS model allows examination of multiple renourishment cycles leading to a complete project life cycle, the effects of beach-fill stabilization structures, the effects of many possible future wave conditions (as defined by the Wave Information Study (WIS) wave hindcast) leading to a suite of possible future shoreline conditions. The numerical approach allows for the evaluation of the project design and its performance within the context of a realistic sediment budget developed for the project reach. Employing a shoreline change model like GENESIS allows the designer to examine project performance under conditions much more representative of the actual project setting than is possible with the analytical approach, and is therefore the recommended approach for final design of major projects.

(a) Simple model application.

- In this section, the GENESIS model is applied in a simplified manner to simulate the evolution of an idealized beach-fill project, throughout an anticipated 50-year project life, to investigate the design issues of advance fill and renourishment requirements. The hypothetical project is 6 km (3.7 miles) long with a design berm width of 20 m (65 ft). Two series of model simulations were performed for each of four renourishment intervals, 3, 5, 7, and 9 years. The first series of simulations were for a hypothetical condition where the project shoreline was subjected to no ambient or background erosion. The second series of simulations were for a project shoreline experiencing a background erosion rate of 0.5 m/year. All simulations were made for the entire 50-year project life. Note that the 3-year renourishment cycle project was simulated as a series of fifteen 3-year cycles plus one 5-year cycle beginning in project year 45. Likewise, the 7-year renourishment cycle project was simulated as a series of six 7-year cycles plus one 8-year cycle, and the 9-year renourishment cycle project was simulated as a series of five 9-year cycles plus one 5-year cycle.

- In the execution of the simulations, the computed shoreline position at the end of each renourishment cycle was used to define the initial shoreline position at the beginning of the next renourishment cycle, except of course in the project area where the required renourishment fill volume was placed with tapered transitions to the existing shoreline adjacent to the project. The incident wave climate was specified as an effective wave condition that approached the project normal to the shoreline and did not change throughout the simulation. The average berm height and depth of closure were specified to be 1.5 and 6 m, respectively, for a total active depth of 7.5 m. The preproject shoreline was straight. The initial construction planform included 2-km-long transitions to the preproject shoreline position adjacent to the project limits, which were added to reduce the rate of end losses from the project. The model was then run for the first renourishment interval, an appropriate nourishment volume was added, the model was run for another renourishment interval, and so on, until the 50-year life was reached. Each prenourishment shoreline within the project limits was advanced seaward a sufficient distance so that the predicted shoreline position at the end of the renourishment cycle was 20 m seaward of the preproject shoreline at all locations within the project, except within 400 m in from both ends of the 6-km-long project. That is, the design width was allowed to be violated only at the lateral limits of the project, and for an alongshore distance of only 400 m. The results of these model simulations bring to light a number of important considerations with respect to beach-fill design.

Plots of the placed advanced fill and renourishment volume throughout the life of each of the projects simulated are shown in Figure V-4-20. Volumes shown in this plot exclude the design fill volume of 960,000 cu m contained within the project limits and small 400-m transitions at the ends of the project. The volume values include the volume contained in the transition zones that are constructed initially, and advance nourishment placed within the project limits needed to see that the design width is not compromised during the first renourishment cycle. As can be seen in Figure V-4-20a, in the absence of background erosion, the required renourishment volume is expected to decrease slightly over the life of the project. With a background erosion rate of 0.5 m/year the required renourishment volume is seen to remain nearly constant throughout the project life. Most project sites experience background erosion.

- Results indicate that the advance fill volumetric requirement is nearly twice the volumetric requirement of subsequent renourishments, and nearly three times as much for the shortest renourishment interval, or 3 years. The advance fill volume includes the volume initially placed in the transition sections. The explanation for this result is that a substantial volume of material is required to provide a natural transition from the adjacent shorelines to the more seaward-advanced project shoreline. This volume of material is required at the time of initial construction, as part of the advanced fill. Without the transition sections, high end losses at the project transitions would have compromised the design berm width over a significant length of the lateral portions of the project. Subsequent renourishments do not require this additional volume because the adjacent beaches are already prograded toward the design beach width. Part V-4-1-h examines the subject of fill transitions in more detail.

- Figure V-4-21 provides plots of the cumulative volume placed for each of the beach nourishment projects simulated. Results indicate that the cumulative beach nourishment volume requirement for a 50-year project life is nearly the same regardless of the renourishment cycle (at least for the renourishment intervals tested, which span the typical range of most beach-fill projects). A detailed examination of the model output indicates that the average annual rate of loss of sand from the project area increases only slightly as the renourishment cycle increases (3 or 4 percent difference between annual loss rates for 3- and 9-year renourishment cycles). Selection of a renourishment cycle for Federal projects is made through an optimization process that optimizes the amortized initial construction costs and the annual cost of periodic renourishment to minimize the total average annual equivalent cost. Selection of renourishment volumes/intervals is typically done based on average expected losses over the life of the project. Selecting a longer renourishment interval, with strict adherence to amortized life-cycle-cost based selection, may reduce flexibility in dealing with annual variations in loss rates, which might be caused by several years of higher than normal storm activity, or design deficiencies discovered within the first few years following construction. From both engineering/design and monitoring/maintenance perspectives, 3- to 4-year renourishment cycles are desirable. If longer renourishment intervals are desired from an economic perspective, it is prudent to plan a short first renourishment interval (about half the optimized interval, or 3 to 4 years, whichever is smaller).

- If the volume remaining within the project area is subtracted from the cumulative placed volume, one can estimate the cumulative spreading losses. In the simulations without background erosion, the cumulative spreading losses range between 2.75 to 2.83 million cu m of sand, depending on the renourishment cycle. However, the simulations that included the effect of a 0.5 m/year background erosion rate indicate substantially higher cumulative losses, between 6.36 to 6.68 million cu m of sand, depending on the renourishment cycle. Some past projects have underestimated renourishment requirements by assuming that a historically based volumetric rate of erosion within the project domain can be used to estimate the required renourishment. This assumption incorrectly neglects the effect of background erosion outside the project on project end losses. For example, the

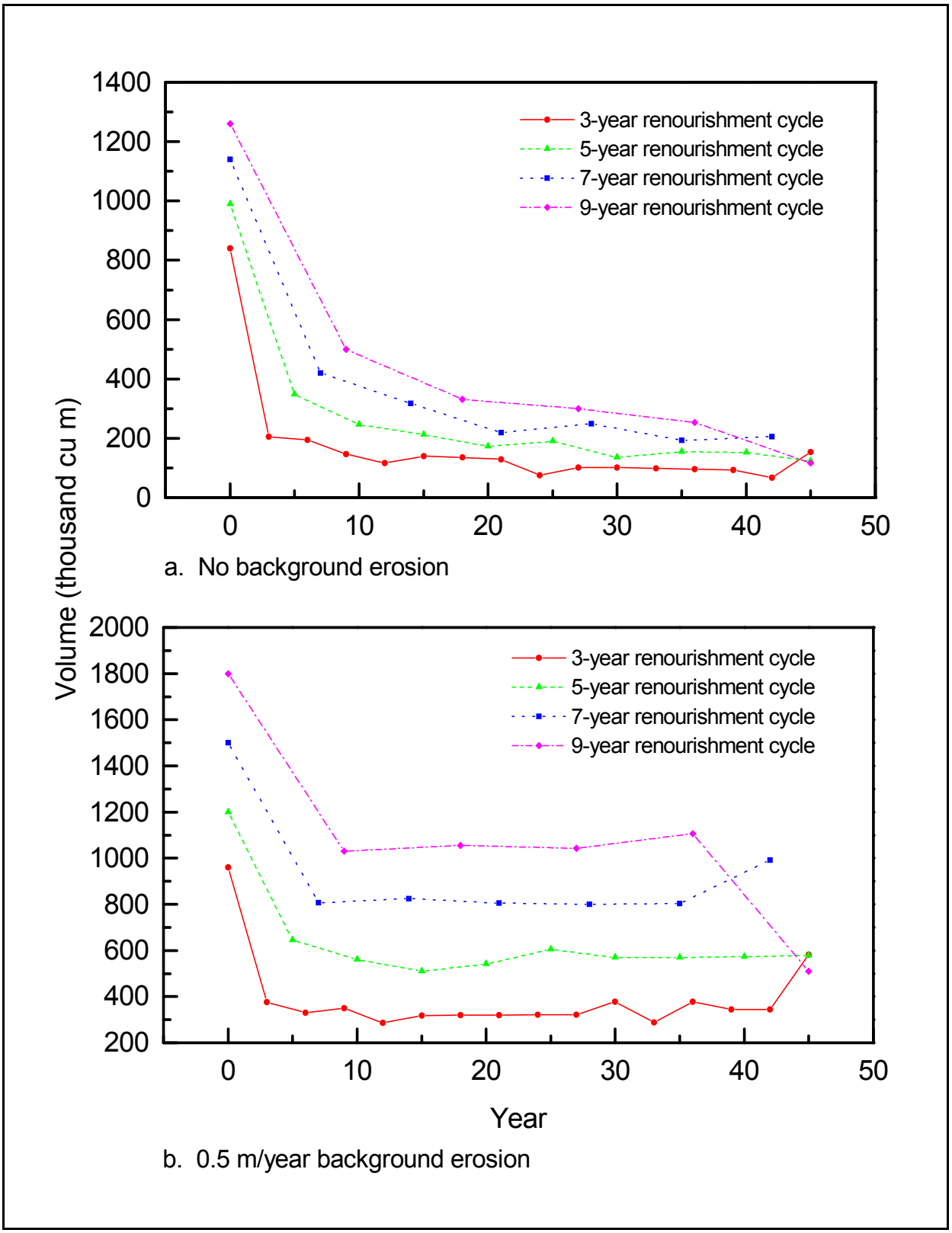

Figure V-4-20. Advanced fill and renourishment volumes

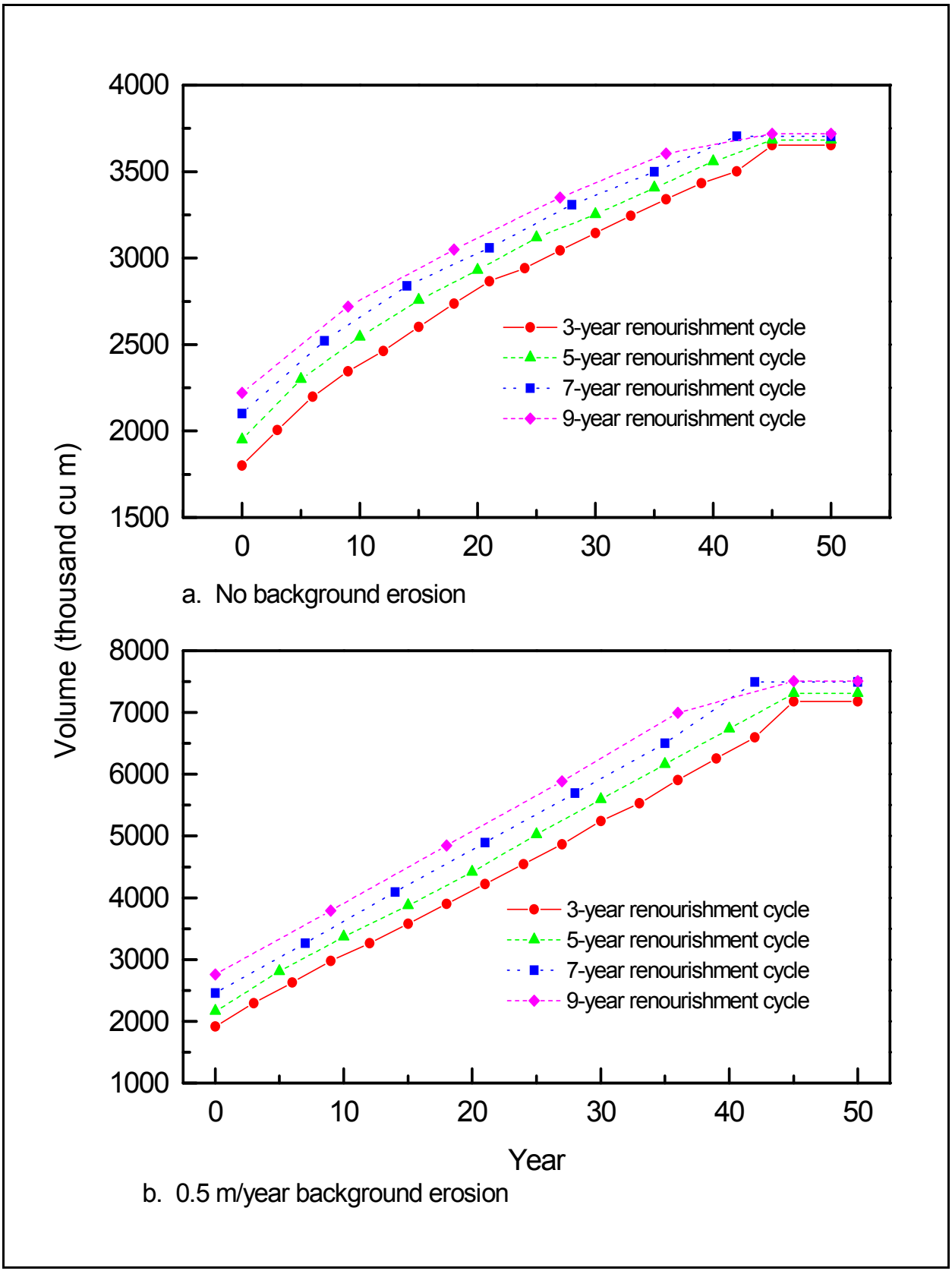

Figure V-4-21. Cumulative beach nourishment volume

volumetric erosion due to a background erosion rate of 0.5 m/year on a 6-km project length with an average berm height of 1.5 m and a depth of closure of 6 m is 1.13 million cu m over a 50-year project life. Adding this volume to the calculated project end loss volume (in the absence of background erosion) of 2.8 million cu m gives a total project volume of 3.93 million cu m which is only about 60 percent of the 6.52 million cu m estimated in the simulations that included a background erosion rate of 0.5 m/year. The explanation for this result is that background erosion outside the project causes the seaward protuberance of the project to become larger each year. At the end of the 50-year project, the design shoreline is 45 m seaward of the adjacent shorelines which are unaffected by the project nourishments; whereas in the absence of background erosion, the protuberance of the design shoreline remains 20 m throughout the 50-year project. The additional nourishment volume is required to provide a natural transition from the eroded adjacent shorelines to the design shoreline. Figure V-4-22 shows the calculated shoreline position at the end of the 50-year nourishment project for each of the project scenarios simulated. It also illustrates the previously discussed requirement for additional nourishment volume in the presence of background erosion. Figure V-4-22 also illustrates the beneficial effects a beach-fill project has on the adjacent shorelines during its lifetime. In the absence of background erosion (Figure V-4-22a) it is seen that the beaches adjacent to the fill project are advanced seaward approximately half the design width for more than a project length on both sides of the fill. With a background erosion rate of 0.5 m/year (Figure V-4-22b) it is seen that the fill project stabilized the shoreline at or seaward of the preproject shoreline position for a distance of approximately one project length on both sides of the fill.

(b) Recommendations for detailed analysis.

- In the previous section, the GENESIS model was applied in a simplified way to estimate volume requirements for an idealized beach-fill project. That application of the GENESIS model was referred to as simplified because the model was not calibrated for the specific project reach nor was a time varying time series of wave information used to represent the environmental forcing. Furthermore, the simplified method of analysis assumes that the project and adjacent beaches can be characterized as long straight beaches with uniform and temporally constant background erosion rates, and that the dominant long-term processes affecting the evolution of the beach-fill project can be captured by examining the alongshore dispersion of the fill by a persistent effective wave condition. However, many if not most projects vary significantly from these assumptions and warrant a more detailed application of the GENESIS model. Gravens, Kraus, and Hanson (1991) and Gravens (1992) provide detailed information concerning the application of the GENESIS model.

- A detailed application involves developing shoreline position and beach profile data sets, analyses of incident wave conditions including detailed nearshore wave transformation, and selection of a time-history of representative wave conditions for use in model calibration, verification, and project forcasting. Typically a detailed wind wave hindcast such as WIS provides the required wave information and serves as the database defining the local and regional characteristics of the offshore wave climate in the vicinity of the project. A long, multiyear record of measured wave data may also suffice.

- A critical aspect of the detailed application is the calibration of the model to site specific project conditions. Calibration involves selection of the domain to be modeled and boundary conditions, evaluation of model accuracy in reproducing historical shoreline change, and net and gross longshore sand transport rates. The calibration and evaluation of the GENESIS model serve to demonstrate the predictive capability of the model at the specific project site. Estimates based on a well-calibrated and verified GENESIS model are considered superior to those based on a simplified application of GENESIS. However, it may be informative to examine the difference between estimates generated

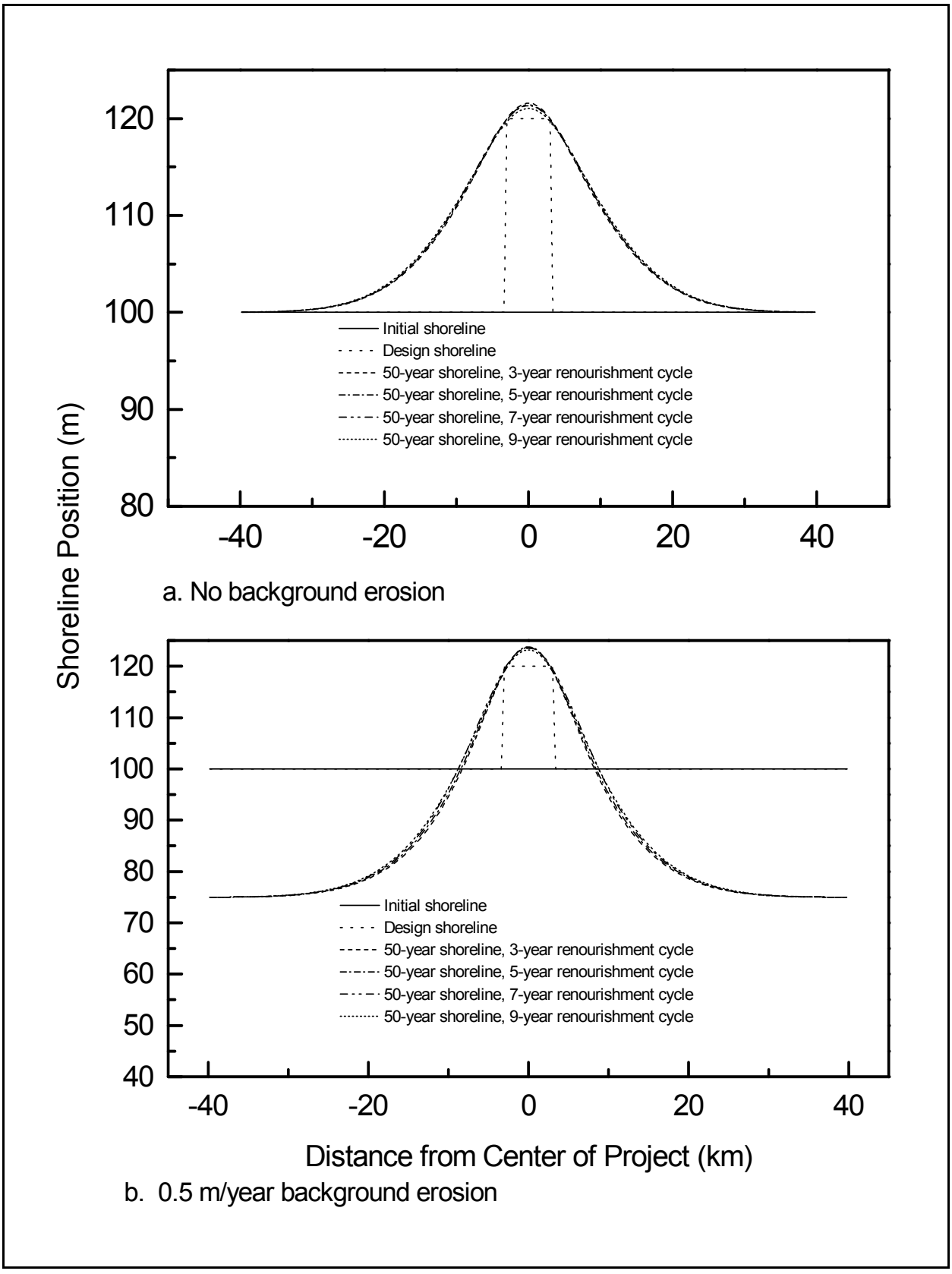

Figure V-4-22. Calculated 50-year shoreline position

through both simplified and detailed applications of GENESIS for a given project to quantify the range of uncertainty between the design methods. Coastal engineering judgement, local coastal experience, and the performance of nearby similarly-situated projects, if any, are important and should be factored into the overall design and specifically the estimates of project volume requirements. The results of a detailed GENESIS model application should always be interpreted in the context of the model calibration and verification. For instance, if the historical rate of erosion was underpredicted in some specific model region of the simulated shoreline in the calibration and verification then it should be expected that the model will continue to underpredict erosion in this area in the simulation of the various design alternatives. Estimates of volume requirements should be adjusted to account for deficiencies in the model calibration and verification.

- One advantage of taking the detailed GENESIS modeling approach in the investigation and prediction of beach-fill project performance is the opportunity to anticipate possible secondary effects that have troubled some past projects. For instance, the excavation of a nearshore borrow area or some preexisting bathymetric feature may significantly alter local breaking wave conditions and result in the development of a localized zone of accelerated erosion along the project shoreline (a hot spot). A detailed application of GENESIS would examine the effects of local bathymetry and project changes in the bathymetry, through the application of nearshore wave transformation models and inclusion of nearshore wave information in the shoreline change calculations. GENESIS model predictions based on this type of data can reveal the potential for the development of shoreline anomalies within the project. Simplified applications of GENESIS or an analysis based on the analytical approach have no chance of revealing possible hot spot development because the processes responsible for their development are ignored or are smoothed over in the analysis.

- If a good calibration of the GENESIS model cannot be achieved because of complex boundary conditions (unstructured inlet, randomly fluctuating shoreline), or insufficient or poor data quality, then a more simplified application of the model is recommended. An alternative to calibrating and verifying the GENESIS model to historical shoreline position data, is to calibrate GENESIS to an accepted existing-condition sediment budget developed through an analysis of the available physical data. In this type of application, a wave time series that reproduces the accepted sediment budget within the model is developed either from hindcast wave information such as WIS, measured wave information, or simply synthesized from observations or general wave and wind information available in a statistical form.

(5) Anticipating hot spots. Hot spots are localized areas within a beach nourishment project that experience a reduction in beach width (corresponding to a loss of sand volume) significantly greater than losses that were predicted and/or are observed throughout the rest of the project. Hot spots are problematic in the sense that the desired level of protection may be compromised locally, whereas the remainder of the project is functioning well. To achieve the desired level of protection, renourishment in the hot spot area may be required on a more frequent basis than the rest of the project. Or, some structural solution may be required to provide the desired level of protection or improve sand retention so that renourishment can be performed on the same schedule as is planned for the rest of the project. Hot spot mitigation measures will probably result in additional unanticipated and undesired costs. The public perception of hot spots that develop shortly after construction can be one of project failure. Therefore, the potential for the occurrence of hot spots should be investigated during the design process. This can be accomplished through, for example, the method used by Smith and Ebersole (1997). The GENESIS model together with detailed nearshore wave conditions can also be used for this purpose (Bodge, Creed, and Raichle 1996).

(a) Hot spots can arise due to a locally strong gradient in longshore sand transport rate, which creates a divergent zone where, in a net sense, more sand is leaving an area than is entering it. Strong longshore transport gradients can develop due to a noticeable change in shoreline/bathymetric contour orientation.

Figure V-4-23 illustrates an example of this type of hot spot at Folly Beach, South Carolina. A beach-fill was constructed along much of the island, and high loss rates were observed locally at the place where the shoreline noticeably changes orientation and creates a convex curve relative to the incident waves (Ebersole, Neilans, and Dowd 1996). Prior to construction of the nourishment project, this area was known as the wash-out area, suggesting an area that previously experienced high erosion rates. Local knowledge or an analysis of historical shoreline change rates may help identify such a zone. However, areas that have historically suffered high sand loss rates may be presently armored with seawalls or revetments, or controlled by some other structures such as groins, thereby pinning the shoreline position and masking the presence of a future hot spot. Any area in which the shoreline has a bulge or convex shape, relative to the incident waves, is a potential candidate for this type of hot spot.

(b) The presence of a submerged offshore shoal, or some other highly irregular bathymetric feature such as an underwater canyon, can also be a cause of erosion hot spots. Morphologic features can alter the propagation of incident waves in a persistent manner, creating strong gradients in net longshore sand transport. Stauble (1994) documented the occurrence of multiple erosional hot spots in a beach nourishment project constructed at Ocean City, Maryland, and hypothesized that the cause of the hot spots was the presence of shore-attached finger shoals that characterize the nearshore bathymetry off Ocean City (see Figure V-4-24). The finger shoals appear as lighter-shaded areas. Stauble also identified corollary cold spots, or areas of unusual sand accumulation, which were formed by the sand that was transported out of the hot spots. Smith and Ebersole (1997) showed that the positions of the hot spots/cold spots were well-correlated to zones of divergent/convergent potential longshore sand transport caused by persistent changes to nearshore wave patterns induced by the shoals. The shoals act to alternately focus and spread wave energy due to the process of wave refraction. Results from the application of a wave transformation model (see Part II-3) were used to compute potential longshore transport rates. Figure V-4-25 shows the variation in transport rates for Ocean City, Maryland. Positive rates are directed to the south, negative to the north. Hot spots correspond to strong uphill gradients (e.g., changes from low southerly transport rates to high southerly transport rates). Cold spots occur at downhill gradients.

(c) Just as natural bathymetric irregularities can lead to the development of a hot spot, an excavated borrow area or a submerged mound constructed out of dredged material can produce the same result. If the manmade feature results in a significant change in bottom relief and is located in water depths where the waves feel the change in depth, persistent longshore sand transport gradients may develop. Hot spots can also form in areas where the incident wave directions are constrained to a narrow window and the area is blocked or sheltered by some land feature or coastal structure, creating a gradient in wave energy and longshore sand transport.

(d) A third type of hot spot can result as a consequence of how a project is designed and built to protect existing structures and infrastructure. Typically beach nourishment projects are built in areas where structures and infrastructure are vulnerable to storm-induced damage. Oftentimes, the project site already has revetments or seawalls that have been built by private landowners. Both protected and unprotected structures may protrude beyond the natural prevailing shoreline position, thereby creating a very irregular, and unnatural, shoreline. It may be difficult to estimate where the prevailing natural shoreline position would be if the structures were not present.

(e) If a project is designed and constructed to "wrap around" protruding structures, in an attempt to create a uniform width of beach in front of each structure, the beach will most likely readjust following construction. The readjustment process will lead to a more stable arrangement of sand in which the design width may not be retained in front of the seaward most structures, whereas the beach width may exceed the design width in other areas. Figure V-4-26 illustrates this process. An offshore depth contour equal to the

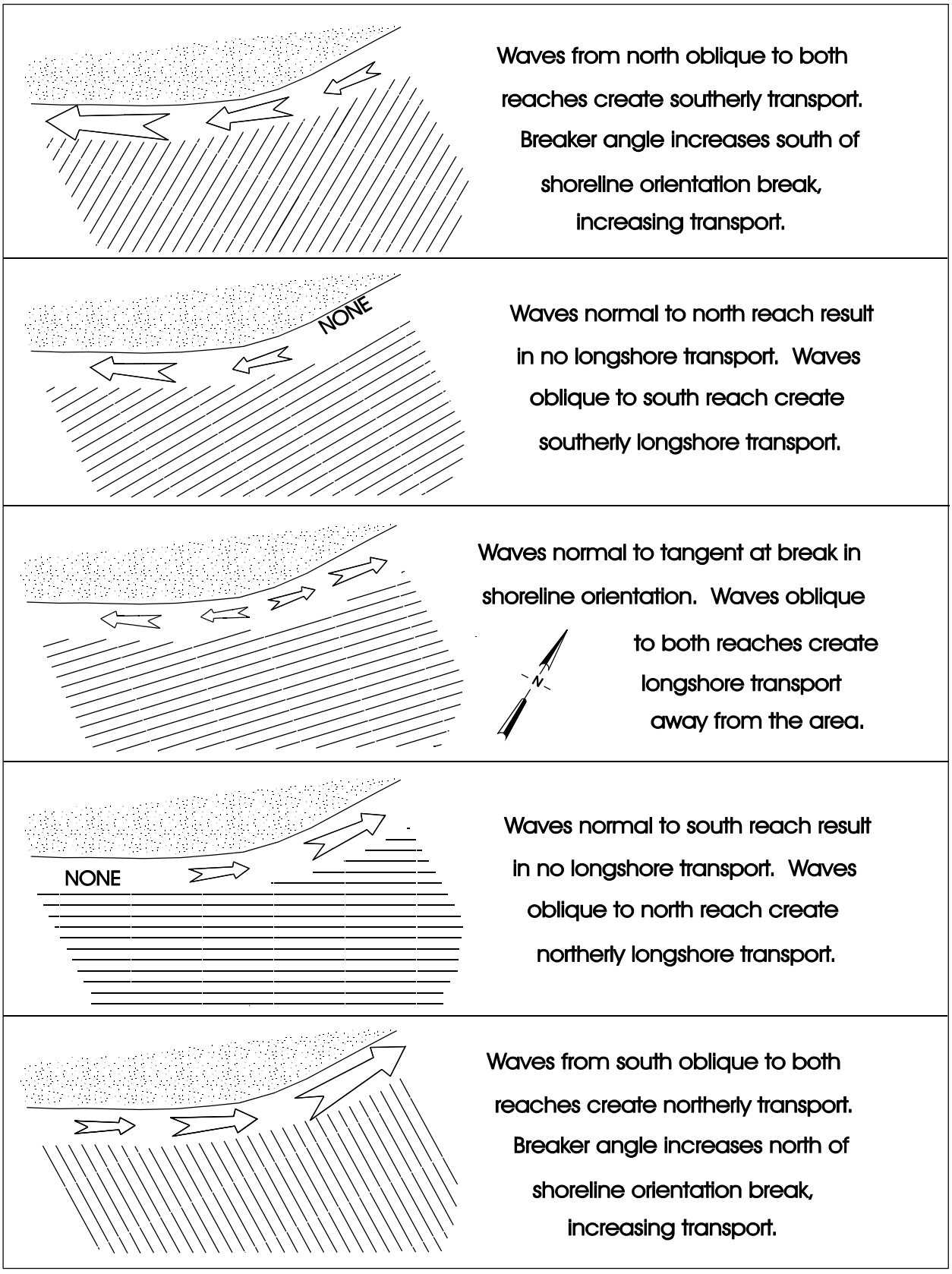

Figure V-4-23. Causes of hot spot formation at a convex shoreline feature

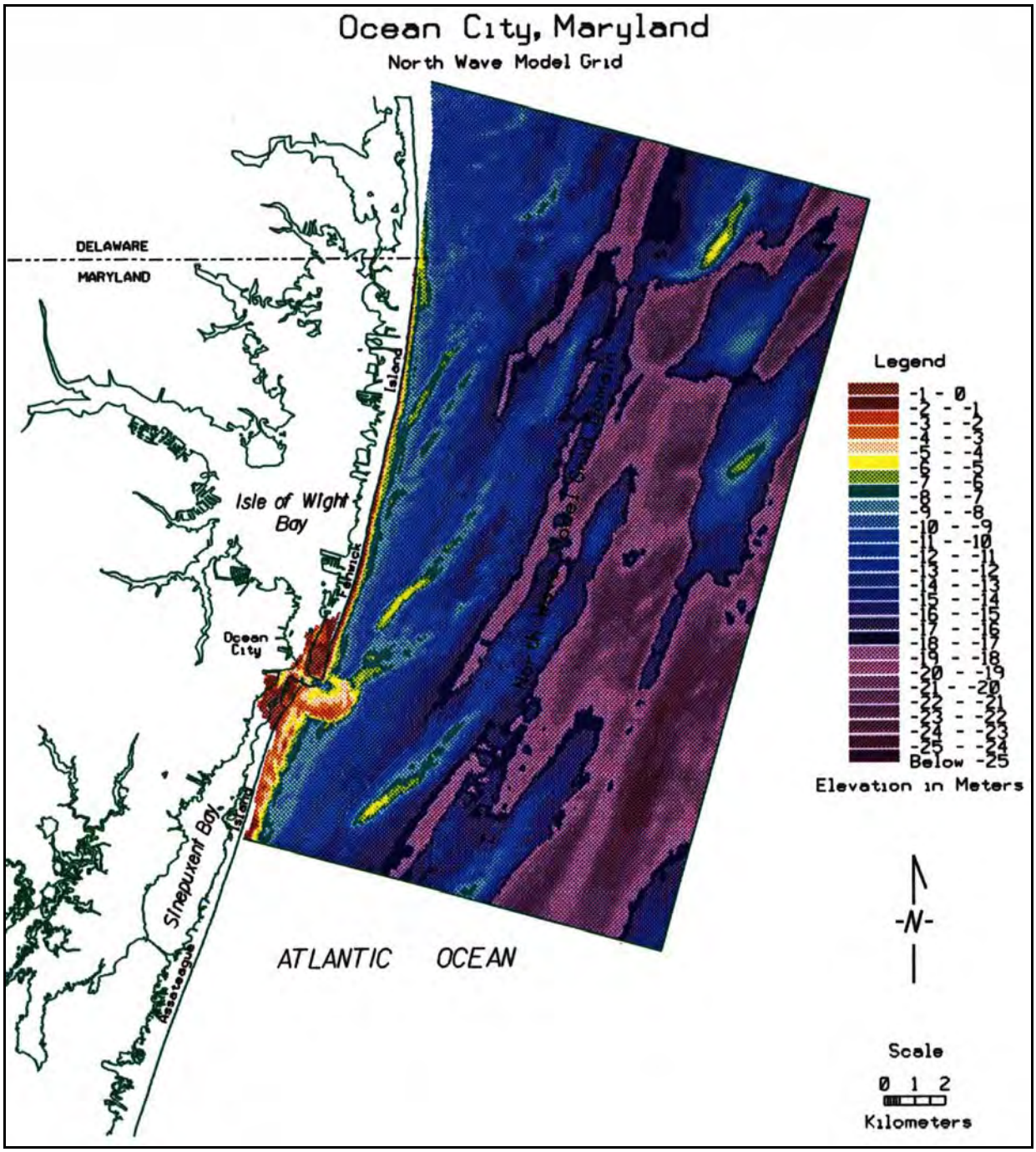

Figure V-4-24. Project shorelines, nearshore bathymetry, wave modeling domain, and position of offshore wave information

breaking wave height associated with frequent storms (2- to 3-m depth contour) may serve as a better indicator of the orientation of the postconstruction, adjusted shoreline.

(f) It may be impossible to maintain the design width in front of some structures without placing a substantially larger volume of sand than is estimated based on "wrapping" the project around the existing structures. It may not be cost-effective to build the entire beach out to the point required to provide the

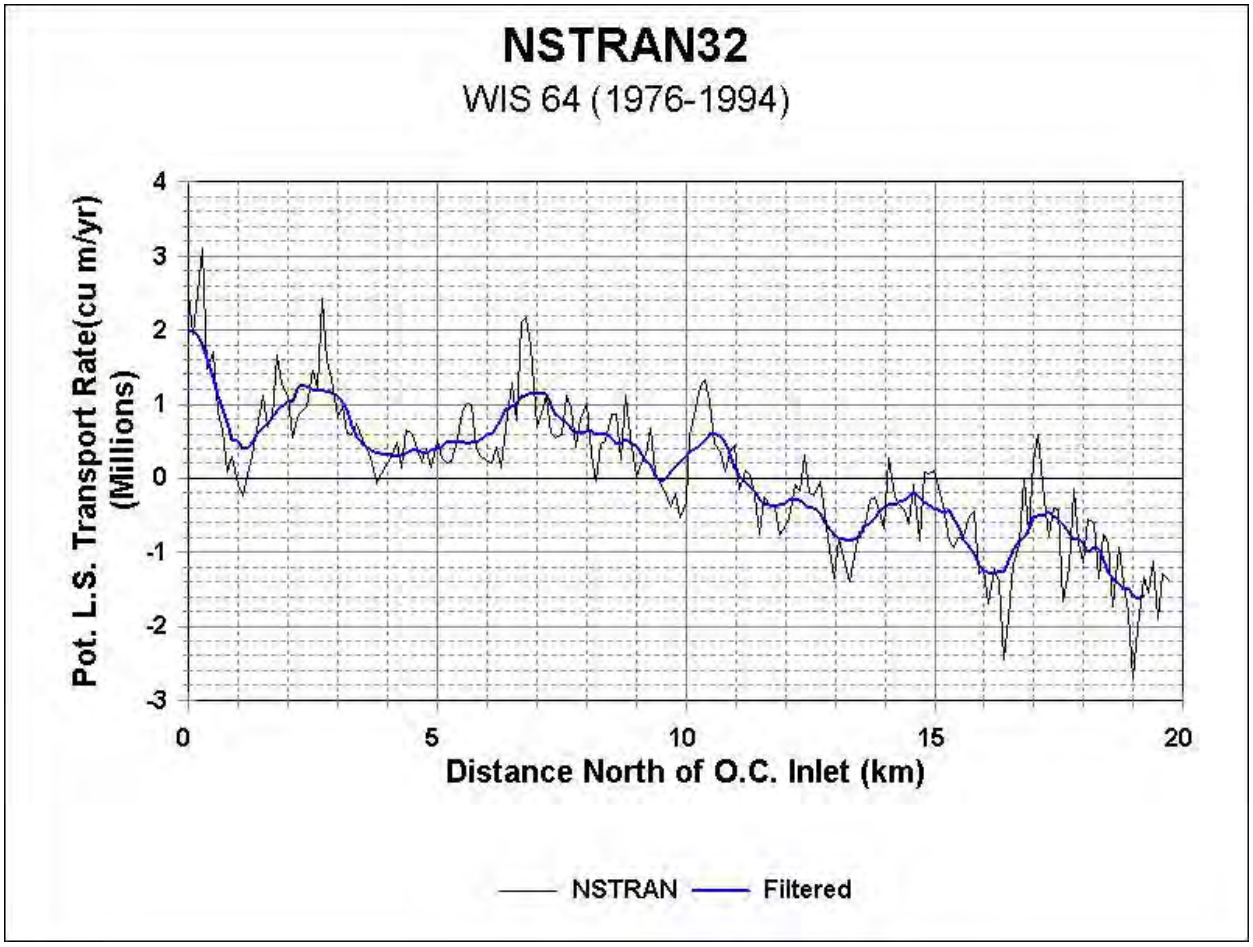

Figure V-4-25. Variations in potential longshore sand transport rates caused by offshore shoals at Ocean City, Maryland

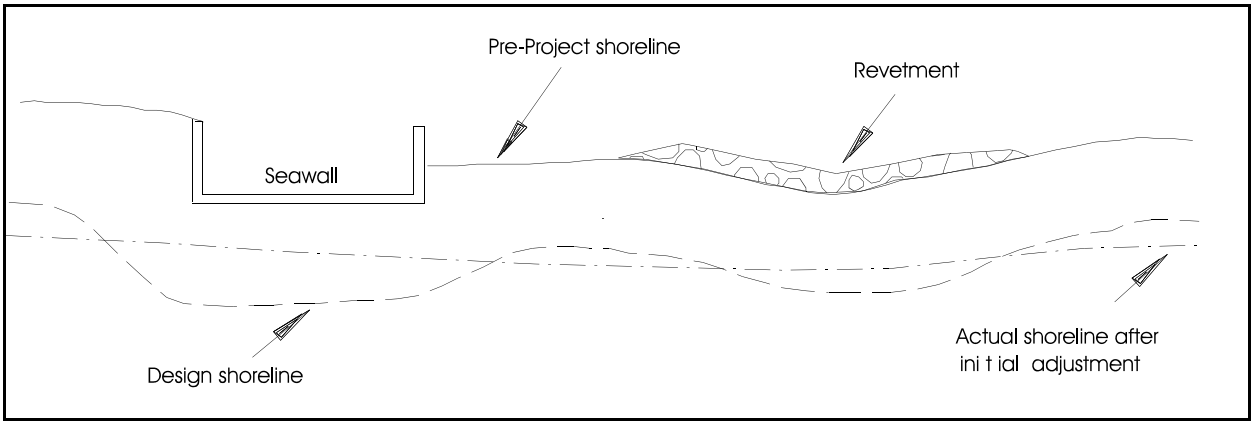

Figure V-4-26. Planform adjustment of a beach-fill project designed to "wrap around" existing coastal structures

desired level of protection to the seaward most structures. If this is the case, other means for achieving the desired level of storm protection in certain local areas, such as more frequent nourishment, use of a feeder beach, a filled groin compartment, or a revetment or seawall, should be considered.

(g) There are probably other less well-understood causes for the development of hot spots. A geologic control such as remnant morphologic feature (relic inlet) with a different sediment composition may cause differential erosion along the project reach. Longshore variation in the sediment characteristics of the borrow material may produce a differential loss rate within sections of the project. However at present, there are no reliable methods for anticipating hot spots caused by these other factors.

h. Fill transitions.

(1) Selection of a method for terminating a beach nourishment project depends on several factors. One important consideration is what lies immediately beyond the project limits. For example, is there an open straight beach or an inlet? On open stretches of coast, transition to the adjacent beach can be accomplished using a fill transition section, which was briefly introduced in the previous section, or using hard structures, such as groins, navigation structures, or breakwaters. Structures placed at the boundaries of a project are called terminal structures. If the project is constructed near an inlet, structures may be desirable to minimize movement of fill material into navigation channels. Hard structures will allow an abrupt termination of the beach-fill section. However, these structures can be costly, and can interfere with the natural longshore transport of sediment along the shoreline. If not designed properly, this interference could result in adverse effects along the unrestored beach and subsequent objections by adjacent-beach property owners.

(2) Another key factor is the purpose for building the project. If the project is built to provide storm protection, what is the reach of shoreline to be protected and what is the desired level of protection within the reach? The desire to maintain a specific design beach width may dictate the design of the transition section. In practice, if a uniform design width is desired for the entire project reach, it will be extremely difficult to maintain that width near the lateral ends of the project, unless a terminal structure is used or the design fill is extended beyond the limits of the design reach. If sand is to be placed outside the design reach, other issues become important. Can the fill provide benefits to the adjacent property, and how will those benefits be factored into the economic justification of design (if at all)? It may be more practical to consider the nourishment project in three sections, one interior section where a desired level of protection will be maintained, and two outer sections of the project where a lesser degree of protection will exist (i.e., the transition sections). In the transition sections, the level of protection will diminish with distance from the main project reach.

(3) If the project is built primarily for recreational purposes, the design goal may be to maximize retention of fill volume within the limits of the project reach. This design objective may dictate whether or not fill transitions are used at all, and if so, how they are designed.

(4) Although sometimes approached as an afterthought in project design, beach-fill termination deserves careful consideration. This is particularly true in terms of its relation to the economics of the project and the level of storm protection that is sought/claimed near the limits of the project. This section discusses use of fill transitions at the ends of a nourishment project. The next section, Part V-4-1-i, discusses use of structures in fill stabilization.

(5) The intent of fill transitions is to minimize the effect of end losses on project integrity. End losses from the main project reach can be reduced by extending the design section past the limits of the reach where protection is desired, or by smoothly tapering the project into the adjacent beaches (i.e., gradually reducing project width from the design width to zero). Tapering the fill ends will decrease the perturbation effects of

the project section. The effect of varying taper length can be estimated with the aid of analytical or numerical shoreline planform response models (Walton 1994; Hanson and Kraus 1989).

(6) The GENESIS model was used in a series of simplified applications to investigate the effect of beach-fill transitions. Figure V-4-27 shows plots of an initial rectangular 6-km-long fill section, and the calculated shoreline at 1-year intervals, for two projects identical in every way except that the project in the top panel has a 400-m-long fill transition and the project in the bottom panel has a 2,000-m-fill transition. The total fill volume is the same in both projects, to allow assessment of how best to utilize a finite volume (or alternatively a fixed cost). The duration for both simulation is 5 years. A single, normally-incident effective wave is considered. The design objective is to maintain a beach width of 20 m throughout the 5-year interval, everywhere within the project reach.

(7) At the end of the 5-year simulation, both projects have beach widths greater than the 20-m design width; and therefore, both projects have satisfied the design objective. It is noted that the average annual volumetric rate of sand loss from the 400-m fill transition project was 148,000 cu m/year; whereas for the 2,000-m fill transition project, the average end losses were 89,000 cu m/year (about a 40 percent reduction in the rate of end losses). However, because approximately 22 percent of the fill volume was placed outside the project reach at the time of construction in the 2,000-m fill transition sections, the percent of total placed fill volume remaining within the 6-km project area is greater for the 400-m fill transition project (58 percent remaining) than for the 2,000-m fill transition project (55 percent remaining). For this case, the example suggests that if there are few or no economic benefits to claim in the transition section, then all the fill volume should be placed within the limits of the project reach (i.e., no use of transition sections). The same conclusion would be reached in this case if maximizing fill volume retention was the primary design goal. However, recall from the previous section that project longevity varies with the square of the project length. Generally, this rule of thumb concerning use of transitions is true for shorter fills. Also, for short fills, it may not be desirable to place sand volume in transition sections which may require a significant percent of the total volume placed within the project.

(8) For longer projects, the design requirement of maintaining the design berm width at the project boundaries throughout the renourishment interval may favor the placement of beach-fill transition sections. Figure V-4-28 provides plots of the initial fill and the calculated shoreline position after 5 years, for 6- and 22-km-long fill projects, with both 400- and 2,000-m fill transition sections. Again, the design berm width is 20 m. In Figure V-4-28a, it is seen that for the 6-km fill project, the 400-m transition project shoreline is seaward of the 2,000-m transition project shoreline after 5 years everywhere within the project domain. However, for the 22-km fill project shown in Figure V-4-28b it is seen that at the project boundaries, the 400-m transition project is landward of the 2,000-m transition project, and more importantly, landward of the design shoreline. This result illustrates the potential value of beach-fill transition sections for long beach-fill projects.

(9) However, even for long projects, the benefit of placing a fill transition section is only realized during the first few years after construction (within the first renourishment cycle, as a rough rule of thumb).

(10) Within only a few years the volume of fill material that has moved from within the project limits onto the adjacent beaches, as a result of alongshore spreading, is likely to be much greater than the volume that was initially placed in the transitions, even with 2,000-m-long transition sections. This conclusion is further illustrated by the results shown in Figure V-4-28, where it is seen that the calculated shoreline position adjacent to the main project after 5 years is for all practical purposes the same for both the project with the 400-m fill transition and the project with the 2,000-m fill transition. The work of Walton (1994) suggests that transition sections have a more lasting significant impact on reducing rates of sand loss from the project only when their length exceeds a value that is 0.25 times the project reach length. In past practice,

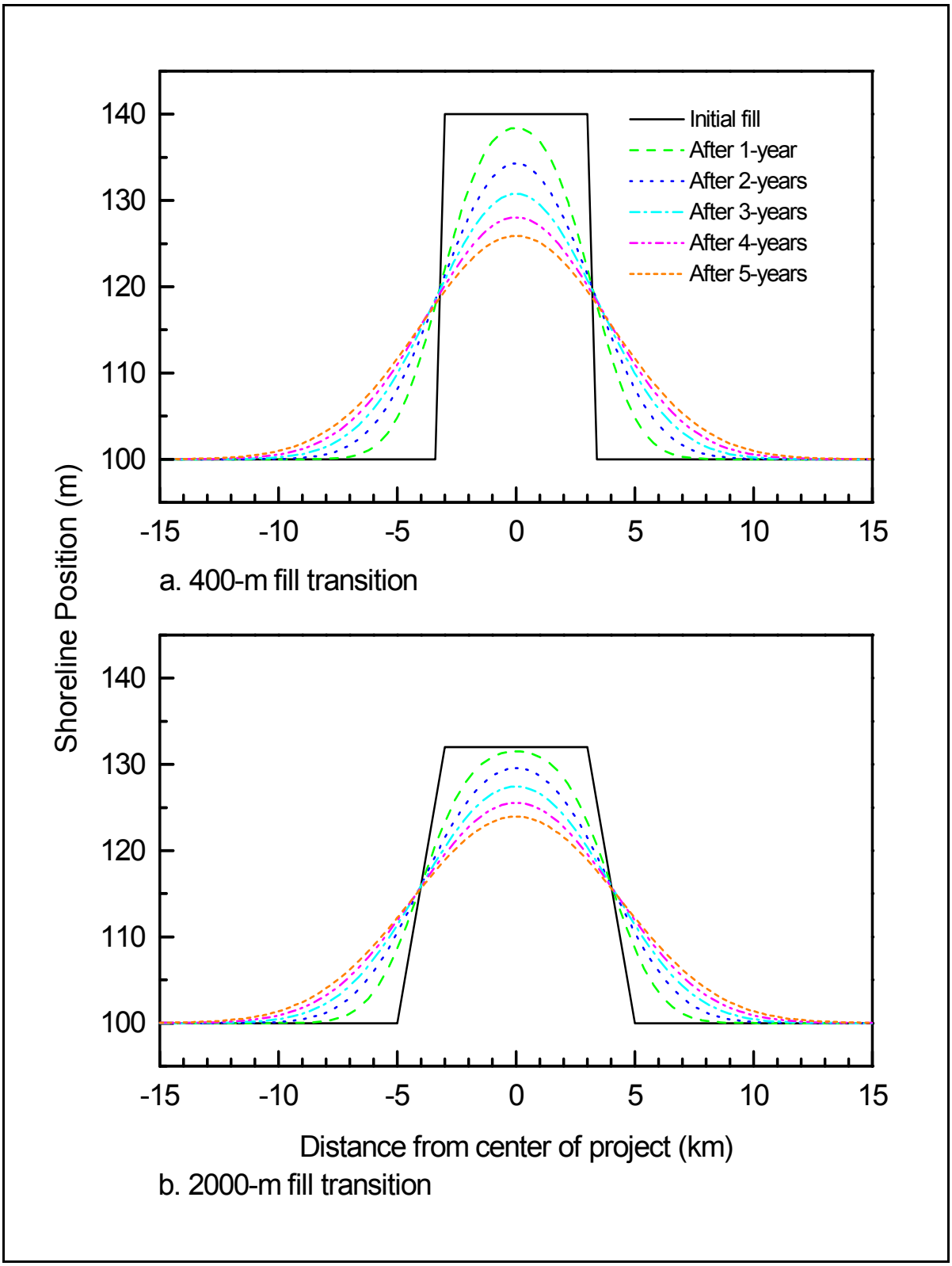

Figure V-4-27. Effect of fill transitions

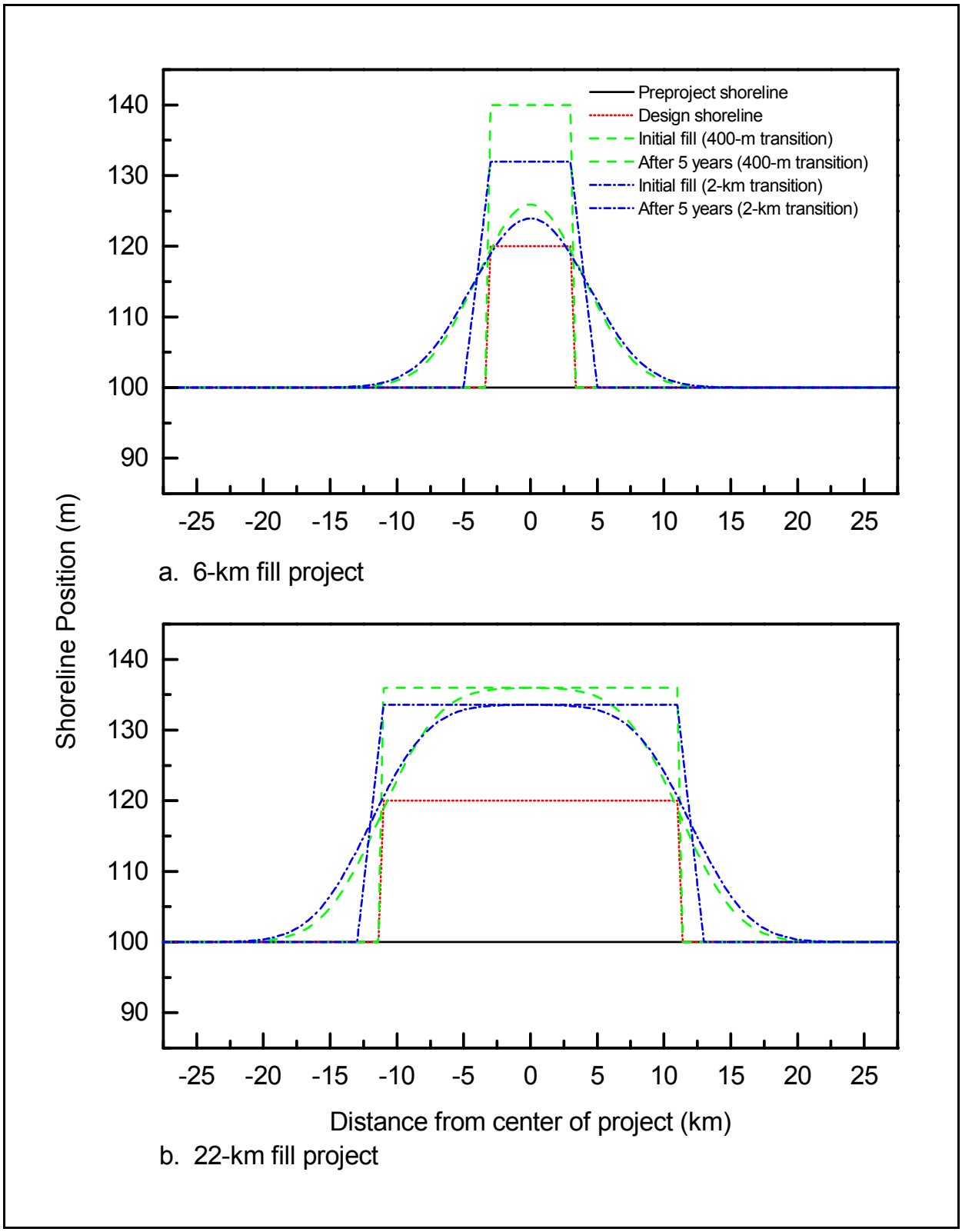

Figure V-4-28. Effect of fill transitions

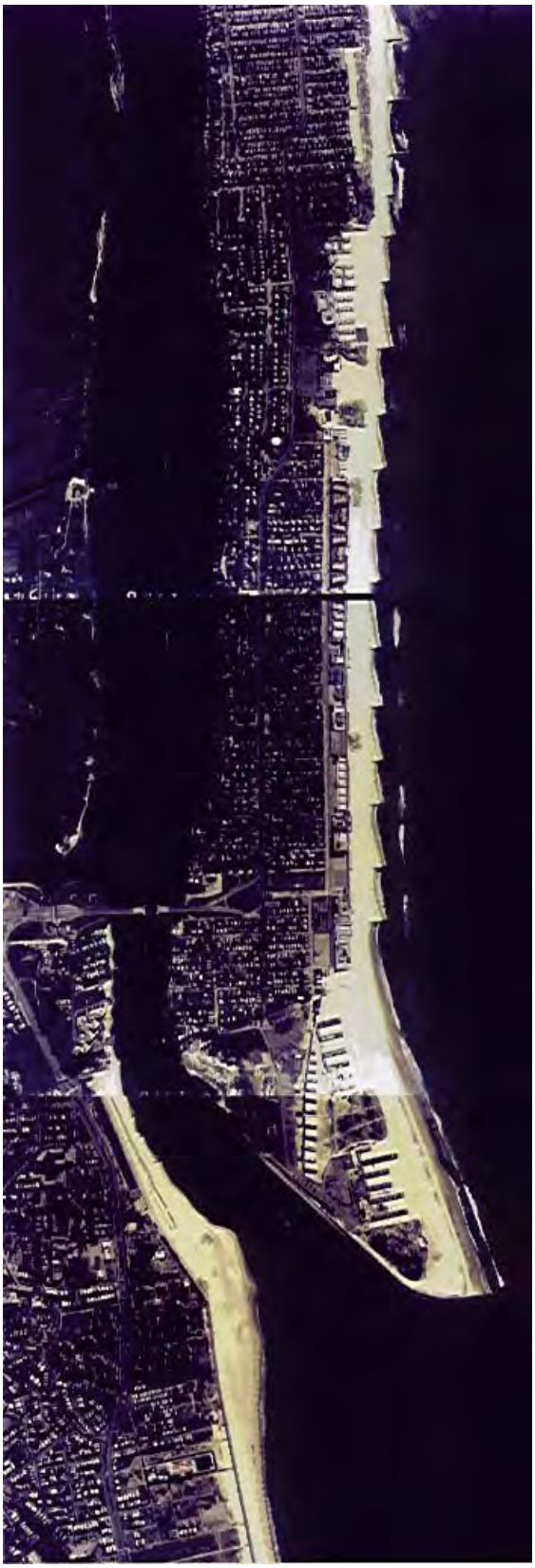

Figure V-4-29. Groin field at Long Beach island, New York

transitions sections have rarely been constructed to this length. In practice, the exact length of the fill transition section does not ultimately matter so long as it is in reasonable proportion to the scale of the project. Typical fill transition lengths for small projects (approximately 1 to 2 km; 100,000 to 200,000 m^3) are on the order of 150 to 300 m (500 to 1000 ft) long, while for larger projects they are on the order of 300 to 600 m (1000 to 1,500 ft) long.

(11) Transition sections do reduce the rate of fill loss from the project; but again, this benefit lasts only for the first few years following construction. Some past project designs have inappropriately estimated the beneficial effects of the beach-fill transitions by computing the reduction in the rate of end loss during the first few years of the project and then projecting these benefits throughout the 50-year project life. The analysis presented here suggests that while benefits associated with reduced loss rates are very high during the first few years, they diminish significantly thereafter.

(12) An analysis of beach-fill transitions should first examine the evolution of the project with transition sections, either tapered sections or lateral extensions of the design section, and then examine evolution of the project with the transition volume distributed within the project economic benefit area. The distribution within the project doesn't have to be uniform, as was the case in the examples shown here. If transitions are a desirable feature, they should be optimized by balancing the reduction in the rate of end losses from the project (which will reduce renourishment costs) with the cost of placing fill volume outside of the project's economic benefit area. Then, costs of the transition sections over the project life should be compared to the cost of using a terminal structure or compartmentalizing the beach-fill material with groins or jetties, including an assessment of any impacts that might be caused by a terminal structure. The most cost-effective approach should be selected. Environmental concerns, land ownership constraints, or other factors may also need to be considered in the selection of the optimum fill transition sections.

i. Beach-fill stabilization measures.

(1) Structures. Different types of structures can be used in conjunction with beach-fill projects to retard fill erosion and thereby reduce periodic renourishment costs. As discussed in the previous section, losses are particularly pronounced at the ends of a project where an offset occurs between the fill section and the adjacent unfilled beach. Structures may be needed in these transition zones to keep fill losses at acceptable levels. In some cases, structures may already be in place on the project beach. Depending on type and location of these structures, it may be advantageous to retain them, and perhaps refurbish them. However, some structures may have a negative effect on the beach, or are undesirable from the standpoint of aesthetics or safety. If existing structures are judged to have a probable negative effect, their removal should be considered. Following is a brief discussion of coastal structures in common use in conjunction with beach-fill projects. A more detailed discussion of their characteristics, effects, and design can be found in Part VI.

(a) Groins.

- Groins are low linear structures which are typically built perpendicular to the shoreline, extending from the beach into shallow nearshore water. Their primary purpose is to trap and retain sand moving in the alongshore direction. Groins can be constructed in groups, or fields, consisting of a series of structures spaced at predetermined intervals along a segment of shore to improve retention of beach-fill material, Figure V-4-29, or as an individual structure intended to provide effective termination of a beach-fill project. Weggel and Sorensen (1991) note that the addition and modification of groins within the Atlantic City, New Jersey, nourishment project, constructed in 1986, improved fill performance when compared to that of previous fills for the same location. The groins acted to retain the fill within the project area and prevented fill losses into the adjacent inlet.

- In the context of beach nourishment projects, the most common use of the groin is as a terminal structure, designed to reduce or eliminate sediment losses out of the project area. The use of a terminal groin is most frequently considered in projects that abut lacks tidal inlets or are adjacent to the beginning or end of a littoral cell. For example, use of a terminal groin at the end of a beach-fill project built next to an unstabilized tidal inlet will not only reduce project end losses but also prevent increased shoaling in the inlet channel caused by deposition of sand lost from the project. Likewise, a terminal groin constructed at the downdrift end of a project built updrift of a submarine canyon can substantially reduce end losses. In both of these cases, the accretionary fillet that develops updrift of the terminal groin can be a renewable source of sediment for maintaining and perhaps renourishing the project. Terminal groins are also appropriate, and should be considered, in projects where the preproject shore lacks existing sandy beach, and in projects where the postproject shoreline will be positioned substantially seaward of the adjacent beaches, particularly in short fills. Federal projects of this type are rare, but private development can often include construction of recreational beaches which depend substantially on terminal structures for their longevity. Figure V-4-30 shows an example of a terminal groin used to terminate a beach nourishment at Oregon Inlet, North Carolina.

Figure V-4-30. Terminal groin, Oregon Inlet, North Carolina

- In littoral cells where there is a dominate net longshore transport direction, a terminal groin centrally located within the cell can exacerbate erosion on the downdrift beach. A terminal groin should not be used within the interior of a littoral cell, unless the downdrift impact of the groin is defined and mitigated. Careful attention must to be given to the design of the groin's profile and length. The terminal groin profile should be a template of the design beach berm and nearshore profile such that the structure blocks littoral transport only to the extent necessary to preserve the design beach cross section, while allowing the ambient net littoral transport to bypass the structure to downdrift beaches. Careful monitoring to assess the structure's impact on the adjacent beaches is recommended. Placing a sacrificial sand fillet downdrift of the terminal groin at the time of initial construction, and perhaps during periodic renourishments, may be necessary to offset any adverse impact to the downdrift beach caused by the groin.

- Groins in general, and groin fields in particular, were commonly used to control erosion and to protect upland development in coastal projects constructed from the 1930s through the 1960s. The experience with groin fields has been checkered with both successes and failures. Groin fields have a proven capacity to provide relief for a local erosion problem by compartmentalization of the shore face and stabilization of the shoreline. However, because the compartments between the groins were rarely filled with beach material at the time of construction, the groin compartments filled over time by capturing, and retaining a portion, if not all, of the longshore sand transport. The result was typically severe erosion downdrift of the groin field. The problem was exacerbated by a chronically increasing deficit of littoral material caused by other upcoast diversions of sand (inlet dredging, breakwaters, hydroelectric dams, etc.). Present coastal engineering knowledge and predictive tools have advanced to the point where competent functional design of groins and groin fields is now possible. However, this design option is often rejected as a matter of policy by many local, state, and Federal agencies with jurisdictional authority.

- Groin fields can provide an effective and economical solution to some coastal erosion problems where shoreline stabilization is the primary project goal. Groins can improve retention of beach fill, but construction of a groin field without concurrent placement of fill is strongly discouraged. As is the case with a terminal groin, groin fields that terminate within a littoral cell, as opposed to at the end of the littoral cell, must provide for sediment bypassing to adjacent shores without interruption. Groin fields should not be terminated in areas with increasing (accelerating) net longshore transport potential. To ensure bypassing, the groin field should be filled during construction and the downdrift groin system should be tapered to provide a smooth transition to the adjacent unprotected shore (see Figure V-4-2). Groin fields have been successfully used together with beach nourishment to stabilize the highly developed southern shorelines of western Long Island at Long Beach Island, New York (see Figure V-4-29). A series of groins were refurbished at Folly Beach, SC, to reduce renourishment requirements for the beach-fill project, which was constructed in 1993 (U.S. Army Engineer District, Charleston, 1987).

- T-head and L-shaped groins are variants of the traditional straight shore-perpendicular groin. These structures include a shore-parallel head section that acts to block and diffract wave energy before it reaches the shoreline. T-head groins can provide a functional improvement over standard groins by reducing the occurrence of rip currents adjacent to the groin and to some extent blocking the offshore movement of sand adjacent to the groin. T-head and L-shape groins are best suited for protecting limited coastal reaches where the mobilizing forces include tidal currents as well as wave-generated currents and where the project objectives are more focused on compartmentalization and stabilization of the coast than on increasing beach width. A series of T-head groins constructed at Ocean Ridge, Florida, downdrift of South Lake Worth Inlet have proven to be effective in local stabilization of the shoreline (U.S. Army Engineer, Charleston, 1987).

(b) Detached breakwaters.

- Detached breakwaters are linear offshore structures generally oriented more or less parallel to the shoreline to which they have no solid connection. They can be built as a single continuous structure or segmented into a series of short sections with gaps. Detached breakwaters provide protection by reducing the wave energy that reaches the shore through dissipation, reflection, and diffraction. Compared to shore-perpendicular structures, such as groins, which provide protection by impoundment of alongshore-moving sediment, detached breakwaters can be designed to allow continued movement of longshore transport through the project area, thus potentially reducing adverse impacts on downdrift beaches. However, as is the case with groins, if fill material is not placed at the time of breakwater construction, then any sediment that accretes in the lee of the breakwaters is sediment that is denied from downdrift beaches, which can be expected to erode. The use of breakwaters for shore protection and in conjunction with beach nourishment in the United States has been primarily limited to littoral sediment-poor regions characterized by a low-energy wave climate. Most projects have been located on the Great Lakes, Chesapeake Bay, or Gulf of Mexico (Chasten et al. 1993). These projects are typically subjected to short-period, steep waves, which tend to approach the shoreline with limited refraction, and generally break at steep angles to the shore.

- While detached breakwaters have several appealing functional characteristics for shore protection, they also have disadvantages that include the following: limited design guidance, high construction and maintenance costs, limited ability to predict and compensate for structure-related phenomena such as adjacent beach erosion, rip currents, scour at the structures base, structure transmissibility, and effects of settlement on project performance. Like groins, detached breakwaters should only be utilized after careful study of the effects they will have on the project area and adjacent beaches.

- Details concerning the uses of detached breakwaters in beach-fill projects and design considerations can be found in Engineer Manual 1110-2-1617, Pope and Dean (1986); Dally and Pope (1986); Rosati (1990); and Chasten et al. 1993. Case studies of interest are contained in Nakashima et al. (1987); Gorecki (1985), and Gravens and Rosati (1994).

(2) Evaluation and optimization of stabilization structures.

(a) As discussed in previous sections, a beach nourishment project requires periodic reconstruction of the beach planform throughout the project life. In this section, use of structures to stabilize a nourishment project and reduce project end losses have been discussed. Structures such as groins and detached breakwaters are comparatively more expensive and permanent than beach-fill material. Project optimization requires an analysis of the cost-effectiveness of incorporating structures to reduce periodic nourishment requirements versus designing the project without the stabilization structures.

(b) During the plan formulation phase of the project, the performance of alternative plans (with and without fill stabilization structures) can be evaluated using a shoreline/beach change model, such as the GENESIS model, to estimate total volume requirements. A model can also provide information for assessing adjacent beach impacts resulting from the inclusion of fill stabilization structures. The effects of structure length and transmissibility can be estimated using the GENESIS model. The physical characteristics of the structure, therefore, can be optimized to best serve specific project requirements and objectives. Physical models can also be utilized to comparatively evaluate the performance of beach-fills with and without structures such as groins and breakwaters (Bottin and Earickson 1984).

(c) Techniques for design of a groin system to reduce beach-fill losses and offshore breakwater design are presented in EM 1110-2-1617. Additional guidance for the functional design of offshore breakwaters for shoreline stabilization is presented in Dally and Pope (1986) and Chasten et al. (1993).

(3) Dune stabilization. Coastal sand dunes are valuable and effective barriers to storm flooding and wave attack; and therefore, they are often an important component of the beach nourishment project. Because of the importance of the dunes to storm protection, and their vulnerability to wind- and wave-induced erosion, it is advisable to stabilize them with sand fences and vegetation. These stabilization measures are relatively inexpensive and serve two beneficial purposes: to enhance the protective nature of the dunes, and to reduce volume losses from the project due to wind blown transport of the fill. Guidelines for estimating the rate of wind blown sediment transport are provided in Part III-4. Beach-fill projects usually involve creating a much wider dry beach, so more sand is available for transport by wind. As a result, if dunes are stabilized with fences and vegetation, they often accrete with time and wind-blown sand losses from the project are minimized.

(a) Fences.

- Various types of fences have been used to create, enlarge, and stabilize coastal dunes. To be successful, the barrier must be porous to wind because a solid barrier creates turbulence that may result in scour rather than accretion. Fencing with a porosity (ratio of area of open space to total projected area) of about 50 percent should be used (Savage and Woodhouse 1969). Open and closed areas should be less than 5-cm in width. The standard slat-type wooden snow fence appears to be the most practical and cost-effective, and it has been widely used for dune stabilization and to promote dune growth. Snow fences are usually installed in single or multiple rows aligned parallel to the shoreline or perpendicular to the predominant wind direction and secured to posts about 3 m (10 ft) apart to improve their stability. If accretion fills the fences, additional fencing can be installed at the new level to promote further growth. Field tests of dune building with sand fences under a variety of conditions have been conducted at Cape Cod, Massachusetts, Core Banks, North Carolina, and Padre Island, Texas. The following are guidelines and suggestions based on these tests.

- Only straight fence alignment is recommended, and the fence should parallel the shoreline. It need not be perpendicular to the prevailing wind direction. Fence will function even if constructed with some angularity to sand-transporting winds. Fence construction with side spurs or a zigzag alignment does not increase the trapping effectiveness enough to be economical (Savage 1962; Knutson 1980). Lateral spurs may be useful for short fence runs of less than 150 m (500 ft), where sand may be lost around the ends (Woodhouse 1978).

- Placement of the fence at the proper distance shoreward of the berm crest may be critical. The fence must be far enough back from the berm crest to be away from frequent wave attack. Efforts have been most successful when the selected fence line coincided with the natural vegetation or foredune line prevalent in the area.

- Dunes are usually built with sand fencing in one of two ways: by installing a single fence and following it with additional single fence lifts as each fence fills (Figure V-4-31); or by installing double fence rows with the individual fences spaced about four times the fence height apart and following these with succeeding double-row lifts as each fills (Figure V-4-32). Single rows of fencing are usually the most cost-effective, particularly at the lower wind speeds, but double fences may trap sand faster at the higher wind speeds.

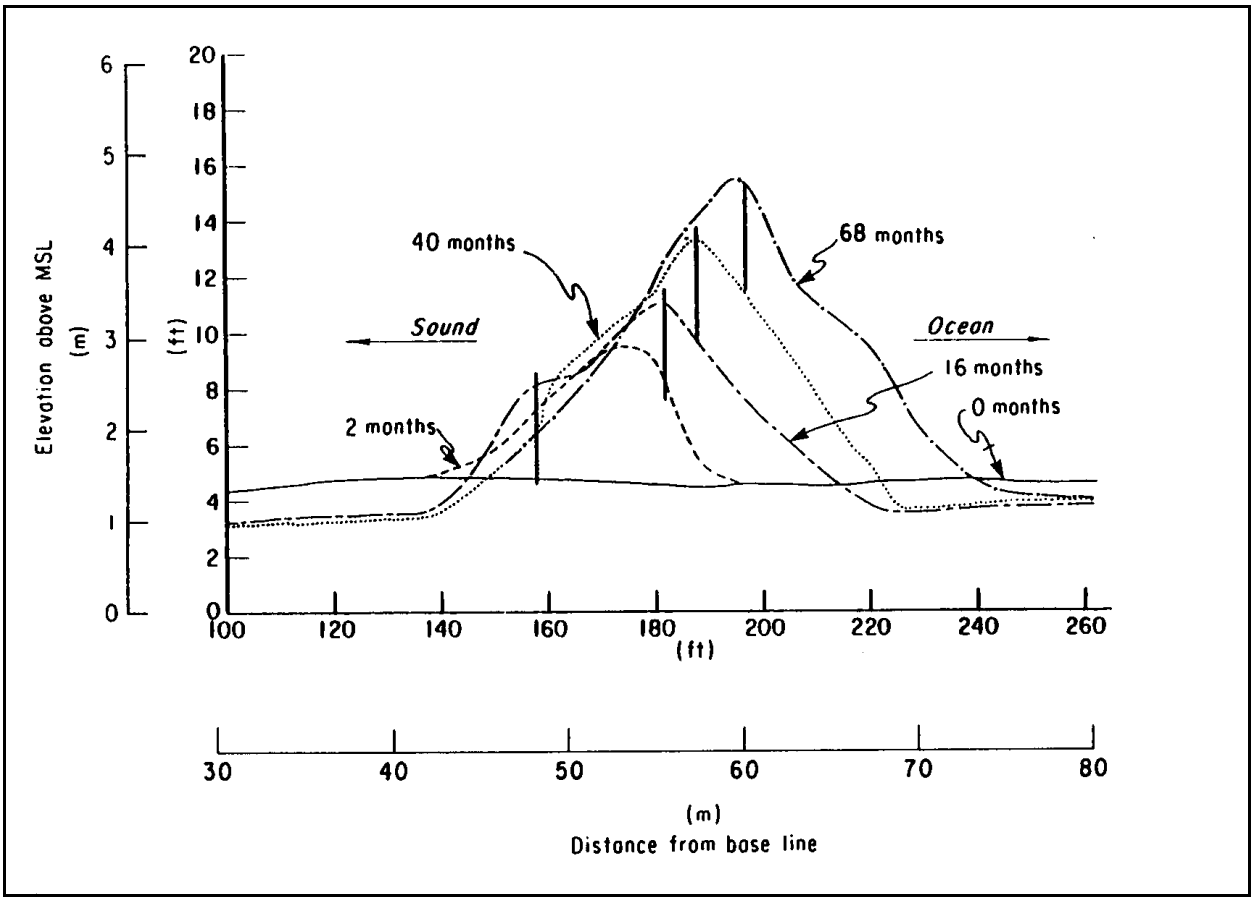

Figure V-4-31. Sand accumulation by a series of four single fence lifts, Outer Banks, North Carolina (Savage and Woodhouse 1969)

- Dune height is increased most effectively by positioning the succeeding lifts near the crest of an existing dune. However, under this system, the effective height of succeeding fences decreases and difficulties may arise in supporting the fence nearest the dune crest as the dune becomes higher and steeper. Dune width is increased by installing succeeding lifts parallel to and about four times the fence height away from the existing fence. The dune may be widened either landward or seaward in this way if the dune is not vegetated.

- Accumulation of sand by fences is not constant and varies widely with the location, the season of the year, and from year to year. Fences may remain empty for months following installation, only to fill within a few days by a single period of high winds. To take full advantage of the available sand, fences must be observed regularly, repaired if necessary, and new fences installed as existing fences fill. With sand moving on the beach, fencing with 50 percent porosity will usually fill to capacity within 1 year (Savage and Woodhouse 1969). The dune will be about as high as the fence. The dune slopes will range from about 1:4 to 1:7, depending on the grain size and wind velocity. The trapping capacity of the initial installation and succeeding lifts of a 1.2-m-high sand fence averages between 5 and 8 cu m/lin m of shoreline (2 to 3 cu yd/lin ft).

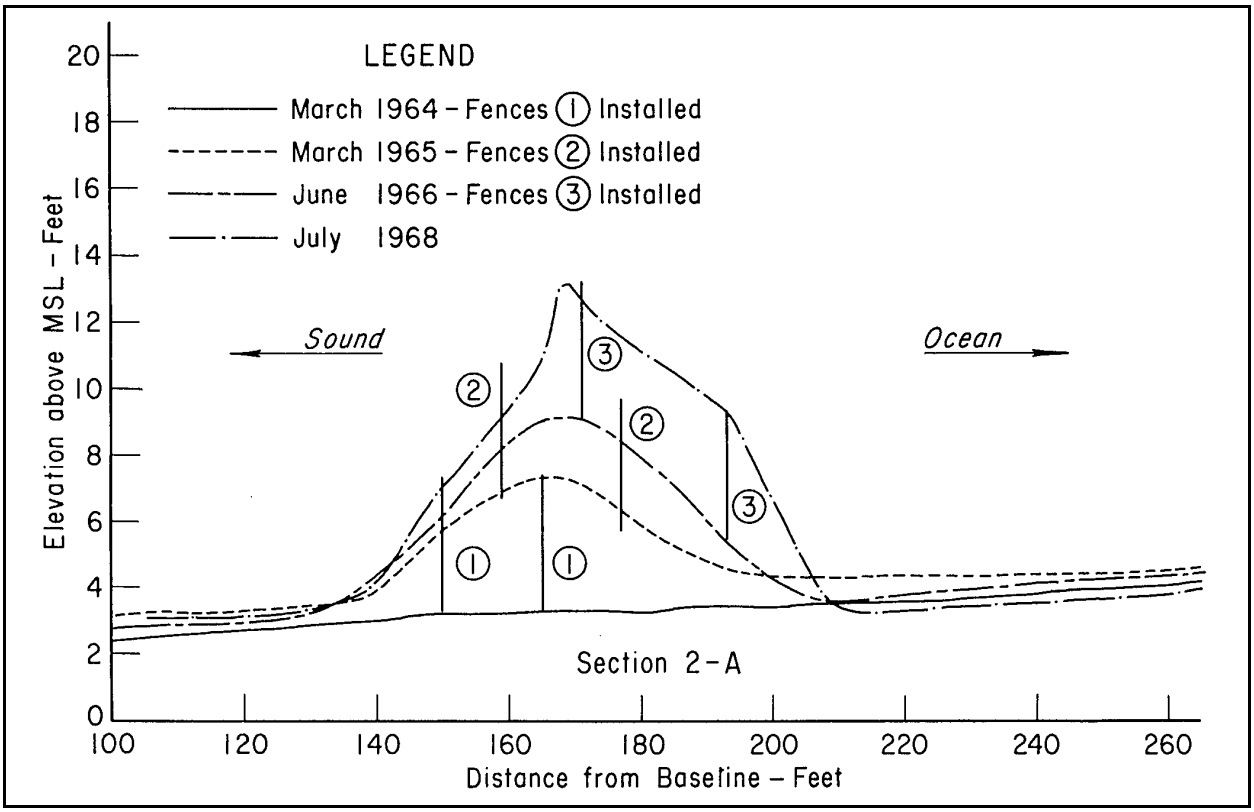

Figure V-4-32. Sand accumulation by a series of three double fence lifts, Outer Banks, North Carolina (Savage and Woodhouse 1969)

- Experience has been that an average of 6 man-hours are required to erect 70 m (230 ft) of wooden, picket-type fence or 60 m (195 ft) of fabric fence when a six-man crew has materials available at the site and uses a mechanical post-hole digger.

- Fence-built dunes must be stabilized with vegetation or the fence will deteriorate and release the sand. While sand fences initially trap sand at a high rate, established vegetation will trap sand at a rate comparable to multiple lifts of sand fence. The construction of dunes with fence alone is only the first step in a two-step operation. Fences have two initial advantages over planting that often warrant their use before or with planting: sand fences can be installed during any season, and the fence is immediately effective as a sand trap once it is installed. There is no waiting for trapping capacity to develop, unlike the vegetative method. Consequently, a sand fence is useful to accumulate sand while vegetation becomes established.

(b) Vegetation. Vegetation is a natural means of shore and dune stabilization that is effective when used under the proper circumstances. Vegetation is relatively economical, and does not detract from, but can enhance environmental quality. On open sea coasts, vegetation is primarily used to enlarge and stabilize dunes. A number of beach grasses and other plants tolerant of a dune environment can be used to create, enlarge, or stabilize dunes. Frequently used species are American beach grass (*Ammophila breviligulata*) in mid- and upper-Atlantic Coast and Great Lakes, European beach grass (*Ammophila arenaria*) on the Pacific Coast, sea oats (*Uniola paniculata*) on the south Atlantic and Gulf Coasts; and the panic grasses (*Panicum amarum*) and (*Panicum amarulum*) on the Atlantic and Gulf Coasts. All of these plants can be propagated by planting suitable stock and are effective in trapping and holding windblown sand. A number of herbaceous and woody plants are also effective in dune areas. The principal considerations in selecting plants

for dune building and stabilization are the suitability of the species for growth in the project area, its probable effects on the existing ecology, availability of stock for transplanting, and economics. Detailed information on suitability of plant species for various regions of the United States, methods of propagation and planting, and protection against disease and physical damage can be found in EM 1110-2-1204, "Environmental Engineering for Coastal Protection"; Knutson (1977); Woodhouse (1978); Savage and Woodhouse (1969); and Knutson (1980). Dune stabilization by vegetation has these advantages. It is capable of growing up through the accumulating dune sand and it can repair itself if damaged, provided the damage is not too extensive and the vegetation was well established prior to being damaged. New plantings will require periodic fertilization the first year or two, and watering the first few months, for the young plants to become well established.

(c) Dune cross-over structures. If newly-constructed or existing dunes are to be stabilized with fences and/or vegetation it is important to protect the stabilization efforts by minimizing traffic through or across the dune. Pedestrian and/or vehicular traffic will damage vegetation and fence lines. Dune walk-over structures for pedestrians and controlled vehicular access points to the beach should be provided in the overall design. Controlled access points provide recreational as well as maintenance access to the beach without damaging the stabilized dune area. Barren low spots (such as caused by trampling) within an otherwise healthy vegetated dune can experience wave overwash and further dune deflation during storms (see Part IV-2). These local areas of overwash and deflation are commonly referred to as a "blow-outs." Blow-outs reduce the dune's reservoir of sand and capability to protect upland areas from flooding. Construction guidelines for dune cross-over structures are provided in U.S. Army Engineer Waterways Experiment Station (1981).

j. Construction issues.

(1) Removal, transfer, and placement of borrow material. Removal, transfer, and placement of borrow material is typically the job for the dredging contractor. However, certain aspects of the dredging work should be understood so that practical design and reasonable specifications can be developed prior to bidding out the dredging job. With regard to the removal and transfer phases of the job, the following points are made:

(a) Offshore borrow areas typically have fine material in the top layers. Hence, if the borrow area is shallow, large losses of fines may occur during the placement operation. Typically, thicker borrow areas are more economical for this reason.

(b) The further offshore the borrow area is located, the more expensive the pumping of material becomes. Direct pumping to the beach may not be economically feasible if the borrow area is located too far offshore.

(c) If a hopper dredge or barge is used to transport fill to the site, many of the borrow material fines are washed out with overflow, hence providing a larger grain size distribution of fill material than that based on in situ samples from the borrow site. This fact and the fact that less dirty material (fines) is provided at the subaerial beach may make this type of placement desirable from an environmental and public satisfaction standpoint.

(d) Borrow areas should not be located too close to shore due to the fact that the equilibrium profile of the beach may be downcut. This could lead to offshore transport of material from the nearshore zone to make up for the deficit. If the borrow site is located too close to shore, and in too shallow water, the irregular bathymetric feature created as a result of the excavation can significantly alter the propagation of incoming waves. This could lead to an erosional hot spot. As a rule of thumb, borrow areas should be located in water depths at least twice the estimated depth of closure (see Part III-3-3-b), or a comparable distance offshore.

(e) For hydraulically-filled projects, there is a minimum practical sectional fill volume. That is, the constructed beach-fill must be of sufficient width for the contractor to erect dikes, move pipeline, and operate equipment for grading the placed fill and building the dune section, etc. Typical sectional fill volumes range from 25 to 63 m^3/m (10 to 25 yd^3/ft) for truck-haul projects and from 75 to greater than 250 m^3/m (30 to greater than 100 yd^3/ft) for hydraulically placed fill projects. Sectional fill volumes between 140 and 215 m^3/m (55 and 85 yd^3/ft) are fairly common; however, Dean and Campbell (1999) recommended a minimum sectional fill volume of 200 m^3/m (80 yd^3/ft) from a performance perspective.

(f) A good overview of various dredging systems which can be applied for beach nourishment from offshore sources is provided by Richardson (1976). If trailing suction hopper dredges are available (loaded draft $\approx$ 9 m for large hopper dredges), long borrow areas may be preferable (for long production runs). Cutterhead pipeline dredges may be more economical where borrow areas are more uniform in dimension (i.e., square) and the deposit is relatively thick (1.5 m or greater) so that the dredge and pipeline do not need to be moved far.

(g) There are four types of material placement for beach-fill purposes. Description and comments on these methods follow:

- Direct placement. In this method, the fill is placed at one time throughout the stretch of shore to be protected. This is the most frequently used method of placement. Usually, fill is pumped as a slurry onto the beach via hydraulic pipeline, then reworked into the desired configuration using earth-moving equipment. Additional pipeline is added in sections to extend the placement zone along the beach. The largest grain sizes in the slurry will settle out closest to the slurry discharge point. Likewise, the finer grain sizes will settle out at greater distances. Hence, locating discharge points in locations of known maximum erosion or hot spot regions may be desirable. Providing a sand dike behind which most of the discharge occurs will reduce loss of fines and provide better water quality in the area.

- Nearshore placement. This method is appealing because large volumes of material can be made available at low costs by hopper dredges or split-haul barges. The principle is that the material, dumped in shallow water is transported towards the beach by wave action. Early tests of this method where the material was dumped in water 6 to 11 m are presented by Hall (1952). In all cases, the results showed that the beaches did not benefit from the dumped sand to any appreciable extent. Hands and Allison (1991) have reviewed a number of offshore dumping projects and found that if disposal depth is less than closure depth, the disposal sediment would be active and move toward the beach. Although nearshore dumping may be more economical, it does not provide the level of protection to upland property that direct placement on the subaerial beach does. It is expected, though, that the nearshore mound will provide some level of wave attenuation. A mound may also change local wave refraction patterns, leading to changes in local longshore sand transport gradients.

- Continuous supply. This method is typically used at a littoral barrier (i.e., navigation channel or inlet) where sand trapped at the updrift side of the barrier is bypassed to the beach on the downdrift side. These operations are more commonly thought of and designed as sand bypassing systems rather than as a method of beach nourishment. The purpose of this approach is to restore the natural flow of littoral transport at the location where such interruption occurs.

- Feeder beaches. Feeder beaches involve the stockpiling of fill at the updrift end of the areas intended to receive the fill as the feeder beach erodes. This method is typically used for smaller projects where sand may be trucked in and/or access to discharge points on the beach is limited. The intent is for the stockpiled material to be distributed by natural littoral processes. Feeder beaches generally work well in areas that serve as a source of material for adjacent beaches. Examples are areas

immediately downdrift from inlets or other man-made structures that form a littoral barrier. An erosional hot spot may be another area where a feeder beach is useful as a means for maximizing sand retention.

- Stockpile. In some projects, sand is stockpiled landward of the primary dune (or elsewhere outside of the normally active littoral system) for use in emergency situations. The intent here is to store a quantity of material at favorable costs at a time when the dredges and equipment are already mobilized. Most often this material is used on an as-required basis to repair or restore dunes following storms, or as fill material to close a breach should one be opened by a storm. Having this material readily available at the time of a breach or when needed to restore an eroded dune line can substantially reduce the time and cost associated with completing the emergency repair. For some projects, it may be possible to anticipate that there will be a need for emergency repairs sometime during the life of the project. In these cases, it may be cost-effective to dredge and stockpile excess material for use in emergency situations at the time of initial project construction.

(2) Construction template.

(a) The construction template is the target cross-sectional profile that the contractor is expected to build to ensure that the proper volume is placed. Two construction approaches are generally used. One is to "over-build" the upper part of the beach profile, stacking the fill material to match the specified template. The second method involves placement of the fill volume over more of the active profile. The over-building method is used most often because of the availability and working limitations of equipment used to place and shape the fill, and the desire to place the material in the most economic manner, which usually means minimizing movement of the discharge point. To a degree, the second construction method involves doing what nature will do on its own anyway, redistribute the volume over more of the active profile. The over-building method relies on wave and current action to redistribute the fill to deeper parts of the active profile.

(b) In the overbuilding method, the dune and/or berm of the design profile is built to the desired elevation. However, the constructed berm width will be much greater than the design berm width for two reasons. First, the volume to be placed includes the advance nourishment volume in addition to the volume needed to create the design profile. Second, and most important, the volume is stacked in the nearshore zone only over a portion of the active depth. Figure V-4-33 shows a typical preproject beach profile, the design profile (which includes a dune), a modified design profile that includes the advance nourishment volume, and the construction template. The construction template reflects a different configuration of the sectional fill volume.

(c) The construction template is usually specified as a simple geometry, like that shown in Figure V-4-33. The dune is usually built with a trapezoidal cross section having the desired crest elevation, crest width, and side slopes (see Part V-4-1-f for guidance on selecting these parameters). The berm may include a gentle slope (1:100) that transitions from the toe of the dune to the seaward end of the berm crest on the design profile. Such a gentle slope is found on many natural benches. Additional material seaward of the design berm that arises from the overbuilding technique should be constructed to the design berm elevation. The design berm is either constructed with a uniform elevation equal to the design crest elevation or with a gentle slope from the toe of the dune to the seaward point on the design berm crest. At the seaward terminus of the constructed berm, the fill should be placed at a constant grade, the upper slope, from the berm crest elevation seaward to the elevation that corresponds to mlw. From this point seaward, the fill is placed on a more gentle slope, the lower slope, in an attempt to match the construction template. Earth-moving equipment can be used to shape the above-water portions of the profile to the desired slope. The submerged portions of the profile are more difficult to control.

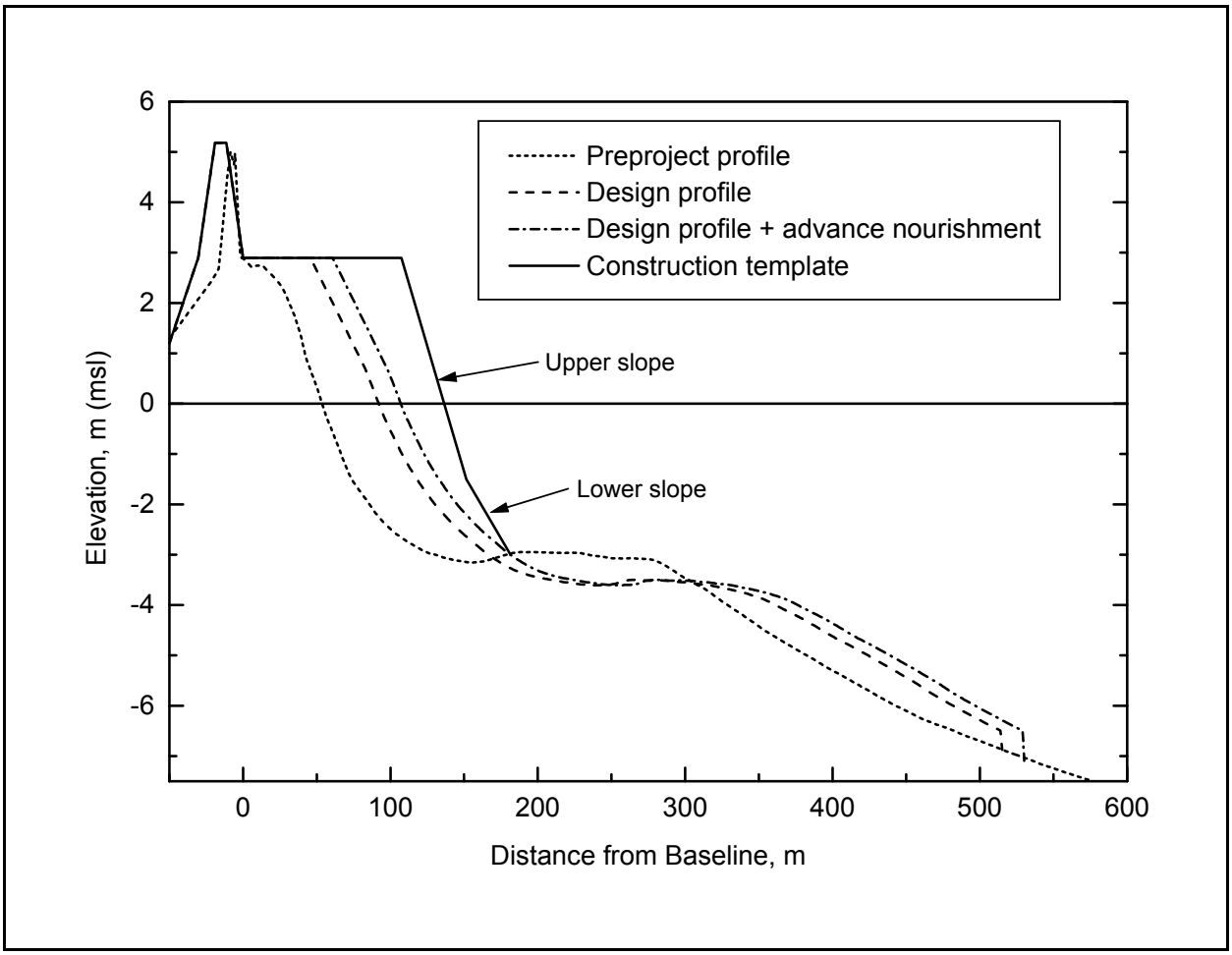

Figure V-4-33. Definition of beach profiles for nourishment projects

(d) To minimize difficulties in constructing the upper and lower slopes of the construction template, they should be defined based on expectations of how the beach will evolve after it is placed. The optimal slopes are primarily a function of the grain size characteristics of the fill and the wave and tide conditions that occur at the site during placement operations. One method for estimating upper and lower slopes involves use of the design profile. Part V-4-1-f-4 discussed methods for estimating the design profile shape. The upper slope of the construction template can be estimated as the average beach slope found on the design profile in the elevation range between the berm crest elevation and the elevation corresponding to mlw. The lower slope of the template can be estimated as an average slope computed from the design profile in the elevation range from mlw to a depth below msl which is approximately equal the typical storm wave height (e.g., 2 to 3 m below msl on the southeastern U.S. coast). The design profile reflects substantial adjustment and equilibration of the placed fill.

- Since the time between fill placement and surveying to assess compliance with the construction template might be short, full equilibration may not be realized. Therefore, the upper and lower slopes of the construction template should be chosen to be slightly steeper than the slopes estimated from the design profile.

- An alternative method is to apply the following rough rules to select both slopes.

Median Grain Size (mm)	Upper Slope	Lower Slope
D_{50} <0.2	1:20 to 1:15	1:35 to 1:20
0.2 <D_{50} <0.5	1:15 to 1:10	1:20 to 1:15
D_{50} > 0.5	1:10 to 1:7.5	1:15 to 1:10

(e) The median grain size corresponds to that of the fill material. Coarser material can be constructed to, and maintain steeper slopes; finer material adjusts to gentler slopes. Additional information on the specification of construction slopes, as a function of grain size, based on design experience in the southeastern United States is provided by Creed, Bodge, and Suter (1999). Example V-4-10 illustrates the procedure for developing a construction template.

(f) During placement, the fill should be monitored to determine actual slopes (particularly the lower slope). Strict adherence to the slope of the construction template is not an absolute requirement if the placed material seeks to attain a different adjusted slope. Adjustments can be made to the berm width of the construction template to allow for differences that occur between assumed and actual slopes. This will prevent unnecessary time being expended to mold the beach in a dynamic region of the profile. Analysis of monitoring data should be performed to ensure the prescribed sectional fill volume (volume per unit length of beach) is placed within the active beach zone. Placement of the prescribed sectional fill volume is more important than exactly matching a construction template.

(g) Scarping is one problem that may be encountered in the overbuilding approach. Scarps may develop at the toe of the fill as waves begin the profile adjustment process. Scarps can pose a threat to human safety, and they also present a problem for nesting sea turtles. Scarps can be mechanically smoothed as part of the construction contract or during regular beach maintenance and cleaning. Designing the berm crest elevation to be equal to the natural berm crest elevation, and selecting an upper slope of the construction template similar to the foreshore slope of the design profile, will minimize the likelihood of severe scarping.

(h) The second construction method involves placing more of the fill offshore, i.e., nourishing more of the active profile rather than stacking the material in the inshore zone. In this method, the target construction template is more or less the design profile. However, emphasis is placed on providing the required volume to the active profile, with less emphasis on achieving an actual construction template. Placement at various points across the profile may be more costly depending on the dredge plant used to construct the project. All material should be placed in depths less than the depth of closure. Accurate surveying is needed to monitor the actual volume of material placed, especially in the deeper portions of the active profile.

(3) Postconstruction profile adjustment. As previously above, construction profiles are generally out of equilibrium with the prevailing coastal processes, and they will begin to change shape during and after placement. This is particularly true for fills placed using the overbuilding method, where sand is “stacked” in the nearshore zone. Sand moved to lower elevations on the profile (eventually down to the depth of closure) is required to create and support the volume of sand visible on the dry beach.

EXAMPLE PROBLEM V-4-10

FIND:

Develop and plot the construction template together with the existing and final design profiles for the design condition discussed in Example V-4-2.

GIVEN:

Existing condition profile (Example V-4-2 Figure A).
Final design profile (Example V-4-2 Figure D).
Sectional fill volume is 298 m^3/m.

SOLUTION:

Develop a schematic construction template with berm elevation of 1.5 m (msl), a 1 on 20 slope from the berm crest to -1 m (msl) and a 1 on 35 slope from -1 m (msl) to the intersection with the existing profile. Translate the schematic construction template such that the volume between the existing profile and the construction template equals the volume difference between the existing profile and the final design profile. The results of this procedure are illustrated below. Note that the msl shoreline is advanced 75 m by the construction template whereas the design condition msl shoreline advances the shoreline only 30 m beyond the existing condition.

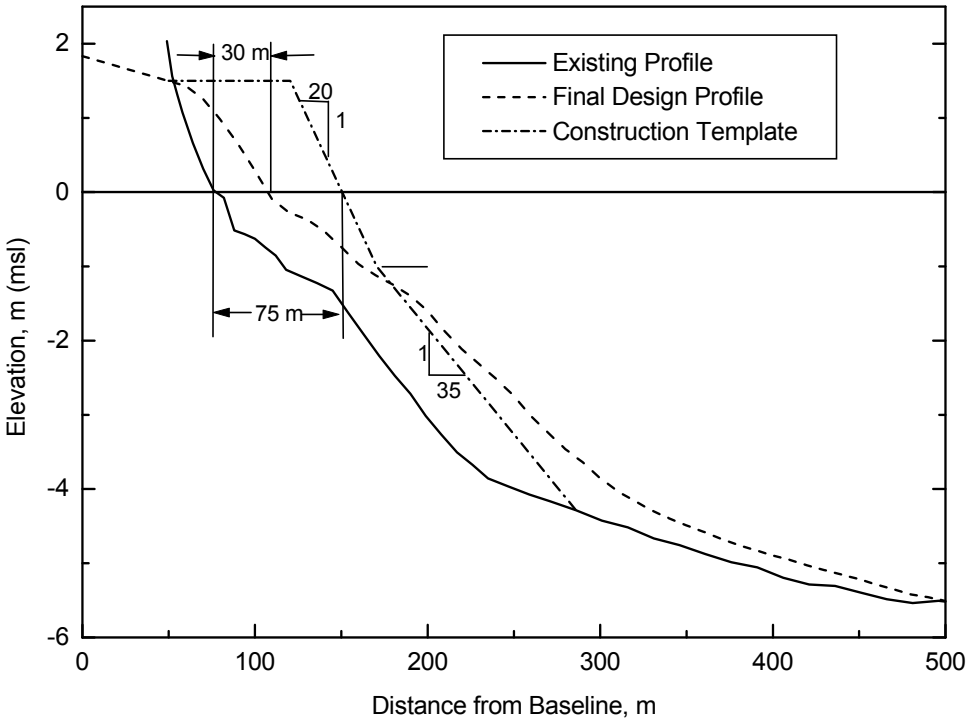

(a) The high water levels and more energetic wave conditions that accompany storms are very effective in adjusting the fill. Usually, the nourished profile will adjust to a shape that is much closer to the expected equilibrium shape during the first full winter season, at least on the portions of the profile that are shallower than the typical winter storm wave breaking depth. However, unless very severe storms are experienced during that first winter season, the fill material may not adjust to elevations equal to the depth of closure. Through the life of the project, as more severe storms are encountered, the material will be transported to deeper depths.

(b) For nourishment projects constructed using the overbuilding method, the initial adjustment process and resulting decrease in beach width can be quite dramatic. A rapid decrease in beach width from the constructed width to the design width (including advance renourishment) is often observed, and is to be expected. As a rule of thumb, decreases in beach width of 40 to 75 percent can be expected within a short period of time (months) immediately following construction if the overbuilding method is used. Projects constructed by placing material across much more of the active profile will see less dramatic adjustment in the width of the placed beach.

(c) The public often perceives this dramatic initial adjustment as project failure, particularly in light of the fact that most of the adjustment occurs either during construction or within a few months after construction. Many projects are built during the winter season (storm season) because of environmental windows imposed on the project, or to avoid the heavy beach-use season. A special effort should be made to educate the public and project sponsors regarding the initial adjustment process, and the differences between constructed profiles and design profiles. If the stacking method of construction is used, it should be explained to the project sponsors and beach users (local community) that the project is less expensive to build utilizing this unnatural construction template, and that the beach berm width will be reduced as natural processes redistribute material to the natural/equilibrium profile. Seasonal, cyclical changes in beach width should also be explained, i.e., loss of beach width during the winter storm season, and subsequent beach recovery during the summer. Seasonal changes in beach width will be masked initially by the much larger changes associated with the initial adjustment process.

k. Plans and specifications

(1) Schedules.

(a) Overall start and completion dates. The contractor is required to commence work under a contract within a specified number of calendar days after the date the contractor receives the notice to proceed. Typically, a period of 10 calendar days is specified. The contractor is directed to prosecute the work diligently and complete all work, ready for use, not later than a specified number of calendar days after receipt of the notice to proceed. The time stated for completion also includes final cleanup of the premises. Time needed to complete the work is directly dependent on the scope and extent of the project, and can vary from as little as 60 to 90 days up to a number of years for large projects. For example, the Atlantic Coast of Maryland Shoreline Protection Project, which included the placement of about 3.5 million cu m of beach-fill and dune construction along about 8 miles of shoreline, required completion within 720 days following the receipt of the notice to proceed (Anders and Hansen 1990). For some projects, start and completion dates may be dictated by environmental considerations such as dredging windows or recreational seasons. Sufficient completion time should be provided to avoid excessively high bids from potential contractors. To enforce the specified completion time for a project, liquidated damages are generally required for each day of delay.

(b) Start and completion dates for specific subtasks. Interim start and completion dates may be required for specific subtasks depending on the scope of the project. For example, an interim completion date for

beach-fill placement between designated stations may be required to enable other project features such as revetment or bulkhead construction to proceed.

- Depending on the scope of the project, the contractor may be required to develop a network analysis system for scheduling the work. The system should consist of diagrams and accompanying analyses that show the order and interdependence of activities and the sequence in which the work is to be accomplished by the contractor. In preparing this system, the scheduling of construction is the responsibility of the contractor. The requirement for the system is included to assure adequate planning and execution of the work and to assist the contracting officer in appraising the reasonableness of the proposed schedule and evaluating progress of the work. An example of one of the numerous acceptable types of network analysis systems is shown in USACE Pamphlet EP 415-1-4 entitled "Network Analysis System Guide."

- A preliminary network defining the contractor's planned operations during the first 60 calendar days after notice to proceed should be submitted soon after the notice to proceed. The contractor's general approach for the balance of the project should be indicated. The complete network analysis system consisting of the detailed network analysis, schedule of anticipated earnings as of the last day of each month, and network diagrams should be submitted within a specified number of calendar days after receipt of notice to proceed. The approved schedule should then be used by the contractor for planning, organizing and directing the work, reporting progress, and requesting payment for work that is completed.

(c) Expenditures. The contractor should submit, at monthly intervals, a report of the actual construction progress. The report should show the activities or portions of activities completed during the reporting period and their total value, which serves as the basis for the contractor's periodic request for payment. Payment made should be based on the total value of activities completed, or partially completed, after verification by the contracting officer. An updated network analysis should be used as a basis for partial payment. The report should state the percentage of work actually completed and scheduled, as of the report date, and the progress along the critical path in terms of days ahead or behind the allowable dates. If the project is behind schedule, progress along other paths with negative slack should also be reported. The contractor should also submit a narrative report which should include but not be limited to a description of the problem areas, current and anticipated factors causing delay, the impact of delay, and an explanation of corrective actions taken or proposed.

(2) Specifications.

(a) Boundaries of the project area. The limit of the geographical area available to the contractor must be shown on the project drawings. Except where indicated, the contractor should confine his work to the area seaward of the construction baseline and between the lateral limits of the project. This area does not generally include access, storage, and staging areas. Access routes and storage and staging areas required to perform the work should be provided by and at the expense of the local sponsor. Sponsors are generally given credit for the cost of obtaining the necessary easements and rights-of-way, which count toward their share of project costs. The contractor should coordinate access to the work area and storage and staging area locations with the contracting officer. Unless otherwise approved by the contracting officer, excess equipment should only be stored in approved storage or staging areas, or in temporary areas, in the immediate vicinity of the fill placement site. Operation of grading and other construction equipment should not be permitted outside the work area limits except for ingress and egress to and from the site at approved locations.

(b) Boundaries of the borrow area. All excavation for beach-fill material should be performed within the borrow area limits shown on the project drawings. Excavation in the borrow areas may be restricted to specified elevations depending on the findings of the geotechnical investigations of the borrow site (see

Part V-4-1-e). For offshore sources, the contractor should be required to set appropriate buoys which should meet U.S. Coast Guard standards to delineate the limits of the borrow areas. The contractor should be required to have electronic positioning equipment capable of achieving Class 1 survey accuracy as specified by EM 1110-2-1003, "Hydrographic Surveying." This accuracy is necessary to locate the dredge when operating in the borrow area. The geographical position of the dredge should be continuously monitored at all times during dredging operations. Locations should be determined with a probable range of error not to exceed 15.24 m (50 ft) to avoid violations of the environmental permits and clearances. Position data should be furnished as a part of the daily report of operations. Prior to initiation of any dredging, the contractor should submit for approval his proposed method of determining the dredge's location. Use of Loran-C positioning systems should be avoided, as output coordinates are not typically repeatable from one machine to the next.

(c) Routes between borrow area and project site. Determination of the route and the method used to transport beach-fill material from the borrow area to the fill site should be at the contractor's option. For offshore borrow sources, the contractor should be required to conduct the work in such manner as to obstruct navigation as little as possible. Upon completion of the work, the contractor should promptly remove his plant, including ranges, buoys, piles, and other marks placed by him under the contract in navigable waters or on shore.

- If a pipeline dredge is utilized in a congested navigation area, the pipeline may have to be submerged except at the dredge or at the location of any booster pumps or pumphouse barges. The contractor should maintain a tight discharge pipeline at all times. The joints of the pipeline should be so constructed as to preclude spillage and leakage. Upon development of a leak, the pipeline should be promptly repaired and the dredge may have to be shut down until a complete repair has been made.

- If a submerged pipeline is placed across a navigable waterway, the contractor should notify the contracting officer in writing. Notification should be received in the District Office prior to the desired closure date. This notification should furnish the following: location and depth (over the top of the pipeline) at which the submerged line should be placed; the desired length of time the navigable water is to be obstructed; the date and hour placement or removal should commence; and the date and hour of anticipated completion.

- It is recommended that a statement concerning submerged pipelines similar to the following be included in the dredging contract:

"Submerged Pipelines. In the event the contractor elects to submerge his pipeline, the top of the submerged pipeline shall be no higher than the required dredging depth for a channel for which the pipeline is placed. The submerged pipeline shall be marked with signs, buoys, and lights as required to the complete satisfaction of the contracting officer."

- Complying with this requirement may require that the contractor excavate a trench in the channel bottom. If it is known during the design phase that a submerged pipeline will cross a navigable waterway, then specifications and provision for the contractor to establish (trench) the crossing should be explicitly provided. The equipment necessary to trench the crossing, and the disposal site for the trenched material will, in all likelihood, be different than that required to construct the beach-fill.

- If the contractor elects to use a hopper dredge or pumpout barge, overflow during loading should be permitted to the extent that designated turbidity and water quality standards are met. The contractor should limit the loading to partial loads, if necessary, to meet turbidity and water quality requirements for the overflow during loading. No overflow or spillage should be permitted during transport to the discharge site.

(d) Placement methods. The contractor should be given the option of starting the beach-fill placement operations at any point and proceeding in any direction along the project beach, unless special conditions exist.

- Acceptance reaches, which are segments of beach measured along the construction baseline between designated stations used to monitor construction of the project, should be defined and identified on the project drawings. For the case of the lateral termini, the acceptance reach is the segment of beach, measured along the construction baseline, between the longitudinal limit of fill and the subsequent designated station.

- Once the contractor begins placement in an acceptance reach, placement in that reach should be completed before proceeding to another acceptance reach. Beach-fill placement operations should proceed in an orderly manner from reach to reach. If more than one dredge and/or pumpout facility is utilized by the contractor, more than one beach-fill operation may be accomplished simultaneously. Placement of beach-fill in multiple locations at any one time should only be allowed if adequate inspection is available.

- Prior to initiation of beach-fill operations, the contractor should submit for approval his proposed plan for beach-fill placement. The plan should include the type of dredge plant to be utilized, the location and type of any booster pump facilities to be utilized, and the sequence of work for beach-fill placement. The contracting officer should reserve the right to reject any scenario which, in his/her opinion, might be detrimental to the stability of the in-place beach-fill, might unduly disrupt access to or use of the beach by the public during placement operations, or for any other credible reason. Excavation of sand from the existing beach for use as beach-fill should not be permitted.

- All materials excavated from the borrow areas should be transported to and deposited on the beach or dune area within the specified lines, grades, and cross sections in a controlled manner so as to maximize sand retention within the beach-fill section and minimize losses to the ocean. This should be accomplished in a manner acceptable to the contracting officer and should include, but not be limited to temporary diking where required, control of the discharge pipe direction and velocity of discharge, and control of the sand and water mixture. Temporary diking included within the dune cross section may be left in place and incorporated into the dune structure.

- For dredged borrow sources, fill placement on the beach can be accomplished by a single or double-pipe system. The double-pipe system consists of a yoke attached to the discharge line, and by use of a double-value arrangement, the discharge slurry is selectively distributed to either one pipe or the other, or to both pipes simultaneously. The beach is built by placing the first discharge pipe at the desired final fill elevation and pumping until the desired elevation is reached. By alternating between the two discharge lines, the beach width is built to the full cross section as they advance. The final placement to the design lines and grades can be accomplished using bulldozers.

- The contractor should be required to maintain and protect the beach-fill in a satisfactory condition at all times until acceptance of the work. Prior to placement of beach-fill, the contractor should remove from the work site all snags, driftwood, and similar foreign debris lying within the limits of the beach-fill section.

- The excavated material should be placed and brought to rest on the beach to the lines, grades, and cross sections indicated on the project drawings, unless otherwise directed by the contracting officer. The beach topography is subject to changes and the elevations on the beach at the time the work is accomplished may vary from the design elevations and the resulting beach-fill quantities may vary from that shown in the unit price schedule. To accommodate this situation, the contracting officer should reserve the right to vary the beach-fill cross sections at any location along the beach.

- The contractor should be responsible for any damage caused by excessive discharge water flowing landward from the beach-fill section. However, the plans and specifications should specify that the contractor will construct sand dikes of a minimum length to control water discharge and promote settlement of the slurry's sediment. Where a pipeline is placed on the beach, sand should be placed around the pipe to form a pedestrian ramp over the pipe at street ends and at midblocks or at locations otherwise directed by the contracting officer. All such ramps should be maintained as long as the pipe is in place.

(e) Final project dimensions. The intent of the contract is to place beach-fill to the lines and grades prescribed in the contract. Tolerances should be provided in the template for the practicality of construction. A tolerance of ±0.2 m (0.5 ft) is usually permitted for the dune and berm design sections. However, in light of the critical nature of beach elevation to shore protection and flood damage reduction, the contractor should be required to provide his best efforts in placing material to the designated lines and grades landward of the influence of waves. Persistent over- or underfilling of the construction template to the plus or minus tolerance should not be permitted. It should be considered that the primary goal of nourishment is to place a specified volume of material per unit length of beach. The required dimensions of the construction template, specifically the width of the construction berm, should not be explicitly specified so that the width of the berm can be adjusted during construction to account for the actual foreshore slope the fill acquires during placement.

- Any material placed above the prescribed cross section, plus the allowable tolerance, should not be included in the pay quantities; however, such material may be left in place at the discretion of the contracting officer. In the event that material placed at any prescribed cross section is below the minus tolerance, the contractor should be required to provide additional sand to the level of the beach-fill template.

- Upon completion of all fill operations in any acceptance reach, the beach should be graded and dressed to eliminate any undrained pockets and abrupt mounds or depressions in the beach-fill surface as necessary to comply with tolerance requirements specified. All temporary dikes not incorporated into the dune cross section should be completely degraded.

- Any material deposited in areas other than those designated or approved by the contracting officer should not be paid for. The contractor should be required to remove such misplaced material and deposit it where directed, at his expense.

(f) Calculating fill volume for payment purposes. Options for calculating fill volumes for payment include: tabulation of the fill delivered by truck load from land borrow sources, comparison of pre- and post-dredging surveys for offshore sources, and measurement of in situ volumes after placement. Of these options, the latter is recommended. With this method, acceptance reaches should be used for the purpose of closely monitoring the cumulative amounts of beach-fill placed. Acceptance reaches should also be used to control the timing for pre- and postplacement surveys. Acceptance for payment by the contracting officer of a reach should not be made until all beach-fill placement is made within the acceptance reach and final surveys have been approved. Separate acceptance for the dune portion of the beach-fill may be made for an acceptance reach upon approval of the contracting officer. In no case, however, should the contractor be paid more than

once for sand placed in any space along any acceptance reach should erosion occur before the entire volume of sand is placed. Unless otherwise approved by the contracting officer, acceptance reach stationing should be as shown on the contract drawings.

- Beach fill, satisfactorily placed, may be measured for payment by use of the average end area method. The quantity computations should be verified from survey data submitted by the contractor in accordance with specified procedures. The basis of measurement should be the preplacement cross sections of the beach and dune area taken by the contractor just prior to the placement of fill and a second set of cross sections of the same area taken by the contractor as soon as practicable after completion of beach-fill placement for any acceptance reach. The plans should depict existing conditions and the construction template at intervals along the shoreline not greater than 150 m (500 ft). Measurement for payment is typically surveyed at more frequent intervals, often at about 30-m (100-ft) spacing. Once postplacement surveys have been taken in an acceptance reach, no removal of beach-fill material should be permitted in that reach unless otherwise directed by the contracting officer. Landward of the wave runup limit (in general, landward of the seaward berm crest position), the area of fill material lying above the plus tolerance (an elevation tolerance of less than ± 0.2 m is typical) template should be deducted from the gross area and the net amount used as a basis for payment. Seaward of the wave runup limit, the quantity of fill material used as a basis for payment should be that determined from the area of fill measured between pre- and postfill cross sections, less any material placed seaward of the intersection of the construction template with the existing sand surface (corrected as necessary for the actual slope taken by the fill material, if deemed appropriate by the contracting officer). Compliance with the construction template should be judged reasonably on the submerged portion of the profile. Success of the placement should also consider placement of the required volume of fill per unit length of beach within the active depth (landward of the design depth of closure).

- Payment for beach-fill should be made at the contract price per unit volume. Such payment should constitute full compensation for furnishing all labor and performing all work necessary to excavate, transport, and place beach-fill material, and all other items of work required by the drawings and the specifications for which separate payment is not provided.

- Survey specifications should indicate that the contractor conduct the original and final surveys, and surveys for any interim period, for which progress payments are requested. All these surveys should be conducted under the direction of the contracting officer, unless the contracting officer waives this requirement in a specific instance. The contractor should employ a registered and licensed land surveyor, experienced in land and hydrographic surveying, to perform the work required for quantity surveys. Prior to initiation of any quantitative beach surveys, the contractor should submit to the contracting officer for approval, a description of his method and type of equipment for performing the surveys.

- The contractor should make such surveys and computations as are necessary to determine the quantities of work performed or sand placed. All original field notes, computations, and other records should be furnished to the contracting officer at the work site.

- The contractor should perform his preplacement surveys of an acceptance reach no more than 5 days prior to placement of beach-fill material within that reach. Prior to placement of fill material the contractor should submit to the contracting officer, all field notes, data disc(s), and computations, with sufficient lead time so that control of quantities, and if necessary, adjustment to the berm width can be made.

- Postplacement surveys should be made as soon as practicable after completion of an acceptance reach. The contractor should use the same survey stations that were used in the preplacement surveys. Postplacement surveys for the next reach should not be conducted until the previous reach is accepted by the contracting officer.

- The contractor should prepare and provide to the contracting officer, immediately after completion of an acceptance reach, cross-sectional drawings showing the preplacement conditions, post-placement conditions, and the design beach-fill template for each section surveyed. The survey cross sections should be taken perpendicular to the construction baseline at specified stations, and at the beginning and ending acceptance reach stations. When unusual site or geographical conditions exist, additional stations and elevations should be taken for greater definition. The pre- and postplacement surveys should extend some distance seaward of the intersection of the construction template with the existing sand surface and that distance should be specified. The scale for the plotted cross sections should be on the order of 1 to 60 in the vertical (1 cm = 0.6 m or 1 in. = 5 ft) and 1 to 240 horizontal (1 cm = 2.4 m or 1 in. = 20 ft). All stations and elevation points taken from field books should be clearly indicated on the cross-section plots.

l. Project monitoring and data analysis. Beach fills are "soft structures" which respond dynamically to changing waves and water levels, similar to natural beaches. Physical responses of a beach-fill include post construction adjustment of the placed sand, seasonal variation and storm-induced changes of the beach profile, and seasonal and long-term change of the project planform. Functional performance of a beach-fill requires that the design cross section and planform be maintained over the life of the project through scheduled periodic renourishment, and emergency maintenance and/or renourishment after severe storms. The dynamic behavior of beach-fills together with the need to ensure project functionality over the design life requires that a systematic monitoring plan be established for beach-fill projects.

(1) Monitoring objectives. Primary objectives of monitoring beach-fill projects are to ensure that project functionality is maintained throughout the design lifetime, and to assess project performance. These objectives involve collection, analysis, and interpretation of data to: evaluate the condition of the project in comparison to design specifications; determine maintenance and renourishment volume requirements; document and assess project performance to determine how well it fulfills the protection requirements for which it was designed; evaluate project impacts on adjacent areas; and address performance problems by identifying causes and developing solutions.

The first two activities listed relate primarily to operational monitoring and provide information required to operate and maintain the project. The latter three activities relate to performance monitoring, and measure the success of the project, identify project problems, and provide information for improving the project design.

(2) Physical monitoring components. A physical monitoring plan for a beach-fill project consists of four major components: beach profile surveys, beach sediment sampling, aerial shoreline photography, and wave and water-level measurements. These four components provide information required to document the physical response and condition of a beach-fill project. A recommended schedule of data collection is presented in Table V-4-1. The schedule is divided in two phases. The initial phase is a period of more-intensive monitoring during the first 3 years of the project that focuses on monitoring the performance of the project. During this phase, data are gathered to confirm that the project design is performing as expected and to identify potential design problems such as erosional hot spots, unexpected project impacts, or inadequate design volumes and cross-section dimensions. If problems are identified, the monitoring data provide information for developing solutions and improving project performance based on an understanding of the physical processes. Assuming the project is functioning properly and design/performance deficiencies are addressed, the monitoring plan presented in Table V-4-1 transitions to a second phase after the third year.

Table V-4-1
Physical Data Collection Schedule for Beach-Fill Monitoring

Phase I: Initial Placement and Project Years 1 to 3[1]

Monitoring Component	Initial Placement		Year 1 Following Initial Placement				Years 2 to 3		Years 1 to 3 Poststorm Contingency
	Pre-fill	Postfill	Mar	Jun	Sep	Dec	Mar	Sep	
Beach profile surveys	X	X	X	X	X	X	X	X	X
Sediment sampling	X	X			X				
Aerial photography	X				X			X	
Waves and water levels	Continuous								

Phase II: Nonconstruction Years for Project Years 4 to N (N= Project Life)

Monitoring Component	Even Number Years Following Each Construction	Odd Number Years Following Each Construction	Years 4 to N Poststorm Contingency
	September	September	
Beach profile surveys	X	X	X
Aerial photography		X	

Phase II: Beach Renourishment

Monitoring Component	Renourishment		Year Following Renourishment
	Prefill	Postfill	September
Beach profile surveys	X	X	X
Sediment sampling	X	X	X
Aerial photography	X		X

[1] Following Year 3, decision is made whether to continue Phase I level of monitoring

The second phase of the plan employs an operational level of monitoring to annually assess the condition of the project. This phase of monitoring also provides information for assessing longer term aspects of project performance. Details of the monitoring components and schedules are discussed in the following paragraphs.

(a) Beach profile surveys. Profile surveys provide data which are used to calculate fill volumes and document changes in the beach cross section. Accurate estimates of fill volume are essential during construction to ensure that required design volumes are placed in the construction template, and to verify payment to contractors. Periodic surveying of profile lines over the project lifetime enable calculation of volume of fill remaining in the project bounds and on the subaerial beach and comparison of the present project condition with the required design template.

- Where practical, profile surveys should be conducted using a sea-sled system. Because of the accuracy, simplicity of design, and wide availability of system components, the sea sled is considered to be the best method for profiling beach nourishment projects (Grosskopf and Kraus 1993). An added advantage is that sea-sled surveys can extend from the upper portion of the dry beach out to the depth of closure. In areas where sea-sled surveys are not practical (e.g., in environments with reefs, rock outcrops, submarine canyons, etc.), offshore surveys should be taken by boat with a properly calibrated fathometer and combined with land-based rod and level surveys performed out to wading depth. When using this combined technique, care must be taken to avoid problems in matching the land-based and fathometer surveys.

- Survey locations should be selected to include profiles within the project limits as well as control profiles some distance up and downdrift of the project boundaries to assess benefits or impact on adjacent shorelines due to longshore spreading of the fill. The number and location of profile surveys is site specific and depends on the length of the fill and the degree of longshore uniformity of the beach morphology. On an essentially straight open-coast beach, longshore profile spacing of approximately 300 m should provide adequate resolution for periodic condition profile surveys. Pre- and postconstruction profile surveys are routinely collected at higher resolution, with spacing of 60 m or less, to accurately determine placement volumes for payment purposes. To reduce costs, profile spacing can be evaluated after several monitoring cycles to determine if the number of profile surveys may be reduced while still adequately characterizing the condition of the project.

- Profile locations should be established along a reference baseline from benchmarks that are documented and recoverable in future years. The project baseline should be set at the beginning of a project study, and all surveys should be referenced to this baseline. The surveys should extend across the entire zone of profile change from the upper profile, landward of any dune, out to beyond the depth of closure.

- In practice, exact timing of beach profile surveys depends on the construction sequence and climatic conditions; but in general, surveys should be conducted as indicated in Table V-4-1. Surveys taken immediately prior to and following construction document fill volumes and cross sections. Quarterly surveys taken during the first year following initial construction document the rapid response of the constructed cross section as it forms a more natural shape. Semiannual surveys measured in years 2 and 3 of the project record the ongoing adjustment of the project cross section. After the third year of the project, survey frequency can be reduced to once a year assuming the project is performing satisfactorily. It is recommended that these annual surveys be performed at the end of summer (or the typical period of low-energy wave conditions) to determine project condition prior to winter (or the typical storm season).

- The monitoring plan should include continency plans to collect surveys immediately after severe storms. Poststorm profile data document storm-induced beach change and poststorm condition of the project.

- Site inspections should be performed concurrently with all beach surveys, and at least once each year. Inspections should document any information relevant to characterizing the condition of the subaerial beach (e.g., level of dune vegetation, evidence of modification or addition of fill material by local property owners, effects of storms such as scarping or overwash, presence of poststorm recovery berm, longshore variability in subaerial beach features). Site inspections should include photographs of the beach, taken looking alongshore, to provide a visual record of the project condition.

(b) Beach sediment samples. Sampling is needed to determine sediment characteristics, such as median grain size and grain-size distribution, which affect the beach profile shape and influence fill volume requirements. Sediment sampling is of particular importance when fill and native material have different characteristics. Sampling of beach sediment provides data that can be used to relate project performance to characteristics of the fill material. This information can then be used to evaluate future borrow-material suitability and determine required fill volumes for renourishment.

- Sediment samples should be collected at selected locations within the project area to account for longshore and cross-shore variability in sediment characteristics. The longshore sample spacing should be approximately 900 m, with sampling locations corresponding to the nearest profile lines.

- Sediment sampling should consist of shallow grab samples at various locations across the beach profile including the dune, berm, midtide level, mlw, and three subaqueous samples spaced uniformly out to the depth of closure (Larson, Morang, and Gorman 1997). This sampling scheme documents cross-shore variability of the median grain size and size distribution which influence profile shape.

- Sediment samples should be collected before and after initial construction and each renourishment, and 1 year following each construction. Sediment sampling should be performed concurrently with beach profile surveying.

(c) Aerial shoreline photography. Aerial photography is an essential monitoring component for documenting long-term performance of beach-fills. Aerial photographs provide a visual record of shoreline position, variations in beach planform, condition of the dune and berm, and subaerial beach width; and do so with a total-project perspective that cannot be obtained by ground photography and beach profile surveys alone. Such information is useful for documenting project planform evolution, evaluating project end effects, and identifying erosional hot spots. Aerial photographs, together with beach profile surveys, provide information on the 3-D characteristics of fill behavior that can be used to better assess condition of the project and renourishment requirements.

- Aerial photography should be taken along a single flight line with 60 percent overlap stereo coverage of the entire project area shoreline, including updrift and downdrift control areas. The scale of the photographs should be sufficient to identify shoreline features. An approximate scale of 1 cm equals 50 m is recommended. All photography should be taken near midday and around low tide to reduce shadows and reflections and to provide the maximum area of exposed intertidal beach.

- Aerial photography should be performed before initial placement and after each construction to document the preproject and postnourishment shoreline. During the first 3 years, aerial photographs should be taken annually to record initial planform spreading and shoreline response to measured wave conditions. After the first 3 years, aerial photographs should be taken once every 2 years between construction and in the year following each construction. It is recommended that aerial photographs be collected in September (prior to the storm season) when the beach is typically in its most-accreted condition. During this time, effects of storms on the observed shoreline are minimized, allowing easier assessment of fill condition from year to year and providing a more consistent measure of long-term project performance.

(d) Wave and water level measurements. Waves and water levels are the principal hydrodynamic forcing parameters controlling beach-fill evolution. Storm waves and water levels erode the upper part of the beach and redistribute sand across the profile. Over the longer term, wave-driven longshore processes reshape the planform and produce shoreline retreat along the project. Establishing a cause-and-effect

relationship between actual waves and water levels and measured beach response is essential for understanding project behavior and formulating solutions when problems occur.

- Wave and water level data also provide valuable information for evaluating project design tools and techniques. Application of design tools with monitoring data may enable more accurate assessment of renourishment intervals and quantities and refinement of the project design to improve performance throughout the remainder of the project life.

- Wave and water level data should be collected using a directional wave gage. The gage should provide a continuous record of information from which significant wave height, peak wave period, peak direction, and mean water level can be determined. Water level (depth) measurements from the gage should be compared with area NOS tide gages or other sources to establish vertical datum control. The wave gage should be placed offshore of the center of the project outside the breaking zone. A depth of 10 m is typically sufficient for gage placement. Hemsley, McGehee, and Kucharski (1991) and Morang, Larson, and Gorman (1997) provide further guidelines for collecting wave and water level data.

- Wave data collection should begin prior to project construction and continue for at least 3 years from the time of initial placement. After 3 years, a decision should be made whether to continue data collection based on sufficiency of information obtained in evaluating project performance. At a minimum, data collection should continue long enough to capture at least one significant storm erosion event and to accurately assess trends in project behavior.

(e) Physical monitoring data analysis. A systematic data analysis plan should be developed as part of the monitoring activities. Pre- and postconstruction beach profile surveys should be analyzed to compute constructed fill volumes and verify compliance with construction template specifications. Sand samples should be analyzed to develop composite measures of median grain size and size distribution from which design profile shapes and fill volumes can be estimated for future construction. Seasonal profile surveys collected during Phase I of the monitoring plan should be used together with aerial shoreline photography to document initial fill adjustment and short-term project behavior. If problems arise such as excessive project erosion rates, erosional hot spots, or unanticipated impacts to adjacent shorelines, a coastal processes study should be performed with the monitoring data to identify causes and develop solutions. Poststorm profiles collected after major erosion events should be analyzed together with storm wave and water level data to verify project performance in light of design criteria. Analysis of Phase II monitoring data should focus on assessing project condition and renourishment requirements. The existing cross section should be compared with the design cross section to identify when dune heights or berm widths fall below design specifications. Shoreline data should be analyzed to determined long-term erosion rates and spreading losses for the project which can be used to fine-tune future renourishment activities.

(3) Borrow area monitoring. Monitoring procedures for the borrow area will depend on the type of borrow area being used. Borrow area types include offshore, inlet shoals, sand traps, bay or lagoons, and terrestrial sources. The principal purpose for monitoring borrow sites is to evaluate borrow fill suitability, borrow area bathymetry, continuing changes in the morphology and sediment characteristics, and biology of the area after completion of the borrow operation. Data collection should include bathymetric and sub-bottom surveying, sediment coring and surface sampling, and biological data acquisition. Baseline data should be collected prior to excavation and periodically thereafter. This section primarily addresses borrow sites in water-covered areas. Terrestrial borrow sites generally exhibit little or no change in topography and sediment characteristics after completion of the borrow operation.

(a) Bathymetric and bottom profiling. Once a borrow site is selected, removal of material from the borrow site will affect its morphology. The nature of the modification depends on whether the material was

obtained by excavating a thin superficial layer over a large area or deep pits in a comparatively small area. One objective of borrow site monitoring is to determine to what extent marine processes restore the original morphology or create new forms. For this reason bathymetric surveys are needed to monitor the site after the borrow operation.

(b) Borrow area sampling scheme. Borrow area sampling time and collection requirements are presented in Table V-4-2. The borrow area monitoring does not require data collection as often as the project site, however a minimum of 1 year between sampling is recommended.

Table V-4-2
Borrow Area Bathymetry and Sediment Sampling Scheme

Year	Times/year	Number of Samples
pre	1	Cores to characterize borrow material and access fill suitability. Bathymetry and subbottom sampling covering expected borrow sites and control areas.
post	1	Surface sediment grab samples to characterize postdredging borrow area sediment distribution. Bathymetry of postdredged surface to assess volume removed.
last	1	Cores to characterize infilling sediment grain size distribution. Bottom surface bathymetry to determine infilling volume.

(c) Changes in processes. Changes in bathymetry due to offshore borrow operations can modify the characteristics of incoming waves. These changes are primarily related to refraction and bottom friction. Dredging fill material from ebb tidal shoals is a likely source of wave modification because these shoals lie close to the shore and their crests are at shallow depths.

- During preproject planning and design, these factors will have been evaluated on the basis of theoretical considerations and indicate wave modification judged to be acceptable. However, it is possible that unforeseen effects may occur. These will usually be indicated by accelerated erosion or accretion of the project beach and/or adjacent shore areas. During postproject monitoring, any unusual erosion or accretion of the project area or adjacent beaches should be investigated with the possibility that it is resulting from modification of offshore borrow sources.

- Another type of process modification can occur where inlets and associated shoals are dredged for borrow material. The strength and distribution of tidal currents in the inlet and shoal areas can be altered by the removal of material. In such cases, provisions should be made for current observations as well as bathymetric and sediment data.

(d) Borrow area data analysis. Analyses should include evaluation of temporal borrow changes, determination of the rate and volume of borrow area infilling, and identification of current patterns in the borrow area channel or basin in cases where inlet shoals are excavated.

(4) Biological monitoring. The excavation and placement of fill material usually impacts the biology of the area that is directly involved. Biological impacts may also be created in adjacent areas from the turbidity created by the excavation process. For this reason, biological surveys of both the beach and borrow area should be performed. Monitoring of the borrow site should include assessment of the infauna, sea grasses, reefs, or other biologically sensitive areas adjacent to the borrow area. The beach project area may also have environmentally sensitive areas such as sea turtle nesting sites, bird nesting areas, beach organisms, nearshore reefs, and sea grasses. Biological sampling should consist of grab samples of the borrow area and quadrate samples of the beach areas to identify the infauna of the borrow and fill locations. Monitoring turbidity in the borrow site and in the surf zone of the fill area may be necessary to assess the impact of

dredging and dumping of fill material on the local biota. A more detailed outline of biological sampling can be found in EM 1110-2-1204, "Environmental Engineering of Coastal Shore Protection."

Data analysis should evaluate fluctuations in the flora and fauna in the beach-fill and adjacent nearshore area, effects of turbidity on fauna at the beach-fill and borrow site, and the effects of the borrow operation on the borrow site organisms. The time and extent of recovery of native organisms should be verified and compared to that of control areas. The absence of native or appearance of new organisms should also be verified and documented.

(5) Structure monitoring. If structures are a component of the project, a periodic inspection and survey report of the structures needs to be performed to assess the condition of the structures. This is especially important after a large storm that might do damage (functional or otherwise) to the structure. If damage is sustained by the structure(s), adequate photography of the structure should be taken to describe the damage and the extent of repairs that will be necessary. As damage photography is best compared to "design built" photography, a baseline set of photography for each structure in the project should be made as soon as possible after the structures are built. Damage photography for any damaged structure should be taken from the same locations as the baseline photography if reasonable and feasible.

At the time of structure inspection, the critical wave conditions (height, period, direction, etc.) under which the structure was damaged (if damaged) or exposed to (if not damaged) should be noted in the report/survey. A detailed survey of the structure may be needed. Last, an assessment of the structure's present and future effectiveness should be made.

m. Operations and maintenance

(1) Purpose. The beach-fill and any structures built for local shore protection, access, and any visitor facilities, must be operated and maintained to obtain the anticipated project benefits. In addition to periodic renourishment, the following types of maintenance work will be needed: mechanical redistribution of sand within the project area, grading, and periodic removal of debris from the project area. Performance and condition monitoring are needed throughout the economic life of the project. As discussed in the previous section, project monitoring and analysis is essential to assuring the project is providing the intended storm protection. In Federal beach nourishment projects, an Operations and Maintenance (O&M) manual specific to the project is prepared upon completion of the initial project construction. The purpose of an O&M manual is to present detailed information to assist the responsible parties in operating and maintaining the project, and to describe the periodic nourishment and monitoring aspects of the project.

(2) Scope of O&M manual. This section will present a possible outline for an O&M manual and briefly describe the contents of each section. A sample outline is provided in Figure V-4-34. The outline should be modified as necessary to meet the specific needs of the project. The manual is divided into four parts. Part I presents general information about the project. Part II provides essential operation and maintenance information necessary to ensure the desired performance of the project. Part III describes the periodic nourishment and monitoring of the project, while Part IV presents information concerning responsibilities of parties involved in the project.

(3) Introduction. This section of the O&M manual provides a concise summary of pertinent information related to the project and generally includes the information discussed in the following paragraphs.

(a) Authority. Cite the authority(ies) which authorized the project construction.

(b) Location. Describe the project location relative to nearby urban centers, water bodies, or other geographic or demographic features. Give the north, east, south, and west project boundaries.

(PROJECT NAME)

(SAMPLE) TABLE OF CONTENTS

PARA.	TITLE	PAGE NO.
	SECTION I - INTRODUCTION	
I-1.	PURPOSE OF THIS MANUAL	
I-2.	AUTHORIZATION	
I-3.	LOCATION	
I-4.	DESCRIPTION OF PROJECT	
I-5.	PROTECTION PROVIDED	
I-6.	CONSTRUCTION HISTORY	
I-7.	LOCAL COOPERATION AGREEMENT	
	SECTION II - OPERATION AND MAINTENANCE	
II-1.	GENERAL	
II-2.	MANAGEMENT	
II-3.	DUTIES	
II-4.	PERIODIC INSPECTIONS	
II-5.	REPORTS	
II-6.	IMPROVEMENTS OR ALTERATIONS	
II-7.	PROJECT FEATURES (Description, Operation, Maintenance)	
	SECTION III - PERIODIC NOURISHMENT	
III-1.	SCOPE	
III-2.	MONITORING (Surveys, Aerial Photography, Sediment Samples, Waves, etc.)	
III-3.	NOURISHMENT	
III-4.	ROUTINE MONITORING ANALYSIS	
III-5.	POSTSTORM ANALYSIS	
III-6.	POSTSTORM MAINTENANCE	
III-7.	POSTSTORM NOURISHMENT	
	SECTION IV - RESPONSIBILITIES	
IV-1.	U.S. ARMY CORPS OF ENGINEERS	
IV-2.	LOCAL SPONSOR	
IV-3.	FINANCIAL	
	APPENDICES	
A.	ENGINEER REGULATION NO. 1110-2-2902	
B.	LOCAL COOPERATION AGREEMENT	
C.	INSPECTION REPORT FORMS	
D.	AS-BUILT DRAWINGS	

Figure V-4-34. Sample Operations and Maintenance manual outline

(c) Brief description. Describe the major features of the project such as dune and berm elevations, widths, and slopes. Give the grain size characteristics of the fill, volume of material placed, type and characteristics of any structures, and lengths of fill, including transitions. Make reference to the availability and location of as-built plans. The anticipated periodic renourishment volume and interval should be briefly discussed.

(d) Protection provided. Discuss the protection provided by the project and if practicable, identify the storm parameters, or combinations thereof, for which the project is expected to limit inland or upland damages to a minor and acceptable level. Alternatively, the expected project response-frequency curves developed from the analysis of the with-project condition could be provided as indicators of expected project responses resulting from the passage of coastal storms.

(e) Local cooperation. Federal beach-fill projects are constructed and maintained by both the Federal government and one or more levels of local government. The partnership established between the various involved parties is detailed in a local cooperation agreement (LCA). The O&M manual should include a copy of the LCA in an appendix and reference to that appendix should be made in this section of the O&M manual. The summary should identify the local sponsor and those represented by the sponsor if more than one entity is involved. The cost-sharing arrangement for periodic nourishment and project monitoring should be stated and the technical document that supports the LCA and cost-sharing agreement should be cited.

(f) Construction history. Review the contracts used in constructing the project indicating the contractor, contract number, award and completion dates, any significant events or circumstances encountered, and the volumes of materials involved.

(4) Operations and maintenance. This part of the O&M manual presents information on general duties and procedures to assist local interests with their responsibilities for operation and maintenance of the beach-fill project (see ER 1110-2-2902, "Prescribed Procedures for the Maintenance and Operation of Shore Protection Works").

(a) Management. The local person or persons that will be responsible for project administration, maintenance, and general operational responsibilities should be identified. The appointment recommendation and approval procedures should be stated.

(b) Duties. Delineate the project management duties related to the project as outlined in ER 1110-2-2902. Some of these duties (in Federal beach-fill projects) include the following: maintain public ownership and use of the beach which formed the basis of Federal participation; prevent unauthorized trespass or encroachment onto the project; ensure alterations are approved by the District Engineer; ensure pedestrian and vehicular traffic are confined to designated access and use areas; and conduct periodic inspections, and operate and maintain the project as specified in this manual.

(c) Periodic inspections. Routine or emergency inspection plans should be identified. The size of the inspection team may vary from the person in charge up to a team of three or four depending on the scale and complexity of the project. Timing and number of routine inspections should be stated along with the features to be inspected, what information to record, and how and when it should be reported. A set of inspection forms should be developed to help ensure needed information is obtained. Inspection procedures to be followed before and after significant storm events should also be included. Notification from the District or some other mechanism should be included to trigger pre- and poststorm action.

(d) Reports. An inspection report is to be completed by the inspection team for each inspection to ensure that no part of the protection project is overlooked. Any item requiring repairs should be noted. Satisfactory items should also be indicated. A completed and signed set of inspection forms, plus any

pertinent photographs taken during the inspection or monitoring effort, will accompany and provide the basis for the report content. In the event that repairs have been made, either temporary or permanent, the nature and date of the repair are pertinent and should be included. The address to which the reports are to be submitted should be given along with the timing of the reports. All reports should indicate project deficiencies discovered during the inspection, and the scheduled remedial measures to correct the reported deficiencies.

(e) Improvements or alterations. Drawings or prints of proposed improvements or alterations are to be submitted to the District Engineer sufficiently in advance of initiation of the proposed construction to ensure that the absence of his approval does not delay construction. As-built drawings will be furnished to the District Engineer and maintained with the original plans.

(f) Project features. This part of the O&M manual provides detailed description of the features and their operational and maintenance requirements. The section will typically cover such features as the dune, beach berm, transitions, crossovers and access ways, and, if included as part of the project, groin(s), nearshore breakwater(s), seawalls(s), and bulkhead(s).

(5) Periodic nourishment. This section of the O&M manual provides procedures for monitoring the condition of the beach-fill portion of the storm protection project, analyzing the monitoring data, evaluating when nourishment will be required, and determining the volumes of nourishment needed. The project must be periodically nourished to ensure that the desired protection is provided throughout its life.

(a) Scope. Refer to the design document and LCA to define periodic renourishment, its anticipated volume, and interval of placement. Explain the concept of advanced nourishment. Discuss the parameters and conditions that will trigger a nourishment event. Direct quotes from the design document provide credibility for the need to renourish the project. If "renourishment is triggered when, in effect, the project reaches its design configuration" is quoted from the design document, then those responsible need to understand that the design section is the minimum section required to provide the protection and not the maximum section desired or constructed. It should be emphasized that the profiles discussed are based on the configuration of the project beach that is expected once the beach has reached its equilibrium state. In most cases, this will be quite different from the configuration shown on the plans and specifications or the profile that was actually constructed. The issue of postconstruction profile adjustment should be discussed, as well as what is to be expected in terms of beach width decreases through time. Expected seasonal changes should also be discussed.

(b) Monitoring. There are various components that need to be considered to understand the performance of a beach-fill project and subsequent nourishment requirements. To ensure that the project is providing at least the design level of protection, knowledge of the project conditions via project monitoring is imperative. Consequently, a monitoring program is designed as part of the periodic nourishment of the project. For Federal projects, the monitoring program is typically administered by the Corps Engineering Division. Data collected during project monitoring will be used to assess the condition of the beach-fill and to determine when to initiate a nourishment operation. Part V-4-1-l provided guidance on the collection of beach profile surveys, sediment samples, aerial photographs, wave data, etc., and additional guidance can be obtained from EM 1110-2-1004, "Coastal Project Monitoring." The application of these monitoring efforts to the project comprise the remaining topic items to be covered in this section of the O&M manual.

(c) Nourishment. Moving material from the foreshore to the higher berm and/or dune area, or from an accreting area within the project limits to an unusually eroded area, is considered maintenance. Artificially adding new material to the beach-fill project is considered renourishment. The need for renourishment is addressed by determining the protection provided by the existing beach-fill project.

(d) Routine monitoring analysis. The O&M manual will require routine inspection and survey of the beach-fill project. Routine analysis will compare existing profile shapes to the design profile shapes. Of specific importance in the comparison of the existing profile with the design profile is the dune elevation and width and the berm elevation and width. If the comparison indicates that the existing condition dune and berm sections are substandard as compared to the design profile, a more detailed and thorough analysis is initiated to determine, for the overall project, the extent of the deficiency and the level of risk associated with delaying nourishment until the next scheduled renourishment. Based on the results of the detailed analysis a decision is made as to whether or not to initiate a project nourishment action or if maintenance (redistribution of sand within the project area) actions can be implemented to alleviate or minimize a localized problem.

(e) Poststorm analysis. This analysis focuses on the protective features of the beach-fill project located on the upper backshore portion of the beach consisting of the dune and/or storm berm. Generally these features, once eroded, are not soon replaced by nature during poststorm beach recovery and therefore must be replaced by maintenance or nourishment of the project beach.

- Inspection and damage assessment will be conducted as soon as possible after the passage of a significant storm. A joint District and local inspection team will assess the project area. Ground photography will be obtained at a minimum and, if warranted, aerial photography and/or video will be obtained to document the poststorm conditions. The inspection will assess the visible part of the project (i.e., dune/berm erosion, damaged fence, destroyed vegetation, etc.)

- If the extent of upper beach erosion is judged to have compromised the integrity of the project, more extensive data collection and analysis will be required. Beach profile surveys should be immediately initiated at the monument locations as described in the monitoring program. Due to the expediency required in reacting to a storm event causing damage to the project and/or upland development, it is recommended that an Indefinite Delivery Type Contract (IDTC) for poststorm surveying be established and maintained.

- Using the water level and wave height data from offshore gages, or other sources, along with other physical data such as storm duration, wind speed and direction, the storm severity should be estimated. Severity should also be assessed in the context of the beach erosion the storm caused, and should include assessment of key project response parameters such as dune crest lowering, landward extent of vertical erosion threshold, volume eroded above National Geodetic Vertical Datum (NGVD), overwash extent and volume, etc. This information should be provided to the local sponsor and used to document the amount of damages that the project prevented. These findings should be reported in an “annual flood damages prevented” report. After collection and analysis of the survey data, a preliminary cost estimate of emergency maintenance and nourishment costs will be made for local use and possible budgeting purposes.

(f) Poststorm maintenance. Using the survey data, volume calculations will be made which will determine the quantity of sand required to restore the dune and/or berm to its design configuration. An assessment will be made as to the vulnerability of specific areas to additional damage during subsequent storms. Appropriate emergency maintenance actions will be identified and performed. Survey data will be used to determine a source of sand within the project boundaries to be used for the repairs. Once the design is completed and a source of material identified, a construction cost estimate will be prepared. Construction will be undertaken by the local sponsor or they may contract with the District to prepare and manage the contract.

(g) Poststorm nourishment. If the above design and survey data indicate a need to obtain material from an outside source and the District and local sponsor determine the vulnerability analysis warrants such action,

an out-of-cycle nourishment contracting procedure will be initiated and the proposed contract will be immediately advertised for bids. Design analysis will determine the required sand quantities and placement areas and the associated construction templates. Construction plans and specifications and cost estimates will be prepared, as well as related contract documents. Advertisement and award of the contract should be accomplished as soon as possible to allow as much flexibility as possible in scheduling the construction.

(6) Responsibilities. This section should define the roles and responsibilities of organizations and organizational elements for implementing the provisions of the O&M manual.

V-4-2. References

Required Publications

EM 1110-1-1802
Geophysical Exploration for Engineering and Environmental Investigations

EM 1110-2-1004
Coastal Project Monitoring

EM 1110-2-1617
Coastal Groins and Nearshore Breakwaters

ER 1110-2-2902
Prescribed Procedures for the Maintenance and Operation of Shore Protection Works

Related Publications

EM 1110-2-1003
Hydrographic Surveying

EM 1110-2-1204
Environmental Engineering of Coastal Shore Protection

EP 415-1-4
Network Analysis System Guide

Anders and Hansen 1990
Anders, F. J., and Hansen, M. 1990. "Beach and Borrow Site Sediment Investigation for a Beach Nourishment at Ocean City, Maryland," Technical Report CERC-90-5, Coastal Engineering Research Center, U.S. Army Engineer Waterways Experiment Station, Vicksburg, MS.

Bodge, Creed, and Raichle 1996
Bodge, K. R., Creed, C. G., and Raichle, A. W., 1996. "Improving Input Wave Data for Use with Shoreline Change Models," *Journal of Waterway, Port, Coastal and Ocean Engineering*, ASCE 122 (5), pp 259-263.

Bodge and Rosen 1988
Bodge, K. R., and Rosen, D. S. 1988. "Offshore Sand Sources for Beach Nourishment in Florida: Part I: Atlantic Coast." *Beach Preservation Technology '88 Proceedings.* Gainesville, FL, pp 175-190.

Bottin and Earickson 1984
Bottin, R. R., Jr., and Earickson, J. A. 1984. "Buhne Point, Humboldt Bay, California, Design for the Prevention of Shoreline Erosion; Hydraulic and Numerical Model Investigation," Technical Report CERC-84-5, Coastal Engineering Research Center, U.S. Army Engineer Waterways Experiment Station, Vicksburg, MS.

Creed, Bodge, and Suter (1999)
Creed, C. G., Bodge, K. R., and Suter, C. L., 1999. "Construction Slopes for Beach Nourishment Projects," *Journal of Waterway, Port, Coastal and Ocean Engineering* 126(1), pp 57–62.

Chasten et al. 1993
Chasten, M. A., Rosati, J. D., McCormick, J. W., and Randall, R.A. 1993. "Engineering Design Guidance for Detached Breakwaters as Shoreline Stabilization Structures," Technical Report CERC 93-19, Coastal Engineering Research Center, U.S. Army Engineer Waterways Experiment Station, Vicksburg, MS.

Dally and Pope 1986
Dally, W. R., and Pope, J. 1986. "Detached Breakwaters for Shore Protection," Technical Report CERC-86-1, Coastal Engineering Research Center, U.S. Army Engineer Waterways Experiment Station, Vicksburg, MS.

Dean 1974
Dean, R. G. 1974. "Compatibility of Borrow Material for Beach Fill." *Proceedings, 14th International Conference on Coastal Engineering*. ASCE, 1319-1333.

Dean 1991
Dean, R. G. 1991. "Equilibrium Beach Profiles: Characteristics and Applications," *Journal of Coastal Research* 7(1), pp 53-84.

Dean 2000
Dean, R. G. 2000. "Beach Nourishment Design: Consideration of Sediment Characteristics," UFL/COEL-2000/002, Department of Civil and Coastal Engineering, University of Florida, Gainesville, FL.

Dean and Campbell 1999
Dean, R. G., and Campbell, T. J. 1999. "Recommended Beach Nourishment Guidelines for the State of Florida and Unresolved Related Issues," UFL/COEL-99/022, Department of Civil and Coastal Engineering, University of Florida, Gainesville, FL.

Dean and Yoo 1992
Dean, R. G., and Yoo, C. H. 1992. "Beach-Nourishment Performance Predictions," *Journal of Waterway, Port, Coastal and Ocean Engineering* 118(6), pp 567-585.

Ebersole, Neilans, and Dowd 1996
Ebersole, B. A., Neilans, P. J., and Dowd, M. W. 1996 "Beach-Fill Performance at Folly Beach, South Carolina (1 Year After Construction) and Evaluation of Design Methods," *Shore & Beach* 64(1), pp 11-26.

Field and Duane 1974
Field, M. E., and Duane, D. B. 1974. "Geomorphology and Sediments of the Inner Continental Shelf, Cape Canaveral, Florida," Technical Memorandum No. 42, Coastal Engineering Research Center, U.S. Army Engineer Waterways Experiment Station, Vicksburg, MS.

Gorecki 1985
Gorecki, R. I. 1985. "Evaluation of Presque Isle Offshore Breakwaters for Beach Stabilization." *Proceedings of 42nd Annual Meeting of the Coastal Engineering Research Board.* Chicago, IL, pp 83-126.

Gravens 1992
Gravens, M. B. 1992. "User's Guide to the Shoreline Modeling System (SMS)," Instruction Report CERC-92-1, Coastal Engineering Research Center, U.S. Army Engineer Waterways Experiment Station, Vicksburg, MS.

Gravens, Kraus, and Hanson 1991
Gravens, M. B., Kraus, N. C., and Hanson, H. 1991. "GENESIS: Generalized Model for Simulating Shoreline Change - Report 2 Workbook and System User's Manual," Technical Report CERC-89-19, Coastal Engineering Research Center, U.S. Army Engineer Waterways Experiment Station, Vicksburg, MS.

Gravens and Rosati 1994
Gravens, M. B., and Rosati, J. D. 1994. "Numerical Model Study of Breakwaters at Grand Isle, Louisiana," Miscellaneous Paper CERC-94-16, Coastal Engineering Research Center, U.S. Army Engineer Waterways Experiment Station, Vicksburg, MS.

Grosskopf and Kraus 1993
Grosskopf, W. G., and Kraus, N. C. 1993. "Guidelines for Surveying Beach Nourishment Projects," Coastal Engeineering Technical Note, CETN II-31, U.S. Army Engineer Waterways Experiment Station, Vicksburg, MS.

Hall 1952
Hall, J. V., Jr. 1952. "Artificially Constructed and Nourished Beaches in Coastal Engineering." *Proceedings, 3rd International Conference on Coastal Engineering*. ASCE, pp 119-133.

Hands and Allison 1991
Hands, E. B., and Allison, M. C. 1991. "Mound migration in deeper water and methods of categorizing active and stable berms." *Proceedings, Coastal Sediments '91*, ASCE, pp 1985-1999.

Hanson 1987
Hanson, H. 1987. "GENESIS, A Generalized Shoreline Change Model for Engineering Use," Report No. 1007, Department of Water Resources Engineering, University of Lund, Sweden.

Hanson and Kraus 1989
Hanson, H., and Kraus, N. C. 1989. "GENESIS: Generalized Model for Simulating Shoreline Change," Technical Report CERC-89-19, Coastal Engineering Research Center, U.S. Army Engineer Waterways Experiment Station, Vicksburg, MS.

Hemsley, McGehee, and Kucharski 1991
Hemsley, J. M., McGehee, D. D., and Kucharski, W. M. 1991. "Nearshore Oceanographic Measurements: Hints on How to Make Them," *Journal of Coastal Research* 7(2), pp 301-315.

James 1974
James, J. R. 1974. "Borrow Material Texture and Beach Fill Stability." *Proceedings, 14th International Conference on Coastal Engineering.* ASCE, pp 1334-1344.

James 1975
James, J. R. 1975. "Techniques in Evaluating Suitability of Borrow Material for Beach Nourishment," Technical Memorandum No. 60, Coastal Engineering Research Center, U.S. Army Engineer Waterways Experiment Station, Vicksburg, MS.

Johnson and Nelson 1985
Johnson, R. O., and Nelson, W. G. 1985. "Biological Effects of Dredging in an Offshore Borrow Area," *Biological Sciences* 3, pp 166-188.

Knutson 1977
Knutson, P. L. 1977. "Planting Guidelines for Dune Creation and Stabilization," CETA 77-4, Coastal Engineering Research Center, U.S. Army Engineer Waterways Experiment Station, Vicksburg, MS.

Knutson 1980
Knutson, P. L. 1980. "Experimental Dune Restoration and Stabilization, Nauset Beach, Cape Cod, Massachusetts," TP 80-5, Coastal Engineering Research Center, U.S. Army Engineer Waterways Experiment Station, Vicksburg, MS.

Krumbein 1957
Krumbein, W. C. 1957. "A Method for Specification of Sand for Beach Fills," Technical Memorandum 102, U.S. Army Corps of Engineers, Beach Erosion Board, Washington, DC.

Krumbein and James 1965
Krumbein, W. C., and James, W. R. 1965. "Spacial and Temporal Variations in Geometric and Material Properties of a Natural Beach," Technical Report No. 44, Coastal Engineering Research Center, U.S. Army Engineer Waterways Experiment Station, Vicksburg, MS.

Larson and Kraus 1989
Larson, M., and Kraus, N. C. 1989. "SBEACH: Numerical Model for Simulating Storm-Induced Beach Change, Report 1 - Empirical Foundation and Model Development," Technical Report CERC-89-9, Coastal Engineering Research Center, U.S. Army Engineer Waterways Experiment Station, Vicksburg, MS.

Larson and Kraus 1998
Larson, M., and Kraus, N. C. 1998. "SBEACH: Numerical Model for Simulating Storm-Induced Beach Change, Report 5 - Representation of Nonerodible (Hard) Bottoms," Technical Report CHL-98-9, Coastal Engineering Research Center, U.S. Army Engineer Waterways Experiment Station, Vicksburg, MS.

Larson, Kraus, and Burns 1990
Larson, M., Kraus, N. C., and Byrnes, M. R. 1990. "SBEACH: Numerical Model for Simulating Storm-Induced Beach Change, Report 2 - Numerical Formulation and Model Tests," Technical Report CERC-89-9, Coastal Engineering Research Center, U.S. Army Engineer Waterways Experiment Station, Vicksburg, MS.

Larson, Morang, and Gorman 1997
Larson, R., Morang, A., Gorman, L. 1997. "Monitoring the Coastal Environment; Part II: Sediment Sampling and Geotechnical Methods," *Journal of Coastal Research,* Vol. 13, No. 2, pp. 308-330.

Meisburger 1990
Meisberger, E. P. 1990. "Exploration and sampling techniques for borrow areas," Technical Report CERC-90-18, Coastal Engineering Research Center, U.S. Army Engineer Waterways Experiment Station, Vicksburg, MS.

Meisburger and Duane 1971
Meisberger, E. P., and Duane, D. B. 1971. "Geomorphology and Sediments of the Inner Continental Shelf, Palm Beach to Cape Kennedy, Florida," Technical Memorandum No. 34, Coastal Engineering Research Center, U.S. Army Engineer Waterways Experiment Station, Vicksburg, MS.

Meisburger and Field 1975
Meisberger, E. P., and Field, M. E. 1975. "Geomorphology, Shallow Structure, and Sediments of the Florida Inner Continental Shelf, Cape Canaveral to Georgia," Technical Memorandum No. 54, Coastal Engineering Research Center, U.S. Army Engineer Waterways Experiment Station, Vicksburg, MS.

Morang, Larson, and Gorman 1993
Morang, A., Larson, R., and Gorman, L. 1997. "Monitoring the Coastal Environment; Part I: Waves and Currents," *Journal of Coastal Research,* Vol 13, No. 1, pp. 111-133.

Morang, Mossa, and Larson 1993
Morang, A., Mossa, J., and Larson, R. J. 1993. "Technologies for Assessing the Geologic and Geomorphic History of Coasts," Technical Report CERC-93-5, Coastal Engineering Research Center, U.S. Army Engineer Waterways Experiment Station, Vicksburg, MS.

Nakashima et al. 1987
Nakashima, L. D., Pope J., Mossa, J., and Dean J. L. 1987. "Initial Response of a Segmented Breakwater System, Holly Beach, Louisiana," *Proceedings, Coastal Sediments '87,* ASCE, pp 1399-1414.

National Research Council 1995
National Research Council. 1995. *Beach Nourishment and Protection*. National Academy Press, Washington, DC.

Nelson 1985
Nelson, W. G. 1985. "Guidelines for Beach Restoration Projects," Report SRG-76, Florida Sea Grant College, Gainesville, FL.

Pope and Dean 1986
Pope, J., and Dean, J. L. 1986. "Development of Design Criteria for Segmented Breakwaters." *Proceedings, 20th International Conference on Coastal Engineering.* ASCE, 2,144-2, pp 158.

Prins 1980
Prins, D. A. 1980. "Data Collection Methods for Sand Inventory-Type Surveys," Technical Report CERC-80-4, Coastal Engineering Research Center, U.S. Army Engineer Waterways Experiment Station, Vicksburg, MS.

Richardson 1976
Richardson, T. W. 1976. "Beach Nourishment Techniques: Report 1, Dredging Systems for Beach Nourishment from Offshore Sources," TR H-76-13, U.S. Army Engineer Waterways Experiment Station, Vicksburg, MS.

Richardson 1977
Richardson, T. W. 1977. "Systems for Bypassing Sand at Coastal Inlets," *Proceedings of the Fifth Symposium of the Waterway, Port, Coastal and Ocean Division*, ASCE, November 1977, pp 67-84.

Rosati 1990
Rosati, J. D. 1990. "Functional Design of Breakwaters for Shore Protection: Empirical Methods," Technical Report CERC-90-15, Coastal Engineering Research Center, U.S. Army Engineer Waterways Experiment Station, Vicksburg, MS.

Rosati et al. 1993
Rosati, J. D., Wise, R. A., Kraus, N. C., and Larson, M. 1993. "SBEACH: Numerical Model for Simulating Storm-Induced Beach Change, Report 3 - User's Manual," Instruction Report CERC-93-2, Coastal Engineering Research Center, U.S. Army Engineer Waterways Experiment Station, Vicksburg, MS.

Savage 1962
Savage, R. P. 1962. "Experimental Study of Dune Building with Sand Fences." *Proceedings, 8th International Conference on Coastal Engineering*. ASCE, pp 671-700.

Savage and Woodhouse 1969
Savage, R. P., and Woodhouse, W. W., Jr. 1969. "Creation and Stabilization of Coastal Barrier Dunes," *Proceedings, 11th International Conference on Coastal Engineering,* ASCE, pp 671-700.

Scheffner and Borgman 1999
Scheffner, N. W., Borgman, L. E. 1999. "Users Guide to the Use and Application of the Empirical Simulation Technique," Technical Report CHL-99-00, U.S. Army Engineer Waterways Experiment Station, Vicksburg, MS.

Schwartz and Musialowski 1980
Schwartz, R. K., and Musialowski, F. R. 1980. "Transport of Dredged Sediment Placed in the Nearshore Zone--Currituck Sand-Bypass Study (Phase I)," Technical Paper CERC-80-1, Coastal Engineering Research Center, U.S. Army Engineer Waterways Experiment Station, Vicksburg, MS.

Shore Protection Manual 1984
Shore Protection Manual. 1984. 4th ed., 2 Vol., U.S. Army Engineer Waterways Experiment Station, U.S. Government Printing Office, Washington, DC.

Smith and Ebersole 1997
Smith, S. J., and Ebersole, B. A. 1997. "Numerical Modeling Evaluation of Hot Spots at Ocean City, Maryland." *Proceedings, 10th National Conference on Beach Preservation Technology*. Florida Shore & Beach Preservation Association, pp 230-245.

Sommerfeld et al. 1994
Sommerfeld, B. G., Mason, J. M., Kraus, N. C., Larson, M. 1994. "BFM: Beach Fill Module, Report 1, Beach Morphology Analysis Package (BMAP) - User's Guide," Instruction Report CERC-94-1, U.S. Army Engineer Waterways Experiment Station, Vicksburg, MS.

Stauble and Nelson 1984
Stauble, D. K., and Nelson, W. G. 1984. "Beach Restoration Guidelines: Prescription for Project Success." *The New Threat to Beach Preservation.* L. Tate, ed., Florida Shore and Beach Preservation Society, Tallahassee, FL, pp 137-155.

Stauble 1994
Stauble, D. K. 1994. "Evaluation of Erosion Hot-spots for Beach Fill Performance." *Proceedings, 7th National Conference on Beach Preservation Technology*. Florida Shore and Beach Preservation Association, pp 198-215.

U.S. Army Corps of Engineers 1991
U.S. Army Corps of Engineers. 1991. "National Economic Development Procedures Manual - Coastal Storm Damage and Erosion," Institute of Water Resources Report No. 91-R-6, Institute for Water Resources, Water Resources Support Center, Fort Belvoir, VA.

U.S. Army Engineer District, Charleston 1987
U.S. Army Engineer District, Charleston. 1987. "Final Detailed Project Report, Charleston Harbor South Carolina, Folly Beach, Section 111 of the River and Harbor Act as Amended, Charleston, SC," Charleston, SC.

U.S. Army Engineer Waterways Experiment Station 1981
U.S. Army Engineer Waterways Experiment Station. 1981. "Beach Dune Walkover Structures," Coastal Engineering Technical Note, CETN-III-5, U.S. Army Engineer Waterways Experiment Station, Vicksburg, MS.

Walton 1994
Walton, T. W., Jr. 1994. "Shoreline Solution for Tapered Beach Fill," *Journal of Waterway, Port, Coastal and Ocean Engineering* 120(6), ASCE, pp 651-655.

Weggel and Sorensen 1991
Weggel, J. R., and Sorensen, R. M. 1991. "Performance of the 1986 Atlantic Atlantic City, New Jersey, Beach Nourishment Project," *Shore and Beach* 59(3), pp 29-36.

Wise, Smith, and Larson 1996
Wise, R. A., Smith S. J., and Larson M. 1996. "SBEACH: Numerical Model for Simulating Storm-Induced Beach Change, Report 4 - Cross-shore Transport Under Random Waves and Model Validation with SUPERTANK and Field Data," Technical Report CERC-89-9, Coastal Engineering Research Center, U.S. Army Engineer Waterways Experiment Station, Vicksburg, MS.

Woodhouse 1978
Woodhouse, W. W. 1978. "Dune Building and Stabilization with Vegetation," SR-3, Coastal Engineering Research Center, U.S. Army Engineer Waterways Experiment Station, Vicksburg, MS.

V-4-3. Definition of Symbols

Δy_o	Initial dry beach width (after cross-shore equilibrium) [length]
ε	Shoreline diffusivity parameter (Equation III-2-26) [length^2/time]
$\sigma_{\varphi b}$	Standard deviation of a borrow sediment sample (Equation III-1-3) [phi units]
$\sigma_{\varphi n}$	Standard deviation of a native sediment sample (Equation III-1-3) [phi units]
φ	Sediment grain diameter in phi units (φ = -log$_2$ D, where D is the sediment grain diameter in millimeters) [phi units]
a	Beach-fill half length [length]
a	One-half the length of the rectangular project [length]
A_F	Nourishment material scale parameter (Table III-3-3) [length$^{1/3}$]
A_N	Native sediment scale parameter (Table III-3-3) [length$^{1/3}$]
A_S	Vessel submerged cross-section area (= BT)[length^2]
B	Design berm elevation [length]
B_R	Channel blockage ratio [dimensionless]
C^n_{go}	Deepwater wave group speed of the nth record [length/time]
C^n_*	Wave speed at breaking of the nth record [length/time]
D_{50}	Median grain size [length]
D_C	Depth of closure [length]
E	Historical shoreline recession rate [length]
H_{eff}	Effective wave height [length]
H^m_s	Significant wave height of the nth record in the time series of N wave records [length]
K_s	Shoaling coefficient [dimensionless]
$M_{\varphi b}$	Estimated mean grain size of a borrow sediment sample (Equation (III-1-2) [phi units]
$M_{\varphi n}$	Estimated mean grain size of a native sediment sample (Equation (III-1-2) [phi units]
R_A	Beach nourishment overfill factor [dimensionless]
R_J	Beach nourishment factor [dimensionless]
t	time
T_{eff}	Effective wave period [time]
V	Volume of material per unit length of shoreline required to produce a beach width of W (Equation V-4-6) [length^3/length]
W	Beach width [length]
W_{add}	Added distance of translation (Equation V-4-5) [length]

V-4-4. Acknowledgments

Authors of Chapter V-4, "Beach-Fill Design:"

Mark B. Gravens, Coastal and Hydraulics Laboratory (CHL), U.S. Army Engineer Research and Development Center, Vicksburg, Mississippi.
Bruce A. Ebersole, CHL
Todd L. Walton, Ph.D., CHL
Randall A. Wise, U.S. Army Engineer District, Philadelphia, Philadelphia, Pennsylvania.

Reviewers:

Nicholas C. Kraus, Ph.D., CHL
Kevin R. Bodge, Ph.D., Olsen Associates, Jacksonville, Florida
Donald K. Stauble, Ph.D., CHL

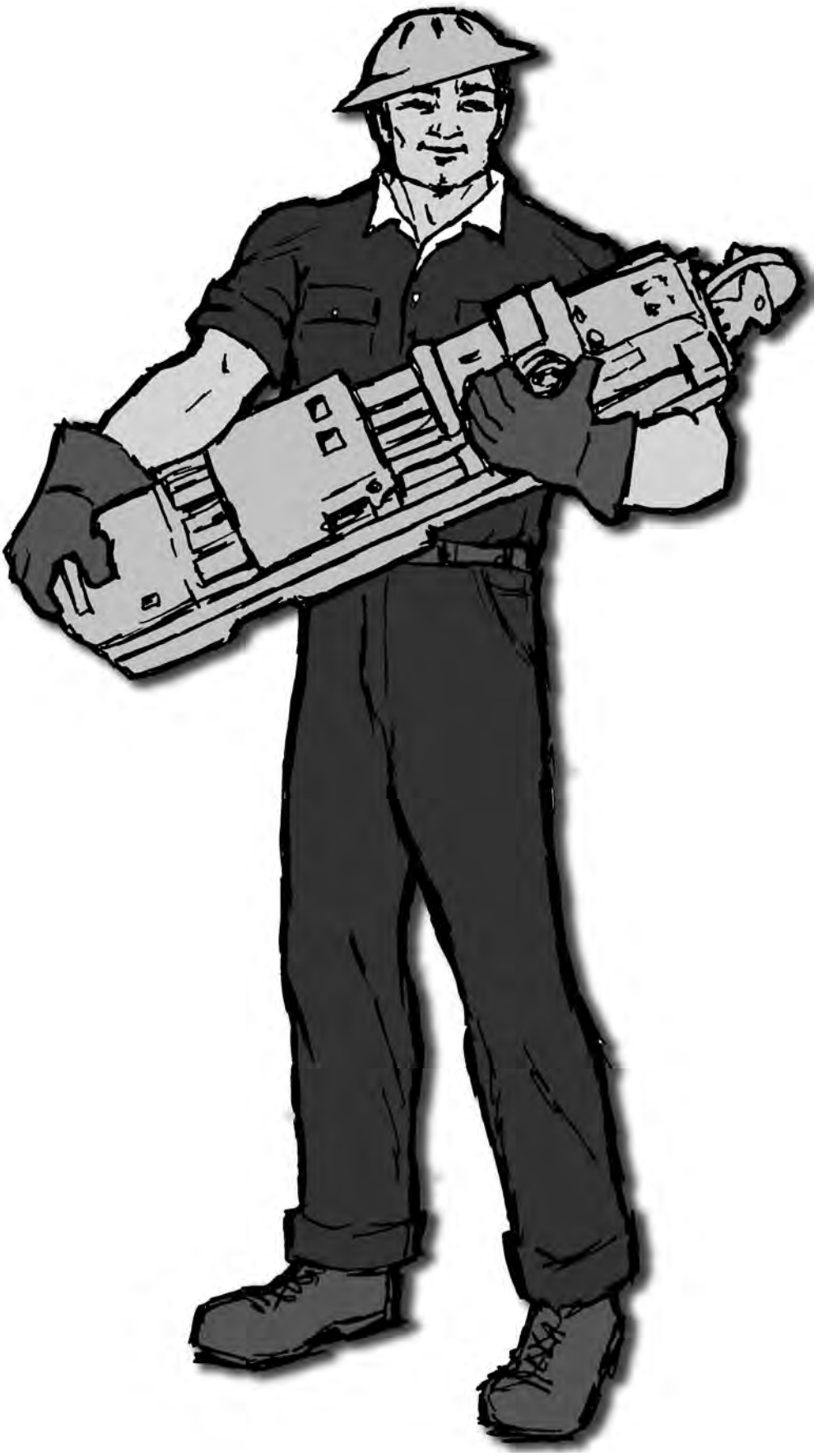

Table of Contents

Page

V-5-1. Project Assessment and Alternative Selection V-5-1
a. Introduction V-5-1
(1) Purpose V-5-1
(2) Contents V-5-1
(3) Relationship to other chapters and parts V-5-1
b. Port and harbor facility issues V-5-2
(1) Motivation V-5-2
(2) Deep- versus shallow-draft projects V-5-2
(3) Organizations related to navigation projects V-5-2
(4) Trends in port and harbor development V-5-3
c. Preliminary planning and design elements V-5-4
d. Policy considerations V-5-5

V-5-2. Defining Vessel Requirements V-5-5
a. Deep-draft ships and shallow-draft vessels V-5-5
(1) Vessel dimensions V-5-5
(2) Cargo capacity V-5-6
(3) Restrictions V-5-8
(4) Vessel characteristics V-5-8
(5) Form coefficients V-5-11
(6) Ship speed V-5-11
(7) Maneuverability V-5-12
b. Vessel operations V-5-12
(1) Navigation system V-5-12
(2) Typical operations V-5-13
(3) Shallow water, restricted channels V-5-14
(4) Ice navigation V-5-17
c. Design considerations V-5-19
(1) Design vessel V-5-19
(2) Design transit and mooring area conditions V-5-20

V-5-3. Data Needs and Sources (Pre-project) V-5-21
a. Introduction V-5-21
b. Currents V-5-21
c. Water levels V-5-21
d. Wind V-5-21
e. Waves V-5-21
f. Water quality V-5-21
g. Sediments V-5-21
h. Bathymetry and sediment transport processes V-5-21
i. Ecological processes V-5-21

j. Local coordination V-5-21
(1) Pilot interviews V-5-21
(2) U.S. Coast Guard V-5-22
(3) Accident records V-5-22

V-5-4. Economic Analysis V-5-22

V-5-5. Channel Depth V-5-24
a. Introduction V-5-24
b. Effect of fresh water V-5-25
c. Vessel motion from waves V-5-25
d. Vessel squat V-5-29
e. Trim V-5-34
f. Shallow-water effects V-5-34
g. Safety clearance V-5-34
h. Advance maintenance V-5-34
i. Dredging tolerance V-5-34
j. Tidal shoals and ship transit concerns example V-5-35

V-5-6. Channel Alignment and Width V-5-38
a. Alignment V-5-38
b. Inner channels (protected waters and harbor areas) V-5-39
(1) Width V-5-39
(2) Berthing areas V-5-44
(3) Special considerations due to ice V-5-44
c. Entrance channels V-5-44
d. Turns and bends V-5-45

V-5-7. Other Project Features V-5-47
a. Turning basins V-5-47
b. Moorage/anchorage areas V-5-49
c. Basin flushing and water quality V-5-49
d. Navigation structures V-5-50
(1) Breakwaters V-5-50
(2) Jetties V-5-55
(3) Training dikes V-5-58
(4) Wave absorbers V-5-58
(5) Revetments, seawalls, and bulkheads V-5-60

V-5-8. Aids to Navigation V-5-60

V-5-9. Operation, Monitoring, and Maintenance V-5-63

V-5-10. Model and Specialized Field Studies V-5-65
a. Harbor modeling V-5-65
(1) Physical modeling as a design tool V-5-65
(2) Example: Dana Point Harbor, California V-5-67
(3) Numerical modeling as a design tool V-5-69
(a) Wind waves, swell, and harbor oscillations V-5-69
(b) Example: Kikiaola Harbor, Kauai, Hawaii V-5-71

(c) Flushing and circulation V-5-78
(d) Example: Maalaea Harbor, Maui, Hawaii V-5-78
(e) Shore response V-5-79
b. Navigation modeling V-5-80
(1) Physical models V-5-80
(a) Example: Barbers Point Harbor, Oahu, Hawaii V-5-80
(b) Additional Information V-5-85
(2) Ship simulations V-5-85
(a) Example: Alafia River Harbor, Florida V-5-87
(b) Example: San Juan Harbor, Commonwealth of Puerto Rico V-5-90
c. Specialized field studies V-5-92
(1) Harbors V-5-92
(a) Example: Kahului Harbor, Maui, Hawaii V-5-92
(b) Data V-5-93
(2) Ship tracking V-5-93

V-5-11. References V-5-96

V-5-12. Definitions of Symbols V-5-103

V-5-13. Acknowledgments V-5-104

List of Figures

Page

Figure V-5-1. Foreign waterborne imports and exports V-5-4

Figure V-5-2. Ship length definitions V-5-7

Figure V-5-3. Midship-section molded-form definitions V-5-7

Figure V-5-4. Block coefficient definition V-5-11

Figure V-5-5. Example ship track, Alafia Channel, Florida V-5-14

Figure V-5-6. Ship wave and flow pattern in a canal V-5-15

Figure V-5-7. Ship-limiting speed in a canal V-5-17

Figure V-5-8. Cold regions of the world V-5-18

Figure V-5-9. Fog over frozen waterway V-5-18

Figure V-5-10. Deep-Draft navigation benefit evaluation procedure V-5-23

Figure V-5-11. Definition of channel types V-5-24

Figure V-5-12. Channel depth allowances V-5-26

Figure V-5-13. Ship motion definitions V-5-27

Figure V-5-14. Ship motion response, mouth of Columbia River V-5-29

Figure V-5-15. Squat analysis definition V-5-30

Figure V-5-16. Example channel cross sections V-5-32

Figure V-5-17. Trench channel definitions V-5-33

Figure V-5-18. Example squat calculations V-5-33

Figure V-5-19. Hypothetical route to a port at head of an estuary V-5-35

Figure V-5-20. Hypothetical distribution of depths for Shoal 2 . . . . . V-5-36

Figure V-5-21. Range of water levels in the Fraser River, British Columbia V-5-37

Figure V-5-22. Components of a ship transit simulation program V-5-38

Figure V-5-23. Ship simulation of deep-draft entrance channel, San Juan Harbor, Commonwealth of Puerto Rico V-5-40

Figure V-5-24. Traditional interior channel width elements V-5-41

Figure V-5-25. Interior channel design width V-5-42

Figure V-5-26. Definition of parameters in channel turn V-5-45

Figure V-5-27. Channel turn configurations V-5-46

Figure V-5-28. Layout of apex-style turn V-5-48

Figure V-5-29. Turning basin alternative designs V-5-48

Figure V-5-30. Alternative anchorage designs V-5-50

Figure V-5-31. Harbor with shore-connected breakwater, Waianae Small Boat Harbor, Oahu, Hawaii (June 1980) V-5-51

Figure V-5-32. View of offshore detached breakwater used to protect harbor entrance, Marina del Rey, California (August 1996) V-5-52

Figure V-5-33. Harbor with both shore-connected and detached breakwaters, Barcelona Harbor, New York (April 1986) V-5-52

Figure V-5-34. Inner breakwater provides protection to small craft mooring area, Port Washington Harbor, Wisconsin (September 1983) V-5-53

Figure V-5-35. Breakwaters protecting small boat harbor from waves and wave-generated crosscurrents on reef, Agana, territory of Guam (May 1978) V-5-54

Figure V-5-36. Dual jetty configuration at a tidal inlet, Murrells Inlet, South Carolina (March 1982) V-5-55

Figure V-5-37. Jetty types, Barnegat Inlet, New Jersey: (a) arrowhead jetties, November-December 1965, and (b) parallel jetties, June 1996 . . . . . V-5-57

Figure V-5-38. Rubble wave absorber at a dock V-5-58

Figure V-5-39. Perforated wall wave absorber at a dock V-5-59

Figure V-5-40. Stacked Igloo model wave absorber units V-5-59

Figure V-5-41. Examples of aids to navigation V-5-61

Figure V-5-42. Designation system of aids to navigation V-5-62

Figure V-5-43. Use of ranges for channel position V-5-63

Figure V-5-44. Deep-draft navigation channel, Brunswick Harbor, Georgia V-5-64

Figure V-5-45. Dana Point Harbor, California (May 1969) V-5-68

Figure V-5-46. Physical model view of Dana Point Harbor, California, under storm wave attack V-5-69

Figure V-5-47. Kikiaola Harbor, Kauai, Hawaii (1998) V-5-72

Figure V-5-48. Kikiaola Harbor alternative plans and model stations V-5-73

Figure V-5-49. Amplification factor and phase contours, 12-sec wave period, 200-deg azimuth approach direction, Kikiaola Harbor V-5-75

Figure V-5-50. Comparison of H_s exceeded 10 percent of the time, Kikiaola Harbor V-5-76

Figure V-5-51. Resonant long wave amplification factor contours, existing Kikiaola Harbor . . . V-5-77

Figure V-5-52. Maalaea Harbor, Maui, Hawaii (March 1984) V-5-78

Figure V-5-53. Station locations and surface layer circulation snapshot at Day 3, Maalaea Harbor, existing plan V-5-79

Figure V-5-54. Time series of conservative tracer concentration at sta 1, Maalaea Harbor, existing plan V-5-80

Figure V-5-55. Barbers Point Harbor, Oahu, Hawaii, location map V-5-81

Figure V-5-56. Barbers Point Harbor, Oahu, Hawaii (August 1994) V-5-81

Figure V-5-57. Physical model of Barbers Point Harbor V-5-82

Figure V-5-58. Bulk carrier *Bunga Saga Empat* V-5-83

Figure V-5-59. Model bulk carrier V-5-84

Figure V-5-60. Model container ship V-5-84

Figure V-5-61. Probability assessment for C9 container ship navigating recommended entrance channel, Barbers Point Harbor V-5-86

Figure V-5-62. USAERDC ship simulator system V-5-86

Figure V-5-63. Ship simulator forces and effects V-5-87

Figure V-5-64. Real-time simulation V-5-88

Figure V-5-65. Existing Alafia River Channel and turning basin V-5-88

Figure V-5-66. Visual scene of Alafia River Harbor ship simulation study, inbound bulk carrier approaching dock V-5-89

Figure V-5-67. San Juan Harbor, Commonwealth of Puerto Rico, location map V-5-90

Figure V-5-68. San Juan Harbor channels V-5-91

Figure V-5-69. Pilot degree of difficulty ratings, inbound container ship, San Juan Harbor V-5-93

Figure V-5-70. Ship tracks, proposed bar channel and turn into Anegado Channel, San Juan Harbor V-5-94

Figure V-5-71. Kahului Harbor, Maui, Hawaii, location map V-5-95

Figure V-5-72. Field gauge locations and bathymetry, Kahului Harbor V-5-95

Figure V-5-73. Components of ship track measurements V-5-96

List of Tables

Page

Table V-5-1. Organization Acronyms Related to Navigation Projects V-5-3

Table V-5-2. Acronyms Commonly Used to Describe Ship Size and Function V-5-6

Table V-5-3. Canal Restrictions on Ship Size V-5-8

Table V-5-4. Characteristics of Large Ships V-5-9

Table V-5-5. Large Tanker Classes V-5-10

Table V-5-6. Depth Allowance for Freshwater Effect V-5-25

Table V-5-7. Squat Allowance for Small Recreational Craft V-5-34

Table V-5-8. Safety Clearance V-5-34

Table V-5-9. Traditional Criteria for Deep-draft Channel Width Design V-5-41

Table V-5-10. One-way Ship Traffic Channel Width Design Criteria V-5-43

Table V-5-11. Two-way Ship Traffic Channel Width Design Criteria V-5-43

Table V-5-12. Recommended Deep-Draft Channel Turn Configurations V-5-47

Table V-5-13. Typical Physical Model Scales for Harbors V-5-66

Table V-5-14. Simple Criteria for Assessing Operational Impact of Harbor Oscillations V-5-77

Table V-5-15. Design Ship Dimensions for Barbers Point Harbor Studies V-5-83

Chapter V-5
Navigation Projects

V-5-1. Project Assessment and Alternative Selection

a. Introduction

(1) Purpose. The purpose of this chapter is to present information and procedures that help in coastal navigation project planning and design. Both deep-draft ports and small boat harbors are included. Navigation channels, turning basins, anchorage areas, and related structures are discussed. Other areas of port and harbor design, such as docks, facilities, terminals, and other land-side requirements, are not included. These areas are generally nonfederal concerns.

Guidance for navigation projects has traditionally been focused on deep-draft project requirements. Modified guidance based on experience has evolved for shallow-draft projects. This chapter follows a similar philosophy, focusing on deep-draft projects with supplementary material for shallow-draft projects, as appropriate. The chapter provides fairly comprehensive coverage, but it is intended to complement, rather than replace, Engineer Manuals 1110-2-1613, "Hydraulic Design Guidance for Deep-Draft Navigation Projects" (USACE 1998), and 1110-2-1615, "Hydraulic Design of Small Boat Harbors" (USACE 1984).

(2) Contents. This section gives an overview of issues and considerations important in assessing navigation projects and in defining and selecting project alternatives. Since navigation projects are designed to satisfy requirements of a target group of vessels, an understanding of vessel types and behavior is given in Part V-5-2. Determination of design vessel and transit conditions is also discussed. Data needs and sources are reviewed in Part V-5-3, with appropriate reference to other CEM chapters. Part V-5-4 is devoted to a brief discussion of economic analysis, which is crucial to every navigation project. Development of navigation project features is addressed in Parts V-5-5 through V-5-8. Features included are channel depth, width, and alignment, turning basins, anchorage areas, navigation-related structures, and aids to navigation. Post-project activities are discussed in Part V-5-9, including operation, monitoring, and maintenance. Part V-5-10 gives a description of physical and numerical modeling tools and specialized field studies which can assist in planning and designing effective navigation projects. A number of specific project examples are presented to illustrate the capabilities and applications of model and field studies. References are given in Part V-5-11.

(3) Relationship to other chapters and parts. Part V provides general guidance on the Planning and Design Process (Part V-1) and Site Characterization (Part V-2), including data needs and sources and monitoring. Part V also contains chapters with more detailed guidance on particular project types frequently encountered in the U.S. Army Corps of Engineers (USACE). This chapter addresses navigation projects. Part V-6, Sediment Management at Inlets/Harbors, is an important complement to this chapter. It deals with sediment processes in the vicinity of inlets and harbor entrances, engineering methods for managing sediment processes to prevent negative project impacts and/or achieve positive benefits, and project experience and lessons learned. Other chapters of particular relevance are Part II-6, Hydrodynamics of Tidal Inlets; Part II-7, Harbor Hydrodynamics (including a section on vessel interactions); and Part VI, Design of Coastal Project Elements, which provides guidance for the detailed structural design needed for navigation and other coastal projects.

b. Port and harbor facility issues

(1) Motivation. Ports and harbors are vital to the nation. Since ports handle about half of U.S. overseas trade by value and nearly all by weight, waterborne commerce directly affects prosperity and richness of life in the United States. Ports and harbors are also vital for military applications because a large percentage of military goods are transported by ship. Finally, harbors provide launching and berthing facilities for commercial fishing boats and a large number of recreational boaters.

(a) The term *harbor* describes a relatively protected area accessible to vessels. The term *port* indicates a location where ships can transfer cargo. A port may be located in a protected harbor or it may be exposed, such as single-point mooring facilities used for petroleum products.

(b) Ports and harbors must be located so that vessels can penetrate coastal waters and interface with land. Ideally, vessels have a relatively short travel distance between port/harbor areas and open water. Vessels must have sufficient water depth and protection to safely enter and exit the harbor/port area. Thus, a well-maintained, clearly identified channel through any shallow areas is needed.

(c) The requirements for access and protection in harbors and ports often lead to dredged channels and engineered structures, such as jetties and breakwaters. These project features can impact dynamic coastal processes and lead to a range of coastal engineering concerns.

(2) Deep- versus shallow-draft projects. The terms *deep-draft* and *shallow-draft* are often used to distinguish between major commercial port projects and recreational or other small boat harbor projects. USACE definitions for these terms are based on authorized navigation project depth:

- Deep draft Channel depth greater than 4.6 m (15 ft)
- Shallow draft Channel depth less than 4.6 m (15 ft)

Defining depth for a deep-draft harbor can vary with context. For example, Federal cost-sharing rules are based on a 6.1-m (20-ft) minimum depth for deep-draft projects. The harbor maintenance tax system is applied to projects with depth greater than 4.3 m (14 ft), while inland fuel taxes apply in shallower-depth projects, excluding entrance channels. Deep-draft U.S. ports serve commercial seagoing ships, Great Lakes freighters, Navy warships, and Army prepositioning ships. Shallow-draft harbors typically serve pleasure craft and fishing boats. The term *small craft* is often used synonymously with *shallow draft*. As part of its mission, USACE has had responsibility for maintaining over 200 deep-draft coastal ports and over 600 shallow-draft harbors. Issues involved in shallow-draft navigation projects have similarities but also significant differences from those in deep-draft projects. For example, shallow-draft boats are typically small and are strongly influenced by wind waves and swell. Thus, wave criteria for safe transit of entrance channels and safe mooring areas are more demanding than for deep-draft vessels. However, large ships typically maneuver with difficulty in confined areas, and channel width is a critical component of deep-draft channels. Deep-draft harbors are more prone to harbor oscillation concerns because resonant periods of moored ship response are typically in the same range as harbor oscillation periods. Flushing is an important issue in many shallow-draft harbors, where numerous users in a confined area can potentially lead to deterioration of water quality. Flushing is usually less critical in deep-draft projects, which require wider entrances and more careful monitoring of vessel discharges. These issues are addressed later in the chapter.

(3) Organizations related to navigation projects. USACE navigation projects involve other organizations, as well. For example, the U.S. Coast Guard is responsible for installing and maintaining the aids to navigation needed to mark Federal channels. Often state and local organizations, such as port authorities, are

part of a navigation project team. Some organizations and acronyms often encountered in navigation projects as team members or information resources are listed in Table V-5-1.

Table V-5-1
Organization Acronyms Related To Navigation Projects

Acronym	Organization
AAPA	American Association of Port Authorities
ABS	American Bureau of Shipping
ASCE	American Society of Civil Engineers
EPA	U.S. Environmental Protection Agency
NAVFAC	U.S. Naval Facilities Engineering Command
NOAA	U.S. National Oceanic and Atmospheric Administration
PIANC	International Navigation Association (formerly, Permanent International Association of Navigation Congresses)
USACE	U.S. Army Corps of Engineers
USCG	U.S. Coast Guard

(4) Trends in port and harbor development. Demand for harbor and port facilities continues to increase while coastal population and other utilization of the coast increases. These competing interests intensify pressures to find mutually agreeable solutions to coastal land and water use. Annual foreign waterborne tonnage (between U.S. and foreign ports) during the years 1987-1996 indicates a clearly increasing trend (Figure V-5-1). Major U.S. ports continue to increase in size and serve larger ships. Dramatic increases in container traffic and a recent trend for container ships to exceed Panama Canal size constraints have helped fuel the need for deeper ports and expanded, modernized terminals. Open terminals and offshore ports have helped accommodate large tankers and bulk carriers, in some markets.

(a) With pressure to serve larger ships, many U.S. ports are faced with costly infrastructure upgrades. Deeper and wider channels, turning basins, and berthing areas are needed. Disposal of large quantities of dredged material, which is often contaminated after many years of harbor operations, can be a major and expensive problem. Dock bulkheads often need to be rebuilt to maintain structural strength in deeper water and with likely higher design loads from ship berthing and apron cargo handling. Landside infrastructure must be capable of efficiently handling cargo from larger ships. This requirement often leads to bigger gantry cranes, single-purpose terminals, larger stockpiling areas, new rail facilities, etc.

(b) Demand for small-craft berthing space is also increasing, mainly to serve recreational boaters. Thus, there is a continuing economic incentive for expansion of existing small-craft harbors and development of new harbors.

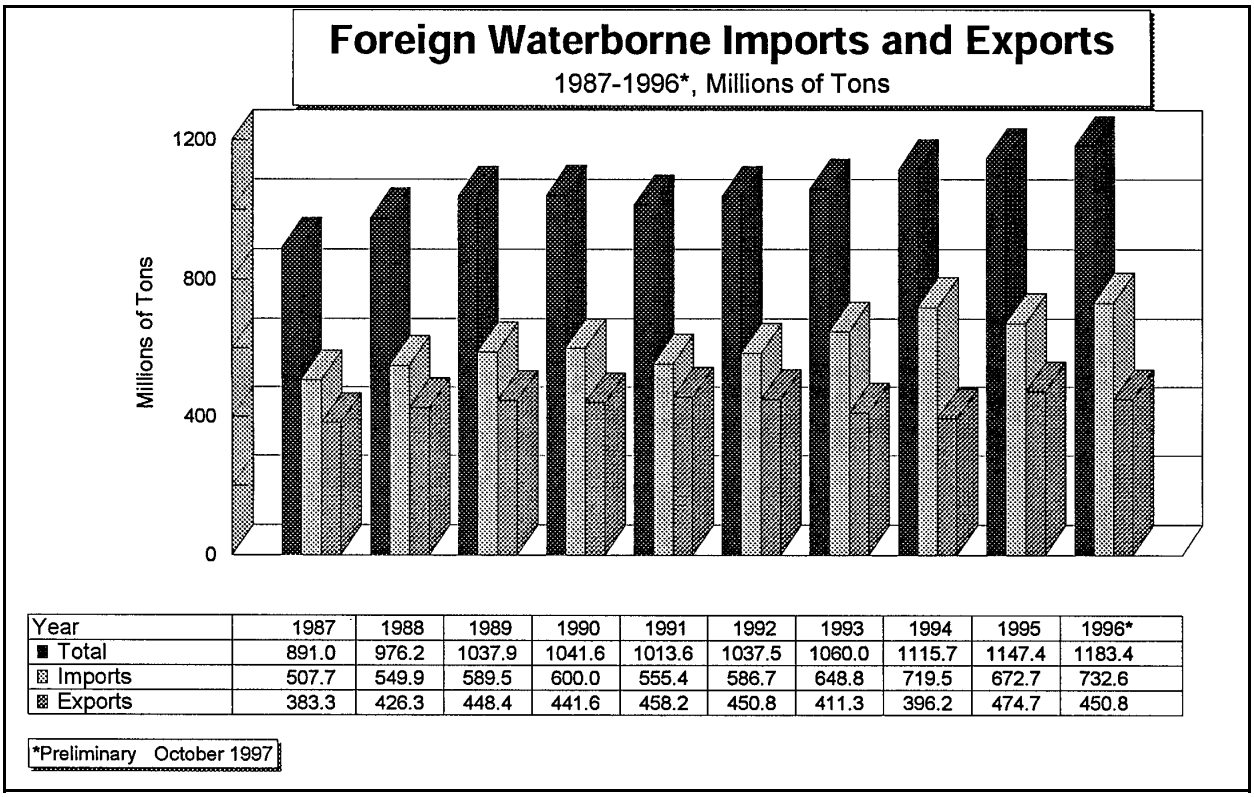

Year	1987	1988	1989	1990	1991	1992	1993	1994	1995	1996*
Total	891.0	976.2	1037.9	1041.6	1013.6	1037.5	1060.0	1115.7	1147.4	1183.4
Imports	507.7	549.9	589.5	600.0	555.4	586.7	648.8	719.5	672.7	732.6
Exports	383.3	426.3	448.4	441.6	458.2	450.8	411.3	396.2	474.7	450.8

Figure V-5-1. Foreign waterborne imports and exports (USACE Waterborne Commerce Statistics Center)

c. Preliminary planning and design elements.

(1) Federal coastal navigation projects are focused on channels and maneuvering areas to allow vessels to transit confined nearshore areas and use ports or harbors. Structures needed to accomplish navigation objectives are also included. Preliminary planning and design may include the following considerations, most of which are discussed in subsequent sections of this chapter:

(a) Site characterization.

(b) Design criteria.

(c) Defining vessel requirements.

(d) Entrance channel configuration.

(e) Inner harbor configuration.

(f) Navigation structures.

(g) Harbor and channel sedimentation and maintenance.

(h) Physical and numerical modeling.

(2) Helpful supplementary references for deep-draft projects include McBride, Smallman, and Huntington (1998); PIANC (1997a, 1997b, 1995); Tsinker (1997); Gaythwaite (1990); Turner (1984); Quinn (1972); and U.S. Navy design manuals. For small-craft projects, references include ASCE (1994), Tobiasson and Kollmeyer (1991), State of California (1980), and Dunham and Finn (1974). References with coverage of both deep-draft and small-craft harbors include Herbich (1992) and Bruun (1990). U.S. Army guidance for military ports is given by USACE (1983).

d. Policy considerations. Federal cost-sharing guidelines are a key concern in U.S. navigation projects. Prior to 1986, the Federal Government paid 100 percent of costs for navigation channel deepening and widening. Under present guidelines for *commercial* harbors, the nonfederal share of general navigation feature construction costs is 10 percent for project depth not exceeding 6.1 m (20 ft), 25 percent for project depth greater than 6.1 m (20 ft) but not exceeding 13.7 m (45 ft), and 50 percent for project depth exceeding 13.7 m (45 ft). The nonfederal sponsor must also pay: (1) an additional 10 percent of construction costs that are cost-shared, and (2) for project depths greater than 13.7 m (45 ft), 50 percent of operation and maintenance costs associated with general navigation features. For *recreational* navigation projects or separable recreational elements of commercial navigation projects, the nonfederal share is 50 percent of construction costs and 100 percent of operation and maintenance costs. Partnering between commercial, recreational, and military interests should always be examined. Cost-sharing guidelines are fully described by USACE (1996).

V-5-2. Defining Vessel Requirements

a. Deep-draft ships and shallow-draft vessels.

(1) Vessel dimensions. Navigation projects are designed to accommodate vessels of a desired size. Key vessel dimensions are length, beam (width), and draft. These dimensions are defined in several different ways to characterize the curved, three-dimensional vessel form. Vessel dimensions, especially for commercial ships, are often presented in terms of standard acronyms defined in Table V-5-2. Terms are explained in the following paragraphs.

(a) The shape of a typical commercial ship is depicted in Figure V-5-2. The LOA is an important measure of length for evaluating ship clearances in confined navigation project areas. For example, a turning basin would be sized based on the design ship LOA. The LBP is a more meaningful measure of the effective length for concerns such as ship displacement and cargo capacity.

(b) Definitions of design draft, freeboard, and beam are illustrated in Figure V-5-3. Molded beam is the maximum width to the outer edges of the ship hull, measured at the maximum cross section (usually at the ship waterline at midship). Design draft is the distance from the design waterline to the bottom of the keel. Ship *depth* is a vertical dimension of the hull, as shown in the figure, and it should not be confused with ship *draft*.

(c) Draft may not be uniform along the vessel bottom for both deep- and shallow-draft vessels. For example, draft near the vessel stern (aft) is often greater than near the bow (fore). Two useful indicators of such variations are:

trim - difference in draft fore and aft

list - difference in draft side to side

Table V-5-2
Acronyms Commonly Used to Describe Ship Size and Function

Acronym	Explanation
LOA	Length overall
LBP	Length between perpendiculars (measured at DWL)
LWL	Length along waterline (usually similar to LBP)
DWL	Design waterline (usually represents full load condition)
B	Beam (maximum width of ship cross section)
D	Draft
D_s	Depth of vessel's hull
FB	Freeboard (=D_s - D)
DT	Displacement tonnage (fully loaded)
l.t.	Long ton; = 1016 kg (2240 pounds)
m.t.	Metric ton: = 1000 kg (2205 pounds); ≈ 1 l.t.
LWT	Lightship weight (empty)
DWT	Dead weight tonnage (= DT - LWT)
GRT	Gross register ton; 1 register ton = 2.83 cu m (100 cu ft) of internal space (may also be stated in cubic meters)
GT	Gross ton
NRT	Net register ton
NT	Net tons
OBO	Ore/bulk/oil combination carrier
TEU	20-ft equivalent units; standardized 6.1 m x 2.4 m x 2.4 m (20 ft x 8 ft x 8 ft) container units

(d) *Maximum navigational draft* (the extreme projection of the vessel below waterline when fully loaded) is needed for navigation channel depth; *mean draft* is preferred for hydrostatic calculations. *Waterline beam* (width of the vessel at the design or fully loaded condition) is needed for navigation channel width.

(e) Maximum dimensions of the above-water part of a vessel are also critical to ensure adequate clearance. *Maximum beam* is the extreme width of the vessel. For a vessel such as an aircraft carrier, maximum beam is much larger than waterline beam. *Lightly loaded draft* is the minimum vessel draft for stability purposes, from which vertical clearance requirements, such as clearance under bridges, can be determined.

(2) Cargo capacity. Cargo capacity of commercial ships is generally indicated by DWT or, in the special case of container ships, by TEU. Units of measure for weight are usually long tons or metric tons (Table V-5-3). Cargo capacity also provides a convenient indicator of ship size, since ship dimensions for a particular type of ship (e.g. tanker) are usually closely correlated with capacity.

(a) Port duties and shipping costs are often figured in terms of register tons, a measure of *volume*. The GRT indicates total internal volume of the ship; NRT indicates volume available for cargo. The GRT is equal to NRT plus volume of space devoted to fuel, water, machinery, living space, etc. The terms GRT and NRT are currently used for older ships, but the terms GT and NT are favored for newer ships. The LWT

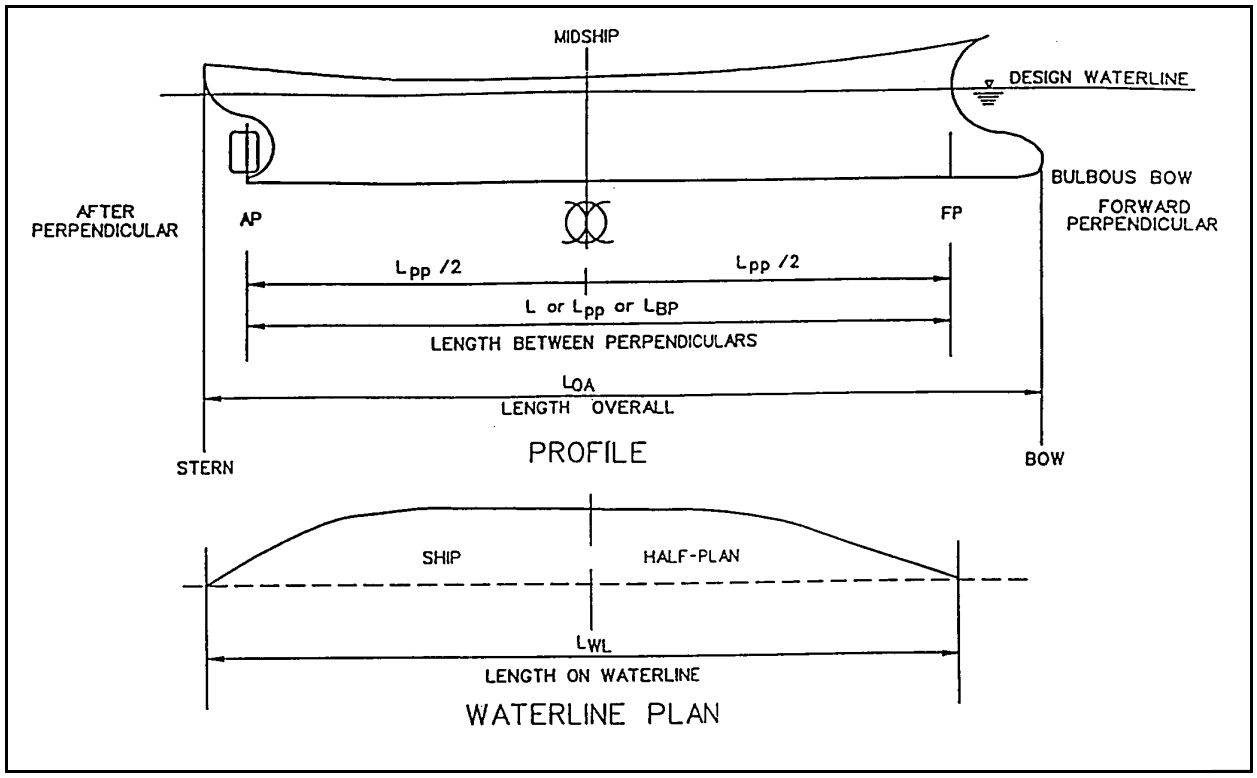

Figure V-5-2. Ship length definitions

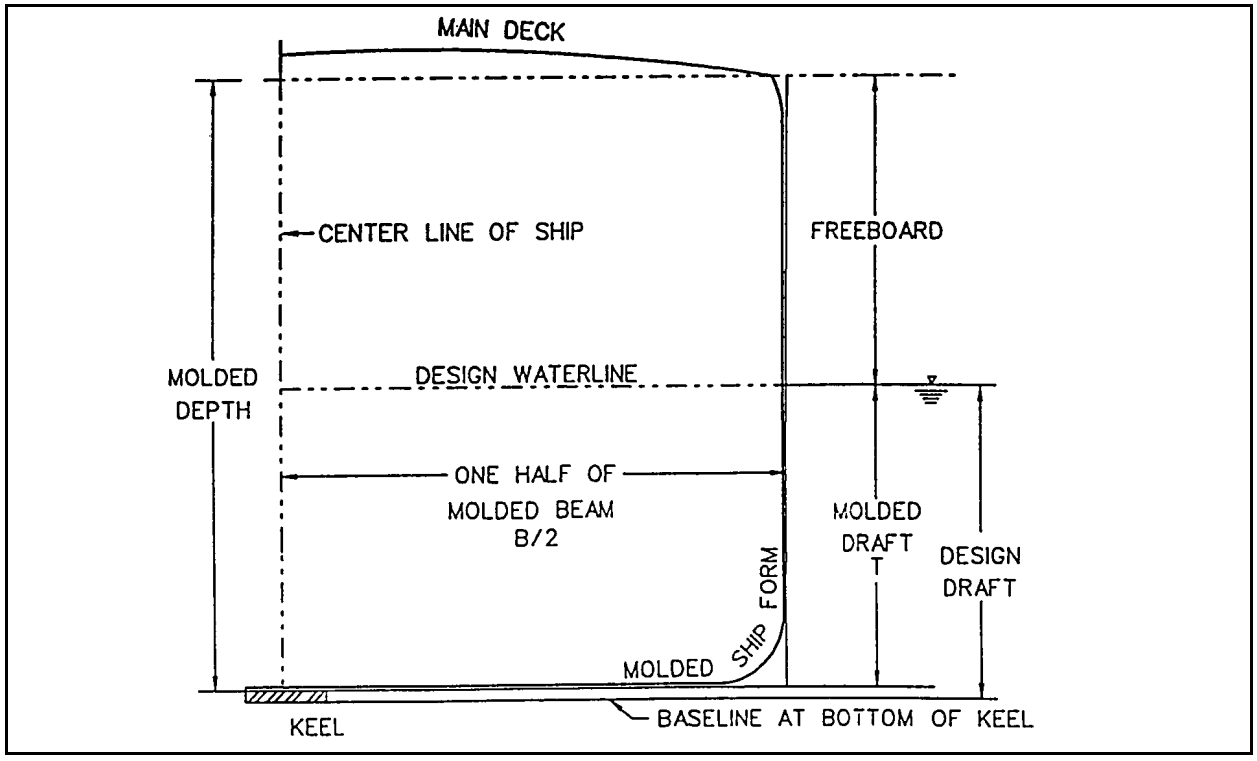

Figure V-5-3. Midship-section molded-form definitions

is the minimum weight a ship can have, such as the weight to be supported in dry dock. In operation, even unloaded ships rarely reach the LWT, as they often take on water, or *ballast*, to increase stability.

(3) Restrictions. Canal and lock sizes can impose distinct restrictions on ship size. The Panama Canal and Suez Canal are the two most critical for oceangoing traffic (Table V-5-3). Ships sized to meet the Panama Canal restrictions are known as *Panamax* vessels. They constitute an important vessel class for navigation projects because many commercial ships fit within the confines of the Panama Canal. Economics associated with some cargos, most notably crude oil, have resulted in ships that cannot pass through the canal. These ships are sometimes referred to as *Post-Panamax* vessels.

Table V-5-3
Canal Restrictions on Ship Size

	Restriction		
Canal	**Draft**	**Beam**	**Length**
Panama	12.0 m (39.5 ft)	32.2 m (105.75 ft)	289.6 m (950.0 ft)
Suez	16.2 m (53.0 ft)	64.0 m (210 ft)	No restriction

(4) Vessel characteristics. Vessels cover a wide range of sizes and shapes. Deep-draft vessels, especially the larger ships that typically dictate navigation project dimensions, may represent a small number of specific ship designs to serve specialized needs and routes. Therefore, deep-draft vessel characteristics are usually presented as a sampling of individual, named vessels. Characteristics of some representative large ships from the world merchant fleet are given in Table V-5-4. Most U.S. ports have controlling depths between 10.7 m (35 ft) and 12 m (40 ft). The deeper ports can accommodate Panamax vessels, but access by larger ships is limited. Common vessel types are briefly reviewed in the following paragraphs. In contrast to deep-draft projects, shallow-draft vessels are usually numerous and their characteristics can be discussed in statistical terms. Also, other factors besides individual vessel characteristics, such as volume of traffic, may be critical to a shallow-draft navigation project.

(a) *Tankers* carry liquid bulk products. Crude oil is by far the most common liquid bulk cargo. Economies of scale have strongly affected tanker design because of the volume and uniformity of product and consistent level of demand. Large tankers are often classified by size (Table V-5-5). The larger vessels far exceed Panamax size, but most can use the Suez Canal in ballast. Loaded tankers less than about 50,000 DWT require a draft of 12 m (40 ft) or less and can enter many U.S. harbors. Supertankers can use partial loading and/or tidal advantage to access U.S. harbors. Navigation projects in the United States generally cannot accomodate the drafts of loaded VLCC and ULCC class tankers. The largest tankers, too big to enter any of the major world ports, ply dedicated trade routes between offshore port facilities.

(b) *Liquid Natural Gas (LNG)* and *Liquid Propane Gas (LPG)* carriers have a highly volatile cargo at very low temperature. They require highly specialized terminals and special safety considerations.

(c) *Dry bulk carriers* carry a wide range of cargoes such as ore, coal, and grain. Size is generally less than 150,000 DWT.

(d) *Combination bulk carriers* are specially configured to carry both liquid and dry bulk cargo. The most common combination is ore/bulk/oil, or *OBO*. Vessel size ranges from 50,000 DWT to 250,000 DWT.

(e) *General cargo ships* carry a wide variety of cargoes packaged in the form of pallets, bales, crates, containers, etc. *Break-bulk* cargo refers to *individually* packaged items that are stowed *individually* in the ship. Size is typically 12,000 to 25,000 DWT.

Table V-5-4
Characteristics of Large Ships

Name	Dead-weight Tonnage	Length		Beam		Draft	
		m	ft	m	ft	m	ft
Tankers							
Pierre Guillaumat	546,265	414.23	1,359.00	62.99	206.67	28.60	93.83
Nisseki Maru	366,812	347.02	1,138.50	54.56	179.00	27.08	88.83
Idemitsu Maru	206,000	341.99	1,122.00	49.81	163.42	17.65	57.92
Universe Apollo	114,300	289.49	949.75	41.28	135.42	14.71	48.25
Waneta	54,335	232.24	761.92	31.70	104.00	12.22	40.08
Olympic Torch	41,683	214.76	704.58	26.92	88.33	12.09	39.67
Ore Carriers							
Kohjusan Maru	165,048	294.97	967.75	47.02	154.25	17.58	57.67
San Juan Exporter	104,653	262.00	859.58	38.05	124.83	15.44	50.67
Shigeo Nagano	80,815	250.02	820.25	36.86	120.92	13.23	43.42
Ore/Oil Carriers							
Svealand	278,000	338.18	1,109.50	54.56	179.00	21.85	71.67
Cedros	146,218	303.51	995.75	43.38	142.33	16.74	54.92
Ulysses	57,829	241.86	793.50	32.39	106.25	12.17	39.92
Bulk Carriers							
Universe Kure	156,649	294.67	966.75	43.33	142.17	17.45	57.25
Sigtina	72,250	250.02	820.25	32.28	105.92	13.36	43.83
Container Ships							
Sally Maersk (6600 TEU)	104,696	347.	1138.	43.	141.	14.5	47.5
Mette Maersk (2933 TEU)	60,639	294.1	964.9	32.3	106.0	13.5	44.3
Korrigan (2960 TEU)	49,690	288.60	946.83	32.23	105.75	13.01	42.67
Kitano Maru (2482 TEU)	35,198	261.01	856.33	32.26	105.83	11.99	39.33
Encounter Bay (1530 TEU)	28,800	227.31	745.75	30.56	100.25	10.69	35.08
Atlantic Crown (TEU)	18,219	212.35	696.67	27.99	91.83	9.24	30.33
Ocean Barges							
SCC 3902	50,800	177.45	582.17	28.96	95.00	12.22	40.08
Exxon Port Everglades	35,000	158.50	520.00	28.96	95.00	9.60	31.50

(Continued)

Table V-5-4 (Concluded)

Name	Dead-weight Tonnage	Length		Beam		Draft	
		m	ft	m	ft	m	ft
Passenger/Cruise Ships							
Voyager of the Seas	142,000 (DT)	310.50	1,018.70	48.00	157.48	8.84	29.00
Grand Princess	101,999 (DT)	285.06	935.24	35.98	118.04	8.00	26.25
Imagination	70,367 (DT)	260.60	854.99	31.50	103.35	7.85	25.75

Table V-5-5
Large Tanker Classes

Name	Approximate Size	Approximate Draft
Supertanker	50,000-150,000 DWT	11-18 m (35-60 ft)
Very Large Crude Carrier (VLCC)	150,000-300,000 DWT	18-24 m (60-80 ft)
Ultra Large Crude Carrier (ULCC)	Greater than 300,000 DWT	24-30 m (80-100 ft)

(f) *Container ships* are designed to carry cargo packaged in standardized steel container boxes. These ships, increasingly dominant in world trade, travel at high speed, and rely on fast turnaround times at port. Container ship speed and size are correlated. The larger container ships cruise at speeds of 46 km/hr (25 knots). Capacity is expressed in twenty-foot equivalent units (TEU), the number of 20-ft-long containers that can be carried. Ships with 4,000-TEU capacity reach loaded drafts of about 12 m (40 ft). Until fairly recently, container ship sizes were constrained by the Panamax limit. Since economics of shipping and terminal facilities have favored a Post-Panamax size, container ships have rapidly increased in scale. The largest container ships in present operation exceed 8,000 TEU, and have limited access to U.S. ports. Vessels of 15,000 TEU are under consideration. These Post-Panamax ships have necessitated new, longer-reach gantry cranes and other new or updated terminal facilities to handle the longer, wider ships and large volumes of cargo.

(g) Other vessel types include: *LASH* (Lighter Aboard Ship), *SEABEE*, and *BARCAT* vessels, designed to transport barges; *Ro/Ro* (Roll on/Roll off) carriers, essentially large, oceangoing ferries that load and unload wheeled cargo (trailers and/or vehicles) via ramps extending from the vessel; conventional ferries; passenger vessels; barges; etc. The *Integrated Tug/Barge (ITB)* is a special adaptation of barge design in which the barge resembles a vessel hull and a tug can be linked to the barge stern to form, in effect, a single vessel. ITB applications are usually dry and liquid bulk cargo transport.

(h) U.S. military vessels generally have maximum drafts of less than 12 m (40 ft). Nimitz class aircraft carriers have maximum draft of 12.5 m (41 ft). U.S. Navy vessel characteristics are available on the Internet (http://www.nvr.navy.mil) and in the NAVFAC Ships Characteristics Database soon to be on the Internet.

(i) Shallow-draft vessels are typically recreational or small fishing vessels. Recreational boats in the United States can range in length from about 3.6 m to 60 m (12 ft to 200 ft), but they are commonly 9-14 m (30-45 ft) in length with beams of 4.6 m (15 ft) or less. Recreational boats often have features protruding from the bow or stern. Although such features may not be included in the nominal boat length, they should be considered as needed in sizing harbor channel and dock clearances. Shallow-draft vessels may be driven by either engine power or sail. In comparison to powerboats, sailboats have narrow beam and require large maneuvering space when under sail.

(5) Form coefficients. Vessel shape is conveniently represented in terms of simple parameters known as *form coefficients*. The most important of these is the *block coefficient*, defined and illustrated in Figure V-5-4. This coefficient usually represents the fully loaded ship. Values of the block coefficient can normally range from around 0.4 for tapered-form, high-speed ships, such as container ships and passenger ferries, to 0.9 for box-shaped, slow-speed ships, such as tankers and bulk carriers. Small craft, sailboats, and power boats, respectively, represent forms with relatively low and high block coefficient.

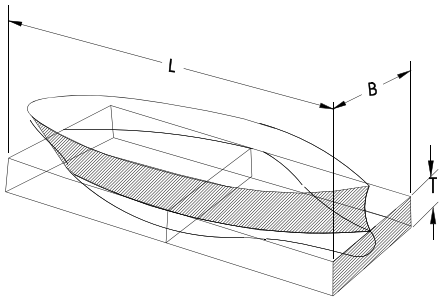

Block coefficient definition

Block coefficient (C_B) = Ratio of the volume of displacement to the volume of a rectangular block having a length, beam, and draft equal to that of the ship.

$$C_B = \frac{\nabla}{LBT}$$

L = Length between perpendiculars

T = Draft to the designed waterline, or molded ship draft

B = Beam amidships at the designed waterline, or molded beam

∇ = Volume of displacement of molded ship form at draft T

Figure V-5-4. Block coefficient definition

(6) Ship speed. Typical transit speeds in deep-draft channels are between 9 and 18 km/hr (5 and 10 knots). Vessel speed in navigation projects often represents a balance between several important considerations, as follows:

(a) Considerations favoring higher vessel speed:

- *Economics*. Vessel productivity increases when transits are faster; loaded vessels may be able to use high tide levels to advantage.

- *Vessel control*. Vessel control in the presence of wind, waves, and/or currents improves when vessel speed is higher.

- *Convenience*. Particularly for small craft, operators and passengers usually prefer quick transits.

(b) Considerations favoring lower vessel speed:

- *Wake effects*. Vessel wakes, directly related to vessel speed, can endanger other vessels and operations and erode banks.

- *Reduction of bank and bottom effects, ship resistance, ship-ship interactions*. Vessels may need to limit speed to avoid creating dangerous, speed-induced pressure differences. The effects are due to constricted clearance between the vessel and other obstacles, such as the bottom, side banks, another vessel in transit, and moored vessels.

- *Safety*. As long as vessels maintain adequate control, lower speeds are generally safer. Typically, vessel speed relative to the water must be at least 4 knots for both deep-draft vessels and small craft.

(7) Maneuverability. Commercial ships are designed primarily for optimum operation in the open ocean. Many of them maneuver poorly in confined areas. A successful navigation project must accommodate the ships using it. Ships are controlled by propellers and rudders at the stern. Some ships are also equipped with bow thrusters or bow and stern thrusters, which aid in control, especially at low speeds. Often, one or more tugs are needed to assist ships in some phases of entering and leaving a port. Control is especially crucial when ships slow to turn, dock, or attach tugs. A navigation project objective is to design ports and approach channels so ships can maintain adequate speed and control and navigate under their own power as much as reasonably possible. Small craft generally respond to engine, sail, and rudder control much more readily than deep-draft vessels. However, as with deep-draft vessels, small craft can encounter conditions in which control is difficult. Factors contributing to loss of control include slow vessel speed, following currents, waves, and cross-wind. Sailboats traveling under sail require extra maneuvering space.

b. Vessel operations. Deep-draft navigation projects are built or improved to enhance safety, efficiency, and productivity of waterborne commerce in U.S. ports and harbors. Shallow-draft projects embody similar concerns and often public recreational access as well. An understanding of vessel operations is critical to successful navigation project design.

(1) Navigation system. Port and harbor operations can be viewed as a system with three main components, as follows:

- Waterway engineering: Navigation channels, environmental factors, dredging and mapping services, shore docking facilities.

- Marine traffic: Operational rules, aids to navigation, pilot and tug service, communications, and vessel traffic services.

- Vessel hydrodynamics: Vessel design, maneuverability and controllability, human factors, navigation equipment.

(a) These components are closely interrelated in a navigation project. Tradeoffs between investment in the components are normal procedure, particularly in deep-draft projects. Thus, for example, channel design is strongly influenced by ship sizes and available accuracy of aids to navigation.

(b) Overall economic optimization of a navigation system can be a complex process. It typically involves crucial tradeoffs between initial investment (e.g. channel dimensions), maintenance, and operational use. For example, a channel that is wide enough for two-way traffic will cost more to dredge and, possibly, to maintain than a one-way channel of the same depth. However, the two-way channel may significantly reduce the amount of time ships must queue while waiting for access to the channel.

(2) Typical operations. Methods of operation must be considered in developing a navigation project. For deep-draft ships, operations depend on interactions between a pilot, captain, crew, and, often, one or more tug captains. On arrival at the entrance to a port, a ship typically is met by a local pilot. The pilot boards the ship near the seaward end of the entrance channel. Boarding is usually accomplished by pulling a small pilot boat next to the ship long enough for the pilot to mount a rope ladder and climb up to the ship deck, a potentially hazardous maneuver during high waves. Local tug services are contacted if needed, and plans finalized for the ship transit. Many tug companies also provide a tug pilot to accompany the local pilot and assist in the tug-aided final phase of transit and docking.

(a) The pilot is stationed on the ship bridge. The pilot effectively takes control of the ship during transit, issuing rudder and engine commands as well as course orders. Transit to a port generally follows a series of straight segments connected by turns. Turn angles greater than about 30 deg require special care because they involve varying currents and changing ship speed and position relative to banks and prevailing wind. Port entrance channels can be especially troublesome due to crosscurrents, waves, shoaling, and wind effects.

(b) A large ship in a confined channel can be difficult to control because ships do not respond quickly to rudder and engine commands. Turning may be sluggish. Bank effects and encounters with passing ships can introduce forces to turn the ship away from the intended travel direction. Such factors, along with human and environmental variability, result in variations in a ship's *swept path* (the envelope of all positions in the channel over which some part of the ship has passed). The swept path is illustrated by a ship simulator study example of ship position at short time increments during transit around a turn, up a channel, and through a turning basin to a dock (see Part V-5-10b for additional discussion of this simulation study) (Figure V-5-5).

(c) The ship must slow down well before approaching the berth or terminal, usually with the assistance of tugs when ship control is lost (at speeds below 6-7 km/hr or 3-4 knots). Often, the ship must pass other port facilities at very slow speed to prevent waves and moored vessel damage. As the ship approaches its berth, tugs typically take full control and push the ship against the dock face while mooring lines are made fast. When the ship departs, operations during a typical outbound run are similar to the inbound run, except in reverse sequence.

(d) Pilots and captains take care to avoid contact between the ship and bottom. However, ship motions and bottom conditions are not entirely predictable, and bottom contact occasionally occurs. Typical consequences are hull abrasion and propeller and rudder damage. Propeller/rudder damage reduces or removes ship control, leaving the ship vulnerable to further damage. It is also costly to repair. Therefore, pilots tend to be very protective of the ship stern when maneuvering in confined channels and turning basins.

(e) Ships may transit in fully loaded, partially loaded, or in ballast condition. The loading condition influences operational concerns. A fully loaded ship has a relatively large fraction of its volume submerged. Hence it is susceptible to currents, shoals, and other bottom influences. A ship in ballast generally has generous bottom clearance, but has a relatively large exposure to wind forces. Some types, including container ships, ferries, and Ro/Ro vessels, have large wind exposure, even in a loaded state.

(f) Sometimes ships approach port with loaded drafts greater than the channel depth, stop in an anchorage area, and offload to smaller vessels (*lighters*). Ships may fully unload to lighters or partially unload to reach an acceptable draft, after which they continue into port.

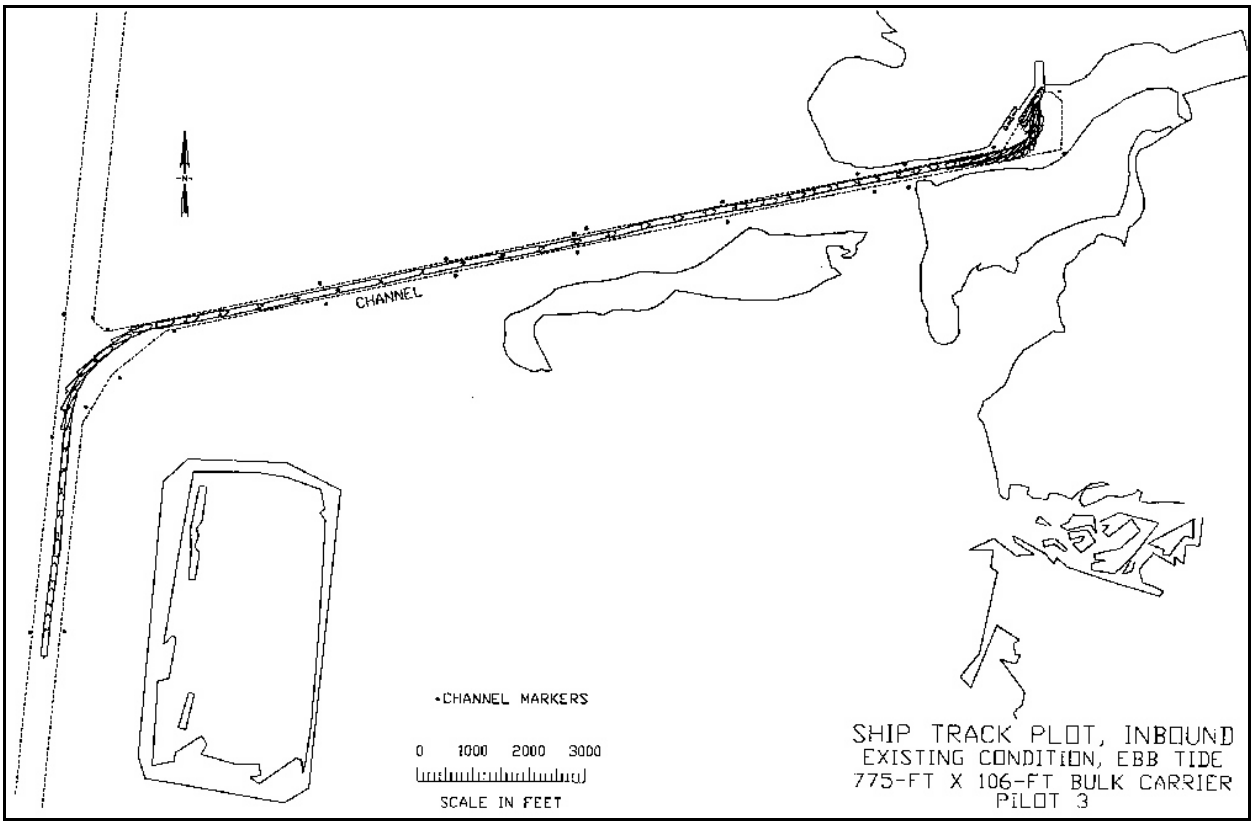

Figure V-5-5. Example ship track, Alafia Channel, Florida

(g) Deep-draft entrance and interior channels are designed for either one-way or two-way traffic. When a ship is entering a port with a one-way channel, any outbound ships must wait until the channel is clear. Two-way channels may accommodate inbound and outbound traffic simultaneously. They may also provide generous horizontal clearance for single ships when passing ships are absent.

(h) For small craft, operational concerns can vary significantly depending on the type of harbor. Small craft travel under their own power, controlled by an operator whose level of expertise and experience can range from novice to seasoned professional. Power boats are typically driven by one or two engines. Sailboats may be equipped with small auxiliary engines for transiting congested harbor areas and for emergency use, but they usually travel under wind power. Depending on wind speed and direction relative to desired travel direction, sailboat operators often must follow a zig-zag course. Small craft operators may take advantage of bays and other protected areas for fishing, sailing, etc., when available, especially if waves along the open coast are rough.

(i) Small craft typically exit the harbor for fishing and/or recreation and return to the same harbor, often on the same day. The number of vessels concurrently using a small-craft harbor during high traffic times can be greater than for deep-draft ports. Level of usage is often affected by holidays, weather, fishing or charter schedules, work schedules, etc. For example, a recreational harbor can be expected to have a higher volume of traffic during fair weather and weekend or holiday times. These same conditions are likely to result in a greater percentage of inexperienced operators and, possibly, a lower level of attention to navigation safety.

(3) Shallow-water, restricted channels. Vessels operating in restricted navigation channels can experience a variety of effects (Figure V-5-6). Large, loaded ships can block much of the channel cross section

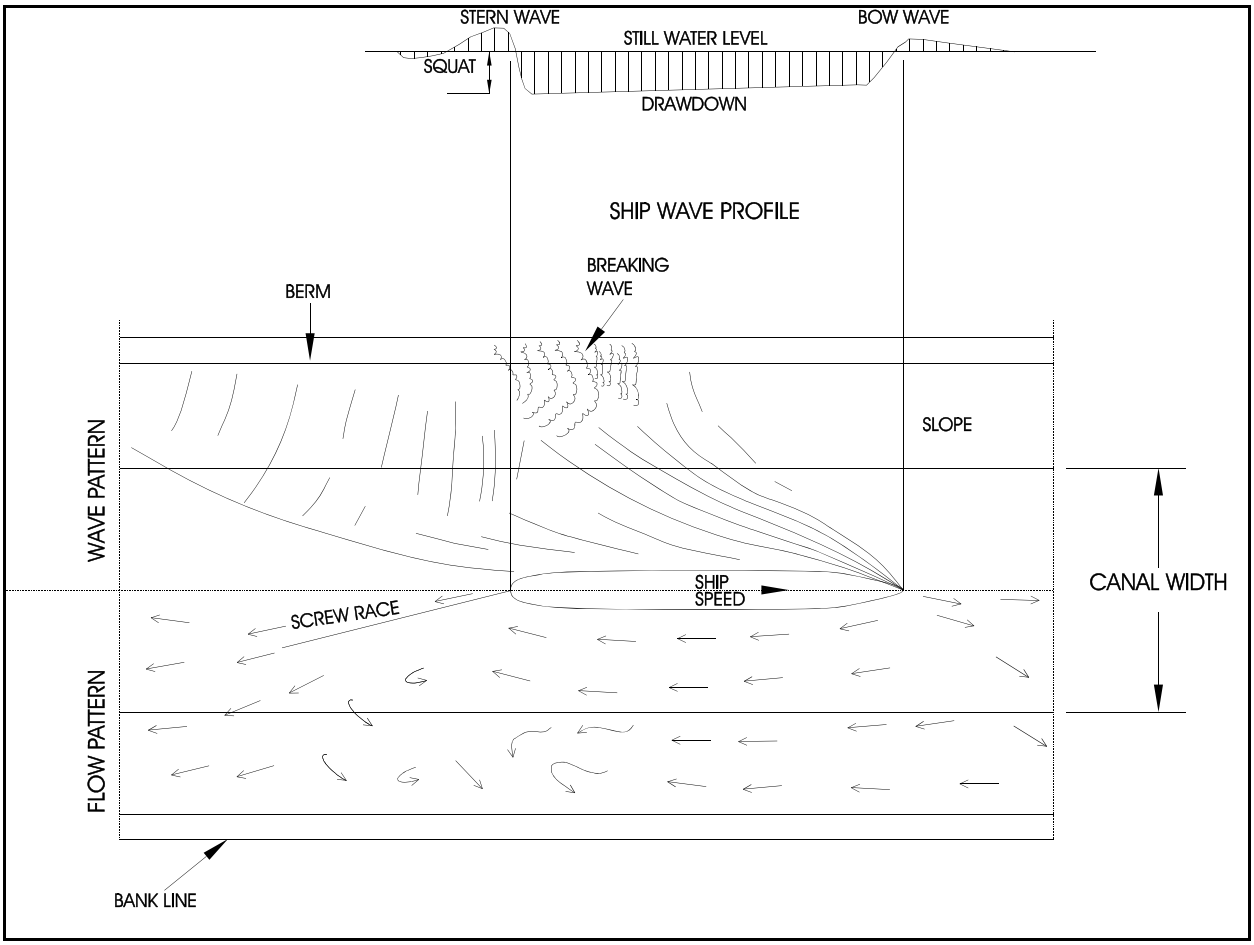

Figure V-5-6. Ship wave and flow pattern in a canal

and encounter very significant hydrodynamic resistance. Much of the water in the channel cross section must flow around the passing ship through highly confined space under the hull and between the hull and channel side slopes. Also, the ship experiences resistance due to the waves it creates as it moves forward.

(a) A moving vessel in a shallow waterway drops in the water relative to its at-rest level. The drop, referred to as *squat*, is due to a reduction in pressure exerted by water flowing around the moving vessel. Squat includes an overall lowering of the vessel *(sinkage*) and a motion-induced trim. Squat further reduces clearance between the vessel hull and the bottom.

(b) The maximum speed a vessel can attain in shallow water is significantly reduced from the typical deepwater speed. An important parameter governing shallow-water effects on a moving vessel (both deep- and shallow-draft vessels) is the depth Froude number

$$F_h = \frac{V}{\sqrt{gh}} \qquad \text{(V-5-1)}$$

where

F_h = channel depth Froude number

V = vessel speed

h = depth of channel or shallow-water area

g = acceleration due to gravity; = 9.80 m/sec^2 (32.2 ft/sec^2)

(c) Consistent units must be used for V, h, and g in the equation. Vessel resistance becomes very high as F_h approaches unity. In practice, a normally self-propelled merchant ship would never operate at F_h greater than about 0.6.

(d) The effect of a restricted, shallow *channel* configuration is to further increase wave effects, squat, and vessel resistance. Relative channel restriction is characterized by the *channel blockage ratio*

$$B_R = \frac{A_C}{A_S} \tag{V-5-2}$$

where

B_R = channel blockage ratio

A_C = channel cross-section area

A_S = vessel submerged cross-section area, = BT

B = vessel beam at midship

T = vessel draft

(e) The channel blockage ratio is illustrated in Figure V-5-7 for the extreme case of a canal with vertical sides. In this case, $A_C = Wh$, where W is channel width. The limiting ship speed for self-propelled vessels in a canal, represented as F_h, is shown as a function of B_R in Figure V-5-7. Typical B_R values range from 2 for very restricted cases to 20 or more for open channels, giving F_h values between 0.2 and 0.7. This effect significantly limits vessel speed in restricted channels. The limit is known as the *Schijf limiting speed*. For example, with B_R = 3 at a 12-m (40-ft) water depth, the maximum ship speed is 11.9 km/hr (6.4 knots). In practice, a ship's engine would not have enough power to drive the ship at the Schijf limiting speed.

(f) Bank effects in a channel can make ship control more difficult by creating suction and/or higher pressures along vessel hulls when vessels are off the channel center line. Forces may differentially affect vessel bow and stern and act to turn the vessel toward a potentially hazardous crosswise position relative to the channel. Bank effects become stronger as *channel overbank depths* (water depth of the natural bottom adjacent to the channel) decrease. Pilots sometimes take advantage of bank effects to assist in turning. Similar differential pressure effects arise when ships pass in a channel and when a ship passes a moored ship adjacent to the channel.

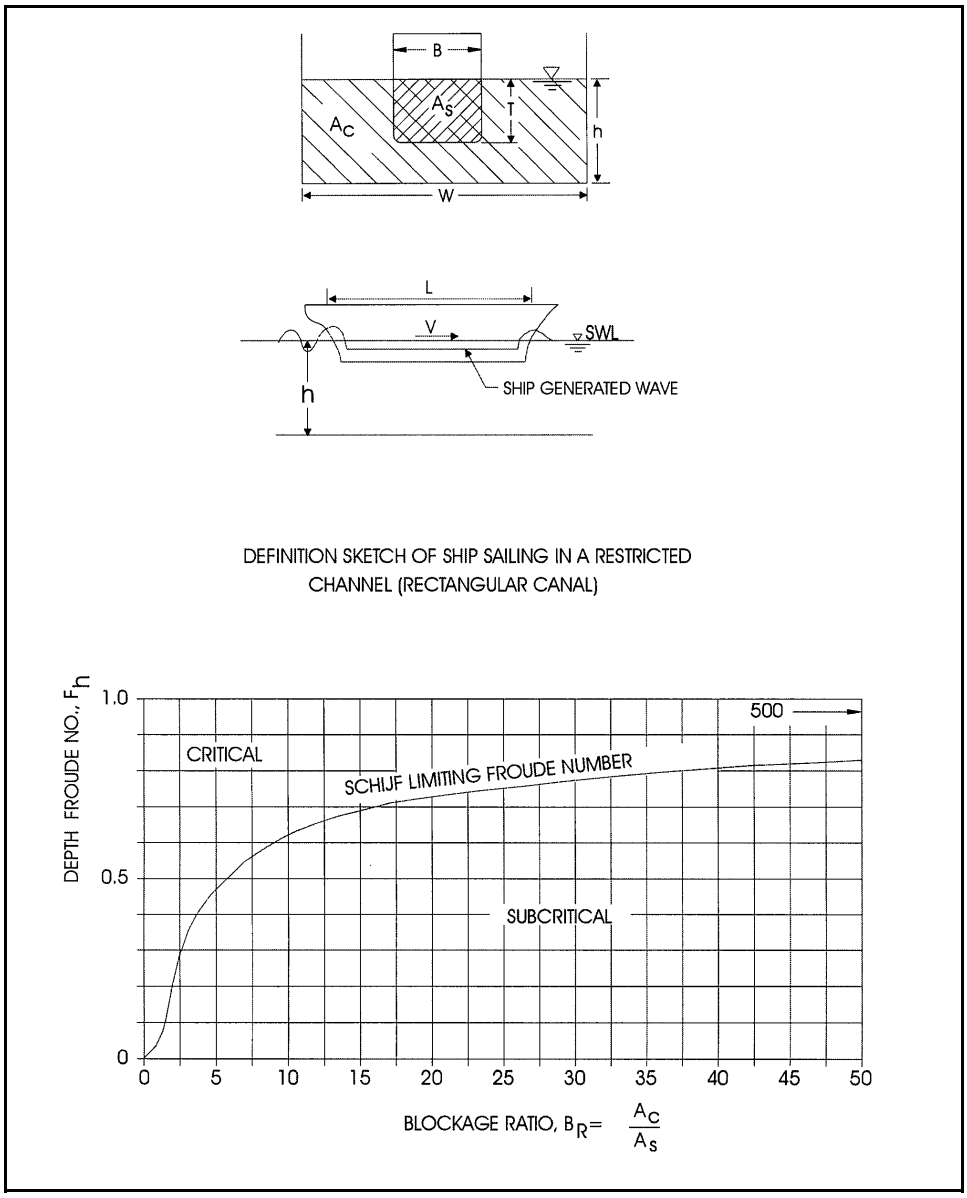

Figure V-5-7. Ship-limiting speed in a canal

(4) Ice navigation. Winter conditions along northern sea coasts, estuaries, and large lakes can cause ice to be an occasional, if not chronic, concern for safe and efficient navigation (PIANC 1984, USACE 1990a). About 42 percent of the earth experiences temperatures below freezing during the coldest month of any year (Figure V-5-8). The presence of ice is accompanied by longer nights and increased fog and precipitation (Figure V-5-9). Shipboard mechanical equipment, instruments, and communications apparatus are less efficient and more prone to failure in cold temperatures. Aids to navigation become less effective, and maneuvering in ice is much more difficult. Navigation projects in northern areas should be designed with consideration of these difficult conditions.

(a) Sea ice nomenclature and map notation symbols are defined by the World Meteorological Organization (WMO 1970). Ice thickness and structure are key concerns. *Multi-year ice*, sea ice more than 1 year in age, can be over 3 m thick, but it is found only in the Arctic Ocean and its marginal seas and near Antarctica.

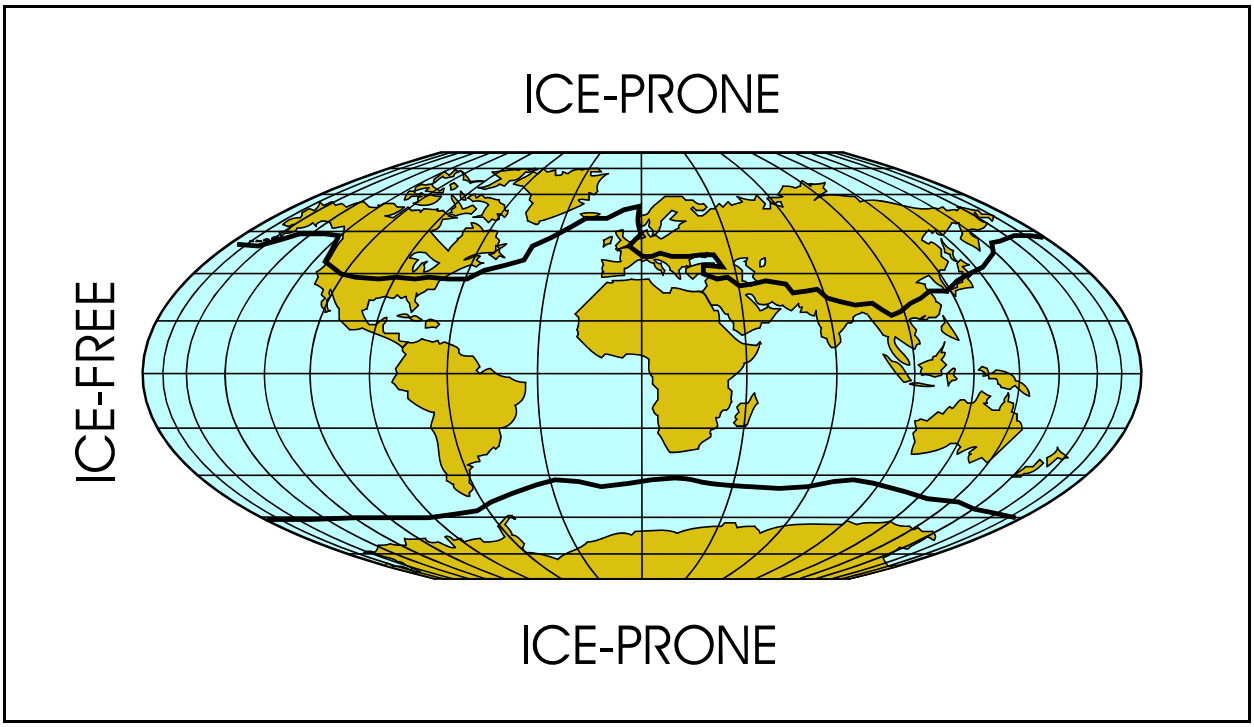

Figure V-5-8. Cold regions of the world

Figure V-5-9. Fog over frozen waterway (photograph, courtesy of Orson P. Smith, University of Alaska, Anchorage, Alaska)

First-year ice is generally classified as *young ice* (0-10 cm), *thin* (10-30 cm), *medium* (30-70 cm), or *thick* (70-120 cm).

(b) Ships that regularly navigate icy waters must have exceptional structural strength and propulsion power for safety of the crew, equipment, cargo, and environment. Special hull, propeller, and rudder designs reduce resistance and help clear lanes. Icebreakers may be needed to escort ice-strengthened cargo vessels or to periodically clear shipping routes. Shallow- and deep-draft ice-strengthened ships are in service around the world, classified for ice navigation by the ABS or several other agencies in Canada, Russia, and Europe.

(c) Factors to be considered for ship operation in ice rather than temperate conditions are:

- Ship maneuverability is retarded.
- Ice forces can divert ships from their intended course.
- Darkness is more common.
- Low visibility is more common (fog and precipitation).
- Winds can be very strong.
- Visual aids to navigation are less effective.
- Shipboard instruments are more prone to malfunction.
- Assistance or rescue by tugs is more difficult.
- Crews are more strained and fatigued in the face of these challenges.

c. Design considerations. Deep-draft navigation projects are typically formulated to provide safe and efficient passage for a selected ship under specified transit conditions. The design ship and transit conditions may be selected to represent the "maximum credible adverse situation," the worst combination of conditions under which the project would be expected to maintain normal operations. A project that successfully accommodates this situation can be expected to perform well with a full range of smaller ships and less difficult transit conditions. If future needs require it, the project may also accommodate ships larger than the design ship under milder transit conditions than the design scenario. Shallow-draft navigation projects are designed to safely accommodate the variety of small craft anticipated during the project design life, typically around 50 years.

(1) Design vessel. For deep-draft projects, the design ship or ships are selected on the basis of economic studies of the types and sizes of the ship fleet expected to use the proposed channel over the project life. The design vessel or vessels are chosen as the maximum or near maximum size ships in the forecast fleet based on the characteristics (length, beam, draft) of the ships being most representative of the potential economic advantage to be found in the forecast ship fleet.

(a) For small craft projects, the design vessel or vessels are selected from comprehensive studies of the various types and sizes of vessels expected to use the project during its design life. Often, different design vessels are used for various project features. For example, sailboats, with relatively deep draft, may determine channel depth design; and fishing boats, with relatively wide beam, may dictate channel width design.

(2) Design transit and mooring area conditions. Operational conditions selected for design can strongly affect a navigation project. A deep-draft project should be designed to allow the design ship to pass safely under design transit conditions. Normally, extreme events are not considered in specifying design transit conditions. Ship operators can usually suspend operations during these rare events without undue hardship. Some important exceptions for which extreme events may need to be considered include ships under construction or in repair facilities, inactive vessels, and USCG vessels.

(a) Operational factors to be specified for design transit include:

- Wind, wave, and current conditions.
- Visibility (day, night, fog, and haze).
- Water level, including possible use of tidal advantage for additional water depth.
- Traffic conditions (one- or two-way, pushtows, cross traffic).
- Speed restrictions.
- Tug assistance.
- Underkeel clearance.
- Ice.

(b) The use of tidal advantage in specifying design transit conditions allows for reduced channel depth, since the design ship would be constrained to transit during a high tide level. Channel length and vessel speed determine vessel transit time. The channel must provide the necessary water depth during at least the transit time period. If tidal advantage is included in design, the optimum design depth may be based on an analysis of water level probabilities, costs (vessel delays, dredging and disposal, etc.), and benefits.

(c) Normal operational conditions are strongly influenced by individual, local pilot, and pilot association rules and practices. For example, pilots usually guide a transit only when conditions allow adequate tug assistance. There may be operational wind, wave, or current limitations on the ability to safely moor a ship at a terminal or berth. Turning operations and maneuvering into a side finger slip may be limited by tide level and current conditions, including river outflow. Energetic wave conditions at the seaward end of the entrance channel may prohibit pilots from safely transferring between the pilot boat and ship. Such operational limitations may well be controlling factors in determining whether or not a safe transit is possible, and navigation project design should be consistent with these limitations.

(d) Design transit conditions for small-craft projects include vessel maneuverability (particularly if parts of the project will accommodate vessels under sail), traffic congestion, wind, waves, water levels, and currents. Design wave criteria are usually expressed as significant wave height, in probabilistic terms, for the entrance and access channels and mooring areas. Typical criteria are:

- Mooring areas: Significant wave height will not exceed 0.3 m (1 ft) more than 10 percent of the time.
- Access channels: Significant wave height will not exceed 0.6 m (2 ft) more than 10 percent of the time.

(e) Final design criteria for small-craft projects should be determined on the basis of economic optimization of the complete project (Part V-5-4).

V-5-3. Data Needs and Sources

a. Introduction. Planning and design of a navigation project are based on a wide range of information about the project area. The necessary data and sources are briefly reviewed in this section. More detailed information about data types and sources is given in Part V-2, "Site Characterization," and Part II-8, "Hydrodynamic Analysis and Design Conditions."

b. Currents. Currents in navigation channels and other project features can strongly affect vessels. Currents may also be important in navigation structure design. Currents of concern are usually tidal circulations or river flows.

c. Water levels. Water levels are essential for determining design depth in channels and other navigation areas. Water level variations are usually due to tides, river discharge, or lake levels. NOAA predicts tides and tidal currents at primary reference stations by the method of harmonic analysis. Phase and amplitude corrections to reference station predictions are available for many other secondary stations (NOAA *Tide Tables* and *Tidal Current Tables*, annual). Interpolation between secondary stations is often practical, if no major constrictions or confluences are present. Commercial software is available that can predict tides at hourly intervals at secondary stations. A similar analysis can be performed by applying the methods of Harris (1981).

d. Wind. Wind forces can strongly influence both vessels under way and moored vessels. Often an airport wind station located in the general area of a project can be used as a source of representative wind data.

e. Waves. Waves can have a major impact on navigation in exposed channels, particularly vertical excursions of the vessel and channel depth requirements. Deep-draft vessels respond to wave periods typically found in exposed ocean and Gulf of Mexico waters. Small craft respond to a wide range of wave periods, and waves can be especially troublesome if they break in the channel. Waves are also important for navigation structure design and for predicting channel shoaling.

f. Water quality. Water quality and potential changes in water quality may become issues for projects creating more enclosed harbor areas, where circulation and flushing may be reduced as a result of the project.

g. Sediments. Sediment characteristics in project and adjacent areas are needed. Bottom materials in any areas to be dredged are especially important. Sediment quality can dictate disposal options and costs ranging from beneficial uses such as beach fill to confined or capped disposal of contaminated material.

h. Bathymetry and sediment transport processes. Bathymetry and sediment transport processes are needed to determine baseline conditions, optimum project location, initial dredging quantities, channel shoaling rate and maintenance needs, and potential project impact on adjacent shorelines. Methods for predicting channel sedimentation are reviewed by Irish (1997).

i. Ecological processes. Navigation projects can have an impact on ecological processes. Baseline conditions may need to be established.

j. Local coordination. Local people familiar with the project area and/or using an existing project regularly can provide valuable insight about present conditions and impact of any modifications.

(1) Pilot interviews. Deep-draft navigation project planners/designers should develop strong coordination with local pilot groups. Pilot interviews can be used to determine users' opinions about existing

channel navigation safety, suitability of design transit conditions, and feasibility and safety of proposed channel design alternatives.

(2) U.S. Coast Guard. The local USCG office should also be contacted early in the project development to solicit their views on channel dimensions and alignment for safe navigation. They can also provide guidance on placement of aids to navigation.

(3) Accident records. Marine accident records are available from the USCG annual compilation of casualty statistics in an automated system called Coast Guard Automated Main Casualty Data Base (CASMAIN). Accident data on existing navigation channel projects proposed for enlargement or improvement should be studied. USCG and National Transportation Safety Board special investigation reports are available for some accidents, which can provide insight on navigation problems.

V-5-4. Economic Analysis

a. A number of alternatives can usually be defined to meet navigation design requirements. Alternatives should generally include a range of channel depths, since depth is one of the major cost-determining parameters. For example, a proposed navigation channel may suffice for the design ship and design transit, but lead to undesirable ship delays and queueing because of heavy ship traffic and limited channel capacity. The adaptability of each alternative for meeting future navigation requirements should also be considered. The final design is usually selected from among the alternatives to maximize economic benefits. USACE navigation project evaluation procedures are described by USACE (1990b).

b. A complete design approach includes consideration and optimization of the full navigation system described in Part V-5-2.b. The comprehensive design process, beyond the scope of this chapter, is discussed by PIANC (1997a).

c. For economic optimization, the cost of each alternative design is estimated. Costs associated with all the elements of developing and maintaining the project should be included. Normally, several alternative channel alignments and widths, as well as depths, are represented. Navigation structures may also be part of some or all alternatives. Costs include initial construction (dredging, dredged material disposal, aids to navigation, breakwaters, jetties, etc.), replacement cost, and operation and maintenance.

d. Benefits for deep-draft projects are determined by transportation savings, considering ship trip time (including loading/unloading time, which may include lightering), cargo capacity, and delays due to project limitations. Benefits are evaluated by determining the transportation costs per ton of commodity for each increment of channel depth. Transportation costs are based on ship annual operating cost for each type of ship, including fixed cost and annual operating expenses. Data on ship operating costs are periodically compiled by the USACE Water Resources Support Center. Benefits may result from:

(1) Use of larger ships.

(2) More efficient use of large ships.

(3) More efficient use of present ships.

(4) Reductions in transit or delay times.

(5) Lower cargo handling costs.

(6) Lower tug assistance costs.

(7) Reduced insurance, interest, and storage costs.

(8) Use of water rather than land transport mode.

(9) Reduction of accident rate and cost of damage.

e. The USACE evaluation procedure to estimate navigation benefits includes nine individual steps (Figure V-5-10). Accurate projection of commodity movements over the proposed alternative project design (steps 3 and 7) is key to evaluation. Details of the procedure are given by USACE (1990b).

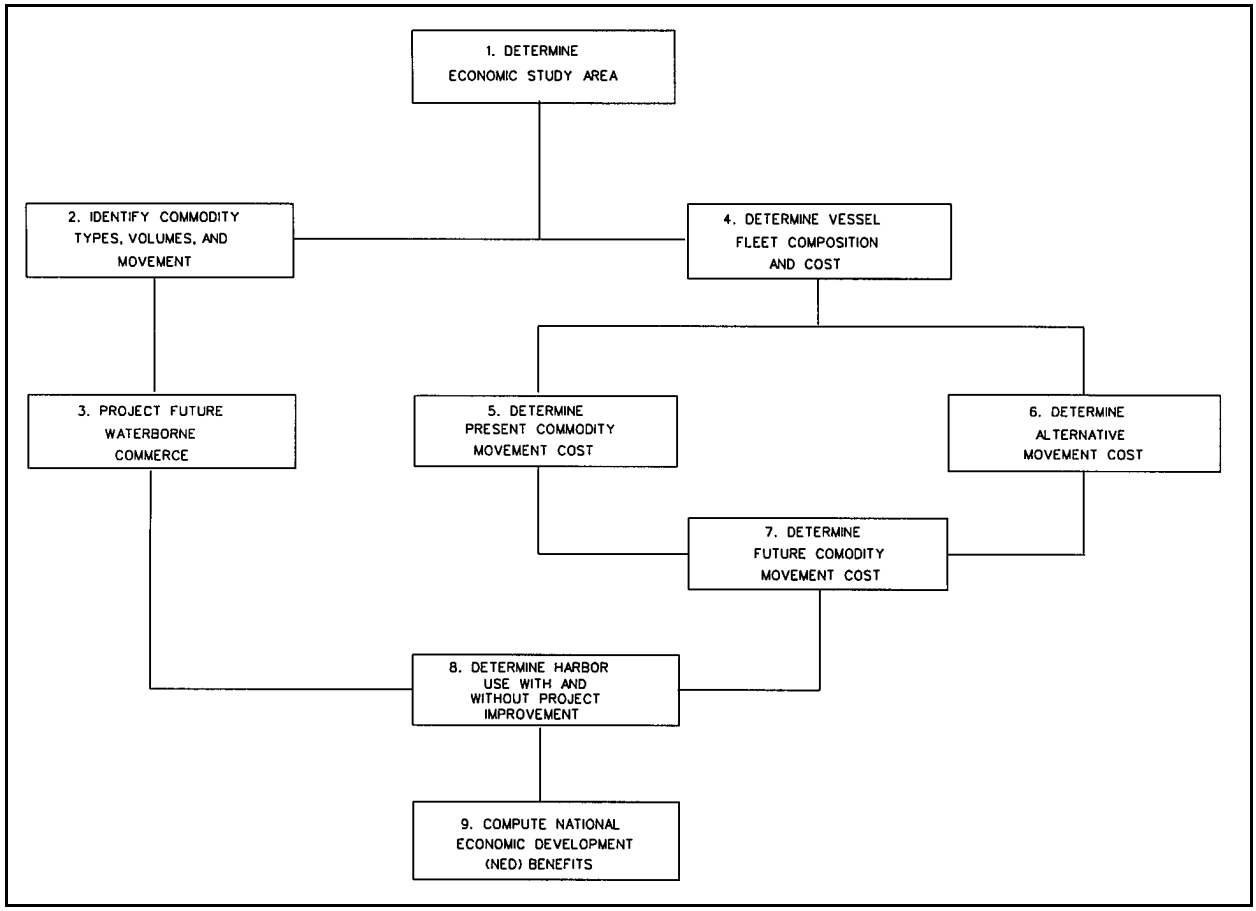

Figure V-5-10. Deep-draft navigation benefit evaluation procedure

f. Small-craft harbor projects follow a similar economic optimization procedure. Generally, several entrance channel and basin configurations are identified as alternatives. The alternatives should provide varying protection and accommodations so an optimal alternative can be selected. The cost for each alternative is estimated, including initial cost, maintenance cost, and social and environmental aspects. Benefits are also estimated. The alternative that maximizes net benefits (difference between benefits and cost) is usually the preferred project plan. After the alternative with optimal level of protection and size has been determined, then the most economical way of providing that protection and size should be developed.

V-5-5. Channel Depth

a. Introduction. Channel depth is a key factor in the cost and usability of a navigation project. It should be adequate to accommodate present and expected traffic. Typically it is chosen on the basis of economic optimization. The design channel depth need not be constant throughout the project. It can, and often does, vary in segments as needed to allow the design vessel or vessels to make safe and efficient transits in a cost-effective project.

(1) Vessels navigating in shallow water encounter a variety of channel cross sections over the length of a navigation project. Since channel cross section can significantly affect natural processes and vessel behavior, it is useful to define characteristic types (Figure V-5-11). A *canal* has an enclosed cross section with exposed land adjacent to both sides of the channel. A *trench* is a deepened passage with submerged overbanks on either side. A *fairway* is a passage with no lateral constraints.

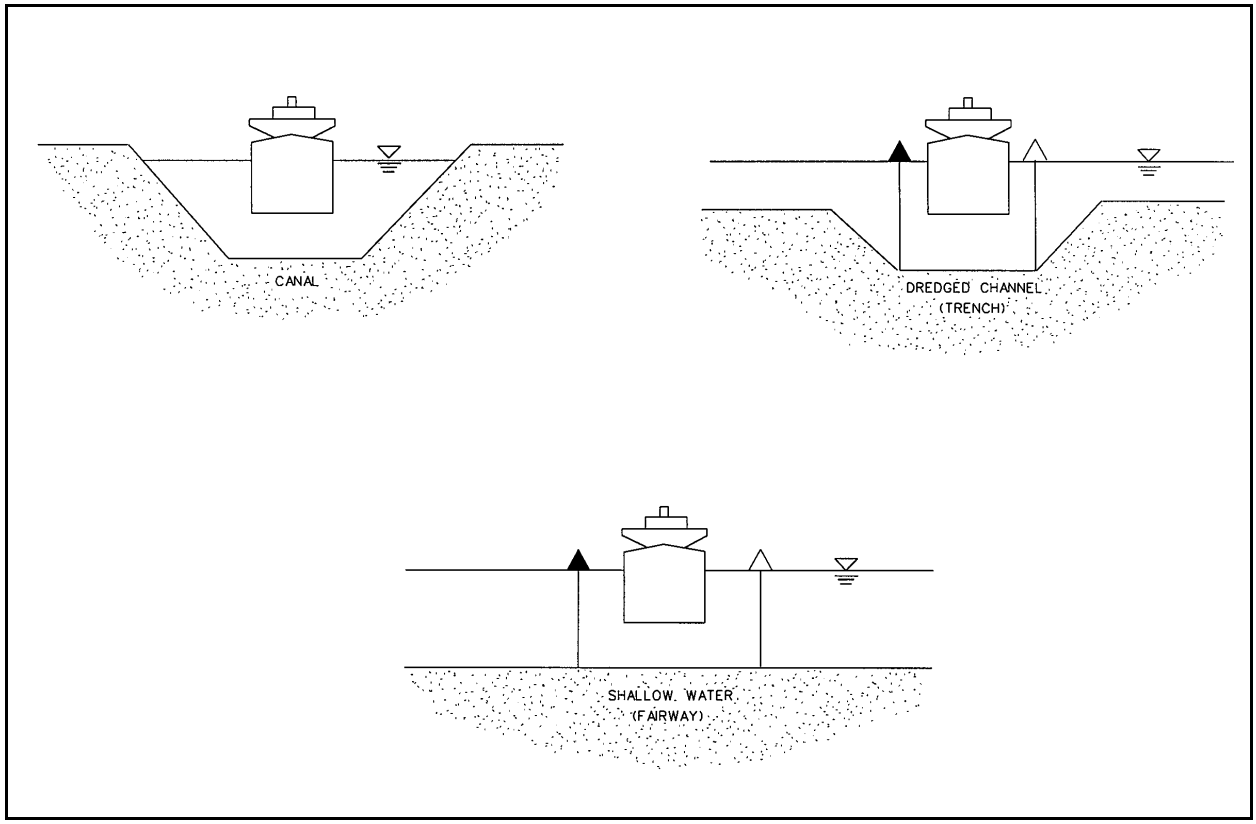

Figure V-5-11. Definition of channel types

(2) Channel depth for both deep- and shallow-draft navigation projects may be determined by figuring a depth increment for each of the important factors affecting vessel underkeel clearance requirements and adding those to the design vessel draft (Figure V-5-12). This depth, required for safe vessel passage, provides a basis for Congressional authorization of Federal channel depth, referred to as the *authorized channel depth*. The dredged channel depth, or *contract depth*, generally exceeds the authorized depth to accommodate potential sedimentation and maintain navigability. In some projects, consideration must also be given to the *permitted depth*, the extreme dredging depth permitted by regulators. The same factors generally apply for both deep- and shallow-draft projects, but their relative importance and estimation procedures differ somewhat, as discussed in the following paragraphs.

b. Effect of fresh water. The nominal draft of seagoing ships usually represents the seawater environment. When ships enter channels and ports in brackish or fresh water, ship draft increases due to the lower water density. The draft increase between ocean and fresh water is 2.6 percent. In USACE practice, a maximum depth allowance of 0.3 m (1 ft) may be included for this effect (Table V-5-6) (see Figure V-5-12). This maximum allowance corresponds to the draft increase between ocean and fresh water for a vessel with an 11.6-m (38-ft) draft. The freshwater effect is generally not considered in small craft navigation projects.

Table V-5-6
Depth Allowance for Freshwater Effect

	Allowance	
Port Location	**m (ft)**	**Percent**
Brackish water	0.15 (0.5)	1.3
Fresh water	0.3 (1.0)	2.6

c. Vessel motion from waves. Vessel vertical motion in response to waves must be considered in design of channel depth at exposed locations (see Figure V-5-12). Entrance channel design depth is typically greater than interior harbor channel depth because of the need to accommodate wave-induced vertical vessel motions. Wave effects tend to increase as wave height increases and decrease with longer vessel length. Maximum vessel response occurs with wavelengths approximately equal to vessel length. Most deep-draft ships are relatively unaffected by very short-period waves but respond when periods are longer than around 6-8 sec.

(1) Vessel motions that affect channel depth are roll, pitch, and heave (Figure V-5-13). Roll is most important when waves are perpendicular to the vessel travel direction (*beam seas*). Pitch and heave are most important when the vessel and wave travel directions are colinear (*head sea* or *following sea*). These motions can have a large impact on deep-draft channel depth requirements. For example, a pitch angle of 1 deg increases the extreme excursion of a 300-m- (1000-ft-) long ship by 2.7 m (9 ft). A 5-deg roll of a ship with a 46-m (150-ft) beam can increase extreme excursion by 2.1 m (7 ft).

(2) Vessel response to waves depends on the combined effects of:

(a) Wave height, period, wavelength, and propagation speed.

(b) Wave direction relative to vessel.

(c) Vessel length and beam.

(d) Vessel speed.

(e) Natural periods of vessel roll, pitch, and heave.

(f) Vessel draft and underkeel clearance.

(g) Channel depth and overbank depth.

(h) Wind and currents (speed and direction relative to vessel).

(i) Pilot strategy.

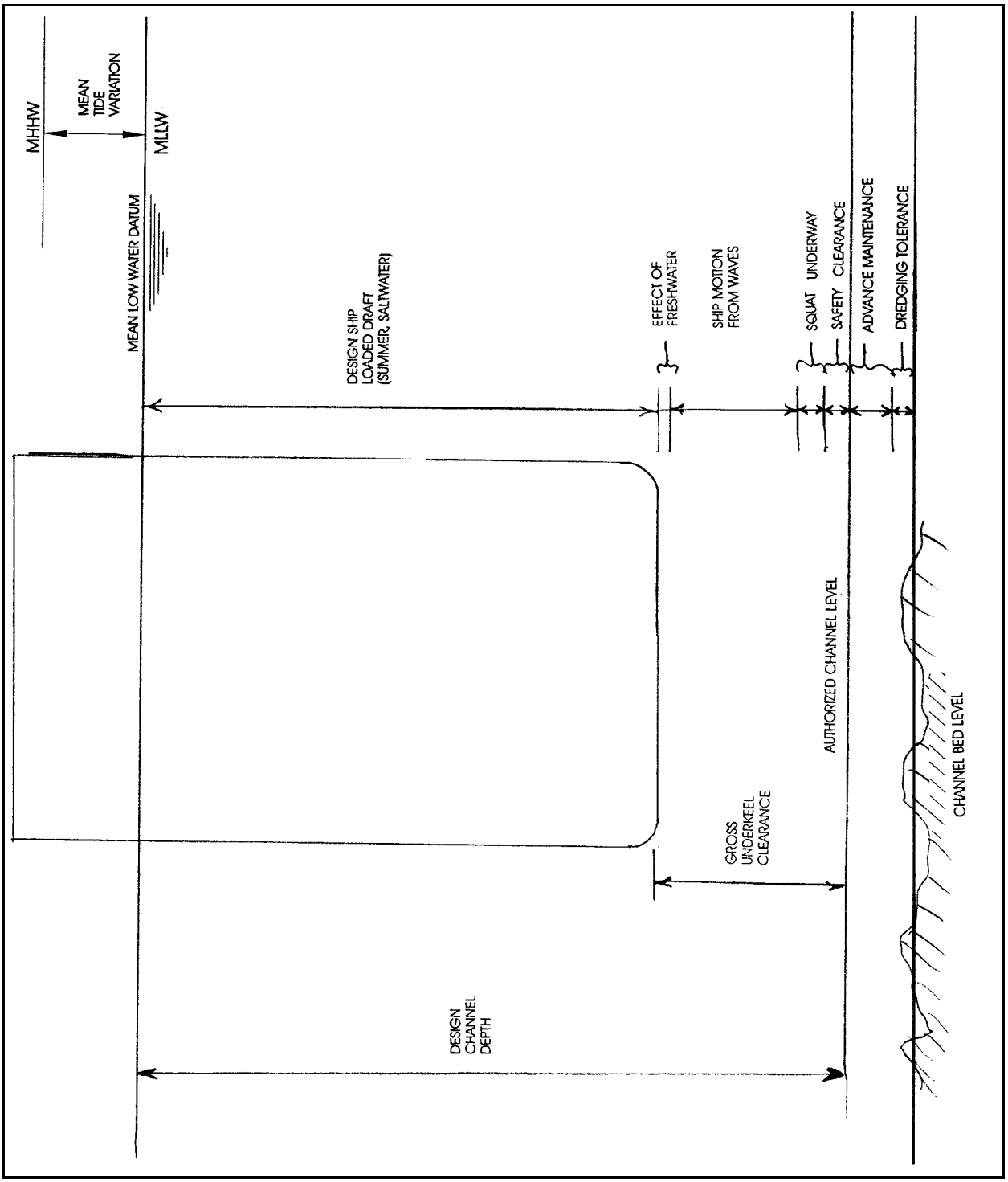

Figure V-5-12. Channel depth allowances

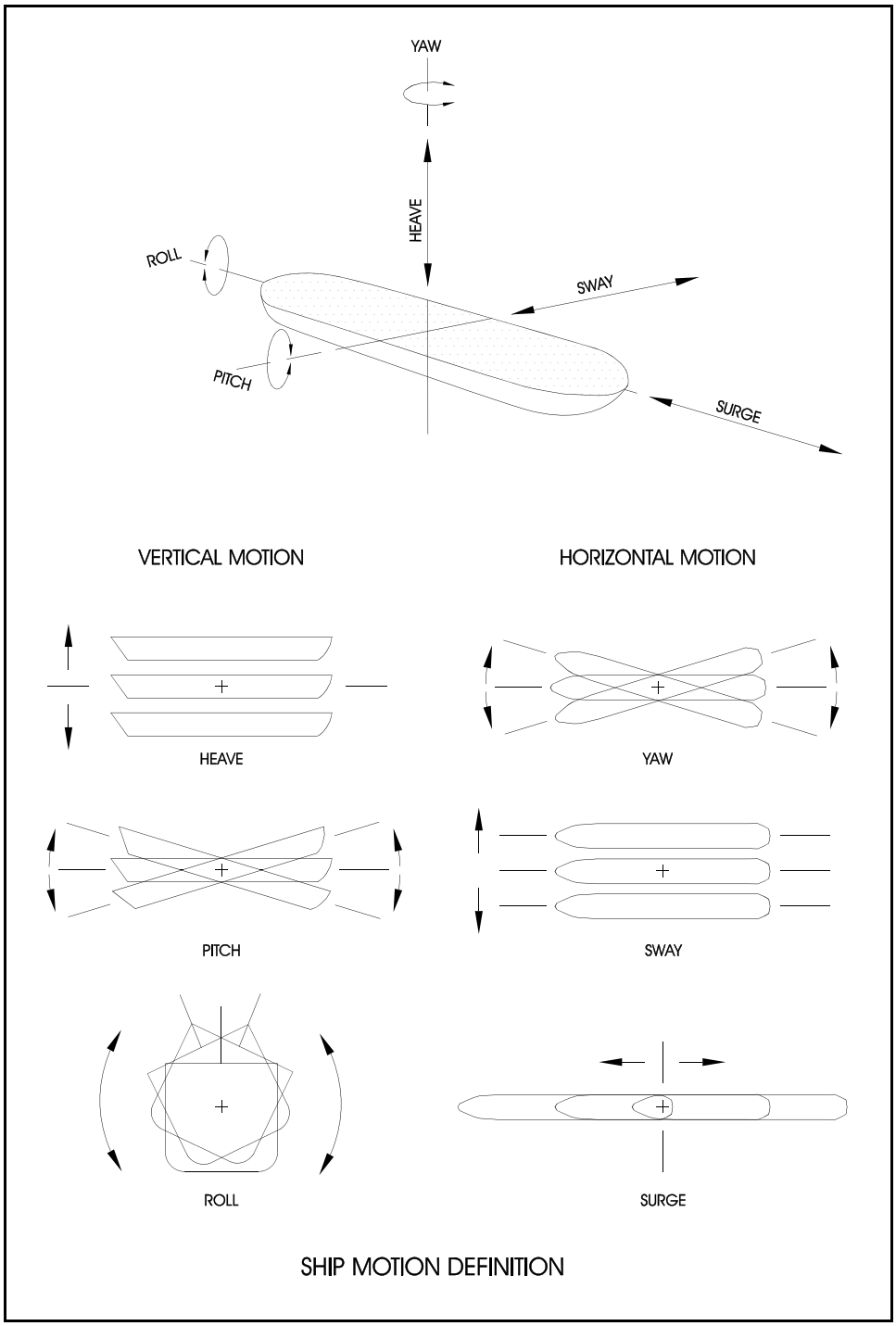

Figure V-5-13. Ship motion definitions

(3) Many of these factors, most notably wave height, vary as a vessel transits a channel. The net effect of these factors on a vessel is difficult to estimate analytically. The design objective is to achieve a channel depth that allows the design vessel to transit the project with a very low probability for any damaging contact with the channel bottom.

(4) For deep-draft projects, the depth allowance needed to accommodate wave-induced ship motions is a major concern for which no easy, accurate solutions are available. Because of the magnitude of depth allowance for waves in many exposed entrance channels and because waves are highly variable, even within a specified sea state, it is prudent for final design to review existing data for similar ships and, in many cases, to conduct studies to develop realistic estimates. Options include (Part V-5-10):

(a) Analytic studies, using strip theory or other theoretical calculation methods as developed by naval architects.

(b) Interactive, real-time ship simulator studies.

(c) Physical model studies, using radio-controlled, free-running scaled ship models with wave response measurements.

(d) Direct, onboard ship measurements while transiting through the entrance channel.

(5) An example of physical model studies to aid in probabilistic navigation channel design is presented in Section V-5-10.b.(1).

(6) Direct field measurements of ship motion are a valuable addition to channel design studies, but extreme conditions controlling design are not easily captured. Field measurements are dependent on available ships and environmental conditions during the limited duration of the measurement program. Figure V-5-14 provides an example of results from a large field measurement program in a high-wave-energy entrance channel. Data were collected over a 2-year period at the mouth of the Columbia River, at the Oregon/Washington border (Wang et al. 1980). The *average* ratio of ship bow/stern response amplitude to wave amplitude on each transit varied between about 0.5 and 2.0 over 29 instrumented voyages.

(7) Simple general guidelines for minimum depth clearance requirements in channels influenced by waves are given by PIANC (1997) as

$$\frac{Water\ depth}{Ship\ draft} \geq 1.3 \qquad \text{when } H \leq 1\text{m (3.3 ft)}$$

$$\frac{Water\ depth}{Ship\ draft} \geq 1.5 \qquad \text{when } H > 1\text{m (3.3 ft) and wave periods and directions are unfavorable}$$

where H = wave height

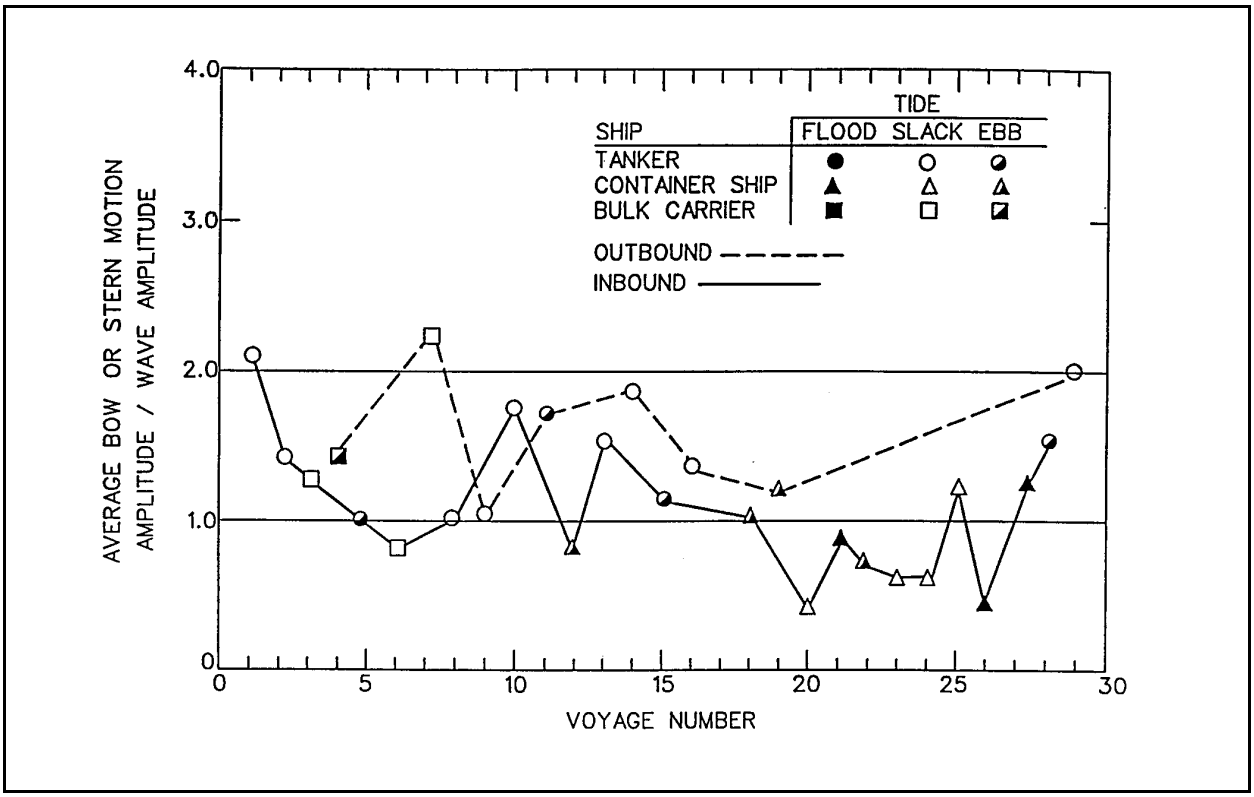

Figure V-5-14. Ship motion response, mouth of Columbia River

(8) For small recreational craft, a depth allowance for waves is also important but difficult to estimate accurately. As with deep-draft vessels, model and measurement studies may be conducted; but such project-specific studies are usually impractical for small-craft channel design. Small craft length and beam are often small relative to wavelengths important for design. It is realistic to consider the maximum vertical drop experienced by a small boat in a wave to occur when the boat is fully contained in the wave trough. The magnitude of this drop below the Swl is then the wave amplitude $H/2$. In practical design, typically one-half the design significant wave height is used.

d. Vessel squat. A depth allowance for squat experienced by vessels under way is included in channel depth design (see Figure V-5-12). The amount of squat experienced by a vessel depends strongly on speed and relative blockage of the channel cross section by the vessel. A small, fast-moving boat in a small channel may experience as much or more squat than a large, slower-moving ship. Squat increases when ships meet and pass in a channel because the total blockage is increased. Squat is an important consideration in both deep- and shallow-draft navigation projects. As with vertical vessel motion due to waves, squat is difficult to estimate accurately and is a subject of present research.

(1) Simplified methods for estimating squat are available. The method presented here is based on equations for squat in fairway and canal channel configurations, with a simple interpolation between these limiting cases to accommodate trench configurations (USACE 1998). A definition sketch of parameters is given in Figure V-5-15.

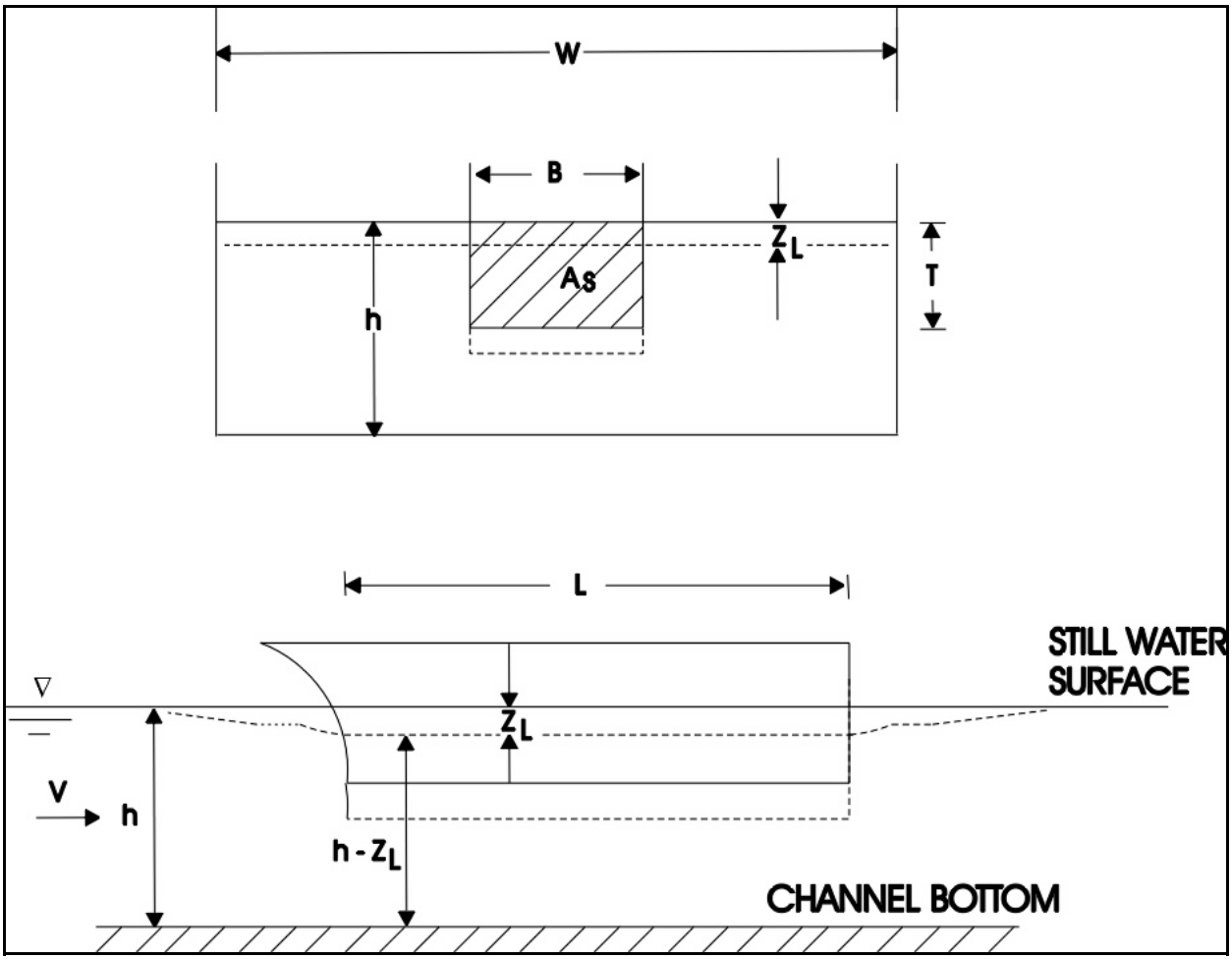

Figure V-5-15. Squat analysis definition

(2) Squat in a fairway can be estimated as (Norrbin 1986)

$$Z = 0.2125\, C_B \frac{B}{L} \frac{T}{h} V^2 \qquad V \text{ in knots, } Z \text{ in ft (fairway)} \tag{V-5-3}$$

$$Z = 0.01888\, C_B \frac{B}{L} \frac{T}{h} V^2 \qquad V \text{ in km/hr, } Z \text{ in m}$$

where

Z = maximum ship squat

C_B = block coefficient (Figure V-5-4)

B = ship beam at midship (Figure V-5-15)

T = ship draft (Figure V-5-15)

L = ship length (Figure V-5-15)

h = depth of shallow-water area (Figure V-5-15)

V = ship speed

This equation is applicable when Froude numbers are less than 0.4.

(3) Squat in a rectangular canal can be related to the Schijf limiting Froude number, which corresponds to the Schijf limiting speed (Part V-5-2-b-(3)). The limiting Froude number is given by (Huval 1980)

$$F_L = \frac{V_L}{\sqrt{gh}} \simeq \left\{ 8 \cos^3 \left[\frac{\pi}{3} + \frac{1}{3} \cos^{-1} \left(1 - \frac{1}{B_R} \right) \right] \right\}^{\frac{1}{2}} \quad \text{(rectangular canal)} \tag{V-5-4}$$

where

F_L = Schijf limiting Froude number

V_L = Schijf limiting ship speed in squat analysis

g = acceleration due to gravity; = 9.80 m/sec^2 (32.2 ft/sec^2)

h = depth of canal (Figure V-5-15)

B_R = channel blockage ratio (Equation V-5-2 and Figure V-5-7)

(4) Maximum ship squat at the Schijf limiting Froude number is given by

$$Z_L = h \left[\frac{F_L^2}{2} \left(F_L^{1/3} - 1 \right) \right] \quad \text{(rectangular canal)} \tag{V-5-5}$$

where

Z_L = maximum squat at Schijf limiting Froude number

An approximate analysis for nonrectangular canal cross sections can be made by replacing the channel depth by a cross-section mean depth.

(5) Trench channels can assume a variety of shapes, including asymmetric overbank depths and different lane depths in two-way channels (Figure V-5-16). The trench configuration is intermediate between the fully

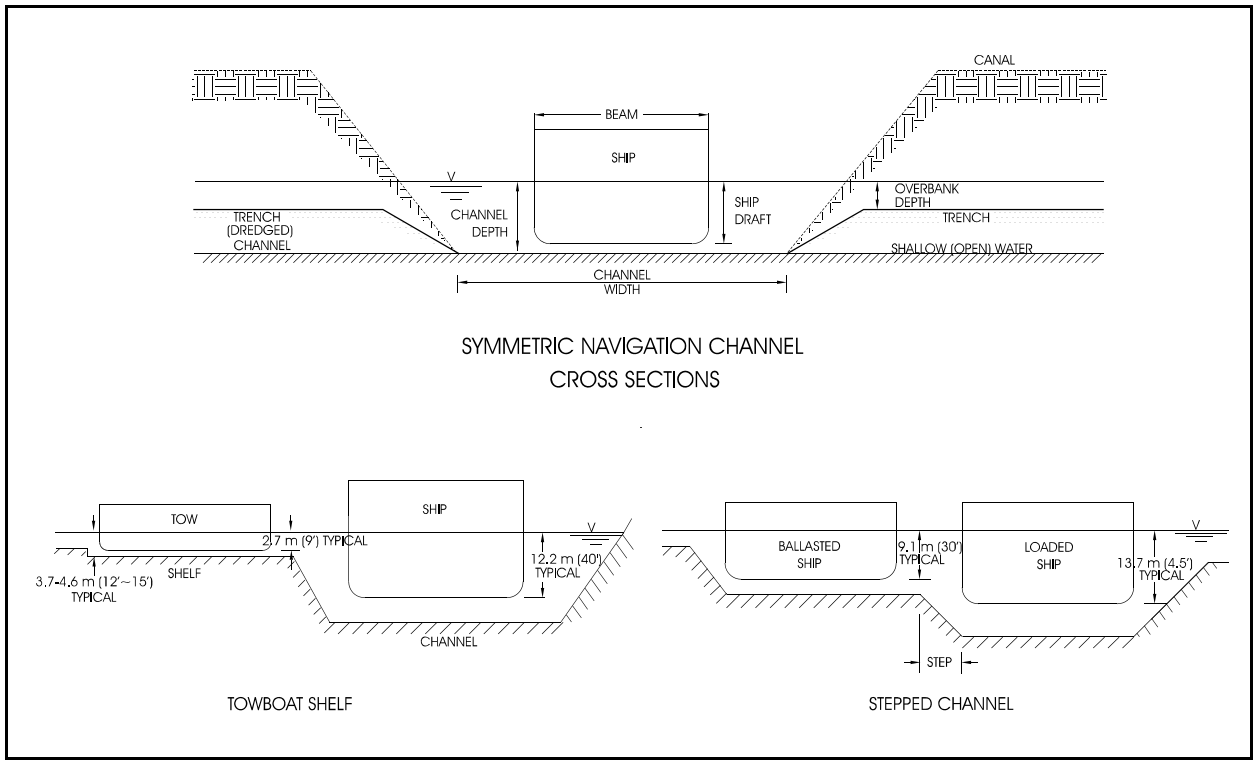

Figure V-5-16. Example channel cross sections

open fairway and fully restricted canal configurations. A first approximation to squat may be made by interpolating between those two extremes, based on the ratio of average overbank depth-to-channel depth (Figure V-5-17)

$$Z_T = \left(\frac{h_1 + h_2}{2h} \right) Z + \left(1 - \frac{h_1 + h_2}{2h} \right) Z_L \qquad \text{(trench)} \tag{V-5-6}$$

where

Z_T = maximum squat in a trench channel

h_1, h_2 = overbank depths

Computational results from a computerized version of this model illustrate squat variation with ship speed and channel type (Figure V-5-18) (Huval 1993). The figure illustrates how a narrow, confined channel can significantly increase squat and, hence, required channel depth.

(6) Squat for small recreational craft is generally less critical than for large displacement, deep-draft ships. However, it should be included in channel design. The usual procedure is to use a fixed depth allowance for squat in entrance channels, where boat speed is relatively high, and a smaller fixed allowance for interior areas, where boat speed is generally low (Table V-5-7).

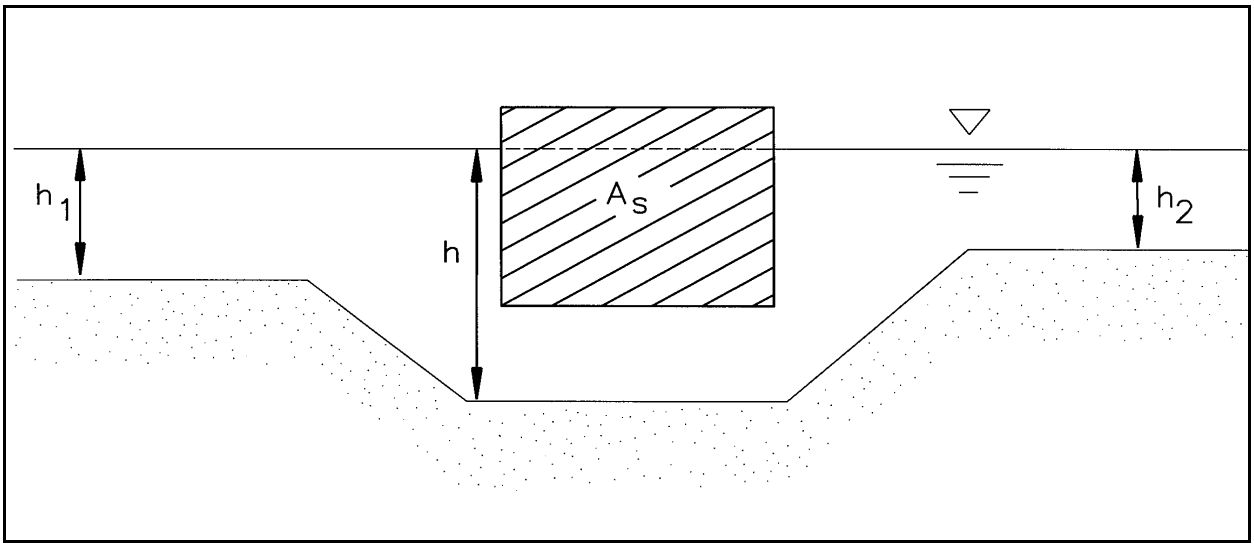

Figure V-5-17. Trench channel definitions

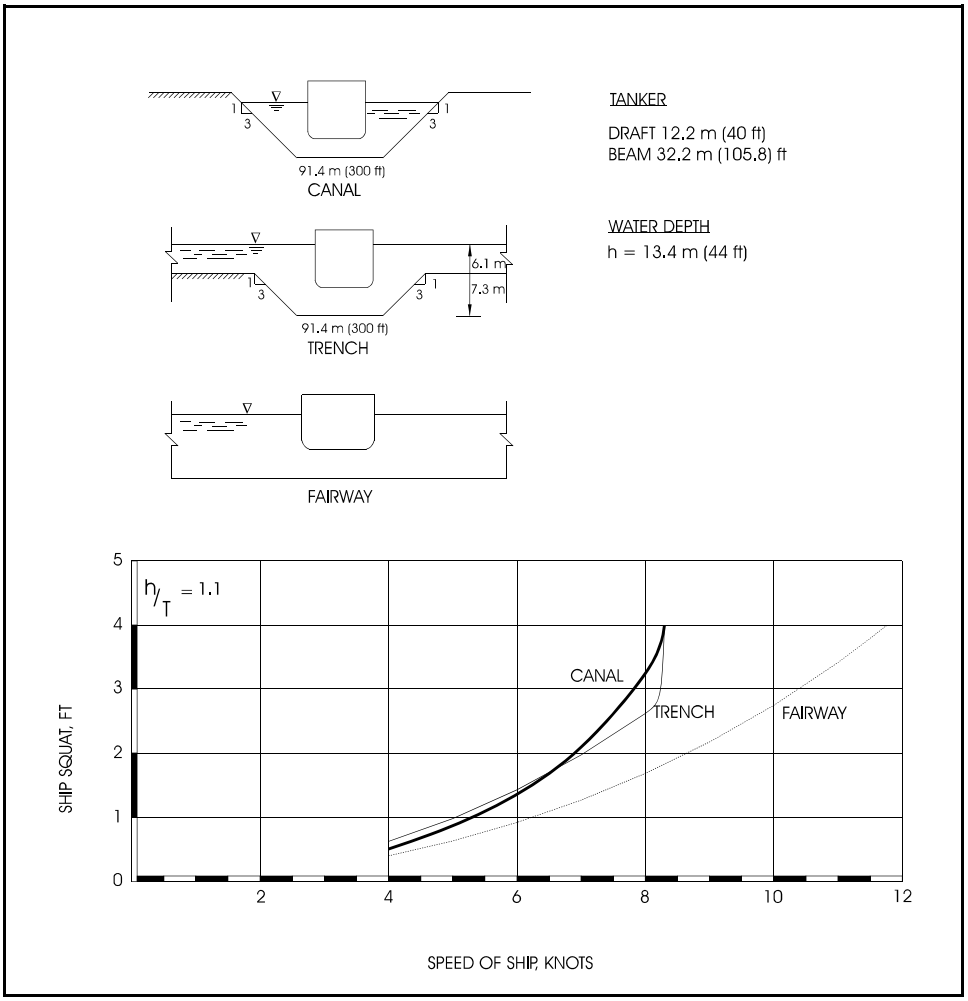

Figure V-5-18. Example squat calculations

Table V-5-7
Squat Allowance for Small Recreational Craft

Location	Allowance
Entrance channels	0.3 m (1.0 ft)
Interior channels, moorage areas, turning basins	0.15 m (0.5 ft)

e. Trim. Deep-draft ships often operate with trim for a variety of reasons. For example, ships may be loaded or ballasted to lower the stern a small amount deeper than the bow, which can improve maneuverability. Ships under way tend to change from the static trim. Small craft in motion can experience significant trim, with the bow rising high and stern dropping low in the water. Because vessel trim conditions are mainly determined by operational decisions, a channel depth allowance for trim is not included.

f. Shallow-water effects. Even when deep-draft ships have sufficient channel depth to avoid hitting bottom, they may experience adverse safety and efficiency effects due to small underkeel clearance. Steering and turning become significantly more difficult, more power is required to maintain speed, and potential for bottom scour and bank failure increases considerably as propeller speed is augmented. Ship cooling systems may ingest benthic organisms or sediment if intakes are too near the bottom. Although these effects can be significant, no depth allowance is included in general channel design to lessen their impact. In some cases, it may be prudent to quantify the location and size of cooling system intakes, evaluate the impacts of small clearances, and perhaps impose a minimum clearance as an added constraint on project design. For example, the U.S. Navy requires a 1.5-m (5-ft) clearance beneath aircraft carrier intakes.

g. Safety clearance. To protect vessel hull, propellers, and rudders from bottom irregularities and debris, a channel depth allowance for safety is included (Table V-5-8). A larger clearance is needed when the channel bottom is hard, such as rock, consolidated sand, or clay (see Figure V-5-12).

Table V-5-8
Safety Clearance

Bottom Type	Minimum Safety Clearance
Soft	0.6 m (2 ft)
Hard	0.9 m (3 ft)

h. Advance maintenance. An additional increment beyond the channel design depth is added to maintain reliable navigable depth between dredge events. This depth increment is to provide for accumulation and storage of sediment. The depth allowance for advance maintenance should be determined by considering several different increments and choosing that which minimizes total channel maintenance cost. Dredge mobilization costs and safety concerns must be balanced against the tendency for a deeper channel to shoal more rapidly. A sediment trap near the entrance may be an economic alternative to reduce advance maintenance requirements in the channel. Depth increments of 0.6-0.9 m (2-3 ft) are normal advance maintenance allowances (see Figure V-5-12).

i. Dredging tolerance. Another depth increment is added beyond the design channel depth to compensate for the inherent mechanical inaccuracies of dredges working in the hostile environment of adverse currents, fluctuating water surface, and non-homogeneous bottom material. A dredging tolerance of 0.3-0.9 m (1-3 ft) is typical (see Figure V-5-12).

j. Tidal shoals and ship transit concerns example. Coastal entrances, bays, and river estuaries typically have meandering natural channels and intermittent shoals. When deeper ship drafts are anticipated, the impact of tidal shoals on schedules and/or margin of safety must be evaluated. Increasing design channel depth over the shoals may eliminate tidal constraints altogether or just improve access to a more economical level. The question, "How deep is deep enough?" must be answered by weighing transportation cost savings against the cost of channel excavation and maintenance. The following example illustrates considerations involved in answering this question and developing an optimum design channel depth.

(1) The example port is located in an estuary, 35 km from the ocean entrance (Figure V-5-19). At a distance of 30 km from port, ships must pass over a shoal with controlling depth of 8 m below mllw (*Shoal 1*). At a distance of 10 km from port, ships encounter another shoal with controlling depth of 7 m below mllw (*Shoal 2*). The port itself has 13 m depth mllw, which is about the average depth available between the two shoals. The diurnal tidal range between mllw and mhhw in this example is amplified from 3 m at the ocean entrance to 4 m at the port, which might correspond to tides in a gradually narrowing bay. Conversely, friction in narrow river estuaries often results in reduced tidal ranges upstream. Tidal datums (e.g., mllw and mhhw) also change as the tidal wave is transformed by the waterway.

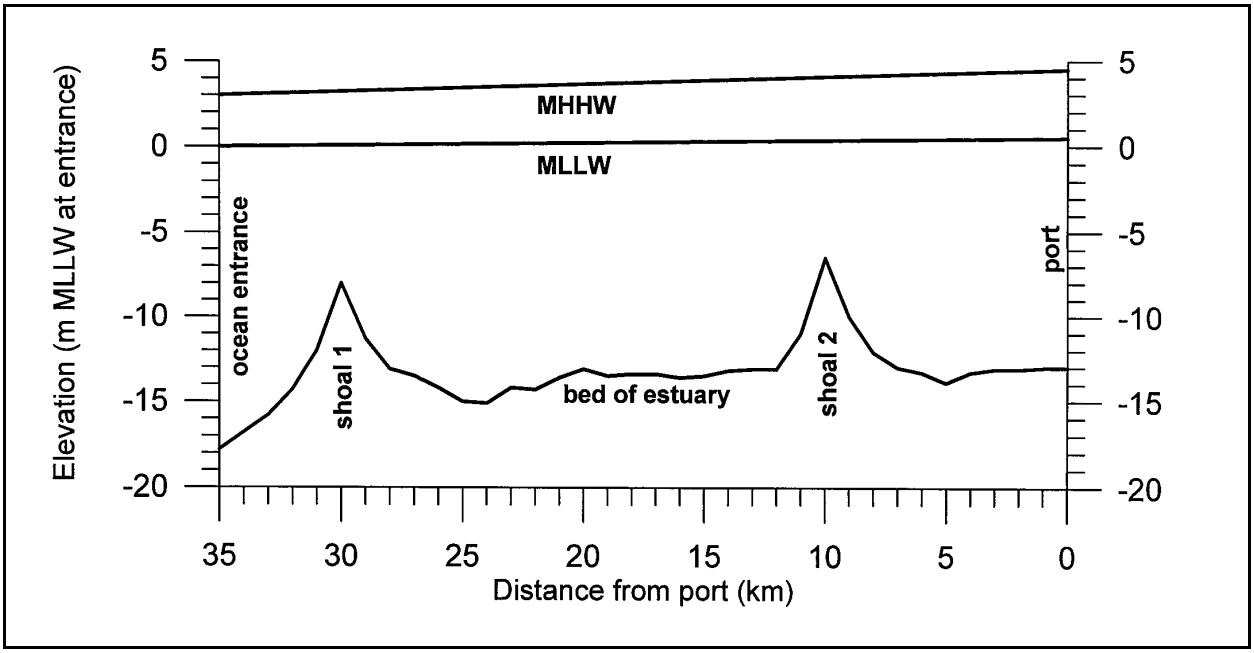

Figure V-5-19. Hypothetical route to a port at the head of an estuary (cross section along channel center line)

(2) The distribution of tidal water levels is estimated by using NOAA primary and secondary tide station data (Part V-5-3). Interpolation between secondary stations is often practical, as needed, if no major constrictions or confluences are present. Figure V-5-20 illustrates the predicted distribution of hourly depths for 1 year at the shallower shoal, Shoal 2. A similar analysis can be performed by applying the methods of Harris (1981).

(3) River discharges and wind-induced water level changes affect water depth over the shoals. Waterway confluences or constrictions and hydrodynamic effects of the shoal itself affect water levels in the vicinity. Seasonal or storm-related changes in elevation of the shoal crest can also affect the depth available to ships. These complications may call for a program of site-specific water level measurements. Numerical modeling

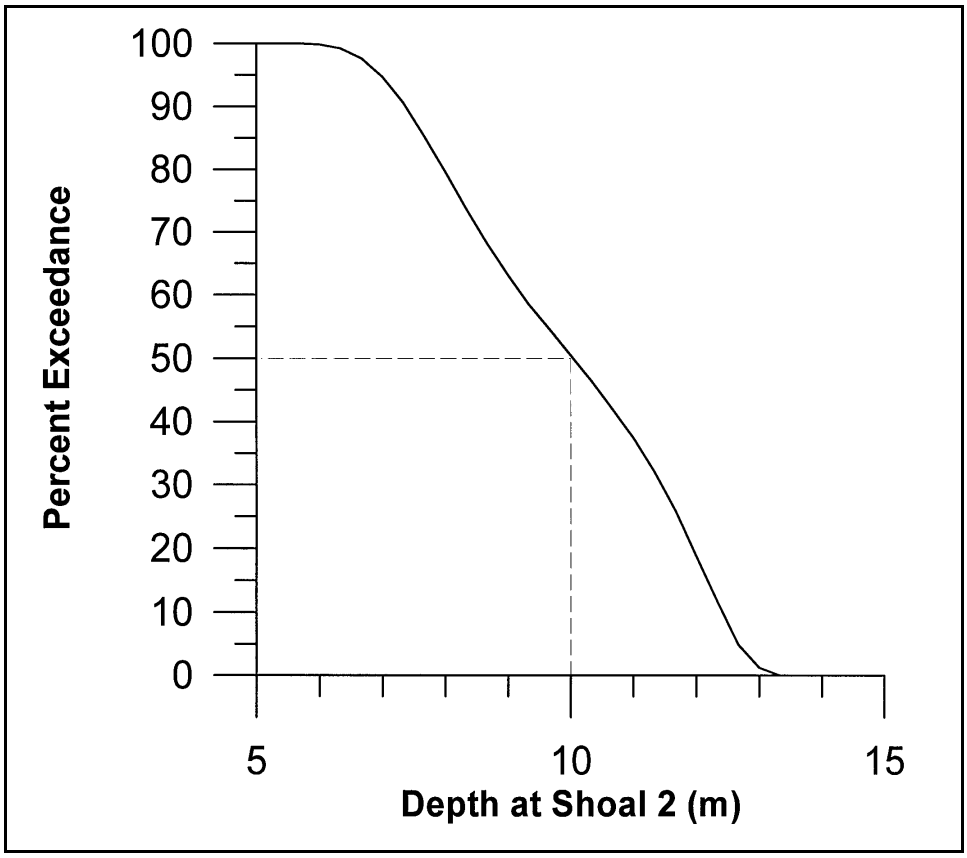

Figure V-5-20. Hypothetical distribution of depths for Shoal 2

of historical conditions (hindcasting) may also be effective for precisely describing water level changes. Figure V-5-21 illustrates water level variations on the main branch of the lower Fraser River near Vancouver, British Columbia, Canada, including tidal and river discharge variations (Ferguson 1991). The transect begins at the river mouth at Sand Heads and continues 35 km up the estuary to New Westminster. Shaded areas show the impact of river outflow on water level for two tide levels (high and low tide). River outflow has little impact on water level at the mouth, but significant impact up into the estuary, especially at low tide. River outflow can add up to 2 m to low tide water depth along this channel. It also affects current. With high river outflow, water level at New Westminster becomes nearly constant over the tidal cycle. Similar processes may need to be considered at the example port.

(4) Figure V-5-20 indicates that ships approaching the example port with draft and keel clearance requirements for a minimum 10-m depth must wait until the upper half of the tidal cycle to cross Shoal 2. Since ships generally arrive on schedules independent of the tide, roughly half the ships of this draft will be delayed. Time spent waiting for the tide, or more likely spent at slow speed offshore, will vary from one arrival to another. Time will also be lost on departure, since ships loaded and ready to depart will have to wait for favorable tide. Deeper ships will lose more time. The shoals of the example are about an hour's sailing apart, so the dangerous possibility exists of crossing one shoal on ebb tide only to find insufficient depth at the second.

(5) The variability of arrival and departure times, ship draft and speed, and water depths is difficult to resolve by multi-variate probability analysis based only on recorded port data. Port arrival and departure times and drafts are usually recorded, but details of shoal-related delays are not. Historical and future delays

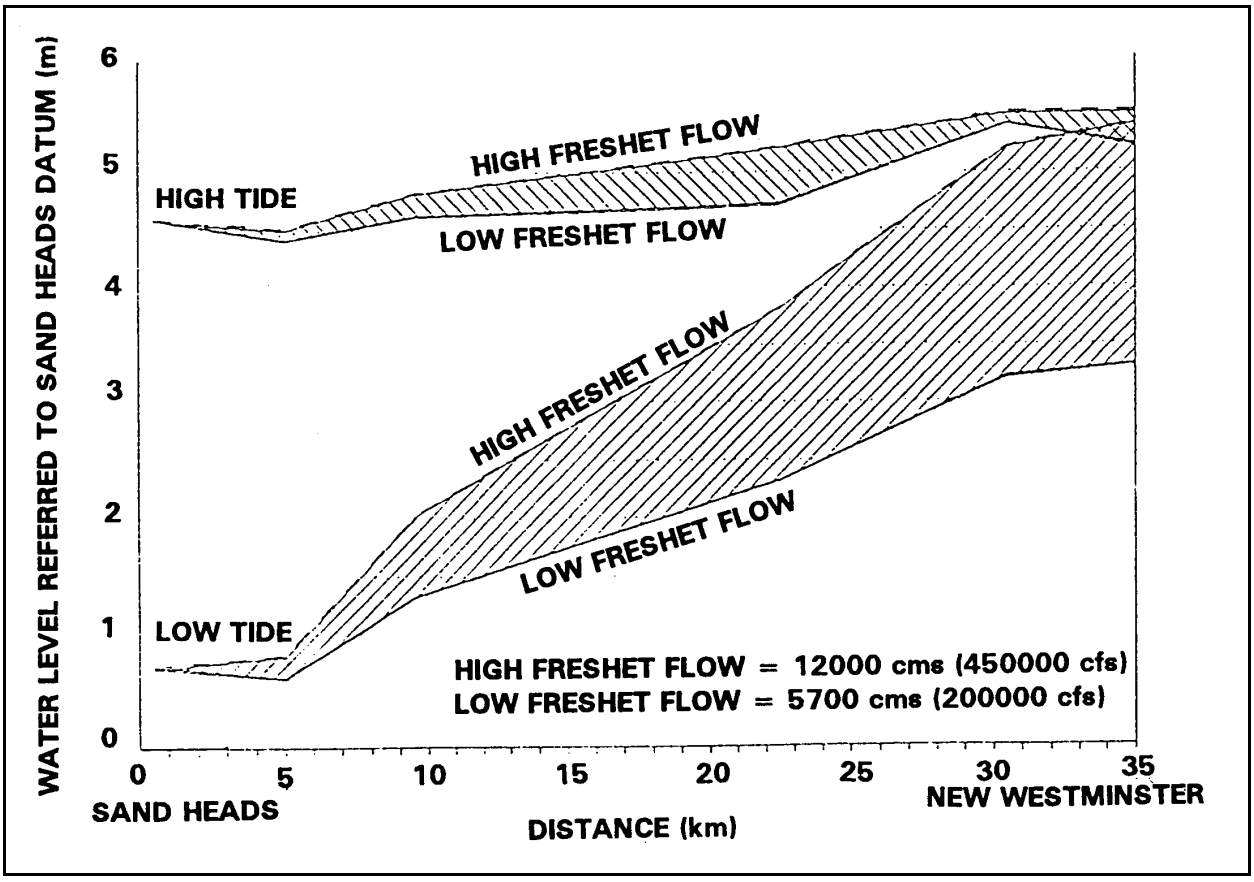

Figure V-5-21. Range of water levels in Fraser River, British Columbia (after Ferguson 1991)

can often be estimated more accurately with numerical simulations. For example, a risk-based system for evaluating channel depth requirements (and for evaluating operational transit safety when coupled with real-time field environmental measurements) is discussed by Silver (1992) and Silver and Dalzell (1997).

(6) Figure V-5-22 illustrates the conceptual approach of a computer program for time-and-motion simulations which applies predicted tides and tidal currents, historical or projected ship cargoes, drafts, and arrival times at the ocean entrance, and cargo transfer rates at port. The same model can simulate ship transit times with various dredged channel geometries. Waiting times are computed as the difference between transit time simulated across the shoals and transit time without shoal restrictions.

(7) Randomly occurring combinations of variables affecting transit times, such as strong winds, river discharge- and wind-induced depth changes, high waves, low visibility, and ice conditions can be added using a Monte Carlo approach. This method requires enough repeated simulations of the same input variables with random values of stochastic variables to encounter the full range of combined extremes. Statistics of transit time, waiting time, and associated costs can be computed from these data. A more complete discussion of vessel traffic flow simulation models is given by PIANC (1997a).

(8) Ship costs are generally proportional to operating time, either under way or at berth. Reductions in time navigating the port approach, at the dock, and departing translate into cost savings. Other cost factors include impacts of ship arrivals on longshoremen, mechanical equipment, and cargo staging at the port. Transportation costs without channel improvement must be estimated as a baseline against which to measure cost-effective optimization of channel excavation. The savings realized by a range of excavation depths and

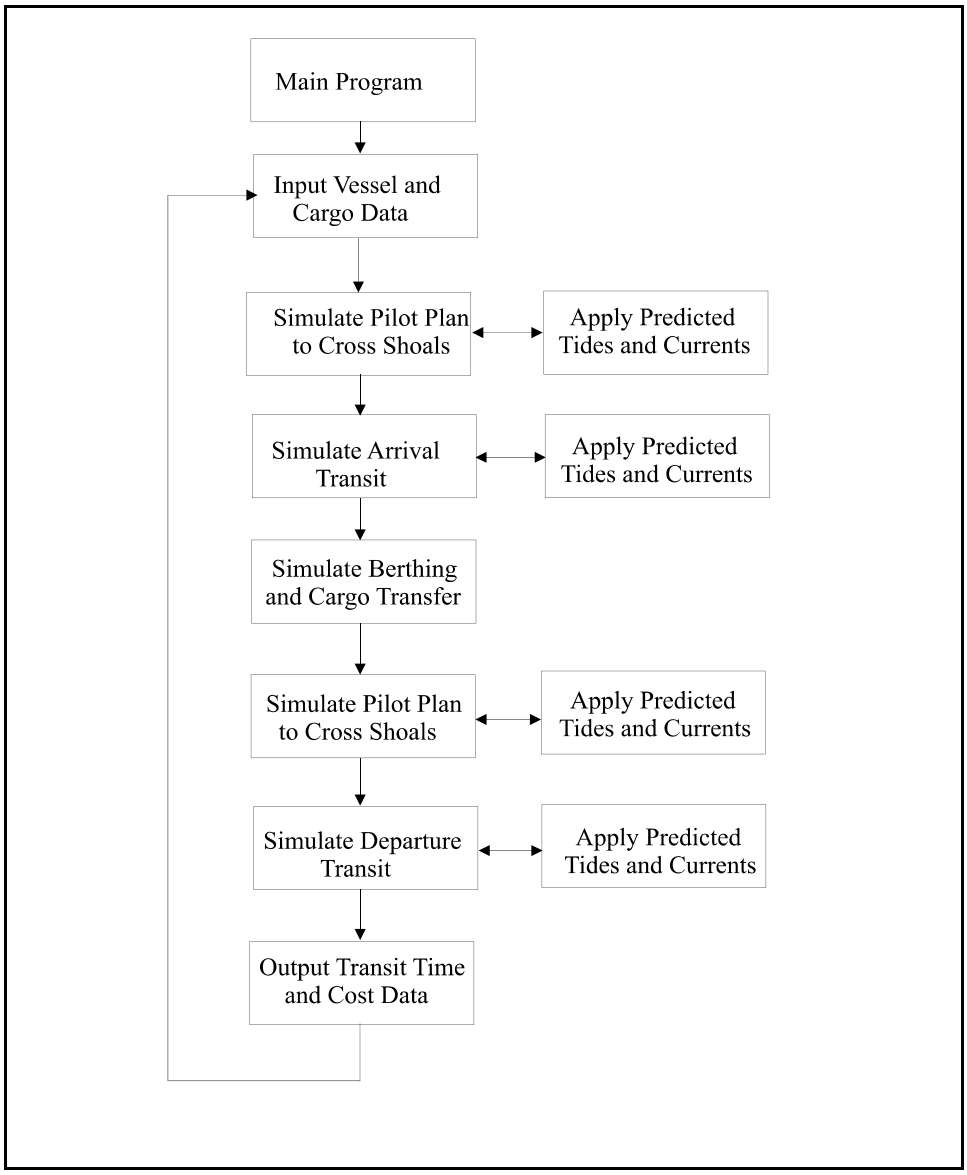

Figure V-5-22. Components of a ship transit simulation program

channel configurations should be compared with corresponding dredging and disposal costs. The ideal optimum will achieve the maximum net savings, but environmental quality effects, financial capabilities, and user preferences can affect the final project design.

V-5-6. Channel Alignment and Width

a. Alignment. Navigation channels are normally aligned as much as possible with natural channels in the pre-project bottom contours. This approach has several important advantages: initial and maintenance dredging are usually minimized; and currents typically take this path in line with the channel, a preferred condition for navigation. The effect of predominant winds and waves, as well as currents, on navigation should be considered. A channel oriented in line with these forces typically serves navigation best.

(1) A straight channel is preferred over a channel with bends. If turning is required, straight reaches with turns between channel segments are preferred over curved alignments. This type of alignment allows the channel to be clearly marked with aids to navigation. Straight segments in a deep-draft channel should be at least five times the length of the design ship. Few turns and small turning angles are best for navigation. Typically, the number of turns introduced in the channel alignment must be balanced against the turning angles to achieve an optimum alignment for navigation purposes. Both deep- and shallow-draft channels should be aligned so that vessels can maintain speed and controllability through areas where they are exposed to potentially damaging winds, waves, and currents. This consideration generally precludes sharp turns in exposed areas.

(2) The entrance channel to San Juan Harbor, Commonwealth of Puerto Rico, helps illustrate the difficulty of turning large ships in design transit conditions (Figure V-5-23). The exposed entrance, or "bar," channel makes a 57-deg turn into Anegado Channel just inside the harbor entrance. A ship simulator was used to model navigation channels in the harbor (Webb 1993). Local pilots from San Juan Harbor conducted simulation runs with two design ships, a tanker and a container ship. Ship tracks from inbound runs with the tanker are shown, where the ship hull outline is plotted at short intervals along each run. The variability of ship track and differences in pilot strategy for making the turn are evident in the figure. Ship track plots such as this clearly show the ship's swept path relative to channel boundaries. The envelope of multiple ship tracks gives valuable information about the navigability of the channel being simulated.

(3) Channel alignment option studies should consist of selecting several alternate routes when viable alternatives are available. Construction and maintenance costs are developed for each alternative. A comparison of annual project costs and benefits then determines the optimum channel alignment.

b. Inner channels (protected waters and harbor areas).

(1) Width. Harbor access channels leading from the bar or entrance channel to the port or harbor area are referred to as *interior channels*. For straight deep-draft channels, the required channel width is based on the following factors, listed in decreasing order of importance:

(a) Traffic pattern (one-way or two-way).

(b) Design ship beam and length.

(c) Channel cross-section shape.

(d) Current speed and direction.

(e) Quality and accuracy of aids to navigation.

(f) Variability of channel and currents.

- Design channel width is defined as the width measured at the bottom of the side slopes on each side of the channel at the design depth. For one-way deep-draft channels, channel width has traditionally been figured as the sum of a maneuvering lane width and bank clearance increments on either side (Figure V-5-24). For two-way channels, an additional maneuvering lane and a ship clearance lane dividing the two lanes of traffic are added. The required width for each increment was given as a factor applied to the design ship beam (Table V-5-9). Factors vary with ship controllability and judgment. Special judgment is required when vessels are exposed to yawing forces.

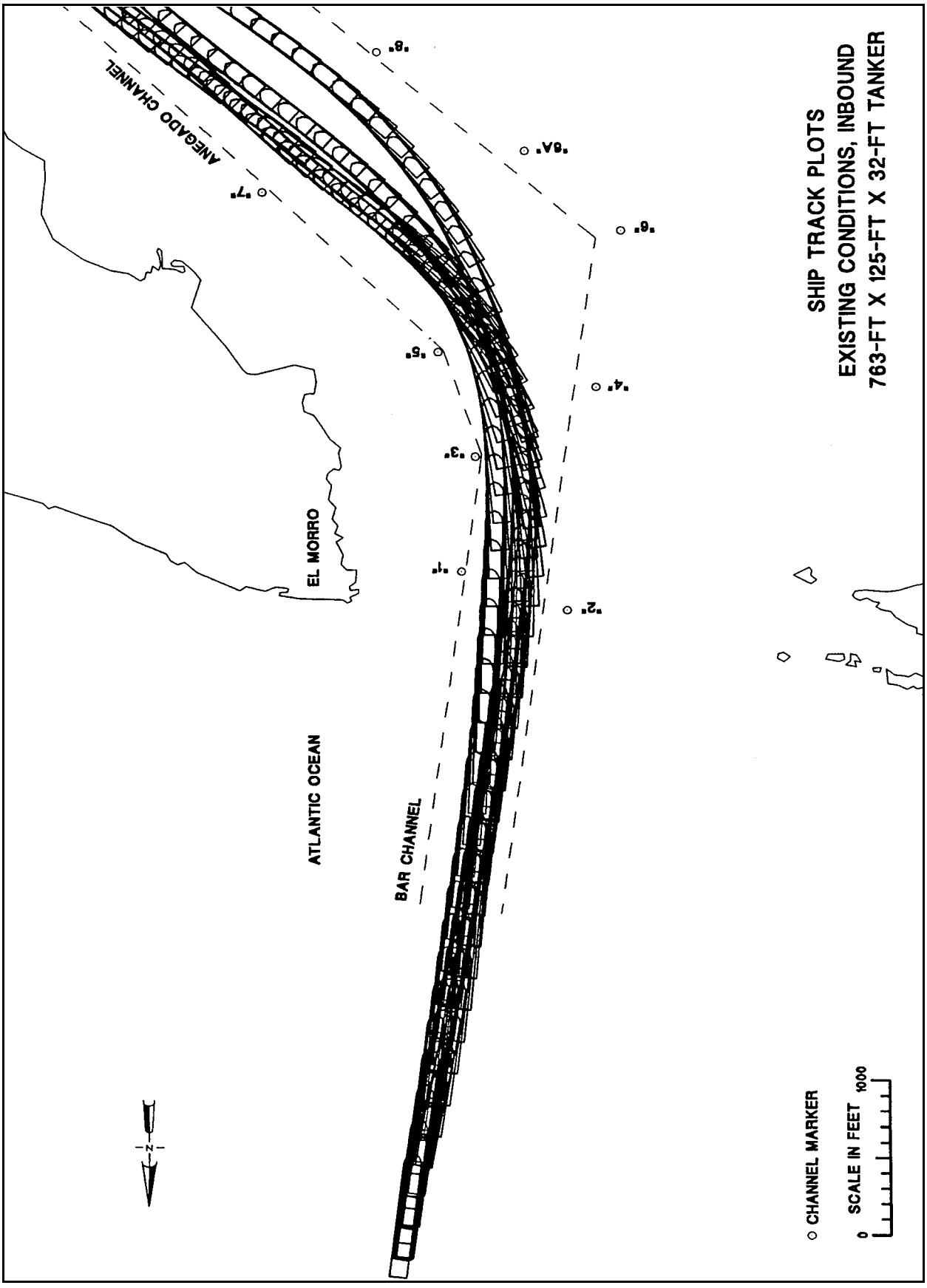

Figure V-5-23. Ship simulation of deep-draft entrance channel, San Juan Harbor, Commonwealth of Puerto Rico

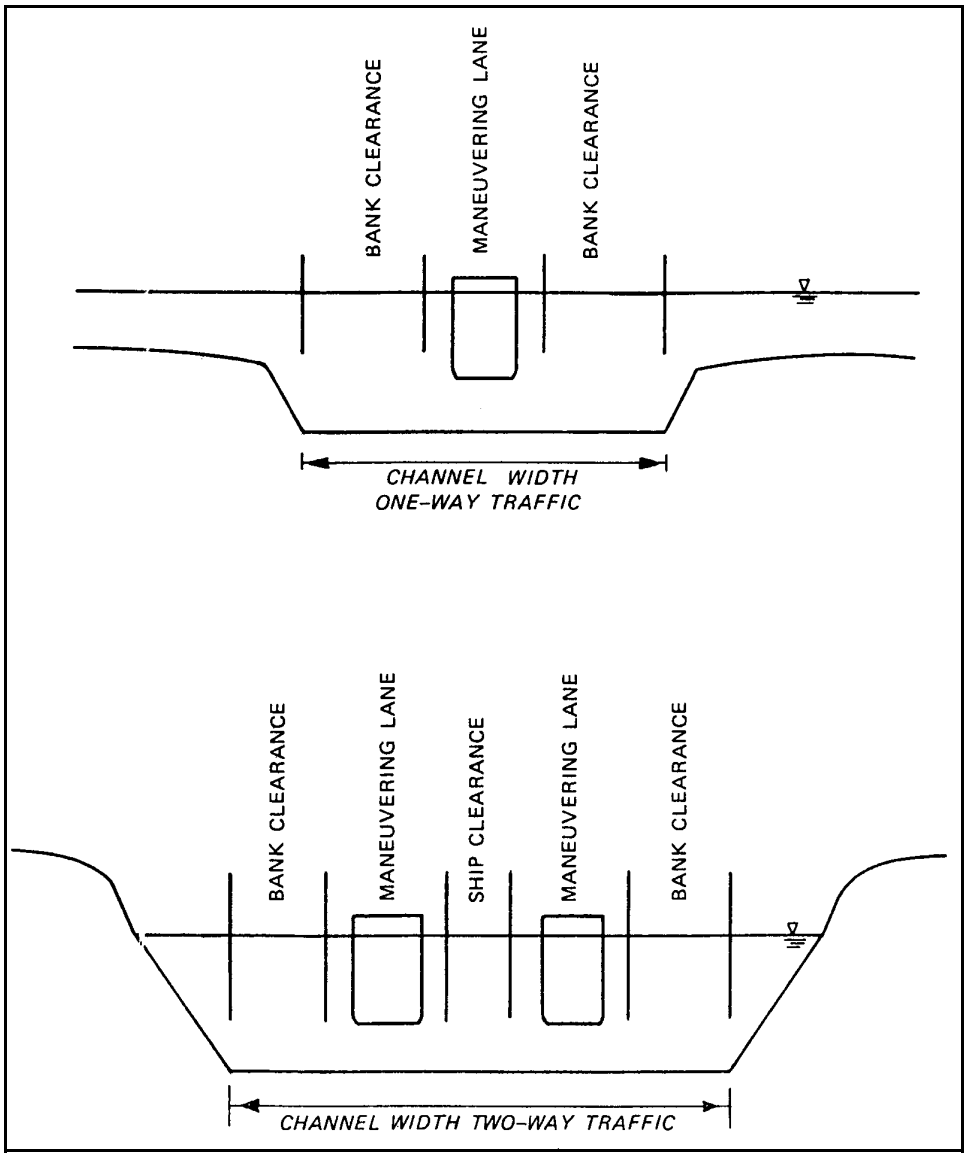

Figure V-5-24. Traditional interior channel width elements

Table V-5-9
Traditional Criteria for Deep-Draft Channel Width Design[1]

	Vessel Controllability			
Location	**Very Good**	**Good**	**Poor**	**Channels with Yawing Forces**
Maneuvering lane, straight channel	1.60	1.80	2.00	Judgment[2]
Bend, 26-deg turn	3.25	3.70	4.15	Judgment[2]
Bend, 40-deg turn	3.85	4.40	4.90	Judgment[2]
Ship clearance	0.80	0.80	0.80	1.00 but not less than 30 m (100 ft)
Bank clearance	0.60	0.60+	0.60+	1.50

[1] Criteria expressed as multipliers of the design ship beam; i.e., W = (factor from table) × B
[2] Judgment is based on local conditions at each project.

- Professional pilots control ships in a way that makes the traditional channel width divisions illogical. For example, they routinely move the ship off center line to use bank effects as a cue in determining ship position. Also, they sometimes use bank effects to assist in turning. Guidance for deep-draft channel width is best expressed as a total channel width based on the design ship beam (e.g., Figure V-5-25). The quality of aids to navigation, type of channel cross section, and current strength impact the required width. Experience with ship simulator studies has indicated that traditional channel width design criteria are overly conservative. Interim guidelines have been developed based on simulator studies (USACE 1998) (Tables V-5-10 and V-5-11). If current speeds are greater than 2.9 m/sec (3.0 knots), design channel width should be developed with the assistance of a ship simulator study (Part V-5-10).

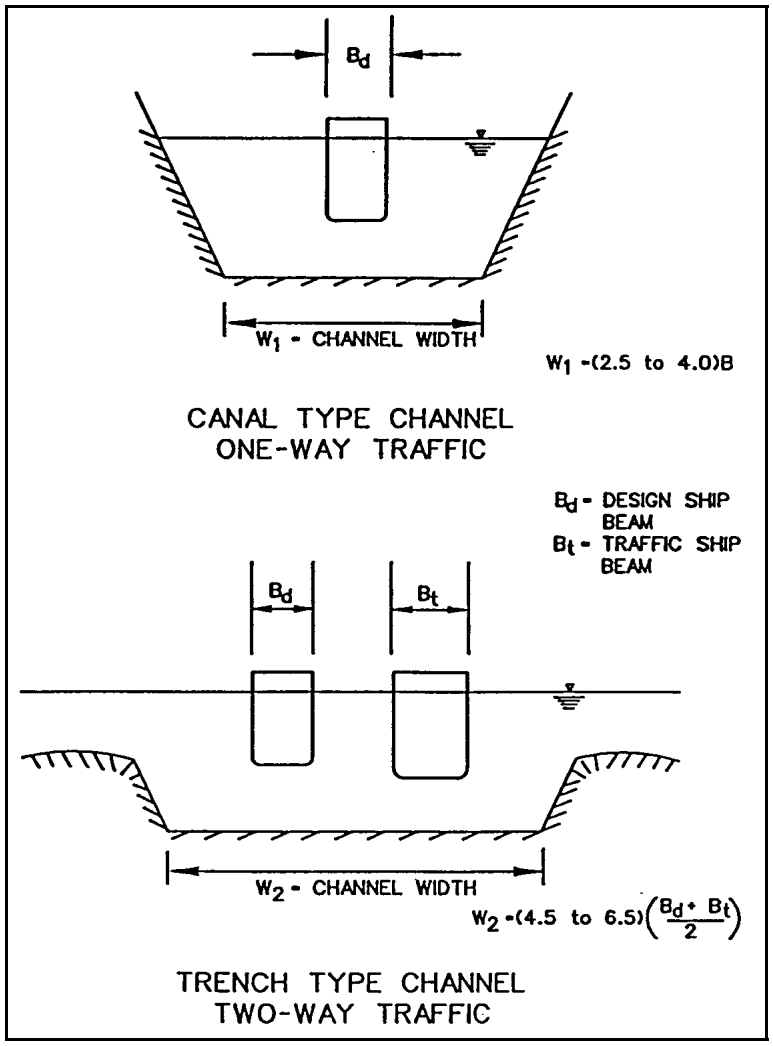

Figure V-5-25. Interior channel design width

- Navigation is more difficult when channel cross section (overbank depths, channel depth and width) varies significantly. Bank effects and currents become less predictable and extra care is needed for vessel control. Table V-5-10 gives channel width factors for a somewhat challenging navigation scenario, with variable cross section and average aids to navigation, and for an ideal scenario with constant cross section and excellent aids to navigation. These two scenarios bracket most channel design projects likely to be encountered in the United States.

Table V-5-10
One-Way Ship Traffic Channel Width Design Criteria[1]

Channel Cross Section	Maximum Current: 0.0 to 0.3 m/sec (0.0 to 0.5 knots)	0.3 to 0.8 m/sec (0.5 to 1.5 knots)	0.8 to 1.5 m/sec (1.5 to 3.0 knots)
Constant Cross Section, Best Aids to Navigation			
Shallow	3.0	4.0	5.0
Canal	2.5	3.0	3.5
Trench	2.75	3.25	4.0
Variable Cross Section, Average Aids to Navigation			
Shallow	3.5	4.5	5.5
Canal	3.0	3.5	4.0
Trench	3.5	4.0	5.0

[1] Criteria expressed as multipliers of the design ship beam; i.e., W = (factor from table) × B

Table V-5-11
Two-Way Ship Traffic Channel Width Design Criteria[1]

Channel Cross Section	Maximum Current: 0.0 to 0.3 m/sec (0.0 to 0.5 knots)	0.3 to 0.8 m/sec (0.5 to 1.5 knots)	0.8 to 1.5 m/sec (1.5 to 3.0 knots)
Constant Cross Section, Best Aids to Navigation			
Shallow	5.0	6.0	8.0
Canal	4.0	4.5	5.5
Trench	4.5	5.5	6.5

[1] Criteria expressed as multipliers of the design ship beam; i.e., W = (factor from table) × B

- Shallow-draft interior channels should be designed to safely handle the expected volume of two-way traffic. Traditional guidance for channel width is the same as for deep-draft channels (Table V-5-9). However, an approach that takes account of the traffic congestion may be preferable. Small-craft channel design guidance is being reevaluated in present research studies. Present recommended simple guidance is a minimum width, generally based on average vessel beam, and an additional width increment based on the number of boats using the project (ASCE 1994, Dunham and Finn 1974)

$$W = W_{\min} + 0.03\ N_B \quad \text{in meters (interior channels)}$$
$$W = W_{\min} + 0.10\ N_B \quad \text{in feet} \qquad \text{(V-5-7)}$$

where

W = design small-craft channel width

W_{min} = minimum width; = 5 B or 15 m (50 ft), whichever is greater

B = average beam

N_B = number of boats using the project

Thus, an interior channel serving 500 small boats with average beam of 5 m would have a minimum width of 5*5 + 0.03*500 = 40 m.

(2) Berthing areas. Although entrance and interior harbor channels and turning basins are usually part of federal navigation projects, berthing areas are typically nonfederal concerns except in military harbors. Normally, a berthing area must have sufficient depth to accommodate the design vessel to be using the berths, which may be smaller than the design vessel for sizing harbor channels, under all or nearly all expected water levels. Typically the design water level for berthing areas is extreme low water. Berthing areas must have sufficient space for safe maneuvering of the appropriate design vessel, often with tug assistance in deep-draft facilities. Guidance for sizing berthing areas to provide adequate access may be found in other references (e.g., Tsinker (1997), Gaythwaite (1990), and U.S. Navy (1981) for deep-draft ports; ASCE (1994), Tobiasson and Kollmeyer (1991), Dunham and Finn (1974), and State of California (1980) for small-craft harbors).

(3) Special considerations due to ice. Increased navigation difficulties in areas with ice may introduce special considerations for channel depth and width. Policies of pilot associations, shipping companies, or vessel insurance underwriters may call for additional keel and bank clearances beyond those allowed in temperate ice-free conditions. These groups and other marine interests, such as the USCG, NOAA, and military operators, should be solicited in the planning process for their views on these matters.

(a) The magnitude and direction of ice forces on ships are random in nature. These forces are combinations of impacts and frictional resistance. Impacts of wind- or current-driven ice forces can be oblique to the course of the ship, causing a sudden diversion. Ship response to such a diversion is slowed by additional oblique impacts and frictional resistance.

(b) Design width for a channel that will be navigated with ice should be increased by as much as 50 to 100 percent over the conventional width. Design depth may also need to be increased. The conventional ice-free design depth including either a standard wave allowance or an additional 0.5-m depth increment, whichever is greater, should be used. Wave allowance can be neglected in ice navigation because ice usually suppresses waves.

c. Entrance channels. Entrance channels are generally wider than interior channels because of many factors complicating navigation at entrances, particularly waves and currents. Intensified waves and currents at entrances make navigation difficult, but they also result in potentially treacherous sediment movement and dynamic shoaling patterns. Often vessels navigate this difficult environment in close proximity to rock or concrete breakwater or jetty structures. Loss of control can result in disastrous collision with these solid structures.

(a) Because of the complexity of processes and vessel responses in entrance channels, experience at the project site or related sites can be an especially helpful guide to determining an acceptable channel width. The traditional simple design approach is to use the guidance in Table V-5-9, choosing factors for a level of

vessel controllability appropriate to the difficulty of the particular entrance channel. Deep-draft entrance channel width design can benefit significantly from comprehensive physical model studies, navigation simulation studies, and field measurements of ship motions (Part V-5-10).

(b) For small-craft harbors, entrance channel width should be a minimum of 23 m (75 ft) (ASCE 1994). Guidance in Table V-5-9 has traditionally been applied. These factors typically exceed those for interior channels, leading to a widened entrance channel design. Small-craft harbor entrance channel design is the subject of a present research study.

(c) USACE practice in southern California, where sailboat usage is accommodated in design, is a minimum width of 90 m (300 ft). Consideration is also given to the number of boats using the project. USACE practice is to increase channel width over the 90-m (300-ft) minimum if the number of boats exceeds 1,000.

$$W = 90 + 0.03\,(N_B - 1000) \quad \text{in meters}$$
$$W = 300 + 0.1\,(N_B - 1000) \quad \text{in feet} \tag{V-5-8}$$

Thus, an entrance channel serving 2,000 small boats would have a minimum width of 90 + 0.03*(2,000-1,000) = 120 m (300 + 0.1*(2,000-1,000) = 400 ft), based on practice in southern California.

d. Turns and bends. Channels with turns and bends are more difficult to navigate than straight channels. Vessel control is reduced and width of the vessel swept path (the envelope around ship hull positions in the horizontal plane) is naturally increased when turning. Therefore, additional width is required in turns and bends for large vessels. Key parameters in a turn are defined in Figure V-5-26. The recommended configuration for widening a turn in a deep-draft channel depends on the deflection angle (Figure V-5-27 and Table V-5-12). Bank conditions, not included in the simple guidance presented here, are important in turn design since pilots often use them to assist in turning.

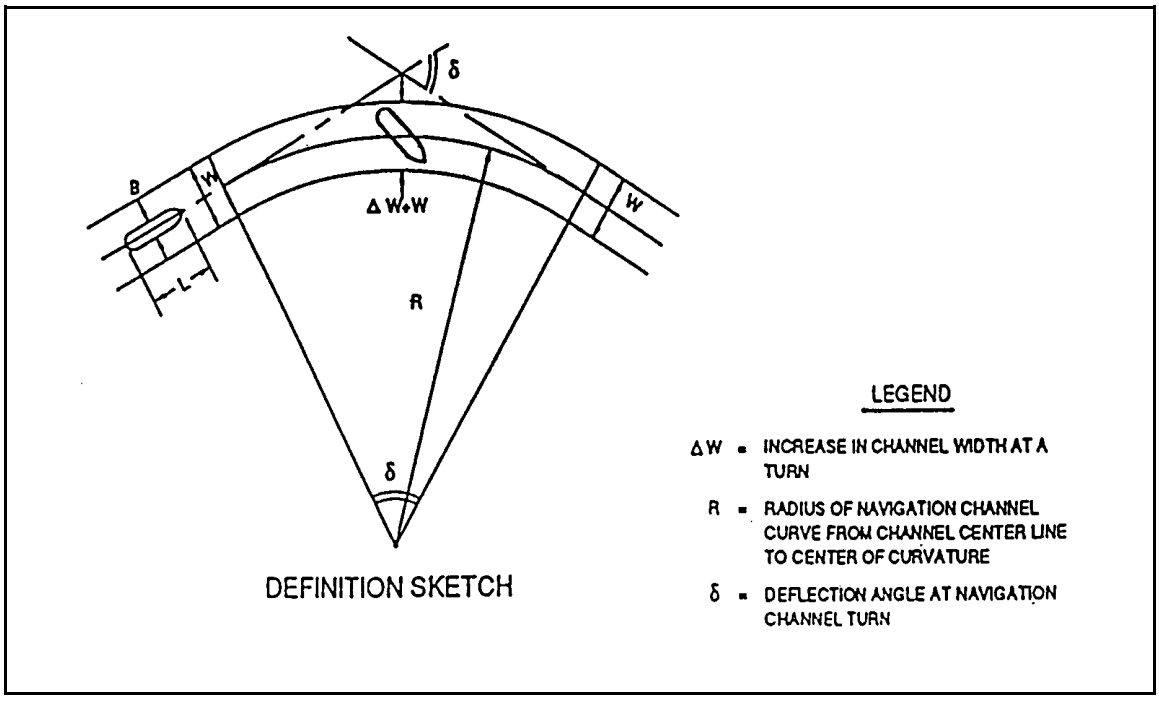

Figure V-5-26. Definition of parameters in channel turn

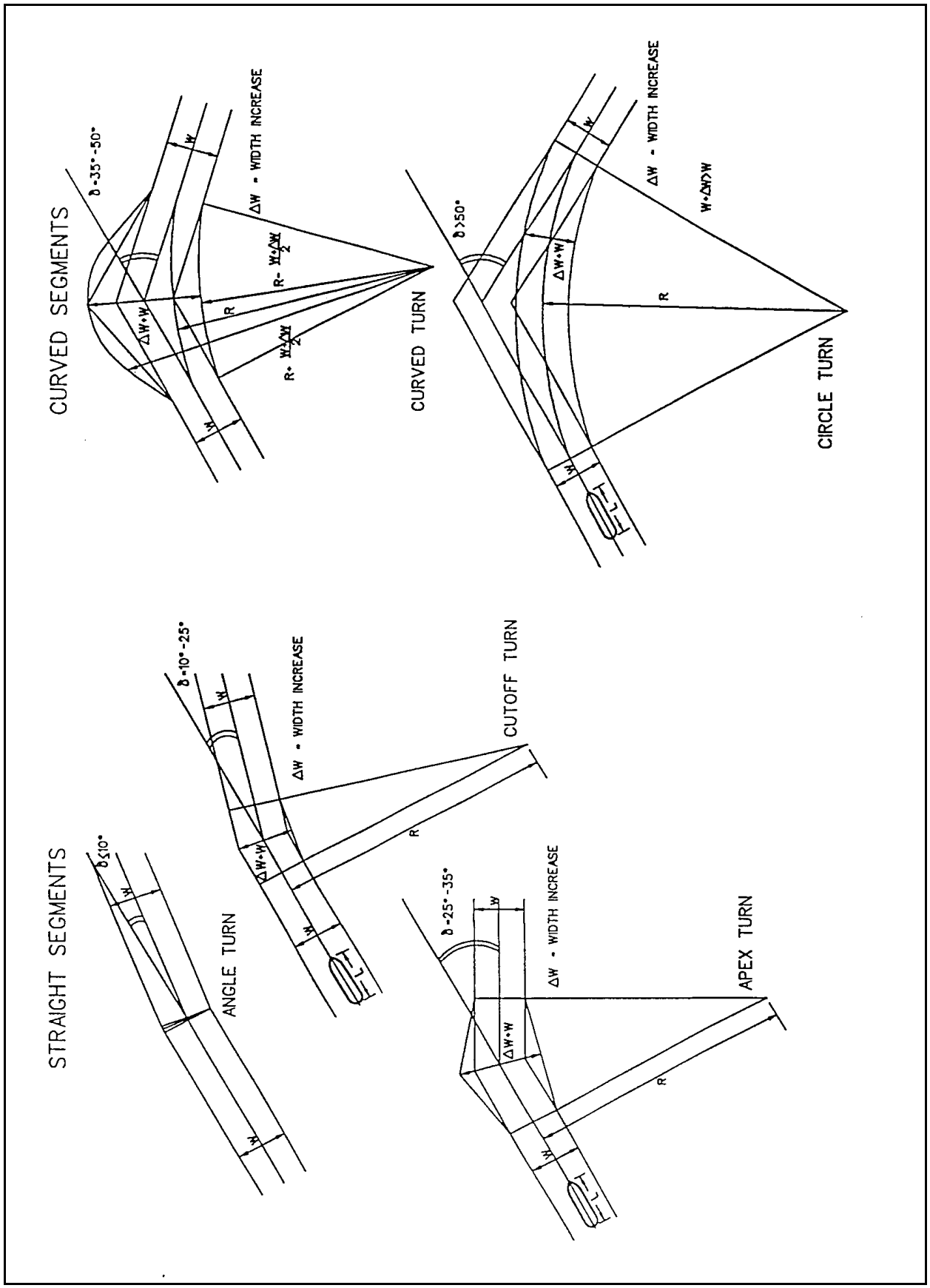

Figure V-5-27. Channel turn configurations

Table V-5-12
Recommended Deep-Draft Channel Turn Configurations

Turn Angle, deg	R/L[1]	Turn Width Increase Factor[2]	Turn Type
0-10	0	0	Angle
10-25	3-5	2.0-1.0	Cutoff
25-35	5-7	1.0-0.7	Apex
35-50	7-10	0.7-0.5	Curved
>50	>10	0.5	Circle

[1] R = curve radius; L = design ship length (see Figure V-5-26).
[2] Expressed as a multiplier of the design ship beam; i.e., ΔW = (factor from table) × B

(1) Apex or cutoff configurations are commonly used because they are simple, easily defined shapes that serve most channel turn requirements. They are easiest to control for dredging, easiest to mark with aids to navigation (usually with two range marker pairs and buoys), and easiest to monitor for maintenance. Some dimensions that are useful for computer drafting are included in Figure V-5-28. Turns should be placed, when possible, in locations easily visible for range markers. A drawback to the apex and cutoff methods is that they can produce difficult current patterns for navigation. In high current areas and/or canals, turns with parallel circular arcs gradually transitioning from straight channel segments into the turn may be warranted.

(2) The impact of channel turns on currents and shoaling and vessel response to wind and waves can be significant. The navigability of a turn design and its shoaling tendencies may merit study with numerical models and a navigation simulator.

(3) Small craft are sufficiently maneuverable that extra channel width in turns is generally not as critical as for deep-draft ships. For large turn angles in the presence of difficult conditions, extra maneuvering space should be provided. A typical situation would be a sharp turn in an exposed entrance channel.

V-5-7. Other Project Features

a. Turning basins. Turning basins are generally provided to allow vessels to reverse direction without having to go backward for long distances. Turning basins provide the extra width needed to comfortably turn. Turning basins are usually located at the upstream end of interior access channels. In long channels accommodating many dock facilities, an extra turning basin may be placed at the upstream end of each group of docks. In normal operations, larger ships turn with pilot and tug assistance.

(1) The minimum turning basin size should allow a turning circle with diameter of 1.2L, where L is the design ship length (Figure V-5-29). Turning difficulty increases significantly when currents are present. If current speed exceeds 0.5 m/sec (0.5 knot), turning basin diameter should be increased as indicated in the figure. If current speed exceeds 0.8 m/sec (1.5 knot), a circular shape no longer suffices. The turning circle should be elongated in the current flow direction, as shown in the figure. Dimensions of the high-current turning basin configuration should be determined with a ship simulator (Part V-5-10). If turning operations will include ships with high sail areas and design wind speeds of greater than 12.9 m/sec (25 knots), a ship simulator design study is also needed.

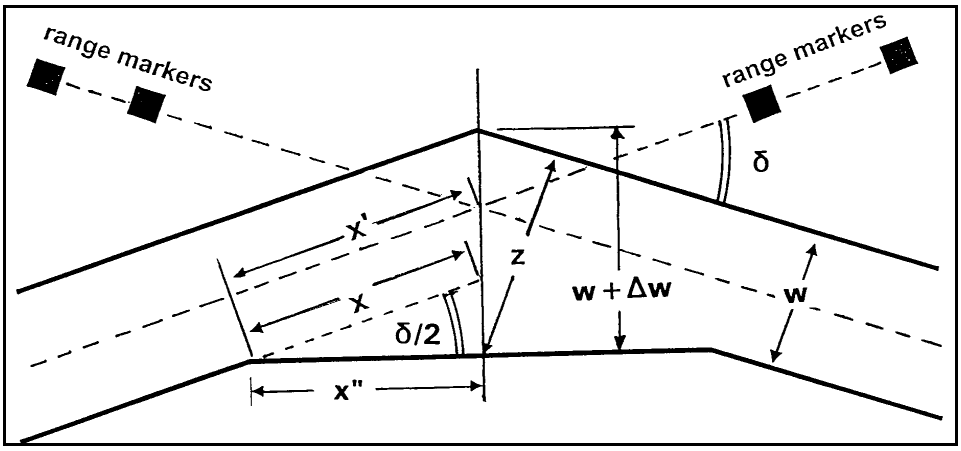

Figure V-5-28. Layout of apex-style turn

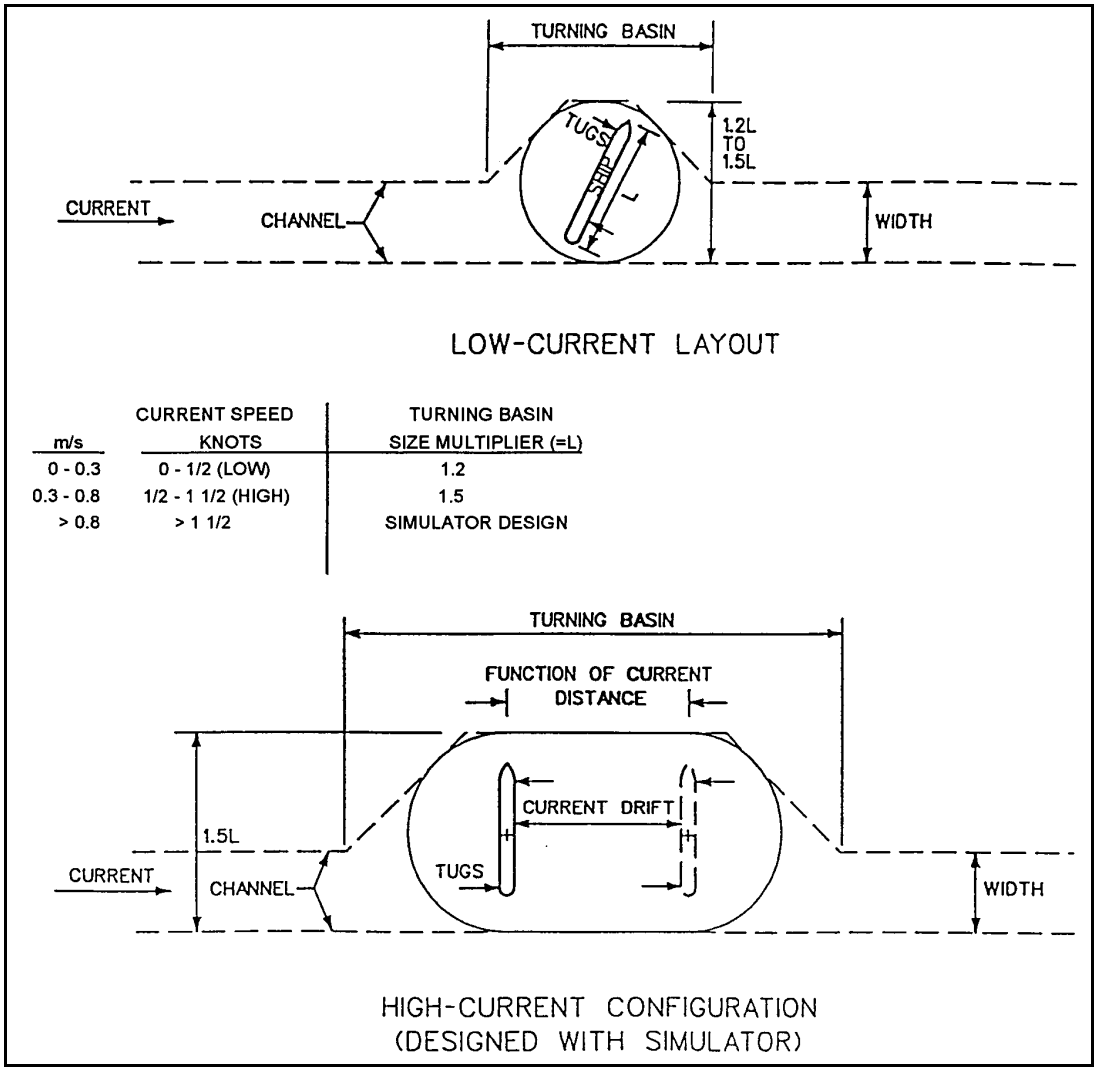

Figure V-5-29. Turning basin alternative designs

(2) Turning space for small boats should be sufficient to allow turning without backing or assistance. The required space depends on the types of boat using the project, but the design channel width usually accommodates turning.

(3) Turning basin design depth normally matches the adjacent channel depth. Turning basins tend to trap sediment because they are wider and typically have lower currents than the navigation channel. Also, being located at the upstream end of the navigation channel, the turning basin is often the first dredged area to intercept river-borne sediment. The potential shoaling problem may be reduced by careful choice of turning basin location and shape to reduce sediment availability and promote flushing.

b. Moorage/anchorage areas. Anchorage areas are provided in some deep-draft ports, typically near the entrance, to accommodate ships awaiting berthing space, undergoing repairs, receiving supplies and crews, awaiting inspection, and lightering off cargo. Anchorage areas may also serve as a refuge for ships during severe storms, since most facilities are designed with the assumption that no ships will be in port during a hurricane or typhoon. Ships may be anchored at the bow and allowed to swing freely or be moored against fixed dolphins. Design guidance is given in Figure V-5-30. Guidance for free-swinging anchorage is approximate, based on a 15-m (50-ft) depth and design ship length of 213 to 305 m (700 to 1,000 ft). The fixed mooring alternative requires a much smaller area for each ship than the free-swinging alternative. If available space is limited or dredging is required, fixed mooring may be the preferred design. Design guidance is available from the U.S. Navy (1998).

c. Basin flushing and water quality. Water quality within a harbor is often a concern with local, state, and Federal agencies. Water quality in a harbor depends on three key factors: quality outside the harbor, substances introduced into the water inside the harbor, and exchange of water between the inside and outside. Although outside water quality is typically beyond the scope of a navigation project, harbor design and operation can have a major impact on the other key factors. Contaminants introduced inside a harbor may include sewage discharge, shower/dishwashing water, bottom paint leaching, fuel and oil spillage, and deck and hull washing. Persistent contaminants may affect bottom sediments as well as water quality, which can increase future dredging costs.

(1) Water movement within a harbor is often restricted by the perimeter design. The extent to which the basin is enclosed, placement of the opening(s), and basin shape all affect water movement in the harbor. Tide, wind, and river flows can help promote circulation in a harbor and exchange between harbor and outside water. For example, a large tidal prism combined with a small low-tide volume gives excellent flushing in a harbor. Flushing processes in harbors are discussed in Part II-7.

(2) Many harbors are located in areas where natural water movement is relatively weak, a desirable condition for navigation but a potential problem for basin flushing. For example, when outside water has a high content of treated sewage, a typical concern, then water should not remain trapped anywhere in the harbor for many days. Methods to promote flushing and prevent stagnation include gaps between perimeter structures and shore, openings within the perimeter structure itself (e.g., segments, baffles, culverts), overlapping wave protective structures to act as scoops to passing water flow, and mechanical agitation. A harbor entrance centrally located along the perimeter is usually preferred over an entrance at one end, which may lead to stagnation at the opposite end.

(3) The flushing characteristics and water quality in a harbor can be predicted with physical and numerical models, as discussed in Part II-7. Both water exchange rates and oxygen or other chemical constituent reactions and replenishment rates should typically be addressed.

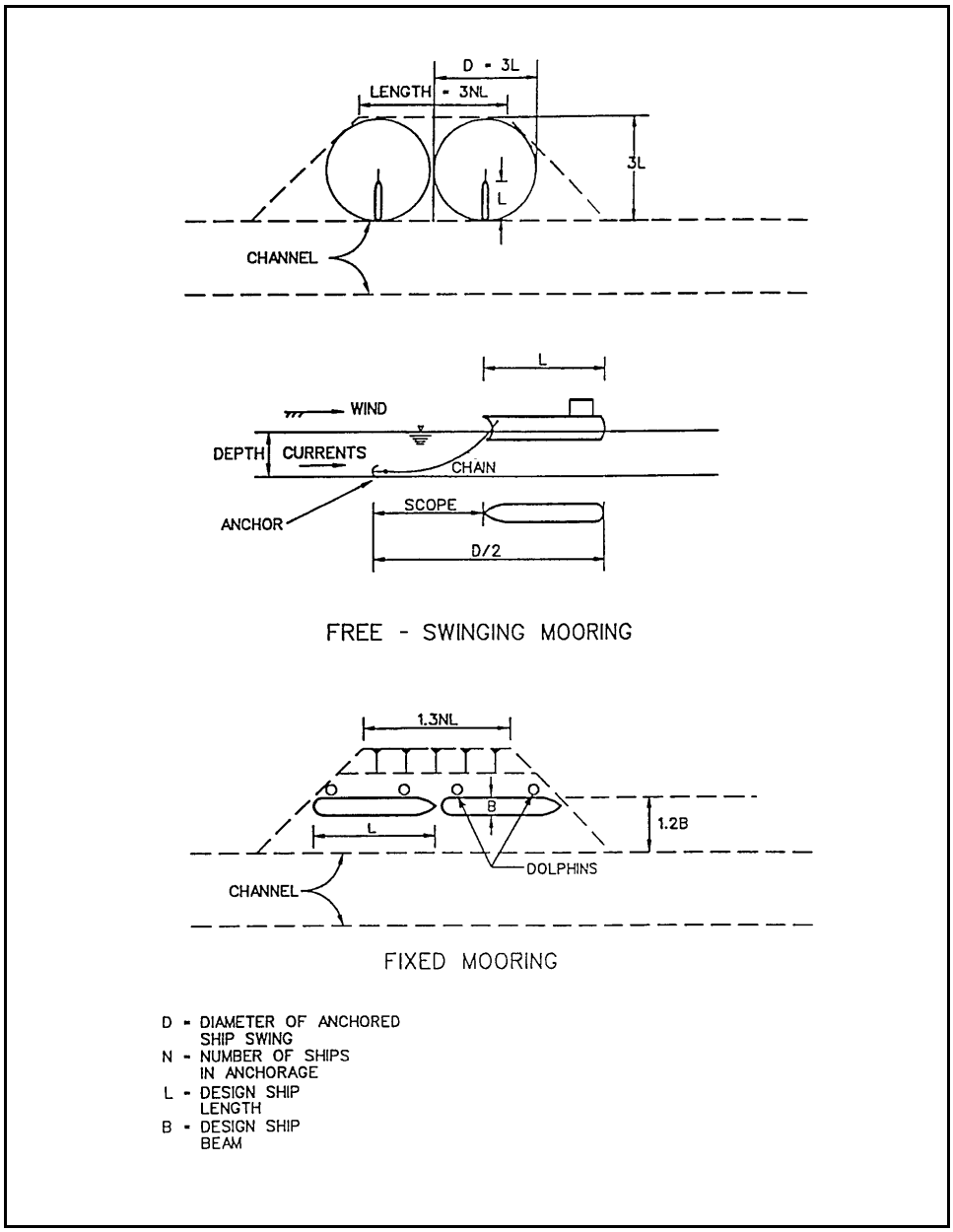

Figure V-5-30. Alternative anchorage designs

d. Navigation structures. Often a navigation project requires one or more engineered structures to accomplish its objectives. Structures can serve a variety of purposes. However, their presence also establishes a major hazard for vessels. Hence, a navigation structure must be designed with regard to several functional concerns. Basic types of structures and functions involved in navigation projects are briefly discussed in this section. Sediment processes and management at inlets and harbors are discussed in Part V-6. Detailed guidance on structure design is given in Part VI.

(1) Breakwaters. Breakwaters are used to protect a harbor, anchorage, basin, or area of shoreline from waves. Breakwaters reflect or dissipate wave energy and thus prevent or reduce wave action in the protected area. Breakwaters must be designed to effectively serve competing requirements for wave blockage and safe vessel passage from fully exposed waters through a constricted entrance into tranquil harbor waters.

(1) For navigation projects, breakwaters are frequently shore-connected and constructed to provide calm waters in a harbor (Figure V-5-31). Shore-connected breakwaters allow access from land for construction, operation, and maintenance, but may have an adverse impact on water quality or sediment movement along the coast.

Figure V-5-31. Harbor with shore-connected breakwater, Waianae Small Boat Harbor, Oahu, Hawaii (June 1980)

(2) If the harbor to be protected is on the open coast and predominant wave crests approach parallel to the coast, a detached offshore breakwater may be a good option. Water quality is preserved with this type structure, but access for construction and maintenance is more difficult than for a shore-connected structure. Offshore structures are sometimes used to provide protection to existing harbor entrances (Figure V-5-32). Accumulation of sediment in the lee of an offshore breakwater must be considered in design (Part V-6).

(3) Many breakwater systems utilize a combination of breakwater types to protect anchorage or mooring areas, such as a shore-connected and a detached structures (Figure V-5-33). Some structures have been constructed with arrowhead entrance configurations, but experience has shown them to be of questionable benefit, and some have been modified to improve performance. The cellular arrowhead breakwater configuration in Figure V-5-33 was modified by adding an overlapping rubble-mound extension to the seaward end of the shore-connected breakwater. In some cases, the primary breakwaters do not provide sufficient protection, and interior breakwaters are needed (Figure V-5-34).

(4) Most breakwaters built on open coasts of the United States are of rubble-mound construction. It is important for harbor tranquility to design such structures to be high enough to prevent excessive wave overtopping and sufficiently impermeable to deter wave transmission through the structure. However, some wave overtopping and/or transmission may be beneficial for harbor flushing. Other structural types include

Figure V-5-32. View of offshore detached breakwater used to protect harbor entrance, Marina del Rey, California (August 1966)

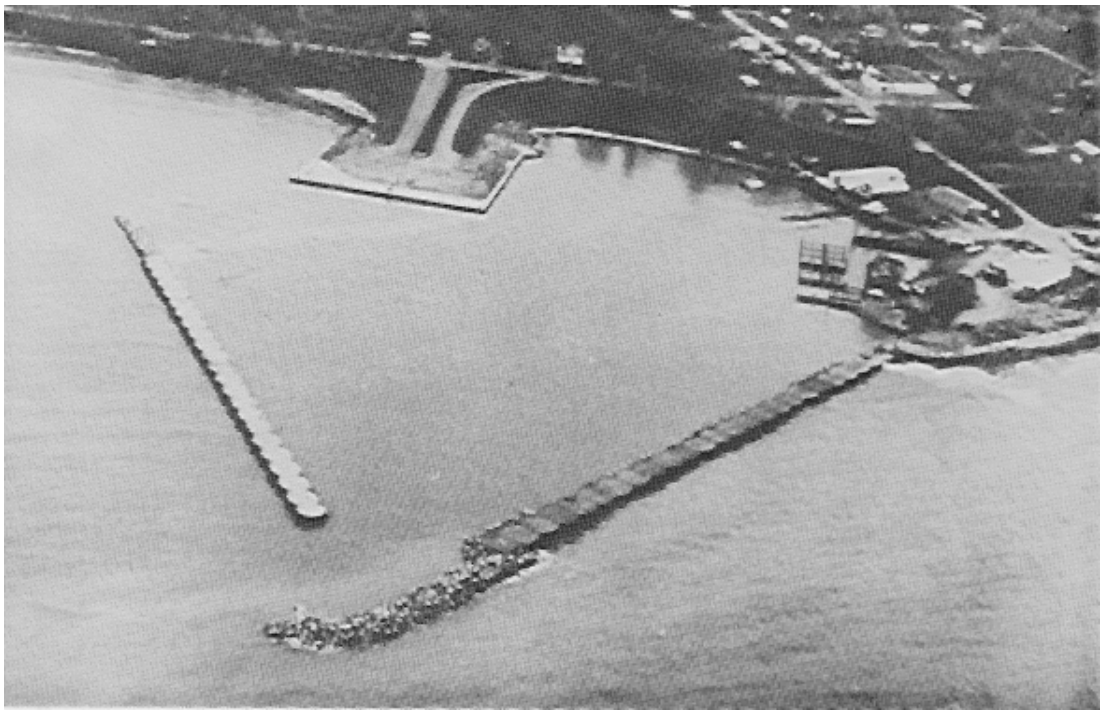

Figure V-5-33. Harbor with both shore-connected and detached breakwaters, Barcelona Harbor, New York (April 1986)

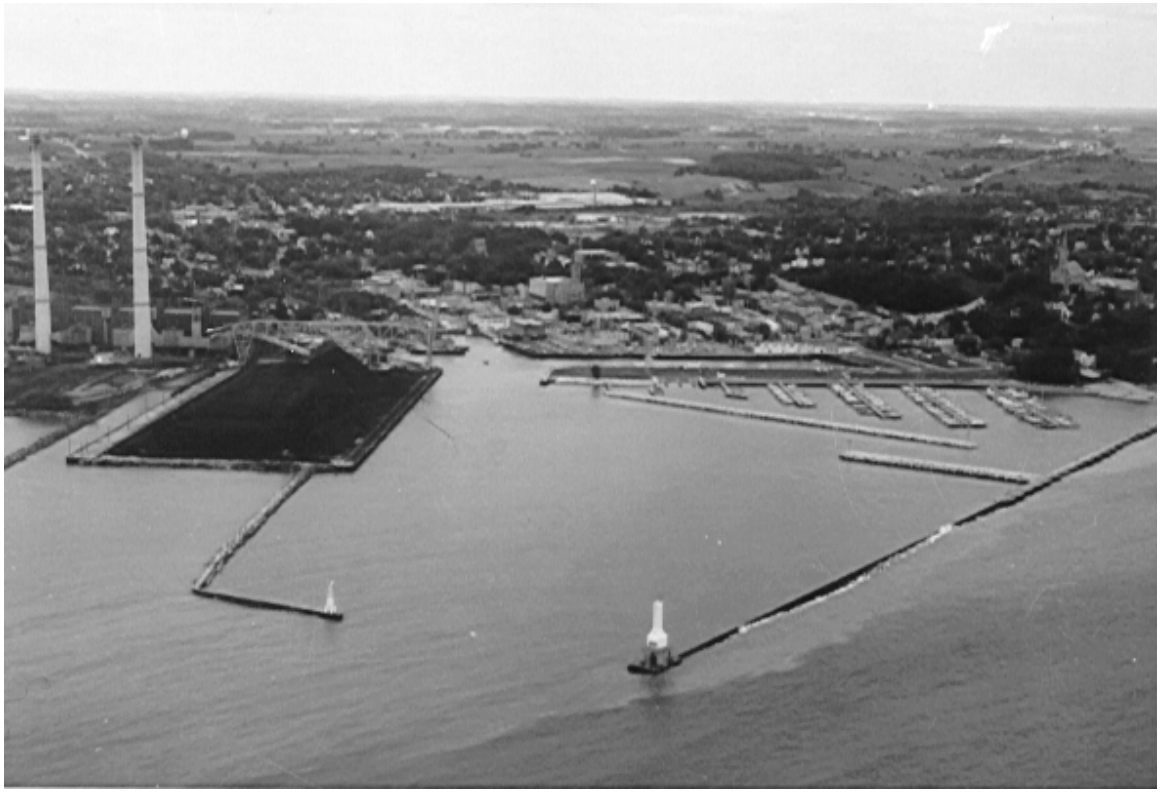

Figure V-5-34. Inner breakwater provides protection to small-craft mooring area, Port Washington Harbor, Wisconsin (September 1983)

concrete caisson, timber crib, sheet pile, cellular steel sheet pile, composite (rubble-mound with concrete cap for stability, etc.), and floating.

(5) The optimum layout of breakwaters for harbor protection is difficult to determine because of the complex conditions typically involved. Waves refract on approaching the entrance, often in the presence of shoals as well as a navigation channel. Wave energy propagates through the entrance, diffracts, and reflects from inner harbor structures. Currents are usually present due to tides, wind, waves, and river flows.

(6) Because they can accurately reproduce many of the complex, interacting hydrodynamic effects on a harbor, physical models provide the most reliable method for optimizing breakwater layout (Part V-5-10). Physical modeling and subsequent monitoring of prototype performance has led to general guidance relative to harbor layout (Bottin 1992). Lessons learned relative to navigation entrance channel and mooring area protection in small boat harbors are:

(a) *Align entrances toward a perpendicular to the incoming wave crests.* It is very dangerous for small craft to travel parallel to high incoming wave crests (*beam seas*). Harbors should be designed to minimize the chance of this condition.

(b) *Block wave energy from the harbor*. It is preferable to prevent wave energy from entering a harbor than to try to dissipate excessive wave energy once inside. Energy entering a harbor can be minimized by using overlapping breakwaters at the entrance, reducing entrance width, minimizing breakwater overtopping, and using impermeable breakwater cores. Breakwaters seaward of the entrance may also be incorporated into a design. If the harbor is at a river mouth, care must be taken to prevent upstream flooding due to flow restriction and/or ice jamming in the harbor.

(c) *Absorb wave energy inside the harbor if necessary*. When physical limitations or costs prevent blocking sufficient wave energy out of the harbor, some energy can be absorbed inside the harbor with judiciously placed rubble slopes and/or spending beaches. Concrete absorber units (e.g. *igloos*) can also be helpful. For long-period wave energy, absorbers installed along harbor slips are essentially ineffective.

(d) *Anticipate Cross Currents on Reefs*. Waves breaking across reefs generally result in very strong currents alongshore. These currents may be hazardous to small craft entering and navigating channels cut through the reef and into harbors. Breakwaters may be used to deflect these currents offshore away from the entrance (Figure V-5-35). Currents also tend to enter the harbor through the entrance. These currents can be used to advantage by laying out interior channels to promote circulation and flushing, as was done with the aid of physical modeling for Agana Small Boat Harbor, Territory of Guam.

Figure V-5-35. Breakwaters protecting small boat harbor from waves and wave-generated crosscurrents on reef, Agana, territory of Guam (May 1978)

(e) *Locate Harbor Facilities and/or Boat Ramps Away from the Entrance Opening*. Wave energy propagating through and diffracting around entrance structures can affect nearby facilities. Facilities can be given further protection by including interior breakwater structures or revetted moles. Although these structures can be very effective, they are expensive and can limit future expansion.

(f) *Avoid vertical walls in high-energy areas of the harbor*. Vertical wall breakwaters and harbor structures are highly reflective. Waves reflecting off entrance structures can result in very confused and hazardous navigation conditions. Reflections inside harbors can cause hazardous anchorage and mooring conditions. Reflected waves from vertical structures have also been found to induce erosion.

(g) *Orient entrances away from the direction of predominant longshore transport*. It is very desirable to promote natural sand bypassing of the harbor entrance. Entrances facing the predominant longshore transport direction are likely to serve as a sediment trap. A typical successful design consists of an outer curved breakwater that overlaps a short shore-connected structure (e.g. Figure V-5-31). The shorter

downcoast structure helps to prevent sediment moving along the shoreline opposite to the dominant direction from coming into the entrance.

(h) *Consider Using Segmented Structures*. Segmented breakwaters are effective in providing wave protection while still allowing tidal circulation through the breakwater openings. They can be effective substitutes for floating or baffled breakwaters. Segmented rubble absorbers inside a harbor, as opposed to a continuous absorber, also have proven to be effective in terms of both performance and cost.

(2) Jetties. A jetty is a shore-connected structure, generally built perpendicular to shore, extending into a body of water to direct and confine a stream or tidal flow to a selected channel and to prevent or reduce shoaling of that channel. Jetties at the entrance to a bay or a river also serve to protect the entrance channel from storm waves and crosscurrents. When located at inlets through barrier beaches, jetties help to stabilize the inlet.

(a) Jetties are usually built in pairs, one on either side of an entrance (Figure V-5-36). Sometimes, jetties are used in combination with a breakwater (Figure V-5-32). A single jetty may also be used, located on the updrift side of the entrance. A disadvantage of the single jetty is that the navigation channel is unconfined and will likely migrate. A typical single jetty problem is the case of an impermeable jetty where the navigation channel migrates to a position immediately beside the jetty, with consequent threats of passing vessels colliding with the structure and undermining of the structure itself. Some jetties have been designed with a low-crested weir section near shore to pass sediment into a deposition basin (Part V-6). The semi-protected waters of the deposition basin are then periodically dredged and sediment is bypassed to the downdrift beach.

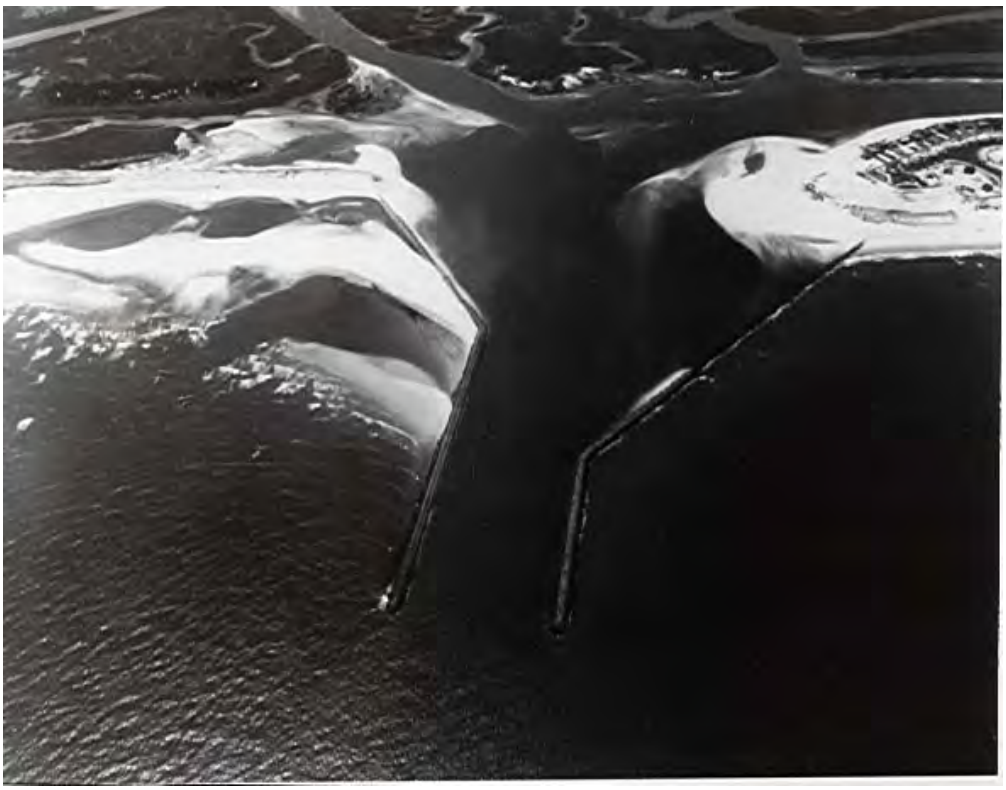

Figure V-5-36. Dual jetty configuration at a tidal inlet, Murrells Inlet, South Carolina (March 1982)

(b) Though jetties have a different function than breakwaters, jetty structural design is similar to breakwaters. Most jetties built on open U.S. coasts are rubble-mound structures. Materials used for jetty construction include stone, concrete, steel, and timber. Unlike breakwaters, jetties are usually designed to allow some wave overtopping. Also, jetty cores may be lower and more permeable than breakwater cores, provided the jetty sufficiently blocks passage of sediment into the navigation channel.

(c) Jetties should be designed to use available construction materials efficiently and effectively to accomplish functional objectives without adversely impacting other physical processes or the environment. Jetties at river or creek mouths, not considering tidal effects, should be spaced close enough together to allow normal river currents to maintain required navigation depths, yet far enough apart to prevent backwater effects and flooding upstream during high river flows. In cold regions, jetties should be oriented to avoid contributing to ice jamming in the entrance, which could cause upstream flooding. In some cases, overlapping jetties have proven to contribute to natural sand bypassing, and they reduce wave energy entering the mouth and lower reaches of the stream. If large quantities of sediment are moving in the area, sand bypassing schemes should be included in the design (Part V-6).

(d) Jetty layout in tidal areas is much more difficult. Interaction of wave-induced currents and tidal currents, sometimes with freshwater discharges, through an inlet connecting the ocean with an embayment, is very complex. A fairly uniform distribution of flow across the entrance is one objective. Dual jetties of equal length usually serve best. The jetties should be parallel if practical; otherwise training dikes or spurs should be added to divert or concentrate flow through the desired channel alignment. If jetty spacing is too wide, shoaling and channel meandering are likely to occur. If jetty spacing is too narrow, structure toes may be undercut and hazardous navigation conditions may occur.

(e) Parallel jetties tend to confine flood and ebb flow, raising flow velocities and providing adequate sediment flushing into the flood and ebb deltas. Arrowhead jetties frequently allow channel shoaling and meandering because ebb flow is not confined enough to produce nondepositional velocities in the widest area between jetties. Barnegat Inlet, New Jersey, is an example where both jetty configurations have been used (Sager and Hollyfield 1974; Seabergh, Cialone, and Stauble 1996) (Figure V-5-37). Arrowhead jetties were built in 1939, and a new south jetty, nearly parallel to the north jetty, was built in 1991. As another general alternative for jetty layout, curved jetties may be designed to produce nondepositional velocities, but flow concentrations on the outside of the curve may cause jetty undermining and a difficult channel alignment for navigation (McCartney, Hermann, and Simmons 1991).

(f) Jetties should be long enough to prevent littoral transport around the jetty ends and into the navigation channel. Jetty orientation for navigation purposes should ensure that the channel is approximately aligned with the approach direction of the more severe waves. Typically, a jetty alignment perpendicular to shore serves this purpose. The ideal jetty alignment for navigation is often a poor alignment for sheltering interior areas from waves. However, waves lose a significant amount of energy in traveling between parallel jetties (energy loss increases with jetty length) or passing through an entrance gap between breakwaters or jetties (Part II-7). The height of waves traveling between parallel jetties may be estimated by treating the jetty entrance as a breakwater gap (Melo and Guza 1991). The inter-jetty propagation distance corresponds to the normal interior distance from the gap and wave height can be estimated from height diffraction contours as given in Part II-7.

(g) Spacing between dual jetties should be determined with consideration of tidal processes, wave protection requirements, river flood discharge requirements, and safe navigation requirements. Jetty spacing for tidal concerns depends on the tidal prism volume or the actual tidal flow exchange through the inlet. Relationships between minimum cross sectional area required at inlet throats as well as detailed design of jettied entrances are presented in Part II-6. Wave protection requirements of interior shorelines and facilities

(a) Arrowhead jetties (November-December 1965)

(b) Parallel jetties (June 1996)

Figure V-5-37. Jetty types, Barnegat Inlet, New Jersey

are specific to each project. A rule of thumb for safe deep-draft navigation is that an entrance width equal to the design ship *length* is satisfactory for two-way traffic. An overbank area between the channel and jetty is needed to protect the structure toes.

(3) Training dikes. Training dikes serve to direct current flow in a desired path. A common application is the use of training dikes interior to a jettied inlet to confine currents to the navigation channel and help prevent channel shoaling and erosion of nearby banks and shores. Dikes are usually constructed of stone, timber pile clusters, or piling with stone fill.

(4) Wave absorbers. Wave energy that penetrates into small boat harbors through entrances or by transmission or overtopping of breakwaters may create serious problems for navigation in interior channels, moored boats, and bank erosion. Excessive wave energy in deep-draft ports can cause similar problems. Wave absorbers are sometimes constructed inside harbors to dissipate this short-period wave energy. Absorbers are generally placed in harbor areas with high concentrations of wave energy.

(a) Beaches are the most effective wave absorbers. Beach slopes dissipate most wind wave and swell energy and reflect very little energy. However, beaches also occupy a relatively large area and may not be practical. More commonly, rubble slopes serve as wave absorbers in navigation projects. For best efficiency, a stone wave absorber should have a rock layer thickness equal to three times the representative diameter of individual rocks used and porosity should be about 30 percent (LeMéhauté 1965).

(b) Sometimes rubble slope absorbers are integrated into a dock to provide wave dissipation without interfering with harbor use. Typical applications are an armored slope under a pile-supported dock face or an absorbing quay wall (PIANC 1997b) (Figure V-5-38). Another approach is a perforated wall along the dock face with a vertical solid-wall fill some distance behind the dock face (Figure V-5-39). The optimum porosity for the perforated wall should be around 30 percent and the optimum set-back of the solid wall should be about one tenth of the wave length to be absorbed (LeMéhauté 1965). Molded concrete wave absorber units may also be used along a vertical dock face. Such units have proven effective in model tests for a Great Lakes site (Bottin 1976) (Figure V-5-40), but have not been used in U.S. harbors.

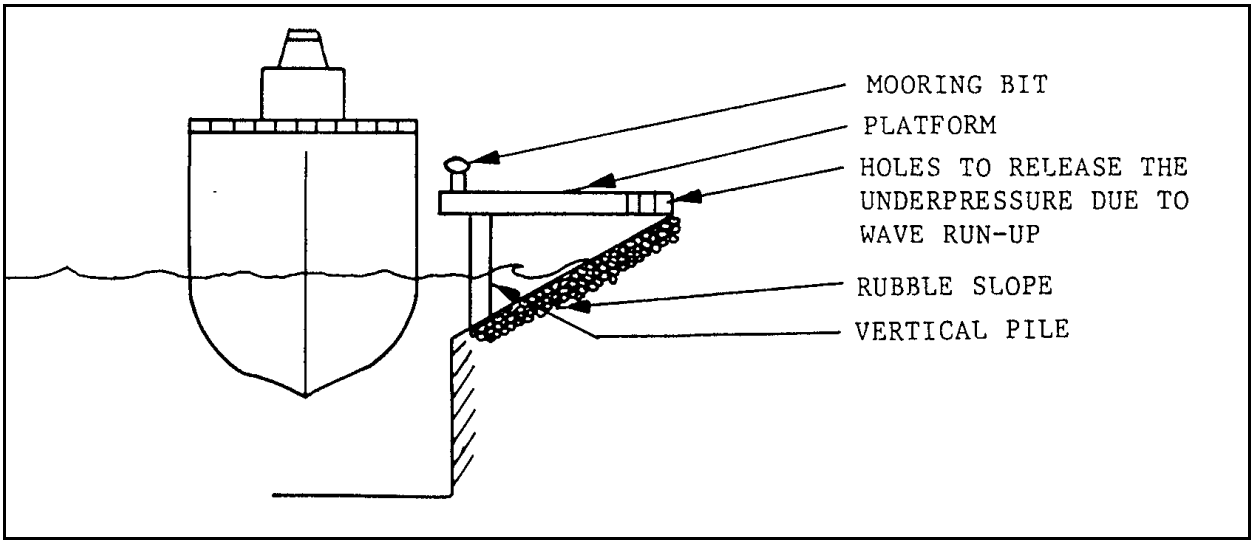

Figure V-5-38. Rubble wave absorber at a dock

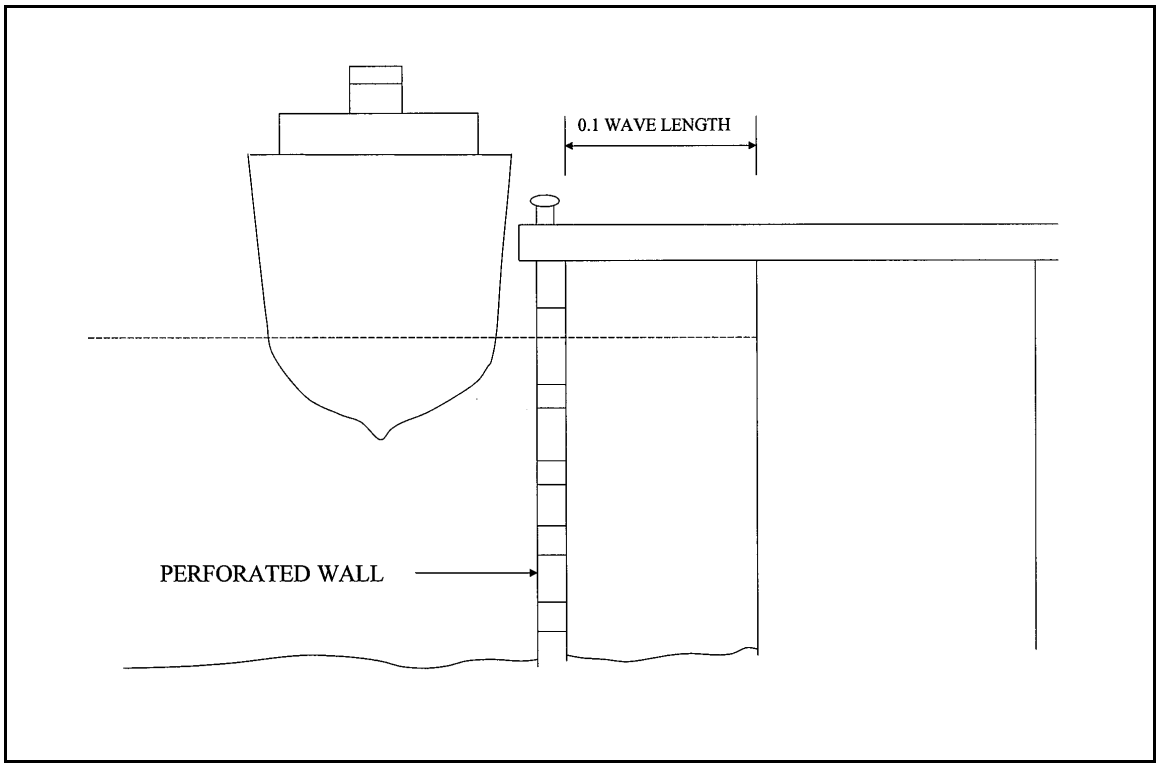

Figure V-5-39. Perforated wall wave absorber at a dock

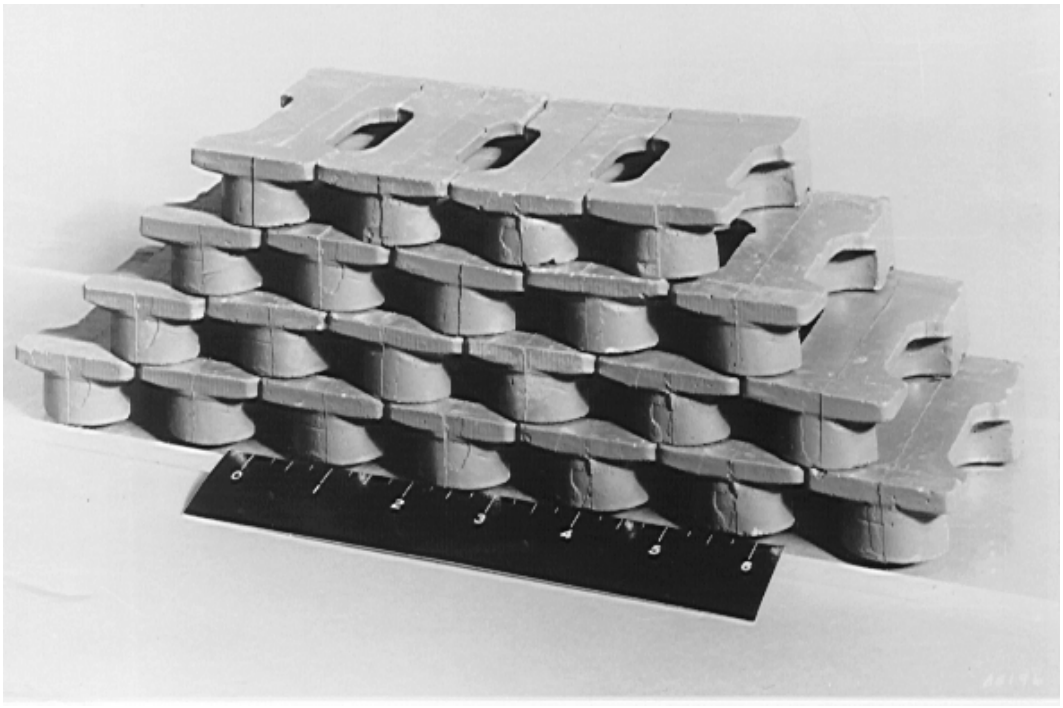

Figure V-5-40. Stacked Igloo model wave absorber units

(5) Revetments, seawalls, and bulkheads. Though not actually navigation structures, revetments, seawalls, and bulkheads are included in, or adjacent to, most harbors. They are briefly reviewed here and discussed in detail in Parts V-3, VI-2, and VI-7. In general, vertical structures are classified as either seawalls or bulkheads, according to their function, while protective materials laid on slopes are called revetments. A seawall is a massive structure that is designed primarily to reduce wave energy and provide wave protection along coastal property. Bulkheads are retaining walls whose primary purpose is to hold or prevent backfill from sliding while providing protection against light-to-moderate wave action.

(a) Revetments, seawalls, and bulkheads are structures placed parallel, or nearly parallel, to the shoreline to separate a land area from a water area. The purpose of the structure dictates which type is used. In harbors, these structures may improve or worsen wave conditions and land access to beaches, depending on the location and design.

(b) Vertical structures (seawalls and bulkheads) are useful as quay walls or docking/mooring areas. Because of potential wave reflection problems, bulkheads to provide vessels with direct access to shore should only be placed in areas with little exposure to wave energy. Wave reflection from vertical structures may create hazardous conditions for small craft, erosion of adjacent shorelines, and beach profile changes.

(c) Revetments are typically less reflective than vertical structures. Rubble revetments may be effective wave absorbers but may hinder access to a beach. Smooth revetments built with concrete blocks generally present little difficulty to pedestrians, but are more reflective than rubble revetments.

(d) On seawalls and bulkheads, convex-curved face and smooth slopes are least effective in reducing wave runup and overtopping. Concave-curved face structures are most effective for reducing wave overtopping when onshore winds are light. Where the structure crest is to be used as a road, promenade, or other such purpose, concave-curved may be the best shape for protecting the crest and reducing spray. If onshore winds occur with high waves, a rubble slope should be considered to reduce runup and overtopping. A stepped-face wall provides the easiest access to beach areas from protected areas, and reduces the scouring of wave backwash. Some seawalls and bulkheads may create access problems and may require the building of stairs.

V-5-8. Aids to Navigation

(1) Aids to navigation are the markers and signals vessels require to safely use a navigation project. The navigation safety of a project is directly related to the clarity and visibility of aids to navigation. Channel design must be planned so that the layout, dimensions, and alignment facilitate clear marking. A reduced width may be possible in a well-marked channel as compared to a poorly marked channel, so a tradeoff between channel widening cost and aids to navigation cost should be considered in design.

(2) The U.S. Coast Guard is responsible for the design, establishment, and maintenance of all aids to navigation in Federal interstate waters (U.S. Coast Guard 1981, 1988a, 1988b). Figure V-5-41 gives two examples of typical devices used to mark U.S. navigation channels. They are uniquely identified by color, shape, and number or letter. They may also include lights, sound, radar reflectors, and electronic signals. Beacons are fixed structures, generally on pilings in shallow water up to about the 5-m (15-ft) depth. Buoys are floating, anchored to the bottom with a chain connected to a concrete block. They mark channel boundaries, hazards, and channel curves or turns, especially in areas where water depth makes beacons impractical. Height above the water, and hence visibility, is more limited for buoys than for beacons. Another limitation of buoys is that their location relative to the channel is imprecise. It can vary over a small distance because buoys are free to move about the anchor point in response to environmental forces.

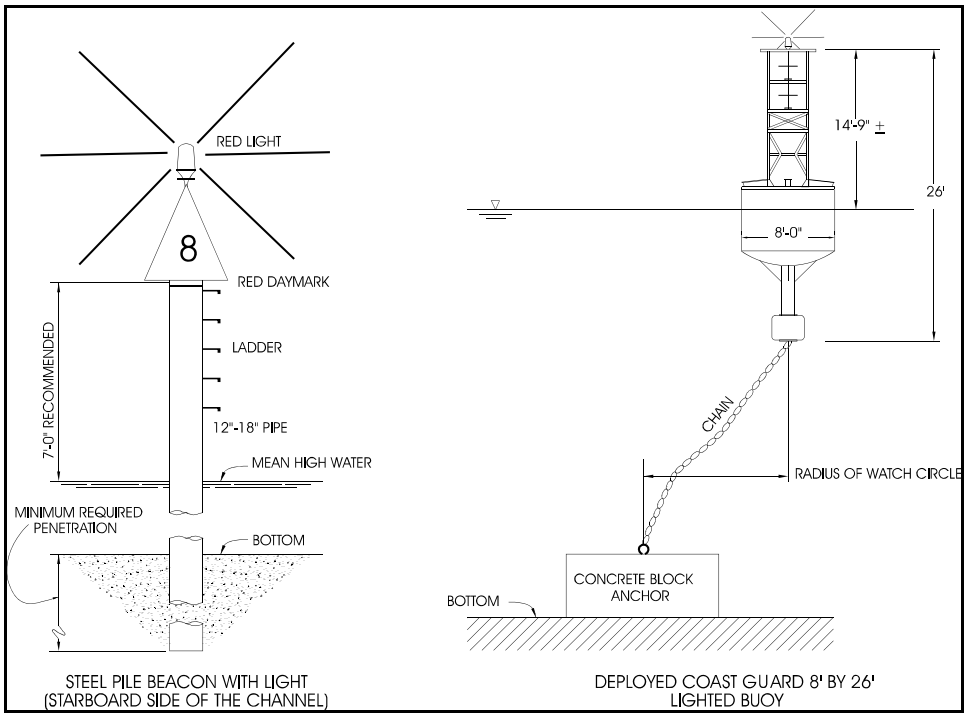

Figure V-5-41. Examples of aids to navigation

(3) Occasionally, buoy/anchor systems are completely moved out of position by strong environmental forces or by vessel impacts. Buoys are also susceptible to sinkage or drifting if mooring connections are lost.

(4) The channel marking system used in U.S. Federal waters is nearly standardized. Conventions for color, shape, numbers/letters, and light characteristics are well-established. Left and right channel sides are relative to an inbound vessel coming from open water into a harbor. Basically, the left side of the channel is signified by green (paint color and/or lights), squares, and odd numbers (Figure V-5-42). The right side is signified by red, triangles, and even numbers. Numbering begins at the seaward end of the channel.

(5) Ranges are pairs of fixed structures usually aligned with the channel center line at one or both ends of straight reaches. They are usually on shore or in very shallow water. The rear marker is always higher than the front marker. They are typically marked with rectangular signs, designated by letters, high-intensity lights, and red and white vertical stripes, as indicated in Figure V-5-42. By observing the placement of front and rear markers relative to each other, mariners can determine vessel position relative to the channel center line (Figure V-5-43).

(6) Additional important aids to navigation along the seacoast include major lights and sea buoys. One or more major lights are located near each harbor entrance. The high-intensity, well-maintained lights are located on fixed structures or towers at heights of up to 60 m (200 ft), sufficient to be visible over a long distance. Electronic aids to navigation are often collocated with major lights. Sea buoys are large, easily visible buoys marking the ocean end of most deep-draft harbor entrance channels. A typical sea buoy is 12 m (40 ft) in diameter and 9 m (30 ft) or more in height, with high-intensity light, electronic aids, and a sound signal. Sea buoys are usually located in deep water on the channel center line extended 2 to 4 km (1 to 2 miles) seaward beyond the channel's seaward end. Often the sea buoy marks an area where inbound ships await local pilot assistance.

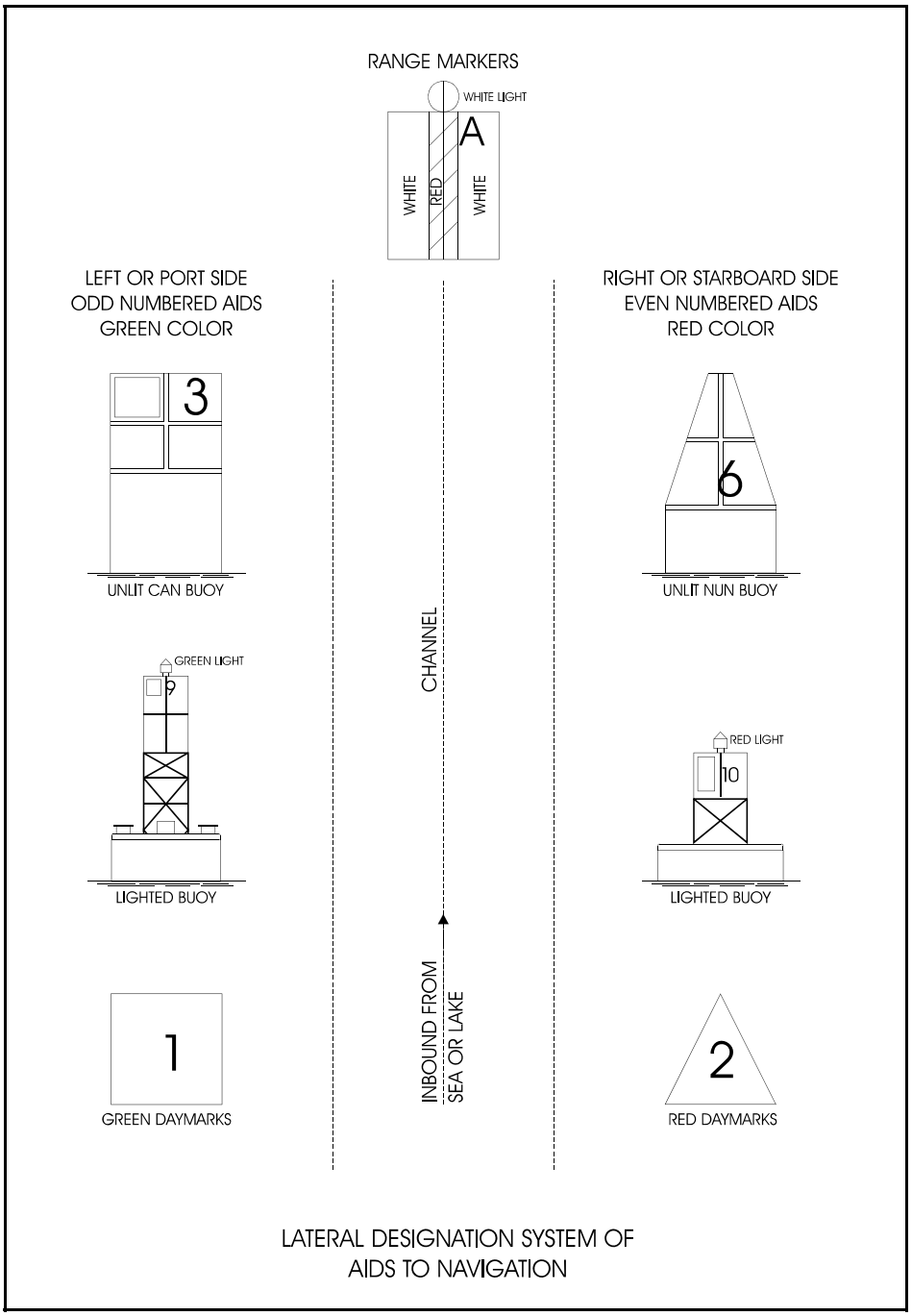

Figure V-5-42. Designation system of aids to navigation

(7) Aids to navigation are normally placed along straight channel reaches so that at least two on either side are always visible. This consideration leads to a practical maximum spacing of about 2.3 km (1.25 n.m.). Range markers must be visible along the entire reach. Practical limitations on range marker height, visibility through fog, and earth curvature effect on line of sight dictate that straight channel reaches should be no longer than about 8 to 10 km (5 to 6 miles). It is good practice to have redundant aids to navigation, such as both range markers and side channel markers, to ensure that failure of a marker will not create a navigation crisis.

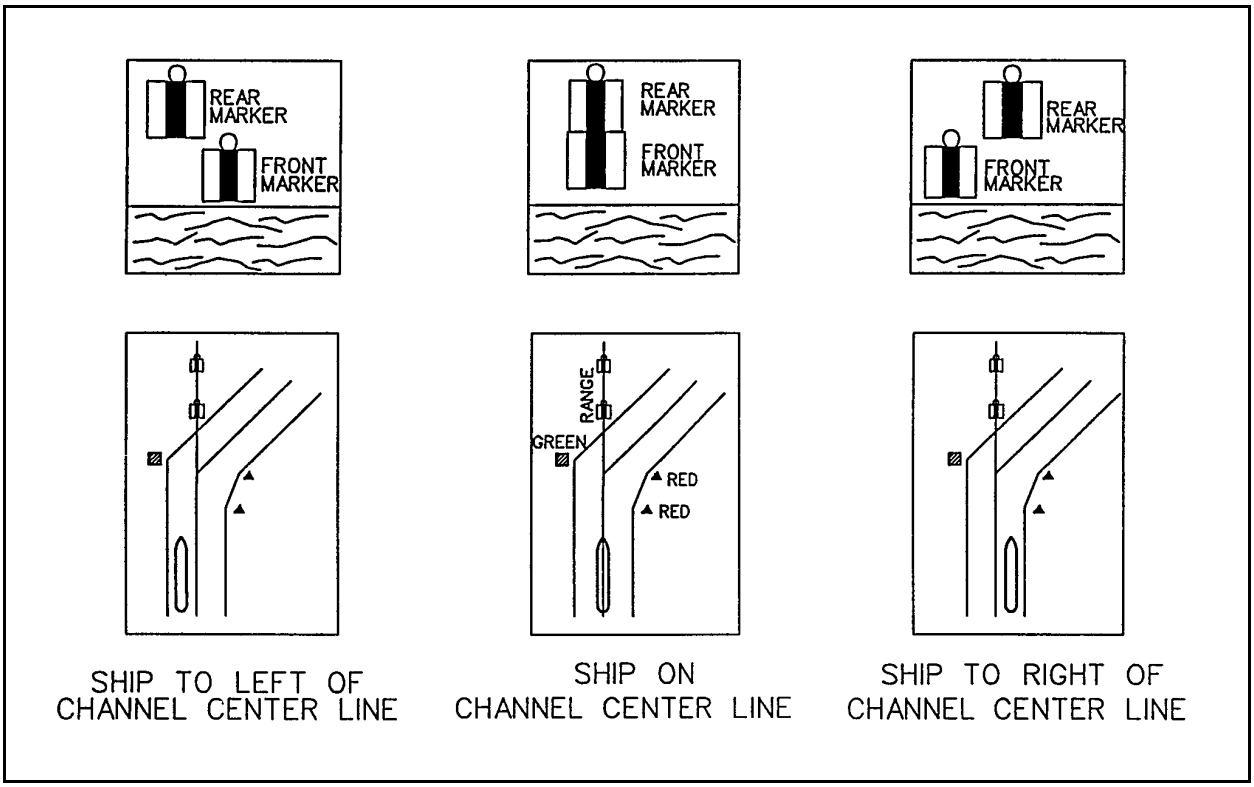

Figure V-5-43. Use of ranges for channel position

(8) An example deep-draft navigation channel at Brunswick Harbor, Georgia, is shown in Figure V-5-44 (Huval and Lynch 1998). The entrance channel begins near a sea buoy in exposed Atlantic Ocean waters, passes between St. Simons and Jekyll Islands, makes a severe turn to pass behind Jekyll Island, and continues with additional turns up the Brunswick River to port facilities at Brunswick. The channel also passes under the Sidney Lanier Bridge. Navigation buoys and range markers are shown.

V-5-9. Operation, Monitoring, and Maintenance

a. After a navigation project has been designed and constructed, operation and maintenance are required to sustain safe and efficient use of the project. Operation and maintenance requirements and costs can be substantial. They are typically estimated with care and optimized against initial construction costs in planning and designing a navigation project. Anticipated maintenance costs are based on predictions of physical changes after the project is constructed.

b. A completed navigation project must be monitored to ensure safe operation and to plan for maintenance activities as needed (see Part V-2-17). Monitoring typically includes hydrographic surveys, beach profile surveys, tide and wave data collection, and navigation structure condition surveys. Surveys are typically done on a planned schedule, such as annually, and before and after periods of maintenance and repair. Surveys should be analyzed comparatively to determine rates of erosion, shoaling, and structure deterioration.

c. Often, periodic dredging to maintain project depths is the major maintenance need. Maintenance dredging intervals depend on factors such as shoaling rate, dredge availability, and dredge mobilization costs.

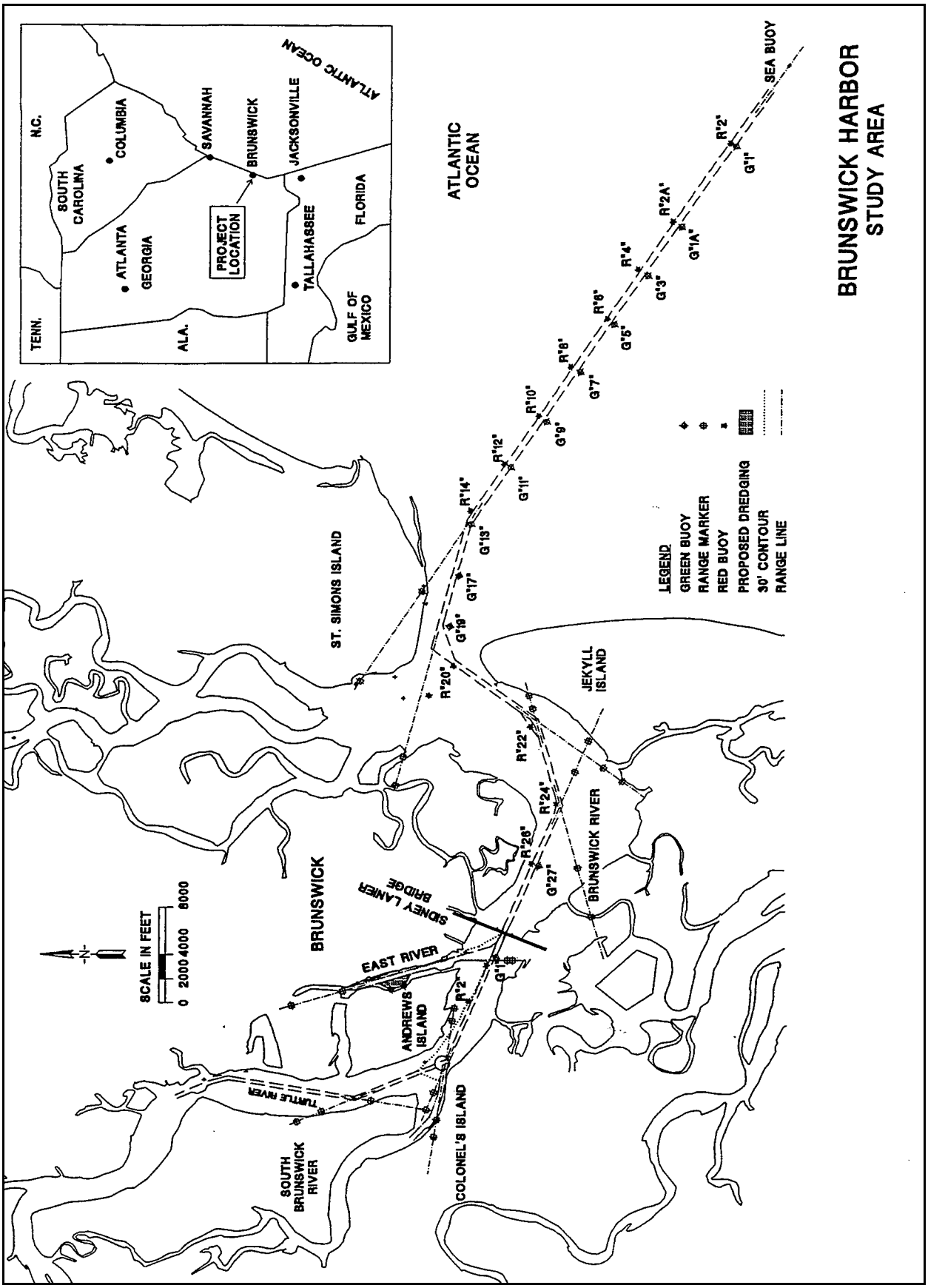

Figure V-5-44. Deep-draft navigation channel, Brunswick Harbor, Georgia

d. Typical maintenance intervals are on the order of 1-3 years at some projects, but maintenance needs are often strongly influenced by storm events. However, environmental forces impacting a navigation project are highly variable. The number and intensity of storms affecting a project each year can only be predicted in terms of probabilities. A single severe storm can cause major shoaling and structure damage. Consequently, monitoring and maintenance activities may occasionally need to respond quickly to maintain project integrity.

e. Project performance should be assessed, based on monitoring data. Actual project performance should be evaluated relative to project expectations during original design. In particular, actual maintenance costs should be compared to those originally predicted. Coordination with local interests, including boaters, pilots, port authorities, etc., should also be part of project performance assessment. Monitoring, maintenance, and performance assessment should continue at an appropriate level for the life of the project.

V-5-10. Model and Specialized Field Studies

a. Harbor modeling. Physical and numerical harbor models are important design tools that can help the designer: Locate the project to ensure maximum wave protection; locate and design breakwaters and/or jetties to provide adequate protection and maintain entrance navigation channels; and locate, orient, and dimension navigation openings to provide vessels safe and easy passage into and out of a harbor without sacrificing wave protection; position spending beaches and other forms of wave absorbers inside the project area. Physical and numerical modeling tools are helpful in developing and optimizing harbor designs. When compounded with problems caused by nearby or adjacent rivers, and/or shoaling problems resulting from littoral transport, and/or harbor oscillation problems relative to long-period wave energy, the designer encounters difficulty in obtaining adequate answers strictly by analytical means. One or both of these tools should be applied when a study has large economic consequences. Even small harbor studies generally benefit from model studies.

(1) Physical modeling as a design tool. Hydraulic scale models are commonly used to plan harbors and to design and lay out breakwaters, jetties, groins, absorbers, etc., to obtain optimum harbor protection and verify suitable project performance. A detailed description of physical modeling related to coastal ports and harbors is given by Hudson et al. (1979). Physical hydraulic model studies may be used to study the following:

- The most economical breakwater and/or jetty configurations that will provide adequate wave protection and navigation channel control for vessels using the harbor.
- Wave heights in the harbor.
- Undesirable wave and current conditions in the harbor entrance.
- Proposals to provide for harbor circulation and/or flushing.
- Qualitative information on the effects of structures on the littoral processes.
- Flood and ice flow conditions.
- Shoaling conditions at harbor entrances.
- River flow and sediment movement in rivers that may enter in or adjacent to the harbor.

- Long-period oscillations (Part II-7).
- Tidal currents or seiche-generated currents in the harbor (Part II-7).
- Inlet entrances.
- Remedial plans for alleviation of undesirable conditions as found necessary.
- Possible design modifications to significantly reduce construction costs and still provide adequate harbor protection.

(a) To ensure accurate reproduction of short-period wave and current patterns (i.e., simultaneous reproduction of both wave refraction and wave diffraction), undistorted models (i.e., vertical and horizontal scales are the same) are necessary for harbor studies. Physical hydraulic models are designed and operated in accordance with Froude's model law (Stevens et al. 1942). Scale relations commonly used for undistorted physical models are shown in Table V-5-13. A scale of 1:100 is used for illustrative purposes.

Table V-5-13
Typical Physical Model Scales for Harbors

Characteristic	Dimension[1]	Scale Relations
Length	L	L_r = 1:100
Area	L^2	$A_r = L_r^2$ = 1:10,000
Volume	L^3	$\forall_r = L_r^3$ = 1:1,000,000
Time	T	$T_r = L_r^{1/2}$ = 1:10
Velocity	L/T	$V_r = L_r^{1/2}$ = 1:10
Roughness (Manning's coefficient, n)	$L^{1/6}$	$n_r = L_r^{1/6}$ = 1:2,154
Discharge	L^3/T	$Q_r = L_r^{5/2}$ = 1:100,000
Force (fresh water)	F	$F_r = L_r^3 \gamma_r$ = 1:1,000,000
Force (salt water)	F	$F_r = L_r^3 \gamma_r$ = 1:1,025,641

[1] Dimensions are in terms of length (L), time (T), and force (F).

(b) Selection of a suitable model scale is an important step in model design. It involves a trade-off between scale effects and construction costs. For short-period wave studies, the model area generally includes enough offshore area and bathymetry to allow waves to refract properly on approaching the harbor and enough upcoast/downcoast area to allow the littoral current to form. Model waves must be large enough to be free from excessive friction and surface tension and to be measured with reasonable accuracy. Typical scales are between 1:75 and 1:150. For long-period wave studies (periods longer than about 25 sec), larger prototype areas are generally needed to include relevant interactions with bay or coastal shelf bathymetry. Also, long-period waves tend to reflect from model basin boundaries and the model harbor should be far from these boundaries. Long-period wave studies usually require distorted-scale models, with unequal horizontal and vertical scales. For example, a USACE model of Los Angeles/Long Beach Harbor, in use since the 1970's has a vertical scale of 1:100 and a horizontal scale of 1:400.

(c) Small-scale models must be constructed very accurately to reproduce conditions in the prototype. The model should reproduce underwater contours to model wave transformation. Shoreline details and irregularities also are important to simulate diffraction, runup, and reflection. The model bed should be as

smooth as possible to minimize viscous scale effects. However, models involving estuary tidal flows and/or river flows typically require the addition of bottom roughness in those areas to correctly simulate flow conditions. When a model involves breakwater or jetty structures, model armor and underlayer stone sizes are adjusted, based on previous research and experience, to reproduce prototype transmission and reflection characteristics. Structure stability is generally not reproduced in harbor models.

(d) The reproduction of river discharges and steady-state tidal flows often is required in wave action model studies. These flows generally are reproduced using circulation systems (i.e., for a river discharge, water is normally withdrawn from the perimeter of the model pit area and discharged in a stilling basin that empties into the upper reaches of the river and flows downstream in the model).

(e) Reproducing the movement of sediment in small-scale coastal model investigations is very difficult (Hudson et al. 1979). Ideally, quantitative, movable-bed models best determine the effectiveness of various project plans with regard to the erosion and accretion of sediment. This type of investigation, however, is difficult and expensive to conduct and entails extensive computations and prototype data. In view of these complexities and due to time and funding constraints, most models are molded in cement mortar (fixed-bed) and a tracer material is selected to qualitatively determine the degree of movement and deposition of sediments in the study area. In past investigations, tracer was chosen in accordance with the scaling relations of Noda (1972), which indicates a relation or model law among the four basic scale ratios: horizontal scale, vertical scale, sediment size ratio (d_{50} model tracer material divided by d_{50} prototype sediment), and relative specific weight ratio. These relations were determined experimentally using a wide range of wave conditions and bottom materials, and they are valid mainly for the breaker zone. This procedure was initiated in the mid-1970's, and has been successful in reproducing aspects of prototype sediment movement as evidenced by the performance of completed projects that have been studied (Bottin 1992). Currently, research is being performed to better understand aspects of sediment movement and improve methods to model it, and scaling relations have been developed for mid-scale, two-dimensional model tests (Hughes and Fowler 1990).

(f) After model construction, representative test conditions must be selected. Wave height and period characteristics, direction of wave approach, and frequency of occurrence are typically needed. Refraction analyses are normally required to transform deepwater waves to shallow water at the location of the model wave generator. From this point, model bathymetry will transform the waves to the harbor area. Still-water levels (swl's) are also important test conditions. Normally more wave energy reaches a harbor with the higher swl's. Lower swl's may result in more seaward movement of longshore sediment (i.e. around a jetty head), since the breaker zone would be moved farther offshore. Dominant movement of wave-induced currents and sediment transport patterns are required for verification of the model. River discharge and/or tidal flow information is also required, if applicable to the study.

(g) Data collected in a physical model include time series measurements at selected points of water surface elevation and, when needed, current. Spatial current patterns and velocities can be estimated by timing the progress of weighted floats over known distances on the model floor. Photographs and videotapes of experiments in progress provide valuable visual documentation of wave transformation patterns, wave breaking, sediment movement, etc.

(2) *Example: Dana Point Harbor, California*. Dana Point Harbor, located on the southern California coast about 64 km (40 miles) southeast of the Los Angeles/Long Beach Harbors, is an example of a small craft harbor designed with the aid of physical modeling (Figure V-5-45). The harbor occupies a small cove in the lee of Dana Point. The harbor consists of a 1,676-m- (5,500-ft-) long west breakwater, a 686-m-(2,250-ft-) long east breakwater, and inner harbor berthing areas partially enclosed by the shoreline and mole sections. The harbor encloses an area of about 0.85 sq km (210 acres) and provides berthing facilities for about 2,150 small boats.

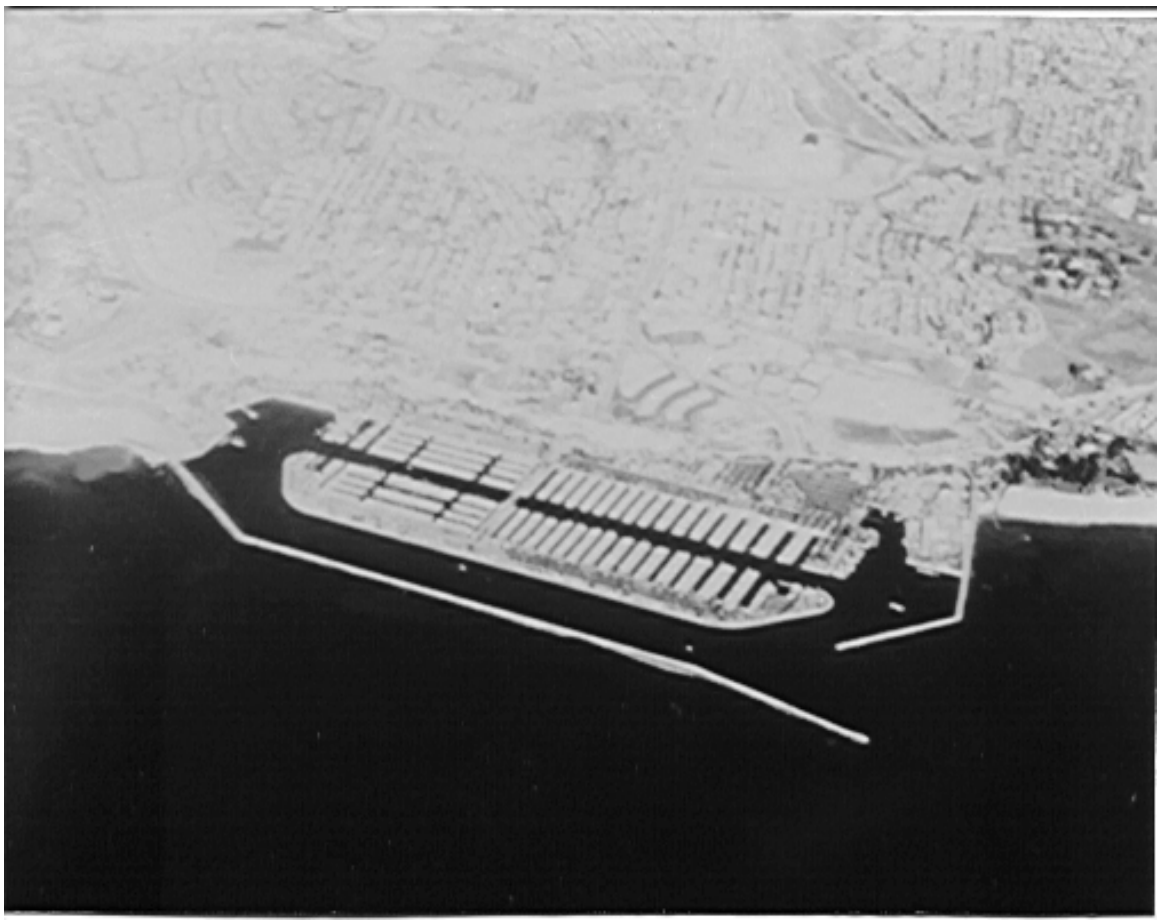

Figure V-5-45. Dana Point Harbor, California (May 1969)

(a) The area is exposed to storm waves from directions ranging from southwest counterclockwise to south-southeast and to ocean swells from the south. Damaging wave energy may reach the berthing areas by passing through the outer navigation entrance and by overtopping and/or passing through the rubble-mound breakwaters.

(b) As part of the original design effort, a 1:100-scale hydraulic model investigation was conducted to determine the optimum breakwater plan and location and size of the navigation opening that would provide adequate protection for mooring areas during storms (Wilson 1966). Waves with periods ranging from 9 to 18 sec and heights ranging from 2.4 to 5.5 m (8 to 18 ft) were generated from eight deepwater directions using an swl of +2.0 m (+6.7 ft) mllw. A wave height acceptance criterion of 0.46 m (1.5 ft) was established in the harbor berthing areas by the sponsor and waves in the fairway were not to exceed 1.2 to 1.5 m (4 to 5 ft).

(c) Experiments were conducted for existing conditions and 13 plans. Results for existing conditions indicated rough and turbulent conditions in the area even for low-magnitude storm waves. The proposed improvement plan involved construction of outer breakwaters and inner-harbor development consisting of east and west basin berthing areas partially enclosed by the shoreline on the north and a mole section on the south, southeast, and southwest (Figure V-5-46).

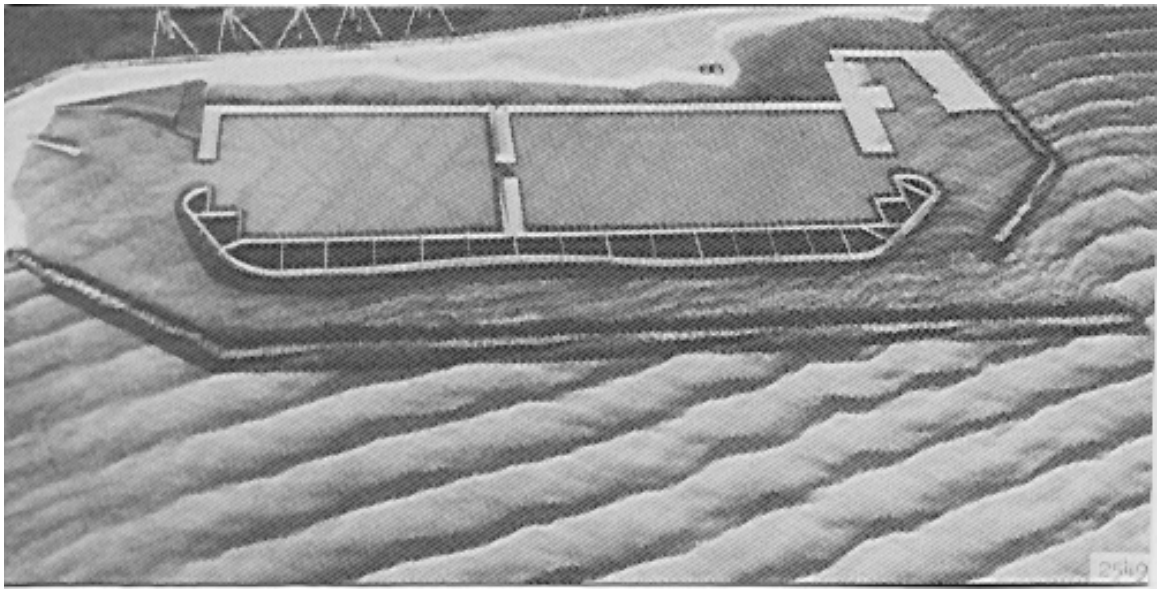

Figure V-5-46. Physical model view of Dana Point Harbor, California, under storm wave attack

(d) Experimental results indicated that wave conditions in the berthing areas were acceptable; however, wave heights in the fairway were about 2.0 m (6.5 ft) for severe storm wave conditions. It was noted that these conditions were due to a standing wave system caused by reflected waves from the mole slopes. Experimental results revealed that modifying the mole slope flanking the fairway, to include a berm, would reduce wave action considerably in the fairway.

(e) The harbor was constructed in accordance with recommendations from the physical model investigation. Post-construction monitoring has shown the harbor is performing as predicted. Mooring areas have experienced no wave problems. The outer west breakwater is overtopped by storm waves, which propagate across the interior channel to the outer revetted mole slope. Vessels in mooring areas behind the moles remain protected. The harbor has successfully endured intense storms, when other southern California small- craft harbor facilities have been severely damaged.

(3) Numerical modeling as a design tool. Numerical modeling requires computerized solution of equations that approximate harbor response to imposed natural forces. Numerical models and computer technology have evolved to the point where useful modeling of actual harbors can often be conveniently done on microcomputers. Numerical models are helpful in harbor studies, even for relatively simple harbor shapes. A combination of physical and numerical modeling is usually preferred for investigating the full range of conditions in a harbor. Numerical modeling related to harbors is best discussed in terms of the natural phenomenon to be modeled, such as waves, circulation, and shore response. Each model's equations and input/output forms are developed for application to particular phenomena. Model systems are now available that provide convenient access to a variety of modeling options under a single user-friendly interface (e.g. SMS 1994).

(a) Wind waves, swell, and harbor oscillations. Numerical wave models can be effectively applied to wave periods ranging from wind waves to long-period harbor oscillations. Numerical models have been useful for: Very long-period wave studies; initial evaluations of harbor conditions; comparative studies of harbor alternatives; and revisiting harbors documented previously with field and/or physical model data.

- For example, numerical models have been used effectively to select locations for field wave gauges (to achieve adequate exposure and avoid oscillation nodes) and to identify from many alternatives a few promising harbor modification plans for fine-tuning in physical model tests. Lillycrop et al. (1993) suggested that numerical modeling is preferable to physical modeling for oscillation periods longer than 400 sec. Both modeling tools can be used effectively for shorter period oscillations.

- Numerical wave modeling concerns are discussed in the following paragraphs, followed by an illustrative example. Additional information on numerical modeling of waves in harbors is available from a number of sources (e.g., Panchang, Xu, and Demirbilek (1998)).

- An initial step in modeling a harbor is to define the area to be covered and required horizontal resolution in the model grid. The coverage area should include the harbor and an area seaward encompassing bathymetry important for waves approaching the harbor. The seaward boundary should be a minimum of several wavelengths away from the harbor entrance, based on the longest wave periods to be modeled. Horizontal resolution is determined by the wavelength of the shortest wave period to be modeled. Typical resolution requirements are between $L/6$ and $L/15$ as the maximum grid element width. If grid elements are uniform in size over the entire grid, L should be based on the shallowest depths of interest. Depending on the particular study and grid-building software available, it may be preferable to build a grid with element sizes varying according to water depth, but still satisfying the wavelength-based maximum size criterion. Computer demands (memory, processing time, storage) in running a harbor model are directly linked to the total number of grid elements. Most harbor studies require a trade-off between coverage area and grid resolution to achieve a workable grid.

- Numerical models applied to harbors are usually based on a form of either the mild slope equation (MSE) or Boussinesq equations. Development of the equations is given by Dingemans (1997), Mei (1983), and others. MSE models are typically steady-state. The MSE model calculates an amplification factor (ratio of local wave height to incident wave height) and phase (relative to the incident wave) for every node in the grid. The MSE does not incorporate spectral processes. Typically, MSE models are run with a representative set of wave height, period, and direction combinations, based on knowledge of incident wave climate. If the MSE is linear, a single wave height for each period/direction combination will suffice. For wind wave and swell applications, regular wave results from the MSE model may be linearly combined, with appropriate weightings, to simulate harbor response to directional wave spectra.

- Boussinesq models are nonlinear and time-dependent. They are forced with an incident wave time series on the seaward boundary and produce a time series of wave response at each node in the grid. The time series may represent regular or irregular wave conditions. Boussinesq models are capable of more accurate representation of harbor wave response than MSE models, at the price of considerably greater computational demands. They are warranted in some practical studies and, with continuing intensive research and development, are likely to become a more workable option in the near future.

- Results from numerical harbor models are in the form of information at selected points or over the entire grid. Point information from Boussinesq models is comparable to time series from field or physical model wave gauges and may be analyzed in similar ways. Spatial information from Boussinesq models can provide animated displays of waves approaching, entering, and interacting with the harbor. Snapshots of waveforms over the harbor at selected times can easily be extracted for still displays. Spatial information from MSE models is in the form of snapshots of amplification factor and phase over the harbor area. Animated displays can be created by expanding amplification factor and phase information into sinusoidal wave time series, if desired.

(b) *Example: Kikiaola Harbor, Kauai, Hawaii*. Kikiaola Harbor is a small, shallow-draft harbor, located along the western part of the Kauai's south shore (Figure V-5-47). The original harbor consisted of west and east breakwaters. The harbor experienced excessive waves, resulting in the addition of inner and outer stub extensions to the east breakwater and a short inner breakwater. A wharf and boat ramp are located along the north boundary of the harbor, east of the inner breakwater.

- Prevailing northeast tradewinds result in a strong predominance of winds from the northeast, east, and southeast at the harbor. Typical wind speeds are 5 to 10 m/sec (10 to 20 mph). Winter storms can generate strong winds from the south. The harbor is exposed to waves approaching from a sector between the 134- and 278-deg azimuths, though the small island of Niihau creates some sheltering in the western exposure. Southern swell, generated by storms in the southern Pacific and Indian Oceans, is a significant part of the wave climate. Also, waves generated by storms in the North Pacific can wrap around the western side of Kauai and affect Kikiaola Harbor. Hurricanes can attack the harbor, which is important for structure design; but they are rare and do not impact operational concerns.

- Use of the existing harbor is limited by two primary factors. First, the harbor is quite shallow. Sediment movement along the local coast, predominantly from east to west, has resulted in shoaling of the entrance and inner harbor. Second, the existing entrance experiences breaking wave conditions that are hazardous to navigation. These two factors are interrelated. Breaking waves are more likely in the existing, shoaled entrance than they would be in a deeper, maintained entrance channel.

- Two plans for modifying the breakwater structures and navigation channels were defined, as follows (Figure V-5-48):

- *Plan 1*. Remove outer stub of east breakwater; remove and reconstruct inner stub of east breakwater a small distance further east; raise crest elevation of exposed portions of east breakwater by 1 m (3-4 ft) and flatten seaward slope to 1:2; widen outer 67 m (220 ft) of west breakwater; dredge 221-m- (725-ft-) long entrance channel with width varying from 32 to 62 m (105 to 205 ft) and maneuvering area to facilitate a 90-deg turn into access channel; dredge 98-m- (320-ft-) long access channel varying in width from 21 to 32 m (70 to 105 ft).

- *Plan 6*. Remove outer and inner stubs of east breakwater; raise crest elevation of exposed portions of east breakwater by 1 m (3-4 ft) and flatten seaward slope to 1:2; extend east breakwater further west to a distance of 33 m (100 ft) past the existing west breakwater location; shorten west breakwater to allow space for access channel; dredge entrance and access channels comparable to those in Plan 1.

- A numerical model study was initiated to investigate wave conditions in the proposed plans relative to the existing harbor and to USACE criteria for channels and berthing areas (Thompson et al. 1998b). An MSE-based numerical model was used to analyze the harbor area (Chen and Houston 1987). Because water depths are shallow (on the order of 1 m in the existing harbor) and the shortest wave period to be modeled was 6 sec, a dense grid was required. To maintain a workable grid size for the model being used, the offshore extent of the grid was significantly limited and could not reach deep water.

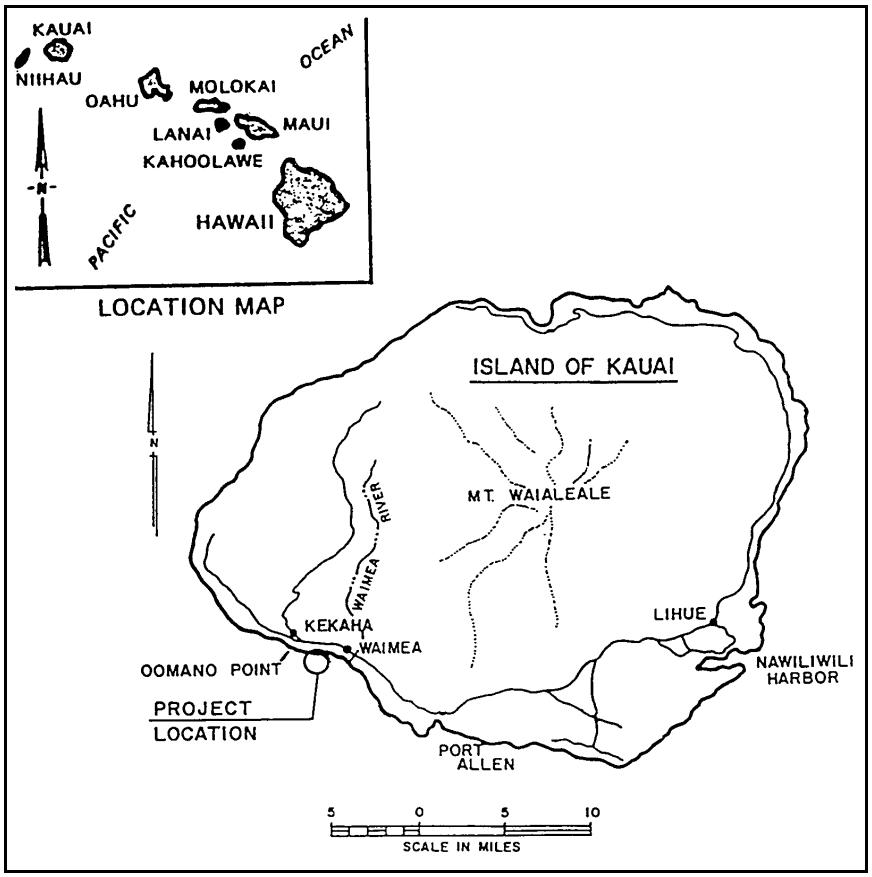

(a) Location map

(b) Photograph (1998)

Figure V-5-47. Kikiaola Harbor, Kauai, Hawaii

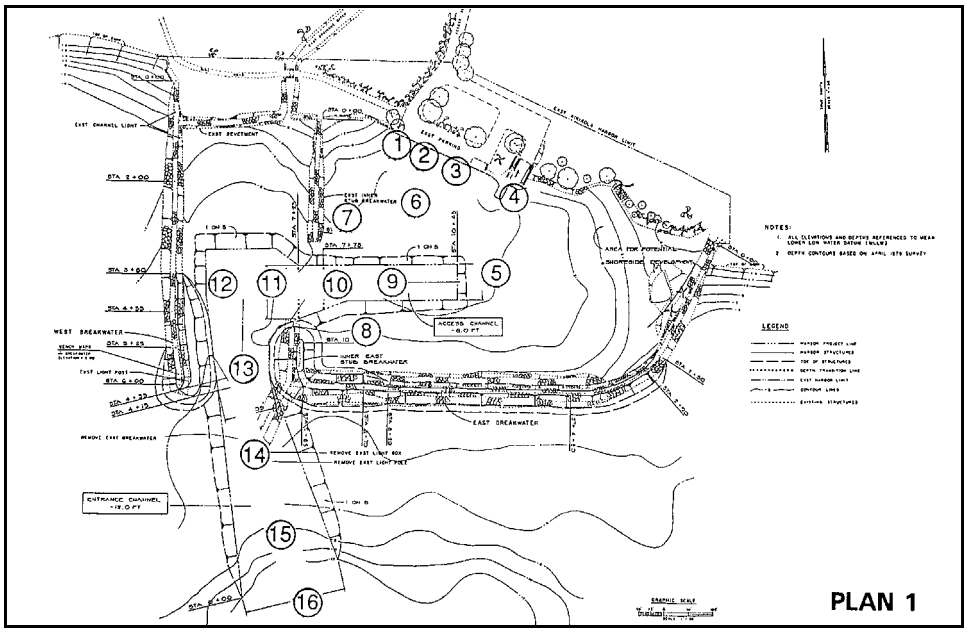

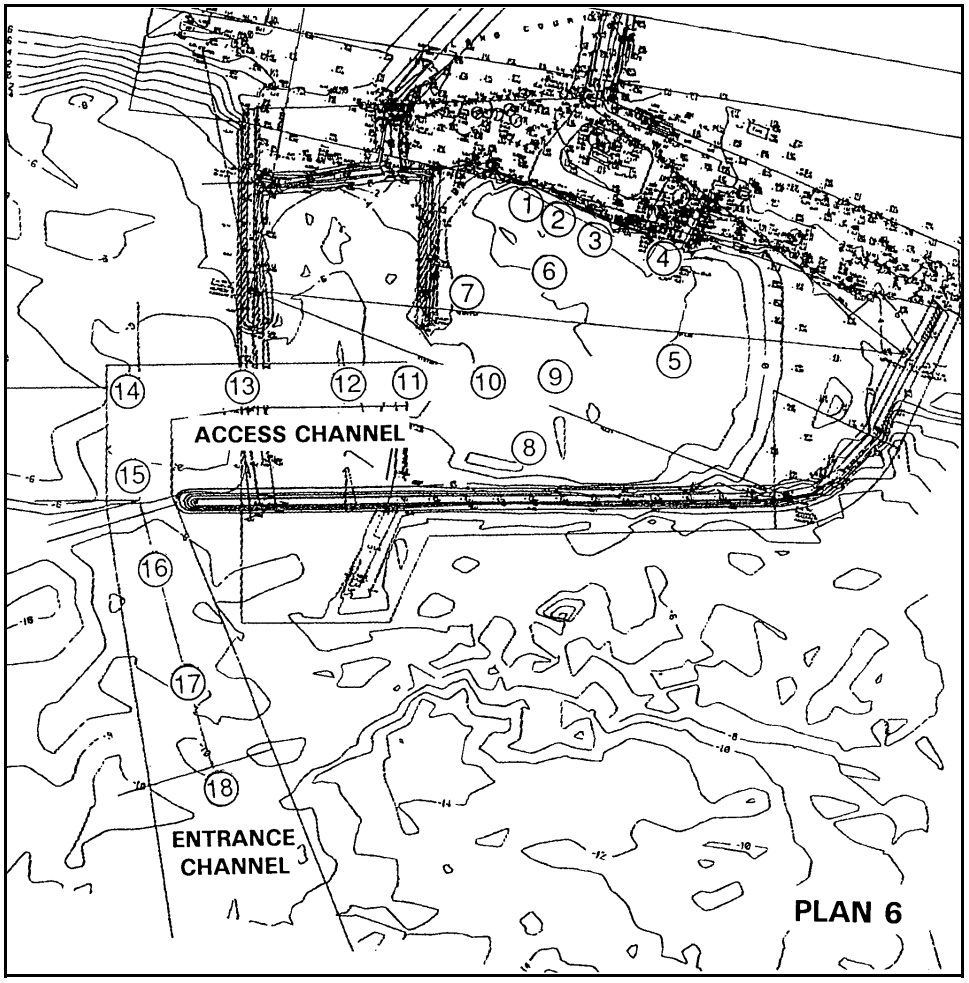

Figure V-5-48. Kikiaola Harbor alternative plans and model stations

- Wave climate at the seaward boundary of the harbor model grid was developed from updated WIS hindcasts in the Pacific OceanAugust 7, 2000. An additional modeling step accounted for sheltering by the islands of Kauai and Niihau as waves approach the harbor. Deepwater wave information was estimated at a point 1.6 km (1 mile) offshore from Kikiaola Harbor. Then, a shallow water transformation model was used to provide wave estimates at the seaward harbor model boundary, at about the 4-m (13-ft) water depth.

- The harbor model grid for the existing harbor consisted of 24,227 elements and 12,461 nodes. Model parameters, including boundary reflection coefficients and bottom friction, were set appropriate to the harbor configuration and model requirements. The tide range at Kikiaola Harbor is about 0.3 m (1 ft). Since harbor response is unlikely to vary much with water level over this small range, a water level of +0.3 m (+1 ft) mllw was used in all runs, representing a high tide condition.

- Wind wave and swell cases were periods ranging from 6 to 22 sec, in 1-sec increments, and approach directions of 164-, 184-, and 204-deg azimuths, representing the range of incident wave directions and entrance exposures. A linear form of the model was used (bottom friction set to zero), so a nominal 0.3-m (1-ft) wave height with each period/direction combination was sufficient. Thus, a total of (17 periods)x(3 directions) = 51 cases was run in the harbor model. Spectral results for each T_p and θ_p needed to represent the incident wave climate were simulated by linearly combining the 51 cases with appropriate weightings based on a JONSWAP spectrum with cos^{2s} directional spreading.

- Snapshots of amplification factor and phase for one incident wave condition illustrate harbor response (Figure V-5-49). A nonspectral condition is shown so that phases can be presented. The amplification factor increases over shoal areas just west of the entrance channel and then steadily decreases as the waves progress through the entrance and into the inner harbor. Plans 1 and 6 provide more shelter to the inner harbor than does the existing plan. Phase lines in the figure show the alignment of wave crests. They give a visual representation of diffraction and shoaling effects on wave direction and length as the 12-sec waves interact with harbor structures and bathymetry.

- Standard operational criteria used by USACE for wind waves and swell in small-craft harbors are:

- H_s in berthing areas will not exceed 0.3 m (1 ft) more than 10 percent of the time.

- H_s in access channels and turning basins will not exceed 0.6 m (2 ft) more than 10 percent of the time.

- To compare with USACE wave criteria, between 15 and 18 stations were selected in each plan, to include the wharf area, berthing area, access channel, and entrance channel (Figure V-5-48). Stations in the existing plan are identical to those shown for Plan 1 except the entrance channel stations are shifted appropriately. Spectral amplification factors were computed and applied to each incident H_s to give a wave climate at each station. The value of H_s exceeded 10 percent of the time was computed at each station. Results for Stations 1-9 are compared to the USACE berthing area criterion and the remaining stations to the USACE access channel criterion (Figure V-5-50). All plans, including the existing, satisfied the berthing criterion at all stations. The inner channel satisfies the channel criterion in all plans. The existing entrance channel does not meet the criterion; and the seaward portions of the Plan 1 and Plan 6 entrance channels slightly exceed the criterion. In conjunction with the increased width of the outer part of the plan entrance channels, the small exceedance of the USACE channel criterion is unlikely to interfere with safe navigation.

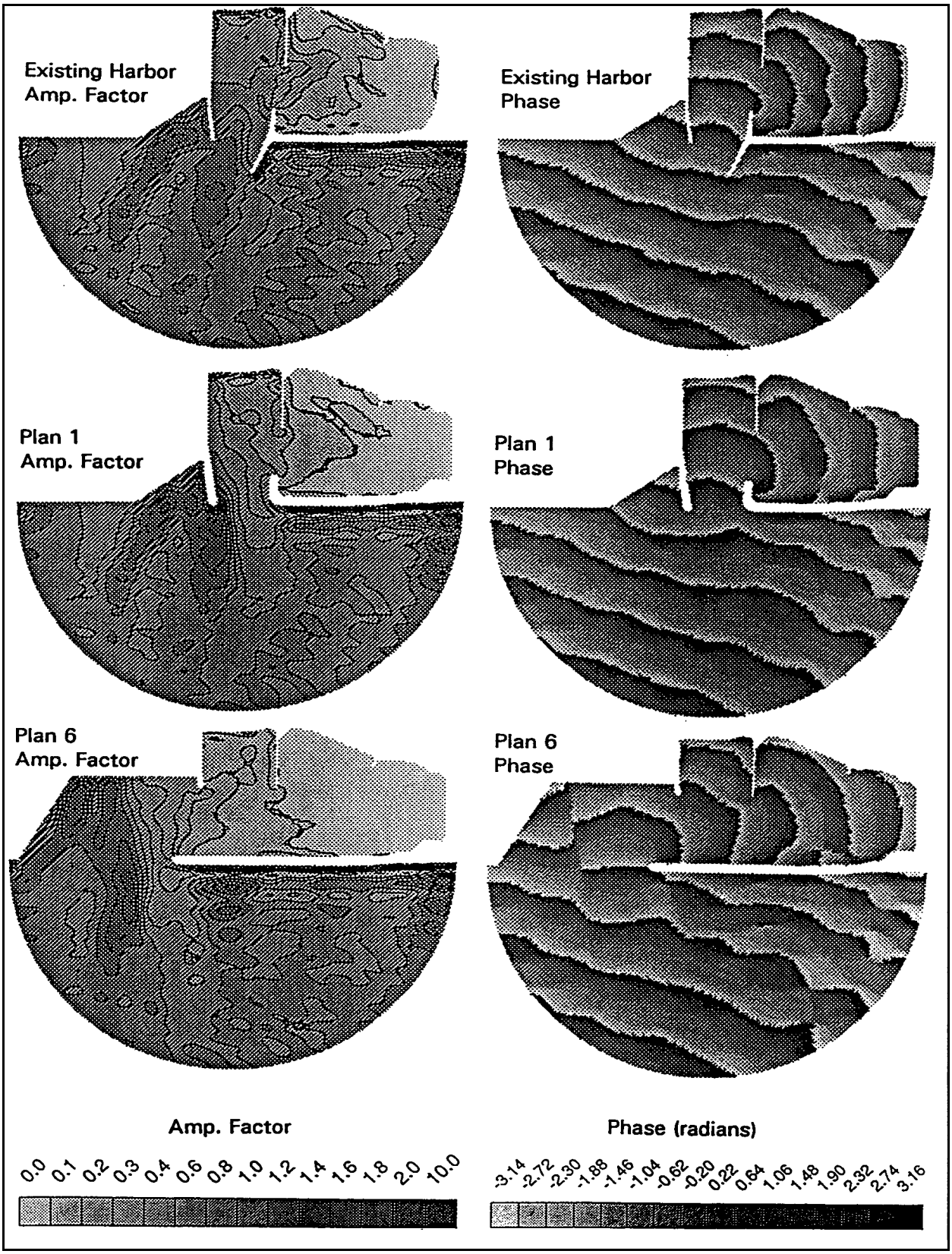

Figure V-5-49. Amplification factor and phase contours, 12-sec wave period, 200-deg azimuth approach direction, Kikiaola Harbor

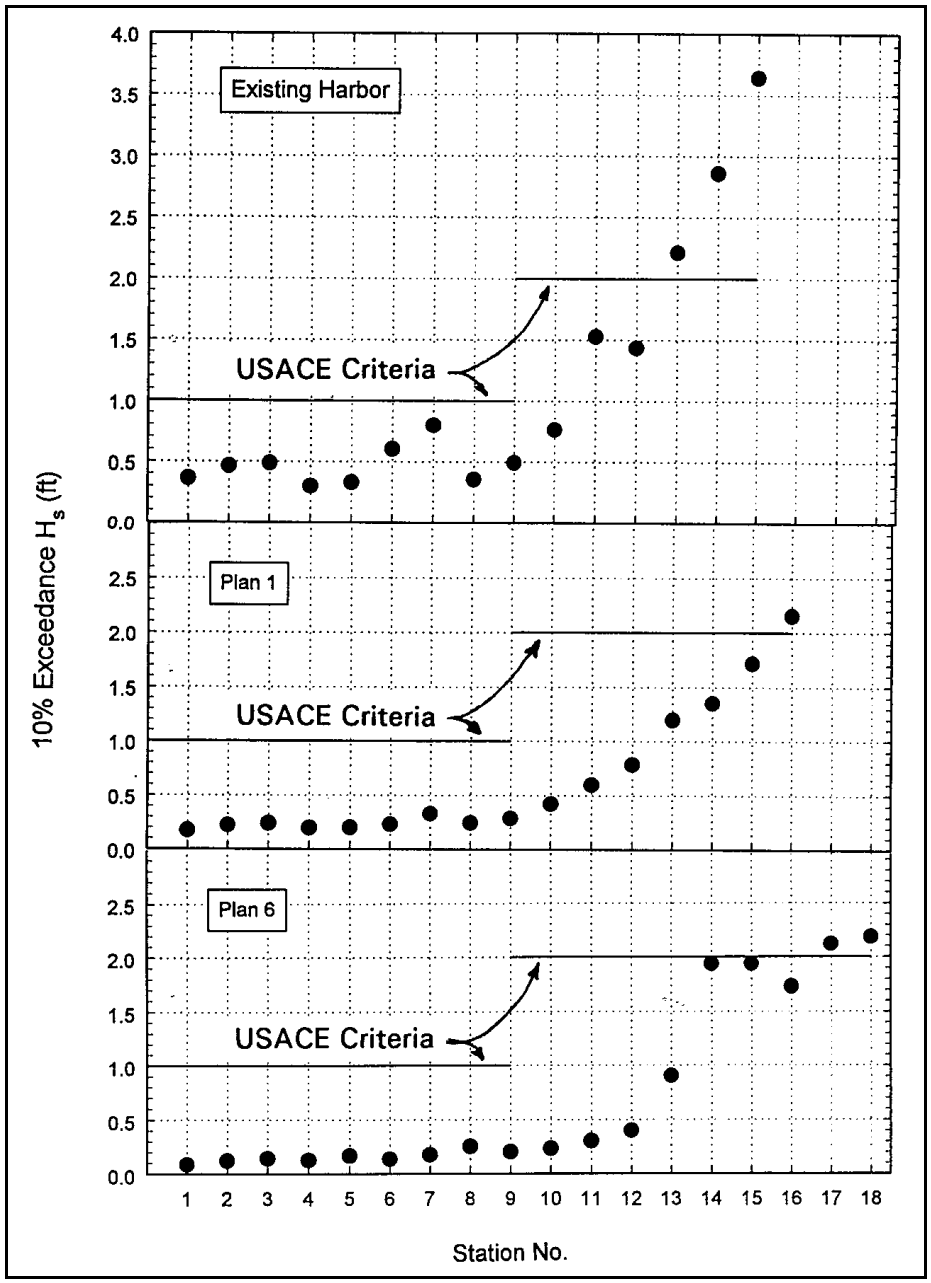

Figure V-5-50. Comparison of H_s exceeded 10 percent of the time, Kikiaola Harbor

- Harbor oscillation characteristics of the existing and plan harbors were also investigated to ensure the plans would not have operational problems due to oscillations. Model parameters were changed to give constant, nonzero bottom friction and full reflection from harbor boundaries. A total of 451 long-wave periods were run, ranging from 25 to 500 sec. The frequency increment between periods was 0.0001 Hz up to a period of 80 sec and 0.00006 Hz for longer periods. Fine resolution in frequency is needed to ensure that resonant peaks are captured. One long wave height is used, representing a moderately energetic long wave case, based on measurements at another Hawaiian harbor. One long wave direction, directly approaching the harbor entrance, is used, since past studies have indicated that harbor response is relatively insensitive to incident long wave direction.

- A snapshot of amplification factors in the existing harbor for a long-period resonance at a period of 150.6 sec represents a simple oscillation between the outer harbor and the east part of the inner harbor (Figure V-5-51). A node (indicated by very low amplification factor) is located a little east of the inner harbor entrance. Considering the most active areas of operational concern, amplification factors at the boat ramp (sta 4) and in the outer harbor (sta 12) were 2 and 3, respectively. A simple basis for judging the operational importance of harbor oscillation amplification factors is given in Table V-5-14 (Thompson, Boc, and Nunes 1998). Thus, the 150.6-sec resonance is not expected to be a problem in operational areas for boats. All amplification factors in all plans across the full range of long-wave periods were significantly less than 5, indicating that harbor oscillations are not a problem in the plan harbors. Additional information on numerical modeling of harbor oscillations is presented in Part II-7-5-f.

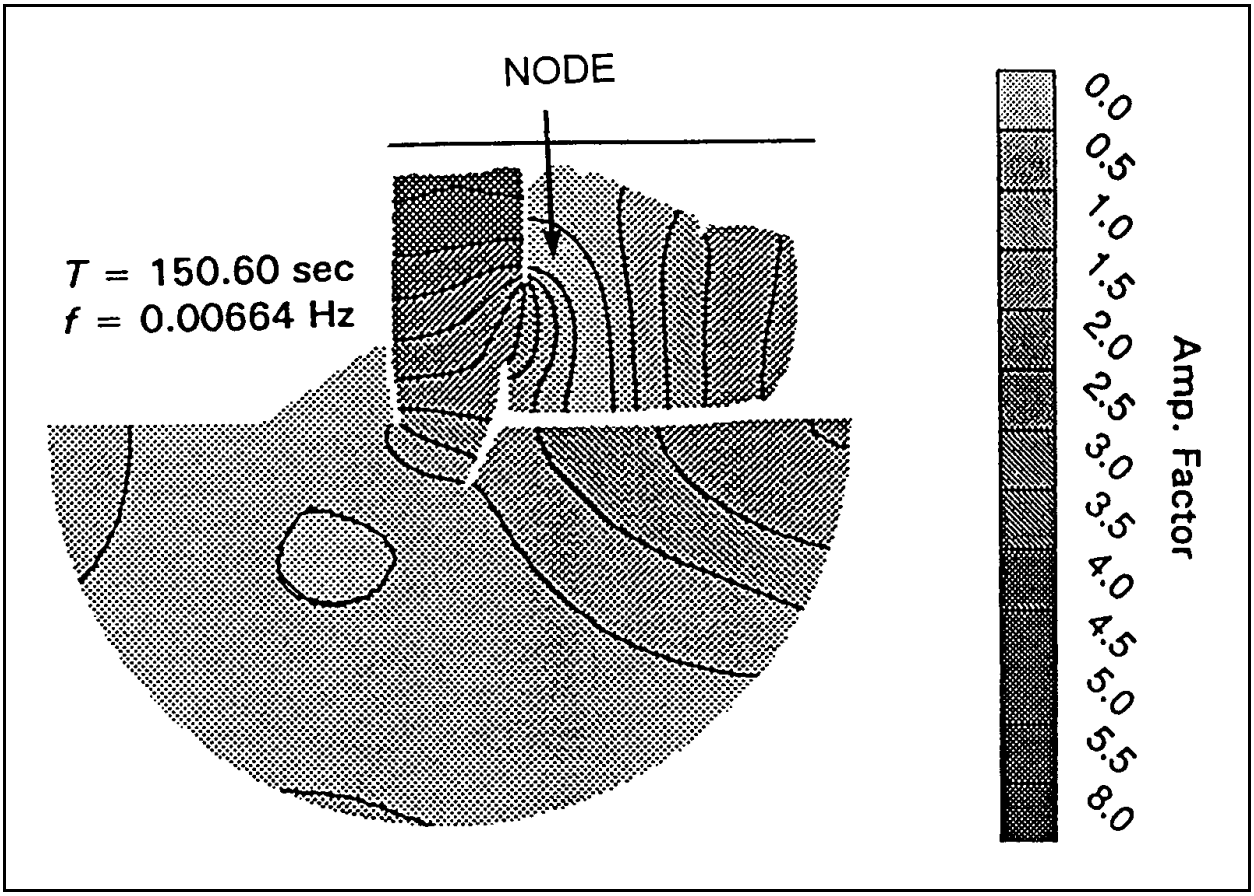

Figure V-5-51. Resonant long wave amplification factor contours, existing Kikiaola Harbor

Table V-5-14
Simple Criteria for Assessing Operational Impact of Harbor Oscillations

Amplification Factor	Operational Impact
> 5	Some problems
> 10	Major problems

(c) Flushing and circulation. Numerical models are effective for evaluating flushing and circulation in harbors and entrances due to forces such as tides and wind. This application is discussed in Part II-7. Numerical models also provide detailed currents along navigation channels needed in ship simulations.

(d) *Example: Maalaea Harbor, Maui, Hawaii.* Maalaea Harbor is a south-facing small-craft harbor located on the southwest coast of the Island of Maui (Figure V-5-52). The harbor facility consists of a 27-m- (90-ft-) wide, 3.7-m- (12-ft-) deep entrance channel and a 0.05-sq-km (11.3-acre) dredged basin. The harbor is protected by a 30-m- (100-ft-) long, 27-m- (90-ft-) wide breakwater on the south side and a 265-m- (870-ft-) long breakwater on the east side. A 91-m- (300-ft-) long paved wharf is located at the shore opposite the entrance. The west and central parts of the harbor are small-craft berthing areas.

Figure V-5-52. Maalaea Harbor, Maui, Harbor (from Air Survey Hawaii, March 1984)

- In response to needs for increased berthing space and better protection during severe wave conditions, the U.S. Army Engineer Division, Pacific Ocean, conducted studies to develop and evaluate harbor modification plans. To evaluate potential impacts on water quality in the harbor, a numerical model circulation and flushing study was conducted for the existing harbor and two proposed plans (Wang and Cialone 1995).

- Circulation in Maalaea Harbor is forced by tide and persistent, often strong winds from the north and northeast. Prototype data were collected over a 9-day period, including currents at two locations and tide. Concurrent wind measurements were available from a nearby airport.

- The numerical model used a curvilinear boundary-fitted coordinate system to generate a computational grid with two vertical layers. It provides current vectors over the harbor and a larger area outside the harbor (Figure V-5-53). The average horizontal grid cell size is 15 m (50 ft). The model is time-dependent, driven with time series of surface elevation along the seaward boundary and wind over the grid surface. Prototype data were used to calibrate the model. Parameters adjusted during calibration include friction, drag, and mixing coefficients.

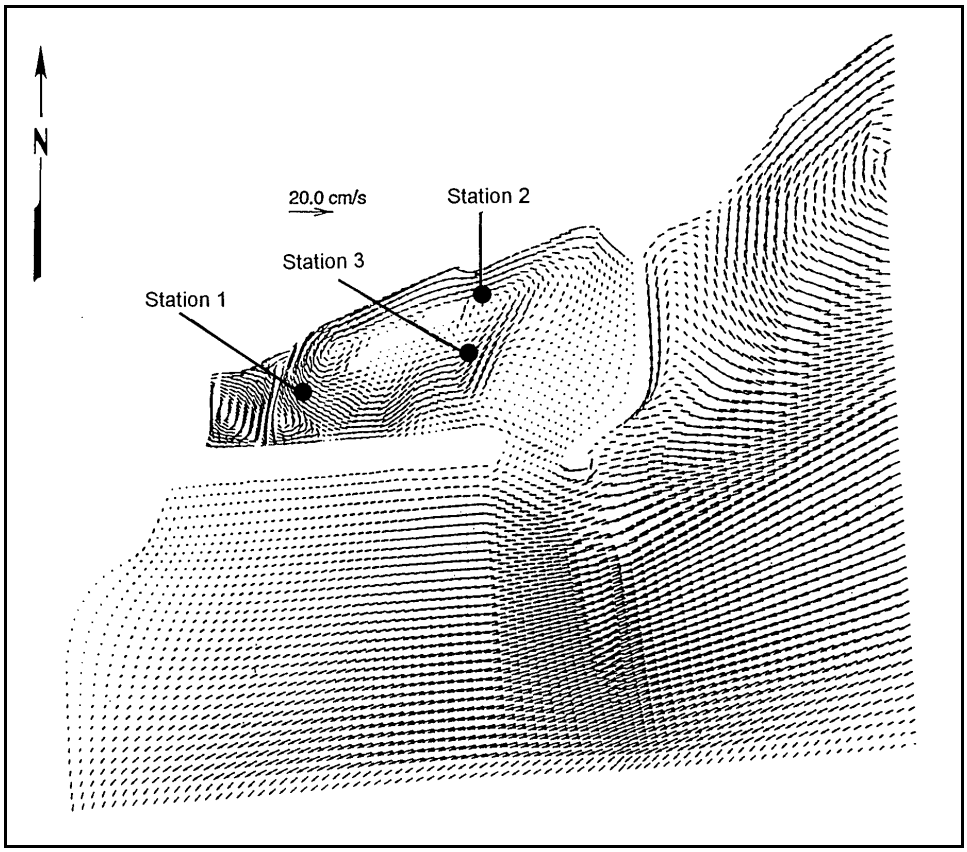

Figure V-5-53. Station locations and surface layer circulation snapshot at Day 3, Maalaea Harbor, existing plan

- Flushing time was defined as the time required for a conservative tracer to decrease to 36.8 percent ($1/e$, $e = 2.71828$) of its initial concentration. This time was evaluated in each plan by beginning a simulation with constant concentration of 100 ppt (parts per thousand) in the harbor and 0 ppt outside the harbor, running the simulation for multiple days, and extracting a concentration time series at three interior harbor stations (Figure V-5-53). Flushing time in the existing harbor was longest at sta 1, in the west part of the harbor and most distant from the entrance (Figure V-5-54). The 2.9-day flushing time was considered acceptable, based on flushing times of 2-4 days as acceptable for design, 4-10 days as marginal, and greater than 10 days as unacceptable (Clark 1983).

(e) Shore response. Possible changes in adjacent shoreline configuration and nearshore bathymetry in response to navigation structures and channel dredging are often a significant concern in navigation projects. Shoreline evolution with and without the project in place can be predicted and analyzed with numerical modeling tools. Guidance on sediment processes at inlets and harbors and numerical modeling options is given in Parts III-2 and V-6.

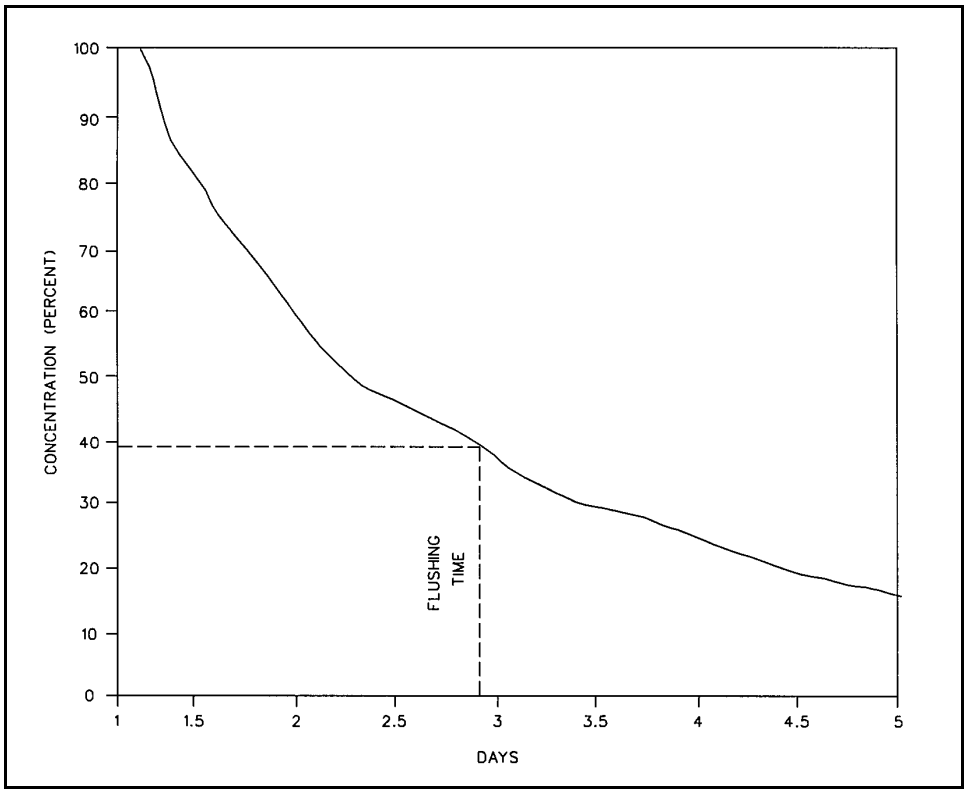

Figure V-5-54. Time series of conservative tracer concentration at sta 1, Maalaea Harbor, existing plan

b. Navigation modeling.

(1) Physical models. Physical models have been used for a variety of navigation studies, with vessel controls such as autopilot, human pilot steering, and free-running vessels with remote control. Physical models are particularly useful for evaluating the behavior of a vessel in the presence of intense, interacting forces, typically involving an entrance channel with ocean waves and possibly harbor or alongshore cross-currents. Waves and human control decisions are statistical processes. Free-running vessel motions in response to many samplings of those processes provide valuable design information about channel depth, width, layout, etc. Vessel position is tracked with high precision relative to channel boundaries in the model. The use of physical models for designing navigation projects is illustrated in the following example.

(a) *Example: Barbers Point Harbor, Oahu, Hawaii*. Barbers Point Harbor is a deep-draft commercial harbor located near the southwest corner of the Island of Oahu, Hawaii (Figures V-5-55 and V-5-56). The harbor was constructed along a previously uninterrupted coastline in 1982. The harbor complex includes a barge basin and small craft marina in addition to the deep-draft basin. The design ship was a general cargo vessel 219 m (720 ft) long with a beam of 29 m (95 ft) and a loaded draft of 10.4 m (34 ft). The entrance channel, designed for one-way traffic, is a constant 137 m (450 ft) in width and 12.8 m (42 ft) mllw in depth over its full length. Just past the coastline, channel depth transitions to 11.6 m (38 ft) mllw, the design depth of the inner channel and deep-draft harbor. The deep-draft basin is approximately 671 m x 610 m (2,200 ft x 2,000 ft) in size, covering an area of 0.37 sq km (92 acres).

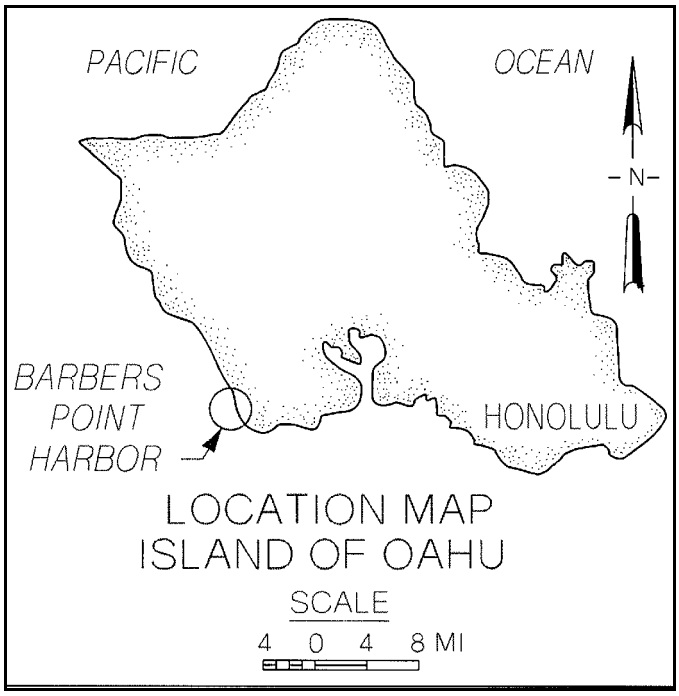

Figure V-5-55. Barbers Point Harbor, Oahu, Hawaii, location map

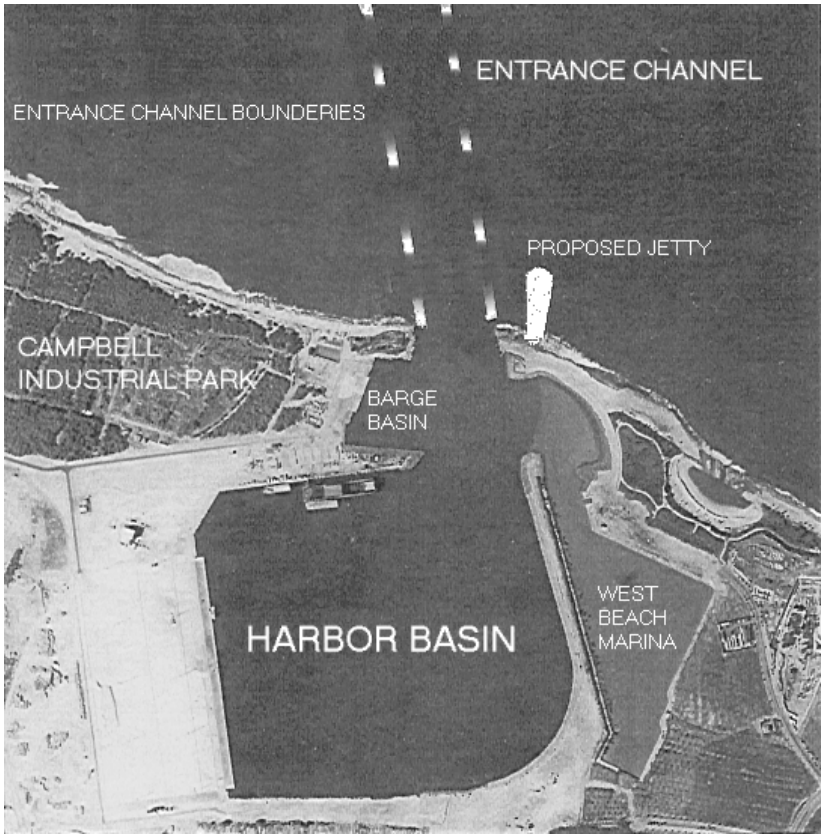

Figure V-5-56. Barbers Point Harbor, Oahu, Hawaii (August 1994)

- Changing economic conditions have created a need for the harbor to serve larger ships. In response to this need, the State of Hawaii and the U.S. Army Engineer Division, Pacific Ocean, sponsored physical and numerical model studies to assist in designing harbor modifications (Briggs et al. 1994, Harkins and Dorrell 1998). The primary study task was to evaluate the navigability of proposed channel and harbor configurations for a larger design ship unaided by tugs.

- A physical model of the harbor complex and adjacent coastal areas was constructed (Figure V-5-57). The model scale, 1:75 undistorted, was selected for proper reproduction of important harbor features, storm waves and longshore currents, and the design ship. Model bathymetry extended to the 30-m (100-ft) mllw bottom contour and a distance of about 1,067 m (3,500 ft) along the coast on either side of the entrance channel. Total area covered by the model was over 1,000 sq m (3,500 sq ft). A directional spectral wave maker was placed seaward of the modeled bathymetry. Longshore currents, which affect navigation in the existing harbor, were created in the model with a system of PVC pipe extending along each lateral boundary (with diffuser ports) and meeting at a pump station located behind the model, landward of the coastline. Pump controls allowed generation of longshore currents in either direction. Diffuser ports were open or plugged as needed to achieve desired current patterns.

Figure V-5-57. Physical model of Barbers Point Harbor

- Two design ships were identified, based on anticipated use of the harbor for container and bulk coal traffic. Existing ships were selected as representative of future harbor traffic, the *President Lincoln*, a C9 container ship with capacity of 2,900 TEU operated by American President Lines, and the *Bunga Saga Empat*, a bulk carrier (Figure V-5-58). The design bulk carrier was a modified version of the *Bunga Saga Empat*, with length increased by 30 m (100 ft). Design ship dimensions are summarized in Table V-5-15.

Figure V-5-58. Bulk carrier *Bunga Saga Empat*

Table V-5-15
Design Ship Dimensions for Barbers Point Harbor Studies

	Prototype Ship Dimensions	
	Container Ship	**Bulk Carrier**
Length Overall	262 m (860 ft)	259 m (850 ft)
Beam	32 m (106 ft)	32 m (106 ft)
Fully Loaded Draft	11.9 m (39 ft)	13.7 m (45 ft)

- Model ships were constructed to match the harbor model scale, 1:75 (Figures V-5-59 and V-5-60). Model ships were self-powered by onboard batteries. Forward and reverse speeds, rudder angle, and, for the container ship, bow thruster direction and speed were remote-controlled.

- A set of design transit conditions was selected for simulation. Prototype measurements of waves and currents near the harbor entrance were available. Wave data were collected over a period of approximately 4 years; currents were collected over a 65-day period. For harbor plan evaluation, the following conditions were used. The highest measured H_s values and a representative range of T_p and θ_p were selected, a total of eight wave conditions. The range of H_s and T_p values was 2.1 to 3.0 m (7.0 to 10.0 ft) and 6 to 18 sec, respectively. Longshore currents were selected to represent average, normal, and extreme conditions from both directions. Extreme currents were 0.41 m/sec (0.80 knot) from the north and 0.33 m/sec (0.65 knot) from the south. Based on data from a nearby airport, severe wind speeds of 10.3, 12.9, and 20.6 m/sec (20, 25, and 40 knots) were selected.

Figure V-5-59. Model bulk carrier

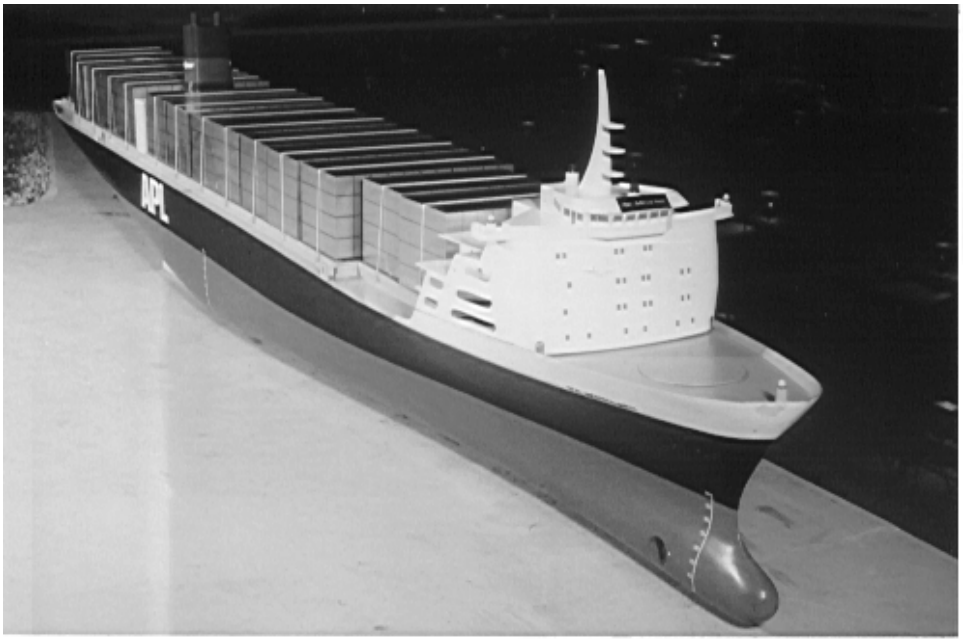

Figure V-5-60. Model container ship

- Six harbor plans were studied with varying combinations of the waves, current, and wind, as selected for design transit conditions. Wind forces were simulated with a ship-mounted fan. Model ships were guided by remote control between deep water and the protected harbor. Both inbound and outbound runs were made. Two experienced local pilots assisted in verifying the model setup and conducting some of the runs. Inbound runs were significantly more difficult than outbound runs. The ship must slow in approaching the entrance and it becomes more difficult to control. Typical inbound ship speeds are 13.0 km/hr (7 knots) at the seaward end of the entrance channel, 7.4-9.3 km/hr (4-5 knots) in the vicinity of the coastline, and 3.7-5.6 km/hr (2-3 knots) in the harbor. After a recommended harbor plan was identified, a number of channel/harbor depth variations were studied to optimize design depths. A total of nearly 2,000 runs were made, of which the majority were inbound.

- Navigability was evaluated by several methods during the course of the model studies. Ship operators recorded their observations after each run, with particular attention to any difficulties during the run. An overhead video camera recorded each run. A commercial motion analysis system was used to collect and analyze model ship motions. The system uses digital cameras and strobes to track reflecting balls. Six balls were mounted on the model ship (e.g., Figure V-5-59) and four were placed at fixed locations around the channel. After processing, the system provides a time series of clearance between ship hull and bottom.

- Physical model data on ship horizontal and vertical clearance in the channel were evaluated in a probabilistic assessment of channel design. The design then includes a consideration of the natural variability of wave, current, wind, ship track, and ship response, which is crucial in realistically assessing the probability of a momentary grounding event during ship transit. Thus risk of design ship contact with channel sides or bottom can be incorporated into the design process. The expected time interval between C9 container ship grounding events as a function of number of transits per year illustrates risk information available for design (Figure V-5-61). Since several different methods for estimating probabilities were applied to the physical model tests, the average from all methods is shown, bracketed by best and worst expected performance based on variability in the methods. Additional details are given by Briggs, Bratteland, and Borgman (2000).

- The recommended plan differs from the existing harbor in the following ways:

- Entrance channel is deepened and flares out at the seaward end to allow ships more maneuvering space during initial approach.

- Transition from entrance channel depth to harbor depth is moved from the coastline to the inner harbor basin opening. This change moves the transition to a lower wave energy environment and gives pilots more space to correct when vessel shear occurs at the depth discontinuity.

- Harbor is deepened and expanded in size by excavation in the east part of the harbor.

(b) Additional information, based on numerical model studies of Barbers Point Harbor oscillation characteristics, is available in Part II-7.

(2) Ship simulations. Increasingly, deep-draft channels are being designed using ship simulators. For example, the USAERDC ship simulator is schematized in Figure V-5-62. Ship simulations typically have pilots operate the steering wheel and ship controls and navigate a realistic course in real time. Pilots give verbal commands for tug assistance as needed, and an assistant operates tug controls. Pilots are drawn from professional pilot associations serving the project area. Their experience and intuition aids in evaluating existing projects as well as refining and studying new alternatives for safe and optimum channels and/or

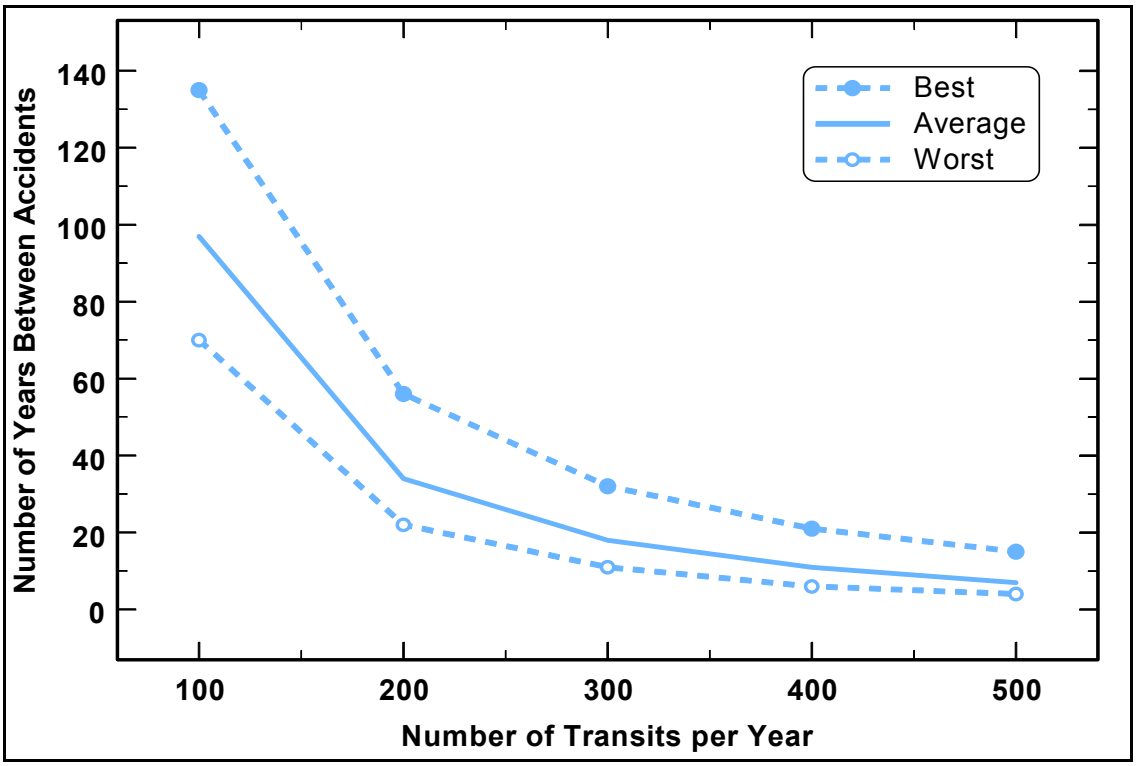

Figure V-5-61. Probability assessment for C9 container ship navigating recommended entrance channel, Barbers Point Harbor

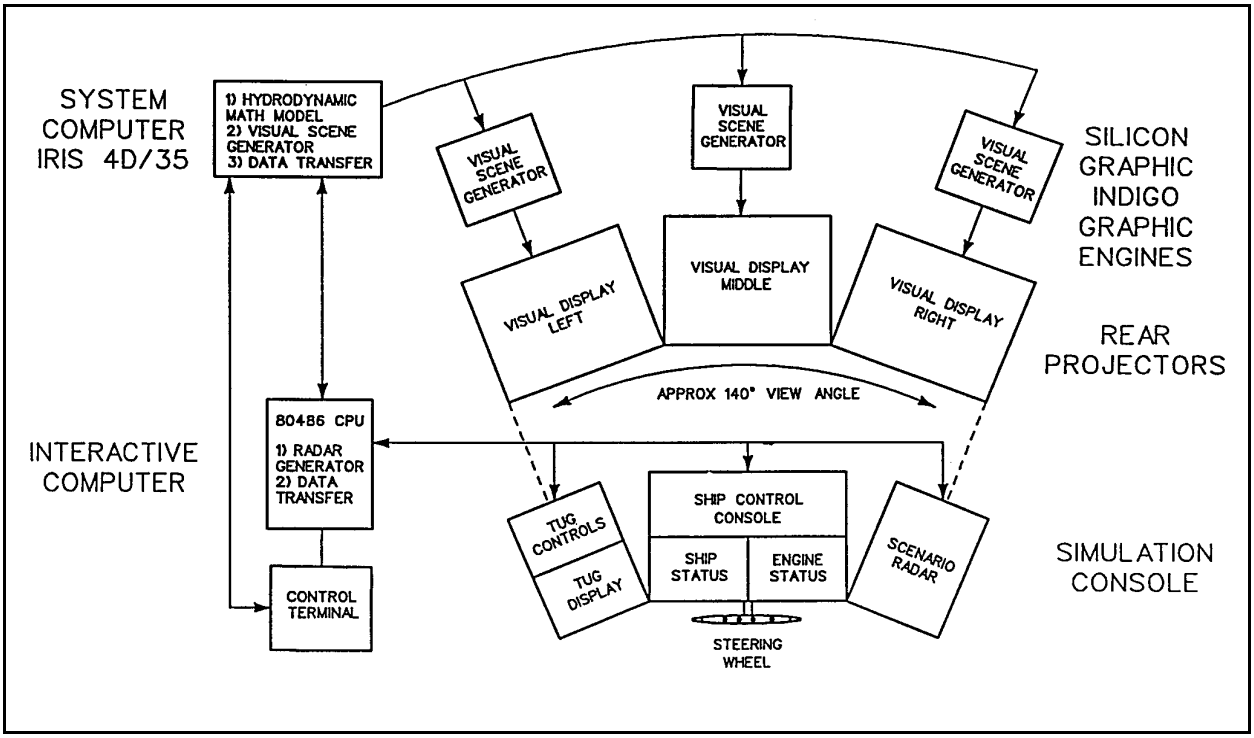

Figure V-5-62. USAERDC ship simulator system

turning basins. At some levels of project design, simulators may be used advantageously for fast-time runs with either autopilot or human control instead of a more comprehensive and costly real-time pilot evaluation program.

- Simulators are special numerical models involving representations of a ship, navigation channel, currents, wind, visual scene (including view over the ship, aids to navigation, bridges, docks, and other visual features needed for piloting cues and adequate realism), radar image, tugs and thrusters, ship bridge controls, and typical bridge instruments. Simulated forces and effects are depicted in Figure V-5-63. The ship model(s) experiences these forces and effects in ways similar to the prototype ship(s).

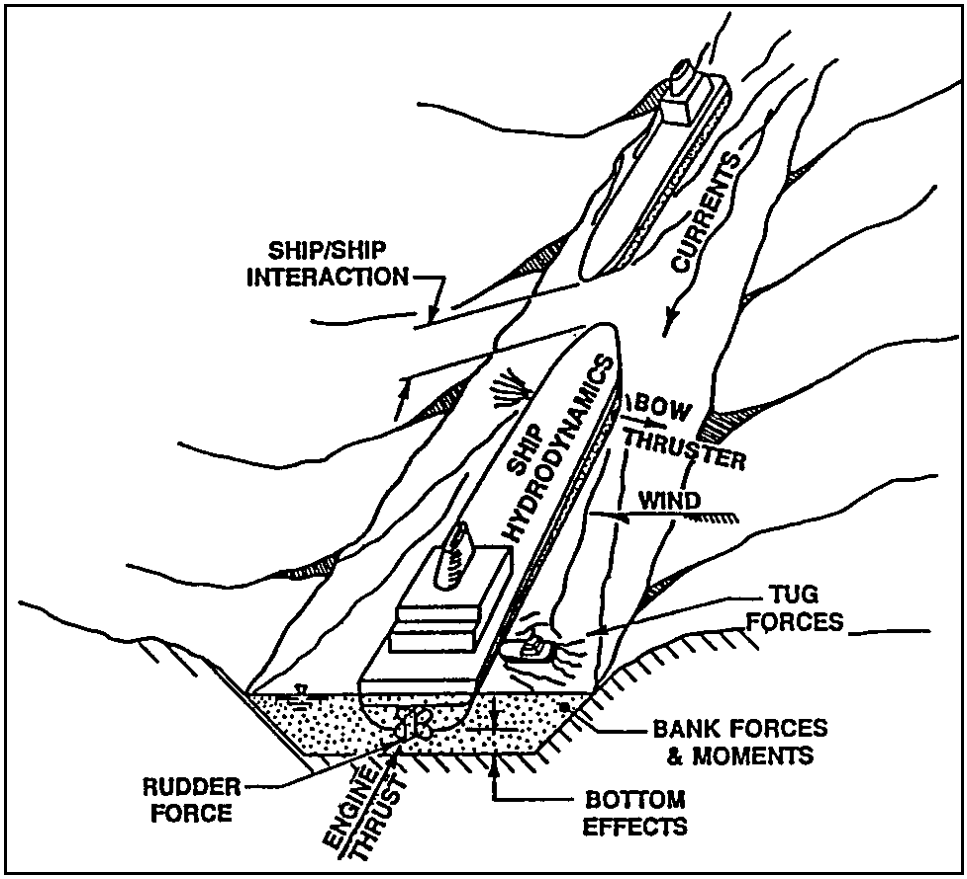

Figure V-5-63. Ship simulator forces and effects

- The key steps in a real-time simulation are shown in Figure V-5-64. Output information saved at selected short time intervals during a simulation includes ship position, engine and rudder settings, ship movement information (speed, heading, rate of turn, drift angle), and minimum clearance relative to channel boundaries. If tugs are used, information on tug forces imposed on the ship may also be saved.

- Two example ship simulator studies are discussed in the following paragraphs. More information on ship simulators is available from USACE (1998), Webb (1994), and PIANC (1997a).

(a) *Example: Alafia River Harbor, Florida*. The Alafia River Harbor is located along the eastern shore of Hillsborough Bay, about 13 km (8 miles) southeast of Tampa, Florida (Figure V-5-65). The

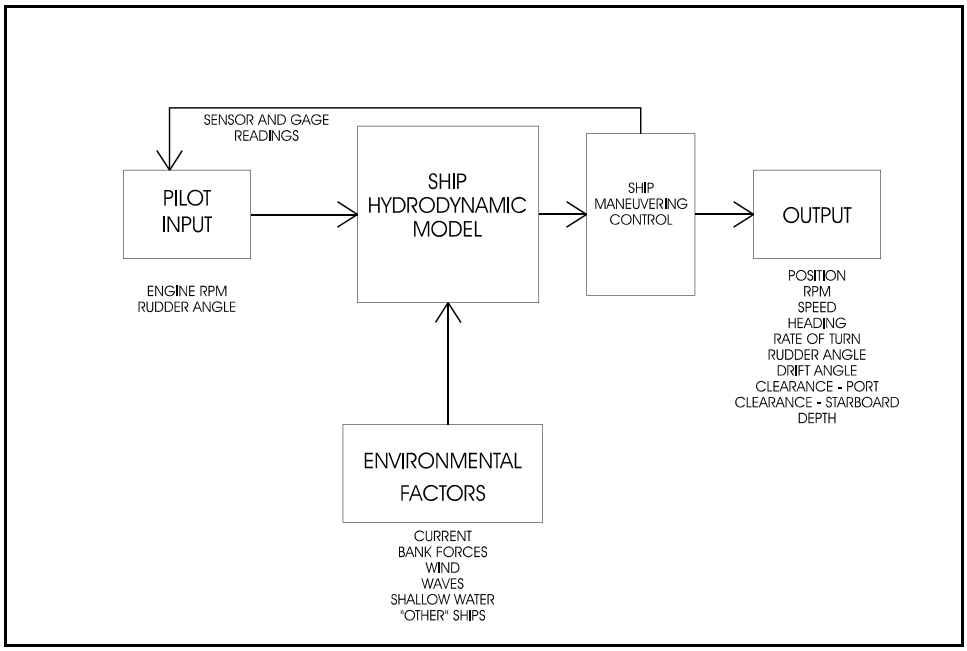

Figure V-5-64. Real-time simulation

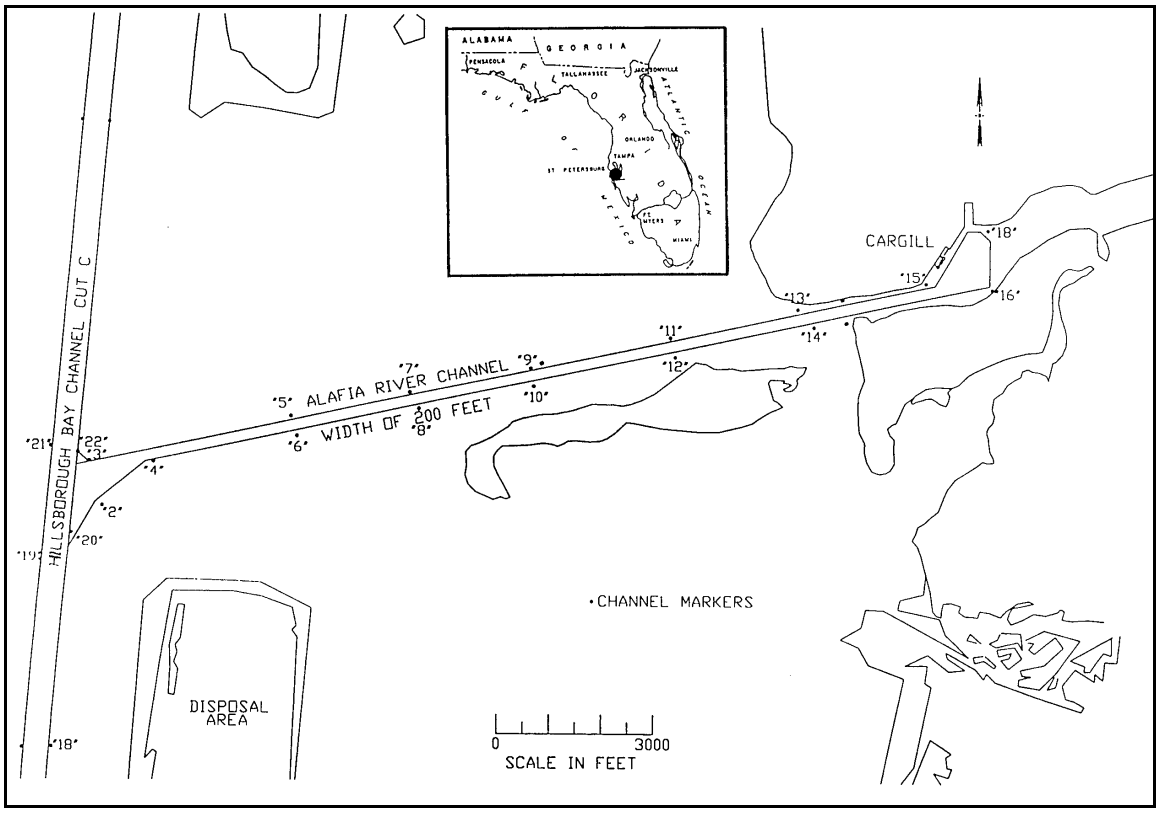

Figure V-5-65. Existing Alafia River Channel and turning basin

existing federally maintained project consists of a turning basin adjacent to the dock facilities and a channel connecting the turning basin to Hillsborough Bay Channel Cut C, the primary north-south shipping channel in Hillsborough Bay. Total length of the federal project is 5.8 km (3.6 miles). Channel depth is 9.1 m (30 ft) mllw. Channel width is 61 m (200 ft). The turning basin is 213 m (700 ft) wide and 366 m (1,200 ft) long.

- Alafia River Harbor is used mainly to ship phosphate rock and bulk phosphate products. Ships typically enter the harbor in ballast and load bulk materials until the ship draft reaches the limit allowed in Alafia River Channel or until the ship is fully loaded. Ships turn in the turning basin at the start of the outbound run, in a loaded condition.

- The U.S. Army Engineer District, Jacksonville, funded ERDC to conduct a ship navigation simulation study to investigate performance of two proposed plans for upgrading the Alafia River Channel and turning basin to accommodate larger ships. A notable part of the study is the detailed visual scene developed to provide pilots with realistic visual cues. The cues are a crucial part of slowing the ship on approach to the turning basin, approaching the dock, and turning the ship for the outbound run. Figure V-5-66 shows two pilots operating a bulk carrier. One pilot is guiding the ship, the other is operating tug controls on command. The ship has just entered the turning basin and turned toward the dock. The view direction (which is easily selected by the pilot) is to starboard, with the ship bow visible at the right side of the scene. The Alafia Channel heading out to Hillsborough Bay is visible at the left side, including a channel marker in the foreground. The dock and dock-side loading facilities are just to the left of the ship bow. Further left are numerous small trees and a line of rail cars. This scene adjusts continuously as ship position or pilot view direction change. Additional details of the study are given by Thompson et al. (1998a).

Figure V-5-66. Visual scene of Alfia River Harbor ship simulation study, inbound bulk carrier approaching dock

(b) *Example: San Juan Harbor, Commonwealth of Puerto Rico*. San Juan Harbor is located on the north coast of Puerto Rico, with open exposure to the Atlantic Ocean (Figure V-5-67). It is the largest port in Puerto Rico and a major container port. Noncontainerized cargo, such as petroleum products, lumber, grain, automobiles, and steel, is also imported to the island by sea. Rum, Puerto Rico's principal export, is shipped in containers. Cruise vessels frequently call on San Juan Harbor.

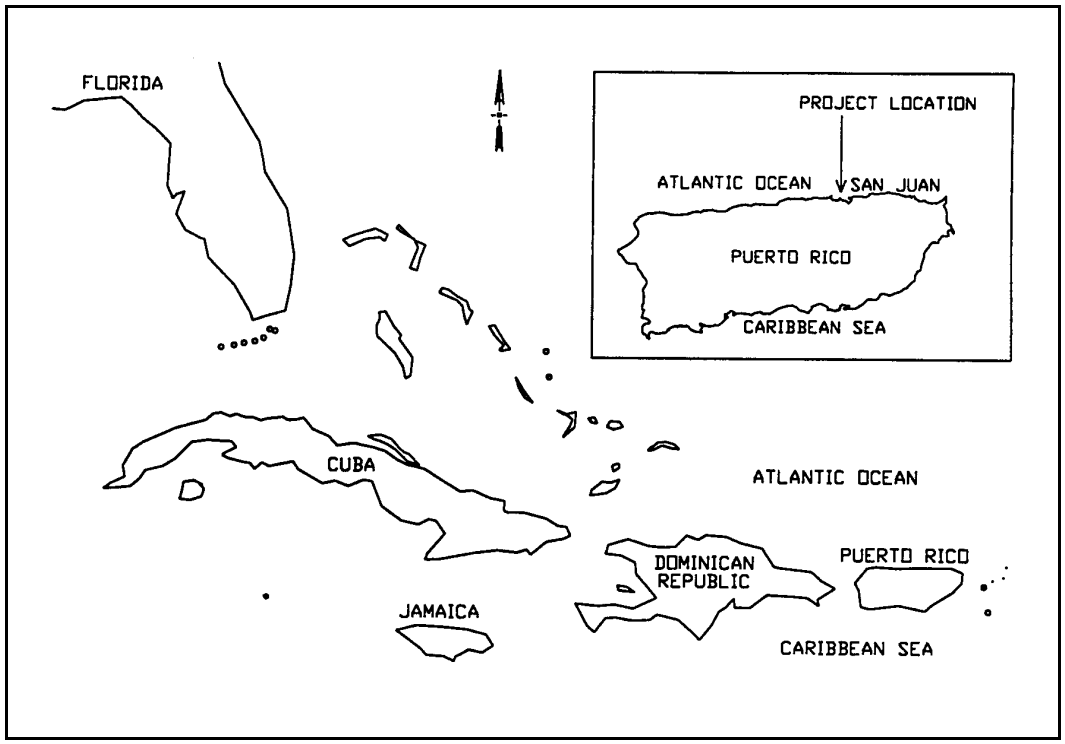

Figure V-5-67. San Juan Harbor, Commonwealth of Puerto Rico, location map

- Federally maintained channels include an entrance channel (Bar Channel), a main interior approach channel to the harbor complex (Anegado Channel), and three interior channels forming a triangular path accessing the principal dock areas (Army Terminal, Puerto Nuevo, and Graving Dock Channels) (Figure V-5-68). Design depth of the outer Bar Channel is 13.7 m (45 ft). The deepest approach to the harbor is the S-shaped path along Bar, Anegado, and Army Terminal Channels, with a controlling depth of 11.0 m (36 ft). Puerto Nuevo and Graving Dock Channels have design depths of 9.8 and 9.1 m (32 and 30 ft), respectively. Bar and Anegado Channel widths are 152 and 305-366 m (500 and 1,000-1,200 ft), respectively. The other three channels have design widths of between 91 and 122 m (300 and 400 ft).

- Wind and waves strongly affect the harbor entrance. Winds are usually steady and are described as being between 8 and 10 m/sec (15 and 20 knots) predominantly from the east and northeast. Waves typically approach the entrance from the north, northeast, and east, with significant heights up to 6-7 m (20-22 ft) during severe events.

- Pilots typically board inbound ships when they are 4.8 km (3 miles) from the harbor entrance. The entrance channel can be difficult to navigate in the presence of wind and wave conditions. Ships must maintain speed in the entrance channel for control, yet they must slow to make the relatively sharp turn into Anegado Channel. All documented accidents in recent years are groundings that have occurred on the south side of this turn. The turn is difficult for outbound ships, too, because of the

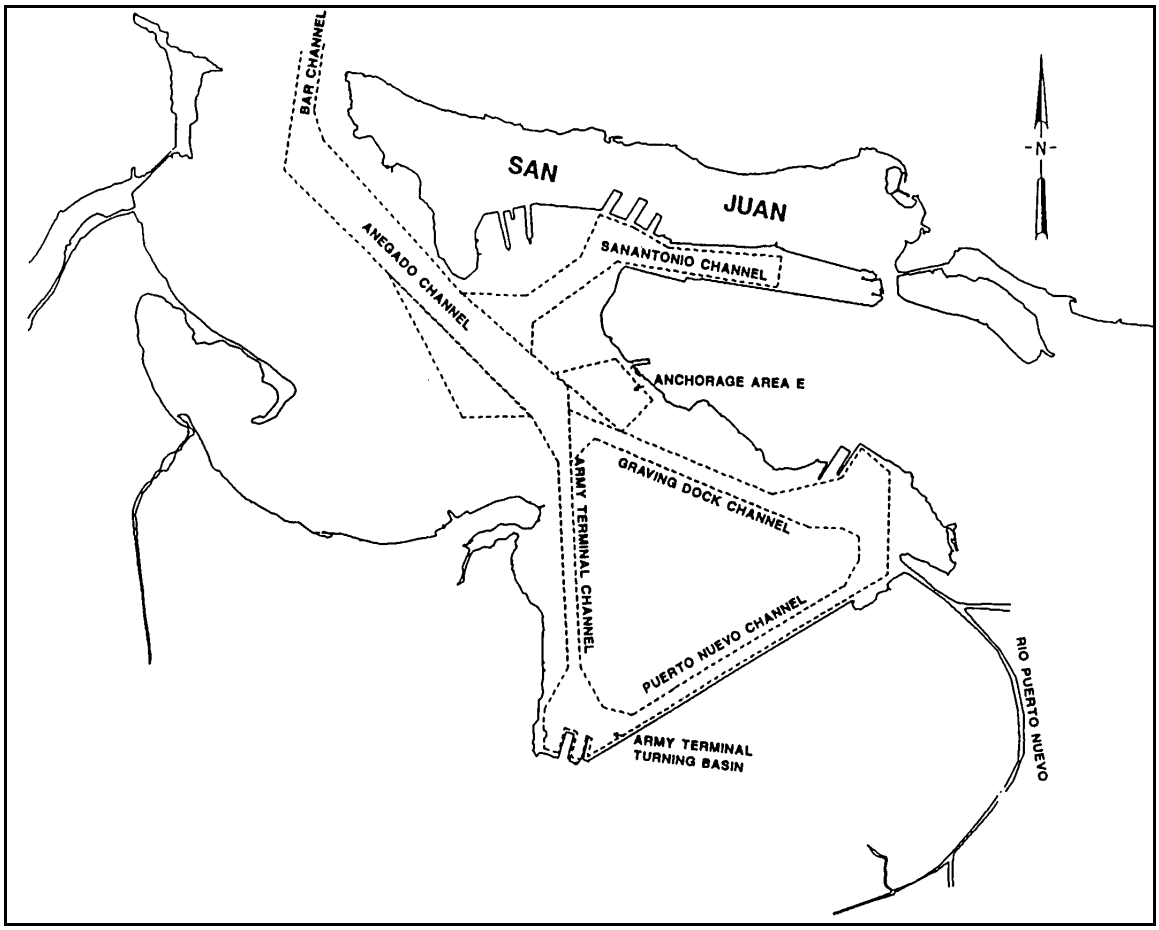

Figure V-5-68. San Juan Harbor channels

relatively narrow entrance channel. Sharp turns associated with the relatively narrow interior channels can also be difficult to navigate.

- The U.S. Army Engineer District, Jacksonville, funded a real-time ship simulator study of existing and two proposed alternative plans to address navigation concerns in San Juan Harbor channels and to allow access to deeper draft ships (Webb 1993). Controlling depth in the proposed plans is 11.9 m (39 ft) in Anegado, Army Terminal, and Puerto Nuevo Channels and 11.0 m (36 ft) in Graving Dock Channel. The purposes of the simulator study were to determine effects of the proposed improvements on navigation, to optimize channel width and alignment for safe and efficient navigation, and to determine necessary depths in Bar and Anegado Channel sections affected by waves.

- Design transit conditions were developed. A wind from the northeast was used with a speed of 10.3 m/sec (20 knots) in the outer entrance. Wind speed was decreased to between 0 and 7.7 m/sec (15 knots) in interior areas sheltered by bluffs and/or tall buildings. Wave information from a 20-year hindcast was used to define incident wave conditions for moderate and heavy seas. A numerical model transformed the selected incident wave conditions to the harbor and through the entrance, giving wave estimates along the channel. For simulation, incident H_s was 4.6 m (15 ft), coming from the northeast. This H_s is about the practical upper limit for ships to enter the harbor. The H_s progressively decreased along Bar Channel to 1.2 m (4 ft) and then to 0 after the turn into Anegado Channel. Tidal currents in the channels were determined with a numerical model of the

harbor embayment. Currents are very small. Since flood tide tends to reduce control of ships entering the harbor, flood tide currents were used with all simulations. A wave-driven cross-current of 0.3 m/sec was added in the more exposed section of the Bar Channel, based on pilot comments.

- Two design ships were used, a tanker 232.6 m (763 ft) in length (LBP) with a 38.1-m (125-ft) beam and a container ship 246.9 m in length (LBP) with a 32.3-m (106-ft) beam. The inbound tanker draft (loaded) was 9.8 m (32 ft) for the existing channels and 11.0 m (36 ft) for proposed channels. The outbound tanker draft (in ballast) was 7.9 m (26 ft). For both inbound and outbound runs, the container ship draft was the same as the inbound loaded tanker draft.

- The simulation was validated with the assistance of two pilots from the San Juan Harbor Pilots Association. Simulations were conducted in three 1-week periods. A total of six licensed San Juan Harbor pilots conducted the simulations (two per week), giving a representative range of experience and piloting strategies. Pilots completed a written questionnaire immediately after each run, including a rating scale of key project features. Some desirable modifications to the proposed plans emerged after the first week of simulations. The plans were adjusted to improve navigation in localized areas with difficult clearance and/or to reduce dredging in areas not needed for navigation.

- Design depths for the wave-influenced Bar and outer Anegado Channels were developed in a separate study component. A range of wave conditions and ship speeds were considered. The sum of vertical ship motion and squat was used to define the required underkeel clearance to be added to the 11.0-m (36-ft) ship draft. Because wave height decreases along the Bar Channel, a stepped design depth was recommended, with depth of 16.8 m (55 ft) at the seaward end of Bar Channel progressively decreasing in three steps to 13.7 m (45 ft) through the turn into Anegado Channel.

- Results from the simulations were summarized to evaluate proposed plans. For example, average pilot ratings for inbound container ship runs indicate the plans will significantly improve harbor access, especially in Puerto Nuevo Channel and at the turn separating it from Army Terminal Channel (Figure V-5-69). The wider entrance channel in the plans gives a significant improvement. Ship track plots from all runs show how the increased width and gentler turn would be used in navigation (Figure V-5-70). An unused area on the outside of the proposed turn is defined by the envelope of ship tracks. Simulations indicated that a ship could not enter this area and still turn safely. Therefore, one study recommendation was that the unused area be deleted from the plan, reducing dredging requirements. Complete results, conclusions, and recommendations are given by Webb (1993).

c. Specialized field studies.

(1) Harbors. As field measurement and data collection techniques have advanced, field studies have become powerful and reliable for documenting the behavior of existing harbors. However, the cost for comprehensive field studies is significant, and such studies are generally practical only for large projects with high economic impact. Typically, field data are used for calibration and validation in physical and numerical model studies. Field data helpful for harbor studies include incident directional waves, water levels, waves and currents at several interior locations, and winds. The data provide valuable information about harbor response to wind waves and swell, entrance channel wave conditions, harbor oscillations, and circulation and flushing. A representative, but extensive, field data collection program in the massive Los Angeles and Long Beach, California, harbor complex is described by Seabergh, Vemulakonda, and Rosati (1992). The program was aimed at enhancing physical and numerical models used in harbor planning.

(a) *Example: Kahului Harbor, Maui, Hawaii*. Kahului Harbor, located on the north shore of the Island of Maui, is the island's only deep-draft harbor and the busiest port in Hawaii outside of the Island of Oahu

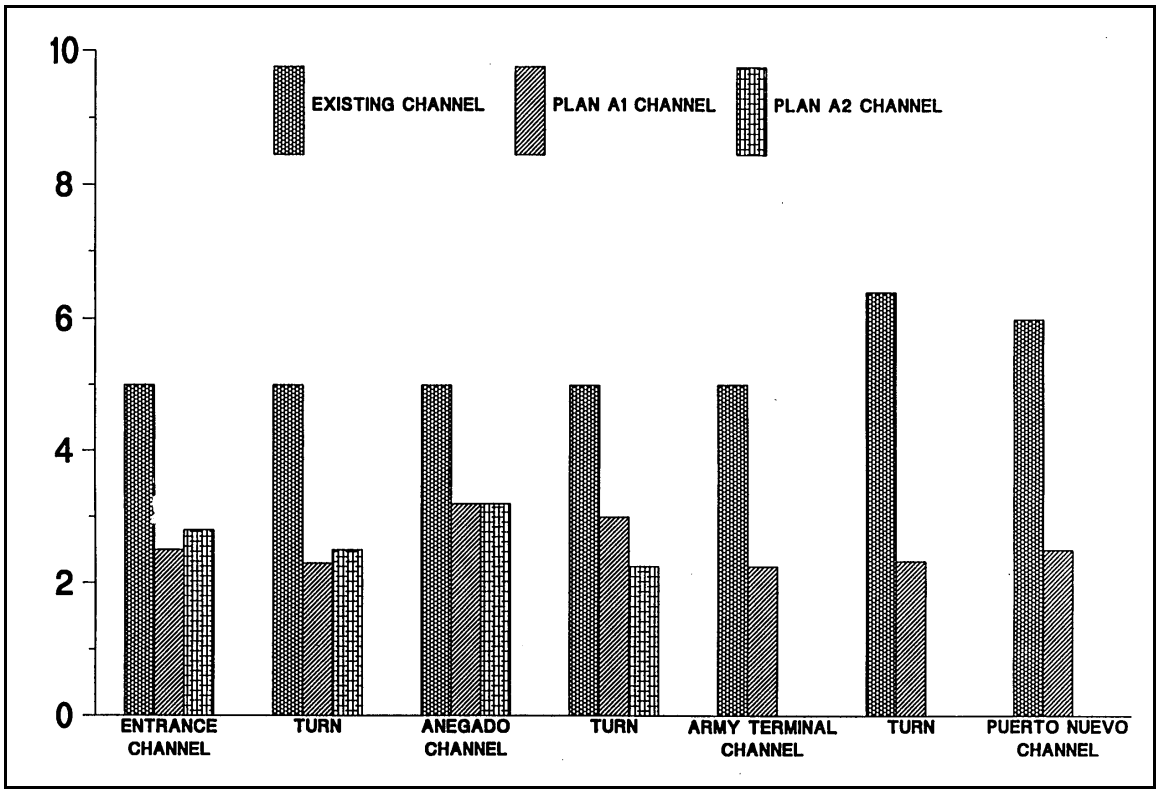

Figure V-5-69. Pilot degree of difficulty ratings, inbound container ship, San Juan Harbor

(Figure V-5-71). Commercial piers are presently on the east side of the harbor. In conjunction with long-term planning for expanded harbor usage, a field wave data collection program was established in the harbor. The program included an offshore directional array to measure incident waves and four pressure gauges in the harbor interior (Figure V-5-72). Interior gauge locations were determined with the assistance of a preliminary numerical model study of harbor wave response (Okihiro et al. 1994).

(b) Data from more than 1 year were collected and proved to be very helpful in subsequent harbor wave response, modeling, and planning studies (Thompson et al. 1996, Okihiro and Guza 1996).

(2) Ship tracking. The optimum depth and width of proposed navigation channel improvements may be determined with increased accuracy by measuring actual ship motions. The measurement program should encompass a significant number of transits of the route during adverse conditions. Availability of differential Global Positioning System (DGPS) apparatus for recording accurate ship fixes (±3 m) at a rapid rate (0.2 Hz or faster) makes this an affordable component of feasibility studies. Commercial software is available for data recording and display in formats applicable to channel design. These systems use standard DGPS receivers compatible with the U.S. Coast Guard network of DGPS radio beacons, as illustrated in Figure V-5-73. A time series of fixes is recorded with concurrent gyrocompass headings and other data, such as engine rpm, rudder angle, and relative wind speed and direction.

(a) Commercial gyrocompasses aboard seagoing cargo vessels usually provide heading accuracy of ±0.3 deg or better. Concurrent time series of position and heading define the swept path of the vessel. Comparison of ship tracks with tidal currents, winds, waves, water levels, visibility conditions, and other environmental conditions present at the time of recording, provide channel designers with realistic parameters for width computations.

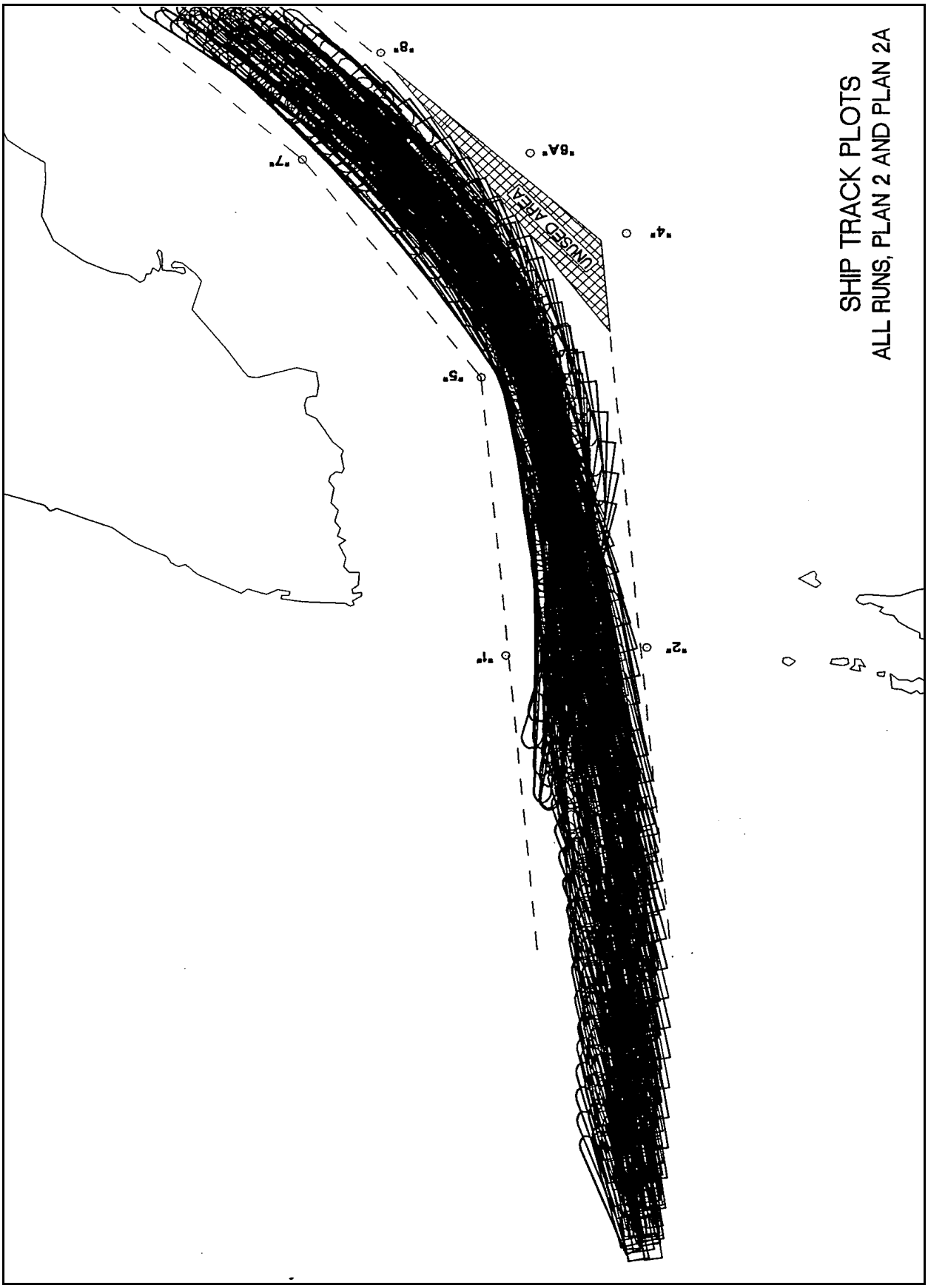

Figure V-5-70. Ship tracks, proposed Bar Channel and turn into Anegado Channel, San Juan Harbor

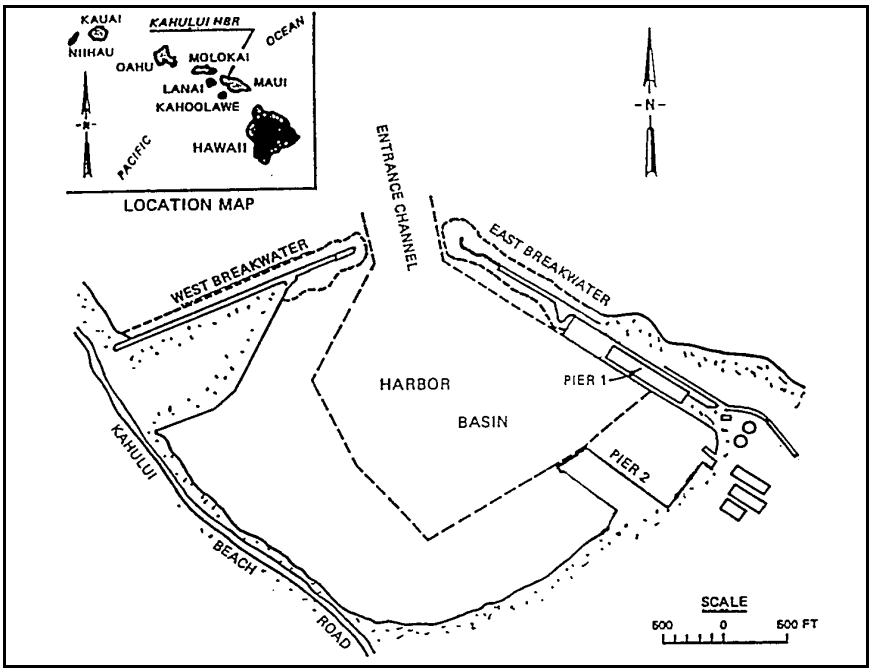

Figure V-5-71. Kahului Harbor, Maui, Hawaii, location map

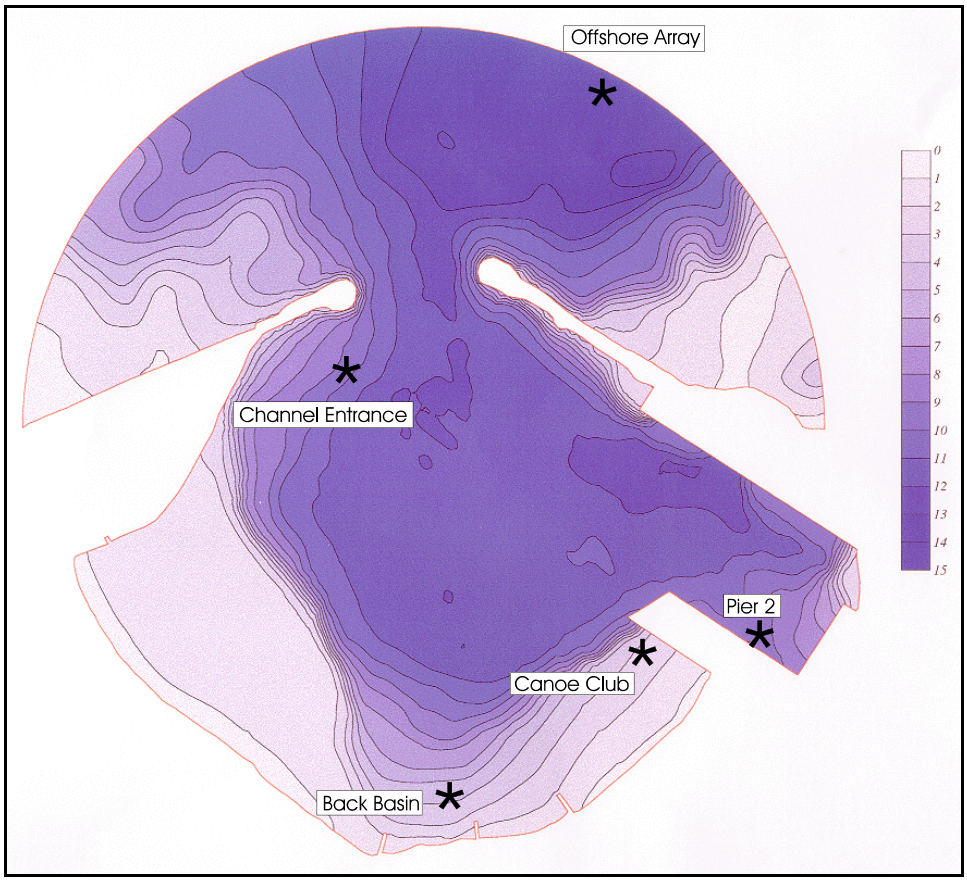

Figure V-5-72. Field gauge locations and bathymetry, Kahului Harbor

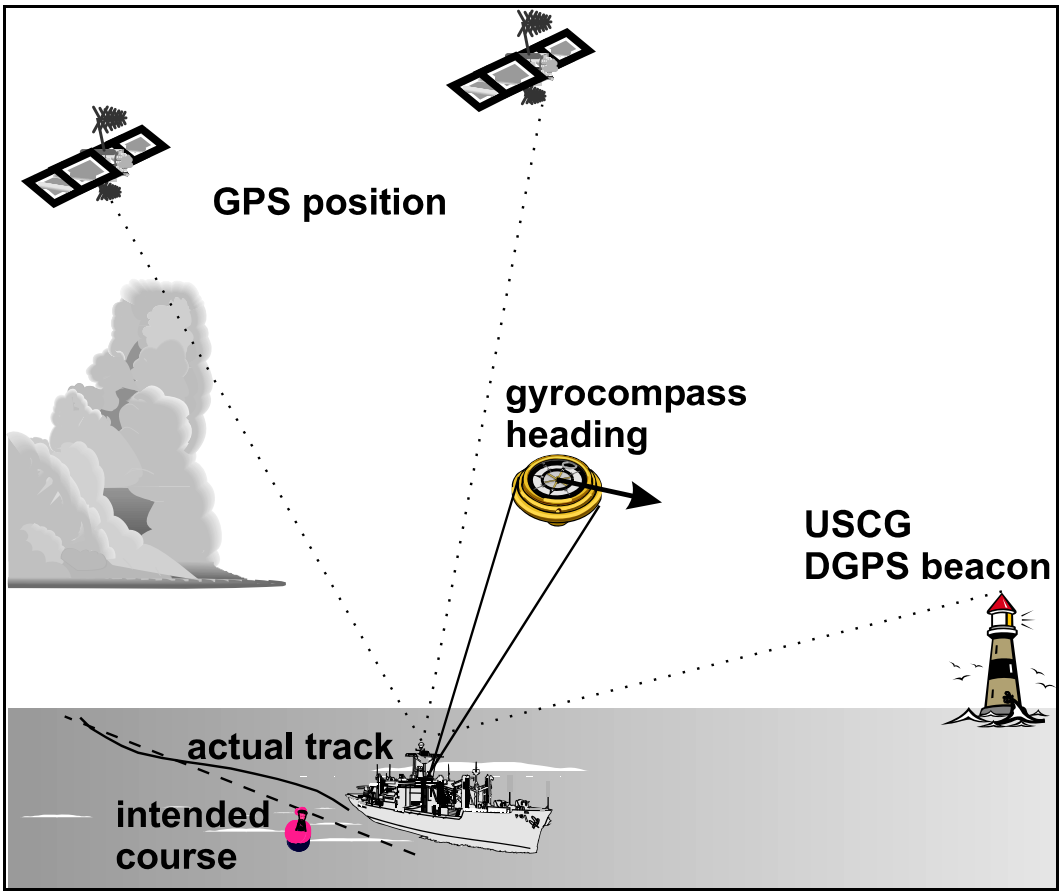

Figure V-5-73. Components of ship track measurements

(b) A dual-frequency DGPS system that measured horizontal and vertical location of ship bow and stern with 1 cm accuracy is described by Webb and Wooley (1998). The data, along with concurrent measurements of current and water level, provided direct calculation of ship squat. The data are useful for evaluating existing navigation conditions, designing modifications, and/or validating ship simulation models to study proposed conditions.

V-5-11. References

EM 1110-2-1615
EM 1110-2-1615, "Hydraulic Design of Small Boat Harbors"

EM 1110-8-1
EM 1110-8-1, "Winter Navigation on Inland Waterways"

EM 1110-2-1613
EM 1110-2-1613, "Hydraulic Design Guidance for Deep-Draft Navigation Projects"

ER 1105-2-100
ER 1105-2-100, "Guidance for Conducting Civil Works Planning Studies"

EP 1165-2-1
EP 1165-2-1, "Digest of Water Resources Policies and Authorities"

American Society of Civil Engineers 1994
American Society of Civil Engineers (ASCE). 1994. *Planning and Design Guidelines for Small Craft Harbors*, ASCE Manual and Reports on Engineering Practice No. 50, New York, NY.

Bottin 1976
Bottin, R. R., Jr. 1976. "Igloo Wave Absorber Tests for Port Washington Harbor, Wisconsin; Hydraulic Model Investigation," Miscellaneous Paper H-76-22, U.S. Army Engineer Waterways Experiment Station, Vicksburg, MS.

Bottin 1992
Bottin, R. R., Jr. 1992. "Physical Modeling of Small-Boat Harbors: Design Experience, Lessons Learned, and Modeling Guidelines," Technical Report CERC-92-12, U.S. Army Engineer Waterways Experiment Station, Vicksburg, MS.

Briggs, Bratteland, and Borgman 2000
Briggs, M. J., Bratteland, E., and Borgman, L. E. 2000. "Probability Assessment of Deep Draft Navigation Channel Design," submitted to *Coastal Engineering Journal*, Elsevier Science, The Netherlands.

Briggs et al. 1994
Briggs, M. J., Lillycrop, L. S., Harkins, G. S., Thompson, E. F., and Green, D. R. 1994. "Physical and Numerical Model Studies of Barbers Point Harbor, Oahu, Hawaii," Technical Report CERC-94-14, U.S. Army Engineer Waterways Experiment Station, Vicksburg, MS.

Bruun 1990
Bruun, P. 1990. *Port Engineering*, Fourth Edition (2 Vols.), Gulf Publishing, Houston, TX.

Chen and Houston 1987
Chen, H. S., and Houston, J. R. 1987. "Calculation of Water Oscillation in Coastal Harbors: HARBS and HARBD User's Manual," Instruction Report CERC-87-2, U.S. Army Engineer Waterways Experiment Station, Vicksburg, MS.

Clark 1983
Clark, J. R. 1983. *Coastal Ecosystem Management: A Technical Manual for the Conservation of Coastal Zone Resources*, John Wiley & Sons, New York, NY.

Dingemans 1997
Dingemans, M. W. 1997. *Water Wave Propagation over Uneven Bottoms*, 2 vols., World Scientific, Singapore.

Dunham and Finn 1974
Dunham, J. W., and Finn, A. A. 1974. "Small-Craft Harbors: Design, Construction, and Operation," Special Report No. 2, U.S. Army Engineer Research and Development Center, Coastal and Hydraulics Laboratory, Vicksburg, MS.

Ferguson 1991
Ferguson, A. 1991. "Navigation, Dredging and Environment in the Fraser River Estuary," Navigation and Dredging Workgroup Report, Fraser River Estuary Management Program, British Columbia, Canada.

Gaythwaite 1990
Gaythwaite, J. W. 1990. *Design of Marine Facilities for the Berthing, Mooring, and Repair of Vessels*, Van Nostrand Reinhold, New York, NY.

Harkins and Dorrell 2000
Harkins, G. S., and Dorrell, C. C. 2000. "Barbers Point Harbor Physical Model Navigation Study," Technical Report ERDC/CHL TR-00-2, U.S. Army Engineer Waterways Experiment Station, Vicksburg, MS.

Harris 1981
Harris, D. L. 1981. "Tides and Tidal Datums in the United States," Special Report No. 7, U.S. Army Engineer Waterways Experiment Station, Vicksburg, MS.

Herbich 1992
Herbich, J. B. 1992. *Handbook of Coastal and Ocean Engineering, Vol. 3, Harbors, Navigational Channels, Estuaries, Environmental Effects*, Gulf Publishing, Houston, TX.

Hudson et al. 1979
Hudson, R. Y., Herrmann, F. A., Jr., Sager, R. A., Whalin, R. W., Keulegan, G. H., Chatham, C. E., Jr., and Hales, L. Z. 1979. "Coastal Hydraulic Models," Special Report SR-5, U.S. Army Engineer Research and Development Center, Coastal and Hydraulics Laboratory, Vicksburg, MS.

Hughes and Fowler 1990
Hughes, S. A., and Fowler, J. E. 1990. "Midscale Physical Model Verification for Scour at Coastal Structures," Technical Report CERC-90-8, U.S. Army Engineer Waterways Experiment Station, Vicksburg, MS.

Huval 1980
Huval, C. J. 1980. "Lock Approach Canal Surge and Tow Squat at Lock and Dam 17, Arkansas River Project; Mathematical Model Investigation," Technical Report HL-80-17, U.S. Army Engineer Waterways Experiment Station, Vicksburg, MS.

Huval 1993
Huval, C. J., ed. 1993. "Planning, Design, and Maintenance of Deep Draft Navigation Channels," PROSPECT Training Course Notes, U.S. Army Engineer Waterways Experiment Station, Vicksburg, MS.

Huval and Lynch 1998
Huval, C. J., and Lynch, G. C. 1998. "Ship Navigation Simulation Study, Brunswick Harbor, Georgia," Technical Report CHL-98-18, U.S. Army Engineer Waterways Experiment Station, Vicksburg, MS.

Irish 1997
Irish, J. L. 1997. "Sensitivity of Channel Sedimentation Prediction to Wave-field Characterization," Bulletin No. 95, PIANC, Brussels, Belgium, pp 5-19.

LeMéhauté 1965
LeMéhauté, B. 1965. "Wave Absorbers in Harbors," Contract Report No. 2-122, U.S. Army Engineer Waterways Experiment Station, Vicksburg, MS, prepared for National Engineering Science Company, Pasadena, CA, under Contract No. DA-22-079-CIVENG-64-81.

Lillycrop et al. 1993
Lillycrop, L. S., Briggs, M. J., Harkins, G. S., Boc, S. J., and Okihiro, M. S. 1993. "Barbers Point Harbor, Oahu, Hawaii, Monitoring Study," Technical Report CERC-93-18, U.S. Army Engineer Waterways Experiment Station, Vicksburg, MS.

McBride, Smallman, and Huntington 1998
McBride, M. W., Smallman, J. V., and Huntington, S. W. 1998. "Guidelines for Design of Approach Channels," *Proceedings, PORTS '98*, ASCE, pp 1315-1324.

McCartney, Hermann, and Simmons 1991
McCartney, B. L., Hermann, F. A., Jr., and Simmons, H. B. 1991. "Estuary Waterway Projects - Lessons Learned," *Journal of Waterway, Port, Coastal, and Ocean Engineering* 117(4), American Society of Civil Engineers, pp 409-421.

Mei 1983
Mei, C. C. 1983. *The Applied Dynamics of Ocean Surface Waves*, John Wiley & Sons, New York, NY.

Melo and Guza 1991
Melo, E., and Guza, R. T. 1991. "Wave Propagation in Jettied Entrance Channels. II: Observations," *Journal of Waterway, Port, Coastal, and Ocean Engineering* 117(5), pp 493-510.

NOAA (Annual)
National Oceanic and Atmospheric Administration (NOAA). (Annual). *Tide Tables* and *Tidal Current Tables*, Rockville, MD.

Noda 1972
Noda, E. K. 1972. "Equilibrium Beach Profile Scale-Model Relationship," *Journal of the Waterways, Harbors, and Coastal Engineering Division* 98(WW4), ASCE, pp 511-528.

Norrbin 1986
Norrbin, N. H. 1986. "Fairway Design with Respect to Ship Dynamics and Operational Requirements," SSPA Research Report No. 102, SSPA Maritime Consulting, Gothenburg, Sweden.

Okihiro and Guza 1996
Okihiro, M. S., and Guza, R. T. 1996. "Observations of Seiche Forcing and Amplification in Three Small Harbors," *Journal of Waterway, Port, Coastal, and Ocean Engineering* 122(5), ASCE, 232-238.

Okihiro et al. 1994
Okihiro, M. S., Guza, R. T., O'Reilly, W. C., and McGehee, D. D. 1994. "Selecting Wave Gauge Sites for Monitoring Harbor Oscillations: A Case Study for Kahului Harbor, Hawaii," Miscellaneous Paper CERC-94-10, U.S. Army Engineer Waterways Experiment Station, Vicksburg, MS.

Panchang, Xu, and Demirbilek 1998
Panchang, V. G., Xu, B., and Demirbilek, Z. 1998. "Wave Models for Coastal Applications," *Handbook of Coastal Engineering*, J. B. Herbich, ed., Vol. 4 (to be published).

PIANC 1984
PIANC. 1984. "Ice Navigation," Supplement to Bulletin No. 46, Permanent International Association of Navigation Congresses, Brussels.

PIANC 1995
PIANC. 1995. "Approach Channels, Preliminary Guidelines," First Report of the Joint PIANC-IAPH Working Group II-30, Permanent International Association of Navigation Congresses, Brussels, Belgium.

PIANC 1997a
PIANC. 1997a. "Approach Channels, a Guide for Design," Supplement to Bulletin No. 95, Permanent International Association of Navigation Congresses, Brussels, Belgium.

PIANC 1997b
PIANC. 1997b. "Guidelines for the Design of Armoured Slopes Under Open Piled Quay Walls," Supplement to Bulletin No. 96, Permanent International Association of Navigation Congresses, Brussels, Belgium.

Quinn 1972
Quinn, A. D. 1972. *Design & Construction of Ports & Marine Structures*, McGraw-Hill.

Sager and Hollyfield 1974
Sager, R. A., and Hollyfield, N. W. 1974. "Navigation Channel Improvements, Barnegat Inlet, New Jersey," Technical Report H-74-1, U.S. Army Engineer Waterways Experiment Station, Vicksburg, MS.

Seabergh, Cialone, and Stauble 1996
Seabergh, W. C., Cialone, M. A., and Stauble, D. K. 1996. "Impacts of Inlet Structures on Channel Location," *Proceedings, 25th International Conference on Coastal Engineering*, ASCE, pp 4531-4544.

Seabergh, Vemulakonda, and Rosati 1992
Seabergh, W. C., Vemulakonda, S. R., and Rosati, J., III. 1992. "Los Angeles-Long Beach Harbors Model Enhancement Program," *Proceedings, PORTS '92*, ASCE, pp 884-897.

Silver 1992
Silver, A. L. 1992. "Environmental Monitoring and Operator Guidance System (EMOGS) for Shallow Water Ports," *Proceedings, PORTS '92*, ASCE, pp 535-547.

Silver and Dalzell 1997
Silver, A. L., and Dalzell, J. F. 1997. "Risk Based Decisions for Entrance Channel Operation and Design," *Proceedings, 7th International Offshore and Polar Engineering Conference*, International Society of Offshore and Polar Engineers, pp 815-822.

SMS 1994
SMS. 1994. "Surface-Water Modeling System," developed by Brigham Young University and USACE, updated periodically.

State of California 1980
State of California. 1980. "Layout and Design Guidelines for Small Craft Berthing Facilities," Department of Boating and Waterways.

Stevens et al. 1942
Stevens, J. C., Bardsley, C. E., Lane, E. W., Straub, L. G., Wright, C. A., Tiffany, J. A., and Warnock, J. E. 1942. *Hydraulic Models*, Manuals of Engineering Practice, No. 25, American Society of Civil Engineers, New York, NY.

Thompson, Boc, and Nunes 1998
Thompson, E. F., Boc, S. J., Jr., and Nunes, F. S. 1998. "Evaluating Operational Impact of Waves Along Proposed Harbor Piers," *Proceedings, PORTS '98*, ASCE, pp 860-869.

Thompson et al. 1996
Thompson, E. F., Hadley, L. L., Brandon, W. A., McGehee, D. D., and Hubertz, J. M. 1996. "Wave Response of Kahului Harbor, Maui, Hawaii," Technical Report CERC-96-11, U.S. Army Engineer Waterways Experiment Station, Vicksburg, MS.

Thompson et al. 1998a
Thompson, E. F., Fong, M. T., Van Norman, P. S., and Brown, B. 1998a. "Ship Navigation Simulation Study, Alafia River, Tampa Bay, Florida," Technical Report CHL-98-13, U.S. Army Engineer Waterways Experiment Station, Vicksburg, MS.

Thompson et al. 1998b
Thompson, E. F., Lin, L., Hadley, L. L., and Hubertz, J. M. 1998b. "Wave Response of Kikiaola Harbor, Kauai, Hawaii," Miscellaneous Paper CHL-98-5, U.S. Army Engineer Waterways Experiment Station, Vicksburg, MS.

Tobiasson and Kollmeyer 1991
Tobiasson, B. O., and Kollmeyer, R. C. 1991. *Marinas and Small-Craft Harbors*, Van Nostrand Reinhold, New York, NY.

Tsinker 1997
Tsinker, G. P. 1997. *Handbook of Port and Harbor Engineering*, Chapman & Hall, New York, NY.

Turner 1984
Turner, H. O., Jr. 1984. "Dimensions for Safe and Efficient Deep-Draft Navigation Channels," Technical Report HL-84-10, U.S. Army Engineer Waterways Experiment Station, Vicksburg, MS.

USACE 1983
U.S. Army Corps of Engineers. 1983. "Engineering and Design of Military Ports," Technical Manual TM 5-850-1, Headquarters, Department of the Army, Washington, DC.

U.S. Coast Guard 1981
U.S. Coast Guard. 1981. "Aids to Navigation Manual - Administration," COMDTINST M16500.7, U.S. Coast Guard, Washington, DC.

U.S. Coast Guard 1988a
U.S. Coast Guard. 1988a. "Aids to Navigation Manual - Seamanship," CG-222.2, U.S. Coast Guard, Washington, DC.

U.S. Coast Guard 1988b
U.S. Coast Guard. 1988b. "Aids to Navigation Manual - Technical," COMDTINST M16500.3, U.S. Coast Guard, Washington, DC.

U.S. Navy 1981
U.S. Navy. 1981. "Harbors," Design Manual 26.1, Naval Facilities Engineering Command, Alexandria, VA.

U.S. Navy 1998
U.S. Navy. 1998. "Handbook for Mooring Design," MIL-HDBK 1026/4, Naval Facilities Engineering Command, Alexandria, VA.

Wang and Cialone 1995
Wang, H. V., and Cialone, A. 1995. "Numerical Hydrodynamic Modeling and Flushing Study at Maalaea Harbor, Maui, Hawaii," Miscellaneous Paper CERC-95-8, U.S. Army Engineer Waterways Experiment Station, Vicksburg, MS.

Wang et al. 1980
Wang, S., Butcher, C., Kimble, M., and Cox, G. D. 1980. "Columbia River Entrance Channel Deep-Draft Vessel Motion Study," Tetra Tech Report No. TC-3925, U.S. Army Engineer District, Portland, OR.

Webb 1993
Webb, D. W. 1993. "Ship Navigation Simulation Study, San Juan Harbor, San Juan, Puerto Rico," Technical Report HL-93-17, U.S. Army Engineer Waterways Experiment Station, Vicksburg, MS.

Webb 1994
Webb, D. W. 1994. "Navigation Channel Design Using Real-Time Marine Simulator," *Proceedings, Dredging '94*, ASCE, pp 1081-1090.

Webb and Wooley 1998
Webb, D. W., and Wooley, R. T. 1998. "Using DGPS Ship Transit Data for Navigation Channel Design," *Proceedings, PORTS '98*, ASCE, pp 1325-1332.

Wilson 1966
Wilson, H. B. 1966. "Design for Optimum Wave Conditions, Dana Point Harbor, Dana Point, California; Hydraulic Model Investigation," Technical Report 2-724, U.S. Army Engineer Waterways Experiment Station, Vicksburg, MS.

WMO 1970
World Meteorological Organization (WMO). 1970. "WMO Sea-ice Nomenclature," WMO/OMM/BMO-No.259.TP.145, as amended, Geneva, Switzerland.

V-5-12. Definitions of Symbols

α_b	Breaking wave angle [deg]
A_C	Channel cross-section area [length^2]
B	Vessel beam at midships [length]
C_B	Block coefficient (Figure V-5-4) [dimensionless]
F_h	Channel depth Froude number [dimensionless]
F_L	Schijf limiting Froude number (Equation V-5-7) [dimensionless]
g	Gravitational acceleration [length/time^2]
h	Depth of channel [length]
h_1, h_2	Overbank depths [length]
L	Ship length [length]
N_B	Number of boats using the project
T	Vessel draft [length]
V	Vessel speed [length/time]
V_L	Schijf limiting ship speed in squat analysis [length/time]
W	Width of channel [length]
Z	Maximum ship squat [length]
Z_L	Maximum ship squat at Schijf limiting Froud number (Equation V-5-8) [length]
Z_T	Maximum squat in a trench channel (Equation V-5-9) [length]

V-5-13. Acknowledgments

Authors of Chapter V-5, "Navigation Projects:"

Edward F. Thompson, Ph.D., Coastal and Hydraulics Laboratory (CHL), U.S. Army Engineer Research and Development Center, Vicksburg, Mississippi.
Carl J. Huval, CHL (retired)
Ray R. Bottin, CHL
Orson P. Smith, Ph.D., U.S. Army Engineer District, Alaska, Anchorage, Alaska, (retired)

Reviewers:

David Curfman, Naval Facilities Engineering Command, Norfolk, Virginia
Lee E. Harris, Ph.D., Department of Marine and Environmental Systems, Florida Institute of Technology, Melbourne, Florida
Mona King, U.S. Army Engineer District, Seattle, Seattle, Washington
John H. Lockhart, Headquarters, U.S. Army Corps of Engineers, Washington, DC, (retired)
J. Richard Weggel, Ph.D., Department of Civil and Architectural Engineering, Drexel University, Philadelphia, Pennsylvania

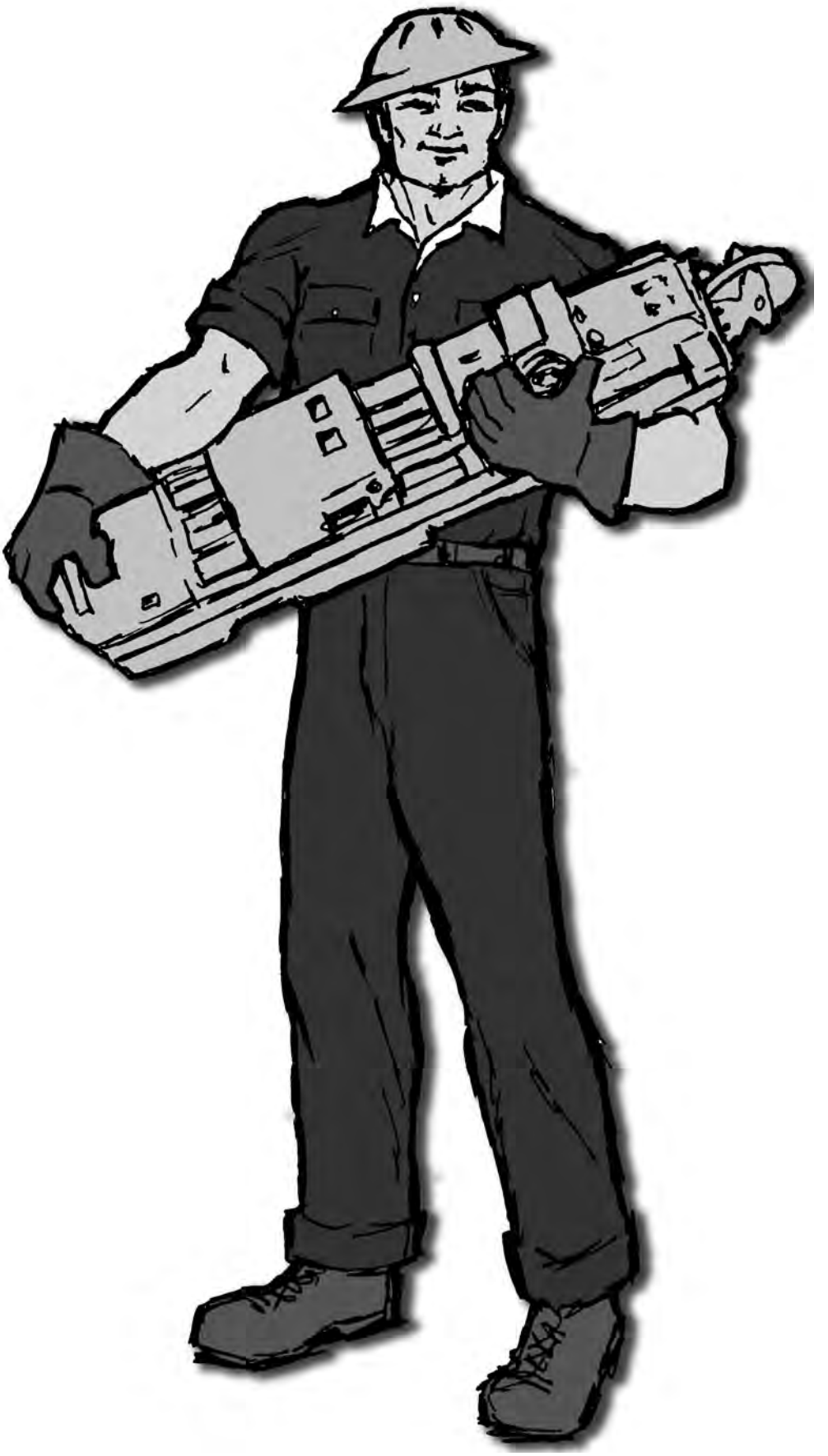

Table of Contents

Page

V-6-1. Introduction V-6-1
- *a. Overview* V-6-1
- *b. Definitions* V-6-1
- *c. Background* V-6-1
- *d. Summary* V-6-5

V-6-2. Regional Sediment Management and Coastal Inlet Processes V-6-5
- *a. Overview* V-6-5
- *b. Regional sediment management* V-6-5
  - (1) Overview V-6-5
  - (2) Critical role of inlets V-6-6
  - (3) Coastal inlet processes V-6-7
- *c. Inlet operation and maintenance activities* V-6-14
- *d. Inlet modifications of longshore transport* V-6-16
- *e. Alongshore extent of inlet influence* V-6-21
- *f. Estimating alongshore extent of inlet influence* V-6-25
- *g. Inlet interactions with adjacent beaches* V-6-56
  - (1) General V-6-56
  - (2) Detection V-6-57

V-6-3. Inlet and Adjacent Beach Sediment Budgets V-6-65
- *a. Overview* V-6-65
- *b. Introduction* V-6-66
- *c. Theory* V-6-66
- *d. Project applications* V-6-68
- *e. History of and procedure for sediment budget formulation* V-6-68
- *f. Data required* V-6-73
- *g. Sediment budget methods and tools* V-6-75

V-6-4. Engineering Approaches V-6-118
- *a. General considerations* V-6-118
- *b. Application of sediment budget to design* V-6-125
- *c. Principles of sand bypassing and backpassing* V-6-130

V-6-5. Engineering Methods V-6-131
- *a. Jetty sand-tightening* V-6-131
- *b. Sand transfer plants* V-6-131
  - (1) Fixed systems V-6-131
  - (2) Mobile systems V-6-132
  - (3) Semimobile systems V-6-132

(4) Equipment for sediment extraction V-6-133
(5) Equipment for discharge V-6-139
c. Sediment traps, deposition basins, and inlet sediment sources V-6-143
(1) Introduction V-6-143
(2) Weirs and weir jetties V-6-143
(3) Sediment traps V-6-145
(4) Channel wideners V-6-146
(5) Flood shoals V-6-147
(6) Ebb shoals V-6-147
d. Bypass system capacity V-6-148
(1) Dredges, jet pumps, and other pumps V-6-148
(2) Excavation craters V-6-149
(3) Productivity V-6-149
(4) Weir jetty systems V-6-151
e. Placement of material V-6-154
(1) Alongshore location V-6-154
(2) Nearshore disposal V-6-156
f. Costs V-6-162

V-6-6. Project Experience V-6-162
a. Overview of existing prototype systems V-6-162
(1) Santa Cruz Harbor, California V-6-162
(2) Santa Barbara Harbor, California V-6-164
(3) Port Hueneme, Channel Islands Harbor, and Ventura marina, California V-6-165
(4) Oceanside Harbor, California V-6-166
(5) Indian River Inlet, Delaware V-6-167
(6) Rudee Inlet, Virginia V-6-168
(7) Masonboro Inlet, North Carolina V-6-169
(8) Ponce de Leon Inlet, Florida V-6-170
(9) Port Canaveral Entrance, Florida V-6-171
(10) South Lake Worth Inlet, Florida V-6-171
(11) Boca Raton Inlet, Florida V-6-172
(12) Hillsboro Inlet, Florida V-6-173
(13) Port Sanilac, Michigan V-6-174
(14) Viareggio Harbor and Marina di Carrara, Italy V-6-174
(15) Nerang River Entrance, Queensland, Austraila V-6-177
(16) Other projects V-6-178
b. Lessons learned V-6-178

V-6-7. References V-6-181

V-6-7. Definition of Symbols V-6-198

V-6-8. Acknowledgments V-6-201

List of Figures

Figure V-6-1a. Conceptual illustration of unstabilized inlet V-6-2

Figure V-6-1b. Conceptual illustration of stabilized inlet V-6-2

Figure V-6-1c. Example of stabilized inlet: Shinnecock Inlet, Long Island, New York (22 April 1997) V-6-3

Figure V-6-1d. Example of entrance: Port Canaveral, Florida, (date unknown) V-6-3

Figure V-6-1e. Example of harbor: Oceanside, California, (12 February 1999, photograph by Eagle Aerial) V-6-4

Figure V-6-2. Conceptual illustration of regions V-6-6

Figure V-6-3. Idealized sediment transport pathways for an unstabilized inlet V-6-8

Figure V-6-4. Idealized sediment transport pathways for stabilized inlet V-6-9

Figure V-6-5. Unstabilized tidal inlets for which (a) longshore current effects dominate, and (b) tidal current effects dominate (adapted from Oertel 1988) V-6-10

Figure V-6-6. Idealized wave-induced bypassing along the ebb tidal shoal ("bypass bar") for (a) unstabilized and (b) stabilized inlets V-6-11

Figure V-6-7. Idealized wave and tidal current bypassing for (a) unstabilized and (b) stabilized inlets V-6-12

Figure V-6-8. Idealized bypassing through migration and welding of bars for an unstabilized inlet (increasing numbers indicate time sequence) V-6-13

Figure V-6-9. Flood and ebb tidal flow in a weir jetty system V-6-16

Figure V-6-10. Example of inlet-adjacent shore erosion associated with (a) a fully-bypassing inlet, and (b) an inlet that is a complete littoral sink V-6-17

Figure V-6-11. Illustration of longshore sediment transport potential computed for three wave conditions incident to inlet's ebb shoal plateau (depths in meters) V-6-19

Figure V-6-12. Solutions of Equation V-6-3 (from Bodge 1994b) V-6-23

Figure V-6-13. Solution of Equation V-6-9 ..... V-6-25

Figure V-6-14. Shoreline change as a function of distance from inlet V-6-32

Figure V-6-15. Even-odd analysis for Example Problem V-6-4 ..... V-6-37

Figure V-6-16. Even-odd analysis for Example Problem V-6-5 ..... V-6-41

Figure V-6-17. Sketch of numerical model results for Example Problem V-6-6 ..... V-6-44

Figure V-6-18. Cumulative volume change with and without beach fill V-6-55

Figure V-6-19. Aerial Photograph of Ocean City Inlet, MD, showing high-water shoreline, berm shoreline, and duneline V-6-59

Figure V-6-20. Nautical chart with and without addition of higher-resolution contours. Arrows indicate sediment transport paths suggested by bathymetry V-6-61

Figure V-6-21. Bathymetric chart of St. Lucie Inlet, FL (c. 1995), digitized and gray-scale enhanced to better define the presence of shoals and channels V-6-62

Figure V-6-22. Historical locations of sandy shoals within Port Canaveral Entrance, Florida (prior to implementation of jetty/inlet improvements). Adapted from Bodge 1994a V-6-63

Figure V-6-23. Bathymetric contours and typical channel sections at Brunswick Harbor Federal Navigation Project, Glynn County, Georgia V-6-64

Figure V-6-24. Average annual volume of maintenance dredging at St. Mary's Entrance Channel and authorized channel depths; 1870 to 1992 ..... V-6-65

Figure V-6-25. Sediment budget parameters as may enter Equation V-6-23 ..... V-6-67

Figure V-6-26. Sediment budget for Example V-6-9 ..... V-6-69

Figure V-6-27. Conceptual sediment budget for Shinnecock Inlet, New York V-6-77

Figure V-6-28. Refined sediment budget for Shinnecock Inlet, New York V-6-78

Figure V-6-29a. SBAS Alternative Window (left) and Topology Window (right) V-6-83

Figure V-6-29b. Zoom-in showing sediment budget cells. Color-coding indicates varying degrees of imbalance V-6-83

Figure V-6-30. SBAS tool bars and button functions V-6-84

Figure V-6-31. Regional view of a sediment budget (zoom-out), with four alternatives V-6-85

Figure V-6-32. Local view of a sediment budget (zoom-in) showing combined (collapsed) sediment budget cells V-6-85

Figure V-6-33. Sediment budget with reinstated (exploded) cells V-6-86

Figure V-6-34. Rate graph feature of SBAS V-6-86

Figure V-6-35. *Volume edit* spreadsheet in SBAS V-6-87

Figure V-6-36. Entering project coordinate system with the *Load map/picture layer* feature on the bottom toolbar V-6-87

Figure V-6-37. Sediment budget for Hillsboro Inlet, Florida V-6-89

Figure V-6-38. Hypothetical shoreline change data for beaches adjacent to Hillsboro Inlet V-6-90

Figure V-6-39. Definition sketch for inlet morphology V-6-91

Figure V-6-40. Pattern of wave breaking on ebb shoal and bar, Ocean City Inlet, Maryland, November 1991 ..... V-6-92

Figure V-6-41. Conceptual design for reservoir model V-6-94

Figure V-6-42. Ebb-shoal planform determined from interpretation of 7-m contour, Ocean City Inlet V-6-98

Figure V-6-43. Volume of ebb-shoal, Ocean City Inlet V-6-99

Figure V-6-44. Volumes of ebb shoal, bypassing bar, and attachment bar, Ocean City Inlet V-6-100

Figure V-6-45. Calculated bypassing rates, Ocean City Inlet V-6-100

Figure V-6-46. Solutions based on linear and quadratic forms for Q_{out} V-6-101

Figure V-6-47. Bypassing bar volume and bypassing rates with/without mining V-6-103

Figure V-6-48. Bypassing rates for simple bidirectional transport V-6-104

Figure V-6-49. Study reach for sediment budget (not to scale, adapted from Jarrett 1991) V-6-106

Figure V-6-50. Sediment budget from Kure Beach (south end of study) to Wrightsville Beach (north end of study), North Carolina, using the wave energy flux method (adapted from Jarrett 1991). Note that the Masonboro Island cell connects to the North end of Masonboro Island cell V-6-107

Figure V-6-51. Sediment transport pathways for Bodge method (1999) V-6-108

Figure V-6-52. Longshore transport potential in vicinity of St. Lucie Inlet, Florida V-6-113

Figure V-6-53. General family of solutions for St. Lucie Inlet, Florida, sediment budget V-6-115

Figure V-6-54. Narrowed family of solutions, per requirements 1-4 ..... V-6-116

Figure V-6-55. Sediment transport rates (1000s cu m/year) computed for modal solution, St. Lucie Inlet, Florida V-6-117

Figure V-6-56. Family of solutions for Example Problem V-6-14 ..... V-6-123

Figure V-6-57. One possible solution for Example Problem V-6-14 ..... V-6-125

Figure V-6-58. Solution for Example Problem V-6-15 ..... V-6-129

Figure V-6-59. Plan and section view of simple fixed bypassing plant (from EM 1110-2-1616) V-6-132

Figure V-6-60. Examples of (a) semimobile and (b) mobile bypassing systems V-6-133

Figure V-6-61. Hopper dredge *McFarland* at Brunswick Harbor entrance, Georgia. Lightly-colored sandy sediment (right-side intake) is mixed with dark colored silt and clay (left-side intake) during dredging V-6-135

Figure V-6-62. Center-drive jet pumps (educators): (a) enclosed nozzle, (b) open nozzle (from EM 1110-2-1616) V-6-136

Figure V-6-63. Typical submersible pump (from EM 1110-2-1616) V-6-137

Figure V-6-64. Examples of Punaise dredging system: (a) in surf zone of a sandy coast, and (b) in a harbor with a trailing suction hopper dredge (after Brouwer, van Berk, and Visser 1992) V-6-138

Figure V-6-65. Example of fluidizers: (a) multiple-pipe, manifold-type (planform view), and (b) single-pipe (seabed view). Adapted from EM 1110-2-1616) V-6-139

Figure V-6-66. Examples of hopper dredge and scow discharge methods V-6-141

Figure V-6-67. Schematic of typical hydrocyclone V-6-142

Figure V-6-68. Weir jetties, weir-groins, and weir deposition basins (a) interior to inlet, and (b) exterior to inlet V-6-144

Figure V-6-69. Inlet sediment traps V-6-146

Figure V-6-70. Sediment borrowing from ebb shoal of an inlet V-6-148

Figure V-6-71. Jet pump operating hours from May 1986 to February 1988; Nerang River bypassing plant; Queensland, Australia (data from Clausner 1988; figure adapted from Bodge 1993) V-6-149

Figure V-6-72. Geometry of a dredge crater (definition sketch) V-6-150

Figure V-6-73. Measured sand bypass rates from South Lake Worth Inlet, Florida, fixed transfer plant: (a) correlated with hindcast longshore transport potential, and (b) depicted as a time-series. "Actual" refers to monthly bypass volumes estimated from plant records. "Computed" refers to the southerly-directed transport, potential as computed from hindcast WIS data for the same 24-year period of record, where the mean value of the computed transport potential was set equal to the mean value of the actual bypass volume over the period of record (Creed 1994) V-6-155

Figure V-6-74. Active and dead sediment storage on a beach adjacent to a weir jetty system (adapted from Weggel 1981) V-6-156

Figure V-6-75. Use of mass curve to predict volumetric capacities required for updrift beach and deposition basins (from Weggel 1981) V-6-157

Figure V-6-76. Method to predict whether sediment placed in a nearshore berm will be active (move landward) or stable (after Hands and Allison 1991) V-6-158

Figure V-6-77. Results for Example Problem V-6-17 ..... V-6-161

Figure V-6-78. Santa Cruz, California V-6-164

Figure V-6-79. Santa Barbara, California V-6-165

Figure V-6-80. Channel Islands and Port Hueneme Harbors, California V-6-166

Figure V-6-81. Oceanside Harbor, California V-6-167

Figure V-6-82. Masonboro Inlet, North Carolina V-6-169

Figure V-6-83. Ponce de Leon Inlet, Florida V-6-170

Figure V-6-84. Historical locations of sandy shoals within Port Canaveral Entrance, Florida (prior to implementation of inlet/jetty improvements). Adapted from Bodge 1994a V-6-173

Figure V-6-85. Boca Raton Inlet, Florida V-6-174

Figure V-6-86. Viareggio Harbor, Italy V-6-175

Figure V-6-87. Original sand bypassing plant at Viareggio Harbor, Italy V-6-175

Figure V-6-88. Existing sand bypass pump system at Viareggio Harbor, Italy V-6-176

Figure V-6-89. Sand bypassing system at Nerang River entrance (schematic) V-6-177

List of Tables

Table V-6-1. Updrift Volume Change V-6-20

Table V-6-2. Downdrift Volume Change V-6-20

Table V-6-3. Calculations for Impoundment and Sand Loss Effects at Inlet V-6-27

Table V-6-4. Volume Change Calculations North and South of Inlet V-6-31

Table V-6-5. Data and Calculations for Even-Odd Analysis V-6-35

Table V-6-6. Data and Calculations for Even-Odd Analysis and Net Volume Change V-6-39

Table V-6-7. Numerical Model Results for Longshore Transport Potential Calculations V-6-43

Table V-6-8. Potential Longshore Transport Rate Information for Fine Grid Columns V-6-48

Table V-6-9. Measured Shoreline Changes and Calculations for Net Sink Effect V-6-52

Table V-6-10. Calculations for Cumulative Volume Change West of Inlet V-6-54

Table V-6-11. Rates of Volume Change for Shinnecock Inlet Sediment Budget, 1938 to 1979 ..... V-6-79

Table V-6-12. Results from Wave Refraction and Transport Rate, Analysis V-6-119

Table V-6-13 Sediment Budget Example Solutions V-6-122

Table V-6-14 Method to Determine D_r', D_b', and D_L' V-6-127

Table V-6-15. Example Calculations for Evaluating Dredging Requirements V-6-128

Table V-6-16. Typical Hydrocyclone Capacities V-6-143

Table V-6-17. Deepwater Wave Data and Calculations to Determine Berm Stability V-6-159

Table V-6-18. Calculations of Maximum Nearbed Orbital Velocity V-6-160

Table V-6-19. Examples of Inlet Sand Bypassing Costs V-6-163

Chapter V-6
Sediment Management at Inlets

V-6-1. Introduction

a. Overview. The U.S. Army Corps of Engineers (USACE) has a mission to provide military and civil works engineering to the nation. Congress authorized the navigation part of this mission in 1824, when USACE was directed to remove sandbars and snags from major navigable rivers. Today, USACE's dredging program involves the planning, design, construction, operation, and maintenance of riverine, estuarine, and coastal passages to meet navigation needs. The most dynamic of these waterways are inlets, entrances, and harbors on oceans, bays, and lakefronts, at which wind waves and tides or seiching of water may combine to transport sediment. The foremost navigation goal is to provide safe passage in these channels for vessels of a given design draft at the least cost. In fiscal year (FY) 1999, USACE dredged approximately 360 million cu m from Federal channels. Maintenance dredging accounted for an average of 85 percent of this volume while new work and emergency dredging made up the remainder. The most efficient means of managing sediment that enters these navigable waterways is the subject of this chapter.

b. Definitions.

(1) For convenience, the term "inlets" will be used herein to encompass all these navigation passages. Inlet generally refers to a short, narrow waterway that connects a lagoon or bay with a larger parent body of water (i.e., ocean or lake), and experiences the inflow and outflow of water due to tidal or seiching. Inlets may be stabilized with shore-perpendicular structures at the mouth, called jetties. Waves and currents at an inlet combine to form ebb- and flood-tidal shoals (Figures V-6-1a, b, and c).

(2) An entrance is the opening to a navigation channel (Figure V-6-1d). A harbor refers to any protected body of water that affords a place of safety for vessels (Figure V-6-1e). Well-situated harbors do not experience significant currents due to tides or seiching and therefore do not have notable ebb- or flood-tidal shoals.

(3) The term "sediment" includes all types of minerals or organic materials that have been deposited by water, wind, or ice. Many navigation channels shoal because of the inflow of sand and finer-grained sediments. If this material impedes navigation, it may be dredged to provide safe passage through the inlet. Littoral pertains to a lake, sea, or ocean. As applied herein, the term "littoral material" refers to sediments (sand, silt, clay, gravel, etc.) that are transported by waves and currents along or near the coast. Note that wind-blown, or eolian, sediment may also contribute to shoaling in navigable waterways. Beach-quality sediment generally refers to sand that is of a sufficient size, color, and composition to be placed on the beach or nearshore. Nonbeach-quality materials can be used in other ways to benefit the coastal zone, e.g., creating wetlands and environmental habitat.

c. Background.

(1) The need to create navigable passage is a direct consequence of the dynamic nature of inlets. As an illustration, imagine a new inlet that is breached from the ocean side of a barrier island during a storm. Waves, an elevated ocean water level, and tidal currents scour sediments from the barrier to form the new inlet. The material is carried landward and seaward to form incipient flood- and ebb-tidal shoals. As tidal cycles pass, a channel is incised into the former barrier bed, thereby establishing the inlet as a coastal feature. Sand and other sediments moving alongshore are entrained by inlet ebb and flood currents, and

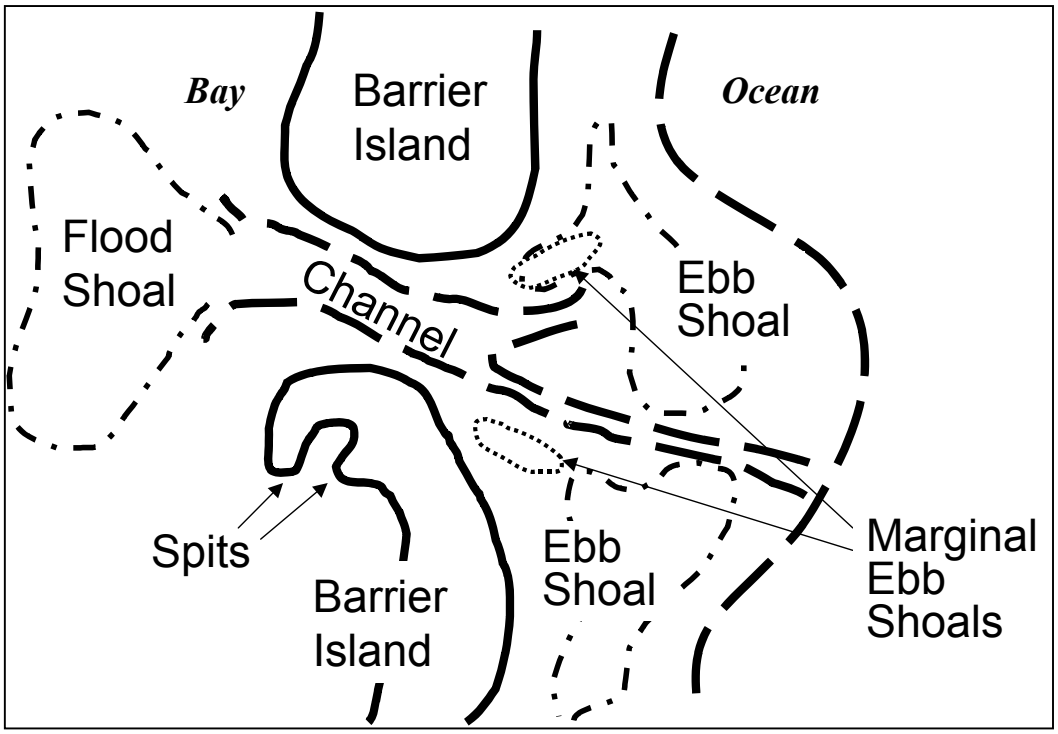

Figure V-6-1a. Conceptual illustration of unstabilized inlet

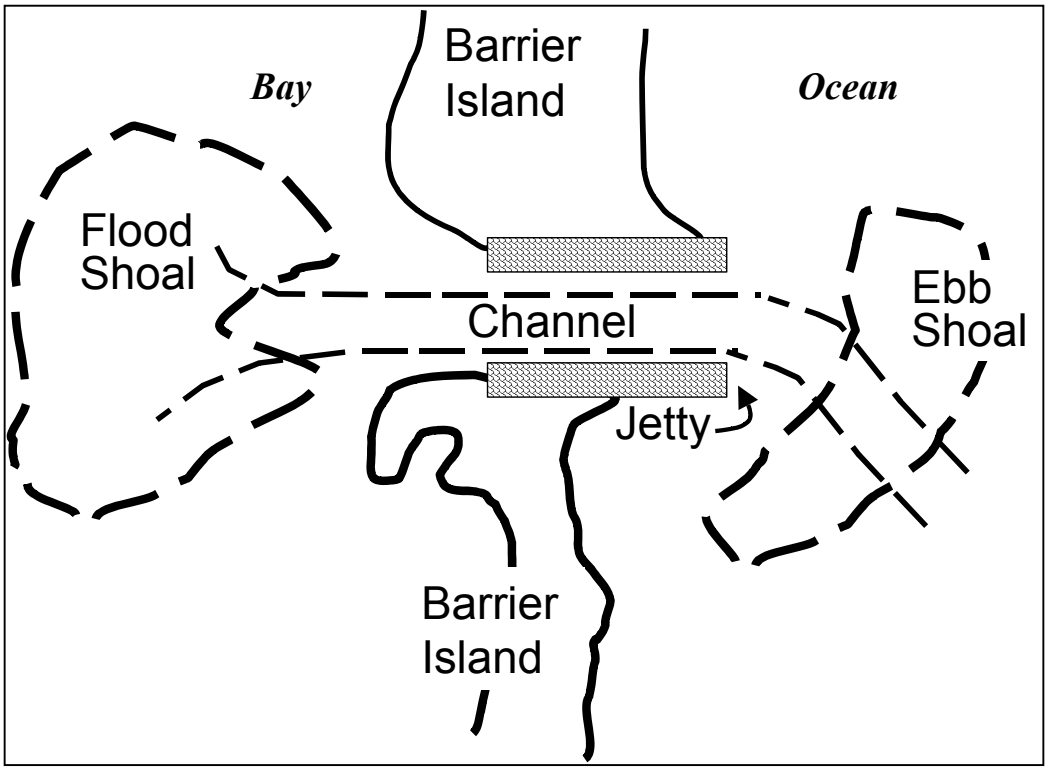

Figure V-6-1b. Conceptual illustration of stabilized inlet

Figure V-6-1c. Example of stabilized inlet: Shinnecock Inlet, Long Island, New York (22 April 1997)

Figure V-6-1d. Example of entrance: Port Canaveral, Forida, (date unknown)

Figure V-6-1e. Example of harbor: Oceanside, California, (12 February 1999, photograph by Eagle Aerial)

may be deposited in the inlet channels. The sediment may remain in the channels or may be jetted to the ebb- and flood-tidal shoals. As the inlet matures, the adjacent beaches may advance and retreat due to the changing waves, currents, and bathymetry in the vicinity of the opening. Volumetrically, the effect of this new inlet is a net loss to the adjacent beach system. Navigability of this new inlet is typically treacherous. Channels may meander and their depths may vary rapidly. Waves may break due to shoaling and due to current-induced wave steepening during ebb flows. Depending on the coastal processes and geologic constrictions, the inlet may migrate alongshore.

(2) The construction of jetties and dredging of channels are navigation controls that seek to promote safe passage through the inlet while minimizing construction and maintenance costs. Jetties stabilize the inlet's location and confine the tidal currents within the channel. In addition, the constricted currents help to clean the channel of shoaled sediment. Dredging improves channel navigability by increasing the depth as required to meet the needs of the design vessel, and straightening channel meanders that make passage through the inlet dangerous. However, the effective removal and disposal of sediment that is removed from the channel and the ebb- and flood-tidal shoals present an ongoing challenge.

(3) The goals of inlet sediment management are multifaceted:

(a) Through design of inlet structures, channels, and other controls (e.g., bypassing plants), to minimize the volume of sediment that accumulates within the navigable waterway.

(b) To remove shoaled sediment and morphologic features that inhibit safety at least cost.

(c) To optimize channel depth such that dredging frequency is reduced while the stability of inlet structures and adjacent beaches are not compromised.

(d) To keep the beach-quality dredged material within the nearshore beach system, effectively bypassing sand around the inlet.

(e) To place beach-quality material within the nearshore system and on adjacent beaches such that it does not cycle back into the inlet.

(f) To assist with other missions of USACE as appropriate, such as using dredged material to enhance environmental habitat, provide flood and storm damage protection, and establish or restore wetlands.

d. Summary. The purpose of this chapter is to discuss engineering works directed towards effective inlet sediment management and review analytical methods that can be applied in the design and evaluation of these projects. Experiences at several sites are reviewed to illustrate approaches to evaluating sediment management problems, the solutions that were implemented, and their performance.

V-6-2. Regional Sediment Management and Coastal Inlet Processes

a. Overview. This section discusses the effects that sediment management activities at inlets have both in the vicinity of the inlet and regionally (on the scale of tens of kilometers along the coast). First, regional sediment management is defined. The relationship between local, inlet-specific activities, and the response of other features within the region is discussed. Next, sediment transport processes at natural and engineered inlets are reviewed, with reference to material contained in Parts II-6 and IV-3.

b. Regional sediment management.

(1) Overview. Regional sediment management refers to the use of littoral, estuarine, and riverine sediment resources in an environmentally beneficial and economical manner. Regional sediment management strives to maintain or enhance the natural exchange of sediment within the boundaries of the physical system. A region may include a variety of geologic features, uplands, beaches, inlets, rivers, estuaries, and bays, and is defined by the sediment transport paths within this physical system (Figure V-6-2). Implementation of regional sediment management recognizes that the physical system and embedded ecosystems are modified and may respond to natural forcing and engineering activities beyond the formal dimensions and time frames of individual projects.

(a) USACE has a central role in the implementation of regional sediment management. The mission areas of USACE include navigation, environmental restoration, storm-damage reduction, and flood reduction. In particular, the mission area ensuring the navigability of our nation's waterways involves removing, transporting, and placing sediment. Some of this material can be used to achieve goals in other mission areas. As opposed to individual homeowners, county and state governments, and other Federal agencies, USACE's role spans both political and geographic boundaries. Although the term "regional sediment management" is new, recognition of the regional nature of coastal processes and the regional

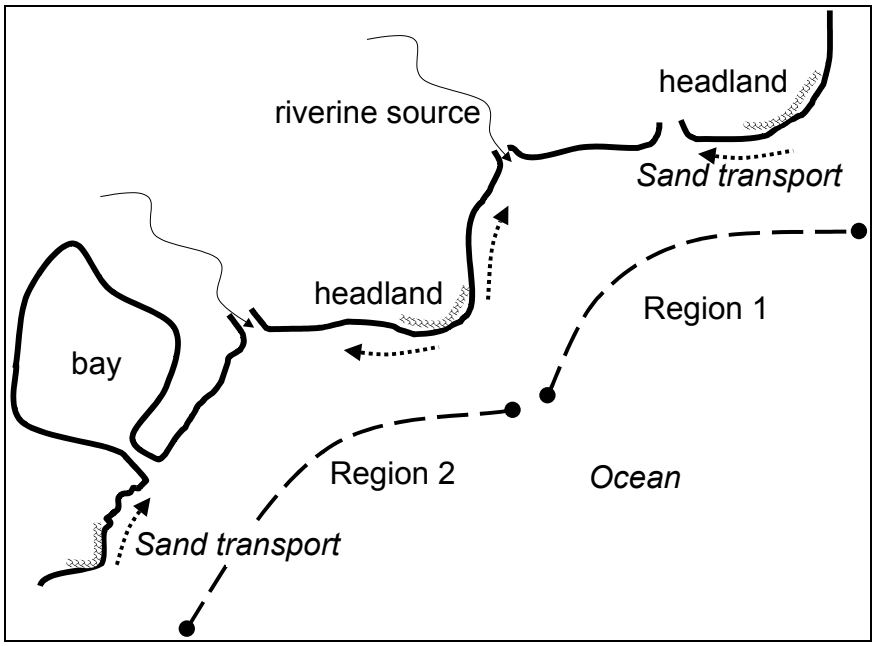

Figure V-6-2. Conceptual illustration of regions

influence of engineering works is not. The interrelationship between coastal navigation projects and contiguous beaches became a Federal interest at least as early as the 1930s (Brooke 1934). The first sand bypassing systems at navigation projects, designed to reinstate net longshore sand transport to downdrift beaches, were put into operation in the mid-1930s at Santa Barbara, California (mobile plant) (Penfield 1960) and South Lake Worth Inlet, Florida (fixed plant) (Caldwell 1951).

(b) Today, USACE is pursuing regional sediment management by collaborating with local and state governments to manage sediments over regions encompassing multiple projects. Schmidt and Schwichtenberg (2000) describe the Jacksonville District's application of regional sediment management principles for proposed improvements to Port Everglades, a deep-draft port on the east coast of Florida. These improvements include widening and deepening existing channels and turning basins, and creating a new turning basin to accommodate larger container ships. Federal shore protection projects along the adjacent three counties will require almost 59 million cu m of beach-quality sand. The District is working with county and state agencies to satisfy the navigational goals at Port Everglades while using the dredged sediments to nourish the adjacent beaches and restore environmental habitat. It is envisioned that beach-quality dredged material can be identified prior to dredging and placed directly on the beach. For mixed sediments, a temporary deposition site on an adjacent beach has been considered. After the dredged slurry has been deposited on the beach, hydrocyclones could separate fine sediments from beach quality sand. The beach-quality sand would be trucked to adjacent beaches, and the silt could be placed and vegetated to build natural berms and dunes.

(2) Critical role of inlets. Inlets are significant elements in controlling sediment movement and its distribution within local and regional domains. They may serve as a source if they funnel riverine, estuarine, and bay sediments to the open coastline. They may also act as a sink by diverting littoral material into the inlet and its bay, harbor, and estuaries. In a manner analogous to water flow through a tidal inlet (see Part II- 6), littoral material may be transported into the inlet on the flood (rising) tide and out of the inlet on the ebb (falling) tide. Flood or ebb dominance of water flow through an inlet, however, does not necessarily determine the net sediment transport direction through the inlet (Stauble et al. 1988; see also Part IV-3-4, or along the adjacent beaches. An inlet in a state of "dynamic equilibrium" indicates

that there is a net long-term (years to decades and longer) balance between water flow through the inlet and sediment transport to and from the inlet. The net, long-term effect is a hydrodynamic field that is sufficient to maintain flow through the inlet and maintain an approximate balance of sediment volume on the beaches to either side of the inlet. In the short term (days to years), cyclical events such as seasonal changes in waves and currents or storms may temporarily disturb the balance. Therefore, although an inlet may be in a state of dynamic equilibrium, it may require dredging to maintain navigability. Inlets that are not in a state of dynamic equilibrium include those that: migrate alongshore, are closing because of shoaling of the channels (either from an upland or ocean source of sediment), and are widening or scouring due to an increasing tidal prism or unstable geologic substrate. For an inlet to remain open, sediment entering the inlet must be diverted from the inlet's principal channels, or the channels must move. If sediment is not bypassed across the inlet, it must be transported by waves or currents away from the inlet throat and into interior shoals, exterior shoals, or beach impoundments; or, it must be removed by dredging. The following section describes hydrodynamic and sediment transport processes at inlets.

(3) Coastal inlet processes.

(a) Inlet features. The following is an overview of principal inlet flow fields and sedimentary features. Parts II-6-1 and IV-3-4 present more detailed descriptions of inlet hydrodynamics and sediment transport/morphology.

Typical elements of nonstabilized and stabilized tidal inlets are illustrated in Figures V-6-1a and b, respectively. An inlet connects a larger, open-water body (the ocean, sea, lake, etc.) with a generally smaller, protected water body (a bay, lagoon, estuary, or river) through a land body such as a barrier spit. The inlet technically includes the entire seabed between the banks of the adjacent barrier shores, measured from the seaward edge of the ebb shoal to the landward edge of the flood shoal (discussed in the following paragraph). The inlet throat is the region with the smallest cross-sectional flow area and highest velocities. The channel (geologically known as a gorge or thalweg) defines the deepest parts of the inlet. There may be several channels in a natural inlet, which may migrate, vanish, or alternate in dominance. The navigable channel is the one that is deepest at a given time or is maintained for navigation by dredging.

A tidal inlet (also known as a lagoonal inlet) connects a tidal water body with the bay, and features significant flow directed both into and out of the inlet throat as a function of water level fluctuations in the ocean and bay. (Riverine mouths or fluvial inlets are dominated by river discharge and minimally affected by flood tide flow). During flood tide, currents are funneled toward the inlet mouth from the ocean (Figures V-6-3a and V-6-4a). In the absence of high, impermeable jetties (Figure V-6-3a), the flood flow is typically most dominant along the ocean shorelines of the adjacent barrier islands, sometimes creating and/or following marginal flood channels. The flood flow converges and accelerates in the throat. Upon its discharge, the flood flow diverges and decelerates beyond the inlet's bayside mouth, depositing sediment in a flood shoal. The flow reverses during ebb current, although rarely symmetrically (Figures V-6-3b and V-6-4b). The ebb flow sweeps sediment from the flood shoal and inlet channels and carries it through the inlet throat. The ebb flow discharges from the inlet's ocean mouth similarly to a free jet, depositing its sediment load in an ebb shoal. The ebb shoal may protrude significantly into the deeper ocean, forming the ebb shoal plateau or terminal lobe.

The coast in the direction from which the majority of offshore wave energy arrives is termed the updrift shoreline (top barrier island in Figures V-6-3c and V-6-4c). The opposite coast is the

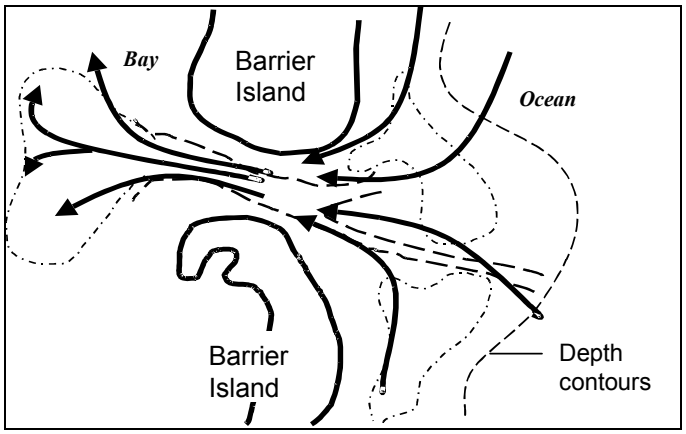

(a) Flood flow

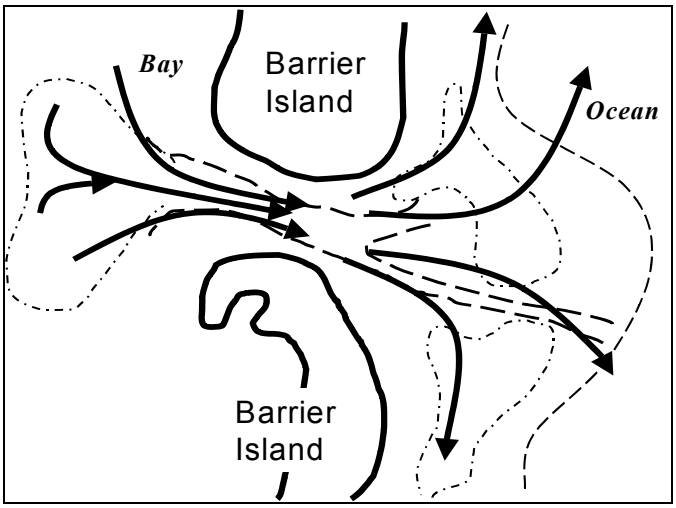

(b) Ebb flow

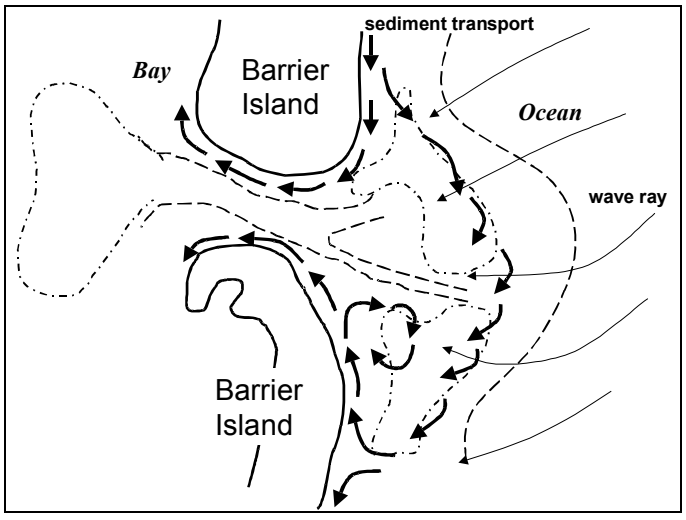

(c) Waves

Figure V-6-3. Idealized sediment transport pathways for unstabilized inlet

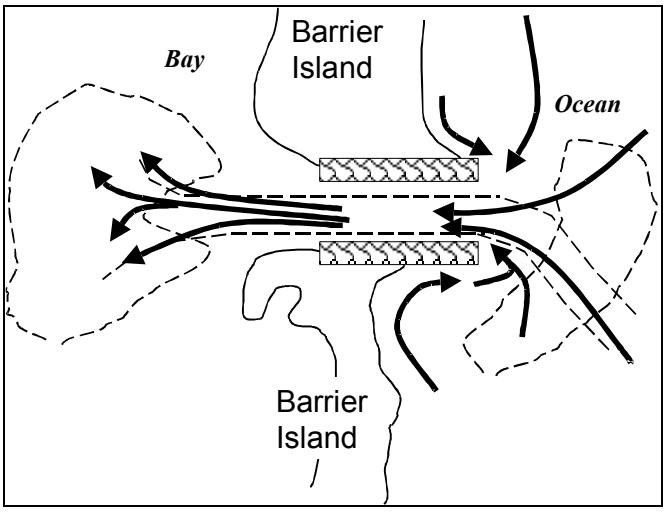

(a) Flood flow

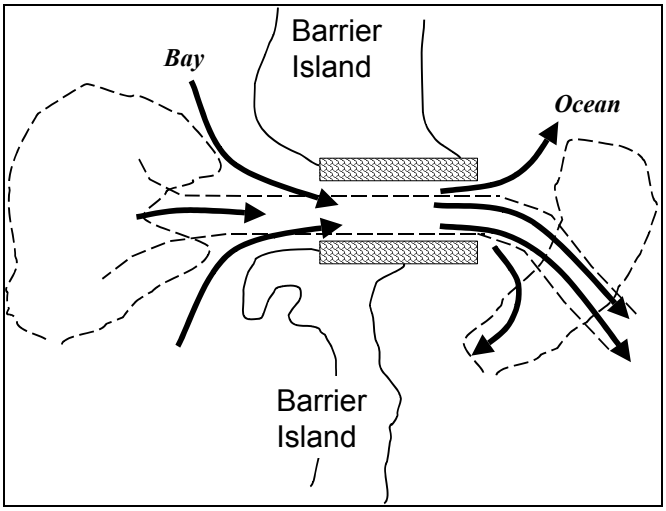

(b) Ebb flow

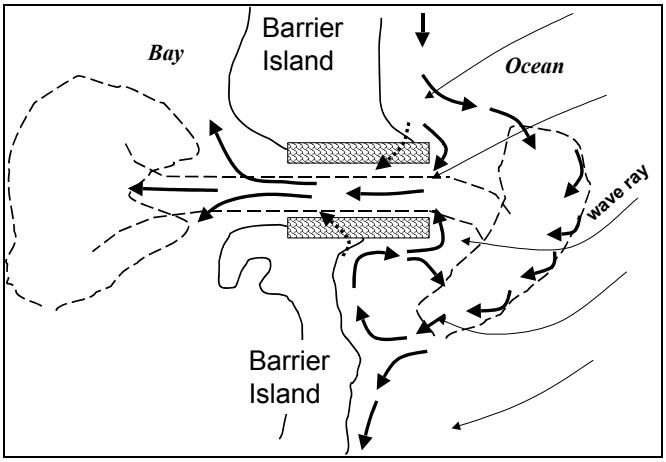

(c) Waves

Figure V-6-4. Idealized sediment transport pathways for stabilized inlet

downdrift shoreline. Along the updrift shoreline, obliquely incident waves transport sediment alongshore and directed toward the inlet. Across the inlet mouth, the waves breaking upon the ebb shoal transport sediment both toward (into) the inlet and toward the downdrift shoreline. The ebb shoal may, in turn, be skewed toward or elongated beyond the downdrift shoreline. Downdrift of the inlet (a distance of anywhere between one-half and 10 km), wave refraction across the ebb plateau decreases the obliquity of the wave's angle and the associated magnitude of the downdrift-directed transport. Closest to the inlet, transport along the shoreline (leeward of the ebb shoal) may even be reversed, so that transport is directed toward the inlet from the downdrift shoreline. This transport is augmented by diffraction currents (resulting from decreased wave energy and water level setup) directed toward the inlet along the immediate downdrift shoreline. The sediment transported toward the inlet from the downdrift shore may be carried into the inlet and/or diverted toward the ebb shoal by gyres or eddies (circular currents) associated with the inlet's tidal currents. If the jetties are not sand-tight, sediment may be transported over or through these structures (dotted lines in Figure V-6-4c).

As illustrated in Figure V-6-5a, inlets where longshore currents dominate are more likely to form an ebb shoal with a shallow, arcuate form across the mouth. If tidal currents dominate littoral transport processes (Figure V-6-5b), marginal ebb shoals (also known as linear bars) are likely, aligned with and bordering the inlet channels. Mixtures of both types of shoals are not uncommon. These characteristics are typically observed at unstabilized inlets.

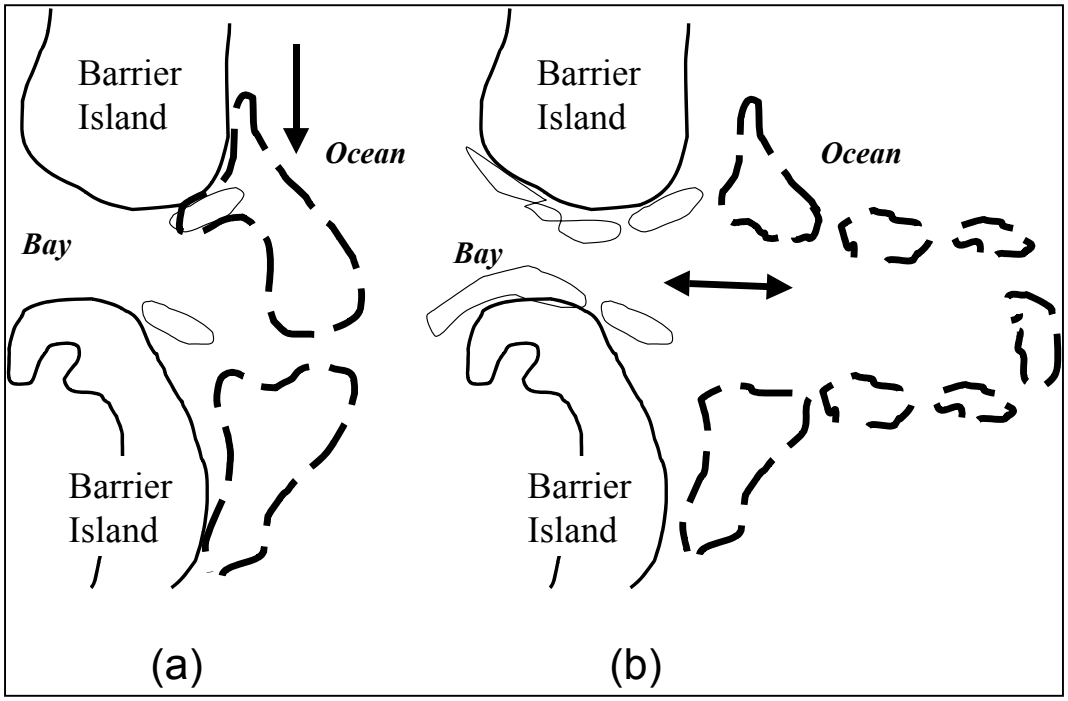

Figure V-6-5. Unstabilized tidal inlets for which (a) longshore current effects dominate, and (b) tidal current effects dominate (adapted from Oertel 1988)

Other sedimentary features include interior spits and channel shoals (see Figure V-6-1a). Spits are emergent landforms that result from the deposition of littoral drift from the adjacent shores. Channel shoals are submerged deposits that encroach upon or cover parts of the inlet seafloor. Spits and channel shoals are usually attached to the barrier island at, or just landward of, the point at which the transport spills from the shoreline into the inlet.

Processes other than just tidal-induced currents and waves can heavily influence inlet dynamics and morphology. These include wind, salinity differences between the ocean and bay waters, wave-current interactions, river discharge, underlying geology, and inlet orientation. These concepts are outlined in Parts II-6 and IV-3.

(b) Bypassing processes. Sediment may be trapped at an inlet or it may also be bypassed by a variety of natural forces. Bruun and Gerritsen (1959) described three principal mechanisms of bypassing for unstabilized inlets: Wave-induced transport along the ebb tidal shoal (bypass bar). Transport into and out of the inlet by tidal currents. Migration and welding of sandbars.

Figure V-6-6 illustrates wave-induced transport along the ebb tidal shoal (termed, in this case, a bypassing bar). Waves transport sand (littoral drift) from the updrift shoreline toward the inlet. Some of the sand is transported (ramped) directly to the ebb shoal (or bar). This sand is temporarily or permanently stored in the shoal, or is transported downdrift by waves. Once outside the principal influence of the inlet's ebb flow, waves transport the sand both landward and further downdrift, where it can rejoin the downdrift shoreline and littoral stream.

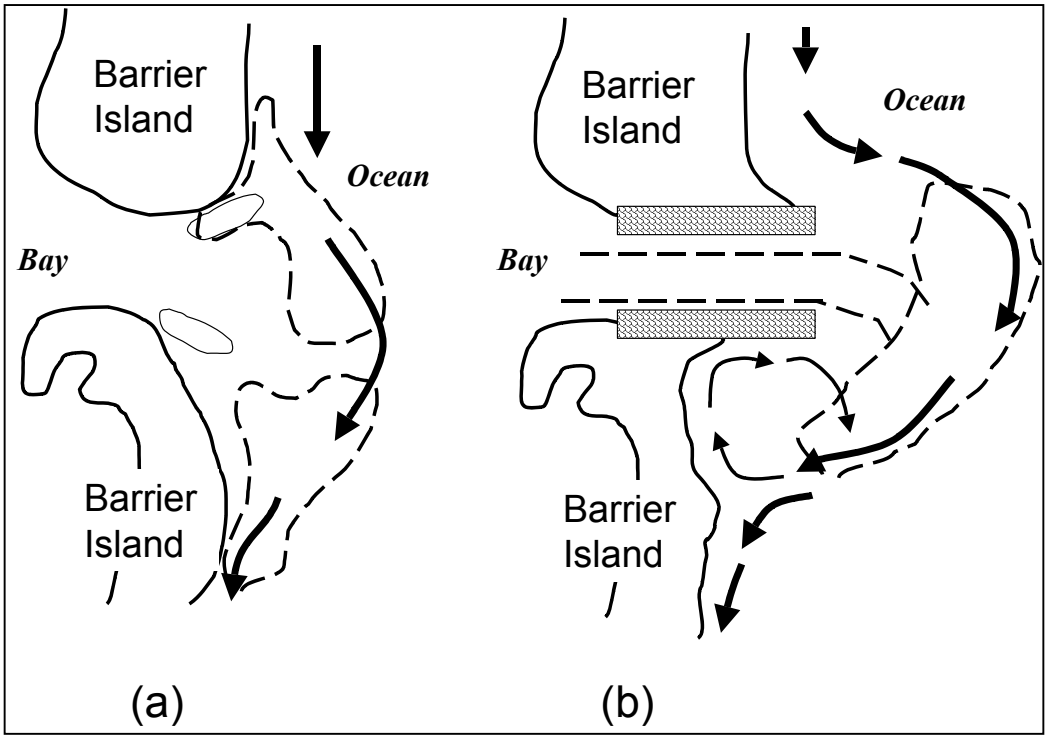

Figure V-6-6. Idealized wave-induced bypassing along the ebb tidal shoal ("bypass bar") for (a) unstabilized and (b) stabilized inlets

Figure V-6-7 illustrates idealized wave and current bypassing. A portion of the littoral drift from the updrift shore may be transported toward the inlet mouth. There, it may be temporarily or permanently stored as part of the updrift beach, creating a bulbous shoreline shape or a shallow plateau at the shoreline's toe, or it may be impounded at the updrift jetty. Or, waves and marginal flood currents may transport the sediment directly into the inlet. Flood currents sweep sand bayward from the inlet's ebb shoals, channels, and interior shoals, and deposit the sand on the flood shoal and along shoals and spits which line the inlet's interior shoreline. Ebb currents, in turn, sweep sand seaward from the flood shoal (and the channels and interior shoals) and deposit it in the ebb shoal. There, the sand may be again swept bayward by flood currents and returned by ebb currents, or may be transported along the ebb shoal by waves, where it can eventually rejoin the downdrift shoreline as previously described.

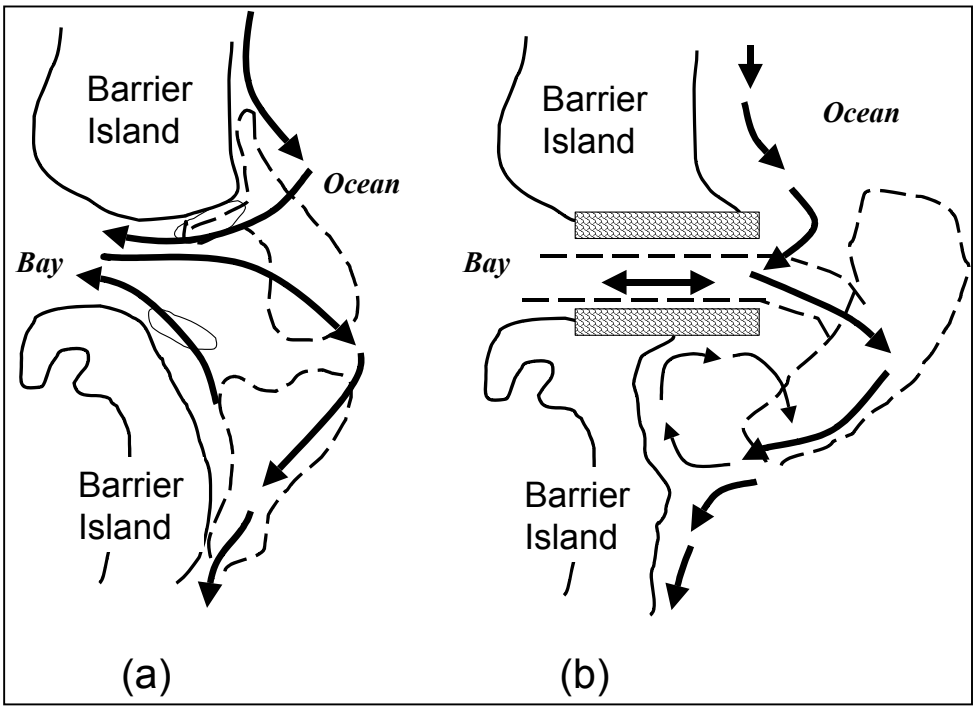

Figure V-6-7. Idealized wave and tidal current bypassing for (a) unstabilized and (b) stabilized inlets

Sand can also be bypassed directly across the ebb shoal in a zig-zag pattern by the combined action of waves and tidal currents. During transport reversals (when the waves approach from the opposite direction), the bypassing pattern can reverse; however, the methods and efficiency of the bypassing are rarely identical, particularly if the inlet and ebb shoal morphology is not symmetrical about the inlet center line. (Lack of symmetry is frequently encountered when one direction of transport dominates). These bypassing mechanisms are generally considered to be a more-or-less steady process, modulated in intensity by periods of increased littoral transport (storms, high waves, etc.).

In Figure V-6-8, increasing numbers indicate the time sequence of bypassing through migration and welding of bars. This process may occur to some degree at stabilized inlets, but it is more common for unstabilized inlets. Waves again transport sand from the updrift shore toward the inlet. Large shoals then form at the edge of the shoreline and the inlet, and/or a spit may develop

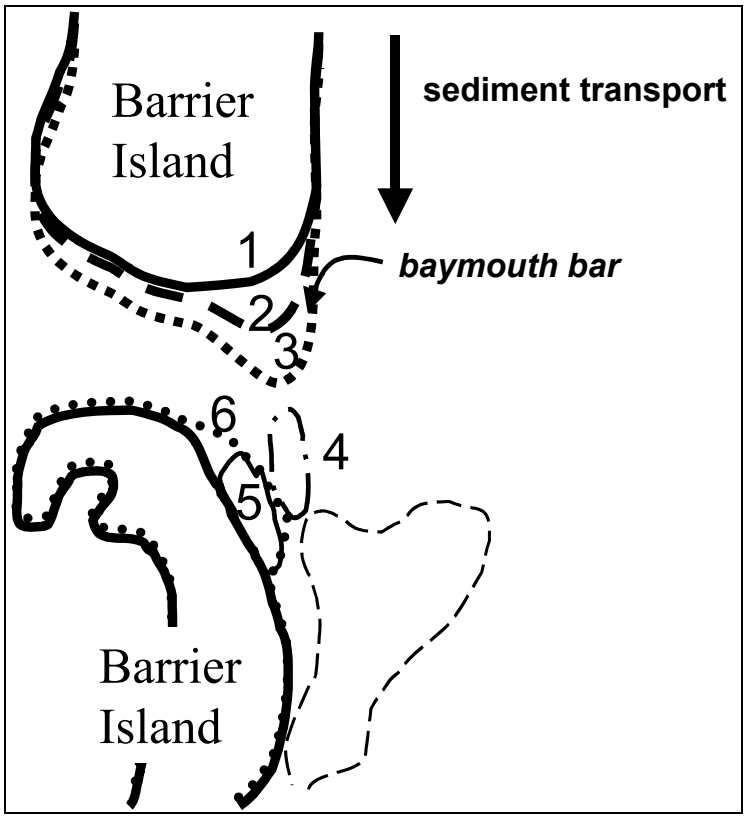

Figure V-6-8. Idealized bypassing through migration and welding of bars for an unstabilized inlet (increasing numbers indicate time sequence)

across the inlet throat (a baymouth bar). Growth of the shoals and spit force the inlet channel to, migrate downdrift. This, in turn leads to channel encroachment upon the downdrift shoreline and conesquent beach erosion. Eventually, the channel's hydraulic efficiency becomes sufficiently poor such that the inlet will close, or the channel will breach the shoals or spit (usually during a storm or flood) near the channel's original location. The shoals or spit, now severed from their direct updrift sediment source, become subject to downdrift-directed transport by waves. These sand bodies, thus, migrate downdrift and shoreward where they eventually weld onto the downdrift shoreline, nourishing the beach which was previously eroded by the inlet channel's earlier migration.

In this way, sand can be naturally bypassed in a cyclical manner, by which the updrift and downdrift shorelines retreat and advance in periodic cycles. The channel shoals and spits are the means of the bypassing mechanism. Their creation, severance, and downdrift attachment can be gradual (quasisteady) or episodic. Time scales of the cycle may range anywhere from 3 to 50 years (FitzGerald 1984, 1988; Fenster and Dolan 1996; Gaudiano and Kana 2001).

In a variation of this pattern for unstabilized inlets (not shown in Figures V-6-6 through V-6-8), waves transport sand from both adjacent shorelines toward the inlet mouth. Strong ebb and flood currents transport the sand into and out of the mouth. The sand is deposited in the ebb tidal plateau as well as large marginal ebb shoals that line the inlet channel. The emerging marginal shoals are ultimately subject to the landward-directed transport of wave action, and eventually migrate toward shore and weld to the beach. The result is a pattern of erosion and deposition along barrier islands marked by the formation of large intertidal bars along the inlet channel, and

apparently little (or at least, uncertain) net sediment bypassing. FitzGerald (1984) and Gaudiano and Kana (2001) described this process as controlling South Carolina's barrier island/inlet shorelines, noting cycles of ebb-tide delta growth and decay (15 to 20 percent changes in volume) which last from 4 to 8 years. Further elaboration of these processes is presented by FitzGerald (1988) and in Part IV-3 and Part IV-4.

Inlets, particularly unstabilized ones, can bypass sand through a combination of the bypassing mechanisms. As part of the bypassing process, unstabilized inlets may migrate, usually in the net downdrift direction, but they can also migrate updrift (see Aubrey and Speer (1984) and Douglass (1991), among others).

Inlets' natural bypassing processes also serve to illustrate the dynamic nature of the shorelines adjacent to an inlet. Roughly, the scale of the bypassing features (and therefore of the directly affected shoreline lengths) can range from 1/2 km updrift and 1-2 km downdrift for a small inlet (for example, 200 m wide), to several kilometers updrift and tens of kilometers downdrift for a large inlet (for example, >1,000 m wide) (The alongshore extent of inlets' influence is discussed in Part V-6) Beach erosion is often manifest if upland development is sited within an inlet's zone of migration or cyclical accretion/erosion associated with natural bypassing and ebb delta fluctuation. This inopportune timing of oceanfront development refers to the platting of land or establishment of construction setback lines, along the oceanfront or the inlet's interior shorefront, at times when the shoreline is at an anomalously advanced location associated with the inlet's cycle.

c. Inlet operation and maintenance activities. To maintain navigable waterways, USACE as well as state and local agencies construct jetties and dredged channels. These activities may change inlet processes (see also Part IV-4).

(1) Dredging of shoals or channels within an inlet, whether with or without structural (jetty) improvements, can increase the inlet's potential to act as a sediment sink. Most simply, the response is analogous to the natural tendency for a depression in the seabed to fill with sediment from the surrounding seabed and the active littoral system. If sand dredged from the inlet during the initial work or its subsequent maintenance is not placed upon the adjacent beaches or otherwise within the active littoral system, then the net long-term effect is expected to be erosion of the adjacent beach on one or both sides of the inlet.

(a) Inlet dredging may also increase the inlet's flow velocities or its tidal prism (the volume of water that flows into or out of the inlet in one-half tide cycle). (See Part II-6.) This may result in enlargement of the inlet shoals, and seaward displacement of the ebb shoal. Enlargement of shoals will remove sediment from the open coast to the inlet channels and on to the flood and ebb shoals. Seaward displacement of the ebb shoal is expected to reduce bypassing capacity of the inlet.

(b) An example of this effect is the 1892 creation of St. Lucie Inlet, Florida, by local residents, who, desiring a convenient channel between Indian River and the Atlantic Ocean, dredged through the sandy barrier island (Sargent 1988). Beach sand was rapidly diverted from the adjacent shores to form large ebb and flood tidal shoals. Within 37 years after the initial cut, the updrift shoreline (Hutchinson Island to the north) retreated up to 540 m from its preinlet location, and the downdrift beach (Jupiter Island) retreated over 650 m (USAED, Jacksonville, 1973). The construction of a 1,010 m-long north jetty in 1929 partially restored the north shoreline's location over the next 30 years by impounding littoral drift, but not before millions of cubic meters of sand had been (mostly irretrievably) diverted from the littoral system (Olsen Associates, Inc. 1995). A 490-m jetty was constructed at the south side in 1980, but does not nearly extend to that shoreline's preinlet location.

(2) Dredging a channel through the ebb tidal platform can also change bypassing mechanisms via the ebb shoal. Initially, portions of the shoal adjacent to the channel are subject to shoreward-directed transport by waves and can simultaneously be deflated by wave- and current-induced erosion. These portions of the shoal may migrate landward and weld to the up- or downdrift shore, resulting in significant accretion of the beach. The welded shoal and its seaward plateau, severed from its bypassing-related sand source, eventually erode and cause the beach to recede from its artificially advanced position. An example of this process may include Bald Head Island, North Carolina, located directly east of the Cape Fear River entrance. The initial stabilization and deepening of the Cape Fear River entrance channel beginning in the 1870s, by dredging, is thought to have severed the inlet's large outer bypassing plateau. The eastern lobe of the ebb shoal (totaling about 4.6 million cu m) migrated shoreward and resulted in a 370- to 600-m advance of the Bald Head Island shoreline directly east of the inlet between 1890 and 1920. The shoreline position then remained relatively stable for about 50 years. At the same time, however, the submerged toe of the severed shoal, which had welded to the shoreline, steadily eroded. Resort and residential development along the accreted, quasi-stable shoreline began in the early 1970s. But by 1974, the shoreline began to rapidly erode toward its earlier location, receding at an average rate of 20 to 30 m/year (Cleary and Hosier 1988; Olsen Associates, Inc. 1989; Jarrett 1990). Similar examples of deflation and landward migration of severed ebb tidal deltas are described for inlet improvement projects at Murrell's Inlet, South Carolina, and Little River Inlet on the North Carolina/ South Carolina border (Douglass 1987; Hansen and Knowles 1988; Chasten 1992).

(3) Structural stabilization of an inlet channel by jetties can have numerous consequences to the sediment-sharing system and adjacent shorelines. Sand-tight jetties may perform much like groins and impound littoral material. Sand may accrete the beach on the updrift shore and, during reversals in longshore transport direction, to a lesser degree on the downdrift beach. If the ebb shoal connects to the beach, construction of the jetty may extend through the bypassing platform, thereby interrupting this bypassing mechanism. Or, jetties may block the formation of bypassing spits and shoals that would otherwise cyclically grow from the updrift shoreline and migrate to the downdrift shoreline.

(a) Jetties can also transport littoral material seaward via offshore-directed (rip) currents that can develop along their updrift face. In some cases, the diverted sand may deposit in the ebb shoal, and it may or may not ever return to the downdrift beach through natural mechanisms.

(b) Jetties displace an ebb shoal seaward as a function of their length and the degree to which they increase the inlet's tidal prism and velocity. For example, the construction of the 3.2-km-long jetties at St. Mary's entrance in the late 1800s is estimated to have caused the net deposition of 92 million cu m of sand across an ebb tidal platform. This platform has been displaced about 4,000 m seaward of the original shoal (Olsen 1977; USAEWES 1995).

(c) Weir jetties, or structures that are low or porous, may increase the degree to which sand is diverted from the adjacent shores. Weir jetties constrict flood currents toward the shoreline, increasing the flow velocity and sediment transport directed into the inlet (Figure V-6-9). The subsequent ebb flow is minimally reduced by the weir's presence and transports the sediment seaward beyond the limit of the weir and jetty structure. (This process can be minimized if the sand falls into a sediment trap and is regularly bypassed by mechanical means to the adjacent shores.) Similarly, low or porous jetties allow flood flow to transport sediment into the inlet from the adjacent seabed, but then act to transport the sediment further seaward during ebb flow by their jetting action upon the ebb current. Dean (1988) has described the latter phenomenon at St. Mary's entrance.

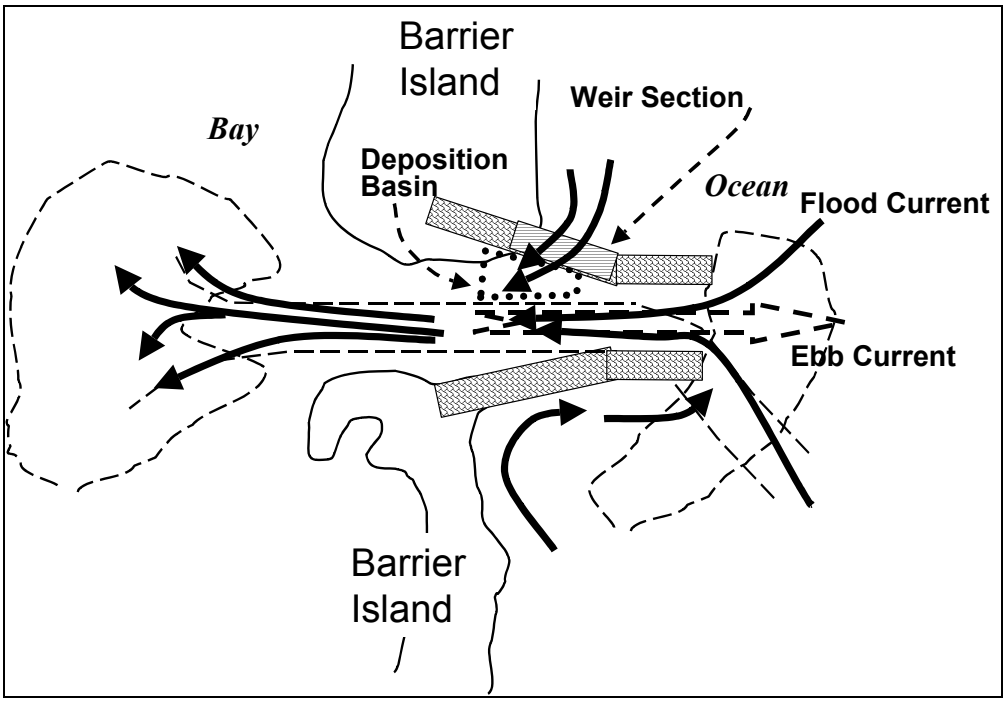

Figure V-6-9. Flood and ebb tidal flow in a weir jetty system

(d) Jetties also influence the littoral transport pattern along adjacent shorelines by developing shadow zones in which the refracted wave field is modified (see Figure V-6-4c). On the downdrift side of a jetty (or in the downdrift lee of an ebb shoal modified by the jetty's presence), sand transport is generally directed into the shadow (i.e., toward the jetty) from the adjacent shoreline by:

Refraction and diffraction of waves about the structure's seaward end.

Diffraction currents associated with a decrease in wave energy within the shadow zone.

The processes can cause a leeward impoundment fillet against the jetty.

d. Inlet modifications of longshore transport.

(1) As discussed in Part III-2, coastal engineering analyses often involve two types of longshore transport rates. (Note that the discussion herein defines rates as positive quantities; the presentation in Part III-2-2(a) applies an alternate definition.) The net longshore transport rate is defined as the difference between the right-directed and left-directed longshore transport over a specified time interval for a seaward-facing observer:

$$Q_{net} = Q_R - Q_L \tag{V-6-1}$$

where the leftward-directed transport rate Q_L and rightward-directed rate Q_R are taken as positive.

(2) The gross longshore transport rate is defined as the sum of the right-directed and left-directed transport rates over a specified time interval for a seaward-facing observer:

$$Q_{gross} = Q_R + Q_L \quad \text{(V-6-2)}$$

Inlets can trap longshore sediment transport from both directions, resulting in a greater amount of transport interruption than simply the net transport rate. That is, inlets are a potential sink to the gross longshore sediment transport in the region. Additionally, tidal currents, ebb-shoal bathymetry, and shoreline morphology can each increase the gross transport directed toward the inlet, increasing the inlet's diversion of littoral drift from the adjacent system. Examples are described in the following paragraphs.

(3) Figure V-6-10(a) depicts a fully-bypassing, equilibrated inlet in which 100 units and 40 units of longshore transport, respectively, are directed toward the inlet from the updrift and downdrift coastlines. The net and gross transport quantities are thus 60 units and 140 units, respectively. As the inlet is assumed to be fully bypassing, there is no net change to the adjacent shorelines.

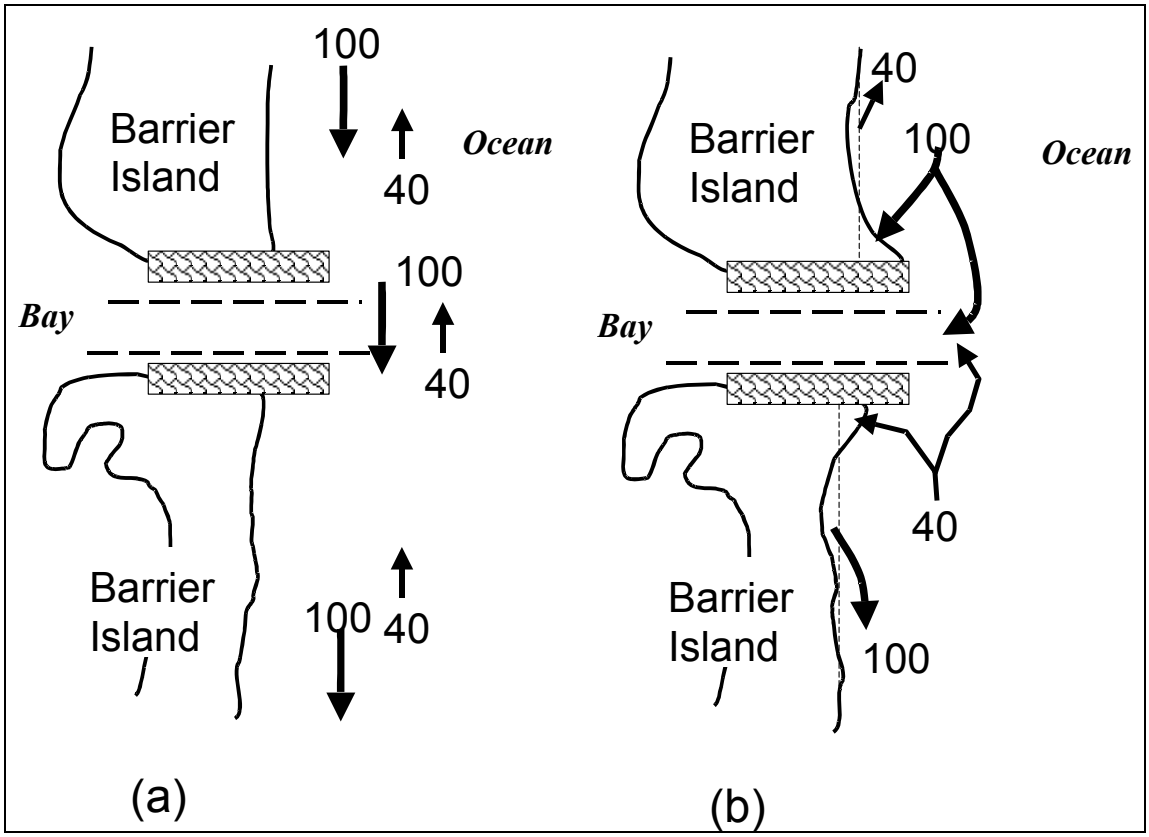

Figure V-6-10. Example of inlet-adjacent shore erosion associated with (a) a fully-bypassing inlet, and (b) an inlet that is a complete littoral sink

(4) Figure V-6-10(b) depicts an inlet which is a complete littoral sink under the same transport conditions as previously described. An inlet may be a complete littoral sink immediately after formation; as it matures, bypassing via the shoal system increases. In Figure V-6-10(b), the incident, updrift transport (100 units) is assumed to be diverted to an updrift impoundment fillet, the inlet channel, and/or shoals. The downdrift shoreline, beyond the jetty's wave shadow and deprived of the 100 units of incident transport, must yield 100 units of beach material in response to the longshore transport potential. During transport reversals, the incident transport (40 units) is likewise assumed to be diverted to a minor impoundment fillet on the other side of the inlet, the

inlet channel, and shoals. If the updrift impoundment fillet is wholly located in the jetty shadow of the reversal waves, or otherwise removed from the littoral stream by refraction effects, then the updrift shoreline, beyond the shadow, must yield 40 units of beach material in response to the longshore transport potential. If impoundment fillets form, the inlet will not shoal and the net effect is the same as the net longshore transport rate: 60 units of accretion (updrift) and erosion (downdrift). However, if no impoundment fillets form, or if the impoundments are already at capacity, the inlet channel and/or shoals may capture the gross transport (140 units), with 40 units of erosion (updrift) and 100 units of erosion (downdrift).

(5) In Figure V-6-10(b), the potential for net updrift erosion associated with the inlet is counterintuitive. Its ultimate manifestation depends upon the degree to which the updrift impoundment fillet is capable of yielding sand to the adjacent shore during transport reversals. In the limit, when there is no impoundment at the updrift jetty and when all of the updrift transport directed toward the inlet is lost therein (and there is no bypassing from the downdrift shoreline), the potential for updrift inlet-related erosion is totally realized.

(6) Wave refraction across the ebb shoal plateau may locally increase the rate of longshore transport directed toward the inlet mouth. Inlet-directed transport may likewise be induced from diffraction currents that result from gradients in breaking wave energy within the wave-shadow of the ebb shoal plateau. Additionally, a shoreline that is curved toward the inlet's mouth, such as that which results from local beach erosion, further exaggerates the local rate of inlet-directed longshore transport. The latter is a result of the increased angle with which waves break along the shoreline. Each of these phenomena can potentially increase the rate at which sand is transported toward the inlet and mouth.

(7) Figure V-6-11 illustrates potential alteration of the pattern of longshore transport by an ebb shoal. Waves 1.0 m in height and 8 sec in period were refracted from deep water across the bathymetry illustrated in the bottom graphic. The incident wave conditions were: From the left (+23 deg), 40 percent annually; from shore-normal (0 deg), 35 percent annually; from the right (-23 deg), 25 percent annually.

(8) The bathymetry is idealized, but is representative of an inlet for which littoral drift dominates tidal flow and for which the net longshore transport direction is from left to right. The upper graphic depicts the potential longshore transport rate computed from each of the three refracted wave cases. The middle graphic depicts the total right-directed, left-directed, and net transport rates that result from the weighted superposition of the individual transport curves. The component transport rates (upper graphic) are normalized by the maximum transport value among the three cases. In the middle graphic, the transport values are normalized by the maximum value of the net transport rate. Only the effect of obliquely incident waves is considered, and transport induced by alongshore gradients in wave height (diffraction currents) and tidal currents are omitted. The methods employed to compute these transport rates are described in Part III-2-2, and, later in this chapter.

(9) In this example, waves from each of the three offshore directions result in transport directed toward the inlet mouth within the alongshore reach of the ebb shoal's refractive influence. Within this region (indicated by asterisks in the middle graphic), no transport is directed away from the inlet. Additionally, the transport magnitude increases significantly beyond that of the ambient transport (i.e., the transport associated with obliquely incident waves outside of the shoal's refractive influence). The result is an increase in transport toward the inlet mouth – with

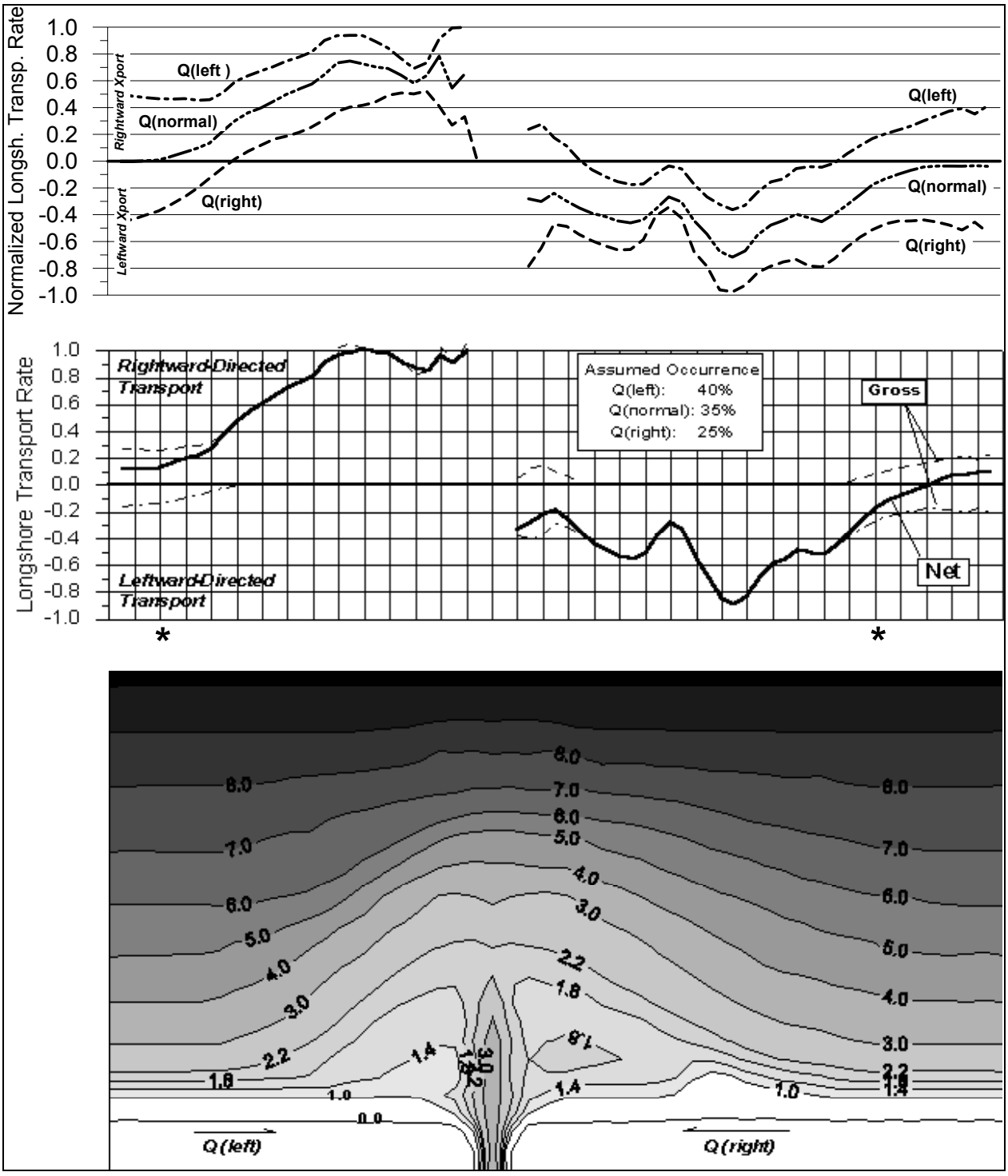

Figure V-6-11. Illustration of longshore sediment transport potential computed for three wave conditions incident to inlet's ebb shoal plateau (depths in meters)

EXAMPLE PROBLEM V-6-1

GIVEN:

The right- and left-directed volume transport rates (volume per unit of time) entering and leaving sections of shoreline upcoast and downcoast of an inlet induced by obliquely incident waves and currents are shown in the following tabulation for each section and for the inlet. Assume the inlet is a total littoral barrier (i.e., no bypassing; material can move into the inlet, but material cannot move out of the inlet).

A	B	C	D	Inlet	E	F	G	H	I
100 → 100	120 →	125 →	125 →	0 →	0 →	0 →	30 →	80 →	100 →
30 ←	30 ←	10 ←	0 ←	0 ←	60 ←	40 ←	50 ←	40 ←	30 ← 30

FIND:

The potential volume rate of change at shoreline sections A through I associated with these transport rates, and the total net volume rate of change on the left (updrift) and right (downdrift) sides of the inlet. Material transported into a section is positive (accretion = +) and material transported out of a section is negative (erosion = -).

SOLUTION:

The volume rate of change at each section A through I is equal to the algebraic sum of all volume transport rates entering and leaving each section. For example, at section C, the volume rate of change is the difference between what goes into section C (+120 + 0 = +120) and what comes out of section C (-125 + (-10) = -135). The algebraic sum of these two numbers (+120 + (-135) = -15) is the volume change per unit of time at section C.

Table V-6-1
Updrift Volume Change

Updrift	Vol. Change
A	0
B	-40
C	-15
D	0
Subtotal	-55
Inlet	+125
Total	+70

Table V-6-2
Downdrift Volume Change

Downdrift	Vol. Change
E	-20
F	+10
G	-40
H	-60
I	-20
Subtotal	-130
Inlet	+60
Total	-70

The total volume rate of transport on the left (updrift) side of the inlet (sections A through D) is equal to the volume rate of material transport entering and leaving through the left face of section A (+100 + (-30) = + 70) plus the volume rate of material transport entering and leaving through the right face of section D (-125 + 0 = -125). The algebraic sum of these two values (+70 + (-125) = -55) is the subtotal of all the changes occurring on the updrift side of the inlet (stations A through D). Thus, the left side of the inlet is eroding at a rate of -55 per unit of time.

(Continued)

EXAMPLE PROBEM V-6-1 (Concluded)

The total volume rate of transport on the right (downdrift) side of the inlet (sections E through I) is equal to the volume rate of material transport entering and leaving through the left face of section E (+0 + (-60) = -60) plus the volume rate of material transport entering and leaving through the right face of section I (-100 + (+30) = -70). The algebraic sum of these two values (-60 + (-70) = -130) is the subtotal of all the changes occurring on the downdrift side of the inlet (sections E through I). Thus, the right side of the inlet is also eroding, but at a rate of -130 per unit of time.

The total volumetric rate of change across the shoreline from sections A through I equals that material entering and leaving the left face of section A (+100 + (-30) = +70) plus that material entering and leaving the right face of section I (-100 + (+30) = -70. Thus, the total volumetric rate of change across sections A through I equals zero since the net amount of material entering the left face of section A is equal to the net amount of material leaving the right face of section I. However, the left (updrift) side of the inlet is eroding at a rate of -55 per unit of time, and the right (downdrift) side of the inlet is eroding at a rate of -130 per unit of time. Since the total erosion rate across sections A through I equals (-55 + (-130) = -185 per unit of time), and the net material rate entering the left face of section A is equal to the net material rate leaving the right face of section I, the material being eroded from the sections to the left and right of the inlet must be accumulating in the inlet. And, indeed, this is the amount of material rate passing through the right face of section D (+125) into the inlet (no material leaves the inlet), plus the amount of material rate passing through the left face of section E (+60) into the inlet (again, no material leaves the inlet), for a total of +185 per unit of time accumulating in the inlet.

no mechanism for reversal. The larger transport gradient erodes sand from the beach and transports it toward the inlet. An inlet's total potential effect is therefore equal to the sum of the ambient gross transport plus additional transport locally directed toward the inlet that is induced by the perturbation caused by the inlet on the local geometry.

e. Alongshore extent of inlet influence.

(1) The length of coastline directly influenced by an inlet is manifest, in large part, by alongshore changes in the nearshore bathymetry (and associated wave field), and alongshore changes in the beach profile shape and magnitudes of historical shoreline fluctuation. The ultimate degree to which an inlet modifies adjacent shores is a function of the volume of sand contained in its other features (Fitzgerald 1988; Bodge 1994b; Fenster and Dolan 1996); that is: impounded by jetties and other structures; captured in the flood and ebb tidal shoals; dredged; placed on adjacent beaches (e.g., dredged material or other source of fill).

(2) Absolute distances of inlet influence remain a subject of study, but may extend further than were previously thought. Shoreline response immediately adjacent to an inlet is typically obvious and erroneously led earlier investigators to conclude that the extent of inlet improvements' influence was limited to short reaches downdrift; usually some multiple (about 3 to 10) of the jetty length away from the inlet. Many, if not most, estimates in the literature of the length of inlet influence were truncated by the limited extent of coast that the investigators examined (Bruun 1995).

(3) Based upon analysis of shoreline change rates, Fenster and Dolan (1996) report the spatial influence for natural inlets along the wave-dominated North Carolina coast as up to 13.0 km, and up to 6.1 km along the mixed-energy, tide-dominated Virginia barrier islands. Dean and Work (1993) report downdrift inlet influence for inlets along Florida's central and southern Atlantic coastlines as at least 2 km

to more than 6 km; however, their analysis was limited to 6 km or less. The erosive effect of the entrance to Lagos, Nigeria, may extend at least 40 to 50 km downdrift (Bruun 1995). Migniot and Granbaulan (1985) report inlet-influenced erosion reaching 50 to 80 km downdrift of river entrances on the southwest coast of France. Bruun (1995) describes inlet-attributable erosion occurring 30 to 35 km downdrift of the Hirtshals navigation works on the North Sea coast of Denmark, 20 to 25 years after the construction of entrance breakwaters and dredging increases. Inlet-adjacent erosion may be particularly severe when the beaches are restricted by geological features, such as pocket beaches on the United States Pacific coast, but this hypothesis needs further research. Terich and Komar (1974) and Komar (1976) describe this effect at the entrance to Tillamook Bay, Oregon.

(4) Outside of the direct influence area (i.e., within the shadow of bypassing bars, jetties, etc.), an inlet's influence appears to decrease exponentially away from the inlet. One example is Port Canaveral Entrance (Bodge 1994a). This effect is also predicted by analytic shoreline-change models, including, for example, the one-line model of Pelnard-Considére (1956) described in Part III-2-2. According to Pelnard-Considére's solution for shoreline change adjacent to a sediment-trapping structure, the shoreline recession y at a distance x downdrift of the structure, at the time t_f at which the structure becomes filled to capacity and begins to bypass sand, is:

$$\frac{y}{Y} = \left[\exp\left(-u^2\right) - \sqrt{\pi} u \; erfc\left(u\right) \right] \tag{V-6-3}$$

where

$$u = \frac{x}{y} \frac{1}{\sqrt{\pi}} \tan \alpha_b \tag{V-6-4}$$

and

$$t_f = \pi \, Y^2 / 4g \, \tan^2(\alpha_b) \tag{V-6-5}$$

(5) The parameter Y is the structure length, *erfc*( ) the error function complement, and α_b is the angle of the breaking wave crests relative to the shoreline (assumed to be quasi-steady). Both y and Y are measured relative to the no-structure shoreline. The longshore diffusivity, ε,

$$\varepsilon = \frac{K H_b^{25} \sqrt{g / \kappa}}{8(s-1)(1-n)(h_* \quad B)} \tag{V-6-6}$$

is a measure of the tendency of wave action to spread out a shoreline perturbation, where K is an empirical coefficient from the longshore transport Equation III-2-5 (of order 1), H_b is the breaking wave height, g is the acceleration of gravity, κ is the ratio of local breaking wave height to local depth (about 0.8), s is the ratio of sediment to water specific gravity (about 2.65), and n is sediment porosity (about 0.4). The value h_* is the depth of active sediment transport (depth of closure) and B is the beach berm height, where B and h_* are positive values above and below the water level, respectively.

(6) Figure V-6-12 presents solutions to Equation V-6-3 for various wave breaking angles. For typical angles on the order of 2 to 8 deg, shoreline recession on the order of 5 percent of the structure's length is predicted between 15 and 50 jetty lengths downdrift. In the case of a 200-m-long jetty, this corresponds to 10 m of recession at locations between 3 and 12 km downdrift of the jetty.

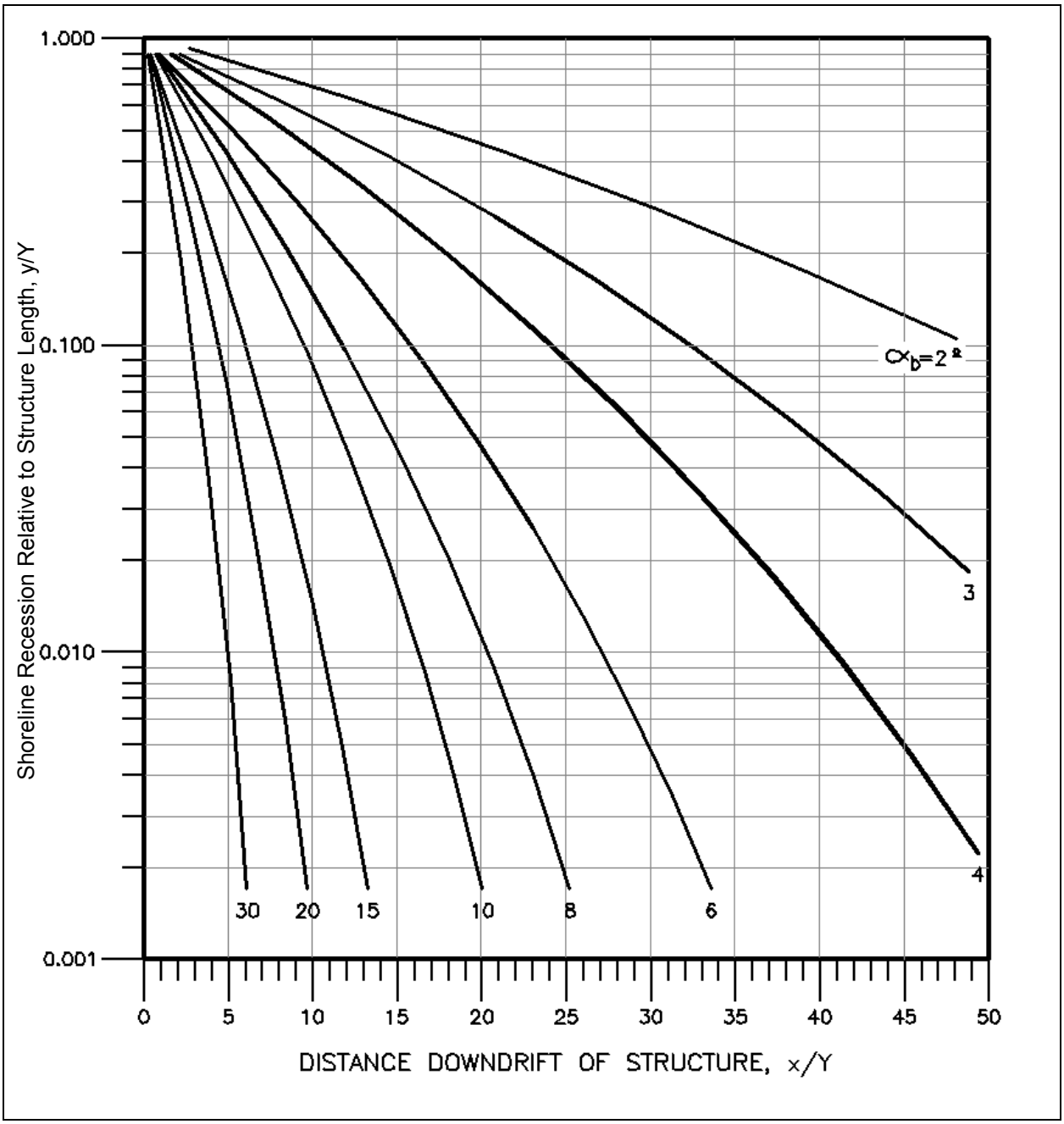

Figure V-6-12. Solutions of Equation V-6-3 (from Bodge 1994b)

(7) Dean and Work (1993) present a solution for Pelnard-Considère's equation for the case where sand is removed from the system at a rate Q_I at the inlet location x = 0:

$$y(x,t) = \frac{2p\,Q_I\sqrt{t}}{(h_* + B)\sqrt{\pi\,\varepsilon}}\,y' \tag{V-6-7}$$

where p describes the degree to which the inlet's sand removal alters each of the inlet's two adjacent shorelines; i.e.,

$$p = \frac{\left(\text{sand lost to inlet from shoreline of interest}\right)}{\left(\text{sand lost to inlet from both shorelines}\right)} \tag{V-6-8}$$

$$y' = \left[\sqrt{\pi}\, v\, erfc\left(v\right) - \exp\left(-\left(v^2\right)\right)\right] \tag{V-6-9}$$

$$v = \frac{|x|}{\sqrt{4gt}} \quad ; \quad |x| = v\sqrt{4gt} \tag{V-6-10}$$

(8) In Equation V-6-8, a value of p = 0.5 implies that the inlet's sink effect (Q_I) is evenly distributed between the two adjacent shorelines; whereas a value of p = 1.0 implies that all of the inlet's sink effect occurs from the shoreline of interest. As another example, p = 0.3 implies that 30 percent of the inlet's sink effect occurs from the shoreline of interest (whereas the other 70 percent occurs as sand losses from the other shoreline).

(9) Figure V-6-13 shows nondimensional solutions of Equation V-6-9. Additional examples and applications of Pelnard-Considère's shoreline change solution are presented in Part III-2-2. As described in that chapter, solutions for $y(x,t)$ can also be linearly added to yield the combined response of shoreline perturbations.

(10) Although Equations V-6-3 and V-6-7 provide useful theoretical insight to the potential response of a shoreline near an inlet, they are generally of limited practical value in assessing real world response. The equations do not readily account for alongshore variabilities in breaking wave angle nor sand impoundment adjacent to inlet jetties. Likewise, cross-shore transport and seasonal reversals in longshore transport direction are not taken into account. Nonetheless, these equations can be examined for order-of-magnitude effects which might be expected for a given inlet situation.

(11) From the Pelnard-Considère equations, Dean (1993) likewise presents solutions of shoreline change adjacent to an inlet for the case where sand is directed toward a dredged inlet by transport induced by ambient oblique waves and by the inlet's perturbative effect to the local shoreline. Dean observes that in the absence of effective jetties, the rate of sand that enters the inlet decreases with the reciprocal square root of time (i.e., $1/T_d^{1/2}$); however, the cumulative amount of sand entering the inlet over time from the adjacent shorelines is infinite. Dean also notes that the equations predict that the location of maximum shore erosion migrates with time away from the inlet. That is, measurements taken at one fixed point along the shoreline would first demonstrate no inlet erosion effect, then a rapid rate of erosion, then a decreasing rate as the shoreline asymptotically approaches an equilibrium, eroded position. Alternately stated, the peak erosion zone would migrate like a wave away from the inlet, and the magnitude of this peak rate would decrease with time.

(12) Bruun (1995) describes numerous examples where erosion downdrift of an inlet appears as an obvious near field effect and as a less obvious, but faster-migrating, far field effect. Bruun concluded that the downdrift shoreline development at a littoral drift barrier may in general, but not always, be described by a short (near field) effect as well as a long distance (far field) effect, both of which move downdrift at various rates. The short distance influence occurs first. After it develops to a certain extent, the long distance effect may appear, gradually moving downdrift faster than the short distance but fading out with distance. The short distance peak of the erosion occurs close to the littoral drift barrier, and moves down-drift at a rate of about 0.3 to 0.5 km/year compared to a rate of 1 to 1.5 km/year for the long distance ero-sional front. Bruun suggests that the short-distance effect is a coastal geomorphological feature, whereas the long-distance effect is a materials-deficit feature.

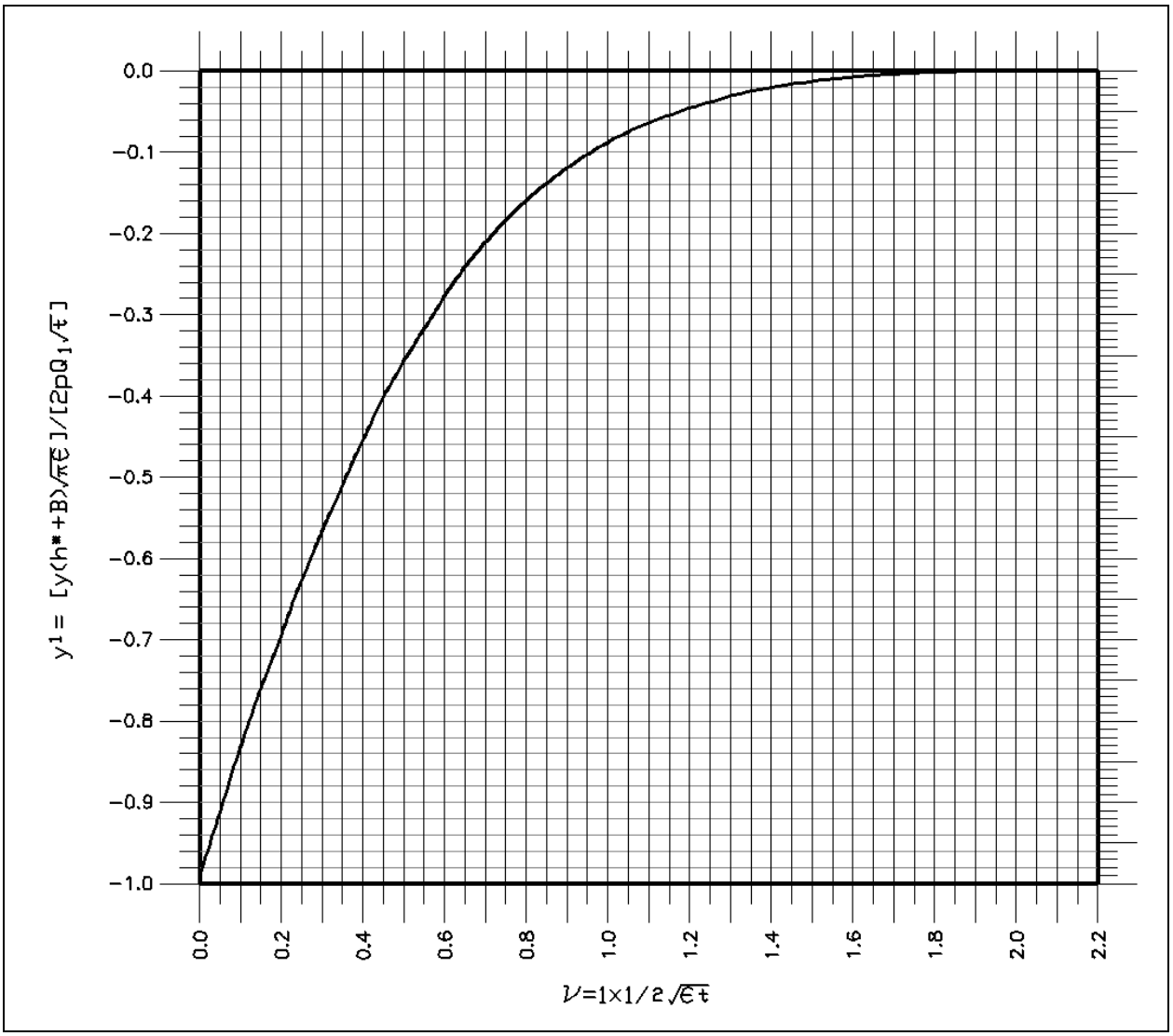

Figure V-6-13. Solution of Equation V-6-9

f. Estimating alongshore extent of inlet influence. Five methods to estimate the alongshore extent of inlet influence are as follows: Examination of historical shoreline changes; even-odd analysis; alongshore variations in beach morphology; wave refraction analysis; examination of inlet's net sink effect.

(1) Of these, Methods 1 and 2 (and to a lesser extent, 5) rely principally upon shoreline change data. Methods 3 and 4 (and, principally 5) rely upon data that are mostly distinct from shoreline change or location data. Methods 2, 3, and 4 typically yield only estimates of direct inlet effect; whereas Methods 1 and 5 potentially yield estimates of both direct and indirect (near field and far field) inlet effects. Method 5 may be the most powerful approach because it first assesses the inlet's littoral impact within the inlet, and then attempts to identify the adjacent shoreline length along which the inlet's volumetric impact is manifest. In practice, some combination of all five methods is typically necessary to assess the volumetric and lineal extent of an inlet's effect upon the adjacent shores.

EXAMPLE PROBLEM V-6-2

GIVEN: An inlet's north jetty is 240 m long (Y). It is estimated that 90 percent (p) of the inlet's net shoaling rate of 55,000 m^3/year (Q_I) is attributable to sand losses from the nonjettied downdrift shoreline. The inlet was created at time t = 0 year, at which time the shoreline was initially straight and in equuilibrium. Assume a beach of typical quartz sand of specific gravity S = 2.65, and with berm elevation B = +2 m and a depth of closure h_* = 6 m, both relative to the same datum. The average breaking wave height H_b = 0.8 m. Assume the ratio of local breaking wave height to local depth to be κ = 0.8, and the constant from the longshore transport Equation III-2-5 is K = 0.5. Assume also that the breaking wave crests typically approach with an angle of breaking $\propto_b$ = 4 deg relative to the shoreline, directed to the south.

FIND: The theoretical shoreline response downdrift of this inlet at the time the updrift jetty initially begins to bypass sand. This response consists of two parts: the impoundment effect, and the sand loss effect. These two components are computed separately and added to determine the total shore recession.

SOLUTION: The maximum recession downdrift of the inlet which is stabilized only by one jetty on the updrift side of the inlet will exist at the time t_f when bypassing begins to occur around the jetty. To determine t_f , the diffusity, ε , must first be obtained from Equation V-6-6:

$$\varepsilon = \frac{KH_b^{2.5}(g/\kappa)^{0.5}}{(8)(S-1)(1-n)(h_* \quad B)}$$

where the gravitational constant g = 9.81 m/sec^{-2} and the sediment porosity n = 0.4 (a typically representataive value).

$$\varepsilon = \frac{(0.5)(0.8m)^{2.5}(9.81m\,\sec^{-2}/0.8)^{0.5}}{(8)(2.65-1)(1-0.4)(6m+2m)}$$

$$\varepsilon = 0.0158m^2/\sec = 498{,}600m^2/year$$

The time at which bypassing is expected to begin can now be determined by Equation V-6-5:

$$t_f = \pi Y^2/4\varepsilon(\tan\alpha_b)^2$$

$$t_f = \frac{(3.1416)(240m)^2}{(4)(0.0158m^2/\sec)(\tan 4.0)^2}$$

$$t_f = 5.85 \text{ x } 10^8 \sec = 18.5 \text{ years}$$

First, compute the erosion due to the impoundment effect. Erosion downcoast of the inlet will be a maximum at the inlet and occur at the time that sand begins to pass around the jetty of length Y = 240 m. This erosion will become asymptotic to the original downcoast shoreline. For convenience, arbitrary multiples of the jetty length in a downcoast x-direction are considered (i.e., x/Y = 1, 2.5, 5, 10, ….., 40 times the jetty length, Y). These computations are tabulated in column 1 of Table V-6-3.

(Continued)

EXAMPLE PROBLEM V-6-2

Table V-6-3
Calculations for Impoundment and Sand Loss Effects at Inlet

Impoundment Effect					Sand Loss Effect		
1	2	3	4	5	6	7	8
x/Y (select)	*y/Y* (Figure V-6-12 for α_b=4°)	*x* (m) (= col. 1 x 240 m)	*y* (m) (= col. 2 x 240 m)	$\nu = \lvert x\rvert/(4\varepsilon t)^{1/2}$	*y'*(from Fig. V-6-13)	*y* (m) (Equation V-6-7)	y_{tot} (m) (Cols. #4 + #7)
1	0.95	240	-228	0.040	-0.93	-40	-268
2.5	0.85	600	-204	0.099	-0.83	-35	-239
5	0.70	1200	-168	0.197	-0.70	-30	-198
10	0.45	2400	-108	0.395	-0.45	-19	-127
15	0.29	3600	-70	0.592	-0.28	-12	-82
20	0.18	4800	-43	0.789	-0.16	-7	-50
25	0.092	6000	-22	0.987	-0.09	-4	-26
30	0.05	7200	-12	1.184	-0.06	-3	-15
35	0.024	8400	-6	1.381	-0.04	-2	-8
40	0.011	9600	-3	1.579	-0.02	-1	-4

For the arbitrary values of x/Y of column 1, the corresponding values of y/Y for α_b = 4 deg are determined from Figure V-6-8. Here y is the impoundment effect component of the total recession. The appropriate y/Y values for the arbitrary x/Y values with α_b = 4 deg are shown in column 2. Column 3 shows the x-distances downcoast for the arbitrary x/Y values of column 1. Next, the Impoundment Effect, y, is obtained by multiplying the y/Y values of column 2 by Y = 240 m, and these results are shown in column 4.

It is now necessary to compute the erosion recession distance associated with the sand loss effect from the downdrift shoreline into the inlet over the 18.5-year period during which the updrift impoundment fillet formed. This erosion distance is a function of two additional parameters (ν and y') which must first be determined.

The parameter ν is defined by Equation V-6-8 as:

$$\nu = \frac{|x|}{(4\varepsilon t_f)^{0.5}}$$

$$\nu = \frac{|x|\, m}{\left[(4)(0.0158 m^2/\sec)(5.85 \times 10^8 \sec)\right]^{0.5}}$$

$$\nu = \frac{|x|}{6080}$$

(Continued)

EXAMPLE PROBLEM V-6-2 (Concluded)

For each of the values of x in column 3, and for the time t_f = 18.5 years (5.85 x 10^8 sec), the corresponding dimensionless value of υ is computed, and displayed in column 5.

The parameter y' can be determined from Equation V-6-7 or from Figure V-6-9, for each of the values of υ from column 5. These values of y' are shown in column 6.

For each of the y' values shown in column 6, the corresponding value of y due to the sand loss effect can be determined from Equation V-6-7:

$$y(x,t) = \frac{2p\,Q_I(t)^{0.5}\,y'}{(h_* + B)(\pi\varepsilon)^{0.5}}$$

At t = t_f = 18.5 years, and for each y' value which is also a function of distance x,

$$y = \frac{(2)(0.9)(55{,}000m^3/year)(18.5years)^{0.5}\,y'}{(6m+2m)\left[(3.1416)(498{,}600m^2/year)\right]^{0.5}}$$

$$y = 42.5y'(m)$$

Thus, for each y' value computed at the alongshore distances x of column 3, the corrresponding recession due to the sand loss effect has been determined, and is shown in column 7.

The total recession at an alongshore location from the inlet, x, is the sum of the recession due to the impoundment effect (column 4) plus the recession due to the sand loss effect (column 7). These total recession values are shown in column 8. For example, at location x = 1,200 m downdrift of the inlet (here x/Y = 5, since Y = 240 m), the shoreline recession is predicted to be -168 m + (-30 m) = -198 m.

(2) The practical utility of the methods that rely upon shoreline change data can be significantly degraded by the limitations of historical shoreline data. Shoreline change data contain temporal and/or survey noise; or, may be biased by artificial manipulation; or, may not adequately characterize the beach profile's behavior as a whole. Three precautions are thus warranted when using adjacent shoreline change data to ensure the best quality conclusions:

(a) *Identify the season and/or storm events that characterize the survey data*. Shoreline locations developed from surveys, charts, or photographs that contain the record of a particular wave event (such as a storm or a period of reversed transport) may not represent the net long-term behavior of the local coastline. If a time series of shoreline positions is available, this problem is often obvious as an anomalous advance of the shoreline followed immediately by a more or less equivalent retreat (or vice versa). Remediation of this problem often requires deleting of the suspect data set.

(b) *Identify the effect of seawalls, beach nourishment, and other artificial manipulations upon the data.* Seawalls or other structures bias data by maintaining the shoreline at more or less constant location. This is often evidenced by an anomalously low (or zero) rate of shoreline change amidst an otherwise erosional coastline. The placement of beach fill by nourishment or bypassing obviously results in a large

initial advance of the shoreline. Less obvious, however, is the fact that shoreline change rates measured within 1 or 2 years after such activity will be anomalously high because of profile equilibration. Failure to recognize the effects of seawalls and beach-fill placement will result in gross overestimation of shoreline stability. Also, failure to recognize the accelerated rate of profile adjustment after beach-fill placement will result in gross overestimation of erosion. Remediation of this problem generally requires deleting (or adjusting) those data that are artificially biased. In the case of beach fill, the estimated effect of the fill's presence can be subtracted from the data; or better, if profile data are available, changes in total beach volume should be considered instead of shoreline location (see the following paragraph).

(c) *Determine the degree to which the elevation selected as the shoreline characterizes the profile behavior as a whole.* The translation of a discrete elevation at which the shoreline is identified may not accurately represent the overall profile's behavior. For example, lower elevations (such as the mean low water line) typically exhibit seaward advance if a profile erodes because of profile flattening. The flatter slopes of lower elevations are highly sensitive to profile change when computing the horizontal location at a given elevation. The mean high water line (mhwl) is typically selected to represent shoreline changes. Particularly along coasts that feature high bluffs or dunes, however, mhwl changes may not reflect beach erosion manifest by dune retreat. For example, 36 percent of the State of Florida's historical beach profiles examined along two of that state's east coast counties exhibited retreat of the dune face and concurrent advancement of the mhwl. For another 36 percent of the profiles, both the dune face and the mhwl exhibited retreat, but in two-thirds of those cases, the rate of dune face recession was over twice as great as that of the mhwl (Savage 1990).

(3) If local shoreline change is not representative of the profile change as a whole, net changes in beach volume should be considered instead of shoreline location. Here, volume changes above the depth of closure (or other sufficiently deep elevation) should be considered; i.e., the volume change per unit alongshore length of shoreline (cu m/m or cu yd/ft, etc.). Alternately, where shoreline change must be specified, as in the case of one-line analytic or numerical models, the local volume change can be converted to an equivalent, artificial shoreline change. This is computed by dividing the volume change (volume/alongshore length) by a specified profile depth (height), where the latter is usually taken as the vertical distance between the berm elevation, B, and the depth of closure, h_*. Precautions regarding the transformation of shoreline changes to volume changes are discussed in the following paragraphs (see Methods 3 and 5).

(a) *Method 1: Examination of historical shoreline changes*. In this method, temporal fluctuations in shoreline location adjacent to an inlet are quantified by comparing (overlaying) historical charts, aerial photographs, profile surveys, etc. Specifically, the cross-shore location of a specific beach elevation (mean high water, etc.) is identified at constant locations along the coast for each time at which data are available. The rates of shoreline change at each location, and between consecutive data sets, are then computed. (Alternately, the change in beach volume above a certain elevation can be quantified at each location for each data set.) Using these methods, Fenster and Dolan (1996) describe three criteria to identify the spatial extent of inlet processes on adjacent shorelines:

> The cessation of abrupt changes in the rates of change alongshore, and/or the reduction in variability of these rates alongshore. Rate-of-change values are deemed no longer abrupt if:

- The difference in rate values between adjacent transects over an X-meter-long reach does not increase or decrease by more than x meters per year (where X and x may be on the order of about 100- to 500 m and 0.2- to 0.3 m, respectively, depending upon the general coastline of interest).

- The standard deviation of a subset of along-the-shore values (neglecting the transects nearest the inlet) is minimized.

The slope of a regression line drawn through a subset of along-the-shore values (neglecting transects nearest the inlet) most closely equals zero.

Changes in the sign of the rate value from erosion to accretion (or vice versa).

A change from less erosional to more erosional (or vice versa); or, from less accretionary to more accretionary (or vice versa).

A change in slope of the cumulative shoreline change or volume change computer along the shoreline.

- For natural inlets located on the wave-dominated North Carolina coast and the mixed-energy, tide-dominated Virginia barrier coast, Fenster and Dolan (1996) found that the first criterion revealed the greatest lineal extent of inlet-related shoreline impact (≤6.1 km). The second criterion generally yielded the next greatest degree of impact (≤5.2 km), and third criterion yielded the most conservative estimate (≤4.3 km). Paraphrasing their results, Fenster and Dolan concluded that there are zones in which inlet-related processes dominate shoreline trends (estimated from the third criterion), and where inlet-related processes influence shoreline trends (estimated from the first criterion). The second criterion yields estimates between the two zones.

- The fourth criterion is a potentially useful synthesis of the first three, particularly where shoreline change data are noisy. In this approach, the shoreline change (or more meaningfully, the local volume change (volume per unit alongshore beach width)), is integrated along the shoreline, starting at the inlet ($x = 0$). The process of integration smoothes fluctuations between adjacent profiles. This allows improved visualization of large-scale trends and easier discrimination of the data points that are dominating the data set. Integrating away from the inlet (and for a positive-valued shoreline axis), positive slopes in the cumulative curve represent shoreline accretion while negative slopes represent erosion.

(b) *Method 2: Even-odd analysis*. Dean and Work (1993) describe the application of the so-called "even-odd" analysis of profile change data (Berek and Dean 1982) for shoreline changes adjacent to inlets in Florida. The total shoreline (or volume) change y at an alongshore distance x from the inlet is considered to be composed of an even (symmetric) component, $y_E(x)$, and an odd (antisymmetric) component, $y_O(x)$:

$$y(x) = y_E(x) + y_O(x) \tag{V-6-11}$$

where $y_E(x) = y_E(-x)$, and $y_O(x) = -y_O(-x)$. The even and odd components are extracted from the total (measured) shoreline (or volume) change signal by

$$y_E(x) = [\, y(x) + y(-x) \,] / 2 \tag{V-6-12a}$$

$$y_O(x) = [\, y(x) - y(-x) \,] / 2 \tag{V-6-12b}$$

The even component is a change that is symmetric about the inlet center line ($x = 0$). Physically, it is interpreted as an ambient, or background change that is common to both shorelines adjacent to the inlet (e.g., storm erosion, relative sea level change), equal placement of fill on both sides of the inlet, or equal transport from the two shorelines into the inlet.

EXAMPLE PROBLEM V-6-3

GIVEN:

Historical charts from 1927 and 1956, sampled at 250-m intervals (x), were used to develop mean high water shoreline changes (y) both north and south of an inlet. These data are shown in columns 1 and 2, respectively, in the following table for directions both north and south of the inlet. Positive values reflect shoreline seaward advance (accretion = +), and negative values reflect shoreline retreat (erosion = -). North of the inlet, the profile's active vertical height $h_* + B = 8.0$ m. Within 1,500 m south of the inlet, $h_* + B = 6.5$ m. Further south, $h_* + B = 7.5$ m. These data are shown in column 3. Here h_* is the depth of profile closure, and B is the berm thickness. The sum of $h_* + B$ is the thickness of sand movement.

Table V-6-4
Volume Change Calculations North and South of Inlet

North of Inlet						South of Inlet					
Given Data			Find (compute)			Given Data			Find (compute)		
1	*2*	*3*	*4*	*5*	*6*	*1*	*2*	*3*	*4*	*5*	*6*
Station *x* (m)	*y* (m)	h_*+B (m)	ΔV cu m/m	$x\,\Delta V$ 1000's of cu m	$\sum x\Delta V$	Station *x* (m)	*y* (m)	h_*+B (m)	ΔV cu m/m	$x\,\Delta V$ 1000's of cu m	$\sum x\Delta V$
2+50	+75.3		602	150.6	150.6	2+50	-8		-52	-13.0	-13.0
5+00	+56.2		450	112.5	263.1	5+00	-86		-559	-139.8	-152.8
7+50	+55.0		440	110.0	373.1	7+50	-99	6.5	-643.5	-160.9	-313.7
10+00	+28.5		228	57.0	430.1	10+00	-66		-429	-107.3	-421.0
12+50	+17.5		140	35.0	465.1	12+50	-42		-273	-68.3	-489.3
15+00	+21.2	8.0	170	42.4	507.5	15+00	-9		-58.5	-14.6	-503.9
17+50	+25.6		205	51.2	558.7	17+50	+3.4		25.5	6.4	-497.5
20+00	+5.4		43.2	10.8	569.5	20+00	-10.		-75	-18.8	-516.3
22+50	+7.4		59.2	14.8	584.3	22+50	-12	7.5	-90	-22.5	-538.8
25+00	+2.1		16.8	4.2	588.5	25+00	-27		-202.5	-50.6	-589.4
27+50	-4.4		-35	-8.8	655	27+50	-27		-202.5	-50.6	-640.0
30+00	+2.0		16	4	659	30+00	-16		-120	-30.0	-670.0
32+50	+3.2		25.6	-6.4	653	32+50	-24		-180	-45.0	-715.0
35+00	-7.5		-60	-15	638	35+00	-18		-135	-33.8	-748.8
37+50	-4.5		-36	-9	629	37+50	-12		-90	-22.5	-771.3

(Continued)

EXAMPLE PROBLEM V-6-3 (Continued)

FIND:

The updrift and downdrift limits of inlet influence upon the adjacent shoreline based upon these historical shoreline change data. Identify the total net volume gained or lost from each adjacent shoreline.

SOLUTION:

The updrift and downdrift inlet effects on the adjacent shorelines are apparent from the data of columns 1 and 2. Here are shown distances alongshore from the inlet, and the corresponding mean high water shoreline changes.

The volume of material V either gained or lost per beach cross section taken at 250-m intervals can be estimated by approximating the cross-sectional area A at each interval and multiplying by the interval distance alongshore x. The cross-sectional area A at a beach section can be approximated as the product of the mean horizontal high water change (y, from column 2) and the section profile's active vertical height ($h_* + B$, from column 3), such that $A = y(h_* + B)$, shown in the Figure V-6-14. When multiplied by x = 1 m alongshore, the resulting volume ΔV is the amount of material being gained or lost per meter of shoreline in the vicinity of that particular beach cross section, and is shown in column 4. When the cross-sectional A is multiplied by the interval distance alongshore (x, from column 1), the resulting volume V is the amount of material being gained or lost between the adjacent cross sections, and is shown in column 5. The summation of the volume of material on both the north and south sides of the inlet are shown in column 6, and these volumes are in Figure V-6-14.

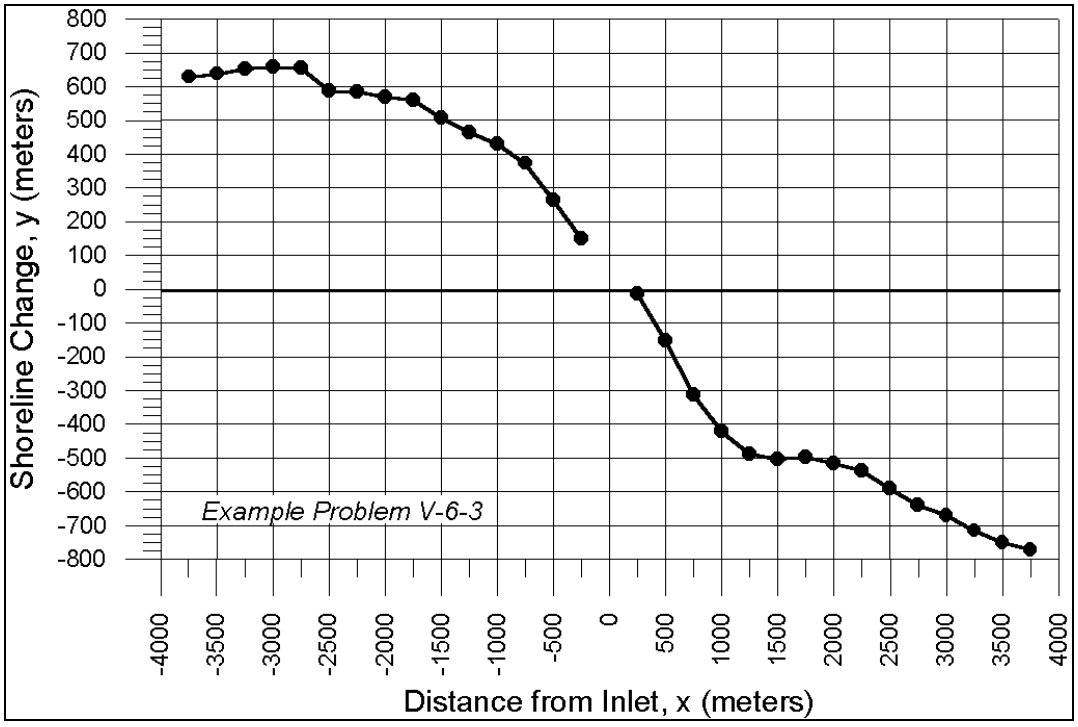

Figure V-6-14. Shoreline change as a function of distance from inlet (Example Problem V-6-3)

EXAMPLE PROBLEM V-6-3 (Concluded)

From this graph, it can be seen that the limit of direct inlet influence is about 2,500 to 2,700 m north of the inlet, and totals about 660,000 cu m of impoundment. Over the period of record, this equates to 660,000 cu m/29 years = 22,800 cu m/year, on average. There is a primary (near field) inlet effect within about 1,500 to 1,700 m south of the inlet, totaling about 500,000 cu m of erosion. There is an apparent far field inlet effect beginning about 2,000 m south of the inlet and extending beyond the 3,750-m limit of data. Within the limit of data, the net volume change downdrift of the inlet is 774,000 cu m of erosion, or about 26,700 cu m/year, on average. The actual downdrift deficit may be greater, as the inlet's influence apparently extends beyond the data limit (indicated by the continuing downward slope of the cumulative-volume curve at the right end of the graph). The fact that the downdrift erosion is greater than the updrift accretion (-774,000 cu m vs. +660,000 cu m) suggests that sand is being lost from the downdrift side by both interruption of the net southerly-directed transport and losses of northerly-directed transport from the south shoreline into the inlet.

The odd component is antisymmetric about the inlet center line. It can be interpreted as the inlet's interruption effect upon the net littoral drift (e.g., impoundment along the updrift shoreline and erosion along the downdrift shoreline), placement of fill on one side of the inlet, accretion of the shoreline due to an attachment of the ebb tidal shoal, etc. Again, volume change (instead of shoreline change) is as aptly used in these equations. Likewise, the difference in shoreline or volume changes before and after a given event in time can be considered by this approach. In this case, the given event may be the creation of, or some modification of, the inlet.

By its nature, the even-odd analysis assumes that shoreline changes (and transport processes) are symmetric/antisymmetric across the inlet center line. Accordingly, the degree to which results from the even-odd analysis accurately reflect actual inlet processes depends upon the degree to which the inlet-adjacent processes are, indeed, symmetric. Imbalances of volume change across the inlet are inherently spread across the inlet (i.e., split between the two shorelines) by the even-odd analysis. In Example ProblemV-6-4, the impoundment effect of both sides of the inlet is equal, while in Example Problem V-6-5, erosion of the downdrift shoreline greatly exceeds the accretion (impoundment) of the updrift shoreline. The result is a significant net deficit of sand in the system.

In Example Problem V-6-5, the total, net value of the inlet's effect is correct for the shoreline lengths considered (at least for the assumed background erosion rate); however, the distribution of the inlet's computed effect may not be correct. That is, the computed distribution assumes that the net inlet-induced loss from the littoral system (-995,000 cu m) is evenly divided between the updrift and downdrift shores. In reality, the net inlet-induced loss from the system may be much greater for one shore than for the other.

The fact that neither the odd- nor even-components tend to zero at the limits of the measurements reveals the net volume deficit in the system. The non-zero values at the analysis' limits also illustrate that the inlet's sediment influence extends beyond the ±4,000-m distance considered in the analysis.

The odd-component is often (incorrectly) assumed to solely represent the inlet's effect. Note, however, that even if the odd-component vanished to zero at the limits of the analysis, the fact that the even-component does not tend to zero indicates that the inlet effect may extend beyond the limits of the analysis. (This is easily demonstrated in this example by setting the measured shoreline change at +4,000 m equal to the shoreline change value at –4,000 m.)

(c) *Method 3: Alongshore variations in beach morphology.* Changes in the beach profile shape and sediment texture may provide evidence of the extent of the inlet's direct effect. For example, in order that adjacent beach profiles close at a common depth across a littoral barrier, accretional shorelines updrift of the barrier must be steeper than erosional shorelines downdrift. The limit of inlet's direct effect may be marked by the point at which variations in the profile shape (steepness) decrease, or when the profile reaches a shape or steepness similar to the remainder of the shore far from the inlet. In practice, profile steepness can be simply expressed as the horizontal length between two fixed elevations on the profile (usually measured from the berm to a depth between the beachface and closure), relative to the fixed elevation difference.

A useful way to compare profile similarity is to compute, for each profile station, the relationship between the change in profile volume and the change in shoreline locations (for some fixed elevation):

$$G_p = \frac{\Delta V}{\Delta y} = \frac{\text{volume change per unit shoreline length}}{\text{change of shoreline location}} \tag{V-6-13}$$

The S.I. units of G_p are cu m/m of shoreline change per meter along the shore; cu m/m/m = m. If the profile shape remains identical as the shoreline advances or retreats, G_p is equal to the height of the active profile; i.e., the vertical height between the top of the berm and the depth of profile closure, $(B + h_*)$. As previously noted, however, profiles steepen as sand is impounded updrift of a barrier (such as a jetty), and flatten as the shoreline recedes due to sediment deficits or the inlet's sink effect. The value of G_p is typically greater for impoundment-type shorelines, and lesser for receding-type shorelines.

The overall practical value of this method is limited because it identifies only the inlet's direct influence. It therefore yields a conservative (short) estimate of inlet effect. Moreover, natural changes in beach morphology, wave climate, or sediment type may obscure those variations that are attributable to the inlet.

(d) *Method 4: Wave refraction analysis.* An inlet's perturbative effect upon nearshore bathymetry strongly influences the transformation (refraction, shoaling, diffraction, etc.) of waves as they approach and break along the shoreline. This, in turn, influences the littoral drift patterns. (See, for example, Figure V-6-11.) Wave refraction analysis is a useful means by which to investigate this effect.

Chapter II-3-2 describes methods to compute wave transformation. Of central importance in the current application is the computation, along the shore, of the wave height and angle at the point of incipient breaking (i.e., immediately at the breakpoint), and the associated longshore sediment transport potential. Use of a grid-based wave refraction model (such as RCPWAVE) is assumed. In order to capture the effect of the inlet's ebb shoals, it is important that the wave transformation be computed all the way to the shoreline or final wave breaking point. That is, computation of breaking wave conditions at the shoreline from the wave conditions at some nearshore reference depth that is along the seaward edge of the ebb shoal plateau will greatly underestimate the inlet's perturbative effect on the wave field (Bodge, Creed, and Raichle 1996).

EXAMPLE PROBLEM V-6-4

GIVEN:

Shoreline surveys spaced 500 m apart both north (+x) and south (-x) of a small inlet were used to identify changes in the location of the mean high water shoreline between 1976 and 1980. These data are shown in columns 1 and 2, respectively, of the table below. Background erosion (i.e., outside the inlet's influence) is thought to be about 0.33 m (1 ft) over this period.

Table V-6-5
Data and Calculations for Even-Odd Analysis

1	2	3	4	5	6	7	8
x **(m)**	***y*** **measured**	y_E **even**	y_O **odd**	***y*** **background**	***y*** **erosion**	***y*** **impoundment**	***y*** **net inlet effect**
-4000	-4	-3.5	-0.5	-0.33	-3.17	-0.5	-3.67
-3500	-5	-3.5	-1.5	-0.33	-3.17	-1.5	-4.67
-3000	-5	-3.5	-1.5	-0.33	-3.17	-1.5	-4.67
-2500	-1	-6	5	-0.33	-5.67	5	-0.67
-2000	5	-2	7	-0.33	-1.67	7	5.33
-1500	22	-2	24	-0.33	-1.67	24	22.33
-1000	35	2	33	-0.33	2.33	33	35.33
-500	50	10	40	-0.33	10.33	40	50.33
-1	45	11.5	33.5	-0.33	11.83	33.5	45.33
1	-22	11.5	-33.5	-0.33	11.83	-33.5	-21.67
500	-30	10	-40	-0.33	10.33	-40	-29.67
1000	-31	2	-33	-0.33	2.33	-33	-30.67
1500	-26	-2	-24	-0.33	-1.67	-24	-25.67
2000	**-9**	**-2**	**-7**	**-0.33**	**-1.67**	**-7**	**-8.67**
2500	-11	-6	-5	-0.33	-5.67	-5	-10.67
3000	-2	-3.5	1.5	-0.33	-3.17	1.5	-1.67
3500	-2	-3.5	1.5	-0.33	-3.17	1.5	-1.67
4000	-3	-3.5	0.5	-0.33	-3.17	0.5	-2.67
Net vol. change (1000's of cu m)							
Vol (-x)	358.5	-8.5	367	-8.5	0	367	367
Vol (+x)	-375	-8.5	-367	-8.5	0	-367	-367
Vol (tot.)	-17	-17	0	-17	0	0	0

(Continued)

EXAMPLE PROBLEM V-6-4 (Continued)

FIND:

The even- and odd-components of the shoreline change signals adjacent to this inlet, and the net effect of the inlet along the shoreline beyond ambient (background) changes.

SOLUTION:

In this example, the even-odd analysis is applied under the assumption that shoreline changes (and transport processes) are symmetric across the inlet center line (i.e., it assumes the shoreline on one side of the inlet is a reverse mirror image of the other side). Therefore, shoreline change data should be obtained at the same corresponding distances on both sides of the inlet to apply the even-odd analysis (i.e., data should be compiled at distance +x on one side of the inlet and -x on the other side of the inlet).

The even and odd components of the shoreline change can be determined by Equations V-6-12a and V-6-12b, respectively, and from the data of columns 1 and 2.

$$y_E(x) = \frac{y(x) + y(-x)}{2}$$

$$y_O(x) = \frac{y(x) - y(-x)}{2}$$

For example, at x = 2,000 m:

$$y_E(2{,}000) = \frac{(-9) + (5)}{2} = -2$$

$$y_O(2{,}000) = \frac{(-9) - (5)}{2} = -7$$

At x = -2,000 m:

$$y_E(-2{,}000) = \frac{(5) + (-9)}{2} = -2$$

$$y_O(-2{,}000) = \frac{(5) - (-9)}{2} = 7$$

The even and odd components for all the x-stations are shown in columns 3 and 4, plotted in Figure V-6-15.

(Continued)

EXAMPLE PROBLEM V-6-4 (Continued)

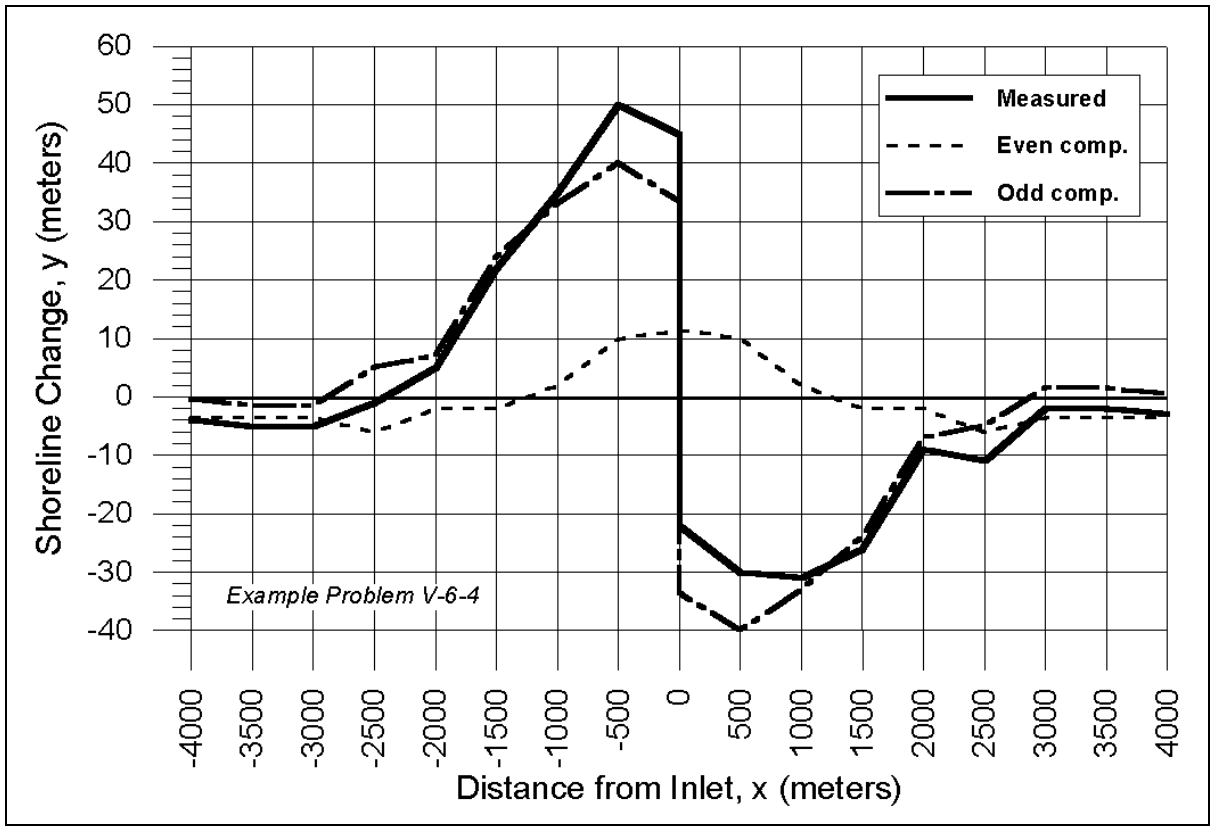

Figure V-6-15. Even-odd analysis for Example Problem V-6-4

From this graph, the positive portion of the even components suggests that there is transport directed towards the inlet within –1,250 to +1,250 m. The odd component reveals the presence of an impoundmnet fillet north of the inlet and a corresponding sediment deficit south of the inlet.

(Continued)

EXAMPLE PROBLEM V-6-4 (Concluded)

The estimated effect of sand transport direct toward the inlet along both shorelines (column 6) is computed as the even component (column 3) minus the estimated background signal of -0.33 m (column 5). For example, at x = +2,000 m, this effect is -2.0 - (-0.33) = - 1.67 m. Values for all the stations are listed in column 6. The estimated impoundment effect of the inlet is simply equal to the odd component (column 4), and is listed again in column 7.

The total net inlet effect relative to the estimated background signal (column 8) is computed as the measured shoreline change (column 2) minus the background signal of -0.33 m (column 5). For example, at x = +2,000 m, the total net inlet-induced effect is -9 - (-0.33) = -8.67 m. Values for all the stations are listed in column 8.

The volume changes associated with the shoreline change data are computed as the shoreline change value multiplied by the active profile depth (6.0 m) multiplied by the alongshore length of beach represented by each station. For example, the measured volume change estimated for the -x stations is:

$$[(-4 - 5 - 5 - 1 + 5 + 22 + 35 + 50)(500) + (45)(250)](6) = 358{,}500 \text{ cu m}$$

The net volume changes are listed at the bottom of each column for the updrift (-x) and downdrift (+x) shorelines, and for the sum of both.

In this example, the total net measured change across both shorelines (-17,000 cu m) is attributed to the area's background erosion rate (column 5). No net erosional effect is computed from transport toward the inlet (column 6), although there is a redistribution of 55,700 cu m of sand from the zone further than 1,000 m away from the inlet to the area within 1,000 m of the inlet. (This volume is computed as the sum of the changes in column 6 within +/-1,000 m of the inlet.) The net volume of the inlet's impoundment effect is computed to be 367,000 cu m (column 7). Neglecting the re-distribution of sand caused by inlet-induced transport (column 6), and neglecting any net accumulation of sand within the inlet's shoals which is not manifest as shoreline erosion within the +/-4-km study area, the inlet's net downdrift deficit beyond background erosion is therefore 367,000 cu m. This effect appears to extend about 3,000 m south of the inlet.

EXAMPLE PROBLEM V-6-5

GIVEN:

Shoreline surveys spaced 500 m apart both north (+x) and south (-x) of a small inlet document changes in the location of the mean high water shoreline between July 1956 and December 1968 (12.5 years). These data are shown in columns 1 and 2 of Table V-6-6. Background retreat (outside of the inlet's influence) is assumed to be 0.8 m/year over this time period, for a total retreat of 10 m.

Table V-6-6
Data and Calculations for Even-Odd Analysis and Net Volume Change

1	2	3	4	5	6	7	8
x **(m)**	***y*** **measured**	y_E **even**	y_O **odd**	***y*** **background**	***y*** **erosion**	***y*** **impoundment**	***y*** **net inlet effect**
-4000	-11	-19	8	-10	-9	8	-1
-3500	-10	-18.5	8.5	-10	-8.5	8.5	0
-3000	-8	-19.5	11.5	-10	-9.5	11.5	2
-2500	-1	-30.5	29.5	-10	-20.5	29.5	9
-2000	-2	-38.5	36.5	-10	-28.5	36.5	8
-1500	22	-36.5	58.5	-10	-26.5	58.5	32
-1000	35	-45	80	-10	-35	80	45
-500	50	-30	80	-10	-20	80	60
-1	45	-26.5	71.5	-10	-16.5	71.5	55
1	-98	-26.5	-71.5	-10	-16.5	-71.5	-88
500	-110	-30	-80	-10	-20	-80	-100
1000	-125	-45	-80	-10	-35	-80	-115
1500	-95	-36.5	-58.5	-10	-26.5	-58.5	-85
2000	-75	-38.5	-36.5	-10	-28.5	-36.5	-65
2500	-60	-30.5	-29.5	-10	-20.5	-29.5	-50
3000	-31	-19.5	-11.5	-10	-9.5	-11.5	-21
3500	-27	-18.5	-8.5	-10	-8.5	-8.5	-17
4000	-27	-19	-8	-10	-9	-8	-17
			Net vol. change (1000's of cu m)				
Vol (-x)	293	-752	1045	-255	-497	1045	548
Vol (+x)	-1797	-752	1045	-255	-497	-1045	-1542
Vol (total)	-1505	-1505	0	-510	-995	0	-995

(Continued)

EXAMPLE PROBLEM V-6-5 (Continued)

FIND:

The even- and odd-components of the shoreline change signals adjacent to the inlet, and the net effect of the inlet beyond ambient (background) shoreline change.

SOLUTION:

As stated earlier, the degree to which results from the even-odd analysis accurately reflect actual inlet processes depends upon the degree to which inlet and adjacent processes are, indeed, symmetric. In this example, retreat of the downdrift shoreline greatly exceeds the advance due to impoundment of the updrift shoreline. The result is a significant deficit of sand in the system.

The even and odd components of the shoreline change are again determined by Equations V-6-12a and V-6-12b, respectively, and from the data of columns 1 and 2.

$$y_E(x) = \frac{y(x) + y(-x)}{2}$$

$$y_O(x) = \frac{y(x) - y(-x)}{2}$$

For example, at x = 2,000 m:

$$y_E(2{,}000) = \frac{(-75) + (-2)}{2} = -38.5$$

$$y_O(2{,}000) = \frac{(-75) - (-2)}{2} = -36.5$$

At x = -2,000 m:

$$y_E(-2{,}000) = \frac{(-2) + (-75)}{2} = -38.5$$

$$y_O(-2{,}000) = \frac{(-2) - (-75)}{2} = 36.5$$

(Continued)

EXAMPLE PROBLEM V-6-5 (Concluded)

The even and odd components for all the x-stations are shown in columns 3 and 4, and plotted in Figure V-6-15.

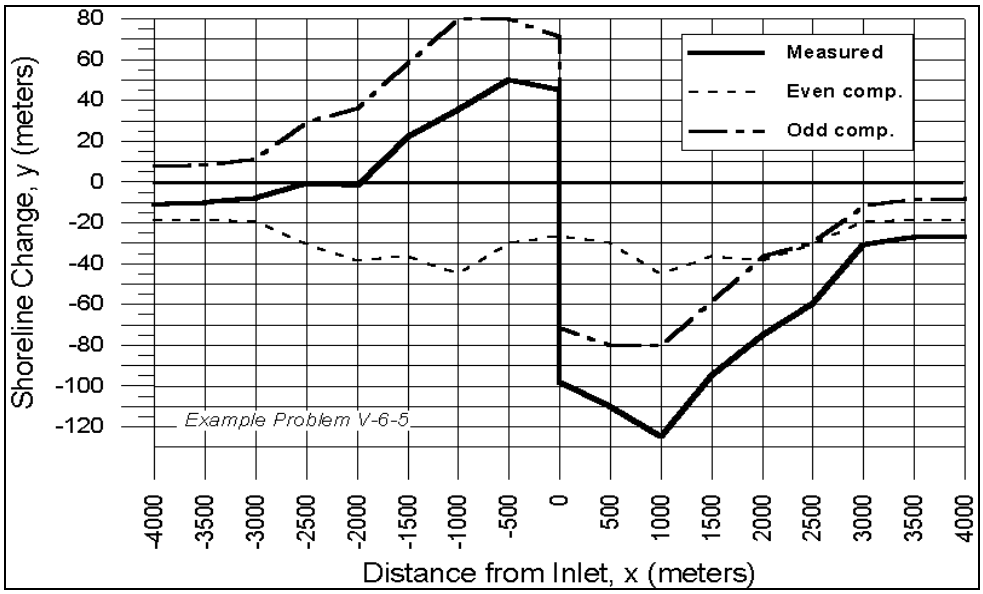

Figure V-6-16. Even-odd analysis for Example Problem V-6-5

The background erosion rate is 0.8 m/year x 12.5 years = 10 m. This value (column 5) is subtracted from the even component (column 3) since this component represents the common (symmetric) signal across both shorelines. The result is listed in column 6.

The even component, adjusted for background erosion effects, suggests that there is transport directed toward the inlet and lost therein. The net effect of this loss is computed as -497,000 cu m from each shoreline, for a total of -995,000 cu m (column 6). The odd component reflects the inlet's gross impoundment effect and the associated downdrift deficit associated with the impoundment's interruption of net littoral drift. This value is computed as -1,045,000 cu m (column 7).

Of the total net volume change estimated from the measured shoreline change data, -1,505,000 cu m (column 2), the -10 m background change accounts for -510,000 cu m (column 5). The balance is the inlet's net effect, -995,000 cu m (column 8). The even-odd analysis distributes this net deficit even across the inlet (i.e., -497,000 cu m for each shoreline, column 6). When added to the impoundment effect, the computed net result is 548,000 cu m of net accretion along the updrift shoreline and -1,542,000 cu m of net erosion along the downdrift shoreline (column 8).

For each alongshore column of the refraction grid, and for each case of interest, the shoreward-most occurrence of a nonbroken wave is identified; i.e., where the wave height H is less than κ times the water depth, h. The breaking index κ is typically equal to about 0.8, or as otherwise specified in the refraction model. Assuming shallow water wave conditions, the breaking wave height H_b and α_b can be estimated from:

$$H_b \sim \frac{A_1}{1 - \frac{1}{5} A_1 A_2} \tag{V-6-14}$$

$$\alpha_b = \sin^{-1}\left[\frac{\sin\hat{\alpha}}{C}\sqrt{g H_b / \kappa}\right] \tag{V-6-15}$$

where

$$A_1 = (\kappa / g)^{1/5} H^{4/5} (C_g \cos\hat{\alpha})^{2/5} \tag{V-6-16a}$$

$$A_2 = g (\sin\hat{\alpha})^2 / C^2 \tag{V-6-16b}$$

The values C and C_g are the wave celerity and group celerity, respectively, at the reference (non-broken wave) location. The value $\hat{\alpha}$ is the wave angle at the reference location measured relative to the local shoreline orientation:

$$\hat{\alpha} = \alpha - \beta \tag{V-6-17}$$

where α is the wave angle relative to the grid at the reference location (i.e., the value output by the wave refraction analysis) and β is the shoreline angle relative to the grid at the alongshore column of interest.

From Part III-2-2, the potential longshore transport rate is computed for each column, and for each wave case, from

$$Q = \mathrm{K}' H_b^{5/2} \sin(2\alpha_b) \tag{V-6-18}$$

where Q has units of volume per time; and where

$$\mathrm{K}' = \frac{K\sqrt{g}}{16(s-1)(1-n)} \tag{V-6-19}$$

and K is the dimensionless coefficient from the CERC Formula (Equation III-2-5).

EXAMPLE PROBLEM V-6-6

GIVEN:

Local water depths, wave heights, and angles were computed by a numerical wave transformation model for five grid elements of one column of a numerical computational grid. The wave period T is 9.0-sec, and the shoreline angle (β) at this column is +2.0 deg relative to the grid. The numerical model's breaking index is $\kappa = H_b/h_b = 0.8$, where H_b is the wave height at breaking and h_b is the water depth where the 9.0 sec wave breaks. Assume the sand specific gravity S = 2.65, the in-place sediment porosity n = 0.4, and the imprecise dimensionless coefficient from the CERC Formula (Equation III-2-18) is taken to be K = 0.5.

Table V-6-7
Numerical Model Results for Longshore Transport Potential Calculations

GIVEN: Numerical Model Results				Compute
Grid Row #	Depth *h* (m)	Wave Ht *H* (m)	Angle α (deg)	κ = *H*/*h*
1	0	0	0	--
2	0.3	0.24	3.5	0.8
3	0.7	0.56	5.4	0.8
4	1.7	0.57	5.6	0.34
5	2.9	0.52	5.8	0.18

FIND:

The incipient breaking wave height and angle, and the longshore transport potential from nearshore wave conditions computed across this numerical wave transformation grid.

(Continued)

EXAMPLE PROBLEM V-6-6 (Continued)

SOLUTION:

The incipient breaking wave height and angle occur in the grid row closest to the shoreline where the breaking index $\kappa = H/h$ is less than 0.8. Here H is the wave height and h is the water depth at a particular cell of the grid. Hence, it is necessary to compute κ for each row of this column of cells, starting at the shoreline and working seaward. At grid row 1, the water depth is 0.0, and H/h is undefined. At grid row 2, H/h = 0.24/0.3 = 0.8 (a broken wave). At grid row 3, H/h = 0.56/0.7 = 0.8 (also a broken wave). At grid row 4, H/h = 0.57/1.7 = 0.34 (a non-broken wave). Thus, the shoreward-most occurrence of a non-breaking wave is at grid row 4 where the water depth is 1.7 m. (Note: The wave height and angle in the above table for grid row 4 are not breaking wave characteristics. Breaking, however, does occur somewhere within grid row 4. Grid row 4 becomes the reference location from which breaking conditions, H_b and α_b, will be computed.) Here this 9.0 sec wave has a non-broken wave height H = 0.57 m and a non-broken wave angle $\alpha = 5.6$ deg relative to the grid. A definition sketch of the layout of the grid relative to the shoreline and approaching wave crests is presented in Figure V-6-17.

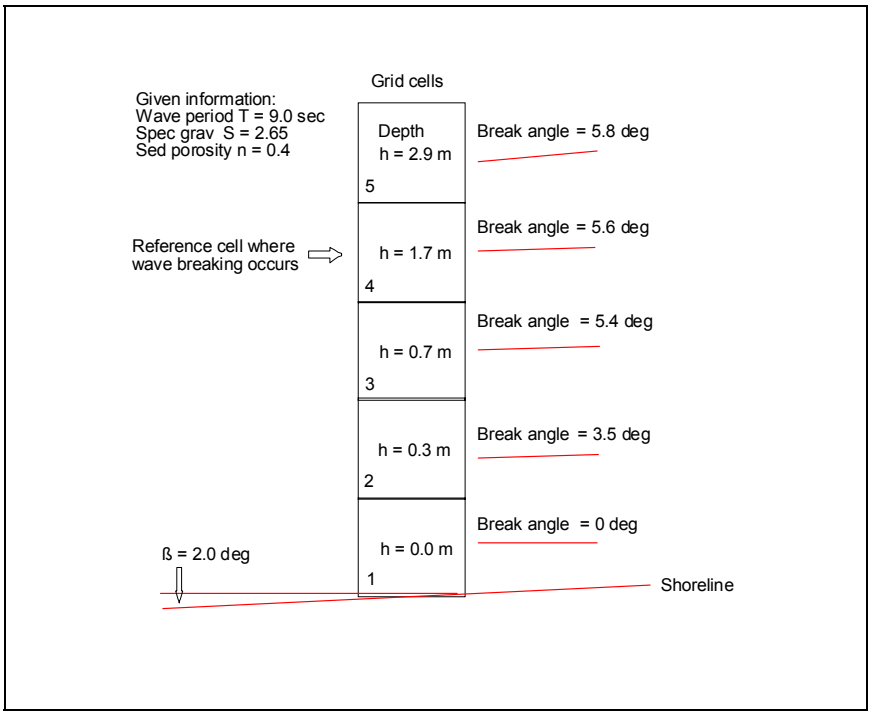

Figure V-6-17. Sketch of numerical model results for Example Problem V-6-6

(Continued)

EXAMPLE PROBLEM V-6-6 (Continued)

The value $\hat{\alpha}$ is the wave angle at the reference location measured relative to the local shoreline orientation. From Equation V-6-17:

$$\hat{\alpha} = \alpha - \beta$$

where α is the wave angle relative to the grid at the reference location (i.e., the output value from the numerical wave transformation model), and β is the shoreline angle relative to the grid at the grid column of interest.

Assuming shallow-water wave conditions, the breaking wave height (H_b) and breaking wave angle α_b can be estimated from Equations V-6-14 and V-6-15, respectively:

$$H_b = \frac{A_1}{1 - \frac{A_1 A_2}{5}}$$

$$\alpha_b = \sin^{-1}\left[\frac{\sin\hat{\alpha}}{C}(gH_b/\kappa)^{0.5}\right]$$

A_1 and A_2 are defined by Equations V-6-16a and V-6-16b, respectively.

where $$A_1 = (\kappa/g)^{0.2} H^{0.8} (C_g \cos\hat{\alpha})^{0.4}$$

and $$A_2 = \frac{g(\sin\hat{\alpha})^2}{C^2}$$

The acceleration due to gravity is g = 9.81 m/sec^2. The values C and C_g are the wave celerity and group celerity, respectively, at the reference (nonbreaking) location where the wave period T = 9.0 sec and the water depth h = 1.7 m. From Equation II-1-7:

$$C = L/T$$

where L is the local wavelength. Hence, it becomes necessary to determine the local wavelength L at this location. From Equation II-1-10:

$$L = \frac{gT^2}{2\pi}\tanh\left(\frac{2\pi h}{L}\right)$$

(Continued)

EXAMPLE PROBLEM V-6-6 (Continued)

The solution of this expression for the local wavelength L involves some difficulty because L occurs on both sides of the equation. There are, however, a number of ways to solve this equation. It can be solved by iteration, or from tabulated values of L and C by Goda (1985), or from tabulated values of h/L_0 and h/L by Wiegel (1954), or by the procedure of Fenton and McKee (1990), or by use of Figure II-1-5 (Part II). From either of these methods, with T = 9 sec and h = 1.7 m, it can be determined that L = 36.27 m. Applying the CEM method (for example), $L_0 = gT^2/2\pi = 9.81(9)^2/2\pi$ = 126.46 m. Thus, h/L_0 = 1.7/126.46 = 0.01344. From Figure II-1-5 at h/L_0 = 0.01344, it can be determined that $\sinh(2\pi d/L)$ = 0.2988, from which $2\pi d/L$ = 0.2945, and from which L = 36.27. Because $C = L/T$, C = 36.27 m/9 sec = 4.03 m/sec.

By Equation II-1-49:

$$C_g = \frac{1}{2}\frac{L}{T}\left[1 + \frac{\frac{4\pi h}{L}}{\sinh\frac{4\pi h}{L}}\right]$$

$$C_g = \frac{1}{2}\frac{36.27m}{9\,\sec}\left[1 + \frac{\frac{(4)(\pi)(1.7m}{36.27m}}{\sinh\frac{(4)(\pi)(1.7m)}{36.27m}}\right]$$

$$C_g = 3.91\,m/\sec$$

Angle α = 5.6 deg (the wave angle relative to the grid), and was determined by the numerical model output at grid row 4. Angle β = 2.0 deg (the shoreline angle relative to the gird) was given. Hence:

$$\hat{\alpha} = \alpha - \beta = 5.6\,\text{deg} - 2.0\,\text{deg} = 3.6\,\text{deg}$$

$$A_1 = (\kappa/g)^{0.2} H^{0.8} (C_g \cos\hat{\alpha})^{0.4}$$

Here κ is the model's breaking wave index, $\kappa = H_b/h_b = 0.8$.

$$A_1 = (0.8/9.81m\sec^{-2})^{0.2}(0.57m)^{0.8}(3.91m\sec^{-1}\cos 3.6\,\text{deg})^{0.4}$$

$$A_1 = 0.677m$$

$$A_2 = g(\sin\hat{\alpha})^2 / C^2$$

(Continued)

EXAMPLE PROBLEM V-6-6 (Concluded)

$$A_2 = 9.81 m \sec^{-2} (\sin 3.6 \deg)^2 / (4.03 m \sec^{-1})^2$$

$$A_2 = 0.00238\ m^{-1}$$

$$H_b = \frac{A_1}{1 - \frac{A_1 A_2}{5}} = \frac{0.0667m}{1 - \frac{(0.667m)(0.00238m^{-1})}{5}}$$

$$H_b = 0.067\ m$$

$$\alpha_b = \sin^{-1}\left[\frac{\sin\hat{\alpha}}{C}(gH_b / \kappa)^{0.5}\right]$$

$$\alpha_b = \sin^{-1}\left(\sin 3.6 \deg / 4.03 m \sec^{-1}\right)\left[(9.81 m \sec^{-2})(0.67m)/0.8\right]^{0.5}$$

$$\alpha_b = 2.56\ deg$$

The potential longshore sediment transport rate can now be determined by Eq. V-6-16:

$$Q = K' H_b^{2.5} \sin(2\alpha_b)$$

where

$$K' = \frac{Kg^{0.5}}{16(S-1)(1-n)}$$

$$K' = \frac{(0.5)(9.81 m \sec^{-2})^{0.5}}{(16)(2.65 - 1)(1 - 0.4)}$$

$$K' = 0.099 m^{0.5} \sec^{-1}$$

from which

$$Q = (0.099 m^{0.5} \sec^{-1})(0.67m)^{2.5}[\sin(2)(2.56 \deg)]$$

$$Q = 0.0033 m^3 \sec^{-1}$$

EXAMPLE PROBLEM V-6-7

GIVEN:

The potential longshore transport rate (Q, in units of volume per time) for each of five alongshore columns of a refraction grid, and for three different wave conditions each during the time period of interest, are presented as lines 1-3 in the Table V-6-8. The percentages of occurrence (P) of the three wave conditions are 22, 25, and 16 percent. There were no waves (calm) during 37 percent of the time period of interest. These percentages of occurrence are shown as lines 4-6 in the table.

Table V-6-8
Potential Longshore Transport Rate Information for Fire Grid Columns

		Grid Column				
Line	Parameter	1	2	3	4	5
1	Q_1 (cu m/hr)	2.9	3.3	5.2	6.4	6.2
2	Q_2 (cu m/hr)	-0.7	-0.4	1.6	1.8	2.1
3	Q_3 (cu m/hr)	-6.8	-6.5	-1.5	0.8	0.2
4	P_1 (%)	0.22	0.22	0.22	0.22	0.22
5	P_2 (%)	0.25	0.25	0.25	0.25	0.25
6	P_3 (%)	0.16	0.16	0.16	0.16	0.16
7	P_1Q_1 (cu m/hr)	0.64	0.73	1.14	1.41	1.36
8	P_2Q_2 (cu m/hr)	-0.18	-0.10	0.40	0.45	0.53
9	P_3Q_3 (cu m/hr)	-1.09	-1.04	-0.24	0.13	0.03
10	Q_R (cu m/hr)	0.64	0.73	1.54	1.99	1.92
11	Q_L (cu m/hr)	-1.27	-1.14	-0.2	0	0
12	$Q_{(NET)}$ (cu m/hr)	-0.63	-0.41	1.30	1.99	1.92
13	Q_{RN} (cu m/hr)	0.32	0.37	0.77	1.00	0.96
14	Q_{LN} (cu m/hr)	-0.64	-0.57	-0.12	0	0
15	$Q_{(NET)N}$ (cu m/hr)	-0.32	-0.21	0.65	1.00	0.96

FIND:

The total rates of right-directed (+), left-directed (-), and net transport potential for the five grid columns along this shoreline. Normalize the results by the net transport maxima.

SOLUTION:

The potential longshore transport rate (Q) can be expressed as some function of the breaking wave height (H_b) and the breaking wave angle (α_b), as given by Equation V-6-18,

$$Q = K' H_b^{2.5} \sin(2\alpha_b)$$

with units of volume per time (e.g., cu m/hr).

(Continued)

EXAMPLE PROBLEM V-6-7 (Concluded)

A numerical simulation wave refraction model was used to determine the breaking wave height (H_b) and breaking wave angle (α_b) for each of the five columns of the refraction grid. Equations V-6-14 through V-6-19 were then used to determine the potential longshore transport rate Q (cu m/hr) for these conditions, and these are GIVEN values shown as lines 1-3. The expression for the potential longshore transport rate Q (cu m/hr) (Equation V-6-18) inherently assumes there is an unlimited supply of sand available for movement. The total amount of sand moved during the time interval of interest is, therefore, the product of the rate of movement Q (cu m/hr) multiplied by the time interval (which may be more or less than 1 hr). The three wave conditions under consideration here existed for P_1 = 22 percent, P_2 = 25 percent, and P_3 = 16 percent of an hour, respectively. These percentages of occurrence are presented as lines 4-6.

The rate of actual material movement per hour by a particular wave climate is determined as the product of the potential longshore transport Q (cu m/hr) and the percentage of occurrence of that particular wave. Hence, the rates of actual material movement are shown as P_1Q_1, P_2Q_2, and P_3Q_3 on lines 7-9, respectively. These are the weighted values of actual (potential) transport rate, weighted based on the percent of time (hour) that a particular wave climate actually existed.

The weighted sum of the actual (potential) transport rates for each column is the sum of all components of transport moving to the right (+), and to the left (-). These values are shown as lines 10 and 11, respectively. For example, for column 1, the weighted sum of the three transports produced by the three different wave climates are 0.64, -0.18, and -1.09 cu m/hr (Lines 7-9 of column 1). The transport to the right Q_R (+) is the only positive value of the three (0.64 cu m/hr), shown as Line 7. The transport to the left Q_L (-) is the sum of the two negative transports (-0.18 and -1.09 cu m/hr), shown as lines 8 and 9. The weighted sum of the actual (potential) transport rates for the five columns of the numerical grid are shown as lines 10 and 11, for right transport Q_R and left transport Q_L, respectively. The weighted net transport $Q_{(NET)}$ is the algebraic sum of the right transport Q_R and the left transport Q_L , and is shown as line 12.

The weighted sums of the actual (potential) longshore transports are then normalized by the maximum value of $Q_{(NET)}$ for all columns as shown in line 12. This maximum value occurs at column 4 (1.99 cu m/hr). All values of lines 10-12 are normalized (divided) by this value, and these right normalized values Q_{RN}, left normalized values Q_{LN}, and net normalized values $Q_{(NET)N}$ are shown as lines 13-15, respectively. These values indicate the relative actual (potential) longshore transport quantities per column of the numerical grid with respect to the maximum value of these parameters occurring within the region of interest.

The total right-directed and left-directed potential transport rates at a given alongshore column are, respectively, the weighted sum of the positive-valued and negative-valued transport estimates for that column:

$$Q_R = \sum p_i Q_i \quad for \quad Q_i \geq 0 \tag{V-6-20}$$

$$Q_L = \sum p_i Q_i \quad for \quad Q_i \leq 0 \tag{V-6-21}$$

where p_i is the fractional occurrence of each wave case i. Likewise, the net transport potential is the weighted sum of all transport values at a given column:

$$Q_{NET} = \Sigma\left(p_i Q_i\right) = Q_R + Q_L \tag{V-6-22}$$

The net, right- and left-directed potential transport rates for each grid column along the shore can then be examined or plotted to assess the alongshore extent and nature of the inlet's influence upon the refracted wave field and the associated littoral transport patterns (see, as an example, Figure V-6-11). The results are also useful in elucidating the inlet's sand transport pathways and for subsequent development of the sediment budget.

This approach is limited in that it does not address transport induced by tidal currents or gradients in wave height. Likewise, it addresses only the inlet's direct effect upon the shoreline and does not reveal far field erosion caused by the inlet's sink effect upon the littoral transport.

(e) *Method 5: Examination of inlet's net sink effect.* Whereas methods 1, 2, and 3 discern an inlet's effect through examination of shoreline change, this method primarily relies upon changes measured at and within the inlet. This is potentially advantageous because shoreline position data are often ambiguous and may reflect engineering activities such as dredged material placement, while, in some cases, the inlet's impoundment of sand adjacent to and within the inlet is more readily discerned (usually with some level of quantifiable uncertainty). Additionally, the assessment of the inlet's impacts is not a priori biased (limited) by the length of shoreline selected for examination.

An inlet's net sink effect is defined as the quantity of material that the inlet has taken from the littoral system. In most cases, natural and stabilized inlets remove sand from the littoral system through accretion of adjacent shores, shoaling in channels, and accretion of ebb- and flood-tidal shoals. However, inlets with riverine input may be the source of littoral material for the coast (e.g., Columbia River, Washington/Oregon).

The net sink effect, or volumetric impact, is first computed by adding: The volume (or rate) of impoundment adjacent to the inlet entrance; the volume (or rate) of net sand accumulation within the inlet's channels and shoals; the volume (or rate) of sand removed from the littoral system by dredging and offshore (or out-of-system) disposal. (If dredged material is placed on the adjacent beaches, it remains within the adjacent littoral system and thus is not added to the total).

Then, the following is subtracted from this total: The volume (or rate) of riverine (or other upland) sedimentary input; the volume (or rate) of barrier removed due to creation (through dredging or breach) of the inlet (if this event is within the time period of consideration).

The resulting value is the volume (or rate) of sand which has been removed from the adjacent shores' littoral systems over the period of examination. Inlet-adjacent volume changes are then examined to discern the minimum distance away from the inlet along which this volumetric impact is manifest.

EXAMPLE PROBLEM V-6-8

GIVEN:

Measured shoreline changes adjacent to an inlet are presented in columns 1 and 2 of Table V-6-9 for the period 1975-1989. Surveys from 1980 and 1988 suggest that the inlet's ebb and interior shoals outside the limits of dredging accreted by 152,000 cu m ±48,000 cu m. The correlation G_p between profile volume change per unit of shoreline length (alongshore) and cross-shore beach width change is estimated to be:

a. Updrift (east) of the inlet: 7.5 cu m/m of shoreline length per meter of cross-shore beach width change (7.5 cu m/m/m).

b. Downdrift (west) of the inlet: 7.2 cu m/m of shoreline length per meter of cross-shore beach width change) (7.2 cu m/m/m).

Profile erosion between 1.5 and 3.5 km downdrift of the inlet is restricted by the presence of seawalls. An average of about 192,000 cu m is dredged from the inlet's entrance channel every 3 years, all of which is disposed in deep water offshore. In 1987, 360,000 cu m of beach fill were placed between 0 and 4.5 km downdrift (west) of the inlet from an offshore sand source. Neglect riverine input of sand. Assume that erosion induced by the inlet along the updrift shoreline is negligible. The total rate at which the inlet removes sand from the littoral system is the sum of:

a. The updrift impoundment rate.

b. The inlet's net shoaling rate (after dredging).

c. The rate at which maintenance-dredging sand is disposed outside the littoral system.

FIND:

The lineal and volumetric extent for which the inlet's net sink effect can be attributed to measured shoreline erosion.

SOLUTION:

The natural inlet and shoreline processes are assumed to be similar over the entire period of interest (1975-1989). The change in shoreline volume per unit of shoreline length (alongshore) ΔV (m^3/m), per unit of change of cross-shore beach width change Δy (m), is denoted by Equation V-6-11:

$$G_p = \frac{\Delta V \text{ (volume change per unit of shoreline length alongshore)}}{\Delta y \text{ (cross - shore beach width change)}}$$

This relationship G_p was previously estimated to be 7.5 m^3/m of shoreline length (alongshore) per meter of cross-shore beach width for the coastal segment immediately updrift of the inlet, and 7.2 m^3/m of shoreline length (alongshore) per meter of cross-shore beach width for the coastal segment immediately downdrift of the inlet. The average annual cross-shore shoreline change data of column 2 with units of m/year can be converted to average annual local volume change data with units of m^3/m/year by using Equation V-6-11.

(Continued)

EXAMPLE PROBLEM V-6-8 (Continued)

Table V-6-9
Measured Shoreline Changes and Calculations for Net Sink Effect

GIVEN			COMPUTE		
1	2	3	4	5	6
Distance from inlet, *x* (km)	Avg. ann'l shoreline change, *dy/dt* 1975-89 (m/year)	Avg. annual local vol. change, *dV/dt* (cu m/m/year)	Reach Length (m)	Avg. annual reach vol. change (cu m/year)	Cum. vol. change - average annual (cu m/year)
7	-0.1	-0.75	1,000	-750	46,825
6	0.2	1.5	1,000	1,500	47,575
5	-0.2	-1.5	1,000	-1,500	46,075
4	0.5	3.8	1,000	3,800	47,575
3	1.2	9	1,000	9,000	43,775
2	1.5	11.3	1,000	11,300	34,775
1	2.0	15	750	11,250	23,475
0.5	2.3	17.3	500	8,650	12,225
0 (east)	1.9	14.3	250	3,575	3,575
0 (west)	-6.2	-44.6	250	-11,150	-11,150
-0.5	-5.3	-38.2	500	-19,100	-30,250
-1	-2.4	-17.3	500	-8,650	-38,900
-1.5	0	0	500	0	-38,900
-2	0	0	500	0	-38,900
-2.5	1.7	12.2	500	6,100	-32,800
-3	3.9	28.1	750	21,075	-11,725
-4	2.1	15.1	1,000	15,100	3,375
-5	0.3	2.2	1,000	2,200	5,575
-6	-1	-7.2	1,000	-7,200	-1,625
-7	-1.7	-12.2	1,000	-12,200	-13,825
-8	-1.9	-13.7	1,000	-13,700	-27,525
-9	-1.3	-9.4	1,000	-9,400	-36,925
-10	-0.6	-4.3	1,000	-4,300	-41,225
-11	-0.3	-2.2	1,000	-2,200	-43,425
-12	-0.4	-2.9	1,000	-2,900	-46,325
-13	-0.5	-3.6	1,000	-3,600	-49,925

(Continued)

EXAMPLE PROBLEM V-6-8 (Continued)

Since $$G_p = \frac{\Delta V}{\Delta y}\ m^3 / m / m$$

then $$\left(G_p\ m^3 / m / m\right)\left(\frac{\Delta y}{\Delta t}\ m / year\right) = m^3 / m / year$$

For example, at x = +7 km,

$$(7.5\ m^3/m/m)(-0.1\ m/year) = -0.75\ m^3/m/year$$

These equivalent average annual local volume change data are shown in column 3.

The effective shoreline reaches for each section updrift and downdrift of the inlet are shown in column 4. Next, the total rate of change along each reach of shoreline was determined by the simple trapezoidal rule (i.e., by multiplying the local volume change rate (column 3) by the local effective shoreline reach (column 4)). For example, the volume change at x = +7 km is

$$(-0.75\ m^3/m/yr)(1{,}000\ m) = -750\ m^3/year$$

These results are shown in column 5. Then the cumulative volume changes along the updrift (east) and downdrift (west) shorelines were determined, starting at the inlet for each direction. These results are shown in column 6. From examination of column 6, the updrift impoundment appears to extend about 4 km east of the inlet, and totals about 47,000 m^3/year (updrift impoundment rate).

The inlet's net shoaling rate between 1980 and 1988 was transformed to an annual average rate as (152,000 m^3 ±48,000 m^3)/8 year = 19,000 ±6,000 m^3/year (inlet net shoaling rate).

The rate of dredging and out-of-system disposal is annualized as 192,000 m^3/3 year = 64,000 m^3/year (maintenance dredging).

Again, the total rate at which the inlet removes sand from the littoral system is the sum of: the updrift impoundment rate; the inlet's net shoaling rate (after dredging); and the rate at which maintenance-dredging sand is disposed outside the littoral system.

Hence, the total rate at which the inlet removes sand from the littoral system is:

47,000 cu m/year + (19,000 ± 6,000) cu m/year + 64,000 cu m/year = 124,000 to 130,000 cu m/year

Hence, in the absence of the beach nourishment project, the downdrift beach is expected to exhibit a loss of between 124,000 and 136,000 cu m/year. Instead, primarily due to the 360,000-cu m-fill, the downdrift beach exhibited a net measured loss of only 49,925 cu m/year along the 13-km reach for which data are given.

To more carefully assess the inlet's actual impact, the beach fill must be included in the analysis. This fill, which was placed on the shore between 0 and 4.5 km downdrift of the inlet, was also removed (eroded) from the beach; therefore, it must be included in the total amount of material removed from the beach. This analysis is performed in the following table. Only the downdrift (west) shoreline is listed in the table since it is only this shoreline that is affected by the beach fill.

(Continued)

EXAMPLE PROBLEM V-6-8 (Continued)

The average annual cumulative volume change downdrift of the inlet (column 6) has been converted to the equivalent total cumulative volume change over the 14-year period between the 1975 and 1989 survey period by multiplying column 6 by 14 years. These data are shown in column 7.

The placed beach fill was also removed (eroded) from the beach. We assume that the 360,000 cu m of beach fill was uniformly distributed over the 4.5-km placement area (i.e., 80 cu m/m of shoreline. Column 8 shows the corresponding fill volume placed within each reach (between each station). From these results, the cumulative alongshore fill volume was computed, and is shown in column 9 as the cumulative placed fill volume along the beach downdrift of the inlet.

The cumulative alongshore volume change over the 14-year survey period, with the beach fill considered, was computed by adding the cumulative placed beach fill volume (column 9) to the cumulative measured beach fill volume change (column 7). These sums are shown in column 10 as the cumulative total volume change. The equivalent average annual cumulative total volume change is computed by dividing these values (column 10) by the survey interval (14 years). These results are shown in column 11. The cumulative updrift and downdrift volume changes, with and without consideration of the fill, are shown in Figure V-6-18.

Table V-6-10
Calculations for Cumulative Volume Change West of Inlet

From previous table			Downdrift volume change with beach fill considered (included)				
1	4	6	7	8	9	10	11
Distance from inlet, *x* (km)	Reach length (m)	Cum. vol. change - average annual (m^3/year)	Cum. vol. Change 1975-1989 (m^3)	Fill vol. placed in reach (m^3) [assumed]	Cum. Placed fill vol. (m^3)	Cum. total vol. change with fill considered; 1975-1989 (m^3)	Cum. total vol. change with fill considered; avg. annual (m^3/year)
0 (west)	-6.2	-11,150	-156,100	20,000	20,000	-176,100	-12,580
-0.5	-5.3	-30,250	-423,500	40,000	60,000	-483,500	-34,540
-1	-2.4	-38,900	-544,600	40,000	100,000	-644,600	-46,040
-1.5	0	-38,900	-544,600	40,000	140,000	-684,600	-48,900
-2	0	-38,900	-544,600	40,000	180,000	-724,600	-51,760
-2.5	1.7	-32,800	-459,200	40,000	220,000	-679,200	-48,510
-3	3.9	-11,725	-164,150	60,000	280,000	-444,150	-31,725
-4	2.1	3,375	47,250	80,000	360,000	-312,750	-22,340
-5	0.3	5,575	78,050	0	360,000	-281,950	-20,140
-6	-1.0	-1,625	-22,750	0	360,000	-382,750	-27,340
-7	-1.7	-13,825	-193,550	0	360,000	-553,550	-39,540
-8	-1.9	-27,525	-385,350	0	360,000	-745,350	-53,240
-9	-1.3	-36,925	-516,950	0	360,000	-876,950	-62,640
-10	-0.6	-41,225	-577,150	0	360,000	-937,150	-66,940
-11	-0.3	-43,425	-607,950	0	360,000	-967,950	-69,140
-12	-0.4	-46,325	-648,550	0	360,000	-1,008,550	-72,040
-13	-0.5	-49,925	-698,950	0	360,000	-1,058,950	-75,640

(Continued)

EXAMPLE PROBLEM V-6-8 (Concluded)

With the effect of the fill included (column 11), the downdrift volume change within the 13-km limit of data equals -75,640 cu m/year. This value is only about 56 to 61 percent of the total net impact (124,000 to 136,000 cu m/year) estimated from the inlet's diversion of sand from the littoral system (i.e., via updrift impoundment, net shoal growth, and out-of-system maintenance dredging disposal). Neglecting any inlet-induced erosion updrift of the inlet, the remaining 39 to 44 percent of the inlet's impact (48,360 to 60,360 cu m/year) must therefore occur further downdrift than 13 km.

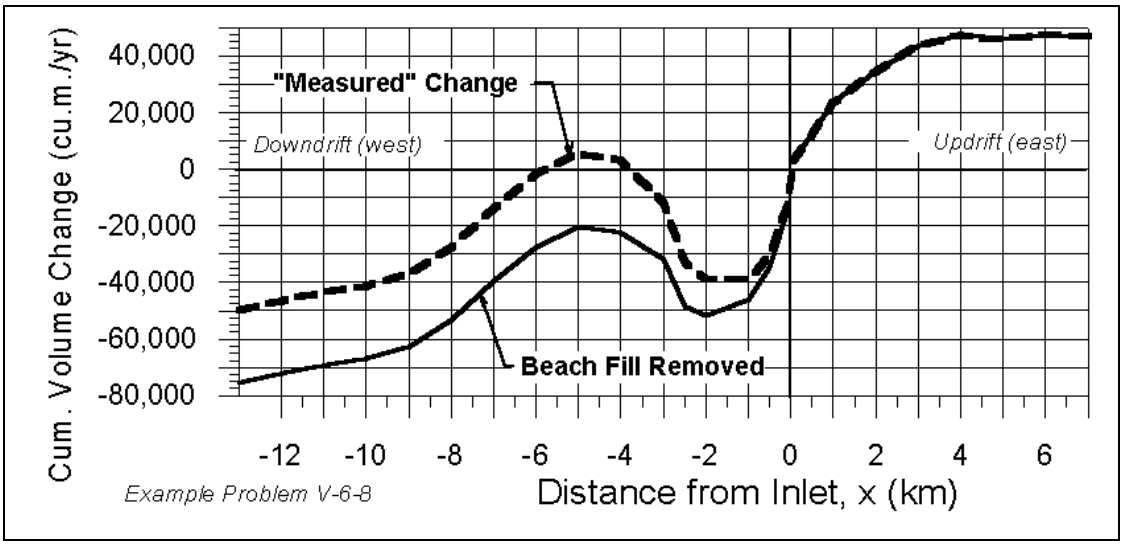

Figure V-6-18. Cumulative volume change with and without beach fill (Example Problem V-6-8)

In summary, the inlet's volumetric impact to the adjacent shorelines is estimated to range from 124,000 to 136,000 cu m/year. About 56 to 61 percent of this quantity (about 75,640 cu m/year) is manifest as erosion within 13 km downdrift (west) of the inlet. The total littoral impact, therefore, extends beyond 13 km from this inlet.

In applying this method, it must be realized that both natural and stabilized inlets have a net volumetric impact. The tendency is to assume that the volumetric impact of a stabilized inlet is entirely due to its stabilization and engineering activities. However, the same inlet in its natural state would also have an impact. The equivalent value for a natural inlet can be estimated by examining volumetric changes at a natural inlet with similar longshore transport rates, tidal range, and wave climate. Then, the volumetric change due to stabilization and engineering activities of the study site can be estimated by subtracting the two volumes.

In practice, the volume of sand impounded at the inlet's entrance (usually by jetties) can be estimated from profile surveys or shoreline-change data using the along-the-shore cumulative approach described above in method 1, criterion No. 4. (See Example Problem V-6-3.) The net volume of sand retained within the inlet shoals is estimated through comparison of bathymetric survey data; or at worse, through comparison of aerial photography with an assumed rate of vertical shoal thickness or accumulation. The volume of sand removed by dredging is estimated from records. Care should be taken to: Avoid double-counting of shoaling volumes and dredging volumes; exclude dredging quantities for new work associated with first-time construction or harbor deepening; exclude nonlittoral fractions (i.e., silt, clay, rock) from the dredging quantities.

Account for dredging quantities placed upon the adjacent shorelines from inlet/harbor maintenance and new work, or offshore sources.

In this fairly typical example, the downdrift shoreline changes, by themselves, do not reveal a clear picture of the inlet's signature. Methods 1 and 2 would therefore be of little value in this example, and methods 3 and 4 would not likely reveal the complete extent of the inlet's influence.

g. Inlet interactions with adjacent beaches.

(1) General.

Sediment may accumulate outside and inside an inlet. Sand storage exterior to the inlet is observed in the form of impoundment fillets along the shorelines adjacent to the inlet entrance. Also, a mature inlet with a well-developed ebb tidal shoal may bypass sand via the ebb shoal, resulting in an attachment zone, or bulge, on the downdrift beach. Interior sand storage occurs in the form of shoals, spits, and shoaling in channels. Mechanisms for this interior storage include (a) leakage of sand over, through, and around the inlet's terminal structures (jetties), and (b) wave- and current-driven transport to the inlet shoals. The effect of inlet-related bathymetry upon the wave field and sediment transport patterns can be observed through examination of wave refraction (discussed in the previous section), and by bathymetric and shoreline influences upon tidal currents.

Understanding the interaction of the inlet with its adjacent beaches is based upon:

(a) The degree to which the inlet's jetties impound, leak, or bypass sand.

(b) The direction, distribution and relative strength of the inlet's tidal currents.

(c) The effect of the inlet's ebb shoal plateau and adjacent bathymetry upon wave transformation (refraction) and littoral transport potential.

(d) The pattern in which shoals form within the inlet.

(e) The location and frequency of maintenance dredging of littoral sediments, and the placement history (location and frequency) and quality (e.g., sediment type and size) of this material.

Methods by which these factors may be examined are outlined in the following paragraphs.

Site observations and data.

There is no substitute for site visits and hours spent observing, walking, and wading along the inlet and its adjacent beaches. Observations should be preferably made during both strong ebb flow and flood flow, and at least once during energetic wave conditions from each of the principal directions of offshore incidence. Site visits should be initiated before commencing detailed studies to better identify those processes and data sources that bear examination. During or after the office analysis, additional site visits are necessary to assess the applicability of the analysis' results and to identify processes that require further study.

Important sources of historical data include:

- Aerial photography.
- Bathymetric surveys and charts.

- Beach profiles and historical shoreline maps.
- Dredging records.
- Discussions with dredging contractors experienced with the inlet's shoaling patterns.
- History of man's improvements and alterations.
- History of storm events.
- Existing reports and anecdotal histories of the inlet and adjacent shores.

If adequate data are not already available, researchers should consider the following new data:

- Controlled, rectified aerial photography.

- Shoreline location survey.

- Bank-to-bank bathymetric survey of the inlet throat, entire flood and ebb shoals, marginal shoals, and nearshore seabed.

- Beach profiles for characterizing the shape of the existing beach as a function of distance from the inlet, and direct comparison to previously collected beach profile data.

- Physical surveys of existing inlet structures (topography, elevations, permeability, etc.).

- Tidal current data focusing upon the horizontal distribution of principal flows and gyres on both the ebb flow and flood flow (dye injections into the water with concomitant aerial photography can be useful in this regard).

- Dye studies to discern jetty leakage (if not otherwise obvious).

- Directional wave data for a meaningful time period (includes hindcast data).

- Jet-probing, vibracore, core-boring, surface grab samples, periodic samples from the dredge plant, and other geotechnical means by which to discern those portions of the inlet's shoals and channels which contain littoral sediments derived from the adjacent shorelines.

- Environmental studies necessary to determine possible effects of disturbing portions of the inlet system for sand management (not discussed herein).

To the greatest extent practical, bathymetric surveys and beach profile surveys should be planned so as to facilitate comparison with existing, historical data. EM 1110-2-1810, "Coastal Geology," lists sources of geographic data in the United States. Other summaries of inlet-related data sources include Barwis (1975, 1976), Weishar and Fields (1985), and Chu, Lund, and Camfield (1987). The local sponsor (in the case of a Federal navigation project) or local interest(s) responsible for managing an inlet, and their private-sector contractors often hold the greatest repository of data specific to a given inlet, most of which is otherwise unavailable.

(2) Detection.

Approaches by which to discern how an inlet interacts with the adjacent beaches are described in the following paragraphs.

(a) Impoundment fillets and attachments. The degree to which sand is stored at an inlet's jetties can be detected by the shoreline signature (anomalous accretion) or the profile shape (anomalous steepness). Identification of these signals is described in Part V-6-2, methods 1, 2, and 3. Impoundment can occur on

either or both sides of a stabilized inlet. Sand may also be stored in the attachment zone, the region in which the inlet bypasses sand via the ebb-tidal shoal. This can be observed through a bulge in the shoreline and an extension of the ebb shoal towards the downdrift beach.

(b) Jetty leakage. Three elements demonstrate a jetty's permeability: its elevation relative to the adjacent beach and seabed; its length relative to the adjacent beach planform; and its porosity.

Elevation. The elevation of most old jetties is typically less than a meter above high water. Jetty crests below the elevation of the berm on the adjacent beach (usually more than 1 to 2 m above high water) allow wave runup to transport sand over the structure and into the inlet. This is typically shown by a high-water shoreline, berm shoreline, or dune line that curves landward immediately adjacent to the inlet (see Figure V-6-19). This local curvature is the result of a sluice that forms between the beach and the jetty. Because the jetty is lower than the beach, a downhill gradient exists from the beach toward the jetty. This promotes return flow of wave runup from the beach toward the jetty, which, in turn, accelerates sand transport from the beach into the inlet beyond that which would be normally transported by tidal currents and oblique incident waves.

Length. In the limit, beach profiles for which the closure depth (the limiting depth of sediment transport) falls seaward of the jetty's end will experience transport from the beach, around the jetty, and into the inlet. Field observation suggests that this effect becomes particularly significant when the beach profile adjacent to the jetty has accreted to the point where the average-annual, low-tide breaking depth (i.e., $h = H_{avg}/\kappa$, low-water datum) is at or seaward of the end of the jetty. In such a condition, it is likely that most, if not all, of the littoral drift that reaches the jetty passes around it. In this instance, the jetty is considered to be saturated.

At the same time, even in the saturated-jetty case, some fraction of the incident littoral drift may still be impounded further updrift of the jetty by the existing impoundment fillet. In this instance, the impoundment fillet continues to grow in a planform shape that may be similar to a backwater curve in classical hydraulics. This signature is sometimes evident in the shoreline's planform, and is predicted by analytic models such as Pelnard-Considère (1956) (see Part III- 2).

(c) Porosity. Jetty porosity is defined by sand transport through the structure. For bulkhead-type jetties, porosity results from cracks, corrosion, nonsealed joints, deterioration of backing (filter) cloth, or other sources of seepage. For rock or other armor-and-core structures, porosity results from insufficient chinking of stable, small rock within the voids between the large rocks or armor units. While this effect may be present within the structure's core, it is most commonly encountered near the top (waterline) of the structure. Here, there is generally minimal or no core, and small stones may have been washed out of the structure. Jetty porosity should be suspected for all rock structures that are low in elevation and/or narrow in profile (i.e., less than three or four armor units' width at the high waterline).

Jetty porosity is also demonstrated by the transmission of waves or current, however small, through the structure. Where transmission is uncertain, dye can be injected on the upwave or upcurrent side of the structure and observed. Porosity may also be evidenced by the occurrence of shoals immediately adjacent to the downwave / downcurrent side of the structure. Similarity between the shoal sediment and that of the adjacent beach is additional evidence of porosity.

In addition to the three factors previously listed, the appearance and growth rate of shoals and spits within the inlet is additional evidence of jetty permeability. This is discussed in item (e) in the following paragraphs.

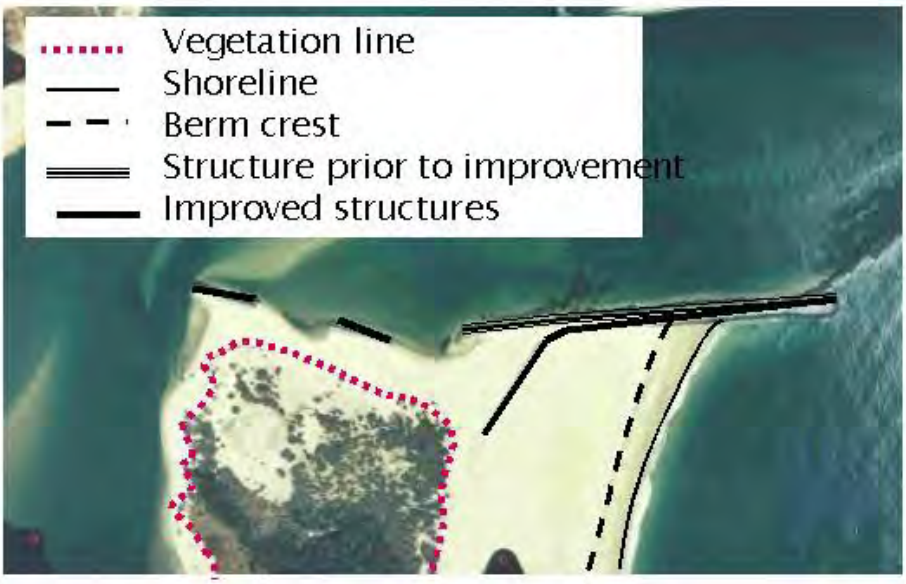

Figure V-6-19. Aerial photograph of Ocean City Inlet, MD, showing high-water shoreline, berm shoreline, and duneline

(d) Jetty rips. Offshore-directed rip currents can form along the upwave side of shore-perpendicular structures (such as jetties). These rip currents divert sand from the beach offshore, where the sand may or may not be transported to or along the inlet's ebb shoal. Rips are visually evident by a seaward-directed flow of water and the steepening of waves that encounter the rip. A modest sluice within 5 to 50 m adjacent to the structure may be visible at low tide. Lifeguards and surfers familiar with the area can be useful sources of data regarding local current and wave patterns.

(e) Inlet bathymetry and shoaling patterns. The location, rate of growth, and direction of movement of inlet shoals and spits, as well as the inlet's overall bathymetry, are excellent indicators of an inlet's sediment transport pathways. Use of bathymetry and shoaling patterns as a diagnostic tool requires, at a minimum, a bank-to-bank bathymetric survey of the inlet throat, flood shoal(s), and entire ebb shoal plateau. The latter should ideally extend outward and alongshore from the inlet entrance to capture the apparent point at which the ebb shoal attaches to the adjacent shorelines (if at all). Diagnostic ability is greatly improved when multiple, comparative surveys collected over time are available. Whenever possible, navigation channel condition surveys should be expanded to include bank-to-bank coverage of the inlet and as much of the inlet's shoals as possible. Pre-dredging, condition surveys are ideal because the shoals have had maximum opportunity to form prior to their removal by dredging. Reliance upon condition surveys that only include the navigation channel risks missing critical elements of the system's sediment transport pathways.

Charts and surveys of the inlet should be contoured at frequent depth intervals in order to illuminate shoaling patterns. Even using traditional, coarse-resolution nautical charts (for which only limited contours are routinely plotted), this technique can offer an enlightening view of the inlet's transport patterns. In the United States, the original National Ocean Service "T-sheets," upon which the printed nautical charts are based, provide additional data. The location and shape of shoals can reveal the potential source of the shoals' sand and the apparent direction of transport. The location of deep areas (outside of dredged areas) indicates apparent, preferred orientation of flow; and, in turn, areas where current-induced erosional stress may be exercised upon the adjacent shore. Figure V-6-20 illustrates an example of an off-the-shelf nautical chart of an inlet, before and after the addition of higher-resolution depth contours.

A particularly effective approach is to digitize, contour, and color-enhance the bathymetric data to more clearly reveal shoaling patterns. Pertinent upland features (jetties, shoreline, channel markers, etc.) should be added to the graphic to allow better visual correlation between the shoals, channels, and the inlet improvements. A prototype example is shown in Figure V-6-21, where lighter shading corresponds to shoals. Shading-enhanced depth contours readily show the leakage of sand through and around both jetties, the subsequent transport of the sand toward the flood shoal, and transport from the flood shoal toward the inlet entrance.

The location, growth, and chronic reappearance of shoals can highlight the paths by which sand enters an inlet. Shoals located near a jetty's seaward end indicate a saturated jetty or jetty rip currents. Shoals near a jetty's landward end suggest a structure that is porous or too low. Shoals and spits that form by sand transport through and over the jetty's landward section are most generally displaced well landward of the adjacent shoreline. These shoals are subject to landward-directed transported by incident waves that sweep along the inlet's interior shorelines. An emergent, sandy shoreline along the inlet's interior, connecting the jetty to the interior shoals, is further evidence of transport through or over the landward section of the jetty, or around the end of a short, saturated jetty. The possibility should also be considered that interior shoals may have been created (or enhanced) by riverine sand that enters the inlet and settles in quiescent water.

Figure V-6-22 illustrates an example in which the chronic reappearance of four distinct shoals along the inlet channel clearly reflects jetty leakage. The seaward two shoals correspond to known transport around the ends of the jetties. The landward two shoals correspond to transport through and over the jetties along the adjacent beaches' shorelines. Diving inspection, core boring, and dredging confirmed that the sediment from all four shoals is distinct from the silts and clays of the channel, but closely matches the adjacent beach sand.

Comparisons of ebb and flood shoal surveys are necessary to estimate the net growth rate of these features. The degree to which these shoals contain nonlittoral material (e.g., silts and clays from rivers) should be considered so that the contributions from the riverine and coastal sources can be properly attributed. Identifying material type is typically based on examining samples from core-boring, dredged material, box-cores, or recovery methods. If only surface samples are available, care should be taken to consider whether silts and clays overlay sandy shoals that originated from the adjacent beaches.

In some locations, sand from shoals (particularly interior shoals) has historically been dredged for upland use. This practice, infrequently recorded or quantified – may have removed significant quantities of sand from many inlet systems (sand which originated from adjacent beaches). Evidence of interior shoal dredging may be offered by the increase of adjacent landfills (readily noted in historical aerial photography) and anecdotal information.

(f) Dredging records. Dredging records may be available from the inlet's managing agency or local sponsor, USACE district offices, and dredging contractors. The date(s), locations of dredging and disposal, purpose (maintenance or new work), and quantity are of central importance. The quantity of dredged littoral (sand) material vs. nonlittoral (silt-clay) material must be identified to differentiate coastal versus upland or riverine origin. Shoaling records (condition surveys) combined with geotechnical data (USAEWES 1995) and/or discussions with dredging contractors and contract managers can be employed for this purpose. Additionally, the location of, and cross-sectional shape of, the shoaling pattern are strong indicators of the source. Shoals that form near shallow, sandy portions of the ambient seabed (such as the ebb shoal) are more likely to be of littoral origin. Shoals that form against one side of the channel, as opposed to those that form uniformly across the channel bottom, are also more likely to be of littoral (beach) origin.

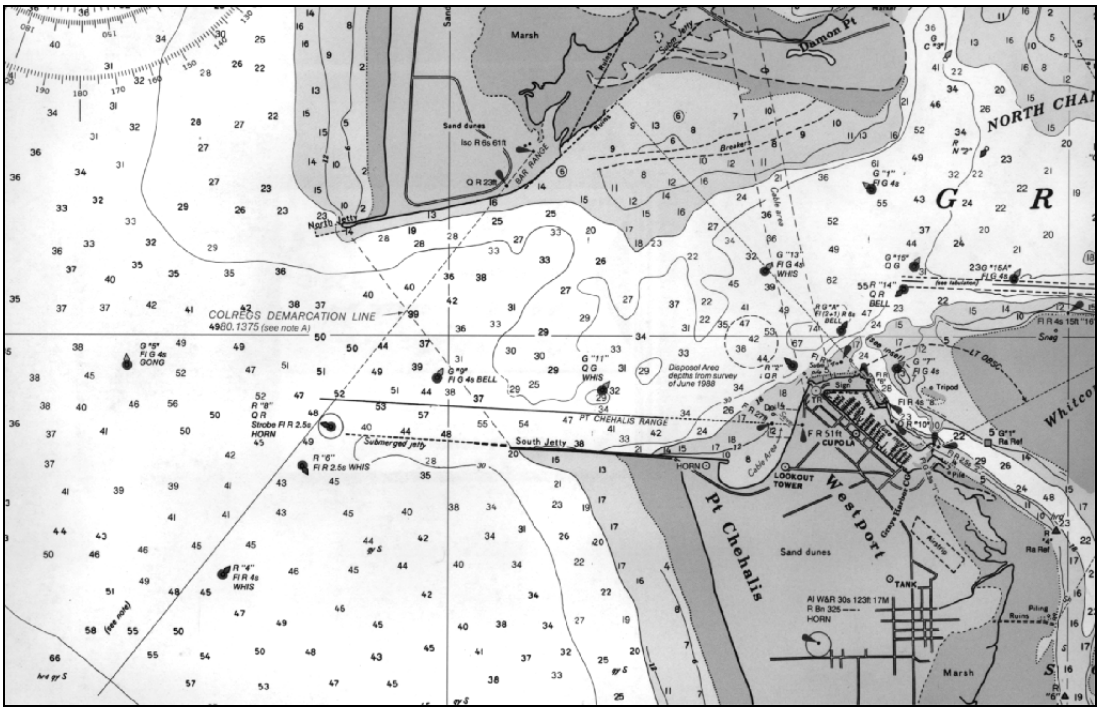

(a)

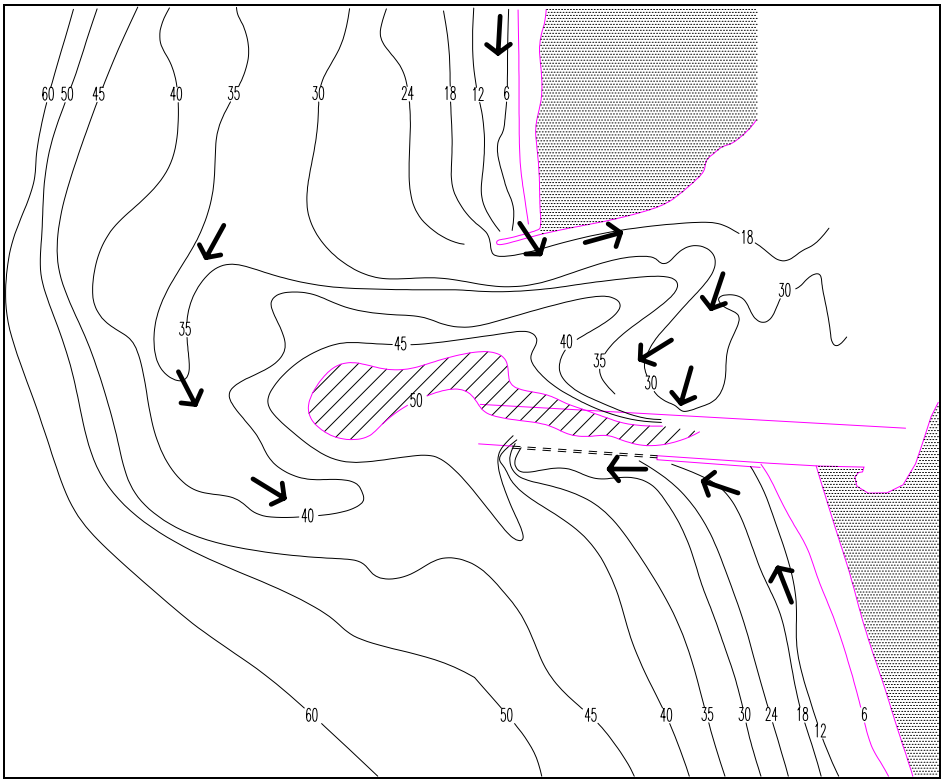

(b)

Figure V-6-20. Nautical chart with and without addition of higher-resolution contours. Arrows indicate sediment transport paths suggested by bathymetry

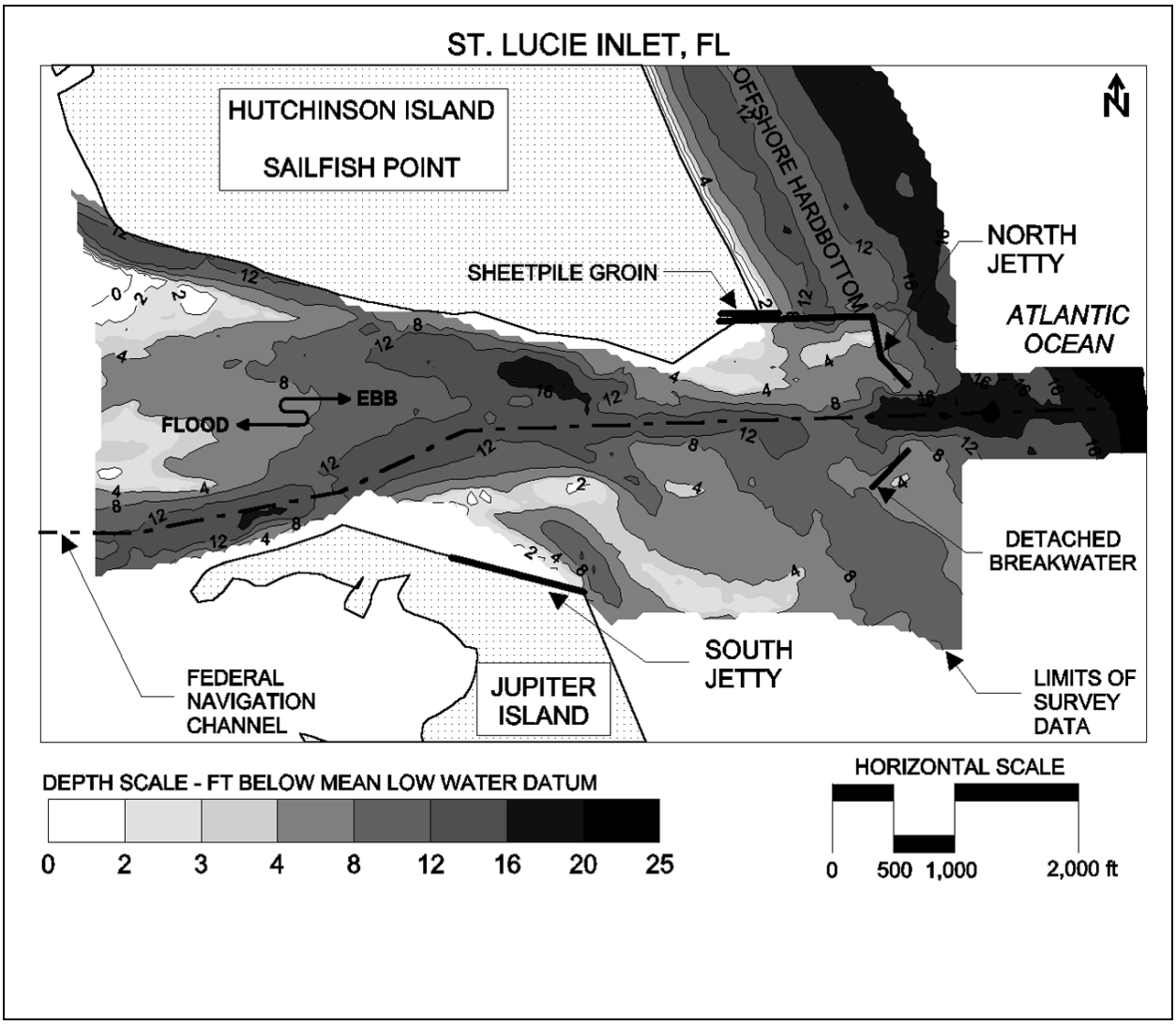

Figure V-6-21. Bathymetric chart of St. Lucie Inlet, Florida (c. 1995), digitized and gray-scale enhanced to better define the presence of shoals and channels

Figure V-6-23 illustrates a classic example of such shoaling signatures. The bar cut of the Brunswick Harbor Federal navigation channel is maintained at a depth of about 10 m (mlw) through an ambient seabed that was historically only 1 to 5 m deep. Material dredged from along the north bank and channel center line in the vicinity of Section A is typically beach-quality sand originating from the area's net southerly littoral drift. Material from the vicinity of Section B is typically silt and clay that settles into the deep channel from the surrounding seabed (slumping), riverine transport (terrigenous source), and oceanic deposition (pelagic settling).

We should note that not all of the littorally-supplied material at an inlet is necessarily sand. Some fraction of the dredged material may consist of silt, clay, gravel or organics of littoral origin. If this material is deposited offshore, it still represents removal of littoral material from the system, and must be included in computations of the inlet's littoral impact.

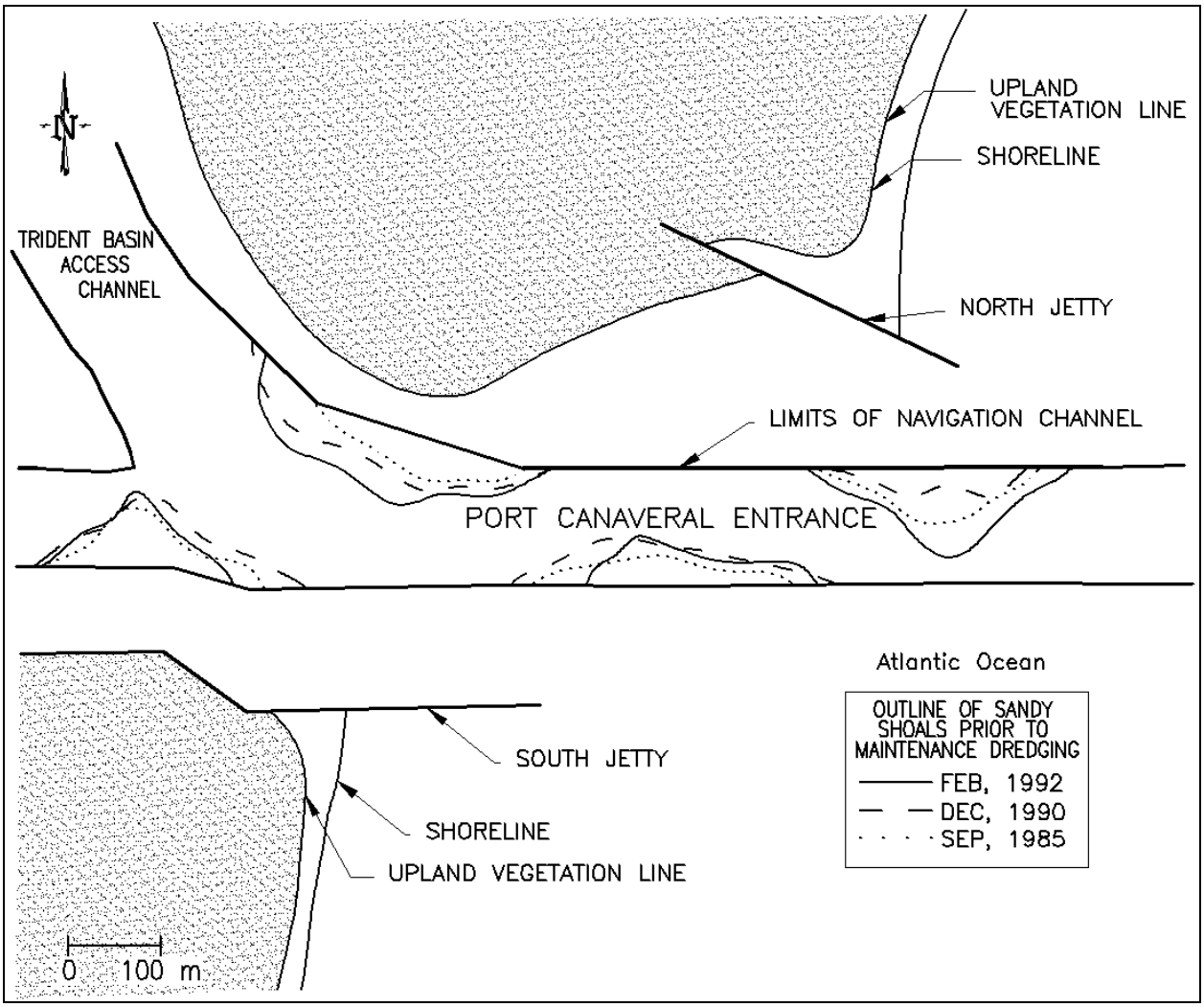

Figure V-6-22. Historical locations of sandy shoals within Port Canaveral Entrance, Florida prior to implementation of jetty/inlet improvements (Adapted from Bodge 1994a)

Dredging for new work (increased channel or harbor dimensions) is typically not included in inlet impact analysis because the material that is dredged is considered to have been a static part of the littoral system. In reality, this exclusion underestimates inlet impacts because some portion of the requisite dredging usually involves removal of beach sand that sloughs into the new channel during initial construction. However, the portion of advance maintenance dredging which features littoral material is included in the inlet impact analysis.

The degree to which increased channel dimensions or other inlet modifications alter dredging requirements can also reveal the degree to which the inlet diverts sand from the littoral system. This, again, requires discrimination of that part of the dredging quantity that was of littoral (beach sand) origin and undertaken for maintenance. Plotting the average-annual or cumulative quantity of maintenance-dredged littoral material as a function of time, and noting those times at which inlet modifications were undertaken, is a potentially useful technique to examine this effect (see Figure V-6-24).

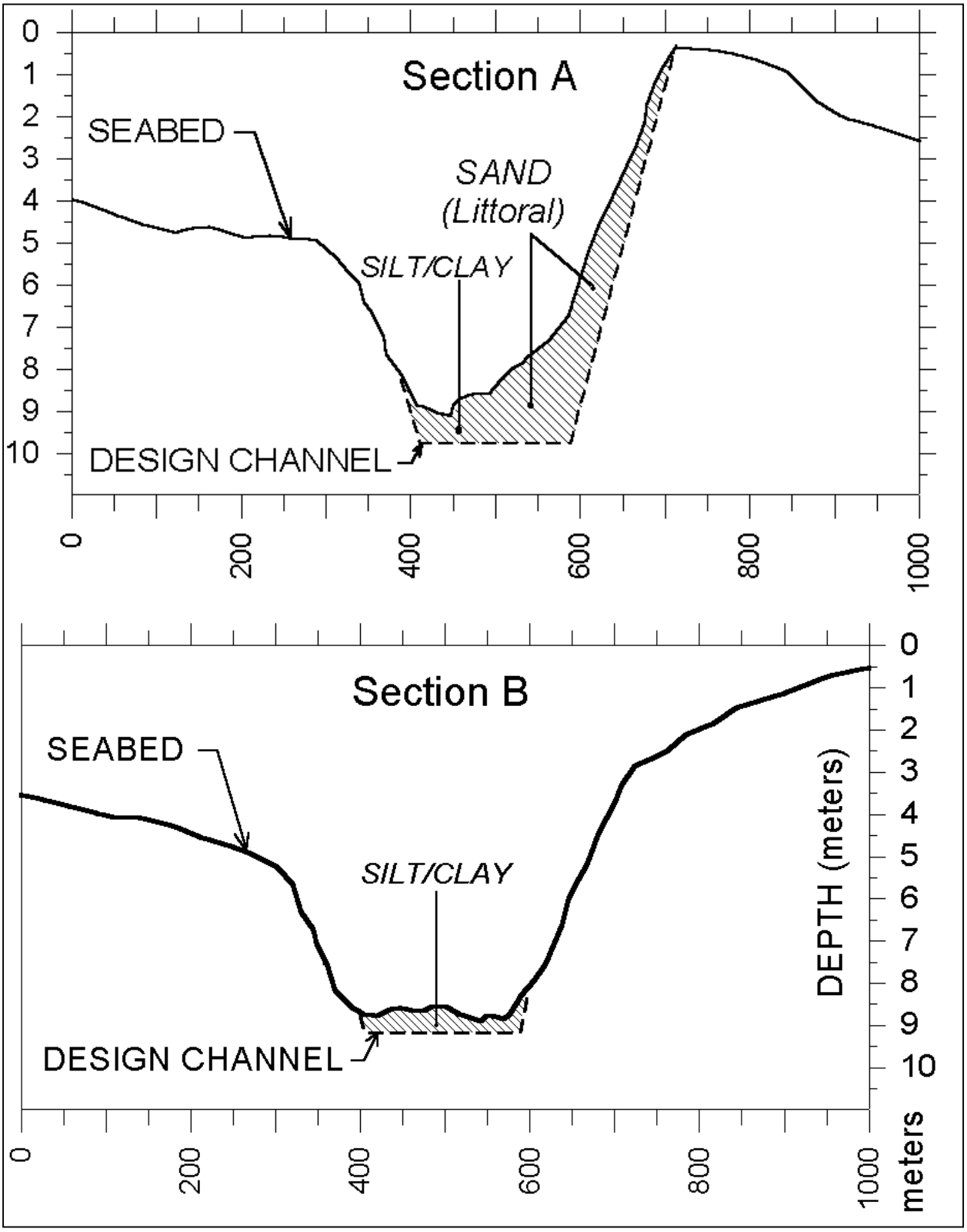

Figure V-6-23. Bathymetric contours and typical channel sections at Brunswick Harbor Federal Navigation Project, Glynn County, Georgia

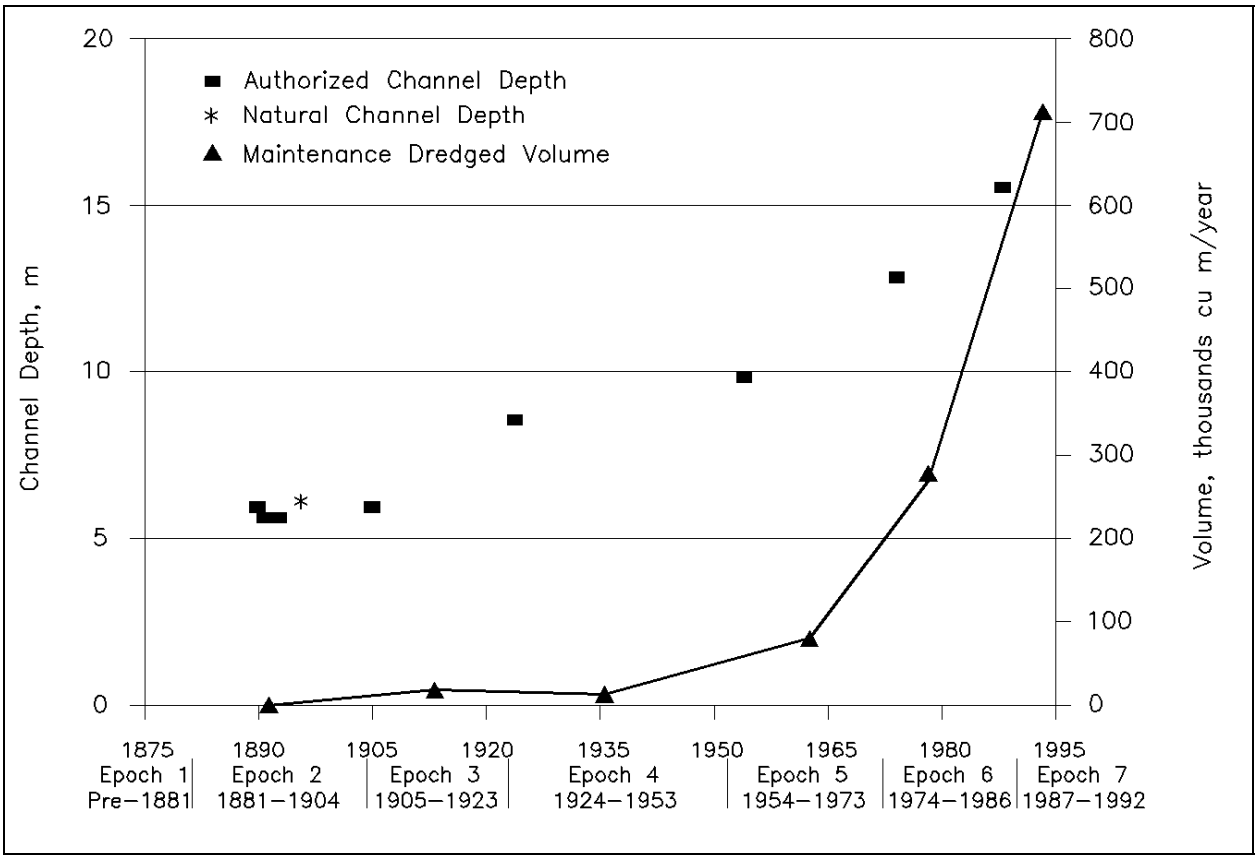

Figure V-6-24. Average annual volume of maintenance dredging at St. Mary's Entrance Channel and authorized channel depths; 1870 to 1992 (from USAEWES 1995)

h. Conclusion. This part of Chapter V-6 has discussed inlet processes and engineering activities at inlets. Inlets and associated engineering activities not only interact with local beaches and morphology, but also have the potential to alter sediment transport patterns and rates over the regional scale, especially over periods of many years. Methods discussed herein allow the coastal researcher to evaluate the impacts of these processes on the inlet morphology and adjacent beaches. These evaluations, together with inlet and adjacent beach sediment budgets (discussed in Chapter V-6-3), will improve the general understanding of the specific inlet's operation, and allow the engineer to optimize the timing and scope of engineering activities at the inlet and along the adjacent beaches.

V-6-3. Inlet and Adjacent Beach Sediment Budgets

a. Overview. This chapter discusses sediment budgets at inlets and their adjacent beaches. First, a history of sediment budgets is provided, followed by the theory of sediment budgets and required data sets to develop an inlet and adjacent beach sediment budget. Examples of previous sediment budgets are presented, and a series of example problems are given. The chapter concludes with a description of recent sediment budget methodologies.

b. Introduction.

(1) A sediment budget is an accounting or tabulation of the inflows and outflows of sediment together with the change in sediment volume within specified boundaries and for the time interval covered by the data. It is similar to a home budget that balances income (source of money), expenses (sinks of money), savings (positive amount), and debts (negative amount). Formulation of a realistic inlet and adjacent beach sediment budget is an essential prerequisite to the development of a successful inlet sand management strategy. Because an inlet's effect upon the adjacent shorelines is a function of the gross transport rates (not just the net rate), it is important to include both right- and left-directed transport in the sediment budget, as well as local, inlet-induced transport. In those cases where transport reversals occur at some time during the period of consideration (i.e., the majority of practical cases), inclusion of only the net transport rate will result in a potentially serious misinterpretation of the inlet's sediment transport pathways and associated volumetric rates of change.

(2) Development of the sediment budget requires that the rates and directions of sand transport adjacent to, within, and through the inlet be "deconvolved" from measured rates of volumetric change within the inlet system; specifically, the updrift and downdrift shorelines, the inlet shoals, and the channels. Allowances for the effects of dredging, beach fill, and other engineering of the inlet features must also be made. Development of the sediment budget is complicated by uncertainties in alongshore sand transport rates, typically incomplete or "noisy" volume-change data, and the fact that the number of transport rates for which values are unknown is greater than the number of equations which define the transport paths. The latter point means that the equations for an inlet sediment budget are almost always underconstrained. Accordingly, a unique solution is rarely possible. The goal, instead, is to develop a suite of possible solutions that is based upon reasonable assumptions of the inlet's processes. In this way, estimates of the practical ranges (or limiting values) of the rates at which sand is transported into or across the inlet from each shoreline can be made for various assumptions of the incident, alongshore transport rate or other physical parameters.

c. Theory.

(1) Since the 1950s, sediment budgets have been created to define the magnitudes and direction of sediment transport within a defined region and to understand, for example, inlet channel sedimentation and patterns of erosion and accretion along the coast. A balanced sediment budget yields an integrated picture of sediment (typically sand) motion, associated beach change, dredging and infilling of navigation channels at inlets, and other engineering activities within the reach covered by the analysis. Typically, the more reliable data form the foundation for the sediment budget, and lesser-known or more uncertain parameters are calculated to balance the budget by applying the principle of conservation of mass of sand (converted to volume or volumetric rate). A balanced sediment budget is a valuable tool for investigating observed coastal change and for forecasting the overall future state of the coast and consequences of management alternatives. Examination of an unbalanced sediment budget provides basic and useful information about the coastal system. An unbalanced budget may indicate a deficiency in the data set forming the budget (Dolan et al. 1987), reveal a misunderstanding in certain physical processes and assumptions (Inman 1991), or give bounds on the uncertainty range for the data sets. Whether or not formally developed, the sediment budget concept is fundamental to coastal engineering and science, usually providing the backdrop by which processes and projects are evaluated and alternatives considered. For additional background discussion, see Komar (1996, 1998).

(2) A sediment budget is a tallying of sediment gains and losses, or sources and sinks, within a specified control volume (or cell), or series of connecting cells, over a given time. There are numerous ways of formulating a sediment budget (e.g., Jarrett 1991; Bodge 1999). The difference between the sediment sources and the sinks in each cell, hence, for the entire sediment budget, must equal the rate of

change in sediment volume occurring within that region, accounting for pertinent engineering activities. The sediment budget equation can be expressed as,

$$\sum Q_{source} - \sum Q_{sink} - \Delta V + P - = R \quad \text{Residual} \tag{V-6-23}$$

in which all terms are expressed consistently as a volume or as a volumetric change rate, Q_{source} and Q_{sink} are the sources and sinks to the control volume (expressed as positive values), respectively, ΔV is the net measured change in volume within the cell, P and R are the amounts of material placed in and removed from the cell, respectively, and Residual represents the degree to which the cell is balanced. For a balanced cell, the residual is zero. Note that the notation for Q_{source} and Q_{sink} due to Longshore Sand Transport (LST) may differ, depending on the application. In Equation V-6-23, Q_{source} and Q_{sink} are expressed as positive values (this differs from that specified in Longshore Sand Transport discussion of Part III-2-2).

(3) Figure V-6-25 schematically illustrates the parameters appearing in Equation V-6-23. For a reach of coast consisting of many contiguous cells, the budget for each cell must balance in achieving a balanced budget for the entire reach.

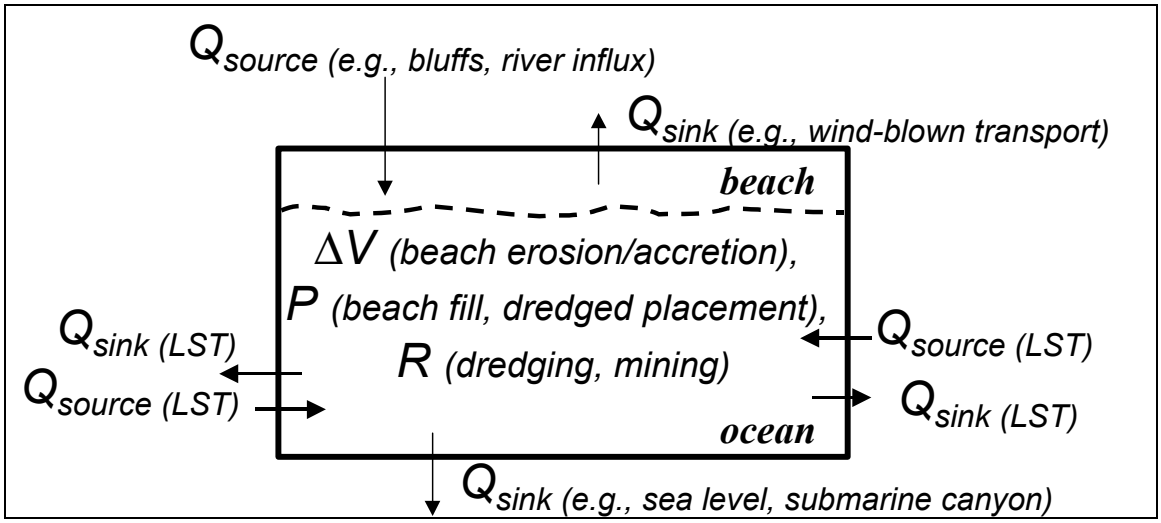

Figure V-6-25. Sediment budget parameters as may enter Equation V-6-23

(4) As noted in Figure V-6-25, sources to the sediment budget include longshore sediment transport, erosion of bluffs, transport of sediment to the coast by rivers, erosion of the beach, beach fill and dredged material placement, and a decrease in relative sea level. Examples of sediment budget sinks are longshore sediment transport, accretion of the beach, dredging and mining of the beach or nearshore, relative sea level rise, and losses to a submarine canyon. If inlets are located within the domain of a coastal sediment budget, they present significant challenges because inlets and the adjacent beaches are connected. Inlets increase the complexity of sediment budgets for several reasons. First, sediment-transport magnitudes and pathways are difficult to define at inlets even in a relative sense. Flood and ebb currents, combined waves and currents, wave refraction and diffraction over complex bathymetry, and engineering activities complicate transport rate directions and may increase or decrease their magnitudes. Because the pathways of sediment movement in the vicinity of an inlet can be circuitous, equations describing the sediment budget of regions directly adjacent to the inlet are not unique (that is, different formulations are possible).

(5) An inlet channel has the potential to capture the left- and right-directed components of the gross longshore transport of sediment, and the inlet system may bypass left- and right-directed longshore transport. Thus, knowledge of the net and gross transport rates, as well as the potential behavior of the inlet with respect to the transport pathways, may be required to correctly represent transport conditions within the vicinity of inlets, as emphasized by Bodge (1993).

d. Project applications.

(1) Sediment budgets can enter at any of four stages in project development:

(a) Existing condition. A sediment budget for the existing condition is the most common type considered. This budget forms the basis for evaluating the impacts of future engineering activities and the natural evolution of the inlet or coast.

(b) Historical (pre-engineering activity) condition. This budget is typically constructed for comparison with the existing-condition budget. A common application using the two budgets is to estimate shore erosion on adjacent beaches attributable to the impacts of inlet-related engineering activities that may warrant mitigation.

(c) Forecast future condition. Adapting and extrapolating the existing-condition sediment budget can assess the potential response to future projects or modifications.

(d) Intermediate condition. Sediment budgets representing other periods create a model of inlet or coastal evolution through time, which may lend insight to interpreting present or future evolution. As examples, intermediate-condition sediment budgets may document evolution of the inlet from initial formation to a quasi-equilibrium state, or may provide a picture of long-term natural bypassing through a cycle of channel migration and welding of a portion of the ebb-tidal shoal to the adjacent beach.

e. History of and procedure for sediment budget formulation.

(1) Consider a regional approach.

(a) For accurate representation of a local project area, especially in the vicinity of inlets, a sediment budget is formulated with its lateral boundaries located well beyond the apparent (expected) local project boundaries. A regional sediment budget might include multiple barrier islands, several inlets or several headlands and pocket beaches to fully capture the past and potential future changes in the sediment transport rate magnitude and direction.

(b) Inlets that have been stabilized by jetties for periods ranging from decades to centuries have the potential to influence the transport of sediment on the adjacent beaches for many kilometers, a distance that may extend well beyond what is considered the direct area of the inlet. Thus, a regional sediment budget that incorporates adjacent barrier islands, bay regions, underlying geology, estuarine and riverine impacts, and perhaps several inlets, may be required to assess the impacts of past and future projects. Engineering activities at navigable inlets and other data required for an inlet sediment budget have a high degree of uncertainty. Examples of these data include dredging quantity, location, and littoral quality; adjacent beach-fill volumes, initial cross-shore and longshore adjustment, and littoral quality; limited ebb-and (more commonly) flood-tidal shoal bathymetric coverage; and assessing the degree to which structures block, reduce, and modify the sediment transport pathways and magnitudes (Kraus and Rosati 1998a, 1999).

EXAMPLE PROBLEM V-6-9

Given:

Referring to figure V-6-26, balance the sediment budget equation given that $Q_{1\ source} = 250$, $Q_{1\ sink} = 100$, $Q_{2\ source} = 100$, $Q_{2\ sink} = 200$, $Q_{4\ source} = Q_{4\ sink} = 0$, $\Delta V = -70$, $P = 130$, and $R = 250$ (all units are thousands of cu m/year).

Find:

Find the value of $Q_{3\ sink}$ that balances the sediment budget (see Equation V-6-23 and Figure V-6-26).

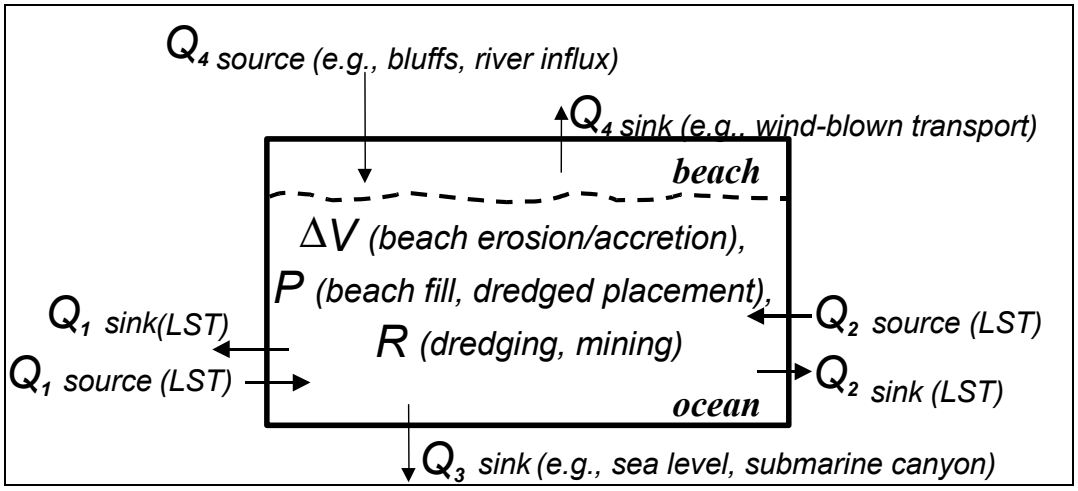

Figure V-6-26. Sediment budget for Example V-6-9

Substituting into Equation V-6-23 gives

$$\sum Q_{source} - \sum Q_{sink} - \Delta V + P - R = Residual$$

$$(250 + 100) - (100 + 200 + Q_{3\ sink}) - (-70) + (130) - 250 = 0$$

$$Q_{3\ sink} = 30$$

The value of $Q_{3\ sink}$ indicates that 30,000 cu m/year are transported out of the littoral cell, in the offshore direction.

(c) In one of the earliest works that may be considered a regional sediment budget, Caldwell (1966) summarizes a study performed in the 1950s by the U.S. Army Engineer District, New York, for the north New Jersey coast (USACE, 1957, 1958). The budget, formulated by examining changes in shoreline position, served as a field laboratory of shore processes with the objective of examining alternatives to mitigate for erosion. This celebrated study deduced a regional divergent nodal point in net longshore transport direction at Mantoloking, located just north of Dover Township. Net longshore transport to the north increased with distance north from Mantoloking because of the sheltering by Long

Island, New York. The budget considered net and gross longshore sand transport for this 190-km reach including 10 inlets over time intervals of 50 to 115 years.

(d) Another example of a regional sediment budget is that of Jarrett (1977, 1991) for the North Carolina shoreline, including three barrier islands and two inlets. Mann (1993) discussed use of a near field versus regional sediment budget. The near field sediment budget represents local (project area) sediment sources, sinks, and pathways. The regional sediment budget combines the near field budget with the sediment-transport processes occurring on the adjacent shorelines. For development of inlet sand management strategies (and estimating the inlet's littoral impacts), Mann recommends consideration of a regional sediment budget so that interactions of the inlet (and any proposed modifications) on the adjacent shorelines can be assessed. Although it may be difficult to define and balance all sources, sinks, and sediment transport pathways within a regional context, this comprehensive approach may allow the practitioner to recognize a source or sink of sediment hundreds of kilometers away that has a potential significance to the project area (Komar 1998).

(2) Develop a conceptual budget. Kana and Stevens (1992) introduced a conceptual sediment budget, which they recommend developing in the planning stage prior to making detailed calculations of individual sources and sinks. The conceptual sediment budget is a qualitative model giving a regional perspective of the inlet interaction with beach processes, containing the effects of offshore bathymetry (particularly shoals and, therefore, wave-driven sources and sinks), and incorporating natural morphologic indicators of net (and gross) sand transport. The conceptual model may be put together in part by adopting sediment budgets developed for other sites in similar settings, and incorporates all sediment sinks, sources, and pathways. The conceptual model should be developed initially, perhaps based upon a reconnaissance study at the site as part of the initial data set. Once the conceptual sediment budget has been completed, data are assimilated to validate the model rather than to develop the model.

(3) Ensure compatibility of temporal and spatial scales. In a discussion of the planning process for coastal projects, Kraus (1989) advocated the concept that the temporal and spatial scales of data used to develop and drive a model (whether a numerical, analytical, physical, or conceptual model) must be commensurate with these scales of the model itself. For example, a sediment budget developed based on pre- and post-storm data representing a day-to-month-length temporal scale within the immediate vicinity of the inlet should not be extrapolated to forecast to temporal scales of years and decades for a region extending over several barrier islands. Similarly, a sediment budget developed based on a 50-year period cannot adequately bracket the seasonal fluctuation observed locally at the project site. Sediment budgets are commonly required to represent periods of engineering and geomorphic significance, from 3-5 years (dredging cycle at inlets) to 30-50 years (project life span; time scale for cyclic ebb shoal welding). Data sets reflecting the longer durations are required to develop the sediment budget for spatial scales reflecting a regional approach. However, seasonal and year-to-year variability should be considered and can contribute to the uncertainty in a sediment budget, or form the basis for a sensitivity analysis.

(4) Delineate littoral cells. A littoral cell (or control volume) defines the boundaries for each sediment budget calculation, and denotes the existence of a complete self-contained sediment budget within its boundaries (Dolan et al. 1987). Bowen and Inman (1966) introduced the concept of littoral cells (Inman and Frautschy 1966) within a sediment budget. The southern California coast lends itself to this concept, with evident sources (river influx, sea cliff erosion), sinks (submarine canyons), and coastal geology (rocky headlands) defining semicontained littoral cells and subcells (Komar 1996, 1998). A littoral cell can also be defined to represent a region bounded by assumed or better-known transport conditions, or natural and engineered features such as the average location of a nodal region (zone in which $Q_{net} \sim 0$) in net longshore transport direction or a long jetty.

(5) Consider net and gross transport rates. For cells of the regional budget that may capture a portion of the left- or right-directed transport, both of these components must enter in the formulation. Examples include submarine canyons and inlet channels that capture both left- and right-directed transport; inlet weirs which may trap a portion of the left- or right-transport rate; and initial beach response at a long groin or headland feature, which may indicate accretion associated with left- and right-directed transport. Caldwell (1966) considered the gross transport rate as a potential indicator of shoaling for inlets in the vicinity of Cape May, New Jersey. Jarrett (1977, 1991) balanced potential longshore energy flux calculations with measured beach and tidal inlet change to solve for net and gross rates of longshore sand transport. Bodge (1993) focussed on the inlet and its adjacent beaches, and emphasized the importance of considering the gross components of longshore sediment transport, especially for inlets that act as sediment sinks. The gross transport rate can also provide an upper limit for the net, left-, and right-directed rates.

(6) Assign values and uncertainties.

(a) Known, estimated, or easily-obtained values and their associated uncertainties are assigned to source, sinks, and engineering activities within the sediment budget. This step should represent a low level of effort to quickly assess the integrity of the macrobudget (discussed in the following paragraphs) and to flush out any problems before detailed analysis begins.

(b) Every measurement has limitations in accuracy and contains a certain error. For coastal and inlet processes, typically direct measurement of many quantities cannot be made, such as the long-term longshore sand transport rate or the amount of material bypassing a jetty. Values of such quantities are obtained with predictive formulas or through estimates based on experience and judgement, which integrate over the system. Therefore, measured or estimated values entering a sediment budget can be considered as consisting of two terms, expressed schematically as

$$\textit{Reported Value} = \textit{Best Estimate} \pm \textit{Uncertainty} \tag{V-6-24}$$

Uncertainty, in turn, consists of error and true uncertainty. A general source of error is limitation in the measurement process or instrument. True uncertainty is the error contributed by unknowns that may not be directly related to the measurement process. Significant contributors to true uncertainty enter through natural variability and unknowns in the measurement process. These include temporal variability (daily, seasonal, and annual beach change); spatial variability (longshore and across shore); definitions (e.g., shoreline orientation, direction of random seas); and inability to quantify a process, such as the volume of material pumped to a beach, or the sediment pathways at an inlet. Other unknowns can enter, such as grain size and porosity of the sediment (especially true in placement of dredged material).

(c) As an example, suppose the variable X is a sum or difference of several independent parameters as $X = x + y - z + \ldots$, then the two common estimates for the uncertainty are:

$$\delta X_{\max} = \delta x + \delta y + \delta z + \ldots \tag{V-6-25a}$$

and

$$\delta X_{\text{best}} = \sqrt{(\delta x)^2 + (\delta y)^2 + (\delta z)^2 + \ldots} \tag{V-6-25b}$$

In both expressions, the errors add, whether or not the variables enter the quantity being reported as a sum or difference. Equation V-6-25a represents an extreme bound for the plausible error. Equation V-6-25b is the root-mean-square (rms) error, and the validity of this expression rests on the assumptions that the

individual uncertainties are independent and random. The rms error accounts for the uncertainty in uncertainty by giving a value that is not an extreme, such as δX_{max}.

(d) Suppose the quantity entering the budget is expressed as a product or quotient of independent variables as $X = xyz$ or as xy/z. In either case, the uncertainty in X is:

$$\left(\frac{\delta X}{X}\right)_{max} = \frac{\delta x}{x} + \frac{\delta y}{y} + \frac{\delta z}{z} \tag{V-6-26a}$$

and

$$\left(\frac{\delta X}{X}\right)_{best} = \sqrt{\left(\frac{\delta x}{x}\right)^2 + \left(\frac{\delta y}{y}\right)^2 + \left(\frac{\delta z}{z}\right)^2} \tag{V-6-26b}$$

and it is seen that the errors are additive whether a variable enters as a product or quotient. These equations state that the relative uncertainty of a product or quotient is equal to the sum of relative uncertainties of each term forming the product or quotient. Kraus and Rosati (1998a, 1999) further discuss uncertainty in coastal-sediment budgets.

(7) Formulate a macrobudget. A macro-budget is a quantitative balance of sediment inflows, outflows, volume changes, and engineering activities within the regional conceptual budget. Essentially, the macrobudget solves the budget with one large cell (perhaps by temporarily combining many interior cells) that encompass the entire longshore and cross-shore extents of interest. Balancing the macro-budget reduces the possibility of inadvertently including potential inconsistencies in a detailed or full budget (Kraus and Rosati 1999).

(8) Refine estimated values and uncertainties. Once the macrobudget has been balanced, detailed analysis for all inflows, outflows, volume changes, and engineering activities pertaining to each individual cell may commence. Originally estimated values used in formulating the macrobudget are used to provide reasonable ranges for each quantity.

(9) Use residuals to balance individual cells. As presented in Equation V-6-23, both a balanced sediment budget cell and the macrobudget have the sum of all sources, sinks, and engineering activities equal to zero. Inman (1991) discussed recording an unbalanced sediment budget cell (a cell with a non-zero residual in Equation V-6-23) as a region requiring more definition and investigation of the unknown processes. Knowledge of the residual may also be useful to bracket the uncertainty range for the data sets (Kraus and Rosati 1999).

(10) Conduct sensitivity testing. Once a sediment budget has been formulated, it can be copied and modified to evaluate the impact of any assumptions on the final sediment budget. Different data sets for the same project site can be applied to evaluate seasonal variations in beach change and transport rate direction and magnitude. A balanced budget representing a historical time period can be copied and altered to represent a potential future with-project condition.

f. Data required. The types of data sets that are available for refining sediment budget quantities are discussed in the following paragraphs. This section supplements the data required for inlet analysis described in Section V-6-2(f).

(1) Aerial photography. Interpretation of aerial photographs offers the best means of obtaining broad qualitative understanding of the site. As examples, photographs of sites with relatively clear water can identify the planform shape of the flood-tidal shoal to estimate its volume if more quantitative data are unavailable. The pattern of wave breaking over the ebb-tidal shoal indicates the planform shape of this feature, which might lend qualitative understanding of its interaction with adjacent beaches and of sediment pathways. Overwash fans on adjacent barrier islands indicate pathways for loss of sediment to the coastal littoral system, from which quantification of volumes might proceed. Shoals adjacent to jetties might indicate sediment-transport over and through the structure as a potential sediment transport pathway. In a more quantitative analysis, controlled and rectified aerial photographs are commonly interpreted to identify the berm or high-water line (HWL) shoreline position (Kraus and Rosati 1998b).

(2) Beach-profile surveys. Volume change, ΔV, in the beach can be obtained accurately through repetitive surveys of the beach profile. The volume change for a given profile is typically assumed to represent the region of beach of length Δx between adjacent profile lines. Both the elevations B of the berm and of the profile closure depth D_C can be estimated from beach-profile surveys if the profile data are sufficiently accurate and well controlled. The active berm crest is a discernible morphologic feature on the profile representing the upward limit reached by the water under normal tide and water-level conditions. The profile may have two berm crests if the beach has recently accreted, and the elevation of the seaward-most feature should be noted. The depth of closure is located where no significant depth changes occur over times of engineering significance (typically, 10 to 50 years) (see Hallermeier 1978; Birkemeier 1985; Wise 1998). Kraus, Larson, and Wise (1999) discuss the depth of closure in detail and extend its definition to cover varied conditions as encountered in engineering practice. Profile surveys performed near structures may indicate their condition. For example, a jetty that allows sediment transport over and through it might be indicated by a berm-crest elevation adjacent to the structure that is comparatively lower than the berm crest further away from the structure. Similarly, surveys close to structures reveal whether the profile deviates from the average shape far from the structures, improving estimates of sand volume. The investigator should be cautious in interpreting beach-profile data near the inlet because of migrating shoal features that may affect the profile shape.

(3) Shoreline-position data. Shoreline-position data may be obtained from analysis of topographic and HWL surveys, aerial photographs, beach-profile surveys, and bathymetric data (Anders and Byrnes 1991; Byrnes and Hiland 1995). In a qualitative manner, beach morphology indicated by shoreline position may imply sediment-transport pathways or controls. As examples, a salient or bulge-type feature in the shoreline downdrift of an inlet may represent the location for ebb shoal bypassing to the adjacent beach. Rocky headlands and outcroppings indicate geologic controls on sediment-transport pathways.

(a) As quantified in a sediment budget, the change in shoreline position Δy averaged over a given longshore distance Δx can be converted to a volume change by assuming that the shoreline translates parallel to itself over an active depth D_A, given by

$$D_A = B + D_C \tag{V-6-27}$$

in which B is the elevation of the seaward-most active berm relative to a datum, and D_C is the depth of closure measured from the same datum. The volume change[1] ΔV over a time interval Δt is given by

$$\Delta V = \frac{\Delta y \Delta x D_A}{\Delta t} \tag{V-6-28}$$

(b) If available, the impoundment rate at a shore-perpendicular structure such as a groin or jetty that is sand tight gives an estimate of the longshore sediment-transport rate.

(4) Bathymetry. Historical and recent bathymetric data sets are a valuable resource for determining the rate of volume change in the inlet channel and on the ebb and flood-tidal shoals. If coverage is sufficient, differences in bathymetric surfaces give the subaqueous volume change on the adjacent beaches and channel and ebb- and flood-tidal shoals. It is noted that, in the past, typical bathymetric coverage has been limited to the inlet channel. However, the benefits of increasing the survey area to include the ebb- and flood-tidal shoals far outweigh the additional costs, particularly in view of reductions in the cost of bathymetric surveys (e.g., SHOALS bathymetric survey system, Parson and Lillycrop 1998). Bathymetric data can also indicate sediment-transport pathways. As examples, a finger shoal extending from the tip of a jetty likely indicates a dominant sediment transport pathway, and the morphologic form of an ebb-tidal shoal that connects to the adjacent beaches may indicate inlet bypassing. Aerial photography of flood-tidal shoals at different, but known tidal elevations can be referenced to create a contour map of the shoals, and thereby to estimate a shoal volume.

(5) Engineering history.

(a) Engineering activities of significance to a sediment budget fall into two categories – those that are of a descriptive nature and must be quantified within the sediment budget; and those that are a priori quantified. Rehabilitation of a jetty is an example of a descriptive activity that requires quantification. The morphology of the inlet and adjacent beach before and after structure rehabilitation, as well as the type of rehabilitation (e.g., raising the jetty crest elevation, inserting a sand-tight core, adding armor stone), and other pertinent data sets indicate the effectiveness of the structure. Consideration should be given as to the degree of sediment transport through, over, and around the structure before and after rehabilitation. Another example of descriptive data is the grain size of dredged material placed on the adjacent beaches. From this information, the engineer must estimate percentage of material that would remain in the active littoral zone.

(b) Engineering activities that are a priori quantified (although sometimes only partially) include the following: volumes, locations, and times of dredged and placed material; volume of material mined from ebb- and flood-tidal shoals, the locations and times of mining; configuration of the placement; volume of fill on adjacent beaches and its placement location and time period of placement; and records of mechanical bypassing (volume, placement location, and time periods). These quantities will enter the sediment budget calculations by adjusting measured volume changes to account for either the removal or placement of material through engineering activities. The adjustment of an initial beach fill can be used to infer rates of longshore and cross-shore sediment transport.

[1] Comparison of a shoreline position derived from aerial photography with a shoreline position derived from beach-profile surveys should account for possible differences in the vertical datums to which each is referenced. For example, it is likely that an aerially-derived shoreline position represents a berm crest or HWL position, whereas a beach-profile shoreline may represent a zero elevation relative to a standard datum (e.g., National Geodetic Vertical Datum, or Mean Sea Level). See Kraus and Rosati 1998b or CEM, Part II, Chapter 5.

(6) Coastal processes. Data on the acting coastal processes are a resource for understanding and quantifying inlet- and sediment-transport pathways and quantitites. Examples are discussed here.

(a) Net, left-, and right-directed potential longshore sand-transport rates can be calculated from wave gauge, Wave Information Study (WIS), and Littoral Environment Observation (LEO, see Schneider (1980)) wave height, period, and direction data. Gravens (1989) discusses the methodology for calculating net potential longshore sand-transport rates from WIS data. The components of the net transport, directed to the left or right as noted by a shore-based observer, can be calculated by using the left- or right-directed waves, respectively, with the methodology as outlined in Gravens (1989). Often the magnitudes of the calculated net, left-, and right-directed potential longshore sand transport rates do not agree with accepted values for the site. However, the relative magnitude between the left- and right-directed transport can be applied in a sediment budget with an accepted value for net longshore sediment transport to adjust the magnitudes. Wave height, period, and direction data allow construction of wave rays or orthogonals as indicators of pathways of sediment transport.

(b) Inlet flow speed and direction data as indicated by current meters or drogue movement give the relative magnitude of sand-transport rates and pathways. For example, measurements of the current from Ocean City Inlet, Maryland, indicated that the flow to the northern part of the bay was considerably greater than that to the southern part (Dean, Perlin, and Dally 1978). This information can be adapted to proportion the relative magnitude of the bay-directed sand transport to different parts of the bay.

(c) The rate of relative sea-level rise may represent a contributing factor to the observed beach change. The long-term beach loss Δy_{sl} because of an increase S in relative sea level is (Bruun 1962; 1988; Komar 1998).

$$\Delta y_{sl} = \frac{L_c}{B + D_c} S \tag{V-6-29}$$

for which L_c is the cross-shore distance from datum to the long-term depth of closure D_c .

(d) Other types of coastal process data useful for formulation of a sediment budget include:

River-flow speed, fluvial sediment grain size and sediment availability as a possible sediment source to the coastal environment.

Wind speed and direction, sediment grain size and availability as a potential aeolian sediment source to or a sink from the coastal environment.

Sediment characteristics (e.g., median size, size distribution, mineral content) as natural tracers for sediment movement.

g. Sediment budget methods and tools. This section discusses sediment budget methods and tools available for inlets and regional studies. The discussion is organized with the simpler methods presented first, followed by the more complex.

EXAMPLE PROBLEM V-6-10

GIVEN:

Develop a conceptual sediment budget for the period 1938 to 1979 for the regional littoral system in the vicinity of Shinnecock Inlet, Long Island, New York. This region extends east of Shinnecock Inlet to Montauk Point and west of Shinnecock Inlet to Moriches Inlet.

BACKGROUND INFORMATION:

Shinnecock Inlet, located on the south shore of Long Island, New York, was formed during a hurricane in September 1938 (Figure V-6-27). The west jetty was initially constructed by New York State in 1947 and was extended from 1953 to 1955, and the east jetty was constructed from 1952 to 1953. Shinnecock Inlet's littoral system is bounded to the east by Montauk Point, a location at which net longshore sediment transport is negligible because of its shoreline orientation and fetch distance from the mid-Atlantic Coast. West of Montauk Point, 10- to 21-m-high bluffs extend for 8 km and are a source of sediment roughly estimated as 35,000 cu m/year based on analysis of profile data. The U.S. Army Engineer District, New York, formulated a sediment budget for the inlet (USAED, New York, 1987). Estimates are available for the net longshore sand-transport rate 1 km east of the inlet (230,000 cu m/year), the ebb-shoal volume change (77,000 cu m/year), the flood-shoal volume change (15,000 cu m/year), and the net longshore sand-transport 1.8 km west of the inlet (189,000 cu m/year).

Nersesian and Bocamazo (1992) developed a preliminary sediment budget in which the net transport east of Shinnecock was 281,000 cu m/year, the ebb and flood shoal captured 77,000 and 15,000 cu m/year, respectively; and transport west of the inlet was 189,000 cu m/year. Kana (1995) estimated net transport rates 3 km east and 2 km west of Shinnecock Inlet as 219,000 and 104,000 cu m/year, respectively. A seaward bulge located approximately 2 km downdrift of Shinnecock Inlet is apparent in the 1979 shoreline position, indicating a possible region of sediment exchange between the ebb-tidal shoal and the downdrift beach. West of Shinnecock Inlet, the Westhampton barrier island extends for 25 km to Moriches Inlet. Moriches Inlet was formed in March 1931 and migrated 1,200 m to the west before it closed naturally in May 1951. Jetties were constructed in 1952 to 1953 at the position of the former inlet, and through dredging and a minor storm, the inlet reopened. Taney (1961a,b) estimated net transport rates at Moriches Inlet as 229,000 cu m/year.

(Continued)

(1) SBAS2000.

(a) Overview. The Sediment Budget Analysis System (SBAS2000) is a PC-based program that utilizes a graphic-based interface to apply Equation V-6-23. The SBAS was developed to allow the engineer and scientist to formulate sediment budgets in areas with complex sediment pathways, such as at inlet entrances, and over a wide regional extent that might encompass several inlets with beaches and infrastructure in between. SBAS can zoom out to reveal a large regional extent, and combine (collapse) sediment budget cells for a macroscale interpretation of sand transport along the coastlines and through rivers. For project-level sediment budgets, SBAS can zoom in to the site-specific area and

EXAMPLE PROBLEM V-6-10 (Concluded)

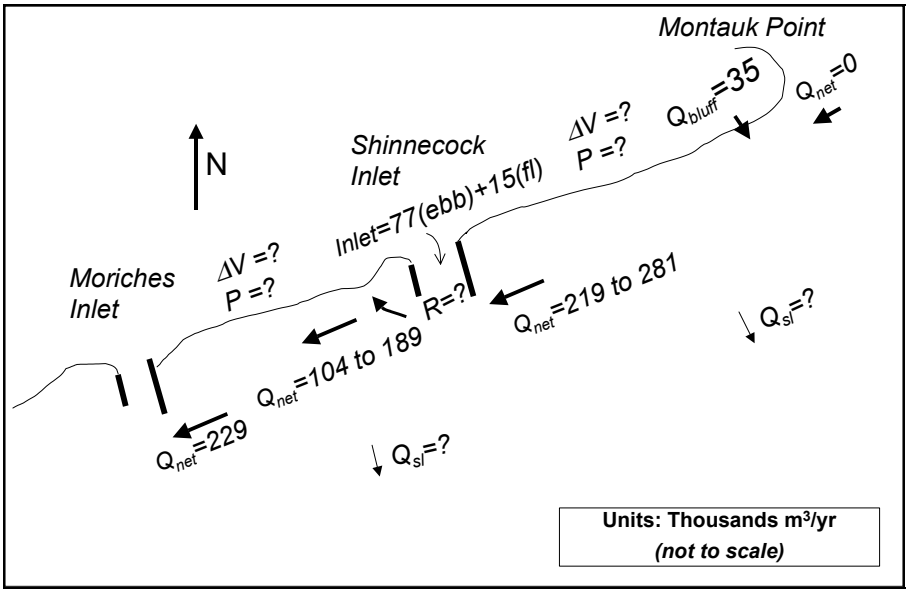

Figure V-6-27. Conceptual sediment budget for Shinnecock Inlet, New York

CONCEPTUAL SEDIMENT BUDGET:

Figure V-6-27 shows the conceptual sediment budget developed from the information presented. Applying this information with Equation V-6-23 indicates that the beaches between Shinnecock Inlet and Montauk Point and between Moriches and Shinnecock Inlets most likely have eroded during the subject period, unless a significant quantity of beach fill was placed. Some volumes are not quantified (e.g., beach losses because of relative sea level rise Q_{sl} ; beach-fill placement rate P; dredging (removal) rate R), but are represented for completeness.

reinstate (explode) sediment budget cells. Through SBAS, numerous sediment budgets can be established, copied, and modified for different project or forcing conditions with internal checks provided by the system. Although SBAS was developed to support regional coastal sediment management, its algorithmic structure and commercial-grade PC interface are independent of application. For example, SBAS can be applied to inland navigation projects or as a general ledger to track funds or products in multiple interactive accounts. Data entry can be accomplished visually or through a spreadsheet, and results can be displayed graphically in a number of ways or as lists, depending on the background and needs of the viewer (management review; engineering detail; overviews to sponsors). Because of the intuitive interface, SBAS can be operated with just a few minutes of training. The system also includes ways to estimate uncertainty, to consider "what if" questions easily, to cut-and-paste graphics, and to obtain hard copy reports.

EXAMPLE PROBLEM V-6-11

GIVEN:

Refine the conceptual budget for Shinnecock Inlet and the beaches ± 3.2 km east and west of the inlet. For this example, uncertainty in the sediment budget will be omitted (refer to Equation V-6-25 and V-6-26 for estimating uncertainty within a sediment budget).

BACKGROUND INFORMATION:

The refined conceptual budget is shown in Figure V-6-28, and details of its formulation are presented here. At 3.2 km east of the inlet, wave refraction modeling indicated that the ratio of Q_R to Q_L was approximately 1.9. The same ratio west of the inlet, also estimated from wave refraction modeling, was 1.8. These ratios indicate a westerly directed net transport that is slightly greater at the eastern boundary as compared with the western boundary. Based on profile-survey data, the berm-crest level was 3.5 m relative to National Geodetic Vertical Datum (NGVD), and the depth of closure was 7.0 m NGVD. The average shoreline change rate $\Delta y \Delta / t$ for Adjacent Beach 1 (from inlet to 3.2 km east, hereafter noted as A1) was 1.40 m/year, and the same quantity for Adjacent Beach 2 (from inlet to 3.2 km west, noted as A2) was –1.43 m/year. Beach-fill placements for A1 and A2 were 13,000 and 25,000 cu m/year, respectively. The rate of relative sea-level rise was 0.003 m/year, and the distance from datum to the depth of closure L_c was approximately 760 m for A1 and A2. The inlet channel and shoals had a net volume change of 111,000 cu m/year, with dredging averaging 2,400 cu m/year (Moffatt and Nichol Engineers and URS Consultants 1999).

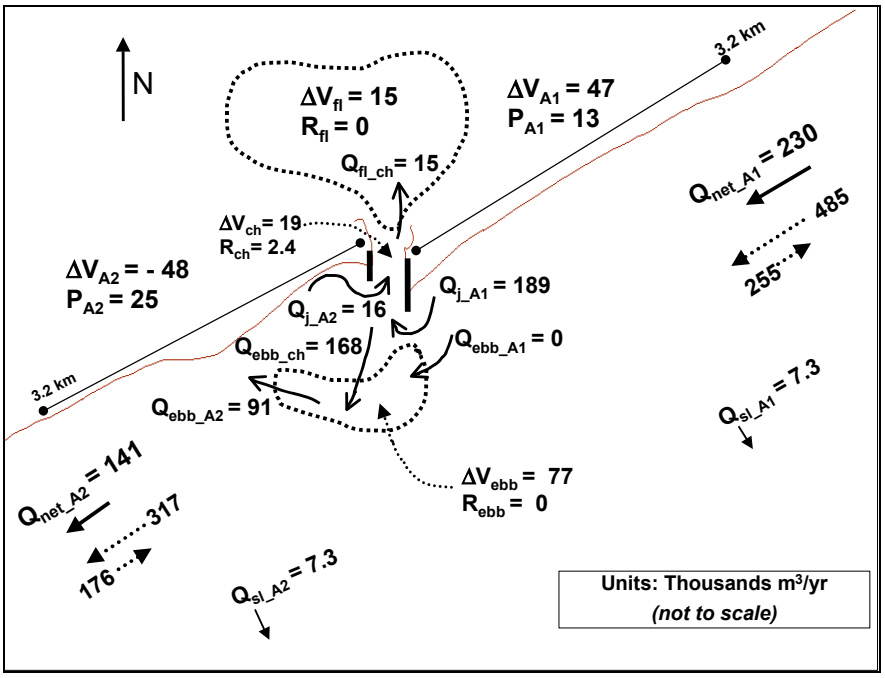

Figure V-6-28. Refined sediment budget for Shinnecock Inlet, New York

(Continued)

EXAMPLE PROBLEM V-6-11 (Continued)

CALCULATIONS:

Applying Equation V-6-27 gives an active depth for A1 and A2,

$$D_A = B + D_C = 3.5 + 7.0 = 10.5 \text{ m}$$

The rate of volume change for A1 and A2 can be calculated with Equation V-6-28,

$$\Delta V_{A1} = \frac{\Delta y \Delta x D_A}{\Delta t} = (1.40 \text{ m/year})\ (3{,}200 \text{ m})\ \ (10.5 \text{ m}) = 47{,}000 \text{ cu m/year}$$

$$\Delta V_{A2} = \frac{\Delta y \Delta x D_A}{\Delta t} = (-1.43 \text{ m/year})\ (3{,}200 \text{ m})\ \ (10.5 \text{ m}) = -48{,}000 \text{ cu m/year}$$

Losses due to relative sea-level rise can be estimated by Equation V-6-29,

$$\Delta y_{sl_A1} = \Delta y_{sl_A2} = \frac{L_c}{B + D_c}\ S = \frac{760}{3 + 7.5}\ (0.003) = 0.22 \text{ m/year}$$

or,

$$Q_{sl_A1} = Q_{sl_A2} = (\Delta y_{sl_A1} \text{ or } \Delta y_{sl_A2})(\Delta x)(D_A) \quad (0.22 \text{ m/year})\ (3{,}200 \text{ m})\ (10.5 \text{ m}) \sim 7{,}300 \text{ cu m/year}$$

The total change in volume for the inlet channel and shoals was given as 111,000 cu m/year. To fully develop the inlet sediment budget, this quantity will be proportioned between the ebb shoal, inlet channel, and flood shoal following the conceptual budget as guidance. Table V-6-11 lists the rate of measured volume change ΔV, beach fill placed P, dredging (removal) R, and losses because of relative sea-level rise Q_{sl}, for A1, each region of the inlet, and A2.

Table V-6-11
Rates of Volume Change for Shinnecock Inlet Sediment Budget, 1938 to 1979 (1,000s cu m/year)

Control Volume	ΔV	P	R	Q_{sl}
A1 (Adjacent Beach 1)	47	13	0	7.3
Inlet: Ebb Shoal	77	0	0	0
Inlet: Channel	19	0	2.4	0
Inlet: Flood Shoal	15	0	0	0
A2 (Adjacent Beach 2)	-48	25	0	7.3

(Continued)

EXAMPLE PROBLEM V-6-11 (Continued)

REFINING CONCEPTUAL SEDIMENT BUDGET:

To formulate the inlet sediment budget, one can assume a rate of net transport at the updrift boundary, Q_{net_A1} = 230,000 cu m/year. This value is within the range identified in the conceptual sediment budget. In a more expanded analysis than presented here, a range of values for Q_{net_A1} can be applied in the sediment budget to examine fully the sensitivity of the inlet sediment-transport magnitudes and pathways to this parameter. The ratio of Q_R and Q_L was given as 1.9, and entering this value into Equation V-6-23 gives,

$$Q_{net_A1} = Q_{R_A1} - Q_{L_A1} = 1.9\ Q_{L_A1} - Q_{L_A1} \quad 0.9\ Q_{L_A1}$$

$$230 = 0.9\ Q_{L_A1}$$

$$Q_{L_A1} = 255 \text{ and } Q_{R_A1} = 485$$

Considering the entire reach as the control volume forms a macrobudget. Applying Equation V-6-23 gives,

$$\sum Q_{source} - \sum Q_{\text{sink}} - \sum \Delta V + \sum P - \sum R = \text{Residual} = 0$$

$$\left(Q_{net_A1}\right) - \left(Q_{sl_A1} + Q_{sl_A2} + Q_{net_A2}\right) - \left(\Delta V_{A1} + \Delta V_{A2} + \Delta V_f + \Delta V_{ch} + \Delta V_{ebb}\right) + \left(P_{A1} + P_{A2}\right) - \left(R_{fl} + R_{ch} + \mathrm{R}_{e\,bb}\right) = 0$$

$$(230) - (7.3 + 7.3 + Q_{net_A2}) - (47 + -48 + 15 + 19 + 77) + (13 + 25) - (0 + 2.4 + 0) = 0$$

$$Q_{net_A2} = 141$$

Applying Equation V-6-23 at the western boundary gives,

$$Q_{net_A2} = Q_{R_A2} - Q_{L_A2}$$

$$141 = 1.8\ Q_{L_A2} - Q_{L_A2}$$

$$Q_{L_A2} = 176 \quad \textit{and} \quad Q_{R_A2} = 317$$

Now, the control volume A1 can be considered. There are two unknowns, the rate of sediment transport around the east jetty, Q_{j_A1}, and sediment transport from A1 to the ebb-tidal shoal, Q_{ebb_A1}. Inspection of bathymetric charts and aerial photography shows no evidence of morphologic pathways (e.g., shoal features) from A1 to the ebb-tidal shoal. Thus, one can assume that $Q_{ebb_A1} \sim 0$ and solve for Q_{j_A1} in Equation V-6-23,

$$\sum Q_{source} - \sum Q_{\sin k} - \sum \Delta V + \sum P - \sum R = \text{Residual} = 0$$

$$\left(Q_{net_A1}\right) - \left(Q_{sl_A1} + Q_{j_A1} + Q_{ebb_A1}\right) - \left(\Delta V_{A1}\right) + \left(P_{A1}\right) = 0$$

$$(230) - (7.3 + Q_{j_A1} + 0) - (47) + (13) = 0$$

$$Q_{j_A1} = 189$$

(Continued)

EXAMPLE PROBLEM V-6-11 (Continued)

gives,

$$\sum Q_{source} - \sum Q_{\text{sink}} - \sum \Delta V + \sum P - \sum R = Residual = 0$$

$$\left(Q_{net_A1}\right) - \left(Q_{sl_A1} + Q_{sl_A2} + Q_{net_A2}\right) - \left(\Delta V_{A1} + \Delta V_{A2} + \Delta V_{fl} + \Delta V_{ch} + \Delta V_{ebb}\right) + \left(P_{A1} + P_{A2}\right) - \left(R_{fl} + R_{ch} + \text{Re}_{bb}\right) = 0$$

$$\left(230\right) - \left(7.3 + 7.3 + Q_{net_A2}\right) - \left(47 + -48 + 15 + 19 + 77\right) + \left(13 + 25\right) - \left(0 + 2.4 + 0\right) = 0$$

$$Q_{net_A2} = 141$$

Next a control volume for A2 is formulated, excluding the ebb-tidal shoal. There are also two unknowns for this control volume, the rate of sediment transport around the west jetty, Q_{j_A2} , and the rate of sediment transport bypassed from the ebb-tidal shoal to A2, Q_{ebb_A2}. A more detailed analysis of the shoreline position and beach-fill placement records for A2 indicates that ΔV - P = –16 for the region east of the bulge in the 1979 shoreline position, and ΔV - P = –58 for the region west of the bulge. As a first estimate, one can set Q_{j_A2} = 16, implying that all sediment lost from the region east of the bulge moved around the west jetty. This assumption also implies that this morphologic feature represents a long-term nodal zone for net longshore sand transport. Using Equation V-6-23 to solve for Q_{ebb_A2} gives,

$$\sum Q_{source} - \sum Q_{sink} - \sum \Delta V + \sum P - \sum R = Residual = 0$$

$$\left(Q_{ebb_A2}\right) - \left(Q_{net_A2} + Q_{j_A2} + Q_{sl_A2}\right) - \left(\Delta V_{A2}\right) + \left(P_{A2}\right) = 0$$

$$\left(Q_{ebb_A2}\right) - \left(141 + 16 + 7.3\right) - \left(-48\right) + \left(25\right) = 0$$

$$Q_{ebb_A2} = 91$$

in units of thousands of cubic meters.

The control volume for the ebb-tidal shoal now has one unknown, the rate of sediment transport from the channel to the ebb-tidal shoal, Q_{ebb_ch}. Applying Equation V-6-23 gives,

$$\sum Q_{source} - \sum Q_{sink} - \sum \Delta V + \sum P - \sum R = Residual = 0$$

$$\left(Q_{ebb_A1} + Q_{ebb_ch}\right) - \left(Q_{ebb_A2}\right) - \left(\Delta V_{ebb}\right) \quad 0$$

$$\left(0 + Q_{ebb_ch}\right) - (91) - (77) \quad 0$$

$$Q_{ebb_ch} = 168$$

(Continued)

EXAMPLE PROBLEM V-6-11 (Concluded)

The final unknown is the rate of sediment transport from the channel to the flood-tidal shoal, Q_{fl_ch}. Equation V-6-23 applied to the inlet channel control volume gives,

$$\sum Q_{source} - \sum Q_{sink} - \sum \Delta V + \sum P - \sum R = Residual = 0$$

$$\left(Q_{j_A1} + Q_{j_A2}\right) - \left(Q_{ebb_ch} + Q_{fl_ch}\right) - \left(\Delta V_{ch}\right) - \left(R_{ch}\right) \quad 0$$

$$(189 + 16) - (168 + Q_{fl_ch}) - (19) - (2.4) \quad 0$$

$$Q_{fl_ch} = 15.6 \sim 15$$

The calculated value of $Q_{fl_ch} = 15.6$ approximately agrees with the assumed change in volume for the flood-tidal shoal, $\Delta V_{fl} = 15$, indicating that there are no other significant sediment sources contributing to the growth of the flood-tidal shoal.

DISCUSSION OF EXAMPLES.

These example problems illustrate one approach that can be taken for formulating a sediment budget. The following assumptions entered:

The net longshore sand transport rate at the updrift boundary of the control volume was assumed to be 230,000 cu m/year.

The rate of sediment transport from A1 to the ebb-tidal shoal was assumed to be negligible.

The rate of sediment transport from A2 around the west jetty was assumed to be 16,000 cu m/year.

Volume change rates for the ebb-tidal shoal, inlet channel, and flood-tidal shoal were assumed to be 77,000, 19,000, and 15,000 cu m/year, respectively.

Uncertainties in quantities forming the sediment budget were omitted for this example problem.

(b) Operation. SBAS has been designed to organize the user's work space and facilitate visualization of sediment budget alternatives. Within the right-hand side of the screen, called the Topology Window, SBAS formulates a sediment budget by allowing the user to create a series of cells and arrows representing sources and sinks that characterize the budget. The user selects items from the upper tool bar to generate elements of the sediment budget. The lower tool bar allows the user to import georeferenced images and data into a desired coordinate system and viewed with the sediment budget in the Topology Window. The user can zoom in to show a detailed area, and zoom out to view the regional sediment

budget. The left-hand side of the screen organizes alternatives within a particular project. Alternatives may represent various time periods, different boundary conditions for the same time period, or modifications to assumptions within the budget reflecting a sensitivity analysis. Once a sediment budget alternative has been defined, and the user has created sediment budget cells with sources and sinks, values can then be assigned to the various components of the sediment-budget topology. Figure V-6-29a shows a screen capture with a georeferenced image of the regional project area, and Figure V-6-29b shows a zoom-in image of a local sediment budget. As shown in Figure V-6-29b, the SBAS indicates by color-coding whether a cell is balanced or not.

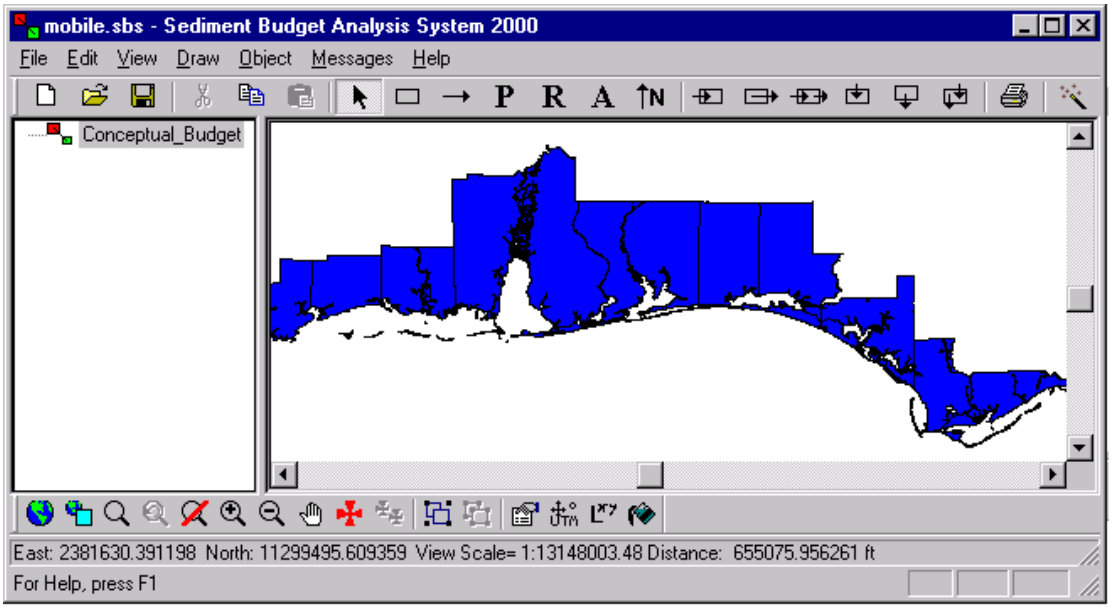

Figure V-6-29a. SBAS Alternative Window (left) and Topology Window (right)

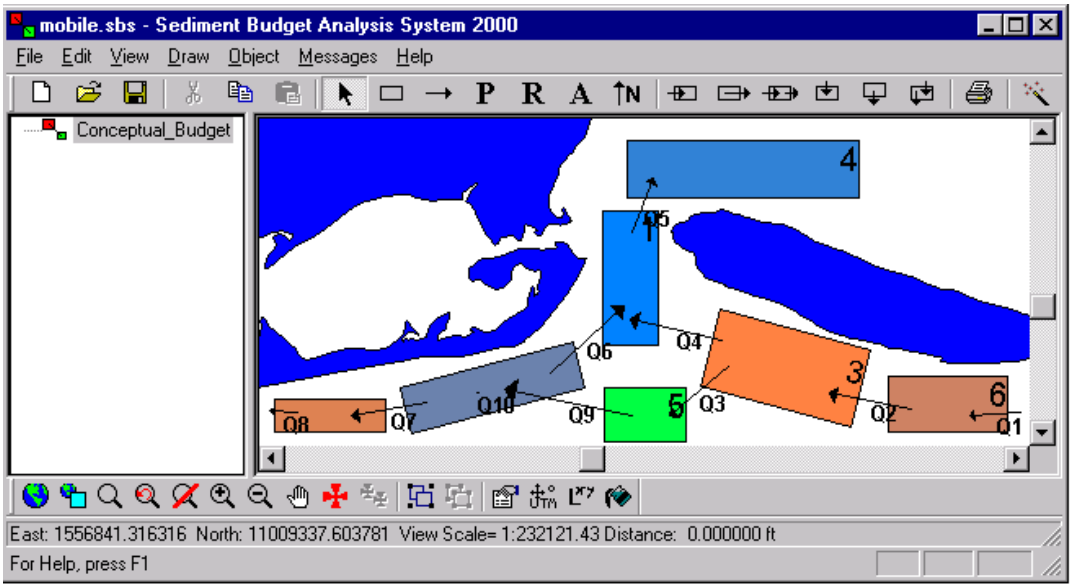

Figure V-6-29b. Zoom-in showing sediment budget cells. Color coding indicates varying degrees of imbalance

The lower tool bar allows the import of georeferenced images and data into a desired coordinate system (Figure V-6-30) and viewed with the sediment budget in the Topology Window. The user can zoom out to view the regional sediment budget (see Figure V-6-31, which shows the Gulf of Mexico shore of Alabama and Florida panhandle), and zoom in to show a detailed area (Figure V-6-32). By dragging the cursor over any combination of cells, sediment budget cells can be combined (collapsed), as shown in Figure V-6-32. Collapsed cells are useful for regional views of a sediment budget. For local, project-level applications, selecting the collapsed cell and choosing an icon from the bottom tool bar will reinstate (explode) the collapsed cell (Figure V-6-33).

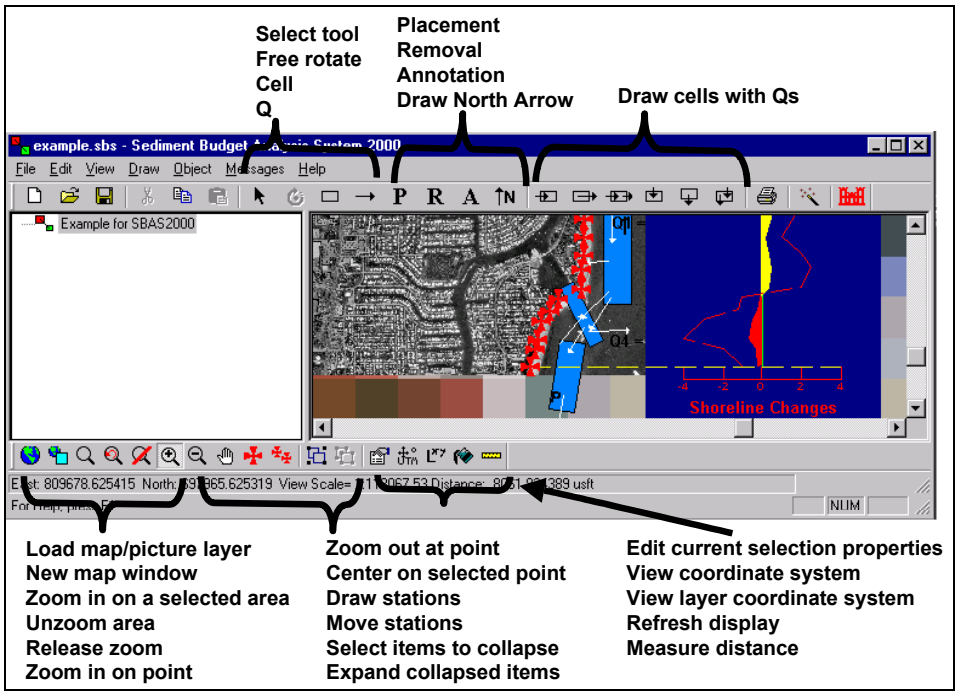

Figure V-6-30. SBAS tool bars and button functions

SBAS can also display data on shoreline change and the rate of volume change associated with stations located along the coast, bay, or river (Figure V-6-34). Location of stations and associated data may be entered directly into SBAS's spreadsheet (Figure V-6-35), or data may be imported using a user-specified format.

Georeferenced images can be imported into SBAS by means of the *Load map/picture layer* on the bottom tool bar. This menu (Figure V-6-36) allows the user to indicate the coordinate system (group, system, datum, and linear unit) in which the sediment budget project will be defined. Next, the maps to be imported are selected, and their coordinate system is selected. SBAS converts the map's coordinate system to the project coordinate system. Multiple images (maps, aerial photographs, contour maps, etc.) can be layered in the sediment budget. SBAS allows for 55 different map coordinate systems.

A demonstration that guides the user through the operation and features of SBAS Version 1.02 available for viewing on the PC, as described in a later section.

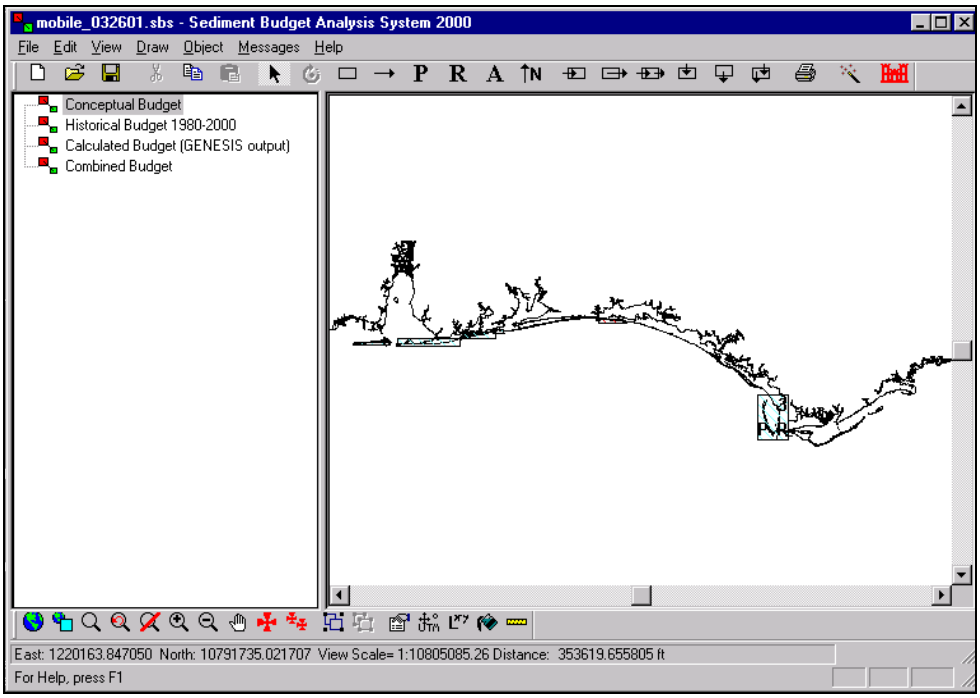

Figure V-6-31. Regional view of a sediment budget (zoom-out), with four alternatives

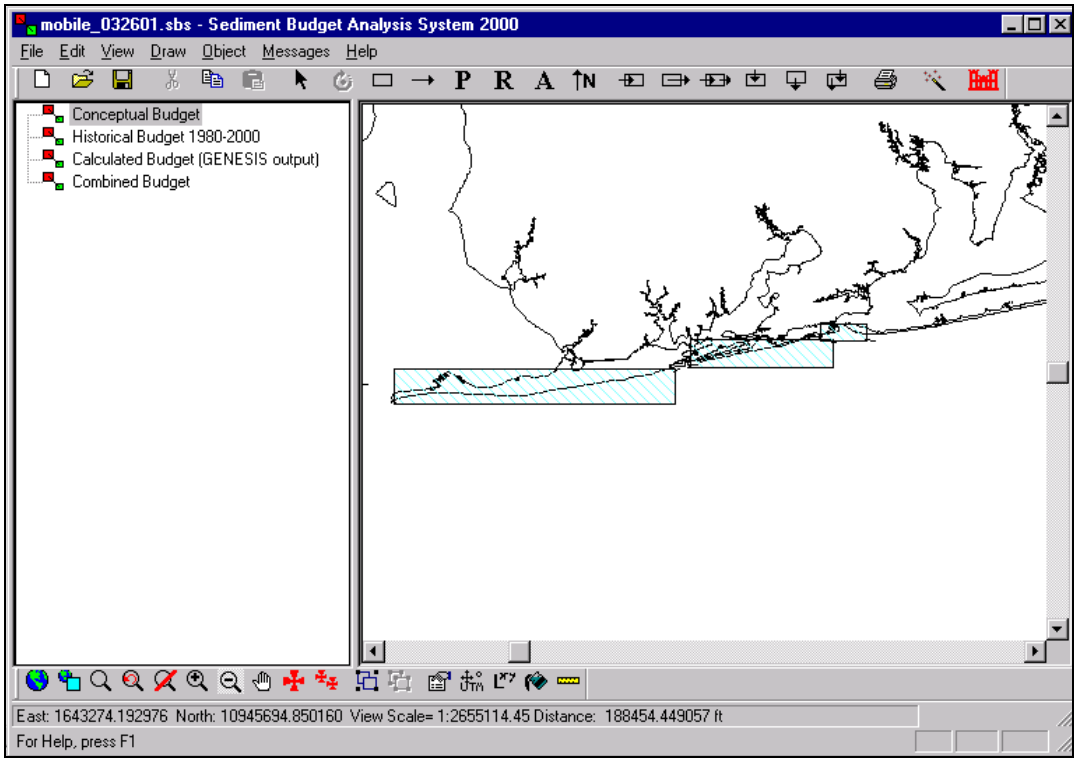

Figure V-6-32. Local view of a sediment budget (zoom-in) showing combined (collapsed) sediment budget cells

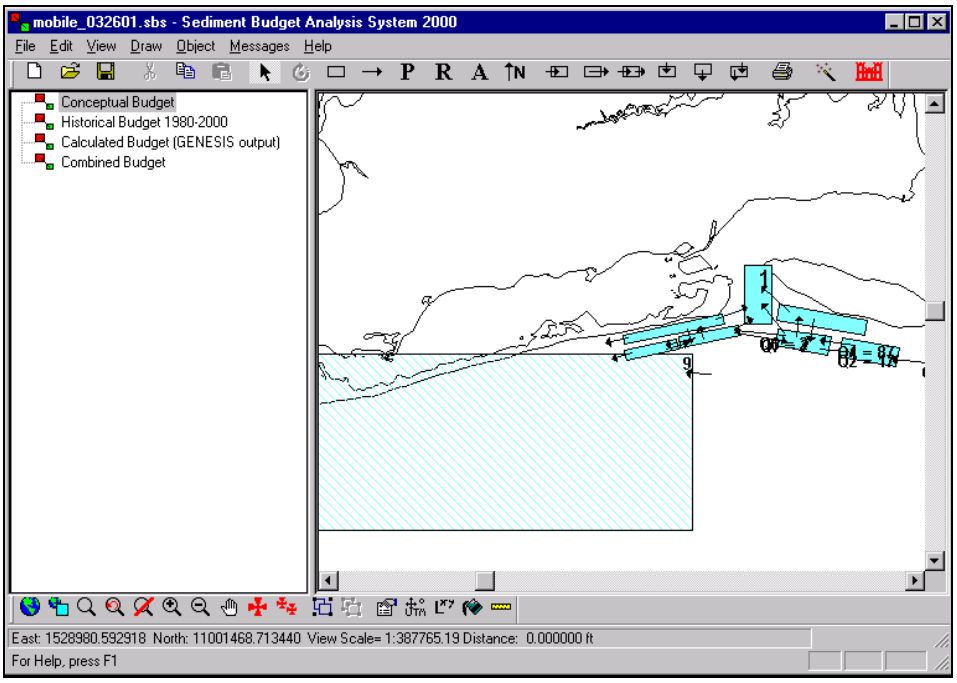

Figure V-6-33. Sediment budget with reinstated (exploded) cells

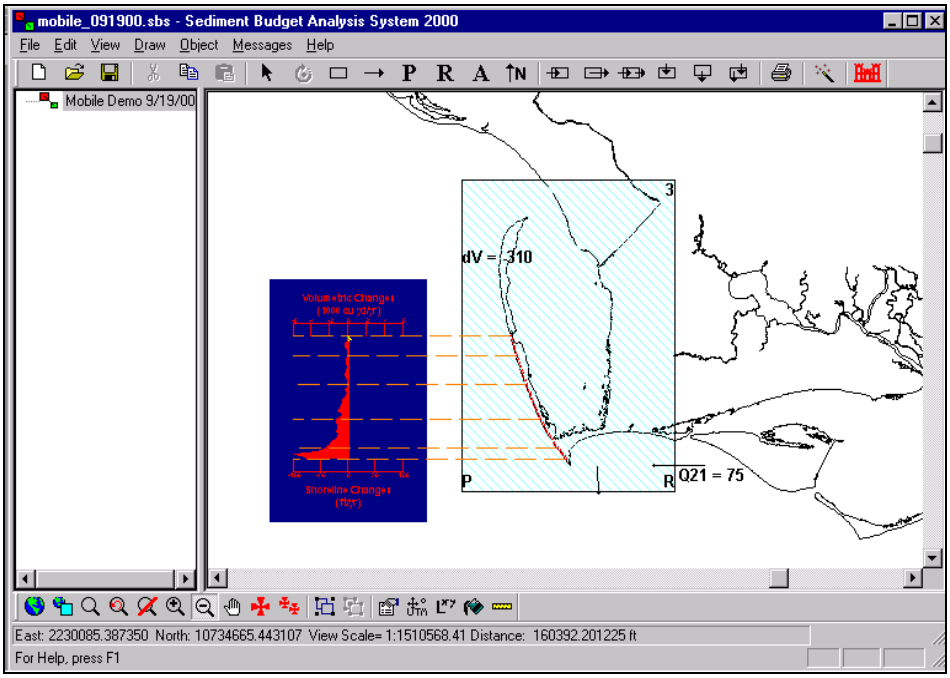

Figure V-6-34. Rate graph feature of SBAS

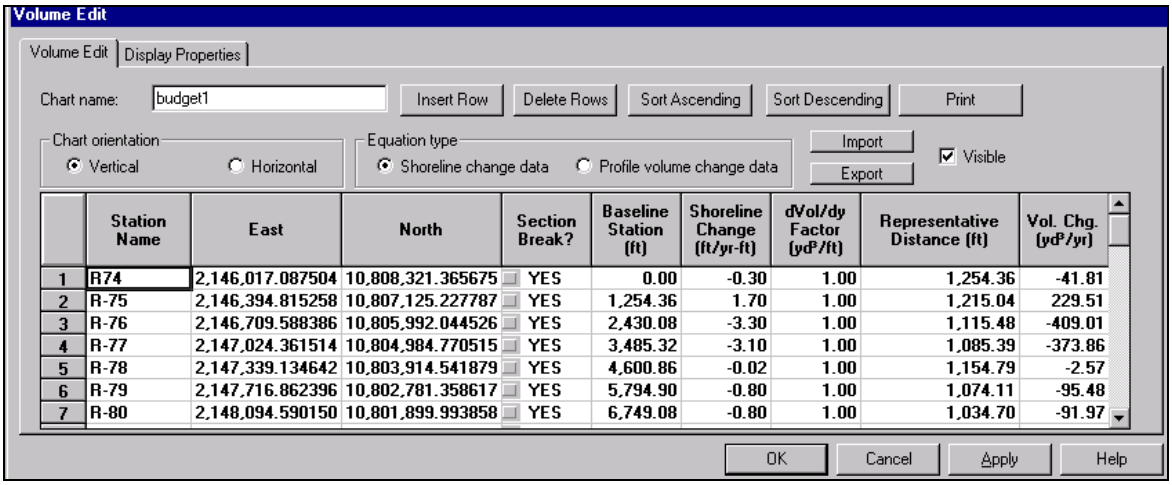

	Station Name	East	North	Section Break?	Baseline Station (ft)	Shoreline Change (ft/yr-ft)	dVol/dy Factor (yd³/ft)	Representative Distance (ft)	Vol. Chg. (yd³/yr)
1	R74	2,146,017.087504	10,808,321.365675	YES	0.00	-0.30	1.00	1,254.36	-41.81
2	R-75	2,146,394.815258	10,807,125.227787	YES	1,254.36	1.70	1.00	1,215.04	229.51
3	R-76	2,146,709.588386	10,805,992.044526	YES	2,430.08	-3.30	1.00	1,115.48	-409.01
4	R-77	2,147,024.361514	10,804,984.770515	YES	3,485.32	-3.10	1.00	1,085.39	-373.86
5	R-78	2,147,339.134642	10,803,914.541879	YES	4,600.86	-0.02	1.00	1,154.79	-2.57
6	R-79	2,147,716.862396	10,802,781.358617	YES	5,794.90	-0.80	1.00	1,074.11	-95.48
7	R-80	2,148,094.590150	10,801,899.993858	YES	6,749.08	-0.80	1.00	1,034.70	-91.97

Figure V-6-35. *Volume Edit* spreadsheet in SBAS

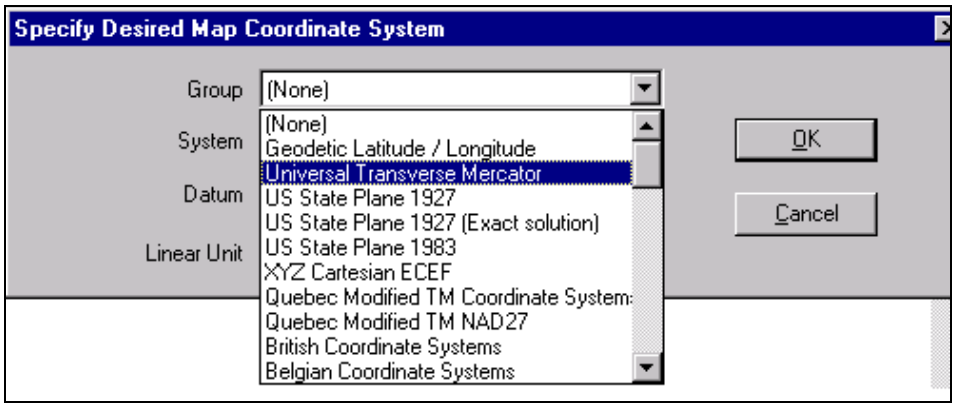

Figure V-6-36. Entering project coordinate system with the *Load map/picture layer* feature on the bottom tool bar

EXAMPLE PROBLEM V-6-12

EXAMPLE:

The SBAS installation includes an example file with georeferenced images, a sediment budget, and rate graph. The following example problem guides the use of these files.

Step 1: Activate SBAS and enter information to the *Document Properties Menu*. Information such as the manager of the project, keywords, units, and type of uncertainty calculation are entered into this menu (see Kraus and Rosati 1998a, for details about the uncertainty calculation). Note: the user should choose the same project coordinate system and consistent units for the transport rate or volume change (e.g., if the project coordinate system will be in U.S. Customary Units, rates should be expressed as cu yd/year and volume as cu yd).

(Continued)

EXAMPLE PROBLEM V-6-12

Step 2: Import georeferenced images. To import the map provided in the installation, activate the Topology Window (right side of the screen) by clicking in this area. Choose the globe on the bottom tool bar. The user first defines the desired project coordinate system as follows:

Group: US State Plane 1927
System: Florida East 901
Datum: NAD 27
Units: USFEET
Select **OK**

Then load the map provided in the installation with the *Connect Map Layer* menu. Select the following files:

Conus12.tif (image) and Conus12.tab (reference file)

On the next menu, indicate that these files are in

Group: Geodetic Latitude/Longitude
System: Latitude/Longitude
Datum: WGS84

(If the image is not visible, select release zoom on the bottom tool bar.)

Step 3: Import a photograph. Choose the globe on the bottom tool bar and import another map layer. Select the following files:

Br21-38.tif (image) and Br21-38.tfw (reference file) (photograph of Hillsboro Inlet, Florida and associated world file)

On the next menu, indicate that these files are in the following coordinate system (same as the project coordinate system):

Group: US State Plane 1927
System: Florida East 901
Datum: NAD27
Units: USFEET

The coordinate system for the layers that have been loaded can be viewed by choosing the **Edit Current Selection Properties** button on the bottom tool bar.

Step 4: Create a sediment budget for Hillsboro Inlet. Accessing the top toolbar, select the cell button and drag and pull sediment budget cells. Cells may be rotated to better represent different areas of the budget (the channel, for instance) by choosing the rotate button on the top tool bar and rotating a corner of a selected cell. Placement and removal in cells may be indicated by choosing the **P** and **R** buttons on the top tool bar, respectively, then clicking on the cell that has the engineering activity. Sediment sources and sinks to and from each cell may be indicated by selecting the **arrow** button on the top tool bar, and dragging arrows into and out of each cell as appropriate. Double clicking on a cell will bring up the *Cell Properties* menu, and values for each sediment budget element can be entered.

(Continued)

EXAMPLE PROBLEM V-6-12 (Continued)

Cells can be collapsed by selecting the **Select Items to be Collapsed** button on the bottom tool bar, and dragging the cursor over the items to be combined. The cells may be reinstated by selecting the collapsed cell, then choosing the **Expand Collapsed Items** on the bottom tool bar. Note: colors of cell balance, gain, and loss, arrows, and other sediment budget elements may be changed by selecting the **Object-Colors** button at the top tool bar.

Hillsboro Inlet Sediment Budget. The sediment budget can be formulated with three cells: updrift, channel, and downdrift. The following text summarizes the sediment budget (Personal Communication, Thomas D. Smith, April 2001, U.S. Army Engineer District, Jacksonville), which has been conceptualized as shown in Figure V-6-37.

Updrift Cell. Net longshore sand transport entering the north boundary of the updrift cell is approximately 120,000 cu yd/year. Sinks from this cell include accretion of the updrift beach at a rate of 6,000 cu yd/year, 54,000 cu yd/year transported over the north jetty weir section to the channel cell, and 60,000 cu yd/year moving around the jetty into the channel cell.

Channel Cell. The source of sediment to this cell is 30,000 cu yd/year moving into the channel from the downdrift cell. Sinks from this cell include 4,000 cu yd/year transported to deep water on ebb flow, 110,000 cu yd/year dredged from the channel and placed within the downdrift cell, and 30,000 cu yd/year which is naturally bypassed from the channel to the downdrift cell.

Downdrift Cell. Dredged material placement into this cell is 110,000 cu yd/year, which is also the value of net longshore transport exiting this cell.

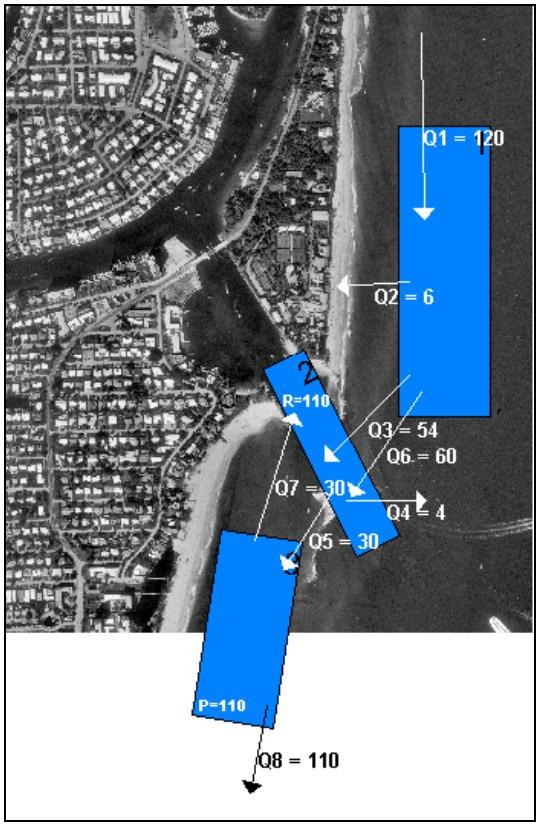

Figure V-6-37. Sediment budget for Hillsboro Inlet, Florida

(Continued)

EXAMPLE PROBLEM V-6-12 (Concluded)

Step 5: Enter shoreline change rate data for Hillsboro Inlet. Select the **Draw Stations** button on the bottom tool bar, and visually place benchmarks for shoreline data on the photograph. (If you have a pre-existing file with data, these station locations may also be imported to the SBAS Rate Graph spreadsheet). Once all stations have been entered, choose the **View-Rate Graph** button on the top tool bar, select the rate graph (named *Untitled* at this point), and choose **Edit**. Shoreline change (or volume change) data may be entered for each benchmark position. SBAS automatically plots these data in the rate graph. Selecting and dragging will move the graph, and deselecting the graph after clicking the **View-Rate Graph** button on the top tool bar can turn it off. An example is shown in Figure V-6-38.

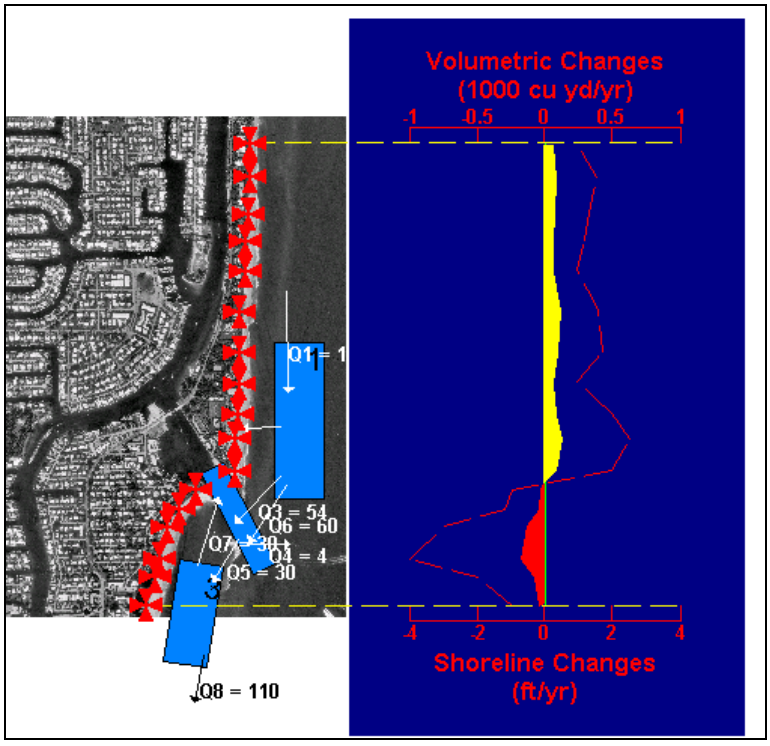

Figure V-6-38. Hypothetical shoreline change data for beaches adjacent to Hillsboro Inlet

SBAS2000 may be obtained by contacting the Coastal and Hydraulics Laboratory, U.S. Army Engineer Research and Development Center, Vicksburg, MS.

(2) Reservoir Model (Kraus 2000)

(a) Kraus developed a time-dependent model of inlet morphology that is mathematically analogous to a reservoir system with known (or estimated) equilibrium volumes for each reservoir and defined transfer rates between reservoirs. The reservoirs represent morphologic features, including the ebb-tidal

shoal, bypassing bar, attachment bar, and flood tidal shoal (Figure V-6-39). Once calibrated, the model predicts a time-dependent sediment budget based on the equilibrium volume of each morphologic feature, and the longshore sand transport characteristics in the region. The following discussion is summarized from Kraus (2000).

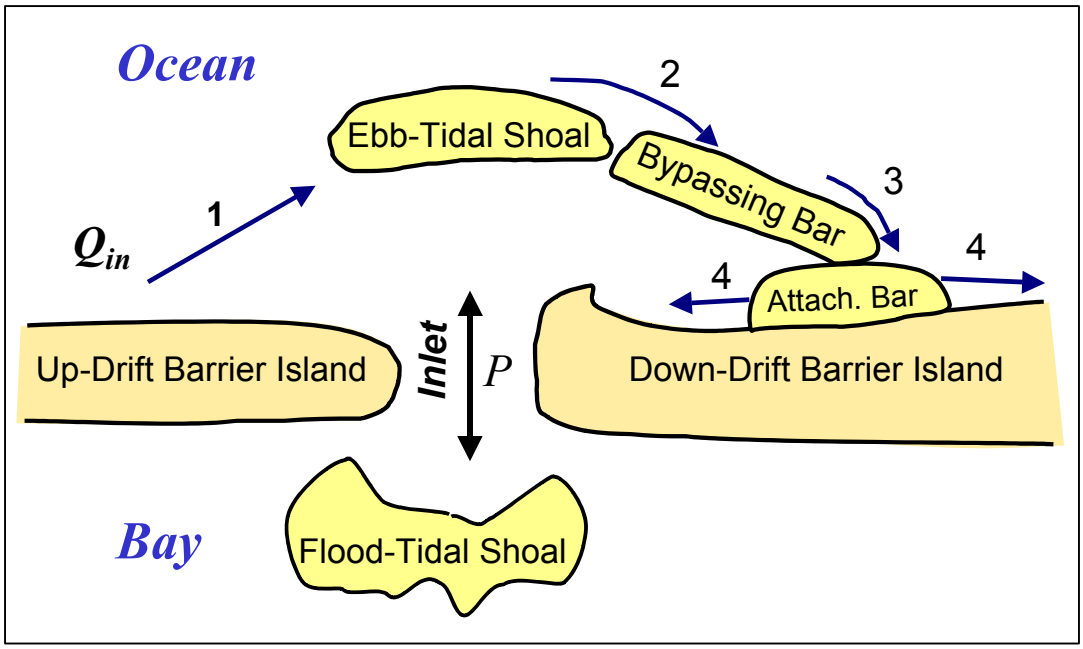

Figure V-6-39. Definition sketch for inlet morphology

(b) The time-dependent Reservoir Model operates on the temporal and spatial scales associated with the entire (aggregated) morphological form of an ebb-tidal shoal. Five assumptions are invoked to arrive at the model:

Mass (sand volume) is conserved.

Morphological forms and the sediment pathways among them can be identified, and the morphologic forms evolve while preserving identity.

Stable equilibrium of the individual aggregate morphologic form(s) exist.

Changes in mesomorphological and macromorphological forms are reasonably smooth.

Material composing the ebb-tidal shoal is predominately transported to and from it through longshore transport.

(a) The ebb-shoal complex is defined as consisting of the ebb shoal proper, one or two ebb-shoal bypassing bars (depending on the balance between left- and right-directed longshore transport), and one or two attachment bars. These features are shown schematically in Figure V-6-39 and the pattern of wave breaking on the crescentic ebb-shoal complex at Ocean City Inlet, Maryland, is shown in Figure V-6-40.

Figure V-6-40. Pattern of wave breaking on ebb shoal and bar, Ocean City Inlet, Maryland, November 1991

The model distinguishes between ebb-tidal shoal proper (hereafter, ebb shoal), typically located in the confine of the ebb-tidal jet, and the ebb-shoal bypassing bar (hereafter, bypassing bar) that grows toward shore from the ebb shoal, principally by the transport of sediment alongshore by wave action. The bar may shelter the leeward beach from incident waves so that a salient might form – similar to the functioning of a detached breakwater (Pope and Dean 1986), initiating creation of the attachment bar.

(b) Previous authors have combined the ebb shoal and the bar(s) protruding from it into one feature referred to as the ebb shoal. Here, the shoal and bypassing bars are distinguished because of the different balance of processes. When a new inlet is formed, the shoal first becomes apparent within the confine of the inlet ebb jet, and bypassing bars have not yet emerged. Bypassing bars are formed by sediment transported off the ebb shoal through the action of breaking waves and the wave-induced longshore current (tidal and wind-induced currents can also play a role). A bar cannot form without an available sediment source, similar to the growth of a spit (as modeled mathematically by Kraus 1999). In this sense, bypassing bars are analogous to the spit platform concept of Meistrell (1972) in which a subaqueous sediment platform develops from the sediment source prior to the visually observed subaerial spit. Bypassing bars grow in the direction of predominant transport as do spits. At inlets with nearly equal left- and right-directed longshore transport or with a small tidal prism, two bars can emerge from the ebb shoal creating a nearly concentric halo about the inlet entrance. As the bypassing bar merges with the shore, an attachment bar is created, thereby transporting sand to the beach. At this point in evolution of the ebb-shoal complex, substantial bypassing of sand can occur from the updrift side of the inlet to the downdrift side.

(c) In this conceptualization, if an inlet is created along a coast, the littoral drift is intercepted to deposit sand first in the channel and ebb shoal. This material joins that volume initially jetted offshore when the barrier island or landmass was breached. Over time, a bar emerges from the shoal and grows in

the predominant direction of drift. After many years, as controlled by the morphologic or aggregate scale of the particular inlet, an attachment bar may form on the downdrift shore. At this stage, significant sand bypassing of the inlet can occur, re-establishing in great part the transport downdrift that existed prior to formation of the inlet. The following model can describe the evolution of an ebb-shoal complex from initial cutting of the inlet, as well as changes in morphologic features and sand bypassing resulting from engineering actions such as mining or from time-dependent changes in wave climate (for example, seasonal shifts).

(f) Reservoir aggregate model. The conceptual model of the ebb-shoal complex described in the preceding section is represented mathematically by analogy to a reservoir system, as shown in Figure V-6-41. It is assumed that sand is brought to the ebb shoal at a rate q_{in}, and the volume v_e in the ebb shoal at any time increases while possibly leaking or bypassing some amount of sand to create a downdrift bypassing bar. The input rate q_{in} typically is the sum of left- and right-directed longshore sand transport. For the analytic model presented, a predominant (unidirectional) rate is taken, but this constraint is not necessary and is relaxed in a numerical example in the following paragraphs.

(g) The volume V_E of sand in the shoal can increase until it reaches an equilibrium volume V_{Ee} (the subscript e denoting equilibrium) according to the hydrodynamic conditions such as given by Walton and Adams (1976). As equilibrium is approached, most sand brought to the ebb shoal is bypassed in the direction of predominant transport. Similarly, the bypassing bar volume V_B grows as it is supplied with sediment by the littoral drift and the ebb shoal, with some of its material leaking to (bypassing to) the attachment bar. As the bypassing bar approaches equilibrium volume V_{Be}, most sand supplied to it is passed to the attachment bar V_A. The attachment bar transfers sand to the adjacent beaches. When it reaches its equilibrium volume V_{Ae}, all sand supplied to it by the bar is bypassed to the downdrift beach. The model thus requires values of the input and output rates of transport from each feature, and their respective equilibrium volumes.

(h) Analytical model. Simplified conditions are considered here to obtain a closed-form solution that reveals the parameters controlling the aggregated morphologic ebb-shoal complex. In the absence of data and for convenience in arriving at an analytical solution, a linear form of bypassing is assumed. The amount of material bypassed from any of the morphological forms is assumed to vary in direct proportion to the volume of the form (amount of material in a given reservoir) at the particular time. Therefore, the rate of sand leaving or bypassing the ebb shoal, $(Q_E)_{out}$, is specified as:

$$(Q_E)_{out} = \frac{V_E}{V_{Ee}} Q_{in} \tag{V-6-30}$$

in which Q_{in} is taken to be constant (average annual rate), although this is not necessary.

The continuity equation governing change in V_E can be expressed as:

$$\frac{dV_E}{dt} = Q_{in} - (Q_E)_{out} \tag{V-6-31}$$

where t = time. For the present situation with Equation V-6-30, it becomes:

$$\frac{dV_E}{dt} = Q_{in}\left(1 - \frac{V_E}{V_{Ee}}\right) \tag{V-6-32}$$

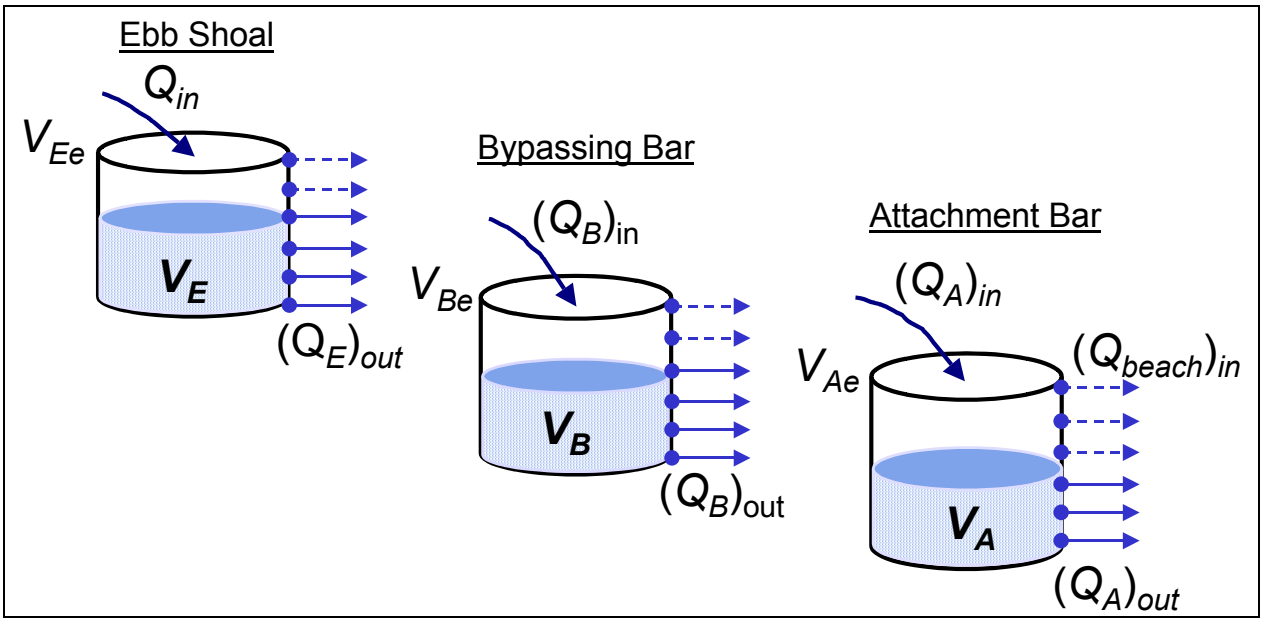

Figure V-6-41. Conceptual design for reservoir model

With the initial condition $V_E(0) = 0$, the solution of Equation V-6-32 is:

$$V_E = V_{Ee}\left(1 - e^{-\alpha t}\right) \tag{V-6-33}$$

in which

$$\alpha = \frac{Q_{in}}{V_{Ee}} \tag{V-6-34}$$

The parameter α defines a characteristic time scale for the ebb shoal. For example, if $Q_{in} = 1\times10^5$ cu m/year and $V_{Ee} = 2\times10^6$ cu m, which are representative values for a small inlet on a moderate-wave coast, then $1/\alpha = 20$ years. The shoal is predicted to reach 50 and 95 percent of its equilibrium volume after 14 and 60 years, respectively, under the constant imposed transport rate. These time frames are on the order of those associated with development of inlet ebb shoals.

The characteristic time scale given by α has a physical interpretation by analogy to the well-known model of bar bypassing introduced by Bruun and Gerritsen (1960) and reviewed by Bruun, Mehta, and Johnsson (1978). Bruun and Gerritsen (1959; 1960); introduced the ratio r as

$$r = \frac{P}{M_{tot}} \tag{V-6-35}$$

in which P = tidal prism, and M_{tot} = average annual littoral sediment brought to the inlet. Inlets with a value of $r > 150$ (approximate) tend to have stable, deep channels and are poor bar bypassers from updrift to downdrift, whereas inlets with $r < 50$ (approximate) tend toward closure and are good bar bypassers.

Because the equilibrium volume of the ebb-tidal shoal is approximately linearly proportional to the tidal prism, $V_{Ee} \propto P$ (Walton and Adams 1976), α is proportional to $1/r$. The reservoir aggregate model therefore contains at its center a concept widely accepted by engineers and geomorphologists. Established here through the continuity equation, the reservoir model gives theoretical justification for the Bruun and Gerritsen ratio by the appearance of α.

The volume of sediment $(V_E)_{out}$ that has bypassed the shoal from inception of the inlet to time t is the difference between the amount that arrived at the shoal and that remaining on the shoal:

$$(V_E)_{out} = Q_{in}t - V_E \tag{V-6-36}$$

The rate of sand arriving at the bypassing bar $(Q_B)_{in}$ equals the rate of that leaving the shoal $(Q_E)_{out} = d(V_E)_{out}/dt$, or

$$\begin{aligned}(Q_B)_{in} &= (Q_E)_{out} = Q_{in} - \frac{dV_E}{dt} \\ &= \frac{V_E}{V_{Ee}} Q_{in}\end{aligned} \tag{V-6-37}$$

which recovers (1) by volume balance. The right side of Equation V-6-37 can be expressed as αV_E, again showing the central role of the parameter α.

Continuing in this fashion, the reservoir aggregate model yields the following equations for the volume of the bypassing bar,

$$V_B = V_{Be}\left(1 - e^{-\beta t'}\right), \qquad \beta = \frac{Q_{in}}{V_{Be}}, \qquad t' = t - \frac{V_E}{Q_{in}} \tag{V-6-38}$$

and for the volume of the attachment bar,

$$V_A = V_{AE}\left(1 - e^{-\gamma t''}\right), \qquad \gamma = \frac{Q_{in}}{V_{AE}}, \qquad t'' = t' - \frac{V_B}{Q_{in}} \tag{V-6-39}$$

The quantities β and γ are analogous to α in representing time scales for the bypassing bar and attachment bar, respectively.

The quantities t' and t'' in Equation V-6-38 and V-6-39 can be interpreted as lag times that delay development of the bar and attachment, respectively. To see this explicitly, Taylor expansions for small relative time give $t' \approx \alpha t^2 / 2$ and $t'' \approx \alpha^2 \beta\, t^4 / 8$, as compared to growth of the ebb shoal given by αt.

The interpretation is that after creation of an inlet, a certain time is required for the bypassing bar to receive a significant amount of sand from the shoal and a longer time for the attachment bar or beach to receive sand. Similarly, modification of, say, the ebb shoal as through sand mining will not be observed immediately in the bypassing at the beach because of the time lags in the system.

A unique crossover time t_c occurs when the volume of material leaving the shoal equals the volume retained, $(V_E)_{out} = V_E$. After the crossover time, the shoal bypasses more sediment than it retains, characterizing the time evolution of the ebb shoal and its bypassing functioning. The crossover time is determined from Equation V-6-36 to be:

$$t_c = \frac{1.59}{\alpha} \tag{V-6-40}$$

Finally, by analogy to (8), the following equations are obtained for the bypassing rate of the bar $(Q_B)_{out}$, which is equal to the input of the attachment $(Q_A)_{in}$, and the bypassing rate of the attachment $(Q_A)_{out}$, which is also the bypassing rate or input to the beach, $(Q_{beach})_{in}$:

$$\left(Q_B\right)_{out} = \frac{V_E}{V_{Ee}} \frac{V_B}{V_{Be}} Q_{in} = \left(Q_A\right)_{in} \tag{V-6-41}$$

$$\left(Q_A\right)_{out} = \frac{V_E}{V_{Ee}} \frac{V_B}{V_{Be}} \frac{V_A}{V_{Ae}} Q_{in} = \left(Q_{beach}\right)_{in} \tag{V-6-42}$$

The quantity $(Q_A)_{out}$ describes the time dependence of the amount of sand reaching the downdrift beach and is, therefore, a central quantity in beach nourishment and shore-protection design.

(i) Validation of model for Ocean City, Maryland. Calculations are compared with observations of the growth in the ebb shoal at Ocean City Inlet, Maryland. Ocean City Inlet was opened by a hurricane in August 1933. Stabilization of the inlet began 1 month later by placement of jetties (Dean and Perlin 1977), with the south and north jetties constructed during 1934 and 1935. Rosati and Ebersole (1996) estimated that between 4.3×10^5 and 9.7×10^5 cu m of sediment were released during the island breach. This material would be apportioned to the flood shoal, ebb shoal, and adjacent beaches. Assateague Island, located to the south and downdrift, began to erode in a catastrophic manner because of interruption of sediment formerly transported from the beaches of Ocean City. Erosion of Assateague Island and growth of the ebb shoal have been well documented (e.g., Dean and Perlin 1977; Leatherman 1984; Underwood and Hiland 1995; Rosati and Ebersole 1996; Stauble 1997).

The location and shape of the ebb shoal and bar at Ocean City can be inferred from the locations of wave breaking, as shown in Figure V-6-40. Numerous bathymetry surveys (Underwood and Hiland 1995; Stauble 1997) confirm this inference. The bypassing bar is skewed to the south and has continued to move to the south (Underwood and Hiland 1995). Several independent authors have noted that much of the longshore sand transport moving to the south along Ocean City is diverted to the ebb shoal. Dean and Perlin (1977) concluded that the north jetty area was fully impounded, and the U.S. Army Engineer District, Baltimore (Personal Communication 1999, G. Bass, Senior Engineer, U.S. Army Engineer District, Baltimore, noted that recent growth of the northern edge of the ebb shoal may be composed of beach fill material placed on Ocean City beaches.

Dean and Perlin (1977) estimated the long-term net (southward) longshore sand transport rate as between approximately 1.15×10^5 and 1.50×10^5 cu m/year, based on impoundment at the north jetty. Underwood and Hiland (1995) estimated the equilibrium volume of the ebb-shoal complex as between 5.8×10^6 and 7.2×10^6 m^3 based on the tidal prism of 2.3×10^7 cu m given by Dean and Perlin (1977) and calculation methods given in Walton and Adams (1976). With M_{tot} estimated

by the upper value of net transport, one finds $r \cong 150$, consistent with lack of a bar across the entrance channel and good navigation. In fact, the entrance channel is rarely dredged.

Bathymetry survey data were available to this study for the dates of 1929/1933 to define the preinlet condition, 1937, 1961/1962, 1977/1978, 1990, and a composite of various surveys conducted in 1995. Underwood and Hiland (1995) developed data sets prior to 1995, and Stauble (1997) assembled the 1995 data set from various sources for the Baltimore District. As part of the present work, the raw data sets were reviewed and vertical datums made consistent.

The seaward boundary of lines unambiguously defining depositional features (ebb shoal, bypassing bar, and attachment bar) were found to be located at the 6-to 7-m National Geodetic Vertical Datum (NGVD) depth contour. Contours lying deeper than 7 m exhibited randomness and loss of identity of the particular feature. Here, to avoid the necessity of employing color to denote relatively complex contours, the landward portions of the bypassing bar and attachment bar polygons are defined by the zone of deposition as given by comparisons of bathymetry change. The lateral and landward boundaries of the ebb shoal polygons are defined by deposition from 1937 to 1962, and by a combination of deposition and depth contours for later time periods. This procedure accounts for the observation that the ebb shoal was fully developed by 1962, whereas changes were observed for the bypassing bar and attachment bar. Based on inspection of several depth contours and the differences in bathymetric surfaces, the ebb shoal was defined as a polygon within the area occupied by the 1962 shoal. As shown in Figure V-6-42a, the 1937 survey revealed a small ebb shoal, evidently located within the confines of the ebb-tidal jet. By 1962, a bypassing bar had formed that emanated southward from the ebb shoal.

The bypassing bar was defined by a polygon located to the south of the ebb shoal, and the attachment bar was defined by the position of the high-water shoreline in the later data sets. By this means, volume change could be calculated for the distinct morphological features as differences between successive surveys, and the evolution of these features is plotted in Figure V-6-42b. Limited data sets were available for the attachment bar. Figure 4b also shows accretion of the shoreline near the south jetty, promoted by sand tightening of the jetty in 1985. In both Figure V-6-42a and V-6-42b, no notable growth to the north of a bypassing bar is evident.

For evaluation of the analytic model, input values were specified based on coastal-processes information from the aforementioned studies, with no optimization of parameters made. The four required parameters were specified as $Q_{in} = 1.50 \times 10^5$ cu m/year corresponding to the upper limit of expected net longshore transport to the south, $V_{Ee} = 3 \times 10^6$ cu m, $V_{Be} = 7 \times 10^6$ cu m, and $V_{Ae} = 5 \times 10^5$ cu m.

The value of V_{Ae} was arbitrarily assigned as an order-of-magnitude estimate. Calculations were made for the 100-year interval 1933-2032.

The measured and calculated volumes of the ebb shoal are plotted in Figure V-6-43, with the dashed lines calculated for values of α for $Q_{in} \pm 50{,}000$ cu m/year to demonstrate sensitivity of the solution to α and to estimate the range of predictions that may be reasonably possible. The trend in the data is well reproduced by Equation V-6-33. Although the Q_{in}-value chosen is at the upper range for the net transport rate, this value must also account for sediment sources other than the net drift to the south. In particular, prior to 1985 when the south jetty was tightened, some sand moving north could pass through it and into the navigation channel (Dean and Perlin 1977), where a portion would be jetted offshore.

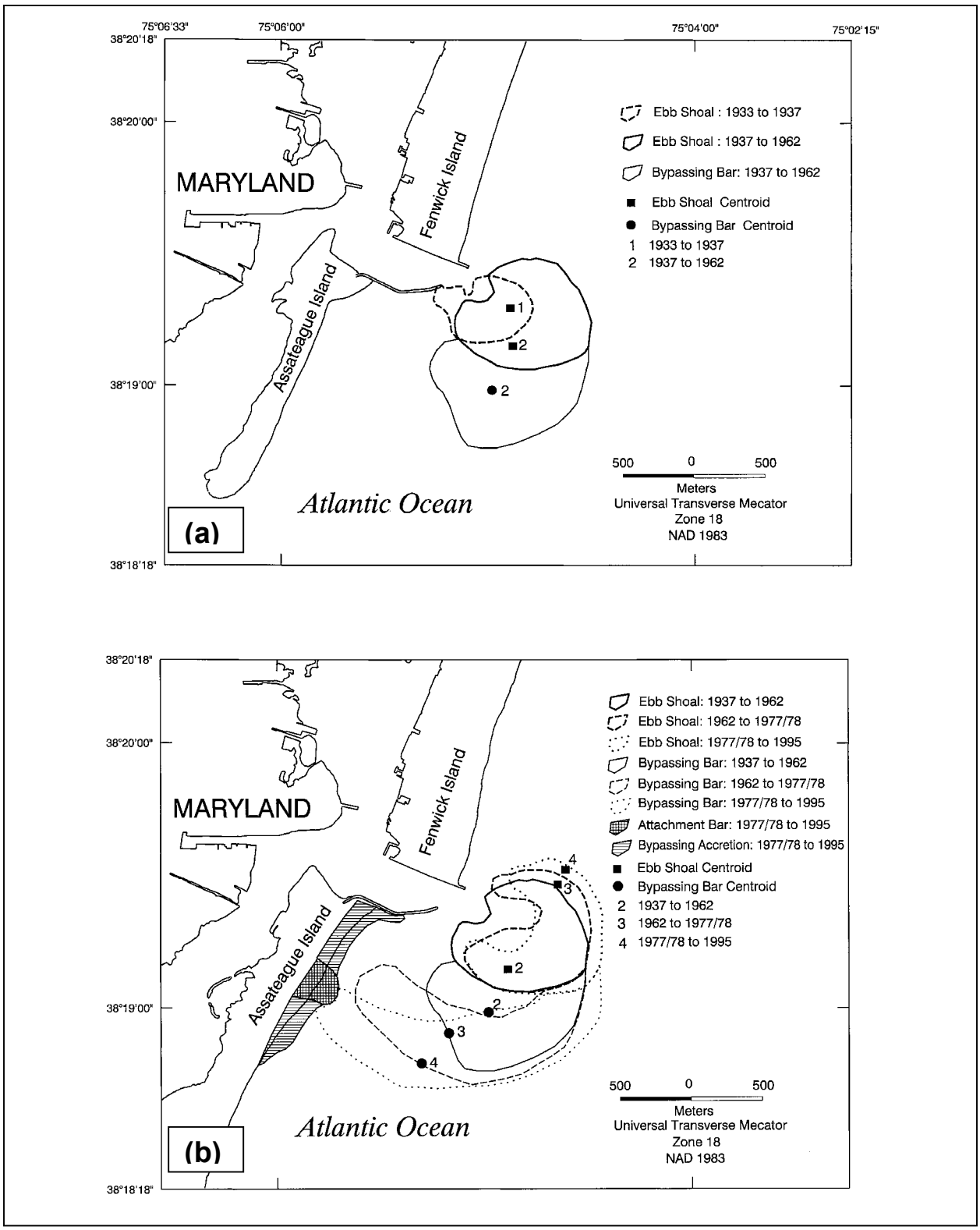

Figure V-6-42. Ebb-shoal planform determined from interpretation of 7-m contour, Ocean City Inlet

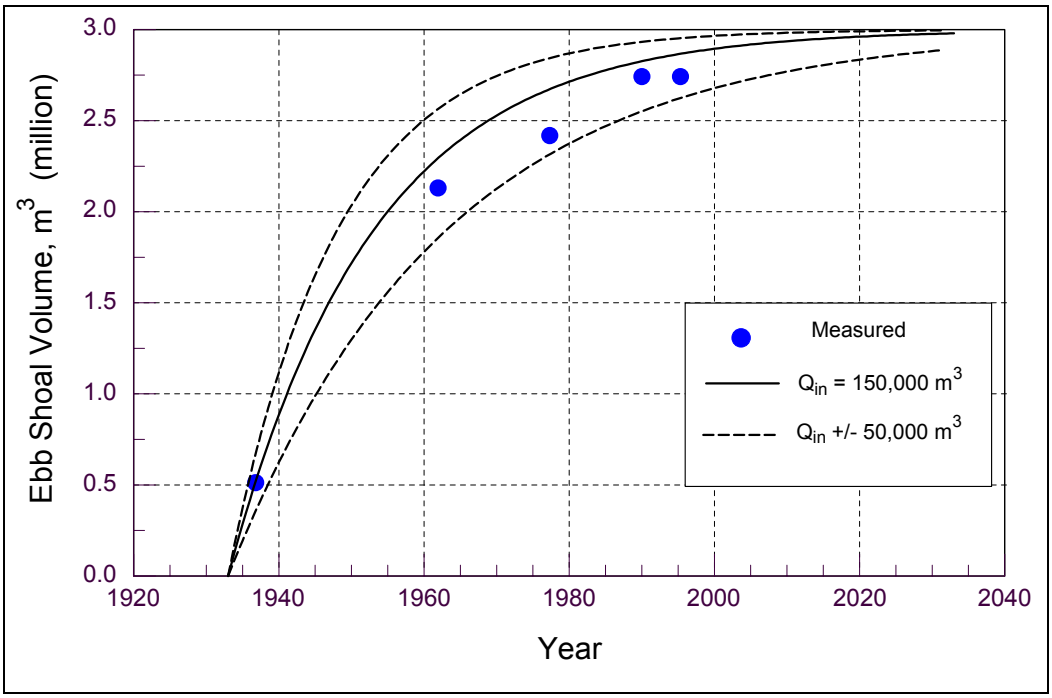

Figure V-6-43. Volume of ebb shoal, Ocean City Inlet

Calculated and measured volumes of the ebb shoal, bypassing bar, and attachment bar are plotted in Figure V-6-44. The calculations exhibit lags in development of the bypassing bar and attachment bar. Based on examination of aerial photographs, Underwood and Hiland (1995) concluded that the attachment had occurred by 1980, when a distinct bulge in the shoreline was seen. The data and model indicate that, although the ebb shoal has achieved equilibrium, the bypassing bar is continuing to grow, so that natural bar bypassing from north to south has not achieved its full potential for sand storage. Bypassing rates calculated with the model, normalized by Q_{in}, are plotted in Figure V-6-45 and indicate the approach to full potential.

The calculations show a substantial lag in sand reaching the bypassing and attachment bars. The bypassing rate at the attachment equals the rate of sand reaching the downdrift beach. Its magnitude as shown in Figure V-6-45 should be interpreted with caution, because the equilibrium volume of the attachment is not presently known. Under the given model input parameters, it appears that in 1999 approximately 60 percent of the net transport is reaching northern Assateague Island. With the stated values, as a simple estimate one can define an effective α for Ocean City through the sum of the ebb shoal and bypassing bar equilibrium volumes. Then the crossover time at which the shoal and bar are predicted to bypass more volume than they retain is t_c = 77 years or in the year 2000, in accord with the 60 percent estimate of bypassing.

(j) Discussion. This section explores sensitivity of the reservoir model to selection of the input and initial conditions, and its extension by numerical solution.

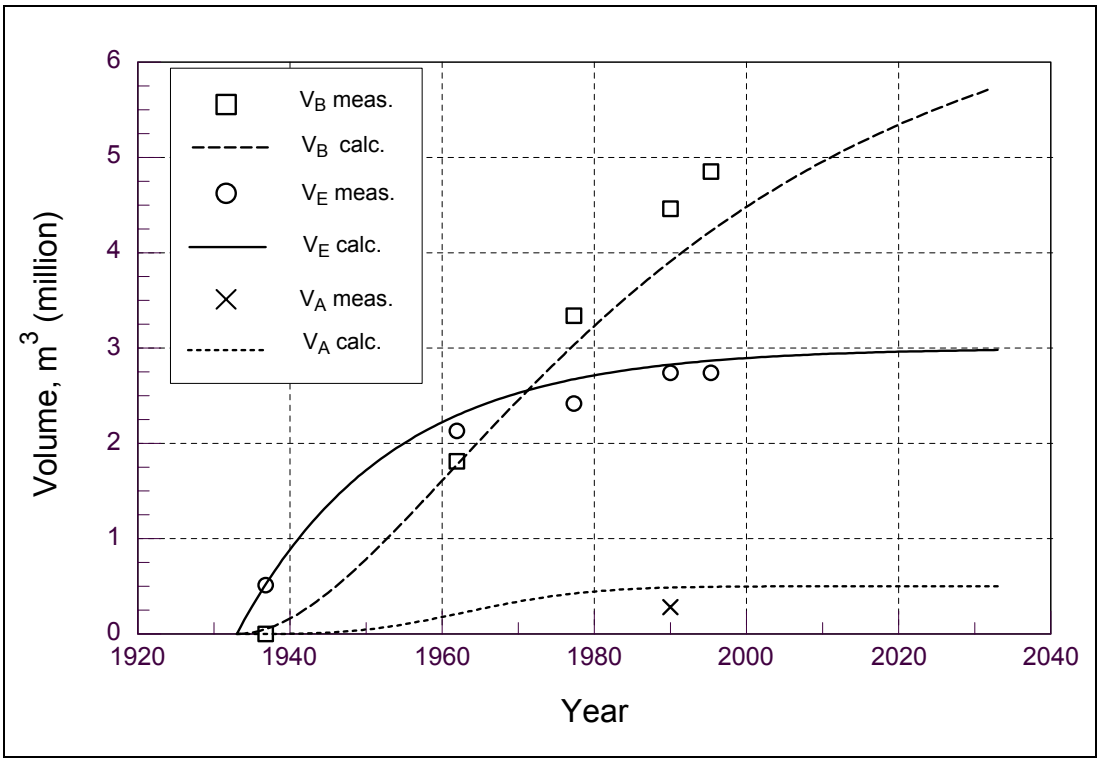

Figure V-6-44. Volumes of ebb shoal, bypassing bar, and attachment bar, Ocean City Inlet

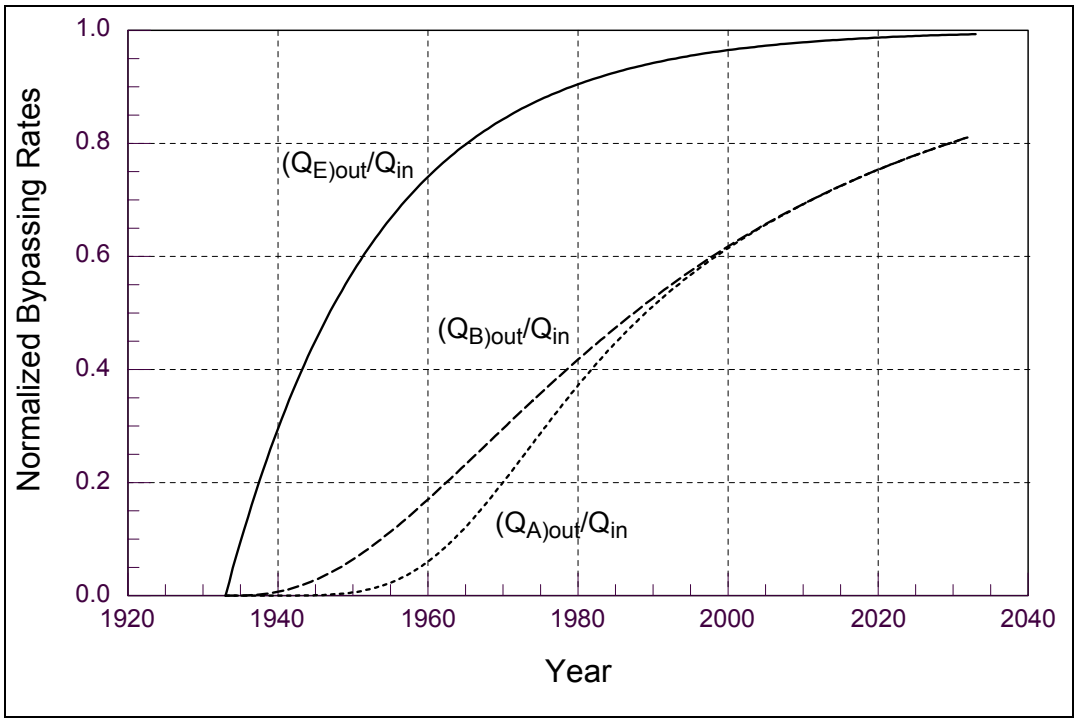

Figure V-6-45. Calculated bypassing rates, Ocean City Inlet

Sensitivity to Q_{out} specification.

- The manner in which the equilibrium volume of an ebb shoal is approached depends upon Q_{out}. Choices other than the linear form of Equation V-6-30 might be made, leading to consideration of the sensitivity of the solution on Q_{out}. As a possible alternative for a quadratic dependence as $Q_{out} = (V_E/V_{Ee})^2 Q_{in}$ can be specified. Then one finds:

$$V_E = V_{Ee} \tanh(\alpha t) \tag{V-6-43}$$

- Equations V-6-33 and V-6-43 are compared in dimensionless form in Figure V-6-46. The quadratic dependence version of Q_{out} produces a more rapid approach to equilibrium. However, the general forms of the solutions are similar, indicating that a substantial change in the manner in which the shoal bypasses sand does not cause a notable change in approach of the shoal to equilibrium. There appear to be no data available to distinguish among such solutions, but specification of Q_{out} is available for improving simulations of all the inlet morphologic forms once adequate observations are made.

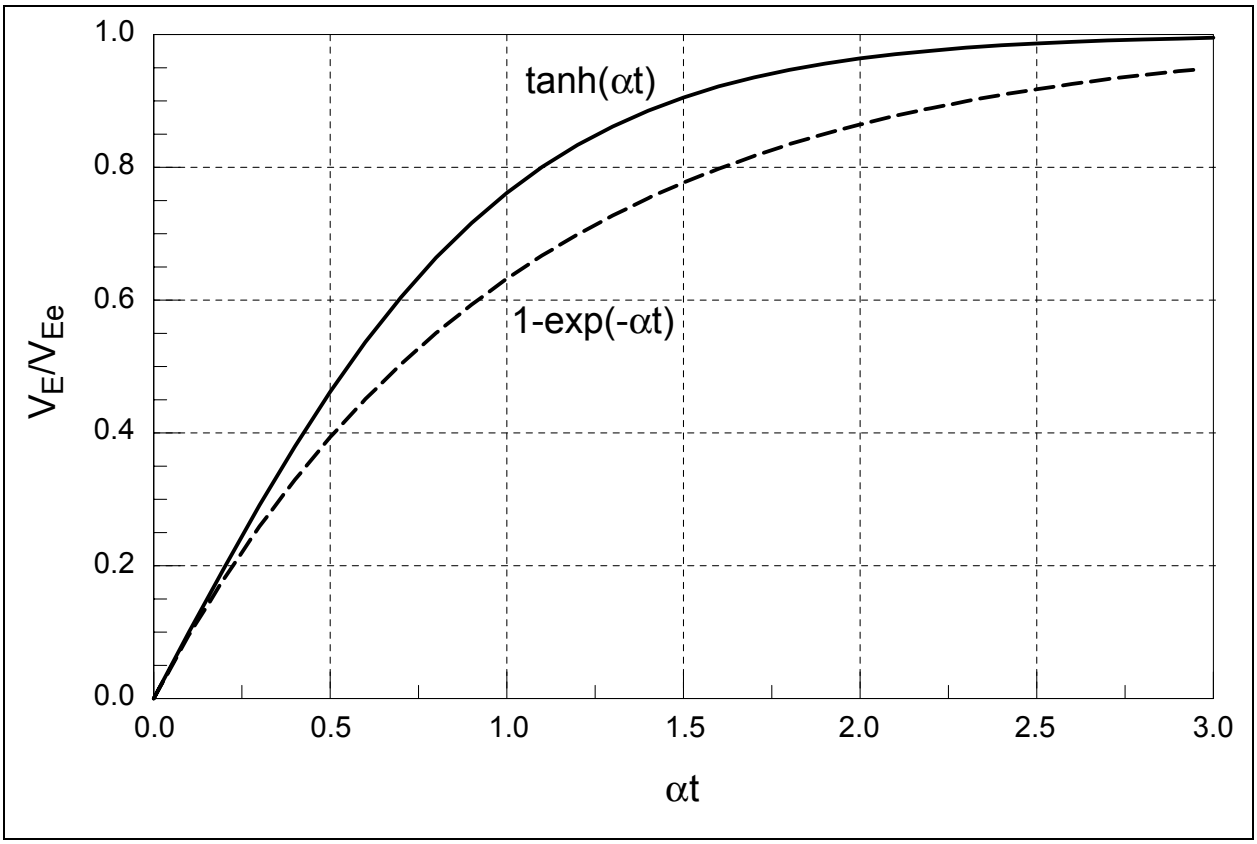

Figure V-6-46. Solutions based on linear and quadratic forms for Q_{out}

Initial breach volume.

- At the initial breach of an inlet, tidal and littoral currents will distribute the released material to adjacent beaches and form a flood shoal and an ebb shoal. Distribution of material among these three areas will depend on the strength and asymmetry of the tidal current and on the incident

wave height and direction, among other factors. The time over which the initial distribution occurs is expected to be much shorter than the time scale $1/\alpha$ and can be approximated by an initial ebb-shoal volume V_{E0} at $t = 0$. With this initial condition, Equations V-6-30 and V-6-31 yield:

$$V_E = V_{Ee}\left(1 - e^{-\alpha t}\right) \quad V_{E0} e^{-\alpha t} \tag{V-6-44}$$

- For a probable overestimate such as $V_{E0} \approx 0.1 V_{Ee}$, inclusion of an initial ebb-shoal volume from the initial breach does not significantly alter the trend of evolution of the shoal, especially considering survey accuracy and temporal and spatial variability in the morphologic system that would obscure minor changes.

Numerical solution.

- The governing equations, such as Equation V-6-31 and related initial condition, can be solved numerically to represent an arbitrary initial condition and time-varying forcing by Q_{in}. For example, assuming Q_{in} is time dependent, a second-order accurate, unconditionally stable solution of Equation V-6-31 is:

$$V_E' = \frac{\Delta t}{2\left(1 + \frac{\Delta t}{2V_{Ee}} Q_{in}'\right)}\left[Q_{in}' + Q_{in} + \left(1 \quad \frac{\Delta t}{2V_{Ee}} Q_{in}\right) V_E\right] \tag{V-6-45}$$

where quantities denoted with a prime indicate values at the next time-step, and Δt = time-step. To validate the solution method, Equation V-6-45 was implemented for Ocean City Inlet. With $\Delta t = 0.1$ year, the analytical and numerical solutions plotted on top of one another. In exploration of the solution scheme, reasonable accuracy was maintained with $\Delta t = 5$ years for the constant input transport rate.

- As an example, engineering application of the numerical model, recovery of the ebb-tidal shoal and alteration of bypassing rates at Ocean City Inlet are calculated in response to hypothetical mining of the bypassing bar. Limited quantitative work has been done to estimate the consequences of ebb-shoal mining (e.g., Mehta, Dombrowski, and Devine 1996; Cialone and Stauble 1998). Walther and Douglas (1993) reviewed the literature and applied an analytical model to three inlets in Florida to estimate recovery time of the shoal and bypassing rates. No time lag was included in their model, however, which yields different responses depending upon depth and location of the mining, factors not included in the present aggregate model.

- For the present example, 750,000 cu m were removed from the bypassing bar in the year 2000, which will be about 25 percent of the material comprising the bar at that time. Figure V-6-47 shows plots of the evolution of bar volume and bypassing rates from the bar and from the attachment bar to the beach. The volume was normalized by V_{Be}, and the bypassing rates by Q_{in}. Mining at the year 2000 stage of development is predicted to effectively translate the bar growth and bypassing rates approximately 20 years back in time, with the bypassing rate to the beach moving from about 0.6 to 0.45 of the potential maximum value of Q_{in}. This example with simplified conditions is not adequate for design, but it does indicate possible applicability of the model in comparison of alternative mining plans. More rigor could be introduced through inclusion of a time-dependent Q_{in} in the present model and estimation of the consequences of ranges of variability in the governing parameters.

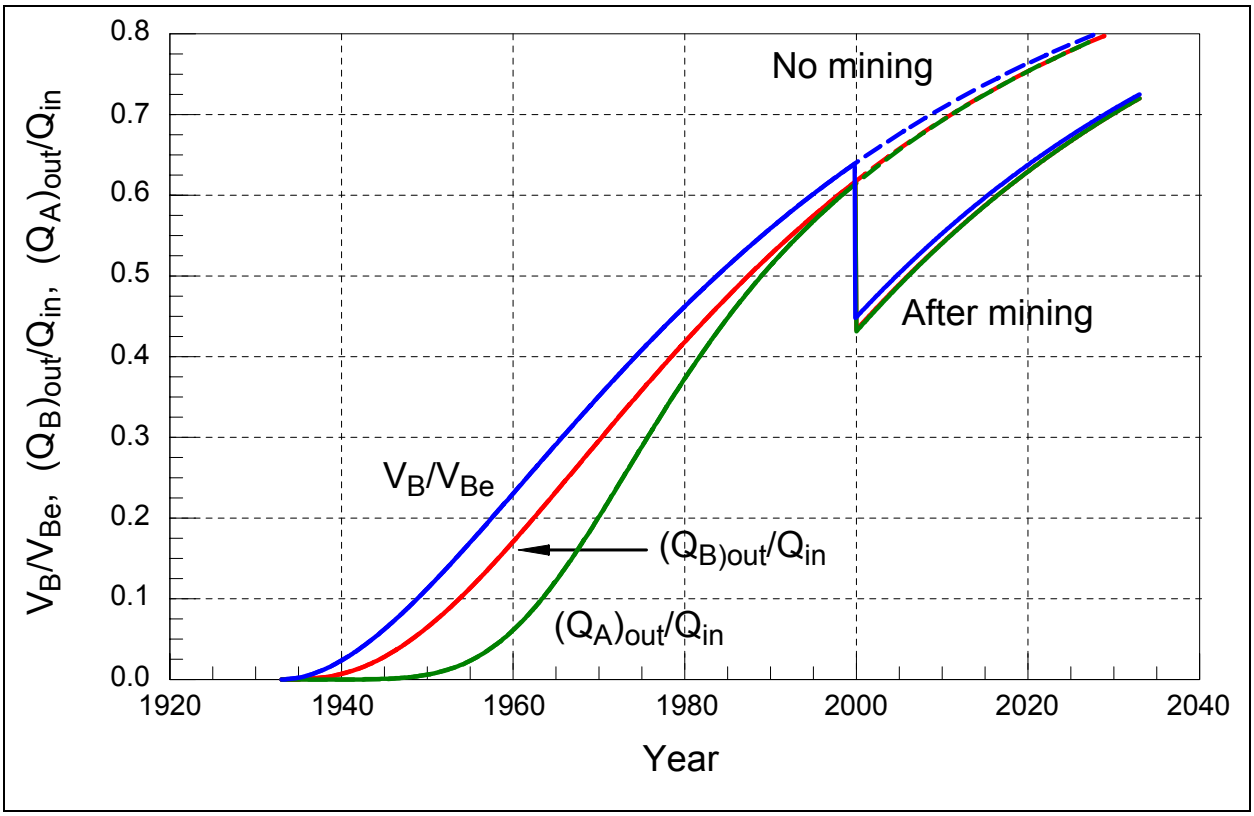

Figure V-6-47. Bypassing bar volume and bypassing rates with/without mining

- Finally, an example involving idealized bidirectional longshore transport is presented. To interpret results readily, the equilibrium volumes of the ebb shoal, bypassing bar, and the attachment bar were set at $V_e = 1 \times 10^6$ cu m, and the magnitude Q the input longshore transport rate was one-tenth of this amount, whether from directed to the right or to the left. Starting from an initial condition of no inlet features, the transport was directed to the right for 25 years and then to the left for 25 years. Time evolution of the normalized volumes and bypassing rates are shown in Figure V-6-48a and V-6-48b, respectively, where subscripts "R" and "L" denote quantities associated with right- and left-directed transport.

- Under the stated condition of equal magnitude but opposite transport, the volume of the ebb shoal grows without discontinuity, because the shoal accepts sand from either direction. With transport directed to the right, the volume of the bypassing bar V_{BR} and of the attachment bar V_{AR} grow while experiencing the characteristic time lag. These features would emerge on the right side of the ebb shoal, for a viewer standing on the shore and facing the water. When the transport rate shifts after 25 years, the volumes V_{BL} and V_{AL} of features on the left side of the ebb shoal begin to grow, but the bypassing bar on the left experiences no time lag because the ebb shoal has a sand supply to contribute immediately. The attachment bar on the left experiences a shorter time lag as compared to its counterpart on the right because transported sand is delayed only by formation of its (left side) bypassing bar and not by the ebb shoal. The bypassing rates show behavior similar to the volumes. In particular, the left-directed bypassing rate on the ebb shoal starts at a large value because of the existence of the shoal created by the right-directed transport. Also, the bypassing rate from the left bypassing bar begins immediately after the switch in transport direction, and the attachment shoal on the left experiences a much shorter lag in receiving sand to bypass than did the attachment shoal on the right.

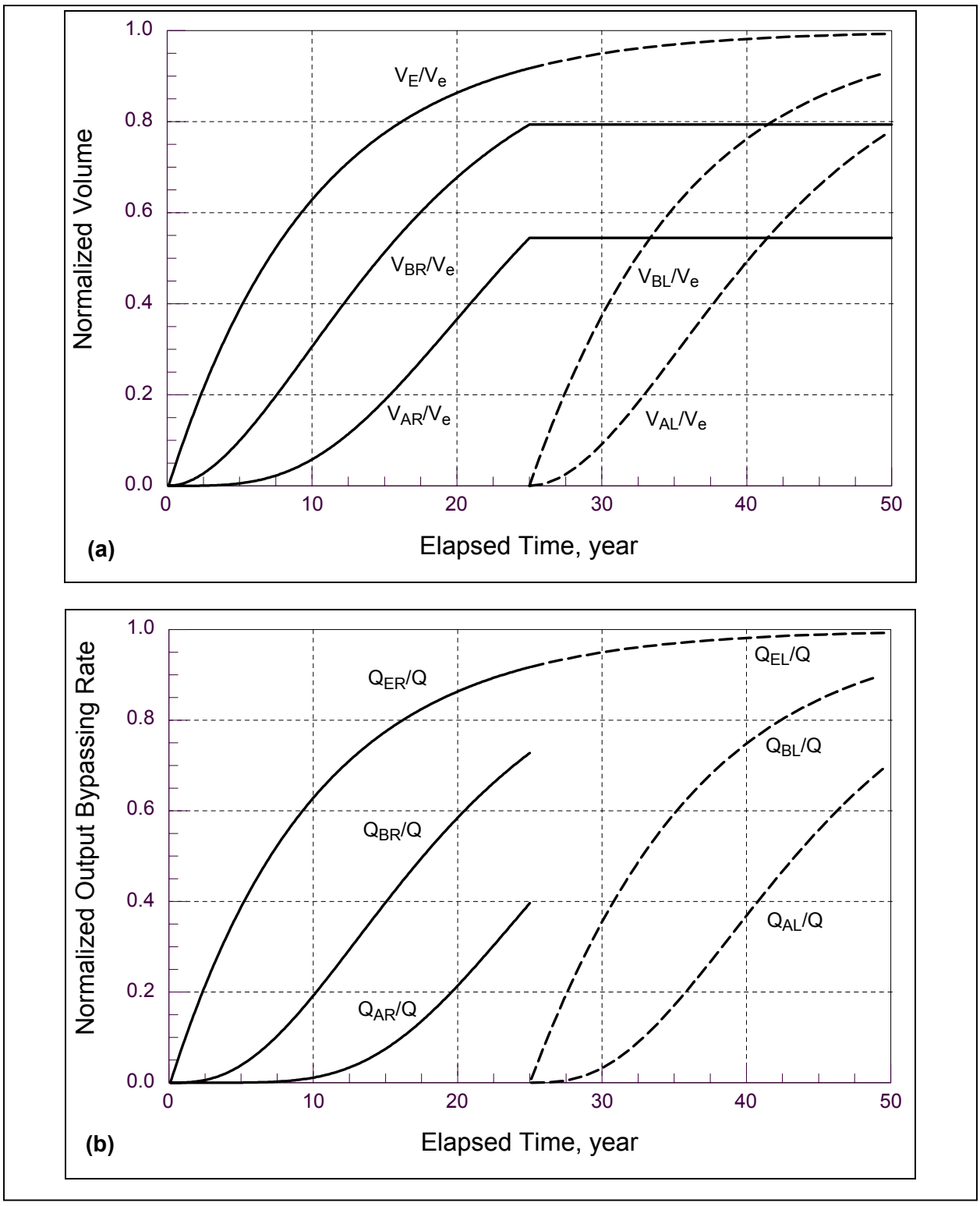

Figure V-6-48. Bypassing rates for simple bidirectional transport

(k) Conclusions. A reservoir model was introduced for describing changes in volume and bypassing rates of morphological components of ebb-tidal shoals. Required inputs for this aggregate model are compatible with the amount and quality of data typically available in engineering and science studies. The model requires estimates of the longshore transport rate, which may be the net or gross rate depending on the inlet configuration; equilibrium volume of the ebb shoal, bypassing bar, and attachment bar; and qualitative understanding of sediment pathways at the particular inlet. The reservoir model is robust in that solutions are bounded. The ratio of the input longshore transport rate and the equilibrium volume of the morphological feature is the main parameter governing volume change and bypassing rates. This parameter is directly related to the widely accepted Bruun and Gerritsen ratio. The reservoir model predicts a delay in sand bypassing to the downdrift beach according to the properties of the morphologic system and longshore transport rate.

The reservoir method requires apportionment of material between the ebb shoal and the bypassing bar, although a simplified version of the model can combine these two sand bodies. A distinction between the shoal and the bypassing bar adds conceptual and quantitative resolution by allowing bypassing bars to develop and evolve according to the properties of the predominant transporting mechanism as either waves (longshore sediment transport) or tidal prism. With constant inputs, the analytic model takes about 1 sec to execute on a standard PC for 100 years of simulation time, allowing numerous runs to be made. The numerical model is also rapid, even if time-dependent rates are involved.

The model as described here does not account for sediment exchange between the inlet channel and flood shoal. However, it can be readily extended both analytically and numerically to include these and similar interactions. The model appears capable of substantial generalization and incorporation of more detailed, processed-based data. In this regard, the reservoir model may serve as a source for preliminary design and provide a framework for generating questions about inlet morphology, sediment pathways, and the fundamental mechanisms of the collective behavior of sand bodies.

(3) Wave energy flux method (Jarrett 1977, 1991).

(a) Jarrett applied sediment budget analysis techniques together with estimates of wave energy flux (derived from wave refraction analysis) to infer longshore sand transport rates for the North Carolina coast (Jarrett 1977, 1991). Data required to apply the method include incident wave climatology, shoreline positions and/or beach profiles, inlet bathymetry, and engineering activities (dredging and placement volumes, beach-fill placement, and sand bypassing rates) for a common time period. Jarrett recommends that the best time period for analysis is one that is free from significant storm events. Storms have the potential to bias the sediment budget, whether it is to reverse the long-term sediment transport direction or cause short-term transport of sediment offshore. The procedure is as follows:

Analyze basic data sets. Calculate volume change associated with the shoreline position, profile, inlet bathymetry, and engineering activity data sets. (see Sections (e) and (f)).

Identify sediment budget cells. Based on the volume changes for each inlet and beach system, identify regions of the study area that appear to behave differently. Potential longshore transport rates will be determined for the boundaries of each of these cells. Jarrett recommends extending inlet cell boundaries several thousand feet up- and downdrift from the inlet to incorporate the effects of the inlet ebb tidal delta and tidal currents within the inlet cell. Natural bypassing across the inlet is left as an unknown that is determined through solving the sediment budget.

Determine the longshore component of wave energy flux in the surf zone. The longshore component of wave energy flux, P_l, is proportional to the amount of sand being transported along the coast through a factor, β, as shown in Equation V-6-46. This quantity can be calculated by transforming incident waves over offshore bathymetry until wave breaking. Then P_l is related to the breaking wave height, depth at breaking, and breaking wave angle (see Part III-3). Longshore energy flux should be calculated for the entire study area both for left- and right-directed transport. Representative values of left- and right-directed P_l for each cell boundary should be determined.

$$Q = \beta P_\ell \tag{V-6-46}$$

Formulate equations between volume change and P_l. For each cell, equations can be written to solve for the relationship between the forcing (longshore energy flux, P_l), and the resulting sediment transport gradient (net volume change within the cell, considering all engineering activities within that cell). Jarrett relates the correlation as follows (notation has been adjusted to be consistent within this chapter):

$$\Delta V - P + R = \beta P_\ell \tag{V-6-47}$$

where β is the unknown constant, and ΔV, P, and R are as defined previously.

Solve for β in the vicinity of the inlets. At the inlet cells, there are three unknowns: bypassing to the updrift beach (during periods of reversal), bypassing to the downdrift beach, and the constant β. Three independent equations can be formulated considering the cell immediately updrift of the inlet, the cell downdrift of the inlet, and the inlet cell. After solving these three cells, a value for the parameter β is obtained which is then used to estimate sand transport between the other cells in the study area.

Optimize the parameter β to best represent volume changes for all cells. Adjustments to the parameter β may be required to develop a balanced sediment budget for the entire region.

- The following example for the North Carolina coast is summarized from Jarrett (1991). Figure V-6-49 shows the study reach with the sediment budget cells identified in bold lettering.

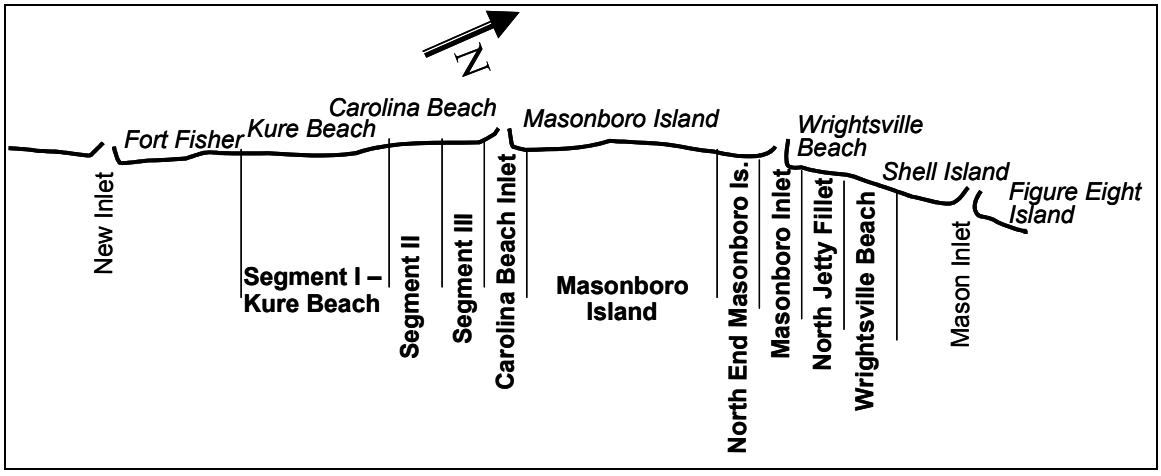

Figure V-6-49. Study reach for sediment budget (not to scale, adapted from Jarrett 1991)

- Segments of the study shoreline with similar trends, as determined from shoreline change data, were defined as sediment budget cells. Cell boundaries in the vicinity of inlets were located several thousand feet from the interior shoreline of the inlet. The inlet boundaries were set so that sediment transport within the inlet cell reflected the combined forcing of waves and tidal currents, with waves having been influenced by the ebb-tidal shoal. Within each shoreline cell, profile and shoreline change data were used to determine the rate of volume change. Sources of sediment, such as beach nourishment or sand bypassing operations, and sinks of sediment, such as inlets and capes, were determined from review of the engineering history, hydrographic surveys, and dredging records. The volume rate of material naturally bypassing each inlet in both the upcoast and downcoast directions were set as unknowns.

- A longshore energy flux analysis was conducted using wave information offshore of the study site, and transforming the waves over the offshore and nearshore bathymetry. Values of the longshore energy flux factor were related to both the left- and right-directed longshore transport rates using Equation V-6-46. These values are shown above each longshore transport rate arrow in Figure V-6-50. Once the transport potential was determined between the various cells, computations using Equation V-6-47 were used to solve for β. As calculations proceeded from cell-to-cell, some adjustments in the computed values of the longshore transport rate were required to develop a completely balanced sediment budget for the study area. The final sediment budget is shown in Figure V-6-50, with the calculated transport rates shown below each arrow.

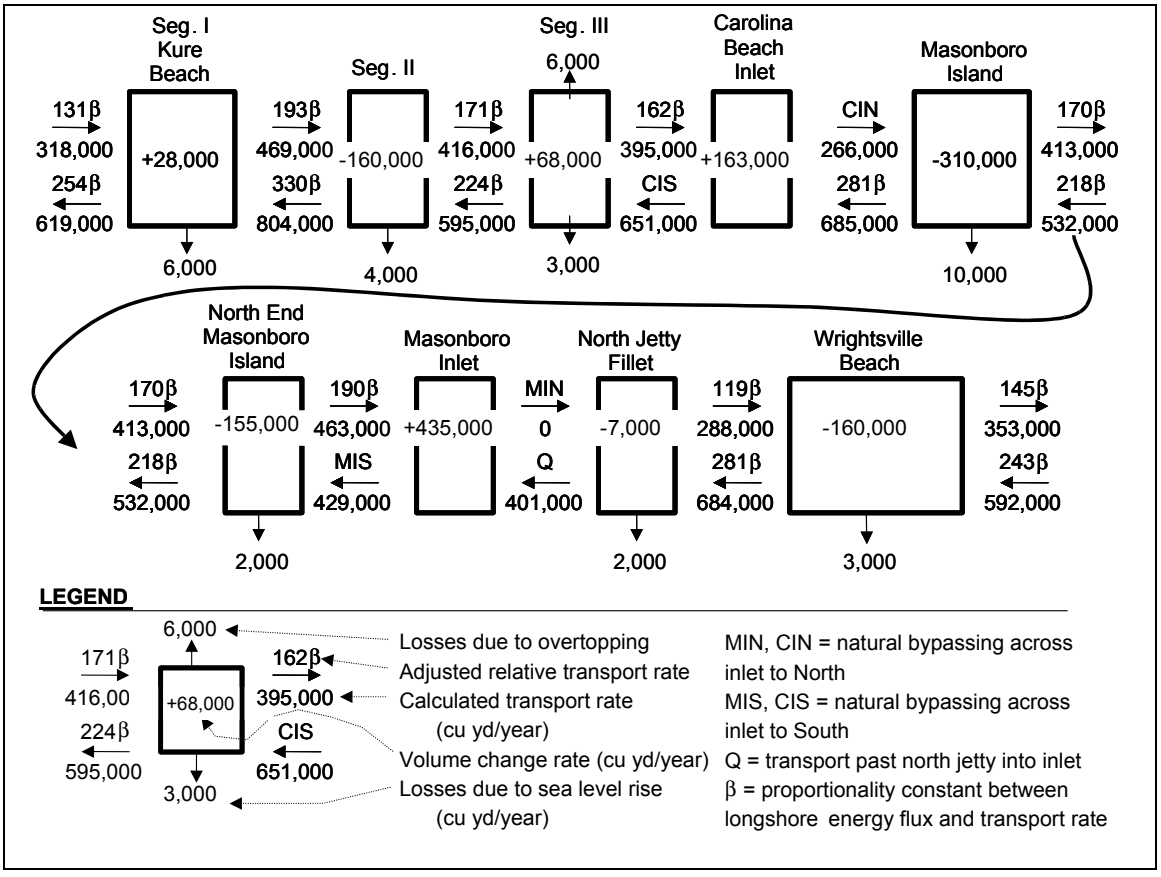

Figure V-6-50. Sediment budget from Kure Beach (south end of study) to Wrightsville Beach (north end of study), North Carolina, using the wave energy flux method (adapted from Jarrett 1991). Note that the Masonboro Island cell connects to the north end of Masonboro Island cell

(4) Bodge's method (1999).

(a) Bodge's approach is an extension of those described by Bruun (1966), Weggel (1981), as well as early case studies by Johnson (1959), Jarrett (1977), among others. Figure V-6-51 illustrates the sediment transport pathways at an idealized inlet for right- and left-directed incident transport, and mechanical transport (dredging and bypassing). Except as noted, all right-directed transport is positive-valued. All left-directed transport is negative-valued. Right- and left-directions are based upon an observer standing at the inlet, facing seaward. The study area boundaries are selected as locations outside of the inlet's direct influence on wave refraction and tidal currents.

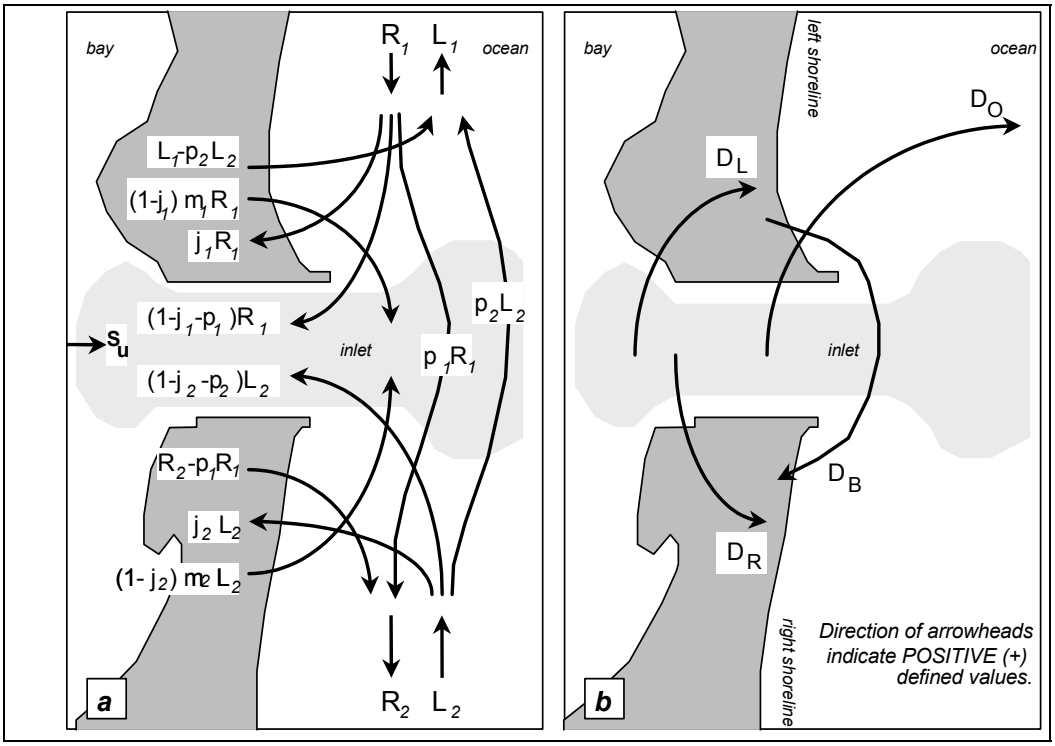

Figure V-6-51. Sediment transport pathways for Bodge method (1999)

(b) In Figure V-6-51a, each transport component is defined as a fraction or multiple of the right- and left-directed longshore transport rates at the boundaries. The subscript "1" refers to transport directed rightward from the left shore, and the subscript "2" refers to transport directed leftward from the right shore. In Figure V-6-51a and V-6-51b, the terms illustrated in the sediment transport pathways are as follows:

R, L = rightward- and leftward-directed incident transport values at the study area's boundaries

j_1, j_2 = fraction of incident transport (R or L) impounded by the inlet's jetties (j_1 = left jetty; j_2 = right jetty; 0.0 = transparent jetty; 1.0 = impermeable jetty)

p_1, p_2 = fraction of incident transport (R or L) naturally bypassed across the inlet (p_1 = from the left, p_2 = from the right; 0.0 = no bypassing; 1.0 = perfect bypassing)

m_1 = local inlet-induced transport from the left shoreline into the inlet (expressed as a fraction or multiple of the right-directed incident transport, R_1)

m_2 = local inlet-induced transport from the right shoreline into the inlet (expressed as a fraction or multiple of the left-directed incident transport, L_2)

S_u = transport of littoral material into the inlet from upland sources (positive value)

D_L, D_R = mechanical transfer of sand from the inlet to the left and right shorelines, respectively

D_B = mechanical transfer of sand from the left shoreline to the right shoreline (defined as positive from left to right; negative from right to left)

D_O = maintenance dredging and out-of-system disposal from the inlet (positive-valued; includes only material of littoral origin; includes deepwater (offshore) and upland disposal; excludes new work)

(c) The transport terms (R, L, Q, S_u, D_L, D_R, D_O) can be expressed as either volume quantities or volumetric rates, so long as the units of each term are consistent with one another. The ratio of left- to right-directed transport magnitude at the study area's boundaries is defined as:

$$r_1 = -L_1 / R_1 \text{ and } r_2 = -L_2 / R_2 \tag{V-6-48}$$

By definition,

$$\begin{array}{ll} 0 \le j_1 \le 1 & 0 \le j_2 \le 1 \\ 0 \le p_1 \le 1 & 0 \le p_2 \le 1 \\ 0 \le p_1 + j_1 \le 1 & 0 \le p_2 + j_2 \le 1 \\ m_1 \ge 0 & m_2 \ge 0 \end{array} \tag{V-6-49}$$

The net volume changes of the left and right shorelines are, respectively,

$$\Delta V_L = (j_1 + j_1 m_1 - m_1) R_1 + L_1 - p_2 L_2 - D_B + D_L \tag{V-6-50}$$

$$\Delta V_R = (m_2 - j_2 m_2 - j_2) L_2 - R_2 + p_1 R_1 + D_B + D_R \tag{V-6-51}$$

where positive ΔV values imply net accretion and negative values imply net erosion. The gross volume of sand that enters the inlet, prior to maintenance dredging, is

$$\Delta V_G = (1 - j_1 - p_1 + m_1 - j_1 m_1) R_1 - (1 - j_2 - p_2 + m_2 - j_2 m_2) L_2 \tag{V-6-52}$$

The inlet's net volume change after dredging, and neglecting upland/offshore input, is

$$\begin{aligned} \Delta V_N &= \Delta V_G - D_L - D_R - D_O - S_U = \left(1 - j_i - p_1 + j_1 m_1\right) \\ & R_1 - \left(1 - j_2 - p_2 + m_2 - j_2 m_2\right) L_2 - D_L - D_R - D_O - S_U \end{aligned} \tag{V-6-53}$$

Combining Equations V-6-50 through V-6-53 yields:

$$\Delta V_L = -(\Delta V_R + D_O + (\Delta V_N - S_u)) + \Delta R + \Delta L \tag{V-6-54}$$

$$\Delta V_R = -(\Delta V_L + D_O + (\Delta V_N - S_u)) + \Delta R + \Delta L \tag{V-6-55}$$

where $\Delta R = R_1 - R_2$ and $\Delta L = L_1 - L_2$.

Physically, if the incident transport rates are identical on both sides of the inlet (that is, $\Delta R = \Delta L = 0$), Equations V-6-50 and V-6-55 demonstrate that the net volume change of an inlet-adjacent shoreline is the negative sum of the other shoreline's net volume change (e.g., impoundment); the volume of sand removed from the inlet by maintenance dredging and out-of-system disposal; and the net growth of the inlet shoal volumes (minus upland/offshore input). This simple and significant result states that an inlet's net volumetric effect to the downdrift shoreline is the sum of: the updrift impoundment; maintenance dredging and out-of-system disposal; and net shoal growth beyond that attributed to upland input. In this way, the global volumetric impact of the inlet to the downdrift shoreline (minus any impoundment fillet, or dead storage on the downdrift side) can be computed without reference to, or assumption of, measured downdrift shoreline changes, ambient longshore transport rates, or detailed mechanics of the inlet's transport pathways. While these data are ultimately useful, Equations (V-6-54) and (V-6-55) demonstrate that such data are not fundamentally required to assess the inlet's downdrift, volumetric impact, at least so long as differences in the ambient transport potential across the inlet are small or known.

Equations V-6-50 through V-6-52 can be solved for p_1 and p_2 and combined to yield two coupled equations containing the volume change terms ΔV_L, ΔV_R, or ΔV_G. In practice, as previously noted, the net volume change of the downdrift beach is often most uncertain or suspect because of the effects of armoring or beach nourishment, or because the length of shoreline to consider is not known a priori. Accordingly, it is advantageous to remove the downdrift volume change term from the coupled equations, and to solve in terms of the volume changes of the updrift beach and the inlet.

If the RIGHT shoreline is downdrift (or of less certain volume change), then from Equations V-6-50, V-6-51, and V-6-52:

$$p_1 = 1 - j_1 (1 + m_1) + m_1 - (L_2/R_1)(1 - j_2 (1+m_2) + m_2 - p_2) - \Delta V_G/R_1 \quad \text{(V-6-56a)}$$

$$p_2 = [(j_1 (1 + m_1) - m_1) R_1 + L_1 - \Delta V_L + D_L - D_B] / L_2 \quad \text{(V-6-56b)}$$

and the corresponding, computed volume change of the right shoreline is:

$$\Delta V_R = (m_2 - j_2 m_2 - j_2) L_2 + p_1 R_1 - R_2 + D_R + D_B \quad \text{(V-6-57)}$$

If the LEFT shoreline is downdrift (or of less certain volume change), then from Equations V-6-50, V-6-51, and V-6-52:

$$p_1 = [(j_2 (1 + m_2) - m_2) L_2 + R_2 + \Delta V_R - D_R - D_B] / R_1 \quad \text{(V-6-58a)}$$

$$p_2 = 1 - j_2 (1 + m_2) + m_2 - (R_1/L_2) (1 - j_1 (1 + m_1) + m_1 - p_1) + \Delta V_G/L_2 \quad \text{(V-6-58b)}$$

and the corresponding, computed volume change of the left shoreline is:

$$\Delta V_L = (j_1 - m_1 + j_1 m_1) R_1 + L_1 - p_2 L_2 + D_L - D \quad \text{(V-6-59)}$$

To solve for the inlet sediment budget, a family of solutions is developed from either Equation V-6-56a,b or V-6-58a,b. Specifically, input values are identified for the updrift volume change (ΔV_L or ΔV_R) and the gross inlet volume change (ΔV_G) and for the dredging/bypassing quantities (D_O, D_L, D_R, D_B) and for upland/offshore inlet volume influx (S_U). A range of physically plausible values for the other transport parameters are additionally identified; i.e., the jetties' impermeability (j_1, j_2 (between 0 and 1)), the local inlet-induced transport (m_1, m_2), the tendency for natural bypassing (p_1 and p_2 (between 0 and 1)), and the incident transport components (R and L). In application, three incident transport components are required: R_1, R_2, and L_1 for Equation V-6-56, and L_1, L_2, and R_1 for Equation V-6-58.

Candidate values for the various parameters, within their identified plausible ranges, are input to Equations V-6-56 or V-6-58. Those combinations of parameters that yield values of p_1 and p_2 within the allowed range of p_1 and p_2 (or, at least, values between 0 and 1), and which likewise satisfy

$$0 \le j_1 + p_1 \le 1 \text{ and } 0 \le j_2 + p_2 \le 1 \tag{V-6-60}$$

are retained as viable discrete solutions of the sediment budget. The set of all such viable, discrete solutions represents the sediment budget's family of solutions.

The family of solutions can be conveniently plotted and inspected in the following way. For each discrete solution, values are computed for the incident (updrift) net transport Q, the natural net bypassing P, and the gross volume that shoals the inlet from the left and right shorelines, S_{LEFT} and S_{RIGHT}, respectively. If Equation V-6-56 is used, where the RIGHT shoreline is downdrift, then

$$Q = Q_1 = R_1 + L_1 \tag{V-6-61a}$$

or if Equation V-6-58 is used, where the LEFT shoreline is downdrift, then

$$Q = Q_2 = R_2 + L_2 \tag{V-6-61b}$$

The net natural bypassing and left- and right- gross inlet shoaling volumes are, respectively,

$$P = p_1 R_1 + p_2 L_2 \tag{V-6-62a}$$

$$S_{\text{LEFT}} = \Delta V_G - S_U - S_{\text{RIGHT}} = (1 - j_1 - p_1 + m_1 - j_1 m_1) R_1 \tag{V-6-62b}$$

$$S_{\text{RIGHT}} = \Delta V_G - S_U - S_{\text{LEFT}} = - (1 - j_2 - p_2 + m_2 - j_2 m_2) L_2 \tag{V-6-62c}$$

The family of solutions can be narrowed by imposing additional constraints; e.g., requiring that the direction of any net natural bypassing, P, be coincident with the incident net transport rate, Q; or, that the jetties' impermeability values (j_1 and j_2) be similar to one another; or, that the shoaling from one side or the other be a minimum percentage of the inlet's total shoaling rate; etc. Or, families of solutions from different time periods can be overlaid, retaining only those subsets of solutions for which the incident transport, Q, solves the sediment budget for both time periods, etc.

Methods to identify the sediment budget's parameters include the following. The volume change of the updrift shoreline (ΔV_L or ΔV_R) can be estimated from the cumulative volume change updrift of the inlet as in Figure V-6-18, where background changes are retained. The gross volume change of the inlet (ΔV_G) can be estimated from surveys and dredging histories, where care is taken to exclude changes due to new-work dredging, datum shifts, etc. The dredging and mechanical bypassing terms (D_R, D_L, D_O, D_B) are estimated from dredging records. The volume influx from upland or offshore sources (S_U) requires some insight as to the inlet's overall geology and/or the influence of, for example, episodic fluvial input, but in many cases can be neglected. A convenient method to identify ranges of values for the incident transport (R and L) is to consider the right- and left-directed transport potential from offshore (hindcast, etc.) wave data. The computed transport rates can be used directly (with ranges bound by some percentage or by standard deviation, etc.). It is additionally useful to compute the ratio of left- to right-directed

transport, r, from Equation V-6-48. In solving the sediment budget equations, this ratio can be held constant, so that the value of L remains a computed, fixed fraction of specified values of R that will be considered. The values of R to be considered should be such that the net incident transport, $Q = R + L$, or $Q = (1\text{-}r)R$, are within a range of physically plausible values, perhaps defined by the range of values of Q for the inlet suggested by prior investigators.

Plausible values for the jetties' impermeabilities (j_1 and j_2) are made from aerial photography, surveyed shoaling patterns, and physical inspection; or, in the limit, can be left to the default uncertainty range of 0 (permeable) to 1 (impermeable). Values for the inlet's net natural bypassing tendency (p_1 and p_2) are typically most uncertain and can be left to the default range of 0 (no bypassing) to 1 (full bypassing). In many cases, however, it might be accepted that an improved inlet is an imperfect bypassing system ($p < 1$) or a complete littoral barrier (p=0), etc.

Values for the local, inlet-induced transport (m_1 and m_2) can be estimated from inspection of computed increases in the inlet-directed longshore transport potential near the inlet mouth. This can be discerned from wave refraction investigation whereby the longshore transport potential is computed from incipient breaking conditions along the shoreline developed for each of several representative offshore wave cases.

The transport potential can be computed by the CERC formula with arbitrary coefficient. For example, an increase in the transport potential, R_1, for example from 0.5 to 0.7 (arbitrary units), induced by refraction across the inlet's ebb shoal, represents a 40 percent inlet-induced increase in local right-directed transport, suggesting a value of $m_1 = 0.4$. Additionally, the parameters m_1 and m_2 can be used to account for inlet-directed transport from the adjacent shorelines induced by tidal currents.

Many other discrete solutions can, of course, be developed from the family of solutions presented in Figures V-6-53 and V-6-54. Those from the latter, narrowed family are more physically plausible, based upon general examination of the inlet. Although even this narrowed family appears broad, one will find that there are not extraordinarily significant differences between discrete solutions within the family, particularly after plotting the results as shown in Figure V-6-55. In particular, there are very modest differences between those solutions that define the central 50 percent of the narrowed family as a whole; i.e., the dark-shaded area in Figure V-6-54.

The methodology described allows the coastal engineer a framework by which to:

- Investigate the volumetric and lineal extent of an inlet's impact upon adjacent shorelines.

- To develop a framework for a conceptual inlet sediment budget based upon ranges of physically plausible input values. The latter results in a family of solutions which bounds those solutions that can mathematically and reasonably solve an inlet sediment budget. This family of solutions inherently accounts for the underconstrained nature of an inlet sediment budget calculation; i.e., where there are more variables than known values. While it allows flexibility of solutions, it provides useful boundaries to the solution. These boundaries can be narrowed, or studied, to the degree that the investigator wishes to prescribe physical constraints to the inlet's transport patterns. The statistics of the values within the family of solutions can be examined to discern the occurrence with which various values of the inlet's transport parameters can solve the sediment budget. This can help to establish the degree to which a given discrete solution lies within the central or outer parts of the most likely (or at least, modal) solutions.

EXAMPLE PROBLEM V-6-13

To illustrate the method's application and utility, an example application at St. Lucie Inlet, Florida, is presented. St. Lucie Inlet is located on Florida's south-central east coast, on the Atlantic Ocean. The inlet was artificially opened in the 1920s, and jetties were later constructed on the north (left) and south (right) shorelines. The north jetty extends across most of the typical surf zone, but is low and permeable. The south jetty is sand-tight, but is very short, and sand is transported around its seaward end. The net incident drift is acknowledged to be from north to south, and is plausibly between 40,000 and 260,000 cu m/year (50,000 to 340,000 cu yd/year). The downdrift (south, or right) shoreline has experienced chronic erosion along a great distance (10's of km), and is it is generally acknowledged that the inlet exhibits some, but far less than perfect, natural sand bypassing.

Values of volume changes and typical dredging practices were identified over a period of 6 to 10 years in the late 1980s, and converted to equivalent annual rates (ATM 1992; USAED, Jacksonville, 1999). These included an updrift (left) shoreline change of ΔV_L = -16,000cu m/year (net erosion); gross inlet shoaling of ΔV_G = 156,000 cu m/year; maintenance dredging and out-of-system disposal of D_O = 33,000 cu m/year; and maintenance dredging and placement to the downdrift (right) shoreline or nearshore of D_R = 60,000 cu m/year. Upland/offshore influx to the inlet shoals is assumed to be neglible; i.e., S_U = 0. From Equation V-6-53, the net inlet shoaling rate is ΔV_N = 63,000cu m/year, representing the estimated net rate of accretion across the inlet's ebb and flood shoals and/or losses to the offshore.

Relevant results of a wave refraction and littoral transport analysis at the inlet (Browder 1996, conducted for USAED, Jacksonville, 1999) are illustrated in Figure V-6-52. Representative wave conditions from various offshore directions were refracted/diffracted to the point of incipient breaking, from which the longshore transport potential was computed. The results were weighted by each wave condition's hindcast occurrence and summed to develop an alongshore estimate of the right- and left-directed transport potential. The values in the figure are normalized by the maximum value of the computed transport potential. Source wave data were WIS Phase II hindcast, 1956-95 (Corson et al. 1982).

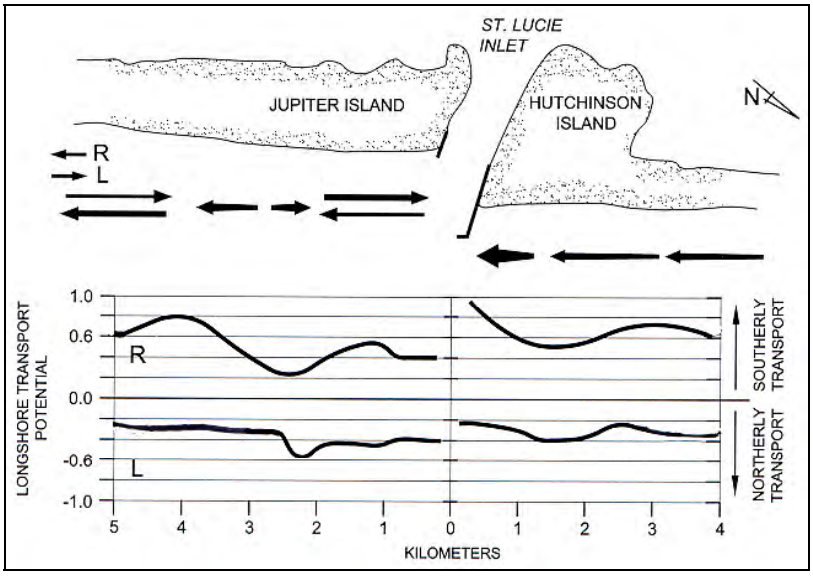

Figure V-6-52. Longshore transport potential in vicinity of St. Lucie Inlet, Florida (after Browder 1996)

(Continued)

EXAMPLE PROBLEM V-6-13 (Continued)

From Figure V-6-52, the ratio of left-to-right-directed transport at the updrift (left) boundary is about $r = -L/R = 0.45$. For an assumed range of net incident transport, Q = 40,000 to 260,000 cu m/year, this implies a range of considered values for the incident, right-directed transport of

$$R_1 = Q/(1-r) = (40{,}000)/(1\text{-}0.45) \text{ to } (260{,}000)/(1\text{-}0.45) = 72{,}700 \text{ to } 472{,}700 \text{ cu m/year}$$

and corresponding incident, left-directed transport of

$$L_1 = -r\,R_1 = (-0.45)(72{,}700) \text{ to } (-0.45)(472{,}700) = 32{,}700 \text{ to } 212{,}700 \text{ cu m/year}$$

Left-directed transport at the downdrift (right) boundary is approximately 90 percent of that at the updrift (left) boundary; hence, it will be presumed that $L_2 = 0.9\,L_1$. Due particularly to shoal and reef features near the inlet mouth, the transport potential directed toward the inlet is computed to increase by about 30 to 50 percent in the immediate vicinity of the inlet. Local transport directed toward the inlet is likewise augmented by tidal (flood) currents, the contributions of which are not included in the figure. It is thus reasonably assumed that the local, inlet-induced increases in right- and left-directed transport, m_1 and m_2, are each in the range of at least 0.3 to 0.5, more or less.

For the sake of generality, no presumptions will be made regarding the jetties' impermeability values (j_1 and j_2) or the natural bypassing tendency (p_1 and p_2). These values, at least initially, will be allowed to range from 0 to 1.

As the right shoreline is downdrift (and of uncertain volume change), Equations V-6-56a and V-6-56b are solved for p_1 and p_2 for the ranges of values described; viz.,

$$p_1 = 1 - j_1\,(1 + m_1) + m_1 - (L_2/R_1)(1 - j_2(1+m_2) + m_2 - p_2) - (156000)/R_1$$

$$p_2 = [\,(j_1\,(1 + m_1) - m_1)\,R_1 + L_1 - (-16000) + 0 - 0\,] \,/\, L_2$$

where $0 \le j_1 \le 1$; $0 \le j_2 \le 1$; $0.3 \le m_1 \le 0.5$; $0.3 \le m_2 \le 0.5$; $72700 \le R \le 472{,}700$; and, $L_1 = 0.45\,R_1$; and $L_2 = L_1$. Only those combinations of values for which $0 \le p_1 \le 1$ and $0 \le p_2 \le 1$, and for which $0 \le p_1 + j_1 \le 1$ and $0 \le p_2 + j_2 \le 1$, are retained as viable solutions. For each of these, the net incident transport, shoaling volume from the left and right shorelines, and the net bypassing volume, are computed from Equations V-6-61a, V-6-62a, V-6-62b, and V-6-62c, respectively.

Figure V-6-53 illustrates the results of these computations; i.e., the general family of solutions. Any point within this family (the shaded area) can solve the sediment budget. The solutions lie along lines of constant net incident transport value (Q_1). The size of the solution family decreases as the local inlet-induced transport term (m_1, m_2) increases. This is indicated by the truncation of the family along its lower right-hand side as m_1 and m_2 increase from 0.3 to 0.5.

(Continued)

EXAMPLE PROBLEM V-6-13 (Continued)

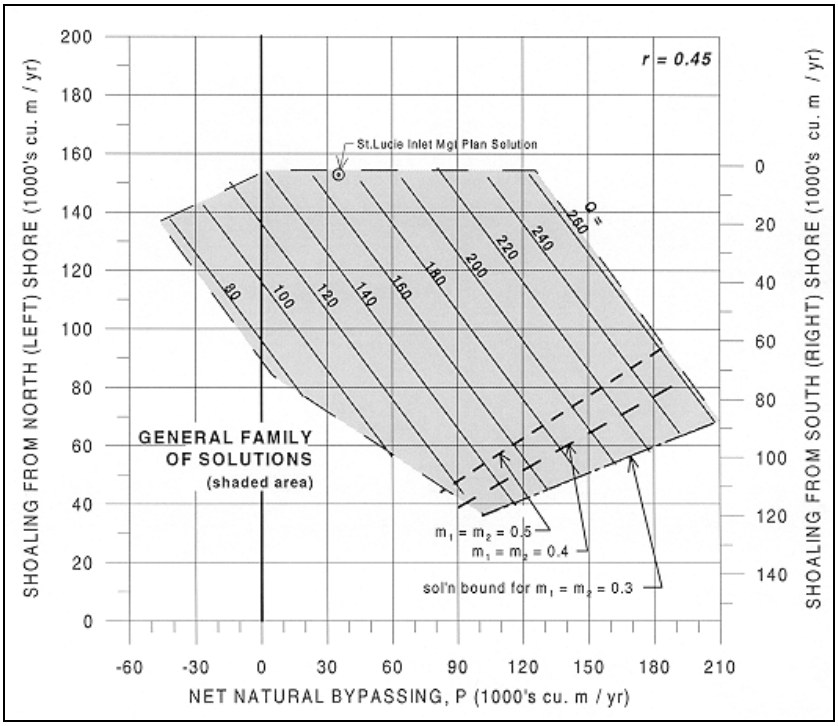

Figure V-6-53. General family of solutions for St. Lucie Inlet, Florida, sediment budget

From Figure V-6-53, it is noted that the minimum net incident transport (Q_1) is about 80,000 cu m/ year in order to solve the sediment budget. A numeric scan of the results demonstrates that the updrift jetty must be at least 25 percent impermeable but not more than 60 percent impermeable ($0.25 < j_1 < 0.6$) to solve the sediment budget; and that the modal impermeability value is about 46 percent ($j_1 = 0.46$). Values for the downdrift jetty's impermeability ranged from 0 to 1, though 90 percent of the values were less than 0.7. Likewise, natural bypassing of the right-directed transport must be less than 69 percent ($p_1 < 0.69$) to solve the sediment budget. A solution proposed in the St. Lucie Inlet Management Plan, prepared for the State of Florida, plots at the top edge of the family. While mathematically viable, it appears as an outlier relative to the bulk of the solution, and was ultimately not adopted by the state.

The family of solutions can be readily narrowed by imposing additional physical constraints, developed through observation of the inlet. For illustration, these shall include:

1. Direction of any net natural bypassing to coincide with the net drift ($P > 0$).
2. Net natural bypassing is not greater than two-thirds of the net incident rate ($P < 0.67\ Q_1$).
3. Shoaling from the right comprises at least one-third of the total inlet shoaling ($S_{RIGHT} > 0.33\ \Delta V_G$).
4. The downdrift, right jetty is not more than 70 percent impermeable ($j_2 \leq 0.7$).

(Continued)

EXAMPLE PROBLEM V-6-13 (Continued)

The resulting, narrowed family is plotted in Figure V-6-54. Requirements No. 1, 2, and 3, respectively, truncated the general solution's left, right, and top boundaries; while No. 4 had little effect in this case, as expected, given that 90 percent of j_2's values were naturally less than 0.7. The bounds of this narrowed family are identical for values of m_1 and m_2 from 0.3 to 0.5. The maximum net, incident transport rate must be less than 250,000 cu m/year in order to solve the sediment budget.

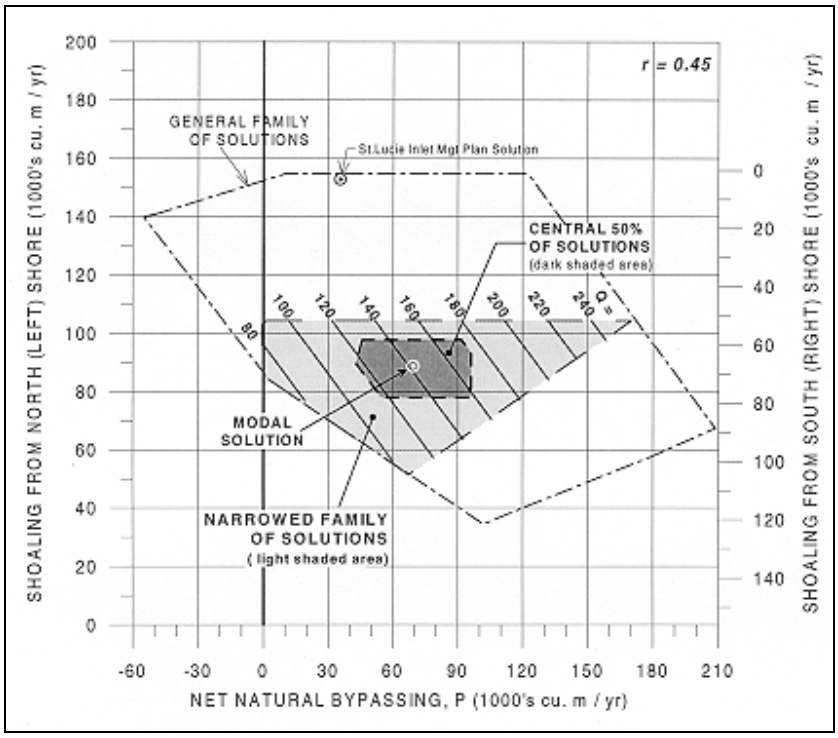

Figure V-6-54. Narrowed family of solutions, per requirements 1-4

A numeric scan of the narrowed family's results reveals the frequency with which values of the various transport parameters can solve the sediment budget for fixed increments of the input values j_1, j_2, and R_1 (or Q_1). For example, the modal (most frequent) value of shoaling from the left shore is 88,600 cu m/year, or 56 percent of the total gross shoaling rate, with half of all of the solutions falling within values of 44,000 cu m/year (28 percent of gross shoaling) to 96,000 cu m/year (62 percent). The modal value of the net incident transport rate is Q_1 = 147,000 cu m/year, with half of all of the solutions defined by values between about 120,000 and 170,000 cu m/year. The modal value of the updrift jetty impermeability is j_1 = 0.47, with half of all solutions described by j_1 = 0.43 to 0.53. The modal value of the downdrift jetty impermeability is j_1 = 0.26, with half of all solutions described by j_1 = 0.13 to 0.43. This suggests that the updrift jetty is about twice as impermeable as the downdrift jetty, a notion that is physically reasonable.

(Continued)

EXAMPLE PROBLEM V-6-13 (Continued)

The dark shaded area in Figure V-6-54 is a subset of solutions that represents the central 50 percent of the narrowed family. That is, it comprises those 50 percent of the solutions distributed about the inlet-parameter values that most frequently solve the sediment budget. Formally, it represents that half of the viable inlet solutions that occur most frequently. The modal solution in the middle indicates the narrowed solutions' weighted average value of computed net bypassing, P, and shoaling, S_{LEFT} and S_{RIGHT}.

As an example, a discrete solution is selected from the family and exploded to develop the corresponding sediment transport pathways. The modal solution is chosen as an illustration, where the most frequently occurring values of the transport parameters are selected as a discrete solution; viz., Q_1 = 142,000 cu m/year (R = 258,200 cu m/year, and L = -116,200 cu m/year); P = 69,400 cu m/year; S_{LEFT} = 88,600 cu m/year, and j_1 = 0.47. The family of solutions is scanned for these discrete conditions (or, a discrete solution can be computed directly for these values). For nominal values of $m_1 = m_2 = 0.4$, the parameters that correspond to these conditions are j_2 = 0.31, p_1 = 0.40, and p_2 = 0.32. For each of these values, and recalling that $L_2 = 0.9\ L_1$, the transport pathways attendant to the inlet are computed with reference to the definition sketch, Figure V-6-51a,b. The results are plotted in Figure V-6-55.

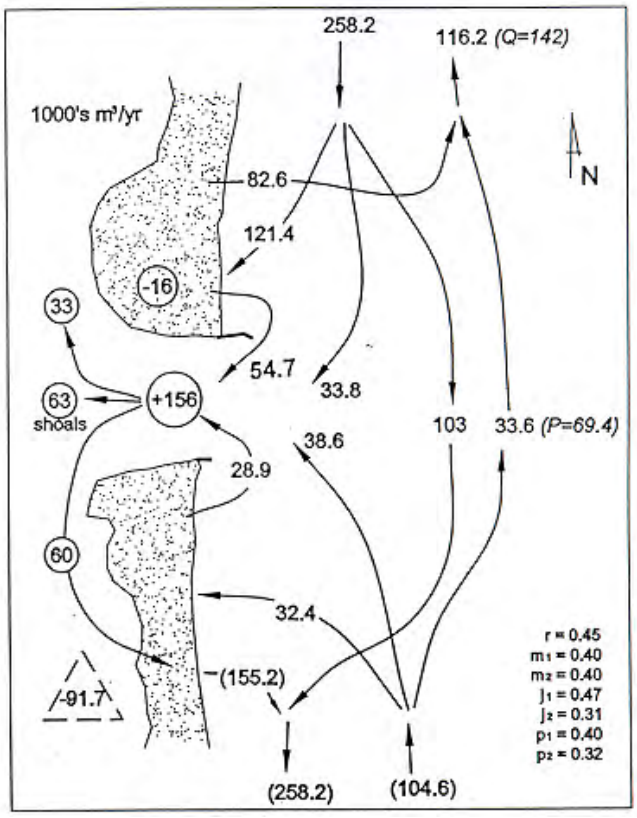

Figure V-6-55. Sediment transport rates (1000s cu m/year) computed for modal solution, St. Lucie Inlet, Florida (figure not to scale)

(Continued)

EXAMPLE PROBLEM V-6-13 (Concluded)

From Equation V-6-57, the volume change of the downdrift shoreline is also computed. This requires presumption of the rightward transport, R_2, directed away from the inlet on the downdrift side, not otherwise needed up to this point. In the present example, and by reference to Figure V-6-51a,b, it is presumed that $R_1 = R_2 =$258,200 cu m/year. This suggests that the downdrift shoreline exhibits an erosion potential of 91,700 cu m/year. From Equation V-6-57, this is the sum of net inlet shoaling (63,000 cu m/year) and out-of-system dredge disposal (33,000 cu m/year) minus net change of the updrift shoreline (-15,900 cu m/year, computed), and accounting for a presumed decrease in the left-directed transport potential across the inlet (11,600 cu m/year).

Measurements of net downdrift volume change vary widely, particularly because of fairly frequent beach nourishment and nearshore (dredge) sand placement of uncertain success. With sand placement to the downdrift shoreline, the observed net volume change is between +67,000 cu m/year to -139,000 cu m/year. (These are the values to which to compare the computed net downdrift volume change, above, ΔV_R = -91,700 cu m/year.) After subracting sand placement, net downdrift erosion is reported on the order of 160,000 to 367,000 cu m/year along 9 km south of the inlet (USAED, Jacksonville, 1999). The great uncertainty in these values is not atypical for downdrift shorelines.

The modal solution depicted presumes a net incident transport rate of 142,000 cu m/year. Prior studies by the Corps estimate this value as about 175,000 cu m/year (USAED, Jacksonville, 1999). The solution, suggests that the transport rates into the inlet from the north and south shorelines are about 88,500 and 67,500 cu m/year, respectively. Corresponding values estimated in USAED, Jacksonville (1999) are about 103,000 and 56,000 cu m/year.

V-6-4. Engineering Approaches

a. General considerations. Development of the inlet sediment budget allows estimation of the degree to which an inlet has historically impacted the adjacent shorelines' littoral system, and is presently bypassing sediment. Mitigation of the first approach may be possible by restoring sand to the affected shores from the inlet's sediment (shoal) resources, although this may aggravate inlet impacts if done improperly or may be otherwise limited by other concerns. Mitigation of the second approach requires that the inlet be improved to decrease its littoral impact as a sediment sink. To the extent that these mitigative approaches are limited, additional mitigation may be required in the form of beach nourishment (or alternate shore protection methods) from sources external to the inlet. In developing mitigative and/or inlet management strategies, the designer must be aware of social and environmental constraints, as well as physical (site) constraints, that can ultimately limit these strategies' feasibility. These include, for example, the presence of natural or historical resources that limit borrowing/sand transfer from inlet shoals; upland property owners' ability to block sand transfer operations that are perceived to remove sand from updrift beaches; questions as to which entity "owns" the sand resource to

EXAMPLE PROBLEM V-6-14

FIND:

The family of solutions that describes an improved inlet's sediment transport pathways.

GIVEN:

The apparent net transport direction across the inlet is from left-to-right. The net volume changes within the inlet's shoals, and along 6 km of the apparent, updrift shoreline, were estimated from survey data for a common period and averaged to annualized rates. Dredging and sand-bypass records are available for the same period. The volume change of the updrift (left) shoreline is -15,000 cu m/year (erosion). Prior to any dredging, the flood shoal accreted at a rate of 237,000 cu m/year and the ebb shoal accreted at a rate of 80,000 cu m/year. An average of about 55,000 cu m/year are dredged from the inlet and disposed of in deep water, offshore. Another 86,000 cu m/year are dredged from the flood shoals, on average, and placed upon the downdrift (right) shoreline. The inlet includes jetties on both shorelines, each of which appears to impound some, but not all, of the incident drift; $0.1 < j < 0.6$, for example. There is a bypassing bar across the inlet mouth that attaches to both shorelines within about 3 to 4 km of the entrance. Results of a wave refraction / transport rate analysis, based upon hindcast wave data, are shown in Table V-6-12. The values of the transport rate potential are normalized by the maximum value of the computed net transport rate. The actual magnitude of the average, net incident drift rate is uncertain, but is thought to be toward the right and on the order of 150,000 to 250,000 cu m/year.

Table V-6-12
Results from Wave Refraction and Transport Rate Analysis

Distance from Inlet (km)	Right-Directed Transport	Left-Directed Transport	Net Transport	Right-Directed Transport	Left-Directed Transport	Net Transport
	Left (updrift) shoreline			Right (downdrift) shoreline		
7	0.85	-0.28	0.57	0.84	-0.28	0.56
6	0.82	-0.28	0.54	0.85	-0.29	0.56
5	0.86	-0.30	0.56	0.82	-0.27	0.55
4	0.92	-0.20	0.72	0.70	-0.30	0.40
3	0.97	-0.11	0.86	0.59	-0.39	0.20
2	1.03	-0.08	0.95	0.33	-0.42	-0.09
1	1.03	-0.03	1.00	0.21	-0.41	-0.20
0.1	1.00	-0.00	1.00	0.15	-0.43	-0.28

SOLUTION:

Step 1. From Table V-6-11 of computed, potential transport rates, the right- and left-directed transport appear to be fairly stable and uniform at 6- to 7-km distance from the inlet. From the given values in the table and Equation V-6-48, the ratio of the right- and left-directed transport potential is about

$$r = - (-0.28) / (0.85) = 0.33$$

EXAMPLE PROBLEM V-6-14 (Continued)

Step 2. From the given data, the range of incident transport rate to be considered shall be Q = 150 to 250, where units of 1,000's of cubic meters per year are assumed throughout.

Step 3. The range of jetty impermeabilities to be considered shall be $0.1 < j_1 < 0.6$ and $0.1 < j_2 < 0.6$.

Step 4. From the table, the right-directed transport rate potential increases from about 0.85 to about 1.0 along the left shoreline adjacent to the inlet. This increase is assumed to reflect the local, inlet-induced transport associated with the term m_1. This represents a localized increase of 0.15 (normalized) units above the incident value of 0.85. Thus,

$$m_1 \approx 0.15 / 0.85 = 0.18$$

Likewise, from the table, the left-directed transport rate potential increases from about -0.29 to -0.42 along the right shoreline adjacent to the inlet. This increase is assumed to reflect the local, inlet-induced transport associated with the term m_2. This is a localized increase of -0.13 units above the incident value of -0.29. Thus,

$$m_2 \approx -0.13 / -0.29 = 0.45$$

Step 5. From the given data, D_O = 55, D_R = 86, D_L = 0, and D_B = 0, where units of 1000's of cu m/year are assumed. Riverine sediment input is assumed to be zero; S_U = 0.

Step 6. From the given data, the inlet's shoal complex accreted by 237 + 80 = 317 (1000's of cu m/year). The net change in inlet shoal volume, subsequent to maintenance dredging, is

$$\Delta V_N = 317 - 55 - 86 = 176 \text{ (1,000's of cu m/year)}$$

Step 7. Given the right-to-left net transport, the LEFT shoreline is the updrift shoreline, where ΔV_L = -15 (1000's of cu m/year).

Step 8. For simplicity, require only that $0 < p_1 < 1$, and $0 < p_2 < 1$.

Step 9 - 10. Develop expressions for p_1 and p_2 for the values previously described. From Equations V-6-56a and V-6-56b), respectively,

$$p_1 = 1 + (0.33)(0.45 - j_2) - ((1-0.33)/Q)\,(0 + 86 + 55 + (-15) + 176 - 0)$$
$$= 1.15 - 0.33\,j_2 - 202.3/Q$$

$$p_2 = 1 + (1/0.33)[0.18 - j_1 + ((1-0.33)/Q)\,(-15 + 0 - 0)$$
$$= 1.55 - 3.03\,j_1 - 30.45/Q$$

(Continued)

EXAMPLE PROBLEM V-6-14 (Continued)

greater than 1; or, if the sum of ($p_1 + j_1$) and/or ($p_2 + j_2$) is less than zero or greater than 1, then the result is unreasonable and is excluded as a possible solution. For example, for the combination of values: $Q = 200$, $j_1 = 0.3$, and $j_2 = 0.2$,

$$p_1 = 1.15 - 0.33\ (0.2) - 202.3/200 = 0.073$$

$$p_2 = 1.55 - 3.03\ (0.3) - 30.45/200 = 0.489$$

Compute the values of p_1 and p_2 for discrete values of Q between 150 and 250 (1000's of cu m/year), and for values of j_1 and j_2 between 0.1 and 0.6. If the the result yields a value of p_1 or p_2 that is less than 0 or

such that

$$p_1 + j_1 = (0.073 + 0.3) = 0.373$$

$$p_2 + j_2 = (0.489 + 0.2) = 0.689$$

This represents a potentially valid solution.

For another example, for the combination of values: $Q = 200$, $j_1 = 0.3$, and $j_2 = 0.5$,

$$p_1 = 1.15 - 0.33\ (0.5) - 202.3/200 = -0.0265$$

$$p_2 = 1.55 - 3.03\ (0.3) - 30.45/200 = 0.489$$

which is an invalid solution because $p_1 < 0$.

Similarly, for the combination of values: $Q = 150$, $j_1 = 0.1$, and $j_2 = 0.5$,

$p_1 = 1.15 - 0.33\ (0.1) - 202.3/150 = -0.232$

$p_2 = 1.55 - 3.03\ (0.5) - 30.45/150 = -0.168$

(Continued)

EXAMPLE PROBLEM V-6-14 (Continued)

which is an invalid solution because both p_1 and p_2 are less than zero. In fact, for this case of Q=150, no reasonable value of j_1 can yield a value of p_1 greater than zero; hence, the value of Q=150 is generally invalid and excluded from the family of solutions. An abbreviated list of additional example solutions is shown in the Table V-6-13.

Table V-6-13
Sediment Budget Example Solutions

Assumed Values			Computed Values				VALID Solution?
Q	j_1	j_2	p_1	p_2	$j_1 + p_1$	$j_2 + p_2$	
210	0.3	0.45	0.038	0.496	0.338	0.946	YES
210	0.3	0.5	0.022	0.496	0.322	0.996	YES
210	0.3	0.55	0.005	0.496	0.305	*1.046*	NO
210	0.35	0.1	0.154	0.345	0.504	0.445	YES
230	0.2	0.1	0.237	0.812	0.437	0.912	YES
230	0.2	0.15	0.221	0.812	0.421	0.962	YES
230	0.2	0.2	0.204	0.812	0.404	*1.012*	NO
230	0.25	0.1	0.237	0.660	0.487	0.760	YES
230	0.25	0.15	0.221	0.660	0.471	0.810	YES

Step 11. For each valid solution, compute total shoaling quantities from the left shoreline, S_{LEFT}, from the right shoreline, S_{RIGHT}; and the net natural bypassing quantities, P. Use Equations V-6-62a), V-6-62b, and V-6-62c, respectively. As an example, for the values listed on the last row of Table V-6-12:

$$S_{LEFT} = (0.18 + 1 - 0.25 - 0.221)\ (230 / (1\text{-}0.33)) = 243.4$$
$$S_{RIGHT} = (0.45 + 1 - 0.15 - 0.660)\ ((0.33)(230)/(1\text{-}.33)) = 72.5$$
$$P = (230/(1\text{-}0.33))\ (0.221 - (0.33)(0.660)) = 1.1$$

each with units of 1,000's of cu m/year. Compute these values for all of the valid solutions and plot, as shown in Figure V-6-56.

(Continued)

EXAMPLE PROBLEM V-6-14 (Continued)

The shaded area in the graph represents the general family of solutions; i.e., all potentially valid solutions. The range of solutions can be narrowed by introducing additional physical restrictions. These might include, for example, requirements that

(1) the direction of net natural bypassing across the inlet be the same as the net incident transport (i.e., from left-to-right, or $P > 0$).

(2) The jetties' impermeabilities are relatively similar (e.g., j_1 and j_2 differ by no more than 50 percent).

(3) The tendency for natural bypassing of incident transport is similar for both shorelines (e.g., p_1 and p_2 differ by no more than 50 percent).

For these example assumptions, the family of solutions is narrowed to the smaller, cross-hatched area in Figure V-6-56

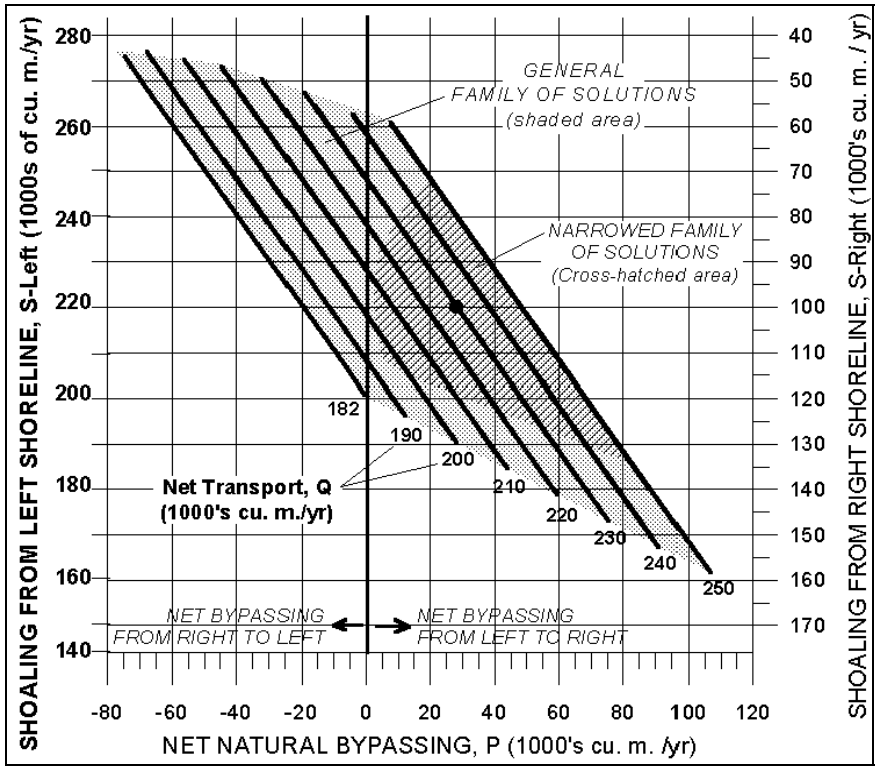

Figure V-6-56. Family of solutions for Example Problem V-6-14

(Continued)

EXAMPLE PROBLEM V-6-14 (Continued)

While any point within this family of solutions is potentially valid (i.e., can satisfy the inlet's sediment budget), it is useful to develop one or more discrete solutions. An example, discrete solution is developed using the values from the approximate center of the narrowed family of solutions (indicated by the bold dot in Figure V-6-56, see Figure V-6-57).

The discrete solution indicated in the figure approximately represents Q = 230, S_{LEFT} = 216, S_{RIGHT} = 100, and P=28.6. Scanning the computed family of solutions for values of j_1, j_2, p_1, and p_2 that result in these quantities yields j_1 = 0.425, j_2 = 0.438, p_1 = 0.126, and p_2 = 0.130. (While these values can be developed algebraically, it is simpler to scan the spreadsheets or other computations in order to identify the combination of input parameters that yield the desired, discrete solution.) For this solution, the components of the sediment transport pathways about the inlet are computed as follows:

Incident, right-directed transport, R (Equation V-6-48 and V-6-61a):
R = (230) / (1-0.33) = 343.3

Incident, left-directed transport, L (Equation V-6-48 and V-6-61a):
L = (-0.33) (230) / (1-0.33) = -113.3

Inlet-induced transport from left shoreline, ($m_1 R$): $m_1 R$ = (0.18) (343.3) = 61.8

Inlet-induced transport from right shoreline, ($m_2 L$): $m_2 L$ = (0.45) (-113.3) = -51.0

Transport impounded by left jetty, ($j_1 R$): $j_1 R$ = (0.425) (343.3) = 145.9

Transport impounded by right jetty, ($j_2 L$): $j_2 L$ = (0.438) (-113.3) = -49.6

Right-directed transport naturally bypassed, ($p_1 R$): $p_1 R$ = (0.126) (343.3) = 43.3

Left-directed transport naturally bypassed, ($p_2 L$): $p_2 L$ = (0.130) (-113.3) = -14.7

where units of 1000's of cu m/year are assumed throughout. The sediment transport pathways, including the given dredging practices, are illustrated in Figure V-6-57. In this example solution, the fraction of the net, incident transport that is naturally bypassed across the inlet is:

$$P / Q = 28.6 / 230 = 0.124 \quad (12.4 \text{ percent}).$$

For the method's assumption that the magnitudes of the left- and right-directed transport are equal at the updrift and downdrift boundaries of the study area, the predicted net volume change on the downdrift (right) side of the inlet is, from Equation V-6-55,

$$\Delta V_R = [(0.437)(0.33)-(0.45)(0.33)-1+0.126)\ (230/(1-0.33))] + 0 + 86 = -215.5 \text{ (1000's cu m/year)}$$

(Continued)

EXAMPLE PROBLEM V-6-14 (Concluded)

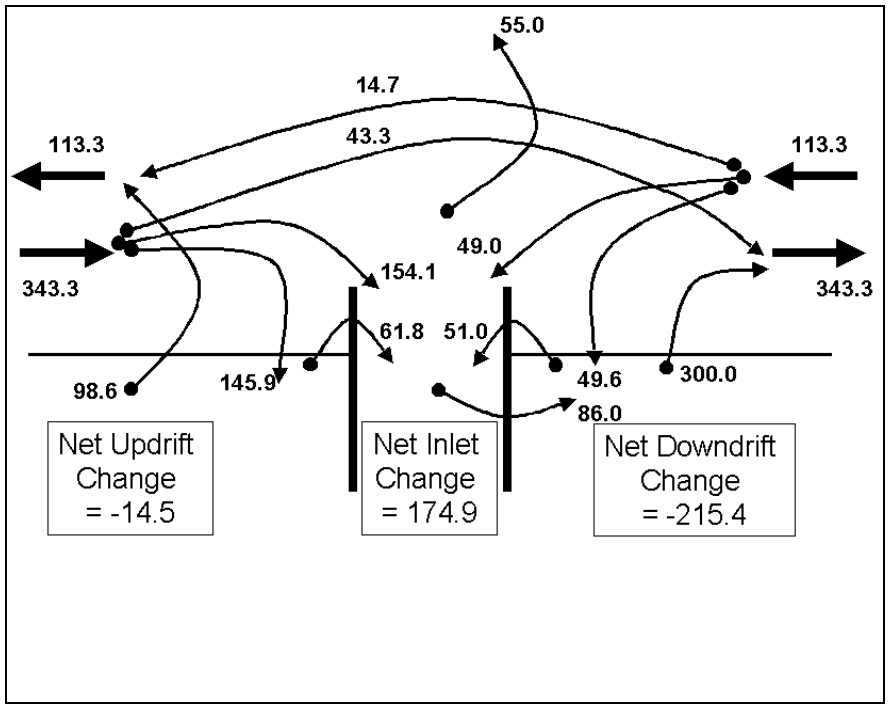

Figure V-6-57. One possible solution for Example Problem V-6-14

be transferred; seasonal restrictions upon dredging activity imposed by marine turtle or bird nesting, storms, tourism, etc.; impacts to surfing and other recreation; inclusion of contaminated sediments; noise and aesthetic impact of sand transfer activity; limited upland access for sand-transfer operations (pipeline, maintenance, pumping stations, etc.); among others. The designer must also consider the ultimate (initial and annual) cost of implementing the proposed sand management strategy versus that of mitigating beach erosion by conventional nourishment from sand sources external to the inlet, assuming that authorization for the latter can be successfully sought and maintained.

b. Application of sediment budget to design. The sediment budget prepared for existing or historical conditions can be utilized to examine potential effects of modifications to the inlet system. The following example illustrates application of the Bodge method (Bodge 1999; see Part V-6-3) to estimate the optimum combination of jetty sand-tightening and mechanical bypassing. This application minimizes the total volume of sand that must be mechanically transferred in order to theoretically yield no net changes to the adjacent shorelines. The same approach can be used to examine the quantities and directions of mechanical sand transfer necessary for any given combination of jetty sand-tightening alternatives.

(1) In the limit, a jetty which is completely sand-tight ($j = 1$) will theoretically allow no transfer of sand past the jetty by either natural bypassing or local, inlet-induced transport; in which case, $p = 0$ and $m = 0$. If it is assumed that the degree to which the sand transfer past a jetty decreases linearly from its present state ($0 < j < 1$) to a completely sand-tightened state ($j = 1$), then the parameters p and m become:

$$p_{1'} = \left(\frac{p_1}{1 - j_1} \right) (1 - j_{1'}) = a (1 - j_{1'}) \tag{V-6-63}$$

$$p_{2'} = \left(\frac{p_2}{1 - j_2} \right) (1 - j_{2'}) = b (1 - j_{2'}) \tag{V-6-64}$$

$$m_{1'} = \left(\frac{m_1}{1 - j_1} \right) (1 - j_{1'}) = c (1 - j_{1'}) \tag{V-6-65}$$

$$m_{2'} = \left(\frac{m_2}{1 - j_2} \right) (1 - j_{2'}) = d (1 - j_{2'}) \tag{V-6-66}$$

where p_1', p_2', m_1', and m_2' are the natural bypassing coefficients and local, inlet-induced transport coefficients for the modified jetty-impoundment coefficients j_1' and j_2'. The nonprimed values of p, m, and j represent the existing (or nonmodified) condition, as determined from measured data and as described in the previous section.

(2) If it is required that there be no net volume change along the left and right shorelines, then from Equations (V-6-50), (V-6-51), and (V-6-63) through (V-6-66), bypass and dredging/beach disposal requirements are:

$$D_B' - D_L' = [Q/(1-r)] [(1+c) j_1' + (r(b-1)-c) - b\, r\, j_2'] \tag{V-6-67}$$

$$D_B' + D_R' = [Q/(1-r)] [a\, j_1' + (1-a+rd) - (r+rd)\, j_2'] \tag{V-6-68}$$

where, from Equations V-6-42 through V-6-45

$$a = p_1 / (1-j_1) \tag{V-6-69a}$$

$$b = p_2 / (1-j_2) \tag{V-6-69b}$$

$$c = m_1 / (1-j_1) \tag{V-6-69c}$$

$$d = m_2 / (1-j_2) \tag{V-6-69d}$$

(3) While this approach prescribes that there be no net volumetric change to each shoreline, there may be local changes (accretion and erosion) caused by redistribution of sand within each shoreline cell.

(4) If $D_B' - D_L' > 0$, then the net requirement is to transfer sand to the right; hence, any interim transfer to the left shoreline (D_L') would be superfluous. In that event, $D_L' = 0$. Likewise, if $D_R' + D_B' < 0$, then the net requirement is to transfer sand to the left; hence, any interim transfer to the right shoreline (D_R') would be superfluous. In that event, $D_R' = 0$. Finally, if $D_B' - D_L' < 0$ and $D_R' + D_B' > 0$, then both shorelines require placement of sand and, hence, any interim bypassing from one to the other (D_B') would be superflous. In that event, $D_B' = 0$. Concisely,

For	$D_B' - D_L' \geq 0$	then $D_L' = 0$	
For	$D_R' + D_B' \leq 0$	then $D_R' = 0$	(V-6-70)
For	$D_B' - D_L' \leq 0$ and $D_R' + D_B' \geq 0$	then $D_B' = 0$	

EXAMPLE PROBLEM V-6-15

FIND:

The requisite, total sand transfer quantities for zero net littoral impact to the adjacent shorelines for the inlet condition in Example Problem V-6-14 for the case of: (a) existing conditions, (b) complete and-tightening of both jetties, and (c) optimum sand-tightening to yield the theoretical, minimum sand transfer quantity.

GIVEN:

Same data as for Problem V-6-14. Assume existing conditions are represented by $j_1 = 0.425$, $j_2 = 0.438$, $m_1 = 0.18$, $m_2 = 0.45$, and $r = 0.33$ with an incident net drift value of $Q = 230{,}000$ cu m/year.

SOLUTION:

For the given values (see Example Problem V-6-14), $p_1 = 0.126$ and $p_2 = 0.130$. From Equation (V-6-69),

$$a = p_1/(1-j_1) = (0.126) / (1-0.425) = 0.219$$
$$b = p_2/(1-j_2) = (0.130) / (1-0.438) = 0.231$$
$$c = m_1/(1-j_1) = (0.18) / (1-0.425) = 0.313$$
$$d = m_2/(1-j_2) = (0.45) / (1-0.438) = 0.801$$

From Equations (V-6-67), (V-6-68) and (V-6-71), where quantities of 1000's of cu m/year are assumed,

$$D_B' - D_L' = A = [230/(1-0.33)]\,[(1+0.313)\,j_1' + (0.33\,(0.231-1) - 0.313) - (0.231)(0.33)\,j_2']$$
$$= A = 450.7\,j_1' - 26.2\,j_2' - 194.6$$

$$D_B' + D_R' = B = [230/(1-0.33)]\,[0.219\,j_1' + (1-0.219 + (0.33)(0.801)) - (0.33 + (0.33)(0.801)\,j_2']$$
$$= B = 75.2\,j_1' - 204.0\,j_2' + 358.9$$

(a) For the case of existing conditions (no jetty sand-tightening), $j_1' = 0.425$ and $j_2' = 0.438$:

$$D_B' - D_L' = A = (450.7)\,(0.425) - (26.2)\,(0.438) - 194.6 = -14.5$$

$$D_B' + D_R' = B = (75.2)\,(0.425) - (204.0)\,(0.438) + 358.9 = 301.5$$

From Table V-6-14, $D_B' = 0$. Thus, $D_L' = 14.5$ and $D_R' = 301.5$. That is, 14,500 cu m/year should be dredged from the inlet and placed upon the updrift (left) shoreline; and, 301,500 cu m/year should be dredged from the inlet and placed upon the downdrift (right) shoreline.

(Continued)

Table V-6-14
Method to Determine D_R', D_B', and D_L'

$A = D_B' - D_L'$	$B = D_R' + D_B'$	D_L'	D_R'	D_B'
+	+	0	*B-A*	*A*
-	+	*-A*	*B*	0
+	-	invalid solution		
-	-	*B-A*	0	*B*

EXAMPLE PROBLEM V-6-15 (Continued)

(b) For the case of total jetty sand-tightening, j_1' = 1.0 and j_2' = 1.0. Therefore,

$$D_B' - D_L' = A = (450.7)(1.0) - (26.2)(1.0) - 194.6 = 230$$

$$D_B' + D_R' = B = (75.2)(1.0) - (204.0)(1.0) + 358.9 = 230$$

From Table V-6-14, $D_L' = 0$. Thus, $D_B' = 230$ and $D_R' = 0$. That is, 230,000 cu m/year should be bypassed across the inlet from left-to-right. This is, as expected, equal to the net incident transport rate.

(c) Neglecting costs of jetty improvements, the optimum (theoretical) jetty sand-tightening alternative is that which minimizes the total quantity of material that must be mechanically transferred across the inlet, and/or from within the inlet to the adjacent shorelines. To investigate this, the dredging quantities ($D_B' - D_L'$) and ($D_B' + D_R'$) are solved for a variety of combinations of j_1' and j_2'. For each, the total requisite dredging quantity ($D_B' + D_L' + D_R'$) is recorded. An abbreviated list of example calculations is shown in Table V-6-15.

Table V-6-15
Example Calculations for Evaluating Dredging Requirements

j_1	j_2	$D_B' - D_L'$	$D_B' + D_R'$	D_B'	D_L'	D_R'	$D_B'+D_L'+D_R'$
0.40	0.6	-30.0	266.6	0.0	30.0	266.6	296.6
0.40	0.8	-35.3	225.8	0.0	35.3	225.8	261.1
0.40	1.0	-40.5	185.0	0.0	40.5	185.0	225.5
0.45	0.6	-7.5	270.3	0.0	7.5	270.3	277.8
0.45	0.8	-12.7	229.5	0.0	12.7	229.5	242.3
0.45	1.0	-18.0	188.7	0.0	18.0	188.7	206.7
0.50	0.6	15.0	274.1	15.0	0.0	259.1	274.1
0.50	0.8	9.8	233.3	9.8	0.0	223.5	233.3
0.50	1.0	4.6	192.5	4.6	0.0	188.0	192.5
0.60	0.6	60.1	281.6	60.1	0.0	221.5	281.6
0.60	0.8	54.9	240.8	54.9	0.0	186.0	240.8
0.60	1.0	49.6	200.0	49.6	0.0	150.4	200.0
0.70	0.6	105.2	289.1	105.2	0.0	184.0	289.1
0.70	0.8	99.9	248.3	99.9	0.0	148.4	248.3
0.70	1.0	94.7	207.5	94.7	0.0	112.9	207.5

(Continued)

EXAMPLE PROBLEM V-6-15 (Concluded)

The total requisite dredging quantity (D_B' + D_L' + D_R') is the value in the last column of the table. This quantity is plotted as a function of the jetties' sand-tightening coefficients on the following graph.

From Figure V-6-58, the minimum dredging quantity is computed at or about j_1' = 0.49 and j_2' = 1.0. From Equations V-6-67, V-6-68 and V-6-71

$$D_B' - D_L' = A = (450.7)(0.49) - (26.2)(1.0) - 194.6 = 0$$

$$D_B' + D_R' = B = (75.2)(0.49) - (204.0)(1.0) + 358.9 = 191.7$$

This implies 100 percent sand-tightening of the right (downdrift) jetty, and minor sand-tightening of the left (updrift) jetty. There would be a theoretical requirement for the placement of 191,700 cu m/year from the inlet to the right shoreline.

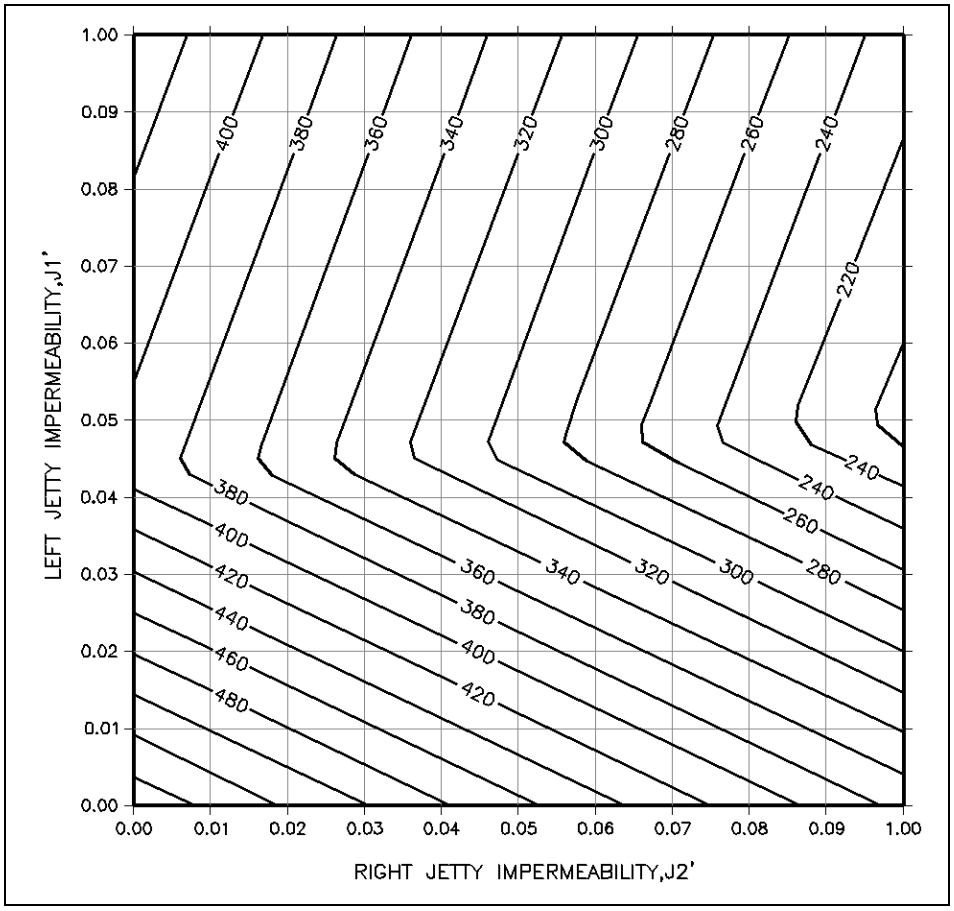

Figure V-6-58. Solution for Example Problem V-6-15

(Note that $D_B' - D_L' \geq 0$ and $D_R' + D_B' \leq 0$ is an invalid solution.) From Equation V-6-70, values of the sand transfer requirements D_L', D_R', and D_B' , for a selected pair of jetty-tightening coefficients, j_1' and j_2', can be computed from Table V-6-14, where

$$A = D_B' - D_L' \quad \text{and} \quad B = D_R' + D_B' \tag{V-6-71}$$

and where a positive (+) value implies a result that is greater than or equal to zero (≥0).

c. Principles of sand bypassing and backpassing. Sand bypassing and backpassing refers to the mechanical transfer of littoral material between the inlet and/or adjacent shorelines to minimize the inlet's erosive impact to the adjacent beaches. Generally, *bypassing* is a transfer of sediment from the updrift shoreline or inlet shoals to the downdrift beach, and also represents a primary means by which to alleviate shoaling within the inlet. *Backpassing* is a transfer of sediment from the inlet shoals (or some portion of the shoreline) to the shoreline from whence the sediment came. The need for either bypassing or backpassing can be identified by the methods previously presented. The majority of sand bypassing/backpassing operations do not involve, nor require, fixed sand transfer plants; instead, they involve more intelligent dredge disposal practice and/or modification of the inlet's structures and channels.

(1) For proper engineering design of an inlet improvement and bypassing/backpassing plan, it is necessary to:

(a) Define the problem (e.g., through inspection and sediment budget approaches).

(b) Determine the need, if any, for jetty improvements or other structure/channel modifications.

(c) Define the requisite quantities and expected seasonal/annual variations thereof, if any.

(d) Define the appropriate physical method(s) for the work.

(e) Define the location(s) of sediment removal.

(f) Define the appropriate location(s) for sediment placement.

The latter four requirements are, ultimately, interrelated.

(2) General classes of bypass/backpass operations include:

(a) Interior vs. exterior traps (i.e., temporary sediment storage within the inlet vs. sediment interception or storage within an updrift or downdrift jetty-fillet).

(b) Periodic vs. continuous (i.e., periodic dredging vs. use of a dedicated plant).

(c) Fixed vs. mobile plant (i.e., fixed plant vs. a conventional, trestle-mounted, or vehicle-mounted dredge plant).

(3) Selection of the most appropriate approach is a function of the unique cirumstances of each inlet. In all cases, however, it is of paramount importance to maintain control of the sediment that enters the inlet system. Sediment can only be transferred if it can be recovered. Examples of transport pathways that, practically speaking, result in a permanent loss of sediment resources include: sediment that is deposited in a thin veneer across the seabed, lost to interior shoals which cannot be dredged for environmental reasons (e.g., high silt content, contaminants, sea grass beds, bird rookeries, etc.),

impounded along shorelines for which dredging cannot be undertaken, dumped offshore in deep water, or dumped nearshore in water depths or configurations that do not promote landward drift. Sand bypassing and backpassing can mitigate inlet impacts to adjacent shorelines only to the degree that sand can be practically recovered from the inlet and transferred. Accordingly, design of inlet and dredging practice that seeks to maximize the degree to which sediment can be intercepted or recovered is central to the development of an effective inlet/harbor sand management plan.

V-6-5. Engineering Methods

a. Jetty sand-tightening. As described in Part V-6-4(b), "Application of Sediment Budget to Design," an inlet's erosive impact to the adjacent shorelines can be reduced, and the requisite sand transfer quantities likewise reduced, with improvements to the terminal structures (jetties) that separate the shorelines and the inlet entrance. Example Problem V-6-15 illustrated the importance of sand-tightening the downdrift jetty in particular. Jetty sand-tightening involves raising the crest elevation, decreasing the porosity, and/or lengthening the structure. (See also Part V-6-3.) Common methods for sand-tightening include:

(1) Overbuilding the structure (i.e., adding armor and/or chinking rock to raise the crest elevation and/or decrease porosity.

(2) Injecting grout into the structure to decrease porosity.

(3) Capping the structure with grout/concrete/asphalt and/or armor units (to increase crest elevation and decrease porosity).

(4) Constructing sheet pile or other bulkhead adjacent to the structure, or placing impermeable barriers within the structure (to increase crest elevation and decrease porosity); and/or

(5) Lengthening the structure.

Specific implementation of these methods is described in Part VI.

b. Sand transfer plants. Selection of methods for sand transfer is described in EM 1110-2-1616, and in Richardson (1990) and Richardson and McNair (1981). The following is a brief overview of equipment and design considerations for facilitating sand transfer.

(1) Fixed systems. Fixed systems are essentially stationary dredging systems designed, built and operated for a specific location (Figure V-6-59). In this case, the sand mover (dredge pump, jet pump, etc.) operates without mobility. System components include the pump and pump motor; a housing to protect the pump and pump motor from waves, spray, and surge; a boom or brace that supports the intake(s); the dredge crater (created by the intake); a discharge pipeline; and booster pumps (depending upon the requisite diameter and length of the discharge pipeline and capacity of the pump). Fixed systems typically employ a conventional suction pump, jet pumps or eductors, submersible pumps, or dedicated dragline. Fluidizers, fixed to the intake or buried in the seabed, can also be employed to increase the sand intake capability. The pumps (or dragline) are generally stationed along the updrift jetty or a trestle immediately updrift of the inlet. Use of fixed systems typically implies the requirement for continuous or high-frequency sand transfer.

(2) Mobile systems. Mobile systems include floating dredge plants, and shore-based plants mounted upon a vehicle. (Figure V-6-60). Use of floating plants typically allows for transfer of greater quantities of sediment and maximum mobility; however, it requires that the area to be dredged is reasonably protected from waves and can be accessed by the plant. Use of shore-based equipment typically involves transfer of smaller quantities, requires that beach access be available, and is limited to sand transfer from along the shore. At the same time, shore-based systems demand less requirement for protected waters and calm weather.

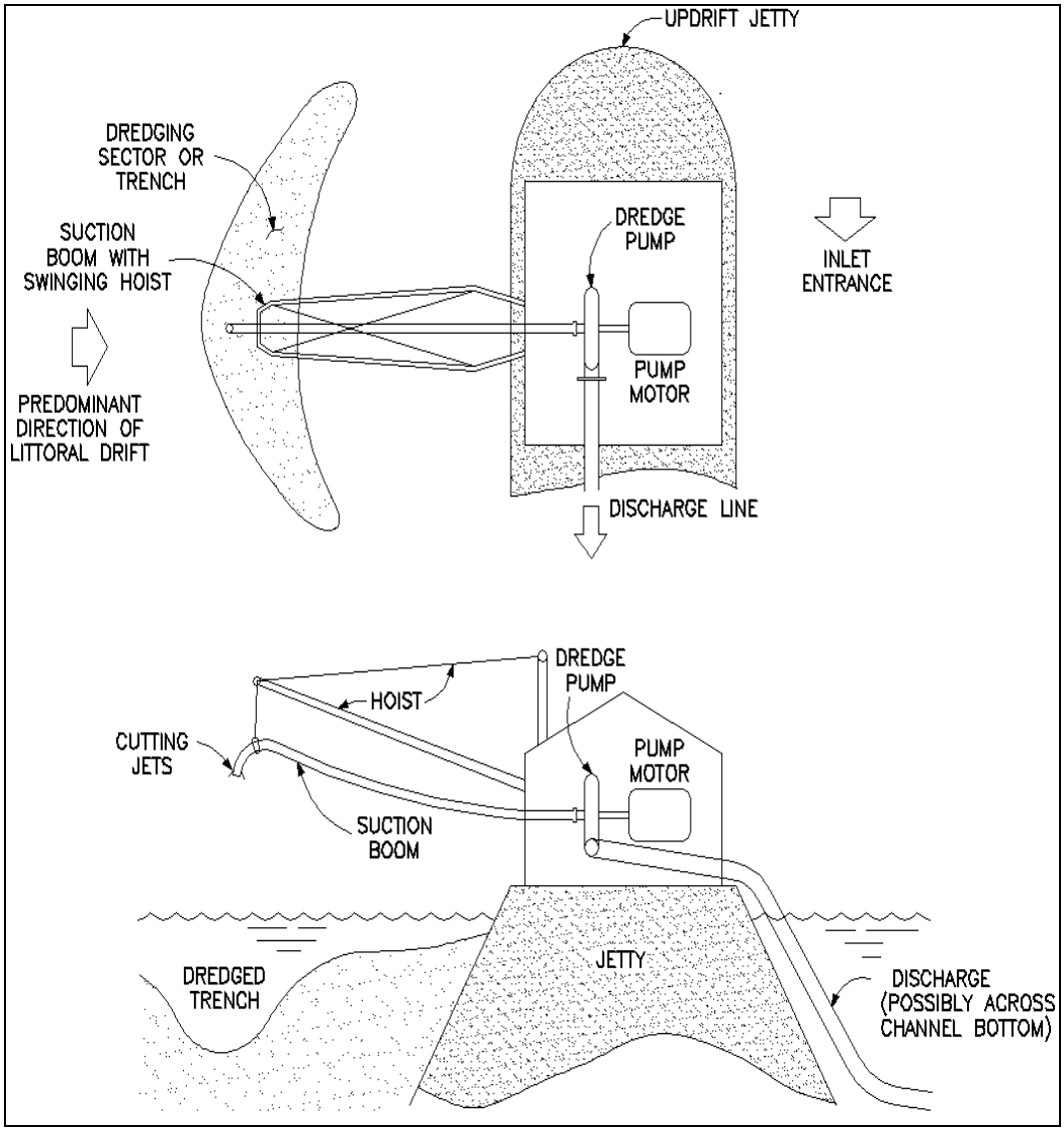

Figure V-6-59. Plan and section view of simple fixed bypassing plant (from EM 1110-2-1616)

(3) Semimobile systems. Semimobile systems include pumps or eductors that are deployed at one location in the inlet for some length of time, then moved to another location. Movement is by barge, truck, boat, etc. Components of mobile and semimobile systems include the dredging equipment (practically unlimited by type) and a temporary or dedicated pipeline or other means to discharge the sand. Use of mobile systems can be considered for either continuous or periodic sand transfer. The dredging equipment can be either contracted for periodic work or purchased (dedicated). The latter is usually considered when the requisite dredging frequency is high or the transfer quantity is modest.

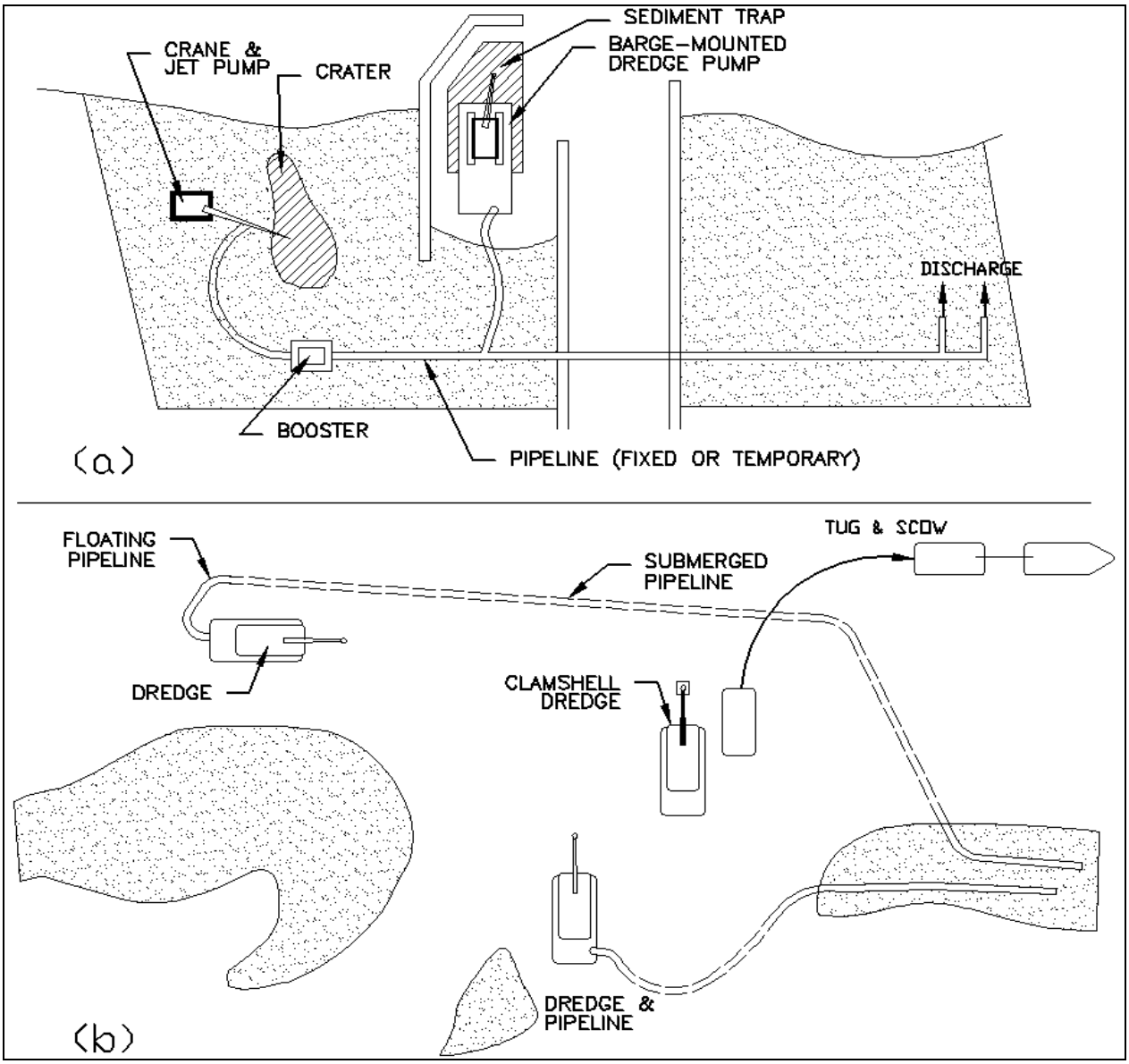

Figure V-6-60. Examples of (a) semimobile and (b) mobile bypassing systems

(4) Equipment for sediment extraction. Equipment most typically used to extract sediment for transfer includes the following systems.

(a) Dredges. Summaries of conventional dredge equipment and their use are presented in McKnight (1966); Bruun (1981); Herbich (1975, 2000); Herbich and Snider (1969); Richardson (1976, 1990); Huston (1970, 1986); and Turner (1984). Mechanical dredges include clamshell (or grapple) buckets, ladder buckets, dipper dredge, and dragline. The dredged material is placed in a hopper, barge or other storage area and is then transported autonomously to the disposal site. Hydraulic (suction) dredges include centrifugal pumps, trash pumps and other suction devices that intake and discharge a slurry mix of sand and water. The discharge is routed to a hopper or scow (from which it is transported to the disposal site) or through a pipeiline to the disposal site. Conventional dredge equipment (mechanical or hydraulic) can be mounted on trucks, trailer, skids, or barges, and are available in a wide variety of sizes and capabilities. As such, they can be incorporated to either fixed or mobile, continuous or periodic,

bypassing strategies. Clark (1983) presents a summary description of commercially available portable hydraulic dredges. Trade magazines (e.g., WODCON) offer monthly reviews of the dredging industry, equipment and technical consultation.

Hopper dredges recover sediment from the seabed through hydraulic means and store it in an onboard hopper for subsequent disposal. Most hopper dredges continuously move as they dredge, working along the channel axis or dredge area. Traditional, large hopper dredges are infrequently suitable for dredging small areas, and often mix littoral material from sandy deposits with silt and clay that is unsuitable for beach/nearshore disposal (Figure V-6-61*)*. Shallow-draft hopper dredges feature loaded drafts of about 3.5 to 4.3 m (11 to 14 ft) with 45- to 60-m (150- to 200-ft) lengths and capacities of about 1,000 to 1,600 cu m (1,300 to 2,000 cu yd). Shallow-draft dredges are more maneuverable than traditional, large hopper dredges, and can work in wave heights of up to about 1.5 m (5 ft) (Bruun 1993).

(b) Jet pumps and eductors. Jet pumps (also known as eductors, ejectors, or injectors), are hydraulically powered pumps with no moving parts (Figure V-6-62). In a simple jet pump, a stream of high-velocity clear water from a supply pump (the motive flow) is forced through a reduction nozzle to create a high-velocity (low-pressure) jet. Upon exiting the nozzle, the jet entrains the surrounding fluid and forces the mixture through a mixing chamber and diffuser, then through the discharge line. When the nozzle/suction opening is buried in the sand, a sand-water (slurry) mixture is drawn into the discharge line. A conventional dredge pump (booster) downstream of the jet pump can be used to help move the slurry through the discharge pipe. Fluidizers are also typically employed near the suction intake to mobilize the seabed sediment and facilitate uptake.

Typical jet pump capacities range from 75 to 300 cu m/hr (100 to 400 cu yd/hr), and feature suction intakes of 10 to 15 cm (4 to 6 in.), although larger pumps have been produced. Use of jet pumps may be ideal where there is a need for continuous or high-frequency bypassing of mostly modest quantities, littoral transport and/or sediment impoundment occurs over a limited (small) area, there are suitable locations for clear-water intake, the area is mostly free of debris, and the material to be moved is free of consolidated cohesive sediment. Clogging by debris is probably the greatest potential limitation of jet pump systems. Like conventional hydraulic (suction) dredges, jet pumps and their discharge pipelines also risk clogging by sediment, usually by excessive solids. Williams, Clausner, and Neilang (1994) and Clausner et al. (1994) provide additional guidance regarding use of jet pumps for sand bypassing.

Jet pumps can be incorporated to either fixed or mobile sand bypass systems. Examples of the latter include jet pumps mounted upon a shore-based crane derrick, deployed from barges, and hauled about by lines and truck-mounted winches. Unlike jet pumps used in mobile systems, which are generally inherently capable of withdrawal from the seabed, jet pumps used in fixed systems should include a mechanism by which to raise the jet pump for purposes of maintenance and/or to remove debris that collects in the suction crater and clogs the intake.

(c) Submersible pumps. Submersible pumps are electrically or hydraulically driven pumps lowered directly into the material to be transferred (Figure V-6-63). In addition to the agitating action of the impeller, submersible pumps can be fitted with jetting rings and/or cutterheads to increase sand flow in compacted material. Most pumps are relatively small (order of 1 m) and weigh between 100 to 1,000 kg (220 to 2,200 lb). Because of their small size, submersible pumps can be deployed with a minimum of support equipment. Performance is comparable to jet pumps, with potential capacities of 40 to 320 cu m/hr (50 to 400 cu yd/hr) in fine to medium sand. Submersible pumps often require a booster pump for discharge distances of greater than about 600 m (2,000 ft). (EM 1110-2-1616). Submersible pumps offer the potential to pump material at higher solids contents than jet pumps or conventional dredges, and require neither a clear water intake, supply pump nor supply lines. On the other hand,

Figure V-6-61. Hopper dredge *McFarland* at Brunswick Harbor entrance, Georgia. Lightly colored sandy sediment (right-side intake) is mixed with dark colored silt and clay (left-side intake) during dredging

the degree to which debris cloggage and rapid wear of the impellers will impede their use is uncertain. Wide prototype experience with submersible pumps for purposes of inlet sand bypassing is limited. Like jet pumps and eductors, submersible pumps are potentially appropriate for either fixed or mobile bypassing systems. The risk of clogging the discharge line is fairly high with submersible pumps due to the high solids-content slurries they are capable of producing. The Punaise is a submersible pump developed

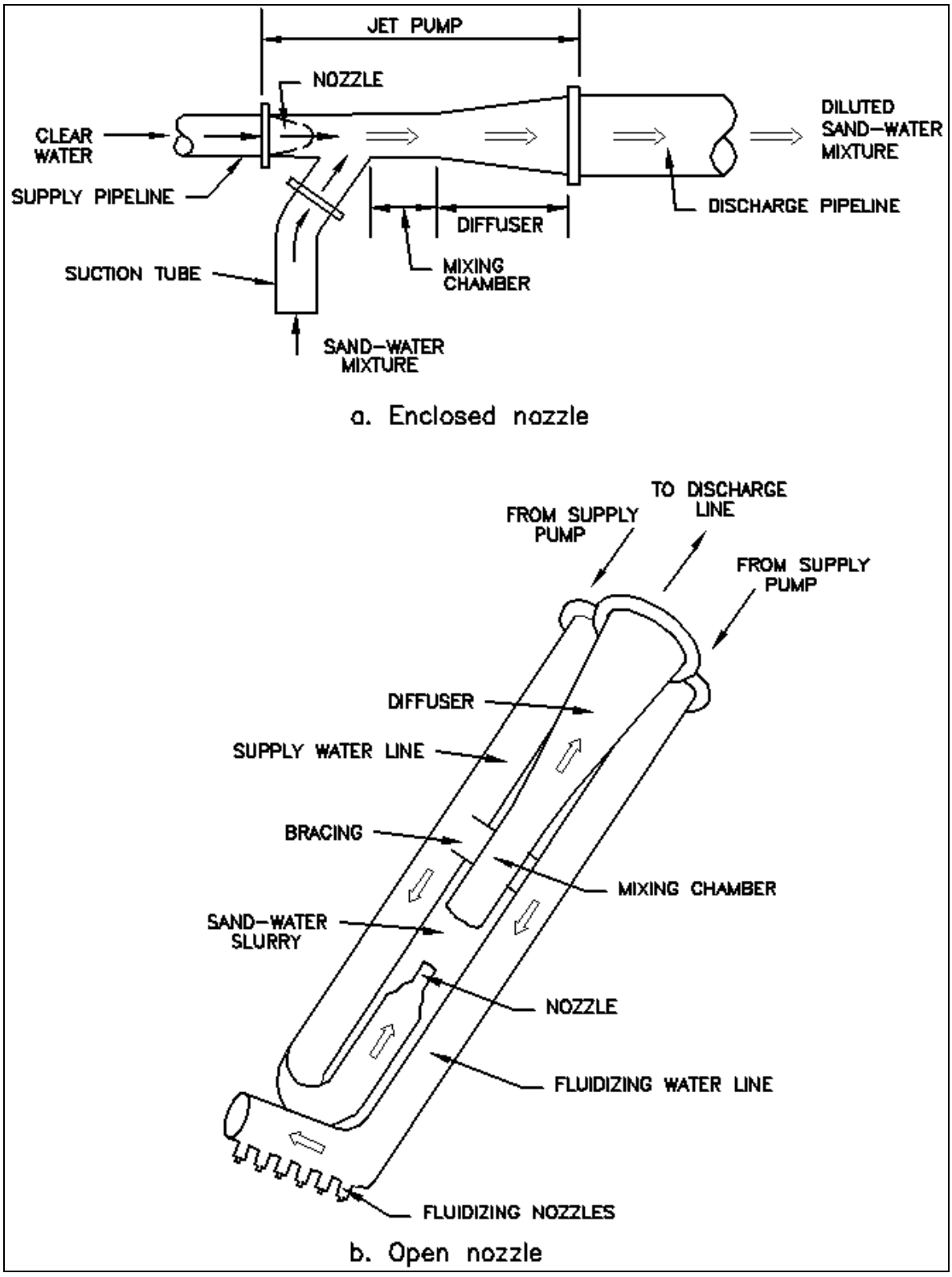

Figure V-6-62. Center-drive jet pumps (educators): (a) enclosed nozzle, (b) open nozzle (from EM 1110-2-1616)

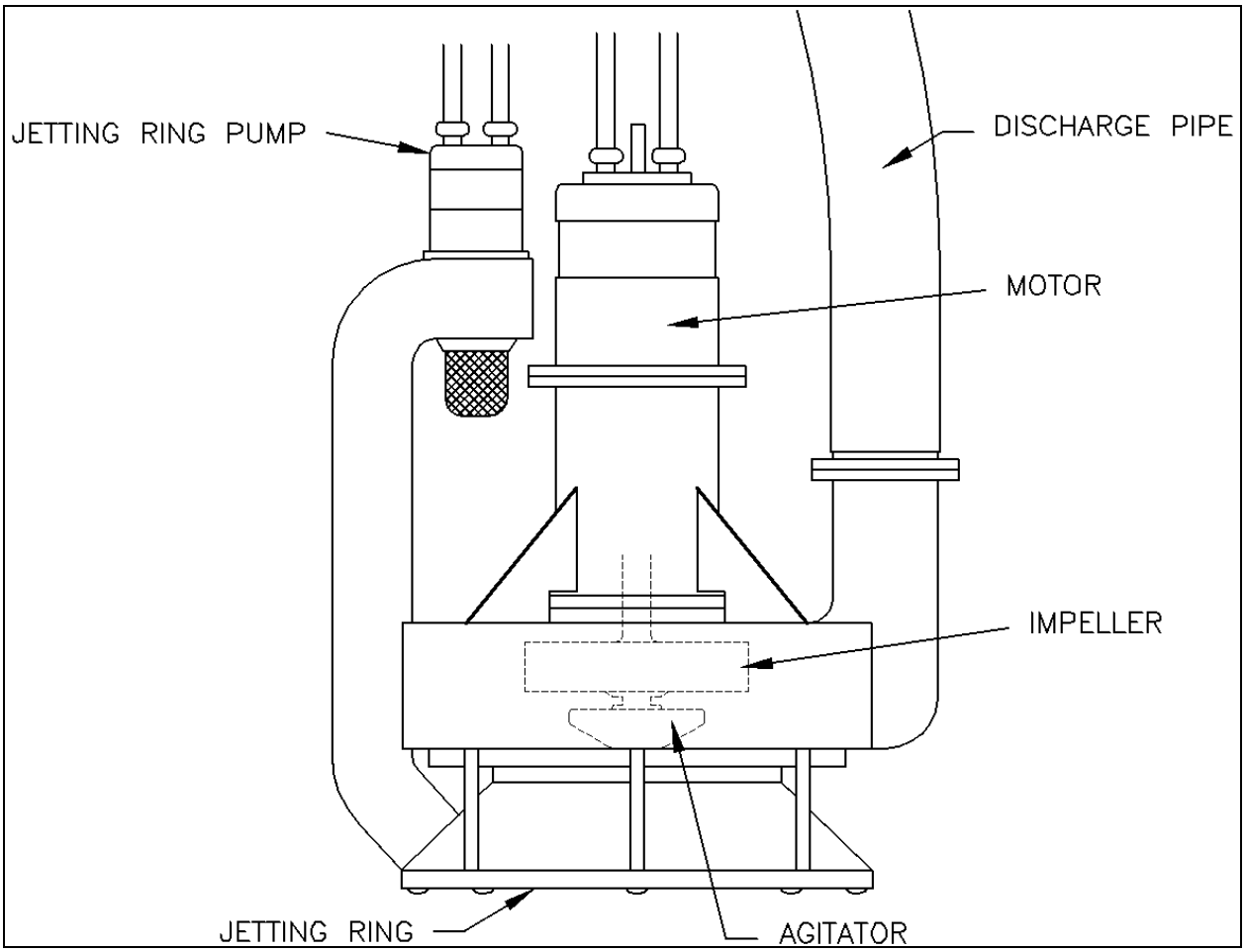

Figure V-6-63. Typical submersible pump (from EM 1110-2-1616)

by the Dutch for pit-dredging of the seabed (Figure V-6-64). Through the use of remotely operated flotation cells, it is designed to be both self-burying and self-emergent. The pump head digs a crater within the seabed and relies upon sediment to be gravity-driven down the crater slopes toward the pump. It is connected to shore or barge by a flexible pipeline (Brouwer, van Berk, and Visser 1992).

(d) Fluidizers. Fluidizers can be used in conjunction with any of the previously mentioned dredging systems to increase the mobility of the seabed sediments, and potentially increase the uptake and production rate of the bypass system (Figure V-6-65). Fluidizers inject clear water near or within the seabed in the vicinity of the suction intake. The fluidizer consists of one or more single jets directed at or around the intake; or, a manifold (a pipe with holes) that slopes downward toward the suction intake. In the former case, their use is intended to agitate, loosen and/or suspend the seabed sediments to facilitate their uptake. In the latter case, the clear-water flow from the fluidizer pipes is intended to mobilize the seabed sediments along each pipe and to induce a gravity flow toward the suction intake. In this way, fluidizers can increase the effective size of the suction crater. The practical benefits of fluidizers mounted directly at the suction intake is well established. On the other hand, long-term prototype experience with

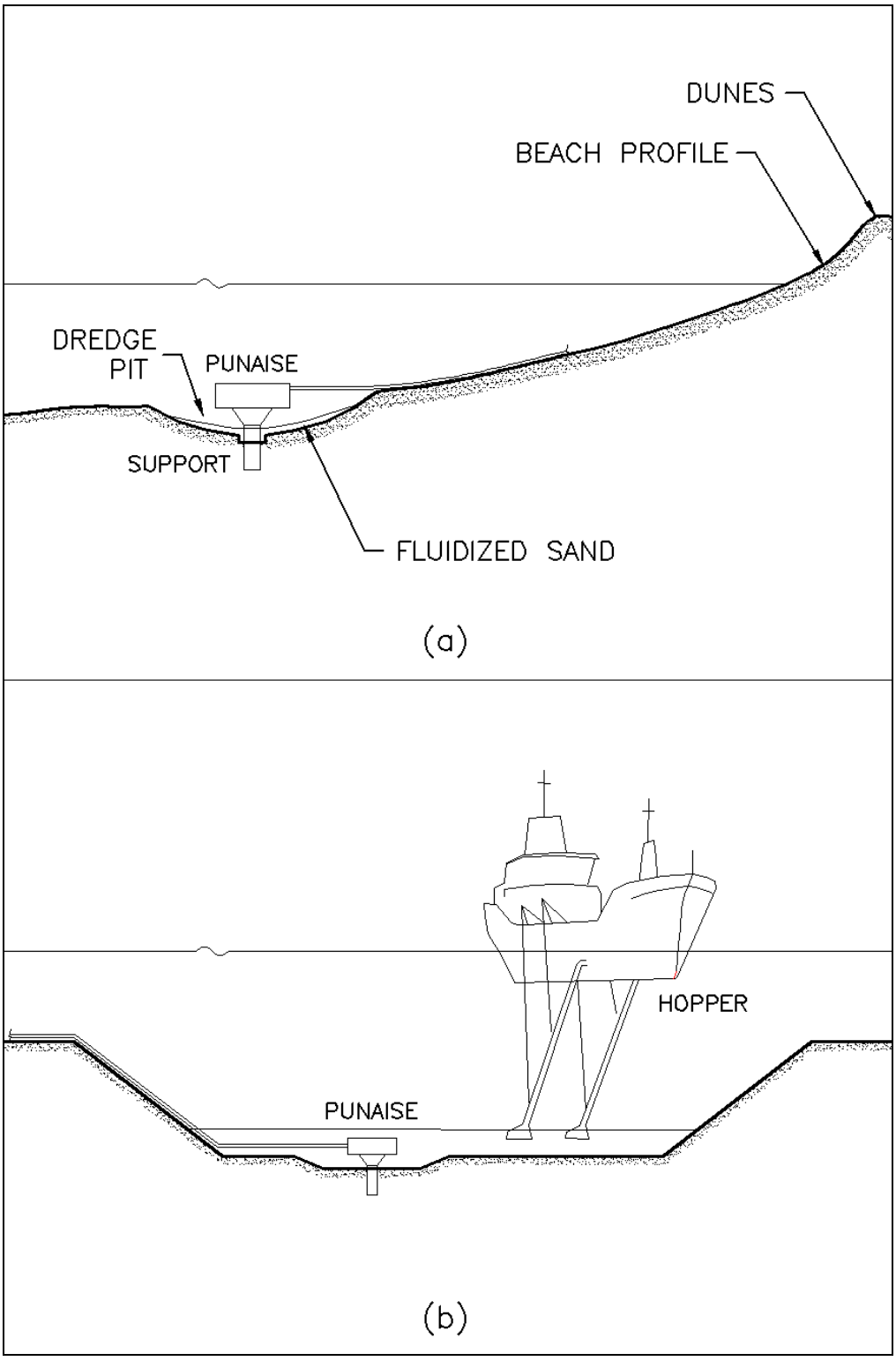

Figure V-6-64. Examples of the Punaise dredging system: (a) in the surf zone of a sandy coast, and (b) in a harbor with a trailing suction hopper dredge (after Brouwer, van Berk, and Visser 1992)

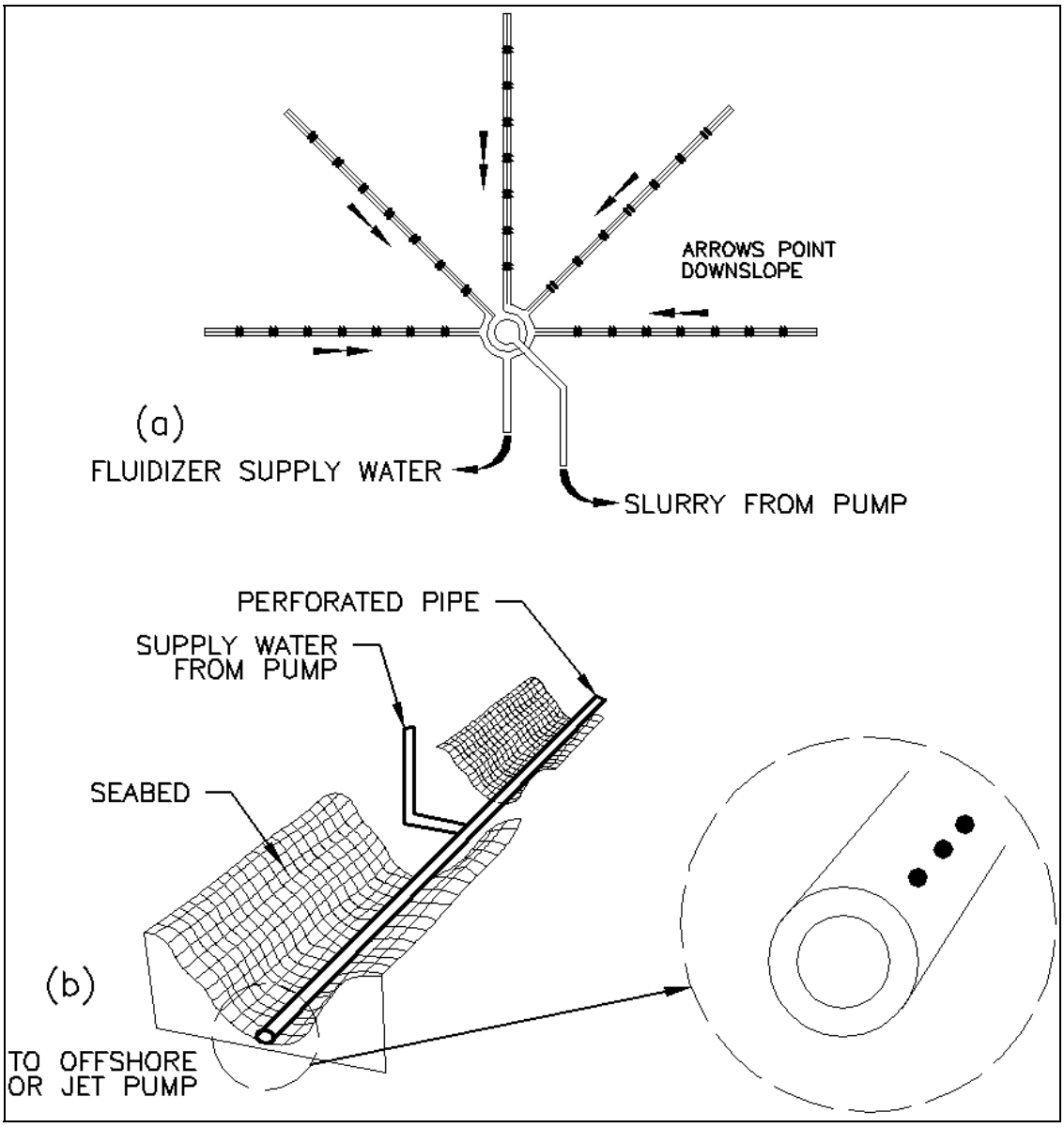

Figure V-6-65. Example of fluidizers: (a) multiple-pipe, manifold-type (planform view), and (b) single-pipe (seabed view). Adapted from EM 1110-2-1616)

manifold-type, seabed-imbedded fluidizers is limited; and there are problems regarding clogging of the fluidizer pipes (Bisher and West 1993). Practical guidance for the use of fluidizers for sand management is presented in Weisman, Lennon, and Clausner (1992, 1996). Methods to minimize clogging of manifold-type fluidizers can also be developed through reference to standard sewage treatment (aeration) equipment, where aerating manifolds, similar in dimension to fluidizers, consist of perforated pipes covered with elastomer membranes. Typical design values for fluidizer pipes include 1/8-in. holes at 2-in. spacing, horizontally opposed, with pipe slopes of about 1:100. To initiate and maintain fluidization, respectively, flow rates of 18 gpm/ft and 11 gpm are indicated (EM 1110-2-1616).

(5) Equipment for discharge. Equipment available for the transport and discharge of the sediment include the following classes.

(a) Hydraulic (pipeline) discharge. For modest transport distances (usually less than 8 km (5 miles), depending upon pump size and capacity), direct hydraulic transfer by fixed, temporary, floating, or submerged pipeline can be used. Sediment recovered by hydraulic means (dredge, jet pump, submersible pump, etc.) can be directly transferred from the intake to the discharge by pipeline, although booster pumps may be necessary en route. Sediment recovered by mechanical means, or otherwise stored in an upland stockpile, barge or scow, can be placed in a hopper, fluidized with clear water, and pumped through a pipeline to the discharge point.

(b) Mechanical, land-based discharge. Sediment recovered by hydraulic or mechanical means can be rehandled by truck transport, assuming that adequate roads and beach access locations are available. Because of its potential impact to roadways, traffic, safety, and noise pollution, this approach is generally suitable only for infrequent operations involving modest quanitites of material (e.g., less than 100,000 cu m (130,000 cu yd)); and typically, should be considered as a method of last resort.

(c) Hopper dredges, barges and scows. Hopper dredges, barges and scows are either closed-hull (also called fixed hull) or open-hull (also called split-hull, bottom-dump, doored, etc.). Closed-hull means that the hopper, barge, or scow can be loaded and emptied only from the top (Figure V-6-66a). Open-hull means that the hopper, barge, or scow can be opened from the bottom, by splitting the hull, opening trap doors on the bottom, or similar means, in order to drop the sediment to the seabed (Figure V-6-66b,c). Sediment recovered in closed-hull vessels must be pumped out or mechanically transferred (rehandled) for either nearshore or beach disposal. Sediment recovered in open-hull vessels can be dropped directly to the seafloor in water depths that accomodate the vessels' draft (bottom-dumping), or discharged to the beach or shallow waters by pump-out or mechanical transfer. Bottom dumping includes nearshore (berm) disposal, discussed in the following paragraphs. In pump-out systems, the sediment is fluidized by clear water and pumped from the vessel via pipeline. For beach disposal, the pipeline (and requisite boosters) are typically fixed, and the hopper/barge/scow ties up to the pipeline's seaward end to discharge its load (Figure V-6-66d). For open-coast pump-out, the pipeline is temporarily secured at the site. Alternately, for pump-out from protected waters, such as within an inlet entrance, harbor or bay, the pipeline might be permanently established (Figure V-6-66e).

(d) Offloaders and rainbow dredges. Offloaders are hydraulic (pump and pipeline) or mechanical (belt-conveyor) systems integral to the hopper, barge, or scow, that are capable of transferring the sediment to the nearshore or beach. Offloader systems vary widely by capacity and mechanism, and can often be customized for a particular application. Up-to-date information regarding such systems is available from the dredging industry, industry consultants and trade magazine (e.g., WODCON). Rainbow dredge discharge (also called over-the-bow discharge) is a hydraulic offloading system whereby a shallow-water hopper dredge offloads sediment by a bow-mounted pipeline that discharges a jet of slurry in an arc toward the shoreline (Bruun and Willekes 1992). (See Figure V-6-66f.) This theoretically enables placement in very shallow depths without need for pipeline or booster placement, but requires that the vessel can maneuver within 50 to 100 m (160 to 330 ft) of the desired placement area. The discharge distance can be theoretically extended with pontoon-floated pipeline deployed from the vessel's bow. To date, typically mild beach slopes combined with relatively deep drafts of existing U.S. hopper dredges greatly limited the application of this method in the United States.

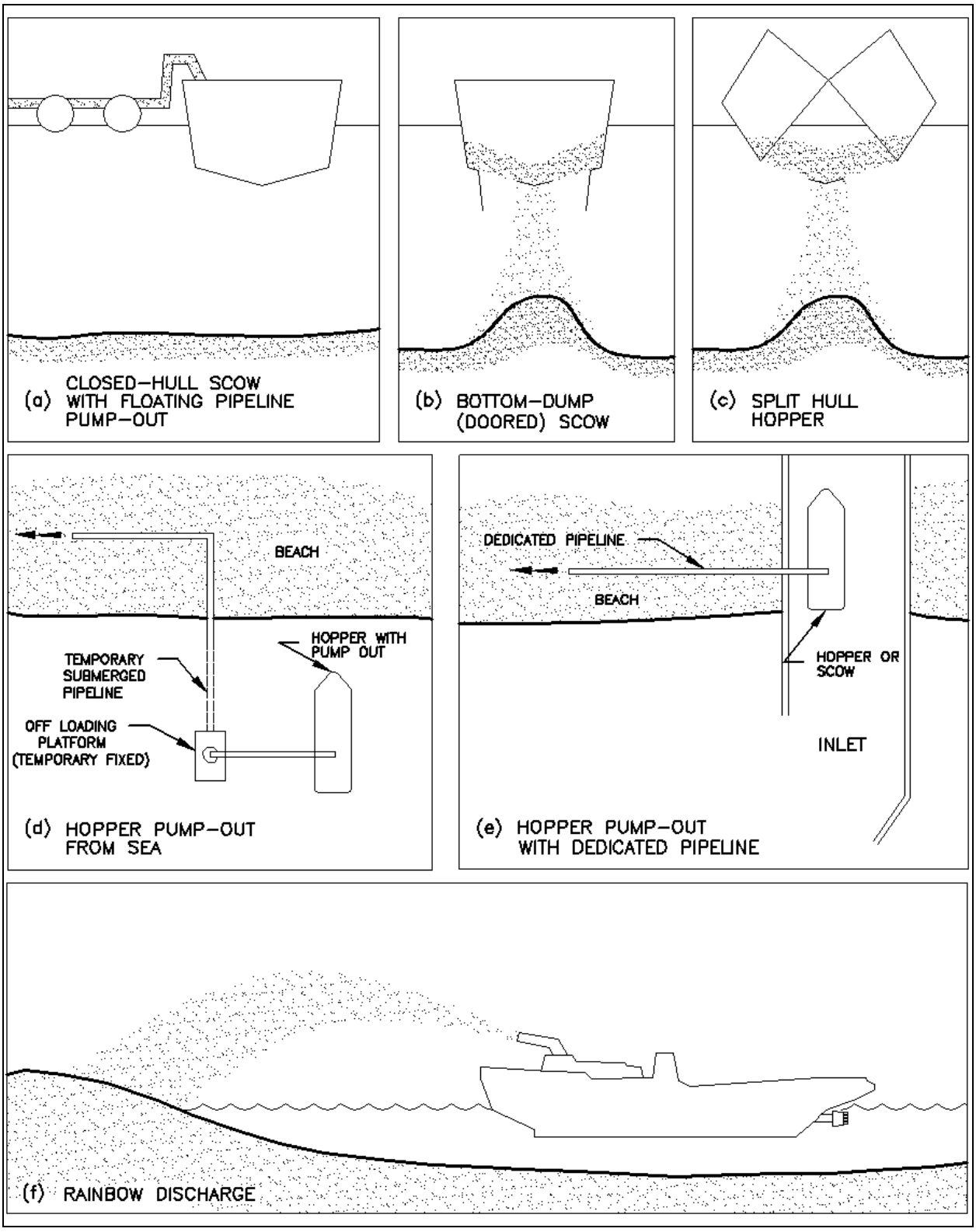

Figure V-6-66. Examples of hopper dredge and scow discharge methods

(e) Hydrocyclones. A hydrocyclone separates coarse- and fine-grained particles within a slurry (Figure V-6-67). It has no moving parts, but instead, uses centrifugal force. The sediment-water slurry is pumped from the dredge or hopper into the hydrocyclone so as to create a vortex within. As the slurry spins within the hydrocyclone chamber, liquid and smaller-grained (lighter) particles migrate toward the inner, air core of the vortex and exit vertically upward as the overflow. Coarser-grained (heavier) particles crowd to the outer wall and exit at the bottom of the chamber as the underflow. Typical operating capacities of a single hydrocyclone are summarized in Table V-6-13. Potential applications of the hydrocyclone in inlet sediment management is to isolate coarser-grained, beach-compatible sediment from unsuitable sediments (silt and clay) dredged during maintenance or expansion of waterways. While widely applied in mining, their protoype use in coastal engineering is, thus far, mostly untested. In practice, their relatively modest capacities reasonably require the use of multiple hydrocyclones, connected in parallel. Limitations on operating pressures usually require use of a gravity-driven slurry supply (as opposed to direct connection to a dredge pump).

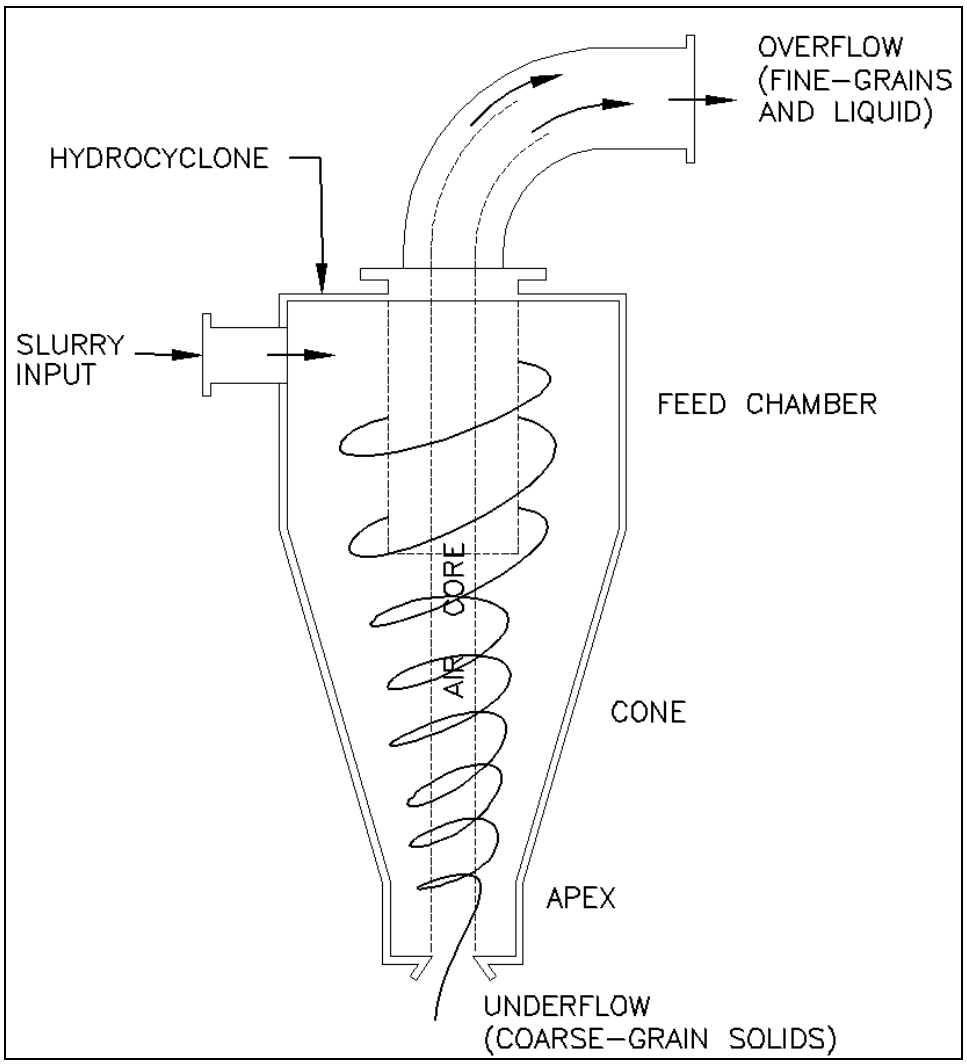

Figure V-6-67. Schematic of a typical hydrocyclone

Table V-6-16
Typical Hydrocyclone Capacities*

Size (in.)	Capacity (gpm)	Operating Pressure (lb/sq in.)	Separation
3	5 - 35	10 - 70	10 to 40 micron
4	20 - 90	10 - 60	10 to 40 micron
6	40 - 200	10 - 50	15 to 40 micron
8	90 - 300	5 - 40	20 to 44 micron
12	200 - 800	5 - 30	30 to 44 micron
18	300 - 1500	5 - 26	200 to 325 mesh
24	800 - 2400	5 - 25	150 to 250 mesh
30	800 - 3500	5 - 25	100 to 150 mesh

* Actual values depend upon suspended ratio and specific gravity of solids in slurry feed, among other factors. Data from Met Pro Refrax lined cyclones; Met Pro Supply, Inc., Bartow, Florida.

c. Sediment traps, deposition basins, and inlet sediment sources.

(1) Introduction. Sediment for bypassing and/or backpassing must be intercepted or temporarily stored to facilitate its extraction and subsequent transfer. Natural sediment traps include the ebb and flood tidal shoals, jetty-adjacent impoundment fillets, and inlet-interior spits. These traps can be augmented or created artificially through the construction of weir jetties, breakwaters, and deposition basins. Such artificial sand traps, if constructed properly and maintained frequently, localize the deposition of drift material and allow a more efficient dredging and/or bypassing operation to be planned. Deposition basins (or sediment traps) are located in regions where the wave climate is mild and the working environment is well suited for dredge or pumping operations; and, where the deposited drift is less likely to interfere with navigation (through shoaling or during dredging) or to be dispersed elsewhere within the inlet. Improperly constructed or maintained traps, on the other hand, can accelerate the inlet's sink effect upon the littoral transport. Sediment can be intercepted interior or exterior to the inlet. Interior traps include the flood shoals, channels, spits, and deposition basins within the jetties. Exterior traps include updrift impoundment fillets, the ebb tidal shoal; and, deposition basins, pumps, dredges, etc. constructed or operated on the outside (beach side) of the jetties. The decision of whether to use interior or exterior traps varies with each inlet; particularly, the size and morphology of the inlet entrance. The design capacity of a deposition basin or bypassing system is described in Part V-6-6.

(2) Weirs and weir jetties. A weir sand-bypassing system is typified by a low section of the updrift jetty (a weir jetty), or a low section of a similar structure built updrift of the updrift jetty (a sand weir or weir groin). A deposition basin, or sand trap, is located downdrift of the weir, from which sand is periodically excavated and then backpassed or bypassed. For wide inlets, the weir and deposition basin can be integral to the jetty and interior to the inlet (Figure V-6-68a). For narrower inlets, at which the deposition basin would interfere with navigation, the weir and deposition basin are located exterior to the inlet (Figure V-6-68b). The purpose of the weir is to: define a restricted area (the trap) into which sediment is transported and held until extracted by dredging or pumping, keep the trap area and sediment accumulation separated from the navigation channel, and ensure that the trap area is protected from waves to facilitate dredging and pumping. The weir also allows flood currents to enter the inlet during rising tide with subsequent channeling of the ebb current during falling tide. While this is intended to improve tidal flushing of the inlet channel, it likewise augments the inlet's sink effect upon the littoral system. That is, additional sediment is swept into the inlet from the adjacent shorelines during flood flow, and subsequently jetted seaward during ebb flow.

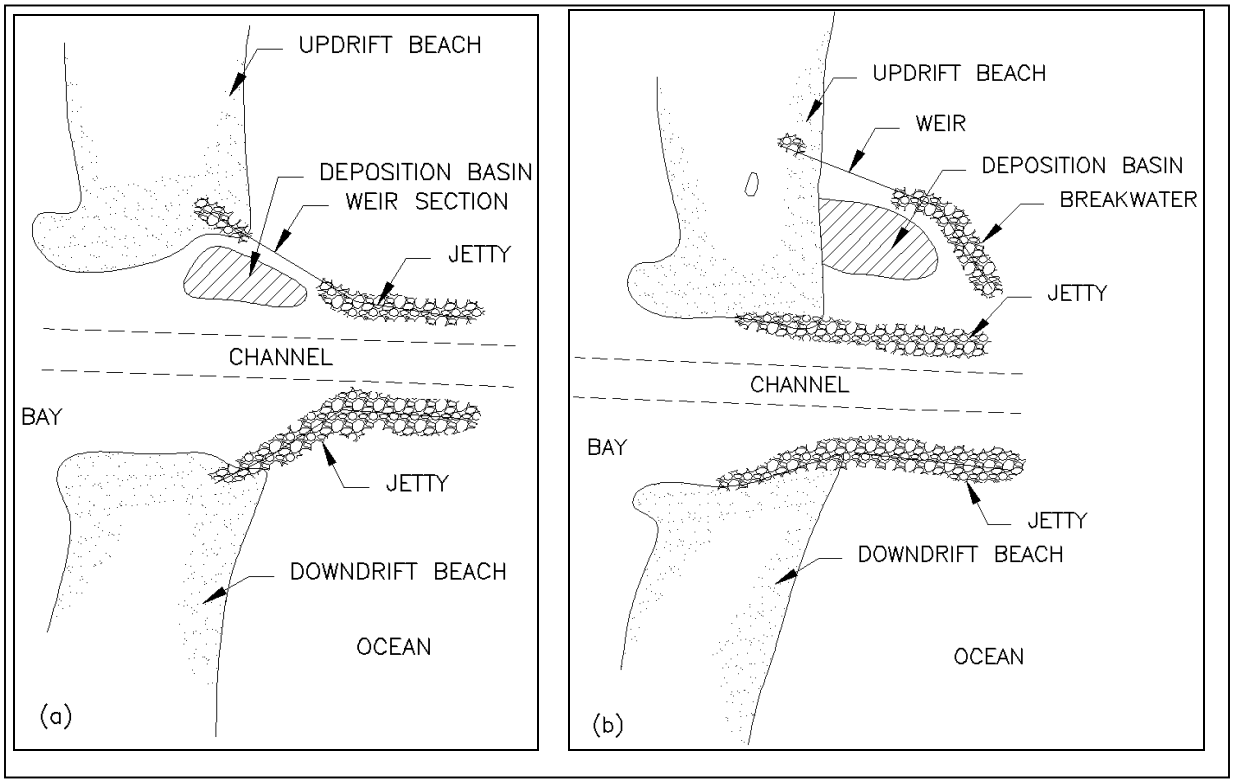

Figure V-6-68. Weir jetties, weir-groins, and weir deposition basins (a) interior to inlet, and (b) exterior to inlet

(a) Weggel (1981) and Seabergh (1983) describe important, specific design principles for weir jetty systems. In general, the weir is designed to allow a quantity of sediment ranging between the total incident sediment transport from the updrift direction and the net littoral drift to deposit in a semiprotected basin in which a dredge or other mechanical byapssing system can operate. Early weirs were constructed with vertical, smooth walls that often included adjustable-height panels. These materials are no longer recommended because of the associated wave reflection and the practical difficulty in adjusting the panels' height. Rubble-mound structures are preferred for weir sections.

(b) Weggel (1981) recommends that weir elevations be set near mean low water for tide ranges less than 0.6 m (2 ft); and, at mean tide level for tide ranges of 0.6 to 1.5 m (2 to 5 ft). Weir performance is poor for greater tide ranges, and weirs are not recommended for tide ranges greater than about 3.6 m (12 ft). Seabergh (1983) describes the effect of lower weir elevations as a function of an inlet's Keulegan "K" repletion coefficient. Weir sections lower than the adjacent beach induce inlet-directed transport, at all stages of the tide, because of the hydaulic gradient that is developed between the energetic, sandy beach outside of the weir and the less-energetic water inside of the weir. The design elevation of a weir should also consider the desired profile of the updrift beach, as the weir will more or less act as a template for that beach.

(c) The majority of sand transported over weirs occurs in the narrow region where the weir, beach, and waterline intersect (Weggel and Vitale 1981; Seabergh 1983). A much smaller portion of the drift moves over the weir as suspended material near the breaker zone. Current guidance is to establish the seaward end of the weir seaward of the normal breaker line (or offshore bars, if applicable), at low tide. This may, however, result in an exceptionally long weir that unintentionally accelerates inlet-directed transport from the updrfit beach via flood currents over the weir. The landward end of the weir is

established at the point where the updrift profile is to be approximately maintained. The landward weir profile should follow the updrift beach profile estimated from existing profiles measured far enough away so as not to be influenced by the inlet. Early weir lengths often extended longer than 350 m (1,000 ft) to account for the possibility of "sanding in" of shorter sectons during severe storms or elevated transport. Weggel (1981) reports instead that this has not occurred and, in fact, the shoreline of the updrfit beach has not typically extended beyond the landward section of the weir. Weir sections which are inappropriately long or low or close to the shoreline can induce anomalously high transport from the updrift beach toward the inlet resulting in net erosion of the updrift shoreline and accelerated shoaling rates and overflow of the deposition basin.

(d) Weir orientation with respect to the updrift shoreline and navigation channel is often determined by individual inlet characteristics and land availability. Weir trapping efficiency is generally independent of the weir orientation relative to the updrift shoreline. From model tests, Seabergh (1983) reported that updrift storage was greatest for weir angles, θ_w, of 90 deg (perpendicular to shore); became progressively less for angles of 60 and 45 deg to shore; and was least for an angle of 30 deg to shore. Likewise, offshore losses were least for 90 deg and greatest for 30 deg. The capability for the updrift storage to move back up the beach during drift reversals was greatest for the 30-deg angle and least for the 90-deg angle. Seabergh's (1983) results suggest that the ideal orientation is a weir section angled 30 to 60 deg from the shoreline, with the seaward ends of the jetties parallel to one another (Figure V-6-68a). It is recommended that the largest (widest and/or deepest) part of the deposition basin be landward of the weir-shoreline connection.

(e) Design of storage capacity is addressed in Part V-6-5, and in Weggel (1981). Likewise, methods to compute the flood tidal flow and wave transmission across the weir are specifically presented in Weggel (1981). Case histories and additional information on weir jetties are presented in Rayner and Magnuson (1966); Snetzer (1969); Magnuson (1967); Purpura (1974, 1977); Parker (1979); Weggel and Vitale (1981), among others. Coastal Tech (1997) describes measured and numerically-modeled flow over a low-weir section at St. Lucie Inlet, Florida.

(3) Sediment traps. Specific areas of an inlet system can be designated, designed, or dredged to serve as deposition basins (sediment traps or sand traps), with or without weir jetties. Examples are illustrated in Figure V-6-69. These "traps" serve as temporary repositories of sediment that enter the inlet. They should be located in areas where natural wave and current processes will readily transport sediment into the trap (but not out of it), in semiprotected waters suitable for periodic operation of a dredge or bypass pump, and so as not to impede navigation. Traps can be located on the downdrift side of a weir section (as described previously), or at other locations where chronic shoaling is observed (e.g., at the seaward ends of jetties, at interior spits, across the flood shoals, etc.), or at locations where shoaling is induced by the construction of breakwaters or other structures. Traps can be located within the inlet (interior traps) or outside the inlet jetties (exterior traps).

(a) Sediment traps can be an overdredged area (or dredge pit) into which sediment is deposited by waves and currents (Figure V-6-69a). Once sediment fills the trap to near the level of the adjacent seabed or channel, the trap must be dredged so as to preclude loss of additional sediment that enters the inlet. The seaward edge of flood shoals, and the interior seabed adjacent to the jetties shoreward ends, are typical locations of overdredged traps. A less typical example is an updrift, exterior trap (also called a nearshore borrow area), which is a pit dredged along the shoreline updrift of an inlet (Figure V-6-69b).

(b) Sediment traps can also be created by breakwaters located near the inlet entrance. Sediment is deposited in the lee of the breakwater and is removed by a dredge or pumps working in the protected waters of the breakwater (Figure V-6-68c).

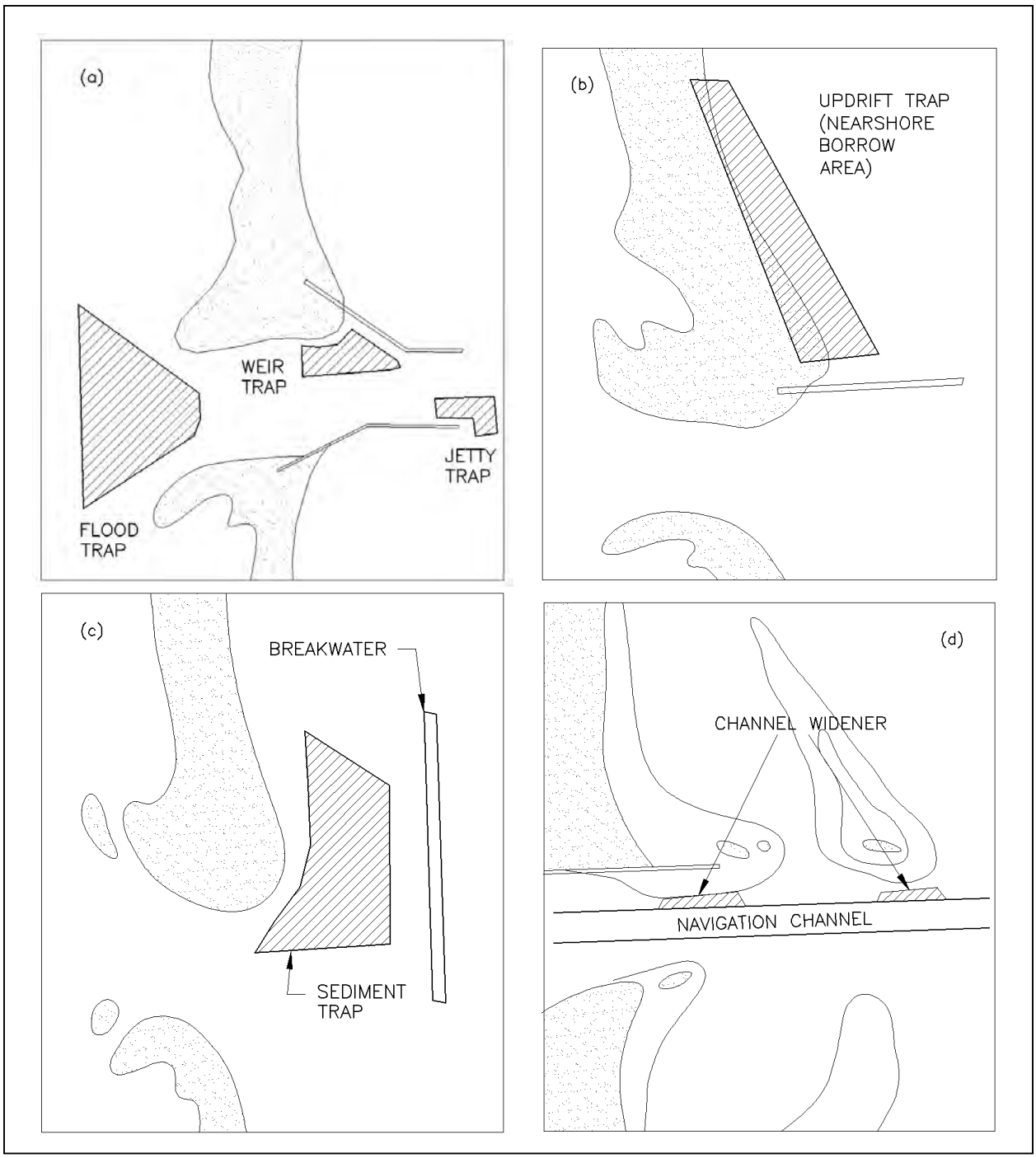

Figure V-6-69. Inlet sediment traps

(4) Channel wideners. The navigation channel can be widened along those areas where chronic shoaling by littoral drift is experienced (Figure V-6-69d). This variation of the sediment trap concept can also be termed advance maintenance, which presents possibilities for funding through Operations and Maintenance (O&M) monies. Channel wideners serve four purposes: they decrease the frequency of requisite maintenance dredging (which, in turn, reduces dredging costs by reducing the number of dredge

mobilizations); they improve the reliability of safe navigation; they provide a designated basin into which littoral sediment can deposit and be less likely to mix with non-beach-compatible sediments of the channel; and they increase the quantity of littoral sediments available for a given dredge job (thereby improving the economic viability of more expensive, beach disposal dredging practices). Methods to estimate the degree to which channel modifications (widening, deepening, etc.) will affect shoaling rates are approximate, at best. Some approaches are presented in O'Conner and Lean (1977); Lean (1980); Trawle (1981); and Galvin (1982). Application of sophisticated, three-dimensional numerical models which estimate sediment transport and shoaling rates from wave, tide and current effects are described in Vemulakonda et al. (1988).

(5) Flood shoals. Interior (flood) shoals present opportunities as a sand source for inlet-adjacent beach nourishment. Practically, however, their use may be limited by the shoal sediments' grain size (typically finer than the native beach sediments) and by the presence of environmentally sensitive resources such as seagrass beds, shellfish beds, or the presence of adjacent aquatic preserves in which dredge-related turbidity is restricted. As in the investigation of all sand borrow sources, core-borings of the flood shoals are critical to define the beach-compatibility and vertical extent of the sediment. Many flood shoals are thin, widespread deposits that overlay lagoonal clays and silts unsuitable for beach placement. The ability of conventional dredge equipment to excavate thin layers of material (i.e., less than 1.3 to 2 m (4 to 6 ft)) is limited, and may instead require the use of small, suction-dredge or jet-pump equipment. Extensive removal of interior shoals will likely increase the inlet's hydraulic efficiency and can be expected to increase the rate of interior shoaling. This may not be problematic so long as the geometry of the shoal borrow area is designed so as to act as a trap (in which the increased flux of sediment can be captured for bypassing/backpassing); and, is designed so as not to undercut or otherwise draw sand directly from the inlet-adjacent beaches. Increases of inlet hydraulic efficiency may also require examination of the hydrologic and biologic effects of increased encroachment of ocean (flood) waters to interior bays and aquifiers.

(6) Ebb shoals. Inlet ebb shoals likewise present attractive, potential opportunities as sand sources for inlet-adjacent beach nourishment. Like the use of flood shoals, borrowing from the ebb shoal for these purposes can be viewed as mitigation for historical inlet impacts. Such retroactive sand bypassing/backpassing is particularly relevant for those cases in which inlet shoal volumes increased as a result of the inlet modifications' erosional effect upon the adjacent beaches.

(a) For those inlets where natural bypassing occurs quasicontinuously via transport along the ebb shoal, care must be taken so as not to overdredge, sever, or otherwise compromise the ebb shoal's ability to transport sand across the inlet's mouth. Improper borrowing would result in a short-term nourishment of the filled beach, followed by an acceleration of erosion, probably on both sides of the inlet, as the ebb shoal and bypassing bar recovers from the dredging event. In these instances, it may be prudent to limit ebb shoal dredging to the outer (seaward) edge of the plateau (Figure V-6-70a).

(b) For those inlets where natural bypassing occurs episodically through the migration of ebb shoals, spits, and baymouth bars, dredging and downdrift placement may simply speed the inlet's natural processes. This is a desirable outcome in those cases where the downdrift erosion stress is so high that the attendant development cannot withstand the time required for the inlet shoals to migrate naturally. The resulting dredge project usually acts to relocate the channel (which is otherwise compromised or forced downdrift by the migrating shoals), and thus results in at least an initial improvement of the inlet's navigability and hydraulic efficiency (Figure V-6-70b).

(c) The potential effect of ebb shoal bypassing to the wave refraction, current and associated littoral transport patterns along the inlet mouth and adjacent shorelines should be evaluated as part of the borrow

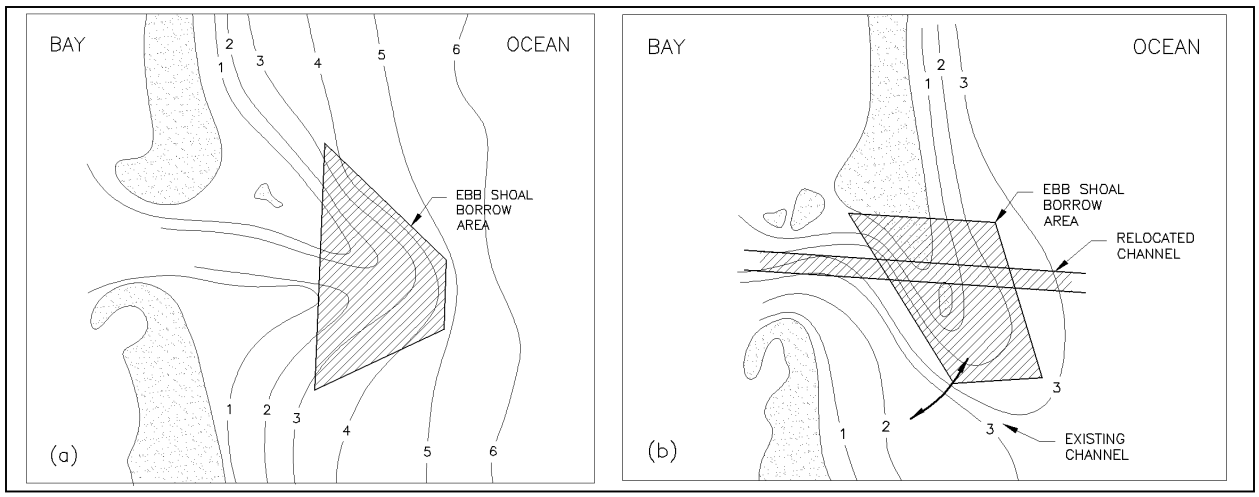

Figure V-6-70. Sediment borrowing from ebb shoal of an inlet

area design. Existing conditions should be compared to simulated post-borrow conditions. It is recommended that the wave height or wave energy density (H or H^2, respectively), be compared at each point across the refraction grid, for various incident wave conditions, to assess the degree to which the borrow activity may locally affect navigation. Likewise, the computed breaking wave energy density and littoral transport potential should be computed at each column of the grid along the adjacent shorelines, for various incident wave conditions, to discern possible changes in the local sediment transport patterns. The approach described in Part V, Chapter 6-2(d), method 4, is applicable in this regard. Like flood shoal borrowing, extensive removal of the ebb shoal may be expected to increase the trapping (shoaling) behavior and hydraulic efficiency of the inlet. Methods to estimate shoaling behavior are similar to those described for channel widening. Methods to examine inlet hydraulic efficiency are described in Part II- 6. Assessment of changes in tidal currents and associated sediment transport patterns is briefly described in Part II-7, and Part II-9.

(d) In the design of projects where ebb shoal dredging may result in channel relocation, it is essential to first understand the natural shoaling and channel-migration cycles of the inlet. Examinations of time-sequences of aerial photographs and bathymetric surveys, supplemented by anecdotal accounts, are valuable means by which to predict the degree to which the dredge project will advance, stagnate, or retard the inlet's natural patterns of sediment transport.

d. Bypass system capacity. Sizing of the requisite pumping equipment and geometry, sediment traps, and weir sections is a function of the gross bypassing requirements and the frequency with which bypassing will be undertaken. Sizing should also consider the potential effect of seasonal fluctuations and storms. Methods to determine the requisite bypass/backpass quantities are described in Part V-6-4 and Part V-6-5.

(1) Dredges, jet pumps, and other pumps. Specific guidance for the selection, layout and design of jet-pump systems is presented in Richardson and McNair (1981) and in EM 1110-2-1616. Introductions to the sizing and selection of conventional dredge equipment are presented in McKnight (1966); Bruun (1981); Herbich (1975, 2000); Herbich and Snider (1969); Richardson (1976, 1990); Huston (1970, 1986); and Turner (1984). Technical consultation is advised early in the design process. The Corps of Engineers' Marine Design Center, as well as industry consultants, are available in this regard.

(2) Excavation craters. Craters created by pumps or fixed dredge systems will remain empty until significant wave activity causes sufficient transport to fill them. Experience demonstrates that those craters located closest to shore fill fastest. For the purposes of intercepting the littoral drift, the apparent dominance of transport at the shoreline and in the swash zone is illustrated by the distribution of pumping hours from the Nerang River fixed bypassing plant in Queensland, Australia (Figure V-6-71). The theoretical yield volume V_C of a typical dredge crater, excluding use of fluidizers, can be estimated as

$$V_C = L_c d_c \left(b + \frac{d_c}{m} \right) + \pi\, d_c \left(\frac{b^2}{4} + \frac{f\, d_c}{2m} + \frac{d_c^2}{3m^2} \right) \tag{V-6-72}$$

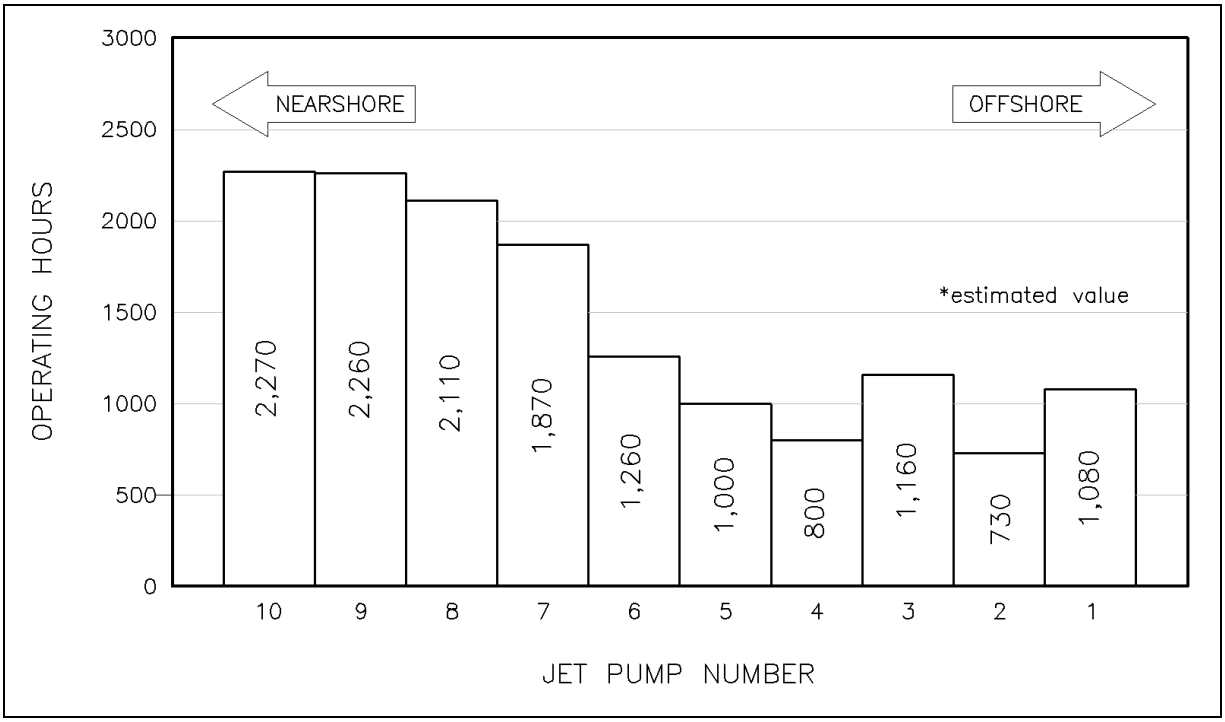

Figure V-6-71. Jet pump operating hours from May 1986 to February 1988; Nerang River bypassing plant; Queensland, Australia (data from Clausner 1988; figure adapted from Bodge 1993)

where L_c is the length (or arc-length) of the crater, d_c is the crater depth below the ambient seabed level, b is the width of the crater at the bottom, and m is the crater side slope as defined in Figure V-6-72. For medium to fine-grained beach sand, and for crater depths of about 1.5 to 2.75 m (5 to 9 ft), m is about 0.5, and b is between 6 and 9 times the diameter of the suction intake. For a circular crater (i.e., that made by a fixed pump), $L_c = 0$.

(3) Productivity. A single jet pump or eductor is typically capable of transferring between 50 and 250 cu m/hr when operating; or, between 50,000 and 150,000 cu m/year. However, average hourly and annual productivity is greatly influenced by mechanical/pipeline limitations, shoaling behavior at the crater, physical mobility of the intake(s), interference by marine debris, etc. considerations. A system's net productivity at any given site is therefore highly dependent upon the physical conditions specific to the site. Example considerations are described in the following paragraphs. See also Richardson and McNair (1981), EM 1110-2-1616, and Clausner et al. (1994).

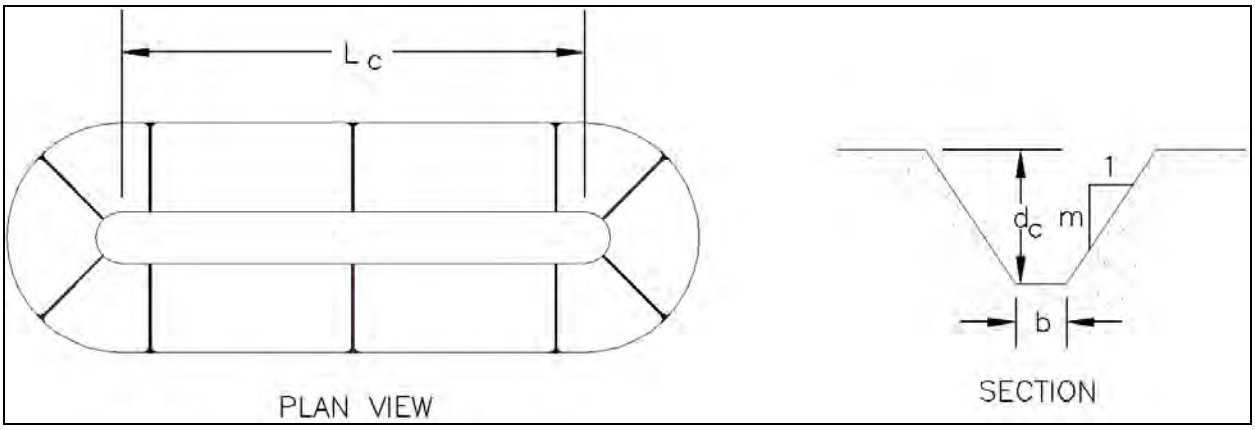

Figure V-6-72. Geometry of a dredge crater (definition sketch)

(a) A bypassing system's ultimate productivity is a function not only of the pumps' mechanical capacity, but also of the time required for the dredged crater(s) to refill. For example, Bodge (1993) observed that the bypass capacity of the fixed sand transfer plant at South Lake Worth Inlet, Florida, is more typically limited by the crater's shoaling rate than by the existing plant's capacity. The time required to excavate the crater, if full, is

$$T_E = V_C / (E - S) \tag{V-6-73}$$

where S is the average volumetric shoaling rate of the crater (volume/time) during and after a given dredging event, and E is the net volumetric capacity of the pump (volume/time) after consideration of all mechanical limitations, shutdown times, etc. The rate at which crater refills, S, will exceed the effective bypass capacity of the plant, E, if

$$S > \frac{1}{2} E \left[1 + \sqrt{1 - \frac{4 V_C}{E T_B}} \right] \tag{V-6-74}$$

where T_B is the elapsed time between the start of subsequent dredging events, For example, for daily operation, T_B = 24 hr. The (+) root implies that pumping continues throughout the interval T_B until the crater is completely emptied. The (-) root implies that pumping is discontinued the first time that the crater is completely emptied during the interval T_B. Undefined values of the radical (i.e., 4 $V_C > E\ T_B$) indicate that the system is limited by the pump's volumetric capacity over the interval T_B, not by the crater volume.

(b) The distribution of crater shoaling rates can be approximated by a Rayleigh distribution centered about the site's mean shoaling rate – at least for the lower 90 percent of the distribution (Bodge 1993). (The Rayleigh distribution likely underestimates the occurrence of the largest 10 percent of the actual shoaling events.) The mean shoaling rate at the inlet can be approximated from existing bypass plant data (i.e., the average value of the volume bypassed divided by the time preceding each bypass event); or, approximated as the gross drift rate at the crater location minus the rate of natural (or other) bypassing around the crater's location. Values for the latter can be estimated from the inlet's sediment budget.

(c) The percentage of time for which Equation V-6-74 holds true, as derived from the distribution of the site's shoaling rates, indicates the percentage of time for which the plant's configuration is limited by mechanical capacity; i.e., that percentage of operating time for which the crater has completely refilled prior to the next start-up of the bypass plant. Alternately stated, the percentage of time for which Equation V-6-74 is false indicates the percentage of operating time for which the crater has not yet re-filled by the time the bypass plant is ready to start up again. For those times, increases in mechanical capacity of the plant are of no net value to overall productivity.

(d) Where sand transfer is limited by crater shoaling rates, net increases in inlet bypassing require that single pumps be moved during the day; or, that multiple pumps be used. Moving a pump implies that the pump assembly is to be physically lifted to another location; or, the pump's intake is mounted on a moveable support (e.g., along a trestle track, from a swinging or articulated boom, etc.) The intent is to increase the crater volume, V_C (precisely, so as to increase b, L_c and/or d_c in Equation V-6-72). It is also noted that the operation of fixed pumps tends to armor the crater's side slopes with coarser material over time, resulting in steeper slopes and smaller crater volumes.

(e) Sediment traps and channel wideners. For the typical case where sediment within a trap is not intended to feed the adjacent shorelines during transport reversals, the capacity of a sediment trap should be sized to accommodate all of the drift incident to that part of the inlet where the trap is located for the entire duration anticipated between bypass events. Accomodation for variations in the annual and/or seasonal transport rates must be made. At a minimum, this should be done by examing the statistical variation of the gross transport rate about the mean, as developed from hindcast wave data. Furthermore, it should not be assumed that deposition within the trap will occur uniformly. That is, accommodation must be made for varying vertical rates of deposition within the trap. Proper use of a sediment trap for effective inlet/harbor sediment management requires that the sediment trap be excavated at or before the time at which it reaches capacity. Accordingly, it is essential that the trap be sized large enough to accommodate periods of elevated transport and/or delays in bypassing operations.

(f) Figure V-6-73 illustrates an example of the temporal fluctuation of bypassing at a fixed sand transfer plant. The plant (South Lake Worth Inlet, Florida) operates whenever there is any sand within the crater and when waves are incident from the north. The record of the plant's bypassing operations is fairly well correlated with the southerly-directed longshore transport rate potential, where the latter was computed from hindcast wave data (Creed 1996).

(g) The ultimate design of a trap's capacity is determined by balancing the decreased cost of bypassing operations associated with larger traps and less frequent equipment mobilization, the increased initial cost of trap construction (if any), the availability of areas within the inlet area(s) in which to create a trap, the uncertainty as to shoaling rates, and in the case of channel wideners and advance nourishment, the decreased costs associated with requisite maintenance dredging to ensure safe navigation. Stochastic methods regarding the latter two issues are presented in Lund (1990).

(4) Weir jetty systems. Weggel (1981) describes the optimum weir-jetty system as one where only the net incident transport ($Q_{NET} = Q_R + Q_L$) enters the deposition basin for ultimate bypassing to the net downdrift beach (see Figure V-6-74). Neglecting local, inlet-induced transport, and assuming net transport directed to the right, the amount of sand carried to the weir from the updrift side is Q_R. An amount of sand equal to (Q_R - Q_{NET}) must be therefore retained in temporary (active) storage on the updrift beach to replace the material trapped by the downdrift jetty and inlet shoals during transport reversals (i.e., an amount equal to Q_L).

EXAMPLE PROBLEM V-6-16

FIND:

The potential net increase in bypassing productivity if a jet pump is changed from a fixed mount to a swinging-boom mount, and/or if the pump's operating schedule is revised.

GIVEN:

An inlet's small, existing 6-in. jet pump bypasses 25,000 cu m/year, operating for about 1,200 hr/year at a fixed location with maximum crater depth of d_c = 2.6 m below the seabed (limited by a clay layer). The plant is operated between 8 a.m. and 5 p.m., each day, as needed, but only when the crater is mostly full. At the beginning of one-quarter of those days for which bypassing is undertaken, the crater has been refilled to capacity overnight after having been mostly excavated the previous day. The proposed system would mount the jet pump at the end of a 5-m-long boom capable of swinging through a horizontal arc of 105 deg.

SOLUTION:

The plant's effective mechanical capacity is:

$$E = (25{,}000 \text{ cu m/year}) / (1{,}200 \text{ hr/year}) = 20.8 \text{ cu m/hr}$$

In SI units, the 6-in. pump diameter is 0.15 m. The crater's base width, b, is six to nine times this diameter, or 0.9 to 1.4 m; for example, if b = 1.2 m. Assume a crater side slope of 1 (vert) : 2 (horiz), or m = 0.5. From Equation V-6-72, and for d_c = 2.6 m and L_c = 0, the crater volume of the existing plant is:

$$V_C = \pi(2.6 \text{ m}) [(1.2 \text{ m})^2 / 4 + (1.2 \text{ m})(2.6 \text{ m}) / (2)(0.5) + (1/3)(2.6 \text{ m} / 0.5)^2) = 102 \text{ cu m}$$

For those events when the crater fills to capacity overnight (from 5 p.m. to 8 a.m., or 15 hr), the crater shoaling rate is at least 102 cu m / 15 hr = 6.8 cu m/hr. From the given data, this represents the 25th percentile of the shoaling rate for those days when bypassing is undertaken. From the Rayleigh distribution (Equation II-1-131), the probability, p, that a value S will exceed some value S_p is:

$$p\ (S > S_p) = \exp\ (-(S_p / S_m)^2)$$

where S_m is the mean value. Taking the natural logarithm of each side and rearranging yields:

$$S_m = [-S_p^2 / \ln\ (p(S_p))]^{1/2}$$

so that

$$S_m = [\ -\ (6.8 \text{ cu m/hr})^2 / \ln\ (0.25)\ ]^{1/2} = 5.8 \text{ cu m/hr}$$

(Continued)

EXAMPLE PROBLEM V-6-16 (Continued)

From Equation V-6-74, assuming that bypassing is undertaken only when the crater is mostly full, the theoretical rate of shoaling which exceeds the existing pump system's capability, based upon no more than 9 hr of operation every 24 hr, is

$$S > (0.5)(20.8 \text{ cu m/hr}) \{ 1 - [1 - (4)(102 \text{ cu m}) / (24 \text{ hr})(20.8 \text{ cu m/hr})]^{1/2} \} = 6.0 \text{ cu m/hr}$$

From Equation V-6-73, this rate of shoaling would require (102 cu m) / (20.8 cu m/hr – 6.0 cu m/hr) = 6.9 hr to excavate the crater. From the Rayleigh distribution, and based upon an assumed mean value of S_m = 5.8 cu m/hr, the probability of shoaling rates exceeding 6.0 cu m/hr is

$$p\,(S > 6.0 \text{ cu m/hr}) = \exp\,(-(6.0 / 5.8)^2) = 0.34 = 34 \text{ percent}$$

Therefore, for operations limited to 9 hr per day, the bypassing quantity could be theoretically increased for 34 percent of the bypassing events by increasing the crater capacity. Note that increases to the pump capacity, E, would not result in a net improvement.

Further, note that the positive (+) root of Equation V-6-74 yields 14.8 cu m/hr. From Equation V-6-73, that rate of shoaling would require (102 cu m) / (20.8 cu m/hr – 14.8 cu m/hr) = 17 hr to excavate the crater. That value exceeds the 9-hr operating window of the plant. On the other hand, if operation beyond 9 hr per day was adopted, the probability of shoaling rates exceeding 14.8 cu m/hr is only

$$p\,(S > 14.8 \text{ cu m/hr}) = \exp\,(-(14.8 / 5.8)^2) = 0.001 = 0.1 \text{ percent}$$

Therefore, adopting bypassing operations beyond the existing 8 a.m. to 5 p.m. window would theoretically increase the bypassing quantity of the existing system without hardware improvements, but only for a small percentage of those days for which bypassing is undertaken.

The proposed hardware improvements (swing-boom) would create an arcuate crater shape of length

$$L_c = (60^o)/(360^o)\ 2\ \pi\ (5 \text{ m}) = 5.2 \text{ m}$$

From Equation V-6-72, the associated crater volume would be

$$V_C = (5.2 \text{ m})\ (2.6 \text{ m})\ (1.2 \text{ m} + (2.6 \text{ m}) / (0.5)) + 102 \text{ cu m} = 189 \text{ cu m}$$

(Continued)

EXAMPLE PROBLEM V-6-16 (Concluded)

From Equation V-6-74,

$S > (0.5)(20.8 \text{ cu m/hr}) \{ 1-[1-(4)(189 \text{ cu m/hr}) / (24 \text{ hr})(20.8 \text{ cu m/hr})]^{1/2} \} = (10.4 \text{ cu m/hr})(1- \sqrt{-0.5}\}$

for which the square root is undefined. Thus, with the proposed enlargement of the crater, the system's capacity would be theoretically limited by the pump capacity, E, instead of the crater volume, V_C.

While the crater volume for the proposed improvement is (189 / 102) = 1.85 times larger than the existing system, the improvements would not yield a 1.85-times increase in bypass capacity. This is because the existing system's bypass performance is limited in only 25 to 34 percent of the existing bypassing events. That is, only some fraction of the 85 percent increased crater capacity would be utilized for only 25 percent to 34 percent of the current bypassing events. Hence, the net increase in bypass quantity provided by the hardware improvements would be, at most, (0.25 to 0.34) x (0.85) = 21 to 29 percent. The decision to improve the plant's hardware or to periodically extend the operating hours (as needed), is a function of economic and other site-specific issues.

(a) Volumetric capacity requirements for the ideal system can be estimated from a mass curve. The mass curve is developed from a plot of the cumulative longshore transport rate versus time (Figure V-6-75). The active storage requirement of the updrift beach is the maximum vertical difference of the cumulative transport curve, as shown in the figure. The minimum storage requirement of the deposition basin is the vertical height of the curve's average slope calculated over the dredging interval of interest.

(b) Allowance on the updrift beach must be made for "dead" storage (Figure V-6-74). This is the impoundment fillet that forms immediately updrift of the weir from which sediment is not transported during reversals. The shape and volume of this dead storage can be approximated from analytic models such as Pelnard-Considère (See Part III-2-2) or numerical models such as GENESIS (See Part III-2-2). In all, the geometry of the weir section should be ideally designed so as to ensure that the requisite active storage will be developed in addition to the dead storage, and so as to ensure that the deposition basin leeward of the weir can be sufficiently sized.

e. Placement of material. In order of priority, placement of bypassed/backpassed sediment should be: upon the beach and beach face; within the typical surf zone (so-called near-nearshore placement); and within the active depth of the beach profile (nearshore disposal). The alongshore placement should be outside of the inlet's direct influence; i.e., so as to minimze the potential for the sediment to return to the inlet and maximize its potential for return to the active littoral system external of the inlet.

(1) Alongshore location. The minimum distance from the inlet for sediment placement can be determined from refraction/transport analysis such as is described in Part V-6-2(c), method 4, in particular, and by Kana and Stevens (1992). Alternately, shoreline change models such as the one-line model of Perlin and Dean (1983) and GENESIS (Hanson and Kraus 1989; see also Part III-2-2, can be employed. Again, the principal objective is to define that distance at which the locally induced transport potential toward the inlet is diminished.

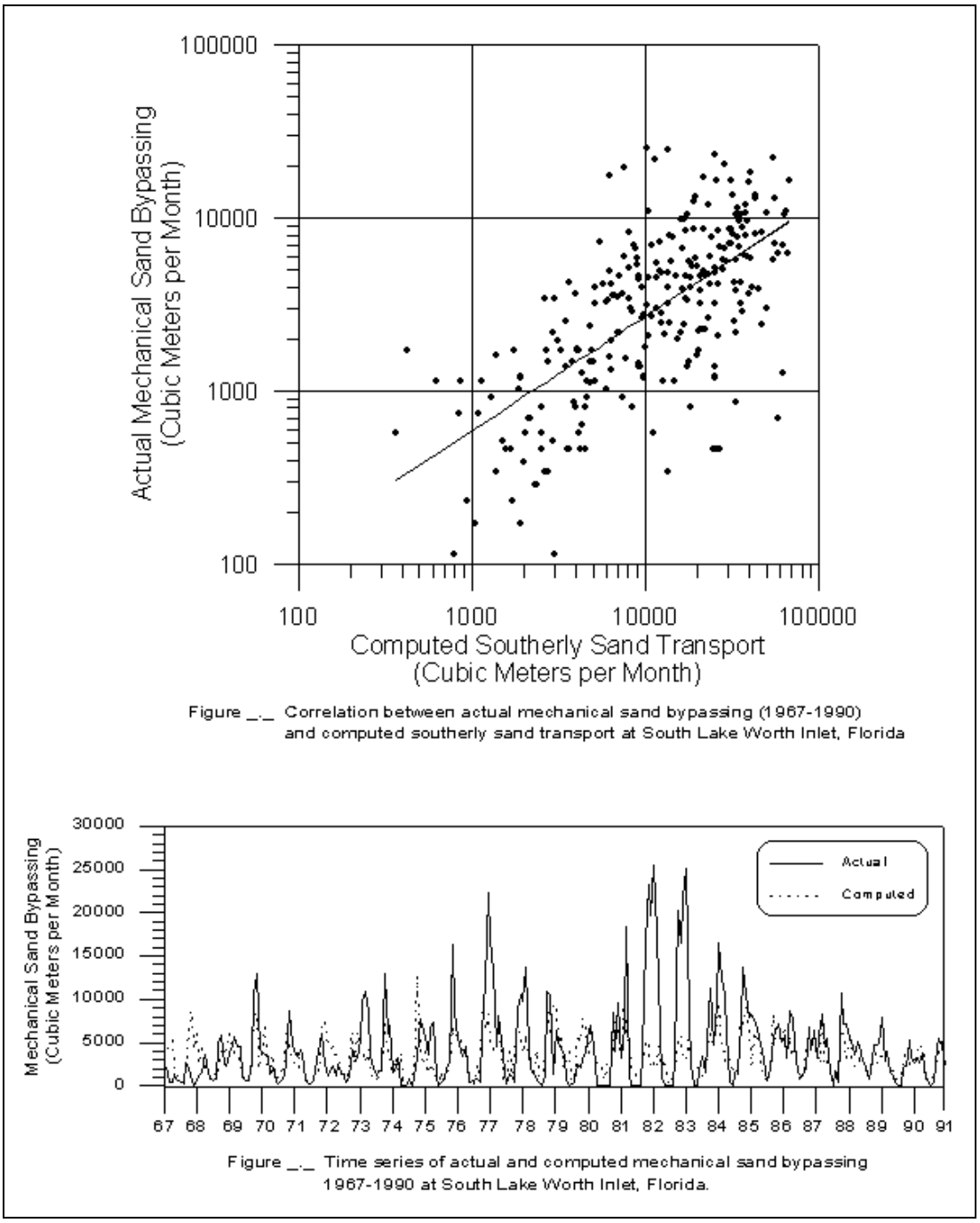

Figure V-6-73. Measured sand bypass rates from the South Lake Worth Inlet, Florida, fixed transfer plant: (a) correlated with hindcast longshore transport potential, and (b) depicted as a time-series. "Actual" refers to monthly bypass volumes estimated from plant records. "Computed" refers to the southerly-directed transport potential as computed from hindcast WIS data for the same 24-year period of record, where the mean value of the computed transport potential was set equal to the mean value of the actual bypass volume over the period of record (Creed 1996)

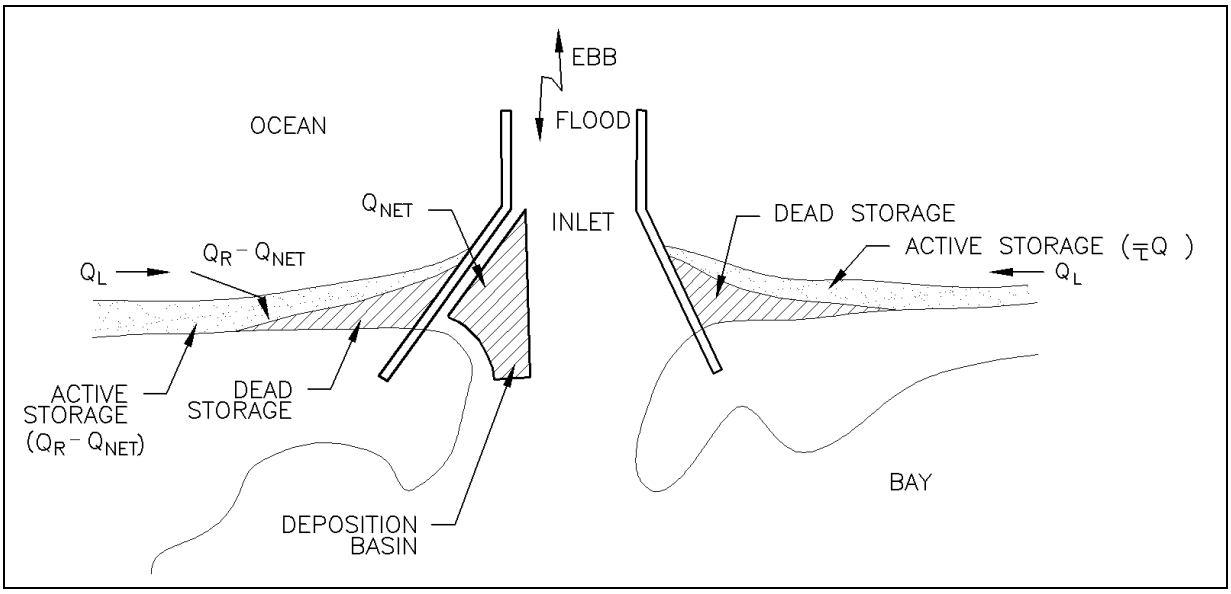

Figure V-6-74. Active and dead sediment storage on a beach adjacent to a weir jetty system (adapted from Weggel 1981)

(2) Nearshore disposal. When placement of the bypassed/backpassed sediment directly on the beach or within very shallow depths is not possible, nearshore disposal (also called nearshore berm disposal) may be considered. In inlet/harbor sediment management, the principal goal is to create an active berm from which the placed sediment will migrate shoreward and return to the shorelines' active littoral system. (A less preferable alternative is to create a stable berm which is intended to provide shore protection through dimunition of wave energy (Zwamborn et al. 1970). The tangible benefits of this strategy are unproven; and, some field studies suggest that nearshore, submerged mounds and structures can induce beach erosion in their lee (USACE 1950; Browder 1995)).

(a) Hands and Allison (1991) present an analytic method by which to predict the seabed placement depth which separates active (shoreward-migrating) from stable berms. In this method, the nonexceedance probability of the maximum nearbed wave-orbital velocity, u_m, is computed and plotted for a given depth, using hindcast wave data for the site of interest. The probability distribution of such plots distinguish stable from active berms (see Figure V-6-76). Most briefly, Hands and Allison (1991) conclude that if the 75-percentile velocity far exceeds 40 cm/sec, or the 95-percentile velocity far exceeds 70 cm/sec, then sand berms should not be expected to remain stable, regardless of the depth or sand size. If the computed velocities are considerably less than these values, a stable sand berm is expected under all but unusual circumstances.

(b) From Equation II-1-22, the maximum nearbed horizontal wave orbital velocity is computed as

$$u_m = \pi \frac{H}{T} \frac{1}{\sinh\left(2\pi h / L\right)} \tag{V-6-75}$$

where T is the (spectral peak) wave period, and H and L are the significant wave height and the wavelength, respectively, in the proposed water depth for berm disposal, *h*. In practice, nearshore or offshore wave data are transformed (refracted and shoaled) to some specified water depth, *h*; the velocity

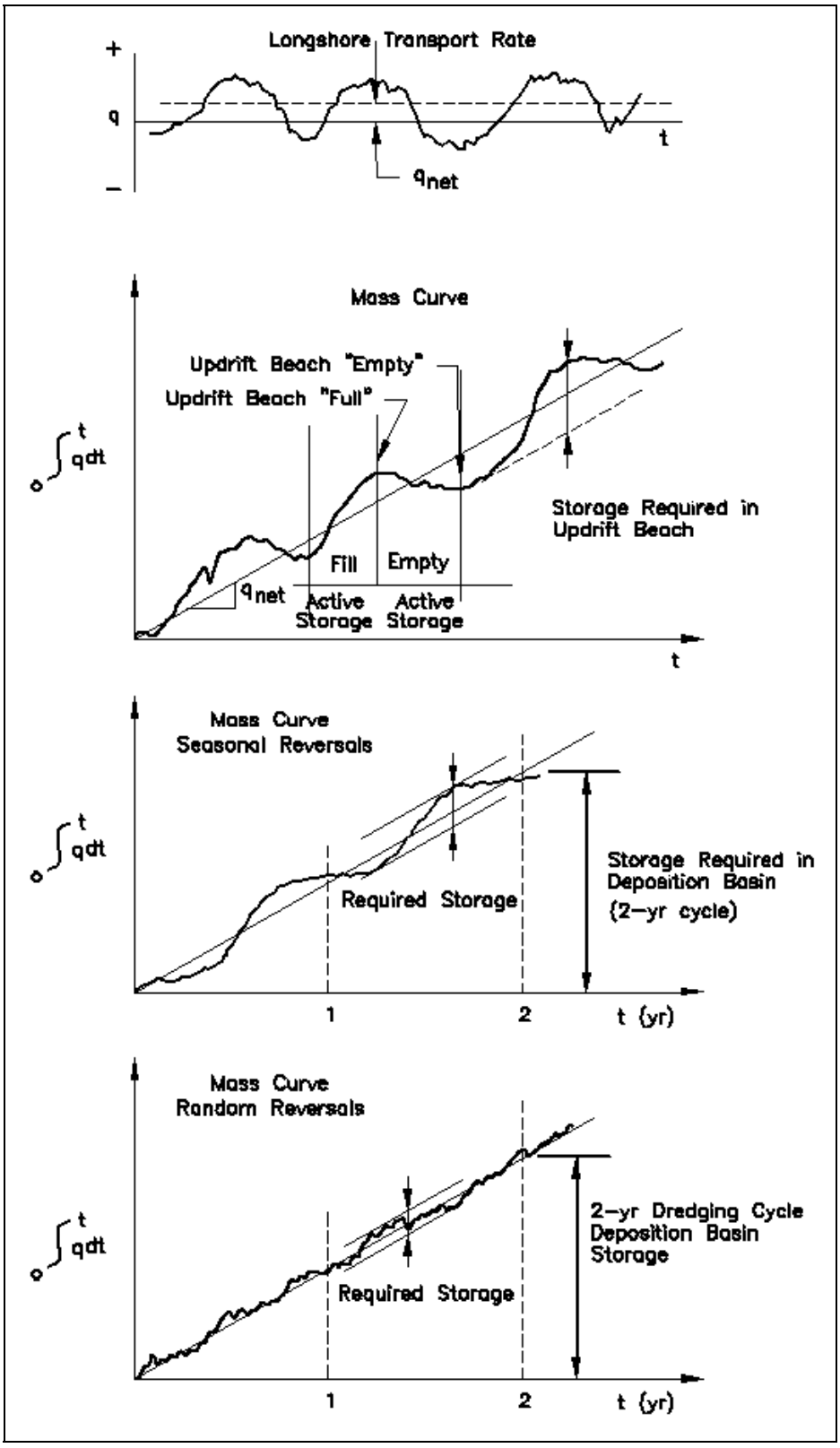

Figure V-6-75. Use of mass curve to predict volumetric capacities required for updrift beach and deposition basins (from Weggel 1981)

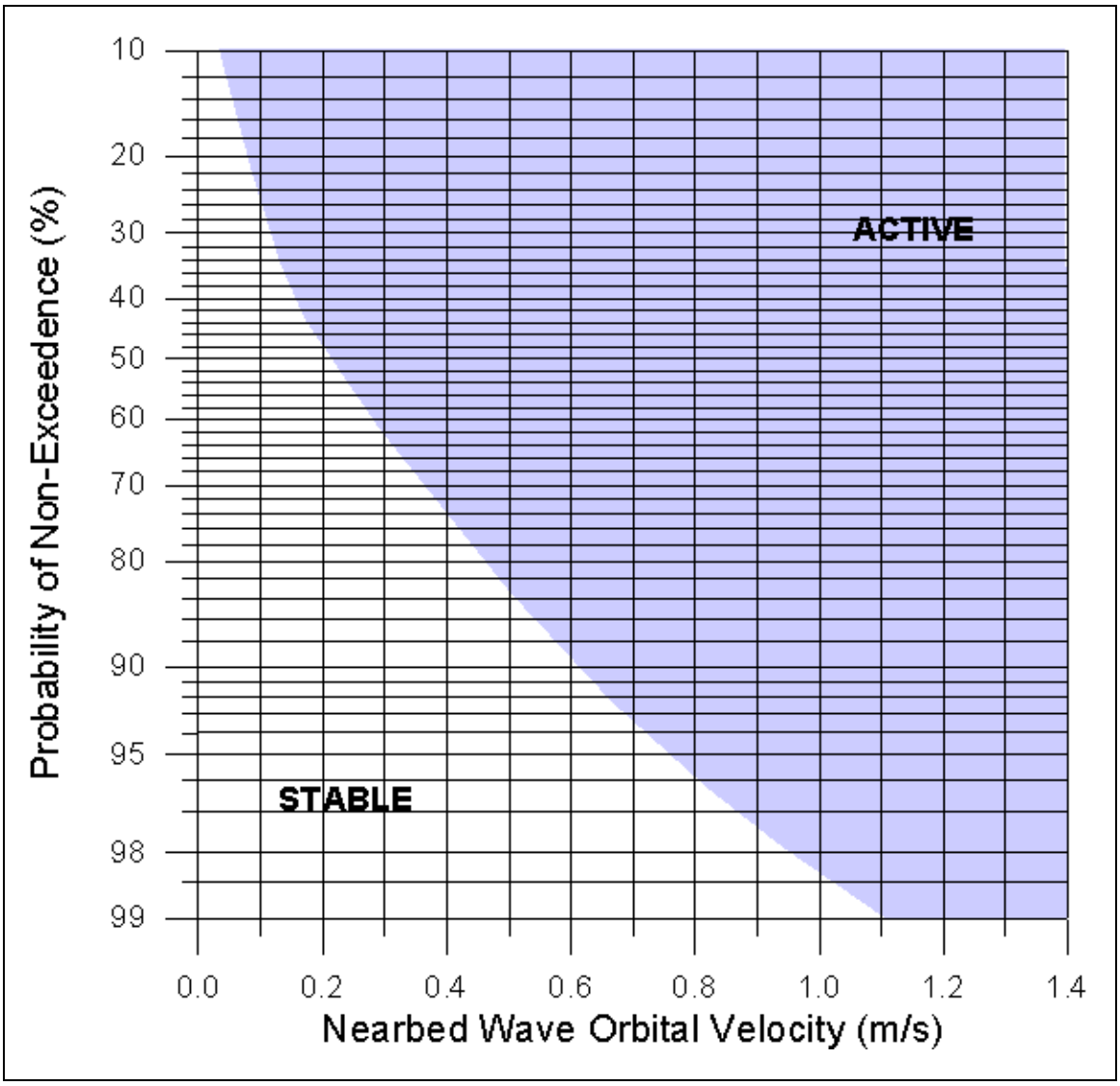

Figure V-6-76. Method to predict whether sediment placed in a nearshore berm will be active (move landward) or stable (after Hands and Allison 1991)

u_m is computed for each transformed wave condition, and the percent-occurrence of each velocity value noted. The velocity values are then ranked, and the percent of nonexceedence computed for each and plotted on a copy of Figure V-6-76. (The nonexceedence is simply the percent occurrence for which the computed velocity values are less than some given value.) If the plotted distribution falls mostly within the active half of the graph, then the berm can be expected to be active; i.e., to migrate shoreward. If not, then a shallower water depth, *h*, should be considered and the computation repeated, etc., until the distribution falls within the active half of the graph. The depth at which the distribution falls generally between the active and stable halves of the graph denotes the maximum seaward depth at which nearshore disposal can be undertaken so as to yield any detectable shoreward migration.

EXAMPLE PROBLEM V-6-17

FIND:

Predict whether a nearshore berm will be stable or active.

GIVEN:

Hindcast, deepwater wave data offshore of a proposed nearshore berm site are given in Table V-6-14. Only onshore-directed waves are tabulated (offshore-directed waves are included under calms). The seabed depth at the proposed berm site is 4 m.

Table V-6-17
Deepwater Wave Data and Calculations to Determine Berm Stability

Given data (deepwater)			Occ. exc. calms	L_o	water depth, h = 4.0 m		
H_o (m)	T (s)	Occ.(%)	(%)	(m)	L (m)	H (m)	u_m (m/s)
calm	--	32.4	--	--	--	--	--
0-0.99	5-7	13.1	19.4	56.2	34.8	0.35	0.23
0-0.99	7-9	25.9	38.3	99.9	48	0.29	0.21
1-1.99	5-7	9.5	14.1	56.2	34.8	1.05	0.7
1-1.99	7-9	7.2	10.7	99.9	48	0.87	0.62
2-2.99	7-9	5.5	8.1	99.9	48	1.44	1.03
2-2.99	9-11	4.9	7.2	156.1	61	1.24	0.92
3-3.99	9-11	1.1	1.6	156.1	61	1.73	1.28
>4	--	0.4	0.6	--	--	--	--

To emulate the empirical results of Hands and Allison (in which the probability of $u_m = 0$ is 0 percent), calm events are excluded. The occurrence of each wave condition is recomputed neglecting calms. For the first noncalm entry in the table:

Percent occurrence excluding calms = (13.1 percent) / (100 percent - 32.4 percent) = 19.4 percent

The wavelength at the reference (hindcast) site is computed for each wave condition. The median height and period values within the ranges given for wave condition are assumed. The wave data are given as deepwater values; hence, from Equation II-1-15, and for the first noncalm entry in the table:

$$L_o = 1.56\,(T^2) = 1.56\,(6.0)^2 = 56.2 \text{ m}$$

The wavelength, L, at the placement depth of h = 4.0 m, is computed from linear theory (see Example Problem Equation II-1-1). The corresponding wave height, H, is computed from Equation V-6-76. For the first noncalm entry in the table:

$$H = (0.5 \text{ m})\,(34.8 \text{ m} / 56.2 \text{ m})^{3/4} = 0.35 \text{ m}$$

(Continued)

EXAMPLE PROBLEM V-6-17 (Concluded)

From Equation V-6-75, for the first noncalm entry in the table:

u_m = (3.14) (0.35 m / 6 sec) / [sinh {(2)(3.14)(4 m)/(34.8 m)}] = (0.183 m/sec) / (0.7862) = 0.23 m/sec

Rank the values of u_m in ascending order, and list the percent-occurrence for each (first two columns in TableV-6-15). Compute the cumulative occurrence for each event (last column in table), which is the same as the probability of nonexceedence. Plot the results atop Figure V-6-77. The plotted curve falls mostly well within the active (shaded) area, suggesting that the proposed berm is more likely to migrate landward than to remain stable.

Table V-6-18
Calculations of Maximum Nearbed Orbital Velocity

u_m, m/sec	Occ., percent	Cumulative Occ., percent
0.21	38.3	38.3
0.23	19.4	57.7
0.62	10.7	68.4
0.70	14.1	82.5
0.92	7.2	89.7
1.03	8.1	97.8
1.28	1.6	99.4

(c) In developing the empirical result illustrated in Figure V-6-76, Hands and Allison (1991) used the wave height transformation:

$$H = H^* \left(\frac{L}{L^*} \right)^{3/4} \tag{V-6-76}$$

where H^* and L^* are the wave height and length at some given water depth (such as the hindcast location), and where the standard dispersion relationship for linear waves was used to compute wavelength (Equation II-1-10).

(d) The propensity for shoreward migration increases with shallower water depths for disposal, and higher, better-defined berm elevations. A principal shortcoming of the Hands and Allison technique (Figure V-6-76) is that it does not consider the crest elevation or width of the berm. The more complicated method of Douglass (1995) demonstrates the importance of these two elements, particularly the former.

(e) Burke and Allison (1992) and Hands and Resio (1994) present additional guidelines on berm disposal geometries and depths, respectively. Douglass (1995) and Sheffner (1996) present analytic methods by which to predict postplacement migration of nearshore berms. Other Corps of Engineers' PC-based numerical methods to predict the fate of disposed dredged material include DIFID, DIFCD, DIFHD, ST-FATE and LT-FATE; described elsewhere. USACE (1950); Uda, Naito, and Kunda (1991); Johnson et al. (1994); Bodge (1994a); Foster, Mealy, and Delange (1996); Mesa (1996), among many others, describe case histories of nearshore berm stability and migration.

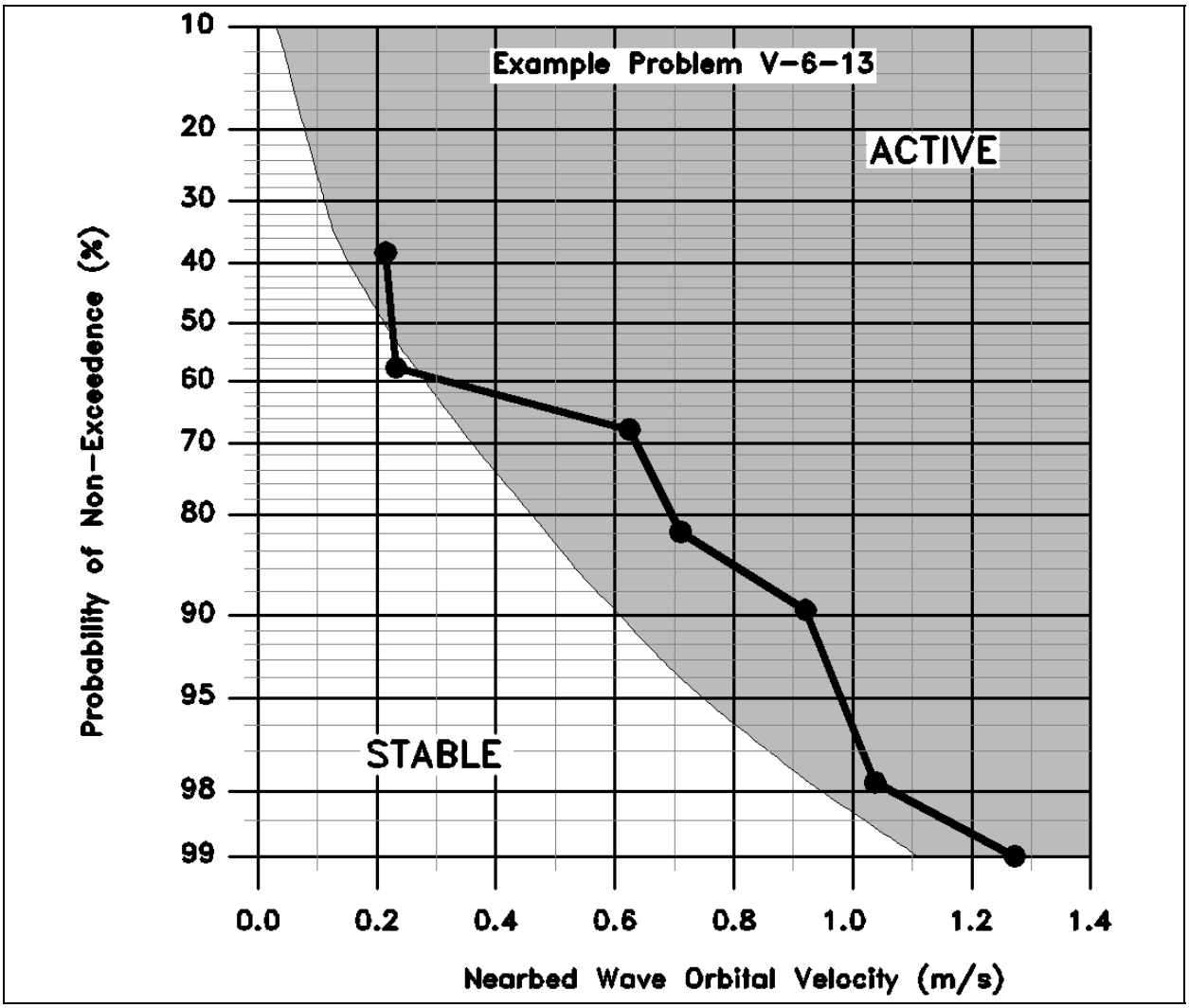

Figure V-6-77. Results for Example Problem V-6-17

(f) The profile zonation technique of Hallermeier (1981), and as described in the *Shore Protection Manual* (1984), generally overpredicts the water depths in which active berms are expected, and results in a wide buffer zone in which berm performance is uncertain (Hands and Allison 1991). The use of the Hallermeier Inner Limits and Outer Limits (HIL and HOL), and the annual seaward limiting depth of the littoral zone, are not recommended for design of nearshore berm disposal criteria.

(g) McLellan and Kraus (1991) present an alternative method by which to predict whether a berm will be active or stable. The work is an extension of onshore/offshore transport predictors employed for beach profile response in the surf zone (see also, Kraus, Larson, and Kriebel 1991); and, as such, may be less appropriate for berms placed in deeper water toward the outer limit of the profiles' active depths. Nonetheless, the application of these transport predictors to berm depths may illuminate the relative degree to which shoreward transport may be anticipated. The simplest such predictor is the so-called "fall-velocity" or "Dean" parameter, N_o

$$N_O = \frac{H_o}{wT} \tag{V-6-77}$$

where H_o is the offshore wave height, w is the sediment's median fall-velocity, and T is the wave period. Concisely, for $N_o < 2.4$, shoreward movement is highly probable; for $N_o < 3.2$, shoreward movement is probable; for $N_o > 3.2$, seaward movement is probable; and for $N_o > 4.0$, seaward movement is highly probable. The utility of this predictor for nearshore berm stability is diminished, as the water depth of the berm placement or crest elevation is not explicitly specified.

f. Costs. Overviews of inlet sand bypassing costs are presented in Jones and Mehta (1977, 1980); EM 1110-2-1616; Bruun (1993), among others. Table V-6-19 presents a brief summary of costs for various inlet sand bypassing projects. It is noted that project costs will vary widely in the prototype as a function of the quantity and complexity of the work, and the potential to combine projects for which similar equipment can be utilized. By far, the greatest economies are to be gained where sediment management strategies (bypassing and backpassing) can be combined with requisite maintance dredging of the inlet/harbor, and can be combined between nearby project sites. Comparative economic analysis is required in those cases where the quantites of sediment bypass/backpass can be minimized by the construction of additional inlet structures, jetty improvements, or channel relocations. Specifically, the short-term (capital) costs of these works must be considered against the long-term reduction in costs associated with decreased dredging requirements. In all cases, the cost of improving inlet/harbor sediment management so as to minimize the erosive impacts to adjacent shorelines should be weighed against the cost of mitigating the erosion through separate beach nourishment projects, and/or the costs of accepting the increased storm damage, legal actions, and loss of recreation, revenue, and habitat should the erosion be left unabated.

V-6-6. Project Experience

a. Overview of existing prototype systems. The methods, mechanical equipment, and success of existing inlet sand management / bypassing systems vary widely, and are dictated by physical, environmental, and social considerations specific to each inlet site. Designers of potential sand management / bypassing systems are urged to consider the history and monitored performance of previous systems; and, whenever possible, to directly consult those engineers and operators that are intimately familiar with these systems' performance. Several prototype systems are summarized. Additional summary descriptions are presented in EM 1110-2-1616.

(1) Santa Cruz Harbor, California. Santa Cruz Harbor is located on the northern coast of Monterey Bay on the Pacific Ocean south of San Francisco (Figure V-6-78). During the project's design in the 1960s, the net longshore transport rate was believed to be less than 230,000 cu m/year, but subsequent studies in 1978 concluded that the rate is between 230,000 and 383,000 cu m/year (Moffatt and Nichol 1978). Within 2-1/2 years after the channel and jetties were constructed in 1962-63, the updrift (west) shoreline had impounded 400,000 cu m of sand, the channel experienced severe shoaling, and the downdrift beach had eroded. Annual channel dredging, usually by 30 cm (12-in.) hydraulic dredge, was begun in 1965 but could not maintain a clear channel against the significant and rapid shoaling experienced in winter. Between 1976-78, an experimental jet-pump system was tested using four mobile pumps and one fixed pump. The severe wave climate and rapid sand shoaling rates buried the jet pumps' supply and discharge lines. This hampered the pumps' mobility and also required frequent backflushing of the supply water lines to clear them of sand. Debris also presented severe problems to the jet pumps. Annual contract dredging was continued, as before, through the mid-1980s; and the channel continued to shoal and mostly close during winter.

Table V-6-19
Examples of Inlet Sand Bypassing Costs (U.S. Dollars in 1995)

Project	Volume (cu yd)	Fre-quency (yr)	Source	Placement	Method	UnitCost ($/cu yd)	Mob/Demob ($)	Total Unit Cost ($/cu yd)
Canaveral Harbor, FL	900,000	6	Updrift beach; -4 to -16 ft mlw)	Beach disposal: 0 to 2 miles downdrift	30" hyd. dredge	$ 4.20	$ 800K	$ 5.10
Canaveral Harbor, FL	200,000	1	Nav. Channel	Nearshore Berm; -20 ft mlw, 6 miles downdrift	Clamshell dredge and 2,500 cu yd dump scow	$ 0.00 (no added cost above offshore disposal)		$ 0.00
Canaveral Harbor, FL	< 200,000	1	Nav. Channel	Nearshore Berm; -10 to -16 ft mlw, 6 miles downdrift	Clamshell dredge and dump scow	< $ 0.25	$ 0 (inc. in basebid)	< $0.25
Masonboro Inlet, NC	696,000	4	Updrift Weir & Dep. Basin	Beach disposal: w/in 2- to 3-miles updrift and downdrift	27"- to 30"-pipeline dredge.	$ 2.76	$ 543K	$ 3.54
Carolina Beach Inlet, NC	517,000	3	Internal Sand Trap	Beach w/in 1 to 2 miles downdrift	Shallow-draft hopper; or pipeline dredge	$ 2.06	$ 310K	$ 2.66
Channel Is., CA	1.5 M	2	Int. Sand Trap	Beach w/in 2 miles downdrift	30"-pipeline dredge	$ 2.20	$ 750K	$ 2.70
Perdido Pass, AL	320,000	2-3	Updrift Weir & Dep. Basin	Beach w/in 1 mile downdrift	24"-pipeline dredge	$ 1.98	$ 132K	$ 2.39
E. Rockaway Inlet, NY	180,000	2	Nav. channel	Nearshore Berm; -16-ft depth, 1 mile downdrift	Hopper dredge (Atchafalaya)	$ 4.16	* $ 164K + $ 342K	$ 5.07
Jones Inlet, NY	380,000	2	Nav. channel	Hempstead Beach; 1- to 2-miles away	Hopper dredge w/ pumpout and 5,000-ft pipeline	$ 7.56		$ 8.46
Indian River Inlet, DE	97,000	cont.	Updrift beach	Beach imm. north of inlet	Mobile crane and jet pump	$ 1.62	$1.7M**	$ 4.98**
Nerang River, Australia	600,000	cont.	Updrift beach	Beach imm. south of inlet	Fixed pier w/ 10 jet pumps	$ 1.20	**Aust.$ 6.3M (1986)	$ 3.24**
So. Lake Worth Inlet, FL	70,000	cont.	Updrift beach	Beach w/in 700 ft south of inlet	Fixed plant w/ suction dredge	$ 2.97	$30K per year maint.	$ 3.40

Projects were contracted jointly.

** Initial Cost to Design and Construct Plant. Total Unit Cost assumes 30-year amortization of initial cost at 9 percent per year.

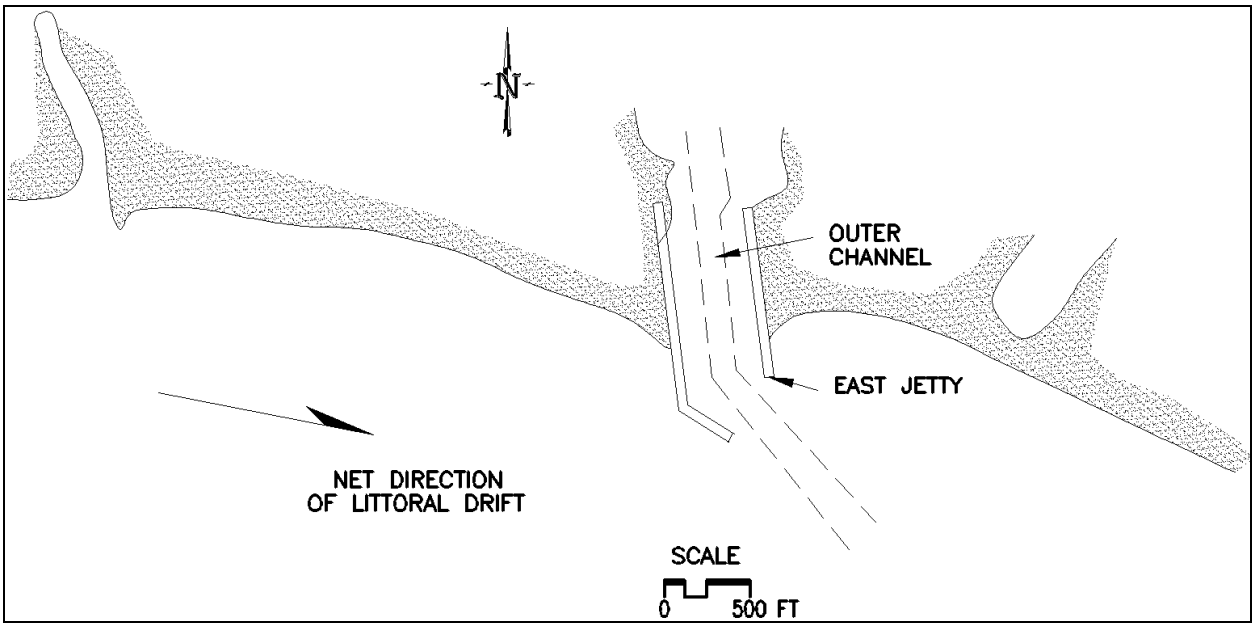

Figure V-6-78. Santa Cruz, California

In 1986, the Santa Cruz Port District obtained its own 40-cm (16-in.) hydraulic dredge. The $2.8 million purchase was 78 percent cost-shared by the Federal government. The dredge bypassed 176,000 cu m to the downdrift (east) beach in its first operational year (1986-87). Subsequently, the harbor has remained open almost continuously. The dredge operates primarily with a jet nozzle suction head and practices pothole dredging, wherein a series of discrete, deep craters is pumped (as opposed to continuous dredge cuts). Significant downtime has been reported due to debris blockage of the pump. Continuing maintenance and operational expenses have also proven to be a problem for the Port District (Walker and Lesnik 1990; EM 1110-2-1616).

(2) Santa Barbara Harbor, California. Santa Barbara Harbor is located on the Pacific Ocean northwest of Los Angeles (Figure V-6-79). The net and gross longshore transport rates are believed to be about 205,000 cu m/year and 282,000 cu m/year, respectively. The harbor's original 550-m-long offshore breakwater, constructed in 1927, was left detached from the coastline in the mistaken belief that this would allow littoral drift to pass through the harbor. The harbor immediately shoaled with sand and the downdrift (east) beach eroded. In 1930, the breakwater was extended 180 m in order to connect it to shore. Sand immediately impounded updrift of the new structure (advancing the beach over 300 m) while the downdrift beach retreated by over 120 m. Sand then bypassed the breakwater and impoundment fillet and shoaled the harbor. In 1935, 154,400 cu m of sand were hopper-dredged and placed in about 7-m water depth offshore of the downdrift beach, but surveys showed little shoreward movement of the sand. Beginning in 1938, hydraulic dredge and pipeline were employed. By 1952, an average of about 488,700 cu m of sand were bypassed every 2 years to the downdrift beach, representing about two-thirds of the area's estimated net littoral drift since the harbor's construction in 1927. In 1966, harbor dredging and sand bypass, by conventional hydraulic dredge and pipeline, became an annual operation. The quantity averages about 267,600 cu m/year or less (Bailard and Jenkins 1982; Walker and Lesnik 1990).

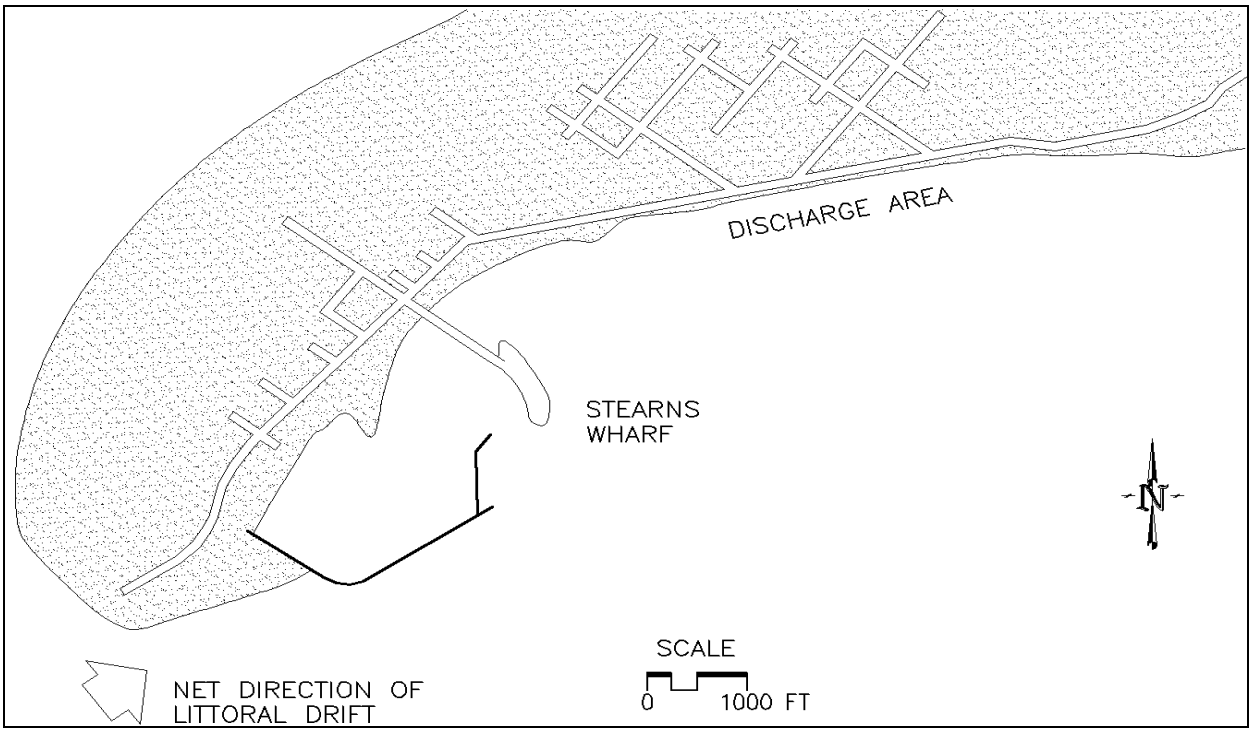

Figure V-6-79. Santa Barbara, California

(3) Port Hueneme, Channel Islands Harbor, and Ventura Marina, California. Port Hueneme is located about 70 km southeast of Santa Barbara Harbor on the Pacific Ocean (Figure V-6-80). The net longshore transport rate is estimated as 612,000 to 920,000 cu m/year. Port Hueneme's ocean entrance was dredged and stabilized by arrowhead jetties in 1938 at the head of the Hueneme submarine canyon. Despite placement of over 2 million cu m of dredged sand to the downdrift (east) shoreline during project construction, these beaches were completely cut off from the net littoral drift and retreated over 210 m within 20 years. Sand was impounded updrift of the inlet's jetties and diverted offshore into the submarine canyon. Coastal sand supply was simultaneously decreased by the construction of upriver dams and additionally by the interruption of littoral drift at Santa Barbara Harbor to the northwest. Between 1953 and 1960, hydraulic dredging of the updrift impoundment fillet and the navigation channel placed about 400,000 cu m to the downdrift beaches, primarily via submerged pipeline; but there remained a 16 million-cu m deficit. In bypassing the updrift impoundment fillet in 1953, the dredge cut into the shoreline and left a narrow barrier of sand seaward in order to provide a temporary wave shelter to the dredge plant. The narrow barrier was then dredged and bypassed at the end of the job.

(a) In 1960, Channel Islands Harbor was constructed about 1 mile northwest (updrift) of Port Hueneme entrance (Figure V-6-80). One intent of the project was to create a sand trap that would reduce losses to Hueneme Canyon and expedite mechanical bypassing to the downdrift beaches. The project consists of two jetties and an offshore, detached 700-m long breakwater, originally constructed in 9-m water depth, which shelter the harbor entrance. The littoral drift that deposits in the lee of the breakwater (i.e., in the trap) is hydraulically dredged by a conventional plant and pipeline and bypassed to the downdrift beach (principally south of Port Hueneme entrance). The equivalent, annual bypass rate has been about 990,000 cu m/year. To save on mobilization costs, bypassing typically takes place every other year (Herron and Harris 1967; Walker and Lesnik 1990).

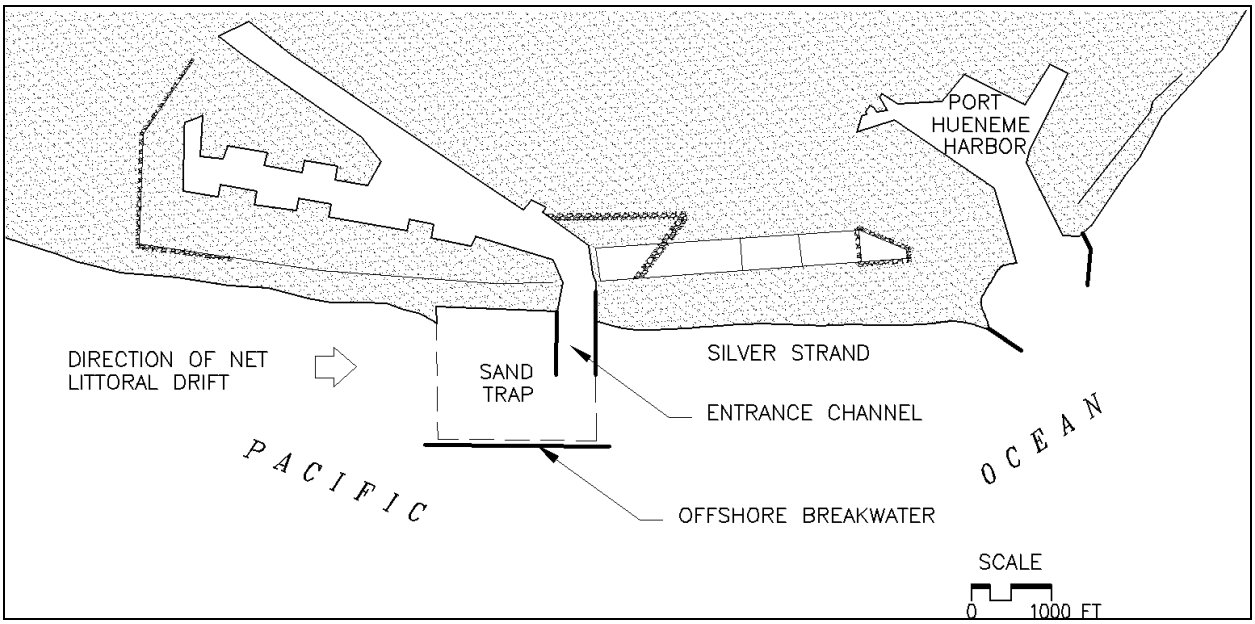

Figure V-6-80. Channel Islands and Port Hueneme Harbors, California

(b) Ventura Marina, located a few kilometers north of Channel Islands Harbor, was constructed by local authorities in 1962-63. Its design included features from the Channel Islands project (dual jetties, offshore breakwater, and leeward sand trap); but failed to recognize the area's high rate of littoral drift and did not plan for sand bypassing. In part because of the deficient length of the jetties and breakwater, sediment accumulates so rapidly that the entrance channel must be frequently dredged, often well before the sand trap is full. There are no measures to control the summer reversal in drift direction, and the resultant transport of sand around the south jetty and into the channel can be significant. While sand has been succesfully dredged from the project and placed upon the adjacent beaches, inlet navigation chronically suffers from rapid channel shoaling and wave inundation.

(4) Oceanside Harbor, California. Oceanside is located on the Pacific Ocean, about 50 km northwest of San Diego (Figure V-6-81). The estimated net littoral drift is small (75,000 to 190,000 cu m/year to the south) relative to the gross drift (on the order of 920,000 cu m/year). The Del Mar boat basin was constructed at the beginning of the 1940s and jetties were constructed in 1942. Shoaling of the entrance channel, updrift impoundment and downdrift erosion rapidly ensued. The north jetty was extended in 1958 and again in 1994. The Oceanside small craft harbor and its south jetty were constructed in the 1960s. Since 1957, the sand dredged from the harbor has been placed on downdrift beaches (about 230,000 cu m/year, on average); nonetheless, downdrift beach erosion continued to be a problem due to the inlet's historical impact to the littoral system and continuing losses associated with the shoreline's large gross transport rate. Mining of the impounded sand updrift (north) of, and between the two harbors, for purposes of bypassing and downdrift placement, was rejected by local interests. In 1982-83, an experimental sand bypass system was proposed consisting of the phased introduction and testing of fixed and mobile jet pumps. The latter, attached to a barge, would operate from locations along the north and south jetties, depending upon wave and sand transport conditions. A dedicated 35-cm pipeline and a shore-based booster station (used for bypassing from the north jetty location) would transport and discharge the sand to the downdrift shoreline.

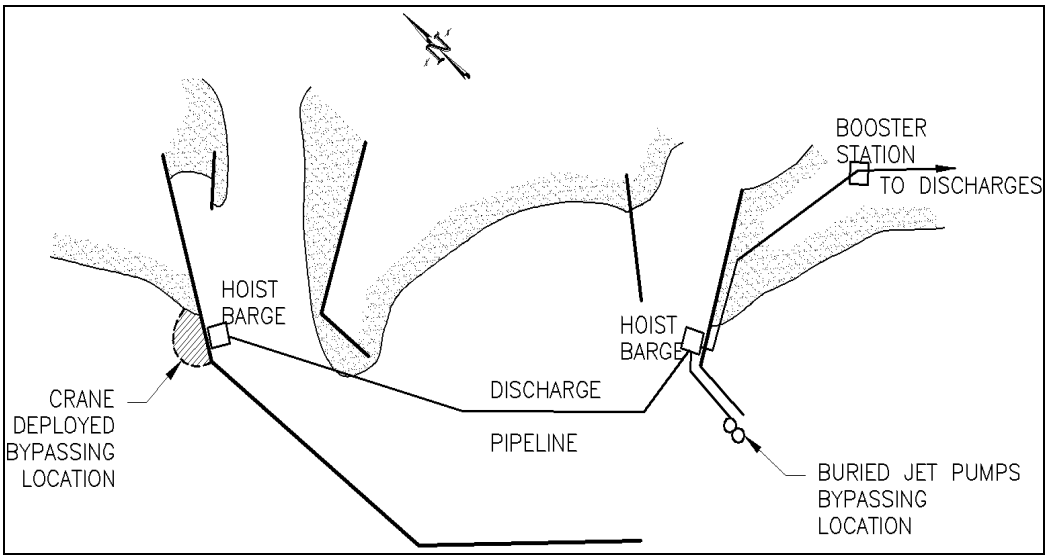

Figure V-6-81. Oceanside Harbor, California

(a) In 1989-90, the system's Phase I evaluation included 3-weeks' testing of a single crane-deployed jet pump operating at the north jetty fillet from upon the barge; and, 11 months' operation of two 4 in. x 4 in. x 6 in. Pekor jet pumps submerged in the entrance channel at the south jetty. Sand was pumped for 305 hr over this period, during which the production rate averaged 48 cu m/hr. The design value was about 150 cu m/hr. Principal difficulties involved continual clogging of the jet pumps (kelp root balls, rope, etc.) and the limited size and infilling rate of each pump's crater (about 4.6 m deep and 25-m diam).

(b) In 1991-92, Phase II evaluation included the addition of a single, pile-supported seabed fluidizer angled downward at about a 1:100 slope toward each of the two fixed jet pump's craters. The two fluidizers were 46 to 61 m in length and 20 to 25-cm diam. During a 13-month period, 81,000 cu m were bypassed with an average production rate of 73 cu m/hr. While the fluidizers appeared to improve productivity, the system exhibited difficulties from continual filling of the fluidizers with sand when the system was not operating. This required backflushing of the fluidizers prior to initiating sand transfer by the jet pumps. Productivity is predicted to improve if a separate fluidizer pump were provided, and if sand entry to the fluidizers could be minimized (Clausner, Patterson, and Rambo 1990; Walker and Lesnik 1990; Patterson, Bisher, and Brodeen 1991; Bottin 1992; Weisman, Lennon, and Clausner 1996).

(5) Indian River Inlet, Delaware. Indian River Inlet is located on the Atlantic Ocean approximately 16 km north of Ocean City, Maryland. The net littoral drift is estimated to be about 84,000 cu m/year to the north. The inlet was improved by dredging and the construction of jetties between 1938 and 1940. This resulted in immediate accretion of the updrift (south) beach and the inlet's ebb and flood shoals, and erosion of the downdrift (north) beach. In 1990, a dedicated, semimobile sand bypassing plant was installed at the inlet. The system consists of a jet pump deployed (suspended) by a 135-ton crawler crane with 37-m boom. The Genflo jet pump has a 6.4-cm nozzle with 15-cm mixing chamber, rated at 152 cu m/hr capacity. Discharge from the jet pump is through a 28-cm HDPE pipe to a booster pump, then through a dedicated pipeline across the inlet with discharge onto the beach at adjustable locations up to 460 m north of the inlet. Both the supply and booster pumps are stationed in a pump house adjacent to the south jetty. The system draws clear water from the inlet and powers the jet pump with a 340-hp supply pump supplying 415 ft of head and 2,500 gpm through a 25-cm supply line. The crane, jet pump, and crater geometry are similar to that shown in Figure V-6-60(a), and the jet pump is as shown in Figure V-6-62.

(a) The system is operated on a 4 day/week schedule with a three-person crew. To start bypassing from a fresh crater, the jet pump is jetted down to about -2.7 m (mlw) within the swash zone and allowed to create a small crater to provide a ready source of clear water to wash out the discharge line in the event of a potential line plug. The jet pump is then lowered to about -5.4 m (mlw), just above an existing clay layer, and kept at that depth for the remainder of the day. During calm surf or falling tide, the pump is raised and laterally moved about 4 m every 15 to 30 min to maximize productivity. Otherwise, little movement is required as wave action continually feeds sand to the crater. The craters produced by the operation are typically 5.5 m deep with 1:1.5 side slopes such that the beach surface diameter is approximately 15 m, and the nominal volume is about 300 cu m. The crane is able to excavate a trench about 3 diam long without moving.

(b) During the nonsummer (energetic) months, the jet pump operates from between 30 and 120 m south of the south jetty. This provides an area available for bypassing of approximately 3,700 cu m. Operation is limited by recreational activity, particularly during the summer months, and by potential nesting of endangered shore birds (piping plover) along the discharge area from March through August. The latter restricts sand discharge from within about 100 m of any observed nest. Productivity is limited by the amount of sand that is naturally transported to the 90-m-long stretch of beach utilized by the crane. Sheltering of this area by the inlet's ebb delta reduces the local rate of transport and the crater infilling rate during periods of low wave energy.

(c) In its first 11 months of operation, the system bypassed 85,500 cu m of sand, thus achieving its design objective. After gaining experience with the system, hourly productivity averaged 280 cu yd/hr. A remote production meter mounted in the crane's cab improved productivity by allowing the operator to monitor the effect of adjusting the pump position. Impacts to the south beach (narrowing) were limited to the area of bypass operation. Final cost of the system, including 610 m of discharge pipeline, was $1.7 million, with estimated annual O&M costs of $210,000/year (1990 dollars) (Rambo, Clausner, and Henry 1991; Clausner et al. 1991; Gebert, Watson, and Rambo 1992).

(6) Rudee Inlet, Virginia. Rudee Inlet, immediately south of Virginia Beach, was essentially non-navigable until 1952 when two short jetties were built and a channel was dredged. The channel immediately began to shoal with sand, and erosion occurred on the downdrift beaches. A fixed bypassing plant with a small capacity was installed in 1955 with little effect, and a floating pipeline dredge was added in 1956. The fixed plant was destroyed by a storm in 1962 and the inlet essentially closed, whereupon sand bypass resumed naturally. In 1968, the inlet was again improved with the construction of a jetty and a breakwater connected to the shore by a sand weir, similar to the geometry shown in Figure V-6-68(b). The weir jetty impoundment basin was never fully dredged initially, and the 25-cm dredge operations were hampered by wave action. From 1968 to 1972, sand bypassing was achieved by dredging sand from the channel and back bay and pumping it to the downdrift beaches. In 1972, 76,000 cu m of sand were removed from the impoundment basin. By 1975, the basin refilled with sand, and bypassing from the basin was repeated by the 25-cm dredge.

(a) Also in 1975, a semimobile jet pump system was added to the impoundment basin. The system consisted of two jet pumps (eductors) attached by flexible rubble hoses to fixed steel pipes. The steel pipes were connected to a pump house equipped with two centrifugal pumps having a combined nominal capacity of 115 cu m/hr. Discharge to the downdrift (north) beach was through a dedicated 20-cm steel pipe. During the system's first 6 months of operation, 60,400 cu m of sand were bypassed by the jet pumps and approximately 23,000 cu m were bypassed from the channel and impoundment basin by the floating dredge.

(b) Since late 1975, the system has been owned and operated by the city of Virginia Beach. Original estimates of pumping capacity were about 38 cu m/hr with effective pumping time of about 113 hr/month.

By 1980, only a single jet pump (eductor) was operated. At that time, it was moved within the impoundment basin by winching and redeploying via a steel cable operated from a truck (Richardson 1977; Dean et al. 1987).

(7) Masonboro Inlet, North Carolina. Masonboro Inlet is located near Wilmington, North Carolina, on the Atlantic Ocean (Figure V-6-82). Net littoral drift is southerly and in excess of 220,000 cu m/year. This natural inlet was first dredged in 1959 and the north (updrift) jetty was constructed in 1965-66. The jetty included a 305-m weir section built of concrete sheet piles with crest elevation at mean tide level. A deposition basin with a 283,000-cu m capacity was dredged along the interior of the weir. Because no south jetty was constructed, the area's strong reversal drift shoaled the inlet from the south and forced the navigation channel northward, undermining the north jetty and cutting through the deposition basin.

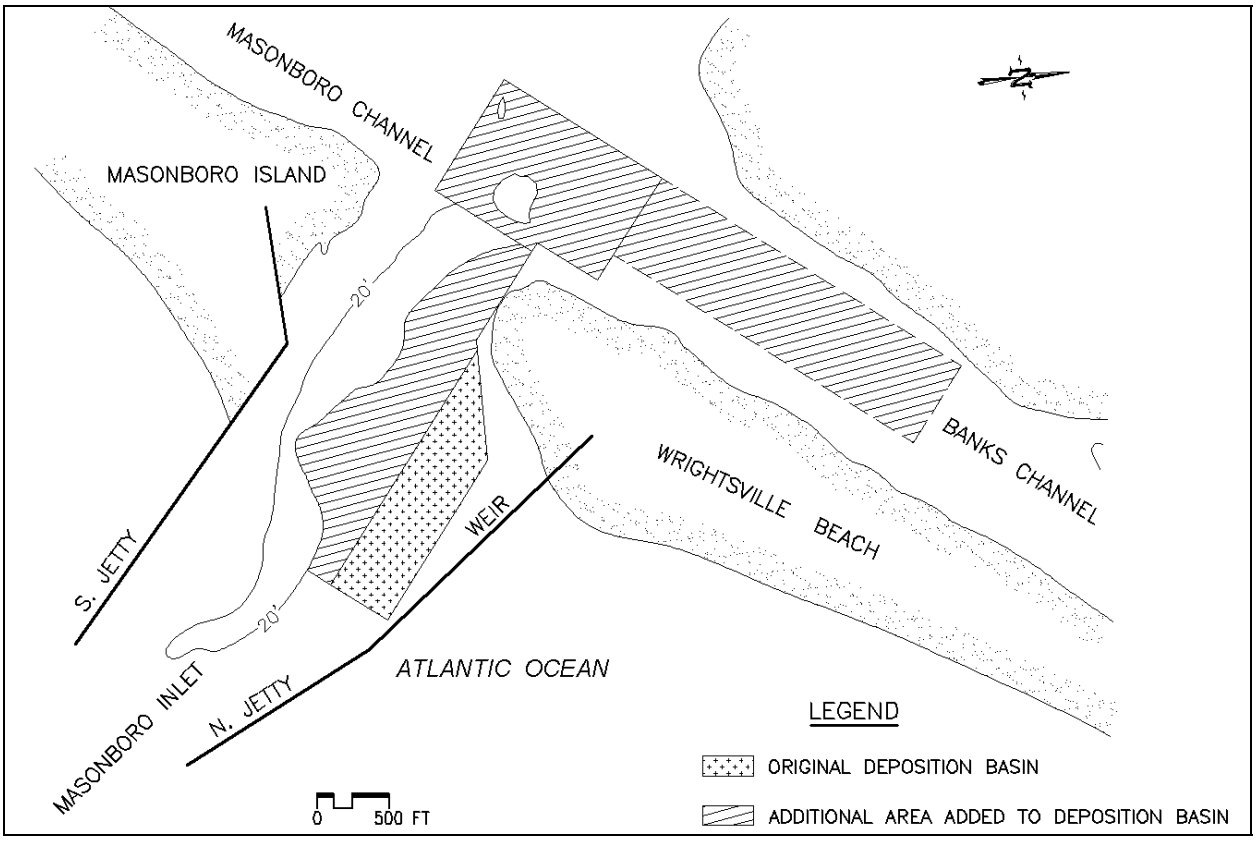

Figure V-6-82. Masonboro Inlet, North Carolina

(a) The south jetty was constructed in 1979-80, at which time 918,000 cu m were dredged from the inlet and placed on the north beach by pipeline. In 1981, dredging centered the channel between the two jetties. Since that time the inlet bathymetry has stabilized, and the need for a proposed training wall (separating the impoundment basin from the channel) has been eliminated. Additionally, the area of deposition expanded considerably to include the original basin, part of the inlet throat, and the inlet interior area. Transport over the weir is principally along the shoreline interface, and deposition is greatest at that area and landward thereof.

(b) Lack of available land along the updrift beach required that the weir-jetty be oriented at about 85 deg from the shoreline (i.e., almost perpendicularly), instead of at the recommended angle of about 60 deg. The latter would have provided greater deposition basin area along the shoreline interface of the

weir, thus improving its capacity and reducing the proclivity of shoaling across the inlet throat and flood shoals. The expanded deposition basin area is typically dredged about every 4 years by contracted floating plant. The dredged material, on the order of 920,000 cu m per event, is bypassed to the south beach and/or backpassed to the north beach depending upon these beaches' conditions. The expansion of the deposition area has proven to be beneficial from the standpoints of both cost (reduced dredging frequency) and the ability to better capture sand within the inlet for purposes of bypassing and backpassing (Rayner and Magnuson 1966; Magnuson 1967; Vallianos 1973).

(8) Ponce de Leon Inlet, Florida. Ponce de Leon Inlet is located near Daytona Beach along east-central Florida's Atlantic coastline (Figure V-6-83). The net littoral drift was originally thought to be southerly-directed. Inlet improvements undertaken between 1968 and 1972 consisted of two jetties (the north jetty being a weir jetty), and the dredging of a navigation channel and an impoundment basin adjacent to the interior of the north weir. The weir was constructed of concrete panels that were to be adjusted in height between king-piles. This was never practicable as loose panels chattered and chipped between the piles, and/or the piles could not be aligned properly to allow adjustment. The impoundment basin adjacent to the weir has never been dredged. Instead, sand rapidly impounded against the south jetty and then created a large, chronic shoal within the inlet interior along the south jetty. The inlet's bypassing scheme was therefore altered. The entrance channel was dredged by hopper and the material placed in an offshore spoil area in about 6-m depth north of the inlet. The south shoal, adjacent to the jetty, was dredged by cutterhead and discharged via pipeline to the north beach. The continued growth of the south shoal forced the channel to migrate northward through the impoundment basin, rendering the basin ineffective and simultaneously acting to undermine the north jetty. The latter effect is exacerbated by the alignment of the north jetty, as the inlet's natural tidal and riverine flow is directed at and against the north jetty. The north jetty's weir section was closed in the 1980s (Partheniades and Purpura 1972; Parker 1979; Jones and Mehta 1980).

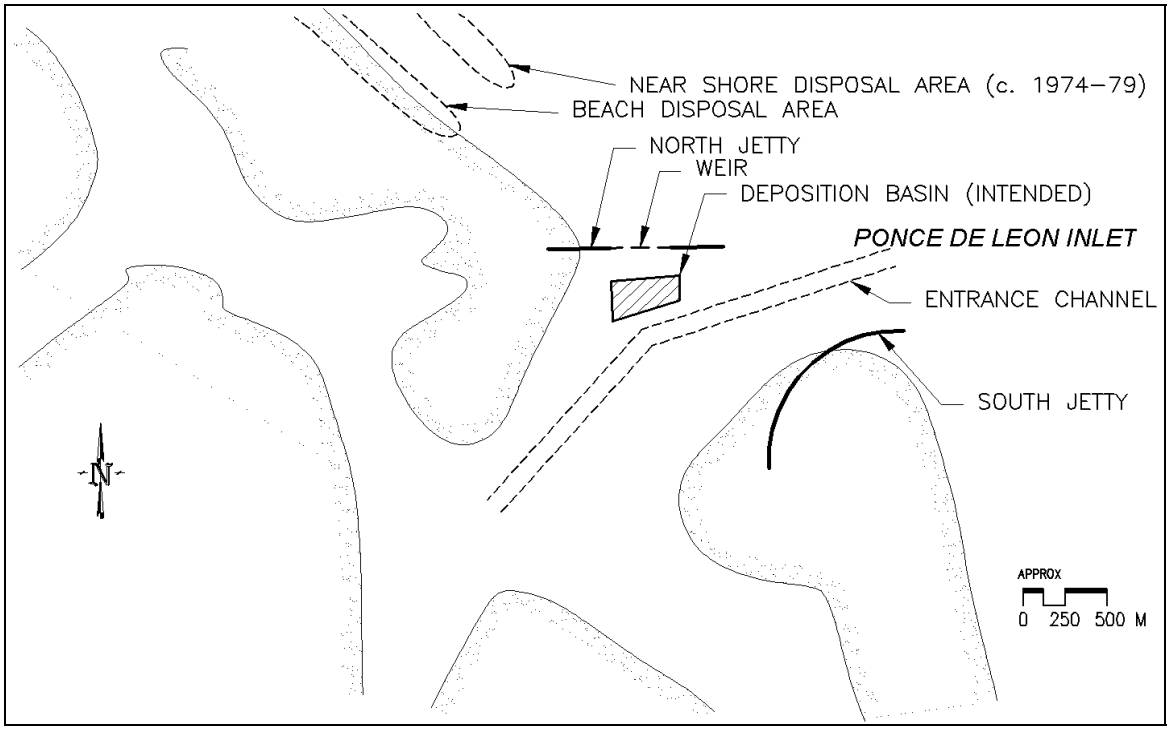

Figure V-6-83. Ponce de Leon Inlet, Florida

(9) Port Canaveral Entrance, Florida. The Canaveral Harbor Federal Navigation Project is located south of the Kennedy Space Center, at Cape Canaveral, along east-central Florida's Atlantic coastline. The net littoral drift is about 152,000 cu m/year to the south. The inlet was artificially created in 1950-52 and stabilized by two rock jetties. The inlet and harbor have always been hydraulically isolated from the interior waters. Tidal flow through the inlet is therefore minimal and there are no ebb or flood tidal shoals. It is estimated that the creation and maintenance dredging of the inlet have resulted in 6 million cu m of updrift impoundment (beyond historical conditions) plus deepwater disposal of another 6 million cu m of littoral material.

(a) Prior to inlet improvements and sand bypassing, sand shoaled the channel in four distinct areas at the seaward and landward ends of the inlet's short, low jetties (Figure V-6-84). The sand from these shoals (typically totaling about 150,000 cu m/year), mixed with up to another 500,000 cu m/year of silt and clay, were annually removed by hopper-dredging and disposed of in deep water, offshore. Beginning in 1992, barge-based clamshell dredging was required in lieu of hopper dredging in order to avoid impacts to marine turtles that loaf at the channel seabed. The mechanically-dredged material, usually placed in 900 to 1,300-cu m scows, was identified in terms of its sand content. Those scow loads containing suitably sandy material (generally less than 10 to 15 percent silt/clay) were placed in a nearshore disposal area about 11 km south (downdrift) of the inlet in 5.5 to 6.5-m water depth (msl). Between 1992 and 1997, about 500,000 cu m of sand were placed in the nearshore disposal area. Attempts to place the material in shallower depths (3.6 to 4.6 m depth) have, to date, been unsuccessful because of the danger and seabed impacts posed to the tugs that tow the scows.

(b) Sand transport over, through, and around the south (downdrift) jetty is estimated to have contributed up to about one-third of the inlet's shoaling and downdrift erosional effects. In 1993, the landward half of the jetty (about 145 m; or, to about -0.5 m, mlw) was temporarily sand-tightened by 1.8-m diam sand-filled geotextile tubes. This resulted in halting about 30,000 cu m/year (about one-third) of the sand transport through the south jetty. In 1995, the south jetty was permanently sand-tightened, raised, and lengthened by driving steel sheet pile immediately adjacent to, and seaward of, the original jetty, and then armoring the sheet pile with boulders. In 1998, the north jetty was sand-tightened by a sand-filled geotextile tube and monitored.

(c) Also in 1995, regular sand bypassing commenced whereby every 6 years, 690,000 cu m (or, 115,000 cu m/year) is dredged by a conventional hydraulic plant and discharged by temporary, submerged pipeline along 3.2 km of shoreline immediately south of the inlet. The dredge area is within the updrift impoundment fillet, along 2.6 km of shoreline immediately north of the inlet, between the mean high waterline and the -5 m-depth contour. The inaugural 1995 operation dredged material from between -1.2 and -5 m (mean sea level) and bypassed very fine sand relative to the native beach (overfill ratio > 2). Monitoring surveys indicate that the 1995 borrow area recovered at a rate equal to or greater than the proposed bypass rate, and that the grain size of the recovering sand is equal to, and sorts itself by depth similarly to, the predredged area. In the first 3 years subsequent to the 1995 bypassing operation and jetty tightening, shoaling of the inlet channel by littoral material appears to have been mostly stopped, and the downdrift beach began to recover toward its preinlet condition (Bodge 1994a, 1994b; Bodge and Hodgens 1997).

(10) South Lake Worth Inlet, Florida. South Lake Worth Inlet (a.k.a. Boynton Inlet) is located on southeast Florida's Atlantic coastline, about 16 km south of Palm Beach. It was opened artificially and stabilized by jetties in 1927 to provide increased flushing of Lake Worth. The net longshore transport rate is about 135,000 cu m/year to the south. By 1932, downdrift erosion prompted local property owners to construct seawalls and groins. By 1936, updrift impoundment saturated the north jetty and led to significant shoaling of the inlet and interior lake. In 1937, a fixed sand transfer plant was constructed atop the north jetty with a dedicated 365-m pipeline discharging sand to the south beach. Between 1937

and 1941, the 15-cm suction intake and 65-hp centrifugal pump bypassed about 55 cu yd/hr; or, 50,400 cu yd/year, on average. The plant was not operated from 1942 through 1945 due to wartime fuel shortages, and the inlet essentially closed. The plant was restarted in 1945 and upgraded in 1948 to a 25-cm suction intake mounted on a swinging boom with 9-m radius, a 20-cm 300-hp centrifugal pump, and 20-cm discharge pipe. The plant's bypassing capacity increased to 76 cu yd/hr. Overall bypassing was also increased by a floating hydraulic dredge that transferred sand from the interior (flood) shoals to the downdrift beach. In 1967, the north and south jetties were extended by 125 m and 20 m, respectively; and, the fixed sand transfer plant was shifted 36 m seaward and increased to a 25-cm pump with 400-hp motor. Portions of the north jetty were sealed in 1971.

(a) The present plant consists of a 30.5-cm suction intake and 25-cm discharge line driven by a 400-hp diesel engine rated to pump 4,000 gpm with up to 20 percent suspended solids. The plant is similar in appearance to that shown in Figure V-6-59. Productivity estimates vary from 95 to 122 cu m/hr. Palm Beach County operates the plant. Local (updrift) interests require that the plant be operated only during wave/transport events from the northeast. Productivity is limited by the crater's size (about 460 cu m) and its sand-infilling rate. The plant's annual bypassing rate averages about 50,000 cu m/year. Of the net incident littoral drift, it is estimated that about 45 percent is naturally bypassed across the ebb-delta plateau, 35 percent is bypassed by the fixed plant, 2 percent is bypassed by periodic hydraulic dredging of the interior (flood) sand trap. The remaining 18 percent is diverted from the littoral system by updrift impoundment and transport to the ebb shoal. It is predicted that the bypassing plant's capacity could be significantly improved by increasing the length of the boom upon which the suction intake is mounted, and by mounting the plant on a mobile platform atop the jetty or adding one or more jet pumps near the jetty's seaward end (Jones and Mehta 1977; Olsen Associates, Inc. 1990).

(b) A similarly-sized, electrically-powered plant operated from the north jetty of Lake Worth Inlet, to the north, from 1957 through the early 1980s. Between 1967 and 1978, the plant is estimated to have bypassed about 102,000 cu m/year (Jones and Mehta 1977).

(11) Boca Raton Inlet, Florida. Boca Raton Inlet is located about 25 km north of Fort Lauderdale on southeast Florida's Atlantic coastline (Figure V-6-84). The net longshore transport rate is estimated as about 124,000 cu m/year to the south. This natural inlet was improved by dredging in 1925-26. Jetties were constructed in 1930-31 and repaired in 1952. These works resulted in erosion of the downdrift (south) beach and promoted the growth of a large ebb shoal that threatened navigation through the inlet. In 1975, the city of Boca Raton undertook a 55-m extension of the north jetty and 165-m sand-tightening of the south jetty. In 1980, a 20-m weir was cut into the north (updrift) jetty to allow sand to enter the inlet throat to facilitate bypassing by the city-owned dredge.

(a) It is estimated that about 36,000 cu m/year enters the inlet through the weir and around the jetty from the north (updrift) shoreline, and that about 4,300 cu m/year enters the inlet from the south (downdrift) shoreline, for a total of 40,300 cu m/year. On average, the city's dedicated, floating hydraulic dredge bypasses this quantity, working mostly year-round, to the south shoreline. In addition, about 176,000 cu m of sand is removed by hydraulic, cutterhead pipeline dredge from the ebb shoal about once every 10 years, and is placed along 1.2 km of shoreline south of the inlet.

(b) Of the 124,000 cu m of net incident drift (approximate), it is estimated that about 30 percent is bypassed by the dedicated floating dredge, 50 percent is naturally bypassed across the ebb-tidal shoal, and 20 percent is diverted to the ebb shoal or offshore. The periodic (10-year) dredging of the ebb shoal is intended to capture at least a portion of the latter quantity for bypassing to the south (Jones and Mehta 1980; Coastal Planning and Engineering 1996; Olsen Associates, Inc. 1997).

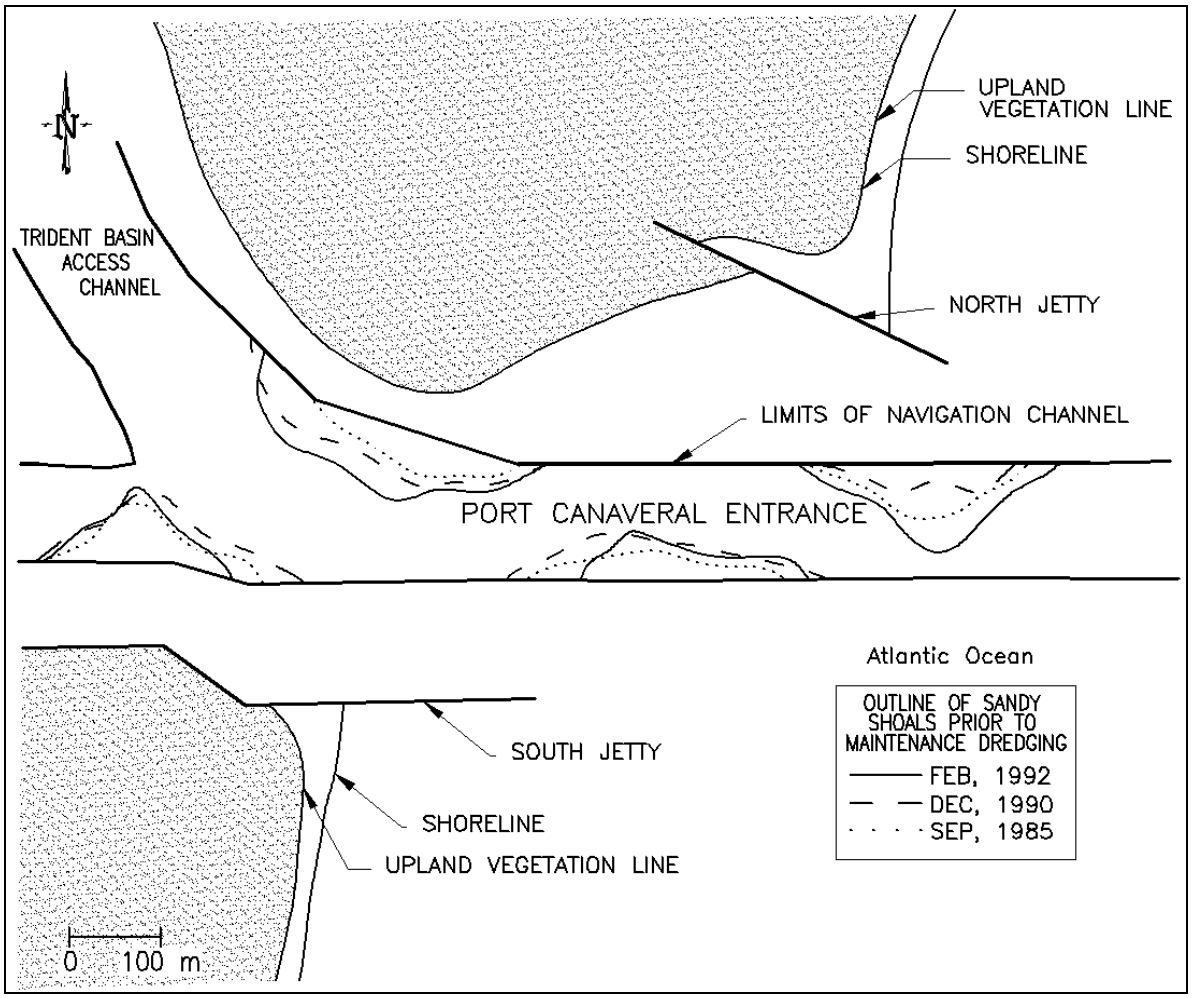

Figure V-6-84. Historical locations of sandy shoals within Port Canaveral Entrance, Florida (prior to implementation of inlet/jetty improvements). Adapted from Bodge 1994a

(12) Hillsboro Inlet, Florida. Hillsboro Inlet, about 9 km south of Boca Raton Inlet, or 16 km north of Ft. Lauderdale, is located on southeast Florida's Atlantic coastline. The net incident littoral drift is estimated as 92,000 cu m/year to the south. This inlet features a natural reef that forms its northern (updrift) boundary. This reef acts as a sand weir; and, in fact, the modern concept of an inlet weir originated at this inlet (Hodges 1955). Sand transported over this reef/weir and around the inlet's two jetties, amounting to about 74,700 cu m/year in total, is bypassed to the south (downdrift) shoreline via a dedicated 20-cm hydraulic dredge and pipeline owned and operated by the inlet's local authority. Of the incident net drift, it is estimated that about 14.5 percent is impounded updrift of the inlet, 64 percent is transported into the inlet (and bypassed by dredging), 18.5 percent is naturally bypassed across the ebb tidal shoal, and 3 percent is lost offshore. Of the net 74,700 cu m dredged and bypassed from the inlet each year, about 78 percent is estimated to originate from the updrift (north) shoreline, while the other 22 percent is sand that returns from the downdrift (south) shoreline into the inlet. Improvements to the south jetty and extending the discharge distance further downdrift of the inlet is predicted to improve sand management at the inlet (Jones and Mehta 1980; Coastal Planning and Engineering 1991; Olsen Associates, Inc. 1997).

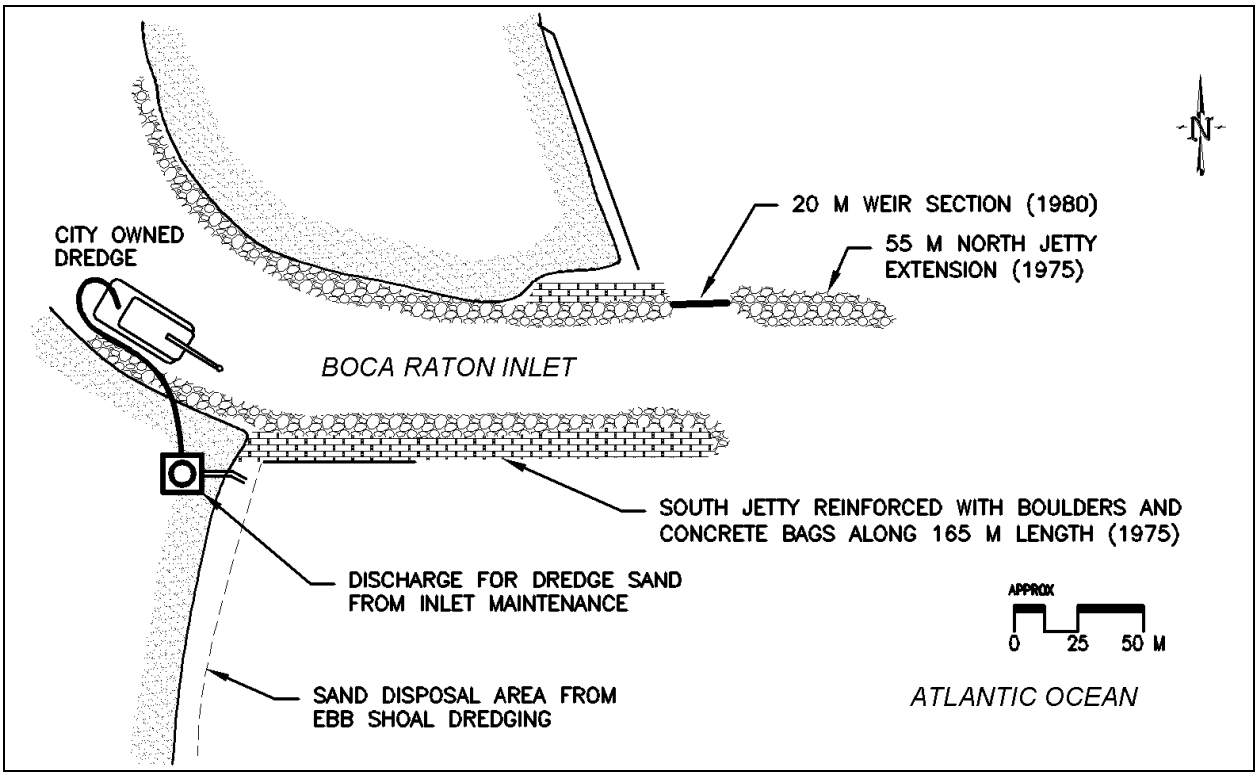

Figure V-6-85. Boca Raton Inlet, Florida

(13) Port Sanilac, Michigan. Port Sanilac is a small-craft harbor on Lake Huron, about 100 km north of Detroit. In the later 1970s, a portable, truck-mounted jet pump system was built by the U. S. Army Waterways Experiment Station (currently the U.S. Army Engineer Research and Development Center) and tested at the harbor for sand bypassing. A 12-m flatbed trailer was outfitted with a fuel tank, generator, air compressor, control room, and water supply and booster pumps with diesel engine drives. The jet pump water supply and slurry discharge lines were supported by foam floats designed to allow the jet pump to sink into the seabed while dredging. To raise the jet pump, air was pumped through the water supply line to a flotation unit attached to the jet pump. The jet pump was steered in the water by diverting water from the supply line through two nozzles attached to the sides of the pump. The system was designed to be driven onto an accretion fillet where the jet pump could be deployed and operated near the shoreline. Discharge from the pump was carried by pipeline along the harbor bottom to the downdrift beach. System technicians reported that the system worked extremely well for its designed purpose. However, resistance by updrift property owners often precluded bypassing operations from the accretion fillet. The system was used mainly as a rehandling device for material released by hopper dredges. For this purpose it was driven onto a barge and operated as a floating dredge. The system was surplused by the U.S. Army Engineer District, Detroit, in 1980, and acquired by the state of Michigan in July 1988 (EM 1110-2-1616).

(14) Viareggio Harbor and Marina di Carrara, Italy. The harbors of Viareggio and Marina di Carrara are located on the northwest coast of Italy on the Mediterranean Sea. The former is about 22 km south of the latter. The net littoral drift at Viareggio is about 200,000 cu m/year toward the north, while the net drift at Marina de Carrara is toward the south.

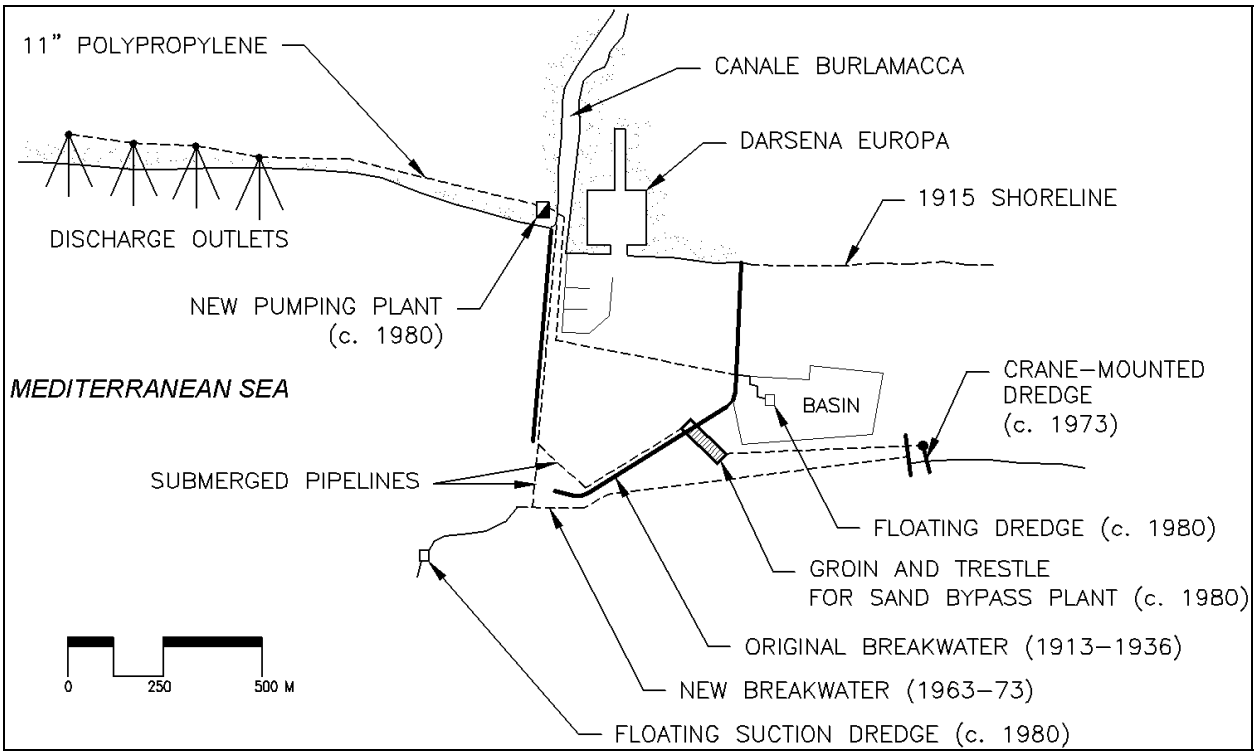

Figure V-6-86. Viareggio Harbor, Italy

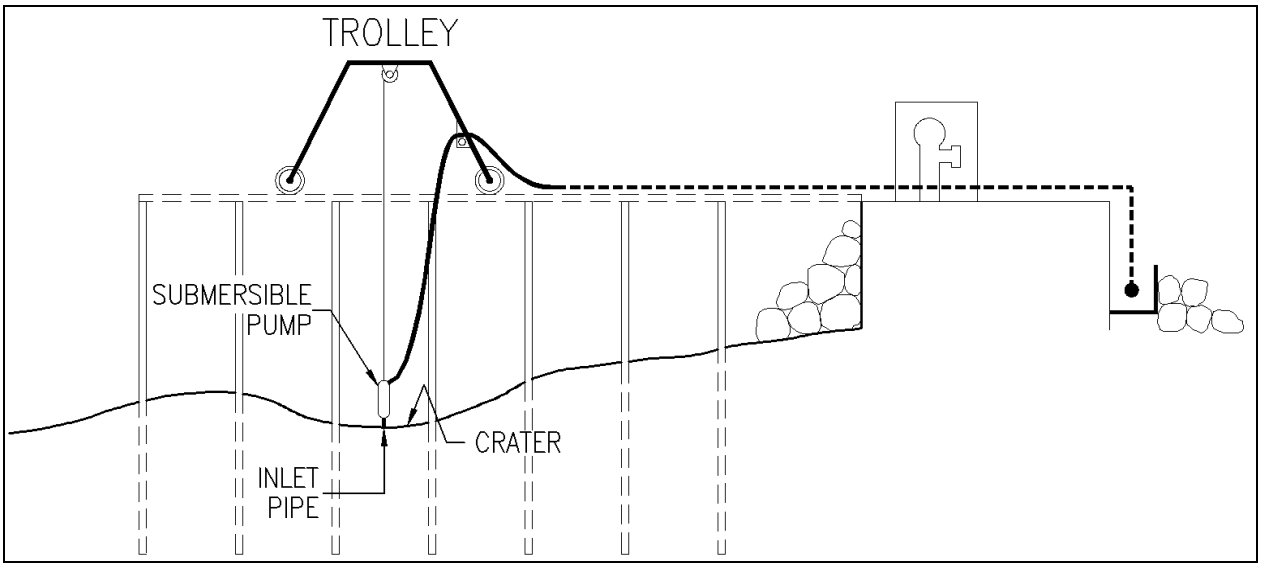

Figure V-6-87. Original sand bypassing plant at Viareggio Harbor, Italy

(a) Navigational improvements at Viareggio date from the Roman Empire. In 1913, an outer harbor was created by the construction of a shore-attached breakwater (Figure V-6-86). As a result, the updrift (south) beach accreted about 20 m/year, the harbor shoaled, and the downdrift beach eroded dramatically. In 1936, 220,000 cu m were dredged from the outer harbor and discharged to the downdrift (north) beach via 60 cm (24 in.) pipeline. This represented the first application of sand bypassing, and artificial beach nourishment, in Italy. In the early 1950s, a spur groin was built along the south breakwater in an

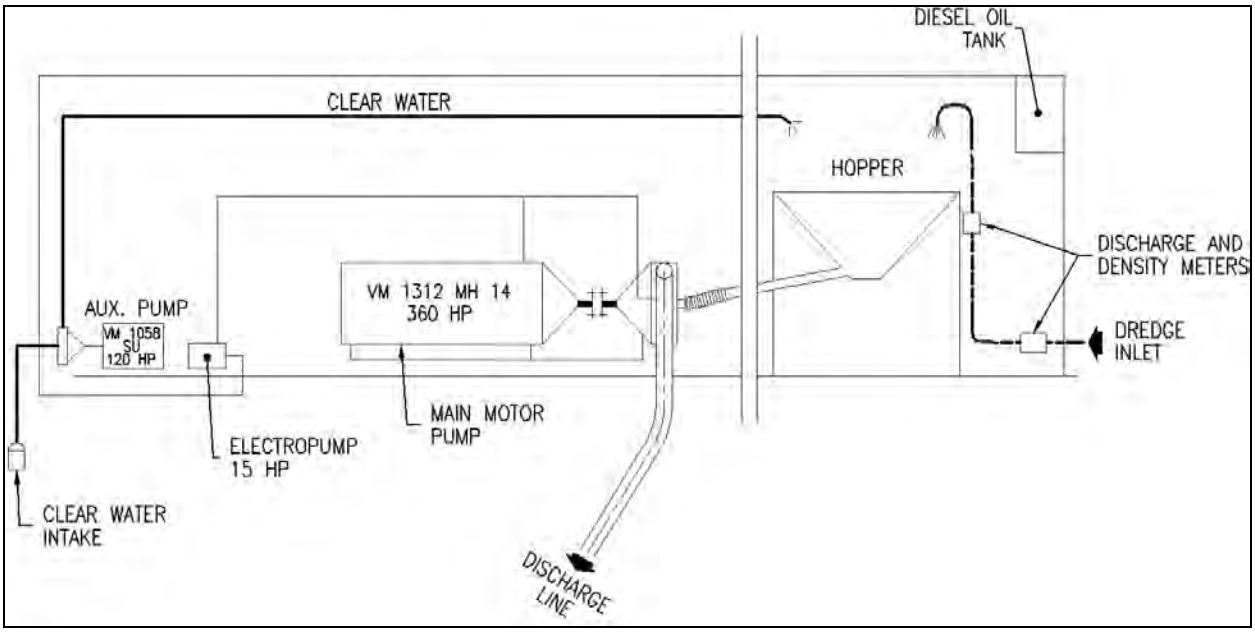

Figure V-6-88. Existing sand bypass pump system at Viareggio Harbor, Italy

attempt to arrest sand transport along the breakwater. A trestle-mounted sand bypassing plant was subsequently built atop this spur groin (Figure V-6-87). The plant consisted of an immersed pump body mounted upon a trolley that ran along tracks. The dredged material was discharged at the root of the north jetty via a 18-cm (7-in.) pipeline. The pump dredged a series of "holes" underneath the installation to serve as traps for the sand. These holes quickly filled with debris and seaweed, and interfered with the plant's intended operation. At the same time, the groin tended to push the sand offshore along a bypassing bar and reduced the rate at which sand reached the plant.

(b) In the early 1970s, a new breakwater was constructed seaward of the original breakwater, and a new basin was excavated into the beach that had been accumulated against the structure. The original sand bypassing plant, now within the uplands of the new breakwater, was relocated to the south. The trolley system was replaced by a crane that would allow sand to be removed from a larger area (i.e., greater potential crater size). The old works were transformed to a booster pump plant. The relocated, crane-mounted bypass plant was never put into operation, however, as the harbor's new authority suspended its operation and the new breakwater caused the updrift beach to rapidly overtake the new plant's location.

(c) In 1980, Viareggio Harbor's existing bypassing system was installed. It is based upon a flexible, mobile scheme to ensure bypassing productivity. Material can be dredged by floating suction dredges from the outer harbor, the new large basin, the updrift beach, or outside the harbor entrance. Suitable dredged material is pumped via submerged pipeline toward the principal pumping station located at the root of the north jetty. The new pumping plant was designed to receive variable sediment discharges and densities, transforming them into suitable slurries for beach discharge. Water-cooled diesel engines are used. An auxiliary plant is used to control the supply of material to the bypassing plant by pumping water into a hopper to compensate for periods when discharge from the dredge platforms is insufficient (i.e., when only one dredge is operating). (See Figure V-6-88). Recent improvements to the plant (combining the discharge from the two dredge platforms) allow up to 1,100 cu m/hr of slurry with 20 percent solids volume. From 1980 to 1985, 380,415 cu m of sand were bypassed over 3,623 operating hours, for an average sand discharge rate of 105 cu m/hr.

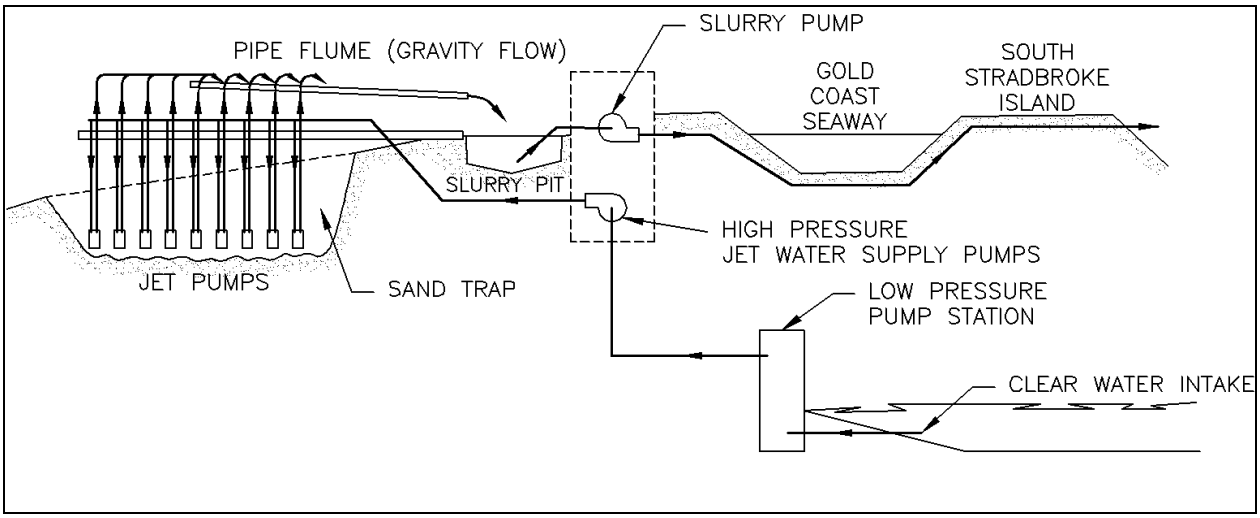

Figure V-6-89. Sand bypassing system at Nerang River entrance (schematic)

(d) Marina di Carrara is similar in geometry to Viareggio Harbor. A pilot bypassing plant was installed in 1965-66 using a floating dredge inside the harbor and five slurry booster pumps onshore along a 6-km-long 14-cm- (5.5-in.) discharge pipeline with multiple outlets. While the system's components reportedly worked well, net productivity was limited, and the material dredged from the harbor was mostly silt and fine sand that was poorly suited for beach placement.

(e) A second bypassing plant was installed in 1967-68. A fixed plant was installed updrift of the harbor entrance, as at Viareggio, but this time a mobile crane could operate on a large-diameter platform in order to reach a wide area far from the platform's foundation piles. After initial success in 1969, productivity declined as the dredged craters filled with debris, and the sand in-filling rate was dependent upon storm conditions. Operation was suspended when the platform collapsed after a ship collision (Fiorentino, Franco, and Noli 1985).

(15) Nerang River Entrance, Queensland, Australia. The Nerang River entrance is located on Queensland's Gold Coast, along Australia's central eastern coastline on the Pacific Ocean. The northerly longshore transport rate is large and dominant (580,000 cu m/year) compared to the southerly transport (84,000 cu m/year). In 1984-85, the inlet entrance, which naturally migrated northward at an average rate of over 36 m/year, was relocated southward by dredging a new navigation channel stabilized by dual rock jetties. In 1985-86, construction of a fixed sand bypassing plant was completed. The plant consists of a 490-m-long pier/trestle located 250 m updrift, and parallel to, the south jetty. Ten jet pumps are spaced approximately every 30 m along the outer 270 m of the pier. The 9-cm (3.5 in.) Genflo "Sand Bug" jet pumps, each rated at 103 cu m/hr (135 cu yd/hr), are attached to wide flange steel beams that slide down a second set of steel support beams attached to the pier's concrete piles. Stops on the beams prevent the pumps from penetrating below their design depth of -10 m (msl).

(a) Supply water to the jet pumps is drawn from the inlet interior via a 122-cm (4-ft) concrete pipe using two low-pressure pumps, each rated at 250 hp and 10,300 gpm (see Figure V-6-89). Water from these pumps flows through a 61-cm (2-ft), 700-m-long pipeline to the main pump house, where it feeds dual 450-hp supply pumps (10,200 gpm each). High pressure water from the supply pumps flows from the pump house through a 36-cm (14-in.) pipeline to the jet pumps. Solenoid-actuated valves control the flow of water to the 15-cm (6-in.) lines that feed each jet pump. Supply water can also be directed to fluidizers on each jet pump. These are used during installation and removal, and to improve transfer capacity when debris has collected around a jet pump. The jet pumps' slurry is discharged through 24-cm

(9-in.) pipes into an elevated pipe flume. The 58-cm- (23-in.-) diam flume, 370 m long and sloped at 2.5 deg, allows gravity flow of the slurry to a conical, 145 cu m-buffering hopper. The flume and hopper were intended to allow the incoming slurry to vary widely in solids content and volume. Make-up water for the flume and hopper, when necessary, can be supplied by clear water from a jet pump. A 950-hp (6,500 gpm) centrifugal booster pump transfers the slurry from the hopper, via pipeline under the inlet entrance, to three discharge points along the uninhabited, downdrift (north) shoreline.

(b) The system is computer controlled, allowing unattended bypassing operations at night to take advantage of lower electric rates. During the day, two full-time employees perform maintenance operations and program the system for the evening's operation as a function of the level of sand within each pump's crater. Should the percent solids fall below a preset value, the computer enables a new series of jet pumps to operate. If a major problem is sensed, the computer telephones an operator at home.

(c) In normal operation, the system bypasses sand at 333 cu m/hr (435 cu yd/hr) at 30.6 percent solids, for a discharge pipeline flow of 6,250 gpm. Under peak conditions, the system bypasses sand at 570 cu m/hr at 40 percent solids. The system was designed for an average yearly transport of about 500,000 cu m, a peak yearly transport of about 750,000 cu m, and maximum 5-day transport of about 100,000 cu m. During the first 22 months after commencing operation, the system bypassed approximately 1 million cu m of sand. The nearshore jet pumps bypass the great majority of the sand volume (see Figure V-6-71). The craters' infilling rate, and therefore overall productivity, is a function of incident wave energy.

(d) Principal problems with the system have included wear on the jet pump nozzles and debris within the craters. Nozzle replacement and periodic debris clearing requires use of a 20-ton crane to remove the jet pumps from their trestle support. In 1987-88, a large-diameter, 23-cm (9-in.) jet pump was introduced to dredge and bypass the debris that chronically collects at the bottom of the craters. This pump is intended for periodic operation at each of the jet pump's craters. Its large size requires the entire output from the supply pump. Experience has suggested that an alternate to the slurry's flume design, and variable (flexible) spacing of the jet pumps along the pier, would improve productivity (Polglase 1987; Pound and Witt 1987; Clausner 1988; Coughlan and Robinson 1990).

(16) Other projects. Numerous other sand bypassing systems have been attempted or incorporated at other tidal inlets that were not described. In the United States these include, among others, Fire Island Inlet, New York; Carolina Beach Inlet, South Carolina; Murrells Inlet, South Carolina; Little River Inlet, South Carolina; Carolina Beach Inlet, North Carolina; Cape Fear River Entrance, North Carolina; St. Marys River entrance, Florida; St. Johns River entrance, Florida; Sebastian Inlet, Florida; Jupiter Inlet, Florida; St. Lucie Inlet, Florida; Mexico Beach, Florida; East Pass, Florida; Perdido Pass, Alabama; and the Colorado River mouth, Texas.

b. Lessons learned.

(1) Inlet shoaling and its impact to navigation is intimately linked to beach response adjacent to inlets. Project planning that fails to recognize and take advantage of this link, that is, planning which isolates the objectives of navigation from those of shore protection, is less likely to develop an inlet sediment management program that is physically, economically, or environmentally optimal. Sand management at inlets is apt to be most successful when inlet improvements are viewed from a holistic approach that examines the inlet's sediment transport pathways, channel alignments and requirements, and adjacent beach processes as an integrated system. This implies that piecewise justification of proposed inlet / navigation project improvements (i.e., benefits based singularly upon navigation benefits or decreased dredging costs or oceanfront storm protection, etc.) should be discouraged in favor of system-wide benefits analysis.

(2) Failure to appreciate the direction, magnitude, and variability of a site's littoral drift, both gross and net, is central to many, if not most, problems of inlet shoaling and inlet-related beach erosion. Realistic evaluation of an inlet improvement project's potential performance requires that the site's transport portfolio be accurately understood. This includes an appreciation of how the littoral drift rates vary in the immediate vicinity of the inlet, particularly due to perturbations associated with the inlet's shoals and other nuances of the nearshore bathymetry. Development of an inlet sediment budget is an important step in determining requisite sand bypassing/backpassing requirements. Measurements of downdrift beach changes, by themselves, may not accurately reflect the magnitude of requisite bypassing. This is because shoreline and volume changes along downdrift beaches, especially those that have suffered chronic erosion, are usually obfuscated by shoreline armoring and beach nourishment projects; and, downdrift impacts may extend much further than expected in alongshore magnitudes that are difficult to perceive from periodic surveys. Beyond knowledge of the global, incident transport rates at an inlet site, understanding the specific transport pathways through and around an inlet, particularly at an improved inlet, is a prerequisite to identifying the most economically and physically effective system for sediment management. In many instances, project designers have failed to recognize the most obvious routes by which sand enters and is dispersed through the inlet and/or by which the adjacent shoreline erodes. Repeated visitation to the site during various wave regimes, discussions with local individuals knowledgeable of the inlet, and scrutiny of surveys that depict the patterns of sedimentation within the inlet are all elementary, but invaluable, means by which to preliminarily accomplish, or verify, this understanding.

(3) Historically, insufficient attention has been given to the height, length and porosity of downdrift jetties. Problems of both shoaling and beach erosion on the downdrift beaches can almost always be improved by sand-tightening the downdrift jetty. Sand-tightening of the updrift jetty, by improving crest elevation, length, and/or impermeability, may also be warranted unless transport through or past the jetty is desired for purposes of interior trapping. In improving an updrift jetty, however, it is important to ensure that updrift impoundment will not result along properties from which the sediment cannot be dredged (recovered) and will not result in an offshore diversion of the sediment.

(4) For sediment management systems that rely upon deposition traps, it is essential that the traps' capacities are large enough to stably contain the material between economically-optimal dredging events; the traps be dredged (downloaded) when they become full or near-full; the geometry and orientation of the traps be configured to intercept the inlet's specific transport pathways; and the traps be located outside of tidal- and wave-induced currents that will move material out of the traps. Poor performance of inlet weir systems, which must include one or more deposition basins (traps) to function properly, can almost always be attributed to a failure to achieve one or more of these four requirements. When a weir system is used, it must include a deposition basin of particularly large capacity, particularly at and landward of the shoreline/weir interface. Provisions must be likewise made to ensure reliable, safe dredging of the basin on a routine basis. In some cases (e.g., Ponce de Leon Inlet, Florida; East Pass, Florida), weirs have been constructed on the incorrect side of the inlet due to a lack of appreciation of the local sediment transport patterns that result from conditions particular to the inlet site.

(5) The productivity of bypassing systems that utilize fixed or semifixed pumps is most typically limited by the rate of crater infilling and debris problems. In most cases, the mechanical or hydraulic capacity of the pumps has not typically limited production; instead, productivity is often ultimately limited by the rate and reliability with which littoral material refills the pumps' dredged craters. Likewise, productivity decreases, and operating expense increases, with the amount of time and effort spent clearing debris from the pumps' craters. Success of these systems requires that that there are sufficiently large dredging areas which the pumps can access, and that these areas are within the zones of highest littoral drift, and that there is a means by which to limit (or remove) the influx of debris. Fluidizers mounted at the pumps' nozzles (intakes) agitate and suspend the seabed sediment. These are of

proven success in improving productivity. Fluidizers constructed across the seabed which are sloped toward the pumps' intake, intended to augment delivery of sediment to the pumps, may be of benefit in increasing the craters' effective size. However, such fluidizers have demonstrated some limitations due to sediment intrusion (blockage) and their use is still considered experimental. Where fluidizers, debris-clearing pumps, and other ancillary devices are used in conjunction with the bypassing pumps, experience demonstrates that there can be a significant net benefit in providing pumps and engines dedicated to these devices; i.e., separate from those used to supply and power the bypassing pumps. Reliable and economic means to lift, remove, and redeploy fixed pumps, for servicing and debris removal, should likewise be considered. Corrosion and wear of the pumps' elements should be given additional consideration beyond normal marine concerns, particularly those elements at and near the sediment intakes.

(6) At most inlets with long-term prototype sand bypassing experience, and at most new sites with dedicated plants, the systems have evolved toward, or have recommended for, increased mobility and flexibility. Because of the dynamic nature of the sediment transport pathways (and the bypassing systems' effects thereupon), and in view of earlier systems' chronic problems with unreliable infilling of dredge craters, modern systems are moving toward multiple pumping locations and/or pumps and dredges mounted on mobile devices. The former includes deployment of jet pumps or similar devices across a variety of areas within the inlet system, with the capability to bypass from one or more of these devices at different times of the year. The latter includes jet pumps or similar devices mounted on mobile cranes, trestles, barges or trucks; or, the use of a dedicated or contracted dredge to intercept sediment across a large (and potentially variable) area.

(7) Other problems encountered with fixed, semifixed, or other dedicated bypassing pumps have included operational limitations imposed by the presence of environmental resources, social (recreational) considerations, and/or upland property owners that protest the transfer of sand. An additional, frequent problem has been the physical reliability and dedication of the operation; i.e., lack of long-term funding, manpower, and/or commitment to operate the system. System interruptions are especially problematic for those plants that have difficulty starting up after extended layoffs or heavy sedimentation.

(8) Where littoral and nonlittoral material mix within an inlet, benefit can be derived by identifying structural means or dredging techniques to separate the material. This includes, for example, training structures that isolate littoral deposition from the influence of ambient silts and clays; or, selective use of smaller or mechanical dredges that can recover the littoral material (in lieu of hopper dredges that mix the material).

(9) The benefit of nearshore disposal of suitable, dredged material is maximized with increasingly shallow depths of placement. Poorly-controlled placement across large seabed areas, and/or in water depths predicted to result in stable berms, do not yield readily discernible benefits to the adjacent shorelines.

(10) The nature and grain sizes of the bypassed material and the adjacent beaches should be examined for compatibility. Sediment intercepted at deeper areas within the inlet system, or from potentially contaminated areas, may not be suitable for beach placement or may not fully represent a one-to-one transfer (bypass) of sediment across the inlet.

(11) As each tidal inlet is more or less unique unto itself, the most appropriate sediment management strategy at a given inlet is unique. A system that is successful at one inlet will not necessarily be viable or successful at another. Often, a combination of structural improvements, dredging equipment and changes in dredging practices will be required, rather than a single modification. Existing or historical practices may require significant revision or abandonment. Such improvements can often be the most difficult to

implement because of resistance to change and/or the perception that such changes are untested, more costly, or inconsistent with policy.

(12) Most generally, successful sediment management at inlets requires that the incident sediment be intercepted for purposes of subsequent handling. Uncontrolled deposition of sediment, or deposition within areas from which recovery is not feasible, is contrary to effective sediment management. When littoral material is transported across a large or dynamic area of the inlet, it is more likely to be mixed with unsuitable material, lost offshore, deposited in thin veneers that are not physically suited to dredging, and/or to interfere with navigation. There are also many areas within inlet systems from which dredging is severely limited. These include areas of environmental sensitivity (seagrass beds, shellfish areas, aquatic preserves, contaminated seabeds, etc.) and areas where upland property owners control or block local dredging activity. If deposition traps are not used to intercept the sediment within or before the inlet, then pumps or other dredging equipment must be positioned so as to reliably intercept, or to move and intercept, the material before it is lost to the inlet. This better ensures that the material will not contribute to navigation problems within the inlet, and that the sediment can be ultimately restored to the littoral system.

V-6-7. References

EM 1110-2-1616
EM 1110-2-1616, "Sand Bypassing System Selection"

EM 1110-2-1810
EM 1110-2-1810, "Coastal Geology"

Anders and Byrnes 1991
Anders, F. J., and Byrnes, M. R. 1991. "Accuracy of Shoreline Change Rates as Determined from Maps and Aerial Photographs," *Shore and Beach*, Vol 59, No. 1, pp 17-26.

Applied Technology Management, Inc. 1992
Applied Technology Management, Inc. (ATM). 1992. "St. Lucie Inlet Management Plan, Comprehensive Master Plan." (Report prepared for Board of County Commissioners, Martin County, Florida, 242 pp.)

Aubrey and Speer 1984
Aubrey, D. G., and Speer, P. E. 1984. "Updrift Migration of Tidal Inlets," *Journal of Geology*, Vol 92, pp 531-545.

Bailard and Jenkins 1982
Bailard, J. A., and Jenkins, S. A. 1982. "City of Carpenteria Beach Erosion and Pier Study," Report prepared for the City of Carpenteria, CA.

Barwis 1975
Barwis, J. H. 1975. "Catalog of Tidal Inlet Aerial Photography," U.S. Army Corps of Engineers, GITI Report 75-2, June 1975.

Barwis 1976
Barwis, J. H. 1976. "Annotated Bibliography on the Geologic, Hydraulic, and Engineering Aspects of Tidal Inlets," U.S. Army Corps of Engineers, GITI Report 4, Jan. 1976.

Berek and Dean 1982
Berek, E. P., and Dean, R. G. 1982. "Field Investigation of Longshore Transport Distribution." *Proceedings of the 18th International Conference on Coastal Engineering.* American Society of Civil Engineers, New York, pp 1620-39.

Birkemeier 1985
Birkemeier, W. A. 1985. "Field Data on Seaward Limit of Profile Change," *Journal of Waterway, Port, Coastal and Ocean Engineering*, ASCE, Vol 111, No. 3, pp 598-602.

Bisher and West 1993
Bisher, D. R., and West, F. W. 1993. "Jet Pumps and Fluidizers Working Together: The Oceanside Experimental Sand Bypass System," *Proceedings of the Beach Preservation Technology.* Florida Shore and Beach Preservation Association, Tallahassee, FL, pp 207-222.

Bodge 1993
Bodge, K. R. 1993. "Gross Transport Effects and Sand Management Strategy at Inlets," *Journal of Coastal Research,* Special Issue 18, Fall 1993, pp 111-124.

Bodge 1994a
Bodge, K. R. 1994a. "Performance of Nearshore Berm Disposal at Port Canaveral, Florida." *Proceedings of Dredging '94.* ASCE, New York.

Bodge 1994b
Bodge, K. R. 1994b. "The Extent of Inlet Impacts upon Adjacent Shorelines," *Proceedings of the 24th International Conference on Coastal Engineering*, ASCE, New York, pp 2943-57.

Bodge 1999
Bodge, K. R. 1999. "Inlet Impacts and Families of Solutions for Inlet Sediment Budgets." *Proceedings, Coastal Sediments '99.* ASCE, Reston, VA, pp 703-718.

Bodge, Creed, and Raichle 1996
Bodge, K. R., Creed, C. G., and Raichle, A. W. 1996. "Improving Input Wave Data for Use with Shoreline Change Models," Vol 122, No. 5, ASCE, New York.

Bodge and Hodgens 1997
Bodge, K. R., and Hodgens, E. 1997. "Recovery of a Nearshore Borrow Area for Inlet Sand Bypassing." *Proceedings of the Conference on Beach Preservation Technology '97.* Florida Shore and Beach Preservation Association, Tallahassee, FL.

Bottin 1992
Bottin, R. R. 1992. "Oceanside Harbor, California: Design for Harbor Improvements," Technical Report CERC-92-14, U.S. Army Engineer Waterways Experiment Station, Vicksburg, MS.

Bowen and Inman 1966
Bowen, A. J., and Inman, D. L. 1966. "Budget of Littoral Sand in the Vicinity of Point Arguello, California," Technical Memorandum No. 19, U.S. Army Coastal Engineering Research Center, 56 pp.

Brooke 1934
Brooke, M. M. 1934. "Shore Preservation in Florida," with discussion, *Shore and Beach*, Vol 2, No. 4, pp 151-154.

Brouwer, van Berk, and Visser 1992
Brouwer, J., van Berk, H., and Visser, K. G. 1992. "The Construction and Nearshore Use of the Punaise: A Flexible Submersible Dredging System," *Proceedings of the XIIIth World Dredging Congress*, Bombay, India, April 1992.

Browder 1995
Browder, A. E. 1995. "Wave Transmission and Current Patterns Associated with Narrow-Crested Submerged Breakwaters." *Proceedings of the Beach Preservation Technology '95*. Florida Shore and Beach Preservation Association, Tallahassee, FL, pp 348-364.

Browder 1996
Browder, A. E. 1996. "Wave Refraction and Littoral Transport Modeling of St. Lucie Inlet, FL." Olsen Associates, Inc., Jacksonville, FL, December, 1996.

Bruun 1962
Bruun, P. 1962. "Sea Level Rise as a Cause of Shore Erosion," *Journal of Waterways and Harbors Division*, ASCE, Vol 88, pp 117-130.

Bruun 1966
Bruun, P. 1966. "Tidal Inlets and Littoral Drift," *Stability of Coastal Inlets.* Vol 2, 193 pp. (Published by the author, copies available from Coastal Engineering Archives, Weil Hall, University of Florida, Gainesville, FL).

Bruun 1981
Bruun, P. 1981. *Port Engineering*. 3rd ed., Gulf Publishing Co., Houston, TX.

Bruun 1988
Bruun, P. 1988. "The Bruun Rule of Erosion by Sea-Level Rise: A Discussion of Large-Scale Two- and Three-Dimensional Usages," *Journal of Coastal Research*, Vol 4, pp 627-648.

Bruun 1993
Bruun, P. 1993. "An Update on Sand Bypassing Procedures and Prices," *Journal of Coastal Research*, Special Issue 18, Fall 1993, pp 277-284.

Bruun 1995
Bruun, P. 1995. "The Development of Downdrift Erosion," *Journal of Coastal Research*, Vol 11, No. 4, Fall 1995, pp 1242-57.

Bruun and Gerritsen 1959
Bruun, P., and Gerritsen, F. 1959. "Natural Bypassing of Sand at Coastal Inlets," *J. Waterways and Harbors Division* ASCE, Vol 85, No. 4, pp 75-107.

Bruun and Gerritsen 1960
Bruun, P., and Gerritsen, F. 1960. *Stability of Coastal Inlets*. North-Holland, Amsterdam, 140 pp.

Bruun, Mehta, and Johnsson 1978
Bruun, P., Mehta, A. J., and Johnsson, I. G. 1978. *Stability of Tidal Inlets*. Developments in Geotechnical Engineering, Vol 23, Elsevier, New York, 510 pp.

Bruun and Willikes 1992
Bruun, P., and Willikes, G. 1992. "Bypassing and Backpassing at Harbors, Navigation Channels, and Tidal Entrances: Use of Shallow-Water Draft Hopper Dredgers with Pump-Out Capabilities," *Journal of Coastal Research*, Vol 8, No. 4, pp 972-977.

Burke and Allison 1992
Burke, C. E., Allison, M. C. 1992. "Design Guidance for Nearshore Berms: Crest Length and End Slope Considerations," *Proceedings of the 1992 National Conference on Beach Preservation Technology*, Florida Shore and Beach Preservation Association, Tallahassee, FL, pp 180-193.

Byrnes and Hiland 1994
Byrnes, M. R., and Hiland, M. W. 1994. "Compilation and Analysis for Shoreline and Bathymetry Data (Appendix B)," In: N. C. Kraus, L. T. Gorman, and J. Pope (ed.) "Kings Bay Coastal and Estuarine Monitoring and Evaluation Program: Coastal Studies," Technical Report CERC-94-09, Coastal Engineering Research Center, Vicksburg, MS, B1-B90.

Caldwell 1951
Caldwell, J. M. 1951. "By-passing Sand at South Lake Worth Inlet, Florida." *Proceedings, First Conference on Coastal Engineering.* Long Beach, California, October 1950, J. W. Johnson, ed., Council on Wave Research, The Engineering Foundation, pp 320-325.

Caldwell 1966
Caldwell, J. M. 1966. "Coastal Processes and Beach Erosion," *Journal of the Society of Civil Engineers*, Vol 53, No. 2, pp 142-157.

Chasten 1992
Chasten, M. A. 1992. "Coastal Response to a Dual Jetty System at Little River Inlet, North and South Carolina," Miscellaneous Paper CERC-92-2, U.S. Army Engineer Waterways Experiment Station, Vicksburg, MS.

Chu, Lund, and Camfield 1987
Chu, Y.-H., Lund, R. B., and Camfield, F. E. 1987. "Sources of Coastal Engineering Information," TR-CERC-87-1, Coastal Engineering Research Center, U.S. Army Engineer Waterways Experiment Station, Vicksburg, MS.

Cialone and Stauble 1998
Cialone, M. A., and Stauble, D. K. 1998. "Historic Findings on Ebb Shoal Mining," *J. Coastal Res.*, Vol 14, No. 2, pp 537-563.

Clark 1983
Clark, G. R. 1983. "Survey of Portable Hydraulic Dredges," Technical Report HL-83-4, U.S. Army Engineer Waterways Experiment Station, Vicksburg, MS.

Clausner 1988
Clausner, J. E. 1988. "Jet Pump Sand Bypassing at the Nerang River Entrance, Queensland, Australia." *Proceedings of the Beach Preservation Technology '88.* Florida Shore and Beach Preservation Association, Tallahassee, FL, pp 345-55.

Clausner, Patterson, and Rambo 1990
Clausner, J. E., Patterson, D. R., and Rambo, A. T. 1990. "Fixed Sand Bypassing Plants -- An Update." *Proceedings of the 1990 National Conference on Beach Preservation Technology.* Florida Shore and Beach Preservation Association, Tallahassee, FL, pp 249-264.

Clausner, Geber, Rambo, and Watson 1991
Clausner, J. E., Gebert, J. A., Rambo, A. T., and Watson, K. D. 1991. "Sand Bypassing at Indian River Inlet, Delaware." *Proceedings of Coastal Sediments '91.* ASCE, New York, pp 1177-1190.

Clausner, Neilans, Welp, and Bishop 1994
Clausner, J. E., Neilans, P. J., Welp, T. L., and Bishop, D. D. 1994. "Controlled Tests of Eductors and Submersible Pumps," Technical Report DRP-94-2, Dredging Research Program, U.S. Army Engineer Waterways Experiment Station, Vicksburg, MS.

Cleary and Hosier 1988
Cleary, W. J., and Hosier, P. E. 1988. "Geomorphology and Shoreline History, Bald Head Island, NC," University of North Carolina, Wilmington, Wilmington, NC.

Coastal Planning and Engineering, Inc. 1991
Coastal Planning and Engineering, Inc. 1991. "Hillsboro Inlet, FL, Inlet Management Plan," Coastal Planning and Engineering, Inc., Boca Raton, FL.

Coastal Planning and Engineering, Inc. 1996
Coastal Planning and Engineering, Inc. 1996. "1995 Monitoring Report of the Boca Raton Inlet and Adjacent Beaches," Report submitted to the city of Boca Raton, FL, Coastal Planning and Engineering, Inc., Boca Raton, FL.

Coastal Tech 1997
Coastal Tech. 1997. "St. Lucie Inlet Hydrodynamic Monitoring and Modeling Study," Coastal Technology Corporation, Vero Beach, FL. Report prepared for Martin County, Stuart, FL.

Corson et al. 1982
Corson, W. D., Resio, D. T., Brooks, R. M., Ebersole, B. A., Jensen, R. E., Ragsdale, D. S., and Tracy, B. A. 1982. "Atlantic Coast Hindcast, Phase II Wave Information," WIS Report 6, Waterways Experiment Station, Vicksburg, MS.

Couglan and Robinson 1990
Couglan, P. M., and Robinson, D. A. 1990. "The Gold Seaway, Queensland, Austrailia," *Shore and Beach,* Vol 58, No. 1, ASBPA, January 1990, pp 9-16.

Creed 1996
Creed, C. G. 1996. "Modelling Inlet Sand Bypassing." *Proceedings, 25th International Conference on Coastal Engineering.* ASCE, New York.

Dean et al. 1987
Dean, R. G., Berek, E. P., Bodge, K. R., Gable, C. G. 1987. "NSTS Measurements of Total Longshore Transport." *Proceedings, Coastal Sediments* '87. ASCE, pp. 652-667.

Dean 1988
Dean, R. G. 1988. "Sediment Interaction at Modified Coastal Inlets: Processes and Policies," Lecture notes on coastal and estuarine studies. *Symposium on Hydrodynamics and Sediment Dynamics of Tidal Inlets*. D. G. Aubrey and L. Weishar, ed., Springer-Verlag, New York.

Dean 1993
Dean, R. G. 1993. "Terminal Structures at Ends of Littoral Systems," *Journal of Coastal Research*, Special Issue 18, Fall 1993, pp 195-210.

Dean and Perlin 1977
Dean, R. G., and Perlin, M. 1977. "Coastal Engineering Study of Ocean City Inlet, Maryland," *Coastal Sediments '77.* ASCE, pp 520-540.

Dean, Perlin, and Dally 1978
Dean, R. G., Perlin, M., and Dally, W. 1978. "A Coastal Engineering Study of Shoaling in Ocean City Inlet," Prepared for U.S. Army Engineer District, Baltimore, under contract with the University of Delaware, Newark, DE, 135 pp.

Dean and Work 1993
Dean, R. G., and Work, P. A. 1993. "Interaction of Navigational Entrances with Adjacent Shorelines," *Journal of Coastal Research*, Special Issue 18, Fall 1993, pp 91-110.

Dolan, Castens, Sonu, and Egense 1987
Dolan, T. J., Castens, P. G., Sonu, C. J., and Egense, A. K. 1987. "Review of Sediment Budget Methodology: Oceanside Littoral Cell, California," *Proceedings, Coastal Sediments '87.* ASCE, Reston, VA, pp 1289-1304.

Douglass 1987
Douglass, S. L. 1987. "Coastal Response to Navigation Structures at Murrells Inlet, South Carolina," Technical Report CERC-87-2, U.S. Army Engineer Waterways Experiment Station, Vicksburg, MS.

Douglass 1991
Douglass, S. L. 1991. "Simple Conceptual Explanation of Down-Drift Offset Inlets," *Journal of Waterway, Port, Coastal and Ocean Engineering*, March/April 1991, pp 44-59.

Douglass 1995
Douglass, S. L. 1995. "Estimating Landward Migration of Nearshore Constructed Sand Mounds," *Journal of Waterway, Port, Coastal and Ocean Engineering*, Vol 121, No. 5, ASCE, New York, pp 247-250.

Fenster and Dolan 1996
Fenster, M., and Dolan, R. 1996. "Assessing the Impact of Tidal Inlets on Adjacent Barrier Island Shorelines," *Journal of Coastal Research*, Vol 12, No. 1, Winter 1996, pp 294-310.

Fenton and McKee 1990
Fenton, J. D., and McKee, W. D. 1990. "On Calculating the Lengths of Water Waves," *Coastal Engineering*. Vol. 14, Amsterdam, The Netherlands, pp 499-513.

Fiorentino, Franco, and Noli 1985
Fiorentino, A., Franco, L., and Noli, A. 1985. "Sand Bypassing Plant at Viareggio, Italy." *Proceedings of the Australian Conference on Coastal and Ocean Engineering.* December 1985, Institute of Engineers, Australia.

FitzGerald 1984
FitzGerald, D. M. 1984. "Interactions Between the Ebb-Tidal Delta and the Landward Shoreline: Price Inlet, SC," *Journal of Sedimentary Petrology*, Vol 54, pp 1303-1318.

FitzGerald 1988
FitzGerald, D. M. 1988. "Shoreline Erosional-Depositional Processes Associated with Tidal Inlets," *Hydrodynamics and Sediment Dynamics of Tidal Inlets*, Vol 29, Lecture Notes on Coastal and Estuarine Studies, D. G. Aubrey and L. Weishar, ed., Springer-Verlag, New York, pp 186-225.

Foster, Healy, and De Lange 1996
Foster, G. A., Healy, T. R., and De Lange, W. P. 1996. "Presaging Beach Renourishment from a Nearshore Dredge Dump Mound, Mt. Maunganui Beach, New Zealand," *Journal of Coastal Research*, Vol 12, No. 2, pp 395-405.

Galvin 1982
Galvin, C. 1982. "Shoaling with Bypassing for Channels at Tidal Inlets," *Proceedings of the 18th International Conference on Coastal Engineering.* ASCE, New York, pp 1496-1513.

Gaudiano and Kana 2001
Gaudiano, D. J., and Kana, T. W. 2001. "Shoal Bypassing in Mixed Energy Inlets: Geomorphic Variables and Empirical Predictions for Nine South Carolina Inlets," *Journal of Coastal Research*, Vol 17, No. 2, pp 280-291.

Gebert, Watson, and Rambo 1992
Gebert, J. A., Watson, K. D., and Rambo, A. T. 1992. "57 Years of Coastal Engineering Practice at a Problem Inlet: Indian River Inlet, Delaware." *Proceedings of Coastal Engineering Practice '92.* ASCE, New York, pp 503-519.

Goda 1985
Goda, Yashimi. 1985. *Random Seas and Design of Maritime Structures*. University of Tokyo Press, Tokyo, Japan.

Gravens 1989
Gravens, M. B. 1989. "Bolsa Bay, California, Proposed Ocean Entrance System Study, Report 2: Comprehensive Shoreline Response Computer Simulation, Bolsa Bay, California," Miscellaneous Paper CERC-98-17, prepared for the State of California, State Land Commission, U.S. Army Engineer Waterways Experiment Station.

Hallermeier 1978
Hallermeier, R. J. 1978. "Uses for a Calculated Limit Depth to Beach Erosion." *Proceedings, 16th International Conference on Coastal Engineering.* ASCE, Hamburg, 1493-1512.

Hallermeier 1981
Hallermeier, R. J. 1981. "A Profile Zonation for Seasonal Sand Beaches from Wave Climate," *Coastal Engineering*, Vol 4, pp 253-277.

Hands and Allison 1991
Hands, E. B., and Allison, M. C. 1991. "Mound Migration in Deeper Waters and Methods of Categorizing Active and Stable Depths." *Proceedings of Coastal Sediments '91.* ASCE, New York, pp 1985-99.

Hands and Resio 1994
Hands, E. B., and Resio, D. T. 1994. "Empirical Guidance for Siting Berms to Promote Stability or Nourishment Benefits." *Proceeding of Dredging '94.* ASCE, New York.

Hansen and Knowles 1988
Hansen, M., and Knowles, S.C. 1988. "Ebb-tidal Response to Jetty Construction at Three South Carolina Inlets," *Hydrodynamics and Sediment Dynamics of Tidal Inlets,* Vol 29, D. G. Aubrey and L. Weishar, ed., Lecture Notes on Coastal and Estuarine Studies, Springer-Verlag, New York, pp 364-381.

Hanson and Kraus 1989
Hanson, H., and Kraus, N. C. 1989. "GENESIS: Generalized Numerical Modeling System for Simulating Shoreline Change, Report 1, Technical Reference Manual," Technical Report CERC-89-19, Coastal Engineering Research Center, U.S. Army Engineer Waterways Experiment Station, Vicksburg, MS.

Herbich 1975
Herbich, J. B. 1975. *Coastal and Deep Ocean Dredging.* Gulf Publishing Co., Houston, TX, 1975.

Herbich 2000
Herbich, J. B. 2000. *Handbook of Dredging Engineering.* 2nd ed., McGraw-Hill, New York.

Herbich and Snider 1969
Herbich, J. B., and Snider, R. H. 1969. "Bibliography on Dredging," Report 112-CDS, Texas A&M University, College Station, TX.

Herron and Harris 1967
Herron, W. J., and Harris, R. L. 1967. "Littoral Bypassing and Beach Restoration in the Vicinity of Point Hueneme, CA." *Proceedings of the 10th Conference on Coastal Engineering.* ASCE, New York, pp 651-75.

Hodges 1955
Hodges, T. K. 1955. "Sand Bypassing at Hillsboro Inlet, FL," *The Bulletin, Beach Erosion Board*, Vol 9, No. 2, Corps of Engineers, Washington, DC, April 1955.

Huston 1970
Huston, J. 1970. *Hydraulic Dredging, Theoretical and Applied.* Cornell Maritime Press, Inc., Cambridge, MD, ISBN 0-87033-142-6, 330 pp.

Huston 1986
Huston, J. 1986. *Hydraulic Dredging: Principles, Equipment, Procedures, Methods*. John Huston, Inc., Corpus Christi, TX, ISBN 0-9616260-0-3, 418 pp.

Inman 1991
Inman D. L. 1991. "Budget of Sediment and Prediction of the Future State of the Coast," State of the Coast Report, San Diego Region, Vol 1, Main Report, Chapter 9, 105 pp.

Inman and Frautschy 1966
Inman, D. L., and Frautschy, J. D. 1966. "Littoral Processes and the Development of Shorelines." *Proceedings, Coastal Engineering Specialty Conference.* ASCE, Reston, VA, 511-536.

Jarrett 1977
Jarrett, J. T. 1977. "Sediment Budget Analysis: Wrightsville Beach to Kore Beach, NC." *Proceedings of Coastal Sediments '77.* ASCE, New York, 1977.

Jarrett 1990
Jarrett, T. 1990. "Wilmington Harbor - Bald Head Island, Evaluation Report, Sec. 933, PL99-662," U.S. Army Engineer District, Wilmington, NC, June 1990, 44 pp plus appendices.

Jarrett 1991
Jarrett, J. T. 1991. "Coastal Sediment Budget Analysis Techniques." *Proceedings, Coastal Sediments '91.* ASCE, Reston, VA, pp 2223-2233.

Johnson 1959
Johnson, J. W. 1959. "The Supply and Loss of Sand to the Coast," *Journal of Waterways and Harbors Division,* Vol 85, No. WW3, ASCE, New York, September 1959, pp 227-251.

Johnson et al. 1994
Johnson, B. H., Scheffner, N. W., Teeter, A. M., Hands, E. B., and Moritz, H. R. 1994. "Analysis of Dredged Material Placed in Open Water." *Proceedings of the 22nd International Conference on Dredging and Dredged Material Placement, Dredging '94.* ASCE, New York.

Jones and Mehta 1977
Jones, C. P., and Mehta, A. J. 1977. "A Comparative Review of Sand Transfer Systems at Florida's Tidal Entrances." *Proceedings of Coastal Sediments ' 77.* ASCE, New York, pp 49-66.

Jones and Mehta 1980
Jones, C. P., and Mehta, A. J. 1980. "Inlet Sand Bypassing Systems in Florida," *Shore and Beach*, Vol 48, No. 1, January 1980, pp 25-33.

Kana 1995
Kana, T. W. 1995. "A Mesoscale Sediment Budget for Long Island, New York, *Marine Geology*, Vol 126, pp 87-110.

Kana and Stevens 1992
Kana, T. W., and Stevens, F. D. 1992. "Coastal Geomorphology and Sand Budgets Applied to Beach Nourishment." *Proceedings of Coastal Engineering Practice '92.* ASCE, New York, pp 29-44.

Komar 1976
Komar, P. D. 1976. *Beach Processes and Sedimentation.* Prentice-Hall, Inc., Englewood Cliffs, New Jersey, 429 pp.

Komar 1996
Komar, P. D. 1996. "The Budget of Littoral Sediments, Concepts and Applications," *Shore and Beach*. Vol 64, No. 3, pp 18-26.

Komar 1998
Komar, P. D. 1998. *Beach Processes and Sedimentation*. Prentice-Hall, Inc., Simon and Schuster, Upper Saddle River, NJ, pp 66-72.

Kraus 1989
Kraus, N. C. 1989. "Beach Change Modeling and the Coastal Planning Process." *Proceedings, Coastal Zone '89*, ASCE, pp 553-567.

Kraus 1999
Kraus, N. C. 1999. "Analytical Model to Spit Evolution at Inlets." *Proc, Coastal Sediments '99.* ASCE, Reston, VA, pp 1739-1754.

Kraus 2000
Kraus, N. C. 2000. "Reservoir Model of Ebb-Tidal Shoal Evolution and Sand Bypassing," *Journal of Waterway, Port, Coastal, and Ocean Engineering*, Vol 126, No. 6, pp 305-313.

Kraus, Larson, and Kriebel 1991
Kraus, N. C., Larson, M., and Kriebel, D. L. 1991. "Evaluation of Beach Erosion and Accretion Predictors," *Coastal Sediments '91*, ASCE, New York, pp 572-87.

Kraus, Larson, and Wise 1999
Kraus, N. C., Larson, M., and Wise, R. A. 1999. "Depth of Closure in Beach-Fill Design." *Proceedings, 12th National Conference on Beach Preservation.* Tallahassee, FL, pp 271-286.

Kraus and Rosati 1998a
Kraus, N. C., and Rosati, J. D. 1998a. "Estimation of Uncertainty in Coastal-Sediment Budgets at Inlets," Coastal Engineering Technical Note CETN-IV-16, U.S. Army Engineer Waterways Experiment Station, Vicksburg, MS.

Kraus and Rosati 1998b
Kraus, N. C., and Rosati, J. D. 1998b. "Interpretation of Shoreline-Position Data for Coastal Engineering Analysis," Coastal Engineering Technical Note CETN-II-39, U.S. Army Engineer Waterways Experiment Station, Vicksburg, MS.

Kraus and Rosati 1999
Kraus, N. C., and Rosati, J. D. 1999. "Estimating Uncertainty in Coastal Inlet Sediment Budgets." *Proceedings, 12th Annual National Conference on Beach Preservation Technology.* Florida Shore and Beach Preservation Association, Tallahassee, FL, pp 287-302.

Lean 1980
Lean, G. H. 1980. "Estimation for Maintenance Dredging for Navigation Channels." Hydraulics Research Station, Wallingford, Oxon, Crown Copyright, 73 pp.

Leatherman 1984
Leatherman, S. P. 1984. "Shoreline Evolution of North Assateague Island, Maryland, *Shore and Beach*, Vol 52, No. 3, pp 3-10.

Lund 1990
Lund, J. 1990. "Scheduling Maintenance Dredging in a Single Reach with Uncertainty," *Journal of Waterway, Port, Coastal and Ocean Engineering*, Vol 116, No. 2, ASCE, New York, pp 211-231.

Magnuson 1967
Magnuson, N. C. 1967. "Planning and Design of a Low-Weir Section Jetty (Masonboro Inlet, N.C.)," *Journal of Waterway and Harbors Division*, ASCE, New York, pp 27-40, 1967.

Mann 1993
Mann, D. W. 1993. "A Note on Littoral Budgets and Sand Management at Inlets," *Journal of Coastal Research*, Special Issue No. 18: 301-308.

McKnight 1966
McKnight, A. L. 1966. "Dredging - past - present and future." *Proceedings of the Coastal Engineering Specialty Conference, Dredging.* ASCE, New York, pp 727-747.

McLellan and Kraus 1991
McLellan, T. N., and Kraus, N. C. 1991. "Design Guidance for Nearshore Berm Construction." *Proceedings of Coastal Sediments '91.* ASCE, New York, pp 2000-2011.

Mehta, Dombrowski, and Devine 1996
Mehta, A. J., Dombrowski, M. R., and Devine, P. T. 1996. "Role of Waves in Inlet Ebb Delta Growth and Some Research Needs Related to Site Selection for Delta Mining," *J. Coastal Res.*, Vol SI 18, pp 121-136.

Meistrell 1972
Meistrell, F. J. 1972. "The Spit-Platform Concept: Laboratory Observation of Spit Development." In: *Spits and Bars.* M. L Schwartz, ed., Dowden, Hutchison, and Ross, Stroudsberg, PA, pp 225-283.

Mesa 1996
Mesa, C. "Nearshore Berm Performance at Newport Beach, CA." *Proceedings of the 25th International Conference on Coastal Engineering.* ASCE, New York, pp 4636-4649.

Migniot and Granboulan 1985
Migniot, C., and Granboulan J. 1985." Travaux de Genie Civil de Long des Cotes Cablonneuses," PIANC, S II-3, pp 47-68.

Moffatt and Nichol Engineers 1978
Moffatt and Nichol Engineers. 1978. "Santa Cruz Harbor Shoaling Study," Moffatt and Nichol Engineers, Prepared for U.S. Army Engineer District, San Francisco, June 1978, Long Beach, CA.

Moffatt and Nichol Engineers and URS Consultants, Inc. 1999
Moffatt and Nichol Engineers and URS Consultants, Inc. 1999. "Storm Damage Reduction Reformulation Study Inlet Dynamics-Existing Conditions," Prepared for U.S. Army Engineer District, New York.

Nersesian and Bocamazo 1992
Nersesian, G. K., and Bocamazo, L. M. 1992. "Design and Construction of Shinnecock Inlets, New York." *Proceedings, Coastal Engineering Practice '92.* ASCE, pp 554-570.

O'Conner and Lean 1977
O'Conner, B.A., and Lean, G. H. 1977. "Estimation of Siltation in Dredged Channels in Open Situations." *Proceedings of the 24th International Nav. Cong.* P.I.A.N.C., Section II, Subject 2, pp 163-177.

Oertel 1988
Oertel, G.F. 1988. "Processes of Sediment Exchange Between Tidal Inlets, Ebb Deltas, and Barrier Islands," *Hydrodynamics and Sediment Dynamics of Tidal Inlets 29.* Lecture notes on coastal and estuarine studies, D. G. Aubrey and L. Weishar, ed, Springer-Verlag, New York, pp 297-318.

Olsen 1977
Olsen, E. J. 1977. "A Study of the Effects of Inlet Stabilization at St. Mary's Entrance, Florida." *Proceedings, Coastal Sediments '77.* ASCE, pp 311-329.

Olsen Associates, Inc. 1989
Olsen Associates, Inc. 1989. "Feasibility Study of Beach Restoration at Bald Head Island, NC," Report prepared for the village of Bald Head Island, NC, Olsen Associates, Inc., Jacksonville, FL, April 1989, 112 pp plus appendices.

Olsen Associates, Inc. 1990
Olsen Associates, Inc. 1990. "South Lake Worth Inlet Sand Management Plan," Report prepared for Palm Beach County, Board of County Commissioners, 31 December 1990, 183 pp plus appendices, Olsen Associates, Inc., Jacksonville, FL.

Olsen Associates, Inc. 1995
Olsen Associates, Inc. 1995. "Sailfish Point Shoreline Stabilization Project, Analysis and Conceptual Design," Report prepared for Sailfish Point Property Owners' Association, November 1995, Olsen Associates, Inc., Jacksonville, FL.

Olsen Associates, Inc. 1997
Olsen Associates, Inc. 1997. "Feasibility Study of Structural Stabilization of Beach Fill in Broward County," Report prepared for Broward County, Department of Environmental Resource Protection, Ft. Lauderdale, FL, December 1997, Olsen Associates, Inc., Jacksonville, FL.

Parker 1979
Parker, N. E. 1979. "Weir Jetties - Their Continuing Evolution," *Shore and Beach*, Vol 47, No. 4, October 1979, pp 15-19.

Parson and Lillycrop 1998
Parson, L. E., and Lillycrop, W. J. 1998. "The SHOALS System: A Comprehensive Survey Tool," Coastal Engineering Technical Note CETN VI-31, U.S. Army Engineer Waterways Experiment Station, Vicksburg, MS.

Partheniades and Purpura 1972
Partheniades, E., and Purpura, J. A. 1972. "Coastline Changes Near a Tidal Inlet." *Proceedings of the 13th Conference on Coastal Engineering.* ASCE, New York, pp 843-864.

Patterson, Bisher, and Brodeen 1991
Patterson, D. R., Bisher, D. R., and Brodeen, M. R. 1991. "The Oceanside Experimental Sand Bypass System." *Proceedings of Coastal Sediments '91.* ASCE, New York, pp 1165-76.

Pelnard-Considére 1956
Pelnard-Considére, R. 1956. "Essai de Th'eorie de l'Evolution des Forms de Rivages en Plage de Sable et de Galets," *4th Journees de l'Hydralique*, les Energies de la Mer, Question III, Rapport No. 1, pp 289-298.

Penfield 1960
Penfield, W. C. 1960. "The Oldest Periodic Beach Nourishment Project," *Shore and Beach*, Vol 28, No. 1, April, pp 9-15.

Perlin and Dean 1983
Perlin, M., and Dean, R. G. 1983 "A Numerical Model to Simulate Sediment Transport in the Vicinity of Coastal Structures," Miscellaneous Report No. 83-10, Coastal Engineer Research Center, U.S. Army Engineer Waterways Experiment Station, Vicksburg, MS.

Polglase 1987
Polglase, R. H. 1987. "The Nerang River Entrance Sand Bypassing System." *Proceedings of the 8th Australian Conference on Coastal and Ocean Engineering.* November 1987.

Pope and Dean 1986
Pope, J., and Dean, J. L. 1986. "Development of Design Criteria for Segmented Breakwaters." *Proceedings, 20th Int'l Coastal Engr. Conference.* Taipei, Taiwan. ASCE, pp 2144-2158.

Pound and Witt 1987
Pound, M. D., and Witt, R. W. 1987. "Nerang River Entrance Sand Bypassing System." *Proceedings of the 8th Australian Conference on Coastal and Ocean Engineering.* November 1987, pp 222-226.

Purpura 1974
Purpura, J. A. 1974. "Performance of a Jetty-Weir Inlet Improvement Plan." *Proceedings of the Fourteenth International Conference on Coastal Engineering.* ASCE, New York, pp 1470-1490.

Purpura 1977
Purpura, J. A. 1977. "Performance of a Jetty-Weir Inlet Improvement Plan." *Proceedings of Coastal Sediments '77.* ASCE, New York, pp 330-349.

Rambo, Clausner, and Henry 1991
Rambo, A., Clausner, J., and Henry, R. 1991. "Sand Bypass Plant: Indian River Inlet, Delaware." *Proceedings of the Conference on Beach Preservation Technology '91.* Florida Shore and Beach Preservation Association, Tallahassee, FL.

Rayner and Magnuson 1966
Rayner, A. C., and Magnuson, N. C. 1966. "Stabilization of Masonboro Inlet," *Shore and Beach*, Vol 34, No. 2, October 1966, pp 36-41.

Richardson 1976
Richardson, T. W. 1976. "Beach Nourishment Techniques, Report 1," Technical Report H-76-13, U.S. Army Engineer Waterways Experiment Station, Vicksburg, MS.

Richardson 1977
Richardson, T. W. 1977. "Systems for Bypassing Sand at Coastal Inlets." *Proceedings of the Fifth Symposium of the Waterway, Port, Coastal, and Ocean Division.* ASCE, New York, November 1977, pp 67-84.

Richardson 1990
Richardson, T. W. 1990. "Sand Bypassing," *Handbook on Coastal and Ocean Engineering*. J. B. Herbich, ed., Gulf Publishing Company, Houston, TX.

Richardson and McNair 1981
Richardson, T. W., and McNair, E. C. 1981. "A Guide to the Planning and Hydraulic Design of Jet Pump Remedial Sand Bypassing Systems," Instruction Report HL-81-1, Hydraulics Laboratory, U.S. Army Engineer Waterways Experiment Station, Vicksburg, MS.

Rosati and Ebersole 1996
Rosati, J. D., and Ebersole, B. A. 1996. "Littoral Impact of Ocean City Inlet, Maryland, USA." *Proc, 25th Coastal Eng. Conf*. ASCE, Reston, VA, pp 2779-2792.

Sargent 1988
Sargent, F. E. 1988. "Case Histories of Corps Breakwater and Jetty Structures, Report 2, South Atlantic Division," Technical Report REMR-CO-3, U.S. Army Engineer Waterways Experiment Station, Vicksburg, MS.

Savage 1990
Savage, R. 1990. "A Comparison of Mean High Water Shoreline Change and Bluff Movement." *Proceedings of the 1990 National Conference on Beach Preservation Technology.* Florida Shore and Beach Preservation Association, Tallahassee, FL, pp 324-338.

Schmidt and Schwichtenberg 2000
Schmidt, D. E., and Schwichtenberg, B. R. 2000. "Regional Sediment Management in Action, Multi-Purpose Project At Post Everglades." *Proceedings, Nat'l Conf. on Beach Preservation Technology.* Florida Shore and Beach Preservation Association, pp 17-24.

Scheffner 1996
Scheffner, N. W. 1996. "Systematic Analysis of Long-Term Fate of Disposed Dredged Material," *Journal of Waterway, Port, Coastal and Ocean Engineering*, Vol 122, No. 3, ASCE, New York, pp 127-133.

Schneider 1980
Schneider, C. 1980. "The Littoral Environment Observation (LEO) Data Collection Program," CETA 80, U.S. Army Engineer Waterways Experiment Station, Vicksburg, MS.

Seabergh 1983
Seabergh, W. C. 1983. "Weir Jetty Performance: Hydraulic and Sedimentary Considerations," Technical Report HL-83-5, U.S. Army Engineer Waterways Experiment Station, Vicksburg, MS.

Shore Protection Manual 1984
Shore protection manual. (1984). 4th ed., 2 Vol, U.S. Army Engineer Waterways Experiment Station, U.S. Government Printing Office, Washington, DC.

Snetzer 1969
Snetzer, R. E. 1969. "Jetty-Weir Systems at Inlets in the Mobile Engineer District," *Shore and Beach*, Vol 37, No. 1, April 1969, pp 28-32.

Stauble 1997
Stauble, D. K. 1997. "Appendix A: Ebb and Flood Shoal Evolution," In: "Ocean City, Maryland, and Vicinity Water Resources Study, Draft Integrated Feasibility Report and Environmental Impact Statement," U.S. Army Engineer District, Baltimore, Baltimore, MD.

Stauble et al. 1988
Stauble, D. K., Da Costa, S. L., Monroe, K. L., and Bhogal, V. K. 1988. "Inlet Flood Tidal Delta Development Through Sediment Transport Processes," *Hydrodynamics and Sediment Dynamics of Tidal Inlets.* Vol 29, Lecture Notes on Coastal and Estuarine Studies, D. G. Aubry and L. Weishar, ed, Springer-Verlag, New York, pp 319-47.

Taney 1961a
Taney, N. E. 1961a. "Geomophology of the South Shore of Long Island, New York," Technical Memorandum 128, U.S. Army Corps of Engineers, Beach Erosion Board, Washington. DC, 97 pp.

Taney 1961b
Taney, N. E. 1961b. "Littoral Materials of the South Shore of Long Island, NewYork," Technical Memorandum 129, U.S. Army Corps of Engineers, Beach Erosion Board, Washington. DC, 97 pp.

Terich and Komar 1974
Terich, T. A., and Komar, P. D. 1974. "Bayocean Spit, Oregon: History of Development and Erosional Destruction," *Shore and Beach*, Vol 42, No. 2, pp 3-10.

Trawle 1981
Trawle, M. J. 1981. "Effects of Depth on Dredging Frequency," Technical Report H-78-5, Report 2, U.S. Army Engineer Waterways Experiment Station, Vicksburg, MS.

Turner 1984
Turner, T. M. 1984. *Fundamentals of Hydraulic Dredging.* Cornell Maritime Press, Centerville, MD.

Uda, Naito, and Kanda 1991
Uda, T., Naito, K., and Kanda, Y. 1991. "Field Experiment on Sand Bypass off the Iioka Coast (Japan)," *Coastal Engineering in Japan*, Vol 34, No. 2, pp 205-221.

Underwood and Hiland 1995
Underwood, S. G., and Hiland, M. W. 1995. "Historical Development of Ocean City Inlet Ebb Shoal and Its Effect on Northern Assateague Island," Report prepared for U.S. Army Engineer Waterways Experiment Station, Coastal Engineering Research Center, Vicksburg, MS.

U.S. Army Corps of Engineers 1950
U.S. Army Corps of Engineers. 1950. "Test of Nourishment of the Shore by Offshore Deposition of Sand, Long Branch, NJ," U.S. Army Corps of Engineers, Beach Erosion Board, Technical Memorandum No. 17, June 1950, 32 pp.

U.S. Army Corps of Engineers 1957
U.S. Army Corps of Engineers. 1957. "Shore of New Jersey from Sandy Hook to Barnegat Inlet, Beach Erosion Control Study," Letter from Secretary of Army, House Document No. 361, 84th Congress, 2nd Session, U.S. Government Printing Office, Washington, DC.

U.S. Army Corps of Engineers 1958
U.S. Army Corps of Engineers. 1958. Shore of New Jersey from Sandy Hook to Bernegat Inlet, Beach Erosion Control Study. Letter from the Secretary of the Army, House Document No. 362, 85th Congress, 2nd Session, U.S. Government Printing Office, Washington, DC.

U.S. Army Engineer District, Jacksonville, 1973
U.S. Army Engineer District, Jacksonville. 1973. "Survey Review Report on St. Lucie Inlet," U.S. Army Engineer District, Jacksonville, Jacksonville, FL.

U.S. Army Engineer District, New York 1987
U.S. Army Engineer District, New York. 1987. "General Design Memorandum – Shinnecock Inlet, Long Island, new York," 2 VOL, revised 1988, New York.

U.S. Army Engineer Waterways Experiment Station 1995
U.S. Army Engineer Waterways Experiment Station. 1995. "Kings Bay Coastal and Estuarine Physical Monitoring and Evaluation Program: Coastal Studies," Technical Report CERC-94-9, Coastal Engineering Research Center, U.S. Army Engineer Waterways Experiment Station, Vicksburg, MS, January 1995.

U.S. Army Engineer District, Jacksonville, 1999
U.S. Army Engineer District, Jacksonville. 1999. "St. Lucie Inlet, FL, Navigation Project, General Design Memorandum," U.S. Army Engineer District, Jacksonville, FL. Rev., March 1999.

Vallianos 1973
Vallianos, L. 1973. "A Recent History of Masonboro Inlet, North Carolina." *Proceedings of the 2nd International Estuarine Research Conference.* ASCE, Columbia, SC.

Vemulakonda 1988
Vemulakonda, S. 1988. "Kings Bay Coastal Processes Numerical Model," Technical Report CERC-88-3, Coastal Engineering Research Center, U.S. Army Engineer Waterways Experiment Station, Vicksburg, MS.

Walker and Lesnik 1990
Walker, J. R., and Lesnik, J. R. 1990. "Impacts of Ocean Entrances on Beaches in Southern California." *Proceedings of the 1990 National Conference on Beach Preservation Technology.* FSBPA, Tallahassee, FL, pp 203-217.

Walther and Douglas 1993
Walther, M. P., and Douglas, B. D. 1993. "Ebb Shoal Borrow Area Recovery," *Journal of Coastal Research*, Vol SI 17, pp 211-223.

Walton and Adams 1976
Walton, T. L., and Adams, W. D. 1976. "Capacity of Inlet Outer Bars to Store Sand." *Proceedings of the 15th Coastal Engineering Conference.* ASCE, New York, pp 1919-1937.

Weggel 1981
Weggel, J. R. 1981. "Weir Sand-Bypassing Systems," Special Report No. 8, Coastal Engineering Research Center, U.S. Army Engineer Waterways Experiment Station, Vicksburg, MS.

Weggel and Vitale 1981
Weggel, J. R., and Vitale, P. 1981. "Sand Transport over Weir Jetties and Low Groins," Symposium on Coastal Physical Modeling, University of Delaware, Newark, DE, pp 163-197.

Weishar and Fields 1985
Weishar, L. L., and Fields, M. L. 1985. "Annotated Bibliography of Sediment Transport Occurring over Ebb-Tidal Deltas," Miscellaneous Paper CERC-85-11, Coastal Engineering Research Center, U.S. Army Engineer Waterways Experiment Station, Vicksburg, MS.

Weisman, Lennon, and Clausner 1992
Weisman, R. N., Lennon, G. P., and Clausner, J. E. 1992. "A Design Manual for Coastal Fluidization Systems," *Proceeding of Coastal Engineering Practice '92.* ASCE, New York, pp 862-878.

Weisman, Lennon, and Clausner 1996
Weisman, R. N., Lennon, G. P., and Clausner, J. E. 1996. "A Guide to the Planning and Hydraulic Design of Fluidizer Systems for Sand Management in the Coastal Environment," Technical Report DRP-96, Dredging Research Program, U.S. Army Engineer Waterways Experiment Station, Vicksburg, MS.

Wiegel 1954
Wiegel, R. L. 1954. *Gravity Waves, Tables of Functions.* University of California, Council on Wave Research, The Engineering Foundation, Berkeley, CA.

Williams, Clausner, and Neilans 1994
Williams, G. L., Clausner, J. E., and Neilans, P. J. 1994. "Improved Eductors for Sand Bypassing," Program Technical Report DRP-94-6, U.S. Army Engineer Waterways Experiment Station, Dredging Research November 1994, 36 pp.

Wise 1998
Wise, R. A. 1998. "Depth of Closure in Beach-Fill Design," Coastal Engineering Technical Note, CETN II-40, U.S. Army Engineer Waterways Experiment Station, Vicksburg, MS.

Zwamborn, Fromme, and Fitzpatrick 1970
Zwamborn, J. A., Fromme, C. A. W., and Fitzpatrick, J. B. 1970. "Underwater Mound for the Protection of Durban's Beaches." *Proceedings of the 12th Coastal Engineering Conference.* ASCE, New York, pp 975-994.

V-6-7. Definition of Symbols

α	Wave angle relative to the grid at the reference point [deg]
α_b	Angle of the breaking wave crests relative to the shoreline [deg]
β	Shoreline angle relative to the grid at the alongshore column of interest [deg]
ε	Longshore diffusivity (Equation V-6-6) [length^2/time]
κ	Ratio of local breaking wave height to local depth [dimensionless]
b	Width of a dredge crater at the bottom [length]
B	Beach berm height [length]
C	Wave celerity [length/time]
C_g	Wave group velocity [length/time]
D_A	Active shoreline depth [length]
D_B	Mechanical transfer of sand from the left shoreline to the right shoreline [length^3/time]
d_c	Dredge crater depth below the ambient seabed level [length]
D_C	Profile closure depth [length]
D_L, D_R	Mechanical transfer of sand from the inlet to the left and right shoreline [length^3/time]
D_O	Maintenance dredging and out-of-system disposal from the inlet [length^3/time]
E	Net volumetric capacity of a dredge pump [length^3/time]
erfc()	Error function complement
g	Gravitational acceleration [length/time^2]
h_*	Depth of active sediment transport (depth of closure) [length]
h	Water depth [length]
H	Wave height [length]
H_b	Breaking wave height [length]
H_O	Offshore wave height [length]
j_1, j_2	Fraction of incident transport impounded by the inlet's jetties [length^3/time]
K	Empirical coefficient from the longshore transport Equation III-2-5 (of order 1) [dimensionless]
L	Wavelength [length]

L	Leftward-directed incident transport values at the study area's boundaries [length^3/time]
L_c	Length (or arc-length) of a dredge crater [length]
L_c	Cross-shore distance from datum to the long-term depth of closure [length]
m	Dredge crater side slope (Figure V-6-72)
m_1, m_2	Local inlet-induced transport from the left and right shoreline into the inlet [dimensionless]
M_{tot}	Average annual littoral brought to the inlet [length^3]
n	Sediment porosity (about 0.4) [dimensionless]
N_O	Fall-velocity or Dean parameter (Equation V-6-77) [dimensionless]
p	Describes the degree to which the inlet's sand removal alters each of the inlet's two adjacent shorelines (Equation V-6-8)
P	Tidal prism [length^3]
P	Beach fill or dredged placement [length^3]
P	Natural net bypassing [length^3/time]
p_1, p_2	Fraction of incident transport naturally bypassed across the inlet [length^3/time]
P_l	Longshore component of wave energy flux
Q	Longshore transport rate [length^3/time]
Q	Incident (updrift) net transport [length^3/time]
Q_R	Annual longshore transport to the right (looking seaward) [length^3/time]
Q_{NET}	Net annual longshore transport [length^3/time]
Q_{GROSS}	Gross annual longshore transport [length^3/time]
Q_L	Annual longshore transport to the left (looking seaward) [length^3/time]
Q_{Aout}	Bypassing rate of the attachment [length^3/time]
Q_{Bout}	Bypassing rate of the bar [length^3/time]
Q_{Eout}	Rate of sand bypassing the ebb shoal [length^3/time]
R	Material removed from a sediment budget cell [length^3]
R	Rightward-directed incident transport values at the study area's boundaries [length^3/time]
s	Ratio of sediment to water specific gravity (about 2.65) [dimensionless]
S	Average volumetric shoaling rate of a dredge crater [length^3/time]

S	Sea level change [length]
S_u	Transport of littoral material into the inlet from upland sources [length^3/time]
T	Wave period [time]
T_B	Elapsed time between the start of subsequent dredging events
t_c	Crossover time [time]
T_E	Time required to excavate a dredge crater (Equation V-6-73)
t_f	Time at which the structure becomes filled to capacity and begins to bypass [time]
t'	Lag time that delays development of the bar
t''	Lag time that delays development of the attachment
u_m	Maximum nearbed horizontal wave orbital velocity [length/time]
V_A	Volume of attachment bar [length^3]
V_B	Bypassing bar volume [length^3]
V_c	Theoretical yield volume of a dredge crater [length^3/time]
V_E	Volume of sand in the shoal [length^3]
∇V	Sediment volume change [length^3]
w	Sediment's median fall velocity [length/time]
x	Distance downdrift of structure [length]
y	Shoreline recession [length]
Y	Structure length [length]
Δy_{st}	Long-term beach loss because of an increase S in relative sea level

V-6-8. Acknowledgments

Authors of Chapter V-6, "Sediment Management at Inlets and Harbors:"

Kevin R. Bodge, Ph.D., Olsen Associates, Jacksonville, Florida.
Julie D. Rosati, Coastal and Hydraulics Laboratory (CHL), U.S. Army Engineer Research and Development Center, Vicksburg, Mississippi.

Reviewers:

Lyndell Z. Hales, Ph.D., CHL
Nicholas C. Kraus, Ph.D., CHL
Andrew Morang, Ph.D., CHL
Gregory L. Williams, U.S. Army Engineer District, Wilmington, North Carolina

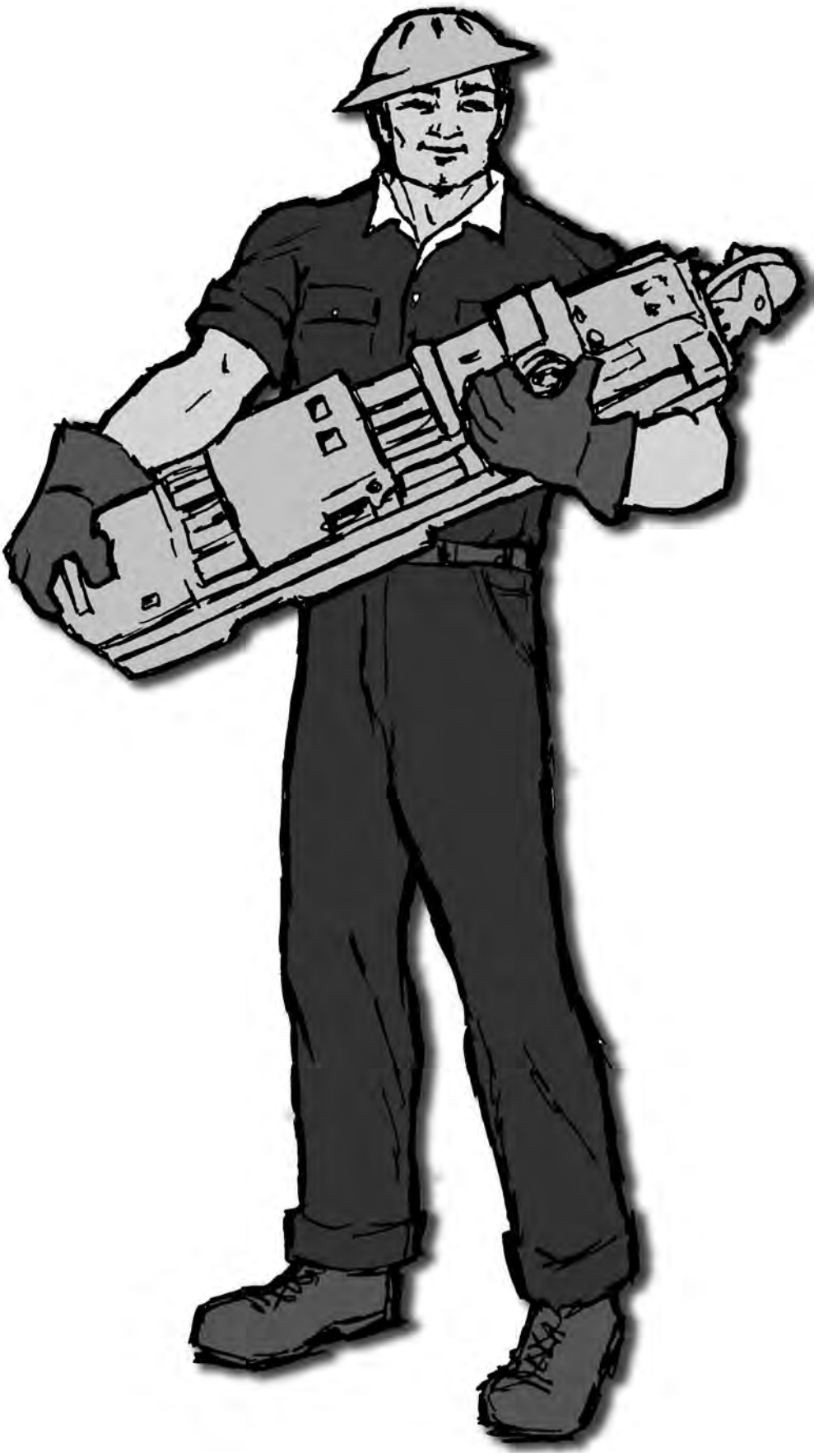

Table of Contents

Page

V-7-1. Introduction V-7-1

V-7-2. Coastal Habitat Projects V-7-1

V-7-3a. Habitat Trade-offs: Issues Associated with Compensatory Mitigation V-7-2

V-7-3b. Habitat Restoration: Issues and Initiatives Beyond Compensatory Mitigation V-7-3

V-7-4. Ecosystem Function and Biodiversity in Coastal Habitat Projects V-7-3

V-7-5. Defining Success and Project Maintenance and Monitoring V-7-4

V-7-6. Adaptive Management V-7-5

V-7-7. Design Considerations and Information Sources for Habitat Projects V-7-5
a. Underwater projects V-7-5
(1) Artificial reefs V-7-5
(2) Oyster reefs V-7-6
(3) Coral reefs V-7-7
(4) Live bottom and worm rock reefs V-7-8
(5) Seagrasses V-7-9
(6) Use of dredged material for creating shallow habitat V-7-11
b. Projects at the land-sea interface V-7-11
(1) Mud/sand flats V-7-11
(2) Intertidal salt and brackish marshes V-7-12
(3) Tidal freshwater wetlands V-7-14
(4) Tidal freshwater marsh restoration V-7-15
(5) Mangroves V-7-16
(6) Rocky intertidal shores V-7-16
c. Projects in coastal uplands V-7-17
(1) Coastal dunes V-7-17
(2) Coastal dune restoration V-7-18
(3) Maritime forests V-7-20
(4) Bird/wildlife islands V-7-20

V-7-8. Environmental Features of Traditional Coastal Engineering Projects V-7-21
a. Example project types V-7-21
(1) Beach nourishment V-7-21
(2) Shoreline structures V-7-22

(a) Breakwaters and sills V-7-23
(b) Groins V-7-23
(c) Seawalls and revetments V-7-24
(3) Navigation, ports, and marinas V-7-24
(a) Construction and maintenance channels V-7-24
(b) Inlets and jetties V-7-25
(c) Piers and docks V-7-25
(d) Boat basins and marinas V-7-26
(e) Port facilities V-7-26
(f) Confined disposal facilities V-7-26

V-7-9. Environmental Issues To Be Considered for All Projects V-7-27
a. In the water V-7-27
(1) Sea turtles V-7-27
(2) Cetaceans V-7-28
(3) Fish and invertebrates V-7-28
b. At the shore/water interface V-7-29
(1) Sea turtles V-7-29
(2) Marine mammals V-7-29
(3) Sea, shore, and wading birds V-7-30
(4) Fish and invertebrates V-7-31
c. Critical areas V-7-31

V-7-10. Information Sources V-7-33

V-7-11. References V-7-34

V-7-12. Acknowledgments V-7-45

List of Figures

Page

Figure V-7-1. Distribution of tidal marsh type along an estuarine salinity gradient V-7-13

Figure V-7-2. Characteristic profile of a mid-Atlantic tidal freshwater marsh V-7-15

Figure V-7-3. Diagram of a sand fence V-7-20

Figure V-7-4. Distribution of the California grunion along the southwest U.S. coast V-7-33

For Geotechnical, Marine or Airport Design and Construction Books, Your Ship Has Come In

Books include classics such as:

- Coastal Engineering Manual (5 volumes)
- NAVFAC DM 7.01—Soil Mechanics, the Classic Reference
- Laboratory Soils Testing
- Bearing Capacity and Settlement
- Mooring Systems: Design, Inspection and Maintenance

...and many more! New titles being added monthly. Competitive prices—always available!

Visit http://www.pz27.net for more information

Part V-7-1
Coastal Engineering for Environmental Enhancement

V-7-1. Introduction

The purpose of this chapter is to provide an overview of coastal habitats and information resources on the creation and restoration of coastal habitats. For the purpose of this report, coastal habitats include both marine nearshore habitats and estuarine (both brackish and freshwater tidal) habitats. Many projects are or can be designed to restore, create, enhance, or protect critical coastal environments and the natural resources (fisheries, wildlife, etc.) that depend on them. Innovative uses of new and traditional coastal engineering technology have enabled scientists, engineers, and resource managers to rehabilitate degraded coastal habitats, create new habitats, better identify habitat needs and opportunities, and manage environmental impacts from development projects. Opportunities to provide environmental enhancements or mitigation in traditional coastal engineering projects (those that do not include habitat creation/restoration or protection as the primary objective) are also presented in this chapter, along with a discussion of potential environmental constraints and issues that may affect coastal engineering projects in general.

V-7-2. Coastal Habitat Projects

a. Individual habitat restoration, creation, or protection projects in the coastal zone provide identifiable benefits onsite. However, in the context of an ecosystem, watershed or landscape, they provide a continuum of benefits which may not be realized at the outset by all project participants. Recent Federal directives and other agency initiatives in restoring coastal habitats have encouraged the implementation of ecosystem-level planning in the design phase of projects (Thom 1997).

b. One example of ecosystem evaluation incorporates the concept of landscape ecology. Landscape ecology focuses on the interaction of three characteristics: (a) structure (the spatial relationship between ecosystem elements), (b) function (the interaction among these elements), and (c) change (the alteration in structure and function over time) (Forman and Gordon 1986). Several components make up natural landscapes and they include: (a) Matrix (the dominant landscape type, in coastal situations this may be water), (b) Patch (a nonlinear surface area differing in appearances from its surroundings, such as a coral reef surrounded by water), (c) Corridor (a narrow strip of habitat that differs from the matrix on either side, such as a band of seagrass), and (d) Node (an intersection of corridors). Individual patches collectively form a heterogeneous mosaic. Organisms within an individual patch (e.g., fish residing in a sub-tropical seagrass bed) may migrate between or among adjacent habitat patches using corridors (e.g., mangrove forests, coral reefs), depending on seasonal, diel, or environmental influences. Effective management of entire ecosystems entails improvements or enhancements to multiple habitat types, with an understanding of the role of habitats. An example of this would be to consider both adjacent and distant habitat types that Pacific salmon are heavily dependent on. That is, near coastal areas and estuaries for juvenile rearing, open ocean areas where they mature and spawning areas located as much as 500 miles upriver in freshwater. Recognition of the interactions between coastal, freshwater, and terrestrial systems, and an understanding of processes occurring in nearby watersheds such as agricultural or industrial activity, are key to planning habitat projects on an ecosystem scale.

c. Several other approaches are valid when considering restoration in the large scale. Examples include the analysis of limiting factors on keystone species. Other restoration efforts have focused on comparison of the historical ecosystem with the current regime to determine what critical elements have been lost. No one single methodology is right for every situation but it is important to evaluate individual restoration efforts in the larger context.

d. Recently, scientists and managers have developed recommendations for improving the state-of-the-art in habitat restoration (Pastorok et al. 1997). These recommendations include refinements in developing goals and objectives, consideration of spatial and temporal scales in design parameters, flexibility and adaptive management in project planning and design, and the importance of establishing long-term monitoring programs to document structural and functional attributes of habitats being restored. Additionally, the concept of ecosystem management is becoming the more common, especially on Federal lands. The primary objective of managing an ecosystem is to maintain its integrity of function, diversity, and structure.

V-7-3a. Habitat Trade-offs: Issues Associated with Compensatory Mitigation

a. Within the last two decades, habitat restoration and creation have increasingly been used as requirements to mitigate for damage to natural resources. This is required in order to compensate for habitat losses as specified in Section 404(b)(1) of the Clean Water Act of 1972 and many state and local regulations. When most of these laws and regulations were passed, wetland and aquatic habitat creation and restoration were still developing technologies. By the mid-1980's, mitigation for human-induced wetland losses became standard practice in the United States.

b. Mitigation is often described as three general types: avoidance, minimization, and compensatory. Under Section 404 of the Clean Water Act, these actions are sequenced in such a way that avoidance is preferred, impacts that cannot be avoided are minimized to the greatest extent practicable, and finally a determination of appropriate levels of compensatory mitigation are determined based on the analysis of lost functions and values. One useful approach to evaluating coastal habitats for mitigation needs has been developed by the U.S. Army Engineer Research and Development Center (ERDC), formerly the U.S. Army Engineer Waterways Experiment Station (Ray 1994).

c. Mitigation may occur at or near the affected habitat (*onsite mitigation)*. It is also considered acceptable to mitigate for damages by creating or restoring habitat elsewhere (*off-site mitigation*), especially when on-site mitigation would be adversely affected by the surrounding development. *In-kind* mitigation is accomplished by restoring/creating the same habitat type (e.g., mitigate for intertidal salt marsh lost by marina construction by creation of salt marsh on nearby dredged material deposit). *Out-of-kind* mitigation involves compensating for the loss of a particular habitat type by replacement with a different habitat type (e.g., creating a salt marsh to mitigate a seagrass bed destroyed by construction of a ferry terminal). The various combinations of mitigation strategies include *onsite in-kind, onsite out-of-kind, off-site in-kind, and off-site out-of-kind*. Preservation of valuable habitats is sometimes used as compensatory mitigation. Yet another alternative involves the use of mitigation banks, large habitat creation projects that developers have the option of contributing funds to in lieu of actually constructing a mitigation wetland. Though many have criticized mitigation banking as a way to skip avoidance and minimization of adverse impacts, in practice, mitigation banking is probably a superior alternative to haphazard construction of small, poorly designed wetland creation projects that are unlikely to be monitored or maintained. In all cases, avoidance and minimization of project impacts are considered preferable to compensatory mitigation.

d. Compensatory mitigation has been criticized and deemed largely unsuccessful in coastal habitats (Race 1985, Zedler 1996a). Restoration of lost ecological functions is difficult to achieve in created wetlands, particularly those that are small and/or isolated and affected by surrounding land use. Even when vastly more

habitat area is created than was lost, it may be insufficient to provide functional equivalency to tidal wetlands lost (Zedler 1996b). In recent years, there has been considerable research on measurement and assessment of functional equivalency in restored and created coastal habitats. The results suggest that even in the case of the most well-designed and carefully executed projects, restoration of certain ecological functions may not occur for decades (Simenstad and Thom 1996).

V-7-3b. Habitat Restoration: Issues and Initiatives Beyond Compensatory Mitigation

a. National policy concerning the protection, restoration, conservation, and management of ecological resources encourages initiatives to go beyond traditional compensatory mitigation concepts and develop environmental projects, including coastal habitat improvements, based purely on environmental benefits. Accordingly, ecosystem restoration has become one of the primary missions of the Civil Works program of the U.S. Army Corps of Engineers. The purpose of Civil Works Ecosystem restoration activities is to restore significant ecosystem function, structure, and dynamic processes that have been degraded. Ecosystem restoration efforts will involve a comprehensive examination of the problems contributing to the system degradation, and the development of alternative means for their solution. The intent of restoration is to partially or fully reestablish the attributes of a naturally functioning and self-regulating system. Study and project authorities through which the Corps can examine ecosystem restoration needs and opportunities are found in Congressionally authorized studies, pursued under General Investigations, i.e., new start reconnaissance and feasibility studies for single-purpose ecosystem restoration or multiple purpose projects that include ecosystem restoration as a primary purpose. Other authorities through which the Corps can participate in the study, design, and implementation of ecosystem restoration and protection projects include: (1) Section 1135, Project Modifications for Improvement of the Environment (Water Resources Development Act (WRDA) of 1986, as amended); (2) Section 206, Aquatic Ecosystem Restoration (WRDA) 1996); (3) Section 204, Beneficial Uses of Dredged Material (WRDA 1992, as amended); and (4) dredging of contaminated sediments under Section 312 of WRDA 1990, as amended. All of these authorities can be used to restore coastal habitats and resources are usually appropriated each year under the specific authority to accomplish such work in the Corps' portion of the Water and Energy budget.

b. Additional opportunities for ecosystem restoration and protection may also be pursued through existing project authorities for the management of operating projects, e.g., through water control changes, or as part of natural resources management.

c. All of these authorities, which vary in their particularities related to specific applications of Corps interest, local cost-sharing, multiple agency participation, etc., are potential tools for developing coastal engineering/environmental projects. Additionally, other Federal agencies provide grants to local jurisdictions or citizen groups to plan, design, and/or construct habitat restoration projects. Examples of alternative means of acquiring and restoring coastal habitats include the National Coastal Wetlands Conservation Grant Program, and North American Wetlands Conservation Grants administered by the U.S. Fish and Wildlife Service; the National Fish and Wildlife Foundation Challenge Grants administered by the National Fish and Wildlife Foundation; and the Wetlands Reserve Program administered by the Natural Resources Conservation Service. Partnering with other agencies is also an effective way of leveraging limited assets in an area that usually has more needs identified than resources to accomplish them.

V-7-4. Ecosystem Function and Biodiversity in Coastal Habitat Projects

a. Coastal habitats are part of a connected ecosystem of freshwater, estuarine, terrestrial, and marine habitats. A primary consideration of habitat restoration is what functions a particular habitat provides and

how those functions relate to functions provided by other parts of the ecosystem. Additionally, it is important to determine what natural physical processes form and change natural habitats and whether these natural processes still exist in an ecosystem. A primary goal of habitat restoration and creation should always be to maintain or recreate natural physical processes because this will help maintain habitats over a much longer time scale.

b. Coastal habitats also contribute substantially to biological diversity, simply defined as the number of species within a habitat, bioregion, or worldwide. Concern over protecting against loss of species in coastal (and terrestrial) habitats is increasing, and environmentally responsible coastal habitat projects should be planned and implemented with maintenance of biological diversity as a key concern. The primary cause of species loss in many areas is the destruction of critical habitat for one or more life-history stages of an organism. In coastal areas, these may include barrier beaches, maritime forests, salt marshes, tidal wetlands, seagrass meadows, and coral reefs. Pollution and loss of water quality may further stress populations, and may contribute to a reduction in genetic diversity due to differential mortality and local extinctions.

c. In certain cases, preservation of biodiversity also may be a primary goal of a habitat restoration, creation, or preservation project, and many projects have attempted to restore or rehabilitate critical habitats in areas that have undergone extensive habitat loss or degradation.

V-7-5. Defining Success and Project Maintenance and Monitoring

a. A key component of designing and implementing habitat restoration or creation projects is to define how and when your project will be considered a success. This requires identifying a project's goals, objectives, and performance standards. Performance standards should be specifically stated in terms such as composition and density of a plant community or number of fish utilizing a site. While such standards can often be difficult to develop, they will provide a clear direction for what parameters must be monitored and how long monitoring will need to be conducted.

b. The most often cited reason for failure of habitat restoration projects is failure to properly monitor site development and implement corrective action as needed. The National Research Council (NRC 1992) has identified a need to develop a systematic approach to improving the state of the art in habitat restoration. A primary area for improvement is in the development and implementation of monitoring programs. A well-designed monitoring program allows project managers to make crucial changes or mid-course corrections to projects, ensuring long-term success. Monitoring data can be used by project managers to demonstrate the ability of the project to meet stated goals and objectives. Monitoring also allows others to learn from previous projects, and avoid pitfalls in future restoration efforts.

c. Recent guidance on monitoring aquatic and marine habitat restoration projects (Thom and Wellman 1996) outlines the components of a monitoring program. A monitoring program should be designed during the planning phase as a direct result of the project objectives and performance standards. Failure to do so may result in the inability to evaluate project performance relative to the stated standards.

d. Baseline data collection helps in setting clear, realistic objectives, provides site-specific information, and guides the development of the monitoring plan. This is considered the initial phase of the monitoring program, and provides pre-project conditions against which to evaluate project performance. During construction, monitoring is carried out to ensure that project design criteria are followed, and to assess any off-site damage that may occur during construction. Upon project completion, performance is assessed and management or modifications to the project can be carried out, as necessary, to achieve the desired project objectives.

e. Reference site selection is often critical to the development of a restoration monitoring program. Reference sites are used as models upon which to base a project design. They provide a target for the development and evaluation of performance standards. Reference sites also provide a control, useful in assessing the degree of natural ecosystem fluctuations. Pre- and post-project conditions can be assessed in the absence of reference sites; however, project performance can only be determined relative to reference conditions (Thom and Wellman 1996).

V-7-6. Adaptive Management

Two of the key elements of success in habitat restoration/creation projects are: (a) clear, technically sound objectives, and (b) the flexibility and capability to deal with unforeseen problems or physical changes. These elements represent the foundation of an adaptive approach to ecosystem management. In recent years, adaptive management plans have been specifically recommended for ecosystem management programs by Federal and State Governments, and other entities (Thom and Wellman 1996). An adaptive management approach literally involves "learning by doing" - a sequential reassessment of system states and dynamic relationships should be an integral part of a well-designed monitoring program (Walters and Holling 1990). Since our knowledge of ecosystems is often incomplete, project managers must rely on continuous assessment and data collection to guide modifications intended to optimize restoration projects. Data collection, comparison with carefully chosen reference sites, and experimentation, where feasible, should be used to indicate the need for adjustments or modifications to the system (and in some cases reevaluation of original goals and project objectives). This can be instrumental in avoiding the pitfalls that typically result from inflexible project designs and represents a "safe-fail" approach, in contrast to the "fail-safe" approach of traditional civil and coastal engineering projects (Pastorok et al. 1997). However, in order for adaptive management to work, or even be utilized at all, there must be a clear mechanism for the monitoring results to be evaluated and a funding source to come back and provide necessary maintenance or construct actual changes to the project.

V-7-7. Design Considerations and Information Sources for Habitat Projects

a. Underwater projects.

(1) Artificial reefs. Artificial reefs have been used to enhance fishing productivity, in both artisanal and highly developed fisheries, for centuries. The National Fishing Enhancement Act of 1984 authorizes states and other government entities to develop and responsibly manage artificial reef programs in coastal waters of the United States. Since the passage of the Act, reef construction in U.S. coastal waters has increased dramatically. There are now over 300 artificial reefs in U.S. waters, most in nearshore waters of the Southern Atlantic and Gulf coasts.

(a) Artificial reefs enhance marine habitat by providing structurally complex substrate and food resources (in the form of encrusting and epiphytic invertebrates) in topographically homogeneous areas of the ocean floor. The new substrate is quickly colonized by epiphytic algae, sponges, bryozoans, and hydroids. In tropical waters, corals are among the initial colonizers. Ultimately, small fish, crustaceans, and larger predatory fish take up residence. Size, vertical relief, structural complexity and location relative to source areas are the primary factors that determine community composition of artificial reefs. Most artificial reefs are constructed to attract and support populations of recreationally or commercially important finfish; however, reefs have also been constructed to specifically target other resource species such as giant kelp, lobsters, and corals.

(b) Engineering and design concerns in artificial reef construction/deployment focus on the following (Bohnsack and Sutherland 1985):

- Material composition.
- Surface texture.
- Shape, height, and profile of the reef.
- Reef size, spatial scale, and dispersion.

(c) Proper placement of artificial reef structures is of critical importance. Most reported failures of artificial reefs are due to improper siting. If deployed too close to an existing natural reef, they may provide little or no enhancement, and may reduce habitat function of the natural reef.

(d) Artificial reefs may be placed at any depth; most reefs in U.S. waters have been deployed at depths of 10-110 m (30-360 ft). Substrate type must also be considered. Hard substrate must be located at or near the surface in order to prevent the artificial reefs from sinking. Natural sedimentation rates in the placement area should be low enough to prevent burial of structures over time. In high-energy coastal waters, reef structures must often be mechanically stabilized to prevent shifting or relocation by waves and storm surges. Water quality parameters in the vicinity of the reef should be assessed prior to deployment. Chronic low oxygen conditions (hypoxia) and rapid changes in salinity, water clarity, temperature, and nutrient concentration will negatively impact reef fish and invertebrate communities.

(e) A variety of materials have been used to construct artificial reefs. Some of the earliest recorded artificial reefs, deployed by Japanese fishermen in the early 18th century, consisted of simple wooden structures weighted with rocks. Bamboo racks (payaos) have been used extensively in artificial reef programs in the Philippines; in recent years these have been replaced with modern concrete structures. Recycled materials are often used to construct artificial reefs. Discarded automobile tires are particularly common due to their low cost and durability. Fly-ash composites and fiber-reinforced plastics have been used. Wooden street cars, automobiles, barges, and ships have been deployed at artificial reef sites in the United States and elsewhere. Concrete structures of various sizes and configurations are also commonly deployed. Quarry rock and rubble derived from demolition activities, such as channel maintenance, have been used extensively in reef construction. Detailed reviews of artificial reef construction and design are provided by Seaman and Sprague (1991), and Sheehy and Vik (1992).

(f) The effectiveness of artificial reefs as a fishery management tool has been questioned by coastal resource managers. It is recognized that artificial reefs can dramatically enhance fish harvests by concentrating fish around discrete, identifiable structures. However, it is often argued that the reefs merely serve to redistribute existing resources from natural sites to artificial sites, and do not actually increase fish production (Bohnsack 1989). Artificial reefs should be considered habitat creation rather than restoration of a naturally occurring habitat type.

(2) Oyster reefs. Harvests of the American oyster (*Crassostrea virginica)* along the U.S. Atlantic coast have declined dramatically during the latter half of the 20th century. In Chesapeake Bay, which historically supported the largest oyster fishery along the Atlantic coast, the principal cause of the decline was overharvesting of the resource (Wennersten 1981). During the early 20th century, yearly harvests declined rapidly as the fishery became more technologically advanced and efficient. Since the early 1960's, oyster diseases and predation, along with reduced environmental quality, have further contributed to the decline. Currently, the oyster fishery in Chesapeake Bay is threatened with economic extinction.

(a) Oysters are filter-feeding bivalves (Phylum Mollusca, Class Bivalvia). They reproduce by shedding eggs and sperm directly into the water column. Oysters are hermaphroditic; they may be either male or female, and change sex at various times during their life cycle. Larval oysters, or veligers, begin to grow shells at approximately two weeks of age and sink to the bottom. If veligers are not able to settle upon a suitable hard substrate (culch), they die. Upon cementing themselves to hard substrate (rock, shell, another oyster) the juvenile oysters (spat) remain sessile for life, filtering the surrounding water, and forming structurally complex reefs. Because they are stationary for life, oysters are susceptible to a wide variety of predators, including gastropod oyster drills, whelks, crabs, boring sponges, and starfish. Most invertebrate oyster predators thrive in salinity above 25 psu. In recent years, oyster populations in the mid-Atlantic have been severely impacted by disease microorganisms. While not harmful to man, these diseases have seriously reduced oyster harvests in Chesapeake Bay and other mid-Atlantic estuaries.

(b) The primary means of increasing oyster populations is by providing additional hard substrate for veligers to settle on. Typically old oyster shells are used, but in some coastal areas this material has become scarce and alternatives such as clamshells, concrete, rubble, or fly-ash (not recommended) composites are used. In recent years, coastal engineers have created experimental oyster reefs by depositing dredged material in areas historically known to support oyster populations, and capping the dredged material mounds with a layer of oyster shell (Earhart, Clarke, and Shipley 1988). This technique holds considerable promise as a tool for enhancement of shellfish resources and as a viable alternative to traditional dredged material disposal options in shallow coastal waters.

(c) Restoring *ecological functions* attributed to oyster reefs, including water-filtration capacity and sediment stabilization, is more likely to provide a self-sustaining ecosystem. Oyster reefs provide structurally complex refuge for a variety of fish and invertebrate species, including many of commercial and recreational significance. The restoration technique is the same; provision of additional hard substrate to increase survivorship of newly recruiting juvenile oysters. However, in the case of restoring oyster reefs as *habitat*, careful attention is given to the structural characteristics of the shell deposits and orientation/spacing of the mounds in order to derive maximum use of the resource by target finfish and macrocrustacean species.

(3) Coral reefs. Coral reefs are very productive ecosystems and occur worldwide along shallow tropical coastlines. The majority of coral reefs occur between 22.5°N and 22.5°S latitude in the tropical Western Pacific and Indian Oceans, and the Caribbean Sea. However, warm ocean currents such as the Gulf Stream in the western Atlantic and the Kuroshio Current in the western Pacific allow limited growth of coral reefs as far north as 34°N latitude (Maragos 1992). Coral assemblages found in waters of the continental United States (South Florida) are dominated by four species: the elkhorn coral (*Acropora palmata*), staghorn coral (*Acropora cervicornia*), common star coral (*Montastraea annularis*), and large star coral (*Montastraea cavernosa*) (Jaap 1984).

(a) Coral reefs are classified according to geomorphic attributes. The most common type of coral reef is the *fringing reef*. Fringing reefs occur slightly below low tide level, occasionally extending into the intertidal zone, and are situated parallel to the shoreline. The proximity of fringing coral reefs to shore increases their susceptibility to human-induced environmental degradation. *Patch reefs* are isolated coral reefs situated shoreward of larger, offshore reefs. Offshore *barrier reefs* are linear in configuration, arising from an offshore shelf, and separated from the mainland by a lagoon. The Great Barrier Reef system of Australia is a well-known example of this reef type. *Atolls* are circular or semicircular reefs that are situated atop subsiding sea floor platforms. They maintain their position above the water column by vertical accretion as the platform subsides.

(b) Coral reefs are the product of a symbiotic association of corals (a colonial invertebrate) and the microscopic vegetative stage of dinoflagellates (zooxanthellae) living within the tissue of the coral animal. Zooxanthellae are responsible for the bulk of primary production within the reef system. The coral animal

and zooxanthellae remove calcium ions from the surrounding seawater and incorporate them into the coral skeleton, forming the reef. A variety of invertebrates and fish utilize the structurally complex reef habitat as a predation refuge and nursery. Because corals grow in oligotrophic waters, nutrients such as nitrogen and phosphorous are recycled within the system. Gross primary production is high due to the presence of the zooxanthellae, but net primary productivity is low due to high rates of respiration within the reef community. Coral reefs function as a sink for nutrients originating from outside the system.

(c) Maragos (1992) lists a number of "functional values" attributed to coral reefs. These include:

- Provision of a food source.
- Shoreline protection.
- Sand and mineral extraction.
- Habitat for rare species.
- Tourism and recreation.
- Scientific, medicinal, and educational resources.

(d) Coral reef ecosystems are fragile and have undergone considerable losses in recent years. Sources of environmental degradation in coral reef systems include mechanical destruction due to channel dredging, vessel groundings, anchors, dynamite fishing, collection for the aquarium industry and trampling by recreational divers and snorkelers.

(e) Coral reef restoration is still very much an experimental technology, and only a few case studies have been documented (Maragos 1992). Coral reef restoration typically occurs in two phases. First, before any physical reconstruction can take place, water quality conditions in the vicinity of the degraded reef must closely approximate that of the system before degradation occurred. Optimal salinity, temperature, water clarity, and hydrological conditions must be met prior to any attempt to mechanically repair or enhance the reef structure. This may be accomplished by cessation or diversion of sewage discharges and runoff, and reestablishment of natural flow regimes in the area being considered for restoration. When the environmental parameters listed above are conducive to reef development, then mechanical repair or restoration of reef structures can be implemented. In the case of physical damage due to ship grounding, it is imperative to salvage as many living corals and sponges as possible. The living surfaces of hard corals die rapidly if allowed to sit on the bare seafloor. Rubble associated with the damaged reef is typically removed and discarded offsite in deep water; occasionally it is feasible to reconstruct portions of the reef structure using cements or epoxies. If the underlying limestone reef platform is damaged, it is often necessary to reconstruct the substrate using limestone boulders. When the underlying reef platform has been reconstructed and the site cleared of debris and rubble, surviving corals and sponges are transplanted using a variety of techniques, including stainless steel wires, nylon cable ties, and epoxy/cement (Maragos 1992).

(4) Live bottom and worm rock reefs. Live bottom habitats are common along all of the coastlines of the United States. They are particularly prevalent along the western coast of Florida and along the North and South Atlantic Coast. Live bottom consists of hard subtidal habitats colonized by sessile and mobile invertebrates, including sponges, hydroids, bryozoans, crustaceans, echinoderms, mollusks, and polychaetes. Typically, these organisms live directly upon submerged rock or fossil reefs. Macroalgal communities (e.g., kelp beds) may dominate in some hard bottom areas. Hard bottom in the surf zone is dominated by low-relief boring and encrusting organisms. As depth increases with distance from shore, species richness and vertical relief increase. Live bottom habitats are known to attract fish and mobile invertebrates, which use the vertical relief as a predation refuge, and prey upon the various organisms that comprise the live bottom community.

In general, nutrient concentrations in the vicinity of live bottom habitats are low, and net primary productivity is also low, due to respiration by resident organisms.

(a) Worm rock reefs are a specific type of hard bottom habitat found along the southeastern Florida Coast (Zale and Merrifield 1989). These reefs are composed of the tubes of the polychaete *Phragmatopoma lapidosa*. The worms construct elaborate, complex aggregations of tubes by cementing sand grains. These structures may extend for hundreds of kilometers. A diverse assemblage of motile and sessile invertebrates, including many other species of polychaetes and crustaceans, are found in association with the worm reefs.

(b) Live bottom habitats are particularly susceptible to changes in sedimentation rates associated with storms, dredging, and artificial beach nourishment. Invertebrate faunas can adapt to periodic burial due to natural processes, but chronic or persistent burial resulting from construction or coastal engineering activities will destroy live bottom. Disturbances due to commercial fishing, such as trawling, are detrimental to live bottom communities. Vessel groundings and anchor scars may also cause permanent physical damage to live bottom habitat.

(c) There are few documented instances of live bottom restoration other than coral reefs (Maragos 1992) and kelp beds (Schiel and Foster 1992). However, many of the general guidelines for coral reef restoration can be applied to restoration of live bottom. Assuming appropriate hydrodynamic and water-quality regimes, restoration involves removal of debris and mechanically rebuilding damaged structures. In the case of worm rock, fragments may be removed from nearby source areas and transplanted onto damaged reefs to speed recolonization.

(5) Seagrasses. Seagrasses are submerged, flowering marine angiosperms, of which approximately 35 species are known worldwide. Seagrass beds occur mainly in low-energy subtidal and intertidal habitats along the Atlantic, Pacific, and Gulf coasts of the United States, with species composition and areal extent varying greatly along each of these coasts. Along the Atlantic coast, eelgrass (*Zostera marina*) beds occur from the Canadian Maritime Provinces south to Albemarle-Pamlico Sound in North Carolina. Along the Pacific coast, eelgrass beds occur from Mexico to Alaska in bays and inlets. Turtle grass (*Thalassia testudinum*) dominates along the east coast of Florida, the Florida Keys, and the Gulf of Mexico, along with shoalgrass (*Halodule wrightii*) and manatee grass (*Syringodium filiforme*). In deeper waters off the Florida continental shelf, two other species (*Halophila engelmanni* and *H. decipiens*) occur. Seagrass communities of the U.S. Pacific coast are comprised of three species of surfgrass (*Phyllospadix scouri*, *P. torreyi*, and *P. serulatus*) and two species of eelgrass (*Zostera marina* and *Z. japonica*).

(a) Seagrass beds are critical nursery areas for many recreational and commercial fishery species, including bay scallop (*Argopecten irradians*), summer flounder (*Paralichthys dentatus*), and blue crab (*Callinectes sapidus*). On the Pacific coast, eelgrass meadows provide nursery habitat for dungeness crab (*Cancer magister*), english sole (*Parophrys vetulus*) and starry flounder (*Platichthys stellatus*). Juveniles of these and other fishery species are afforded refuge from predators and benefit from abundant food within the complex seagrass canopy. Eelgrass beds are also important as spawning substrate for bait fish species such as herring (*Clupea pallasi*).

(b) Critical environmental parameters for seagrass beds include wave energy, salinity, temperature, water clarity, and nutrient concentrations. Depth and water clarity exert the primary controls over seagrass zonation and the degree of colonization by epiphytes. Redistribution of sediments by waves and storm surges can severely impact seagrass beds. Diseases can have a catastrophic effect on seagrass communities. During the 1930's, widespread infection by the slime mold *Labryinthula macrocystis* decimated Atlantic coast eelgrass populations (Short, Muehlstein, and Porter 1987). Many coastal areas have not yet recovered from this "wasting disease."

(c) Seagrass beds are susceptible to an array of human-induced degradations. Dredge and fill operations associated with navigation channel maintenance have taken a toll. Deterioration of water quality conditions associated with human population in coastal areas remains a primary cause of seagrass bed degradation. Physical damage to seagrass beds may be caused by recreational boating in shallow waters. This type of chronic disturbance is common in populated areas and is persistent; turtle grass beds in Florida Bay may require upwards of a decade to recover from propeller scarification (Zieman 1976).

(d) There has been considerable interest and effort expended to devise effective methods of creating or restoring seagrass beds, primarily by transplantation. Most efforts have failed, usually because site conditions are not suitable. The parameters of the transplant site must closely match those of the donor, or reference site, if restoration is to be successful.

(e) The earliest recorded eelgrass transplant efforts along the U.S. Atlantic coast were documented by Addy (1947). The first successful transplantation of turtle grass was reported by Kelly, Fuss, and Hall (1971) in Boca Ciega Bay, Florida. Attempts to reestablish subtropical seagrasses on dredged material deposits in Port St. Joe, Florida, are described by Phillips (1980).

(f) Thorhaug and Austin (1976) discuss types of coastal engineering projects that could benefit from transplantation of seagrass beds. These include (a) dredging of canals where both sides can be replanted, (b) stabilization of the shallow subtidal and intertidal portions of dredged material islands, and (c) other miscellaneous dredge and fill impact projects (road, bridge construction, marinas, etc.). Transplantation of turtle grass, manatee grass, and shoalgrass beds in Biscayne Bay, Florida, and other locations in the Caribbean are documented by Thorhaug (1985, 1986). Darovec et al. (1975) described transplant techniques for seagrasses along Florida's west coast. Lewis (1987) reviews seagrass restoration in the southeast United States, and discusses reasons for failures, as well as success, using well-documented case studies in south Florida.

(g) Recent efforts to reestablish eelgrass in lower Chesapeake Bay are documented by Moore and Orth (1982). Thom (1990) reviewed eelgrass transplanting projects in the Pacific Northwest and Wyllie-Echeverria, Olson, and Hershman (1994) documented the state of seagrass science in policy in the Pacific Northwest.

(h) Planting techniques, along with cost and labor estimates for establishment of eelgrass, shoalgrass, manatee grass, and turtle grass on dredged material and other unvegetated substrates are documented by Fonseca, Kenworthy, and Thayer (1987). Fonseca (1994) reviews all aspects of seagrass restoration, including planting guidelines and monitoring programs for the Gulf of Mexico; however, this information is applicable to seagrass restoration in general.

(i) A variety of transplant methods have been used to restore seagrasses, including broadcast seeding, seed tapes, stapling of individual plants, and use of "peat pots" or sediment plugs containing whole plants. The latter method appears to be most successful (Fonseca 1994). Fertilizer applications have been tried in some instances, although performance has been inconclusive (Fonseca 1994). Careful attention must be paid to spacing of individual planting units in order to achieve site coalescence. Subtropical seagrass beds in Florida Bay and the eastern Gulf of Mexico have achieved coalescence in as little as 9 months, or as long as 3-4 years, depending on planting distance between individual units. In high-energy areas, beds may never fully coalesce.

(j) Careful monitoring is critical to the success of any seagrass restoration project. Performance indicators should include survival rates of planting units, areal coverage, and number of shoots per planting unit. Fonseca (1994) recommends quarterly monitoring intervals during the first year following planting and semi-annual intervals for the next 2 years. Areal coverage should be monitored in successive years.

Assessment of ecological functions (e.g., nutrient cycling, primary production, utilization by benthic invertebrate and fishery species), should also be conducted, and more recent studies have focused on restoration of specific functions of seagrass beds, including the ability of seagrasses to modify their surrounding hydrodynamic environment (Fonseca and Fisher 1986) and their potential for utilization as a nursery by fishes and invertebrates (Homziak, Fonseca, and Kenworthy 1982, Fonseca et al. 1990).

(6) Use of dredged material for creating shallow habitat. In the face of increasing restrictions on open-water disposal of dredged material and limited capacity in existing disposal facilities, coastal engineers have proposed placing dredged material in nearshore waters. In highly developed bay and harbors where shallow intertidal or subtidal habitat is limited, the placement of clean dredged material can create or restore important nearshore habitat. Shallow coastal waters are often home to seagrass beds, macroalgae beds, and other communities.

b. Projects at the land-sea interface.

(1) Mud/sand flats. Intertidal mud and sand flats are a conspicuous coastal habitat type present along all coasts of North America. They are most abundant and expansive in high tidal range areas such as Puget Sound and the New England coast. A variety of fish and invertebrate species, many of commercial and recreational importance, depend on intertidal and shallow subtidal unvegetated marine habitat, particularly during early life stages. Along the U.S. Atlantic coast these include the sandworm (*Nereis virens*) and bloodworm (*Glycera dibranchiata*). These two species represent an important bait industry in the northeast (Wilson and Ruff 1988). Bivalves, which occupy mud and sand flats along the Atlantic coast, include the hard clam (*Mercenaria mercenaria*) and softshell clam (*Mya arenaria*); both are harvested commercially. On the west coast, several commercially important species are associated with mud and sand flats, including the Pacific razor clam (*Saliqua patula*), littleneck clam (*Protothaca saminea*), pismo clam (*Tivela stultorum*), Pacific oyster (*Crassostrea gigas*) and dungeness crab (*Cancer magister*).

(a) Mud and sand flats are also very productive for benthic and epibenthic invertebrates and algae. They are an important source of nutrients to the entire coastal ecosystem. In virtually all estuarine and coastal areas, mud and sand flats are important forage sites for a myriad of resident and migratory waterfowl as well as wading bird species, which feast on the abundance of invertebrate prey items (worms, small crustaceans, bivalves) available at low tide.

(b) Restoration and creation of unvegetated intertidal habitats has not received the level of attention given to restoration/creation of vegetated intertidal habitats, such as salt marshes and mangrove forests. However, deposition of fine dredged material in shallow coastal waters may inadvertently result in the creation of intertidal mud and sandflats. Many such artificial habitats were created prior to the implementation of the National Environmental Protection Act (NEPA) and therefore, are not well-documented. A study by the U.S. Army Engineer Division, New England and ERDC compared benthic invertebrate community dynamics at a recently constructed mudflat with a nearby natural mudflat at Jonesport, Maine (Ray et al. 1994). A diverse infaunal assemblage was present 2 years after construction and included commercially important species such as sandworms and softshell clams. As with most shallow-water habitat creation and restoration projects, habitat tradeoffs must be considered. In certain geographic areas (e.g., coastal New England) creation of intertidal mud or sand flats may represent an attractive beneficial use alternative to conventional dredged material disposal. Mud and sand flats can also be restored or created by the removal of fill material that may have been placed in the nearshore zone to create uplands for development. When industrial areas adjacent to the water are abandoned, it provides a perfect opportunity to remove fill and recreate aquatic habitat. Another technique used in highly modified shorelines (such as ports) in the Pacific Northwest includes the creation of intertidal benches that are surrogates for once prevelent mudflats. Long linear stretches of riprap bankline are altered to accommodate a rock crib that is lined with filter fabric. These cribs are filled with fine-grained material (50 percent sand, 25 percent silt, and 25 percent clay) and become sites

for benthic recruitment and algae attachment. These intertidal benches are also placed at specific tidal elevations for epibenthic production as well. As juvenile fish migrate downstream to the ocean, they follow the shoreline through the developed port areas and can feed during their migration.

(2) Intertidal salt and brackish marshes. Intertidal marshes are found in all coastal areas of the United States, except for the southern half of Florida, where they are replaced by mangroves; and certain areas of the Western Gulf of Mexico, where they are replaced by wind-tidal flats. They are a conspicuous landscape feature along the gently sloping Atlantic coastal plain, from New England to east-central Florida, in association with drowned river-valley estuaries and back-barrier lagoons. Intertidal marshes are ubiquitous in the lower Mississippi Delta and back-barrier systems of the Gulf of Mexico, ranging from west-central Florida to Southwest Texas. Intertidal marshes are found along the Pacific coast from Baja, Mexico to Alaska, but are less extensive than those along the Atlantic and Gulf coasts. Large Pacific coast estuaries (e.g., San Francisco Bay and Puget Sound) historically supported large areas of intertidal marsh, but have experienced dramatic losses. In the past, the losses were primarily due to the building of dikes and reclamation of the marshes as farmland, but more recently have primarily been due to dredge and fill activities.

(a) Intertidal marshes occur along the entire estuarine salinity gradient from tidal freshwater (<0.5 psu) to polyhaline (>20 psu) conditions (Figure V-7-1). Ecological functions attributed to intertidal wetlands include shoreline stabilization, storage of surface waters, maintenance of surface water and groundwater quality, and the provision of nursery habitat for estuarine-dependent finfish and shellfish species.

(b) Vegetation communities in intertidal wetlands are dominated by grasses (Poaceae), rushes (Juncaceae), or a combination of the two. Variability in environmental factors (e.g., nutrient availability, duration and depth of intertidal flooding, and pore water salinity) limits plant species diversity in intertidal salt and brackish marshes. The spatial extent of the major zones of intertidal marsh vegetation is largely determined by elevation and its effect on the tidal flooding regime.

(c) Intertidal marshes provide habitat for a variety of organisms, including many commercially important fish species. Examples of marsh-dependent fish and crustaceans along the Atlantic and Gulf coasts include blue crab, brown, white and pink shrimp (*Penaeus* spp.), red drum (*Sciaenops ocellatus*), and spotted sea trout (*Cynoscion ocellatus*). Early life stages of these organisms are afforded refuge from predators and benefit from abundant prey resources in shallow tidal marsh habitats. Prey species include various killifishes (*Fundulus* spp.) and caridean shrimp (*Palaemonetes* spp.) commonly encountered on the vegetated intertidal marsh surface and in shallow subtidal creeks and pools. Characteristic marsh invertebrates include fiddler crabs (*Uca* spp.), amphipod and isopod crustaceans, terrestrial insects and arachnids, various bivalve and gastropod mollusks, and annelids. Wading birds, such as egrets and herons, prey upon resident fishes and invertebrates of intertidal marshes. Many other birds, both arboreal and aquatic, feed and nest in upper intertidal marsh habitats. A variety of mammals, including deer, fox, raccoon, and otter, use intertidal marshes for foraging, breeding, and refuge.

(d) The restoration and creation of intertidal salt and brackish marshes have received much attention in coastal engineering. This is likely due to the considerable acreage of salt marsh that has been lost along U.S. coastlines, recognition of the functions provided by intertidal marshes, and the relative ease in which salt marsh vegetation can be propagated upon dredged material. Restoration of tidal marsh environments may involve removal or breaching of dikes and berms, or installation of culverts under roads to reestablish the natural tidal prism. Hydrologic restoration of tidal marshes has occurred in New England (Sinicrope et al. 1990), the mid-Atlantic (Shisler 1990), central Florida (Rey et al. 1990), central and southern California (Niesen and Josselyn 1981), and the Pacific Northwest (Frenkel and Morlan 1991). Reestablishing tidal conduits increases accessibility of previously impounded or restricted wetlands to estuarine-dependent finfish and wildlife. Invasive plant species such as common reed (*Phragmites australis*), which often predominate in hydrologically altered wetlands, may be controlled via reestablishment of historical tidal regimes (Roman, Niering, and Warren 1984).

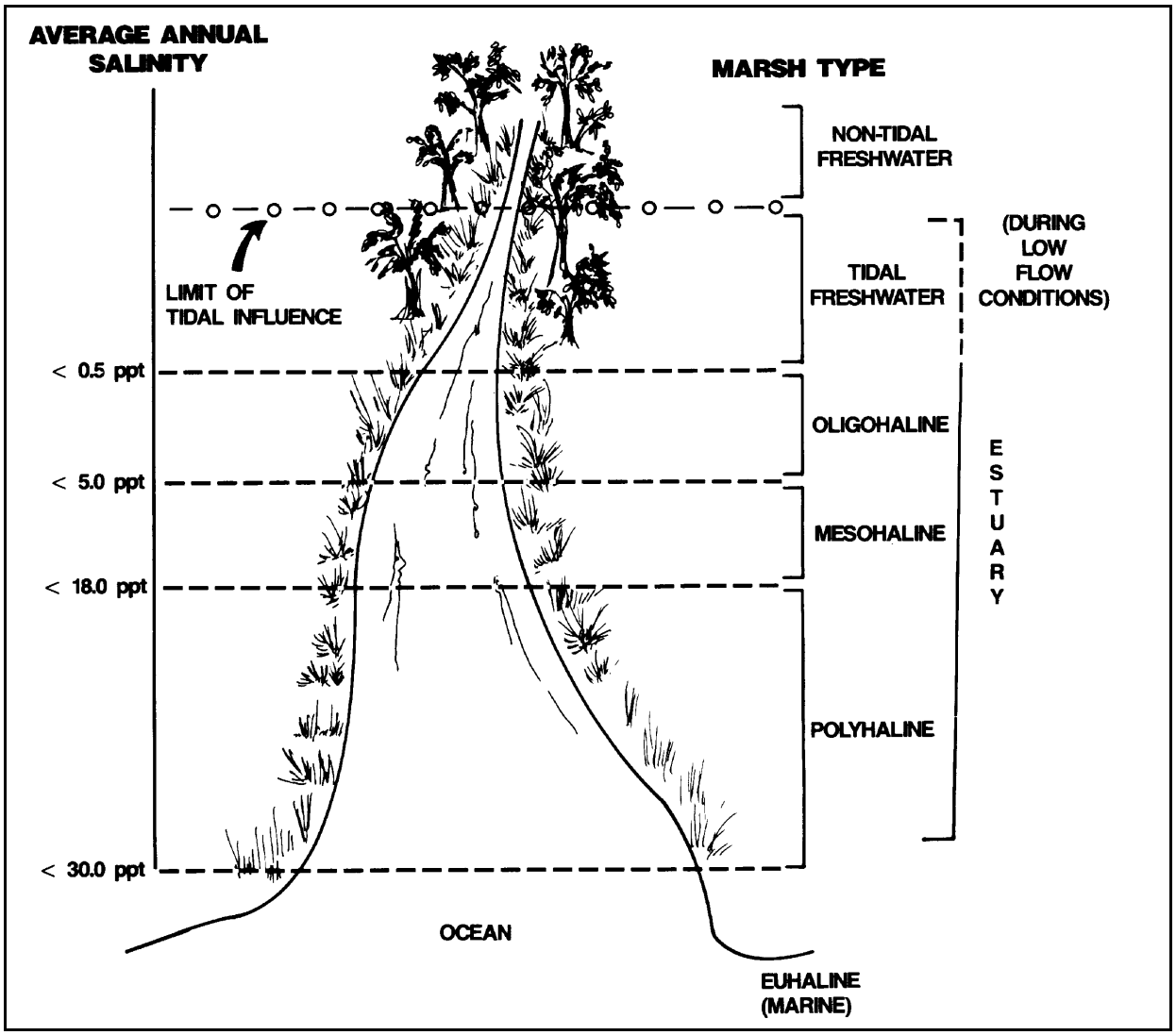

Figure V-7-1. Distribution of tidal marsh type along an estuarine salinity gradient

(e) Marsh *creation* is often a component of the restoration process, especially in projects involving the removal of fill and/or regrading of adjacent uplands to intertidal elevations. However, it is important to recognize that marshes can often be created in upland or shallow subtidal areas that have not historically supported intertidal vegetation.

(f) Techniques for establishing *Spartina alterniflora* marshes on dredged material deposits along the south Atlantic coast were pioneered by researchers at North Carolina State University in the late 1960's to early 1970's (Seneca 1974, Seneca et al. 1976). The objective of these early studies was to provide stabilization of shorelines and dredged materials, and to recoup some of the losses to coastal habitats that had occurred as a result of human population growth in coastal areas. The U.S. Army Corps of Engineers Dredged Material Research Program (DMRP) pioneered large-scale salt marsh establishment on all three U.S. coastlines in the 1970's (Barko et al. 1977, Smith 1978). Tidal marshes established under the DMRP were monitored from 1974-1987 (Landin, Webb, and Knutson 1989). Parameters studied include plant propagation success, shoreline stabilization properties, and utilization by fish and wildlife species. Successive research has focused on refining the techniques developed by the DMRP, and in recent years, increased attention has focused on replication of ecological function in created or restored intertidal marshes.

(g) Tidal marsh creation/restoration, with emphasis on planting techniques, is discussed by Broome, Seneca, and Woodhouse (1988). Darovec et al. (1975) provide guidance on planting salt marsh vegetation, including information on handling of seed stock, transplant units, planting intervals, and elevation requirements, with emphasis on the Florida coast. Roberts (1991) evaluated the habitat value of 22 created coastal marshes in northern and central Florida, concluding that the basic habitat requirements of fish, bird, and mammal species that use natural marshes in this region were being met by the majority of the man-made habitats. Marsh shape and size were critical features determining the degree of use by fish and wildlife species. Minello, Zimmerman, and Medina (1994) determined that geomorphic features such as tidal creek edges strongly influenced the abundance and distribution of fishes and invertebrates on the surfaces of intertidal marshes created from dredged materials in Galveston Bay, Texas.

(h) Salt marsh creation/restoration has been conducted at a number of sites in central and southern California during the last two decades. There has been considerable debate on the benefits of marsh creation/restoration as mitigation for destruction of natural wetlands along the west coast and elsewhere (Race 1985, Zedler 1996a). Josselyn and Bucholz (1982) provide a detailed overview of marsh restoration projects in the San Francisco Bay estuary, including case histories and monitoring studies. Zedler (1988) reviews salt marsh restoration in Southern California, and discusses the importance of hydrologic concerns, and the value of experimentation in planning and monitoring marsh restoration projects. Several "lessons" from restoration efforts in California are outlined, including the importance of planning for the maintenance of rare or endangered plant and animal species in tidal marsh restoration projects, and a recommendation against the use of offsite mitigation for development projects that impact natural wetlands. Recently, the San Francisco District has taken dike breaching to large scale. The Sanoma Baylands project incorporated both levee breaching of an old salt evaporation pond and beneficial uses of dredged material. The salt pond had been in use for almost 100 years and as a result the original marsh elevation had greatly subsided. In order to offset the subsidence, dredged material was spread out over the 117-ha (289-acre) project area to reestablish tidal marsh elevations. Two other larger scale dike breaches are planned for Hamilton Army Airfield (a 364-ha (900-acre) abandoned facility) and Napa Marsh. Similar projects also have taken place in the Pacific Northwest. Trestel Bay, a project in the Portland District, restored over 202 ha (500 acres) by a dike breach in five separate locations. The ability of created/restored tidal wetlands to perform the functions attributed to natural tidal wetlands is addressed by Simensted and Thom (1996) in their study of a restored brackish intertidal wetland in the Puyallup River, Washington. These authors contend that only a few of 16 functions investigated displayed a tendency toward equivalency with natural tidal wetlands in the Pacific Northwest in the first several years subsequent to construction. Natural variability among reference sites was cited as an impediment to assessing the degree of functional equivalence between restored and natural marshes.

(3) Tidal freshwater wetlands. Tidal freshwater wetlands occur along the upper reaches of rivers characterized by moderate to strong tidal influence. They are most extensive along the Atlantic coast between Georgia and New England, especially in the mid-Atlantic/Chesapeake Bay region and along the coastal rivers of South Carolina and Georgia. Tidal freshwater wetlands are also common in the Pacific Northwest, where considerable freshwater influence and high-amplitude tides prevail (Odum et al. 1984). The vegetation community of tidal freshwater marshes is diverse, in comparison to salt and brackish marshes (Figure V-7-2). Rarely does any one species dominate, and notable changes in plant community structure can occur within a single growing season. Freshwater tidal marshes can be dominated by emergent herbaceous species, shrubs, or trees (particularly in the Pacific Northwest), or a combination of all three. As with salt and brackish marshes located downstream, tidal freshwater marshes support populations of both resident and migratory fishes, many of which have recreational or commercial significance, including salmon and trout (*Oncorhynchus sp.*), striped bass (*Morone saxatilis*), yellow perch (*Perca flavescens*), and black bass (*Micropterus* spp.). Wildlife, including mammals, reptiles, and amphibians reside or forage in tidal freshwater marshes. Many arboreal and aquatic bird species are temporary or year-round residents of tidal freshwater marshes.

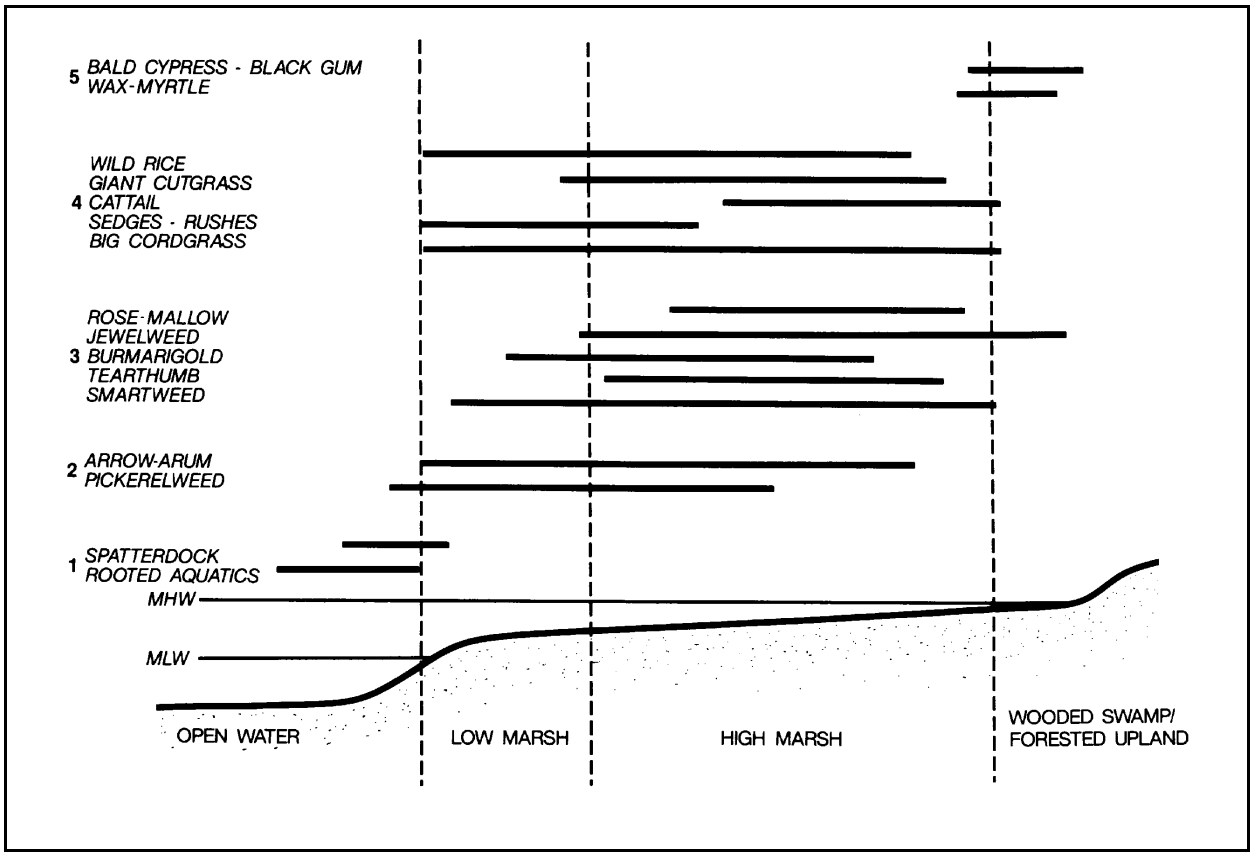

Figure V-7-2. Characteristic profile of a mid-Atlantic tidal freshwater marsh

(4) Tidal freshwater marsh restoration. Restoration and creation of tidal freshwater marshes is technically similar to that of salt and brackish marshes. One of the earliest of the Corps' DMRP wetland creation efforts was the Windmill Point Marsh project conducted in the James River, Virginia (Lunz et al. 1978; Landin, Webb, and Knutson 1989). In 1974, fine-grained dredged material from the James River was used to construct an 8-ha (20-acre) island surrounded by a temporary sand dike. Upon completion of the island, the dike was breached to allow natural formation of tidal channels. Vegetation colonization occurred within one growing season without planting, attesting to the value of seed banks in tidal freshwater sediments. Information collected on fisheries use and benthic invertebrate communities at Windmill Point represents some of the most comprehensive data available on faunal utilization of tidal freshwater habitats. Ultimately, much of the original island site was lost due to erosion and subsidence; however, a spatially complex system of intertidal marsh and shallow subtidal habitat persists in providing nursery habitat for resident and migratory fish and wildlife. Several smaller tidal freshwater marsh restoration projects have also been conducted in upper Chesapeake Bay (Garbisch and Coleman 1978).

(a) Another DMRP project involving the creation/restoration of tidal freshwater wetlands is the Miller Sands Island habitat development project in the lower Columbia River, near Astoria, Oregon (Clairain et al. 1978). This large island/wetland complex was also constructed in 1974 and monitored extensively to document vegetation and soils development, and utilization by fisheries and wildlife (Landin, Webb, and Knutson 1989). This represents one of the few published efforts to date documenting faunal utilization of tidal freshwater wetlands in the Pacific northwest.

(b) On the west coast, a common method of restoring tidal freshwater wetlands is to breach dikes or levees constructed for farmland creation in the past. The Sacramento District breached dikes at Cache Slough

to create approximately 8.9 ha (22 acres) of freshwater marsh habitat (Stevens and Rejmankova 1995). The Seattle District restored over 162 ha (400 acres) of freshwater wetlands to tidal influences in a WRDA 1986, Section 1135 project. The Deepwater Slough project used explosives experts from the Army's 168th Division to detonate charges to create some of the breaches. Forested tidal freshwater wetlands are relatively rare habitats and should be considered an important habitat to restore. Unfortunately, it may take 25-100 years, as they are not yet mature.

(5) Mangroves. Mangroves are woody trees and shrubs of the family Rhizophoracea, and represent a tropical/subtropical analog to herbaceaous intertidal vegetation of temperate regions. In the United States, mangroves occur primarily in southern Florida, especially along the southwest coast, and in scattered locations in Louisiana, Texas, and Hawaii.

(a) Like salt marshes, mangrove forests provide critical nursery and foraging habitat for resident and transient fish populations, many of which are recreationally and commercially significant, including red drum (*Sciaenops occelatus*), tarpon (*Megalops atlantica)*, and Snook (*Centropomus undecimalis*). A variety of wildlife and avifauna, including American alligator (*Alligator mississippiensis*), American crocodile (*Crocodylus acutus*), Roseate spoonbill (*Ajaia ajaja*), white ibis (*Eudocimus albis*) and several species of herons and egrets use mangroves as refuge and breeding habitats. Important tropic linkages have been established between mangrove forests and adjacent ecosystems, such as seagrass beds and coral reefs. Mangroves, like intertidal marshes, provide shoreline stabilization. Mangroves intercept and retain nutrients moving downstream and maintain water quality via filtration of tidal surface waters.

(b) Loss and degradation of mangrove forests has resulted from hydrologic alteration, industrial and agricultural land use, dredge and fill activities, and, in some areas, direct harvest for wood products (Cintron-Molero 1992).

(c) Mangrove restoration. Mangrove restoration is typically accomplished by transplanting individual propagules (seedlings) along unvegetated intertidal shorelines. Important factors to consider in attempting to transplant mangroves include plant size and source of donor plantings, salinity, shoreline energy, and tidal flooding depth (elevation). The latter factor is of considerable importance, particularly when transplantation is being conducted on dredged material deposits, which may settle over time. Commonly cited reasons for failure of mangrove restoration efforts include excess wind/wave energy at the transplant site, improper hydrologic regime (inadequate tidal flushing), and failure to replace planting units lost to mortality (Cintron-Molero 1992).

(d) The earliest documented efforts to restore mangroves date back to the early 1970's in Florida. There are anecdotal reports of earlier attempts to transplant mangroves for soil stabilization in the early 1900's (Pulver 1976). Teas (1977) describes the life history of various mangrove species in Florida, with implications for their restoration. Pulver (1976) describes transplant techniques for red, black, and white mangroves in southwest Florida. Darovec et al. (1975) provide detailed planting guidelines for mangroves in South Florida, including information on elevation requirements, planting unit height, age and spacing of planting units, soil types, and fertilization. Lewis (1982) discusses a variety of mangrove restoration projects from Florida and the U.S. Virgin Islands, with recommendations for improving the success of mangrove projects. A more recent assessment of the state of the art in mangrove restoration is provided by Cintron-Molero (1992) with examples from Puerto Rico and other Caribbean locales.

(6) Rocky intertidal shores. Rocky intertidal shorelines are found worldwide, primarily in high-energy littoral environments. Biotic assemblages of rocky intertidal shores include macroalgae, particularly brown algae (*Fucus* spp.); various mollusks, including limpets, mussels, and gastropods; and barnacles. The complex interactions among these organisms along rocky shores of the east and west coasts of North America have been the subject of numerous experimental studies in the last several decades, forming the basis for

much of our understanding of the structure and function of shallow marine communities (Connel 1972, Paine and Levin 1981). Shallow rocky habitats along the U.S. west coast are used as spawning sites for juvenile fishes, including some commercially important species such as Pacific herring (*Clupea harengus pallasi*). Shorebirds forage extensively along rocky shorelines and in tidepools. Marine mammals such as sea lions, otters, and seals breed and reside along rocky shores.

c. Projects in coastal uplands.

(1) Coastal dunes. Coastal dunes are highly dynamic sand deposits located landward of beaches. They occur along all coasts of the United States, including the Great Lakes. They are especially common along the Atlantic and Gulf barrier island shores, and also dominate in some Pacific coast areas (California, Oregon). Dunes supply sand to beaches during erosive storm events, and act as buffers to wave energy. Removal of dunes from coastal areas can result in significant economic loss from damage to homes, businesses, and natural areas (Woodhouse 1978).

(a) In general, dunes and other transient lands such as spits are highly desired by developers, because of their proximity to the shoreline. This practice should be strongly discouraged as the forces causing the dynamic nature of the land masses do not cease once houses are built on a spit, etc. Engineering structures such as steel sheet piles and stone revetments are a temporary solution and frequently cause harm to downdrift properties.

(b) Dunes may be vegetated, and, therefore, relatively stable, or they may be naturally unvegetated. Three types of vegetated dunes are recognized:

- *Foredune Ridges* are linear, low-amplitude sand ridges oriented parallel to the beach. These are common along the Atlantic and Gulf coasts.

- *Parabolic Dunes* are sparsely vegetated, U-shaped dunes, open to the direction of prevailing winds. These generally form behind foredunes and are common along the lower shoreline of Lake Michigan, Cape Cod, and northwest Florida.

- *Precipitation Dunes* are blown sand deposits which intrude onto adjacent forested uplands. These commonly occur along the U.S. Pacific coast.

(c) Unvegetated dunes are the most dynamic and also vary considerably in morphology. *Transverse Dunes* are sand deposits that lie perpendicular to the prevailing winds. *Longitudinal Dunes* are oriented parallel to prevailing winds. *Transverse Dunes* are rapidly migrating dunes that move landward in response to prevailing winds. Transverse dunes may be straight or sinuous in shape and may persist for up to 1 km (0.6 mile) in length.

(d) Wave climate and local wind regimes are the primary physical factors responsible for dune establishment. Littoral processes (longshore drift) and storm-associated overwash events provide the sand; dune morphology is determined by wind climate (the direction of prevailing winds relative to the orientation of the beach).

(e) Characteristic perennial grass species that grow on dunes are instrumental in maintaining dune integrity and stabilization function. Sea oats (*Unionicola paniculata*) are the dominant dune grass along most of the south Atlantic and Gulf coasts. This and other dune-building species are able to withstand high salinity, wind, evaporation, and periodic burial by drifting sand. Other dune-building plants include American beach grass (*Ammophila breviligulata*), bitter panic grass (*Panicum amarum*), saltmeadow cordgrass (*Spartina patens*), and seacoast bluestem (*Schizachyrium maritinum*). European beach grass

(*A.arenaria*) has been widely introduced, especially in the Pacific Northwest, and has displaced native American dunegrass (*Elymus molli*) throughout much of this region.

(f) Dunes are fragile coastal habitats and are subject to destruction by trampling, vehicular traffic, construction, and livestock grazing. Once disturbed, the dunes become unstable, and sand is distributed via wind and wave action either into adjacent waters, or inland.

(2) Coastal dune restoration. In recognition of the potential importance of dunes as shoreline stabilizers, considerable research has been conducted to develop restoration techniques. Historically, dunes have been stabilized with vegetative plantings in many coastal areas; however, this frequently led to a loss of dune processes (longshore movement, etc.), and may even eliminate unvegetated habitat used by native wildlife such as snowy plovers on the west coast. Early settlers on Cape Cod, Massachusetts, planted American beach grass to stabilize dunes. European beach grass was introduced to the San Francisco Bay area at the turn of the century for dune and shoreline stabilization purposes. During the 1930's, dune restoration projects were completed by the Civilian Conservation Corps in the Pacific Northwest and along the Outer Banks of North Carolina. Dune creation/restoration has also been conducted in Europe, Israel, Australia, and South Africa (Dahl et al. 1975). Recent efforts have sought to improve the state of the art of dune restoration with regard to appropriate selection of native plant species, improved planting techniques, removal of nonnative invasive species, and the use of new technology. Much of the research to develop effective methods of dune building was conducted at the U.S. Army Engineer Waterways Experiment Station's Coastal Engineering Research Center (CERC) in the mid-1960's. These techniques have been applied to dune creation and restoration in coastal areas throughout the United States, and elsewhere (Gage 1970, Darovec et al. 1975). Knutson (1977) provides a general overview of dune restoration, including a discussion of specific applications and recommendations for transplant species. Woodhouse (1978) reviews the ecology of dune plants and provides detailed guidelines for planting, fertilization, and maintenance of artificial dunes, on a region-specific basis.

(a) Typically, dunes are constructed mechanically using earth-moving equipment, or sand fences are used to trap sand in desired areas. Transplant units can be obtained from nursery stocks, or removed from nearby intact dune systems (this may be illegal in some areas). The most commonly used species in dune transplantation are American beach grass, European beach grass, sea oats, and bitter panic grass. Plantings are done by hand or with a strawberry or tobacco planter. Irrigation can be used to stabilize unconsolidated sand prior to planting. Fertilization is usually necessary to establish plant growth in these nutrient-poor systems. Typically, nitrogen, phosphorous, and potassium fertilizers are broadcast by hand or applied using a mechanical spreader.

(b) Once the primary species are established, additional species will eventually grow due to natural colonization processes. Vegetative planting serves two functions: (a) it stabilizes sand deposits, and (b) it provides a baffle that encourages deposition of wind-blown sand on the dune surface. The ability of the various transplant species to perform the two functions varies widely among geographic regions.

(c) Removal of nonnative vegetation is another technique for dune restoration, particularly on the west coast. Methods include manual pulling/removal of plants, mowing, or grubbing with equipment. Often these treatments need to be repeated over several seasons to ensure removal of all or most of the non-native plants. Pickart, Miller, and Duebendorfer (1998) and Pickart et al. (1998) removed yellow bush lupine from northern California dune systems and investigated how the nutrient input from the lupine influenced colonization of the dunes by both nonnative and native plant species.

(d) Sand fences (longitudinal wooden or fabric fence erected along the beach face to encourage deposition of sand) can be used to initially create dunes in the absence of vegetation (Figure V-7-3). This is typically done in an area where dunes do not currently exist, and must be established prior to vegetative stabilization. Sand fences may be constructed in successive "lifts" in order to encourage the accretion of large

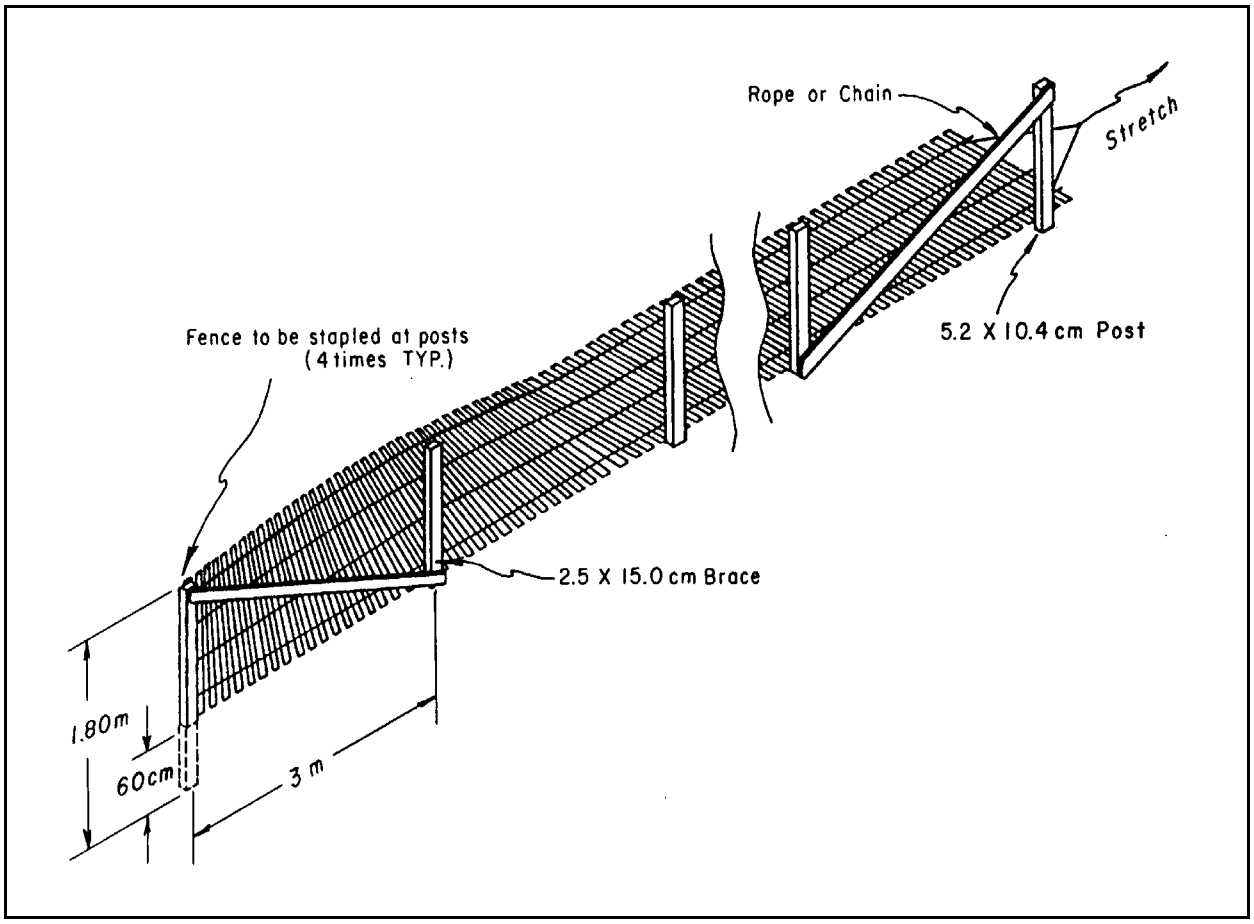

Figure V-7-3. Diagram of a sand fence

dunes (Woodhouse 1978). Most constructed dunes are linear. However, in some cases, it may be advantageous to attempt to replicate the sinuous contours often observed in natural dune systems. Sand fences are advantageous because they trap sand at a rapid rate. Once established, dune-building plants can trap sand at a rate comparable to that of sand fences (Knutson 1980).

(e) Although benefits to reestablishing or stabilizing coastal dunes are considerable, environmental issues need to be considered (Knutson and Finkelstein 1987). Dune construction may interfere with natural geomorphological processes, such as barrier island migration and salt marsh development. Overwash provides the sediment necessary for the maintenance of salt marshes, and periodically provides new substrate for the formation of new marshes. Large-scale dune establishment along barrier islands could potentially interfere with natural cycles of marsh burial and reestablishment associated with overwash events.

(f) Another environmental concern involves changes in natural plant communities as a result of artificial dune construction. Dunes provide protection from salt spray, flooding, and wind/wave energy. A reduction in environmental stress may induce rapid and unwanted changes in vegetation communities behind the primary dunes. Dense growth of shrubs is the most commonly encountered result, with a resulting change in microclimate. This may or may not be considered ecologically desirable, depending on the relative abundance and perceived importance of this habitat type in a specific region. Many coastal wildlife species (arboreal birds, small mammals) will readily inhabit coastal shrub thickets. However, most colonial waterbirds (gulls, terns) prefer to nest in sparsely vegetated dunes.

(3) Maritime forests. Maritime forests are evergreen tree and shrub systems that occur in a narrow discontinuous band along barrier islands and low-lying mainland areas. In the United States, they are most common from North Carolina to Florida. Maritime forests support a distinct fauna and flora adapted to a unique set of environmental parameters, including high soil salinities resulting from periodic storm-induced seawater inundation, wind, and limited fresh water. Canopy height is often restricted from the effects of near-continuous salt spray. Bellis (1995) described the following maritime forest sub-community types based on dominant vegetation and hydrologic patterns:

- Maritime Shrub
- Maritime Evergreen Forest
- Maritime Deciduous Forest
- Coastal Fringe Evergreen Forest
- Coastal Fringe Sandhill
- Maritime Swamp Forest
- Maritime Shrub Swamp
- Interdune Pond

(a) Common plants of eastern maritime forests include wax myrtle (*Myrica cerifera*), live oak (*Quercus virginiana*), and loblolly pine (*Pinus taeda*); on the west coast common species include shore pine (*Pinus contorta*) and Sitka spruce (*Picea sitchensis*). Exposure to salt aerosols is the primary factor that determines species composition and canopy height. As distance from the ocean increases, the floristic composition of maritime forests more closely resembles a typical mainland forest community. Maritime forests provide habitat for wildlife, and stabilize barrier island soils. A diverse assemblage of terrestrial and semi-terrestrial invertebrates inhabit maritime forests, but these communities have not been well-studied. Wildlife species richness can be high, especially on large barrier island systems or on islands that are periodically connected to the mainland and provide dispersal corridors.

(b) Maritime forests have been lost or decimated by timber harvesting and livestock grazing since colonial times. They are subject to development impacts and are becoming increasingly fragmented. Recent recognition of maritime forests as a rare and unusual habitat type has led to various protection initiatives along the U.S. Atlantic coast. As of yet, there have been no documented attempts to restore or create maritime forests in areas where significant acreage has been lost. Certain maritime forest species, such as wax myrtle, are known to rapidly recolonize protected areas behind man-made dunes, suggesting the potential for large-scale creation or restoration of these unique habitats.

(4) Bird/wildlife islands. Terrestrial islands and coastal uplands are often created using dredged material specifically to provide nesting and refuge habitats for birds and other wildlife. Many of the Corps DMRP habitat development sites included bird/wildlife islands as part of the overall habitat mosaic created (Buckley and McCaffrey 1978, Chaney et al. 1978, Soots and Landin 1978). Dredged-material islands are used extensively as rookeries by various birds, including terns, gulls, pelicans, skimmers, stilts, willets, and oystercatchers. Maximum utilization by a diverse bird and wildlife assemblage is attained when habitat heterogeneity is maximized. Creation of terrestrial islands will require careful consideration of the environmental consequences. It is important to focus on the system as a whole; not benefitting one species over another. This becomes apparent during the last few years when Sand Island created in the lower Columbia estuary from dredged material for nesting terns required extensive modification to discourage birds

from using the project. Pit tag analysis (these are small markers placed on young fish) at the nesting site of the terns revealed that they had taken an enormous amount of juvenile salmon as they migrated down the Columbia River to the ocean. Several species of the salmon are listed as threatened or endangered under the Endangered Species Act and it seems that the nesting terns were one of many factors that have led to salmon decline.

(a) Dunes, vegetated swales, ponds, and mud/sandflats are all important components of a well-functioning bird/wildlife island. Tree and shrub species rapidly colonize created dredged material islands, providing rookeries for species that nest in canopies. Small mammals, such as mice, shrews, and voles will readily colonize these islands, especially if nearby upland habitats are available to provide dispersal corridors. Deer, fox, raccoon, and other species are typical residents of created upland habitats in coastal areas.

(b) Studies along the North Carolina coast (Parnell, DuMond, and Needham 1978; Parnell, DuMond, and McCrimmon 1986) suggest that the presence or absence of retaining dikes is an important determinant of plant colonization rates and subsequent utilization by wildlife. The earlier constructed wildlife islands in North Carolina (prior to the mid-1970's) were mostly undiked, while islands constructed after 1975-76 were diked. Diked islands were not used as extensively by colonial waterbirds compared to the undiked islands. Terrestrial plant species colonize diked islands more rapidly than undiked islands; species which prefer dense vegetative cover (some small mammals, arboreal birds) benefit at these sites; however, most colonial waterbirds prefer to nest along sparsely vegetated beachfront, which is available mainly at older, undiked islands. Nest sites located behind dikes are subject to flooding following heavy rain. Although many previously undiked islands have been diked at a later date for stability and longevity, this has decreased available nesting habitat for colonial waterbirds.

V-7-8. Environmental Features of Traditional Coastal Engineering Projects

The majority of coastal engineering projects will no doubt be required to provide habitat mitigation or restoration as a result of regulatory requirements and there are many opportunities and considerations for habitat protection in the planning and implementation phase of traditional coastal engineering projects. Consideration of sound environmental design criteria and potential environmental benefits can be invaluable in generating public and agency approval in high-profile or controversial coastal engineering projects.

a. Example project types.

(1) Beach nourishment. The dynamic nature of the littoral environment ensures that beaches will remain an ephemeral resource in many areas. Wave, wind, and tidal action combine to continually erode or accrete beach landscapes; these processes occur on a variety of temporal and spatial scales. In areas experiencing relative sea level rise, the net result is gradual loss of beach environment. Given the penchant for man to live, work, and recreate near the beach, maintenance of some steady state is considered economically desirable. Thus, considerable effort has been expended to stabilize and maintain beaches and counteract the effects of beach erosion.

(a) Artificial renourishment of beaches is considered to be the most cost-effective and environmentally desirable method of maintaining beaches in the short term (NRC 1995); however, recreating natural beach processes is likely to be much more successful ecologically, over longer time scales. The most appropriate sources of artificial beach fill are generally (a) dynamic accreting shorelines, such as those located around inlets, (b) channel maintenance dredging, and (c) offshore sand deposits at a depth of greater than about 15 m. These sand reserves are generally located far enough from shore such that they do not affect littoral processes and, in most cases, do not represent critical habitats (Hobson 1981). Sand from upland or riverine sources

may also be used as beach fill; however, this material may vary considerably in quality and the costs of transporting large volumes over land or downstream may be prohibitive (NRC 1995).

(b) Many of the beaches in the Great Lakes are composed of a relatively thin layer of sand over glacial or lacustrine clay. When the sand supply is interrupted, the clay is exposed and eroded, thus allowing (larger) higher energy waves to impact the bluff. The Detroit District has observed that beach nourishment fills that contain a coarse fraction (gravel to cobble-sized material) would lag the underlying clay, reducing the lake bed downcutting of the clays.

(c) Excessive siltation and increased turbidity associated with the sand mining process can cause serious environmental impacts to marine organisms (Auld and Schubel 1978, Snyder 1976). Siltation and burial of benthic organisms and reef/hard bottom habitat is an issue of concern, because the increase in turbidity affects both filter-feeding organisms and fishes. Larval and juvenile fish, in particular, are especially sensitive to dredging-induced turbidity as their gills may become clogged or abraded by floating particulates. Feeding ability of larval and juvenile fishes is decreased due to a reduction in available light. Sand mining activities must be timed properly so that they do not coincide with recruitment or migration of larval and juvenile marine organisms, especially at inlets, where these organisms are often concentrated.

(d) Substrate factors, especially grain size, are of critical importance in planning beach nourishment. It is important to match grain size of the donor sites with that of the beach site being nourished (James 1975). Analysis of grain size using standard sediment testing sieves is preferred. Generally, a single beach fill will not maintain a beach indefinitely; replenishment must be conducted over the long term in a gradual series of nourishment events. The amount of fill used will vary depending on location and severity of loss; however, a rule of thumb is to provide enough material to offset losses occurring naturally. Often, it is desirable to place excess material at the upper end of an eroding beach, allowing natural littoral processes (longshore drift) to naturally redistribute material over time.

(e) A variety of marine organisms are potentially affected by placing fill on intertidal or subtidal portions of the beachface. In general, these organisms are able to persist in the dynamic beach environment because they have adapted to conditions such as high wind and wave energy and periodic burial. The ability of most benthic invertebrates to survive a fill event depends on their ability to burrow up into the newly deposited substrate. Therefore, substrate composition and depth are the major factors determining survival rates of beach invertebrates subjected to instantaneous burial (Culter and Mahadevan 1982, Nelson 1985). Although benthic invertebrate communities on beaches are generally able to recover rapidly from fill events, the time between mortality and recovery represents a decrease in available prey resources for wildlife (primarily shore birds) which utilize the lower intertidal zone as foraging habitat.

(f) Sea turtles may be affected by beach nourishment activities (Nelson 1988; Nelson, Mauck, and Fletemeyer 1987). Spring through late summer is the primary sea turtle nesting period along the U.S. southeast and Gulf coasts. Although nourishment programs can potentially result in greater available nesting habitat for sea turtles, most of the construction activity associated with beach nourishment is likely to deter nesting females. Physical properties of the newly deposited fill (grain size, density, shear strength, color, temperature, moisture content) have been demonstrated to influence incubation, and hatching success (Nelson, Mauck, and Fletemeyer 1987). Various nesting relocation programs have been attempted to minimize the impacts associated with beach nourishment during nesting seasons.

(2) Shoreline structures. Hard structures used in beach stabilization include breakwaters, groins, revetments, seawalls, and bulkheads. These are costly to build compared to beach filling alone, but are often necessary along developed shorelines. In most cases, “hard” structures are used in combination with an artificial beach nourishment program to maintain their effectiveness in reducing beach loss in coastal communities. Environmental impacts associated with breakwaters, groins and sills are largely related to the

interruption of natural littoral drift processes and the necessity of periodically replacing or bypassing sand. The environmental impacts of shore protection structures are not limited to the beach being stabilized. When longshore drift is interrupted by stabilization structures, the effect is manifested downdrift. Animals which rely on the beach or surf zone for all or part of their lives are directly impacted by both soft and hard beach stabilization techniques (e.g., sea turtles, mole crabs and other invertebrates, grunion). Nesting and feeding shorebirds are deterred by noise and construction. Construction of shoreline stabilization structures typically involves excavation, installation of piles, backfilling, and material transport. These activities can induce temporary conditions of high turbidity in nearby waters, which may result in increased mortality to larval and juvenile finfish and shellfish. Increased turbidity may impact sensitive habitats nearby, such as coral reefs and seagrass beds. The presence of shoreline structures may alter natural patterns of circulation, resulting in altered flushing rates and scour/deposition patterns.

(a) Breakwaters and sills. Offshore breakwaters are linear structures placed parallel to the beach. Their purpose is to diminish wave energy and reduce beach erosion, while still providing for longshore transport of sand along the beach. Both single and multiple nearshore breakwater systems have been employed. In some cases, breakwaters are connected to the shoreline via a jetty. Shore-connected breakwaters may interrupt longshore transport processes and require increased maintenance (e.g., sand-bypassing) in order to maintain the integrity of downdrift shorelines (NRC 1995).

- Submerged offshore sills provide a similar function to breakwaters; they diminish some wave energy and thus reduce erosive forces acting upon the beach. Sills interrupt movement of sediments offshore, resulting in a “perched” beach; however, the characteristics of a sill which reduce loss of sand during erosive episodes also function as an impediment to sand being deposited on the beach during periods of accretion. A sill provides some environmental and aesthetic advantages relative to breakwaters, because the sill is rarely located above the high-tide mark.

- Breakwaters and sills function by modifying the nearshore wave environment. This may result in undesirable habitat changes for species which have adapted to the high-energy surf zone. However, species adapted to low-energy sheltered environments may colonize the area in the shadow of the breakwater/sill. In addition, the addition of hard substrate provides habitat for fouling organisms, and shelter for fish and motile invertebrates. Exposed portions of detached breakwaters may be used by colonial seabirds. In some areas, these structures may represent the only form of hard-bottom habitat available, resulting in an increase in local biodiversity.

(b) Groins. Groins are oriented perpendicular to the beach and extend into the surf zone. They are most commonly constructed of rubble (quarrystone) but may also be made from timber, steel, or concrete. They are typically constructed in series, commonly referred to as a groin field, along a beach. The purpose of a series of groins is to prevent sand from being transported off the beach via longshore drift. However, the presence of groins can lead to increased erosion downdrift due to interruption of longshore drift patterns. An advantage of groins over parallel nearshore structures is that wave energy is not affected by perpendicular structures, although the prevalence of rip currents is increased. Subtidal benthic invertebrate communities are not likely to be affected, because species which persist in the surf zone are adapted to dynamic patterns of scour and deposition. Sea turtles and shore birds are not likely to be deterred by the presence of groins, although initial construction and maintenance activities must be timed so as to avoid critical nesting periods for these special concern species. As with other rubble-mound protective structures, the submerged rock surfaces can function effectively as fish habitat, resulting from the provision of shelter and the abundance of epifaunal invertebrates which colonize exposed rock surfaces.

(c) Seawalls and revetments. Some seawalls are vertical structures (bulkheads) intended to protect developed shorelines or fill from wave erosion. They should only be used in situations where reflected wave energy can be tolerated. This generally eliminates bodies of water where the reflected wave energy may

interfere with or impact on harbors, marinas, or other developed shore areas. A revetment is protective armour placed on an existing bank and therefore are sloped. They are typically employed to absorb the direct impact of waves more effectively than a vertical seawall. Although revetments displace intertidal beach habitat, a potential environmental benefit may be realized by the colonization of the submerged portions of the structures (particularly rock revetments) by fouling and motile epifaunal invertebrates. Juvenile finfish and shellfish may use the submerged rocks as a feeding area and to avoid predators. In time, revetments are undermined or flanked, resulting in failure. Both seawalls and revetments eliminate the supply of literal material from the protected bluff.

(3) Navigation, ports, and marinas.

(a) Construction and maintenance channels**.** Channel construction and deepening to facilitate passage of vessels may result in a variety of potential impacts to shallow coastal habitats. The severity and extent of dredging-related impacts depends on the type of dredging equipment used, and the susceptibility of nearby habitat types and aquatic biota. *Mechanical dredging* involves the use of dragline/bucket dredges, or clamshell dredges. *Hydraulic dredging* involves the use of suction pumps and pipelines, which may or may not be equipped with rotating cutterheads. Mechanical dredging operations generate localized, pulsed, conditions of high turbidity as the bucket or clamshell apparatus is deployed. Hydraulic dredging may generate continuous conditions of high turbidity, and the area affected may be large, relative to that of mechanical dredging operations, especially if mobile equipment (e.g., hopper dredge) is used (McClellan et al. 1989, Raymond 1984).

- Both mechanical and hydraulic dredging may result in direct and indirect impacts to a variety of aquatic fauna. Benthic invertebrate communities are subject to direct mortality and burial (Hirsch, DiSalvo, and Peddicord 1978); however, these organisms usually recover from disturbance in a relatively short time. Direct impacts and disturbance are usually confined to within a few hundred meters of the dredging equipment while in operation. Initially, invertebrate species diversity may increase in dredged channels, as opportunistic species rapidly colonize the denuded or disturbed area. Elevated turbidity associated with dredging and channel construction activities has adverse secondary impacts on a variety of organisms, including filter-feeding bivalves, and fishes; the larval and juvenile forms of many species are susceptible to mortality induced by gill-clogging and abrasion. If underwater blasting is necessary to remove rocks, this may result in fish kills due to rupturing of swim bladders.

- Dissolved oxygen levels may be substantially decreased during dredging operation, due to the resuspension of oxidizable particulates (Brown and Clark 1968). However, dissolved oxygen levels may improve considerably following cessation of dredging due to the removal of organic sediments from the system. Deepening of navigation channels may result in increased saltwater intrusion into inland waterways, potentially altering the distribution and abundance of freshwater, estuarine and marine organisms.

- Channel construction in tropical and sub-tropical locales can directly impact valuable seagrass and coral reef communities. Recovery of damaged seagrass or reef communities can take decades, and in some cases they may never recover. These sensitive habitats are also subject to indirect impacts resulting from increased turbidity, as they depend on adequate light penetration for survival. Floating silt curtains can be used to partially alleviate the effects of dredging on critical habitats and organisms, however, careful attention must be given to critical or special-concern habitats, seasonal migration patterns of non-resident fishery species, and spawning seasons of resident species in the specification of optimal windows for conducting maintenance dredging.

(b) Inlets and jetties. Inlets are dynamic coastal features primarily associated with barrier islands. Most inlets shift continuously in response to short and long-term physical factors, such as storms and near-shore sediment distribution patterns. Coastal engineers are faced with the difficult challenge of stabilizing inlets in order to provide for safe and efficient navigation. Accumulation of sediments in inlets necessitates frequent maintenance dredging in order to maintain navigation conditions. Sand stored in inlets may reduce the volume available for downdrift beaches.

- Inlet dredging can cause burial or direct mortality of benthic organisms and chronic turbidity. However, many of the organisms adapted to life in inlets are minimally impacted by maintenance dredging. Recolonization by benthic organisms generally occurs within a short time following disturbance. Dredging windows (seasonal restrictions) are used to reduce the level of impacts to migratory organisms such as sea turtles and marine mammals. Avoidance of dredging during the known spawning seasons of marine and estuarine finfish and shellfish is critical to reducing impacts to the delicate early life stages (eggs, larvae, juveniles) of these organisms.

- Jetties are used to protect and maintain inlets, marinas, and port facilities. They serve multiple purposes, including protecting vessels entering a port/marina from dangerous waves and controlling the movement of sand into dredged channels and harbor entrances. Like groins, jetties will induce accretion of sand on the updrift side, with consequent erosion of sand on the downdrift shoreline. Environmental considerations for jetties are similar to those outlined previously for groin systems. These are primarily associated with the interruption of natural longshore sediment transport. In addition, scour on the downdrift side of a jetty may adversely affect colonization by benthic invertebrates. A major environmental concern associated with jetty construction involves disruption of natural transport patterns of ichthyoplankton (fish eggs and larvae). Eggs and larvae which are naturally transported into estuaries via longshore drift may become entrained into harbors via disruption of normal hydrodynamics. The inherently poor water quality and increased turbidity in harbors may result in significant mortality of ichthyoplankton.

(c) Piers and docks. A common environmental problem in urban coastal areas is habitat and water quality degradation in abandoned pier and dock basins (Hawkins et al. 1992). These degraded habitats, abundant in industrialized areas, may date back to colonial times in large U.S. cities (e.g., New York, Boston, Philadelphia) and even earlier in European cities. Many older docks were abandoned in the latter half of the 20th century as larger seagoing vessels were unable to access them, and newer, modern port facilities were established. Most abandoned docks are polluted from decades or centuries of unregulated dumping and discharge from vessels and shore facilities. Poor tidal circulation in docks, in part due to the prevalence of numerous dead-end canals and deep basins, combined with the prevalence of organic matter in the sediments, results in near continuous hypoxia or anoxia. Benthic invertebrate communities of docks and basins are species depauparate, and dominated by a few opportunistic taxa, mostly annelid worms or insect larvae. Bacterial mats and noxious algal blooms are prevalent. Certain blue-green algae and dinoflagellates associated with these blooms produce toxins known to cause significant mortality in fishes, and may cause sickness in humans. Heavy metals and other industrial contaminants are also often found in high concentrations in abandoned basin sediments.

- A variety of technologies have been applied to the problem of dock and pier restoration (Hawkins et al. 1992). The first step is to identify and curtail discharges of industrial and human wastes. Following cessation of discharge, there are several possible means of improving water and habitat quality. Mechanical aeration of anoxic basin sediments has been used to promote mixing and oxygenation. Hydraulic pumps and paddles are used to promote mixing in enclosed areas. Bivalve mollusks have been transplanted in dock/pier areas as biological filters to improve water quality. Dead-end canals and deep basins can be filled in or recontoured to improve circulation. Decaying piers and pilings are removed, primarily for aesthetic purposes. However, this activity may reduce

overall habitat quality because epifauna associated with piers and pilings provide a food resource for fish.

- The complex structure of the piers and pilings provide a predation refuge for juvenile fishes. Some commercially significant species along the U.S. Atlantic coast (e.g., striped bass) may be found in high concentrations in and among piers in urban reefs which can provide habitat diversity, along with the visual appeal of an unobstructed waterfront.

(d) Boat basins and marinas**.** Construction of marinas, or basins for small boats measuring less than 31 m (102 ft) constitutes a significant coastal engineering issue worldwide. The environmental effects of marina construction and maintenance are many, and sound construction practice and management are necessary to prevent serious environmental degradation. Critical shallow-water habitats, which may be present in the vicinity of marinas, include intertidal marshes and mudflats, seagrass beds, shellfish beds, and, in tropical locations, mangroves and coral reefs. Pollution (from both point and non-point sources) is a potentially serious environmental problem associated with marinas. Construction of boat-launching facilities and parking lots may cause in chronic turbidity in the vicinity due to increased runoff. Discharge of fuels and engine oils, garbage, paints, and other waste materials directly impacts water quality. Noise pollution associated with the day-to-day activities of the marina will affect use of the area by wading birds and other wildlife. Wakes caused by the constant movement of small vessels in and out of the area lead to increased shoreline erosion and may disrupt life-cycle larval and juvenile fishes and invertebrates. Construction of a basin increases the residence time of water in the area, inhibiting the natural pollution abatement function attributed to tidal flushing. Use of breakwaters in the vicinity of the marina may further increase residence time of water in the area.

- Mitigation of direct impacts resulting from marine construction is often attempted by creation/restoration of shallow, vegetated habitats elsewhere. However, the success rate of these projects is unacceptably low in many cases (e.g., seagrass projects). The U.S. Army Corps of Engineers provides detailed guidelines for marina construction in order to minimize environmental impacts (USACE 1993). These include construction of the marina to avoid dead-end canals, thereby reducing the likelihood of creating stagnant pools of water. Square or rectangular basins are not recommended, and it is imperative that basins not be constructed such that they are deeper than the associated access channels.

- Wide access channels are recommended, and gradual slopes from channel to harbor are best. Floating, rather than fixed breakwaters situated at the marina entrance are preferred for maintaining adequate flushing. Giannio and Wang (1974) provide a number of recommendations to reduce adverse environmental effects in small boat basins. These include implementation of designs which promote tidal flushing and control water quality, use of structures which encourage colonization by fouling communities as a food source for fishery species, use of sloping, rather than vertical sidewalls for channels where feasible, and provision to beneficially use material removed by dredging of the marina(e.g., habitat development projects).

(e) Port facilities. Many of the environmental concerns associated with the construction and maintenance of small boat basins are applicable to larger commercial and industrial port facilities, albeit at a much greater scale. Elimination of significant acreage of critical spawning and nursery habitats, such as intertidal marsh and seagrass beds is one major problem, and numerous attempts have been made to mitigate for the detrimental effects of port construction and expansion on critical shallow coastal habitats. The environmental effects of shoreline protective structures such as jetties on early life stages of finfish and invertebrates should be addressed in port facility projects. Point and non-point source pollution effects are a primary concern in port construction/expansion projects, especially considering the variety and magnitude of hazardous materials which continuously pass through ports in the United States and elsewhere.

(f) Confined disposal facilities. Confined disposal facilities (CDFs) are structures designed to store dredged materials. Approximately 30 percent of total material dredged from U.S. waters is placed in confined aquatic disposal facilities, the remaining 70 percent being disposed of at unconfined disposal areas or used in beach nourishment or beneficial-use programs (USACE 1987). In recent years, environmental issues associated with open-water disposal of dredged material has increased the demand for confined disposal. This demand is expected to increase in the future (Averett, Palermo, and Wade 1988).

- A typical confined disposal facility is a diked containment area. The design is such that solids can be retained while carrier water is released from the containment facility (Palermo, Montgomery, and Poindexter 1978). Dikes are constructed in order to form a confined area. Dredged materials are hydraulically pumped in the form of a slurry into the containment area. After solids have settled out of suspension, clarified water is released from the facility through a weir. Filtration and or chemical treatment of effluent may be necessary in some cases in order to meet water quality criteria for suspended solids concentrations (Schroeder 1983). The projected functional life span of a confined disposal area ranges from years to decades.

- Environmental considerations in the construction of confined disposal facilities are varied. Critical habitats such as intertidal marsh, seagrass, mangroves, and coral reefs should be avoided in the site selection phase. Near-shore or on-shore CDF's are more likely to displace critical shallow water habitats than CDF's which are constructed in deeper, open waters. Nursery grounds and migratory pathways for fishes and marine vertebrates should be identified and avoided. Ground-water impacts are of primary importance. Leachates may eventually work their way into aquifers and even in uncontaminated dredged materials may contain elevated levels of chloride, potassium, sodium, calcium, iron, and manganese, especially when marine or estuarine sediments are deposited over a freshwater aquifer. Contaminated dredged materials may leach a variety of metals and organic contaminants (e.g., PCB's, pesticides). These materials may also be present in effluent water discharged from the CDF. Engineering considerations to reduce groundwater impacts include site location, topography and slope, underlying stratigraphy, subsurface hydrology, climatological factors, soil properties, and the degree of use of the aquifer by humans. Aquifer recharge areas should be avoided. In some cases, either natural (clay) or artificial liners are necessary to prevent introduction of potentially contaminated leachate into sensitive aquifers.

V-7-9. Environmental Issues To Be Considered for All Projects

Certain critical habitats and individual species may be of particular importance in coastal engineering projects, regardless of whether or not the project is intended to provide environmental benefits. Threatened and endangered (T&E) species of fish, birds, mammals, and reptiles are high-profile issues, and merit special consideration and accommodations during the reconnaissance, planning, implementation, and monitoring phases of projects. The following are specific examples of T& E species considerations or habitats of special concern encountered in the coastal zone.

a. In the water.

(1) Sea turtles. Maintenance dredging of navigable waterways can potentially induce mortality of threatened or endangered sea turtles. Relatively little is known about the distribution and abundance of sea turtles in navigable waterways and harbors, but there have been documented cases of sea turtle mortality during hopper dredging in channels of the southeastern United States (Dickerson et al. 1995). The three species which are at risk along the South Atlantic and Gulf coasts are the loggerhead (*Caretta caretta*), green (*Chelonias mydas*), and Kemp's ridley (*Lepidochelys kempi*). Since 1980, an observer program has been in effect during dredging operations in the southeast U.S., in accordance with the Endangered Species Act of

1973. Observation and documentation of sea turtle mortality is essential to develop technical and management solutions to dredging-related impacts. Mortality has decreased substantially since inception of the observer program. This may be due to improved management and operations, but may also reflect long-term fluctuations in turtle abundance in southeast U.S. Waters (Dickerson et al. 1995). Management and operations alternatives which can help reduce mortality include seasonal restriction on dredging, relocation of individual live turtles, and improvement to dredging equipment which minimizes turtle entrainment. Comprehensive surveys have been conducted in several channel/harbor areas where sea turtle mortality due to maintenance dredging has occurred (Butler, Nelson, and Henwood 1987, Dickerson et al. 1995, Van Dolah and Maier 1993). Results of these and similar studies are critical in specifying seasonal dredging windows, when sea turtles are least likely to be present and dredging may be conducted with minimal risk.

(2) Cetaceans. Whales, dolphins, and porpoises are large mammals which have adapted completely to the marine environment. They spend their entire lives at sea, although a few species are known to migrate into freshwater rivers and lakes. Some 80 species of cetaceans are recognized worldwide; many of these are in serious decline due to harvesting. Cetaceans are divided into two functional groups based on feeding morphology. The Mysticeti are the ten species of baleen whales, which feed by filtering water through a bony sieve (the baleen). The Odontoceti (toothed cetaceans) include some 70 species of whales, porpoises and dolphins.

(a) Many cetaceans have a large home range and undergo extensive seasonal movements. Dolphins and porpoises do not have set migration patterns, but larger cetaceans do. Cetaceans usually reproduce in warmer tropical waters, but food availability is greater in temperate waters, and extensive feeding journeys are undertaken.

(b) Because many cetacean populations are in decline, it is important to consider potential detrimental effects of coastal engineering projects on these animals. In general, whales are not likely to be encountered in shallow nearshore waters, where most coastal engineering projects are likely to occur. Occasionally, however, an individual will become disoriented and enter channels and harbor areas, or become stranded along a beach. Dolphins and porpoises are common in shallow coastal waters, and may be seen riding the bow waves of supertankers and other large commercial vessels entering and leaving harbors. These animals are strong and graceful swimmers, but nonetheless, they are occasionally killed by large commercial vessels.

(c) Dredging operations in channel harbor areas are potentially threatening to small cetaceans. The turbidity plume associated with maintenance dredging interferes with feeding, since these animals are visual predators. Dolphins and porpoises are known to frequent highly polluted estuaries and harbors; thus, poor water quality and high contaminant levels can pose serious threats to their health. In recent years, there have been increasing numbers of mass dolphin strandings along the southeast U.S. coast. It is not known to what extent chronic pollution has contributed to this phenomenon.

(3) Fish and invertebrates. A number of marine and estuarine fish species, many of commercial or recreational significance, have undergone population declines in the latter half of the 20th century, primarily due to overharvesting and loss of shallow-water spawning and nursery habitat. Some species, such as striped bass on the U.S. Atlantic coast and red drum on the Gulf coast, have rebounded dramatically in the last decade, as a result of wise management practices, including a moratorium on commercial harvests in some areas. Many other species continue to decline, and some, such as the shortnose sturgeon (*Acipenser brevirostrum*) along the Atlantic coast, and multiple species of Pacific salmon, are listed as federally threatened or endangered.

(a) Coastal engineering projects should consider potential effects on fish and the aquatic food web. Construction activities, especially those that include dredging and the resultant increase in turbidity, should

be timed so as not to interfere with critical spawning or migration times. Spawning and nursery areas are known for most species; these should be identified and avoided if possible.

(b) A number of marine and estuarine invertebrate species have also undergone significant declines in the latter half of the 20th century. American oyster populations have been completely decimated in many coastal areas, particularly along the Atlantic coast. Current harvests are but a fraction of what was historically taken in once-productive estuaries such as Chesapeake and Narragansett Bays. Blue crab harvests have declined in the mid-Atlantic region in recent years, likely a result of overfishing. Improved management practices may provide some relief, but destruction of habitat remains a critical issue. Other invertebrate communities are valued not for their commercial significance but for aesthetics and recreational value (e.g., coral reef communities). Coastal engineering projects should seek to avoid or minimize impacts on invertebrate populations. Construction activities that involve dredging are most detrimental. Many crustaceans (shrimp, blue crabs) burrow and overwinter in channels and are likely to be encountered during maintenance dredging. Sessile invertebrates (oysters, mussels, clams) are subject to burial and subsequent mortality from dredging. Even if burial does not occur, increased turbidity associated with nearby dredging activity is detrimental to these filter-feeding invertebrates. Corals and other hard-bottom invertebrate communities are subject to direct mechanical damage and burial effects from construction projects that include dredging. Projects that result in periodic or chronic conditions of poor water quality (including turbidity, elevated nutrient levels, low dissolved oxygen) are detrimental to both sessile and motile invertebrate communities.

a. At the shore/water interface.

(1) Sea turtles. A primary concern related to beach nourishment along the southeast Atlantic and Gulf coasts is the nesting activity of sea turtles. Several species of threatened and endangered sea turtles commonly nest on beaches in the southeast United States, including the loggerhead, leatherback, and green turtles (Nelson 1988; Nelson, Mauck, and Fletemeyer 1987). Nesting season occurs from late spring through summer, although there is considerable variation within and between regions. Sea turtles ascend the beach at night, lay eggs in a nest cavity in the zone between MHW and the top of the primary dune, and return to the ocean. Beach nourishment and restoration activities can disrupt the nesting patterns of sea turtles, but effective beach nourishment can also provide additional nesting habitat in areas where beaches have eroded. The issue of beach nourishment vs. turtle nesting has sparked contentious debate in heavily populated coastal areas of the southeast, particularly in Florida.

(a) Specific activities that interfere with turtle nesting include direct burial of existing nest cavities with new fill and placement of barriers along the beach (e.g., pipelines), which deter or impede migration of nesting females. Bright lights, noise, and vehicles disrupt nesting activity of female turtles, and may interfere with the orientation of hatchlings as they migrate towards the ocean. Disturbance may cause a nesting female to return to the water without digging a nest cavity, or she may abandon a cavity without depositing eggs. Minimization of construction activities and illumination along beaches at night is recommended. In some cases, turtle nests have been successfully relocated to undisturbed areas of beach.

(b) Post-construction effects of beach nourishment may also impact sea turtle nesting success. If the topography of the resulting beach differs from that found in nature (e.g., formation of false scarps), nesting females may be deterred. Compacted sands typical of newly filled beaches may inhibit nest excavation by sea turtles. This can be mediated to some extent by tilling, and by mandating the use of wide-tracked vehicles during construction. Differences in grain size, color, shear resistance, density and gas exchange potential of newly deposited sand vs. natural sand may negatively affect hatching success and/or hatchling sex ratios. New fill material can be placed seaward of the primary nesting area and graded to a gentle slope to facilitate access by nesting turtles. Timing of nourishment activities should be outside of the nesting season, when possible. Appropriate timing, minimization of light and noise disturbance, and an effort to properly replicate

natural conditions can potentially reduce impacts to nesting turtles, and many beach nourishment projects have actually increased suitable sea turtle nesting habitat in the southeast United States.

(2) Marine mammals. Coastal engineering projects can potentially affect marine mammals that use coastal habitats as breeding areas or rookeries. Several marine mammals are commonly found near populated shorelines in the United States and worldwide. Many of these species are threatened or endangered. Most marine mammals frequent temperate waters, although a few species are known to exist in tropical or subtropical waters. Seals, sea lions, and walruses (Pinnipedia) are amphibious mammals that rely on isolated, protected shorelines to mate and bear young. Three pinniped groups are recognized and include the walrus (Odobenidae), the eared seals (Otaridae), and true seals (Phocidae). Eared seals include the northern fur seal and sea lion and are distinguished by the presence of small but visible external ears and the ability to rotate the hind flippers for increased mobility on land. The true seals (Phocidae) include the ringed, harbor, and elephant seals. All pinnipeds are strong swimmers and effective divers. Direct mortality to these animals due to construction activity is unlikely in most cases, but destruction of breeding habitat may be a significant concern in some areas.

(a) River otters (*Lutra canadensis*) are common in shallow coastal habitats, including intertidal wetlands. Unlike pinnipeds, which have evolved specifically for life in the marine environment, otters are highly mobile on land and water. Destruction of shallow coastal habitats in populated areas is likely the primary threat to this species. The sea otter (*Enhydra lutris*) was once common along the entire Pacific coast of North America, but was hunted nearly to extinction during the 19th century. Populations have recovered during the last half-century, but destruction of breeding and refuge habitats remains a potential threat to this species.

(b) Mammals that belong to the order Sirena include the three species of manatee (Trichechidae), and dugongs (Dugongidae). These large, slow-moving vegetarians are highly vulnerable due to their gentle, gregarious nature; the Caribbean sea cow and the Stellers sea cow (a cold water species) are now extinct. Populations of the manatee (*Trichechus manatus*) in southern Florida and the Caribbean are seriously threatened by coastal development. Manatees are frequently injured or killed in collisions with recreational or commercial vessels, and many bear tell-tale propeller scars from such encounters. The largest concentration of manatees occurs in sub-tropical waters of south and central Florida, and they are known to occasionally migrate as far as North Carolina and Virginia, presumably in search of food. Manatees are listed as Federally endangered in U.S. waters and many areas have implemented restrictions on use of motorized vessels in canals and other areas frequented by these animals. Coastal engineering projects that may potentially impact manatee populations include dredge and fill projects that result in destruction of critical habitat (e.g., seagrass beds), and any activity that may result in an increase in boat traffic.

(3) Sea, shore, and wading birds. Aquatic birds rely on shallow coastal habitats such as mudflats, intertidal wetlands, and both natural and man-made islands as critical breeding grounds and forage sites. True *seabirds* are those species that spend most of their time at sea, primarily foraging on surface waters by diving or skimming for food, but rely on shore habitats for breeding. These birds have evolved various adaptations to an exclusively marine existence, notably the presence of a salt gland, which regulates blood salinity. True seabirds include gulls, terns, pelicans, albatrosses, cormorants, and the frigate birds and tropic birds of warm regions. Many of these species, notably the albatross, are wide-ranging travelers, and fly vast distances over open ocean in search of food. Others, such as gulls and pelicans, spend most of their time near the coast.

(a) Waterfowl, including diving and dabbling ducks, geese, and swans are common in saline and freshwater tidal marshes and shallow tidal embayments. These habitats provide abundant food and refuge for these birds, especially during winter. Seeds and rhizomes of emergent marsh vegetation are the preferred food of most waterfowl species.

(b) *Shorebirds* forage along intertidal margins and *wading birds* forage primarily on invertebrate prey in shallow waters or on sand/mudflats. During fall migration, many shorebirds switch to a diet of seeds of tidal marsh plants, such as wild rice. Shorebirds include sandpipers, rails, and soras; these birds are found on intertidal flats and in both saline and fresh tidal marshes. Wading birds include herons, egrets, ibises, and bitterns. These are commonly encountered on intertidal flats and in marshes. Wading birds feed on small fish and invertebrates captured in tidal shallows.

(c) Coastal engineering projects that may potentially affect sea, shore, and wading birds are those that result in habitat destruction, alteration, and disturbance. Construction activities should be timed so as not to occur during critical nesting seasons. Beach nourishment activities can deter shorebirds from feeding and nesting; however, if carefully timed, beach nourishment may potentially improve shorebird habitat via increased beach width. Dredge and fill projects which result in destruction of seagrass or marsh habitat will negatively impact waterfowl, and wading/shore birds that use these habitats. Chronic noise and human activity will deter seabirds, shorebirds, and wading birds from using an area. Long-term pollution impacts such as eutrophication and contaminant input can have both immediate and long-term effects on the viability of sea, shore-, and wading bird populations in coastal areas.

(4) Fish and invertebrates. Many important fishery species rely on coastal wetlands as nurseries and as feeding and refuge areas (Boesch and Turner 1984, Rozas and Hackney 1983, Weinstein 1979). Along the Atlantic and Gulf coasts of the United States, species such as blue crab, summer flounder, red drum, and penaeid shrimp (*Penaeus* spp.) depend on shallow tidal marsh creeks, which provide refuge from predators and an abundant food source in the form of zooplankton and benthic invertebrates. These estuarine-dependent fishery species grow rapidly during their temporary stay in coastal wetlands before migrating back to deeper coastal waters. Adults of these and other transient species periodically enter tidal wetlands in search of food. Loss of valuable coastal wetland habitat is a primary concern for marine fisheries managers, and habitat destruction is considered as serious a threat to the integrity of many coastal fisheries as is overharvesting.

(a) In the Pacific northwest, all of the Pacific salmonids (trout and salmon) are known to directly utilize estuarine tidal wetlands as critical nursery habitat for feeding and avoiding predators (Shreffler, Simenstad, and Thom 1992), as well as migratory corridors along the shorelines. Other species, such as dungeness crab and various flatfish, rely on the extensive tidal flats and shallows as a primary nursery habitat. Bivalve mollusks, including the pismo clam (*Tivela stultorum*), littleneck clam (*Protothaca staminea*), and Pacific razor clam (*Siliqua patula*) are found in shallow intertidal sand/mudflats. These species are the basis for important commercial and recreational fisheries.

(b) The California grunion, which spawns in burrows dug in saturated sand, is directly threatened by coastal habitat destruction throughout its range along the central and southern California coast (Figure V-7-4). This species is harvested by recreational fishermen throughout most of its range. Disturbance resulting from an increase in human activity along the coastline is a potential threat to this unusual fish (Fritzsche, Chamberlain, and Fisher 1985).

e. Critical areas.

(1) Many marine habitats and other areas of special concern are subject to degradation from coastal engineering activities. These include, but are not restricted to, intertidal wetlands, shallow-water nursery habitats, and cultural/archeological resources. In many cases, the actual project "footprint" may not encroach upon the habitat in question; however, both short- and long-term impacts may affect critical areas. For example, a dredge and fill project may create a turbidity plume that could reduce light penetration in a nearby seagrass bed. Beach nourishment projects may affect nearby offshore areas, including coral reefs and other hard-bottom habitats by anchoring dredges or placement of pipelines. Prolonged beach nourishment or

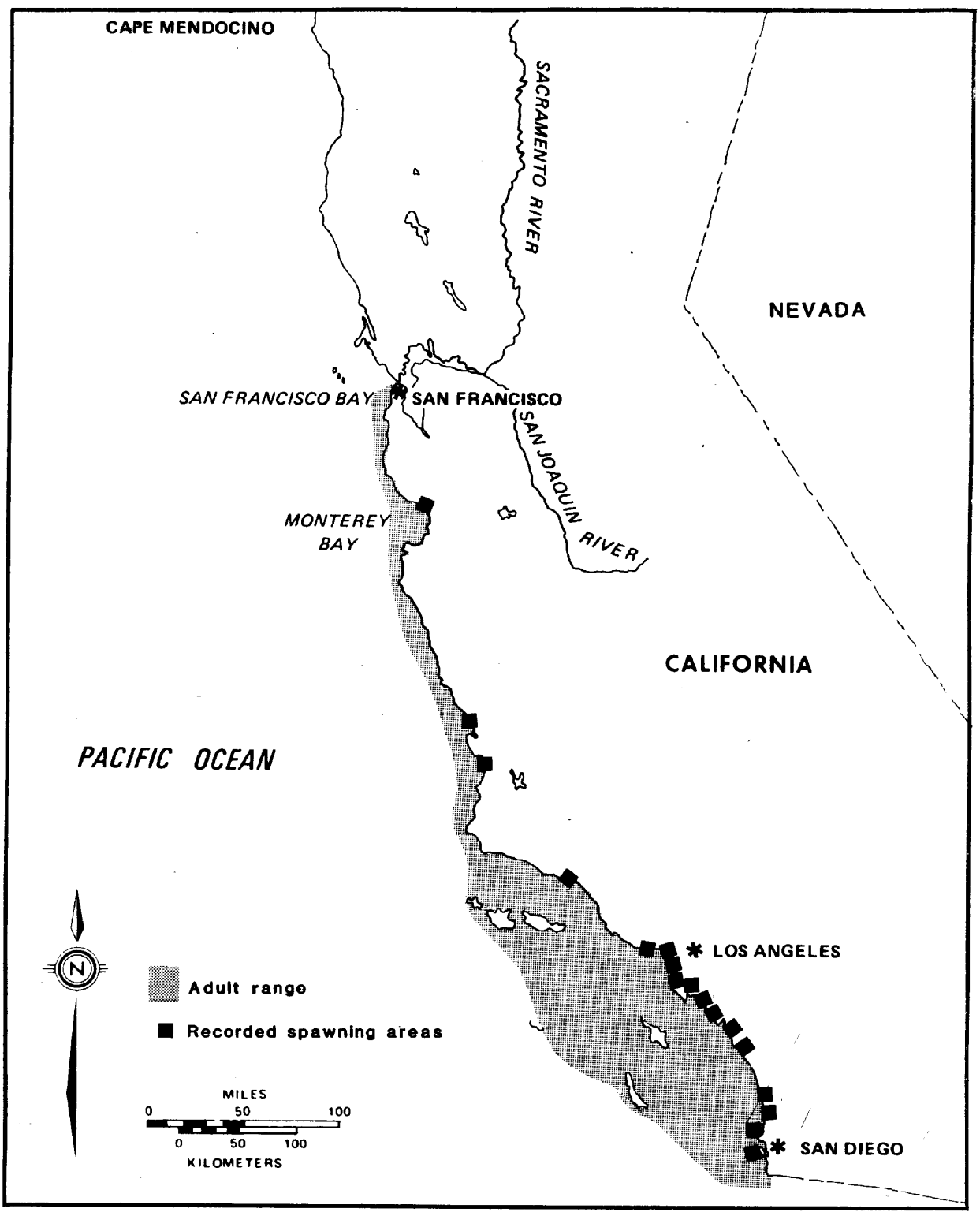

Figure V-7-4. Distribution of the California grunion along the southwest U.S. coast

excessive erosion of recently nourished beaches may result in chronic conditions of high turbidity or smothering in offshore habitats. Marine construction may result in chronic nutrient or contaminant loading, which could affect biota in adjacent tidal wetlands or other nursery areas. The timing of coastal engineering projects should consider known spawning and migration patterns of fishes and invertebrates. Many commercially important fishery species enter shallow coastal waters during spring and summer as larvae or juveniles, and are especially susceptible to environmental disturbances associated with coastal engineering projects. Similarly, beach nourishment and shoreline stabilization projects should not be conducted during the nesting season for shorebirds or sea turtles (typically late spring through summer).

(2) Sites of known or potential cultural or archaeological importance are frequently encountered in coastal areas. Cultural and archaeological resources provide valuable physical evidence (e.g., structures, sites, artifacts) of past human history. This information can be used to assess historic and prehistoric use of an area for habitation, fishing, agriculture, and navigation. Native Americans and early European colonists made extensive use of coastal areas in North America, and archaeological remains associated with Indian middens and early colonial settlements can often be encountered in coastal habitat or engineering projects. Construction can potentially disrupt or destroy valuable cultural or archaeological remains. Offshore dredging projects may encounter historic shipwrecks. Pre-construction site assessments using divers, side-scan sonar, and magnetometers will identify potential cultural resources prior to construction or dredging. The potential of a project site to support such artifacts should be assessed prior to initiation of projects in coastal areas. The National Historic Preservation Act of 1966 directs the Federal Government to preserve, restore, and maintain historic or cultural sites; coastal engineering and construction activities associated with Federal navigation or shore protection projects must coordinate with Federal, state, or local historic preservation authorities.

(3) Avoidance or minimization of adverse effects to critical areas and habitats need not be viewed as an impediment to coastal engineering projects. Rather, these issues can be viewed as opportunities to apply innovative technology to environmental problem-solving in the coastal zone. Multi-disciplinary partnerships between scientists, resource managers, and engineers, and the continued development of comprehensive, regional management plans in coastal areas are necessary to ensure the success of both habitat restoration projects and traditional shoreline protection projects. Institutional and regulatory authorities are increasingly recognizing the need for adaptive management, design flexibility, and applications of new engineering technology in coastal areas; future efforts will surely benefit from these opportunities, and result in improved management of coastal resources.

V-7-10. Information Sources

a. An important part of any coastal habitat project is doing the proper research. First steps usually involve talking with local resource agencies that are familiar with the area. Sometimes a watershed analysis or restoration plan for the area has already identified specific needs. Corps libraries have a wealth of information on historic conditions, hydraulic analyses, and coastal project descriptions.

b. Several scientific societies are partially or wholly dedicated to habitat restoration issues. Some of these are:

- Society for Ecological Restoration (SER). The SER hosts conferences, provides proceedings, and has a journal. They maintain a Web site at http://ser.org/.

- National Estuarine Research Federation (ERF). The ERF hosts conferences, provides proceedings , and has a journal. They maintain a Web site at http://www.erf.org/.

- Society for Conservation Biology (CB). The CB hosts conferences, provides proceedings, and has a journal. They maintain a Web site at http://conbio.rice.edu/scb/.

- Society of Wetland Scientist (SWS). The SWS hosts conferences, provides proceedings, and has a journal. They maintain a Web site at http://www.sws.org.

In addition, the Corps offers some good information through its Web sites:

- Institute for Water Resources, http://www.wrsc.usace.army.mil.iwr.

- U.S. Army Engineer Research and Development Center http://www.erdc.usace.army.mil.

- U.S. Army Corps of Engineers Headquarters policy homepage, http://www.usace.army.mil.

V-7-11. References

EM 1110-2-5027
EM 1110-2-5027, "Confined Disposal of Dredged Material"

EM 1110-2-1206
EM 1110-2-1206, "Environmental Engineering for Small Boat Basins"

Addy 1947
Addy, C. E. 1947. "Eelgrass Planting Guide," *Maryland Conservationist*, Vol 24, pp 16-17.

Auld and Schubel 1978
Auld, A. H., and Schubel, J. R. 1978. "Effects of Suspended Sediment on Fish Eggs and Larvae: A Laboratory Assessment," *Estuarine and Coastal Marine Science*, Vol 6, pp 153-64.

Averett, Palermo, and Wade 1988
Averett, D. E., Palermo, M. R., and Wade, R. 1988. "Verification of Procedures for Designing Dredged Material Containment Areas for Solids Retention," Technical Report D-88-2, U.S. Army Engineer Waterways Experiment Station, Vicksburg, MS.

Barko et al. 1977
Barko, J. W., Smart, R. M., Lee, C. R., Landin, M. C., Sturgis, T. C., and Gordon, R. N. 1977. "Establishment and Growth of Selected Freshwater and Coastal Marsh Plants in Relation to Characteristics of Dredged Sediments," Technical Report D-77-2, U.S. Army Engineer Waterways Experiment Station, Vicksburg, MS.

Bellis 1995
Bellis, V. J. 1995. "Ecology of Maritime Forests of the Southern Atlantic Coast: A Community Profile," Biological Report 30, U.S. Department of the Interior, National Biological Service, Washington, DC.

Boesch and Turner 1984
Boesch, D. F., and Turner, R. E. 1984. "Dependence of Fishery Species on Salt Marshes: The Role of Food and Refuge," *Estuaries*, Vol 7, pp 460-68.

Bohnsack 1989
Bohnsack, J. A. 1989. "Are High Densities of Fishes at Artificial Reefs the Result of Habitat Limitation or Behavioral Preference?" *Bulletin of Marine Science*, Vol 44, pp 631-645.

Bohnsack and Sutherland 1985
Bohnsack, J. A., and Sutherland, S. P. 1985. "Artificial Reef Research: A Review with Recommendations for Future Priorities," *Bulletin of Marine Science*, Vol 37, pp 11-39.

Broome, Seneca, and Woodhouse 1988
Broome, S. W., Seneca, E. D., and Woodhouse, W. W., Jr. 1988. "Tidal Salt Marsh Restoration," *Aquatic Botany*, Vol 32, pp 1-22.

Brown and Clark 1968
Brown, C. L., and Clark, R. 1968. "Observations on Dredging and Dissolved Oxygen in a Tidal Waterway," *Water Resources Research*, Vol 4, pp 1381-1384.

Buckley and McCaffrey 1978
Buckley, F. G., and McCaffrey, C. A. 1978. "Use of Dredged Material Islands by Colonial Seabirds and Wading Birds in New Jersey," Technical Report D-78-1, U.S. Army Engineer Waterways Experiment Station, Vicksburg, MS.

Butler, Nelson, and Henwood 1987
Butler, R., Nelson, W. A., and Henwood, T. A. 1987. "A Trawl Survey Method for Estimating Loggerhead Turtle, *Caretta caretta*, Abundance in Five Eastern Florida Channels and Inlets," *Fishery Bulletin*, Vol 85, pp 447-453.

Chaney et al. 1978
Chaney, A. H., Chapman, B. R., Karges, J. P., Nelson, D. A., Schmidt, R. R., and Thebeau, L. C. 1978. "Use of Dredged Material Islands by Colonial Seabirds and Wading Birds in Texas," Technical Report D-78-8, U.S. Army Engineer Waterways Experiment Station, Vicksburg, MS.

Cintron-Molero 1992
Cintron-Molero, G. 1992. "Restoring Mangrove Systems." *Restoring the Nation's Marine Environment*. G. W. Thayer, ed., Maryland Sea Grant, College Park, MD, pp 223-278.

Clairain et al. 1978
Clairain, E. J., Jr., Cole, R. A., Diaz, R. J., Ford, A. W., Huffman, R. T., Hunt, L. J., and Wells, B. R. 1978. "Habitat Development Field Investigations, Miller Sands Marsh and Upland Habitat Development Site, Columbia River, Oregon. Summary Report," Technical Report D-77-38, U.S. Army Engineer Waterways Experiment Station, Vicksburg, MS.

Connel 1972
Connel, J. H. 1972. "Community Interactions on Marine Rocky Intertidal Shores," *Annual review of Ecology and Systematics*, Vol 3, pp 169-192.

Culter and Mahadevan 1982
Culter, J. K., and Mahadevan, S. 1982. "Long-Term Effects of Beach Nourishment on the Benthic Fauna of Panama City Beach, Florida," Miscellaneous Report No. 82-2, Coastal Engineering Research Center, U.S. Army Engineer Research and Development Center, Vicksburg, MS.

Dahl et al. 1975
Dahl, B. E., Fall, B. A., Lohse, A., and Appan, S. G. 1975. "Construction and Stabilization of Coastal Foredunes with Vegetation: Padre Island Texas," Miscellaneous Paper No. No. 9-75, Coastal Engineering Research Center, U.S. Army Engineer Research and Development Center, Vicksburg, MS.

Darovec et al. 1975
Darovec, J. E., Jr., Carleton, J. M, Pulver, T. R., Moffler, M. D., Smith, G. B., Whitfield, W. K., Jr., Willis, C. A., Steidinger, K. A., and Joyce, E. A., Jr. 1975. "Techniques for Coastal Restoration and Fishery Enhancement in Florida," Florida Marine Research Publication No. 15, Bureau of Marine Research, Florida Department of Natural Resources.

Dickerson et al. 1995
Dickerson, D. D., Reine, K. J., Nelson, D. A., and Dickerson, C. E., Jr. 1995. "Assessment of Sea Turtle Abundance in Six South Atlantic U.S. Channels," Miscellaneous Paper EL-95-5, U.S. Army Engineer Waterways Experiment Station, Vicksburg, MS.

Earhart, Clarke, and Shipley 1988
Earhart, G., Clarke, D., and Shipley, J. 1988. "Beneficial Uses of Dredged Material in Shallow Coastal Waters; Chesapeake Bay Demonstrations," Environmental Effects of Dredging Information Exchange Bulletin D-88-6, U.S. Army Engineer Waterways Experiment Station, Vicksburg, MS.

Fonseca 1994
Fonseca, M. S. 1994. "A Guide to Planting Seagrasses in the Gulf of Mexico," Texas A&M University Sea Grant College Program, TAMU-SG-94-601.

Fonseca and Fisher 1986
Fonseca, M. S., and Fisher, J. S. 1986. "A Comparison of Canopy Friction and Sediment Movement Between Four Species of Seagrass with Reference to Their Ecology and Restoration," *Marine Ecology Progress Series*, Vol 29, pp 15-22.

Fonseca, Kenworthy, and Thayer 1987
Fonseca, M. S., Kenworthy, W. J., and Thayer, G. W. 1987. "Transplanting of the Seagrasses *Halodule wrightii*, *Syringodium filiforme*, and *Thalassia testudinum* for Sediment Stabilization and Habitat Development in the Southeast Region of the United States," Technical Report EL-87-8, U.S. Army Engineer Waterways Experiment Station, Vicksburg, MS.

Fonseca et al. 1990
Fonseca, M. S., Kenworthy, W. J., Colby, D. R., Rittmaster, K. A., and Thayer, G. W. 1990. "Comparisons of Fauna Among Natural and Transplanted Eelgrass *Zostera marina* Meadows: Criteria for Mitigation," *Marine Ecology Progress Series*, Vol 55, pp 251-264.

Forman and Gordon 1986
Forman, R. T., and Gordon, M. 1986. "Landscape Ecology," John Wiley and Sons.

Frenkel and Morlan 1991
Frenkel, R. E., and Morlan, J. C. 1991. "Can We Restore Our Salt Marshes? Lessons from the Salmon River, Oregon," *The Northwest Environmental Journal*, Vol 7, pp 119-135.

Fritzsche, Chamberlain, and Fisher 1985
Fritzsche, R. A., Chamberlain, R. H., and Fisher, R. A. 1985. "Species Profiles: Life Histories and Environmental Requirements of Coastal Fishes and Invertebrates (Pacific southwest) - California Grunion," U.S. Fish and Wildlife Service Biological Report 82 (11.28), Technical Report EL-82-4, U.S. Army Engineer Waterways Experiment Station, Vicksburg, MS.

Gage 1970
Gage, B. O. 1970. "Experimental Dunes of the Texas Coast," Miscellaneous Paper No. 1-70, U.S. Army Engineer Waterways Experiment Station, Coastal Engineering Research Center, Vicksburg, MS.

Garbisch and Colemen 1978
Garbisch, E. W., Jr., and Coleman, L. B. 1978. "Tidal Freshwater Marsh Establishment in Upper Chesapeake Bay." *Freshwater Wetlands: Ecological Processes and Management Potential.* R.E. Good, D.F. Whigham, and R.L Simpson, eds., Academic Press, New York, pp 285-298.

Giannio and Wang 1974
Giannio, S. P., and Wang, H. 1974. "Engineering Considerations for Marinas in Tidal Marshes," Report No. DEL-SG-9-74, College of Marine Studies, University of Delaware, Newark, DE.

Hawkins et al. 1992
Hawkins, S. J., Allen, J. R., Russell, G., White, K. N., Conlan, K., Hendry, K., and Jones, H. D. 1992. "Restoring and Managing Disused Docks in Inner City Areas," *Restoring the Nation's Marine Environment.* G. W. Thayer, ed., Maryland Sea Grant, College Park, MD, pp 473-582

Hirsch, DiSalvo, and Peddicord 1978
Hirsch, N. D., DiSalvo, L. H., and Peddicord, R. 1978. "Effects of Dredging and Disposal on Aquatic Organisms," Technical Report DS-78-5, U.S. Army Engineer Waterways Experiment Station, Vicksburg, MS.

Hobson 1981
Hobson, R. D. 1981. "Beach Nourishment Techniques; Report 3: Typical U.S. Beach Nourishment Projects Using Offshore Sand Deposits," Technical Report H-76-13, U.S. Army Engineer Waterways Experiment Station, Coastal Engineering Research Center, Vicksburg, MS.

Homziak, Fonseca, and Kenworthy 1982
Homziak, J., Fonseca, M. S., and Kenworthy, W. J. 1982. "Macrobenthic Community Structure in a Transplanted Eelgrass Meadow," *Marine Ecology Progress Series*, Vol 9, pp 211-221.

Jaap 1984
Jaap, W. C. 1984. "The Ecology of South Florida Coral Reefs: A Community Profile," U.S. Fish and Wildlife Service, Division of Biological Services, Washington, DC, FWS/OBS-82/32.

James 1975
James, W. R. 1975. "Techniques in Evaluating Suitability of Borrow Material for Beach Nourishment," Technical Manual 60, U.S. Army Engineer Waterways Experiment Station, Coastal Engineering Research Center, Vicksburg, MS.

Josselyn and Buzholz 1982
Josselyn, M., and Bucholz, J. 1982. "Summary of Past Wetland Restoration Projects in California." *Wetland Restoration and Enhancement in California, Proceedings of a Conference, February 1982, California State University, Hayward.* M. Josselyn, ed., California Sea Grant Report T-CSGCP-007, Tiburon Center for Environmental Studies, Tiburon, CA, 1-10.

Kelly, Fuss, and Hall 1971
Kelly, J. A., Jr., Fuss, C. M., Jr., and Hall, J. R. 1971. "The Transplanting and Survival of Turtle Grass, *Thalassia testudinum*, in Boca Ciega Bay, Florida," *Fishery Bulletin*, Vol 69, pp 273-280.

Knutson 1977
Knutson, P. L. 1977. "Planting Guidelines for Dune Creation and Stabilization," Coastal Engineering Technical Aid No. 77-4, U.S. Army Engineer Waterways Experiment Station, Coastal Engineering Research Center, Vicksburg, MS.

Knutson 1980
Knutson, P. L. 1980. "Experimental Dune Restoration and Stabilization, Nauset Beach, Cape Cod, Massachusetts," Technical Paper No. 80-5, U.S. Army Engineer Waterways Experiment Station, Coastal Engineering Research Center, Vicksburg, MS.

Knutson and Finkelstein 1987
Knutson, P. L., and Finkelstein, K. 1987. "Environmental Considerations for Dune-Stabilization Projects," Technical Report EL-87-2, U.S. Army Engineer Waterways Experiment Station, Vicksburg, MS.

Landin, Webb, and Knutson 1989
Landin, M. C., Webb, J. W., and Knutson, P. L. 1989. "Long-Term Monitoring of Eleven Corps of Engineers Habitat Development Field Sites Built of Dredged Material, 1974-1987," Technical Report D-89-1, U.S. Army Engineer Waterways Experiment Station, Vicksburg, MS.

Lewis 1982
Lewis, R. R., III. 1982. "Mangrove Forests." *Creation and Restoration of Coastal Plant Communities*. R.R. Lewis, III, ed., CRC Press, Inc., Boca Raton, FL, pp 153-172.

Lewis 1987
Lewis, R. R., III. 1987. "The Restoration and Creation of Seagrass Meadows in the Southeast United States." *Proceedings of the Symposium on Subtropical-Tropical Seagrasses of the Southeastern United States*. M. J. Durako, R. C. Phillips, and R. R. Lewis, III, eds., Research Publication No. 42, Bureau of Marine Research, Florida Department of Natural Resources, pp 153-173.

Lunz et al. 1978
Lunz, J. D., Zeigler, T. W., Huffman, R. T., Diaz, R. J., Clairain, E. J., Jr., and Hunt, L. J. 1978. "Habitat Development Field Investigations, Windmill Point Marsh Development Site, James River, Virginia. Summary Report," Technical Report D-77-23, U.S. Army Engineer Waterways Experiment Station, Vicksburg, MS.

Maragos 1992
Maragos, J. E. 1992. "Restoring Coral Reefs with Emphasis on Pacific Reefs." *Restoring the Nation's Marine Environment.* G. W. Thayer, ed., Maryland Sea Grant, College Park, MD, pp 141-222.

McClellan et al. 1989
McClellan, T. N., Havis, R. N., Hayes, D. F., and Raymond, G. L. 1989. "Field Studies of Sediment Resuspension by Selected Dredges," Technical Report HL-89-9, U.S. Army Engineer Waterways Experiment Station, Vicksburg, MS.

Minello, Zimmerman, and Medina 1994
Minello, T. J., Zimmerman, R. J., and Medina, R. 1994. "The Importance of Edge for Natant Macrofauna in a Created Salt Marsh," *Wetlands*, Vol 14, pp 184-198.

Moore and Orth 1982
Moore, K. A., and Orth, R. J. 1982. "Transplantation of *Zostera marina* L. into Recently Denuded Areas." *The Biology and Propagation of* Zostera marina*, Eelgrass, in the Chesapeake Bay, Virginia*. R.J. Orth and K.A. Moore, eds., Special Report No. 265 in applied Marine Science and Ocean Engineering, Virginia Institute of Marine Science, Gloucester Point, VA, pp 92-148.

NRC 1992
National Research Council. 1992. *Restoration of Aquatic Ecosystems: Science, Technology, and Public Policy*. National Academy Press, Washington, DC.

NRC 1995
National Research Council. 1995. *Beach Nourishment and Protection*. National Academy Press, Washington, DC.

Nelson 1988
Nelson, D. A. 1988. "Life History and Environmental Requirements of Loggerhead Turtles," U.S. Fish and Wildlife Service Biological Report 88(23), Technical Report EL-86-2, U.S. Army Engineer Waterways Experiment Station, Vicksburg, MS.

Nelson, Mauck, and Fletemeyer 1987
Nelson, D. A., Mauck, K., and Fletemeyer, J. 1987. "Physical Effects of Beach Nourishment on Sea Turtle Nesting, Delray Beach, Florida," Technical Report EL-87-15, U.S. Army Engineer Waterways Experiment Station, Vicksburg, MS.

Nelson 1985
Nelson, W. G. 1985. "Guidelines for Beach Restoration Projects, Part 1: Biological Guidelines," Report No. 76, Florida Sea Grant College Program, Gainesville, FL.

Niesen and Josselyn 1981
Niesen, T., and Josselyn, M. 1981. "The Hayward Regional Shoreline Marsh Restoration: Biological Succession During the First Year Following Dike Removal," Technical Report No. 1, Tiburon Center for Environmental Studies, Tiburon, CA.

Odum et al. 1984
Odum, W. E., Smith, T. J., III., Hoover, J. K., and McIvor, C. C. 1984. "The Ecology of Tidal Freshwater Marshes of the United States East Coast: A Community Profile," U.S. Fish and Wildlife Service, Division of Biological Services, Washington, DC, FWS/OBS-83/17.

Paine and Levin 1981
Paine, R. T., and Levin, S. A. 1981. "Intertidal Landscapes: Disturbance and the Dynamics of Pattern," *Ecological Monographs*, Vol 51, pp 145-178.

Palermo, Montgomery and Poindexter 1978
Palermo, M. R., Montgomery, R. L., and Poindexter, M. 1978. "Guidelines for Designing, Operating, and Managing Dredged Material Containment Areas," Technical Report DS-78-10, U.S. Army Engineer Waterways Experiment Station, Vicksburg, MS.

Parnell, DuMond, and McCrimmon 1986
Parnell, J. F., DuMond, D. M., and McCrimmon, D. A. 1986. "Colonial Waterbird Habitats and Nesting Populations in North Carolina Estuaries: 1983 Survey," Technical Report D-86-3, U.S. Army Engineer Waterways Experiment Station, Vicksburg, MS.

Parnell, DuMond, and Needham 1978
Parnell, J. F., DuMond, D. M., and Needham, R. N. 1978. "A Comparison of Plant Succession and Bird Utilization on Diked and Undiked Dredged Material Islands in North Carolina Estuaries," Technical Report D-78-9, U.S. Army Engineer Waterways Experiment Station, Vicksburg, MS.

Pastorok et al. 1997
Pastorok, R. A., MacDonald, A., Sampson, J. R., Wilber, P., Yozzo, D. J., and Titre, J. P. 1997. "An Ecological Decision Framework for Environmental Restoration Projects," *Ecological Engineering*, Vol 9, pp 89-107.

Phillips 1980
Phillips, R. C. 1980. "Planting Guidelines for Seagrasses," Coastal Engineering Technical Aid 80-2, U.S. Army Engineer Waterways Experiment Station, Coastal Engineering Research Center, Vicksburg, MS.

Pickart, Miller, and Duebendorfer 1998
Pickart, A. J., Miller, L. M., and Duebendorfer, T. E. 1998. "Yellow Bush Lupine Invasion in Northern California Coastal Dunes; I: Ecological Impacts and Manual Restoration Techniques," *Restoration Ecology*, Vol 6, No. 1, pp 59-68.

Pickart et al. 1998
Pickart, A. J., Theiss, K. C., Stauffer, H. B., and Olsen, G. T. 1998. "Yellow Bush Lupine Invasion in Northern California Coastal Dunes; II: Mechanical Restoration Techniques," *Restoration Ecology*, Vol 6, No. 1, pp 69-74.

Pulver 1976
Pulver, T. R. 1976. "Transplant Techniques for Sapling Mangrove Trees, *Rhizophora mangle*, *Laguncularia racemosa*, and *Avicennia germinans*, in Florida," Florida Marine Research Publication No. 22, Bureau of Marine Research, Florida Department of Natural Resources.

Race 1985
Race, M. S. 1985. "Critique of Present Wetlands Mitigation Policies in the United States Based on Analysis of Past Restoration Projects in San Francisco Bay," *Environmental Management*, Vol 9, pp 71-82.

Ray 1994
Ray, G. L. 1994. "A Conceptual Framework for the Evaluation of Coastal Habitats," Technical Report EL-94-33, U.S. Army Engineer Waterways Experiment Station, Vicksburg, MS.

Ray et al. 1994
Ray, G. L., Clarke, D., Wilber, P., and Fredette, T. J. 1994. "Ecological Evaluation of Mud Flat Habitats on the Coast of Maine Constructed of Dredged Material," Environmental Effects of Dredging Information Exchange Bulletin D-94-3, U.S. Army Engineer Waterways Experiment Station, Vicksburg, MS.

Raymond 1984
Raymond, G. L. 1984. "Techniques to Reduce the Sediment Resuspension Caused by Dredging," Miscellaneous Paper HL-84-3, U.S. Army Engineer Waterways Experiment Station, Vicksburg, MS.

Rey et al. 1990
Rey, J. R., Shaffer, J., Tremain, D., Crossman, R. A., and Kain, T. 1990. "Effects of Re-establishing Tidal Connections in Two Impounded Subtropical Marshes on Fishes and Physical Conditions," *Wetlands*, Vol 10, pp 27-45.

Roberts 1991
Roberts, T. H. 1991. "Habitat Value of Man-Made Coastal Marshes in Florida," Technical Report WRP-RE-2, U.S. Army Engineer Waterways Experiment Station, Vicksburg, MS.

Roman, Niering, and Warren 1984
Roman, C. T., Niering, W. A., and Warren, R. S. 1984. "Salt Marsh Vegetation Change in Response to Tidal Restriction," *Environmental Management*, Vol 8, pp 141-150.

Rozas and Hackney 1983
Rozas, L. P., and Hackney, C. T. 1983. "The Importance of Oligohaline Estuarine Wetland Habitats to Fisheries Resources," *Wetlands*, Vol 3, pp 77-89.

Schiel and Foster 1992
Schiel, D. R., and Foster, M. S. 1992. "Restoring Kelp Forests." *Restoring the Nation's Marine Environment.* G.W. Thayer, ed., Maryland Sea Grant, College Park, MD, pp 279-342.

Schroeder 1983
Schroeder, P. R. 1983. "Chemical Clarification Methods for Confined Dredged Material Disposal," Technical Report D-83-2, U.S. Army Engineer Waterways Experiment Station, Vicksburg, MS.

Seaman and Sprague 1991
Seaman, W., Jr., and Sprague, L. M. 1991. *Artificial Habitats for Marine and Freshwater Fisheries*, Academic Press, San Diego, CA.

Seneca 1974
Seneca, E. D. 1974. "Stabilization of Coastal Dredge Spoil with *Spartina alterniflora*." *Ecology of Halophytes.* R. J. Reimold and W. H. Queen, eds., Academic Press, New York, pp 525-529.

Seneca et al. 1976
Seneca, E. D., Broome, S. W., Woodhouse, W. W., Jr., Cammen, L. M., and Lyon, J. T., III. 1976. "Establishing *Spartina alterniflora* marsh in North Carolina," *Environmental Conservation*, Vol 3, pp 185-188.

Sheehy and Vik 1992
Sheehy, D. J. and Vik, S. F. 1992. "Developing Prefabricated Reefs: An Ecological and Engineering Approach." *Restoring the Nation's Marine Environment*. G. W. Thayer, ed., Maryland Sea Grant, College Park, MD, pp 543-582.

Shisler 1990
Shisler, J. K. 1990. "Creation and Restoration of the Coastal Wetlands of the Northeastern United States." *Wetland Creation and Restoration: the Status of the Science.* J. A. Kusler and M. E. Kentula, eds., Island Press, Washington, DC, pp 143-170.

Short, Muehlstein, and Porter 1987
Short, F. T., Muehlstein, L. K., and Porter, D. 1987. "Eelgrass Wasting Disease: Cause and Recurrence of a Marine Epidemic," *Biological Bulletin*, Vol 173, pp 557-562.

Shreffler, Simenstad, and Thom 1992
Shreffler, D. K., Simenstad, C. A., and Thom, R. M. 1992. "Foraging by Juvenile Salmon in a Restored Estuarine Wetland," *Estuaries*, Vol 15, pp 204-213.

Simenstad and Thom 1996
Simenstad, C. A., and Thom, R. M. 1996. "Functional Equivalency Trajectories of the Restored Gog-Le-Hi-Te Estuarine Wetland," *Ecological Applications*, Vol 6, pp 38-56.

Sinicrope et al. 1990
Sinicrope, T. L., Hine, P. G., Warren, R. S., and Neiring, W. A. 1990. "Restoration of an Impounded Salt Marsh in New England," *Estuaries*, Vol 13, pp 25-30.

Smith 1978
Smith, H. K. 1978. "An Introduction to Habitat Development on Dredged Material," Technical Report DS-78-19, U.S. Army Engineer Waterways Experiment Station, Vicksburg, MS.

Snyder 1976
Snyder, G. R. 1976. "Effects of Dredging on Aquatic Organisms with Special Application to Areas Adjacent to the Northeastern Pacific Ocean," *Marine Fisheries Review*, Vol 38, pp 34-38.

Soots and Landin 1978
Soots, R. F, Jr., and Landin, M. C. 1978. "Development and Management of Avian Habitat on Dredged Material Islands," Technical Report D-78-18, U.S. Army Engineer Waterways Experiment Station, Vicksburg, MS.

Stevens and Rejmankova 1995
Stevens, M. L., and Rejmankova, E. 1995. "Cache Slough/Yolo Bypass Ecosystem Monitoring Study to Determine Wetland Mitigation Success." Technical Report WRP-RE-11, U.S. Army Engineer Waterways Experiment Station, Vicksburg, MS.

Teas 1977
Teas, H. J. 1977. "Ecology and Restoration of Mangrove Shorelines in Florida," *Environmental Conservation*, Vol 4, pp 51-58.

Thom 1990
Thom, R. M. 1990. "A Review of Eelgrass (*Zostera marina* L.) Transplanting Projects in the Pacific Northwest," *The Northwest Environmental Journal*, Vol 6, pp 121-137.

Thom 1997
Thom, R. M. 1997. "System-Development Matrix for Adaptive Management of Coastal Ecosystem Restoration Projects," *Ecological Engineering*, Vol 8, pp 219-232.

Thom and Wellman 1996
Thom, R. M., and Wellman, K. F. 1996. "Planning Aquatic Ecosystem Restoration Monitoring Program," IWR Report 96-R-23, U.S. Army Corps of Engineers Institute for Water Resources, Alexandria, VA.

Thorhaug 1985
Thorhaug, A. 1985. "Large-Scale Seagrass Restoration in a Damaged Estuary," *Marine Pollution Bulletin*, Vol 16, pp 55-62.

Thorhaug 1986
Thorhaug, A. 1986. "Review of Seagrass Restoration Efforts," *Ambio*, Vol 15, pp 110-117.

Thorhaug and Austin 1976
Thorhaug, A., and Austin, C. B. 1976. "Restoration of Seagrasses with Economic Analysis," *Environmental Conservation*, Vol 3, pp 259-268.

Van Dolah and Maier 1993
Van Dolah, R. F., and Maier, P. P. 1993. "The Distribution of Loggerhead Turtles (*Caretta caretta*) in the Entrance Channel of Charleston Harbor, South Carolina, U.S.A.," *Journal of Coastal Research*, Vol 9, pp 1004-1012.

Walters and Holling 1990
Walters, C. J., and Holling, C. S. 1990. "Large-Scale Management Experiments and Learning by Doing," *Ecology*, Vol 71, pp 2060-2068.

Weinstein 1979
Weinstein, M. P. 1979. "Shallow Marsh Habitats as Primary Nurseries for Fishes and Shellfish, Cape Fear River, North Carolina," *Fishery Bulletin*, Vol 77, pp 339-357.

Wennersten 1981
Wennersten, J. R. 1981. *The Oyster Wars of Chesapeake Bay.* Tidewater Publishers, Inc., Centreville, MD.

Wilson and Ruff 1988
Wilson, W. H., and Ruff, R. E. 1988. "Species Profiles: Life Histories and Environmental Requirements of Coastal Fishes and Invertebrates (North Atlantic) - Sandworm and Bloodworm," U.S. Fish and Wildlife Service Biological Report 82 (11.80), U.S. Army Engineer Waterways Experiment Station, Technical Report EL-82-4, Vicksburg, MS.

Woodhouse 1978
Woodhouse, W. W., Jr. 1978. "Dune Building and Stabilization with Vegetation," Special Report No. 3., U.S. Army Engineer Waterways Experiment Station, Coastal Engineering Research Center, Vicksburg, MS.

Wyllie-Echeverria, Olson, and Hershman 1994
Wyllie-Echeverria, S., Olson, A. M., and Hershman, M. J. 1994. "Seagrass Science and Policy in the Pacific Northwest," Proceedings of a Seminar Series SMA 94-1), EPA 910/R-94-004.

Zale and Merrifield 1989
Zale, A. V., and Merrifield, S. G. 1989. "Species Profiles: Life Histories and Environmental Requirements of Coastal Fishes and Invertebrates (south Florida) - Reef-Building Tube Worm," U.S. Fish and Wildlife Service Biological Report 82 (11.115), U.S. Army Engineer Waterways Experiment Station, Technical Report TR EL-82-4, Vicksburg, MS.

Zedler 1988
Zedler, J. B. 1988. "Salt Marsh Restoration: Lessons for California," *Rehabilitating Damaged Ecosystems*. 2nd ed., J. Cairns, Jr., ed., CRC Press, Inc., Boca Raton, FL, pp 75-96.

Zedler 1996a
Zedler, J. B. 1996a. "Coastal Mitigation in Southern California: The Need for a Regional Restoration Strategy," *Ecological Applications*, Vol 6, pp 84-93.

Zedler 1996b
Zedler, J. B. 1996b. "Tidal Wetland Restoration: A Scientific Perspective and Southern California Focus," Report T-038, California Sea Grant College, University of California, La Jolla, CA.

Zieman 1976
Zieman, J. C. 1976. "The Ecological Effects of Physical Damage from Motorboats on Turtle Grass Beds in Southern Florida," *Aquatic Botany*, Vol 2, pp 127-139.

V-7-9. Acknowledgments

Authors of Chapter V-7, "Coastal Engineering for Environmental Enhancement:"

David J. Yozzo, Ph.D., Barry A. Vittor & Associates, Kingston, New York
Jack E. Davis, Ph.D., Coastal and Hydraulics Laboratory (CHL), U.S. Army Engineer Research and Development Center, Vicksburg, Mississippi
Patrick T. Cagney, U.S. Army Engineer District, Seattle, Seattle, Washington

CHAPTER VI-1

Introduction to Coastal Project Element Design

TABLE OF CONTENTS

Page

VI-1-1. Introduction to Part VI VI-1-1

a. Part VI Overview VI-1-1
b. Comparison between Part VI and the Shore Protection Manual VI-1-2
c. Logical Connections to Other Coastal Engineering Manual Parts VI-1-4
d. Using Part VI in the Design Process VI-1-4

VI-1-2. References VI-1-5

VI-1-3. Acknowledgements VI-1-5

VI-1-4. Symbols VI-1-5

List of Tables

Table VI-1-1. Topic Coverage in Part VI Compared to *Shore Protection Manual* (1984) VI-1-3

CHAPTER VI-1

Introduction to Coastal Project Element Design

VI-1-1. Introduction to Part VI. Part VI is the second of two engineering-based parts oriented toward design of coastal projects. Part V (Coastal Project Planning and Design) focuses on aspects related to overall coastal project design and development, whereas Part VI contains specific information and procedures for designing the structural elements used in coastal navigation and shore protection projects.

a. Part VI Overview. Part VI contains eight chapters as described below.

(1) Chapter VI-1 briefly overviews and summarizes the contents of each Part VI chapter and provides overall guidance on using the design procedures.

(2) Chapter VI-2, "Types and Functions of Coastal Structures," begins with brief descriptions of the various types and functions of coastal structures most often used in coastal projects. Typical cross sections and layouts are illustrated in the second section along with descriptions of the usual construction for each structure type. The third section introduces the types of concrete armor units used on coastal structures. The chapter ends with a comprehensive overview of failure modes associated with each structure type. Understanding potential failure modes is critical for design, and this understanding is aided by many figures in the chapter illustrating the various failure modes.

(3) Chapter VI-3, "Site-Specific Design Conditions" focuses on site-specific design information that may need to be considered during preliminary and final design. Whereas several project sites might experience similar design wave and water-level conditions, there may be unique conditions at each site that could significantly influence final design. Site specific design conditions and considerations discussed in this chapter include foundation and geotechnical requirements, seasonal profile variation, structure flanking, seismic activity, ice, environmental considerations, aspects related to construction, maintenance, aesthetics, etc.

(4) Chapter VI-4, "Materials and Construction Aspects," begins with a section discussing general requirements of materials used in coastal projects such as material properties, durability, adaptability, cost, availability, handling, and maintenance requirements. More detail and specific design guidance and considerations are given in individual sections for earth and sand, stone, concrete, steel and other metals, wood, geotextiles, and plastics. Each section overviews typical use of the material in coastal projects, lists the physical and mechanical properties of the material, and discusses placement considerations and potential environmental impacts.

(5) Chapter VI-5, "Fundamentals of Design," is the heart of Part VI, and contains most of the guidance and methodology needed for designing coastal structure cross sections (with the exception of hydrodynamic criteria, which are presented in Part II, "Coastal Hydrodynamics"). A brief introduction is followed by a section giving guidance related to the hydraulic response of the waves at the structure (i.e., wave runup, overtopping, transmission, and reflection). Next are two sections containing methodology for determining loading and response for sloping-front

rubble-mound structures and vertical-front structures, respectively. Foundation loads are also reviewed in this chapter. The intention is to generate awareness of when geotechnical aspects should be considered in the design process. Estimation of scour for different situations is covered next along with procedures for designing scour protection. Methods for estimating wave forces on slender cylindrical piles are followed by the final section, which summarizes briefly impact forces and ice forces that might occur at structures.

(6) Chapter VI-6 introduces reliability-based design of coastal structures. Familiar deterministic design equations are cast into the form of "failure functions," which can be evaluated in terms of random loading and response variables. Sophisticated probability methods are overviewed, but application requires the distribution of the random variables be reasonably well established. The partial safety factor system is presented that permits a less rigorous, but still useful, reliability analysis based on tabulated coefficients for specific design formulas. Overall system reliability can be analyzed based on failure probability of system components.

(7) Chapter VI-7, "Example Problems," illustrates application of design guidance and formulations given in previous chapters through case studies and example problems. The examples cover the most common applications such as wave runup, wave overtopping, armor layer stability, and stability of vertical-walled bulkheads and caissons, and forces on cylindrical piles.

(8) Chapter VI-8 begins with an overview of coastal project maintenance followed by a section on project monitoring and inspection. Condition monitoring occurs over the life of the structure whereas performance monitoring is usually short-term monitoring to access project performance. Each type of monitoring has different elements, but often shares the same instrumentation or techniques. Coverage includes evaluation of structure condition, types of instruments, and monitoring plan considerations. Repair and rehabilitation of rubble-mound structures after damage or deterioration is needed to assure continued functionality. Techniques for different levels of repair are discussed.

b. Comparison between Part VI and the *Shore Protection Manual*. Part VI corresponds mainly to the topics covered in Chapter 7 of the *Shore Protection Manual* ("Structural Design: Physical Factors"). Part VI is substantially larger than the equivalent portions of the older document, with most topics receiving expanded coverage. Several topics not included in the *Shore Protection Manual* have been added to Part VI. Table VI-1-1 shows the main topics of Part VI and how coverage compares with similar content in the *Shore Protection Manual*.

(1) The two main organizational differences between the *Coastal Engineering Manual* and *Shore Protection Manual* relate to presentation of design guidance and example calculations. Much of the design guidance in the CEM is presented in the form of tables. Each table applies to a specific design formula or procedure. Typically the table includes all the information needed for applying the formula or procedure to a specific structure type including necessary coefficients, variables, range of applicability, and when necessary, a cross-section or planview sketch illustrating the specific structure for which the methodology applies. The tables contain only minimal discussion and background information about the methodology so that Part VI

could be kept to a manageable length. If additional information is needed, see the provided reference to the original source material.

Table VI-1-1
Topic Coverage in Part VI Compared to *Shore Protection Manual* (1984)

Section	Topic	Changes from *Shore Protection Manual* (1984)
VI-2-1	Structure types	Similar coverage
VI-2-4	Failure modes	New topic
VI-3	Site-specific design criteria	Revised/updated
VI-4	Construction materials and procedures	New topic
VI-5-2	Wave runup and overtopping	Revised/updated
VI-5-2	Wave transmission and reflection	Revised/updated
VI-5-3	Rubble-mound structures	Revised/expanded
VI-5-4	Vertical-front structures	Revised
VI-5-5	Marine foundations	New topic
VI-5-6	Scour and scour protection	New topic
VI-5-7	Forces on piles	Same/revised
VI-5-8	Other forces on structures	Revised
VI-6	Reliability in design	New topic
VI-7	Design of specific project elements	Same/new examples using new guidance
VI-8	Monitoring, maintenance and repair	New topic

(2) In the *Shore Protection Manual*, some of the design guidance was immediately illustrated by example problems embedded in the text at that location, whereas in the *Coastal Engineering Manual* example applications of various design formulas are collected separately in Part VI-7. Separation of examples from the tables of design guidance is part of the modular design of Part VI. Many of the *Coastal Engineering Manual* example problems use the same conditions given for the corresponding problems in the *Shore Protection Manual*. This allows side-by-side comparison to show how the new guidance of the *Coastal Engineering Manual* differs from the older *Shore Protection Manual* results.

(3) Even with the increased number of pages, there are several instances where specific guidance contained in the *Shore Protection Manual* has not been included in the *Coastal Engineering Manual*. Decisions on whether or not to include certain material were based on considerations of guidance reliability and usefulness, with priority given to more common design needs. For those few situations where no guidance is included in the *Coastal Engineering Manual*, it should be acceptable to use the older guidance found in the *Shore Protection Manual* (or other sources) subject to the restrictions and caveats noted and provided improved procedures are not available in other design manuals. For example, the *Shore Protection Manual* contains provisional guidance for estimating slamming forces on vertical walls caused by breaking waves (Minikin method). This procedure produces high forces, and it is viewed with skepticism by some. Because no commonly accepted procedure was available at the time of writing to replace Minikin's method, it was decided to not include this topic. In other cases, the guidance was

deemed sound, but the application was considered fairly rare compared to the included procedures. These were tough decisions, but the important point to remember is that the *Coastal Engineering Manual* is not all-inclusive; and just because a particular design formula or procedure is not given in the *Coastal Engineering Manual*, this does not imply that it is not valid. That judgment must be made separately based on available information. However, where design guidance provided in the *Shore Protection Manual* differs from newer design methods contained in the *Coastal Engineering Manual*, strong justification is needed before choosing the *Shore Protection Manual* guidance over the preferred *Coastal Engineering Manual* recommendation.

c. Logical Connections to Other *Coastal Engineering Manual* Parts. Part VI is most closely linked with Part V, "Coastal Project Planning and Design" and Part II, "Coastal Hydrodynamics." Part V guides the engineer in selecting and evaluating alternatives to solve coastal problems, and Part VI tells how to design the specific elements (structures) that comprise each alternative. For each alternative, functional project design results in planform dimensions and multiple design objectives related to the purpose and intended function of the structure types used in the project. Contained in these design objectives are specific structure performance criteria such as whether to allow overtopping, permissible wave transmission, allowable damage levels, etc. Some information on general design criteria related to individual structure types can also be found in Part V.

(1) Hydrodynamic loading (i.e., wave parameters, design water levels, currents, etc.) related to specific structure geographic location and exposure are estimated using information provided in *Coastal Engineering Manual* Part II. These estimates form the hydrodynamic design criteria for each structure that is part of the coastal project. Hydrodynamic input requirements are specified for each design formula, and some parameters may vary between formulas. For example, design waves may be specified as significant wave height (H_s or $H_{1/3}$), zeroth-moment wave height (H_{mo}), or some other statistical representative wave height such as $H_{10\%}$ or $H_{1\%}$. Therefore, it is necessary to determine from Part VI what form the hydrodynamic criteria take when estimating the criteria from Part II.

(2) **Important note:** Part II was authored several years before Part VI, and in Part II-7, "Harbor Hydrodynamic," older guidance related to wave reflection and transmission was included that has since been superseded by the updated design guidance provided in Part VI. Although the older guidance provides reasonable estimates, using the formulas for wave reflection and transmission provided in Part VI-5-2 is recommended.

d. Using Part VI in the Design Process. In some cases more than one procedure is available for estimating the result of wave loading on a specific structure type, and separate tables are given for each methodology. Usually, similar results are produced by the different methods, but the range of applicability may differ. Therefore, it is important to first verify the appropriateness of a selected procedure for the specific design problem. If more than one set of guidelines is appropriate, it is wise to perform the calculation by both methods and compare results. Results that are nearly the same indicate either method can be used with confidence. In cases where answers from two methodologies diverge, the engineer must investigate further the background of the competing methods with primary focus on extent and range of experimental measurements on which the method is based, and the general acceptance of the method in the

coastal community. For example, one method might be based primarily on shallow water conditions, whereas the other method examined deeper water conditions. An older formula might be based on monochromatic wave experiments, but cover a wide range of incident wave conditions, whereas a newer formula might have been developed with a small number of irregular wave observations. At the end of the day, engineering judgment based on past experience may be needed, and that is acceptable provided concerns and caveats are made known to those with a stake in the project.

VI-1-2. References.

Shore protection manual. (1984). 4th ed., 2 Vol, U.S. Army Engineer Waterways Experiment Station, U.S. Government Printing Office, Washington, DC.

VI-1-3. Acknowledgements.

Author: Steven A. Hughes, PhD, Coastal and Hydraulics Laboratory (CHL), Engineer Research and Development Center, Vicksburg, Mississippi.

Reviewer: Frank A. Santangelo, U.S. Army Engineer District, New York.

VI-1-4. Symbols.

H_{mo}	Zeroth-moment wave height
H_s or $H_{1/3}$	Significant wave height (length)
$H_{10\%}$ or $H_{1\%}$	Statistical representative wave heights

CHAPTER 2

Types and Functions of Coastal Structures

TABLE OF CONTENTS

Page

VI-2-1. Applications VI-2-1

a. Sea dikes VI-2-1
b. Seawalls VI-2-1
c. Revetments VI-2-1
d. Bulkheads VI-2-2
e. Groins VI-2-3
f. Detached breakwaters VI-2-4
g. Reef breakwaters VI-2-5
h. Submerged sills VI-2-5
i. Beach drains VI-2-6
j. Beach nourishment and dune construction VI-2-6
k. Breakwaters VI-2-6
l. Floating breakwaters VI-2-7
m. Jetties VI-2-7
n. Training walls VI-2-7
o. Storm surge barriers VI-2-7
p. Pipelines VI-2-7
q. Pile structures VI-2-8
r. Scour protection VI-2-8

VI-2-2. Typical Cross Sections and Layouts VI-2-8

a. Sea dikes VI-2-8
b. Seawalls and revetments VI-2-9
c. Groins VI-2-12
d. Detached breakwaters VI-2-14
e. Rubble-mound breakwaters VI-2-15
f. Reshaping rubble-mound breakwaters VI-2-18
g. Reef breakwaters VI-2-19
h. Vertical-front breakwaters VI-2-19
i. Piled breakwaters VI-2-23
j. Jetties VI-2-23
k. Storm surge barriers VI-2-23

VI-2-3. Main Types of Concrete Armor Units VI-2-24

VI-2-4. Failure Modes of Typical Structure Types VI-2-26

a. Failure VI-2-26
b. Sloping-front structures VI-2-27
c. Vertical-front structures VI-2-42
d. Floating structures VI-2-54
e. Beach fills VI-2-54
f. Scour potential and toe failure VI-2-55

VI-2-5. References VI-2-55

VI-2-6. Acknowledgments VI-2-56

List of Figures

Page

Figure VI-2-1. Example of asphalt-armored sea dike VI-2-9

Figure VI-2-2. Example of grass-armored sea dike design from the North Sea coast of Denmark VI-2-9

Figure VI-2-3. Examples of sloping front rubble-mound seawall/revetment structures VI-2-10

Figure VI-2-4. Examples of sloping-front seawalls/revetments with pattern-placed concrete armor units VI-2-11

Figure VI-2-5. Examples of sloping front seawalls/revetments with fixed surfaces of asphalt and in situ cast concrete VI-2-12

Figure VI-2-6. Examples of sloping front revetment designs from the Danish North Sea coast (Danish Coast Authority) VI-2-13

Figure VI-2-7. Example of a vertical front seawall VI-2-13

Figure VI-2-8. Typical beach configuration with groins VI-2-14

Figure VI-2-9. Examples of groin structures VI-2-15

Figure VI-2-10. Typical beach configurations with detached nearshore breakwaters VI-2-16

Figure VI-2-11. Conventional multilayer rubble-mound breakwater VI-2-17

Figure VI-2-12. Rubble-mound structures with S-shaped and bermed fronts VI-2-17

Figure VI-2-13. Example of rubble-mound breakwater with concrete superstructure VI-2-18

Figure VI-2-14. Reshaping rubble-mound breakwater VI-2-18

Figure VI-2-15. Example of a reef breakwater VI-2-19

Figure VI-2-16. Conventional caisson breakwater with vertical front VI-2-20

Figure VI-2-17. Vertical composite caisson breakwater VI-2-20

Figure VI-2-18. Horizontal composite caisson breakwater VI-2-21

Figure VI-2-19. Sloping-top caisson breakwater VI-2-21

Figure VI-2-20. Perforated front wall caisson breakwater VI-2-22

Figure VI-2-21. Example of blockwork breakwater VI-2-22

Figure VI-2-22. Example of piled breakwater VI-2-23

Figure VI-2-23. Storm surge barrier proposed for the Venice Lagoon VI-2-24

Figure VI-2-24. Examples of concrete armor units VI-2-24

Figure VI-2-25. Overview of rubble-mound breakwater failure modes VI-2-28

Figure VI-2-26. Main armor layer instability VI-2-28

Figure VI-2-27. Rear side erosion of crest VI-2-29

Figure VI-2-28. Hydraulic instability on steep slopes VI-2-29

Figure VI-2-29. Armor unit breakage VI-2-30

Figure VI-2-30. Armor unit deterioration VI-2-31

Figure VI-2-31. Sliding of superstructure VI-2-32

Figure VI-2-32. Failure due to armor unit breakage VI-2-32

Figure VI-2-33. Forward tilting of superstructure VI-2-33

Figure VI-2-34. Rear-side erosion due to overtopping VI-2-33

Figure VI-2-35. Erosion due to venting VI-2-34

Figure VI-2-36. Failure due to toe berm erosion VI-2-34

Figure VI-2-37. Scour-induced armor displacement VI-2-35

Figure VI-2-38. Block subsidence due to liquefaction VI-2-35

Figure VI-2-39. Toe instability on hard bottoms VI-2-36

Figure VI-2-40. Washout of underlayer material VI-2-36

Figure VI-2-41. Slip surface failure VI-2-37

Figure VI-2-42. Structure settlement failure VI-2-37

Figure VI-2-43. Scour due to overtopping VI-2-38
Figure VI-2-44. Toe erosion failure of rubble slope VI-2-38
Figure VI-2-45. Failure of sheet-pile toe wall VI-2-39
Figure VI-2-46. Pressure blowout of slab elements VI-2-39
Figure VI-2-47. Erosion of dike slope protection VI-2-40
Figure VI-2-48. Toe scour erosion of dike VI-2-40
Figure VI-2-49. Dike crest erosion by overtopping VI-2-41
Figure VI-2-50. Dike backscouring due to piping VI-2-41
Figure VI-2-51. Dike slip surface failure VI-2-41
Figure VI-2-52. Sliding of caisson on foundation VI-2-43
Figure VI-2-53. Caisson settlement VI-2-43
Figure VI-2-54. Soil foundation slip surface failure VI-2-44
Figure VI-2-55. Slip surface failure of rubble foundation VI-2-44
Figure VI-2-56. Caisson overturning VI-2-45
Figure VI-2-57. Seaward tilting and settlement due to erosion of rubble base VI-2-45
Figure VI-2-58. Seaward tilting and settlement due to scour VI-2-46
Figure VI-2-59. Loss of foundation material due to caisson motion VI-2-46
Figure VI-2-60. Failure of fronting armor units VI-2-47
Figure VI-2-61. Caisson front wall failure VI-2-47
Figure VI-2-62. Displacement of individual blocks VI-2-48
Figure VI-2-63. Seaward sliding of gravity wall VI-2-48
Figure VI-2-64. Seaward overturning of gravity wall VI-2-49
Figure VI-2-65. Gravity wall settlement VI-2-49

Figure VI-2-66. Rotational slip failure of gravity wall VI-2-50

Figure VI-2-67. Landward overturning of gravity wall VI-2-50

Figure VI-2-68. Displacement of individual gravity wall components VI-2-51

Figure VI-2-69. Failure due to toe scour VI-2-51

Figure VI-2-70. Rotational slip surface failure VI-2-52

Figure VI-2-71. Failure of thin wall construction material VI-2-52

Figure VI-2-72. Failure due to anchor pullout VI-2-53

Figure VI-2-73. Back scour and thin wall failure VI-2-53

List of Tables

Page

Table VI-2-1. Types and Functions of Coastal Structures.....VI-2-2

Table VI-2-2. Failure Modes of Caisson and Blockwork Breakwaters.....VI-2-42

CHAPTER VI-2

Types and Functions of Coastal Structures

VI-2-1. Applications. Coastal structures are used in coastal defense schemes with the objective of preventing shoreline erosion and flooding of the hinterland. Other objectives include sheltering of harbor basins and harbor entrances against waves, stabilization of navigation channels at inlets, and protection of water intakes and outfalls. An overview of the various types of coastal structures and their application is given in Table VI-2-1. Overall planning and development of coastal projects is covered in Part V.

a. Sea dikes. Sea dikes are onshore structures with the principal function of protecting low-lying areas against flooding. Sea dikes are usually built as a mound of fine materials like sand and clay with a gentle seaward slope in order to reduce the wave runup and the erodible effect of the waves. The surface of the dike is armored with grass, asphalt, stones, or concrete slabs.

b. Seawalls.

(1) Seawalls are onshore structures with the principal function of preventing or alleviating overtopping and flooding of the land and the structures behind due to storm surges and waves. Seawalls are built parallel to the shoreline as a reinforcement of a part of the coastal profile. Quite often seawalls are used to protect promenades, roads, and houses placed seaward of the crest edge of the natural beach profile. In these cases a seawall structure protruding from the natural beach profile must be built. Seawalls range from vertical face structures such as massive gravity concrete walls, tied walls using steel or concrete piling, and stone-filled cribwork to sloping structures with typical surfaces being reinforced concrete slabs, concrete armor units, or stone rubble.

(2) Erosion of the beach profile landward of a seawall might be stopped or at least reduced. However, erosion of the seabed immediately in front of the structure will in most cases be enhanced due to increased wave reflection caused by the seawall. This results in a steeper seabed profile, which subsequently allows larger waves to reach the structure. As a consequence, seawalls are in danger of instability caused by erosion of the seabed at the toe of the structure, and by an increase in wave slamming, runup, and overtopping. Because of their potential vulnerability to toe scour, seawalls are often used together with some system of beach control such as groins and beach nourishment. Exceptions include cases of stable rock foreshores and cases where the potential for future erosion is limited and can be accommodated in the design of the seawall.

c. Revetments. Revetments are onshore structures with the principal function of protecting the shoreline from erosion. Revetment structures typically consist of a cladding of stone, concrete, or asphalt to armor sloping natural shoreline profiles. In the Corps of Engineers, the functional distinction is made between seawalls and revetments for the purpose of assigning project benefits; however, in the technical literature there is often no distinction between seawalls and revetments.

d. Bulkheads. Bulkhead is the term for structures primarily intended to retain or prevent sliding of the land, whereas protecting the hinterland against flooding and wave action is of secondary importance. Bulkheads are built as soil retaining structures, and in most cases as a vertical wall anchored with tie rods. The most common application of bulkheads is in the construction of mooring facilities in harbors and marinas where exposure to wave action is minimized. Some reference literature may not make a distinction between bulkheads and seawalls.

Table VI-2-1
Types and Functions of Coastal Structures

Type of Structure	Objective	Principal Function
Sea dike	Prevent or alleviate flooding by the sea of low-lying land areas	Separation of shoreline from hinterland by a high impermeable structure
Seawall	Protect land and structures from flooding and overtopping	Reinforcement of some part of the beach profile
Revetment	Protect the shoreline against erosion	Reinforcement of some part of the beach profile
Bulkhead	Retain soil and prevent sliding of the land behind	Reinforcement of the soil bank
Groin	Prevent beach erosion	Reduction of longshore transport of sediment
Detached breakwater	Prevent beach erosion	Reduction of wave heights in the lee of the structure and reduction of longshore transport of sediment
Reef breakwater	Prevent beach erosion	Reduction of wave heights at the shore
Submerged sill	Prevent beach erosion	Retard offshore movement of sediment
Beach drain	Prevent beach erosion	Accumulation of beach material on the drained portion of beach
Beach nourishment and dune construction	Prevent beach erosion and protect against flooding	Artificial infill of beach and dune material to be eroded by waves and currents in lieu of natural supply
Breakwater	Shelter harbor basins, harbor entrances, and water intakes against waves and currents	Dissipation of wave energy and/or reflection of wave energy back into the sea
Floating breakwater	Shelter harbor basins and mooring areas against short-period waves	Reduction of wave heights by reflection and attenuation
Jetty	Stabilize navigation channels at river mouths and tidal inlets	Confine streams and tidal flow. Protect against storm water and crosscurrents

Training walls	Prevent unwanted sedimentation or erosion and protect moorings against currents	Direct natural or man-made current flow by forcing water movement along the structure
Storm surge barrier	Protect estuaries against storm surges	Separation of estuary from the sea by movable locks or gates
Pipeline outfall	Transport of fluids	Gravity-based stability
Pile structure	Provide deck space for traffic, pipelines, etc., and provide mooring facilities	Transfer of deck load forces to the seabed
Scour protection	Protect coastal structures against instability caused by seabed scour	Provide resistance to erosion caused by waves and current

e. Groins.

(1) Groins are built to stabilize a stretch of natural or artificially nourished beach against erosion that is due primarily to a net longshore loss of beach material. Groins function only when longshore transport occurs. Groins are narrow structures, usually straight and perpendicular to the preproject shoreline. The effect of a single groin is accretion of beach material on the updrift side and erosion on the downdrift side; both effects extend some distance from the structure. Consequently, a groin system (series of groins) results in a saw-tooth-shaped shoreline within the groin field and a differential in beach level on either side of the groins.

(2) Groins create very complex current and wave patterns. However, a well-designed groin system can arrest or slow down the rate of longshore transport and, by building up of material in the groin bays, provide some protection of the coastline against erosion. Groins are also used to hold artificially nourished beach material, and to prevent sedimentation or accretion in a downdrift area (e.g., at an inlet) by acting as a barrier to longshore transport. Deflecting strong tidal currents away from the shoreline might be another purpose of groins.

(3) The orientation, length, height, permeability, and spacing of the groins determine, under given natural conditions, the actual change in the shoreline and the beach level. Because of the potential for erosion of the beach downdrift of the last groin in the field, a transition section of progressively shorter groins may be provided to prevent the formation of a severe erosion area. Even so, it might be necessary to protect some part of the downdrift beach with a seawall or to nourish a portion of the eroded area with beach material from an alternative source.

(4) Groins are occasionally constructed non-perpendicular to the shoreline, can be curved, have fishtails, or have a shore-parallel T-head at their seaward end. Also, shore-parallel spurs are provided to shelter a stretch of beach or to reduce the possibility of offshore sand transport by rip currents. However, such refinements, compared to the simple shape of straight perpendicular groins, are generally not deemed effective in improving the performance of the groins.

(5) In most cases, groins are sheet-pile or rubble-mound constructions. The latter is preferably used at exposed sites because of a rubble-mound structure's ability to withstand severe wave loads and to decrease wave reflection. Moreover, the risk of scouring and formation of strong rip currents along rubble groins is reduced.

(6) The landward end of the groins must extend to a point above the high-water line in order to stay beyond the normal zone of beach movement and thereby avoid outflanking by back scour. The groins must, for the same reason, reach seawalls when present or connect into stable back beach features. The position of the seaward end is determined such that the groin retains some proportion of the longshore transport during more severe wave conditions. This means that the groin must protrude some distance into the zone of littoral transport, the extent of which is largely determined by surf zone width. Groins can be classified as either *long* or *short*, depending on how far across the surf zone they extend. Groins that transverse the entire surf zone are considered *long*, whereas those that extend only part way across the surf zone are considered *short*. These terms are relative, since the width of the surf zone varies with water level, wave height, and beach profile. Most groins are designed to act as *short* structures during severe sea states and as *long* structures under normal conditions. Groins might also be classified as *high* or *low*, depending on the possibility of sediment transport across the crest. Significant cost savings can be achieved by constructing groins with a variable crest elevation that follows the beach profile rather than maintaining a constant crest elevation. These groins would maintain a constant cross section and allow increasing amounts of sand to bypass as water depth increases. At some point the crest of the groin becomes submerged. *Terminal groins* extend far enough seaward to block all littoral transport, and these types of groins should never be used except in rare situations, such as where longshore transported sand would be otherwise lost into a submarine canyon.

(7) Some cross-groin transport is beneficial for obtaining a well-distributed retaining effect along the coast. For the same reason *permeable groins,* which allow sediment to be transported through the structure, may be advantageous. Examples of permeable groins include rubble-mound structures built of rock and concrete armor units without fine material cores, and structures made of piles with some spacing. Most sheet-pile structures are impermeable. Low and permeable groins have the benefit of reduced wave reflection and less rip current formation compared with high and impermeable groins.

f. Detached breakwaters.

(1) Detached breakwaters are small, relatively short, nonshore-connected nearshore breakwaters with the principal function of reducing beach erosion. They are built parallel to the shore just seaward of the shoreline in shallow water depths. Multiple detached breakwaters spaced along the shoreline can provide protection to substantial shoreline frontages. The gaps between the breakwaters are in most cases on the same order of magnitude as the length of one individual structure.

(2) Each breakwater reflects and dissipates some of the incoming wave energy, thus reducing wave heights in the lee of the structure and reducing shore erosion. Beach material transported along the beach moves into the sheltered area behind the breakwater where it is deposited in the lower wave energy region. The nearshore wave pattern, which is strongly

influenced by diffraction at the heads of the structures, will cause *salients* and sometimes *tombolos* to be formed, thus making the coastline similar to a series of pocket beaches. Once formed, the pockets will cause wave refraction, which helps to stabilize the pocket-shaped coastline.

(3) Like groins, a series of detached breakwaters can be used to control the distribution of beach material along a coastline. Just downdrift of the last breakwater in the series there is an increased risk of shoreline erosion. Consequently, it might be necessary to introduce a transition section where the breakwaters gradually are made smaller and placed closer to the shoreline. In addition, seawall protection of the downdrift stretch of beach might be necessary.

(4) Detached breakwaters are normally built as rubble-mound structures with fairly low crest levels that allow significant overtopping during storms at high water. The low-crested structures are less visible and help promote a more even distribution of littoral material along the coastline. Submerged detached breakwaters are used in some cases because they do not spoil the view, but they do represent a serious nonvisible hazard to boats and swimmers.

(5) Properly designed detached breakwaters are very effective in reducing erosion and in building up beaches using natural littoral drift. Moreover, they are effective in holding artificially nourished beach material.

(6) Optimizing detached breakwater designs is difficult when large water level variations are present, as is the case on coastlines with a large tidal range or in portions of the Great Lakes, which may experience long-term water level fluctuations.

g. Reef breakwaters. Reef breakwaters are coast-parallel, long or short submerged structures built with the objective of reducing the wave action on the beach by forcing wave breaking over the *reef*. Reef breakwaters are normally rubble-mound structures constructed as a homogeneous pile of stone or concrete armor units. The breakwater can be designed to be stable or it may be allowed to reshape under wave action. Reef breakwaters might be *narrow crested* like detached breakwaters in shallow water or, in deeper water, they might be *wide crested* with lower crest elevation like most natural reefs that cover a fairly wide rim parallel to the coastline. Besides triggering wave breaking and subsequent energy dissipation, reef breakwaters can be used to regulate wave action by refraction and diffraction. Reef breakwaters represent a nonvisible hazard to swimmers and boats.

h. Submerged sills. A submerged sill is a special version of a reef breakwater built nearshore and used to retard offshore sand movements by introducing a structural barrier at one point on the beach profile. However, the sill may also interrupt the onshore sand movement. The sill introduces a discontinuity into the beach profile so that the beach behind it becomes a *perched* beach as it is at higher elevation and thus wider than adjacent beaches. Submerged sills are also used to retain beach material artificially placed on the beach profile behind the sill. Submerged sills are usually built as rock-armored, rubble-mound structures or commercially available prefabricated units. Submerged sills represent a nonvisible hazard to swimmers and boats.

i. Beach drains. Beach drains are installed for the purpose of enhancing accumulation of beach material in the drained part of the beach. In principal, the drains are arranged at an elevation just beneath the lowest seasonal elevation of the beach profile in the swash zone. Pumping water from the drains causes local lowering of the groundwater table, which helps reduce the backwash speed and the groundwater outflow in the beach zone. This allows more beach material to settle out on the foreshore slope. Beach drains are built like normal surface drain systems consisting of a stable granular filter, with grain sizes ranging from that of the beach material to coarse materials like pebbles, arranged around closely spaced perforated pipes. The drain pipes are connected to few shore-normal pipelines leading to a pump sump in the upper part of the beach profile. Replacing the granular filter with geotextiles is not recommended because of the increased tendency to clog the drainage system.

j. Beach nourishment and dune construction.

(1) Beach nourishment is a *soft structure* solution used for prevention of shoreline erosion. Material of preferably the same, or larger, grain size and density as the natural beach material is artificially placed on the eroded part of the beach to compensate for the lack of natural supply of beach material. The beachfill might protect not only the beach where it is placed, but also downdrift stretches by providing an updrift point source of sand.

(2) Dune construction is the piling up of beach quality sand to form protective dune fields to replace those washed away during severe storms. An essential component of dune reconstruction is planting of dune vegetation and placement of netting or snow fencing to help retain wind-blown sand normally trapped by mature dune vegetation. Storm overwash fans may be a viable source of material for dune construction.

k. Breakwaters.

(1) Breakwaters are built to reduce wave action in an area in the lee of the structure. Wave action is reduced through a combination of reflection and dissipation of incoming wave energy. When used for harbors, breakwaters are constructed to create sufficiently calm waters for safe mooring and loading operations, handling of ships, and protection of harbor facilities. Breakwaters are also built to improve maneuvering conditions at harbor entrances and to help regulate sedimentation by directing currents and by creating areas with differing levels of wave disturbance. Protection of water intakes for power stations and protection of coastlines against tsunami waves are other applications of breakwaters.

(2) When used for shore protection, breakwaters are built in nearshore waters and usually oriented parallel to the shore like *detached breakwaters*. The layout of breakwaters used to protect harbors is determined by the size and shape of the area to be protected as well as by the prevailing directions of storm waves, net direction of currents and littoral drift, and the maneuverability of the vessels using the harbor. Breakwaters protecting harbors and channel entrances can be either detached or shore-connected.

(3) The cost of breakwaters increases dramatically with water depth and wave climate severity. Also poor foundation conditions significantly increase costs. These three environmental factors heavily influence the design and positioning of the breakwaters and the harbor layout.

(4) Breakwaters can be classified into two main types: *sloping-front* and *vertical-front* structures. Sloping-front structures are in most cases rubble-mound structures armored with rock or concrete armor units, with or without wavewall superstructures. Vertical-front structures are in most cases constructed of either sandfilled concrete caissons or stacked massive concrete blocks placed on a rubble stone bedding layer. In deep water, concrete caissons are often placed on a high mound of quarry rock for economical reasons. These breakwaters are called *composite structures*. The upper part of the concrete structure might be constructed with a sloping front to reduce the wave forces. For the same reason the front wall might be perforated with a wave chamber behind to dissipate wave energy. Smaller vertical structures might be constructed of steel sheetpiling backfilled with soil, or built as a rock-filled timber cribwork or wire cages. In milder wave climates sloping reinforced concrete slabs supported by batter piles is another possibility.

l. Floating breakwaters. Floating breakwaters are used in protected regions that experience mild wave climates with very short-period waves. For example, box-shaped reinforced concrete pontoons are used to protect marinas in sheltered areas. Floating docks affixed to piles are also used in marinas.

m. Jetties. Jetties are used for stabilization of navigation channels at river mouths and tidal inlets. Jetties are shore-connected structures generally built on either one or both sides of the navigation channel perpendicular to the shore and extending into the ocean. By confining the stream or tidal flow, it is possible to reduce channel shoaling and decrease dredging requirements. Moreover, on coastlines with longshore currents and littoral drift, another function of the jetties is also to arrest the crosscurrent and direct it across the entrance in deeper water where it represents less hazard to navigation. When extended offshore of the breaker zone, jetties improve the maneuvering of ships by providing shelter against storm waves. Jetties are constructed similar to breakwaters.

n. Training walls. Training walls are structures built to direct flow. Typical training wall objectives might be to improve mooring conditions in an estuary or to direct littoral drift away from an area of potential deposition. Most training walls are constructed using sheet piles.

o. Storm surge barriers. Storm surge barriers protect estuaries against storm surge flooding and related wave attack. These barriers also prevent excessive intrusion of salt-water wedges during high-water episodes. In most cases the barrier consists of a series of movable gates that normally stay open to let the flow pass but will be closed when storm surges exceed a certain level. The gates are sliding or rotating steel constructions supported in most cases by concrete structures on pile foundations. Scour protection on either side of the barrier sill is an important part of the structure because of high flow velocities over the sill.

p. Pipelines. Pipelines in the coastal zone are typically used for outlet of treated sewage, transport of oil and gas from offshore fields, and water supply between islands/mainlands and across inlets. Typical types of pipelines are small-diameter flexible PVC pipes used for water supply and small sewage outfalls, large low-pressure sewage outfalls constructed of stiff reinforced concrete pipe elements up to several meters in diameter, and semi-flexible concrete-covered steel pipes used for high-pressure transport of oil and gas. Diffusers at the offshore terminal of sewage outlets are in most cases concrete structures placed on or in the seabed.

Pipelines might be buried or placed on the seabed with or without surface protection, depending on the risk of damage caused by scour and flow-induced instability, or damage by surface loads from collision with ships, anchors, and fishing gear. Where significant changes in the seabed are expected, e.g., surf zones and eroding beaches, it is common to bury the pipelines to depths below the expected maximum eroded profile. In some cases it is prudent to provide scour protection due to uncertainty in predicting the eroded beach profile.

q. Pile structures. The most common pile structures in coastal engineering are bridge piers extending from the shore into the water where they are exposed to loads from waves, currents, and in cold regions, ice loads. The purpose of pile structures might be to provide open coast moorings for vessels, in which case the deck and the piles must carry loads from traffic, cranes, goods, and pipeline installations. Piers are also used for recreational purposes by providing space for fishing, outlook platforms, restaurants, shops, etc. The supporting pile structure might consist of slender wood, steel or reinforced concrete piles driven into the sea-bed, or of large diameter piles or pillars placed directly on the seabed or on pilework, depending on the bearing capacity and settlement characteristics of the seabed. Large diameter piles would commonly be constructed of concrete or be steel pipes filled with mass concrete. Pillars would most commonly be constructed as concrete caissons, concrete blockwork, or backfilled steel sheet piling.

r. Scour protection. The function of scour protection of the seabed is to prevent instability of coastal structures with foundations that rely on stable seabed or beach levels. Both granular material and clay can be eroded by the action of waves and currents. Scour potential is especially enhanced by a combination of waves and currents. In most cases scour protection consists of a rock bed on stone or geotextile filter; however, several specially designed concrete block and mattress systems exist. Scour protection is commonly used at the toe of seawalls and dikes; and in some instances scour protection is needed around piles and pillars, at the toe of vertical-front breakwaters, and at groin heads. Scour protection might also be needed along structures that cause concentration of currents, such as training walls and breakwaters extending from the shoreline. Highly reflective structures like impermeable vertical walls are much more susceptible to near-structure scour than sloping rubble-mound structures.

VI-2-2. Typical Cross Sections and Layouts.

a. Sea dikes. Sea dikes are low-permeability (watertight) structures protecting low-lying areas against flooding. As a consequence fine materials such as sand, silty sand, and clay are used for the construction. The seaside slope is usually very gentle in order to reduce wave runup and wave impact. The risks of slip failures and erosion by piping determine the steepness of the rear slope. The seaward slope is armored against damage from direct wave action. Steeper slopes require stronger armoring. Figure VI-2-1 shows asphalt armoring on slopes of 1:5 and 1:3, while Figure VI-2-2 shows grass armoring on a slope of 1:10. When risk of lowering of the foreshore is present, it is important either to design an embedded toe or a flexible toe that can sink and still protect the slope when the foreshore is eroded as illustrated in Figure VI-2-1.

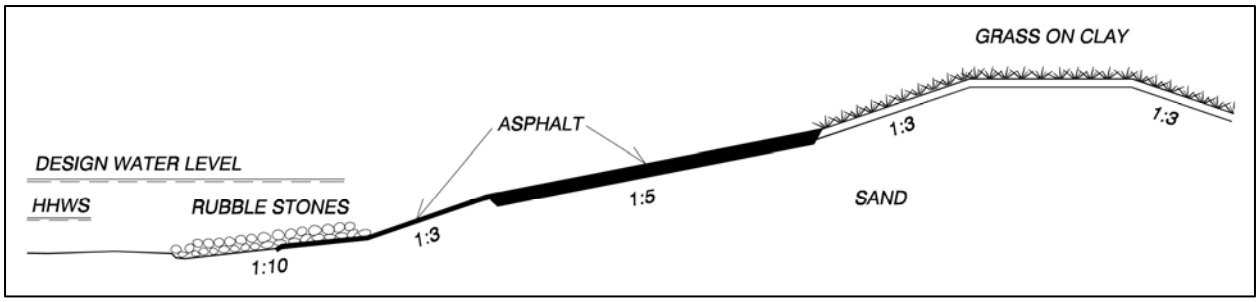

Figure VI-2-1. Example of asphalt-armored sea dike

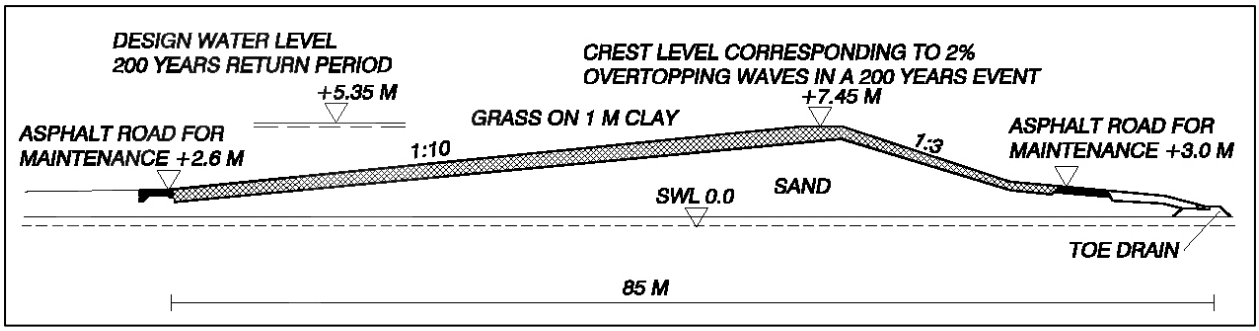

Figure VI-2-2. Example of grass-armored sea dike design from the North Sea coast of Denmark

b. Seawalls and revetments.

(1) Although seawalls and revetments differ by function, they often are similar in construction detail. Seawalls and revetments can be classified as sloping-front and vertical-front structures. Sloping-front structures might be constructed as flexible rubble-mound structures which are able to adjust to some toe and crest erosion. Figure VI-2-3 shows three examples with randomly placed armor. Figure VI-2-4 shows sloping-front structures with pattern-placed concrete armor units. In the United States pattern-placed block slopes are more commonly found on revetments. The stability of the slope is very dependent on an intact toe support. In other words, loss of toe support will likely result in significant armor layer damage, if not complete failure of the armored slope.

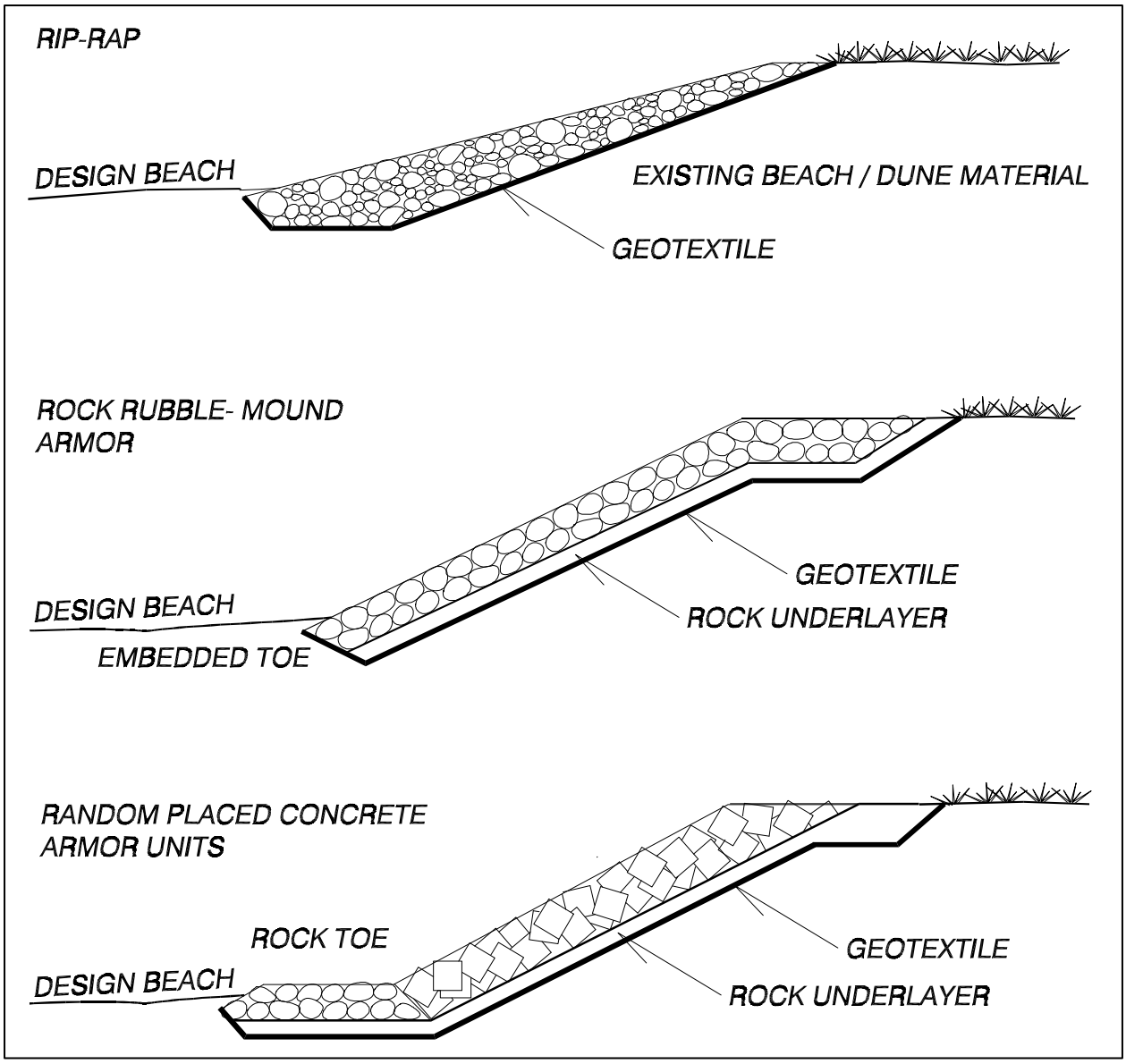

Figure VI-2-3. Examples of sloping front rubble-mound seawall/revetment structures

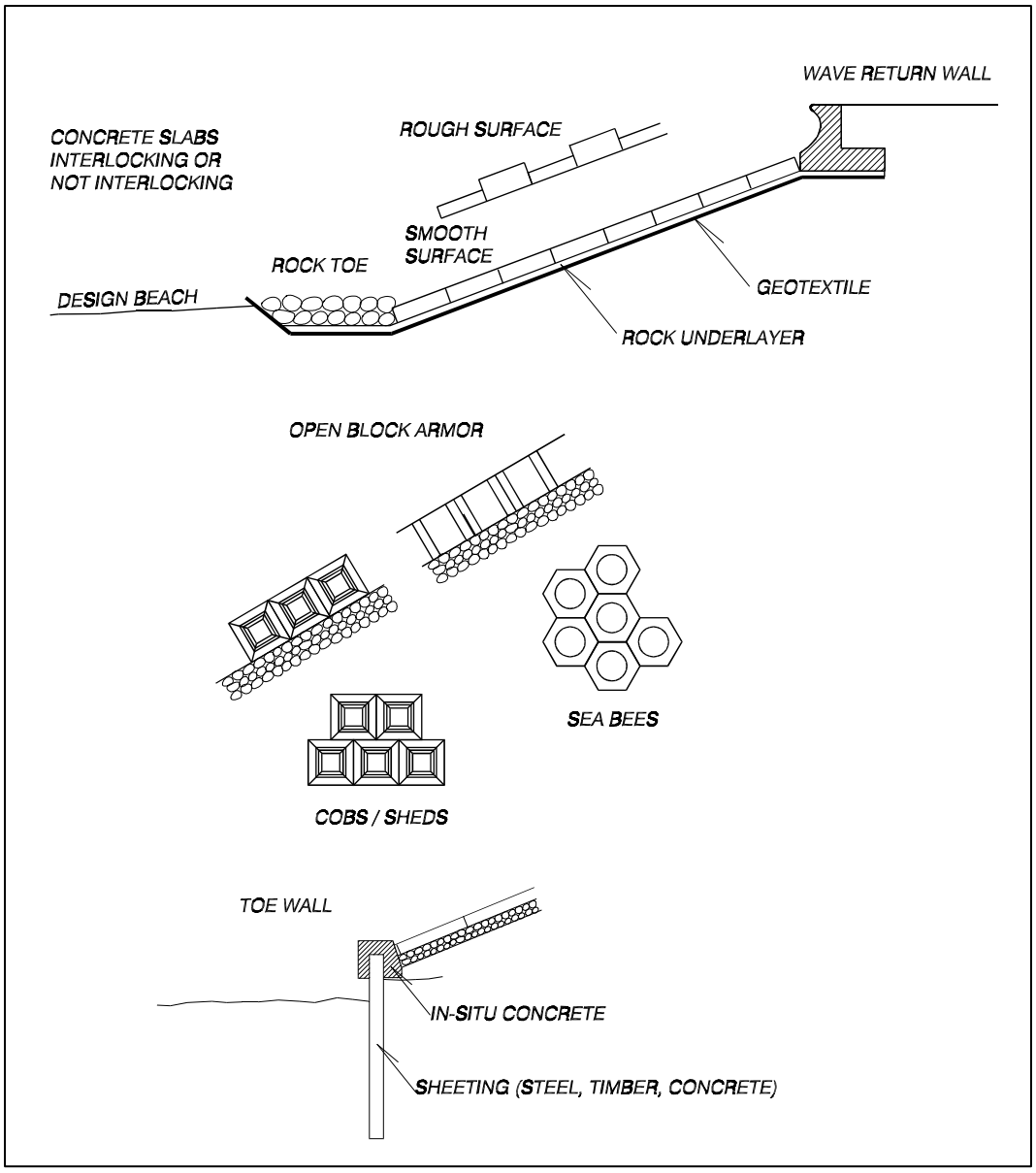

Figure VI-2-4. Examples of sloping-front seawalls/revetments with pattern-placed concrete armor units

(2) The top portion of Figure VI-2-5 shows an example of a sloping front revetment with fixed asphalt layer surface and the bottom portion shows a seawall with a sloping front of in situ cast concrete. Asphalt structures with either rubble toes or thin asphalt carpet toes are flexible structures able to survive rather substantial beach erosion, whereas the rigid concrete structures are vulnerable to any form of undermining. Figure VI-2-6 shows examples of sloping front revetment designs from the Danish North Sea coast. Vertical-front seawalls can be constructed as tied walls using steel, concrete, and timber piling; as stone-filled cribwork; and as massive gravity concrete walls. Figure VI-2-7 is an example of a gravity wall structure.

c. Groins. Groins are in most cases constructed as sloping-front structures or as piled vertical face structures. Figure VI-2-8 shows a typical beach configuration with groins. Figure VI-2-9 shows examples of groin structure designs. Timber groins are used for smaller and less exposed applications, whereas rubble-mound groins are used for all conditions. On very exposed coastlines the armor is often concrete armor units. The timber planking groin is weaker and much more vulnerable to scour failure than the timber pile groin.

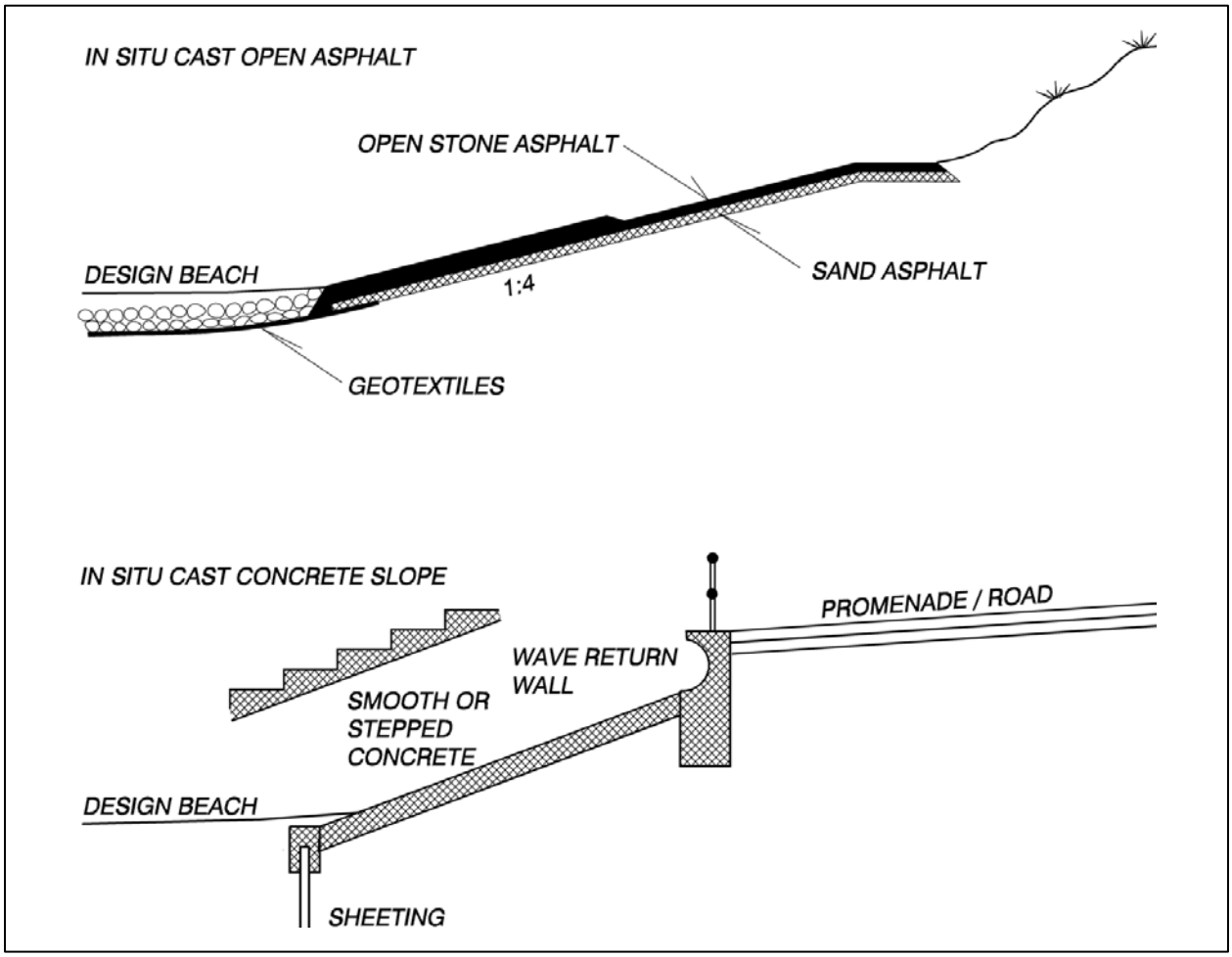

Figure VI-2-5. Examples of sloping front seawalls/revetments with fixed surfaces of asphalt and in situ cast concrete

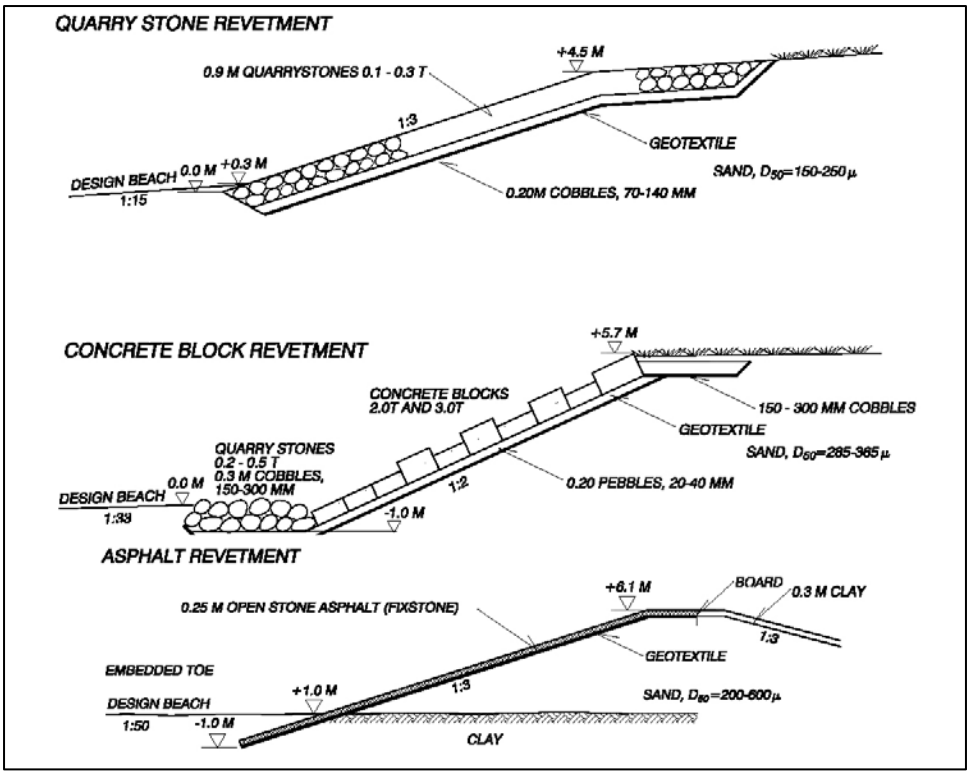

Figure VI-2-6. Examples of sloping front revetment designs from the Danish North Sea coast (Danish Coast Authority)

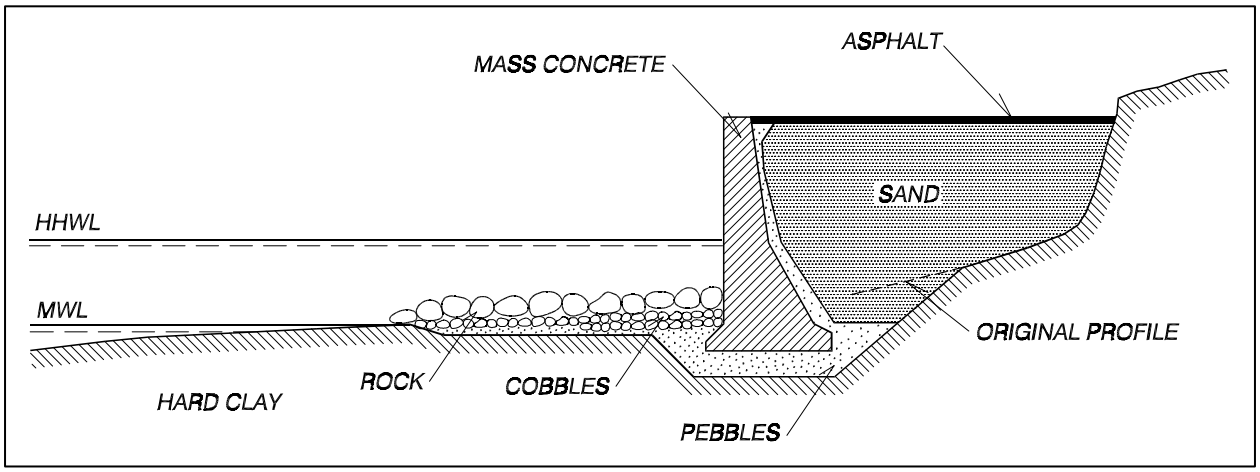

Figure VI-2-7. Example of a vertical front seawall

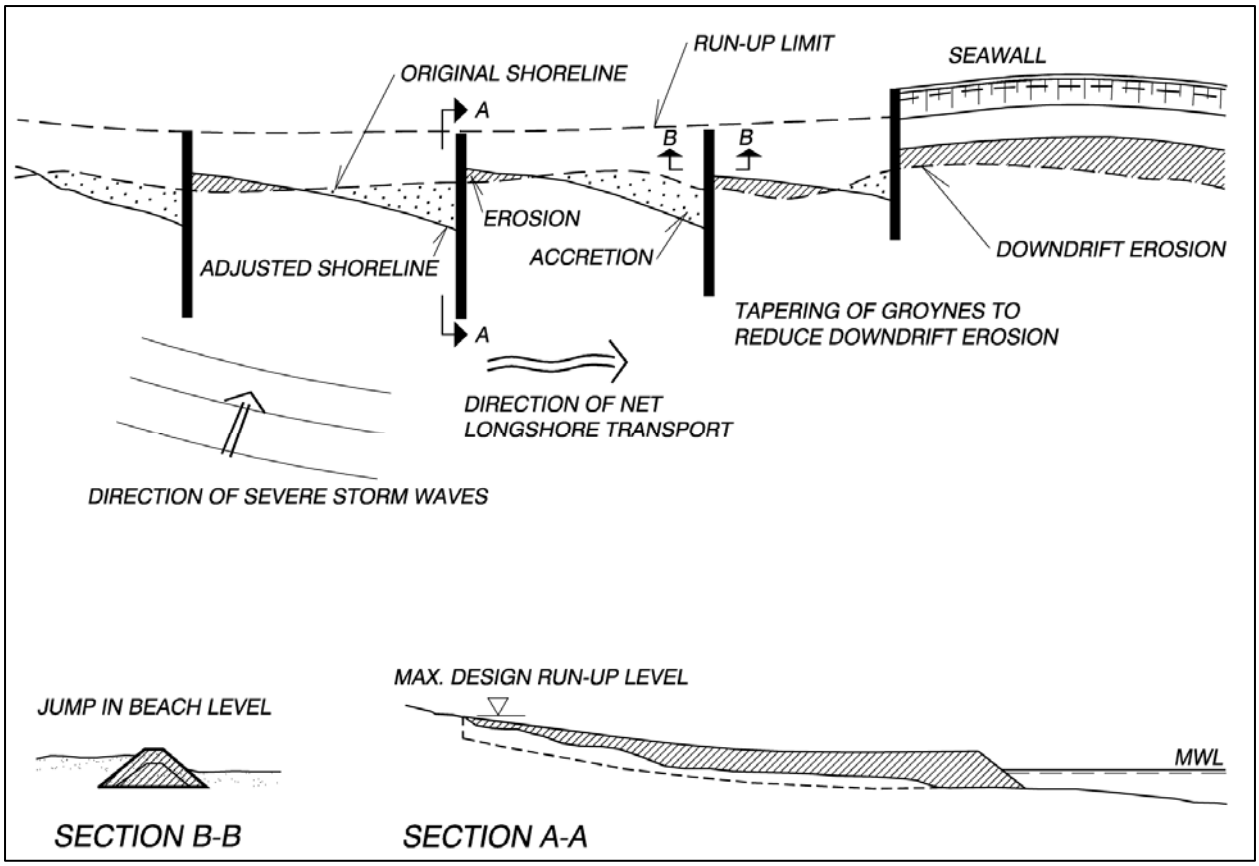

Figure VI-2-8. Typical beach configuration with groins

d. Detached breakwaters. Detached breakwaters are almost always built as rubble-mound structures. Typical cross sections are as shown for the rubble-mound groin in Figure VI-2-9. Typical beach configurations with detached nearshore breakwaters are shown in Figure VI-2-10. Whether or not the detached breakwaters become attached to shore is a function of placement distance offshore. Tombolos are more likely to form when breakwaters are constructed within the surf zone. The two examples of detached breakwaters shown in Figure VI-2-10 serve different functions. See Part V-4 for functional design guidance on detached breakwaters.

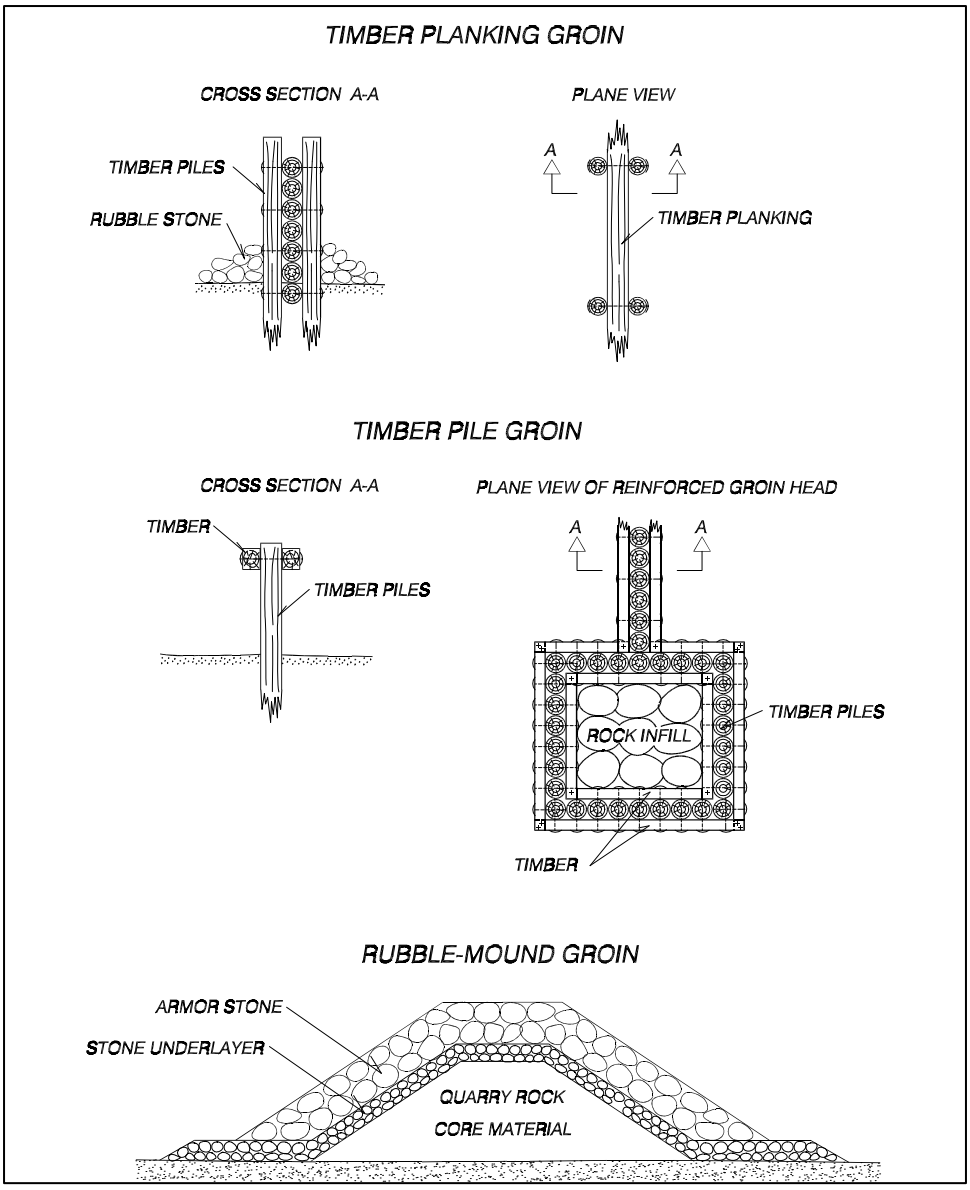

Figure VI-2-9. Examples of groin structures

e. Rubble-mound breakwaters.

(1) Rubble-mound breakwaters are the most commonly applied type of breakwater. In its most simple shape it is a mound of stones. However, a homogeneous structure of stones large enough to resist displacements due to wave forces is very permeable and might cause too much penetration not only of waves, but also of sediments if present in the area. Moreover, large stones are expensive because most quarries yield mainly finer material (quarry run) and only relatively few large stones. As a consequence the conventional rubble-mound structures consist of a core of finer material covered by big blocks forming the so-called armor layer. To prevent finer material being washed out through the armor layer, filter layers must be provided. The filter layer just beneath the armor layer is also called the underlayer. Structures consisting of armor layer, filter layer(s), and core are referred to as multilayer structures. The lower part of the armor

layer is usually supported by a toe berm except in cases of shallow- water structures. Figure VI-2-11 shows a conventional type of rubble-mound breakwater.

(2) Concrete armor units are used as armor blocks in areas with rough wave climates or at sites where a sufficient amount of large quarrystones is not available. Main types of armor units are discussed in Part VI-2-3.

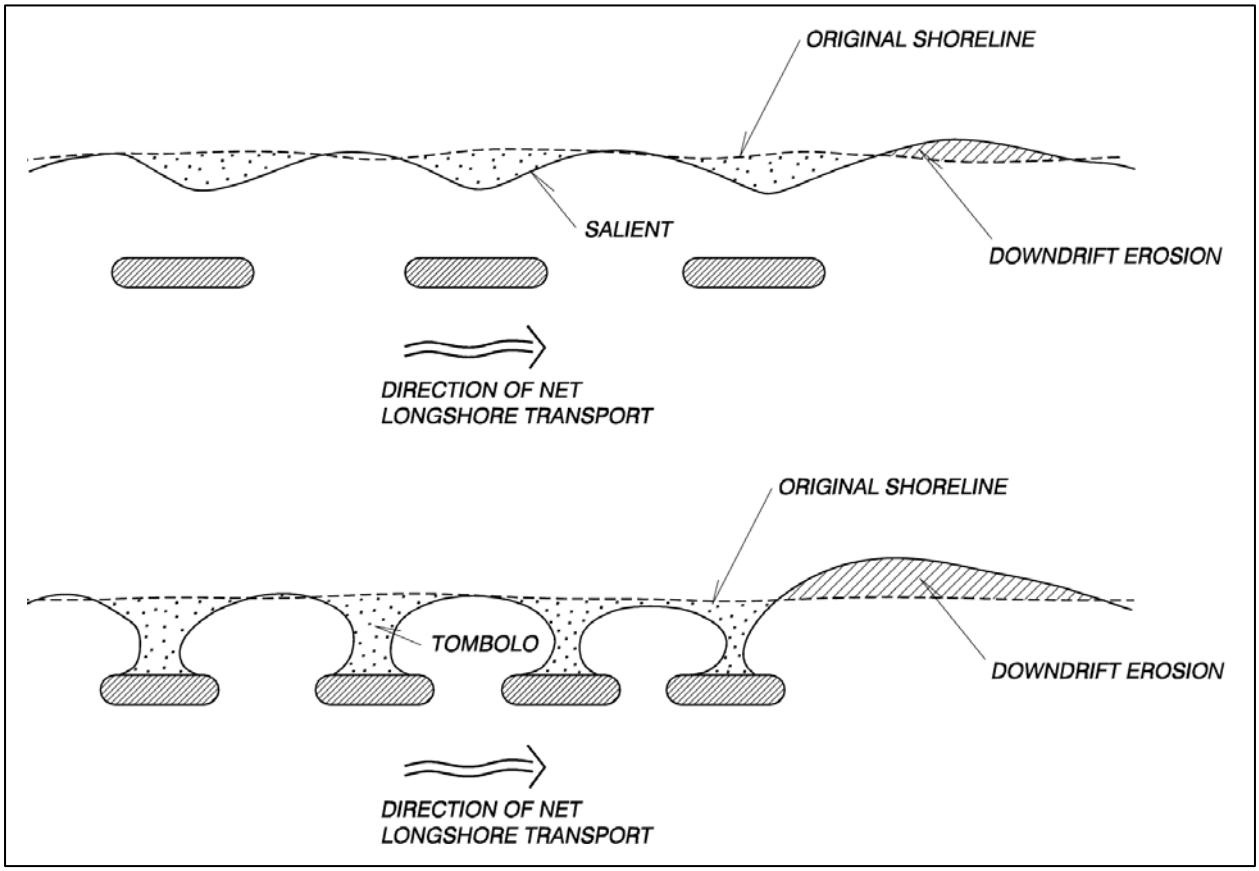

Figure VI-2-10. Typical beach configurations with detached nearshore breakwaters

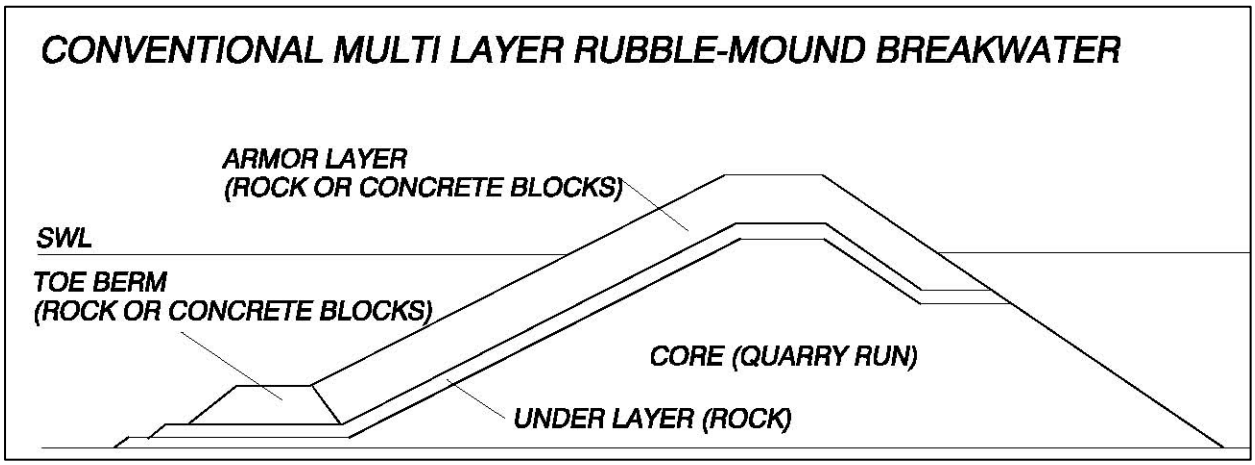

Figure VI-2-11. Conventional multilayer rubble-mound breakwater

(3) The front slope of the armor layer is in most cases straight. However, an S-shaped front or a front with a horizontal berm might be used to increase the armor stability and reduce overtopping. For these types of structures, optimization of the profiles might be difficult if there are large water level variations. Figure VI-2-12 illustrates these types of front profiles.

(4) Overtopping can be reduced by a wave-wall superstructure as shown in Figure VI-2-13.

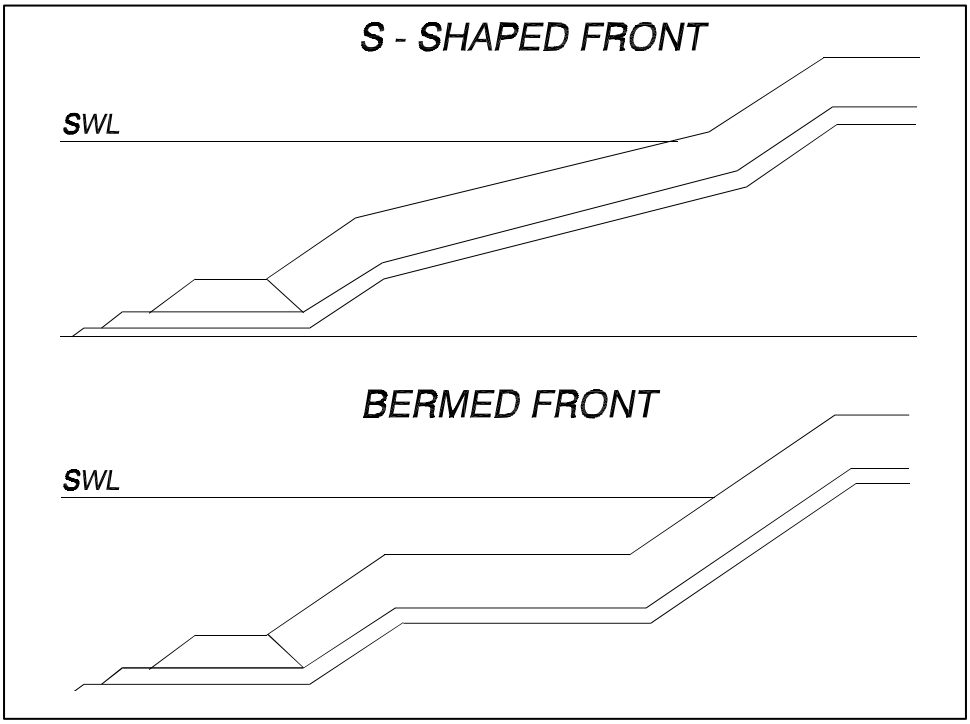

Figure VI-2-12. Rubble-mound structures with S-shaped and bermed fronts

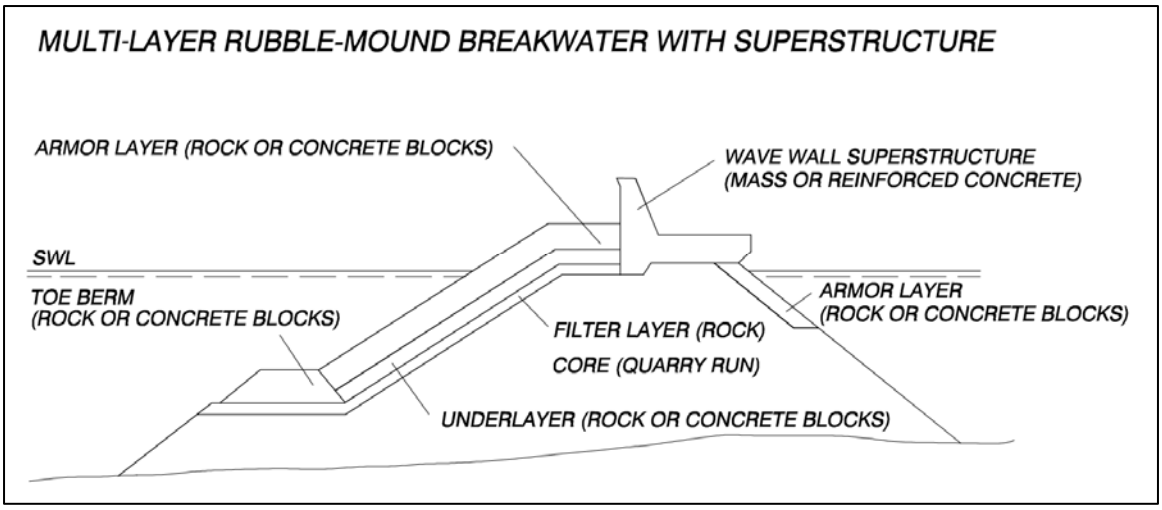

Figure VI-2-13. Example of rubble-mound breakwater with concrete superstructure

(5) Superstructures can serve several purposes, e.g., providing access for vehicles, including cranes for maintenance and repair, and accommodation of installations such as pipelines.

(6) The armor units in conventional multilayer structures are designed to stay in place as built, i.e., the profile remains unchanged with displacement of only a minor part of the armor units.

f. Reshaping rubble-mound breakwaters.

(1) Reshaping rubble-mound breakwaters is based on the principle of natural adjustment of the seaward profile to the actual wave action, as illustrated by Figure VI-2-14. In this way the most efficient profile in terms of armor stability (and possibly minimum overtopping) is obtained for the given size and quantity of armor stone.

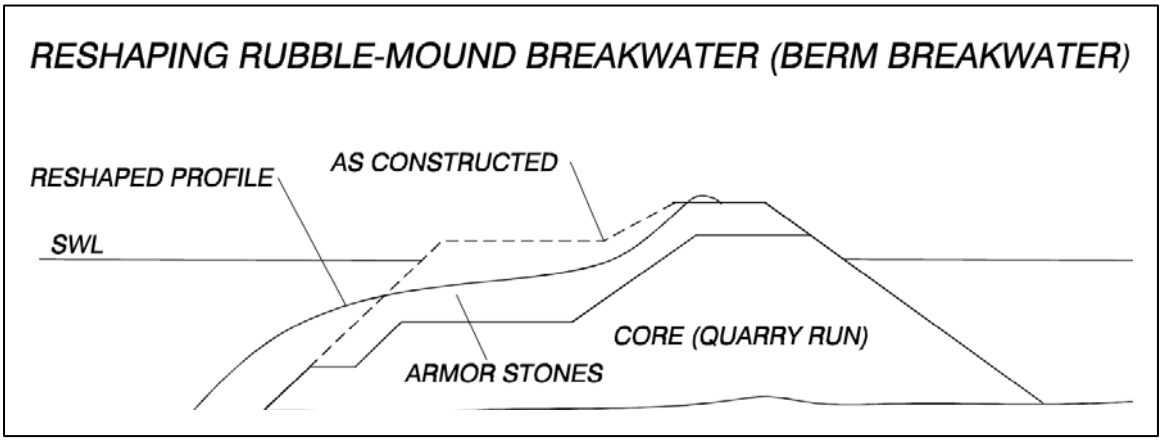

Figure VI-2-14. Reshaping rubble-mound breakwater

(2) Because of natural reshaping, the structure can be built in a very simple way by first dumping the core material consisting of quarry run, and then dumping the armor stones in a berm profile with seaward slope equal to the natural angle of repose for the stone material. Due to the initial berm profile, this type of structure is also known as a berm breakwater.

(3) The natural adjusted S-profile allows smaller armor stones to be used compared to the armor stones in conventional rubble structures. The smaller the armor stones, the flatter the S-profile will be. The minimum size of the armor stones is often selected to limit transport of stones along the structure under oblique wave attack.

g. Reef breakwaters. Reef breakwaters are in principle designed as a rubble-mound structure with submerged crests, as shown in Figure VI-2-15. Both homogeneous and multilayer structures are used. This example shows a mound of smaller stones protected by an armor layer of larger stones.

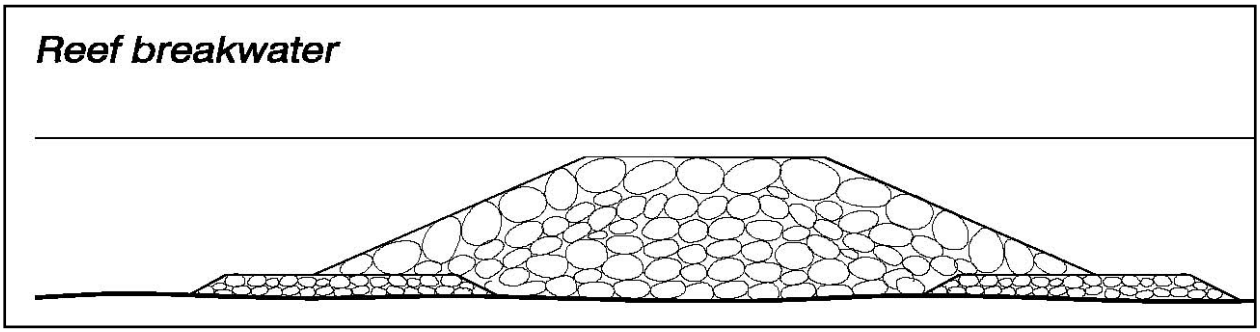

Figure VI-2-15. Example of a reef breakwater

h. Vertical-front breakwaters. Vertical-front breakwaters are another major class of breakwater structures. The basic structure element is usually a sandfilled caisson made of reinforced concrete, but blockwork types made of stacked precast concrete blocks are also used. Caisson breakwaters might be divided into the following types:

(1) Conventional, i.e., the caisson is placed on a relatively thin stone bedding layer (Figure VI-2-16).

(2) Vertical composite, i.e., the caisson is placed on a high rubble-mound foundation (Figure VI-2-17). This type is economical in deep waters. Concrete caps may be placed on shore-connected caissons.

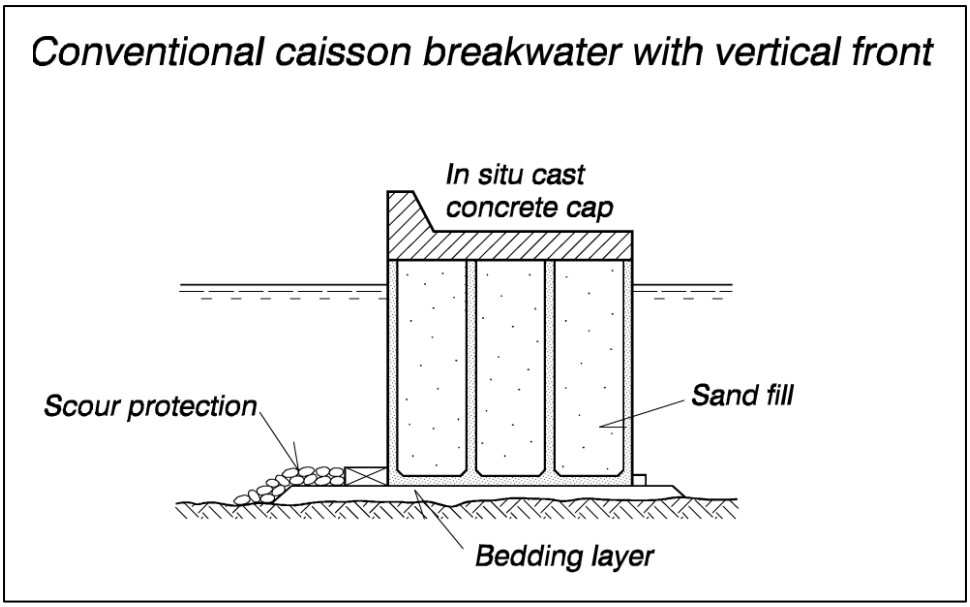

Figure VI-2-16. Conventional caisson breakwater with vertical front

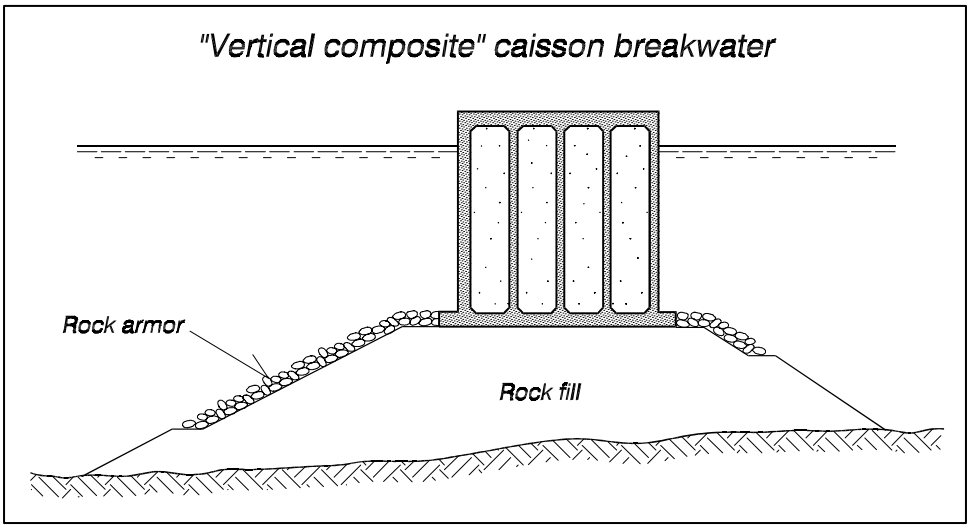

Figure VI-2-17. Vertical composite caisson breakwater

(3) Horizontal composite, i.e., the front of the caisson is covered by armor units or a rubble-mound structure (multilayered or homogeneous) (Figure VI-2-18). This type is typically used in shallow water; however, there have been applications in deeper water where impulsive wave pressures are likely to occur. The effects of the mound are reduction of wave reflection, wave impact, and wave overtopping. Depending on bottom conditions, a filter layer may be needed beneath the rubble-mound portion.

(4) Sloping top, i.e., the upper part of the front wall above still-water level is given a slope with the effect of a reduction of the wave forces and a much more favorable direction of the wave forces on the sloping front (Figure VI-2-19). However, overtopping is larger than for a vertical wall of equal crest level.

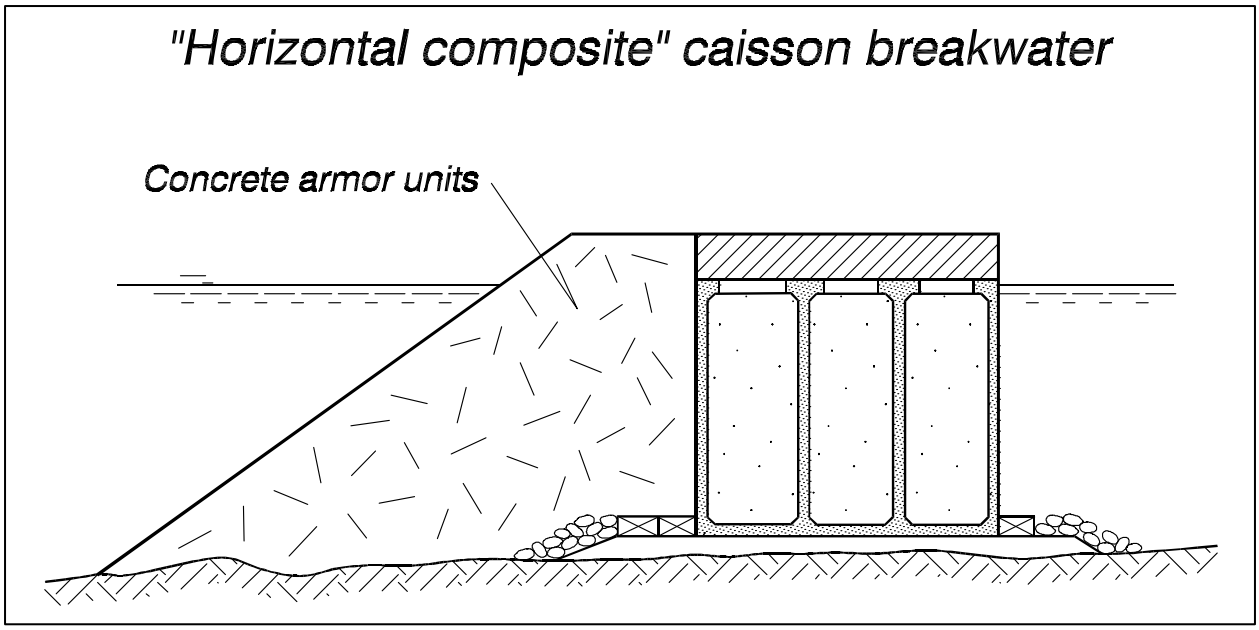

Figure VI-2-18. Horizontal composite caisson breakwater

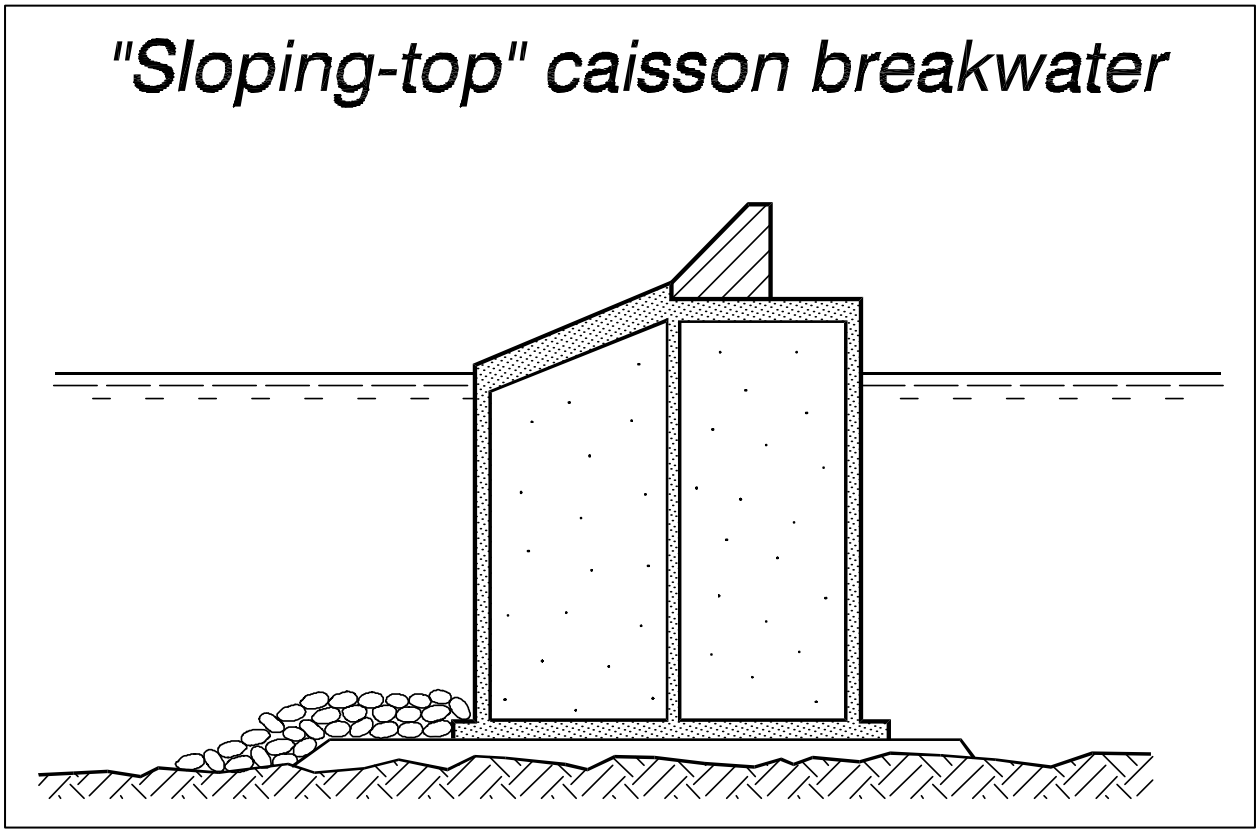

Figure VI-2-19. Sloping-top caisson breakwater

(5) Perforated front wall, i.e., the front wall is perforated by holes or slots with a wave chamber behind (Figure VI-2-20). Dissipation of energy reduces both wave forces on the caisson and wave reflection. Caisson breakwaters are generally less economical than rubble-mound structures in shallow water. Moreover, they demand stronger seabed soils than rubble structures. In particular, the blockwork type needs to be placed on rock seabeds or on very strong soils due to very high foundation loads and sensitivity to differential settlements (Figure VI-2-21).

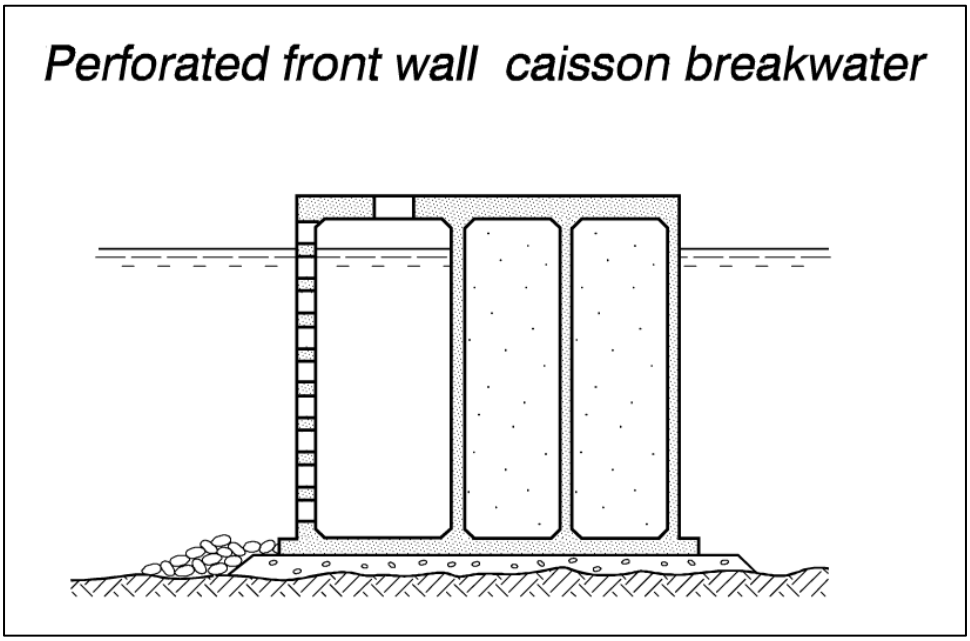

Figure VI-2-20. Perforated front wall caisson breakwater

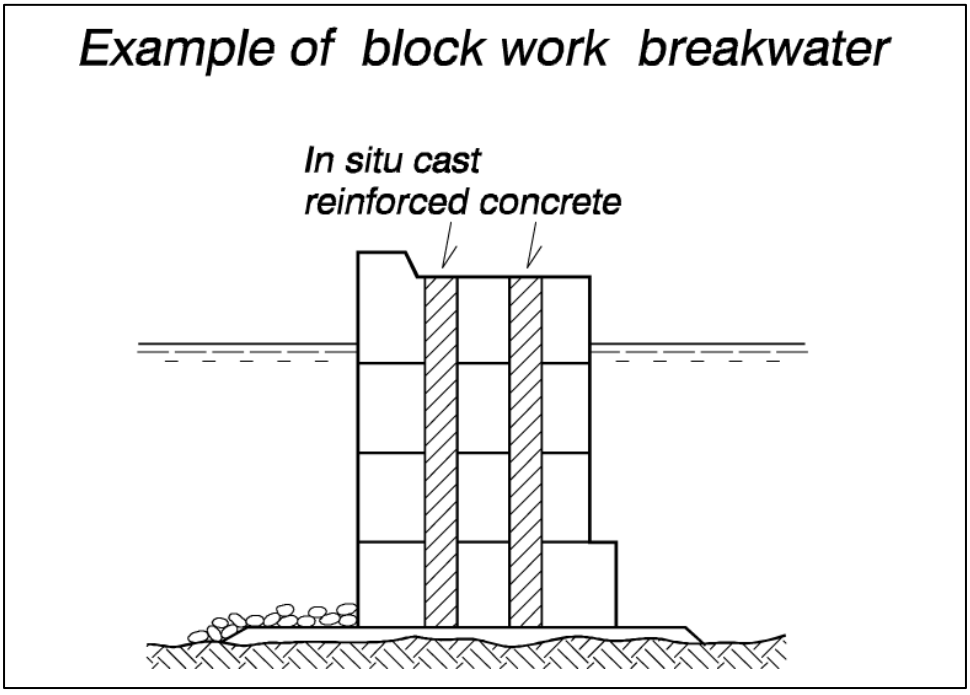

Figure VI-2-21. Example of blockwork breakwater

i. Piled breakwaters. Piled breakwaters consist of an inclined or vertical curtain wall mounted on pile work (Figure VI-2-22). This type of breakwater is applicable in less severe wave climates on sites with weak and soft subsoils.

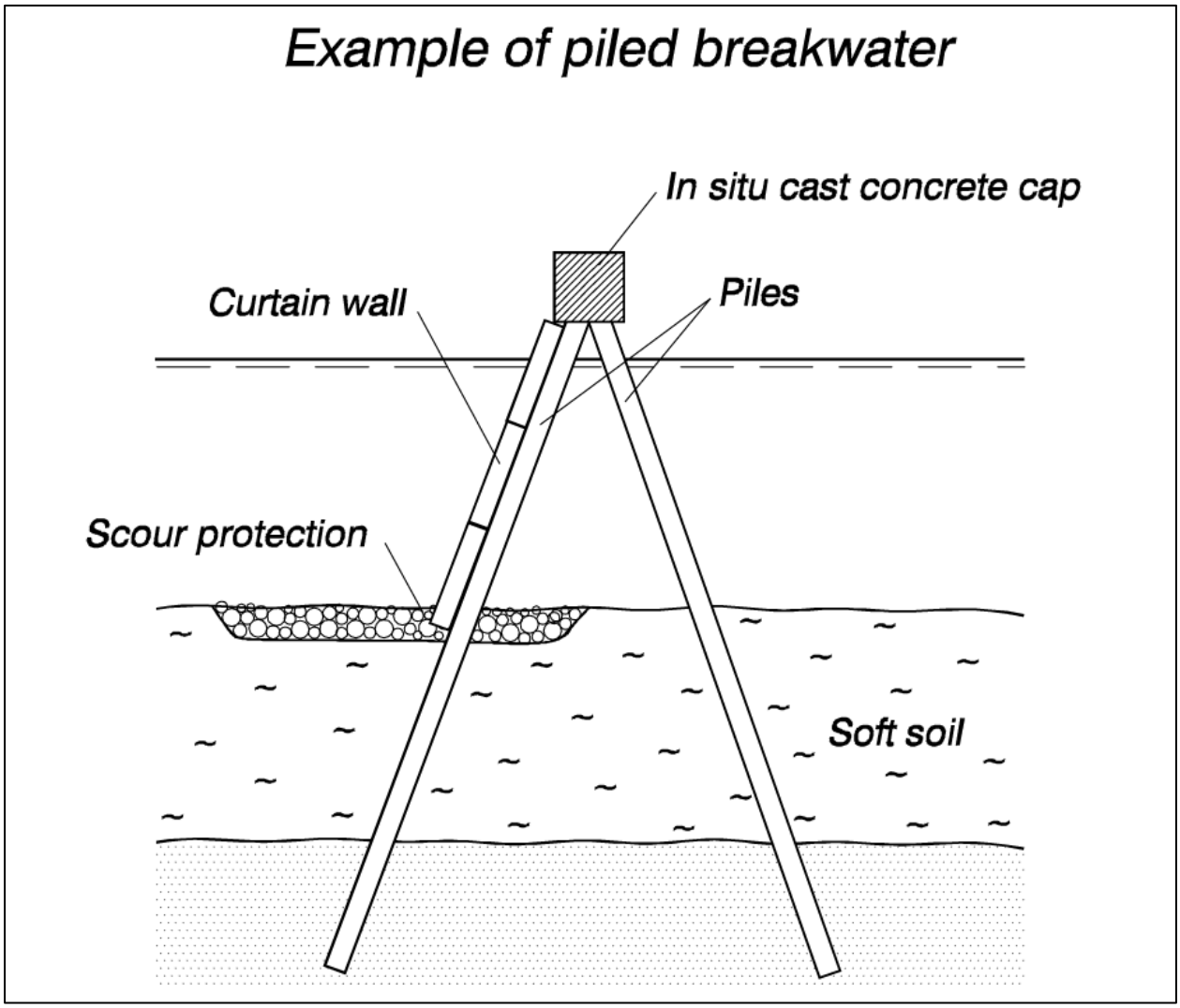

Figure VI-2-22. Example of piled breakwater

j. Jetties. Jetties are in most cases designed as rubble-mound structures (breakwaters and groins) except that the outer part must be armored on both sides.

k. Storm surge barriers. Storm surge barriers are generally designed as movable segmented gates made of steel. The segments might span between caisson structures, either hinged to be the caisson sidewalls or hanging in a hoist arrangement. A solution with no visible structures was proposed for the protection of the Venice Lagoon where the segments are hinged to a concrete foundation placed in the seabed as sketched in Figure VI-2-23. This structure had not been built as of this writing.

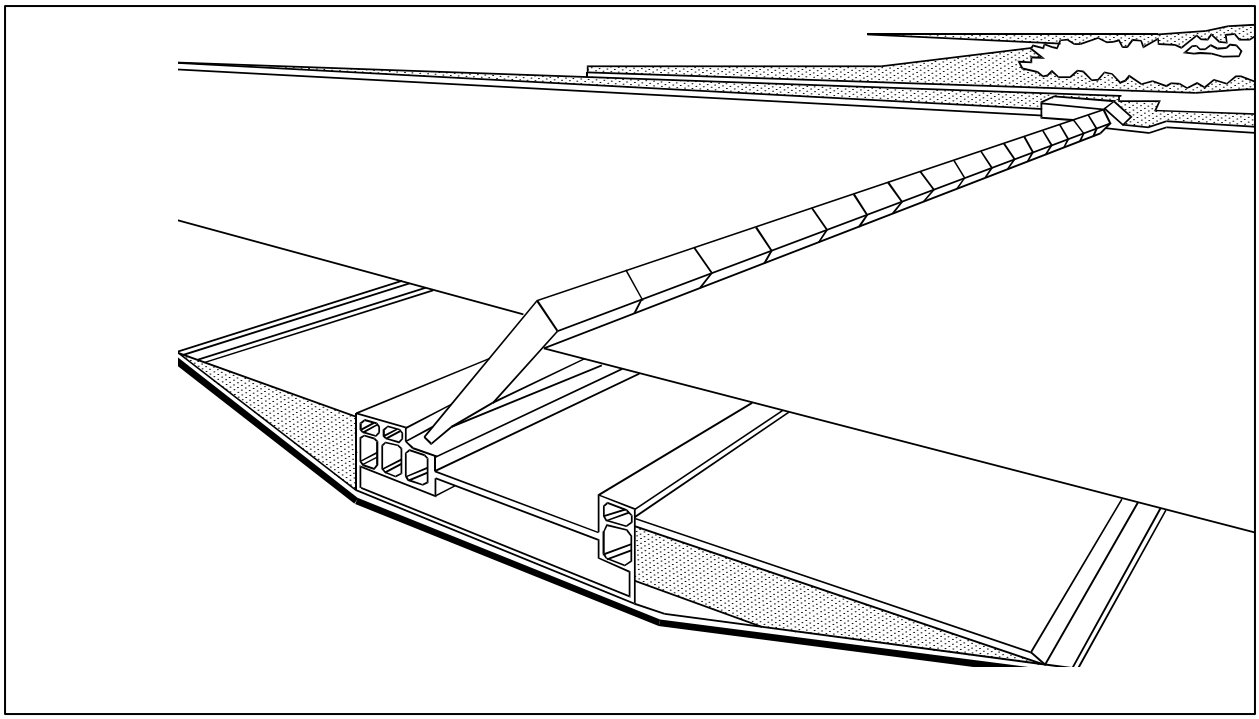

Figure VI-2-23. Storm surge barrier proposed for the Venice Lagoon

VI-2-3. Main Types of Concrete Armor Units.

a. Figure VI-2-24 shows examples of the many existing types of concrete armor units.

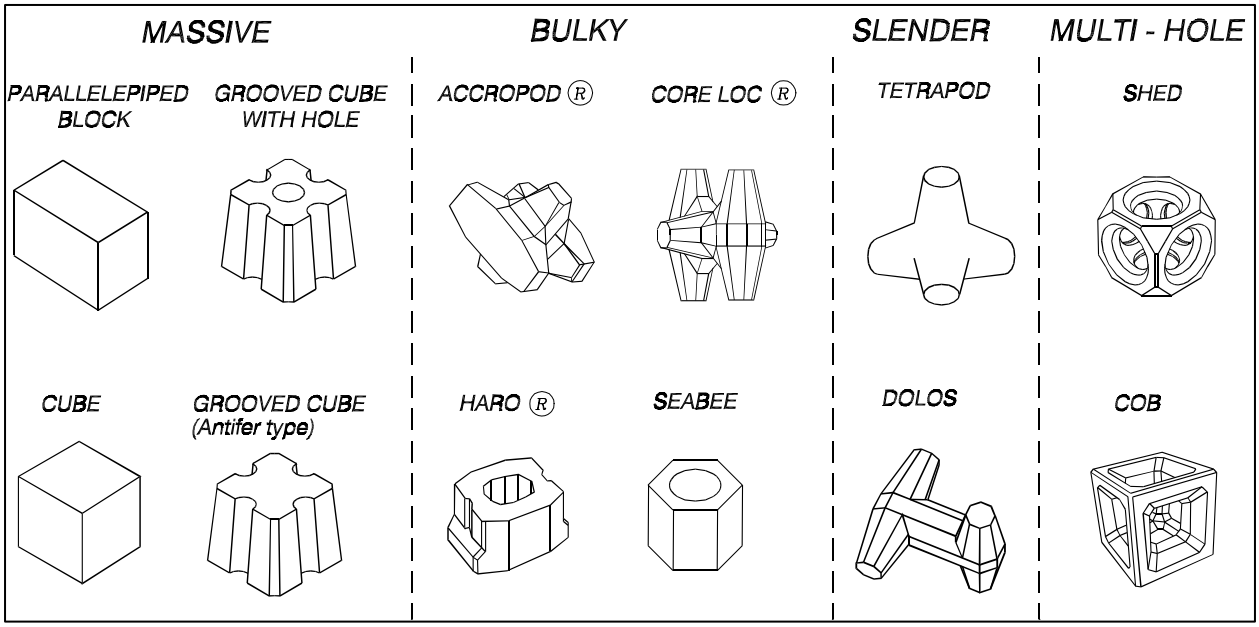

Figure VI-2-24. Examples of concrete armor units

The units can be divided into the following categories related to the structural strength:

(1) Massive or blocky (e.g., cubes incl. grooved types, parallelepiped block)

(2) Bulky (e.g., Accropode7, Core Loc7, Haro7, Seabee)

(3) Slender (e.g., Tetrapod, Dolos)

(4) Multi-hole cubes (e.g., Shed, Cob)

b. The hydraulic efficiency might be expressed in terms of the resistance against movements per volume of concrete required to armor a unit area of the slope. The hydraulic efficiency increases from massive units to slender units to multi-hole cubes. Because the porosity of randomly placed armor also increases in the same way (Price 1979), there appears to be an explainable correlation between hydraulic stability and porosity (Burcharth and Thompson 1983).

c. Concrete armor units are almost always placed randomly on the slope in a layer that has a thickness of two armor units. Exceptions are Accropodes[7] and Core Locs[7], which are placed in a layer having thickness of one armor unit, and multi-hole cubes which are placed orderly in a regular pattern where each unit rests against adjacent units.

d. Generally, concrete armor units are made of conventional unreinforced concrete except for some of the multi-hole cubes where fiber reinforcement is used. For slender units, such as Dolos with small waist ratios, various types of high-strength concrete and reinforcement (conventional bars, prestressing, fibers, scrap iron, steel profiles) have been considered. But these solutions are generally less cost-effective, and they are seldom used.

e. The hydraulic stability of armor layers is decreased if the armor units disintegrate because this reduces the stabilizing gravitational force acting on the unit, and possibly decreases interlocking effects. Moreover, broken armor unit pieces can be thrown around by wave action and thereby trigger accelerated breakage. In order to prevent breakage it is necessary to ensure the structural integrity of the armor units.

f. Unreinforced concrete is a brittle material with a low *tensile strength* S_T (on the order of 2-5 MPa) and a *compressive strength* S_C that is one order of magnitude larger than S_T. Consequently, crack formation and breakage are nearly always caused by load-induced *tensile stresses* σ_T exceeding S_T. Therefore, the magnitude of S_T is more critical to concrete armor unit design than S_C, and this fact should be reflected in specifications for armor unit concretes. It is important to note that S_T decreases with repeated load due to *fatigue* effects (Burcharth 1984). The different categories of concrete armor units are not equally sensitive to breakage.

g. *Slender units* are the most vulnerable to cracking and breaking because the limited cross-sectional areas give rise to relatively large tensile stresses. Many failures of breakwaters armored with Tetrapods and Dolosse were caused by breakage of the units before the hydraulic stability of the unbroken units was exceeded. Much of the damage could have been avoided if design diagrams for concrete armor unit structural integrity had been available during design.

h. These failures caused a decline in the use of slender armor units and a return to the use of massive blocks, especially the Antifer Cube types. This also led to the development of bulky units like the Haro[7], the Accropode[7], and the Core Loc[7]. The tendency toward massive blocks will not change until reliable design strength diagrams exist for the slender units. Presently, structural integrity diagrams are available only for Dolos (Burcharth 1993, Melby 1993) and Tetrapod armor (Burcharth et al. 1995).

i. *Massive units* generally will have the smallest tensile stresses due to the large cross-sectional areas. However, breakage can take place if the units experience impacts due to application of less restrictive hydraulic stability criteria and if the concrete quality is poor in terms of a low tensile strength. Cracking can also occur in larger units where temperature differences during the hardening process can create tensile stresses that exceed the strength of the weak young concrete, resulting in microcracking of the material, also known as *thermal stress cracking* (Burcharth 1983). If massive units are made of good quality concrete, units are not damaged during handling, and if the units are designed for marginal displacements, there will be no breakage problems. With the same precautions the *bulky units* are also not expected to have breakage problems. No structural integrity design diagrams exist for the massive concrete armor units.

j. *Multi-hole cubes* will experience very small solid impact loads provided they are placed correctly in patterns that exclude significant relative movements of the blocks. Due to the slender structural members with rather tiny cross sections, the limiting factors (excluding impacts) for long-term durability are material deterioration, abrasion on sandy coasts, and fatigue due to wave loads.

VI-2-4. Failure Modes of Typical Structure Types.

a. Failure.

(1) For many people, the word “failure” implies a total or partial collapse of a structure, but this definition is limited and not accurate when discussing design and performance of coastal structures. In the context of design reliability, it is preferable to define failure as:

> FAILURE: Damage that results in structure performance and functionality below the minimum anticipated by design.

Thus, partial collapse of a structure may be classified as “damage” provided the structure still serves its original purpose at or above the minimum expected level. For example, subsidence of a breakwater protecting a harbor would be considered a failure if it resulted in wave heights within the harbor that exceed operational criteria. Conversely, partial collapse of a rubble-mound jetty head might be classified as damage if resulting impacts to navigation and dredging requirements are minimal or within acceptable limits.

(2) Coastal project elements fail for one or more of the following reasons:

(a) Design failure occurs when either the structure as a whole, including its foundation, or individual structure components cannot withstand load conditions within the design criteria. Design failure also occurs when the structure does not perform as anticipated.

(b) Load exceedance failure occurs because anticipated design load conditions were exceeded.

(c) Construction failure arises due to incorrect or bad construction or construction materials.

(d) Deterioration failure is the result of structure deterioration and lack of project maintenance.

(3) New or innovative coastal project design concepts are more susceptible to design failure due to lack of previous experience with similar designs. In these situations, allowances should be made for unknown design effects, and critical project elements should be extensively tested using laboratory and/or numerical model techniques before finalizing the design.

(4) Practically all projects accept some level of failure probability associated with exceedance of design load conditions, but failure probability increases at project sites where little prototype data exist on which to base the design. These cases may require a conservative factor of safety (for information on probabilistic design see Part V-1-3, “Risk Analysis and Project Optimization,” and Part VI-6, “Reliability in Design”).

(5) In the design process all possible failure modes must be identified and evaluated in order to obtain a balanced design. An overview of the most important and common failure modes for the main types of fixed coastal structures is given in this chapter. Some failure modes are common to several types of structures. Examples include displacement of armor stones and toe erosion which are relevant to most rubble structures such as seawalls, groins, and breakwaters. It should be noted that in this chapter the common failure modes are shown only for one of the relevant structures. The most comprehensive sets of failure modes are related to breakwaters, and for this reason they are discussed first.

b. Sloping-front structures.

(1) Breakwaters. Figure VI-2-25 provides an overview of the failure modes relevant to rubble-mound breakwaters. The individual failure modes are explained in more detail in Figures VI-2-26 to VI-2-42.

(2) Seawalls/revetments. Typical failure modes for seawalls and revetments are shown in Figures VI-2-43 to VI-2-46.

(3) Dikes. Figures VI-2-47 through VI-2-51 illustrate dike failure modes.

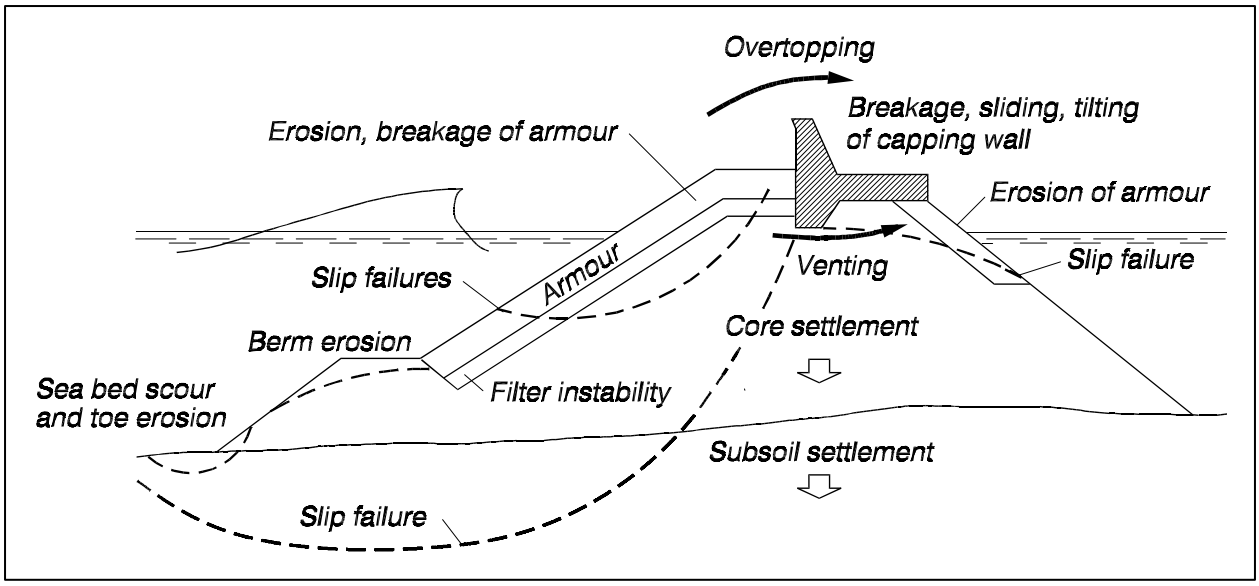

Figure VI-2-25. Overview of rubble-mound breakwater failure modes

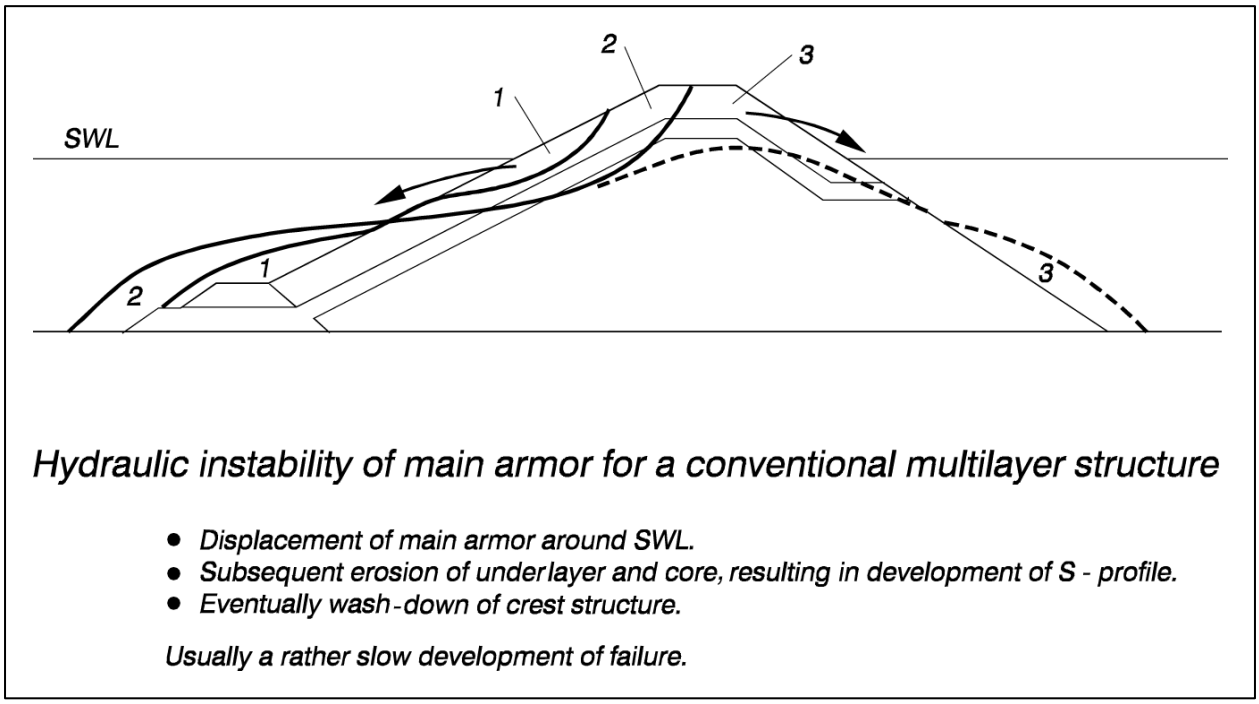

Figure VI-2-26. Main armor layer instability

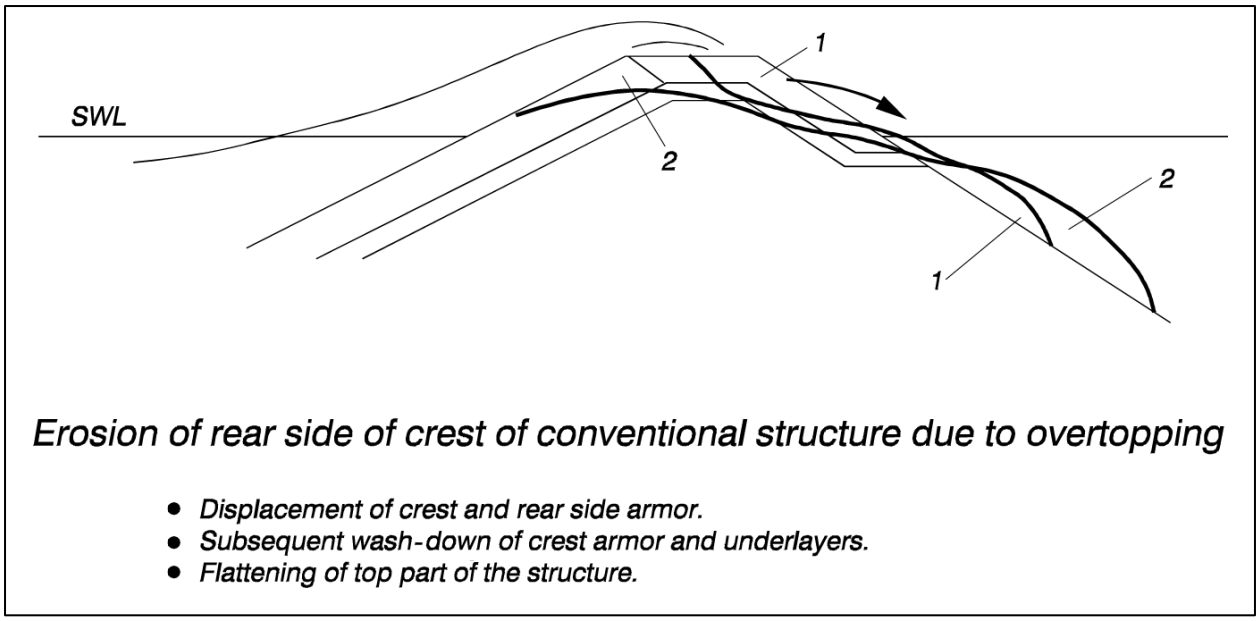

Figure VI-2-27. Rear side erosion of crest

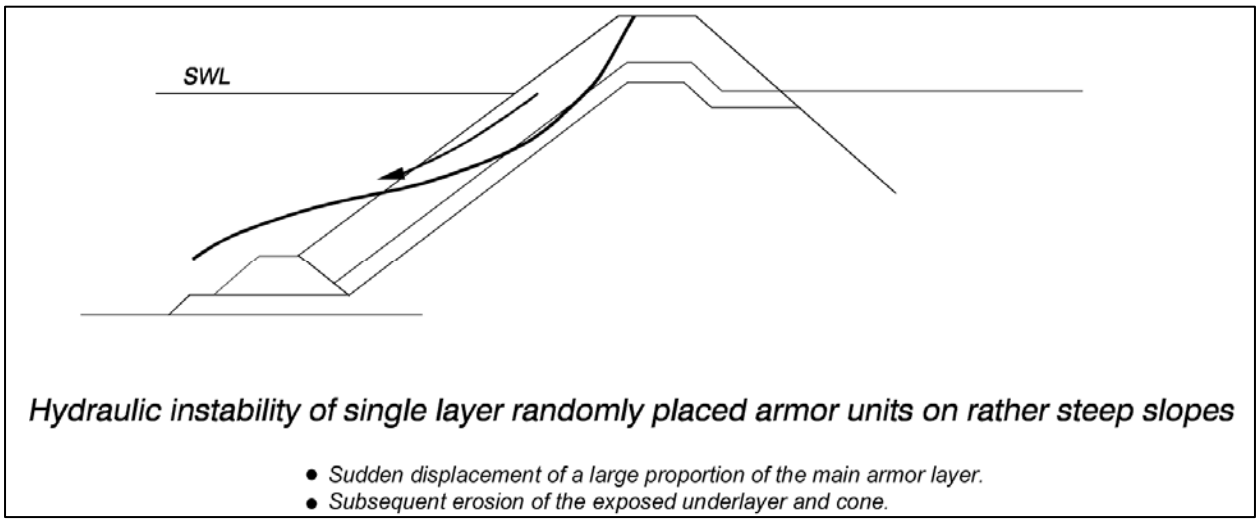

Figure VI-2-28. Hydraulic instability on steep slopes

Breakage of armor units

- *The armor units break when the stresses caused by gravity and wave-induced forces exceed the strength of the concrete.*
- *Breakage of complex types of armor units causes collapse of the armor layer if a substantial proportion of the units (say more than 15%) break.*

Figure VI-2-29. Armor unit breakage

Deterioration of rock and concrete armor blocks

- *Weathering caused by chemical reactions, temperature variations (including freeze - thaw) and abrasion results in loss of strength and mass.*
- *Subsequently there is a higher risk of breakage and in reduced hydraulic stability.*

Figure VI-2-30. Armor unit deterioration

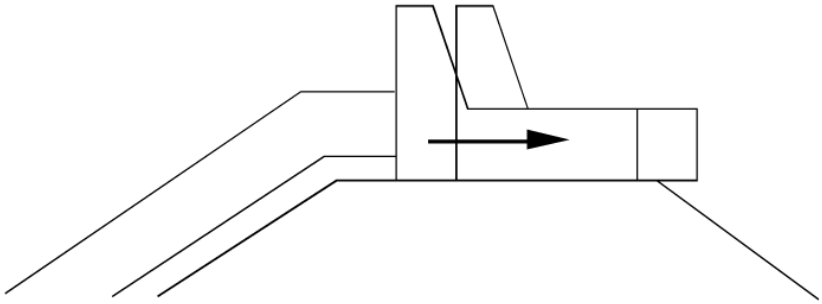

Sliding of wave wall superstructure

The superstructure slides backwards when the horizontal wave force exceeds the friction forces underneath the base plate.

Large displacements lead to tilting and wash-down of the superstructure.

Figure VI-2-31. Sliding of superstructure

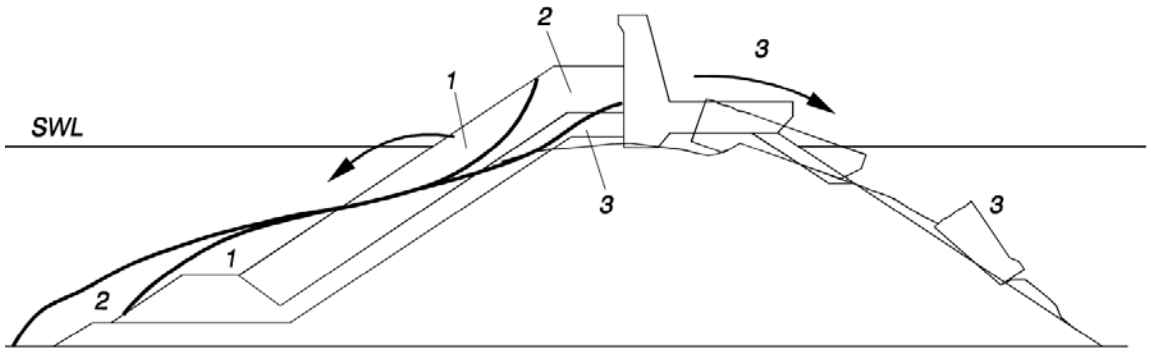

Hydraulic instability and/or breakage of complex types of armor units leading to failure of wave wall superstructure

- *Displacement of intact or broken units.*
- *Subsequent exposure of the wave wall to large wave impacts and uplift pressures.*
- *Eventual breakage and wash-down of superstructure.*

The failure can proceed rather fast if the armor unit breakage is extensive.

Figure VI-2-32. Failure due to armor unit breakage

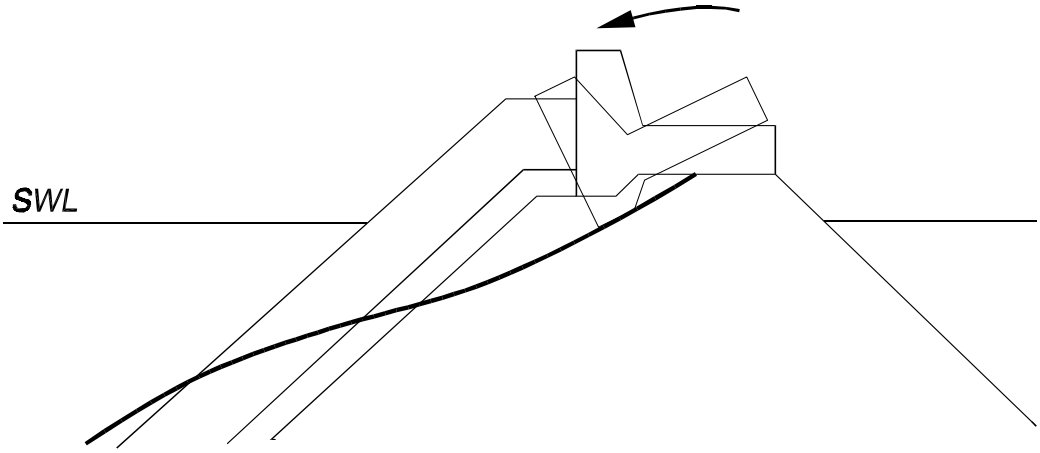

Forward tilt of superstructure due to undermining

- *Displacement of main armor and erosion of filter layers and core material in front of a superstructure might lead to a forward tilt of the superstructure.*

Figure VI-2-33. Forward tilting of superstructure

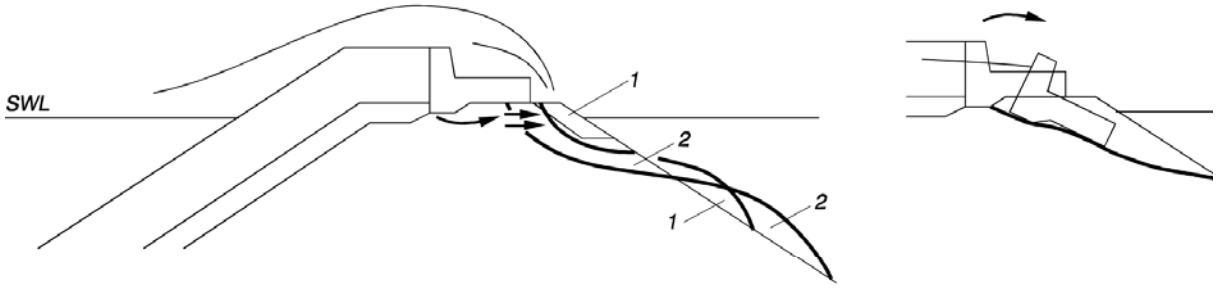

Erosion of rear side armor due to overtopping of a structure with capping

- *Displacement of rear-side armor.*
- *Subsequent pushout of bedding material under superstructure due to increased venting.*
- *Possible slip failure in bedding material, causing displacement of superstructure.*

Figure VI-2-34. Rear-side erosion due to overtopping

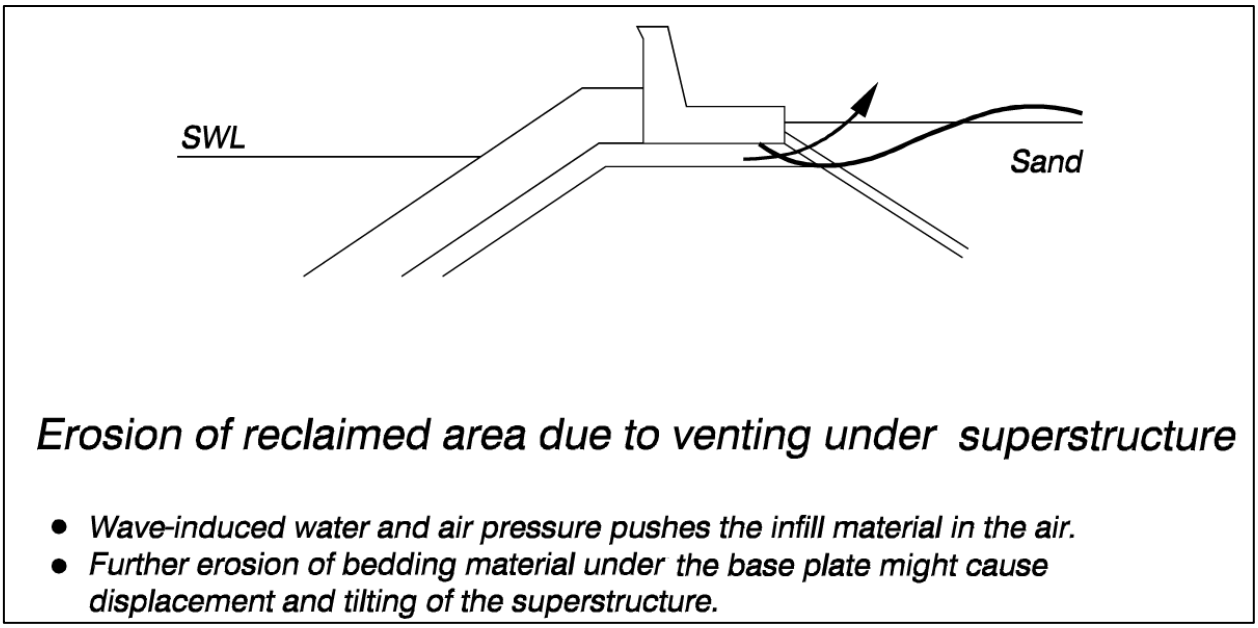

Figure VI-2-35. Erosion due to venting

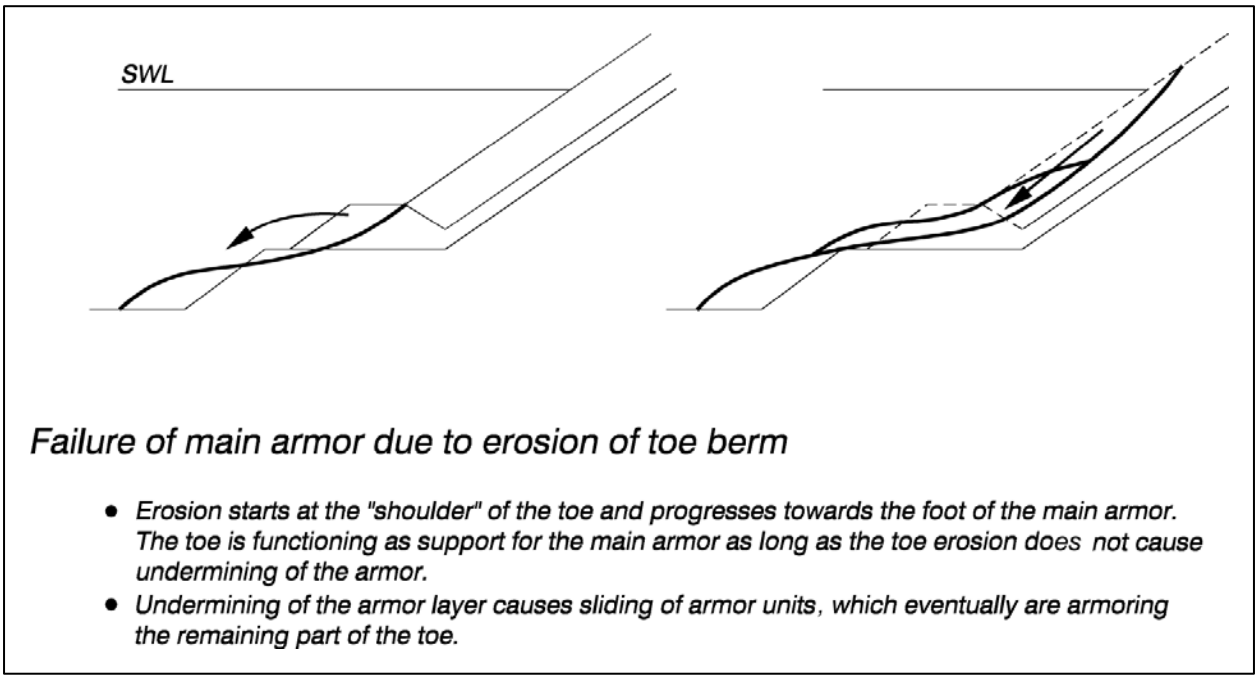

Figure VI-2-36. Failure due to toe berm erosion

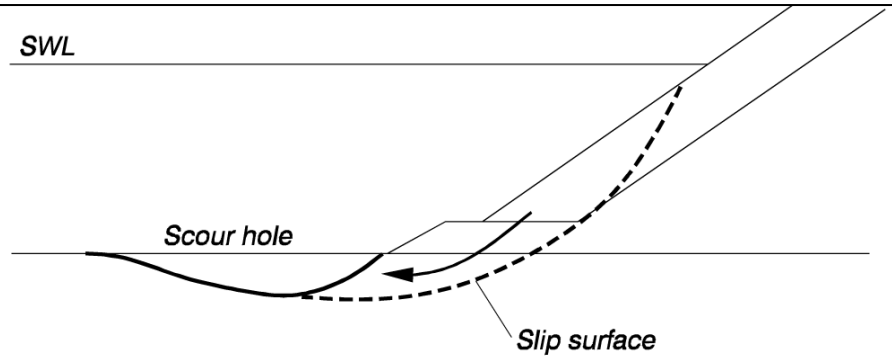

Sliding of main armor due to seabed scour

- *Formation of scour hole close to the foot of the structure due to wave and current action. The toe is functioning as support for the main armor as long as the toe erosion does not cause undermining of the armor.*
- *Reduced stabilizing forces causes slip failure, which results in sliding of armor.*

Figure VI-2-37. Scour-induced armor displacement

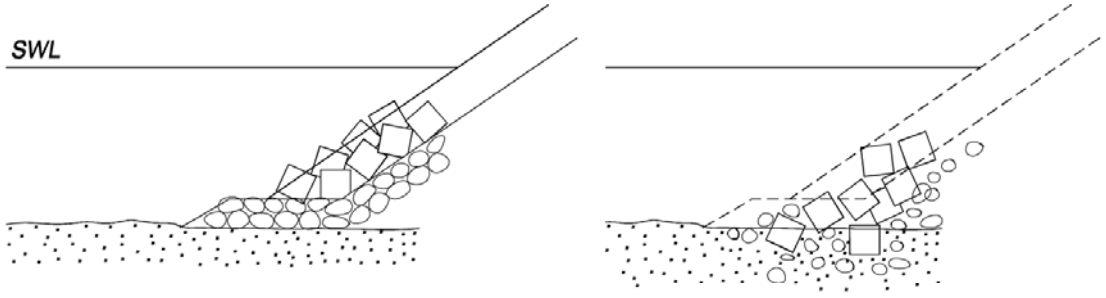

Subsidence of blocks into fine material seabeds due to wave-induced liquefaction

- *Wave-induced pore pressure built - up in sandy seabeds reduces the bearing capacity of the seabed material.*
- *Underlayer stones and armor units sink into the seabed, eventually causing an armoring which stops further subsidence.*

Figure VI-2-38. Block subsidence due to liquefaction

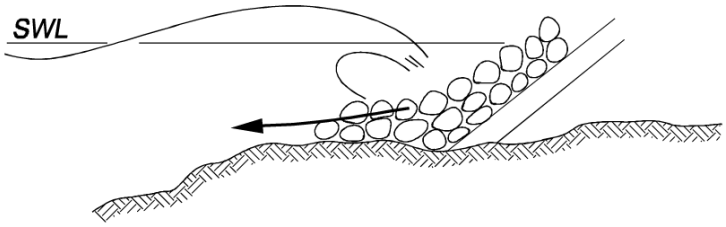

Instability of toe and foot of armor in shallow water when placed on hard seabeds and exposed to wave breaking

- *The forces from breaking waves cause displacement of the blocks unless they are several times heavier than conventional toe blocks and heavier than the main armor blocks. On smooth rock surfaces it is necessary to bolt or anchor the toe block if a trench is not made.*

Figure VI-2-39. Toe instability on hard bottoms

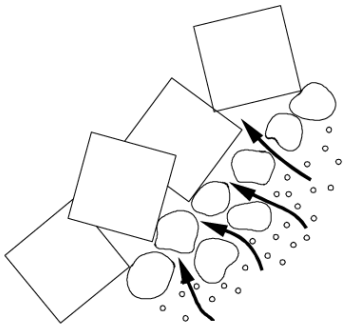

Washout of fine material

- *The wave-induced pressure gradients cause washout of finer material through coarser material if the criteria for stable filters are not met.*
- *Washout causes cavites and local collapse of the structure.*

Figure VI-2-40. Washout of underlayer material

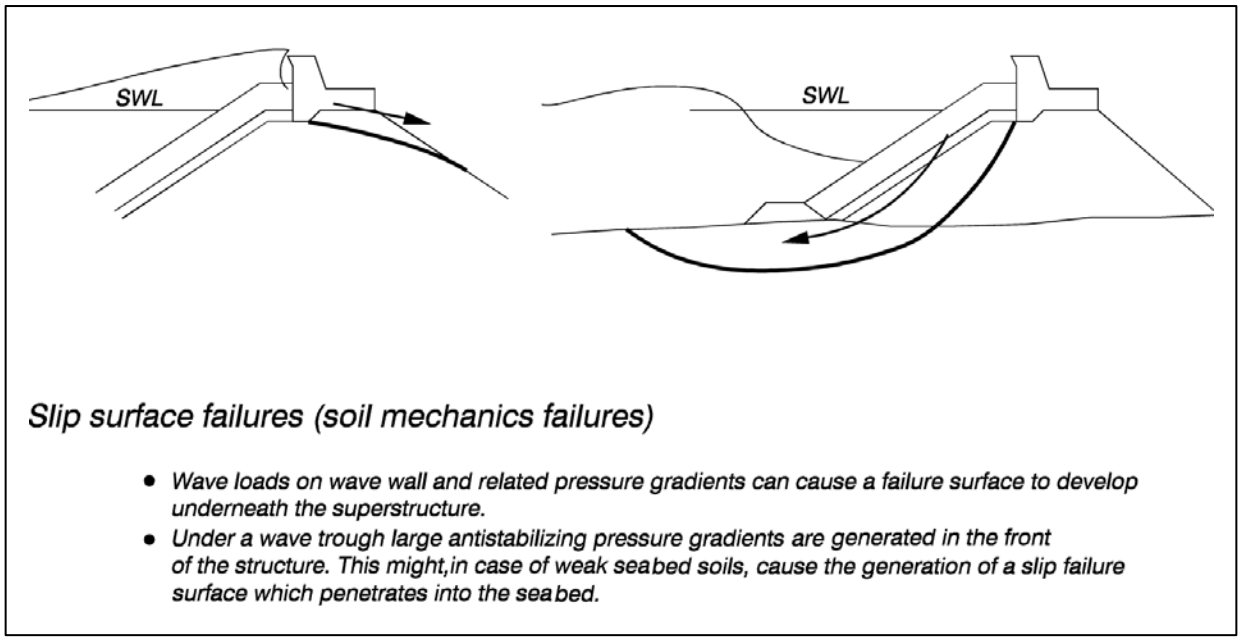

Figure VI-2-41. Slip surface failure

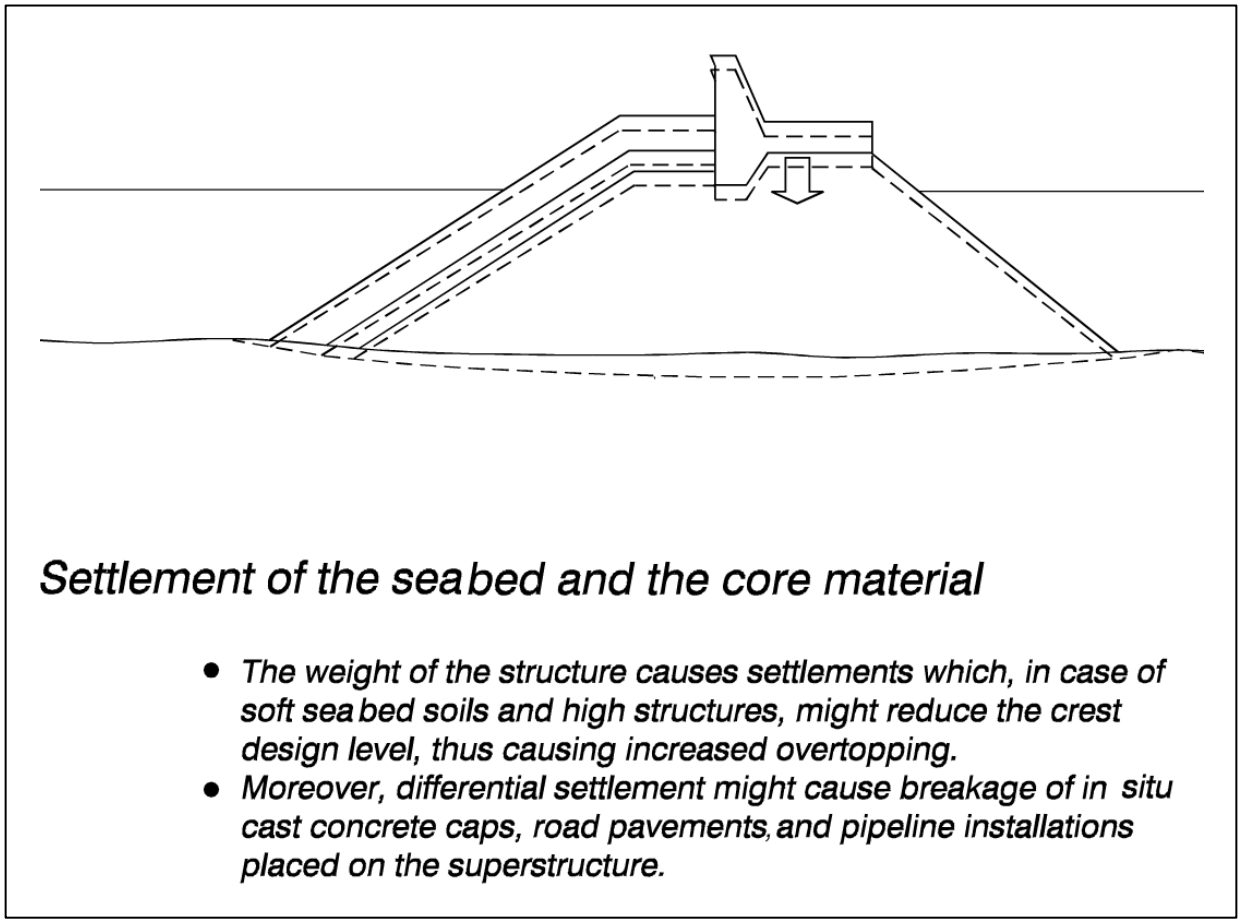

Figure VI-2-42. Structure settlement failure

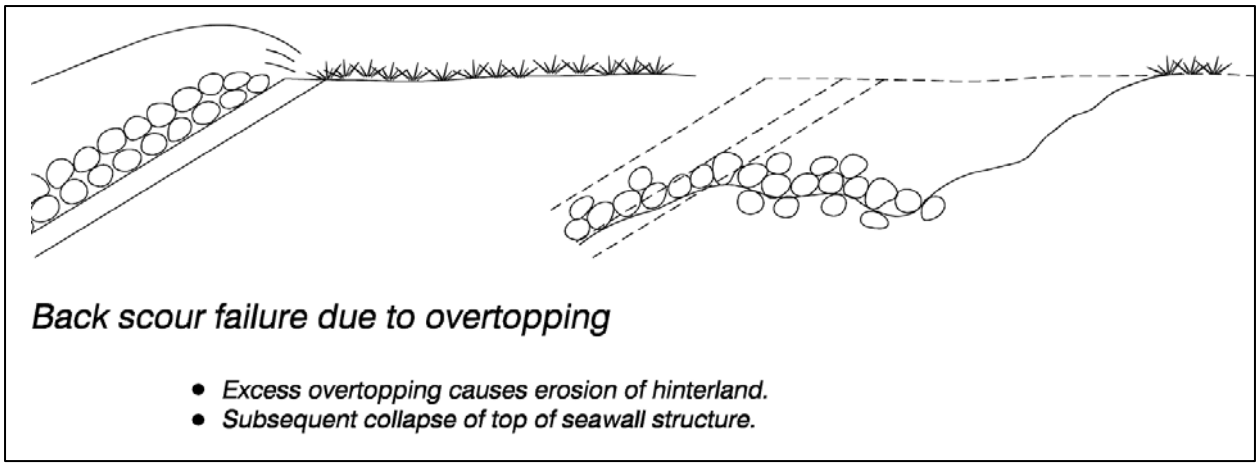

Figure VI-2-43. Scour due to overtopping

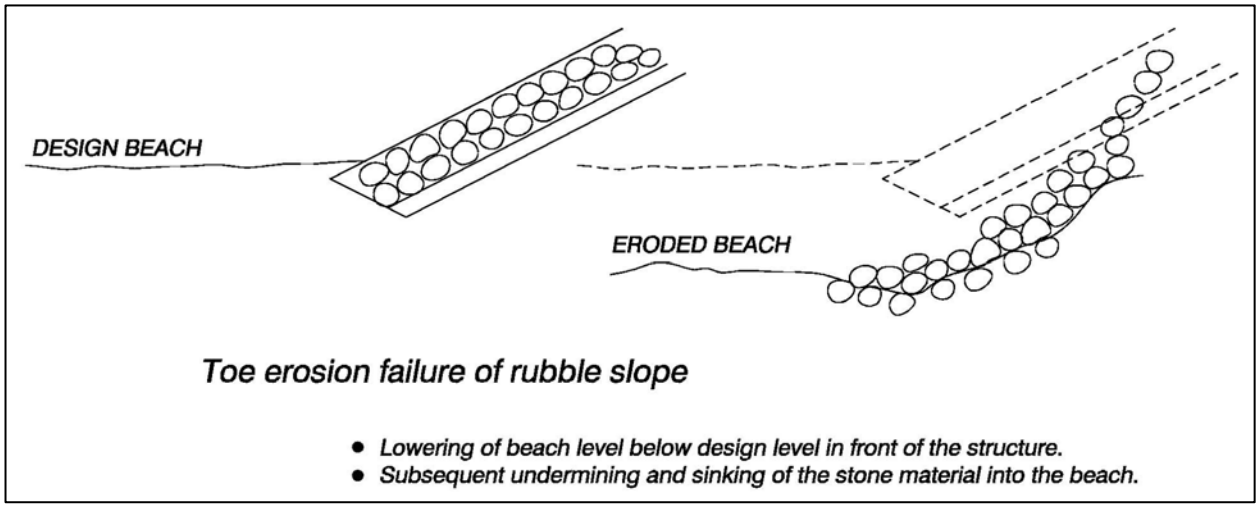

Figure VI-2-44. Toe erosion failure of rubble slope

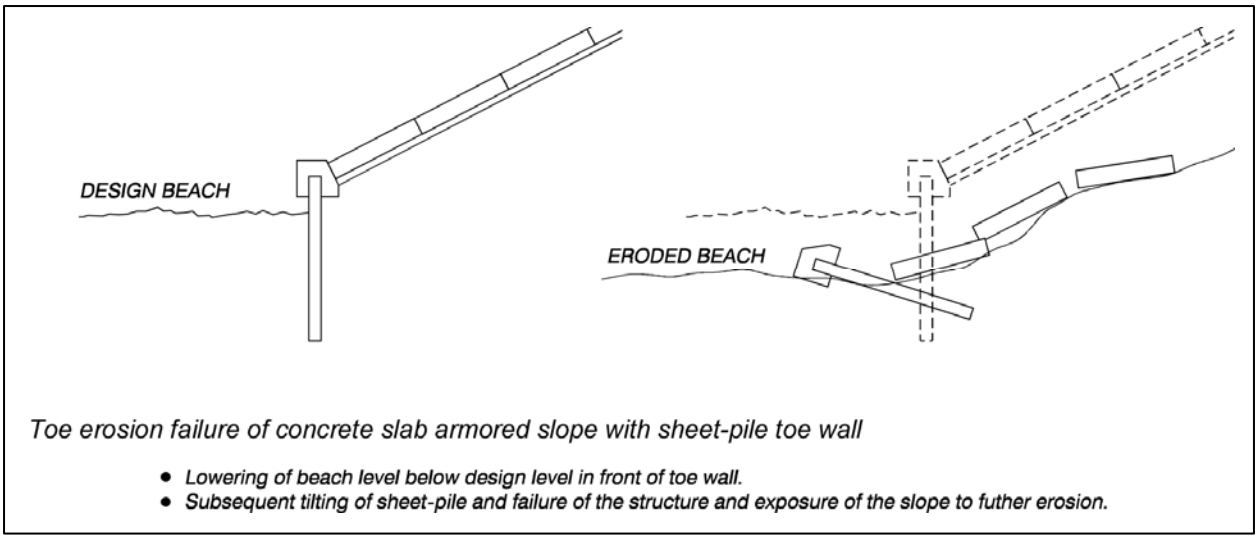

Figure VI-2-45. Failure of sheet-pile toe wall

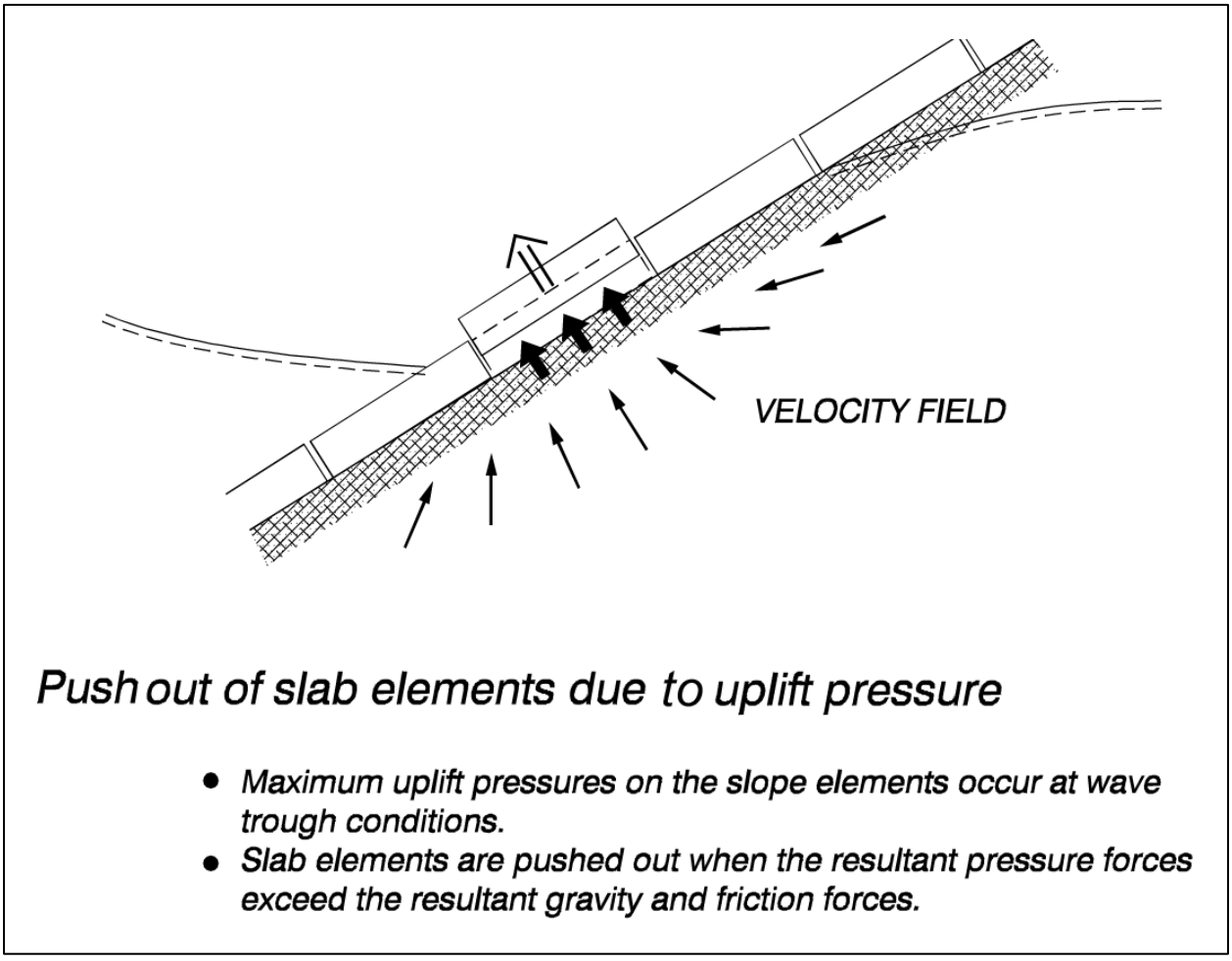

Figure VI-2-46. Pressure blowout of slab elements

Erosion and lifting of front slope surface armor

- *Weakness in the surface armor (grass, asphalt, concrete slabs) might allow the waves to erode the surface.*
- *The internal water pressure might, during the presence of deep wave troughs (max. rundown situations), cause lifting of impermeable surface armor layers.*
- *The most exposed zone is the zone of impact by breaking waves down to a level just below that of maximum wave rundown.*
- *After exposure of the dike core material,a rather fast erosion and subsequent breach will take place.*

Figure VI-2-47. Erosion of dike slope protection

Seabed scour and toe erosion

- *An unprotected seabed at the toe of the dike might be eroded.*
- *Subsequently erosion at the toe of the dike will take place, unless the dike armoring is flexible and able to retain its integrity.*

Figure VI-2-48. Toe scour erosion of dike

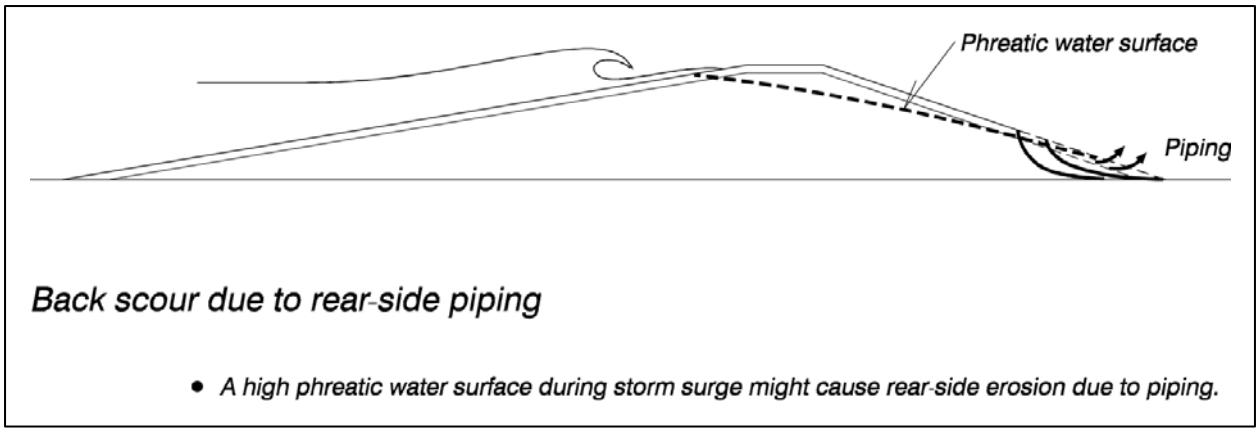

Figure VI-2-49. Dike crest erosion by overtopping

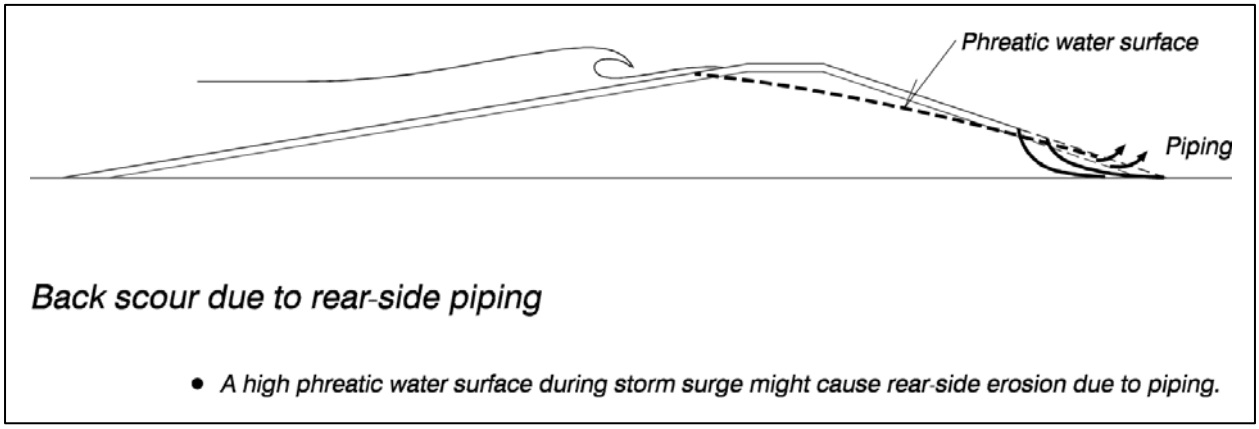

Figure VI-2-50. Dike backscouring due to piping

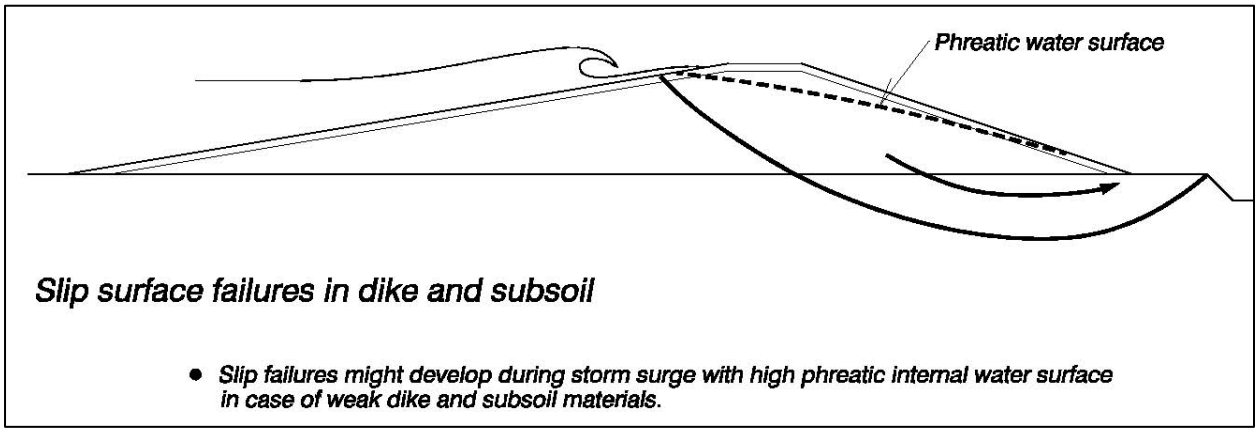

Figure VI-2-51. Dike slip surface failure

c. Vertical-front structures.

(1) Caisson and Blockwork Breakwaters. Failure modes can be classified based on Table VI-2-2.

Table VI-2-2
Failure Modes of Caisson and Blockwork Breakwaters

Overall (global) instability of monoliths	Foundation failure modes: Slip surface failures Excess settlement Overturning Lateral displacement or sliding on foundation
Local instability	Hydraulic instability of rubble foundation Hydraulic instability of rubble-mound slope protection in front of caissons and breakage of blocks Seabed scour in front of the structure Breakage and displacement of structural elements

The local stability failure modes can trigger the overall stability failure modes. Figures VI-2-52 to VI-2-62 illustrate the failure modes for caisson and blockwork breakwaters.

(2) Seawalls/revetments.

(a) Gravity walls. Figures VI-2-63 to VI-2-68 illustrate common failure modes for gravity-type seawalls/revetments.

(b) Tied walls. Failure modes of thin walls supported by tie-backs are shown in Figures VI-2-69 through VI-2-73.

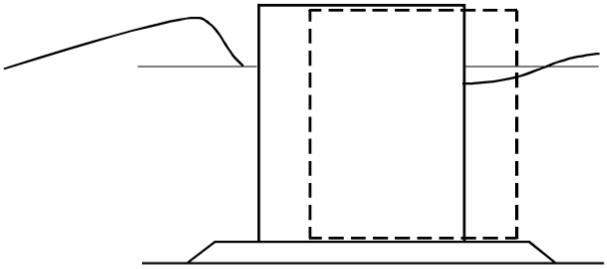

Shoreward sliding of caisson

- *Resulting horizontal wave force in seaward direction exceeds the friction force between the caisson baseplate and the bedding layer.*
  Large resulting shoreward wave force occurs when wave crests hit the caisson front simultaneously with wave troughs at the rear of the caisson.

Figure VI-2-52. Sliding of caisson on foundation

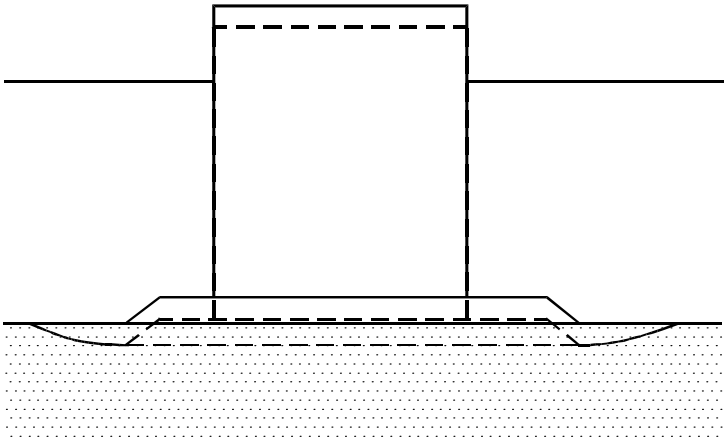

Settlement

- *Vertical settlements occur when soil consolidation takes place.*

Figure VI-2-53. Caisson settlement

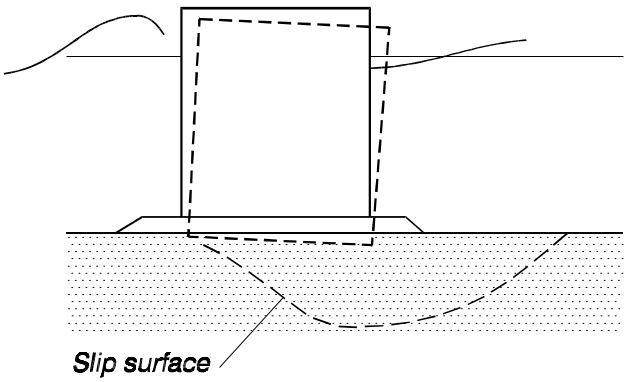

Slip failure in subsoil

- *The caisson base plate load on the subsoil creates stresses which exceed the strength of the soil.*
  The strength of the soil is influenced by possible pore pressure built up due to the cyclic wave induced pressure variations in the soil.
- *The slip surface failure causes the caisson to rotate and settle.*

Figure VI-2-54. Soil foundation slip surface failure

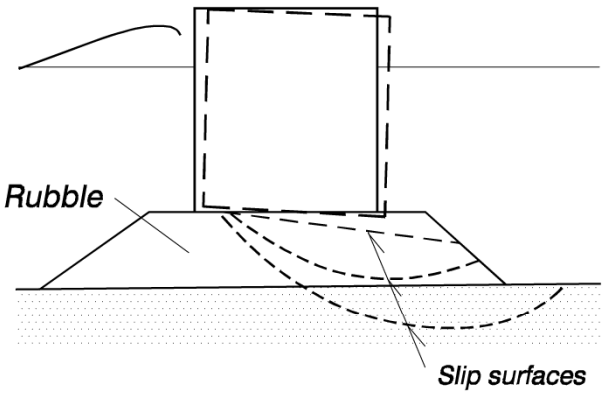

Slip failures in rubble foundation and subsoil

- *The caisson baseplate load on the rubble foundation creates stresses that exceed the strength of the rubble material and possibly also that of the subsoil. Subsoil strength might be influenced by wave-induced pore pressure buildup.*

Figure VI-2-55. Slip surface failure of rubble foundation

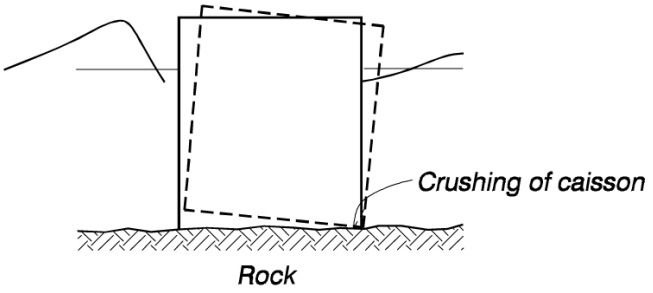

Overturning of caisson around heel

- *Tilting of the caisson takes place when the wave-induced resulting moment exceeds the gravity-based stabilizing moments.*
  The failure mode is relevant only to cases where ground failure does not occur, i.e., in case of rocky seabeds and very strong subsoils.
  Tilting of a caisson will in most cases cause local crushing of the caisson heel and cracking in the caisson walls.

Figure VI-2-56. Caisson overturning

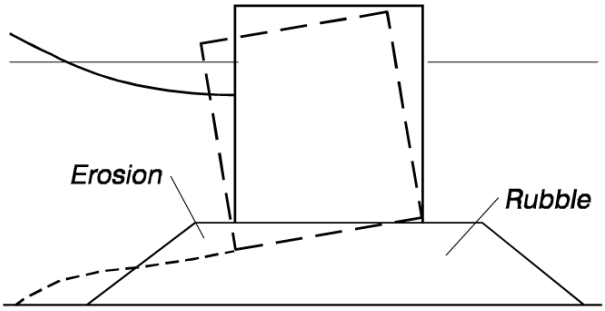

Erosion of rubble foundation, seaward tilt,and settlement

- *Wave-induced erosion of the seaward rubble foundation might cause seaward tilt and subsequent settlement of the caisson.*
- *Critical wave load situations exist when deep wave troughs occur at the caisson front.*

Figure VI-2-57. Seaward tilting and settlement due to erosion of rubble base

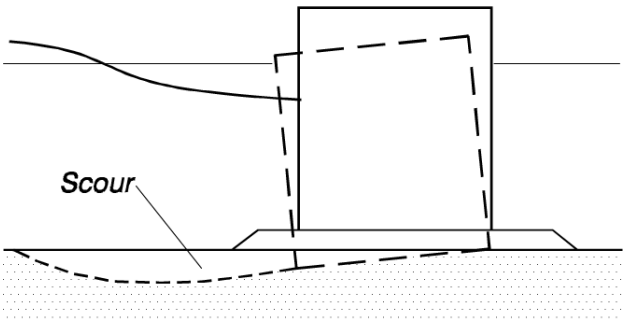

Scour in seabed, seaward tilt,and settlement

- *Scour in front of a caisson due to waves and currents might cause seaward tilt and settlement of the caisson.*
- *Critical wave load situations exist when deep troughs occur at the caisson front.*

Figure VI-2-58. Seaward tilting and settlement due to scour

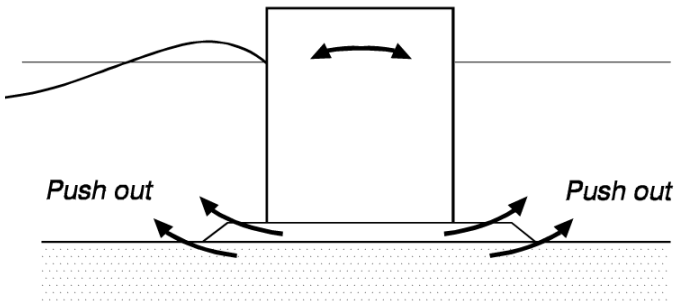

Pushout of base material due to rocking motion of the caisson

- *Wave-induced rocking motion of a caisson causes oscillatory porous flow in the bedding layer and the subsoil.*
- *In case of relatively fine materials,a pushout of material might take place resulting in increased rocking motion and subsequent possible ground failure and tilt of the caisson.*

Figure VI-2-59. Loss of foundation material due to caisson motion

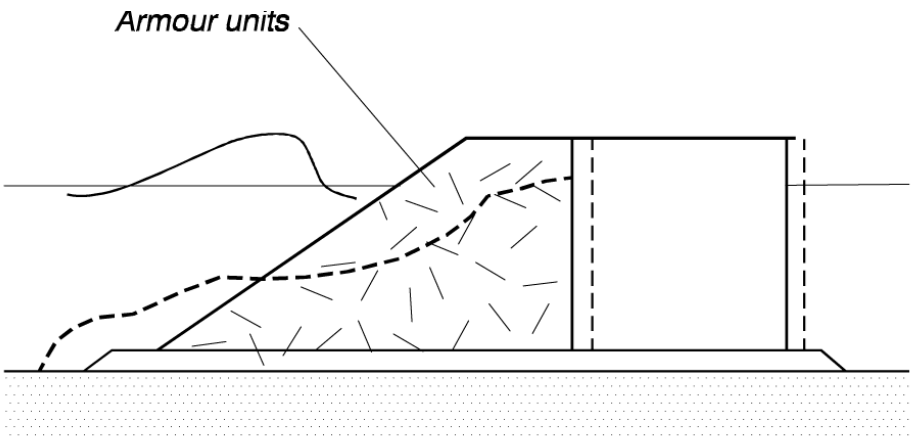

Breakage and displacement of armor units in front of caisson

- *Wave action might lead to breakage and/or displacement of the armor units.*
- *The subsequent increase in the wave forces on the caisson front wall might cause the caisson to slide.*
- *Damage to the armor protection might increase the overtopping.*

Figure VI-2-60. Failure of fronting armor units

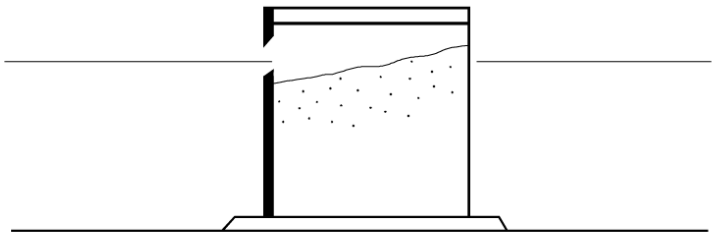

Failure of caisson front wall

- *Failures might be caused by excess wave loads, deteriorated reinforced concrete, and ship impact.*
- *If the caisson fill is leaking, the caisson might slide and/or tilt due to decreased gravitational stability.*

Figure VI-2-61. Caisson front wall failure

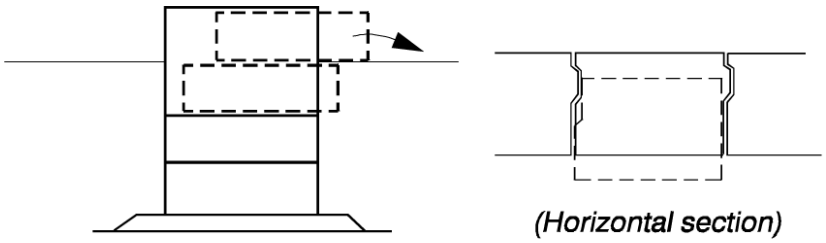

Push out of elements in blockwork structures and failure of shear keys between blocks and caissons

- *Wave-induced loads might cause elements in blockwork structures to be pushed out of position with subsequent failure of the wall.*
- *Failure of shear keys between blocks and caissons due to large differential wave loads or due to differential settlements in case of caisson will lead to displacements of blocks and caissons.*

Figure VI-2-62. Displacement of individual blocks

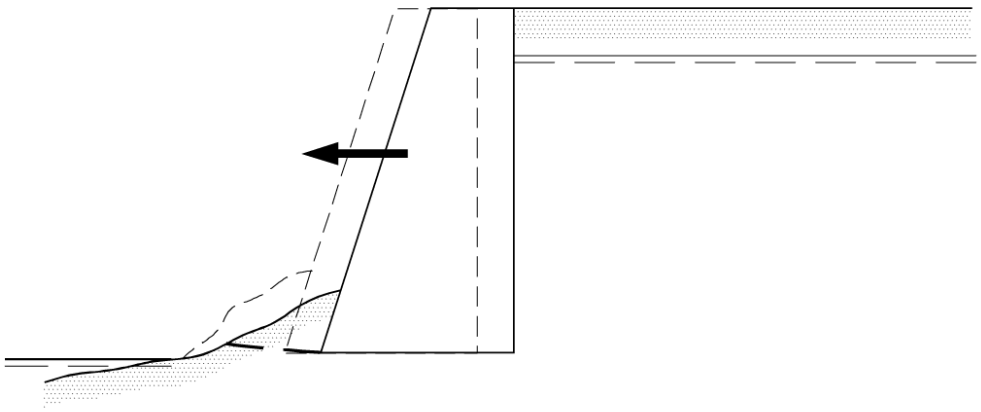

Sliding of gravity wall

- *The wall slides when the resulting pressure on the rear of the wall from active soil pressure and the groundwater exceeds the sum of the frictional resistance over the base of the wall and the passive resistance at the toe.*

Figure VI-2-63. Seaward sliding of gravity wall

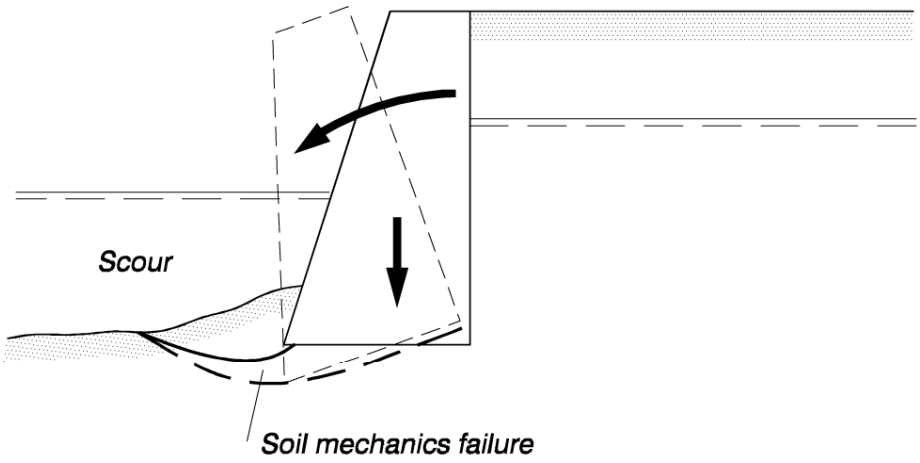

Seaward overturning and settlement of gravity wall

- *Scour in front of the wall reduces both the passive resistance and the bearing capacity of the foundation soil.*
- *The resulting load from the active backfill pressure, the high groundwater table, and the weight of the wall cause a bearing capacity failure in the soil resulting in a forward overturning and some settlement of the wall.*

Figure VI-2-64. Seaward overturning of gravity wall

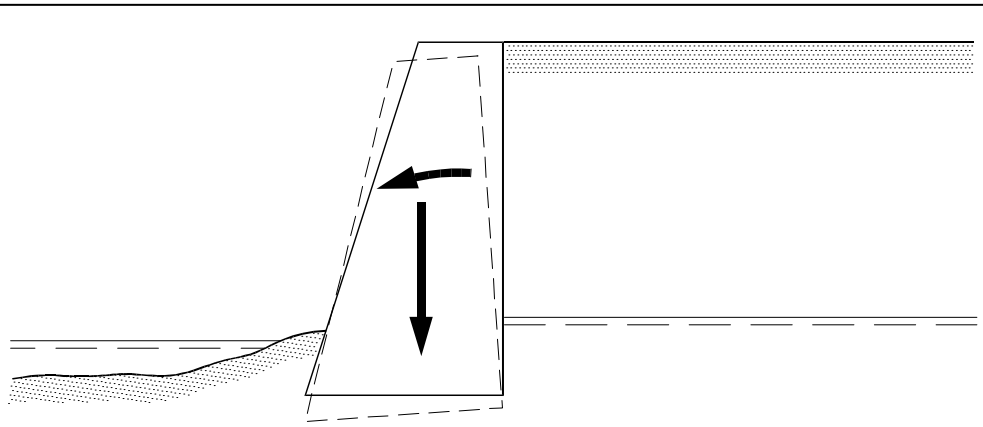

Settlement of gravity wall

- *Settlement might be caused by consolidation of the foundation soil or by soil mechanics failures when the foundation load exceeds the bearing capacity of the soil.*

Figure VI-2-65. Gravity wall settlement

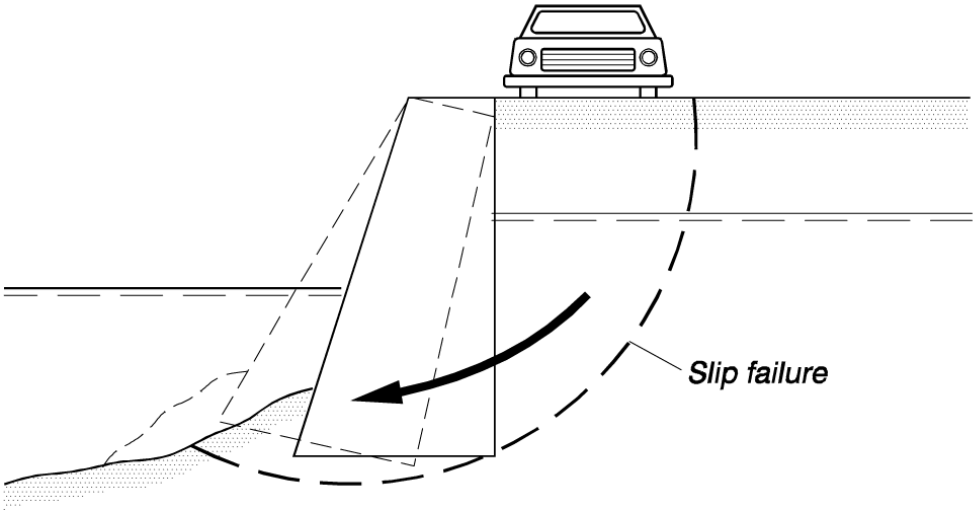

Rotational slip failure

- *Rotational slip failure occurs when the driving moment caused by the weight of soil, groundwater, and surface loads exceeds the restoring moment given by the soil strength.*

Figure VI-2-66. Rotational slip failure of gravity wall

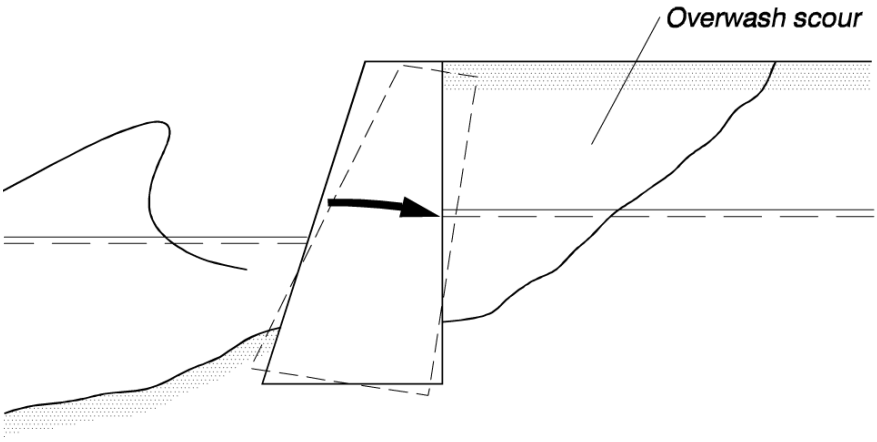

Landward overturning of gravity wall due to overwash scour

- *Heavy overtopping might cause rear-side scour and thereby loss of passive resistance from the backfill.*
- *Wave loads on the front might cause a landward tilt of the wall.*

Figure VI-2-67. Landward overturning of gravity wall

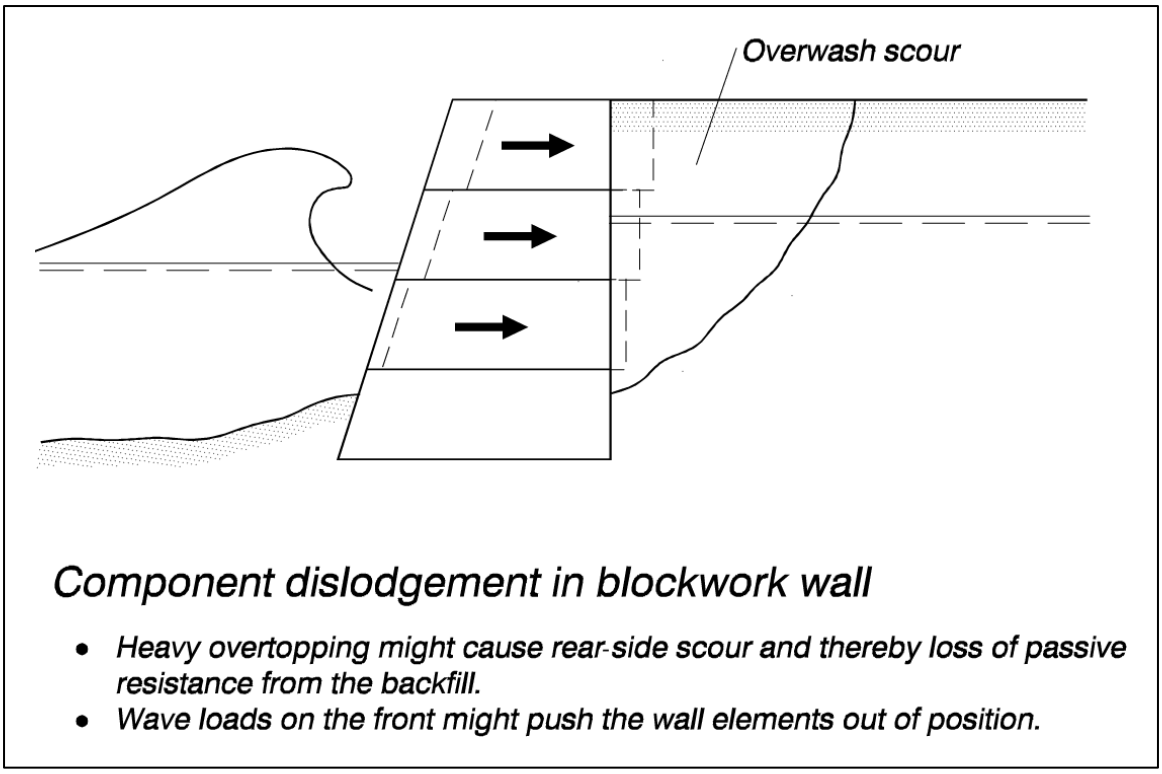

Figure VI-2-68. Displacement of individual gravity wall components

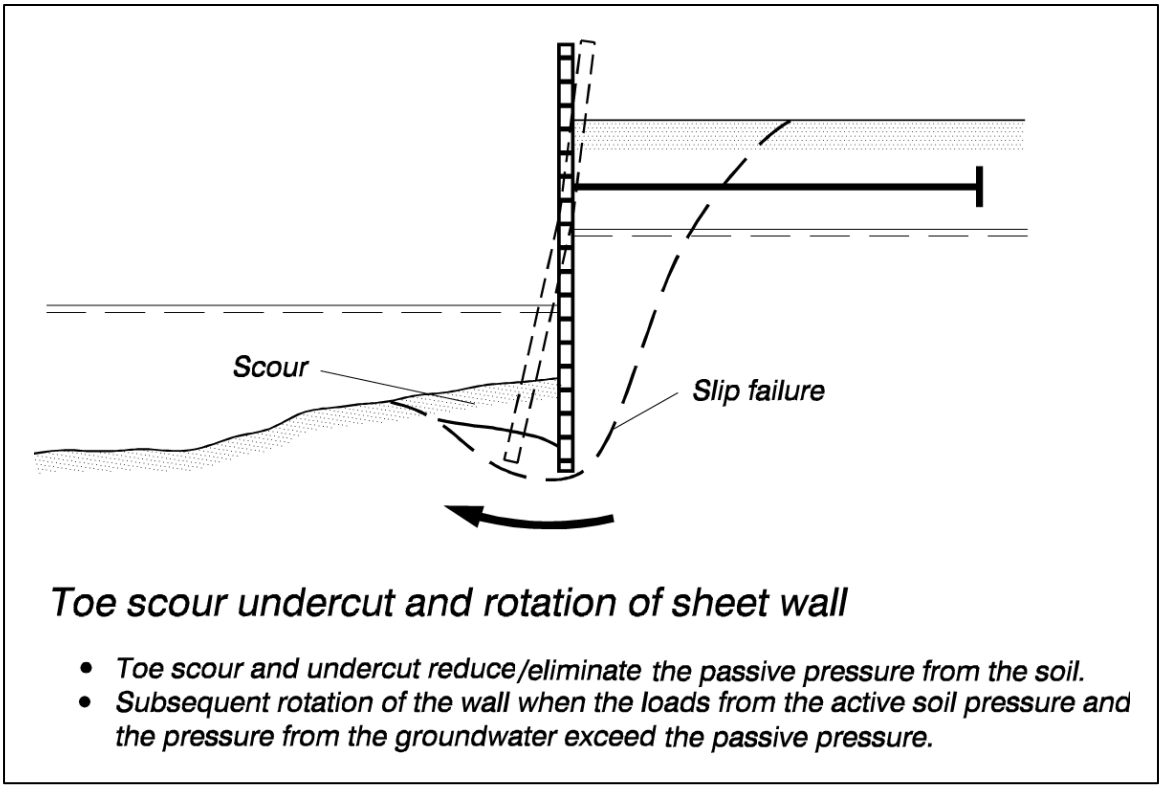

Figure VI-2-69. Failure due to toe scour

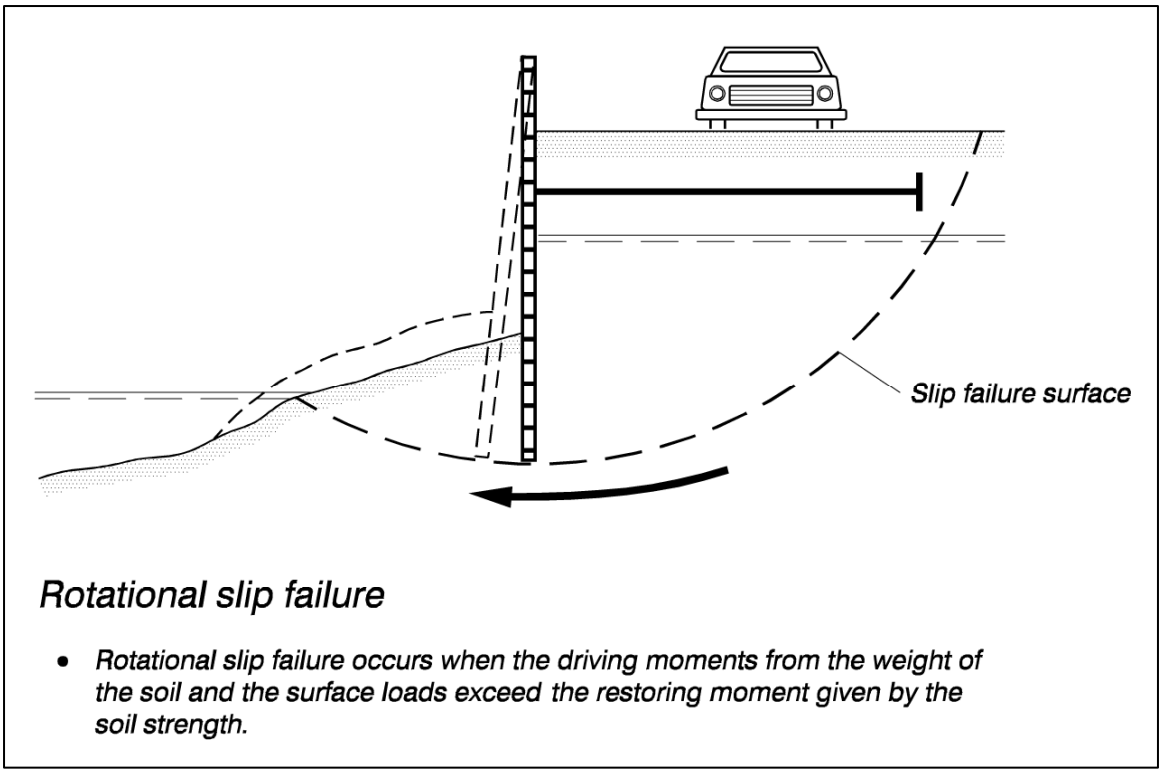

Figure VI-2-70. Rotational slip surface failure

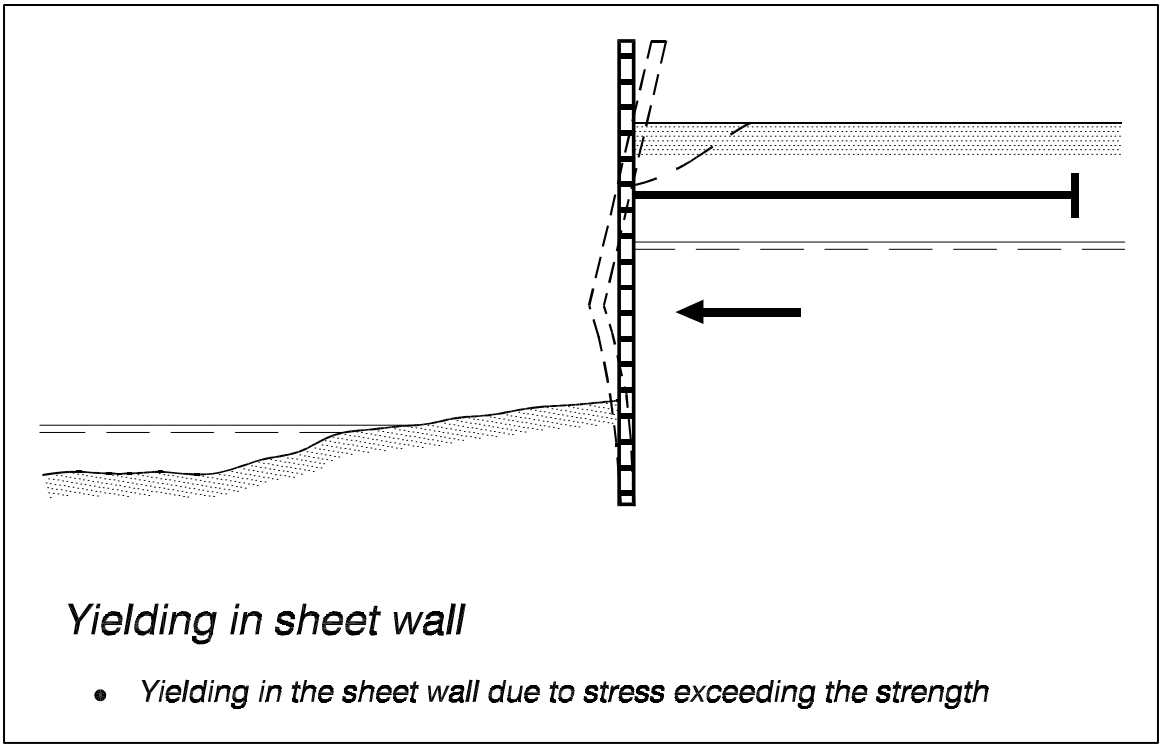

Figure VI-2-71. Failure of thin wall construction material

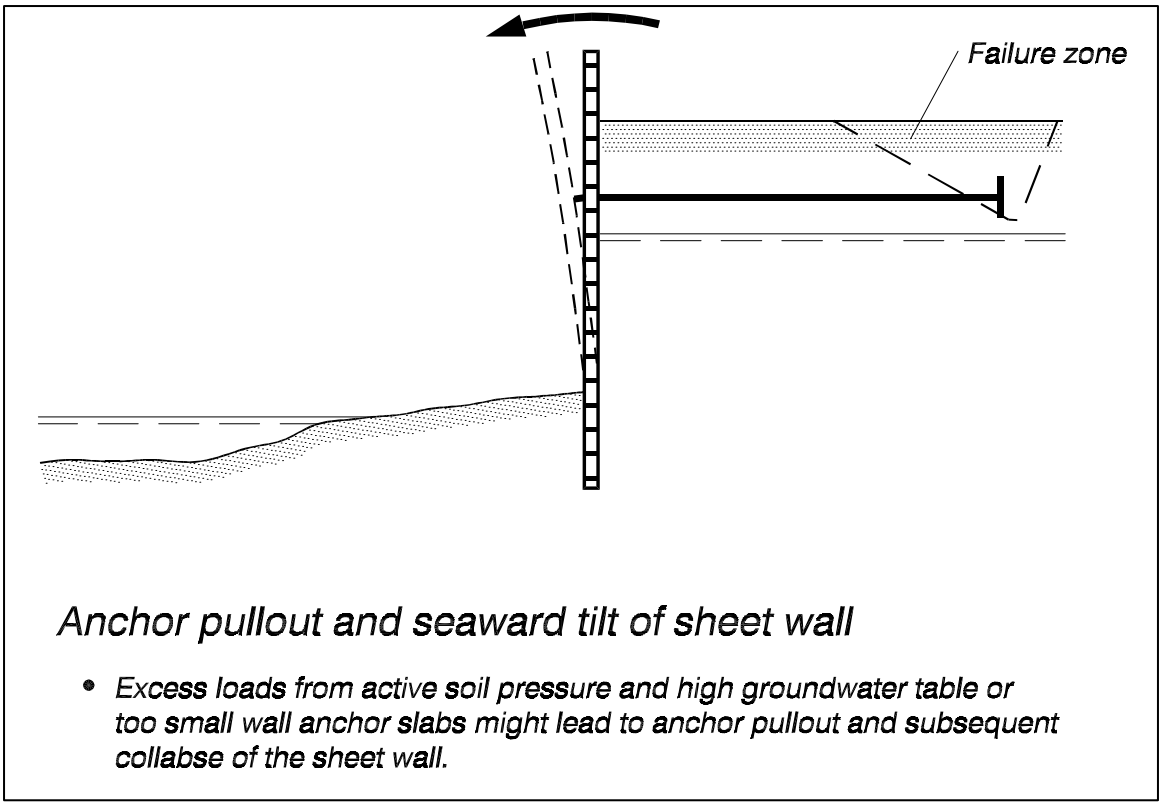

Figure VI-2-72. Failure due to anchor pullout

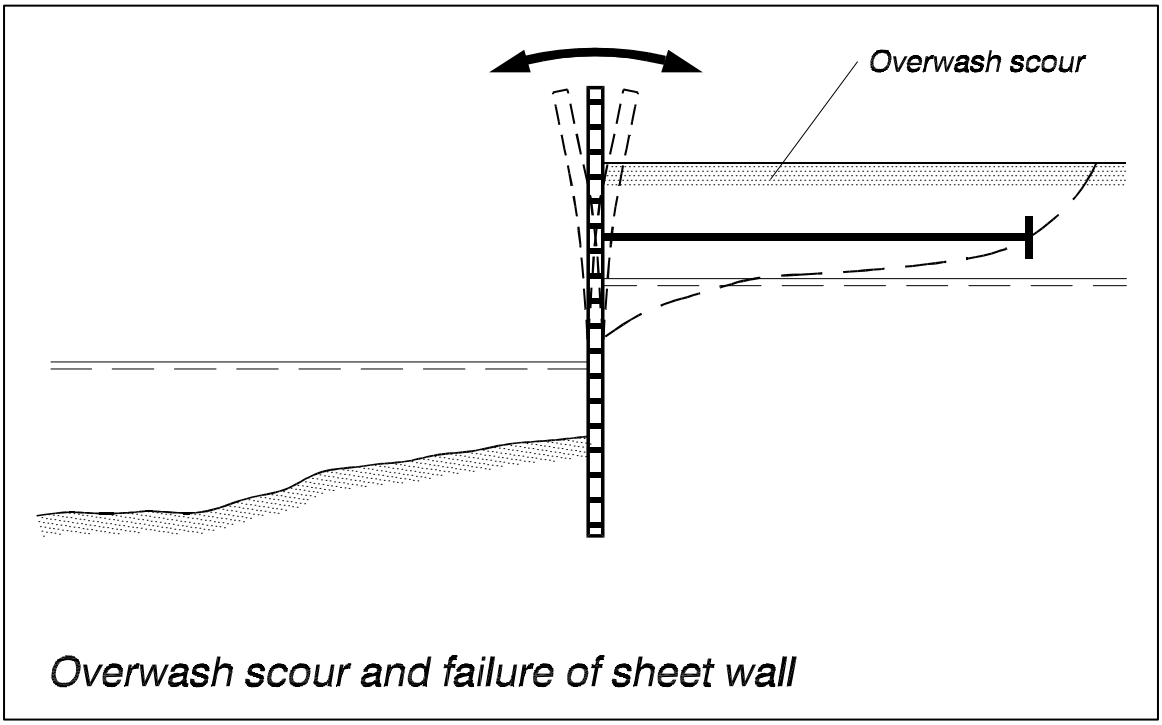

Figure VI-2-73. Back scour and thin wall failure

d. Floating structures.

(1) Floating structures used in coastal engineering applications have four different failure modes associated with structural design:

(a) Failure of floating sections.

(b) Failure of floating section connectors.

(c) Failure of anchor system or pile supports.

(d) Flooding and sinking.

(2) Material used to fabricate individual floating sections must be able to withstand wave slamming forces, vessel impacts, marine corrosion, and concentrated loading at connection points and mooring points. Floating sections fabricated with concrete must withstand deterioration. Damage to the floating section construction material may lead to flooding of the unit, displacement of the section from its moored location, or rendering of the section unsafe for traffic.

(3) Many floating structures consist of several units joined with flexible connections. These connectors must be able to resist transmitted force and moment loads induced by environmental loading and differential movements between floating sections. Failure of the connectors results in a substantial decrease in the structure=s functionality.

(4) The mooring/anchoring system of a floating structure is critical to a successful design. Mooring systems fail when the mooring lines break or separate from the connection points, or when the anchoring method does not resist the mooring loads. Dead weight anchors rely primarily on anchor mass with additional help from frictional resistance between the anchor and soil. Penetration anchors rely on soil shear strength to resist Apullout@ under load conditions. Extreme loads may cause anchors to drag or pullout, but the floating structure may survive intact at a displaced location. Failure occurs if the structure displacement results in the floating structure breaking up, suffering impact damage, or becoming unretrievable. Similar damage can occur to pile-supported floating structures when the piles fail or the floating structure breaks free of the pilings.

(5) Many floating structures have compartments of entrapped air that provide necessary buoyancy. If these compartments flood, the structure may sink. Flooding can occur because of impact damage, construction material failure, excessive structure tilting, or wave overtopping.

(6) Finally, floating structures may fail because they do not perform at the expected level. For example, a floating breakwater that does not reduce wave heights sufficiently and a floating boat slip with excessive motion would both be considered failures.

e. Beach fills.

(1) Judging the success or failure of beach fill projects is somewhat subjective and arises more from a political position rather than an assessment in terms of the beach fill project's original design goals. Beach fill projects are usually built in areas that experience shoreline erosion, and it is expected that the beach fill will gradually disappear in time as erosion continues. Part of the design process is estimating how long the beach fill will serve its function under typical wave conditions. Such estimates are difficult, at best, because of wave climate uncertainty and the complexity of beach fill response to storm conditions. A new project may suffer a severe storm immediately upon completion, resulting in massive fill losses, or the beach fill may serve for many years without ever being exposed to design storm conditions.

(2) Despite the controversy about failure or success of beach fill projects, there are several recognized failure modes for beach fills:

(a) Failure to protect upland property or structures during storm events.

(b) Movement of fill material to undesired locations, such as into inlets or harbors.

(c) Loss of fill material at a rate greater than anticipated for some reason other than design wave exceedance.

(3) When used to protect upland property, beach fills are sacrificial soft structures, somewhat analogous to automobile fenders that are designed to crumple on impact to absorb the energy.

f. Scour potential and toe failure. Any coastal structure resting on, driven into, or otherwise founded on soil or sand is susceptible to scour and possible toe failure when exposed to waves and currents. Generally, scour potential around impermeable structures is enhanced in regions of flow concentration due to directed currents, high wave reflection, etc. Scour potential is decreased around sloping permeable structures. Failure modes due to scour for specific structure types are illustrated in the figures of this section.

VI-2-5. References.

Burcharth 1983
Burcharth, H. F. 1983. "Materials, Structural Design of Armour Units," *Proceedings of Seminar on Rubble Mound Breakwaters*, Royal Institute of Technology, Stockholm, Sweden, Bulletin No. TRITA-VBI-120.

Burcharth and Thompson 1983
Burcharth, H. F., and Thompson, A. C. 1983. "Stability of Armour Units in Oscillatory Flow," *Proceedings of Coastal Structures '83*, American Society of Civil Engineers, pp 71-82.

Burcharth 1984
Burcharth, H. F. 1984. "Fatigue in Breakwater Concrete Armour Units," *Proceedings of the 19th International Conference on Coastal Engineering*, American Society of Civil Engineers, Vol. 3, pp 2592-2607.

Burcharth 1993
Burcharth, H. F. 1993. "Structural Integrity and Hydraulic Stability of Dolos Armour Layers," Doctoral Thesis (Series Paper 9), Department of Civil Engineering, Aalborg University, Aalborg, Denmark.

Burcharth, et al. 1995
Burcharth, H. F., Jensen, M. S., Liu, Z., Van der Meer, J. W., and D'Angremond, K. 1995. "Design Formula for Tetrapod Breakage," *Proceedings of the Final Workshop, Rubble Mound Breakwater Failure Modes*, Sorrento, Italy.

Melby 1993
Melby, J. A. 1993. "Dolos Design Procedure Based on Crescent City Prototype Data," Technical Report CERC-93-10, U.S. Army Engineer Waterways Experiment Station, Coastal Engineering Research Center, Vicksburg, MS.

Price 1979
Price, W. A. 1979. "Static Stability of Rubble Mound Breakwaters," Dock and Harbour Authority, Vol. LX (702).

VI-2-6. Acknowledgments.

Authors: Dr. Hans F. Burcharth, Department of Civil Engineering, Aalborg University, Aalborg, Denmark; Dr. Steven A. Hughes, Coastal and Hydraulics Laboratory (CHL), U.S. Army Engineer Research and Development Center, Vicksburg, MS.

Reviewers: Han Ligteringen, Delft University of Technology, The Netherlands; John H. Lockhart, Headquarters, U.S. Army Corps of Engineers, Washington, DC (retired); Joan Pope, U.S. Army Engineer Research and Development Center, Vicksburg, MS.

CHAPTER 3

Site Specific Design Conditions

TABLE OF CONTENTS

Page

VI-3-1. Foundation/Geotechnical Requirements VI-3-1

a. Introduction VI-3-1
b. Foundation loads VI-3-1
c. Foundation soil responses VI-3-2
d. Geotechnical investigations VI-3-3
e. Geotechnical design criteria for shallow foundations VI-3-6

VI-3-2. Seasonal Profile Variation VI-3-8

VI-3-3. Flanking Possibility VI-3-9

VI-3-4. Seismic Activity VI-3-10

VI-3-5. Ice VI-3-11

a. Ice loading VI-3-11
b. Ice on sloping-sided (rubble-mound) structures VI-3-12
c. Ice on vertical-wall structures VI-3-13
d. Ice on the shoreline and shore protection structures VI-3-14
e. Ice on floating breakwaters VI-3-14
f. Ice on piles and piers VI-3-14

VI-3-6. Environmental Considerations VI-3-14

VI-3-7. Construction Considerations VI-3-15

VI-3-8. Other Design Considerations VI-3-19

a. Regulatory compliance VI-3-19
b. Project maintenance VI-3-19
c. Disposal of dredged materials VI-3-20
d. Aesthetics VI-3-20
e. Aids to navigation VI-3-20
f. Fishing platforms VI-3-20

g. Vandalism and theft VI-3-21

VI-3-9. References VI-3-21

VI-3-10. Acknowledgments VI-3-22

List of Figures

Figure VI-3-1. Bayside erosion and protective revetment at east jetty of Moriches Inlet..VI-3-10

List of Tables

Table VI-3-1. Soil Data Required to Evaluate Foundation Failure Modes VI-3-5

Table VI-3-2. Ice Effects in Coastal Project Design VI-3-13

CHAPTER VI-3

Site-Specific Design Conditions

VI-3-1. Foundation/Geotechnical Requirements. This section presents an overview of site-specific design information that may be required to complete preliminary and final foundation design for coastal projects. Foundation failure modes are overviewed in Part VI-2-4, "Failure Modes of Typical Structure Types," and foundation design procedures are discussed in Part VI-5-5, "Foundation Loads."

a. Introduction.

(1) Most man-made coastal project elements are designed to be built or placed directly on top of the natural soil, sand, or other bottom material of the project site (the major exceptions are pile-supported structures). Depending on the particular functional requirements of the coastal project element, it may be subjected to environmental loadings that include waves, currents, fluctuating water levels, and seismic vibrations, along with specific loadings such as vessel impacts and ice surcharge.

(2) The interaction between a coastal project and the soil upon which it is placed may be a critical aspect of a project=s performance. The underlying soil, or *foundation*, must be capable of resisting that portion of the loading that is transferred to the foundation in addition to supporting the weight of the structure. Resistance to the total imposed time-dependent loading and resultant changes in soil stresses within the soil layers must be achieved without undue structure deformation and with sufficient reserve soil strength to assure that the probability of soil instability is sufficiently low.

(3) Foundation design for coastal structures requires the engineer to make reasonable estimates of the expected loading conditions, to determine the appropriate site-specific foundation soil engineering properties, and to understand reasonably the structure/soil interaction. Geotechnical investigations are conducted to gather necessary information about the soil layers beneath the project so the engineer can complete the foundation design to a level commensurate with each stage of project design.

b. Foundation loads.

(1) For typical coastal structures exposed to waves and currents, the underlying foundation soils must contend with static, dynamic, and impact force loads. Static loads are caused by the structure and foundation soil self-weight; and in most cases, these forces are relatively constant over the life of the project. It is important to remember that buoyancy effectively reduces the weight of that portion of the structure beneath the water surface. Consequently, the structure self-weight load on the foundation soil will vary with tide elevation.

(2) A structure=s weight distribution and the differential loading applied to the foundation must be evaluated, particularly for gravity-type structures extending into greater depths or spanning different soil types. Lateral forces due to imbalanced hydrostatic pressure must also be considered.

(3) Waves, currents, tides, storm surges, and wind are the primary dynamic forces acting on coastal structures; however, in some regions of the world earthquake ground motions may also induce severe dynamic loads. Dynamic loads vary greatly in time, duration, and intensity, and the worst likely load combinations should be examined during foundation design.

(4) Impact loads on structures may arise from ship or ice collisions, partial failure of some portion of the structure, or even from breaking waves slamming into the structure. Importance of impacts depends on the type of structure and magnitude of impact. Structures such as rubble-mound breakwaters are somewhat flexible and can absorb a portion of the impact load, whereas monolithic structures are more likely to transmit a greater portion of the impact load to the foundation as lateral shear or overturning forces. However, the large mass and natural frequency of monolithic structures help to reduce the transmitted loads. Finally, the proposed project construction method should be examined to determine if any significant construction loads might adversely affect the foundation soil stability.

c. Foundation soil responses. Structure static loads applied to the foundation soil, along with dynamic and impulsive force loads transmitted by a coastal structure to the foundation, can evoke several soil responses that concern design engineers.

(1) Soil consolidation may occur due to the structure=s weight. Consolidation is a reduction in soil void space that occurs over time as compressive loads force water out of the voids. This results in a denser soil with increased soil strength properties. Densification of the soil may result in structure settlement or differential settlement that could impact the structure’s functionality. Other factors that influence settlement include compression of softer subsoil layers, squeezing of very soft sublayers, or collapse of underground cavities (Construction Industry Research and Information Association/Centre for Civil Engineering Research and Codes (CIRIA/CUR) 1991). Estimates of potential settlement are used to assess the need for structure crest overbuild or to determine stability of structures sensitive to differential movement.

(2) Soil shear stresses are induced when lateral forces and overturning moments on the structure are transferred to the foundation. If soil strength is exceeded, foundation damage may occur which can be either localized or widespread, such as in the case of slip-surface failure of a soil slope. Rapid soil stress loading will cause excess pore pressures and a corresponding decrease in soil shear strength which may lead to soil liquefaction. Cyclic loading of noncohesive sand can also cause excess pore pressure buildup, and when combined with strong accelerations from earthquakes, liquefaction of the foundation and consequent failure of the foundation may be catastrophic.

(3) Finally, the design engineer needs to consider the possibility that foundation material will be eroded from beneath the structure or immediately adjacent to the structure (scour). Induced excess pore pressures or pressure gradients within the soil can contribute to this loss. Steps must be taken to provide adequate protection to keep the foundation material in place (See Part VI-5-6, “Scour and Scour Protection”).

d. Geotechnical investigations.

(1) The wide variety of soil conditions encountered in the coastal regime, coupled with the range of coastal projects, precludes standardization of the study components comprising geotechnical investigations. A general guiding criterion is that the investigations should include sufficient subsurface investigations, lab testing, and analysis to assure the adequacy of project design and constructability. This may involve discovering answers for these questions:

(a) What are the soil types and strata at the site?

(b) What are the mechanical properties of the soil relative to its strength and deformation under loading?

(c) What is the range of conditions to which the soil might be exposed? (For example, flooding/drying or freeze/thaw cycles might be important for land-based structures.)

(d) Is the soil condition expected to degrade over the project life?

(e) Is the soil fissured or weathered?

(2) The three overlapping phases of a geotechnical investigation are site reconnaissance, preliminary exploration, and detailed design exploration. Determining what information is to be gathered in the latter phases depends, in part, on findings from previous investigation phases.

(a) The **Site Reconnaissance Phase** is primarily a desk study that seeks to assemble existing geological data to characterize the nature of the proposed project site. The results of this phase are important in helping to establish data collection requirements for subsequent phases. The goal of the site reconnaissance is to glean from available data an understanding of the geological stratification, formation, and history; the groundwater regime; and possibly the seismicity of the site (Pilarczyk 1990). Sources of information for this phase include: topographic and geologic maps, aerial photography, groundwater maps, past geotechnical studies at the proposed site and at adjacent locations, local observations and reports in the local media, recorded ground movements, published geotechnical and geological descriptions, and historical records of previous coastal projects in the vicinity. In particular, it is important to note partial removal of previous coastal structures because structure remnants in the foundation area may cause construction difficulty for new projects.

- Toward the end of the site reconnaissance phase it is essential for the engineer responsible for planning the geotechnical investigation to conduct a field trip to the project site. This trip allows the engineer to reconcile the assembled information with existing site conditions and to uncover any previously unrevealed factors (Eckert and Callender 1987). The focus of the trip should be on surface evidence of subsoil conditions such as existing cuts, landslides, surrounding geology, etc.

- The final step of the site reconnaissance phase is to develop a program for the preliminary exploration phase that will best fill remaining information gaps vital for site selection, planning, and preliminary design decisions. A major challenge is to optimize the data collection within the constraints of the project budget.

(b) The goals of the **Preliminary Exploration Phase** are the following: (1) to recognize potential geotechnical problems, (2) to obtain sufficient geotechnical information at alternative project sites so that the final site selection can be made, and (3) to determine adequately those geotechnical parameters necessary for preliminary project design. Results from the preliminary exploration generally form the basis of a Corps of Engineers survey report that is used to obtain project authorization. Therefore, the exploration should be sufficient to reveal any soil condition that might adversely influence project cost and constructability. Project size, cost, and importance all factor into the extent of the investigation. See Eckert and Callender (1987) for three useful examples that span the typical range of coastal projects.

- During the preliminary exploration it is necessary to collect site information to determine the following over the project area: (1) the approximate depth, thickness, and composition of the various soil strata, (2) depth to the soil-bedrock interface, (3) variations in the groundwater level, (4) estimates of critical soil parameters, and (5) potential sources of construction borrow materials.

- A variety of geophysical investigation methods can be employed to obtain these data over a wide area at a reasonable cost. Continuous seismic reflection surveys are commonly utilized for marine investigations. The seismic waves are reflected by the boundaries between soil strata, and the depth to each strata is determined by the arrival time of the reflected pulse. Different seismic frequencies provide varying depth coverage. Side-scan sonar images can provide information about the seafloor surface soil characteristics adjacent to the trackline of the survey vessel. Concurrent bathymetric soundings aid the interpretation of side-scan sonar images. Dry-land geophysical investigation methods include electro-resistivity, electromagnetic, and seismic refraction and reflection. Interpretation of most geophysical survey results requires an experienced professional.

- When feasible, geophysical survey results should be supplemented with a small number of in situ borings to aid in calibrating survey results. Ideally, the borings should be obtained at critical locations along the proposed project alignment, but often severe environmental conditions make coring at these locations dangerous or expensive. The core samples confirm the geophysical survey interpretation.

- Information collected during the preliminary exploration should be sufficient to make the final site selection and to develop a preliminary design. Once this has been achieved and the project receives final approval, planning for necessary detailed geophysical measurements can proceed.

(c) The purpose of the **Detailed Design Exploration Phase** is to collect and analyze specific soil data (beyond that gathered in the preliminary phases) to determine those geotechnical parameters necessary for completing the final foundation design. Critical to this phase is specifying which soil parameters need to be determined, at what locations and depths the determinations should be made, and how best to collect and analyze the data to achieve desired results within the time and monetary allowance. Secondary considerations include when to conduct the investigation, who will perform the work, and who will be responsible for the laboratory analyses and data interpretation. A well-planned exploration program that provides realistic soil parameters can often save more than it cost. Uncertainties about soil strength may

result in unnecessary structure overdesign, or conversely, a detailed site investigation may reveal a soil weakness that could result in structure failure if adequate provisions are not enacted. The decision about which soil parameters must be determined depends on the anticipated foundation failure modes. Table VI-3-1 (from CIRIA/CUR (1991)) lists the main foundation failure modes and identifies those soil parameters that are useful in evaluating each mode.

Table VI-3-1
Soil Data Required to Evaluate Foundation Failure Modes (CIRIA/CUR 1991)

Macro-Instability			Macro-Failure Settlements	Micro-Instability Filter Erosion	Parameter
Slip Failure	Liquefaction	Dynamic Failure			
A	A	A	A	A	Soil profile
A	A	A	A	A	Classification/grain size
A	A	A	B	A	Piezometric pressure
B	B	B	A	A	Permeability
A	B	B	A	B	Dry/wet density
-	A	B	-	-	Relative density, porosity
A	B	B	-	C	Drained shear strength
A	-	-	-	C	Undrained shear strength
B	-	-	A	-	Compressibility
A	-	-	A	-	Rate of consolidation
B	B	A	A	-	Moduli of elasticity
B	A	A	A	-	In situ stress
-	A	B	A	-	Stress history
B	A	A	B	-	Stress/strain curve

NOTE: A - Very important.
B - Important.
C - Less important.

- Spacing, depth, and location of soil samples and borings are specified for each site based on the known geology and particular type of project. When soil conditions are relatively uniform, the number of borings can be decreased and the spacing can be increased. Conversely, areas where geotechnical problems have been identified will require denser boring spacing to delineate the problem area=s geotechnical parameters. Boring depth is a function of the estimated project surcharge loading and the in situ soil profile.

- Field tests conducted on the in situ soil include (Eckert and Callender 1987):

– Penetration and vane shear devices to estimate in situ soil strength.

– Pressure meters and plate load equipment to estimate load-deformation characteristics.

– Nuclear densimeters and sand cone devices to measure density.

– Specialized equipment to measure permeability and pore pressure.

– Test loading of piles.

– Instrumentation of embankments and foundations.

– Monitoring of soils during vibratory and impulse loading.

- Modified versions of these tests (with an additional cost factor) are used for subaqueous bottom investigations.

- Laboratory tests conducted on soil samples can include the use of triaxial or related apparatus to test for strength, compressibility, and dynamic response; consolidation test devices; and equipment to measure parameters such as water content, gradation, plasticity, permeability, and relative density (see Part VI-4-2, “Earth and Sand”).

- The information presented above is little more than a brief introduction to a coastal project’s geotechnical design needs. Geotechnical engineers responsible for the foundation design will have the knowledge and information resources to guide the geotechnical design from the initial site reconnaissance phase through to the final design. Eckert and Callender (1987) and CIRIA/CUR (1991) provide additional guidance specifically related to coastal project geotechnical investigations, including details on soil collection and testing methods. Other more general information sources include Engineer Manual (EM) 1110-1-1802, EM 1110-1-1804, EM 1110-2-1906, EM 1110-1-1906; textbooks; and various soil testing standards.

e. Geotechnical design criteria for shallow foundations.

(1) Foundations are classed as either shallow or deep depending on the depth of the soil strata at which the structure=s load is to be supported. Most coastal structures rely on shallow foundations for support, i.e., the load is supported by the soil just beneath the bottom. The exceptions are pile-supported structures and piers, which require deep foundations. Shallow foundations (e.g., spread footings, mats) effectively widen the bearing area over which the load is distributed so the underlying soil can safely carry the burden.

(2) Environmental factors that may influence design of shallow foundations in coastal projects include currents, tides/storm surges, waves, and seismic activity. These loads (individually or in combination) may induce lateral or vertical forces, excess pore pressures, dynamic forces, or scour. Specific site considerations include soil type and strength, topography, water depth, and structure positioning. Other considerations related to foundation design include construction materials, construction techniques, and the anticipated foundation load distribution. Not all of the factors listed above will pertain to all foundation designs, so the geotechnical engineer must determine which factors are important for the particular site and foundation type.

(3) In shallow foundation design, ultimate bearing capacity and expected foundation settlement are calculated separately, and the in situ soil properties will largely determine whether the design is governed by bearing capacity or settlement criteria. Shallow foundation design on cohesionless soils is generally controlled by total and differential settlements because ultimate bearing capacity is very high for sand. Both settlement and bearing capacity must be considered when designing shallow foundations on cohesive soils, because either or both may be critical for the specific coastal project foundation.

(4) Allowable settlement depends on the rigidity and intended function of the supported project element. For example, a rubble-mound structure will tolerate more differential settlement without damage than a caisson-type structure. Internal structural stresses are less severe during uniform settlement; however, the overall decrease in crest elevation may impact the structure's functionality.

(5) Settlement in cohesionless soils is rapid with little time-delayed soil consolidation. In fact, much of the settlement occurs during construction, allowing onsite correction to achieve desired structure crest elevation. Total settlement in cohesive soils occurs in three steps. *Immediate settlement* is the soil distortion that occurs concurrently with soil loading. *Primary consolidation* occurs over time as water is pushed from the soil=s voids. Finally, *secondary compression* occurs as the soil structure adjusts to the effective applied load after consolidation.

(6) Coastal project elements situated on slopes or embankments may be susceptible to slip-surface failures passing through or under the structure. This applies mainly to retaining-type structures like bulkheads, seawalls, revetments, and earthen dikes. Design parameters related to the pore pressure distribution in the subsoil are needed to complete slip-failure analyses. Slip-surface failures are seldom a concern for subaqueous foundations such as those supporting navigation structures, breakwaters, and groins, unless these structures are built on weak soils. However, slip-surface damage could occur at channel structures if the navigation channel meanders too close to the structure toe.

(7) A key design criteria for retaining structures is determining the earth pressure caused by the backfill. The backfill pressure might be increased due to saturation by wave overtopping or rainfall runoff, or the pressure might be decreased by backfill erosion under certain conditions. Scour potential at the retaining structure toe should also be examined (see Part VI-5-6, "Scour and Scour Protection").

(8) The prospect of project damage by seismic activity should be evaluated for projects located in high seismic risk zones. Generally, seismic-related damage to rubble-mound structures does not result in catastrophic failure, and it is possible for earthquake-damaged rubble-mound structures to continue to fulfill their intended function. (The possible exception might be structures armored with nonreinforced slender concrete armor units that could experience significant breakage during an earthquake.) Potential repair costs resulting from seismic damage should be factored into the project selection criteria if conditions warrant. Seismic design of waterfront retaining structures is covered by Ebeling and Morrison (1993).

VI-3-2. Seasonal Profile Variation.

a. Many shore-normal cross-sectional beach profiles exhibit a distinct variation with season, characterized by a lowering of the profile at the shoreline during the stormy winter months and a building up of the profile at the shoreline during calmer summer months. The winter wave conditions contribute to movement of sand in a seaward direction and a general flattening of the profile. Winter profile erosion occurs fairly rapidly during storms, and some periods of beach recovery may occur between storm events. The calmer wave conditions typical of summer months contribute to the shoreward movement of sediment and a rebuilding of the beach at the shoreline with a steepening of the profile. Beach recovery occurs fairly continuously, but at a slow rate. Thus, complete recovery from a series of severe winter storms may not occur during the following summer season.

b. Seasonal weather patterns may also influence the direction and magnitude of net sediment transport at a project site, resulting in beach profile changes as longshore sediment supply increases or diminishes according to the site characteristics. Of course, pronounced profile changes beyond the seasonal variations can occur during any season in conjunction with strong storm wave conditions, and some profiles may be experiencing long-term erosional changes that are more subtle than seasonal variations.

c. The extent of seasonal cross-shore profile variations can be an important design consideration for shore protection projects, such as seawalls, revetments, beachfills, pipelines, and offshore breakwaters. For example, knowledge of the seasonal lowering of the beach profile fronting a seawall will be a factor when evaluating the type and extent of toe protection needed for seawall stability. Cross-shore profile seasonal variations are of lesser importance in the design of navigation structures such as breakwaters and jetties.

d. Seasonal variations in alongshore transport may influence design of coastal projects constructed normal to the shoreline, such as groins, jetties, piers, beachfills, and sand bypassing plants. For example, a groin at the boundary of a beach renourishment project might be needed to retain a beachfill during seasons of high longshore sediment movement.

e. As discussed in Part V, functional project design considers the potential impacts a coastal project may have on adjacent or fronting beaches. Conversely, the design of specific project components must anticipate whether or not the expected post-construction shoreline or profile changes will impact the component design. The type and location of a coastal project may cause substantial changes to the seasonal cross-shore and alongshore beach profile variations due to the influence of the project on the before-project coastal processes.

f. The seasonal extent of beach profile variations at a location can be approximated from historical profile data or with periodic site inspections over several years provided the yearly wave climatology during the observation period is typical for the site. Reliability of seasonal profile change estimated from measured beach profile data is a function of yearly profiling frequency, the number of years represented in the profile records, and the accuracy of the surveys. Judging seasonal variations using a few isolated profiles is not likely to produce a meaningful result. Always be aware that a single extraordinary storm could cause profile

variation and beach recession several times that of a typical year, thus masking the true seasonal variation.

g. Profile variations due to seasonal changes in longshore sediment transport are more difficult to estimate than profile changes caused by storm activity. Generally, the coastal engineer needs to be aware of time periods when the supply of longshore sediment may be curtailed, which would result in a lowering of the profile.

VI-3-3. Flanking Possibility.

a. Some coastal projects, particularly shore protection projects located on or near the active shoreline, may be vulnerable to flanking damage due to continued beach erosion beyond the project boundaries. Flanking of a coastal structure, if left unchecked, will eventually lead to progressive damage of the project; and eventually periodic maintenance or rehabilitation will be required. Special attention should be given to designing suitable transitions between the project and adjacent non-project areas.

b. Ideally, shore protection projects should extend shoreward past the zone of active erosion to a stable portion of the beach or should be tied into a less erodible feature, such as a low bluff or dune. However, this is often not feasible due to increased costs, property boundaries, or other practical reasons. End transition sections for coastal structures should retreat landward and include enhanced toe protection in anticipation of increased erosion at the project terminus.

c. Possibility of flanking should also be considered when designing shore-connected structures such as jetties and groins. Navigation channel jetty structures are vulnerable to breaching on their landward end due to erosion on the seaward side and/or the interior bay side, as illustrated in Figure VI-3-1. This problem is usually associated with jetties stabilizing barrier island tidal inlets. The landward extent of the shore-connected structure must be sufficient to preclude the possibility of breaching due to shoreline recession, and it may be necessary to armor the bay-side shoreline with revetment (as shown on Figure VI-3-1) to stem potential erosion.

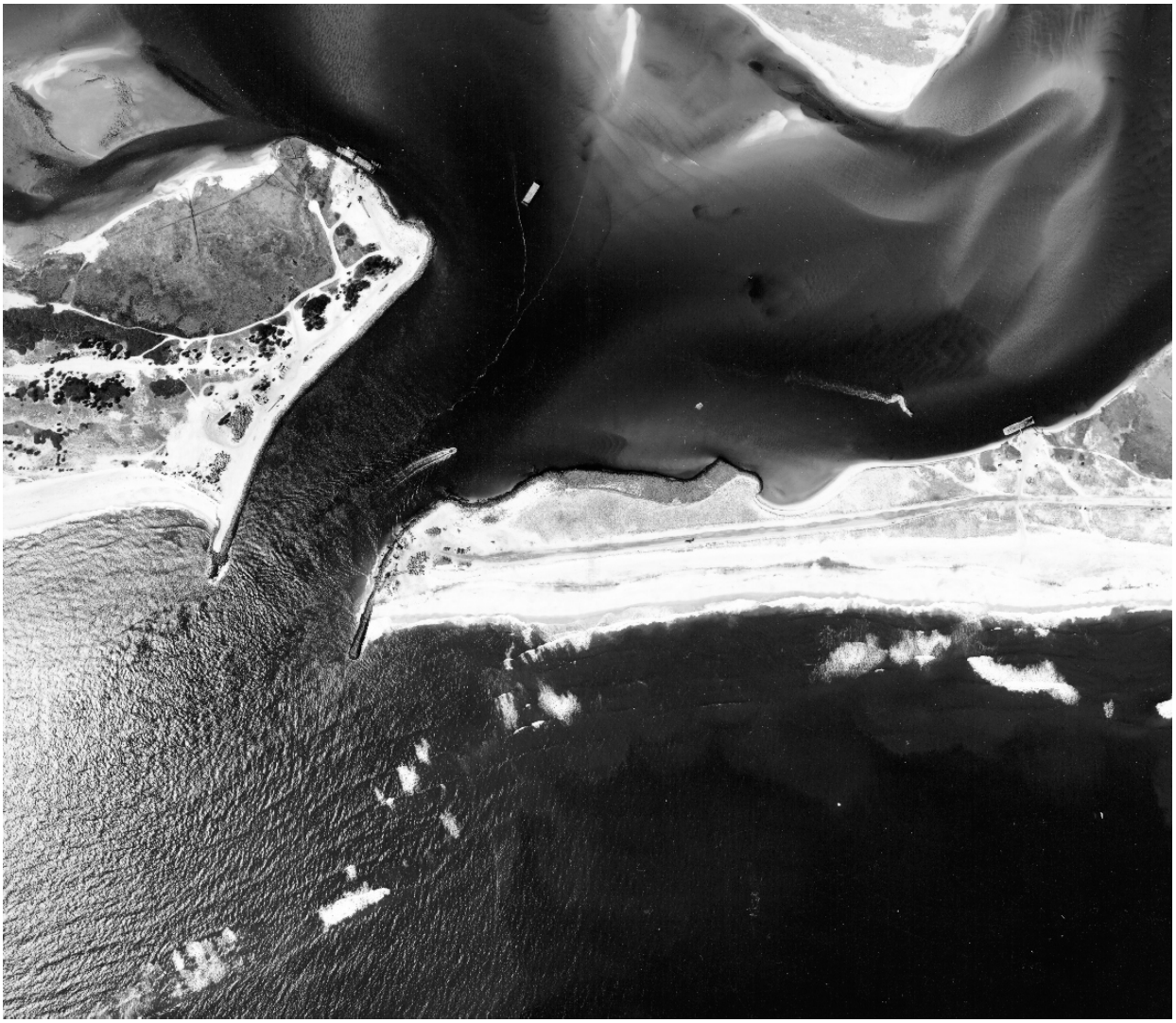

Figure VI-3-1. Bayside erosion and protective revetment at east jetty of Moriches Inlet

VI-3-4. Seismic Activity.

a. Coastal projects constructed in regions known to experience seismic activity may need to consider potential impacts related to ground deformation and severe liquefaction. Seismic loading may also be a concern in design of confined dredged material berms (subaerial) and caps (subaqueous) where liquefaction could release contaminated sediments.

b. Designing for seismic activity depends largely on the type and function of the project. For example, partial or complete failure of a breakwater or jetty during an earthquake probably will not result in catastrophic damage or loss of lives; therefore, these structures are usually not designed to withstand seismic loadings. Conversely, seismic failure of some coastal structures may carry substantial consequences if human life is at risk, repair costs are high, or vital services or commerce might be interrupted. Port and harbor facilities in particular fall into this category. The earthquake that struck Kobe, Japan in 1994 (magnitude about 7.0 on the Richter scale) resulted in ground motions and liquefaction so severe that quay walls sunk, gantry cranes were

toppled, and 179 of 186 berths at the port had to be shut down (Matso 1995). In addition to direct damage of coastal project elements, engineers must consider potential damage to adjacent facilities that could result from failure or partial collapse of a coastal structure. In Kobe, an approach span to a harbor bridge collapsed when liquefaction resulted in a 2-m lateral movement of a seawall and highway column foundations being supported on the retained fill. Monolithic coastal structures in Japan are designed to resist earthquakes.

c. Until 1994, Corps of Engineers= experience with earthquake effects on coastal structures generally had indicated relatively minor damage to Corps-maintained rubble-mound breakwaters and jetties in Southern California. However, a 6.7-magnitude earthquake (Richter scale) at Northridge in 1994 was thought to have caused additional damage to the Channel Islands north jetty that had been previously damaged by a storm (Department of the Army 1995). The relative flexibility of rubble-mound structures makes them more suitable for withstanding earthquake loads with usually only minor settlement or damage to the armor layers. Monolithic-type structures are less likely to survive seismic loading unscathed.

d. Waterfront retaining structures typical of ports and harbors often have cohesionless soils beneath and behind them with relatively high water tables. During strong ground vibrations, there is a possibility of pore pressure buildup and associated liquefaction. Designing for such an occurrence is still an evolving art, with past experience and empirical results forming a substantial portion of the design guidance. Ebeling and Morrison (1993) provide a useful overview of specific design procedures applicable to the design of waterfront retaining structures.

e. The decision to allow for seismic loadings in coastal project design should be made on a case-by-case basis. When loss of life and interruption of vital services are not considerations, the decision to design for seismic loading may hinge on such factors as estimated repair costs versus replacement costs, or the risk of damage versus increased initial construction costs.

VI-3-5. Ice.

a. Ice loading.

(1) At some latitudes, freshwater lakes and coastal regions experience annual ice formation during portions of the year. Thus, in planning stages it is important to determine if the presence of ice adversely impacts the project=s functionality; and during design, it is important to consider the effect that ice loads and impacts might have on individual coastal project elements. (Also see Part V-3-13-d.)

(2) Most cases of ice action on coastal project elements fall into one of the below categories:

(a) **Dynamic ice forces** from floating ice sheets and floes driven by winds or currents are normally the most critical for coastal marine structures. At vertical structures the ice fails by crushing and/or splitting, which develops horizontal loads on the vertical face of the structure. At

sloping structures the ice fails by bending and/or shear, which produces both vertical and horizontal loads on the sloping face of the structure.

(b) **Static ice forces** are developed when more or less intact ice sheets encompassing structures undergo thermal expansion and contraction, or when the ice mass exerts a steady pressure due to winds or water currents. The ice undergoes plastic deformation around the structure rather than failing outright.

(c) **Broken ice forces** occur when a mass of broken pack ice is driven against a structure much like a river ice jam or ice piling up along a lakeshore. This condition may be crucial in the design of small isolated structures. Because of flexibility within a broken ice field, loading pressures on structures usually are less than pressures developed by solid ice sheets.

(d) **Uplift and drawdown forces** are associated with ice that has frozen to a structure, such as a vertical pile, or with ice that rests atop a structure such as a breakwater. Changes in water level that suspend or submerge a portion of the ice create gravity or buoyancy loads, respectively.

(3) The above-listed forces pertain to the structural loading on the larger coastal project elements. Smaller additions to the project, such as railings, navigation aids, lights, or other relatively fragile structures, are easily damaged by ice riding over the structure.

(4) Table VI-3-2 summarizes the effects ice may have on the design of coastal project elements. Design guidance and appropriate references for use in estimating ice loads are given in Part VI-5-8-b, “Ice Forces.” Additional information can be found in a monograph from the ASCE Technical Council on Cold Regions Engineering (Chen and Leidersdorf 1988) and in proceedings of the *International Offshore and Polar Engineering Conference* series sponsored by the International Society of Offshore and Polar Engineers.

b. Ice on sloping-sided (rubble-mound) structures.

(1) Sackinger (1985) distinguished several categories of ice action that could occur at rubble-mound structures:

(a) rideup of sheet ice on the structure slope,

(b) piling up of fractured ice fragments on the slope,

(c) ice sheets or fragments overriding the structure crest,

(d) dislocation of individual armor units by a moving ice sheet,

(e) damage to individual armor units by ice fragments,

(f) lateral forces on the entire structure by an ice sheet, and

(g) grounded ice rubble adjacent to the structure that could impede functionality.

(2) Massive rubble-mound structures, such as breakwaters and jetties built to protect harbors on open coasts are seldom affected to any great extent by ice loading. In these cases, the design wave loads are comparable in magnitude to the maximum possible pressure that could be developed in an ice sheet; and because maximum wave loads and ice thrust cannot occur at the same time, no special provision is made in the design. Smaller armor stones and concrete armor units may be frozen into the ice and displaced vertically with the ice during periods of water level increase (e.g., tides or seiche). However, small displacements of individual armor units should not adversely impact structure stability due to the random nature of rubble-mound armor layers. Increased breakage of 1,800-kg (2,000-lb) dolos on the Cleveland East Breakwater during winter months was attributed to a combination of increased wave action and ice forces (Pope, Bottin, and Rowen 1993).

Table VI-3-2
Ice Effects in Coastal Project Design (after Peyton (1968))

Direct Results of Ice Forces on Structures	
Horizontal forces on structures caused by:	Failure of laterally moving ice sheets by crushing.
	Failure of laterally moving ice sheets by bending.
	Impact by large floating ice masses.
	Plucking of individual armor units frozen to ice.
Vertical forces on structures caused by:	Weight of ice frozen to structure and suspended at low tide.
	Buoyancy of ice frozen to structure and submerged at high tide.
	Vertical component of ice sheet bending failure induced by ice breakers.
	Diaphragm bending forces during water level change of ice sheets frozen to structural elements.
	Weight of ice on superstructure elements caused by ice spray.
Second-order effects on structures caused by:	Movement during thawing of ice frozen to structure elements.
	Expansion during freezing of entrapped water.
	Jamming of ice rubble between structural framing members.
Indirect Results of Ice Forces on Structures	
Mooring loads caused by impingement of ice sheets on moored vessels.	
Ship impacts during mooring that are greater than normally expected.	
Abrasion and subsequent corrosion of structural elements.	
Low-Risk, But Catastrophic Considerations	
Collision by a ship caught in fast-moving, ice-covered waters.	
Collision by an extraordinarily large ice mass of very low probability of occurrence.	

c. Ice on vertical-wall structures.

(1) Vertical-wall structures must account for lateral ice loads caused by wind or currents acting on ice sheets. Heavy ice in the form of solid ice sheets or floating ice fields may exert sufficient lateral loads to dislodge monolithic structures off their base, and adequate precautions should be taken to secure the structure against sliding on its base. Generally, this should only be a concern for smaller structures designed for mild wave conditions, and in these cases it may be necessary to operate ice breakers to avoid potential buildup of large ice sheets. Lateral ice loads also could cause high overturning moment loads on the foundation.

(2) Uplift forces can occur with changes in water level when ice freezes to the structure, and additional ice surcharge needs to be included in the foundation design loading. Abrasion of the vertical face by ice rubble could lead to spalling of concrete or damage to timber wales. Large ice floes may ground on any submerged rubble berm structure, resulting in damage to the rubble mound.

d. Ice on the shoreline and shore protection structures. Occasionally, ice formations can cause damage to the shoreline and shoreline protective structures, but often the net ice effects are largely beneficial. Freezing spray on banks and structures covers them with a protective ice layer; however, thawing of frozen bluffs may contribute to bluff collapse. Ice driven ashore and piled up on beaches and structures generally does not cause serious damage, and in many instances the ice provides additional protection against winter storm waves. Ice formations may cause abrasion of timber or poorly fabricated concrete structures, and individual structural members may be bent or broken by the weight of the ice.

e. Ice on floating breakwaters. Floating breakwaters are particularly susceptible to ice impact, ice buoyancy lifting, and lateral ice loads. An additional concern is the transfer of ice loads to the floating structure=s mooring system, and the possibility of mooring line breakage or anchor dragging. Many floating structures are used seasonally and removed during winter months. Because most floating structures are not designed for severe wave loading conditions, ice loading may be the most critical design condition for those floating structures that serve through the winter.

f. Ice on piles and piers. Lightly loaded (tapered) piles can be lifted when ice that is frozen to the pile undergoes upward motion due to water level fluctuations caused by tides, or in some cases, passing vessels. Lifting of the pile is contingent on the ice sheet freezing to the pile in a relatively short time, and the force necessary to lift the pile is less than the force that would fracture the ice sheet. Lowering of the tide level does not return the pile to its original position because driving a pile takes more force. This problem can be alleviated by placing fiberglass, PVC, or plastic sleeves around piles to cover the region from high water to below the depth of freezing. When ice freezes to the sleeve, the ice sheet can oscillate freely without exerting vertical loads on the pile. An alternate method is to keep the region around the pile free of ice by using “bubble curtains” that continually circulate the warmer water at the bottom up to the surface. This is accomplished by forcing compressed air through perforated pipes placed on the bottom. Piles and pier structures are also subject to lateral ice loads, impacts, and abrasion by ice floes. For example, ships maneuvering in an ice field can induce lateral displacement of ice, resulting in lateral forces on nearby piles.

VI-3-6. Environmental Considerations.

a. Understanding and mitigating environmental impacts of coastal projects are key considerations throughout the planning, design, construction, and maintenance phases of all projects. Potential environmental impacts need to be identified early in the planning process and proactively addressed during subsequent functional design. Parts V-3-12, “Environmental Considerations,” and V-4-1, “Project Assessment and Alternative Selection,” provide details about environmental aspects that could influence the coastal project design.

b. Once environmental concerns have been identified and project alternatives have been developed to minimize environmental impacts, the engineer must design individual project elements to conform to the environmental guidelines established for each alternative. Each project site will have its own unique environmental considerations, so it is difficult to generalize what allowances will have to be made in project element design. Often design parameters that best fulfill the environmental requirements may not result in a project that is the most cost-effective or easiest to construct. For example, crest elevation for a seawall might be established so as not to block the view of the fronting beach and water; however, this could lead to unacceptable wave overtopping during storm events. In this case, the coastal engineer must consider structure alternatives, such as a milder structure slope or recurved seawall face, to compensate for the lowering of crest elevation.

c. Another environmental consideration that might influence the actual design of individual project elements relates to project construction. Concern for various species may constrain the time periods when construction can occur. For example, beach nourishment projects cannot be constructed during turtle nesting season, and dredging activities should avoid fish spawning periods. Construction during acceptable periods may expose the partially constructed project to adverse weather conditions, and the design should allow for these increased loads during construction. Construction methods that cause significant dust, noise, water turbidity, or disruption to local activities may need to be altered to comply with environmental standards. Some changes in construction procedure could result in changes to the project design.

d. In general most environmental design parameters are established during project functional design and carried over into design of individual project elements. The engineer must develop a viable design that meets the environmental design criteria or state compelling reasons why this is not feasible.

VI-3-7. Construction Considerations.

a. Fundamental to engineering design is the skillful combination of design elements necessary to resist the imposed loads along with practical elements related to project construction. This is particularly true of many coastal engineering projects where construction often involves massive quantities of material that must be accurately placed into the water when environmental conditions are less than ideal. Design optimization of coastal project elements without factoring in construction considerations will likely result in an elegant design that is expensive and difficult (if not impossible) to build.

b. Availability of construction material, equipment, and skilled labor determine, in part, the project construction procedure. Practical knowledge and/or experience about how construction will proceed helps the engineer to evaluate the possibilities and modify the design to best accommodate construction needs. Severe constraints in construction procedures will impact the design accordingly. Depending on the type of coastal project, construction may require land-based plant, floating plant, or some combination thereof. In cases where either option is viable, this becomes an important decision that should be weighed carefully. The following sections highlight some of the construction factors that influence or modify engineering design of coastal project elements.

(1) Availability of materials. The primary materials used in construction of coastal projects are stone, concrete, beach sand, steel, timber, and geotextiles (Part VI-4, "Materials and Construction Aspects," provides a more in-depth examination of materials and material properties). Large material quantities are required for many coastal projects, and considerable savings in transportation cost and future maintenance costs can be achieved if suitable materials can be obtained locally, or if the design can be adapted to use the locally available materials. For example, it may be less expensive to armor a coastal structure using concrete armor units if no local quarries can produce sufficient quantities of required stone sizes. Other considerations include methods of material transport and whether the required material quantities can be delivered when needed for construction.

(a) Rubble-mound structures depend on availability of large amounts of suitably sized stone at low cost. Source and availability of stone should be investigated during design, not after the design has been completed. If possible, the design should be tailored to the known output capability of the quarry expected to be used as the supplier. Quarry production records are helpful in assessing rock quality, density, durability, sizes, and gradation. Part V-3-15, "Availability of Materials," contains information and references on quarry inspection and stone quality.) If the quarry is unable to deliver the ideal stone size and gradation at a reasonable cost, it may be necessary to design a structure with milder slopes that can be protected with smaller stone. Alternately, a dynamic-slope structure could be specified with the initial slope being reshaped by the waves into an equilibrium profile.

(b) Designs specifying significant amounts of concrete require an affordable source of quality aggregates and sand. Beachfill projects rely on nearby sources of inexpensive, beach-quality sand. Beachfill construction techniques, and possibly the construction sequence, may depend on whether the selected sand source is inland or offshore of the project.

(c) When possible, construction of project components should use standard off-the-shelf items rather than custom manufactured components. Typical components might include sheet piles, piles, timbers, anchoring systems, steel members, prestressed concrete beams, etc. Substantial cost savings can be realized if minor design modifications result in the use of standard components.

(2) Availability of construction equipment. Coastal engineering construction can involve highly specialized equipment, such as heavy-duty cranes, barges, dredges, pipeline dredges, and large trucks. If a vital piece of equipment is unavailable, construction schedules and delays will add significantly to the costs. When the option exists for either land-based or floating construction, the availability and capacity of plants to handle the selected materials and construction procedure are key factors in the decision. Construction time can be decreased if the design permits more equipment to work in tandem.

(a) Additional equipment-related considerations are the time and costs associated with mobilization and demobilization of construction equipment. Land-based equipment mobilization time is generally shorter than the time needed to mobilize floating equipment. This is especially true if terminal facilities have to be constructed (CIRIA/CUR 1991). Barges and floating construction equipment and the skilled labor needed to operate the equipment are not as readily available as for land-based equipment.

(b) Placement of armor stones on rubble-mound structures is critically dependent on the capacity of the crane, which is determined by the maximum armor stone weight at the longest reach. Therefore, placement of toe stone and berm armor will impose the worst loads on the crane. For large rubble-mound structures the design engineer should consider the ramifications of decreasing structure slope and reducing the armor stone size accordingly, if the change facilitates use of a smaller crane. In situations where the stone size cannot be reduced and the capacity of existing cranes is inadequate, floating equipment can be employed to place the armor units beyond the safe reach of land-based cranes.

(c) Concrete armor units are used where stone of sufficient size is unavailable. Casting of the units requires a nearby concrete plant, a ready supply of materials, a casting yard large enough to stockpile enough units to keep abreast of construction, and a good supply of concrete forms. Economics may justify using existing forms for concrete armor units, even if the forms are larger than the size determined by the design analysis. The increased cost in materials is offset by not having to fabricate new forms. For information on availability of existing concrete armor unit forms used in previous construction, check with contractors and the Government agency or construction firm responsible for the project.

(d) Regardless of the type of coastal project being constructed, it is important for the design engineer to be aware of the types of equipment that will be required and to consider the entire construction sequence. Design modifications that avoid any obvious weak links related to availability of equipment may be crucial to project success.

(3) Constructability. Certain types of coastal projects can be constructed using either land-based or water-based construction techniques. The project design may need to be altered to facilitate one method over the other, and the best alternative might be a combination of both techniques. Land-based equipment is almost always preferred to floating equipment, and barge dumping is often more expensive. Therefore, when feasible, land-based construction should be used.

(a) Project construction with a floating plant depends primarily on water depth, tide range, currents, wave conditions, structure configuration, and equipment availability. Construction using floating equipment is possible for placing materials at levels deeper than 3 m below the low water level relative to vessel draft (CIRIA/CUR 1991). This allows rapid and efficient barge dumping of the core material. Long structures extending into deeper water are better suited to construction using floating equipment, and work can progress at several project locations simultaneously. Existing terminal facilities at the project site help to reduce costs when loading material and equipment onto barges.

(b) Cranes on floating platforms may have difficulty accurately placing heavy loads on the higher portion of structures like breakwaters and jetties because of the long reach. Likewise, underwater placement is also difficult. In areas with a large tide range, it may be possible to plan the construction procedure to take advantage of the differing water levels. Risk of damage to floating equipment is an important concern, and water-based construction has a greater probability of work stoppage during harsh wave and wind conditions.

(c) Land-based construction requires sufficient maneuvering space for the construction equipment. For shore protection structures located on the shoreline, access to the immediate area behind the structure is usually required. Construction of shore protection structures can proceed at more than one location, but care must be taken to avoid weakness where different sections join.

(d) Breakwaters and jetties can be built out seaward from dry land equipment located on a road built on the structure crest; generally construction can proceed on only one front. Crest elevation may need to be increased over that established to meet the overtopping criterion to assure the safety of construction equipment and personnel during heavy wave action, and sufficient crest width is needed for trucks and other equipment to pass or to accommodate special equipment. It may be necessary to add special turnaround areas to the structure. Some of the changes to accommodate land-based construction may increase the structure cross section beyond that required for stability and functionality. Risk of damage to land-based equipment is usually less than for water-based construction, and there will tend to be less work interruption due to storm wave conditions. Care must be taken to protect equipment from vandalism and theft.

(e) Accurate underwater placement of construction materials is a function of water depth, water clarity, wave conditions, and equipment. If accurate placement under water is expected to be difficult, design of that portion of the project will have to compensate for less than optimal construction. Placing geotextiles under water in a wave and current environment is also difficult, and the engineer should consider how the placement will be accomplished. Land-based construction of the underwater portion of rubble-mound structures and toes is difficult, and there may be a tendency to oversteepen the underwater slope.

(f) Construction of coastal projects requires experienced contractors, crane operators, and labor crews. Contractors should be given some leeway in fulfilling the essential aspects of constructing the project according to design specifications. Novel or unique projects will challenge even experienced contractors, and the engineer should be open to design modifications suggested by the winning bidder on the project. Experienced construction inspectors also may have good suggestions based on practices they have witnessed on previous projects.

(4) Design requirements during construction. Most completed coastal projects are expected to withstand severe environmental conditions with little or no damage (beachfills are a notable exception), but these same projects may be quite vulnerable to damage if exposed to high waves during the construction phase when not yet fully armored. Although large tide ranges can be beneficial to construction, there is also the possibility that storm waves could break on the partially completed structure during some stage of the tide.

(a) Land-based construction is concentrated around the crane position, so it is usually possible to build the structure to its full strength as construction progresses. Therefore, only a small portion of the unprotected project is exposed at any one time. Temporary stability of placed materials is necessary, and an approaching storm may necessitate temporary protection of incomplete construction in order to withstand the storm with minimum damage. Project construction may concentrate currents at the structure head and cause scour holes to develop. Infilling of the holes will add additional expense and delay construction.

(b) Water-based construction can proceed over a wider area and the risk of damage to uncompleted portions can be limited by not exposing the underlayers to breaking waves unless it can be immediately protected by the primary armor. Likewise, scour hole development can be curtailed by providing scour protection well in advance of the structure.

(c) Temporary roads, construction access, or construction supports on the project should be anticipated and allowed for as part of the design loads (also see Part V-3-16, "Accessibility"). In addition, removal of temporary engineering works must be undertaken so as not to damage or weaken the structure. Project construction may disrupt ongoing activities in the vicinity, such as navigation, dredging, beach recreation, etc. These construction impacts should be minimized if possible. Onsite facilities and storage areas for materials and equipment should be sufficiently large to supply the project at all times. Limited storage areas or supply lines may necessitate a construction procedure that reduces risk of damage to partially completed structures. Floating breakwaters require a means of transporting project components to the site and a safe method of connecting the modules into a continuous floating breakwater.

VI-3-8. Other Design Considerations.

a. Regulatory compliance. As discussed in Part V-2-1, "Planning and Design Process," and Part V-3-13, "Regional Considerations," coastal projects require regulatory approval from Federal, state, and local agencies. These approvals will likely be contingent upon the project meeting certain criteria. For example, local permitting agencies may be unwilling to grant construction approval for a seawall if the crest elevation blocks the view from a popular boardwalk or if adequate beach access is lacking. Likewise, construction of a project may require additional work to mitigate project impacts to an acceptable level. Fulfilling the regulatory requirements may impact the project design, the method of construction, the transportation of materials to the site, or even the choice of construction materials. Therefore, the design engineer must have a clear understanding of provisions expected to appear in various permits and approvals so that the design will meet all approval criteria. Failure to consider these important aspects will result in delays, added expenses, or possibly a nonviable project.

b. Project maintenance. The design engineer should be aware of maintenance requirements for each project element and assure that the design permits necessary maintenance to take place. Accommodating maintenance is particularly important for coastal projects, such as beachfills and rubble-mound structures, which are expected to suffer some degree of damage over the life of the project.

(1) Projects built using floating equipment will generally require floating equipment for maintenance activities. Projects constructed with land-based equipment may have adequate access for maintenance using land-based equipment, but this will depend on costs to mobilize the necessary equipment. For example, jetties with an installed concrete cap and road provide easy access and mobilization costs would be low, whereas jetties without a cap would require construction of a road over the structure crest before equipment could be moved into place. In the latter case it might be more economical to perform maintenance and repair using floating equipment.

(2) Monitoring and periodic inspections of coastal projects may be required to determine when maintenance should be performed (Part VI-8-2, "Inspecting and Monitoring Coastal Structures"). If the type of expected monitoring has been determined, it may be wise to include monitoring aids as part of the design. Such aids might include surveying targets, aerial photogrammetry targets, in situ monitoring instruments, etc.

(3) Maintenance considerations for floating structures include replacing connections and anchoring system components, removing marine growth which could affect the flotation height of the structure, replacing unsafe guardrails, and taking steps to prevent concrete deterioration. The designer should anticipate how the maintenance can be accomplished without subjecting the structure to additional risk. Design of super-structure, guardrails, walkways, etc., on coastal projects should strive for low maintenance requirements.

c. Disposal of dredged materials. Dredging may be required to gain access to the project site, for entrenching toe materials, for backfilling higher quality foundation material, or for other reasons. When dredging is to occur, dredging volumes should be estimated, and the method of dredged material transport and disposal should be determined. Beneficial uses of the dredged material should be considered, particularly if the displaced material consists primarily of beach-quality sediment. Guidance on dredging disposal and beneficial uses of dredged material can be found in Engineer Manuals 1110-2-5025 (Department of the Army 1983) and 1110-2-5026 (Department of Army 1987). Also, papers from technical specialty conferences, e.g., *Dredging '94* (American Society of Civil Engineers 1994), provide useful information.

d. Aesthetics. Coastal projects should be pleasing in form as well as functional. Good workmanship and close adherence to design contribute to project aesthetics. Repair sections should be geometrically similar to the original structure, and transitions between new and existing project elements should be made attractive, if possible. Public reaction to existing projects can serve as input to new designs and modifications. Examples of projects that require aesthetic consideration are low-cost shore protection devices, which may be viewed as unsightly, or high-crested structures, which may block a scenic ocean view.

e. Aids to navigation. Prior to construction of any coastal project that may impact navigation, or interrupt any existing aids to navigation, complete project information should be provided to local authorities (Coast Guard District Commander). This information should include details about project authorization, the proposed construction schedule, and a detailed drawing showing the project location relative to existing features. Local authorities may require a set of "as-built" plans after the project has been completed, and it may be necessary to include new aids to navigation as part of the project design.

f. Fishing platforms. Coastal structures normally provide excellent habitat for fish, which in turn attract recreational fishermen to the structures. Where safe and justified, project designs should include accommodations for recreational fishing. However, recognize that many coastal structures, such as low-crested rubble-mound breakwaters and jetties, are inherently unsafe during larger waves and higher water levels, and there is a substantial risk of fishermen being swept into the water. This risk, combined with the difficulty of providing guardrails on rubble-mound structures, may preclude fishing activities at the project, and provisions may be needed to prevent site access to unauthorized personnel.

g. Vandalism and theft. At some project sites it may be necessary to consider the potential consequences of vandalism and theft of materials. If vandalism and theft are potential threats to a project, construction materials must be chosen that cannot be easily cut, carried away, dismantled, or damaged. For example, sand-filled geotextile bags can be cut, small concrete blocks can be stolen, and wire gabions can be opened with wire cutters. Such damage could initiate considerable damage to the structure. On the other hand, there are no documented thefts of 30-ton armor stones.

VI-3-9. References.

EM 1110-1-1802
Geophysical Exploration for Engineering and Environmental Investigations

EM 1110-1-1804
Geotechnical Investigations

EM 1110-1-1906
Soil Sampling

EM 1110-2-1906
Laboratory Soils Testing

EM 1110-2-5025
Dredging & Dredged Material Disposal

EM 1110-2-5026
Beneficial Uses of Dredged Material

American Society of Civil Engineers 1994
American Society of Civil Engineers. 1994. *Proceedings of the Second International Conference on Dredging and Dredged Material Placement*, E. Clark McNair, ed., two volumes, American Society of Civil Engineers, New York.

Chen and Leidersdorf 1988
Chen, A. T., and Leidersdorf, C. B., eds. 1988. “Arctic Coastal Processes and Slope Protection Design,” Technical Council on Cold Regions Engineering Monograph, American Society of Civil Engineers, New York.

CIRIA/CUR 1991
Construction Industry Research and Information Association (CIRIA) and Centre for Civil Engineering Research and Codes (CUR). 1991. “Manual on the Use of Rock in Coastal and Shoreline Engineering,” CIRIA Special Publication 83/CUR Report 154, CIRIA, London and CUR, The Netherlands.

Department of the Army 1995
U.S. Army Engineer District, Los Angeles. 1995. “Channel Islands Harbor, Ventura County, CA: Basis for Design, North Jetty Repair,” Los Angeles, CA.

Ebeling and Morrison 1993
Ebeling, R. M., and Morrison, E. E. 1993. “The Seismic Design of Waterfront Retaining Structures,” NCEL Technical Report R-939, Naval Civil Engineering Laboratory, Port Hueneme, CA.

Eckert and Callender 1987
Eckert, J., and Callender, G. 1987. “Geotechnical Engineering in the Coastal Zone,” Instruction Report CERC-87-1, U.S. Army Engineer Waterways Experiment Station, Coastal Engineering Research Center, Vicksburg, MS.

Matso 1995
Matso, K. 1995. “Lessons from Kobe,” *Civil Engineering*, American Society of Civil Engineers, Vol. 65, No. 4, pp 42-47.

Peyton 1968
Peyton, H. R. 1968. “Ice and Marine Structure,” *Ocean Industry Magazine*, Parts 1-3, March, September, and December.

Pilarczyk 1990
Pilarczyk, K. W. 1990. “Design of Seawalls and Dikes - Including Overview of Revetments,” in *Coastal Protection*, K. Pilarczyk, ed., A. A. Balkema Publishers, Rotterdam, The Netherlands.

Pope, Bottin, and Rowen 1993
Pope, J., Bottin, R. R., Jr., and Rowen, D. 1993. “Monitoring of East Breakwater Rehabilitation at Cleveland Harbor, Ohio,” Miscellaneous Paper CERC-93-5, U.S. Army Engineer Waterways Experiment Station, Coastal Engineering Research Center, Vicksburg, MS.

Sackinger 1985
Sackinger, W. 1985. “Ice Action Against Rock Mound Structure Slopes,” *Design and Construction of Mounds for Breakwaters and Coastal Protection*, P. Bruun, ed., Elsevier, Amsterdam.

VI-3-10. Acknowledgments.

Author: Dr. Steven A. Hughes, Coastal and Hydraulics Laboratory (CHL), U.S. Army Engineer Research and Development Center, Vicksburg, MS.

Reviewers: Dr. Hans F. Burcharth, Department of Civil Engineering, Aalborg University, Aalborg, Denmark; Han Ligteringen, Delft University of Technology, The Netherlands; John H. Lockhart, Headquarters, U.S. Army Corps of Engineers, Washington, DC (retired); Charlie Johnson, U.S. Army Engineer District, Chicago, Chicago, IL (retired); Michael C. Mohr, U.S. Army Engineer District, Buffalo, Buffalo, NY; and Joan Pope, U.S. Army Engineer Research and Development Center, Vicksburg, MS.

CHAPTER 4

Materials and Construction Aspects

TABLE OF CONTENTS

Page

VI-4-1. Material Requirements VI-4-1

a. Material properties and strength VI-4-1
b. Material durability VI-4-2
c. Material adaptability VI-4-4
d. Material costs VI-4-4
e. Material availability VI-4-4
f. Material handling requirements VI-4-6
g. Material maintenance requirements VI-4-7
h. Material environmental impacts VI-4-8

VI-4-2. Earth and Sand VI-4-9

a. Uses of earth and sand in coastal construction VI-4-9
b. Physical and mechanical properties of earth and sand VI-4-10
c. Placement considerations for earth and sand VI-4-15
d. Environmental effects on earth and sand VI-4-15

VI-4-3. Stone VI-4-16

a. Use of stone in coastal construction VI-4-16
b. Physical and mechanical properties of rock VI-4-17
c. Quarrystone procurement and inspection guidelines VI-4-22
d. Placement considerations for stone VI-4-23
e. Environmental effects on stone VI-4-27

VI-4-4. Portland Cement Concrete and Bituminous Concrete VI-4-28

a. Use of concrete and asphalt in coastal construction VI-4-28
b. Physical and mechanical properties of concrete VI-4-30
c. Physical and mechanical properties of asphalt VI-4-35
d. Concrete construction practices VI-4-36
e. Concrete for armor units VI-4-38
f. Environmental effects on concrete and asphalt VI-4-39

VI-4-5. Steel and Other Metals VI-4-40

a. Use of metal in coastal construction VI-4-40
b. Physical and mechanical properties of metals VI-4-41
c. Design values for structural metals VI-4-43
d. Metal protective treatments VI-4-46
e. Metal fasteners and connections VI-4-46
f. Environmental effects on metal VI-4-47

VI-4-6. Wood VI-4-47

a. Use of wood in coastal construction VI-4-47
b. Physical and mechanical properties of wood VI-4-48
c. Design values for structural lumber VI-4-50
d. Wood preservatives and treatment VI-4-51
e. Wood fasteners and connectors VI-4-51
f. Environmental effects on wood VI-4-52

VI-4-7. Geotextiles and Plastics VI-4-53

a. Use of plastics in coastal construction VI-4-53
b. Physical and mechanical properties of plastics VI-4-55
c. Design requirements for geotextile fabrics VI-4-57
d. Geotextile installation considerations VI-4-61
e. Environmental effects on geotextiles and plastics VI-4-64

VI-4-8. References VI-4-65

VI-4-9. Acknowledgements VI-4-68

VI-4-10. Symbols VI-4-69

List of Figures

Figure VI-4-1. Uniform placement VI-4-25

Figure VI-4-2. Random placement VI-4-25

Figure VI-4-3 Selective placement VI-4-26

Figure VI-4-4 Special placement VI-4-27

Figure VI-4-5 Typical use of geotextile fabric in coastal revetment VI-4-54

List of Tables

Table VI-4-1. Soil Density Parameters VI-4-11

Table VI-4-2. Typical Soil Permeability Coefficients VI-4-14

Table VI-4-3. Engineering Characteristics of Unweathered Common Rocks VI-4-18

Table VI-4-4. Durability Ranking for Common Stone VI-4-21

Table VI-4-5. Approximate Criteria for Evaluating Stone VI-4-22

Table VI-4-6. Typical Compressive Strengths of Concrete VI-4-31

Table VI-4-7. Concrete Compressive Strength for Different Water-Cement Ratios VI-4-32

Table VI-4-8. Recommended Concrete Slump for Various Types of Construction VI-4-34

Table VI-4-9. Average Unit Weight of Fresh Concrete VI-4-35

Table VI-4-10. Specifications and Applications for Steel Suitable for Marine Service VI-4-42

Table VI-4-11. Galvanic Series in Flowing Seawater at Ambient Temperature VI-4-44

Table VI-4-12. Tensile Stress Limits for Selected Metals and Alloys VI-4-45

Table VI-4-13. General Characteristics of Common Wood VI-4-51

Table VI-4-14. Comparative Properties of Geotextile Materials VI-4-56

Table VI-4-15. Minimum Geotextile Fabric Physical Property Requirements VI-4-59

Table VI-4-16. Determination of EOS and POA for Geotextiles VI-4-60

Table VI-4-17. Construction Limitations: Quarrystone Revetment VI-4-62

Table VI-4-18. Construction Limitations: Block Revetments and Subaqueous Applications VI-4-63

CHAPTER VI-4

Materials and Construction Aspects

VI-4-1. Material Requirements. Materials used to construct coastal engineering projects are critically important to the success and longevity of the project. Selected construction materials often must withstand the rigors of relentless wave pounding in a corrosive environment that may undergo freeze-thaw cycles. Primary material selection criteria are physical properties and strength, durability, adaptability, cost, availability, handling requirements, maintenance requirements, and environmental impact. Knowledge of past material performance on similar coastal projects is an important consideration for the design engineer. Much of the information presented in the following sections was condensed from a comprehensive Special Report entitled A*Construction Materials for Coastal Structures*@ by Moffatt and Nichol (1983).

a. Material properties and strength. In practically all cases, common materials having well- documented physical properties and strengths are used in construction of coastal project elements. Sections in this chapter, beginning with Part VI-4-2, give properties for widely used construction materials. General aspects of key material physical properties are listed below.

(1) Specific gravity. Specific gravity is a fundamental property for all coastal construction materials. Coastal structures, such as breakwaters, rely on self-weight of the structure to resist applied loads. Thus, materials with high specific gravity, like rock and concrete, are ideally suited for these types of applications, particularly for submerged portions where water buoyancy decreases effective structure weight. Specific gravity is also important for structures such as surge barriers and piers, which must be designed to support the weight of the component structural members. Materials with lower specific gravities, such as wood and plastics, also have uses in coastal construction. Beach renourishment projects function best if the placed beach fill material has a specific gravity the same as, or greater than, the native beach sand.

(2) Strength. Depending on the application, materials used in coastal construction may need to resist tension, compression, and flexure stresses. Material strength properties help determine the size, shape, and stability of component structural members. Structures built of stone, earth, concrete, and asphalt are capable of withstanding compression, shear, and impact loading; but they generally cannot resist tensile loads. Tensile loads in concrete structures can be tolerated provided there is sufficient steel reinforcing or prestressing of the member to carry the tensile stress. Geosynthetics add tensile strength to the soil mass.

(a) Steel, and most other metals, can accommodate high levels of tensile, compressive and torsional stresses and impact. Often steel structural members undergo considerable flexing or displacement when subjected to bending moments, and this displacement must be considered in the design. Metals also expand and contract with temperature change, which can introduce additional stress into the structure.

(b) Wood also exhibits good tensile and compressive strengths, but wood is not isotropic and its strength depends on orientation of the wood grain relative to the applied loads. Wood components can tolerate significant deflection and movement without failing.

(c) Geotextile fabrics are subjected mainly to tension, impacts, flexing, and fatigue. Synthetic structural components can resist compression, tension, shear, and torsion to varying degrees depending on the particular synthetic. Some plastics will undergo enormous deflection before yielding, whereas some plastics have very little elongation prior to failure. Strength characteristics of some synthetic materials will decrease in time due to ultraviolet radiation or other environmental factors, and precautions must be taken when using these materials. Also plastics can experience a slow, permanent deformation under constant load.

(3) Resistance to cyclic, impact, and seismic loads. Coastal engineering project elements are often exposed to continual cyclic wave loading, impact loading from waves or vessels, and occasionally accelerations due to seismic activity. Surviving these load conditions may require that portions of rigid structures be able to absorb the load without exceeding the elastic yield limit of the materials. Stone or earth structures resist these types of loads by providing stress relief through differential settlement, nesting of stone layers, or local areas of damage.

(4) Flexibility. Flexibility is the property of a material that allows it to bend without breaking. Materials with good flexibility will help absorb cyclic and impact loads, but continual flexing might eventually lead to fatigue failure, plastic deformation, and crack formation. Material flexibility is a relative term, and it depends on both the material and the shape of the structural member. For example, steel columns and beams can be designed for little deformation whereas steel rods and cables can be highly flexible. Generally, concrete and stone are considered to have little flexibility, followed by the more flexible steel and wood. Rubber and some synthetic materials are highly flexible. Flexibility can also be used to describe the response of coastal projects. For instance, the individual armor stones on a jetty have no flexibility, but the entire armor layer is capable of movement and settlement to a new position without undue loss of functionality, thus making it a “flexible” structure. Likewise, beach fills can be termed flexible structures even though the individual sand grains are rigid.

(5) Compatibility. Many projects combine different materials, and compatibility problems may arise due to differences in material physical or chemical properties. The constituent materials in composites such as concrete and asphalt must be compatible to attain adequate strength. Rigidly combining structural components of different flexibilities or different expansion coefficients may induce additional stresses or component failure. Different materials (or materials in which properties vary) undergo abrasion at different rates. For example, armor stones of different hardness may degrade at different rates, which may lead to weak spots in the armor layer. Contact between different types of metals in the marine environment can cause a galvanic reaction and rapid corrosion. Corrosion can also stem from contact with chemicals. For example, materials used to contain contaminated sediment must be able to withstand any chemical reactions that may result from direct contact with the contaminant.

b. Material durability. Durability is a relative term describing how well a material withstands the rigors of the environment into which it is placed. The durability of a particular coastal project element is a combination of the durability of the construction materials and the capability of the project to continue functioning at an acceptable level even after the construction material has begun to degrade. Therefore, material durability needs to be considered in terms of the project’s design life, first costs, and projected maintenance expenses. Projects with short

design lives can tolerate less durable materials at a reduced cost. Factors that affect a material's durability include its ability to resist abrasion, chemical attack and corrosion, marine biodegradation, wet/dry cycles, freeze/thaw cycles, and temperature extremes.

(1) Earth and sand. Earth is generally considered durable unless changes in water content or chemistry reduce grain size to the range of silts and clays. Quartz sand is very durable, but sand mixtures with high carbonate content from shell material will be more vulnerable to chemical attack if the water is acidic. Also shell particles are not as hard as quartz and are more susceptible to abrasion.

(2) Stone. Igneous rock is considered to be the most durable, but this depends partially on the geology of the rock. Sedimentary rock is usually stratified and subject to failure through shear stress, impact, chemical deterioration, or changes in water content. Sedimentary armor stones generally are more easily worn down by abrasion. Any armor stone that develops small cracks may eventually fracture due to freeze/thaw cycles, irrespective of the type of rock.

(3) Concrete and asphalt. Concrete is considered to be durable and is usually expected to last throughout the lifetime of most coastal projects, provided the concrete is not exposed to adverse chemicals or excessive abrasion, and loads are within design limits. Cracks in concrete may lead to spalling of the surface and exposure of steel reinforcement, which will immediately begin to rust. Rough handling of individual concrete armor units during placement may result in chipping or cracking of slender members. Asphalt it not considered to be a durable material because it has low strength in both compression and tension, it is subject to chemical reaction, its stiffness changes with temperature, and it is not resistant to impact or abrasion.

(4) Steel. Standard grade steel is considered very durable if properly protected from rust and corrosion throughout the project lifetime. Bare steel will rapidly deteriorate in the corrosive coastal environment. Sacrificial anodes should be provided to protect steel exposed to seawater. Abrasion of steel components by sand, particularly near the seabed, is also a problem. Stainless steel is more durable, but this advantage is often offset by increased cost.

(5) Wood. Although wood is considered less durable than concrete, lengthy service life can be obtained for wood components. Wood durability depends on the characteristics of the wood, its usage and exposure to the elements, and project maintenance. Wood is an organic material that can be attacked by plants and marine animals if precautions are not taken. Fasteners and connectors, such as bolts, nails, etc., must also be protected from corrosion to assure wood structure longevity. Dry wood is the least fire-resistant material commonly used in coastal projects.

(6) Geotextiles and plastics. Geotextiles and many plastics are generally resistant to chemical and biological attack, but will deteriorate when exposed to ultraviolet radiation. The rate of deterioration can be reduced by adding UV inhibitors, coatings, or by covering the geosynthetic with soil, sand, water, or even algal growth. Use of synthetic materials in coastal construction projects is relatively new, thus long-term durability of some synthetic materials in the coastal environment has yet to be determined. Some synthetic materials are vulnerable to fire and can generate toxic fumes when ignited. For these reasons and other functional requirements, geotextiles are generally covered with soil.

c. Material adaptability. Non-rigid mound-type stone and earthen structures can be constructed in a variety of shapes and sizes, and these structures can accommodate changes in foundation elevation and structure slope without losing functionality and structural stability. Stone and earth can be used in most weather conditions and temperature extremes without significant consequences.

(1) Concrete is very adaptable for use in coastal projects; however, cost often limits its usage to applications that cannot be effectively constructed using less expensive materials such as stone. For example, concrete vertical caisson breakwaters are used when water depths are too great for conventional rubble-mound structures or when mooring facilities are needed adjacent to the structure. Concrete is also viable for use as rubble-mound structure armor units, piles, and sheetpiling.

(2) Steel is very adaptable for complex structures, support frameworks, structures with movable parts, floating structures, and structure components. Except in the above cases, costs generally limit steel usage to piles, sheetpiling, and beams.

(3) Wood is considered to be fairly adaptable for use in smaller structures and as structure components, and it is easily stored and handled during construction. Synthetic materials usually have specific functions determined by their hydraulic and strength properties, such as geotechnical filter, separation of soil reinforcement. Geotextile tubes are finding a variety of uses due to their capability to retain fine-grained material.

d. Material costs. Because of the large quantities of material needed for most coastal projects, material cost is an important design consideration. Historically, coastal structures have been built using common, readily available materials that were obtained locally at low cost. When evaluating material costs, the cost of transporting the material to the job site must be included. If the material is not locally available, transportation costs could equal or exceed material costs per unit volume. Consequently, a more expensive local source may be preferable to a less expensive alternative located further away from the project site. Any material selection based on cost must include consideration of further maintenance expenses associated with the selection. For example, selecting a local source of lesser-quality stone for a breakwater may result in initial construction cost savings, but this choice may result in increased maintenance expense due to stone fracturing and stone abrasion. At every juncture of the design process, the coastal engineer should evaluate the costs associated with material specification. Significant cost savings can be realized for bulk materials because of the vast quantities required. However, practical choices are somewhat limited for most coastal projects. Any project design that requires fabricated components should attempt to specify common “off-the-shelf” items rather than custom-made parts. When feasible, this will result in both cost and time savings. Finally, consider the costs associated with any special material handling requirements (see below). These costs may more than offset any material cost savings.

e. Material availability. Availability of suitable materials for coastal project construction and future maintenance is an important design consideration. Lack of viable local sources for primary construction materials may limit design options or significantly increase construction costs and time of construction. For example, use of concrete in remote locations may not be feasible unless good quality sand and aggregate are locally available for onsite

mixing. The projected rate of material usage must be matched with the rate that material can be supplied. It may be necessary to stockpile material onsite to compensate for an intermittent supply and to avoid slack work periods (Thomas and Hall 1992). If plans call for future project replacement, modification, or maintenance, sufficient sources of similar (or required) materials should be determined a priori. (See Part VI-3-7, "Construction Considerations," for site-specific design factors related to material availability.)

(1) Earth and sand. In most locations an adequate local source of earth exists for use in dikes, fills, and foundations. Exceptions include areas characterized by deltaic deposits of silts and clay and some rocky coastal regions. Less common are local sources of high-quality beach sand for use in placed beach fills.

(2) Stone. Stone is generally abundant in most regions of the continental United States. However, some locations, such as the coastline of the Gulf of Mexico and South Atlantic, can be as far as 250 km or more from stone sources. Other locations may have huge quantities of stone, but the quality may not be adequate for coastal projects because of low density or low strength. An example is volcanic rock on Pacific islands. Along high wave energy coasts, coastal projects may require huge stones that are difficult to produce from local quarries.

(3) Concrete and asphalt. Cement, stone aggregate, and sand suitable for use in concrete mixtures are available in all coastal regions in the United States. Concrete materials may have to be transported to some remote locations, such as some of the smaller Pacific islands. Also, difficult local access to material sources in remote regions may make importation of concrete materials economically feasible. Generally, asphalt is available at most project sites in the United States, but use of asphalt at other locations depends on availability of the asphalt components and handling equipment.

(4) Steel. Standard grades of steel in common cross sections and stock lengths are generally available for coastal projects. Special cross sections or less-common steel specifications (such as high strength steel or even stainless steel) are less likely to be available locally and may require substantial transportation costs between the mill and construction site. Availability of prefabricated steel components depends largely on the project's proximity to qualified steel fabrication yard.

(5) Wood. In the past, wood was one of the most available materials for construction of coastal projects. However, in recent years certain types and sizes of durable hardwoods have become more difficult to obtain. This has resulted in fewer coastal projects in the United States being constructed with wood as the primary construction material. Where available locally, hardwood often compares favorably in terms of cost and utility to other construction materials for projects such as bulkheads and piers.

(6) Geotextiles and plastics. It is unlikely that most coastal project sites will have a local source of manufactured geotextiles and plastics. However, these materials are economically transported to all regions of the United States. Availability of large quantities of synthetics may require special orders to the factory with plenty of lead time to assure ontime delivery.

f. Material handling requirements. A substantial portion of project construction cost involves material handling. Included in handling costs are transportation of materials to the construction site, onsite storage of materials, onsite material mixing and component fabrication, and placement of materials to build the project. Projects in isolated locations must consider site access and availability of equipment to handle materials. Conversely, projects in urbanized coastal regions must consider impacts of large-sized material transport vehicles on congested streets and space requirements for onsite material storage. Most materials can be transported by conventional methods such as rail, barge, truck, or ship. Special allowances are needed for oversized loads and loads exceeding usual United States highway load limits of 180-215 kN (20-24 tons) per truck. Another important transportation consideration is projected future site access for bringing in materials needed for long-term maintenance or rehabilitation. Just as important is the ease with which materials can be handled either by hand or with conventional equipment. Materials that are awkward to handle, require special handling techniques and equipment, or require particular labor skills and specialized training add to project costs.

(1) Earth and sand. Earth is easily handled with conventional earth-moving equipment and transportation methods. The availability of earth compaction equipment will determine how earth fills will be compacted, which in turn factors into design load bearing capacity. If earth handling results in formation of dust clouds, workers must wear some sort of breathing filters. Sand from land-based sources is handled similarly to earth. However, sand obtained from offshore sources must be dredged and pumped or transported to the project site. In these cases, material handling will be a substantial portion of the project cost. Cost of earth and sand will increase if sorting into acceptable grain size ranges is required.

(2) Stone. Stone handling limitations arise primarily with large armor stone sizes. Availability of adequate handling equipment at quarries is a critical factor, as well as the cost of quarrying and transporting large armor stones. Some quarries have equipment capable of handling stones larger than allowed on public highways. Road weight limitations not only influence armor layer design, but careful planning is also required to maximize usage of trucks or rail transportation. Equipment must be available for handling of large armor stones at the project site. Cranes must have sufficient lift capacity and must be able to reach outward sufficient distances to place armor stones accurately at the toe of the structure. Approach roads and staging areas must be able to support the heavy truck loads.

(3) Concrete and asphalt. Handling requirements for concrete and asphalt beyond normal batch processing, truck hauling, and truck placement are a function of the particular structure design. Some designs may require special handling equipment, such as cranes with buckets, pumps, or roller compaction equipment. Availability of this equipment may influence the structural design. Air or water temperature and underwater placement may have an impact on concrete and asphalt handling requirements. Forms are needed to cast concrete armor units, and special equipment is needed to fabricate reinforced or prestressed concrete piles. Consideration should be given to whether special equipment, such as concrete forms, is reusable. Time should be allowed for concrete armor units to cure before placing them on the structure.

(4) Steel. Conventional steel members and framework can be fabricated for easy transport and handling using conventional equipment; however, some site assembly may be

required. Unusual steel fabrications, or very heavy steel components, may require specially designed or modified handling equipment.

(5) Wood. Typical wooden structural components present no difficulty in transporting and handling. Application of chemical preservatives may require special equipment to assure sufficient wood penetration.

(6) Geotextiles and plastics. Most synthetic materials can be transported by conventional means. Special handling equipment and techniques may be required to place geotextile fabrics, particularly in underwater applications. If the geotextile has specific weight less than water, provisions must be made to hold the fabric in place until it is overlain with denser material. Similarly, in above-water applications wind can lift sections of geotextile fabric unless it is weighted.

g. Material maintenance requirements. Project maintenance requirements depend in part on how selected materials deteriorate over time due to physical and chemical processes.

(1) Earth and sand. It is not necessary to protect earth and sand used in coastal projects from physical or chemical deterioration, but it is necessary to prevent or retard removal of material by wind or water erosion. The only maintenance costs will be associated with replacing eroded material, and this cost will be affected by access to the earth and/or sand portions of the project.

(2) Stone. The main concern with stone is reduction in size through abrasion and splitting. Armor stones broken into smaller pieces can be removed from a structure by wave action. Maintenance consists of replacing damaged or missing stones, which can entail significant mobilization costs. Preservation of stone material is generally not feasible.

(3) Concrete and asphalt. Concrete quality is determined by the quality of its component materials and the method of mixing and placement. Like stone, the main maintenance requirement is periodically taking steps to prevent deterioration, or mending portions that have cracked, broken, spalled, etc. Protective coatings can be applied to exposed concrete surfaces to help prevent flaking and to seal cracks that might allow water to penetrate the surface and cause corrosion of steel reinforcement. Some concrete sealants may become less effective when exposed to certain chemicals that react with the sealant. Broken concrete armor units should be replaced with new units. Care must be taken to assure replacement armor units are interlocked into the armor layer rather than simply placed on top. During original construction, future maintenance costs can be reduced by casting a suitable number of replacement armor units and stockpiling them onsite. Maintenance of asphalt structures consists primarily of patching or replacing damaged areas. Underlying earth materials may shift and settle, opening large cracks in the asphalt cover layer. These cracks must be repaired before the fill material erodes. Also, repeated cycles of large temperature change may open significant cracks in the asphalt. Continuous maintenance of asphalt roadway surfaces is required to avoid damage to vehicles and equipment.

(4) Steel. Steel must be protected from chemical and galvanic corrosion, unless it is made of special alloys such as stainless steel. Exposed steel surfaces corrode very rapidly in coastal

settings, especially in the wet-dry regions and at the sandline where sand particles continually abrade the paint and protective rust. Most steel maintenance involves reapplying protective coatings like paint, replacing corroded structural members and fasteners, and servicing the cathodic protection system by replacing sacrificial anodes. Steel structural members damaged by vessel impacts or debris should be replaced as soon as possible if the damage is severe enough to threaten structural integrity. For example, a buckled steel strut could result in failure of adjacent members at loads considerably below design values. Cosmetic damage, such as dents, can be addressed during scheduled maintenance.

(5) Wood. Wood structure components are susceptible to biological attack at all places except below the mud line. Most wood deterioration occurs in the wet and dry tidal range. Wood maintenance consists of reapplying protective surface coatings such as paint and replacing deteriorated wood portions with new material. It is usually not practical to re-treat deteriorated pressure-treated, chemical-impregnated wood. These members should be replaced. Surface coatings consist of antifouling paints or coating materials that resist borer penetration, such as a 0.5-mm-thick coating of epoxy. Maintenance of wood structures also involves replacement of wood members damaged by vessel or wave impacts, fire, or exposure to harmful chemicals. Broken structural members should be immediately replaced to avoid additional damage to adjacent structure components. Pollutants in some harbors may be harmful to wood, but a side benefit is the almost complete absence of marine life harmful to wood structures.

(6) Geotextiles and plastics. Maintenance requirements of synthetic materials vary widely, depending on the material and its application. Maintenance of geotextiles may be warranted if the fabric is exposed for a period of time. For example, loss of armor stone and underlayer stone might expose the geotextile filter cloth, which could then be damaged by debris or sunlight. Geotextiles used in sand-filled bags can usually withstand ultraviolet radiation, but the bags can be torn or vandalized, requiring immediate repair. Repair can be accomplished by sewing, overlapping, or gluing a patch to the damaged geotextile. Plastics can withstand practically all naturally occurring chemicals found in coastal regions. However, pollutants or spilled fuels may react with some plastics, causing rapid deterioration or change in the material's characteristics. Plastics can be physically damaged by impacts and by fatigue brought about by cyclic loading. Determining whether or not broken plastic components is needed will depend upon the importance of the plastic component to overall structural integrity.

h. Material environmental impacts. Long-term project success relies on the ability of the selected construction materials to resist attacks from the surrounding environment by such diverse factors as force loadings, corrosive chemicals, marine organisms, abrasion, fire, wet/dry cycles, freeze/thaw cycles, etc. Equally important is minimizing effects that construction materials may have on the natural environment in which they are placed. Strong justification is needed to use any construction material that introduces adverse chemicals into the environment that might impact plant and animal life in the immediate project vicinity. Coastal construction can produce nonchemical adverse impacts such as high levels of turbidity from earth and sand placement or from foundation dredging. Impacts also arise from burying or displacing species during construction, although many mobile animal species simply migrate out of the area temporarily. Completed coastal projects often provide viable habitat, thus offsetting somewhat the negative environmental consequences of construction. An evaluation of potential

environmental impacts of a project should consider future impacts that could arise from project deterioration, vandalism, and subsequent repair or maintenance. Environmental impacts may be reduced during repair and rehabilitation if materials from the original construction can be reused. Finally, present and future visual impacts of the project definitely should not be ignored.

VI-4-2. Earth and Sand.

a. Uses of earth and sand in coastal construction. Coastal projects tend to be fairly large and require a significant volume of construction materials. When feasible, structures are designed to use earth or sand as an economical filler material, and in many cases the mechanical strength properties of the soil are an integral part of the design. Below are some of the common uses of earth and sand in coastal construction:

(1) Rubble-mound breakwaters. Sand may be used as core material to provide a structure with a nearly impervious core, although sand-only cores are not common practice. The sand can contain clays, but cohesive clay-like materials alone are unsuitable for breakwater cores. Sand cores must be protected by geotextile or gravel filters and successively larger stone layers to prevent loss of sand due to piping under wave and current action.

(2) Caissons. Sand or soil is used to fill the compartments of concrete caissons and "cell-type" structures made of steel sheetpiles. Sand is preferred if the filler material is expected to support road works. Fill material must be protected from wave action that could wash away the soil.

(3) Bulkheads and vertical-front seawalls. Sand and soil are most often used as backfill or as foundation material for bulkheads and seawalls. The backfill usually is compacted to provide supportive soil pressure to resist wave loads and hydrostatic pressures. Soil may be needed to level the working area for foundations, or in weak soil conditions, to replace unsatisfactory in situ soil. Some circumstances may require coarser backfill material to promote rapid draining.

(4) Dikes. Earthen dikes constructed of sand, clay, or a combination of both, are used as dredged material containment structures and as storm protection structures. Dikes exposed to wave action need to be protected against erosion, i.e., armored like a revetment.

(5) Beach and dune restoration. Beach-quality sand from either land or offshore sources is the key ingredient for successful beach nourishment and dune restoration projects. Constructed sand dunes can be temporarily stabilized using snow fencing while dune vegetation is being established. Useful guidelines on stabilizing dunes with vegetation were given by Woodhouse (1978).

(6) Land reclamation. Construction of coastal facilities such as harbors and marinas often involves creation of new above-water land areas. Earth and sand used in these projects may come from dredging or from inland sources. Soils used in most reclamation projects are expected to have some degree of load- bearing capacity, depending on project requirements.

(7) Construction roads. Access to coastal projects may require construction of temporary or permanent roads using earth, sand, and gravel. Initial construction or major rehabilitation of shore-connected rubble-mound structures requires a roadway along the structure crest capable of supporting a crane and heavy trucks. If a permanent crest road is not part of the structure design, a temporary gravel road can be constructed that will eventually be washed away by storm waves.

(8) Concrete aggregate. Sand and gravel are essential ingredients in concrete and grouts used in coastal construction.

b. Physical and mechanical properties of earth and sand. Part III-1 (Coastal Sediment Properties) provides a thorough overview of sand composition, properties, and engineering applications. The following sections cover a broader range of soils.

(1) General soil properties and classification. The terms “earth” and “soil” are used to describe mixtures of a large assortment of materials comprised of various size particles. Soils are classified according to grain size into groups that share similar engineering characteristics. One such system is the widely used Unified Soil Classification System (USCS) as presented in Table III-1-2 of Part III-1, “Coastal Sediment Properties.” This classification system spans the particle size range that includes boulders, cobbles, gravels, sands, silts, and clays. Listed below are some general engineering characteristics of soils classified according to the USCS (Eckert and Callender 1987):

(a) **Boulders and cobbles**. “Boulders” and “cobbles” are rounded to angular, bulky, hard rock particles. Boulders have an average diameter greater than 300 mm, whereas cobbles have diameters spanning the range between 75 and 300 mm. Boulders and cobbles are very stable components for fill and for stabilizing slopes, particularly when the particles are angular. Including these larger particles as aggregates in finer grained soils helps improve the soil capacity to support foundation loads.

(b) **Gravels and sands**. Gravels and sands are rounded to angular bulky, hard, rock particles that can be naturally occurring or made by crushing larger stones. Gravels span the range of grain diameters from 4.76 to 75 mm, and sands cover grain sizes in the range from 0.074 to 4.75 mm. Within each category there are further divisions such as “coarse” and “fine.” Gravel and sand have essentially the same engineering properties; they differ mainly in degree. They are easily compacted, little affected by moisture content, and unaffected by frost. Gravels are more permeable than sands, and they are generally more resistant to erosion and piping. Stability of sands and gravels generally decreases as the grain-size distribution becomes narrower.

(c) **Silts and clays**. Soil particles with diameters less than 0.074 mm are silts or clays, and the distinction between the two arises from its behavior under certain conditions. Silts are inherently unstable, particularly when moisture content is increased, and they may reach a “quick” state when saturated. Silts are difficult to compact, highly susceptible to frost heave, and are easily eroded. Clays exhibit plastic behavior and have cohesive strength, which increases as moisture content decreases. Clays have low permeability, are difficult to compact when wet, and are difficult to drain. Clays resist erosion and piping when compacted, and they are not susceptible to frost heave. However, clays do expand and contract with changes in moisture

content. In general, highly expansive clays should not be used to backfill coastal structures. The most important engineering properties of soils are density, shear strength, compressibility, and permeability. These properties are used to estimate slope stability, bearing capacity, settlement, and erosion rate. Some of the basic soil properties can be determined using field and laboratory tests. For other properties it is necessary to correlate the soil parameters with results from previous experience. In the sections that follow, several key soil parameters are discussed. More detailed information on these and other soil properties such as water content and grain-size distribution are given in Eckert and Callender (1987) or in any geotechnical engineering textbook.

(2) Soil density. Soil is a multiphase mixture composed of solid particles and void spaces that are filled with water and/or gas. Consequently, in soil mechanics the term "*density*" describes the overall soil density as a function of particle density and the relative proportion of solids and voids in the sample. Table VI-4-1 shows a number of density-related parameters commonly used by geotechnical engineers. Note that specific gravity G is determined using the unit weight of fresh water. Typically, G ranges between 2.5 and 2.8 with preliminary calculation "default" values of 2.65 for sand and 2.70 for clays. Void ratio and porosity are indicators of soil compressibility and permeability. Geotechnical engineers prefer using void ratio because the volume of solids remains constant during any soil volume change. Void ratio can range from 0.15 for well-compacted soils having a wide grain-size distribution to 4.0 for very loose clays with high organic material content. Densely packed uniform spheres have a minimum void ratio of 0.35. Table III-1-4 in Part III-1 gives typical density values for common coastal sediments.

Table VI-4-1
Soil Density Parameters

Name	Symbol	Defining Equation
Basic Parameters		
Weight of solids	W_s	
Weight of water	W_w	
Volume of solids	V_s	
Volume of voids	V_v	
Total volume	V	$V_s + V_v$
Water unit weight	γ_w	
Derived Parameters		
Dry soil Unit weight	γ_d	$\frac{W_s}{V}$
Moist soil Unit weight	γ	$\frac{W_s + W_w}{V}$
Saturated soil Unit weight	γ_{sat}	$\frac{W_s + V_v \gamma_w}{V}$
Immersed soil Unit weight	γ_{sub}	$\frac{W_s - V_s \gamma_w}{V}$
Specific gravity	G	$\frac{\gamma_d}{\gamma_w}$

Void ratio	e	$\frac{V_v}{V_s}$ or $\frac{n}{100-n}$
Porosity	n	$\frac{V_v}{V}\times 100\%$ or $\frac{e}{1+e}\times 100\%$

(3) Soil relative density and relative compaction. These two parameters give a measure of a soil's in situ density relative to the range of possibilities for that particular soil.

(a) **Relative density** is used for noncohesive sands, and it is defined as the percentage given by the expression

$$D_r = \frac{e_{\max} - e}{e_{\max} - e_{\min}} \times 100\% \qquad \text{(VI-4-1)}$$

where the numerator is "*the difference between the void ratio of a cohesionless soil in the loosest state (e_{max}) to any given void ratio, e,*" and the denominator is "*the difference between void ratios in the loosest and densest (e_{min}) states*." Relative density provides a measure of the compactness of granular materials used in coastal projects such as sand backfill or dike cores. In the field, relative density is found using standard penetration tests or Dutch cone penetration tests. Actual estimation of relative density should follow the American Society for Testing and Materials (ASTM) Standards (ASTM D-4254 1994) or EM 1110-2-1906 (Department of the Army 1986). However, because of the difficulty in establishing the loosest and densest states of cohesionless soils, significant variations occur in determination of relative density, and correlations with other soil engineering properties should be avoided except for use in preliminary calculations.

(b) **Relative compaction** describes the relative density of *compacted* soils, and it is defined as "the ratio of the unit dry weight of an in situ material (γ_d) to the unit dry weight of the soil when compacted to its maximum density ($\gamma_{d\max}$)," or

$$R_c = \frac{\gamma_d}{\gamma_{d\max}} \times 100\% \qquad \text{(VI-4-2)}$$

The Standard Proctor Method, given in EM 1110-2-1906 (Department of the Army 1986) is recommended for determining maximum unit dry weight for coastal fills and embankment applications. Relative compaction is normally used to describe cohesive soils (placed or pre-existing) that have been stabilized or improved using compaction techniques.

(4) Soil shear strength. Soil fails when shear displacement occurs along a plane on which soil stress limit is exceeded. For all but preliminary design, soil strength should be determined using appropriate in situ or laboratory testing procedures as described in EM 1110-2-1906 (Department of the Army 1986) or ASTM Standards. Commonly performed tests are the Unconsolidated-Undrained triaxial test, Consolidated- Undrained triaxial test, and the Consolidated-Drained triaxial test. These tests produce stress-strain curves for the tested loading condition, and the shear strength is defined as the first maximum that occurs on the curve. The

tests also reveal conditions of failure for the soil. Soil strength is usually presented in terms of Mohr circles and Mohr failure envelopes. This allows shear strength to be expressed in terms of cohesion, maximum stress, and the angle of internal friction. Noncohesive, granular soils (i.e. sand) resist shearing through two mechanisms: (a) the frictional resistance between particles due to the normal force acting at the point of contact; and (b) the interlocking of particles as they attempt to shift past one another during strain. Frictional resistance is the principal source of soil strength, and it is a function of the soil confining stress. Soil shear strength increases with increases in confining stress. Highly compacted soils with low void ratios have increased strength due to particle interlocking. The shear strength of placed or backfilled cohesive soil will depend to a large extent on the moisture content (pore-pressure) and the compaction the soil receives. Tests should be conducted after compaction to verify that design strength levels have been achieved or surpassed. Shear strength of in situ cohesive soils depends on the method of original deposition and the past overburden history. Undisturbed clays may be over-consolidated, normally consolidated, or under-consolidated. Shear strength is determined using the triaxial tests mentioned above.

(5) Soil compressibility. Soil compressibility is an indication of settlement that will occur over time due to a given load condition or a change in groundwater level. Compressibility of noncohesive materials is governed by the relative density of the soil, and estimates of soil settlement are straightforward. Consolidation of cohesive soils is more complex and occurs in three stages. Immediate settlement is compression of the soil matrix without any dissipation of pore pressure or water expulsion. Some immediate settlement may be due to compression of trapped gases in the soil. Primary consolidation occurs over time as increased pore pressures force water from the soil voids. This process continues until all the excess pore pressure is relieved. The rate of consolidation depends on soil permeability and the drainage characteristics of the adjacent soil. After primary consolidation, Secondary compression can occur in soils having higher plasticity or significant organic content, such as soft marine or estuarine deposits. Consolidation tests are used to establish the coefficients necessary to estimate settlement of silts and clays. Eckert and Callender (1987) describe the test and analysis methods, and they provide an example application.

(6) Soil permeability. Permeability is a soil parameter related to laminar (viscous) flow of water through the soil under the influence of gravity. Coastal geotechnical problems affected by soil permeability include seepage through beach sand, consolidation of backfills and hydraulically placed fills, and settlement of foundations. Viscous flow through soils is calculated with an empirical relationship known as Darcy's Law, which is applicable for soils from clays and silts up to coarse sands. In its simplest form, Darcy=s equation for steady flow through uniform soil is

$$Q = K\,A\frac{\Delta h}{L} \tag{VI-4-3}$$

where

Q = discharge

A = flow cross-sectional area

L = length of flow path

Δh = head difference over the flow length

The empirical coefficient K in Darcy's equation is called the *coefficient of permeability*, and it is a function of both the soil and the pore fluid. Soil particle size and gradation have the largest influence on the coefficient of permeability. Soil permeability is best determined in the field using pumping tests (see Eckert and Callender (1987) for an overview and references). Less accurate permeability coefficients can be obtained with laboratory tests using falling- or constant-head permeameters as described in EM 1110-2-1906 (Department of the Army 1986) or ASTM Standards. Many empirical equations have been proposed to relate permeability to characteristics of the soil such as effective grain size. However, these equations are generally suited only for compacted, clean, coarse soils, whereas naturally occurring soils will exhibit significant variation. Table VI-4-2 gives typical coefficients of permeability for common soils. These values are suitable for use in preliminary design calculations.

Table VI-4-2
Typical Soil Permeability Coefficients (from Eckert and Callender (1987))

	Particle Size Range, cm		"Effective" Size D_{10},	Permeability Coefficient, k	
Soil Types	D_{max}	D_{min}	mm	(cm/sec)	(ft/yr)
Uniform, coarse sand	0.2	0.05	0.6	0.4	0.4×10^{6}
Uniform, medium sand	0.05	0.025	0.3	0.1	0.1×10^{6}
Clean, well-graded sand and gravel	1.0	0.0005	0.1	0.01	0.01×10^{6}
Uniform, fine sand	0.025	0.005	0.06	40×10^{-4}	4,000
Well-graded, silty sand and gravel	0.5	0.001	0.02	4×10^{-4}	400
Silty sand	0.2	0.0005	0.01	1×10^{-4}	100
Uniform silt	0.005	0.0005	0.006	0.5×10^{-4}	50
Sandy clay	0.10	0.0001	0.002	0.05×10^{-4}	5
Silty clay	0.005	0.0001	0.0015	0.01×10^{-4}	1
Clay (30 to 50 percent clay sizes)	0.005	0.00005	0.0008	0.001×10^{-4}	0.1

(7) Soil mixtures. Depending on the borrow source, backfill material may be composed of a mixture containing some fraction of gravel, sand, silt, or clay, along with a significant percentage of organic materials such as vegetable matter or shell fragments. Soil properties of soil mixtures containing a wide range of components will vary tremendously, and the soil should be tested to assure compliance with specified strength and density requirements. Soil mixtures containing organic materials are usually considered detrimental and should not be used because they tend to be more compressible and have lower shear strengths.

c. Placement considerations for earth and sand. The method chosen for earth placement depends on such factors as location of material borrow source (land or offshore), type of fill, availability of suitable equipment, environmental impacts of the method, and project economics.

(1) Dumped placement. Earth or sand obtained from upland sources or dredged from the sea bottom can be transported to the construction site and dumped into place. For land-based construction the mode of transport can be trucks, scrapers, conveyor belts, or other means, depending on the transport distance. Typical land-based projects include backfilling seawalls and bulkheads, placing foundation material, and placing the cores of shore-connected rubble-mound structures. Offshore earth and sand can be placed by dumping from barges or by using draglines and buckets for more precision. Dumped material that is not compacted will have low relative densities, and settlement should be expected to occur over time. Barge dumping at sea creates turbulence that will segregate material by grain size as it falls and increase turbidity as fine particles are suspended in the water column.

(2) Hydraulic placement. Soils dredged from the sea or lake bottom can be transported and placed hydraulically by moving the material as a slurry through a pipeline. The pipeline may extend directly from the dredge to the project site, as in the case of some beach nourishment projects; or barges that bring the material to the construction site can be emptied with hydraulic pumping. Hydraulic placement offers greater accuracy than dumping for offshore applications such as the cores of rubble-mound structures. Material placed underwater, either hydraulically or by dumping, may be moved by waves and currents before it can be adequately protected with overlying filters and armor layers. Land placement of earth and sand by hydraulic means involves a large amount of wash water runoff that can erode sediment along the drainage path or leave segregated pockets of fine-grained sediment that have engineering characteristics vastly different from the rest of the fill.

(3) Compaction. Above water, earth and sand fills can be compacted by a number of methods depending on the degree of compaction necessary to reach the specified soil parameters. Construction documents should specify the required density, moisture limits, and lift thickness. In situ testing is needed to verify that the compacted fill meets specifications. Mechanical compaction of soils placed underwater is not practical; however, in some situations cyclic wave loading will help compact placed sand.

d. Environmental effects on earth and sand.

(1) Effects of soils on the environment. Polluted soils should not be used in coastal projects because contaminants may be released in coastal waters either by leeching out of the placed fill material or through project damage and erosion of the fill material during storms. Potential soil contaminants include industrial wastes such as toxic heavy metals (mercury, cadmium, lead, and arsenic), chlorinated organic chemicals (DDT and PCB=s), and pathogens (bacteria, viruses, and parasites) (Eckert and Callender 1987). Use of dredged materials in coastal construction must be limited to good quality materials free of toxic wastes. See Engineer Manual 1110-2-1204 (Department of the Army 1989) and Engineer Manual 1110-2-5025 (Department of the Army 1998) for related design guidance. Also examine recent Federal and state environmental regulations pertaining to use of dredged material.

(2) Effects of the environment on soils. The particles comprising mixtures of earth and sand are generally unaffected by the natural environment over the project life span. However, structural components constructed using earth and sand are subject to natural forces that can degrade the performance and functionality of the project. Erosion of materials and subsequent decrease in fill volume can be caused by wind, rain, ice, currents, waves, burrowing animals, or human activities. This may reduce the capacity of the soil to resist applied loads and result in project damage. For example, vertical seawall designs often rely on the backfilled soil to help resist wave impacts and water pressures. Unconsolidated sands and silts are most susceptible to erosion. Gravel is more stable against erosion due to the size of the particles, and clays are more stable because of tractive forces between particles. Liquefaction of submerged loose fine sand and silts can occur in areas of high seismic activity or high wave action.

VI-4-3. Stone.

a. Use of stone in coastal construction. In the context of coastal engineering, "stone" refers to individual blocks, or to fragments that have been broken or quarried from bedrock exposures or obtained from boulders and cobbles in alluvium (Moffatt and Nichol 1983). Commercial-grade stone can be classified according to size, shape, size distribution, and various physical properties of the material. Stone is used extensively to construct coastal structures, and it is by far the most common material used in the United States for breakwaters, jetties, groins, revetments, and seawalls. Larger projects may contain more than a million tonnes of stone; 80 percent in the core and 20 percent in the armor layers (CIRIA/CUR 1991). Stone used as aggregate and riprap is crushed, broken, or alluvial stone in which the shape of individual stones has not been specified and the size distributions are fairly wide. Quarrystones are larger rock pieces that are "blocky" in shape rather than elongated or "slabby." A principal use of quarrystone is in the armor layer of rubble-mound structures. Below are listed the major uses of stone in coastal construction. Undoubtedly there are additional uses not mentioned. For example, quarrystones make great gifts for your geologist friends.

(1) **Rubble-mound structures**. Large quarrystone with specified weight, density, and durability are used for the primary armor layer of most rubble-mound structures. Underlayers are composed of progressively smaller stone sizes; and in many cases, the rubble-mound core material may be riprap or "*quarry-run*" stone. Quarry stone is also used to construct the base of "*composite structures*" where a monolithic, vertical-front structure is placed on a rubble-mound base.

(2) **Riprap structures**. Riprap is used more for shore and bank protection structures that are not exposed to high waves or strong currents. The wider size distribution of riprap provides a less uniform armor layer that is more susceptible to damage by strong waves and currents. Riprap is less expensive than uniform stone, and placement on the slope is usually less precise (e.g., dumping from trucks).

(3) **Toe protection**. Graded stone is used to protect the toes of sloping- and vertical-front structures from undermining by scour. Stable stone sizes are selected based on the anticipated maximum waves or currents.

(4) **Scour blankets**. Stone blankets are placed on the seafloor in areas subject to scour by waves and/or currents. Often the scour blanket is a remediation response to scour that was not anticipated in the original project design. Protection of bridge and pier pilings with scour blankets is a routine application.

(5) **Stone fill**. Stone is used as a filler material for coastal structures such as cribs, caissons, and gabions. (Gabions are steel wire cages filled with small stones that can be stacked to form steep revetments and bank protection.)

(6) **Filter layers**. Smaller stones are used for filter layers over the foundation soil or in drainage applications. Placement is usually by dumping. Selection of stone for a particular project depends on the purpose of the project, design loads, and local availability of suitable stone. In some cases, it may be necessary to evaluate the benefits of using inferior locally available stone as opposed to transporting higher-quality stone from a distant source.

b. Physical and mechanical properties of rock. The paragraphs below provide an overview of rock properties crucial for coastal engineering applications. These and other rock properties are covered in much greater detail in the *Manual on the Use of Rock in Coastal and Shoreline Engineering* (CIRIA/CUR 1991).

(1) Types of rock. Rock, as it occurs in nature, is classified into three distinct groups. **Igneous rocks** are formed by crystallization and solidification of molten silicate magma. **Sedimentary rocks** are formed by sedimentation (usually underwater) and subsequent lithification of mineral grains. **Metamorphic rocks** are transformed igneous or sedimentary rocks in which textures and minerals have been altered by heat and pressure over geological time periods (CIRIA/CUR 1991). Within each major rock category are additional subdivisions based mainly on composition and texture (Table VI-4-3). Some of the more common stone types are described below:

(a) **Granite** is a term applied to medium- and coarse-grained igneous rocks consisting mainly of feldspar and quartz. Mica may also exist in small quantities, but large amounts of mica may result in fracture planes within the rock. Most granites are dense, hard, strong, have low porosity, and are resistant to abrasion and impacts. These characteristics make granite a good choice for riprap and armor stone.

(b) **Basalt** is a term applied to various dense, fine-grained, volcanic rocks (dacite, andesite, trachyte, latite, basalt). Basaltic rock was formed by cooling lava, and it is composed primarily of feldspar and ferromagnesian minerals. Some basalts may not be suitable for concrete aggregates if they contain reactive substances in the pores. Basalts are generally very dense, hard, tough, and durable, and they are good choices for aggregates, riprap, and armor stone.

Table VI-4-3
Engineering Characteristics of Unweathered Common Rocks (from CIRIA/CUR (1991))

Rock Group Name	Rock Specific Weight (kN/m^3)	Unconfined Compressive Strength (MPa) x 10^8	Water Absorption (%)	Porosity (%)
		Igneous		
Granite	24.5-27.5	160-260	0.2-2.0	0.4-2.4
Diorite	25.5-30.4	160-260	---	0.3-2.7
Gabbro	27.5-31.4	180-280	0.2-2.5	0.3-2.7
Rhyolite	22.6-27.5	100-260	0.2-5.0	0.4-6.0
Andesite	23.5-29.4	160-260	0.2-10	0.1-10
Basalt	24.5-30.4	160-280	0.1-1.0	0.1-1.0
		Sedimentary		
Quartzite	25.5-27.5	220-260	0.1-0.5	0.1-0.5
Sandstone	22.6-27.5	15-220	1.0-15	5-20
Siltstone	22.6-27.5	60-100	1.0-10	5-10
Shale	22.6-26.5	15-60	1.0-10	5-30
Limestone	22.6-26.5	30-120	0.2-5.0	0.5-20
Chalks	14.7-22.6	5-30	2.0-30	20-30
		Metamorphic		
Phyllite	22.6-26.5	60-90	0.5-6.0	5-10
Schist	26.5-31.4	70-120	0.4-5.0	5-10
Gneiss	25.5-27.5	150-260	0.5-1.5	0.5-1.5
Marble	26.5-27.5	130-240	0.5-2.0	0.5-2.0
Slate	26.5-27.5	70-120	0.5-5.0	0.5-5.0

(c) **Carbonate** is a broad term applied to limestone, dolomite, and marble. These rocks contain varying amounts of calcite and span the range from fine-grained to very coarse-grained. Often a high percentage of clays make some carbonate rock unsuitable for use as stone in coastal construction. Conversely, high sand or silica content may harden carbonates. Marble is limestone or dolomite transformed by metamorphic processes into a harder, more crystalline structure. Carbonate stone that is physically sound, dense, tough, and strong is suitable for concrete aggregate, riprap, and armor stone.

(d) **Sandstone** is sedimentary rock composed of small (0.25-6.0 mm) particles cemented together. Strength and durability of sandstone varies greatly depending on the cementing material. Rock cemented by silica or calcite is suitable for use as crushed and broken stone, whereas rock cemented with clay or iron oxide is inadequate for most applications. Sandstone is more porous than granite and basalt. Other less common rocks may be available for use in coastal construction, and many types have attributes necessary for use as armor stone and riprap. Moffatt and Nichol (1983) and CIRIA/CUR (1991) describe several additional rock types.

(2) Specific weight. Most coastal applications of stone require that the stones remain stable and stationary under all imposed wave and current forces. For structures in which the armor layer stones are not bound together by concrete or asphalt, stability is achieved through the relatively high specific weight of stone, assisted to some degree by the friction and mechanical interlocking that occurs between adjacent stones. Table VI-4-3 includes typical ranges of specific weight for common stone. Stones with high specific weight are best for primary layer armor units, but less dense stones can be used successfully. Specific weight is not as important for core material and underlayer stones, which are held in place by the primary armor layer. Design methods used to calculate stable armor stone weight depend on stone specific weight. Therefore, once the design is complete and stone specific weight has been specified, it is important to ensure stones used in the project meet or exceed the assumed specific weight used in design. Armor stones are usually purchased by weight, whereas core and secondary layer stones may be specified according to volume.

(3) Stone size and distribution. Quarries produce crushed and broken stone in sizes ranging from small gravel to huge blocks that cannot be handled and transported without special equipment. A rough estimate of stone size for a somewhat round stone is given as the diameter of an equivalent-volume sphere, i.e.,

$$D_s = 1.24\left(\frac{W_s}{\gamma_s}\right)^{1/3} \tag{VI-4-4}$$

where

W_s = stone weight

γ_s =stone specific weight in compatible units

Quarry output can be categorized according to median stone diameter and size distribution about the median. Categories of stone based on size and gradation include the following:

(a) **Armor stones** are selected by weight and density to resist wave loads. Ideally, all armor stones are blocky in shape and nearly uniform in size. The largest stone dimension on an individual stone should be no more than three times the shortest dimension.

(b) **Underlayer stones** are smaller stones randomly placed in a layer to support the primary armor layer. The size distribution of underlayer stone can be reasonably wide, provided the smallest stones in the distribution are still too large to pass through voids in the covering layer of larger stones.

(c) **Quarry-run** or quarry-waste materials are often used for cores of rubble-mound breakwaters and jetties. Generally the material should be sound and reasonably well-graded with no more than 10 percent fines. Smaller median sizes and wider distributions produce less porous structures.

(d) **Riprap** is comprised of heavy irregular stone fragments having a fairly wide size distribution. Riprap is used to protect slopes from erosion in less severe wave conditions. Riprap is also used in emergency repairs because sufficient quantities are usually readily available.

(e) **Bedding and filter layer stones** are typically smaller stones with narrow gradations. These layers prevent piping loss of underlying soils.

The above stone classifications are general. Specific guidance on median sizes and allowable size distributions for stone used in coastal structures is given in Part VI-5-2, "Wave/Structure Interactions" and Part VI-7, "Design of Specific Project Elements."

(4) Stone shape. Stone shape is an important factor in stability of armor stones. Angular, blocky stones are preferred for armor layers because they wedge and interlock well with adjacent stones when placed randomly, they can be placed on steeper slopes, and they provide a more porous armor layer that more effectively dissipates wave energy. Well-rounded armor stones are less stable, cannot be placed on steep slopes, and are more difficult to handle than angular stones. In addition, dislodged round stones will tend to roll downslope to the structure toe, whereas angular stones are more likely to find a new resting place on the armor slope. Quarry-produced stones are typically angular, whereas stones from glacial deposits and alluvial sources are usually rounded. Stones mined from older coastal structures could have become more rounded from years of service and weathering. Examples of stone shape and classification are given in CIRIA/CUR (1991). Many examples exist of coastal structures constructed of closely fitted blocky stones that resemble the work of stone masons. Gaps between stones can be grouted to provide a more impervious structure; however, sufficient openings must be left in the armor layer to relieve hydrostatic uplift pressures. Underlayers also should have sufficient angularity to be stable on the slope during construction. Underlayer stone angularity helps lessen the discontinuity between armor and underlayer. Highly angular stones placed directly on geotextile fabric are more likely to puncture the fabric during placement or subsequent movement.

(5) Durability. Stone durability is a qualitative measure of the stone's ability to retain its physical and mechanical properties throughout its service in an engineering project. Stone durability is related to properties of the basic rock from which the stones were produced (texture, structure, mineral composition, etc.), method of quarrying (blasting or cutting), handling of the stone prior to final placement, environmental conditions to which the stone is exposed, and loads applied to the stone (Magoon and Baird 1991). Generally, stone that is dense or fine-textured, hard, and tough is the most durable. Durability of stone placed in a coastal structure is a very important design consideration. However, stone durability is not well understood, and best durability estimates for stones from a particular quarry may come from past performance of stone from the same quarry that was placed in similar environments. Stone degradation by cracking or chipping reduces the average weight and angularity of armor stone resulting in a less stable armor layer. Stones that are expected to degrade rapidly lead to higher maintenance costs and may necessitate initial overdesign of armor stone size and placement on milder slopes. Economics may dictate using higher-quality stone from a distant site if local stone is not sufficiently durable. Useful information on stone durability experience in the United States was presented at the specialty conference *Durability of Stone for Rubble Mound Breakwaters*

(Magoon and Baird 1991). Papers in this conference covered theoretical and laboratory analysis of stone durability, engineering and design practices, quarry and construction topics, and case histories of stone durability. In one of the conference papers, Lutton (1991) gave the relative stone durability rankings shown on Table VI-4-4 for use in preliminary planning. Lutton also presented "approximate" criteria for evaluating stone durability shown on Table VI-4-5 (also given in Department of the Army (1990)). Descriptions of various tests used to quantify durability characteristics of stone are beyond the scope of the manual. See CIRIA/CUR (1991), Department of the Army (1990), Latham (1991), and Lienhart (1991) for information on these testing procedures. These sources also cite applicable testing standards of the American Society for Testing and Materials.

TableVI-4-4
Durability Ranking for Common Stone

Most Durable to Least Durable
1. Granite
2. Quartzite
3. Basalt
4. Limestone and Dolomite
5. Rhyolite and Dacite
6. Andesite
7. Sandstone
8. Breccia and Conglomerate

(6) Strength. Stone used in coastal projects is usually selected according to its specific weight, durability, and shape properties. Seldom are there any tensile or compressive strength requirements. Generally, stones must be sufficiently strong in compression to support the load of any overlying stone or structure without crushing. Table VI-4-3 gives compressive strength ranges for the listed stone. Generally, high density stone is also very strong in compression. Fittings such as ringbolts can be epoxied into holes drilled into stone, and usually the tensile stone strength is sufficient to withstand substantial loads on the fitting.

(7) Porosity and water absorption. **Stone porosity** is the volume of voids contained in a unit volume of stone. This term should not be confused with **bulk porosity** of a stone armor layer (which is related to the volume of voids between stones). **Water absorption** is the mass of water absorbed per unit of dry stone mass at atmospheric pressure, and it will be less than the absorption that would occur if all the voids of the stone were saturated. Values of stone porosity and water absorption are listed in Table VI-4-3. Stone water absorption is the single most important indicator of stone durability, particularly in applications where the stones undergo cyclic stresses caused by freeze/thaw cycles. Primary armor layer stones should have low values of water absorption to help ensure good weathering characteristics and less stone breakage. A limit of 1 percent absorption is considered reasonable (Department of the Army 1990).

Table VI-4-5
Approximate Criteria[1] for Evaluating Stone

Test	Approximate Criterion for Suitability
Petrography	Fresh, interlocking crystalline, with few pores, no clay minerals, and no soluble minerals
Bulk specific gravity (saturated, surface dry)	Greater than 2.60
Absorption	Less than 1.2 percent[2]
$MgSO_4$ soundness	Less than 2 percent loss in five cycles[1]
Glycol soundness	No deterioration except minor crumbs from surface
Abrasion	Less than 25 percent loss in 1,000 revolutions[2]
Freezing-thawing	Largely unaffected in 20 cycles
Wetting-drying	No major progressive cracking in 35 cycles
Field visual	Distinctions based on color, massiveness, and other visual characteristics
Field index	Distinctions based on scratch, ring, and other physical characteristics
Field drop test	No breakage or cracking
Field set-aside	No loss or cracking in 12-month exposure

[1] Criteria are broad generalizations useful for preliminary judgment only rather than being reflective of any official standard.
[2] Coarse aggregate sizes.

(8) Abrasion and soundness. Resistance to abrasion is an important stone property for materials handled in bulk such as core material, riprap, filter stone, etc. Weaker stones will break into smaller pieces as the materials are loaded into trucks, dumped, and rehandled onsite. This could result in changed size distributions by the time the stone is placed. Waterborne sand and cobbles can slowly wear away at weak armor stone, but this is not an overriding design concern. Dynamic armor layers that are reshaped by wave action should be constructed using abrasion-resistant stone. Stone soundness depends on the amount of fissures, fractures, laminations, and other discontinuities in the stone. Some stone fissures may be the result of blasting in the quarry, other weaknesses may develop with multiple handling and stockpiling of larger stones.

c. Quarrystone procurement and inspection guidelines. The following are suggested general guidelines for specifying and inspecting quarrystone for coastal projects. It will be necessary to supplement these guidelines on a case-by-case basis. Additional guidance is provided in EM 1110-2-2301 (Department of the Army 1994), CIRIA/CUR (1991), and Moffatt and Nichol (1983).

(1) Contractor bids should be reviewed to ensure bid items are not underpriced in anticipation of potential claims for extra payments.

(2) Any environmental, historic preservation, and biologic constraints on quarrying must be resolved by obtaining all relevant Federal, state, and local permits.

(3) Inspection visits to the quarry during production are needed to ensure adequate stone quality and gradation.

(4) Over-blasting, which may lead to unacceptable fracturing of armor stones, should be avoided.

(5) Well-trained inspectors familiar with blasting procedures, stone quality, and stone inspection techniques should be employed.

(6) A record of stone quality from known quarries should be maintained for reference. Quarries with records of producing unsatisfactory stone should be disqualified up front.

(7) Qualified personnel (e.g., a geologist) should identify specific areas of unacceptable in situ stone within the quarry and make the inspector aware of its location. This prevents the manufacture of potentially unsuitable stone.

(8) Stones representing the approved rock type in several different weights should be set aside and clearly marked for visual reference by the inspector and contractor.

(9) Stones should be spread out in the quarry for inspection prior to loading for transport. Armor stones should be rotated to inspect all sides.

(10) Weights of delivered stone should be checked periodically to ensure contract compliance, and an adequate supply of stone across the specified gradation should be maintained at the construction site.

d. Placement considerations for stone. The success of any coastal project built using stone depends critically on careful stone placement conforming to design specifications. Structures in which stones are carelessly placed will inevitably suffer damage at loads below design levels. The following stone placement guidelines (condensed from Moffatt and Nichol (1983)) are based on Corps of Engineers' experience in building rubble structures. These guidelines are intended to be general in nature with the recognition that Corps Districts and other entities may prefer their own specifications based on past experience and local knowledge.

(1) General placement considerations. On slopes, stone placement should begin at the toe and proceed upslope to produce a layer with maximum interlocking of stones and minimum voids. Larger stones that are individually placed should be oriented so the longest axis is approximately perpendicular to the structure slope. Armor stones should be "seated" on the underlayer stones to avoid slipping, rocking, or displacement under wave action or weight of overlying stones. Some settlement of the armor layer is expected, but ideally this will be a tightening of the matrix without significant lateral stone movements. Controlled stone placement provides improved armor layer stability, but it depends on skilled and experienced equipment operators and personnel. Typical extreme tolerances for rubble slopes are ∀30 cm (12 in.) from the design finished surface for underwater placement, and ∀15 cm (6 in.) for above-water portions. Underlayer and bedding layer tolerances may be as tight as ∀8 cm (3 in.), whereas up to ∀45 cm (18 in.) may be allowed for large armor stones. Rubble-mound structures exposed to wave action during construction should be completed and armored in short sections to minimize

damage risk from storms. Structures built through the surf zone may require stone blankets placed in advance of construction to reduce scour effects. Toe protection armor should be evenly distributed over the area with a minimum percentage of voids.

(2) Filters, bedding, and core materials. Stone used for rubble-mound cores, filter layers, and bedding layers should be handled and placed in a manner that minimizes segregation of the material size distribution. Material placed by clamshell, dragline, or similar equipment should not be dropped distances greater than 0.6 m (2 ft) above the bottom or previously placed stone. Self-unloading vessels like bottom dump scows (when permitted) should proceed along lines directly over the final dumping location and parallel to the structure center line. Placing bedding material over soft and organic bottom materials should force the soft material outward toward the edges of the bedding layer. When finished, filter and bedding layers should be free of mounds and windrows and coverage should be complete.

(3) Underlayer stone. Underlayer stone should be placed to full underlayer thickness in a manner that does not displace underlying materials or soil as construction progresses from the toe up the slope. The goal is to achieve an even distribution of the graded material with minimum voids in the underlayer. For smaller structures like revetments, unsegregated stone may be lowered in buckets and placed directly on the underlying material. Placing stone in any manner that results in stone segregation is not permitted. Drop heights for underlayer stone generally cannot exceed 0.6 m (2 ft).

(4) Armor layer stone. Armor layer stone can be placed uniformly, randomly, and by a special placement method.

(a) **Uniform placement** is used only for cut or dressed stones that are uniform in size and shape. Uniform stones are placed in an orderly pattern or arrangement in which the stones are closely spaced. Such arrangements make it more difficult for individual stones to be dislodged, but it also provides a less permeable structure with more runup and overtopping. This is the most expensive method of armor placement. Figure VI-4-1 illustrates uniform placement.

(b) **Random placement** covers a range of placement techniques from careful placement of individual angular quarrystones in a random pattern to underwater dumping of stones from barges. In the case of armor stones, significant variations in stability are likely to occur between underwater and above-water placement even when placement is by crane. Furthermore, the degree of armor interlocking achieved varies between crane operators, and even between structures constructed by the same crane operator. Figure VI-4-2 illustrates random placement. Placing individual armor stones should not displace underlayer stones and should not result in any armor damage other than minor chipping. Stone armor layers are at least two stones in thickness, and the layer should be constructed to this thickness as armoring progresses up the slope from the toe. This provides better interlocking than placing first one layer of stone and then covering it with a second layer. Placed armor stone should be stable, keyed, and interlocked with neighboring stones. "*Floater*" stones having minimal contact or not wedged against adjacent stones are more likely to be dislodged during storms. During construction, the crane operator should be able to select the best sized stone for a particular position from a number of armor stones stockpiled nearby. Smaller stones in the allowed size distribution should be used to fill

Figure VI-4-1. Uniform placement

Figure VI-4-2. Random placement

gaps between larger stones. In this way skilled operators are able to build "*tight*" armor layers. Equipment used for placing armor stones should be capable of positioning the stones to their final position before release (even at the toe), and the crane should be able to pick up and reposition stones after initial placement. Dropping stones more than 30 cm (1 ft) or pushing stones downslope should not be permitted. Final shaping of the armor layer slope to design grade should be achieved during stone placement.

(c) **Selective placement** is used by some Corps of Engineer field offices to increase structure stability. Selective placement is the careful selection and placement of individual armor stones to achieve a higher degree of interlocking. Although careful selective placement increases armor layer stability, the variation expected between projects does not warrant increasing the values of stability coefficients. In some respects selective placement is simply carefully constructed random placement. Figure VI-4-3 illustrates selective placement.

Figure VI-4-3. Selective placement

(d) **Special placement** applies only to parallelepiped-shaped stones, and this method of placement requires special efforts to align the longest axis of parallelepiped-shaped stones perpendicular to the structure slope. Special placement also requires careful supervision during construction with clear communication to the contractor about proper placement procedures. If feasible, construction supervisors with previous special placement experience should be employed. Special placement requires more time for selection, handling, and placement of the armor, along with increased costs of construction. Figure VI-4-4 illustrates special placement. Construction techniques for special placement have been suggested to supplement the recommendations given above for random placement. The lowest tier of armor stones should be keyed into the seafloor or bedding layer. Subsequent tiers should be placed in the saddle points of the next lower tier. Construction should proceed upslope and diagonally toward the crane operator. Spotters should be used to help direct placement and ensure grade line is maintained. Each stone should be oriented so the heavier end of the parallelepiped-shaped stone is closer to the underlayer, and stones should be keyed and fitted so there are at least three points of contact with adjacent stones. All capstone should be placed closely together. The top tier of armor stones on the seaward side should extend slightly above the level of the capstone to protect the cap from wave forces, whereas on the lee side the top tier should be slightly lower than the capstone. No stone should protrude out of the armor face more than one fifth of its major dimension. This is

particularly important for single layer construction. Armor gradation should be fairly uniform, and stone on the landward face of breakwaters should not be reduced in size because wave transmission through permeable structures may dislodge leeside armor stones. In general, turbid water conditions do not allow special placement below the water level. Stones placed on underwater portions of the structure must be placed by "feel," and this results in a more random placement. Stones must be carefully fitted at the transition between random and special placement (around the low water level). In addition, care must be taken with special placement around the waterline because damage by breaking waves is more likely to occur in this region.

Figure VI-4-4. Special placement

(5) Riprap. Placement of riprap is less precise than armor stone, but the basic objectives are similar. Placement should not disturb underlying materials or damage geotextile fabric, and dumping should not segregate the riprap distribution. Dumping into chutes is likely to produce unacceptable segregation, and this practice should not be allowed. Riprap placement should be to full layer thickness in one operation; placing in multiple layers should not be permitted. After placement the riprap gradation should be similar throughout the structure with no obvious weak spots, with even distribution of larger stones, and with a minimum of voids. Rearrangement of individual stones with equipment or by hand may be needed to provide a reasonable gradation of stone sizes or to reinforce layer weaknesses. Pushing riprap up or down the slope is not allowed because it segregates the material and may damage the underlayer. Chink stones should be forced into voids in the riprap layer by rodding, spading, or similar methods.

e. Environmental effects on stone. Stone selected for use in coastal structures is very durable and is little affected by the natural environment.

(1) Wave action. Hydrodynamic forces caused by wave action on stone structures generally do not damage individual stones. However, waves which cause stone movement and

impacts between stones can lead to chipping and breakage. Waves also carry abrasive particles that can deteriorate weak stone over long time periods.

(2) Temperature and fire. Stone expands and contracts with temperature change, but most stone has reasonable tolerance to normal environmental temperature changes. Stone will be damaged to some degree by high temperatures caused by fire, and granite is particularly vulnerable to cracking and spalling caused by unequal expansion of differentially heated stone. This is due to its irregular crystalline structure and mineral composition. At temperatures greater than 100EC limestones start to decompose. Sandstones and other sedimentary stone will tend to crack along lamination planes after an extreme heating and cooling cycle.

(3) Freezing and thawing. Water that freezes in stone cracks produces stresses that may lead to stone breakage or spalling after a number of cycles. This problem increases with the porosity of the stone.

(4) Chemical attack. Calcareous stones are subject to decomposition by acids that may be formed by the combination of moisture and naturally occurring gases such as sulfur dioxide. This may cause disintegration of sandstones, which are cemented by calcium carbonate (Moffatt and Nichol 1983).

VI-4-4. Portland Cement Concrete and Bituminous Concrete. The sections below are intended to give a brief overview of portland cement concrete, and to a much lesser extent bituminous concrete, with emphasis on those characteristics important to coastal projects. Following common usage, the term “concrete” will be used to denote portland cement concrete, and “asphalt” will be used to denote bituminous concrete. Additional information is available in any of the literally hundreds of textbooks and design manuals that cover nearly all aspects of concrete and asphalt and their use as a construction material.

a. Use of concrete and asphalt in coastal construction.

(1) Concrete. Concrete is one of the most common and adaptable materials used in coastal construction. Suitable aggregates and sand for mixing concrete are usually available near coastal project sites, and the widespread use of concrete in conventional land-based construction usually assures a nearby source for cement and steel reinforcement. Concrete components of coastal projects can consist of: (a) huge cast-in-place gravity structures, such as re-curved seawalls and roadways; (b) large components that are cast and then moved into position, such as caissons that are floated into position and sunk; (c) smaller components that are assembled into a larger coastal structure, such as armor layers constructed of concrete armor units or revetment blocks; and (e) prestressed beams, columns, and piles. Some of the more important coastal applications of concrete include the following:

(a) Seawalls, Revetments, Bulkheads. Massive cast-in-place concrete seawalls have survived many decades with need of only minor repair. Solid vertical-faced, recurved, or stepped concrete seawalls provide excellent protection of upland property from severe wave action. Specially shaped concrete blocks can be placed as an armor layer on sloping revetments. The interlocking block layer can tolerate minor movement without damage. Poured concrete cover layers can only be used for above-water revetments or when the slope has been dewatered.

Bulkheads can be constructed in numerous configurations using poured concrete or concrete sheet-piles.

(b) Jetties and Breakwaters. Concrete can be used as a grout in rubble-mound structures to reduce permeability or as a binder to hold stones together. Concrete is often used to construct rib caps for jetties. In milder wave climates, cellular jetties and breakwaters can be constructed of concrete, filled with earth or rocks, and capped with concrete. Weir sections in jetties can be constructed of prestressed concrete sheet piles.

(c) Groins. Groins can be constructed using prestressed concrete sheet piles or keyed kingpiles supporting concrete panels. A cast-in-place concrete cap ties the prestressed components together. Concrete-filled bags are also used as groins in low-wave climates.

(d) Caissons. In deeper water, concrete caissons are used as breakwaters and jetties. The caissons are placed either directly on the seafloor foundation or atop a rubble-mound base structure. Concrete is used to cap the filled caissons and to build additional structural features such as parapet walls or mooring and port facilities.

(e) Concrete Armor Units. Concrete is used to fabricate reinforced and unreinforced armor units of various sizes and shapes. Concrete armor units are used when suitably sized stone is unavailable or when the higher stability offered by many concrete armor units is needed to resist high wave loads.

(f) Piles. Reinforced or prestressed concrete piles are used for piers and wharfs and to support the foundations of other coastal structures such as concrete seawalls placed on soil with low bearing capacity. Concrete piles exceed 36 m (118 ft) in length, and typically the piles have round, square, octagonal, or hollow cross sections (Moffatt and Nichol 1983).

(g) Floating Structures. Concrete pontoons are used for floating pontoon bridges, floating breakwaters in short-wave environments, wharfs, boat slips, and floating dry docks. In these applications, the individual units often are linked together to form the structure.

(h) Other Applications. Concrete is used extensively in construction of conventional land-based facilities that may be part of a coastal project. This may include roadways, bridges, foundations, drainage ponds, pipelines, ocean outfalls, and discharge structures. Concrete is also used to encase wooden or steel structural components to provide protection against biological and corrosive agents in seawater.

(2) Asphalt. Bituminous concrete (referred to as "*asphalt*" because asphalt is a primary ingredient) can be used in coastal construction as a binder or filler to stabilize rubble mounds or soils, as a sealer to reduce or prevent water flow, or as a wearing surface that can be repaired easily. Asphalt is also used as a preservative treatment or coating to protect wood and metal. Typical project elements that may use asphalt include the following:

(a) **Dikes**. Although asphalt is not widely used in the United States for coastal protection structures, the Dutch have made good use of asphalt to protect the slopes of earthen dikes.

(b) **Jetties and Breakwaters**. In the United States asphalt is used only as a binder or filler for rubble-mound structures, or as part of the crest roadway.

(c) **Revetments**. Asphalt can be used to bind revetment riprap together to form a stronger, impermeable armor layer. When wave action is slight, an asphalt layer alone is adequate to protect the revetment slope.

(d) **Roadways and Slope Protection**. Bituminous concrete is used extensively for road construction and surfaces supporting vehicular traffic, such as surfaces on wharfs and quays. Asphalt may be suitable for protecting eroding mild slopes against erosion or for lining drainage ponds and ditches.

b. Physical and mechanical properties of concrete. Portland cement concrete exists in a semi-liquid state while being mixed, transported, and placed into forms. The concrete then undergoes irreversible hardening into a durable form having excellent compressive strength properties and resistance to the harsh coastal environment. The materials used to manufacture concrete are reasonably inexpensive and exist in relative abundance throughout the world. Concrete has two main ingredients: aggregates, which comprise between 60 and 80 percent of the concrete volume; and paste, which makes up most of the remaining volume. Coarse aggregates (e.g., gravel) have diameters greater than 6 mm, whereas fine aggregates (e.g., sand) have diameters usually much less than 6 mm. The relative proportions of fine and coarse aggregates help determine concrete properties. Cement paste is portland cement and water mixed in proportions that relate directly to strength. Entrained air or special additives may occupy up to 8 percent of the volume of a concrete mixture. Aggregates should be hard, nonporous materials; and the water used in mixing should be reasonably clean and nearly free of silts or harmful chemicals, such as sulfates and alkalies. Seawater can be used if no freshwater source is available and no steel reinforcement is used in the concrete. However, concrete made with seawater has less strength than equivalent concrete made with fresh water. Several important concrete properties are listed below. Generally, the design engineer will not specify concrete mixture proportions, additives, etc.; but instead will request certain properties and minimum strengths, and the contractor will provide an appropriate concrete. Field tests and tests on sample cylinders are used to verify concrete compliance with specifications.

(1) Strength. Concrete strength is based on its capability to withstand compressive stresses. Concrete has only minor resistance to tensile stress (ranging between 7 and 10 percent of the compressive strength), and any structural member subjected to bending moments must contain steel reinforcement to resist tensile stresses. Usually the steel reinforcement is designed with the assumption that the concrete will not carry any of the applied tensile load. What little tensile strength concrete has is useful in reducing cracks that form due to shrinkage. For a particular type of portland cement, concrete strength is largely determined by the ratio of water to cement (by weight) used in mixing. Generally, concrete strength increases as water content decreases. Variations in strength for a given water-to-cement mixture are caused by aggregate properties such as maximum size, grading, shape, and strength; by entrained air content; and by types of concrete additives (called admixtures). Compressive strength is best determined by testing sample cylinders of the proposed concrete mixture, and most experienced concrete suppliers can provide accurate test results for their standard concrete mixtures. Five types of

Portland cement are available for use in coastal projects. They have the following general characteristics, as specified by ASTM Standard C-150 (ASTM C-150 1994). Other, more exotic types of concrete are available for specialized purposes.

(a) **Type I**. Cement used for ordinary structural concrete for foundations, roads, and foundations not subject to freezing/thawing conditions or marine exposure. Type IA concrete specifies air entrainment for freezing conditions.

(b) **Type II**. Mild sulphate-resisting cement that can be used in nonfreezing marine environments. Not as durable as Type V cement in seawater. Air entrainment in Type IIA concrete helps it tolerate freezing conditions.

(c) **Type III**. This cement provides high strength earlier in the curing process. After 7 days, Type III concrete reaches the same strength as Type I after 28 days. Type III should NOT be used for marine construction.

(d) **Type IV**. Provides low heat of hydration for use in structures such as dams or where heat buildup is undesirable.

(e) **Type V**. This cement has the greatest resistance to sulfates and should be used in all marine environments. Air entrainment is essential in freezing environments.

Typical compressive strengths of the above five types of concrete are shown on Table VI-4-6. Use of the tabulated values should be limited to preliminary design calculations, because actual strengths will vary greatly with materials, proportions, and curing conditions.

Table VI-4-6
Typical Compressive Strengths of Concrete (from CRC (1976))

	Compressive Strength in MPa (lb/in.^{2})				
ASTM Type	7 days	28 days	3 months	1 year	5 years
I	20.7 (3000)[1]	29.6 (4300)	35.2 (5100)	37.9 (5500)	39.3 (5700)
II	17.9 (2600)	29.0 (4200)	35.8 (5200)	40.7 (5900)	44.1 (6400)
III	26.2 (3800)	32.4 (4700)	35.2 (5100)	37.2 (5400)	37.9 (5500)
IV	10.3 (1500)	24.1 (3500)	35.8 (5200)	41.4 (6000)	44.8 (6500)
V	17.2 (2500)	28.3 (4100)	36.5 (5300)	42.1 (6100)	46.2 (6700)

[1] Note that values in parentheses are of lb/in.^{2}

As mentioned, water content in concrete mixtures is an important factor in concrete compressive strength. Table VI-4-7 presents the American Concrete Institute's (ACI 1986) suggested

maximum permissible water-to-cement ratios for concrete when strength data from field experience or trial mixes are unavailable.

Table VI-4-7
Concrete Compressive Strength for Different Water-Cement Ratios (from Mehta (1991))

Compressive Strength (at 28 days)		Water-Cement Ratio (by weight)	
(MPa)	(lb/in.^{2})	Non-Air-Entrained Concrete	Air-Entrained Concrete
41.4	6,000	0.41	------
34.5	5,000	0.48	0.40
27.6	4,000	0.57	0.48
20.7	3,000	0.68	0.59
13.8	2,000	0.82	0.74

Concrete modulus of elasticity E_c, used in calculating compressive stresses due to bending, can be estimated by the following empirical formula (ACI 1986)

$$E_c = 33 (w_c)^{3/2} (f_c)^{1/2} \qquad \text{English Units} \qquad \text{(VI-4-5)}$$

where

w_c = specific weight of concrete in lb/ft^3 (must be in the range 90-150 lb/ft^3)

f_c = compressive strength of concrete in lb/in.^{2}

E_c = modulus of elasticity in lb/in.^{2}

A metric equivalent of this nonhomogeneous equation is

$$E_{cm} = 1392 (w_{cm})^{3/2} (f_{cm})^{1/2} \qquad \text{SI Units} \qquad \text{(VI-4-6)}$$

where

w_{cm}= specific weight of concrete (must be in the range 14-24 kN/m^3)

f_{cm} = compressive strength of concrete in kPa

E_{cm}= modulus of elasticity in kPa

The modulus of elasticity for non-prestressed steel reinforcement is generally equal to 200,000 MPa (29,000,000 lb/sq in.). In addition to portland cement, there are compounds known as *blended hydraulic cements* that are covered by the Standard Specification for Blended Hydraulic Cements (ASTM C-595, 1997). Blended cements in commercial production in the United States are Type IS, which contains 30 to 65 percent rapidly cooled, finely pulverized, blast-furnace slag, and Type IP, which contains 15 to 30 percent fine pozzolan (Mehta 1991). Blended cements have lower heat of hydration (resistance to thermal cracking), lower rate of strength development, and better chemical resistance than ordinary portland cement. However,

Mehta (1991) noted that these characteristics can be obtained by using ground granulated blast-furnace slag or pozzolan as a mineral admixture into portland cement mixtures. Another attraction of blended cements is lower cost.

(2) Durability. Durability is the capability of concrete to withstand the deteriorating effects of the environment without loss of functionality. The primary factors causing deterioration of concrete are weathering, chemical action, and wear.

(a) Damage by weathering is caused mainly by freeze/thaw cycles and by restrained expansion and contraction due to wetting and drying and temperature changes. Weathering resistance is better for air-entrained concrete because the air pockets relieve pressures developed by expanding water. High-density concrete with low permeability also has better weathering resistance.

(b) Chemical reactions between alkalies in cement and mineral constituents of concrete aggregates can cause large-scale random cracking, excessive expansion, and formation of large cracks. Concrete is also affected by acids, sulfates, chlorides, salt brine at high temperatures, and hot distilled water. Steel reinforcement will rust if cracks in the covering concrete allow water and oxygen to reach the steel. Steel corrosion is particularly problematic if exposed to salt water, often causing spalling of the concrete and exposure of the reinforcement.

(c) Wearing away of concrete is caused primarily by flow cavitation, abrasion by particles in flowing water, traffic, wind blasting, and floating ice impacts (Department of the Interior 1975). Low pressure areas can develop on concrete exposed to high-velocity flows, leading to cavitation erosion of the concrete surface. Even the highest strength concretes can succumb to cavitation, and the only solution is to avoid abrupt transitions adjacent to rapid flows.

Portions of concrete structures in proximity to active sand transport are susceptible to wear by abrasion. Wind-blown sand can also erode concrete, but this process occurs slowly. Impacts by floating ice, vessels, debris, or even waves can chip concrete surfaces, possibly weakening the structure or exposing steel reinforcement. Wear resistance against abrasion and impacts increases proportionally with compressive strength. Also, wear resistance increases with curing age up to 28 days, and special precautions may be needed to protect concrete while it is curing. Some special situations might require protecting the concrete surface with a layer of a less erosive material or a material more capable of absorbing impacts. Wear resistance is not appreciably affected by hydrated lime or inert powdered admixtures up to 20 percent of the concrete volume (La Londe and Janes 1961). Mehta (1991) provides a thorough overview of factors causing deterioration of concrete in the marine environment.

(3) Consistency. Water content in wet concrete is a key factor in how well the concrete flows when being poured into formwork. Other factors include aggregate angularity, size, and texture. Increasing water content produces concrete that flows easier and is less likely to leave voids in the concrete. However, the ease of handling is offset by reduced compressive strength and the potential for aggregate segregation during placement. Concrete consistency is judged by its "*slump*." Wet concrete is placed in a special container which is then upturned and removed, leaving a free-standing mass of concrete. Slump is the vertical distance between the original

height of the container and the final resting height of the concrete pile. Large slump values correspond to wetter concrete mixtures and larger aggregates. The American Concrete Association recommends the minimum and maximum slump values shown in Table VI-4-8.

Table VI-4-8
Recommended Concrete Slump for Various Types of Construction (from Mehta (1991))

	Slump			
	Maximum		Minimum	
Types of Construction	(cm)	(in.)	(cm)	(in.)
Reinforced foundation walls and footings	7.6	3	2.5	1
Plain footings, caissons, and substructure walls	7.6	3	2.5	1
Beams and reinforced walls	10.2	4	2.5	1
Building columns	10.2	4	2.5	1
Pavements and slabs	7.6	3	2.5	1
Mass concrete	5.1	2	2.5	1

(4) Workability. Concrete "workability" is a qualitative term used to describe a mixture's capability to be handled, transported, placed, and properly finished without any harmful segregation of the aggregates. Concrete plasticity and uniformity have much influence on the functionality and appearance of the finished structural component. The type of structure and concrete placement requirements determine to some extent what workability is needed. Heavily reinforced structures require a mixture that will totally encase the reinforcement when worked using conventional techniques (e.g., vibrated). Workability is influenced by properties of the aggregate (grading, shape, proportions), amount of cement, entrained air, admixtures, and consistency (Moffatt and Nichol 1983). Practical field experience is paramount in judging concrete workability.

(5) Watertightness. As concrete cures, small voids are created by water evaporation and by shrinkage of the cement paste. Additional cavities are present in air-entrained concretes. These tiny voids may be sufficiently interlinked to allow water to pass through under capillary action or hydrostatic pressure. Concrete can be made to be virtually impervious by exercising care in mixing and placement. Aggregates must be nonporous and surrounded by impervious cement paste, and the mixture must have a low water-to-cement ratio and have no purposely entrained air. During placement, the concrete should be worked thoroughly to eliminate any pockets of entrapped air. Care should be taken to avoid contaminating the concrete with foreign matter such as dirt clods, dry leaves, or discarded trash. Concrete becomes more impervious if it cures at a slow rate. Normal concrete should be kept moist for at least 7 days, and high-early-strength concrete should be wetted for at least 3 days to assure watertightness (La Londe and Janes 1961). Admixtures are available to enhance structure watertightness.

(6) Specific weight. The specific weight of typical concrete mixtures varies between 22-25 kN/m^3 (140-160 lb/ft^3). Reinforced concrete has a nominal specific weight of 23.6 kN/m^3 (150 lb/ft^3), stone concrete is 22 kN/m^3 (140 lb/ft^3), and cinder concrete is about 15.7 kN/m^3 (100 lb/ft^3). Specific weights of concretes made with lightweight aggregates depend on the weight and proportion of lightweight aggregate. Table VI-4-9 (Department of the Interior 1975)

shows average specific weights of normal fresh concrete for given water content and aggregate size and specific gravity. English units are provided in the top table, and metric equivalents (direct conversion of English unit values) are provided on the lower table.

Table VI-4-9
Average Unit Weight of Fresh Concrete (from Department of the Interior (1975))

	Average Values			Aggregate Specific Gravity Unit Weight				
Maximum Aggregate Size	Air Content (%)	Water Content	Cement Content	2.55	2.60	2.65	2.70	2.75
			Unit Weight in lb/ft^3					
0.75 (in.)	6.0	283 (lb/yd^3)	566 (lb/yd^3)	137	139	141	143	145
1.5 (in.)	4.5	245 (lb/yd^3)	490 (lb/yd^3)	141	143	146	148	150
3.0 (in.)	3.5	204 (lb/yd^3)	408 (lb/yd^3)	144	147	149	152	154
6.0 (in.)	3.0	164 (lb/yd^3)	282 (lb/yd^3)	147	149	152	154	157
			Unit Weight in kN/m^3					
20 (mm)	6.0	1.65 (kN/m^3)	3.29 (kN/m^3)	21.5	21.8	22.2	22.5	22.8
40 (mm)	4.5	1.43 (kN/m^3)	2.85 (kN/m^3)	22.2	22.5	22.9	23.3	23.6
75 (mm)	3.5	1.19 (kN/m^3)	2.37 (kN/m^3)	22.6	23.1	23.4	23.9	24.2
150 (mm)	3.0	0.95 (kN/m^3)	1.64 (kN/m^3)	23.1	23.4	23.9	24.2	24.7

(7) Volume change. Concrete shrinks as it cures and hardens, and it also expands and contracts with temperature and moisture content. Generally, expansion is not too serious a problem because it induces compressive stresses. However, overall expansion must be considered for structural components like constrained slender beams and slabs, which could buckle unless some allowance is made for excessive expansion. Contraction of concrete is a more serious problem because of the material's low tolerance of tensile stresses. Contraction cracks form in the surface, allowing water to penetrate the concrete. If water between the cracks freezes, the cracks are enlarged and damage occurs. Steel reinforcement helps distribute the concrete contraction more uniformly, resulting in smaller cracks. Most shrinkage occurs as new concrete cures because of the large amount of water in the paste. Shrinkage increases with increases in initial water content and entrained air and with compressibility of the aggregates. A 1-percent increase in water quantity increases shrinkage by 2 percent (La Londe and Janes 1961). Shrinkage that occurs in average concrete while curing to complete dryness is about equivalent to the shrinkage that would occur due to a temperature drop of 56EC (100EF).

c. Physical and mechanical properties of asphalt. Combining asphalt cement with various types of aggregates in different proportions can produce a wide range of bituminous concretes exhibiting different characteristics. This versatility makes Aasphalt@ a useful construction material for coastal projects. Usually, the aggregates used in bituminous concrete are durable, so the physical properties of the mixture stem largely from the properties of the asphalt cement. Asphalt is not affected by most chemicals, with the notable exception of other

petroleum-based products that can act as solvents. The flexibility of asphalt allows bituminous concrete to conform to uneven surfaces and to adjust to differential movements. Asphalt mixtures can be made to be porous or impervious when placed. Impervious mixtures are often used to line drainage ditches or to waterproof structures. Asphalt mixtures have both plastic and elastic properties that are mainly a function of temperature. Asphalt mixes must be designed to achieve project objectives at an economical cost. Some of the factors considered when blending asphalt and aggregates include the following:

(1) There must be sufficient quantities of asphalt cement to ensure mixture durability under design load conditions.

(2) Proper type and size distribution of aggregates is needed to ensure a bituminous concrete that can tolerate loads without excessive deformation.

(3) Sufficient voids in the mixture are necessary to allow for a slight amount of additional compaction without loss of stability and without loss of impermeability.

(4) Good workability of the initial heated mixture allows easy placement of the asphalt compound without segregation of the aggregates.

Moffatt and Nichol (1983) provide additional descriptions of bituminous concrete and asphaltic compounds. Specific design guidance for various types of asphalt mixtures can be found in publications from the Asphalt Institute or from local asphalt contractors.

d. Concrete construction practices. An important and essential reference for the design and construction of concrete structures is the American Concrete Institute's *Manual of Concrete Practice* (ACI 1986), which is revised annually. Standard ACI 318 in the ACI manual provides building code requirements, along with a detailed commentary on code provisions.

(1) Transport and placement. Concrete can be mixed onsite or batched offsite and transported to the site by a number of different means including revolving drum trucks, barges, rail cars, conveyor belts, and pipelines. In all cases the objective is deliver the mix to the site without significantly altering the concrete's water-cement ratio, slump, air content, and distribution of aggregates.

(a) Concrete placement should strive to achieve the same objectives as stated above for transportation, and handling equipment should be chosen accordingly. Transport and placing capacity must allow the concrete to be kept plastic and free of cold joints while it is being placed in forms. Horizontal layers should not exceed 0.6 m (2 ft) in depth; and for monolithic structures, successive layers should be placed while the underlayer can still be vibrated to join the layers together, thus avoiding cold joints. When possible, concrete should be placed directly into the forms with minimum lateral movement, as the lateral movement tends to segregate the aggregates. Placement on sloping surfaces should begin at the toe and proceed upslope.

(b) Placement techniques should avoid high-velocity discharge or long drops, both of which contribute to aggregate segregation. Requests for addition of water to assist concrete flow down the chute should not be routinely granted without an assessment of how the concrete

strength will be affected. Water should not be added to concrete that retains good workability and can be properly consolidated in place. Concrete with slump in excess of specifications should be rejected by the supervising engineer. Contractors should provide handling equipment sufficient to place concrete of specified consistency.

(c) Consolidation by screeding and vibrating removes air bubbles that are entrapped during placement. Vibrating also provides a more uniform distribution of solids and water in the concrete. (However, it is possible to over-vibrate concrete, which could result in a less homogeneous mixture.)

(d) Floor surfaces are more durable if steel troweling machines are used to finish the concrete as it sets. Troweling produces a low-maintenance, dense surface layer free of surface voids. Good vibrating adjacent to forms helps assure reasonably smooth surface finishes for nonhorizontal surfaces.

(2) Curing and formwork removal.

(a) Proper curing is essential for concrete to reach its design strength. Rapid loss of moisture must be prevented because water is needed for cement hydration, and the temperature should be controlled to assure the concrete attains its mature strength. In above-freezing conditions, water can be ponded on horizontal surfaces, and structural members such as columns can be covered with wet burlap or kept under constant “misting” with water. Where ambient temperatures are below freezing, fresh concrete must be protected from freezing with insulating blankets and cured with steam or electrically heated forms or infrared lamps (Mehta 1991). An alternate method is to raise the temperature of the mixture by heating the water and aggregates. Seawater should not be used to cure reinforced concrete; however, high-strength concrete can be exposed to seawater after 3 days of curing because by this time it is considered impermeable.

(b) Formwork should not be removed until the concrete has cured sufficiently to support the dead load and any live load that may be imposed during subsequent construction. To prevent damage to the surface, formwork should have been properly oiled or treated, and the concrete should be hard before forms are removed. Form removal may expose warm concrete to chilly winds that may cause cracks to form as contraction occurs.

(3) Reinforcement cover thickness. *The Manual of Concrete Practice* (ACI 1986) specifies minimum cover thicknesses for conventional and prestressed concrete structural elements. For coastal and offshore structures, steel reinforcing bars should have a minimum concrete cover of 50 mm (2 in.) for portions submerged or exposed to the atmosphere. The cover should be increased to 65 mm (2.5 in.) for portions of the structure in the splash zone or exposed to salt spray. Submerged prestressed members should have 75 mm (3 in.) of minimum cover, and 90 mm (3.5 in.) of cover in the splash zone. Stirrups may have 13 mm (0.5 in.) less cover than the minimums for reinforcement.

(4) Joints and sealants. Most concrete structural elements contain construction joints to compensate for volume changes, to allow for construction sequence, or to serve some other design purpose.

(a) **Contraction Joints** are control joints used to control the amount of cracking that occurs during contraction of the concrete. They are most commonly used to subdivide large, thin members like slabs into smaller units. The intent is for cracking to occur at the joint which can later be sealed with a flexible sealant.

(b) **Expansion Joints** are placed between concrete members to allow for expansion, thus avoiding crushing, buckling, or warping of slender members. Expansion joints also serve to isolate adjacent members so loads are not transferred between structural components, allowing differential movement between members. The joint is typically a clear space between member cross sections with keyways or dowels sometimes used to prevent lateral displacements of components. The joint can be sealed with a flexible sealant.

(c) **Construction Joints** are predetermined discontinuities in concrete to facilitate construction sequence. They can resemble either expansion or contraction joints. When continuous structural integrity is required, reinforcement is carried through the joint and efforts are made to bond adjacent components at the joint. Sealing of joints, particularly contraction joints, may be necessary to prevent water from entering the concrete and causing deterioration. In other cases, joint sealing is necessary to help retain backfill soil, contain a liquid, or prevent ice from forming in the joint. A variety of sealants are available for use in joints and cracks. These include sand grout, epoxies, oil-based mastics, bituminous compounds, metallic materials, thermoplastics, and others. Moffatt and Nichol (1983) give an overview of common sealants and their properties.

(5) Repairs. Post-construction repairs may be needed to seal curing cracks that are excessively wide or to repair damage incurred during form removal. Cracks can be filled with an appropriate epoxy, and surface voids left by entrapped air can be filled using concrete grout or mortar. Repair of deteriorating concrete structures is covered in Part VI-8, “Monitoring, Maintenance, and Repair of Coastal Projects.”

e. Concrete for armor units. A unique application of concrete in coastal structures is artificial armor units placed as protection on rubble-mound structures in lieu of stone. Concrete armor units are cast in a variety of sizes and shapes (see Part VI-2-3, “Main Types of Armor Units.” Because concrete armor units are usually unreinforced, they become vulnerable to tension breakage above a certain size, depending on type of unit (slender versus bulky) and other parameters. Steel reinforcement has been used in the past, but the cost of reinforcement is high. Large, slender, unreinforced concrete armor units have low reserve strength in tension beyond simply supporting their own self-weight, and any movement of placed units could cause breakage. Consequently, engineers strive to design the armor unit layer for no movement of the units after placement. High-strength concrete helps lower the risk of breakage, and methods are now available to access stress probabilities in terms of concrete strength (see Part VI-5-3-c, “Structural Integrity of Concrete Armor Units.” Special precautions should be followed to ensure uniform, high-quality concrete is used in casting concrete armor units. The concrete should be properly vibrated to remove all voids which could substantially weaken the armor unit. Units must be cured properly before placing them on the armor layer. In particular, it is important to avoid formation of thermal cracks due to rapid curing. Any means to reduce high temperature

gradients in the curing concrete will help reduce crack formation. Special equipment will be needed to handle, transport, and place the armor units.

f. Environmental effects on concrete and asphalt.

(1) Pollutants. Some pollutants may contain chemicals (sulfates and acids) in sufficient quantities to damage concrete. The chemicals must be in solution form to do harm. Naturally occurring sulfates may be present in soil or dissolved in groundwater adjacent to concrete structures. In general, concrete is not significantly affected by most pollutants found in the coastal zone. Bituminous asphalt is resistant to most chemicals with the exception of petroleum solvents, which can cause deterioration of the asphalt.

(2) Water penetration. Water itself is not harmful to concrete, but it may carry sulfates or acids in solution that can have a detrimental effect. Salt water that penetrates to steel reinforcement causes the steel to corrode, weakening the structure. Also, the products of corrosion can expand and cause spalling. Periodic wetting and drying may cause cracks to form. Asphalt is usually considered to be impermeable and resistant to water penetration.

(3) Waves and currents. Concrete structures designed under correct loading assumptions will not be affected by waves and currents. High flow velocities at abrupt transitions may cause flow cavitation, which can lead to deterioration of the concrete surface. Asphalt is not affected by waves and currents unless the waves are large enough to damage the asphalt layer directly or carry floating bodies that impact the asphalt.

(4) Ice and temperature changes. Ice can damage concrete structures in two ways. Water that freezes in cracks will enlarge the cracks and eventually damage the concrete through spalling or outright fracturing. Impacts by floating ice or stresses induced by ice riding up on a structure can also damage concrete. Temperature changes cause expansion and contraction, but these effects are countered by proper design. Temperature control is a critical aspect of the curing process in order to obtain specified strength. Exposure of asphalt to temperatures above 163EC causes solvents to dissipate, resulting in deterioration. Ice does not cause problems with asphalt other than damage caused by floating ice. However, cold temperatures cause asphalt to become brittle.

(5) Marine organisms. Concrete is one of the toughest materials used in coastal construction and has no food value for marine organisms. Neither marine organisms nor larger land animals have any effect on good concrete made with strong aggregates. Barnacles and marine plants can attach to concrete surfaces, but they have little effect outside of causing additional drag resistance to flows. The softness of bituminous asphalt makes it susceptible to damage from crustaceous organisms; but because asphalt is petroleum-based, it has no attraction for other animals.

(6) Abrasion. Hard particles carried by wind and water can wear down concrete surfaces over time, but this process is so slow that it usually is inconsequential over the life of the structure. Bituminous asphalt resists wearing by small waterborne particles quite well; however, impacts by larger particles can cause damage.

(7) Seismic activity. Accelerations from earthquakes can be detrimental to concrete structures through direct inducement of stresses in the structure or through differential settlement caused by foundation damage. The *Manual of Concrete Practice* (ACI 1986) describes special provisions for the design of earthquake- resistant structures. The plasticity of asphalt allows it to flex and deform with earthquake motions rather than resisting through a rigid structure. This flexibility helps reduce damage to the asphalt project elements.

(8) Other effects. Concrete is not affected by sunlight, and it has good resistance to fire or extremely high temperatures. Human activity has little effect on the performance of concrete structures, and concrete is difficult to damage through vandalism. However, coastal structures provide ample canvas for graffiti artists, which may cause noticeable visual pollution. Fire is a real hazard for bituminous asphalt because it is petroleum-based. Usually there is not enough solvent in the asphalt binder to sustain fire; but in the presence of other combustible materials, asphalt will burn.

VI-4-5. Steel and Other Metals.

a. Use of metal in coastal construction. Many components of coastal projects are well-suited for fabrication using common metals. Construction requirements such as strength, availability, ease of construction, durability, and adaptability can often be met with metals such as steel, aluminum, copper, or various metal alloys. Consideration should be given to the economic benefits of yard fabrication of structural components as opposed to site fabrication.

(1) Steel.

(a) Steel has been used in marine construction since the late 1800s. Perhaps the most common use of steel is as concrete reinforcement in such structures as caissons, seawalls and bulkheads, paved working surfaces and roadways, and pretensioned piles. Steel reinforcement should be placed to provide adequate concrete coverage to protect it from the corrosive effects of water. (see Part VI-4-4-d-(3), “Reinforcement Cover Thickness”).

(b) Another important marine application of steel is pilings. Pipe piles and H-piles are used to support foundations or as supports for coastal structures or fendering systems. Steel H-piles can be driven into hard strata or through soils containing obstructions such as rocks. Site-welding steel H-piles end to end allows deep penetration through soft soils down to bedrock. Pilings are sometimes encased in concrete to prevent corrosion. Steel sheet piles are used extensively in port and harbor facilities to construct seawalls and wharfs.

(c) Conventional steel framing is used for building construction in the marine environment in the same manner as inland; however, more attention is given to preventing corrosion. Steel is also used for fabricating specialty components such as fendering and mooring system components, structural framework, supports for navigation aids, chains, flow control gates, and storm surge barriers. Steel wire is used to construct wire cages for gabions and chain-link fencing. Steel bolts, plates, and fasteners are used to connect structure components of similar or different materials. Steel rods are used as bracing and as vertical retaining wall tiebacks. Steel wire rope is used to lash batter piles and for other purposes.

(d) In special applications, high-strength steel may be specified; but the cost will be greater, and there may be restrictions regarding onsite modification with cutting torches, which could weaken the steel. Drilling holes will also be more difficult. Stainless steel is not used in great quantities, but it is an important material for components that are openly exposed to salt water and must remain free of corrosion. Cast iron is used to fabricate special shapes such as mooring bollards.

(2) Aluminum alloys. Many aluminum alloys are resistant to corrosion, which makes them ideally suited for low-maintenance applications in exposed coastal regions. These applications include door and window frames in buildings, building roofing and siding, tread plates, decking, catwalks, railings, support framework, and architectural trim such as gutters and downpipes, facia, etc. Aluminum fasteners can be used in corrosive environments, but consideration must be given to aluminum's reduced strength capacity and fatigue characteristics when compared to steel. Aluminum alloys are also used as electrical conductors and in constructing specialty components, where light weight is an important criterion.

(3) Other metals and metal alloys. Other metals and alloys are used to a much lesser extent in coastal construction. Copper is used in electrical wiring and buses and for piping and sheathing. Because of its relatively noncorrosive nature, brass (copper and zinc) is used for hardware fittings and fasteners and often as survey monument marker plates. More exotic metals and alloys, such as monel (nickel-copper) and titanium are found only in project components that require the unique capabilities offered by these materials.

b. Physical and mechanical properties of metals. Much of the versatility of metals stems from their strength, durability, "workability," and competitive cost. Metals have a crystalline structure that results in a very homogeneous material with consistent strength properties throughout. During manufacture, metal can be formed into a variety of shapes and sizes, and a wide assortment of metal "stock" is available for design. Depending on the metal, its manufacture, and its shape, metal properties vary from rigid to flexible, ductile to brittle, soft to hard, and weak to strong. Undoubtedly, metals offer numerous options as design materials.

(1) Steel. Steel is the most commonly used metal, and it is available in a wide assortment of grades and sizes. Steel is an ideal material for construction because is can be easily joined, has high tensile strength, good ductility, and good toughness. Physical and mechanical properties of steel are well-documented in material handbooks, standards from the ASTM, and the *Manual of Steel Construction* (AISC 1980). Table VI-4-10, is an abbreviated list of steel specifications used in the United States along with typical applications for each grade of steel. Each ASTM specification sets out manufacturing guidelines such as steel ingredients and quantities, manufacturing processes, quality control, etc. Other countries may have similar steel specifications or have adopted those of the ASTM.

Table VI-4-10
Specifications and Applications for Steel Suitable for Marine Service (from Moffatt and Nichol (1983))

ASTM Designation	Title of Standard	Application
A36-93a	Standard specification for structural steel.	Bridges, bulkheads, general structures.
A252-93	Standard specification for welded and seamless steel pipe piles.	Structures, forms for cast-in-place concrete piles.
A328-93	Standard specification for steel sheetpiling.	Sheetpiling, dock walls, and cofferdams.
A573-93	Standard specification for structural carbon steel plates of improved toughness.	Steel plates and sheetpiling.
A690-93	Standard specification for high-strength, low-alloy steel H-piles and sheetpiling for use in marine environments.	Dock walls, seawalls, bulkheads; providing 2 to 3 times greater resistance to seawater splash zone than ordinary carbon steel.
A709-93a	Standard specification for structural steel for bridges.	Carbon and high-strength, low-alloy steel plates and sheets.

(2) Aluminum alloys. Pure aluminum is soft and ductile and does not have sufficient strength for most commercial applications. Other metal elements are added to aluminum to create alloys having a variety of physical properties. Many alloys of aluminum have high corrosion resistance to marine atmosphere as well as good strength-to-weight ratios. Aluminum alloys are identified by numbers that are grouped together according to alloy components and manufacturing process.

(a) **1000 Series**. This series contains alloys that contain at least 99 percent aluminum. These alloys have high thermal and electrical conductivity, excellent corrosion resistance and workability, but they have the lowest structural strength. These alloys can only be hardened by cold working. Aluminum alloy 1350 is used for electrical wiring.

(b) **2000 Series**. This group contains alloys in which copper is the major alloying element. These alloys have less corrosion resistance than most other aluminum alloys.

(c) **3000 Series**. Alloys in which manganese is the major alloying element are in this series. These alloys generally cannot be heat-treated, but they can be hardened by cold working. Roofing and siding are usually 3004 aluminum.

(d) **4000 Series**. This group contains alloys in which silicon is the major alloying element. These alloys have a lower melting point, and thus they are used in welding and brazing wire to weld other aluminum alloys.

(e) **5000 Series**. This series contains alloys in which magnesium is the major alloying element. These alloys have moderate to high strength, good corrosion resistance in marine environments, and good welding characteristics.

(f) **6000 Series**. Aluminum alloys containing silicon and magnesium in about equal proportion comprise this group. These alloys are heat-treatable, have medium strength, and have good corrosion resistance. Windows, door frames, and lampposts are usually 6063 aluminum. Tread plate is usually heat-treated 6061 aluminum.

(g) **7000 Series**. This group contains alloys in which zinc is the major alloying element. These are heat-treatable alloys that have very high strength.

Aluminum alloys 5083, 5086, 5052, and 6061 are commonly used in marine environments. Although the 5000 series has best corrosion resistance, alloys from the 1000, 3000, and 6000 series are also used in coastal applications. Aluminum alloys can be used in the splash zone, but they are not recommended for continuous immersion. In addition to the numerical series specification, aluminum alloy designations also have a letter indicating the method of tempering.

(3) Other metals and metal alloys. Copper has high electrical and thermal conductivity, excellent corrosion resistance under normal atmospheric conditions, and it has good workability. Copper can be alloyed with other metals to improve strength, and to provide better corrosion and creep resistance. Well- known copper alloys include brass and monel. Best corrosion resistance in seawater comes from copper alloys that form thin corrosion films that protect the metal from further corrosion, even in flowing water. Metals and metal alloys other than those mentioned above are not commonly used in coastal engineering projects, but may appear in special applications.

(4) Galvanic reactions. When two dissimilar metals in electrical contact are placed in salt water, an electric potential is established and a process occurs that is referred to as “galvanic corrosion.” The more galvanically active metal (anode) will corrode at a faster rate than it would by itself. The more noble metal of the pair (cathode) is protected from corrosion by the galvanic coupling. Table VI-4-11 lists common metals and alloys in a “*galvanic series*” for flowing seawater at ambient temperature. In the table, the most active metal is at the top and the entries are in decreasing order to the least active metal at the bottom. If two dissimilar metals must come in contract, several steps can be taken to reduce galvanic corrosion: (a) choose metals close together in Table VI-4-11; (b) electrically insulate the two metals at the point of contact; (c) coat the anode metal (higher in the galvanic series); and (d) place a more active third metal in electrical contact with the other two metals to provide cathodic protection via a sacrificial anode. Zinc is commonly used for sacrificial anodes. Periodically inspecting and replacing sacrificial anodes will extend the working life of components that have potential for galvanic corrosion.

c. Design values for structural metals. Industry adherence to uniform quality standards in the manufacture of metals and metal alloys has led to reliable design values. Table VI-4-12 presents recommended allowable tensile strengths and yield strengths for some grades of steel, aluminum, and other metals. Values for metals not listed in the table can usually be found in the ASTM Standards or in design manuals prepared by industry associations. Most designs utilize metal fabricated into standard cross sections, such as I-beams, H-beams, box sections, angles,

pipe sections, etc. These “standard sections” have allowable design loads associated with particular loading conditions. For example, unbraced slender columns will fail in buckling before allowable compressive strength is exceeded. Design handbooks are available covering most of the standard structural cross sections. For structural steel, the *Manual of Steel Construction*, produced by the American Institute of Steel Construction (AISC (1980 or more recent edition)) is widely used by engineers in the United States.

Table VI-4-11
Galvanic Series in Flowing Seawater (2.4 TO 4.0 m/s) at Ambient Temperature (from Moffatt and Nichol (1983))

Magnesium
Zinc
Aluminum alloys
Calcium
Carbon steel
Cast iron
Austenitic nickel cast iron
Copper - nickel alloys
Ferritin and mortensitic stainless steel (passive)
Nickel copper alloys, 400, K-500
Austenitic stainless steels (passive)
Alloy 20
Ni - Cr - Mo alloy C
Titanium
Graphite
Platinum

Table VI-4-12
Tensile Stress Limits for Selected Metals and Alloys

Name or ASTM Code	Grade	Min. Yield Stress MPa (ksi)	Tensile Strength MPa (ksi)
	Steel		
A36		250 (36)	400-550 (58-80)
A252	1	205 (30)	345 (50)
	2	240 (35)	414 (60)
	3	310 (45)	455 (66)
A328		270 (39)	485 (70)
A573	58	220 (32)	400-490 (58-71)
	65	240 (35)	450-530 (65-77)
	70	290 (42)	485-620 (70-90)
A690		345 (50)	485 (70)
A709	36	250 (36)	400-550 (58-80)
	50	345 (50)	450 (65)
	50W	345 (50)	485 (70)
	70W	485 (70)	620-760 (90-110)
	100-100W	620-690 (90-100)	690-895 (100-130)
	Aluminum Alloys		
B209	3004-0	55 (8)	145-193 (21-28)
	5052-0	65.5 (9.5)	172-214 (25-31)
	5083-0	124 (18)	276-352 (40-51)
	5086-0	97 (14)	241-304 (35-44)
	6061-0	83 (12)	138 (20)
B241	6063-0	(18)	(19)
	Copper Alloys		
Copper, B152, B124, B133	Annealed	69 (10)	221 (32)
	Cold-drawn	276 (40)	310 (45)
Yellow Brass, B36, B134, B135	Annealed	124 (18)	331 (48)
	Cold-drawn	379 (55)	483 (70)
Naval Brass, B21	Annealed	152 (22)	386 (56)
	Cold-drawn	276 (40)	448 (65)
Alum. Bronze, B169, B124, B150	Annealed	172 (25)	483 (70)
	Hard	448 (65)	724 (105)
	Nickel Alloys		
Cast Nickel	As cast	172 (25)	393 (57)
A Nickel, B160, B161, B162	Annealed	138 (20)	483 (70)
	Cold-drawn	483 (70)	655 (95)
K Monel	Annealed	310 (45)	690 (100)
	Spring	965 (140)	1034 (150)

d. Metal protective treatments. Corrosion is the primary cause of steel deterioration in the coastal zone. Other metals suffer corrosion to a lesser extent. If steel corrosion is allowed to continue, structural steel will eventually weaken to a point where allowable stresses will be exceeded and the structure may fail. Exposed steel must be covered with a protective coating; and as the Navy is well aware, painting (and regular repainting) will help fight steel corrosion by seawater and salt air. In extreme cases, a thick coating of tar may provide adequate protection. Other protection methods include encasing the steel in concrete, such as in pier pilings; protecting the steel with a plastic coating, such as used for chain-link fencing; and applying a protective layer such as galvanizing or chrome plating. Abrasion by sand particles or vessel contact will strip away protective metal coatings with time, necessitating field maintenance where feasible or replacement in situations where the protective coating is factory-applied and cannot be mended in the field. Aluminum alloys can be "anodized" to provide greater corrosion resistance and some degree of galvanic protection when placed in contact with other metals. Copper, brass, and some other metals and metal alloys provide their own corrosion protection by forming a thin layer of corroded material. For example, brass will tarnish to a dull finish without losing any structural functionality.

e. Metal fasteners and connections. Metal structural components are usually fitted together in the factory or at the project site using a variety of methods including machine screws, bolts and bolted connector plates, electric arc welding, and brazing.

(1) Rivets and Bolts.

(a) Advances in welding and high-strength bolts have lessened the use of riveting in steel structure connections during the construction phase. However, riveting is an important option during the manufacturing of structural components. The ASTM Standards (ASTM A-502 (1994)) provide guidelines for the use of steel structural rivets in fabrication. Riveting is more common for joining aluminum structural components, particularly for heat-treated alloys, which could be weakened by welding. Aluminum riveting requires less skill than welding and it is a relatively fast method for making connections. Rivets are particularly useful for connecting dissimilar metals.

(b) Bolts are typically used in construction when welding is impractical or when the connections may need to be disassembled for maintenance or replacement. Less skill is needed to make bolted connections than for welding. Common practice is to oversize bolts exposed to corrosive marine environments to compensate for excessive corrosion. Bolts are made of carbon structural steel or high strength steel. Resistance of high- strength bolts to atmospheric corrosion is about twice that of carbon structural steel, which is an advantage in coastal construction. Allowable stresses for standard and high-strength bolts are given in the *Manual of Steel Construction* (AISC 1980) or other appropriate design manuals.

(2) Welding. Factory and onsite welding of metals is usually accomplished using either gas welding or arc welding. Oxyacetylene is suitable for welding carbon and alloy steel, cast iron, copper, nickel, aluminum, and zinc alloys. Hydrogen, methane, or propane gases are used to weld metal with lower melting temperatures such as aluminum, magnesium, zinc, and lead. Welding flux is needed for oxyacetylene welding of stainless steel, cast iron, and most nonferrous metals. Arc welding provides strong connections for structural carbon steel; and for

critical connections, welding quality can be checked using x-ray techniques. Underwater arc welding is feasible, but not recommended except in emergency situations or for temporary repairs. Underwater welds in mild steel develop about 80 percent of the strength of comparable dry welds, but they are only half as ductile. Underwater welding surfaces must be free of marine growth, rust, mill scale, and paint to assure high-quality welds.

f. Environmental effects on metal. Metals and metal alloys are very durable and stand up reasonably well to the coastal environment. Most metals are unaffected by ultraviolet radiation; however, sunlight may contribute to stress corrosion cracking in stainless steel. Toughness of carbon steel and some steel alloys decreases as temperature decreases; and in regions of extreme temperature change, design allowances for expansion and contraction must be made. Although metal is fire-resistant, yield strength is reduced as temperature rises, which may result in structure collapse.

(1) Abrasion. Metals can suffer abrasion by sand particles carried by water or wind. Although loss of metal through abrasion will be minor, a more critical problem is stripping of protective coatings or corrosion films down to bare metal, which then leads to rapid corrosion.

(2) Corrosion. Metal corrosion due to freshwater and saltwater exposure is a primary concern in coastal designs. Corrosiveness of water is dependent on water acidity, electrical conductivity, and most importantly, oxygen content. Fresh water polluted with acidic compounds may be more corrosive to carbon steel than seawater. Salt ions in seawater cause localized destruction of the protective oxide films (e.g., rust), thus reducing the corrosion resistance of the metal. Corrosion rates for carbon steel exposed to the air at the shoreline are 10 times greater than rates at locations 500 m inland from the shoreline. Pilings located in the splash zone can achieve two to three times the corrosion resistance of carbon steel if they are fabricated of high-copper-bearing, high-strength, low-alloy steel conforming to ASTM Standards (ASTM A-690 (1994)).

(3) Marine fouling. Fouling of immersed metal by marine plants and animals increases corrosion rates in some metals, such as carbon steel, stainless steel, and aluminum. In addition, marine growth may increase flow resistance, which induces greater loads on the structure. Copper and copper-nickel alloys have the best resistance to biofouling, and brass and bronze have good resistance. Biofouling can be decreased by application of antifouling paints. Metal placed in contact with soil can suffer corrosion due to either anaerobic or aerobic bacteria in the soil.

(4) Seismic effects. Properly designed metal structures can withstand seismic accelerations with little damage. Structural steel is well-suited for seismic designs because of its high tensile strength, good ductility, and consistent yield stress properties when loaded in tension, shear, and compression.

VI-4-6. Wood.

a. Use of wood in coastal construction. Wood can be used in coastal projects such as seawalls, revetments, bulkheads, piers, wharfs, sand fences, and floating platforms. Wood is also used for temporary constructions such as formwork, bracing, blocking, etc.

(1) Untreated lumber. Stock untreated lumber is typically used only during project construction or when the wooden components are expected to survive for only a few months. Typical short-term applications include concrete formwork, temporary bracing, machinery supports, and dunnage. Untreated lumber can be used as a permanent part of a project provided it is protected by a covering (e.g., interior framework) or painted and maintained for the life of the project. However, untreated wood will rapidly decay if it comes into direct contact with soil or seawater.

(2) Treated lumber. Stock treated lumber is used in situations where the wood comes into direct contact with the ground or water. Contact with soil leads to rot, fungus, or insect attack. A typical wood pressure treatment consists of chromated copper arsenate, but local project conditions and intended application may dictate a different treatment to prolong project life. Lumber submerged or periodically immersed in seawater should be pressure-treated with coal-tar creosote or a similar protective treatment.

(3) Piles and poles. Wood piles are frequently used in coastal construction in applications such as pile dolphins (clusters of wood piles lashed together), guide piles for floating structures, piles for channel markers, pile-supported seawalls and bulkheads, building foundations, piers, wharfs, fendering systems, trestles, jetties, and groins. Practically all wood piles are pressure-treated with coal-tar creosote to resist insects, marine borers, limnoria, rot, and fungus. Untreated wood piles are used only as temporary supports or to carry electric power and communication lines to the project site.

(4) Beams and stringers. Treated lumber beams and stringers are used to build load-bearing structures such as groins, bulkheads, jetties, pier decks, wharfs, bracing, and other structures related to shipborne commerce. Untreated beams are used only as support members within protected areas (e.g., buildings), when protected by paint, or as temporary support members.

(5) Plywood and laminated wood.

(a) Practically all plywood used in coastal projects is designed to withstand the effects of humidity and water immersion. Wet-use plywood can be used as building flooring and sheathing, wood-frame gusset plates, concrete forms, and sign boards. Special plywood treatment is needed in extreme conditions like saltwater immersion.

(b) Glued laminated wood provides stronger load-bearing structural members because of better quality control and ability to size members to a specific need. Laminated structural members may be suitable as columns, beams, and trusses, particularly in larger sizes and lengths that are difficult to find in stock lumber. Laminating glue must be waterproof and the wood must be treated with preservatives except in protected or sheltered applications.

b. Physical and mechanical properties of wood. Trees are classified either as hardwoods or softwoods. Hardwoods are typically broad-leafed trees which shed their leaves in the fall; whereas most softwoods are evergreens, which have needles or scale-like leaves. The physical and mechanical properties of wood vary significantly between different tree species. Solid wood substance has a specific gravity of about 1.5 regardless of species. However, part of the volume

of dry wood consists of air-filled cavities, giving variation to the density of wood construction materials. In general, wood strength increases with density. The *Timber Construction Manual* (AITC 1985) provides tables listing unit weight and specific gravity for commercial lumber species at different moisture contents.

(1) Directional strength characteristics. Mechanical properties of wood are specified according to three principal axes: (a) longitudinal axis (parallel to the grain), (b) tangential axis (perpendicular to the grain and tangential to the growth rings), and (c) radial axis (perpendicular to the grain and growth rings). For design purposes, stresses are usually determined parallel to and perpendicular to the grain because there is little difference between tangential and radial stress properties.

(2) Loading configurations. Because wood strength differs along each of its three principal axes, structural design of load-bearing members must consider grain orientation when determining appropriate member dimensions necessary to resist the applied loads. Wood has the greatest strength when loaded so as to produce tension or compression parallel to the grain. The following stress conditions are likely to occur in wood structures:

(a) Tension and compression parallel to grain. Wood structures are commonly designed so the primary force loadings produce tension or compression parallel to the wood grain in structural members. Columns, piles, struts, and beams typically have the grain parallel to the longest dimension. The strength capacity will be reduced if the load is applied at an angle to the grain or if knots are present in the wood.

(b) Tension and compression perpendicular to grain. Wood has the least strength in resisting loads that induce tension stresses perpendicular to the wood grain. This type of loading should be avoided for all load-bearing members. Compression forces perpendicular to the wood grain tend to compress the wood at the surface, but generally this can be tolerated provided the displacement of adjoining members does not cause difficulties.

(c) Shear parallel to grain. Wood has the capacity to resist shearing forces parallel to the wood grain, but this capacity is greatly reduced by shakes, checks, and splits that may occur in wood members as they dry. Consequently, allowable shear stress design limits are reduced to compensate for the likelihood of imperfections in the wood.

(d) Shear perpendicular to grain. Solid wood components can withstand substantial shear stresses when loads are applied perpendicular to the grain. In most loading configurations, safe stress limits will be exceeded by compression perpendicular to the grain well before shear perpendicular to the grain becomes critical.

(3) Temperature and moisture effects. Wood does expand and contract with changes in temperature, but in most cases this expansion is not sufficient to create significant stresses. Wood shrinks as it dries and swells as moisture content increases. The amount of shrinkage or swelling is different in the radial, tangential, and longitudinal directions relative to the wood grain, with the most shrinkage occurring in the tangential direction. Generally, dimensional changes due to moisture content are greater for hardwoods than for softwoods. Allowances for swelling should be made when using kiln-dried lumber for project components that will usually

be saturated with water. Average shrinkage in the three principal axes for various wood species when kiln-dried is given in the *Timber Construction Manual* (AITC 1985).

c. Design values for structural lumber. Structural lumber is classified according to wood species, size, and intended use. Dimension lumber refers to rectangular-shaped pieces of smaller dimensions typically used as framing materials, joists, planks, etc. Dimension lumber is usually graded for strength in bending edgewise or flatwise, but it is also used in applications requiring tensile or compressive strength. Beams and stringers are larger rectangular cross-section pieces used primarily in construction that is more robust than simple house framing. Nominal cross-section dimensions are greater than 150 mm, and the members are graded for strength in bending in the widest dimension. Posts and timbers have square or nearly square cross sections with dimensions greater than 150 by 150 mm. Grading is based on the intended use as columns and posts with compression as the primary loading condition. Structural lumber design parameters are based on the natural strength of the wood species along with reductions to account for factors such as knots and their location, grain slope, location of checks and splits, and seasoning. Most lumber is visually graded according to specifications set forth by the American Society for Testing and Materials (ASTM D-2555 (1994) and ASTM D-245 (1994)). The *National Design Specification for Wood Construction* (National Forest Products Association 1991) is the principal reference for determining lumber engineering parameters for use in design. The *Timber Construction Manual* (AITC 1985) provides comprehensive guidance for designing wooden structures and structural components. Allowable working stresses for timber in coastal projects should be those for wood that is continuously wet or damp. Table VI-4-13 lists some general engineering characteristics for the more common softwoods and hardwoods found in the United States.

Table VI-4-13
General Characteristics of Common Wood (from Moffat and Nichol (1983))

Softwoods					
General Characteristics	Douglas Fir	Redwood	Cedar	Spruce	Southern Pine
Shrinkage in volume from green to ovendry (pct)	10.9	11.5	11.2	10.4	12.4
Modulus of rupture (MPa)	43.7 (green)	51.4 (green)	41.6 (green)	31.4 (green)	44.1 (green)
Modulus of elasticity (GPa)	7.798 (green)	7.591 (green)	5.199 (green)	5.971 (green)	7.860 (green)
Hardwoods					
General Characteristics	Oak	Maple	Ash	Birch	Greenheart
Shrinkage in volume from green to ovendry (pct)	12.7 to 17.7	12.0 to 14.5	11.7	15.0 to 16.8	3
Modulus of rupture (MPa)	49.5 to 73.8 (green)	40.1 to 62.5 (green)	41.4 to 68.9 (green)	59.2 (green)	123.4 (green)
	54.2 to 77.3 (dry)	105.2 (dry)	108.0 (dry)	133.8 (dry)	206.8 (dry)
Modulus of elasticity (GPa)	6.047 to 11.63 (green)	6.502 to 10.16 (green)	7.102 to 10.20 (green)	10.27 to 10.64 (green)	20.00 (green)
	9.108 to 14.36 (dry)	12.14 to 12.95 (dry)	9.618 to 12.26 (dry)	16.52 (dry)	

d. Wood preservatives and treatment. Wood that has been correctly treated with preservative can increase the service life of the wood member by a factor of four to five over untreated wood. Wood treatment is practical and highly recommended for coastal projects, particularly in regions populated by marine borers and other natural enemies of wood. The most effective injected wood preservative for timber exposed to seawater or in direct contact with the ground appears to be creosote oil with a high phenolic content. Piles subject to marine-borer attack need a maximum creosote penetration and retention, and coal-tar solutions are recommended. If the borer infestation is severe, it may also be necessary to treat the pile with a waterborne salt preservative. Thorough descriptions of wood preservative treatments and standards are given in the Wood Preservers' *Book of Standards* (American Wood Preservers' Association 1984) and in Moffatt and Nichol (1983). Untreated timber piles should not be used unless the piles are protected from exposure to marine-borer attack. In some applications, untreated piles can be encased in a protective armor such as gunite. Field boring and cutting of treated lumber or piles should be avoided if possible. When unavoidable, cut surfaces should receive a careful field treatment of similar preservative to prevent (or at least retard) the onset of dry rot.

e. Wood fasteners and connectors. Except in rare occasions, wood structures in the coastal zone are held together by either metal fasteners and connectors or by adhesives.

(1) The most common metal connectors are nails, spikes, and bolts which are often used in conjunction with metal plates and brackets. Metal is also used for spike grids and split ring connectors to increase shear capacity at joints, and for miscellaneous components like bearing plates and straps. Chain, wire rope, and metal rods are sometimes used to secure and brace wood construction or to anchor wood portions to other parts of the structure. Metal connectors and fasteners are subject to rapid corrosion by water and damp air. Some metals will experience galvanic corrosion if placed in seawater. Protecting metal fasteners used in wood construction requires the same precautionary steps as detailed in Part VI-4-5, "Steel and Other Metals." Abrasion by sand particles or floating debris and chafing by objects such as mooring lines can quickly strip away protective coatings applied to corrodible metals. The process of selecting a protection system must consider these factors and recognize that any metal protection has a limited life in the marine environment. Periodic inspection and maintenance of metal fasteners and connectors is recommended, particularly for critical connections.

(2) Field use of adhesives in coastal wood construction is limited primarily to framework and sheathing for house-like structures in which the adhesive is protected from the harsh environment. Field application of adhesives to exposed wood construction should be limited to secondary joints where failure would not be catastrophic. Wooden components, such as plywood and laminated beams, use adhesives which are applied during manufacture in controlled factory settings. This assures well-mated surfaces, uniform adhesive application, and proper curing of the glued surfaces. Factory-fabricated wood components should use waterproof glue if the piece is expected to be immersed in water. Additional information on application and use of wood adhesives is given in Moffatt and Nichol (1983) and in several standards from the American Society for Testing and Materials (ASTM D-2559 (1994)).

f. Environmental effects on wood. Wood reacts to a number of environmental conditions encountered in the coastal zone.

(1) Water will penetrate wood and cause swelling with a corresponding strength reduction, and extended immersion will soften the wood fibers. Periodic wetting and drying causes uneven drying and may lead to development of cracks or provide conditions favorable to fungi that cause dry rot. Strong acids will hydrolyze wood and severely impact strength, but exposure to strong acids is rare and limited to accidental spills in places such as cargo handling areas.

(2) Water pollution may help preserve wood structures by reducing the oxygen that supports wood-attacking marine biota.

(3) Marine organisms are the principal cause of wood destruction for immersed timbers and piles, and the concentration of damaging biota will vary with location. Application of proper preservatives is essential for longer service life in these conditions. Marine plants also grow on immersed wood, but flora growth does not seem to harm the strength characteristics of the wood. However, slippery marine growth on wood decking may be hazardous to pedestrians.

(4) Dry wood can catch fire, but larger structural wood members will retain a substantial portion of their strength for a period of time as fire slowly chars the wood inward from the surface.

(5) Abrasion of wood by wind and sand can eventually lead to a reduction in strength due to a decrease in cross section; however, this process takes a long time to occur. Rubbing of wood surfaces by a harder material, such as a steel vessel, will also wear down the wood. Although such wear eventually damages the wood, the relative softness of wood compared to other materials is a beneficial design feature in some applications.

(6) The resilience of wood allows wood structures and structural members to absorb impact energy and rebound better than more rigid structures. This flexibility helps wood structures withstand wave and vessel impact loads and seismic accelerations.

(7) Many wood structures are constructed to serve human activities such as harbor facilities, wharfs, piers, etc. Eventually wood will begin to show wear from human and vehicular traffic, accidental impacts, vandalism, and other causes. Periodic monitoring is needed to assure that normal wear from human activities does not weaken a structure beyond a safe level. Immediate inspection is needed after any accident that may have caused structural damage.

VI-4-7. Geotextiles and Plastics.

a. Use of plastics in coastal construction. The term “plastic” is a generic label for a large number of synthetic materials composed of chainlike molecules called polymers. Plastics can be easily molded into shapes during manufacture. The most common use for plastic in coastal construction is in the form of geotechnical fabrics, which are the main focus of this section.

(1) Geotextile fabrics. Plastic filaments or fibers can be woven or needlepunched into strong fabrics called “geotextiles” that are often used as filter cloth beneath hard armor systems. Other names for these types of fabrics include filter fabrics, construction fabrics, plastic filter cloth, engineering fabrics, and geotechnical fabrics. The most frequent use of geotextiles in coastal construction is as a filter between fine granular sands or soils and overlying gravel or small stone that forms the first underlayer of a coastal structure such as a revetment. The purpose of the geotextile is to retain the soil while permitting flow of water through the fabric. Figure VI-4-5 illustrates typical usage of a geotextile fabric in coastal construction. Geotextile filters have several general advantages over conventional gravel filters (Barrett 1966):

(a) Filtering characteristics are uniform and factory controlled.

(b) Geotextile filter fabrics can withstand tensile stresses.

(c) Geotextile placement is more easily controlled, and underwater placement is likely to be more successful than comparable gravel filters.

(d) Inspection and quality control are quick and accurate.

(e) Local availability of filter materials is not a cost consideration, and often substantial savings can be realized.

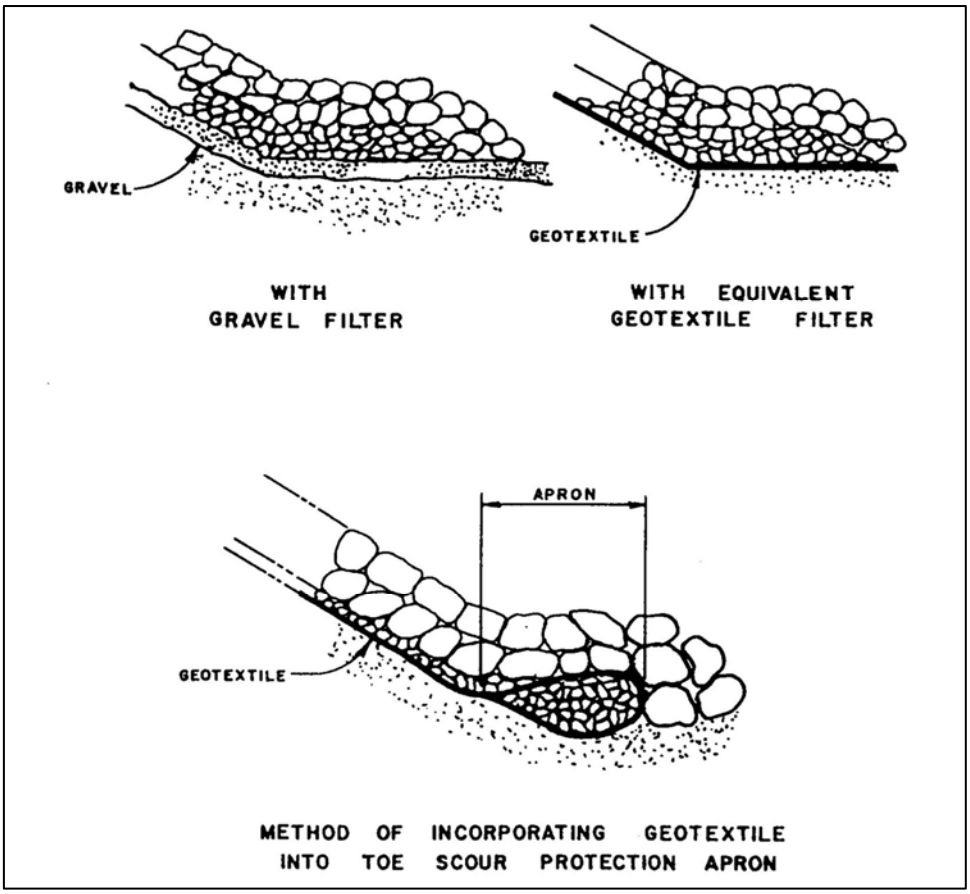

Figure VI-4-5. Typical use of geotextile fabric in coastal revetment (from Moffatt and Nichol (1983))

(2) Some potential disadvantages of geotextile filter fabrics are the following: (1) it is difficult to repair damaged fabric that underlays several layers of stone, (2) if improperly designed, some fabrics can be relatively impervious to rapid hydraulic transients, which could lead to uplift pressures over the fabric surface, and (3) the fabric is susceptible to undermining at the structure toe if not properly anchored. Coastal application of woven geotextile fabric began in the mid-1950s. In the United States geotextiles were first used as a filter for an ocean-front concrete block revetment in 1958. Dutch coastal engineers first used geotextiles in 1956, and they continued development of geotextiles as work began on the massive Delta Works Scheme (John 1987). During the 1960s, geotextiles became well-established as replacements for granular filters due in part to extensive use in the Delta Works Scheme. It is estimated that over 10 million cu m of geotextile were used in the Dutch flood protection project. Initially, use of geotextiles was not cost-effective, and applications were limited to sites that lacked local sources of good granular fill material. Presently, the use of geosynthetics has become more widespread. Although the most common geotextile application is to serve as a filter, these fabrics can also serve the following functions:

(a) Separate different soil layers.

(b) Reinforce soil banks against lateral movement.

(c) Control erosion of banks.

(d) Provide drainage.

(e) Cap and/or contain contaminated dredged material.

Generally, geotextile filter fabrics should allow water to flow through while retaining the soil. Other coastal applications, such as bank reinforcement, rely on high fabric tensile strength. Examples of geotextile use in coastal construction can be found in Barrett (1966), Dunham and Barrett (1974), Koerner and Welsh (1980), and John (1987).

(3) Other forms of plastic. High-strength plastic fabric such as nylon has been used successfully as flexible forms for concrete. Two layers of cloth are injection-filled with concrete or grout to form a mattress-like structure for slope protection. Similarly, grout-filled plastic tubes have been used in various shore protection schemes. Examples of the above applications are given by Koerner and Welsh (1980) and by Moffatt and Nichol (1983). Impervious plastic sheets made of polyethylene, vinyl, or rubber compounds are used as liners and covers to control water seepage or to contain pollutants. During construction, plastic sheets can be used to shield unprotected metal components from corrosive effects of salt air and rainwater or to keep lumber (or other construction materials) dry. Highly porous plastic mesh can be used as dune fencing to trap windblown sediment. High-strength plastics can be molded into almost any shape for specialized applications. For example, high- density polyethylene is often used for mooring fenders and guards because it has low surface friction, good toughness, and it resists abrasion and impact damage. Plastic is also used to line and protect pilings from corrosion and from attack by marine borers. Special fiber-reinforced polyester pipe can replace steel pipe in some applications, but at a greater cost. Standard polyvinyl chloride (PVC) pipe up to 25 cm in diameter can be used for applications such as electrical conduit, water supply, and drainage. Finally, epoxy resins can be used to affix bolts in concrete or stone, or the resin can be mixed with sand to produce a chemical grout for patching concrete.

b. Physical and mechanical properties of plastics.

(1) General characteristics. Most plastics are synthetic, carbon-based products of a chemical reaction that alters the characteristics of the original component materials. The resulting plastics are high polymers composed of monomer atoms joined together in molecular aggregations. During some stage of production, plastics are soft and can be formed into shapes by application of heat, pressure, or both.

(a) *Thermoplastics* can be repeatedly softened (up to melting) and hardened again by heating and cooling without changing the plastic properties. At low temperatures the material becomes brittle. Included in the thermoplastics group are polyethylene, polyvinyl chloride, acrylics, nylon, and polystyrene.

(b) *Thermosets* are plastics that go through a soft, pliable stage only once before irreversibly transforming to a permanently hardened material. Heating thermosets breaks down the plastic. Polyesters, epoxies, silicones, phenol-formaldehydes, and melamine-formaldehydes are examples of thermosetting plastics.

Physical characteristics of some plastics can be modified by combining various additives such as plasticizers and stabilizers with the plastic during manufacture. Plasticizers make plastics that are rigid or brittle at normal temperatures softer and more pliable. Stabilizers help to decrease the deteriorating effects of weather and ultraviolet light on plastics. Different plastics can be combined during manufacture to form *copolymers* that exhibit some of the beneficial properties of both components. Most structural plastic components are copolymers. Plastics can also be reinforced with high-strength fibers to attain greater yield strength. Plastic is a good construction material because it can be shaped into practically any form. In addition, there are several other characteristics that make plastic a good construction material. These are its corrosion, wear, and impact resistance; its light weight; its flexibility and energy absorption capability; and its electrical and thermal insulating qualities. Some properties vary greatly over the range of commonly available plastics.

(2) Geotextiles. Most geotextiles are made from one of the four main polymer families: polyester, polyamide, polypropylene, or polyethylene. Polyethylene has one of the simplest molecular structures, and its main attractions include low cost and chemical resistance. Polyamides (e.g., nylon) are roughly three times more expensive than polyethylene, and they exhibit moderate strength and chemical resistance characteristics. Polypropylenes are low cost and currently comprise the most widely used group of geotextiles (John 1987). Polyesters have the best tensile strength characteristics, the least long-term creep and high inherent ultraviolet light resistance, but these attributes come at a high cost. The relative differences between the four polymer families in terms of important physical properties are shown Table VI-4-14. Within each main group there are many subgroups that can have significantly different characteristics than those attributed to the group as a whole. In particular, strength properties vary with manufacturing method.

Table VI-4-14
Comparative Properties of Geotextile Materials (from John (1987))

Characteristic		Polyester	Polyamide	Polypropylene	Polyethylene
Comparative Properties					
Tensile strength		High	Medium	Low	Low
Elastic modulus		High	Medium	Low	Low
Strain at failure		Medium	Medium	High	High
Creep		Low	Medium	High	High
Unit weight		High	Medium	Low	Low
Cost		High	Medium	Low	Low
Resistance Properties					
U-V Light:	Stabilized	High	Medium	High	High
	Unstabilized	High	Medium	Medium	Low
Alkalis		Low	High	High	High
Fungus, vermin, insects		Medium	Medium	Medium	High
Petroleum products		Medium	Medium	Low	Low
Detergents		High	High	High	High

Engineering properties and overall suitability of geotextiles for specific applications depend as much on the fabric manufacture as the properties of the polymer. Fabrics are either woven, nonwoven, or a combination of the two. Several weaving methods are used in the manufacture of geotextiles, and each method achieves different results in the fabric. Fabrics made of monofilament yarns have relatively regular and uniform pore sizes and are more reliable for critical filtration applications where the higher cost is justified. Nonwoven geotextiles are made of discrete fibers bonded together by some method that often allows for a somewhat thicker porous fabric. Porosity may be achieved by punching holes in the fabric with needles to attain a more uniform filtering capability. Both woven and nonwoven fabrics have been used in coastal applications, but woven monofilament geotextiles are overwhelmingly preferred for coastal structures.

c. Design requirements for geotextile fabrics.

(1) General design requirements. Use of a geotextile as a filter cloth requires that the fabric be permeable to water without allowing passage of retained soil particles or clogging. Flow of water through the geotextile must be at a rate that prevents excessive head loss or buildup of hydrostatic pressure. An effective filter requires a geotextile suited to the retained soil grain size and slope, groundwater, wave and water level loading, and particulars of the overlying stone layers. Selection of a geotextile may be difficult because of the wide range of fabrics available from a number of manufacturers; however, the specification should be based on properties such as transmissivity, porosity, etc. It may help to examine past performance of particular geotextiles in similar projects. Some combination of the factors listed below may influence the selection of a suitable geotextile fabric (Moffatt and Nichol 1983).

(a) *Tensile strength*. Fabric tensile strength is needed to resist tearing when subjected to dynamic loads from waves, currents, and constant movement of structure underlayers. For rubble structures, strong fabrics allow placement of larger stones directly on the geotextile, thus reducing the overall structure thickness. However, if large voids occur in the overlying structure layers, soil pressure and/or hydrostatic pressure may rupture the fabric. Fabrics that have sufficient Aburst strength@ will continue to retain the soil, thus reducing rehabilitation costs.

(b) *Elongation at failure*. Excessive elongation will distort and enlarge the pores, changing the filtering characteristics and perhaps resulting in soil loss.

(c) *Puncture resistance*. Geotextiles need good puncture resistance to survive placement of materials over the fabric during construction. The fabric also needs to resist puncturing due to movement of armor stone and underlayer stone as the structure settles or as it responds dynamically to wave action.

(d) *Abrasion resistance*. Constant wave action on a coastal structure causes movement of materials adjacent to the geotextile, and the fabric must withstand this abrasion over the life of the structure. Special care must be taken during construction to avoid fabric abrasion as materials are placed on the geotextile.

(e) *Durability*. Geotextiles must perform consistently over the life of the structure. Durability depends on the chemical composition and construction of the fabric, physical

properties of the finished fabric, exposure to deteriorating environmental conditions, and physical abuse experienced during service.

(f) *Site-specific factors*. Some coastal applications may subject geotextile fabrics to freeze/thaw conditions or to high or low temperatures. It may be necessary to test the geotextile for survivability under these conditions. Also, fabric selection should account for any anticipated exposure to chemicals, acids, alkalis, or fuels.

(g) *Construction factors*. Placement of geotextiles in severe wave environments may be difficult, and fabric may be damaged or severely abraded during placement attempts. Excessive movement of underlayer materials by waves may severely damage the fabric before more stable armor layers can be placed. Construction methods may need to be modified to minimize adverse wave exposure.

(2) Recommended minimum geotextile physical properties. Moffatt and Nichol (1983) presented recommended minimum values for various geotextile engineering parameters under three different loading conditions for coastal projects. These recommendations are reproduced in Table VI-4-15. “Severe dynamic loading” refers to continued abrasive movement of materials adjacent to the fabric due to wave action. “Dynamic and static loading” results from more restrictive placement procedures that limit abrasion. “Stringent placement and drainage” refers to applications where placement and service life are nearly free of any abrasive movement of adjacent materials. Design values for specific candidate geotextiles should be determined according to test procedures given in the referenced ASTM standards in Table VI-4-15 (also summarized in Moffatt and Nichol (1983)).

(3) Design properties of commercial geotextile fabrics. There are numerous commercial manufacturers of geotextiles, and each manufacturer produces a variety of fabrics having differing engineering properties. The best listing of currently available geotechnical fabrics and their associated design properties is the annual Specifier’s Guide of the *Geotechnical Fabrics Report* published by the Industrial Fabrics Association International. The annual *Specifier’s Guide* details property specifications of over 500 geosynthetic products from more than 50 international producers. Some textbooks and manuals also list commercial products. For example, Koerner (1986) provides tables from the *1985 Geotechnical Fabrics Report*, and Ingold and Miller (1988) provide addresses, distributors, product lines, and design parameters for European-based producers of geotechnical fabric.

(4) Geotextile filtering and clogging criteria. Geotextile filters in coastal structures may be exposed to rapid flow fluctuations including turbulent flows, high hydrodynamic pressure differentials, and sudden or periodic runup and rundown. The selected geotextile must be able to retain the soil, yet have openings large enough to permit rapid drainage without clogging. Calhoun (1972) conducted extensive tests to develop engineering criteria for geotextile fabrics, and these criteria have been verified through numerous field applications. The capability of a geotextile to retain soil while allowing water to pass is termed the “*piping resistance.*” Calhoun developed a procedure for determining the piping resistance based on the size of the retained soil and the *equivalent opening size* (EOS) of the geotextile. He also developed clogging criteria based on the fabric “*percent of open area*” (POA). Values of EOS and POA are determined using the procedures described in Table VI-4-16.

Table VI-4-15
Minimum Geotextile Fabric Physical Property Requirements (from Moffatt & Nichol (1983))

Property		Test Method	Category A Severe Dynamic Loading	Category B Dynamic & Static Loadings	Category C Stringent Placement & Drainage
Tensile strength[4]	SPD[1]	ASTM D-4632	1.56 kN		0.89 kN
	BPD[2]			0.89 kN	
	WPD[3]		0.98 kN		0.44 kN
Elongation at failure		ASTM D-4632	<36 percent	36 percent	36 percent
Seam strength[4]		ASTM D-4884	0.87 kN	0.80 kN	0.36 kN
Puncture resistance		ASTM D-4883	0.53 kN	0.53 kN	0.29 kN
Burst strength		ASTM D-3786	3450 kPa	3790 kPa	1650 kPa
Abrasion resistance[4]	SPD	ASTM D-4886	0.44 kN		0.27 kN
	BPD			0.29 kN	
	WPD		0.29 kN		0.15 kN
Optional Requirements					
Freeze-thaw resistance		ASTM D-5034	90 percent of required strength		
High temperature survivability		ASTM D-5034	80 percent of required strength		
Low temperature survivability		ASTM D-5034	85 percent of required strength		
Effects of acids		ASTM D-5034	90 percent of required strength		
Effects of alkalies		ASTM D-5034	90 percent of required strength		
Effects of JP-4 fuel		ASTM D-5034	85 percent of required strength		

[1] SPD = Stronger principal direction.
[2] BPD = Both principal directions.
[3] WPD = Weaker principal direction.
[4] In accordance with the specifications for the tests for these properties, these forces are applied over a width of 25.4 mm (1 in.).

Table VI-4-16
Determination of EOS and POA for Geotextiles (from Moffatt and Nichol (1983))

Equivalent Opening Size (EOS)
Based on the Calhoun (1972) method, five unaged samples shall be tested. Obtain about 150 gm of each of the following fractions of a sand composed of sound, rounded-to-subrounded particles: U.S. Standard Sieve Numbers Sample 1. Passing #10 and Retained on #20 Sample 2. Passing #20 and Retained on #30 Sample 3. Passing #30 and Retained on #40 Sample 4. Passing #40 and Retained on #50 Sample 5. Passing #50 and Retained on #70 Sample 6. Passing #70 and Retained on #100 Sample 7. Passing #100 and Retained on #120 The cloth shall be affixed to a standard sieve having openings larger than the coarsest sand used, in such a manner that no sand can pass between the cloth and the sieve wall. The sand shall be oven-dried. Shaking of the sample will continue for 20 min. Determine by sieving (using successively coarser fractions) that fraction of sand of which 5 percent or less by weight passes the cloth. The equivalent opening size of the cloth sample is the Aretained on@ U.S. Standard Sieve number of this fraction.
Percent of Open Area (POA)
Each of five unaged samples should be placed separately in a 50- x 50-mm (2- x 2-in.) glass slide holder and the image projected with a slide projector on a screen. Select a block of 25 openings near the center of the image and measure to the nearest 25.4 microns (0.001 in.) the length and width of each of the 25 openings and the widths of two fibers adjacent to each opening. The percent open area is determined by dividing the sum of the open areas of the 25 openings by the sum of the total area of the 25 openings and their adjacent fibers.

For retention of coarse-grained soils containing 50 percent or less by weight of particles passing U.S. No. 200 sieve (0.074 mm diameter), the piping resistance *(PR)* for woven geotextile fabric is given by

$$PR = \frac{D_{85}\ of\ \ protected\ soil}{EOS} \qquad \text{(VI-4-7)}$$

where D_{85} is the effective grain size (in mm) for which 85 percent of the soil (by weight) has smaller grain size. (Note *EOS* is expressed in millimeters.) Ideally, the value of the piping resistance should be unity or slightly greater to promote drainage and prevent clogging. As values of *PR* increase, flow resistance through the fabric also increases. Adequate clogging resistance is provided by geotextiles having an effective POA equal to or greater than 4 percent. If a percentage of the geotextile's surface is covered by flat smooth materials (e.g., patio-type blocks) without an intervening gravel layer, the necessary fabric POA must be increased

proportionately. For example if one third of the fabric is to be covered by flat blocks, then the necessary geotextile POA must be increased by a factor of 3 to 12 percent to give an effective POA of 4 percent. Geotextiles adjacent to finer soils in which more than 50 percent of the grains (by weight) pass through the U.S. No. 200 sieve should have an EOS no larger than a U.S. No. 70 sieve (0.210 mm). Geotextiles with an EOS smaller than a U.S. No. 100 sieve (0.149 mm) should not be used as filter in coastal projects.

d. Geotextile installation considerations. Practical experience with geotextile filters in coastal projects has provided general guidelines for geotextile installation and maintenance. However, unique site conditions may dictate alternate techniques.

(1) Geotextile placement. Successful use of geotextiles in coastal projects depends critically on initial placement of the fabric. The sequence of geotextile placement is determined somewhat by the specific project and application, but in general the following guidelines should be followed.

(a) Geotextiles should be laid loosely, free of wrinkles, creases, and folds. This allows the fabric to conform to irregularities in the soil when heavier materials are placed on the fabric. Placing the geotextile in a stretched condition under tensile stress should be avoided.

(b) Fabric placement on slopes subjected to wave action should begin at the slope toe and proceed upslope with the upslope panel overlapping the downslope panel. For slopes subjected to along-structure currents, upstream panels should overlap downstream panels.

(c) When the slope continues beyond the protective armor layers, the filter should be keyed into a trench at the upper portion of the structure. Similar termination of the filter can be used at the structure toe as illustrated in Figure VI-4-5.

(d) Horizontal underwater fabric placement should start at the shoreward end and proceed seaward. For scour protection the placement should start adjacent to the protected structure and proceed to the outer limit of the protection.

(e) Any overlying gravel layers must have sufficient permeability so as not to reduce flow through the geotextile.

(f) Steel securing pins (when needed) should be 5 mm (3/16 in.) in diameter and have a head capable of retaining a steel washer having a 3.8-cm outside diameter. Pin length should be a minimum of 45 cm (1.5 ft) for medium to high density soil, and longer for looser soils. Pins should be placed at the overlap mid-point. Pin spacing along the overlap should be a maximum of 0.6 m (2 ft) for slopes steeper than 1-on-3, 1.0 m (3 ft) for slopes between 1-on-3 and 1-on-4, and 1.5 m (5 ft) for slopes flatter than 1-on-4. Additional pins should be used as necessary to prevent geotextile slippage.

(g) Placement of overlying stones should begin at the toe and proceed upslope. Some projects may require stone placement in conjunction with geotextile placement to hold the fabric against wave or current action.

(h) Care must be exercised in placing the overlying stone layers to avoid puncturing the geotextile. Tables VI-4-17 and VI-4-18 provide construction drop height limitations for quarrystone revetments, block revetments, and subaqueous applications. Loading conditions are the same as described for Table VI-4-15. No stones over 440 N (100 lb) should be rolled downslope over the fabric.

Table VI-4-17
Construction Limitations: Quarrystone Revetment[1] (from Moffatt and Nichol (1983))

Parameter	Category A	Category B	Category C
Steepest slope	1V on 2H	1V on 2.5H	1V on 3H
Min. gravel thickness above filter	None	None	20 cm
Stone Adjacent to Geotextile			
Max. stone weight[3]	1.1 kN	0.78 kN	Gravel
Max. drop height	1 m	1 m	1.5 m
Max. stone weight	1.8 kN	1.3 kN	
Riprap weight range[4]	0.89 - 3.3 kN	0.22 - 2.2 kN 0.61 m	NA[2]
Max. drop height	0.61 m		
Max. stone weight	1.8 - 8.9 kN	1.3 - 8.9 kN	
Max. drop height	placed	placed	NA
Subsequent Stone Layer			
Max. stone weight	NA	NA	0.67 kN
Max. drop height			1.2 m
Max. stone weight	NA	NA	1.3 kN
Max. drop height	NA	NA	1 m
Max. stone weight	44 kN	44 kN	4.4 kN
Max. drop height	3 m	2.5	placed
Max. stone weight	> 44 kN	> 44 kN	> 4.4 kN
Max. drop height	placed	placed	placed

NOTE:
a. Stronger principal direction (SPD) and seams of the geotextile should be perpendicular to the shoreline.
b. There is no limit to the number of underlayers between the armor and the geotextile.

[1] This table may also be used for sand core breakwaters (a jetty, groin, or breakwater in which the core material consists of sand rather than stone).
[2] Not applicable.
[3] Weight of quarrystone armor units of nearly uniform size.
[4] Weight limits of riprap, quarrystone well-graded within wide size limits.

Table VI-4-18
Construction Limitations: Block Revetments and Subaqueous Applications
(from Moffatt and Nichol (1983))

Block Revetment[1]	Category		
	A	B	C
Precast Cellular Block[2]			
Steepest slope			
Individual blocks	1V on 2H	1V on 3H	NA[3]
Cabled blocks[4]	1V on 1.5H	1V on 2H	NA
Max. block weight	>3.1 kPa	3.1 kPa	NA
Interlocking Concrete Block[2]			
Steepest slope	NA	1V on 2H	1V on 2.5H
Min. gravel thickness above filter	NA	15.2 cm	15.2 cm
Max. block weight	NA	>3.1 kPa	3.1 kPa
Subaqueous Applications[5]			
Steepest slope	1V on 15H	1V on 15H	1V on 15H
Stone adjacent to geotextile:			
Max. stone weight	8.9 kN	8.9 kN	3.3 kN
Min. drop through water	1.5 m	1.5 m	1.5 m
Max. stone weight	>13.3 kN	>13.3 kN	>3.3 kN
Max. drop height	placed	placed	placed
Subsequent stone layer (s)			
Max. stone weight	No limit	No limit	No limit
Max. drop height	NCP[6]	NCP	NCP

[1] Stronger principal direction (SPD) and seams of the geotextile should be perpendicular to the shoreline.
[2] With flat base.
[3] Not applicable.
[4] Precast cellular blocks cabled together in a horizontal plane.
[5] No limit to the number of underlayers between the armor and the geotextile.
[6] As in normal construction practice: the geotextile does not require special limitations in these layers.

(2) Geotextile seams and joins. Geotextiles can be obtained in fairly long lengths, but width is limited by practical considerations related to manufacture and transportation. Wider panels reduce the number of fabric overlaps (which is the most probable cause of error during placement). Overlaps that are not subjected to tensile loading should be at least 45 cm (1.5 ft) and staggered in above water applications where placement can be well-controlled. Underwater geotextile overlaps should be at least 1 m (3 ft). Geotextile panels can be joined before or during placement by either sewing or cementing the panels together at the seams. Generally, sewing is preferred for onsite joins. The most appropriate guidance on field joining of specific geotextile fabrics should be available from the manufacturer. More general guidance is given in various geotextile textbooks (e.g., Ingold and Miller (1988), John (1987)).

(3) Geotextile repairs. Construction damage to geotextile filters is easily repaired by trimming out the damaged section and replacing it with a section of fabric that provides a minimum of 0.6 m (2 ft) overlap in all directions. The edges of the replacement fabric should be placed under the undamaged geotextile. If damage occurs to geotextile panels in which the fabric tensile strength is needed to reinforce soil slopes, the entire fabric panel should be replaced. Repairing damaged fabric underlying a rubble-mound structure is more difficult because the overlying stone layers must first be removed to expose the damaged filter cloth.

e. Environmental effects on geotextiles and plastics.

(1) Chemical and biological effects. Plastics are generally considered not biodegradable, and they are relatively unaffected by chemicals found in normal concentrations in the coastal zone. However, some chemicals, such as alkalis and fuel products, can rapidly destroy some plastic compounds. Although plastics are impervious to biological attack, marine growth on plastic structure components may induce additional drag forces or hinder smooth operation of moving parts. Bacterial activity in the interstices of geotextiles can clog the fabric and increase its piping resistance.

(2) Ultraviolet radiation. Unless stabilizers have been added during manufacture, plastics will deteriorate when exposed to ultraviolet (UV) radiation. For most coastal structure filtering applications, geotextiles are exposed to sunlight for only a short period during construction before placement of overlayers, and the effects of UV radiation are minor. In some cases, it may be prudent to sequence construction to minimize exposure of geotextile fabric to sunlight. Geotextiles can be exposed to UV radiation if the armor layer is relatively thin, allowing sunlight to penetrate through voids in the armor layer. Similarly, precast armoring blocks may have holes that allow light penetration. Storm damage to structure armor layers can expose geotextile filters to sunlight for extended periods before repairs can be initiated. In the above situations, UV radiation will ultimately destroy the geotextile unless the fabric has been stabilized. The relative ultraviolet radiation resistance of untreated polymer types is shown in Table VI-4-14.

(3) Fire. Plastics will burn or disintegrate if exposed to fire or high temperatures, often releasing very poisonous gases. Some plastics will burn easily, some slowly, and others with great difficulty. Flame-retardant chemicals can be combined into the molecular structure of the plastic materials. Temperatures above the polymer’s melting point will alter the filtering characteristics of geotextile fabrics.

(4) Other factors. Abrasion by overlying material (or debris in the case of exposed fabric) can tear fibers in geotextiles, weakening the fabric. Impact loading by waves, vessels, or other objects may puncture geotextile fabric, and ice formation may induce tensile stresses exceeding the material yield strength. Excessive ground motion accelerations due to seismic events may cause differential shifting of the armor layer or soil slope, resulting in tension failure of the geotextile filter. Finally, exposed geotextile or high- strength fabrics may be damaged by vandalism.

VI-4-8. References.

EM 1110-2-1204
Environmental Engineering for Coastal Shore Protection

EM 1110-2-1601
Hydraulic Design of Flood Control Channels

EM 1110-2-1612
Ice Engineering

EM 1110-2-1906
Laboratory Soils Testing

EM 1110-2-2301
Test Quarries and Test Fills

EM 1110-2-2302
Construction with Large Stone

EM 1110-2-5025
Dredging & Dredged Material Disposal

ACI 1986
American Concrete Institute. 1986 (revised annually). *Manual of Concrete Practice*, Part 3, Detroit, MI.

AISC 1980
American Institute of Steel Construction, Inc. 1980. *Manual of Steel Construction*, 8th ed., Chicago, IL.

AITC 1985
American Institute of Timber Construction. 1985. *Timber Construction Manual*, John Wiley and Sons, New York.

American Wood Preservers' Association 1984
American Wood Preservers' Association. 1984. *Book of Standards*, Stevensville, Maryland.

ASTM C-150
American Society for Testing and Materials. 1994. "Standard Specification for Portland Cement," ASTM C-150, *Annual Book of ASTM Standards*, Philadelphia, PA, Vol. 04.01, pp 125-129.

ASTM C-595
American Society for Testing and Materials. 1997. "Standard Specification for Blended Hydraulic Cement," ASTM C-595, *Annual Book of ASTM Standards*, Philadelphia, PA, Vol. 04.01, pp 301-306.

ASTM D-245
American Society for Testing and Materials. 1994. "Practice for Establishing Structural Grades and Related Allowable Properties for Visually Graded Lumber," ASTM D-245, *Annual Book of ASTM Standards*, Philadelphia, PA, Vol. 04.10, pp 88-105.

ASTM D-502
American Society for Testing and Materials. 1994. "Specification for Steel Structural Rivets," ASTM D-503, *Annual Book of ASTM Standards*, Philadelphia, PA, Vol. 15.08, pp 113-115.

ASTM D-690
American Society for Testing and Materials. 1994. "Specification for High-Strength Low-Alloy Steel H-Piles and Sheet Piling for Use in Marine Environments," ASTM D-690, *Annual Book of ASTM Standards*, Philadelphia, PA, Vol. 01.04, pp 349-350.

ASTM D-2555
American Society for Testing and Materials. 1994. "Standard Test Methods for Establishing Clear Wood Strength Values," ASTM D-2550, *Annual Book of ASTM Standards*, Philadelphia, PA, Vol. 04.10, pp 371-384.

ASTM D-2559
American Society for Testing and Materials. 1994. "Specification for Adhesives for Structural Laminated Wood Products for Use Under Exterior (Wet Use) Exposure Conditions," ASTM D-2559, *Annual Book of ASTM Standards*, Philadelphia, PA, Vol. 15.06, pp 154-158.

ASTM D-4254
American Society for Testing and Materials. 1994. "Test Method for Minimum Index Density and Unit Weight of Soils and Calculation of Relative Density," ASTM D-4254, *Annual Book of ASTM Standards*, Philadelphia, PA, Vol. 04.08, pp 543-550.

Barrett 1966
Barrett, R. J. 1966. "Use of Plastic Filters in Coastal Structures," *Proceedings of the 10th International Conference on Coastal Engineering*, American Society of Civil Engineers, Vol. 2, pp 1048-1067.

Calhoun 1972
Calhoun, C. C., Jr. 1972. "Development of Design Criteria and Acceptance Specifications for Plastic Filter Cloth," Technical Report S-72-7, U.S. Army Engineer Waterways Experiment Station, Vicksburg, MS.

CIRIA/CUR 1991
Construction Industry Research and Information Association (CIRIA) and Centre for Civil Engineering Research and Codes (CUR). 1991. "Manual on the Use of Rock in Coastal and Shoreline Engineering," CIRIA Special Publication 83/CUR Report 154, CIRIA, London and CUR, The Netherlands.

CRC 1976
Chemical Rubber Company. 1976. *Handbook of Tables for Applied Engineering Science*, 2nd ed., CRC Press, Cleveland, OH.

Department of the Interior 1975
Bureau of Reclamation. 1975. *Concrete Manual, A Manual for the Control of Concrete Construction*, 8th ed., U.S. Government Printing Office, Washington, DC.

Dunham and Barrett 1974
Dunham, J. W, and Barrett, R. J. 1974. "Woven Plastic Cloth Filters for Stone Seawalls," *Journal of the Waterways, Harbors, and Coastal Engineering Division*, American Society of Civil Engineers, Vol. 100, No. WW1, pp 13-22.

Eckert and Callender 1987
Eckert, J., and Callender, G. 1987. "Geotechnical Engineering in the Coastal Zone," Instruction Report CERC-87-1, U.S. Army Engineer Waterways Experiment Station, Coastal Engineering Research Center, Vicksburg, MS.

Ingold and Miller 1988
Ingold, T. S., and Miller, K. S. 1988. *Geotextiles Handbook*, Thomas Telford, Limited, London.

John 1987
John, N. W. 1987. *Geotextiles*, Blackie and Sons, Ltd., London.

Koerner 1986
Koerner, R. M. 1986. *Designing with Geosynthetics*, Prentice-Hall, Englewood Cliffs, NJ.

Koerner and Welsh 1980
Koerner, R. M., and Welsh, J. P. 1980. *Construction and Geotechnical Engineering Using Synthetic Fabrics*, John Wiley and Sons, New York.

La Londe and Janes 1961
La Londe, W. S., Jr., and Janes, M. F. 1961. *Concrete Engineering Handbook*, McGraw-Hill Book Company, New York.

Latham 1991
Latham, J. P. 1991. "In-Service Durability Evaluation of Armourstone," *Durability of Stone for Rubble Mound Breakwaters*, O. T. Magoon and W. F. Baird, eds., American Society of Civil Engineers, pp 6-18.

Lienhart 1991
Lienhart, D. A. 1991. "Laboratory Testing of Stone for Rubble Mound Breakwaters: An Evaluation," *Durability of Stone for Rubble Mound Breakwaters*, O. T. Magoon and W. F. Baird, eds., American Society of Civil Engineers, pp 19-33.

Lutton 1991
Lutton, R. J. 1991. "U.S. Experience with Armor-Stone Quality and Performance," *Durability of Stone for Rubble Mound Breakwaters*, O. T. Magoon and W. F. Baird, eds., American Society of Civil Engineers, pp 40-55.

Magoon and Baird 1991
Magoon, O. T., and Baird, W. F. 1991. "Durability of Armor Stone for Rubble Mound Coastal Structures," *Durability of Stone for Rubble Mound Breakwaters*, O. T. Magoon and W. F. Baird, eds., American Society of Civil Engineers, pp 3-4.

Mehta 1991
Mehta, P. K. 1991. *Concrete in the Marine Environment*, Elsevier Science Publishers, Ltd., London, England.

Moffatt and Nichol 1983
Moffatt and Nichol, Engineers. 1983. "Construction Materials for Coastal Structures," Special Report SR-10, U.S. Army Engineer Waterways Experiment Station, Coastal Engineering Research Center, Vicksburg, MS.

National Forest Products Association 1991
National Forest Products Association. 1991. *National Design Specification for Wood Construction: Structural Lumber, Glued Laminated Timber, Timber Piles, Connections; Recommended Practice*, Washington, DC.

Thomas and Hall 1992
Thomas, R. S., and Hall, B. 1992. *Seawall Design*, Butterworth-Heinemann, Ltd., Oxford.

Woodhouse 1978
Woodhouse, W. W., Jr. 1978. "Dune Building and Stabilization with Vegetation," Special Report SR-3, U.S. Army Engineer Waterways Experiment Station, Coastal Engineering Research Center, Vicksburg, MS.

VI-4-9. Acknowledgments.

Author: Dr. Steven A. Hughes, Coastal and hydraulics Laboratory (CHL), U.S. Army Engineer Research and development Center, Vicksburg, MS.

Reviewers: Dr. Hans F. Burcharth, Department of Civil Engineering, Aalborg University, Aalborg, Denmark; Douglas A. Gaffney, private consultant; Han Ligteringen, Delft University of Technology, The Netherlands; John H. Lockhart, Headquarters, U.S. Army Corps of Engineers, Washington, DC (retired); and Charlie Johnson, U.S. Army Engineer District, Chicago, Chicago, IL (retired).

VI-4-10. Symbols.

γ_d	Unit dry weight of an in situ material (force/length^3)
γ_s	Specific weight of stone (force/length^3)
A	Cross-sectional area (length^2)
D_{85}	Effective grain size for which 85 percent of the soil (by weight) has a smaller grain size (length)
D_r	Relative density of noncohesive sands (Equation VI-4-1)
D_s	Diameter of an equivalent-volume sphere (Equation VI-4-4)
e	Void ratio of a cohesionless soil
E_c	Concrete modulus of elasticity (force/length^2)
f_c	Compressive strength of concrete (force/length)
Δh	Head difference over the flow length (length)
K	Empirical coefficient of permeability (length/time)
L	Length of flow path (length)
PR	Piping resistance (Equation VI-4-7)
Q	Discharge through a uniform soil (Equation IV-4-3) (length^3/time)
R_c	Relative soil compaction (Equation VI-4-2)
w_c	Specific weight of concrete, (force/length^3)
W_s	Stone weight (force)

CHAPTER 5

Fundamentals of Design

TABLE OF CONTENTS

Page

VI-5-1. Introduction VI-5-1
a. Overview VI-5-1
b. Wave/structure interaction VI-5-2

VI-5-2. Structure Hydraulic Response VI-5-3
a. Wave runup and rundown on structures VI-5-3
b. Wave overtopping of structures VI-5-22
c. Wave reflection VI-5-38
d. Wave transmission VI-5-50

VI-5-3. Rubble-Mound Structure Loading and Response VI-5-59
a. Armor layer stability VI-5-59
b. Granulated filters and geotextile filter stability VI-5-94
c. Structural integrity of concrete armor units VI-5-98
d. Toe stability and protection VI-5-111
e. Design of structure cross section VI-5-125
f. Blanket stability in current fields VI-5-140

VI-5-4. Vertical-Front Structure Loading and Response VI-5-145
a. Wave forces on vertical walls VI-5-145
b. Wave-generated forces on vertical walls and caissons VI-5-149
c. Wave-generated forces on concrete caps VI-5-174
d. Stability of concrete caps and caissons against sliding and overturning VI-5-181
e. Waves at structure convex and concave corners VI-5-184
f. Uplift forces VI-5-188

VI-5-5. Foundation Loads VI-5-192
a. Introduction VI-5-192
b. Soil and rock properties VI-5-194
c. Strength parameters VI-5-204
d. Hydraulic gradient and flow forces in soils VI-5-212
e. Cyclic loading of soils VI-5-217
f. Dynamic loading of soils under monolithic structures VI-5-231
g. Slip surface and zone failures VI-5-234

h. Settlement VI-5-250

VI-5-6. Scour and Scour Protection VI-5-252
a. Scour problems in coastal engineering VI-5-252
b. Prediction of scour VI-5-257
c. Design of scour protection VI-5-274

VI-5-7. Wave Forces on Slender Cylindrical Piles VI-5-278
a. Introduction VI-5-278
b. Vertical cylindrical piles and nonbreaking waves VI-5-280
c. Selection of hydrodynamic force coefficients C_D, C_M, and C_L VI-5-301
d. Safety factors in pile design VI-5-307
e. Other considerations related to forces on slender cylindrical piles VI-5-308

VI-5-8. Other Forces and Interactions VI-5-309
a. Impact forces VI-5-309
b. Ice forces VI-5-310

VI-5-9. References VI-5-320

VI-5-10. Acknowledgements VI-5-352

VI-5-11. Symbols VI-5-353

List of Figures

Page

Figure VI-5-1. Illustration of runup and rundown VI-5-4

Figure VI-5-2. Typical velocity field for the porous flow in a breakwater. Numerical calculation VI-5-5

Figure VI-5-3. $R_{u2\%}$ for head-on waves on smooth slopes VI-5-9

Figure VI-5-4. R_{us} for head-on waves on smooth slopes VI-5-10

Figure VI-5-5. $R_{u2\%}$ for long-crested head-on waves on smooth slopes VI-5-11

Figure VI-5-6. Parameters in berm test program at Delft Hydraulics VI-5-13

Figure VI-5-7. Definition of α_{eq} and α in Equation VI-5-9 ..... VI-5-14

Figure VI-5-8. Evaluation of the use of ξ_{eq} to account for the influence of a berm VI-5-14

Figure VI-5-9. Test program for wave runup on smooth slopes conducted at Delft Hydraulics, de Waal and van der Meer (1992) VI-5-15

Figure VI-5-10. Influence of angle of incidence β and directional spreading on runup on smooth slopes conducted at Delft Hydraulics; de Waal and van der Meer (1992) VI-5-16

Figure VI-5-11. Notational permeability coefficients VI-5-18

Figure VI-5-12. 2 percent and significant runup of irregular head-on waves on impermeable and permeable rock slopes VI-5-20

Figure VI-5-13. Definition of crest freeboard, R_c VI-5-23

Figure VI-5-14. Structure profile geometrical parameters related to overtopping VI-5-25

Figure VI-5-15. Wave overtopping data as basis for Equations VI-5-24 and VI-5-25 ..... VI-5-35

Figure VI-5-16. Vertical wall wave overtopping data plotted with $\gamma_s = 1.0$ VI-5-36

Figure VI-5-17. Vertical wall wave overtopping data with fitted mean and 95 percent confidence bands VI-5-37

Figure VI-5-18. Reflection coefficients for concrete armor unit slopes VI-5-41

Figure VI-5-19. Wave reflection coefficients for rock armored slope with berm at SWL VI-5-42

Figure VI-5-20. Wave reflection coefficients for plain vertical breakwater on 1:50 seabed VI-5-43

Figure VI-5-21. Wave reflection coefficients for plain vertical breakwater on rubble-mound foundation VI-5-44

Figure VI-5-22. Wave reflection coefficients for horizontal composite breakwaters with tetrapod slope 1:1.5 ..... VI-5-45

Figure VI-5-23. Wave reflection coefficients for sloping top breakwaters VI-5-46

Figure VI-5-24. Wave reflection coefficients for perforated caissions VI-5-46

Figure VI-5-25. Wave reflection coefficients for single perforated screen VI-5-47

Figure VI-5-26. Wave reflection coefficients for impermeable and permeable vertical breakwaters exposed to oblique, nonbreaking, short-crested waves VI-5-48

Figure VI-5-27. Measured versus estimated u_{rms} near smooth, impermeable 1:2 slope VI-5-50

Figure VI-5-28. Wave transmission diagram by Allsop (1983) and Powell and Allsop (1985) VI-5-52

Figure VI-5-29. Example of total wave transmission coefficients, Ct, for conventional and reef type low-crested and submerged breakwaters, calculated from the van der Meer and d=Angremond (1991) formula given by Equation VI-5-54 ..... VI-5-54

Figure VI-5-30. Wave transmission by overtopping of horizontal composite breakwaters armored with tetrapods VI-5-57

Figure VI-5-31. Wave transmission by overtopping of sloping top structures VI-5-58

Figure VI-5-32. Wave transmission through perforated single wall VI-5-59

Figure VI-5-33. Typical armor layer failure modes VI-5-60

Figure VI-5-34. Illustration of influence of slope angle on the stabilizing effects of gravitational force, interlocking and surface friction VI-5-63

Figure VI-5-35. Damage parameters for structure armor layer VI-5-69

Figure VI-5-36. Illustration of supersturcture designs causing insignificant and significant reduction in front slope armor stability VI-5-71

Figure VI-5-37. Illustration of critical areas for damage to armor layers in the round head VI-5-90

Figure VI-5-38. Illustration of improvement of round head stability by change of geometry VI-5-93

Figure VI-5-39. Convex and concave bends and corners VI-5-93

Figure VI-5-40. Examples of concrete armor units VI-5-99

Figure VI-5-41. Breakage formula for dolosse VI-5-103

Figure VI-5-42. Breakage formula for tetrapods VI-5-103

Figure VI-5-43. Wave height versus maximum flexural tensile stress for several dolos waist ratios VI-5-106

Figure VI-5-44. Dolos mass versus maximum flexural tensile stress for several dolos waist ratios VI-5-106

Figure VI-5-45. Example of calculation of thermal stresses and cracked regions in a 70-tonne cube 100 hr after casting VI-5-110

Figure VI-5-46. Examples of temperature development during curing in 30-tonne modified cubes with and without a hole VI-5-112

Figure VI-5-47. Typical toe and toe berm solutions in rubble-mound breakwater design VI-5-114

Figure VI-5-48. Example of potential instability of the stones placed on rock seabed ... VI-5-115

Figure VI-5-49. Support of the stones by a trench or anchor bolts VI-5-115

Figure VI-5-50. Typical seawall toe designs where scour is foreseen VI-5-116

Figure VI-5-51. Illustration of foot protection blocks for vertical structures VI-5-123

Figure VI-5-52. Example of Japanese foot protection block VI-5-123

Figure VI-5-53. Design of foot protection blocks according to Japanese practice VI-5-124

Figure VI-5-54. Rubble-mound section for seaward wave exposure with zero-to-moderate overtopping conditions VI-5-127

Figure VI-5-55. Rubble-mound section for wave exposure on both sides with moderate overtopping conditions VI-5-130

Figure VI-5-56. Logic diagram for preliminary design of rubble-mound structures VI-5-133

Figure VI-5-57. Illustration of vertical wall wave forces from nonbreaking and breaking waves VI-5-148

Figure VI-5-58. Identification of types of total horizontal wave loadings on vertical wall structure exposed to head-on long-crested irregular waves VI-5-149

Figure VI-5-59. Pressure distributions for nonbreaking waves VI-5-150

Figure VI-5-60. Pressure distributions on overtopped vertical wall VI-5-151

Figure VI-5-61. Wave barrier definition sketch VI-5-162

Figure VI-5-62. Best-fit to wave barrier force data VI-5-163

Figure VI-5-63. Power curve exponents VI-5-164

Figure VI-5-64. Comparison of Equation VI-5-139 to data used in empirical curve fits VI-5-165

Figure VI-5-65. Variation of wave height along a semi-infinite, fully reflecting breakwater exposed to head-on, long-crested waves VI-5-167

Figure VI-5-66. Peak-delay force reduction for oblique regular waves VI-5-168

Figure VI-5-67. Numerical simulation of peak-delay reduction, long-crested waves. Example of uncertainty calculation for wave train with 500 waves VI-5-169

Figure VI-5-68. Example of peak-delay force reduction for short-crested waves VI-5-170

Figure VI-5-69. Nondimensional amplitude of horizontal turning moment around the center of the caisson exposed to oblique nonbreaking regular waves ... VI-5-171

Figure VI-5-70. Example of force reduction from model tests with short-crested breaking waves VI-5-172

Figure VI-5-71. Broken wave forces on wall seaward of shoreline VI-5-172

Figure VI-5-72. Broken wave forces on wall landwater of shoreline VI-5-174

Figure VI-5-73. Illustration of forces on a superstructure VI-5-175

Figure VI-5-74. Illustration of comparison between base plate pore pressure distributions (under quasi-static porous flow conditions) and the approximated linear distribution VI-5-176

Figure VI-5-75. Impulsive pressure force caused by wave breaking on the wave wall... VI-5-177

Figure VI-5-76. Typical crown wall configurations VI-5-177

Figure VI-5-77. Comparison of predictions to measurements using the methods in Table VI-5-61 ..... VI-5-180

Figure VI-5-78. Convex and concave corners and bends at vertical walls VI-5-184

Figure VI-5-79. Mach reflection at a vertical wall VI-5-186

Figure VI-5-80. Total stresses in a soil element VI-5-197

Figure VI-5-81. Illustration of shear modulus *G* and bulk modulus *K* for granular soils exposed to initial and repeated (cyclic) loadings VI-5-200

Figure VI-5-82. In-situ secant values of shear modulus *G* for quasi-static loaded saturated clays VI-5-202

Figure VI-5-83. Static and secant cyclic shear modulus, *G*, for Drammen clay VI-5-203

Figure VI-5-84. Values of G/G_{max} for sands and gravels VI-5-205

Figure VI-5-85. Damping ratios for sands and saturated clays VI-5-206

Figure VI-5-86. Mohr envelope for stresses of failure VI-5-207

Figure VI-5-87. Illustration of straight-line approximations to curved Mohr envelopes corresponding to drained conditions VI-5-207

Figure VI-5-88. Angle of friction in rock fill of different grading and porosity with maximum diameter in the range 70-200 mm VI-5-208

Figure VI-5-89. Crude visualization of dilatancy and angle of dilation ψ VI-5-209

Figure VI-5-90. Failure criterion for a water-saturated clay in undrained condition defined from Mohr envelope VI-5-211

Figure VI-5-91. Representation of flow regimes for stationary porous flow based on a Forchheimer equation formulation VI-5-213

Figure VI-5-92. Illustration of wave induced forces on caisson foundation and related stress variations in the subsoil VI-5-221

Figure VI-5-93. Illustration of approximate cyclic wave loading and related cyclic shear stress variation in a subsoil element during a storm sequence VI-5-222

Figure VI-5-94. Simplified stress conditions for some elements along a potential failure surface VI-5-223

Figure VI-5-95. Illustration of (a) stabilization and pore pressure build-up, and (b) liquefaction undrained triaxial test on sand VI-5-224

Figure VI-5-96. Illustration of effective stress paths for clay samples in undrained triaxial tests VI-5-227

Figure VI-5-97. Stress strain behavior of Drammen clay (I_p = 27 percent) under various cyclic loading conditions corresponding to OCR = 4 ..... VI-5-228

Figure VI-5-98. Result of cyclic tests on normally consolidated Drammen clay with OCR = 1, and I_p = 27 percent VI-5-229

Figure VI-5-99. Example of normalized diagrams for cyclic loading of Drammen clay with OCR = 1, in triaxial tests (a), and DSS tests (b) VI-5-230

Figure VI-5-100. Cyclic shear strength of Drammen clay with OCR = 1 ..... VI-5-231

Figure VI-5-101. Approximation to horizontal wave load history for waves breaking directly on vertical walls VI-5-232

Figure VI-5-102. Definition of translatory and rotational motions and dimensions for caisson structure and parapet wave wall exposed to dynamic loading .. VI-5-233

Figure VI-5-103. Amplification factors for translatory and rotational motions for caisson structure with square footing and triangular load shape VI-5-234

Figure VI-5-104. Illustration of flow nets in a homogeneous isotropic breakwater for two instantaneous wave load situations VI-5-237

Figure VI-5-105. Illustration of instantaneous flow net in a homogeneous isotropic seabed under wave action VI-5-239

Figure VI-5-106. Illustration of forces to be considered in slope stability analysis VI-5-240

Figure VI-5-107. Illustration of logarithmic spiral VI-5-241

Figure VI-5-108. Illustration of failure surface in case of weak stratum VI-5-242

Figure VI-5-109. Illustration of forces on a soil slice in the method of slices slope stability analysis VI-5-242

Figure VI-5-110. Illustration of safety factor F for three-dimensional slope failure VI-5-244

Figure VI-5-111. Illustration of fictitious footing to replace real footing under eccentric loading conditions VI-5-249

Figure VI-5-112. Simplified base and rear slope geometries to be applied in the general bearing capacity formula Table VI-5-86 ..... VI-5-249

Figure VI-5-113. Illustration of passive earth pressure P to be included in the determination of the foundation load resultant R in place of the depth coefficients in Equations VI-5-248 and VI-5-250 ..... VI-5-250

Figure VI-5-114. Coastal scour problems VI-5-255

Figure VI-5-115. Regular and irregular wave-scoured profiles at a vertical-front structure VI-5-258

Figure VI-5-116. Scour prediction for nonbreaking waves at vertical wall VI-5-260

Figure VI-5-117. Scour due to breaking waves at a vertical seawall VI-5-262

Figure VI-5-118. Relative scour depth as a function of relative depth at a vertical wall VI-5-263

Figure VI-5-119. Correction factor, k_1, for pile/pier shape VI-5-268

Figure VI-5-120. Wave-induced equilibrium scour depth at a vertical pile VI-5-269

Figure VI-5-121. Wave and current scour around large vertical piles VI-5-272

Figure VI-5-122. Pipeline scour and pipeline embedment VI-5-272

Figure VI-5-123. Scour apron for vertical pile in a current VI-5-277

Figure VI-5-124. Stone blanket scour protection for submerged pipelines VI-5-278

Figure VI-5-125. Definition sketch of wave forces on a vertical cylinder VI-5-279

Figure VI-5-126. K_{im} versus relative depth, d/gT^2 ..... VI-5-286

Figure VI-5-127. K_{Dm} versus relative depth, d/gT^2 ..... VI-5-287

Figure VI-5-128. Inertia force moment arm S_{im} versus relative depth, d/gT^2 ..... VI-5-288

Figure VI-5-129. Drag force moment arm S_{Dm} versus relative depth, d/gT^2 ..... VI-5-289

Figure VI-5-130. Breaking wave height and regions of validity of various wave theories VI-5-290

Figure VI-5-131. Isolines of φ_m versus H/gT^2 and d/gT^2 (W = 0.05) VI-5-291

Figure VI-5-132. Isolines of φ_m versus H/gT^2 and d/gT^2 (W = 0.10) VI-5-292

Figure VI-5-133. Isolines of φ_m versus H/gT^2 and d/gT^2 (W = 0.50) VI-5-293

Figure VI-5-134. Isolines of φ_m versus H/gT^2 and d/gT^2 (W = 1.0) VI-5-294

Figure VI-5-135. Isolines of α_m versus H/gT^2 and d/gT^2 (W = 0.05) VI-5-297

Figure VI-5-136. Isolines of α_m versus H/gT^2 and d/gT^2 (W = 0.10) VI-5-298

Figure VI-5-137. Isolines of α_m versus H/gT^2 and d/gT^2 (W = 0.5) VI-5-299

Figure VI-5-138. Isolines of α_m versus H/gT^2 and d/gT^2 (W = 1.0) VI-5-300

Figure VI-5-139. Drag coefficient C_D as a function of KC and constant values of R_c or β for smooth cylinders VI-5-302

Figure VI-5-140. Inertia coefficient C_M as a function of KC and constant values of R_e or β for smooth cylinders VI-5-303

Figure VI-5-141. Lift coefficient C_L as a function of KC and constant values of R_e or β for smooth cylinders VI-5-304

Figure VI-5-142. Drag coefficient C_D as a function of Reynolds number for rough cylinders VI-5-305

Figure VI-5-143. Inertia coefficient C_M as a function of Reynolds number for rough cylinders VI-5-306

Figure VI-5-144. Ice riding up on structure slope VI-5-314

Figure VI-5-145. Vertical ice forces on a cylindrical pile VI-5-317

List of Tables

Page

Table VI-5-1. Types of Wave Breaking on Impermeable Slopes and Related ξ_o Values....VI-5-7

Table VI-5-2. Coefficients in Equation VI-5-3 for Runup of Long-Crested Irregular Waves on Smooth Impermeable Slopes....VI-5-10

Table VI-5-3. Surface Roughness Reduction Factor γ_r in Equation VI-5-3, Valid for $1 < \xi_{op} < 3$-4....VI-5-12

Table VI-5-4. Test Program....VI-5-17

Table VI-5-5. Coefficients in Equations VI-5-12 and VI-5-13 for Runup of Irregular Head-On Waves on Impermeable and Permeable Rock Armored Slopes....VI-5-21

Table VI-5-6. Critical Values of Average Overtopping Discharges....VI-5-24

Table VI-5-7. Models for Average Overtopping Discharge Formulae....VI-5-28

Table VI-5-8. Overtopping Formula by Owen (1980, 1982)....VI-5-29

Table VI-5-9. Overtopping Formula by Bradbury and Allsop (1988)....VI-5-30

Table VI-5-10. Coefficients by Aminti and Franco (1988) for Overtopping Formula by Bradbury and Allsop in Table VI-5-9....VI-5-31

Table VI-5-11. Overtopping Formula by van der Meer and Janssen (1995)....VI-5-32

Table VI-5-12. Overtopping Formula by Pedersen and Burcharth (1992), Pedersen (1996)....VI-5-33

Table VI-5-13. Overtopping Formula by Franco and Franco (1999)....VI-5-34

Table VI-5-14. Wave Reflection Coefficients for Non-Overtopped Sloping Structures Based on Seelig (1983) Equation....VI-5-40

Table VI-5-15. Wave Transmission Formula by van der Meer and d=Angremond (1991) for Rock Armored Low-crested, Submerged, and Reef Breakwaters....VI-5-53

Table VI-5-16. Wave Transmission Formula by Goda (1969)....VI-5-55

Table VI-5-17. Wave Transmission Formula by Takahashi (1996)....VI-5-56

Table VI-5-18. Parameters Influencing Hydraulic Stability of Armor Layers....VI-5-62

Table VI-5-19. Definition of Damage Parameters *D, N_{od}* and *S* VI-5-65

Table VI-5-20. Examples of Experimentally Determined Relationships Between N_{od} and *S* VI-5-67

Table VI-5-21. Damage Classification and Related Values of the Damage Parameters *D, N_{od}* and *S* VI-5-68

Table VI-5-22. Rock, Two-Layer Armored Non-Overtopped Slopes (Hudson 1974) VI-5-73

Table VI-5-23. Rock, Two-Layer Armored Non-Overtopped Slopes (van der Meer 1988) VI-5-74

Table VI-5-24. Rock, Two-Layer Armored Overtopped, but Not Submerged, Low-Crested Slopes VI-5-75

Table VI-5-25. Rock, Submerged Breakwaters with Two-Layer Armor on Front, Crest and Rear Slope (van der Meer 1991) VI-5-76

Table VI-5-26. Rock, Two-Layer Armored Low-Crested and Submerged Breakwaters (Vidal et al. 1992) VI-5-77

Table VI-5-27. Rock, Low-Crested Reef Breakwaters Built Using Only One Class of Stone VI-5-78

Table VI-5-28. Rock, Rear Slope Stability of Two-Layer Armored Breakwaters Without Superstructures (Jensen 1984) VI-5-79

Table VI-5-29. Concrete Cubes, Two-Layer Armored Non-Overtopped Slopes VI-5-80

Table VI-5-30. Tetrapods, Two-Layer Armored Non-Overtopped Slopes VI-5-81

Table VI-5-31. Dolos, Non-Overtopped Slopes (Burcharth and Liu 1992) VI-5-82

Table VI-5-32. ACCROPODE7 (van der Meer 1988b) VI-5-84

Table VI-5-33. ACCROPODE7, Non-Overtopped or Marginally Overtopped Slopes (Burcharth et al. 1998) VI-5-85

Table VI-5-34. CORE-LOC7, Non or Marginally Overtopped Slopes (Melby and Turk 1994; Turk and Melby 1997) VI-5-86

Table VI-5-35. Tetrapods, Horizontally Composite Breakwaters (Hanzawa et al. 1996) VI-5-87

Table VI-5-36. Tribars, Non-Overtopped or Minor Overtopped Slopes, Random and Uniform Placement VI-5-88

Table VI-5-37. Rock and Dolos Breakwater Head Stability, No Overtopping (Carver and Heimbaugh 1989) VI-5-91

Table VI-5-38. Tetrapod and Tribar Breakwater Head Section Stability, No Overtopping VI-5-92

Table VI-5-39. Types and Origins of Loads on Armor Units (Burcharth 1993b) VI-5-101

Table VI-5-40. Breakage Formula for Dolosse and Tetrapods VI-5-102

Table VI-5-41. Stress Prediction Formulae for Dolosse VI-5-104

Table VI-5-42. Approximate Values of Ultimate Rigid Body Impact Velocities For Concrete Armor Units VI-5-109

Table VI-5-43. Drawbacks Related to Crack-Reducing Procedures VI-5-111

Table VI-5-44. Fatigue for Conventional Unreinforced Concrete Exposed to Uniaxial and Flexural Stress Conditions With Zero Mean Stress VI-5-113

Table VI-5-45. Stability of Toe Berm Tested in Regular Waves VI-5-117

Table VI-5-46. Stability of Toe Berm Formed by 2 Layers of Stone Having Density 2.68 tonnes/m^3. Variable Berm Width, and Sloping Structures VI-5-118

Table VI-5-47. Stability of Toe Berm Formed by Two Layers of Stones or Parallellepiped Concrete Blocks VI-5-120

Table VI-5-48. Stability of Toe Berm Formed by Two Layers of Stones in Front of Vertical Impermeable Wall Structure VI-5-121

Table VI-5-49. Stability Under Combined Waves and Currents VI-5-126

Table VI-5-50. Weight and Size Selection Dimensions of Quarrystone VI-5-129

Table VI-5-51. Layer Coefficient and Porosity for Various Armor Units VI-5-136

Table VI-5-52. The Sainflou Formula for Head-on, Fully Reflected, Standing Regular Waves VI-5-153

Table VI-5-53. Goda Formula for Irregular Waves VI-5-154

Table VI-5-54. Goda Formula Modified to Include Impulsive Forces from Head-on Breaking Waves VI-5-155

Table VI-5-55. Resulting Wave Induced Forces and Moments, and Related Uncertainties and Bias When Calculated from Wave Load Equations by Goda and Takahashi VI-5-156

Table VI-5-56. Wave Loads on Impermeable Inclined Walls VI-5-157

Table VI-5-57. Wave Loads on Sloping Top Structures VI-5-158

Table VI-5-58. Wave Loads on Vertical Walls Protected by a Rubble-Mound Structure VI-5-159

Table VI-5-59. Wave Pressures from Regular Head-on Waves on Caissons with Vertical Slit Front Face and Open Wave Chamber VI-5-160

Table VI-5-60. Horizontal Wave Force on Concrete Caps VI-5-178

Table VI-5-61. Horizontal Wave Force, Uplift Wave Pressure and Turning Moment on Concrete Caps VI-5-179

Table VI-5-62. Experimental Test Results of Friction Coefficient Conducted in Japan VI-5-182

Table VI-5-63. Experimental Test Results of Friction Coefficient VI-5-182

Table VI-5-64. Dynamic Friction Coefficient Between Caisson Bottom and Rubble-Mound VI-5-183

Table VI-5-65. Fractional Limits of Grain Sizes According ISO/CEN VI-5-194

Table VI-5-66. Typical Bulk Density Values VI-5-195

Table VI-5-67. Typical Values of Void Ratio *e* and Porosity *n* for Granular Soils VI-5-195

Table VI-5-68. Density Characterization of Granular Soils VI-5-196

Table VI-5-69. Deformation of Moduli for Elastic Material VI-5-199

Table VI-5-70. Typical Values of Poisson's Ratio, ν VI-5-199

Table VI-5-71. Example Values of Secant Young's Modulus *E* in MN/m^2 for Sand VI-5-201

Table VI-5-72. Typical Values of Secant Young's Modulus, *E*, for Clay VI-5-201

Table VI-5-73. Typical Secant Values of Deformation-Moduli *G, K* and *M* for Quasi-Static Loaded Quartz Sand VI-5-201

Table VI-5-74. Typical Values of Triaxial Test Friction Angle ν_s for Quartz Sand VI-5-208

Table VI-5-75. Critical Value of Angle of Friction, νN_{crit} VI-5-210

Table VI-5-76. Typical Values of ψ_{max} for Quartz Sand and Quarried Granitic Gneiss VI-5-210

Table VI-5-77. Classification of Clay According to Undrained Shear Strength, c_u VI-5-211

Table VI-5-78. One-Dimensional Porous Flow Equation VI-5-214

Table VI-5-79. Typical Values of Permeability, *k*, for Fine Materials VI-5-215

Table VI-5-80. Typical Values of Permeability, *k*, for Stone Materials VI-5-215

Table VI-5-81. Wave Induced Set-up in Sloping Rubble Mound Structures VI-5-216

Table VI-5-82. Horizontal Wave Induced Pore Pressure Gradients in the Core of Rubble-Mound Breakwaters VI-5-217

Table VI-5-83. Classification of Loading and Soil Conditions VI-5-219

Table VI-5-84. Example of Consolidation Times for Sand VI-5-220

Table VI-5-85. Wave and Tide Induced Pore Pressures in Permeable Seabeds VI-5-238

Table VI-5-86. Bearing Capacity Formula for Rectangular Concentrically Statically Loaded Horizontal Footings VI-5-245

Table VI-5-87. Bearing Capacity Formula[1] for Rectangular Statically Loaded Horizontal Footing VI-5-246

Table VI-5-88. General Bearing Capacity Formula for Rectangular Statically Loaded Inclined Footing on Cohesionless Soil in Vicinity of Slope VI-5-248

Table VI-5-89. Values of Skin Friction Coefficient, C_{sf} VI-5-311

Table VI-5-90. Values of Effective Ice Crushing Strength, σ_c VI-5-313

CHAPTER VI-5

Fundamentals of Design

VI-5-1. Introduction.

a. Overview.

(1) Planning and design procedures for coastal projects are described in Part V-1, "Planning and Design Process." The engineering design steps related to a specific type of coastal structure can be schematized as follows:

(a) Specification of functional requirements and structure service lifetime.

(b) Establishment of the statistics of local short-term and long-term sea states as well as estimation of possible geomorphological changes.

(c) Selection of design levels for the hydraulic responses: wave runup, overtopping, wave transmission, wave reflection (e.g., 20 percent probability of overtopping discharge exceeding 10^{-5} m^3/s A m during 1 hr in a 50-year period).

(d) Consideration of construction equipment and procedures, and of availability and durability of materials (e.g., only land based equipment operational and available at reasonable costs, rock of sufficient size easily available).

(e) Selection of alternative structure geometries to be further investigated (e.g., composite caisson structures, rubble structures with and without crown walls).

(f) Identification of all possible failure modes for the selected structures (e.g., armor layer displacement).

(g) Selection of design damage levels for the identified failure modes (e.g., 50 percent probability of displacement of 5 percent of the armor units within 50 years).

(h) Conceptual design of the structural parts based on the chosen design levels for failure mode damage and hydraulic responses (e.g., determination of armor layer block size and crest height for a breakwater).

(i) Evaluation of costs of the alternative structures and selection of preferred design(s) for more detailed analysis and optimization.

(j) Detailed design including economical optimization and evaluation of the overall safety of the structure. This stage will involve scale model tests and/or advanced computational analyses for non-standard and major structures.

(2) Items *c* and *g* are closely related to item *a*, and the failure modes mentioned in item *f* are dealt with in Part VI-2-4, "Failure Modes of Typical Structure Types."

(3) The previous steps are a brief summary of the flow chart given as Figure V-1-2 in Part V-1-1. They are the steps most related to actual design of project structure elements. In all steps, the outlined design procedure should preferably involve a probabilistic approach which allows implementation of safety based on reliability assessments. The principles are explained in Part VI-6, "Reliability Based Design of Coastal Structures." The present Part VI-5 discusses the basic tools available for conceptual design related to wave-structure interactions (item *h* in the design process).

(4) Wave-structure interaction can be separated into hydraulic responses (such as wave runup, wave overtopping, wave transmission and wave reflection), and loads and response of structural parts. Each interaction is described by a formula, which in most cases is semiempirical in nature with the form based on physical considerations but the empirical constants determined by fitting to experimental data.

(5) The uncertainty and bias of the formula are given when known. Tables of available partial safety factors and the related design equations which show how the partial safety factors are implemented are given in Part VI-6, "Reliability Based Design of Coastal Structures."

b. Wave/structure interaction.

(1) Hydraulic response.

(a) Design conditions for coastal structures include acceptable levels of hydraulic responses in terms of wave runup, overtopping, wave transmission, and wave reflection. These topics are covered in Part VI-5-2, "Structure Hydraulic Response."

(b) The wave runup level is one of the most important factors affecting the design of coastal structures because it determines the design crest level of the structure in cases where no (or only marginal) overtopping is acceptable. Examples include dikes, revetments, and breakwaters with pedestrian traffic.

(c) Wave overtopping occurs when the structure crest height is smaller than the runup level. Overtopping discharge is a very important design parameter because it determines the crest level and the design of the upper part of the structure. Design levels of overtopping discharges frequently vary, from heavy overtopping of detached breakwaters and outer breakwaters without access roads, to very limited overtopping in cases where roads, storage areas, and moorings are close to the front of the structure.

(d) At impermeable structures, wave transmission takes place when the impact of overtopping water generates new waves at the rear side of the structure. With submerged structures, the incident waves will more or less pass over the structure while retaining much of the incident wave characteristics. Permeable structures like single stone size rubble mounds and slotted screens allow wave transmission as a result of wave penetration. Design levels of transmitted waves depend on the use of the protected area. Related to port engineering is the question of acceptable wave disturbance in harbor basins, which in turn is related to the movements of moored vessels. Where groins are included as part of a coastal protection scheme, it is desirable to ensure wave transmission (sediment transport) across the groins.

(e) Wave reflection from the boundary structures like quay walls and breakwaters determines to a large extent the wave disturbance in harbor basins. Also, maneuvering conditions at harbor entrances are highly affected by wave reflection from the breakwaters. Reflection causing steep waves and cross waves can be very dangerous to smaller vessels. Moreover, breakwaters and jetties can cause reflection of waves onto neighboring beaches and thereby increase wave impacts on beach processes.

(2) Wave loadings and related structural response.

(a) An important part of the design procedure for structures in general is the determination of the loads and the related stresses, deformations, and stability conditions of the structural members.

(b) In the case of rubble-mound structures exposed to waves, such procedures cannot be followed because the wave loading on single stones or blocks cannot be determined by theory, by normal scale model tests, or by prototype recordings. Instead a black box approach is used in which experiments are used to establish relationships between certain wave characteristics and the structural response, usually expressed in terms of armor movements. The related stresses, e.g., in concrete armor blocks, are known only for a few types of blocks for which special investigations have been performed. Rubble-mound structures are covered in Part VI-5-3, "Rubble-Mound Structure Loading and Response."

For vertical-front monolithic structures like breakwater caissons and seawalls it is possible either from theory or experiments to estimate the wave loadings and subsequently determine stresses, deformations, and stability. Vertical-front structures are covered in Part VI-5-4, "Vertical-Front Structure Loading and Response."

VI-5-2. Structure Hydraulic Response.

a. Wave runup and rundown on structures.

(1) Introduction.

(a) Wind-generated waves have wave periods which trigger wave breaking on almost all sloping structures. The wave breaking causes runup, R_u, and rundown, R_d, defined as the maximum and minimum water-surface elevation measured vertically from the still-water level (SWL), see Figure VI-5-1a.

(b) R_u and R_d depend on the height and steepness of the incident wave and its interaction with the preceding reflected wave, as well as the slope angle, the surface roughness, and the permeability and porosity of the slope. Maximum values of flow velocities and values of R_u and R_d for a given sea state and slope angle are reached on smooth impermeable slopes.

(c) Figure VI-5-1a illustrates the variation of the flow velocity vectors along an impermeable slope over the course of a wave cycle. Figure VI-5-1b illustrates this variation for a permeable slope. Both the magnitude and direction of the velocity vectors are important for stability of the armor units. Generally, the most critical flow field occurs in a zone around and

just below still-water level (swl) where down-rush normally produces the largest destabilizing forces. Exceptions are slopes flatter than approximately 1:3.5 in which cases up-rush is more vulnerable. The velocity vectors shown in Figure VI-5-1b explain why reshaping breakwaters attain S-profiles.

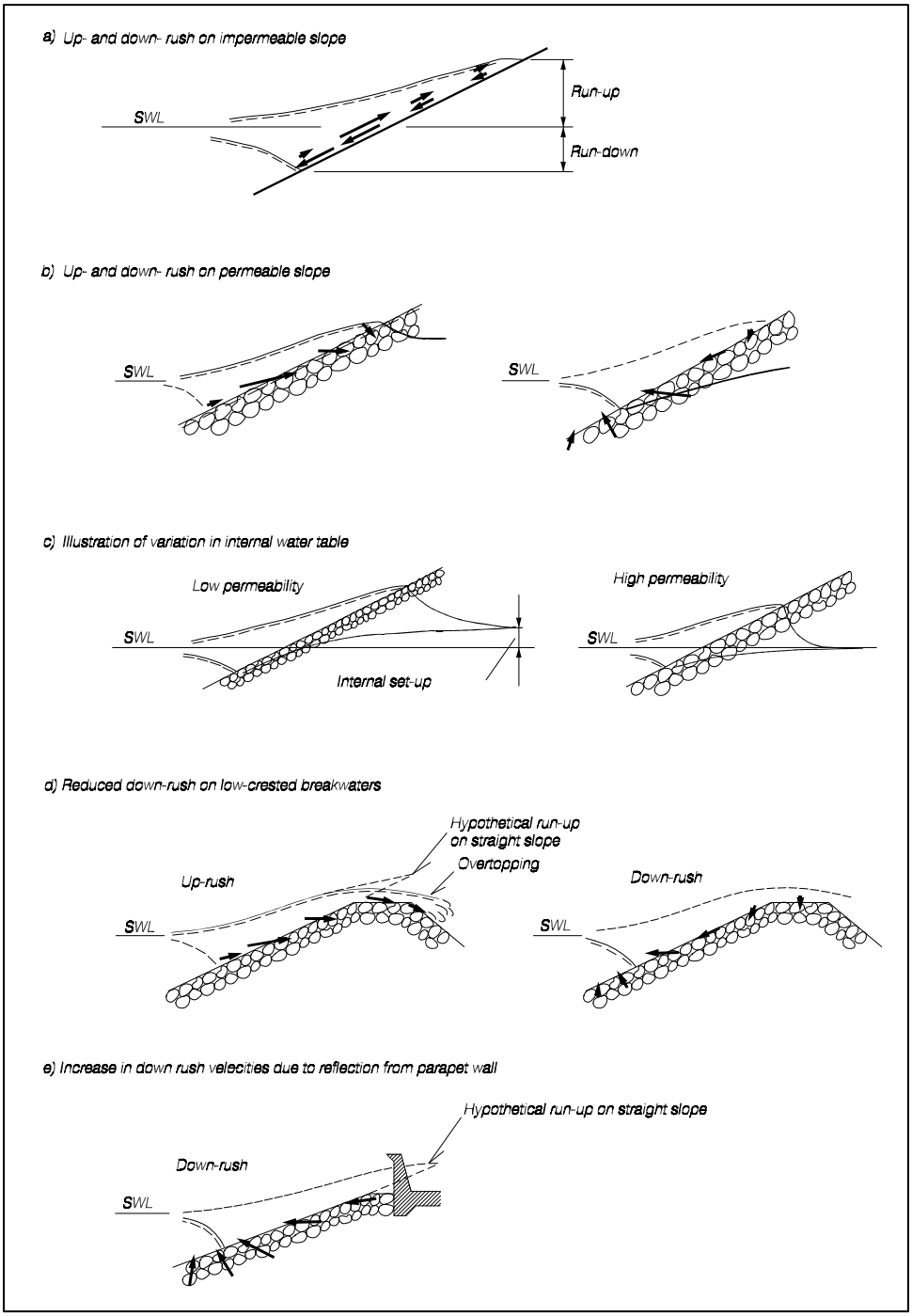

Figure VI-5-1. Illustration of runup and rundown (Burcharth 1993)

(d) Increase in permeability of the slope reduces the flow velocities along the slope surface because a larger proportion of the flow takes place inside the structure. The wave action will cause a rise of the internal water level (phreatic line) indicated in Figure VI-5-1c, leading to an increase in the mean pore pressures. The internal setup is due to a greater inflow surface area during wave runup than the outflow surface area during rundown. The mean flow path for inflow is also shorter than that for outflow. The rise of the phreatic line will continue until the outflow balances the inflow. The lower the permeability of the structure, the higher the setup as indicated on Figure VI-5-1c.

(e) Barends (1988) suggested practical formulae for calculation of the penetration length and the maximum average setup which occurs after several cycles. Two cases are considered: a conventional breakwater structure with open (permeable) rear side, and a structure with a closed (impermeable) rear side. The latter case causes the largest setup.

(f) An example of a numerical calculation of the internal flow patterns in a breakwater exposed to regular waves is shown in Figure VI-5-2. The strong outflow in the zone just below SWL when maximum rundown occurs is clearly seen.

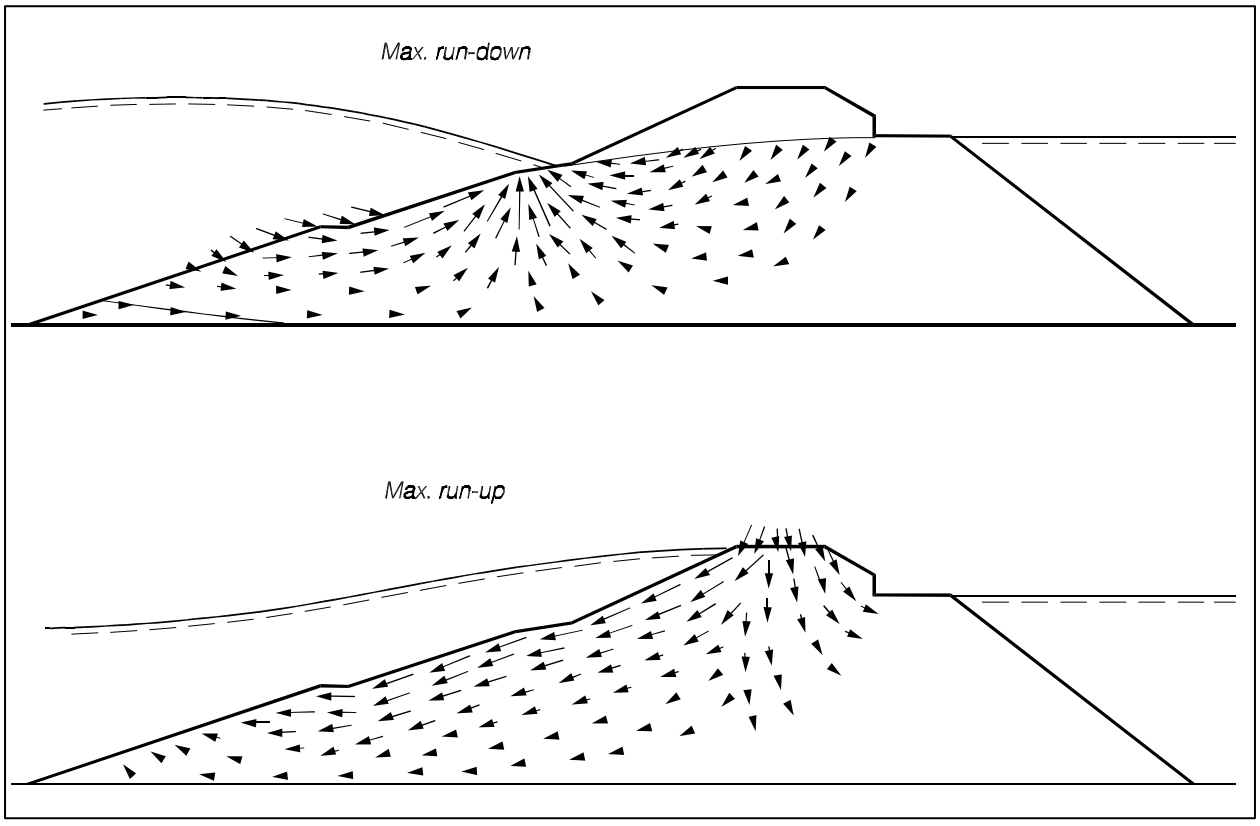

Figure VI-5-2. Typical velocity field for the porous flow in a breakwater. Numerical calculation (Barends et al. 1983)

(g) Increasing structure porosity also reduces the overflow velocities because a larger portion of the incoming water volume can be stored in the pores which then act as reservoirs.

The destabilizing forces on armor units are thereby reduced. This positive reservoir effect is reduced in the case of a large internal setup of the water table.

(h) Breakwaters with crest levels lower than the runup level are called low-crested breakwaters. Although the runup velocities are almost unchanged compared to nonovertopped slopes, the rundown velocities are reduced due to the overtopping of some part of the incoming wave as seen in Figure VI-5-1d. Greater overtopping reduces rundown, and thus, lessens the destabilizing flow forces on the armor units. Parapet walls which cut off the hypothetical runup wedge (shown in Figure VI-5-1e) will increase the down-rush velocities and thereby increase the destabilizing flow forces on the armor units.

(2) Surf similarity parameter (Iribarren number).

(a) Wave runup and rundown on a structure depend on the type of wave breaking. Breaker types can be identified by the so-called surf-similarity parameter, ξ (Battjes 1974b). The parameter ξ is also referred to as the breaker parameter or Iribarren number. The surf-similarity parameter was originally defined for regular waves as

$$\xi_o = \frac{\tan \alpha}{\sqrt{s_o}} \tag{VI-5-1}$$

where

α = slope angle

s_o = deepwater wave steepness (= H_o / L_o)

H_o = deepwater wave height

L_o = deepwater wavelength (= $gT^2/2\pi$)

T = wave period

g = acceleration due to gravity

(b) The wave height H_b at the breaking point is sometimes substituted for H_o in which case the parameter is denoted by ξ_b. Breaker types and related ranges of ξ_o-values are given for impermeable slopes in Table VI-5-1. The boundaries of transition from one type of breaker to another are approximate.

Table VI-5-1
Types of Wave Breaking on Impermeable Slopes and Related ξ_o-Values

	SPILLING $\xi_o < 0.5$
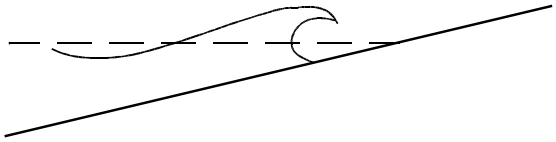	PLUNGING $0.5 < \xi_o < 3$
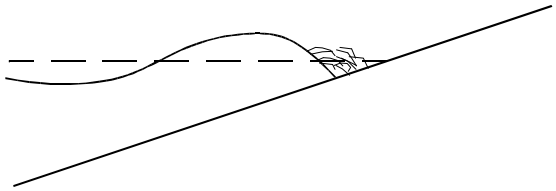	COLLAPSING $\xi_o \approx 3$ à 3.5
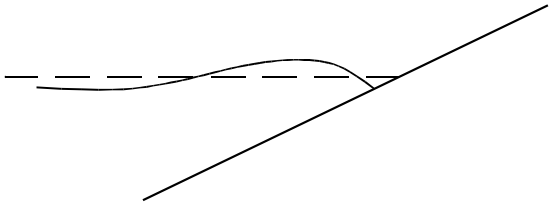	SURGING $\xi_o > 3.5$

(c) For irregular waves the surf--similarity parameter is defined as

$$\xi_{om} = \frac{\tan\alpha}{\sqrt{s_{om}}} \quad \text{or} \quad \xi_{op} = \frac{\tan\alpha}{\sqrt{s_{op}}} \tag{VI-5-2}$$

where

$$s_{om} = \frac{H_s}{L_{om}} = \frac{2\pi}{g}\frac{H_s}{T_m^2}$$

$$s_{op} = \frac{H_s}{L_{op}} = \frac{2\pi}{g}\frac{H_s}{T_p^2}$$

and

H_s = significant wave height of incident waves at the toe of the structure

T_m = mean wave period

T_p = wave period corresponding to the peak of the wave spectrum

Note that s_{om} and s_{op} are fictitious wave steepnesses because they are ratios between a statistical wave height at the structure and representative deepwater wavelengths.

(d) The relative runup R_u /H is a function of ξ, the wave angle of incidence, and the slope geometry (profile, surface roughness, porosity). Differences in runup characteristics make it convenient to distinguish between impermeable and permeable slopes. Impermeable slopes belong to dikes, revetments, and breakwaters with either impermeable surfaces (e.g., asphalt, concrete) or rough surfaces (e.g., rubble stones, concrete ribs) on fine core materials. Permeable slopes belong typically to rubble-mound structures with secondary armor layers, filter layers, and quarryrun core.

(3) Wave runup and rundown on impermeable slopes. Runup on impermeable slopes can be formulated in a general expression for irregular waves having the form (Battjes 1974)

$$\frac{R_{ui\%}}{H_s} = \left(A\xi + C\right)\gamma_r\gamma_b\gamma_h\gamma_\beta \tag{VI-5-3}$$

where

$R_{ui\,\%}$ = runup level exceeded by i percent of the incident waves

ξ = surf-similarity parameter, ξ_{om} or ξ_{op}

A, C = coefficients dependent on ξ and i but related to the reference case of a smooth, straight impermeable slope, long-crested head-on waves and Rayleigh-distributed wave heights

γ_r = reduction factor for influence of surface roughness (γ_r = 1 for smooth slopes)

γ_b = reduction factor for influence of a berm (γ_b = 1 for non-bermed profiles)

γ_h = reduction factor for influence of shallow-water conditions where the wave height distribution deviates from the Rayleigh distribution (γ_h = 1 for Rayleigh distributed waves)

γ_β = factor for influence of angle of incidence β of the waves (γ_β = 1 for head-on long-crested waves, i.e., $\beta = 0^o$). The influence of directional spreading in short-crested waves is included in γ_β as well

(a) Smooth slope, irregular long-crested head-on waves. Van Oorschot and d'Angremond (1968) tested slopes of 1:4 and 1:6 for $\xi_{op} < 1.2$. Ahrens (1981a) investigated slopes between 1:1 and 1:4 for $\xi_{op} > 1.2$. Figure VI-5-3 shows the range of test results and the fit of Equation VI-5-3 for $R_{u2\,percent}$. Considerable scatter is observed, most probably due to the fact that the runs for ξ_{op}

> 1.2 contained only 100-200 waves. The coefficient of variation, $\sigma_{Ru} / \overline{R_u}$, seems to be approximately 0.15.

- The significant runup level $R_{us} = R_{u33\,\%}$ depicted in Figure VI-5-4 does not contain data for $\xi_{op} < 1.2$. The coefficient of variation appears to be approximately 0.1.

- The coefficients A and C together with estimates of the coefficient of variation for R_u are given in Table VI-5-2. It should be noted that data given in Allsop et al. (1985) showed runup levels considerably smaller than given here.

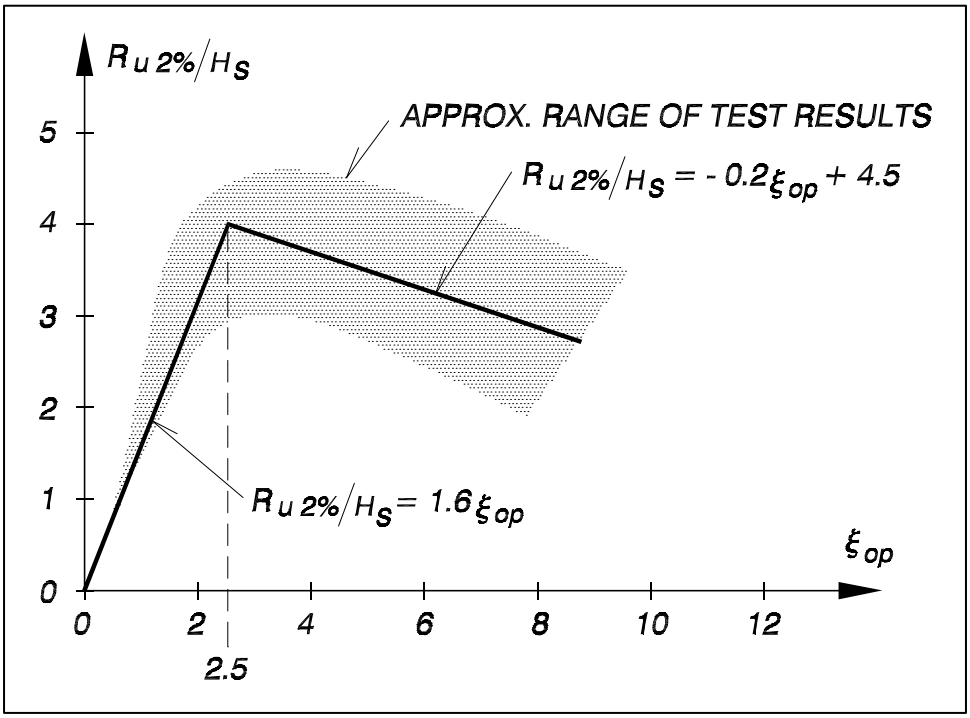

Figure VI-5-3. $R_{u2\%}$ for head-on waves on smooth slopes. Data by Ahrens (1981a) and Van Oorschot and d'Angremond (1968)

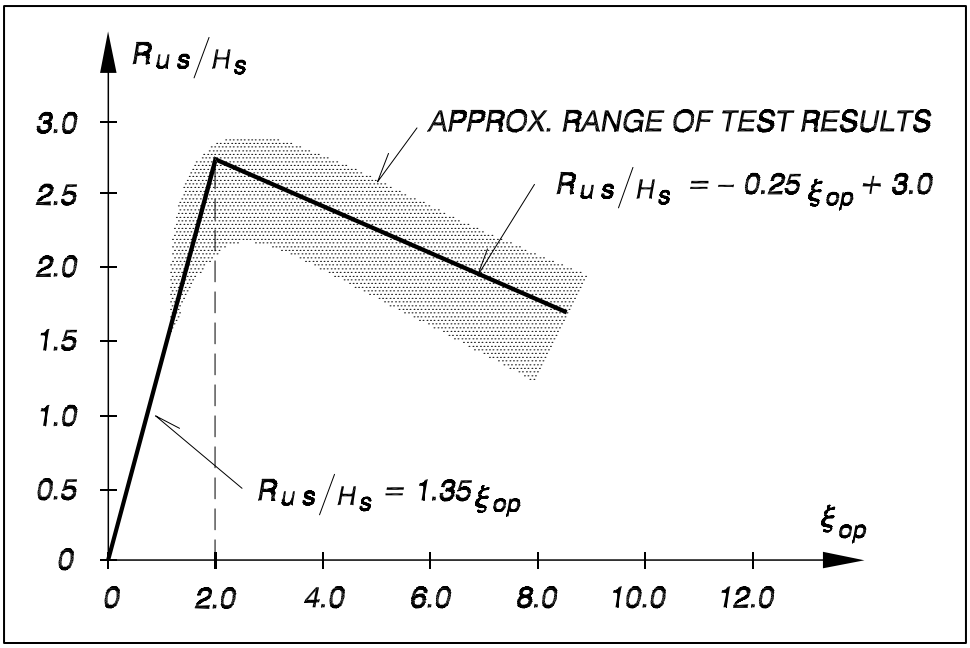

Figure VI-5-4. R_{us} for head-on waves on smooth slopes. Data by Ahrens (1981a)

Table VI-5-2
Coefficients in Equation VI-5-3 for Runup of Long-Crested Irregular Waves on Smooth Impermeable Slopes

ξ	R_u	ξ-Limits	A	C	σ_{Ru}/R_u
ξ_{op}	$R_{u2\ percent}$	$\xi_p \le 2.5$ $2.5 < \xi_p < 9$	1.6 -0.2	0 4.5	≈ 0.15
	R_{us}	$\xi_p \le 2.0$ $2.0 < \xi_p < 9$	1.35 -0.15	0 3.0	≈ 0.10

- Generally less experimental data are available for rundown. Rundown corresponding to $R_{d2\ percent}$ from long-crested irregular waves on a smooth impermeable slope can be estimated from

$$\frac{R_{d2\%}}{H_s} = \begin{cases} 0.33\xi_{op} & \text{for} \quad 0 < \xi_{op} \le 4 \\ 1.5 & \text{for} \quad \xi_{op} > 4 \end{cases} \qquad \text{(VI-5-4)}$$

- In the Dutch publication by Rijkswaterstaat Slope Revetments of Placed Blocks, 1990, the following expression was given for rundown on a smooth revetment of placed concrete block

$$\frac{R_{d2\%}}{H_s} = 0.5\xi_{op} - 0.2 \qquad \text{(VI-5-5)}$$

- Another set of runup data for long-crested head-on waves on smooth slopes was presented by de Waal and van der Meer (1992). The data cover small scale tests for slopes 1:3, 1:4, 1:5, 1:6 and large scale tests for slopes 1:3, 1:6, 1:8. The surf-similarity parameter range for the small scale tests is $0.6 < \xi_{op} < 3.4$, and for the large scale tests $0.6 < \xi_{op} < 2.5$. The data are shown in Figure VI-5-5 and were used by de Waal and van der Meer (1992) and van der Meer and Janssen (1995) as the reference data for the evaluation of the γ-factors defined by Equation VI-5-3.

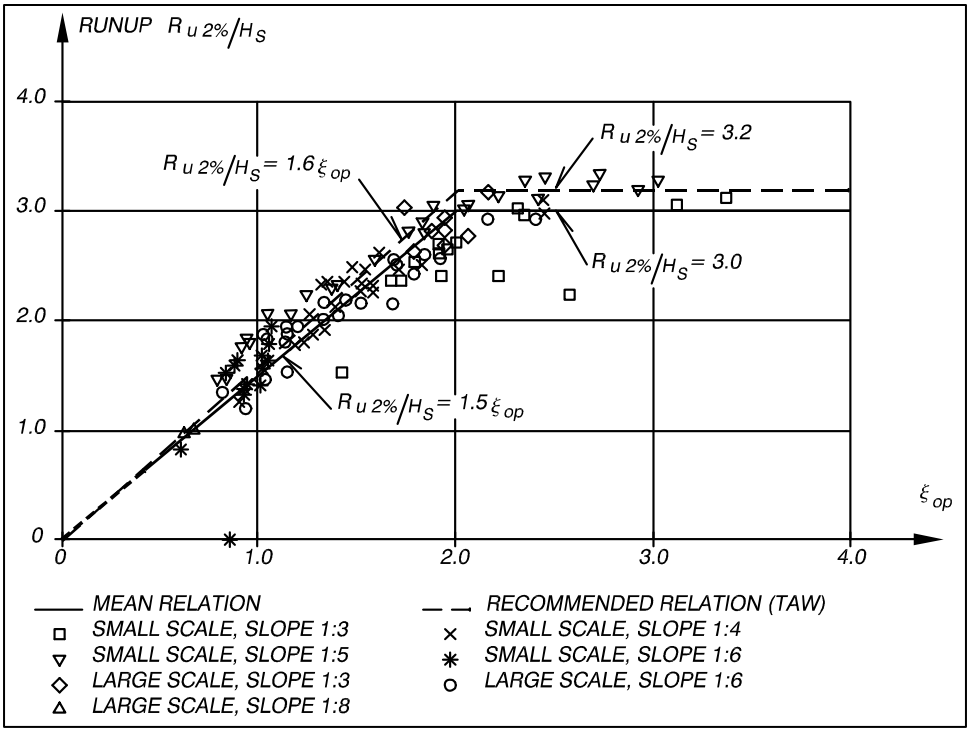

Figure VI-5-5. $R_{u2\%}$ for long-crested head-on waves on smooth slopes.
From de Waal and van der Meer (1992)

- The mean relationship, taken as the reference case for Equation VI-5-3, is shown with the solid line and is represented by the expression

$$\frac{R_{u2\%}}{H_s} = \begin{cases} 1.5\xi_{op} & \text{for} \quad 0.5 < \xi_{op} \le 2 \\ 3.0 & \text{for} \quad 2 < \xi_{op} < 3-4 \end{cases} \tag{VI-5-6}$$

- The dotted line includes a small safety factor, and this relationship is recommended for design by the Technical Advisory Committee on Water Defence in Holland.

- Based on a somewhat reduced data set compared to Figure VI-5-5, the uncertainty on Equation VI-5-6 is described by de Waal and van der Meer (1992) by assuming the factor 1.5 as a stochastic variable with a normal distribution and a coefficient of variation of 0.085.

– Influence of surface roughness on runup. The original values for γ_r given in Dutch publications and in the old *Shore Protection Manual* have been updated based on experiments

including large-scale tests with random waves. These factors are given in Table VI-5-3. The new γ_r values taken from de Waal and van der Meer (1992) are valid for $1 < \xi_{op} <$ 3-4. For larger ξ_{op}-values the γ_r factors will slowly increase to 1.

Table VI-5-3
Surface Roughness Reduction Factor γ_r in Equation VI-5-3, Valid for $1 < \xi_{op} <$ 3-4

Type of Slope Surface	γ_r
Smooth, concrete, asphalt	1.0
Smooth block revetment	1.0
Grass (3 cm length)	0.90 - 1.0
1 layer of rock, diameter D, (H_s/D = 1.5 - 3.0)	0.55 - 0.6
2 or more layers of rock, (H_s/D = 1.5 - 6.0)	0.50 - 0.55
Roughness elements on smooth surface (length parallel to waterline = P, width = b, height = h)	
Quadratic blocks, $P = b$	
h/b b/H_s area coverage	
0.88 0.12 - 0.19 1/9	0.70 - 0.75
0.88 0.12 - 0.24 1/25	0.75 - 0.85
0.44 0.12 - 0.24 1/25	0.85 - 0.95
0.88 0.12 - 0.18 1/25 (above SWL)	0.85 - 0.95
0.18 0.55 - 1.10 1/4	0.75 - 0.85
Ribs	
1.00 0.12 - 0.19 1/7.5	0.60 - 0.70

– Influence of a berm on runup. A test program at Delft Hydraulics was designed to clarify the influence of a horizontal or almost horizontal berm on wave runup. Figure VI-5-6 shows the range of tested profiles and sea states.

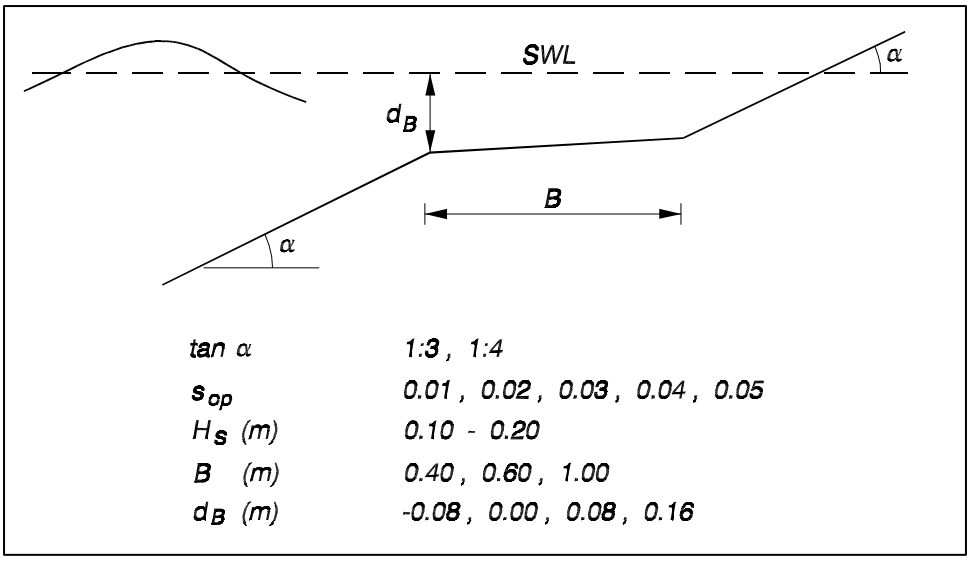

Figure VI-5-6. Parameters in berm test program at Delft Hydraulics

- According to de Waal and van der Meer (1992) the effect of a berm can be taken into account by the following formulation of the reference Equation VI-5-6

$$\frac{R_{u2\%}}{H_s} = \begin{cases} 1.5\xi_{op}\gamma_r\gamma_b\gamma_h\gamma_\beta = 1.5\xi_{eq}\gamma_r\gamma_h\gamma_\beta & \text{for} \quad 0.5 < \xi_{eq} \le 2 \\ 3.0\gamma_r\gamma_h\gamma_\beta & \text{for} \quad \xi_{eq} > 2 \end{cases} \tag{VI-5-7}$$

where ξ_{eq} is the breaking wave surf similarity parameter based on an equivalent slope (see Figure VI-5-7). The berm influence factor γ_b is defined as

$$\gamma_b = \frac{\xi_{eq}}{\xi_{op}} = 1 - r_B\left(1 - r_{dB}\right), \quad 0.6 \le \gamma_b \le 1.0 \tag{VI-5-8}$$

where

$$r_B = 1 - \frac{\tan\alpha_{eq}}{\tan\alpha}$$
$$r_{dB} = 0.5\left(\frac{d_B}{H_s}\right)^2, \quad 0 \le r_{dB} \le 1 \tag{VI-5-9}$$

and the *equivalent* slope angle α_{eq} and the *average* slope angle α are defined in Figure VI-5-7.

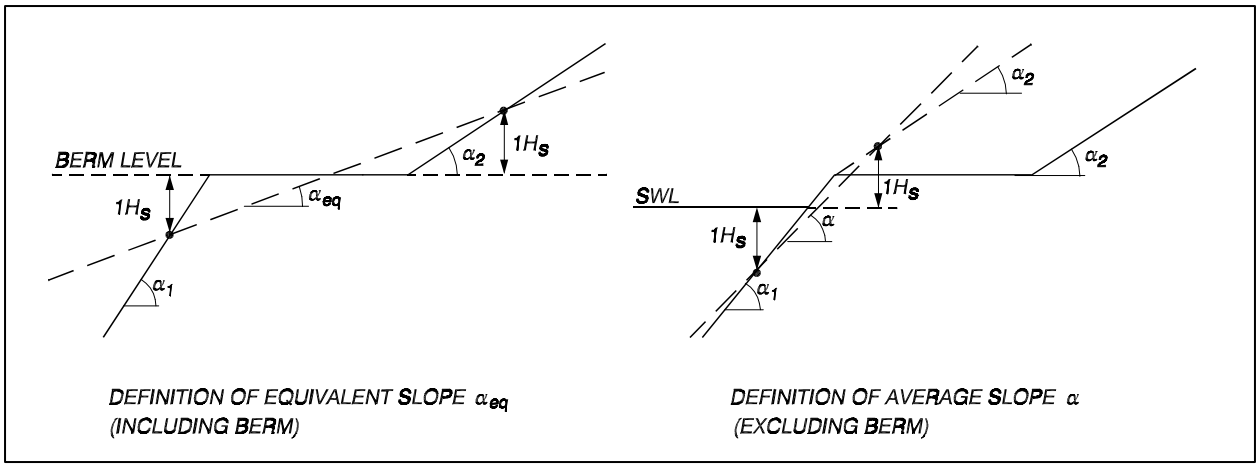

Figure VI-5-7. Definition of α_{eq} and α in Equation VI-5-9

- The influence of the berm can be neglected when the berm horizontal surface is positioned more than $H_s\sqrt{2}$ below SWL. If the berm horizontal surface lies higher than $d_B = H_s\sqrt{2}$ above SWL, then the runup can be set to $R_{u2\%} = d_B$ if $B/H_s \geq 2$. The berm is most effective when lying at SWL, i.e., $d_B = 0$. An optimum berm width B, which corresponds to $\gamma_b = 0.6$, can be determined from the formulae given by Equations VI-5-8 and VI-5-9.

- The use of ξ_{eq} in Equation VI-5-7 is evaluated in Figure VI-5-8 on the basis of the test program given in Figure VI-5-6, which implies $\gamma_r = \gamma_h = \gamma_\beta = 1$.

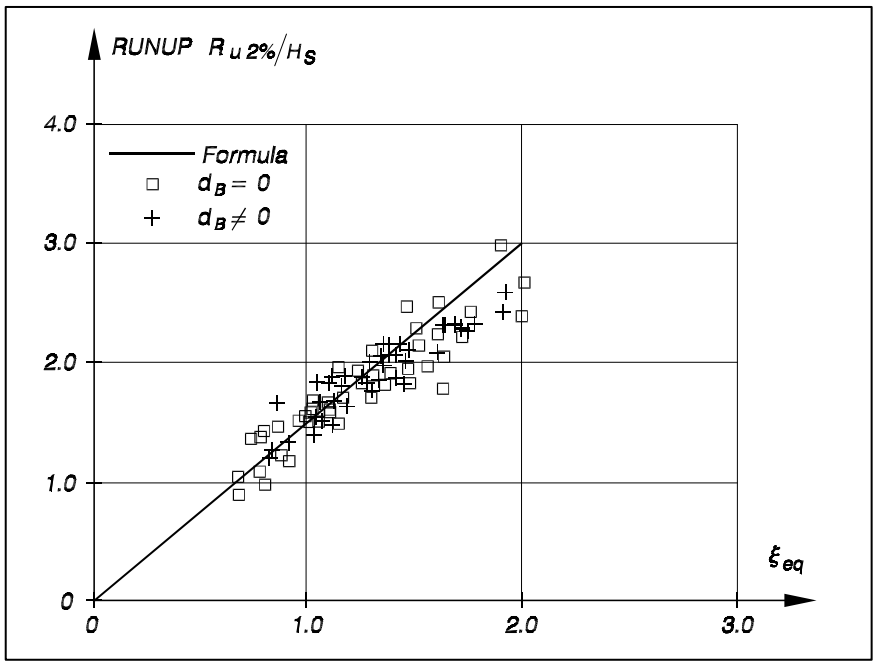

Figure VI-5-8. Evaluation of the use of ξ_{eq} to account for the influence of a berm

– Influence of shallow water on runup. Wave heights in Equation VI-5-7 are characterized by H_s which provides a unique definition for deep water conditions where wave heights are Rayleigh distributed. In shallow water where some waves break before they reach the structure, the wave heights will no longer be Rayleigh distributed. According to de Waal and van der Meer (1992), the influence factor can be estimated as

$$\gamma_h = \frac{H_{2\%}}{1.4 H_s} \tag{VI-5-10}$$

where the representative wave heights are specified for the water depth at the toe of the structure ($H_{2\%}/H_s$ = 1.4 for Rayleigh distributed wave heights).

– Influence of angle of wave attack on runup. Both the angle of incidence and the directional spreading of the waves influence the runup. A test program for runup on smooth slopes at Delft Hydraulics, as specified in Figure VI-5-9, revealed the variations in the influence factor γ_β as given by Equation VI-5-11 and depicted in Figure VI-5-10.

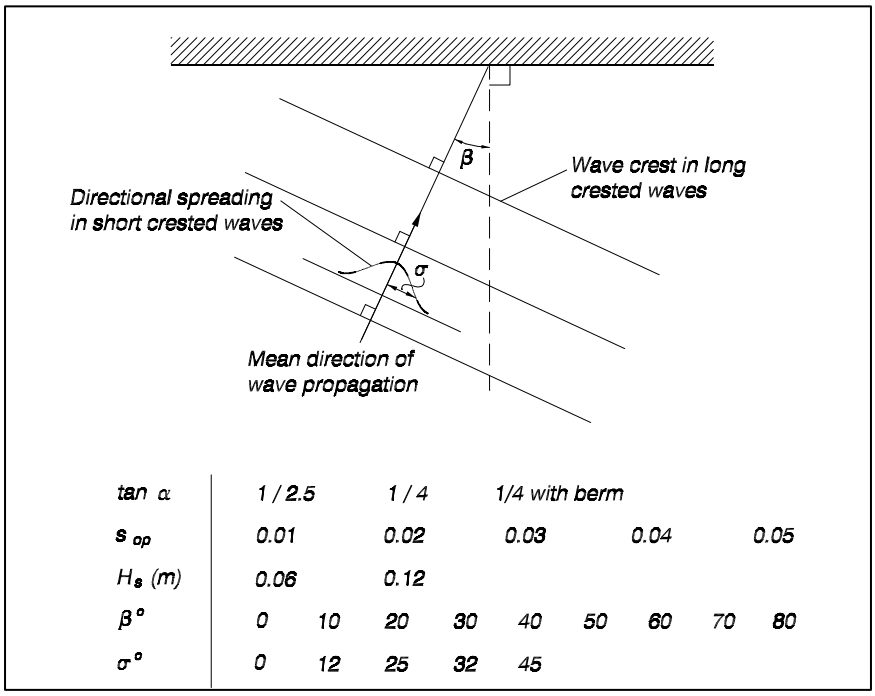

tan α	1 / 2.5		1 / 4		1/4 with berm				
s_{op}	0.01		0.02		0.03		0.04		0.05
H_s (m)	0.06		0.12						
β°	0	10	20	30	40	50	60	70	80
σ°	0	12	25	32	45				

Figure VI-5-9. Test program for wave runup on smooth slopes conducted at Delft Hydraulics, de Waal and van der Meer (1992)

- Note that γ_β-values larger than 1 were obtained for long-crested waves in the range $10^o \le \beta \le 30^o$, and that values very close to 1 were obtained for short-crested waves for β up to 50^o.

- Based on the results, the following formulas for mean values of γ_β were given

Long-crested waves	$= 1.0$	for $0^o \leq \beta \leq 10^o$	
(mainly swell)	$\gamma_\beta = \cos(\beta - 10^o)$	for $10^o < \beta \leq 63^o$	
	$= 0.6$	for $\beta > 63^o$	(VI-5-11)
Short-crested waves	$\gamma_\beta = 1 - 0.0022\,\beta$		

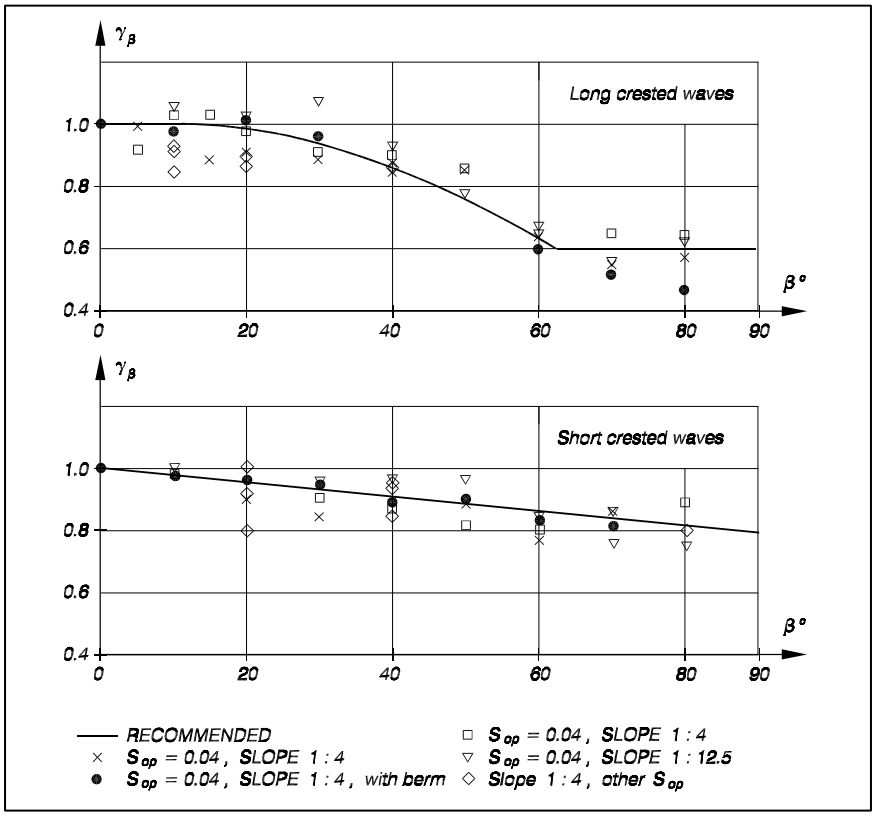

Figure VI-5-10. Influence of angle of incidence β and directional spreading on runup on smooth slopes conducted at Delft Hydraulics; de Waal and van der Meer (1992)

(b) Rock armored slopes, irregular long-crested head-on waves. Runup on rock armored impermeable and permeable slopes was studied by Delft Hydraulics in the test program given in Table VI-5-4.

Table VI-5-4
Test Program(van der Meer 1988)

Slope Angle cot α	Grading D_{85} / D_{15}	Spectral Shape	Core Permeability	Relative Mass Density	Number of Tests	Range $H_s/\Delta D_{n50}$	Range s_{om}
2	2.25	PM	none	1.63	1.9e+31	0.8-1.6	0.005-0.016
3	2.25	PM	none	1.63		1.2-2.3	0.006-0.024
4	2.25	PM	none	1.63		1.2-3.3	0.005-0.059
6	2.25	PM	none	1.63		1.2-4.4	0.004-0.063
3*	1.25	PM	none	1.62		1.4-2.9	0.006-0.038
4	1.25	PM	none	1.62		1.2-3.4	0.005-0.059
3	2.25	narrow	none	1.63		1.0-2.8	0.004-0.054
3	2.25	wide	none	1.63		1.0-2.4	0.004-0.043
3[1]	1.25	PM	permeable	1.62		1.6-3.2	0.008-0.060
2	1.25	PM	permeable	1.62		1.5-2.8	0.007-0.056
1.5	1.25	PM	permeable	1.62		1.5-2.6	0.008-0.050
2	1.25	PM	homogeneous	1.62		1.8-3.2	0.008-0.059
2	1.25	PM	permeable	0.95		1.7-2.7	0.016-0.037
2	1.25	PM	permeable	2.05		1.6-2.5	0.014-0.032
2[2]	1.25	PM	permeable	1.62		1.6-2.5	0.014-0.031
2[3]	1.25	PM	permeable	1.62		1.4-5.9	0.010-0.046

PM Pierson Moskowitz spectrum
[1] Some tests repeated in Delta Flume
[2] Foreshore 1:30
[3] Low-crested structure with foreshore 1:30

- The core permeability in Table VI-5-4 refers to the structures shown in details *a*, *c* and *d* of Figure VI-5-11, taken from van der Meer (1988). The figure provides definition of a notational permeability parameter P which is used in various formulae by van der Meer to take into account the effect of permeability on response to wave action. The value $P = 0.4$ in Figure VI-5-11, detail *b*, is not identified by tests, but instead is an estimated value.

- The runup results from the test program described in Table VI-5-4 are presented in Figure VI-5-12.

- Note that $\xi_{om} = \tan \alpha / (2\pi H_s / g T_{om}^2)^{1/2}$, where T_{om} is the mean wave period, is used instead of ξ_{op}. By using T_{om} instead of T_{op} variations in the width of the wave spectrum are taken into account. The ratio $T_{om} / T_{op} = \xi_{om} / \xi_{op} = 0.79 - 0.87$ for Joint North Sea Wave Program (JONSWAP) spectra and 0.71 - 0.82 for Pierson-Moskowitz spectra.

- The central fit to the data for impermeable rock slopes was given by Delft Hydraulics (1989) as

$$\frac{R_{ui\%}}{H_s} = \begin{cases} A\xi_{om} & \text{for} \quad 1.0 < \xi_{om} \le 1.5 \\ B\left(\xi_{om}\right)^C & \text{for} \quad \xi_{om} > 1.5 \end{cases} \tag{VI-5-12}$$

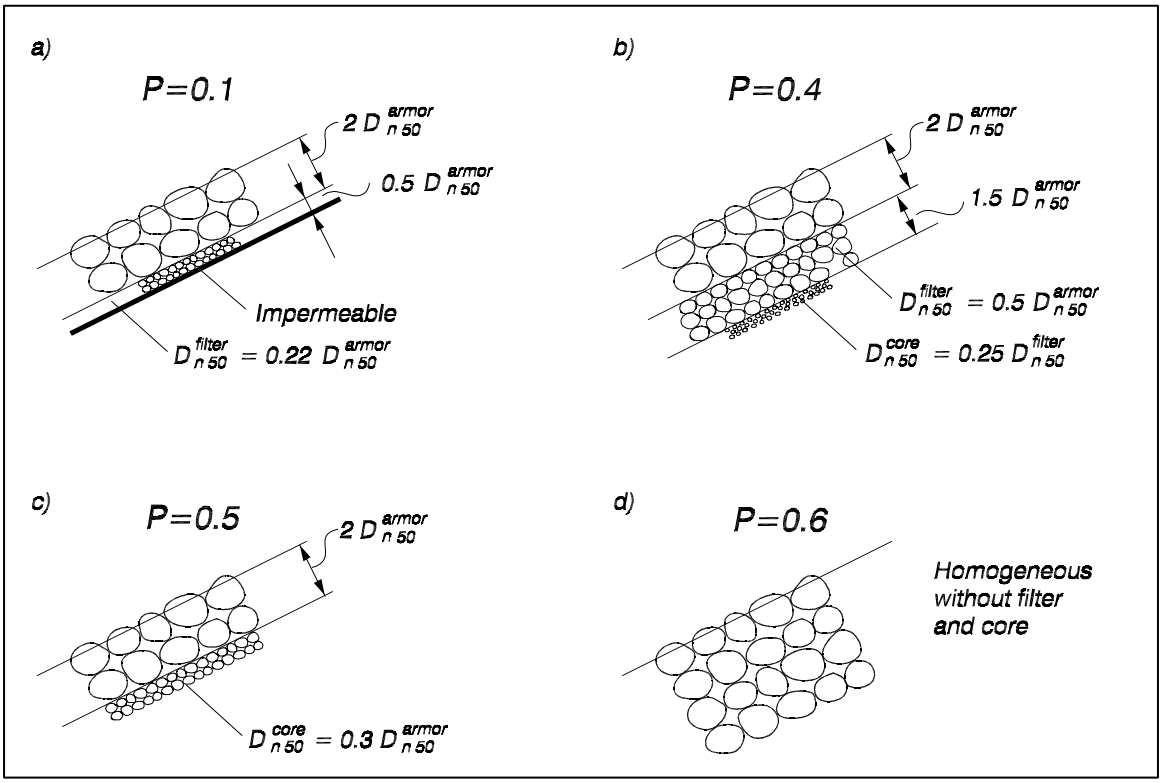

Figure VI-5-11. Notational permeability coefficients (van der Meer 1988)

- The coefficients A, B and C are given in Table VI-5-5. For impermeable slopes the coefficient of variation for A, B and C is 7 percent. Data presented by Ahrens and Heinbaugh (1988a) for maximum runup on impermeable riprap slopes are in agreement with the data represented by Equation VI-5-12.

- Equation VI-5-12 is valid for relatively deep water in front of a structure where the wave height distribution is close to the Rayleigh distribution. Wave breaking on a foreshore results in a truncation in the runup distribution which mainly results in lower runup heights for small exceedence probability levels. However, sometimes higher runup may occur according to observations in the Delft Hydraulics tests and recent tests conducted at Texas A&M University.

(4) Wave runup and rundown on permeable slopes. With respect to runup, permeable structures are defined as structures with core material of such permeability that wave induced porous flow and fluctuations of the internal phreatic line do vary with the frequencies of the waves. The storage capacity of the structure pores results in maximum runup that is smaller than for an equivalent structure with an impermeable core.

(a) Rock armored slopes, irregular long-crested head-on waves. Rock armored permeable slopes with notational permeability $P = 0.5$, as shown in detail *c* of Figure VI-5-11, were tested in irregular head-on waves by Delft Hydraulics in the program specified in Table VI-5-4. The results are shown in Figure VI-5-12, and the corresponding equation for the central fit to the data is given by

$$R_{ui\,\%}/H_s \begin{cases} = A\,\xi_{om} & \text{for } 1.0 < \xi_{om} \le 1.5 \\ = B\,(\xi_{om})^C & \text{for } 1.5 < \xi_{om} \le (D/B)^{1/C} \\ = D & \text{for } (D/B)^{1/C} \le \xi_{om} < 7.5 \end{cases} \qquad \text{(VI-5-13)}$$

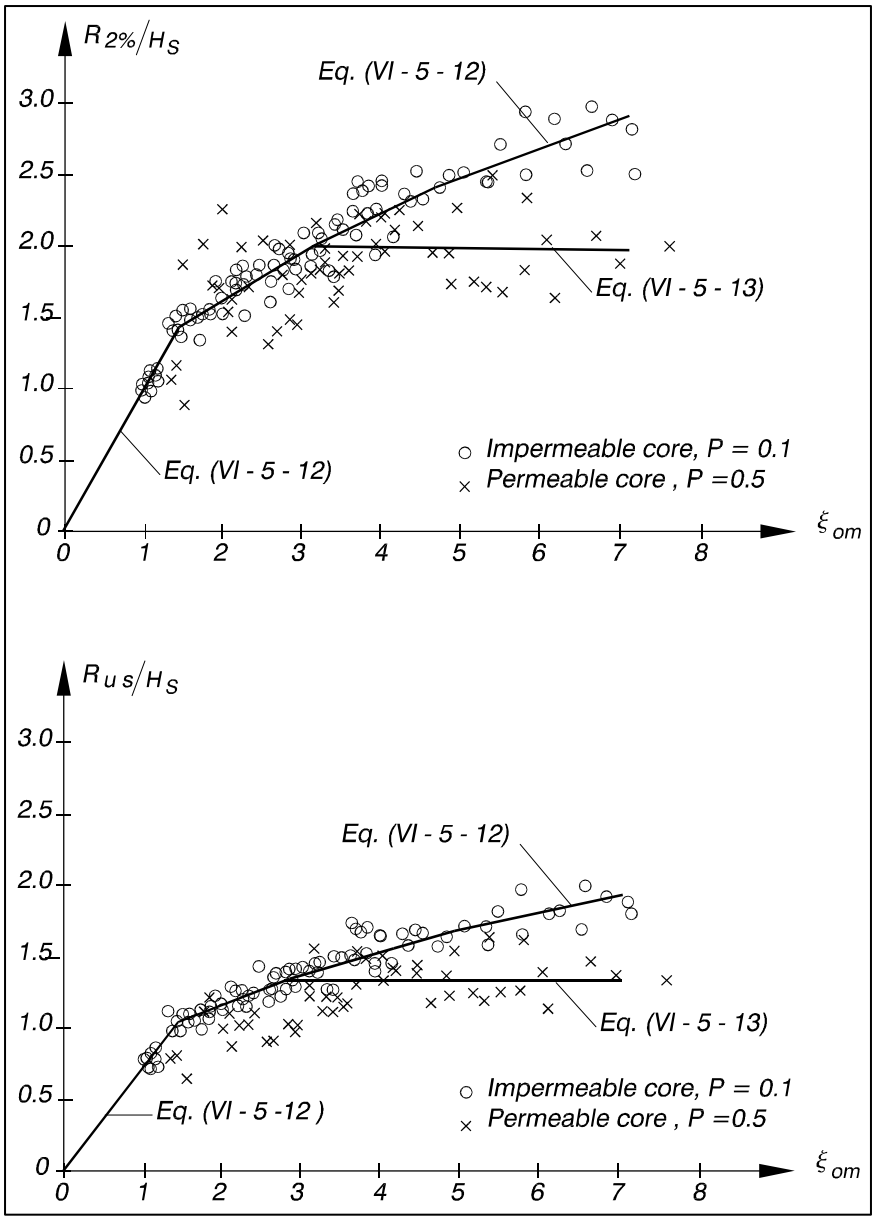

Figure VI-5-12. 2 percent and significant runup of irregular head-on waves on impermeable and permeable rock slopes. Delft Hydraulics (1989)

Table VI-5-5
Coefficients in Equations VI-5-12 and VI-5-13 for Runup of Irregular Head-On Waves on Impermeable and Permeable Rock Armored Slopes

Percent [1]	A	B	C	D [2]
0.1	1.12	1.34	0.55	2.58
2.0	0.96	1.17	0.46	1.97
5	0.86	1.05	0.44	1.68
10	0.77	0.94	0.42	1.45
(significant)	0.72	0.88	0.41	1.35
50 (mean)	0.47	0.60	0.34	0.82

[1] Exceedence level related to number of waves
[2] Only relevant for permeable slopes

- The coefficients *A*, *B*, *C* and *D* are listed in Table VI-5-5. For permeable structures the coefficient of variation for *A*, *B*, *C* and *D* is 12 percent. Tests with homogeneous rock structures with notational permeability $P = 0.6$, as shown in detail *d* of Figure VI-5-11, showed results almost similar to the test results corresponding to $P = 0.5$ as shown in Figure VI-5-12.

- Equation VI-5-13 is valid for relatively deepwater conditions with wave height distributions close to a Rayleigh distribution. Wave breaking due to depth limitations in front of the structure cause truncation of the runup distribution and thereby lower runup heights for small exceedence probability levels. However, higher runup might also occur according to observations in the Delft Hydraulics tests, van der Meer and Stam (1992). The influence on runup for the shallow-water conditions included in the test program given in Table VI-5-4 were investigated for the rock armored permeable slope. However, no systematic deviations from Equation VI-5-13 were observed.

(b) Statistical distribution of runup. The runup of waves with approximately Rayleigh distributed wave heights on rock armored permeable slopes with $\tan \alpha \exists 2$ were characterized by van der Meer and Stam (1992) with a best-fit two-parameter Weibull distribution as follows:

$$Prob\left(R_u > R_{up\%}\right) = \exp\left[-\left(\frac{R_{up\%}}{B}\right)^C\right] \text{ or} \tag{VI-5-14}$$

$$R_{up\%} = B\left(-\ln p\right)^{1/C} \tag{VI-5-15}$$

where

$R_{up\%}$ = Runup level exceeded by p % of the runup

$$B = H_s\left[0.4\left(s_{om}\right)^{-1/4}\left(\cot\alpha\right)^{-0.2}\right] \tag{VI-5-16}$$

$$C = \begin{cases} 3.0\left(\xi_{om}\right)^{-3/4} & \text{for} \quad \xi_{om} \le \xi_{omc} \left(\text{plunging waves}\right) \\ 0.52P^{-0.3}\left(\xi_{om}\right)^{P}\sqrt{\cot\alpha} & \text{for} \quad \xi_{om} > \xi_{omc} \left(\text{surging waves}\right) \end{cases} \tag{VI-5-17}$$

$$\xi_{omc} = \left(5.77P^{0.3}\sqrt{\tan\alpha}\right)^{\left[1/(P+0.75)\right]} \tag{VI-5-18}$$

$$s_{om} = \frac{2\pi H_s}{gT_{om}^2}$$

P = notational permeability, see Figure VI-5-11.

- It follows from Equation VI-5-15 that the scale parameter B is equal to $Ru_{37\,\%}$ ($\ln p = -1$ for $p = 0.37$). If the shape parameter C is equal to 2, then Equation VI-5-14 becomes a Rayleigh distribution. The uncertainty on B corresponds to a coefficient of variation of 6 percent for $P < 0.4$ and 9 percent for $P \ge 0.4$.

- Rundown on rock slopes in the Delft Hydraulics test program listed in Table VI-5-4 gave the following relationship which includes the effect of structure permeability P (see Figure VI-5-11).

$$\frac{R_{d\,2\%}}{H_s} = 2.1\sqrt{\tan\alpha} - 1.2P^{0.15} + 1.5e^{-(60s_{om})} \tag{VI-5-19}$$

b. Wave overtopping of structures. Wave overtopping occurs when the highest runup levels exceed the crest freeboard, R_c as defined in Figure VI-5-13. The amount of allowable overtopping depends on the function of the particular structure. Certain functions put restrictions on the allowable overtopping discharge. For example access roads and installations placed on the crest of breakwaters and seawalls, berths for vessels as well as reclaimed areas containing roadways, storage areas, and buildings located just behind the breakwater are overtopping design considerations. Design criteria for overtopping should include two levels: Overtopping during normal service conditions and overtopping during extreme design conditions where some damage to permanent installations and structures might be allowed. Very heavy overtopping might be allowed where a breakwater has no other function than protection of harbor entrances and outer basins from waves. However, significant overtopping can create wave disturbances which could lead to damage of moored vessels. Fortunately, waves generated by overtopping usually have much shorter periods than the incident wave train.

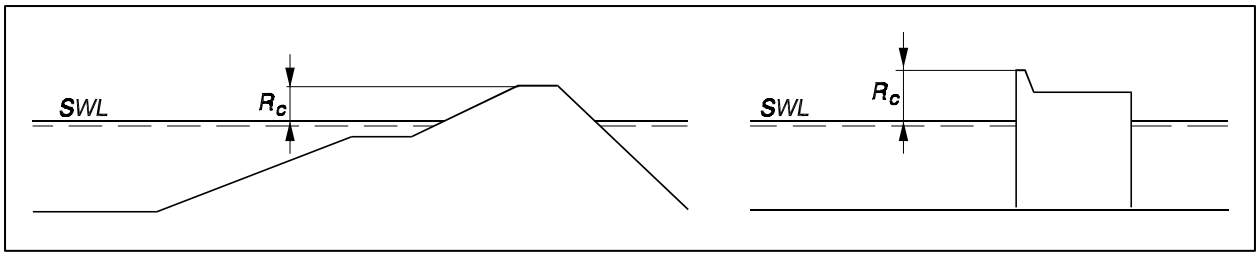

Figure VI-5-13. Definition of crest freeboard, R_c

(1) Admissible average overtopping discharge.

(a) The overtopping discharge from wind-generated waves is very unevenly distributed in time and space because the amount varies considerably from wave to wave. The major part of the overtopping discharge during a storm is due to a small fraction of the waves. In fact the local overtopping discharge (in m^3/s per meter structure) from a single wave can be more than 100 times the average overtopping discharge during the storm peak. Nevertheless, most information on overtopping is given as the time averaged overtopping discharge, q, expressed in m^3/s per meter of structure length. However, some limited information exists on the probability distribution of the volume of overtopping water per wave.

(b) Field studies of tolerable overtopping limits of dikes and revetments have been performed by Tsuruta and Goda (1968), Goda (1970), and Fukuda, Uno, and Irie (1974). Some critical values for overtopping of a breakwater were discussed by Jensen (1984), and Dutch Guidelines on river dikes indicated allowable overtopping rates for inner slopes. Delft Hydraulics tested admissible overtopping rates for grass dikes (Smith, Seijffert, and van der Meer 1994). De Gerloni et al. (1991), and Franco, de Gerloni, and van der Meer (1994) studied the effect of falling water jets on a person, simulating the conditions on breakwater crests. Endoh and Takahashi (1994) performed full-scale tests as well as numerical modeling of overtopping rates which endanger people.

(c) The information from these various studies is condensed in Table VI-5-6, which presents critical values of the average overtopping discharge, q. The values given in this table must be regarded only as rough guidelines because, even for the same value of q, the intensity of water hitting a specific location is very much dependent on the geometry of the structure and the distance from the front of the structure. The maximum intensities might locally be up to two orders of magnitude larger than the value of q. Moreover, what is regarded as acceptable conditions is to a large extent a matter of local traditions and individual opinions.

Table VI-5-6
Critical Values of Average Overtopping Discharges

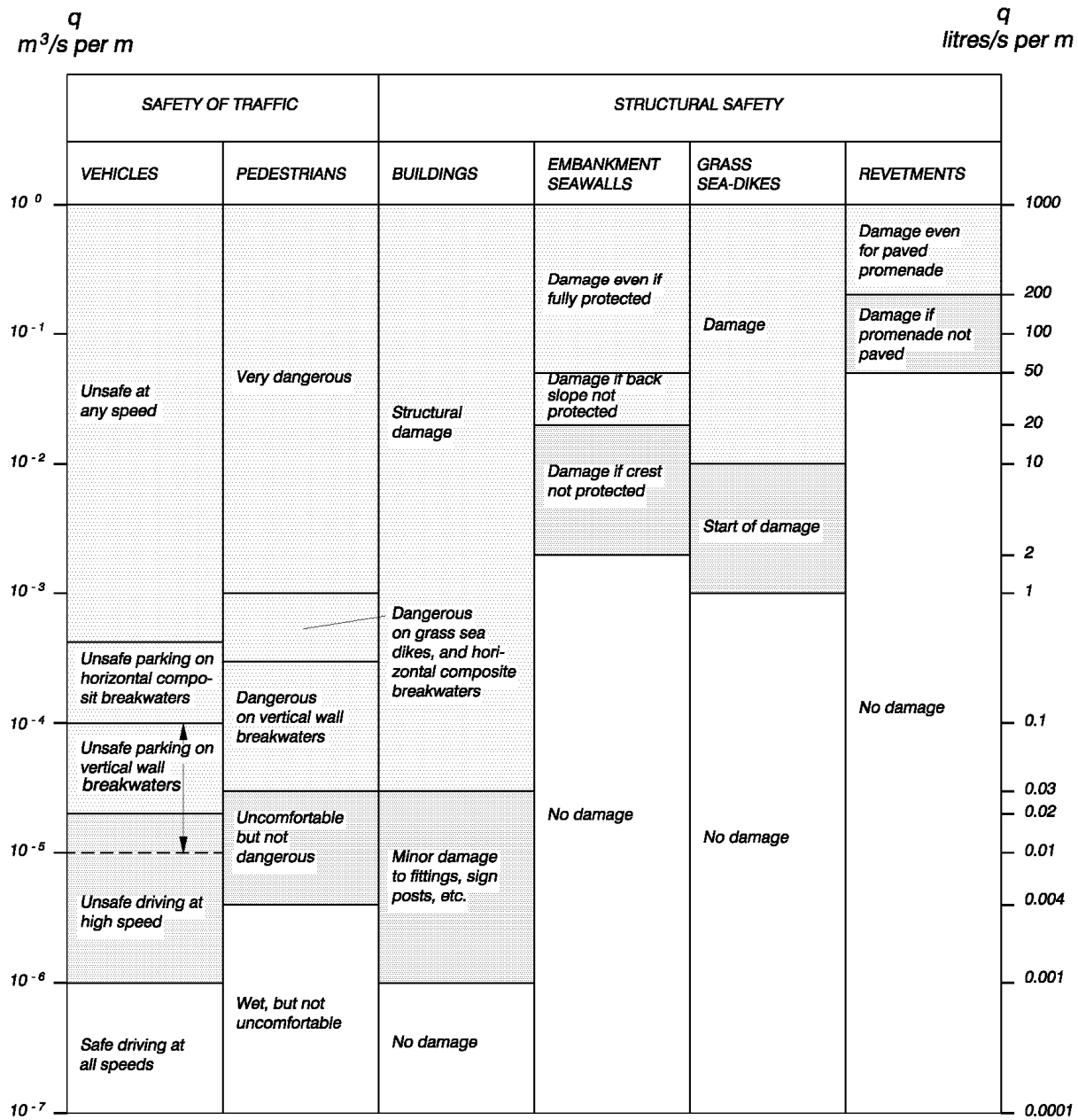

(d) The wind can carry spray long distances whereas solid (green) water is practically unaffected by the wind. It is important to consider spray because it can cause damage to goods placed on storage areas and can cause icing of vessel superstructures in cold regions.

(e) Overtopping occurs only if the runup level exceeds the freeboard, R_c, of the structure. Figure VI-5-14 shows the notation used to describe profile geometry for several structure types.

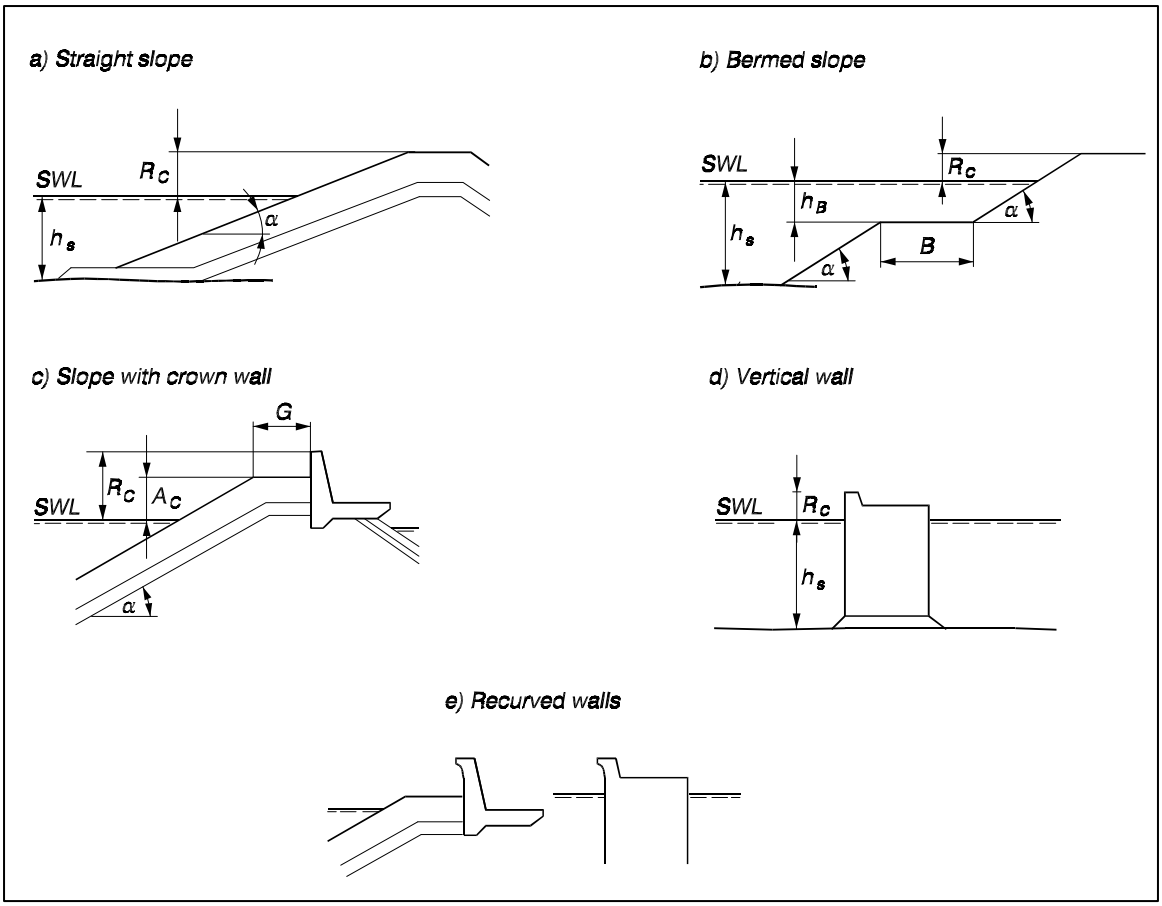

Figure VI-5-14. Structure profile geometrical parameters related to overtopping

(f) The relative freeboard, R_c / H_s, is a simple, but very important, dimensionless parameter for the prediction of overtopping. However, the wave period or wave steepness is also a significant parameter as are geometric parameters related to structure permeability, porosity and surface roughness. Under certain conditions a recurved wave wall as shown in Figure VI-5-14 e is effective in reducing overtopping. For small values of R_c / H_s (< 0.3) when the overtopping is excessive, the detailed geometry of the crest part of the structure becomes less important because the waves just travel over the structure.

(2) Average overtopping discharge formulas.

(a) Sloping structures. Formulae for overtopping are empirical because they are fitted to hydraulic model test results for specific breakwater geometries. In general the average overtopping discharge per unit length of structure, q, is a function of the standard parameters:

$$q = \text{function}\left(H_s, T_{op}, \sigma, \beta, R_c, h_s, g, \text{structure geometry}\right)$$

where

H_s = significant wave height

T_{op} = wave period associated with the spectral peak in deep water (alternately T_{om})

σ = spreading of short-crested waves

β = angle of incidence for the waves

R_c = freeboard

h_s = water depth in front of structure

g = gravitational acceleration

Two types of mathematical formulatons (models) for dimensionless overtopping dominate the literature, i.e.,

$$Q = a_e^{-(bR)} \tag{VI-5-20}$$

and

$$Q = aR^{-b} \tag{VI-5-21}$$

where Q is a dimensionless average discharge per meter and R is a dimensionless freeboard. Table VI-5-7 gives an overview of the models used in recent overtopping formulae along with the associated definitions for dimensionless discharge and freeboard.

(b) The fitted coefficients a and b in Equations VI-5-20 and VI-5-21 are specific to the front geometry of the structure and must be given in tables. So far no general model for the influence of front geometry exists except for rubble-mound slopes with a seawall (Pedersen 1996), in which case the front geometry (described by the front berm width B, berm crest height A_c , and slope angle α), as well as R_c, enters into R.

(c) Some formulae take into account the reduction in overtopping due to slope surface roughness, berm, shallow water, angle of wave incidence and shortcrestedness, and specific front geometries by dividing R by the respective reduction coefficients: γ_r (Table VI-5-3), γ_b (Equation VI-5-8), γ_h (Equation VI-5-10), γ_β (Equations VI-5-11, VI-5-26, VI-5-29), and γ_s (Table VI-5-13).

(d) Goda (1985) presented diagrams for wave overtopping of vertical revetments and block-mound seawalls on bottom slopes of 1:10 and 1:30. The diagrams are based on model tests with irregular long-crested head-on waves and express average discharge per meter width as a function of wave height, wave steepness, freeboard, and water depth.

- Sloping structures. Tables VI-5-8 to VI-5-12 pertain to sloping-front structures.

- Figure VI-5-15 shows the data basis for Equations VI-5-24 and VI-5-25 which includes the data of Owen (1980, 1982) for straight slopes, data of Führböter, Sparboom, and

Witte (1989) and various data sets of Delft Hydraulics. It is seen that Equation VI-5-24 contains some bias for small values of q.

- Vertical front structures.

– Figure VI-5-16 shows the data used to establish Equation VI-5-28. Appropriate values of γ_β from Table VI-5-13 were used in plotting Figure VI-5-16; however γ_s was taken as unity (plain impermeable wall).

Table VI-5-7
Models for Average Overtopping Discharge Formulae

Authors	Structures	Overtopping model	Dimensionless discharge Q	Dimensionless freeboard R
Owen (1980,1982)	Impermeable smooth, rough, straight and bermed slopes	$Q = a\ exp(-b\,R)$	$\frac{q}{g\,H_s\,T_{om}}$	$\frac{R_c}{H_s}\left(\frac{s_{om}}{2\,\pi}\right)^{0.5}\frac{1}{\gamma}$
Bradbury and Allsop (1988)	Rock armored impermeable slopes with crown walls	$Q = a\ R^{-b}$	$\frac{q}{g\,H_s\,T_{om}}$	$\left(\frac{R_c}{H_s}\right)^2\left(\frac{s_{om}}{2\,\pi}\right)^{0.5}$
Aminti and Franco (1988)	Rock, cube, and Tetrapod double layer armor on rather impermeable slopes with crown walls, (single sea state)	$Q = a\ R^{-b}$	$\frac{q}{g\,H_s\,T_{om}}$	$\left(\frac{R_c}{H_s}\right)^2\left(\frac{s_{om}}{2\,\pi}\right)^{0.5}$
Ahrens and Heimbaugh (1988b)	7 different seawall/revetment designs	$Q = a\,exp(-b\,R)$	$\frac{q}{\sqrt{g\,H_s^3}}$	$\frac{R_c}{(H_s^2\,L_{op})^{1/3}}$
Pedersen and Burcharth (1992)	Rock armored rather impermeable slopes with crown walls	$Q = a\,R$	$\frac{q\,T_{om}}{L_{om}^2}$	$\frac{H_s}{R_c}$
van der Meer and Janssen (1995)	Impermeable smooth, rough straight and bermed slopes	$Q = a\,exp(-b\,R)$	$\frac{q}{\sqrt{g\,H_s^3}}\sqrt{\frac{s_{op}}{\tan\alpha}}$ for $\xi_{op} < 2$	$\frac{R_c}{H_s}\frac{\sqrt{s_{op}}}{\tan\alpha}\frac{1}{\gamma}$ for $\xi_{op} < 2$
			$\frac{q}{\sqrt{g\,H_s^3}}$ for $\xi_{op} > 2$	$\frac{R_c}{H_s}\frac{1}{\gamma}$ for $\xi_{op} > 2$
Franco et al. (1994)	Vertical wall breakwater with and without perforated front	$Q = a\,exp(-b\,R)$	$\frac{q}{\sqrt{g\,H_s^3}}$	$\frac{R_c}{H_s}\frac{1}{\gamma}$
Pedersen (1996)	Rock armored permeable slopes with crown walls	$Q = R$	$\frac{q\,T_{om}}{L_{om}^2}$	$3.2\cdot 10^{-5}\frac{H_s^5\,\tan\alpha}{R_c^3\,A_c\cdot B}$

Table VI-5-8
Overtopping Formula by Owen (1980, 1982)

Straight and bermed impermeable slopes, Figures VI-5-14 *a* and *b*.
Irregular, head–on waves.

$$\frac{q}{g\,H_s\,T_{om}} = \mathbf{a}\;exp\left(-\mathbf{b}\;\frac{R_c}{H_s}\sqrt{\frac{s_{om}}{2\,\pi}}\;\frac{1}{\gamma_r}\right) \qquad (\text{VI}-5-22)$$

Coefficients in Eq VI-5-22
Straight smooth slopes.
Non-depth limited waves.

Slope	**a**	**b**
1 : 1	0.008	20
1 : 1.5	0.010	20
1 : 2	0.013	22
1 : 3	0.016	32
1 : 4	0.019	47

Surface roughness reduction factor γ_r.
Updated γ_r-values are given in Table VI-5-3.

Smooth impermeable (including smooth concrete and asphalt)	1.0
One layer of stone rubble on impermeable base	0.8
Gravel, gabion mattresses	0.7
Rock riprap with thickness greater than $2\,D_{n50}$	0.5 - 0.6

Coefficients in Eq VI-5-22
Bermed smooth slopes.
Non-depth limited waves.

Slope	h_B (m)	B (m)	$\mathbf{a}\cdot 10^4$	**b**
1 : 1	−4.0	10	64	20
1 : 2			91	22
1 : 4			145	41
1 : 1	−2.0	5	34	17
1 : 2			98	24
1 : 4			159	47
1 : 1	−2.0	10	48	19
1 : 2			68	24
1 : 4			86	46
1 : 1	−2.0	20	8.8	15
1 : 2			20	25
1 : 4			85	50
1 : 1	−2.0	40	3.8	23
1 : 2			5.0	26
1 : 4			47	51
1 : 1	−1.0	5	155	33
1 : 2			190	37
1 : 4			500	70
1 : 1	−1.0	10	93	39
1 : 2			340	53
1 : 4			300	80
1 : 1	−1.0	20	75	46
1 : 2			34	50
1 : 4			39	62
1 : 1	−1.0	40	12	49
1 : 2			24	56
1 : 4			1.5	63
1 : 1	0	10	97	42
1 : 2			290	57
1 : 4			300	80

Table VI-5-9
Overtopping Formula by Bradbury and Allsop (1988)

Straight rock armored slope with berm in front of crown wall, Figure VI-5-14c. Slope 1:2. Impermeable membrane at various depths as shown in the following figure. Berm width G is three or six stone diameters. Irregular, head–on waves.

$$\frac{q}{g\,H_s\,T_{om}} = \mathbf{a}\left[\left(\frac{R_c}{H_s}\right)^2 \sqrt{\frac{s_{om}}{2\,\pi}}\right]^{-\mathbf{b}} \qquad \text{(VI–5–23)}$$

Coefficients in Eq VI-5-23. Non–depth limited waves.

Note: "a" coefficients are shown multiplied by 10^9. For example, a value of 6.7 in the table represents $6.7(10)^{-9}$.

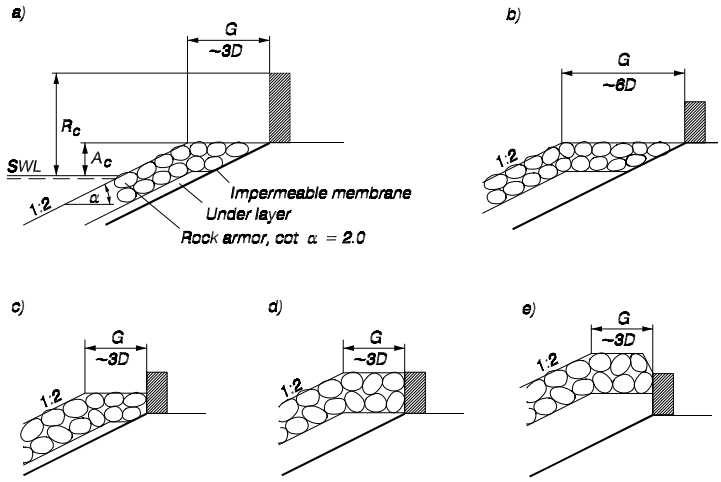

Section	G/H_s	G/R_c	A/R_c	$a \cdot 10^9$	b
a	0.79 - 1.7	0.75	0.28	6.7	3.5
		0.58	0.21	3.6	4.4
		1.07	0.39	5.3	3.5
		0.88	0.32	1.8	3.6
b	1.6 - 3.3	2.14	0.39	1.0	2.8
c	0.79 - 1.7	1.07	0.71	1.6	3.2
d	0.79 - 1.7	1.07	1.00	0.37	2.9
e	0.79 - 1.7	0.83	1.00	1.30	3.8

Table VI-5-10
Coefficients by Aminti and Franco (1988) for Overtopping Formula by Bradbury and Allsop in Table VI-5-9

Straight slope with berm in front of crown wall, Figure VI-5-14c. Rock, cube, and tetrapod armor on rather impermeable core. Only one sea state tested (JONSWAP spectrum). Non–depth limited waves. Irregular, head–on waves.

Note: "a" coefficients are shown multiplied by 10^8. For example, a value of 17 in the table represents $17(10)^{-8}$.

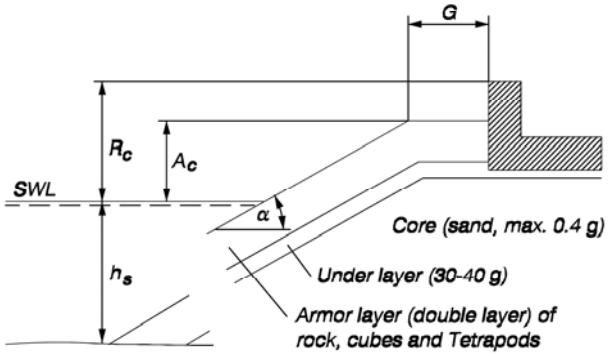

Tested ranges:
H_s = 0.136 m
T_{om} = 1.33 s
S_{om} = 0.05
h_s / H_s = 2.9
cot α 1.33 , 2.0
R_c / H_s 0.6 - 2.0
A_c / H_s 0.6 , 0.75 , 1.05
G / H_s 1.1 , 1.85 , 2.6 corresponding to width of 3, 5 and 7 stone diameters.

ARMOR	cot	G/H_s	$a \cdot 10^8$	b
ROCK	2.00	1.10	17	2.41
		1.85	19	2.30
		2.60	2.3	2.68
	1.33	1.10	5.0	3.10
		1.85	6.8	2.65
		2.60	3.1	2.69
CUBES	2.00	1.10	8.3	2.64
		1.85	15	2.43
		2.60	84	2.38
	1.33	1.10	62	2.20
		1.85	17	2.42
		2.60	1.9	2.82
TETRAPODS	2.00	1.10	1.9	3.08
		1.85	1.3	3.80
		2.60	1.1	2.86
	1.33	1.10	5.6	2.81
		1.85	1.7	3.02
		2.60	0.92	2.98

Table VI-5-11
Overtopping Formula by van der Meer and Janssen (1995)

Straight and bermed impermeable slopes including influence of surface roughness, shallow foreshore, oblique, and short-crested waves, Figures VI-5-14a and VI-5-14b.

$\underline{\xi_{op} < 2}$

$$\frac{q}{\sqrt{g\,H_s^3}}\sqrt{\frac{s_{op}}{\tan\alpha}} = 0.06\,exp\left(-5.2\,\frac{R_c}{H_s}\,\frac{\sqrt{s_{op}}}{\tan\alpha}\,\frac{1}{\gamma_r\,\gamma_b\,\gamma_h\,\gamma_\beta}\right) \qquad \text{(VI}-5-24\text{)}$$

application range: $0.3 < \dfrac{R_c}{H_s}\,\dfrac{\sqrt{s_{op}}}{\tan\alpha}\,\dfrac{1}{\gamma_r\,\gamma_b\,\gamma_h\,\gamma_\beta} < 2$

Uncertainty: Standard deviation of factor 5.2 is $\sigma = 0.55$ (See Figure VI-5-15).

$\underline{\xi_{op} > 2}$

$$\frac{q}{\sqrt{g\,H_s^3}} = 0.2\,exp\left(-2.6\,\frac{R_c}{H_s}\,\frac{1}{\gamma_r\,\gamma_b\,\gamma_h\,\gamma_\beta}\right) \qquad \text{(VI}-5-25\text{)}$$

Uncertainty: Standard deviation of factor 2.6 is $\sigma = 0.35$ (See Figure VI-5-15).

The reduction factors references are

γ_r Table VI-5-3

γ_b Eq VI-5-8

γ_h Eq VI-5-10

$$\left.\begin{array}{l}\text{Short-crested waves}\\ \gamma_\beta = 1 - 0.0033\,\beta\\ \text{Long-crested waves (swell)}\\ \gamma_\beta = \begin{cases} 1.0 & \text{for } 0^\circ \le \beta \le 10^\circ \\ \cos^2(\beta - 10^\circ) & \text{for } 10^\circ < \beta \le 50^\circ \\ 0.6 & \text{for } \beta > 50^\circ \end{cases}\end{array}\right\} \qquad \text{(VI}-5-26\text{)}$$

The minimum value of any combination of the γ-factors is 0.5.

Table VI-5-12
Overtopping Formula by Pedersen and Burcharth (1992), Pedersen (1996)

Rock armored permeable slopes with a berm in front of a crown wall, Figure VI-5-14c. Irregular, head-on waves.

$$\frac{qT_{om}}{L_{om}^2} = 3.2 \cdot 10^{-5} \left(\frac{H_s}{R_c}\right)^3 \frac{H_s^2}{A_c\, B\, \cot\alpha} \qquad \text{(VI−5−27)}$$

Notational permeability $P = 0.4$.

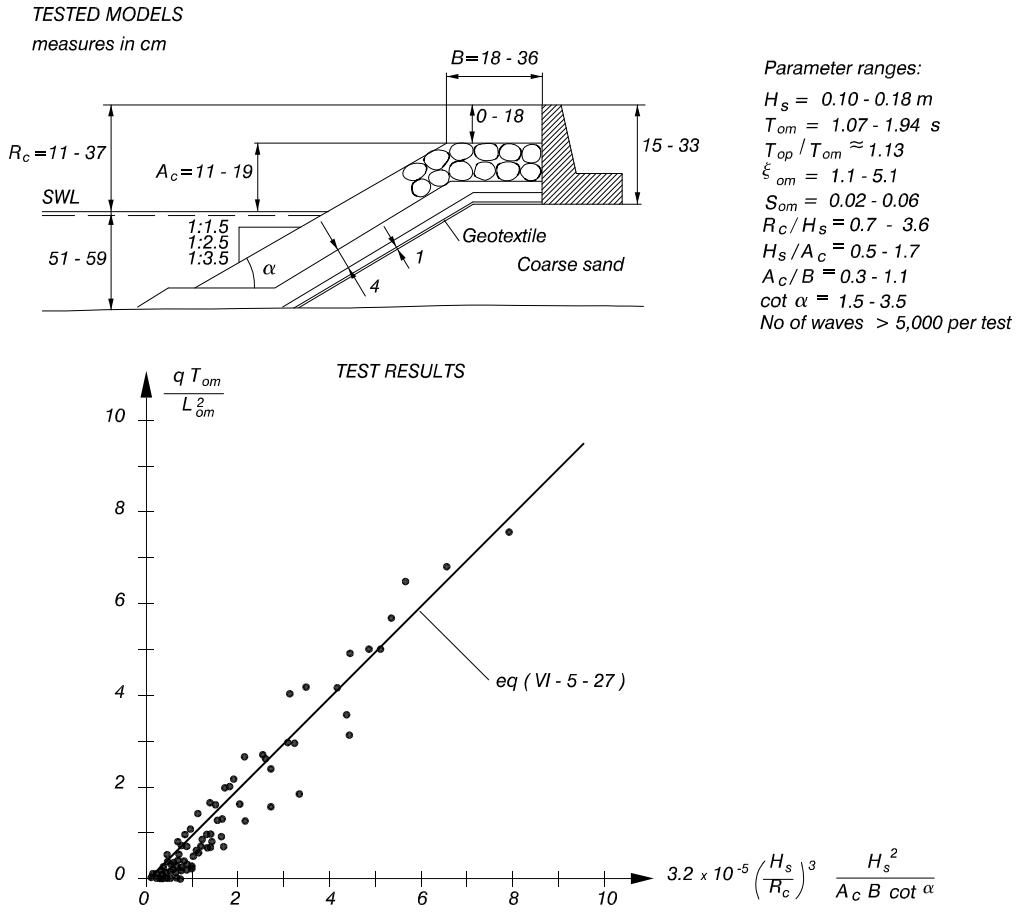

Some conservative bias of Eq VI-5-27 for small values of q is observed.

Table VI-5-13
Overtopping Formula by Franco and Franco (1999)

Impermeable and permeable vertical walls. Non-breaking, oblique, long- and short-crested waves.

$$\frac{q}{\sqrt{gH_s^3}} = 0.082 \exp\left(-3.0 \frac{R_c}{H_s} \frac{1}{\gamma_\beta \gamma_s}\right) \qquad \text{(VI−5−28)}$$

Uncertainty: Standard deviation of factor 3.0 = 0.26 (see Figure VI-5-16).

Tested range:

H_s = 12.5 – 14.0 cm
s_{op} = 0.04 (wave steepness)
$\beta = 0° - 60°$ (angle of incidence)
σ = app. 22° and app. 28° (directional spreading)
R_c/H_s = 1.2 and 1.6
h_s/H_s = app. 4.4
h_b/h_s = 0.21

Tested cross sections:

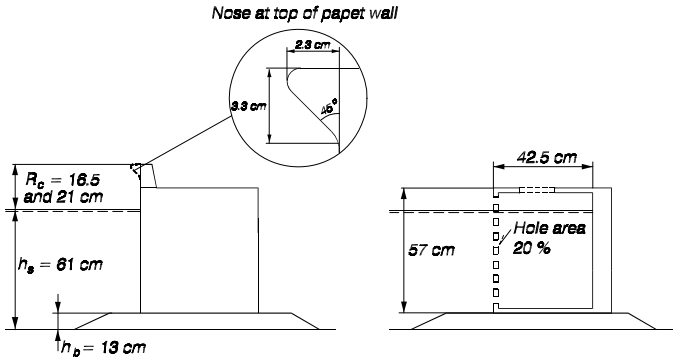

$$\gamma_\beta = \begin{cases} \left.\begin{array}{ll} \cos\beta & \text{for } 0° \le \beta \le 37° \\ 0.79 & \text{for } \beta > 37° \end{array}\right\} \text{Long-crested waves} \\ \\ \left.\begin{array}{ll} 0.83 & \text{for } 0° \le \beta \le 20° \\ 0.83\cos(20° - \beta) & \text{for } \beta > 20° \end{array}\right\} \begin{array}{l} \text{Short-crested waves} \\ \sigma = 22° \text{ and } 28° \end{array} \end{cases} \qquad \text{(VI−5−29)}$$

Front geometry	γ_s
Plain impermeable wall	1.00
Plain impermeable wall with recurved nose	0.78
Perforated front (20% hole area) and deck	0.72 – 0.79
Perforated front (20% hole area) and open deck	0.58

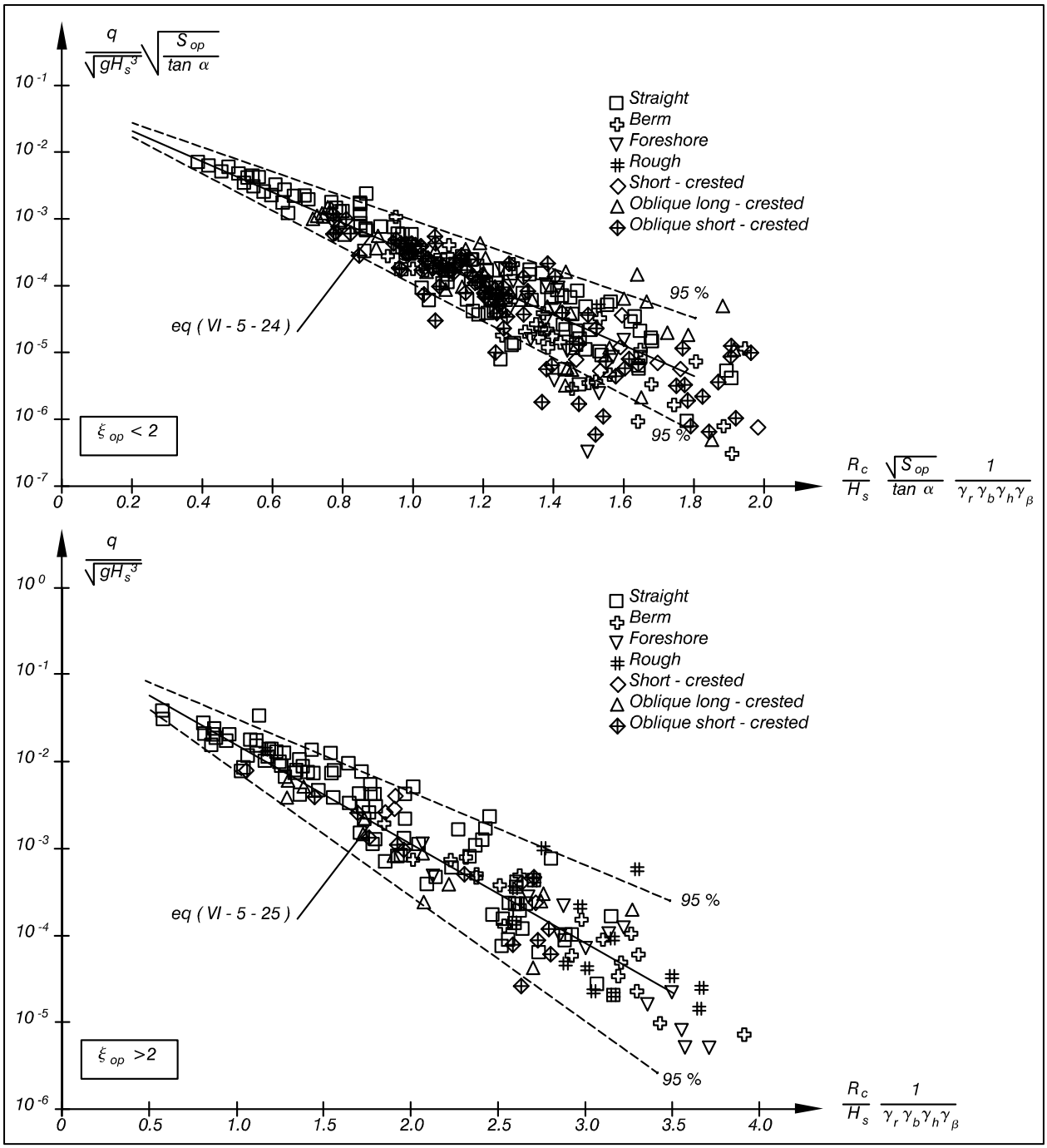

Figure VI-5-15. Wave overtopping data as basis for Equations VI-5-24 and VI-5-25. Fitted mean and 95 percent confidence bands (van dere Meer and Janssen 1995)

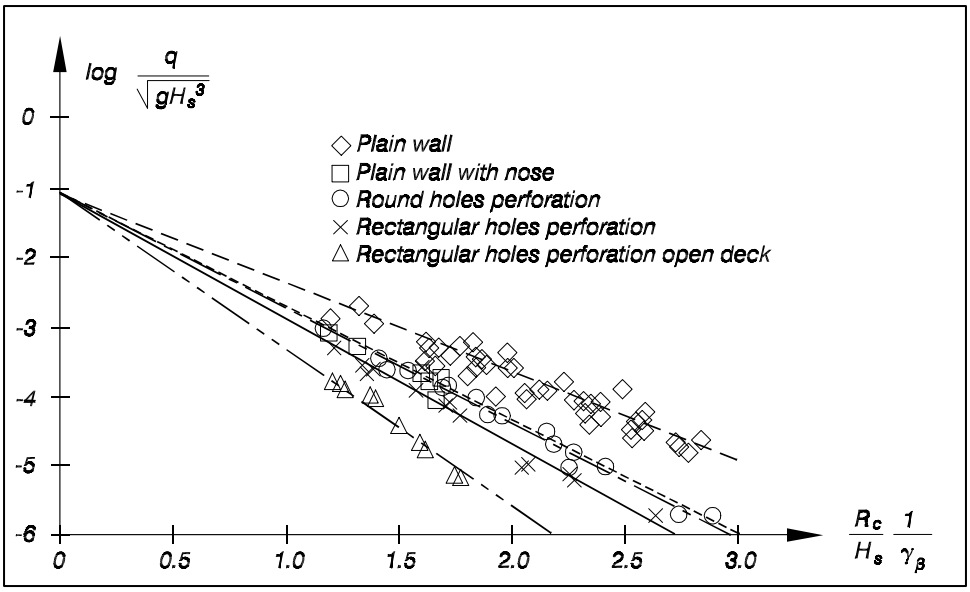

Figure VI-5-16. Vertical wall wave overtopping data plotted with $\gamma_s = 1.0$ (Franco and Franco 1999)

– Figure VI-5-17 shows the same vertical wall overtopping data plotted with appropriate values of γ_β and γ_s from Table VI-5-13. The solid line is Equation VI-5-28.

(3) Overtopping volumes of individual waves. The average overtopping discharge q provides no information about the discharge intensity of the individual overtopping waves. However, such information is important because most damaging impacts on persons, vehicles, and structures are caused by overtopping of large single waves. The overtopping volume per wave has been recorded in model tests and it was found that the probability distribution function for overtopping volume per wave per unit width (V m^3/m) follows a Weibull distribution as given in Equation VI-5-30 (Franco, de Gerloni, and van der Meer 1994; van der Meer and Jansson 1995).

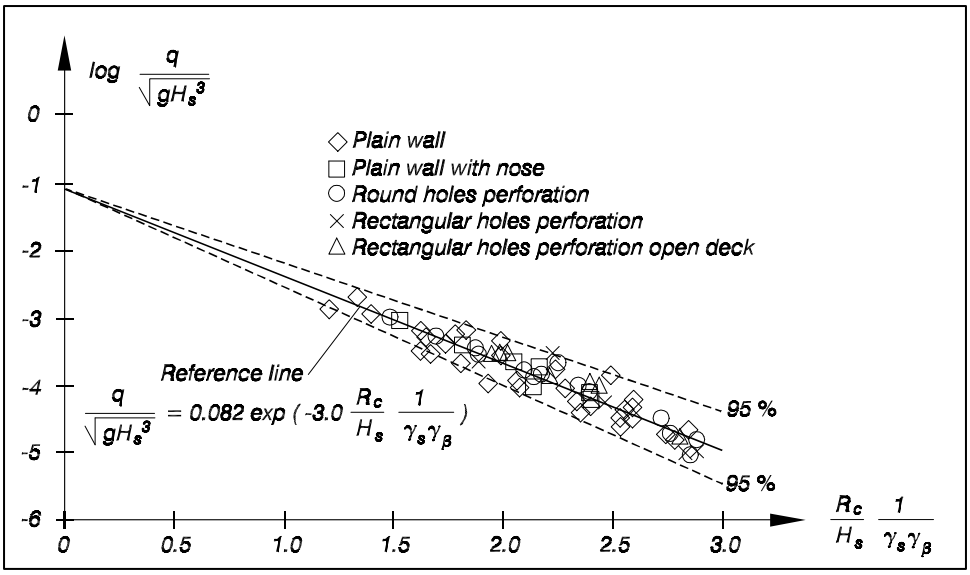

Figure VI-5-17. Vertical wall wave overtopping data with fitted mean and 95 percent confidence bands (Franco and Franco 1999)

$$prob\left(v > V\right) = \exp\left[-\left(\frac{V}{B}\right)^{3/4}\right] \text{ or} \tag{VI-5-30}$$

$$V = B\left(-\ln\left[prob\left(v > V\right)\right]\right)^{4/3} \tag{VI-5-31}$$

with

$$B = 0.84\frac{T_m q}{P_{ow}} \tag{VI-5-32}$$

where

$prob(v > V)$ = probability of individual wave overtopping volume per unit width, v, being larger than the specified overtopping volume per unit width, V

T_m = average wave period (in units of seconds)

q = average overtopping discharge per unit width (in units of m^3/s per m)

P_{ow} = probability of overtopping per incoming wave (= N_{ow} / N_w)

N_{ow} = number of overtopping waves

N_w = number of incoming waves

If the runup levels follow a Rayleigh distribution, the probability of overtopping per incoming wave can be estimated as

$$P_{ow} = \exp\left[-\left(\frac{R_c}{cH_s}\right)^2\right] \quad \text{(VI-5-33)}$$

where

For sloping structure, irregular waves:
$c = 0.81\,\xi_{eq}\,\gamma_r\,\gamma_h\,\gamma_\beta$ with a maximum of $c = 1.62\,\gamma_r\,\gamma_h\,\gamma_\beta$
For vertical wall structure, irregular, impermeable, long-crested, nonbreaking, head-on waves:
$c = 0.91$ (VI-5-34)

and

R_c = structure crest height relative to swl

H_s = significant wave height

A first estimate of the maximum overtopping volume per unit width produced by one wave out of the total number of overtopping waves can be calculated using the expression

$$V_{\max} = B\left(\ln N_{ow}\right)^{4/3} \quad \text{(VI-5-35)}$$

c. Wave reflection.

(1) Introduction.

(a) Coastal structures reflect some proportion of the incident wave energy. If reflection is significant, the interaction of incident and reflected waves can create an extremely confused sea with very steep waves that often are breaking. This is a difficult problem for many harbor entrance areas where steep waves can cause considerable maneuvering problems for smaller vessels. Strong reflection also increases the sea bed erosion potential in front of protective structures. Waves reflected from some coastal structures may contribute to erosion of adjacent beaches.

(b) Non-overtopped impermeable smooth vertical walls reflect almost all the incident wave energy, whereas permeable, mild slope, rubble-mound structures absorb a significant portion of the energy. Structures that absorb wave energy are well suited for use in harbor basins.

(c) In general incident wave energy can be partly dissipated by wave breaking, surface roughness and porous flow; partly transmitted into harbor basins due to wave overtopping and penetration; and partly reflected back to the sea, i.e.

$$E_i = E_d + E_t + E_r \tag{VI-5-36}$$

where E_i , E_d , E_t , and E_r are incident, dissipated, transmitted, and reflected energy, respectively.

(d) Reflection can be quantified by the bulk reflection coefficient

$$C_r = \frac{H_{sr}}{H_s} = \left(\frac{E_r}{E_i} \right)^{1/2} \tag{VI-5-37}$$

where H_s and H_{sr} are the significant wave heights of incident and reflected waves, respectively, at that position; and E_i and E_r are the related wave energies.

(2) Reflection from non-overtopped sloping structures.

(a) Very long waves such as infragravity and tidal waves are almost fully reflected by any type of impervious structure. Wind-generated waves generally break on slopes (see Table VI-5-1) with the type of wave breaking given as a function of the surf-similarity parameter ξ, defined by Equation VI-5-2. Wave energy dissipation by wave breaking is much greater than dissipation due to surface roughness and porous flow for conventional coastal structures. Therefore, it is relevant to relate the bulk reflection coefficient, C_r, to ξ, (Battjes 1974b; Seelig 1983).

(b) The bulk reflection coefficient for straight non-overtopped impermeable smooth slopes and conventional rubble-mound breakwaters can be estimated from Equation VI-5-38 (Seelig 1983) given in Table VI-5-14. Figure VI-5-18 shows the fitting of the model test results by Allsop and Hettiarachichi (1988). Some scatter in the fitting can be seen.

Table VI-5-14
Wave Reflection Coefficients for Non-Overtopped Sloping Structures Based on Seelig (1983) Equation

Head-on waves

$$C_r = \frac{a\,\xi^2}{(b+\xi^2)} \qquad \xi = \frac{\tan\alpha}{\sqrt{\frac{2\pi H}{gT^2}}} \qquad \text{(VI–5–38)}$$

For irregular wave H is replaced by H_s, T is replaced either by T_p (ξ_{op}) or T_m (ξ_{om}).

Fitted coefficients in Eq VI-5-38

Author	Structure	a	b
Seelig (1983) $2.5 \le \xi \le 6$	Impermeable, smooth, straight slopes, regular waves	1.0	5.5
Allsop and Hettiarachchi (1988) range of ξ or ξ_{op} shown in Figure VI-5-18	Dolosse, regular waves (ξ) Slope 1:1.5, 1:2, 1:3	0.56	10.0
	Cobs, regular waves (ξ) Slope 1:1.5, 1:2, 1:3	0.50	6.54
	Tetrapods and Stabit, irregular waves (ξ_{om}) Slope 1:1.33, 1:1.5, 1:2	0.48	9.62
	Shed and Diode, irregular waves (ξ_{om}) Slope 1:1.33, 1:1.5, 1:2	0.49	7.94
Allsop (1990) $3 \le \xi_{om} \le 6$	Smooth and impermeable	0.96	4.8
	1 layer rock and stone underlayer on impermeable slope (P=1)	0.64	7.22
	2 layer rock and stone underlayer on impermeable slope (P=1)	0.64	8.85
Benoit and Teisson (1994) $2.7 \le \xi_{op} \le 7$	2 layer rock armor $H_s : 0.03 - 0.09m$, $T_p = 1.3s$, $d = 0.4m$ Slope 1:1.33, 1:1.5, 1:2	0.6	6.6
Davidson, et al (1994) $8 \le \xi_{op} \le 50$	Field measurement on rock slope 1:1.1 Water depth h in meters		
	$h > 3.25$	0.65	25
	$2.5 \le h \le 3.25$	0.60	35
	$h < 2.5$	0.64	80

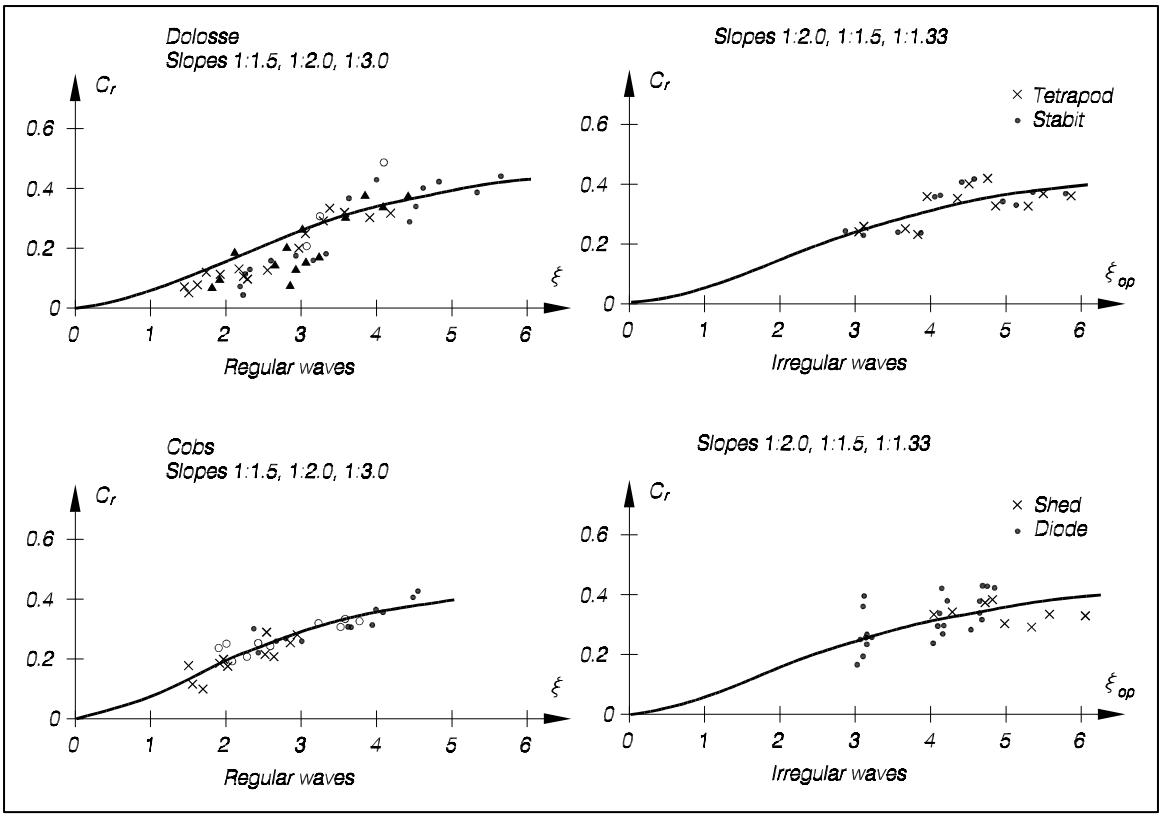

Figure VI-5-18. Reflection coefficients for concrete armor unit slopes. Head-on waves (Allsop and Hettiarachchi 1988)

(c) An alternative formula to Equation VI-5-38 was given by Postma (1989), who analyzed van der Meer's (1988) reflection data (see Table VI-5-4) for non-overtopped rock slopes. Postma introduced the notational permeability P (shown on Figure VI-5-11), the slope angle α and the wave steepness s_{op} in the formula

$$C_r = 0.071(P)^{-0.082}(\cot\alpha)^{-0.62}(s_{op})^{-0.46} \quad \text{(VI-5-39)}$$

(d) The uncertainty of Equation VI-5-39 corresponds to a variational coefficient of 0.036.

(e) The effect of a berm in a slope is generally a reduction in C_r. Figure VI-5-19 shows C_r values for a rubble-mound structure with berms of varying width at SWL (Allsop 1990).

(3) Reflection from vertical walls.

(a) Bulk reflection coefficients for plain vertical breakwaters on seabed, for plain vertical breakwaters on rubble foundation, for horizontal composite breakwaters, for sloping top caissons, for single perforated screens, and for perforated caissions are given in Figures VI-5-20, VI-5-21, VI-5-22, VI-5-23, VI-5-24, and VI-5-25, respectively. They were obtained from scaled model tests with irregular, head-on waves. The effect of oblique waves and wave shortcrestedness on plain and perforated vertical wall caissons is shown in Figure VI-5-26.

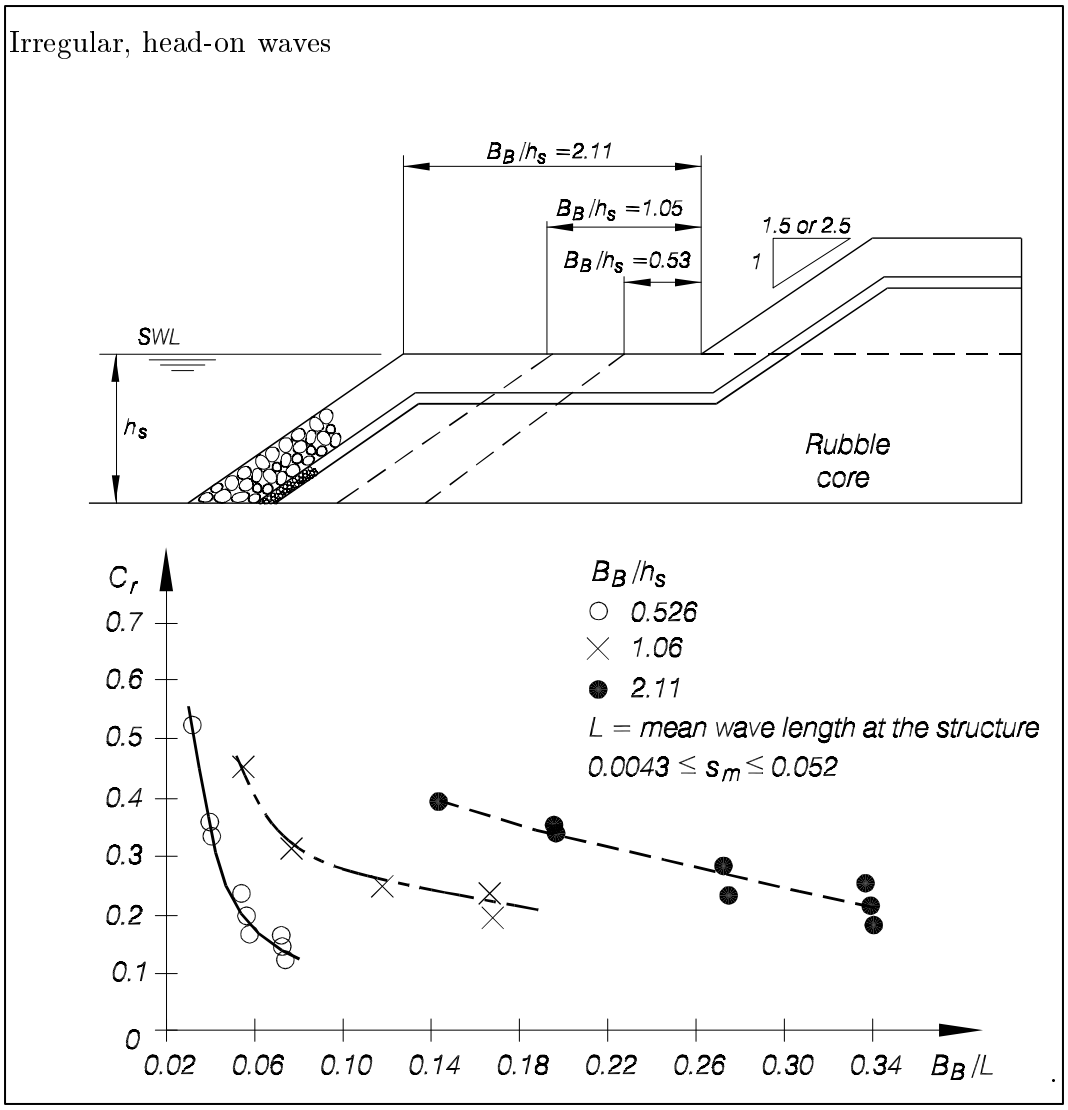

Figure VI-5-19. Wave reflection coefficients for rock armored slope with berm at SWL (Allsop 1990)

(b) The influence of wave shortcrestedness and oblique wave approach on reflection from plain impermeable and perforated vertical caissions is illustrated by Figure VI -5-26.

(4) Kinematics of reflected irregular waves.

(a) Close to highly reflective coastal structures incident and reflected waves interact with some degree of "phase locking." This result is a partially standing wave field characterized by nodes and antinodes. For the extreme case of perfectly reflected regular waves, a standing wave field occurs with stationary nodes and antinodes. Reflecting irregular waves create a less noticeable spatial variation of partially standing nodes and antinodes that decrease in magnitude with distance from the structure.

Irregular, head-on waves

$$C_r = \begin{cases} 0.79 + 0.11 \frac{R_c}{H_s} & \frac{R_c}{H_s} \le 1.0 \\ 0.90 & \frac{R_c}{H_s} > 1.0 \end{cases} \qquad \text{(VI-5-40)}$$

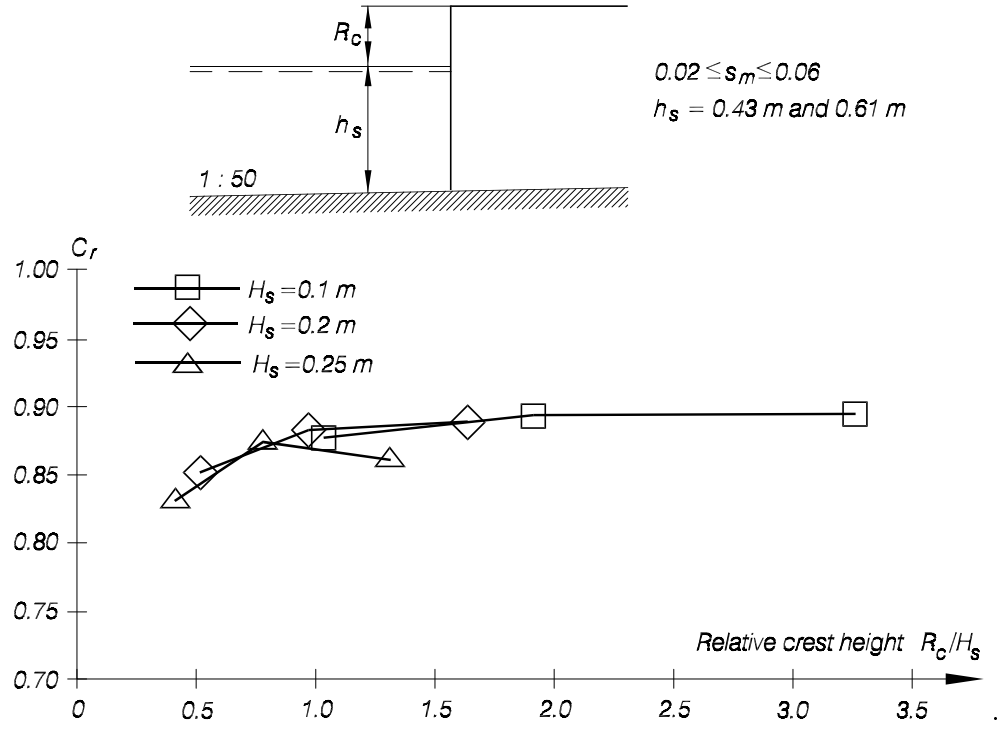

Figure VI-5-20. Wave reflection coefficients for plain vertical breakwater on 1:50 seabed (Allsop, McBride, and Columbo 1994)

(b) Assuming that the sea surface is comprised of a large number of linear wave trains that can be superimposed, the sea surface elevation adjacent to a reflective structure can be written as

$$\eta = \sum_{i=1}^{\infty} a_i \sqrt{1 + C_{ri}^2 + 2C_{ri} \cos\left(2k_i x + \theta_i\right)} \cos\left(\sigma_i t - \varepsilon_i\right) \qquad \text{(VI-5-42)}$$

and the horizontal component of the wave orbital velocity is given as

$$u = \sum_{i=1}^{\infty} a_i \left(\frac{gk_i}{\sigma_i}\right) \frac{\cosh\left[k_i\left(h+z\right)\right]}{\cosh\left(k_i h\right)} \sqrt{1 + C_{ri}^2 - 2C_{ri} \cos\left(2k_i x + \theta_i\right)} \cos\left(\sigma_i t - \varepsilon_i\right) \qquad \text{(VI-5-43)}$$

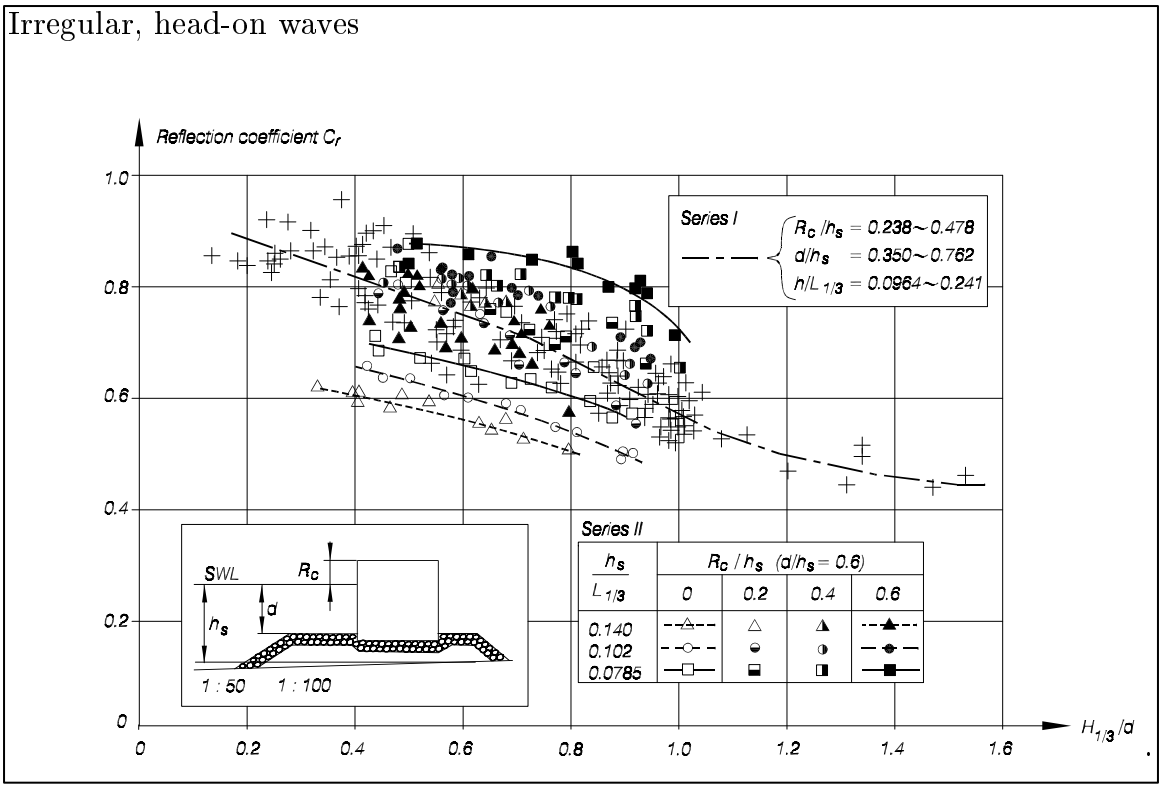

Figure VI-5-21. Wave reflection coefficients for plain vertical breakwater on rubble-mound foundation (Tanimoto, Takahashi, and Kimura 1987)

where

a_i = amplitude of ith incident wave component

k_i = wave number of ith incident wave component

σ_i = angular wave frequency of the ith incident wave component

g = gravitational acceleration

h = water depth

x = horizontal coordinate with positive toward the structure and x=0 located at the structure toe

z = vertical coordinate with z=0 at swl and z=-h at bottom

C_{ri} = reflection coefficient of ith incident wave component

θ_i = reflection phase angle of ith incident wave component

ε_i = random wave phase angle of ith incident wave component

Irregular, head-on waves

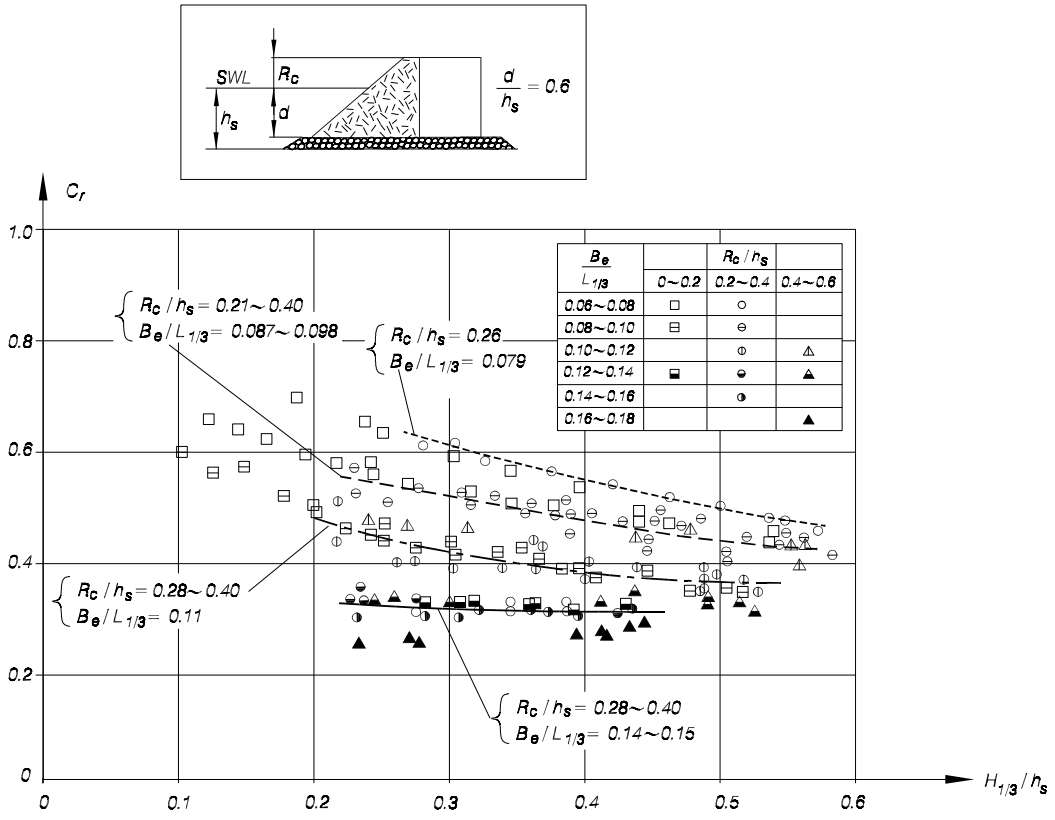

$$B_e = b_0 - \left(\frac{\cot\alpha}{h_s + R_c}\right)\left(\int_{-d}^{R_c} \frac{cosh^2 2\pi(h_s+z)/L}{cosh^2 2\pi h_s/L} z dz + 0.5R_c^2\right) \qquad \text{(VI-5-41)}$$

where b_0 covering width at the still water level

α slope angle of the structure measured from horizontal

z upward distance away from the still water level

Figure VI-5-22. Wave reflection coefficients for horizontal composite breakwaters with tetrapod slope 1:1.5 (Tanimoto, Takahashi, and Kimura 1987)

(c) These two equations strictly apply to the case of two-dimensional, nonbreaking, irregular waves propagating over a flat bottom and approaching normal to reflective structures. Similar expressions can be written for the case of oblique reflection of irregular, long-crested waves.

(d) The corresponding equation for estimating the root-mean-squared sea surface elevations is (Goda and Suzuki 1976)

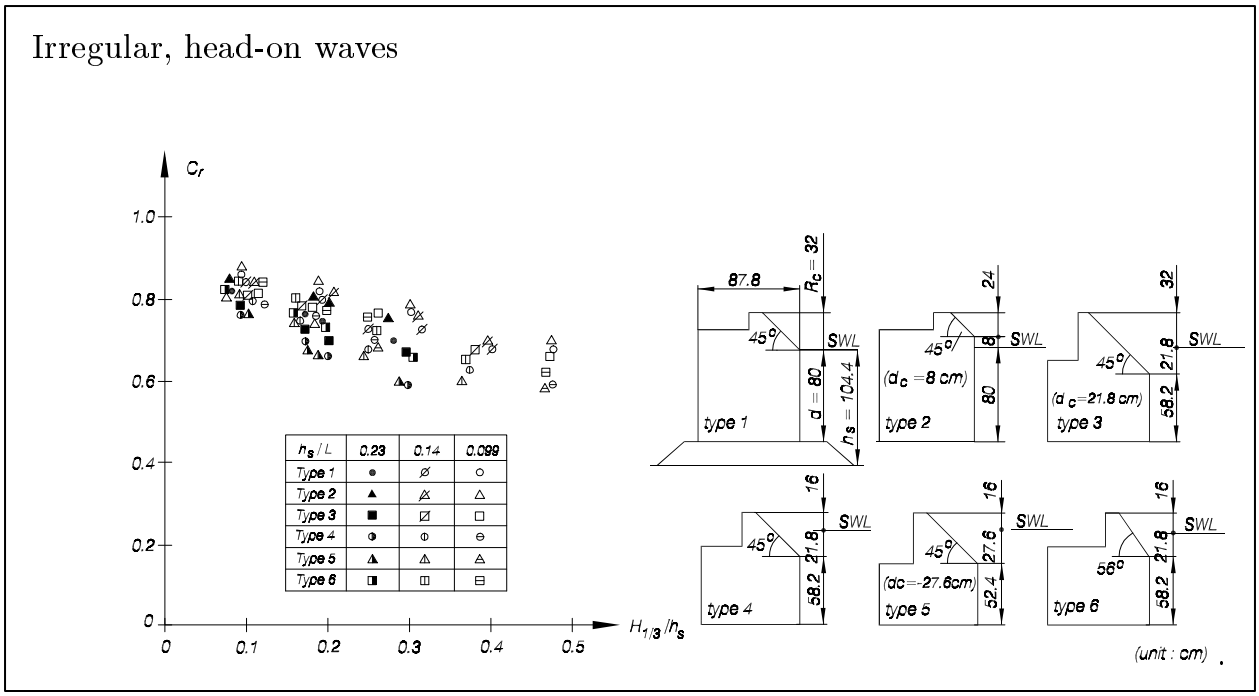

Figure VI-5-23. Wave reflection coefficients for sloping top breakwaters (Takahashi 1996)

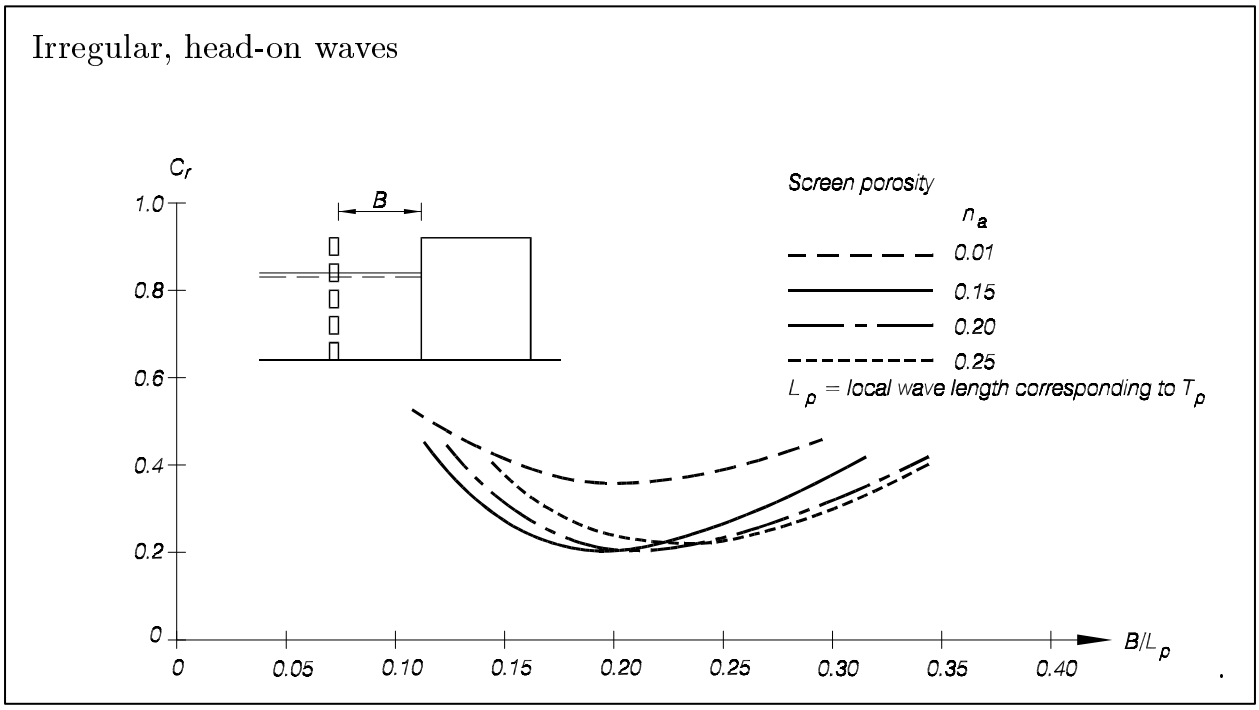

Figure VI-5-24. Wave reflection coefficients for perforated caissions (Allsop and Hettiarachchi 1988)

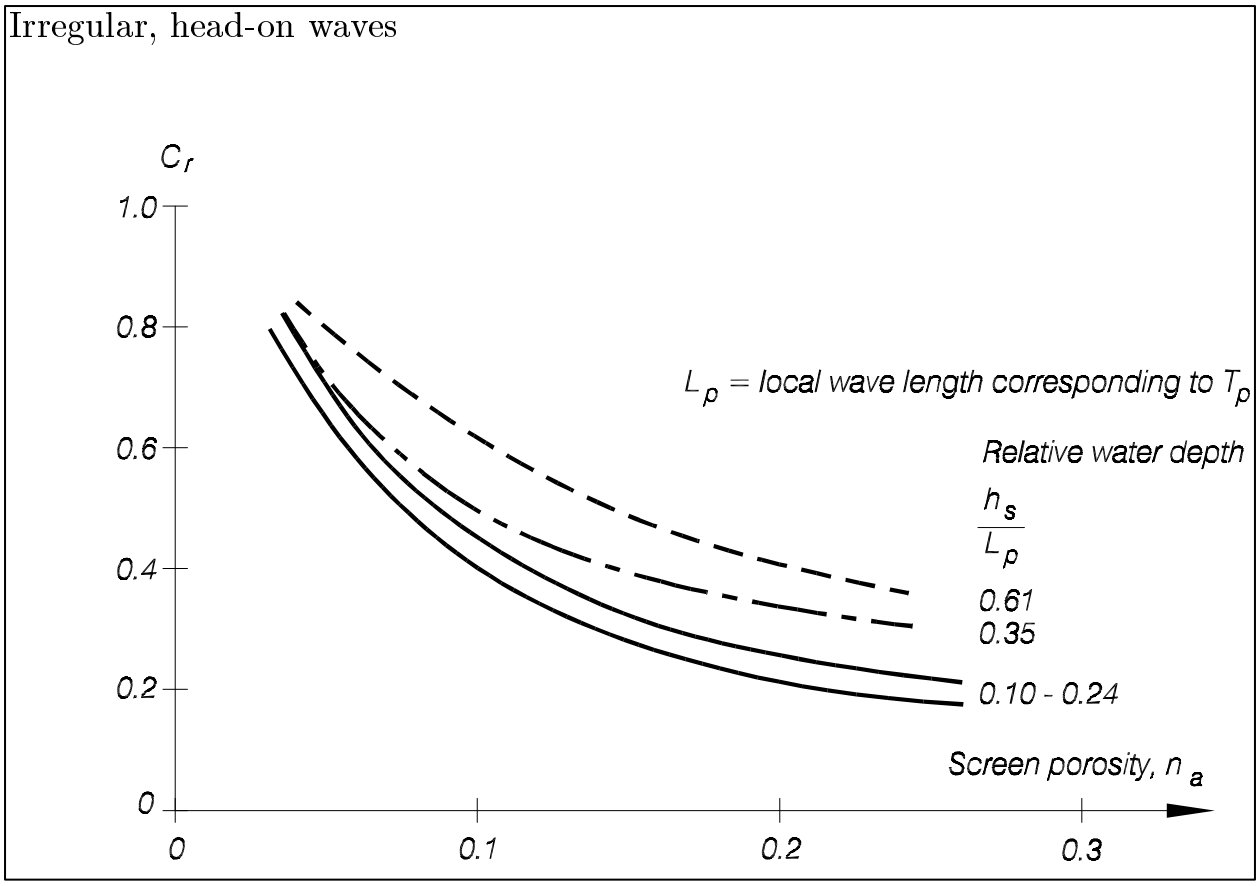

Figure VI-5-25. Wave reflection coefficients for single perforated screen (Allsop and Hettiarachchi 1988)

$$\eta_{rms}^2 = \sum_{i=1}^{\infty} \left[1 + C_{ri}^2 + 2C_{ri} \cos\left(2k_i x + \theta_i\right) \right] \frac{a_i^2}{2} \tag{VI-5-44}$$

and the root-mean-squared horizontal wave velocity is (Hughes 1992)

$$u_{rms}^2 = \sum_{i=1}^{\infty} \left(\frac{gk_i}{\sigma_i} \right) \frac{\cosh^2\left[k_i\left(h+z\right)\right]}{\cosh^2\left(k_i h\right)} \left[1 + C_{ri}^2 - 2C_{ri} \cos\left(2k_i x + \theta_i\right) \right] \frac{a_i^2}{2} \tag{VI-5-45}$$

(e) The root-mean-squared sea surface elevations and horizontal velocities are functions of the incident wave spectrum (a_i, k_i, σ_i), water depth (h), location in the water column relative to the structure toe (x, z), and the reflection coefficient (C_{ri}) and reflection phase angle (θ_i) associated with each wave component in the incident spectrum.

(f) For impermeable vertical walls the reflection coefficient C_{ri} is equal to unity for all wave componets and the reflection phase shift is $\theta_i = 0, 2\pi, 4\pi, \ldots$. However, for sloping structures reflection is less than perfect, and it is necessary to estimate the reflection coefficient and phase angle as functions of wave component frequency.

Test set-up

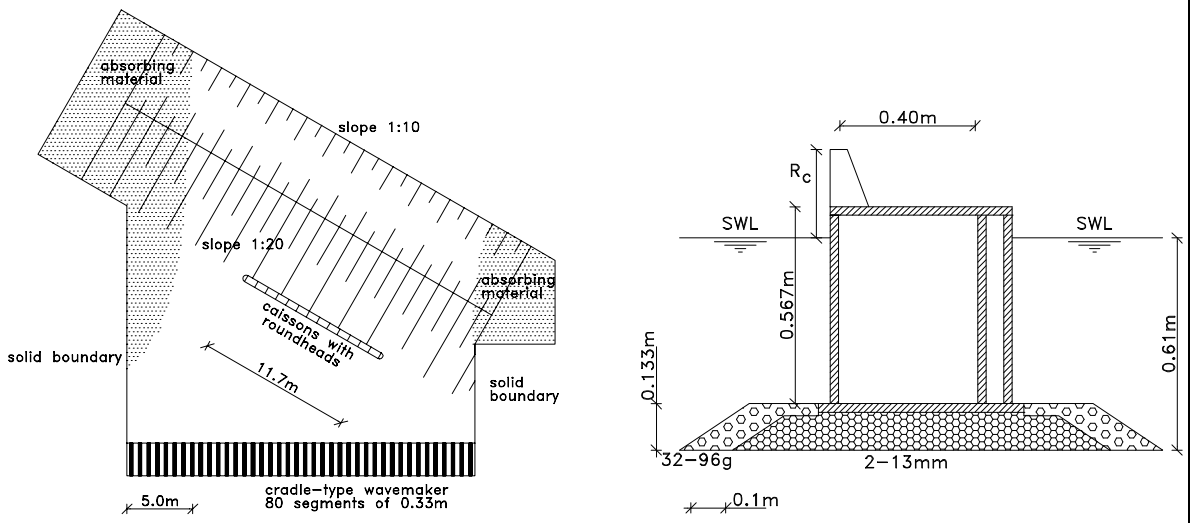

JONSWAP spectrum; H_s=14 cm, T_p =1.5 s
Gaussian spreading function; Spreading angle: 0^0(long-crested), 15^0, 30^0
Mean incident direction: 0^0 (head-on), 10^0, 20^0, 40^0, 60^0
Impermeable plain and perforated (porosity 25%, chambe width 0.4 m) vertical front

---

Test results

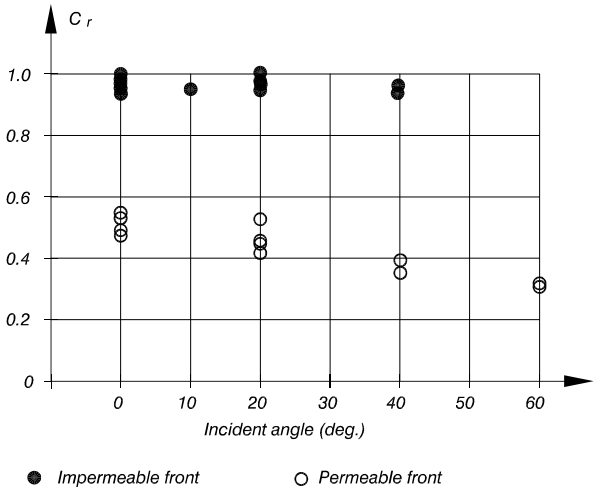

The data on the figure show that the reflection coefficients are almost independent of the wave short-crestedness within the tested range. The reflection coefficients for an impermeable plain vertical caisson are independent of wave obliquity, while it is decreasing with wave incident angle for a perforated caission.

Figure VI-5-26. Wave reflection coefficients for impermeable and permeable vertical breakwaters exposed to oblique, nonbreaking, short-crested waves (Helm-Petersen 1998)

(g) Empirical expressions for θ_i and C_{ri} for sloping impermeable and rubble-mound structures have been developed based on laboratory experiments (Hughes and Fowler 1995; Sutherland and O'Donoghue 1998a; Sutherland and O'Donoghue 1998b). The reflection phase for each incident wave component can be estimated from the following expression presented by Sutherland and O'Donoghue (1998a)

$$\theta_i = -8.84\pi\chi^{5/4} \tag{VI-5-46}$$

where

$$\chi = \frac{\sigma_i}{2\pi \tan\alpha}\sqrt{\frac{d_t}{g}} \tag{VI-5-47}$$

and

d_t = depth at the toe of the sloping structure

α = structure slope

The reflection coefficient for each incident wave component is estimated from recent results of Sutherland and O'Donoghue (1998b) by the empirical expressions

$$C_{ri} = \frac{\xi_\sigma^{2.58}}{7.64 + \xi_\sigma^{2.58}} \text{ for smooth impermeable slopes} \tag{VI-5-48}$$

$$C_{ri} = \frac{0.82\xi_\sigma^2}{22.85 + \xi_\sigma^2} \text{ for rubble-mound slopes} \tag{VI-5-49}$$

where

$$\xi_\sigma = \frac{\tan\alpha}{\sigma_i}\sqrt{\frac{2\pi g}{H_s}} \tag{VI-5-50}$$

and H_s is the significant wave height of the incident spectrum.

Figure VI-5-27 compares measured data to estimates of u_{rms} at middepth adjacent to a smooth, impermeable laboratory structure on a 1:2 slope. The estimates were made using the measured incident wave spectrum.

Sutherland and O'Donoghue (1997) showed that the two-dimensional expression for root-mean-square velocity can be extended to include the case of obliquely incident, long-crested waves.

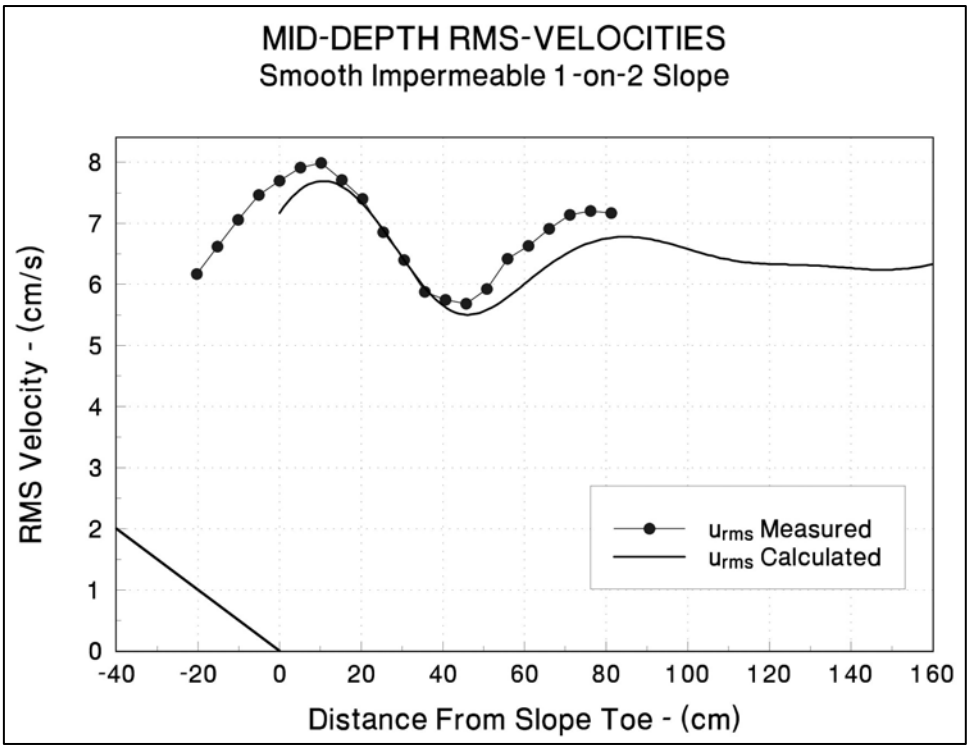

Figure VI-5-27. Measured versus estimated u_{rms} near smooth, impermeable 1:2 slope (Hughes and Fowler 1995)

d. Wave transmission.

(1) Introduction.

(a) Wave action behind a structure can be caused by wave overtopping and also by wave penetration if the structure is permeable. Waves generated by the falling water from overtopping tend to have shorter periods than the incident waves. Generally the transmitted wave periods are about half that of the incident waves.

(b) Wave transmission can be characterized by a transmission coefficient, C_t, defined either as the ratio of transmitted to incident characteristic wave heights (e.g., H_{st} and H_s) or as the square root of the ratio of transmitted to incident time-averaged wave energy (e.g., E_t and E_i) as given in Equation VI-5-51.

$$C_t = \frac{H_{st}}{H_s} = \left(\frac{E_t}{E_i} \right)^{1/2} \tag{VI-5-51}$$

(c) Specific transmission coefficients for wave overtopping (C_{to}) and wave penetration (C_{tp}) could be defined as follows

$$C_{to} = \frac{H_{st}^{overtop}}{H_s} \tag{VI-5-52}$$

$$C_{tp} = \frac{H_{st}^{penetr.}}{H_s} \quad \text{(VI-5-53)}$$

(d) However, in practice it is difficult to distinguish between $H_{st}^{overtop}$ and $H_{st}^{penetr.}$, and consequently, usual practice is to calculate C_t as defined by Equation VI-5-51.

(e) Values of C_t given in the literature are almost all from laboratory experiments, many of which were conducted at rather small scales. Some scale effects might have influenced the results, especially for the proportion of C_t related to wave penetration.

(2) Wave transmission through and over sloping structures.

(a) The total coefficient of wave transmission, C_t, for rock armored low-crested and submerged breakwaters, and reef breakwaters under irregular head-on waves are given in Figure VI-5-28 and Table VI-5-15.

(b) Figure VI-5-29 shows an example of the use of Equation VI-5-54.

(c) Breakwaters with complex types of concrete armor units, such as tetrapods or CORE-LOCS7 hereafter referred to as Core-Locs, generally have a more permeable crest than rock armored breakwaters, and this results in larger transmission coefficients.

(d) Detached breakwaters for coastal protection are placed in very shallow water and are often built entirely of armor blocks without underlayer and core. Such breakwaters are very permeable and C_{tp} can reach 0.8 in the case of complex armor units and small wave steepnesses.

(3) Wave transmission for vertical structures. Wave transmission for vertical breakwaters is mainly the result of wave overtopping. Therefore the ratio of the breakwater crest height (R_c) to the incident wave height (H_s) is the most important parameter. Wave transmission coefficients for plain vertical breakwaters, horizontal composite breakwaters, sloping top breakwaters and perforated walls are given in Table VI-5-16, Table VI-5-17, Figure VI-5-30, Figure VI-5-31, and Figure VI-5-32, respectively.

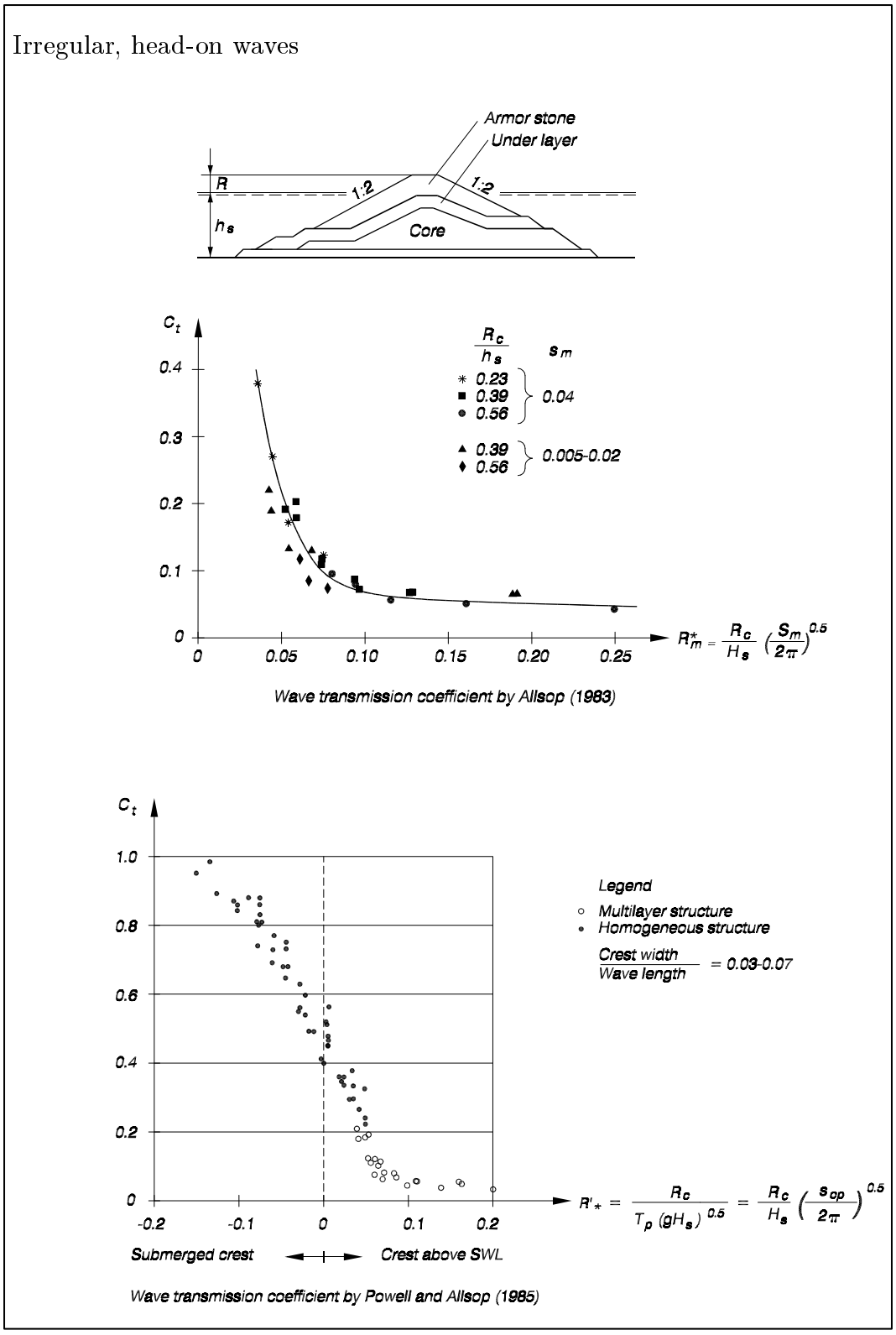

Figure VI-5-28. Wave transmission diagram by Allsop (1983) and Powell and Allsop (1985)

Table VI-5-15
Wave Transmission Formula by van der Meer and d'Angremond (1991) for Rock Armored Low-crested, Submerged, and Reef Breakwaters

Conventional rock armored low-crested breakwaters with their crests above and below still water level, and reef breakwaters, i.e., a homogenous rock structure without filter layers and core. Irregular, head–on waves.

$$C_t = \left(0.031 \frac{H_s}{D_{n50}} - 0.24\right) \frac{R_c}{D_{n50}} + b \qquad \text{(VI−5−54)}$$

maximum $C_t = 0.75$, minimum $C_t = 0.075$ conventional structure
maximum $C_t = 0.60$, minimum $C_t = 0.15$ reef type structure

where

$$b = \begin{cases} -5.42\, s_{op} + 0.0323 \frac{H_s}{D_{n50}} - 0.0017 \left(\frac{B}{D_{n50}}\right)^{1.84} + 0.51 & \text{conventional structure} \\ -2.6\, s_{op} - 0.05 \frac{H_s}{D_{n50}} + 0.85 & \text{reef type structure} \end{cases}$$

H_s – significant wave height of incident waves
D_{n50} – median of nominal diameter of rocks for design conditions
R_c – freeboard, negative for submerged breakwater
B – width of the crest
s_{op} – deepwater wave steepness corresponding to peak period.

The maximum and minimum limits of C_t must be interpreted as the valid ranges of Equation VI-5-54 and not as general limits since it is obvious that C_t can exceed these limits when the crest is deeply submerged. For example when the crest is deeply submerged ($R_c/D_{n50} < -6$) then C_t becomes close to unity.

The formula is based on model test results of Seelig (1980), Powell and Allsop (1985), Daemrich and Kahle (1985), Ahrens (1987), van der Meer (1988) and Daemen (1991).
Tested ranges : $1 < \frac{H_s}{D_{n50}} < 6$ $0.01 < s_{op} < 0.05$ $-2 < R_c/D_{n50} < 6$

Comparison between model test results and results calculated by Eq VI-5-54 gives a standard deviation of $\sigma(C_t) = 0.05$ corresponding to the 90% confidence limits given by $C_t \pm 0.08$.

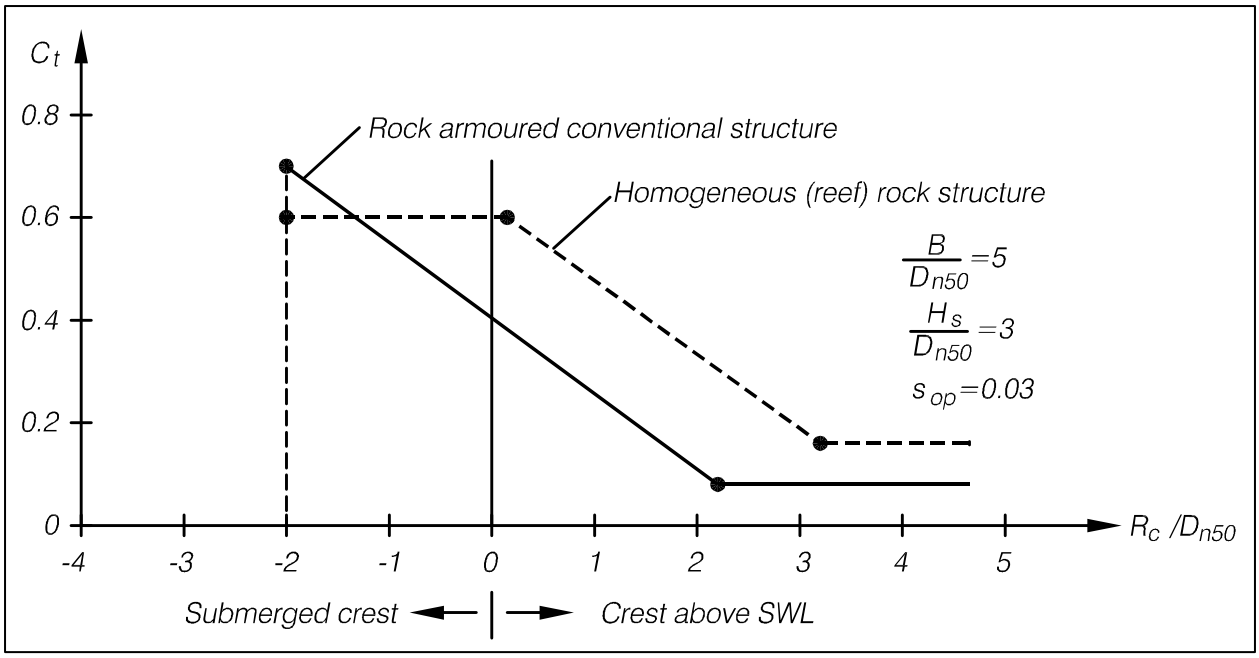

Figure VI-5-29. Example of total wave transmission coefficients, C_t, for conventional and reef type low-crested and submerged breakwaters, calculated from the van der Meer and d'Angremond (1991) formula given by Equation VI-5-54

Table VI-5-16
Wave Transmission Formula by Goda (1969)

Regular, head-on waves

$$C_t = \begin{cases} \left(0.25\left(1-\sin\left(\frac{\pi}{2\alpha}\right)\ \left(\frac{R_c}{H}+\beta\right)\right)^2 + 0.01\left(1-\frac{h_c}{h_s}\right)^2\right)^{0.5} & \beta-\alpha < \frac{R_c}{H} < \alpha-\beta \\ 0.1\left(1-\frac{h_c}{h_s}\right) & \frac{R_c}{H} \geq \alpha-\beta \end{cases} \quad \text{(VI–5–55)}$$

$\alpha = 2.2$

β is given by the figure

h_c is the vertical distance from water level to the bottom of caissons.

Formula is based on regular wave tests, but can be applied to irregular waves by using H_s for H

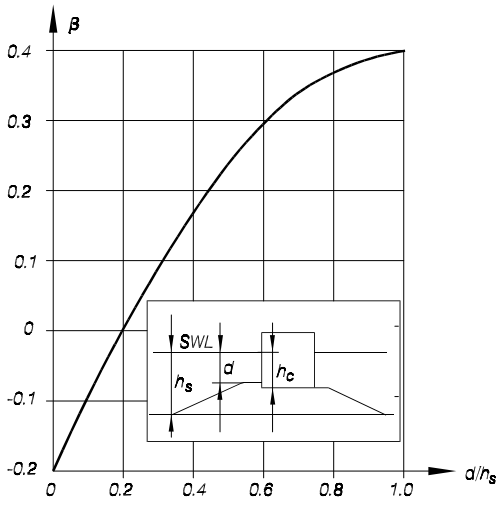

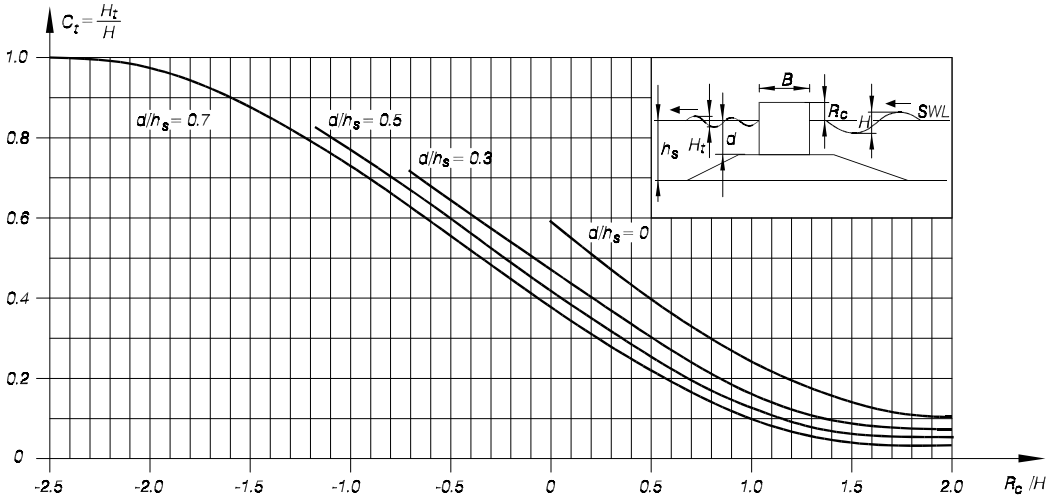

Table VI-5-17
Wave Transmission Formula by Takahashi (1996)

Irregular, head-on and oblique long-crested waves

$$C_t = \left[0.25\left[\left(1-sin\frac{\pi}{4.4}\right)\left(\frac{R_c}{H_{1/3}}+\beta+\beta_s\right)\right]^2+0.01\left(1-\frac{h_c}{h_s}\right)^2\right]^{0.5}$$

$$\text{valid for } \beta+\beta_s-2.2<\frac{R_c}{H_{1/3}}<2.2-\beta-\beta_s \qquad \text{(VI-5-56)}$$

$$C_t = 0.1\left(1-\frac{h_c}{h_s}\right) \qquad \text{valid for } \frac{R_c}{H_{1/3}}\geq 2.2-\beta-\beta_s$$

where

$\beta_s = -0.3\left[(R_c - 2\,d_c)\,/\left(H_{1/3}\,tan\theta\right)\right]^{0.5}$

β is given by the figure

d_c is the elevation of the lower edge of the sloping face relative to still-water level, i.e., positive if over SWL and negative if under SWL.

θ is angle of wave incidence with 0^o being normal incidence

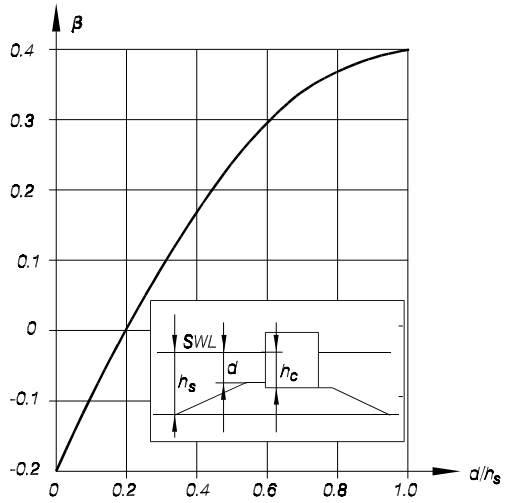

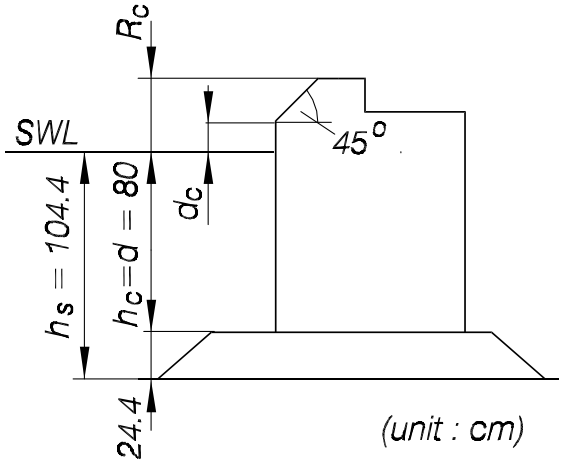

.

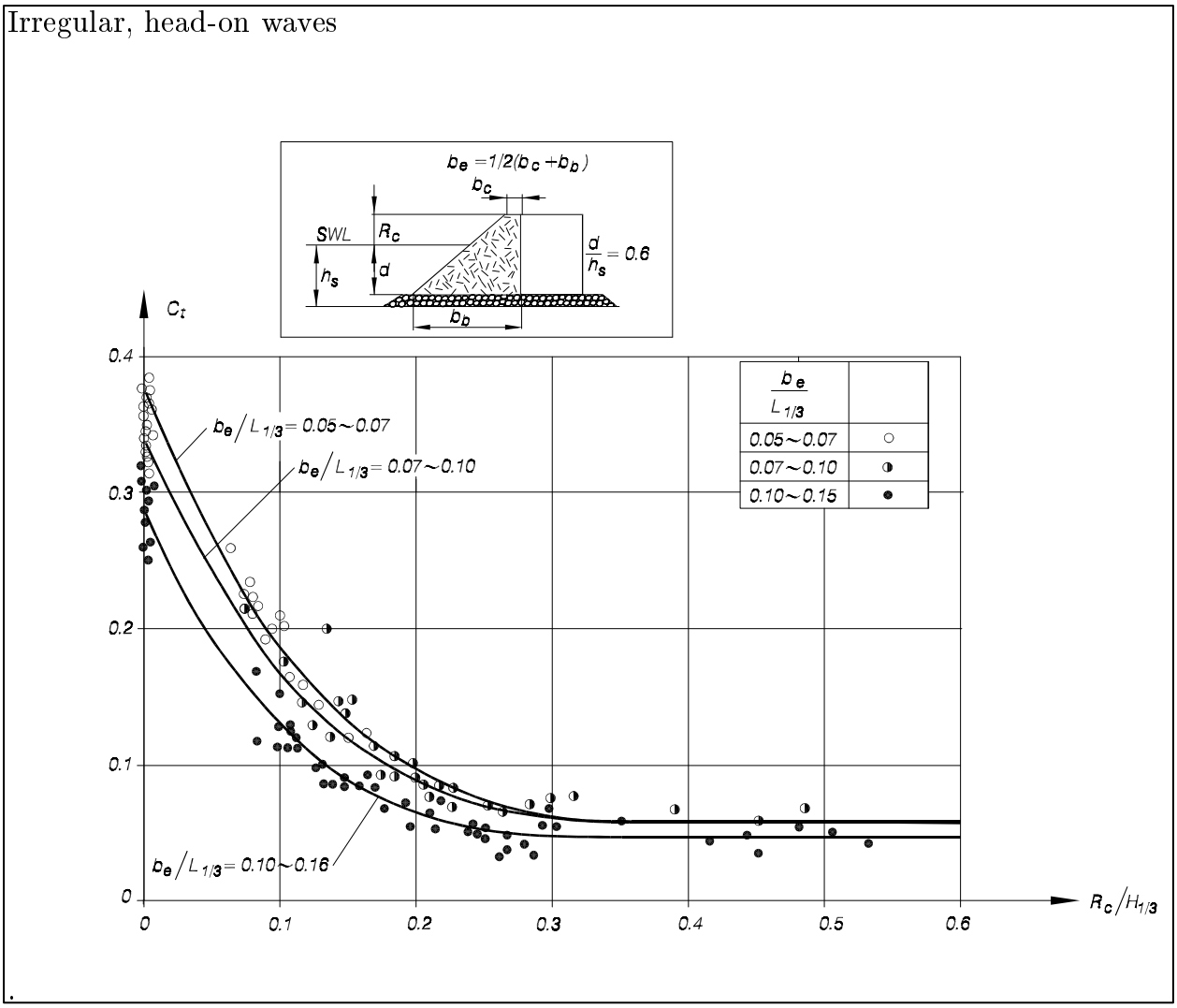

Figure VI-5-30. Wave transmission by overtopping of horizontal composite breakwaters armored with tetrapods (Tanimoto, Takanashi, and Kimura 1987)

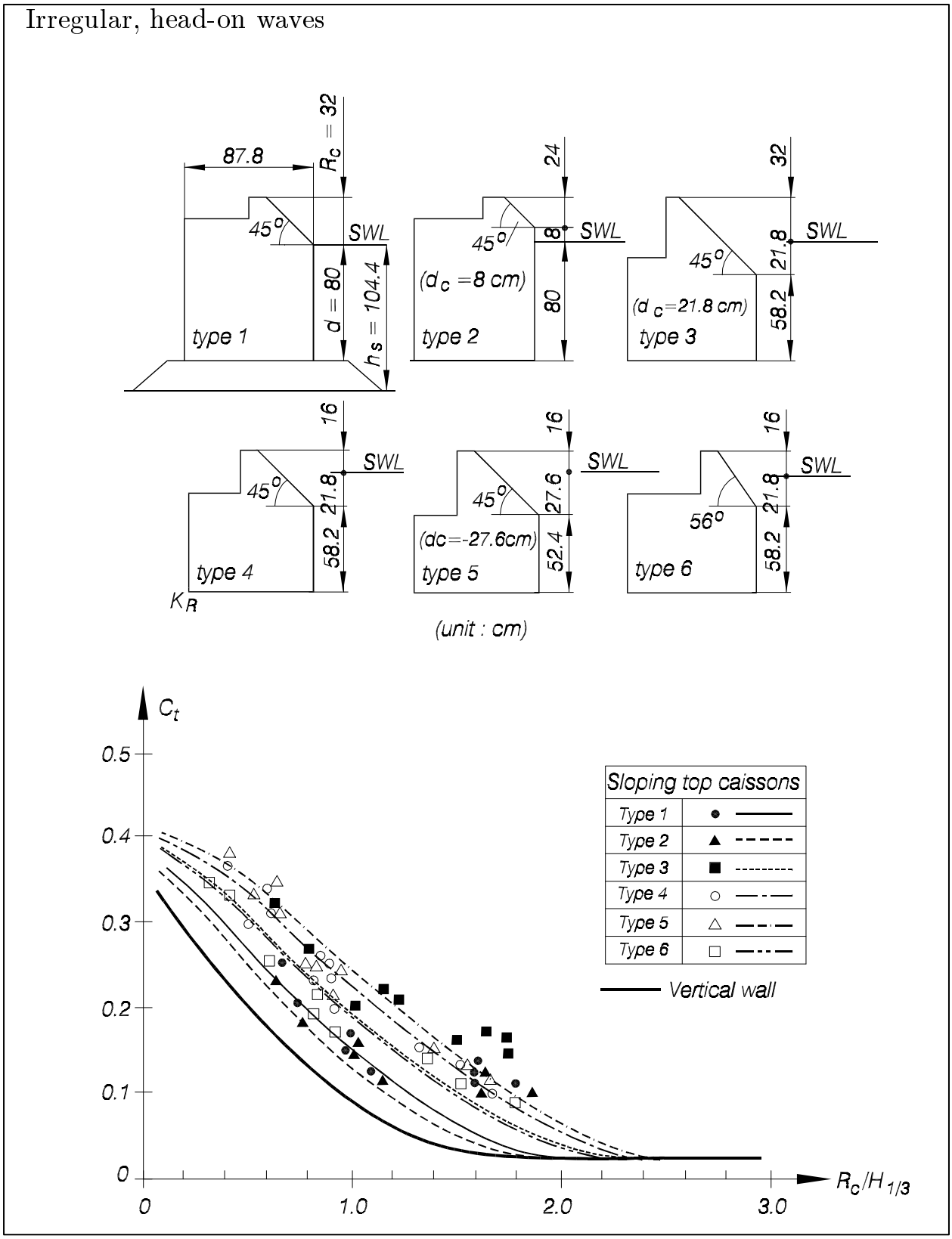

Figure VI-5-31. Wave transmission by overtopping of sloping top structures (Takahashi and Hosoyamada 1994)

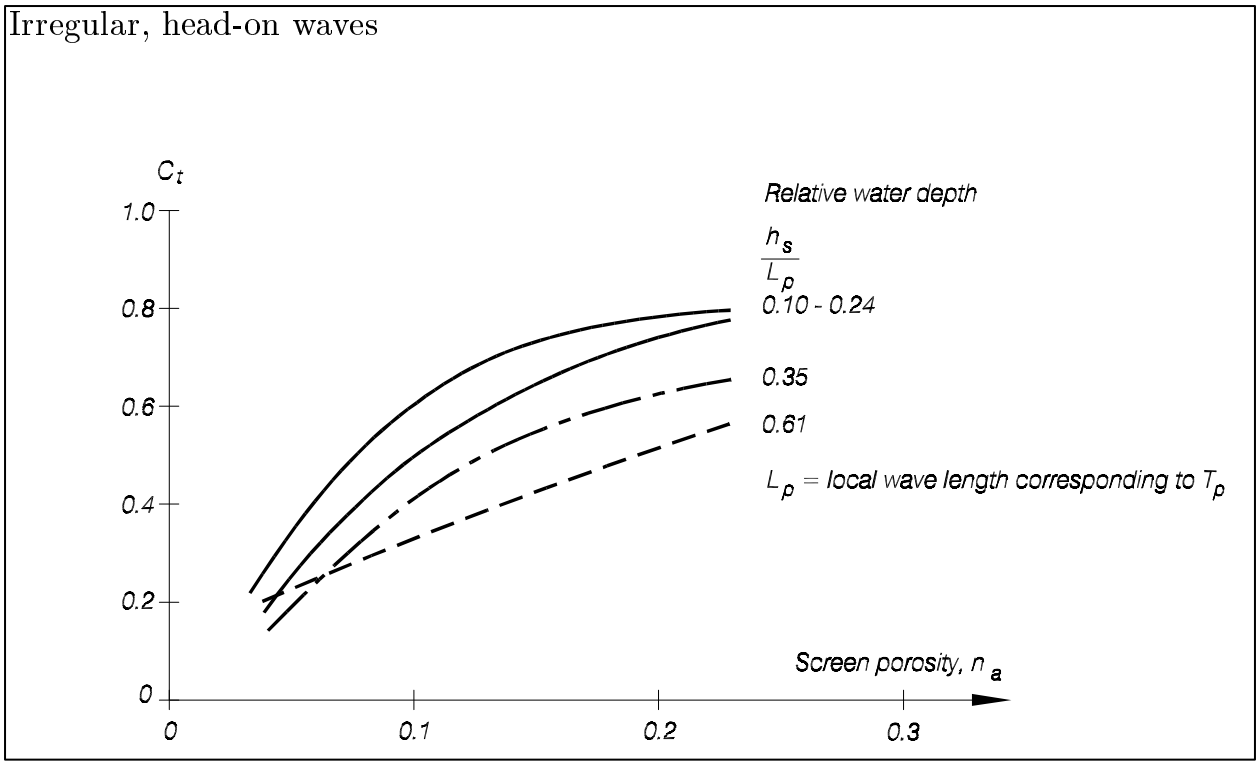

Figure VI-5-32. Wave transmission through perforated single wall (Allsop and Hettiarachchi 1988)

VI-5-3. Rubble-Mound Structure Loading and Response.

a. Armor layer stability.

(1) Introduction.

(a) Wave forces acting on a rubble-mound slope can cause armor unit movement. This is called hydraulic instability. Breakage of armor units is another type of instability which is discussed in Part VI-5-3*c*, "Structural integrity of concrete armor units."

(b) Armor unit movements can be rocking, displacement of units out of the armor layer, sliding of a blanket of armor units, and settlement due to compaction of the armor layer. Figure VI-5-33 shows the most typical armor layer failure modes.

(c) The complicated flow of waves impacting armor layers makes it impossible to calculate the flow forces acting on armor units. Moreover, the complex shape of units together with their random placement makes calculation of the reaction forces between adjacent armor units impossible. Consequently, deterministic calculations of the instantaneous armor unit stability conditions cannot be performed, which is why stability formulae are based on hydraulic model tests. The response of the armor units in terms of movements are related directly to parameters of the incident waves, while treating the actual forces as a "black box" transfer function. However, some qualitative considerations of the involved forces can be used to explore the structure of stability formulae.

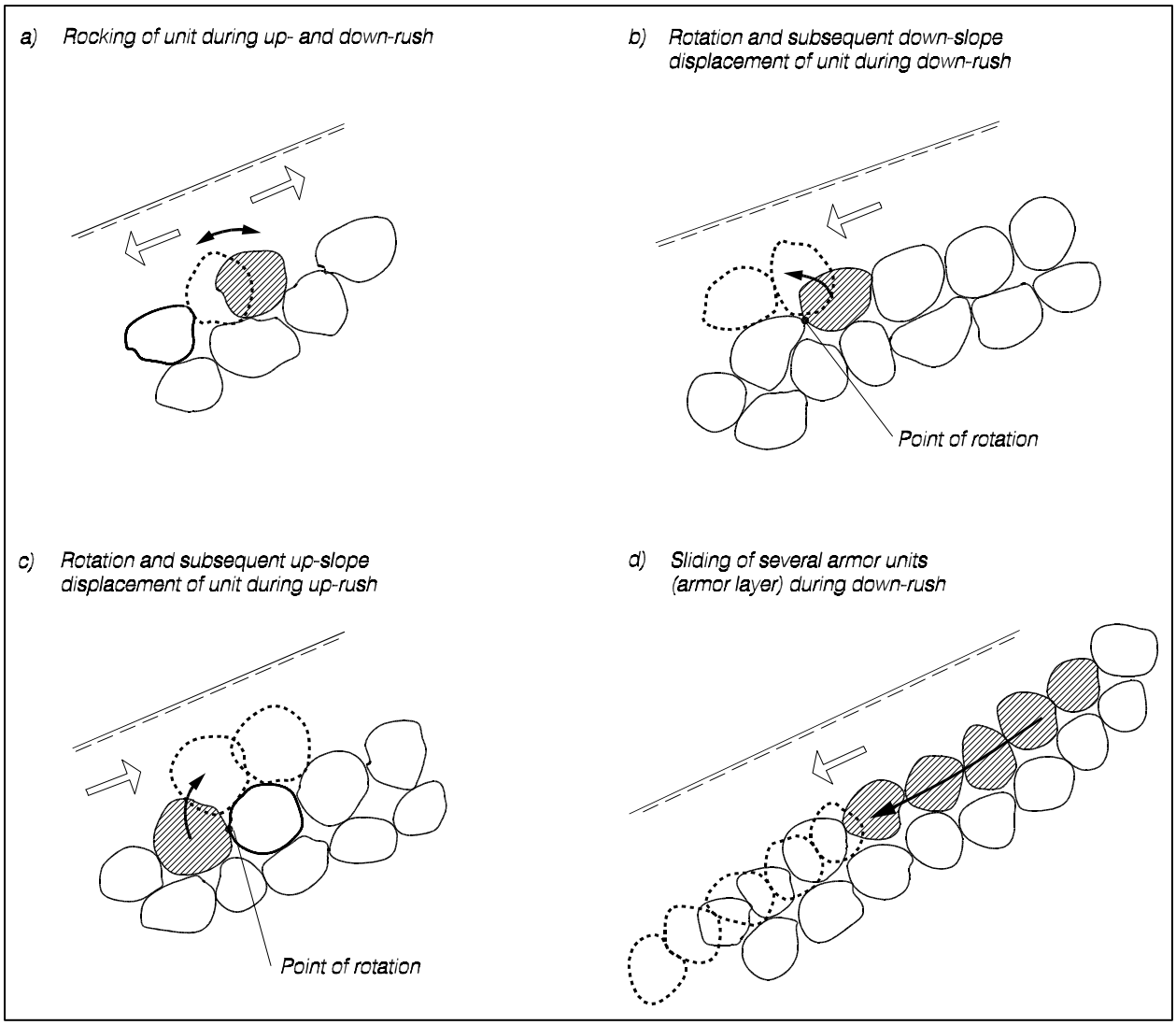

Figure VI-5-33. Typical armor layer failure modes (Burcharth 1993)

(2) Stability parameters and structure of stability formulae.

(a) The wave-generated flow forces on armor units might be expressed by a Morison equation containing a drag force F_D, a lift force F_L and an inertia force F_I. The stabilizing force is the gravitational force F_G. Assuming that at the stage of instability drag and lift force dominates the inertia force, a qualitative stability ratio can be formulated as the drag force plus the lift force divided by the gravity force

$$\frac{F_D + F_L}{F_G} \approx \frac{\rho_w D_n^2 v^2}{g\left(\rho_s - \rho_w\right) D_n^3} = \frac{v^2}{g \Delta D_n} \tag{VI-5-57}$$

where D_n = (armor unit volume)$^{1/3}$ is the equivalent cube length, ρ_s and ρ_w are the mass densities of armor units and water, respectively, and v is a characteristic flow velocity. By inserting v .

$(gH)^{1/2}$ for a breaking wave height of H in Equation VI-5-57 the following stability parameter, N_s, is obtained.

$$N_s = \frac{H}{\Delta D_n} \tag{VI-5-58}$$

where $\Delta = (\rho_s / \rho_w - 1)$. Non-exceedence of instability, or a certain degree of damage, can then be expressed in the general form

$$N_s = \frac{H}{\Delta D_n} \le K_1^a K_2^b K_c^3 \ldots \tag{VI-5-59}$$

where the factors depend on all the other parameters, except H, Δ and D_n, influencing the stability. Table VI-5-18 gives an overview of the sea state and structural parameters influencing armor layer stability. Also given are the combined parameters including wave height-period parameters commonly used in stability formulae. Stability formulae do not contain explicitly all the parameters shown in Table VI-5-18. This together with the stochastic nature of wave load and armor response introduces uncertainty in any stability formula. This uncertainty is in most cases included in Equation VI-5-59 in the form of a Gaussian distributed stochastic variable with a specified mean value and standard deviation.

(b) Simple geometrical considerations of the balance of the forces acting on an armor stone have been used to explore the right-hand side of Equation VI-5-59. Examples are:

$$\frac{H}{\Delta D_n} = K \cos\alpha \qquad \text{Svee (1962)}$$

$$\frac{H}{\Delta D_n} = \left(K \cot\alpha\right)^{1/3} \qquad \text{Hudson (1958, 1959)}$$

$$\frac{H}{\Delta D_n} = K\left(\tan\varphi \cos\alpha - \sin\alpha\right) \qquad \text{Iribarren (1938), Iribarren and Nogales (1954)}$$

where φ is the angle of repose of the armor. The coefficient K includes some level of damage as well as all other influencing parameters not explicitly included in the formulae.

(c) For armor units of complex shape and interlocking capability it is more difficult to make simple realistic force balance models. Qualitatively the difference between interlocking and noninterlocking armor is illustrated in the graphs of Figure VI-5-34, which show the influence of slope angle on the stabilizing effects of gravitational force, interlocking and surface friction. The interlocking effect is significant only for steeper slopes. Price (1979) performed dolos armor pullout tests in the dry that indicated maximum resistance occurs at slope of $cot\ \alpha = 2$. As a further demonstration Burcharth and Thompson (1983) showed that dolos armor placed on a horizontal bed and exposed to oscillatory flow is not more stable than rock armor of similar weight.

Table VI-5-18
Parameters Influencing Hydraulic Stability of Armor Layers

Sea state parameters

- Characteristic wave heights: H_s, $H_{1/3}$, H_{mo}, $H_{1/10}$, etc.
- Characteristic wave length: L_m, L_{om}, L_p, etc.
- Characteristic wave steepness: s_m, s_{om}, s_p, etc.
- Wave assymmetricity
- Shape of wave spectrum: JONSWAP, P-M, TMA etc. and double peak spectra.
- Wave grouping
- Water depth, h
- Wave incident angle, β
- Number of waves, N_z
- Mass density of water, ρ_w

Structural parameters

- Seaward profile of the structure, including armor layer slope angle α, freeboard, etc.
- Mass density of armor units, ρ_s
- Grading of rock armor, d_{n50}, d_{n15}, d_{n85}
- Mass M and shape of armor units
- Packing density, placement pattern and layer thickness of main armor
- Porosity and permeability of underlayers, filter layer(s) and core

Combined parameters

$\Delta = \frac{\rho_s}{\rho_w} - 1$

$N_s = \frac{H_s}{\Delta D_n}$ Shore Protection Manual (1984)

$N_s^* = N_s \, s_p^{-1/3}$ Ahrens (1987)

$H_0 \, T_0 = N_s \, T_m \sqrt{\frac{g}{D_n}}$ van der Meer (1988)

$\xi_m = \frac{\tan \alpha}{\sqrt{s_{om}}}$ Battjes (1974b)

where s_p the local wave steepness

T_m mean wave period

$s_{om} = \frac{2\pi H_s}{g T_m^2}$

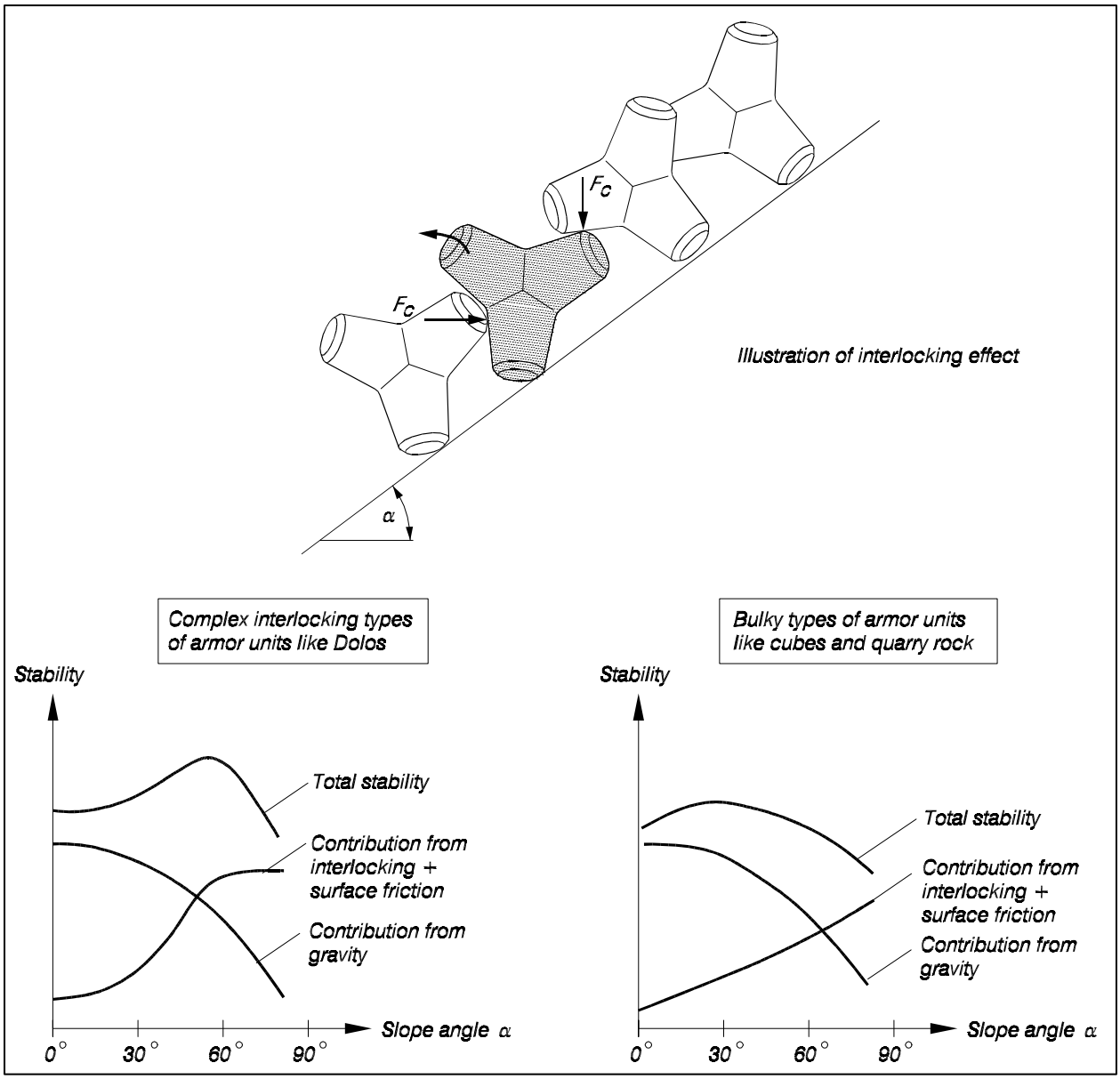

Figure VI-5-34. Illustration of influence of slope angle on the stabilizing effects of gravitational force, interlocking and surface friction (Burcharth 1993)

(3) Definition of armor layer damage.

(a) Damage to armor layers is characterized either by counting the number of displaced units or by measurement of the eroded surface profile of the armor slope. In both cases the damage is related to a specific sea state of specified duration. The counting method is based on some classification of the armor movements, for example:

- No movement.
- Single armor units rocking.

- Single armor units displaced from their original position by a certain minimum distance, for example D_n or h_a, where h_a is the length (height) of the unit

(b) Displacements can be in terms of units being removed out of the layer or units sliding along the slope to fill in a gap. In case of steep slopes, displacements could also be sliding of the armor layer due to compaction or loss of support.

(c) Damage in terms of displaced units is generally given as the relative displacement, D, defined as the proportion of displaced units relative to the total number of units, or preferably, to the number of units within a specific zone around swl. The reason for limiting damage to a specific zone is that otherwise it would be difficult to compare various structures because the damage would be related to different totals for each structure. Because practically all armor unit movements take place within the levels $\forall H_s$ around swl, the number of units within this zone is sometimes used as the reference number. However, because this number changes with H_s it is recommended specifying a H_s-value corresponding to a certain damage level (as proposed by Burcharth and Liu 1992) or to use the number of units within the levels swl $\forall$ n D_n, where n is chosen such that almost all movements take place within these levels. For example for dolosse $n = 6$ is used.

(d) Damage D can be related to any definition of movements including rocking. The relative number of moving units can also be related to the total number of units within a vertical strip of width D_n stretching from the bottom to the top of the armor layer. For this strip displacement definition, van der Meer (1988) used the term N_{od} for units displaced out of the armor layer and N_{or} for rocking units. The disadvantage of N_{od} and N_{or} is the dependence of the slope (strip) length.

(e) Damage characterization based on the eroded cross-section area A_e around swl was used by Iribarren (1938) and Hudson (1958) (Table VI-5-19). Hudson defined D as the percent erosion of original volume. Iribarren defined the limit of severe damage to occur when erosion depth in the main armor layer reached D_n.

(f) Broderick (1983) defined a dimensionless damage parameter for riprap and rock armor given as

$$S = \frac{A_e}{D_{n50}^2} \tag{VI-5-60}$$

which is independent of the length of the slope and takes into account vertical settlements but not settlements and sliding parallel to the slope. S can be interpreted as the number of squares with side length D_{n50} which fit into the eroded area, or as the number of cubes with side length D_{n50} eroded within a strip width D_{n50} of the armor layer. The damage parameter S is less suitable in the case of complex types of armor like dolosse and tetrapods due to the difficulty in defining surface profile. An overview of the damage parameters is given in Table VI-5-19.

Table VI-5-19
Definition of Damage Parameters D, N_{od} and S

1)	Relative displacement within an area	$D = \frac{\text{number of displaced units}}{\text{total number of units within reference area}}$ Displacement has to be defined, e.g., as position shifted more than distance D_n, or displacements out of the armor layer. The reference area has to be defined, e.g., as the complete armor area, or as the area between two levels, e.g., $SWL \pm H_s$, where H_s corresponds to a certain damage, or $SWL \pm nD_n$, where $\pm nD_n$ indicates the boundaries of armor displacements.
2)	Number of displaced units within a strip with width D_n (van der Meer 1988)	$N_{od} = \frac{\text{number of units displaced out of armor layer}}{\text{width of tested section / } D_n}$
3)	Relative number of displaced units within total height of armor layer (van der Meer 1988)	$\frac{N_{od}}{N_a}$, where N_a is the total number of units within a strip of horizontal width D_n $\frac{N_{od}}{N_a} = D$ if in D the total height of the armor layer is considered, and no sliding $> D_n$ of units parallel to the slope surface takes place
4)	Percent erosion of original volume (Hudson 1958)	$D = \frac{\text{average eroded area from profile}}{\text{area of average original profile}}$ x 100%
5)	Relative eroded area (Broderick 1983)	$S = A_e / D_{n50}^2$

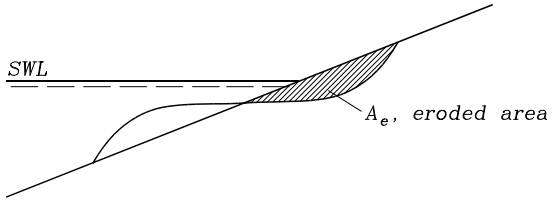

If settlements are disregarded the following relationship between N_{od} and S is valid:

$$N_{od} = G(1-p)S \tag{VI-5-61}$$

where p is the porosity of the armor layer and G is a factor dependent on the armor layer gradation. The range of p is approximately 0.4 - 0.6 with the lowest values corresponding to rock and the highest to dolosse. $G = 1$ for uni-size concrete armor and 1.2 - 1.6 for stone armor. It is seen that N_{od} is roughly equal to $S/2$. Unfortunately Equation VI-5-61 is not generally applicable because experience shows that the relationship depends on the armor slope angle. Table VI-5-20 shows examples of relationships between N_{od} and S as determined from model tests.

(g) A conventional damage level classification and the related values of the damage parameters D, N_{od} and S are given in Table VI-5-21.

(4) Armor layer damage progression.

(a) During the projected service life of a rubble-mound structure, damage to the armor layer may occur if design wave conditions are exceeded or the structure is exposed to repeated storms near the design conditions. Often it is not possible to mobilize and repair armor layer damage before the structure is impacted by additional severe storm waves that could worsen damage and possibly result in structure failure. A method for assessing armor layer damage progression due to multiple storms of differing wave conditions was developed by Melby and Kobayashi (1998a, 1998b) and Melby (1999). The method is based on seven long-duration physical model tests simulating various combinations of successive storms. The 1:2 sloping structure was protected with uniform armor stone (five tests) or wide-graded riprap (two tests). Irregular breaking wave conditions generally exceeding the design wave condition were used with the highest wave conditions causing moderate overtopping of the structure. Two water depths were used in the testing. The average damage as a function of time was given by Melby (1999) in terms of time domain wave parameters as

$$\overline{S}(t) = \overline{S}(t_n) + 0.025 \frac{(N_s)_n^5}{(T_m)_n^{1/4}} \left(t^{1/4} - t_n^{1/4}\right) \qquad \text{for } t_n \le t \le t_{n+1} \tag{VI-5-62}$$

or in terms of frequency domain wave parameters

$$\overline{S}(t) = \overline{S}(t_n) + 0.0202 \frac{(N_{mo})_n^5}{(T_p)_n^{1/4}} \left(t^{1/4} - t_n^{1/4}\right) \quad \text{for} \quad t_n \le t \le t_{n+1} \tag{VI-5-63}$$

with

$$\overline{S} = \frac{A_e}{D_{n50}^2} \qquad N_s = \frac{H_s}{\Delta D_{n50}} \qquad N_{mo} = \frac{H_{mo}}{\Delta D_{n50}} \qquad \Delta = \frac{\rho_a}{\rho_w} - 1 \tag{VI-5-64}$$

Table VI-5-20
Examples of Experimentally Determined Relationships Between N_{od} and S

van der Meer (1988)	Cubes, slope 1:1.5	$N_{od} = (S - 0.4)/1.8$
	Tetrapod, slope 1:1.5	$N_{od} = (S - 1)/2$
	Accropode, slope 1:1.33	$N_{od} = (S - 1)/2$
Holtzhausen and Zwamborn (1991)	Accropodes	

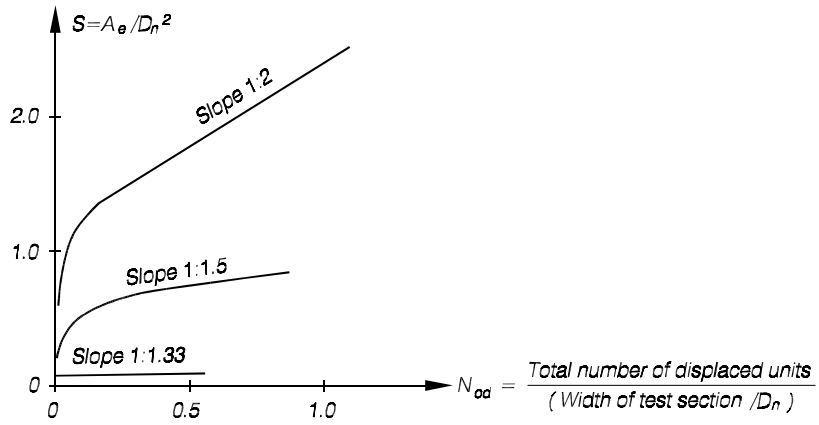

where t_n is the time at start of storm n, and t is time at end of storm n. (Time has the same units as wave period.) The wave parameters are local incident wave conditions not too far seaward of the structure toe, and the subscript n refers to those wave parameters associated with storm n. The standard deviation of average damage was given by the expression

$$\sigma_s = 0.5\overline{S}^{0.65} \tag{VI-5-65}$$

(b) For a specified sequence of storms of given duration Equation VI-5-62 or VI-5-63 is solved with the damage result from the previous storm being the initial damage for the next storm. Reasonable sequences of wave parameters and storm durations must be estimated using probabilistic methods based on long-term wave measurements or hindcasts.

Table VI-5-21
Damage Classification and Related Values of the Damage Parameters D, N_{od} and S

No damage	No unit displacement. Note that S might not be equal to zero due to settlement
Initial damage	Few units are displaced. This damage level corresponds to the *no-damage* level used in *Shore Protection Manual* 1977 and 1984 in relation to the Hudson formula stability coefficient, where the *no-damage* level is defined as 0-5% displaced units within the zone extending from the middle of the crest height down the seaward face to a depth below SWL equal to a H_s-value which causes the damage 0-5%.
Intermediate damage ranging from moderate to severe damage	Units are displaced but without causing exposure of the under or filter layer to direct wave attack
Failure	The underlayer or filter layer is exposed to direct wave attack

Damage level by D for two-layer armor

Unit	Slope	Initial damage	Intermediate damage	Failure	Reference
Rock[1]	1:2-1:3	0-5%	5-10%	≥20%	Jackson (1968)
Cube[2]	1:1.5-1:2		4%		Brorsen et al. (1974)
Dolosse[2]	1:1.5	0-2%		≥15%	Burcharth and Liu (1992)
Accropode[2,3]	1:1.33	0%	1-5%	≥10%	Burcharth et al. (1998)

[1] D is defined as percentage of eroded volume.
[2] D is defined as percentage of units moved more than D_n within the following level restricted areas: For rock see definition under initial damage, for cube $SWL \pm 6D_n$, for Dolosse $SWL \pm 6D_n$, for Accropodes between levels $SWL + 5D_n$ and $-9D_n$.
[3] One-layer armor cover layer.

Damage level by N_{od} for two-layer armor (van der Meer 1988)

Unit	Slope	Initial damage	Intermediate damage	Failure
Cube	1:1.5	0		2
Tetrapods	1:1.5	0		1.5
Accropode	1:1.33	0		0.5

Damage level by S for two-layer armor (van der Meer 1988)

Unit	Slope	Initial damage	Intermediate damage	Failure
Rock	1 : 1.5	2	3–5	8
Rock	1 : 2	2	4–6	8
Rock	1 : 3	2	6–9	12
Rock	1 : 4 – 1 : 6	3	8–12	17

Melby and Kobayashi also noted that average damage was related to the armor layer eroded depth, d_e , cover depth, d_c , and the upslope eroded length, l_e as defined in Figure VI-5-35.

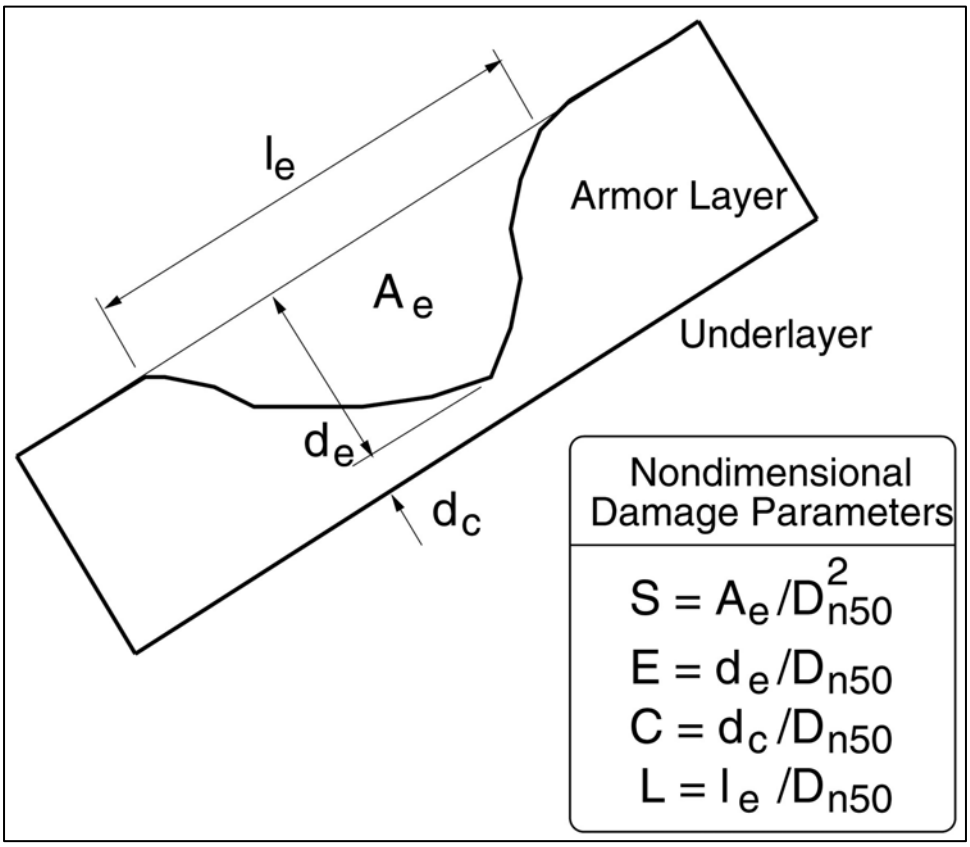

Figure VI-5-35. Damage parameters for structure armor layer (after Melby and Kobayashi 1998b)

In terms of the nondimensional parameters presented in Figure VI-5-35, these relationships were given as

$$\overline{E} = 0.46\overline{S}^{0.5} \qquad \sigma_E = 0.26 - 0.00007\left(\overline{S} - 7.8\right)^4$$

$$\overline{C} = C_o - 0.1\overline{S} \qquad \sigma_C = \sigma_{C_o} + 0.098 - 0.002\left(\overline{S} - 7\right)^2 \tag{VI-5-66}$$

$$\overline{L} = 4.4\overline{S}^{0.5}$$

where σ_e and σ_c are the standard deviations of the average nondimensional eroded depth and cover depth, respectively; and C_o is the zero-damage cover layer thickness.

(c) The nondimensional eroded depth in Equation VI-5-66 could be used to estimate average damage in rock armor from an observed eroded depth after a severe storm. This estimate could then be used in Equation VI-5-62 or VI-5-63 to predict damage progression from subsequent storms.

(d) Although the previous damage progression relationships are based on a small number of laboratory experiments, they were formulated to be conservative in the estimates. The more difficult problem is to develop good realizations of storm sequences.

(5) Practical formulae for hydraulic stability of armor layers.

(a) Formulae for hydraulic stability of armor layers are almost exclusively based on small scale model tests. Large scale model tests for verification of small scale model test results have been performed in few cases. Adjustment of formulae due to prototype experience seems not to be reported in the literature.

(b) Generally small scale hydraulic tests of armor layer stability are assumed to be conservative if any bias is present. Nevertheless, armor stability formulae should be applied only for conceptual design, and the uncertainty of the formulae should be considered. When the formulae do not cover the actual range of structure geometries and sea states, preliminary designs should be model tested before actual construction. Major structures should always be tested in a physical model.

(c) Some of the factors by which armor stability formulae can be classified are as follows:

- Type of armor unit.
- Deep or shallow-water wave conditions.
- Armor layers crest level relative to wave runup and swl.
- Structures with and without superstructure.

(d) Type of armor unit distinguishes between rock armor, for which shape and grading must be defined, and uni-size concrete armor units.

(e) Deepwater conditions correspond to Rayleigh distributed wave height at the structure, i.e., depth-limited wave breaking does not take place. Shallow-water conditions correspond to non-Rayleigh distributed wave heights at the structure, i.e., depth limitations cause wave breaking in front of, or in the worst case, directly upon the structure.

(f) Overtopping affects the armor stability. When the crest is lower than the runup level, wave energy can pass over the structure. Thus, the size of the front slope armor can be reduced while the size of the crest and rear slope armor must be increased compared to non-overtopped structures. With respect to armor stability it is common to distinguish between

- Non-overtopped or marginally overtopped structures.
- Low-crested structures, i.e., overtopped structures but with crest level above swl.
- Submerged structures, i.e., the crest level is below swl.

(g) This section presents armor layer stability formulae for use in designing coastal structures. These stability formulae can be used in the context of reliability based design using the partial safety factors given in the tables of Part VI-6-6, "Partial Safety Factor System for Implementing Reliability in Design." Guidance for designing structure cross sections is given in Part VI-5-3*e*, "Design of Structure Cross Section," and complete design examples for specific structure types are given in Part VI-7, "Example Problems."

- Structure trunk stability. Stability formulae for front slope armor on structure trunks are presented in the following tables outlined as follows:

Armor Unit	Non-Overtopped	Overtopped	Submerged
Rock	Tables VI-5-22/23	Tables VI-5-24/26	Tables VI-5-25/26
Concrete cubes	Table VI-5-29		
Tetrapods	Table VI-5-30		
Dolosse	Table VI-5-31		
ACCROPODES [7]	Tables VI-5-32/33		
CORE-LOC [7]	Table VI-5-34		
Tribars	Table VI-5-36		

- Rear side armor stability. Information on rear side armor stability is given in Table VI-5-28. A formula for stability of reef breakwater is presented in Table VI-5-27. A formula for stability of armor in front of a vertical wall is presented in Table VI-5-35. Rubble-mound structure head stability is given in Tables VI-5-37/38. Parapet walls are placed on top of rubble-mound structures to reduce overtopping by deflecting the uprushing waves back into the sea. This generally reduces the front slope armor stability. A low wall behind a wide front armor berm will hardly affect the armor stability (see Figure VI-5-36a). On the other hand a high wall with a relatively deep foundation situated behind a narrow front armor berm will significantly reduce the armor stability (see Figure VI-5-36b).

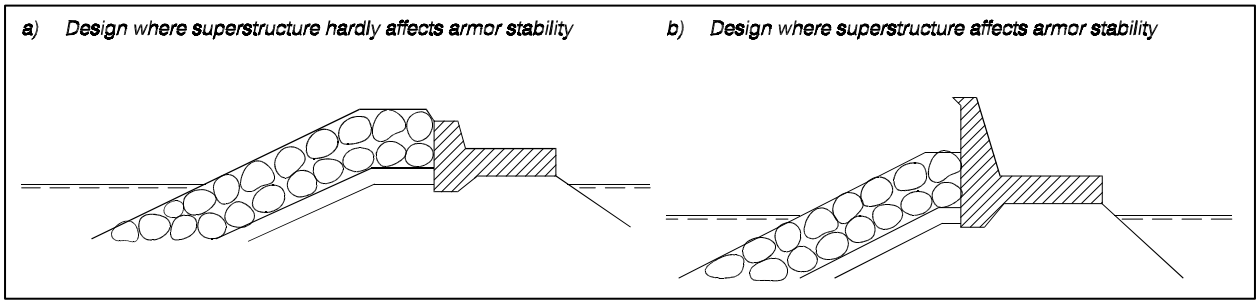

Figure VI-5-36. Illustration of superstructure designs causing insignificant and significant reduction in front slope armor stability

- Front slope armor stability. No generally applicable formulae are available for reduction in front slope armor stability caused by parapet walls.

(h) All of the various armor stability criteria represented by the equations and empirical coefficients in Tables VI-5-22 to VI-5-36 were developed in laboratory physical models, most often at reduced scale. Although field experience has added validation to some of these stability formulae, designers should be aware of the following limitations when applying laboratory stability results to prototype conditions.

- Some of the earlier results were obtained using monochromatic waves, whereas most of the more recent model tests used irregular waves. Numerous studies have suggested that the monochromatic wave height leading to armor instability roughly corresponds to the significant wave height of irregular waves; however, not all studies have found this correspondence. For preliminary design for nonbreaking wave conditions always use a stability formula based on irregular wave testing if possible. For breaking wave conditions monochromatic wave stability results will be conservative.

- It is generally thought that the higher waves associated with wave groups are responsible for armor layer damage. Typically irregular wave stability model tests use wave trains with assumed random phasing of the spectral components. Over the course of the testing wave groups of differing characteristics impact the structure, and the assumption is that these wave groups are representative of nature. However, it is possible that nonrandom phasing occurs in nature, particularly in shallow water (Andrews and Borgman 1981). Therefore, use of regular wave stability results will be appropriate in some cases.

- Hand-built armor layers on laboratory structures could be tighter than are armor layers typically constructed in the prototype. This leads to unconservative stability results. In particular special placement of armor in the laboratory is unlikely to be reproduced as well on the job site, especially below the water surface where placement will be much more random. For this reason it may be advisable to use stability criteria for random placement as a basis for design.

- Armor stability formulae are intended for use in preliminary design phases and for estimating material quantities. When feasible, preliminary designs should be confirmed and optimized with hydraulic model tests.

Table VI-5-22
Rock, Two-Layer Armored Non-Overtopped Slopes (Hudson 1974)

Irregular, head-on waves

$$\frac{H}{\Delta D_{n50}} = (K_D \cot\alpha)^{1/3} \quad \text{or} \quad M_{50} = \frac{\rho_s H^3}{K_D \left(\frac{\rho_s}{\rho_w} - 1\right)^3 \cot\alpha} \qquad \text{(VI-5-67)}$$

where

H	Characteristic wave height (H_s or $H_{1/10}$)
D_{n50}	Equivalent cube length of median rock
M_{50}	Medium mass of rocks, $M_{50} = \rho_s D_{n50}^3$
ρ_s	Mass density of rocks
ρ_w	Mass density of water
Δ	$\left(\rho_s/\rho_w\right) - 1$
α	Slope angle
K_D	Stability coefficient

K_D-values by SPM 1977, $H = H_s$, for slope angles $1.5 \leq \cot\alpha \leq 3.0$. (Based entirely on regular wave tests.)

Stone shape	Placement	Damage, D [4]			
		0-5%		5-10%	10-15%
		Breaking waves [1]	Nonbreaking waves [2]	Nonbreaking waves	Nonbreaking waves
Smooth, rounded	Random	2.1	2.4	3.0	3.6
Rough angular	Random	3.5	4.0	4.9	6.6
Rough angular	Special [3]	4.8	5.5		

K_D-values by SPM 1984, $H = H_{1/10}$.

Stone shape	Placement	Damage, D [4] = 0-5%	
		Breaking waves [1]	Nonbreaking waves [2]
Smooth rounded	Random	1.2	2.4
Rough angular	Random	2.0	4.0
Rough angular	Special [3]	5.8	7.0

[1] Breaking waves means depth-limited waves, i.e., wave breaking takes place in front of the armor slope. (Critical case for shallow-water structures.)

[2] No depth-limited wave breaking takes place in front of the armor slope.

[3] Special placement with long axis of stone placed perpendicular to the slope face.

[4] D is defined according to SPM 1984 as follows: The percent damage is based on the volume of armor units displaced from the breakwater zone of active armor unit removal for a specific wave height. This zone extends from the middle of the breakwater crest down the seaward face to a depth equivalent to the wave height causing *zero* damage below still-water level.

Shore Protection Manual (1977) versus *Shore Protection Manual* (1984): When considering that $H_{1/10} = 1.27 H_s$ for Rayleigh distributed wave heights (non-depth-limited waves) it is seen that the recommendations of *Shore Protection Manual* (1984) introduce a considerable safety factor compared to the practice based on *Shore Protection Manual* (1977).

Uncertainty of the formula: The coefficient of variation of Eq VI-5-67 is estimated to be 18% by van der Meer (1988). Melby and Mlaker (1997) reported a coefficient of variation for K_D of 25% for stone and 20% for Dolosse.

Table VI-5-23
Rock, Two-Layer Armored Non-Overtopped Slopes (van der Meer 1988)

Irregular, head-on waves

$$\frac{H_s}{\Delta D_{n50}} = 6.2 \cdot S^{0.2}\, P^{0.18}\, N_z^{-0.1}\, \xi_m^{-0.5} \qquad \text{Plunging waves}: \ \xi_m < \xi_{mc} \qquad \text{(VI}-5-68\text{)}$$

$$\frac{H_s}{\Delta D_{n50}} = 1.0 \cdot S^{0.2}\, P^{-0.13}\, N_z^{-0.1} (\cot\alpha)^{0.5}\, \xi_m^{P} \qquad \text{Surging waves}: \ \xi_m > \xi_{mc} \qquad \text{(VI}-5-69\text{)}$$

$$\xi_m = s_m^{-0.5} \tan\alpha \qquad\qquad \xi_{m\,c} = \left(6.2\, P^{0.31}\, (\tan\alpha)^{0.5}\right)^{1/(P+0.5)}$$

where	H_s	Significant wave height in front of breakwater
	D_{n50}	Equivalent cube length of median rock
	ρ_s	Mass density of rocks
	ρ_w	Mass density of water
	Δ	$(\rho_s/\rho_w) - 1$
	S	Relative eroded area (see Table VI-5-21 for nominal values)
	P	Notional permeability (see Figure VI-5-11)
	N_z	Number of waves
	α	Slope angle
	s_m	Wave steepness, $s_m = H_s/L_{om}$
	L_{om}	Deepwater wavelength corresponding to mean wave period

Validity:

1) Equations VI-5-68 and VI-5-69 are valid for non-depth-limited waves. For depth-limited waves H_s is replaced by $H_{2\%}/1.4$.
2) For $\cot\alpha \geq 4.0$ only Eq VI-5-68 should be used.
3) $N_z \leq 7,500$ after which number equilibrium damage is more or less reached.
4) $0.1 \leq P \leq 0.6 \quad , \quad 0.005 \leq s_m \leq 0.06 \quad , \quad 2.0\ tonne/m^3 \leq \rho \leq 3.1\ tonne/m^3$
5) For the 8 tests run with depth-limited waves, breaking conditions were limited to spilling breakers which are not as damaging as plunging breakers. Therefore, Eqs VI-5-68 and VI-5-69 may not be conservative in some breaking wave conditions.

Uncertainty of the formula: The coefficient of variation on the factor 6.2 in Eq VI-5-68 and on the factor 1.0 in Eq VI-5-69 are estimated to be 6.5% and 8%, respectively.

Test program: See Table VI-5-4.

Table VI-5-24
Rock, Two-Layer Armored Overtopped, but Not Submerged, Low-crested Slopes

Powell and Allsop (1985) analyzed data by Allsop (1983) and proposed the stability formula

$$\frac{N_{od}}{N_a} = a \exp\left[b\, s_p^{-1/3}\, H_s / (\Delta\, D_{n50})\right] \quad \text{or} \quad \frac{H_s}{\Delta D_{n50}} = \frac{s_p^{1/3}}{b} \ln\left(\frac{1}{a}\frac{N_{od}}{N_a}\right) \qquad \text{(VI−5−70)}$$

where values of the empirical coefficients a and b are given in the table as functions of freeboard R_c and water depth h. N_{od} and N_a are the number of units displaced out of the armor layer and the total number of armor layer units, respectively.

Values of coefficients a and b in Eq VI-5-70.

R_c/h	$a \cdot 10^{-4}$	b	wave steepness H_s/L_p
0.29	0.07	1.66	<0.03
0.39	0.18	1.58	<0.03
0.57	0.09	1.92	<0.03
0.38	0.59	1.07	>0.03

van der Meer (1991) suggested that the van der Meer stability formulae for non-overtopped rock slope, Eqs VI-5-68 and VI-5-69, be used with $f_i D_{n50}$ substituted for D_{n50} . The reduction factor f_i is given as

$$f_i = \left(1.25 - 4.8\, \frac{R_c}{H_s} \sqrt{\frac{s_{op}}{2\pi}}\right)^{-1} \qquad \text{(VI−5−71)}$$

where R_c is the freeboard, $s_{op} = H_s/L_{op}$, and L_{op} is deepwater wavelength corresponding to the peak wave period. Limits of Eq VI-5-71 are given by

$$0 < \frac{R_c}{H_s} \sqrt{\frac{s_{op}}{2\pi}} < 0.052$$

Table VI-5-25
Rock, Submerged Breakwaters with Two-Layer Armor on Front, Crest and Rear Slope
(van der Meer 1991)

Irregular, head-on waves

$$\frac{h_c'}{h} = (2.1 + 0.1\ S)\ \exp(-0.14\ N_s^*) \qquad \text{(VI-5-72)}$$

where h Water depth

h_c' Height of structure over seabed level ($h - h_c'$ is the water depth over the structure crest).

S Relative eroded area

N_s^* Spectral stability number, $N_s^* = \frac{H_s}{\Delta D_{n50}} s_p^{-1/3}$

Uncertainty of the formula: The uncertainty of Eq VI-5-72 can be expressed by considering the factor 2.1 as a Gaussian distributed stochastic variable with mean of 2.1 and standard deviation of 0.35, i.e., a coefficient of variation of 17%.

Data source: Givler and Sorensen (1986): regular head-on waves, slope 1:1.5

van der Meer (1991): irregular head-on waves, slope 1:2

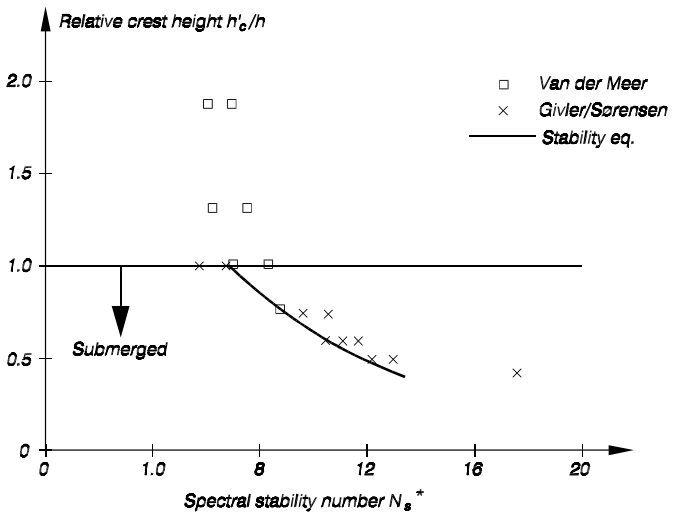

Table VI-5-26
Rock, Two-Layer Armored Low-Crested and Submerged Breakwaters (Vidal et al. 1992)

Tested trunk cross section

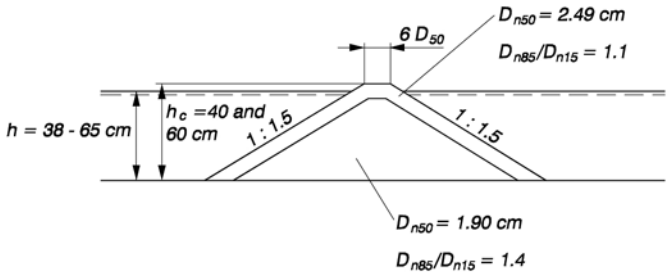

Tested ranges

Irregular, head-on waves

Spectral H_s=5-19 cm, T_p= 1.4 and 1.8 sec.

Free board : $-5\text{cm} \leq R_c = h_c - h \leq 6\text{cm}$

Dimensionless freeboard: $-2 \leq R_c/D_{n50} \leq 2.4$

Stability corresponding to initiation of damage, S=0.5-1.5

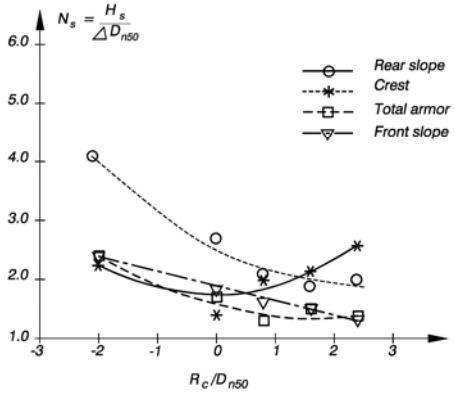

Stability corresponding to extraction of some rocks from lower layer , S=2.0-2.5.

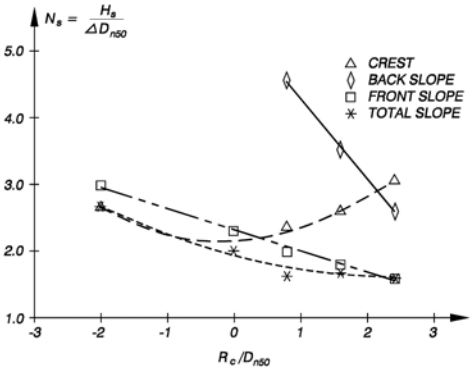

Table VI-5-27
Rock, Low-Crested Reef Breakwaters Built Using Only One Class of Stone

Irregular, head-on waves

van der Meer (1990)

Trunk cross section of reef breakwater

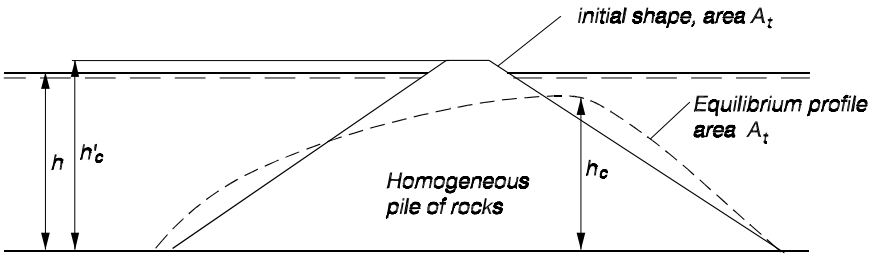

The equilibrium height of the structure

$$h_c = \sqrt{\frac{A_t}{\exp\left(aN_s^*\right)}} \quad \text{with a maximum of } h_c' \qquad \text{(VI−5−73)}$$

where A_t area of initial cross section of structure

h water depth at toe of structure

h_c' initial height of structure

$N_s^* = \frac{H_s}{\Delta D_{n50}} s_p^{-1/3}$

$a = -0.028 + 0.045 \frac{A_t}{(h_c')^2} + 0.034 \frac{h_c'}{h} - 6 \times 10^{-9} \frac{A_t^2}{D_{n50}^4}$

Data source: Ahrens (1987), van der Meer (1990)

Powell and Allsop (1985) analyzed data by Ahrens, Viggosson, and Zirkle (1982) and Ahrens (1984) and proposed the stability formula

$$\frac{N_{od}}{N_a} = a \exp\left[b\, H_s / \left(\Delta D_{n50}\right)\right] \quad \text{or} \quad \frac{H_s}{\Delta D_{n50}} = \frac{1}{b} \ln\left(\frac{1}{a}\frac{N_{od}}{N_a}\right) \qquad \text{(VI−5−74)}$$

where values of the empirical coefficients a and b are given in the table as functions of freeboard R_c and water depth h. N_{od} and N_a are the number of displaced rocks and the total number of rocks in the mound, respectively.

Values of coefficients a and b in Eq (VI-5-74).

R_c/h	$a \cdot 10^4$	b
0.0	15	0.31
0.2	17	0.33
0.4	4.8	0.53

Valid for $0.0012 < H_s/L_p < 0.036$

Table VI-5-28
Rock, Rear Slope Stability of Two-Layer Armored Breakwaters Without Superstructures
(Jensen 1984)

Irregular, head-on waves

Jensen (1984) reported results from two case studies of conventional rock armored rubble-mound breakwaters with the main armor carried over the crests and the upper part of the rear slope. Crest width was approximately 3–4 stone diameters. Although Jensen points out that the results are very project dependent, these results could be useful for preliminary estimates. Wave steepness significantly influences the rear side damage.

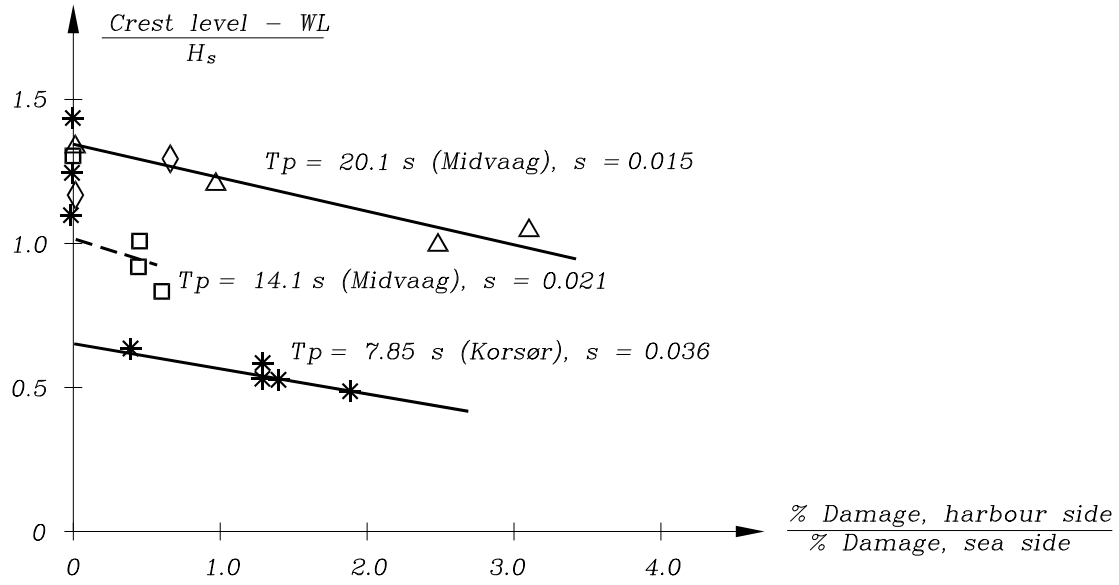

.

Table VI-5-29
Concrete Cubes, Two-Layer Armored Non-Overtopped Slopes

van der Meer (1988b)

$$N_s = \frac{H_s}{\Delta D_n} = \left(6.7\, N_{od}^{0.4}/N_z^{0.3} + 1.0\right)\, s_m^{-0.1} \qquad \text{(VI}-5-75\text{)}$$

where
- H_s Significant wave height in front of breakwater
- ρ_s Mass density of concrete
- ρ_w Mass density of water
- Δ $\left(\rho_s/\rho_w\right) - 1$
- D_n Cube length
- N_{od} Number of units displaced out of the armor layer within a strip width of one cube length D_n
- N_z Number of waves
- s_{om} Wave steepness, $s_{om} = H_s/L_{om}$

Valid for: Non-depth-limited wave conditions. Irregular head-on waves

Two layer cubes randomly placed on 1:1.5 slope

Surf similarity parameter range $3 < \xi_m < 6$

Uncertainty of the formula: corresponds to a coefficient of variation of approximately 0.10

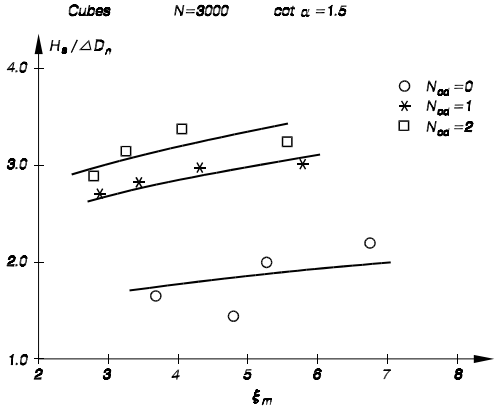

Brorsen, Burcharth, and Larsen (1974)

Brorsen, Burcharth, and Larsen gave the following average N_s and corresponding K_D-values for a two layer concrete cube armor, random placement, slope angles $1.5 \leq \cot\alpha \leq 2.0$ and non-depth-limited irregular waves

Damage level	$N_s = \frac{H_s}{\Delta D_n}$	K_D	
		slope 1 : 1.5	slope 1 : 2
Onset, $D = 0\%$	1.8 - 2.0	3.9 - 5.3	2.9 - 4.0
Moderate, $D = 4\%$	2.3 - 2.6	8.1 - 12	6.1 - 8.8

Table VI-5-30
Tetrapods, Two-Layer Armored Non-Overtopped Slopes

van der Meer (1988b) for non-depth-limited waves

$$N_s = \frac{H_s}{\Delta D_n} = \left(3.75\, N_{od}^{0.5}/N_z^{0.25} + 0.85\right) s_{om}^{-0.2} \qquad \text{(VI−5−76)}$$

where

H_s	Significant wave height in front of breakwater
ρ_s	Mass density of concrete
ρ_w	Mass density of water
Δ	$(\rho_s/\rho_w) - 1$
D_n	Equivalent cube length, i.e., length of cube with the same volume as Tetrapods
N_{od}	Number of units displaced out of the armor layer within a strip width of one cube length D_n
N_z	Number of waves
s_{om}	Wave steepness, $s_{om} = H_s/L_{om}$

Valid for: Non-depth limited wave conditions, Irregular head-on waves
Two layer tetrapods on 1:1.5 slope

Surf similarity parameter range $3.5 < \xi_m < 6$

Uncertainty of the formula: corresponds to a coefficient of variation of approximately 0.10

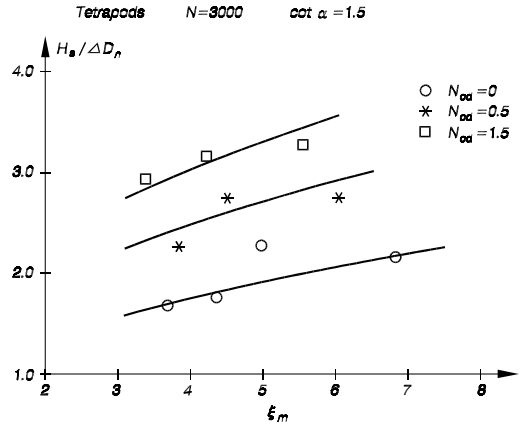

d'Angremond, van der Meer, and van Nes (1994) for depth-limited waves

$$N_s = \frac{H_{2\%}}{\Delta D_n} = 1.4\left(3.75\, N_{od}^{0.5}/N_z^{0.25} + 0.85\right) s_{om}^{-0.2} \qquad \text{(VI−5−77)}$$

In deep water the ratio $H_{2\%}/H_s = 1.4$ for Rayleigh distributed waves. In shallow water this ratio decreases with decreasing relative water depth due to wave breaking.

Table VI-5-31
Dolos, Non-Overtopped Slopes (Burcharth and Liu 1992)

$$N_s = \frac{H_s}{\Delta D_n} = (47 - 72\,r)\,\varphi_{n=2} D^{1/3} N_z^{-0.1}$$

$$= (17 - 26\,r)\,\varphi_{n=2}^{2/3} N_{od}^{1/3} N_z^{-0.1} \qquad \text{(VI-5-78)}$$

where

H_s	Significant wave height in front of breakwater
ρ_s	Mass density of concrete
ρ_w	Mass density of water
Δ	$(\rho_s/\rho_w) - 1$
D_n	Equivalent cube length, i.e., length of cube with the same volume as dolosse
r	Dolos waist ratio
φ	Packing density
D	Relative number of units within levels SWL $\pm$ 6.5 Dn displaced one dolos height h, or more (e.g., for 2% displacement insert $D = 0.02$)
N_{od}	Number of displaced units within a strip width of one equivalent cube length D_n
N_z	Number of waves. For $N_z \geq 3000$ use $N_z = 3000$

Valid for: Breaking and nonbreaking wave conditions
Irregular head-on waves, two layer randomly placed dolosse with a 1:1.5 slope

$0.32 < r < 0.42$

$0.61 < \varphi < 1$

$1\% < D < 15\%$

$2.49 < \xi_0 < 11.7$

Slope angle: The effect of the slope angle on the hydraulic stability is not included in Eq VI-5-78. Brorsen, Burcharth, and Larsen (1974) found only a marginal influence for slopes in the range 1:1 to 1:3.

Uncertainty of the formula: corresponds to a coefficient of variation of approximately 0.22.

(continued)

Table VI-5-31 (Concluded)

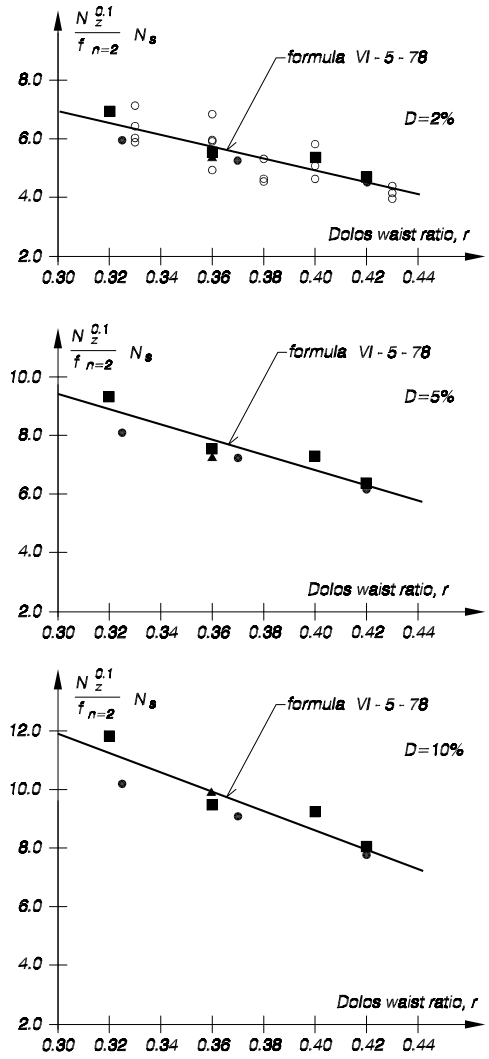

Legend:

Reference	$\phi_{n=2}$	Repeated No	Duration (min.)	ξ_{mo}
▲ Brorsen et al. (1974)	1 (App.)	2	60	2.49-5.37
■ Burcharth et al. (1986)	0.61-0.7	5 or 15	20	3.04-4.49
○ Holtzhausen et al. (1990)	1	3 or 8	60	2.91-7.6
● Burcharth et al. (1992)	0.74	20	5	3.23-11.7

Fit of hydraulic stability formula for a two-layer randomly placed dolos armor on a slope of 1:1.5. Damage levels, $D = 2\%$, 5% and 10% displaced units within levels SWL $\pm$ $6.5D_n$.

Table VI-5-32
ACCROPODE 7 (van der Meer 1988b)

$$N_s = \frac{H_s}{\Delta D_n} = \begin{cases} 3.7 & \text{no damage} \\ 4.1 & \text{failure} \end{cases} \qquad \text{(VI-5-79)}$$

where H_s Significant wave height in front of breakwater

ρ_s Mass density of concrete

ρ_w Mass density of water

Δ $(\rho_s/\rho_w) - 1$

D_n Equivalent cube length, i.e., length of cube with the same volume as Accropode

Valid for: Irregular, head-on waves
Nonbreaking wave conditions
One layer of Accropodes on slope 1:1.33 placed in accordance with SOGREAH recommendations

No influence of number of waves were found except after start of failure.

Uncertainty of the formula: The standard deviation of the factors 3.7 and 4.1 is approximately 0.2.

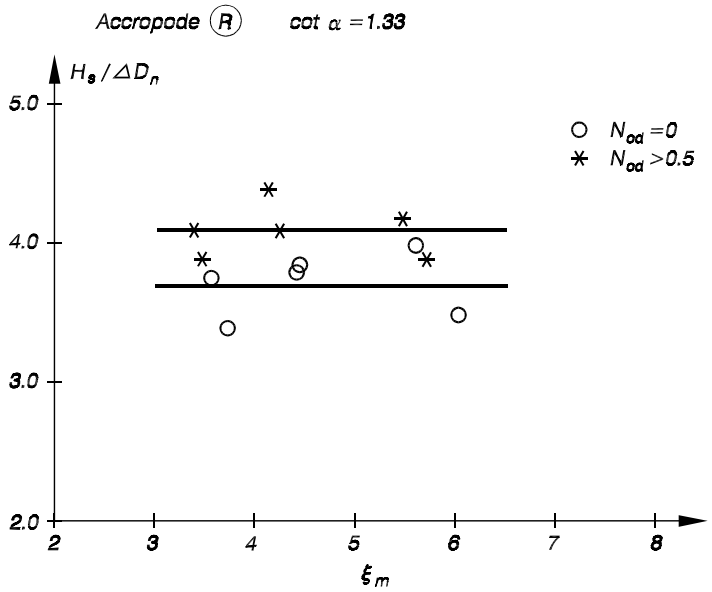

Table VI-5-33
ACCROPODE 7, Non-Overtopped or Marginally Overtopped Slopes (Burcharth et al. 1998)

$$N_s = \frac{H_s}{\Delta D_n} = A\left(D^{0.2} + 7.70\right) \quad \text{or} \quad D = 50\left(\frac{H_s}{\Delta D_n} - 3.54\right)^5 \qquad \text{(VI-5-80)}$$

where	H_s	Significant wave height in front of breakwater
	ρ_s	Mass density of concrete
	ρ_w	Mass density of water
	Δ	$\left(\rho_s/\rho_w\right) - 1$
	D_n	Equivalent cube length, i.e., length of cube with the same volume as Accropode
	D	Relative number of units displaced more than distance D_n
	A	Coefficient with mean value $\mu = 0.46$ and coefficient of variation $\sigma/\mu = 0.02 + 0.05(1 - D)^6$, where σ is the standard deviation

Valid for: Irregular, head-on waves

Breaking and nonbreaking wave conditions

One layer of Accropodes on 1:1.33 slope placed in accordance with SOGREAH recommendations

Accropodes placed on filter layer and conventional quarry rock run

$3.5 < \xi_m < 4.5$ (minimum stability range, see figure)

No influence of number of waves were found except after start of failure.

Uncertainty of the formula: see figure and explanation of A.

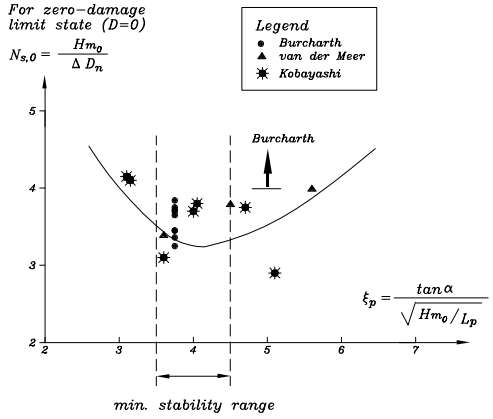

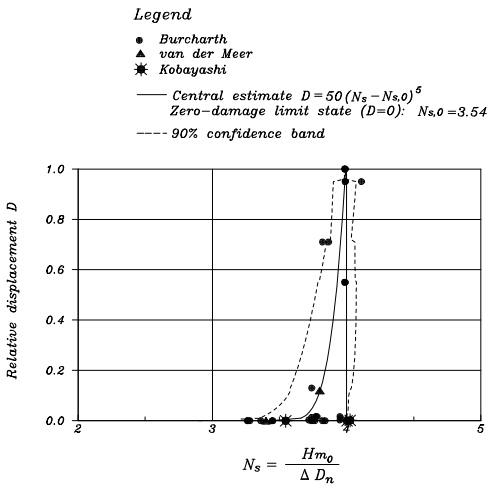

SOGREAH recommends for preliminary design the following K_D-values to be used in Eq VI-5-67.

$$K_D = \begin{cases} 15 & \text{Nonbreaking waves} \\ 12 & \text{Breaking waves} \end{cases}$$

Table VI-5-34
CORE-LOC 7, Non or Marginally Overtopped Slopes
(Melby and Turk 1994; Turk and Melby 1997)

Irregular, head-on waves

$$\frac{H}{\Delta D_{n50}} = (K_D \cot \alpha)^{1/3} \quad or \quad M_{50} = \frac{\rho_c H^3}{K_D (\frac{\rho_c}{\rho_w} - 1)^3 \cot \alpha} \tag{VI-5-81}$$

where H Characteristic wave height (H_s)
D_{n50} Equivalent length of cube having same mass as Core-Loc, $D_{50} = (M_{50}/\rho_c)^{1/3}$
M_{50} Mass of Core-Loc armor unit, $M_{50} = \rho_c (D_{n50})^3$
ρ_c Mass density of concrete
ρ_w Mass density of water
Δ $(\rho_c/\rho_w) - 1$
α Slope angle
K_D Stability coefficient

Trunk section stability. Melby and Turk (1994) found no reasonable ($K_D < 50$) irregular breaking or nonbreaking wave conditions that would destabilize the layer. For an armor layer exposed to regular depth-limited plunging to collapsing waves, $K_D = 16$ in Equation VI-5-81 is recommended for preliminary design of all trunk sections. The recommended value of K_D is conservative, and it represents a zero-damage condition with little to no armor unit rocking. Site specific physical model tests will usually yield higher values.

Head section stability. $K_D = 13$ is recommended for preliminary design of head sections exposed to both breaking and nonbreaking oblique and head-on waves.

Stability test parameters

Model parameters	M_{50} = 219 g; Depths: 36 and 61 cm; Height: 90 cm
Wave parameters	4.6 # H_{mo} # 36 cm; 1.5 # T_p # 4.7 sec
Structure slope, α	1V:1.33H and 1V:1.5H
Surf similarity parameter	2.13 # ξ_o # 15.9
Relative depth	0.012 # d/L_o # 0.175
Wave steepness	0.001 # H_{mo}/L_o # breaking

Placement. Core-Locs are intended to be randomly placed in a single-unit thick layer on steep or shallow slopes. They are well suited for use in repairing existing dolos structures because they interlock well with dolosse when properly sized (length of Core-Loc central flume is 92 percent of the dolosse fluke length).

Table VI-5-35
Tetrapods, Horizontally Composite Breakwaters (Hanzawa et al. 1996)

$$N_s = \frac{H_s}{\Delta D_n} = 2.32 \left(N_{od} / N_z^{0.5} \right)^{0.2} + 1.33 \qquad \text{(VI−5−82)}$$

where
- H_s Significant wave height in front of breakwater
- ρ_s Mass density of concrete
- ρ_w Mass density of water
- Δ $(\rho_s/\rho_w) - 1$
- D_n Equivalent cube length, i.e., length of cube with the same volume as Tetrapods
- N_{od} Number of units displaced out of the armor layer within a strip width of one cube length D_n
- N_z Number of waves

Test range: The formula was obtained by fitting of earlier model test results and five real project model tests

Irregular head-on waves
Water depth: 0.25 - 0.50 cm
Slope: 1:1.5
Foreshore : 1:15 - 1:100
Mass of Tetrapods: 90 - 700 g
H_s: 8 - 25.9 cm; T_s: 1.74 - 2.5 s; s_{om}: 0.013 - 0.04

Uncertainty of the formula: Not given. Tanimoto, Haranaka, and Yamazaki (1985) gave the standard deviation of N_{od} equal to $0.36 N_{od}^{0.5}$

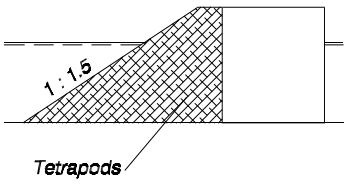

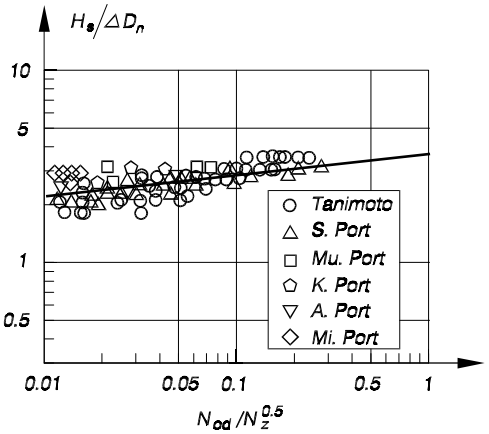

Table VI-5-36
Tribars, Non-Overtopped or Minor Overtopped Slopes, Random and Uniform Placement

Regular, head-on waves

$$\frac{H}{\Delta D_{n50}} = \left(K_D \cot\alpha\right)^{1/3} \quad \text{or} \quad M_{50} = \frac{\rho_s H^3}{K_D \left(\frac{\rho_s}{\rho_w} - 1\right)^3 \cot\alpha} \tag{VI-5-83}$$

where
H Characteristic wave height (H_s)
D_{n50} Equivalent cube length of median rock
M_{50} Median mass of stone armor unit, $M_{50} = \rho_s (D_{n50})^3$
ρ_s Mass density of stone
ρ_w Mass density of water
Δ $(\rho_s/\rho_w) - 1$
α Slope angle
K_D Stability coefficient

Trunk section stability

K_D-values by *Shore Protection Manual* (1984), $H - H_{1/10}$, 0% to 5% damage

Placement	Layers	Breaking waves[1]	Nonbreaking waves[2]	Slope angle cot α
Random	2	9.0	10.0	1.5 – 3.0
Pattern-placed	1	12.0	15.0	(not given)

[1] Depth-limited breaking with waves breaking in front of and on the armor slope.
[2] No depth-limited breaking occurs in front of the armor slope.

- Design wave height considerations. In shallow water the most severe wave condition for design of any part of a rubble-mound structure is usually the combination of predicted water depth and extreme incident wave height and period that produces waves which would break directly on the structure. In some cases, particularly for steep foreshore wlopes, waves breaking offshore will strike directly on the structure. Goda (1985) recommended computing the design wave height a distance $5H_s$ from the structure toe to account for the travel distance of large breakers. A shallow-water coastal structure exposed to a variety of water depths, especially a shore-perpendicular structure such as a groin, should have wave conditions investigated for each range of water depths to determine the highest breaking wave that might impact any part of the structure. For example, a groin that normally experiences wave forces on its armor layer near the seaward end might become submerged during storm surges, and the worst breaking wave condition could occur on a more landward portion of the groin. The effect of oblique wave approach on armor layer stability has not yet been sufficiently quantified. Tests in the European Marine Science and Technology (MAST) program seemed to indicate relatively little reduction

in damage for rock armored slopes subjected to oblique wave approach angles up to 60 deg compared to waves of normal incidence (Allsop 1995). The stability of any rubble-mound structure exposed to oblique wave attack should be confirmed with physical model tests.

(6) Structure head section stability.

(a) Under similar wave conditions the round head of a rubble-mound structure normally sustains more extensive and more frequent damage than the structure trunk. One reason is very high cone-overflow velocities, sometimes enhanced in certain areas by wave refraction. Another reason is the reduced support from neighboring units in the direction of wave overflow on the lee side of the cone as shown in Figure VI-5-37. This figure also illustrates the position of the most critical area for armor layer instability. The toe within the same area is also vulnerable to damage in shallow-water situations, and a toe failure will often trigger failure of the armor layer see Part VI-5-6*b*(2), "Scour at sloping structures."

(b) Table VI-5-37 presents stability criteria for stone and dolos rubble-mound structure heads subjected to breaking and nonbreaking waves without overtopping, and Table VI-5-38 gives stability criteria for tetrapod and tribar concrete armor units.

(c) The stability in the critical area of the roundhead might be improved by increasing the head diameter or adding a tail as shown in Figure VI-5-38. Besides obtaining better support from neighboring units, a reduction in wave heights by diffraction is also achieved before the waves reach the vulnerable rear side. Optimization of the slope angle and the layout geometry of cone roundheads can only be achieved by physical model tests because quantitative information on roundhead stability is limited.

(d) The armor layer at bends and corners is generally more exposed than in straight trunk sections. A convex bend or corner will often follow the seabed contours because construction in deeper water increases costs dramatically. Refraction might then cause an increase of the wave height as illustrated in Figure VI-5-39, which in turn increases wave runup and overtopping. Moreover, in sharper convex corners and bends the lateral support by neighbor blocks is reduced as in the case of roundheads. A concave bend or corner will often be exposed to larger waves than the neighboring trunk sections due to the concentration of wave energy by oblique reflection on the slope (Figure VI-5-39). Consequently, runup and overtopping will also be increased.

(7) Riprap armor stability.

(a) The previous armor stability formulations are intended for fairly uniform distributions of armor stone or for uniform size concrete armor units. Riprap armor is characterized by fairly wide gradations in rock size with a large size difference between the largest and smallest stones in the distribution. Use of graded riprap cover layers is generally more applicable to revetments than to breakwaters or jetties. A limitation on the use of graded riprap is that the design wave height should be less than about 1.5 m. At higher design wave heights uniform-size armor units are usually more economical.

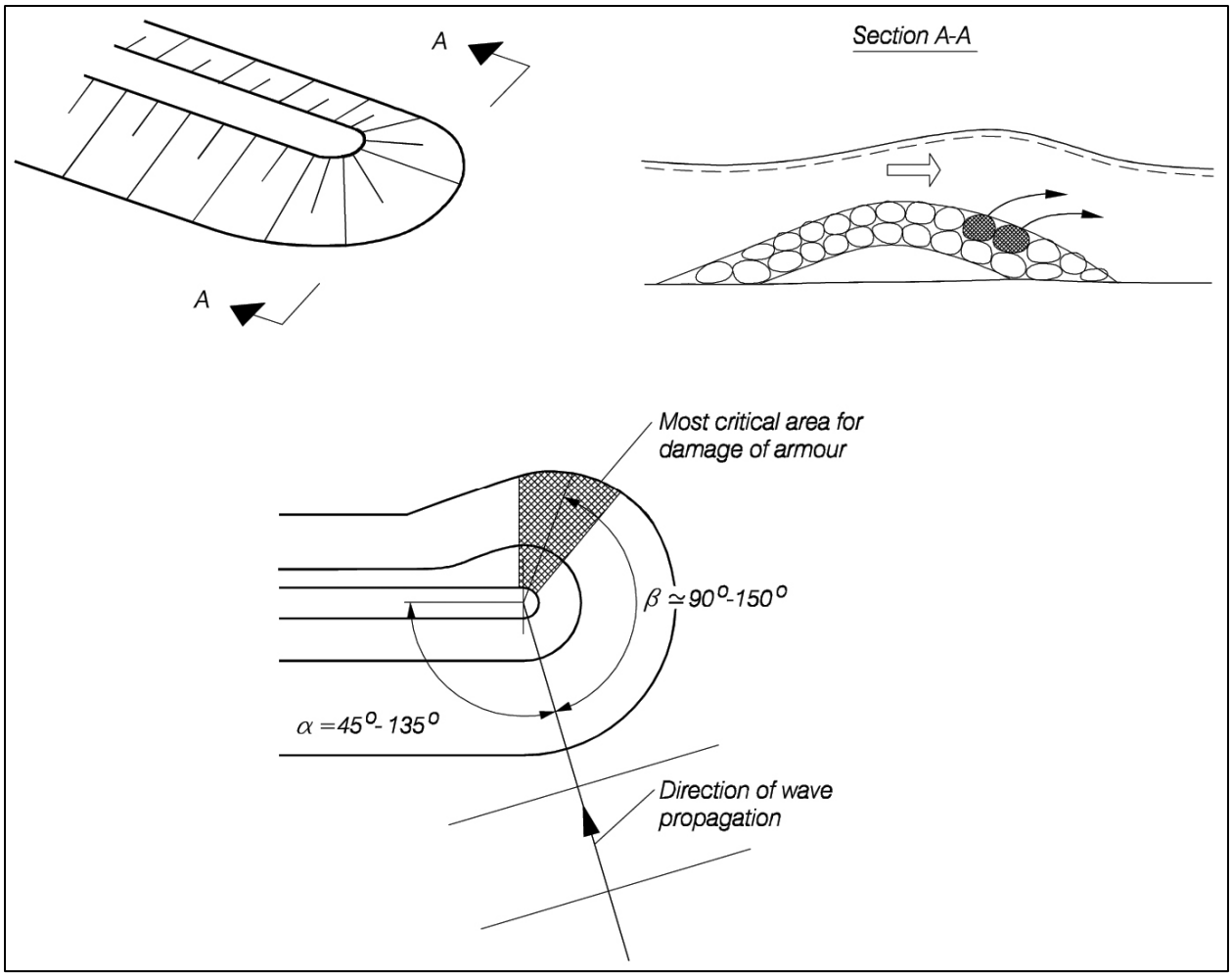

Figure VI-5-37. Illustration of critical areas for damage to armor layers in the round head (Burcharth 1993)

Table VI-5-37
Rock and Dolos Breakwater Head Stability, No Overtopping (Carver and Heimbaugh 1989)

Rock and dolos armor, monochromatic waves

Mostly monochromatic waves with a few irregular wave cases

Breaking and nonbreaking waves

Incident wave angles: 0^o, 45^o , 90^o, 135^o (note: 0^o is wave crests perpendicular to trunk)

$$\frac{H}{\Delta D_{n50}} = A\xi^2 + B\xi + C_C \qquad \text{(VI-5-84)}$$

where

$$\xi = \frac{\tan\alpha}{\left(H/L\right)^{1/2}}$$

and
H Characteristic wave height
D_{n50} Equivalent cube length of median rock
ρ_s Mass density of stone
ρ_w Mass density of water
Δ $(\rho_s / \rho_w) - 1$
L Local wavelength at structure toe
α Structure armor slope
A,B,C_c Empirical coefficients

Table of coefficients for use in Equation VI-5-84

Armor Type	A	B	C_c	Slope	Range of ξ
Stone	0.272	-1.749	4.179	1V to 1.5H	2.1 – 4.1
Stone	0.198	-1.234	3.289	1V to 2.0H	1.8 – 3.4
Dolos	0.406	-2.800	6.881	1V to 1.5H	2.2 – 4.4
Dolos	0.840	-4.466	8.244	1V to 2.0H	1.7 – 3.2

Notes: The curves giving the best fit to the data were lowered by two standard deviations to provide a conservative lower envelope to the stability results.

A limited number of tests using irregular waves produced corresponding results with T_p equivalent to the monochromatic period and H_{mo} equal to the monochromatic wave height.

Table VI-5-38
Tetrapod and Tribar Breakwater Head Section Stability, No Overtopping

Regular, head-on waves

$$\frac{H}{\Delta D_{n50}} = \left(K_D \cot\alpha\right)^{1/3} \quad \text{or} \quad M_{50} = \frac{\rho_s H^3}{K_D \left(\frac{\rho_s}{\rho_w} - 1\right)^3 \cot\alpha} \tag{VI-5-85}$$

where H Characteristic wave height (H_s)
D_{n50} Equivalent cube length of median rock
M_{50} Median mass of stone armor unit, $M_{50} = \rho_s (D_{n50})^3$
ρ_s Mass density of stone
ρ_w Mass density of water
Δ $(\rho_s / \rho_w) - 1$
α Slope angle
K_D Stability coefficient

Head Section Stability.

K_D-values by *Shore Protection Manual* (1984), H = $H_{1/10}$, 0 percent to 5 percent damage

Armor Unit	Placement	Layers	Breaking Waves[1]	Nonbreaking Waves[2]	Slope Angle cot α
Tetrapod	Ramdom	2	5.0[3]	6.0	1.5
			4.5	5.5	2.0
			3.5	4.0	3.0
Tribar	Random	2	8.3	9.0	1.5
			7.8	8.5	2.0
			6.0	6.5	3.0
Tribar	Pattern	1	7.5	9.5	(not given)

[1] Depth-limited breaking with waves breaking in front of and on the armor slope.
[2] No depth-limited breaking occurs in front of the armor slope.
[3] K_D values shown in italics are unsupported by tests results and are provided only for preliminary design purposes.

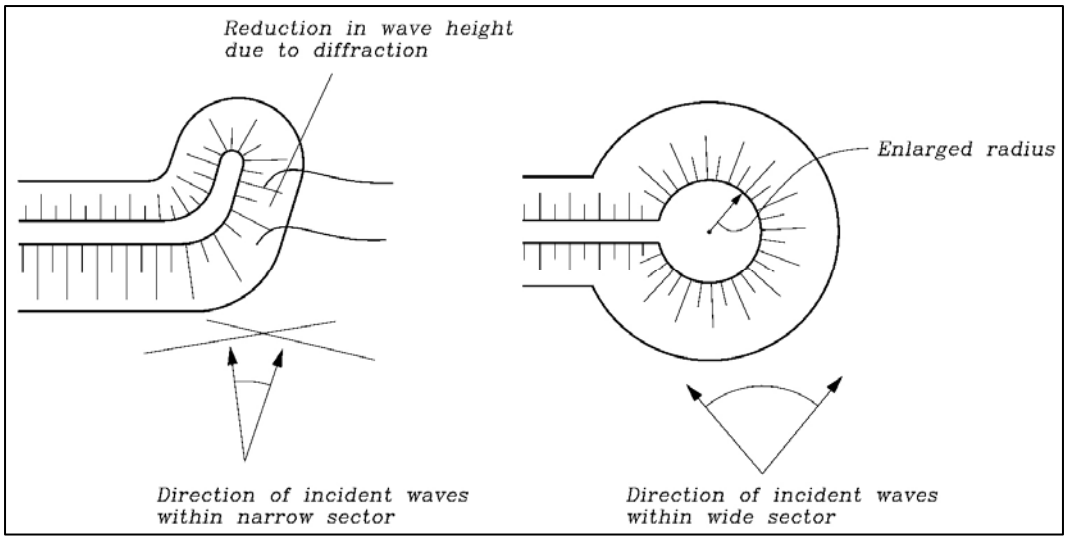

Figure VI-5-38. Illustration of improvement of round head stability by change of geometry (Burcharth 1993)

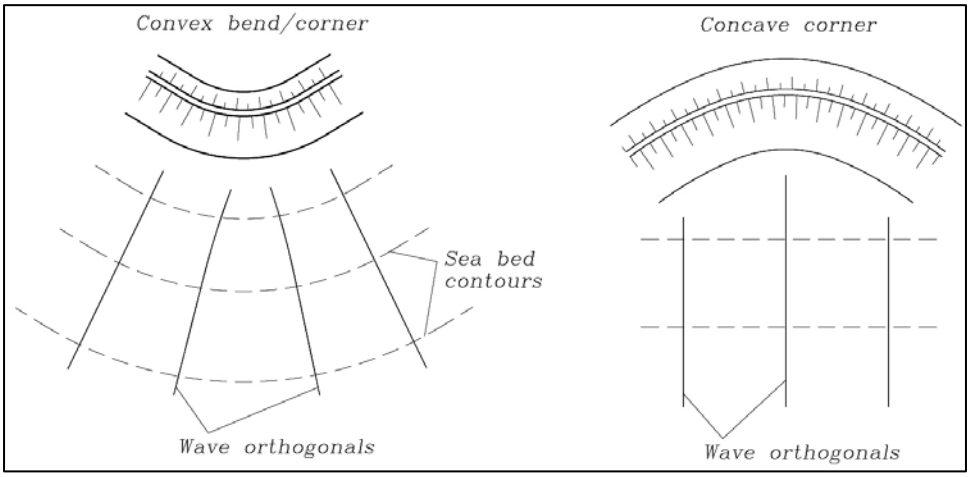

Figure VI-5-39. Convex and concave bends and corners

Generally, the maximum and minimum stone weights in riprap gradations should be limited to

$$W_{\max} = 4.0W_{50} \qquad W_{\min} = 0.125W_{50}$$

where W_{50} is the median stone weight. The median stone mass for a stable riprap distribution can be determined using the Hudson equation

$$M_{50} = \frac{\rho_r H_{10\%}^3}{K_{RR}\left(\frac{\rho_r}{\rho_w} - 1\right)^3 \cot\alpha} \tag{VI-5-86}$$

where ρ_r is the mass density of the riprap, K_{RR} is the riprap stability coefficient, and the other variables are as defined for Equation VI-5-67 in Table VI-5-22. Recommended conservative stability coefficients (0 percent to 5 percent damage) are K_{RR} = 2.2 for breaking waves and K_{RR} = 2.5 for nonbreaking waves (Ahrens 1981b). Melby and Kobayashi (1998b) showed that deterioration of riprap and uniform armor with equivalent median stone weights was similar. Therefore, Equation VI-5-62 through VI-5-66 could be used to estimate damage progression for both narrow gradations and riprap. The van der Meer (1988) equation (see Table VI-5-23) can also be used to design riprap armor.

(b) An examination of riprap field performance at 14 different dams across the La Grande Hydroelectic complex in Quebec, Canada, generally confirmed the validity of Equation VI-5-86 (Belfadhel, Lefebvre, and Rohan 1996; also see discussion of this paper by van der Meer 1997). Design of riprap armor layer cross sections is covered in Part VI-5-3e, "Design of structure cross section." A complete design example for a riprap armored slope is included in Part VI-7, "Example Problems."

b. Granulated filters and geotextile filter stability. In coastal engineering, filter layers are defined as layers that protect the underlying base material or soil from erosion by waves and currents without excessive buildup of pore pressure in the underlying material. Filter functions can be achieved using either one or more layers of granulated material such as gravel or small stone of various grain sizes, geotextile fabric, or a combination of geotextile overlaid with granulated material. This section covers the function and design of granulated filters. Design criteria for geotextile filter cloth used in filter application are given in Part VI-4-7, "Geotextiles and Plastics." Design of rubble-mound structure underlayers is covered in Part VI-5-3*e*, "Design of structure cross section."

(1) Filter layer functions. Filter layers are designed to achieve one or more of the following objectives in coastal structures. They can prevent the migration of underlying sand or soil particles through the filter layer voids into the overlying rubble-mound structure layers. Leeching of base material could be caused by turbulent flow within the structure or by excessive pore pressures that can wash out fine particles. Without a filter layer, foundation or underlayer material would be lost and the stones in the structure layer over the filter would sink into the void resulting in differential settlement and decreased structure crest elevation.

Filter layers can aid in the distribution of structure weight. A bedding filter layer helps to distribute the structure's weight over the underlying base material to provide more uniform settlement. A levelled bedding layer also ensures a more uniform baseplate load on caisson structures.

Filter layers can also reduce the hydrodynamic loads on a structure's outer stone layers. A granular filter layer can help dissipate flow energy whereas a geotextile filter will not be as effective in this regard.

(a) Granulated filters are commonly used as a bedding layer on which a coastal structure rests, or in construction of revetments where the filter layer protects the underlying embankment. Filter layers are also needed in rubble-mound structures having cores composed of fine materials like sand or gravel. Stone blankets (used to prevent erosion due to waves and currents) also

reduce leeching of the underlying sand or soil, but in this situation stability of the stone blanket material in waves and currents is an important design concern. Design of stone blankets is covered in Part VI-5-3*f*, "Blanket stability in current fields."

(b) It is advisable to place coastal structures on a bedding layer (along with adequate toe protection) to prevent or reduce undermining and settlement. When rubble structures are founded on cohesionless soil, especially sand, a filter blanket should be provided to prevent differential wave pressures, currents, and groundwater flow from creating an unstable foundation condition through removal of particles. Even when a filter blanket is not needed, bedding layers may be used to prevent erosion during construction, to distribute structure weight, or to retain and protect a geotextile filter cloth. Bedding layers are not necessary where depths are greater than about three times the maximum wave height, where the anticipated bottom current velocities are below the incipient motion level for the average-size bed material, or where the foundation is a hard, durable material such as bedrock.

(c) In some situations granular filters have several advantages over geotextile filters in coastal construction (Permanent International Association of Navigation Congresses (PIANC) 1992).

- The filter elements (stone, gravel, sand, etc.) are usually very durable.

- Granular filters provide a good contact interface between the filter and base material below and between the filter and overlying layers. This is important for sloping structures.

- Granular bedding layers can help smooth bottom irregularities and thus provide a more uniform construction base.

- The porosity of granular filters help damp wave energy.

- Self-weight of the filter layer contributes to its stability when exposed to waves and currents during construction whereas geotextiles may have to be weighted under similar conditions.

- The loose nature of the filter elements allows the filter to better withstand impacts when larger stones are placed on the filter layer during construction or the stones shift during settlement.

- Granular filter layers are relatively easy to repair, and in some instances may be self-healing.

- Filter materials are widely available and inexpensive.

(d) The major disadvantage of granular filters is the difficulty of assuring uniform construction underwater to obtain the required thickness of the filter layer.

(e) Placing larger armor stone or riprap directly on geotextile filter cloth is likely to puncture the fabric either during placement or later during armor settlement. Placing a granular

filter layer over the geotextile fabric protects it from damage. In this application there is more flexibility in specifying the filter stone gradation because the geotextile is retaining the underlying soil.

(2) Granulated filter failure modes. Granular filter layers fail their intended function when:

(a) The base layer is eroded through the filter layer. Erosion can occur either by outgoing flow washing out particles perpendicular to the base/filter interface or by wave- and current-induced external flows parallel to the interface.

(b) The filter layer becomes internally unstable. Instability occurs in filters having a very wide gradation when the finer fraction of the filter grain-size distribution is flushed out of the layer between the coarser material. This could result in compaction of the filter layer, differential settlement of the overlayers, and gradual increase in layer permeability.

(c) The interface between adjacent granular layers becomes unstable, and lateral shearing motion occurs between layers constructed on a slope.

(d) The filter layer fails to protect the underlying geotextile fabric from punctures and loss of soil through the filter cloth.

(3) Granulated filter design criteria.

(a) Design criteria for granular filters were originally based on the geometry of voids between packed, uniform spheres. Allowances for grain-size distributions (and many successful field applications) led to the following established geometric filter design criteria. (Design guidance for exposed filter layers must also consider instability due to flow as discussed in Part VI-5-3f, “Blanket stability in current fields.”

- Retention criterion. To prevent loss of the foundation or core material by leeching through the filter layer, the grain-size diameter exceeded by 85 percent of the filter material should be less than approximately four or five times the grain-size diameter exceeded by the coarsest 15 percent of the foundation or underlying material, i.e.,

$$\frac{d_{15(\text{filter})}}{d_{85(\text{foundation})}} < (4 \text{ to } 5) \tag{VI-5-87}$$

The coarser particles of the foundation or base material are trapped in the voids of the filter layer, thus forming a barrier for the smaller sized fraction of the foundation material. The same criterion can be used to size successive layers in multilayer filters that might be needed when there is a large disparity between void sizes in the overlayer and particle sizes in the material under the filter. Filter layers overlying coarse material like quarry spall and subject to intense dynamic forces should be designed similar to a rubble-mound structure underlayer with

$$\frac{W_{50(\text{filter})}}{W_{50(\text{foundation})}} < (15 \text{ to } 20) \tag{VI-5-88}$$

- Permeability criterion. Adequate permeability of the filter layer is needed to reduce the hydraulic gradient across the layer. The accepted permeability criterion is

$$\frac{d_{15(\text{filter})}}{d_{15(\text{foundation})}} > (4 \text{ to } 5) \tag{VI-5-89}$$

- Internal stability criterion. If the filter material has a wide gradation, there may be loss of finer particles causing internal instability. Internal stability requires

$$\frac{d_{60(\text{filter})}}{d_{10(\text{filter})}} < 10 \tag{VI-5-90}$$

- Layer thickness. Filter layers constructed of coarse gravel or larger material should have a minimum thickness at least two to three times the diameter of the larger stones in the filter distribution to be effective. Smaller gravel filter layer thickness should be at least 20 cm, and sand filter layers should be at least 10 cm thick (Pilarczyk 1990). These thickness guidelines assume controlled above-water construction. In underwater placement, bedding layer thickness should be at least two to three times the size of the larger quarrystones used in the layer, but never less than 30 cm thick to ensure that bottom irregularities are completely covered. Considerations such as shallow depths, exposure during construction, construction method, and strong hydrodynamic forces may dictate thicker filters, but no general rules can be stated. For deeper water the uncertainty related to construction often demands a minimum thickness of 50 cm.

- Bedding layer over geotextile fabric. In designs where a geotextile fabric is used to meet the retention criterion, a covering layer of quarry spalls or crushed rock (10-cm minimum and 20-cm maximum) should be placed to protect against puncturing by the overlying stones. Recommended minimum bedding layer thickness in this case is 60 cm, and filtering criteria should be met between the bedding layer and overlying stone layer.

(b) Examples of typical granular filters and bedding layers are illustrated in Lee (1972), who discussed and illustrated applications of granular and geotextile filters in coastal structures. Design of filters for block-type revetments with large holes in the cover layer can be found in the PIANC (1992) reference.

(c) The previous geometric granular filter criteria are widely accepted in practice, and they are recommended in cases when an appreciable pressure gradient is expected perpendicular to the soil/filter interface. However, these rules may be somewhat conservative in situations without significant pressure gradients and when flow is parallel to the filter layer.

(d) The need for reliable granular filter design guidance under steady flow and cyclic design conditions fostered research by Delft Hydraulics Laboratory in support of the Oosterschelde Storm Surge Barrier in The Netherlands. Stationary and cyclic flow both parallel to and perpendicular to the filter layer were investigated by de Graauw, van der Meulen, and van der Does de Bye (1984). They developed hydraulic filter criteria based on an expression for critical hydraulic gradient parallel to the filter/soil interface. This method assumes that erosion of base material is caused by shear stresses rather than groundwater pressure gradients; and where this is the case, the geometric filter requirements can be relaxed.

(e) The filter design guidance of de Graauw et al. was expressed in terms of the filter d_{15}, base material d_{50}, filter porosity, and critical shear velocity of the base material; and acceptable values for the critical gradient were given by graphs for each of the flow cases. Design of a hydraulic granular filter requires good understanding of the character of flow within the filter layer, e.g., steady flow in channels. In these cases the method of de Graauw et al. (1984) can be used. More recent research aimed at improving granular filter design criteria was reported by Bakker, Verheij, and deGroot (1994).

(4) Granulated filter construction aspects.

(a) Granular filter construction above water creates no special problems, and accurate placement is straightforward. However, constructing a filter beneath the water surface is somewhat more problematic. If small-size filter material with a wide gradation is dropped into place, there is a risk of particle segregation by size. This risk can be decreased by using more uniform material and minimizing the drop distance. Another problem is maintaining adequate layer thickness during underwater placement. This has led to the recommended layer thickness being greater than required by the geometric filter criteria. Finally, filter or bedding layers placed underwater are exposed to eroding waves and currents until the overlayers are placed. Depending on site-specific conditions, this factor may influence the construction sequence or the time of year chosen for construction.

(b) It is common practice to extend the bedding layer beneath rubble-mound structures at least 1.5 m beyond the toe of the cover stone to help reduce toe scour. Some low rubble-mound structures have no core, and instead are composed entirely of armor layer and underlayers. These structures should have a bedding layer that extends across the full width of the structure.

c. Structural integrity of concrete armor units.

(1) Introduction.

(a) Figure VI-5-40 shows examples of the wide variety of existing concrete armor units. These might be divided into the following categories related to the structural strength:

Massive or blocky	(e.g., cubes including Antifer type, parallelepiped block, grooved cube with hole)
Bulky	(e.g., seabee, Core-Loc®, Accropode®, Haro®, dolos with large waist ratios)
Slender	(e.g., tetrapod, dolos with smaller waist ratios)
Multi-hole cubes	(e.g., shed, cob)

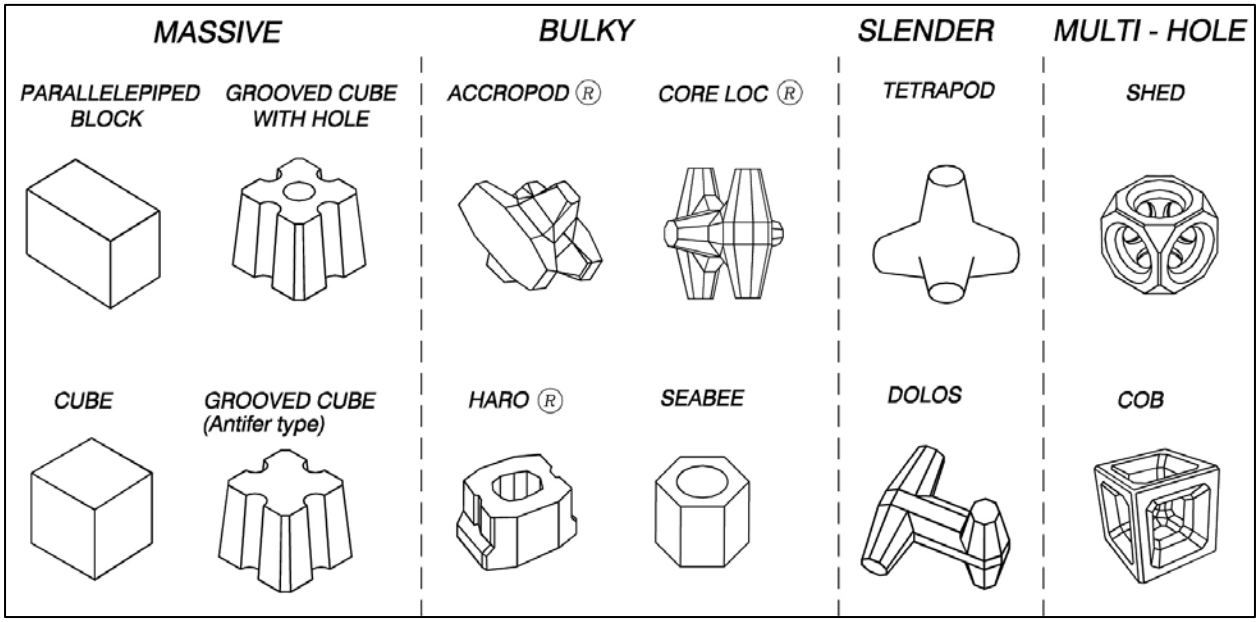

Figure VI-5-40. Examples of concrete armor units

(b) The units are generally made of conventional unreinforced concrete except the multi-hole cubes where fiber reinforcement is sometimes used.

(c) For slender units such as dolos with small waist ratios, various types of high-strength concrete and reinforcement (conventional rebars, prestressing, fibers, scrap iron, steel profiles) have been considered. However, reinforcement has only been used in few cases because it generally seems to be less cost-effective and because of the risk of rapid corrosion of the steel reinforcement.

(d) Hydraulic stability of armor layers is reduced if the armor units disintegrate causing reduction of the stabilizing gravitational force and possible interlocking effects. Moreover, broken armor unit pieces might be thrown around by wave action and thereby trigger additional breakage at an increased rate. In order to prevent this, it is necessary to ensure structural integrity of the armor units.

(e) Unreinforced concrete is a brittle material with a low tensile strength, f_T, on the order of 2-6 MPa and a compressive strength, f_C, which is one order of magnitude larger than f_T. Consequently, crack formation and breakage is nearly always caused by load induced tensile stresses, σ_T, that exceed f_T. The magnitude of f_T is therefore more important than f_C in armor unit concrete, and specifications should focus on achieving adequate values of f_T. It is important to note that f_T decreases with repeated load due to fatigue effects.

(f) The different categories of concrete armor units are not equally sensitive to breakage. Slender units are the most vulnerable because the limited cross-sectional areas give rise to relatively large tensile stresses. Some recent failures of breakwaters armored with tetrapods and dolosse were caused by breakage of the units into smaller pieces having less hydraulic stability than the intact armor units.

(g) Massive units will generally have the smallest tensile stresses due to the distribution of loads over large cross-sectional areas. However, breakage can take place if the units experience impacts due to less restrictive hydraulic stability criteria and if the concrete quality is poor with a low f_T. This latter point is related mainly to larger units where temperature differences during the hardening process can create tensile stresses which exceed the strength of the weak young concrete, thus resulting in microcracking of the material (thermal cracking). If massive units are made of good quality concrete and not damaged during handling, and if the armor layer is designed for marginal displacements, there will be no breakage problems. This statement also holds for the bulky units under the same precautions.

(h) The different types of loads on armor units and load origins are listed in Table VI-5-39.

(2) Structural design formulae for dolosse and tetrapods. Based on model tests with instrumented units, Burcharth (1993b), Burcharth and Liu (1995) and Burcharth et al. (1995b) presented a dimensional formula for estimation of the relative breakage of dolosse and tetrapods (fraction of total units) as presented in Table VI-5-40. Figures VI-5-41 and VI-5-42 compare the formulae to breakage data. Design diagrams for dolos were also presented in Burcharth and Liu (1992).

(a) Stress determination. Sturctural design methodologies for dolosse have also been proposed by Anglin et al. (1990) (see Table VI-5-41); Melby (1990, 1993); Zwamborn and Phelp (1990); and Melby and Turk (1992). The methods of Zwamborn and Phelp are based primarily on prototype failure tests, and therefore, are site specific.

- Melby (1990, 1993) provided a method to determine the design tensile stress for a dolos layer and discussed a computer program to compute this design stress. Figure VI-5-43 shows wave height in meters versus maximum flexural tensile stress in MPa for several dolos waist ratios and several Hudson stability coefficients. In this case, the wave height was used to determine a dolos weight using the Hudson stability equation. Figure VI-5-44 shows dolos weight in metric tons versus maximum flexural tensile stress in MPa for several dolos waist ratios. Both figures were generated using a tensile stress exceedance value of E=2 percent for the condition where the given stress level is exceeded in approximately 2 percent of the units on the slope. In addition, a structure slope of 1V:2H and a specific gravity of ρ_a / ρ_w = 2.40 were used to

compute the stress level, although the effect of these parameters on the stress was negligible over typical ranges of these parameters. Further, Figure VI-5-44 was not affected by the choice of stability coefficient.

Table VI-5-39
Types and Origins of Loads on Armor Units (Burcharth 1993b)

TYPES OF LOADS		**ORIGIN OF LOADS**
Static		Weight of units Prestressing of units due to wedge effect and arching caused by movement under dynamic loads
Dynamic	Pulsating	Gradually varying wave forces Earthquake loads
	Impact	Collisions between units when rocking or rolling, collision with underlayers or other structural parts Missiles of broken units Collisions during handling, transport, and placing High-frequency wave slamming
Abrasion		Impacts of suspended sand, shingle, etc.
Thermal		Temperature differences during the hardening (setting) process after casting Freeze – thaw cycles
Chemical		Alkali-silica and sulphate reactions, etc. Corrosion of steel reinforcement

Table VI-5-40
Breakage Formula for Dolosse and Tetrapods (Burcharth 1993b, Burcharth and Liu 1995, Burcharth et al. 1995b, Burcharth et al. 2000)

$$B = C_0 \, M^{C_1} \, f_T^{C_2} \, H_s^{C_3} \qquad \text{(VI-5-91)}$$

where B Relative breakage
M Armor unit mass in ton, $2.5 \leq M \leq 50$
f_T Concrete static tensile strength in MPa, $2 \leq f_T \leq 4$
H_s Significant wave height in meters
C_0, C_1, C_2, C_3 Fitted parameters

The effects of static, pulsating, and impact stresses are included in the formula.

Fitted parameters for the breakage formula

	Waist ratio	Variational Coef. of C_0	C_0	C_1	C_2	C_3
Trunk of dolosse	0.325	0.188	0.00973	-0.749	-2.58	4.143
	0.37	0.200	0.00546	-0.782	-1.22	3.147
	0.42	0.176	0.01306	-0.507	-1.74	2.871
Round-head of dolosse	0.37	0.075	0.025	-0.65	-0.66	2.42
Trunk of tetrapods		0.25	0.00393	-0.79	-2.73	3.84

Summary of the hydraulic model tests

	Dolos trunk	Dolos round-head	Tetrapod trunk
Breakwater slope α	1.5	1.5	1.5
Foreshore	1:20	horizontal	1:50
Water depth at toe (cm)	23	50	30 and 50
Height of breakwater (cm)	60	70	55 and 75
Mass of units (kg)	0.187	0.187	0.290
Concrete density (tons/m^2)	2.3	2.3	2.3
Spectral peak period T_p (s)	1.5-3	1.5-2.5	1.3-2.8
Significant wave height H_s (cm)	5.7-17.7	5-13	8.8-27.3
Surf similarity parameter $\xi = (H_s/L_p)^{-0.5} \tan\alpha$	3-7.5	3.8-7.5	2.7-4.1

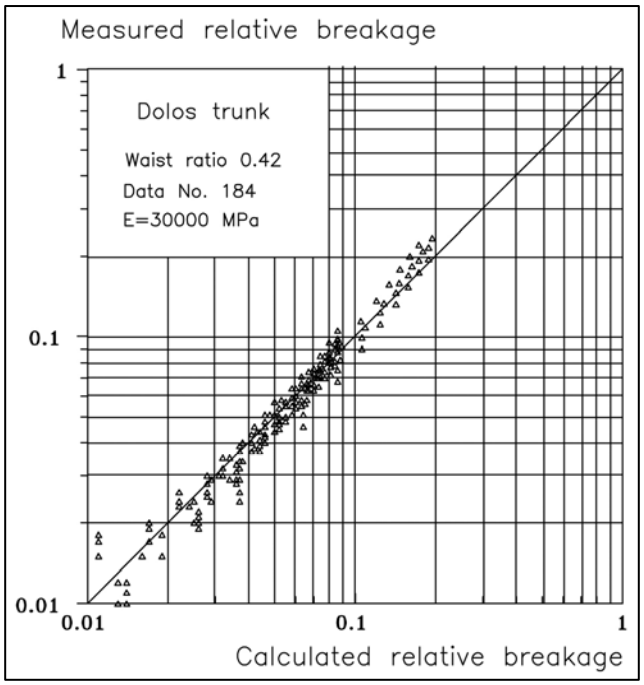

Figure VI-5-41. Breakage formula for dolosse (Burcharth 1993b; Burcharth and Liu 1995; Burcharth et al. 1995b)

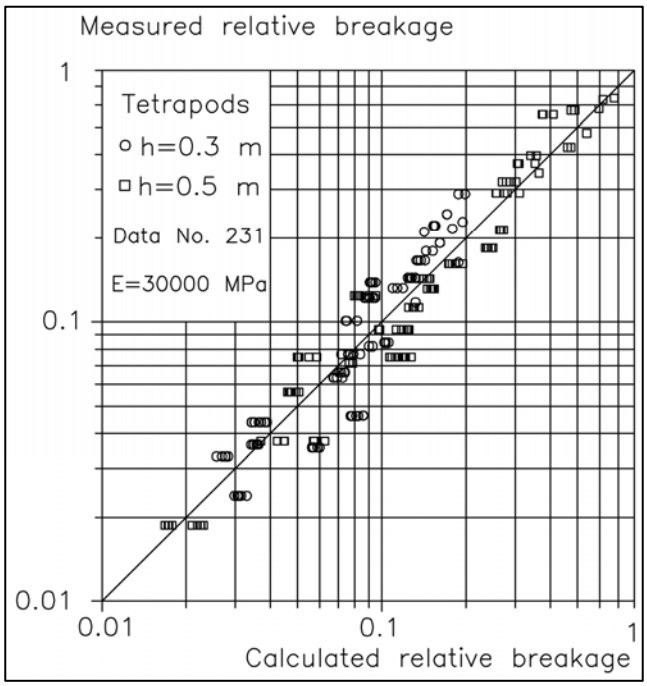

Figure VI-5-42. Breakage formula for tetrapods (Burcharth 1993b, Burcharth and Liu 1995, Burcharth et al. 1995b)

Table VI-5-41
Stress Prediction Formulae for Dolosse (Anglin et al. 1990)

Anglin et al. (1990) developed a dolos structural design methodology based on small scale measurements of strain in laboratory hydraulic models. Only the static stresses were considered. The criterion for allowable static tensile stress in a dolos at a vertical distance D_v down from the crest on a dry structure was proposed as

$$n\left(\sigma_s\right)_p < f_T \tag{VI-5-92}$$

where

f_T = Prototype concrete static tensile strength (MPa)

$(\sigma_s)_p$ = Static principal stress in model dolos with probability of exceedance, p

n = Model scale factor

The static principal stress is estimated as

$$\left(\sigma_s\right)_p = 10^{\left(\log(\sigma_s)_{est} + 0.31\left[\Phi^{-1}(p)\right]\right)} \tag{VI-5-93}$$

with

$$\log\left(\sigma_s\right)_{est} = -2.28 + 0.91\alpha + 0.30\left(\frac{D_v}{n} - 0.45\right) + 0.34l \tag{VI-5-94}$$

and the model scale factor was given as

$$n = 9.43\left(\frac{W}{0.1549 w_a}\right)^{1/3} \tag{VI-5-95}$$

and

α = Tangent of seaward armor slope

l = Layer (0 for top; 1 for bottom)

D_v = Vertical distance from crest to stressed dolos location

$\Phi^{-1}(p)$ = Tabulated inverse normal variate (see next page)

W = Prototype armor unit weight

w_a = Armor concrete specific weight

(Continued)

Table VI-5-41 (Concluded)

Values for the inverse normal variate in Eq VI-5-93 are given in the box to the right.

Probability of exceedance	$\Phi^{-1}(p)$
0.1	1.28
0.05	1.65
0.02	2.05
0.01	2.33

Equations VI-5-92 through VI-5-95 are limited to the range of values:

$0.4 \# \alpha \# 0.67$; $0.3 \text{ m} \# D_v/n \# 0.6 \text{ m}$;
r = 0.32 where *r* is the dolos waist ratio

Another model study examined the combined effects of static and quasistatic (wave-induced pulsating loads) under nonbreaking regular wave conditions, but did not include impact stresses. The criterion for allowable tensile stress in a dolos located a vertical distance, D_{swl}, from the swl was given as

$$n(\sigma_t)_p < f_T \tag{VI-5-96}$$

where

$$(\sigma_t)_p = (\sigma_t)_{est} + 0.001\left[\Phi^{-1}(p)\right] \tag{VI-5-97}$$

$$(\sigma_t)_{est} = 0.905\,(\sigma_s)_{est} + 0.639\,(\sigma_q)_{est} \tag{VI-5-98}$$

$$\log(\sigma_q)_{est} = -2.36 + 0.15\alpha + 0.01\left(\frac{T}{\sqrt{n}}\right) + 0.29\left(\frac{D_{swl}}{n}\right) + 2.20\left(\frac{H}{n}\right) \tag{VI-5-99}$$

and

$(\sigma_t)_p$ = Total static and pulsating principal stress in model armor unit with probability of occurrence,
$(\sigma_q)_p$ = Pulsating principal stress in model armor unit with probability of occurrence, *p*
$(\sigma_s)_p$ = Static principal stress with probability of occurrence, *p*, from Eq VI-5-94
H = Regular wave height
T = Regular wave period
D_{swl} = Vertical distance from swl to location of stressed dolos. (Positive above swl, negative below swl.)
n = Model scale factor from Eq VI-5-95
α = Tangent of seaward armor slope
$\Phi^{-1}(p)$ = Tabulated inverse normal variate from the preceding box

Equations VI-5-96 through VI-5-99 are limited in application to the range of values:
$0.05 \text{ m} \# H/n \# 0.25 \text{ m}$; $0.4 \# \alpha \# 0.67$; $0.3 \text{ m} \# D_v/n \# 0.6 \text{ m}$;
$1.25 \text{ s} \# T/(n)^{1/2} \# 2.5 \text{ s}$; $-0.1 \text{ m} \# D_{swl}/n \# +0.1 \text{ m}$

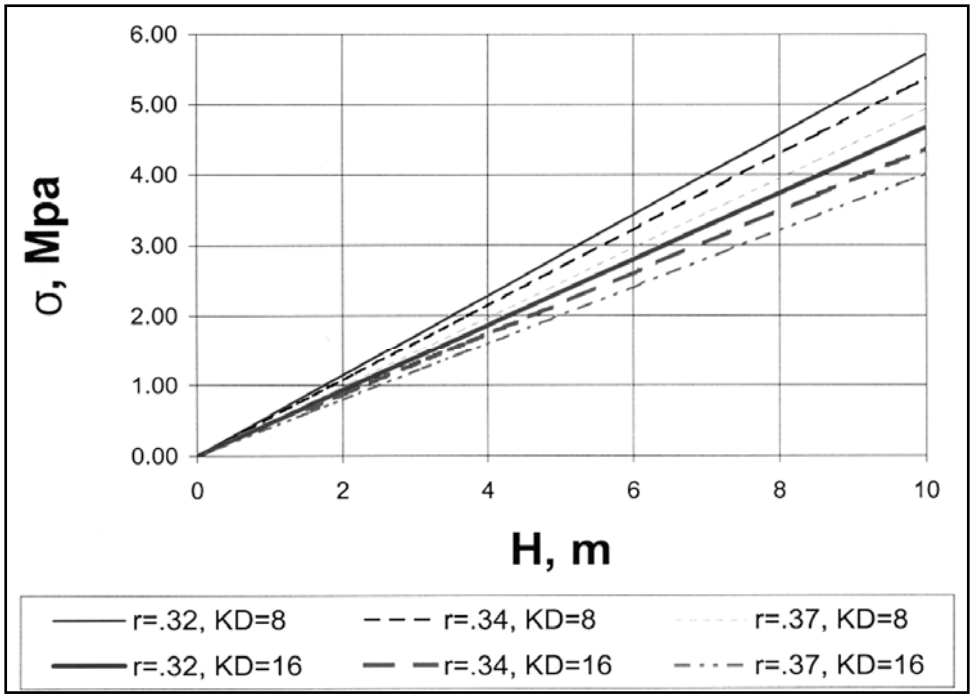

Figure VI-5-43. Wave height versus maximum flexural tensile stress for several dolos waist ratios

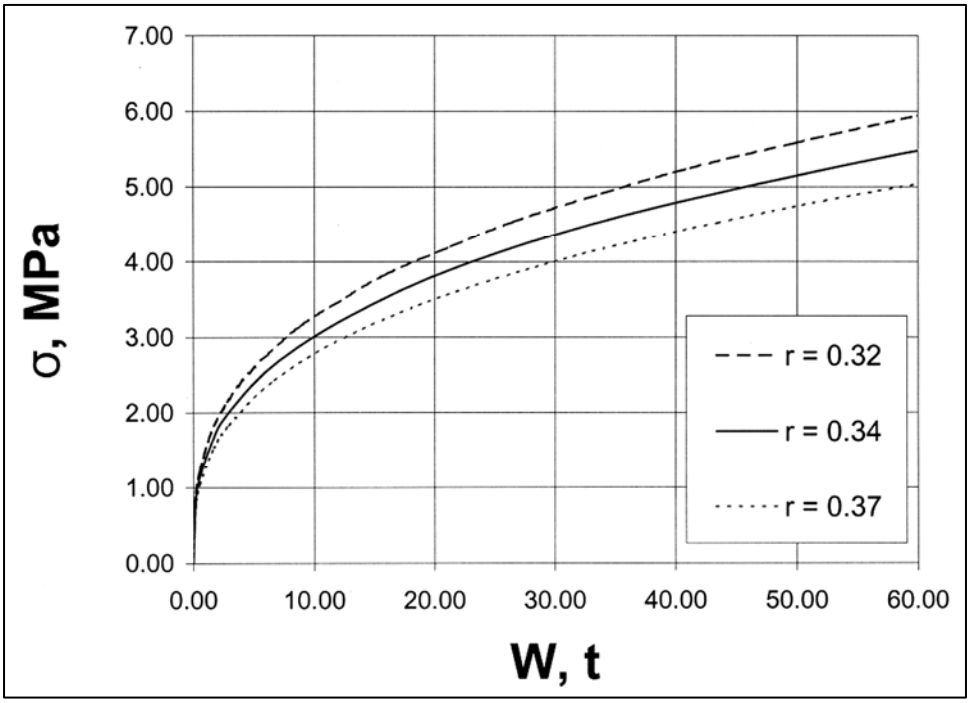

Figure VI-5-44. Dolos mass versus maximum flexural tensile stress for several dolos waist ratios

(b) Reinforced dolos design. Melby and Turk (1992) extended the method of Melby (1993) to include a level I reliability analysis and conventional reinforced concrete design methodology (American Concrete Institute (ACI) 1989). The following technique utilizes a probabilistic principal stress computed using any of the previous methods. These methods allow the designer to consider unreinforced concrete, conventional steel rebar reinforcement, or prestressing in a unified format. The basic design equation, following structural concrete design conventions, equates a factored strength with a factored load as

$$\gamma Q_n = \phi R_n \tag{VI-5-100}$$

where γ and φ are the load and strength factors, respectively, to account for uncertainty in nominal load Q_n and nominal strength R_n. Melby and Turk noted that the load factor ranges from 1.0 to 1.2 for typical values of exceedance probability for stress. American Concrete Institute (ACI) (1989) recommends $\varphi = 0.85$ for torsion. To facilitate reinforcement design, Melby and Turk assumed a circular cross section and decomposed Equation VI-5-100 into a flexure equation

$$\gamma S_M k_M \sigma_1 < \phi\left(0.7 M_{cr}\right) \tag{VI-5-101}$$

and a torsional equation

$$\gamma S_T k_T \sigma_1 < \phi\left(0.7 T_{cr} + T_s\right) \tag{VI-5-102}$$

where σ_1 is the principal stress, $S_M = 0.1053(rC)^3$ and $S_T = 0.2105(rC)^3$ are the section moduli for flexure and torsion, r is the dolos waist ratio, C is the dolos fluke length, and $k_M = k_T = 0.6$ are the moment and torque contribution factors, $M_{cr} = T_{cr} = 0.7 f_{ct}$ are the critical strengths of the concrete in moment and torque, f_{ct} is the concrete splitting tensile strength, and T_s is the strength contribution from the torsional steel reinforcement. The inequality in Equations VI-5-101 and VI-5-102 assures that the factored tensile strength will be greater than the factored tensile load.

- The technique for steel reinforcement design utilizes conventional structural design techniques. Torsional steel is specified first, and it is only required in the shank because the flukes are not likely to be twisted. Details are given in ACI 318-89 (ACI 1989). Assuming a circular section for the dolos shank, the amount of torsional steel is given as $T_s = R_h A_s f_y$, where R_h is the distance to the center of the section, A_s is the total area of steel intersecting the crack, and f_y is the yield strength of the steel. Substituting T_s into Equation VI-5-102 yields the equation for required torsional steel, i.e.,

$$A_s > \frac{\gamma\left(S_T k_T \sigma_1\right) - \phi\left(0.7 T_{cr}\right)}{\phi f_y R_h} \tag{VI-5-103}$$

- The number of bars required is then given by $n = A_s / A_b$, where A_b is the cross-sectional area of hoop reinforcing bars, and the spacing is $s = 1.5\pi R_h / n$, assuming the crack extends three-fourths of the distance around the circumference.

- For flexural reinforcement design, it is assumed that the concrete offers no resistance in tension. Nominal strength is reached when the crushing strain in the outer fiber of the concrete is balanced by the yield strain in the steel rebar. The balanced failure condition using the Whitney rectangular stress block is prescribed in ACI 318-89, Part 10 (ACI 1989). The solution requires an iterative approach because the neutral axis is a priori unknown. Assuming a rebar size, the neutral axis is located by solving the quadratic equation that results from balancing the compressive force moment from the Whitney stress block with the tensile force moment from the steel. Once the neutral axis is determined, the nominal moment from the steel can determined and substituted into Equation VI-5-101 to determine if the quantity of steel is adequate to balance the flexural design load. After determining the amount of flexural steel required, typical checks of compressive stress, shear, bond, minimum reinforcement, and temperature steel should be made as per ACI 318-89.

(c) Prestressed dolos design. Prestressing acts reduce principal stress. The principal stress reduction factor is given by

$$\xi = 0.5\left(\left(k_M - \lambda \right) + \sqrt{\left(k_M - \lambda \right)^2 + 4k_T^2} \right) \tag{VI-5-104}$$

where λ is the ratio of applied precompressive stress to design principal stress. This equation was substituted into the moment-torque interaction relations to get design equations for torsion and flexure as follows:

$$\gamma \xi k_T \sigma_1 = 0.5\phi \sqrt{\frac{f_c}{1 + 4\left(\frac{k_M S_M}{k_T S_T} \right)^2}} \tag{VI-5-105}$$

$$\gamma \xi k_M \sigma_1 = 0.5\phi \sqrt{\frac{f_c}{1 + 0.25\left(\frac{k_T S_T}{k_M S_M} \right)^2}} \tag{VI-5-106}$$

where f_c is the concrete compressive strength. These equations are similar to Equations VI-5-101 and VI-5-102, but they are for prestressed concrete design. Details for determining prestressing steel requirements are given in ACI 318-89 (ACI 1989).

(3) Ultimate impact velocities end equivalent drop height.

(a) For evaluation of the placing technique during construction it is important to consider the ultimate impact velocities. The lowering speed of the crane at the moment of positioning of the units must be much slower than the values given in Table VI-5-42. The values of ultimate impact velocities given in Table VI-5-42 are rough estimates corresponding to solid body impact against a heavy rigid concrete base which causes breakage resulting in a mass loss of 20 percent or more. If the armor units are not dropped on a hard rigid surface but instead on soil or a rock

underlayer, the ultimate impact velocities can be significantly higher than those given in Table VI-5-42.

Table VI-5-42
Approximate Values of Ultimate Rigid Body Impact Velocities for Concrete Armor Units (Burcharth 1993b)

Armor Unit	Impact Velocity of the Unit's Center (m/s)	Equivalent Drop Height of the Unit's Center (m)
Cube < 5 tonne	5 - 6	1.2 - 1.8
20 tonne	4 - 5	0.8 - 1.2
50 tonne	3 - 4	0.4 - 0.8
Tetrapod	2	0.2
Dolos, waist ratio 0.42	2	0.2
Dolos, waist ratio 0.32	1 - 1.5	0.05 - 0.12

(b) When placing units underwater, a heavy swell might impose rather large horizontal velocities on a unit suspended from a crane. It is obvious from the values in Table VI-5-42 that free-fall dropping of concrete armor units by quick release from a crane should be avoided because even small drop heights can cause breakage. This is also true for underwater placement because the terminal free-fall velocity underwater exceeds the limiting values given in Table VI-5-42 except for very small massive types of units.

(4) Thermal stresses.

(a) As concrete cures, the heat of hydration increases the temperature. Because of the fairly low thermal conductivity of concrete and because of the poor insulation of conventional formwork (e.g., steel shutter), a higher temperature will be reached in the center part of the armor unit than on the concrete surface. The temperature difference will create differential thermal expansion, and internal thermal stresses will develop in the concrete. The temperature differences and resulting thermal stresses increase with the distance between the armor unit center and the surface of the unit. Tensile stresses can easily exceed the limited strength of the fresh young concrete thus causing formation of microcracks. Unfortunately, it is not possible to see thermal cracks because they will close at the surface due to the thermal contraction of the concrete as it cools.

(b) The curing process is very complicated and theoretically it can only be dealt with in an approximate manner, mainly because the description of creep and relaxation processes of the hardening concrete are not precise enough to avoid large uncertainties in the calculations. Calculations are performed by the use of special finite element computer programs for three-dimensional bodies. Necessary input is data on the concrete mix including the composition (type) of the cement, the concrete temperature when poured, the geometry of the units, the type of formwork (conductivity/insulation), the environmental climate (air temperature and wind velocities as function of time), and the cycling time for removal of the formwork. The output of the calculations is the development of stresses and related crack formation as function of time. Figure VI-5-45 shows an example of such a calculation for a 70-tonne cube.

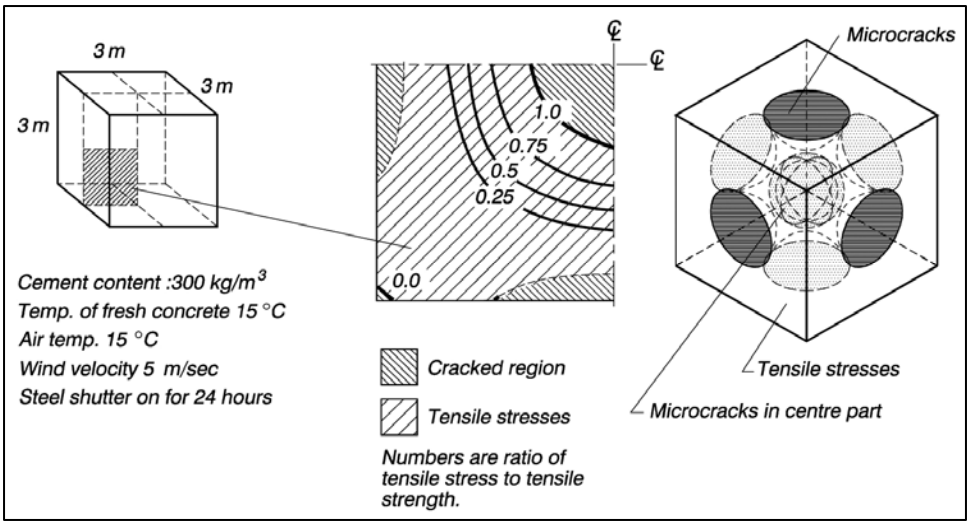

Figure VI-5-45. Example of calculation of thermal stresses and cracked regions in a 70-tonne cube 100 hr after casting (Burcharth 1993b)

(c) The cube will have no visible sign of weakness, but it will be fragile and brittle because the cracked regions at the surfaces and in the center will have almost zero tensile strength and the noncracked regions will be in tension. This means that not only the strength, but also the fatigue life and the resistance to deterioration, will be reduced.

(d) Thermal stress calculations are complicated and must be performed using numerical models described in the concrete literature. However, a very important rule of thumb for avoiding thermal cracks is that the temperature difference during curing should not exceed 20^{o} *C* between any two points within the concrete element. The temperature difference is easy to monitor by placing/casting copper-constanting thermo-wire (e.g., 2 x 0.7 mm^2) in the concrete. The wire insulation must be removed at the tips which are placed at positions in the center and near the surface of the units where the temperatures are maximum and minimum, respectively. Temperature readings can then be monitored by connecting a pocket instrument to the free wire ends.

(e) There are several measures related to concrete technology for the prevention of damaging thermal stresses, but they all involve some drawbacks as described by Table VI-5-43.

(f) Another way of dealing with the thermal stress problem is to keep the effective dimensions of the armor units as small as possible. For cubes it can be done by making a hole as was done in the hot-climate Bosaso Harbor project in Somalia. Figure VI-5-46 shows examples of the temperature development in 30-tonne blocks with and without a hole. The reduced temperature difference introduced by the hole is clearly seen by comparison of the two blocks casted during winter time. In fact it was easier to keep the 20^{o} *C* temperature difference limit in a 30-tonne unit with a hole than in a 7-tonne unit without a hole.

Table VI-5-43
Drawbacks Related to Crack-Reducing Procedures

Measure to Reduce Thermal Stresses	Drawback
Use of less cement	Reduced long-term durability due to higher porosity. Slower development of strength, longer cycle time for forms
Use of low-heat cement or retarder	Higher production costs due to slower development of strength, longer cycle time for forms, larger casing and stockpiling area needed
Cooling of water and aggregates	Higher production costs
Use of insulation during part of the curing period	Higher production costs

(5) Fatigue in concrete armor units.

(a) The strength of concrete decreases with the number of stress cycles. Each stress cycle larger than a certain stress range will cause partial fracture in some parts of the material matrix resulting in a decreased yield strength. Repeated loads cause an accumulative effect which might result in macro cracks, and ultimately, breakage of the structural element.

(b) The number of stress cycles caused by wave action will be in the order of 200 million during 50 years structural life in the North Atlantic area. About 10 million cycles will be caused by larger storm waves. In subtropical and tropical areas the number of storm wave cycles is generally one or two orders of magnitude less.

(c) Fatigue for conventional unreinforced concrete exposed to uniaxial and flexural stress conditions with zero mean stress is given in Table VI-5-44.

d. Toe stability and protection.

(1) Introduction.

(a) The function of a toe berm is to support the main armor layer and to prevent damage resulting from scour. Armor units displaced from the armor layer may come to rest on the toe berm, thus increasing toe berm stability. Toe berms are normally constructed of quarry-run, but concrete blocks can be used if quarry-run material is too small or unavailable.

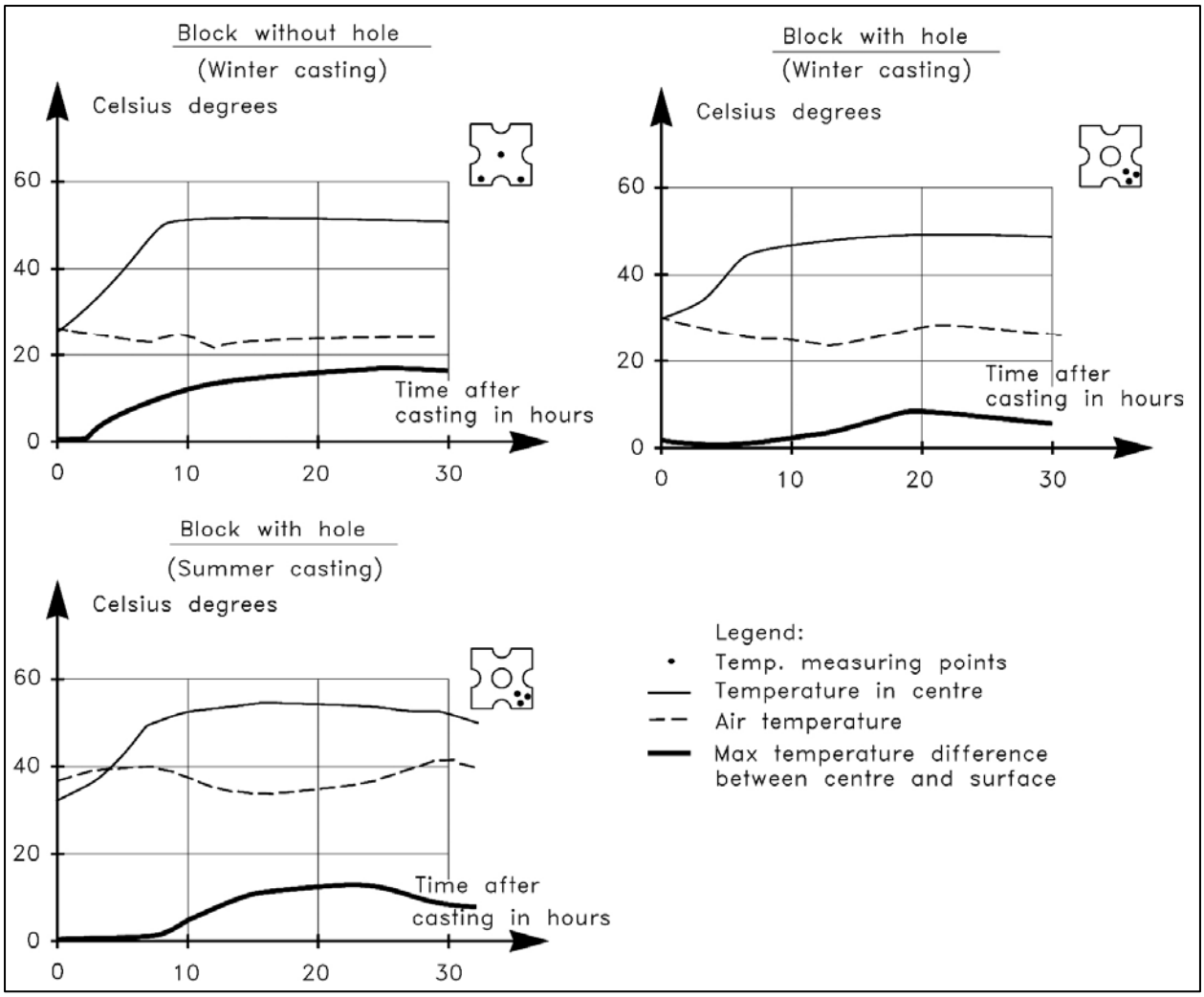

Figure VI-5-46. Examples of temperature development during curing in 30-tonne modified cubes with and without a hole (Burcharth et al. 1991)

(b) In very shallow water with depth-limited design wave heights, support of the armor layer at the toe is ensured by placing one or two extra rows of main armor units at the toe of the slope as illustrated in Figure VI-5-47a. This is a stable solution provided that scour does not undermine the toe causing the armor layer to slide as illustrated by Figure VI-5-48. In shallow water it is usually possible to use stones or blocks in the toe that are smaller than the main armor, as shown in Figure VI-5-47 b. In deep water, there is no need for the main armor to cover the slope at greater depths, and the toe berm can be constructed at a level above the seabed as illustrated by Figure VI-5-47c.

(c) Toe berm stability is affected by wave height, water depth at the top of the toe berm, width of the toe berm, and block density. However, wave steepness does not appear to be a critical toe berm stability parameter.

Table VI-5-44
Fatigue for Conventional Unreinforced Concrete Exposed to Uniaxial and Flexural Stress Conditions With Zero Mean Stress (Burcharth 1984)

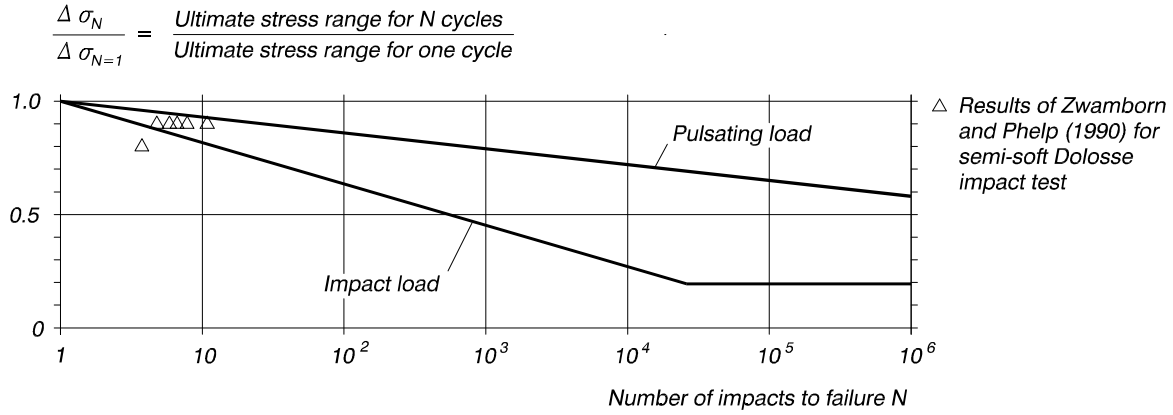

It should be noted that the ultimate impact load strength for one stress cycle is on the order of 1.4 to 1.5 times the ultimate pulsating load strength in the case of uniaxial tension and compression, respectively. For flexural stresses a factor of approximately 1.4 should be applied. The ultimate pulsating load strength properties for one cycle can be taken to be equal to those found for static load conditions.

Data basis for fatigue curve

Author(s)	Loading condition	Specimens
Tepfers and Kutti (1979)	pulsating tension and compression	cubes of 150 mm length
Tait and Mills (1980)	pulsating tension	Dolosse of 300 mm height
Fagerlund and Larsson (1979)	impact compression	cylinders of 100 mm diameter
Zielinski, Reinhardt, and Körmeling (1981)	impact tension	cylinders of 74 mm diameter
Burcharth (1984)	impact flexural stress	Dolosse of 790 mm height

Zwamborn and Phelp (1990) performed drop tests with 9-ton Dolosse on a horizontal underlayer of quarry rock. This relatively soft base created a milder dynamic response than the solid rigid concrete base used by other authors. As seen from the figure Zwamborn and Phelp's data are in between the two curves which might be regarded as upper and lower limits for the fatigue effect.

(d) Model tests with irregular waves indicate that the most unstable location is at the shoulder between the slope and the horizontal section of the berm. The instability of a toe berm will trigger or accelerate the instability of the main armor. Lamberti (1995) showed that moderate toe berm damage has almost no influence on armor layer stability, whereas high damage of the toe berm severly reduces the armor layer stability. Therefore, in practice it is economical to design toe berms that allow for moderate damage.

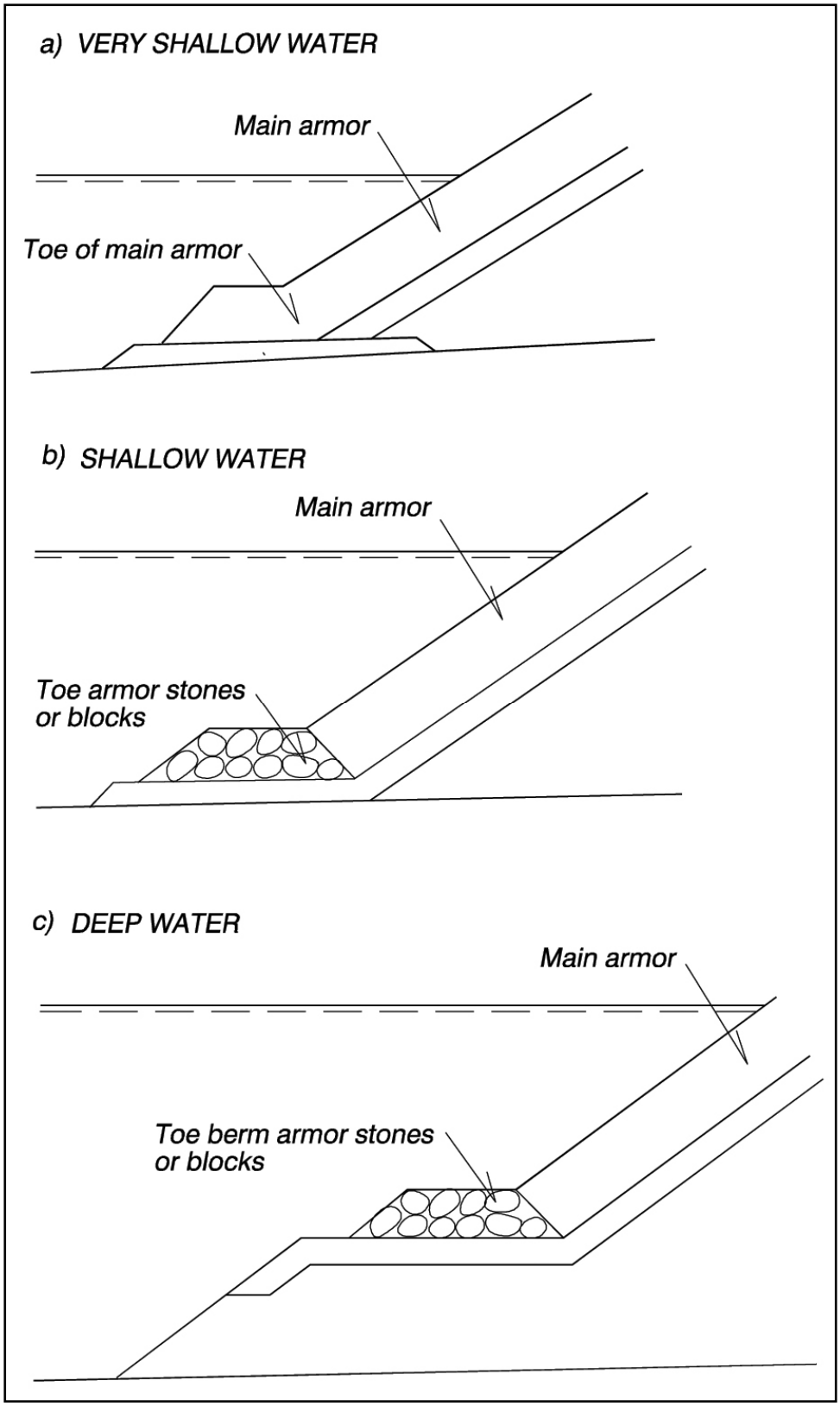

Figure VI-5-47. Typical toe and toe berm solutions in rubble-mound breakwater design

(e) Rock seabeds often provide a poor foundation for the toe berm because of seaward sloping and/or rather smooth surfaces. Toe stability will be difficult to obtain, especially in shallow water with wave breaking at the structure (see Figure VI-5-48). Toe stones placed on hard bottoms can be supported by a trench or anchor bolts as sketched in Figure VI-5-49.

(f) Scour in front of the toe berm can also trigger a failure. The depth of toe protection required to prevent scour can be estimated from the scour depth prediction methods discussed in Part VI-5-6, "Scour and Scour Protection." Typical forms of scour toe protection are illustrated in Figure VI-5-50.

(2) Practical toe stability formulas for waves. Toe berm stability formulas are based exclusively on small scale physical model tests. These formulas are presented in the following tables.

Waves	Structure	Table
Regular, head-on and oblique	Sloping and vertical, trunk and head section	VI-5-45
Irregular, head-on	Trunk of sloping structure	VI-5-46 & VI-5-47
Irregular, head-on	Trunk of vertical structure	VI-5-48

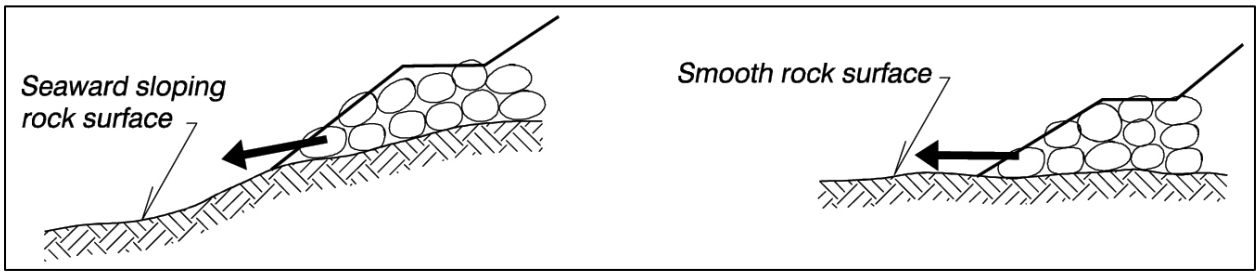

Figure VI-5-48. Example of potential instability of the stones placed on rock seabed

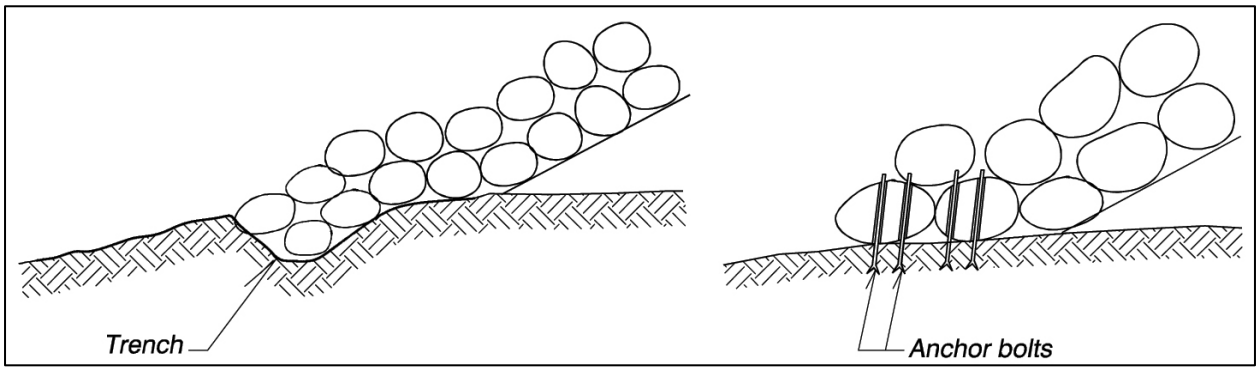

Figure VI-5-49. Support of the stones by a trench or anchor bolts

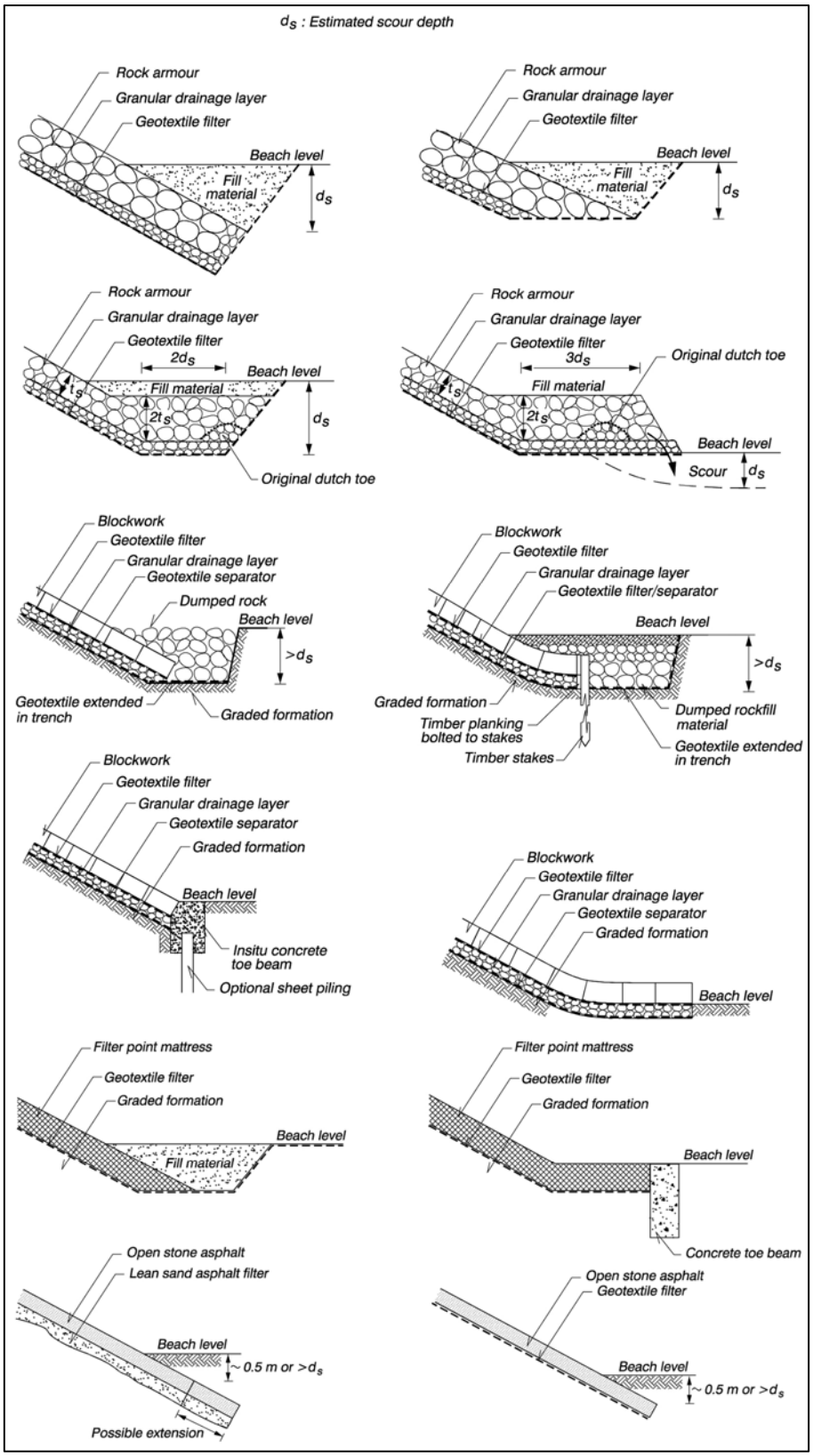

Figure VI-5-50. Typical seawall toe designs where scour is foreseen (McConnell 1998)

Table VI-5-45
Stability of Toe Berm Tested in Regular Waves (Markle 1989)

Regular waves, head-on and oblique

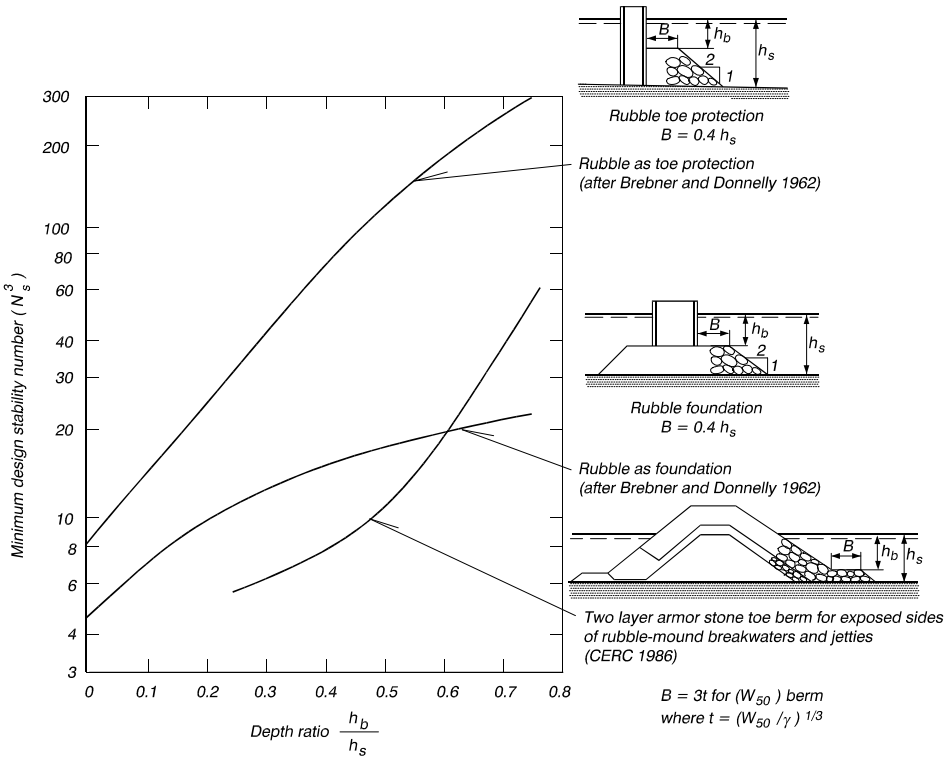

where N_s $N_s = H/(\Delta D_{n50})$
H Wave height in front of breakwater
Δ $(\rho_s/\rho_w) - 1$
ρ_s Mass density of stones
ρ_w Mass density of water
D_{n50} Equivalent cube length of median stone

Remarks: The curves in the figure are the lower boundary of N_s-values associated with acceptable toe berm stability (i.e., some stone movement occurs; but the amount of movement is minor and acceptable, which shows that the toe is not overdesigned)

(3) Foot protection blocks.

(a) Foot protection blocks have been applied to prevent foundation erosion at the toe of vertical structures as shown in Figure VI-5-51.

(b) According to Japanese practice the blocks are rectangular concrete blocks with holes (approximately 10 percent opening ratio) to reduce the antistabilizing pressure difference between the top and bottom of the blocks. Figure VI-5-52 shows a typical 25-tonne block.

Table VI-5-46
Stability of Toe Berm Formed by 2 Layers of Stone Having Density 2.68 tonnes/m^3. Variable Berm Width, and Sloping Structures (van der Meer, d=Angremond, and Gerding 1995)

$$N_s = \frac{H_s}{\Delta D_{n50}} = \left(0.24 \frac{h_b}{D_{n50}} + 1.6\right) N_{od}^{0.15} \qquad \text{(VI-5-107)}$$

where H_s Significant wave height in front of breakwater

Δ $(\rho_s/\rho_w) - 1$

ρ_s Mass density of stones

ρ_w Mass density of water

D_{n50} Equivalent cube length of median stone

h_b Water depth at top of toe berm

N_{od} Number of units displaced out of the armor layer within a strip width of D_{n50}. For a standard toe size of about 3-5 stones wide and 2-3 stones high:

$$N_{od} = \begin{cases} 0.5 & \text{no damage} \\ 2 & \text{acceptable damage} \\ 4 & \text{severe damage} \end{cases}$$

For a wider toe berm, higher N_{od} values can be applied.

Tested cross sections

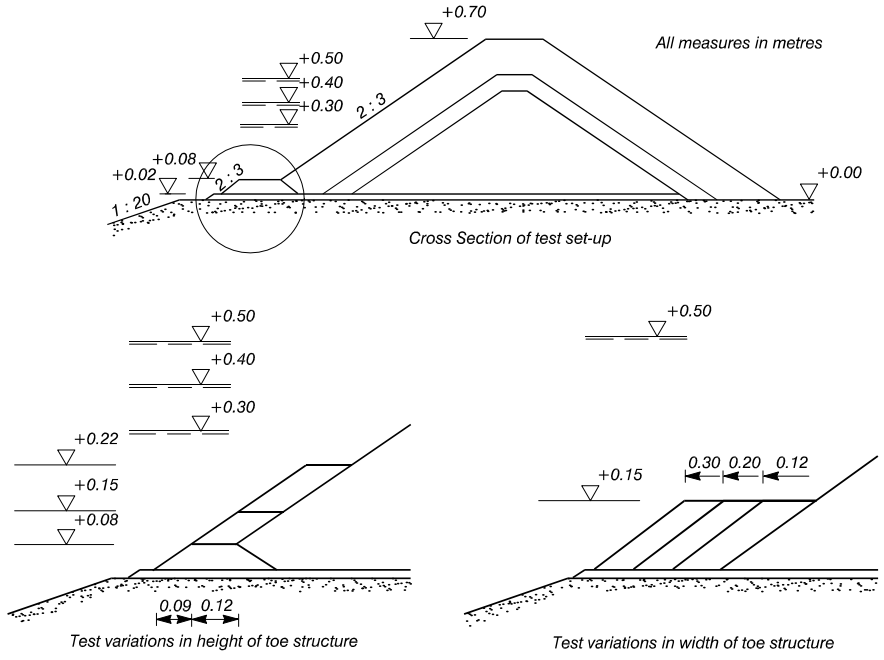

(Continued on next page)

Table VI-5-46 (Concluded)

Valid for: Irregular head-on waves; nonbreaking, breaking and broken

Toe berm formed of two layers of stones with $\rho_s = 2.68\ tonnes/m^3$ $(168\ lb/ft^3)$

$0.4 < h_b/h_s < 0.9, \quad 0.28 < H_s/h_s < 0.8, \quad 3 < h_b/D_{n50} < 25$

where h_s is the water depth in front of the toe berm

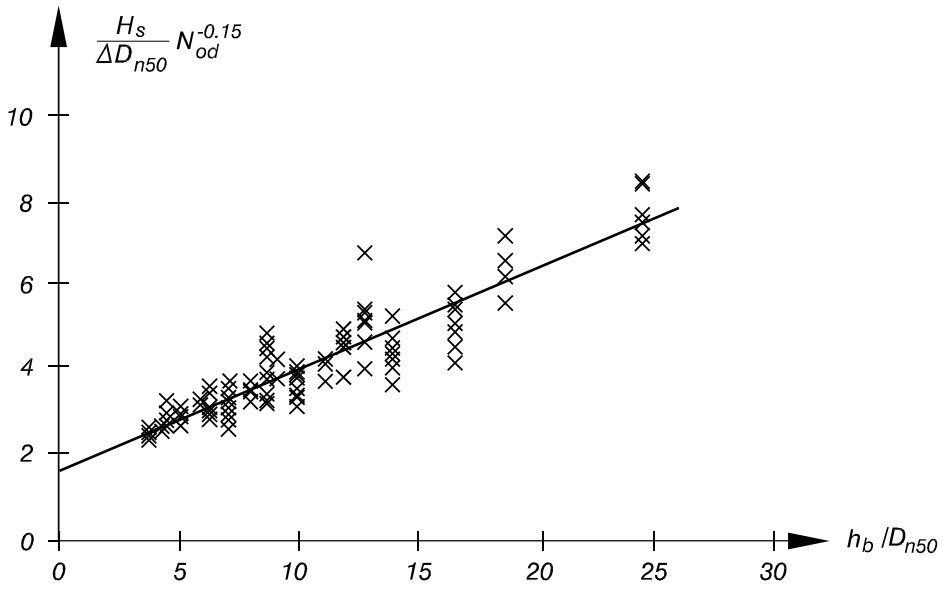

Uncertainty of the formula: corresponding to a coefficient of variation of approximately 0.10.

Table VI-5-47
Stability of Toe Berm Formed by Two Layers of Stones or Parallellepiped Concrete Blocks
(Burcharth et al. 1995a)

Equation VI-5-107 was modified so that it can be applied to the toe berm formed of stones having other densities or to parallellepiped concrete blocks.

$$N_s = \frac{H_s}{\Delta D_{n50}} = \left(0.4\,\frac{h_b}{\Delta D_{n50}} + 1.6\right) N_{od}^{0.15} \quad \text{or} \quad \frac{H_s}{\Delta D_{n50}} = \frac{1.6}{N_{od}^{-0.15} - 0.4\,h_b/H_s} \qquad \text{(VI−5−108)}$$

Results of the stability tests with a toe berm made of 16.5-tonne parallellepiped concrete blocks are shown below. The negative influence of a high reflecting wave wall superstructure on the toe stability is demonstrated.

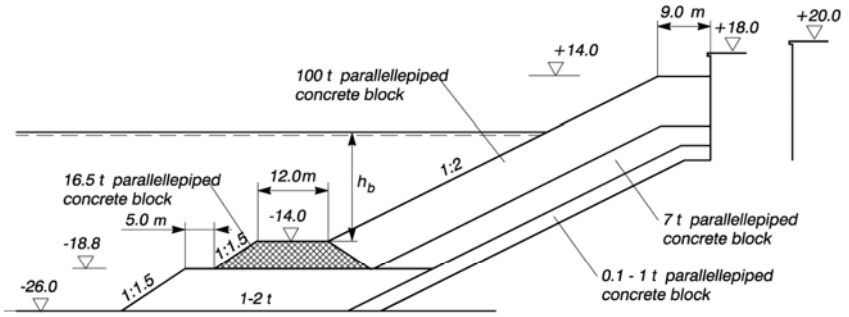

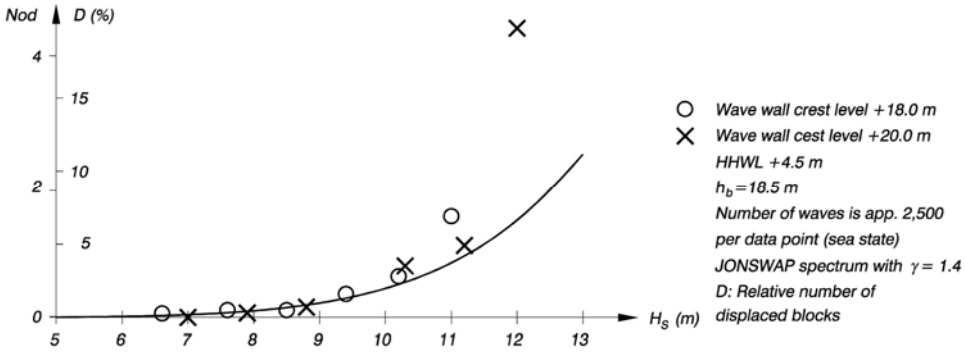

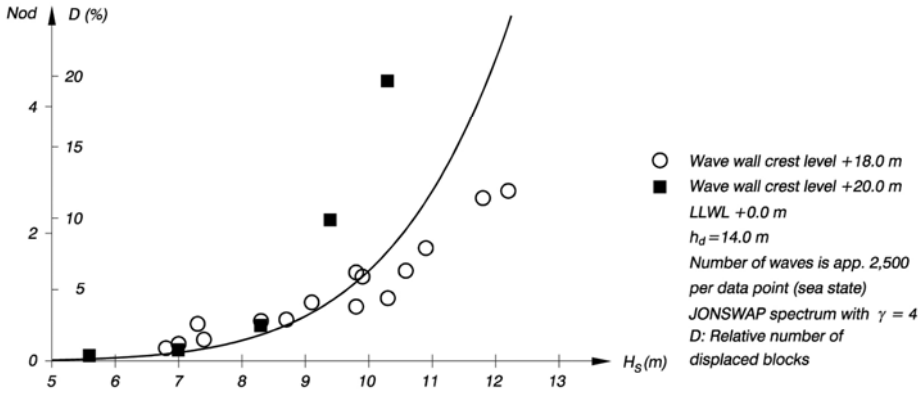

Table VI-5-48
Stability of Toe Berm Formed by Two Layers of Stones in Front of Vertical Impermeable Wall Structure

Madrigal and Valdés (1995) for two layers of quarrystones

$$N_s = \frac{H_s}{\Delta D_{n50}} = \left(5.8\,\frac{h'}{h_s} - 0.6\right) N_{od}^{0.19} \qquad \text{(VI−5−109)}$$

where
H_s	Significant wave height in front of breakwater
Δ	$(\rho_s/\rho_w) - 1$
ρ_s	Mass density of stones
ρ_w	Mass density of water
D_{n50}	Equivalent cube length of median stone
h'	Water depth at top of toe berm
h_s	Water depth in front of toe berm
N_{od}	Number of units displaced out of the armor layer within a strip width of D_{n50}

$$N_{od} = \begin{cases} 0.5 & \text{start of damage (1-3\% of units displaced)} \\ 2 & \text{acceptable damage (5-10\% of units displaced)} \\ 5 & \text{severe damage (20-30\% of units displaced)} \end{cases}$$

Tested cross sections

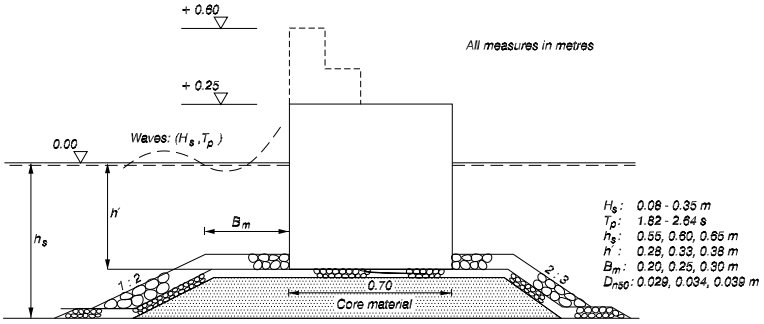

Valid for: Irregular head-on waves. Toe berm formed of two layers of stones with $\Delta = 1.65$
$0.5 < h_b/h_s < 0.8$; $7.5 < h_b/D_{n50} < 17.5$; $0.3 < B_m/h_s < 0.55$

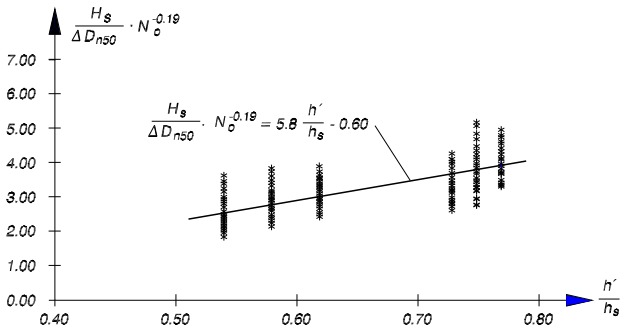

Uncertainty of the formula: Not given

(Continued)

Table VI-5-48 (Concluded)

Tanimoto, Yagyu, and Goda (1982), Takahashi, Tanimoto, and Shimosako (1990) for two layers of quarrystones

$$N_s = \frac{H_s}{\Delta D_{n50}} = \max\left\{1.8,\ 1.3\ \frac{1-\kappa}{\kappa^{1/3}}\frac{h'}{H_s} + 1.8\exp\left(-1.5\frac{(1-\kappa)^2}{\kappa^{1/3}}\frac{h'}{H_s}\right)\ \right\} \qquad \text{(VI-5-110)}$$

$$\begin{aligned}
\kappa &= \kappa_1\ \kappa_2 \\
\kappa_1 &= 2kh'/\sinh(2kh') \\
\kappa_2 &= \max\left\{0.45\sin^2\theta\cos^2(kB\cos\theta),\ \cos^2\theta\sin^2(kB\cos\theta)\ \right\}
\end{aligned}$$

where

H_s	Significant wave height in front of breakwater
Δ	$(\rho_s/\rho_w) - 1$
ρ_s	Mass density of stones
ρ_w	Mass density of water
D_{n50}	Equivalent cube length of median stone
h'	Water depth on top of toe berm (excluding armor layer)
B	Width of toe berm
k	Wave number $k = 2\pi/L_p$
θ	Wave incident angle ($\theta = 0^0$ for head-on)

Valid for: Irregular head-on and oblique waves
Toe berm formed by two layers of quarrystones
$\Delta = 1.65$

Uncertainty of the formula: Not given

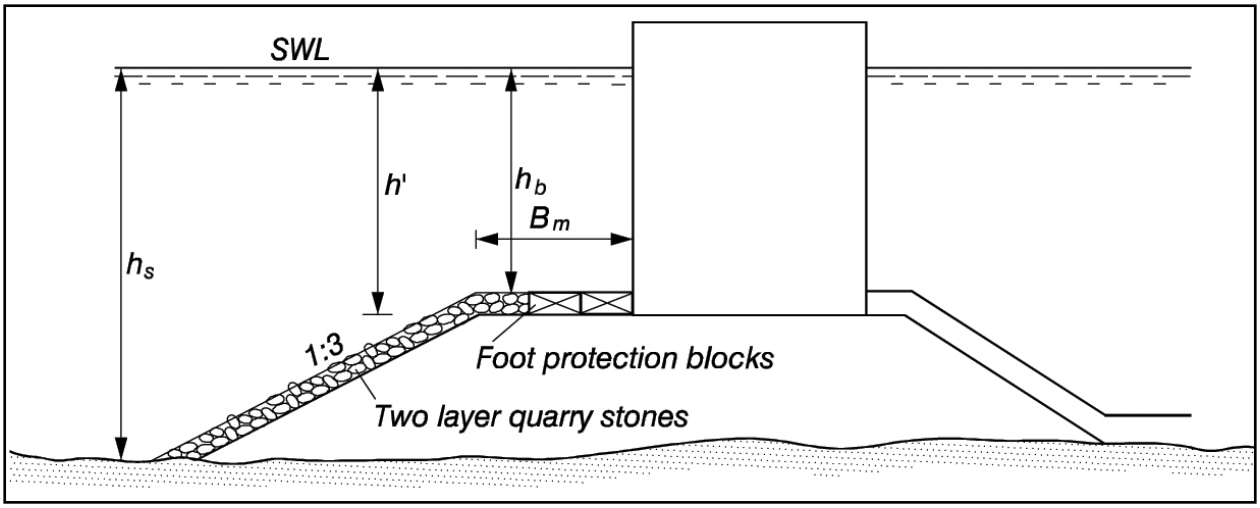

Figure VI-5-51. Illustration of foot protection blocks for vertical structures

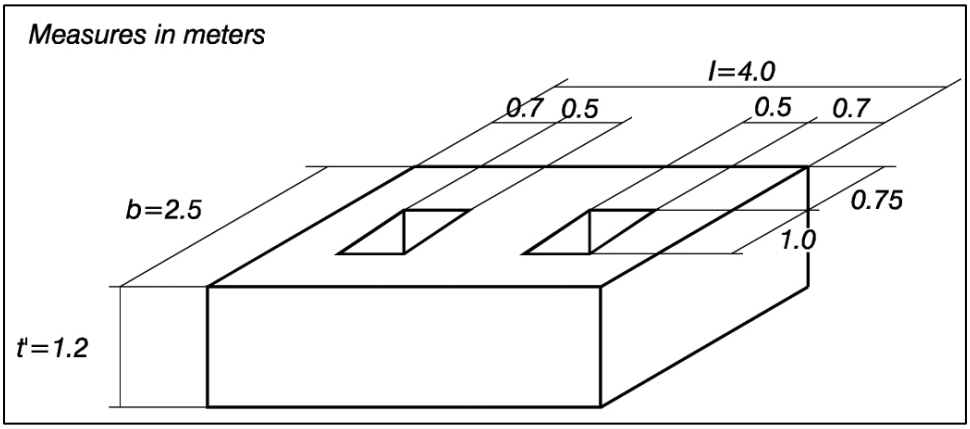

Figure VI-5-52. Example of Japanese foot protection block

Figure VI-5-53 shows a diagram taken from Takahashi (1996) for the determination of the necessary block thickness *t'* as functions of wave height *H* and the ratio of water depths h_b/h_s at the berm and in front of the structure as shown back on Figure VI-5-51.

(c) Stable foot protection blocks do reduce the pressure induced current in the mound, even when there are 10 percent openings in the blocks. Thus the risk of erosion of a sandy seabed underneath a thin rubble mound bedding layer is reduced too.

(4) Toe stability in combined waves and currents.

(a) Coastal structures, such as entrance jetties, are exposed to waves combined with currents running parallel to the structure trunk. In certain circumstances toe stability may be decreased due to the vectorial combination of current and maximum wave orbital velocity. For normal wave incidence the combined wave and current vector magnitude is not greatly increased. However, in the case of jetties where waves approach the jetty trunk at large oblique angles (relative to the normal), the combined velocity magnitude becomes large, and toe stability is jeopardized.

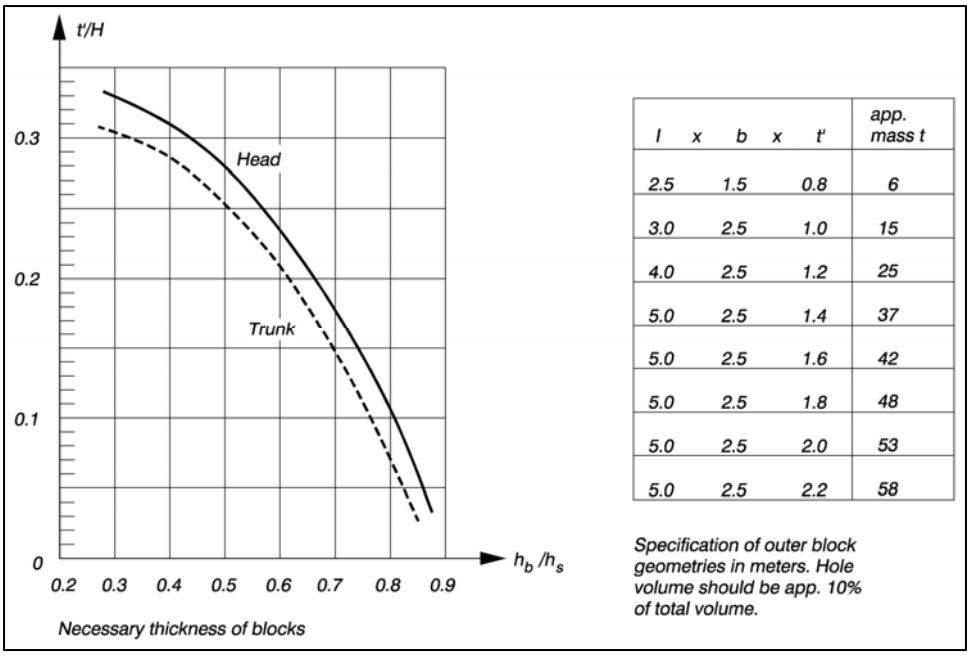

Figure VI-5-53. Design of foot protection blocks according to Japanese practice

(b) Smith (1999) conducted 1:25-scale laboratory experiments to develop design guidance for jetty structures where oblique waves combine with opposing (ebb) currents. Smith found that small current magnitudes did not destabilize toes designed in accordance with guidance given by Markle (1989) and presented in Table VI-5-45. But damage did occur as currents were increased, and a pulsating effect was observed in the wave downrush as the wave orbital velocity combined with the ebb current.

(c) The test configuration had waves approaching at an angle of 70 deg from the normal to the structure trunk, and wave heights were adjusted until breaking occurred on the structure. This is fairly typical scenaro for jettied entrance channels. Both regular and irregular wave conditions were used in the tests. Generally, less damage was recorded for equivalent irregular waves, but this was attributed to the relatively short duration of the wave runs during the experiments. The range of model parameters tested, and the prototype equivalents for the 1:25-scale model, are shown in the following tabulation. Generally, currents less than 15 cm/s in the model (0.75 m/s prototype) did not affect toe stability.

Parameter	Model Value	Prototype Equivalent
Depth	24 cm and 30 cm	6.1 m and 7.6 m
Wave Period	1.7 - 3.0 s	8.5 - 15.0 s
Ebb Current	0.0 - 46 cm/s	0.0 - 2.3 m/s
Wave Height	Breaking	Breaking

(d) Smith developed a procedure to modify Markle's toe stability criterion to account for currents flowing parallel to the structure. Strictly, the method is intended for situations where

waves approach at a large angle from the normal (55-80 deg). Application to situations with wave approach more normal to the structure will yield conservative design guidance. The iterative procedure is outlined in Table VI-5-49.

e. Design of structure cross-section.

(1) Introduction.

(a) A rubble-mound structure is normally composed of a bedding layer and a core of quarry-run stone covered by one or more layers of larger stone and an exterior layer or layers of large quarrystone or concrete armor units. Typical rubble-mound cross sections are shown in Figures VI-5-54 and VI-5-55. Figure VI-5-54 illustrates cross-section features typical of designs for breakwaters exposed to waves on one side (seaward) and intended to allow minimal wave transmission to the other (leeward) side. Breakwaters of this type are usually designed with crests elevated to allow overtopping only in very severe storms with long return periods. Figure VI-5-55 shows features common to designs where the breakwater may be exposed to substantial wave action from both sides, such as the outer portions of jetties, and where overtopping is allowed to be more frequent. Both figures show a more complex idealized cross section and a recommended cross section. The idealized cross section provides more complete use of the range of materials typically available from a quarry, but it is more difficult to construct. The recommended cross section takes into account some of the practical problems involved in constructing submerged portions of the structure.

(b) Figures VI-5-54 and VI-5-55 include tables giving average layer rock size in terms of the stable primary armor unit weight, W, along with the gradation of stone used in each layer (right-hand column). To prevent smaller rocks in the underlayer from being pulled through an overlayer by wave action, the following criterion for filter design may be used to check the rock-size gradations given in Figures VI-5-54 and VI-5-55.

$$D_{15}\left(\text{cover}\right) \le 5D_{85}\left(\text{under}\right) \tag{VI-5-114}$$

where D_{85} *(under)* is the diameter exceeded by the coarsest 15 percent of the underlayer and D_{15} *(cover)* is the diameter exceeded by the coarsest 85 percent of the layer immediately above the underlayer.

(c) Stone sizes are given by weight in Figures VI-5-54 and VI-5-55 because the armor in the cover layers is selected by weight at the quarry, but the smaller stone sizes are selected by dimension using a sieve or a grizzly. Thomsen, Wohlt, and Harrison (1972) found that the sieve size of stone corresponds approximately to

$$D_{sieve} \approx 1.15\left(\frac{W}{w_a}\right)^{1/3} \tag{VI-5-115}$$

Table VI-5-49
Stability Under Combined Waves and Currents (Smith 1999)

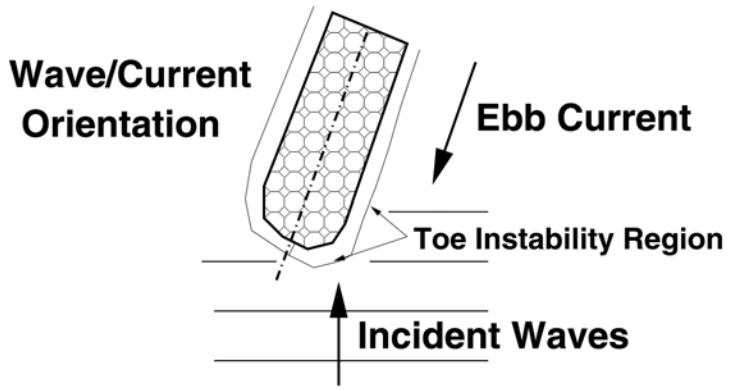

The current-modified stability number is caculated by the formula

$$(N_s)_c = a\left(\frac{U+u}{\sqrt{gh_s}}\right) \tag{VI-5-111}$$

where

$$u = \frac{g\,H\,T}{2\,L} \tag{VI-5-112}$$

$$a = 51.0\left(\frac{h_b}{h_s}\right) - 26.4 \tag{VI-5-113}$$

and

u = m aximum wave orbital velocity in shallow water
U = current magnitude
g = gravity
h_s = total water depth
h_b = water depth over toe berm
H = breaking wave height
T = wave period
L = local wavelength

Procedure: For a given wave condition, first calculate the stability number, N_s, using Markle's method from Table VI-5-45 for sloping rubble-mound structures. Then calculate a current-modified stability number from Equation VI-5-111. If $(N_s)_c > N_s$, the toe stone is unstable, and the procedure is repeated using a larger toe stone to calculate new values of N_s and h_b.

Uncertainty of the Formula: Unknown

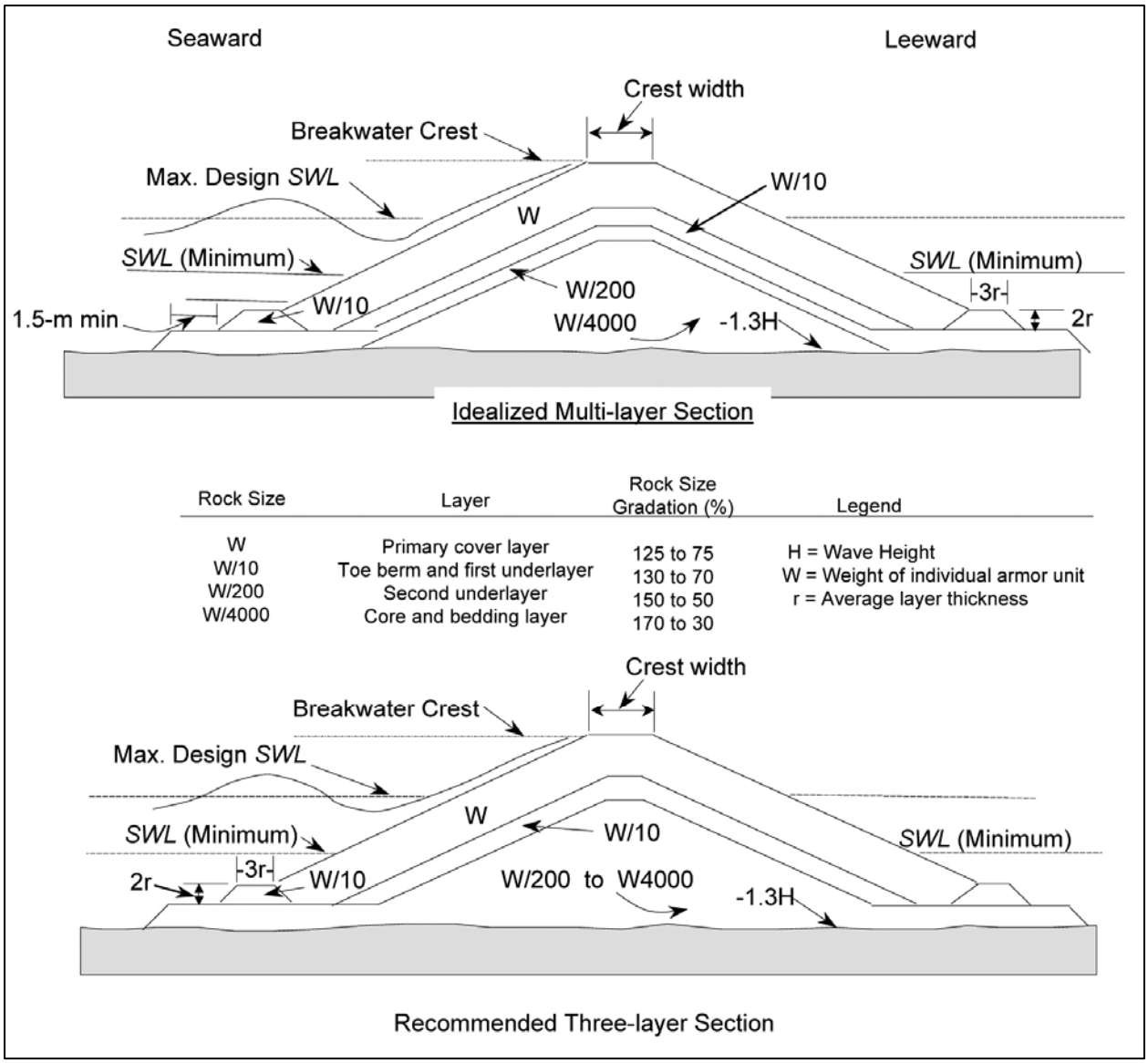

Figure VI-5-54. Rubble-mound section for seaward wave exposure with zero-to-moderate overtopping conditions

where W is the stone weight and w_a is the stone unit weight. Table VI-5-50 lists weights and approximate dimensions for a wide range of stone sizes having stone specific weight of 25.9 kN/m^3 (165 lb/ft^3). The dimensions listed for stone weighing several tons corresponds to the approximate size of the stone determined from visual inspection. Layer thickness should not be estimated as multiples of the dimensions given in Table VI-5-50 because that does not allow for stone intermeshing. Layer thickness is correctly estimated using Equation VI-5-117.

(d) Structure design is part of the overall project planning and design process as illustrated by the generic design diagrams given in Figures V-1-1 through V-1-3 in Part V-1-1-h. Figure VI-5-56 presents a logic diagram for preliminary design of rubble-mound structures.

Included in the diagram are three phases: structure geometry, evaluation of construction technique, and evaluation of design materials.

(e) As part of the design analysis indicated in the logic diagram of Figure VI-5-56, the following structure geometric features should be investigated:

- Crest elevation and width.
- Concrete cap for rubble-mound structures.
- Thickness of armor layer and underlayers.
- Bottom elevation of primary cover layer.
- Toe berm for cover layer stability.
- Structure head and leeside cover layer.
- Secondary cover layer.
- Underlayers.
- Bedding layers and filter blanket layer (see Part VI-5-3*b*, "Granulated and geotextile filter stability."
- Scour protection at toe see Part VI-5-6, "Scour and Scour Protection."
- Toe berm for foundation stability see Part VI-5-3*d*, "Toe stability and protection," and Part VI-5-5, "Foundation Loads."

(f) The following sections describe design aspects for the previously listed geometric features.

(2) Crest elevation and width.

Table VI-5-50
Weight and Size Selection Dimensions of Quarrystone[1]

Weight		Dimension		Weight		Dimension		Weight		Dimension		Weight		Dimension		Weight		Dimension	
mt	**(tons)**	**m**	**ft**	**kg**	**(lb)**	**m**	**(ft)**	**kg**	**(lb)**	**cm**	**(in)**	**kg**	**(lb)**	**cm**	**(in.)**	**kg**	**(lb)**	**cm**	**(in.)**
0.907	(1)	0.81	(2.64)	45.36	(100)	0.30	(0.97)	2.27	(5)	10.92	(4.30)								
1.814	(2)	1.02	(3.33)	90.72	(200)	9.38	(1.23)	4.54	(10)	13.77	(5.42)	0.23	(0.5)	5.08	(2.00)	0.01	(0.025)	1.88	(0.74)
2.722	(3)	1.16	(3.81)	136.08	(300)	0.43	(1.40)	6.81	(15)	15.77	(6.21)								
3.629	(4)	1.28	(4.19)	181.44	(400)	9.50	(1.54)	9.07	(20)	17.35	(6.83)	0.45	(1.0)	6.40	(2.52)	0.02	(0.050)	2.36	(0.93)
4.536	(5)	1.38	(4.52)	226.80	(500)	0.51	(1.66)	11.34	(25)	18.70	(7.36)								
5.443	(6)	1.46	(4.80)	272.16	(600)	0.54	(1.77)	13.61	(30)	19.86	(7.82)	0.68	(1.5)	7.32	(2.88)	0.03	(0.75)	2.70	(1.06)
6.350	(7)	1.54	(5.05)	317.52	(700)	0.57	(1.86)	15.88	(35)	20.90	(8.23)								
7.258	(8)	1.61	(5.28)	362.88	(800)	0.60	(1.95)	18.14	(40)	21.84	(8.60)	0.91	(2.0)	8.05	(3.17)	0.04	(0.100)	2.97	(1.17)
8.165	(9)	1.67	(5.49)	408.24	(900)	0.62	(2.02)	20.41	(45)	22.73	(8.95)								
9.072	(10)	1.73	(5.69)	453.60	(1000)	0.64	(2.10)	22.68	(50)	23.55	(9.27)	1.13	(2.5)	8.66	(3.41)	0.06	(0.125)	3.20	(1.26)
9.979	(11)	1.79	(5.88)	498.96	(1100)	0.66	(2.16)	24.95	(55)	24.31	(9.57)								
10.866	(12)	1.84	(6.05)	544.32	(1200)	0.68	(2.23)	27.22	(60)	25.02	(9.85)	1.36	(3.0)	9.22	(3.63)	0.07	(0.150)	3.40	(1.34)
11.793	(13)	1.89	(6.21)	589.68	(1300)	0.70	(2.27)	29.48	(65)	25.70	(10.12)								
12.700	(14)	1.94	(6.37)	635.04	(1400)	0.72	(2.35)	31.75	(70)	26.34	(10.37)	1.59	(3.5)	9.70	(3.82)	0.08	(0.175)	3.58	(1.41)
13.608	(15)	1.98	(6.51)	680.40	(1500)	0.73	(2.40)	34.02	(75)	26.95	(10.61)								
14.515	(16)	2.03	(6.66)	725.76	(1600)	0.75	(2.45)	36.29	(80)	27.53	(10.84)	1.81	(4.0)	10.13	(3.99)	0.09	(0.200)	3.73	(1.47)
15.422	(17)	2.07	(6.79)	771.12	(1700)	0.76	(2.50)	38.56	(85)	28.09	(11.06)								
16.330	(18)	2.11	(6.92)	816.48	(1800)	0.78	(2.55)	40.82	(90)	28.65	(11.28)	2.04	(4.5)	10.54	(4.15)	0.10	(0.225)	3.89	(1.53)
17.237	(19)	2.15	(7.05)	861.84	(1900)	0.80	(2.60)	43.09	(95)	29.16	(11.48)								
18.144	(20)	2.19	(7.17)	907.20	(2000)	0.81	(2.64)	45.36	(100)	29.54	(11.63)	2.27	(5.0)	10.92	(4.30)	0.11	(0.250)	4.04	(1.59)

[1] Dimensions correspond to size measured by sieve, grizzly, or visual inspection for stone of 25.9 kilonewtons per cubic meter unit weight. Do not use for determining structure crest width or layer thickness.

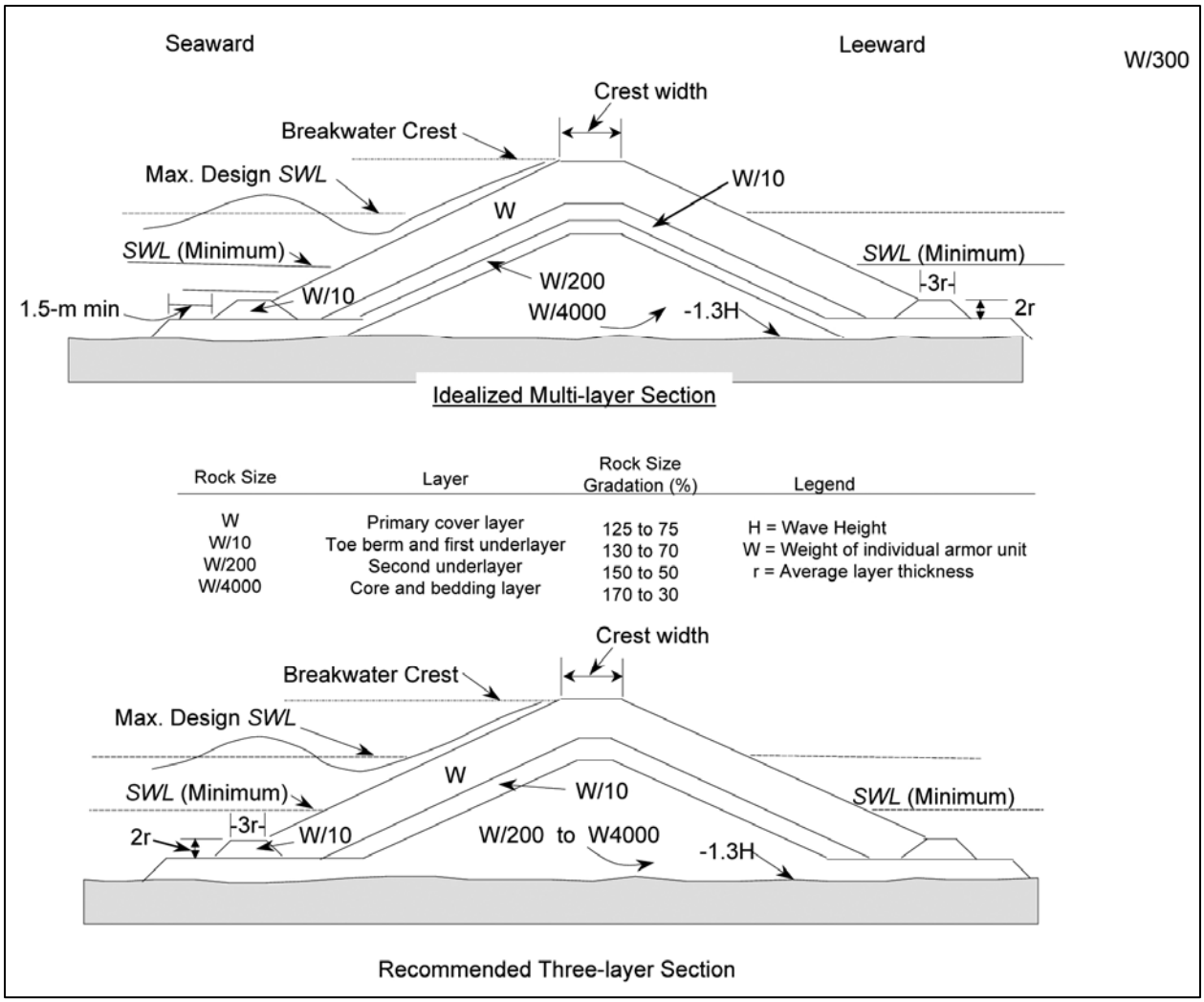

Figure VI-5-55. Rubble-mound section for wave exposure on both sides with moderate overtopping conditions

(a) Overtopping of a rubble-mound structure such as a breakwater or jetty usually can be tolerated if the waves generated by the overtopping do not cause damage behind the structure. Overtopping will occur if the crest elevation is lower than the wave runup, as estimated using the procedures in Part VI-5-2*a*, "Wave runup and rundown on structures." If the armor layer is chinked, or in other ways made smoother or less permeable, maximum runup will be increased.

(b) The selected crest elevation should be the lowest that provides the protection required. Excessive overtopping of a breakwater or jetty can cause choppiness of the water surface behind the structure and can be detrimental to harbor operations such as small craft mooring and most types of commercial cargo transfer. Overtopping of a rubble seawall or revetment can cause serious erosion behind the structure and flooding of the backshore area. Jetty overtopping is tolerable if it doesn't affect navigation in the channel. Signs warning pedestrians of overtopping dangers should be prominently posted on any publicly accessible structure designed for occasional wave overtopping.

(c) Crest width depends greatly on the degree of allowable overtopping; however, this dependency has not been quantified into general design guidance. The general rule of thumb for overtopping conditions is that minimum crest width should equal the combined widths of three armor units (n = 3) as determined by the formula

$$B = nk_{\Delta}\left(\frac{W}{w_a}\right)^{1/3} \qquad \text{(VI-5-116)}$$

where

B = crest width

n = number of stones (n = 3 is recommended minimum)

k_{Δ} = layer coefficient from Table VI-5-51

W = primary armor unit weight

w_a = specific weight of armor unit material

Where there is no overtopping, crest width is not critical; but in either case the crest must be wide enough to accommodate any construction and maintenance equipment that might operate directly on the structure.

(d) The sketches in Figures VI-5-54 and VI-5-55 show the primary armor cover layer extending over the crest. Armor units designed according to the non-overtopping stability formulas in Part VI-5-3*a*, "Armor layer stability," are probably stable on the crest for minor overtopping. For low-crested structures where frequent, heavy overtopping is expected, use the appropriate stability formula given in the Part VI-5-3*a* tables for preliminary design. Physical model tests are strongly recommended to confirm the stability of the crest and backside armor under heavy overtopping conditions. Model testing is almost imperative to check the overtopping stability of concrete armor units placed on the crest which may be less stable than equivalent stone armor.

(3) Concrete cap for rubble-mound structures.

(a) Placed concrete may be added to the cover layer of rubble-mound jetties and breakwaters for purposes such as filling the interstices of stones in the cover layer crest and side slopes as far down as wave action permits, or as large monolithic blocks cast in place. Placed concrete may serve any of four purposes: to strengthen the crest, to deflect overtopping waves away from impacting directly on the leeside slope, to increase the crest height, and to provide roadway access along the crest for construction or maintenance purposes.

(b) Massive concrete caps have been used with cover layers of precast concrete armor units to replace armor units of questionable stability on an overtopped crest and to provide a rigid backup to the top rows of armor units on the slopes. To accomplish this dual purpose, the

cap can be a slab with a solid or permeable parapet (Czerniak and Collins 1977; Jensen 1983) a slab over stone grouted to the bottom elevation of the armor layer, or a solid or permeable block (Lillevang 1977; Markle 1982). Massive concrete caps must be placed after a structure has settled or must be sufficiently flexible to undergo settlement without breaking up (Magoon et al. 1974).

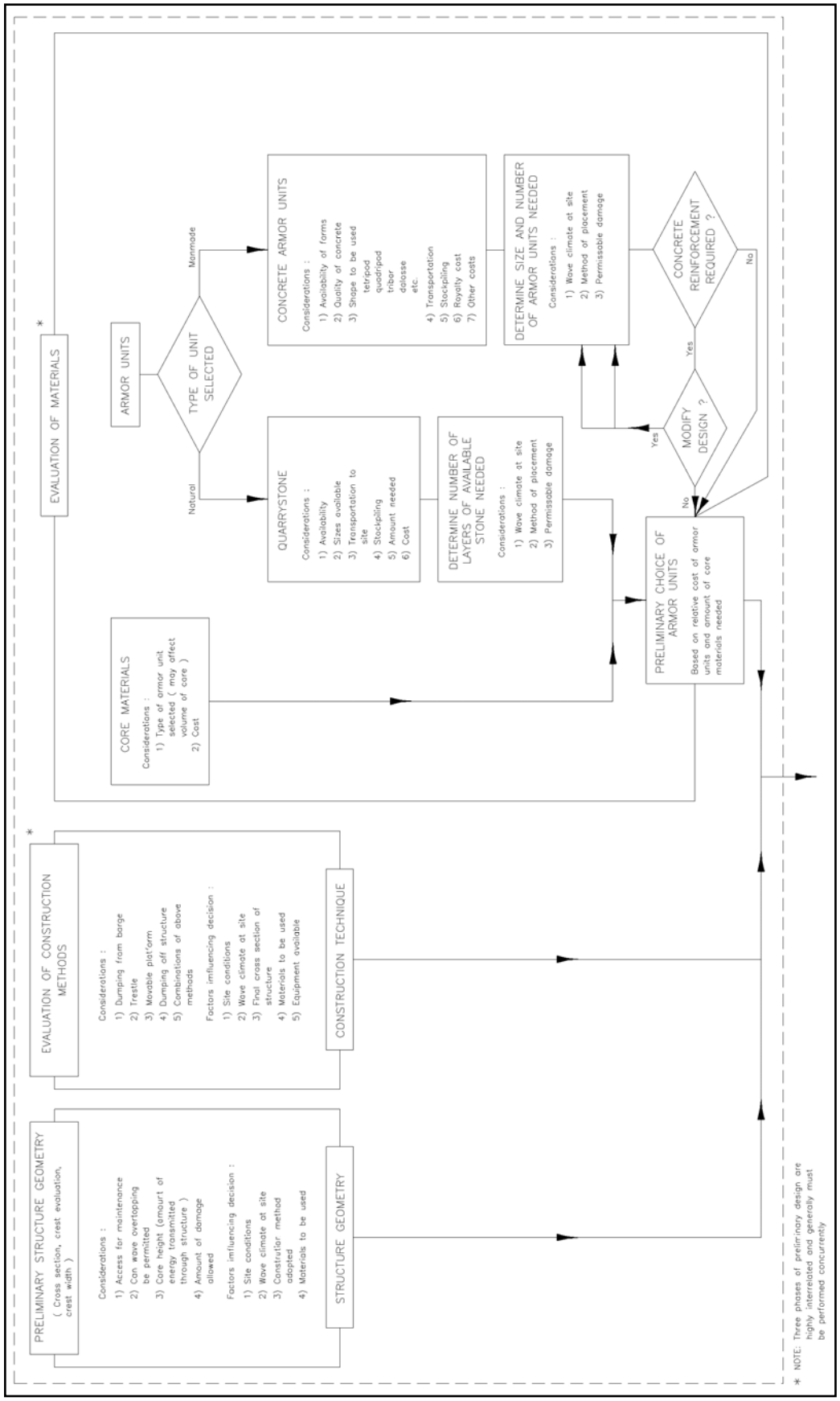

Figure VI-5-56. Logic diagram for preliminary design of rubble-mound structures

(c) Concrete caps with solid vertical or sloped walls reflect waves out through the upper rows of armor units, perhaps causing loss of those units. Solid slabs and blocks can trap air beneath them, creating uplift forces during heavy wave action that may crack or tip the cap (Magoon et al. 1974). A permeable cap decreases both of these problems. A parapet can be made permeable, and vertical vents can be placed through the slab or block itself (Mettam 1976). Lillevang (1977) designed a breakwater crest composed of a vented block cap placed on an unchinked, ungrounted extension of the seaward slope's underlayer, a permeable base reaching across the crest.

(d) Ribbed caps are a compromise between the solid block and a covering of concrete armor units. The ribs are large, long, rectangular members of reinforced concrete placed perpendicular to the axis of a structure in a manner resembling railroad ties. The ribs are connected by reinforced concrete braces, giving the cap the appearance of a railroad track running along the structure crest. This cap serves to brace the upper units on the slopes, yet is permeable in both the horizontal and vertical directions.

(e) Ribbed caps have been used on U.S. Army Corps of Engineers breakwaters at Maalea Harbor (Carver and Markle 1981), at Kahului (Markle 1982), on Maui, and Pohoiki Bay, all in the State of Hawaii.

(f) Waves overtopping a concrete cap can damage the leeside armor layer. The width of the cap and the shape of its lee side can be designed to deflect overtopping waves away from the structure's lee side (Czerniak and Collins 1977; Lillevang 1977; and Jensen 1983). Ribbed caps help dissipate waves.

(g) High parapet walls have been added to caps to deflect overtopping seaward and allow the lowering of the crest of the rubble mound itself. These walls present the same reflection problems described above and complicate the design of a stable cap (Mettam 1976; Jensen 1983). Hydraulic model tests by Carver and Davidson (1976, 1983) have investigated the stability of caps with high parapet walls proposed for Corps structures. Part VI-5-4*d*, “Stability of concrete caps and caissons against sliding and overturning,” provides design guidance.

(h) To evaluate the need for a massive concrete cap to increase structural stability against overtopping, consideration should be given to the cost of including a cap versus the cost of increasing dimensions to prevent overtopping and for construction and maintenance purposes. A massive concrete cap is not necessary for the structural stability of a structure composed of concrete armor units when the difference in elevation between the crest and the limit of wave runup on the projected slope above the structure is less than 15 percent of the total wave runup. For this purpose, an all-rubble structure is preferable, and a concrete cap should be used only if substantial savings would result. Maintenance costs for an adequately designed rubble structure are likely to be lower than for any alternative composite-type structure. The cost of a concrete cap should also be compared to the cost of covering the crest with flexible, permeable concrete armor units, perhaps larger than those used on the slopes, or large quarrystone armor. Hydraulic model tests are recommended to determine the most stable and economical crest designs for major structures.

(i) Experience indicates that concrete placed in the voids on the structure slopes has little structural value. By reducing slope roughness and surface porosity, the concrete increases wave runup. The effective life of the concrete is short, because the bond between concrete and stone is quickly broken by structure settlement. Such filling increases maintenance costs. For a roadway, a concrete cap can usually be justified if frequent maintenance of armor slopes is anticipated. A smooth surface is required for wheeled vehicles; tracked equipment can be used on ribbed caps.

(4) Thickness of armor layer and underlayers.

(a) The thickness of the cover layer and underlayers is calculated using the formula

$$r = nk_{\Delta}\left(\frac{W}{w_a}\right)^{1/3} \tag{VI-5-117}$$

and the placing density (number of armor units per unit area) is estimated using the equation

$$\frac{N_a}{A} = nk_{\Delta}\left(1-\frac{P}{100}\right)\left(\frac{w_a}{W}\right)^{2/3} \tag{VI-5-118}$$

where r is the average layer thickness, n is the number of quarrystone or concrete armor units in the thickness (typically $n = 2$), W is the weight of individual armor units, w_a is the specific weight of the armor unit material, and N_a is the required number of individual armor units for a given surface area, A. The layer coefficient (k_{Δ}) and cover layer average porosity (P) in percent were experimentally determined, and values are given in Table VI-5-51. Equations VI-5-117 and VI-5-118 can be used with either metric or English units.

(b) The specified placing or packing density must be strictly maintained during construction to assure proper interlocking, and therefore hydraulic stability, of the armor layer. During placement, packing density can be maintained by specifying a mean and allowable deviation for the centroidal distance (in three dimensions) between units, or it can be maintained by counting units in a specified area. For grid placement, each subsequent row of armor units is typically offset laterally from the previous lower row to avoid failure planes. To specify the placement grid, D_H is the distance between the centroids of two adjacent units on the same horizontal row and D_U is the distance between the centroids of units upslope in the plane of the structure slope. Values of D_H and D_U for specific armor sizes and packing density coefficients appropriate for Core-Loc and Accropod units can be obtained from the vendor or license holder. Within any matrix of armor units, every effort should be made to achieve maximum interlocking. The maximum centroidal distance D_{max} should not exceed 110 percent of the values specified. Greater spacing may jeopardize interlocking and the integrity of the armor layer.

Table VI-5-51
Layer Coefficient and Porosity for Various Armor Units

Armor Unit	n	Placement	Layer Coefficient k_Δ	Porosity P (percent)
Quarrystone (smooth)[1]	2	Random	1.02	38
Quarrystone (rough)[2]	2	Random	1.00	37
Quarrystone (rough)[2]	∃3	Random	1.00	40
Quarrystone (parallepiped)[3]	2	Special	--	27
Quarrystone[4]	Graded	Random	--	37
Cube (modified)[1]	2	Random	1.10	47
Tetrapod[1]	2	Random	1.04	50
Tribar[1]	2	Random	1.02	54
Tribar[1]	1	Uniform	1.13	47
dolos[5]	2	Random	0.94	56
Core-Loc[6] Vol. < 5 m^3 5 < Vol. < 12 m^3 12 < Vol. < 22m^3	1	Random	1.51	60 63 64
Accropod[7] Vol. < 5 m^3 5 < Vol. < 12 m^3 12 < Vol. < 22m^3	1	Random	1.51	57 59 62

[1] Hudson (1974)
[2] Carver and Davidson (1983)
[3] Layer thickness is twice the average long dimension of the parallelepiped stones. Porosity is estimated from tests on one layer of uniformly placed modified cubes (Hudson 1974).
[4] The minimum layer thickness should be twice the cubic dimension of the W_{50} riprap. Check to determine that the graded layer thickness is ∃1.25 the cubic dimension of the W_{max} riprap (see Equations VI-5-119 and VI-5-120).
[5] Carver and Davidson (1977)
[6] Turk and Melby (1997)
[7] Accropod informational brochure

(c) The thickness r of a layer of riprap is the greater of either 0.3 m, or one of the following, whichever of the three is greatest:

$$r = 2.0\left(\frac{W_{50}}{w_a}\right)^{1/3} \tag{VI-5-119}$$

where W_{50} is the weight of the 50-percent size in the riprap gradation, or

$$r = 1.25\left(\frac{W_{\max}}{w_a}\right)^{1/3} \tag{VI-5-120}$$

where W_{max} is the heaviest stone in the gradation. The specified layer thickness should be increased by 50 percent for riprap placed underwater if conditions make placement to design dimensions difficult. The placing density of riprap is defined as the total weight of riprap placed (W_T) per unit area (A) of structure slope. Riprap placing density can be estimated as

$$\frac{W_T}{A} = rw_a\left(1 - \frac{P}{100}\right) \tag{VI-5-121}$$

(5) Bottom elevation of primary cover layer.

(a) When water depth is greater than 1.5 H (where H is the irregular wave height parameter used to determine a stable primary armor unit weight), the armor units in the cover layer should be extended downslope to an elevation below minimum SWL equal to the design wave height H as shown in Figure VI-5-54. For water depths less than 1.5 H extend the cover layer armor units to the toe as shown in Figure VI-5-55. Model tests to determine the bottom elevation of the primary cover layer and the type of armor placement should be conducted when feasible. Revetment cover layers located in shallow water should be extended seaward of the structure toe on sandy bottoms to serve as scour protection.

(b) Increased stability for special-placement parallelepiped stone (see higher K_D values in Table VI-5-22) can only be obtained if a toe mound is carefully placed to support the quarrystones with their long axes perpendicular to the structure slope. For dolosse it is recommended that the bottom rows of units in the primary cover layer be Aspecial placed@ on top of the secondary cover layer as shown in Figure VI-5-54, on top of the toe berm as shown in Figure VI-5-55, or on the bottom itself. This placement is highly dependent on wave conditions and water clarity. Site-specific model studies have placed the bottom layer of dolosse with vertical flukes away from the slope and the second row placed so that the units overlap the horizontal flukes of the bottom layer. This helps assure interlocking with the random-placed units farther up the slope (Bottin, Chatham, and Carver 1976), and provides better toe stability than random placement. The seaward dolosse in the bottom row should be placed with the bottom of the vertical flukes one-half the length of the units back from the design surface of the primary armor layer to produce the design layer thickness.

(c) Core-Loc units can be placed randomly along the toe, but experiments indicate a pattern placement along the toe is more stable and should be used when the breakwater is built in shallow, depth-limited conditions. For the bottom layer, individual Core-Loc units are set in a three-point stance in cannon fashion with the central fluke pointing seaward, up at a 45-deg angle like the cannon barrel. All toe units are placed side-by-side with minimal space between adjacent units. The second course of units is laid atop of the toe units such that they straddle each toe unit. Once the second row has been placed, all subsequent Core-Loc armor units are placed in a random matrix. While placing these units in a variety of random orientations, care must be taken to assure that all overlying units are interlocked with and constrain underlying units.

(6) Toe berm for cover layer stability.

(a) Structures exposed to breaking waves should have a quarrystone toe berm to protect the toe of the primary armor layer (see Figure VI-5-55). Design guidance for toe berm dimensions and stone size is given in Part VI-5-3*d*, "Toe stability and protection."

(b) The toe berm may be placed before or after the adjacent cover layer. For special-placement quarrystone or uniform-placement tribars, the toe berm serves as a base, and it must be placed first. When placed after the cover layer, the toe berm must be high enough to provide bracing up to at least half the height of the toe armor units. Usually, this requirement is exceeded by the design guidance recommended in Part VI-5-3*d*.

(7) Structure head and leeside cover layer.

(a) Armoring of the head of a breakwater or jetty should be the same on the leeside slope as on the seaside slope for a distance of about 15 to 45 m from the structure end. This distance depends on such factors as structure length and crest elevation at the seaward end. (See Tables VI-5-37 and VI-5-38 for sizing stable armor units for heads.)

(b) Design of leeside cover layers depends on the extent of wave overtopping, any waves or surges acting directly on the lee slope, structure porosity, and differential hydrostatic head resulting in uplift forces that may dislodge armor units on the back slope. If the crest elevation is established to prevent possible overtopping, the weight of armor units and the bottom elevation of the back slope cover layer should depend on the lesser wave action on the lee side (if any) and the porosity of the structure. Under minor overtopping the armor weight calculated for the seaward side primary cover layer should be used on the lee side down to at least the SWL or -0.5 *H* for preliminary designs. However, model testing may be needed to determine stable armor weights for overtopping wave impacts.

(c) For heavy overtopping of breaking waves in shallow water, the primary armor layer on the lee side should be extended to the bottom as shown in Figure VI-5-55. Where concrete caps are employed, stability of the leeside armor during overtopping should be verified with model tests. When both sides of a structure are exposed to similar wave action (groins and jetties), both slopes should have similar designs.

(8) Secondary cover layer.

(a) If the armor units in the primary and secondary cover layers are of the same material, the weight of armor units in the secondary cover layer, between -1.5 *H* and -2.0 *H*, should be greater than about one-half the weight of armor units in the primary cover layer. Below -2.0 *H*, the weight requirements can be reduced to about *W*/15 for the same slope condition (see Figure VI-5-54). If the primary cover layer is quarrystone, the weights for the secondary quarrystone layers should be ratioed from the weight of quarrystone that would be required for the primary cover layer. The use of a single size of concrete armor unit for all cover layers (i.e., upgrading the secondary cover layer to the same size as the primary cover layer) may prove to be economically advantageous when the structure is located in shallow water as shown in Figure VI-5-55 where the primary cover layer is extended down the entire slope.

(b) The secondary cover layer (shown in Figure VI-5-54 from elevation -1.5 *H* to the bottom) should be as thick as, or thicker than, the primary cover layer. As an example, cover layers of quarrystone of two-stone thickness ($n = 2$) will require a secondary cover layer thickness of $n = 2.5$ for the slope between elevations -*H* and -2.0 *H*, and a thickness of $n = 5$ for the slope below an elevation of -2.0 *H*. These layer thicknesses are based on the armor unit weight ratios given in Figure VI-5-54.

(c) The interfaces between the secondary cover layers and the primary cover layer are shown at the slope of 1-to-1.5 on Figure VI-5-54. Steeper slopes for the interfaces may contribute to the stability of the cover armor, but material characteristics and site wave conditions during construction may require using a flatter slope than shown in the figure.

(9) Underlayers.

(a) The first underlayer directly beneath the primary armor units (see Figures VI-5-54 and VI-5-55) should have a minimum thickness of two quarrystones ($n = 2$). The first underlayer stones should weigh about one-tenth of the weight of the overlying armor units (*W*/10) if the cover layer and first underlayer are both quarrystone, or the first underlayer is quarrystone and the cover layer is concrete armor units with a stability coefficient of K_D □ 12 (see Tables VI-5-29, VI-5-33, VI-5-34, VI-5-36). When the cover layer armor unit $K_D > 12$ (dolosse, Core-Loc, and uniformly-placed tribars) the first underlayer quarrystone weight should be about one-fifth the weight of the overlying unit (*W*/5). The larger size promotes increased interlocking between the first underlayer and the concrete armor units of the primary cover layer. Hydraulic model tests (Carver and Davidson 1977; Carver 1980) indicate for quarrystone armor units and dolosse on a breakwater trunk exposed to nonbreaking waves that the underlayer stone size could range from *W*/5 to *W*/20 with little effect on armor stability, wave runup or rundown. If the underlayer stone proposed for a given structure is available with a gradation in the range of *W*/5 to *W*/20, the structure should be model tested with that underlayer gradation to determine if this economical material will support a stable primary cover layer of planned armor units when exposed to the site design conditions.

(b) The second underlayer beneath the primary cover layer and upper secondary cover layer (above -2.0 *H*) should have a minimum equivalent thickness of two quarrystones and a weight about 1/20 the weight of the stones in the first underlayer. In terms of primary armor unit

weight this is approximately 1/20 H $W/10 = W/200$ for quarrystone and some concrete armor units.

(c) The first underlayer beneath the lower secondary cover layer (below -2.0 H on Figure VI-5-54) should also have a minimum of two thicknesses of quarrystone. Stones in this layer should weigh about 1/20 of the immediately overlying armor unit weight. In terms of primary armor unit weight this is approximately 1/20 x $W/15 = W/300$ for units of the same material. The second underlayer for the secondary armor below -2.0 H can be as light as $W/6000$, or equal to the core material size.

(d) For the recommended cross section in Figure VI-5-54 when the primary armor is quarrystone and/or concrete units with K_D □ 12, the first underlayer and the cover layer below -2.0 H should have quarrystone weights between $W/10$ and $W/15$. If the primary armor is concrete armor units with $K_D > 12$, the first underlayer and cover armor below -2.0 H should be quarrystone with weights between $W/5$ and $W/10$.

(e) For graded riprap cover layers the minimum requirement for the underlayers (if one or more are required) is

$$D_{15}\left(\text{cover}\right) \le 5D_{85}\left(\text{under}\right) \qquad \text{(VI-5-122)}$$

where D_{15} *(cover)* is the diameter exceeded by the coarsest 85 percent of the riprap or underlayer on top and D_{85} *(under)* is the diameter exceeded by the coarsest 15 percent of the underlayer or soil below (Ahrens 1981b). For a revetment where the riprap and the underlying soil satisfy the size criterion, no underlayer is necessary. Otherwise, one or more of the following is required.

(f) The size criterion for riprap is more restrictive than the general filter criterion given in Part VI-5-3*b*, "Granulated and geotextile filter stability." The riprap criterion requires larger stone in the lower layer to prevent the material from washing through the voids in the upper layer as cover layer stones shift during wave action. A more conservative underlayer than required by the minimum criterion may be constructed of stone with a 50-percent size of about $W_{50}/20$. This larger stone will produce a more permeable underlayer and should reduce runup and increase interlocking between the cover layer and underlayer. However, be sure to check the underlayer gradation against the underlying soil to assure the minimum criterion of Equation VI-5-122 is met.

(g) The underlayers should be at least three thicknesses of the W_{50} stone, but never less than 0.23 m (Ahrens 1981b). The thickness can be calculated using Equation VI-5-119 with a coefficient of 3 rather than 2. Because a revetment is placed directly on the soil or fill material of the bank it protects, a single underlayer also functions as a bedding layer or filter blanket.

f. Blanket stability in current fields. Stone blankets constructed of randomly-placed riprap or uniformly sized stone are commonly used to protect areas susceptible to erosion by fast-flowing currents. Blanket applications include lining the bottom and sloping sides of flow channels and armoring regions of tidal inlets where problematic scour has developed. Design of stable stone or riprap blankets is based on selecting stone sizes such that the shear stress required

to dislodge the stones is greater than the expected shear stress at the bottom developed by the current.

(1) Boundary layer shear stress.

(a) Prandl established a universal velocity profile for flow parallel to the bed given by

$$\frac{u}{v_*} = \frac{1}{\kappa} \ln\left(\frac{y}{k_s}\right) + B \qquad \text{(VI-5-123)}$$

where

κ = von Karman constant (= 0.4)

y = elevation above the bed

u = velocity at elevation y

k_s = boundary roughness

B = function of Reynolds number (= 8.5 for fully rough, turbulent flow)

v_* = shear velocity (= $(\tau_o / \rho_w)^{1/2}$)

τ_o = shear stress acting on the bed

ρ_w = density of water

Equation VI-5-123 can be expressed in terms of the mean flow velocity, $\bar{u}$, by integrating over the depth, i.e.,

$$\frac{\bar{u}}{v_*} = \frac{1}{h}\int_0^h \frac{u}{v_*} dy = \frac{1}{\kappa} \ln\left(\frac{h}{k_s}\right) + B - \frac{1}{\kappa} \qquad \text{(VI-5-124)}$$

or

$$\frac{\bar{u}}{v_*} = 2.5 \ln\left(\frac{11h}{k_s}\right) \qquad \text{(VI-5-125)}$$

when fully rough turbulent flow is assumed, which is usually the case for flow over stone blankets. Equation VI-5-125 assumes uniform bed roughness and currents flowing over a distance sufficient to develop the logarithmic velocity profile over the entire water depth.

(b) Bed roughness k_s over a stone blanket is difficult to quantify, but it is usually taken to be proportional to a representative diameter d_a of the blanket material, i.e., $k_s = C_1\, d_a$. Substituting for k_s and v_* in Equation VI-5-125 and rearranging yields an equation for shear stress given by

$$\tau_o = \frac{w_w}{g}\left[\frac{\overline{u}}{2.5\ln\left(\frac{11h}{C_1 d_a}\right)}\right]^2 \tag{VI-5-126}$$

where $w_w = \rho_w g$ is the specific weight of water.

(2) Incipient motion of stone blankets.

(a) Stone blankets are stable as long as the individual armor stones are able to resist the shear stresses developed by the currents. Incipient motion on a horizontal bed can be estimated from Shield's diagram (Figure III-6-7) for uniform flows. Fully rough turbulent flows occur at Reynolds numbers where Shields parameter is essentially constant, i.e.,

$$\Psi = \frac{\tau}{(\rho_a - \rho_w) g d_a} \approx 0.04 \tag{VI-5-127}$$

where

τ = shear stress necessary to cause incipient motion

ρ_a = density of armor stone

Rearranging Equation VI-5-127 and adding a factor K_1 to account for blankets placed on sloping channel side walls gives

$$\tau = 0.04 K_1 (w_a - w_w) d_a \tag{VI-5-128}$$

where w_a is the specific weight of armor stone (= $\rho_a g$), and

$$K_1 = \sqrt{1 - \frac{\sin^2\theta}{\sin^2\varphi}} \tag{VI-5-129}$$

with

θ = channel sidewall slope

φ = angle of repose of blanket armor [. 40^o for riprap]

(b) Equating Equations VI-5-126 and VI-5-128 gives an implicit equation for the stable blanket diameter d_a. However, by assuming the logarithmic velocity profile can be approximated by a power curve of the form

$$\ln\left(\frac{11h}{C_1 d_a}\right) \approx C_2 \left(\frac{h}{d_a}\right)^{\beta}$$

an explicit equation is found having the form

$$\frac{d_a}{h} = C_T \left[\left(\frac{w_w}{w_a - w_w}\right)^{\frac{1}{2}} \left(\frac{\bar{u}}{\sqrt{K_1 g h}}\right)\right]^{\frac{2}{(1-2\beta)}} \tag{VI-5-130}$$

where all the constants of proportionality have been included in C_T . Equation VI-5-130 implies that blanket armor stability is directly proportional to water depth and flow Froude number, and inversely proportional to the immersed specific weight of the armor material. The unknown constants, C_T and β, have been empirically determined from laboratory and field data.

(3) Stone blanket stability design equation.

(a) Stable stone or riprap blankets in current fields should be designed using the following equation from Engineer Manual 1110-2-1601.

$$\frac{d_{30}}{h} = S_f C_s \left[\left(\frac{w_w}{w_a - w_w}\right)^{\frac{1}{2}} \left(\frac{\bar{u}}{\sqrt{K_1 g h}}\right)\right]^{\frac{5}{2}} \tag{VI-5-131}$$

where

d_{30} = stone or riprap size of which 30 percent is finer by weight

S_f = safety factor (minimum = 1.1) to allow for debris impacts or other unknowns

C_s = stability coefficient for incipient motion
= 0.30 for angular stone
= 0.38 for rounded stone

(b) EM 1110-2-1601 presents additional coefficients for channel bends and other situations where riprap size must be increased due to flow accelerations. The methodology is also summarized in Maynord (1998). Equation VI-5-131 is based on many large-scale model tests and available field data, and the exponent and coefficients were selected as a conservative envelope to most of the scatter in the stability data. Riprap stone sizes as specified by Equation

VI-5-131 are most sensitive the mean flow velocity, so good velocity estimates are needed for economical blanket designs.

(c) Alternately, Equation VI-5-131 can be rearranged for mean flow velocity to give the expression

$$\bar{u} = \left(\frac{1}{s_f C_s} \right)^{\frac{2}{5}} \left(\frac{h}{d_{30}} \right)^{\frac{1}{10}} \left[g K_1 \left(\frac{w_a - w_w}{w_w} \right) d_{30} \right]^{\frac{1}{2}} \tag{VI-5-132}$$

(d) Equation VI-5-132, which is similar to the well-known Isbash equation, can be used to determine the maximum mean velocity that can be resisted by riprap having d_{30} of a given size. The main difference between Equation VI-5-132 and the Isbash equation is that the Isbash equation multiplies the term in square brackets by a constant whereas Equation VI-5-132 multiplies the square-bracketed term by a depth-dependent factor that arises from assuming a shape for the boundary layer. The Isbash equation is more conservative for most applications, but it is still used for fast flows in small water depths and in the vicinity of structures such as bridge abutments.

(e) By assuming the blanket stones are spheres having weight given by

$$W_{30} = \frac{\pi}{6} w_a d_{30}^3 \tag{VI-5-133}$$

where W_{30} is the stone weight for which 30 percent of stones are smaller by weight, Equation VI-5-131 can be expressed in terms of stone weight as

$$\frac{W_{30}}{w_a h^3} = \frac{\pi}{6} (S_f C_s)^3 \left[\left(\frac{w_w}{w_a - w_w} \right)^{\frac{1}{2}} \left(\frac{\bar{u}}{\sqrt{K_1 g h}} \right) \right]^{\frac{15}{2}} \tag{VI-5-134}$$

(4) Stone blanket gradation.

(a) All graded stone distributions (riprap) used for stone blankets should have distributions conforming to the weight relationships given below in terms of W_{30} or $W_{50\,min}$ (EM 1110-2-1601).

$$W_{50\,\min} = 1.7\, W_{30} \tag{VI-5-135}$$

$$W_{100\,\max} = 5 W_{50\,\min} = 8.5 W_{30} \tag{VI-5-136}$$

$$W_{100\,\min} = 2\, W_{50\,\min} = 3.4\, W_{30} \tag{VI-5-137}$$

$$W_{50\,\max} = 1.5\, W_{50\,\min} = 2.6\, W_{30} \tag{VI-5-138}$$

$$W_{15\,\max} = 0.5\,W_{50\,\max} = 0.75\,W_{50\,\min} = 1.3\,W_{30} \quad \text{(VI-5-139)}$$

$$W_{15\,\min} = 0.31\,W_{50\,\min} = 0.5\,W_{30} \quad \text{(VI-5-140)}$$

(b) Recommended thickness of the blanket layer, *r*, depends on whether placement is submerged or in the dry as specified by the following formulas.

(c) For blankets placed above water, the layer thickness should be

$$r = 2.1\left(\frac{W_{50\,\min}}{w_a}\right)^{\frac{1}{3}} = 2.5\left(\frac{W_{30}}{w_a}\right)^{\frac{1}{3}} \quad \text{(VI-5-141)}$$

with a minimum blanket thickness of 0.3 m. Blankets placed below water should have layer thickness given by

$$r = 3.2\left(\frac{W_{50\,\min}}{w_a}\right)^{\frac{1}{3}} = 3.8\left(\frac{W_{30}}{w_a}\right)^{\frac{1}{3}} \quad \text{(VI-5-142)}$$

with a minimum blanket thickness of 0.5 m.

VI-5-4. Vertical-Front Structure Loading and Response.

a. Wave forces on vertical walls.

(1) Wave-generated pressures on structures are complicated functions of the wave conditions and geometry of the structure. For this reason laboratory model tests should be performed as part of the final design of important structures. For preliminary designs the formulae presented in this section can be used within the stated parameter limitations and with consideration of the uncertainties. Three different types of wave forces on vertical walls can be identified as shown in Figure VI-5-57.

(a) Nonbreaking waves: Waves do not trap an air pocket against the wall (Figure VI-5-57a). The pressure at the wall has a gentle variation in time and is almost in phase with the wave elevation. Wave loads of this type are called pulsating or quasistatic loads because the period is much larger than the natural period of oscillation of the structures. (For conventional caisson breakwaters the period is approximately one order of magnitude larger.) Consequently, the wave load can be treated like a static load in stability calculations. Special considerations are required if the caisson is placed on fine soils where pore pressure may build up, resulting in significant weakening of the soil.

(b) Breaking (plunging) waves with almost vertical fronts: Waves that break in a plunging mode develop an almost vertical front before they curl over (see Figure VI-5-57b). If this almost vertical front occurs just prior to the contact with the wall, then very high pressures are generated having extremely short durations. Only a negligible amount of air is entrapped,

resulting in a very large single peaked force followed by very small force oscillations. The duration of the pressure peak is on the order of hundredths of a second.

(c) Breaking (plunging) waves with large air pockets: If a large amount of air is entrapped in a pocket, a double peaked force is produced followed by pronounced force oscillations as shown in Figure VI-5-57c. The first and largest peak is induced by the wave crest hitting the structure at point A, and it is similar to a hammer shock. The second peak is induced by the subsequent maximum compression of the air pocket at point B, and is it is referred to as compression shock, (Lundgren 1969). In the literature this wave loading is often called the ABagnold type.@ The force oscillations are due to the pulsation of the air pocket. The double peaks have typical spacing in the range of milliseconds to hundredths of a second. The period of the force oscillations is in the range 0.2-1.0 sec.

(2) Due to the extremely stochastic nature of wave impacts there are no reliable formulas for prediction of impulsive pressures caused by breaking waves. Determination of impact pressures in model tests is difficult because of scale effects related to the amount and size of air bubbles and size and shape of air pockets. Also the instrumentation, data sampling, and analyses need special attention to avoid bias by dynamic amplification and misinterpretation when scaling to prototype values. Another problem related to model tests is the sensitivity of the shock loads on the shape and kinematics of the breaking waves. This calls for a very realistic and statistically correct reproduction of natural waves in laboratory models.

(3) Impulsive loads from breaking waves can be very large, and the risk of extreme load values increases with the number of loads. Therefore, conditions resulting in frequent wave breaking at vertical structures should be avoided. Alternatives include placing a mound of armor units in front of the vertical wall structure to break the waves before they can break directly on the wall, or using a rubble-mound structure in place of the vertical wall structure.

(4) Frequent wave breaking at vertical structures will not take place for oblique waves with angle of incidence larger than 20 deg from normal incidence. Nor will it take place if the seabed in front of the structure has a mild slope of about 1:50 or less over a distance of at least several wavelengths, and the vertical wall has no sloping foundation at the toe of the wall.

(5) The use of a sloping-front face from about still-water level (swl) to the crest is very effective in reducing large impact pressures from breaking waves. In addition, the direction of the wave forces on the sloping part (right angle to the surface) helps reduce the horizontal force and the tilting moment. Structures with sloping tops might be difficult to optimize where large water level variations are present. Also, a sloping-front structure allows more overtopping than a vertical wall structure of equivalent crest height.

EXAMPLE PROBLEM VI-5-1

FIND:
Riprap distribution for a stable scour blanket over a nearly horizontal bottom

GIVEN:
The following information is known (English system units shown in parentheses)

Specific weight of riprap, w_a = 25.9 kN/m^3 (165 lb/ft^3)
Specific weight of water, w_w = 10.05 kN/m^3 (64 lb/ft^3)
Bottom slope, θ = 0 deg i.e., K_1 = 1.0
Water depth, h = 6 m (19.7 ft)
Depth-averaged mean velocity, $\bar{u}$ = 2.5 m/s (8.2 ft/s)
Stability coefficient, C_s = 0.38 i.e., rounded stone
Factor of safety, S_f = 1.1
Gravitational acceleration, g = 9.81 m/s^2 (32.2 ft/s^2)

SOLUTION:
From Equation VI-5-134

$$\frac{W_{30}}{w_a h^3} = \frac{\pi}{6}\left[(1.1)(0.38)\right]^3 \left[\left(\frac{10.05 kN/m^3}{[25.9-10.05]kN/m^3}\right)^{\frac{1}{2}}\left(\frac{2.5 m/s}{\sqrt{(1.0)(9.81 m/s^2)(6m)}}\right)\right]^{\frac{15}{2}} = 1.54(10)^{-6}$$

The W_{30} weight is found as

$$W_{30} = 1.54(10)^{-6}\, w_a h^3 = 1.54(10)^{-6}\left(25.9 kN/m^3\right)(6m)^3 = 0.0086 kN = \underline{8.6 N}\,(1.9 lb)$$

The rest of the riprap distribution is found using Equations VI-5-135 - VI-5-140, i.e.,

$W_{50\,\max} = 2.6\,(8.6\ N) = 22.4\ N\ \ (5.0\ lb)$ $\qquad$ $W_{50\,\min} = 1.7\,(8.6\ N) = 14.6\ N\ \ (3.3\ lb)$
$W_{100\,\max} = 8.5\,(8.6\ N) = 73.1\ N\ \ (16.4\ lb)$ $\qquad$ $W_{100\,\min} = 3.4\,(8.6\ N) = 29.2\ N\ \ (6.6\ lb)$
$W_{15\,\max} = 1.3\,(8.6\ N) = 11.2\ N\ \ (2.5\ lb)$ $\qquad$ $W_{15\,\min} = 0.5\,(8.6\ N) = 4.3\ N\ \ (1.0\ lb)$

Blanket layer thickness for underwater placement is found using Equation VI-5-142

$$r = 3.8\left(\frac{0.0086 kN}{25.9 kN/m^3}\right)^{\frac{1}{3}} = 0.26 m\,(0.86 ft)$$

The calculated value for blanket thickness is less than the minimum value, so use $\underline{r = 0.5\ m}$ (1.6 ft).

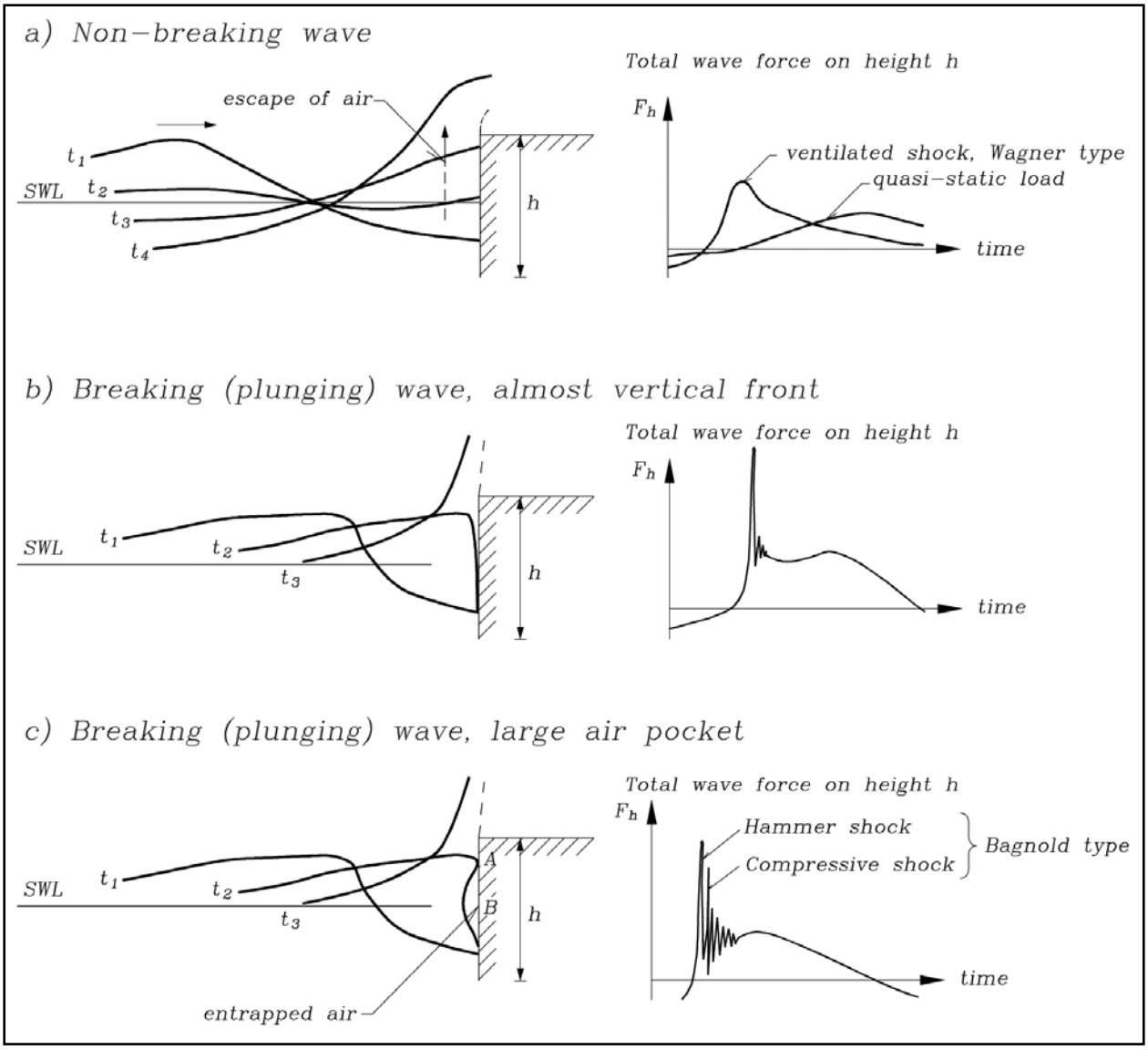

Figure VI-5-57. Illustration of vertical wall wave forces from nonbreaking and breaking waves

(6) It is important to investigate the effect of sloping rubble protection or any rubble foundation that extends in front of a vertical wall to make sure the slope does not trigger wave breaking, causing frequent impact loads on the wall.

(7) Figure VI-5-58 shows a system for identifying types of total horizontal wave loadings on the vertical-front structures as a function of structure geometry and wave characteristics (Kortenhaus and Oumeraci 1998). The system is based on two-dimensional model tests with irregular head-on waves. It should be noted that conditions for three-dimensional waves and oblique waves are different. Also note that the diagram does not cover situations where wave breaking takes place in a wider zone in front of the structure, i.e., typical shallow-water situations with depth-limited waves and seabeds flatter than 1:50.

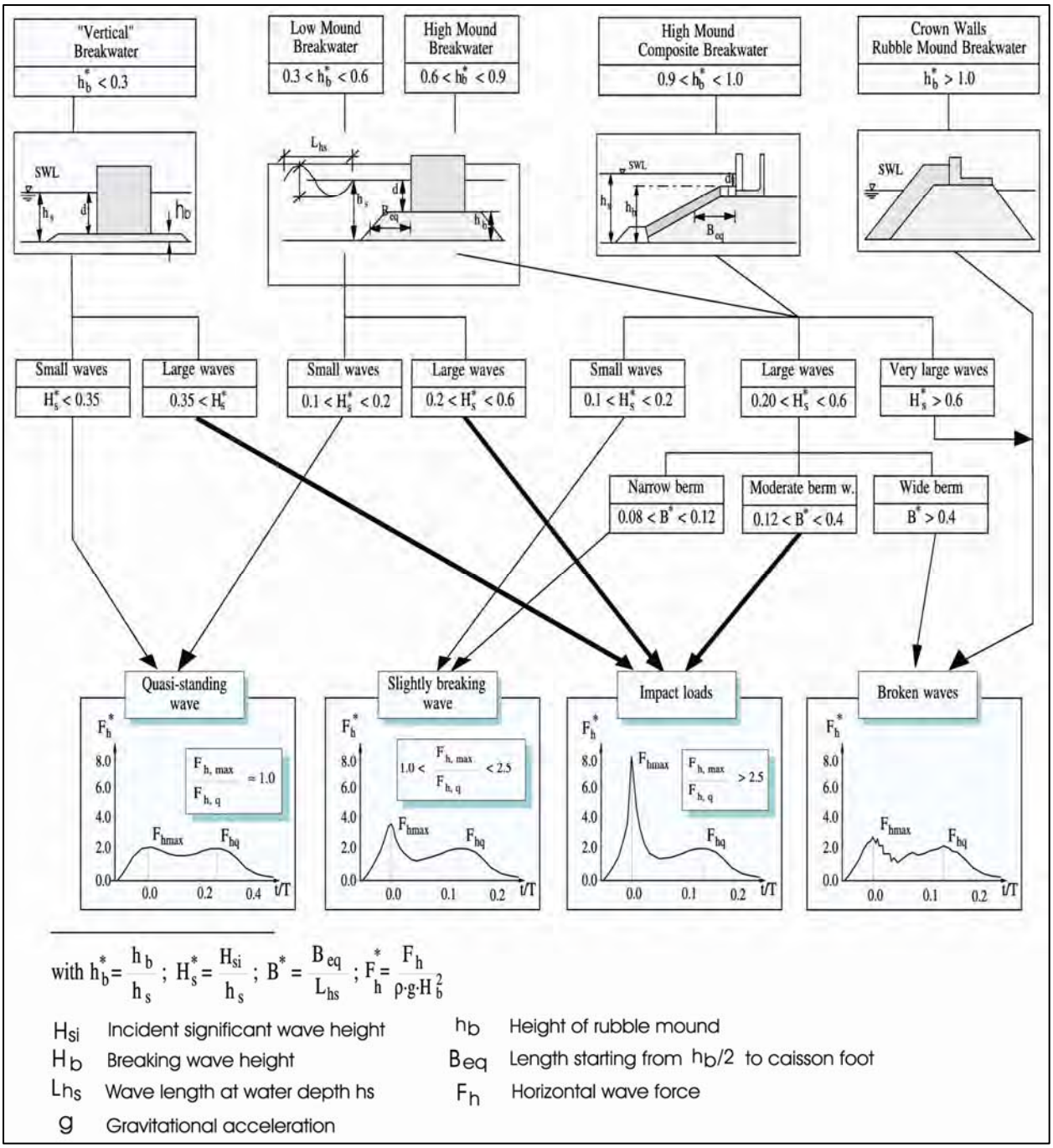

Figure VI-5-58. Identification of types of total horizontal wave loadings on vertical wall structure exposed to head-on long-crested irregular waves (Kortenhaus and Oumeraci 1998). Not valid if breaker zone is present in front of the structure

b. Wave-generated forces on vertical walls and caissons.

(1) Two-dimensional wave forces on vertical walls. Nonbreaking waves incident on smooth, impermeable vertical walls are completely reflected by the wall giving a reflection coefficient of 1.0. Where wales, tiebacks, or other structural elements increase the wall surface

roughness and retard the vertical water motion at the wall, the reflection coefficient will be slightly reduced. Vertical walls built on rubble bases will also have a reduced reflection coefficient.

(a) The total hydrodynamic pressure distribution on a vertical wall consists of two time-varying components: the hydrostatic pressure component due to the instantaneous water depth at the wall, and the dynamic pressure component due to the accelerations of the water particles. Over a wave cycle, the force found from integrating the pressure distribution on the wall varies between a minumum value when a wave trough is at the wall to a maximum values when a wave crest is at the wall as illustrated by Figure VI-5-59 for the case of nonovertopped walls or caissons.

(b) Notice in the right-hand sketch of Figure VI-5-59 the resulting total hydrodynamic load when the wave trough is at the vertical wall is less than the hydrostatic loading if waves were not present and the water was at rest. For bulkheads and seawalls this may be a critical design loading because saturated backfill soils could cause the wall to fail in the seaward direction (see Figures VI-2-63 and VI-2-71). Therefore, water level is a crucial design parameter for calculating forces and moments on vertical walls.

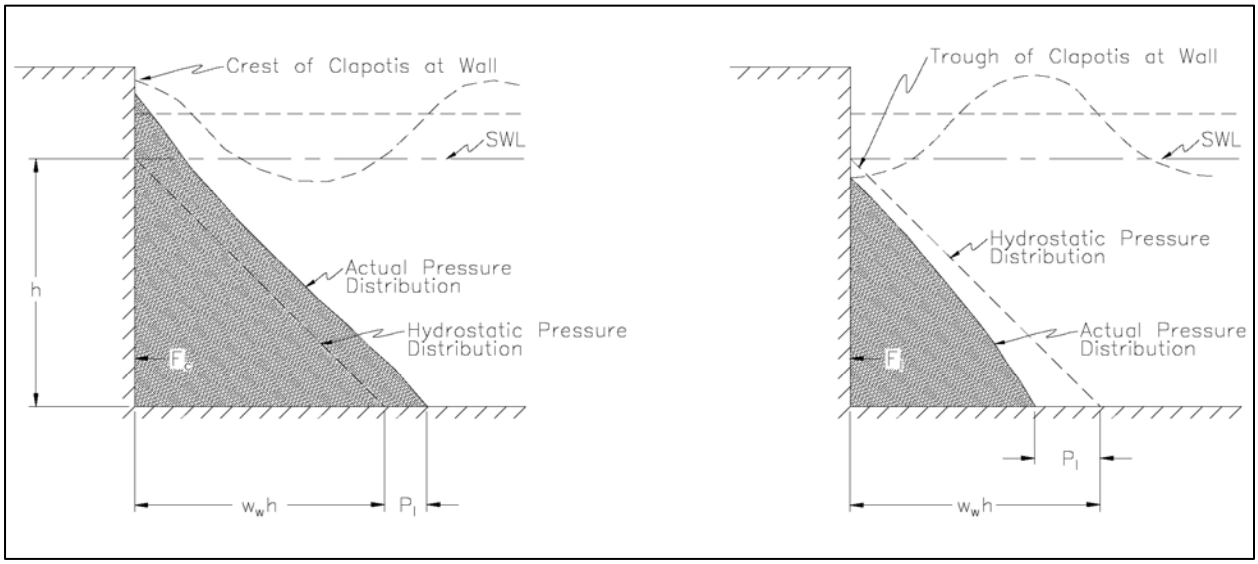

Figure VI-5-59. Pressure distributions for nonbreaking waves

(c) Wave overtopping of vertical walls provides a reduction in the total force and moment because the pressure distribution is truncated as shown schematically in Figure VI-5-60. Engineers should consider the ffect overtopping might have on land-based vertical structures by creating seaward pressure on the wall caused by saturated backfill or ponding water.

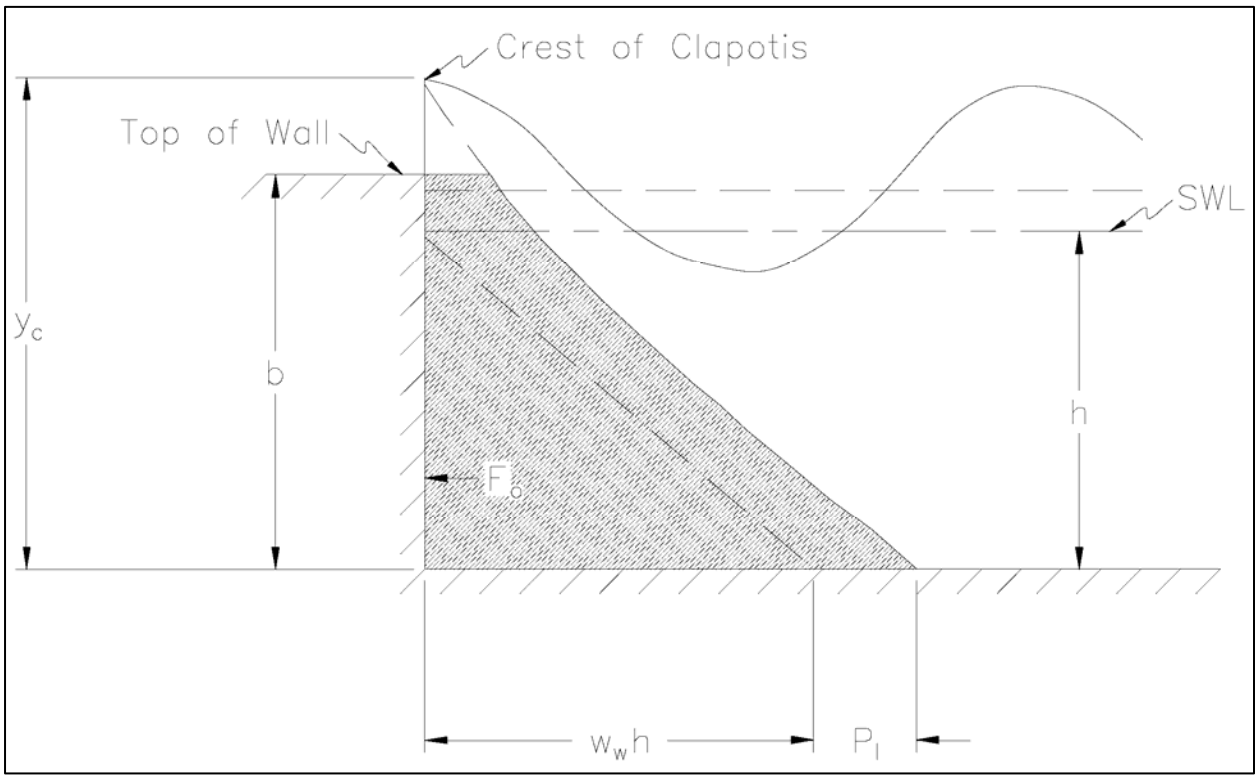

Figure VI-5-60. Pressure distributions on overtopped vertical wall

(d) This section provides formulae for estimating pressure distributions and corresponding forces and overturning moments on vertical walls due to nonbreaking and breaking waves. Most of the methodology is based on the method presented by Goda (1974) and extended by others to cover a variety of conditions. These formulae provide a unified design approach to estimating design loads on vertical walls and caissons.

(e) Important Note: All of the methods in this section calculate the pressure distribution and resulting forces and moments for only the wave portion of the hydrodynamic loading. The hydrostatic pressure distribution from the swl to the bottom is excluded (see Figure VI-5-59). For a caisson structure, the swl hydrostatic forces would exactly cancel; however, it will be necessary to include the effect of the swl hydrostatic pressure for vertical walls tied into the shoreline or an embankment.

(f) The formulae given in the following tables are exclusively based on small-scale model tests. They are presented as follows:

Formula	Waves	Structure	Table
Sainflou formula	Standing	Impermeable vertical wall	VI-5-52
Goda formula	2-D oblique	Impermeable vertical wall	VI-5-53
Goda formula, modified by Takahashi, Tanimoto, and Shimosako 1994a	Provoked breaking	Impermeable vertical wall	VI-5-54
Goda formula forces and moments	Provoked breaking	Impermeable vertical wall	VI-5-55
Goda formula modifed by Tanimoto and Kimura 1985	2-D head-on	Impermeable inclined wall	VI-5-56
Goda formula modified by Takahashi and Hosoyamada 1994	2-D head-on	Impermeable sloping top	VI-5-57
Goda formula modified by Takahashi, Tanimoto, and Shimosako 1990	2-D head-on	Horizontal composite structure	VI-5-58
Goda formula modifed by Takahashi, Tanimoto, and Shimosako 1994b	3-D head-on	Vertical slit wall	VI-5-59

Table VI-5-52
The Sainflou Formula for Head-on, Fully Reflected, Standing Regular Waves (Sainflou 1928)

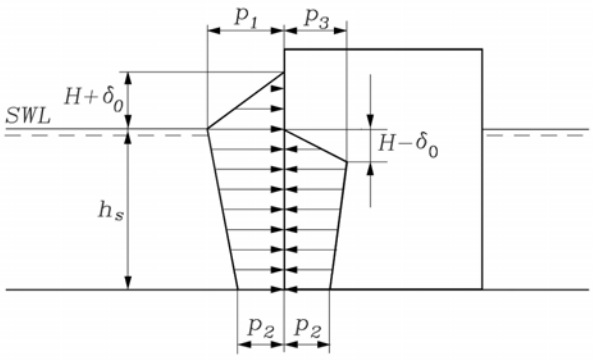

$$p_1 = (p_2 + \rho_w g h_s)\frac{H + \delta_o}{h_s + H + \delta_o} \qquad \text{(VI−5−143)}$$

$$p_2 = \frac{\rho_w g H}{\cosh(2\pi h_s / L)} \qquad \text{(VI−5−144)}$$

$$p_3 = \rho_w g (H - \delta_o) \qquad \text{(VI−5−145)}$$

$$\delta_o = \frac{\pi H^2}{L}\coth\frac{2\pi h_s}{L} \qquad \text{(VI−5−146)}$$

where H Wave height. In case of irregular waves, H should be taken as a characteristic wave height. In Japan $H_{1/3}$ is used, while in other countries $H_{1/10}$ might be used.

p_1 Wave pressure at the still water level, corresponding to wave crest

p_2 Wave pressure at the base of the vertical wall

p_3 Wave pressure at the still water level, corresponding to wave trough

δ_o Vertical shift in the wave crest and wave trough at the wall

ρ_w Water density

h_s Water depth at the foot of the structure

L Local wave length.

Remarks. The Sainflou formula for conditions under wave crest and wave trough were derived theoretically for the case of regular waves and a vertical wall. The formula cannot be applied in cases where wave breaking and/or overtopping takes place.

Table VI-5-53
Goda Formula for Irregular Waves (Goda 1974; Tanimoto et al. 1976) (Continued)

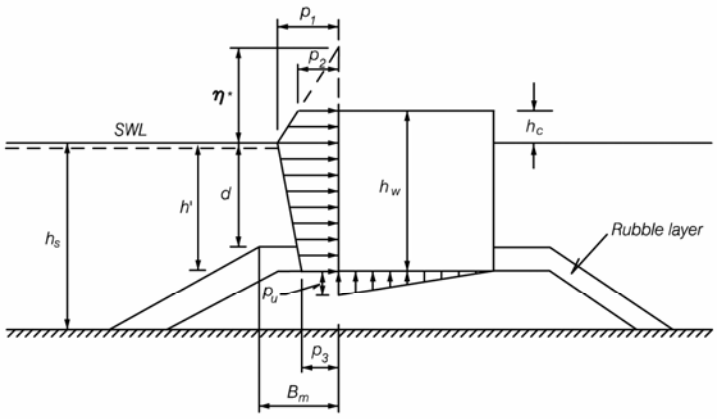

$$\eta^* = 0.75(1 + cos\beta)\,\lambda_1 H_{design} \qquad \text{(VI-5-147)}$$

$$p_1 = 0.5(1 + cos\beta)(\lambda_1\alpha_1 + \lambda_2\alpha_* cos^2\beta)\,\rho_w\, g\, H_{design} \qquad \text{(VI-5-148)}$$

$$p_2 = \begin{cases} \left(1 - \frac{h_c}{\eta^*}\right) p_1 & \text{for } \eta^* > h_c \\ 0 & \text{for } \eta^* \le h_c \end{cases} \qquad \text{(VI-5-149)}$$

$$p_3 = \alpha_3\, p_1 \qquad \text{(VI-5-150)}$$

$$p_u = 0.5(1 + cos\beta)\lambda_3\alpha_1\alpha_3\rho_w g\, H_{design} \qquad \text{(VI-5-151)}$$

where

β Angle of incidence of waves (angle between wave crest and front of structure)

H_{design} Design wave height defined as the highest wave in the design sea state at a location just in front of the breakwater. If seaward of a surf zone Goda (1985) recommends for practical design a value of 1.8 H_s to be used corresponding to the 0.15% exceedence value for Rayleigh distributed wave heights. This corresponds to $H_{1/250}$ (mean of the heights of the waves included in 1/250 of the total number of waves, counted in descending order of height from the highest wave). Goda's recommendation includes a safety factor in terms of positive bias as discussed in Table VI-5-55. If within the surf zone, H_{design} is taken as the highest of the random breaking waves at a distance $5H_s$ seaward of the structure.

$$\alpha_* = \alpha_2$$

$$\alpha_1 = 0.6 + 0.5\left[\frac{4\pi\, h_s/L}{sinh\,(4\pi\, h_s/L)}\right]^2$$

$$\alpha_2 = \text{the smallest of } \frac{h_b - d}{3\, h_b}\left(\frac{H_{design}}{d}\right)^2 \text{ and } \frac{2d}{H_{design}}$$

$$\alpha_3 = 1 - \frac{h_w - h_c}{h_s}\left[1 - \frac{1}{cosh\,(2\pi\, h_s/L)}\right]$$

L Wavelength at water depth h_b corresponding to that of the significant wave $T_s \simeq 1.1T_m$, where T_m is the average period.

h_b Water depth at a distance of $5H_s$ seaward of the breakwater front wall.

λ_1, λ_2 and λ_3 are modification factors depending on the structure type. For conventional vertical wall structures, $\lambda_1 = \lambda_2 = \lambda_3 = 1$. Values for other structure types are given in related tables.

(Continued)

Table VI-5-53. (Concluded)

Uncertainty and bias of formulae: See Table VI-5-55.

Tested ranges:	water depth (cm)	wave height (cm)	wave period (s)	mound height (cm)
	35	7.1-31.2	2	0 & 15
	45	6.7-41.6	1.7	0 & 25
	45	7.6-32.8	1.3	0 & 25
	45	9.2-22.9	1	0 & 25

The formulae have been calibrated with the cases of 21 slidings and 13 nonslidings of the upright sections of the prototype breakwaters in Japan.

Table VI-5-54
Goda Formula Modified to Include Impulsive Forces from Head-on Breaking Waves
(Takahashi, Tanimoto, and Shimosako 1994a)

The modification of Goda's formula concerns the formula for the pressure p_1 at the still water level (SWL). The coefficient α_* is modified as

$$\alpha_* = \text{largest of } \alpha_2 \text{ and } \alpha_I$$

$$\alpha_2 = \text{the smallest of } \frac{h_b - d}{3\,h_b}\left(\frac{H_{design}}{d}\right)^2 \text{ and } \frac{2d}{H_{design}}$$

$$\alpha_I = \alpha_{I0} \cdot \alpha_{I1}$$

$$\alpha_{I0} = \begin{cases} H_{design}/d & \text{for} \quad H_{design}/d \le 2 \\ 2.0 & \text{for} \quad H_{design}/d > 2 \end{cases}$$

$$\alpha_{I1} = \begin{cases} \frac{\cos\delta_2}{\cosh\delta_1} & \delta_2 \le 0 \\ \frac{1}{\cosh\delta_1 \cdot (\cosh\delta_2)^{\frac{1}{2}}} & \delta_2 > 0 \end{cases}$$

$$\delta_1 = \begin{cases} 20 \cdot \delta_{11} & \text{for} \quad \delta_{11} \le 0 \\ 15 \cdot \delta_{11} & \text{for} \quad \delta_{11} > 0 \end{cases}$$

$$\delta_{11} = 0.93\left(\frac{B_m}{L} - 0.12\right) + 0.36\left(\frac{h_s - d}{h_s} - 0.6\right)$$

$$\delta_2 = \begin{cases} 4.9 \cdot \delta_{22} & \text{for} \quad \delta_{2\,2} \le 0 \\ 3 \cdot \delta_{22} & \text{for} \quad \delta_{22} > 0 \end{cases}$$

$$\delta_{22} = -0.36\left(\frac{B_m}{L} - 0.12\right) + 0.93\left(\frac{h_s - d}{h_s} - 0.6\right)$$

where H_{design}, L, d, h_s, h_b, B_m are given in the figure and text of Table VI-5-53.

Range of tested parameters:	Regular waves	
	bottom slope 0.01	$h_s = 42\,\text{cm}$ and $54\,\text{cm}$
	$d = 7 - 39\,\text{cm}$	$B_m = 2.5 - 200\,\text{cm}$
	$H = 17.2 - 37.8\,\text{cm}$	T - 1.8 – 3 sec.

Table VI-5-55
Resulting Wave Induced Forces and Moments, and Related Uncertainties and Bias When Calculated From Wave Load Equations by Goda and Takahashi

Per running meter of the breakwater the wave induced horizontal force, F_H, the uplift force, F_U, and the reduced weight of the vertical structure due to buoyancy, F_G, can be calculated from equations by Goda and Takahashi as follows:

$$F_H = U_{F_H}\left[\frac{1}{2}(p_1+p_2)h_c+\frac{1}{2}(p_1+p_3)h'\right] \quad \text{(VI−5−152)}$$

$$F_U = U_{F_U}\cdot\frac{1}{2}p_u\cdot B \quad \text{(VI−5−153)}$$

$$F_G = \rho_c\cdot g\,B\cdot h_w-\rho_w\cdot g\,B\cdot h' \quad \text{(VI−5−154)}$$

where ρ_c Mass density of the structure
ρ_w Mass density of the water
U_{F_H} Stochastic variable signifying the bias and the uncertainty related to the horizontal force
U_{F_U} Stochastic variable signifying the bias and the uncertainty related to the uplift force
h' Submerged height of the wall from the toe to the still water level.
B Vertical structure width

The corresponding moments at the heel of the caisson breakwater are:

$$M_H = U_{M_H}\left[\frac{1}{6}(2p_1+p_3)h'^2+\right.$$
$$\left.+\frac{1}{2}(p_1+p_2)h'h_c+\frac{1}{6}(p_1+2p_2)h_c^2\right] \quad \text{(VI−5−155)}$$

$$M_U = U_{M_U}\cdot\frac{1}{3}p_u\cdot B^2 \quad \text{(VI−5−156)}$$

$$M_G = \frac{1}{2}B^2g\,(\rho_c h_w-\rho_w h') \quad \text{(VI−5−157)}$$

where U_{M_H} Stochastic variable signifying the bias and the uncertainty of the horizontal moment
U_{M_U} Stochastic variable signifying the bias and the uncertainty of the uplift moment.

Uncertainty and bias of the Goda formulae in Table VI-5-53. Based on reanalysis by Juhl and van der Meer (1992), Bruining (1994), and van der Meer, Juhl, and van Driel (1994) of various model tests performed at Danish Hydraulic Institute and Delft Hydraulics. The mean values and standard deviations of the stochastic variables U are given as

Uncertainty and bias of horizontal wave induced force, uplift force, horizontal moment and uplift moment (vertical composite type)

Stochastic variable	Mean value	no model tests		model test performed	
		Stand. dev.		Stand. dev.	
X_i	μ_{X_i}	σ_{X_i}	$\frac{\sigma_{X_i}}{\mu_{X_i}}\%$	σ_{X_i}	$\frac{\sigma_{X_i}}{\mu_{X_i}}\%$
U_{F_H}	0.90	0.25	0.22	0.05	0.055
U_{F_U}	0.77	0.25	0.32	0.05	0.065
U_{M_H}	0.81	0.40	0.49	0.10	0.12
U_{M_U}	0.72	0.37	0.51	0.10	0.14

Table VI-5-56
Wave Loads on Impermeable Inclined Walls (Tanimoto and Kimura 1985)

Tanimoto and Kimura (1985) performed model tests and demonstrated that the Goda formula can be applied by projection of the Goda wave pressures calculated for a vertical wall with the same height (crest level) as illustrated in the figure.

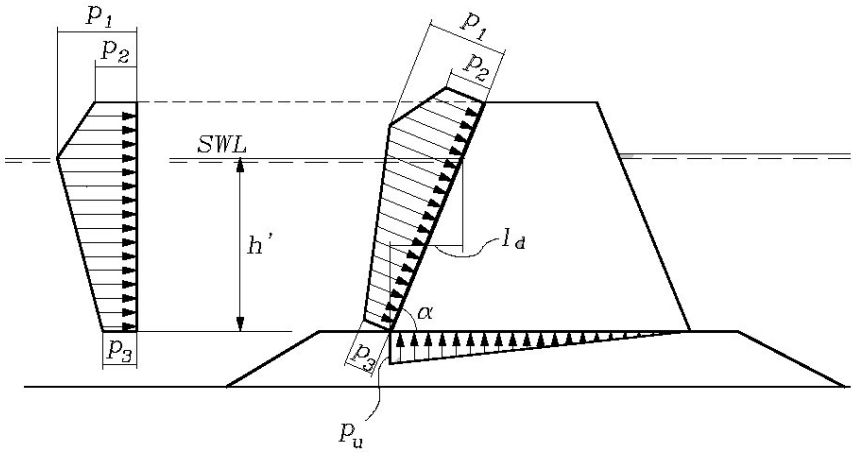

The wave induced uplift pressure on the base plate is reduced compared to the vertical face case. Consequently λ_3 for the calculation of p_u in the Goda formula is modified as

$$\lambda_3 = exp\left[-2.26(7.2\,\ell_d\,/L)^3\right] \qquad \text{(VI-5-158)}$$

where $\ell_d = h' \cot\alpha$ and L is the wavelength.

Eq VI-5-158 is valid for $\alpha \geq 70°$ and $\ell_d < 0.1L$.

Table VI-5-57
Wave Loads on Sloping Top Structures (Takahashi and Hosoyamada 1994)

Tested cross sections

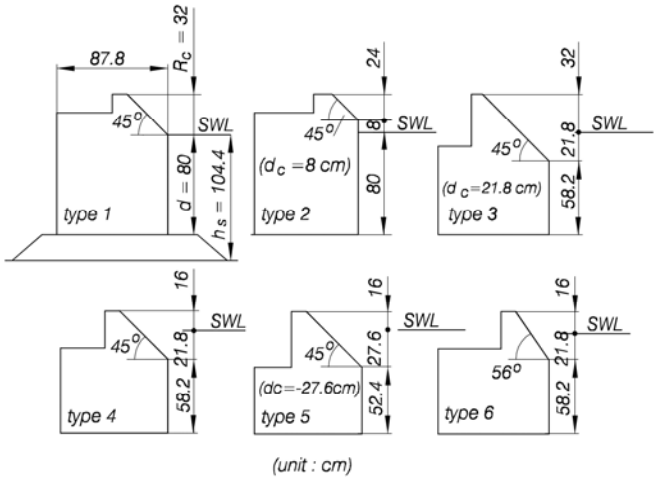

Pressure distribution

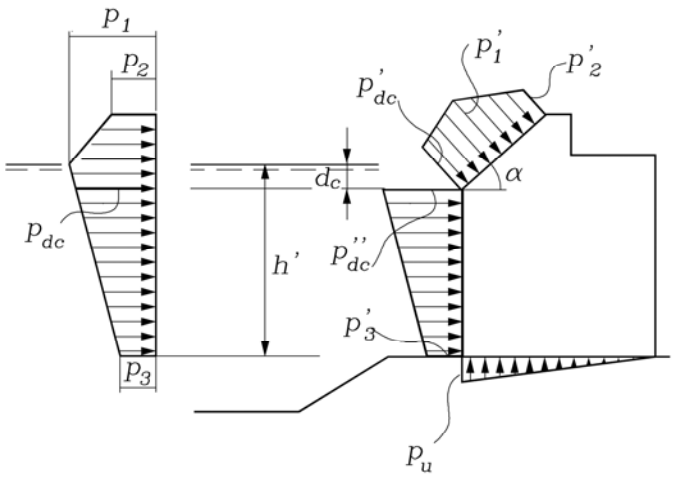

$$p_1' = \lambda_{SL}\, p_1 \sin\alpha \ , \ p_2' = \lambda_{SL}\, p_2 \sin\alpha \ , \ p_{dc}' = \lambda_{SL}\, p_{dc} \sin\alpha \qquad \text{(VI-5-159)}$$

$$p_{dc}'' = \lambda_V\, p_{dc} \ , \ p_3' = \lambda_V\, p_3$$

where

$$\lambda_{SL} = \frac{1}{\sin^2\alpha}\, min[1.0 \ , \ max(\sin^2\alpha \ , \ 1 + 0.46\cos^2\alpha - 23\cos^2\alpha H/L)]$$

$$\lambda_V = min[1.0 \ , \ max(1.1. \ , \ 1.1 + 11 d_c/L) - 5.0 H/L]$$

$p_1,\ p_2,\ p_3,\ p_{dc}$ & p_u are calculated from the Goda formula (Table VI-5-53)

Table VI-5-58
Wave Loads on Vertical Walls Protected by a Rubble-Mound Structure (Takahashi, Tanimoto, and Shimosako 1990)

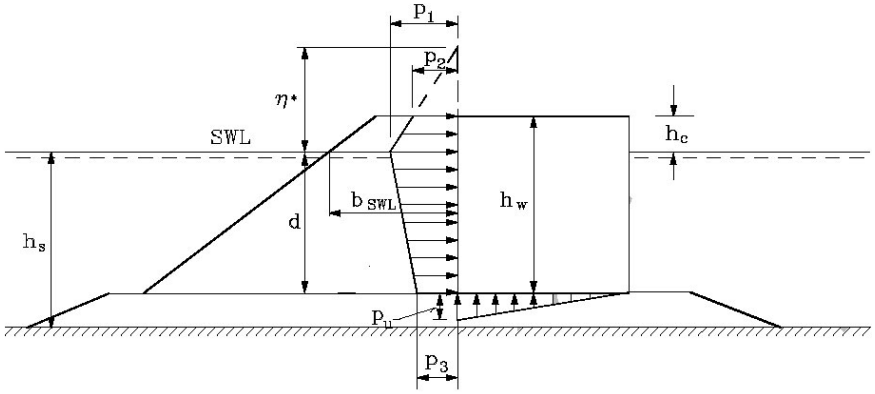

λ_1, λ_2 and λ_3 in the Goda formula are modified as:

$$\lambda_1 = \lambda_3 = \begin{cases} 1.0 & H_{design}/h_s < 0.3 \\ 1.2 - 0.67\,(H_{design}/h_s) & 0.3 \le H_{design}/h_s \le 0.6 \\ 0.8 & H_{design}/h_s > 0.6 \end{cases} \qquad \text{(VI-5-160)}$$

$$\lambda_2 = 0$$

Validity range: These values presume that the rubble consists of blocks of the complex types like Tetrapods and Dolosse. Also, the width of the block section at the top of the vertical wall should be no less than twice the height of a block. The front slope is approximately 1 : 1.5. The model tests cover the parameter intervals: $h_s/L_{1/3} = 0.07 - 0.11$ and $b_{SWL}/L_{1/3} = 0.046 - 0.068$.

Uncertainty and bias: From the test results the mean value, μ_{λ_1}, and the variational coefficient, $\frac{\sigma_{\lambda_1}}{\mu_{\lambda_1}}$, of λ_1 are estimated to be approximately

$$\mu_{\lambda_1} = \begin{cases} 0.90 & H_{design}/h_s < 0.4 \\ 0.90 - (H_{design}/h_s - 0.4) & 0.4 \le H_{design}/h_s \le 0.7 \\ 0.60 & 0.7 < H_{design}/h_s < 0.8 \end{cases} \qquad \text{(VI-5-161)}$$

and

$$\frac{\sigma_{\lambda_1}}{\mu_{\lambda_1}} = 5\% - 10\%$$

Table VI-5-59
Wave Pressures from Regular Head-on Waves on Caissons with Vertical Slit Front Face and Open Wave Chamber (Tanimoto, Takahashi, and Kitatani 1981; Takahashi, Shimosako, and Sakaki 1991) (Continued)

Cross sections

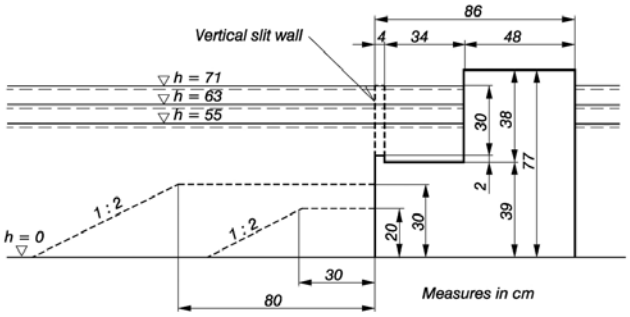

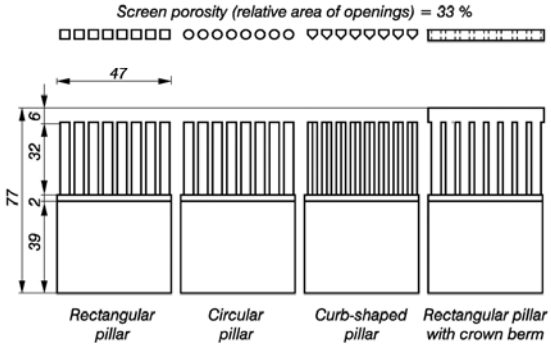

Tested wave range: Regular head-on waves
Incident wave height: 10-30 cm
Wave period: 1.5, 2.0, 2.5 s

Considered wave crest faces

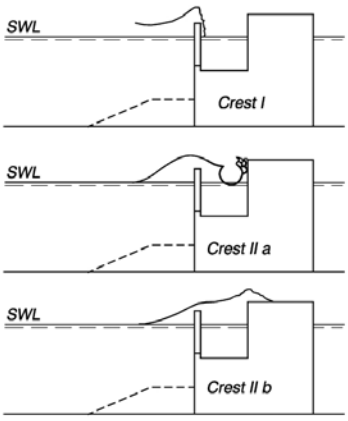

(Continued)

Table VI-5-59. (Concluded)

Pressure distribution

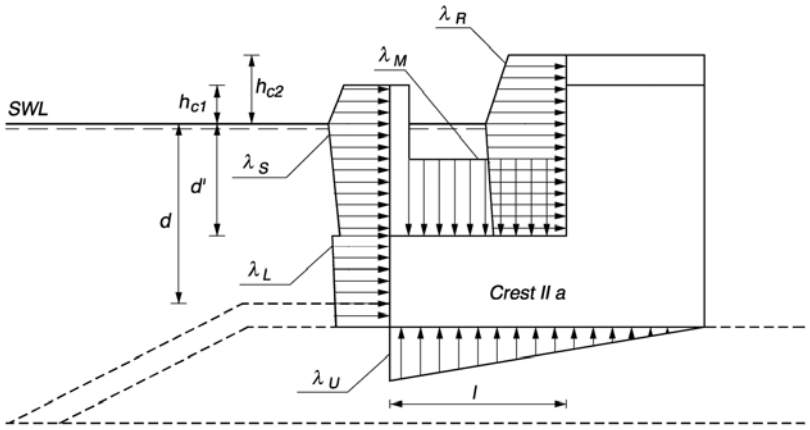

Pressure calculation: Use the Goda formulae with modified λ_1, λ_2 and λ_3 as given in the following table. For example, the wave pressure on the slit wall in the case of Crest-I is calculated by the Goda formulae with λ_1 and λ_2 replaced by λ_{S1} and λ_{S2}, respectively.

Modification factors for vertical slit wall caisson (From Takahashi et al. 1994b).

		Crest-I	Crest-IIa	Crest-IIb
Slit wall	λ_{S1}	0.85	0.7	0.3
	λ_{S2}	0.4 ($\alpha^* \le 0.75$) $0.3/\alpha^*$ ($\alpha^* > 0.75$)	0	0
Impermeable part of front wall	λ_{L1}	1	0.75	0.65
	λ_{L2}	0.4 ($\alpha^* \le 0.5$) $0.2/\alpha^*$ $\alpha^* > 0.5$)	0	0
Wave chamber rear wall	λ_{R1}	0	$20l/3L'$ $l/L' \le 0.15$) 1.0 ($1/L' > 0.15$)	1.4 $H/h \le 0.1$) 1.6 - $2H/h$ ($0.1 < H/h < 0.3$) 1.0 ($H/h \ge 0.3$)
	λ_{R2}	0	0.56 ($\alpha^* \le 25/28$) $0.5/\alpha^*$ ($\alpha^* > 25/28$)	0
Wave Chamber bottom slab	λ_{M1}	0	$20l/3L'$ ($l/L' \le 0.15$) 1.0 ($l/L' > 0.15$)	1.4 ($H/h \le 0.1$) 1.6 - $2H/h$ ($0.1 < H/h < 0.3$) 1.0 ($H/h \ge 0.3$)
	λ_{M2}	0	0	0
Uplift force	λ_{U3}	1	0.75	0.65

In the calculation of α^* for the rear wall, α_1 should be replaced by α_1' which is obtained with the parameters d', L' and B_M' instead of d, L and B_M respectively, where d' is the depth in the wave chamber, L' is the wavelength at water depth d, $B_M' = l - (d - d')$, and l is the width of the wave chamber including the thickness of the perforated vertical wall.

(g) Wave pressure distributions for breaking waves are estimated using Table VI-5-54, and the corresponding forces and moments are calculated from Table VI-5-55. Not included in this manual is the older breaking wave forces method of Minikin as detailed in the *Shore Protection Manual* (1984). As noted in the Shore Protection Manual the Minikin method can result in very high estimates of wave force, Aas much as 15 to 18 times those calculated for nonbreaking waves.@ These estimates are too conservative in most cases and could result in costly structures.

(h) On the other hand, there may be rare circumstances where waves could break in just the right manner to create very high impulsive loads of short duration, and these cases may not be covered by the range of experiment parameters used to develop the guidance given in Table VI-5-54. In addition, scaled laboratory models do not correctly reproduce the force loading where pockets of air are trapped between the wave and wall as shown in Figure VI-5-57. For these reasons, it may be advisable to design vertical-front structures serving critical functions according to Minikin's method given in *Shore Protection Manual* (1984).

(2) Vertical wave barriers.

(a) A vertical wave barrier is a vertical partition that does not extend all the way to the bottom as illustrated by the definition sketch in Figure VI-5-61. Wave barriers reduce the transmitted wave height while allowing circulation to pass beneath the barrier. A useful application for vertical wave barriers is small harbor protection.

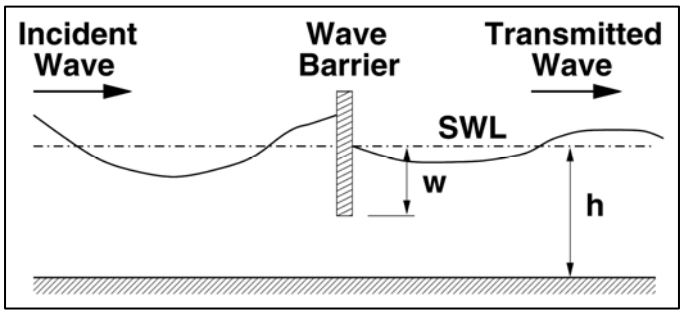

Figure VI-5-61. Wave barrier definition sketch

(b) Kriebel, Sollitt, and Gerken (1998) presented small- and large-scale laboratory measurements of forces on vertical wave barriers and found that existing methods for estimating wave forces on wave barriers overpredicted measured forces by about a factor of 2. They also presented an eigenvalue expansion method for calculating theoretical wave forces, and the predicted forces matched the experiment measurements within 10-20 percent. Both regular and irregular wave experiments were used in the analysis.

(c) Estimation of wave forces using the eigenvalue expansion method involves solving matrix equations for unknown coefficients under the physical constraints of no flow through the barrier and matching dynamic pressure in the gap beneath the barrier. However, this method must be programmed on a computer to obtain force estimates.

(d) An empirical equation for estimating forces on vertical wave barriers was developed for this manual based on the large-scale laboratory irregular wave measurements presented in Kriebel et al. (1998). Their experiments used solid vertical plates having penetration values of w/h = 0.4, 0.5, 0.6, and 0.7 placed in a 3-m water depth. Time series of total force on the plate were recorded, and significant force amplitudes per unit width of barrier were calculated from the zeroth-moment of the force spectra as

$$F_{mo} = \frac{1}{2}\left(4\sqrt{m_o}\right)\frac{1}{B} \tag{VI-5-162}$$

where m_o is the area beneath the measured force spectrum and B is the horizontal width of the barrier. The 1/2-factor arises because the force spectrum also includes forces directed seaward, which are approximately the same magnitude as the landward directed forces (Kriebel et al. 1998).

(e) The relative force measurements per unit width of barrier are shown in Figure VI-5-62. The significant force per unit width (F_{mo}) is nondimensionalized by the significant force per unit width (F_o) for a vertical wall extending over the entire depth, given by the equation

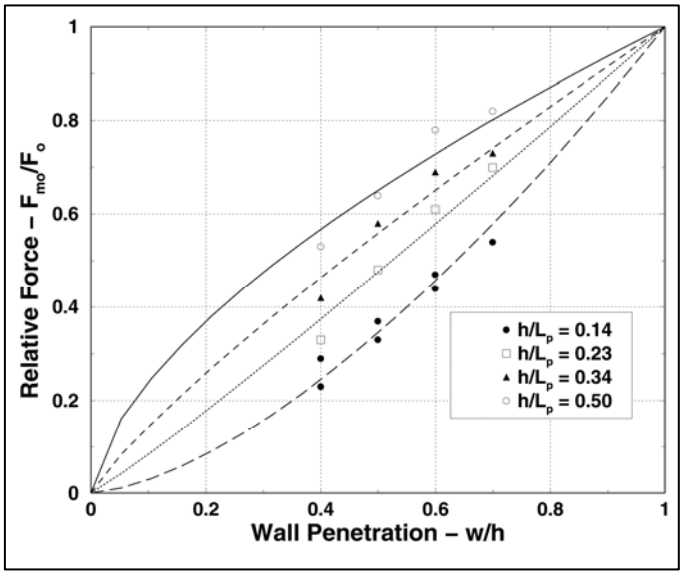

Figure VI-5-62. Best-fit to wave barrier force data

$$F_o = \rho g\, H_{mo}\, \frac{\sinh k_p h}{k_p \cosh k_p h} \tag{VI-5-163}$$

where

ρ = water density

g = gravity

H_{mo} = incident significant wave height

k_p = wave number associated with the spectral peak period, T_p

h = water depth at the barrier

(f) The lines in Figure VI-5-62 are best-fit curves of the form $F_{mo}/F_o = (w/h)^m$. The exponents (m) are plotted in Figure VI-5-63 as a function of relative depth, h/L_p, along with a best-fit power curve.

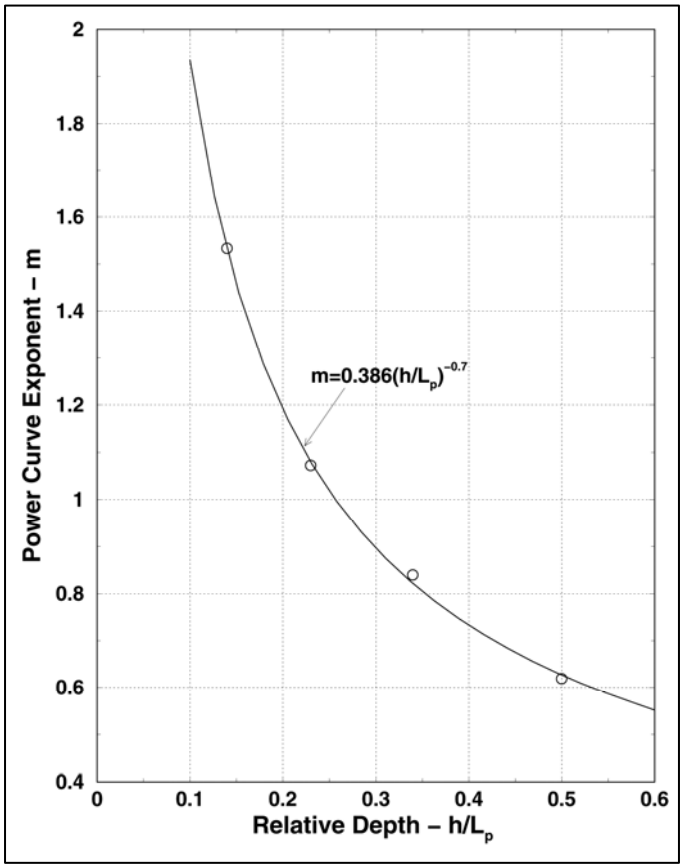

Figure VI-5-63. Power curve exponents

(g) The resulting empirical predictive equation is then given by

$$F_{mo} = F_o \left(w/h\right)^{0.386\left(h/L_p\right)^{-0.7}} \qquad \text{(VI-5-164)}$$

where

F_{mo} = significant force per unit width of barrier

F_o = significant force per unit width of vertical wall (Equation VI-5-163)

w = barrier penetration depth

h = water depth

L_p = local wavelength associated with the peak spectral period, T_p

(h) A comparison of the measured force values versus estimates based on the empirical Equation VI-5-164 is shown in Figure VI-5-64.

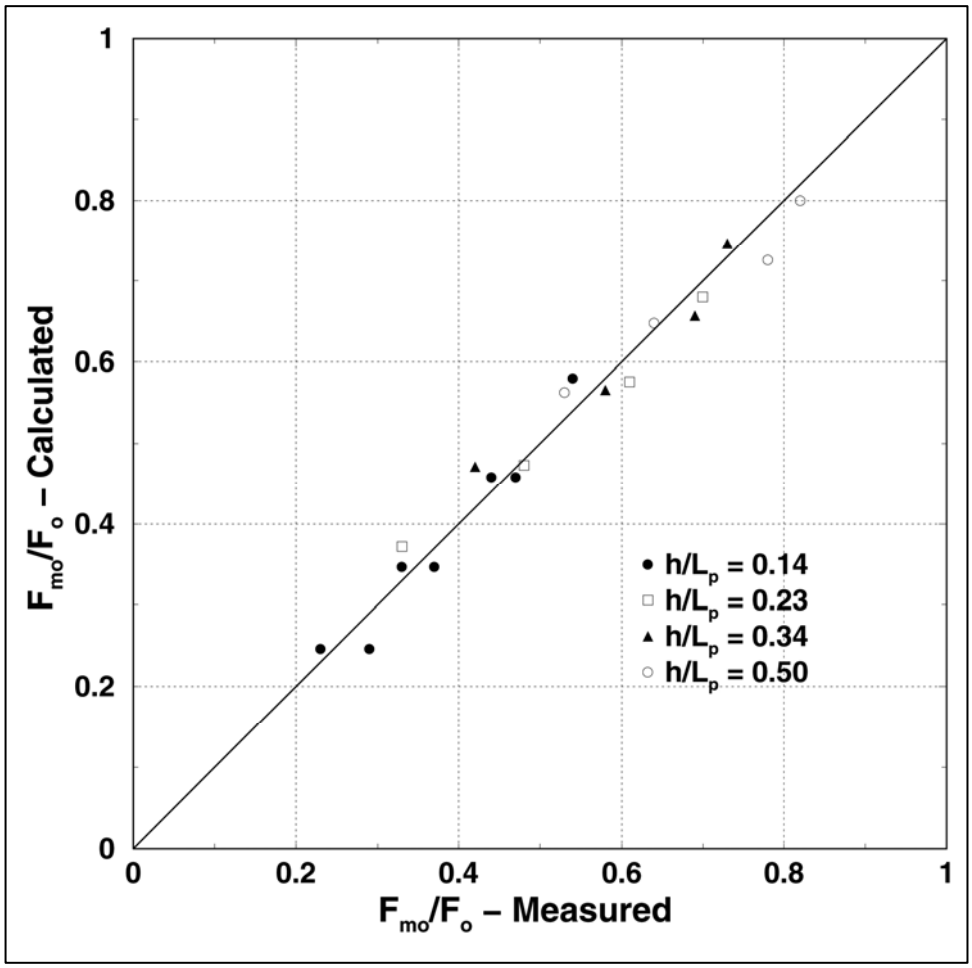

Figure VI-5-64. Comparison of Equation VI-5-139 to data used in empirical curve fits

(i) Use of Equation VI-5-164 should be limited to the range $0.4 < w/h < 0.7$ and $0.14 < h/L_p < 0.5$; however, estimates slightly outside the strict bound of the laboratory data are probably reasonable.

(j) The design force load on the vertical barrier should be the load corresponding to the design wave height, $H_{design} = 1.8\ H_s$ as recommended by Goda (1985). For Rayleigh distributed

waves, $H_{design} = H_{1/250}$; and by linear superposition, we can assume that force amplitudes will also be Rayleigh distributed. Thus, the design force load is determined as

$$F_{design} = 1.8F_{mo} \tag{VI-5-165}$$

(3) Structure length and alignment effects on wave height.

(a) Diffraction at the head of a structure creates variations in wave heights along the structure. For a semi-infinite, fully reflecting structure exposed to nonbreaking long-crested regular waves, Ito, Tanimoto, and Yamamoto (1972) calculated the ratio of the wave height along the structure, H, to the incident wave height, H_I, as

$$\frac{H}{H_I} = \sqrt{\left(C + S + 1\right)^2 + \left(C - S\right)^2} \tag{VI-5-166}$$

where

$$C = \partial_0^u \cos\left(\frac{\pi}{2}t^2\right)dt,\ S = \partial_0^u \sin\left(\frac{\pi}{2}t^2\right)dt,\ u = 2\sqrt{\frac{2x}{L}}\sin\left(\frac{\alpha}{2}\right) \tag{VI-5-167}$$

and x is the distance from the tip of the structure, L is the wavelength and α is the angle between the direction of wave propagation and the front alignment of the structure.

(b) Figure VI-5-65 shows an example of the wave height variation for regular head-on waves of period T = 10 s. Shown with the dotted line is the wave height variation calculated for nonbreaking long-crested irregular (random) waves (Bretschneider-Mitsuyasu spectrum, $T_{1/3}$ = 10 s). The smoothing effect of random seas is clearly seen. At some locations the wave height exceeds twice the incident wave height expected for infinitely long vertical wall structures.

(c) For short-length breakwaters, the diffraction from both ends of the structure influences the wave height variation (see Goda 1985). Also note that experiments indicate that the theoretical assumption of complete reflection of waves from smooth vertical walls appears not fulfilled, because reflection coefficients on the order of 0.95 have been measured. (However, the methods for measuring reflection are less than perfect, as well.) Oblique waves create wave height variations different from those created by head-on waves. Concave and convex corners also affect the wave height variation along the structure (see Part VI-5-4*e*).

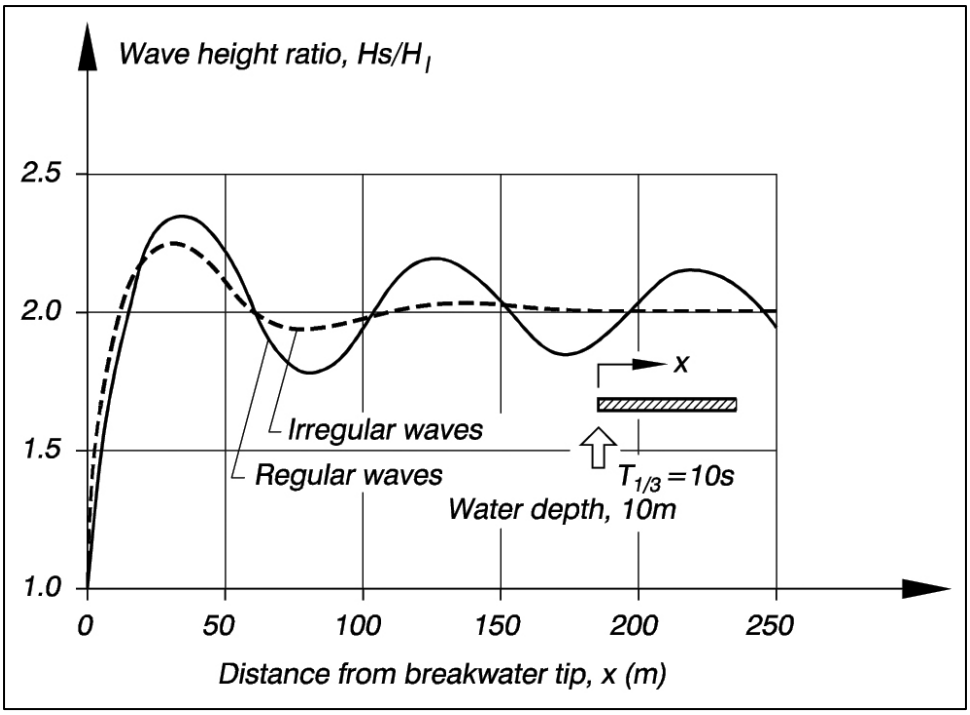

Figure VI-5-65. Variation of wave height along a semi-infinite, fully reflecting breakwater exposed to head-on, long-crested waves (from Goda 1985)

(4) Horizontal wave force reduction for nonbreaking waves.

(a) The effect of incident wave angle on the horizontal wave force exerted on a caisson is twofold. One effect is a force reduction, compared to head-on waves, due to the reduction of point pressure on the caisson, referred to as point-pressure force reduction. The second effect is a force reduction due to the fact that peak pressures do not occur simultaneously along the caisson, referred to as peak-delay force reduction. These two-force reduction effects will be present in short-crested waves because of spreading of the wave energy over a range of incident angles. Model test results Franco, van der Meer, and Franco (1996) with long-crested waves indicate that the point-pressure reduction can be estimated by the Goda formula.

(b) The peak-delay force reduction for oblique nonbreaking regular waves can be predicted by the Battjes formula (Battjes 1982)

$$r_F\left(L,\theta\right)=\frac{\text{max. force, wave incident angle }\theta}{\text{max. force, head-on wave}\left(\theta=0°\right)}=\frac{\sin\left(\frac{\pi L_s}{L}\sin\theta\right)}{\frac{\pi L_s}{L}\sin\theta} \tag{VI-5-168}$$

where L and L_s are the wavelength and the structure length, respectively, and θ is the wave incident angle. Equation VI-5-168 is depicted in Figure VI-5-66. (In the figure β is used instead of θ.)

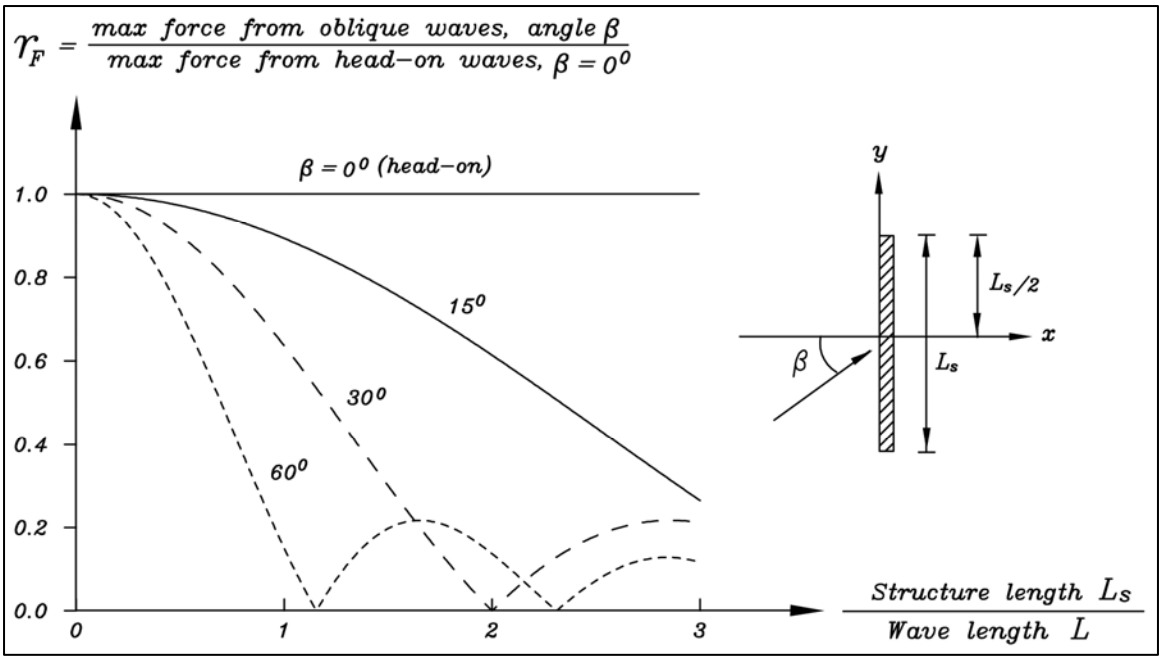

Figure VI-5-66. Peak-delay force reduction for oblique regular waves (Burcharth and Liu 1998)

(c) The peak-delay force reduction for oblique nonbreaking long-crested irregular waves can be estimated by the formula (Burcharth and Liu 1998)

$$r_F\left(L_p,\theta\right)=\frac{\text{characteristic wave force, wave incident angle }\theta}{\text{characteristic wave force, head-on wave }\left(\theta=0°\right)}=\left|\frac{\sin\left(\frac{\pi L_s}{L_p}\sin\theta\right)}{\frac{\pi L_s}{L_p}\sin\theta}\right| \qquad \text{(VI-5-169)}$$

where L_p is the wavelength corresponding to the peak frequency. For example, the characteristic wave force can be chosen as F_{max}, $F_{1/250}$, $F_{1\ percent}$, $F_{10\ percent}$, etc.

(d) In order to investigate the uncertainty and bias of Equation VI-5-169, a real-time calculation of the wave force on a caisson by nonbreaking long-crested irregular waves was performed by Burcharth and Liu (1998). The result is given in Figure VI-5-67.

(e) Figure VI-5-67 shows that Equation VI-5-169 gives a close estimate of the mean value of the peak-delay reduction. However, a large variation of the peak-delay force reduction factor corresponding to a low exceedence probability, e.g., $F_{1/250}$, was observed.

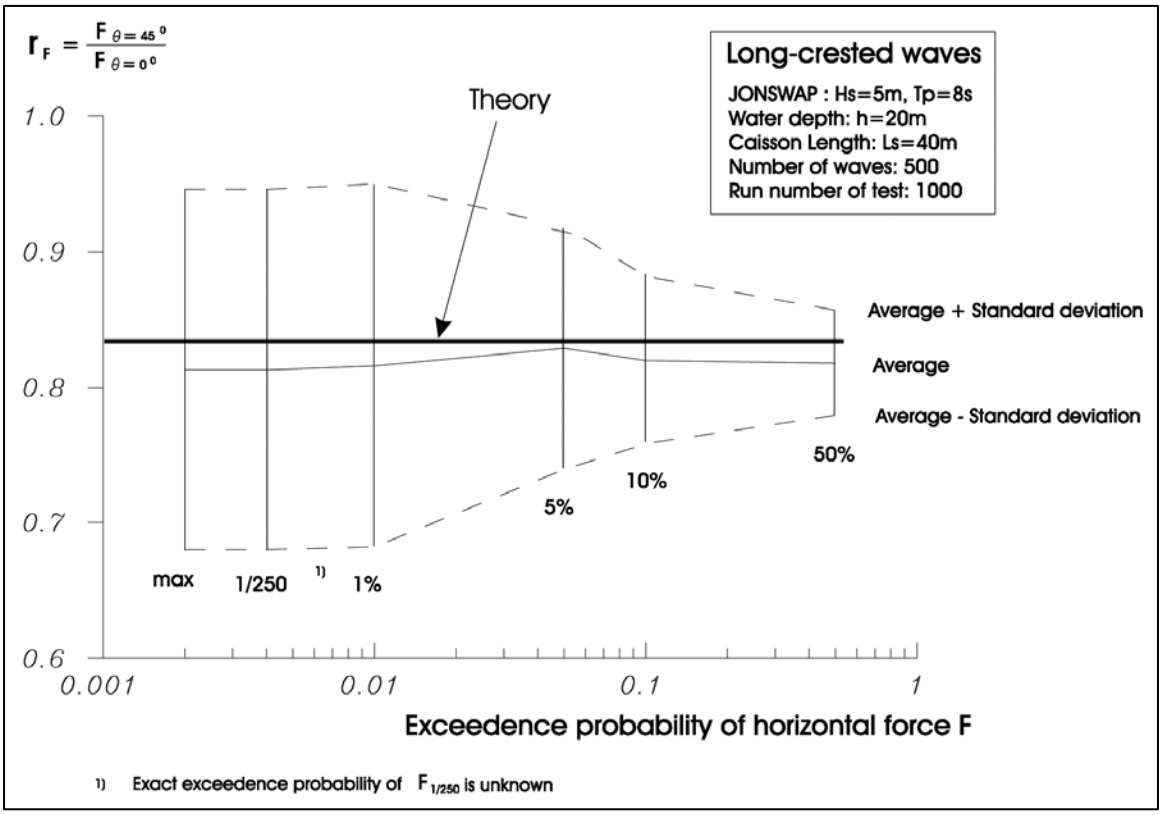

Figure VI-5-67. Numerical simulation of peak-delay reduction, long-crested waves. Example of uncertainty calculation for wave train with 500 waves (Burcharth and Liu 1998)

(f) The peak-delay force reduction for oblique nonbreaking short-crested waves can be estimated by the formula (Burcharth and Liu 1998)

$$r_F(\sigma,\theta_m) = \frac{\text{characteristic wave force, short-crested wave}}{\text{characteristic wave force, head-on long-crested wave}} \approx \approx \left(\int_{-\pi}^{\pi} r_F(L_p,\theta) D(\sigma,\theta_m)\, d\theta\right)^{1/2} \quad \text{(VI-5-170)}$$

where $r_F(L_p,\theta)$ is given by Equation VI-5-169 and $D(\sigma,\theta_m)$ is the wave directional spreading function with the wave energy spreading angle σ and the mean wave incident direction θ_m. An example of Equation VI-5-170 is depicted in Figure VI-5-68.

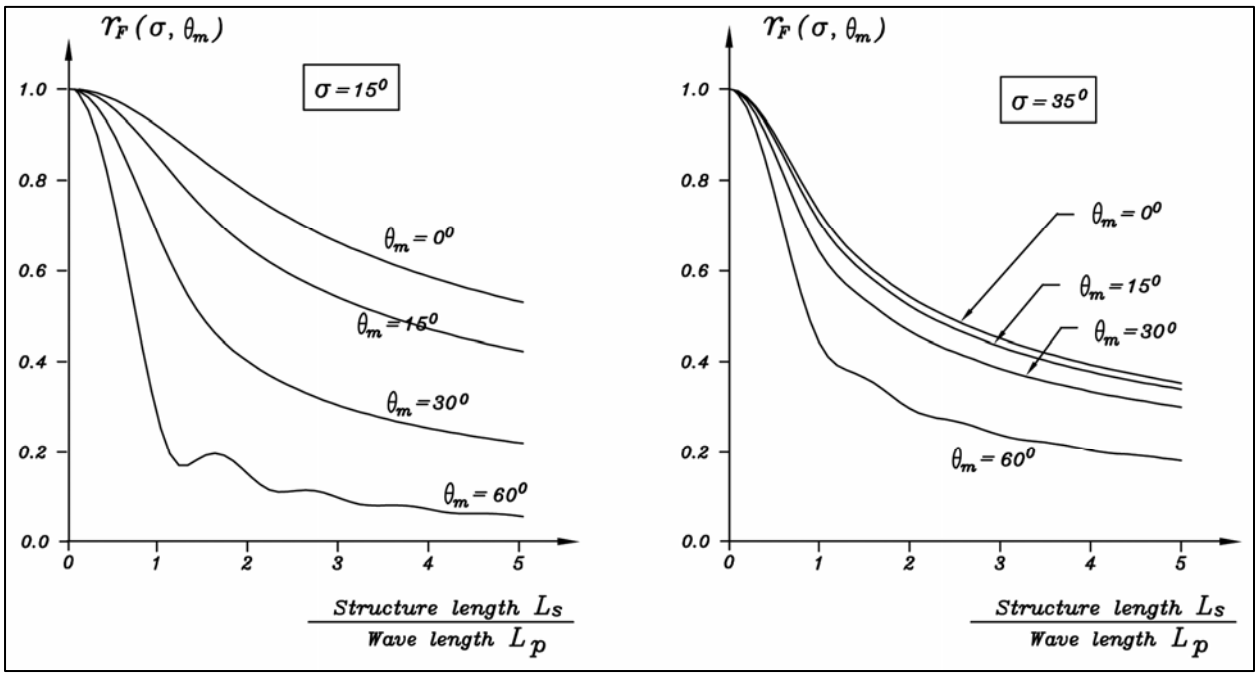

Figure VI-5-68. Example of peak-delay force reduction for short-crested waves (Burcharth and Liu 1998)

(5) Horizontal turning moment for nonbreaking waves. Oblique wave attack generates resultant wave forces acting eccentrically on the caisson front. The horizontal turning moment around the caisson center caused by oblique regular waves can be estimated by the formula (Burcharth 1998)

$$r_M = \frac{\text{max. moment, wave incident angle } \theta}{(\text{head-on max. force}) \times (\text{structure length})} = \frac{1}{2}\left| \frac{\cos\left(\frac{\pi L_s}{L}\sin\theta\right)}{\frac{\pi L_s}{L}\sin\theta} - \frac{\sin\left(\frac{\pi L_s}{L}\sin\theta\right)}{\left(\frac{\pi L_s}{L}\sin\theta\right)} \right| \quad \text{(VI-5-171)}$$

Equation VI-5-171 is depicted in Figure VI-5-69. The maximum horizontally turning moment around caisson center under arbitrary wave incident angle is

$$M_{\max} = 0.22 F_{\theta=0^\circ} L_s \quad \text{(VI-5-172)}$$

where $F_{\theta=0^\circ}$ is the maximum head-on wave force.

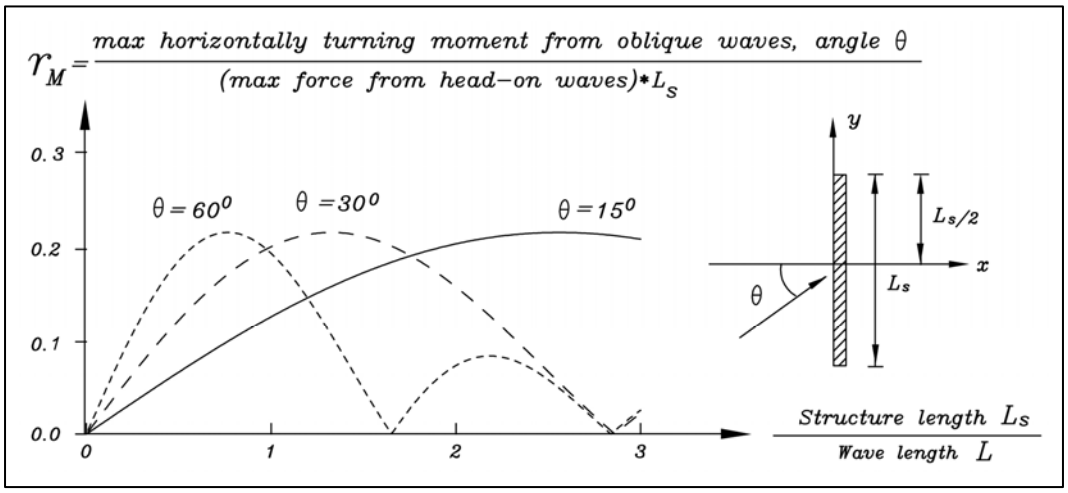

Figure VI-5-69. Nondimensional amplitude of horizontal turning moment around the center of the caisson exposed to oblique nonbreaking regular waves

(6) Horizontal wave force reduction for breaking waves. Short-crested waves break in a limited area and not simultaneously along the whole caisson, which results in an even larger force reduction in comparison with nonbreaking waves. Figure VI-5-70 shows an example of force reduction from model tests with short-crested, breaking, head-on waves, where the force reduction r_F is defined as

$$r_F = \frac{F_{1/250}, \text{ short-crested wave, mean wave incident angle } \theta_m}{F_{1/250}, \text{ long-crested head-on wave}} \quad \text{(VI-5-173)}$$

(7) Broken wave forces.

(a) Shore structures may be located where they are only subjected to broken waves under the most severe storm and tide condition. Detailed studies relating broken wave forces to incident wave parameters and beach slope are lacking; thus simplifying assumptions are used to estimate design loads. Critical designs should be confirmed with physical model tests.

(b) Model tests have shown approximately 78 percent of the breaking wave height (0.78 H_b) is above the still-water line when waves break on a sloping beach (Wiegel 1964). The broken wave is assumed to decay linearly from the breakpoint to the intersection of the swl with the beach slope, where the wave height is reduced to a height of $H_{swl} = 0.2\ H_b$ for beach slopes in the range $0.01 \# \tan \beta \# 0.1$ (Camfield 1991). The water mass in the broken wave is assumed to move shoreward with velocity equal to the breaking wave celery by linear theory, i.e., $C = (gh_b)^{1/2}$.

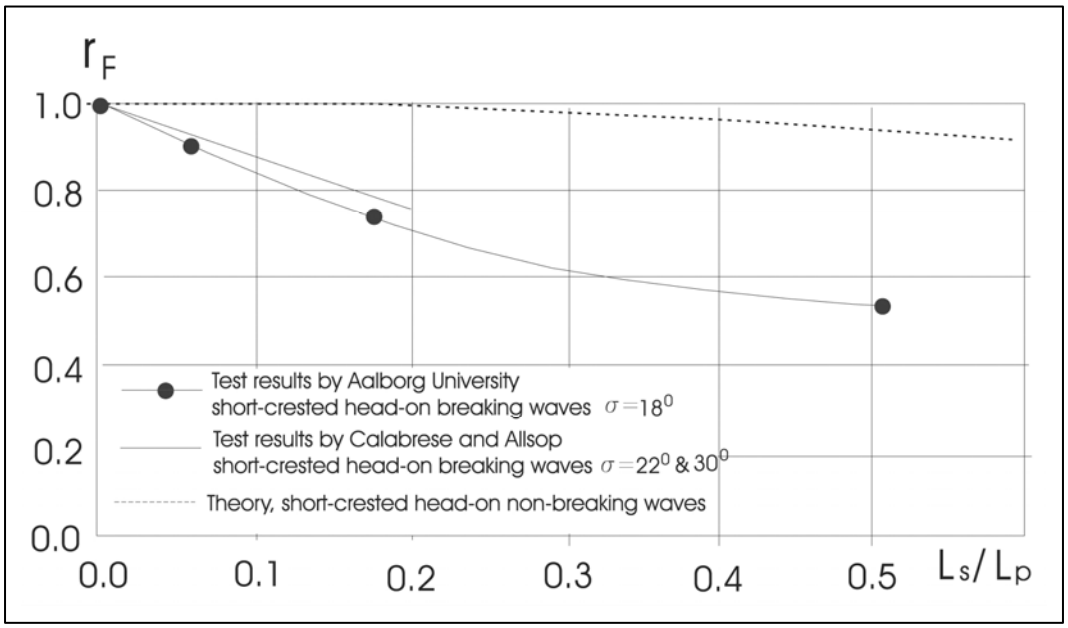

Figure VI-5-70. Example of force reduction from model tests with short-crested breaking waves (Burcharth 1998, Calabrese and Allsop 1997)

- Vertical wall seaward of the shoreline. Vertical walls situated seaward of the SWL/beach intersection are subjected to wave pressures composed of dynamic and hydrostatic pressures as illustrated in the sketch of Figure VI-5-71. The wave height at the wall, H_w, is determined by similar triangles to be

$$H_w = \left(0.2 + 0.58\frac{h_s}{h_b}\right) H_b \tag{VI-5-174}$$

where h_s is the water depth at the wall, and h_b is the water depth at wave breaking.

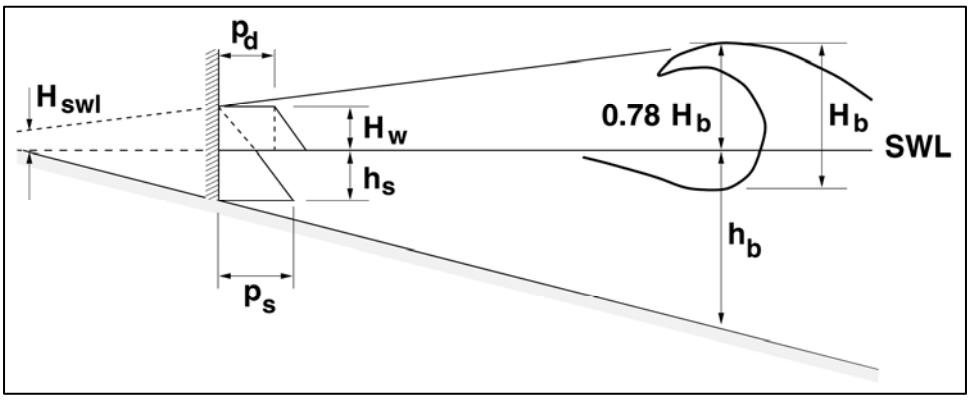

Figure VI-5-71. Broken wave forces on wall seaward of shoreline

- Above the swl, the dynamic component of the pressure is given as

$$p_d = \frac{1}{2}\rho C^2 = \frac{1}{2}\rho g h_b \tag{VI-5-175}$$

and the corresponding force per unit horizontal length of the wall is

$$R_d = p_d H_w = \frac{\rho g h_b H_w}{2} \tag{VI-5-176}$$

where ρ is the density of water. The overturning moment per unit horizontal length about the toe of the wall due to the dynamic pressure is given by

$$M_d = R_d\left(h_s + \frac{H_w}{2}\right) \tag{VI-5-177}$$

- The hydrostatic pressure varies from zero at a height H_w above the SWL to a maximum at the base of the wall given by

$$P_s = \rho g\left(h_s + H_w\right) \tag{VI-5-178}$$

- The hydrostatic force per unit horizontal width of the wall is calculated as

$$R_s = \frac{\rho g}{2}\left(h_s + H_w\right)^2 \tag{VI-5-179}$$

and the corresponding hydrostatic overturning moment per unit width is

$$M_s = R_s\left(\frac{h_s + H_w}{3}\right) = \frac{\rho g}{6}\left(h_s + H_w\right)^3 \tag{VI-5-180}$$

- The total force and moment per unit horizontal width of wall is the summation of dynamic and hydrostatic components, i.e.,

$$R_T = R_d + R_s \tag{VI-5-181}$$

$$M_T = M_d + M_s \tag{VI-5-182}$$

- Any backfilling with sand, soil or stone behind the wall will help resist the hydrodynamic forces and moments on the vertical wall.

- Vertical wall landward of the shoreline. Landward of the intersection of the SWL with the beach and in the absence of structures, the broken wave continues running up the beach slope until it reaches a maximum vertical runup height, R_a, that can be estimated using the procedures given in Part II-4-4, "Wave Runup on Beaches." If a vertical wall is located in the

runup region, as shown in Figure VI-5-72, the surging runup will exert a force on the wall that is related to the height, H_w, of the surge at the wall.

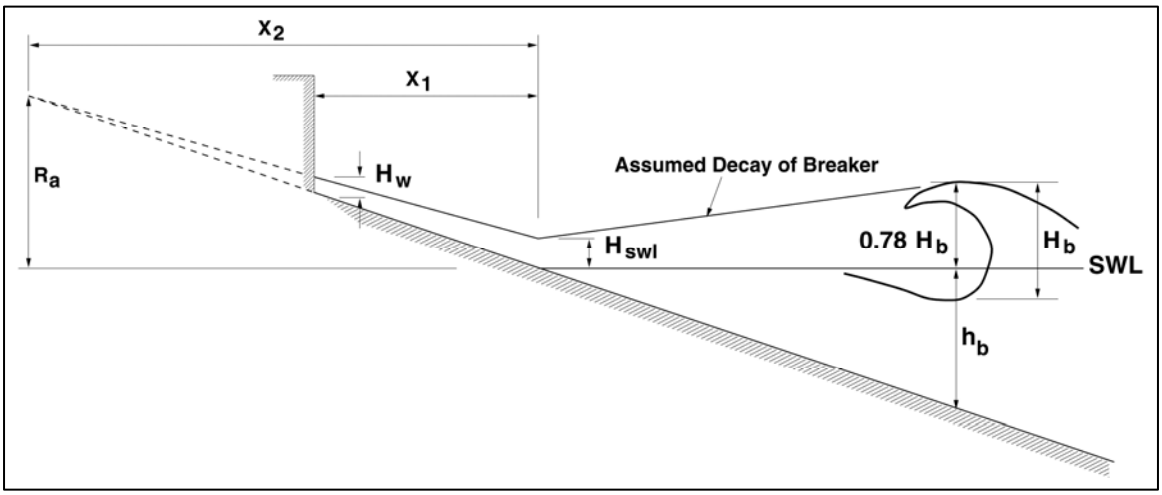

Figure VI-5-72. Broken wave forces on wall landwater of shoreline

- Camfield (1991) assumed a linear decrease in the runup surge over the distance X_2 shown in Figure VI-5-72 which yielded the following expression for surge height at the wall

$$H_w = H_{SWL}\left(1-\frac{X_1}{X_2}\right) = 0.2H_b\left(1-\frac{X_1\tan\beta}{R_a}\right) \qquad \text{(VI-5-183)}$$

where H_{SWL} . 0.2 H_b and β is the beach slope angle. The force of the surge per unit horizontal width of the vertical wall was approximated by Camfield (1991) based on the work of Cross (1967) to be

$$F_{surge} \approx 4.5\rho g H_w^2 \qquad \text{(VI-5-184)}$$

or when combined with Equation VI-5-158

$$F_{surge} \approx 0.18\rho g H_b^2\left(1-\frac{X_1\tan\beta}{R_a}\right)^2 \qquad \text{(VI-5-185)}$$

- This approximate method is intended for use on plane slopes in the range 0.01 # tan β # 0.1. The methodology does not apply to steeper slopes or composite slopes. No estimates are given for the pressure distribution or the resulting overturning moment on the vertical wall.

c. Wave-generated forces on concrete caps.

(1) Wave loads on concrete caps occur only if the runup reaches the wall. The load is very dependent, not only on the characteristics of the waves, but also on the geometry (including the porosity) of the seaward face of the structure.

(2) The wave forces on a monolithic superstructure exposed to irregular waves are of a stochastic nature. The pressure distributions and the related resultant forces at a given instant are schematized in Figure VI-5-73. Not included in the figure is the distribution of the effective stresses on the base plate.

(3) The wave-generated pressure, p_w, acting perpendicular to the front of the wall is the pressure that would be recorded by pressure transducers mounted on the front face. The distribution of p_w is greatly affected by very large vertical velocities and accelerations which often occur. F_w is the instantaneous resultant of the wave generated pressures.

(4) The instantaneous uplift pressure, p_b, acting perpendicular to the base plate is equal to the pore pressure in the soil immediately under the plate. The resultant force is F_b. At the front corner (point f) the uplift pressure p_b^f, equals the pressure on the front wall. At the rear corner (point r) the uplift pressure, p_b^r, equals the hydrostatic pressure at point r. The actual distribution of p_b between p_b^f and p_b^r depends on the wave-generated boundary pressure field and on the permeability and homogeneity of the soil.

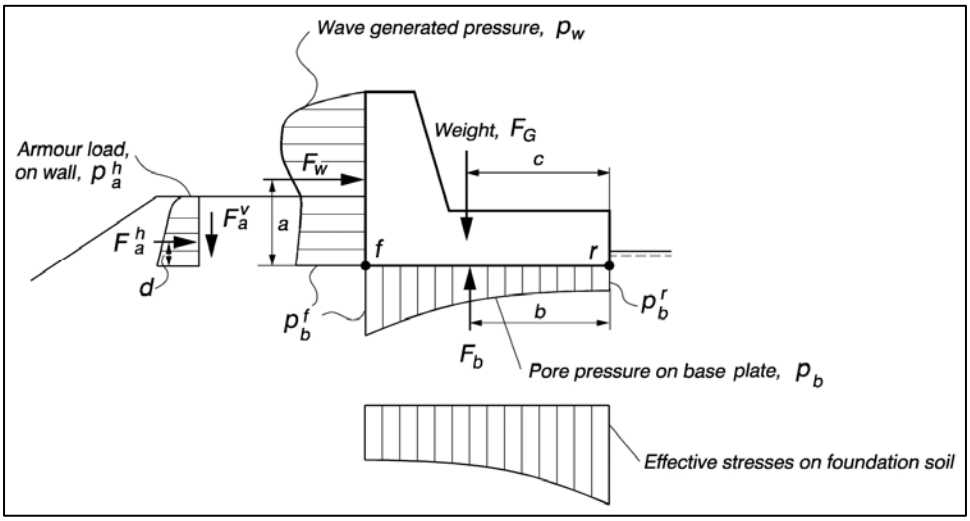

Figure VI-5-73. Illustration of forces on a superstructure

The distribution cannot be determined in normal wave flume scale tests because of strong scale effects related to porous flow. However, the corner pressures p_b^f and p_b^r can be measured or estimated, and in case of homogeneous and rather permeable soils and quasi-static conditions, a safe estimate on the most dangerous uplift can be found assuming a linear pressure distribution between a maximum value of p_b^f and a minimum value of p_b^r as shown in Figure VI-5-74a. If a blocking of the porous flow is introduced on the seaside of the base, the assumption of a linear distribution will be even safer as illustrated by Figure VI-5-74b. On the other hand a blockage under the rear end of the base plate might cause the linear assumption to be on the unsafe side as illustrated by Figure VI-5-74c. Note, that in case b and c the resultant of the base plate pressure is not vertical.

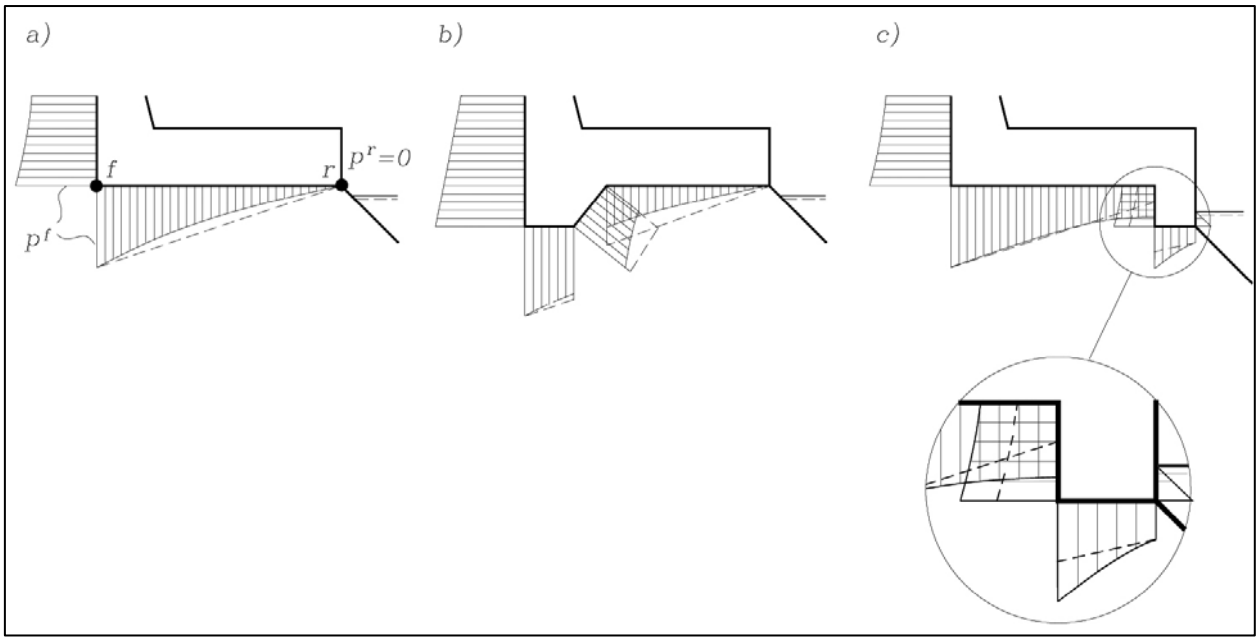

Figure VI-5-74. Illustration of comparison between base plate pore pressure distributions (under quasi-static porous flow conditions) and the approximated linear distribution

(5) Armor and filter stones resting against the front of the wave wall will introduce an armor load, p_a, on the front through the contact points. Both a normal soil mechanics load and a proportion of the dynamic wave loads on the armor contribute to p_a. The resultant force F_a is generally not perpendicular to the front wall due to friction between the soil and the wall, and must be split into the two orthogonal components F_a^h and F_a^v. In the case of high walls (low front berms) F_a is insignificant compared to the wave load, F_w.

(6) The load will in general be dynamic but is normally treated as quasi-static due to a rather smooth variation in time over a wave period. However, if wave breaking takes place directly on the wall face some short duration, but very large, slamming forces can occur, especially if the front face is almost vertical at the moment when the wave collides with the wall as shown in Figure VI-5-75. Such forces are also called impact or impulsive forces.

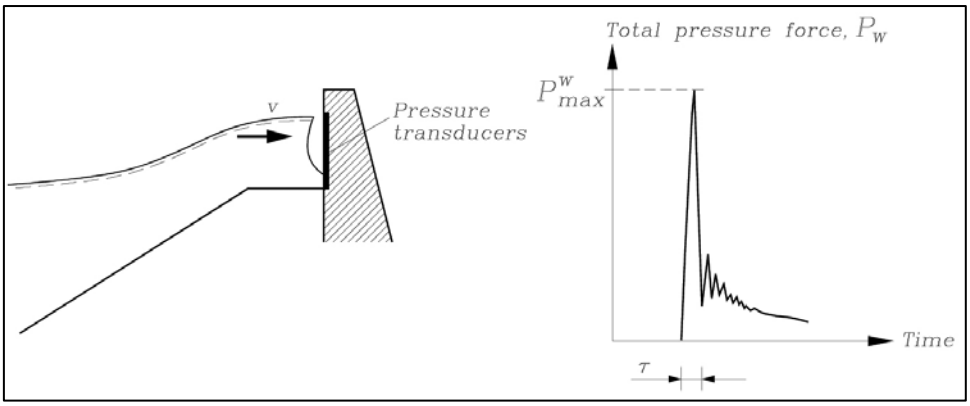

Figure VI-5-75. Impulsive pressure force caused by wave breaking on the wave wall

(7) Wave slamming on the wall can be avoided and the quasi-static wave loads reduced by increasing the crest level and/or the width of the front berm as shown by Figure VI-5-76. Wave slamming on the front of the wall will not occur in configurations *c* and *d*.

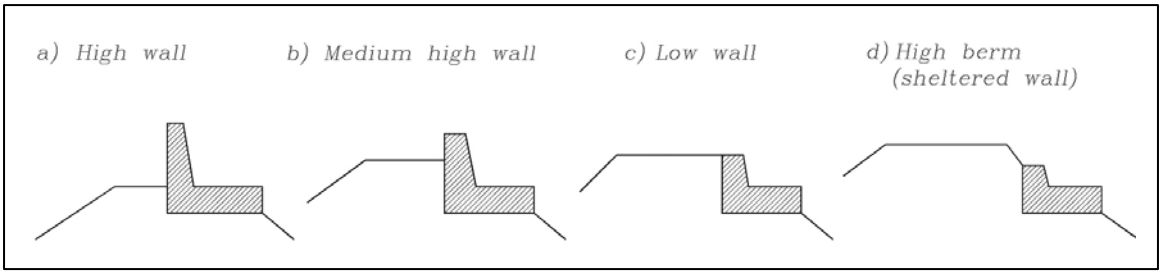

Figure VI-5-76. Typical crown wall configurations

(8) The wave loadings on a crown wall can be assessed only by physical model tests or by prototype recordings. However, no prototype results have been reported in the literature and most model test results are related to specific crown wall configurations.

(9) Table VI-5-60 shows an empirical formula for horizontal wave load given by Jensen (1984) and Bradbury et al. (1988). Table VI-5-61 shows empirical formulae for horizontal wave load, turning moment and uplift pressure presented by Pedersen (1996). The formulae are based on small scale model tests with head-on irregular waves. Predictions are compared to measurements in Figure VI-5-77.

Table VI-5-60
Horizontal Wave Force on Concrete Caps (Jensen 1984; Bradbury et al. 1988)

$$\frac{F_{h,0.1\%}}{\rho_w\, g\, h_w\, L_{op}} = \alpha + \beta \frac{H_s}{A_C} \qquad \text{(VI-5-186)}$$

where $F_{h,0.1\%}$ Horizontal wave force per running meter of the wall corresponding to 0.1% exceedence probability
ρ_w Mass density of water
h_w Crown wall height
L_{op} Deepwater wavelength corresponding to peak wave period
H_s Significant wave height in front of breakwater
A_c Vertical distance between MWL and the crest of the armor berm
α, β Fitted coefficient, see table

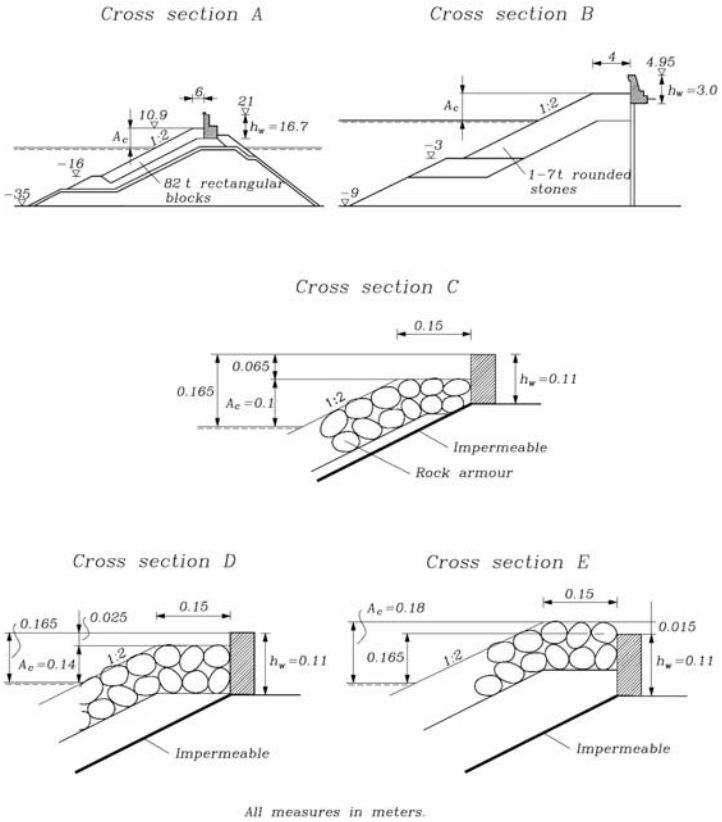

Cross section	Parameter ranges in tests			0.1% exceedence values of coefficients in Eq (VI-5-186)		Coefficient of variation	Reference
	A_c (m)	$s_{op} = \frac{H_s}{L_{op}}$	$\frac{H_s}{A_c}$	α	β		
A	5.6 - 10.6	0.016 - 0.036	0.76 - 2.5	−0.026	0.051	0.21	Jensen (1984)
B	1.5 - 3.0	0.05 - 0.011	0.82 - 2.4	−0.016	0.025	0.46	—
C	0.10	0.023 - 0.07	0.9 - 2.1	−0.038	0.043	0.19	Bradbury, et al. (1988)
D	0.14	0.04 - 0.05	1.43	-0.025	0.028		—
E	0.18	0.04 - 0.05	1.11	-0.088	0.011		—

Table VI-5-61
Horizontal Wave Force, Uplift Wave Pressure and Turning Moment on Concrete Caps
(Pedersen 1996)

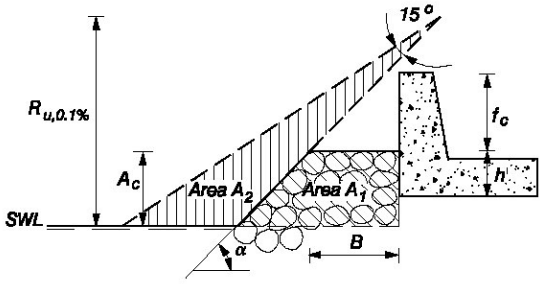

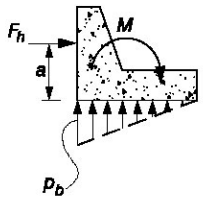

$$F_{h,0.1\%} = 0.21\sqrt{\frac{L_{om}}{B}}\left(1.6 p_m y_{eff} + A\frac{p_m}{2}h'\right) \quad \text{(VI−5−187)}$$

$$M_{0.1\%} = a \times F_{h,0.1\%} = 0.55(h' + y_{eff})F_{h,0.1\%} \quad \text{(VI−5−188)}$$

$$p_{b,0.1\%} = 1.00\ A\ p_m \quad \text{(VI−5−189)}$$

where

$F_{h,0.1\%}$	Horizontal wave force per running meter of the wall corresponding to 0.1% exceedence probability
$M_{0.1\%}$	Wave generated turning moment per running meter of the wall corresponding to 0.1% exceedence probability
$p_{b,0.1\%}$	Wave uplift pressure corresponding to 0.1% exceedence probability
L_{om}	Deepwater wavelength corresponding to mean wave period
B	Berm width of armor layer in front of the wall
p_m	$p_m = \rho_w g(R_{u,0.1\%} - A_c)$
$R_{u,0.1\%}$	Wave runup corresponding to 0.1% exceedence probability

$$R_{u,0.1\%} = \begin{cases} 1.12 H_s \zeta_m & \zeta_m \le 1.5 \\ 1.34 H_s \zeta_m^{0.55} & \zeta_m > 1.5 \end{cases}$$

$$\zeta_m = \tan\alpha / \sqrt{H_s / L_{om}}$$

α	Slope angle of armor layer
A_c	Vertical distance between MWL and the crest of the armor berm
A	$A = \min\{A_2/A_1, 1\}$, where A_1 and A_2 are areas shown in the figure
y_{eff}	$y_{eff} = \min\{y/2, f_c\}$

$$y = \begin{cases} \frac{R_{u,0.1\%} - A_c}{\sin\alpha}\frac{\sin 15^0}{\cos(\alpha - 15^0)} & y > 0 \\ 0 & y \le 0 \end{cases}$$

h'	Height of the wall protected by the armor layer
f_c	Height of the wall not protected by the armor layer

Uncertainty of the formulae

factor in the formulae	0.21	1.6	0.55	1.00
standard deviation σ	0.02	0.10	0.07	0.30

Tested range: See Table VI-5-12

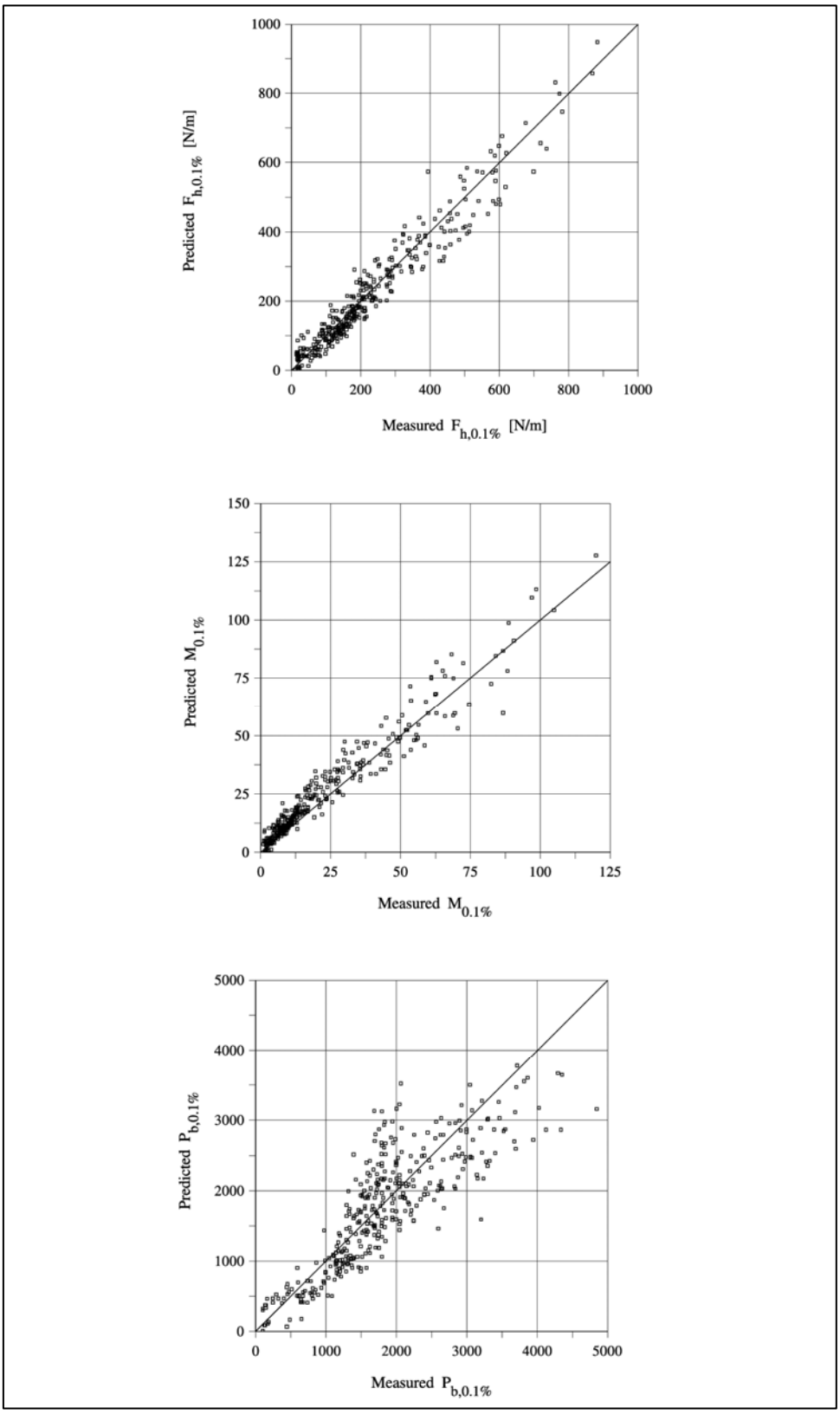

Figure VI-5-77. Comparison of predictions to measurements using the methods in Table VI-5-61 (from Pedersen 1996)

d. Stability of concrete caps and caissons against sliding and overturning.

(1) Stability against sliding between the caisson base and the rubble foundation requires

$$(F_G - F_U)\,\mu \geq F_H \qquad \text{(VI-5-190)}$$

where

μ = friction coefficient for the base plate against the rubble stones

F_G = buoyancy-reduced weight of the caisson

F_U = wave induced uplift force

F_H = wave induced horizontal force

(2) Overturning can take place only when the heel pressure under the caisson is less than the bearing capacity of the foundation. If the caisson is placed on rubble stones and sand it is unlikely that overturning will occur. Instead there will be soil mechanics failure. Overturning is a realistic failure mode only if the caisson is placed on rock or on very strong clay, in which case breakage of the caisson is likely to occur.

(3) Stability against overturning is maintained if

$$M_{FG} \geq M_{FU} + M_{FH} \qquad \text{(VI-5-191)}$$

where

M_{FG} = stabilizing moment around the heel by buoyancy-reduced weight of the caisson

M_{FU} = antistabilizing moment by wave induced uplift force

M_{FH} = antistabilizing moment by wave induced horizontal force

(4) The value of the friction coefficient μ has been investigated in models and in prototype studies. For a plane concrete slab resting on quarried rubble stones, Takayama (1992) found as an average a static friction coefficient of $\mu = 0.636$ and a coefficient of variation of 0.15. Table VI-5-62 taken from Stückrath (1996), presented experimental test results of friction coefficients conducted in Japan.

(5) French tests (Cété-Laboratoire Régional Norde-Pas de Calais 1990) give a somewhat lower friction coefficient as shown in Table VI -5-63.

(6) Morihira, Kihara, and Horikawa[1] investigated the dynamic friction coefficient between caissons with different bottom patterns and rubble foundation with different levelling as shown in Table VI-5-64.

Table VI-5-62
Experimental Test Results of Friction Coefficient Conducted in Japan
(taken from Stückrath 1996)

No.	Stone type	Stone size (mm)	Condition of mound	μ	Average of μ
1	Crushed stone	30	Screeded surface	0.460-0.801	-
2	Rubble stone	120	Not screeded	0.564-0.679	0.624
3	Rubble stone	50	Surface smoothed with smaller stone	0.45-0.69	-
4	Rubble stone	30-80	Screeded	0.77-0.89	0.82
5	Cobble stone	30-50	Not screeded	0.69-0.75	0.70
6	Crushed stone	20-30	Not screeded	0.607-0.790	0.725
7	Crushed stone	10-50	Not screeded	0.486-0.591	0.540
8	Crushed stone	13-30	Not uniform	0.41-0.56	-

Table VI-5-63
Experimental Test Results of Friction Coefficient
(Cété-Laboratoire Régional Norde-Pas de Calais 1990)

Vertical Load (tonne)	Normal Stress (tonne/m^2)	Horizontal Force (tonne)		Friction Coefficient μ	
		Smooth	Corrugated	Smooth	Corrugated
Natural Sea Gravel 20-80 mm					
24.1	10.5	12.6	13.7	0.53	0.58
18.4	8	10.3	11.3	0.56	0.62
Crushed Gravel 0-80 mm					
24.1	10.5		10.4		0.43
18.4	8		8.6		0.47

[1] Personal Communication, 1998, M. Marihira, T. Kihara, and H. Horikawa. "On the Friction Coefficients Between Concrete Block Sea Walls and Rubble-Mound Foundations."

Table VI-5-64
Dynamic Friction Coefficient Between Caisson Bottom and Rubble-Mound (Morihira, Kihara, and Harikawa, personal communication 1998)

Levelling method for rubble mound

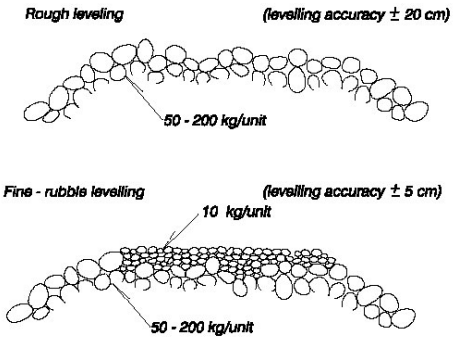

Bottom pattern of caissons

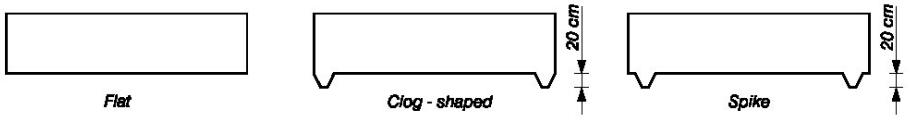

Table of Dynamic friction coefficients

Levelling	Bottom pattern	μ_{max}	$\overline{\mu_{max}}$	μ_{const}	μ			
					S=5 cm	S=10 cm	S=20 cm	S=30 cm
rough	flat	0.75	0.70	0.70	0.53	0.59	0.65	0.70
		0.73	0.70	0.70	0.70	0.70	0.70	0.70
	clog-shaped	1.19	1.13	1.16	0.76	0.91	0.98	1.08
		1.11	1.02	1.01	0.76	0.90	1.01	1.00
	spike	0.85	0.79	0.80	0.62	0.80	0.80	0.80
		0.97	0.81	0.84	0.70	0.70	0.83	0.95
	clog-shaped with foot protection	1.45	1.36	>1.4	1.11	1.30	1.41	
		1.34	1.19	>1.3	0.94	1.09	1.28	
fine	flat	0.68	0.63	0.65	0.63	0.64	0.64	0.55
		0.70	0.60	0.60	0.59	0.60	0.60	0.60
	clog-shaped	1.18	1.08	1.08	0.95	1.03	1.08	1.08
		1.15	1.01	1.06	0.90	0.94	0.97	1.04
	spike	0.87	0.78	0.82	0.72	0.72	0.75	0.82
		1.04	0.87	0.82	0.78	0.95	1.01	0.85

μ_{max} dynamic friction coefficient corresponding to maximum tensile load
$\overline{\mu_{max}}$ dynamic friction coefficient corresponding to the average of the peak tensile loads
μ_{const} dynamic friction coefficient corresponding to constant tensile load
μ dynamic friction coefficient corresponding to caisson displacement S
S caisson displacement

e. Waves at structure convex and concave corners. Many projects have coastal structures featuring concave or convex bends or sharp corners corresponding to structure realignment. Usually, the location and curvature of corners are determined by functional design factors, such as harbor layout or proposed channel alignment, or by site considerations, such as bathymetry. Regardless of the functional design motivation, structure bends and corners must meet or exceed the same design criteria as the rest of the structure. The orientation of bends and corners relative to the incident waves may cause changes in the local wave characteristics due to refraction, reflection, and focusing effects. Changes in wave heights could affect armor stability on the corner section, and local crest elevation may have to be heightened to prevent increased overtopping. Convex corners and bends are defined as having an outward bulge facing the waves, whereas concave corners and bends have a bulge away from the waves. Figure VI-5-78 illustrates convex and concave configurations for vertical-wall structures. Similar definitions are used for sloping-front structures.

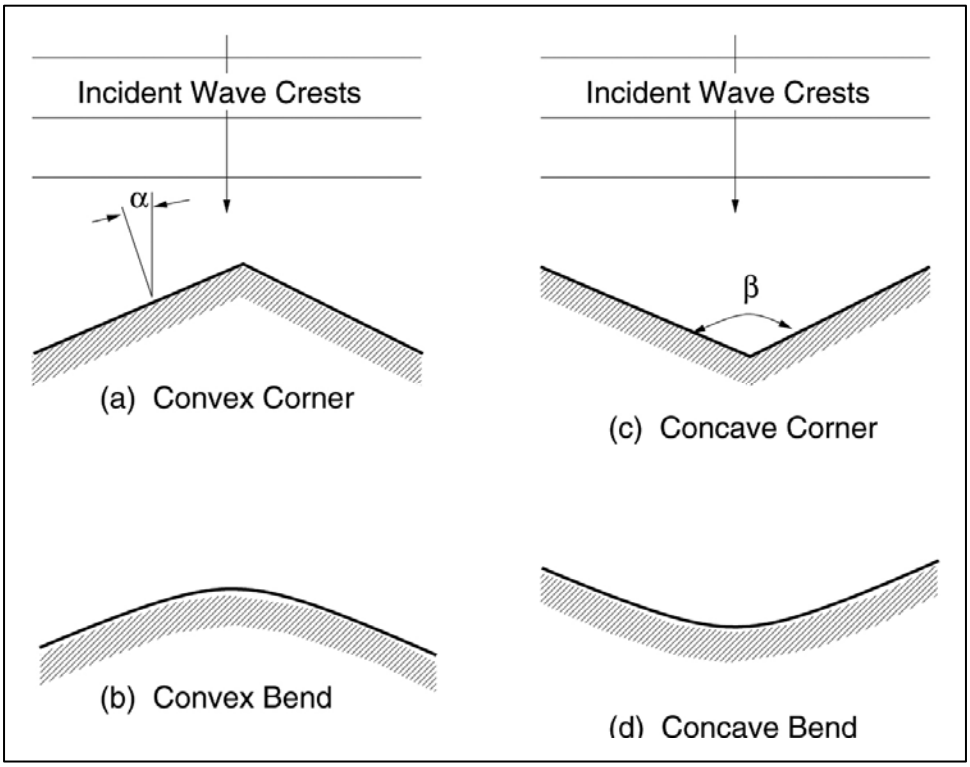

Figure VI-5-78. Convex and concave corners and bends at vertical walls

(1) Waves at convex corners.

(a) Vertical structures with convex corners. Waves approaching vertical walls with sharp convex corners such as depicted in Figure VI-5-78a will be almost perfectly reflected if the wall is impervious. This results in a diamond-like wave pattern of incident and reflected waves with the wave crests and troughs at the wall appearing to move along the wall. The maximum wave height at the wall depends on the incident wave height, H_i, angle of wave approach, α, and wave nonlinearity.

- Perroud (1957) performed laboratory tests of solitary waves obliquely reflected by a vertical wall. He observed "normal reflection" with the angle of reflection nearly the same as the incident wave angle for cases where the incident wave angle, α (defined in Figure VI-5-78), was less than about 45 deg. This is the same result given by linear wave theory for oblique reflection. The reflected wave height was just slightly less than the incident wave height for small incident angles, and it decreased as angle of incidence increased. This is contrary to linear wave theory. The maximum wave height at the wall was about twice the incident wave height up to $\alpha = 45$ deg, similar to linear wave theory for oblique reflection.

- For wave incident angles between about 45 deg and 70 deg Perroud observed a phenomenon referred to as "Mach reflection" in acoustics. Mach reflection of water waves is a nonlinear effect characterized by the presence of a reflected wave and a "Mach" wave with its crest propagating perpendicular to the vertical wall. The reflected wave height is significantly less than the incident wave height, and the angle of the reflected wave becomes less than the incident wave angle. The Mach reflection wave grows in length as it moves along the wall, and the maximum wave height, known as the "Mach stem" occurs at the wall.

- Figure VI-5-79 presents Perroud's (1957) averaged results for solitary waves obliquely reflected by a vertical wall. The upper plot shows the wave height at the wall in terms of the incident wave height for increasing angle of wave incidence. The ratio of reflected to incident wave height is shown in the lower plot. These plots are also given by Wiegel (1964) along with additional plots showing the decrease in reflected wave angle for Mach reflection and the increasing length of the Mach reflection wave with distance along the wall. (Note: In Wiegel (1964) the plots are given in terms of a differently defined angle of wave incidence i which is related to α via ($i = 90^o - \alpha$).)

- The speed of the Mach stem, C_M, was given as (Camfield 1990)

$$C_M = \frac{C}{\sin \alpha} \tag{VI-5-192}$$

where C is the incident wave celerity.

- For angles of incidence greater than 70 deg from normal, Perroud observed that the wave crest bends so it is perpendicular to the vertical wall, and no discernible reflected wave appears. The wave height at the wall decreases with continuing increase in angle of incidence as indicated in Figure VI-5-79a.

- Keep in mind that the experimental results were obtained for Mach reflection of solitary waves. This implies that the results represent the shallow-water limiting case. The Mach reflection effect will decrease for smaller amplitude waves in deeper water.

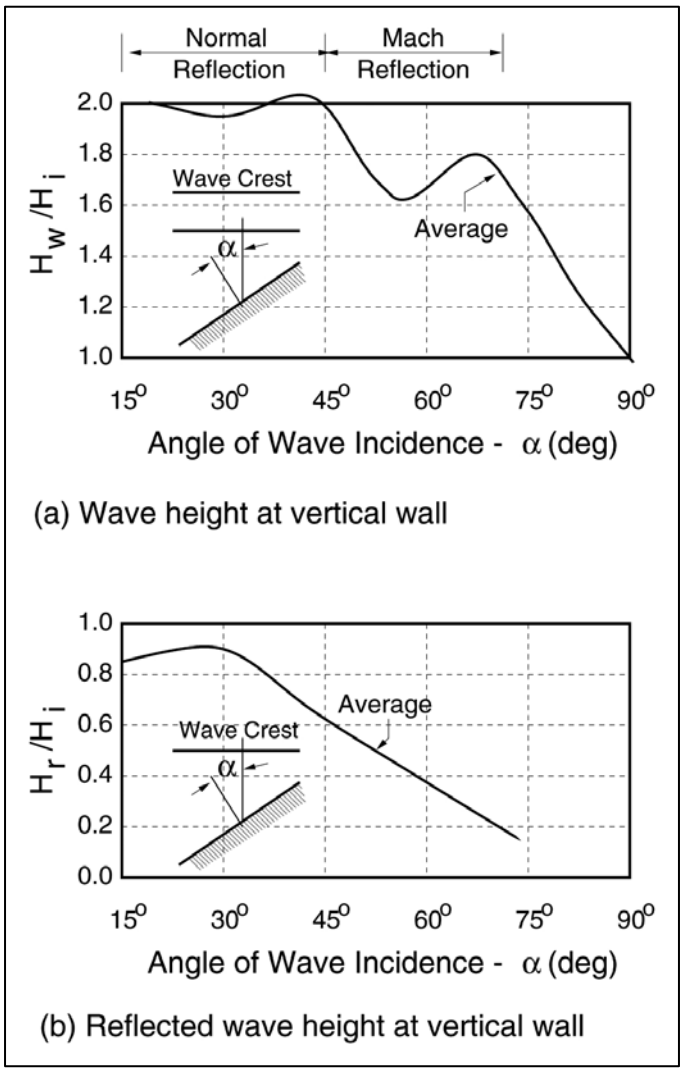

Figure VI-5-79. Mach reflection at a vertical wall
(after Wiegel 1964)

- Vertical walls with bends rather than sharp corners (Figure VI-5-78b) produce somewhat more complicated wave reflection patterns. Along the structure bend, the local angle of wave incidence varies, as does the reflected wave angle. Consequently, accurate estimates of maximum wave height along the vertical bend are best accomplished using laboratory tests or capable numerical wave models. Estimates from Figure VI-5-79 using the local angle of wave incidence should provide a reasonable approximation for mild bends. Vertical walls with very short radii bends are analogous to the seaward portion of large diameter vertical cylinders, and wave estimation techniques used in the offshore engineering field should be appropriate.

(b) Sloping structures with convex corners. The majority of coastal structures have impermeable or rubble-mound sloping fronts. Convex corners and bends for sloping-front structures are defined the same as illustrated in Figure VI-5-78 for vertical walls. Sharp corners are more likely on smooth, impermeable slopes whereas rubble-mound structures will have more rounded bends. Chen (1961) conducted experiments with solitary waves approaching smooth,

impermeable slopes at oblique angles. For steep slopes the resulting wave behavior was similar to vertical walls with the onset of Mach reflection at larger angles of wave incidence. As the wall slope decreased, a large horizontal eddy formed over the slope. Further decreasing of the structure slope led to wave breaking along the slope. Generally, the onset of wave breaking depends on structure slope, incident wave angle, and the ratio of wave height to water depth (*H/h*). Chen's experiments used only one value of *H/h* so this relationship was not quantified. Rubble-mound structures with convex corners and bends may have armor stability problems for short-radius bends. In this case the bend is similar to the head section of a breakwater or jetty structure. Sakaiyama and Kajima (1997) conducted model tests of armor stability at convex bends in a structure protecting a manmade island. They found that armor stability increased as the bend radius increased. In many cases, armor stability at bends and corners is confirmed with physical model tests before construction begins. For short-radius bends an alternative is to use armor stability guidance developed for head sections. Increasing the bend radius will increase armor stability, but the tradeoff is greater quantities of construction materials.

(2) Waves at concave corners.

(a) Vertical structures with concave corners. Goda (1985) provided a simple formula for estimating the increased wave height at the apex of a concave corner of angle β formed by two impermeable vertical walls as illustrated by Figure VI-5-78c. A horizontal bottom is assumed. Provided the walls are sufficiently long, the wave height is estimated as

$$\frac{H_c}{H_i} = \frac{2\pi}{\beta} \tag{VI-5-193}$$

where H_c is the wave height in the corner, H_i is the incident wave height, and the angle β is expressed in radians. For $\beta = \pi$ the corner becomes a straight wall, and $H_c / H_i = 2$. However, as β becomes small, H_c increases to unreasonable values, and steepness-limited wave breaking will occur. Therefore, estimates of maximum waves at concave corners using Equation VI-5-193 should never be greater than the steepness-limited wave at that location. Goda stated the formula is also applicable to random waves. The wave height varies greatly along the walls due to interference between incident and reflected waves. For certain combinations of wall angle β and incident wave angle, the wave height at some position along the wave may be greater than at the corner apex (Goda 1985). Goda also described a more involved procedure for estimating wave heights associated with directionally spread irregular waves. Perfectly reflecting vertical structures with concave bends (see Figure VI-5-78d) will have higher wave heights than straight walls with normal wave incidence. Wave height will depend on the radius of curvature, with greater heights expected for smaller radius bends. No simple formulas are available to estimate wave heights at concave bends; but a conservative estimate can be made by approximating the bend as a corner formed by two straight walls, and then applying Equation VI-5-193. Alternately, wave heights could be determined using an appropriate numerical model.

(b) Sloping structures with concave corners. There do not appear to be any simple, reliable engineering procedures for estimating wave height variations at sloping structures with concave corners or bends. For steep-sloped, impermeable structures, the previously described method for vertical walls will provide a conservative estimate. For milder slopes, the engineer

should expect wave runup on the slope to be higher than would occur on straight structures because of the convergence of the incident wave crests. Generally, milder structure slopes, longer radii of curvature, and increased structure porosity will all contribute to a decrease in wave runup on the slope. Critical bends and corners should be tested in a physical model. If available, appropriate numerical models could also be used.

f. Uplift forces. The fluid induced force on a structure/object in the vertical (z-coordinate) direction is typically referred to as the "uplift" force (or "lift' force). The uplift force derives from various physical reasons depending on whether the structure is submerged or above water.

(1) Submerged or partially submerged structure.

(a) In the case of submerged or partially submerged structures in nonmoving fluids (i.e., a horizontal cylinderical object such as a timber cross-bracing in a pier or an outfall pipe), there is a buoyancy force which is equal to the volume of the fluid displaced by the structure/object times the specific weight of the fluid. This buoyancy force acts through the center of gravity of the displaced fluid volume in a vertically upward direction. The point through which the buoyant force acts is referred to as the center of buoyancy. The equation for this force component is given (Fox and McDonald 1985) as the integration over the volume of displaced fluid, i.e.,

$$F_B = \int_V (\rho_w g)\, dV \tag{VI-5-194}$$

where

F_B = buoyancy force (positive upwards)

ρ_w = density of water

g = acceleration of gravity

V = volume of displaced fluid

(b) For example, the buoyancy force acting on a fully submerged 1-m-diameter sphere is

$$F_B = \gamma_w \left(\frac{\pi D^3}{6}\right) = (10.1\, kN/m^3)\,(0.524\, m^3) = 5.29\, kN$$

where D is the sphere diameter and γ_w is the specific weight of salt water. The buoyancy force is directly countered by the gravitational force (weight) acting on the object. A net upward force occurs if the density of the submerged body is less than the water in which it is submerged.

(c) Additional vertically directed forces on the submerged or partially submerged solid body in the case of a moving fluid are due to the integration of the vertical component of pressure forces over the surface of the structure while neglecting elevation changes (Fox and McDonald 1985), i.e.,

$$F_L = -\int_S p_s (\vec{dA} \bullet \vec{n}_z) \qquad \text{(VI-5-195)}$$

where

F_L = lift force (positive upwards)

p_s = pressure on solid body surface due to moving fluid (does not include hydrostatic pressure difference due to elevation changes over the surface

$\vec{dA}$ = differential surface area element of solid body with direction outward normal to surface

$\vec{n}_z$ = normal unit vectory in the positive z-direction (upwards)

(d) In the case of steady flow in the horizontal x-direction, an uplift force (often referred to as a lift force) develops when the flow field around the solid body has streamlines that are closer together above the body than below it (i.e., the "Bernoulli effect") creating a lower pressure above than below the solid body. This uplift force is analogous to the aerodynamic lift force that keeps an airplane aloft. Pipelines or outfalls lying on the seabed are examples of objects that could experience an uplift force due to the distortion of streamlines created by the protrusion of the pipeline/outfall in the flow field. Where the structure/object is only partially submerged and there is no flow over the top of the structure/object, the lift force will be acting vertically downward (i.e., negative lift force) due to the compression of streamlines (and hence lower pressure) under the structure/object.

(e) Uplift force computations on solid objects can be made via potential flow theory for simple geometry cases where there is low velocity flow (i.e., no flow separation). For the more typical design situation of turbulent flow over a solid body with flow separation, vortex shedding, and possibly a complex boundary imposed flow field, experimental laboratory measurements must be relied on to evaluate the uplift force. For steady flow situations, empirical uplift force coefficients (lift coefficients) are a function of the flow Reynold=s number, "roughness" of the solid body, and the boundary imposed flow field around the body.

(f) When the fluid is unsteady, (e.g., oscillatory wave motion) the time-varying uplift force is estimated in the same manner as for steady flow only the computation becomes even more intractable due to the unsteady nature of the flow. In oscillatory flow over a solid body, vortices are shed with frequency and phase shifting that is dependent on the Keulegan-Carpenter number. For this situation uplift force computations and determination of empirical uplift force coefficients for the solid bodies in the flow are based on experimental laboratory measurements, often combined with numerical calculations.

(g) Oscillatory flow empirical uplift force coefficients are a function of the Keulegan-Carpenter number of the flow, the Reynolds number, "roughness of the structure/object, and boundary imposed flow field" (e.g., Sarpkaya and Isaacson 1981). Where vortex shedding occurs at or near the natural frequency of the object in the flow, a large amplitude dynamic response,

called vortex-induced vibration, may occur, causing much larger forces than predicted by the static approach previously discussed.

(h) Uplift forces induced by both steady and oscillatory currents need to be considered where the characteristic width of structure to wavelength ratio is small (e.g., $D/L < 0.2$ in the case of circular cylinders of diameter, D). The equation for calculation of lift force in this situation is simplified as given in the following equation (Fox and McDonald 1985, Rouse 1950; and Sarpkaya and Isaacson 1981):

$$F_L = C_L A_n \gamma_w \left(\frac{u^2}{2g} \right) \tag{VI-5-196}$$

where

C_L = empirical lift coefficient

A_n = projected area of solid body normal to the flow direction

γ_w = specific weight of water

g = gravitational acceleration

u = magnitude of flow velocity (lift will be perpendicular to flow direction)

(i) In the case of both steady and oscillatory currents, the velocity components of the currents must be added vectorially to provide the velocity to utilize in the previous equation.

(j) When the size of the solid structure/object is large enough to modify the incident wave field by wave diffraction and/or wave scattering, Equation VI-5-196 cannot be used to determine lift forces. For large structures, transverse and inline forces must be computed using diffraction theory (Wiegel 1964, Sarpkaya and Isaacson 1981). Typically, diffraction theory is implemented using numerical models that determine the pressure on the solid body surface and then integrate over the surface to determine the total force.

(2) Emergent structures.

(a) In the situation where the structure/object is above water (i.e., a horizontal structural member) and subjected to oscillatory wave action, intermittant approximately vertical directed impact forces occur when the level of the water reaches the structure/object. The uplift force on a structure/object in this scenerio cannot be theoretically derived due to the complex fluid structure interaction. Instead, engineers must rely on laboratory measurements or empirical impact force ("slamming") coefficients derived from laboratory testing. The uplift force for this situation is approximated as

$$F_U = C_U A_z \gamma_w \left(\frac{w^2}{2g} \right) \tag{VI-5-197}$$

where

C_U = laboratory derived slamming coefficient

A_z = projected area of solid body in the horizontal plane

w = vertical component of flow velocity at level of object

(b) A slamming coefficient approach to calculation of this type of uplift force is utilized primarily for slender members (for which the Morrison equation is utilized for the inline force computation). The wave theory utilized to calculate the vertical velocity at the level of the structure may depend on what level of approximation is desired and/or whether a monochromatic wave theory or irregular (linear) wave theory is utilized for the computation. A particular problem in evaluation of Equation VI-5-197 is estimating the velocity field at the structure. For even the most simple calculations an assumption that the structure does not influence the wave flow field must be made. Most uplift impact (slamming) force coefficients are derived from experimental laboratory measurements. Sarpkaya and Isaacson (1981) discussed experimental results for rigidly mounted horizontal circular cylinders subject to slamming forces, and they noted laboratory measured slamming force coefficients (C_U) ranging from 4.1 to 6.4.

(c) Typical coastal structures on which uplift forces may need to be calculated that do not fit into any of the previous catagories are caisson or monolithic concrete type breakwaters. These structures have additional complications with regard to calculation of uplift forces because they are situated on permeable foundations of rock or sand making theoretical calculations for the uplift forces very difficult. In this situation, empirical or semiempirical formula (based on laboratory testing) are utilized to provide preliminary design calculations. Typically, design conditions will not be the same as tested in past laboratory tests; therefore, uplift forces may need to be determined by testing the design in a physical model.

(d) Goda (1985) provided empirical formulae with which to make simple (uplift) dynamic component wave force calculations on the base of composite foundation vertical caisson (or monolithic concrete) breakwaters. The dynamic component of uplift force is assumed to be triangular over the base of the structure. The empirical formulae utilized are based on a limited number of laboratory tests and should only be utilized for preliminary calculations. Variables not in the empirical guidance but very important to the pressure distribution under the structure base are foundation permeability and structure width. High permeability and narrow structure widths could lead to uplift forces considerably in excess of Goda=s (1985) empirical guidance.

(e) Uplift forces on docks and piers are also of concern to coastal engineers although limited information exists for the computation of forces on these types of structures. When the wave crest height exceeds the underside level of the pier or dock, the structure will be subjected to uplift forces in both transverse directions. The computation of uplift force in this situation is difficult due to the modification of the flow field by the structure and the nonlinear boundary conditions at the water surface that must be accommodated. Typically, laboratory experiments augmented by numerical modeling must be utilized to evaluate these types of uplift forces.

French (1969) measured (in a laboratory experiment) transverse (positive and negative uplift) forces due to a solitary wave moving perpendicular to a pier and found that negative uplift forces often exceeded the positive uplift forces for the situations addressed. Lee and Lai (1986) utilized a numerical model to calculate wave uplift forces on a pier; and they noted that under certain conditions of bottom slope and solitary wave height to water depth combinations, positive uplift pressures can be larger than those calculated utilizing hydrostatic pressure for the given depth of immersion. In the situation where a vertical wall abuts the platform and wave reflection takes place (e.g., a dock structure), the positive uplift appears to be significantly increased while the negative uplift is reduced compared to the pier (i.e., no wave reflection) case.

(f) Bea et al. (1999) examined wave forces on the decks of offshore platforms in the Gulf of Mexico. They summarized results from a performance study of platforms that had been subjected to hurricane wave loadings on their lower decks. Modification to guidelines of the American petroleum industry were discussed and validated. Bea et al. provides up-to-date references related to wave forces on decks of offshore platforms that may be useful for similar calculations for docks and piers.

VI-5-5. Foundation Loads.

a. Introduction.

(1) This section assumes the reader has a general knowledge about soil mechanics and foundation design because only limited basic information is given with emphasis on coastal structure foundations. The soil parameter values and empirical expressions given in this section are suitable for feasibility studies and preliminary design calculations prior to any direct soil parameter measurements being performed in the field or laboratory. The same applies for final design calculations in small projects where specific geotechnical investigations cannot be performed. In general, calculations for detailed design should be based on specific analysis of the local soil mechanics conditions. Moreover, the most relevant and accurate methods of analysis should be applied.

(2) The main objective of this section is to present two important geotechnical aspects related to the design and geotechnical stability of breakwaters, dikes and seawalls:

(a) Assurance of safety against failure in soils contained within structures, rubble-mound structures, and in foundation soils.

(b) Assurance of limited (acceptable) deformations in soils contained within structures, rubble-mound structures, and in the foundation soil during structure lifetime.

(3) Related to these two aspects are the geotechnical failure modes illustrated in Part VI-2-4:

(a) Slip surface and zone failures, causing displacement of the structure and/or the subsoil.

For rubble-mound structures and dikes see Figures VI-2-25, VI-2-41, and VI-2-51.
For monolithic structures see Figures VI-2-54, VI-2-55, VI-2-64, and VI-2-66.
For tied wall structures see Figures VI-2-69, VI-2-70, VI-2-71, and VI-2-72.

(b) Excess settlement due to consolidation of subsoil and rubble foundation, causing lowering of the crest of the structure as shown in Figures VI-2-42 and VI-2-53.

(4) Slip surface and zone failures are the result of insufficient soil bearing capacity caused by unforeseen external loadings and/or degradation of soil strength. Such failures generally lead to pronounced settlement and damage or collapse of the structure. Potential for such failure makes it important to implement proper safety factors in the design.

(5) Excess settlement due to consolidation is caused by misjudgment of subsoil characteristics and, in the case of larger rubble-mound structures, the core materials. If evenly distributed, the settlement lowers the crest level, which causes an increase in overtopping and might reduce structure functionality. Differential settlements can cause damage to the structure itself, for example breakage of concrete superstructures, cracking of long concrete caissons, or creating weaknesses in the armor layer.

(6) A significant difference between geotechnical stability of coastal structures and common land based structures is the presence of wave action on the structure and its foundation. Another difference is the wave- induced pore pressure variation which will be present in wave exposed porous structures and seabed soils. The wave load introduces stress variations in the soils that can lead to degradation in soil strength due to pore pressure build-up. The designer has to show that at any stage throughout the structure lifetime the soil stresses should not exceed the soil strength. This calls for prediction of short and long-term stress and strength development in the soils. Distinction is made between cases with gradually varying wave forces caused by nonbreaking waves and cases with short-duration impulsive wave forces due to waves breaking directly on the structure. The first case is referred to as cyclic loading; the second case is dynamic loading, which includes dynamic amplication.

(7) This section is organized into the following sections containing basic information about the soil and related hydromechanic processes:

Part/Chapter/Section Heading	Section Topic
VI-5-5-b. Soil and Rock Properties	Basic definitions and related typical parameter values. Deformation characteristics of soils are discussed as well.
VI-5-5-c. Strength Parameters	Soil parameter definitions and typical soil strength values.
VI-5-5-d. Hydraulic Gradients and Flow Forces in Soils.	Includes the Forchheimer equation and estimates on wave induced internal set-up and pore pressure gradients in breakwater cores.
VI-5-5-e. Cyclic loading of soils.	Discussion of drainage conditions, transmission of wave loads to the foundation soil, and degradation of soil strength and generation of residual pore pressure when exposed to wave induced cyclic loading.
VI-5-5-f. Dynamic Loading of Soils Under Monolithic Structures.	Evaluation of dynamic amplification of foundation forces and deformations caused by impulsive wave forces.
VI-5-5-g. Slip Surface and Zone Failures.	Stability of slopes, bearing capacity of quarry rock foundations and subsoils. Stability of soil retaining structures is not discussed.
VI-5-5-h. Settlement.	Short discussion of immediate and consolidation settlement.

b. Soil and rock properties.

(1) Grain sizes. Table VI-5-65 gives the fractional limits according to International Standards Organization (IS), and Comité Européen de Normalisation (CEN).

Table VI-5-65
Fractional Limits of Grain Sizes According to ISO/CEN

Main Group	Grain Size, mm	Sub-Groups	Grain Size, mm
Boulders	> 200		
Cobbles	60 – 200		
		Coarse	20 - 60
Gravel	2 – 60	Medium	6 - 20
		Fine	2 - 6
		Coarse	0.6 - 2.0
Sand	0.06 - 2.0	Medium	0.2 - 0.6
		Fine	0.06 - 0.2
		Coarse	0.02 - 0.06
Silt	0.002 - 0.06	Medium	0.006 - 0.02
		Fine	0.002 - 0.006
Clay	< 0.002		

(2) Bulk density. The bulk density is defined by the relation

$$\rho = m / V \tag{VI-5-198}$$

where m is total mass and V is total volume. Typical bulk densities are given in Table VI-5-66.

Table VI-5-66
Typical Bulk Density Values

	Bulk Density, ρ (tonne/m^3)	
Soil Type	Water-Saturated	Above Water Table
Peat	1.0 - 1.1	(often water-saturated)
Dy and gyttja	1.2 - 1.4	(often water-saturated)
Clay and silt	1.4 - 2.0	(often water-saturated)
Sand and gravel	2.0 - 2.3	1.6 - 2.0
Till	2.1 - 2.4	1.8 - 2.3
Rock fill	1.9 - 2.2	1.4 - 1.9

The unit weight is given by

$$\gamma = \rho\, g = \rho\,(9.81\, kN/m^3)$$

(3) Volume of voids. The volume of voids is either expressed in terms of

$$\textit{porosity}\ \ n = V_p / V \qquad \textit{or} \qquad \textit{void ratio}\ \ e = V_p / V_s \tag{VI-5-199}$$

where V is the total volume and V_p and V_s are the volume of voids and solids, respectively.

(a) The porosity of coarse-grained soils is strongly dependent on the grain size distribution, the shape of the grains, and the compaction. Typical values of e and n for granular soils are given in Table VI-5-67.

Table VI-5-67
Typical Values of Void Ratio e and Porosity n for Granular Soils

	Void Ratio		Porosity	
Material	e_{min}	e_{max}	n_{min}	n_{max}
Uniform spheres	0.35	0.92	0.26	0.48
Uniform sand	0.40	1.00	0.29	0.50
Sand	0.50	0.80	0.33	0.44
Silty sand	0.30	0.90	0.23	0.47
Uniform silt	0.40	1.1	0.29	0.52

(b) For cohesive soils the range of e (and n) is much larger than for granular soils. For clays e can range between 0.2 and 25.

(4) Relative density. The relative density is defined as

$$D_r = \frac{e_{\max} - e}{e_{\max} - e_{\min}} 100\% \qquad \text{(VI-5-200)}$$

where

e_{min} = void ratio of soil in most dense condition

e_{max} = void ratio of soil in loosest condition

e = in-place void ratio

Table VI-5-68 provides a density characterization of granular soils on the basis of D_r.

Table VI-5-68
Density Characterization of Granular Soils

Relative Density D_r (percent)	Descriptive Term
0 - 15	very loose
15 – 35	loose
35 - 65	medium
65 – 85	dense
85 – 100	very dense

(5) Plasticity index. The plasticity index I_p relates to cohesive soils and indicates the magnitude of water content range over which the soil remains plastic. The plasticity index is given by

$$I_p = w_l - w_p \qquad \text{(VI-5-201)}$$

where w is the water content, i.e., the ratio of weight of water to the weight of solids in a soil element, and subscripts l and p refer to liquid and plastic limits, respectively.

(6) Total and effective stresses. The total stresses on a section through a soil element can be decomposed into a normal stress σ, and a shear stress τ as illustrated by Figure VI-5-80.

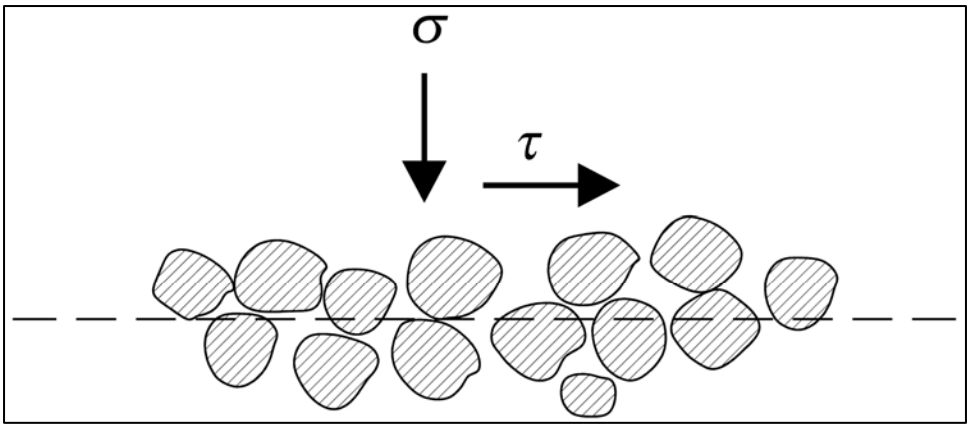

Figure VI-5-80. Total stresses in a soil element

(a) Because the soil is a three-phase medium consisting of solids and voids filled with water and/or gas it is seen that the total normal force is the sum of the contact forces between the grains and the pore pressure, u. In terms of stresses (force per unit area) we define

$$\sigma = \sigma' + u \tag{VI-5-202}$$

where σ is total stress, σN is effective stress and u the pore pressure. Because of the small area of the contact points it can be assumed that u is acting over the whole unit area of the section.

(b) Water and gas cannot resist shear stress so the total shear stress, τ, is set equal to the effective shear stress, τN, i.e., the stress carried by the grains,

$$\tau = \tau' \tag{VI-5-203}$$

(c) It follows from Equation VI-5-202 and Equation VI-5-203 that the ability of the soil to resist failure depends on the strength of the grain skeleton, which in turn depends on the effective stresses. This means that under constant normal stress, an increase in the pore pressure will lower the soil strength. For coastal structures changes in pore pressure are normally caused by changes in seawater level and by wave action.

(7) Geostatic stress. The geostatic stress is the stress caused by the weight of the soil when the ground surface is horizontal and the nature of the soil has only slight variation in the horizontal directions. For homogeneous soil the vertical geostatic stress is given by

$$\begin{aligned} &\sigma_v = z\,\gamma\,, \quad \textit{based on total stress} \\ &\sigma'_v = z\,\gamma'\,, \quad \textit{based on effective stress} \end{aligned} \tag{VI-5-204}$$

where z is the depth, and γ and γN are the total and the submerged unit weights of the soil, respectively. In other words, σ_v and σN_v vary linearly with depth.

(8) Stresses within soil deposits. The coefficient of lateral stress, K, is the ratio of horizontal to vertical effective stress, i.e.,

$$K = \frac{\sigma_h - u}{\sigma_v - u} = \frac{\sigma'_h}{\sigma'_v} \qquad \text{(VI-5-205)}$$

K_o is the coefficient of lateral stress at rest. For sand deposits created by sedimentation values of K_o are typically in the range 0.4 - 0.5.

(9) Stresses due to externally applied surface loads. Although soil is an elastic plastic material, the theory of elasticity is often used to compute stresses from externally applied loads. (Examples are settlement calculations and verification of deformation amplification by dynamic loading.) Furthermore, most of the useful solutions from this theory assume that the soil is homogeneous and isotropic. Soil seldom, if ever, fulfills these assumptions. However, the engineer has little choice but to use the results from the elasticity theory together with engineering judgement. The assumption of elastic behavior is rather good if the applied stresses are low compared to stresses at failure. Diagrams for estimation of stresses induced by uniform loading on circular areas, rectangular areas and strip areas are given in most geotechnical textbooks, see for example Hansbo (1994) and Lambe and Whitman (1979).

(10) Overconsolidation ratio. A soil element that is at equilibrium under the maximum stress it has ever experienced is normally consolidated, whereas a soil at equilibrium under a stress less than the maximum stress to which it was once consolidated is termed overconsolidated. The ratio between the maximum past pressure and the actual pressure is the overconsolidation ratio (OCR). A value of OCR = 1 corresponds to normally consolidated clay where the soil tries to reduce volume (contract) when loaded further, whereas $OCR > 1$ corresponds to overconsolidated clay which tends to increase volume (dilate) under applied loads.

(11) Deformation moduli. Although soils generally exhibit plastic deformations during failure, the theory of elasticity is still widely used (for example relating soil response to dynamic loadings and stress distributions under static loads). Assuming soil behaves as an elastic material, the deformation characteristics can be expressed in terms of the moduli given in Table VI-5-69.

(a) Typical values of Poisson's ratio, v, for conditions after initial loading are given in Table VI-5-70. Exact determination of v is of less importance, because practical engineering solutions are generally not sensitive to v.

(b) The nonlinear deformation characteristics of soil makes it necessary to use secant values of the deformation moduli, as shown in Figure VI-5-81 which illustrates results from shear and compression tests. Uniaxial and confined compression tests exhibit a similar reaction. Secant values relate to stress levels being some fraction of the maximum (failure) stress. Distinction is made between initial loading where relative large deformations occur, and repeated (cyclic) loading where permanent deformations decrease and eventually disappear.

Table VI-5-69
Deformation of Moduli for Elastic Material

Young's modulus

$$E = \frac{\sigma_1}{\varepsilon_1}$$

Poisson' ratio

$$\nu = -\frac{\varepsilon_2}{\varepsilon_1}$$

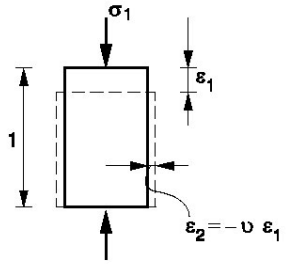

Uniaxial loading of elastic cylinder

Shear modulus

$$G = \frac{\tau}{\gamma} = \frac{E}{2(1+\nu)}$$

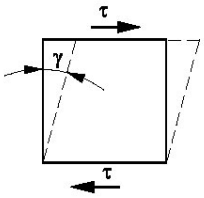

Shear applied to elastic cube

Bulk modulus

$$K = \frac{\sigma}{\varepsilon_{vol}} = \frac{2G(1+\nu)}{3(1-2\nu)}$$

ε_{vol} is volumetric strain, i.e. the relative change in volume V

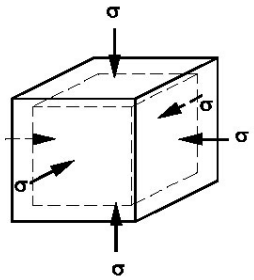

Isotropic compression of elastic cube

Constrained modulus
(Oedometer modulus)

$$M = \frac{\sigma_1}{\varepsilon_1} = \frac{2G(1-\nu)}{1-2\nu}$$

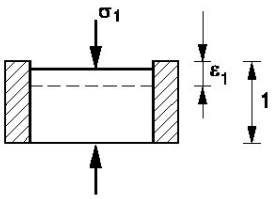

Confined compression

Table VI-5-70
Typical Values of Poisson's Ratio, *v*

Soil	v
Dry Sand	0.35
Partially saturated sand and clay	0.4
Saturated sand and clay	0.5

(c) Young modulus for sand varies with the void ratio, strength and shape of the grains, the stress history and the loading rate. Table VI-5-71 gives some example values of the secant Young's modulus corresponding to quasi-static loadings of 50 percent of the peak deviator stress and 101.3 kN/m^2 (1 atm) confining stress (Lambe and Whitman 1979).

(d) Young's modulus for clay varies with stress level, level of consolidation, and rate of strain. Table VI-5-72 provides typical values given by Richardson and Whitman (1964) corresponding to quasi-static loadings.

(e) It follows from Figure VI-5-81 that the deformation moduli depend on the strain level and the type of loading.

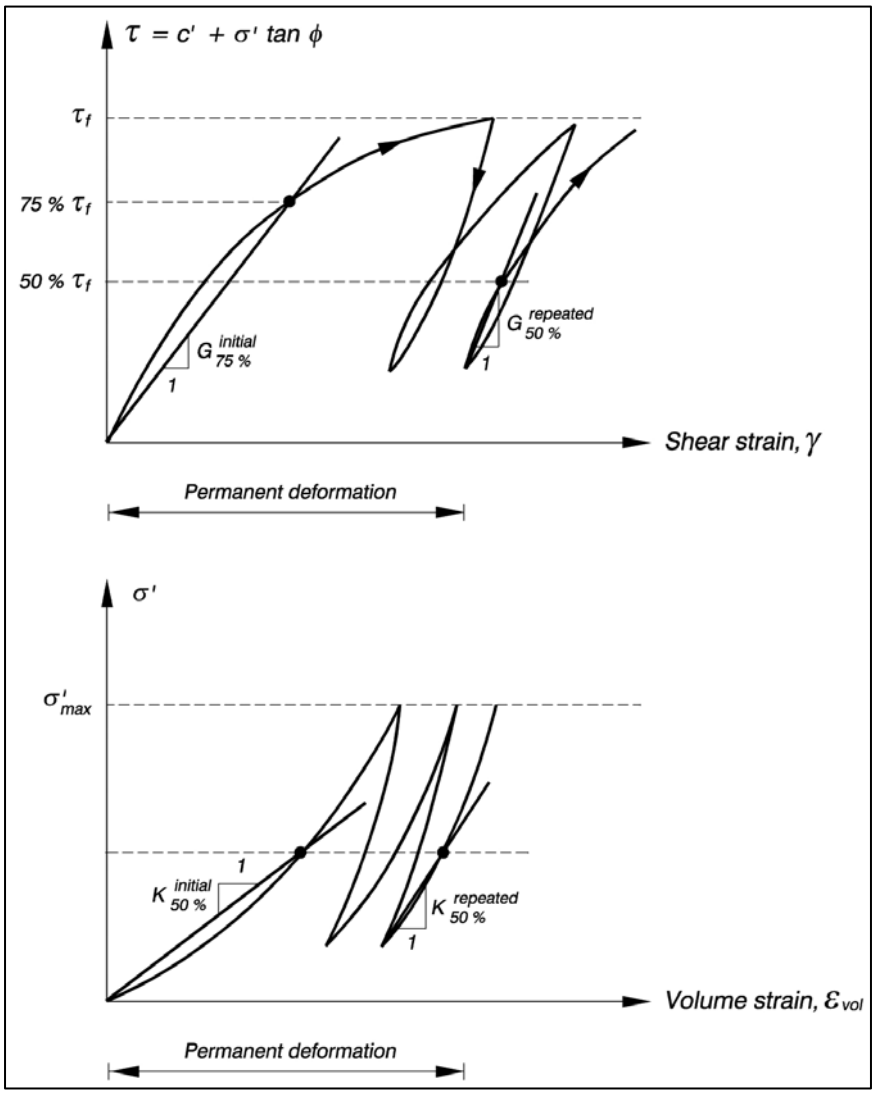

Figure VI-5-81. Illustration of shear modulus *G* and bulk modulus *K* for granular soils exposed to initial and repeated (cyclic) loadings

(f) Typical values of shear modulus G, bulk modulus K and oedometer modulus M for quartz sand is given in Table VI-5-73 corresponding to initial loading (σN# 300 kN/m^2) and subsequent unloading and reloading (mean σN= 100 kN/m^2).

Table VI-5-71
Example Values of Secant Young's Modulus E in MN/m^2 for Sand

Material	Loading	Packing Density	
		Loose	Dense
Angular	Initial	15	35
	Repeated	120	200
Rounded	Initial	50	100
	Repeated	190	500

Table VI-5-72
Typical Values of Secant Young's Modulus, E, for Clay

Level of Consolidation	Strain Rate	E/σ	
		Safety Level 3[1]	Safety Level 1.5
Normal	1 percent / 1 min.	250	160
	1 percent / 500 min.	120	60
Over	1 percent / 1 min.	450	200
	1 percent / 500 min.	250	140

[1] Deviator stress equal to 33 percent of peak deviator stress.

Table VI-5-73
Typical Secant Values of Deformation-Moduli G, K and M for Quasi-Static Loaded Quartz Sand (Centre for Civil Engineering Research and Codes (CUR) 1995)

Parameter	Initial Loading	Repeated Loading
G (MN/m^2)	4 - 40	20 - 400
K (MN/m^2)	10 - 100	50 - 1000
M (MN/m^2)	15 - 150	80 - 500

Note: Higher values valid for dense sand, lower values valid for very loose sand.

(g) The shear modulus G is independent of drained or undrained conditions, and the value of G for clays is dependent on the type of clay (plasticity index), the type of loading, the stress level, and the OCR. Figure VI-5-82 shows the range of G over the static undrained shear strength, c_u, as a function of the shear strain for some saturated clays (not further characterized).

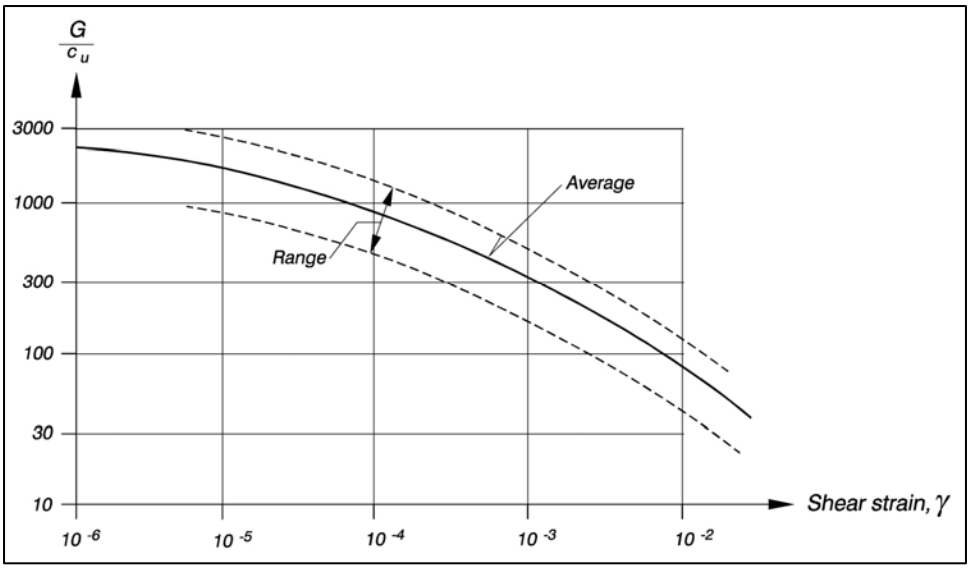

Figure VI-5-82. In-situ secant values of shear modulus *G* for quasi-static loaded saturated clays (after Seed and Idriss 1970)

(h) The significant influence of *OCR* and cyclic loading on *G* is shown in Figure VI-5-83 which presents results for Norwegian Drammen clay with plasticity index I_p of 27 percent and a clay content of 45-55 percent. These results were based on stress controlled DSS tests and resonant column tests. In Figure VI-5-83 the parameter σ_u^{DSS} is the undrained static DSS shear strength for two hours of loading to failure. The stress τ_{cy} is the shear stress amplitude in the symmetric cyclic loading. *N* is number of load cycles.

(i) The shear modulus *G* is an important parameter in soil response to dynamic loadings that might be caused by waves and earthquakes. In quasi-static loading tests, such as simple shear and triaxial tests, the lower limit for strain measurements is approximately 10^{-3}, whereas in bender element and resonant column tests strains down to 10^{-6} can be recorded. Thus in practice, the maximum value G_{max} which can be identified corresponds to a shear strain of approximately 10^{-6}. Formulae for G_{max} are given as follows:

- Sand (Hardin and Black 1968)

$$G_{\max} = \begin{cases} \dfrac{6908\,(2.17 - e)^2}{1+e}\sqrt{p'} & round-grained \\ \dfrac{3230\,(2.97 - e)^2}{1+e}\sqrt{p'} & angular-grained \end{cases} \qquad \text{(VI-5-206)}$$

- Gravel (Seed et al. 1986). They found G_{max} values approximately 2.5 times larger than for sand.

- Clay (Hardin and Drnevich 1972)

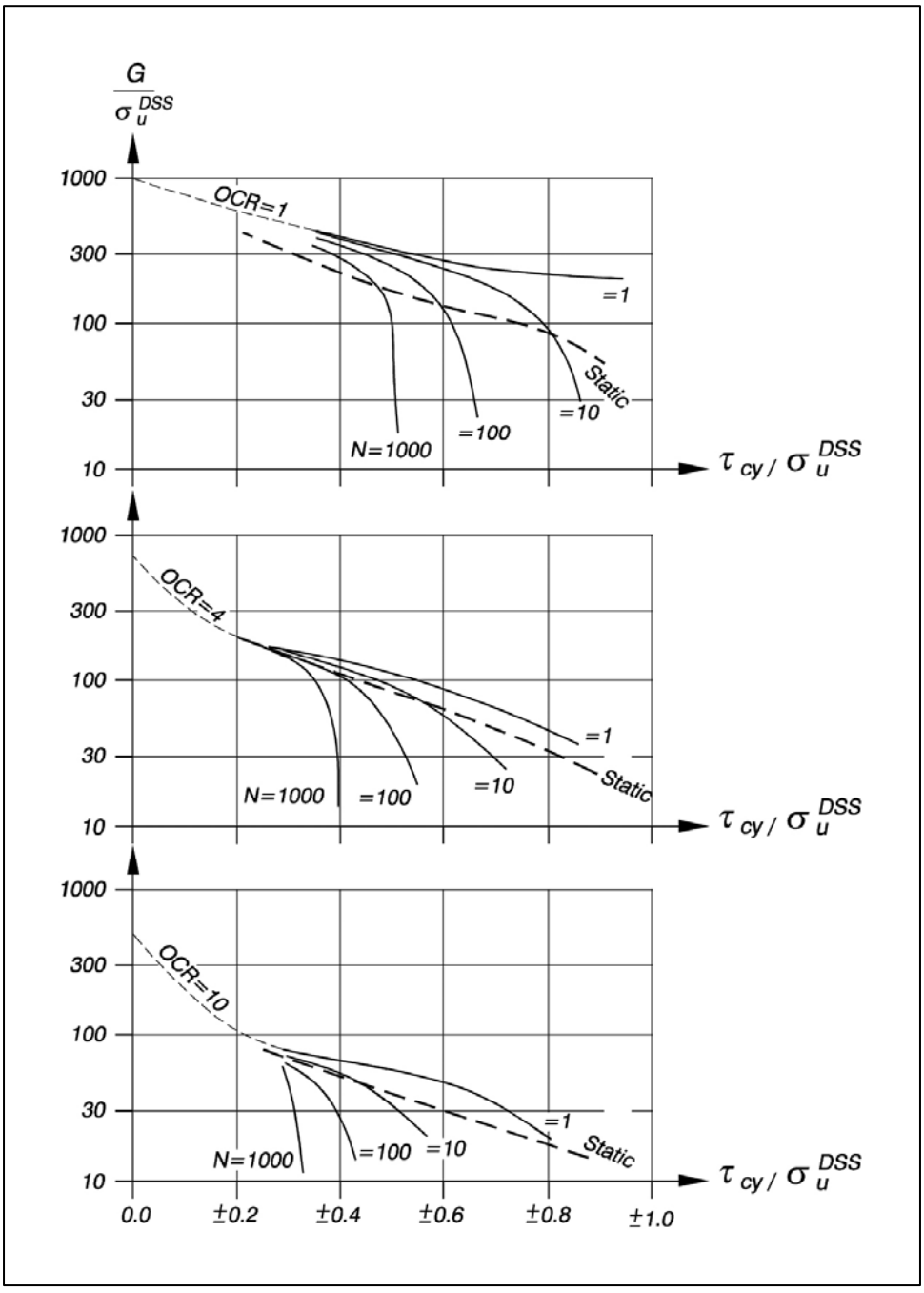

Figure VI-5-83. Static and secant cyclic shear modulus, *G*, for Drammen clay (Andersen, Kleven, and Heien 1988)

$$G_{\max} = \frac{3230\,(2.97 - e)^2}{1 + e}\,(OCR)^K \sqrt{p'} \qquad \text{(VI-5-207)}$$

where

e = void ratio

p' = mean effective stress, $1/3(\sigma_1 N + \sigma_2 N + \sigma_3 N)$ to be inserted in kN/m^2 to obtain G_{max} in kN/m^2

OCR = overconsolidation ratio

K = constant dependent on the plasticity index

Plasticity Index (percent)	0	20	40	60	80	∃ 100
K	0	0.18	0.30	0.41	0.48	0.50

Hardin (1978) proposed for both granular and cohesive soils that

$$G_{\max} = \frac{625}{0.3 + 0.7\, e^2} (OCR)^K \sqrt{p_a\, p'} \qquad \text{(VI-5-208)}$$

where p_a is atmospheric pressure (101.3 kN/m^2). The ratio between G and G_{max} as function of the shear strain for sand and gravel is given in Figure VI-5-84.

(12) Damping ratio. The damping ratio D signifies the decrease in the displacement amplitude z_n of the oscillations and is defined by

$$D = \frac{\delta}{2\pi} = \frac{1}{2\pi} \ln\left(\frac{z_n}{z_n + 1}\right) \qquad \text{(VI-5-209)}$$

where δ is the logarithmic decrement. Figure VI-5-85 shows damping ratios for sands and clays.

c. Strength parameters.

(1) Mohr-Coulomb failure criterion.

(a) The strength parameters of soil and rock fill constitute the basis for analysis of soil bearing capacity and wall pressures. Failure occurs when shear stresses reach an upper limit represented by the envelope to the Mohr failure circles, as shown in Figure VI-5-86.

(b) The Mohr envelope is generally curved for drained conditions. Figure VI-5-87 shows two commonly applied straight-line approximations to curved envelopes found from drained triaxial tests. Figure VI-5-87 demonstrates that the straight-line approximation is good only in the vicinity of the σN_f-value for which the tangent to the circle is constructed. The approximation in Figure VI-5-87a is given by the Mohr-Coulomb equation

$$\tau_f = c' + \sigma_{f'} \tan \varphi_{t'} \qquad \text{(VI-5-210)}$$

where cN is the cohesion intercept, $\nu_t N$ is the effective tangent angle of friction, and $\sigma_f N$ is the effective stress at failure as specified by Equation VI-5-204.

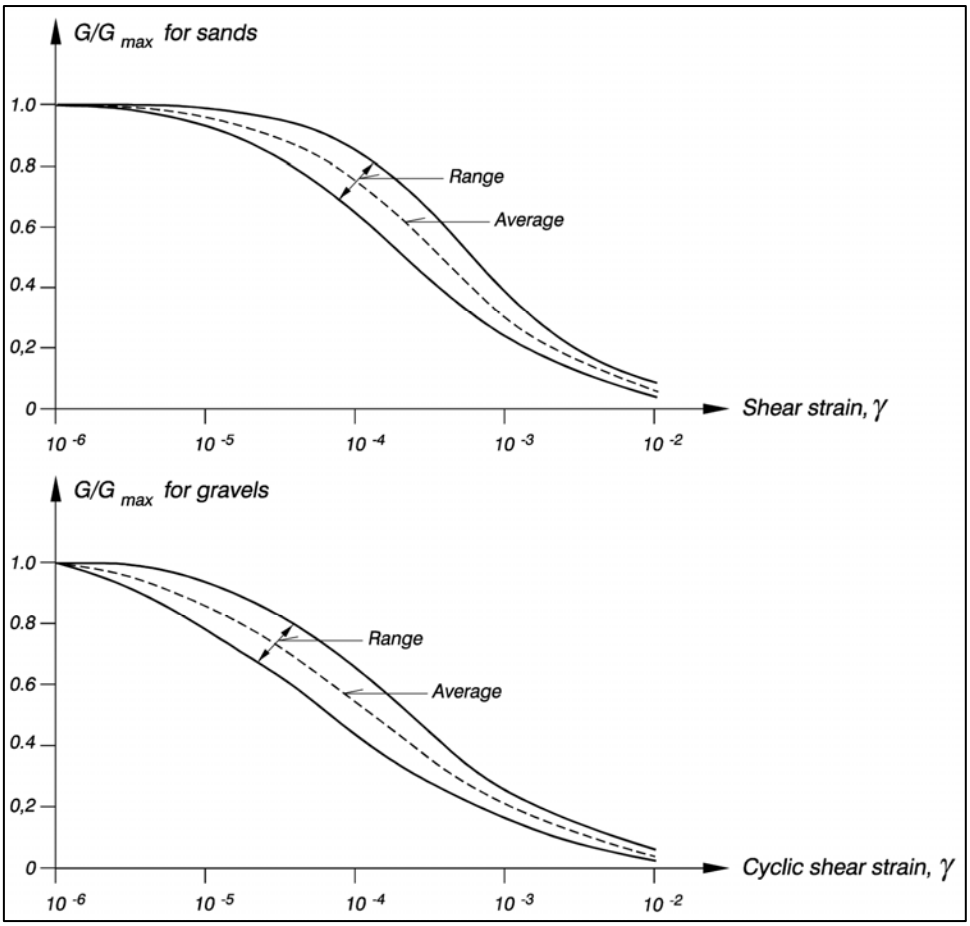

Figure VI-5-84. Values of G/G_{max} for sands and gravels
(after Seed et al. 1986)

(2) Noncohesive soils.

(a) The failure criterion approximation shown in Figure VI-5-87b corresponding to the equation

$$\tau_f = \sigma_{f'} \tan \varphi_{s'} \qquad \text{(VI-5-211)}$$

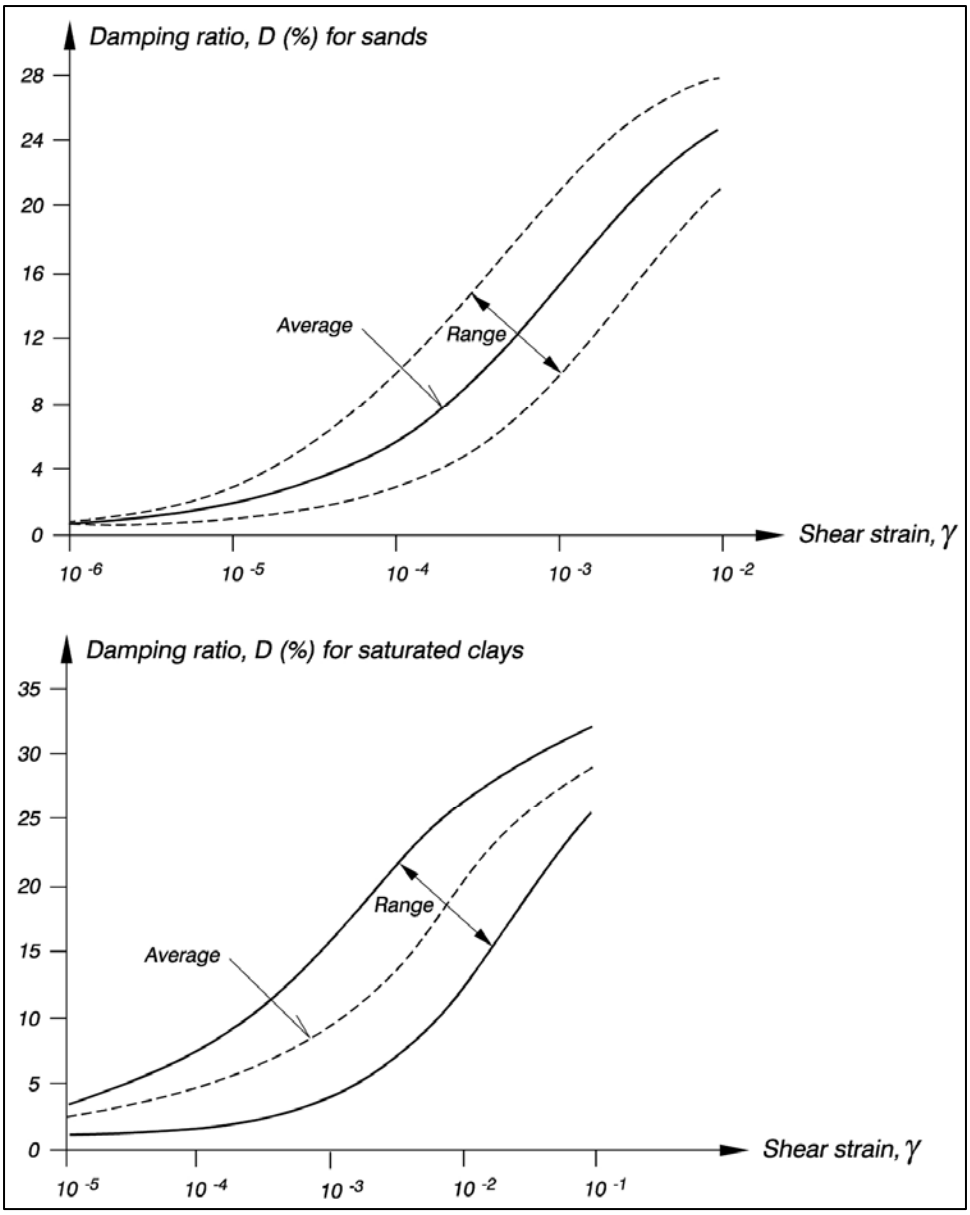

Figure VI-5-85. Damping ratios for sands and saturated clays (Seed 70)

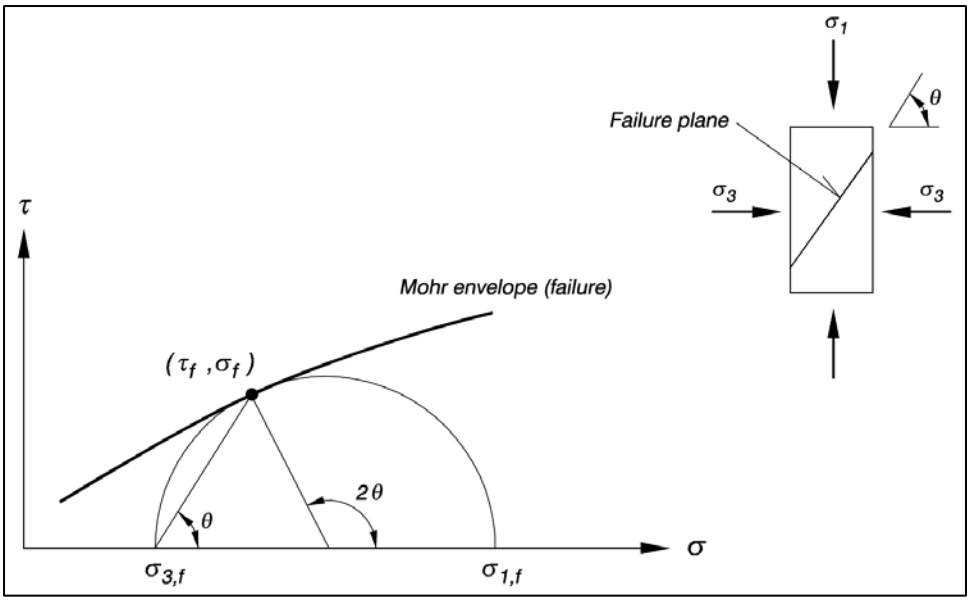

Figure VI-5-86. Mohr envelope for stresses of failure

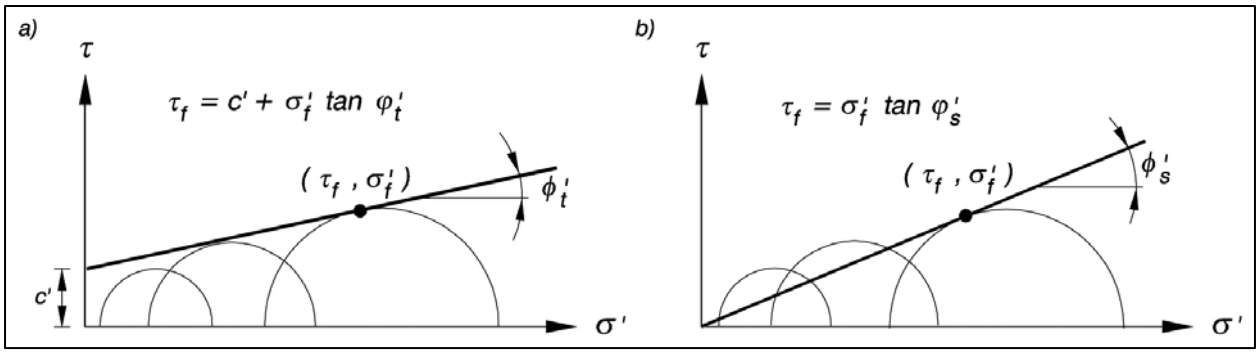

Figure VI-5-87. Illustration of straight-line approximations to curved Mohr envelopes corresponding to drained conditions: (a) Tangent formulation, (b) Secant formulation

where $\nu_s N$ is the effective secant angle of friction, has been applied to granular soils ever since the early studies by Coulomb. The equation is accurate only for relatively small values of $\sigma_f N$. However, for well graded quartz sand the limit for reasonable accuracy may be as high as 1,000 kN/m^2. In general the equation should be applied only to a limited stress range around the $\sigma_f N$ value corresponding to $\nu_s N$. Otherwise, for very high stress ranges the strength of a granular soil or rockfill can only be satisfactorily represented by Equation VI-5-210, or a curved Mohr envelope. Another way to represent the nonlinear strength relation is to treat $\tan \nu N$ as a variable that depends on the confining pressure as indicated in Figure VI-5-87, which shows that νN is a function of the actual effective stress level.

(b) The angle of friction νN in granular materials depends on the grain-size distribution, size and shape of the grains, and on the porosity. Well graded materials exhibit higher friction than uniformly graded materials. Sharp edged angular grains give higher friction than rounded grains, and the friction angle will be higher in densely packed than it is in loose soils.

(c) Typical angles of friction for granular soils like quartz sand and quarried granite rock fill are given in Table VI-5-74 and Figure VI-5-88.

Table VI-5-74
Typical Values of Triaxial Test Friction Angle ν_s for Quartz Sand

Relative Density	Friction Angle from Triaxal Tests ν_s (degrees)
Very loose	-
Loose	29 - 35
Medium	33 - 38
Dense	37 - 43
Very dense	-

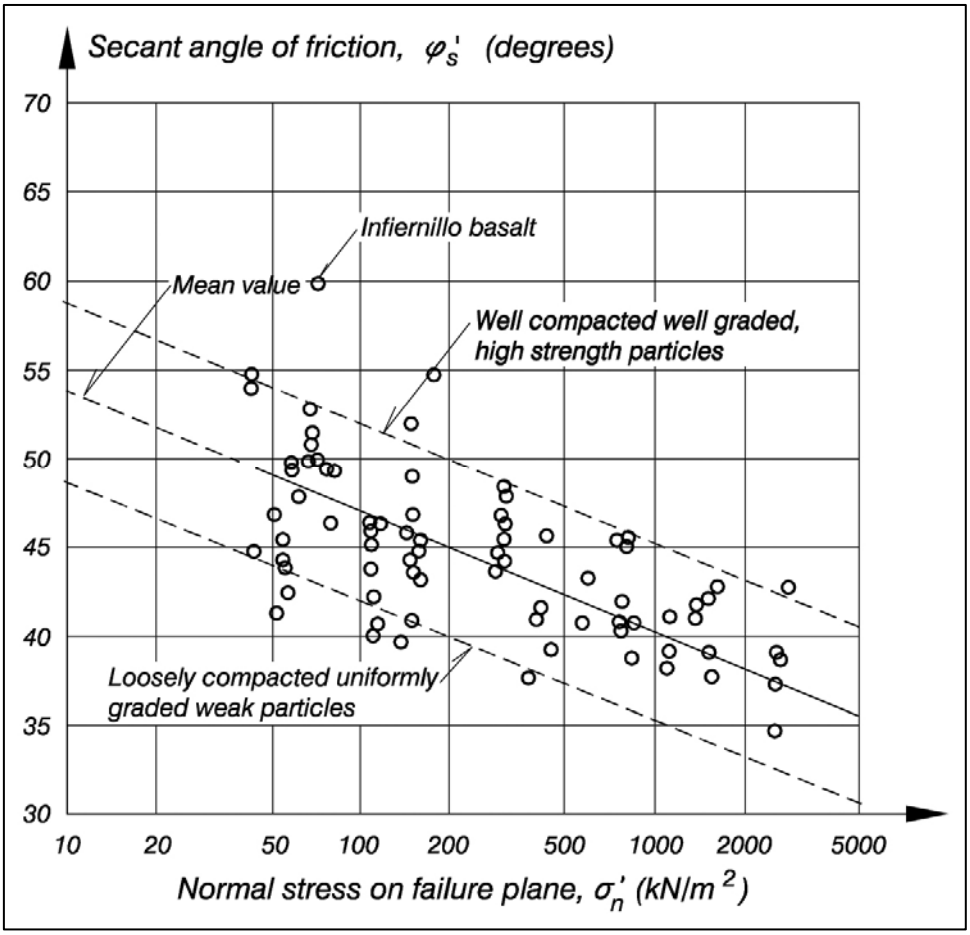

Figure VI-5-88. Angle of friction in rock fill of different grading and porosity with maximum diameter in the range 70-200 mm (after Leps 1970 and Kjaernsli, Valstad, and Høeg 1992)

(d) Steenfelt and Foged (1994) reported secant angles of friction $\nu_s N = 45^o$ - 62.2^o at normal stress on failure plane σ_nN = 77 - 273 kN/m^2 for Hyperite crushed stone of mass density

3.1 tonne/m^3, d_{50} = 15 - 16 mm and d_{max} = 64 mm. This compares well with the Infiernillo basalt data in Figure VI-5-88.

(3) Dilatancy.

(a) Shearing of frictional soils under drained conditions generally involves volume changes in terms of dilation or contraction. A crude visualization of dilatancy in plane strain is shown in Figure VI-5-89.

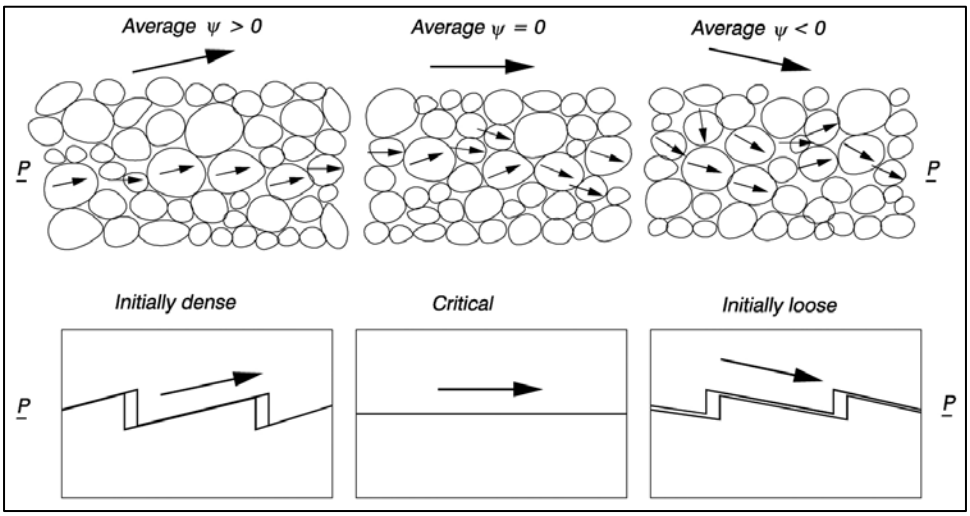

Figure VI-5-89. Crude visualization of dilatancy and angle of dilation ψ (Bolton 1979)

(b) The volume changes associated with stress as it increases toward maximum strength (see $\nu_s N$ in Equation VI-5-211) depend on the effective stress level and the initial density, which is given by porosity n or void ratio e. The volume changes are quantified by the angle of dilation, ψ, defined by

$$\sin \psi = -\frac{\dot{\varepsilon}_1 + \dot{\varepsilon}_3}{\dot{\varepsilon}_1 - \dot{\varepsilon}_3} = \frac{\dot{\varepsilon}_{vol}}{\dot{\varepsilon}_{vol} - 2\dot{\varepsilon}_3} \qquad \text{(VI-5-212)}$$

where $\dot{\varepsilon}_1$, and $\dot{\varepsilon}_3$ are strain rates in principal stress directions 1 and 3, and $\dot{\varepsilon}_{vol}$ is the volume strain rate. The strain rates can be found from triaxial tests.

(c) The angle of friction corresponding to the critical (also called ultimate) condition where the soil strains without volume changes (see Figure VI-5-89) is denoted the critical angle of friction, νN_{crit}. The parameter νN_{crit} appears to be a material constant because it depends on the mineralogy, grading and shape of the grains for the soil in question, but seems independent on the relative density or porosity. Typical values of νN_{crit} are given in Table VI-5-75.

(d) An average value of νN_{crit} for sand is 32 deg. For quarried rockfill a somewhat higher value is found. Steenfelt (1992) stated that a simple bench test for νN_{crit}, offering an accuracy of

about 1^o, is the angle of repose of a loosely tipped heap of dry material subjected to excavation at the foot.

The contribution of dilation to the strength of the material is suggested as follows by Bolton (1986)

$$\varphi_{m'ax} - \varphi_{c'rit} = 0.8\,\psi_{max} = \begin{cases} 5^o\, I_r & \textit{plane strain} \\ 3^o\, I_r & \textit{triaxial strain} \end{cases} \qquad \text{(VI-5-213)}$$

Table VI-5-75
Critical Value of Angle of Friction, νN_{crit} (Steenfelt 1992)

Material	d_{50} (mm)	d_{max} (mm)	νN_{crit} (deg)
Quartz sand,	0.17	-	27.5 - 32
dry and saturated	0.24	-	29 - 33.3
	0.52 - 0.55	-	33.5
	0.88	-	31.9
Rock fill, quarried granitic gneiss	-	9.5 - 80	39.1

where

$$I_R = D_r\ (A - \ln\ p') - 1 \qquad \text{(VI-5-214)}$$

and

$\nu N_{max} = \nu N_s$ for triaxial strain, as given by Equation VI-5-211

D_r = relative density

pN = mean effective stress, $1/3(\sigma_1 N + \sigma_2 N + \sigma_3 N)$ in kN/m

A = material constant, 10 for quartz and feldspar, and 8 for limestone

Typical values of ψ_{max} for quartz granular materials are given in Table VI-5-76.

Table VI-5-76
Typical Values of ψ_{max} for Quartz Sand and Quarried Granitic Gneiss

Relative Density	Angle of Dilation, ψ_{max} (deg)
Loose	-2 to +3
Medium	+3 to +8
Dense	+8 to +13

(4) Cohesive soils.

(a) The shear strength of cohesive soils like clay and organic mineral soils is due to both friction (between coarser grains and between aggregates formed by clay particles) and cohesion within the material (sorption forces). The shear strength of clay normally refers to the static shear strength from undrained strain controlled tests with a monotonic load increase lasting 1-3 hours to failure. This so-called undrained shear strength, c_u and the related failure envelope are illustrated in Figure VI-5-90.

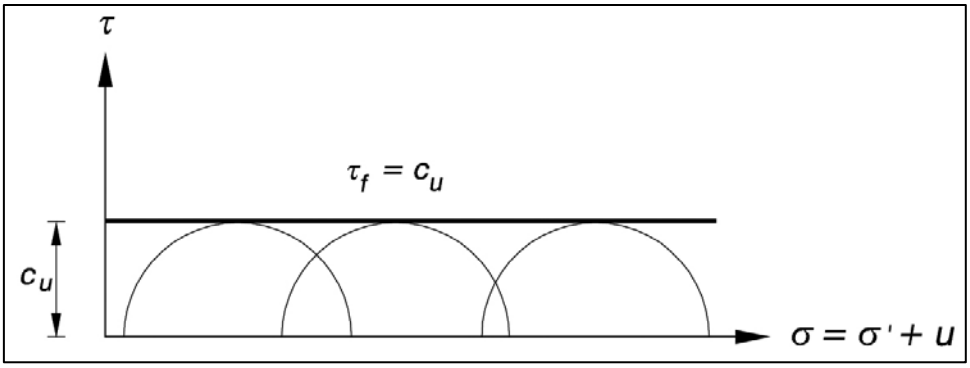

Figure VI-5-90. Failure criterion for a water-saturated clay in undrained condition defined from Mohr envelope

(b) For a specific clay with a given stress history, c_u depends solely on the initial effective stress conditions before the loading. Thus, the increase in σ in Figure VI-5-90 is equal to the increase in the pore pressure, u. In addition, the c_u-value and the deformation characteristics depend on the overconsolidation ratio, *OCR*, defined in Part VI-5-5*b*, as well as on the rate and number of loadings, as discussed in Part VI-5-5*e* on cyclic loading. Failure analysis related to cohesive soils in undrained conditions is performed on the basis of total stresses, σ, as opposed to analysis of noncohesive soils which is based on effective stresses, σN.

(c) The relative density of cohesive types of soils cannot be determined, and for this reason these soils are usually classified according to shear strength properties (see Table VI-5-77).

Table VI-5-77
Classification of Clay According to Undrained Shear Strength, c_u

Descriptive Term	c_u (kN/m^2) (Hansbo 1994)	c_u (kN/m^2) (Tomlinson 1980)
Very soft	< 20	< 25
Soft	20 - 40	25 - 50
Firm	40 - 75	50 - 100
Stiff	75 - 150	100 - 200
Very stiff	> 150	> 200

(d) It should be noted that development of large shear stresses often involves soil deformations which might be damaging to the function of the structure. This is true especially for normally consolidated clay. For such cases the failure criterion must be defined as a strain level instead of the stress level, c_u.

(e) Cohesive soils are also classified according to their sensitivity to loss of strength when disturbed. The sensitivity, S_t, is defined as the ratio between the undrained shear strength of a specimen in undisturbed and in remoulded states. S_t is important for the estimation of shear strength reduction in case of disturbance due to activities such as piling and excavation. Fall-cone tests can be used to determine values of S_t. Soils are termed slightly sensitive when $S_t < 8$, moderately sensitive when $8 \# S_t \# 30$, and highly sensitive when $S_t > 30$. The last range includes quick clays for which $S_t \exists 50$.

d. Hydraulic gradient and flow forces in soils.

(1) Hydraulic gradient.

(a) If the seawater level and the groundwater level are horizontal and not moving, the pore water will be in static equilibrium corresponding to the hydrostatic pressure distribution and constant head, h. Any deviation from this stage causes a change in h, and generates a flow governed by the hydraulic gradient i, which is given by

$$i = \frac{\Delta h}{\Delta l} \tag{VI-5-215}$$

where Δh is the difference in hydraulic head over the distance Δl. The hydraulic head is defined as

$$h = z + \frac{u}{\gamma_w} \tag{VI-5-216}$$

where z is a vertical coordinate, u is the pore pressure, and $\gamma_w = \rho_w g$ is the unit weight of the water (ρ_w is the mass density of water and g is gravity).

(b) A flow force of $i\gamma_w$ will act on the grains in the direction of the hydraulic gradient, i. The effective unit weight, $\gamma_s N$, of a saturated soil can then be defined as

$$\gamma_{s'} = \gamma - \gamma_w \pm i\,\gamma_w \tag{VI-5-217}$$

where γ = unit weight of dry soil, the plus sign is used for vertical downward flow, and the minus sign is used for vertical upward flow. For an upward flow, if $i = (\gamma - \gamma_w) / \gamma_w$, then $\gamma_s N = 0$, corresponding to a total loss of soil bearing capacity, referred to as the limit stage of fluidization or liquifaction. The flow forces in the soil have to be included in the work or force balance equations for the failure limit states, either by including the flow force $i\gamma_w$ on all internal parts of the soil elements, or by including the pore pressures along the boundaries of the soil elements.

(c) The bulk flow velocity v introduced by i may be calculated by the one-dimensional extended Forchheimer equation

$$i = Av + B|v|v + C\frac{\delta v}{\delta t} \tag{VI-5-218}$$

where the coefficients A, B and C depend on the soil and water characteristics, i.e., grain size and shape, gradation, porosity, viscosity and the Reynolds number. The last term in Equation VI-5-218 can be neglected because it has only minor influence for wave-induced flow in cores, subsoils and rubble foundations related to coastal structures.

(d) Figure VI-5-91 illustrates the variation of A and B in Equation VI-5-218. Table VI-5-78 presents expressions of A and B as well as related flow coefficients found from experiments as listed in Burcharth and Anderson (1995). Considerable scatter in the flow coefficients is observed.

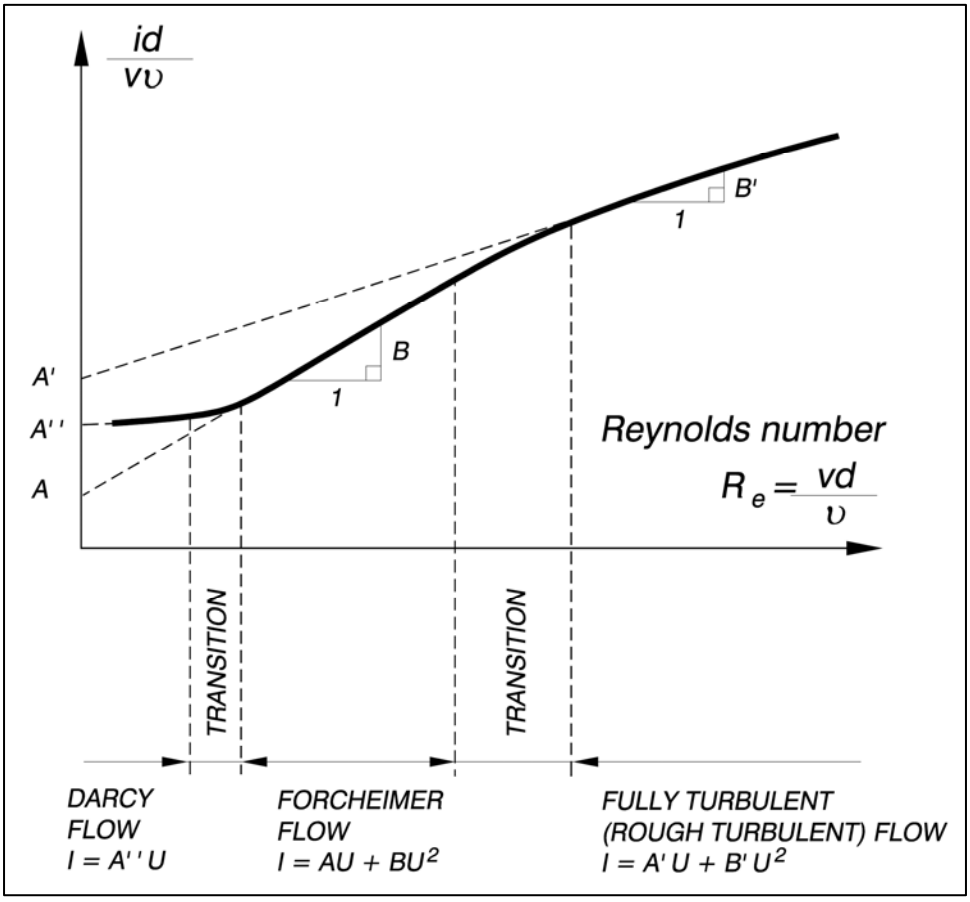

Figure VI-5-91. Representation of flow regimes for stationary porous flow based on a Forchheimer equation formulation (Burcharth and Anderson 1995)

(2) Permeability.

(a) For $R_e < 1$, Equation VI-5-219 in Table VI-5-78 is most often presented as the Darcy equation

$$v = k\, i \tag{VI-5-220}$$

where k is a dimensional quality referred to as the permeability coefficient. Comparing the first term in Equation VI-5-219 with Equation VI-5-220 gives

$$k = \frac{n^3}{\alpha\,(1-n)^2}\,\frac{g\,d^2}{\nu} \tag{VI-5-221}$$

(b) Equation VI-5-221 can be applied for fine materials like clay, silt, and fine sand ($d \leq$ 0.2 mm) whereas for coarser material the nonlinear Equation VI-5-219 must be applied. It should be noted that α (and thereby k) depends on the Reynolds number and the soil gradation.

(c) Typical values of k are given in Table VI-5-79 for rather uniform sands. Order of magnitude values of k for stone materials are given in Table VI-5-80.

Table VI-5-78
One-Dimensional Porous Flow Equation

One-dimensional steady porous flow equation and related coefficients. Burcharth and Anderson (1995).

$$i = \alpha\frac{(1-n)^2}{n^3}\frac{\nu}{gd^2}v + \beta\,\frac{1-n}{n^3}\frac{1}{gd}v^2 \qquad \text{(VI}-5-219\text{)}$$

where
- n Porosity
- d Characteristic grain diameter, e.g. d_{50}
- ν Kinematic viscosity ($1.3.10^{-6}\ m^2/s$ for water at 10^oC)
- g Gravitational constant
- v Bulk flow velocity

Typical values of α and β in Eqn. VI-5-219 for uniform sand and quarried rock materials

$$\frac{d_{85}}{d_{15}} = 1.3 - 1.9$$

Flow range	$\boldsymbol{Re = \frac{dv}{\nu}}$	α	β
Darcy	< 1	300 - 400	0
Forchheimer	10 - 150	300	3.0 - 3.6
Fully turbulent	1,000 - 12,000	1,000 - 10,000	3.6 - 2.4[1]

[1] Smallest values of β correspond to largest R_e.

Table VI-5-79
Typical Values of Permeability, *k*, for Fine Materials

Material	Packing	*k* (m/s)
Coarse sand	loose	10^{-2}
	dense	10^{-3}
Medium sand	loose	10^{-3}
	dense	10^{-4}
Fine sand	loose	10^{-4}
	dense	10^{-5}
Silty sand	-	10^{-6}
Sandy clay	-	10^{-7}

Table VI-5-80
Typical Values of Permeability, *k*, for Stone Materials

Gradation Diameter Range (mm)	*k* (m/s)
100 - 300	0.3
10 - 80	0.1

(3) Wave-induced internal setup. Wave action on a pervious slope causes a fluctuating internal water table (phreatic surface) and a setup as indicated in the figure in Table VI-5-81. The reason for the setup is that inflow dominates outflow due to larger surface area and longer duration. The setup increases if the shore side of the structure is impermeable, e.g., a rubble revetment built in front of a clay cliff.

(a) The setup can be estimated by a method (Barends 1988) presented in Table VI-5-81. The method is based on a linearization of the Forchheimer equation, where the permeability *k* for sands can be estimated from Table VI-5-79. For quarry-run materials, where linearization is less suitable, Equation VI-5-219 should be used. Order of magnitude values are given in Table VI-5-80.

(b) Besides storage of water due to internal setup of the phreatic level, also some storage due to compressibility of the soil rock skeleton and water-air mix can occur. However, for conventional structures such elastic storage will be insignificant compared to the phreatic setup storage.

(4) Pore pressure gradients in sloping rubble-mound structures.

(a) The horizontal wave-induced pressure gradient in the core of a rubble-mound breakwater can be estimated by the method of Burcharth, Liu, and Troch (1999) as presented in Table VI-5-82. The method is mainly based on pore pressure recordings from a prototype and large and small scale model tests.

Table VI-5-81
Wave Induced Set-up in Sloping Rubble Mound Structures (Barends 1988)

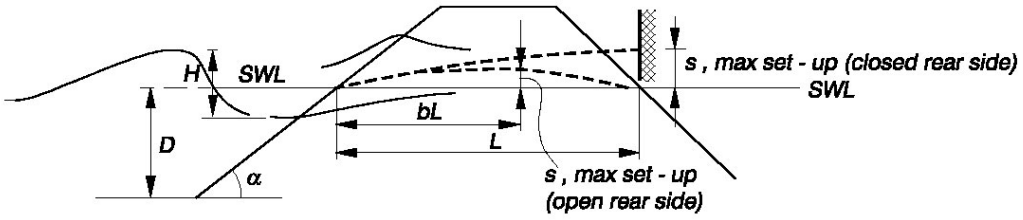

$$s/D = \sqrt{(1 + \xi\ F)} - 1 \qquad \text{for large waves, i.e. } H \leq D$$

$$s/H = \sqrt{(1 + \xi\ F)} - 1 \qquad \text{for small waves, i.e. } H \ll D$$

where $\xi = 0.1cH^2/(n\lambda\ D \tan\alpha)$
H = Height of incoming wave
n = Porosity of structure
c = Infiltration factor > 1. The magnitude is uncertain (Barends 1988) used $c \simeq 1.3$ to make calculations fit to conventional scale model test results
$\lambda = 0.5\sqrt{c\ k\ DT\ /n}$
α = Slope angle
k = Average permeability
T = Wave period
F = Function dependent on rear side conditions (open or closed) as given in diagram. The parameter b in the diagram defines position of maximum setup in the open case.

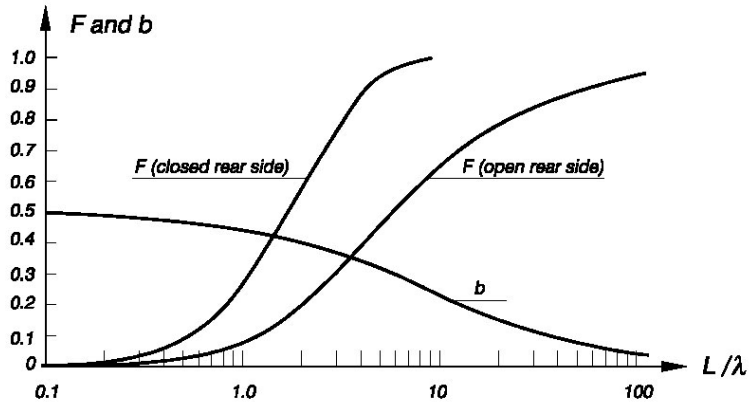

Table VI-5-82
Horizontal Wave Induced Pore Pressure Gradients in the Core of Rubble-Mound Breakwaters
(Burcharth, Liu, and Troch 1999)

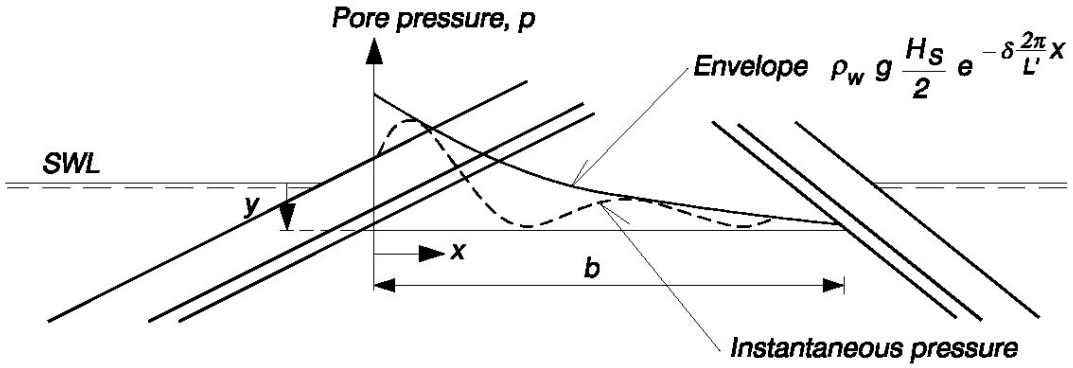

The horizontal pressure gradient

$$I_x = \frac{1}{\rho_w g}\frac{d_p}{dx}$$

$$= -\frac{\pi H_s}{L'} e^{-\delta \frac{2\pi}{L'} x} \left[\delta \cos\left(\frac{2\pi}{L'} x + \frac{2\pi}{T_p} t\right) + \sin\left(\frac{2\pi}{L'} x + \frac{2\pi}{t_p} t\right)\right] \qquad \text{(VI-5-222)}$$

where
- H_s Significant height of incoming waves
- δ $0.014 \frac{n^{0.5} L_p^2}{H_s b}$, damping coefficient
- n Porosity
- L_p Wavelength corresponding to peak of spectrum
- b Width of core at the level of interest
- L' $L_p/\sqrt{1.4}$, wave length in core valid for $h/L_p < 0.5$ (where h is the water depth)
- x Horizontal coordinate, $x = o$ at the seaward core boundary
- T_p Period corresponding to peak of the wave spectrum
- t Time
- ρ_w Mass density of water

(b) Equation VI-5-222 is valid only for rather permeable core materials (d_{50} ∃ 50 mm) and for normal breakwater cross sections with open rear side, i.e., no excess pressure. Additionally, Equation VI-5-222 holds for the region between swl and level $SWL + 2H_s$, i.e., 0 # y # $2H_s$. In each point within this region the larger pressure gradients will be of the same order of magnitude as the horizontal gradient.

e. Cyclic loading of soils. An essential part of the design of monolithic coastal structures is to ensure that the foundation soil or rubble base has sufficient capacity to carry both the static gravity loads and the wave-induced loads with an adequate safety margin and without excessive deformations. The bearing capacity under combined static and cyclic loads may be

significantly smaller than under purely static loads. The strength of soils exposed to cyclic loading is influenced not only by the stress level and the stress variations but also by the soil drainage capability. Pore pressure build-up and related loss of strength might take place in rather impervious soils where the time scale of drainage or consolidation is larger than the time scale of the load cycles. The following sections discuss evaluation of drainage conditions under cyclic loading, approximation of wave- induced irregular loading in terms of equivalent cyclic loading, and estimation of strength and deformation of soils exposed to cyclic loading.

(1) Time scale of drainage and consolidation.

(a) In saturated soil, the immediate effect of a load-induced stress increment will be a similar increase in the total stress σ and the pore pressure u (see Equation VI-5-202), i.e., the loading will be carried solely by the pore water. The soil skeleton will not carry the extra load until it has rearranged itself. This can happen only if some pore water is squeezed out, due to the very small compressibility of the water compared to that of the skeleton. In permeable materials such as stone blankets this happens immediately, while in clay it can be a very slow process. The related decrease in volume is termed consolidation.

(b) The degree of consolidation is defined as

$$U = \frac{s_t}{s_\infty} \tag{VI-5-223}$$

where s_t is the settlement (decrease in layer thickness) at time t, and s_4 is the final settlement reached when the soil skeleton is fully carrying the load. For coastal structures the dominating live load is caused by wave loading that varies in time. The time scale of consolidation has to be compared to the time scale of the loading to estimate U and thereby the effective stress in the soil.

(c) For the one-dimensional case Terzaghi showed that U in terms of average degree of consolidation is a function of the dimensionless time factor (Terzaghi and Peck 1944)

$$T_c = \frac{k\,M}{\gamma_w H^2} t = \frac{C_V}{H^2} t \tag{VI-5-224}$$

where

C_V = coefficient of consolidation (= kM/γ_w)

k = permeability (see Table VI-5-79)

M = oedometer modulus

γ_w = unit weight of water

t = time

H = drainage distance, which is equal to layer thickness for one side drainage, and equal to half the layer thickness for double side drainage.

(d) Full consolidation (i.e., U=100 percent) is in principle never reached. Consolidation of U=99 percent corresponds to T_c-. 2, whereas U=95 percent corresponds to T_c . 1.2. The necessary time for almost 100 percent consolidation is approximated in practice as

$$t_{U(100\%)} = \frac{2\gamma_w H^2}{k M} \tag{VI-5-225}$$

(e) By comparing t_U with the rise time of the wave-induced load, t_{rise} , it is possible to classify the wave loading and to estimate whether drained, partially drained or undrained conditions will be present. This criterion is given in Table VI-5-83.

Table VI-5-83
Classification of Loading and Soil Conditions

$\frac{t_{rise}}{t_{U(100\ percent)}}$	Type of Loading	Soil Condition
>> 1	Quasi-stationary	Completely drained
– 1	Nonstationary	Partially drained
<< 1	Nonstationary	Undrained

(f) Typical wave loadings from nonbreaking waves on coastal structures have periods in the range T . 2(t_{rise}) = 3-20 sec. Using the $t_{U(100\ percent)}$ values in Table VI-5-84, if follows from Table VI-5-83 that sand subsoil under virgin loading should generally be regarded as undrained, except for coarse sand which in some cases might be regarded as partially drained. Under subsequent wave loadings fine sand should still be regarded as undrained, whereas medium sand typically might be regarded as partially drained, and coarse sand would be considered drained.

(g) Very short duration impulsive loadings from waves breaking on structures have load rise times on the order of t_{rise} = 0.01 - 0.05 s (see Figure VI-5-101); and in this case all soils, including quarry-rock rubble foundations, have to be regarded as undrained.

(2) Wave load transmission to monolithic structure foundations.

(a) Wave loads transmitted to the foundation soil/rubble by monolithic structures, such as caissons and superstructure parapet walls, depend on the period of the wave load as well as the mass of the structure and the deformation characteristics of the soil/rubble.

Example 5-2. Calculation of $t_{U(100\ percent)}$ for quartz sand.

The elastic plastic component of M for initial loading corresponding to mean normal effective stress $\sigma N\#$ 300 kPa is found to be

$$M = \begin{cases} 15 \quad MPa & loose\ sand \\ 150 \quad MPa & dense\ sand \end{cases}$$

The elastic component of M found by unloading and reloading at σN= 100 kPa is found to be

$$M = \begin{cases} 80 \quad MPa & loose\ sand \\ 500 \quad MPa & dense\ sand \end{cases}$$

The drainage distance H is given as 5 m. Using these typical M-values together with the k-values given in Table VI-5-79, Equation VI-5-225 gives the consolidation times presented in Table VI-5-84.

Table VI-5-84
Example of Consolidation Times for Sand

		$t_{U(100\ percent)}$ (s)	
Material	Packing	Initial Deformation	Elastic Deformation
Coarse sand	loose	3	0.6
	dense	3	1
Medium sand	loose	30	6
	dense	30	10
Fine sand	loose	300	60
	dense	300	100

(b) The natural period $T_{n,s}$ of typical monolithic structures would normally be in the range 0.2 - 2 sec. If the period of the loading, T, is close to $T_{n,s}$ then dynamic amplification occurs resulting in increased loading of the foundation. Design wave loading can be separated into pulsating loads from nonbreaking waves and impulsive loads from waves breaking on the structure (see Figure VI-5-57). The pulsating loads have periods corresponding to the wave period, i.e., normally in the range 5-20 sec, which is much larger than $T_{n,s}$. Consequently, such low frequency loading is assumed to be transmitted to the foundation with unchanged frequency.

(c) Figure VI-5-92 illustrates how the resultant foundation load force of a wave-loaded caisson changes size, direction, and position during the wave cycle. The variation of the force resultant can be given by fully correlated time series of a tilting moment and a horizontal force. Figure VI-5-92 also illustrates the wave- induced stress variations in two soil elements (shown as hatched boxes).

(d) The initial shear stress τ_i prior to the installation of the structure is assumed to act under drained conditions, and the soil is assumed fully consolidated under this stress. $\Delta\tau_s$ is the change in the average shear stress due to the submerged weight of the structure. Depending on the type of soil, $\Delta\tau_s$ will initially act under undrained conditions, but as the soil consolidates, this

shear stress will also be applied under drained conditions. In the case of rubble-mound foundations the consolidation will be instantaneous. For sand foundations drainage will occur rapidly, as indicated by Table VI-5-84, and it is reasonable to assume that the soil will consolidate before the structure experiences design wave loading. In addition, it is unlikely that pore pressures will accumulate from one storm to the next. For clays, consolidation occurs much more slowly, varying from months for silty-sandy very stiff clays to many years for soft clays. The amount of settlement and the corresponding increase in effective stresses, is calculated by ordinary consolidation theory the same as for structures on dry land.

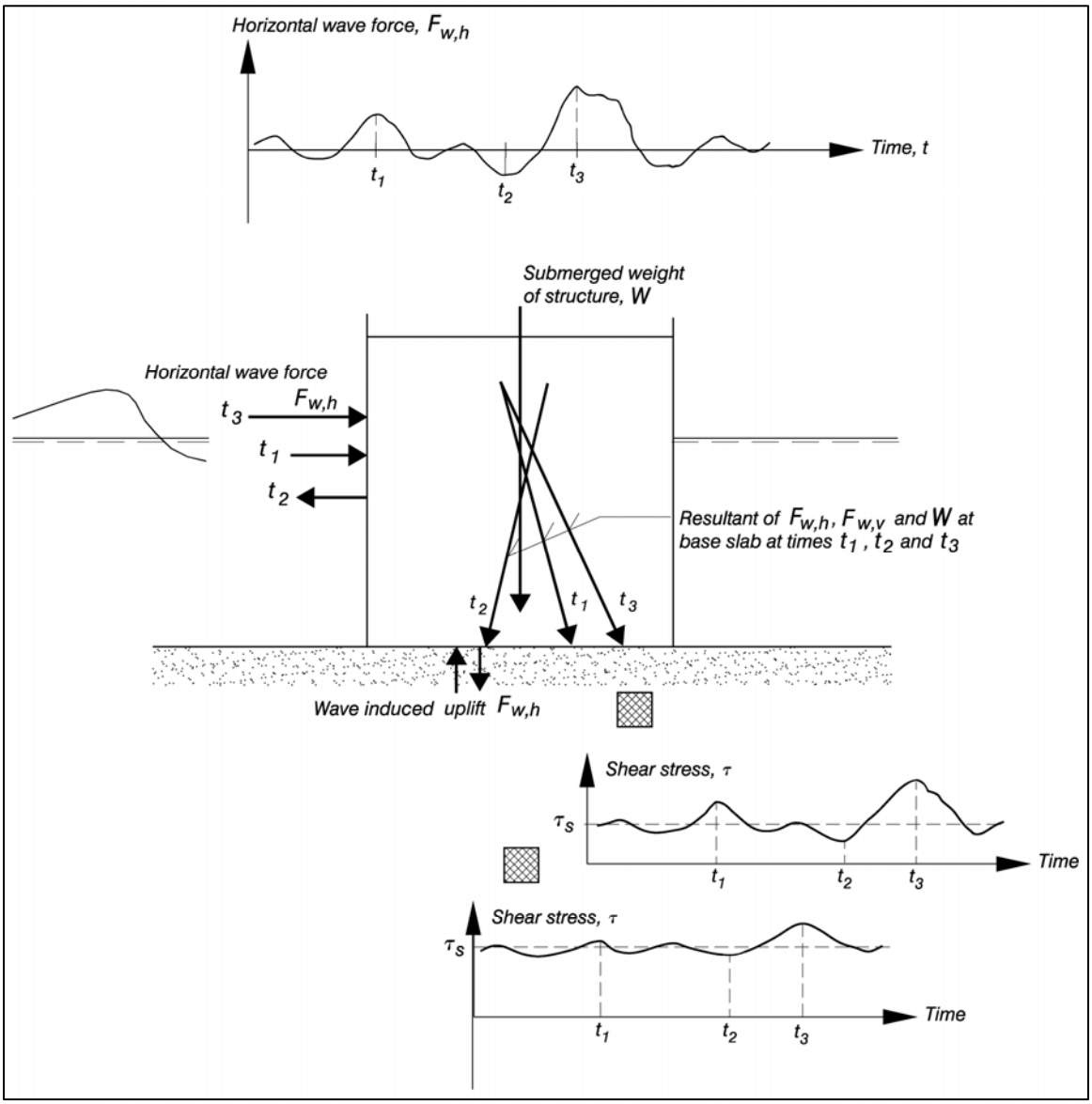

Figure VI-5-92. Illustration of wave induced forces on caisson foundation and related stress variations in the subsoil

(e) The effective static shear stress before wave loading is given by

$$\tau_s = \tau_i + \Delta\tau_s \qquad \text{(VI-5-226)}$$

(f) The initial shear stress, τ_i, is determined by the submerged weight of the soil as τ_i = 0.5 (1 - K_o) $p_o N$, where K_o is the coefficient of earth pressure at rest, and $p_o N$ is the vertical effective overburden pressure. $\Delta\tau_s$ can be estimated from Newmark's influence diagrams, assuming homogeneous, isotropic and elastic soil (e.g., see Hansbo 1994 and Lambe and Whitman 1979). This is usually a good approximation if the soil is not close to failure. A rough rule of thumb is a load spreading of 1 (horizontal) to 2 (vertical).

(g) The behavior of the soil when exposed to the cyclic loading can be studied in triaxial tests or direct simple shear (DSS) tests. The irregular wave loading F_W during the design storm might be approximated by equivalent cyclic wave loadings, causing cyclic shear stress variations with amplitude τ_{cy} as given in Figure VI-5-93. However, it is more correct if the real stress variations in the subsoil, as illustrated in Figure VI-5-92, are approximated by an equivalent cyclic variation. The stress τ_{cy} should be determined by finite element analysis.

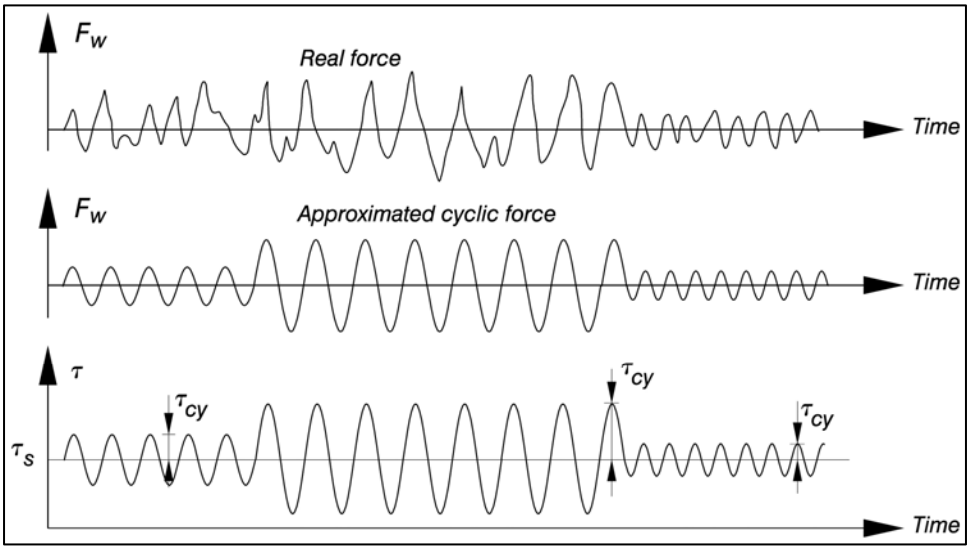

Figure VI-5-93. Illustration of approximate cyclic wave loading and related cyclic shear stress variation in a subsoil element during a storm sequence

(h) The criterion for determination of the equivalent cyclic stress in terms of τ_{cy} and number of cycles $N_{eqv,}$ is that the approximation gives the same effect as the actual load history. Procedures to determine N_{eqv} were presented by Andersen (1981, 1983). For sands, N_{eqv} may be computed by accumulating the permanent pore pressure generated during the cyclic load history, taking into account that drainage is likely to occur during the design storm. Calculation of the pore pressure accumulation can be performed using pore pressure diagrams established from cyclic stress-controlled laboratory tests. The dissipation of the permanent pore pressure due to both drainage towards free boundaries and grain redistribution can be determined by finite element analysis or, for idealized situations, by closed-form solutions. In principle, the cyclic

shear strength of clays could also be computed by accumulating the permanent pore pressure. However, measurements in clays are more difficult to acquire than in sands. In addition, short-term drainage will not take place in clays; consequently, it is preferable to use the shear strain as a measure of the cyclic strength for clays. Moreover, for situations where the cyclic shear moduli under undrained conditions are of primary interest, the shear strain will also be a more direct parameter than the pore pressure.

(i) The stress conditions in the soil beneath structures subjected to combinations of static and cyclic loads are very complex even though the irregular loadings are approximated by equivalent cyclic loadings. Advanced finite element numerical modeling is the obvious tool for calculation of stress and strain development provided the model is carefully verified against documented test cases. As an alternative, a practical approximate method is presented by Andersen (1991) and Andersen and Høeg (1991). This method is based on the stress path philosophy in which laboratory tests are performed to simulate the stress conditions in few typical soil elements along potential failure surfaces as illustrated in Figure VI-5-94. The elements follow various stress paths which might be approximated to triaxial or direct simple shear (DSS) types of loading corresponding to various conditions of average stresses, τ_s and cyclic shear stresses, τ_{cy}. Additionally, the number of cycles to failure, N_f, and the shear strains are determined in the tests.

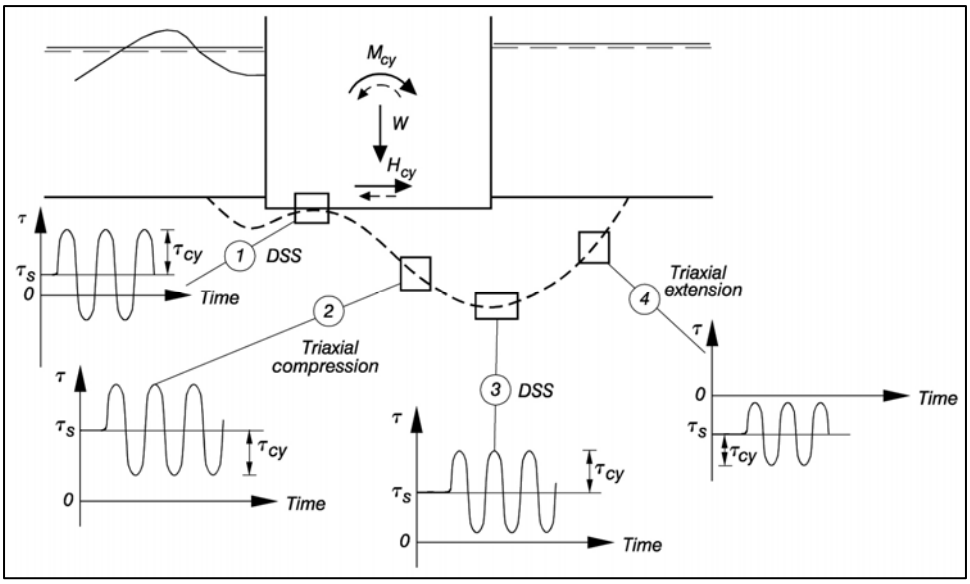

Figure VI-5-94. Simplified stress conditions for some elements along a potential failure surface (Andersen 1991)

(3) Noncohesive soil exposed to wave-induced cyclic loadings.

(a) For noncohesive soils, cyclic stress variations can either lead to strengthening of the soil or to soil weakening and eventual liquefaction due to pore pressure build-up. The outcome depends on soil permeability, average shear stress τ_s, wave-induced shear stress variations, and soil compaction. Pore pressure build-up does not happen in coarse materials like gravel and

rubble foundation materials because of almost instant drainage. Consequently, only sand-sized noncohesive soils will be considered in the following discussion.

(b) Cyclic loading of soil specimens can be performed in undrained triaxial tests using a cell height-to-width ratio of one and lubricated cap and base, thus assuring uniform stress-strain conditions in the sample (Rowe and Barden 1964; Bishop and Green 1965; and Jacobsen 1967). From such tests the phenomena depicted in Figure VI-5-95 can be observed.

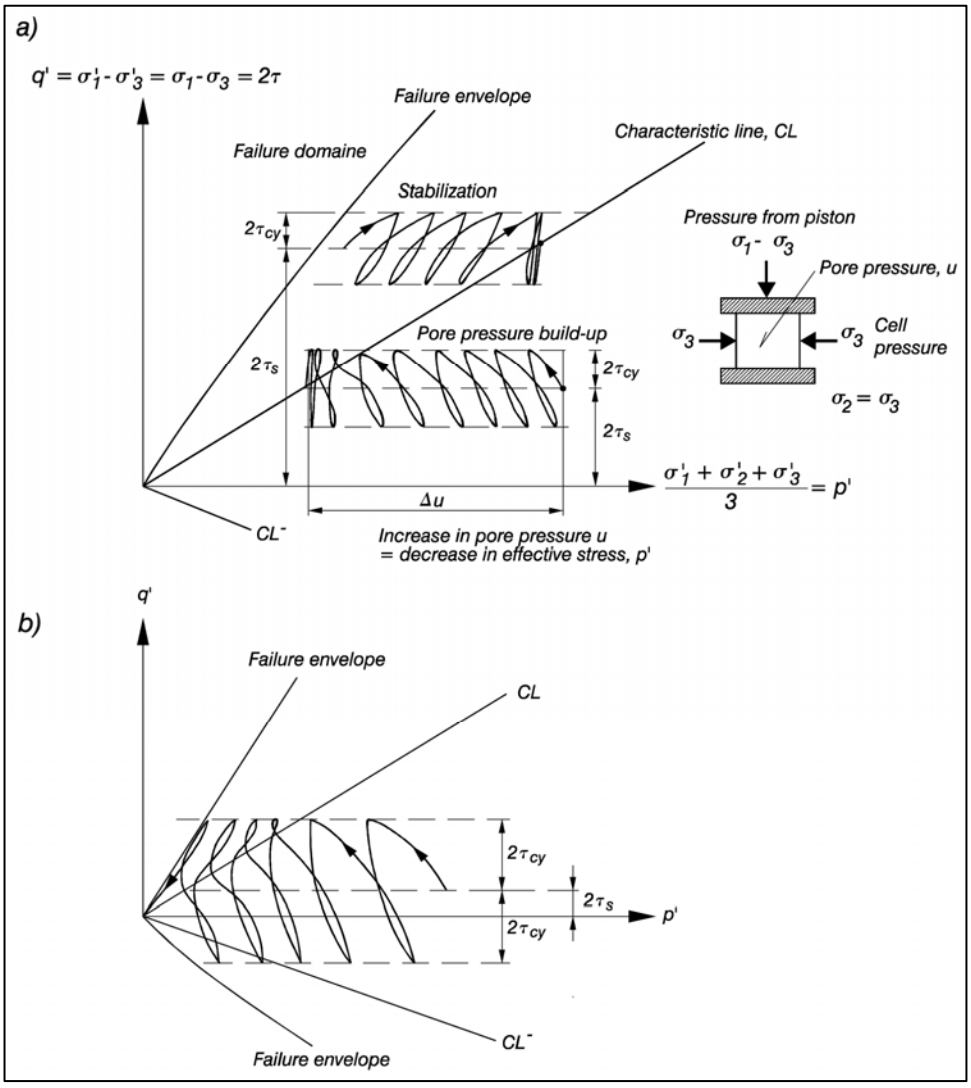

Figure VI-5-95. Illustration of (a) stabilization and pore pressure build-up, and (b) liquefaction undrained triaxial test on sand

(c) The shear stress τ is given by

$$\tau = \frac{\sqrt{3}}{2}\sqrt{J_2} \tag{VI-5-227}$$

where

$$J_2 = \frac{1}{6}\left[(\sigma_{1'} - \sigma_{2'})^2 + (\sigma_{2'} - \sigma_{3'})^2 + (\sigma_{1'} - \sigma_{3'})^2 \right] \quad \text{(VI-5-228)}$$

and $\sigma_1 N\exists$ $\sigma_2 N\exists$ $\sigma_3 N$ are the effective stresses in three orthogonal directions.

(d) The average effective stress level is given by

$$p' = \frac{\sigma_{1'} + \sigma_{2'} + \sigma_{3'}}{3} = \frac{\sigma_1 + \sigma_2 + \sigma_3}{3} - u \quad \text{(VI-5-229)}$$

where σ is total stress and u is the pore pressure, as in Equation VI-5-202. In undrained triaxial tests with cell pressure $\sigma_2 N = \sigma_3 N$ the piston generated stress (deviator stress) is

$$q' = \sigma_{1'} - \sigma_{3'} = \sigma_1 - \sigma_3 = 2\,\tau \quad \text{(VI-5-230)}$$

(e) In the $qN - pN$ diagram of Figure VI-5-95 the characteristic line (CL) separates stress domains where deviator stress fluctuations cause dilation and contraction. The CL signifies a stable state where further cyclic loadings will not lead to hardening or softening of the soil. Figure VI-95a shows that if the average stress τ_s is situated above the CL, the cyclic test will generate negative pore pressures leading to stabilization (hardening) of the soil.

(f) If τ_s is situated below the CL, cyclic tests will generate positive pore pressures and decreasing effective stress (softening). With small τ_s and large stress fluctuations τ_{cy}, liquefaction will occur as shown in Figure VI-5-95b if the stress path touches the CLΓ line.

The equations for the CL and CLΓ lines are

$$\text{CL:}\quad q' = \frac{6 \sin \varphi_{c'rit}}{3 - \sin \varphi_{c'rit}}\, p' \quad \text{(VI-5-231)}$$

$$\text{CL}^-\text{:}\quad q' = \frac{-6 \sin \varphi_{c'rit}}{3 + \sin \varphi_{c'rit}}\, p' \quad \text{(VI-5-232)}$$

where νN_{crit} is the critical angle of friction, as given in Table VI-5-75. νN_{crit} is independent of the relative density or porosity and is very close to 30 deg for sand in the range d_{50} = 0.14 - 0.4 mm (Ibsen and Lade 1998). The number of cycles to failure can be determined from a series of triaxial or DSS laboratory tests conducted with various combinations of τ_s and $\tau_{cy.}$

(g) The previous discussion of the effect of cyclic loading is related to undrained conditions in laboratory tests. The assumption of undrained conditions is either true or on the safe side with respect to soil strength properties. However, sands in nature may experience partial drainage during a storm. The amount of drainage depends upon the permeability of the sand and the drainage boundary conditions. The drainage can be significant and should be

considered in design because experience from laboratory tests has shown that the soil structure and the resistance to further pore pressure generation may be significantly altered when the excess pore pressure due to cyclic loading dissipates (Bjerrum 1973; Andersen et al. 1976; Smits, Anderson, and Gudehus 1978). Cyclic loading with subsequent pore pressure dissipation is referred to as precycling.

(h) Moderate precycling in sands may lead to significant reduction in pore pressure generation under further cyclic loading, even in dense sands. Precycling may occur during the first part of the design storm. The beneficial effect of precycling might be taken into account in cyclic testing of sand in the laboratory by applying some precycling prior to the main cycling. As previously mentioned, the shear strength that the soil can mobilize to resist the maximum load (wave) depends on the effective stresses in the soil, and thus on the excess pore pressure that is generated during the storm. The shear strength also depends on whether the soil is contractive or dilative. If the soil is dilative and saturated, a negative pore pressure is generated when the soil is sheared under undrained conditions. This will give higher shear strength than achieved for drained conditions. However, for sands one should be careful about relying fully on higher shear strength caused by negative pore pressure due to uncertainty about the amount of drainage that might take place. The amount of drainage during a cycle and the residual pore pressure at the end of a storm might be estimated from calculations with finite element programs. Examples of design diagrams based on such calculations are pressented in de Groot et al. (1996). A method valid for the estimation of the changes in pN in sand as function of the number of cycles was given in Ibsen (1999).

(4) Cohesive soil exposed to wave-induced cyclic loadings.

(a) The shear strength, c_u, of clay normally refers to undrained strain controlled tests of approximately 1-3 hr duration to reach failure. Clays will be practically undrained during a storm, and possibly also over a seasonal period including several storms. Because c_u for a specific clay in undrained conditions depends solely on the initial effective stress conditions before the loading, there will be only insignificant changes in c_u as long as drainage of the clay has not taken place.

(b) The stress-strain behavior of a specific clay determined from samples is affected by the test method, OCR, τ_s, τ_{cy}, N and the stress rate (load frequency). During the cyclic loading the pressure build-up causes a reduction of the effective stresses as illustrated in Figure VI-5-96. Figures VI-5-96a and VI-5-96b show development of failure by cyclic loading. Figure VI-5-96c shows stabilization of effective stress after 25 cycles.

(c) After a certain number of cycles, the failure envelope will be reached and large shear strains developed. The cyclic shear strength can be defined as

$$\tau_{f,cy} = (\tau_s + \tau_{cy}) \tag{VI-5-233}$$

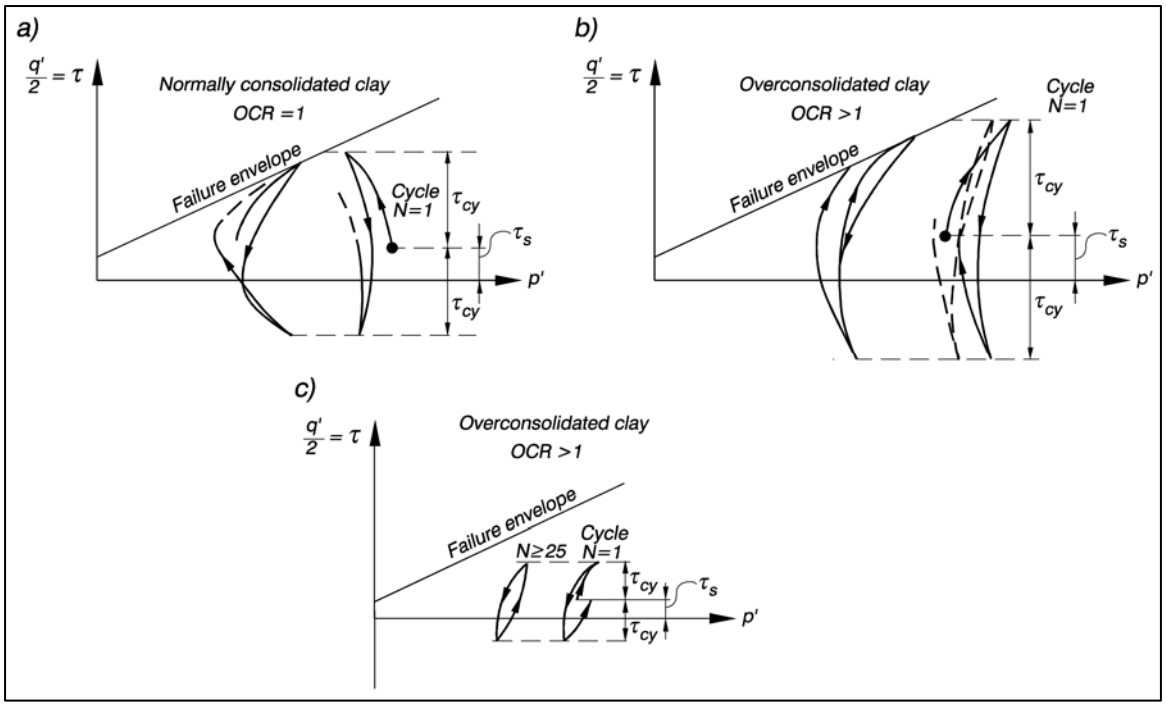

Figure VI-5-96. Illustration of effective stress paths for clay samples in undrained triaxial tests

(d) It is very difficult to determine accurately the change in pore pressure, and therefore, also the change in effective stresses in triaxial and DSS tests. Consequently, to determine the relationship between the shear strength c_u and τ_s, τ_{cy}, and number of cycles, N, it is better to examine the load increase to failure in normal static tests for samples already exposed to various ranges of cyclic loadings. From the load increase the actual c_u-value after a specific exposure in terms of τ_s, τ_{cy}, and N can then be estimated. Examples and information on such post-cyclic static shear strength are presented in Andersen (1988). For Norwegian Drammen clay, being a plastic clay with plasticity index I_p = 27 percent, it was found that cyclic loading causing large cyclic shear strains also caused significant reduction in the static shear strength. The reduction increases with the number of cycles. It was also found that the reduction is generally less than 25 percent as long as the cyclic shear strains are less than 3 percent and the number of cycles less than 1,000. This holds for *OCR*-values of 1, 4, and 10. Figure VI-5-97 shows an example of stress-strain behavior of Drammen clay. This example shows the importance of modeling the type of loading correctly when trying to determine the stress-strain behavior or the shear modulus in situ from laboratory tests.

(e) The number of cycles to failure, N_f, can be determined from a series of triaxial or DSS laboratory tests applying various combinations of τ_s and τ_{cy}. Due to the very large shear strain at failure, it is often appropriate to define failure as a lower strain level, the value of which must depend on the type and function of the structure. The test results can conveniently be plotted in diagrams as shown in Figure VI-5-98, where failure is taken when either the cyclic strain, γ_{cy}, or the average strain, γ_s, reaches 15 percent.

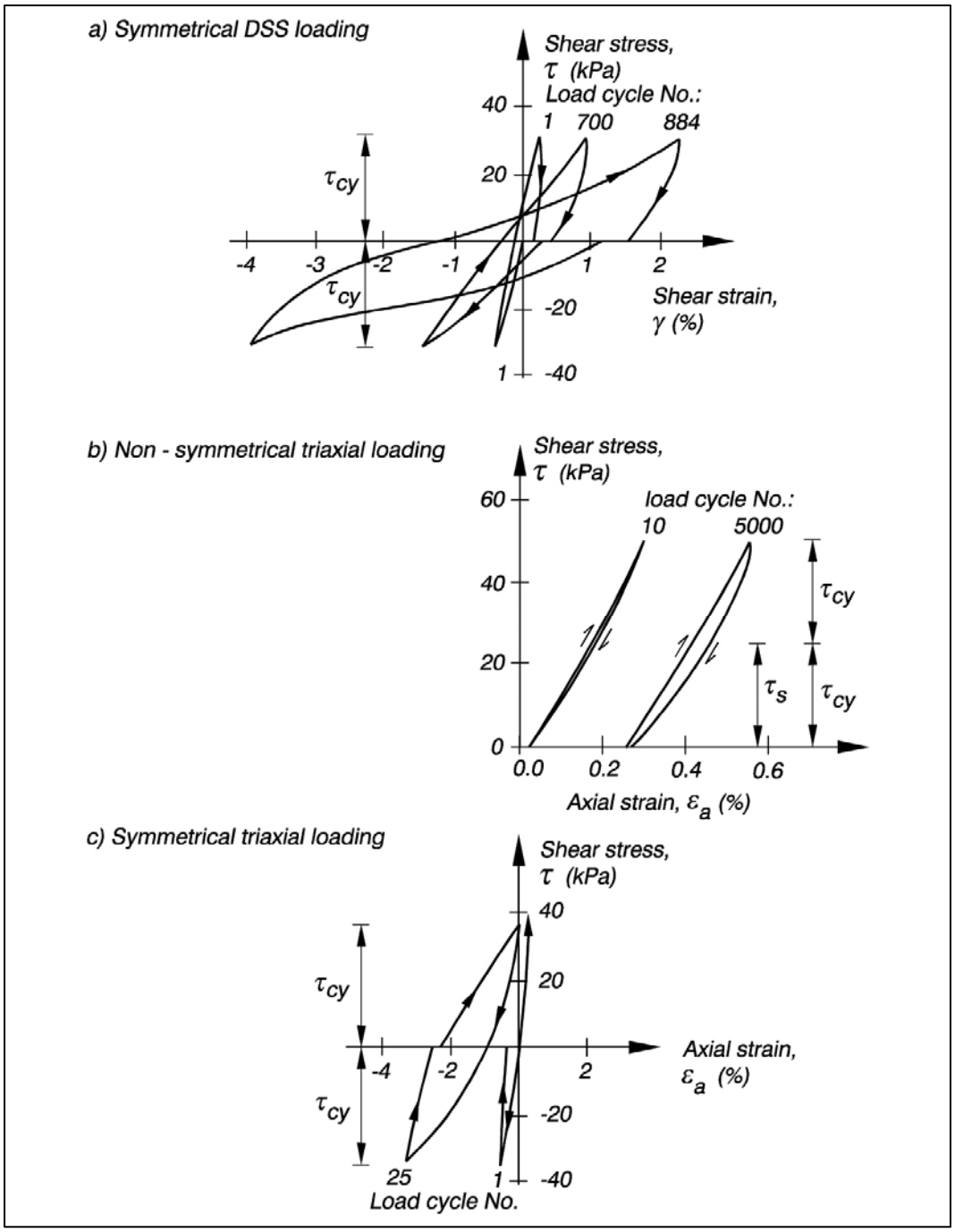

Figure VI-5-97. Stress strain behavior of Drammen clay (I_p = 27 percent) under various cyclic loading conditions corresponding to *OCR* = 4 (from Norwegian Geotechnical Institute 1992)

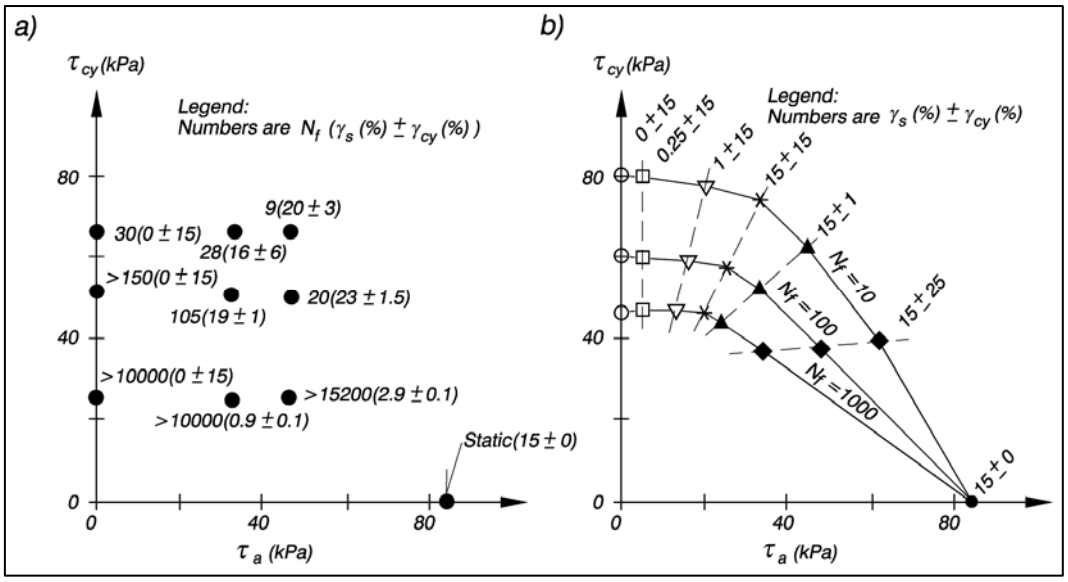

Figure VI-5-98. Result of cyclic tests on normally consolidated Drammen clay, with *OCR* = 1 and I_p = 27 percent (from Norwegian Geotechnical Institue 1992)

(f) In Figure VI-5-98 N_f is number of cycles to failure defined as either the cyclic strain γ_{cy} or the average strain γ_s reaching 15 percent. Figure VI-5-98a shows individual test results, and Figure VI-5-98b shows interpolated curves based on the individual tests. A diagram like Figure VI-5-98b can be transformed to normalized form using the vertical effective stress σ_{vc}N at the end of the cycling (consolidation), and the undrained static shear strength, $\sigma_{u,}$ measured in strain-controlled tests. Figure VI-5-99 shows an example based on both triaxial and DSS tests.

(g) In Figure VI-5-99 σ_u^E, σ_u^C, and σ_u^{DSS} are undrained static shear strength in triaxial compression and extension tests and in DSS tests, respectively.

(h) By replotting the data from Figure VI-5-99 it is possible to show the relationship between the cyclic shear strength, $\tau_{f,cy}$, as defined by Equation VI-5-233, and N_f, $\sigma_{vc}N$ and the undrained static shear strengths. An example is shown in Figure VI-5-100.

(i) A simple diagram for approximate correction of the static failure load to take into account the effect of cyclic loading in static calculations is presented in de Groot et al. (1996) for Drammen clay (*OCR* = 1, = 4 and = 40).

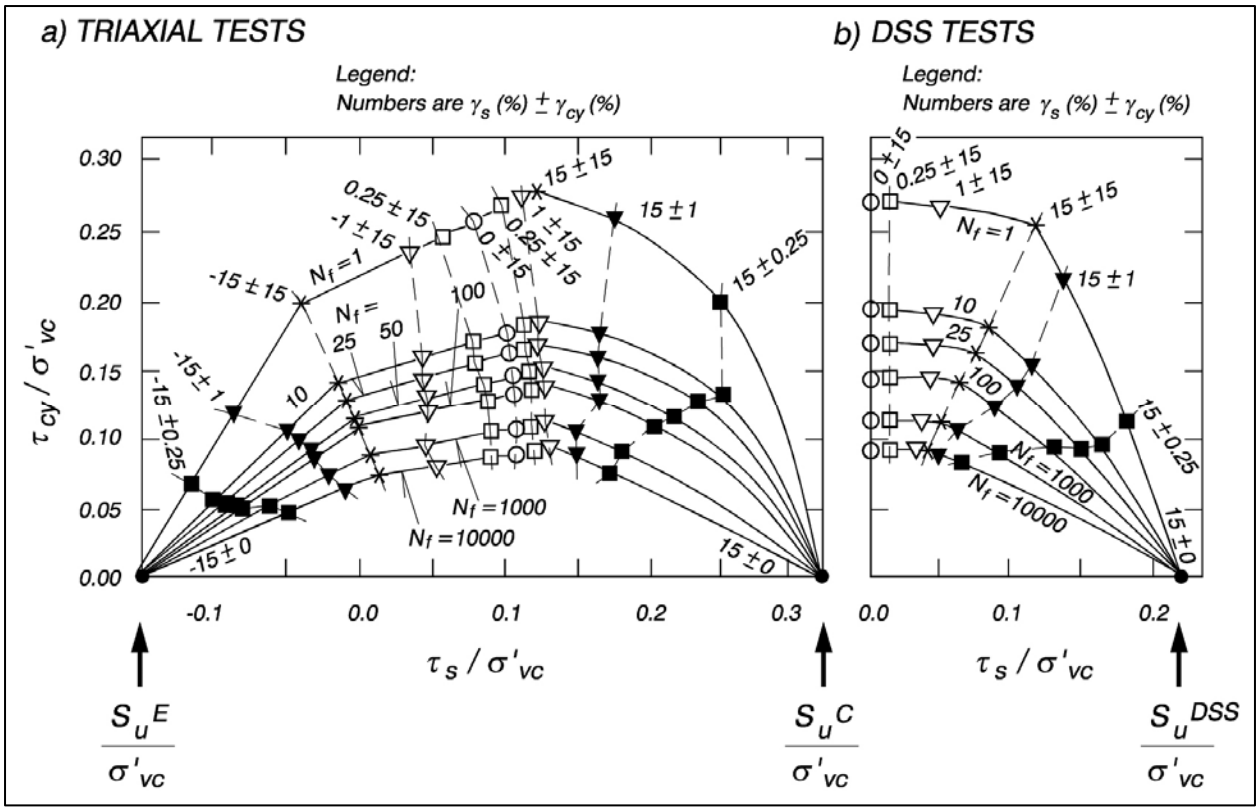

Figure VI-5-99. Example of normalized diagrams for cyclic loading of Drammen clay with *OCR* = 1, in triaxial tests (a), and DSS tests (b) (from Norwegien Geotechnical Institute 1992)

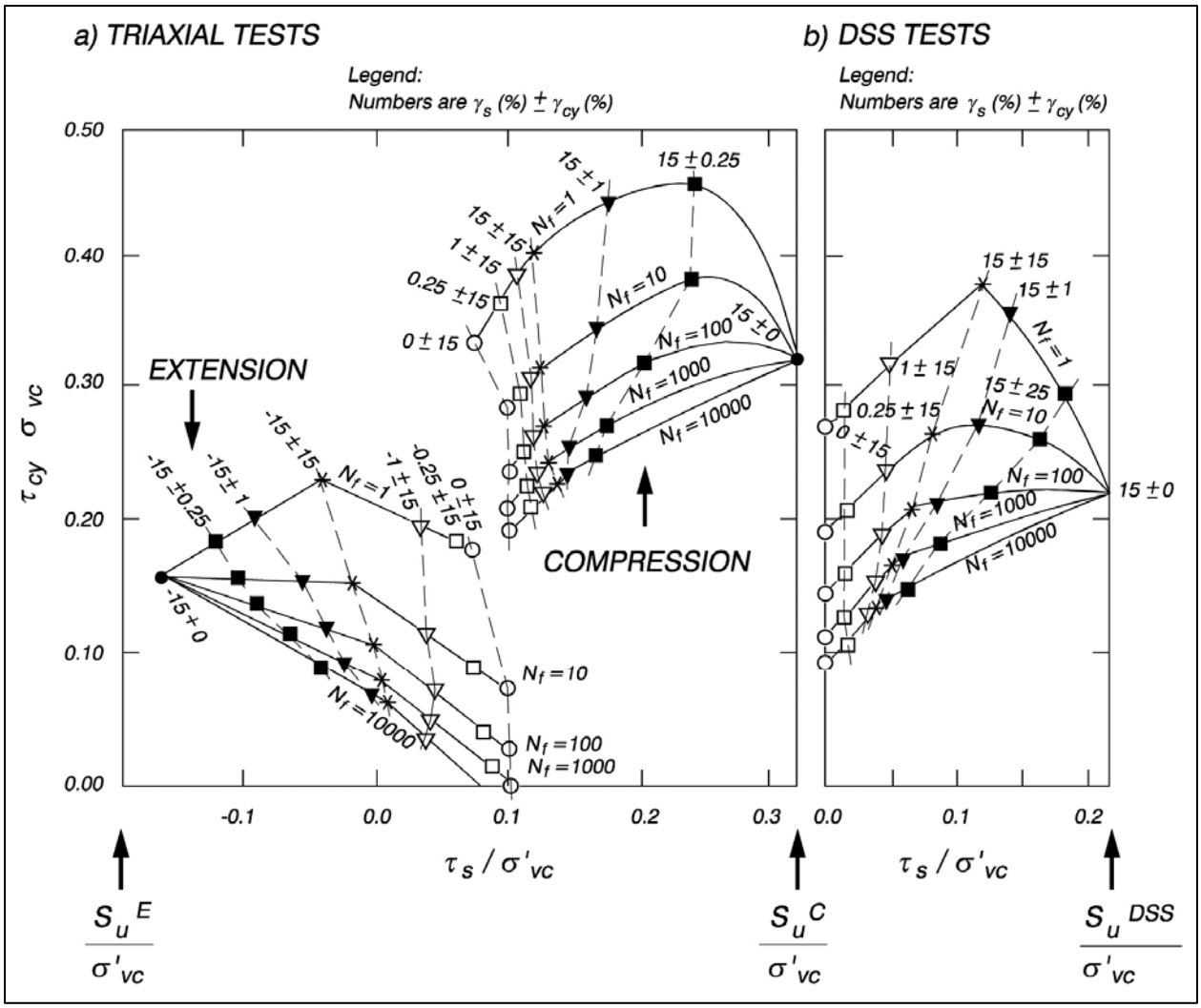

Figure VI-5-100. Cyclic shear strength of Drammen clay with *OCR* = 1
(from Norwegian Geotechnical Institute 1992)

f. Dynamic loading of soils under monolithic structures.

(1) Dynamic loading of soils and rubble rock foundations occurs when wave wall superstructures and vertical wall breakwaters are exposed to impulsive loads from waves breaking at the structures, as shown in Figure VI-5-56. The impulsive load magnitude can be very large, but the loads have very short durations with load periods in the range 0.1-1.0 sec for the peaked part of the loading. Because the natural period of some structures often are within (or close to) the same period range, dynamic amplification of the wave load and corresponding structure movements might occur.

(2) When moderately loaded, the soil and rubble rock will react approximately as an elastic material; whereas under severe loading, permanent deformations will occur, corresponding to plastic behavior.

(3) Determination of impulsive wave forces caused by waves breaking directly on vertical wall structures is extremely uncertain. The same can be said about the related loading on the foundation. In addition, breaking wave loads can be very large; therefore, direct wave breaking on the structure should be avoided. If necessary, the geometry or position of the structure should be changed to avoid large impulsive wave forces. In cases where the wave load is known, it is possible to obtain some estimates of the effect on the foundation as explained in the following paragraphs.

(4) The actual time of the wave loading is an important factor in the dynamic amplification. Model studies by Bagnold (1939) and Oumeraci (1991) showed that the load history of forces from waves breaking on vertical walls can be approximated with a church-roof like time-history as sketched in Figure VI-5-101.

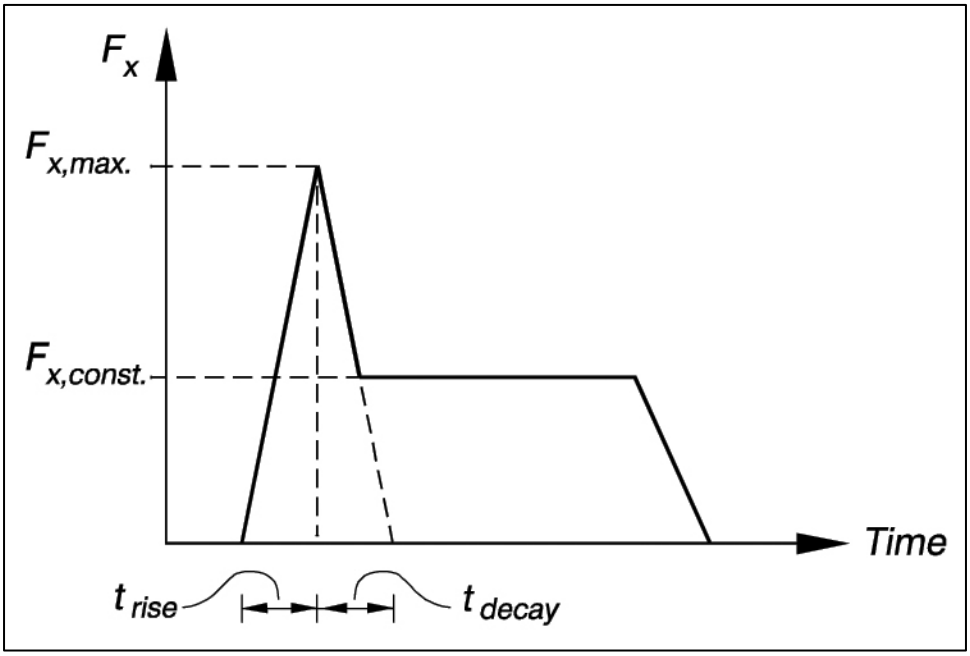

Figure VI-5-101. Approximation to horizontal wave load history for waves breaking directly on vertical walls

(5) For the elastic case it is possible to get a crude estimate on the dynamic amplification by modeling the soil-structure system as a rigid body resting on a linear elastic half-space, idealized by a lumped mass system where the geodynamic response is represented by a spring-dashpot model. A two-degrees-of-freedom system allowing only translatory motion, x, in the horizontal direction and rotation, ν, about the center of gravity, C_g, is commonly considered (see Figure VI-5-102).

(6) The effect of any impulsive loading can be found by solving the equations of motion for the complete translatory and rotational motion, provided the stiffness and damping coefficients are known. However, for practical design purposes a simple static approach can be accomplished by assuming an equivalent static load which will induce the same motions of the structure as those found from a dynamic calculation. The following definitions of dynamic load

factors, Ω, show how the equivalent static force and motions are related to the dynamic force and motions.

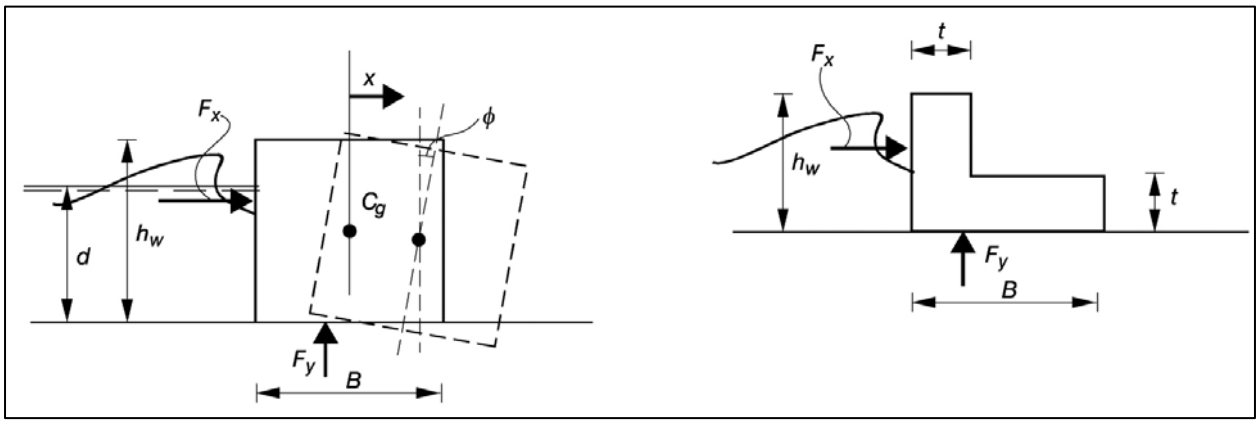

Figure VI-5-102. Definition of translatory and rotational motions and dimensions for caisson structure and parapet wave wall exposed to dynamic loading

$$\Omega_x = \frac{\max\ dynamic\ translation}{\max\ static\ translation} = \frac{\max\{x\}}{F_{x,\max}/kx} = \frac{F_{x,equiv}}{F_{x,\max}}$$

(VI-5-234)

$$\Omega_\varphi = \frac{\max\ dynamic\ rotation}{\max\ static\ rotation} = \frac{\max\{\varphi\}}{M_{\max}/k_\varphi} = \frac{M_{equiv}}{M_{\max}}$$

where $F_{x,\max}$ is defined in Figure VI-5-101, k_x and k_ν are stiffness coefficients, and $M_{\max}$ is the maximum wave-load-induced moment around the center of gravity. The moment also includes wave-generated uplift forces, F_y. If Ω_x, Ω_ν, k_x, k_ν, and the maximum wave loading F_x and M_ν are known, then the maximum motions and related equivalent static wave loadings can be determined. The vertical motion is of little interest for monolithic structures under predominantly horizontal wave loading.

(7) Pedersen (1996, 1997) presented diagrams of Ω_x and Ω_ν for caissons and wave wall superstructures with square footings (i.e., B x B shown in Figure VI-5-102) exposed to the type of loading shown in Figure VI-5-101. The soil was modeled as a linear elastic half-space. Pedersen used results of Lysmer and Richardt (1966) and Hall (1967) to obtain expressions for optimized constant values of stiffness and damping coefficients. An example of Pedersen's diagrams for caisson structures is shown in Figure VI-5-103 for load history $t_{rise}/t_{decay} = 1$ under triangular loading. T_{nd} is the coupled, damped natural period of the caisson. Pedersen showed that the constant part of the wave loading following the peak has little influence on the response if $F_{x,const} \# 0.5\ F_{x,max}$.

(8) Due to the many uncertainties and simplifying assumptions, diagrams such as shown in Figure VI-5-103 should be used only for judging the possibility of dynamic amplification. If dynamic amplification factors are found to be close to or greater than 1, then a detailed dynamic analysis should be performed or the structure design should be changed.

g. Slip surface and zone failures.

(1) Slip surface and zone failure calculations are based on limit state calculations related to assumed or approximate rupture figures. Two different solutions are applied:

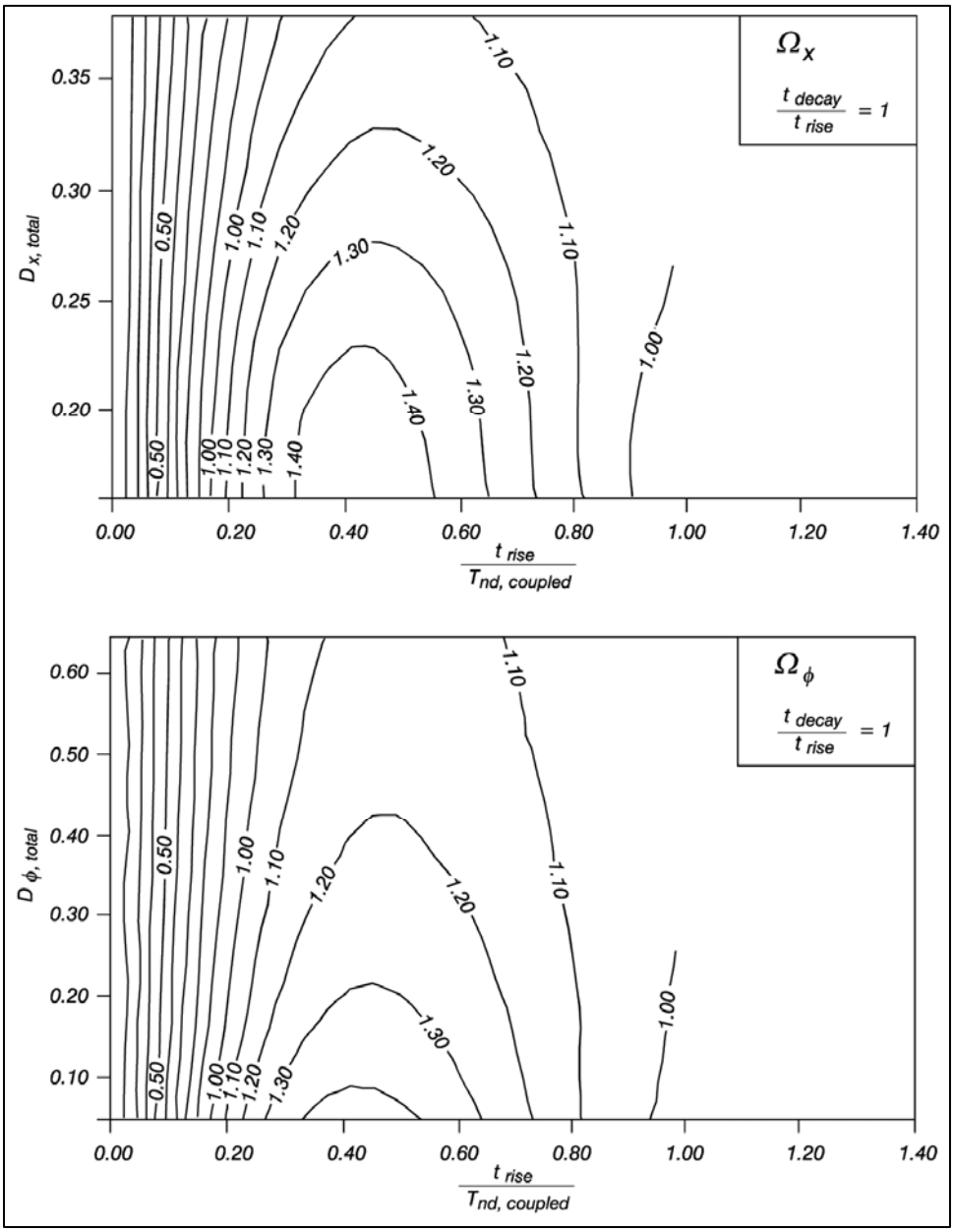

Figure VI-5-103. Amplification factors for translatory and rotational motions for caisson structure with square footing and triangular load shape (Pedersen 1997)

(a) Statically admissible solutions are defined by stress distributions that satisfy equilibrium for stresses and loads for all involved soil elements. In homogeneous soils with sufficiently simple boundary conditions, e.g., straight and uniformly loaded boundaries, these

types of approximate solutions may represent a simple and efficient solution technique. Many standard formulas and calculation methods in soil mechanics for bearing capacity and earth pressure problems are derived from statically admissible solutions. However, even slight modifications of the boundary conditions, and especially the introduction of inhomogeneous soil properties, may make a realistic solution of this type extremely complicated. Consequently, statically admissible solutions do not represent a generally applicable solution method, even if a limited number of standard cases are known and are widely used.

(b) Kinematically admissible solutions are defined by displacement fields that satisfy the boundary conditions for displacements as well as the associated flow rule (normality condition) within the theory of plasticity. Satisfying the flow rule makes the use of work equations possible. The flow rule requires the angle of friction ν and the angle of dilation ψ to be equal, although this is not true for frictional materials. To overcome this problem Hansen (1979) proposed to set $\psi = \nu = \nu_d$ where the modified angle of friction ν_d is defined by

$$\tan \varphi_d = \frac{\sin \varphi \cos \psi}{1 - \sin \varphi \sin \psi} \tag{VI-5-235}$$

(c) When applying ν_d it follows that both statically and kinematically admissible solutions will always be on the safe side. Otherwise statically admissible solutions will either be correct or on the safe side, whereas kinematically admissible solutions, according to the upper bound theorem, will either be correct or on the unsafe side.

(2) Experience indicates that solutions based on realistic rupture figures are in both cases generally close to the true situaton.

(3) For a given structure it is necessary to identify the most critical rupture figure, defined as the one which provides the lowest bearing capacity. For example, if work equations are used, then the rupture figure corresponding to the lowest ratio of work of stabilizing forces W_s to work of destabilizing forces W_d is the critical rupture figure. In any case in order to prevent failure and to have some safety the condition

$$\min\left(\frac{W_s}{W_d}\right) \geq 1 \tag{VI-5-236}$$

must be fulfilled. If not, the structure design has to be modified or the soil strength improved (by preloading, compaction, or installation of drains), or the soil must be replaced.

(4) For a number of standard cases the rather complicated equations related to statically and kinematically admissible solutions have been simplified to practical force equations, formulae, and diagrams (e.g., the determination of foundation bearing capacity and soil pressures on walls). The formulae and diagrams are based not only on the basis of theoretical solutions but also on model tests and field experience. This compensates for non-exact kinematically admissible solutions.

(a) Stability of slopes.

- Slope instability failure modes for coastal structures are schematized by the various slip failure surfaces shown in the figures in Part VI-2-4*b*. Slope instability is a conventional soil mechanics problem which is dealt with in almost every handbook on geotechniques and foundation engineering, e.g., Terzaghi and Peck (1944), Taylor (1958), Lambe and Whitman (1979), Anderson and Richards (1985), and Hansbo (1994). However, the conventional treatment of the subject does not pay attention to wave loadings which characterize the special conditions for coastal structures.

- Direct wave action on a permeable slope increases the antistabilizing forces because the runup presents an extra load and creates fluctuating pore pressures and related antistabilizing hydraulic gradients in the structure. In addition, both waves and tides create pore pressure gradients in porous seabeds.

- Slope instability rarely occurs in conventionally designed rubble-mound structures. Stability problems can occur if the structure is placed on weak soils or on soil with weak strata because the slip failure plane passes through weaker materials. Very large breakwaters with steep slopes might be suspectable to stability problems within the structure itself especially if exposed to earthquake loading. Another type of failure related to rubble-mound slopes is sliding of one layer over another layer which is caused by reduced shear strength at the interface between two layers of narrow graded materials of different particle size and shape, e.g., armor layer and filter layer. If geotextiles are used, the interface shear strength is significantly reduced.

- The two load categories pertinent to coastal structure slope stability are listed below:

Long-term stability	Permanent loads, i.e., weight of structure and soils, permanent surface loads, and average loads from groundwater.
Short-term stability	Permanent loads as well as variable loads from waves (direct wave loading and seepage forces), seismic activity and vehicles. Ice loads are usually not dangerous to slope stability.

- For each of the load cases it is important to apply the relevant soil strength parameters. This includes consideration of soil strength degradation related to variable loadings, as discussed in Part VI-5-5*e* of this chapter.

- Variable loads from waves and the related seepage forces should be considered for the two instantaneous load situations depicted in Figure VI-5-104. The pore pressures and the related hydraulic pressure gradient and seepage forces in a homogeneous, isotropic breakwater structure can be estimated from flow nets if the Darcy equation (Equation VI-5-220) is taken as valid, or calculated using advanced numerical models. In Figure VI-5-104 the seabed is assumed to be impermeable compared to the breakwater. This is usually a good approximation for rubble-mound structures built of quarry materials.

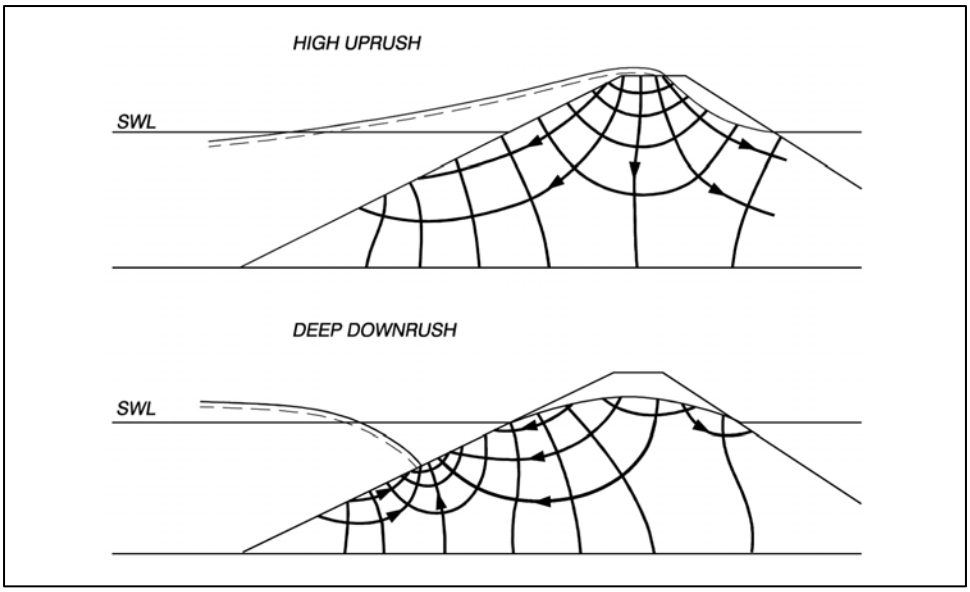

Figure VI-5-104. Illustration of flow nets in a homogeneous isotropic breakwater for two instantaneous wave load situations

- The pore pressure variation in a homogeneous seabed due to water level changes caused by tides and waves can be estimated by the method of de Rouck (1991) as shown in Table VI-5-85. The pore pressure in deeper strata corresponds to the hydrostatic pressure at mean water level. However, some seepage forces are created due to the reduction in pressure at the seabed surface beneath a wave trough during low tide. Tidal variations only cause vertical seepage forces due to the long tidal wavelength. However, short waves also cause horizontal seepage forces that are generally smaller than the vertical seepage forces. Figure VI-5-105 illustrates the flow net related to wave action.

- Equation VI-5-238 in Table VI-5-85 assumes that the compressibility of seawater is negligible compared to that of the grain skeleton, which is almost always the case. The pore pressure variations in the seabed underneath a rubble-mound structure can be determined from Equation VI-5-238 by estimating u_0 along the seabed surface using flow nets similar to those illustrated in Figure VI-5-104.

- It follows from Equation VI-5-238 that the attenuation of u with depth z decreases with more permeable and stiffer soil and with longer wave periods. Pore pressure variations due to tides (T = 12h 25 min) are only very slightly attenuated in sand, but there is a significant attenuation in clay. Pore pressure variations due to wind generated waves (T < 20 s) are strongly attenuated, even in sand.

- Seismic loads are usually taken into account by adding the seismic related horizontal inertia forces to the forces acting on the soil along with additional hydrodynamic forces which might result from the displacement of the soil body. Possible seabed scour should be taken into account when defining the bottom topography.

Table VI-5-85
Wave and Tide Induced Pore Pressures in Permeable Seabeds (de Rouck 1991)

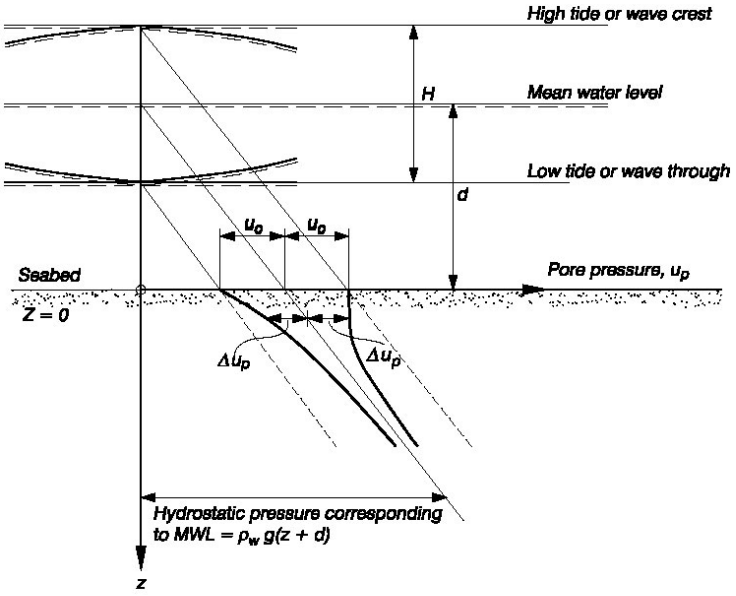

The pore pressure in depth z is given by

$$u_p = \rho_w g(z+d) + \Delta u_p \qquad \text{(VI−5−237)}$$

$$\Delta u_p = u_0 e^{-Az} \cos\left(\frac{2\pi X}{L} + \frac{2\pi t}{T} - Az\right) \qquad \text{(VI−5−238)}$$

where

Δu_p	Pore pressure deviation caused by wave or tide
u_0	Bottom pore pressure amplitude $= \rho_w g \frac{H}{2}$ for tides $= \frac{\rho_w g H}{2\cosh\left(\frac{2\pi d}{L}\right)}$ for waves assuming linear wave theory
ρ_w	Mass density of water
g	Gravitational acceleration
d	Mean water depth
x	Horizontal coordinate
L	Wavelength
t	Time
T	Wave period
$A =$	$\left(\frac{\rho_w g \pi}{k E_{oed} T}\right)^{0.5}$
k	Darcy permeability coefficient
E_{oed}	Oedometric compression modulus of soil

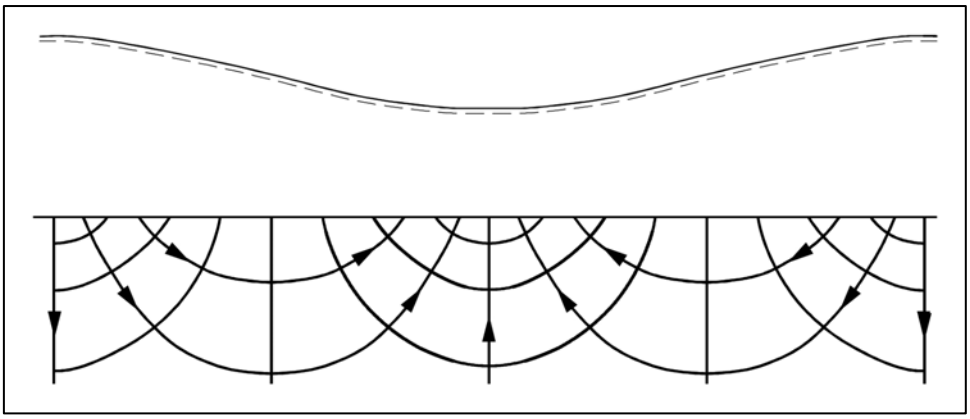

Figure VI-5-105. Illustration of instantaneous flow net in a homogeneous isotropic seabed under wave action

- For the two-dimensional case, simple methods of estimating slope stability have been developed. The stability can be investigated by considering the equilibrium of the soil body confined by the failure surface as illustrated in Figure VI-5-106. The ratio between the "stabilizing" and "driving" rotational moments, M_s and M_D, determined from all forces acting on the free soil body, is a measure of the stability.

- In Figure VI-5-106, W is the total weight of the soil element including pore water, S is the horizontal seismic inertia force, τ and σN are shear stress forces and effective normal stress forces, respectively, u_s is the water pressure along the surface of the slope, and u_p is the pore water pressure along the failure circle. The variables τ and σN usually vary along the failure circle. The parameter u_s is determined by the mean water level and the wave action. At the time of maximum runup a good approximation would be a hydrostatic pressure distribution, i.e., $u_s = \rho_w h$ where ρ_w is the water mass density and h is the local instantaneous water depth. The variable u_p can be determined from flow nets sketched for the instantaneous wave action situation, or from numerical models (Barends et al. 1983). Another, but in fact identical, formulation of the force balance indicated in Figure VI-5-106 would be to subtract the effect of hydrostatic water pressure corresponding to the mean water level from W, u_s and u_p.

- A safety factor F for the slope stability can be expressed as

$$F = \frac{M_s}{M_D} = \frac{moment\ of\ stabilizing\ forces}{moment\ of\ driving\ forces} \tag{VI-5-239}$$

or as

$$F = \frac{available\ shear\ strength}{shear\ strength\ required\ for\ stability} \tag{VI-5-240}$$

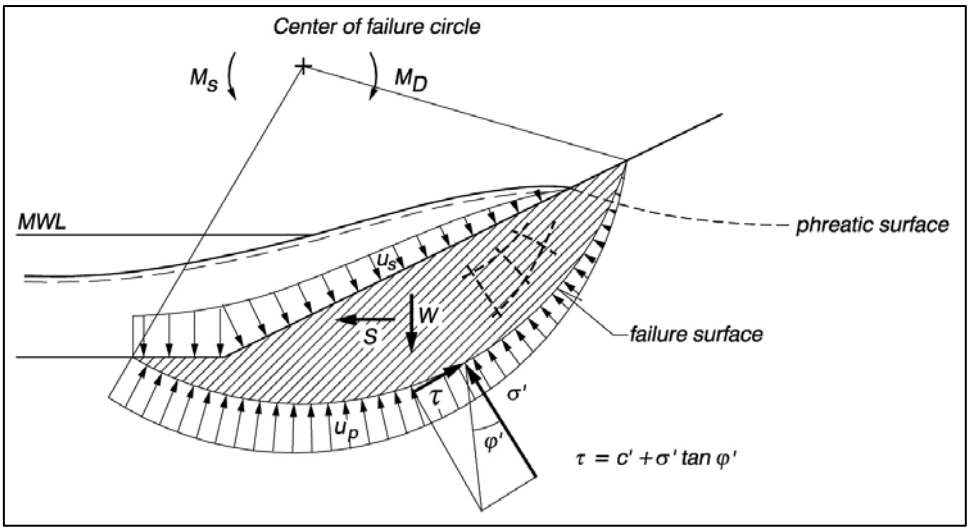

Figure VI-5-106. Illustration of forces to be considered in slope stability analysis

- If the failure surface is circular then the resultant force of the pore pressure u_p goes through the center of the circle and will not contribute to M_D. In this case it is common to define a safety factor as

$$F = \frac{moment\ of\ shear\ strength\ along\ failure\ circle}{moment\ of\ weight\ of\ failure\ mass\ and\ surface\ loads} \tag{VI-5-241}$$

- The minimum value of F has to be identified by varying the position of the center of the failure circle and the radius. Also, F must be larger than unity to assure stability. The determination of the actual (minimum) safety factor for a given slope requires usually many trial failure surfaces calculations. It is important to notice that F is not a general safety factor because it depends on the applied definition. A specific value of F does not express a unique safety level.

- Various hydraulic load situations must be evaluated, such as a rapid run-down situation in which the phreatic surface in the slope material remains in a high position due to slow drainage (see Figure VI-5-104). This load situation, which occurs when rather impermeable materials are used, might be approximated and treated like rapid (instantaneous) drawdown known from earth dam design. Morgenstern and Price (1965) provide stability charts of F (Equation VI-5-239) as a function of slope angle, ratio of drawdown height over water depth, and soil strengths cN and νN.

- The critical circular failure surface and the related safety factor F can be determined directly following the method of Janbu (1954a, 1954b) for the case of homogeneous soil, stationary water table and undrained conditions, i.e., the soil strength is given by the undrained shear strength c_u. Hansbo (1994) presented diagrams for determination of F as function of slope geometry, water level, c_u, and surface load.

- A unique solution when determining slope stability for soils with an internal angle of friction, ν, cannot be obtained because of four unknowns and only three equations of static

equilibrium. If νN is constant along the failure surface, one solution to the problem is to substitute the circle with a logarithmic spiral, i.e.,

$$r = r_1 \exp(\omega \tan _') \tag{VI-5-242}$$

in which the radius vector forms an angle νN with its normal at each point of the curved surface. The unknown frictional forces along the failure surface now pass through the center of the spiral as shown in Figure VI-5-107.

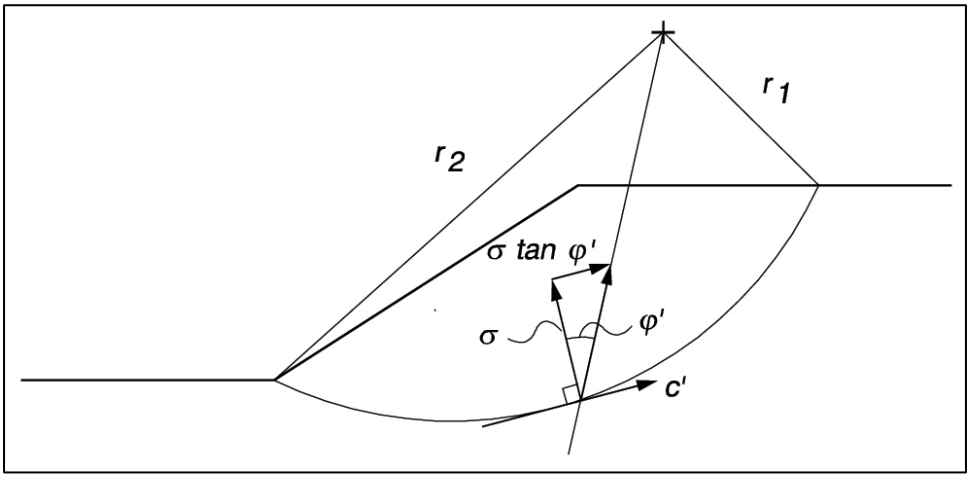

Figure VI-5-107. Illustration of logarithmic spiral

The stabilizing moment due to friction and cohesion, both taken as constants, is given by

$$M_s = \frac{1}{2} c' (r_1^2 - r_2^2) \cot \varphi' \tag{VI-5-243}$$

- The logarithmic spiral is not kinematically admissible as is the case for a circular (or straight line) failure plane. However, the deviation between the two curves is not significant in most cases.

- The simple methods illustrated in Figures VI-5-106 and VI-5-107 cannot be applied to inhomogeneous soils in which the soil strength parameters cN and νN vary along the failure surface. This situation arises when the slip surface goes through both the rubble-mound and seabed soil, or through layered parts of the rubble structure where the interfacial friction angles are different (smaller) from the friction angle of the rubble. Moreover, if weak strata are present, then the slip surface will not be circular or log-spiral shaped because the failure surface tends to go through the weak layers as illustrated in Figure VI-5-108.

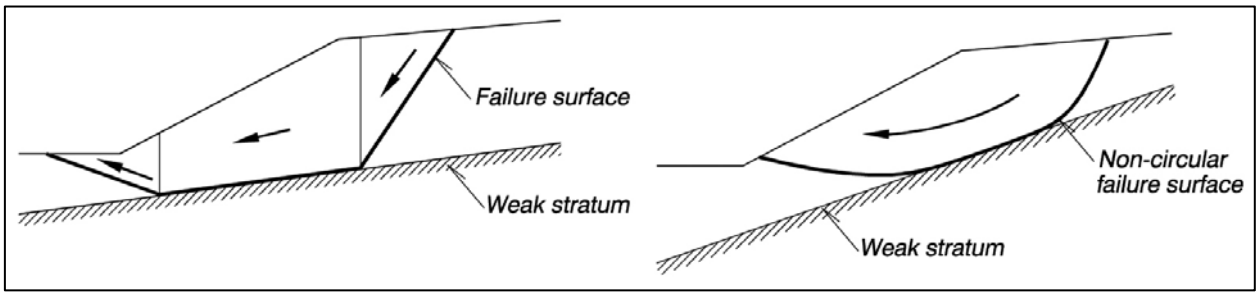

Figure VI-5-108. Illustration of failure surface in case of weak stratum

- For inhomogeneous conditions, slope stability is generally analyzed by the method of slices. The soil body is separated into fictitious vertical slices having widths that are determined such that cN and νN can be assumed constant within a slice. Slope stability is analyzed by considering all the forces acting on each slice, as shown by Figure VI-5-109. The failure surface that gives the lowest stability has to be identified by trial calculations. In Figure VI-5-109, W is the total weight of the slice including surface load, u_p is the total pore water pressure at the bottom of the slice, and the parameters P and T are the horizontal and vertical forces, respectively, on the sides of the slice.

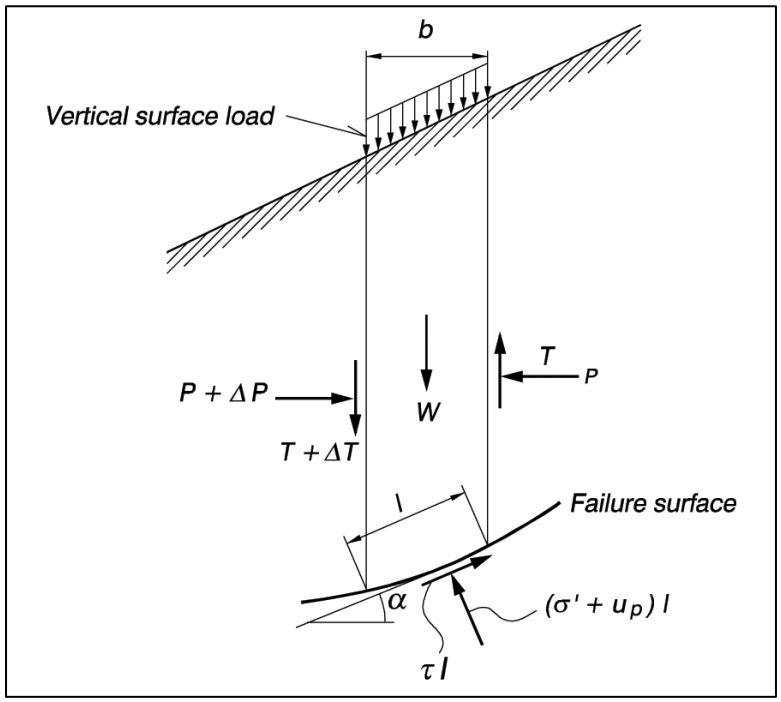

Figure VI-5-109. Illustration of forces on a soil slice in the method of slices slope stability analysis

- Several approximate methods exist for determining F, as defined by Equation VI-5-241. The most commonly applied methods are the ordinary method of slices and the simplified method of slices by Bishop. Both methods are based on the assumption of

circular-cylindrical failure surfaces. The reasonableness of this assumption should be considered in light of the comments about weak strata.

- The Ordinary Method of Slices, also known as the method of Fellinius (1936), assumes that the resultant of the forces *P* and *T* acting upon the sides of any slice have zero resultant force in the direction normal to the failure direction are for that slice. It is also assumed that the failure surface is circular-cylindrical. The related safety factor is given by

$$F = \frac{\sum_{i=1}^{n}\left[c_{i'} l_i + \left(W_i \cos\alpha_i - u_{pi} l_i \right) \tan\varphi_{i'} \right]}{\sum_{i=1}^{n} W_i \sin\alpha_i} \tag{VI-5-244}$$

If cN and νN are taken as constants, Equation VI-5-244 simplifies to

$$F = \frac{c'L + \tan\varphi' \sum_{i=1}^{n}\left(W_i \cos\alpha_i - u_{pi} l_i \right)}{\sum_{i=1}^{n} W_i \sin\alpha_i} \tag{VI-5-245}$$

where *L* is the total length of the circular failure surface. The values of *F* calculated by Equations VI-5-244 or VI-5-245 fall below the lower bound of solutions that satisfy static analysis. Thus, the method is on the safe side. The method of slices was further developed by Janbu (1954a) and Bishop (1955).

- The Simplified Method of Slices by Bishop (1955) is valid for a circular-cylindrical failure surface, and it assumes that the forces acting on the sides of any slice have zero resultant in the vertical direction, i.e., ΔT in Figure VI-5-109 is zero. The related safety factor, defined by Equation VI-5-241, is

$$F = \frac{R\sum_{i=1}^{n}\left[c_{1'} b_i + \left(W_i - u_{pi} b_i \right) \tan\varphi_{i'} \right] \Big/ \left[\left(1 + \tan\alpha_i \tan\varphi_{i'} / F \right) \cos\alpha_i \right]}{M_D + R\sum_{i=1}^{n} W_i \sin\alpha_i} \tag{VI-5-246}$$

where *R* is the radius of the failure surface circle and M_D is the driving moment of any load not included in Figure VI-5-109. Because *F* is implicitly given, an iteration procedure must be used; however, convergence of trials is very rapid.

- The Method of Slices by Janbu (1954a, 1973) is for more complicated situations where circular-cylindrical slip surfaces cannot be used, and a method for composite failure surfaces of arbitrary shape must be applied. The method is based on a combination of equations expressing moment and force equilibrium of each slice, and an iteration method for calculating *F* must be used.

- Most slope failures are three-dimensional. An approximate treatment of a three-dimensional slope failure is illustrated in Figure VI-5-110. The safety factors, F_1, F_2, and F_3, for three parallel cross-sections are computed. An estimate of the safety factor, F, for the whole body can then be estimated as the weighted safety factor using the total free body soil weights, W_1, W_2, and W_3, above the failure surface in each cross section as the weighting factors.

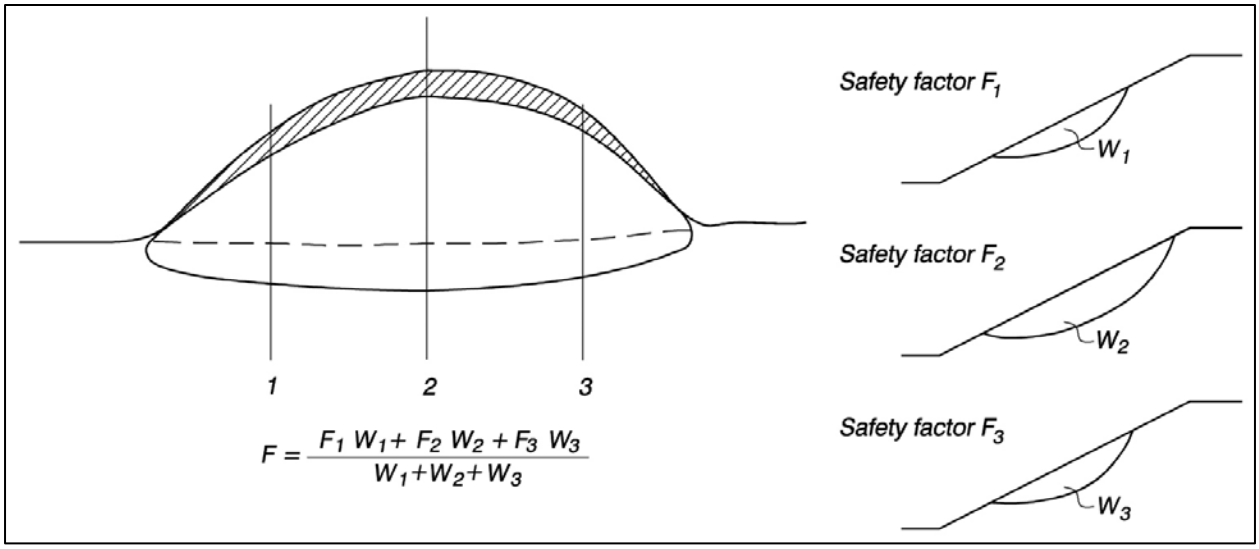

Figure VI-5-110. Illustration of safety factor F for three-dimensional slope failure

(b) Bearing capacity.

- The bearing capacity of a foundation is the load, transferred through the foundation - soil interface, that will initiate soil failure. Thus, bearing capacity is related to the ultimate limit state. The bearing capacity of the foundation of monolithic structures or structure elements like caissons and parapet concrete superstructures must be analyzed, and sufficient safety must be implemented in the design. Typical bearing capacity failure modes are shown in Part VI-2-4, "Failure Modes of Typical Structure Types."

- Rubble-mound breakwater structures placed on weak seabed soils might suffer from insufficient seabed bearing capacity. This can be investigated by the slip surface analysis explained in the previous section on slope stability.

- Bearing capacity calculations are based on zone failure analysis. In the case of homogeneous soil conditions the vertical bearing capacity of strip footings and individual rectangular footings can be estimated by formulae developed by Meyerhof (1951, 1963) and Brinch Hansen (1961, 1970), presented in Tables VI-5-86 and VI-5-87. The formulae, which represent a further development of Prandtl's and Terzaghi's theories for concentrically loaded horizontal footings, are valid for static loading and homogeneous soil conditions within the space of the zone failures.

Table VI-5-86
Bearing Capacity Formula for Rectangular Concentrically Statically Loaded Horizontal Footings (Meyerhof 1951, 1963)

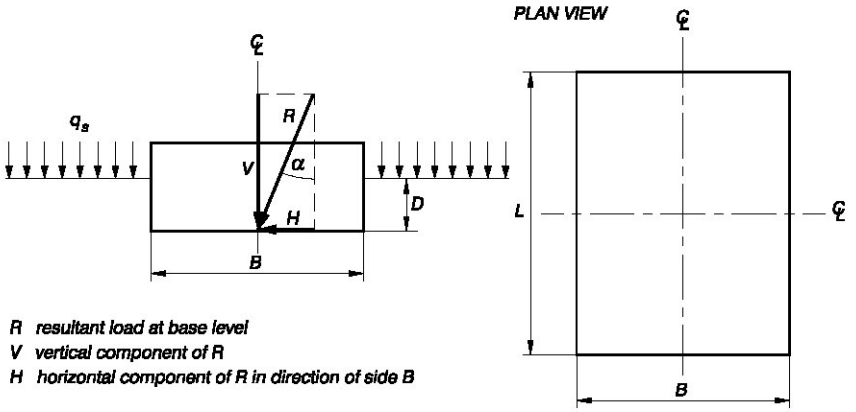

Ultimate vertical bearing capacity per unit area of the footing:

$$q_u = \frac{Q^{N_u}}{BL} = \frac{1}{2}\,\bar{\gamma}'\,B\,N_\gamma\,s_\gamma\,d_\gamma\,i_\gamma + q'\,N_q\,s_q\,d_q\,i_q + c\,N_c\,s_c\,d_c\,i_c \qquad \text{(VI-5-247)}$$

Q_u	Ultimate (maximum) value for the vertical component of the load
B	Width of footing
L	Length of footing, always $\geq B$
D	Minimum depth of footing below soil surface
$\bar{\gamma}'$	Average effective weight of soil from base level to depth B under base level
q'	Effective overburden pressure at base level (contribution from surface load q_s and effective weight of soil above base level)
c	Shear strength of soil. c_u for undrained conditions, and c' (effective) for drained conditions
φ'	Effective friction angle of soil determined by plain strain tests. Friction angle φ'_{triax} determined by triaxial test should be replaced by $\varphi' = (1.1 - 0.1\ B/L)\varphi'_{triax}$

Bearing capacity factors:

$$N_\gamma = (N_q - 1)\tan(1.4\,\varphi')$$
$$N_q = \exp(\pi\tan\varphi')\tan^2(45^0 + \varphi'/2) = \exp(\pi\tan\varphi')(1+\sin\varphi')/(1-\sin\varphi')$$

$$N_c = \begin{cases} (N_q - 1)\cot\varphi' \\ \pi + 2 \end{cases} \quad \text{for undrained conditions } (\varphi' = 0)$$

Shape coefficients:

$$s_\gamma = s_q = \begin{cases} 1.0 & \text{for } \varphi' = 0^0 \\ 1 + 0.1\,(B/L)\tan^2(45^0 + \varphi'/2) & \text{for } \varphi' \geq 10^0 \end{cases}$$

$$s_c = 1 + 0.2\,(B/L)\tan(45^0 + \varphi'/2)$$

Depth coefficients:

$$d_\gamma = d_q = \begin{cases} 1.0 & \text{for } \varphi' = 0 \\ 1 + 0.1\,(D/B)\tan(45^0 + \varphi'/2) & \text{for } \varphi' \geq 10^0 \end{cases}$$

$$d_c = 1.0 + 0.2\,(D/B)\tan(45^0 + \varphi'/2)$$

Inclination coefficients:

$$i_\gamma = \begin{cases} 1.0 & \text{for } \varphi' = 0 \\ (1 - \alpha/\varphi')^2 & \text{for } \varphi' \geq 10^0 \end{cases} \qquad \alpha = \arctan(H/V)$$

$$i_q = i_c = (1 - \alpha/90^0)^2$$

Table VI-5-87
Bearing Capacity Formula[1] for Rectangular Statically Loaded Horizontal Footing
(Brinch Hansen 1961, 1970)

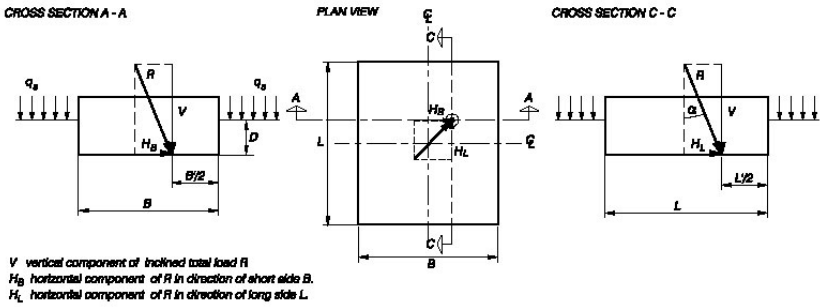

Ultimate vertical bearing capacity per unit area of effective footing:

$$q_u = \frac{Q_u}{B'L'} = \frac{1}{2}\,\bar{\gamma}'\,B'\,N_\gamma\,s_\gamma\,d_\gamma\,i_\gamma + q'\,N_q\,s_q\,d_q\,i_q + c\,N_c\,s_c\,d_c\,i_c \qquad \text{(VI-5-248)}$$

Q_u Ultimate (maximum) value for the vertical component of the load

$B' =$ $B - 2e_B$, effective width of footing, $B' \geq 0.4B$

$L' =$ $L - 2e_L$, effective length of footing, $L' \geq 0.4L$

D Minimum depth of footing below soil surface

$\bar{\gamma}'$ Average effective weight of soil from base level to depth B under base level

q' Effective overburden pressure at base level (contribution from surface load q_s and effective weight of soil above base level)

c Shear strength of soil. c_u for undrained conditions, and c' (effective) for drained conditions.

φ' Effective friction angle of soil determined by plain strain tests. Friction angle, φ'_{triax}, determined by triaxial tests should be replaced by $\varphi' = 1.1\varphi'_{triax}$.

Bearing capacity factors:

$$N_\gamma = 1.5(N_q - 1)\tan\varphi'$$

$$N_q = \exp(\pi\tan\varphi')\tan^2(45^0 + \varphi'/2) = \exp(\pi\tan\varphi')(1+\sin\varphi')/(1-\sin\varphi')$$

$$N_c = \begin{cases} (N_q - 1)\cot\,\varphi' \\ \pi + 2\,, \end{cases} \qquad \text{for undrained conditions } (\varphi' = 0)$$

Shape coefficients:

$$s_\gamma = 1 - 0.4\;B'/L' \quad \text{, must always be} \geq 0.6$$

$$s_q = 1 + \sin\,\varphi'\;B'/L'$$

$$s_c = 1 + 0.2\;B'/L'$$

Depth coefficients:

$$d_\gamma = 1$$

$$d_q = 1 + 2\tan\varphi'(1-\sin\varphi')^2\;\arctan(D/B')$$

$$d_c = 1 + 0.4\;\arctan(D/B')$$

Inclination coefficients:

$$\left.\begin{array}{l} i_\gamma = (1 - \frac{0.7H_B}{V + B'\,L'\,c'\,\cot\varphi'})^5 \\ i_q = (1 - \frac{0.5H_B}{V + B'\,L'\,c'\,\cot\varphi'})^5 \end{array}\right\} \quad \text{if the quantity inside the bracket becomes negative then the bearing capacity is negligible.}$$

$$i_c = \begin{cases} i_q - \frac{1-i_q}{N_q - 1} \;\simeq\; i_c & \text{for } \varphi' \neq 0 \\ 0.5(1 + (1 - \frac{H_B}{B'\,L'\,c_u})^{0.5}) & \text{for } \varphi' = 0 \end{cases}$$

[1] Failure can take place either along the long side or the short side of the footing. The formulae given above correspond to the first case. For the second case substitute L' for B', B' for L', and H_L for H_B.

- Brinch Hansen (1970) extended his formula to cover also the bearing capacity of statically loaded footings with inclined base in the vicinity of a slope. The formula which is termed the general bearing capacity formula is presented in Table VI-5-88 as an addition to the formula in Table VI-5-87.

- If foundation zone failures penetrate into more than one type of uniform soil then the formulae given in Tables VI-5-86, VI-5-87 and VI-5-88 cannot be applied, and the bearing capacity must be estimated by trial and error calculations in which the most critical rupture figure providing the lowest bearing capacity is identified.

- Eccentricity of the load, R, can, according to Meyerhof (1953), be taken into account by calculating the ultimate bearing capacity for a fictitious centrically loaded footing with width BN and length LN given by

$$B' = B - 2\,e_B \qquad and \qquad L' = L - 2\,e_L \tag{VI-5-249}$$

where e_B and e_L are the eccentricity of R in the directions of the width and length of the footing, respectively, as shown in Figure VI-5-111. Values of BN must always be smaller than LN in the calculation of q_u when using Equation VI-5-247. Moreover, the eccentricities are limited to $BN \exists$ 0.4 B and $LN \exists$ 0.4 L corresponding to e smaller than 0.3 times the width of the footing. Otherwise a failure configuration underneath the unloaded part of the footing might develop. This situation is not covered by Equation VI-5-247. For the case of inclined loading, the method does not apply if horizontal sliding of the foundation occurs.

- For the case of nonhorizontal foundation base and ground surface, Brinch Hansen (1967, 1970) introduced a base inclination coefficient, b, and a ground inclination coefficient, g, in his bearing capacity formula to obtain a more general formula. In the context of coastal structures, sloping base and sloping ground surface are mostly relevant for cohesionless rubble materials as indicated by Figure VI-5-112, which shows a wave wall superstructure and a caisson on a high rubble-mound foundation. Also shown is the simplified geometry of the wave wall superstructure base and of the rear side of the mound foundation to be applied in the Brinch Hansen formula for cohesionless materials given in Table VI-5-88.

- Where the foundation inclined loading has a large horizontal component, the passive pressure P indicated in Figure VI-5-113 should be included in the force balance instead of using the depth coefficients in the calculation of the bearing capacity with Equations VI-5-248 and VI-5-250.

- Note that the bearing capacity formulae given in Tables VI-5-86, VI-5-87, and VI-5-88 are all approximations. Consequently, for final design more detailed bearing capacity calculations are recommended.

Table VI-5-88
General Bearing Capacity Formula for Rectangular Statically Loaded Inclined Footing on Cohesionless Soil in Vicinity of Slope (Brinch Hansen 1961, 1967, 1970)

R foundation load
V foundation load component normal to the base
H foundation load component in plane of the base

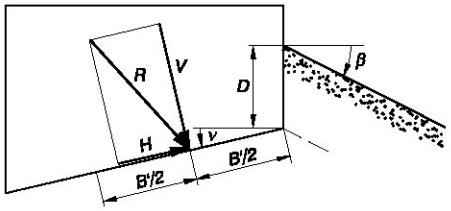

Ultimate bearing capacity per unit area of the footing:

$$q_u = \frac{Q_u^N}{B'\ L'} = \frac{1}{2}\ \bar{\gamma}'\ B'\ N_\gamma\ s_\gamma\ d_\gamma\ i_{\gamma b}\ b_\gamma\ g_\gamma\ + q'\ N_q\ s_q\ d_q\ i_q\ b_q\ g_q \qquad \text{(VI-5-250)}$$

Q_u^N is the ultimate (maximum) value for the load component normal to the base.

The formula is identical to Eq VI-5-248 except for the missing c-term ($c_u = 0$) and for the addition of the coefficients b and g, and a modified i_γ - coefficient.

Base inclination coefficients:

$$b_\gamma = \exp(-2.7\ \nu\ \tan\varphi')$$

$$b_q = \exp(-2\ \nu\ \tan\varphi')$$

Ground inclination coefficients:

$$g_\gamma = g_q = (1 - 0.5\tan\beta)^5$$

Modified load inclination coefficients:

$$i_{\gamma_b} = (1 - (0.7 - \nu^0/450^0)\ H/V)^5$$

Limitations:

The angles ν and β must be possitive but $\nu + \beta$ must not exceed 90^0. β must be smaller than φ'.

- Publications of PIANC provide the limit state equations for rupture figures related to the two-dmensional case of a statically loaded monolithic structure with horizontal base placed on a rubble foundation overlaying a seabed of sand or clay.

- Following Equation VI-5-236, the limit state equations are defined as

$$g = W_s - W_d \geq 0 \qquad \text{(VI-5-251)}$$

- A related measure of safety can be defined as

$$F = \frac{W_s}{W_d} \tag{VI-5-252}$$

- For more accurate estimations of three-dimensional bearing capacity, it is necessary to use advanced finite element calculations.

- The given bearing capacity formulae for statically loaded foundations could be applied for dynamic loadings using a dynamic amplification factor on the load as discussed in Part VI-5-5*f*, Equation VI-5-234. Such simplified methods can be used in conceptual design, but detailed design of large structures should use more accurate methods if there is a risk of dynamic load amplification.

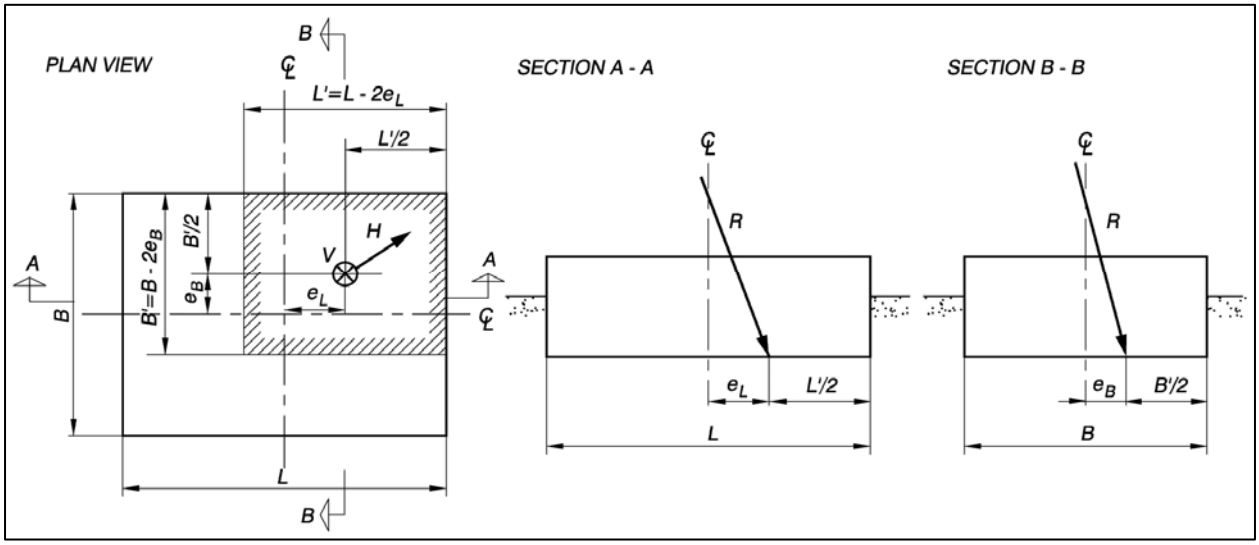

Figure VI-5-111. Illustration of fictitious footing to replace real footing under eccentric loading conditions

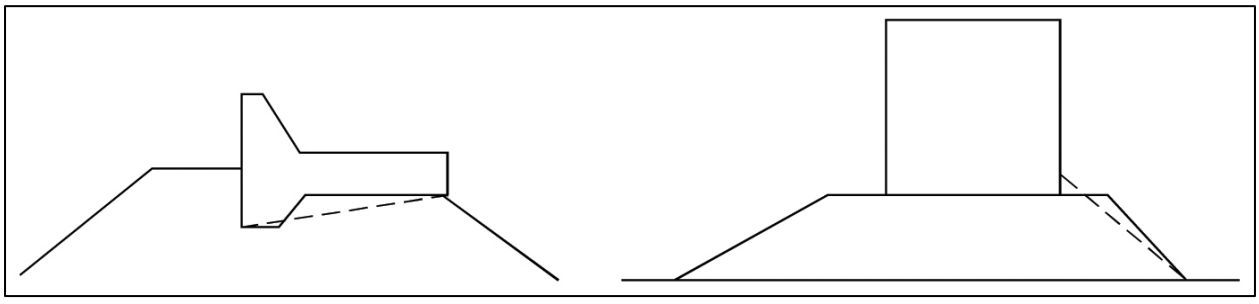

Figure VI-5-112. Simplified base and rear slope geometries to be applied in the general bearing capacity formula Table VI-5-86

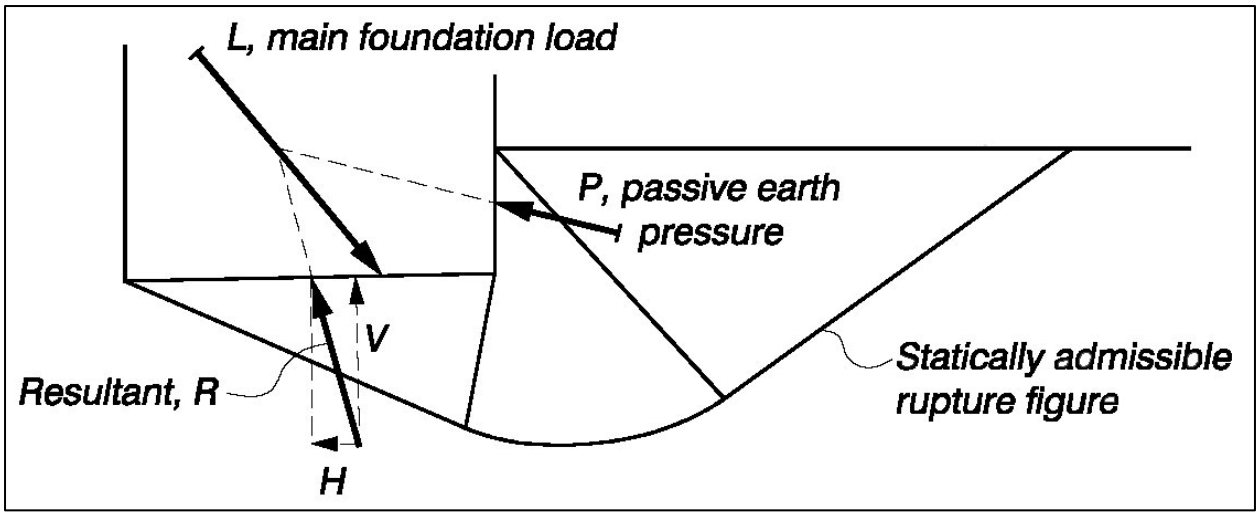

Figure VI-5-113. Illustration of passive earth pressure *P* to be included in the determination of the foundation load resultant *R* in place of the depth coefficients in Equations VI-5-248 and VI-5-250

h. Settlement.

(1) For coastal structures, settlement is related both to the seabed soils and to the structure mound materials. The mound materials are generally cohesionless permeable materials such as quarrystones, quarry-run, gravel, and coarse sand. The seabed soils are in most cases fine and less permeable materials such as sand, silt, and clay, quite often layered. Soft and muddy deposits exist in many places, especially in estuaries, deltas, and river outlets. Settlement is the direct result of volume reduction of the soil mass, and it is caused by escape of water from the voids between particles and compression of the particle skeleton.

(a) Vertical settlement of coastal structures is generally of concern where the foundation is on soft seabed materials, or at deepwater mound structures where the high mound can settle significantly. The latter case is also a concern for the foundation of caissons on high rubble mounds.

(b) Differential settlement is a problem where it might lead to damage of roads and installations placed on the structures. Damage to joints between caissons could also be due to differential settlements.

(2) Structure settlement increases vulnerability to wave overtopping by lowering the crest level of the structure. Thus, the expected total vertical settlement during the structure service lifetime has to be estimated, and the construction crest level increased accordingly.

(3) Poor seabed materials which cause large settlement and stability problems might necessitate soil improvement by methods such as preloading, compaction, installation of drains, or soil replacement. Also, it may be possible to select the type and design of structure that gives a minimum foundation load.

(4) The consequence of foundation loading on settlement depends to a great extent on the loading time relative to the consolidation time. The following three categories can be identified:

(a) Drained loading, when the consolidation time is much less than the loading time.

(b) Undrained loading, when the consolidation time is much greater than the loading time.

(c) Partially drained loading, when the consolidation time and the loading time are of the same order of magnitude.

(5) This description of the loading corresponds to the classification given in Table VI-5-83 in Part VI-5-5*e*(1) where consolidation time is discussed.

(6) Foundation loads related to coastal structures are given as follows:

(a) Loads from the weight of structure materials or structure elements placed during the construction phases. The expected loading time would be in the range from minutes to days to months.

(b) Weight of the completed structure including permanent external loads.

(c) Loads from wave action, traffic loads, and other live loads. The loading times would be in the range from seconds to hours. The wave loads will be cyclic.

(7) Generally the permeability of stone materials and coarse sand is so large that deformation problems related to the previously listed loadings can be handled as drained problems. On the other hand, the permeability of clay is so low that the conditions will always be undrained. For fine sand and silt with permeabilities between coarse sand and clay, it is not possible to make such general statements as each case must be examined. However, it is most likely that conditions during wave loadings will be undrained.

(8) Settlements are usually devided into immediate (instantaneous) settlement, primary consolidation settlement, and creep (also denoted secondary consolidation).

(a) Instantaneous settlement occurs rapidly almost in phase with the application of the load.

(b) Primary consolidation settlement is the deformation that occurs in saturated or partially saturated low permeability soils when the load carried by excess pore water pressure is gradually transferred to the soil skeleton with corresponding simultaneous excess pore water dissipation.

(c) Secondary consolidation settlement is a long-term creep phenomenon due to shear. It might continue for a long time after completion of primary consolidation.

(9) All three settlement components are relevant to low permeability materials, whereas only immediate and secondary consolidation settlements occur with high permeability materials with drained soil conditions.

(10) The starting point in calculation of settlement of the seabed soils is understanding the in situ stress distributions just after the loading is applied and estimating the relationship between stresses and soil deformations. The in situ stress distributions are generally calculated assuming elastic material and using methods such as the procedure given by Steinbrenner (1936) or by means of the influence diagrams by Newark (1942). The empirical 2:1 load spreading method might also be used. It should be noted that fill material used for rubble-mound structures is completely flexible whereas a caisson constitutes a stiff footing.

(11) Instantaneous settlement is estimated from the deformation moduli determined either by laboratory experiments with representative small soil specimens or by in situ tests such as plate loading tests, pressure meter tests, or other standard test procedures.

(12) Primary consolidation settlement is generally determined from consolidation theory by the use of the oedometer modulus and the permeability. During the construction phase, the load on the foundation is time-varying. Because the consolidation due to every load increment proceeds independently of the preceding load increment, the total settlement can be computed by superposition. Consolidation and the related settlement within the structure lifetime are caused almost entirely by the weight of the structure. Occasional loading from waves and other live loads can normally be disregarded in this context except where the wave-generated cyclic loadings cause significant volume changes of the soil (see Part VI-5-5*e*).

(13) Secondary settlement of seabed soils is difficult to estimate. It will usually be much smaller than the sum of the instantaneous and the primary consolidation settlements.

(14) Mound material such as quarrystones and quarry-run used for the construction of rubble-mound breakwaters is usually tipped from dumpers or barges. Most of the anticipated settlement takes place during the construction phase, especially if heavy vehicles such as dumpers pass over the already placed material. Settlement will then typically be in the order of 2 - 5 percent of the height of the mound. High quarrystone foundations for caisson breakwaters might need compaction to reduce the risk of unacceptable differential settlements.

VI-5-6. Scour and Scour Protection. Any coastal project built on erodible sand or soil may be susceptible to damage resulting from scour. This section describes scour problems that affect coastal projects, gives procedures for estimating maximum depth of scour for specific situations, and presents design guidance for scour protection. The available scour prediction methods presented here assume the erodible bed is composed of noncohesive sediment.

a. Scour problems in coastal engineering. In the most general definition, scour is the erosive force of moving water. This broad definition of scour includes any erosion of sediment under any circumstances, such as beach profile change and inlet channel migration. A more specific definition of scour is used in reference to coastal engineering projects: Scour is the removal by hydrodynamic forces of granular bed material in the vicinity of coastal structures. This definition distinguishes scour from the more general erosion; and as might be expected, the

presence of a coastal structure most definitely contributes to the cause of scour. Scour that occurs at coastal projects can lead to partial damage, or in some cases, complete failure of all or portions of the structure. Scour-induced damage happens at sloping-front structures when scour undermines the toe so it can no longer support the armor layer, which then slides downslope (see Figure VI-2-37). Scour impacts vertical-front caissons and other gravity-type structures if the structure is undermined to the point of tilting as illustrated by Figure VI-2-58. Monolithic gravity seawalls can also settle and tilt as a result of scour (see Figure VI-2-64). Scour at vertical sheetpile walls can result in seaward rotation of the sheetpile toe due to pressure of the retained soil as shown by Figure VI-2-69. Coastal structure damage or failure brought about by scour impacts coastal projects in several ways including: project functionality is decreased; costs will be incurred to repair or replace the structure, and scour related damage is often difficult and expensive to repair; upland property being protected by the structure may be lost or inundated; clients and cost-sharing partners will lose confidence in the project's capability to perform as required.

(1) Physical processes of scour.

(a) Scour will occur anywhere the hydrodynamic shear stresses on the bottom are high enough to initiate sediment transport. Clear water scour occurs when bottom shear stresses are high only in a localized portion of the bed; outside the local region sediment is not moving. This occurs mostly in uniform, steady flow situations. In live bed scour bottom shear stresses over the entire bed exceed the level for incipient motion with locally higher shear stresses where greater scour occurs. An equilibrium is reached when the volume of sediment being removed from the scour hole is exactly equal to sediment being deposited in its place. Understanding the physical processes involved in scour is difficult because the shear stresses responsible for scour are developed by waves, currents, or combined waves and currents, that usually are heavily influenced by the presence of a coastal structure. Because of the distinct influence coastal structures exert on the hydrodynamics, structural aspects such as geometry, location, and physical characteristics (roughness, permeability, etc.) impact the scour process. Therefore, modifying some physical characteristic of a structure may reduce scour potential.

(b) Typical structure and hydrodynamic conditions leading to scour include the following (acting singularly or in combination):

- Localized increases in peak orbital wave velocities due to combined incident and reflected waves

- Particular structure orientations or configurations that focus wave energy and increase wave velocity or initiate wave breaking

- Structure orientations that direct currents along the structure or cause a flow acceleration near the structure

- Flow constrictions that accelerate the fluid

- Breaking wave forces that are directed downward toward the bed or that generate high levels of turbulence capable of mobilizing sediment

- Wave pressure differentials and groundwater flow that produce a "quick" condition, allowing material to be carried off by currents

- Flow separation and creation of secondary flows such as vortices

- Transitions from hard bottom to erodible bed

(c) Even if the hydrodynamic aspects of scour were fully understood, there remains the difficulty of coupling the hydrodynamics with sediment transport. Consequently, most scour prediction techniques consist of rules of thumb and fairly simplistic empirical guidance developed from laboratory and field observations.

(d) Depending on the circumstances, scour can occur rapidly over short time spans (e.g., energetic storm events), or as a gradual loss of bed material over a lengthy time span (months to years). In the short-term case sediment is probably transported primarily as suspended load, whereas bedload transport is more likely during episodes of long-term scour. Scour may be cyclic with infilling of the scour hole occurring on a regular basis as the flow hydrodynamics undergo seasonal change.

(e) Most scour holes and trenches would eventually reach a stable configuration if the same hydrodynamic conditions persisted unchanged over a sufficient time span. Such an equilibrium is more likely to occur for scour induced primarily by current regimes than by wave action. It is difficult to determine if observed scour development at a particular coastal project represents an equilibrium condition. The scour might be the result of energetic flow conditions that subsided before the full scour potential was realized. Or it is possible the scour was initially greater, and infilling of the scour hole occurred prior to measurement. Finally, there is the possibility that the observed scour is simply the partial development of an ongoing long-term scour process.

(2) Common scour problems. Common coastal engineering situations where scour may occur are illustrated on Figure VI-5-114 and described as follows.

(a) Scour at coastal inlet structures.

- Kidney-shaped scour holes are sometimes present at the tip of one or both inlet jetty structures. These scour holes are usually permanent features of the inlet structure system, but there have been instances where seasonal infilling occurs due to longshore sediment transport. In some cases scour holes have been deep enough to result in partial collapse of the jetty head, while in other cases the scour holes have resulted in no structure damage. Hughes and Kamphuis (1996) observed in movable-bed model experiments that the primary hydrodynamic process responsible for kidney-shaped scour holes appears to be flood currents rounding the jetty head and entering the channel. Sediment mobilization, rate of scour, and extent of scour are increased by wave action, particularly waves that are diffracted around the jetty tip into the navigation channel. Waves breaking across the jetty head in the absence of currents will also cause scour of a lesser magnitude (Fredsøe and Sumer 1997).

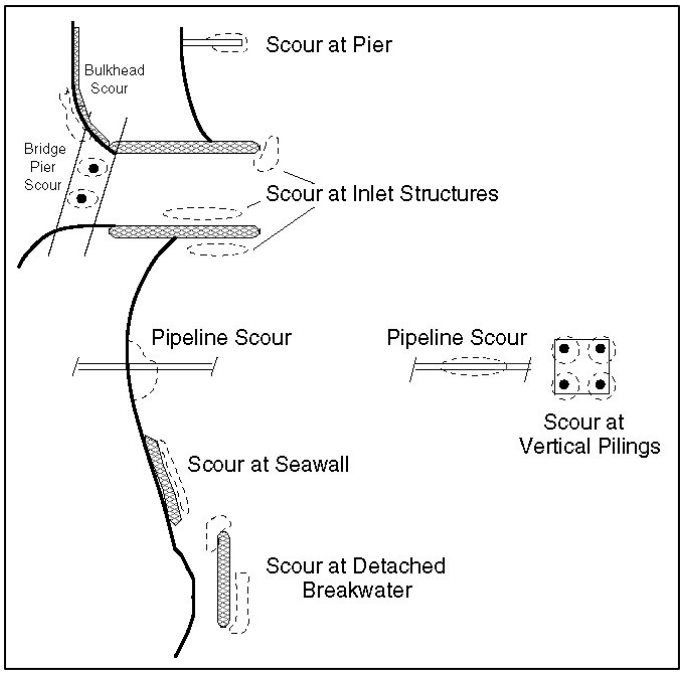

Figure VI-5-114. Coastal scour problems

- Substantial scour trenches are known to form along the channel-side toes of jetty structures. These trenches are caused either by migration of the navigation channel (by unknown causes) to a position adjacent to the jetty toe or by ebb-flow currents that are redirected by the jetty structure. Hughes and Kamphuis (1996) argued that ebb flows deflected by a jetty are analogous to plane jet flow exiting a nozzle with similar geometry. As the flow cross section decreases, the flow velocity increases proportionately to maintain the ebb flow discharge.

- Scour trenches can also form along the outside toe of the updrift jetty. These trenches might be formed by the seaward deflection of longshore currents that causes a local flow acceleration adjacent to the jetty toe, or the scour may stem from high peak orbital velocities resulting from the interaction of obliquely incident and reflected waves. A likely scenario is scour hole formation due to both hydrodynamic processes with the waves mobilizing sediment and the current transporting the material seaward. Scour trenches on the outside toe of a jetty may be seasonal at locations experiencing seasonal reversal of predominant wave direction.

- Scour holes occur regularly around bridge pilings and piers that span coastal inlets. Generally, this situation is similar to scour that plagues bridge piers on inland waterways. Additional factors complicating scour at inlet bridge piers are the unsteady and reversing nature of tidal flows, and the possible exposure to waves and storm surges.

(b) Scour at structures in deeper water.

- Scour can occur at the toes of vertical-faced breakwaters and caissons placed in deeper water. Wave-induced scour results from high peak orbital velocities developed by the interaction of incident and reflected waves. If a particular structure orientation results in increased currents along the structure toe, scour potential will be significantly enhanced.

Localized liquefaction due to wave pressure differentials and excess pore pressure within the sediment may cause sediment to be removed by reduced levels of bottom fluid shear stress.

- Characteristic scour patterns may occur around the vertical supporting legs (usually cylinders) of offshore platforms. Under slowly-varying boundary layer flow conditions, the platform leg interrupts the flow causing formation of a horseshoe vortex wrapped around the structure just above the bed. This secondary flow intensifies the bottom fluid shear stresses, and erodes sediment. The quasi-equilibrium scour hole closely resembles the shape of the horseshoe vortex. In the absence of currents, waves can cause scour in the shape of an inverted, truncated cone around the vertical cylinder provided the bottom orbital velocities are sufficiently high.

- Pipelines laid on the sea bottom are susceptible to scour action because the pipe cross section obstructs the fluid particle motion developed by waves and currents.

(c) Scour at structures in shallow water.

- Piers and pile-supported structures in shallow water react to currents and waves just as in deep water. However, the shallow depth means that orbital velocities from shorter period waves can cause scour. Therefore, vertical piles are vulnerable to scour caused by a wider range of wave periods than in deeper water.

- Scour can occur along the seaward toe of detached breakwaters due to wave reflection. The scour process will be enhanced in the presence of transporting currents moving along the breakwater. Scour holes may be formed at the ends of the breakwater by diffracted waves. In shallow water, breaking waves can create high turbulence levels at the structure toe.

- Vertical-front and sloping-front seawall and revetments located in the vicinity of the shoreline can be exposed to energetic breaking waves that produce downward-directed flows and high levels of turbulence which will scour the bed. Scour could also be produced by flows associated with wave downwash at less permeable sloping structures.

- Vertical bulkheads are usually not exposed to waves capable of producing scour; however, it is possible for scour to occur by local current accelerations.

- Scour around pipelines will occur by the same mechanisms as in deeper water with shorter period waves becoming more influential as water depth decreases. Buried pipelines traversing the surfzone can be at risk if beach profile erosion exposes the pipeline to pounding wave action and strong longshore currents.

- Depending on specific design details, coastal outfalls may develop scour patterns that jeopardize the structure.

(d) Other occurrences of scour.

- Any type of flow constriction caused by coastal projects has the potential to cause scour. For example, longshore currents passing through the gap between a jetty and a detached

breakwater at Ventura Harbor, CA, accelerated and caused scour along the leeside toe of the detached breakwater (Hughes and Schwichtenberg 1998).

- Storm surge barriers, sills, and other structures founded on the sea floor can experience scour at the downstream edge of the structure. Small pad foundations can be undermined by waves and currents.

- Structure transition points and termination points may produce local flow accelerations or may focus wave energy in such a way that scour occurs.

- Scour may occur as a transient adjustment to new construction. For example, Lillycrop and Hughes (1993) documented scour that occurred during construction of the terminal groin at Oregon Inlet, North Carolina. Despite maintenance of a scour blanket in advance of construction, the project required 50 percent more stone because of the scour.

b. Prediction of scour. There have been many theoretical and laboratory studies conducted examining various aspects of scour related to coastal projects. Some studies focussed on discovering the physical mechanisms responsible for scour, whereas other studies were directed at developing engineering methods for predicting the location and maximum depth of scour. In the following sections usable engineering prediction methods are presented for estimating scour for specific coastal structure configurations and hydrodynamic conditions. To a large extent the predictive equations have been empirically derived from results of small-scale laboratory tests, and often the guidance is fairly primitive. In some situations the only predictive capability consists of established rules of thumb based on experience and field observation. A comprehensive discussion of scour mechanisms, theoretical developments, and experiment descriptions is well beyond the scope of this manual. However, there are several publications containing detailed overviews of scour knowledge for many situations of interest to coastal engineers (e.g., Hoffmans and Verheij 1997; Herbich 1991; and Sumer and Fredsøe 1998a). In the following sections, appropriate citations of the technical literature are provided for more in-depth study.

(1) Scour at vertical walls. Occurrence of scour in front of vertical walls can be conveniently divided into two cases: nonbreaking waves being reflected by a vertical wall, and breaking waves impacting on a vertical wall. In either case, waves can approach normal to the wall or at an oblique angle.

(a) Nonbreaking waves. Nonbreaking waves are more prevalent on vertical-front structures located in deeper water and at bulkhead structures located in harbor areas. Almost all the energy in incident waves reaching a vertical-front structure is reflected unless the structure is porous. Close to the structure, strong phase locking exists between incident and reflected waves, and this sets up a standing wave field with amplified horizontal particle velocities beneath the water surface nodes and minimal horizontal velocities beneath the antinodes. The bottom sediment responds to the fluid velocities by eroding sediment where bottom shear stresses are high and depositing where stresses are low.

- Normally incident nonbreaking waves. Researchers have identified two characteristic scour patterns associated with nonbreaking waves reflected by a vertical wall (de Best, Bijker,

and Wichers 1971; Xie 1981; Irie and Nadaoka 1984; Xie 1985). Fine sand is transported primarily in suspension, and in this case scour occurs at the nodes of the sea surface elevation with deposition occurring at the antinodes. Coarse sediment is moved primarily as bed load so that scour occurs midway between the sea surface nodes and antinodes with deposition usually centered on the nodes of the standing wave pattern.

– Uniform, regular waves produce a repeating pattern of scour and deposition as a function of distance from the toe of the vertical wall as illustrated in the upper portion of Figure VI-5-115. For fine sand maximum scour nearest the wall occurs a distance $L/4$ from the wall where L is the wavelength of the incident wave. Irregular waves produce a similar scour pattern for fine sand as shown in the lower portion of Figure VI-5-115. However, phase-locking between incident and reflected irregular waves decreases with distance from the wall with the maximum scour depth for fine sand approximately located a distance $L_p/4$ from the vertical wall, where L_p is the wavelength associated with the peak spectral frequency using linear wave theory.

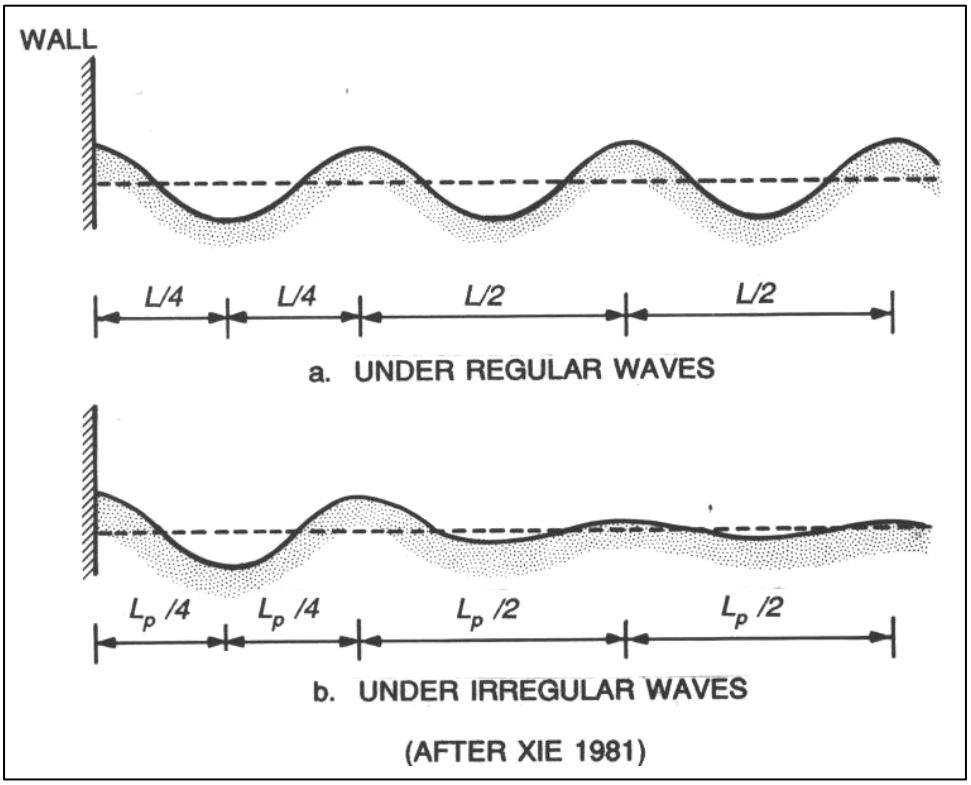

Figure VI-5-115. Regular and irregular wave-scoured profiles at a vertical-front structure

– Based on results from 12 movable-bed model tests, Xie (1981, 1985) proposed an empirically-based equation to estimate maximum scour for normally incident, nonbreaking, regular waves incident upon an impermeable vertical wall. The equation was given as:

$$\frac{S_m}{H} = \frac{0.4}{[\sinh(kh)]^{1.35}} \qquad \text{(VI-5-253)}$$

where

S_m = maximum scour depth at node ($L/4$ from wall)

H = incident regular wave height

h = water depth

k = incident regular wave number ($k = 2\pi/L$)

L = incident regular wavelength

– A similar laboratory-based prediction empirical equation for the more appropriate case of normally incident, nonbreaking irregular waves was given by Hughes and Fowler (1991) as

$$\frac{S_m}{(u_{rms})_m T_p} = \frac{0.05}{[\sinh(k_p h)]^{0.35}} \tag{VI-5-254}$$

where

T_p = wave period of the spectral peak

k_p = wave number associated with the spectral peak by linear wave theory

$(u_{rms})_m$ = root-mean-square of horizontal bottom velocity

– The value of $(u_{rms})_m$ was given by Hughes (1992) as

$$\frac{(u_{rms})_m}{g\, k_p T_p H_{mo}} = \frac{\sqrt{2}}{4\pi \cosh(k_p h)}\left[0.54 \cosh\left(\frac{1.5 - k_p h}{2.8}\right)\right] \tag{VI-5-255}$$

where H_{mo} is the zeroth-moment wave height, and g is gravity. (Equation VI-5-255 is empirically based and should not be applied outside the range $0.05 < k_p h < 3.0$.)

– Equation VI-5-255 is plotted on Figure VI-5-116 along with the movable-bed model experiment results. The dashed line is an equivalent to Equation VI-5-254. Scour predicted for irregular waves is significantly less than scour predicted for regular waves, and in many cases the predicted maximum scour does not represent a threat to the structure toe due to its location $L_p/4$ from the wall. Also, any effect related to sediment size is missing from these formulations (other than the stipulation of fine sand). Therefore, sediment scale effects may have influenced laboratory results causing less scour than might occur at full scale.

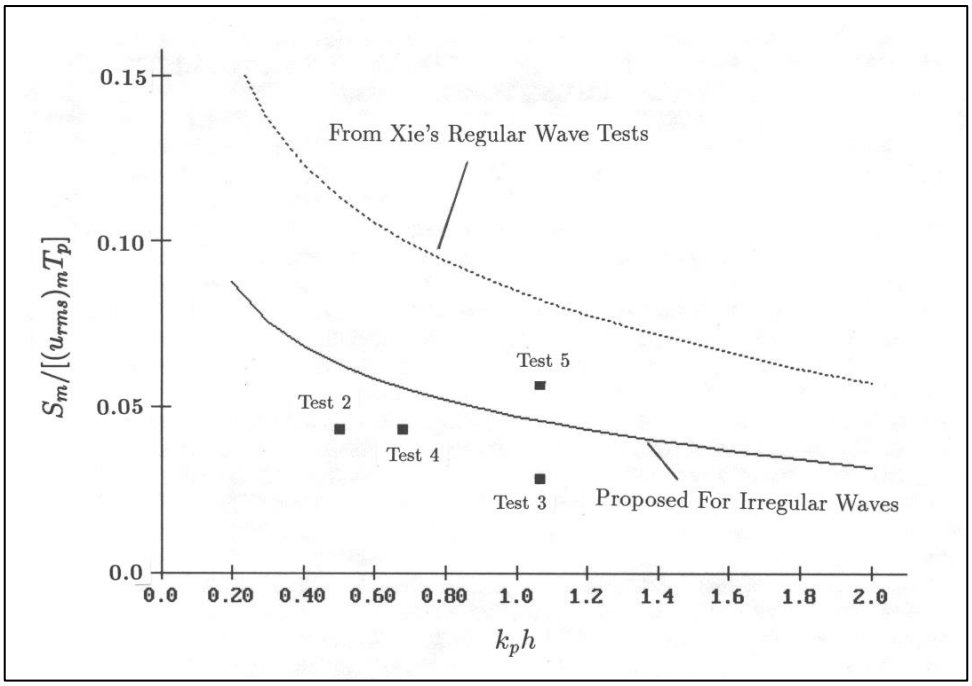

Figure VI-5-116. Scour prediction for nonbreaking waves at vertical wall (Hughes and Fowler 1991)

– The relatively minor scour depths predicted for nonbreaking waves may be a direct result of scale effects or it may be related to the two-dimensionality of the laboratory experiments. In the wave flume an equilibrium profile is reached even though sediment is still constantly in motion. At an actual project site strong currents running parallel to a vertical-front structure could remove sediment put into motion by the standing wave pattern. If this occurs, scour will continue until a new live-bed equilibrium is reached. Sato, Tanaka, and Irie (1968) gave field examples of scour attributed to along-structure currents acting in conjunction with bed agitation by waves. Unfortunately, there are no scour prediction methods covering this possibility.

- Obliquely incident nonbreaking waves. Obliquely approaching incident nonbreaking waves will also be nearly completely reflected by a vertical wall. The resulting combined incident and reflected waves resemble a short-crested, diamond pattern that propagates in a direction parallel to the wall. (See Hsu (1991) for development of theories related to obliquely reflected long-crested waves.) Just as in the case of normal wave incidence, partial nodes and antinodes develop on lines parallel to the structure at distances that are a function of the wave properties and incident wave angle. However, obliquely reflected waves also generate a mass transport component parallel to the vertical structure which may contribute to enhanced scour along the structure. Silvester (1991) summarized laboratory results of scour at highly reflective (but not necessarily vertical-front) structures caused by obliquely incident long-crested regular and irregular waves. It was observed that obliquely incident waves tended to scour more than equivalent normally incident waves, and irregular waves scour at a slower rate and somewhat more uniformly than regular waves. No engineering methods are presently available to estimate scour caused by obliquely incident, nonbreaking irregular waves reflected by a vertical wall.

- Scour at the head of a vertical breakwater. Sumer and Fredsøe (1997) conducted small-scale movable-bed experiments to investigate scour around the circular head of a vertical breakwater aligned parallel to the wave crests. They discovered that scour around the breakwater head is due mainly to the lee-wake vortices, similar to wave-induced scour at vertical piles. Maximum scour depths from different sized breakwaters corresponded remarkably well with the associated Keulegan-Carpenter number, which is defined as

$$KC = \frac{U_m T}{B} \tag{VI-5-256}$$

where

U_m = maximum wave orbital velocity at the bed (in the absence of a structure)

T = regular wave period

B = diameter of the vertical breakwater circular head

– Sumer and Fredsøe presented the following empirical equation to predict maximum scour depth (S_m) as a function of the Keulegan-Carpenter number and diameter of the breakwater head:

$$\frac{S_m}{B} = 0.5\, C_u \left[1 - e^{-0.175\,(KC-1)} \right] \tag{VI-5-257}$$

in which C_u is an uncertainty factor with a mean value of unity and a standard deviation of σ_u = 0.6. This empirical expression was developed for the data range $0 < KC < 10$. However, beyond $KC = 2.5$, data from only one breakwater diameter were used. Irregular waves will probably not scour as deeply, so the empirical equation could be considered conservative.

– Sumer and Fredsøe (1997) also investigated scour at the heads of squared-ended vertical breakwaters, perhaps representative of caissons. They found similar planform extent of scour, but depth of scour was greater by about a factor of 2. No empirical design equation was given for this situation, but it is possible to make estimates directly from the curve in their paper or from the simple equation

$$\frac{S_m}{B} = -0.09 + 0.123\, KC \tag{VI-5-258}$$

which fits the data reasonably well. However, this expression is based on very limited laboratory data, and scour estimates should be considered tentative.

– The angle of obliquely incident waves on scour around the vertical breakwater head was also shown to be a factor in scour magnitude, and the addition of even small currents moving in the direction of wave propagation significantly increased depth of scour. No design guidance was suggested that included currents and wave angle. Sumer and Fredsøe analyzed

scale effects in their laboratory experiments and concluded that scour holes at full scale will be slightly smaller than equivalent scaled-up model results. Design of scour protection for vertical breakwater heads is discussed in Part VI-5-6*c*, "Design of scour protection."

(b) Breaking waves. Scour caused by waves breaking on vertical-front structures has been a topic of numerous studies. (See Powell 1987; Kraus 1988; and Kraus and McDougal 1996 for overviews of the literature.) Scour caused by breaking waves is generally greater than for nonbreaking waves, and there is more likelihood of scour leading to structure damage. Spilling or plunging breaking waves can break directly on the vertical wall or just before reaching the wall. The physical mechanisms responsible for scour by breaking waves are not well understood, but it is generally thought that the breaking process creates strong downward directed flows that scour the bed at the base of the wall. For example, the re-entrant tongue of a plunging wave breaking before it reaches the structure generates a strong vortex motion that will mobilize sediment at the toe. A wave impacting directly on the vertical face will direct water down at the toe in the form of a jet. Sediment mobilization and transport is dominated by turbulent fluid motions rather than fluid shear stresses, and air entrained in the breaking wave also influences the erosion process (Oumeraci 1994). Figure VI-5-117 illustrates scour and profile change fronting a vertical seawall.

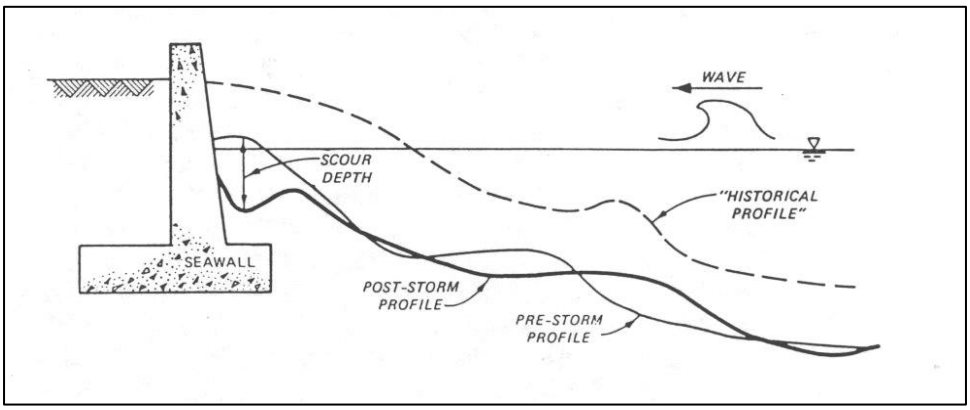

Figure VI-5-117. Scour due to breaking waves at a vertical seawall (Kraus 1988)

- Rules of thumb. There are several accepted rules-of-thumb pertaining to scour of noncohesive sediment at vertical walls. For the case of normally incident breaking waves with no currents:

  – The maximum scour depth at a vertical wall (S_m) is approximately equal to the nonbreaking wave height (H_{max}) that can be supported by the water depth (h) at the structure, i.e.,

$$S_m = H_{\max} \quad \text{or} \quad S_m \approx h \tag{VI-5-259}$$

  – Maximum scour occurs when the vertical wall is located around the plunge point of the breaking wave.

  – Reducing the wall reflection reduces the amount of scour.

- Irregular breaking wave scour prediction. Predictive equations for estimating maximum scour at vertical walls due to normally incident regular breaking waves were proposed by Herbich and Ko (1968) and Song and Schiller (1973). Powell (1987) discussed shortcomings of these two methods and concluded the empirical equations were not useful for design purposes.

– Fowler (1992) also examined the Song and Schiller relationship using data from midscale movable-bed model tests using irregular waves, and reasonable correspondence was noted between measurements and predictions. Fowler then combined his irregular wave scour data with regular wave data from Barnett and Wang (1988) and from Chesnutt and Schiller (1971) as shown in Figure VI-5-118.

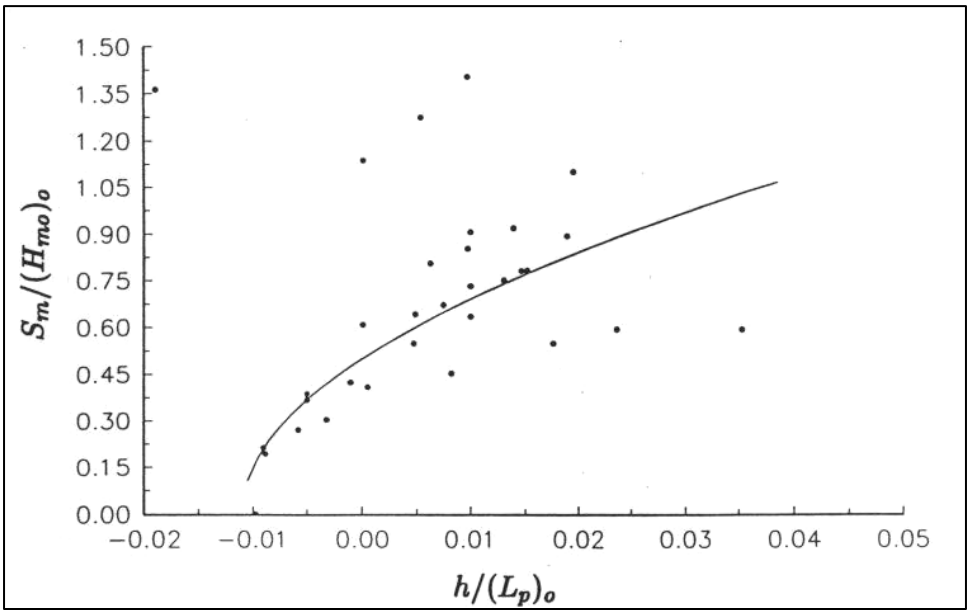

Figure VI-5-118. Relative scour depth as a function of relative depth at a vertical wall (Fowler 1992)

– The following empirical equation (solid line on Figure VI-5-118) was proposed for estimating maximum scour of noncohesive sediment due to normally incident breaking irregular waves with a mild approach slope.

$$\frac{S_m}{(H_{mo})_o} = \sqrt{22.72 \frac{h}{(L_p)_o} + 0.25} \tag{VI-5-260}$$

where

S_m = maximum scour depth

$(H_{mo})_o$ = zeroth-moment wave height in deep water

h = pre-scour water depth at the vertical wall

$(L_p)_o$ = deepwater wavelength associated with the peak spectral wave period, T_p, i.e., $(L_p)_o = (g/2\pi)\ T_p^2$

– Fowler noted that application of this empirical equation is limited by the data to values of relative depth and relative steepness within the ranges

$$0.011 < \frac{h}{(L_p)_o} < 0.045 \qquad and \qquad 0.015 < \frac{(H_{mo})_o}{(L_p)_o} < 0.040 \tag{VI-5-261}$$

– Fowler's predictive equation does not include any parameters relating to sediment properties, which are expected to have some influence in the scouring process. However, sediment transport induced by waves breaking against a vertical wall will not be very dependent on Shields parameter due to the turbulent nature of the entraining flow, and this would decrease the influence of sediment grain size. Also, the previous scour estimation method assumes no current flow along the vertical wall.

– Scour of cobble (or shingle) beaches fronting vertical walls is discussed by Carpenter and Powell (1998). They provided dimensionless design graphs to predict maximum scour depth as a function of significant wave height, wave steepness, and local water depth. Their results were based on laboratory movable-bed model tests, which were correctly scaled due to the relatively large size of cobbles compared to sand.

(2) Scour at sloping structures. Scour at the toe of sloping-front structures is thought to be a function of structure slope and porosity, incident wave conditions, water depth, and sediment grain-size. Despite considerable research into the processes responsible for wave-induced scour at sloping structures, there are no generally accepted techniques for estimating maximum scour depth or planform extent of scour (Powell 1987; Fowler 1993). However, progress is being made in development of numerical models to predict scour at sloping-front structures. Engineering use of such numerical models should consider model input requirements, representation of structure characteristics (particularly reflection parameters), and documented validation against field or laboratory experiments conducted at larger scales. Nonbreaking irregular waves impinging on a sloping structure will create a standing wave field similar to a vertical structure except the variation between the sea surface elevation nodes and antinodes is less pronounced, and the location of the node nearest the structure toe varies with wave condition and structure reflection properties (Hughes and Fowler 1995; O'Donoghue and Goldsworthy 1995; Losada, Silva, and Losada 1997). Erosion of fine sediment is expected to occur at the nodal location, but no empirical estimation method has been proposed.

(a) Rules of thumb. In lieu of easily applied semi-empirical scour estimation tools, simple rules-of-thumb serve as engineering guidelines for scour at sloping-front structures.

- Maximum scour at the toe of a sloping structure is expected to be somewhat less than scour calculated for a vertical wall at the same location and under the same wave condition. Therefore, a conservative scour estimate is provided by the vertical wall scour prediction equations, i.e., $S_m < H_{max}$.

- Depth of scour decreases with structure reflection coefficient. Therefore, structures with milder slopes and greater porosity will experience less wave-induced scour.

- Scour depths are significantly increased when along-structure currents act in conjunction with waves.

- Obliquely incident waves may cause greater scour than normally incident waves because the short-crested waves increase in size along the structure (Lin et al. 1986) due to the mach-stem effect. Also, oblique waves generate flows parallel to the structure.

(b) Scour at head of sloping breakwater. Fredsøe and Sumer (1997) conducted small-scale movable-bed model experiments to investigate mechanisms responsible for wave-induced scour around the conical heads of sloping-front breakwater structures. The experiments were similar in many respects to the companion study of scour at the ends of vertical breakwaters (Sumer and Fredsøe 1997). For most tests the rubble-mound breakwater head was approximated as an impermeable, smooth structure constructed of steel frames covered with sheet metal and having a slope of 1:1.5. The breakwater head was aligned parallel to the incident irregular waves. Observed scour was attributed to two different mechanisms; steady streaming of flow around the breakwater head, and waves breaking across the breakwater head and impinging on the leeside bed.

- Scour holes caused by steady streaming formed at the breakwater toe on the seaward curve of the breakwater head. An estimation of maximum scour depth (S_m) was developed as a function of the Keulegan-Carpenter number (KC) and given by Fredsøe and Sumer (1997) as

$$\frac{S_m}{B} = 0.04\, C_u \left[1 - e^{-4.0\,(KC - 0.05)} \right] \tag{VI-5-262}$$

in which C_u is an uncertainty factor with a mean value of unity and a standard deviation of $\sigma_u = 0.2$. The Keulegan-Carpenter number is calculated as given by Equation VI-5-256 using the peak spectral wave period, T_p, as the period, T, and the breakwater head diameter at the bed as B.

- Fredsøe and Sumer suggested that U_m be calculated from linear wave theory as the bottom velocity found using a wave height of

$$H = \frac{1}{\sqrt{2}} H_s \tag{VI-5-263}$$

where H_s is the significant wave height. A similar expression for predicting deposition was also presented.

- The second scour mechanism is caused by waves breaking across the sloping front of the breakwater head. The geometry of the steep breakwater face causes lateral water motion that forms the tongue of the plunging breaker into a rounded re-entrant jet that impacts the bed at a steep angle and mobilizes sediment. This creates a scour hole at the breakwater toe on the leeside of the rounded head with the maximum depth located approximately at the intersection of

breakwater head and trunk. Fredsøe and Sumer presented the following empirical equation for maximum scour depth (S_m) due to plunging breaking waves

$$\frac{S_m}{H_s} = 0.01\, C_u \left(\frac{T_p \sqrt{g\, H_s}}{h} \right)^{3/2} \tag{VI-5-264}$$

where C_u is an uncertainty factor with a mean value of unity and a standard deviation of σ_u = 0.34, h is water depth, and the other parameters are as defined previously.

- As noted by Fredsøe and Sumer, these equations were developed for impermeable, smooth breakwater heads. The permeability and roughness of rubble-mound breakwaters will effectively decrease both scour mechanisms, thus scour estimates may be somewhat conservative. The previous empirical expressions for predicting maximum scour depths are based on a limited number of data points derived primarily from laboratory experiments, and the equations should be considered tentative until additional studies are conducted. Also, scour is caused by waves only; superimposed currents are expected to increase appreciably maximum scour depth. Design of scour protection for sloping-front breakwater heads is discussed in Part VI-5-6*c*, "Design of scour protection."

(3) Scour at piles. The majority of methods for estimating scour at vertical piles were developed for piles with circular cross section, which are widely used in coastal and offshore engineering applications. However, there are estimation techniques for piles with noncircular cross sections and for specialized structures such as noncircular bridge piers and large bottom-resting structures. Scour at small vertical piles (pile diameter, D, is less than one-tenth of the incident wavelength) is caused by three simultaneously acting mechanisms: formation of a horseshoe-shaped vortex wrapped around the front of the pile; vortex shedding in the lee of the pile; and local flow accelerations due to streamline convergence around the pile. The pile does not significantly affect the incident wave. Large diameter piles, in which the diameter is greater than one-tenth of the incident wavelength, do have an impact on the incident waves which are reflected by the pile and diffracted around the pile. The key parameters governing scour formation appear to be current magnitude, orbital wave velocity, and pile diameter. Less important parameters are sediment size and pile shape (if the pile has noncircular cross section). For detailed descriptions of the physical mechanisms responsible for scour at vertical piles see Niedoroda and Dalton (1986) or some of the following references. A general, and somewhat conservative, rule-of-thumb is: Maximum depth of scour at a vertical pile is equal to twice the pile diameter. This rule-of-thumb appears to be valid for most cases of combined waves and currents. Smaller maximum scour depths are predicted by the equations in the following sections. Estimation formulas for maximum scour depth have been proposed for the cases of currents only, waves only, and combined waves and currents. The flow problem and associated sediment transport are beyond a complete theoretical formulation, and even numerical modeling attempts have not been able to describe fully the scour process at vertical piles (see Sumer and Fredsøe 1998a for a summary of numerical modeling approaches).

(a) Scour at small diameter vertical piles. Vertical piles with diameter, *D,* less than one-tenth of the incident wavelength constitute the vast majority of pile applications in coastal engineering. Even cylindrical legs of some offshore oil platforms may fall into this category.

- Pile scour by currents. Many scour estimation formulas have been proposed for scour caused by unidirectional currents without the added influence of waves. A formulation widely used in the United States is the Colorado State University (CSU) equation developed for bridge piers (e.g., Richardson and Davis 1995) given by the expression

$$\frac{S_m}{h} = 2.0\, K_1 K_2 \left(\frac{b}{h}\right)^{0.65} F_r^{\,0.43} \tag{VI-5-265}$$

where

S_m = maximum scour depth below the average bottom elevation

h = water depth upstream of the pile

b = pile width

F_r = flow Froude number [$F_r = U/(gh)^{1/2}$]

U = mean current velocity magnitude

K_1 = pile shape factor

K_2 = pile orientation factor

– Equation VI-5-265 is a deterministic formula applicable for both clear water scour and live bed scour, and it represents a conservative envelope to the data used to establish the empirical coefficients. The shape factor, K_1, is selected from Figure VI-5-119, and the orientation factor, K_2, can be determined from the following equation given by Froehlich (1988).

$$K_2 = (\cos\theta + \frac{L}{b}\sin\theta)^{0.62} \tag{VI-5-266}$$

where L/b is defined in Figure VI-5-119 and θ is the angle of pile orientation. K_2 equals unity for cylindrical piles. Other modifying factors have been proposed to account for sediment gradation and bed forms, but these factors have not been well established. An additional factor is available for use when piles are clustered closely together. See Richardson and Davis (1995) and Hoffmans and Verheij (1997) for details.

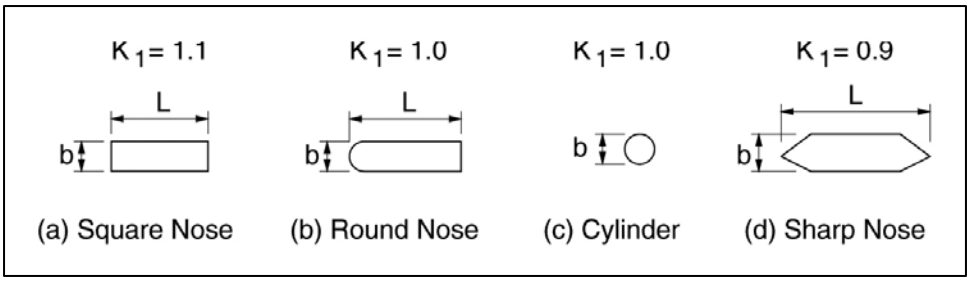

Figure VI-5-119. Correction factor, K_1, for pile/pier shape

– Johnson (1995) tested seven of the more commonly used scour prediction equations against field data and found that the CSU equation (Equation VI-5-265) produced the best results for $h/b > 1.5$. At lower values of h/b a different empirical formulation offered by Breusers, Nicollet, and Shen (1977) provided better results.

– Johnson (1992) developed a modified version of the CSU empirical equation for use in reliability analysis of failure risk due to scour at cylindrical piles. Her formula represents a best-fit to the data rather than a conservative envelope. An application example is included in her 1992 paper.

- Pile scour by waves. The physical processes associated with wave-only scour around vertical piles are reasonably well described qualitatively (See Sumer and Fredsøe (1998a) for a comprehensive review and listing of many references.)

– In an earlier paper Sumer, Christiansen, and Fredsoe (1992a) established an empirical equation to estimate scour at a vertical pile under live bed conditions. They used small- and large-scale wave flume experiments with regular waves, two different sediment grain sizes, and six different circular pile diameters ranging from 10 cm to 200 cm. Maximum scour depth (S_m) was found to depend only on pile diameter and Keulegan-Carpenter number (KC), as expressed by Equation VI-5-256 with pile diameter, D, as the denominator. The experimental data of Sumer, Christiansen, and Fredsoe (1992a) are shown plotted in Figure VI-5-120, and the solid line is the predictive equation given by

$$\frac{S_m}{D} = 1.3\left[1 - e^{-0.03(KC-6)}\right] \tag{VI-5-267}$$

where D is cylindrical pile diameter. No live-bed scour occurs below values of $KC = 6$, which corresponds to onset of horseshoe vortex development. At values of $KC > 100$, $S_m/D \rightarrow 1.3$, representing the case of current-only scour.

– Independent confirmation of Equation VI-5-267 was presented by Kobayashi and Oda (1994) who conducted clear water scour experiments. They stated that maximum scour depth appeared to be independent of Shields parameter, grain size diameter, and whether scour is clear-water or live-bed.

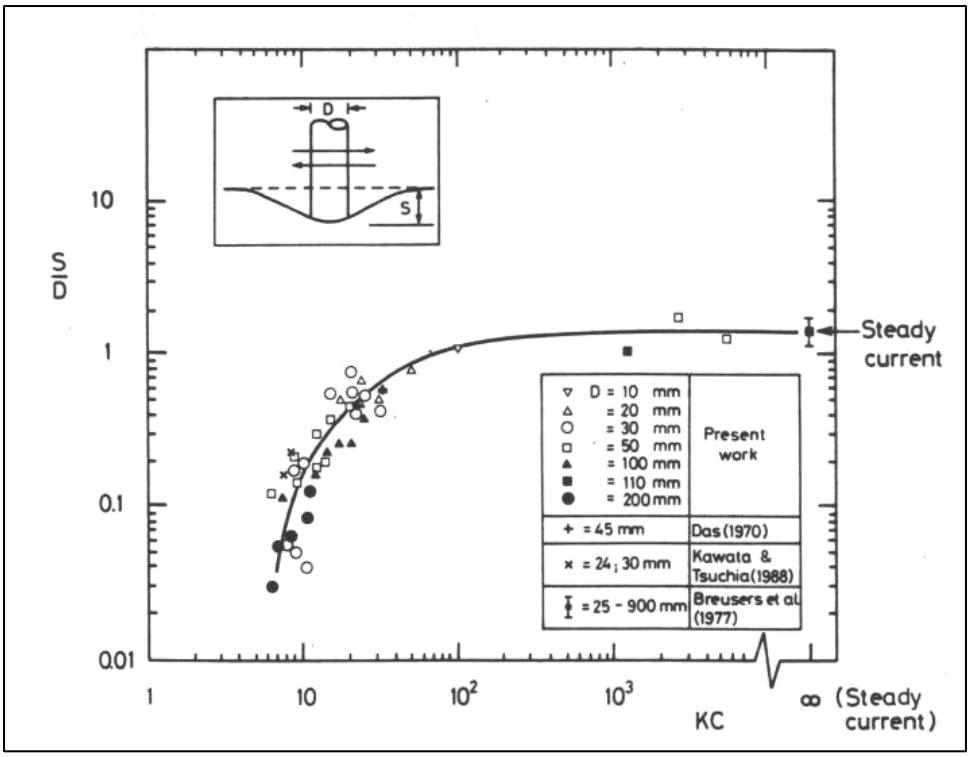

Figure VI-5-120. Wave-induced equilibrium scour depth at a vertical pile

– In an extension to their 1992 study, Sumer, Christiansen, and Fredsoe (1993) conducted additional regular wave live-bed scour experiments using square piles oriented with the flat face 90 deg and 45 deg to the waves. The following empirical equations for maximum scour were obtained as best-fits to the observed results:

Square pile 90 deg to flow:

$$\frac{S_m}{D} = 2.0\left[1 - e^{-0.015(KC-11)}\right] \qquad for\ KC _ 11 \tag{VI-5-268}$$

Square pile 45 deg to flow:

$$\frac{S_m}{D} = 2.0\left[1 - e^{-0.019(KC-3)}\right] \qquad for\ KC _ 3 \tag{VI-5-269}$$

– Scour for the square pile oriented at 45 deg begins at lower values of *KC*, but the maximum scour at large *KC* values approaches $S_m/D = 2$ regardless of orientation.

– Studies on the time rate of scour development were reported by Sumer, Christiansen, and Fredsoe (1992b), Sumer et al. (1993), and Kobayashi and Oda (1994). Recent research on wave scour around a group of piles was summarized by Sumer and Fredsøe (1998a, 1998b).

- Pile scour by waves and currents. Kawata and Tsuchiya (1988) noted that local scour depths around a vertical pile were relatively minor compared to scour that occurs when even a small steady current is added to the waves. Eadie and Herbich (1986) conducted small-scale laboratory tests of scour on a cylindrical pile using co-directional currents and irregular waves. They reported the rate of scour was increased by adding wave action to the current, and the maximum scour depth was approximately 10 percent greater than what occurred with only steady currents. This latter conclusion contradicts Bijker and de Bruyn (1988) who found that nonbreaking waves added to steady currents slightly decreased ultimate scour depth whereas adding breaking waves caused increased scour to occur. Eadie and Herbich also noted that the inverted cone shape of the scour hole was similar with or without wave action, and the use of irregular versus regular waves appeared to influence only scour hole geometry and not maximum scour depth. They developed a predictive equation using results from approximately 50 laboratory experiments, but no wave parameters were included in the formulation. Finally, they pointed out that their conclusions may hinge on the fact that the steady current magnitude exceeded the maximum bottom wave orbital velocity, and different results may occur with weak steady currents and energetic waves.

- Earlier work by Wang and Herbich (1983) did provide predictive equations that included wave parameters along with current, pile diameter, sediment properties, and water depth. However, there were some unanswered questions about scaling the results to prototype scale. Consequently, until further research is published, maximum scour depth due to waves and currents should be estimated using the formulations for scour due to currents alone (Equation VI-5-265).

(b) Scour at large diameter vertical piles. Rance (1980) conducted laboratory experiments of local scour at different shaped vertical piles with diameters greater than one-tenth the incident wavelength. The piles were exposed to coincident waves and currents. Rance provided estimates of maximum scour depth as functions of pile equivalent diameter, D_e, for different orientations to the principal flow direction. (D_e is the diameter of a cylindrical pile having the same cross-sectional area as the angular pile.) These formulas are given in Figure VI-5-121.

(c) Maximum scour occurs at the corners of the square piles. Estimates of extent of scour are useful for design of scour blankets. Sumer and Fredsøe (1998a) provided additional information about flow around large piles.

(4) Scour at submerged pipelines. Waves and currents can scour material from beneath pipelines resting on the bottom, leading to partial or even complete burial of the pipeline. In most situations pipeline burial is usually considered a desirable end result. However, if the pipeline spans soil types having different degrees of erodibility, differential scour may result in sections of the pipeline being suspended between bottom hard points, and this could lead to pipeline failure. Onset of scour beneath a pipeline resting on, or slightly embedded in, the bottom occurs initially as piping when seepage beneath the pipeline increases and a mixture of sediment and water breaks through (Chiew 1990). Onset of scour is followed by a phase of rapid scour called tunnel erosion in which the bed shear stresses are increased four times above that of the undisturbed sand bed. Tunnel erosion is followed by lee-wake erosion in which the lee-wake of

the pipeline appears to control the final equilibrium depth and shape of the downstream scour. Equilibrium depth of scour beneath the pipeline is usually defined as the distance between the eroded bottom and the underside of the pipeline as illustrated on Figure VI-5-122. Overviews of pipeline scour knowledge and citations to the extensive literature are included in Sumer and Fredsøe (1992, 1998a) and Hoffmans and Verheij (1997). Only the established empirical equations for estimating scour depth are included in the following:

(a) Pipeline scour by currents. In steady currents the equilibrium scour depth beneath a pipeline is thought to be a function of pipe diameter, pipe roughness, pipe Reynolds number, and Shields parameter. For clear water scour, when mean flow velocity, U, is less than the critical velocity, U_c, maximum scour depth can be calculated using the following equation from Hoffmans and Verheij (1997)

$$\frac{S_m}{D} = \frac{\mu}{2}\left(\frac{U}{U_c}\right) \tag{VI-5-270}$$

where

$$\mu = \left(\frac{k_s}{12\,D}\right)\ln\left(\frac{6\,D}{k_s}\right) \tag{VI-5-271}$$

and

D = pipe diameter

h = water depth

U = depth averaged flow

U_c = critical depth-averaged flow velocity

k_s = effective bed roughness, $k_s = 3\,d_{90}$ (k_s must have the same units as D)

When $U/U_c > 1$, live-bed scour occurs, and in this case Sumer and Fredsøe (1992) stated that pipe Reynolds number only influences flow around smooth pipes and the influence of Shields parameter is minor. They recommended the simple equation for predicting maximum equilibrium scour depth. The 0.1-value represents the standard deviation of the data, so a conservative estimate of scour would be S_m/D=0.7.

$$\frac{S_m}{D} = 0.6 \pm 0.1 \tag{VI-5-272}$$

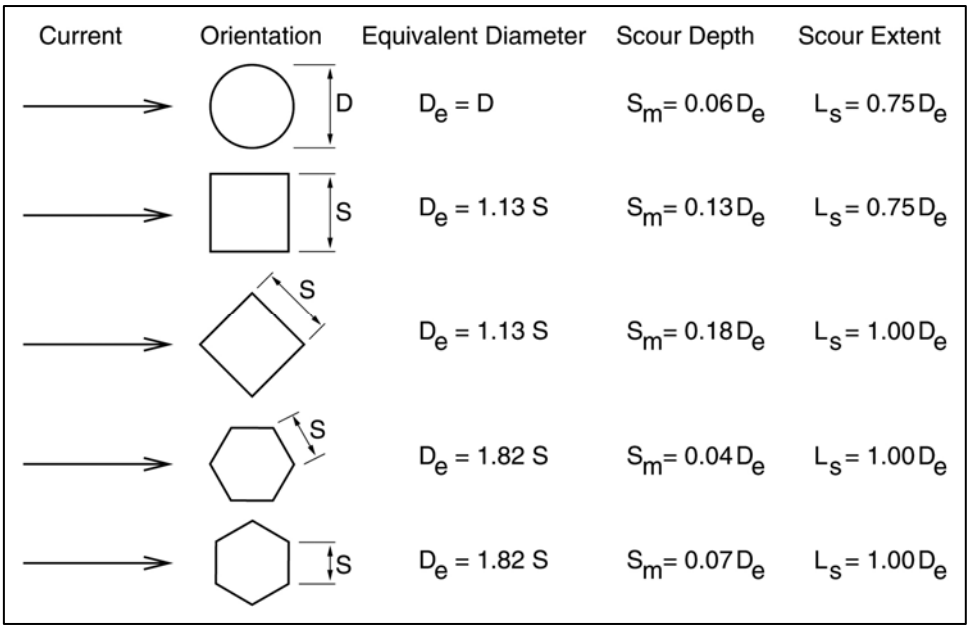

Figure VI-5-121. Wave and current scour aroundlarge vertical piles (Rance 1980)

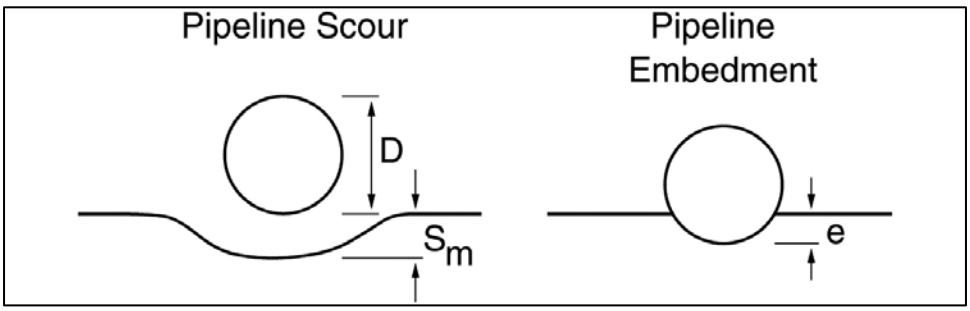

Figure VI-5-122. Pipeline scour and pipeline embedment

(b) Pipeline scour by waves. Oscillatory bottom velocities under waves create piping conditions beneath pipelines in the same manner as steady currents. Sumer and Fredsøe (1991) gave a criterion for onset of scour under waves based on a small number of laboratory experiments. This criterion is

$$\frac{e_{cr}}{D} = 0.1 \ln(KC) \tag{VI-5-273}$$

where e_{cr} is the critical embedment (depth of pipeline burial beyond which no scour occurs), and KC is the Keulegan-Carpenter number, given by Equation VI-5-256 with D as the denominator. Scour is unlikely to occur for values of $e_{cr}/D > 0.5$ (half buried pipe). Sumer and Fredsøe (1990) studied scour beneath a bottom-resting pipeline under wave action. Their laboratory data, combined with that of an earlier researcher, indicated that live-bed scour was strongly related to Keulegan-Carpenter number and pipe diameter, while only weakly influenced by Shields parameter and pipe roughness. The data were well represented over a wide range of Keulegan-Carpenter number ($2 < KC < 300$) by the empirical expression

$$\frac{S_m}{D} = 0.1\sqrt{KC} \tag{VI-5-274}$$

Klomb and Tonda (1995) presented a modified version of Equation VI-5-274 that included allowance for partial embedment, *e*, of the pipeline, i.e.,

$$\frac{S_m}{D} = 0.1\sqrt{KC}\left(1 - 1.4\frac{e}{D}\right) + \frac{e}{D} \tag{VI-5-275}$$

with scour depth taken relative to the undisturbed bed. Equation VI-5-275 is valid for values of $e/D < 0.5$ (Hoffmans and Verheij 1997).

(c) Pipeline scour by waves and currents. Sumer and Fredsøe (1996) conducted laboratory tests of pipeline scour due to combined waves and currents covering a range of *KC* from 5 to about 50 with codirectional currents. The general trend, regardless of the value of *KC*, was for scour depth to initially decrease as current is increased from zero. At higher values of current, maximum scour depth approaches the value given by Equation VI-5-272 for currents alone. Sumer and Fredsøe (1996) provided empirical design equations based on the laboratory experiments; but for values of *KC* between 40 and 50 maximum scour depth is almost the same as the estimate for currents alone.

(d) Pipelines in the nearshore. Pipelines traversing the surfzone may be damaged if exposed to breaking waves and strong longshore currents. Little design guidance is available other than the fact that additional scour will occur once the pipeline is exposed. The burial depth for a pipeline through the nearshore should exceed in all places the expected bottom profile lowering that might occur over the life of the pipeline. This can be estimated using profile-change models or from long-term beach profile data.

(5) Other scour problems. Some coastal projects may include structural elements or hydrodynamic flow conditions that are typically associated with inland waterways or estuaries. Structures such as storm surge barriers, discharge control structures, or large pad footings may experience scour around their foundations due to currents or combined waves and currents.

(a) Hoffmans and Verheij (1997) provided a summary of techniques for estimating maximum scour for a number of situations that may be applicable to coastal projects:

- Scour downstream of sills and stone blankets due to currents.
- Scour downstream of hard bottoms due to horizontal submerged jets.
- Scour at control structures due to plunging jets.
- Scour at two- and three-dimensional culverts.
- Scour at abutments and spur dikes.

(b) See Hoffmans and Verheij (1997) for further details and associated technical literature.

c. Design of scour protection. Toe protection in the form of an apron is needed to prevent toe scour which may destabilize or otherwise decrease the functionality of a coastal structure. The apron must remain intact under wave and current forces, and it should be flexible enough to conform to an initially uneven sea floor. Scour apron width and required stone size for stability are related to wave and current intensity, bottom material, and structure characteristics such as slope, porosity, and roughness. Design guidance for scour protection is based largely on past successful field experience combined with results from small-scale laboratory tests. Special attention is needed where scour potential is enhanced such as at structure heads/ends, at transitions in structure composition, or at changes in structure alignment. This section provides general design guidance for scour aprons; however, this guidance should be considered preliminary. Projects requiring absolutely stable scour blankets should have proposed designs tested in a physical model. Hales (1980) surveyed scour protection practices in the United States and found that the minimum scour protection was typically an extension of the structure bedding layer and any filter layers. The following minimum rules-of-thumb resulted from this survey: minimum toe apron thickness - 0.6 m to 1.0 m (1.0 m to 1.5 m in northwest U.S.); minimum toe apron width - 1.5 m (3 m to 7.5 m in northwest U.S.); material - quarrystone to 0.3 m diameter, gabions, mats, etc. These rules-of-thumb are inadequate when the water depth at the toe is less than two times the maximum nonbreaking wave height at the structure or when the structure reflection coefficient is greater than 0.25 (structures with slopes greater than about 1:3). Under these more severe conditions use the scour protection methods summarized in the following sections for specific types of coastal structures.

(1) Scour protection for vertical walls.

(a) Vertical-front structures consist of large caisson-type gravity structures, gravity retaining walls, and cantilevered or anchored sheet-pile retaining walls. Toe protection design for larger vertical-front gravity structures subjected to waves is covered in Part VI-5-3*d*, "Toe stability and protection."

(b) For cantilevered or anchored retaining walls, Eckert (1983) proposed toe protection in the form of a scour apron constructed of quarrystone. The main purpose of the apron is to retain soil at the toe and/or to provide sufficient weight to prevent slip failure (see Figures VI-2-69 and VI-2-70). From geotechnical considerations the width (W) of the scour apron should be approximately

$$W = \frac{d_e}{\tan\left(45^o - \phi/2\right)} \approx 2.0\, d_e \qquad \text{(VI-5-276)}$$

where d_e is the depth of sheet-pile penetration below the seabed, and φ is the angle of internal friction of the soil (varies from about 26 deg to 36 deg). The width of the scour apron based on hydrodynamic criteria was given by Eckert as the greater of

$$W = 2.0\, H_i \qquad or \qquad W = 0.4\, d_s \qquad \text{(VI-5-277)}$$

where H_i is the incident wave height and d_s is the depth at the structure toe. Selected scour apron design width will be the greater of Equations VI-5-276 and VI-5-277.

(c) Eckert (1983) noted that gravity retaining walls do not require the apron to be as wide as needed for cantilevered walls. In this case, he recommended that scour apron width be about the same as the nonbreaking incident wave height.

(d) Determining the toe apron quarrystone size depends on the hydrodynamic conditions. They are as follows:

- Waves. If retaining walls are exposed to vigorous wave conditions, the toe quarrystone should be sized using the guidance given by Figure VI-5-45 (Part VI-5-3*d* "Toe stability and protection," and the apron thickness should be equal to either two quarrystone diameters or the minimum given in the prior rules-of-thumb, whichever is greater.

- Currents. If strong currents flow adjacent to the wall, toe quarrystone should be sized using the guidance provided in Part VI-5-3*f*, "Blanket stability in current fields."

- Waves and Currents. If both waves and strong currents impact the toe adjacent to a vertical retaining wall, estimate the size of the apron quarrystone for the waves alone and for the current alone. Then increase whichever is larger by a factor of 1.5 (Eckert 1983).

(e) In Sumer and Fredsøe's (1996) study of scour around the head of a vertical breakwater, laboratory tests were conducted to establish a relationship for the width of a scour apron that provides adequate protection against scour caused by wave-generated lee-wake vortices. Their empirical formula was given as

$$\frac{W}{B} = 1.75\,(KC - 1)^{1/2} \tag{VI-5-278}$$

where B is the diameter of the vertical breakwater circular head and KC is the Keulegan-Carpenter number given by Equation VI-5-256. Sumer and Fredsøe cautioned that this estimation of apron width may be inadequate in the presence of a current or for head shapes other than circular. Scour apron stone sizes are determined using the methods outlined in Part VI-5-3*d*, "Toe stability and protection."

(2) Scour protection for sloping structures.

(a) Scour protection for sloping structures exposed to waves is typically provided by the toe protection. Part VI-5-3*d*, "Toe stability and protection," presents guidance on the design of toe protection. Additional scour protection is sometimes needed at sloping-front structures to prevent scour by laterally-flowing currents. Strong tidally-driven currents adjacent to navigation jetties can scour deep trenches that may destabilize the jetty toe and result in slumping of the armor layer. Because prediction of the location and extent of potential scour is not well advanced, scour blankets are often not installed until after realization that scour has occurred. Depending on the scour hole configuration, it may be necessary to backfill the scour hole before placing a scour blanket, and the necessary extent of the protection is determined in part by the

extent of the existing scour, by past experience, and by the judgment of the engineer. An understanding of the flow regime will help assure that the scour problem will not reoccur downstream of the scour protection blanket. Stone size for scour protection from currents is given in Part VI-5-3*f*, "Blanket stability in current fields." Bass and Fulford (1992) described the design and installation of scour protection along the south jetty of Ocean City Inlet in Maryland.

(b) Fredsøe and Sumer's (1997) laboratory study of wave-induced scour at the rounded heads of rubble-mound structures included design suggestions for scour protection. The width of the scour apron from the structure toe to outer edge was given by

$$\frac{W}{B} = A_1 (KC) \tag{VI-5-279}$$

where B is the breakwater head diameter at the bed and KC is given by Equation VI-5-256. Complete scour protection is provided with $A_1 = 1.5$ whereas a value of $A_1 = 1.1$ will result in relatively minor scour at the outer edge with a depth equal to about 0.01 B. Scour apron stone size are determined using the methods outlined in Part VI-5-3*d*, "Toe stability and protection."

(3) Scour protection for piles.

(a) Vertical piles and piers exposed only to currents can be protected against scour by placement of scour aprons constructed of stone or riprap, gabions, concrete mattresses, or grout-filled bags. Riprap aprons should be designed according to the relationships given in Part VI-5-3*f*, "Blanket stability in current fields." Options other than riprap or stone should be tested in physical models.

(b) Based on an earlier report by Bonasoundas (in German), Hoffmans and Verheij (1997) recommended that minimum width for the horizontal extent of the scour apron around circular piers be specified as a function of pile diameter, B. Upstream of the pile, and to both sides, apron width is 2.5 B. Downstream the apron elongates to a width of 4.0 B as illustrated on Figure VI-5-123. Elongation in both directions is necessary for alternating tidal currents.

(c) An alternative recommendation was given by Carstens (1976) who found that scour apron width was a function of maximum scour depth (S_m) at the pile, i.e.,

$$\frac{W}{S_m} = \frac{F_s}{\tan \phi} \tag{VI-5-280}$$

where φ is the bed material angle of repose and F_s is a factor of safety.

(d) General recommendations for specifying apron width for different shaped piers and pilings, or for groups of piles, are lacking. In these cases laboratory model tests are needed to assure adequate scour protection. Past experience on other successful projects or case histories reported in the literature can also serve as design guidance (e.g., Edge et al. 1990; Anglin et al. 1996).

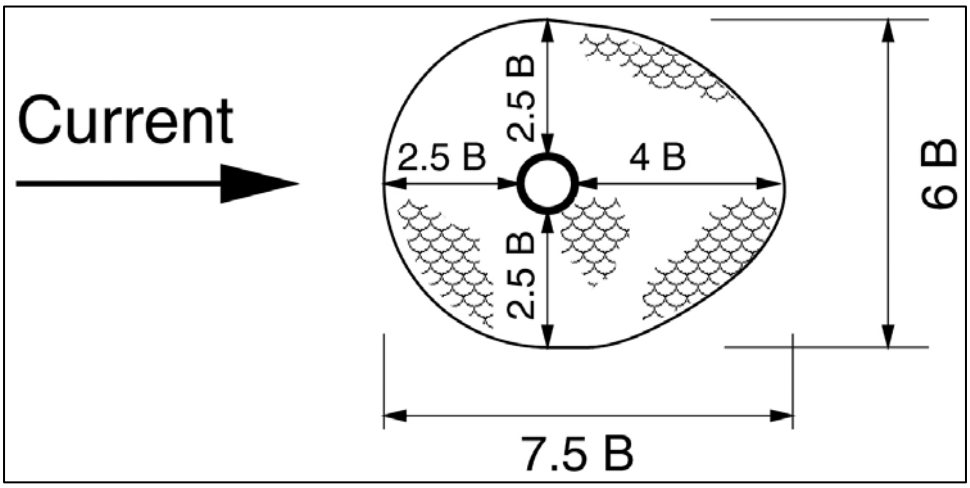

Figure VI-5-123. Scour apron for vertical pile in a current

(e) Similar protective measures can be deployed to prevent scour around piles by wave action. However, guidance is also lacking on how to design stable scour aprons in wave environments (Sumer and Fredsøe 1998a), and the best recourse is site-specific model tests. As a rule-of-thumb, the horizontal extent of the apron should be approximately twice the predicted scour depth.

(4) Scour protection for submerged pipelines.

(a) Submerged pipelines can be protected by either burying the pipeline in a trench or by covering the pipeline with a stone blanket or protective mattress. Protected pipelines are less susceptible to trawler damage and less likely to suffer damage caused by differential scour that leaves portions of the pipeline suspended between support points.

(b) Outside the active surfzone, burial depth is a function of local wave and current climate, sediment properties, and liquefaction potential. Usually the excavated material can be used as backfill provided it is sufficiently coarse to avoid buildup of excessive pore pressures which could lead to liquefaction and vertical displacement of the pipeline (Sumer and Fredsøe 1998a). Pipelines traversing the surfzone should be buried at an elevation lower than the anticipated erosion that would occur over the projected service life of the pipeline. Generally, stone blankets or mattresses are not considered effective protection in the surfzone because the elements must be designed to withstand the intense action of breaking waves.

(c) Pipelines resting on the bottom can be protected from being undermined by stabilizing the adjacent bed with a stone blanket having a horizontal width less than the extent of expected scour. Hjorth (1975) reported that covering at least the bottom half of the pipeline, as shown in the upper part of Figure VI-5-124, provides sufficient protection as evidenced by field experience. The alternative is to cover the pipeline completely with a stone blanket consisting of two or more filter layers as illustrated by the lower sketch of Figure VI-5-124. Stability of the uppermost stone layer requires that the shields parameter (Equation III-6-43) based on stone diameter must be less than the critical value for incipient motion. Stone blanket placement can be

accomplished by dumping stone from the surface, provided the falling stones are not so large as to damage the pipeline on impact.

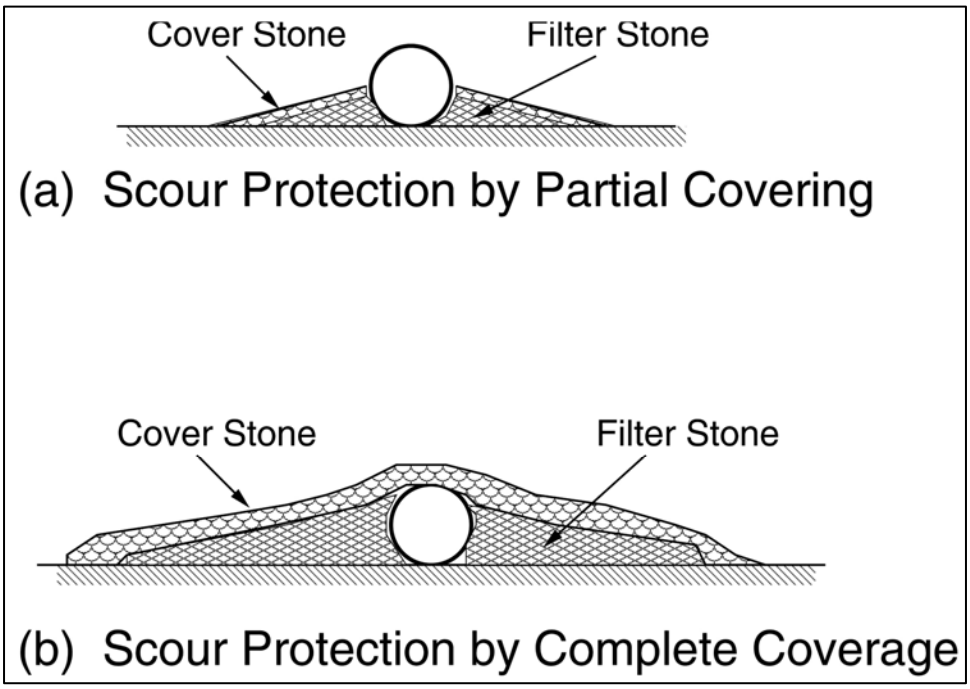

Figure VI-5-124. Stone blanket scour protection for submerged pipelines

(d) Various types of scour mattresses have also been used effectively to protect pipelines. Mattresses may be economical when stone is not readily available; however, special mattress placing equipment is usually required. Hoffmans and Verheij (1997) illustrated several types of mattresses.

VI-5-7. Wave Forces on Slender Cylindrical Piles.

a. Introduction.

(1) Frequent use of pile-supported coastal and offshore structures makes the interaction of waves and piles of significant practical importance. The basic problem is to predict forces on a pile due to the wave-associated flow field. Because wave-induced flows are complex, even in the absence of structures, solution of the complex problem of wave forces on piles relies on empirical coefficients to augment theoretical formulations of the problem. This section is meant to be only an introduction to estimating forces and moments on slender cylindrical piles. For more detailed analysis see the literature related to ocean engineering and the design of offshore facilities.

(2) Variables important in determining forces on circular piles subjected to wave action are shown in Figure VI-5-125. Variables describing nonbreaking, monochromatic waves are the wave height H, water depth d, and either wave period T, or wavelength L. Water particle velocities and accelerations in wave-induced flows directly cause the forces. For vertical piles the horizontal fluid velocity u and acceleration du/dt and their variation with distance below the

free surface are important. The pile diameter D and a dimension describing pile roughness elements k are important variables describing the pile. In this discussion the effect of the pile on the wave-induced flow is assumed negligible. Intuitively, this assumption implies that the pile diameter D must be small with respect to the wavelength L. Significant fluid properties include the fluid density ρ and the kinematic viscosity ν. In dimensionless terms, the important variables can be expressed as follows:

$\frac{H}{gT^2}$ = dimensionless wave steepness

$\frac{d}{gT^2}$ = dimensionless water depth

$\frac{D}{L}$ = ratio of pile diameter to wavelength (assumed small)

$\frac{k}{D}$ = relative pile roughness

$\frac{HD}{T\nu}$ = a form of the Reynolds number

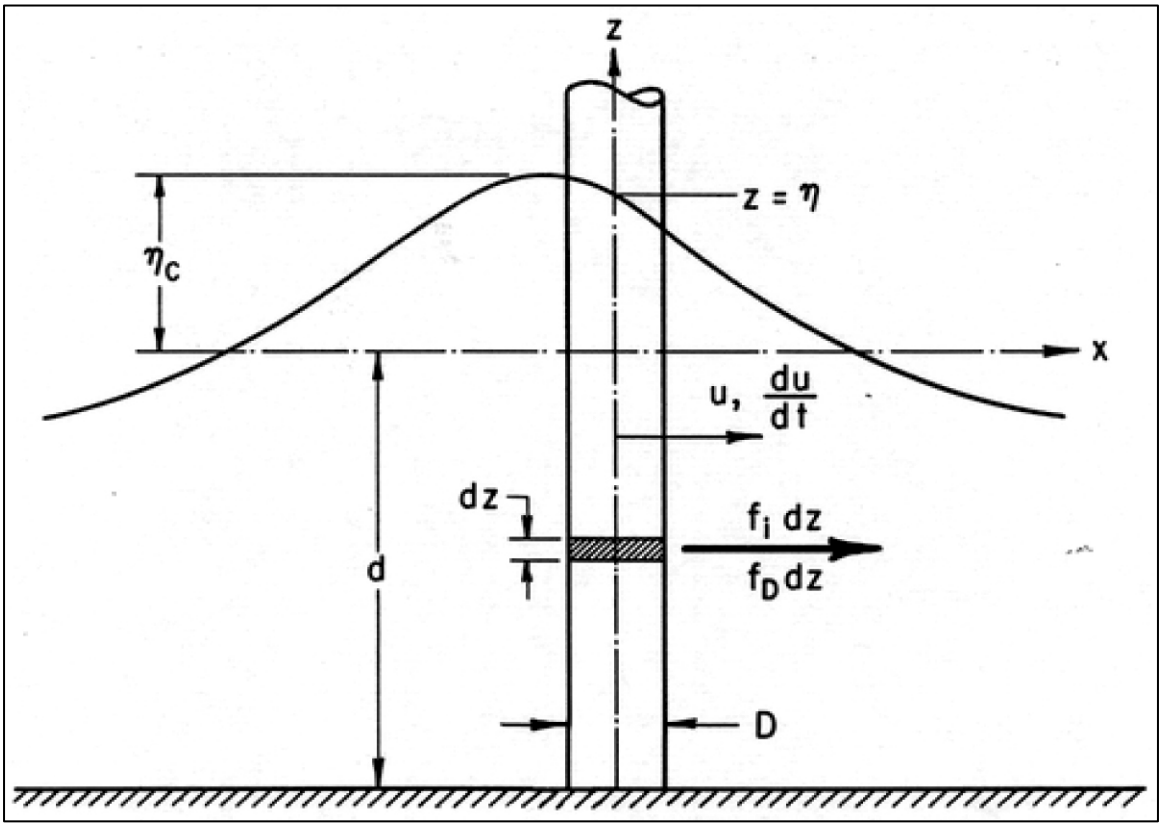

Figure VI-5-125. Definition sketch of wave forces on a vertical cylinder

(3) Given the orientation of a pile in the flow field, the total wave force acting on the pile can be expressed as a function of these dimensionless parameters. The variation of force over the length of the pile depends on the mechanism by which the water particle velocities and accelerations cause the forces. The following analysis relates the local forces acting on a section of pile element of length *dz* to the local fluid velocity and acceleration that would exist at the center of the pile if the pile were not present. Two dimensionless force coefficients, an inertia (or mass) coefficient C_M and a drag coefficient C_D, are used to establish the wave-force relationships. These coefficients are determined by experimental measurements of force, velocity, and acceleration or by measurement of force and water surface profiles, with accelerations and velocities inferred by assuming an appropriate wave theory.

(4) In the following section it is initially assumed that the force coefficients C_M and C_D are known to illustrate calculation of forces on vertical cylindrical piles subjected to monochromatic waves. Selection of C_M and C_D follows in Part VI-5-7*c*. Experimental data are available primarily for the interaction of nonbreaking waves and vertical cylindrical piles; and consequently, specific design guidance can be given for this common situation.

b. Vertical cylindrical piles and nonbreaking waves.

(1) Basic concepts. Morison et al. (1950) suggested that the horizontal force per unit length of a vertical cylindrical pile subjected to waves is analogous to the mechanism by which fluid forces on bodies occur in unidirectional flow, and this force can be expressed by the formulation

$$f = f_i + f_D = C_M \rho \frac{\pi D^2}{4} \frac{du}{dt} + C_D \frac{1}{2} \rho D u \mid u \mid \qquad \text{(VI-5-281)}$$

where

f_i = inertial force per unit length of pile

f_D = drag force per unit length of pile

ρ = mass density of fluid

D = pile diameter

u = horizontal water particle velocity at the axis of the pile (calculated as if the pile were absent) total

$\frac{du}{dt}$ = horizontal water particle acceleration at the axis of the pile (calculated as if the pile were absent)

C_D = drag hydrodynamic force coefficient

C_M = inertia or mass hydrodynamic force coefficient

(a) The inertia force term f_i is of the form obtained from an analysis of the force on a body in an accelerated flow of an ideal nonviscous fluid. The drag force term f_D is the drag force exerted on a cylinder in a steady flow of a real viscous fluid. The drag force f_D is proportional to u^2 and acts in the direction of the velocity u. To retain the correct direction sign, u^2 is written as $u|u|$. Although these remarks support the soundness of the formulation of the problem as given by Equation VI-5-281, it should be emphasized that expressing total force by the terms f_i and f_D is an assumption justified only if it leads to sufficiently accurate predictions of wave force as evidenced by ample measurements.

(b) Because the quantities u and du/dt in Equation VI-5-281 are defined as the values of these parameters at the axis of the pile, it is apparent that the influence of the pile on the flow field a short distance away from the pile has been neglected. Using linear wave theory MacCamy and Fuchs (1954) analyzed theoretically the problem of waves passing a circular cylinder. Their analysis assumed an ideal nonviscuous fluid and led to an inertia force having the form given for f_i under special conditions. Although their theoretical result is valid for all ratios of pile diameter to wavelength, D/L, the inertia force was found to be nearly proportional to the acceleration du/dt for small values of D/L (where L is wavelength calculated by linear theory). This theoretical result provides an indication of how small the pile should be for Equation VI-5-281 to apply, and the restriction is given as

$$\frac{D}{L} < 0.05 \tag{VI-5-282}$$

where L is calculated by linear wave theory. This restriction will seldom be violated for slender pile force calculations; however, the restriction may be important when applying Equation VI-5-281 to larger structures such as cylindrical caissons.

(c) To apply Equation VI-5-281 it is necessary to choose an appropriate wave theory for estimating u and du/dt from values of wave height H, wave period T, and water depth d; and for that particular wave condition appropriate values of C_D and C_M must be selected.

(2) Calculation of forces and moments. For structural design of a single vertical pile, it is often unnecessary to know in detail the distribution of forces over the height of the pile. Instead, the designer needs to know the total maximum force and the total maximum moment about the mud line ($z = -d$) acting on the pile. The total time-varying force and the time-varying moment acting about the mud line is found by integrating Equation VI-5-281 between the bottom and the free surface, i.e.,

$$F = \int_{-d}^{\eta} f_i \, dz + \int_{-d}^{\eta} f_D \, dz = F_i + F_D \tag{VI-5-283}$$

$$M = \int_{-d}^{\eta} (z + d) \, f_i \, dz + \int_{-d}^{\eta} (z + d) \, f_D \, dz = M_i + M_D \tag{VI-5-284}$$

In general form these quantities may be written

$$F_i = C_M \rho g \frac{\pi D^2}{4} H K_i \tag{VI-5-285}$$

$$F_D = C_D \frac{1}{2} \rho g D H^2 K_D \tag{VI-5-286}$$

$$M_i = C_M \rho g \frac{\pi D^2}{4} H K_i d S_i = F_i d S_i \tag{VI-5-287}$$

$$M_D = C_D \frac{1}{2} \rho g D H^2 K_D d S_D = F_D d S_D \tag{VI-5-288}$$

in which C_D and C_M have been assumed constant, and where K_i, K_D, S_i, and S_D are dimensionless parameters that depend on the specific wave theory used in the integrations. In the following sections values of the inertia coefficient C_M and drag coefficient C_D are assumed to be known constants. (Part VI-5-7*c* covers estimation of C_M and C_D.)

(a) Linear wave theory. The force on a slender cylindrical pile can be estimated using linear wave theory, but the result is limited to situations where linear wave theory provides a reasonable approximation of the wave kinematics. This implies small amplitude waves and greater depths. Also recall that any wave force on the pile above the swl will not be included in the estimate. Nevertheless, it is instructive to examine Equation VI-5-281 when linear wave theory is applied.

- With the pile center line located at $x = 0$, as shown in Figure VI-5-125, the equations from Part II-1, "Water wave mechanics" for surface elevation (Equation II-1-19), horizontal component of local fluid velocity (Equation II-1-22), and horizontal component of local fluid acceleration (Equation II-1-24) are respectively

$$\eta = \frac{H}{2} \cos\left(\frac{2\pi t}{T}\right) \tag{VI-5-289}$$

$$u = \frac{H}{2} \frac{gT}{L} \frac{\cosh[2\pi(z+d)/L]}{\cosh[2\pi d/L]} \cos\left(\frac{2\pi t}{T}\right) \tag{VI-5-290}$$

$$\frac{du}{dt} \approx \frac{\partial u}{\partial t} \approx \frac{g\pi H}{L} \frac{\cosh[2\pi(z+d)/L]}{\cosh[2\pi d/L]} \sin\left(-\frac{2pit}{T}\right) \tag{VI-5-291}$$

- Introducing Equations VI-5-290 and VI-5-291 for *u* and *du/dt* into Equation VI-5-281 gives the following expressions for the inertia force and drag force.

$$f_i = C_M \rho g \frac{\pi D^2}{4} H \left[\frac{\pi}{L} \frac{\cosh[2\pi(z+d)/L]}{\cosh[2\pi d/L]}\right] \sin\left(-\frac{2pit}{T}\right) \tag{VI-5-292}$$

$$f_D = C_D \frac{1}{2} \rho g D H^2 \left[\frac{gT^2}{4L^2} \left(\frac{\cosh[2\pi(z+d)/L]}{\cosh[2pid/L]} \right)^2 \right] \cos\left(\frac{2\pi t}{T}\right) \left| \cos\left(\frac{2\pi t}{T}\right) \right| \qquad \text{(VI-5-293)}$$

- Equations VI-5-292 and VI-5-293 show that the two force components vary with elevation z on the pile and with time t. The inertia force f_i is maximum for sin $(-2\pi t/T) = 1$, which corresponds to $t = -T/4$ for linear wave theory. Thus, the maximum inertia force on the pile occurs $T/4$ seconds before the passage of the wave crest that occurs at $t = 0$ (see Equation VI-5-289). The maximum value of the drag force component f_D coincides with passage of the wave crest at $t = 0$.

- The magnitude of the maximum inertia force per unit length of pile varies with depth the same as the horizontal acceleration component (Equation VI-5-291). The maximum value occurs at the swl ($z = 0$) and decreases with depth. The same trend is true for the maximum drag force per unit length of pile except the decrease with depth is more rapid because the depth attenuation factor (cosh $[2\pi(z+d)/L\}$/cosh$[2\pi d/L]$) is squared in Equation VI-5-293.

- The total time-varying force and the time-varying moment acting about the mudline is found for linear wave theory by integrating Equations VI-5-283 and VI-5-284 between the bottom and the swl ($z = 0$) using the expressions for f_i and f_D given by Equations VI-5-292 and VI-5-293, respectively. The integration results in total force and moment components given by Equations VI-5-285 through VI-5-288 with values of the dimensionless parameters K_i, K_D, S_i, and S_D given by

$$K_i = \frac{1}{2} \tanh\left(\frac{2\pi d}{L}\right) \sin\left(-\frac{2\pi t}{T}\right) \qquad \text{(VI-5-294)}$$

$$\begin{aligned} K_D &= \frac{1}{8}\left(1 + \frac{4\pi d/L}{\sinh[4\pi d/L]}\right) \cos\left(\frac{2\pi t}{T}\right) \left| \cos\left(\frac{2\pi t}{T}\right) \right| \\ &= \frac{1}{4} n \cos\left(\frac{2\pi t}{T}\right) \left| \cos\left(\frac{2\pi t}{T}\right) \right| \end{aligned} \qquad \text{(VI-5-295)}$$

$$S_i = 1 + \frac{1 - \cosh[2\pi d/L]}{(2\pi d/L)\sinh[2\pi d/L]} \qquad \text{(VI-5-296)}$$

$$S_D = \frac{1}{2} + \frac{1}{2n}\left(\frac{1}{2} + \frac{1 - \cosh[4\pi d/L]}{(4\pi d/L)\sinh[4\pi d/L]}\right) \qquad \text{(VI-5-297)}$$

where

$$n = \frac{C_g}{C} = \frac{1}{2}\left(1 + \frac{4\pi d/L}{\sinh[4\pi d/L]}\right) \qquad \text{(VI-5-298)}$$

- The maximum values for total inertia force and moment are found by taking $t = -T/4$ in Equations VI-5-294 and VI-5-296, respectively. Likewise, the maximum values for total drag force and moment are found by taking $t = 0$ in Equations VI-5-295 and VI-5-297, respectively. A conservative design approach would be to sum the individual maximum inertia and drag components that occur during a wave cycle to get total maximum force and moments. However, the individual maximums do not occur simultaneously, so the real maximum total force and moment wil be somewhat less. The correct method is to calculate the time-varying sum of inertia and drag components, and then use the maximum sum that occurs over the wave cycle. The time at which the maximum occurs may vary depending on the selected values for C_M and C_D.

- Although linear wave theory provides a nice closed-form solution for forces and moments on slender cylindrical piles, in practice the hydrodynamics associated with the steeper design wave conditions will not be well predicted by linear wave theory. Even more critical is the fact that linear theory provides no estimate of the force caused by that portion of the wave above the swl, an area where the horizontal velocities and accelerations are the greatest. An ad hoc adjustment is to assume a linear force distribution having a maximum value of force estimated at the still-water line and a value of zero at the crest location of the linear wave ($H/2$ above the swl). Most likely, the design wave will be nonlinear with steep wave crests and with much of the wave height above the swl, and it would be well advised to use an appropriate nonlinear wave theory in the force and moment calculation.

(b) Nonlinear wave theory.

- Design conditions for vertical cylindrical piles in coastal waters will most likely consist of nonlinear waves characterized by steep crests and shallow troughs. For accurate force and moment estimates, an appropriate nonlinear wave theory should be used to calculate values of u and du/dt corresponding to the design wave height, wave period, and water depth.

- The variation of f_i and f_D with time at any vertical location on the pile can be estimated using values of u and du/dt from tables such as Stoke's fifth-order wave theory (Skjelbriea et al. 1960) or stream-function theory (Dean 1974). Computer programs based on higher order monochromatic wave theories may be available to ease the task associated with using tabulated wave kinematics.

- The separate total maximum inertia force and moment and total drag force and moment on a vertical cylindrical pile subjected to nonlinear waves can be estimated using Equations VI-5-285 through VI-5-288. Values for K_i, K_D, S_i, and S_D in Equations VI-5-285 - VI-5-288 are given by K_{im}, K_{Dm}, S_{im}, and S_{Dm}, respectively, in the nomograms shown in Figures VI-5-126 through VI-5-129. (Note: In the nomograms the subscript m is used to denote maximum.) These nomograms were constructed using stream-function theory (Dean 1974), and they provide the maximum total force and total moment for the inertia and drag components considered separately rather than the combined total force and moment. The curves in Figures VI-5-126 to VI-5-129 represent wave height as a fraction of the breaking wave height. For example, curves labeled 1/2 H_b represent $H/H_b = 1/2$. Breaking wave height is obtained from Figure VI-5-130 for values of d/gT^2 using the curve labeled Breaking Limit.

- For linear waves, the maximum inertia force occurs at t = -T/4 and the maximum drag force occurs at $t = 0$. However, for nonlinear waves the times corresponding to maximum inertia and drag forces are phase dependent and not separated by a constant quarter wavelength as in linear wave theory.

- The total maximum force F_m, where the sum of the inertia and drag components is maximum, can be estimated using Figures VI-5-131 to VI-5-134. These figures were also constructed using stream-function theory. Figure selection is based on the nondimensional parameter

$$W = \frac{C_M D}{C_D H} \tag{VI-5-299}$$

and the drawn curves give values of φ_m corresponding to the known parameters H/gT^2 and d/gT^2.

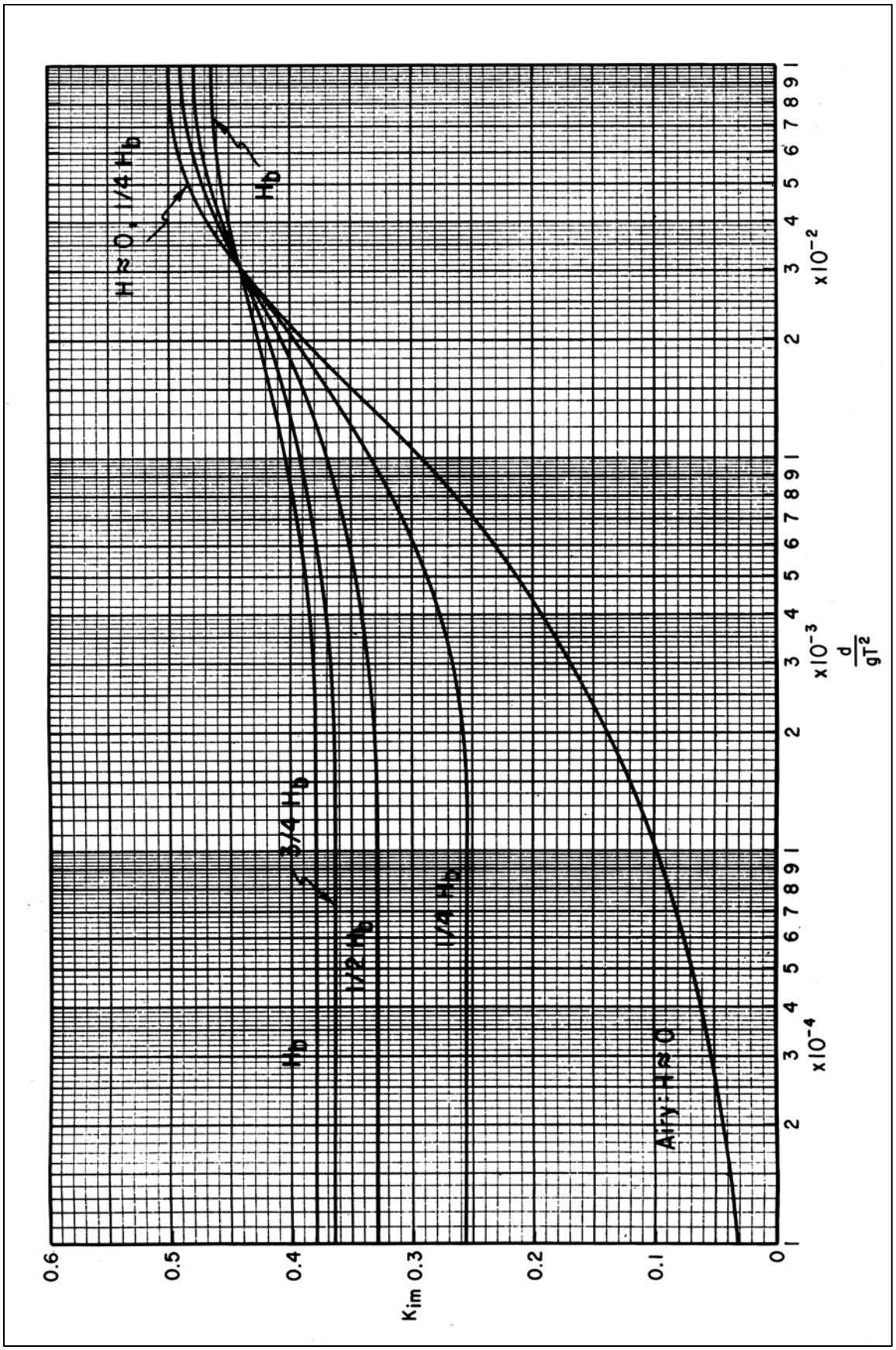

Figure VI-5-126. K_{im} versus relative depth, d/gT^2

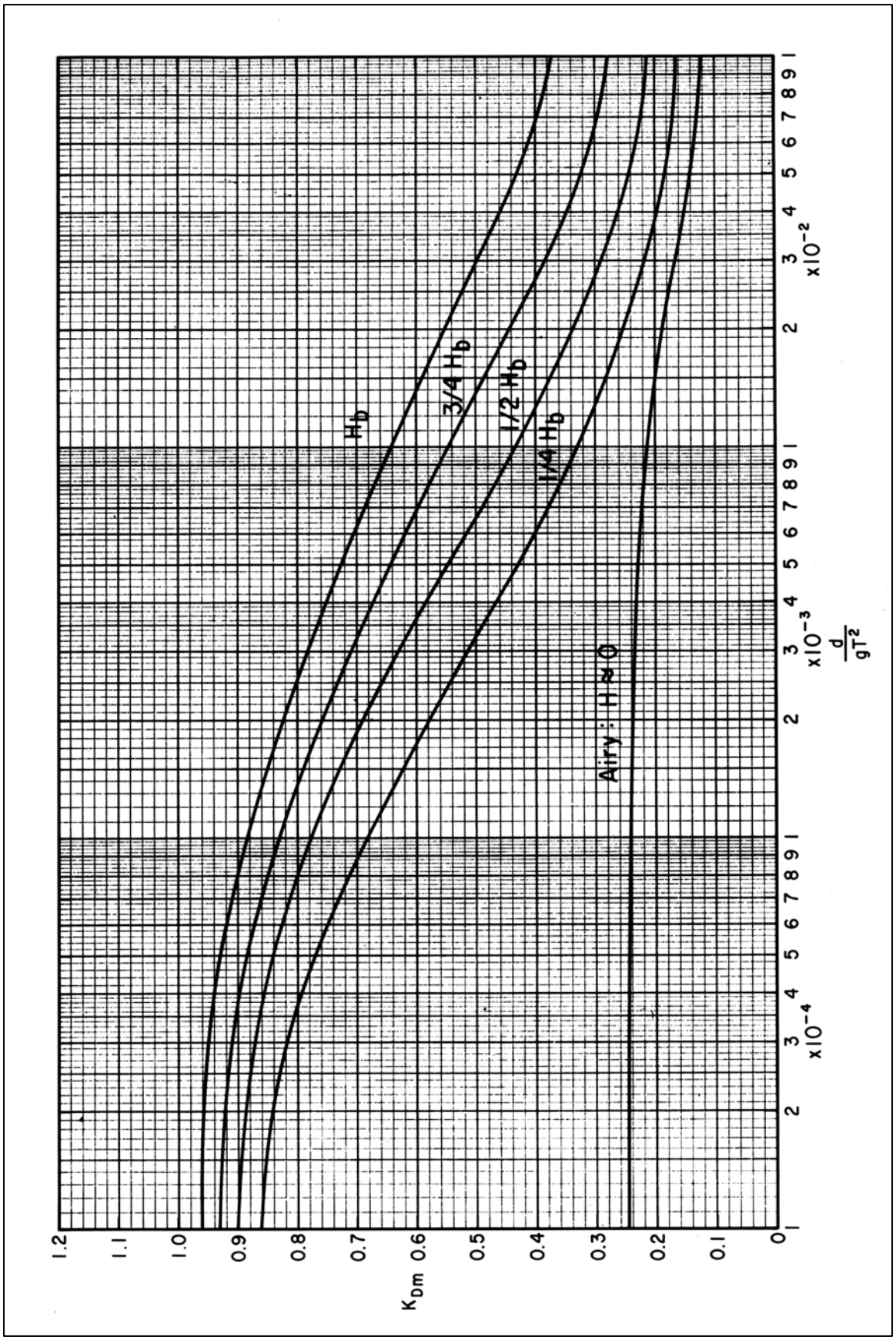

Figure VI-5-127. K_{Dm} versus relative depth, d/gT^2

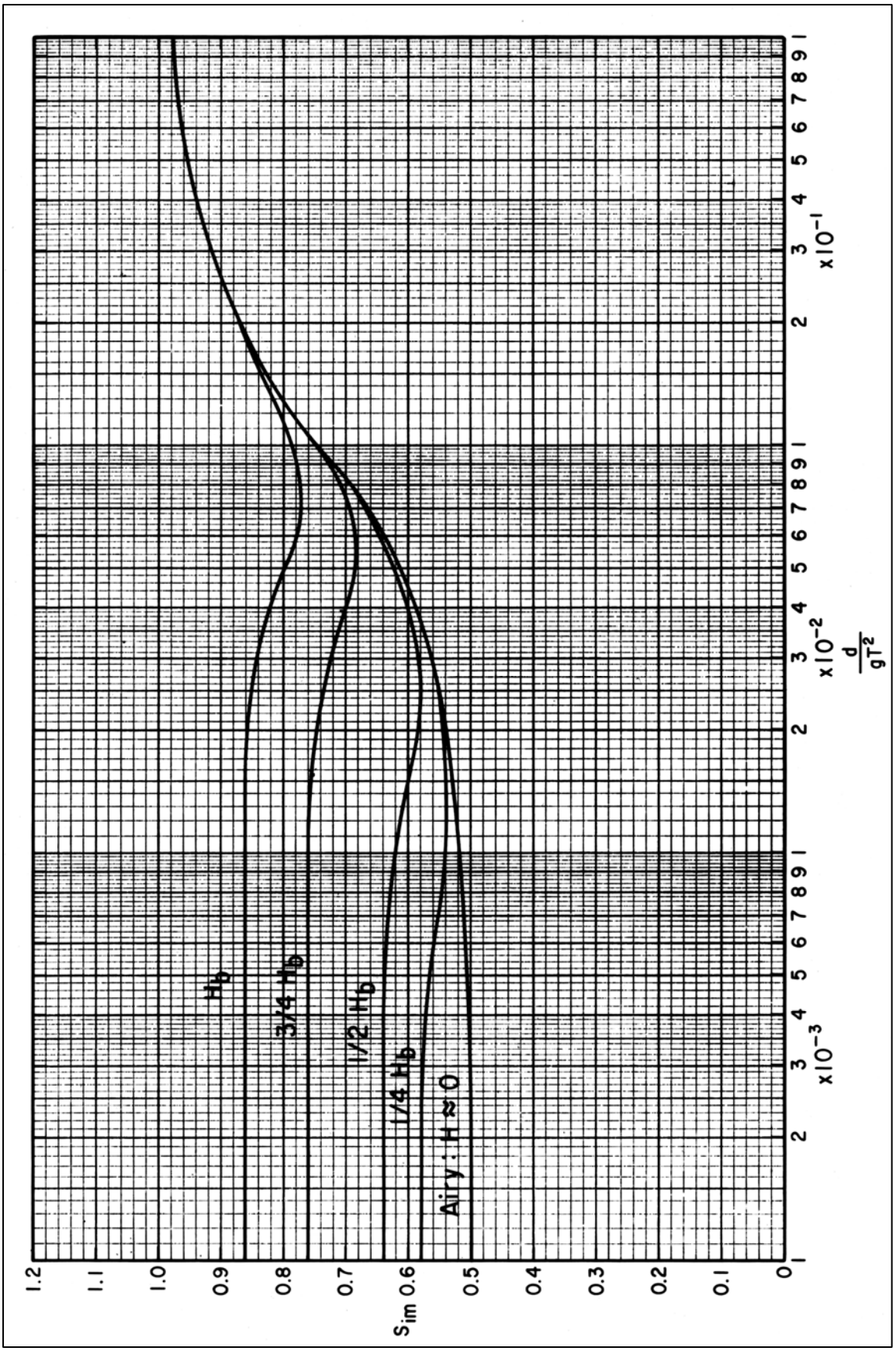

Figure VI-5-128. Inertia force moment arm S_{im} versus relative depth, d/gT^2

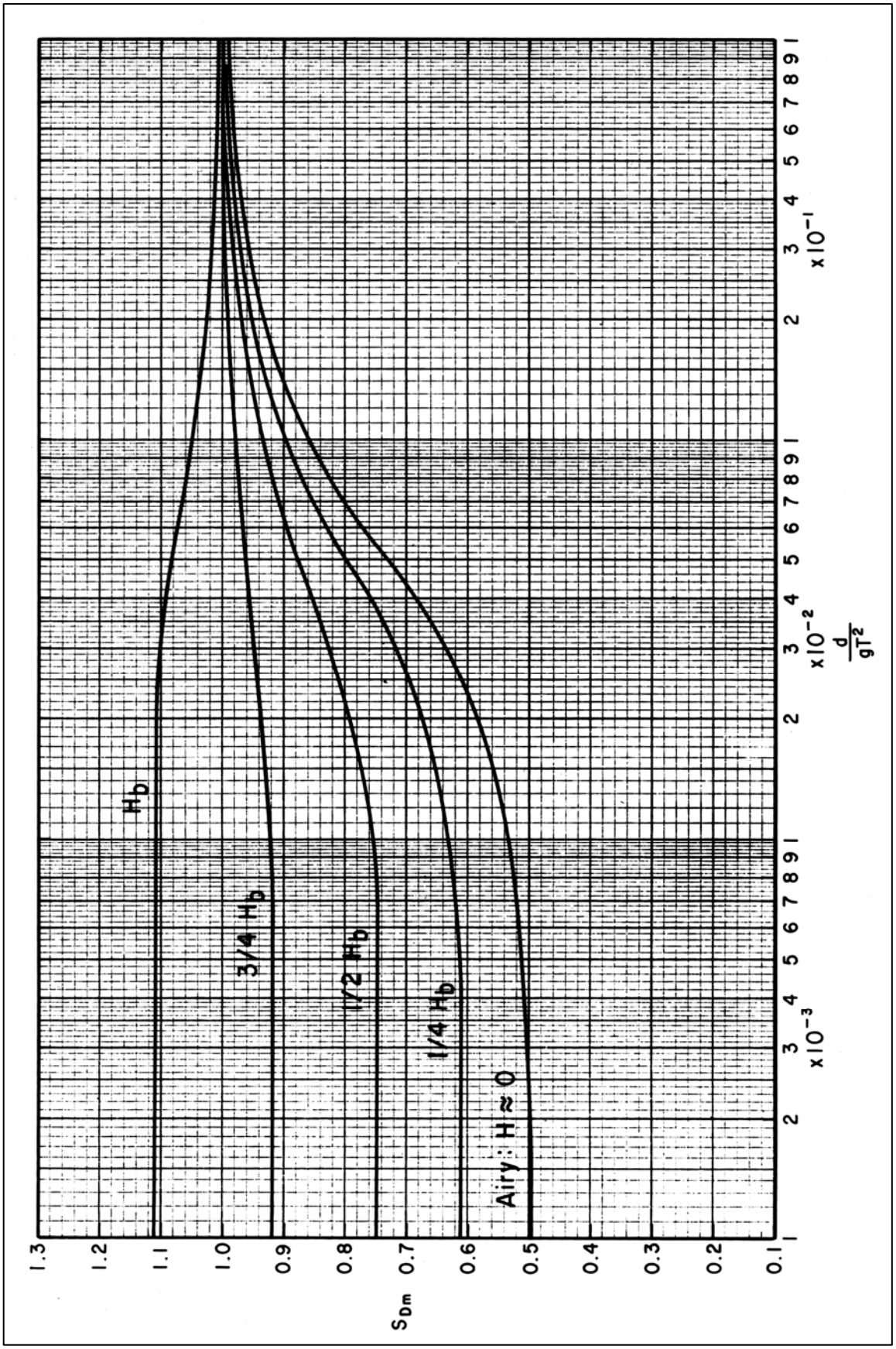

Figure VI-5-129. Drag force moment arm S_{Dm} versus relative depth, d/gT^2

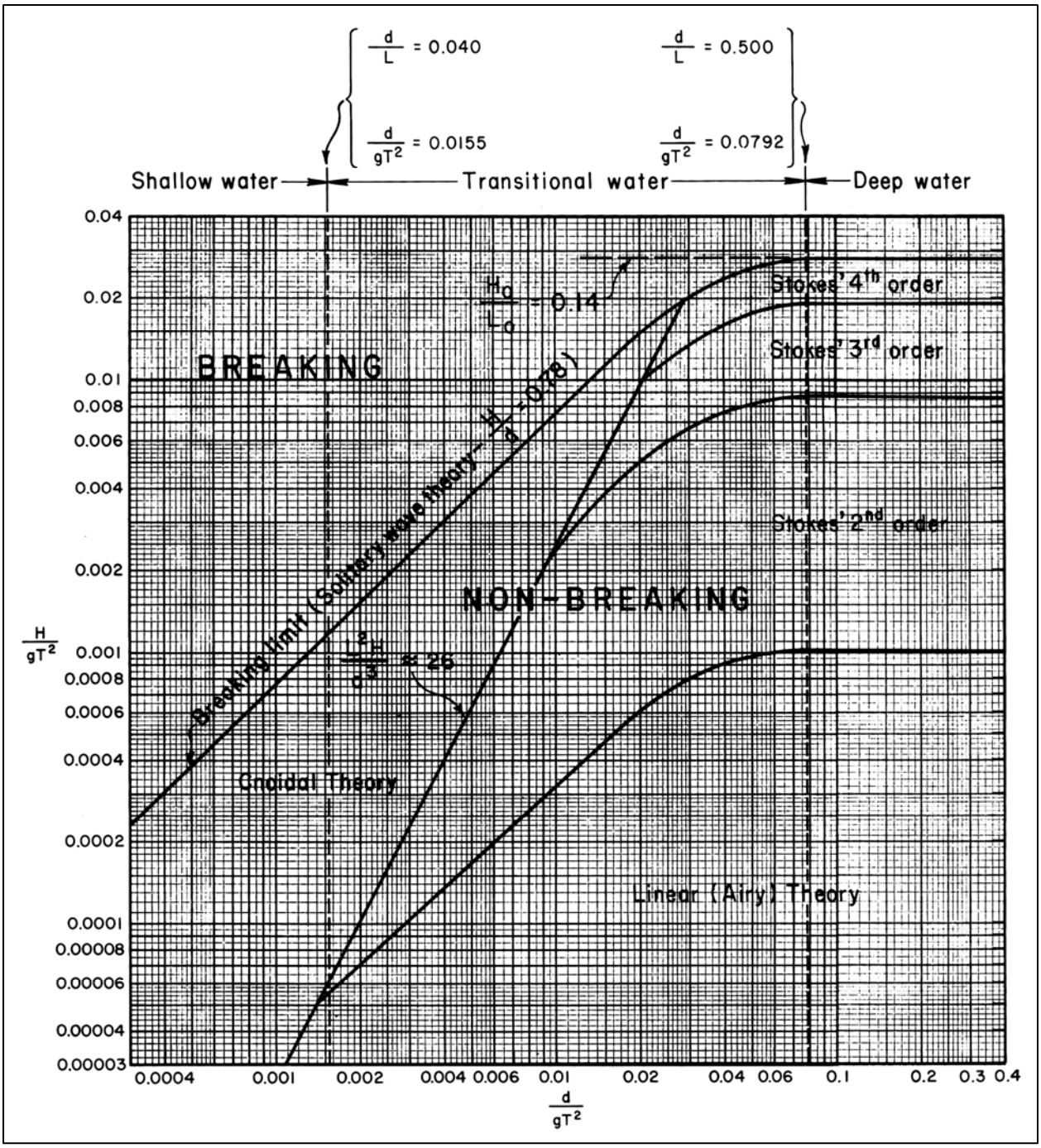

Figure VI-5-130. Breaking wave height and regions of validity of various wave theories

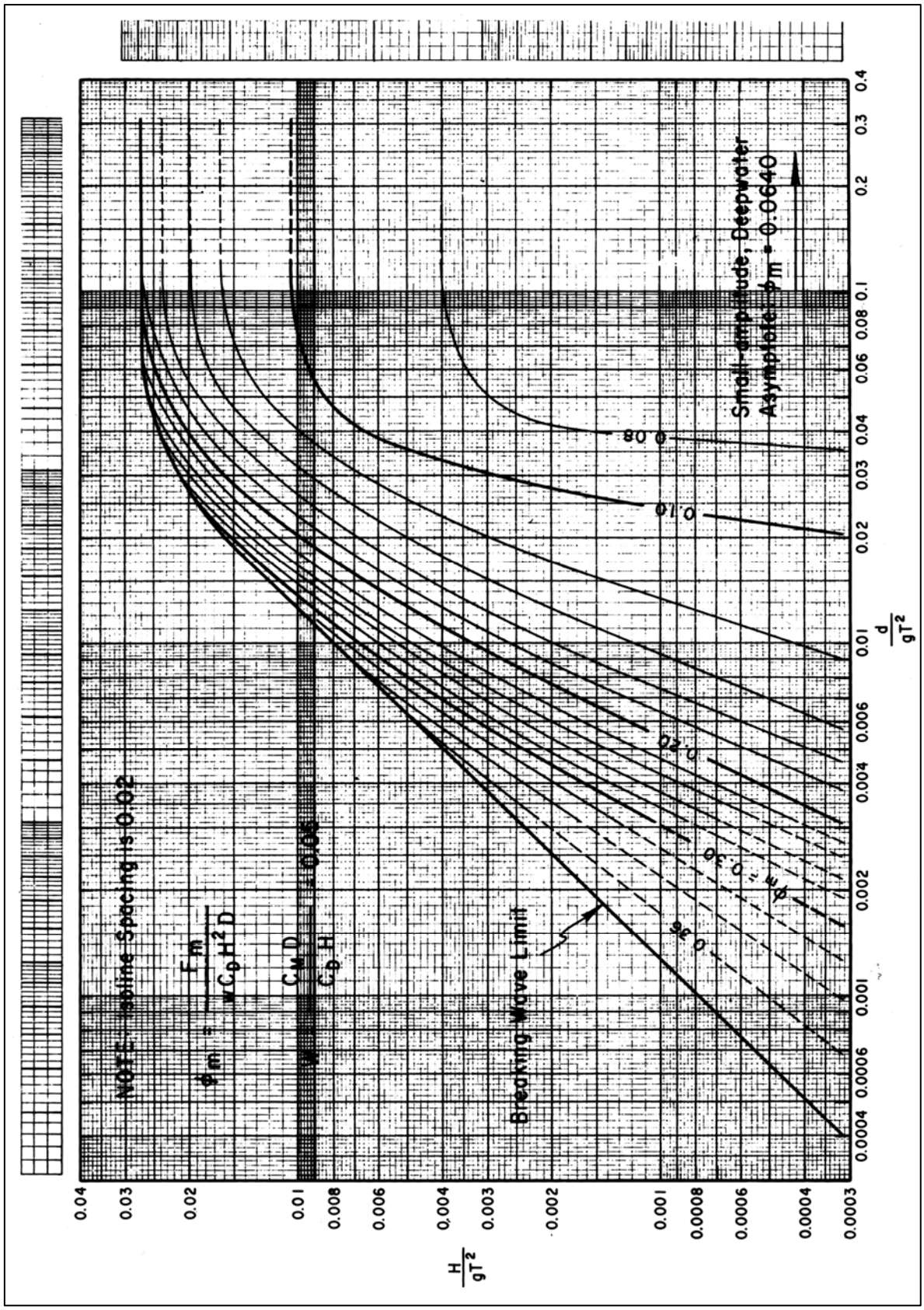

Figure VI-5-131. Isolines of φ_m versus H/gT^2 and d/gT^2 ($W = 0.05$)

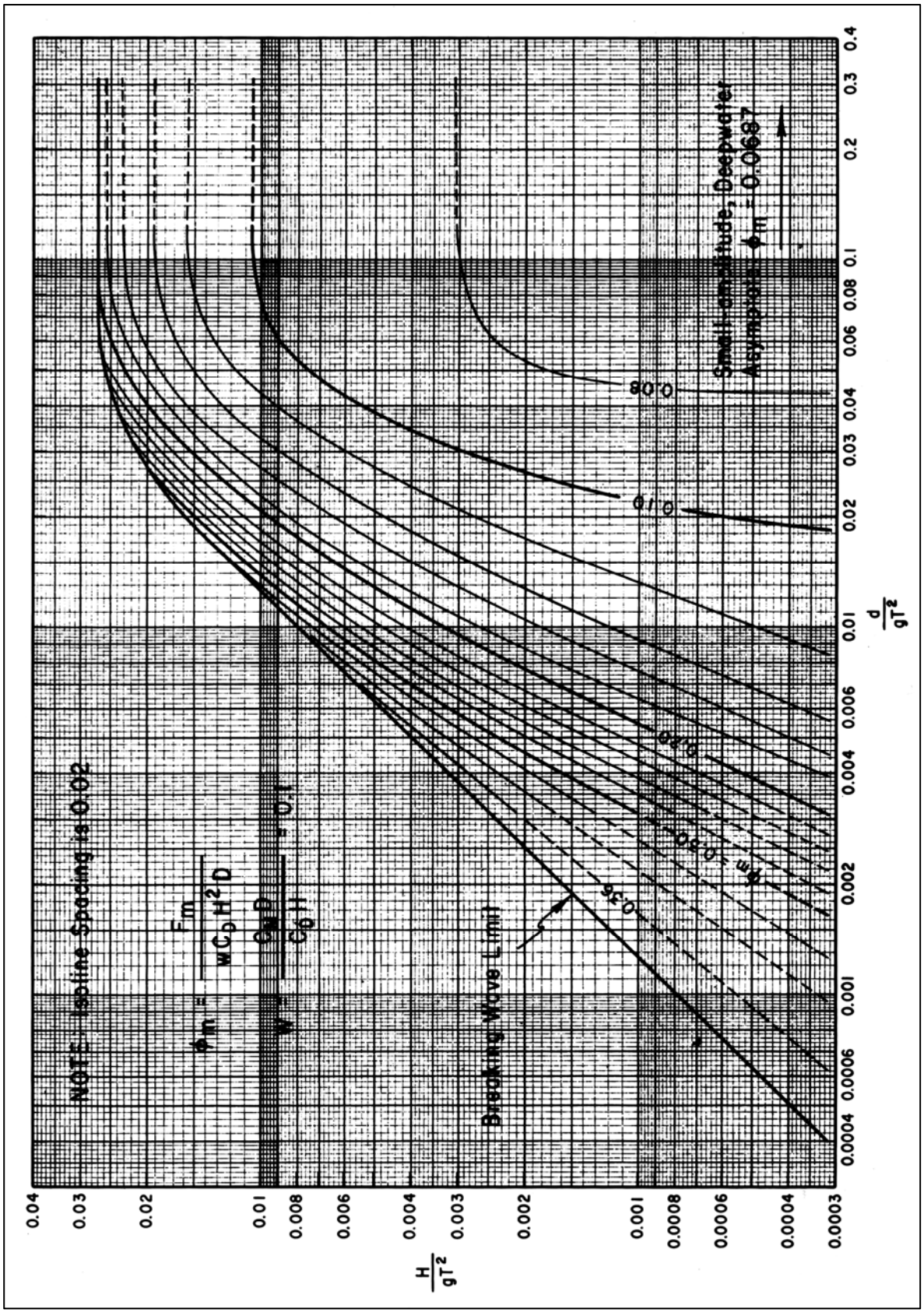

Figure VI-5-132. Isolines of φ_m versus H/gT^2 and d/gT^2 ($W = 0.10$)

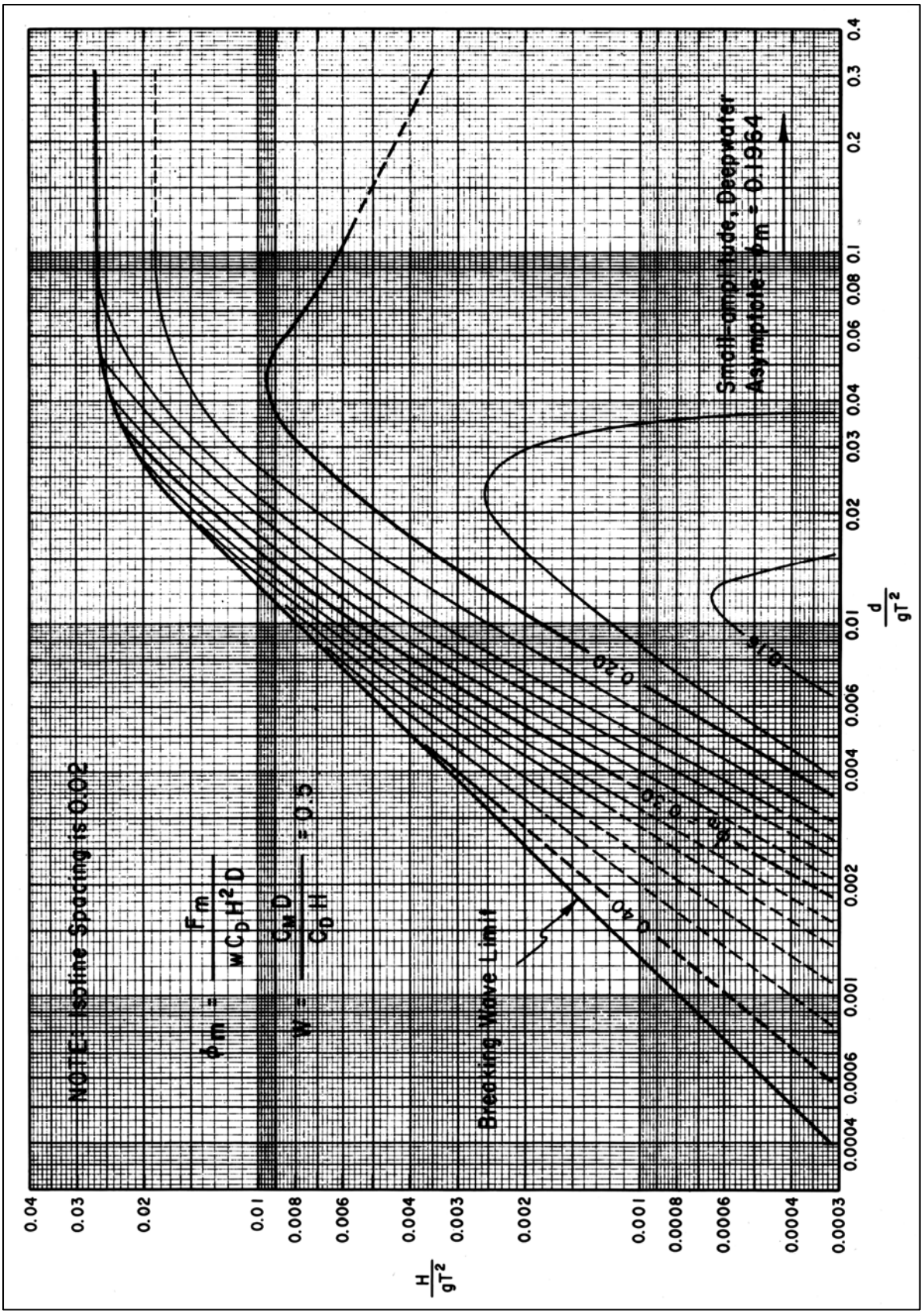

Figure VI-5-133. Isolines of φ_m versus H/gT^2 and d/gT^2 ($W = 0.50$)

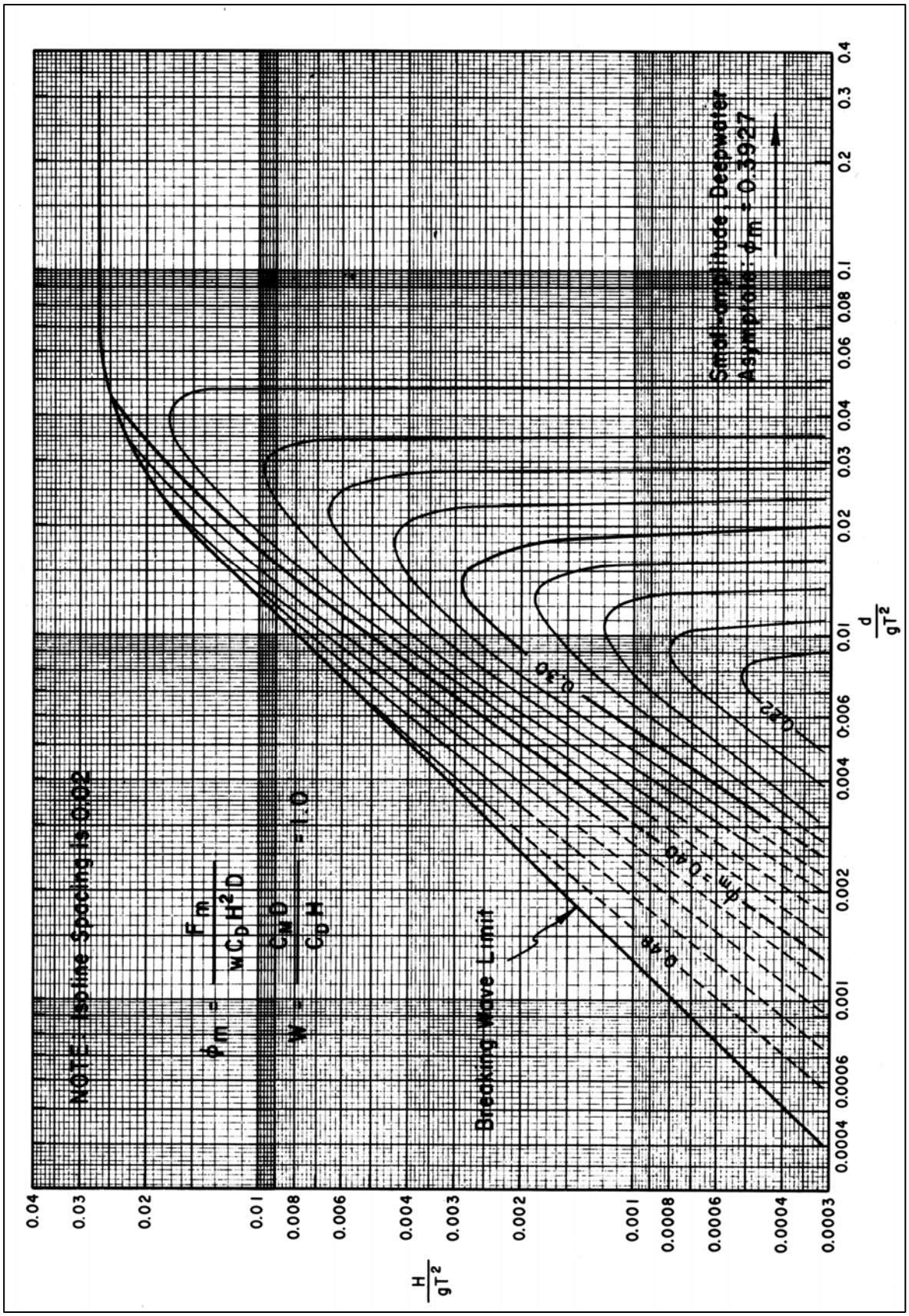

Figure VI-5-134. Isolines of φ_m versus H/gT^2 and d/gT^2 ($W = 1.0$)

- The maximum force is calculated as

$$F_m = \phi_m C_D \rho g H^2 D \quad \text{(VI-5-300)}$$

- Similarly, the total maximum moment M_m can be estimated using Figures VI-5-135 through VI-5-138 which were also constructed using stream-function theory. Choice of figure is based on the value of W given by Equation VI-5-299, and values for α_m are corresponding to the parameters H/gT^2 and d/gT^2. The moment about the mudline is given by

$$M_m = \alpha_m C_D \rho g H^2 D d \quad \text{(VI-5-301)}$$

- For both the total force and total moment calculations, the calculated value of W will likely lie between the values for which the figures are drawn. In this case, determine values of φ_m and α_m from the plots on either side of the W-value, then use linear interpolation to estimate values of φ_m and α_m for the calculated value of W.

- The maximum moment is calculated at the mudline, and the corresponding moment arm is the maximum moment divided by the maximum force, or

$$r_a = \frac{M_m}{F_m} \quad \text{(VI-5-302)}$$

- If the surrounding soil does not provide any lateral resistance, or if there has been scour around the pile, the effective moment arm must be increased and a new maximum total moment calculated. For example, if the scour depth beneath the surrounding bed is S_m, the modified maximum total moment will be

$$M_{m'} = (r_a + S_m) F_m \quad \text{(VI-5-303)}$$

- See Part VI-7, "Design of Specific Project Elements," for an example illustrating calculation of forces and moments on a vertical cylinder.

(3) Transverse forces due to eddy shedding.

(a) In addition to drag and inertia forces that act in the direction of wave advance, transverse forces may arise. Transverse forces are caused by vortex or eddy shedding on the downstream side of the pile. Eddies are shed alternately from each side of the pile resulting in a laterally oscillating force. Transverse forces act perpendicular to both wave direction and pile axis, and they are often termed lift forces because they are similar to aerodynamic lift acting on an airfoil.

(b) Laird, Johnson, and Walker (1960) and Laird (1962) studied transverse forces on rigid and flexible oscillating cylinders. In general, lift forces were found to depend on the dynamic response of the structure. For structures with a natural frequency of vibration about twice the wave frequency, a dynamic coupling between the structure motion and fluid motion occurs, resulting in large lift forces. Transverse forces have been observed 4.5 times greater than

the drag force. However, for rigid structures a transverse force equal to the drag force is a reasonable upper limit. Larger transverse forces can occur where there is dynamic interaction between the waves and cylindrical pile. The design guidance in this section pertains only to rigid piles.

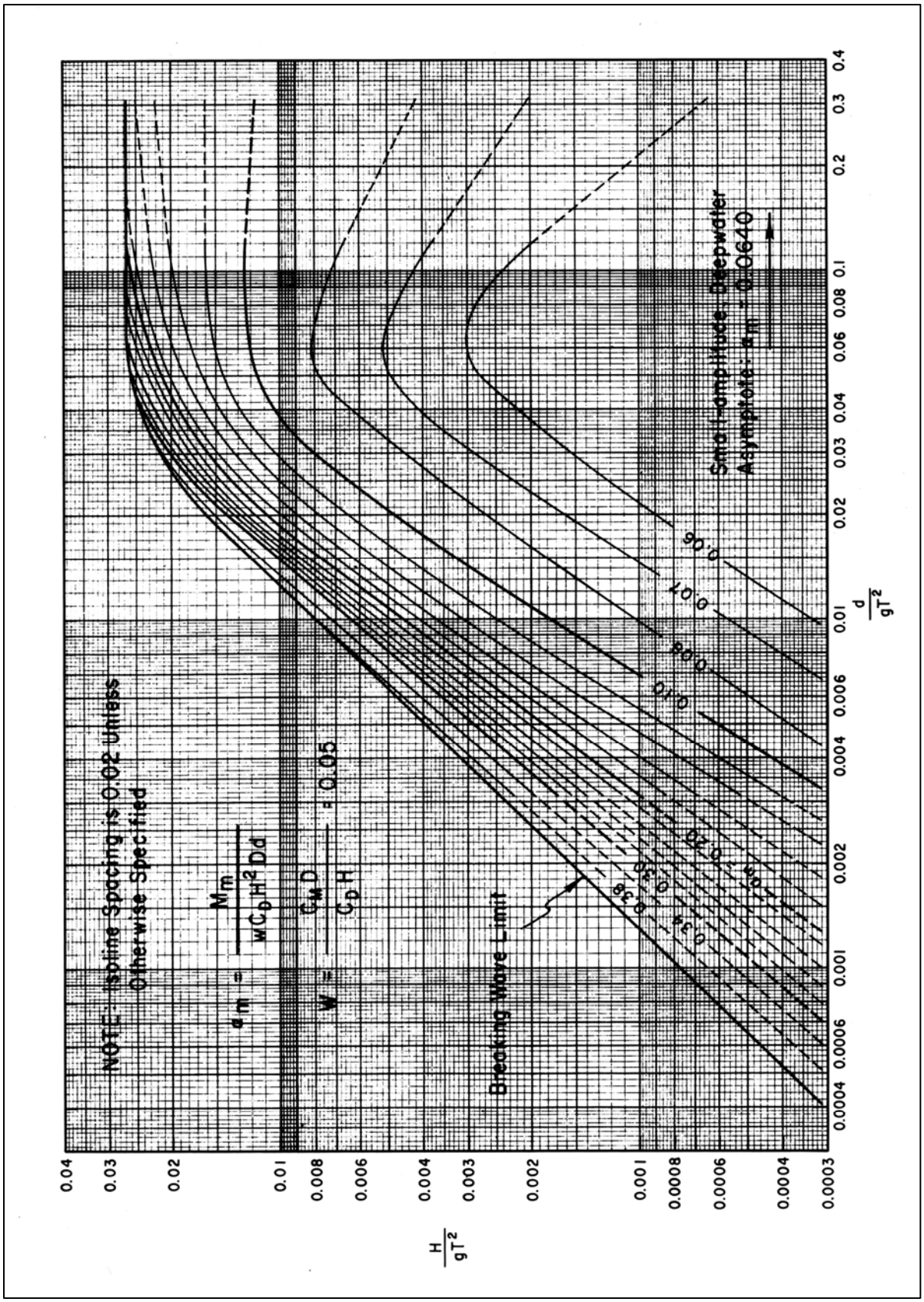

Figure VI-5-135. Isolines of α_m versus H/gT^2 and d/gT^2 ($W = 0.05$)

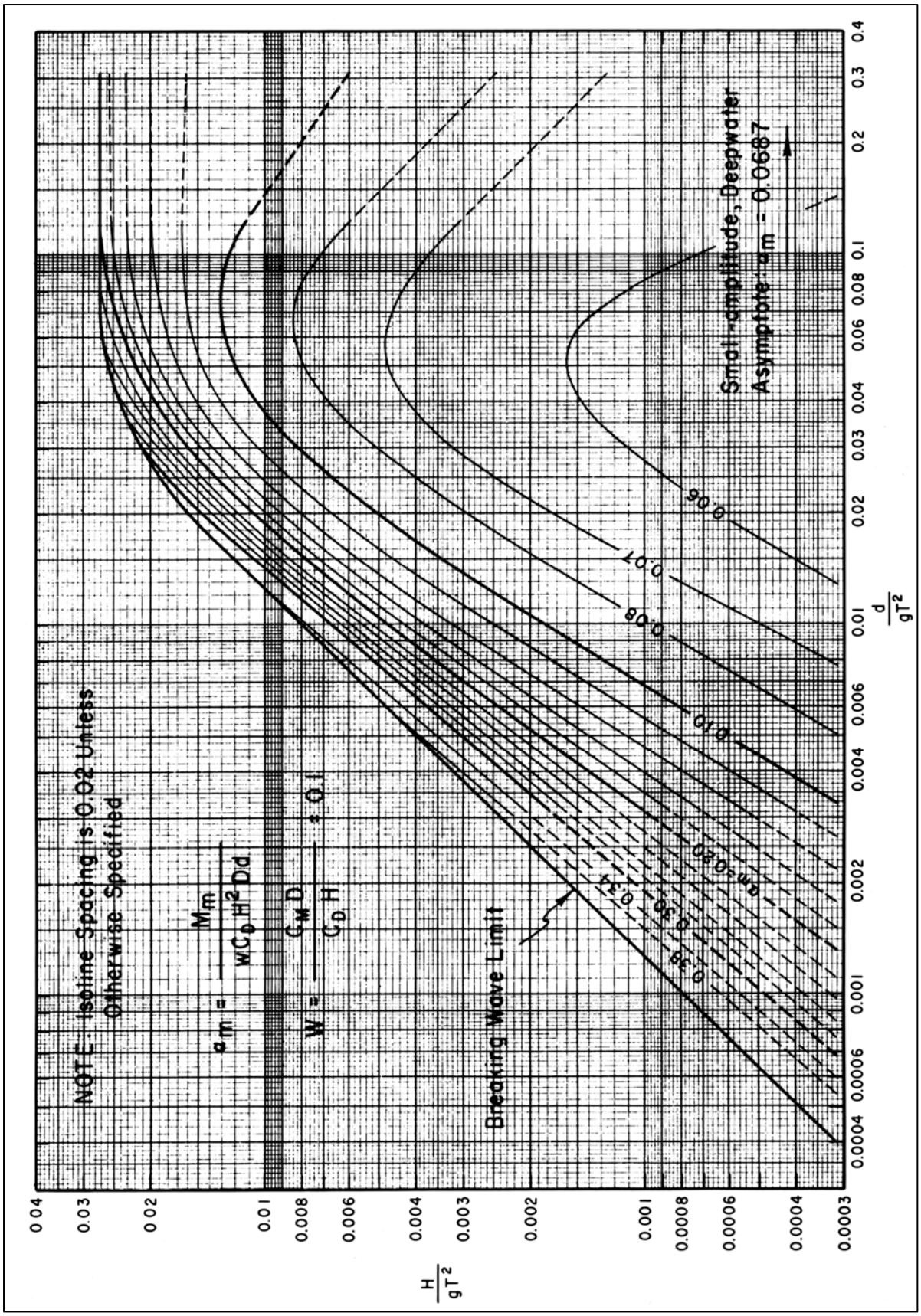

Figure VI-5-136. Isolines of α_m versus H/gT^2 and d/gT^2 ($W = 0.10$)

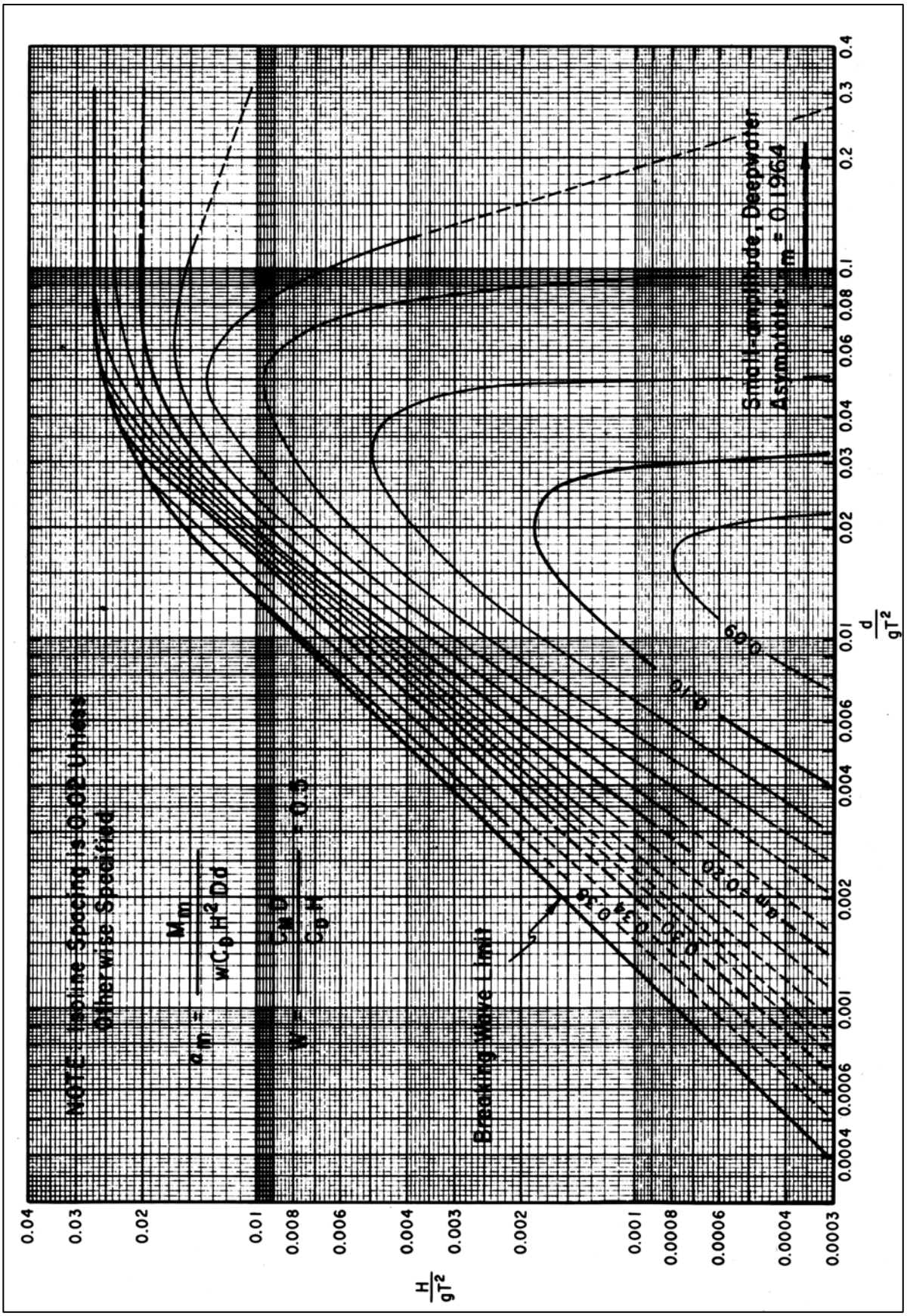

Figure VI-5-137. Isolines of α_m versus H/gT^2 and d/gT^2 ($W = 0.5$)

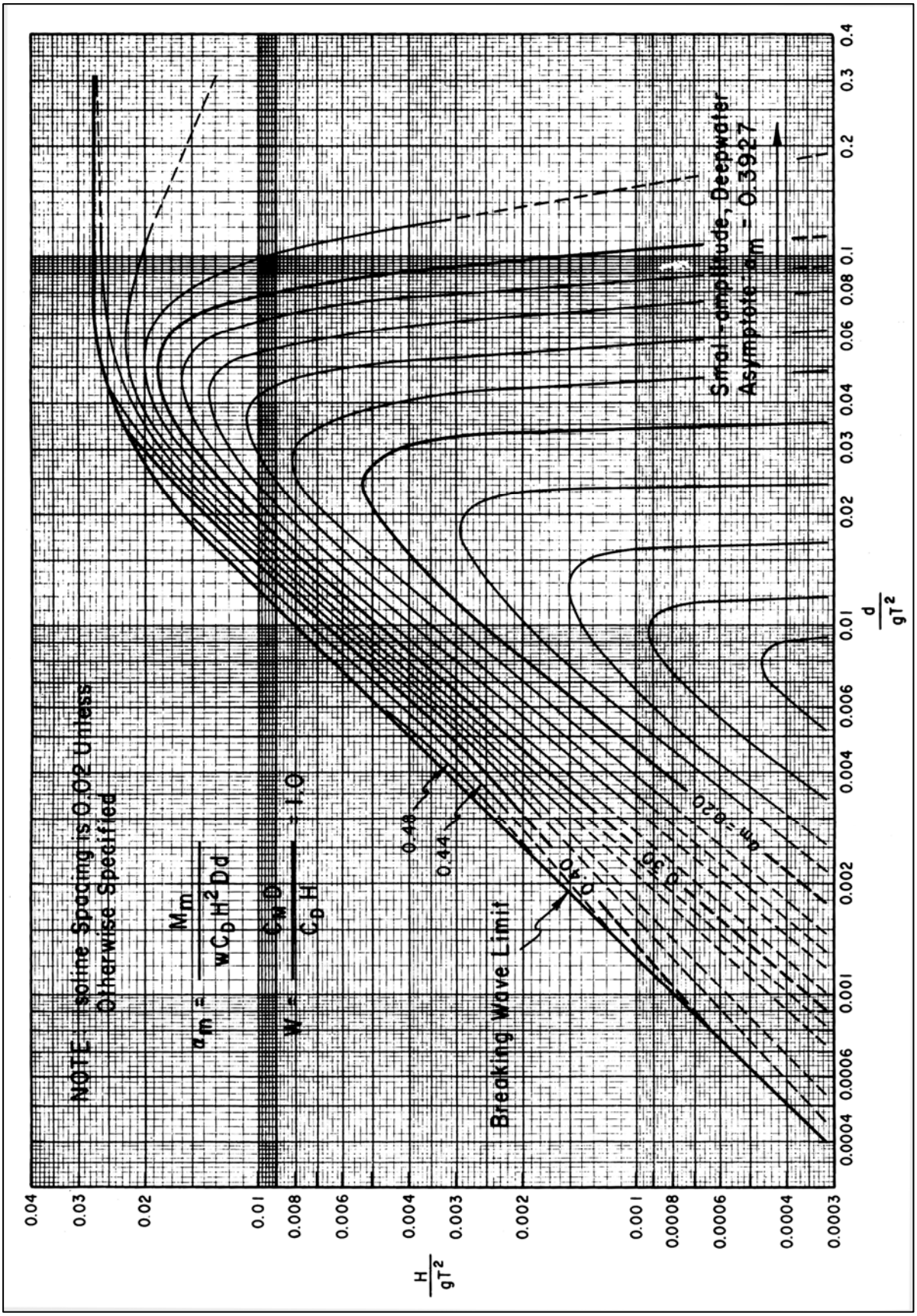

Figure VI-5-138. Isolines of α_m versus H/gT^2 and d/gT^2 ($W = 1.0$)

(c) Chang (1964) found in laboratory investigations that eddies are shed at a frequency that is twice the wave frequency. Two eddies are shed after passage of the wave crest (one on each side of the pile), and two are shed on the return flow after passage of the wave trough. The maximum lift force is proportional to the square of the horizontal wave-induced velocity in much the same way as the drag force. Consequently, for design estimates of the lift force the following equation can be applied.

$$F_L = F_{Lm} \cos 2\theta = C_L \frac{\rho g}{2} D H^2 K_{Dm} \cos 2\theta \qquad \text{(VI-5-304)}$$

where F_L is the time-varying transverse (lift) force, F_{Lm} is the maximum transverse force, θ is the wave phase angle ($\theta = 2\pi x/L - 2\pi t/T$), C_L is an empirical lift coefficient analogous to the drag coefficient in Equation VI-5-286, and K_{Dm} is the dimensionless parameter given in Figure VI-5-127. Chang found that C_L depends on the average Keulegan-Carpenter number given as

$$KC_{ave} = \frac{(u_{\max})_{ave} T}{D} \qquad \text{(VI-5-305)}$$

where $(u_{max})_{ave}$ is the maximum horizontal velocity averaged over the depth. When KC_{ave} is less than 3, no significant eddy shedding occurs and no lift forces are developed. As KC_{ave} increases, C_L increases until it is approximately equal to C_D for rigid piles. Consequently, it must be recognized that: the lift force can represent a major portion of the total force acting on a pile and therefore should not be neglected in the design of the pile.

c. Selection of hydrodynamic force coefficients C_D , C_M , and C_L .

(1) Sarpkaya (1976a, 1976b) conducted an extensive experimental investigation of the inertia, drag, and transverse forces acting on smooth and rough circular cylinders. The experiments were performed in an oscillating U-tube water tunnel for a range of Reynolds numbers up to 700,000 and Keulegan-Carpenter numbers up to 150. Relative roughness of the cylinders k/D varied between 0.002 and 0.02 (where k is the average height of the roughness element). Forces were measured on stationary cylinders, and the corresponding drag and inertia coefficients were determined using a technique of Fourier analysis and least-squares best fit of the Morison equation (Equation VI-5-281) to the measured forces.

(2) The results were presented as plots of the force coefficients versus Keulegan-Carpenter number

$$KC = \frac{u_m T}{D} \qquad \text{(VI-5-306)}$$

for given values of Reynolds number

$$R_e = \frac{u_m D}{\nu} \qquad \text{(VI-5-307)}$$

or the frequency parameter

$$\beta = \frac{R_e}{KC} = \frac{D^2}{\nu T} \qquad \text{(VI-5-308)}$$

(3) In Equations VI-5-306 - VI-5-308 u_m is the maximum horizontal wave velocity, T is the wave period, D is the cylinder diameter, and ν is the fluid kinematic viscosity.

(4) Figures VI-5-139 through VI-5-141 present Sarpkaya's (1976a, 1976b) experimental results for the force coefficients C_D, C_M, and C_L for smooth cylinders. In each figure the force coefficient is plotted versus Keulegan-Carpenter number for constant values of Reynolds number (dotted lines) and frequency parameter (solid lines). Drag and inertia force coefficients versus Reynolds number for rough cylinders are plotted on Figures VI-5-142 and VI-5-143, respectively, for selected values of relative roughness k/D. Sarpkaya cautioned that the force coefficients were developed for oscillatory flow with zero mean velocity, and it is possible that waves propagating on a uniform current may have different force coefficients.

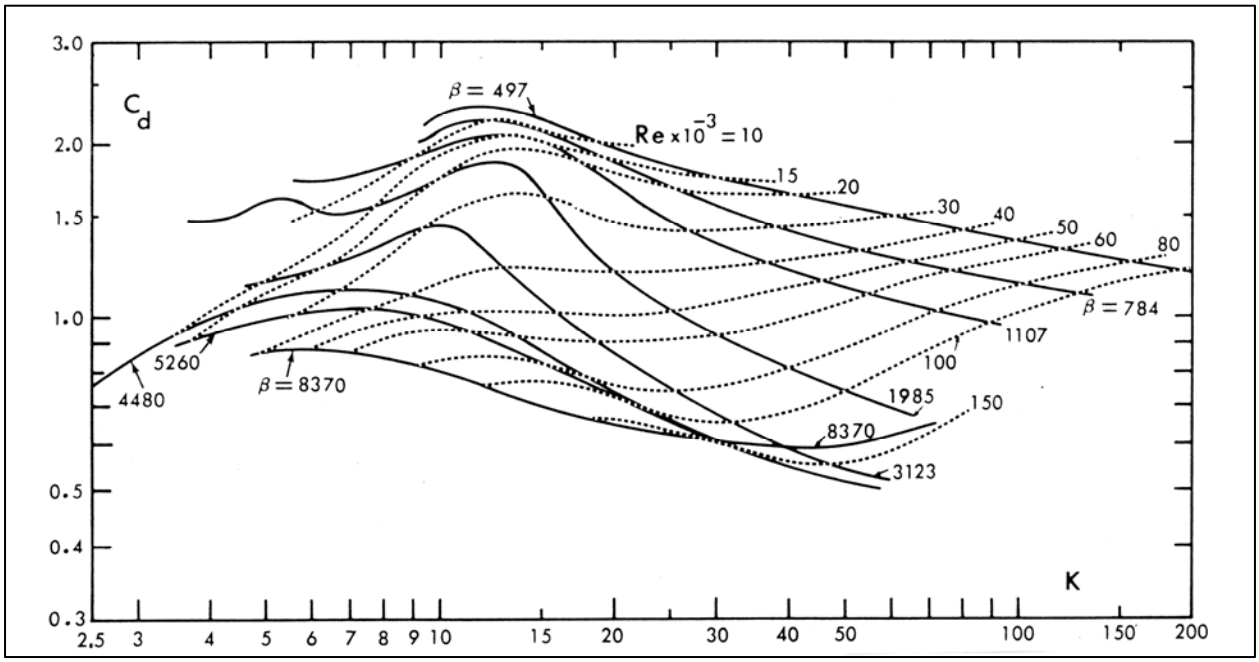

Figure VI-5-139. Drag coefficient C_D as a function of KC and constant values of R_e or β for smooth cylinders (from Sarpkaya 1976a)

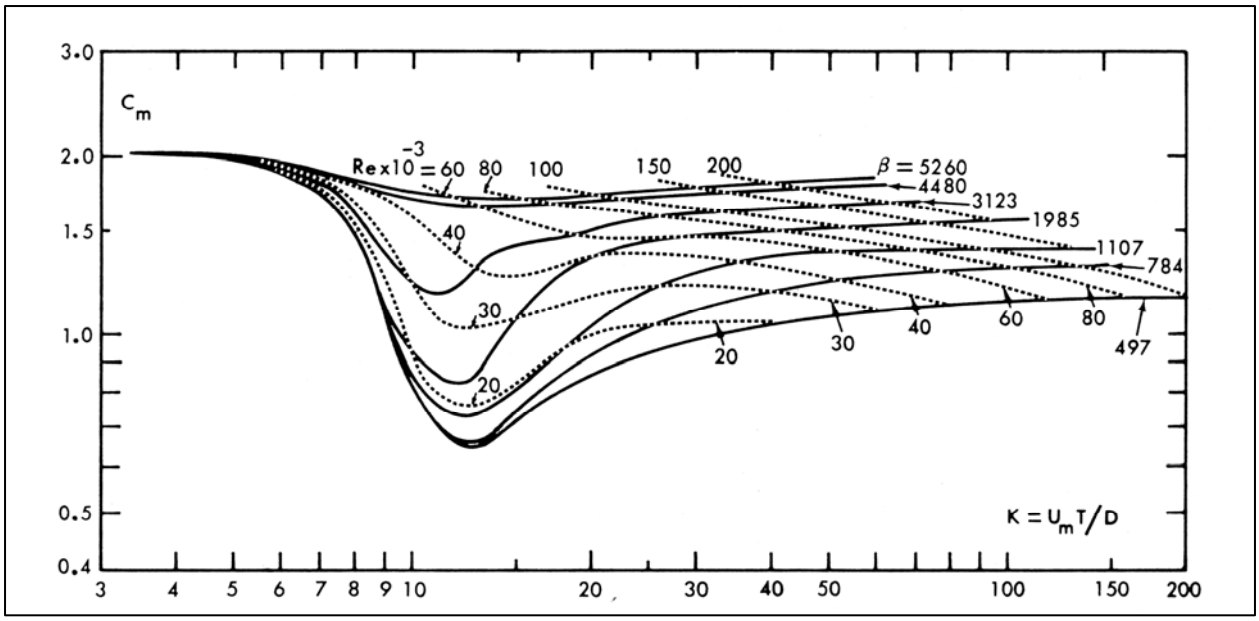

Figure VI-5-140. Inertia coefficient C_M as a function of KC and constant values of R_e or β for smooth cylinders (from Sarpkaya 1976a)

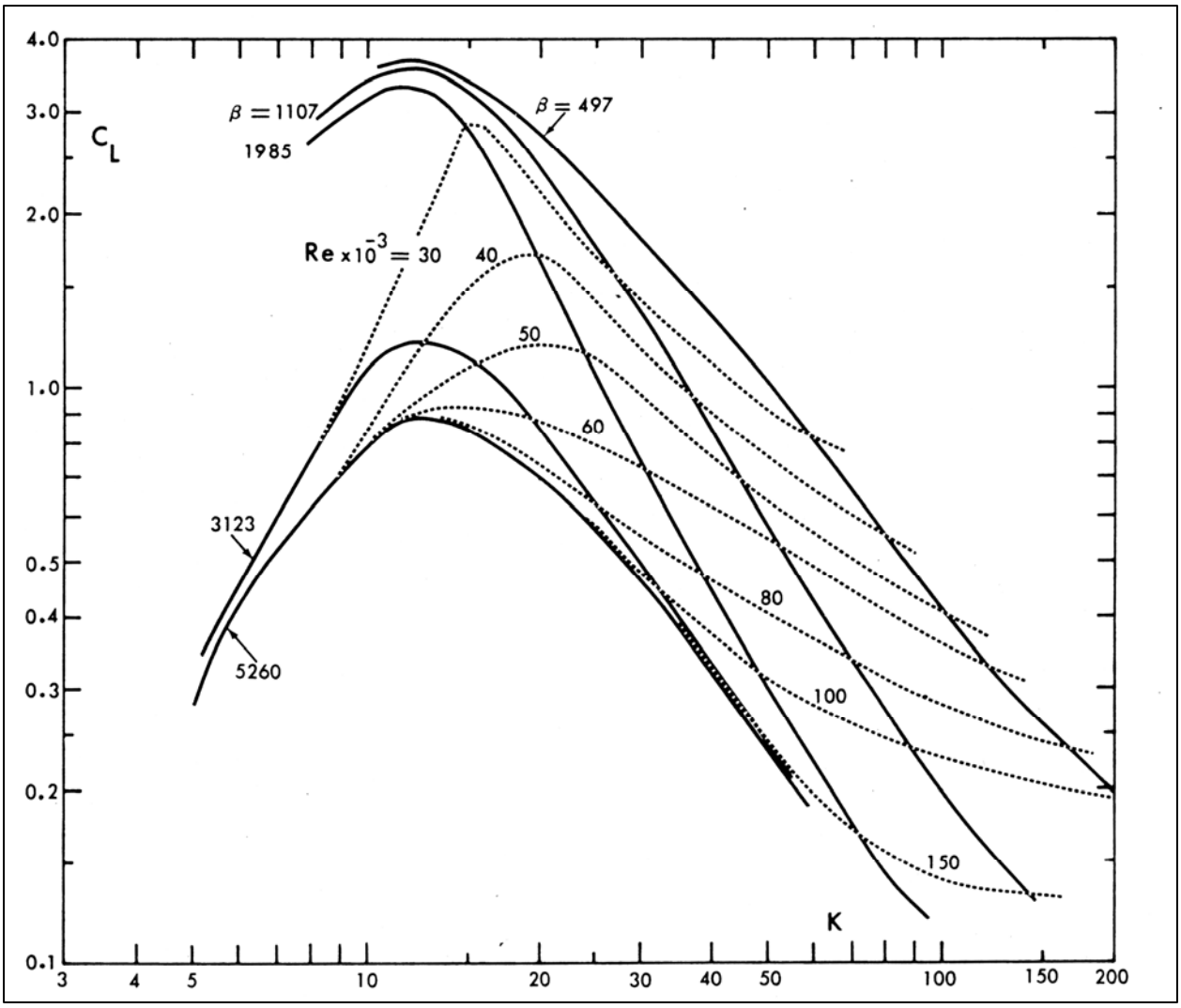

Figure VI-5-141. Lift coefficient C_L as a function of KC and constant values of R_e or β for smooth cylinders (from Sarpkaya 1976a)

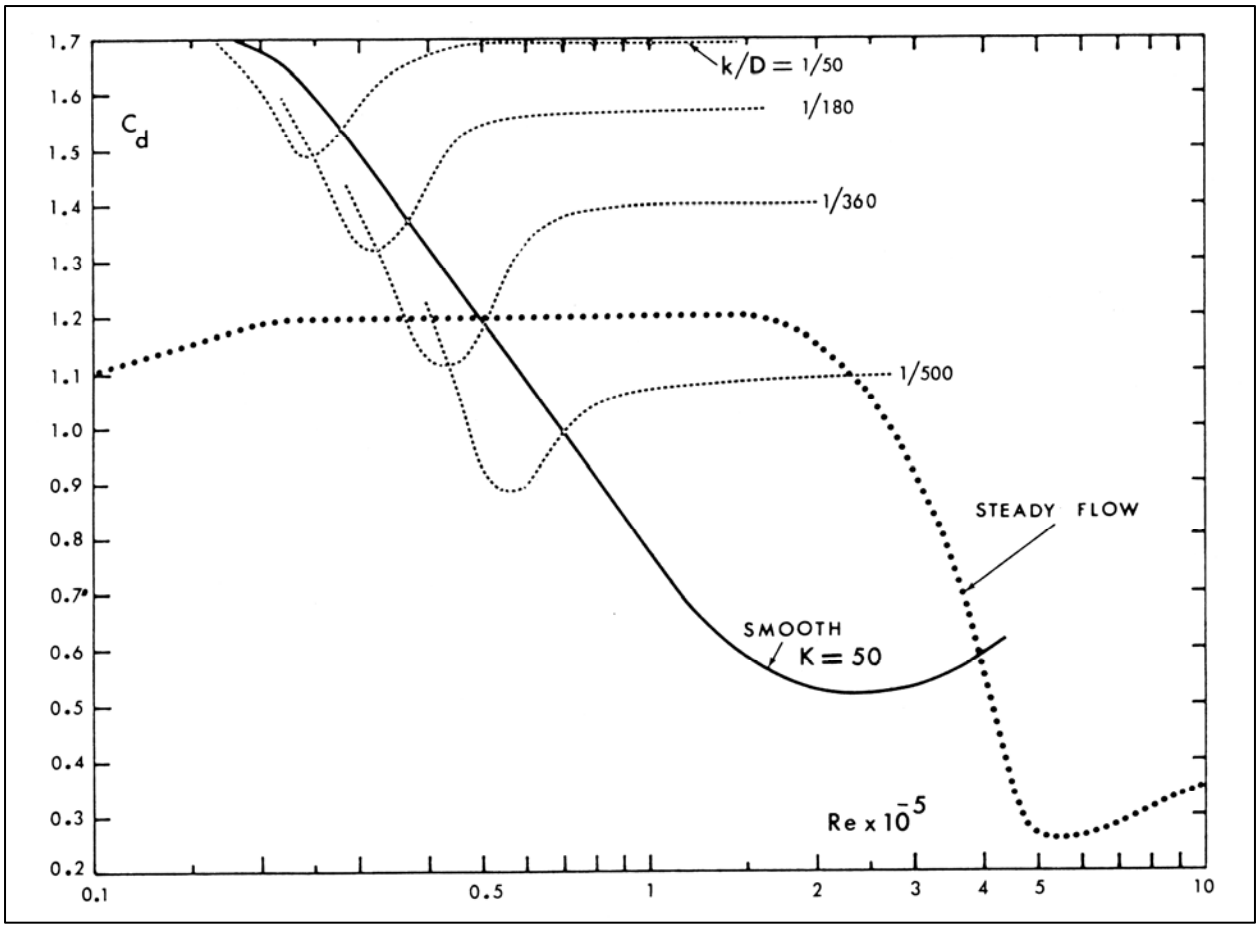

Figure VI-5-142. Drag coefficient C_D as a function of Reynolds number for rough cylinders (from Sarpkaya 1976a)

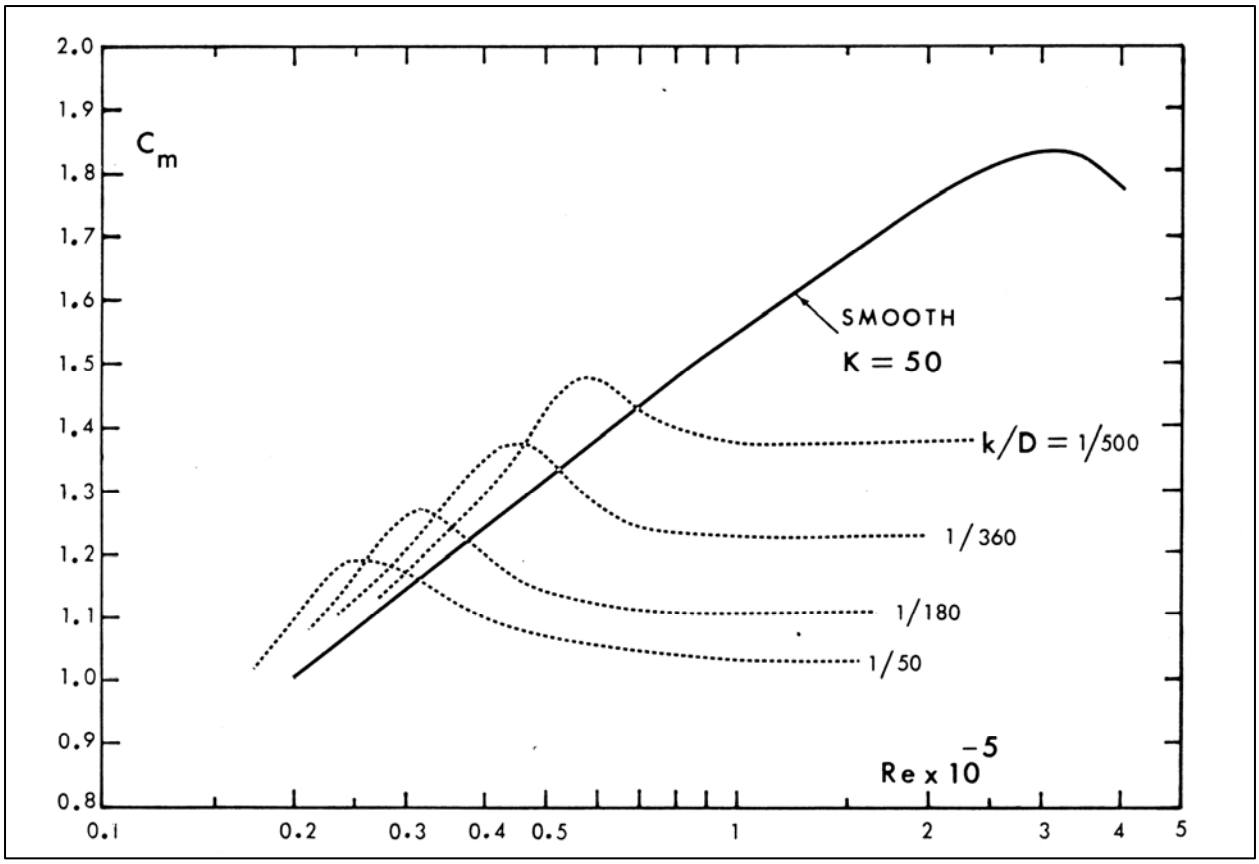

Figure VI-5-143. Inertia coefficient C_M as a function of Reynolds number for rough cylinders (from Sarpkaya 1976a)

(5) The force coefficients given in Figures VI-5-139 through VI-5-143 should give reasonable force estimates when used with the design figures based on stream function theory given in the previous section. However, the design engineer should be aware of the limitations of assuming the force coefficients are constant over the water depth and throughout the wave cycle.

(6) Sarpkaya's experimental apparatus gave uniform values of Reynolds number and Keulegan-Carpenter number over the entire test pile. For a vertical pile exposed to waves, the maximum horizontal velocity will vary from its largest value at the sea surface to a somewhat smaller value near the bottom. Consequently, both R_e and KC will vary over the depth of the pile. For design purposes, it is reasonable to calculate R_e and KC based on the average value of u_m over the water depth in shallow water because the variation will not be too significant. In deeper water it may be wise to investigate the variation of force coefficients with depth to determine if using R_e and KC based on average u_m is appropriate.

(7) Sarpkaya=s experimental data do not cover the range of Reynolds numbers likely to be encountered with bigger waves and larger pile diameters. For larger calculated Reynolds numbers use the following guidance that has been repeated from the old *Shore Protection Manual* (1984).

$$C_D = \begin{cases} 1.2 - \dfrac{(R_e - 2(10)^5}{6(10)^5} & for\ \ 2(10)^5 < R_e - 5(10)^5 \\ 0.7 & for\ \ 5(10)^5 < R_e \end{cases}$$

$$C_M = \begin{cases} 2.5 - \dfrac{R_e}{5(10)^5} & for\ \ 2.52(10)^5 < R_e - 5(10)^5 \\ 1.5 & for\ \ 5(10)^5 < R_e \end{cases}$$

Bear in mind the above recommendations for higher Reynolds number are based on older experimental results, and more accurate estimates might be available from the offshore engineering literature for critical applications.

d. Safety factors in pile design.

(1) Before the pile is designed or the foundation analysis is performed, a safety factor is usually applied to calculated forces. Reasons for uncertainty to the design include approximations in applying the wave theory, estimated values for the force coefficients, potential loss of pile strength over time, and the probability that the design wave will be exceeded during the life of the structure.

(2) The following recommendations for safety factors are offered as general rules of thumb. In situations where pile failure could lead to loss of life or catastrophic failure of supported infrastructure, safety factors should be increased.

(a) When the design wave has low probability of occurrence, it is recommended that a safety factor of 1.5 be applied to calculated forces and moments that are to be used as the basis for structural and foundation design.

(b) If the design wave is expected to occur frequently, such as in depth-limited situations, a safety factor of at least 2.0 should be applied to the calculated forces and moments.

(3) In addition to the safety factor, changes occurring during the expected life of the pile should be considered in design. Such changes as scour about the pile base and added pile roughness due to marine growth may be important.

(4) The design procedure presented in the previous sections is a static procedure; forces are calculated and applied to the structure statically. The dynamic nature of forces from wave action must be considered in the design of some offshore structures. When a structure's natural frequency of oscillation is such that a significant amount of energy in the wave spectrum is available at that frequency, the dynamics of the structure must be considered. In addition, stress reversals in structural members subjected to wave forces may cause failure by fatigue. If fatigue problems are anticipated, the safety factor should be increased or allowable stresses should be decreased. Evaluation of these considerations is beyond the scope of this manual.

(5) Corrosion and fouling of piles also require consideration in design. Corrosion decreases the strength of structural members. Consequently, corrosion rates over the useful life of an offshore structure must be estimated and the size of structural members increased accordingly.

(6) Fouling of a structural member by marine growth increases the roughness and effective diameter of the pile and also changes the values of the force coefficients. The increased diameter must be carried through the entire design procedure to determine forces on the fouled member.

e. Other considerations related to forces on slender cylindrical piles.

(1) Wave forces on pile groups. For a group of piles supporting a structure such as a platform or pier, the methods given in the previous sections can be used provided the piles are sufficiently separated so that flow around one pile does not influence the flow around adjacent piles. One approach is to assume waves are long crested and of permanent form. Given the relative orientation of the piles to each other and to the incoming wave, forces can be estimated on each pile at different times during the wave passage. Typically, the maximum force on individual piles occurs at different times unless all the piles are parallel to the wave crest. Therefore, numerous calculations throughout the wave passage are needed to determine the worst loading on the overall structure. Because the tops of the piles are connected by the superstructure, and the connections may provide some rigidity; it may be necessary to analyze the pile group as a frame.

(a) As the distance between piles becomes small relative to the wavelength, maximum forces and moments on pile groups may be conservatively estimated by summing the maximum forces and moments on each pile.

(b) The assumption that piles are unaffected by neighboring piles is not valid when the distance between piles is less than about three times the pile diameter. Chakrabarti (1991) presented design graphs giving maximum force on a pile in a linear pile group (piles aligned in a row) as a function of Keulegan-Carpenter number and relative separation distance *S/D* where *S* is the distance between center lines of adjacent piles. Graphs were provided for pile groups consisting of two, three and five piles with waves approaching parallel and perpendicular to the line of piles. Graphs were also given for estimating C_D, C_M, and C_L for pile groups of three and five piles exposed to waves parallel and perpendicular to the pile line.

(2) Wave forces on nonvertical piles. Forces and moments on nonvertical cylindrical piles can be estimated using Morison's equation (Equation VI-5-281) where the values for velocity *u* and acceleration *du/dt* are given as the velocity and acceleration components perpendicular to the pile. Calculations will need to be performed using an appropriate wave theory along with the force coefficients given in Part VI-5-7*c*, "Selection of hydrodynamic force coefficients C_D, C_M, and C_L." Do not use the curves provided in design Figures VI-5-126 through VI-5-129 and VI-5-131 through VI-5-134 because these figures are only for vertical piles. For nonvertical piles, the pile self weight (immersed and above water) will contribute to the overturning moment and must be included in the calculation.

(3) Broken wave forces. Forces resulting from action of broken waves on piles are much smaller than forces due to breaking waves. When pile-supported structures are constructed in the surf zone, lateral forces from the largest wave breaking on the pile should be used for design. Although breaking-wave forces in the surf zone are great per unit length of pile, the pile length actually subjected to wave action is usually short. Hence, the resulting total force and moment are small. Pile design in the surf zone is usually governed primarily by vertical loads acting along the pile axis.

VI-5-8. Other Forces and Interactions.

a. Impact forces. Impact force loading on coastal projects occurs when waves or solid objects collide with typically stationary coastal structure elements. Only solid body impacts are discussed in this section. Impact loads between shifting concrete armor units are discussed in Part VI-5-3*c*, "Structural integrity of concrete armor units."

(1) Certain coastal structures such as thin-walled flood barriers, sheet-pile bulkheads, mooring facilities, coastal buildings, or other infrastructure may be subject to impact damage by solid objects carried by waves, currents, or hurricane-force winds. During severe storms, high winds may propel small pleasure craft, barges, and floating debris which can cause significant horizontal impact loads on structures. Likewise, floating ice masses can also cause great impact loads. Impact loads are an important consideration in design of vessel moorings and fendering systems.

(2) Designing a structure to resist impact loads during extreme events is difficult because of uncertainty associated with impact speed and duration. In situations where impact damage by large floating objects could cause catastrophic loss, it may be prudent to limit adjacent water depth by constructing sloping rubble-mound protection fronting the structure or by placing submerged breakwaters seaward of the structure to ground large floating masses and eliminate the hazard.

(3) Impact forces are evaluated using impulse-momentum and energy considerations found in textbooks on fundamental dynamics. However, application of these principles to particular impact problems is difficult unless reliable estimates can be made of object mass (including added mass in water), the mass initial and final velocities, duration of impact loading, and distribution of impact force over time. In addition, some evaluation must be made on whether the collision of the floating object with a coastal structure results in purely elastic behavior in which momentum is conserved, purely plastic impact with all the kinetic energy of the impact being absorbed, or some combination of the two.

(4) Fendering systems in ports and harbors are designed to absorb low-velocity impacts by vessels during docking maneuvers and seiching motions. Design of fendering systems is adequately covered by numerous textbooks and design standards. Examples of typical design references in the coastal engineering literature include Quinn (1972) and Costa (1973). The modes of kinetic energy absorption by fendering systems were studied theoretically by Hayashi and Shirai (1963). Otani, Horii, and Ueda (1975) presented field measurements related to absorption of impact kinetic energy of 50 large tankers. They observed that most berthing velocities are generally below 6 cm/s, and that measured impact energy was substantially larger

than calculated using the design standards that existed at that time. Kuzmanovic and Sanchez (1992) discussed protective systems for bridge piers and pilings, and they gave procedures for accessing the equivalent static force acting on bridge piers due to vessel impacts.

b. Ice forces. A description of ice loading and how it may impact various types of coastal structures in the context of site-specific design criteria is given in Part VI-3-5, "Ice." Other general references include Chen and Leidersdorf (1988); Gerwick (1990); and Leidersdorf, Gadd, and Vaudrey(1996). The following section presents methods for calculating ice forces under specific loading conditions.

(1) Horizontal ice forces.

(a) Solid ice forces.

- Large horizontal forces can result when solid sheet ice, or large chunks of solid ice that have broken free, come in contact with vertical-front coastal structures. Most ice sheets are large enough that impact forces are limited by ice failure in the weakest mode permitted by the mechanics of interaction as the structure penetrates the ice, i.e., crushing, splitting, shear, or bending. For smaller ice blocks or wide structures, the maximum impact force may be limited by the kinetic energy available at the moment of impact (HQUSACE 1982). Ice impact calculations should be based on impulse-momentum considerations, but such calculations will be difficult because of uncertainty in estimating a value for ice block velocity.

- Wind and water current drag acting on large floating blocks of ice press the ice blocks against structures creating large pressures at the points of contact. The force due to drag on a block of ice can be calculated for wind and water currents using the following formula (PIANC 1992)

$$F_d = C_{sf} \rho A (u - u_i)^2 \qquad \text{(VI-5-309)}$$

where

C_{sf} = coefficient of skin friction between wind and ice or water and ice (see Table VI-5-89).

ρ = fluid density (air or water)

A = horizontal area of ice sheet

u = fluid velocity (10 m above ice for air or 1 m below ice for water)

u_i = velocity of ice in the direction of u

Table VI-5-89
Values of Skin Friction Coefficient, C_{sf} (PIANC 1992)

	Smooth Ice	Rough (Pack) Ice
Wind drag	0.001 - 0.002	0.002 - 0.003
Water drag	0.002 - 0.004	0.005 - 0.008

- Separate drag calculations should be performed for both wind and water currents with the results treated as vector forces on the ice mass. Because drag force is directly proportional to ice surface area, larger ice sheets will exert greater forces.

- Once an ice sheet has come to rest against a structure, u_i is zero, and the total drag force can be calculated. Intact ice sheets should be treated as solid bodies with the resultant loads vectorially distributed among the structure/ice contact points using force and moment balance. The total force may be somewhat uniformly distributed along a lineal vertical wall. However, if the ice block comes in contact at only a few discrete points, the contact pressure may be very large. In these cases, the calculated force due to drag may exceed the force necessary for local crushing of the ice, in which case the local crushing strength becomes the limiting force applied to the structure.

(b) Localized ice crushing forces.

- The limiting ice force on a vertical structure is determined by the crushing failure strength of the ice in compression. A theoretical expression for the horizontal ice crushing force was given in Korzhavin in a 1962 Russian publication (Ashton 1986) as

$$\frac{F_c}{bh_i} = m\, I\, k\, x\, \sigma_c \qquad \text{(VI-5-310)}$$

where

F_c = horizontal crushing force

b = structure horizontal width or diameter

h_i = thickness of ice sheet

m = plan shape coefficient

I = indentation coefficient

k = contact coefficient

x = strain rate function

σ_c = ice compressive failure strength in crushing

- This formula is usually applied to piles and pier structures rather than long vertical walls. The plan shape coefficient, m, is 1.0 for flat surfaces, 0.9 for circular piles, and 0.85[$sin(\beta/2)$]$^{1/2}$ for wedge-shaped structures having a wedge angle of β. The indentation coefficient, I, has been found experimentally to be a function of the aspect ratio, b/h_i, and it is usually presented in graphical form. The contact coefficient, k, is a function of ice velocity and width of structure, and it varies between values of 0.4 to 0.7 for ice velocities between 0.5 and 2.0 m/s. The strain rate coefficient is also a function of ice speed. Ashton (1986) provided further details about the theoretical development of Equation VI-5-310 and its associated coefficients.

- In a Russian publication, Afansev (Ashton 1986) combined the coefficients I, k, and x of Equation VI-5-310 into a single coefficient, C, giving the formula

$$\frac{F_c}{bh_i} = C\, m\, \sigma_c \tag{VI-5-311}$$

- Afansev established the following empirical relationship for C based on model tests using laboratory-grown, saline ice.

$$C = \left(5\frac{h_i}{b} + 1 \right)^{1/2} \qquad for\ \ 1 < \frac{b}{h_i}$$
$$C = 4.17 - 1.72\left(\frac{b}{h_i}\right) \qquad for\ \ 0.1 < \frac{b}{h_i} < 1 \tag{VI-5-312}$$

- The lower formula in Equation VI-5-312 is a linear interpolation as recommended in Ashton (1986).

- In Equation VI-5-311 values of the shape coefficient are the same as given for the Korzhavin formula (Equation VI-5-310).

- The Canadian Standards Association Bridge Code (Canadian Standards Association 1978) recommended an even more simplified version of Equation VI-5-310 given by

$$\frac{F_c}{bh_i} = \sigma_c \tag{VI-5-313}$$

using the range of values for sheet ice compressive crushing strength shown in Table VI-5-90. Equation VI-5-313 and the crushing strength values of Table VI-5-90 were also adopted by the American Association of State Highway and Transportation Officials.

- Use of Equation VI-5-313 implies that the product $C\ A\ m = 1$ in Equation VI-5-311, which corresponds to large values of b/h_i. This is a realistic assumption for large bridge piles and piers, but ice crushing forces on smaller diameter piles should be calculating using the appropriate strength values from Table VI-5-90 in Equation VI-5-311.

Table VI-5-90
Values of Effective Ice Crushing Strength, σ_c

Ice Crushing Stress	Environmental Situation
0.7 MPa (100 psi)	Ice breakup occurs at melting temperatures and the ice moves in small pieces that are essentially disintegrated.
1.4 MPa (200 psi)	Ice breakup occurs at melting temperatures, but the ice moves in large pieces that are generally sound.
2.1 MPa (300 psi)	Ice breakup consists of an initial movement of the entire ice sheet or large sheets of sound ice impact piers.
2.8 MPa (400 psi)	Ice breakup occurs with an ice temperature significantly below the melting point and ice movement consists of large sheets.

(c) Thermal ice forces. Equations are available for predicting ice temperature based on an energy balance between the atmosphere and the ice sheet. However, the required parameters (air temperature, air vapor pressure, wind, and cloud cover) needed to calculate thermal expansion are difficult to estimate. Thermal strain is equal to the ice thermal expansion coefficient times the change in ice temperature. For restrained or partially restrained ice sheets a nonlinear, time dependent stress-strain law is used to predict thermal stresses (HQUSACE 1982). Because of stress relaxation due to creep, the rate of thermal change is an important factor; and even a thin snow cover can drastically reduce thermal stresses in ice sheets.

- A design rule-of-thumb for thermal expansion loads per unit horizontal length on dams and other rigid structures is 145 - 220 kN/m (10,000 - 15,000 lbs/ft) (HQUSACE 1982). Movable structures should allow for 73 kN/m (5,000 lbs/ft). These values are based on field measurements.

- Thermal expansion of water frozen between elements of a coastal structure can result in dislocation of individual elements or cracking of armor units making the protection vulnerable to wave attack.

(2) Ice forces on slopes.

(a) Ride-up of ice on slopes.

- When horizontally moving ice encounters a sloping structure, a component of the horizontal force pushes the ice up the slope. This action induces a bending failure in the ice sheet at loads less than required for ice crushing failure. Ashton (1986) showed the derivation of a simple two-dimensional theory for calculating the horizontal force exerted by ice on a sloping structure as illustrated in Figure VI-5-144. (Ashton also included discussion and analysis of the more complex case of ice ride-up on three-dimensional structures).

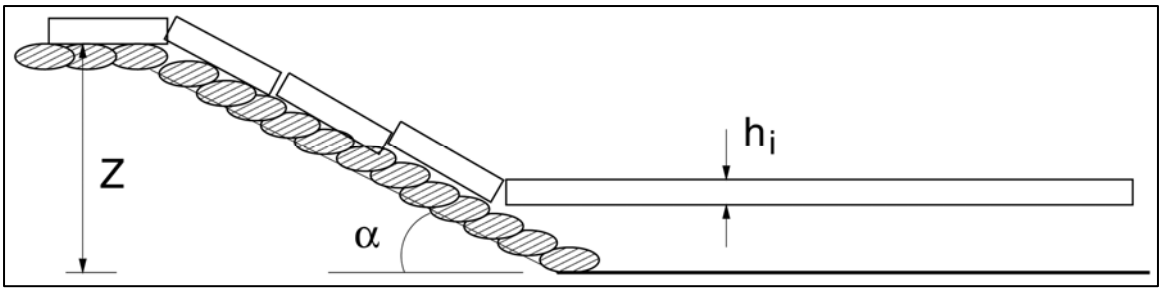

Figure VI-5-144. Ice riding up on structure slope

- For the two-dimensional case the horizontal force per unit width of structure was given by the expression

$$\frac{F_h}{b} = C_1 \sigma_f \left(\frac{\rho_w g h_i^5}{E} \right)^{1/4} + C_2 Z \rho_i g h_i \qquad \text{(VI-5-314)}$$

with

$$C_1 = 0.68 \left[\frac{\sin \alpha + \mu \cos \alpha}{\cos \alpha - \mu \sin \alpha} \right] \qquad \text{(VI-5-315)}$$

and

F_h = total horizontal force

$$C_2 = \left[\frac{(\sin \alpha + \mu \cos \alpha)^2}{\cos \alpha - \mu \sin \alpha} + \frac{\sin \alpha + \mu \cos \alpha}{\tan \alpha} \right] \qquad \text{(VI-5-316)}$$

b = horizontal width of structure contact zone

h_i = ice sheet thickness

σ_f = flexural strength of ice (0.5 = 1.5 MPa)

ρ_w = water density

ρ_i = ice density (915 = 920 kg/m^3)

E = modulus of elasticity of ice (1,000 = 6,000 MPa)

Z = maximum vertical ice ride-up distance

g = gravitational acceleration

α = structure slope angle relative to horizontal

μ = structure slope friction factor (0.1 = 0.5)

- The first term in Equation VI-5-314 is interpreted as the force necessary to break the ice in bending, and the second term is the force that pushes the ice blocks up the sloping structure. The modulus of elasticity varies from 1,000 MPa for very salty water up to about 6,000 MPa for fresh water (Machemehl 1990). Ashton (1986) warned that this simple two-dimensional theory will be inadequate for narrow structures because the zone of ice failure will be wider than the structure.

- Low values of friction factor (μ = 0.1) are associated with smooth slopes such as concrete or carefully layed block protection, whereas high values (μ = 0.5) are applicable for randomly-placed stone armor, riprap, or filled geotextile bags. For slopes steeper than 1:1, the horizontal ice force increases rapidly for the higher friction factors, and there is a risk of the dominant failure mode being crushing or buckling rather than bending. Milder slopes with smooth surfaces are much more effective in reducing horizontal ice forces. Croasdale, Allyn, and Roggensack (1988) discussed several additional aspects related to ice ride-up on sloping structures.

- Quick "rough" estimates of horizontal forces on sloping structures can be made using a variation of Equation VI-5-313 as proposed in Ashton (1986), i.e.,

$$\frac{F_h}{b} = K_h h_i \sigma_c \tag{VI-5-317}$$

where K_h is approximated from a curve given in Ashton (1986) by the formula

$$K_h = 1 - 0.654 f^{0.38} \tag{VI-5-318}$$

with

$$f = \frac{1 - \mu \tan \alpha}{\mu + \tan \alpha} \tag{VI-5-319}$$

and σ_c is the ice compressive strength as given in Table VI-5-90. As slope angle increases, K_h approaches a value of unity which represents failure by crushing. For decreasing slope angles, K_h decreases because of the increasing tendency of the ice to fail in bending. Values of K_h less than 0.2 should never to used in Equation VI-5-317.

(b) Adfreeze loads. When ice that is in contact with a coastal structure is stationary for a sufficient time, the ice will freeze to the structure or its elements. Adfreeze loads result if the ice then moves either horizontally by dynamic ice thrust or vertically due to changing water level. This is more of a problem in lakes with slowly varying water levels than in tidal waters.

- Little guidance is available on adfreeze stresses with adhesion strength varying between 140 kPa to 1050 kPa for freshwater ice (PIANC 1992). Adfreeze may dislodge individual armor stones on rubble-mound slopes creating a weakness in the armor layer. This can be prevented by using oversized stones or interlocking armor on the slope. A survey of riprap structures at Canadian hydropower reserviors concluded that plucking of individual stones frozen to ice could be largely prevented by sizing the riprap median diameter (d_{50}) greater than the expected maximum winter ice thickness (Wuebben 1995).

(3) Vertical ice forces. Ice frozen to coastal structures can create vertical forces due to ice buoyancy effects when water level rises, or by ice weight when water level falls. These vertical forces will persist until the ice sheet fractures due to bending or the adfreeze force is exceeded.

(a) Cylindrical piles.

- In cases where the ice sheet freezes around a pile, forces will be exerted on the pile if the water level rises or falls. A rising water level will lift the ice sheet, and under certain conditions the uplift force on the pile may be sufficient to pull the pile free. Similarly, during falling water levels the weight of the ice sheet will exert a downward force on a pile which may be sufficient to buckle a slender pile.

- Kerr (1975) studied vertical loads on cylindrical piles and presented equations for calculating loads under the conservative assumption that the water level change is rapid enough to assure elastic ice behavior before failure. A closed-form solution to the governing equation was obtained in terms of Bessel functions, and Kerr presented a numerically evaluated solution in graphical form as shown on Figure VI-5-145. The graphical solution is dimensional, and it has the functional form of

$$P = f\ (a, h, E_{av}, \Delta, \nu) \tag{VI-5-320}$$

where

P = uplift force in metric tons (tonnes)

a = pile radius (cm)

h = ice plate thickness (cm)

E_{av} = averaged Young's modulus for ice (kg/cm^2)

Δ = water level rise (cm) up to the thickness of the ice

ν = Poisson's ratio

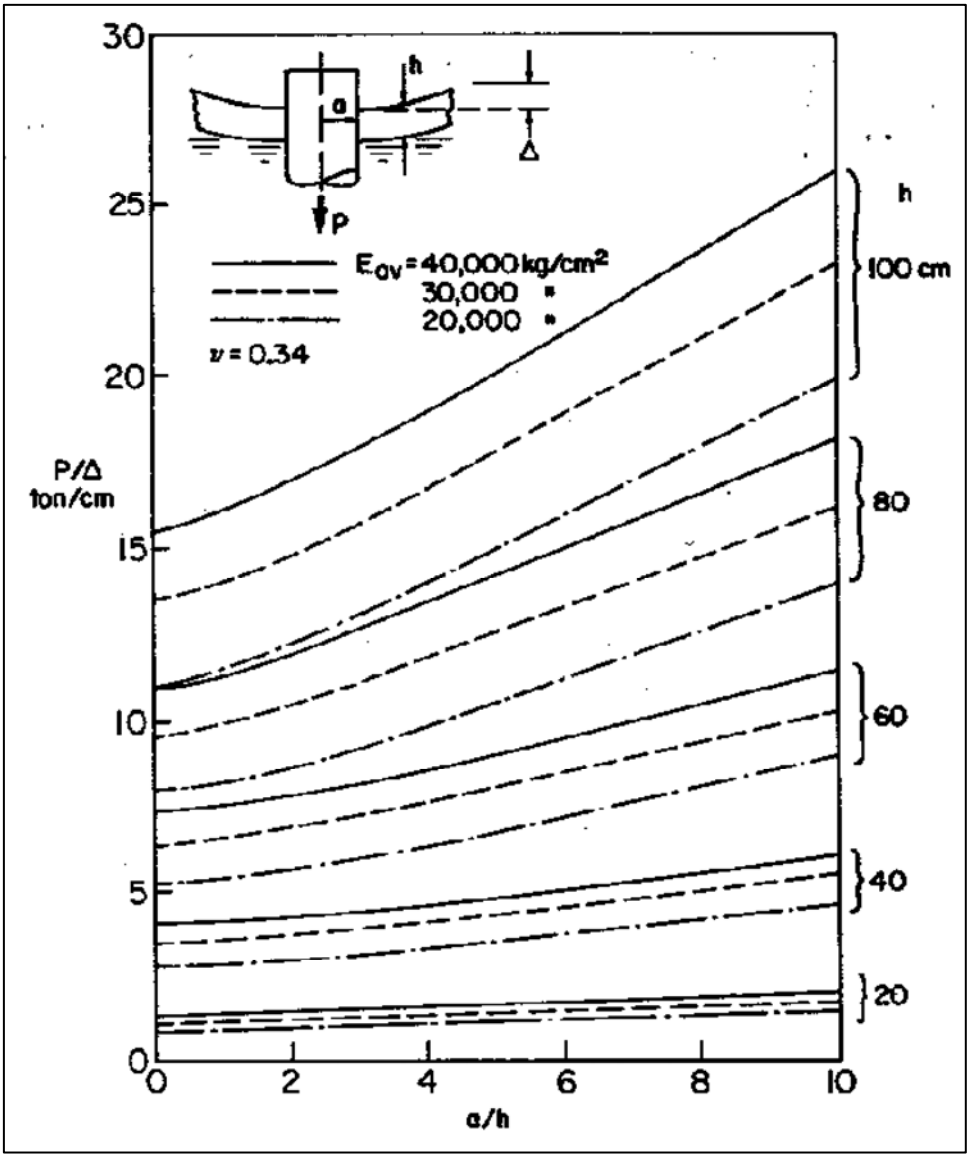

Figure VI-5-145. Vertical ice forces on a cylindrical pile (Kerr 1975)

- Kerr's solution gives estimates of the maximum vertical load assuming the ice sheet does not fail in shear or bending before the maximum load on the pile is reached. For example, the maximum uplift force on a pile with radius a = 100 cm surrounded by a 40-cm-thick ice sheet having an average Young's modulus of 30,000 kg/cm^2 would be estimated from Figure VI-5-145 using a value of a/h = 2.5 giving $P_{max} = 3.7\,\Delta$. The total maximum force for a 5-cm water level rise would be

$$P_{\max} = 3.7\,\Delta = 3.7\,(5\,cm) = 18.5\,tonnes$$

- Kerr (1975) pointed out that the same analysis applied for falling water levels with only a sign change, thus Figure VI-5-145 can also be used decreasing water levels.

(b) Vertical walls.

- Uplift or downward forces per unit horizontal length caused by vertical movement of ice sheets frozen to vertical walls can be approximated using the following formula (PIANC 1992)

$$\frac{F_v}{b} = \rho_w g \, \Delta h \, L_c \tag{VI-5-321}$$

where the characteristic length L_c is given as

$$L_c = \left[\frac{E h_i^3}{12 \rho_w g \left(1 - \nu^2\right)} \right]^{1/4} \tag{VI-5-322}$$

and

F_v = total vertical force acting on the wall

b = horizontal length of wall

Δh = change in water level

ρ_w = density of water

g = gravitational acceleration

E = modulus of elasticity of ice

h_i = ice thickness

ν = Poisson's ratio (0.31-0.35)

- As previously mentioned, the modulus of elasticity for ice varies with brine volume from about 1,000 MPa for very salty water to about 6,000 MPa for freshwater ice. For freshwater ice, L_c is typically between 15 to 20 times the ice thickness with a reasonable rule-of-thumb being $L_c = 17 \, h_i$.

(c) Sloping structures. The additional vertical load caused by the ride-up and piling of ice on sloping structures needs to be evaluated for the local conditions and specific type of structure. Ice piled up on the slope could initiate slumping of the armor layer on steeper slopes. During rising waters, individual armor stones or revetment units might be lifted out by adfreeze forces.

(4) Aspects of slope protection design.

(a) Much of our understanding of successful slope protection design in cold coastal regions stems from practical experience as documented in the technical literature. In general the

design philosophy recognizes that little can be done to prevent ice contact with slope protection structures. Therefore, emphasis is placed on minimizing potential ice damage using a variety of techniques.

(b) Leidersdorf, Gadd, and McDougal (1990) reviewed the performance aspects of three types of slope protection used for coastal projects related to petroleum activities in the Beaufort Sea. For water depths less than 2 m, sacrificial beaches appeared to function well. In water depths ranging from 7 m to 15 m, gravel-filled geotextile bags were able to withstand the larger wave forces, but they were susceptible to ice damage and required regular maintenance. Linked concrete mat armor (Leidersdorf, Gadd, and McDougal 1988; Gadd and Leidersdorf 1990) withstood both wave and ice loads in depths up to about 14 m. Mats were recommended for projects with a lengthy service life so that high initial capital costs would be offset by lower maintenance expenses. Wuebben (1995) reviewed the effects of ice on riprap structures constructed along ice-prone waterways. This paper provided a good summary of successful riprap revetment design and construction practices based on actual field experience. Numerous useful references documenting ice effects on riprap are included in Wuebben's paper. The following rules-of-thumb for arctic slope protection were given in Chen and Leidersdorf (1988) and summarized in PIANC (1992).

- Cover layers and underlayers should be strong enough to withstand local penetration by thick ice sheets.

- Smooth slopes without protrusions will reduce loads and allow the ice to ride up more easily without plucking out individual armor elements. (However, wave runup will be greater.)

- Flexible cover layers consisting of graded riprap may help absorb impacts by smaller ice blocks during wave action without appreciable damage. Sand bags are effective for structures with intended short service lives.

- Mild structure slopes are essential because they reduce the risk of ice penetration into the slope. Maximum slope 15 deg is recommended in the zone of ice attack.

- Compound slopes with a nearly horizontal berm above the swl provide a platform for piled-up ice in regions which experience frequent ride-up of ice sheets.

- Maximum ice loads will not occur at the same time as maximum expected wave loads. Therefore, slope design can consider each load condition separately.

VI-5-9. References.

EM 1110-2-1601
Hydraulic Design of Flood Control Channels

EM 1110-2-1612
Ice Engineering

ACI 1989
American Concrete Institute. 1989 (revised annually). *Manual of Concrete Practice*, Part 3, Detroit, MI.

Ahrens 1981a
Ahrens, J. P. 1981a. "Irregular Wave Runup on Smooth Slopes," Technical Aid No. 81-17, U.S. Army Engineer Waterways Experiment Station, Coastal Engineering Research Center, Vicksburg, MS.

Ahrens 1981b
Ahrens, J. P. 1981b. "Design of Riprap Revetments for Protection Against Wave Attack," Technical Paper TP-81-5, U.S. Army Engineer Waterways Experiment Station, Coastal Engineering Research Center, Vicksburg, MS.

Ahrens 1984
Ahrens, J. P. 1984. "Reef Type Breakwaters," *Proceedings of the 19th International Coastal Engineering Conference*, American Society of Civil Engineers, Vol 3, pp 2648-2662.

Ahrens 1987
Ahrens, J. P. 1987. "Characteristics of Reef Breakwaters," Technical Report CERC-87-17, U.S. Army Engineer Waterways Experiment Station, Vicksburg, MS.

Ahrens and Heinbaugh 1988a
Ahrens, J. P., and Heinbaugh, M. S. 1988a. "Approximate Upper Limit of Irregular Wave Runup on Riprap," Technical Report CERC-88-5, U.S. Army Engineer Waterways Experiment Station, Coastal Engineering Research Center, Vicksburg, MS.

Ahrens and Heinbaugh 1988b
Ahrens, J. P., and Heinbaugh, M. S. 1988b. "Seawall Overtopping Model," *Proceedings of the 21st International Coastal Engineering Conference*, American Society of Civil Engineers, Vol 1, pp 795-806.

Ahrens, Viggosson, and Zirkle 1982
Ahrens, J. P., Viggosson, G., and Zirkle, K. P. 1982. "Stability and Wave Transmission Characteristics of Reef Breakwaters," Interim Report, U.S. Army Engineer Waterways Experiment Station, Coastal Engineering Research Center, Vicksburg, MS.

Allsop 1983
Allsop, N. W. 1983. "Low-Crest Breakwaters, Studies in Random Waves," *Proceedings of Coastal Structures '83*, American Society of Civil Engineers, pp 94-107.

Allsop 1990
Allsop, N. W. 1990. "Reflection Performance of Rock Armoured Slopes in Random Waves," *Proceedings of the 22nd International Coastal Engineering Conference*, American Society of Civil Engineers, Vol 2, pp 1460-1472.

Allsop 1995
Allsop, N. W. 1995. "Stability of Rock Armour and Riprap on Coastal Structures," *River, Coastal and Shoreline Protection: Erosion Control Using Riprap and Armourstone,* C. R. Thorne, S. R. Abt, F. B. Barends, S. T. Maynord, and R. W. Pilarczyk, eds., John Wiley and Sons, New York, pp 213-226.

Allsop and Hettiarachchi 1988
Allsop, N. W., and Hettiarachchi, S. S. 1988. "Reflections from Coastal Structures," *Proceedings of the 21st International Coastal Engineering Conference*, American Society of Civil Engineers, Vol 1, pp 782-794.

Allsop et al. 1985
Allsop, N. W., Hawkes, P. I., Jackson, F. A., and Franco, L. 1985. "Wave Run-Up on Steep Slopes - Model Tests Under Random Waves," Report No. SR2, Hydraulics Research Station, Wallingford, England.

Allsop, McBride, and Colombo 1994
Allsop, N. W., McBride, M. W., and Colombo, D. 1994. "The Reflection Performance of Vertical Walls and Low Reflection Alternatives: Results of Wave Flume Tests," *Proceedings of the 3rd MCS Project Workshop, MAS2-CT92-0047, Monolithic (Vertical) Coastal Structures,* De Voorst, The Netherlands.

Aminti and Franco 1988
Aminti, P., and Franco, L. 1988. "Wave Overtopping on Rubble Mound Breakwaters," *Proceedings of the 21st International Coastal Engineering Conference*, American Society of Civil Engineers, Vol 1, pp 770-781.

Andersen 1981
Andersen, K. H. 1981. Discussion of "Cyclic Simple Shear Behaviour of Fine Grained Soil," Dyvik, Zimme, and Schimelfenjg, *International Conference on Recent Advances in Geotechnical Earthquake Engineering and Soil Dynamics*, St. Louis, MO, pp. 920-921.

Andersen 1983
Andersen, K. H. 1983. "Strength and Deformation Properties of Clay Subjected to Cyclic Loading," Report 52412-8, Norwegian Geotechnical Institute.

Andersen 1988
Andersen, K. H. 1988. "Properties of Soil Clay Under Static and Cyclic Loading," *Proceedings of the International Conference on Engineering Problems of Regional Soils*, Beijing, China, pp 7-26.

Andersen 1991
Andersen, K. H. 1991. "Foundation Design of Offshore Gravity Structures," *Cyclic Loading of Soils*, M. P. O'Reilly and S. F. Brown, eds., Blackie and Son Ltd., Glasgow, Scotland.

Andersen and Høeg 1991
Andersen, K. H., and Høeg, K. 1991. "Deformation of Soils and Displacements of Structures Subjected to Combined Static and Cyclic Loads," *Proceedings 10th European Conference on Soil Mechanics and Foundation Engineering*, Florence, Italy, Vol 4, pp 1147-1158.

Andersen and Richards 1985
Andersen, M. G., and Richards, K. S. 1985. *Slope Stability*, John Wiley & Sons, New York, NY.

Anderson et al. 1976
Anderson, K. H., Brown, S. F., Foss, I., Pool, J. H., and Rosenbrand, F. W. 1976. "Effect of Cyclic Loading on Clay Behavior," *Proceedings of the Conference on Design and Construction of Offshore Structures*, Institution of Civil Engineers, London, UK, pp 75-79.

Andersen, Kleven, and Heien 1988
Andersen, K. H., Kleven, A., and Heien, D. 1988. "Cyclic Soil Data for Design of Gravity Structures," *Journal of Geotechnical Engineering*, American Society of Civil Engineers, Vol 114, No. 5, pp 517-539.

Andrews and Borgman 1981
Andrews, M. E., and Borgman, L. E. 1981. "Procedures for Studying Wave Grouping in Wave Records from the California Coastal Data Collection Program," Statistics Laboratory Report No. 141, University of Wyoming, Laramie, WY.

Anglin et al. 1990
Anglin, C. D., Scott, R. D., Turcke, D. J., and Turke, M. A. (1990). "The Development of Structural Design Criteria for Breakwater Armor Units," *Stresses in Concrete Armor Units*, American Society of Civil Engineers, pp 123-148.

Anglin et al. 1996
Anglin, C. D., Nairn, R. B., Cornett, A. M., Dunaszegi, L, Turnham, J, and Annandale, G. W. 1996. "Bridge Pier Scour Assessment for the Northumberland Strait Crossing," *Proceedings of the 25th International Coastal Engineering Conference*, American Society of Civil Engineers, Vol 2, pp 2230-2243.

Ashton 1986
Ashton, G. D. 1986. *River and Lake Ice Engineering*. Water Resources Publications, Littleton, CO.

Bagnold 1939
Bagnold, R. A. 1939. "Interim Report on Wave-Pressure Research," *Journal of Institution of Civil Engineers*, Vol 12, pp 202-226.

Bakker et al. 1994
Bakker, K. J., Verheij, H. J., and de Groot, M. B. 1994. "Design Relationship for Filters in Bed Protection," *Journal of Hydraulic Engineering*, American Society of Civil Engineers, Vol 120, No. 9, pp 1082-1088.

Barends 1988
Barends, F. B. 1988. Discussion of "Pore Pressure Response and Stability of Rubble-Mound Breakwaters," Simm and Hedges, *Proceedings of the Breakwaters '88 Conference: Design of Breakwaters,* Institution of Civil Engineers, Thomas Telford, London, UK, pp 85-88.

Barends et al. 1983
Barends, F. B., van der Kogel, H., Uijttewall, F. J., and Hagenaar, J. 1983. "West Breakwater - Sines: Dynamic-Geotechnical Stability of Breakwaters," *Proceedings of Coastal Structures '83*, American Society of Civil Engineers, pp 31-43.

Barnett and Wang 1988
Barnett, M. R., and Wang, H. 1988. "Effects of a Vertical Seawall on Profile Response," *Proceedings of the 21st International Coastal Engineering Conference*, American Society of Civil Engineers, Vol 2, pp 1493-1507.

Bass and Fulford 1992
Bass, G. P, and Fulford, E. T. 1992. "South Jetty Scour Hole Stabilization, Ocean City, Maryland," *Proceedings of Coastal Engineering Practice '92*, American Society of Civil Engineers, pp 583-597.

Battjes 1974
Battjes, J. A. 1974. "Computation of Set-Up, Longshore Currents, Run-Up, and Overtopping Due to Wind-Generated Waves," Report 74-2, Committee on Hydraulics, Department of Civil Engineering, Delft University of Technology, The Netherlands.

Battjes 1974b
Battjes, J. A. 1974b. "Surf Similarity," *Proceedings of the 14th International Coastal Engineering Conference*, American Society of Civil Engineers, Vol 1, pp 466-479.

Battjes 1982
Battjes, J. A. 1982. AEffects of Short-Crestedness on Wave Loads on Long Structures," *Applied Ocean Research*, Vol 4, No. 3, pp 165-172.

Bea et al. 1999
Bea, R. G., Xu, T., Stear, J., and Ramos, R. 1999. "Wave Forces on Decks of Offshore Platforms," *Journal of Waterway, Port, Coastal, and Ocean Division*, American Society of Civil Engineers, Vol 125, No. 3, pp 136-144.

Belfadhel, Lefebvre, and Rohan 1996
Belfadhel, M. B., Lefebvre, G., and Rohan, K. 1996. "Comparison and Evaluation of Different Riprap Stability Formulas Using Field Performance," *Journal of Waterway, Port, Coastal and Ocean Engineering*, American Society of Civil Engineers, Vol. 122, No. 1, pp 8-15.

Benoit and Teisson 1994
Benoit, M. and Teisson, C. 1994. "Laboratory Study of Breakwater Reflection - Effect of Wave Obliquity, Wave Steepness and Mound Slope," *International Symposium: Waves - Physical and Numerical Modelling,* Vol 2, pp 1021-1030.

Bijker and de Bruyn 1988
Bijker, E. W., and de Bruyn, C. A. 1988. "Erosion Around a Pile Due to Current and Breaking Waves," *Proceedings of the 21st International Coastal Engineering Conference*, American Society of Civil Engineers, Vol 2, pp 1368-1381.

Bishop 1955
Bishop, A. W. 1955. "The Use of the Slip Circle in the Stability Analysis of Slopes," *Geotechnique*, Vol V, No. 1, pp 1-17.

Bishop and Green 1965
Bishop, A. W., and Green, G.E. 1965. "The Influence of End Restraint on the Compression Strength of a Cohesionless Soil," *Geotechnique*, Vol 15, No. 3, pp. 243-266.

Bjerrum 1973
Bjerrum, L. 1973. "Problems of Soil Mechanics and Construction on Soft Clays," State-of-the-Art Report to Session IV, *Proceedings of the International Conference on Soil Mechanics and Foundation Engineering 3*, pp 111-159.

Bolton 1979
Bolton, M. D. 1979. *A Guide to Soil Mechanics.* Macmillan Press Ltd., London, UK.

Bolton 1986
Bolton, M. D. 1986. "The Strength and Dilatancy of Sands," *Geotechnique,* Vol 36, No. 1, pp 65-78.

Bottin, Chatham, and Carver 1976
Bottin, R., Chatham, C., and Carver, R. 1976. "Waianae Small-Boat Harbor, Oahu, Hawaii, Design for Wave Protection," TR H-76-8, U.S. Army Engineer Waterways Experiment Station, Vicksburg, MS.

Bradbury and Allsop 1988
Bradbury, A. P., and Allsop, N. W. 1988. "Hydraulic Effects of Breakwater Crown Walls," *Proceedings of the Breakwaters '88 Conference,* Institution of Civil Engineers, Thomas Telford Publishing, London, UK, pp 385-396.

Bradbury et al. 1988
Bradbury, A. P., Allsop, N. W., and Stephens, R. V. 1988. "Hydraulic Performance of Breakwater Crown Walls," Report No. SR146, Hydraulics Research, Wallingford, UK.

Breusers, Nicollet, and Shen 1977
Breusers, H. N. C., Nicollet, G., and Shen, H. W. 1977. "Local Scour Around Cylindrical Piers," *Journal of Hydraulic Research*, Vol 15, No. 3, pp 211-252.

Brinch Hansen 1961
Brinch Hansen, J. 1961. "A General Formula for Bearing Capacity," Bulletin No. 11, Danish Geotechnical Institute, Copenhagen, Denmark.

Brinch Hansen 1967
Brinch Hansen, J. 1967. "Støttemures Bæreevne (The Bearing Capacity of Retaining Walls)," B-undervisning og Forskning 67, Danmarks Ingeniørakademi, Copenhagen, Denmark, pp 307-320.

Brinch Hansen 1970
Brinch Hansen, J. 1970. "A Revised and Extended Formula for Bearing Capacity," Bulletin No. 28, Danish Geotechnical Institute, Copenhagen, Denmark.

Broderick 1983
Broderick, L. L. 1983. "Riprap Stability A Progress Report," *Proceedings of Coastal Structures '83*, American Society of Civil Engineers, pp 320-330.

Brorsen, Burcharth, and Larsen 1974
Brorsen, M., Burcharth, H. F., and Larsen, T. 1974. "Stability of Dolos Slopes," *Proceedings of the 14th International Coastal Engineering Conference*, American Society of Civil Engineers, Vol 3, pp 1691-1701.

Bruining 1994
Bruining, J. W. 1994. "Wave Forces on Vertical Breakwaters. Reliability of Design Formula," Delft Hydraulics Report H 1903, MAST II contract MAS2-CT92-0047.

Burcharth 1984
Burcharth, H. F. 1984. "Fatigue in Breakwater Concrete Armour Units," *Proceedings of the 19th International Coastal Engineering Conference*, American Society of Civil Engineers, Vol 3, pp 2592-2607.

Burcharth 1993
Burcharth, H. F. 1993. "The Design of Breakwaters," Department of Civil Engineering, Aalborg University, Denmark.

Burcharth 1993b
Burcharth, H. F. 1993b. "Structural Integrity and Hydraulic Stability of Dolos Armor Layers," Series Paper 9, Department of Civil Engineering, Aalborg University, Denmark.

Burcharth 1998
Burcharth, H. F. 1998. "Breakwater with Vertical and Inclined Concrete Walls: Identification and Evaluation of Design Tools," Report of Sub-group A, Working Group 28, PIANC PTCII.

Burcharth and Andersen 1995
Burcharth, H.F., and Andersen, O.H. 1995. "On the One-Dimensional Unsteady Porous Flow Equation," *Coastal Engineering,* Vol 24, pp. 233-257.

Burcharth and Brejnegaard-Nielsen 1986
Burcharth, H. F., and Brejnegaard-Nielsen, T. 1986. "The Influence of Waist Thickness of Dolosse on the Hydraulic Stability of Dolosse Armour," *Proceedings of the 20th International Coastal Engineering Conference*, American Society of Civil Engineers, Vol 2, pp 1783-1796.

Burcharth and Liu 1992
Burcharth, H. F., and Liu, Z. 1992. "Design of Dolos Armour Units," *Proceedings of the 23rd International Coastal Engineering Conference*, American Society of Civil Engineers, Vol 1, pp 1053-1066.

Burcharth and Liu 1995
Burcharth, H. F., and Liu, Z. 1995. "Design Formula for Dolos Breakage," *Proceedings of the Final Workshop, Rubble Mound Breakwater Failure Modes,* Sorrento, Italy.

Burcharth and Liu 1998
Burcharth, H. F., and Liu, Z. 1998. "Force Reduction of Short-Crested Non-Breaking Waves on Caissons," Section 4.3, Part 4, Class II Report of MAST II Project: PROVERBS, Technical University of Braunschweig, Germany, ed.

Burcharth and Thompson 1983
Burcharth, H. F., and Thompson, A. C. 1983. "Stability of Armour Units in Oscillatory Flow," *Proceedings of Coastal Structures '83*, American Society of Civil Engineers, pp 71-82.

Burcharth et al. 1991
Burcharth, H. F., Toschi, P. B., Turrio, E., Balestra, T, Noli, A., Franco, L., Betti, A., Mezzedimi, S. 1991. "Bosaso Harbour, Somalia. A New Hot-Climate Port Development," *Third International Conference on Coastal & Port Engineering in Developing Countries*, Vol 1, pp 649-666.

Burcharth et al. 1995a
Burcharth H. F., Frigaard, P., Uzcanga, J., Berenguer, J. M., Madrigal, B. G., and Villanueva, J. 1995a. "Design of the Ciervana Breakwater, Bilbao," *Proceedings of the Advances in Coastal Structures and Breakwaters Conference*, Institution of Civil Engineers, Thomas Telford, London, UK, pp 26-43.

Burcharth et al. 1995b
Burcharth, H. F., Jensen, M. S., Liu, Z., van der Meer, J. W., and D'Angremond, K. 1995b. "Design Formula for Tetrapod Breakage," *Proceedings of the Final Workshop, Rubble Mound Breakwater Failure Modes*, Sorrento, Italy.

Burcharth et al. 1998
Burcharth, H. F., Christensen, M., Jensen, T. and Frigaard, P. 1998. "Influence of Core Permeability on Accropode Armour Layer Stability," *Proceedings of International Conference on Coastlines, Structures, and Breakwaters '98*, Institution of Civil Engineers, London, UK, pp 34-45.

Burcharth, Liu, and Troch 1999
Burcharth, H.F., Liu, Z., and Troch, P. 1999. "Scaling of Core Material in Rubble Mound Breakwater Model Tests," *Proceedings of Fifth International Conference on Coastal and Port Engineering in Developing Countries*, Cape Town, South Africa, pp 1518-1528.

Burcharth et al. 2000
Burcharth, H. F., d'Angremond, K, van der Meer, J. W., and Liu, Z. 2000. "Empirical Formula for Breakage of Dolosse and Tetrapods," *Coastal Engineering*, Elsevier, Vol 40, No. 3, pp 183-206.

Calabrese and Allsop 1997
Calabrese, M., and Allsop, N. W. 1997. "Impact Loading on Vertical Walls in Directional Seas," Contribution to the 1st Task, MAST III Workshop (PROVERBS), Edinburgh.

Camfield 1990
Camfield, F. E. 1990. "Tsunami," *Handbook of Coastal and Ocean Engineering - Volume 1: Wave Phenomena and Coastal Structures*. John B. Herbich, ed., Gulf Publishing Company, Houston, TX, pp 591-634.

Camfield 1991
Camfield, F. E. 1991. "Wave Forces on Wall," *Journal of Waterway, Port, Coastal, and Ocean Engineering*, American Society of Civil Engineers, Vol 117, No. 1, pp 76-79.

Canadian Standards Association 1978
Canadian Standards Association. 1978. "Design of Highway Bridges," Standard CAN3-56-M78.

Carpenter and Powell 1998
Carpenter, K. E., and Powell, K. A. 1998. "Toe Scour at Vertical Walls: Mechanisms and Prediction Methods," Report No. SR506, HR Wallingford, UK.

Carstens 1976
Carstens, T. 1976. "Seabed Scour by Currents Near Platforms," Proceedings of the 3rd International Conference on Port and Ocean Engineering Under Arctic Conditions, pp 991-1006.

Carver 1980
Carver, R. D. 1980. "Effects of First Underlayer Weight on the Stability of Stone-Armored, Rubble-Mound Breakwater Trunks Subjected to Nonbreaking Waves with No Overtopping," Technical Report HL-80-1, U.S. Army Engineer Waterways Experiment Station, Vicksburg, MS.

Carver and Davidson 1977
Carver, R. D., and Davidson, D. D. 1977. "Dolos Armor Units Used on Rubble-Mound Breakwater Trunks Subjected to Nonbreaking Waves with No Overtopping," Technical Report H-77-19, U.S. Army Engineer Waterways Experiment Station, Vicksburg, MS.

Carver and Davidson 1983
Carver, R. D., and Davidson, D. D. 1983. "Jetty Stability Study, Oregon Inlet, North Carolina," Technical Report CERC-83-3, U.S. Army Engineer Waterways Experiment Station, Vicksburg, MS.

Carver and Heimbaugh 1989
Carver, R. D., and Heimbaugh, M. S. 1989. "Stability of Stone- and Dolos-Armored Rubble-Mound Breakwater Heads Subjected to Breaking and Nonbreaking Waves with No Overtopping," Technical Report CERC-89-4, U.S. Army Engineer Waterways Experiment Station, Coastal and Hydraulics Laboratory, Vicksburg, MS.

Carver and Markle, 1981
Carver, R. D., and Markle, D. G. 1981. "Stability of Rubble-Mound Breakwater; Maalea Harbor, Maui, Hawaii," Miscellaneous Paper HL-81-1, U.S. Army Engineer Waterways Experiment Station, Vicksburg, MS.

Chakrabarti 1991
Chakrabarti, S. K. 1991. "Wave Forces on Offshore Structures," *Handbook of Coastal and Ocean Engineering - Volume 2: Offshore Structures, Marine Foundations, Sediment Processes, and Modeling*. John B. Herbich, ed., Gulf Publishing Company, Houston, TX. pp 1-54.

Chang 1964
Chang, K. S. 1964. "Transverse Forces on Cylinders Due to Vortex Shedding in Waves," M.A. thesis, Department of Civil Engineering, Massachusetts Institute of Technology, Cambridge, MA.

Chen 1961
Chen, T. C. 1961. "Experimental Study on the Solitary Wave Reflection Along a Straight Sloped Wall at Oblique Angle of Incidence," Technical Memorandum No. 124, U.S. Army Corps of Engineers, Beach Erosion Board, Washington, DC.

Chen and Leidersdorf 1988
Chen, A. T., and Leidersdorf, C. B., ed. 1988. "Arctic Coastal Processes and Slope Protection Design," Technical Council on Cold Regions Engineering Monograph, American Society of Civil Engineers, New York, NY.

Chesnutt and Schiller 1971
Chesnutt, C. B., and Schiller, R. E. 1971. "Scour of Simulated Gulf Coast Sand Beaches Due to Wave Action in Front of Sea Walls and Dune Barriers," COE Report No. 139, *TAMU-SG-71-207*, Texas A&M University, College Station, TX.

Chiew 1990
Chiew, Y-M. 1990. "Mechanics of Local Scour Around Submarine Pipelines," *Journal of Hydraulic Engineering*, American Society of Civil Engineers, Vol 116, No. 4, pp 515-539.

Cété-Laboratoire Régional Nord - Pas de Calais 1990
Cété-Laboratoire Régional Nord - Pas de Calais. 1990. "Le Havre - Route du Mole Central - Essais de Frottement Beton Ondulé-Grave Concassée," Laboratoire Régional Nord - Pas de Calais.

Costa 1973
Costa, F. V. 1973. "Berthing Maneuvers of Large Ships," *Port Engineering*. Gulf Publishing Company, Houston, TX, pp 401-417.

Croasdale, Allyn, and Roggensack 1988
Croasdale, K. R., Allyn, N., and Roggensack, W. 1988. "Arctic Slope Protection: Considerations for Ice," *Arctic Coastal Processes and Slope Protection Design*. A. T. Chen and C. B. Leidersdorf, ed., American Society of Civil Engineers, pp 216-243.

Cross 1967
Cross, R. H. 1967. "Tsunami Surge Forces," *Journal of the Waterways and Harbors Division*, American Society of Civil Engineers, Vol 93, No. ww4, pp 201-231.

Centre for Civil Engineering Research and Codes 1995
Centre for Civil Engineering Research and Codes. 1995. "Manual on the Use of Rock in Hydraulic Engineering," CUR/RWS Publication 169, CUR, Gouda, The Netherlands.

Czerniak and Collins 1977
Czerniak, M. T., and Collins, J. I. 1977. "Design Considerations for a Tetrapod Breakwater," *Proceedings of Ports '77*, American Society of Civil Engineers, New York, pp 178-195.

d'Angremond, van der Meer, van Nes 1994
d'Angremond, K., van der Meer, J. W., and van Nes, C. P. 1994. "Stresses in Tetrapod Armour Units Induced by Wave Action," *Proceedings of the 24th International Coastal Engineering Conference*, American Society of Civil Engineers, Vol 2, pp 1713-1726.

Daemrich and Kahle 1985
Daemrich, K. F., and Kahle, W. 1985. "Shutzwirkung von Unterwasserwellen Brechern Unter Dem Einfluss Unregelmassiger Seeganswellen," Eigenverlag des Franzius-Instituts fur Wasserbau und Kusteningenieurswesen, Heft 61 (in German).

Daemen 1991
Daemen, I. F. 1991. "Wave Transmission at Low-Crested Breakwaters," M.S. thesis, Delft University of Technology, The Netherlands.

Davidson et al. 1994
Davidson, M. A., Bird, P. A., Bullock, G. N., and Huntley, D. A. 1994. "Wave Reflection: Field Measurements, Analysis and Theoretical Developments," *Proceedings of Coastal Dynamics '94*, American Society of Civil Engineers, pp 642-655.

Dean 1974
Dean, R. G. 1974. "Evaluation and Development of Water Wave Theories for Engineering Application," Special Report 1, Vols I and II, U.S. Army Coastal Engineering Research Center, Stock Nos. 008-022-00083-6 and 008-022-00084-6, U.S. Government Printing Office, Washington, DC.

de Best, Bijker, and Wichers 1971
de Best, A., Bijker, E. W., and Wichers, J. E. W. 1971. "Scouring of a Sand Bed in Front of a Vertical Breakwater," *Proceedings of the 1st International Conference on Port and Ocean Engineering Under Artic Conditions*, Vol II, pp 1077-1086.

de Gerloni et al. 1991
de Gerloni, M, Cris, E., Franco, L., and Passoni, G. 1991. "The Safety of Breakwaters Against Wave Overtopping," *Proceedings of the Coastal Structures and Breakwaters Conference*, Institution of Civil Engineers, Thomas Telford, London, UK, pp 335-342.

de Graauw, van der Meulen, and van der Does de Bye 1984
de Graauw, A. F., van der Meulen, T., and van der Does de Bye, M. R. 1984. "Granular Filters: Design Criteria," *Journal of Waterway, Port, Coastal, and Ocean Engineering*, American Society of Civil Engineers, Vol 110, No. 1, pp 80-96.

de Groot et al. 1996
de Groot, M. M., Andersen, K. H., Burcharth, H. F., Ibsen, L. B., Kortenhaus, A., Lundgren, H., Magda, W., Oumeraci, H., and Richwien, W. 1996. "Foundation Design of Caisson Breakwaters," Publication No. 198, Norwegian Geotechnical Institute, Oslo, Norway.

de Rouck 1991
de Rouck, J. 1991. "De Stabilitet Van Stortsteengolfbrekers. Algemeen Glijdingsevenwicht - Een Nieuw Deklaagelement," Hydraulic Laboratory, University of Leuven, Belgium.

de Waal and van der Meer 1992
de Waal, J. P., and van der Meer, J. W. 1992. "Wave Run-Up and Overtopping on Coastal Structures," *Proceedings of the 23rd International Coastal Engineering Conference*, American Society of Civil Engineers, Vol 2, pp 1758-1771.

Delft Hydraulics 1989
Delft Hydraulics. 1989. "Slopes of Loose Materials: Wave Run-Up on Statistically Stable Rock Slopes Under Wave Attack," Report M 1983 (in Dutch), Delft Hydraulics Laboratory, The Netherlands.

Eadie and Herbich 1986
Eadie, R. W., and Herbich, J. B. 1986. "Scour About a Single Cylindrical Pile Due to Combined Random Waves and a Current," *Proceedings of the 20th International Coastal Engineering Conference*, American Society of Civil Engineers, Vol 3, pp 1858-1870.

Eckert 1983
Eckert, J. W. 1983. "Design of Toe Protection for Coastal Structures," *Proceedings of Coastal Structures '83*, American Society of Civil Engineers, pp 331-341.

Edge et al. 1990
Edge, B. L., Crapps, D. K., Jones, J. S., and Dean, W. L. 1990. "Design and Installation of Scour Protection for the Acosta Bridge," *Proceedings of the 22nd International Coastal Engineering Conference,* American Society of Civil Engineers, Vol 3, pp 3268-3280.

Endoh and Takahashi 1994
Endoh, K., and Takahashi, S. 1994. "Numerically Modelling Personnel Danger on a Promenade Breakwater Due to Overtopping Waves," *Proceedings of the 24th International Coastal Engineering Confernece*, American Society of Civil Engineers, Vol 1, pp 1016-1029.

Fagerlund and Larsson 1979
Fagerlund, G., and Larsson, B. 1979. "Betongs Slaghallfasthed." (in Swedish), Swedish Cement and Concrete Research Institute, Institute of Technology, Stockholm, Sweden.

Fellenius 1936
Fellenius, W. 1936. "Calculation of the Stability of Earth Dams," *Proceeding of the 2nd International Conference on Large Dams*, Washington DC, Vol 4, pp 445-449.

Fowler 1992
Fowler, J. E. 1992. "Scour Problems and Methods for Prediction of Maximum Scour at Vertical Seawalls," Technical Report CERC-92-16, U.S. Army Engineer Waterways Experiment Station, Coastal Engineering Research Center, Vicksburg, MS.

Fowler 1993
Fowler, J. E. 1993. "Coastal Scour Problems and Methods for Prediction of Maximum Scour," Technical Report CERC-93-8, U.S. Army Engineer Waterways Experiment Station, Coastal Engineering Research Center, Vicksburg, MS.

Fox and McDonald 1985
Fox, R. W., and McDonald, A. T. 1985. *Introduction to Fluid Mechanics*. Third ed., John Wiley and Sons, New York, NY.

Franco and Franco 1999
Franco, C., and Franco, L. 1999. "Overtopping Formulas for Caisson Breakwaters with Nonbreaking 3D Waves," *Journal of Waterway, Port, Coastal, and Ocean Engineering*, American Society of Civil Engineers, Vol 125, No. 2, pp 98-108.

Franco, de Gerloni, and van der Meer 1994
Franco, L., de Gerloni, M., and van der Meer, J. W. 1994. "Wave Overtopping on Vertical and Composite Breakwaters," *Proceedings of the 24th International Coastal Engineering Conference*, American Society of Civil Engineers, Vol 1, pp 1030-1045.

Franco, van der Meer, and Franco 1996
Franco, C., van der Meer, J. W., and Franco, L. 1996. "Multidirectional Wave Loads on Vertical Breakwaters," *Proceedings of the 25th International Coastal Engineering Conference*, Vol 2, pp 2008-2021.

Fredsøe and Sumer 1997
Fredsøe, J., and Sumer, B. M. 1997. "Scour at the Round Head of a Rubble-Mound Breakwater," *Coastal Engineering*, Elsevier, Vol 29, No. 3, pp 231-262.

French 1969
French, J. A. 1969. "Wave Uplift Pressure on Horizontal Platforms," Report No. KH-R-19, W. M. Keck Laboratory of Hydraulics and Water Resources, California Institute of Technology, Pasadena, CA.

Froehlich 1988
Froehlich, D. C. 1988. "Analysis of Onsite Measurements of Scour at Piers," *Hydraulic Engineering- Proceedings of the 1988 National Conference*, American Society of Civil Engineers, pp 534-539.

Führböter, Sparboom, and Witte 1989
Führböter, A., Sparboom, U., and Witte, H. H. 1989. "Großer Wellenkanal Hannover: Versuchsergebnisse über den Wellenauflauf auf Glatten und Rauhen Deichböschungen mit der Neigung 1:6," Die Küßte. Archive for Research and Technology on the North Sea and Baltic Coast.

Fukuda, Uno, and Irie 1974
Fukuda, N., Uno, T., and Irie, I. 1974. "Field Observations of Wave Overtopping of Wave Absorbing Revetment," *Coastal Engineering in Japan*, Vol 17, pp 117-128.

Gadd and Leidersdorf 1990
Gadd, P. E., and Leidersdorf, C. B. 1990. "Recent Performance of Linked Concrete Mat Armor Under Wave and Ice Impact," *Proceedings of the 22nd International Conference on Coastal Engineering*, American Society of Civil Engineers, Vol 3, pp 2768-2781.

Gerwick 1990
Gerwick, B. C., Jr. 1990. "Ice Forces on Structures," *The Sea: Ocean Engineering Science*. B. Le Mehaute and D. M. Hanes, eds., Vol 9, Part B, pp 1263-1301.

Givler and Sorensen 1986
Givler, L. D., and Sorensen, R. M. 1986. "An Investigation of the Stability of Submerged Homogeneous Rubble-Mound Structures Under Wave Attack," Report IHL 110-86, H.R. IMBT Hydraulics, Lehigh University, Philadelphia, PA.

Goda 1969
Goda, Y. 1969. "Reanalysis of Laboratory Data on Wave Transmission Over Breakwaters," *Report of Port and Harbour Research Institute*, Japan, Vol 8, No. 3, pp 3-18.

Goda 1970
Goda, Y. 1970. "Estimation of the Rate of Irregular Overtopping of Seawalls," *Report of Port and Harbor Research Institute*, Vol 9, No 4, 1970 (in Japanese).

Goda 1974
Goda, Y. 1974. "New Wave Pressure Formulae for Composite Breakwaters," *Proceedings of the 14th International Coastal Engineering Conference*, Vol 3, pp 1702-1720.

Goda 1985
Goda, Y. 1985. *Random Seas and Design of Maritime Structures,* University of Tokyo Press, Tokyo, Japan.

Goda and Suzuki 1976
Goda, Y., and Suzuki, Y. 1976. "Estimation of Incident and Reflected Waves in Random Wave Experiments," *Proceedings of the 15th International Coastal Engineering Conference*, American Society of Civil Engineers, Vol 1, pp 828-845.

Hales 1980
Hales, L. Z. 1980. "Erosion Control of Scour During Construction," Technical Report HL-80-3, U.S. Army Engineer Waterways Experiment Station, Coastal Engineering Research Center, Vicksburg, MS.

Hall 1967
Hall, J. R. 1967. "Coupled Rocking and Sliding Oscillations of Rigid Circular Footings," *Proceedings of the International Symposion on Wave Propagation and Dynamic Properties of Earth Materials*, American Society of Civil Engineers, pp 139-167.

Hansbo 1994
Hansbo, S. 1994. *Foundation Engineering*. Elsevier. The Netherlands.

Hansen 1979
Hansen, B. 1979. "Definition and Use of Friction Angles," *Seventh European Conference on Soil Mechanics and Foundation Engineering*, Brighton, Vol 1, pp 173-176.

Hanzawa et al. 1996
Hanzawa, M., Sato, H., Takahashi, S., Shimosako, K., Takayama, T., and Tanimoto, K. 1996. "New Stability Formula for Wave-Dissipating Concrete Blocks Covering Horizontally Composite Breakwaters," *Proceedings of the 25th International Coastal Engineering Conference*, American Society of Civil Engineers, Vol 2, pp 1665-1678.

Hardin 1978
Hardin, B. O. 1978. "The Nature of Stress-Strain Behaviour of Soils," *Earthquake Engineering and Soil Dynamics*, American Society of Civil Engineers, Vol I, pp 3-90.

Hardin and Black 1968
Hardin, B. O., and Black, W. L. 1968. "Vibration Modulus of Normally Consolidated Clays," *Journal of the Soil Mechanics and Foundations Division*, American Society of Civil Engineers, Vol 94, No. SM2, pp 353-369.

Hardin and Drnevich 1972
Hardin, B. O., and Drnevich, V. P. 1972. "Shear Modulus and Damping in Soils: Design Equations and Curves," *Journal of the Soil Mechanics and Foundations Division*, American Society of Civil Engineers, Vol 98, No. SM7, pp 667-692.

Hayashi and Shirai 1963
Hayashi, T., and Shirai, M. 1963. "Force of Impact at the Moving Collision of a Ship with the Mooring Construction," *Coastal Engineering in Japan*, Japan Society of Civil Engineering, Vol 6, pp 9-19.

Helm-Petersen 1998
Helm-Petersen, J. 1998. "Estimation of Wave Disturbance in Harbours," Ph.D. diss., Department of Civil Engineering, Aalborg University, Denmark.

Herbich 1991
Herbich, J. B. 1991. "Scour Around Pipelines, Piles, and Seawalls," Handbook of Coastal and Ocean Engineering - Volume 2: Offshore Structures, Marine Foundations, Sediment Processes, and Modeling. John B. Herbich, ed., Gulf Publishing Company, Houston, TX, pp 867-958.

Herbich and Ko 1968
Herbich, J. B., and Ko, S. C. 1968. "Scour of Sand Beaches in Front of Seawalls," *Proceedings of the 11th International Coastal Engineering Conference*, American Society of Civil Engineers, Vol 1, pp 622-643.

Hjorth 1975
Hjorth, P. 1997. "Studies on the Nature of Local Scour," Department of Water Resources Engineering Bulletin, Series A, No. 46, University of Lund, Sweden.

Hoffmans and Verheij 1997
Hoffmans, G.J.C.M., and Verheij, H. J. 1997. *Scour Manual*. A. A. Balkema, Rotterdam, The Netherlands.

Holtzhausen and Zwamborn 1990
Holtzhausen, A. H., and Zwamborn, J. A. 1990. "Stability of Dolosse with Different Waist Thicknesses for Irregular Waves," *Proceedings of the 22nd International Coastal Engineering Conference*, American Society of Civil Engineers, Vol 2, pp 1805-1818.

Holtzhausen and Zwamborn 1991
Holtzhausen, A. H., and Zwamborn, J. A. 1991. "Stability of Accropode7 and Comparison with Dolosse," *Coastal Engineering*, Vol 15, pp 59-86.

Hsu 1991
Hsu, J. R. 1991. "Short-Crested Waves," *Handbook of Coastal and Ocean Engineering - Volume 1: Wave Phenomena and Coastal Structures*. John B. Herbich, ed., Gulf Publishing Company, Houston, TX, pp 95-174.

Hudson 1958
Hudson, R. Y. 1958. "Design of Quarry-Stone Cover Layers for Rubble-Mound Breakwaters; Hydraulic Laboratory Investigation," Research Report No. 2-2, U.S. Army Engineer Waterways Experiment Station, Vicksburg, MS.

Hudson 1959
Hudson, R. Y. 1959. "Laboratory Investigation of Rubble-Mound Breakwaters," *Journal of the Waterways and Harbors Division*, American Society of Civil Engineers, Vol 85, No. WW3, pp 93-121.

Hudson 1974
Hudson, R. Y. (editor). 1974. "Concrete Armor Units for Protection Against Wave Attack," Miscellaneous Paper H-74-2, U.S. Army Engineer Waterways Experiment Station, Vicksburg, MS.

Hughes 1992
Hughes, S. A. 1992. "Estimating Wave-Induced Bottom Velocities at Vertical Wall," *Journal of Waterway, Port, Coastal and Ocean Engineering*, American Society of Civil Engineers, Vol 118, No. 2, pp 175-192.

Hughes and Fowler 1991
Hughes, S. A., and Fowler, J. E. 1991. "Wave-Induced Scour Prediction at Vertical Walls," *Proceedings of Coastal Sediments '91*, American Society of Civil Engineers, Vol. 2, pp 1886-1900.

Hughes and Fowler 1995
Hughes, S. A., and Fowler, J. E. 1995. "Estimating Wave-Induced Kinematics at Sloping Structures," *Journal of Waterway, Port, Coastal and Ocean Engineering*, American Society of Civil Engineers, Vol 121, No. 4, pp 209-215.

Hughes and Kamphuis 1996
Hughes, S. A., and Kamphuis, J. W. 1996. "Scour at Coastal Inlet Structures," *Proceedings of the 25th International Coastal Engineering Conference*, American Society of Civil Engineers, New York, Vol 2, pp 2258-2271.

Hughes and Schwichtenberg 1998
Hughes, S. A., and Schwichtenberg, B. R. 1998. "Current-Induced Scour Along a Breakwater at Ventura Harbor, California - Experimental Study," *Coastal Engineering*, Elsevier, Vol 34, No. 1-2, pp 1-22.

Ibsen 1999
Ibsen, L. B. 1999. "Cyclic Fatique Model," Geotechnical Engineering Papers, Aalborg University.

Ibsen and Lade 1998
Ibsen, L. B., and Lade, P.V. 1998. The Role of the Characteristic Line in Static Soil Behaviour," *Localization and Bifurcation Theory for Soils and Rocks*. Adachi and Yashima, Balkema, ed., Rotterdam.

Iribarren 1938
Iribarren, R. 1938. "Una Formula Para el Cálculo de los Digues de Escollera," Technical Report HE 116-295, Fluid Mechanics Laboratory, University of California, Berkeley, CA (Translated by D. Heinrich in 1948).

Iribarren and Nogales 1954
Iribarren, R., Nogales, C. 1954. "Other Verifications of the Formula for Calculating Breakwater Embankments," PIANC Bulletin No. 39, Permanent International Association of Navigation Congresses.

Irie and Nadaoka 1984
Irie, I., and Nadaoka, K. 1984. "Laboratory Reproduction of Seabed Scour in Front of Breakwaters," *Proceedings of the 19th International Coastal Engineering Conference*, American Society of Civil Engineers, Vol 2, pp 1715-1731.

Ito, Tanimoto, and Yamamoto 1972
Ito, Y., Tanimoto, K., and Yamamoto, S. 1972. "Wave Height Distribution in the Region of Ray Crossings - Application of Numerical Analysis Method of Wave Propagation," Report of Port and Harbour Research Institute, Vol 11, No.3, pp 87-109 (in Japanese).

Jackson 1968
Jackson, R. A. 1968. "Design of Cover Layers for Rubble-Mound Breakwaters Subjected to Nonbreaking Waves," Research Report No. 2-11, U.S. Army Engineer Waterways Experiment Station, Vicksburg, MS.

Jacobsen 1967
Jacobsen, M. 1967. "The Undrained Shear Strength of Preconsolidated Boulder Clay," *Proceedings of Geotechnical Conference*, Oslo, Norway, Vol I, pp 119-122.

Janbu 1954a
Janbu, N. 1954. "Application of Composite Slip Surfaces for Stability Analysis," *Proceedings of the Conference on Stability*, Vol III, p. 43, Stockholm, Sweden.

Janbu 1954b
Janbu, N. 1954. "Stability Analysis of Slopes with Dimensionless Parameters," Ph.D. diss., Harvard University, Cambridge, MA.

Janbu 1973
Janbu, N. 1973. "The Generalized Procedure of Slices," *Embankment Dam Engineering*, Casagrande Volume, pp 47-86.

Jensen, 1983
Jensen, O. J. 1983. "Breakwater Superstructures," *Proceedings of Coastal Structures '83*, American Society of Civil Engineers, New York, pp 272-285.

Jensen 1984
Jensen, O. J. 1984. "A Monograph on Rubble Mound Breakwaters," Danish Hydraulic Institute, Denmark.

Johnson 1992
Johnson, P. A. 1992. "Reliability-Based Pier Scour Engineering," *Journal of Hydraulic Engineering*, American Society of Civil Engineers, Vol 118, No. 10, pp 1344-1358.

Johnson 1995
Johnson, P. A. 1995. "Comparison of Pier-Scour Equations Using Field Data," *Journal of Hydraulic Engineering*, American Society of Civil Engineers, Vol 121, No. 8, pp 626-630.

Juhl and van der Meer 1992
Juhl, J. and van der Meer, J. W. 1992. "Quasi-Static Forces on Vertical Structures. Re-Analysis of Data at the Danish Hydraulic Institute and Delft Hydraulics," Report MAST G6-S, Coastal Structures, Project 2.

Kawata and Tsuchiya 1988
Kawata, Y., and Tsuchiya, Y. 1988. "Local Scour Around Cylindrical Piles Due to Waves and Currents Combined," *Proceedings of the 21st International Coastal Engineering Conference*, American Society of Civil Engineers, Vol 2, pp 1310-1322.

Kerr 1975
Kerr, A. D. 1975. "Ice Forces on Structures Due to a Change of the Water Level," *Proceedings IAHR 3rd International Symposium on Ice Problems*, Interational Association for Hydraulic Research, pp 419-427.

Kjærnsli, Valstad, and Høeg 1992
Kjærnsli, B., Valstad, T., and Høeg, K. 1992. "Rockfill Dams," Norwegian Institute of Technology, Division of Hydraulic Engineering, Trondheim, Norway.

Klomb and Tonda 1995
Klomb, W. H. G., and Tonda, P. L. 1995. "Pipeline Cover Stability," *Proceedings of the 5th International Conference on Offshore Mechanics and Arctic Engineering*, American Society of Mechanical Engineering, Vol 2, pp 15-22.

Kobayashi and Oda 1994
Kobayashi, T., and Oda, K. 1994. "Experimental Study on Developing Process of Local Scour Around a Vertical Cylinder," *Proceedings of the 24th International Coastal Engineering Conference*, American Society of Civil Engineers, Vol 2, pp 1284-1297.

Kortenhaus and Oumeraci 1998
Kortenhaus, A., and Oumeraci, H. 1998. "Classification of Wave Loading on Monolithic Coastal Structures," *Proceedings of the 26th International Coastal Engineering Conference*, Vol 1, pp 867-880.

Kraus 1988
Kraus, N. C. 1988. "The Effects of Seawalls on the Beach: An Extended Literature Review," *Journal of Coastal Research*, The Coastal Education and Research Foundation, Special Issue No. 4, N. C. Kraus and O. H. Pilkey, eds., pp 1-28.

Kraus and McDougal 1996
Kraus, N. C., and McDougal, W. G. 1996. "The Effects of Seawalls on the Beach: Part I, An Updated Literature Review," *Journal of Coastal Research*, The Coastal Education and Research Foundation, Vol 12, No. 3, pp 691-701.

Kriebel, Sollitt, and Gerken 1998
Kriebel, D., Sollitt, C, and Gerken, W. 1998. "Wave Forces on a Vertical Wave Barrier," *Proceedings of the 26th International Coastal Engineering Conference*, American Society of Civil Engineers, Vol 2, pp 2069-2081.

Kuzmanovic and Sanchez 1992
Kuzmanovic, B. O., and Sanchez, M. R. 1992. "Design of Bridge Pier Pile Foundations for Ship Impact," *Journal of Structural Engineering*, American Society of Civil Engineers, Vol 118, No. 8, pp 2151-2167.

Laird 1962
Laird, A. D. K. 1962. "Water Forces on Flexible Oscillating Cylinders," *Journal of the Waterways and Harbor Division*, American Society of Civil Engineers, Vol 88, No. WW3, pp 125-137.

Laird, Johnson, and Walker 1960
Laird, A. D. K., Johnson, C. A., and Walker, R. W. 1960. "Water Eddy Forces on Oscillating Cylinders," *Journal of the Hydraulics Division*, American Society of Civil Engineers, Vol 86, No. HY9, pp 43-54.

Lambe and Whitman 1979
Lambe, T. W., and Whitman, R. V. 1979. *Soil Mechanics* (SI version). John Wiley and Sons.

Lamberti 1995
Lamberti, A. 1995. "Preliminary Results on Main Armour - Toe Berm Interaction," Final Proceedings of MAST II Project, *Rubble Mound Breakwater Failure Modes*, Vol 2, Aalborg University, ed.

Lee 1972
Lee, T. T. 1972. "Design of Filter System for Rubble-Mound Structures," *Proceedings of the 13th International Conference on Coastal Engineering*, American Society of Civil Engineers, Vol 3, pp 1917-1933.

Lee and Lai 1986
Lee, J. J., and Lai, C. P. 1986. "Wave Uplift on Platforms or Docks," *Proceedings of the 20th International Coastal Engineering Conference*, American Society of Civil Engineers, Vol 2, pp 2023-2034.

Leidersdorf, Gadd, and McDougal 1988
Leidersdorf, C. B., Gadd, P. E., and McDougal, W. G. 1988. "Articulated Concrete Mat Slope Protection," *Proceedings of the 21st International Conference on Coastal Engineering*, American Society of Civil Engineers, Vol 3, pp 2400-2415.

Leidersdorf, Gadd, and McDougal 1990
Leidersdorf, C. B., Gadd, P. E., and McDougal, W. G. 1990. "Arctic Slope Protection Methods," *Proceedings of the 22nd International Conference on Coastal Engineering*, American Society of Civil Engineers, Vol 2, pp 1687-1701.

Leidersdorf, Gadd, and Vaudrey 1996
Leidersdorf, C. B., Gadd, P. E., and Vaudrey, K. D. 1996. "Design Considerations for Coastal Protection Projects in Cold Regions," *Proceedings of the 25th International Conference on Coastal Engineering*, American Society of Civil Engineers, Vol 4, pp 4397-4410.

Leps 1970
Leps, T. M. 1970. "Review of Shearing Strength of Rockfill," *Journal of the Soil Mechanics and Foundation Division*, American Society of Civil Engineers, Vol 96, No. SM4, pp 1159-1170.

Lillevang 1977
Lillevang, O. V. 1977. "Breakwater Subjected to Heavy Overtopping; Concept Design, Construction, and Experience," *Proceedings of Ports '77*, American Society of Civil Engineers, New York, pp 61-93.

Lillycrop and Hughes 1993
Lillycrop, W. J., and Hughes, S. A. 1993. "Scour Hole Problems Experienced by the Corps of Engineers; Data Presentation and Summary," Miscellaneous Paper CERC-93-2, U.S. Army Engineer Waterways Experiment Station, Coastal Engineering Research Center, Vicksburg, MS.

Lin et al. 1986
Lin, M-C., Wu, C-T., Lu, Y-C., and Liang, N-K. 1986. "Effects of Short-Crested Waves on the Scouring Around the Breakwater," *Proceedings of the 20th International Coastal Engineering Conference*, American Society of Civil Engineers, Vol 3, pp 2050-2064.

Losada, Silva, and Losada 1997
Losada, I. J., Silva, R, and Losada, M. A. 1997. "Effects of Reflective Vertical Structures Permeability on Random Wave Kinematics," *Journal of Waterway, Port, Coastal, and Ocean Engineering*, American Society of Civil Engineers, Vol 123, No. 6, pp 347-353.

Lundgren 1969
Lundgren, H. 1969. "Wave Shock Forces: An Analysis of Deformations and Forces in the Wave and in the Foundation," *Proceedings of the Symposium on Research on Wave Action*, Delft Hydraulics Laboratory, Emmeloord, The Netherlands, Vol II, Paper 4.

Lysmer and Richart 1966
Lysmer, J., and Richart, F. E. 1966. "Dynamic Response of Footings to Vertical Loading," *Journal of Soil Mechanics and Foundations Division*, American Society of Civil Engineers, Vol 92, No. SM 1, pp 65-91.

MacCamy and Fuchs 1954
MacCamy, R. C., and Fuchs, R. A. 1954. "Wave Forces on Piles: A Diffraction Theory," Technical Memorandum TM-69, U.S. Army Corps of Engineers, Beach Erosion Board, Washington, DC.

Machemehl 1990
Machemehl, J. L. 1990. "Wave and Ice Forces on Articicial Islands and Arctic Structures," *Handbook of Coastal and Ocean Engineering - Volume 1: Wave Phenomena and Coastal Structures*. John B. Herbich, ed., Gulf Publishing Company, Houston, TX, pp 1081-1124.

Madrigal and Valdés 1995
Madrigal, B. G., and Valdés, J. M. 1995. "Study of Rubble Mound Foundation Stability," Proceedings of the Final Workshop, MAST II, MCS-Project.

Magoon et al. 1974
Magoon, O. T., Sloan, R. L., and Foote, G. L. 1974. "Damages to Coastal Structures," *Proceedings of the 14th International Coastal Engineering Conference*, American Society of Civil Engineers, Vol 3, pp 1655-1676.

Markle, 1982
Markle, D. G. 1982. "Kahului Breakwater Stability Study, Kahului, Maui, Hawaii," Technical Report HL-82-14, U.S. Army Engineer Waterways Experiment Station, Vicksburg, MS.

Markle 1989
Markle, D. G. 1989. "Stability of Toe Berm Armor Stone and Toe Buttressing Stone on Rubble-Mound Breakwaters and Jetties; Physical Model Investigation," Technical Report REMR-CO-12, U.S. Army Engineer Waterways Experiment Station, Vicksburg, MS.

Maynord 1998
Maynord, S. T. 1998. "Corps of Engineers Riprap Design For Bank Stabilization," *Proceedings of the International Water Resources Engineering Conference*, American Society of Civil Engineers, pp 471-476.

McConnell 1998
McConnell, K. 1998. *Revetment Systems Against Wave Attack - A Design Manual,* Thomas Telford Publishing, London, UK.

Melby 1990
Melby, J. A. 1990. "An Overview of the Crescent City Dolos Design Procedure," *Stresses in Concrete Armor Units*, American Society of Civil Engineers, pp 312-326.

Melby 1993
Melby, J. A. 1993. "Dolos Design Procedure Based on Crescent City Prototype Data," Technical Report CERC-93-10, U.S. Army Engineer Waterways Experiment Station, Coastal Engineering Research Center, Vicksburg, MS.

Melby 1999
Melby, J. A. 1999. "Damage Progression on Rubble-Mound Breakwaters," Technical Report CHL-99-17, U.S. Army Engineer Waterways Experiment Station, Coastal and Hydraulics Laboratory, Vicksburg, MS.

Melby and Kobayashi 1998a
Melby, J. A., and Kobayashi, N. 1998a. "Progression and Variability of Damage on Rubble-Mound Breakwaters," *Journal of Waterway, Port, Coastal, and Ocean Engineering*, American Society of Civil Engineers, New York, Vol 124, No. 6, pp 286-294.

Melby and Kobayashi 1998b
Melby, J. A., and Kobayashi, N. 1998b. "Damage Progression on Breakwaters," *Proceedings of the 26th International Coastal Engineering Conference*, American Society of Civil Engineers, Vol 2, pp 1884-1897.

Melby and Mlaker 1997
Melby, J. A., and Mlaker, P. R. 1997. "Reliability Assessment of Breakwaters," Technical Report CHL-97-9, U.S. Army Engineer Waterways Experiment Station, Vicksburg, MS.

Melby and Turk 1992
Melby, J. A., and Turk, G. F. 1992. "Dolos Design Using Reliability Methods," *Proceedings of the 23rd International Coastal Engineering Conference*, American Society of Civil Engineers, Vol 2, pp 1385-1399.

Melby and Turk 1994
Melby, J. A., and Turk, G. F. 1994. "The CORE-LOC: Optimized Concrete Armor," *Proceedings of the 24th International Coastal Engineering Conference*, American Society of Civil Engineers, Vol 2, pp 1426-1438.

Mettam 1976
Mettam, J. D. 1976. "Design of Main Breakwater at Sines Harbor," *Proceedings of the 15th International Coastal Engineering Conference*, American Society of Civil Engineers, Vol 3, pp 2499-2518.

Meyerhof 1951
Meyerhof, G. G. 1951. "The Ultimate Bearing Capacity of Foundations," *Geotechnique*, Vol 2, pp 301-332.

Meyerhof 1953
Meyerhof, G. G. 1953. "The Bearing Capacity of Foundations Under Eccentric and Inclined Loads," *Proceedings of the 3rd International Conference on Soil Mechanics*, Zurich, Vol 1, pp 440-445.

Meyerhof 1963
Meyerhof, G. G. 1963. "Some Recent Research on the Bearing Capacity of Foundations," *Canadian Geotechnique* I., Vol 1, No. 1, pp 16-26.

Morgenstern and Price 1965
Morgenstern, N. R., and Price, V. E. 1965. "The Analysis of the Stability of Slip Surfaces," *Geotechnique*, Vol 15, No 1, pp 79-93.

Morison et al. 1950
Morison, J. R., O'Brien, M. P., Johnson, J. W., and Shaff, S. A. 1950. "The Force Exerted by Surface Waves on Piles," *Petroleum Transactions*, AIME, Vol 189, pp 149-154.

Newark 1942
Newark, N. M. 1942. "Influence Charts for Computation of Stresses in Elastic Foundations," Bulletin No. 45, University of Illinois, Urbana-Champaign, IL.

Norwegian Geotechnical Institute 1992
Norwegian Geotechnical Institute. 1992. Publication No. 185, Norwegian Geotechnical Institute, Oslo, Norway.

Niedoroda and Dalton 1986
Niederoda, A. W. and Dalton, C. 1986. "A Review of the Fluid Mechanics of Ocean Scour," *Ocean Engineering*, Vol 9, No. 2, pp.159-170.

O'Donoghue and Goldsworthy 1995
O'Donoghue, T., and Goldsworthy, C. J. 1995. "Random Wave Kinematics in Front of Sea Wall," *Proceedings of Breakwaters '95*, Institution of Civil Engineering, London, UK, pp 1-12.

Otani, Horii, and Ueda 1975
Otani, H., Horii, O., and Ueda, S. 1975. "Field Study on the Impact Energy of Large Tankers," *Coastal Engineering in Japan*, Japan Society of Civil Engineering, Vol 18, pp 185-194.

Oumeraci 1991
Oumeraci, H. 1991. "Dynamic Loading and Response of Caisson Breakwaters - Results of Large-Scale Model Tests," MAST G6-S, Project 2 Report, Franzius Institute, University of Hannover, Hannover, Germany.

Oumeraci 1994
Oumeraci, H. 1994. "Scour in Front of Vertical Breakwaters - Review of Problems," *Proceedings of International Workshop on Wave Barriers in Deepwaters*, Port and Harbor Research Institute, Japan, pp 281-307.

Owen 1980
Owen, M. W. 1980. "Design of Seawalls Allowing for Wave Overtopping," Report No. 924, Hydraulics Research Station, Wallingford, UK.

Owen 1982
Owen, M. W. 1982. "The Hydraulic Design of Seawall Profiles," *Proceedings of the Coastal Protection Conference*, Institution of Civil Engineers, Thomas Telford Publishing, London, UK, pp 185-192.

Pedersen 1996
Pedersen, J. 1996. "Experimental Study of Wave Forces and Wave Overtopping on Breakwater Crown Walls," Series paper 12, Hydraulics & Coastal Engineering Laboratory, Department of Civil Engineering, Aalborg University, Denmark.

Pedersen 1997
Pedersen, J. 1997. "Dynamic Response of Caisson Breakwaters Subjected to Impulsive Wave Loading - Design Diagrams for Dynamic Load Factors," *Proceedings*, Annex 2 C, 1st overall Workshop, EU-MASTIII project PROVERBS, Las Palmas, Gran Canaria, Spain.

Pedersen and Burcharth 1992
Pedersen, J., and Burcharth, H. F. 1992. "Wave Forces on Crown Walls," *Proceedings of the 23rd International Coastal Engineering Conference*, American Society of Civil Engineers, Vol 2, pp 1489-1502.

Perroud 1957
Perroud, P. H. 1957. "The Solitary Wave Reflection Along a Straight Vertical Wall at Oblique Incidence," Ph.D. diss., University of California, Berkeley, CA.

Permanent International Association of Navigation Congresses 1992
Permanent International Association of Navigation Congresses. 1992. "Guidelines for the Design and Construction of Flexible Revetments Incorporating Geotextiles in Marine Environment," Report of Working Group No. 21 of the Permanent Technical Committee II, Supplement to Bulletins No. 78/79.

Pilarczyk 1990
Pilarczyk, Krystian, W. 1990. "Design of Seawalls and Dikes - Including Overview of Revetments," *Coastal Protection*, K. Pilarczyk, ed., A.A. Balkema Publishers, Rotterdam, The Netherlands.

Postma 1989
Postma, G. M. 1989. "Wave Reflection from Rock Slopes Under Random Wave Attack," M.S. thesis, Delft University of Technology, The Netherlands.

Powell 1987
Powell, K. A. 1987. "Toe Scour at Sea Walls Subject to Wave Action," Report SR 119, Hydraulic Research Limited, Wallingford, UK.

Powell and Allsop 1985
Powell, K. A., and Allsop, N. W. 1985. "Low-Crest Breakwaters, Hydraulic Performance and Stability," Report No. SR 57, Hydraulics Research Station, Wallingford, England.

Price 1979
Price, A. W. 1979. "Static Stability of Rubble Mound Breakwaters," *Dock and Harbour Authority*, Vol LX, No. 702, pp 2-7.

Quinn 1972
Quinn, A. D. 1972. *Design and Construction of Ports and Marine Structures*. McGraw-Hill, New York.

Rance 1980
Rance, P. J. 1980. "The Potential for Scour Around Large Objects," *Scour Prevention Techniques Around Offshore Structures*, London Seminar, Society for Underwater Technology, pp 41-53.

Richardson and Davis 1995
Richardson, E. V., and Davis, S. R. 1995. "Evaluating Scour at Bridges," *Hydraulic Engineering Circular No. 18*, FHWA-IP-90-017, Federal Highway Administration, Washington, DC.

Richardson and Whitman 1964
Richardson, A. M., Jr., and Whitman, R. V. 1964. "Effect of Strain Rate Upon Undrained Shear Resistance of Saturated Remolded Fat Clay," *Geotechnique*, Vol 13, No. 4, pp 310-346.

Rouse 1950
Rouse, H., ed. 1950. *Engineering Hydraulics*, John Wiley and Sons, New York, NY.

Rowe and Barden 1964
Rowe, P.W., and Barden, L. 1964. "Importance of Free Ends in Triaxial Testing," *Journal of the Soil Mechanics and Foundation Division*, American Society of Civil Engineers, Vol 90, No. SM1, pp 1-17.

Sainflou 1928
Sainflou, M. 1928. "Treatise on Vertical Breakwaters," *Annals des Ponts et Chaussee*, Paris, France (Translated by W. J. Yardoff, U.S. Army Corps of Engineers.)

Sakaiyama and Kajima 1997
Sakaiyama, T., and Kajima, R. 1997. "Stability of Armor Units at Concave Section of Man-Made Island," *Proceedings of the Combined Australasian Coastal Engineering and Ports Conference - Pacific Coasts and Ports '97,* Center for Advanced Engineering, Vol 1, pp 213-218.

Sarpkaya 1976a
Sarpkaya, T. 1976a. "Vortex Shedding and Resistance in Harmonic Flow About Smooth and Rough Circular Cylinders at High Reynolds Numbers," Report No. NPS-59SL76021, Naval Postgraduate School, Monterey, CA.

Sarpkaya 1976b
Sarpkaya, T. 1976b. "In-Line and Transverse Forces on Cylinders in Oscillatory Flow at High Reynolds Number," *Proceedings of the Eighth Offshore Technology Conference*, Houston, TX, Paper No. OTC 2533, Vol 2, pp 95-108.

Sarpkaya and Isaacson 1981
Sarpkaya, T., and Isaacson, M. 1981. *Mechanics of Wave Forces on Offshore Structures,* Van Nostrand Reinhold.

Sato, Tanaka, and Irie 1968
Sato, S., Tanaka, N., and Irie, I. 1968. "Study on Scouring at the Foot of Coastal Structures," *Proceedings of the 11th International Coastal Engineering Conference*, American Society of Civil Engineers, Vol 1, pp 579-598.

Seed and Idriss 1970
Seed H. B., and Idriss, I. M. 1970. "Soil Moduli and Damping Factors for Dynamic Response Analysis," Report No. EERC 75-29, Earthquake Engineering Research Center, University of California, Berkeley, CA.

Seed et al. 1986
Seed H. B., Wong, R. T., Idriss, I. M., and Tokimatsu, K. 1986. "Moduli and Damping Factors for Dynamic Analyses of Cohesive Soils," *Journal of Geotechnical Engineering*, American Society of Civil Engineers, Vol 112, No. GT 11, pp 1016-1032.

Seelig 1980
Seelig, W. N. 1980. "Two-Dimensional Tests of Wave Transmission and Reflection Characteristics of Laboratory Breakwaters," Technical Report No. 80-1, U.S. Army Engineer Waterways Experiment Station, Vicksburg, MS.

Seelig 1983
Seelig, W. N. 1983. "Wave Reflection from Coastal Structures," *Proceedings of Coastal Structures '83*, American Society of Civil Engineers, pp 961-973.

Shore Protection Manual 1977
Shore Protection Manual. 1977. 3rd ed., U.S. Army Engineer Waterways Experiment Station, U.S. Government Printing Office, Washington, DC.

Shore Protection Manual 1984
Shore Protection Manual. 1984. 4th ed., U.S. Army Engineer Waterways Experiment Station, U.S. Government Printing Office, Washington, DC.

Silvester 1991
Silvester, R. 1991. "Scour Around Breakwaters and Submerged Structures," *Handbook of Coastal and Ocean Engineering - Volume 2: Offshore Structures, Marine Foundations, Sediment Processes, and Modeling*. John B. Herbich, ed., Gulf Publishing Company, Houston, TX, pp 959-996.

Skjelbriea et al. 1960
Skjelbriea, L., Hendrickson, J. A., Grogg, W., and Webb, L. M. 1960. "Loading on Cylindrical Pilings Due to the Action of Ocean Waves," Contract NBy-3196, 4 Volumes, U.S. Naval Civil Engineering Laboratory.

Smith 1999
Smith, E. R. 1999. "Toe Stability of Rubble-Mound Structures in a Breaking Wave and Ebb Flow Environment," Technical Report REMR-CO-20, U.S. Army Engineer Waterways Experiment Station, Coastal and Hydraulics Laboratory, Vicksburg, MS.

Smith, Seijffert, and van deer Meer 1994
Smith, G. M., Seijffert, J. W., and van der Meer, J. W. 1994. "Erosion and Overtopping of a Grass Dike: Large Scale Model Tests," *Proceedings of the 24th International Coastal Engineering Conference*, American Society of Civil Engineers, Vol 3, pp 2639-2652.

Smits, Anderson, and Gudehus 1978
Smits, F. P., Andersen, K. H., and Gudehus, G. 1978. "Pore Pressure Generation," *International Symposium on Soil Mechanics Research and Foundation Design for the Oosterschelde Storm Surge Barrier*, Vol 1, paper II-3.

Song and Schiller 1973
Song, W. O., and Schiller, R. E. 1973. "Experimental Studies of Beach Scour," COE Report No. 166, Texas A&M University, College Station, TX.

Steenfelt 1992
Steenfelt, J. S. 1992. "Strength and Dilatancy Revisited," Miscellaneous Papers in Civil Engineering, 35th Anniversary of the Danish Engineering Academy, Lyngby, Denmark, pp 157-188. (Also published by the Danish Geotechnical Institute, Lyngby, Denmark).

Steenfelt and Foged 1994
Steenfelt, J. S., and Foged, N. 1994. "Dilational Behaviour of Crushed Stone," *Proceedings of the 7th International IAEG Congress*, Lisbon, Portugal, Vol V, pp 3357-3364.

Steinbrenner 1936
Steinbrenner, W. 1936. "A Rational Method for Determination of the Vertical Normal Stresses Under Foundations," *Proceedings of the International Conference on Soil Mechanics and Foundation Engineering*, Cambridge, MA, Vol 2, pp 142-143.

Stückrath 1996
Stückrath, T. 1996. "Recommendation for the Construction of Breakwaters With Vertical and Inclined Concrete Walls," Report of Sub-Group C, Working Group 28, PIANC PTC II.

Sumer and Fredsøe 1990
Sumer, B. M., and Fredsøe, J. 1990. "Scour Below Pipelines in Waves," *Journal of Waterway, Port, Coastal, and Ocean Engineering*, American Society of Civil Engineers, Vol 116, No. 3, pp 307-323.

Sumer and Fredsøe 1991
Sumer, B. M., and Fredsøe, J. 1991. "Onset of Scour Below a Pipeline Exposed to Waves," *International Journal of Offshore and Polar Engineering*, Vol 1, No. 3, pp 189-194.

Sumer and Fredsøe 1992
Sumer, B. M., and Fredsøe, J. 1992. "A Review of Wave/Current-Induced Scour Around Pipelines," *Proceedings of the 23rd International Coastal Engineering Conference*, American Society of Civil Engineers, Vol 3, pp 2839-2852.

Sumer and Fredsøe 1996
Sumer, B. M., and Fredsøe, J. 1996. "Scour Around Pipelines in Combined Waves and Currents," *Proceedings of the 7th International Conference on Offshore Mechanics and Arctic Engineering*, American Society of Mechanical Engineering, Vol 5, pp 595-602.

Sumer and Fredsøe 1997
Sumer, B. M., and Fredsøe, J. 1997. "Scour at the Head of a Vertical-Wall Breakwater," *Coastal Engineering*, Elsevier, Vol 29, No. 3, pp 201-230.

Sumer and Fredsøe 1998a
Sumer, B. M., and Fredsøe, J. 1998a. "Wave Scour Around Structures," *Advances in Coastal Engineering,* Phillip Liu, ed., Vol 4, World Scientific, Singapore.

Sumer and Fredsøe 1998b
Sumer, B. M., and Fredsøe, J. 1998b. "Wave Scour Around Group of Vertical Piles," *Journal of Waterway, Port, Coastal, and Ocean Engineering Division*, American Society of Civil Engineers, Vol 124, No. 5, pp 248-256.

Sumer, Christiansen, and Fredsøe 1992a
Sumer, B. M., Christiansen, N., and Fredsøe, J. 1992a. "Scour Around Vertical Pile in Waves," *Journal of Waterway, Port, Coastal, and Ocean Engineering Division*, American Society of Civil Engineers, Vol 118, No. 1, pp 15-31.

Sumer, Christiansen, and Fredsøe 1992b
Sumer, B. M., Christiansen, N., and Fredsøe, J. 1992b. "Time Scale of Scour Around a Vertical Pile," *Proceedings of the 2nd International Offshore and Polar Engineering Conference*, International Society of Offshore and Polar Engineers, Vol 3, pp 308-315.

Sumer, Christiansen, and Fredsøe 1993
Sumer, B. M., Christiansen, N., and Fredsøe, J. 1993. "Influence of Cross Section on Wave Scour Around Piles," *Journal of Waterway, Port, Coastal, and Ocean Engineering Division*, American Society of Civil Engineers, Vol 119, No. 5, pp 477-495.

Sutherland and O'Donoghue 1997
Sutherland, J., and O'Donoghue, T. 1997. "CRF Study of Wave Kinematics in Front of Coastal Structures," *Proceedings of Coastal Dynamics '97*, American Society of Civil Engineers, pp 694-703.

Sutherland and O'Donoghue 1998a
Sutherland, J., and O'Donoghue, T. 1998a. "Wave Phase Shift at Coastal Structures," *Journal of Waterway, Port, Coastal and Ocean Engineering*, American Society of Civil Engineers, Vol 124, No. 2, pp 90-98.

Sutherland and O'Donoghue 1998b
Sutherland, J., and O'Donoghue, T. 1998b. "Characteristics of Wave Reflection Spectra," *Journal of Waterway, Port, Coastal and Ocean Engineering*, American Society of Civil Engineers, Vol 124, No. 6, pp 303-311.

Svee 1962
Svee, R. 1962. "Formulas for Design of Rubble Mound Breakwaters," *Journal of the Waterways and Harbours Division,* American Society of Civil Engineers, Vol 88, No. WW2, pp 11-21.

Tait and Mills 1980
Tait, R. B., and Mills, R. D. 1980. "An Investigation into the Material Limitations of Breakwater Dolosse," ECOR Newsletter, No. 12.

Takahashi 1996
Takahashi, S., 1996. "Design of Vertical Breakwaters," Reference Documents, No. 34, Port and Harbour Research Institute, Japan.

Takahashi and Hosoyamada 1994
Takahashi, S., and Hosoyamada, S. 1994. "Hydrodynamic Characteristics of Sloping Top Caissions," *Proceedings of International Conference on Hydro-Technical Engineering for Port and Harbour Construction*, Port and Harbour Research Institute, Japan, Vol 1, pp 733-746.

Takahashi, Tanimoto, and Shimosako 1990
Takahashi., S., Tanimoto, K., and Shimosako, K. 1990. "Wave and Block Forces on a Caisson Covered With Wave Dissipating Blocks," Report of Port and Harbour Research Institute, Yokosuka, Japan, Vol 30, No. 4, pp 3-34 (in Japanese).

Takahashi, Shimosako, and Sasaki 1991
Takahashi, S., Shimosako, K., and Sasaki, H. 1991. "Experimental Study on Wave Forces Acting on Perforated Wall Caisson Breakwaters," Report of Port and Harbour Research Institute, Yokosuka, Japan, Vol 30, No. 4, pp 3-34 (in Japanese).

Takahashi, Tanimoto, and Shimosako 1994a
Takahashi, S., Tanimoto, K., and Shimosako, K. 1994a. "A Proposal of Impulsive Pressure Coefficient for Design of Composite Breakwaters," *Proceedings of the International Conference on Hydro-Technical Engineering for Port and Harbor Construction,* Port and Harbour Research Institute, Yokosuka, Japan, pp 489-504.

Takahashi, Tanimoto, and Shimosako 1994b
Takahashi, S., Tanimoto, K., and Shimosako, K. 1994. "Wave Pressure on Perforated Wall Caissons," *Proceeding of International Conference on Hydro-Technical Engineering for Port and Harbor Construction*, Port and Harbour Research Institute, Yokosuka, Japan, pp 747-764.

Takayama 1992
Takayama, T. 1992. "Estimation of Sliding Failure Probability of Present Breakwaters for Probabilistic Design," Port and Harbour Research Institute, Vol 31, No.5, pp 80-96.

Tanimoto and Kimura 1985
Tanimoto, K., and Kimura, K. 1985. "A Hydraulic Experimental Study on Trapezoidal Caisson Breakwaters," Technical Note No. 528, Port and Harbour Research Institute, Yokosuka, Japan (in Japanese).

Tanimoto, et al. 1976
Tanimoto, K., Moto, K., Ishizuka, S., and Goda Y. 1976. "An Investigation on Design Wave Force Formulae of Composite-Type Breakwaters," *Proceedings of the 23rd Japanese Conference on Coastal Engineering*, pp 11-16 (in Japanese).

Tanimoto, Takahashi, and Kitatani 1981
Tanimoto, K., Takahashi, K., and Kitatani, T. 1981. "Experiment Study of Impact Breaking Wave Forces on a Vertical Wall Caisson of Composite Breakwater," Report of Port and Harbour Research Institute, Vol 20, No. 2, pp 3-39 (in Japanese).

Tanimoto, Yagyu, and Goda 1982
Tanimoto, T., Yagyu, T., and Goda, Y. 1982. "Irregular Wave Tests for Composite Breakwater Foundations," *Proceedings of the 18th International Coastal Engineering Conference*, American Society of Civil Engineers, Vol 3, pp 2144-2163.

Tanimoto, Haranaka, and Yamazaki 1985
Tanimoto, K, Haranaka, S., and Yamazaki, K. 1985. "Experimental Study of Wave Dissipating Concrete Blocks Against Irregular Waves," *Report of the Port and Harbour Research Institute*, Vol 24, No. 2, pp 85-121 (in Japanese).

Tanimoto, Takahashi, and Kimura 1987
Tanimoto, K., Takahashi, S., and Kimura, K. 1987. "Structures and Hydraulic Characteristics of Breakwaters - The State of the Art of Breakwater Design in Japan," *Report of the Port and Harbour Research Institute*, Japan, Vol. 26, No. 5, pp 11-15.

Taylor 1958
Taylor, D. W. 1958. *Fundamentals of Soil Mechanics*, John Wiley & Sons, New York, NY.

Tepfers and Kutti 1979
Tepfers, R., and Kutti, T. 1979. "Fatigue Strength of Plain Ordinary and Lightweight Concrete," *ACI Journal*, May 1979, pp 635-652.

Terzaghi and Peck 1944
Terzaghi, K., and Peck, R. B. 1944. *Soil Mechanics in Engineering Practice*, John Wiley & Sons, New York, NY.

Thomsen, Wohlt, and Harrison 1972
Thomsen, A. L., Wohlt, P. E., and Harrison, A. S. 1972. "Riprap Stability on Earth Embankments Tested in Large- and Small-Scale Wave Tanks," TM-37, U.S. Army Corps of Engineers, Coastal Engineering Research Center, Washington, DC.

Tomlinson 1980
Tomlinson, M. J. 1980. *Foundation Design and Construction*. Pitman Publishing Ltd., London.

Tsuruta and Goda 1968
Tsuruta, S., and Goda, Y. 1968. "Expected Discharge of Irregular Wave Overtopping," *Proceedings of the 11th International Coastal Engineering Conference*, American Society of Civil Engineers, Vol 2, pp 833-852.

Turk and Melby 1997
Turk, G. F., and Melby, J. A. 1997. "CORE-LOC^7 Concrete Armor Units: Technical Guidelines," Miscellaneous Paper CHL-97-6, U.S. Army Engineer Waterways Experiment Station, Coastal and Hydraulics Laboratory, Vicksburg, MS.

van der Meer 1988
van der Meer, J. W. 1988. "Rock Slopes and Gravel Beaches Under Wave Attack," Ph.D. diss., Delft University of Technology, The Netherlands. (Also Delft Hydraulics Publication No. 396)

van der Meer 1988b
van der Meer, J. W. 1988b. "Stability of Cubes, Tetrapodes and Accropode," *Proceedings of the Breakwaters '88 Conference; Design of Breakwaters*, Institution of Civil Engineers, Thomas Telford, London, UK, pp 71-80.

van der Meer 1990
van der Meer, J. W. 1990. "Low-Crested and Reef Breakwaters," Report H198/Q638, Delft Hydraulics Laboratory, The Netherlands.

van der Meer 1991
van der Meer, J. W. 1991. "Stability and Transmission at Low-Crested Structures," Delft Hydraulics Publication No. 453, Delft Hydraulics Laboratory, The Netherlands.

van der Meer 1997
van der Meer, J. W. 1997. Discussion of "Comparison and Evaluation of Different Riprap Stability Formulas Using Field Performance," Belfadhel et al., *Journal of Waterway, Port, Coastal and Ocean Engineering*, American Society of Civil Engineers, Vol. 123, No. 3, pp 147-148.

van der Meer and d'Angremond 1991
van der Meer, J. W., and d'Angremond, K. 1991. "Wave Transmission at Low Crested Structures," *Proceedings of the Coastal Structures and Breakwaters Conference*, Institution of Civil Engineers, Thomas Telford Publishing, London, UK, pp 25-41.

van der Meer and Janssen 1995
van der Meer, J. W., and Janssen, W. 1995. "Wave Run-Up and Wave Overtopping at Dikes," In *Wave Forces on Inclined and Vertical Wall Structures*, Kobayashi and Demirbilek, eds., American Society of Civil Engineers, pp 1-27.

van der Meer and Stam 1992
van der Meer, J. W., and Stam C. M. 1992. "Wave Run-Up on Smooth and Rock Slopes of Coastal Structures," *Journal of Waterway, Port, Coastal and Ocean Engineering*, American Society of Civil Engineers, Vol. 118, No. 5, pp 534-550.

van der Meer, d=Agremond, and Juhl 1994
van der Meer, J. W., d=Angremond, K., and Juhl, J. 1994. "Probabilistic Calculation of Wave Forces on Vertical Structures," *Proceedings of the 24th International Coastal Engineering Conference*, American Society of Civil Engineers, Vol 2, pp 1754-1769.

van der Meer, d=Angremond, and Gerding 1995
van der Meer, J. W., d'Angremond, K., and Gerding, E. 1995. "Toe Structure Stability of Rubble Mound Breakwaters," *Proceedings of the Advances in Coastal Structures and Breakwaters Conference*, Institution of Civil Engineers, Thomas Telford Publishing, London, UK, pp 308-321.

van Oorschot and d'Angremond 1968
van Oorschot, J. H., and d'Angremond, K. 1968. "The Effect of Wave Energy Spectra on Wave Run-Up," *Proceedings of the 11th International Coastal Engineering Conference*, American Society of Civil Engineers, Vol 2, pp 886-900.

Vidal et al. 1992
Vidal, C., Losada, M. A., Medina, R., Mansard, E. P., and Gomez-Pina, G. 1992. "A Universal Analysis for the Stability of Both Low-Crested and Submerged Breakwaters," *Proceedings of the 23rd International Coastal Engineering Conference*, American Society of Civil Engineers, Vol 2, pp 1679-1692.

Wang and Herbich 1983
Wang, R. K., and Herbich, J. B. 1983. "Combined Current and Wave Produced Scour Around a Single Pile," Report No. COE 269, Texas Engineering Experiment Station, Texas A&M University, College Station, TX.

Wiegel 1964
Wiegel, R. L. 1964. *Oceanographical Engineering*, Prentice-Hall, New Jersey.

Wuebben 1995
Wuebben, J. L. 1995. "Ice Effects on Riprap," *River, Coastal and Shoreline Protection: Erosion Control Using Riprap and Armourstone*. C. R. Thorne, S. R. Abt, F. B. Barends, S. T. Maynord, and R. W. Pilarczyk, eds., John Wiley & Sons, Ltd., Chichester, UK, pp 513-530.

Xie 1981
Xie, S.-L. 1981. "Scouring Patterns in Front of Vertical Breakwaters and their Influences on the Stability of the Foundations of the Breakwaters," Department of Civil Engineering, Delft University of Technology, Delft, The Netherlands.

Xie 1985
Xie, S.-L. 1985. "Scouring Patterns in Front of Vertical Breakwaters," *Acta Oceanologica Sinica*, Vol 4, No. 1, pp 153-164.

Zielinski, Reinhardt, and Körmeling 1981
Zielinski, A. J., Reinhardt, H. W., and Körmeling, H. A. 1981. "Experiments on Concrete Under Repeated Uniaxial Impact Tensile Loading," RILEM, Materials and Structures, Vol 14, No. 81.

Zwamborn and Phelp 1990
Zwamborn, J. A., and Phelp, D. 1990. "Structural Tests on Dolosse," *Proceedings of Stresses in Concrete Armor Units*, American Society of Civil Engineers, pp 40-60.

VI-5-10. Acknowledgements.

Authors: Dr. Hans F.Burcharth, Department of Civil Engineering, Aalborg University, Aalbort, Denmark; and Dr. Steven A. Hughes, Coastal and Hydraulics Laboratory (CHL), U.S. Army Engineer Research and Development Center, Vicksburg, MS.

Reviewers:
H. Lee Butler, CHL (retired)
Dr. David R. Basco, Department of Civil Engineering, Old Dominion University, Norfolk, VA
Students Han Ligteringen, Delft University of Technology, The Netherlands; Jorgen Fredsøe and Mutly Sumer, Institute of Hydrodynamics and Hydraulic Engineering, Technical University of Denmark, Lyngby, Denmark.

VI-5-11. Symbols.

α (alpha)	
α	Angle a surface-piercing sloped plane forms with the horizontal [deg]
α	Angle of wave approach [deg]
α	Tangent of seaward armor slope
β (beta)	
β	Angle of incidence of waves [deg]
β	Concave angle at vertical walls [radians]
β	Frequency parameter [dimensionless]
γ (gamma)	
γ	Load factor [dimensionless]
γ_β	Factor for influence of angle of incidence β of the waves [dimensionless]
γ_b	Reduction factor for influence of a berm [dimensionless]
γ_h	Reduction factor for influence of shallow-water conditions where the wave height distribution deviates form the Rayleigh distribution [dimensionless]
γ_r	Reduction factor for influence of surface roughness [dimensionless]
γ_w	Specific weight of water or salt water [force/length^3]
_*!*	Average effective weight of soil from base to depth *B* under base level [force]
δ (delta)	
δ	Logarithmic decrement
δ_0	Vertical shift in the wave crest and wave trough at the wall [length]
Δ (delta)	
Δ	(= ρ_s / ρ_w) - 1
Δ	Water level rise up to the thickness of the ice [length]
$\Delta\tau_s$	Change in the average shear stress due to the submerged weight of the structure [force/length^2]
ε (epsilon)	
ε_i	Random wave phase angle of the *i*th incident wave component [deg]
$\dot{\varepsilon}_1, \dot{\varepsilon}_3$	Strain rates in principal stress directions 1 and 3
$\dot{\varepsilon}_{vol}$	Volume strain rate
η (eta)	
η	Sea surface elevation adjacent to a reflective structure [length]
η^2_{rms}	Root-mean-squared sea surface elevation [length^2]
θ (theta)	
θ	Angle of wave incidence [deg]
θ	Bottom slope [deg]

θ	Channel side wall slope [degrees]
θ	Wave phase angle (= $2\pi x/L$ - $2\pi t/T$) [radians]
θ_i	Reflection phase angle of the ith incident wave component [deg]
κ (kappa)	
κ	von Karman constant (= 0.4) [dimensionless]
λ (lamda)	
$\lambda_{1,2,3}$	Modification factors depending on the structure type [dimensionless]
μ (mu)	
μ	Dynamic friction coefficient corresponding to caisson displacement S [dimensionless]
μ	Friction coefficient for the base plate against the rubble stones [dimensionless]
μ	Structure slope friction factor [dimensionless]
ν (nu)	
ν	Kinematic viscosity [length^2/time]
ν	Poisson= ratio [dimensionless]
v_*	Shear velocity
ξ (xi)	
ξ	Principal stress reduction factor
ξ_0	Surf similarity parameter for regular waves (Equation VI-5-1)
ξ_{0m}	Surf similarity parameter for irregular waves (Equation VI-5-2)
ξ_{0p}	Surf similarity parameter for irregular waves (Equation VI-5-2)
ξ_{eq}	Breaking wave surf similarity parameter
ρ (rho)	
ρ	Bulk density [force/length^3]
ρ_a	Mass density of armor units [force/length^3]
ρ_c	Mass density of the structure [force/length^3]
ρ_i	Ice density [force/length^3]
ρ_s	Mass density of armor units [force/length^3]
ρ_w	Mass density of water (salt water = 1,025 kg/m^3 or 2.0 slugs/ft^3; fresh water = 1,000 kg/m^3 or 1.94 slugs/ft^3) [force-time^2/length^4]
σ (sigma)	
σ	Normal stress on a section through a soil element [force/length^2]
σ	Spreading of short-crested waves
σ_1	Principal stress [force/length^2]
σ_c	Ice compressive failure strength in crushing [force/length^2]
σ_c	Standard deviation of the average non-dimensional cover armor depth
σ_e	Standard deviation of the average non-dimensional eroded armor depth

σ_f	Flexural strength of ice
σ_f'	Effective stress at failure [force/length^2]
σ_i	Angular wave frequency of the *i*th incident wave component [time^{-1}]
σ_n'	Normal stress on failure plane [force/length^2]
σ_S	Standard deviation of average damage
τ (tau)	
τ	Shear stress on a section through a soil element [force/length^2]
τ_0	Shear stress acting on the bed [force/length^2]
Ψ (psi)	
Ψ	Angle of dilation [degrees]
Ψ	Shields parameter
Ω (omega)	
Ω	Dynamic load factor [dimensionless]
ν	
ν	Angle of internal friction of the soil [degrees]
ν	Angle of repose of the armor [degrees]
ν	Strength factor [dimensionless]
ν'	Angle of friction in granular material [degrees]
ν'_{crit}	Critical angle of friction [degrees]
ν'_s	Effective secant angle of friction
ν'_t	Effective tangent angle of friction
A	
a	Pile radius [length]
a_i	Amplitude of the *i*th incident wave component [length]
A	Area of structure slope [length^2]
A	Horizontal area of ice sheet [length^2]
A_c	Berm crest height [length]
A_e	Area of eroded armor layer [length^2]
A_n	Projected area of solid body normal to the flow direction [length^2]
A_s	Total area of steel intersecting the crack [length^2]
A_t	Area of initial cross section of structure [length^2]
A_z	Projected area of solid body in the horizontal plane [length^2]
B	
b	Pile width [length]
b	Structure horizontal width or diameter [length]

B	Berm width [length]
B	Diameter of the vertical breakwater circular head [length]
B	Function of Reynolds number (= 8.5 for fully rough, turbulent flow)
B	Horizontal width of the barrier [length]
B	Relative breakage
B	Width of footing [length]
B	Width of structure crest [length]
C	
c	Infiltration factor [dimensionless]
c	Shear strength of soil [force/length^2]
c_u	Undrained shear strength [force/length^2]
$c!$	Cohesion intercept
C	Damage parameter for structure armor layer [dimensionless]
C	Dolos fluke length [length]
C_0	Zero-damage cover layer thickness [length]
C_D	Drag hydrodynamic force coefficient [force/length]
C_L	Empirical lift coefficient
C_M	Inertia or mass hydrodynamic force coefficient [force/length]
C_r	Bulk reflection coefficient [dimensionless]
C_{ri}	Reflection coefficient of the *i*th incident wave component [dimensionless]
C_s	Stability coefficient for incipient motion [dimensionless]
C_{sf}	Coefficient of skin friction between wind and ice or water and ice [dimensionless]
C_t	Wave transmission coefficient [dimensionless]
C_{to}	Wave transmission coefficient for overtopping [dimensionless]
C_{tp}	Wave transmission coefficient for wave penetration [dimension]
C_u	Uncertainty factor [dimensionless]
C_U	Laboratory derived slamming coefficient [dimensionless]
C_V	Coefficient of consolidation
D	
d	Grain diameter [length]
d_B	Berm horizontal surface above the still-water line [length]
d_c	Depth of armor cover [length]
d_c	Elevation of the lower edge of the sloping face relative to the SWL [length]
d_e	depth of sheet-pile penetration below the seabed [length]
d_e	Depth of eroded armor layer [length]

d_i	Depth at the toe of the sloping structure [length]
d_s	Water depth at the structure toe [length]
D	Cylindrical pile diameter [length]
D	Damping ratio [dimensionless]
D	Minimum depth of footing below soil surface [length]
D	Pipe diameter [length]
D	Sphere diameter [length]
D_e	Equivalent pile diameter [length]
D_H	Distance between centroids of two adjacent units on the same horizontal row [length]
D_n	Cube length [length]
D_{n50}	Median of nominal diameter of rocks for design conditions [length]
D_r	Relative density of soils [percent]
D_{swl}	Vertical distance from SWL to location of stressed dolos [length]
D_U	Distance between the centroids of units upslope in the plane of the structure slope [length]
E	
e	In-place void ratio [dimensionless]
e_{cr}	Critical embedment [length]
e_{max}	Void ratio of soil in loosest condition [dimensionless]
e_{min}	Void ratio of soil in most dense condition [dimensionless]
E	Damage parameter for structure armor layer [dimensionless]
E	Modulus of elasticity of ice
E	Young=s modulus
E_{av}	Averaged Young=s modulus for ice [force/length^2]
E_d	Dissipated wave energy in one wavelength per unit crest width [length-force/length^2]
E_i	Incident wave energy in one wavelength per unit crest width [length-force/length^2]
E_r	Reflected wave energy in one wavelength per unit crest width [length-force/length^2]
E_t	Transmitted wave energy in one wavelength per unit crest width [length-force/length^2]
F	
f_c	Concrete compressive strength [force/length^2]
f_c	Height of wall not protected by the armor layer [length]
f_{ct}	Concrete splitting tensile strength [force/length^2]
f_D	Drag force per unit length of pile [force/length]

f_i	Inertial force per unit length of pile [force/length]
f_i	Reduction factor [dimensionless]
f_T	Concrete static tensile strength [force/length]
f_y	Yield strength of the steel
F	Safety factor [dimensionless]
F_0	Significant force per unit width for a vertical wall [force/length]
F_B	Buoyancy force [force]
F_c	Horizontal crushing force [force]
F_D	Drag force [force]
F_G	Gravitational force [force]
F_G	Reduced weight of the vertical structure due to buoyancy [force]
F_H	Wave induced horizontal force [force]
F_I	Inertia force [force]
F_L	Lift force [force]
F_L	Time-varying transverse (lift) force
F_{Lm}	Maximum transverse force [force]
F_{m0}	Significant force per unit width of barrier [force/length]
F_r	Flow Froude number [dimensionless]
F_U	Wave induced uplift force [force]
F_v	Total vertical force acting on the wall [force]
F_W	Irregular wave loading [force]
G	
g	Gravitational acceleration [length/time^2]
G	Berm width [length]
G	Factor dependent on the armor layer gradation [dimensionless]
G	Shear modulus
H	
h	Ice plate thickness [length]
h	Pre-scour water depth at the vertical wall [length]
h	Water depth [length]
h_b	Water depth at a distance of $5H_s$ seaward of the breakwater front wall [length]
h_b	Water depth at top of toe berm [length]
h_c	Equilibrium height of the structure [length]
h_i	Thickness of ice sheet [length]
h_s	Water depth in front of structure [length]
$h!$	Height of wall protected by the armor layer [length]

$h!$	Submerged height of the wall from the toe to the still water line [length]
$h!_c$	Initial height of structure over seabed level [length]
Δh	Change in water level [length]
H	Characteristic wave height [length]
H	Drainage distance [length]
H_0	Deepwater wave height [length]
H_b	Breaking wave height [length]
H_c	Wave height in the corner [length]
H_i	Incident wave height [length]
H_I	Incident wave height [length]
H_{m0}	Zeroth-moment wave height [length]
H_S	Significant wave height [length]
H_{sr}	Significant reflected wave height [length]
H_w	Wave or surge height at the wall [length]
I	
i	Hydraulic gradient [length/length]
I	Indentation coefficient [dimensionless]
I_p	Plasticity index
K	
k	Contact coefficient [dimensionless]
k	Permeability coefficient
k	Wave number ($= 2\pi/L = 2\pi/CT$) [length^{-1}]
k_i	Wave number of the ith incident wave component [length^{-1}]
k_M	Moment contribution factor
k_p	Wave number associated with the spectral peak by linear wave theory [length^{-1}]
k_p	Wave number associated with the spectral peak period T_p [length^{-1}]
k_s	Boundary or bed roughness
k_T	Torque contribution factor [dimensionless]
k_x	Stiffness coefficient
k_v	Stiffness coefficient
k_Δ	Layer coefficient (Table VI-5-51)
K	Bulk modulus
K	Coefficient of lateral stress [dimensionless]
K	Factor to account for blankets plaved on sloping channel side walls [dimensionless]
K_1	Pile shape factor [dimensionless]
K_2	Pile orientation factor [dimensionless]

KC	Keulegan-Carpenter number [dimensionless]
K_D	Stability coefficient
K_o	Coefficient of lateral stress at rest [dimensionless]
L	
l_e	Upslope eroded length [length]
L	Damage parameter for structure armor layer [dimensionless]
L	Length of footing [length]
L	Local wave length [length]
L_0	Deepwater wave length (= $gT^2/2\pi$) [length]
L_{0m}	Deepwater wave length corresponding to mean wave period [length]
L_{0p}	Deepwater wave length corresponding to the peak of the wave spectrum [length]
L_p	Local wavelength associated with the peak spectral period T_p [length]
M	
m	Plan shape coefficient [dimensionless]
m	Total mass [force]
m_0	Area beneath the measured force spectrum [length^2]
M	Armor unit mass [force]
M	Constrained modulus
M_{50}	Medium mass of rocks; mass of Core-Loc armor unit (= $\rho_s (D_{n50})^3$) [force]
M_{cr}	Critical strength of concrete in moment
M_d	Overturning moment per unit horizontal length about the toe of the wall due to the dynamic pressure [length-force/length]
M_{FG}	Stabilizing moment around the heel by buoyancy-reduced weight of the caisson [length-force]
M_{FH}	Antistabilizing moment by wave induced horizontal force [length-force]
M_{FU}	Antistabilizing moment by wave induced uplift force [length-force]
M_{max}	Maximum wave-load-induced moment around the center of gravity [length-force]
M_s	Hydrostatic overturning moment per unit width [length-force/length]
M_s	Stabilizing moment due to friction and cohesion [length-force]
N	
n	Model scale factor [dimensionless]
n	Porosity
$\underline{n_z}$	Normal unit velocity in the positive z-direction [length/time]
N_{0w}	Number of overtopping waves
N_a	Total number of armor layer units or number of rocks in the mound
N_f	Number of cycles to failure

N_{od}	Number of units displaced out of the armor layer
N_{or}	Number of rocking units
N_S	Stability parameter [dimensionless]
N_w	Number of incoming waves
N_z	Number of waves
N^*_S	Spectral stability number [dimensionless]
P	
p	Porosity of the armor layer [dimensionless]
p_a	Atmospheric pressure [force/length^2]
p_s	Pressure on solid body surface due to moving fluid [force/length^2]
$p_{1,2,3}$	Wave pressure at the SWL corresponding to wave crest, at the base, at the SWL, corresponding to wave trough [force/length^2]
$p!$	Mean effective stress [force/length^2]
$p!_o$	Vertical effective overburden pressure [force/length^2]
P	Notational permeability parameter (Figure VI-5-11)
P	Uplift force in metric tons
P_{ow}	Probability of overtopping per incoming wave
P_s	Hydrostatic pressure [force/length^2]
Q	
q	Average overtopping discharge per unit length of structure [length^3/time/length]
$q!$	Effective overburden pressure [force/length^2]
Q	Dimensionless average discharge per meter (Equations VI-5-20 and VI-5-21)
Q_n	Nominal load [force]
R	
r	Dolos waist ratio [dimensionless]
r	Thickness of armor cover or under layer [length]
R_a	Maximum vertical runup height [length]
R_c	Crest freeboard (Figure VI-5-13) [length]
R_d	Force per unit horizontal length of wall [force/length]
R_d	Minimum rundown or water-surface elevation measured vertically from the still-water level [length]
R_e	Reynolds number [dimensionless]
R_h	Distance to the center of the section [length]
R_n	Nominal strength
R_s	Hydrostatic force per unit horizontal width of wall [force/length^2/length]
R_u	Maximum runup or water-surface elevation measured vertically from the still-water level [length]

$R_{ui\%}$	Runup level exceeded by *i* percent of the incident waves (Equation VI-5-3) [length]
R_{us}	Significant runup level [length]
S	
s_0	Deepwater wave steepness (=H_0/L_0) [dimensionless]
s_{0m}	Deepwater mean wave steepness (=H_s/L_{0m})
s_{0p}	Deepwater wave steepness corresponding to the peak of the wave spectrum [dimensionless]
s_m	Wave steepness (= H_s / L_{0m})
s_p	Local wave steepness [dimensionless]
s_t	Settlement (decrease in layer thickness) at time *t* [length]
s_4	Final settlement reached when the soil skeleton is fully carrying the load [length]
S	Caisson displacement [length]
S	Horizontal seismic inertia force
S	Relative eroded area or damage parameter for structure armor layer [dimensionless]
S_f	Safety factor at allow for debris impacts or other unknowns [dimensionless]
S_m	Maximum scour depth [length]
S_M	Section moduli for flexure
S_t	Cohesive soil sensitivity (ratio between the undrained shear strength of a specimen in undisturbed and in remoulded states)
S_T	Section moduli for torsion
T	
t	Time at end of storm *n*
t_n	Time at start of storm *n*
T	Wave period [time]
T_{0m}	Wave period associated with the spectral peak in deep water [time]
T_{0p}	Wave period associated with the spectral peak in deep water [time]
T_{cr}	Critical strength of concrete in torque
T_m	Average or mean wave period [time]
T_p	Wave period corresponding to the peak of the wave spectrum [time]
T_s	Strength contribution from the torsional steel reinforcement
U	
u	Horizontal component of the wave orbital velocity [length/time]
u	Magnitude of flow velocity [length/time]
u	Pore pressure [force/length^2]
u_i	Velocity of ice [length/time]

u_p	Pore water pressure [force/length^2]
u_s	Water pressure along the surface of the slope [force/length^2]
u^2_{rms}	Root-mean-squared horizontal wave velocity [length^2]
U	Current magnitude [length/time]
U	Degree of consolidation [dimensionless]
U_c	Critical depth-averaged flow velocity [length/time]
U_m	Maximum wave orbital velocity at the bed [length/time]
V	
v	Bulk flow velocity [length/time]
V	Overtopping volume per wave per unit width [length^3/length]
V	Total volume [length^3]
V_p	Volume of voids [length^3]
V_s	Volume of solids [length^3]
W	
w	Barrier penetration depth [length]
w	Vertical component of flow velocity at level of object [length/time]
w_a	Specific weight of armor material [force/length^3]
W	Stone or armor weight [force]
W	Total weight of the slice including surface load [force]
W	Width of scour apron [length]
W_T	Total weight of riprap [force]
X	
x	Horizontal coordinate with positive toward the structure and $x = 0$ located at the structure toe [length]
x	Strain rate function
Y	
y	Elevation above the bed [length]
Z	
z	Vertical coordinate with $z = 0$ at the SWL and $z = -h$ at bottom [length]
Z	Maximum vertical ice ride-up distance [length]

CHAPTER 6

Reliability Based Design of Coastal Structures

TABLE OF CONTENTS

Page

VI-6-1. Introduction VI-6-1

VI-6-2. Failure Modes and Failure Functions VI-6-2

VI-6-3. Single Failure Modes Probability Analysis VI-6-3
a. Level III methods VI-6-3
b. Level II methods VI-6-5

VI-6-4. Failure Probability Analysis of Failure Mode Systems VI-6-15

VI-6-5. Parameter Uncertainties in Determining the Reliability of Structures VI-6-22

a. Uncertainty related to failure mode formulae VI-6-22
b. Uncertainty related to environmental parameters VI-6-22
c. Uncertainty related to structural parameters VI-6-25

VI-6-6. Partial Safety Factor System for Implementing Reliability in Design VI-6-26

a. Introduction to partial safety factors VI-6-26
b. Uncertainties and statistical models VI-6-27
c. Format for partial safety factors VI-6-30
d. Tables of partial safety factors VI-6-30

VI-6-7. References VI-6-49

VI-6-8. Acknowledgments VI-6-50

VI-6-9. Symbols VI-6-50

List of Figures

Figure VI-6-1. Illustration of the two-dimensional joint probability density function for loading and strength VI-6-4

Figure VI-6-2. Illustration of failure probability in case of two independent variables, S and R VI-6-6

Figure VI-6-3. Illustration of reliability index VI-6-7

Figure VI-6-4. Illustration of β in normalized coordinate system VI-6-8

Figure VI-6-5. Definition of the Hasofer and Lind reliability index, β_{HL} VI-6-9

Figure VI-6-6. Illustration of a first-passage problem VI-6-15

Figure VI-6-7. Example of simplified fault tree for a breakwater VI-6-16

Figure VI-6-8. Example of cause-consequence diagram for a rubble-mound breakwater VI-6-17

Figure VI-6-9. Series and parallel systems VI-6-17

Figure VI-6-10. Decomposition of the fault tree into series and parallel systems VI-6-18

Figure VI-6-11. Example of simplified fault tree for a breakwater VI-6-21

Figure VI-6-12. Decomposition of the fault tree into series and parallel systems VI-6-21

List of Tables

Table VI-6-1. Typical Variational Coefficients $\sigma N = \sigma / \mu$ (standard deviation over mean value) for Measured and Calculated Sea State Parameters VI-6-24

Table VI-6-2. Wave Data from Different Locations Fitted to a Weibull Distribution VI-6-28

Table VI-6-3. Partial Safety Factor Tables VI-6-31

Table VI-6-4. Partial Safety Factors for Stability Failure of Rock Armor, Hudson Formula, Design Without Model Tests VI-6-32

Table VI-6-5. Partial Safety Factors for Stability Failure of Rock Armor, Plunging Waves, van der Meer Formula, Design Without Model Tests VI-6-32

Table VI-6-6. Partial Safety Factors for Stability Failure of Rock Armor, Surging Waves, van der Meer Formula, Design Without Model Tests VI-6-33

Table VI-6-7. Partial Safety Factors for Stability Failure of Cube Block Armor, van der Meer Formula, Design Without Model Tests VI-6-33

Table VI-6-8. Partial Safety Factors for Stability Failure of Tetrapods, van der Meer Formula, Design Without Model Tests VI-6-34

Table VI-6-9. Partial Safety Factors for Stability Failure of Dolosse, Without Superstructure, Burcharth Formula, Design Without Model Tests VI-6-34

Table VI-6-10. Partial Safety Factors for Stability Failure of Dolosse, With Superstructure, Burcharth and Liu (1995a), Design Without Model Tests VI-6-35

Table VI-6-11. Partial Safety Factors for Stability Failure of Trunk of Hollowed Cubes, Slope 1:1.5 and 1:2, Berenguer and Baonza (1995), Design Without Model Tests VI-6-36

Table VI-6-12. Partial Safety Factors for Stability Failure of Roundhead of Hollowed Cubes, Slope 1:1.5 and 1:2, Berenguer and Baonza (1995), Design Without Model Tests VI-6-37

Table VI-6-13. Partial Safety Factors for Stability Failure of Toe Berm, Parallelepiped Concrete Blocks and Rocks., Burcharth Formula, Design Without Model Tests VI-6-38

Table VI-6-14. Partial Safety Factors for Trunk Dolos Breakage, Burcharth Formula, Design Without Model Tests VI-6-38

Table VI-6-15. Partial Safety Factors for Roundhead Dolos Breakage, Burcharth Formula, Design Without Model Tests VI-6-39

Table VI-6-16. Partial Safety Factors for Trunk Tetrapod Breakage, Burcharth Formula, Design Without Model Tests VI-6-39

Table VI-6-17. Partial Safety Factors for Runup, Rock Armored Slopes, De Waal and van der Meer (1992), Design Without Model Tests VI-6-40

Table VI-6-18. Partial Safety Factors for Runup, Hollowed Cubes, Slopes 1:1.5 and 1:2, Berenguer and Baonza (1995), Design Without Model Tests VI-6-41

Table VI-6-19. Partial Safety Factors for Runup, Dolosse, Slopes 1:1.5, Burcharth and Liu (1995b), Design Without Model Tests VI-6-42

Table VI-6-20. Partial Safety Factors for Steady Stream Scour Depth in Sand at Conical Roundheads, Fredsøe and Sumer (1997), Design Without Model Tests VI-6-43

Table VI-6-21. Partial Safety Factors for Scour Depth in Sand at Conical Roundheads in Breaking Wave Conditions, Fredsøe and Sumer (1997), Design Without Model Tests VI-6-43

Table VI-6-22. Partial Safety Factors for Foundation Failure of Vertical Wall Caissons - Sand Subsoil VI-6-44

Table VI-6-23. Partial Safety Factors for Foundation Failure of Vertical Wall Caissons - Clay Subsoil VI-6-45

Table VI-6-24. Partial Safety Factors for Sliding Failure of Vertical Wall Caissons VI-6-46

Table VI-6-25. Partial Safety Factors for Overturning Failure of Vertical Caissons VI-6-47

Table VI-6-26. Partial Safety Factors for Scour at Circular Vertical Wall Roundheads, Sumer and Fredsøe (1997), Design Without Model Tests VI-6-48

Table VI-6-27. Partial Safety Factors for Toe Berm Rock Armor Failure in Front of Vertical Wall Caissons, Design Without Model Tests VI-6-48

CHAPTER VI-6

Reliability Based Design of Coastal Structures

VI-6-1. Introduction.

a. Conventional design practice for coastal structures is deterministic in nature and is based on the concept of a design load which should not exceed the resistance (carrying capacity) of the structure. The design load is usually defined on a probabilistic basis as a characteristic value of the load, for example the expectation (mean) value of the 100-year return period event. However, this selection is often made without consideration of the involved uncertainties. In most cases the resistance is defined in terms of the load that causes a certain design impact or damage to the structure, and it is not given as an ultimate force or deformation. This is because most of the available design formulae only give the relationship between wave characteristics and some structural response, such as runup, overtopping, armor layer damage, etc. An example is the Hudson formula for armor layer stability.

b. Almost all coastal structure design formulae are semiempirical and based mainly on central fitting to model test results. The often considerable scatter in test results is not considered in general because the formulae normally express only the mean values. Consequently, the applied characteristic value of the resistance is then the mean value and not a lower fractile as is usually the case in other civil engineering fields. The only contribution to a safety margin in the design is inherent in the choice of the return period for the design load. (The exception is when the design curve is fitted to the conservative side of the data envelope to give a built-in safety margin.) It is now more common to choose the return period with due consideration of the encounter probability, i.e., the probability that the design load value is exceeded during the structure lifetime. This is an important step towards a consistent probabilistic approach.

c. In addition to design load probability, a safety factor (as given in some national standards) might be applied as well, in which case the method is classified as a Level I (deterministic/quasi-probabilistic) method. However, this approach does not allow determination of the reliability (or the failure probability) of the design; and consequently, it is not possible to optimize structure design or avoid overdesign of a structure. In order to overcome this problem, more advanced probabilistic methods must be applied where the uncertainties (the stochastic properties) of the involved loading and strength variables are considered.

d. Methods where the actual distribution functions for the variables are taken into account are denoted as Level III methods. Level II methods generally transform correlated and non-normally distributed variables into uncorrelated and standard normal distributed variables, and reliability indices are used as measures of the structural reliability. Both Level II and III methods are discussed in the following sections. Also described is an advanced partial coefficient system which takes into account the stochastic properties of the variables and makes it possible to design a structure for a specific failure probability level.

VI-6-2. Failure Modes and Failure Functions.

a. Evaluation of structural safety is always related to the structural response as defined by the failure modes. Failure modes for various structures are presented in Part VI-2-4, "Failure Modes of Typical Structure Types."

b. Each failure mode must be described by a formula, and the interaction (correlation) between the failure modes must be known. As an illustrative example consider only one failure mode, "hydraulic stability of the main armor layer" described by the Hudson formula

$$D_n^3 = \frac{H_s^3}{K_D \Delta^3 \cot \alpha} \tag{VI-6-1}$$

where

D_n = nominal block diameter

$\Delta = \rho_s / \rho_w - 1$

ρ_s = block density

ρ_w = water density

α = armor slope angle

H_s = significant wave height

K_D = coefficient signifying the degree of damage (movements of the blocks)

c. The formula can be split into load variables X_i^{load} and resistance variables, X_i^{res}. Whether a parameter is a load or a resistance parameter can be seen from the failure function. If a larger value of a parameter results in a safer structure, it is a resistance parameter; and if a larger value results in a less safe structure, it is a load parameter.

d. According to this definition one specific parameter can in one formula act as a load parameter while in another formula the same parameter can act as a resistance parameter. An example is the wave steepness parameter in the van der Meer formulas for rock, which is a load parameter in the case of surging waves, but a resistance parameter in the case of plunging waves. The only load variable in Equation VI-6-1 is H_s while the others are resistance variables.

e. Equation VI-6-1 is formulated as a failure function (performance function)

$$g = A \bullet \Delta \bullet D_n (K_D \cot \alpha)^{1/3} - H_s \begin{cases} < 0 \ \ failure \\ = 0 \ \ limit\ state\ (failure) \\ > 0 \ \ no\ failure\ (safe\ region) \end{cases} \tag{VI-6-2}$$

f. All the involved parameters are regarded as stochastic variables, X_i, except K_D, which signifies the failure, i.e., a specific damage level chosen by the designer. The factor A in Equation VI-6-2 is also a stochastic variable signifying the uncertainty of the formula. In this case the mean value of A is 1.0.

g. In general Equation VI-6-2 is formulated as

$$g = R - S \tag{VI-6-3}$$

where R stands for resistance and S for loading. Usually R and S are functions of many random variables, i.e.,

$$R = R\left(X_1^{res}, X_2^{res}, \ldots, X_m^{res}\right) \quad and \quad S = S\left(X_{m+1}^{load}, \ldots, X_n^{load}\right) \quad or \quad g = g\left(\overline{X}\right)$$

The limit state is given by

$$g = 0 \tag{VI-6-4}$$

which is denoted the *limit state equation* and defines the so-called *failure surface* which separates the safe region from the failure region.

h. In principle, R is a variable representing the variations in resistance between nominally identical structures, whereas S represents the maximum load effects within a period of time, for instance T successive years. The distributions of R and S are both assumed independent of time. The *probability of failure*, P_f, during any reference period of duration T years is then given by

$$P_f = \text{Prob}\left(g \le 0\right) \tag{VI-6-5}$$

i. The reliability R_f is defined as

$$R_f = 1 - P_f \tag{VI-6-6}$$

VI-6-3. Single Failure Modes Probability Analysis.

a. Level III methods.

(1) A simple method (in principle) of estimating P_f is the Monte Carlo method where a very large number of realizations x of the variables X are simulated. P_f is then approximated by the proportion of the simulations where $g \# 0$. The reliability of the Monte Carlo method depends on a realistic assessment of the distribution functions for the variables X and their correlations.

(2) Given $f_{\overline{X}}$ as the joint probability density function (*jpdf*) of the vector $\overline{X} = (X_1, X_2, \ldots, X_n)$, then Equation VI-6-5 can be expressed by

$$P_f = \int_{R \le S} f_{\bar{X}}(\bar{x})\, d\bar{x} \tag{VI-6-7}$$

(3) Note that the symbol x is used for values of the random variable X. If only two variables R and S are considered then Equation VI-6-7 reduces to

$$P_f = \int_{R \le S} f_{(R,S)}(r,s)\, dr\, ds \tag{VI-6-8}$$

which is conceptually illustrated in Figure VI-6-1. If more than two variables are involved it is not possible to describe the *jpdf* as a surface but requires an imaginary multidimensional description.

(4) Figure VI-6-1 also shows the so-called design point which is the point of failure surface where the joint probability density function attains the maximum value, i.e., the most probable point of failure.

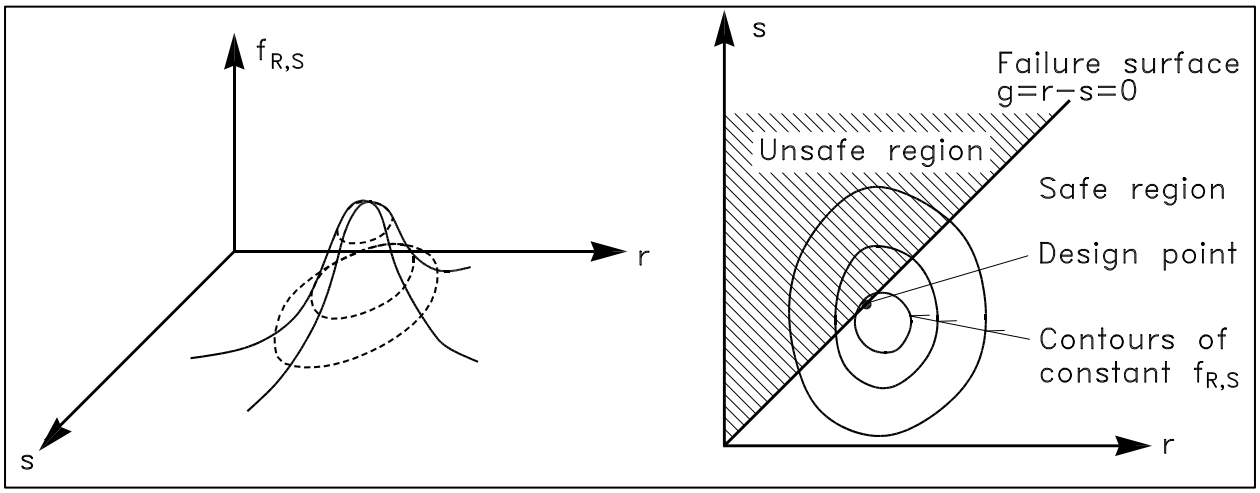

Figure VI-6-1. Illustration of the two-dimensional joint probability density function for loading and strength

(5) Unfortunately, the *jpdf* is seldom known. However, the variables can often be assumed independent (noncorrelated) in which case Equation VI-6-7 is given by the n-fold integral

$$P_f = \iiint_{R \le S} \cdots \int f_{X_1}(x_1) \ldots f_{X_n}(x_n)\, d\, x_1 \ldots d\, x_n \tag{VI-6-9}$$

where f_{Xi} are the marginal probability density function of the variables X_i. The amount of calculations involved in the multidimensional integration Equation VI-6-9 is enormous if the number of variables, n, is larger than 5.

(6) If only two independent variables are considered, e.g., *R* and *S*, then Equation VI-6-9 simplifies to

$$P_f = \iint_{R \le S} f_R(r)\, f_S(s)\, dr\, ds \tag{VI-6-10}$$

which by partial integration can be reduced to a single integral

$$P_f = \int_0^{\infty} F_R(x)\, f_S(x)\, dx \tag{VI-6-11}$$

where F_R is the cumulative distribution function for *R*. Formally the lower integration limit should be -4, but it is replaced by 0 since, in general, negative strength is not meaningful.

(7) Equation VI-6-11 represents the product of the probabilities of two independent events, namely the probability that *S* lies in the range *x, x+dx* (i.e., $f_S(x)\, dx$) and the probability that *R # x* (i.e., $F_R(x)$), as shown in Figure VI-6-2.

b. Level II methods. This section gives a short introduction to reliability calculations at Level II. Only the so-called first-order reliability method (FORM), where the failure surface is approximated by a tangent hyberplane at some point, is presented. A more accurate method is the second-order reliability method (SORM), which uses a quadratic approximation to the failure surface.

(1) Linear failure functions of normally-distributed random variables.

(a) Assume the loading *S(x)* and the resistance *R(x)* for a single failure mode to be statistically independent and with density functions as illustrated in Figure VI-6-2. The failure function is given by Equation VI-6-3 and the probability of failure is expressed by Equation VI-6-10 or Equation VI-6-11.

(b) However, in many cases these functions are not known, but under certain assumptions the functions might be estimated using only the mean values and standard deviations. If *S* and *R* are assumed to be independent normally distributed variables with known means and standard deviations, then the linear failure function $g = R - S$ is normally distributed with mean value,

$$\mu_g = \mu_R - \mu_S \tag{VI-6-12}$$

and standard deviation

$$\sigma_g = \sqrt{(\sigma_R^2 + \sigma_S^2)} \tag{VI-6-13}$$

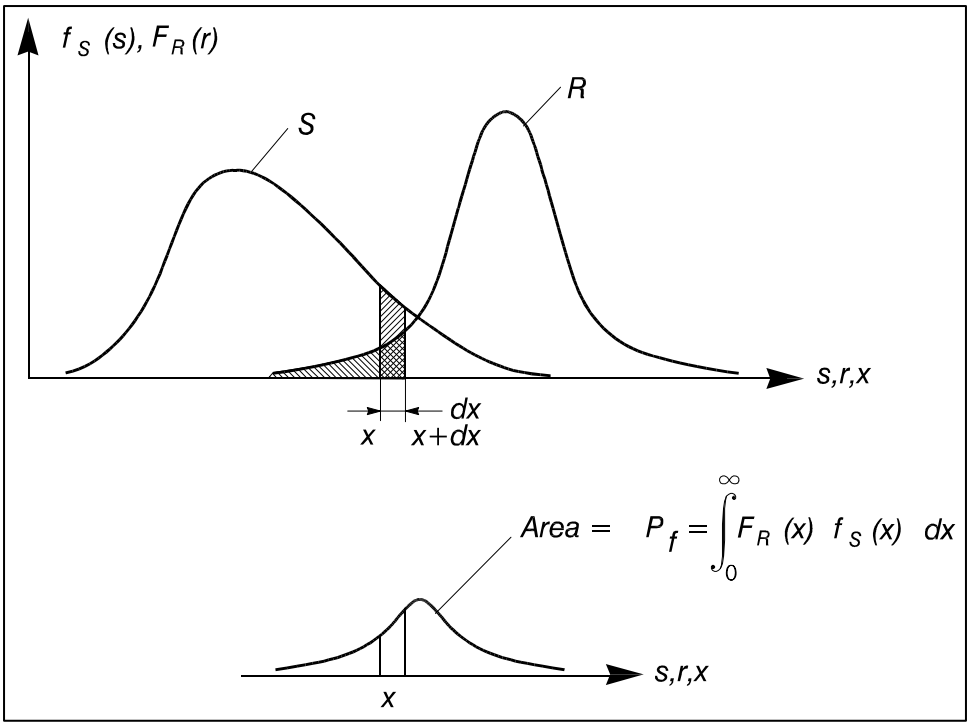

Figure VI-6-2. Illustration of failure probability in case of two independent variables, *S* and *R*

The quantity $(g - \mu_g) / \sigma_g$ will be unit standard normal, and consequently,

$$P_f = prob\,(\,g \le 0) = \int_{-\infty}^{0} f_g(x)\,dx = \Phi\left(\frac{0 - \mu_g}{\sigma_g}\right) = \Phi\,(-\beta) \qquad \text{(VI-6-14)}$$

where

$$\beta = \frac{\mu_g}{\sigma_g} \qquad \text{(VI-6-15)}$$

is a measure of the probability of failure referred to as the reliability index (Cornell 1969). Figure VI-6-3 illustrates β and the reliability index. Note that β is the inverse of the coefficient of variation, and it is the distance (in terms of number of standard deviations) from the most probable value of *g* (in this case the mean) to the failure surface, $g = 0$.

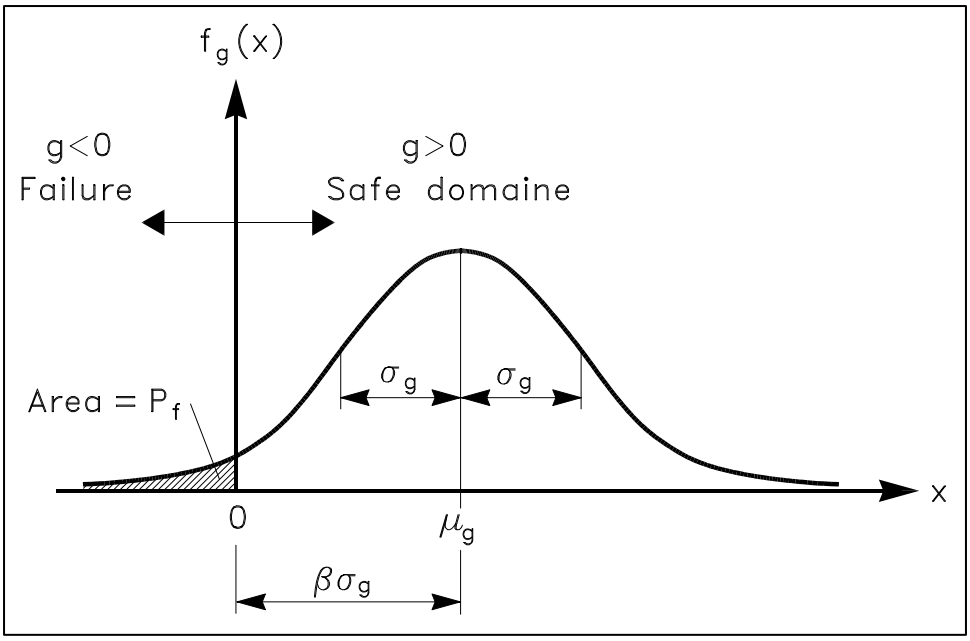

Figure VI-6-3. Illustration of reliability index

(c) If R and S are normally distributed and "correlated," then Equation VI-6-14 still holds, but σ is given by

$$\sigma_g = \sqrt{(\sigma_R^2 + \sigma_S^2 + 2\ \rho_{RS}\,\sigma_R\,\sigma_S\ )} \tag{VI-6-16}$$

where ρ_{RS} is the *correlation coefficient*

$$\rho_{RS} = \frac{Cov\,(R,S)}{\sigma_R\,\sigma_S} = \frac{E\,[(R - \mu_R\ )\ (S - \mu_S\ )]}{\sigma_R\,\sigma_S} \tag{VI-6-17}$$

R and S are said to be uncorrelated if $\rho_{RS} = 0$.

(d) In addition to the illustration of β in Figure VI-6-3, a simple geometrical interpretation of β can be given in the case of a linear failure function $g = R - S$ of the independent variables R and S by a transformation into a normalized coordinate system of the random variables $RN = (R - \mu_R) / \sigma_R$ and $SN = (S - \mu_S) / \sigma_S$, as shown in Figure VI-6-4.

(e) With these variables the failure surface $g = 0$ is linear and given by

$$R'\,\sigma_R - S'\,\sigma_S + \mu_R - \mu_S = 0 \tag{VI-6-18}$$

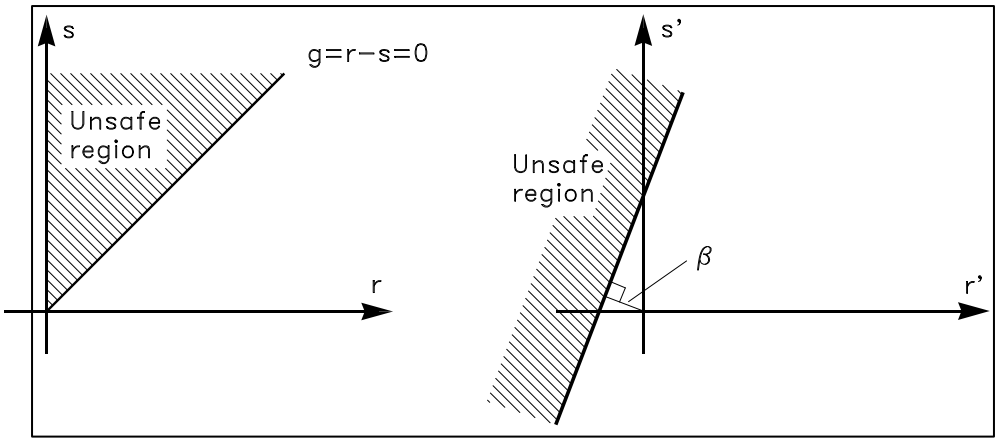

Figure VI-6-4. Illustration of β in normalized coordinate system

(f) By geometrical considerations it can be shown that the shortest distance from the origin to this linear failure surface is equal to in which Equations VI-6-12 and VI-6-13 are used.

$$\beta = \frac{\mu_g}{\sigma_g} = \frac{\mu_R - \mu_S}{\sqrt{\sigma_R^2 + \sigma_S^2}} \tag{VI-6-19}$$

(2) Nonlinear failure functions of normally-distributed random variables.

(a) If the failure function $g = g(\overline{X})$ is *nonlinear*, then approximate values for μ_g and σ_g can be obtained by using a linearized failure function. Linearization is generally performed by retaining only the linear terms of a Taylor-series expansion about some point. However, the values of μ_g and σ_g, and thus the value of β, depend on the choice of linearization point. Moreover, the value of β defined by Equation VI-6-15 will change when different, but functionally equivalent, nonlinear failure functions are used.

(b) To overcome these problems, a transformation of the basic variables $\overline{X} = (X_1, X_2, \ldots, X_n)$ into a new set of normalized variables $\overline{Z} = (Z_1, Z_2, \ldots, Z_n)$ is performed. For uncorrelated normally distributed basic variables $\overline{X}$ the transformation is

$$Z_i = \frac{X_i - \mu_{X_i}}{\sigma_{X_i}} \tag{VI-6-20}$$

in which case $\mu_{Zi} = 0$ and $\sigma_{Zi} = 1$. By this linear transformation the failure surface g = 0 in the *x*-coordinate system is mapped into a failure surface in the *z*-coordinate system which also divides the space into a safe region and a failure region as illustrated in Figure VI-6-5.

(c) Figure VI-6-5 introduces the Hasofer and Lind reliability index β_{HL} which is defined as the distance from the origin to the nearest point, *D*, of the failure surface in the *z*-coordinate system (Hasofer and Lind 1974). This point is called the design point. The coordinates of the

design point in the original *x*-coordinate system are the most probable values of the variables $\overline{X}$ at failure. β_{HL} can be formulated as

$$\beta_{HL} = \min_{g(\bar{z})=0} \left(\sum_{i=1}^{n} z_i^2 \right)^{1/2} \qquad \text{(VI-6-21)}$$

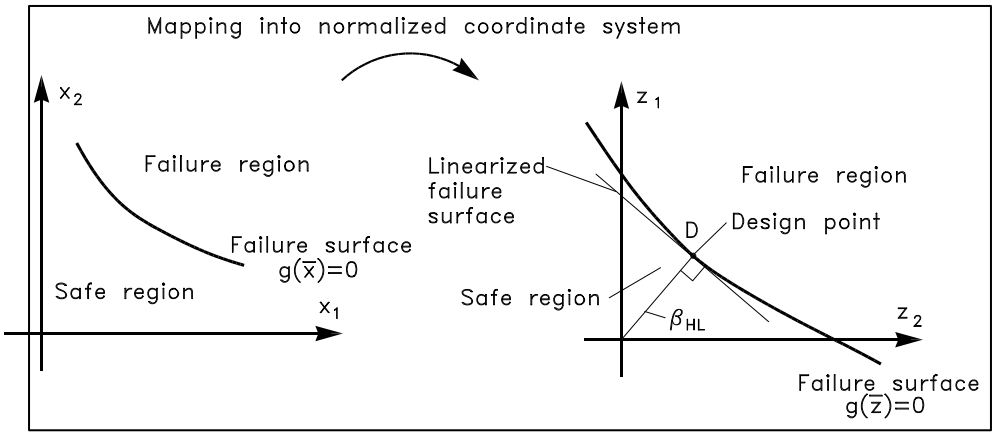

Figure VI-6-5. Definition of the Hasofer and Lind reliability index, β_{HL}

(d) The special feature of β_{HL}, as opposed to β, is that β_{HL} is related to the failure "surface" $g(\bar{z}) = 0$ which is invariant to the failure function because equivalent failure functions result in the same failure surface.

(e) The calculation of β_{HL} and the design point coordinates can be undertaken in a number of different ways. An iterative method must be used when the failure surface is nonlinear. A widely used method of calculating β_{HL} is

- Step 1. Select some trial coordinates of the design point in the *z*-coordinate system

$$\bar{z}^d = (z_1^d, z_2^d, \ldots, z_n^d)$$

- Step 2. Calculate α_i $i = 1, 2, \ldots, n$ by

$$\alpha_i = \left. \frac{\partial g}{\partial z_i} \right|_{\bar{z} = \bar{z}^d}$$

- Step 3. Determine a better estimate of $\bar{z}^d$ by

$$z_i^d = \alpha_i \frac{\sum_{i=1}^{n} \left(\alpha_i z_i^d\right) - g\big|_{\bar{z}=\bar{z}^d}}{\sum_{i=1}^{n} \left(\alpha_i\right)^2}$$

- Step 4. Repeat Steps 2 and 3 to achieve convergence

- Step 5. Evaluate β_{HL} by

$$\beta_{HL} = \left(\sum_{i=1}^{n} \left(z_i^d\right)^2 \right)^{1/2}$$

The method is based on the assumption of the existence of only one minimum. However, several "local" minima might exist. In order to avoid convergence toward a local minima (and thereby overestimation of β_{HL} and the reliability) several different sets of trial coordinates might be tried.

(3) Nonlinear failure functions of non-normal random variables.

(a) It is not always a reasonable assumption to consider the random variables normally distributed. For example, parameters characterizing the sea state in long-term wave statistics, such as H_s, will in general follow extreme distributions (e.g., Gumbel and Weibull). These distributions are quite different from the normal distribution and cannot be described using only the mean value and the standard deviation.

(b) For such cases it is still possible to use the reliability index β_{HL}, but an extra transformation of the non-normal basic variables into normal basic variables must be performed before β_{HL} can be determined as previously described.

(c) A commonly used transformation is based on the substitution of the non-normal distribution of the basic variable X_i by a normal distribution in such a way that the density and distribution functions f_{Xi} and F_{Xi} are unchanged at the design point.

(d) If the design point is given by $x_1^d, x_2^d, \ldots, x_n^d$, then the transformation reads

$$F_{X_i}(x_i^d) = \Phi\left(\frac{x_i^d - \mu_{X_i'}}{\sigma_{X_i'}}\right)$$
$$f_{X_i}(x_i^d) = \frac{1}{\sigma_{X_i'}} \varphi\left(\frac{x_i^d - \mu_{X_i'}}{\sigma_{X_i'}}\right) \qquad \text{(VI-6-22)}$$

where μN_{Xi} and σN_{Xi} are the mean and standard deviation of the approximate (fitted) normal distribution.

(e) Equation VI-6-22 yields

$$\sigma_{X_i'} = \frac{\varphi\left(\Phi^{-1}\left(F_{X_i}(x_i^d)\right)\right)}{f_{X_i}(x_i^d)}$$
$$\mu_{X_i'} = x_i^d - \Phi^{-1}\left(F_{X_i}(x_i^d)\right)\sigma_{X_i'} \quad \text{(VI-6-23)}$$

(f) Equation VI-6-22 can also be written

$$F_{X_i}(x_i^d) = \Phi\left(\frac{x_i^d - \mu_{X_i'}}{\sigma_{X_i'}}\right) = \Phi(z_i^d) = \Phi(\beta_{HL}\ \alpha_i)$$

(g) Solving with respect to x_i^d gives

$$x_i^d = F_{X_i}^{-1}[\Phi(\beta_{HL}\,\alpha_i)] \quad \text{(VI-6-24)}$$

(h) The iterative method presented above for calculation of β_{HL} can still be used if for each step of iteration the values of μN_{Xi} and σN_{Xi} given by Equation VI-6-24 are calculated for those variables where the transformation (Equation VI-6-22) has been used. For correlated random variables the transformation into noncorrelated variables is used before normalization.

(4) Time-variant random variables. The failure functions within breakwater engineering are generally of the form

$$g = f_1(\overline{R}) - f_2(H_s, W, T_m) \quad \text{(VI-6-25)}$$

where $\overline{R}$ represents the resistance variables and H_s, W, and T_m are the load variables signifying the wave height, the water level, and the wave period. The random variables are in general time-variant.

(a) Discussion of load variables:

- The most important load parameter in breakwater engineering is the wave height. It is a time-varying quantity which is best modeled as a stochastic process. Distinction is made between short-term and long-term statistics of the wave heights. Short-term statistics deal with the distribution of the wave height H during a stationary sequence of a storm, i.e., during a period of constant H_s (or any other characteristic wave height). The short-term wave height distribution follows the Rayleigh distribution for deepwater waves and some truncated distribution in the case of shallow-water waves.

- Long-term statistics deal with the distribution of the storms which are then characterized by the maximum value of H_s occurring in each storm. The storm history is given as the sample (H_{s1}, H_{s2},... , H_{sn}) covering a period of observation, Y. Extreme-value distributions like the Gumbel and Weibull distributions are then fitted to the data sample. For strongly depth-

limited wave conditions a normal distribution with mean value as a function of water depth might be appropriate.

- The true distribution of H_s can be approximated by the distribution of the maximum value over T years, which is denoted as the distribution of H_s^T. The calculated failure probability then refers to the period T (which in practice might be the lifetime of the structure) if distribution functions of the other variables in Equation VI-6-25 are assumed to be unchanged during the period T.

- As an example, consider a sample of n independent storms, i.e., H_{s1} , H_{s2}, ... , H_{sn} , obtained within Y years of observation. Assume that H_s follows a Gumbel distribution given by

$$F(H_s) = \exp\left[-e^{-\alpha(H_s-\beta)}\right] \tag{VI-6-26}$$

which is the distribution of H_s over a period of Y years with average time span between observations of Y/n.

- The distribution parameters α and β can be estimated from the data using techniques such as the maximum likelihood method or the methods of moments. Moreover, the standard deviations of α and β, signifying the statistical uncertainty due to limited sample size, can also be estimated.

- The sampling intensity is $\lambda = n / Y$. Within a T-year reference period the number of data will be λT. The probability of the maximum value of H_s within the period T is then

$$F\ (H_s^T) = [F\ (H_s)]^{\lambda T} = \left[\ \exp\left(-e^{-\alpha(H_s-\beta)}\right)\right]^{\lambda T} \tag{VI-6-27}$$

- The expectation (mean) value of H_s^T is given by

$$\mu_{H_s^T} = \beta - \frac{1}{\alpha}\ln\left[-\ln\left(1-\frac{1}{\lambda T}\right)\right] \tag{VI-6-28}$$

and the standard deviation of H_s^T (from maximum likelihood estimates) is

$$\sigma_{H_s^T} = \left[\frac{1}{n\alpha^2}\left\{1.109 + 0.514\left(-\ln\left[-\ln\left(1-\frac{1}{\lambda T}\right)\right]\right) + 0.608\left(-\ln\left[-\ln\left(1-\frac{1}{\lambda T}\right)\right]\right)^2\right\}\right]^{1/2} \tag{VI-6-29}$$

- Equation VI-6-29 includes the statistical uncertainty due to limited sample size. Some uncertainty is related to the estimation of the sample values H_{s1} , H_{s2} , ... , H_{sn} arising from measurement errors, errors in hindcast models, etc. This uncertainty corresponds to a coefficient

of variation σ_{Hs} / μ_{Hs} on the order of 5 - 20 percent. The effect of this might be implemented in the calculations by considering a total standard deviation of

$$\sigma = \sqrt{\sigma_{H_s^T}^2 + \sigma_{H_s}^2} \tag{VI-6-30}$$

- In Level II calculations, Equation VI-6-27 is normalized around the design point, and Equations VI-6-28 and VI-6-29 or VI-6-30 are used for the mean and the standard deviation.

- Instead of substituting H_s in Equation VI-6-25 with H_s^T, the following procedure might be used: Set T in Equations VI-6-27 to VI-6-29 to be 1 year. The outcome of the calculations will then be the probability of failure in a 1-year period, $P_f\,(1\ year)$. If the failure events of each year are assumed independent for all variables then the failure probability in T years is

$$P_f\,(T\ years) = 1 - [\,1 - P_f\ (1\ year)]^T \tag{VI-6-31}$$

- This assumption simplifies the probability estimation somewhat, and for some structures it is reasonable to assume failure events are independent, e.g., rubble-mound stone armor stability. However, for some resistance variables, such as concrete strength, it is unrealistic to assume the events of each year are independent. The calculated values of the failure probability in T-years using $H_s^{1\ year}$ and H_s^T will be different. The difference will be very small if the variability of H_s is much larger than the variability of other variables.

- The water level W is also an important parameter because it influences the structure freeboard and limits wave heights in shallow-water situations. Consequently, for the general case it is necessary to consider the joint distribution of H_s, W, and T_m. However, for deepwater waves W is often almost independent (except for barometric effects) of H_s and T_m and can be approximated as a noncorrelated variable that might be represented by a normal distribution with a certain standard deviation. The distribution of W is assumed independent of the length of the reference period T. In shallow water, W will be correlated with H_s due to storm surge effects.

- The *wave period* T_m is correlated to H_s. As a minimum the mean value and the standard deviation of T_m and the correlation of T_m with H_s should be known in order to perform a Level II analysis. However, the linear correlation coefficient is not very meaningful because it gives an insufficient description when the parameters are non-normally distributed. Alternatively the following approach might be used: From a scatter diagram of H_s and T_m a relationship of the form $T_m = A\ f(H_s)$ is established in which the parameter A follows a normal distribution (or some other distribution) with mean value $\mu_A = 1$ and a standard deviation σ_A which signifies the scatter. T_m can then be replaced by the variable A in Equation VI-6-25. The variable A is assumed independent of all other parameters.

- Generally, the best procedure for coping with the correlations between H_s, W, and T_m is to work on the conditional distributions. Assume the distribution of the maximum value of H_s within the period T is given as $F_1(H_s^T)$. Furthermore, assume the conditional distributions $F_2(W|H_s^T)$ and $F_3(T_m|H_s^T)$ are known. Let Z_1, Z_2 and Z_3 be independent standard normal variables and

$$\Phi(z_1) = F_1(H_s^T)$$
$$\Phi(z_2) = F_2(W|H_s^T)$$
$$\Phi(z_3) = F_3(T_m|H_s^T)$$

- The inverse relationships are given by

$$H_s^T = F_1^{-1}[\Phi(z_1)]$$
$$W = F_2^{-1}[\Phi(z_2)|H_s^T]$$
$$T_m = F_3^{-1}[\Phi(z_3)|H_s^T]$$

- By converting the resistance variables $\overline{R}$ into standard normal variable $\overline{Z}_o$, i.e., the resistance term is written $f_1(\overline{R}) = f_3(\overline{z}_o)$, then the failure function Equation VI-6-25 becomes

$$g = f_3(\overline{z}_o) - f_2\left(F_1^{-1}[\Phi(z_1)]\ ,\ F_2^{-1}[\Phi(z_2)|H_s^T]\ ,\ F_3^{-1}[\Phi(z_3)|H_s^T]\right) = 0$$

- Because g now comprises only independent standard normal variables, the usual iteration methods for calculating β_{HL} can be applied.

(b) Discussion of resistance parameters:

- The service life of coastal structures spans anywhere between 20 to 100 years. Over periods of this length a decrease in the structural resistance is to be expected because of various types of material deterioration. Chemical reaction, thermal effect, and repeated loads (fatigue load) can cause deterioration of concrete and natural stone leading to disintegration and rounding of elements. Also the resistance against displacements of armor layers made of randomly placed armor units will decrease with the number of waves (i.e., with time) due to the stochastic nature of the resistance. Consequently, for armor layers this means a reduction over time of the D_n and K_D parameters in the Hudson equation.

- Although material effects can greatly influence reliability in some cases, they are not easy to include in reliability calculations. The main difficulty is the assessment of the variation with time which depends greatly on the intrinsic characteristics of the placed rock and concrete. At this time only fairly primitive methods are available for assessment of the relevant material characteristics. In addition, the variation with time depends very much on the load-history which can be difficult to estimate for the relevant period of structural life.

- Figure VI-6-6 illustrates an example situation representing the tensile strength of concrete armor units where a resistance parameter $R(t)$ decreases with time t. $R(t)$ is assumed to

be a deterministic function. The load *S(t)* (the tensile stress caused by wave action) is assumed to be a stationary process. The probability of failure, *P(S > R)*, within a period *T* is

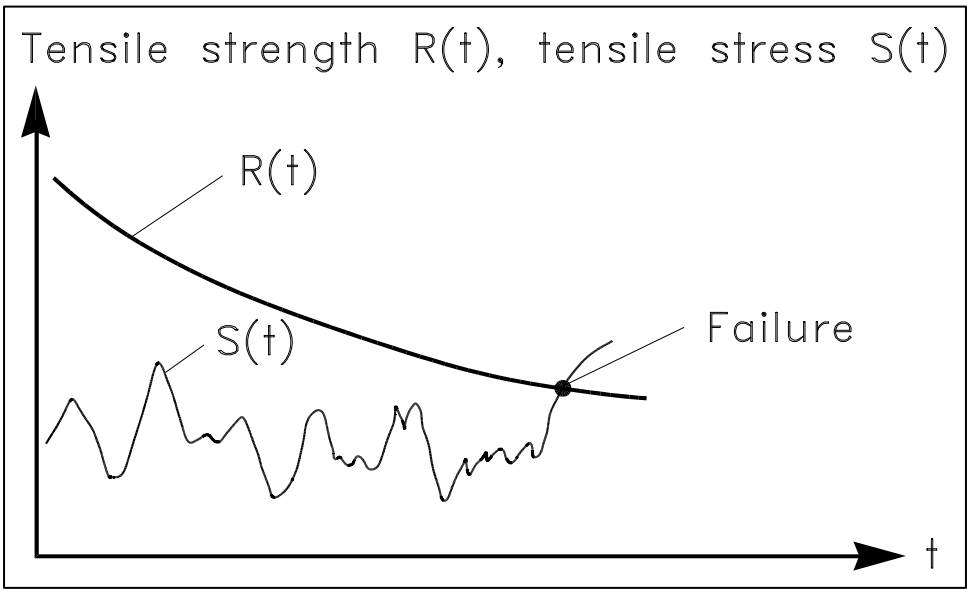

Figure VI-6-6. Illustration of a first-passage problem

$$P_f(T) = 1 - \exp\left[-\int_0^T \nu^+[R(t)]\,dt\right] \qquad \text{(VI-6-32)}$$

where $\nu^+[R(t)]$ is the mean-upcrossing rate (number of upcrossings per unit time) of the level *R(t)* by the process *S(t)* at time *t*. ν^+ can be computed by Rice's formula

$$\nu^+[R(t)] = \int_{\dot{R}}^{\infty} (\dot{S} - \dot{R})\, f_{S\dot{S}}[R(t), \dot{S}]\,d\dot{S}$$

in which $f_{S\dot{S}}$ is the joint density function for $S(t)$ and $\dot{S}(t)$. Implementation of time-variant variables into Level II analyses is rather complicated. For further explanation, see Wen and Chen (1987).

VI-6-4. Failure Probability Analysis of Failure Mode Systems.

a. A coastal structure can be regarded as a system of components which can either function or fail. Due to interactions between the components, failure of one component may impose failure of another component and even lead to failure of the system. A so-called fault tree is often used to clarify the relationships between the failure modes.

b. A fault tree describes the relationships between the failure of the system (e.g., excessive wave transmission over a breakwater protecting a harbor) and the events leading to this failure. Figure VI-6-7 shows a simplified example based on some of the failure modes of a rubble-mound breakwater.

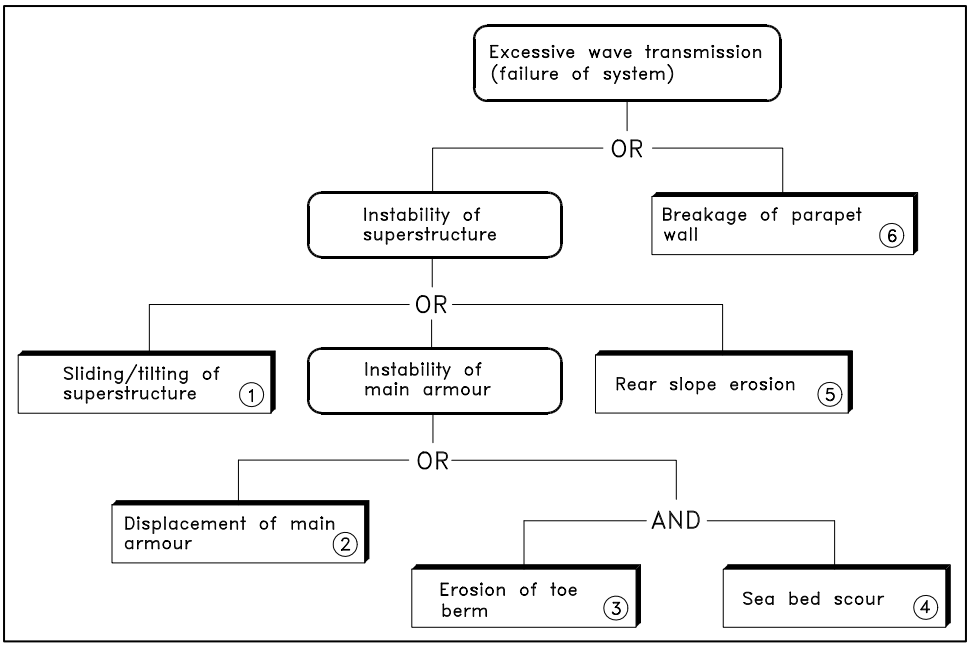

Figure VI-6-7. Example of simplified fault tree for a breakwater

c. A fault tree is a simplification and a systematization of the more complete so-called cause-consequence diagram that indicates the causes of partial failures as well as the interactions between the failure modes. An example is shown in Figure VI-6-8.

d. The failure probability of the system (for example, the probability of excessive wave transmission in Figure VI-6-7) depends on the failure probability of the single failure modes and on the correlation and linking of the failure modes. The failure probability of a single failure mode can be estimated by the methods described in Part VI-6-3. Two factors contribute to the correlation, namely physical interaction, such as sliding of main armor caused by erosion of a supporting toe berm, and correlation through common parameters like H_s. The correlations caused by physical interactions are not yet quantified. Consequently, only the common-parameter-correlation can be dealt with in a quantitative way. However, it is possible to calculate upper and lower bounds for the failure probability of the system.

e. A system can be split into two types of fundamental systems, namely series systems and parallel systems as illustrated by Figure VI-6-9.

(1) Series systems.

(a) In a series system, failure occurs if any of the elements $i = 1, 2, \ldots, n$ fails. The upper and lower bounds of the failure probability of the system, P_{fS} are

$$\textit{Upper bound} \quad P_{fS}^{U} = 1 - (1 - P_{f1})\,(1 - P_{f2}) \ldots (1 - P_{fn}) \tag{VI-6-33}$$

$$\textit{Lower bound} \quad P_{fS}^{L} = \max[P_{fi}] \tag{VI-6-34}$$

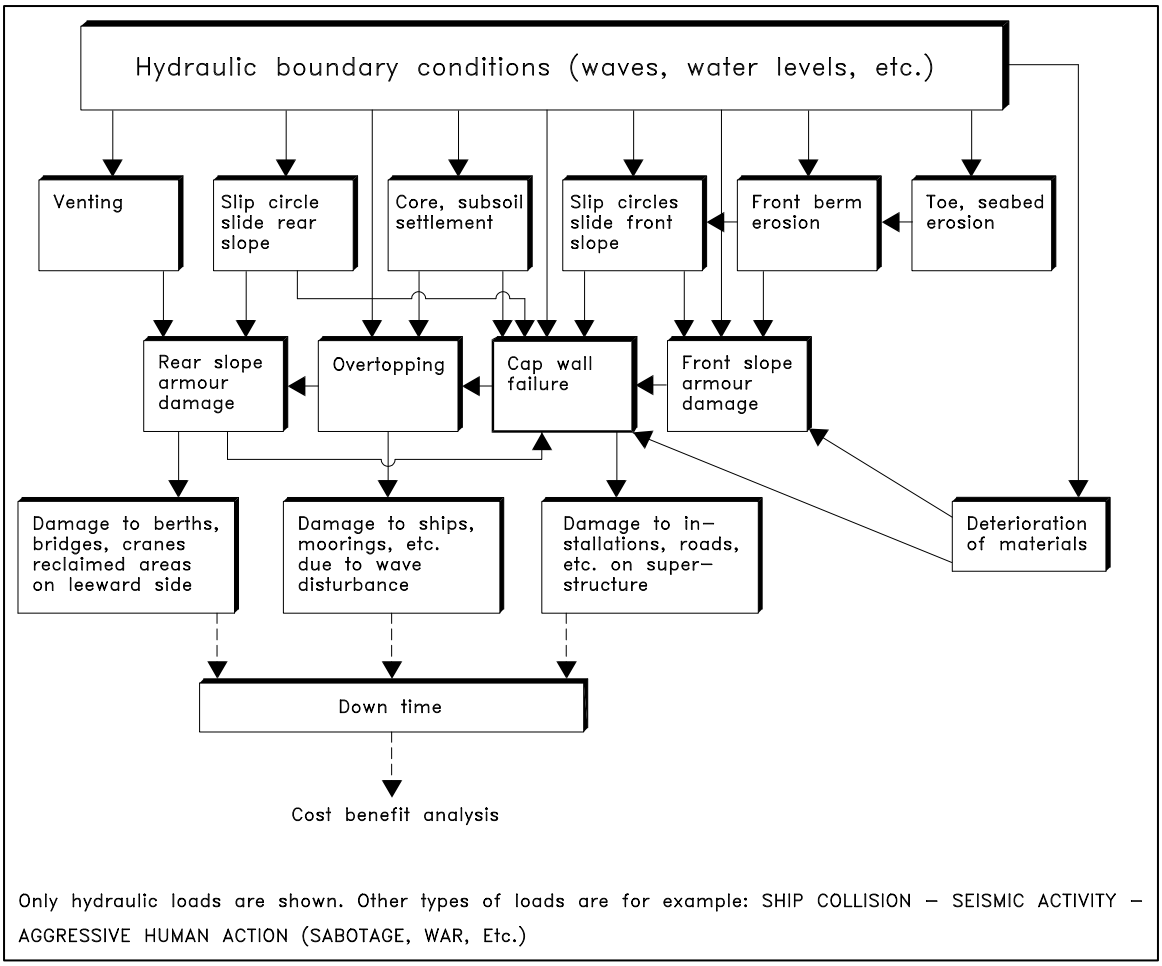

Figure VI-6-8. Example of cause-consequence diagram for a rubble-mound breakwater

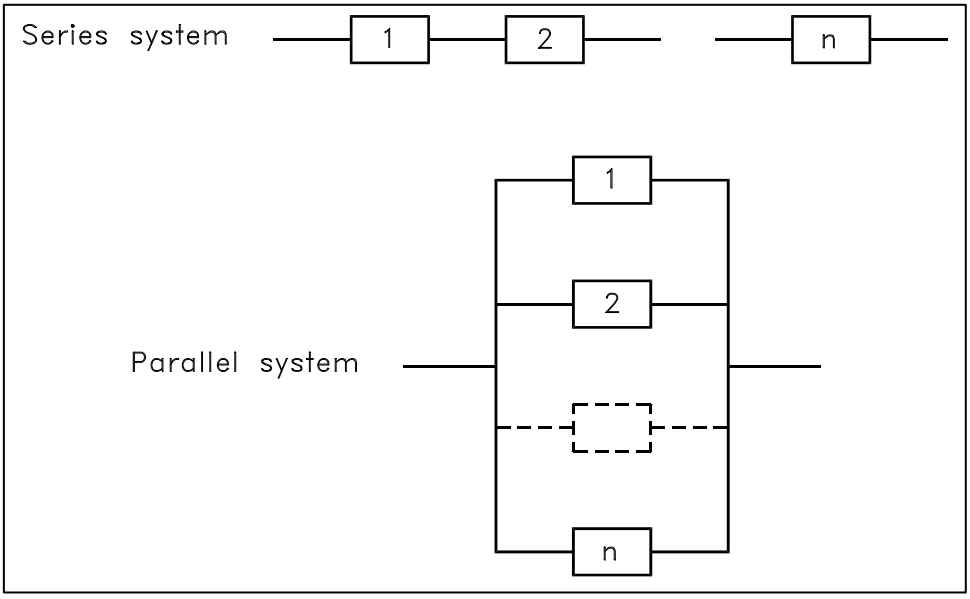

Figure VI-6-9. Series and parallel systems

where max [P_{fi}] is the largest failure probability among all elements. The upper bound corresponds to no correlation between the failure modes and the lower bound to full correlation.

Equation VI-6-33 is sometimes approximated by $P_{fS}^{U} = \sum_{i=1}^{n} P_{fi}$ which is applicable only for small P_{fi} because P_{fS}^{U} should not be larger than 1.

(b) The OR-gates in a fault tree correspond to series components. Series components are dominant in breakwater fault trees. In fact, the AND-*gate* shown in Figure VI-6-7 is included for illustration purposes, and in reality it should be an OR-gate.

(2) Parallel systems.

(a) A parallel system fails only if all the elements fail.

Upper bound $P_{fS}^{U} = \min [\, P_{fi} \,]$ (VI-6-35)

Lower bound $P_{fS}^{L} = P_{f1} \bullet P_{f2} \ldots P_{fn}$ (VI-6-36)

(b) The upper bound corresponds to full correlation between the failure modes, and the lower bound corresponds to no correlation.

- The AND-gates in a fault tree represent parallel components. To calculate upper and lower failure probability bounds for a system, it is convenient to decompose the overall system into series and parallel systems. Figure VI-6-10 shows a decomposition of the fault tree (Figure VI-6-7).

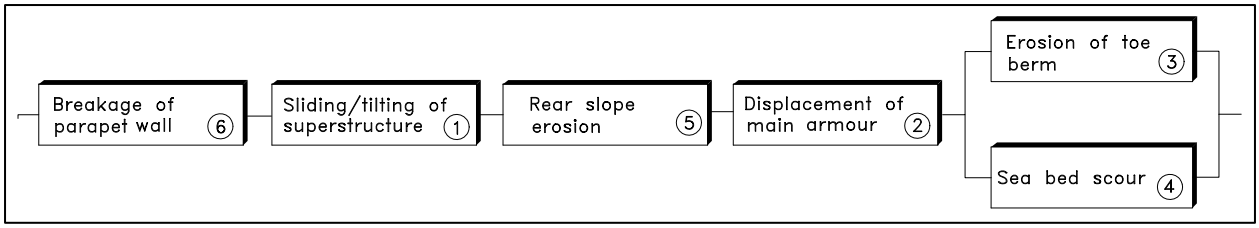

Figure VI-6-10. Decomposition of the fault tree into series and parallel systems

- To obtain correct P_{fS}-values it is very important that the fault tree represents precisely the real physics of the failure development. This is illustrated by Example VI-6-2 where a fault tree alternative to Figure VI-6-7 is analyzed. In Example VI-6-2 the same failure mode probabilities as given in Example VI-6-1 are used.

- The real failure probability of the system P_{fS} will always be in between P_{fS}^{U} and P_{fS}^{L} because some correlation exists between the failure modes due to the common loading represented by the sea state parameters, e.g., H_s.

EXAMPLE PROBLEM VI-6-1

The Level II analysis of the single failure modes for a specific breakwater schematized in Figure VI-6-10 revealed the following probabilities of failure in a 1-year period

i	1	2	3	4	5	6
P_{fi} %	3	6	4	3	0.5	1

Note that these P_{fi}-values cannot be used in general because they relate to a specific structure. However, they are typical for conventionally designed breakwaters with respect to order of magnitude and large variations.

The simple failure probability bounds for the system are given by Equations VI-6-33, VI-6-34, VI-6-35, and VI-6-36:

Upper bound (no correlation):

$$P_{fS}^{U} = 1 - (1 - P_{f6})\ (1 - P_{f1})\ (1 - P_{f5})\ (1 - P_{f2})\ (1 - \min\ [P_{f3},\ P_{f4}]) = 12.9\,\%$$

or alternately for small values of P_{fi}

$$P_{fS}^{U} = P_{f6} + P_{f1} + P_{f5} + P_{f2} + \min\ [P_{f3},\ P_{f4}]) = 13.5\,\%$$

Lower bound (full correlation):

$$P_{fS}^{L} = \max\ [P_{f6}, P_{f1}, P_{f5}, P_{f2}, (P_{f3} \bullet\ P_{f4})] = 6\,\%$$

The simple bounds corresponding to T-years structural life might be approximated by the use of Equation VI-6-31[1]

	Structure life in years		
	20	50	100
P_{fs}^{U} %	94	100	100
P_{fs}^{L} %[1]	71	95	100

[1] It is very important to notice that the use of Equation VI-6-31, which assumes independent failure events from one year to another, can be misleading. This will be the case if some of the parameters which contribute significantly to the failure probability are time-invariant, i.e., are not changed from year to year. An example would be the parameter signifying a large uncertainty of a failure mode formula, such as the parameter A in Equation VI-6-2. If all parameters were time-invariant then the correct lower bound would be

$$P_{fS}^{L} = \max_{i=1-n} [P_{fi}]$$

independent of T, i.e., 6% for all T in the example. It follows that use of Equation VI-6-31 results in values of P_{fS}^{L} for $T > 1$ year that are too large.

EXAMPLE PROBLEM VI-6-2

Figure VI-6-11 shows a fault tree that differs from the fault tree in Figure VI-6-7. In Figure VI-6-11 only failure mode 6 can directly cause system failure, whereas in Figure VI-6-7 each of the failure modes 6, 5, 1, 2 and (3+4) can cause system failure.

The decomposition of the fault tree is shown in two steps in Figure VI-6-12. Note that the same failure mode can appear more than once in the decomposed system.

The simple bounds for the system are given by Equations VI-6-33, VI-6-34, VI-6-35, and VI-6-36:

Upper bound:

$$P_{fS}^{U} = 1 - (1 - P_{f6})\ (1 - \min\ [P_{f1}, P_{f5}])\ \ [P_{f1},\ P_{f2},\ P_{f3},\ P_{f4}] = 4.5\,\%$$

or for smaller values of P_{fi}

$$P_{fS}^{U} = P_{f6} + \min\ [P_{f1}, P_{f5}] + \min\ [P_{f1},\ P_{f2},\ P_{f3},\ P_{f4}] = 4.5\,\%$$

Lower bound:

$$P_{fS}^{L} = \max\ [P_{f6}, (P_{f1} \bullet P_{f5}), (P_{f1} \bullet\ P_{f2} \bullet\ P_{f3} \bullet\ P_{f4})] = 1\,\%$$

Using the same P_{fi}-values and procedure as given in Example VI-6-1 the following system failure probabilities are obtained

	Structure life in years		
	20	50	100
P_{fs}^{U} %	60	90	99
P_{fs}^{L} %[1]	18	39	63

These values are quite different from the values of Example VI-6-1 which emphasizes the importance of a correct fault tree.

[1] See note in Example VI-6-1.

- It would be possible to estimate P_{fS} if the physical interactions between the various failure modes were known and described by formulae, and if the correlations between the involved parameters were known. However, the procedure for determining such correlations are complicated and are not yet fully developed for practical use.

- The probability of failure cannot in itself be used as the basis for an optimization of a design. Optimization must be related to a kind of measure (scale), which for most structures is the economy, but can include other measures such as loss of human life.

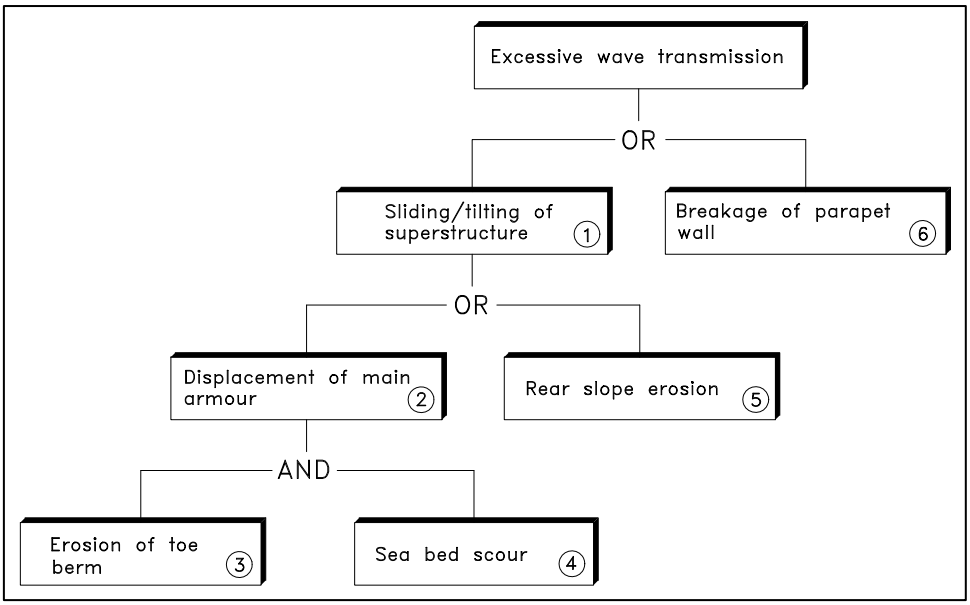

Figure VI-6-11. Example of simplified fault tree for a breakwater

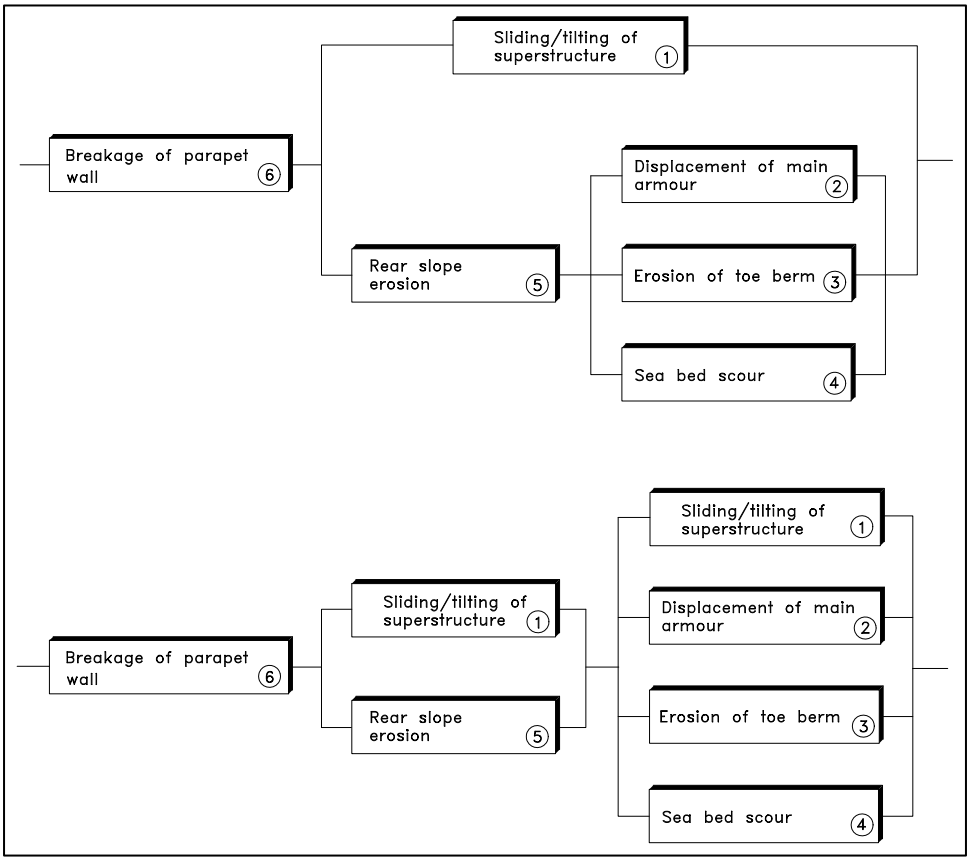

Figure VI-6-12. Decomposition of the fault tree into series and parallel systems

- The so-called risk, defined as the product of the probability of failure and the economic consequences, is used in optimization considerations. The economic consequences

must cover all kinds of expenses related to the failure in question, i.e., cost of replacement, downtime costs, etc.

VI-6-5. Parameter Uncertainties in Determining the Reliability of Structures. Calculation of reliability or failure probability of a structure is based on formulae describing the structure's response to loads and on information about the uncertainties related to the formulae and relevant parameters. Basically, uncertainty is best given by a probability distribution; but because the true distribution is rarely known, it is common to assume a normal distribution and a related coefficient of variation, defined as

$$\sigma' = \frac{\sigma}{\mu} = \frac{standard\ deviation}{mean\ value} \tag{VI-6-37}$$

as the measure of the uncertainty. The term "uncertainty" is used in this chapter as a general term referring to errors, to randomness, and to lack of knowledge.

a. Uncertainty related to failure mode formulae. The uncertainty associated with a formula can be considerable. This is clearly seen from many diagrams presenting the formula as a smooth curve shrouded by a wide scattered cloud of data points (usually from experiments) that are the basis for the curve fitting. Coefficients of variation of 15 - 20 percent or even larger are quite normal. The range of validity and the related coefficient of variation should always be considered when using a design formula.

b. Uncertainty related to environmental parameters. The sources of uncertainty contributing to the total uncertainties in environmental design values are categorized as follows:

(1) Errors related to instrument response (e.g., from accelerometer buoy and visual observations).

(2) Variability and errors due to different and imperfect calculations methods (e.g., wave hindcast models, algorithms for time-series analysis).

(3) Statistical sampling uncertainties due to short-term randomness of the variables (variability within a stochastic process, e.g., two 20-min. records from a stationary storm will give two different values of the significant wave height)

(4) Choice of theoretical distribution as a representative of the unknown long-term distribution (e.g., a Weibull and a Gumbel distribution might fit a data set equally well but can provide quite different values for a 200-year event).

(5) Statistical uncertainties related to extrapolation from short samples of data sets to events of low probability of occurrence.

(6) Statistical vagaries of the elements.

(a) Distinction must be made between short-term sea state statistics and long-term (extreme) sea statistics. Short-term statistics are related to the stationary conditions during a sea

state, e.g., wave height distribution within a storm of constant significant wave height, H_s. Long-term statistics deal with the extreme events, e.g., the distribution of H_s over many storms.

(b) Related to the short-term sea state statistics the following aspects must be considered:

- The distribution for individual wave heights in a record in deepwater and shallow-water conditions, i.e., Rayleigh distribution and some truncated distributions, respectively.

- Variability due to short samples of single peak spectra waves in deep and shallow water based on theory and physical simulations.

- Variability due to different spectral analysis techniques, i.e., different algorithms, smoothing and filter limits.

- Errors in instrument response and influence of measurement location. For example, floating accelerometer buoys tend to underestimate the height of steep waves. Characteristics of shallow-water waves can vary considerably in areas with complex seabed topography. Wave recordings at positions with depth-limited breaking waves cannot produce reliable estimates of the deepwater waves.

- Imperfection of deep and shallow-water numerical hindcast models and quality of wind input data.

(c) Estimates of overall uncertainties for short-term sea state parameters (first three items) are presented in Table VI-6-1 for use when more precise site specific information is not available.

(d) Evaluation of the uncertainties related to the long-term sea state statistics, and use of these estimates for design, involves the following considerations:

- The encounter probability.

- Estimation of the standard deviation of a return-period event for a given extreme distribution.

- Estimation of extreme distributions by fitting to data sets consisting of uncorrelated values of H_s from

  – Frequent measurements of H_s equally spaced in time.

  – Identification of the largest H_s in each year (annual series).

  – Maximum values of H_s for a number of storms exceeding a certain threshold value of H_s using peak over threshold (POT) analysis.

The methods of fitting are the maximum likelihood method, the method of moments, the least square method, and visual graphical fit.

- Uncertainty on extreme distribution parameters due to limited data sample size.

- Influence on the extreme value of H_s on the choice of threshold value in the POT analysis. (The threshold level should exclude all waves which do not belong to the statistical population of interest).

- Errors due to lack of knowledge about the true extreme distribution. Different theoretical distributions might fit a data set equally well, but might provide quite different return period values of H_s . (The error can be estimated only empirically by comparing results from fits to different theoretical distributions).

Table VI-6-1
Typical Variational Coefficients $\sigma N = \sigma / \mu$ (standard deviation over mean value) for Measured and Calculated Sea State Parameters (Burcharth 1992)

Parameter	Methods of Determination	Estimated Typical Values		Comments
		ΣN	Bias	
Significant wave height, OFFSHORE	Accelerometer buoy, pressure cell, vertical radar	0.05 - 0.1	–0	
	Horizontal radar	0.15	–0	
	Hindcast numerical models	0.1 - 0.2	0 - 0.1	Very dependent on quality of weather maps
	Hindcast, SMB method	0.15 - 0.2	?	Valid only for storm conditions in restricted sea basins
Significant wave height NEARSHORE determined from offshore significant wave height accounting for shallow-water effects	Visual observations from ships	0.2	0.05	
	Numerical models	0.1 - 0.20	0.1	σN can be much larger in some cases
	Manual calculations	0.15 - 0.35		
Mean wave period offshore on condition of fixed significant wave height	Accelerometer buoy	0.02 - 0.05	–0	
	Estimates from ampl. Spectra	0.15	–0	
	Hindcast, numerical models	0.1 - 0.2	–0	

Duration of sea state with significant wave height exceeding a specific level	Direct measurements	0.02	–0
	Hindcast numerical models	0.05 - 0.1	–0
Spectral peak frequency offshore	Measurements	0.05 - 0.15	–0
	Hindcast numerical models	0.1 - 0.2	–0
Spectral peakedness offshore	Measurements and hindcast numerical models	0.4	–0
Mean direction of wave propagation offshore	Pitch-roll buoy	5 degrees	
	Measurements η, u, v or p, u, v [1]	10 degrees	
	Hindcast numerical models	15 - 30 degrees	
Astronomical tides	Prediction from constants	0.001 - 0.07	–0
Storm surge	Numerical models	0.1 - 0.25	∀0.1

[1] Two horizontal velocity components and water-level elevation or pressure.

- Errors due to applied plotting formulae in the case of graphical fitting. Depending on the applied plotting formulae quite different extreme estimates can be obtained. The error can only be empirically estimated.

- Climatological changes.

- Physical limitations in extrapolation to events of low probability. The most important example might be limitations in wave heights due to limited water depths and fetch restrictions.

- The effect of measurement error on the uncertainty related to an extreme event.

(e) It is beyond the scope of this chapter to discuss in more detail the mentioned uncertainty aspects related to the environmental parameters. Additional information is given in Burcharth (1992).

c. Uncertainty related to structural parameters. The uncertainties related to material parameters (such as density) and geometrical parameters (such as slope angle and size of structural elements) are generally much smaller than the uncertainties related to the environmental parameters and to the design formulae.

VI-6-6. Partial Safety Factor System for Implementing Reliability in Design.

a. Introduction to partial safety factors.

(1) The objective of using partial safety factors in design is to assure a certain reliability of the structures. This section presents the partial safety factors developed by the Permanent International Association of Navigation Congresses (PIANC) PTCII Working Group 12 (Analysis of Rubble-Mound Breakwaters) and Working Group 28 (Breakwaters with Vertical and Inclined Concrete Walls), Burcharth (1991) and Burcharth and Sørensen (1999).

(2) The partial safety factors, γ_i, are related to characteristic values of the stochastic variables, $X_{i,ch}$. In conventional civil engineering codes the characteristic values of loads and other action parameters are often chosen to be an upper fractile (e.g., 5 percent), while the characteristic values of material strength parameters are chosen to be a lower fractile. The values of the partial safety factors are uniquely related to the applied definition of the characteristic values.

(3) The partial safety factors, γ_i, are usually larger than or equal to 1. Consequently, if we define the variables as either load variables X_i^{load} (for example H_s) or resistance variables X_i^{res} (for example the block volume) then the related partial safety factors should be applied as follows to obtain the design values:

$$X_i^{design} = \gamma_i^{load} \bullet X_{i,ch}^{load}$$
$$X_i^{design} = \frac{X_{i,ch}^{res}}{\gamma_i^{res}} \qquad \text{(VI-6-38)}$$

(4) The magnitude of γ_i reflects both the uncertainty of the related parameter X_i, and the relative importance of X_i in the failure function. A large value, e.g., $\gamma_{Hs} = 1.4$, indicates a relatively large sensitivity of the failure probability to the significant wave height, H_s. On the other hand, $\gamma \approx 1$ indicates little or negligible sensitivity, in which case the partial coefficient should be omitted. Bear in mind that the magnitude of γ_i is not (in a mathematical sense) a stringent measure of the sensitivity of the failure probability of the parameter, X_i.

(5) As an example, when partial safety factors are applied to the characteristic values of the parameters in Equation VI-6-2, a design equation is obtained, i.e., the definition of how to apply the coefficients. The partial safety factors can be related either to each parameter or to combinations of the parameters (overall coefficients). The design equation obtained when partial safety factors are applied to each parameter is given by

$$G = \frac{A_{ch}}{\gamma_A}\frac{\Delta_{ch}}{\gamma_\Delta}\frac{D_{n,ch}}{\gamma_{D_n}}\left(K_D \frac{\cot\alpha_{ch}}{\gamma_{\cot\alpha}}\right)^{1/3} - \gamma_{H_s} H_{s,ch} \geq 0$$
$$or \qquad \text{(VI-6-39)}$$
$$D_{n,ch} \geq \gamma_A \gamma_\Delta \gamma_{D_n} \gamma_{\cot\alpha}^{1/3} \gamma_{H_s} \frac{H_{s,ch}}{A_{ch}\,\Delta_{ch}\,K_D \cot\alpha_{ch}}$$

(6) If the partial safety factors are applied to combinations of parameters, there may be only γ_{Hs} and an overall coefficient γ_Z related to the first term on the right-hand side of Equation VI-6-39. The design equation would then become

$$G = \frac{A_{ch}}{\gamma_Z}\Delta_{ch} D_{n,ch}\left(K_D \cot\alpha\right)^{1/3} - \gamma_{H_s} H_{s,ch} \geq 0$$

or (VI-6-40)

$$D_{n,ch} \geq \gamma_Z \gamma_{H_s} \frac{H_{s,ch}}{A_{ch}\Delta_{ch}\left(K_D \cot\alpha_{ch}\right)^{1/3}}$$

(7) Equations VI-6-39 and VI-6-40 express two different "code formats." By comparing the two equations it is seen that the product of the partial coefficients is independent of the chosen format if the other parameters are equal. A goal is to have a system which is as simple as possible, i.e., with as few partial safety factors as possible, but without invalidating the accuracy of the design equation beyond acceptable limits. Fortunately, it is often possible to use overall coefficients, such as γ_A in Equation VI-6-40, without losing significant accuracy within the realistic range of parameter value combinations. This is the case for the partial safety factors system presented in this chapter where only two partial safety factors, γ_{Hs} and γ_Z, are used in each design formula.

(8) Usually several failure modes are relevant to a particular design. The relationship between the failure modes are characterized either as series systems or parallel systems. A fault tree can be used to illustrate the complete system. The partial safety factors for failure modes associated with a system having a failure probability, P_f, are different from the partial safety factors for single failure modes having the same failure probability, P_f. Therefore, partial safety factors for single failure modes and multifailure mode systems must be treated separately.

b. Uncertainties and statistical models. Uncertainties in relation to rubble-mound breakwaters can be divided in uncertainties related to the following three groups:

(1) Load uncertainties (wave modeling).

(2) Soil strength uncertainties (modeling of soil strength parameters).

(3) Model uncertainties (both wave load models and models for bearing capacity of the foundation).

(a) Wave modeling.

- For calibration of partial safety factors the maximum significant wave height in T years is denoted as $F_{H_S^T}$, and it is modeled (for example) by the extreme Weibull distribution, given as

$$F_{H_S^T}(H_s) = \left\{ 1 - \exp\left[-\left(\frac{H_s - H_{\bar{s}}}{\beta} \right)^{\alpha} \right] \right\}^{\lambda T} \qquad \text{(VI-6-41)}$$

where λ is the number of observations per year, H_SN is the threshold level, and α and β are the Weibull distribution parameters.

- For calibration of the PIANC partial safety factor system, wave data from four quite different geographical locations were selected as presented in Table VI-6-2. In Table VI-6-2, N is the number of data samples and h is the water depth in meters.

Table VI-6-2
Wave Data from Different Locations Fitted to a Weibull Distribution
(β, H_SN and h are in meters)

	N	λ	α	β (m)	H_SN(m)	h (m)
Bilbao	50	4.17	1.39	1.06	4.9	25
Sines	15	1.25	1.78	2.53	7.1	25
Tripoli	15	0.75	1.83	3.24	2.9	25
Fallonica	46	5.94	1.14	0.58	2.7	10

- The wave data from Bilbao, Sines and Tripoli correspond to deepwater waves, whereas the wave data from Fallonica corresponds to shallow-water waves. To model the statistical uncertainty, α and β are modeled as independent and normally distributed.

- The model uncertainty related to the quality of the measured wave data is modeled by a multiplicative stochastic variable F_{Hs} which is assumed to be normally distributed with expected value 1 and standard deviation $\sigma_{F_{Hs}}$. High quality and low quality wave data could be represented by $\sigma_{F_{Hs}}$ = 0.05 and 0.2, corresponding to accelerometer buoy and fetch diagram estimates, respectively, as given by Table VI-6-1.

(b) Soil strength modeling.

- Statistical modeling of the soil strength (sand and/or clay) is generally difficult, and only few models are available in the literature that can be used for practical reliability calculations. In general the material characteristics of the soil have to be modeled as a stochastic field. The parameters describing the stochastic field have to be determined on the basis of the measurements which are usually performed to characterize the soil characteristics. Because these measurements are only performed in a few locations, statistical uncertainty due to the sparse data is introduced, and this uncertainty must be included in the statistical model. Furthermore, the

uncertainty in the determination of the soil properties and the measurement uncertainty must also be included in the statistical model.

- Because breakwaters are composed of loose material in frictional contact, and it is assumed that the foundation failure modes are developed in the core; only statistical models for the effective friction angle and the angle of dilation are needed. Usually these angles are modeled by normal or lognormal distributions.

- The bearing capacities related to the geotechnical failure modes are estimated using the upper bound theorem of classical plasticity theory where an associated flow rule is assumed. However, the friction angle and the dilation angle for the rubble-mound material and the sand subsoil are usually different. Therefore, in order to use the theory based on an associated flow rule, the following reduced effective friction angle ν_d is used (Hansen 1979):

$$\tan \varphi_d = \frac{\sin \varphi' \cos \psi}{1 - \sin \varphi' \sin \psi} \tag{VI-6-42}$$

where νN is the effective friction angle and ψ is the dilation angle.

(c) Model uncertainties.

- In general, model uncertainties related to a given mathematical model can be evaluated on the basis of:

– Comparisons between experimental tests/measurements and numerical model calculations.

– Comparisons between numerical calculations with the given mathematical model and a more advanced/complex model.

– Expert opinions.

– Information from the literature.

- Many laboratory experiments have been performed for most of the failure modes related to hydraulic instability of the armor layer. Based on these experiments the model uncertainty can be estimated. Model uncertainty connected with extrapolation from laboratory to a real structure can be judged on the basis of expert opinions, information from the literature, and observations of similar existing structures.

- For soil strength models no similar measurements models are available. However, if "simple" rotation and translation failure models based on the upper bound theorem of plasticity theory are used, then these can be evaluated by comparison with results from more refined numerical calculations using nonlinear finite element programs. Estimates of the model uncertainties can thus be obtained.

c. Format for partial safety factors.

(1) The PIANC partial safety factors are calibrated with the following input:

(a) Design lifetime T_L (= 20, 50 or 100 years).

(b) Acceptable probability of failure P_f (= 0.01, 0.05, 0.10, 0.20, or 0.40).

(c) Coefficient of variation $\sigma_{F_{H_s}}$ = (0.05 and 0.20).

(d) Deep or shallow-water conditions.

(e) Wave loads determined with or without hydraulic model tests.

(2) The partial safety factors are as follows:

(a) A load partial safety factor γ_P to be applied to the mean value of the permanent load (= 1).

(b) A load partial safety factor γ_H to be applied to $\hat{H}_s^{T_L}$ (the central estimate of the significant wave height which, in average, is exceeded once every T_L years).

(c) A partial safety factor to be used to the combination of the mean values of the resistance variables as shown in the design equation. γ_Z is to be used with friction materials in rubble-mound and/or subsoils (tangent to the mean value of the friction angle is divided by γ_Z).

(d) A partial safety factor γ_C to be used with the mean value of the undrained shear strength of clay materials in the subsoil (the mean value of the undrained shear strength is divided by γ_C).

d. Tables of partial safety factors.

(1) Partial safety factors are presented in Table VI-6-3.

(2) In the case of vertical walls, wave forces are calculated from the Goda formula. Furthermore, the following factors are used to compensate for the positive bias inherent in the Goda formula (see Table VI-5-55):

$\hat{U}_{Hor.Force}$ = 0.90, bias factor to be applied to the Goda horizontal wave force

$\hat{U}_{Ver.Force}$ = 0.77, bias factor to be applied to the Goda vertical wave force

$\hat{U}_{Hor.Moment}$ = 0.81, bias factor to be applied to the moment from the Goda horizontal wave forces around the shoreward heel of the base plate

$\hat{U}_{Ver.Moment}$ = 0.72, bias factor to be applied to the moment from the Goda vertical wave forces around the shoreward heel of the base plate

A carrot symbol (^) over the variable indicates a mean value.

Table VI-6-3
Partial Safety Factor Tables

Structure	Failure	Armor	Table(s)
Rubble-mound structures	Armor stability	Rocks	VI-6-4 - VI-6-6
		Cubes	VI-6-7
		Tetrapods	VI-6-8
		Dolosse	VI-6-9 & VI-6-10
		Hollowed Cubes	VI-6-11 & VI-6-12
	Toe berm		VI-6-13
	Breakage	Dolosse	VI-6-14 & VI-6-15
		Tetrapods	VI-6-16
	Runup	Rock	VI-6-17
		Hollowed Cubes	VI-6-18
		Dolosse	VI-6-19
	Scour		VI-6-20 & VI-6-21
Vertical-wall caisson structures	Foundation: sand subsoil		VI-6-22
	Foundation: clay subsoil		VI-6-23
	Sliding failure		VI-6-24
	Overturning failure		VI-6-25
	Scour		VI-6-26
	Toe berm		VI-6-27

(3) Part VI-7, “Example Problems,” contains worked design examples for the most common coastal structures. Some of these examples include a reliability analysis based on the information contained in Tables VI-6-4 to VI-6-27 either as part of the design or as an alternative to deterministic methods based on a single return period of occurrence. The Part VI-7 examples provide coastal engineers with guidance on selection of partial safety factors γ_{Hs} and γ_Z for various levels of P_f and $\sigma_{F_{Hs}}$.

Table VI-6-4
Partial Safety Factors for Stability Failure of Rock Armor, Hudson Formula, Design Without Model Tests

Design equation (cf. Table VI-5-22)

$$G = \frac{1}{\gamma_Z}\hat{\Delta}\hat{D}_n(K_D\ c\hat{o}t\ \alpha)^{1/3} - \gamma_H \hat{H}_S^T \qquad (\text{VI}-6-43)$$

	$\sigma'_{FH_S} = 0.05$		$\sigma'_{FH_S} = 0.2$	
P_f	γ_H	γ_Z	γ_H	γ_Z
0.01	1.7	1.04	2.0	1.00
0.05	1.4	1.06	1.6	1.02
0.10	1.3	1.04	1.4	1.06
0.20	1.2	1.02	1.3	1.00
0.40	1.0	1.08	1.1	1.00

Table VI-6-5
Partial Safety Factors for Stability Failure of Rock Armor, Plunging Waves, van der Meer Formula, Design Without Model Tests

Design equation (cf. Table VI-5-23)

$$G = \frac{1}{\gamma_Z} 6.2\ \hat{S}^{0.2}\ \hat{P}^{0.18}\ \hat{\Delta}\hat{D}_n\hat{f}\ (c\hat{o}t\ \alpha)^{0.5}\ (\hat{s}_{om})^{0.25}\ \hat{N}_z^{-0.1} - \gamma_H \hat{H}_S^T \qquad (\text{VI}-6-44)$$

where the factor f models the effect of low crested breakwaters:

$$\hat{f} = \frac{1}{1.25 - 4.8\frac{R_c}{\hat{H}_S^T}\sqrt{\frac{\hat{s}_{op}}{2\pi}}}$$

	$\sigma'_{FH_S} = 0.05$		$\sigma'_{FH_S} = 0.2$	
P_f	γ_H	γ_Z	γ_H	γ_Z
0.01	1.6	1.04	1.9	1.00
0.05	1.4	1.02	1.5	1.06
0.10	1.3	1.00	1.3	1.10
0.20	1.2	1.00	1.2	1.06
0.40	1.0	1.08	1.0	1.10

Table VI-6-6
Partial Safety Factors for Stability Failure of Rock Armor, Surging Waves, van der Meer Formula, Design Without Model Tests

Design equation (cf. Table VI-5-23)

$$G = \frac{1}{\gamma_Z}\hat{S}^{0.2}\,\hat{P}^{-0.13}\,\hat{\Delta}\,\hat{D}_n\,\hat{f}\,(c\hat{o}t\,\alpha)^{(0.5-P)}(\hat{s}_{om})^{-0.5P}\,\hat{N}_z^{-0.1} - \gamma_H\hat{H}_S^T \qquad \text{(VI−6−45)}$$

where

$$\hat{f} = \frac{1}{1.25 - 4.8\frac{R_c}{\hat{H}_S^T}\sqrt{\frac{\hat{s}_{op}}{2\pi}}}$$

	$\sigma'_{FH_S} = 0.05$		$\sigma'_{FH_S} = 0.2$	
P_f	γ_H	γ_Z	γ_H	γ_Z
0.01	1.7	1.00	1.9	1.02
0.05	1.3	1.10	1.6	1.00
0.10	1.3	1.02	1.4	1.04
0.20	1.1	1.10	1.2	1.08
0.40	1.0	1.08	1.1	1.00

Table VI-6-7
Partial Safety Factors for Stability Failure of Cube Block Armor, van der Meer Formula, Design Without Model Tests

Design equation (cf. Table VI-5-29)

$$G = \frac{1}{\gamma_Z}\left(6.7\,\frac{(\hat{N}_{od})^{0.4}}{(\hat{N}_z)^{0.3}} + 1.0\right)(\hat{s}_{om})^{-0.1}\hat{\Delta}\hat{D}_n - \gamma_H\hat{H}_S^T \qquad \text{(VI−6−46)}$$

	$\sigma'_{FH_S} = 0.05$		$\sigma'_{FH_S} = 0.2$	
P_f	γ_H	γ_Z	γ_H	γ_Z
0.01	1.5	1.10	1.8	1.04
0.05	1.3	1.08	1.5	1.04
0.10	1.3	1.00	1.4	1.02
0.20	1.2	1.00	1.2	1.06
0.40	1.0	1.08	1.0	1.10

Table VI-6-8
Partial Safety Factors for Stability Failure of Tetrapods, van der Meer Formula, Design Without Model Tests

Design equation (cf. Table VI-5-30)

$$G = \frac{1}{\gamma_Z}\left(3.75\,\frac{(\hat{N}_{od})^{0.5}}{(\hat{N}_z)^{0.25}} + 0.85\right)(\hat{s}_{om})^{-0.2}\,\hat{\Delta}\hat{D}_n - \gamma_H \hat{H}_S^T \qquad \text{(VI}-6-47\text{)}$$

	$\sigma'_{FH_S} = 0.05$		$\sigma'_{FH_S} = 0.2$	
P_f	γ_H	γ_Z	γ_H	γ_Z
0.01	1.7	1.02	1.9	1.04
0.05	1.4	1.06	1.5	1.08
0.10	1.3	1.04	1.4	1.04
0.20	1.2	1.02	1.3	1.00
0.40	1.0	1.08	1.1	1.00

Table VI-6-9
Partial Safety Factors for Stability Failure of Dolosse, Without Superstructure, Burcharth Formula, Design Without Model Tests

Design equation (cf. Table VI-5-31)

$$G = \frac{1}{\gamma_Z}\hat{\Delta}\hat{D}_n(47 - 72\hat{r})\,\hat{\varphi}\,\hat{D}^{1/3}\,\hat{N}_z^{-0.1} - \gamma_H \hat{H}_S^T \qquad \text{(VI}-6-48\text{)}$$

	$\sigma'_{FH_S} = 0.05$		$\sigma'_{FH_S} = 0.2$	
P_f	γ_H	γ_Z	γ_H	γ_Z
0.01	2.1	1.08	2.4	1.02
0.05	1.7	1.00	1.7	1.08
0.10	1.5	1.00	1.6	1.00
0.20	1.3	1.00	1.3	1.04
0.40	1.0	1.10	1.1	1.02

Table VI-6-10
Partial Safety Factors for Stability Failure of Dolosse, With Superstructure, Burcharth and Liu (1995a), Design Without Model Tests

Design equation

$$G = \frac{1}{\gamma_Z}\hat{\Delta}\hat{D}_n(43 - 66\hat{r})\,\hat{\varphi}\,\hat{D}^{1/3}\,\hat{N}_z^{-0.1} - \gamma_H \hat{H}_S^T \qquad \text{(VI-6-49)}$$

	$\sigma'_{FH_S} = 0.05$		$\sigma'_{FH_S} = 0.2$	
P_f	γ_H	γ_Z	γ_H	γ_Z
0.01	1.9	1.10	2.2	1.04
0.05	1.6	1.02	1.7	1.04
0.10	1.4	1.04	1.5	1.04
0.20	1.2	1.06	1.3	1.04
0.40	1.0	1.10	1.1	1.02

H_s^T	Significant wave height with return period T
ρ_s	Mass density of concrete
ρ_w	Mass density of water
Δ	$(\rho_s/\rho_w) - 1$
D_n	Equivalent cube length, i.e., length of cube with the same volume as Dolosse
r	Dolos waist ratio
φ	Packing density
D	Relative number of units within levels SWL $\pm$ 6.5 Dn displaced one Dolos height h, or more (e.g., for 2% displacement insert $D = 0.02$)
N_z	Number of waves. For $N_z \geq 3000$ use $N_z = 3000$

Table VI-6-11
Partial Safety Factors for Stability Failure of Trunk of Hollowed Cubes, Slope 1:1.5 and 1:2, Berenguer and Baonza (1995), Design Without Model Tests

Design equation

$$G = \frac{1}{\gamma_Z}\hat{\zeta}_p^{-0.1}(3.3 + 0.7\hat{N}_{0d}^{0.4})\hat{\Delta}\hat{D}_n - \gamma_H \hat{H}_S^T \qquad \text{(VI-6-50)}$$

where

$$\hat{\zeta}_p = (\hat{cot}\ \alpha)^{-1}\ (\hat{s}_{op})^{-0.5}$$

	$\sigma'_{FH_S} = 0.05$		$\sigma'_{FH_S} = 0.2$	
P_f	γ_H	γ_Z	γ_H	γ_Z
0.01	3.5	1.10	3.5	1.10
0.05	2.3	1.08	2.5	1.02
0.10	1.8	1.06	1.9	1.04
0.20	1.4	1.06	1.5	1.02
0.40	1.1	1.04	1.1	1.04

H_s^T	Significant wave height with return period T
ρ_s	Mass density of concrete
ρ_w	Mass density of water
Δ	$(\rho_s/\rho_w) - 1$
D_n	Equivalent cube length, i.e., length of cube with the same volume as Dolosse
N_{od}	Number of displaced units within a strip width of one equivalent cube length D_n

Table VI-6-12
Partial Safety Factors for Stability Failure of Roundhead of Hollowed Cubes, Slope 1:1.5 and 1:2, Berenguer and Baonza (1995), Design Without Model Tests

Design equation

$$G = \frac{1}{\gamma_Z}(1.8 + 6.6\hat{D}^{0.33}\,\hat{\zeta}_p^{-0.1})\hat{\Delta}\hat{D}_n - \gamma_H \hat{H}_S^T \qquad \text{(VI-6-51)}$$

where

$$\hat{\zeta}_p = (\hat{cot}\ \alpha)^{-1}(\hat{s}_{op})^{-0.5}$$

	$\sigma'_{FH_S} = 0.05$		$\sigma'_{FH_S} = 0.2$	
P_f	γ_H	γ_Z	γ_H	γ_Z
0.01	1.8	1.00	1.9	1.06
0.05	1.5	1.00	1.5	1.10
0.10	1.3	1.06	1.4	1.06
0.20	1.2	1.02	1.3	1.00
0.40	1.0	1.08	1.1	1.00

H_s^T	Significant wave height with return period T
ρ_s	Mass density of concrete
ρ_w	Mass density of water
Δ	$(\rho_s/\rho_w) - 1$
D_n	Equivalent cube length, i.e., length of cube with the same volume as Dolosse
D	Relative number of displaced units
s_{op}	Wave steepness, Hs/L_{op}
L_{op}	Deepwater wave length corresponding to peak wave period

Table VI-6-13
Partial Safety Factors for Stability Failure of Toe Berm, Parallelepiped Concrete Blocks and Rocks., Burcharth Formula, Design Without Model Tests

Design equation (cf. Table VI-5-47)

$$G = \frac{1}{\gamma_Z}(0.4\frac{\hat{h}_b}{\hat{\Delta}\hat{D}_{n50}} + 1.6)\,(\hat{N}_{od})^{0.15}\hat{\Delta}\hat{D}_{n50} - \gamma_H\hat{H}_S^T \qquad \text{(VI}-6-52\text{)}$$

	$\sigma'_{FH_S} = 0.05$		$\sigma'_{FH_S} = 0.2$	
P_f	γ_H	γ_Z	γ_H	γ_Z
0.01	1.6	1.06	1.8	1.06
0.05	1.3	1.10	1.5	1.06
0.10	1.3	1.02	1.4	1.04
0.20	1.1	1.10	1.2	1.08
0.40	1.0	1.08	1.0	1.10

Table VI-6-14
Partial Safety Factors for Trunk Dolos Breakage, Burcharth Formula, Design Without Model Tests

Design equation (cf. Table VI-5-40)

$$G = \frac{1}{\gamma_Z}B - C_0\,\hat{M}^{C_1}\,\hat{f}_T{}^{C_2}\,(\gamma_H\hat{H}_S^T)^{C_3} \qquad \text{(VI}-6-53\text{)}$$

	$\sigma'_{FH_S} = 0.05$		$\sigma'_{FH_S} = 0.2$	
P_f	γ_H	γ_Z	γ_H	γ_Z
0.01	1.9	1.00	2.1	1.00
0.05	1.5	1.04	1.6	1.10
0.10	1.4	1.00	1.5	1.00
0.20	1.2	1.10	1.3	1.00
0.40	1.1	1.00	1.1	1.02

Table VI-6-15
Partial Safety Factors for Roundhead Dolos Breakage, Burcharth Formula, Design Without Model Tests

Design equation (cf. Table VI-5-40)

$$G = \frac{1}{\gamma_Z} B - 0.025\, \hat{M}^{-0.65}\, \hat{f_T}^{-0.66}\, (\gamma_H \hat{H}_S^T)^{2.42} \qquad (\text{VI}-6-54)$$

	$\sigma'_{FH_S} = 0.05$		$\sigma'_{FH_S} = 0.2$	
P_f	γ_H	γ_Z	γ_H	γ_Z
0.01	1.8	1.02	2.0	1.00
0.05	1.4	1.10	1.6	1.00
0.10	1.3	1.06	1.4	1.08
0.20	1.2	1.02	1.3	1.00
0.40	1.1	1.00	1.1	1.00

Table VI-6-16
Partial Safety Factors for Trunk Tetrapod Breakage, Burcharth Formula, Design Without Model Tests

Design equation (cf. Table VI-5-40)

$$G = \frac{1}{\gamma_Z} B - 3.39(10)^{-3}\, \hat{M}^{-0.79}\, \hat{f_T}^{-2.73}\, (\gamma_H \hat{H}_S^T)^{3.84} \qquad (\text{VI}-6-55)$$

	$\sigma'_{FH_S} = 0.05$		$\sigma'_{FH_S} = 0.2$	
P_f	γ_H	γ_Z	γ_H	γ_Z
0.01	1.9	1.10	2.1	1.06
0.05	1.6	1.00	1.7	1.00
0.10	1.4	1.04	1.5	1.04
0.20	1.2	1.10	1.3	1.06
0.40	1.1	1.00	1.1	1.04

Table VI-6-17
Partial Safety Factors for Runup, Rock Armored Slopes, De Waal and van der Meer (1992), Design Without Model Tests

Design equation

For $\zeta_m = (\cot \alpha)^{-1}(s_{om})^{-0.5} \leq 1.5 \quad : \quad R_u/H_s = a\,\zeta_m$

$$G = \frac{1}{\gamma_Z}\hat{R}_u\,\hat{a}^{-1}\,(cot\ \hat{\alpha})(\hat{s}_{om})^{0.5} - \gamma_H \hat{H}_s^T \qquad \text{(VI−6−56)}$$

	$\sigma'_{FH_S} = 0.05$		$\sigma'_{FH_S} = 0.2$	
P_f	γ_H	γ_Z	γ_H	γ_Z
0.01	1.7	1.04	2.0	1.00
0.05	1.4	1.06	1.6	1.02
0.10	1.3	1.04	1.4	1.06
0.20	1.2	1.02	1.3	1.00
0.40	1.0	1.08	1.1	1.00

For $\zeta_m = (\cot \alpha)^{-1}(s_{om})^{-0.5} > 1.5 \quad : \quad R_u/H_s = b\,(\zeta_m)^c$

$$G = \frac{1}{\gamma_Z}\hat{R}_u\,\hat{b}^{-1}[\cot\,\hat{\alpha}\,(\hat{s}_{om})^{0.5}]^{\hat{c}} - \gamma_H \hat{H}_s^T \qquad \text{(VI−6−57)}$$

	$\sigma'_{FH_S} = 0.05$		$\sigma'_{FH_S} = 0.2$	
P_f	γ_H	γ_Z	γ_H	γ_Z
0.01	1.5	1.08	1.8	1.02
0.05	1.3	1.06	1.4	1.10
0.10	1.2	1.06	1.3	1.08
0.20	1.1	1.08	1.2	1.06
0.40	1.0	1.06	1.0	1.10

For permeable structures, $P > 0.4$, the upper limit of R_u is given by $R_u/H_s = d$

α	Slope angle
s_{om}	Wave steepness, Hs/L_{om}
L_{om}	Deepwater wave length corresponding to mean wave period
R_u	Wave runup
H_s^T	Significant wave height with return period T
P	Notational permeability, cf. Figure VI-5-11

Values of a, b, c, *and* d coefficients.

exceedence probability (%)	a	b	c	d
0.1	1.12	1.34	0.55	2.58
2	0.96	1.17	0.46	1.97
Significant	0.72	0.88	0.41	1.35

Table VI-6-18
Partial Safety Factors for Runup, Hollowed Cubes, Slopes 1:1.5 and 1:2, Berenguer and Baonza (1995), Design Without Model Tests

Design equation

$$G = \frac{1}{\gamma_z}\hat{R}_u - \gamma_H \hat{H}_S^T \, (0.78 + 0.17\,\hat{\zeta}_p) \qquad \text{(VI-6-58)}$$

where

$$\hat{\zeta}_p = (\cot\,\alpha)^{-1}(\hat{s}_{op})^{-0.5}$$

	$\sigma'_{FH_S} = 0.05$		$\sigma'_{FH_S} = 0.2$	
P_f	γ_H	γ_Z	γ_H	γ_Z
0.01	1.8	1.02	2.0	1.04
0.05	1.4	1.10	1.7	1.00
0.10	1.3	1.08	1.5	1.02
0.20	1.2	1.06	1.3	1.02
0.40	1.0	1.10	1.1	1.02

α	Slope angle
s_{op}	Wave steepness, Hs/L_{op}
L_{op}	Deepwater wavelength corresponding to peak wave period
R_u	Wave runup
H_s^T	Significant wave height with return period T

Table VI-6-19
Partial Safety Factors for Runup, Dolosse, Slopes 1:1.5, Burcharth and Liu (1995b), Design Without Model Tests

Design equation

$$G = \frac{1}{\gamma_z}\hat{R}_u - \gamma_H \hat{H}_S^T \, (0.75 + 0.11 \, \hat{\zeta}_p) \qquad \text{(VI-6-59)}$$

where

$$\hat{\zeta}_p = (\cot \alpha)^{-1} \, (\hat{s}_{op})^{-0.5}$$

	$\sigma'_{FH_S} = 0.05$		$\sigma'_{FH_S} = 0.2$	
P_f	γ_H	γ_Z	γ_H	γ_Z
0.01	1.5	1.10	1.8	1.04
0.05	1.4	1.00	1.5	1.04
0.10	1.3	1.00	1.4	1.02
0.20	1.2	1.00	1.2	1.06
0.40	1.0	1.08	1.0	1.10

α	Slope angle
s_{op}	Wave steepness, Hs/L_{op}
L_{op}	Deepwater wavelength corresponding to peak wave period
R_u	Wave runup
H_s^T	Significant wave height with return period T

Table VI-6-20
Partial Safety Factors for Steady Stream Scour Depth in Sand at Conical Roundheads, Fredsøe and Sumer (1997), Design Without Model Tests

Design equation, cf. Eqn. VI-5-262

$$G = \frac{1}{\gamma_z}\frac{\hat{S}}{\hat{B}} - 0.04\left(1 - \frac{1}{\exp[4(\hat{KC} - 0.05)]}\right) \qquad \text{(VI-6-60)}$$

where

$$KC = \frac{U_m T_p}{B}$$

In calculation of U_m (maximum wave orbital velocity at the bed with no structure) use the wave height $\gamma_H \hat{H}_s^T$

	$\sigma'_{FH_S} = 0.05$		$\sigma'_{FH_S} = 0.2$	
P_f	γ_H	γ_Z	γ_H	γ_Z
0.01	1.7	1.10	1.9	1.10
0.05	1.4	1.10	1.6	1.08
0.10	1.3	1.10	1.4	1.10
0.20	1.2	1.06	1.2	1.10
0.40	1.0	1.10	1.1	1.02

Table VI-6-21
Partial Safety Factors for Scour Depth in Sand at Conical Roundheads in Breaking Wave Conditions, Fredsøe and Sumer (1997), Design Without Model Tests

Design equation, cf. Eqn. VI-5-264

$$G = \frac{1}{\gamma_z}\hat{S} - 0.01\left(\frac{\hat{T}_p\sqrt{g\gamma_H \hat{H}_S^T}}{\hat{h}}\right)^{1.5} \qquad \text{(VI-6-61)}$$

	$\sigma'_{FH_S} = 0.05$		$\sigma'_{FH_S} = 0.2$	
P_f	γ_H	γ_Z	γ_H	γ_Z
0.01	1.6	1.08	1.8	1.10
0.05	1.4	1.02	1.5	1.10
0.10	1.3	1.02	1.4	1.06
0.20	1.2	1.00	1.3	1.00
0.40	1.1	1.00	1.1	1.00

Table VI-6-22
Partial Safety Factors for Foundation Failure of Vertical Wall Caissons - Sand Subsoil

Design equation

$$G = G(\gamma_H \hat{H}_S^T,\ \hat{\rho}_c,\ \hat{U}_{Hor.Force},\ \hat{U}_{Ver.Force},\ \hat{U}_{Hor.Moment},\ \hat{U}_{Ver.Moment},\ \hat{\zeta},\ \frac{1}{\gamma_Z}\hat{\tan}\,\varphi_{d_1},\ \frac{1}{\gamma_Z}\hat{\tan}\,\varphi_{d_2},\ B) \quad \text{(VI−6−62)}$$

Deep water. Design without model tests. γ_Z is used for both rubble-mound and sand subsoil.

	$\sigma'_{FH_S} = 0.05$		$\sigma'_{FH_S} = 0.2$	
P_f	γ_H	γ_Z	γ_H	γ_Z
0.01	1.4	1.3	1.4	1.3
0.05	1.3	1.2	1.3	1.2
0.10	1.2	1.2	1.2	1.2
0.20	1.1	1.1	1.1	1.2
0.40	1.1	1.0	1.1	1.0

Deep water. Wave load determined by model tests. γ_Z is used for both rubble-mound and sand subsoil.

	$\sigma'_{FH_S} = 0.05$		$\sigma'_{FH_S} = 0.2$	
P_f	γ_H	γ_Z	γ_H	γ_Z
0.01	1.3	1.2	1.4	1.2
0.05	1.3	1.1	1.4	1.1
0.10	1.2	1.1	1.3	1.1
0.20	1.1	1.1	1.1	1.1
0.40	1.1	1.0	1.1	1.0

Shallow water. Design without model tests. γ_Z is used for both rubble-mound and sand subsoil.

	$\sigma'_{FH_S} = 0.05$		$\sigma'_{FH_S} = 0.2$	
P_f	γ_H	γ_Z	γ_H	γ_Z
0.01	1.3	1.4	1.3	1.4
0.05	1.2	1.3	1.3	1.3
0.10	1.2	1.2	1.2	1.2
0.20	1.1	1.1	1.1	1.2
0.40	1.1	1.0	1.1	1.0

Shallow water. Wave load determined by model tests. γ_Z is used for both rubble-mound and sand subsoil.

	$\sigma'_{FH_S} = 0.05$		$\sigma'_{FH_S} = 0.2$	
P_f	γ_H	γ_Z	γ_H	γ_Z
0.01	1.3	1.2	1.4	1.2
0.05	1.3	1.1	1.4	1.1
0.10	1.2	1.1	1.3	1.1
0.20	1.1	1.1	1.1	1.1
0.40	1.1	1.0	1.1	1.0

H_s^T	Significant wave height with return period T
B	Width of caisson
$\hat{U}_{Hor.Force}$	0.90, bias factor to be applied to the Goda horizontal wave force
$\hat{U}_{Ver.Force}$	0.77, bias factor to be applied to the Goda vertical wave force
$\hat{U}_{Hor.Moment}$	0.81, bias factor to be applied to the moment from the Goda horizontal wave forces around the shoreward heel of the base plate
$\hat{U}_{Ver.Moment}$	0.72, bias factor to be applied to the moment from the Goda vertical wave forces around the shoreward heel of the base plate
φ_d	$\frac{\sin\varphi' \cos\psi}{1-\sin\varphi' \sin\psi}$
φ'	Effective friction angle of friction material (sand or rubble stone)
ψ	Dilation angle of friction material (sand or rubble stone)
ρ_c	Mass density of caisson

Table VI-6-23
Partial Safety Factors for Foundation Failure of Vertical Wall Caissons - Clay Subsoil

Design equation

$$G = G(\gamma_H \hat{H}_S^T,\ \hat{\rho}_c,\ \hat{U}_{Hor.Force},\ \hat{U}_{Ver.Force},\ \hat{U}_{Hor.Moment},\ \hat{U}_{Ver.Moment},\ \hat{\zeta},\ \frac{1}{\gamma_Z}\hat{\tan}\,\varphi_{d_1},\ \frac{1}{\gamma_c}\hat{c}_u,\ B) \qquad \text{(VI−6−63)}$$

Deep water. Design without model tests. γ_Z is used for rubble-mound and γ_C clay subsoil.

	$\sigma'_{FH_S} = 0.05$			$\sigma'_{FH_S} = 0.2$		
P_f	γ_H	γ_Z	γ_C	γ_H	γ_Z	γ_C
0.01	1.3	1.5	1.6	1.4	1.5	1.6
0.05	1.2	1.4	1.5	1.3	1.4	1.5
0.10	1.1	1.3	1.5	1.2	1.3	1.5
0.20	1.0	1.3	1.4	1.0	1.3	1.5
0.40	1.0	1.1	1.1	1.0	1.1	1.2

Deep water. Wave load determined by model tests. γ_Z is used for rubble-mound and γ_C clay subsoil.

	$\sigma'_{FH_S} = 0.05$			$\sigma'_{FH_S} = 0.2$		
P_f	γ_H	γ_Z	γ_C	γ_H	γ_Z	γ_C
0.01	1.2	1.5	1.6	1.3	1.5	1.6
0.05	1.1	1.3	1.5	1.2	1.3	1.5
0.10	1.0	1.3	1.5	1.1	1.3	1.4
0.20	1.0	1.2	1.3	1.0	1.3	1.3
0.40	1.0	1.1	1.1	1.0	1.1	1.1

Shallow water. Design without model tests. γ_Z is used for rubble-mound and γ_C for clay subsoil.

	$\sigma'_{FH_S} = 0.05$			$\sigma'_{FH_S} = 0.2$		
P_f	γ_H	γ_Z	γ_C	γ_H	γ_Z	γ_C
0.01	1.2	1.5	1.6	1.3	1.5	1.6
0.05	1.1	1.4	1.5	1.2	1.4	1.5
0.10	1.1	1.3	1.3	1.2	1.3	1.3
0.20	1.0	1.3	1.3	1.1	1.2	1.3
0.40	1.0	1.1	1.1	1.1	1.1	1.1

Shallow water. Wave load determined by model tests. γ_Z is used for rubble-mound and γ_C for clay subsoil.

	$\sigma'_{FH_S} = 0.05$			$\sigma'_{FH_S} = 0.2$		
P_f	γ_H	γ_Z	γ_C	γ_H	γ_Z	γ_C
0.01	1.2	1.3	1.4	1.3	1.3	1.4
0.05	1.1	1.2	1.4	1.2	1.2	1.4
0.10	1.1	1.2	1.3	1.1	1.2	1.3
0.20	1.0	1.1	1.3	1.1	1.1	1.2
0.40	1.0	1.0	1.0	1.1	1.0	1.0

H_s^T	Significant wave height with return period T
B	Width of caisson
$\hat{U}_{Hor.Force}$	0.90, bias factor to be applied to the Goda horizontal wave force
$\hat{U}_{Ver.Force}$	0.77, bias factor to be applied to the Goda vertical wave force
$\hat{U}_{Hor.Moment}$	0.81, bias factor to be applied to the moment from the Goda horizontal wave forces around the shoreward heel of the base plate
$\hat{U}_{Ver.Moment}$	0.72, bias factor to be applied to the moment from the Goda vertical wave forces around the shoreward heel of the base plate
φ_d	$= \frac{\sin\varphi' \cos\psi}{1-\sin\varphi' \sin\psi}$
φ'	Effective friction angle of friction material (sand or rubble stone)
ψ	Dilation angle of friction material (sand or rubble stone)
ρ_c	Mass density of caisson
c_u	Undrained shear strength of clay

Table VI-6-24
Partial Safety Factors for Sliding Failure of Vertical Wall Caissons

Design equation

$$G = G(\gamma_H \hat{H}_s^T,\ \hat{\rho}_c,\ \hat{U}_{Hor.Force},\ \hat{U}_{Ver.Force},\ \hat{\zeta},\ \frac{1}{\gamma_Z}\hat{f},\ B)$$

$$= (\hat{F}_G - \hat{U}_{Ver.Force}\ \hat{F}_U)\frac{1}{\gamma_Z}\hat{f} - \hat{U}_{Hor.Force}\ \hat{F}_H \qquad \text{(VI−6−64)}$$

In calculation of $\hat{F_U}$ and $\hat{F_H}$ use wave height $\gamma_H \hat{H}_s^T$.

Deep water. Design without model tests.

	$\sigma'_{FH_S} = 0.05$		$\sigma'_{FH_S} = 0.2$	
P_f	γ_H	γ_Z	γ_H	γ_Z
0.01	1.4	1.7	1.5	1.7
0.05	1.3	1.4	1.4	1.4
0.10	1.3	1.2	1.4	1.3
0.20	1.2	1.2	1.3	1.2
0.40	1.1	1.0	1.1	1.1

Deep water. Wave load determined by model tests.

	$\sigma'_{FH_S} = 0.05$		$\sigma'_{FH_S} = 0.2$	
P_f	γ_H	γ_Z	γ_H	γ_Z
0.01	1.3	1.5	1.4	1.5
0.05	1.2	1.4	1.3	1.4
0.10	1.2	1.2	1.3	1.2
0.20	1.1	1.2	1.2	1.2
0.40	1.0	1.2	1.1	1.0

Shallow water. Design without model tests.

	$\sigma'_{FH_S} = 0.05$		$\sigma'_{FH_S} = 0.2$	
P_f	γ_H	γ_Z	γ_H	γ_Z
0.01	1.3	1.9	1.4	1.9
0.05	1.2	1.6	1.3	1.6
0.10	1.2	1.4	1.3	1.4
0.20	1.1	1.3	1.2	1.3
0.40	1.0	1.2	1.0	1.2

Shallow water. Wave load determined by model tests.

	$\sigma'_{FH_S} = 0.05$		$\sigma'_{FH_S} = 0.2$	
P_f	γ_H	γ_Z	γ_H	γ_Z
0.01	1.2	1.6	1.3	1.6
0.05	1.1	1.5	1.2	1.5
0.10	1.1	1.3	1.2	1.3
0.20	1.1	1.2	1.1	1.2
0.40	1.0	1.1	1.0	1.1

H_s^T	Significant wave height with return period T
B	Width of caisson
$\hat{U}_{Hor.Force}$	0.90, bias factor to be applied to the Goda horizontal wave force
$\hat{U}_{Ver.Force}$	0.77, bias factor to be applied to the Goda vertical wave force
$\hat{U}_{Hor.Moment}$	0.81, bias factor to be applied to the moment from the Goda horizontal wave forces around the shoreward heel of the base plate
$\hat{U}_{Ver.Moment}$	0.72, bias factor to be applied to the moment from the Goda vertical wave forces around the shoreward heel of the base plate
ρ_c	Mass density of caisson
F_G	Buoyancy reduced weight of caisson
F_H	Horizontal wave force calculated by the Goda formula
F_U	Wave induced uplift force calculated by the Goda formula
f	Friction coefficient

Table VI-6-25
Partial Safety Factors for Overturning Failure of Vertical Caissons

Design equation

$$G = G(\gamma_H \hat{H}_S^T,\ \hat{\rho}_c,\ \hat{U}_{Hor.Moment},\ \hat{U}_{Ver.Moment},\ \hat{\zeta},\ B)$$
$$= (\hat{M}_G - \hat{U}_{Ver.Moment}\ M_U) - \hat{U}_{Hor.Moment}\ M_H \qquad \text{(VI−6−65)}$$

In calculation of $\hat{M}_U$ and $\hat{M}_H$ use wave height $\gamma_H \hat{H}_s^T$.

Design without model tests.

	$\sigma'_{FH_S} = 0.05$	$\sigma'_{FH_S} = 0.2$
P_f	γ_H	γ_H
0.01	-	-
0.05	2.7	-
0.10	2.0	2.5
0.20	1.6	1.7
0.40	1.2	1.2

Wave load determined by model tests.

	$\sigma'_{FH_S} = 0.05$	$\sigma'_{FH_S} = 0.2$
P_f	γ_H	γ_H
0.01	2.1	2.3
0.05	1.7	1.9
0.10	1.4	1.6
0.20	1.3	1.4
0.40	1.1	1.2

H_s^T	Significant wave height with return period T
B	Width of caisson
$\hat{U}_{Hor.Force}$	0.90, bias factor to be applied to the Goda horizontal wave force
$\hat{U}_{Ver.Force}$	0.77, bias factor to be applied to the Goda vertical wave force
$\hat{U}_{Hor.Moment}$	0.81, bias factor to be applied to the moment from the Goda horizontal wave forces around the shoreward heel of the base plate
$\hat{U}_{Ver.Moment}$	0.72, bias factor to be applied to the moment from the Goda vertical wave forces around the shoreward heel of the base plate
ρ_c	Mass density of caisson
M_G	Moment of F_G around heel of caisson
M_H	Moment of F_H around heel of caisson
M_U	Moment of F_U around heel of caisson
F_G	Buoyancy reduced weight of caisson
F_H	Horizontal wave force calculated by the Goda formula
F_U	Wave induced uplift force calculated by the Goda formula

Table VI-6-26
Partial Safety Factors for Scour at Circular Vertical Wall Roundheads, Sumer and Fredsøe (1997), Design Without Model Tests

Design equation, cf. Equation VI-5-257

$$G = \frac{1}{\gamma_Z}\frac{\hat{S}}{\hat{B}} - 0.5\left[1 - \exp(-0.175\left[\hat{KC} - 1\right])\right] \qquad \text{(VI−6−66)}$$

where

$$KC = \frac{U_m T_p}{B}$$

In calculation of U_m (maximum wave orbital velocity at the bed with no structure) use the wave height $\gamma_H \hat{H}_s^T$.

Deep water.

	$\sigma'_{FH_S} = 0.05$		$\sigma'_{FH_S} = 0.2$	
P_f	γ_H	γ_Z	γ_H	γ_Z
0.01	2.0	2.4	2.0	2.4
0.05	2.0	2.0	2.0	2.0
0.10	2.0	1.8	2.0	1.8
0.20	2.0	1.5	2.0	1.5
0.40	2.0	1.2	2.0	1.2

Shallow water.

	$\sigma'_{FH_S} = 0.05$		$\sigma'_{FH_S} = 0.2$	
P_f	γ_H	γ_Z	γ_H	γ_Z
0.01	2.0	2.4	2.0	2.4
0.05	2.0	2.0	2.0	2.0
0.10	2.0	1.8	2.0	1.8
0.20	2.0	1.5	2.0	1.5
0.40	2.0	1.2	2.0	1.2

Table VI-6-27
Partial Safety Factors for Toe Berm Rock Armor Failure in Front of Vertical Wall Caissons, Design Without Model Tests

Design equation (cf. Table VI-5-48)

$$G = \frac{1}{\gamma_Z}\hat{\Delta}\,\hat{D}_n\left(5.8\,\frac{\hat{h}_b}{\hat{h}_s} - 0.60\right)(N_{od})^{0.19} - \gamma_H \hat{H}_S^T \qquad \text{(VI−6−67)}$$

Deep water.

	$\sigma'_{FH_S} = 0.05$		$\sigma'_{FH_S} = 0.2$	
P_f	γ_H	γ_Z	γ_H	γ_Z
0.01	1.6	1.3	1.7	1.3
0.05	1.4	1.2	1.5	1.2
0.10	1.3	1.2	1.4	1.2
0.20	1.2	1.1	1.3	1.1
0.40	1.1	1.0	1.2	1.0

Shallow water.

	$\sigma'_{FH_S} = 0.05$		$\sigma'_{FH_S} = 0.2$	
P_f	γ_H	γ_Z	γ_H	γ_Z
0.01	1.5	1.5	1.6	1.5
0.05	1.3	1.3	1.4	1.3
0.10	1.2	1.2	1.3	1.2
0.20	1.1	1.2	1.2	1.2
0.40	1.1	1.0	1.2	1.0

VI-6-7. References.

Berengu□r and Baonza 1995
Berengu□r, J. M., and Baonza, A. 1995. "Hollowed Cube Research," Final Proceedings, EU-MAST 2 Project MAS 2- CT92 - 0042, Rubble-Mound Breakwater Failure Modes, Aalborg University, Denmark.

Burcharth 1991
Burcharth, H. F. 1991. "Introduction of Partial Coefficient in the Design of Rubble Mound Breakwaters," *Proceedings of the Conference on Coastal Structures and Breakwaters*, Institution of Civil Engineers, London, Thomas Telford Publishing, London, UK, pp 543-565.

Burcharth 1992
Burcharth, H. F. 1992. "Uncertainty Related to Environmental Data and Estimated Extreme Events," Final Report of PIANC Working Group 12, Group B, June 1992.

Burcharth and Liu 1995a
Burcharth, H. F., and Liu, Z. 1995a. "2-D Model Tests of Dolos Breakwater," Final Proceedings, EU-MAST 2 project MAS 2 - CT92 - 0042, Rubble Mound Breakwater Failure Modes, Aalborg University, Denmark.

Burcharth and Liu 1995b
Burcharth, H. F., and Liu, Z. 1995b. "Design Formulae for Hydraulic Stability and Structural Integrity of Dolos Breakwater Roundheads," Final Proceedings, EU-MAST 2 project MAS 2 - CT92 -0042, Rubble Mound Breakwater Failure Modes, Aalborg University, Denmark.

Burcharth and Sørensen 1999
Burcharth, H. F., and Sørensen, J. D. 1999. "The PIANC Safety Factor System for Breakwaters," *Proceedings of Coastal Structures' 99*, J. J. Losada and A. A. Balkema, eds., Vol 2, pp 1125-1144.

Cornell 1969
Cornell, C. A. 1969. "A Reliability-Based Structural Code," *ACI-Journal*, Vol 66, pp 974-985.

De Waal and van der Meer 1992
De Waal, J. P., and van der Meer, J. W. 1992. "Wave Run-Up and Overtopping of Coastal Structures," *Proceedings of the 23rd International Coastal Engineering Conference*, Vol 2, pp 1758-1771.

Fredsøe and Sumer 1997
Fredsøe, J., and Sumer, B. M. 1997. "Scour at the Roundhead of a Rubble Mound Breakwater," *Coastal Engineering,* Elsevier, Vol. 29, No 3-4, pp 231-262.

Hasofer and Lind 1974
Hasofer, A. M., and Lind, N. C. 1974. "Exact and Invariant Second-Moment Code Format," *Journal of Engineering Mechanics Division*, American Society of Civil Engineers, Vol 100, No. EM1, pp 111-121.

Hansen 1979
Hansen, B. 1979. "Definition and Use of Friction Angles," Proceedings of the Seventh European Conference on Soil Mechanics and Foundation Engineering, Brighton, UK.

Sumer and Fredsøe 1997
Sumer, B. M., and Fredsøe, J. 1997. "Scour at the Head of a Vertical-Wall Breakwater," *Coastal Engineering*, Elsevier, Vol 29, No. 3-4, pp 201-230.

Wen and Chen 1987
Wen, Y. K., and Chen, H. C. 1987. "On Fast Integration for Time Variant Structure Reliability," *Probabilistic Engineering Mechanics*, Vol 2, pp 156-162.

VI-6-8. Acknowledgments.

Author: Dr. Hans F. Burcharth, Department of Civil Engineering, Aalborg University, Aalborg, Denmark.

Reviewers: H. Lee Butler (CHL retired), Dr. Steven A. Hughes, and Jeffrey A. Melby, Coastal and Hydraulics Laboratory (CHL), U.S. Army Engineer Research and Development Center (ERDC), Vicksburg, MS.

VI-6-9. Symbols.

α	Weibull distribution parameter
α	Armor slope angle
ß	Weibull distribution parameter
β_{HL}	Hasofer and Lind reliability index
β	Reliability index
γ_i	Partial safety factors
λ	Number of observations per year
μ	Mean value
ρ_c	Mass density of caisson [force/length^3]
ρ_w	Mass density of water (salt water = 1,025 kg/m^3 or 2.0 slugs/ft^3; fresh water = 1,000 kg/m^3 or 1.94 slugs/ft^3) [force-time^2/length^4]
ρ_s	Mass density of concrete [force/length^3]
ρ_s	Block density
$\sigma!_{FHs}$	Coefficient of variation
σ	Standard deviation
Ψ	Angle of dilation [degrees]

ν	Packing density
$\nu!$	Angle of friction in granular material [degrees]
B	Width of caisson [length]
c_u	Undrained shear strength of clay [force/length^2]
D	Relative number of units
D_n	Nominal block diameter [length]
f	Friction coefficient [dimensionless]
F_U	Wave induced uplift force [force]
F_H	Horizontal wave force [force]
F_G	Buoyancy reduced weight of caisson [force]
g	Failure function
H^T_s	Significant wave height with return period T
h	Water depth [length]
$h_S!$	Threshold level
H_S	Significant wave height [length]
K_D	Coefficient signifying the degree of damage [dimensionless]
L_{om}	Deepwater wave length corresponding to mean wave period [length]
L_{op}	Deepwater wave length corresponding to the peak wave period [length]
M_G	Moment around the heel of caisson by buoyancy-reduced weight of the caisson [length-force]
M_H	Moment around the heel of caisson by wave induced horizontal force [length-force]
M_U	Moment around the heel of caisson by wave induced uplift force [length-force]
N_{od}	Number of units displaced out of the armor layer
N_z	Number of waves
N	Number of data points
P	Notational permeability parameter (Figure VI-5-11)
P_f	Probability of failure
R_u	Maximum runup or water-surface elevation measured vertically from the still-water level [length]
r	Dolos waist ratio [dimensionless]

R_f Reliability

R Variable representing the variations in resistance between nominally identical structures

s_{om} Wave steepness ($=H_s/L_{om}$)

s_{op} Deepwater wave steepness [dimensionless]

$\boldsymbol{S}$ Represents the maximum load effects within a period of time

T_L Design lifetime [years]

T_m Wave period [time]

U_m Maximum wave orbital velocity at the bed with no structure [length/time]

W Water level [length]

CHAPTER 7

Example Problems

TABLE OF CONTENTS

Page

VI-7-1. Introduction VI-7-1

VI-7-2. Wave Runup VI-7-2

VI-7-3. Wave Overtopping VI-7-21

VI-7-4. Armor Layer Stability VI-7-29

VI-7-5. Stability of Vertical Walled Bulkheads and Caissons VI-7-70

VI-7-6. Forces on Cylindrical Piles VI-7-86

VI-7-7. References VI-7-89

VI-7-8. Acknowledgements VI-7-91

VI-7-9. List of Symbols VI-7-91

List of Figures

Page

Figure VI-7-1. Smooth faced levee VI-7-18

Figure VI-7-2. Overtopping of an impermeable structure VI-7-25

Figure VI-7-3. Percent damage curve for CBBT South Island revetment VI-7-44

Figure VI-7-4. Homogeneous breakwater cross section VI-7-58

Figure VI-7-5. Variations in design water level and breakwater crest elevations VI-7-60

CHAPTER VI-7

Example Problems

VI-7-1. Introduction.

a. "Only the application makes the rod into a lever" is the famous remark of the philosopher Ludwig Wittgenstein (Pitcher 1964). All engineers remember their university days (and nights) doing homework problems that turned the lectures (rod) into useful information and tools (lever) by the application of the materials presented. Those textbooks with many example problems (and answers to the homework problems) always rate as the best.

b. The *Coastal Engineering Manual* (CEM) is divided into six parts. The first four parts mainly cover the science surrounding the subject while the remaining Parts V and VI summarize the latest engineering knowledge, studies, designs, and constructions. Part VI-7 has been set aside for example problems. This chapter includes wave runup, wave overtopping, armor-layer stability, and forces on vertical-front structures.

c. The single, most important coastal engineering advance has been the use of irregular water-wave spectra in the analytical treatment, physical (laboratory) experiments, and numerical model simulations to study wave runup, overtopping, and armor-layer stability. Coastal engineers must adopt this new technology quickly to prepare more cost-effective and safe designs in the future.

d. Throughout the example problems chapter, several references to the *Shore Protection Manual* (1984) are made. By referencing the older document, an attempt has been made to identify differences in engineering practice between the older *Shore Protection Manual* and the newer *Coastal Engineering Manual*.

VI-7-2. Wave Runup.

EXAMPLE PROBLEM VI-7-1

FIND: The surf-similarity parameter (also called the Iribarren number) for use in wave runup and wave overtopping calculations for long-crested, irregular waves on impermeable (without water penetration) and permeable slopes.

GIVEN: An impermeable structure has a smooth slope of 1 on 2.5 and is subjected to a design significant wave, H_s = 2.0 m (6.6 ft) measured at a gauge located in a depth, d = 4.5 m (14.8 ft). Design wave peak period is T_p = 8 s. Water depth at structure toe at high water is d_{toe} = 3.0 m (9.8 ft). (Assume no change in the refraction coefficient between the structure and the wave gauge.)

SOLUTION: The surf-similarity parameter for irregular waves depends on the wave steepness and structure slope. Two definitions are given in Equation VI-5-2 formulated with either the peak wave period, T_p or the mean wave period, T_m; but both use the significant wave height at the toe of the structure.

(Sheet 1 of 5)

EXAMPLE PROBLEM VI-7-1 (Continued)

Ideally, a spectral wave model would be used to shoal the irregular wave H_s to the structure toe. However, for purposes of illustration, it is assumed that H_s will shoal according to linear wave theory. For swell-type spectra this is reasonable assumption, but linear shoaling overestimates shoaling of fully saturated storm spectra.

Item 1. Linear, regular wave shoaling (illustrated by several of the available methods).

(a) Deep water.

First calculate the deep water, unrefracted wave height, H_o' from where measured back out to deep water. Using the depth where waves measured, and assuming $T = T_p = 8$ s and $H = H_s$ gives

$$\frac{d}{L_o} = \frac{2\pi d}{gT^2} = \frac{2\pi(4.5\text{ m})}{(9.81\text{ m/s}^2)(8\text{ s})^2} = 0.0450$$

(1) From the *Shore Protection Manual* (1984), Table C-1, Appendix C for $d/L_o = 0.0450$.

$$\frac{H}{H_o'} = 1.042, \text{ the shoaling coefficient, } k_s$$

Therefore,

$$H_o' = \frac{2.0\text{ m}}{1.042} = 1.92\text{ m}(6.3\text{ ft})$$

(2) or, using ACES (Leenknecht et al. 1992), Snell's Law, crest angle = 0.0°

$H_o' = 1.92$ m (6.3 ft)

(3) or, using explicit approximations (e.g., Nielsen 1984)

$$\frac{C_g}{C_o} = \sqrt{k_o d}\left[1 - \frac{1}{2}k_o d + \frac{7}{72}(k_o d)^2\right]$$

$$k_o = \frac{2\pi}{L_o} = \frac{4\pi^2}{gT^2}$$

$$K_s = \sqrt{0.5\,C_o / C_g}$$

EXAMPLE PROBLEM VI-7-1 (Continued)

gives

$$k_o d = 0.28296$$

$$\frac{C_g}{C_o} = 0.46082$$

$$K_s = 1.0416$$

$$H_o ¢= 1.920 \text{ m} \left(6.3 \text{ ft}\right)$$

(b) Toe of structure

Next, shoal the deepwater wave to a depth, d = 3.0 m (9.8 ft) at the toe of the structure

(1) From the *Shore Protection Manual* (1984), Table C-1, Appendix C for

$$\frac{d_{toe}}{L_o} = \frac{2\pi d_{toe}}{gT^2} = \frac{2\pi\left(3.0\ m\right)}{\left(9.81\ m/s^2\right)\left(8\ s\right)^2} = 0.030023$$

$$K_s = \frac{H_{toe}}{H_o'} = 1.125$$

$$H_{toe} = 1.92\ m\ \left(1.125\right) = 2.16\ m \left(7.09\ ft\right)$$

(2) From ACES, Snell's law, crest angle = 0.0°.

H_{toe} = 2.161 (7.09 ft)

(3) From explicit approximations

$$k_o d = 0.18864$$

$$\frac{C_g}{C_o} = 0.39486$$

$$K_s = 1.1253$$

$$H_{toe} = 2.161 \text{ m} \left(7.09 \text{ ft}\right)$$

(Sheet 3 of 5)

EXAMPLE PROBLEM VI-7-1 (Continued)

Item 2. Deepwater wave steepness, s_{op}

$$\left(s_{op}\right)_{toe} \equiv \frac{\left(H_s\right)_{toe}}{L_{op}} = \frac{2\pi H_{toe}}{gT_p^{\,2}} = \frac{2\pi\left(2.16\text{ m}\right)}{9.81\text{ m/s}^2\left(8\text{ s}\right)^2}$$

$$s_{op} = 0.02162$$

Item 3. Surf-similarity parameter, ξ_{op}

Finally, the surf-similarity parameter, ξ_{op} as defined by Equation VI-5-2 gives

$$\xi_{op} \equiv \frac{\tan\alpha}{\sqrt{s_{op}}} = \frac{1/2.5}{\sqrt{0.02162}} = \frac{0.4}{0.1469}$$

Therefore,

$$\xi_{op} = 2.72$$

Note that the subscript notation means using the deepwater wavelength, L_o, and the peak wave period, T_p, to calculate ξ_{op}.

Item 4. Surf-similarity parameter, ξ_{om}

The mean wave period, T_m, requires knowledge of variations in the width of the wave spectrum. From Section VI-5-2-a-(3)-(b) for the theoretical spectrums

JONSWAP spectra $T_m/T_p = 0.79$ to 0.87

or

PIERSON-MOSKOWITZ spectra $T_m/T_p = 0.71$ to 0.82

Therefore, assuming $T_m/T_p = 0.76$, gives $T_m = 6.1$ s, hence

$$s_{om} = \frac{H_{toe}}{\frac{g}{2\pi}T_m^{\,2}} = \frac{\left(2\pi\right)\left(2.16\text{ m}\right)}{9.81\text{ m/s}^2\left(6.1\text{ s}\right)^2} = 0.03718$$

(Sheet 4 of 5)

EXAMPLE PROBLEM VI-7-1 (Continued)

Therefore,

$$\xi_{om} \equiv \frac{\tan\alpha}{\sqrt{s_{om}}} = \frac{1/2.5}{\sqrt{0.03718}} = \frac{0.4}{0.1928}$$

$$\xi_{om} = 2.07$$

Both ξ_{op} and ξ_{om} are employed in wave runup and overtopping formulations.

DISCUSSION: In general (for either ξ_{op} or ξ_{om})

$$\xi_o \equiv \frac{\tan\alpha}{\sqrt{s_o}}$$

$$s_o \equiv \frac{H_s}{L_o} = \frac{2\pi H_s}{gT^2}$$

$$\xi_o \equiv \frac{(\tan\alpha)T}{\left(\frac{2\pi}{g}\right)^{1/2}(H_s)^{1/2}}$$

or

$$\xi_o \equiv \frac{T}{(K)\cot\alpha(H_s)^{1/2}}$$

where k is a constant.

(1) As T increases, ξ_o increases

(2) As cot α increases (flatter slope), ξ_o decreases

(3) As H_s increases, ξ_o decreases, nonlinearly

(Sheet 5 of 5)

EXAMPLE PROBLEM VI-7-2

FIND:
(a) The height above the still-water level (SWL) to which a new revetment must be built to prevent wave overtopping by the design wave. The structure is to be impermeable.

(b) The reduction in required structure height if uniform-sized armor stone is placed on the slope.

GIVEN: An impermeable structure has a smooth slope of 1 on 2.5 and is subjected to a design, significant wave H_s = 2.0 m (6.6 ft) measured at a gauge located in a depth d = 4.5 m (14.8 ft). Design wave peak period is T_p = 8 s. Water depth at structure toe at high water is d_{toe} = 3.0 m (9.8 ft).

SOLUTION: From Example Problem VI-7-1, linear wave theory estimates the wave height due to wave shoaling as

$$\left(H_s\right)_{toe} = 2.16 \text{ m} \left(7.1 \text{ ft}\right)$$

and the surf-similarity parameter as

$$\xi_{op} = 2.72$$

To prevent wave overtopping, the wave runup value at the 2 percent probability of exceedance level is calculated. Figure VI-5-3 displays the considerable scatter in the data for smooth slopes, irregular, long-crested, head-on waves and Table VI-5-2 gives the coefficients for use in Equation VI-5-3 when

$$\xi_{op} > 2.5$$

Namely

$$\frac{R_{u2\%}}{\left(H_s\right)_{toe}} = -0.2\xi_{op} + 4.5$$

$$= -0.2\left(2.72\right) + 4.5 = -0.544 + 4.5 = 3.956$$

R_{u2}% = 3.956 (2.16 m) = 8.545 m (28.0 ft)

(Sheet 1 of 4)

EXAMPLE PROBLEM VI-7-2 (Continued)

So that,

(a) Smooth slopes

(1) To prevent overtopping; $R_{u2\%}$ = 8.55 m (28.1 ft)
(Note that $\gamma_r = \gamma_b = \gamma_h = \gamma_\beta = 1.0$ are taken in Equation VI-5-3 for smooth, no berm, Rayleigh distribution, and zero incidence angle conditions, respectively.)
Another set of runup data for smooth slopes is presented in Figure VI-5-5 and Equation VI-5-6 (from de Waal and van der Meer 1992). When

$$\xi_{op} > 2.0$$

namely

$$\frac{R_{u2\%}}{(H_s)_{toe}} = 3.0$$

hence,

(2) To prevent overtopping; $R_{u2\%}$ = 3.0 (2.18 m) = 6.48 m (21.3 ft)
Note that the data in Figure VI-5-5 is for slopes milder than 1 on 2.5, and thus may not be appropriate for this example.

(b) Rough slopes
The surface roughness reduction factor γ_r for Equation VI-5-3 is given in Table VI-5-3 and lies in the range, γ_r = 0.5-0.6 for one or more layers of rock.

Use γ_r = 0.55 to get

(1) Equation VI-5-3 $\frac{R_{u2\%}}{(H_s)_{toe}} = 3.956\,\gamma_r = 3.956(0.55) = 2.176$

hence

$R_{u2\%}$ = 2.176 (2.16 m) = 4.70 (15.4 ft)

(Sheet 2 of 4)

EXAMPLE PROBLEM VI-7-2 (Continued)

and

(2) Equation VI-5-6 $\frac{R_{u2\%}}{(H_s)_{toe}} = 3.0\ \gamma_r = 3.0(0.55) = 1.65$

$R_{u2\%}$ = 1.65 (2.16 m) = 3.56 m (11.7 ft)

(3) The Delft Hydraulics test program (Table VI-5-4) also provided data for impermeable rock slopes. Here, the surf-similarity parameter based on mean wave period, ξ_{om}, is employed to develop design Equation VI-5-12 with coefficients in Table VI-5-5 for a wide range of exceedance probabilities. The ξ_{om}-value for this example (ξ_{om} = 2.07) was estimated in Example Problem VI-7-1.

When $\xi_{om} > 1.5$

$$\frac{R_{u2\%}}{(H_s)_{toe}} = 1.17(\xi_{om})^{0.46}$$

$$= 1.17(2.07)^{0.46} = 1.635$$

Therefore, $R_{u2\%}$ = 1.635 (2.16 m) = 3.353 m (11.6 ft) using coefficients for B and C at the 2% exceedance probability level. This result is very close to that in the preceding Equation VI-5-6 (2) taking γ_r = 0.55.

(4) Partial safety factors, γ_H and γ_z and $\hat{R}_{u2\%}$. The Delft Hydraulics data set has been analyzed for partial safety factors as discussed in Part VI-6 and presented in Table VI-6-17.

Assume the annual failure probability P_f = 0.10 (90% reliability). For relatively low uncertainty in knowledge of the wave height (σ'_{FHS} = 0.05) the values associated with Equation VI-6-57 yield

$\gamma_H\ \gamma_z$ = 1.2 (1.06) = 1.272

(Sheet 3 of 4)

EXAMPLE PROBLEM VI-7-2 (Concluded)

and a probabilistic estimate, $\hat{R}_{u2\%}$ = 1.272 (3.53 m) = 4.49 m (14.7 ft). If the uncertainty is higher regards wave height (σ'_{FHS} = 0.2) then

$$\gamma_H \gamma_z = 1.3\ (1.08) = 1.404$$

and a probabilistic estimate, $\hat{R}_{u2\%}$ = 1.404 (3.53 m) = 4.96 m (16.3 ft).

The range of $\hat{R}_{u2\%}$ = 4.5-5.0 m (14.8-16.4 ft) brackets the estimate of $\hat{R}_{u2\%}$ = 4.7 m (15.4 ft) as found from Equation VI-5-3. The higher estimate of the $\hat{R}_{u2\%}$ value found from Equation VI-5-3 could also be explained as being reliable at the 90-percent annual level.

DISCUSSION: As seen in Figure VI-5-3, at ξ_{op} = 2.5, $R_{u2\%}/H_s$ reaches a maximum value. Solving for the variables involved in ξ_{op} gives approximately

Metric system

$$\frac{(\tan\alpha)\,T_p}{\left(H_{toe}\right)^{1/2}} = 2.0$$

English system

$$\frac{(\tan\alpha)\,T_p}{\left(H_{toe}\right)^{1/2}} = 1.10$$

For the preceding example, keeping tanα = 0.4, H_{toe} = 2.16 m gives

(T_p) = 7.35 s for maximum runup

For the preceding example, keeping T_p = 8.0 s, H_{toe} = 2.16 m gives

tan α = 0.36, cot α = 2.7 for maximum runup.

Using a steeper or flatter slope will reduce the wave runup, all else being equal.

(Sheet 4 of 4)

EXAMPLE PROBLEM VI-7-3

FIND: The height above the SWL to which a rock-armored structure (permeable) should be built to prevent wave overtopping by the design wave.

GIVEN: The same information for Example Problem VI-7-2 as summarized as follows, but now for a permeable breakwater (jetty) structure

slope = 1:2.5
H_s = 2.0 m (6.6 ft)
measured at d = 4.5 m (14.8 ft)
T_p = 8 s
d_{toe} = 3.0 m (9.8 ft)
ξ_{om} = 2.07
$(H_s)_{toe}$ = 2.16 m

SOLUTION: Core permeability may significantly influence wave runup. Notational permeability coefficients are defined in Figure VI-5-11. The previous Example Problem VI-7-2 was for P = 0.1 defined as impermeable. Test results shown in Figures VI-5-12 are with $P = 0.1$ and $P = 0.5$ and clearly reveal the runup reduction when $\xi_{om} > 3$ for permeable structures. Equation VI-5-13 has been developed as the central fit to the permeable data with coefficients again found in Table VI-5-5. For $R_{u2\%}$, $B = 1.17$, $C = 0.46$, and $D = 1.97$. Selection of the appropriate equation requires calculation of

$$\left(D/B\right)^{1/C} = \left(\frac{1.97}{1.17}\right)^{\frac{1}{0.46}} = \left(1.68\right)^{2.17} = 3.10$$

Because $1.5 < \xi_{om} < (D/B)^{1/C}$, use the equation

$$\frac{R_{u2\%}}{\left(H_s\right)_{toe}} = B\left(\xi_{om}\right)^C$$

$$= 1.17\left(2.07\right)^{0.46} = 1.635$$

Therefore, $R_{u2\%} = 1.635$ (2.16 m) = 3.53 m (11.6 ft), and this is a similar result as for $P = 0.1$, impermeable slopes.

For the 2% runup exceedence level a value of

$$\xi_{om} \equiv \frac{\tan\alpha}{\sqrt{s_{om}}} \geq 3.10$$

EXAMPLE PROBLEM VI-7-3 (Concluded)

is the point where the permeable core begins to reduce wave runup. Longer period waves will increase ξ_{om}, but the runup remains constant because of the structure permeability. At this limit,

$$\frac{R_{u2\%}}{\left(H_s\right)_{toe}} = D = 1.97 \text{ (see Table VI-5-5)}$$

Therefore,

$$\left(R_{u2\%}\right)\max = 1.97 \text{ (2.16 m)} = 4.25 \text{ m (13.9 ft) for } T_m \geq 9.1 \sec \left(T_p \approx 12s\right)$$

for a slope of 1 to 2.5.

(Sheet 2 of 2)

EXAMPLE PROBLEM VI-7-4

FIND: The height above the still-water level to which a revetment must be built to prevent wave overtopping by the design wave (same as Example Problem VI-7-2) but for the following conditions:

(a) Statistical distributions of wave runup

(b) Influence of shallow water on wave runup

(c) Influence of wave angle and directional spreading on wave runup

GIVEN: Same conditions as Example Problem VI-7-2 for smooth slope

SOLUTION: Equation VI-5-3 holds in general for any $R_{ui\%}$ defined as the runup level exceeded by *i%* of the incident waves. Coefficients A and C depend on both ξ_{op} and i for Rayleigh distributed wave heights.

(a) Statistical distributions

(1) Significant runup. Figure VI-5-4 displays the data scatter and Table VI-5-2 provides coefficients to calculate the significant wave runup, R_{us}. Again from Example Problem VI-7-1

$$\left(H_s\right)_{toe} = 2.16 \text{ m } (7.1 \text{ ft})$$

and

$$\xi_{op} = 2.72$$

For R_{us} in the range $2 < \xi_{op} < 9$

$$\frac{R_{us}}{\left(H_s\right)_{toe}} = -0.25\,\xi_{op} + 3.0$$

$$= -0.25\left(2.72\right) + 3.0 = -0.68 + 3.0 = 2.32$$

therefore,

$$R_{us} = 2.32\ (2.16 \text{ m}) = 5.01 \text{ m } (16.4 \text{ ft})$$

(Sheet 1 of 5)

EXAMPLE PROBLEM VI-7-4 (Continued)

The *Shore Protection Manual* (1984) calculated a runup value of 5.6 m (18.4 ft) for Example Problem No. 4 for the same data taking the design wave as the significant wave height. The Rayleigh distribution for wave heights gives the following relationships for extreme events

$$\frac{H_{0.1}}{H_{0.135}} = \frac{H_{0.1}}{H_s} = 1.072$$

$$\frac{H_{0.02}}{H_s} = 1.398$$

$$\frac{H_{0.01}}{H_s} = 1.516$$

If the wave runup also followed a Rayleigh distribution, then it might be expected that

$$\frac{R_{u0.2}}{R_{us}} = 1.398$$

gives

$R_{u0.2}$ = 1.398 (5.01 m) = 7.0 m (23.0 ft)

This result is much lower than $R_{u2\%}$ = 8.55 m (28.1 ft) calculated in Example Problem-7-2 for the smooth slope. In general, values for R_{us} and $R_{u2\%}$ calculated from Equation VI-5-3 and coefficients in Table VI-5-2 do not follow a Rayleigh distribution for wave runup.

(2) Statistical distribution of runup on permeable slopes

For the following restrictions: (1) Rayleigh distributed wave heights
(2) Permeable, rock armored slopes
(3) Slope, cot α > 2

Equation VI-5-15 says

$$R_{up\%} = B\ (-ln\ p)^{1/C}$$

where

$R_{up\%}$ = runup level exceeded by p% of runup

and

B, C are calculated from Equation VI-5-16 and 17, respectively

[1] See discussion, p. VI-7-16.

(Sheet 2 of 5)

EXAMPLE PROBLEM VI-7-4 (Continued)

From Example Problem VI-7-1

$\xi_{om} = 2.07$ ($S_{om} = 0.03718$)

and using the values for the permeable slope in Example Problem VI-7-3

$P = 0.5$

$\tan\alpha = 0.4$

Equation VI-5-18 gives

$$\xi_{omc} = \left(5.77\, P^{0.3}\sqrt{\tan\alpha}\right)^{\left[1/(P+0.75)\right]}$$

$$= \left(5.77(0.5)^{0.3}\sqrt{0.4}\right)^{\left[1/(1.25)\right]}$$

$$= (2.964)^{0.8}$$

$$= 2.385$$

Because

$$\xi_{om} < \xi_{omc}$$

The value of C in Equation VI-5-17 is given for plunging waves as

$$C = 3.0(\xi_{om})^{-3/4}$$

$$= 3.0(2.07)^{-3/4} = 1.738$$

and

$$\frac{1}{C} = 0.5754$$

(NOTE: When $C = 2$, Equation VI-5-15 becomes the Rayleigh distribution)

The scale parameter from Equation VI-15-16 becomes

$$B = H_s\left[0.4(s_{om})^{-1/4}(\cot\alpha)^{-0.2}\right]$$

or

(Sheet 3 of 5)

EXAMPLE PROBLEM VI-7-4 (Continued)

$$= 2.16 \text{ m}\left[0.4\left(0.03718\right)^{-1/4}\left(2.5\right)^{-0.2}\right]$$
$$= 2.16 \text{ m}\left[0.4\left(2.2773\right)\left(0.83255\right)\right]$$
$$= 2.16 \text{ m}\left[0.7584\right]$$
$$B = 1.638 \text{ m}$$

Now check previous results using the above values for B and C in Equation VI-5-15

$$R_{u2\%} = 1.638 \text{ m } \left[-\ln\left(0.02\right)\right]^{1/1.738}$$
$$R_{u2\%} = 1.638 \text{ m } \left(3.912\right)^{0.5754}$$
$$= 1.638 \text{ m } \left(2.192\right)$$
$$R_{u2\%} = 3.59 \text{ m (11.8 ft) } \left[\text{(From Example Problem VI-7-3, } R_{u2\%} = 3.53 \text{ m (11.6 ft)}\right]$$

and

$$R_{us} = 1.638 \text{ m } \left[-\ln\left(0.135\right)\right]^{0.5754}$$
$$R_{us} = 1.638 \text{ m } \left(2.002\right)^{0.5754}$$
$$= 1.638 \text{ m } \left(1.491\right)$$
$$R_{us} = 2.44 \text{ m (8.0 ft)}$$

now

$$\frac{R_{u2\%}}{R_{us}} = \frac{3.59 \text{ m}}{2.44 \text{ m}} = 1.47$$

which does not give the same ratio as the Rayleigh distribution for wave heights where $H_{2\%} = 1.398\ H_s$.

(Sheet 4 of 5)

EXAMPLE PROBLEM VI-7-4 (Concluded)

At the 1 percent level

$$R_{u1\%} = 1.638 \text{ m } \left[-\ln(0.01)\right]^{0.5754}$$
$$= 1.638 \text{ m } (4.605)^{0.5754}$$
$$= 1.638 \text{ m } (2.4079) = 3.94 \text{ m (12.9 ft)}$$

For design, wave runup values calculated at the 2 percent exceedance probability level are considered a reasonable upper limit ". . . to prevent wave overtopping."

(b) Influence of shallow water on wave runup

Assuming the breaker index for shallow-water wave breaking is given by the ratio

$$\left(\frac{H}{d}\right)_b = 0.78$$

then

$$H_b = 0.78\, d = 0.78\ (3.0) = 2.34 \text{ m (7.7 ft)}$$

Therefore, because $H_s = 2.16$ m < H_b, no breaking occurs. Therefore, assuming $_h = 1.0$ is justified.

Note that if the design water depth at the structure toe dropped to 2.8 m (9.2 ft), then breaking begins. Equation VI-5-10 can only be applied where $H_{2\%}$ and H_s are known from field data or numerical model results.

(c) Influence of wave angle and directional spreading

As seen in Equation VI-5-11, the previous results hold for wave angles, β less than 10 deg from normal incidence of long-crested swell-type, wave spectrums. Angles of incidence larger than 10 deg will reduce the wave runup ($\gamma_\beta < 1.0$).

DISCUSSION: For other conditions, the statistical distribution of the wave runup has not been analyzed.

(Sheet 5 of 5)

EXAMPLE PROBLEM VI-7-5

FIND: Determine the wave runup at the 2 percent exceedance probability level for a composite slope shown in the following.

GIVEN: A smooth-faced breakwater of composite slope (m) shown with water depth, d_{toe} = 1.2 m (3.9 ft) is subjected to a significant wave height in deep water H_o' = 1.5 m (4.9 ft) and T_p = 8 s. The offshore slope is 1:20.

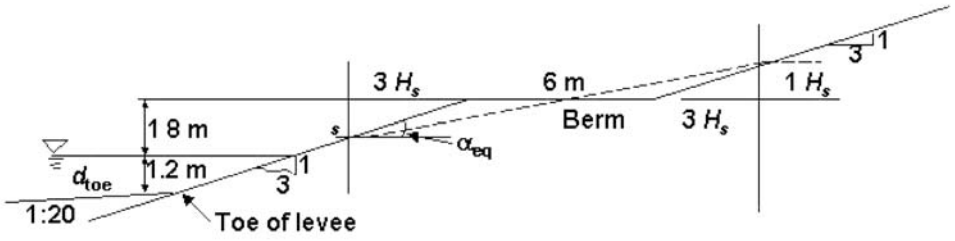

Figure VI-7-1. Smooth faced levee

SOLUTION:
(1) Wave height, *(H_s) toe*

(a) SPM (1984)

$$\frac{H_o'}{gT^2} = \frac{1.5 \text{ m}}{9.81 \text{ m/s}^2 (8 \text{ s})^2} = 0.0024$$

From Figure 7-3 (*Shore Protection Manual* 1984), at m = 0.05

$$\frac{H_b}{H_o'} = 1.46 \text{ or } H_b = 1.46 \text{ (1.5 m)} = 2.19 \text{ m (7.19 ft)}$$

From Figure 7-2, *Shore Protection Manual* (1984), for m = 0:05 and

$$\frac{H_b}{gT^2} = \frac{2.19 \text{ m}}{9.81 \text{ m/s}^2 \left(8 \text{ s}\right)^2} = 0.0035$$

(Sheet 1 of 3)

EXAMPLE PROBLEM VI-7-5 (Continued)

$$\frac{d_b}{H_b} = 0.93$$

$d_b = 0.93\ (2.19\ \text{m}) = 2.04\ \text{m}\ (6.68\ \text{ft})$

and occurs about 17 m (56 ft) in front of toe

(b) ACES (Leenknecht et al. 1992)
Goda method not applicable for $d < 3.048$ m (10 ft)

Linear theory/Snell's law - Wave broken, $H_b = 2.41$ m, $d_b = 2.33$ m gives

$$\frac{d_b}{H_b} = \frac{2.33}{2.41} = 0.97 \qquad \text{(Checks okay)}$$

(c) Assume wave energy decay continues from $d_b = 2.1$ - 2.3 m to toe of levee, hence,

$$\left(H\right)_{\text{toe}} = \frac{d_b}{0.93} = \frac{1.2}{0.93} = 1.29\ \text{m}\ (4.2\ \text{ft})$$

Use $(H_s)_{\text{toe}} = 1.29$ m at toe of levee

(2) Berm influence factor, γ_b

(a) Breaking wave surf similarity parameter based on an equivalent slope, ξ_{eq}.
(See Figure VI-7-1)

equivalent structure slope $\alpha_{eq} = \tan^{-1}\left[\frac{1.29}{3+3(1.29)}\right] = \tan^{-1} 0.188 = 10.63°$ (1:5.3 slope)

average slope

$$\alpha = \tan^{-1} 0.333 = 18.43°$$

$$s_{op} \equiv \frac{\left(H_s\right)_{toe}}{L_{op}} = \frac{2\pi\left(H_s\right)_{toe}}{gT_p^2} = \frac{2\pi\left(1.29\right)}{9.81\ \text{m/s}^2\,(8\ \text{s})^2} = 0.01291$$

EXAMPLE PROBLEM VI-7-5 (Concluded)

therefore

$$\xi_{eq} = \frac{\tan \alpha_{eq}}{\sqrt{s_{op}}} = \frac{0.188}{\sqrt{0.01291}} = 1.65$$

$$\xi_{op} = \frac{\tan \alpha}{\sqrt{s_{op}}} = \frac{0.333}{\sqrt{0.01291}} = 2.93$$

From Equation VI-5-8

$$\gamma_b = \frac{\xi_{eq}}{\xi_{op}} = \frac{1.65}{2.93} = 0.56$$

Since $0.6 < \gamma_b$ 1.0, use $\gamma_b = 0.6$

For $\xi_{eq} \leq 2$ from Equation VI-5-7

$$\frac{R_{u2\%}}{(H_s)_{toe}} = 1.5 \xi_{op} \gamma_r \gamma_b \gamma_h \gamma_\beta$$

Take,

$\gamma_r = 1.0$ (smooth)

$\gamma_b = 0.6$ berm influence

$\gamma_h = 0.9$ (since wave breaking begins 19 m (59 ft) from toe, assume some reduction in γ_h

$\gamma_\beta = 1.0$ ($\theta = 0°$)

gives

$$\frac{R_{u2\%}}{(H_s)_{toe}} = 1.5(2.93)(1.0)(0.6)(0.9)(1.0)$$

$$= 2.37$$

$$R_{u2\%} = 2.37(1.29 \text{ m}) = 3.06 \text{ m} (10.0 \text{ ft})$$

[NOTE: By composite method, *Shore Protection Manual* (1984) gave R_{us} = 1.8 m (5.9 ft). Assuming Rayleigh distribution

$R_{u2\%}/R_{us}$ = 1.4 m (4.6 ft) so $R_{u2\%}$ = 2.5 m (8.2 ft)].

(Sheet 3 of 3)

VI-7-3. Wave Overtopping.

EXAMPLE PROBLEM VI-7-6

FIND: Estimate the average overtopping discharge rate for the given wave, water level, and structure geometry.

GIVEN: An impermeable structure with a smooth slope of 1-on-2.5 ($\tan \alpha = 0.4$) is subjected to waves having a deepwater, significant height $H_o' = 1.5$ m (4.9 ft) and a period $T = 8$ s. Water depth at the structure toe is $d_{toe} = 3.0$ m (9.8 ft) relative to design still-water level (SWL). The crest elevation, R_L is 1.5 m (4.9 ft) above the design, SWL. Onshore winds of 18 m/s (35 knots) are assumed.

SOLUTION: Table VI-5-7 lists two models applicable for this example, to determine the average overtopping discharge rate, q (cu m/s per meter) from two formulas, namely Owen (1980, 1982) and van der Meer and Janssen (1995). Both require knowledge of the wave height, H_s at the toe of the structure.

Assume wave direction is shore normal to the structure.

(1) Wave height, H_s at structure toe

(a) Linear wave theory

$$L_o = \frac{g}{2\pi} T^2 = \frac{9.81 \text{ m/s}^2}{2\pi} (8 \text{ s})^2 = 99.92 \text{ m (327.8 ft)}$$

$$\frac{d}{L_o} = \frac{3.0}{99.92} = 0.0300$$

$$\frac{H}{H_o'} = 1.125$$

(Table C-1, Shore Protection Manual 1984)

Assume $H = H_s = 1.125(1.5 \text{ m}) = 1.69$ m (5.5 ft) (nonbreaking)

(b) Irregular wave, Goda method, see ACES (Leenknecht et al. 1992)

$H_s = 1.6$ m (5.2 ft) (Checks okay)

(Sheet 1 of 4)

EXAMPLE PROBLEM VI-7-6 (Continued)

(c) Use $(H_s)_{toe}$ = 1.69 m (5.5 ft) (conservative)

(2) Table VI-5-8, Owen (1980, 1982)

Using Equation VI-5-22

$$\frac{q}{gH_sT_{om}} = a\exp\left(-b\frac{R_c}{H_s}\sqrt{\frac{s_{om}}{2\pi}}\frac{1}{\gamma_r}\right)$$

requires knowledge of T_{om}. As discussed in VI-5-2-a-(3)-(b), the relation between T_m and T_p can be estimated from

JONSWAP spectra T_m/T_p = 0.79 - 0.87

or in deep water

Pierson-Moskowitz spectra T_m/T_p = 0.71 - 0.82

here, take $T_m = 0.8\ T_p$ so that T_m = 6.4 sec = T_{om}

Therefore,

$$L_{om} = \frac{g}{2\pi}T_m^2 = \frac{9.81\ \text{m/s}^2}{2\pi}(6.4\ \text{s})^2 = 63.9\ \text{m (210 ft)}$$

and

$$s_{om} = \frac{H_s}{L_{om}} = \frac{1.69\ \text{m}}{63.9\ \text{m}} = 0.02645$$

Now from the coefficients table for smooth slopes shown in Table VI-5-8

Slope	a	b
1:2.0	0.0130	22
1:2.5	0.0145	27 ← by linear interpolation
1:3.0	0.0160	32

Therefore, with γ_r = 1.0 (smooth slope)

$$\frac{q}{(9.81\ \text{m/s}^2)(1.69\ \text{m})(6.4\ \text{s})} = 0.0145\exp\left(-27\frac{1.5\ \text{m}}{1.69\ \text{m}}\sqrt{\frac{0.02645}{2\pi}}\frac{1}{1.0}\right)$$

$$= 0.0145\exp(-1.5549)$$

$$= 0.0145(0.21122) = 0.003063$$

(Sheet 2 of 4)

EXAMPLE PROBLEM VI-7-6 (Continued)

or

$$q = \left(9.81 \text{ m/s}^2\right)\left(1.69 \text{ m}\right)\left(6.4 \text{ s}\right)\left(0.003063\right)$$
$$= \left(106.10\right)\left(0.003063\right)$$
$$= 0.325 \text{ m}^3\text{/s per meter width } (3.5 \text{ ft}^3\text{/s per foot width})$$

(3) Table VI-5-11, van der Meer and Janssen (1995)

The data used to develop Equation VI-5-24 are shown in Figure VI-5-15 (top plot) for $\xi_{op} < 2$. This is a comprehensive data set showing the 95 percent confidence bands for the data.

Using $T_p = 8$ s gives:

$$s_{op} = \frac{H_s}{L_{op}} = \frac{1.69 \text{ m}}{99.92 \text{ m}} = 0.01691$$

so that

$$\xi_{op} = \frac{\tan\alpha}{\sqrt{s_{op}}} = \frac{0.4}{\sqrt{0.01691}} = \frac{0.4}{0.13} = 3.08$$

Therefore:

$$\xi_{op} > 2$$

so that Equation VI-5-25 (see bottom plot of Figure VI-5-15) governs.

Using Equation VI-5-25

$$\frac{q}{\sqrt{9.81 \text{ m/s}^2 \left(1.69 \text{ m}\right)^3}} = 0.2 \exp\left(-2.6 \frac{1.5 \text{ m}}{1.69 \text{ m}} \ \frac{1}{\left(1.0\right)\left(1.0\right)\left(1.0\right)\left(1.0\right)} \right)$$

with all the reduction factors as unity.

(Sheet 3 of 4)

EXAMPLE PROBLEM VI-7-6 (Concluded)

or

$$q = \sqrt{\left(9.81 \text{ m/s}^2\right)\left(1.69 \text{ m}\right)^3} \cdot 0.2 \exp\left(-2.30769\right)$$

$$q = 6.88 \text{ m}^3\text{/s (0.0199)}$$

$$q = 0.137 \text{ m}^3\text{/s per meter width (1.47 ft}^3\text{/s per foot width)}$$

This result is considerably lower than that found from Table VI-5-8 by Owen (1980, 1982). However, a check of this result by examining the data scatter in the lower plot of Figure VI-5-15 provides some insight.

For a value on the horizontal axis of

$$\frac{R_c}{H_s}\frac{1}{\gamma_r\gamma_b\gamma_h\gamma_\beta} = \frac{1.5 \text{ m}}{1.69 \text{ m}}\frac{1}{1.0} = 0.89$$

the range covered on the vertical axis by the data is about

$$\frac{q}{\sqrt{gH_3^3}} = \begin{cases} 5\left(10^{-2}\right) \\ 1\left(10^{-2}\right) \end{cases} 0.0199 \approx 2\left(10^{-2}\right) \text{ (mean)}$$

Therefore

$$q = \begin{cases} 0.344 \\ 0.136 \leftarrow \text{ mean, m}^3\text{/s per meter} \\ 0.069 \end{cases} \quad \begin{cases} 3.7 \\ 1.46 \leftarrow \text{ mean, ft}^3\text{/s per foot} \\ 0.74 \end{cases}$$

The range of q at the 95 percent confidence level is about 0.07 to 0.34 m^3/s per meter. The result from Table VI-5-8 with q = 0.32 m^3/sec per meter (3.44 ft^3/sec per foot) now seems reasonable.

This example problem is identical to Example Problem 8 in Chapter 7 of the *Shore Protection Manual* (1984) where the average overtopping rate $\bar{Q}$ = 0.3 m^3/s per meter (3.23 ft^3/s per foot) was found. The *Shore Protection Manual* result included a factor for wind that is not included. Because of the range of variability in the time-average overtopping discharge rate, the rate of

q = 0.3 m^3/s per meter width

indicates a potential danger for vehicles, pedestrians, and the safety of structures as illustrated in Table VI-5-6. Therefore, raising the crest elevation should be considered.

(Sheet 4 of 4)

EXAMPLE PROBLEM VI-7-7

FIND:
a. Estimate the overtopping volumes of individual waves, and overtopping distributions for the given wave, water level, and structure geometry.

b. What effect does the structure permeability have on the results?

GIVEN: The identical conditions of Example Problem VI-7-6 (see sketch)

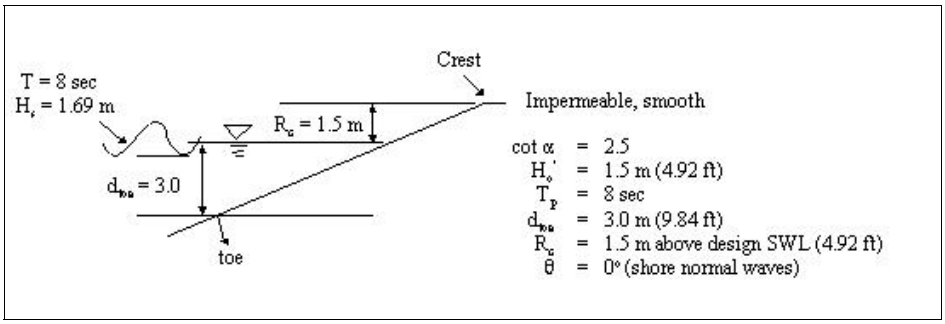

Figure VI-7-2. Overtopping of an impermeable structure

SOLUTION: From Example Problem VI-7-6

q = 0.3 m^3/s per meter (3.23 ft^3/s per foot)

is the *average* overtopping discharge rate for waves with $(H_s)_{toe}$ = 1.69 m (5.54 ft) and T_m = 6.4 s.

Equation VI-5-30 (or VI-5-31) with coefficient B (Equation VI-5-32) depend on P_{ow}, probability of overtopping per incoming wave.

(1) Rayleigh distribution for runup on smooth, impermeable slopes.

Assuming the runup levels follow a Raleigh distribution, Equation VI-5-33 gives for the probability of overtopping per incoming wave,

$$P_{ow} = \exp\left[-\left(\frac{R_c}{c\,H_s}\right)^2\right]$$

(Sheet 1 of 4)

EXAMPLE PROBLEM VI-7-7 (Continued)

and Equation VI-5-34 gives

$$c = 0.81\ \xi_{eq}\ \gamma_r\ \gamma_h\ \gamma_\beta$$

From Example Problem VI-7-6, taking

$\xi_{eq} = \xi_{op} = 3.07$ (i.e., $\gamma_b = 1$, no berm)

and all other reduction factors of unity, gives

$$c = 0.81\ (3.07)\ (1.0)\ (1.0)\ (1.0) = 2.49$$

and

$$P_{ow} = \exp\left[-\left(\frac{1.5\text{ m}}{2.49(1.69\text{ m})}\right)^2\right]$$

$$P_{ow} = 0.88 = \frac{\text{number of overtopping waves}}{\text{number of incoming waves}}$$

This large percentage is due to the relatively low, crest elevation of the structure.

(2) Other distributions

As shown in Example Problem VI-7-4, the relation between

$$\frac{R_{u2\%}}{R_{us}} = \frac{8.55}{5.01} = 1.71$$

for smooth, impermeable slopes is much different than the Rayleigh distribution for wave heights where $H_{0.02}/H_s = 1.398$. Until further research is conducted, however, it must be assumed that wave runup on smooth, impermeable slopes can be approximated by the Rayleigh distribution.

(a) Overtopping volumes of individual wave, V

From Equation VI-5-32

$$B = 0.84\frac{T_m q}{P_{ow}} = 0.84\frac{(6.4\text{ s})(0.3\text{ m}^3/\text{s/m})}{0.88}$$

$$B = 1.833\text{ m}^3/\text{m}$$

(Sheet 2 of 4)

EXAMPLE PROBLEM VI-7-7 (Continued)

as the scale factor for the one-parameter, Weibull distribution given by Equation VI-5-31, so that

$$V = (1.833\ m^3/m)\ [-\ln (p_>)]^{4/3}$$

where $p_>$ is the probability of an individual wave overtopping volume (per unit width) exceeding the specified overtopping volume, V (per unit width), for some representative probabilities of exceedance for individual waves,

$P>$	V (m3/m)	V (ft3/ft)
0.5	1.12	12.1
0.135	4.62	49.7
0.10	5.57	60.0
0.05	7.92	85.3
0.02	11.29	121.5
0.01	14.04	151.1
0.001	24.11	259.5

The maximum overtopping volume per unit width, V_{max} produced by one wave can be estimated from Equation VI-5-35 with B = 1.833 m^3/m, i.e., $V_{max} = 1.833\ (ln\ N_{ow})^{4/3}$ which depends on storm duration, t.

Assuming T_m = 6.4 s over the storm duration, t, and P_{ow} = 0.88

t			*Vmax*		
hr	N_w	N_{ow}	m^3/m	ft^3/ft	Remarks
1	563	495	20.9	225	
2	1125	990	24.7	266	Similar to $P> = 0.001$
5	2813	2475	28.4	306	
10	5630	4954	31.8	342	
15	8438	7425	33.8	364	
20	11250	9900	35.3	380	
24	13500	11880	36.3	391	Gives $P> = 0.0001$

EXAMPLE PROBLEM VI-7-7 (Concluded)

Storm surge hydrographs with varying design water levels and accompanying wave condition variability during the storm will modify these results, considerably.

(b) Effect of structure permeability

No data exist for permeable, straight and bermed slopes as summarized in Table VI-5-7, to estimate average wave overtopping discharge rates. However, as shown in Example VI-7-2 for a rough, impermeable slope

$R_{u2\%}$ = 4.70 m (15.4 ft) (Equation VI-5-3) $\gamma = 0.55$

= 3.56 m (11.7 ft) (Equation VI-5-6) $\gamma = 0.55$

= 3.53 m (11.6 ft) (Equation VI-5-12) (Table VI-5-5) $P = 0.1$

using various models. And, as shown in Example VI-7-3 for rock-armored, permeable-slopes ($P = 0.5$).

$R_{u2\%}$ = 3.53 m (11.6 ft) (Equation VI-5-3) (Table VI-5-5)

The runup elevation at the 2% exceedance level for this example is about the same for permeable and impermeable slopes.

Statistical distribution for wave runup on rock-armored, permeable slopes are discussed in Part VI-5-2-b.(4)(b) and best-fit, by a two-parameter Weibull distribution (Equation VI-5-14). Structure permeability absorbs the higher frequency runup components to modify the distribution from that given by the Rayleigh distribution.

Research is needed for the probability distribution of wave overtopping per incoming waves on permeable slopes.

(Sheet 4 of 4)

VI-7-4. Armor Layer Stability.

EXAMPLE PROBLEM VI-7-8

FIND: The weight of uniform-sized armor stone placed on an impermeable revetment slope with nonovertopping waves.

GIVEN: An impermeable structure (revetment) on a freshwater shore has a slope of 1 on 2.5 and is subjected to a design, significant wave height, H_s = 2.0 m (6.6 ft) measured at a gauge located in a depth, d = 4.5 m (14.8 ft). Design wave peak period, T_p = 8 s. Design depth at structure toe at high water is d_{toe} = 3.0 m (9.8 ft).

SOLUTION: From Example Problem VI-7-1, linear wave theory gives the wave height due to shoaling at the structure toe as:

$(H_s)_{toe}$ = 2.16 m (7.0 ft)

ASSUMPTIONS: (See Tables VI-5-22 and VI-5-23)

1. Fresh water, ρ_w = 1,000 kg/m^3
2. Rock, ρ_s = 2,650 kg/m^3
3. Two layers, n = 2, random placement
4. Quarry stone, rough angular
5. No damage criteria (see Table VI-5-21 for damage values, D and S)

Item 1. Hudson (1974), *Shore Protection Manual* (1984)
Use $H = H_{0.1}$ = 1.27 H_s for the Rayleigh distributed wave heights and related K_D-values for stability coefficient. These recommendations of *Shore Protection Manual* (1984) introduce a factor of safety compared to that recommended in the *Shore Protection Manual* (1977). The no-damage range is D = 0-5 percent.

From Equation VI-5-67, rearranged for the median rock mass

$$M_{50} = \frac{\rho_s H^3}{K_D \left(\rho_s / \rho_w - 1\right)^3 \cot \alpha}$$

Noting

$W_{50} = M_{50}$g

(Sheet 1 of 6)

EXAMPLE PROBLEM VI-7-8 (Continued)

this equation becomes

$$W_{50} = \frac{\rho_s g H^3}{K_D \left(\rho_s / \rho_w - 1\right)^3 \cot \alpha}$$

By definition

$\gamma_s = \rho_s g$ = unit weight of rock

and

ρ_s/ρ_w = s, the specific gravity for rock

so

$$W_{50} = \frac{\gamma_s H^3}{K_D \left(s - 1\right)^3 \cot \alpha}$$

which is the more familiar form of the Hudson formula. K_D is the Hudson stability coefficient.

At the toe, $\frac{H_s}{d} = \frac{2.16 \text{ m}}{3.0 \text{ m}} = 0.7$, and the wave condition is close to breaking for shallow water.

If H_s is assumed to be equivalent to the energy-based significant wave height, H_{mo}, then the maximum depth-limited H_{mo} 0.6 d. Therefore, the maximum breaking wave at the structure toe would be the maximum monochromatic breaking wave.

If H_s is taken equal to $H_{1/3}$, then $H_s > H_{mo}$ near the point where a significant portion of waves in the distribution are breaking. In this case, calculate $H_{0.1}$ to see if it is greater than the maximum breaking wave at the structure toe, then use the lesser of the two.

In summary, determination of wave breaking depends on which definition of significant wave height (H_{mo} or $H_{1/3}$) is used to transform the waves to the toe of the structure.

For this example, assume $H_s = H_{mo}$. Therefore, linear shoaling has given an unrealistically large estimate of H_s. So assume $H_s = 0.6\ d = 0.6$ (3.0 m) = 1.8 m (5.9 ft).

The maximum breaking wave height at this depth (assuming a horizontal approach slope) is

$H_b = 0.78\ d = 0.78$ (3.0 m) = 2.34 m (7.7 ft)

(Sheet 2 of 6)

EXAMPLE PROBLEM VI-7-8 (Continued)

For breaking waves on randomly-placed, rough angular stone, use $K_D = 2.0$ in Hudson's equation

$$W_{50} = \frac{\left(2{,}650\ kg/m^3\right)\left(9.81\ m/s^2\right)\left(2.34\ m\right)^3}{2.0\left(2.65-1\right)^3\left(2.5\right)} = 14{,}830\ \text{N (3,334 lb)}$$

The equivalent cube length is given by

$$D_{n50} = \left(\frac{W_{50}}{\rho_s g}\right)^{1/3} = \left[\frac{14{,}830\ \text{kg - m/s}^2}{\left(2{,}650\ \text{kg/m}^3\right)\left(9.81\ \text{m/s}^2\right)}\right] = 0.83\ \text{m}\ \left(2.7\ \text{ft}\right)$$

Item 2. Van der Meer (1988), Table VI-5-23
Additional assumptions and data input are required. See Table VI-5-23.

(a) Notational permeability coefficient, P.
As shown on Figure VI-5-11 for impermeable, rock revetments,
$P = 0.1$

(b) Number of waves, N_z
This value depends on the length of the storm and average wave period during the storm. For example, a 13-14 hr storm with average wave period, $T_m = 6.6$ s would produce about 7,500 waves. When $N_z > 7{,}500$, the equilibrium damage criteria is obtained.
Let $N_z = 7{,}500$

(c) Relative eroded (damage) area, S. This variable is defined by Equation VI-5-60.

$$S \equiv \frac{A_e}{D_{n50}^2}$$

where A_e is the eroded cross-section area around the SWL. Thus, S is a dimensionless damage parameter, independent of slope length. Table VI-5-21 presents damage levels (initial, intermediate, failure) for a two-layer armor layer (n=2). For a slope 1:2.5 (interpolate between 1:2 and 1:3).

Initial damage, $S = 2$
Intermediate damage, $S = 5.0\text{-}7.5$
Failure, $S \geq 10$

(Sheet 3 of 6)

EXAMPLE PROBLEM VI-7-8 (Continued)

Hence, for initial or no damage condition, use

$S = 2$ (nominal value)

For irregular waves striking the revetment at 90 deg (normal), the applicable formulas of van der Meer (1988) are found in Table VI-5-23. Two cases exist depending on whether the waves are (1) plunging or (2) surging against the revetment slope.

(1) Plunging waves: $\xi_m < \xi_{mc}$ (Equation VI-5-58)

Recall Example VI-7-1 where the surf-similarity parameter, ξ_m was defined and discussed. Here, it is determined for a mean wave period, T_m using the wave height at the toe, H_{toe}. Therefore, using $H_s = 1.8$ m and $T_m = 6.6$ s,

$$s_{om} = \frac{H_{toe}}{\frac{g}{2\pi}\left(T_m\right)^2} = \frac{1.8\text{ m}\left(2\pi\right)}{9.81\text{ m/s}^2\left(6.6\text{ s}\right)^2} = 0.02647$$

Here, it is assumed that $T_m = 0.82\ T_p$, which is an average relation and slightly different than that employed for Example Problem VI-7-1.

Now it is found that

$$\xi_m = \frac{\tan\alpha}{\sqrt{s_{om}}} = \frac{1/2.5}{\sqrt{0.02647}} = 2.46$$

As discussed in Table VI-5-23, if $\square_m < \square_{mc}$ where

$$\xi_{mc} \equiv \left[6.2P^{0.31}\left(\tan\alpha\right)^{0.5}\right]^{1/(P+0.5)}$$

then, the plunging waves Equation VI-5-68 is applicable. Hence,

$$\xi_{mc} = \left[6.2\left(0.1\right)^{0.31}\left(0.4\right)^{0.5}\right]^{1/0.6}$$

gives

$\xi_{mc} = 2.97$

(Sheet 4 of 6)

EXAMPLE PROBLEM VI-7-8 (Continued)

Therefore, $\xi_m < \xi_{mc}$ so that the plunging wave conditions apply. It is convenient to apply the stability paramater, N_z form (see Equation VI-5-58) to give

$$\frac{H_s}{\Delta D_n} = 6.2\, S^{0.2} P^{0.18} N_z^{-0.1} \xi_m^{-0.5}$$

from Table VI-5-23. Or,

$$\frac{H_s}{\Delta D_n} = 6.2(2)^{0.2}(0.1)^{0.18}(7500)^{-0.1}(2.46)^{-0.5} = 1.23$$

which gives for $H = H_s = 1.8$ m, $\Delta = (s - 1) = 1.65$

$$D_{n50} = \frac{H_s}{1.23\Delta} = \frac{1.8\text{ m}}{1.23(1.65)} = 0.89\text{ m (2.9 ft)}$$

and

$$W_{50} = \rho_s g\,(D_{n50})^3 = (2{,}650\text{ kg/m}^3)\,(9.81\text{ m/s}^2)\,(0.89\text{ m})^3 = 18{,}327\text{ N (4,120 lb)}$$

The stability number is $N_s = 1.23$. Statically stable breakwaters have this stability parameter in the range 1-4 for $H_o\, T_o < 100$ (van der Meer 1990).

DISCUSSION: In summary, for the breaking wave, storm, and damage conditions, i.e.,

$H_s = 1.8$ m
$H_b = 2.34$ m
$T_p = 8$ s
$S = 2$
$N_z = 7{,}500$ (13-14 hr storm)

Hudson (1974) $W_{50} = 14{,}830$ N (3,334 lb) breaking wave
van der Meer (1988) $W_{50} = 18{,}327$ N (4,120 lb) plunging wave

and it can be said that both methods give simular results.

EXAMPLE PROBLEM VI-7-8 (Concluded)

The Hudson (1974) formula and therefore, the *Shore Protection Manual* (1984) method limitations include:

no wave period effects
no storm duration effects
damage level limited to range 0-5%

and others as discussed in subsequent examples. The wave period effects have long been discussed as an important missing element in the Hudson (1974) formulation. For example, as shown in Example VI-7-1, as T increases, the surf similarity parameter increases. If the period in the preceding example was increased, the following results would be obtained from the van der Meer (1988) formulation for plunging waves (Table VI-5-23).

Period, s			
T_p	T_m	W_{50}, N	Remarks
9.0	7.38	21, 478	Plunging Waves formula okay
10.0	8.2	23, 865	Use Surging Wave formula, Equation VI-5-69
11.0	9.02	23, 194	Use Surging Wave formula, Equation VI-5-69

Example VI-7-9 demonstrates the practical importance of wave period on armor layer stability.

(Sheet 6 of 6)

EXAMPLE PROBLEM VI-7-9

FIND:
1. The design wave height for a stable, uniform-sized armor stone placed on an impermeable revetment slope with non-overtopping waves.

2. Study the evolution in armor stability design since the 1960's including such factors as alteration in coefficients, wave period, and partial safety factors for design.

GIVEN: In the early 1960's, the Chesapeake Bay Bridge Tunnel (CBBT) islands were constructed with 10 ton (U.S. units) armor stones on a 1:2 slope (single layer) as a revetment for storm protection. The CBBT revetments have been relatively stable and survived many northeasters and hurricanes.

On 31 October 1991, the famous Halloween storm caused severe damage to the revetment. (This storm has been the subject of a best selling novel "The Perfect Storm," Junger (1997) and a Hollywood movie "The Storm of the Century"). Hydrographic surveys determined the extent of damage as discussed in Example Problem VI-7-10.

Wave conditions measured at the U.S. Army Engineers Field Research Facility (FRF) located 65 miles south in 8 m (26.2 ft) water depth were H_s = 4.6 m (15.1 ft), T_p = 22 sec. At the Virginia Beach wave gauge VA001 also located in 8 m depth, H_s = 2.6 m (8.53 ft) and T_p about 23 sec under peak conditions. These waves came from 90 deg (True North) direction and lasted about 12 hours. The measured storm surge at Hampton Roads tide gauge (Sewells Pt.) was 0.85 m (2.8 ft).

ASSUMPTIONS: (See Tables VI-5-22 and VI-5-23)
1. Sea water, ρ_w = 1,030 kg/m^3.
2. Rock, ρ_s = 2,650 kg/m^3.
3. One layer, n = 1, rough angular, random placement.
4. No-damage criteria (see Table VI-5-21 for D and S damage values).

SOLUTION:
Item 1. Hudson (1974), SPM (1977)
Estimate the stable design wave height $H = H_s$. From Equation VI-5-67.

$$\frac{H}{\Delta D_{n50}} = \left(K_D \cot\alpha\right)^{1/3}$$

Knowing $W_{50} = (\rho_s g)(D_{n50})^3$ = 10 tons = 20,000 lbs (89,000 N), and
$\rho_s g = \gamma_s$ = (5.14 slugs/ft^3) (32.2 ft/s^2) = 165.6 lb/ft^3 (26,000 N/m^3)

(Sheet 1 of 7)

EXAMPLE PROBLEM VI-7-9 (Continued)

The equivalent cube length is given as:

$$D_{n50} = \left(\frac{20{,}000 \text{ lbs}}{165.6 \text{ lb/ft}^3} \right)^{1/3} = 4.94 \text{ ft } (1.51 \text{ m})$$

Now, considering only wave breaking events on the revetment, as seen in Table VI-5-22, K_D values employed in 1977 were $K_D = 3.5$ for randomly-placed, rough, angular stone. Rearranging Equation VI-5-67

$$H_b = \Delta D_{n50} \left(K_D \cot \alpha \right)^{1/3} = \left(\frac{\rho_s}{\rho_w} - 1 \right) (4.94 \text{ m}) (3.5 \square 2.0)^{1/3}$$

$$H_b = (1.57)(4.94 \text{ m})(1.913)$$

$$H_b = 14.8 \text{ ft } (4.5 \text{ m})$$

If the stones were smooth and rounded, $K_D = 2.1$ giving $H_b = 12.5$ ft (3.8 m). These 10-ton stones would be less stable.

Item 2. Hudson (1974), SPM (1984)
The SPM (1984) took $H_{1/10} = 1.27\ H_s$ from the Rayleigh Distribution for a non-breaking conditions and reduced the Hudson coefficients as a result of additional testing using irregular waves. For breaking wave conditions, use H_b as the wave height.

$$H_b = \Delta D_{n50} \left(K_D \square \cot \alpha \right)^{1/3}$$

$$H_b = 1.57 (4.94) (2.0 \square 2.0)^{1/3}$$

$$H_b = 12.3 \text{ ft } (3.76 \text{ m})$$

so that $H_b = 12.3$ ft (3.76 m) for the stable conditions

Note also that for smooth stones ($K_D = 1.2$) gives $H_b = 10.4$ ft (3.17 m).

These results should be interpreted to demonstrate that for a given armor stone weight the design wave height for the stable, no-damage condition has decreased by about 22 percent using the SPM (1984) for breaking waves. Assuming the breaking wave height is approximately equal to $H_{1/10}$, the corresponding significant wave height is

$H_s = H_b / 1.27 = 12.3 \text{ ft}/1.27 = 9.7 \text{ ft } (2.96 \text{ m})$

(Sheet 2 of 7)

EXAMPLE PROBLEM VI-7-9 (Continued)

Wave heights measured at Duck, NC (H_s = 4.6 m) and at Virginia Beach, VA, during the storm event exceeded the design wave height, so it reasonable to assume waves at the CBBT site also exceed the design wave height.

The Halloween Storm event was unique to the Atlantic Ocean, East Coast for the very long period swell waves (T_p > 20 sec) generated and recorded. Wave period is not a variable in the Hudson formula.

Item 3. van der Meer (1988), Table VI-5-23

Now consider for irregular, head-on waves on rock, non-overtopping slopes, the formulas of van der Meer (1988) as shown in Table VI-5-23.

Assume as additional, needed variables

P = 0.1 for impermeable, rock revetments

$$N_z = \frac{t}{T_m} = \frac{\text{12 hrs (3,600 s/hr)}}{\text{18.3 sec}} = \text{ 2,360 waves}$$

S = 2 (nominal value) for the initial, no-damage condition

T_p = 22.0 sec (T_m = 18.3 sec)

(a) Determine which stability equation is applicable.

Because of the very long wave period, T_p = 22 sec giving $T_m \approx$ 18.3 sec, the surf-similarity parameter, ξ_m given by

$$\xi_m = \frac{\tan\alpha}{\sqrt{S_m}}$$

with

$$s_m = \frac{H_{toe}}{\frac{g}{2\pi}\left(T_m\right)^2}$$

gives a relatively large value of ξ_m. For example, taking H_s = 5.75 ft (1.75 m) gives ξ_m = 8.63. But the critical ξ_{mc} is found from Table VI-5-23.

(Sheet 3 of 7)

EXAMPLE PROBLEM VI-7-9 (Continued)

$$\xi_{mc} = \left(6.2\ P^{0.31}\left(\tan\alpha\right)^{0.5}\right)^{1/(P+0.5)} = \left(6.2\ (0.1)^{0.31}\ (0.5)^{0.5}\right)^{1/0.6}$$

$$\xi_{mc} = 3.57$$

Therefore, since $\xi_m > \xi_{mc}$, Table VI-5-23 requires that the Surging Waves, Equation VI-5-69 be employed.

(b) Use Surging Waves, Equation VI-5-69 ($\xi_m > \xi_{mc}$)

The stability parameter, N_s form in Table VI-5-23 is

$$\frac{H_s}{\Delta D_{n50}} = 1.0\ S^{0.2} P^{-0.13} N_z^{-0.1} \left(\cot\alpha\right)^{0.5} \xi_m^P$$

giving

$$= 1.0\left(2\right)^{0.2}\left(0.1\right)^{-0.13}\left(2360\right)^{-0.1}\left(2.0\right)^{0.5}\left(\xi_m\right)^{0.1} = 1.008\left(\xi_m\right)^{0.1}$$

Substituting D_{n50} = 4.94 ft (1.51 m) and Δ = 1.57 and expanding ξ_m yields

$$H_s = 1.57\ (4.94\ \text{ft})(1.008)\left[\sqrt{\frac{2\pi\ H_s}{g\ T_m^{\ 2}}}^{\tan\alpha}\right]^{0.1}$$

$$H_s = 7.82\left[\sqrt{\frac{2\pi}{32.2\ \text{ft/s}^2\left(18.3\ \text{s}\right)^2}}^{0.5}\right]^{0.1}\left[\frac{1}{H_s}\right]^{0.05}$$

$$H_s^{1.05} = 10.58$$

$$H_s = (10.58)^{1/1.05} = 9.5\ \text{ft}\ (2.9\ \text{m})$$

which is comparable to the value estimated by the Hudson equation.

(Sheet 4 of 7)

EXAMPLE PROBLEM VI-7-9 (Continued)

The stability number, N_s = 1.22, i.e., N_s > 1 for stable conditions.

Now for this same wave height, H_s = 9.5 ft (2.90 m), what armor layer weight, W_{50} is required for shorter wave periods, T_p to remain stable?

Wave period (sec)		Weight W_{50}		
T_p	T_M	lbs	(kN)	Remarks
20.0	16.7	20,770	(92.4)	OK - Surging Equation VI-5-69
15.0	12.5	22,640	(100.7)	OK - Surging Equation VI-5-69
12.0	10.0	24,206	(107.7)	OK - Surging Equation VI-5-69
10.0	8.3	19,140	(85.1)	Use Plunging Equation VI-5-68

Now we see that for surging waves, lowering the wave period increases the stone weight, W_{50}, for stability up to some point where the conditions for the Surging Wave Equation are no longer applicable. This is the opposite trend as shown in Example VI-7-8 for the case where the Plunging Wave Equation was applicable. In general, each equation is only applicable for the special conditions.

$\xi_m < \xi_{mc}$ Use Plunging Waves, Equation VI-5-68

$\xi_m > \xi_{mc}$ Use Surging Waves, Equation VI-5-69

and the wave period, T_p is an important variable in the equation for ξ_m.

All the above does not address the need for some safety factors in applying the van der Meer formulas for design.

Item 4. Partial Safety Factors (VI-6-6)

The theory behind the inclusion of partial safety factors for the stable design of armor stone is found in VI-6-6. In general, the safety factors increase:

1. as our knowledge of the wave height conditions decreases, and
2. as our desire for a risk free, low failure probability increases.

Table VI-6-6 presents the Partial Safety Factors ranging up to 1.9 for Surging Wave conditions on non-overtopping slopes using the van der Meer, 1988 Equation VI-6-45.

(Sheet 5 of 7)

EXAMPLE PROBLEM VI-7-9 (Continued)

Here, we consider the influence of the partial safety factors on the wave heights for a stable armor stone weight, 10 tons on a 1:2 slope for this example. In all cases, also take $P = 0.1$, $S = 2$, and $N_z = 2360$ waves for $T_p = 22.0$ sec. Consider two cases:

(a) Excellent Knowledge of Wave Conditions (= 0.05) at site.

Failure Probability	P_f	γ_H	γ_z	H_s, ft (m)
Low	0.01	1.7	1.00	5.73 (1.75)
Medium	0.10	1.3	1.02	7.25 (2.21)
High	0.40	1.0	1.08	8.85 (2.70)
No. S.F.	?	1.0	1.0	9.5 (2.90)

Decreasing the degree of risk of failure (i.e., including safety factors) means lowering the wave height design conditions for the same armor stone weight and revetment slope.

(b) Relatively Poor Knowledge of Wave Conditions ($\sigma = 0.2$) at site

Failure Probability	P_f	γ_H	γ_z	*Hs* ft (m)
Low	0.01	1.9	1.02	5.05 (1.54)
Medium	0.10	1.4	1.04	6.65 (2.03)
High	0.40	1.1	1.00	8.70 (2.65)

To ensure a low failure probability means using 10-ton armor stone on a 1:2 slope in regions with long period waves but wave heights only in the 5-6 ft range.

Clearly, since these armor stones were severly damaged in the 31 October 1991 storm, the storm wave heights must have been greater than all those calculated above.

(Sheet 6 of 7)

EXAMPLE PROBLEM VI-7-9 (Concluded)

5. SUMMARY:
Given:

$W_{50} = 10$ tons = 20,000 lbs (89,000 N)
$D_{n50} = 4.94$ ft (1.51 m)
P = 0.1
S = 2
$N_z = 2,360$
$T_p = 22$ sec ($T_m = 18.3$ sec)

Armor-Layer Stability Formula	Stable, Significant Wave Height, H_s		Remarks
	feet	meters	
Hudson (1974) SPM (1977)	14.9	4.5	No period effects, breaking waves No safety factor
Hudson (1974) SPM (1984)	9.7	2.32	No period effects, breaking waves Revised coefficients, conservative
van der Meer (1988) (no safety factor)	9.5	2.90	T_p = 22.0 sec, surging waves No safety factor
van der Meer (1988) (with safety factor)	5-9	1.5-2.7	T_p = 22.0 sec, surging waves Includes partial safety factors, Part VI, Chapter 6

With such long wave periods, it is possible that waves did not break on the revetment, and Hudson's equation could be applied with nonbreaking wave $K_D s$.

Clearly a wide range of wave heights are possible based on these formulas. Example VI-7-10 considers the damage experience by the CBBT island revetments to determine the design wave conditions. Example VI-7-11 considers the size (weight) of the armor stones for repair.

(Sheet 7 of 7)

EXAMPLE PROBLEM VI-7-10

FIND: The damage curve relationship for wave energy above the design wave height for uniform-sized armor stone placed on an impermeable revetment slope with nonovertopping waves.

GIVEN: The same condition as found in Example VI-7-9 for the Cheasapeake Bay Bridge Tunnel (CBBT) island revetments with 1:2 sloped revetment, T_p = 22.0 s, but uncertain knowledge of the wave height, H_s.

SOLUTION: Method 1. Based on van der Meer (1988)

Table 7-9 (in the *Shore Protection Manual* (1984), (Volume II, p. 7-211) presented the following generic, H/H_d - vs - damage D in percent relationships for rough/quarrystone revetments. (Two layers, random placed, nonbreaking waves, minor overtopping.) This table was not well supported by data, so it was not included in the *Coastal Engineering Manual*. The value of H depends on what level $H_{D=0}$ is used for a stable design.

$H/H_{D=0}$	Damage. D Percent
1.0	0-5
1.08	5-10
1.19	10-15
1.27	15-20
1.37	20-30
1.47	30-40
1.56	40-50

(Sheet 1 of 3)

EXAMPLE PROBLEM VI-7-10 (Continued)

Now apply van der Meer's (1988) Equation VI-5-69 for surging waves with $H_s(S=2)$ = 9.5 ft (2.90 m), and vary the significant wave height, H_s to calculate S, the damage level. We keep D_{n50} = 4.95 ft (1.51 m) and W_{50} = 10 tons (20,000 lb). This assumes adequate depth exists at the structure toe to support the increased significant wave heights without depth-limited breaking.

H_s feet	H_s (m)	$H/H_s(S=2)$	S	Relative Damage Level	Remarks
9.5	(2.90)	1.00	2.018	1.009	Slight rounding error, S = 2
10.0	(3.05)	1.05	2.643	1.32	
11.0	(3.35)	1.16	4.36	2.18	Intermediate damage level, S = 4 - 6
11.5	(3.51)	1.21	5.51	2.76	
12.0	(3.66)	1.26	6.89	3.45	
12.5	(3.81)	1.32	8.54	4.27	
13.0	(3.96)	1.37	10.5	5.25	Failure, S = 8 m, armor layer damaged, underlayer exposed to direct wave attack
14.0	(4.27)	1.47	15.5	7.75	
15.0	(4.57)	1.58	22.2	11.1	
16.0	(4.88)	1.68	31.2	15.6	

From Table VI-5-21, van der Meer (1988) gives the following guidelines for 1:2 slopes.

Initial damage	S = 2	Initial damage - no displacement
Intermediate damage	S = 4 - 6	Units displaced but without underlayer exposure
Failure (of armor layer	S = 8	The underlayer is exposed to direct wave attack

Values of H/H_s (S = 2) - vs - S are plotted in Figure VI-7-3. Also, approximate percentage damage, D scales from *Shore Protection Manual* (1984) are constructed for comparison.

(Sheet 2 of 3)

EXAMPLE PROBLEM VI-7-10 (Concluded)

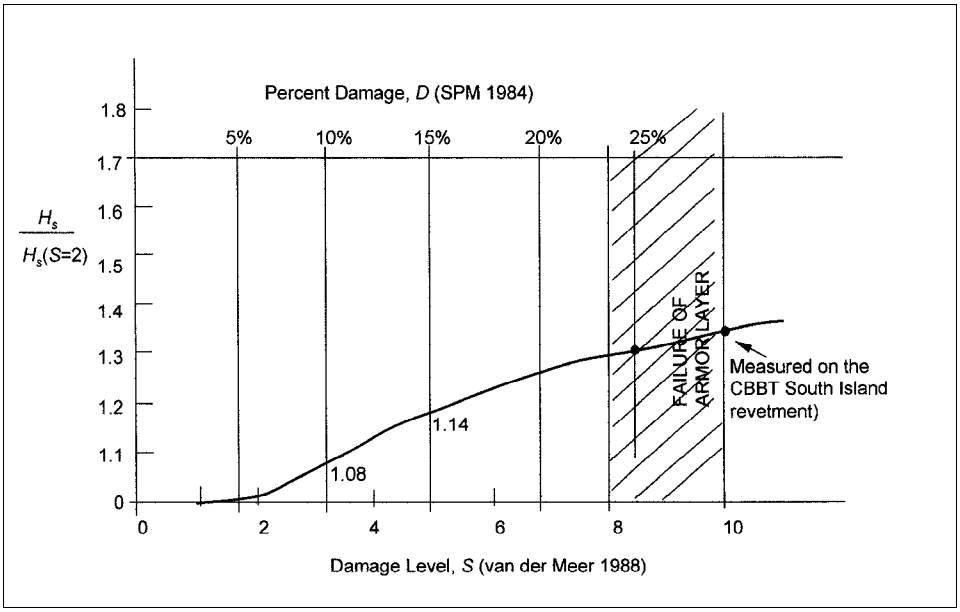

Figure VI-7-3. Percent damage curve for CBBT South Island revetment

Method 2. Damage measurements on CBBT Islands

Damage profile surveys taken by the engineering staff, CBBT District have been analyzed to learn that $S = 10$ from the 31 October 1991 Halloween Storm northeaster. Some underlayers were exposed and this level of the damage parameter is consistent with the criteria for "failure" as shown in Table VI-5-21.

This damage occurred on South Island on a curved section where the armor stones are more vulnerable, i.e., on the head of the structure rather than within the trunk section. Table VI-5-37 presents a method to estimate stability of rock breakwaters as proposed by Carver and Heimbaugh (1989).

From the analysis for $S = 10$, the ratio $H/H_s(S = 2) = 1.35$ giving a significant wave height of

$$H_s = 1.35\ (9.5\ \text{ft}) = 12.8\ \text{ft}\ (3.9\ \text{m})$$

necessary to produce this level of damage using the van der Meer (1988) formulation for surging waves. As shown in Example Problem VI-7-9, wave heights were measured at Duck, North Carolina, as 15.1 ft (4.6 m). These wave conditions are possible at the Chesapeake Bay entrance with relatively deep ($d = 12$ m (39.4 ft)) water.

Example VI-7-11 considers what value of H_s should be used to determine the size and weight of armor stone for repairs of the CBBT island.

(Sheet 3 of 3)

EXAMPLE PROBLEM VI-7-11

FIND: The weight of armor stone to repair the damage to the CBBT Island revetment.

GIVEN:
The results of Example Problems VI-7-9 and VI-7-10
Wave Information Study (WIS) hindcast information for nearby locations
Other extreme wave condition measurements/criteria
Appropriate partial safety factors for wave conditions

Method 1. WIS Station 2059 (Brooks and Brandon 1995)

d = 14 m (46.0 ft) Lat. 37.00°N - Long. 75.75°W

Extreme Prob. Dist. Fisher-Tippett	Spectral Significant Wave Height, H_{mo} (m) Recurrence Interval, T_r, years					
	2	5	10	20	25	50
Type I	5.87	6.67	7.22	7.76	7.93	8.46
Type II	5.87	6.98	7.90	8.90	9.25	10.41

Method 2. Virginia Beach Hurricane Protection Project (U.S. Army Corps of Engineers)

1% chance storm each year (100-year recurrence interval)

d = 30 ft (9.1 m)
H_s = 15.8 ft (4.8m)
T_p = 13.7 sec

Storm surge elevation = 8.7 ft (2.65 m) above NGVD (1929)

SOLUTION: As shown in Example Problem VI-7-10, when H_s = 12.8 ft (3.90 m), the damage level parameter, S, in the van der Meer (1988) for surging waves was about 10 and this was also the average damage level measured by survey. For redesign, consider the following four cases:

a. Wave height, H_s = 13.0 ft (3.96 m)
Wave period, T_p = 22.0 s

b. Consider what effect different wave periods will have on the armor stone size, keeping H_s = 13.0 ft.

(Sheet 1 of 4)

EXAMPLE PROBLEM VI-7-11 (Continued)

c. Consider what effect storm duration up to N_{max} = 7,500 waves will have on the stone size for H_s = 13.0 ft (3.96 m) and the critical periods.

d. Consider what effect some increase in allowable damage level, S, has on these results.

Case a. From Equation VI-6-45 in Table VI-6-6, for H_s = 13.0 ft and T_p = 22.0 s (T_m = 18.3 s).

W_{50} = 54, 236 lb (241,250 N)
D_{n50} = 6.9 ft (2.10 m)

with no safety factor, i.e., $\gamma_H = \gamma_Z = 1.0$

Assuming our knowledge of wave conditions is fairly good (σ_w = 0.05) and using a failure probability (P_f) of 0.10 gives γ_H = 1.3 and γ_z = 1.02. Using these partial safety factors in Equation VI-6-45 gives

W_{50} = 126,490 lb (562,650 N)
D_{n50} = 9.1 ft (2.77 m)

This is not a practical size in the quarry and for construction.

Case b. From Equation VI-6-45 for H_s = 13.0 ft and other wave periods, T_p with no partial safety factors.

Mean Wave Period, T_m s	Peak Wave Period , T_p s	Armor Layer		van der Meer Formula S = Surging P = Plunging	N_z = 2,360 Storm Duration t, hr	Remarks
		Stone wt, W_{50}, lb	Stone diam, D_n, ft (m)			
18.3	22	54,340	6.90 (2.10)	S	12.0	The Hudson formula does not consider wave period
16.7	20	55,852	6.96 (2.12)	S	10.4	
14.9	18	57,796	7.04 (2.15)	S	9.8	
13.3	16	59,799	7.12 (2.17)	S	8.7	
11.6	14	62,304	7.22 (2.20)	S	7.6	
10.0	12	51,585	6.78 (2.07)	P	6.6	
8.3	10	39,007	6.18 (1.88)	P	5.4	

(Sheet 2 of 4)

EXAMPLE PROBLEM VI-7-11 (Continued)

Lowering the wave period with H_s = 13.0 ft (3.96 m) slightly *increases* the armor stone weight by 15 percent for T_p from 22 - 14 s. The surging equations govern.

Case c. As noted in Table VI-5-23 for N_z = 7,500 waves, the equilibrium damage level is approximately reached.

Wave Period, T_p s	Armor Stone Weight, W50 lbs				Remarks
	N_z = 2,360 (t = hr)	N_z = 3,500 (t = hr)	N_z = 5,000 (t = hr)	N_z = 7,500 (t = hr)	
22	54.340 (12.0)	61,159 (17.8)	68,066 (25.4)	76,871 (38.1)	The very long durations are not physically realistic. Long durations at long periods also not realistic
18	57,796 (9.8)	65,049 (14.5)	72,396 (20.7)	81,760 (31.0)	
14	62.304 (7.6)	70,123 (11.3)	78,042 (16.1)	88,137 (24.2)	

Again, as expected, increasing the storm duration increases the weight of the armor stone required for stable weight at the S = 2 level. Note however, that some storm durations (t > 18 hr) are physically unrealistic for sustained, long period waves and wave heights, Hs = 13.0 ft (3.96 m).

Case d. Consider realistic wave periods, T_p = 14-22 s for storms lasting 8 to 18 hr with H_s = 13.0 ft (3.96 m). Now vary the damage level allowable to the intermediate range, S = 4 - 6 (say S = 5) for rock on slopes with cot θ = 2:

Damage Parameter S	Armor Stone Weight, W_{50} lb					
	N_z = 2,360			N_z = 3,500		
	T_p = 22 s	T_p = 18 s	T_p = 14 s	T_p = 22 s	T_p = 18 s	T_p = 14 s
2	54,340	57,796	62,304	61,159	65,049	70,123
3	42,605	45,315	48,849	47,952	51,002	54,980
4	35,851	38,131	41,105	40,350	42,916	46,264
5	31,358	33,353	35,954	35,294	37,539	40,467
6	28,109	29,897	32,229	31,637	33,649	36,273
7	25,626	27,256	29,381	28,842	30,676	33,069

EXAMPLE PROBLEM VI-7-11 (Concluded)

Allowing the damage level to rise up to $S = 6$ in effect means using roughly one-half the weight of armor stone needed when $S = 2$. This is a tremendous reduction and cost savings for initial construction costs and repair costs in a balanced design.

(Note that using the Hudson (1977) formula and *Shore Protection Manual* (1984) methodology $H_{1/10} = 1.27\ H_s$, $K_D = 2.0$, gives $W_{50} = 48{,}036$ lb. This is roughly equivalent to that previously obtained for $T_p = 14$ s, $S = 3$ with an 11+ hr storm event.)

The CBBT island revetment was repaired in August 1994. The W_{50} was 13.5 tons (27,000 lb) with allowable range 12-15 tons. No stones $W_{50} < 12$ tons were allowed. As already demonstrated, this repair stone weight, $W_{50} = 13.5$ tons (35 percent increase in weight) is on the order required but with some damage expected in the future. All of the preceding is with no partial safety factors in the design.

Alternatives for repair would be to use artifically manufactured concrete cubes (Table VI-5-29), tetrapods (Table VI-5-30) or the Corps of Engineers' new Core-Loc® design (Table VI-5-34). These units have greater interlocking abilities and are stable with less weight. A detailed cost analysis is necessary to justify the additional repair expense.

SUMMARY:
Item 1. All of the preceding was calculated keeping $H_s = 13.0$ ft (3.96 m) for design. Wave period, storm duration, and allowable damage level are all additional, important factors, but are not considered in the Hudson formula (1977) nor in the *Shore Protection Manual* (1984).

Item 2. As shown in Table VI-6-6 for Equation VI-6-45 surging waves and van der Meer (1988) formulation, not including any partial safety factors (i.e., taking $\gamma_H = \gamma_F = 1.0$) implies:

a. Our knowledge of wave height conditions is good ($\sigma_w = 0.05$) and

b. A damage probability, $P_f > 40$ percent is expected sometime during the lifetime of the structures. This is acceptable if the damage can be repaired (economically) and if the additional risk is understood.

Item 3. Using artifically manufactured units (concrete cubes, tetrapods, Core-Loc®, etc.) can greatly reduce the level of risk by allowing P_f to decrease (say $P_f = 0.05$) including the appropriate γ_H and γ_F factors and repairing the damage on the CBBT island revetments. This will be shown in Example Problem VI-7-15.

(Sheet 4 of 4)

EXAMPLE PROBLEM VI-7-12

FIND: The weight of armor stone placed as a permeable, nearshore breakwater with overtopped wave conditions.

GIVEN: A permeable structure (nearshore, detached breakwater) has a slope of 1 on 2.5 and is subject to a design, significant wave height, H_s of 2.0 m (6.56 ft) measured at a gauge located in a depth, d = 4.5 m (14.8 ft). Design wave peak period, T_p = 8 s. Design water depth at the structure toe, d_{toe} = 3.0 m (9.8 ft). From Example Problem, VI-7-2 for these conditions, runup, R_{U2}% is 3.5-4.5 m above the SWL, hence some wave overtopping occurs.

SOLUTION: From Example Problem VI-7-1, linear wave theory shoaling to the structure toe gave: $(H_s)_{toe}$ = 2.16 m (7.09 ft). However, it was noted in Example Problem VI-7-8 that this value of H_s exceeded the depth-limited energy-based wave height. So a value of $(H_s)_{toe}$ = 0.6 d = 0.6 (3.0 m) = 1.8 m (5.9 ft) was used.

ASSUMPTIONS: (See Tables VI-5-22, VI-5-24, and VI-5-25 for conventional, two-layer armor stone designs. Also see Figure VI-5-11 for notational permeability coefficients.)

1. Fresh water ρ_w = 1,000 kg/m^3
2. Rock ρ_r = 2,650 kg/m^3
3. Two-layers n = 2, random placement
4. Quarrystone, rough, angular
5. No-damage criteria (see Table VI-5-21 for valves, D and S)

Item 1. Hudson (1974), *Shore Protection Manual* (1984)

See Example Problem VI-7-8 for results which do not change for rubble-mound revetment or nearshore breakwaters:

1. Nonbreaking waves K_D = 4, $H_{1/10}$ = 1.27 (1.8 m) = 2.28 m (7.5 ft)
   W_{50} = 6,859 N (1,542 lb)
   D_{n50} = 0.64 m (2.1 ft)

2. Breaking waves, K_D = 2, H_b = 2.34 m (7.7 ft)
   W_{50} = 14,830 N (3,334 lb)
   D_{n50} = 0.83 m (2.7 ft)

(Sheet 1 of 6)

EXAMPLE PROBLEM VI-7-12 (Continued)

The Hudson formula was originally developed for nonovertopped slopes, but has been often applied to cases with moderate to substantial wave overtopping. In these cases, stone weights estimated with the Hudson equation will be conservative.

Item 2. Van der Meer (1991) Table VI-5-24.

Van der Meer (1991) developed an overtopping reduction factor, f_i given by Equation VI-5-71 in Table VI-5-24 to modify the original van der Meer (1988) stability formulas (Equations VI-5-68 and VI-5-69. The calculated D_{n50} value is reduced by f_i, and the relative freeboard R_c/H_s plays an important role in the factor, f_i . Here, R_c is the same as defined for overtopping depicted in Figure VI-5-14.

1. Nonovertopping conditions - impermeable revetment

Recall from Example Problem VI-7-8 when

P = 0.1 (impermeable)
N_z 7,500 (t = 16-17 hr)
S = 2 (no damage condition)
$\xi_m < \xi_{mc}$

then for plunging wave conditions

D_{n50} = 0.89 m (2.9 ft)
W_{50} = 18,327 N (4,120 lb)

2. Overtopping conditions

The van der Meer (1991) equations can be written

$$\frac{f_i H_s}{\Delta D_{n50}} = 6.2\, S^{0.2} P^{0.18} N_z^{-0.1} \xi_m^{-0.5} \qquad \text{plunging } (\xi_m < \xi_{mc})$$

and

$$\frac{f_i H_s}{\Delta D_{n50}} = 1.0\, \mathrm{S}^{-0.2} P^{-0.13} N_z^{-0.1} \left(\cot\alpha\right)^{0.5} \xi_m^{P} \qquad \text{surging } (\xi_m > \xi_{mc})$$

(Sheet 2 of 6)

EXAMPLE PROBLEM VI-7-12 (Continued)

where:

$$f_i = \left(1.25 - 4.8 \frac{R_c}{H_s} \sqrt{\frac{s_{op}}{2\pi}} \right)^{-1} \qquad \text{(VI-5-71)}$$

within limits

$$0 < \frac{R_c}{H_s} \sqrt{\frac{s_{op}}{2\pi}} < 0.052$$

Note that now, the peak period wave steepness, s_{op}, is employed. It is convenient to set up a spreadsheet solution to investigate how D_{n50} and W_{50} vary with relative freeboard, R_c/H_s. First consider the case (unlikely) for an impermeable, nearshore breakwater design.

(a) Impermeable, $P = 0.1$

Relative Freeboard, R_c/H_s	R_c		D_{n50}		W_{50}		f_i	Remarks
	m	(ft)	m	(ft)	N	(tons)		
1.0	1.8	(5.9)	0.89	(2.9)	18,327	(2.06)	1.000	Exceeds Limit 0.052
0.85	1.53	(5.02)	0.86	(2.82)	16,556	(1.86)	0.969	
0.75	1.35	(4.43)	0.84	(2.75)	15,377	(1.73)	0.946	
0.50	0.90	(2.95)	0.79	(2.60)	12,883	(1.45)	0.892	
0.0	0	(0)	0.71	(2.33)	9,304	(1.05)	0.800	Limit Value = 0

As the relative freeboard, R_c/H_s decreases, more wave overtopping occurs, and the stable armor-layer weight also decreases, over the limiting factor range $0.8 < f_i < 1.0$.

(b) Permeable, $P = 0.4$ or 0.5

The primary application of the original van der Meer (1988) formulation with modification by the reduction factor, f_i, is for permeable structures such as nearshore breakwaters. The following tables illustrate application to permeable structures using the same wave and structure parameters.

EXAMPLE PROBLEM VI-7-12 (Continued)

Relative Freeboard, R_c/H_s	R_c m	R_c (ft)	D_{n50} m	D_{n50} (ft)	W_{50} N	W_{50} (tons)	f_i	*Limit Parameter*	*Remarks*
P = 0.4 (see Figure VI-5-11)									
1.0	NOT APPLICABLE							>0.052	
0.85	1.53	(5.02)	0.67	(2.20)	7,830	(0.88)	0.969		Going from P = 0.1 (impermeable to P = 0.4 (permeable) produces a 50% or one-half lower weight requirement
0.80	1.44	(4.73)	0.66	(2.17)	7,545	(0.85)	0.957		
0.75	1.35	(4.43)	0.65	(2.15)	7,274	(0.82)	0.946		
0.50	0.90	(2.95)	0.62	(2.02)	6,094	(0.68)	0.891		
0.25	0.45	(1.48)	0.58	(1.91)	5,156	(0.58)	0.843		
0.10	0.18	(0.59)	0.56	(1.85)	4,684	(0.53)	0.817		
0.05	0.09	(0.30)	0.56	(1.85)	4,540	(0.51)	0.808		
0	0	(0)	0.55	(1.82)	4,400	(0.49)	0.800	0	
P = 0.5 (Permeable, D core = 0.3 D armor									
1.0	NOT APPLICABLE							>0.052	Going from P = 0.4 to P = 0.5 gives a 11.3% drop in W_{50}
0.85	1.53	(5.02)	0.64	(2.11)	6,942	(0.78)	0.969		
0.80	1.44	(4.73)	0.66	(2.09)	6,689	(0.75)	0.957		
0.75	1.35	(4.43)	0.63	(2.06)	6,448	(0.72)	0.946		
0.50	0.90	(2.95)	0.59	(1.94)	5,402	(0.61)	0.891		
0.25	0.45	(1.48)	0.56	(1.84)	4,570	(0.51)	0.843		
0.10	0.18	(0.59)	0.54	(1.78)	4,152	(0.47)	0.817		
0.05	0.09	(0.30)	0.53	(1.76)	4,024	(0.45)	0.808		
0	0	(0)	0.53	(1.76)	3,901	(0.44)	0.800	0	

The value of P =0.6 is reserved for permeable breakwaters built with no core and homogeneous sized units as discussed in Example Problem VI-7-13.

(Sheet 4 of 6)

EXAMPLE PROBLEM VI-7-12 (Continued)

Note the significant (50% or more) reduction in the stable armor weight requirements due to the permeability, P, of the typical nearshore breakwater designs with a core.

SUMMARY:

Item 1. The Hudson formula is not applicable for wave overtopping conditions because it gives conservative results.

Item 2. Use the van der Meer (1991) formula to determine D_{n50}, then reduce D_{n50} by the factor, f_i.

Item 3. The reduction factor lies in the range $0.8 < f_i < 1.0$ where

$f_i = 0.8$ at $R_c / H_s = 0$ zero freeboard

and

$f_i = 1.0$ at $\frac{R_c}{H_s}\sqrt{\frac{s_{op}}{2\pi}} = 0.052$ limit

Item 4. At limit of zero freeboard, $R_c = 0$, $f_i = 0.8$.

$$W_{50} = D_{n50}^3$$

Weight reduction = $(0.8)^3 = 0.512$ or almost a 50% drop.

Item 5. At limit $f_i = 1.0$ with

$$s_{op} = \frac{H_s}{L_{op}} = \frac{H_s}{\frac{g}{2\pi}T_p^2}$$

the limit for Equation VI-5-71 is

$$\frac{R_c}{H_s}\left(\frac{H_s}{\frac{g}{2\pi}T_p^2 2\pi}\right)^{1/2} < 0.052$$

$$\frac{R_c}{H_s}\left(\frac{H_s}{gT_p^2}\right)^{1/2} < 0.052$$

(Sheet 5 of 6)

EXAMPLE PROBLEM VI-7-12 (Concluded)

Thus, for a range of practical wave heights $1.0 < H_s < 10.0$ m and peak periods, $3 < T_p < 21$ s, a table can be prepared to calculate the maximum values of R_c/H_s at the 0.052 limit. This gives a practical range of $(R_c/H_s)_{max}$ values as shown in the table below.

H_s		$(R_c/H_s)_{max}$ Values at Limit = 0.052						
		Peak Period, *Tp*						
m	(ft)	3	6	9	12	15	18	21
1.0	(3.28)	0.49	0.98	1.49	1.95	2.44	2.93	3.42
2.0	(6.56)	0.35	0.69	1.04	1.38	1.73	2.07	2.42
3.0	(9.84)	0.28	0.56	0.85	1.13	1.41	1.69	1.97
4.0	(13.1)	0.24	0.49	0.73	0.98	1.22	1.47	1.71
5.0	(16.4)	0.22	0.44	0.66	0.88	1.09	1.31	1.53
7.0	(23.0)	0.19	0.37	0.55	0.74	0.92	1.11	1.29
10.0	(32.8)	0.15	0.31	0.46	0.61	0.77	0.93	1.08

For (R_c/H_s) values greater than in the table, nonovertopping conditions prevail.

(Sheet 6 of 6)

EXAMPLE PROBLEM VI-7-13

FIND: The weight of armor stone placed as a permeable, nearshore breakwater with submerged water-level conditions.

GIVEN: The same data as for Example Problem VI-7-12 except now the design water depth, d_{toe} increases to submerge the structure. Assume H_s does not change as water level increases.

$\cot \alpha$ = 2.5
$(H_s)_{toe}$ = 1.8 m (5.9 ft)
T_p = 8 s
ρ_w = 1,000 kg/m^3 (fresh water)
ρ_r = 2,650 kg/m^3 (rock)
n = 2 layers, random placement quarrystone, rough angular, no-damage criteria, $S = 2$
d_{toe} = varies

SOLUTION:

Method 1. van der Meer (1991) Table VI-5-25

For irregular, head-on waves and data for $\cot \alpha = 1.5$, 2 slopes, van der Meer (1991) developed the formula

$$h_c'/h = (2.1 + 0.1\,S) \exp(-0.14\,N_s^*) \quad \text{(Equation VI-5-72)}$$

where

h_c' = crest height of structure above sea level
h = water depth
$h - h_c'$ = water depth over the structure crest
S = relative eroded area, (damage level)

and

N_s^* = spectral stability number

$$= \frac{H_s}{\Delta D_{n50}} s_p^{-1/3}$$

(Sheet 1 of 3)

EXAMPLE PROBLEM VI-7-13 (Continued)

with

$$s_p = H_s/L_p$$

where L_p is the local wavelength based on peak spectral period, T_p.

To determine the stable, armor stone diameter and weight, Equation VI-5-72 is solved first for a given h_c'/h ratio and s_p value to calculate N_s^*. Then rearrange N_s^* to solve for D_{n50}, i.e.,

$$N_s^* = -\frac{1}{0.14}\ln\left[\frac{(h_c')/h}{(2.1+0.1S)}\right]$$

A spreadsheet solution aids the calculation process. Note that the slope does not enter into the calculation and the empirical formula VI-5-72 has only been developed for two slopes.

ASSUMPTIONS:

1. Assume VI-5-72 also applicable when cot $\alpha = 2.5$.
2. Using $S = 2$ gives the no-damage results.
3. Assume crest height, $h_c' = 3.0$ m above seabed.

		Water Depth, h		Diameter, D_{n50}		Weight, W_{50}			
h_c'/h	h/h_c'	m	(ft)	m	(ft)	N	(tons)	N_s^*	Remarks
1.1	Overtopped, not submerged, use Equation VI-5-71, $h_c' = 3.0$								
1.000	1.0	3.0	9.8	0.52	1.72	3,742	0.42	5.95	$R_c = 0$
0.909	1.1	3.3	10.8	0.48	1.57	2,826	0.32	6.63	
0.833	1.2	3.6	11.8	0.44	1.45	2,249	0.25	7.25	
0.769	1.3	3.9	12.8	0.41	1.36	1,858	0.21	7.82	
0.714	1.4	4.2	13.8	0.39	1.29	1,579	0.18	8.35	
0.667	1.5	4.5	14.8	0.38	1.23	1,372	0.15	8.85	
0.625	1.6	4.8	15.7	0.36	1.18	1,212	0.14	9.31	
0.588	1.7	5.1	16.7	0.35	1.14	1,087	0.12	9.74	
0.556	1.8	5.4	17.7	0.34	1.10	985	0.11	10.15	
0.526	1.9	5.7	18.7	0.33	1.07	902	0.10	10.53	
0.500	2.0	6.0	19.7	0.32	1.04	832	0.09	10.90	

The inverse of the h_c'/h ratio in Equation VI-5-72 is the relative submergence ratio $h/h_c' > 1.0$. At $h/h_c' = 1.0$ the water level is at the structure crest and this condition is equal to $R_c = 0$ as relative freeboard, R_c/H_s in Equation VI-5-71 when $f_i = 0.8$ (see previous Example Problem VI-7-12). Because the given data are the same for both Example Problem VI-7-12 and this problem VI-7-13, then the rock size D_{n50} and weight W_{50} should coincide at these extreme limits of these equations.

(Sheet 2 of 3)

EXAMPLE PROBLEM VI-7-13 (Concluded)

From Equation VI-5-71, at the limit when $R_c/H_s = 0$ (zero freeboard) the following values were obtained in Example Problem VI-7-12. These are compared to the W_{50} of 3,742 N (0.42 tons) found in this example for $h_c'/h = 1.0$.

P	D_{n50} (m)	(ft)	W_{50}, (N)	(tons)	Remarks
0.1	0.71	2.33	9,304	(1.05)	Substantially higher
0.4	0.55	1.82	4,400	(0.49)	Little higher
0.5	0.53	1.76	3,901	(0.44)	nearly the same

Therefore, it can be concluded that Equation VI-5-72 applies to permeable structures and may not be appropriate for submerged, impermeable structures.

(Sheet 3 of 3)

EXAMPLE PROBLEM VI-7-14

FIND: Select the armor stone size to withstand the design water level and wave conditions for a rubble-mound, nearshore breakwater constructed of homogeneous units with no core, i.e., permeable.

GIVEN: Breakwater crest elevations +4.0 ft, +5.0 ft, +6.0 ft (MLW) (1.22, 1.52, 1.83 m)

Design Water Levels			Design Wave Conditions			
Recurrence Interval, T_r, years	Storm Surge, S ft		Wave Height, H_s		Wave Period, T (sec)	Remarks
	(MLW)	(m)	ft	(m)		
1	3.6	(1.10)	5.0	(1.52)	5.6	Storm surge and waves at structure toe
10	4.5	(1.37)	5.6	(1.71)	6.5	
25	5.2	(1.58)	6.5	(1.98)	7.6	
50	6.0	(1.83)	7.2	(2.19)	9.7	

(See Figure VI-7-4)

Tidal range, MTR = 1.0 ft (0.3 m)
Elevation at BW location = -3.5 ft (MLW) = Z (-1.07 m)
Vertical datum, MLW = 0.0 ft
Assume crest width, B = 5.0 ft (1.52 m)

Note: Values of H_s determined by numerical model. In some cases ratio of H_s to design water depth exceeds 0.6, which is the depth-limit value to use when more accurate methods are not available.

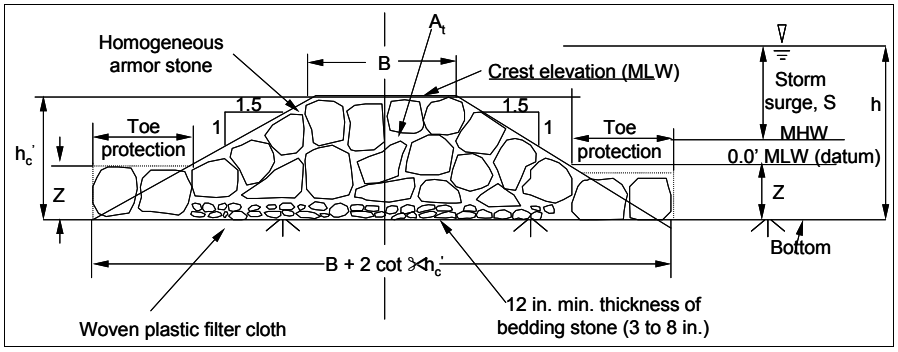

Figure VI-7-4. Homogeneous breakwater cross section

(Sheet 1 of 5)

EXAMPLE PROBLEM VI-7-14 (Continued)

Overtopping and submergence

Because of storm surge, some conditions will produce complete submergence so the breakwater acts as a low-crested reef. Table VI-5-27 gives Equation VI-5-73 as proposed by van der Meer (1990) using data by Ahrens (1987) and van der Meer (1990).

$$h_c = \sqrt{\frac{A_t}{\exp\left(aN_s^*\right)}}$$

where $h_c = h_c^{'}$ is the no-damage condition. The equilbrium profile changes when wave energy reshapes the cross section to give a lower crest elevation height, h_c (damaged). The equilibrium area, A_t remains unchanged. The stability number is defined as

$$N_s^* = \frac{H_s}{\Delta D_{n50}} s_p^{-1/3}$$

where s_p is the wave steepness based on T_p and local wavelength.

Also, the parameter, *a,* is given by

$$a = -0.028 + 0.045\frac{A_t}{\left(h_c^{'}\right)^2} + 0.034\frac{h_c^{'}}{h} - \left(6\times10^{-9}\right)\frac{A_t^2}{D_{n50}^4}$$

Note that the stable stone size, D_{n50}, hence stable weight, W_{50}, is found by:

1. Specifying the reef breakwater dimensions, h_c', B, and cot α, so the cross-sectional area A_t can be calculated.

2. Calculating a for a given water depth, h. (The formula for a is truncated, omitting the small last term.)

3. Calculating N_s^* when $h_c = h_c'$.

4. Calculating $s_p = H_s/L_p$, the local wave steepness.

5. Calculating D_n, i.e.

$$D_{n50} = \frac{H_s}{\Delta N_s^*} s_p^{-1/3}$$

(Sheet 2 of 5)

EXAMPLE PROBLEM VI-7-14 (Continued)

6. and finally, calculating the homogeneous stone weight, W, from

$$W = \rho_s g (D_n)^3$$

Again, a spreadsheet solution aids the calculation process. Figure VI-7-5 illustrates the possible cases for design calculation. Calculations on the following table assumed rock specific weight of 165 lb/ft^3 and $\Delta = 1.58$ (salt water).

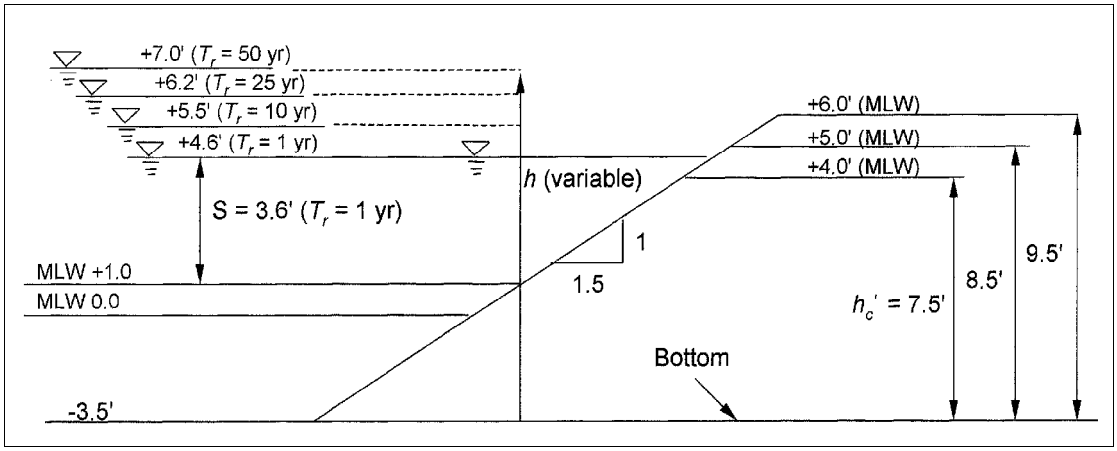

Figure VI-7-5. Variations in design water level and breakwater crest elevations

As expected, the rarer events with low exceedance probabilities each year (higher recurrence intervals) with larger wave heights require larger stones for stability. The crest elevation selected depends upon economics, allowable wave transmission, and resulting shoreline adjustment in the lee of each nearshore breakwater structure.

EXAMPLE PROBLEM VI-7-14 (Continued)

Case 1. Crest Elevation +4.0 ft (MLW) $h_c^* = 7.5$ ft						
Recurrence Interval T_r, years	Water Depth h ft	Wave Conditions		Reef (Homogenous)		Remarks
		H_s ft	T_p, sec (T_m)	D_n ft	W lbs	
1.0	8.1	5.0	5.6	1.07	199	Sub
10.0	9.0	5.6	6.5	1.19	281	Sub
25.0	9.7	6.5	7.6	1.38	436	Sub
50.0	10.5	7.2	9.7	1.60	674	Sub
Case 2. Crest Elevation +5.0 ft (MLW) $h_c' = 8.5$ ft						
1.0	8.1	5.0	5.6	1.13	236	Overtop
10.0	9.0	5.6	6.5	1.26	328	Sub
25.0	9.7	6.5	7.6	1.45	504	Sub
50.0	10.5	7.2	9.7	1.67	773	Sub
Case 3. Crest Elevation +6.0 ft (MLW) $h_c' = 9.5$ ft						
1.0	8.1	5.0	5.6	1.19	278	Overtop
10.0	9.0	5.6	6.5	1.32	383	Overtop
25.0	9.7	6.5	7.6	1.52	584	Sub
50.0	10.5	7.2	9.7	1.75	889	Sub

This example problem was taken from Appendix A "Case Design Example of a Detached Breakwater Project" in Chasten et al. (1993). It is a real, constructed project for the community of Bay Ridge, Anne Arundel County, Maryland, on the western shore of the Chesapeake Bay near Annapolis. Example Problem V-3-1 in the cited report described the functional design of the breakwater layout (spacing distance offshore, length, etc.). A crest elevation of +4.0 ft (MLW) was selected for design. Structural stability design conditions were also given for the homogenous sized stone. Design conditions selected were:

T_r = 25 years
H_s = 6.5 ft
T_p = 7.6 s
DSWL = +5.2 ft (MLW)
h = 9.7 ft (MLW)

The Hudson (1974) formula and *Shore Protection Manual* (1984) coefficients were used in the analysis. The breaking wave Hudson coefficient, $K_D = 2.0$ gives

D_n = 2.85 ft
W = 3,830 lb

(Sheet 4 of 5)

EXAMPLE PROBLEM VI-7-14 (Concluded)

The range of stone sizes accepted was 2,500-4,500 lb. The cross-sectional sketch of Figure VI-7-4 was taken from Chasten et al. (1993) Appendix A. It shows the large stone placed at the bottom for toe protection. The crest width *B* was 9.0 ft using three stone widths.

Use of the Hudson formula for Case 1 with completely submerged conditions gives stone weights over eight times heavier than required for these design conditions (436 lb – vs. – 3,830 lb). Even for the 50-year recurrence interval conditions, the Hudson formula results are roughly five times heavier. The crest width, based on three stone widths could also be reduced (6 ft – vs. – 9 ft which translates into less stone volume required and less costs).

SUMMARY: The Hudson formula was not meant to be applied for these conditions and is far too conservative.

The *Coastal Engineering Manual* presents stone stability formulations that give practical information for a range of water depths and waves impacting nearshore breakwaters.

(Sheet 5 of 5)

EXAMPLE PROBLEM VI-7-15

FIND: The weight and type (natural or artificial, concrete units) for repair of the north jetty at Barnegat Inlet, New Jersey.

GIVEN: The "Information Report on Effects of the North Jetty Repair on Navigation," especially Chapter 4, 'Hydraulic Analysis' (U.S. Army Engineer District, Philadelphia, 2001). Bathymetry from field surveys and numerical modeling of storm surge, water levels and wave conditions produced parameters with a range of frequency distributions. These permitted "sensitivity testing" for combined storm surge and wave conditions.

The design criteria specified less than 5 percent armor displacement or less than 0.5-ft crest elevation reduction for "storm conditions" at the 2 percent exceedance probability level in any one year, i.e., the 50-year recurrence interval. These criteria resulted in:

Storm surge = +8.1 ft (MLLW)
Wave height, H_{m0} = 13.8 ft (near structure head and toe)
Seabed elevation = -24ft (MLLW) (near structure head)

The raised jetty crest elevation was to be at +7.8 ft (MLLW).

SOLUTION:
Additional Assumptions: Sea water, $\rho = 1.99$ slugs/ft^3, $\gamma = 64$ lb/ft^3
Rock, $\rho_s = 5.14$ slugs/ft^3

$$\frac{\rho_s}{\rho} = 2.58$$

Use English System of units as given in USACE (2002).

Item 1. Natural Stone Armor Layer – Trunk

Assume quarrystone is available for all sizes required and construction equipment available for placement.

a. Hudson (1974) – Nonovertopped slopes

(1) Assume rough, angular, two layers
(2) Use no partial safety factors (Table VI-6-4)
(3) Assume nonbreaking wave conditions (H_{m0}/h) <0.6
(4) Use $K_D = 4.0$
(5) Use $H_{0.1} = 1.27\ H_{m0}$ for design wave
(6) Use Eq. VI-6-43,
(7) $W_{50} = \rho_s\ g\ D_{n50}^3$

(Sheet 1 of 7)

EXAMPLE PROBLEM VI-7-15 (Continued)

cot α	W_{50} (lb)
1.5	37,646
2.0	28,235
2.5	22,588

No wave period, structure permeability, or storm duration effects are considered in the Hudson method. Damage is assumed to be between 0-5 percent.

b. van der Meer (1988) – Nonovertopped slopes

Additional assumptions include:
(1) Rock jetty, notational permeability, $P = 0.4$
(2) Nominal damage level, $S = 2$ (investigate W for $S = 5$)
(3) Number of waves, $N_z = 2{,}500$ (investigate W for $N_z = 5{,}000$, 7,500)
(4) Wave period, $T_p = 14$ s (investigate W for $T_p = 11$ s, 9 s)
(5) Use H_{m0} for design wave

The wave periods are taken from Table 4-11 for storm conditions as investigated in the report (Corps 2002). The results are found as follows when surging or plunging formulas are applicable, again with no partial safety factors. Mean period, T_m, was assumed to be 0.83 T_p.

T_p	cot α	W (lb)	Type	Applicable Eq.
14.0 sec	1.5	45,080	Surging	VI-6-45
	2.0	34,788	Plunging	VI-6-44
	2.5	24,892	Plunging	VI-6-44

Effects of wave period

T_p	cot α	W (lb)	Type	Applicable Eq.
11.0 sec	1.5	37,402	Plunging	VI-6-44
	2.0	24,291	Plunging	
	2.5	17,381	Plunging	
9.0 sec	1.5	27,680	Plunging	VI-6-44
	2.0	17,977	Plunging	
	2.5	12,863	Plunging	

It is clear that the longer period, $T_p = 14$ s ($T_m = 11.6$ s) requires heavier natural stones from the quarry. All are plunging type, except for cot $\alpha = 1.5$ and $T_p = 14$ s. But the storm surge will cause wave overtopping of the relatively low jetty crest.

(Sheet 2 of 7)

EXAMPLE PROBLEM VI-7-15 (Continued)

c. van der Meer (1991) – Overtopping slopes

Now the relative freeboard (water depth – jetty crest) must be considered. This will vary as the total water level (storm surge, hydrograph plus local tidal range) changes during a storm event. Consider a freeboard range, 8 ft, 5 ft, 3 ft, 1 ft, 0 ft and Equation VI-5-71 used to reduce the values determined from van der Meer's Equations VI-6-44 and VI-6-45. To begin, assume design wave height, H_{m0} = 13.8 ft remains constant as the storm surge increases, and T_p = 14 s.

	Stone Weights, W for Freeboard, R_c (ft)					
cot α	8 ft	5 ft	3 ft	1 ft	0 ft	Type
1.5	32,057	28,209	25,980	23,890	23,056	S
2.0	24,817	21,838	20,113	18,564	17,849	P
2.5	17,739	15,610	14,377	13,270	12,759	P

The results reveal how overtopping reduces the stone weight requirements as formulated by van der Meer (1991). The largest freeboard possible is actually +7.8 ft at MLLW with no storm surge present. At the other extreme, with the design storm surge condition of +8.1 ft (MLLW), the structure actually becomes submerged.

d. van der Meer (1991) – Submerged conditions

The crest height, h_c' = 7.8 ft + 24 ft water depth = 31.8 ft (from sea bottom).
The design storm surge water depth, h = 8.1 ft + 24 ft water depth = 32.1 ft (from sea bottom).

The van de Meer (1991) formulation, Equation VI-5-72, uses the relative submergence, h_c'/h, and all results are independent of structure slope, α.

The required stone weights decrease slightly with minor increases in submergence as illustrated as follows for H_{m0} = 13.8 ft, T_p = 14.0 s.

	Stone Weights, W (lb) for Submergence Levels h - h_c' (ft)				
cot α	0 ft	0.1 ft	0.2 ft	0.3 ft	0.5 ft
1.5	und	16,266	16,109	15,953	15,801
2.0	und	16,266	16,109	15,953	15,801
2.5	und	16,266	16,109	15,953	15,801

The design case is for 0.3-ft submergence = $h_{design} - h_c$ = 32.1 - 31.8 ft.

e. Effect of storm duration, t (hr)

All of the preceding results are for N_z = 2,500 waves and for T_p = 14 s which is roughly, T_m = 11.6 and t = 8-hr storms. It is instructive to consider increased storm durations shown as follows. Armor weights are in pounds

(Sheet 3 of 7)

EXAMPLE PROBLEM VI-7-15 (Continued)

cot α	N_z = 2,500 t = 8 hr	N_z = 5,000 t = 16 hr	N_z = 7,500 t = 24 hr	Type
1.5	45,080	55,500	62,679	S
2.0	34,788	42,829	48,369	*P*
2.5	24,892	30,646	34,610	*P*

These results return to the basic, nonovertopping formulations (Equations VI-6-44 and VI-6-45), for illustration purposes only. The longer storms may produce increased levels of the related damage parameter, *S*, as illustrated as follows.

The longest storm duration is recommended at N_z = 7,500 waves, beyond which, no increased effects are found.

f. Effect of damage parameter, *S*

All the preceding results are for S = 2.0, which is the nominal, almost zero-level damage parameter recommended. Increasing the damage parameter S to 5.0 will reduce the stable stone weight required, as illustrated as follows. This level is more consistent with longer storms with more waves. Armor weghts are given in pounds, and Eqs. VI-6-44 and VI-6-45 were used.

cot α	N_z = 2,500 t = 8 hr	N_z = 5,000 t = 16 hr	N_z = 7,500 t = 24 hr	Type
1.5	26,015	32,028	36,171	S
2.0	20,075	24,716	27,913	*P*
2.5	14,365	17,685	19,973	*P*

Again, these results return to the basic, nonovertopping formulations, for illustrative purposes.

The nominal stone diameter for cot α = 1.5, N_z = 7,500 waves, S = 5.0, and under surging conditions with W_{50} = 36,171 lb is:

D_{nom} = 6.02 ft

(Sheet 4 of 7)

EXAMPLE PROBLEM VI-7-15 (Continued)

g. Discussion/Summary

Point 1. The time phase relationship between storm surge hydrograph (including local tidal range) and the wave energy variation is important because the required stable stone weight varies considerably under nonovertopping, overtopping, and submerged conditions. Design for the combination that gives the largest armor stone weight.

Point 2. Increased storm duration increases armor weight requirements. A compromise is to accept more damage by increasing the nominal damage parameter from $S = 2$ to $S = 5$.

Point 3. Many factors not considered in the Hudson formulation can be included in the van der Meer formulation to give design insight regarding their importance.

Point 4. Partial safety factors can also be included to increase the stable stone weights required and increase the corresponding reliability. These should be studied for overtopped to submerged conditions.

Point 5. For design, consider for TRUNK SECTION ONLY the following values.

cot α	W, lb	W, tons	Remarks
1.5 2.0 2.5	36,000 28,000 20,000	18 14 10	These recommended values include overtopping, $S = 5\%$, long storms, and are similar to Hudson (1974)

Point 6. Physical model studies should be conducted for verification. This is especially true for the head section.

Point 7. Artificial, concrete armor units, e.g., Core-Loc®, must also be considered, as discussed as follows.

Item 2. Artificial, concrete armor units

a. Core-Loc® Non – or marginally-overtopped slopes
These units are discussed in Table VI-5-34 and in Melby and Turk (1994). Hereafter, referred to as Core-Loc, they have been under development since July 1992 by the U.S. Army Corps of Engineers. They incorporate all the following features that were previously distinct weaknesses of existing armor unit shapes (Melby and Turk 1994):

(1) High hydraulic stability when placed in a single-unit thickness at any slope angle

(2) Reserve stability for wave conditions that exceed the design event

EXAMPLE PROBLEM VI-7-15 (Continued)

(3) No tendency for units to rock on slope

(4) Continued stability when broken or following renesting resulting from local instability

(5) Efficient combination of porosity and slope roughness to dissipate the maximum wave energy (and reduce wave runup)

(6) Maximum performance with a minimum concrete armor unit volume

(7) Hydraulically stable when placed as a repair with other shapes

(8) Low internal stresses, so no reinforcement required

(9) Easy to cast

(10) Easily constructed armor layer (single-unit-thickness), even in low visibility water

(11) Uses minimal casting yard or barge space

(12) Utilizes conventional construction materials and techniques

b. Example of a single-unit-thickness concrete armor layer, randomly placed:

For irregular, head-on waves, the Hudson formula has been applied, i.e.,

$$W = \frac{\rho_c \, g \, H_s^3}{K_D \left(\frac{\rho_c}{\rho_w} - 1 \right)^3 \cot \alpha}$$

as Equation VI-5-81 multiplied by the gravity constant, *g*, where:

H_s = the significant wave height
ρ_c = mass density of concrete
$\rho_c g$ = γ_c = unit weight concrete (assume = 140 lb/ft^3)
ρ_w = mass density of water in which unit is placed

For irregular, depth limited, breaking waves (plunging to collapsing), and the zero-damage condition (little or no rocking),

K_D = 16 is recommended for trunk section stability
K_D = 13 is recommended for head section stability

(Sheet 6 of 7)

EXAMPLE PROBLEM VI-7-15 (Concluded)

Results for the trunk section with $K_D = 16$ are:

cot α	*W*, lb	*W*, tons
1.333	10,302	5.2
1.5	9,155	4.6
2.0	6,866	3.4
2.5	5,493	2.8

and, for the head section with $K_D = 13$

cot α	*W*, lb	*W*, tons
1.333	12,680	6.3
1.5	11,268	5.6
2.0	8,450	4.2
2.5	6,760	3.4

Note that Core-Loc® units have been tested and remain stable on steeper slopes (3V:4H, cot $\alpha = 1.333$) which can be very important economically for deepwater applications requiring large stone volumes.

The weight of the Core-Loc® units are roughly 3.5 to 4 times less than the rubble-mound stone armor units. But many other factors are involved in selecting the type (natural or concrete units) for repair of the north jetty at Barnegat Inlet, New Jersey. These factors include primarily:

Factor 1. Cost Data
Price of rock-fill per ton (including quarrying, transport, and positioning on structures)
Price of concrete armor unit, Core-Loc®, per cubic yard (including manufacture, handling, and positioning on structure)

and

Factor 2. Construction Method/Available Equipment
From land or using offshore equipment
Crane capacity for lifting and span

c. Other Artificial Concrete Unit Types
Many other types (dolos, tetrapod, tribar, accropode, etc.) have been successfully applied, but all have weaknesses in one or more of the areas previously cited as strengths of the Core-Loc® design. None have been specifically designed to be used as repair units. For these reasons, it is recommended to use the Core-Loc® unit.

(Sheet 7 of 7)

VI-7-5. Stability of Vertical Walled Bulkheads and Caissons.

EXAMPLE PROBLEM VI-7-16

FIND: The width of a vertical walled, caisson-type breakwater/jetty structure for the north jetty site at Barnegat Inlet, New Jersey.

GIVEN: The same information as found in Example Problem VI-7-15 summarized here (using non-SI units as given in the report):

Recurrence interval for design, T_r = 50 years.
Spectral significant wave height for design, H_{m0} = 13.8 ft.
Peak wave period, T_p = 14 s (consider also 11 s, 9 s).
Water depth near structure head, h = 24 ft (MLLW to seabed).
Storm surge for design, s = +8.1 ft (MLLW).
Structure crest elevation = +9.0 ft (MLLW).
Wave direction for design, β = 0 deg.
Seawater, γ_w = 64 lb/ft^3.
Concrete, γ_c = 140 lb/ft^3.
Sand, γ_s = 125 lb/ft^3.

SOLUTION:
Item 1. Additional assumptions.

A suitable, rubble-mound foundation (core layer) with toe protection armor layer will support the concrete/sand-filled caisson structure. Assume the bottom of the caisson structure h^* is located at 0.85 h water depth below datum (MLLW), so take

h^* = caisson bottom depth (MLLW)
h^* = 0.85 (h) = 0.85 (24 ft) = 20.4 ft

assume

h^* = 20 ft. This leaves 4 ft for suitable rubble-foundation.

Adding the structure crest elevation above MLLW gives the total caisson structure height, h_w

h_w = 20 ft +9.0 ft = 29.0 ft

(Sheet 1 of 12)

EXAMPLE PROBLEM VI-7-16 (Continued)

The caisson concrete wall thickness, t, and concrete cap height, nt, can be varied where n is cap height multiplier of the wall thickness.

assume

$t = 2.0$ ft

$n = 2$

The rock thickness, r, for the toe armor layer can be specified as some fraction of the core layer depth, $(h - h^*)$. Assume

$r = 0.75\ (h - h^*) = 0.75\ (4) = 3.0$ ft

Finally, the rock berm width, B_m, can be taken as some multiplier of the rock thickness, say $2r$ (ASSUME).

$B_m = 2r = 6.0$ ft

Item 2. Calculated dimensions

See the sketch in Table VI-5-53 (Goda formula for irregular waves) for additional, dimensions.

Total water depth,

$h_s = \text{h} + \text{s}$

$h_s = 24.0$ ft $+ 8.1$ ft $= 32.1$ ft

Structure submerged depth,

$h' = h^* + s$

$h' = 20$ ft $+ 8.1$ ft $= 28.1$ ft

Armor rock depth,

$d = h' - r$

$d = 28.1$ ft $- 3.0$ ft $= 25.1$ ft

Freeboard

$h_c = h_w - h' = 29.0$ ft $- 28.1$ ft $= 0.9$ ft

Item 3. Calculated coefficients and pressures

3.1. Wave height for design, H_{design}

(Sheet 2 of 12)

EXAMPLE PROBLEM VI-7-16 (Continued)

As seen in Table VI-5-53, most of the coefficients (α_i) and pressures (p) for the net wave pressure distribution against the vertical wall depend on H_{design}. If seaward of the surf zone, Goda (1985) recommends for practical design.

$$H_{design} = 1.8\ H_s = 1.8\ (13.8\ \text{ft}) = 24.8\ \text{ft}$$

This is the wave height with only 0.15 percent exceedence of Rayeigh distributed waves or $H_{1/250}$.

3.2. Coefficients

The coefficients, α_1, α_2, and α_3 depend upon the local wavelength, L, at a water depth, h_b, and at a distance of 5 H_s seaward of the front wall of the vertical caisson. This requires a further assumption of the bottom slope, m, seaward of the wall.

Take

$$m = 1/100$$

and also assume

$$H_s = H_{m0}$$

Thus

$$h_b = 5\ (H_s)\ m + h_s$$
$$h_b = 5\ (13.8\ \text{ft})\ (0.01) + 32.1\ \text{ft}$$
$$h_b = 32.8\ \text{ft}$$

For $T_p = 14$ s and $h_b = 32.8$ ft, the local wavelength is

$$L = 439.1\ \text{ft}$$

Now find the coefficients α_1, α_2, and α_3.

$$\alpha_1 = 0.6 + 0.5\left[\frac{4\pi\ h_s / L}{\sinh\left(4\pi\ h_s / L\right)}\right]^2$$

$$= 0.6 + 0.5\left[\frac{4\pi\left(32.1\ \text{ft} / 439.1\ \text{ft}\right)}{\sinh\ 4\pi\left(32.1\ \text{ft} / 439.1\ \text{ft}\right)}\right]^2$$

$$\alpha_1 = 0.980$$

EXAMPLE PROBLEM VI-7-16 (Continued)

and

$$\alpha_2 = \text{ smallest of } \left[\frac{(h_b - d)}{3h_b}\left(\frac{H_{design}}{d}\right)^2\right] \text{ and } \frac{2d}{H_{design}}$$

Therefore,

$$\alpha_2 = \text{ smallest of } \left[\frac{(32.8 \text{ ft} - 25.1 \text{ ft})}{3(32.8 \text{ ft})}\left(\frac{24.8 \text{ ft}}{25.1 \text{ ft}}\right)^2\right] \text{ and } \frac{2(25.1 \text{ ft})}{24.8 \text{ ft}}$$

α_2 = smallest of 0.0764 and 2.024

so $\alpha_2 = 0.0764$

and

$$\alpha_3 = 1 - \frac{h_w - h_c}{h_s}\left[1 - \frac{1}{\cosh(2\pi\, h_s / L)}\right]$$

$$\alpha_3 = 1 - \frac{(29.0 \text{ ft} - 0.9 \text{ ft})}{32.1 \text{ ft}}\left[1 - \frac{1}{\cosh(2\pi\,(32.1 \text{ ft} / 439.1 \text{ ft}))}\right]$$

$$\alpha_3 = 0.9151$$

and note

$\alpha_* = \alpha_2$

so that

$\alpha_* = 0.0764$

Now, the pressures against the vertical wall are calculated.

3.3. Pressures

The theoretical, zero pressure is at a vertical distance, η^*, above the design water level. This distance and the pressures, p_1, p_2, p_3, and p_u, all include a coefficient λ (λ_1, λ_2, λ_3) that are "modification" factors depending on the structure type (i.e., inclined, curved, etc.). For conventional, vertical wall structures,

$\lambda_1 = \lambda_2 = \lambda_3 = 1$

(Sheet 4 of 12)

EXAMPLE PROBLEM VI-7-16 (Continued)

$$\eta^* = 0.75(1+\cos\beta)\lambda_1 H_{design}$$
$$= 0.75(1+\cos 0^o)(1.0)(24.8 \text{ ft})$$
$$\eta^* = 37.2 \text{ ft}$$

and

$$p_1 = 0.5(1+\cos\beta)(\lambda_1\alpha_1 + \lambda_2\alpha_* \cos^2\beta)(\rho_w g) H_{design}$$
$$= 0.5(1+\cos 0^o)(1.0 \cdot 0.980 + 1.0 \cdot 0.0764 \cos^2 O^o)(64 \text{ lb/ft}^3)(24.8 \text{ ft})$$
$$p_1 = 1,677 \text{ lb/ft}^2$$

and

$$p_2 = \begin{cases} \left(1 - \frac{h_c}{\eta^*}\right) p_1 & \text{for } \eta^* > h_c \\ 0 & \text{for } \eta^* \le h_c \end{cases}$$

and clearly $\eta^* > h_c$ so that

$$p_2 = \left[1 - (0.9 \text{ ft}/37.2 \text{ ft})\right](1,677 \text{ lb/ft}^2)$$
$$p_2 = 1,636 \text{ lb/ft}^2$$

and

$$p_3 = \alpha_3 p_1$$
$$= 0.9151(1,677 \text{ lb/ft}^2)$$
$$= 1,535 \text{ lb/ft}^2$$

(Sheet 5 of 12)

EXAMPLE PROBLEM VI-7-16 (Continued)

The bottom uplift pressure, p_u, is not equal to p_3 but found from

$$p_u = 0.5\left(1+\cos\beta\right)\lambda_3\alpha_1\alpha_3\left(\rho_w g\right)H_{design}$$
$$= 0.5\left(1+\cos 0^{o}\right)\left(1.0\right)\left(0.980\right)\left(0.9151\right)\left(64\text{ lb/ft}^3\right)\left(24.8\text{ lb/ft}\right)$$
$$p_u = 1,423\text{ lb/ft}^2$$

These pressures could be plotted to create the pressure distribution diagrams, similar to that shown in Table VI-5-53.

Item 4. Calculated forces and moments

Specifying a structure width, B, is now needed which is the horizontal dimension normal to h_w (not shown in Table VI-5-53). For illustration purposes of the calculations, assume

$B = 40$ ft

This structure width will significantly influence the structure weight (in air and water) and the uplift force on the bottom.

Table VI-5-55 presents the resulting wave induced forces and moments (including uncertainty factors) when calculated from the wave load equations by Goda (Table VI-5-53), and Takahashi, et al. (Table VI-5-54).

The formulas assume that the hydrostatic, horizontal pressures are in balance on both sides of the structure and are per running length of the structure (i.e., per unit length).

4.1.Forces

The horizontal force, F_H is:

$$F_H = U_{FH}\left[\frac{1}{2}\left(p_1+p_2\right)h_c+\frac{1}{2}\left(p_1+p_3\right)h'\right]$$

Use the mean values of the uncertainty and bias factors as presented in Table VI-5-56. So $U_{FH} = 0.90$ and $U_{FU} = 0.77$

$$F_H = 0.9\left[\frac{1}{2}\left(1,677\text{ lb/ft}^2+1,636\text{ lb/ft}^2\right)\left(0.9\text{ ft}\right)+\frac{1}{2}\left(1,677\text{ lb/ft}^2+1,535\text{ lb/ft}^2\right)28.1\text{ ft}\right]$$
$$F_H = 41,958\text{ lb/ft}$$

(Sheet 6 of 12)

EXAMPLE PROBLEM VI-7-16 (Continued)

The uplift force, F_U, depends on caisson width, B.

$$F_U = U_{FH}\left[\frac{1}{2}p_u(B)\right]$$
$$F_U = 0.77\left[\frac{1}{2}\left(1{,}423 \text{ lb/ft}^2\right)(40 \text{ ft})\right]$$
$$F_U = 21{,}914 \text{ lb/ft}$$

The structure submerged weight is more complicated. The formula in Table VI-5-55 for F_G says

$$F_G = (\rho_c g)\, B \cdot h_w - (\rho_w g)\, B \cdot h'$$

where

$\rho_c g$ = unit weight of the combined, concrete/sand structure

The first term is the total weight and the second term is the buoyant uplift force.

Because the walls are concrete (γ_c = 140 lb/ft^3) and the caisson is filled with sand (γ_s = 125 lb/ft^3), clearly the total weight (per lineal foot) will depend on the wall thickness, t, and the cap dimension, nt. Using the values

t = 2.0 ft
n = 2
B = 40 ft

gives

$$W_{\text{concrete}} = 140 \text{ lb/ft}^3\ [(40 \text{ ft})(29 \text{ ft}) - (36 \text{ ft})(23 \text{ ft})] = 46{,}480 \text{ lb/ft}$$
$$W_{\text{sand}} = 125 \text{ lb/ft}^3\ [(36 \text{ ft})(23 \text{ ft})] = 103{,}500 \text{ lb/ft}$$
$$W_{\text{Total}} = 46{,}480 \text{ lb/ft} + 103{,}500 \text{ lb/ft} = 149{,}980 \text{ lb/ft}$$

Therefore,

$$F_G = 149{,}980 \text{ lb/ft} - \left(64 \text{ lb/ft}^3\right)(40 \text{ ft})(28.1 \text{ ft})$$
$$F_G = 149{,}980 \text{ lb/ft} - 71{,}936 \text{ lb/ft}$$
$$F_G = 78{,}044 \text{ lb/ft}$$

(Sheet 7 of 12)

EXAMPLE PROBLEM VI-7-16 (Continued)

4.2.Moments about heel of the caisson

Using the recommended uncertainty and bias factors from Table VI-5-55 (U_{MH} = 0.81 and U_{MU} = 0.72), the overturning moment due to the horizontal force is

$$M_H = U_{MH}\left[\frac{1}{6}(2p_1 + p_3)h'^2 + \frac{1}{2}(p_1 + p_2)h'h_c + \frac{1}{6}(p_1 + 2p_2)h_c^2\right]$$

$$= 0.81\left[\begin{array}{l}\frac{1}{6}\left(2\left(1{,}677\ \text{lb/ft}^2\right) + 1{,}535\ \text{lb/ft}^2\right)\left(28.1\ \text{ft}\right)^2 + \\ \frac{1}{2}\left(1{,}677\ \text{lb/ft}^2 + 1{,}636\ \text{lb/ft}^2\right)28.1\ \text{ft}\cdot\left(0.9\ \text{ft}\right) \\ + \frac{1}{6}\left(1{,}677\ \text{lb/ft}^2 + 2\left(1{,}636\ \text{lb/ft}^2\right)\right)\left(0.9\ \text{ft}\right)^2\end{array}\right]$$

$$M_H = 555{,}630\ \text{lb-ft/ft}$$

The overturning moment of the uplift force is given by

$$M_U = U_{MU}\ \frac{1}{3}p_u \cdot B^2$$

$$M_U = 0.72(1/3)\left(1{,}423\ \text{lb/ft}^2\right)\left(40\ \text{ft}\right)^2 = 546{,}430\ \text{lb-ft/ft}$$

The compensating moment of the structure weight (net)

$$M_G = \frac{1}{2}B^2 g\left(\rho_c h_w - \rho_w h'\right)$$

is the moment formula found in Table VI-5-55 where again, the composite structure unit weight, ($\rho_c g$) is required. However, because the caisson cross section is symmetrical, the total force, F_G, is assumed to act at a horizontal distance $B/2$ from the back side, so

$$M_G = \frac{1}{2}B \cdot F_G$$

$$= \frac{1}{2}\left(40\ \text{ft}\right)\left(78{,}044\ \text{lb/ft}\right)$$

$$M_G = 1{,}560{,}880\ \text{lb-ft/ft}$$

This completes the basic calculation of forces and moments (per unit length) due to the wave loading formulations of Goda and Takahashi. Further analysis requires basic design practices, safety factors, and codes, i.e., DESIGN CRITERIA for the engineering evaluation of the assumed structure width, B.

(Sheet 8 of 12)

EXAMPLE PROBLEM VI-7-16 (Continued)

5. Safety against sliding, overturning, and heal bearing pressures.

5.1.Design criteria
Goda (1985) gave the following coefficients, safety factors as practiced by coastal engineers in Japan. Others are possible (see Tables VI-5-62 and VI-5-63).

Sliding friction coefficient, $\mu = 0.6$
Safety factor against sliding, $SF_s \geq 1.2$
Safety factor against overturning, $SF_o \geq 1.2$
Heal bearing pressures, $P_e < 8000 - 10{,}000$ lb/ft^2
P_e max = 12,000 lb/ft^2

5.2.Sliding from Equation VI-5-190

$$SF_s \equiv \frac{\mu\left(F_G - F_U\right)}{F_H}$$

and is simply the ratio of frictional resistance force to the applied force in the horizontal direction.

$$SF_s = \frac{0.6\left(78{,}044 \text{ lb/ft} - 21{,}914 \text{ lb/ft}\right)}{41{,}958 \text{ lb/ft}}$$

$$= \frac{33{,}678}{41{,}958}$$ (WARNING: Structure unstable in sliding mode)

$$SF_s = 0.80$$

The structure width with $B = 40$ ft is too narrow to prevent sliding because $SF_s < 1.2$.

5.3.Overturning from Equation VI-5-191

$$SF_O \equiv \frac{M_G}{M_U + M_H}$$

which is the ratio of resistive moment due to self-weight to overturning moments.

$$SF_O = \frac{1{,}560{,}880 \text{ lb-ft/ft}}{\left(546{,}430 + 555{,}630\right) \text{ lb-ft/ft}}$$

$$SF_O = \frac{1{,}560{,}880}{1{,}102{,}060}$$

$$SF_O = 1.42$$

(Sheet 9 of 12)

EXAMPLE PROBLEM VI-7-16 (Continued)

which is stable against overturning because SF_O exceeds the allowable safety factor, i.e., $SF_O \geq 1.2$.

5.4.Heel bearing pressure, Pe
See Goda (1985) and other marine foundation design references for eccentric, inclined loadings. Assume the seafloor is dense sand and the supporting, core layer material of good bearing capacity.

Define:
$W_e \equiv$ net vertical force
$W_e \equiv F_G - F_u = 78{,}044$ lb/ft $- 21{,}914$ lb/ft $= 56{,}130$ lb/ft
and
$M_e \equiv$ net moment about heel (positive counterclockwise)
$M_e \equiv M_G - M_u - M_H = (1{,}560{,}880 - 546{,}430 - 555{,}630)$ lb-ft/ft $= 458{,}820$ lb-ft/ft

Then $M_e = W_e \cong t_e$
or
$t_e \equiv M_e/W_e$
where t_e is the moment arm of the net vertical force.

so

$$t_e = \frac{458{,}820 \text{ lb-ft/ft}}{56{,}130 \text{ lb/ft}} = 8.17 \text{ ft}$$

Because $t_e \leq B/3$, assume a triangular bearing pressure distribution, with

$$P_e = \frac{2W_e}{3t_e}$$

$$P_e = \frac{2(56{,}130 \text{ lb/ft})}{3(8.17 \text{ ft})} = 4{,}580 \text{ lb/ft}^2$$

which is within safe bearing capacity.

Note: If $t_e > B/3$ a trapezodal bearing pressure distribution would be assumed with

$$P_e = \frac{2W_e}{B}\left(2\text{-}3\frac{t_e}{B}\right)$$

EXAMPLE PROBLEM VI-7-16 (Continued)

5.5. Summary, B = 40 ft caisson width (T_p = 14.0 s)

For the design wave, $H_{design} = 1.8\ H_{m0}$ and structure dimensions, h_w = 29.0 ft, B = 40 ft, this vertical, caisson-type jetty is unstable against sliding and stable against overturning. Heel bearing pressures are acceptable. Several design modifications could be considered to determine a stable caisson width.

Structure width, B, is the key variable because wider structures provide more weight for stability against sliding and overturning. However, the uplift forces and moments also increase, and cost per unit structure length also increase.

For the preceding example, keeping everything constant, it turns out that B must be increased to about 60.3 ft width for

$(SF)_s = 1.2$

5.6. Additional considerations for increased stability.

a. Increasing the jetty crest elevation, h_c. The structure weight could be increased by increasing the crest elevation, which was previously set at +9.0 ft (MLLW). Increasing by 1.0 ft increments, +10.0 ft, 11.0 ft, etc., produces ever decreasing stable width, B in a nonlinear trend.

b. Increasing the unit weight of the fill material, γ_s. The only practical way remaining is to find a suitable caisson fill material, e.g., slag from blast furnaces that is more dense and has a higher unit weight, γ_s, than saturated sand (γ_s = 125 s/ft^3).

c. Reliability analyses. Chapter VI-6 contains tables with partial safety factors for:

Sliding failure, Table VI-6-25
Overturning failure, Table VI-6-26
Foundation failure (Heel bearing pressure)
    Table VI-6-23, sand subsoil
    Table VI-6-24, clay subsoil

The width of the foundation sublay can be extended seaward and the vertical-walled, concrete caisson protected by a rubble-mound structure, seaward. Table VI-5-58 presents changes in the λ_1, λ_2, λ_3 coefficients in the Goda formula for this case.

EXAMPLE PROBLEM VI-7-16 (Continued)

The caisson sections exposed to wave breaking directly on the structure in the surf zone should be checked to ensure stability. Wave heights will be lower so that the same cross-sectional design may be sufficient.

6.0. Summary: In general, for relatively shallow-water depths, vertical-walled concrete caisson structures are not economically competitive with the rubbble-mound structures, but each site is different and should be checked.

(Sheet 12 of 12)

EXAMPLE PROBLEM VI-7-17

FIND: Find the total force per unit lateral length on a vertical baffle breakwater having penetration depths of 1/3 and 2/3 of the water depth. The breakwater will protect a mooring facility on Lake Michigan.

GIVEN: The following baffle breakwater parameters are defined in Part VI-5, Figure VI-5-61.

Water depth, h = 15.0 ft.
Wall penetration relative to SWL, w = 5.0 ft, 10 ft.
Specific weight of fresh water, $\rho_w g$ = 62.4 lb/ft^3.
Zeroth-moment wave height at breakwater, H_{mo} = 3.0 ft.
Wave period associated with the spectral peak, T_p = 5.0 s.

SOLUTION: The appropriate wavelength is found using linear wave theory with a depth of h = 15 ft and a wave period of T_p = 5 s, i.e., L_p = 96.3 ft. The corresponding wave number is

$$k_p = \frac{2\pi}{L_p} = \frac{2\pi}{96.3\text{ft}} = 0.0652 \quad 1/\text{ft}$$

Force on a Partially Penetrating Wall:

The first step is to calculate the parameter F_o which represents the significant force per unit length on a vertical wall extending all the way to the bottom as determined using linear wave theory. F_o is calculated using Eq. VI-5-163.

Important Note: The F_o-factor should only be used as part of the calculation for partially-penetrating walls (it is a normalizing factor). Estimates for forces on full-depth walls should be calculated using the Goda method detailed in Table VI-5-53.

(Sheet 1 of 2)

EXAMPLE PROBLEM VI-7-17 (Continued)

$$F_o = \rho_w \quad g \quad H_{mo}\left[\frac{\sinh\ \left(k_p h\right)}{k_{\ p}\ \cosh\ \left(k_p h\right)}\right]$$

$$F_o = \left(62.4 \quad \text{lb/ft}^3\right) \quad (3 \quad ft) \quad \left[\frac{\sinh\ \left[\left(0.0652 \quad 1/\text{ft}\right)\ \left(15 \quad \text{ft}\right)\right]}{\left(0.0652 \quad 1/\text{ft}\right)\ \cosh\left[\left(0.0652 \quad 1/\text{ft}\right)\ \left(15 \quad \text{ft}\right)\right]}\right]$$

$$F_o = 2{,}159 \quad \text{lb}/\text{ft}$$

Substituting given values of h and L_p and the calculated value of F_o into total force empirical formula for partially penetrating vertical walls given by Eq. VI-5-164 yields

$$F_{mo} = F_o \ \left(\frac{w}{h}\right)^{0.386\left(h/L_p\right)^{-0.7}}$$

$$F_{mo} = \left(2{,}159 \ \text{lb/ft}\right) \left(\frac{w}{h}\right)^{0.386\left(15\ \text{ft}/96.3\ \text{ft}\right)^{-0.7}}$$

$$F_{mo} = \left(2{,}159 \ \text{lb/ft}\right) \left(\frac{w}{h}\right)^{1.419}$$

Now substitute the different wall penetration values to find the significant total force at each depth.

w = 5 ft

$$F_{mo} = \left(2{,}159 \ \text{lb/ft}\right) \left(\frac{5 \ \text{ft}}{15 \ \text{ft}}\right)^{1.419} = 454.2 \ \text{lb/f}t$$

w = 10 ft

$$F_{mo} = \left(2{,}159 \ \text{lb/ft}\right) \left(\frac{10 \ \text{ft}}{15 \ \text{ft}}\right)^{1.419} = 1{,}214.4 \ \text{lb/ft}$$

Recall for final design it is recommended that the significant total force be increased by a factor of 1.8,

$$F_{design} = 1.8 \ F_{mo}$$

This increase corresponds roughly to the Goda-recommended design wave

$$H_{design} = H_{1/250} = 1.8\, H_{mo}$$

(Sheet 2 of 2)

EXAMPLE PROBLEM VI-7-18

FIND: Find the total force and moment per unit lateral length on a vertical seawall located inside the surf zone on an ocean beach.

GIVEN: The following parameters are defined in Part VI-5, Figure VI-5-71.

Water depth at breaking, h_b = 8.0 ft.
Breaking wave height, H_b = 7.0 ft.
Still-water depth at vertical wall toe, h_s = 5.0 ft.
Specific weight of salt water, $\rho_w g$ = 64.0 lb/ft^3.

SOLUTION: The broken wave height at the structure, as represented by the turbulent bore rushing up the beach, is estimated using Eq. VI-5-174, i.e.,

$$H_w = \left(0.2 + 0.58 \ \frac{h_s}{h_b} \right) \ H_b$$

$$H_w = \left[0.2 + 0.58 \ \frac{(5 \ \text{ft})}{(8 \ \text{ft})} \right] \ (7 \ \text{ft}) = 3.94 \ \text{ft}$$

The total horizontal force (excluding backfill soil or standing water pressure behind the wall) is the sum of the dynamic pressure force (Eq. VI-5-176) and the static pressure force (Eq. VI-5-179), i.e.,

$$R_T = \frac{\rho_w g \ h_b \ H_w}{2} + \frac{\rho_w g}{2} (h_s + H_w)^2$$

$$R_T = \frac{(64.0 \ \text{lb/ft}^3) \ (8 \ \text{ft}) \ (3.94 \ \text{ft})}{2} + \frac{(64.0 \ \text{lb/ft}^3)}{2} \ (5 \ \text{ft} + 3.94 \ \text{ft})^2$$

$$R_T = 1,008.6 \ \text{lb/ft} + 2,557.6 \ \text{lb/ft} = 3,566 \ \text{lb/ft}$$

(Sheet 1 of 2)

EXAMPLE PROBLEM VI-7-18 (Continued)

The total moment about the toe of the wall (excluding backfill soil or standing water pressure behind the wall) is the sum of the moments due to the dynamic pressure force (Eq. VI-5-177) and the static pressure force (Eq. VI-5-180), i.e.,

$$M_T = R_d \left(h_s + \frac{H_w}{2} \right) + R_s \left(\frac{h_s + H_w}{3} \right)$$

$$M_T = \left(1{,}008.6 \text{ lb/ft}\right) \left(5 \text{ ft} + \frac{3.94 \text{ ft}}{2} \right) + \left(2{,}557.6 \text{ lb/ft}\right) \left(\frac{5 \text{ ft} + 3.94 \text{ ft}}{3} \right)$$

$$M_T = 7{,}030 \ \frac{\text{ft-lb}}{\text{ft}} + 7{,}622 \ \frac{\text{ft-lb}}{\text{ft}} = 14{,}652 \ \frac{\text{ft-lb}}{\text{ft}}$$

(Sheet 2 of 2)

VI-7-6. Forces on Cylindrical Piles.

EXAMPLE PROBLEM VI-7-19

FIND: Find the total force and moment on a small-diameter cylindrical vertical pile situated in the nearshore area of the Atlantic Ocean (salt water).

GIVEN:
Water depth, d = 16.4 ft.
Wave height, H = 9.5 ft (approx. ¾ H_b).
Wave period, T = 8.0 s
Cylindrical pile diameter, D = 2.3 ft.
Specific weight of salt water, $\rho_w g$ = 64.0 lb/ft^3.
Kinematic viscosity of salt water, $\nu = 1.076(10)^{-5}$ ft^2/s

SOLUTION:
1. Estimate drag and inertia force coefficients.
An estimate of the maximum horizontal velocity under the prescribed wave is found from Stream Function theory to vary between

u_m = 13.1 ft/s (at crest of wave)
u_m = 6.1 ft/s (at the seabed)

The average maximum velocity of

u_m = 9.5 ft/s (average)

is used for calculation of the pile Reynolds number.

From Eqn. VI-5-307 the pile Reynolds number is calculated as

$$R_e = \frac{u_m \ D}{\nu} = \frac{(9.5 \text{ ft/s}) \ (2.3 \text{ ft})}{1.076 \ (10)^{-5} \text{ ft}^2/\text{s}} = 2.03 \ (10)^6$$

Figures VI-5-139 to VI-5-143 give plots for drag and inertia coefficients for Reynolds much lower than the previous calculation. In this case, use the guidance given after Figure VI-5-143 for higher Reynolds number. Because $R_e = 2.03(10)^6$ is greater than $5(10)^5$, the drag and inertia coefficients are assumed to have constant values given by

C_D = 0.7
C_M = 1.5

(Sheet 1 of 3)

EXAMPLE PROBLEM VI-7-19 (Continued)

2. Estimate force and moment coefficients from nomograms.
The *Coastal Engineering Manual* provides two methods for estimating the maximum force and moment acting on a cylindrical pile. One method estimates the individual maximums for the drag and inertia forces and moments, and then sums the values. This method is conservative because the two maximums are out of phase. The preferred method is to estimate the maximum combined drag and inertia forces and moment forces using Equations VI-5-300 and VI-5-301, reproduced as follows.

$$F_m = \varphi_m \; C_D \; \rho_w g \; H^2 \; D$$
$$M_m = \alpha_m \; C_D \; \rho_w g \; H^2 \; D \; d$$

Values for the nondimensional coefficients φ_m and α_m are taken from the appropriate nomograms contained in Figures VI-5-131 to VI-5-138 based on the nondimensional parameter W given by Eqn. VI-5-299. For the values of drag and inertia coefficients in this example,

$$W = \frac{C_M}{C_D} \; \frac{D}{H} = \frac{1.5}{0.7} \; \frac{(2.3 \text{ ft})}{(9.5 \text{ ft})} = 0.52$$

Also needed are values of relative wave steepness and relative water depth that are the ordinate and abscissa, respectively, of the nomograms. For this example

$$\frac{H}{gT^2} = \frac{9.5 \text{ ft}}{(32.2 \text{ ft/s}^2)\,(8 \text{ s})^2} = 0.0046$$
$$\frac{d}{gT^2} = \frac{16.4 \text{ ft}}{(32.2 \text{ ft/s}^2)\,(8 \text{ s})^2} = 0.0080$$

Figure VI-5-133 was constructed for a value of $W = 0.5$, and it is the closest to the value of $W = 0.52$ calculated for this example. Using the values for $H/(gT^2)$ and $d/(gT^2)$, the force coefficient in found from Figure VI-5-133 to be

$$\varphi_m = 0.32$$

Similarly, the moment coefficient for $W = 0.5$ is found from Figure VI-5-137 as

$$\alpha_m = 0.30$$

(Sheet 2 of 3)

EXAMPLE PROBLEM VI-7-19 (Continued)

3. Estimate maximum total force and moment.

Finally, the total maximum force and total maximum moment are calculated as

$$F_m = \varphi_m \, C_D \, \rho_w g \, H^2 \, D$$

$$F_m = 0.32 \, \left(0.7\right) \, \left(64.0 \ \text{lb/ft}^3\right) \, \left(9.5 \ \text{ft}\right)^2 \, \left(2.3 \ \text{ft}\right) = 2{,}976 \ \text{lb}$$

and

$$M_m = \alpha_m \, C_D \, \rho_w g \, H^2 \, D \, d$$

$$M_m = 0.30 \, \left(0.7\right) \, \left(64.0 \ \text{lb/ft}^3\right) \, \left(9.5 \ \text{ft}\right)^2 \, \left(2.3 \ \text{ft}\right) \, \left(16.4 \ \text{ft}\right) = 45{,}752 \ \text{ft-lb}$$

The corresponding moment arm is found simply as

$$\text{Moment Arm} = \frac{M_m}{F_n} = \frac{45{,}752 \ \text{ft-lb}}{2{,}976 \ lb} = 15.4 \ \text{ft}$$

which is one foot below the still waterline.

NOTE: In this example the calculated value of W was reasonably close to that of Figures VI-5-133 and VI-5-137. For cases when W falls between nomograms, finds values of φ_m and α_m from the bracketing nomograms and linearly interpolate.

(Sheet 3 of 3)

VI-7-7. References.

Ahrens 1987
Ahrens, J. P. 1987. "Characteristics of Reef Breakwaters," Technical Report CERC-87-17, Coastal Engineering Research Center, U.S. Army Engineer Waterways Experiment Station, Vicksburg, MS.

Brooks and Brandon 1995
Brooks, R. M., and Brandon, W. A. 1995. "Hindcast Wave Information for the U.S. Atlantic Coast: Update 1976-1993." WIS Report 33, Coastal Engineering Research Center, U.S. Army Engineer Waterways Experiment Station, Vicksburg, MS.

Carver and Heimbaugh 1989
Carver, R. D., and Heimbaugh, M. S. 1989. "Stability of Stone- and Dolos-Armored Rubble-Mound Breakwater Heads Subjected to Breaking and Nonbreaking Waves with No Overtopping," Technical Report CERC-89-4, Coastal Engineering Research Center, U.S. Army Engineer Waterways Experiment Station, Vicksburg, MS.

Chasten et al. 1993
Chasten, M. A., Rosati, J. D., McCormick, J. W., and Randall, R. E. 1993. "Engineering Design Guidance for Detached Breakwaters as Shoreline Stabilization Structure," Technical Report CERC-93-19, Coastal Engineering Researach Center, U.S. Army Engineer Waterways Experiment Station, Vicksburg, MS.

de Waal and van der Meer 1992
de Waal, J. P., and van der Meer, J. W. 1992. "Wave Run-Up and Overtopping on Coastal Structures, *Proceedings 23rd International Coastal Engineering Conference*, American Society of Civil Engineers (ASCE), Vol. 2, 1,758-1,771.

Goda 1985
Goda, Y. 1985. *Random Seas and Design of Maritime Structures*. University of Tokyo Press, Tokyo, Japan.

Hudson 1974
Hudson, R. Y. (editor). 1974. "Concrete Armor Units for Protection Against Wave Attack," Miscellaneous Paper H-74-2, U.S. Army Engineer Waterways Experiment Station, Vicksburg, MS.

Junger 1997
Junger, S. 1997. *The Perfect Storm: A True Story of Men Against the Sea*. W.W. Norton & Co., New York, 227 pp.

Leenknecht et al. 1992
Leenknecht, D. A., Szuwalski, A., and Sherlock, A. R. 1992. "Automated Coastal Engineering System: User Guide and Technical Reference, Version 1.07," U.S. Army Engineer Waterways Experiment Station, Vicksburg, MS.

Melby and Turk 1994
Melby, J. A. and Turk, G. F. 1994. "The CORE-LOC: Optimized Concrete Armor," *Proceedings 24th International Coastal Engineering Conference*, ASCE, Vol. 2, 1,426-1,438.

Nielsen 1984
Nielson, P. 1984. "Analytical Determination of Wave Height Variation," *Journal of Waterway Port, Coastal, and Ocean Engineering*, ASCE, Vol. 110, No. 2, pp. 283-287.

Owen 1980
Owen, M. W. 1980. "Design of Seawalls Allowing for Wave Overtopping," Report No. 924, Hydraulics Research Station, Wallingford, England.

Owen 1982
Owen, M. W. 1982. "The Hydraulic Design of Seawall Profiles," *Proceedings of Coastal Protection Conference*, Institution of Civil Engineers, Thomas Telford, London, 185-192.

Pitcher 1964
Pitcher, G. 1964. *The Philosophy of Wittgenstein, Part I*. Prentice-Hall, Inc., Englewood Cliffs, NJ.

Shore Protection Manual 1977
Shore protection manual. 1977. 3rd ed., 3 Vol, U.S. Army Engineer Waterways Experiment Station, U.S. Government Printing Office, Washington, DC.

Takahashi, Tanimoto, and Shimosako 1994
Takahashi, S., Tanimoto, K., and Shimosako, K. 1994. "A Proposal of Impulsive Pressure Coefficient for Design of Composite Breakwaters," *Proceedings of the International Conference on Hydro-Technical Engineering for Port and Harbor Construction*, Port and Harbour Research Institute, Yokosuka, Japan, pp. 489-504.

Shore Protection Manual 1984
Shore protection manual. 1984. 4th ed., 2 Vol, U.S. Army Engineer Waterways Experiment Station, U.S. Government Printing Office, Washington, DC.

U.S. Army Engineer District, Philadelphia 2001
U.S. Army Engineer District, Philadelphia. 2001. "Information Report on Effects of the North Jetty Weir on Navigation, Barnegat Inlet, New Jersey: Chapter 4, Hydraulic Analysis," Draft Report, February 2001.

van der Meer 1988
van der Meer, J. W. 1988. "Rock Slopes and Gravel Beaches Under Wave Attack," Ph.D. diss., Delft Hydraulics Publication No. 396, Delft University of Technology, The Netherlands.

van der Meer 1990
van der Meer, J. W. 1990. "Low-Crested and Reef Breakwaters," Report H198/Q638, Delft Hydraulics Laboratory, The Netherlands.

van der Meer 1991
van der Meer, J. W. 1991. "Stability and Transmission at Low-Crested Structures," Delft Hydraulics Publication No. 453, Delft Hydraulics Laboratory, The Netherlands.

van der Meer and Janssen 1995
van der Meer, J. W., and Janssen, W. 1995. "Wave Run-Up and Wave Overtopping at Dikes," in *Wave Forces on Inclinded and Vertical Wall Structures*. N. Kobayashi and Z. Demirbilek, ed., ASCE, pp. 1-27.

VI-7-8. Acknowledgements.

Authors: Dr. David R. Basco, Department of Civil Engineering, Old Dominion University, Norfolk, VA; and Dr. Steven A. Hughes, Coastal and Hydraulics Laboratory (CHL), U.S. Army Engineer Research and Development Center, Vicksburg, MS.

Reviewers: H. Lee Butler, CHL (retired); Dr. Lyndell Z. Hales, CHL; and Dr. Lee E. Harris, Department of Marine and Environmental Systems, Florida Institute of Technology, Melbourne, FL.

VI-7-9. List of Symbols.

Symbols have been defined in each example problem at the time they are first used or derived. Also see VI-5 for symbols.

CHAPTER 8

Monitoring, Maintenance, and Repair of Coastal Projects

TABLE OF CONTENTS

Page

VI-8-1. Maintenance of Coastal Projects....VI-8-1
a. Aging of coastal projects....VI-8-1
b. Project maintenance....VI-8-2

VI-8-2. Inspecting and Monitoring Coastal Structures....VI-8-3
a. Introduction and overview....VI-8-3
b. Project condition monitoring....VI-8-4
c. Project performance/function monitoring....VI-8-27
d. Monitoring plan considerations....VI-8-30

VI-8-3. Repair and Rehabilitation of Coastal Structures....VI-8-37
a. General aspects of repair and rehabilitation....VI-8-37
b. Repair and rehabilitation of rubble-mound structures....VI-8-40

VI-8-4. References....VI-8-60

VI-8-5. Acknowledgments....VI-8-67

VI-8-6. Symbols....VI-8-67

List of Figures

Figure VI-8-1. Dolos breakage on Crescent City, California, breakwater VI-8-6

Figure VI-8-2. Interior of Great Sodus east breakwater, Lake Ontario, New York VI-8-8

Figure VI-8-3. Aerial photogrammetry image of Yaquina, Oregon, north jetty VI-8-10

Figure VI-8-4. Multibeam scanner mounted on survey vessel VI-8-12

Figure VI-8-5. Major reaches and structure functions for typical jetty VI-8-18

Figure VI-8-6. Damage at Redondo Harbor breakwater looking from inside harbor VI-8-42

Figure VI-8-7. Cleveland Harbor breakwater rehabilitation, 1980 ..... VI-8-47

Figure VI-8-8. Cleveland Dike 14 before rehabilitation VI-8-49

Figure VI-8-9. Cleveland Dike 14 after rehabilitation VI-8-50

Figure VI-8-10. North jetty at entrance to Humboldt Bay, California VI-8-60

List of Tables

Table VI-8-1. Frequency of Walking Inspections VI-8-6
Table VI-8-2. General Condition Index Scale VI-8-13
Table VI-8-3. Steps in Condition and Performance Rating System VI-8-14
Table VI-8-4. Functional and Structural Rating Categories VI-8-14
Table VI-8-5. Functional Rating Guidance for Navigation Channel VI-8-19
Table VI-8-6. Structural Index Scale for Coastal Structures VI-8-21
Table VI-8-7. Rating Guidance for Armor Loss VI-8-23
Table VI-8-8. Functional Index Scale for Coastal Structures VI-8-24
Table VI-8-9. When Coastal Project Might Need Repairs or Rehabilitation VI-8-38
Table VI-8-10. Case Histories of USACE Breakwater and Jetty Structures VI-8-41
Table VI-8-11. Construction Equipment for Repair of Rubble-Mound Structures VI-8-43
Table VI-8-12. Options for Repairing Rubble-Mound Structures VI-8-44
Table VI-8-13. Summary of Stability Results for Dissimilar Armor Overlays VI-8-46
Table VI-8-14. Buhne Point Cementitious Sealant VI-8-57

CHAPTER VI-8

Monitoring, Maintenance, and Repair of Coastal Projects

VI-8-1. Maintenance of Coastal Projects. This chapter covers maintenance requirements of coastal engineering projects. Ongoing maintenance at some level is necessary for most existing coastal projects to assure continued acceptable project performance. Major topics included in this chapter are monitoring of projects, evaluation of project condition, repair and rehabilitation guidelines, and project modifications. Available guidance related to specific repair and rehabilitation situations is included. However, in many cases design guidance suitable for new construction is used to design repairs.

a. Aging of coastal projects.

(1) The U.S. Army Corps of Engineers (USACE) has responsibility for constructing and maintaining federally authorized coastal engineering projects in the United States. These include navigation channels, navigation structures, flood-control structures, and erosion control projects. Pope (1992) summarized a series of reports (see Table VI-8-10) on Corps-maintained breakwaters and jetties and noted that 77 percent of the 265 navigation projects constructed in the United States were over 50 years old. Even more revealing is the fact that about 40 percent of the breakwaters and jetties originated in the 1800s. This means that a majority of the Corps' structures were designed and built before the introduction of even rudimentary design guidance and armor stability criteria, and in many cases the structures have survived well beyond their intended service life because they have been properly maintained. Most developed countries undoubtedly have a similar situation.

(2) Over the projected life of a project, the structural components are susceptible to damage and deterioration. Damage is usually thought of as structure degradation that occurs over a relatively short period such as a single storm event, a unique occurrence, or perhaps a winter storm season. Damage might be due to storm events that exceed design levels, impacts by vessels, seismic events, unexpected combinations of waves and currents, or some other environmental loading condition.

(3) Deterioration is a gradual aging of the structure and/or its components over time. Deterioration can progress slowly, and often goes undetected because the project continues to function as originally intended even in its diminished condition. However, if left uncorrected, continual deterioration can lead to partial or complete failure of the structure.

(4) Pope (1992) distinguished between two types of aging processes that occur at coastal projects. Structure aging is a change to a portion of the structure that affects its function. Examples of structure aging include: settlement or lateral displacement of the structure, loss of slope toe support, partial slope failure, loss of core or backfill material, and loss of armor units.

(5) Unit aging is defined as deterioration of individual components which could eventually affect the structure's function. Examples of unit aging include: breakage of concrete armor units, fracturing of armor stone, below-water deterioration of wood or sheet metal pilings,

corrosion of metal supports and fittings, concrete spalling, ripping of geotextile bags, and failure of individual gabion or timber crib units.

(6) Because coastal structure aging is a slow process, and the severity of deterioration may be hidden from casual inspection, rehabilitation often is given a low priority and may be postponed if the structure is still functioning at an acceptable level. Saving money by neglecting needed repairs runs the risk of facing a far more expensive (and possibly urgent) repair later.

b. Project maintenance.

(1) Project maintenance is a continuous process spanning the life of the coastal project. The goal of maintenance is to recognize potential problems and to take appropriate actions to assure the project continues to function at an acceptable level.

(2) Maintenance consists of the following essential elements (Vrijling, Leeuwestein, and Kuiper 1995):

(a) Periodic project inspection and monitoring of environmental conditions and structure response.

(b) Evaluation of inspection and monitoring data to access the structure's physical condition and its performance relative to the design specifications.

(c) Determining an appropriate response based on evaluation results. Possible responses are

- Take no action (no problems identified or problems are minor)
- Rehabilitate all or portions of the structure
- Repair all or portions of the structure

(3) Rehabilitation is defined in the dictionary as ARestoring to good condition, operation, or capacity.” This implies that steps are taken to correct problems before the structure functionality is significantly degraded. For example, replacing broken concrete armor units, filling and capping scour holes, replacing corroded steel sheet pile, or patching spalled concrete might be considered structure rehabilitation. Rehabilitation can also be thought of as preventative maintenance. There are two types of preventative maintenance: condition-based maintenance which is rehabilitation based on the observed condition of the project; and periodic maintenance which is rehabilitation that occurs after a prescribed time period or when a particular loading level is exceeded.

(4) Repair is defined in the dictionary as “Restoring to sound condition after decay, damage, or injury.” The major implication in this definition for repair is that damage has occurred and structure functionality is significantly reduced. For example, rebuilding a slumped armor slope, resetting breakwater crown blocks, rebuilding damaged pier decks, repairing vertical seawall, and backfilling eroded fill could be considered structure repair. Repair can also

be thought of as corrective maintenance. Obviously there are many situations where it is difficult to distinguish between repair and rehabilitation. The concepts behind coastal structure maintenance are straightforward; the difficulties lie in determining

(a) What to monitor.

(b) How to evaluate the monitoring data.

(c) Whether or not to undertake preventative or corrective action.

(d) How to access the economic benefits of the possible responses.

(5) Because of the wide variety of coastal structures and the varied environments in which they are sited, development of a generic project maintenance plan is difficult. Perhaps the best source of guidance is past experience maintaining similar projects.

(6) In addition to repair and rehabilitation, a third response that might arise during maintenance is a decision to modify a project even if it shows no damage or deterioration. Monitoring might reveal the project is not performing as expected, or the goals of the project might have changed or expanded, necessitating structure additions or modification. Examples include raising breakwater crest elevation to reduce overtopping into a harbor, modifying jetty length to reduce downdrift erosion problems, and sand tightening jetties to block passage of sediment.

VI-8-2. Inspecting and Monitoring Coastal Structures.

a. Introduction and overview.

(1) Project monitoring is a vital part of any successful maintenance program. The complexity and scope of a monitoring effort can vary widely from simple periodic onsite visual inspections at the low end of the scale to elaborate and expensive long-term measurement programs at the other extreme. The most important aspect in any monitoring and inspection program is to determine carefully the purpose of the monitoring. Without a clear definition of the monitoring goals, resources and instruments will not be used in the most beneficial manner; and most likely, the monitoring information will be insufficient to evaluate the project and recommend appropriate maintenance responses.

(2) Project monitoring can be divided into two major categories:

(a) Project condition monitoring consists of periodic inspections and measurements conducted as part of project maintenance. Condition monitoring provides the information necessary to make an updated assessment of the structure state on a periodic basis or after extreme events.

(b) Project performance/function monitoring consists of observations and measurements aimed at evaluating the project's performance relative to the design objectives. Typically, performance monitoring is a short-duration program relative to the life of the project.

(c) There are substantial differences between monitoring plans developed for project condition monitoring and plans developed for monitoring project performance. However, when developing either type of plan, several guidelines should be followed.

- First, establish the goals of the monitoring. Once the goals are known, every component suggested for the monitoring program can be assessed in terms of how it supports the goals. If a proposed element does not support the goals, there is little justification for including it.

- Second, review the project planning and design information to identify the physical processes that affect the project. These processes are then ranked in order of importance with respect to the monitoring goals. For some situations this step will be difficult because of uncertainties about the interaction between project elements and the environmental loadings. Once the monitoring goals are determined and the principal physical processes are identified, it is then possible to proceed with developing a plan to acquire the necessary monitoring data.

- An essential component of any plan is a provision for gathering sufficient project baseline data. Baseline data provide the basis for meaningful interpretation of measurements and observations. Elements of the baseline data collection are determined directly from the monitoring plan. For example, if the cross-section profile of a rubble-mound structure is to be monitored, it is necessary to establish the profile relative to known survey monuments at the start of the monitoring period. The as-built drawings often serve as part of the baseline survey information for project condition monitoring. Note that as-built drawings based on after-construction surveys are not always prepared. Thus, original design drawings may have to serve as baseline information.

b. Project condition monitoring. Project condition monitoring and inspection are necessary only for preventative maintenance programs. Failure-based maintenance does not require a monitoring program (Vrijling, Leeuwestein, and Kuper 1995). However, even failure-based maintenance must have some means of discovering whether or not severe damage or failure has occurred. If damage is not reported, there is a risk that additional damage or complete failure may occur, resulting in more costly repairs. Choosing which aspects of the project to inspect and monitor should be based on an understanding of the potential damage and failure modes for that particular type of project. This includes understanding the failure modes and deterioration traits of individual project components, as well as the project as a whole. Some failure modes may have a higher likelihood of occurrence, but may occur gradually without immediate impact to project functionality. On the other hand, there may be other failure modes with lower probability of occurrence that cause immediate, catastrophic damage. Just as important as identifying failure modes is knowing the physical signs of impending failure associated with each particular mode. For example, loss of armor stone from a slope or armor unit breakage may be a precursor to slope failure. The monitoring plan should outline what signs to look for, and if possible, how to quantify the changes. Some identified failure modes may give no warning signs of impending doom; and in these cases, monitoring will not help. Past experience with similar projects is beneficial in establishing what aspects of the project to monitor for change. Project condition monitoring always involves at least visual inspection of the project, and in some cases the inspection is augmented with measurements meant to quantify

the current structure condition relative to the baseline condition. These observations are then used to evaluate the current project condition and make decisions on the course of action. Condition monitoring should be performed when changes are most likely to occur. Most changes happen during construction and in the first year or two after a project is completed. During this period, there can be dynamic adjustments such as structure settlement, armor units nesting, and bathymetry change. After initial structure adjustment, most significant changes occur during storm events. The monitoring plan should provide enough flexibility in scheduling to accommodate the irregularity of severe storms.

(1) Periodic inspections. The Corps of Engineers' policy relative to periodic inspection of navigation and flood-control structures is as follows:

(a) "Civil Works structures, whose failure or partial failure could jeopardize the operational integrity of the project, endanger the lives and safety of the public, or cause substantial property damage shall be periodically inspected and evaluated to ensure their structural stability, safety, and operation adequacy."

(b) The major USACE District and Division commands have responsibility for establishing periodic inspection procedures, intervals, etc., for civil works projects. However, standardized inspection methodology across all USACE Field Offices is lacking due to specific guidance, credentials of the individuals performing the inspections as well as the wide diversity in projects, sites, and environmental conditions.

(c) Above-water visual inspection of structural components can be accomplished by walking on the structure, or viewing it from a boat or an airplane. The effectiveness of visual inspection depends heavily on knowing what symptoms of deterioration to look for and being able to gauge changes that have occurred since the previous inspection. For example, broken armor units and displaced stone are obvious signs of potential problems (Figure VI-8-1).

(d) Visual inspections are subjective by nature; and, as in most practical aspects of coastal engineering, experience is paramount in recognizing potential problems. Inexperienced engineers, new to the inspection process, should accompany the seasoned engineers during inspection tours so they can learn to recognize the important signs of deterioration. This also helps provide monitoring continuity over the life of the structure as senior personnel retire and younger engineers move into senior positions.

(e) When observations indicate the need to quantify the structure changes, a few simple, inexpensive techniques can be used during the onsite inspection. These measures include: counting broken armor units, spray paint marking of cracks or suspected displacements, using a tape to measure distances between established points on the structure, shooting the elevation of selected locations using a level, and repeated photo-documentation from the same vantage point (Pope 1992).

(f) Frequency of periodic walking inspections of coastal structures varies a great deal across the USACE District and Division offices and even between different structures in the same jurisdiction. Typical options are included in Table VI-8-1.

Figure VI-8-1. Dolos breakage on Crescent City, California, breakwater

Table VI-8-1
Frequency of Walking Inspections

Annual walking inspections
Annual walking inspections for recently completed structures and repairs; less frequent inspections for older structures
Walking inspections every 2 years
Walking inspections every 3 years if the structure has not changed for 4 consecutive years
Walking inspections only after major storm events
Walking inspections only when personnel are in the region for other purposes and time permits
Walking inspections only after local users report a problem

(g) In general, the frequency of inspection of a particular structure should be determined on a case-by case basis. Factors that influence inspection frequency, along with recommended general guidelines, are listed in the following paragraphs:

- Geographic location. Structures situated in exposed locations on high-energy shores (e.g., northwest coast of the U.S.) should be inspected annually. Structures in sheltered areas or

on low-energy coasts can stretch the inspection interval to 2 or 3 years. If no significant damage occurs for 5 years, inspections can be less frequent. Structures that undergo seasonal ice loading and freeze/thaw conditions should be inspected at least once every other year with particular emphasis on stone integrity or armor displacement.

- Structure age. Recently constructed, rehabilitated, or repaired structures should be inspected annually. Older structures with a good stability record for at least 5 years can be inspected less often. Frequently repaired structures should have annual inspections, but chronic damage should be addressed by a more robust design.

- Storm damage. Structures should be inspected after major storm or other events that might cause damage (e.g., earthquake or ship collision). Annual inspections are warranted in cases where damaged structures would impact navigation, property, and life. Reports of damage by local users of the project should be investigated immediately.

- Available funds. Sufficient funds and available personnel dictate both the frequency and priority of periodic inspections, particularly in Districts with many coastal structures. Past experience will help establish an inspection schedule that optimizes available funds.

(h) In summary, periodic inspection methods and frequency are determined based on repair history, past experience, engineering judgment, and available funding and manpower.

(i) All inspections should be documented to provide information and guidance for future assessments, and careful consideration should be given as to how the inspection information is to be preserved. Even the most observant visual inspection has little value if others cannot review the information and understand what was observed. Cryptic shorthand notes, rough sketches, etc., should be translated and expanded shortly after the inspection.

(j) Aerial visual inspection of coastal projects by fixed-wing or rotor-wing aircraft is an option that has several advantages. Aircraft provide easier access to remote project sites and to structures that are not attached to shore. They also allow the inspector to witness structure performance during wave conditions that would be unsafe for a walking inspection. Finally, several individual projects along a stretch of coastline can be inspected from the air in a short time span. During the aerial inspection, still photographs and video can be taken to augment the inspection notes. These images can be compared to previous photographs to see if obvious changes have occurred.

(k) The major disadvantage of aerial inspections is that only obvious changes can be identified whereas subtle changes and signs of deterioration may go unnoticed, even when inspecting enlarged aerial photographs. Nevertheless, aerial inspections make economic sense for projects with good performance histories and for making quick assessments after major storms to determine which projects need closer inspection.

(l) Underwater and interior visual inspection of structure condition is difficult, if not impossible, for many projects. These inspections require professional divers who also understand the signs of damage and deterioration for the particular type of structure. Water visibility plays a big role in underwater inspection. Some inspections, such as examining the condition of piers

and piles, can be performed during poor visibility. However, other visual inspections, such as assessing the integrity of armor slopes beneath the surface, require sufficient visibility to see enough of the slope to recognize missing armor and slope discontinuities. Even in the best of conditions, information from diver surveys is subjective and spatial detail is sparse. Around tidal inlets, underwater inspections can only take place during the slack water. Above all, safety for both the divers and their support crew on the surface is the most important criterion for underwater visual inspections. Figure VI-8-2 shows the interior of the concrete parapet of the Great Sodus east breakwater, Lake Ontario, New York. Notice the missing timber and interior fill. Further information on diver inspections is given in Thomas (1985).

Figure VI-8-2. Interior of Great Sodus east breakwater, Lake Ontario, New York

(m) In some circumstances, it may be possible to use video cameras lowered into the water or mounted on remotely-controlled vehicles to inspect underwater portions of a structure. Other methods for quantifying underwater portions of structures are listed in the next section.

(2) Measurements. Measurements to quantify specific aspects of a coastal project that cannot be judged from a visual inspection may be included as part of the long-term project condition monitoring. Such measurements may be acquired concurrently with the visual inspection, or they may be part of longer-duration monitoring. Generally, project condition measurements focus on physical changes of the structure and its foundation. Examples include

repeated elevation surveys of selected structure cross sections to quantify settlement or loss of armor, bathymetry soundings to document scour hole development, quantifying underwater structure profiles with sensors, and spot testing of materials undergoing deterioration, such as concrete, timber, and geosynthetics. Basically, any measurement that aids in evaluating structure condition can be considered for the condition monitoring program. Most measurements require baseline data for comparison, and sequential measurements help to assess the rate of change for the monitored property.

(a) Photogrammetry. Photogrammetry is a term applied to the technique of acquiring and analyzing aerial photography to quantify the three-dimensional (3-D) geometry of objects in the photographs relative to a fixed coordinate system. One area particularly well suited to photogrammetry techniques is profiling rubble-mound structure cross sections and monitoring movement of armor units on exposed structures based on properly acquired aerial photography (Kendell 1988; Hughes et al. 1995a,b). Traditionally, this task was accomplished by surveying targets placed on individual armor units, a difficult, expensive, and often very dangerous undertaking. Naturally, photogrammetric analysis can only be applied to that portion of the structure visible above the waterline; hence, aerial overflights are scheduled to coincide with low tide level to maximize the benefits. An example is shown in Figure VI-8-3.

- The first step in photogrammetric monitoring of a rubble-mound structure is establishing permanent benchmarks on or near the structure that can be easily recognized in the aerial photographs. The horizontal and vertical position of these benchmarks are established using conventional ground surveying techniques, and they are used in the photogrammetry analysis to correct for aircraft tilt, roll, and yaw; to determine the camera position and orientation relative to ground features; and to compensate for the earth's curvature. Next, high-quality, low-level stereo photographs of the structure are obtained using standard stereo-mapping equipment and techniques. The photographic stereo pairs are used along with the ground survey information to establish a stereo-model, which is a 3-D representation of the study area that is free of geometric distortion. Stereo-models are usually constructed using a computer. Annual flights of the same structure using the same control reference points facilitate comparisons between stereo-models to extract information such as stone movement and yearly structure profile change above water level.

- Several requirements for successful monitoring using aerial photogrammetry are as follows:

  – Good quality equipment and experienced personnel must be employed. If possible the same equipment and personnel should be retained throughout the entire monitoring program.

  – The pilot should be experienced in low-level, low-speed flight in order to obtain blur-free, high resolution photographic images.

  – Best results come during calm weather with clear visibility and low water levels to maximize coverage of the structure. The sun should be nearly overhead to minimize shadows.

  – Photograph forward overlap should be at least 60 percent.

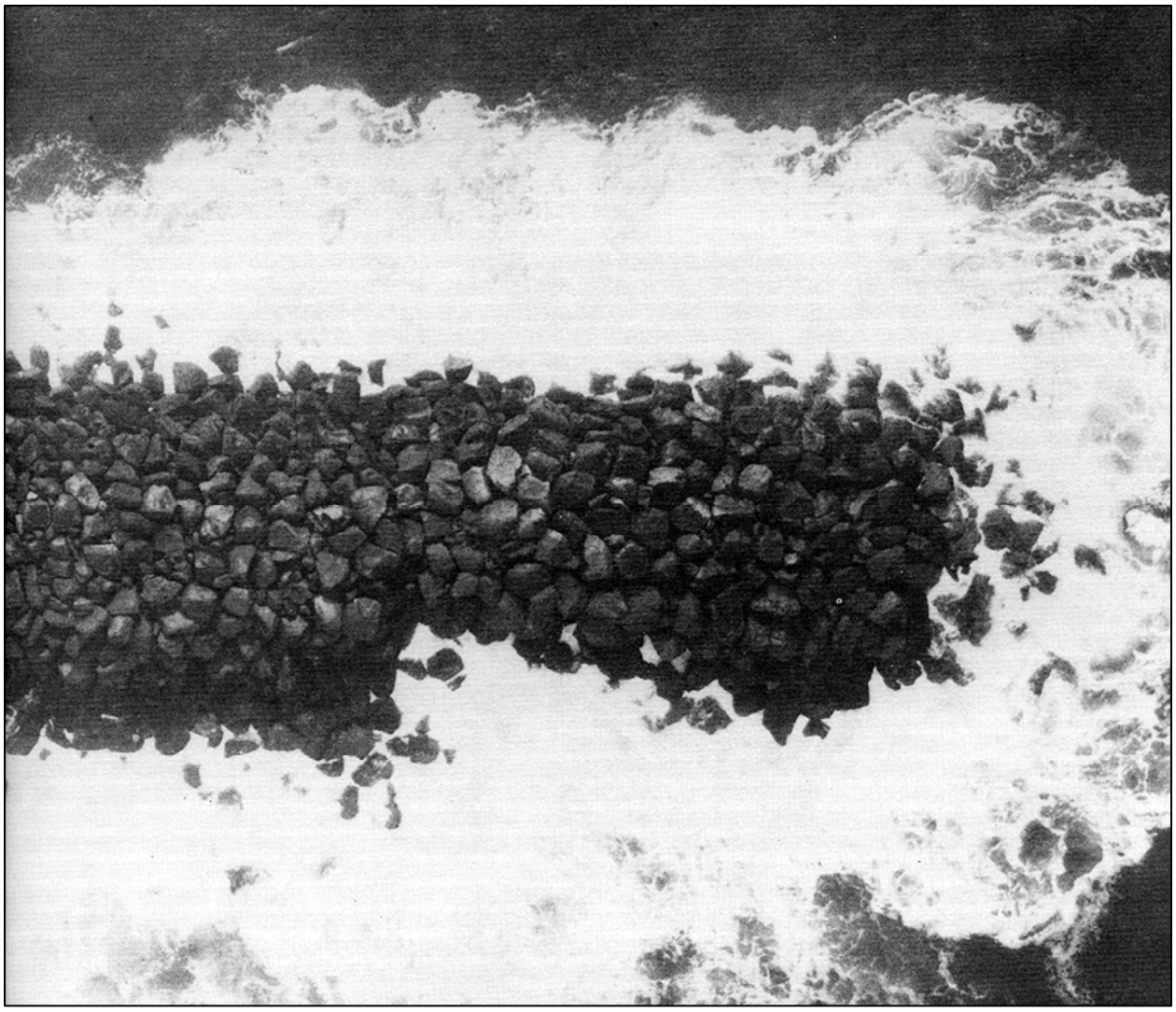

Figure VI-8-3. Aerial photogrammetry image of Yaquina, Oregon, north jetty

– There should be at least five or six evenly distributed control points in each photographic stereo pair in order to remove geometric distortions.

- Additional information on photogrammetry related to rubble-mound structures can be found in Cialone (1984) and U.S. Army Engineer Waterways Experiment Station (1991). Corps monitoring of the Crescent City breakwater using aerial photogrammetry was described by Kendall (1988); monitoring of the Yaquina north breakwater was documented in Hughes et al. (1995a,b).

(b) Underwater inspection. Quantifying underwater changes to coastal structures is difficult, but it is an important part of monitoring structure condition. Underwater problems that go undetected can lead to sudden, unexpected failures. At least four measuring systems (not including visual inspection) are available for obtaining information about the underwater condition of coastal structures.

- The most limited method for sloping-front structures is using a crane situated on the structure crest to make soundings of the underwater portions of the structure. Horizontal and vertical position of the survey lead can be established using modern Global Positioning Systems (GPS). This method is contingent on crane availability/capability and access to the structure crest. Similar techniques have been attempted using a sounding line attached to a helicopter. See McGehee (1987) for additional information.

- Side-scan sonar returns obtained by towing the instrument off a vessel running parallel to the structure can be interpreted to give general information of underwater structure condition, particularly near the seabed. The main advantage of side-scan sonar is the coverage and the speed of surveying. The disadvantage of this technology is the skill needed to interpret the record in a meaningful way. Side-scan is perhaps best used to identify structure portions that need to be examined using more sophisticated instruments. Additional information and operating rules-of-thumb are given by Kucharski and Clausner (1989, 1990) and Morang, Larson, and Gorman (1997b).

- For accurate mapping of the underwater portions of rubble-mound structures, the best solution to date is a commercial system named SeaBat®. The SeaBat is a portable, downward and side-looking single-transducer multibeam sonar system. The instrument is mounted to a vessel with the sonar head positioned to transmit on a plane perpendicular to the vessel's heading. The sonar transmits 60 sonar beams on radials spaced at 1.5 deg, giving total swath coverage of 90 deg. By tilting the sonar head, the instrument can provide data for mapping almost the entire underwater portion of a sloping rubble-mound structure from just below the sea surface to the structure toe as illustrated on Figure VI-8-4. SeaBat data must be synchronized with simultaneous readings of vessel position, heading, and motion (heave, pitch, and roll). The final analyzed product is a spatially rectified map of the structures below-water condition. Although it is difficult to identify individual armor displacement, any slope irregularities due to construction or subsequent damage are easily spotted on the map. SeaBat systems have been extensively tested by Corps Districts, and the technology is considered quite mature and highly reliable. Additional information on SeaBat multibeam sonars can be found in EM 1110-2-1003 and in Prickett (1996, 1998).

- The final method for mapping, which can be used for both the underwater and above-water portions of sloping structures, is the airborne lidar technologies as provided by the Scanning Hydrographic Operational Airborne Lidar Survey (SHOALS) system (Parsons and Lillycrop 1998). Normally a SHOALS survey is not conducted with the sole purpose of examining structures; instead the structure mapping is an added benefit that occurs during the survey of a much larger portion of the surrounding area.

- Typically, the spatial distribution of SHOALS data will not be sufficient to recognize smaller irregularities in the armor layer, such as individual movements. However, larger problems in the armor slope and details of adjacent scour holes are readily apparent in SHOALS topography/bathymetry. It is impractical to include a SHOALS component when planning structure condition monitoring unless SHOALS surveys are planned as part of the overall project monitoring.

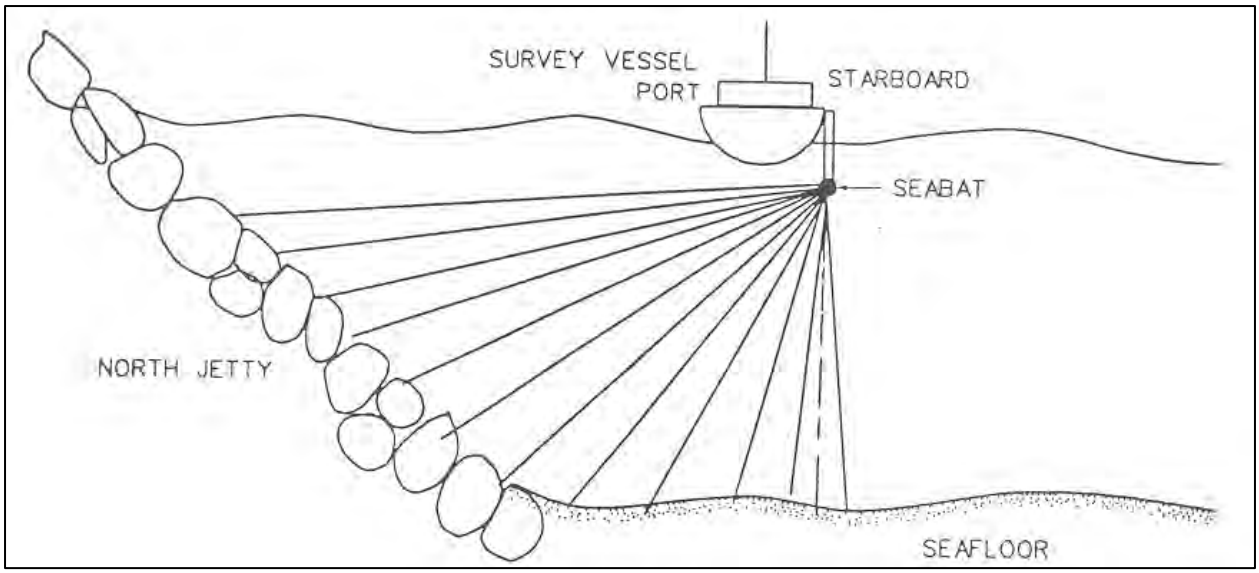

Figure VI-8-4. Multibeam scanner mounted on survey vessel

(3) Evaluating structure condition. Inspections are highly subjective, and the overall assessment of structure condition given by one observer may differ substantially from the opinion of another. Many factors can influence structure condition assessment with experience and previous visits to the site perhaps being the most important. In the 1990s, USACE developed guidelines aimed at providing a more uniform and consistent method for evaluating the physical condition and functional performance of coastal structures. These procedures, while still subjective, give a more meaningful evaluation by quantifying inspection observations in terms of uniform condition and performance criteria. The resulting numerical ratings allow better comparisons of condition and performance between similar structures, and better tracking of structure condition over time. A major benefit of a consistent condition rating system is the prospect of obtaining similar evaluations from different observers over the life of the structure. The procedure described in this section is a condition and performance rating system for rubble-mound breakwaters and jetties armored with stone or concrete armor units. Similar methods could be adopted for other coastal structures (revetments, bulkheads, monolithic structures, etc.) but have not yet been formally developed. The primary source for the information given in this section was a technical report (Oliver et al. 1998) available in Portable Document Format (PDF) from the Web site of the Repair, Evaluation, Maintenance, and Rehabilitation (REMR) Research Program (see Oliver et al. 1998 citation in this chapter=s References for Web address). A few tables from the REMR report are reproduced in this section, but application of the methodology requires obtaining a copy of the complete report, which also includes useful examples. An associated software program is also available at the REMR Web site.

(a) Condition and performance rating system for breakwaters and jetties. The condition and performance rating system is a performance-based evaluation system where emphasis is placed more on the question “how well is the structure functioning?” than on “what is the physical condition relative to the as-built structure?” This emphasis recognizes that coastal structures have some level of deterioration tolerance before significant loss of functionality, thus condition alone is not sufficient justification for rehabilitation.

- The end result of a performance evaluation is structure ratings given in terms of condition index numbers ranging between 0 and 100. Table VI-8-2 lists the general condition index range along with corresponding descriptions of the structure condition and damage levels. The different categories in Table VI-8-2 are fairly generic because the general condition index scale is intended to apply to a variety of USACE navigation and control structures, not just coastal breakwaters and jetties. For coastal structures the condition index (CI) is determined from a functional index (FI) and a structural index (SI). The FI indicates how well a structure (or a portion of the structure) is performing its intended functions, whereas the SI for a structure (or structure component) indicates the level of physical condition and structural integrity.

Table VI-8-2
General Condition Index Scale (from Oliver et al. 1998)

Observed Damage Level	Zone	Index Range	Condition Level	Description
Minor	1	85 to 100	EXCELLENT	No noticeable defects. Some aging or wear may be visible.
		70 to 84	GOOD	Only minor deterioration or defects are evident.
Moderate	2	55 to 69	FAIR	Some deterioration or defects are evident, but function is not significantly affected.
		40 to 54	MARGINAL	Moderate deterioration. Function is still adequate.
Major	3	25 to 39	POOR	Serious deterioration in at least some portions of the structure. Function is inadequate.
		10 to 24	VERY POOR	Extensive deterioration. Barely functional.
		0 to 9	FAILED	No longer functions. General failure or complete failure of a major structural component.

- The condition index is primarily a planning tool, with the index value serving as an indicator of the structure's general condition level. A series of condition index evaluations can be used to judge likely future functional performance degradation based on the trend of the condition index. For this reason, it is critical that all evaluations reflect the condition of the structure at the time of inspection, and not the condition that is expected at some future time. The condition ratings and index values are simply a numerical shorthand for describing structure physical condition and functional performance, and they represent only one part of the information required to make decisions about when, where, and how to spend maintenance dollars. Other necessary factors include knowledge of the structure's history, budget constraints, policies, etc. Furthermore, the condition index system is not intended to replace the detailed investigations which are needed to document fully structure deficiencies, to identify their causes, and to formulate plans for corrective action (see CEM, Part VI-8-2, “Project performance/ function monitoring”).

(b) Initial procedures for rubble-mound breakwaters and jetties. The condition and performance rating system involves eight steps as shown in Table VI-8-3. Steps 1-5 are initial procedures that are performed once for a given structure. The only other time some or all of steps 1-5 will need to be repeated is after major rehabilitation or project alteration. Steps 6-8 are performed for each condition assessment based on structure inspection. Each of the steps in Table VI-8-3 is discussed in greater detail in the following paragraphs.

- Steps 1-2: Determining structure functions and dividing into major reaches. The functions served by a structure can vary over different portions of the structure. Division of a structure into major reaches by function is performed as an office study using authorizing documents and project history in combination with the functional descriptions given in Table VI-8-4.

Table VI-8-3
Steps in Condition and Performance Rating System (after Oliver et al. 1996)

Step	Description
Steps 1-5 are Initial (One-Time Only)	
1	Determine structure function
2	Divide structure into major reaches based on function
3	Subdivide major reaches into subreaches by structural and length criteria
4	Establish functional performance criteria
5	Establish structural requirements
Steps 6-8 are Repeated as Necessary	
6	a) Inspect structure
	b) Produce structural rating
7	a) Produce functional rating
	b) Calculate condition index
8	Review structural requirements

Table VI-8-4
Functional and Structural Rating Categories (from Oliver et al. 1996)

Functional Area	Functional Rating Categories	Structural Rating Categories
Harbor area	Harbor navigation harbor use	Breach
Navigation channel	Entrance use channel	Core-exposure
Sediment management	Ebb shoal	Armor loss
	Flood shoal	Loss of armor contact and interlock
	Harbor shoal	Armor quality defects
	Shoreline impacts	Slope defects
Structure protection	Nearby structures	
	Toe erosion[1]	
	Trunk protection[1]	

[1] Not included in condition index calculation.

- The four functional areas and associated 11 rating categories are described as follows.

- Harbor area. How well the structure controls waves and currents to allow full use of the harbor area during all conditions and for all vessels, as compared with design expectations or current requirements.

- *Harbor navigation*. Indicates how well navigable conditions are maintained within the harbor itself. Difficulty in maneuvering and restrictions on vessel drafts or lengths are indications of problems.

- *Harbor use*. Normal usage may be restricted by waves, currents, or seiches at support facilities, such as docks and mooring facilities. Problematic conditions may be seasonal. Three subcategories are considered.

  – Moored vessels. How well moored vessels are protected from damage, and the degree to which portions of the harbor are unusable during certain conditions. Functional deficiency can be measured by the frequency and degree to which vessels sustain damage from excessive waves or currents.

  – Harbor structures. How well the harbor infrastructure is kept usable and free from damage. Structures include mooring facilities, docks, slips, bulkheads, revetments, etc. Functional deficiency exists if waves or currents damage or impair use of these facilities.

  – Other facilities. This subcategory includes facilities set back from the water's edge and facilities that are part of the surrounding commercial and recreational infrastructure.

- Navigation channel. How well the structure controls waves and currents to allow full use of the navigation channel and entrance during all conditions and for all vessels.

- *Entrance use*. This category indicates the success of the structure in maintaining a safe channel by controlling waves and currents as stipulated by authorizing documents. Functional deficiencies are indicated if certain sizes or types of vessels are unable to navigate the channel safely or are delayed in entering.

- *Channels*. This category indicates how well the structure controls waves and currents in the channel through which vessels may operate without difficulty, delay, or damage. Functional deficiencies include strong cross-channel currents or crossing wave trains, channel obstructions, grounding occurrences, and vessel collisions with structures or other vessels.

- Sediment management. How well the structure controls the depth, character, and pattern of sedimentation in the navigation channel; the depth of ebb and flood shoals in tidal entrances; and the buildup or loss of sediments on nearby shorelines.

- *Ebb shoal.* This category indicates the impact of the ebb shoal on navigation depths and widths in the approach channel. Functional deficiency is indicated by vessel delays, groundings, or maneuvering difficulties. Currents and wave transformation caused by the ebb shoal are evaluated under "Entrance use."

- *Flood shoal.* This category covers the impact flood shoals may have on navigation channel depth and location. Negative impacts due to modification of hydrodynamic conditions by flood shoals are evaluated under the "Channels" category.

- *Harbor shoal.* This category applies to shoaling in mooring and maneuvering areas, and a functional rating is developed for structures designed to prevent or limit shoaling.

- *Shoreline impacts.* This category indicates the structure's impact on the adjacent shore. Functional deficiency occurs where profiles and shoreline location are not maintained within acceptable limits. Separate shoreline maintaining systems, such as bypassing plants, are not considered in this rating.

- Structure protection. How well the structure protects nearby structures, or portions of itself, from wave attack or erosion damage.

- *Nearby structures.* This category indicates the protection provided to other structures located in the lee or in the diffraction zone from damaging waves and currents. This is the only item included in the functional rating.

- *Toe erosion.* This category indicates the structure's level of resistance to toe scour and subsequent undermining of the toe by waves and currents. Toe erosion is accounted for in the structure rating.

- *Trunk protection.* This category mostly applies to structure heads, and it indicates the success of the head in preventing unraveling of the structure trunk.

- Figure VI-8-5 illustrates the division of a jetty structure into major functional regions along with identification of structure functions for each reach.

- Step 3: Subdivision of major reaches by structural and length criteria.

- Further division of a structure into more manageable lengths is based primarily on changes in construction characteristics. Examples include changes in type of construction, type or size of armor, change in cross-sectional dimensions or geometry, and rehabilitated sections. Final subdivisions are based on length where function and construction are uniform over long reaches. Generally, each final division length should be between 60 and 150 m (200 to 500 ft) with the head section always being considered as a separate reach with a length of at least 30 m (100 ft) unless construction differences dictate otherwise.

- Subdivisions within major reaches are illustrated in Figure VI-8-5. The recommended numbering scheme begins at the shoreward end and proceeds seaward with the digit representing the major functional reach and the second letter corresponding subdivisions within the reach. Both structural and functional ratings use the same demarcations. Permanent markers should be established delineating the structure reaches to assure uniformity in future evaluations.

- Step 4: Establishing functional performance criteria.

- Once structure functions have been determined for each structure reach, the next step is to determine the expected performance level for each rating category. These criteria must be based on how well the structure could perform when in perfect physical condition. (Note: Design deficiencies cannot be corrected through the maintenance and repair process, and thus, should not be considered in this analysis.) Begin by reviewing the authorizing documents and structure history. Check if the original expectations have been changed, or if they need to be changed based on past observations.

- Defining performance requirements for each structure reach should be done using the rating tables provided in the report by Oliver et al. (1998). An extracted portion from the functional rating tables for the functional subcategory of ANavigation channels@ is shown in Table VI-8-5 as an example.

- Notice in Table VI-8-5 that the functional performance descriptions are given for three different wave conditions defined as:

– Design storm condition. The design storm is the largest storm (or most adverse combination of storm conditions) that the structure (or project) is intended to withstand without allowing disruption of navigation or harbor activities, or damage to the structure or shore facilities. Design storm conditions include: wave height, direction, and period; water level; storm duration; and combinations of these factors. The design storm is usually designated by frequency of occurrence or probability of occurrence. Authorizing documents, design notes, project history, and present-day requirements should be used to confirm the appropriate design storms for a project.

– Intermediate storms. This level refers to storms (or combinations of adverse conditions) of intermediate intensity that occur on the order of twice as often as the design storm. This level is intended to represent a midway point between the maximum storm levels (design storm) and small or minor intensity storms that may occur more frequently, especially during certain periods of the year.

– Low intensity storm conditions. This level refers to storms (or combinations of adverse conditions) of low intensity that may occur frequently throughout the year, and includes common rainstorms or periods of above normal winds. This level is the next stage above normal nonstorm conditions.

- Establishing the functional performance criteria essentially means determining to what extent the structure should control: waves, currents, and seiches; sediment movement; and shoreline erosion and accretion at the project.

- Factors that help decide how much control of waves, currents, and sediment movements is needed include:

– Determining the normal dredging frequencies and sand bypassing requirements.

– Deciding what size ships should be able to pass through the entrance and channel under normal conditions and during higher wave or storm conditions.

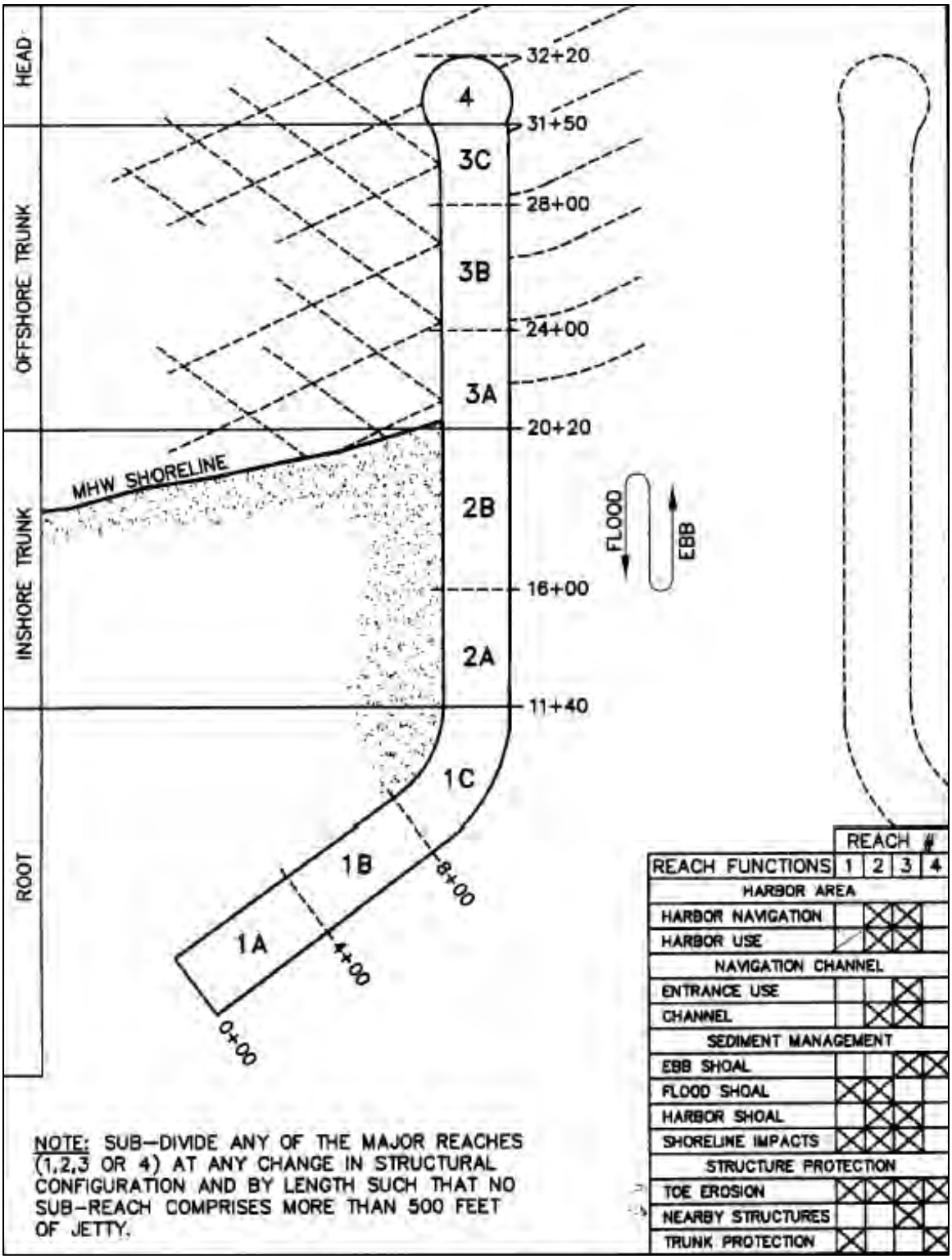

Figure VI-8-5. Major reaches and structure functions for typical jetty

Table VI-8-5
Functional Rating Guidance for Navigation Channel (partial table extract from Oliver et al. 1998)

Rating	Rating Category	Design Storm Conditions	Intermediate Storms (2X Design Storm Frequency)	Low Intensity Storm Conditions
Moderate Functional Loss				
55 to 69	Entrance Use	Vessels generally have little difficulty in the entrance when seeking shelter.	Vessels generally have no difficulty in the entrance when seeking shelter.	Vessels experience no difficulties in the entrance.
	Channel	There are generally few vessel delays in the channel within the shelter of the breakwaters or jetties, except in a few exposed locations. Some vessels using the harbor do not have enough water under the keel to go safely. Small vessels have some problems with conditions at exposed locations.	There are generally no vessel delays in the channel within the shelter of the breakwater or jetties, except at exposed locations.	There are no vessel delays in the channel within the shelter of the breakwaters or jetties. No vessels using the harbor are limited by either insufficient depth or by severe wave conditions.
40 to 54	Entrance Use	Vessels generally have some difficulty in the entrance when seeking shelter. Vessel entrance may be delayed until flood tide.	Vessels generally have no difficulty in the entrance when seeking shelter	Vessels have little or no difficulty in the entrance.
	Channel	There are vessel delays, in the channel, within the shelter of the breakwaters or jetties. In a few locations the delays can be significant for larger vessels that do not have enough water under the keel to proceed safely. Small vessels have problems with wave conditions at a number of locations.	There are some vessel delays in the channel within the shelter of the breakwaters or jetties. A few vessels that would normally use the harbor are limited by either insufficient depth or severe wave conditions.	Vessels experience little or no difficulty in the channel.

– Determining if any flooding of shoreline facilities should be expected during storm events, and if so, to what extent.

- Step 5: Establishing structural requirements. Structural ratings are produced by comparing the current physical condition, alignment, and cross-sectional dimensions of a structure to that of a “like new” structure built as intended, according to good practice, and with good quality materials. Because rubble-mound structures tolerate a degree of damage before loss of functionality, structural damage does not automatically equate to loss of function.

- The structural requirements are established by determining what minimum structure cross-sectional dimensions, crest elevation, and level of structural integrity are needed to meet the functional performance requirements. Initial efforts in determining these structural dimensions can be aided by estimating the impact on project functionality if the reach under study were to be completely destroyed. Project history, authorizing documents, public input, and analysis may be required to identify these dimensions. As this is not an exact science, and some engineering judgment is necessary to produce reasonable estimates. Once established, these structural requirements are used to help identify sources of functional deficiencies in the existing structure. Structural rating categories are shown in the right-hand column of Table VI-8-4 and briefly summarized in the following section.

(c) Recurring procedures. Once a structure has been divided into reaches, and the functional performance criteria and associated structural requirements have been established, the condition of the structure can be evaluated after each periodic inspection in a logical and consistent manner. Forms designed for use with this evaluation method are available in Oliver et al. (1998). Filling out these forms during inspection assures that key aspects of the rating system are evaluated.

- Step 6a: Inspection process. The inspector (or inspection team) should be familiar with the structure and past inspection reports before the inspection begins. The beginning and end of each reach should also be known. A copy of the most recent inspection report should be brought to the work site to help judge changes in condition.

– Other items to help conduct an effective inspection and document findings include: project maps and photographs, still and video cameras, tape measures, hand levels, and tide information. Ratings may be best determined by first walking the length of the structure and making notes of observed defects, their station location, and their severity. On the return walk, ratings may then be selected based on having seen the whole structure and on a second opportunity to scrutinize defects.

– Providing thorough comments on the rating form is a very important part of the process. Comments should note the location, character, size, and actual or potential effects of structure defects. The comments serve as backup and explanation for the ratings and suggested actions chosen by the inspector. Comments also provide a good record for future reference.

- Step 6b: Producing a structural rating. The result of the structural rating procedure is an index (SI) that can be generally related to structure condition by Table VI-8-6.

Table VI-8-6
Structural Index Scale for Coastal Structures (from Oliver et al. 1998)

Observed Damage Level	Zone	Structural Index	Condition Level	Description
Minor	1	85 to 100	Excellent	No significant defects - only slight imperfections may exist.
		70 to 84	Good	Only minor deterioration or defects are evident.
Moderate	2	55 to 69	Fair	Deterioration is clearly evident, but the structure still appears sound.
		40 to 54	Marginal	Moderate deterioration.
Major	3	25 to 39	Poor	Serious deterioration in some portions of the structure.
		10 to 24	Very poor	Extensive deterioration.
		0 to 9	Failed	General failure.

- The form for rating structures includes sections for rating the six categories described in the following paragraphs. Illustrative figures for each of the previously described categories are given in Oliver et al. (1998).

- Breach/loss of crest elevation. A breach is a depression (or gap) in the crest of a rubble-mound structure to a depth at or below the bottom of the armor layer due to armor displacement. A breach is not present unless the gap extends across the full width of the crest. Loss of crest elevation is primarily due to settlement of the structure or foundation. Both result in a reduced structure height.

- Core (or underlayer) exposure or loss. Core exposure is present when the underlayer or core stones can be readily seen through gaps between the primary armor stones. Core loss occurs when underlayer or core stone is removed from the structure by waves passing through openings or gaps in the armor layer. Movement and separation of armor often result in the exposure of the underlayer or core stone.

- Armor loss. Three cases of armor loss are considered on the inspection form:

– *Displacement* is most likely to occur near the still-water line where dynamic wave and uplift forces are greatest. Localized loss of armor (up to 4 or 5 armor stones in length) is typically like a pocket in the armor layer at the waterline with the displaced stones having moved downslope to the toe of the structure. (If the area is longer than 4 or 5 armor stones, use the rating for “Slope defects.”

– *Settling* may occur along or transverse to the slope, and may be caused by consolidation or settlement of underlayer stones, core, or foundation soils.

– *Bridging* is a form of armor loss that may apply to the side slopes or crest of a rubble-mound structure. Bridging occurs when the underlying layers settle but the top armor layer remains in position (at or near its original elevation) by bridging over the resulting cavity much like an arch.

- Loss of armor contact or armor interlock. Armor contact is the edge-to-edge, edge-to-surface, or surface-to-surface contact between adjacent armor units, particularly large quarrystones. Armor interlock refers to the physical containment by adjacent armor units. Good contact and interlock tie adjoining units together into a larger interconnected mass. Certain types of concrete armor units are designed to permit part of one unit to nest with its neighbors. In this arrangement, one or more additional units would have to move significantly to free any given unit from the matrix. Any special armor placement should be stated in the inspection notes.

- Armor quality defects. This rating category deals with structural damage to the armor units. It is not a rating of potential armor durability, but rather a reflection of how much damage or deterioration has already occurred. Four kinds of armor quality defects are defined in the following paragraphs.

– *Rounding* of armor stones, riprap, or concrete armor units with angular edges is caused by cyclic small movements or by abrasion. The result is edges that are worn into smoother, rounded contours. This reduces the overall stability of the armor layer because edge-to-edge or edge-to-surface contact between units is less effective and movement is easier when the edges become rounded.

– *Spalling* is the loss of material from the surface of the armor unit. Spalling can be caused by mechanical impacts between units, stress concentrations at edges or points of armor units, deterioration of both rock and concrete by chemical reactions in seawater, freeze-thaw cycles, ice abrasion, or other causes.

– *Cracking* involves visible fractures in the surface of either rock or concrete armor units. Cracks may be either superficial or may penetrate deep into the body of the armor unit. Cracking is potentially most serious in slender concrete armor units such as dolosse.

– *Fracturing* occurs where cracks progress to the stage that the armor unit breaks into at least two major pieces. Fracturing has serious consequences on armor layer stability, and it brings a risk of imminent and catastrophic failure.

- Slope defects. When armor loss or settlement occurs over a large enough area that the shape or angle of the side slope is effectively changed at that section, then a slope defect exists. Slope defects occur when many adjacent armor units (or underlayer stones) appear to have settled or slid as if they were a single mass. Two forms of slope defects are described in the following paragraphs.

– *Slope Steepening* is a localized process where the surface appears to have a steeper slope than for which it was designed or constructed, and it is evidence of a failure in progress on a rubble-mound structure slope.

– *Sliding* is a general loss of the armor layer directly down the slope. Unlike slope steepening, this problem is usually caused by more serious failures at the toe of the structure. Slope failure can be caused by severe toe scour, such as can occur at a tidal inlet with strong currents, or by failure within weak, cohesive soils when soil shear strength is exceeded.

- Rating tables are provided in Oliver et al. (1998) for each of the six structural rating categories. These tables are structured like Table VI-8-6, but they are specific for each category to help guide the inspector while assigning an appropriate rating number. Ratings are based on a comparison of existing structure condition with the Aperfect@ condition for that particular structure. The structural rating table for armor loss is reproduced in Table VI-8-7 as an example. The other five rating tables have similar format.

Table VI-8-7
Rating Guidance for Armor Loss

Structural Rating	Description
Minor or No Damage	
85 to 100	At most, slight movement of the armor in a few isolated spots. Movement has left a depression no larger than 1/4 of one armor stone (or unit) diameter.
70 to 84	Armor movement has caused some waviness along the slope surface with depressions less than 3/4 the armor layer thickness. Any bridging is over a void less than 1/2 of the armor diameter. Underlayer may be seen in spots, but none have been lost.
Moderate Damage	
55 to 69	Some loss of armor in spots, leaving voids or depressions about the size of an armor unit. Units surrounding the void may be rocking or gradually moving out of place. Underlayer or core might be seen at these spots, but armor position still prevents loss of this material. Bridging to a diameter of an armor stone may be visible in several places.
40 to 54	Armor units have been lost or displaced in some portions of the reach length. Voids are just large enough to allow loss of underlayer.
Major Damage	
25 to 39	Armor units have been fully displaced or lost. Voids are large enough to easily allow underlayer and core loss.
10 to 24	Armor units have been fully displaced or lost. Underlayer loss is evident.
0 to 9	Armor units are gone or fully displaced. Structure is unraveling.

- The numerical ratings are used to calculate the structural index according to the formulae given in Step 7b (Calculating the condition index).

- Step 7a: Producing a functional rating. The structure's functional performance is the most critical portion of the condition index for coastal structures. Functional index (FI) values

are expressed as numbers from 0 to 100 and have the general interpretation as shown in Table VI-8-8.

Table VI-8-8
Functional Index Scale for Coastal Structures

Functional Loss Level	Zone	Functional Index	Condition Level	Description
Minor	1	85 to 100	EXCELLENT	Functions well, as intended. May have slight loss of function during extreme storm events.
		70 to 84	GOOD	Slight loss of function generally.
Moderate	2	55 to 69	FAIR	Noticeable loss of function, but still adequate under most conditions.
		40 to 54	MARGINAL	Function is barely adequate in general and inadequate under extreme conditions.
Major	3	25 to 39	POOR	Function is generally inadequate.
		10 to 24	VERY POOR	Barely functions.
		0 to 9	FAILED	No longer functions.

- For each designated reach of the structure, functions were assigned during step 4 from the four major functional categories containing 11 subcategories (see Table VI-8-4). The assigned functions should not change unless major changes are made to the structure or project. The functional index for each reach will then be based on the same selected functional rating categories every time a functional rating is done.

- Special forms are used for completing the functional ratings which are determined using rating tables provided in Oliver et al. (1998). Table VI-8-5 is a partial example showing the functional rating descriptions extracted from one of the 11 categories. The process of producing a functional rating for each reach will involve:

  – Reviewing original authorizing documents.

  – Reviewing previously established functional performance criteria.

  – Examining available inspection reports, dredging records, project history, and other office records relating to project performance.

  – Reviewing the structural ratings and comments.

  – Reviewing the environmental setting in and around the project.

  – Gathering information from vessel operators, harbor masters, the U.S. Coast Guard, etc., on any known navigation difficulties, facility damage, or other project deficiencies.

- Further guidance on determining the functional rating is provided in the report by Oliver et al. (1998) along with examples that detail how to use the rating forms and tables.

- The key point to remember is that functional ratings are made in reference to structure performance criteria. Any detected design deficiencies are not included in the rating, but should be reported for separate action. Thus, to affect the ratings, functional deficiencies must be caused by structural deterioration, or in some cases, changed requirements. In any case, situations that a structure could not reasonably correct or control should not be taken into account. Also, functional ratings must be based on the condition of the structure at the time it was inspected.

- Step 7b: Calculating the condition index. Calculation of the structural index, functional index, and overall condition index can be performed using BREAKWATER, a DOS-based computer program available for downloading (Aguirre and Plotkin 1998). The equations used by the computer program for determining the indices are listed in the following paragraphs.

- *Structure index*. For each reach of the structure a reach index is calculated by first determining individual structure indices for the crest, sea-side, and harbor-side components of the structure cross section using the same formula

$$\left.\begin{matrix} CR \\ SE \\ CH \end{matrix}\right\} = R_5 + 0.3(R_1 - R_5)\left(\frac{R_2 + R_3 + R_4}{300}\right) \tag{VI-8-1}$$

where

CR = structural index for crest/cap

SE = structural index for sea-side slope

CH = structural index for channel/harbor-side slope

R_5 = lowest of the five ratings for the cross-section component

R_1 = highest of the five ratings for the cross-section component

R_2, R_3, R_4 = values for the second, third, and forth highest ratings

- For a reach that forms a structure head, the channel/harbor-side (CH) index does not apply. The individual component indices are then combined using the following equation to create a structural index for the reach

$$SI_R = I_L + 0.3(I_H - I_L)\frac{I_M}{100} \tag{VI-8-2}$$

where

SI_R = structural index for the reach

I_L = lowest of the three cross-sectional indices

I_H = highest of the three cross-sectional indices

I_M = middle value of the three cross-sectional indices

- For a reach that forms a structure head, there will be just two cross-sectional index values, and the term (I_M/100) becomes 1.

- Finally, the structural index for the entire structure is determined by the formula

$$SI = I_L + 0.3(I_H - I_L)\left[\frac{\%1}{100}\left(\frac{S1}{100}\right) + \frac{\%2}{100}\left(\frac{S2}{100}\right) + \frac{\%3}{100}\left(\frac{S3}{100}\right) + \bullet\bullet\bullet\right] \quad \text{(VI-8-3)}$$

where

SI = structural index for the structure

I_L = lowest of the reach structural indices

I_H = highest of the reach sectional indices

%1, %2, %3, ... = percentage of the structure length occupied by reaches 1, 2, 3, ...

S1, S2, S3,... = structural indices for reaches 1, 2, 3, ...

- *Functional index*. The functional index is calculated using rating values determined for categories within the harbor area, navigation channel, sediment management, and nearby structures functional areas. First, a functional index is calculated for each reach of the structure using the formula

$$FI_R = R_L + 0.3(R_H - R_L)\left[\frac{\left(R_2/100 + R_3/100 + R_4/100 + \bullet\bullet\bullet\right)}{N}\right] \quad \text{(VI-8-4)}$$

where

FI_R = structural index for the reach

R_L = lowest of the functional ratings for the reach

R_H = highest of the functional ratings for the reach

R_2, R_3, R_4,... = values for the second, third, fourth, etc., highest ratings

N = number of rated functions for the reach

- Functional indices for all the reaches are combined to create the overall functional index for the entire structure using the formula

$$FI = I_L + 0.3(I_H - I_L)\left[\frac{\left(I_2/100 + I_3/100 + I_4/100 + \bullet\bullet\bullet\right)}{N}\right] \quad \text{(VI-8-5)}$$

where

FI = structural index for the structure

I_L = lowest of the reach functional indices

I_H = highest of the reach functional indices

I_2, I_3, I_4,... = values for the second, third, fourth, etc., highest reach indices

N = number of reaches in the structure

- The *condition index* for a reach or structure is the same as the functional index.

- Step 8: Reviewing structural requirements.

- This final step in the condition and performance rating system is to assess the structural requirements previously established for each reach in view of the structural and functional performance ratings determined after the inspection. It may be necessary to modify the structural requirements for several reaches as knowledge about the structure increases with repeated condition evaluations.

- This review can also result in recommendations related to preventative maintenance or repair. It may be possible to project any trends identified over a number of inspection periods to the future to obtain estimates of future maintenance requirements so appropriate funding can be requested.

c. Project performance/function monitoring.

(1) Project performance/function monitoring consists of measurements and observations that are used to evaluate actual project performance relative to expected design performance. Typically, performance monitoring programs are implemented early in a project's life, and monitoring duration is short (several years) relative to the project's design life.

(2) In the broadest sense, performance monitoring is making observations and acquiring measurements necessary to document the project's response to environmental forcing. Four of the most common reasons for project performance monitoring are the following:

(a) Provide a basis for improving project goal attainment. The uncertainties involved in coastal engineering design may result in a project that is not performing as well as originally anticipated. Before corrective actions can be taken, a monitoring program is needed to establish the circumstances under which the project performance is below expectation. For example, if wave action in a harbor exceeds design criteria, it is necessary to determine the incident wave conditions (forcing) and the mechanisms (refraction/diffraction/transmission) that cause unacceptable waves action (response) in the harbor.

(b) Verify and improve design procedures. Much design guidance was developed based on systematic laboratory testing combined with practical experience gained from earlier projects. However, most coastal projects have some degree of uniqueness, such as location, exposure to waves and currents, available construction materials, combined functions, and existing project features. Consequently, the generic design guidance may not be entirely applicable for a specific

structure or project, and in many cases physical modeling is either too expense or not appropriate. Performance monitoring will verify whether the design is functioning as intended, and it will also provide data that can be used to improve existing design procedures or extend the design guidance over a wider range of applicability. For example, estimates can be made regarding the rate of infilling expected for a deposition basin serving a jetty weir section. Short-term monitoring will provide verification of the shoaling rate, and this could lead to cost savings associated with scheduled maintenance dredging.

(c) Validate construction and repair methods. Construction techniques for coastal projects vary depending on the specific project, availability of suitable equipment, contractor experience, environmental exposure, and whether the construction is land-based or from floating plant. Careful construction is paramount for project success. In addition, there is little guidance for designing repairs to deteriorated structures. In these cases the practical experience of the engineers can be as important as the available design guidance formulated for new construction. Performance monitoring may be needed to validate the procedures and to spot problems before serious damage can occur in these particular situations. For example, monitoring might be needed to evaluate the impacts of repairing a stone-armored rubble-mound structure with concrete armor units.

(d) Examine operation and maintenance procedures. Many coastal projects entail ongoing postconstruction operation procedures, and periodic project maintenance is usually required. Performance monitoring is useful for evaluating the efficiencies and economy associated with specific operating procedures. For example, if periodic navigation channel maintenance results in beach quality sand being placed on downdrift beaches, monitoring could be established to determine the best location for sand discharge to provide the most benefit with minimum amounts of sand re-entering the channel during episodes of littoral drift reversal.

(3) Performance/function monitoring is very project specific so there is no exact set of ingredients that constitute the perfect monitoring plan. A wide variation in monitoring plans arises from the different target goals and objectives for each project. Some performance monitoring plans are one-time, comprehensive postconstruction efforts spanning several months of continuous data collection and analyses. Other monitoring plans consist of repetitive data collection episodes spanning several years, perhaps augmented with continuous recording of environmental parameters such as wave and wind data. Comprehensive guidance for developing monitoring plans is available in EM-1110-2-1004, and several of the key points are summarized in the following paragraphs.

(4) The success of a performance monitoring program depends on developing a comprehensive and implementable plan. Several key steps for monitoring plan development are listed in the following paragraphs. (Elements contained in several of the steps are discussed in greater detail in the following section.)

(a) Identify monitoring objectives. This is the single most important step because it provides a basis for justifying every component of the monitoring plan. If there are multiple objectives, attempt to prioritize the objectives in terms of maximum benefits to the project (or to future similar projects). Whether or not a particular objective is achievable will be evident later in the plan development process.

(b) Ranking physical processes. Review the project planning and design documents carefully to identify the dominant physical processes (forcing) affecting the project. The identified physical processes should be ranked in order of importance with regard to project performance of its required functions, and each process should be linked to one or more of the monitoring objectives. Higher ranking physical processes that have significant influence on the project and adjacent shorelines are strong candidates for measurement, whereas less emphasis should be placed on lower ranked processes.

(c) Monitoring parameters. Decisions have to be made regarding which parameters of each physical process must be measured or otherwise observed. This requires knowledge of which parameters best characterize the particular aspect of the physical processes affecting the project. For instance, wave height and period might be most useful when monitoring wave runup or harbor agitation, but wave orbital bottom velocities may be most important for scour and deposition problems. A partial listing of measurable aspects of coastal projects is given in Table V-2-4, CEM Part V-2-17, “Site Characterization - Monitoring.” Completing this step requires knowledge about which parameters can be reasonably estimated with instrumentation or quantified through visual or photographic observations.

(d) Scope of data collection. For each physical parameter consideration must be given to the duration and frequency of measurement. Some environmental parameters vary in time and space so that decisions must be made on where to collect information and over what duration. For example, wave parameters might be collected continuously throughout the monitoring, whereas tidal elevations need only be collected for a few months, and aerial photography may only be needed once or twice. Be sure to consider availability of skilled personnel to install and service equipment and analyze results. Fiscal constraints of the monitoring program factor heavily during this step.

(e) Instrument selection. There may be several different instruments available to accomplish measurement of a particular physical parameter. Selection of the appropriate instrument depends on factors such as accuracy, reliability, robustness, expense, availability, and installation/servicing requirements (more about this in the next section). Instruments with shore-based electronics require secure and environmentally protected locations at the monitoring site. Local troubleshooting capability is also beneficial.

(f) Implementation. Adequate funding is necessary to implement a comprehensive performance monitoring program. If funding is lower than needed for an optimal plan covering all the objectives, it is usually better to scale back the objectives rather than attempting to meet all the objectives by scaling back the measurements associated with each objective. Performance monitoring seldom last longer than 5 years except for unusual projects or situations where longer data records are needed for statistical stability. Decisions on the length and extent of a monitoring effort must be made with a realistic evaluation of the importance of the data to the objectives. No plan should be implemented until it is clear that essential data can be obtained.

(5) To be effective, performance monitoring should be implemented when changes to the project are most likely to occur. For new construction, this period is during and immediately after construction, when the project and adjacent shoreline undergoes significant adjustment. Often, this means the monitoring plan should be completed before construction starts in order to

obtain preconstruction bathymetry and measurements of physical parameters likely to be impacted by the project. The importance of preconstruction information cannot be stressed enough as it provides a basis for evaluating changes brought about by the project. After an initial adjustment of one to several years, performance monitoring can be terminated or reduced in scope and converted to condition monitoring.

(6) Performance monitoring plans implemented after problems are identified or after project repair/rehabilitation may not have good baseline data for comparison, and this must be factored into the data collection scheme. An inventory of existing data should be conducted, and data quality should be assessed to determine what baseline data are needed to meet monitoring goals.

(7) The Corps has maintained an ongoing program of monitoring completed and repaired coastal and navigation structures (Hemsley 1990) with the purpose of obtaining information that can be applied to future projects. Numerous reports have been prepared evaluating functional and structural performance for projects on the Atlantic, Pacific, Gulf, and Great Lakes coasts. The following project types and physical processes have been monitored at one or more locations:

(a) Jettied inlets (inlet hydraulics, sedimentation, and structure evaluation).

(b) Harbors (harbor waves, currents, and resonance).

(c) Breakwaters (wave and shoreline interaction and structural stability).

(d) Beach fills (longshore and cross-shore sediment motion).

(8) Lessons learned from the monitoring program, grouped by project type, are given in Camfield and Holmes (1992, 1995). The individual project reports, published by the Corps' monitoring program, are a good source of information for use when developing monitoring plans for similar projects. The bibliography section of Camfield and Holmes (1995) lists references for reports completed before 1995.

d. Monitoring plan considerations. Condition monitoring and project performance/function monitoring are distinctly different in goals and execution. However, many elements of both monitoring types have similar considerations, particularly those aspects related to measurements. This section covers those considerations most commonly encountered when developing and implementing monitoring plans. The main reference for this section is EM-1110-2-1004, “Coastal Project Monitoring.”

(1) Fiscal constraints. The single most important major consideration for both condition monitoring and performance monitoring is the availability of funding because fiscal constraints impact the level of data collection. Generally, performance monitoring requires greater fiscal resources per year because of the emphasis on quantifying measurements. Condition monitoring is less expensive on a yearly basis, but often may continue for decades or longer, adding up to a substantial sum over the life of the project. Realistic funding is essential for a successful

monitoring effort, and monitoring costs should be included in the overall project budget, instead of being funded separately after project completion.

(a) Determining an appropriate funding level for project monitoring is not an easy task. A typical approach is to first determine the monitoring goals and then outline the components necessary to achieve those goals. For example, monitoring excessive wave agitation in a harbor would require one or more wave gauges outside the harbor to establish the forcing condition and several strategically-placed gauges inside the harbor to measure response. In addition, there must be analyses performed on the measurements, and there might be a numerical modeling effort or a physical modeling component that makes use of the measured wave data along with bathymetric data inside and outside the harbor. If initial evaluation indicated that wave transmission through a breakwater is contributing to the excessive harbor wave heights, then measurements are needed to quantify this aspect.

(b) The cost estimate for each major activity could vary widely, depending on factors such as the duration of data collection, instrument quality, level of analysis applied, variations in conditions examined by the models, etc. The result is a range of monitoring cost estimates from an inadequate bare-bones minimum to an expensive feature-packed plan. Available funding will tend to be much less than the highest estimate. If funding is less than the minimum estimate, then something will have to be eliminated from the plan or the monitoring goals will have to be adjusted. Attempting to accomplish all the original monitoring goals with an inadequate budget increases the likelihood of not achieving any of the goals. It is better to eliminate tasks in order to fund the remaining tasks at an appropriate level. This requires a realistic evaluation of every measurement's importance. Don't waste funding collecting data that falls into the category of Amight be useful.@ Each measurement must contribute directly to the monitoring goal, and it must have an associated analysis component. If funds appear inadequate to achieve monitoring goals, it may be wise not to attempt any monitoring because improperly collected data can lead to conclusions that are worse than those drawn when no data are available.

(2) Data considerations. There are three overriding considerations that apply to data in general: accuracy, quality, and quantity.

(a) Data accuracy is an assessment of how close the value of a recorded piece of information is to the true value that occurred at the time of observation. Data accuracy relates directly to the means of measuring or observing the physical process. As an extreme example, visual estimates of wave height and period are much less accurate than similar estimates obtained using bottom-mounted pressure transducers that infer sea surface elevation through pressure change. In turn, surface-piercing wave gauges that measure directly the change in sea surface elevation are likely to be more accurate than the pressure gauge. Generally, expect greater accuracy to carry greater cost, although this is not an absolute truth.

(b) Data quality is more encompassing than data accuracy because it includes site specific factors as well as other influences such as instrument calibration. High-quality, accurate instrumentation is necessary for quality data, but instrumentation alone does not guarantee data quality. For example, the best acoustic Doppler current meter will return poor-quality data if air bubbles pass through the sampling volume (breaking wave zone). Similarly, the methods used to analyze measurements can compromise data quality, such as using linear wave theory to

interpret bottom pressures under highly nonlinear waves. Finally, data quality is jeopardized if the wrong instrument is selected, or incorrect parameters are set on an appropriate instrument. For example, sampling waves at a 1-Hz rate may not adequately resolve the shorter waves or waves with steep crests.

(c) Data quantity can greatly influence the bottom line cost for obtaining data. For some measurements, well established guidelines exist detailing necessary data quantity for success. For example, one month of tidal elevation data will suffice for many tidal circulation studies. On the other hand, greater uncertainty exists concerning the duration necessary to measure waves in order to establish reasonable wave climatology for a location. For specific measurements, rely on past experience or advice from experts familiar with measuring that particular parameter. A realistic evaluation of data quantity will need to balance multiple factors such as cost, importance of the data, instrument reliability, and natural (and seasonal) variability of the measured parameter.

- For each measurement included in a monitoring plan, the maximum range of the measured physical parameters must be estimated to assure an appropriate instrument or procedure is selected. The maximum parameter value is often most important for coastal projects because of potential adverse impacts stemming from storms. Therefore, if available measurement technology cannot span the entire range of anticipated parameter values, it may be wise to focus on the portion of the range most likely to influence project performance or cause damage.

- When feasible, data should be recorded in digital form to reduce handling and translation errors, and to simplify data reduction and analysis. Data recorded in manual or analog format should be converted to digital form (if appropriate) as soon as practical. Both the raw and transferred data should be stored together with a description of the data type, measurement location and other pertinent information (e.g., water depth), period of measurement, and a statement of data quality and completeness. A detailed description of the format of both the raw and processed data is important for future processing and analyses.

- Data reduction is a term encompassing: conversion of raw data into engineering units by applying calibration and conversion factors, identifying and correcting erroneous data (e.g., data spikes), flagging or removing obviously corrupt data that cannot be recovered, and possibility converting to digital format. Data reduction can be difficult and expensive, particularly if the raw data are noisy, erratic, incomplete, or poorly documented. Unique measurements may involve developing new data reduction techniques which may be more susceptible to errors than previously tested techniques. Of course, even using established methodology for data reduction can introduce errors if applied inappropriately.

- Data reduction costs can be significant for some types of measurements, and considerable thought should be given to data reduction during monitoring plan formulation. This includes determining the final form of the data for analysis and reporting purposes. Ideally, acquired data will be reduced and inspected for quality often, particularly near the start of data acquisition. This will catch potential measurement problems while there is still time to make corrections. The worst scenario is waiting until the end of data collection to begin data reduction and analysis. In cases where there is no possibility of interim data checking (e.g. internally

recording wave gauges without shore connection), carefully select the instrument based on its reliability record.

- The complexity, and associated expense, of data analysis varies widely with the type of measurement. For example, analysis of current meter data is relatively straightforward using computer programs supplied with the instrument or programs previously developed. Conversely, photogrammetric analysis of rubble-mound structures still requires several steps, along with human intervention and interpretation of the data. Automated analysis of data has greatly increased our ability to display and interpret large quantities of data, and it has also eliminated much human error. But by automating much of the mundane data reduction, we have also lessened some of the human quality control that was present when data were reduced and manipulated by hand. Therefore, it is imperative that automatically reduced and analyzed measurements be subjected to some form of quality assurance before being used to form conclusions. Simple mistakes such as using the wrong calibration input will produce errant results. In other words, be suspect of the analyses until you have assured yourself the values are reasonable. The corollary is that unbelievable results are more likely analysis error than abnormal physical processes.

(3) Frequency of monitoring. Previous sections discussed the differences between condition monitoring and performance monitoring and the corresponding general monitoring approaches. Generally, the tasks within a condition monitoring plan tend to be somewhat evenly spaced in time over the structure service life. Some tasks may be more frequent for several years immediately after construction to assure the structure is reacting as intended. The frequency of tasks conducted as part of performance monitoring usually are more closely spaced in time in order to collect sufficient data to judge project performance and functionality. It is difficult to estimate the frequency of monitoring tasks that are conducted only after major storm events.

(a) There are few rules-of-thumb suggesting appropriate intervals between repetitive monitoring tasks, and once again past experience with similar projects is the best guideline. When monitoring project aspects where seasonal change occurs, such as beach profiles, the monitoring frequency needs to be at least semiannual to separate long-term change from seasonal variations. The data should also be collected at the same time during the year.

(b) The conduct of monitoring elements associated with potential failure modes may increase in frequency if the monitoring indicates deterioration that could put the structure at risk. Conversely, if monitoring indicates some aspect of the project is holding up better than anticipated, the interval between periodic monitoring tasks can be increased. The important point is that monitoring plans should allow flexibility in scheduling repetitive monitoring elements to react to evolving circumstances.

(c) In addition to the frequency of monitoring considerations related to the overall monitoring plan, there are also several considerations that must be determined for each type of instrument or measurement technique. These include sampling rate, sample length, sampling interval, and measurement duration.

- Sampling rate is the rate at which measurements of a specific parameter are made during a measurement interval. Most importantly, the sampling rate must be rapid enough to

describe completely the physical phenomenon being measured. For example, waves must be sampled at one or more samples per second, whereas tides may be sampled at rates of several samples per hour.

- Sample length refers to the period over which samples are taken at a selected sample rate. The sample length depends on the length of time needed to determine the various components of a given phenomenon. A typical sample length for waves is 20 to 40 min in order to collect enough waves to give stable statistics, but tides are recorded for at least 28 days to cover a full lunar tidal cycle.

- Sampling interval is the time between measurement samples. This interval depends on how the measured parameter changes with time. Waves are typically sampled hourly or every 3 hr because during storms the sea condition can change fairly rapidly. Other parameters such as water temperature change at slower rates, allowing a greater sampling interval.

- Measurement duration depends on the physical process being measured and the monitoring goals. For example, it may be necessary to measure waves continuously over a 1- or 2-year period to establish average wave climatology; but if the wave measurements are to be used to validate a harbor response numerical model, the measurement duration can be shorter, provided the target condition occurs.

(d) Recommendations on appropriate sampling parameters for specific types of instruments and techniques are given in Morang, Larson, and Gorman (1997a,b); Larson, Morang, and Gorman (1997), and Gorman, Morang, and Larson (1998). Also, EM-1110-2-1004 contains specific sampling information.

(4) Instrument selection. Instrument selection can be a challenging task if several options exist for measuring the same physical parameter. In the broadest sense, instrument selection is a tradeoff between data quality/quantity and cost. In the following paragraphs are listed somewhat general considerations for instrument selection. Not every item applies to every monitoring instrument or technique, and the considerations are not in any specific order of importance.

(a) Initial instrument cost factors heavily into the aforementioned budgetary constraints of the monitoring effort if instrumentation is to be purchased or leased. Bear in mind that instruments placed in an ocean environment may be lost or damaged beyond repair.

(b) Instrument accuracy corresponds to measurement accuracy, which in turn depends on how the data will be used. Although accuracy is important, it might be overshadowed by other considerations. For example, it might be prudent to opt for an instrument giving less accuracy, but greater reliability in situations where loss of data would have a greater impact than less accurate data.

(c) Instrument reliability is usually a critical consideration for instruments that are installed at a monitoring site and left unattended for some length of time. For internally recording instruments, very high reliability is necessary to prevent loss of the entire measurement sequence. High reliability is also needed for any instruments where failure and subsequent replacement would involve substantial mobilization costs. Less reliable instruments

can be used for measurements during site visits or other situations where a failure can be overcome by using a backup instrument or returning to the site later to obtain the measurement.

(d) Instrument ruggedness should be evaluated in the context of where the instrument will be deployed, and under what circumstances. Delicate instruments must be well protected during transport, and they may require special handling. Instruments mounted on the seabed must be able to resist such hazards as trawlers, anchors, etc. Instrument buoys should be able to sustain impacts from vessels or debris.

(e) Instrument stability usually refers to the capability of the instrument to give consistent output for the same input over a range of environmental conditions, such as air and water temperature fluctuations. Unexpected linear trends in data records almost always point to stability problems with electronic circuits.

(f) Type and capacity of data recording associated with an instrument will dictate data sampling rates and duration. Some instruments record data onboard for later processing, some transmit the data stream via cable or telemetry to a receiving station in either analog or digital form, and some instruments have dual capability.

(g) Instrument calibration procedures must be considered, and a clear understanding of how the calibration is applied to the recorded data is essential. The cost of calibrating instruments at special calibration facilities must be included in the budget. When practical, postcalibration of the instrument after retrieval adds veracity to collected data.

(h) Requirements for instrument installation must be known before selecting the instrument because field mobilization, installation, and retrieval can be a major portion of the cost for acquiring data with that instrument.

(i) Instruments placed in water may become fouled with marine growth. For locations where fouling is likely to occur, either avoid using instruments that suffer loss of functionality when fouled, or plan to periodically remove marine growth before data quality degrades.

(j) Some instruments, either in the water or mounted on a structure, transmit data through cables to data loggers. Consideration must be given to where and how to route the cables so they are protected from damage. Typical hazards include boat anchors, harsh environmental conditions, and vandals. Cables coming ashore through the surf zone must be buried.

(k) Decisions on instrument location are often made giving consideration to the type of instrument that will be deployed. Locations that expose the instrument to harsh conditions or other hazards require robust equipment, whereas protected locations can use less rugged instruments.

(l) Any instrument maintenance will factor into monitoring costs. For remote locations, select instruments requiring minimal maintenance to reduce site visits. Also consider the skills necessary to perform field maintenance. If special training or tools are required, maintenance costs will be higher.

(m) Security is a very important consideration for any instrument location that might be accessible by thieves and vandals. At high risk locations, choose inexpensive equipment that is easily replaced and immediately stream data to a secure location offsite. This will help minimize data loss if the equipment is stolen or damaged. Similarly, shore-based electronics for instruments placed in the water need to be in a secure, environmentally protected enclosure.

(n) If feasible, establish a local source for troubleshooting onsite instrumentation if problems develop. A local contact that has access to the instrument and can perform basic tasks will save substantial costs. Examples include reconnecting severed power lines, changing fuses and resetting breakers, periodically replacing recording media, and reporting on equipment status. A competent local contact may be able to correct a problem successfully via telephone under guidance of an expert.

(o) A strong consideration in instrument selection is the ease of data handling and analysis. Some instruments have companion analysis software that simplifies the analysis and significantly shortens the time it takes to have results for interpretation. If no such software exists, or the instrument provides data that cannot be reduced and analyzed by computer, be certain that necessary analysis procedures and equipment are available. Attempting to develop appropriate analysis techniques after the data have been acquired is not recommended.

(5) Other considerations. A concern of paramount importance is the safety and well-being of the personnel involved onsite during monitoring activities and instrument installation and retrieval. The coastal environment is harsh and deadly at times. Do not include monitoring elements that inherently require risky behavior either during installation or during routine observation. Monitoring elements that may periodically involve risk to personnel should be carefully explained to the monitoring personnel so they know when they can and cannot perform that monitoring element. Examples of unacceptable risky behavior include walking on structures when wave overtopping is occurring, being on a rubble-mound structure at night, snorkeling adjacent to a structure in adverse wave, current or surge conditions, and many more too numerous to mention. Diving operations must be conducted according to established USACE procedures and regulations.

(a) The effect of project monitoring on the environment must be considered in the development of a monitoring plan. This includes the effects of personnel, equipment, and techniques on the environment. Minimizing environmental impacts may influence sensor selection and instrument location, and it may limit site access for the monitoring personnel. The plan should incorporate methods and approaches that will reduce or eliminate adverse effects that the monitoring might have on the environment. This may result in seasonal windows for monitoring operations.

(b) The monitoring plan should consider the logistics required to install and maintain the monitoring equipment, and to perform onsite inspections. Contracting of services such as aerial photography or geophysical surveys should be carefully considered, particular for repeated work over an extended time period.

(c) Any monitoring equipment that might interfere with normal navigation, such as bottom-mounted instruments or instrument buoys, should be clearly marked with warning signs,

and a description of the hazard should be published as a “Notice to Mariners.” Some equipment installations may require a permit from the U.S. Coast Guard or other state or local authorities.

VI-8-3. Repair and Rehabilitation of Coastal Structures. In the United States and other developed countries, most of the coastal infrastructure is already in place. Thus, emphasis has shifted from developing coastal protection projects and navigation facilities to maintaining or expanding these facilities to accommodate future growth. Most of the cost associated with maintaining existing projects is either completing repairs after damage occurs or rehabilitating projects that have deteriorated. Project condition monitoring (Part VI-8-2-b) is essential for knowing when maintenance is required. The first part of this section presents general guidance useful for planning repair or rehabilitation of coastal structures. This general introduction is followed by more specific design guidance, suggested methodologies, and literature references for repairing and rehabilitating sloping-front rubble-mound structures. Finally, several case histories are presented that illustrate repairs and rehabilitations that have been successful for rubble-mound structures.

a. General aspects of repair and rehabilitation.

(1) Design guidance related to structure repair and rehabilitation is not as abundant as it is for new project construction. Part of the difficulty in developing general design guidance is that often damage or deterioration is localized, and possibly quite specific to a particular project. Conducting repairs or rehabilitating a coastal structure is analogous to repairing a house damaged by a fallen tree. The success depends greatly on assessing what needs to be repaired, knowing how much needs to be removed and what can be salvaged, and mating the repaired portion with existing structure in a way that minimizes weaknesses.

(2) Earlier in this chapter, general definitions are given for repair and rehabilitation. Without changing the general meaning, the same definitions are given as follows, tailored to coastal projects.

(a) Repair: Fixing portions of a structure that have been damaged by waves, winds, currents, surges, impacts, or seismic activity.

(b) Rehabilitation: Renovation of deteriorated structure components to original condition or upgrading the structure to withstand greater design loads.

(3) One of the hardest questions to answer is, “When should a structure or coastal project be repaired or rehabilitated?” This, of course, depends on what functions are served by the project, and how critical the project is relative to other projects in need of repair. Usual indications that a project needs some type of repair or rehabilitation are listed in Table VI-8-9.

(4) Repair and rehabilitation of coastal projects is costly, and the uncertainty in predicting when projects might need repair or rehabilitation precludes detailed advanced budget planning. Usually, critical repairs that must be completed immediately can be funded from contingency funds established for emergency operations. Less critical repairs, where loss of functionality is not great and additional damage is unlikely to occur, can be included in future budgets as a specific cost item. The same caveat applies to project rehabilitation. Once included

in a proposed budget, the repair or rehabilitation must compete with other funding priorities. Thus, those projects serving vital functions have a higher likelihood of being repaired quickly, whereas less critical ones may be left in a damaged or deteriorated condition for many years until funding is available.

Table VI-8-9
When Coastal Project Might Need Repairs or Rehabilitation

After damaging storms or other events that cause damage such as vessel impacts, earthquakes, etc.
If periodic condition inspections indicate progressive deterioration to the point where functionality is jeopardized.
If performance monitoring indicates the project is not functioning as planned.
If the project is suffering chronic damage from underestimation of design loads.
If the intended structure function is modified to provide new or enhanced service that was not originally in the design.

(5) There are distinct differences between designing new projects and repairing or rehabilitating existing projects of similar type. Implementation considerations relate to specific structure type, such as rubble-mound structures, monolithic concrete structures, etc., and these are discussed in the subsections related to specific types of structures. Design environment considerations encompass differences between new design and repair/rehabilitation design that include both the physical environment that provides the forcing and the societal environment in which the design occurs. Listed in the following paragraphs are several general design environment considerations that might apply to the design of a coastal project repair or rehabilitation.

(a) In general there will be no difference in the actual design parameters (waves, water levels, storm frequency) from when the project was originally constructed to the time when repairs are needed. In other words, the physical environment has not changed in time. Exceptions might occur where exposure to the wave climate has been altered (e.g., construction of an offshore breakwater) or where bathymetry has been altered (e.g., growth of an ebb-shoal bar, profile deepening/steepening, etc.).

(b) In some circumstances there may be more reliable estimates of the design parameters than were available during original construction, or during the previous repair/rehabilitation. For example, several years of wave measurements from a nearby wave gauge will provide better representations of wave climate than might have been available previously. This is particularly true if the measurements include the storm or series of storms thought to have caused the damage. In the case of general project deterioration, this will be a less important consideration.

(c) Designers of repairs and rehabilitations can draw on whatever available knowledge exists about past project performance, including performance of similar projects. Monitoring data collected before damage occurs can be crucial in understanding why the project was damaged and how to prevent a reoccurrence in the future.

(d) Depending on the age of the project, there may be new regulations or environmental restrictions that did not exist at the time of original construction. Consequently, it may not be feasible to repair or rehabilitate the project using the same construction methods or materials. Similarly, design standards may have changed or have been implemented for certain types of structures or structural components.

(e) Availability of materials and construction plant may be considerations. For example, a local quarry that produced the original armor stone may not be in operation, and there might not be any other local suppliers of adequate armor stone. This may require using concrete armor units in lieu of stone.

(f) Access to the project site for construction and staging materials could be significantly different due to surrounding development since previous work on the project. This, in turn, will influence the design by limiting construction sequence options.

(6) Every repair or rehabilitation of a coastal project will be unique. However, the general guidelines listed in the following paragraphs apply to many projects.

(a) Review the original design criteria, plans, and specifications. These documents, if available, will provide valuable insight into what the original designers held to be most important in the project design. As-built drawings are especially important because they document what was actually constructed, and thus, captured any onsite changes dictated by circumstances at the time. For older structures, the original environmental forcing design criteria become less important because the environmental forcing was probably not well characterized.

(b) Determine the cause of the problem. At times the cause will be obvious, such as in the case of a vessel impact. Other times, the cause will not be so easily determined. For example, loss of concrete armor units from a breakwater might be due to extreme wave events, breakage of units into smaller pieces, or slumping of the entire armor layer. Examine the failure modes given in CEM Part VI-2 for the structure type, and try to determine how the structure sustained damage. Bear in mind that damage or failure may have been caused by a combination of circumstances rather than to any single factor. If the true cause of damage is not identified, there is a risk of future damage caused in the same manner as previous damage.

(c) If damage can be attributed to a single storm or series of storms, estimate the severity of the events to the extent possible using available data and observations. Accurate estimates are critical in designing a repair that will withstand future events of similar strength.

(d) Investigate the present project relative to the as-built plans and locate discrepancies. This may help isolate problem areas as well as identify regions where future problems might develop.

(e) Devise a solution for the problem. If possible, propose several different solutions and develop each one to the point that reasonable cost estimates can be made. Be sure to factor in any costs associated with testing or optimizing the final design using a physical model. For large repairs or rehabilitation, physical modeling will be a small fraction of the total cost, and the

modeling will more than pay for itself in cost savings. For smaller projects, potential cost savings may not justify extensive laboratory testing.

(f) Design a repair that fixes the problem without extensive modification. If a project needs extensive modifications in order to regain (or initially achieve) functionality, it may be that the project was not well designed in the first place, and the designer should reconsider the project in its entirety.

(7) An intangible factor in developing a plan for repairing or rehabilitating a structure is past history of the structure as captured through condition monitoring or through corporate memory. The quality and quantity of corporate memory varies greatly depending on how well documentation was completed originally and how well it survived through the years. Case histories of breakwater and jetty structures were reported in a series of nine reports produced by the USACE REMR Program. Table VI-8-10 lists the reports by Corps Division along with the general geographical coverage in the United States. Besides providing structure histories, in many cases these reports discuss repairs or modifications completed and the variety of repair methods that have been used.

b. Repair and rehabilitation of rubble-mound structures.

(1) General considerations.

(a) One of the advantages of rubble-mound structures is that they are relatively flexible and can tolerate slight movement caused by settlement or wave action without noticeable change in function. Damage to rubble-mound structures generally consists of armor unit wearing or breakage, dislocation of armor units, or removal of a section of the armor layer as shown on Figure VI-8-6. Generally, repairs of rubble-mound structures consist primarily of rebuilding the stone structure or replacing the stone with new material. In some cases repair can be achieved with concrete or asphalt grout.

(b) In addition to the general design environment considerations listed in the previous section, there are several implementation considerations that distinguish the design of repairs to rubble-mound structures from the design of new structures.

- The repairs are made to an existing rubble-mound structure that may be deflated with lowered crest elevation and milder slopes than originally built.

- Original armor may be mixed with underlayer stone.

- Changing armor slope to suit design parameters is difficult.

- Embedding and securing a new armor slope toe is more difficult than new construction.

- Transitions between the repair section and the existing undamaged slope must be accomplished without creating weaknesses in the armor layer.

Table VI-8-10
Case Histories of USACE Breakwater and Jetty Structures

Corps Division	States Covered	Projects	Author(s)
New England	Maine, New Hampshire, Massachusetts, Rhode Island, Connecticut	52	Sargent and Bottin 1989a
North Atlantic	New York, Vermont, New Jersey, Pennsylvania, Delaware, Maryland, Virginia	58	Smith 1988
North Central	Minnesota, Wisconsin, Michigan, Illinois, Indiana, Ohio, Pennsylvania, New York	107	Bottin 1988b
South Atlantic	North Carolina, South Carolina, Georgia, Florida, Alabama	32	Sargent 1988
Lower Mississippi Valley	Louisiana	10	Sargent and Bottin 1989b
Southwestern	Texas	12	Sargent and Bottin 1989c
South Pacific	California	28	Bottin 1988a
North Pacific	Alaska, Washington, Oregon	48	Ward 1988
Pacific Ocean	Hawaii, Am. Samoa, Guam	14	Sargent, Markle, and Grace 1988

- Repairs to armor slopes may involve mixing of armor unit sizes and types (e.g., overlaying rock with concrete armor units, overlaying laid-up cut stone with rubble-mound, etc.).

- It may be necessary to remove part or all of a damaged armor slope in order to begin repairs. In some instances broken armor units may need to be removed. This will temporarily expose the underlayers to wave action, and it requires either removing material from the site or stockpiling it for reuse during the repair.

- Spot repairs to isolated damage on armor slopes require substantial mobilization of equipment, and thus might be postponed unless economical methods can be devised.

- Importing small quantities of armor stone is expensive, particularly if the source quarry is not local. (Stockpiling spare material onsite should be considered during initial construction.)

- There will be fewer options regarding equipment and site access for repairing rubble-mound structures. For example, the original structure might have been constructed from an access road atop the structure crest, whereas the repair might have to be accomplished from floating plant. Table VI-8-11 lists construction equipment that can be used for repair of rubble-mound structures.

Figure VI-8-6. Damage at Redondo Harbor breakwater looking from inside harbor (circa 1988)

(c) Depending on the extent of damage or deterioration on a rubble-mound structure, repair options range from minor redressing of the primary armor layer to complete replacement of the structure. Pope (1992) listed the common options for repairing rubble-mound structures shown in Table VI-8-12.

(2) Armor and underlayers. There are four general categories of armor layer repair: spot replacement of broken or dislodged armor units; overlaying existing armor layers; replacing armor layers, and rebuilding the structure. Each of these categories is discussed in the following subsections. Design guidance for armor layer repairs is sparse, and most of the following discussion consists of common sense rules of thumbs that can be applied along with consideration of those unique aspects of each particular repair. As always, past repair experience on the same or similar structures is valuable design input.

(a) Spot replacement of broken or dislodged armor units. If damage to the primary armor layer consists of displaced individual armor units, and the percentage of displaced units is less than 5 percent, the armor layer can be repaired by replacing the dislodged armor units with units of similar type and size (Groeneveld, Mol, Nieuwenhuys 1984). Reusing displaced armor units, supplemented with new units is acceptable practice provided the old armor units are still sound and have not been broken into smaller pieces.

- It is important to establish that the damage occurred as a result of forcing conditions that were similar to the design event. If damage was caused by lesser storm events, then

repairing with similar units may not provide adequate long-term protection. Therefore, repair by spot replacement should be considered on a case-by-case basis.

Table VI-8-11
Construction Equipment for Repair of Rubble-Mound Structures (from CIRIA/CUR 1991)

Equipment	Handling Attachment	Comment	Access
Tracked hydraulic excavator	Bucket	Positive pickup and placement. Limited placement and movement. Drops stone.	Suitable for beaches, over crest stones
	Fixed-arm	Positive pickup and placement.	As above
	Orange peel grab	Non-positive pickup and placement. Difficult to pick up individual stones from face.	As above
Wheeled hydraulic excavator	Bucket grapple grab	As above	Only suitable for hard smooth traffic surfaces, small stones, and limited reach.
Crawler crane	Orange peel grab	As above, slower than excavator because of attachment	Suitable for remote areas of structure where hard traffic surface available adjacent to damage.
Jack-up pontoon with crane or excavator	Bucket grapple grab	As above	Suitable for non-drying sites without access from structure.
Cranes and excavator for reinforcing failed sections by other means	Buckets and skips	Applicable to areas where importing large stones is difficult.	Need good access close to structure to reinforce sections with concrete or asphalt grout
Block and tackle	Chains and lifting eyes	Suitable where rock does not have to be moved far distances.	Access for large plant materials difficult.

- Spot replacement of dislodged armor units is the least expensive of the repair options because of shorter time onsite, less new material costs, and less rehandling of existing armor. Individual armor units are generally dislodged in the vicinity of the still-water line, and repairs can be achieved using cranes perched on the structure crest if accessible. For structures where crest access in unavailable or where building temporary construction roads is too expensive, repairs can be made from floating plant.

Table VI-8-12
Options for Repairing Rubble-Mound Structures (Pope 1992)

Problem Area	Options
Slope and crest repair	Chinking, resurfacing Addition of dissimilar armor Layer reconstruction Crest raising Burial
Toe and foundation repair	Toe reconstruction Scour apron Addition of a berm or toe trench
Core repair or void sealing	Precast concrete blocks Filter cloth Grout
Replace original structure	Type of structure Entirely remove existing structure

- Different techniques for replacing armor stones in a damaged layer were examined using 2-D and 3-D small-scale laboratory tests (Ward and Markle 1990). Three different localized repair methods were tried using replacement stone that was similar in size to the original. For each repair method, loose armor stones (usually one to three units) were removed from the damaged area before commencing repairs.

  – Voids above the still-water level (SWL) were filled with new armor stone without handling any of the surrounding undisturbed armor stones.

  – Voids about SWL were filled with new armor stone, and adjacent undisturbed armor stones were reoriented to provide better seating of the new stones. Up to two stones away from the void were handled to assure the voids were completely filled and the armor was well keyed in the layer.

  – Existing stones from the armor layer above the void were used to fill the void, progressively moving the void upslope to the crest where new stones were added. This method helped assure good contact between stones in the repaired area and in the slope above the repair. This method also eliminates multiple handling of armor stone and the need to stockpile existing armor stones.

- Intuitively, repair method 3 would seem better than method 2 which, in turn, would be better than method 1. However, the model tests proved inconclusive. As expected, the tests did indicate that achieving interlocking of armor stones is critical for stability of the spot repair. If an existing damaged armor layer has good interlocking in the undamaged portions, reseating or shifting those stones during spot repairs may introduce new weaknesses in the armor layer and reduce the armor stability. Similarly, new stone placed on the structure must be well seated with maximum contact with surrounding stones to achieve a stable repair.

- For interlocking concrete armor units, such as dolos or Core-Locs J, stability is based on the strong interlocking between adjacent units. Groeneveld, Mol, and Nieuwenhuys (1984) recommended that repair of damage to concrete armor unit layers should precede by removing both damaged and undamaged units from the repair location all the way up the slope to the crest, and then replacing the entire area with undamaged units. This assures proper interlocking throughout the armor slope.

- Turk and Melby (1997) suggested two methods for repairing concrete armor slopes. The spot repair method is used to repair a small cluster of broken armor units. The broken units are removed from the slope and replaced with new units. Because there is little handling of adjacent undamaged units, care must be taken to achieve good interlocking of the new units with the existing units. The AV-notch@ method of repair is more extensive because armor is removed from the point of damage up the slope in a V-shape that widens as it approaches the structure crest. The notch is then filled in using either all new units or a combination of new and original armor units. It was noted that any spot repair is only as stable as the surrounding original armor unit matrix. The report provides guidelines for repairing dolos armor layers using the Core-Loc concrete armor unit.

(b) Overlaying damaged armor layers. If an existing structure experiences widespread armor layer damage resulting in large sections of the armor being displaced or slumped, it may be feasible to repair the structure by adding an overlay consisting of similar or dissimilar armor units. Overlays can also be used to increase crest elevation to reduce overtopping, or to decrease the armor slope for more stability. Constructing an overlay repair is expensive because of the quantity of new armor units required, but an overlay is not as expensive as replacing the armor layer completely. Degradation of the structure cross section might be caused by dislodging of armor stones, loss of underlayer materials, or toe failure and slumping of the slope armor. In some cases the remaining structure cross section has a lower crest elevation and milder side slopes than originally built. A key factor in designing the overlay is determining what caused the damage. If the damage is a result of armor instability, the overlay will need to consist of armor units capable of resisting the wave loading. For rubble-mound structures armored with stone, this implies overlying stone armor must be larger than the original armor or placed at a flatter slope. Where sufficiently large stone is unavailable, concrete armor units are the only option. There are some significant concerns related to the design and construction of rubble-mound structure overlays. These are listed as follows in no particular order of importance.

- *Single-layer stone overlays.* There are no established stability coefficients that can be used in stability formulas for single-layer rock overlays placed on existing structures. It is inappropriate to use published stability coefficients intended either for two-layer armor layers or for single-layer new construction. Physical model tests should be used to verify and optimize a stable one-layer overlay design. Wolf (1989) presented an overview of new breakwater construction in the Detroit District using one layer of armor stone. Although this is not the same as an overlay, the report provides useful guidance on armor placement and stability requirements for single layers.

- *Two-layer stone overlays.* Most stability coefficients for stone are based on two-layer design, and these coefficients should be adequate for two-layer overlays provided sufficient care

is taken to interface with the underlying existing armor slope. For large projects physical model tests are warranted.

- *Overlays using dissimilar armor units.* Typically, this refers to overlaying an existing stone-armored structure with an armor layer composed of concrete armor units. Concrete armor units are used to obtain increased stability through increased interlocking due to unit shape (dolos, accropode, Core-Loc), increased mass (cubes), or a combination of both.

- Carver (1989a) surveyed existing USACE projects where dissimilar armor was used for repairs. In all cases design of the overlayer was based on:

  – Design guidance for new construction.

  – Prototype experience.

  – Engineering judgment.

  – Evaluation of model tests of similar structures.

  – Site-specific model tests.

- The total lack of appropriate design guidance for dissimilar armor overlays led to a series of laboratory model studies investigating various types of dissimilar armor overlays. Table VI-8-13 briefly summarizes the results.

Table VI-8-13
Summary of Stability Results for Dissimilar Armor Overlays

Overlay Type	Stability Coef., K_D	Comments[1]	Reference
Dolos over stone (trunk)	12	Randomly placed. Minimum stability for long waves in shallow water.	Carver and Wright (1988a)
Dolos over stone (head)	8	Slope 1:1.5	Carver (1989b)
	7	Slopes 1:2 thru 1:3.5	
	6	Slopes 1:4 thru 1:5	
Tribar over stone (trunk)	9	Randomly placed on slopes no steeper than 1:2	Carver and Wright (1988a)
	7	Uniformly placed on slopes as steep as 1:1.5	
Dolos over dolos (trunk)	15.6	Randomly placed. Minimum stability for long waves in shallow water.	Carver and Wright (1988b)
Dolos over tribars (Trunk and head)	15	Randomly placed. Exceeds stability of new construction.	Carver and Wright (1988c)

[1] Slopes are given as Avertical rise: horizontal run,@ e.g., 1:2 means A1 vertical to 2 horizontal.@

- *Armor interface with existing armor.* During placement, care is needed to maximize interlocking between the new armor layer and the existing armor stones lying beneath. Typically, the profile of the underlying armor stone will be irregular as shown in Figure VI-8-7. Thus, in some places the new armor stones may rest directly on existing armor, and in other places new underlayer stone may be needed to restore the existing slope to a uniform grade. Construction of underwater portions of armor slopes is always difficult, but this difficulty is compounded when the existing slope is irregular. Care must be taken to assure the underwater portion of the armor overlay is reasonably uniform and free of gaps.

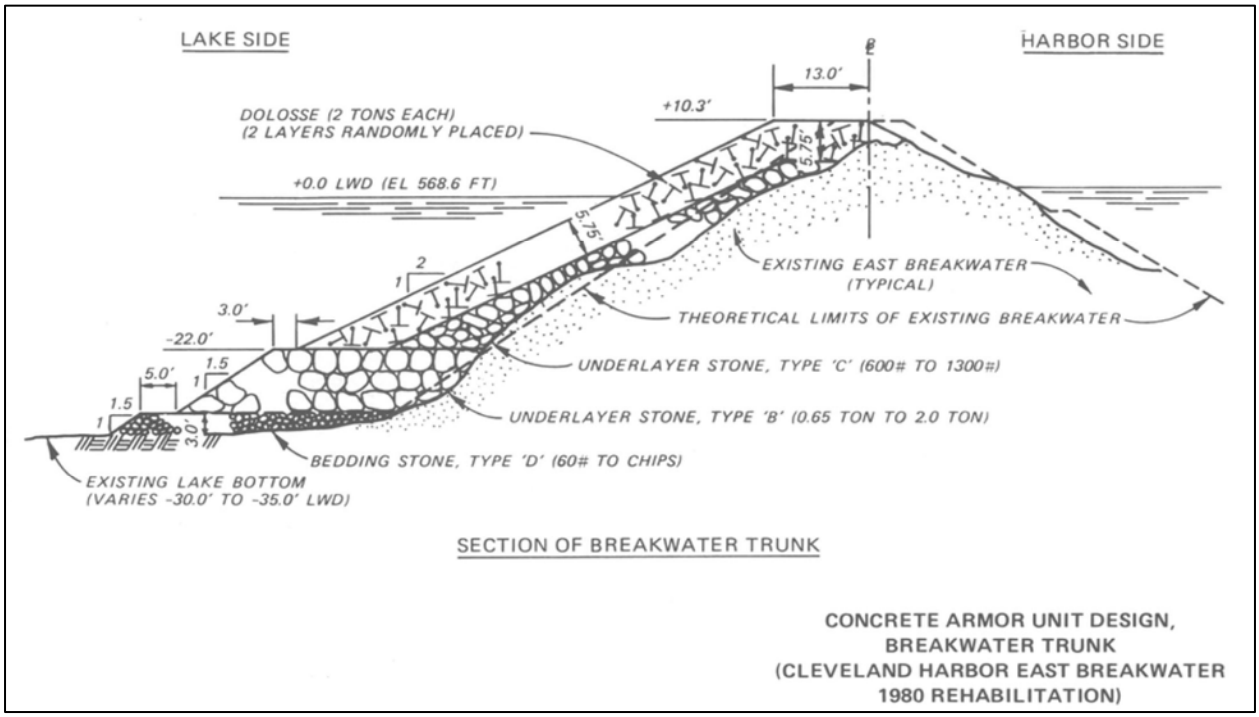

Figure VI-8-7. Cleveland Harbor breakwater rehabilitation, 1980 (from Carver 1989a)

- *Leeside crest armor units.* If heavy overtopping of the new overlay or transmission through the structure is expected, care must be taken to assure the leeside crest armor units are securely keyed into the existing structure. Otherwise, the leeward most armor units might be lost, initiating unraveling of the crest.

- *Overlay toe.* The new overlay toe must be securely positioned and adequately protected by either a toe berm or toe trench. This may range from construction of a new toe berm as illustrated on Figure VI-8-7 to excavation of a toe trench for a shallow-water structure. Difficulties arise where dislodged armor stones litter the toe region. It may be necessary to remove some displaced armor stones to clear the area for construction of the new toe.

- *Construction methods.* Constructing an overlay is quite similar to new construction in that armor placement begins at the toe and proceeds upslope. Where the existing slope is irregular, extra effort is needed to achieve good interlocking between the overlayer and existing

armor. In some cases, it may be necessary to remove or relocate existing armor units. As always, past experience on similar projects is very helpful.

(c) Replacement of armor layer. A more expensive alternative than constructing an overlay is entirely replacing or rebuilding the armor layer over a portion of the structure. Replacing the armor layer might be necessary where the original armor protection has proven to be inadequate either structurally or functionally. Example situations that might warrant armor layer replacement include excessive broken armor units, undersized armor units, excessive wave overtopping, or excessive wave transmission. Rebuilding the armor layer is only advisable when it can be determined that damage was caused by something other than armor instability. Examples include faulty construction or damage due to seismic events. Although very expensive, armor layer replacement or rebuilding is justified if anticipated future maintenance costs of the existing structure (based on past performance) are projected to be higher than the replacement cost.

- Replacement armor layers should be designed using the guidance available for new construction. Be certain that the existing underlayer on which the new armor will be placed meets proper specifications to prevent loss of underlayer through voids in the primary armor. Construction of replacement armor layers requires removing all existing armor units in the section to be repaired, and replacing with new armor units or a similar or dissimilar type. Construction typically will begin at the toe and work up the slope. Disposing of the removed original armor units is a substantial expense. If possible, minimize handling costs by recycling the old armor units on a nearby project for which they are adequate. One alternative might be to place the damaged and undersized armor units at the toe of the structure to create an elevated berm that serves as a base for the new armor layer. In general, broken pieces of armor (especially rounded concrete pieces) should not be used to fill in as underlayer material.

- To rebuild a damaged armor layer, a construction plan must be devised for removing the existing stone over a section of the structure, then replacing the armor units starting with the toe and working upslope. Depending on the particular projects, efficient stockpiling of armor units and minimizing rehandling of armor can help reduce costs for rebuilding.

- Armor layer rebuilding or replacing is similar to new construction except that the core and underlayers already exist. Depending on the extent of damage, it may be necessary to replace, add to, or adjust portions of the first underlayer to accept the new armor layer. The underlayer should be checked for correct thickness and compaction. If the new armor layer consists of much larger armor units, the stone sizes in the first underlayer may have to be increased to avoid loss of material through the voids. The slope of the new primary armor layer can be decreased by placing additional underlayer stone on the existing slope. Figure VI-8-8 shows a section of Cleveland dike 14 that was typical of damage caused by severe stone cracking and deterioration. The original armor layer consisted of large blocky stones placed on a 1V-to-1.5H slope. Repair to the armor layer involved removing existing armor stones and placing them downslope (where practical) to form a new underlayer at a 1V-to-2H slope which was then covered with a new armor layer as shown in Figure VI-8-9.

(d) Reconstruction of rubble mound. Structures that sustain catastrophic damage where the integrity of the structure has been lost, or where repair can only be realized through a major redesign, will need to be entirely rebuilt. If the project function requires the structure to be rebuilt at the same location, it may be necessary to bury or completely remove the existing structure. Burial of an existing structure probably means that a larger cross section will result (Pope 1992). In cases where the same functionality can be achieved by construction of a new structure adjacent to the damaged structure, it may be possible to abandon the old structure pursuant to regulatory approvals. Design of replacement structures follows the same guidance as new construction. If the new structure is to be placed atop the remnants of the existing structure, special attention is needed preparing the existing structure to serve as the rubble base of the new construction. This may involve removing material, preparing a new toe, and laying down new bedding material. Removing materials from the old structure will be a major expense, and consideration should be given to the possible reuse of the material in the new construction. Otherwise, reconstruction will be more costly than building a new structure.

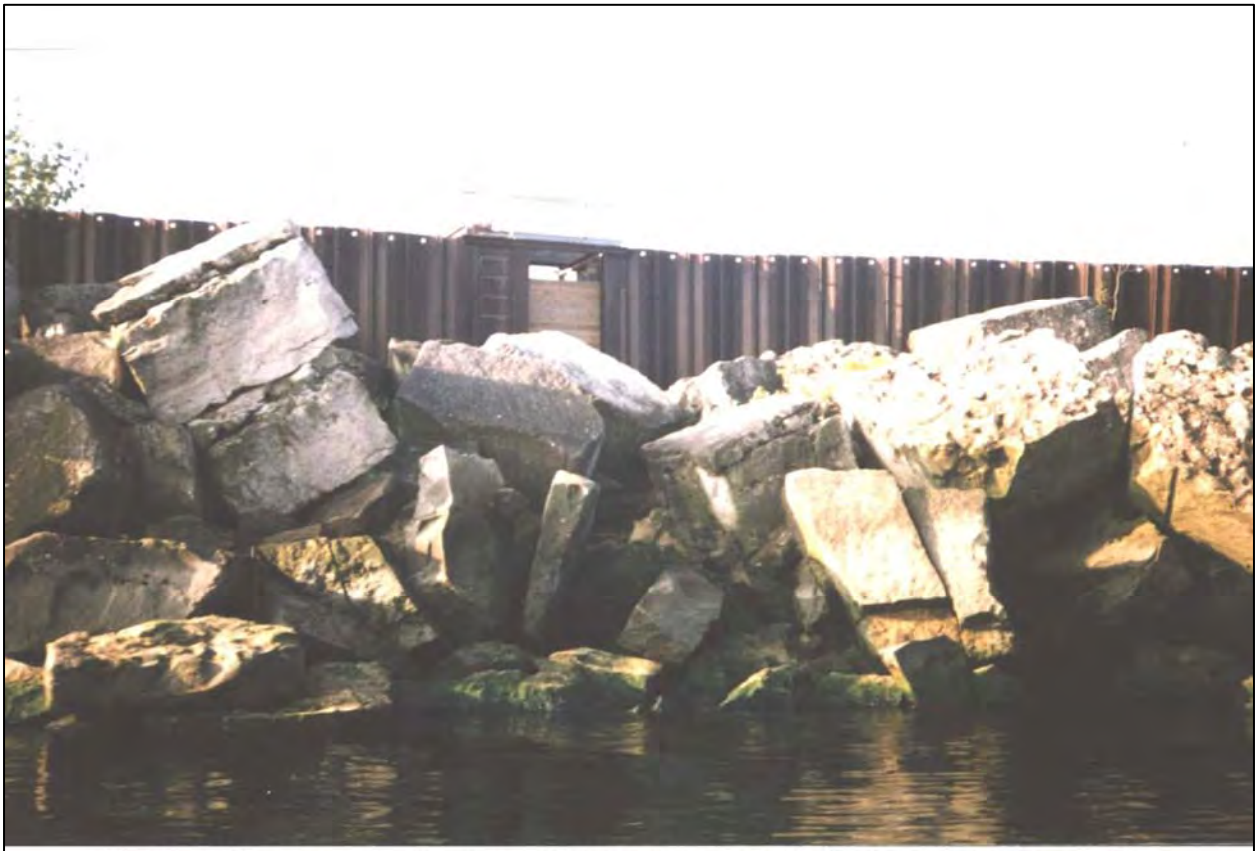

Cleveland Dike 14, Looking South from Water at Overflow Weir, Station 25+00, 15 Sept. 1997.

Figure VI-8-8. Cleveland dike 14 before rehabilitation

Figure VI-8-9. Cleveland dike 14 after rehabilitation

(3) Caps and crowns. Some structures have caps or crown walls placed on the crest. Usually the purpose for these crest structures is one or more of the following: to increase structure integrity of the rubble mound, reduce core loss, enhance safe public access, increase crest height to reduce overtopping, or provide harbor and ship loading facilities. Caps and crown walls come in a variety of configurations, but usually they are constructed of concrete. It is possible to cast a cap in place after construction of the structure crest, but provision must be made to prevent poured concrete from running through voids in the crest. When cured, the new cap conforms to the irregularities of the crest. Some caps are constructed of prefabricated concrete units that are placed on the rubble crest.

(a) Damage to structure caps and crown walls (excluding concrete deterioration) occurs when the concrete sections are dislodged or displaced by wave action, the supporting underlying armor stones are lost, or differential settlement distorts portions of the structure (see Figures VI-2-31 to VI-2-34, CEM Part VI-2-4, “Failure Modes of Typical Structure Types”). The displaced cap elements might remain intact, or they may break into smaller pieces depending on the cap design, the extent of movement, and the load configuration and support in the new position.

(b) Repair methods for displaced or broken caps and crown walls are not well established, and depend primarily on the specifics of the structure and damage. Minor displacements or settlements might be corrected with hydraulic jacks or cranes, or by lifting and repositioning the cap elements. In cases where the supporting armor layer is removed, it may be necessary to remove the surviving cap or crown elements, then replace them after the armor layer has been reconstructed. Caps that have been cast in place are less likely to be reused, especially if underlying crest armor has moved or has been replaced. Cap or crown elements broken during movement may not be usable, and will have to be removed from the structure and

replaced with new elements. Adding a new cap or crown wall as part of a rehabilitation or enhancement of an existing rubble-mound structure will proceed much like new construction. Consideration must be given to structure access for equipment and materials required for the addition. The design should include provision for upward venting through the cap, just as in new design.

(4) Toes and berms. Damaged rubble-mound berms may still provide some degree of protection for the primary armor layer. Because berm crests are typically submerged, repairing a berm is most effectively accomplished by adding new material atop of the existing berm to restore the berm to design cross section. If damage is minor and thought to be caused by exceedence of the design condition, the new material can be the same size or slightly larger than originally placed.

(a) If berm damage is severe, it may be necessary to redesign the berm using larger armor units. It may be possible to place the new berm on the remnants of the damaged one, but in some cases it will be necessary to remove some or all of the existing berm material. Removal of scattered material may be necessary if it encroaches on the navigation channel or otherwise interferes with navigation or other activities. Existing projects can be upgraded by adding a berm to reduce wave energy and increase stability of the primary armor layer. A berm also can decrease wave runup and overtopping on projects which are not functioning as intended.

(b) Stability problems with rubble-mound breakwater and jetty toes experienced by the USACE were documented by Markle (1986). Twelve of 21 Corps Districts reported existing or past problems with rubble-mound structure toe stability, and Markle=s report includes numerous case histories. Most toe instability was related to both inadequate sizing and placing of the toe stones, or due to undermining of the toe berm by scour. Subsequent to the field survey, a small-scale laboratory test program was conducted at the U.S. Army Engineer Waterways Experiment Station (currently the U.S. Army Engineer Research and Development Center) to develop appropriate design guidance for toe berms (Markle 1989). The resulting design guidance for rubble berms and toes is given in CEM Part VI-5-3-d, “Toe Stability and Protection,” and this same guidance should be used for repairing damaged toe berms if the problem appears related to toe stone stability.

(c) Toe instability caused by waves and currents scouring the seabed adjacent to the structure toe is more problematic. Additional toe material can be placed to rebuild the toe profile that has been degraded by materials falling into the scour hole, or a scour blanket can be constructed to protect the toe from damage by scour. A third, more expensive solution is to excavate and reconstruct the structure toe, but care must be taken not to initiate a slope failure of the main armor layer during repair. If warranted, it may be advantageous to reconstruct the damaged toe berm to a larger size than originally designed in order to reduce runup and overtopping and to increase armor stability.

(5) Scour holes and bed protection. Some initial designs include provisions for scour protection, usually in the form of a stone apron extending some distance from the structure toe. More often, however, scour protection is added to a project after monitoring has revealed formation of scour holes or trenches due to currents, waves, or a combination of both. For

example, in situations where scour has undermined the structure toe berm, the repair plan should include some type of scour protection to prevent future occurrences.

(a) Prediction of where scour may occur at a coastal project is rudimentary at best, with past experience being the best gauge. There is little difference between designing scour protection as part of a structure repair or rehabilitation and designing the protection for a new project. See CEM Part VI-5-6, “Scour and Scour Protection,” for appropriate design guidance for estimating scour and designing scour protection. Design of scour blankets in a current field is given in CEM Part VI-5-3-f, “Blanket Stability in Current Fields.”

(b) One of the main decisions facing the designer of scour protection after scour has occurred is whether or not to fill in the scour hole before placing the protective stone blanket. If the scour hole is close to the structure toe and has relatively steep side slopes, there is a risk of the toe falling into the scour hole either by armor slope failure or slip-circle failure. (See Figures VI-2-37, VI-2-64, VI-2-69, CEM Part VI-2-4, “Failure Modes of Typical Structure Types.” This is a hard design decision because no guidance exists regarding armor slope instability relative to scour hole side slopes adjacent to the structure toe. In addition, deep scour holes indicate strong local currents, and filling in these scour holes may substantially increase currents and cause scour in adjacent, unprotected portions of the seabed. When judging qualitatively the risk a scour hole may have on the stability of the adjacent rubble-mound structure, be sure to examine only cross sections that have been drawn without distortion of the vertical axis which makes the scour hole side slopes appear steeper than they actually are.

(6) Void sealing. Rubble-mound breakwaters, jetties, and groins have some degree of permeability that varies significantly with cross-section design. Rubble-mound permeability helps absorb wave energy, reduce wave runup and overtopping, decrease wave reflection, and generally increase armor layer stability. However, wave transmission through the structure increases with increased permeability, and excessive wave transmission can affect vessel navigation, mooring, and harbor activities. For projects where rubble-mound structures are placed within active littoral zones, sand can flow through permeable rubble mounds and deposit in shoals on the leeside of the structure. If the shoals result in depths less than the authorized project depths, maintenance dredging is required to assure continued project functionality. Permeability of newly constructed rubble-mound structures might decrease slightly as the structure Anests@ and stones shift into the voids. Conversely, it is possible for rubble-mound permeability to increase over time if smaller core material is washed out of the structure by wave action or if portions of the armor layer suffer damage. In situations where structure permeability is causing problems, it may be possible to decrease permeability by a process called void sealing where grout or some type of sealant is injected into the structure to fill the voids. Using techniques developed in civil and mining engineering, it is possible to fill interior voids on the order of 1 m in diameter. However, the longevity of grouts and sealants placed in coastal structures is unknown due to lack of long-term field experience. The following paragraphs summarize a study conducted as part of the REMR Program that was documented in a series of four reports (Simpson 1989; Simpson and Thomas 1990; Rosati and Denes 1990; and Simpson et al. 1990). These reports should be consulted for more thorough information before undertaking feasibility studies related to breakwater or jetty void sealing.

(a) Determining need for structure sealing. Void sealing of rubble-mound structures is an alternative where project functionality is impacted by excessive wave transmission through the structure or by sand moving through the structure and infilling the navigation channel or mooring areas. Measurements should be made to establish the existing degree of wave transmission through the structure for a range of typical operational wave conditions. Also note the variation of wave transmission along the structure with a view toward minimizing the distance to be sealed.

- If sand transmission through the structure is suspected, it must be shown that deposition results from sand actually passing through the structure rather than moving over or around the structure. If dye released in the water on the sea side of a structure appears on the lee side of the rubble mound in less than 1 min, it is safe to assume that sand can easily flow through the structure and deposit in a shoal. Hydrographic surveys scheduled in concert with dredging activities or storm events will reveal the location of sand leakage and the rate of shoal growth due to sand transport through the structure. Dyed tracer sand may provide an indication of sediment pathways and the upstream source of sediment. This information can be used to assess alternate solutions that may be less costly than void sealing. For example, it may be feasible to trap some of littoral sediment before it reaches the leaky structure.

- Simpson et al. (1990) stated: “The quantity of material moving through the structure which contributes to the shoal must be of such a magnitude that the cost of its elimination is offset by the savings in mobilization, demobilization, and dredging which would otherwise be attributed to it.”

- Alternately, if shoaling caused by sand movement through the structure does not affect navigation significantly between regularly scheduled channel maintenance dredging, then void sealing of the structure would not be cost-effective relative to the small additional cost of dredging the shoal as part of the regular dredging cycle. Structures that are nearly at the end of their service life or are scheduled for rehabilitation are not likely candidates for void sealing. In the case of structure rehabilitation, it may be cost-effective to include provisions for reducing sediment transmission as part of the rehabilitation. Benefits gained by reduction of future maintenance dredging may offset the additional cost of a rehabilitation that includes reduction of sand transmission.

- An important consideration in determining the viability of void sealing is the engineering practicality of sealing a particular structure. Factors such as equipment (drilling and sealing) availability and site accessibility should be investigated early in the planning process. Sealing structures requires placing drilling and other equipment on the structure. Low crested, frequently overtopped structures present a higher risk of equipment damage or loss, and this risk must be included in the economic analysis. In addition, fully successful void sealing of rubble-mound structures is difficult to achieve, and field experience with this type of remedy is sparse.

- Finally, void filling of a permeable rubble-mound structure will alter how waves interact with the structure. An assessment must be made as to whether these changes will have any impact on the overall project functionality. The primary concerns are increased wave runup

and possibly overtopping, increased wave reflection from the structure, and the possibility of decreased armor unit stability.

(b) Determining extent of structure void sealing. The lateral extent proposed for void sealing should cover the area where wave and/or sand transmission is a problem. In addition, attempt to determine additional locations where transmission may become a problem after sealing the structure due to altered wave characteristics or breaker angles. The sealed structure may cause sand accretion on the seaward side that eventually could flank the sealed portion as a new equilibrium shoreline develops adjacent to the structure. For prevention of sand transmission the existing sand layer should be stabilized (sealant is injected into the sand bed, displacing the sand), and then the void sealant is injected to an elevation greater than the expected elevation of sand accretion on the seaward side of the structure. To decrease wave transmission the void sealant barrier should be placed to approximately the mean high-water level (Simpson et al. 1990).

(c) Sealing techniques. Two cementitious sealants and two sodium silicate sealants were shown to be potentially effective for permeable coastal structures. Correct mixing and handling of these grouting materials is essential for good bonding and reasonable durability. See the previous referenced reports for further details on the mixtures and correct application.

- The general procedure for grouting a permeable structure is to drill primary grouting holes along the rubble-mound structure center line at about 3-m (10-ft) spacings. The pumping nozzle is placed into the hole and an estimated volume of grout/sealant needed to create the barrier is injected starting near the bottom. After an estimated quantity of sealant has been placed, the nozzle is raised vertically a specified distance and another volume of sealant is placed. This procedure continues until the grout reaches final elevation. The quantities injected at each elevation must be determined from a few test injections or by monitoring the filling of the first few grout holes. The resulting grout structure will have a somewhat conical shape with low “valleys” between the adjacent peaks.

- After the primary holes are filled, the gaps between the injection points are filled via secondary holes that are evenly spaced between the primary holes. Again, the amount of sealant injected has to be estimated a priori. Depending on the particular application, additional holes may be needed between the secondary holes.

- Simpson et al. (1990) described four types of sealing treatment that might be considered in coastal engineering applications: barrier curtain sealing, cavity filling, soil sealing, and riprap sealing. They also discussed equipment commonly used for sealing operations such as drills, sealant pumps, concrete pumps, mixers, sealant lines, and monitoring equipment.

(d) Sealing design parameters. A preliminary field investigation is crucial for designing an appropriate sealing strategy.

- Factors to be evaluated during the investigation include the following:

– An estimate of stone size and type in the section to be sealed. Stone size provides information about the void sizes and the degree of communication with other voids. Stone type gives a preliminary indication of drilling difficulty.

– The water flow rate through the structure which factors into the type of grout or sealant suitable for the conditions. Higher flow rates dictate faster setting sealant mixtures.

– The present sand level beneath the structure should be estimated so that sealant quantities can be calculated. This may require drilling of exploratory holes through the structure. (Note: Exploratory drilling also reveals the drilling difficulty that can be expected.)

– Water chemistry (pH, salinity, and temperature) can affect the stability and durability of the sealant mixture.

- The main factors affecting a sealant mix intended for rubble-mound structure void filling are listed as follows.

– Potential for dilution and dispersion of the sealant by water movement through the structure during emplacement

– Consistency of the sealant and the homogeneity of the rubble mound

– Size of the voids within the rubble-mound structure

– Top elevation of the grout curtain

– Permanence of the grout mass

- Satisfying these criteria requires a grout or sealant mixture that is highly viscous very soon after placement, but still fluid enough under low pumping pressure to be placed at a rate much greater than the water flow rate through the cavities. The mixture must set fast and be durable and stable under cyclic wetting/drying conditions. Finally, the mixture must be economical for batching in large quantities. Sealants injected to stabilize the sand bed must penetrate the sand mass for a distance of around half a meter at low pressure.

- According to Simpson et al. (1990): “The most important part of the entire sealing operation is retaining a contractor who is competent in this type of work and conscientious enough to understand the indications of what is occurring below the surface and make necessary adjustments. The flow of sealant to adjacent holes or out the sides of a structure must be monitored to adjust the mix or injection procedures.”

- Detailed guidance on void sealing field procedures, quantity estimation, contract specification, contracting procedures, and site supervision/inspection of grouting operations is included in the REMR reports cited at the beginning of this section. The summary report (Simpson et al. 1990) also includes results of a sealant durability study where specimens were exposed to the elements.

(e) Field experience. Seven completed void sealing projects, including four USACE projects, were summarized in Simpson et al. (1990). A more detailed description of void sealing at Port Everglades, Florida, was given by Rosati and Denes (1990). The Port Everglades study included pre- and postconstruction monitoring to gauge the effectiveness of the void sealing operation.

- Sodium silicate-cement and sodium silicate-diacetin chemical sealants were used to seal man-sized voids in the Port Everglades south jetty. The purpose of the grouting was to reduce sand flow through the structure. Dye injection and measurement of dye concentrations at sealed and unsealed portions of the jetty indicated that the void sealing was successful in reducing water flow transmission by a factor of 2. The unsealed jetty was estimated to be 4.0 percent transmissible whereas the sealed structure reduced this value to about 1.9 percent. It was also noted that the structure was reflecting more wave energy as indicated by a shift in the average current vector measured adjacent to the jetty. Doubts were expressed about the long-term viability of the sealants used in this project based on exposure tests conducted as part of the REMR Program.

- Sand moving through the south jetty at Palm Beach Harbor, Florida, was depositing in a channel-side shoal that interfered with navigation and required expensive dredge mobilization each year. The south jetty was sealed in 1984 by the U.S. Army Engineer District, Jacksonville, using a mixture of cement and silicate. This sealing mixture was suggested by the contractor after initial efforts using the two originally specified sealants were unsuccessful. The final hole spacing was about 1 m (3 ft), and it was during this project the alternate hole filling sequence was seen to produce better buildup of sealant. After completion of the sealing, samples of the void barrier were extracted from exploratory holes, and these samples indicated that design objectives had been met. The jetty sealing significantly reduced shoaling into the channel to the point that no dredging mobilization has been required specifically to remove the shoal.

- In 1985 the U.S. Army Engineer District, San Francisco, sealed a newly constructed groin and a new extension of an existing groin at the Buhne Point, California, Shoreline Erosion Demonstration Project. On the new groin the sealing was accomplished in three phases with the initial holes drilled at about 3-m (10-ft) centers. After filling the first set of holes, holes spaced at the midpoints between the initial holes were drilled and filled. Finally, another set of midpoint holes were drilled giving a final hole spacing of about 0.75 m (2.5 ft). The groin extension was drilled at 1.5-m (5-ft) centers. The originally specified sealant was a cementitious mixture that proved difficult to pump, and the mixture was modified, as shown in Table VI-8-14.

- Holes spaced at 3 m (10 ft) on the Buhne Point groin took about 5.4 m^3 (7 yd^3) on average. The holes were 4.4 m (14.5 ft) deep. The holes centered between the first set of holes had an average intake of 3.8 m^3 (5 yd^3). Examination during high tide and 1.2-m (4-ft) seas revealed that a third set of holes centered between existing holes were needed to prevent leaks at the +1.8-m (+6-ft) mlw elevation and above. Sealant intake for the final set of holes at 0.75-m (2.5-ft) centers was about 0.8 m^3 (1 yd^3).

Table VI-8-14
Buhne Point Cementitious Sealant (recipe for 1 yd^3)

Component	Specified Weight (lbs)	Modified Weight (lbs)
Coarse aggregate	1,000	1,115
Fine aggregate	1,450	1,655
Cement	705	705
Clay	305	37
Water	500	371
Calcium chloride	15	15
Air	B	0.41

- Inspection after completion of the project revealed 25 to 30 possible leaks in the total groin length of 365 m (1,200 ft). None of the leaks were thought to be below an elevation of 1.5 m (+5 ft mlw), and there did not appear to be any problems related to sand leakage through the groin. Based on experience from sealing of the Buhne Point groins it was recommended that drill holes to be at least 15 cm (6 in.) in diameter to facilitate injection operations and visual inspection.

- Several other void sealing projects are summarized in Simpson et al. (1990). Engineers involved with a project of this nature should study the REMR reports for additional insights. One very obvious conclusion from the REMR study was that much work is needed in the area of developing ways to estimate the quantity of mixture per unit length of structure.

(7) Rubble-mound structure repair case histories. Many rubble-mound structures have a history of rehabilitation, repair, and modification as witnessed by the narratives contained in the REMR reports listed in Table VI-8-10. Lessons learned from previous experience at the same or similar structures are a valuable source of ideas and methodologies that can be considered when a structure needs repair or maintenance. However, each structure is unique in its location, exposure, construction, and intended functionality, so it is important to not adopt blindly a repair procedure without first carefully evaluating all aspects of the project. With the exception of the Sines west breakwater, documented case histories of damage and repair of rubble-mound structure are not abundant in the literature. Several papers reporting on three repair case histories are summarized in the following paragraphs. Engineers with similar repair projects may avoid unforeseen situations by examining the cited literature.

(a) Port of Sines, Portugal, west breakwater. Numerous papers have documented the failure and subsequent repair of the west breakwater at the Port of Sines, Portugal. This 1.7-km-long breakwater was armored with 40-tonne dolosse, and it was nearing completion in February 1978 when the structure was hit by a moderate storm (H_s estimated to be 8.5 - 9.0 m) that caused serious damage. A year later a storm with H_s estimated near the 11-m design wave height caused near catastrophic failure of the armor slope and concrete superstructure (Weggel et al. 1994).

- Baird et al. (1980) summarized the final report of the Port Sines Investigating Panel (PSIP 1982) which examined possible causes of failure, and they presented their own hypothesis on the series of events leading to failure. Several Sines-related papers were presented in the Coastal Structures '83 conference. Toppler et al. (1983) overviewed rehabilitation studies for the west breakwater which included wave climatology, geotechnical studies, and hydraulic stability analyses. Details of study components were given in companion papers. Mynett, de Voogt, and Schmeltz (1983) presented numerical hindcast results for 20 major storms spanning a 25-year period at Sines. Barends et al. (1983) examined geotechnical stability of large breakwaters with reference to quantified results from physical model tests of the Sines west breakwater and from emergency repairs. Groeneveld, Mol, Zwetsloot (1983) compared structural strength of dolos, tetrapods, and cubes and concluded that beyond a certain size the residual static strength of dolos and tetrapods disappears. Armor stability of the emergency repair and rehabilitation of the outer breakwater portion were examined in hydraulic model tests described by Mol et al. (1983).

- Reconstruction of the Sines west breakwater was completed in December 1992, and the engineering aspects of the new breakwater design and construction were documented in the proceedings of a seminar held in September 1993 (RMSC 1994). The seminar proceedings contain 17 papers covering history, rehabilitation studies, geotechnical issues, construction, inspection, monitoring, and maintenance of the new Sines west breakwater and other port constructions. A short summary of the breakwater reconstruction was given by Weggel et al. (1994).

- The Sines west breakwater is fairly unique because of its size, exposure, and 45-m water depth at the toe. The failure and subsequent reconstruction is the most documented in history, and the lessons learned from Sines have benefited our engineering understanding of large rubble-mound structures.

(b) Jetty rehabilitation at Humboldt Bay, California. Edge et al. (1994) and Bottin (1988a) described the historical development of the two jetties protecting the entrance to Humboldt Bay on the northern California coast. Original construction began in 1888, and over the course of the next 80 years the structures have undergone several damage/repair cycles. By 1970 both jetty heads were destroyed and in need of reconstruction. A 1-to-50 scale model was used at WES (Davidson 1971) to develop a stable head section. Tests were conducted using armor slopes constructed of concrete blocks, tribars, tri-longs, tetrapods, and dolos, and the final recommended head section consisted of reinforced 42-ton dolos; the first application of this armor unit in the United States (see Figure VI-8-10). Since reconstruction of the two jetties, the heads have remained generally stable with occasional maintenance needed to repair damage caused by severe storms. Keen insight into the process of actually building the new jetty heads at Humboldt Bay was given by Hanson (1994). He was the USACE construction manager for the project, and his paper presented an interesting chronological record of the complex, and at times, adversarial relationship between the contractor and client. From bidding issues through to the end of the contract, Hanson presented an inside view of what types of issues arise, how they sometimes are resolved, and what can be learned from the experience. A focus of this paper is on the controversy surrounding the use of reinforcement in the dolos. It was decided to use the prototype construction as a testing opportunity by placing some unreinforced and fiber-reinforced dolos in the armor layer. Subsequent examination in 1993 indicated less than

1 percent dolos breakage on both jetties. No conclusions about the value of reinforcement could be drawn from this small sample other than the steel reinforcing prevented the broken pieces from becoming smaller projectiles that could impact and break intact units (Melby and Turk 1994).

(c) Breakwaters at a port in northern Spain. Groeneveld, Mol, Zwetsloot (1984) presented a case study examining options for repairing two dolos-armored breakwaters protecting an unidentified port on the northern coast of Spain. The structures were built in water depths up to 20 m. Shortly after original construction, breakage of 50-ton dolosse armor units occurred under not particularly severe wave conditions. The concrete armor units were placed on slopes of 1:1.5 and 1:2. Three years after construction 17 percent (3,000 units) of the total placed armor on one breakwater and 25 percent of the units on the other were broken. Differential settlement of the south breakwater caused large cracks in the crown wall.

- Six alternative repair options were considered for the north breakwater, and relative cost was determined in terms of the most conventional repair option, which was given as option 1. The options with the relative cost given in brackets are as follows:

  – Remove 50-ton dolosse armor layer and replace with two layers of 81,646.6-kg (90-ton) cube. New rock underlayers would also be placed.

  – Fill in existing voids with quarry-run material, then cover the existing dolos layer with a new berm-like layer consisting of 81,646.6-kg (90-ton) cubes. (140 percent of option 1).

  – Repair the damaged armor layer with 45,359.2-kg (50-ton) dolos and construct a toe berm to a level of about one-third of the water depth. New armor (unspecified) would be placed above the berm. (165 percent of option 1).

  – Install a wide berm (approximately 100-m length) to reduce wave energy. Dolos left in place, but new 60-ton cubes added to slope above the berm. (65 percent of option 1).

  – Leave breakwater unrepaired, but install a new submerged rubble-mound breakwater at some distance seaward to break up the incident waves. Waves reaching the damaged breakwater would not cause additional damage. (105 percent of option 1).

  – Same concept as option 5, with the submerged structure being concrete caissons resting on a rubble base. (200 percent of option 1).

- Costs for option 2 were increased by the need to pump gravel into the existing dolos layer to provide proper sublayer porosity for the armoring system. Higher costs for option 6 included the need to repair the head section using the option 1 technique because the berm would not protect the head adequately. The north breakwater was repaired using option 1, and the risk associated with exposing the underlayer during rehabilitation was acknowledged and accepted.

- The south breakwater needed both armor layer repair and general strengthening for geotechnical stability. The two alternatives considered were the following:

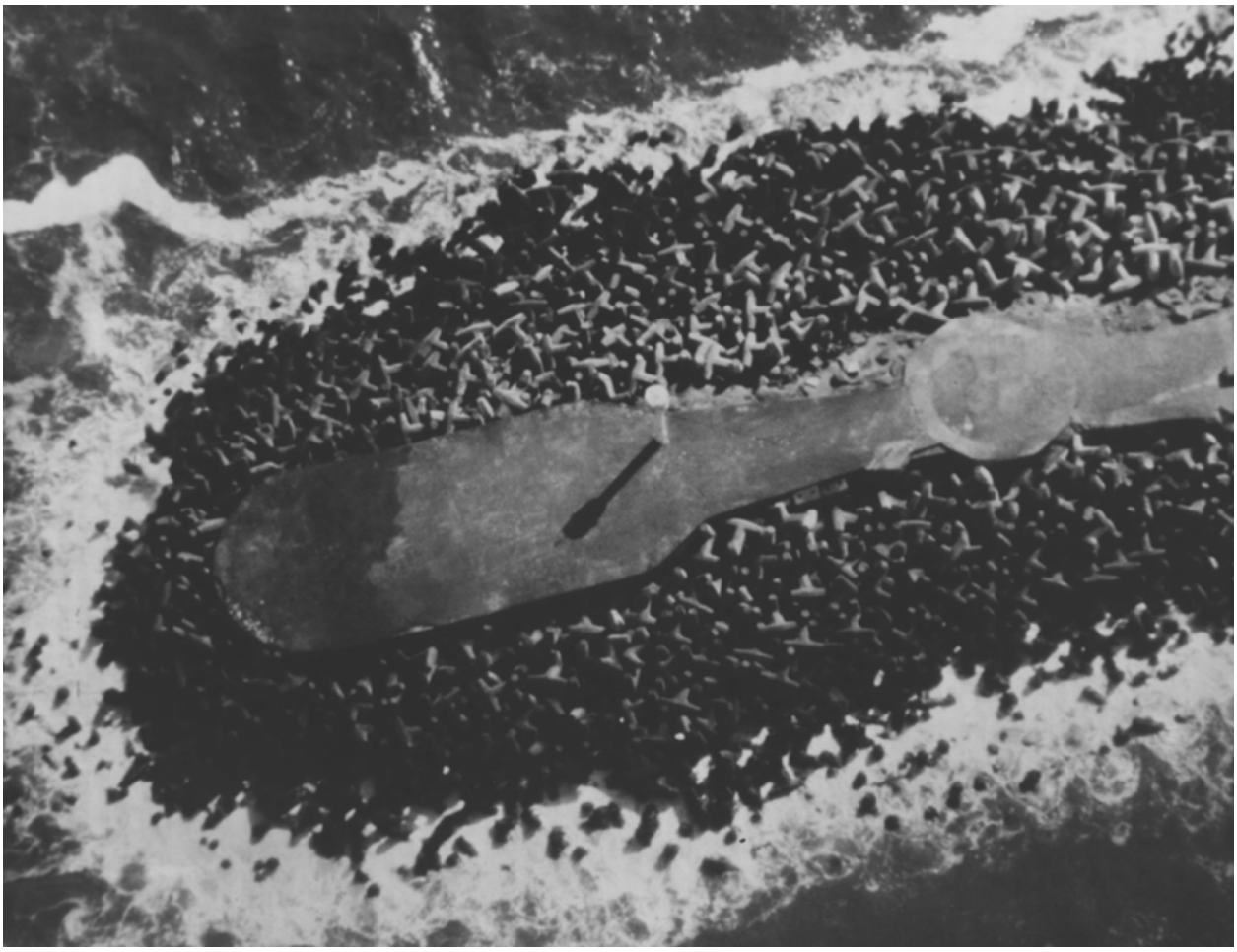

Figure VI-8-10. North jetty at entrance to Humboldt Bay, California

– Removal of the dolosse armor layer and placement of filter material over the existing core at 1:2 slope. A new underlayer would be placed, protected by concrete cubes varying between 45,359.2 to 81,646.6 kg (50 to 90 tons).

– Similar to option 1, but the new filter, underlayer, and armor layer would be placed at a 1:3 slope. Primary armor would be smaller than option 1, and a toe berm would be included.

- Groeneveld, Mol, Nieuwenhuys (1984) stated that the cost of option 2 would be 50 percent higher than option 1. No details were given about repair of the concrete crown wall.

VI-8-4. References.

EM 1110-2-1003
Hydrographic Surveying

EM 1110-2-1004
Coastal Project Monitoring

Aguirre and Plotkin 1998
Aguirre, R., and Plotkin, D. 1998. "REMR Management Systems - BREAKWATER Computer Program User Manual (Version 1.0)," Technical Report REMR-OM-20, U.S. Army Construction Engineering Research Laboratory, Champaign, IL.
(*http://owww.cecer.army.mil/fl/remr/break.html*)

Baird et al. 1980
Baird, W. F., Caldwell, J. M., Edge, B. L., Magoon, O. T., and Treadwell, D. D. 1980. "Report on the Damage to the Sines Breakwater, Portugal." *Proceedings of the 17th International Coastal Engineering Conference*. American Society of Civil Engineers, Vol 3, pp 3063-3077.

Barends et al. 1983
Barends, F. B., van der Kogel, H., Uijttewaal, F. J., and Hagenaar, J. 1983. "West Breakwater - Sines, Dynamic-Geotechnical Stability of Breakwaters." *Proceedings of Coastal Structures '83.* ASCE, pp 31-44.

Bottin 1988a
Bottin, R. R., Jr. 1988a. "Case Histories of Corps Breakwater and Jetty Structures: Report 1, South Pacific Division," Technical Report REMR-CO-3, U.S. Army Engineer Waterways Experiment Station, Vicksburg, MS.

Bottin 1988b
Bottin, R. R., Jr. 1988b. "Case Histories of Corps Breakwater and Jetty Structures: Report 3, North Central Division," Technical Report REMR-CO-3, U.S. Army Engineer Waterways Experiment Station, Vicksburg, MS.

Camfield and Holmes 1992
Camfield, F. E., and Holmes, C. M. 1992. "Monitoring Completed Coastal Projects - Lessons Learned I," Coastal Engineering Technical Note, CETN-III-50, U.S. Army Engineer Waterways Experiment Station, Vicksburg, MS.

Camfield and Holmes 1995
Camfield, F. E., and Holmes, C. M. 1995. "Monitoring Completed Coastal Projects," *Journal of Performance of Constructed Facilities*, ASCE, Vol 9, No. 3, pp 161-171.

Carver 1989a
Carver, R. D. 1989a. "Prototype Experience with the Use of Dissimilar Armor for Repair and Rehabilitation of Rubble-Mound Coastal Structures," Technical Report REMR-CO-2, U.S. Army Engineer Waterways Experiment Station, Vicksburg, MS.

Carver 1989b
Carver, R. D. 1989b. "Stability of Dolos Overlays for Rehabilitation of Stone-Armored Rubble-Mound Breakwater Heads Subjected to Breaking Waves," Technical Report REMR-CO-9, U.S. Army Engineer Waterways Experiment Station, Vicksburg, MS.

Carver and Wright 1988a
Carver, R. D., and Wright, B. J. 1988a. “Stability of Dolos and Tribar Overlays for Rehabilitation of Stone-Armored Rubble-Mound Breakwater and Jetty Trunks Subjected to Breaking Waves,” Technical Report REMR-CO-4, U.S. Army Engineer Waterways Experiment Station, Vicksburg, MS.

Carver and Wright 1988b
Carver, R. D., and Wright, B. J. 1988b. “Stability of Dolos Overlays for Rehabilitation of Dolos-Armored Rubble-Mound Breakwater and Jetty Trunks Subjected to Breaking Waves,” Technical Report REMR-CO-5, U.S. Army Engineer Waterways Experiment Station, Vicksburg, MS.

Carver and Wright 1988c
Carver, R. D., and Wright, B. J. 1988c. “Stability of Dolos Overlays for Rehabilitation of Tribar-Armored Rubble-Mound Breakwater and Jetty Trunks Subjected to Breaking Waves,” Technical Report REMR-CO-6, U.S. Army Engineer Waterways Experiment Station, Vicksburg, MS.

Cialone 1984
Cialone, M. A. 1984. “Monitoring Rubble-Mound Coastal Structures with Photogrammetry,” Coastal Engineering Technical Note, CETN III-21, U.S. Army Engineer Waterways Experiment Station, Vicksburg, MS.

CIRIA/CUR 1991
Construction Industry Research and Information Association (CIRIA) and Centre for Civil Engineering Research and Codes (CUR). 1991. “Manual on the Use of Rock in Coastal and Shoreline Engineering,” CIRIA Special Publication 83/CUR Report 154, CIRIA, London and CUR, The Netherlands.

Davidson 1971
Davidson, D. D. 1971. “Proposed Jetty Head Repair Sections, Humboldt Bay, California,” Technical Report H-71-8, U.S. Army Engineer Waterways Experiment Station, Vicksburg, MS.

Edge et al. 1994
Edge, B. L., Magoon, O. T., Davidson, D. D., Hanson, D., and Sloan, R. L. 1994. “The History of the Humboldt Jetties, Eureka, California, 1880 to 1994.” *Proceedings of Case Histories of the Design Construction, and Maintenance of Rubble Mound Structures*. ASCE, pp 172-194.

Gorman, Morang, and Larson 1998
Gorman, L., Morang, A, and Larson, R. 1998. “Monitoring the Coastal Environment; Part III: Mapping, Shoreline Changes, and Bathymetric Analysis,” *Journal of Coastal Research*, Vol 14, No. 1, pp 61-92.

Groeneveld, Mol, and Zwetsloot 1983
Groeneveld, R. L., Mol, A., and Zwetsloot, P. A. 1983. “West Breakwater - Sines, New Aspects of Armor Units.” *Proceedings of Coastal Structures '83*. ASCE, pp 45-56.

Groeneveld, Mol, and Nieuwenhuys 1984
Groeneveld, R. L., Mol, A., and Nieuwenhuys, E. H. 1984. "Rehabilitation Methods for Damaged Breakwaters." *Proceedings of the 19th International Coastal Engineering Conference*. ASCE, Vol 3, pp 2467-2486.

Hanson 1994
Hanson, D. 1994. "Dolosse Repair of Humboldt Bay Breakwaters: Construction Management Aspects." *Proceedings of Case Histories of the Design Construction, and Maintenance of Rubble Mound Structures.* ASCE, pp 195-210.

Hemsley 1990
Hemsley, M. J. 1990. "Monitoring Completed Coastal Projects - Status of a Program," *Journal of Coastal Research,* Vol 6, No. 2, pp 253-263.

Hughes et al. 1995a
Hughes, S. A., Prickett, T. L., Tubman, M. W., and Corson, W. D. 1995a. "Monitoring of the Yaquina Bay Entrance North Jetty at Newport, Oregon; Summary and Results," Technical Report CERC-95-9, U.S. Army Engineer Waterways Experiment Station, Vicksburg, MS.

Hughes et al. 1995b
Hughes, S. A., Peak, R. C., Carver, R. D., Francis, J. D., and Bertrand, G. M. 1995b. "Investigation of Damage at the Yaquina Bay North Jetty." *Proceedings of Case Histories of the Design, Construction, and Maintenance of Rubble Mound Structures*. ASCE, New York, pp 227-249.

Kendall 1988
Kendall, T. R. 1988. "Analysis of 42-ton Dolos Motions at Crescent City." *Proceedings of the 21st International Coastal Engineering Conference*. ASCE, New York, Vol 3, pp 2129-2143.

Kucharski and Clausner 1989
Kucharski, W. M., and Clausner, J. E. 1989. "Side Scan Sonar for Inspection of Coastal Structures," REMR Technical Note CO-SE-1.4, U.S. Army Engineer Waterways Experiment Station, Vicksburg, MS.

Kucharski and Clausner 1990
Kucharski, W. M., and Clausner, J. E. 1990. "Underwater Inspection of Coastal Structures Using Commercially Available Sonars," REMR Technical Report CO-11, U.S. Army Engineer Waterways Experiment Station, Vicksburg, MS.

Larson, Morang, and Gorman 1997
Larson, R., Morang, A., and Gorman, L. 1997. "Monitoring the Coastal Environment; Part II: Sediment Sampling and Geotechnical Methods," *Journal of Coastal Research*, Vol 13, No. 2, pp 308-330.

Markle 1986
Markle, D. G. 1986. “Stability of Rubble-Mound Breakwater and Jetty Toes; Survey of Field Experience,” Technical Report REMR-CO-1, U.S. Army Engineer Waterways Experiment Station, Vicksburg, MS.

Markle 1989
Markle, D. G. 1989. “Stability of Toe Berm Armor Stone and Toe Buttressing Stone on Rubble-Mound Breakwaters and Jetties,” Technical Report REMR-CO-12, U.S. Army Engineer Waterways Experiment Station, Vicksburg, MS.

McGehee 1987
McGehee, D. D. 1987. “Crane Survey of Submerged Rubble-Mound Coastal Structures,” REMR Technical Note CO-SE-1.2, U.S. Army Engineer Waterways Experiment Station, Vicksburg, MS.

Melby and Turk 1994
Melby, J. A., and Turk, G. F. 1994. “Concrete Armor Unit Performance in Light of Recent Research Results.” *Proceedings of Case Histories of the Design Construction, and Maintenance of Rubble Mound Structures*. ASCE, pp 48-67.

Mol et al. 1983
Mol, A., Ligeringen, H., Groeneveld, R. L., and Pita, C. R. 1983. “West Breakwater - Sines, Study of Armour Stability.” *Proceedings of Coastal Structures '83*. ASCE, pp 57-70.

Morang, Larson, and Gorman 1997a
Morang, A., Larson, R., and Gorman, L. 1997a. “Monitoring the Coastal Environment; Part I: Waves and Currents,” *Journal of Coastal Research*, Vol 13, No. 1, pp 111-133.

Morang, Larson, and Gorman 1997b
Morang, A., Larson, R., and Gorman, L. 1997b. “Monitoring the Coastal Environment; Part III: Geophysical and Research Methods,” *Journal of Coastal Research*, Vol 13, No. 4, pp 1064-1085.

Mynett, de Voogt, and Schemltz 1983
Mynett, A. E., de Voogt, W. J., and Schmeltz, E. J. 1983. “West Breakwater - Sines, Wave Climatology.” *Proceedings of Coastal Structures '83*. ASCE, pp 17-30.

Oliver et al. 1996
Oliver, J., Plotkin, D., Lesnik, J., Pirie, D. 1996. “Condition and Performance Rating System for Breakwaters and Jetties.” *Proceedings of the 25th International Coastal Engineering Conference.* ASCE, New York, Vol 2, pp 1852-1861.

Oliver et al. 1998
Oliver, J., Plotkin, D., Lesnik, J., Pirie, D. 1998. “Condition and Performance Rating Procedures for Rubble Breakwaters and Jetties,” Technical Report REMR-OM-24, U.S. Army Construction Engineering Research Laboratory, Champaign, IL.
(*http://owww.cecer.army.mil/techreports/plorub/plorubb.remr.post.pdf*)

Parsons and Lillycrop 1988
Parsons, L. E., and Lillycrop, W. J. 1988. “The SHOALS system - A Comprehensive Surveying Tool,” Coastal Engineering Technical Note, CETN VI-31, U.S. Army Engineer Waterways Experiment Station, Vicksburg, MS.

Pope 1992
Pope, J. 1992. “Our Ageing Coastal Infrastructure.” *Proceedings of Coastal Engineering Practice >92*. ASCE, New York, pp 1055-1068.

Prickett 1996
Prickett, T. L. 1996. “Coastal Structure Underwater Inspection Technologies,” Coastal Engineering Technical Note, CETN III-62, U.S. Army Engineer Waterways Experiment Station, Vicksburg, MS.

Prickett 1998
Prickett, T. L. 1998. “Coastal Structure Inspection Technologies; Investigation of Multibeam Sonars for Coastal Structure Surveys,” REMR Technical Report CO-19, U.S. Army Engineer Waterways Experiment Station, Vicksburg, MS.

PSIP 1982
Port Sines Investigation Panel. 1982. *Failure of the Breakwater at Port Sines, Portugal.* ASCE, New York.

RMSC 1994
Rubble Mound Structures Committee, ASCE. 1994. Reconstruction of the West Breakwater at Port Sines, Portugal. ASCE, New York.

Rosati and Denes 1990
Rosati, J. D., and Denes, T. A. 1990. “Field Evaluation of Port Everglades, Florida, Rehabilitation of South Jetty by Void Sealing,” Technical Report REMR-CO-15, U.S. Army Engineer Waterways Experiment Station, Vicksburg, MS.

Sargent 1988
Sargent, F. E. 1988. “Case Histories of Corps Breakwater and Jetty Structures: Report 2, South Atlantic Division,” Technical Report REMR-CO-3, U.S. Army Engineer Waterways Experiment Station, Vicksburg, MS.

Sargent and Bottin 1989a
Sargent, F. E., and Bottin, R. R., Jr. 1989a. “Case Histories of Corps Breakwater and Jetty Structures: Report 7, New England Division,” Technical Report REMR-CO-3, U.S. Army Engineer Waterways Experiment Station, Vicksburg, MS.

Sargent and Bottin 1989b
Sargent, F. E., and Bottin, R. R., Jr. 1989b. “Case Histories of Corps Breakwater and Jetty Structures: Report 8, Lower Mississippi Valley Division,” Technical Report REMR-CO-3, U.S. Army Engineer Waterways Experiment Station, Vicksburg, MS.

Sargent and Bottin 1989c
Sargent, F. E., and Bottin, R. R., Jr. 1989c. "Case Histories of Corps Breakwater and Jetty Structures: Report 9, Southwestern Division," Technical Report REMR-CO-3, U.S. Army Engineer Waterways Experiment Station, Vicksburg, MS.

Sargent, Markle, and Grace 1988
Sargent, F. E., Markle, D. G., and Grace, P. J. 1988. "Case Histories of Corps Breakwater and Jetty Structures: Report 4, Pacific Ocean Division," Technical Report REMR-CO-3, U.S. Army Engineer Waterways Experiment Station, Vicksburg, MS.

Simpson 1989
Simpson, D. P. 1989. "State-of-the-Art Procedures for Sealing Coastal Structures with Grouts and Concretes," Technical Report REMR-CO-8, U.S. Army Engineer Waterways Experiment Station, Vicksburg, MS.

Simpson and Thomas 1990
Simpson, D. P., and Thomas, J. L. 1990. "Laboratory Techniques for Evaluating Effectiveness of Sealing Voids in Rubble-Mound Breakwaters and Jetties with Grouts and Concretes," Technical Report REMR-CO-13, U.S. Army Engineer Waterways Experiment Station, Vicksburg, MS.

Simpson et al. 1990
Simpson, D. P., Rosati, J. D., Hales, L. Z., Denes, T. A., and Thomas, J. L. 1990. "Rehabilitation of Permeable Breakwaters and Jetties by Void Sealing: Summary Report," Technical Report REMR-CO-16, U.S. Army Engineer Waterways Experiment Station, Vicksburg, MS.

Smith 1988
Smith, E. R. 1988. "Case Histories of Corps Breakwater and Jetty Structures: Report 5, North Atlantic Division," Technical Report REMR-CO-3, U.S. Army Engineer Waterways Experiment Station, Vicksburg, MS.

Thomas 1985
Thomas, J. 1985. "Diver Inspection of Coastal Structures," REMR Technical Note CO-SE-1.1, U.S. Army Engineer Waterways Experiment Station, Vicksburg, MS.

Toppler et al 1983
Toppler, J. F., Steenmeyer, A., Goncalves da Silva, M. A., Ligteringen, H., and Silverira Ramos, F. 1983. "West Breakwater - Sines, Overview of Rehabilitation and Synthesis of Project." *Proceedings of Coastal Structures '83*. ASCE, pp 3-16.

Turk and Melby 1997
Turk, G. F., and Melby, J. A. 1997. "Preliminary 3-D Testing of CORE-LOC™ as a Repair Concrete Armor Unit for Dolos-Armored Breakwater Slopes," Technical Report REMR-CO-18, U.S. Army Engineer Waterways Experiment Station, Vicksburg, MS.

U.S. Army Engineer Waterways Experiment Station 1991
U.S. Army Engineer Waterways Experiment Station. 1991. "Surveys of Coastal Structures," Coastal Engineering Technical Note, CETN III-41, U.S. Army Engineer Waterways Experiment Station, Vicksburg, MS.

Vrijling, Leeuwestein, and Kuiper 1995
Vrijling, J. K., Leeuwestein, W., and Kuiper, H. 1995. "The Maintenance of Hydraulic Rock Structures," in *River, Coastal and Shoreline Protection; Erosion Control Using Riprap and Armourstone*, Thorne, Abt, Barends, Maynord, and Pilarczyk, ed., John Wiley & Sons, Inc., New York, pp 651-666.

Ward 1988
Ward, D. L. 1988. "Case Histories of Corps Breakwater and Jetty Structures: Report 6, North Pacific Division," Technical Report REMR-CO-3, U.S. Army Engineer Waterways Experiment Station, Vicksburg, MS.

Ward and Markle 1990
Ward, D. L., and Markle, D. G. 1984. "Repair of Localized Armor Stone Damage on Rubble-Mound Structures," Technical Report REMR-CO-14, U.S. Army Engineer Waterways Experiment Station, Vicksburg, MS.

Weggel et al. 1994
Weggel, J. R., Baird, W. F., Edge, B., Magoon, O. T., Mansard, E., Threadwell, D. D., and Whalin, R. W. 1994. "Sines Breakwater Revisited - Repair and Reconstruction." *Proceedings of Case Histories of the Design Construction, and Maintenance of Rubble Mound Structures.* ASCE, pp 272-280.

Wolf 1989
Wolf, J. R. 1989. "Study of Breakwaters Constructed with one Layer of Armor Stone; Detroit District," Technical Report REMR-CO-10, U.S. Army Engineer Waterways Experiment Station, Vicksburg, MS.

VI-8-5. Acknowledgments.

Author: Dr. Steven A. Hughes, Coastal and Hydraulics Laboratory (CHL), U.S. Army Engineer Research and Development Center, Vicksburg, MS.

Reviewers: Donald D. Davidson and Lyndell Z. Hales, Coastal and Hydraulics Laboratory (CHL), U.S. Army Engineer Research and Development Center, Vicksburg, MS.

VI-8-6. Symbols.

CH	Structural index for channel/harbor-side slope
CR	Structural index for crest or cap
FI	Structural index for the structure
FI_R	Structural index for the reach

H_s	Significant wave height (length)
I_H	Highest of the reach sectional indices
I_L	Lowest of the three cross-sectional indices
I_L	Lowest of the reach structural indices
I_M	Middle value of the three cross-sectional indices
I_2, I_3, I_4, ...	Values for the second, third, fourth, etc., highest reach indices
N	Number of rated functions for the reach
N	Number of reaches in the structure
R_H	Highest of the functional ratings for the reach
R_I	Highest of the five ratings for the cross-section component
R_L	Lowest of the functional ratings for the reach
R_2, R_3, R_4, …	Values for the second, third, fourth, etc., highest ratings
R_5	Lowest of the five ratings for the cross-section component
SE	Structural index for sea-side slope
SI	Structural index for the structure
SI_R	Structural index for the reach

APPENDIX A
GLOSSARY OF COASTAL TERMINOLOGY

Table of Contents

A-1. Glossary A-1

A-2. Sources A-92

A-3. Acknowledgments A-94

Usage note: CAPITALIZATION within a definition indicates that the term is defined elsewhere in the glossary. Figure numbers refer to the main text of the *Coastal Engineering Manual*.

A

ABRASION
The mechanical wearing away by rock material transported by wind or water

ABRASION PLATFORM
A rock or clay platform which has been worn by the processes of abrasion.

ACCELEROMETER
A device used in wave buoys for measuring acceleration.

ACCRETION
May be either natural or artificial. Natural accretion is the buildup of land, solely by the action of the forces of nature, on a beach by deposition of water- or airborne material. Artificial accretion is a similar buildup of land by reason of an act of man, such as the accretion formed by a GROIN, BREAKWATER, or beach fill deposited by mechanical means. Also AGGRADATION.

ACTIVE MARGIN
A margin of a continental plate consisting of a continental shelf and slope, and an oceanic trench or basin.

ADJUSTABLE GROIN
A GROIN whose permeability can be changed, usually with gates or removable sections.

ADVANCE (of a beach)
(1) A continuing seaward movement of the shoreline. (2) A net seaward movement of the shoreline over a specified time. Also PROGRESSION.

ADVECTION
Changes in a sea water property (salinity, temperature, oxygen content, etc.) that take place in the presence of currents. Also, changes in atmospheric properties in the earth's atmosphere.

AEOLIAN
See EOLIAN.

AGE, WAVE
The ratio of wave velocity to wind velocity (in wave forecasting theory).

AGGRADATION
See ACCRETION.

ALIGNMENT
The course along which the center line of a channel, canal or drain is located.

ALLUVIAL DEPOSITS
Detrital material which is transported by a river and deposited – usually temporarily – at points along the flood plain of a river. Commonly composed of sands and gravels.

ALLUVIAL PLANE
A plain bordering a river, formed by the deposition of material eroded from areas of higher elevation.

ALLUVIUM
Soil (sand, mud, or similar detrital material) deposited by streams, or the deposits formed.

ALONGSHORE
Parallel to and near the shoreline; LONGSHORE.

ALTIMETER
An instrument that determines its distance above a particular surface.

ALTIMETER, LASER
An instrument that determines altitude by measuring the length of time needed for a pulse of coherent light to travel from the instrument to the surface and back, and multiplies half this time by the speed of light to get the straight-line distance to the surface.

ALTIMETER, LIDAR
See ALTIMETER, LASER.

AMPLITUDE, WAVE
(1) The magnitude of the displacement of a wave from a mean value. An ocean wave has an amplitude equal to the vertical distance from still-water level to wave crest. For a sinusoidal wave, the amplitude is one-half the wave height. (2) The semirange of a constituent tide.

ANCHOR ICE
Spongy underwater ice formed on a submerged object or attached to the bottom of a shallow body of water which is itself not frozen; syn. bottom ice

ANGLE OF REPOSE
The maximum slope (measured from the horizontal) at which soils and loose materials on the banks of canals, rivers or embankments will stay stable.

ANISOTROPIC
Having properties that change with changing directions.

ANOXIC
Refers to an environment that contain little or no dissolved oxygen and hence little or no benthic marine life. These conditions arise in some basins or fjords where physical circulation of seawater is limited.

ANTIDUNES
BED FORMS that occur in trains and are in phase with, and strongly interact with, gravity water-surface waves.

ANTINODE
See LOOP.

APRON
Layer of stone, concrete or other material to protect the toe of a structure.

AQUATIC MATERIAL PLACEMENT
Comprises all placement options under which the dredged material is submerged under water and remains water-saturated after placement terminates.

AQUIFER
A geologic formation that is water-bearing, and which transmits water from one point in the formation to another.

ARCHIPELAGO
A sea that contains numerous islands; also the island group itself.

ARMOR LAYER
Protective layer on a BREAKWATER or SEAWALL composed of armor units.

ARMOR UNIT or STONE
A relatively large quarrystone or concrete shape that is selected to fit specified geometric characteristics and density. It is usually of nearly uniform size and usually large enough to require individual placement. In normal cases it is used as primary wave protection and is placed in thicknesses of at least two units.

ARTIFICIAL NOURISHMENT
The process of replenishing a beach with material (usually sand) obtained from another location.

ASTRONOMICAL TIDE
The tidal levels and character which would result from gravitational effects, e.g. of the Earth, Sun and Moon, without any atmospheric influences.

ATOLL
A ring-shaped coral REEF, often carrying low sand islands, enclosing a shallow LAGOON. The reef is surrounded by deep water of the open sea.

ATTENUATION
(1) A lessening of the amplitude of a wave with distance from the origin. (2) The decrease of water-particle motion with increasing depth. Particle motion resulting from surface oscillatory waves attenuates rapidly with depth, and practically disappears at a depth equal to a surface wavelength.

AUTOCHTHONOUS
A term applied to shelves on which older shelf sediments are primarily being reworked by modern shelf processes.

AUTOMATIC TIDE GAGE
An instrument that automatically registers the rise and fall of the tide. In some instruments, the registration is accomplished by printing the heights at regular intervals, in others by a continuous graph in which the height of the tide is represented by the ordinates of the curve and the corresponding time by the abscissae.

AVULSION
(1) Rapid EROSION of the shore land by waves during a storm. (2) A sudden cutting off of land by flood, currents or change in course of a body of water.

AWASH
Situated so that the top is intermittently washed by waves or tidal action. Condition of being exposed or just bare at any stage of the tide between high water and chart datum.

B

BACK BARRIER
Pertaining to the lagoon-marsh-tidal creek complex in the lee of a coastal barrier island, barrier spit, or baymouth barrier.

BACKBEACH
See BACKSHORE.

BACKRUSH
The seaward return of the water following the uprush of the waves. For any given tide stage the point of farthest return seaward of the backrush is known as the Limit of backrush or limit backwash.

BACKSHORE
That zone of the shore or beach lying between the foreshore and the coastline comprising the BERM or BERMS and acted upon by waves only during severe storms, especially when combined with exceptionally high water. Also BACKBEACH. (See Figure A-1)

BACKWASH
(1) See BACKRUSH. (2) Water or waves thrown back by an obstruction such as a ship, BREAKWATER, or cliff.

BACKWASH RIPPLES
Low amplitude ripple marks formed on fine sand beaches by the Backwash of the waves.

BACKWATER CURVE
The longitudinal profile of the water surface in an open channel where the depth of flow has been increased by an obstruction as a weir or a dam across the channel, by increase in channel roughness, by decrease in channel width or by a decrease of the bed gradient

BANK
(1) The rising ground bordering a lake, river, or sea; or of a river or channel, for which it is designated as right or left as the observer is facing downstream. (2) An elevation of the sea floor or large area, located on a continental (or island) shelf and over which the depth is relatively shallow but sufficient for safe surface navigation (e.g., Georges Bank); a group of shoals. (3) In its secondary sense, used only with a qualifying word such as “sandbank,” “gravelbank,” or “spoil bank,” a shallow area consisting of shifting forms of silt, sand, mud, and gravel.

BAR
A submerged or emerged embankment of sand, gravel, or other unconsolidated material built on the sea floor in shallow water by waves and currents. See BAYMOUTH BAR, CUSPATE BAR.

BARRIER BEACH
A bar essentially parallel to the shore, the crest of which is above normal high water level. Also called offshore barrier and BARRIER ISLAND.

BARRIER FLAT
The flat area, often marshy and populated with low vegetation, on the bay or lagoon side of a barrier island

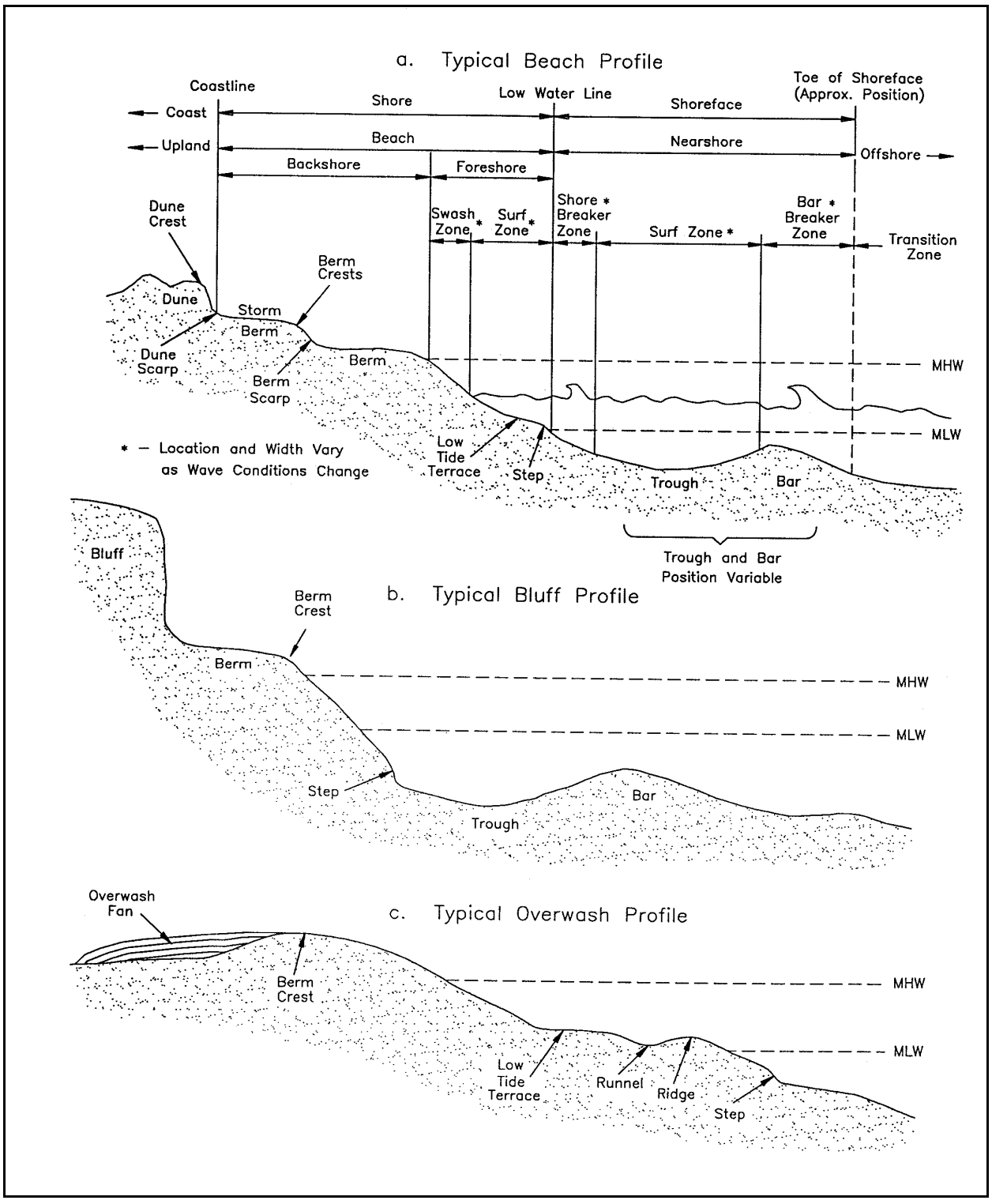

Figure A-1. Definition of terms and features describing the coastal zone

BARRIER ISLAND

A detached portion of a barrier beach between two inlets. It commonly has DUNES, vegetated areas, and swampy terranes (see BARRIER FLAT) extending from the beach into the lagoon. Example: Outer Banks, North Carolina.

BARRIER LAGOON

A bay roughly parallel to the coast and separated from the open ocean by barrier islands. Also, the body of water encircled by coral islands and REEFS, in which case it may be called an ATOLL lagoon.

BARRIER REEF

A coral REEF parallel to and separated from the coast by a lagoon that is too deep for coral growth. Generally, barrier reefs follow the coasts for long distances and are cut through at irregular intervals by channels or passes. Example: Great Barrier Reef, Queensland, Australia.

BARRIER SPIT

Similar to a BARRIER ISLAND, but connected to the mainland.

BASIN

A depressed area with no surface outlet, such as a lake basin or an enclosed sea.

BASIN, BOAT

A naturally or artificially enclosed or nearly enclosed harbor area for small craft.

BASTION

A massive groin, or projecting section of seawall normally constructed with its crest above water level.

BATHYMETRIC CHART

A topographic map of the bed of the ocean, with depths indicated by contours (isobaths) drawn at regular intervals.

BATHYMETRY

The measurement of water depths in oceans, seas, and lakes; also information derived from such measurements.

BAY

A recess in the shore or an inlet of a sea between two capes or headlands, not as large as a gulf but larger than a cove. See also BIGHT, EMBAYMENT.

BAYMOUTH BAR

A bar extending partly or entirely across the mouth of a bay .

BAYOU

A minor sluggish waterway or estuarial creek, tributary to, or connecting, other streams or bodies of water, whose course is usually through lowlands or swamps. Sometimes called SLOUGH. Term is commonly used in the southern United States.

BEACH

The zone of unconsolidated material that extends landward from the low water line to the place where there is marked change in material or physiographic form, or to the line of permanent vegetation (usually the effective limit of storm waves). The seaward limit of a beach--unless otherwise specified--is the mean low water line. A beach includes foreshore and backshore. (See Figure A-1) See also SHORE, SUSTAINABLE BEACH, and SELF-SUSTAINING BEACH, and TIDELANDS.

BEACH ACCRETION

See ACCRETION.

BEACH BERM
A nearly horizontal part of the beach or backshore formed by the deposit of material by wave action. Some beaches have no berms, others have one or several. (See Figure A-1)

BEACH CREST
The point representing the limit of normal HIGH TIDE wave run-up (see BERM CREST)

BEACH CUSP
See CUSP.

BEACH EROSION
The carrying away of beach materials by wave action, tidal currents, littoral currents, or wind.

BEACH FACE
The section of the beach normally exposed to the action of the wave uprush. The FORESHORE of a BEACH. (Not synonymous with SHOREFACE.)

BEACH FILL
Material placed on a beach to renourish eroding shores, usually pumped by dredge but sometimes delivered by trucks.

BEACH HEAD
The cliff, dune or sea wall looming above the land ward limit of the active beach

BEACH MATERIAL
Granular sediments, usually sand or shingle moved by the sea.

BEACH NOURISHMENT
See BEACH FILL.

BEACH PLAN SHAPE
The shape of the beach in plan; usually shown as a contour line, combination of contour lines or recognizable features such as beach crest and/or the still water line

BEACH PROFILE
A cross-section taken perpendicular to a given beach contour; the profile may include the face of a dune or sea wall, extend over the backshore, across the foreshore, and seaward underwater into the NEARSHORE zone.

BEACH RIDGE
See RIDGE, BEACH.

BEACH SCARP
See SCARP, BEACH.

Table A-1
Beaufort Wind Scale

Beaufort Number	Wind Speed (knots)	WMO Description [1]
0	< 1	Calm
1	1 - 3	Light air
2	4 - 6	Light breeze
3	7 - 10	Gentle breeze
4	11 - 16	Moderate breeze
5	17 - 21	Fresh breeze
6	22 - 27	Strong breeze
7	28 - 33	Near gale
8	34 - 40	Gale
9	41 - 47	Strong Gale
10	48 - 55	Storm
11	56 - 63	Violent storm
12	≥ 64	Hurricane

[1] World Meteorological Organization, from http://www.crh.noaa.gov/lot/webpage/beaufort/ (28 Aug. 2001)

BEACH WIDTH

The horizontal dimension of the beach measured normal to the shoreline and landward of the higher-high tide line (on oceanic coasts) or from the still water level (on lake coasts)

BEAUFORT SCALE

Classification of the force of the winds in accordance with a scale established by Rear-Admiral, Sir Francis Beaufort in which the range of intensity varies in integers from 0 to 12, with a description of the state and behavior of a "well-conditioned man-of-war."

BED

The bottom of a watercourse, or any body of water.

BED FORMS

Any deviation from a flat bed that is readily detectable by eye and higher than the largest sediment size present in the parent bed material; generated on the bed of an alluvial channel by the flow.

BED LOAD
Sediment transport mode in which individual particles either roll or slide along the bed as a shallow, mobile layer a few particle diameters deep, the part of the load that is not continuously in suspension.

BED PROTECTION
A (rock) structure on the bed in order to protect the underlying bed against erosion due to current and/or wave action.

BED SHEAR STRESS
The way in which waves (or currents) transfer energy to the sea bed.

BEDDING PLANE
A surface parallel to the surface of deposition, which may or may not have a physical expression. The original attitude of a *bedding plane* should not be assumed to have been horizontal.

BEDROCK
The solid rock that underlies gravel, soil, and other superficial material. Bedrock may be exposed at the surface (an outcrop) or it may br buried under a few centimeters to thousands of meters of unconsolidated material.

BENCH
(1) A level or gently sloping erosion plane inclined seaward. (2) A nearly horizontal area at about the level of maximum high water on the sea side of a dike.

BENCH MARK, TIDAL
A bench mark whose elevation has been determined with respect to MEAN SEA LEVEL at a nearby tide GAUGE; the *tidal bench mark* is used as reference for that tide gauge.

BENCH MARK
A permanently fixed point of known elevation. A primary bench mark is one close to a tide station to which the tide staff and tidal datum originally are referenced.

BENEFICIAL USE OF DREDGED MATERIAL
Placement or use of dredged material for some productive purpose. Examples: BEACH FILL or NEARSHORE BERM construction.

BENEFITS
The asset value of a scheme, usually measured in terms of the cost of damages avoided by the scheme, or the valuation of perceived amenity or environmental improvements

BENTHIC
Pertaining to the sub-aquatic bottom.

BENTHOS
Those animals who live on the sediments of the sea floor, including both mobile and non-mobile forms.

BERM
(1) On a beach: a nearly horizontal plateau on the beach face or backshore, formed by the deposition of beach material by wave action or by means of a mechanical plant as part of a beach renourishment scheme. Some natural beaches have no berm, others have several. (2) On a structure: a nearly horizontal area, often built to support or key-in an armor layer.

BERM, BEACH
See BEACH BERM.

BERM BREAKWATER
Rubble mound structure with horizontal berm of armor stones at about sea level, which is allowed to be (re)shaped by the waves.

BERM CREST
The seaward limit of a BERM. Also called BERM EDGE. (See Figure A-1)

BIGHT
A bend in a coastline forming an open BAY. A BAY formed by such a bend.

BIOTURBATION
The disturbance of sediment bedding by the activities of burrowing organisms.

BIRDFOOT DELTA
A river DELTA formed by many levee-bordered DISTRIBUTARIES extending seaward and resembling in plan the outstretched claws of a bird. Example: Mississippi River delta.

BLANKET (FOUNDATION or BEDDING)
A layer or layers of graded fine stones underlying a BREAKWATER, GROIN or rock embankment to prevent the natural bed material from being washed away.

BLOWN SANDS
See EOLIAN SANDS.

BLOWOUT
A depression on the land surface caused by wind erosion.

BLUFF
A high, steep bank or cliff.

BOG
A wet, spongy, poorly drained area which is usually rich in very specialized plants, contains a high percentage of organic remnants and residues and frequently is associated with a spring, seepage area, or other subsurface water source. A *bog* sometimes represents the final stage of the natural processes of eutrophication by which lakes and other bodies of water are very slowly transformed into land areas.

BOIL
An upward flow of water in a sandy formation due to an unbalanced hydrostatic pressure resulting from a rise in a nearby stream, or from removing the overburden in making excavations.

BOLD COAST
A prominent landmass that rises steeply from the sea.

BORE
A very rapid rise of the tide in which the advancing water presents an abrupt front of considerable height. In shallow estuaries where the range of tide is large, the high water is propagated inward faster than the low water because of the greater depth at high water. If the high water overtakes the low water, an abrupt front is presented, with the high-water crest finally falling forward as the tide continues to advance. Also EAGER.

BOTTOM (nature of)
The composition or character of the bed of an ocean or other body of water (e.g., clay, coral, gravel, mud, ooze, pebbles, rock, shell, shingle, hard, or soft). (See Figure A-1)

BOTTOM BOUNDARY LAYER
The lower portion of the water flow that experiences frictional retardation based on its proximity to the bed.

BOTTOMSET
One of the horizontal or gently inclined sediment layers deposited in front of the advancing forest beds of a delta.

BOULDER
A rounded rock more than 256 mm (10 inch) in diameter; larger than a cobblestone. See SOIL CLASSIFICATION.

BOUNDARY CONDITIONS
Environmental conditions, e.g. waves, currents, drifts, etc. used as boundary input to physical or numerical models

BOX GAGE
A tide GAUGE that is operated by a float in a long vertical box to which the tide is admitted through an opening in the bottom. In the original type of *box gauge* the float supported a graduated rod which rose and fell with the tide.

BRAIDED RIVER
A river type with multiple channels separated by shoals, bars and islands

BREACHING
(1) Formation of a channel through a barrier spit or island by storm waves, tidal action, or river flow. Usually occurs after a greater than normal flow, such as during a hurricane. (2) Failure of a dike allowing flooding.

BREAKER
A wave breaking on a shore, over a REEF, etc. Breakers may be classified into four types (See Figure II-4-1):

COLLAPSING--breaking occurs over lower half of wave, with minimal air pocket and usually no splash-up. Bubbles and foam present.

PLUNGING--crest curls over air pocket; breaking is usually with a crash. Smooth splash-up usually follows.

SPILLING--bubbles and turbulent water spill down front face of wave. The upper 25 percent of the front face may become vertical before breaking. Breaking generally occurs over quite a distance.

SURGING--wave peaks up, but bottom rushes forward from under wave, and wave slides up beach face with little or no bubble production. Water surface remains almost plane except where ripples may be produced on the beachface during runback.

BREAKER DEPTH
The still-water depth at the point where a wave breaks. Also called BREAKING DEPTH.

BREAKER INDEX
Ratio of breaking wave height to DEEPWATER wave height

BREAKER ZONE
The zone within which waves approaching the coastline commence breaking, typically in water depths of between 5 and 10 meters for ocean coasts, but sometimes in shallower water.

BREAKING
Reduction in wave energy and height in the surf zone due to limited water depth

BREAKWATER
A man-made structure protecting a shore area, harbor, anchorage, or basin from waves. A harbor work.

BREASTWORK

Vertically-faced or steeply inclined structure usually built with timber and parallel to the shoreline, at or near the beach crest, to resist erosion or mitigate against flooding.

BUFFER AREA

A parcel or strip of land that is designed and designated to permanently remain vegetated in an undisturbed and natural condition to protect an adjacent aquatic or wetland site from upland impacts, to provide habitat for wildlife and to afford limited public access.

BULKHEAD

A structure or partition to retain or prevent sliding of the land. A secondary purpose is to protect the UPLAND against damage from wave action.

BULK DENSITY

Identical to apparent specific gravity, Ga = soil density ÷ density of water. "Apparent" means that the basis of measurement is the total soil volume including voids, not just the individual soil particles.

BULL NOSE

Substantial lip or protuberance at the top of the seaward face of a wall, to deflect waves seaward.

BUOY

A float; especially a floating object moored to the bottom, to mark a channel, anchor, shoal rock, etc. Some common types include: a *nun* or *nut* buoy is conical in shape; a *can* buoy is squat and cylindrical above water and conical below water; a *spar* buoy is a vertical, slender spar anchored at one end; a *bell* buoy, bearing a bell, runs mechanically or by the action of waves, usually marks shoals or rocks; a *whistling* buoy, similarly operated, marks shoals or channel entrances; a *dan* buoy carries a pole with a flag or light on it.

BUOYANCY

The resultant of upward forces, exerted by the water on a submerged or floating body, equal to the weight of the water displaced by this body.

BYPASSING, SAND

Hydraulic or mechanical movement of sand from the accreting updrift side to the eroding downdrift side of an inlet or harbor entrance. The hydraulic movement may include natural movement as well as movement caused by man.

C

CAISSON
Concrete box-type structure.

CALCAREOUS
Containing calcium carbonate ($CaCO_3$), chiefly as the minerals calcite and aragonite. When applied to rock, it implies that as much as 50 percent of the rock is carbonate (e.g., calcareous sand).

CALM
The condition of the water surface when there is no WIND WAVES or SWELL.

CANAL
An artificial watercourse cut through a land area for such uses as navigation and irrigation.

CANYON
A relatively narrow, deep depression with steep slopes, the bottom of which grades continuously downward. May be underwater (submarine) or on land (SUBAERIAL).

CAPE
A land area jutting seaward from a continent or large island which prominently marks a change in, or interrupts notably, the coastal trend; a prominent feature. Examples: Cape Cod, Massachusetts; Cape Hatteras, North Carolina.

CAPILLARY WAVE
A wave whose velocity of propagation is controlled primarily by the surface tension of the liquid in which the wave is traveling. Water waves of length less than about 1 inch are considered capillary waves. Waves longer than 1 inch and shorter than 2 inches are in an indeterminate zone between capillary and gravity waves. See RIPPLE.

CARTOGRAPHY
The science and art of making maps.

CATCHMENT AREA
The area which drains naturally to a particular point on a river, thus contributing to its natural discharge.

CAUSEWAY
A raised road across wet or marshy ground, or across water.

CAUSTIC
In refraction of waves, the name given to the curve to which adjacent orthogonals of waves refracted by a bottom whose contour lines are curved, are tangents. The occurrence of a caustic always marks a region of crossed orthogonals and high wave convergence.

CAY
See KEY.

CELERITY
Wave speed.

CENTRAL PRESSURE INDEX (CPI)
The estimated minimum barometric pressure in the eye (approximate center) of a particular hurricane. The CPI is considered the most stable index to intensity of hurricane wind velocities in the periphery of the storm; the highest wind speeds are associated with storms having the lowest CPI.

CHANNEL

(1) A natural or artificial waterway of perceptible extent which either periodically or continuously contains moving water, or which forms a connecting link between two bodies of water. (2) The part of a body of water deep enough to be used for navigation through an area otherwise too shallow for navigation. (3) A large strait, as the English Channel. (4) The deepest part of a stream, bay, or strait through which the main volume or current of water flows (see THALWEG).

CHANNEL CAPACITY

The maximum flow which a channel is capable of transmitting without its banks being overtopped.

CHANNEL-MOUTH BAR

A bar built where a stream enters a body of standing water, resulting from decreased flow velocity.

CHARACTERISTIC WAVE HEIGHT

See SIGNIFICANT WAVE HEIGHT.

CHART

A special-purpose map, esp. one designed for navigation such as a *bathymetric chart*.

CHART DATUM

The plane or level to which soundings (or elevations) or tide heights are referenced (usually LOW WATER DATUM). The surface is called a tidal datum when referred to a certain phase of tide. To provide a safety factor for navigation, some level lower than MEAN SEA LEVEL is generally selected for hydrographic charts, such as MEAN LOW WATER or MEAN LOWER LOW WATER. See DATUM PLANE.

CHEMICAL WEATHERING

Disintegration of rocks and sediments by chemical alteration of the constituent minerals or of the cementing matrix. It is caused by exposure, oxidation, temperature changes, and biological processes.

CHENIER

A long, narrow wooded beach ridge or sandy hummock forming roughly parallel to a prograding shore, usually seaward of marsh and mud-flat deposits (as along the south coast of Louisiana)

CHOP

The short-crested waves that may spring up quickly in a moderate breeze, and which break easily at the crest. Also WIND CHOP.

CHOPPY SEA

Short, rough waves tumbling with a short and quick motion. Short-crested waves that may spring up quickly in a moderate breeze, and break easily at the crest.

CLAPOTIS

The French equivalent for a type of STANDING WAVE. In American usage it is usually associated with the standing wave phenomenon caused by the reflection of a nonbreaking wave train from a structure with a face that is vertical or nearly vertical. Full clapotis is one with 100 percent reflection of the incident wave; partial clapotis is one with less than 100 percent reflection.

CLASTIC ROCKS

Rocks built up of fragments which have been produced by weathering and erosion of pre-existing rocks and minerals and, typically, transported mechanically to their point of deposition.

CLAY

A fine grained, plastic, sediment with a typical grain size less than 0.004 mm. Possesses electromagnetic properties which bind the grains together to give a bulk strength or cohesion. See SOIL CLASSIFICATION.

CLIFF

A high, steep face of rock; a precipice. See also SEA CLIFF.

CLIMATE

The characteristic weather of a region, particularly regarding temperature and precipitation, averaged over some significant internal of time (years).

CLOSING LINE

The line dividing inland waters and the territorial sea at the mouth of a river, bay, or harbor.

CLOSURE DEPTH

The water depth beyond which repetitive profile or topographic surveys (collected over several years) do not detect vertical sea bed changes, generally considered the seaward limit of littoral transport. The depth can be determined from repeated cross-shore profile surveys or estimated using formulas based on wave statistics. Note that this does not imply the lack of sediment motion beyond this depth.

CNOIDAL WAVE

A type of wave in shallow water (i.e., where the depth of water is less than 1/8 to 1/10 the wavelength). The surface profile is expressed in terms of the Jacobian elliptic function cn u; hence the term cnoidal.

CO-TIDAL LINES

Lines which link all the points where TIDE is at the same stage (or phase) of its cycle.

COAST

(1) A strip of land of indefinite width (may be several kilometers) that extends from the SHORELINE inland to the first major change in terrain features. (See Figure A-1.) (2) The part of a country regarded as near the coast.

COASTAL AREA

The land and sea area bordering the SHORELINE. (See Figure A-1)

COASTAL CURRENTS

(1) Those currents which flow roughly parallel to the shore and constitute a relatively uniform drift in the deeper water adjacent to the surf zone. These currents may be tidal currents, transient, wind-driven currents, or currents associated with the distribution of mass in local waters. (2) For navigational purposes, the term is used to designate a current in coastwise shipping lanes where the tidal current is frequently rotary.

COASTAL DEFENSE

General term used to encompass both coast protection against erosion and sea defense against flooding.

COASTAL FORCING

The natural processes which drive coastal hydro- and morphodynamics (e.g.winds, waves, tides, etc).

COASTAL PLAIN

The plain composed of horizontal or gently sloping strata of clastic materials, generally representing a strip of sea bottom that has emerged from the sea in recent geologic time. May extend inland many km.

COASTAL PROCESSES

Collective term covering the action of natural forces on the SHORELINE, and near shore seabed

COASTAL STRIP

A zone directly adjacent to the waterline, where only coast related activities take place. Usually this is a strip of some 100 m wide. In this strip the coastal defense activities take place. In this strip often there are restrictions to land use.

COASTAL ZONE

The transition zone where the land meets water, the region that is directly influenced by marine and lacustrine hydrodynamic processes. Extends offshore to the continental shelf break and onshore to the first major change in topography above the reach of major storm waves. On barrier coasts, includes the bays and LAGOONS between the BARRIER and the mainland.

COASTAL ZONE MANAGEMENT

The integrated and general development of the coastal zone. Coastal Zone Management is not restricted to coastal defense works, but includes also a development in economical, ecological and social terms. Coastline Management is a part of Coastal Zone Management.

COAST LINE

The term used in the Submerged Lands Act to describe the low-water line and closing lines across the mouths of inland water bodies.

COASTLINE

(1) Technically, the line that forms the boundary between the coast and the shore. (2) Commonly, the line that forms the boundary between the land and the water, esp. the water of a sea or ocean. The SHORELINE. A more general term than COAST LINE.

COBBLE (COBBLESTONE)

A rock fragment between 64 and 256 mm in diameter, usually rounded. See SOIL CLASSIFICATION.

COFFERDAM

A temporary watertight structure enclosing all or part of the construction area so that construction can proceed in the dry.

COHESIVE SEDIMENT

Sediment containing significant proportion of clays, the electromagnetic properties of which cause the sediment to bind together.

COLLOID

As a size term refers to particles smaller than 0.00024 mm, smaller than clay size.

COMBER

(1) A DEEPWATER wave whose crest is pushed forward by a strong wind; much larger than a whitecap. (2) A long-period breaker.

COMPETENCE

The ability of a wind or water current to transport detritus, in terms of particle size rather than amount, measured as the diameter of the largest particles.

COMPLEX SPIT

A large RECURVED SPIT with secondary spits developed at its end. Example: Sandy Hook, New Jersey.

CONFLUENCE

The junction of two or more river reaches or channels (the opposite of a bifurcation) .

CONSOLIDATION

The gradual, slow compression of a cohesive soil due to weight acting on it, which occurs as water is driven out of the voids in the soil. Consolidation only occurs in clays or other soils of low permeability.

CONTINENTAL SHELF

(1) The zone bordering a continent extending from the line of permanent immersion to the depth, usually about 100 m to 200 m, where there is a marked or rather steep descent toward the great depths of the ocean. (2) The area under active littoral processes during the HOLOCENE period. (3) The region of the oceanic bottom that extends outward from the shoreline with an average slope of less than 1:100, to a line where the gradient begins to exceed 1:40 (the CONTINENTAL SLOPE).

CONTINENTAL SLOPE

The declivity from the offshore border of the CONTINENTAL SHELF to oceanic depths. It is characterized by a marked increase in slope.

CONTOUR

A line on a map or chart representing points of equal elevation with relation to a DATUM. It is called an ISOBATH when connecting points of equal depth below a datum. Also called DEPTH CONTOUR.

CONTROLLING DEPTH

The least depth in the navigable parts of a waterway, governing the maximum draft of vessels that can enter.

CONVERGENCE

(1) In refraction phenomena, the decreasing of the distance between orthogonals in the direction of wave travel. Denotes an area of increasing wave height and energy concentration. (2) In wind-setup phenomena, the increase in setup observed over that which would occur in an equivalent rectangular basin of uniform depth, caused by changes in planform or depth; also the decrease in basin width or depth causing such increase in setup.

CORAL

(1) (Biology) Marine coelenterates (Madreporaria), solitary or colonial, which form a hard external covering of calcium compounds or other materials. The corals which form large REEFS are limited to warm, shallow waters, while those forming solitary, minute growths may be found in colder waters to great depths. (2) (Geology) The concretion of coral polyps, composed almost wholly of calcium carbonate, forming reefs and tree-like and globular masses. May also include calcareous algae and other organisms producing calcareous secretions, such as bryozoans and hydrozoans.

CORAL REEF

A coral-algal mound or ridge of in-place coral colonies and skeletal fragments, carbonate sand, and organically-secreted calcium carbonate. A coral reef is built up around a wave-resistant framework, usually of older coral colonies.

CORE

(1) A cylindrical sample extracted from a beach or seabed to investigate the types and depths of sediment layers. (2) An inner, often much less permeable portion of a BREAKWATER or BARRIER BEACH

CORIOLIS EFFECT

Force due to the Earth's rotation, capable of generating currents. It causes moving bodies to be deflected to the right in the Northern Hemisphere and to the left in the Southern Hemisphere. The "force" is proportional to the speed and latitude of the moving object. It is zero at the equator and maximum at the poles.

COVE

A small, sheltered recess in a COAST, often inside a larger EMBAYMENT.

COVER LAYER

The outer layer used in a rubble system as protection against external hydraulic loads

CREEK

(1) A stream, less predominant than a river, and generally tributary to a river. (2) A small tidal channel through a coastal MARSH.

CREEP
Very slow, continuous downslope movement of soil or debris.

CRENULATE
An indented or wavy shoreline beach form, with the regular seaward- pointing parts rounded rather than sharp, as in the cuspate type.

CREST
Highest point on a beach face, BREAKWATER, or SEAWALL.

CREST LENGTH, WAVE
The length of a wave along its crest. Sometimes called CREST WIDTH.

CREST OF WAVE
(1) the highest part of a wave. (2) That part of the wave above still-water level. (See Figure II-1-4.)

CREST OF BERM
The seaward limit of a berm. Also called BERM EDGE. (See Figure A-1.)

CREST WIDTH, WAVE
See CREST LENGTH, WAVE.

CROSS-BEDDING
An arrangement of relatively thin layers of rock inclined at an angle to the more nearly horizontal BEDDING PLANES of the larger rock unit. Also referred to as cross-stratification.

CROSS-SHORE
Perpendicular to the SHORELINE.

CROWN WALL
Concrete superstructure on a rubble mound.

CURRENT
(1) The flowing of water, or other liquid or gas. (2) That portion of a stream of water which is moving with a velocity much greater than the average or in which the progress of the water is principally concentrated. (3) Ocean currents can be classified in a number of different ways. Some important types include the following: (1) *Periodic* - due to the effect of the tides; such Currents may be rotating rather than having a simple back and forth motion. The currents accompanying tides are known as tidal currents; (2) *Temporary* - due to seasonal winds; (3) *Permanent* or *ocean* - constitute a part of the general ocean circulation. The term DRIFT CURRENT is often applied to a slow broad movement of the oceanic water; (4) *Nearshore* - caused principally by waves breaking along a shore.

CURRENT, COASTAL
One of the offshore currents flowing generally parallel to the shoreline in the deeper water beyond and near the surf zone; these are not related genetically to waves and resulting surf, but may be related to tides, winds, or distribution of mass.

CURRENT, DRIFT
A broad, shallow, slow-moving ocean or lake current. Opposite of CURRENT, STREAM.

CURRENT, EBB
The tidal current away from shore or down a tidal stream. Usually associated with the decrease in the height of the tide.

CURRENT, EDDY
See EDDY.

CURRENT, FEEDER
Any of the parts of the nearshore current system that flow parallel to shore before converging and forming the neck of the RIP CURRENT.

CURRENT, FLOOD
The tidal current toward shore or up a tidal stream. Usually associated with the increase in the height of the tide.

CURRENT, INSHORE
See INSHORE CURRENT.

CURRENT, LITTORAL
Any current in the littoral zone caused primarily by wave action; e.g., LONGSHORE CURRENT, RIP CURRENT. See also CURRENT, NEARSHORE.

CURRENT, LONGSHORE
The littoral current in the breaker zone moving essentially parallel to the shore, usually generated by waves breaking at an angle to the shoreline.

CURRENT METER
An instrument for measuring the velocity of a current

CURRENT, NEARSHORE
A current in the NEARSHORE ZONE. (See Figure A-1)

CURRENT, OFFSHORE
See OFFSHORE CURRENT.

CURRENT, PERIODIC
See CURRENT, TIDAL.

CURRENT, PERMANENT
See PERMANENT CURRENT.

CURRENT, RIP
See RIP CURRENT.

CURRENT, STREAM
A narrow, deep, and swift ocean current, as the Gulf Stream. CURRENT, DRIFT.

CURRENT SYSTEM, NEARSHORE
See NEARSHORE CURRENT SYSTEM.

CURRENT, TIDAL
The alternating horizontal movement of water associated with the rise and fall of the tide caused by the astronomical tide-producing forces. Also CURRENT, PERIODIC. See also CURRENT, FLOOD and CURRENT, EBB.

CURRENT-REFRACTION
Process by which wave velocity, height, and direction are affected by a current

CUSP
One of a series of short ridges on the FORESHORE separated by crescent-shaped troughs spaced at more or less regular intervals. Between these *cusps* are hollows. The *cusps* are spaced at somewhat uniform distances along beaches. They represent a combination of constructive and destructive processes. Also BEACH CUSP. (See Figure III-2-23.)

CUSPATE BAR

A crescent-shaped bar uniting with the shore at each end. It may be formed by a single spit growing from shore and then turning back to again meet the shore, or by two spits growing from the shore and uniting to form a bar of sharply cuspate form.

CUSPATE SPIT

The spit that forms in the lee of a shoal or offshore feature (BREAKWATER, island, rock outcrop) by waves that are refracted and/or diffracted around the offshore feature. It may eventually grow into a TOMBOLO linking the feature to the mainland.

CUTTERHEAD DREDGE

A hydraulic dredge that uses a rotating steel head consisting of hardened cutting blades and a backing ring to dislodge bottom material. The head is mounted at the suction entrance of the hydraulic pipeline, and fluidized material is picked up by suction and carried away through the pipe.

CYCLOIDAL WAVE

A steep, symmetrical wave whose crest forms an angle of 120 degrees and whose form is that of a cycloid. A trochoidal wave of maximum steepness. See also TROCHOIDAL WAVE.

CYCLONE

A system of winds that rotates about a center of low atmospheric pressure. Rotation is clockwise in the Southern Hemisphere and anti-clockwise in the Northern Hemisphere. In the Indian Ocean, the term refers to the powerful storms called HURRICANES in the Atlantic.

D

DAM
Structure built in rivers or estuaries, basically to separate water at both sides and/or to retain water at one side.

DATUM
Any permanent line, plane or surface used as a reference datum to which elevations are referred.

DATUM, CHART
See CHART DATUM.

DATUM, PLANE
The horizontal plane to which soundings, ground elevations, or water surface elevations are referred. Also REFERENCE PLANE. The plane is called a TIDAL DATUM when defined by a certain phase of the tide. The following datums are ordinarily used on hydrographic charts:

MEAN LOW WATER--Atlantic coast (U. S.), Argentina, Sweden, and Norway.

MEAN LOWER LOW WATER--Pacific coast (U. S.).

MEAN LOW WATER SPRINGS--United Kingdom, Germany, Italy, Brazil, and Chile.

LOW WATER DATUM--Great Lakes (U. S. and Canada).

LOWEST LOW WATER SPRINGS--Portugal.

LOW WATER INDIAN SPRINGS--India and Japan (See INDIAN TIDE PLANE).

LOWEST LOW WATER--France, Spain, and Greece.

A common datum used on United States topographic maps is MEAN SEA LEVEL. See also BENCH MARK.

DAVIDSON CURRENT
Deep-ocean boundary current off the west coast of the U.S. which brings warmer, saltier, low oxygen, high phosphate equatorial type water from low to high latitudes.

DEBRIS LINE
A line near the limit of storm wave uprush marking the landward limit of debris deposits.

DECAY AREA
Area of relative CALM through which waves travel after emerging from the generating area.

DECAY DISTANCE
The distance waves travel after leaving the generating area (FETCH).

DECAY OF WAVES
The change waves undergo after they leave a generating area (FETCH) and pass through a calm, or region of lighter winds. In the process of decay, the significant wave height decreases and the significant wavelength increases.

DEEP WATER
Water so deep that surface waves are little affected by the ocean bottom. Generally, water deeper than one-half the surface wavelength is considered deep water. Compare SHALLOW WATER.

DEEP WATER WAVES
A wave in water the depth of which is greater than one-half the WAVE LENGTH.

DEFLATION
The removal of loose material from a beach or other land surface by wind action.

DEGRADATION
The geologic process by means of which various parts of the surface of the earth are worn away and their general level lowered, by the action of wind and water.

DELTA
(1) An ALLUVIAL DEPOSIT, usually triangular or semi-circular, at the mouth of a river or stream. The delta is normally built up only where there is no tidal or current action capable of removing the sediment at the same rate as it is deposited, and hence the delta builds forward from the coastline. (2) A TIDAL DELTA is a similar deposit at the mouth of a tidal INLET, the result of TIDAL CURRENTS that flow in and out of the inlet.

DELTA PLAIN
The nearly-level surface composing the landward portion of a large DELTA.

DENSITY
Mass (in kg) per unit of volume of a substance; kg/m^3. For pure water, the density is 1000 kg/m^3, for seawater the density is usually more. Density increases with increasing salinity, and decreases with increasing temperature. More information can be found in "properties of seawater". For stone and sand, usually a density of 2600 kg/m^3 is assumed. Concrete is less dense, in the order of 2400 kg/m^3. Some types of basalt may reach 2800 kg/m^3.
For sand, including the voids, one may use 1600 kg/m^3, while mud often has a density of 1100 - 1200 kg/m^3.

DENSITY CURRENT
Phenomenon of relative flow within water due to difference in density. For example, the salt-water wedge is a density current, as is a volcanic *nuée ardente*.

DENSITY STRATIFICATION
The lateral expansion of a sediment plume as it moves out of the distributary mouth, where salt and fresh water mix. This is most likely to occur where the speed of the river flow is moderate to low and the distributary mouth is relatively deep.

DENSITY-DRIVEN CIRCULATION
Variations in salinity create variations in density in estuaries. These variations in density create horizontal pressure gradients, which drive estuarine circulation.

DEPRESSION
A general term signifying any depressed or lower area in the ocean floor.

DEPTH
The vertical distance from a specified datum to the sea floor.

DEPTH CONTOUR
See CONTOUR, also ISOBATH.

DEPTH, CONTROLLING
See CONTROLLING DEPTH.

DEPTH FACTOR
See SHOALING COEFFICIENT.

DEPTH OF BREAKING
The still-water depth at the point where the wave breaks. Also BREAKER DEPTH.

DERRICK STONE
See STONE, DERRICK.

DESIGN HURRICANE
See HYPOTHETICAL HURRICANE.

DESIGN STORM
A hypothetical extreme storm whose waves coastal protection structures will often be designed to withstand. The severity of the storm (i.e. return period) is chosen in view of the acceptable level of risk of damage or failure. A DESIGN STORM consists of a DESIGN WAVE condition, a design water level and a duration.

DESIGN WAVE
In the design of HARBORS, harbor works, etc., the type or types of waves selected as having the characteristics against which protection is desired.

DESIGN WAVE CONDITION
Usually an extreme wave condition with a specified return period used in the design of coastal works.

DETACHED BREAKWATER
A BREAKWATER without any SUBAERIAL connection to the shore.

DETRITUS
Small fragments of rock which have been worn or broken away from a mass by the action of water or waves.

DIFFERENTIAL EROSION / WEATHERING
These features develop in rocks which have varying resistance to the agencies of erosion and/or weathering so that parts of the rock are removed at greater rates than others. A typical example is the removal of soft beds from between harder beds in a series of sedimentary rocks. The term may be applied to any size of feature, from small-scale ‘etching’ to the regional development of hills and valleys controlled by hard and soft rocks.

DIFFRACTION (of water waves)
The phenomenon by which energy is transmitted laterally along a wave crest. When a part of a train of waves is interrupted by a barrier, such as a BREAKWATER, the effect of diffraction is manifested by propagation of waves into the sheltered region within the barrier's geometric shadow. (See Figure II-7-2)

DIFFRACTION COEFFICIENT
Ratio of diffracted wave height to DEEPWATER wave height.

DIFFUSION
The distributing or spreading-out of molecules, atoms, or substances into a vacuum, fluid, or porous medium so that the concentration equalizes in all parts of the system

DIKE
Earth structure along sea or river in order to protect low lands from flooding by high water; dikes along rivers are sometimes called LEVEES. Sometimes written as DYKE

DISCHARGE
The volume of water per unit of time flowing along a pipe or channel.

DISPERSION
(1) Pattern of geographic distribution of individuals within a species. (2) Distortion of the shape of a seismic wave train or ocean wave train because of variations of velocity with frequency.

DISTRIBUTARIES
Multiple branches of a river.

DITCH
A channel to convey water for irrigation or drainage.

DIURNAL
Having a period or cycle of approximately one TIDAL DAY.

DIURNAL CURRENT
The type of tidal current having only one FLOOD and one EBB period in the tidal day. A ROTARY CURRENT is diurnal if it changes its direction through all points of the compass once each tidal day.

DIURNAL INEQUALITY
The difference in height of the two high waters or of the two low waters of each day. Also, the difference in velocity between the two daily flood or EBB CURRENTS of each day.

DIURNAL TIDE
A tide with one high water and one low water in a tidal day. (See Figure II-5-16)

DIVERGENCE
(1) In refraction phenomena, the increasing of distance between orthogonals in the direction of wave travel. Denotes an area of decreasing wave height and energy concentration. (2) In wind-setup phenomena, the decrease in setup observed under that which would occur in an equivalent rectangular basin of uniform depth, caused by changes in planform or depth. Also the increase in basin width or depth causing such decrease in setup.

DIVERGING WAVE
Waves that move obliquely out from a vessel's sailing line. (See Figure II-7-40)

DIVERSION CHANNEL
A waterway used to divert water from its natural course. The term is generally applied to a temporary arrangement e.g. to by-pass water around a dam site during construction.

DOCK
The slip or waterway between two piers, or cut into the land, for the reception of ships.

DOLPHIN
A cluster of piles.

DOWNDRIFT
The direction of predominant movement of littoral materials.

DOWNSTREAM
Along coasts with obliquely approaching waves there is a longshore (wave-driven) current. For this current, one can define an upstream and a DOWNSTREAM direction. For example, on a beach with an orientation west-east, the sea is to the north. Suppose the waves come from NW, then the current flows from West to East. Here, UPSTREAM is west of the observer, and east is *downstream* of the observer.

DOWNWELLING

A downward movement (sinking) of surface water caused by onshore Ekman transport, converging CURRENTS, or when a water mass becomes more dense than the surrounding water.

DRAINAGE BASIN

Total area drained by a stream and its tributaries.

DREDGED CHANNEL

An artificially maintained sea lane extending from an inland water body into the marginal sea to accomodate vessel traffic through coastal shallows.

DREDGED MATERIAL PLACEMENT SITE

Designated area for dredged material placement. In the United States, designated areas must be coordinated with the Environmental Protection Agency and resource agencies such as the U. S. Fish and Wildlife Service and the National marine Fisheries Service for environmental compliance and with local interests for capacity and acceptability.

DREDGING

The practice of excavating or displacing the bottom or shoreline of a water body. *Dredging* can be accomplished with mechanical or hydraulic machines. Most is done to maintain channel depths or berths for navigational purposes; other *dredging* is for shellfish harvesting, for cleanup of polluted sediments, and for placement of sand on beaches.

DRIFT (noun)

(1) Sometimes used as a short form for LITTORAL DRIFT. (2) The speed at which a current runs. (3) Floating material deposited on a beach (driftwood). (4) A deposit of a continental ice sheet; e.g., a DRUMLIN.

DRIFT CURRENT

A broad, shallow, slow-moving ocean or lake current.

DRIFT SECTOR

A particular reach of marine shore in which LITTORAL DRIFT may occur without significant interruption, and which contain any and all natural sources of such drift, and also any accretion shore forms accreted by such drift.

DROMOND

A large medieval fast-sailing galley or cutter.

DROWNED COAST

A shore with long, narrow channels, implying that subsidence of the coast has transformed the lower portions of river valleys into tidal estuaries.

DRUMLIN

A low, smoothly-rounded, elongate hill of compact glacial till built under the margin of the ice and shaped by its flow.

DRYING BEACH

That part of the beach which is uncovered by water (e.g. at low tide). Sometimes referred to as 'SUBAERIAL' beach.

DUNES

(1) Ridges or mounds of loose, wind-blown material, usually sand. (See Figure IV-2-11.) (2) Bed forms smaller than bars but larger than ripples that are out of phase with any water-surface gravity waves associated with them.

DURABILITY

The ability of a rock to retain its physical and mechanical properties (i.e. resist degradation) in engineering service.

DURATION
In wave forecasting, the length of time the wind blows in nearly the same direction over the FETCH (generating area).

DURATION, MINIMUM
The time necessary for steady-state wave conditions to develop for a given wind velocity over a given fetch length.

DURATION OF EBB
The interval of time in which a tidal current is ebbing, determined from the middle of the slack waters.

DURATION OF FALL
The interval from high water to low water.

DURATION OF FLOOD
The interval of time in which a tidal current is flooding, determined from the middle of slack waters.

DURATION OF RISE
The interval from low water to high water.

DYNAMIC EQUILIBRIUM
Short term morphological changes that do not affect the morphology over a long period.

DYNAMIC VISCOSITY
In fluid dynamics, the ratio between the shear stress acting along any plane between neighboring fluid elements and the rate of deformation of the velocity gradient perpendicular to this plane.

E

EAGER
See BORE.

EBB
Period when tide level is falling; often taken to mean the ebb current which occurs during this period.

EBB CURRENT
The movement of a tidal current away from shore or down a tidal stream. In the semidiurnal type of reversing current, the terms greater ebb and lesser ebb are applied respectively to the ebb currents of greater and lesser velocity of each day. The terms of *maximum ebb* and *minimum ebb* are applied to the maximum and minimum velocities of a continuously running *ebb current*, the velocity alternately increasing and decreasing without coming to a slack or reversing. The expression maximum ebb is also applicable to any *ebb current* at the time of greatest velocity.

EBB INTERVAL
The interval between the transit of the moon over the meridian of a place and the time of the following strength of ebb.

EBB SHIELD
High, landward margin of a flood-tidal shoal that helps divert ebb-tide currents around the shoal.

EBB STRENGTH
The EBB CURRENT at the time of maximum velocity.

EBB TIDAL DELTA
The bulge of sand formed at the seaward mouth of TIDAL INLETS as a result of interaction between tidal currents and waves. Also called inlet-associated bars and estuary entrance shoals.

EBB TIDE
The period of tide between high water and the succeeding low water; a falling tide. (See Figure II-5-16.)

ECHO SOUNDER
An electronic instrument used to determine the depth of water by measuring the time interval between the emission of a sonic or ultrasonic signal and the return of its echo from the bottom.

ECOSYSTEM
The living organisms and the nonliving environment interacting in a given area, encompassing the relationships between biological, geochemical, and geophysical systems.

EDDY
A circular movement of water formed on the side of a main current. Eddies may be created at points where the main stream passes projecting obstructions or where two adjacent currents flow counter to each other.

EDDY CURRENT
See EDDY.

EDGE WAVE
An ocean wave parallel to a coast, with crests normal to the shoreline. An edge wave may be STANDING or PROGRESSIVE. Its height diminishes rapidly seaward and is negligible at a distance of one wavelength offshore.

EKMAN TRANSPORT
Resultant flow at right angles to and to the right of the wind direction (in the northern hemisphere) referred to as UPWELLING and DOWNWELLING.

ELEVATION

The vertical distance from mean sea level or other established datum plane to a point on the earth's surface; height above sea level. Although sea floor elevation below msl should be marked as a negative value, many charts show positive numerals for water depth.

EL NIÑO

Warm equatorial water which flows southward along the coast of Peru and Ecuador during February and March of certain years. It is caused by poleward motions of air and unusual water temperature patterns in the Pacific Ocean, which cause coastal downwelling, leading to the reversal in the normal north-flowing cold coastal currents. During many *El Niño* years, storms, rainfall, and other meteorological phenomena in the Western Hemisphere are measurably different than during non-*El Niño* years.

ELUTRIATION

The process by which a granular material can be sorted into its constituent particle sizes by means of a moving stream of fluid (usually air or water). *Elutriators* are extensively used in studies of sediments for determining Particle size distribution. Under certain circumstances wind, rivers and streams may act as elutriating agents.

EMBANKMENT

Fill material, usually earth or rock, placed with sloping sides and with a length greater than its height. Usually an embankment is wider than a dike.

EMBAYMENT

An indentation in the shore forming an open bay.

EMERGENT COAST

A coast in which land formerly under water has recently been exposed above sea level, either by uplift of the land or by a drop in sea level.

ENDEMIC

Native or confined to a specific geographic area.

ENERGY COEFFICIENT

The ratio of the energy in a wave per unit crest length transmitted forward with the wave at a point in shallow water to the energy in a wave per unit crest length transmitted forward with the wave in deep water. On refraction diagrams this is equal to the ratio of the distance between a pair of orthogonals at a selected shallow-water point to the distance between the same pair of orthogonals in deep water. Also the square of the REFRACTION COEFFICIENT.

ENTRANCE

The avenue of access or opening to a navigable channel or inlet.

EOLIAN (also AEOLIAN)

Pertaining to the wind, esp. used with deposits such as loess and dune sand, and sedimentary structures like wind-formed ripple marks.

EOLIAN SANDS

Sediments of sand size or smaller which have been transported by winds. They may be recognized in marine deposits off desert coasts by the greater angularity of the grains compared with waterborne particles.

EQUATORIAL CURRENTS

(1) Ocean currents flowing westerly near the equator. There are two such currents in both the Atlantic and Pacific Oceans. The one to the north of the equator is called the North Equatorial Current and the one to the south is called the South Equatorial Current. Between these two currents there is an easterly flowing stream known as the Equatorial Countercurrent. (2) Tidal currents occurring semimonthly as a result of the moon being over the equator. At these times the tendency of the moon to produce DIURNAL INEQUALITY in the current is at a minimum.

EQUATORIAL TIDES

Tides occurring semimonthly as the result of the moon being over the equator. At these times the tendency of the moon to produce a DIURNAL INEQUALITY in the tide is at a minimum.

EROSION

The wearing away of land by the action of natural forces. On a beach, the carrying away of beach material by wave action, tidal currents, littoral currents, or by deflation.

ESCARPMENT

A more or less continuous line of cliffs or steep slopes facing in one general direction which are caused by erosion or faulting. Also SCARP. (See Figure A-1)

ESTUARY

(1) The part of a river that is affected by tides. (2) The region near a river mouth in which the fresh water of the river mixes with the salt water of the sea and which received both fluvial and littoral sediment influx.

EUSTATIC SEA LEVEL CHANGE

Change in the relative volume of the world's ocean basins and the total amount of ocean water.

EYE

In meteorology, usually the "eye of the storm" (hurricane): the roughly circular area of comparatively light winds and fair weather found at the center of a severe tropical cyclone.

F

FAIRWAY
The parts of a waterway that are open and unobstructed for navigation. The main traveled part of a waterway; a marine thoroughfare.

FAR-INFRAGRAVITY
The frequency band (nominally 0.001 - 0.02 Hz) occupied by SHEAR INSTABILITIES of the longshore current. This band falls both below and in the lower part of the Infragravity band occupied by Infragravity waves.

FATHOM
A unit of measurement used for soundings equal to 1.83 meters (6 feet).

FATHOMETER
The copyrighted trademark for a type of ECHO SOUNDER.

FAULT
A fracture in rock along which there has been an observable amount of displacement. Faults are rarely single planar units; normally they occur as parallel to sub-parallel sets of planes along which movement has taken place to a greater or lesser extent. Such sets are called fault or fracture-zones.

FAUNA
The entire group of animals found in an area.

FEEDER BEACH
An artificially widened beach serving to nourish downdrift beaches by natural littoral currents or forces.

FEEDER CURRENT
The currents which flow parallel to shore before converging and forming the neck of a RIP CURRENT.

FEEDER CURRENT
See CURRENT, FEEDER.

FEELING BOTTOM
The initial action of a deepwater wave, in response to the bottom, upon running into shoal water.

FETCH
The area in which SEAS are generated by a wind having a fairly constant direction and speed. Sometimes used synonymously with FETCH LENGTH. Also GENERATING AREA.

FETCH LENGTH
The horizontal distance (in the direction of the wind) over which a wind generates seas or creates a WIND SETUP.

FETCH-LIMITED
Situation in which wave energy (or wave height) is limited by the size of the wave generation area (fetch).

FILTER
Intermediate layer, preventing fine materials of an underlayer from being washed through the voids of an upper layer.

FIORD (FJORD)
A narrow, deep, steep-walled inlet of the sea, usually formed by entrance of the sea into a deep glacial trough.

FIRTH

A narrow arm of the sea; also, the opening of a river into the sea.

FLOOD

(1) Period when tide level is rising; often taken to mean the flood current which occurs during this period (2) A flow beyond the carrying capacity of a channel.

FLOOD CHANNEL

Channel located on ebb-tidal shoal that carries the flood tide over the tidal flat into the back bay or lagoon.

FLOOD CURRENT

The movement of a tidal current toward the shore or up a tidal stream. In the semidiurnal type of reversing current, the terms *greater flood* and *lesser flood* are applied respectively to the flood currents of greater and lesser velocity each day. The terms *maximum flood* and *minimum flood* are applied to the maximum and minimum velocities of a flood current the velocity of which alternately increases and decreases without coming to slack or reversing. The expression *maximum flood* is also applicable to any flood current at the time of greatest velocity.

FLOOD GATE

A gravity outlet fitted with vertically-hinged doors, opening if the inner water level is higher than the outer water level, so that drainage takes place during low water.

FLOOD INTERVAL

The interval between the transit of the moon over the meridian of a place and the time of the following flood.

FLOOD MARK

Proof of any kind on the shoreline, or on structures like bridge abutments, used to determine the highest level attained by the water surface during the flood (note: the height of the flood mark usually includes the wave run-up).

FLOOD PLAIN

1) A flat tract of land bordering a river, mainly in its lower reaches, and consisting of ALLUVIUM deposited by the river. It is formed by the sweeping of the meander belts downstream, thus widening the valley, the sides of which may become some kilometers apart. In time of flood, when the river overflows its banks, sediment is deposited along the valley banks and plains. (2) Synonymous with 100-year *floodplain*. The land area susceptible to being inundated by stream derived waters with a 1 percent chance of being equaled or exceeded in any given year.

FLOOD RAMP

Seaward-dipping sand platform dominated by flood-tidal currents, located on ebb-tidal shoal near the opening to the inlet.

FLOOD ROUTING

The determination of the attenuating effect of storage on a river-flood passing through a valley by reason of a feature acting as control (e.g. a reservoir with a spillway capacity less than the flood inflow, or the widening or narrowing of a valley).

FLOOD TIDAL DELTA

The bulge of sand formed at the landward mouth of TIDAL INLETS as a result of flow expansion.

FLOOD TIDE

The period of tide between low water and the succeeding high water; a rising tide. (See Figure II-5-16.)

FLOOD WALL, SPLASH WALL

Wall, retired from the seaward edge of the seawall crest, to prevent water from flowing onto the land behind.

FLORA

The entire group of plants found in an area.

FLUVIAL
Of or pertaining to rivers; produced by the action of a river or stream (e.g., *fluvial* sediment).

FLUSHING TIME
The time required to replace all the water in an ESTUARY, HARBOR, etc., by action of current and tide.

FOAM LINE
(1) The front of a wave as it advances shoreward, after it has broken. (2) Lines of foam such as those which move around the head of a RIP.

FOLLOWING WIND
Generally, the same as a tailwind; in wave forecasting, wind blowing in the direction of ocean-wave advance.

FOREDUNE
The front DUNE immediately behind the backshore.

FORERUNNER
Low, long-period ocean SWELL which commonly precedes the main swell from a distant storm, especially a tropical cyclone.

FORESHORE
The part of the shore, lying between the crest of the seaward berm (or upper limit of wave wash at high tide) and the ordinary low-water mark, that is ordinarily traversed by the uprush and backrush of the waves as the tides rise and fall. See BEACH FACE. (See Figure A-1)

FORE REEF
The seaward side of a REEF (usually coral); in places a steep slope covered with reef talus.

FORWARD SPEED (hurricane)
Rate of movement (propagation) of the hurricane eye in meters per second, knots, or miles per hour.

FREEBOARD
At a given time, the vertical distance between the water level and the top of the structure. On a ship, the distance from the waterline to main deck or gunwale.

FRINGING ISLANDS
A series of islands that fringe, or mask, a mainland coast often known as BARRIER ISLANDS. The waters landward of such islands are sometimes treated as high seas enclaves or as inland waters.

FRINGING REEF
A coral REEF attached directly to an insular or continental shore. There may be a shallow channel or lagoon between the reef and the adjacent mainland.

FRONT OF THE FETCH
In wave forecasting, the end of the generating area toward which the wind is blowing.

FROUDE NUMBER
The dimensionless ratio of the inertial force to the force of gravity for a given fluid flow. It may be given as $F_r = V/Lg$ where V is a characteristic velocity, L is a characteristic length, and g the acceleration of gravity - or as the square root of this number.

FULLY-DEVELOPED SEA
The waves that form when wind blows for a sufficient period of time across the open ocean. The waves of a *fully developed sea* have the maximum height possible for a given wind speed, FETCH and duration of wind.

G

GABION
(1) Steel wire-mesh basket to hold stones or crushed rock to protect a bank or bottom from erosion. (2) Structures composed of masses of rocks, rubble or masonry held tightly together usually by wire mesh so as to form blocks or walls. Sometimes used on heavy erosion areas to retard wave action or as a foundation for BREAKWATERS or JETTIES.

GALE
A wind between a strong breeze and a storm. A continuous wind blowing in degrees of moderate, fresh, strong, or whole *gale* and varying in velocity from 28 to 47 nautical miles per hour (see BEAUFORT SCALE).

GAUGE (GAGE)
Instrument for measuring the water level relative to a datum or for measuring other parameters.

GENERATING AREA
In wave forecasting, the continuous area of water surface over which the wind blows in nearly a constant direction. Sometimes used synonymously with FETCH LENGTH. Also FETCH.

GEOGRAPHICAL INFORMATION SYSTEM (GIS)
Database of information which is geographically referenced, usually with an associated visualization system.

GEOGRAPHIC MILE
Unit of linear measure equal to one minute of latitude at the equator. See NAUTICAL MILE.

GEOMETRIC MEAN DIAMETER
The diameter equivalent of the arithmetic mean of the logarithmic frequency distribution. In the analysis of beach sands, it is taken as that grain diameter determined graphically by the intersection of a straight line through selected boundary sizes, (generally points on the distribution curve where 16 and 84 percent of the sample is coarser by weight) and a vertical line through the median diameter of the sample.

GEOMETRIC SHADOW
In wave diffraction theory, the area outlined by drawing straight lines paralleling the direction of wave approach through the extremities of a protective structure. It differs from the actual protected area to the extent that the diffraction and refraction effects modify the wave pattern.

GEOMORPHOLOGY
(1) That branch of physical geography which deals with the form of the Earth, the general configuration of its surface, the distribution of the land, water, etc. (2) The investigation of the history of geologic changes through the interpretation of topographic forms.

GEOPHYSICS
The study of the physical characteristics and properties of the earth, usually employing quantitative physical methods.

GEOTEXTILE
A synthetic fabric which may be woven or non-woven used as a filter.

GLACIER
A large body of ice moving slowly down a slope of valley or spreading outward on a land surface (e.g., Greenland, Antarctica) and surviving from year to year.

GLACIO-ISOSTACY
The state of hydrostatic equilibrium of the earth's crust as influenced by the weight of glacier ice.

GLOBAL POSITIONING SYSTEM (GPS)

A navigational and positioning system developed by the U.S. Department of Defense, by which the location of a position on or above the Earth can be determined by a special receiver at that point interpreting signals received simultaneously from several of a constellation of special satellites.

GORGE

(1) The deepest portion of an inlet, the THROAT. (2) A narrow, deep valley with nearly vertical rock walls.

GRADED BEDDING

An arrangement of particle sizes within a single bed, with coarse grains at the bottom of the bed and progressively finer grains toward the top of the bed.

GRADIENT

(1) A measure of slope (soil- or water-surface) in meters of rise or fall per meter of horizontal distance. (2) More general, a change of a value per unit of distance, e.g. the *gradient* in longshore transport causes erosion or accretion. (3) With reference to winds or currents, the rate of increase or decrease in speed, usually in the vertical; or the curve that represents this rate.

GRADING

Distribution, with regard to size or weight, of individual stones within a bulk volume; heavy, light and fine grading are distinguished.

GRADUAL CLOSURE METHOD

Method in which the final closure gap in a dam is closed gradually either by the vertical or horizontal closure method; this in contradiction with a sudden closure.

GRANULAR FILTER

Band of granular material which is incorporated in an embankment, dam, dike, or bottom protection and is graded so as to allow seepage to flow across or down the filter zone without causing the migration of the material adjacent to the filter.

GRAVEL

Unconsolidated natural accumulation of rounded rock fragments coarser than sand but finer than pebbles (2-4 mm diameter).

GRAVITY WAVE

A wave whose velocity of propagation is controlled primarily by gravity. Water waves more than 5 cm long are considered gravity waves. Waves longer than 2.5 cm and shorter than 5 cm are in an indeterminate zone between CAPILLARY and GRAVITY WAVES. See RIPPLE.

GROIN (British, GROYNE)

Narrow, roughly shore-normal structure built to reduce longshore currents, and/or to trap and retain littoral material. Most groins are of timber or rock and extend from a SEAWALL, or the backshore, well onto the foreshore and rarely even further offshore. See T-GROIN, PERMEABLE GROIN, IMPERMEABLE GROIN.

GROIN BAY

The beach compartment between two groins.

GROIN SYSTEM

A series of groins acting together to protect a section of beach. Commonly called a GROIN field.

GULF

A relatively large portion of the ocean or sea extending far into land; the largest of various forms of inlets of the sea (e.g., Gulf of Mexico, Gulf of Aqaba).

GUT

A tidal stream connecting two larger waterways.

H

HALCOCLINE
A zone in which salinity changes rapidly.

HALF-TIDE LEVEL
A plane midway between MEAN HIGH WATER and MEAN LOW WATER, also called MEAN TIDE LEVEL.

HARBOR (British, HARBOUR)
Any protected water area affording a place of safety for vessels. See also PORT. A harbor may be natural or man-made.

HARBOR OSCILLATION (HARBOR SURGING)
The nontidal vertical water movement in a harbor or bay. Usually the vertical motions are low; but when oscillations are excited by a tsunami or storm surge, they may be quite large. Variable winds, air oscillations, or surf beat also may cause oscillations. See SEICHE.

HARD DEFENSES
General term applied to impermeable coastal defense structures of concrete, timber, steel, masonry, etc, which reflect a high proportion of incident wave energy.

HEAD OF RIP
The part of a rip current that has widened out seaward of the breakers. See also CURRENT, RIP; CURRENT, FEEDER; and NECK (RIP).

HEADLAND (HEAD)
(1) A comparatively high promontory with either a CLIFF or steep face extending out into a body of water, such as a sea or lake. An unnamed HEAD is usually called a *headland*. (2) The section of RIP CURRENT which has widened out seaward of the BREAKERS, also called HEAD OF RIP. (3) Seaward end of BREAKWATER or dam.

HEADWATER LEVEL
The level of water in the reservoir.

HEAVE
(1) The vertical rise or fall of the waves or the sea. (2) The translational movement of a craft parallel to its vertical axis. (3) The net transport of a floating body resulting from wave action.

HIGH SEAS
This term, in municipal and international law, denotes the continuous body of salt water in the world that is navigable in its character and that lies outside territorial waters and maritime belts of the various countries.

HIGH TIDE, HIGH WATER (HW)
The maximum elevation reached by each rising tide. See TIDE. (See Figure II-5-16.)

HIGH WATER (HW)
Maximum height reached by a rising tide. The height may be solely due to the periodic tidal forces or it may have superimposed upon it the effects of prevailing meteorological conditions. Nontechnically, also called the HIGH TIDE.

HIGH WATER LINE
In strictness, the intersection of the plane of mean high water with the shore. The shoreline delineated on the nautical charts of the National Ocean Service is an approximation of the high water line. For specific occurrences, the highest elevation on the shore reached during a storm or rising tide, including meteorological effects.

HIGH WATER MARK
A reference mark on a structure or natural object, indicating the maximum stage of tide or flood.

HIGH WATER OF ORDINARY SPRING TIDES (HWOST)
A tidal datum appearing in some British publications, based on high water of ordinary spring tides.

HIGHER HIGH WATER (HHW)
The higher of the two high waters of any tidal day. The single high water occurring daily during periods when the tide is diurnal is considered to be a higher high water. (See Figure II-5-16.)

HIGHER LOW WATER (HLW)
The higher of two low waters of any tidal day. (See Figure II-5-16.)

HIGHEST ASTRONOMICAL TIDE (HAT)
The highest level of water which can be predicted to occur under any combination of astronomical conditions. This level may not be reached every year.

HINDCASTING
In wave prediction, the retrospective forecasting of waves using measured wind information.

HINTERLAND
The region lying inland from the coast. Also the inland area served by a port.

HISTORIC EVENT ANALYSIS
Extreme analysis based on hindcasting typically ten events over a period of 100 years.

HOLOCENE
An epoch of the QUATERNARY period, from the end of the PLEISTOCENE, about 8,000 years ago, to the present time. Syn: Recent.

HOMOPYCNAL FLOW
A condition in which the outflow jet from a river or coastal inlet and the water in the receiving basin are of the same density or are vertically mixed.

HOOK
A spit or narrow cape of sand or gravel which turns landward at the outer end; a RECURVED SPIT.

HOPPER DREDGE
Self-propelled floating plant which is capable of dredging material, storing it onboard, and transporting and placing the material at a specified disposal site. Often used to dredge inlets and then deposit the material along the open coast or offshore.

HORIZONTAL CLOSURE METHOD
Construction of a dam by dumping the materials from one or both banks, thus constricting the channel progressively laterally until the dam is closed. This method is also known as end dumping and point tipping

HURRICANE
An intense tropical cyclone in which winds tend to spiral inward toward a core of low pressure, with maximum surface wind velocities that equal or exceed 33.5 m/sec (75 mph or 65 knots) for several minutes or longer at some points. TROPICAL STORM is the term applied if maximum winds are less than 33.5 m/sec but greater than a whole gale (63 mph or 55 knots). Term is used in the Atlantic, Gulf of Mexico, and eastern Pacific.

HURRICANE PATH or TRACK
Line of movement (propagation) of the eye through an area.

HURRICANE STAGE HYDROGRAPH

A continuous graph representing water level stages that would be recorded in a gage well located at a specified point of interest during the passage of a particular hurricane, assuming that effects of relatively short-period waves are eliminated from the record by damping features of the gage well. Unless specifically excluded and separately accounted for, hurricane surge hydrographs are assumed to include effects of astronomical tides, barometric pressure differences, and all other factors that influence water level stages within a properly designed gage well located at a specified point.

HURRICANE WIND PATTERN or ISOVEL PATTERN

An actual or graphical representation of near-surface wind velocities covering the entire area of a hurricane at a particular instant. Isovels are lines connecting points of simultaneous equal wind velocities, usually referenced 9 meters (30 feet) above the surface, in meters per second, knots, or meters per hour; wind directions at various points are indicated by arrows or deflection angles on the isovel charts. Isovel charts are usually prepared at each hour during a hurricane, but for each half hour during critical periods.

HYDRAULIC DREDGE

Floating or (occasionally) truck-based plant which lifts the material through a suction pipe. It requires dilution water for material pickup, lift, and transportation. Often used to renourish beaches when material is pumped onto the shore from an offshore sand source.

HYDRAULIC RADIUS

Quotient of the wetted cross-sectional area and the wetted perimeter.

HYDRAULICALLY EQUIVALENT GRAINS

Sedimentary particles that settle at the same rate under the same conditions.

HYDROGRAPHY

(1) The description and study of seas, lakes, rivers and other waters. (2) The science of locating aids and dangers to navigation. (3) The description of physical properties of the waters of a region.

HYDROGRAPHIC PRESSURE

The pressure exerted by water at any given point in a body of water at rest.

HYPOPYCNAL FLOW

Outflow from a river or coastal inlet in which a wedge of less dense water flows over the denser sea water.

HYPOTHETICAL HURRICANE ("HYPOHURRICANE")

A representation of a hurricane, with specified characteristics, that is assumed to occur in a particular study area, following a specified path and timing sequence.

TRANSPOSED--A hypohurricane based on the storm transposition principle, assumed to have wind patterns and other characteristics basically comparable to a specified hurricane of record, but transposed to follow a new path to serve as a basis for computing a hurricane surge hydrograph that would be expected at a selected point. Moderate adjustments in timing or rate of forward movement may also be made, if these are compatible with meteorological considerations and study objectives.

HYPOHURRICANE BASED ON GENERALIZED PARAMETERS--Hypohurricane estimates based on various logical combinations of hurricane characteristics used in estimating hurricane surge magnitudes corresponding to a range of probabilities and potentialities. The STANDARD PROJECT HURRICANE is most commonly used for this purpose, but estimates corresponding to more severe or less severe assumptions are important in some project investigations.

STANDARD PROJECT HURRICANE (SPH)--A hypothetical hurricane intended to represent the most severe combination of hurricane parameters that is reasonably characteristic of a specified region, excluding extremely rare combinations. It is further assumed that the SPH would approach a given project site from such direction, and at such rate of movement, to produce the highest HURRICANE SURGE HYDROGRAPH, considering pertinent hydraulic characteristics of the area. Based on this concept, and on extensive meteorological studies and probability

analyses, a tabulation of "Standard Project Hurricane Index Characteristics" mutually agreed upon by representatives of the U. S. Weather Service and the Corps of Engineers, is available.

PROBABLE MAXIMUM HURRICANE--A hypohurricane that might result from the most severe combination of hurricane parameters that is considered reasonably possible in the region involved, if the hurricane should approach the point under study along a critical path and at optimum rate of movement. This estimate is substantially more severe than the SPH criteria.

DESIGN HURRICANE--A representation of a hurricane with specified characteristics that would produce HURRICANE SURGE HYDROGRAPHS and coincident wave effects at various key locations along a proposed project alinement. It governs the project design after economics and other factors have been duly considered. The design hurricane may be more or less severe than the SPH, depending on economics, risk, and local considerations.

I

ICE AGE
A loosely-used synonym of glacial epoch, or time of extensive glacial activity; specifically of the latest period of widespread continental glaciers, the PLEISTOCENE Epoch.

ICE FRONT
The floating vertical cliff forming the seaward edge of an ICE SHELF or other glacier that enters the sea.

ICE SHELF
A extensive sheet of ice which is attached to the land along one side but most of which is afloat and bounded on the seaward side by a steep cliff (ICE FRONT) rising 2 tp 50+ m above sea level. Common along polar coasts (Antarctica, Greenland), and generally of great breadth and sometimes extending tens or hundreds of km seaward from the continental coastline.

IMPERMEABLE GROIN
A GROIN constructed such that sand cannot pass through the structure (but sand may still move over or around it).

INCIDENT WAVE
Wave moving landward.

INDIAN SPRING LOW WATER
The approximate level of the mean of lower low waters at spring tides, used principally in the Indian Ocean and along the east coast of Asia. Also INDIAN TIDE PLANE.

INDIAN TIDE PLANE
The datum of INDIAN SPRING LOW WATER.

INFRAGRAVITY WAVE
Long waves with periods of 30 seconds to several minutes.

INLAND WATERS
Waters landward of the baseline (COASTLINE) from which the marginal seas are measured and over which complete sovereignty is exercised. Also known as “internal waters.”

INLET
(1) A short, narrow waterway connecting a bay, lagoon, or similar body of water with a large parent body of water. (2) An arm of the sea (or other body of water) that is long compared to its width and may extend a considerable distance inland. See also TIDAL INLET.

INLET GORGE
Generally, the deepest region of an inlet channel.

INSHORE (ZONE)
In beach terminology, the zone of variable width extending from the LOW WATER LINE through the BREAKER ZONE. Also SHOREFACE. (See Figure A-1)

INSHORE CURRENT
Any current in or landward of the BREAKER ZONE.

INSULAR SHELF
The zone surrounding an island extending from the LOW WATER LINE to the depth (usually about 183 m; 100 fathoms) where there is a marked or rather steep descent toward the great depths.

INTERNAL WAVES

Waves that occur within a fluid whose density changes with depth, either abruptly at a sharp surface of discontinuity (an interface), or gradually. Their amplitude is greatest at the density discontinuity or, in the case of a gradual density change, somewhere in the interior of the fluid and not at the free upper surface where the surface waves have their maximum amplitude.

INTERTIDAL

The zone between the high and low water tides.

IRREGULAR WAVES

Waves with random wave periods (and in practice, also heights), which are typical for natural wind-induced waves.

IRROTATIONAL WAVE

A wave with fluid particles that do not revolve around an axis through their centers, although the particles themselves may travel in circular or nearly circular orbits. Irrotational waves may be PROGRESSIVE, STANDING, OSCILLATORY, or TRANSLATORY. For example, the Airy, Stokes, cnoidal, and solitary wave theories describe irrotational waves. Compare TROCHOIDAL WAVE.

ISOBATH

A contour line connecting points of equal water depths on a CHART.

ISOPACHYTE

Line connecting points on the seabed with an equal depth of sediment.

ISOVEL PATTERN

See HURRICANE WIND PATTERN.

ISTHMUS

A narrow strip of land, bordered on both sides by water, that connects two larger bodies of land.

J

JET
To place (a pile, slab, or pipe) in the ground by means of a jet of water acting at the lower end.

JETTY
(1) (United States usage) On open seacoasts, a structure extending into a body of water, which is designed to prevent shoaling of a channel by littoral materials and to direct and confine the stream or tidal flow. Jetties are built at the mouths of rivers or tidal inlets to help deepen and stabilize a channel. (2) (British usage) WHARF or PIER. See TRAINING WALL.

JOINT PROBABILITY
The probability of two (or more) things occurring together.

JOINT PROBABILITY DENSITY
Function specifying the joint distribution of two (or more) variables.

JOINT RETURN PERIOD
Average period of time between occurrences of a given joint probability event.

JONSWAP SPECTRUM
Wave spectrum typical of growing deep water waves developed from field experiments and measurements of waves and wave spectra in the Joint North Sea Wave Peoject

K

KATABATIC WIND
Wind caused by cold air flowing down slopes due to gravitational acceleration.

KEY
A cay, esp. one of the low, insular banks of sand, coral, and limestone off the southern coast of Florida.

KINEMATIC VISCOSITY
The dynamic viscosity divided by the fluid density.

KINETIC ENERGY (OF WAVES)
In a progressive oscillatory wave, a summation of the energy of motion of the particles within the wave.

KNOLL
A submerged elevation of rounded shape rising less than 1000 meters from the ocean floor and of limited extent across the summit. Compare SEAMOUNT.

KNOT
The unit of speed used in navigation equal to 1 nautical mile (6,076.115 ft or 1,852 m) per hour.

L

LAGGING OF TIDE
The periodic retardation in the time of occurrence of high and low water due to changes in the relative positions of the moon and sun.

LAGOON
A shallow body of water, like a pond or sound, partly or completely separated from the sea by a BARRIER ISLAND or REEF. Sometimes connected to the sea via an INLET. (See Figure IV-1-6.)

LAMINAR FLOW
Slow, smooth flow, with each drop of water traveling a smooth path parallel to its neighboring drops. Laminar flow is characteristic of low velocities, and particles of sediment in the flow zones are moved by rolling or SALTATION.

LAND BREEZE
A light wind blowing from the land to the sea, caused by unequal cooling of land and water masses.

LAND-SEA BREEZE
The combination of a land breeze and a sea breeze as a diurnal phenomenon.

LANDLOCKED
Enclosed, or nearly enclosed, by land--thus protected from the sea, as a bay or a harbor.

LANDMARK
A conspicuous object, natural or artificial, located near or on land, which aids in fixing the position of an observer.

LEAD LINE
A line, wire, or cord used in sounding (to obtain water depth). It is weighted at one end with a plummet (sounding lead). Also SOUNDING LINE.

LEDGE
A rocky formation forming a ridge or REEF, especially one underwater or near shore

LEE
(1) Shelter, or the part or side sheltered or turned away from the wind or waves. (2) (Chiefly nautical) The quarter or region toward which the wind blows.

LEEWARD
The direction toward which the wind is blowing; the direction toward which waves are traveling.

LENGTH OF WAVE
The horizontal distance between similar points on two successive waves measured perpendicularly to the crest.

LEVEE
(1) A ridge or EMBANKMENT of sand and silt, built up by a stream on its flood plain along both banks of its channel. (2) A large DIKE or artificial EMBANKMENT, often having an access road along the top, which is designed as part of a system to protect land from floods.

LIGHT BREEZE
A wind with velocity from 4 to 6 KNOTS.

LIMIT OF BACKRUSH (LIMIT OF BACKWASH)
See BACKRUSH, BACKWASH.

LITTORAL

Of or pertaining to a shore, especially of the sea. Often used as a general term for the coastal zone influenced by wave action, or, more specifically, the shore zone between the high and low water marks.

LITTORAL CELL

A reach of the coast that is isolated sedimentologically from adjacent coastal reaches and that features its own sources and sinks. Isolation is typically caused by protruding headlands, submarine canyons, inlets, and some river mouths that prevent littoral sediment from one cell to pass into the next. Cells may range in size from a multi-hundred meter POCKET BEACH in a rocky coast to a BARRIER ISLAND many tens of kilometers long.

LITTORAL CURRENT

See CURRENT, LITTORAL.

LITTORAL DEPOSITS

Deposits of littoral drift.

LITTORAL DRIFT, LITTORAL TRANSPORT

The movement of beach material in the littoral zone by waves and currents. Includes movement parallel (long shore drift) and sometimes also perpendicular (cross-shore transport) to the shore.

LITTORAL TRANSPORT RATE

Rate of transport of sedimentary material parallel or perpendicular to the shore in the littoral zone. Usually expressed in cubic meters (cubic yards) per year. Commonly synonymous with LONGSHORE TRANSPORT RATE.

LITTORAL ZONE

In beach terminology, an indefinite zone extending seaward from the shoreline to just beyond the breaker zone.

LOAD

The quantity of sediment transported by a current. It includes the suspended load of small particles and the BED LOAD of large particles that move along the bottom.

LONG WAVES

Waves with periods above about 30 seconds; can be generated by wave groups breaking in the surf zone. See also INFRAGRAVITY WAVES.

LONGSHORE

Parallel to and near the shoreline; ALONGSHORE.

LONGSHORE BAR

A sand ridge or ridges, running roughly parallel to the shoreline and extending along the shore outside the trough, that may be exposed at low tide or may occur below the water level in the offshore.

LONGSHORE CURRENT

See CURRENT, LONGSHORE.

LONGSHORE DRIFT

Movement of (beach) sediments approximately parallel to the coastline.

LONGSHORE TRANSPORT RATE

See LITTORAL TRANSPORT RATE.

LONGSHORE TROUGH

An elongate DEPRESSION or series of depressions extending along the lower BEACH or in the offshore zone inside the BREAKERS.

LOOP

That part of a STANDING WAVE where the vertical motion is greatest and the horizontal velocities are least. Loops (sometimes called ANTINODES) are associated with CLAPOTIS and with SEICHE action resulting from wave reflections. Compare NODE.

LOW TIDE (LOW WATER, LW)

The minimum elevation reached by each falling tide. See TIDE. (See Figure II-5-16.)

LOW TIDE TERRACE

A flat zone of the beach near the low water level.

LOW WATER (LW)

The minimum height reached by each falling tide. Nontechnically, also called LOW TIDE.

LOW WATER DATUM

An approximation to the plane of mean low water that has been adopted as a standard reference plane. See also DATUM, PLANE and CHART DATUM.

LOW WATER LINE

The line where the established LOW WATER DATUM intersects the shore. The plane of reference that constitutes the LOW WATER DATUM differs in different regions.

LOW WATER OF ORDINARY SPRING TIDES (LWOST)

A tidal datum appearing in some British publications, based on low water of ordinary spring tides.

LOWER HIGH WATER (LHW)

The lower of the two high waters of any tidal day. (See Figure II-5-16.)

LOWER LOW WATER DATUM

An approximation to the plane of MEAN LOWER LOW WATER that has been adopted as a standard reference plane for a limited area and is retained for an indefinite period regardless of the fact that it may differ slightly from a better determination of MEAN LOWER LOW WATER from a subsequent series of observations.

LOWER LOW WATER (LLW)

The lower of the two low waters of any tidal day. The single low water occurring daily during periods when the tide is diurnal is considered to be a lower low water. (See Figure II-5-16.)

LOWEST ASTRONOMICAL TIDE (LAT)

The lowest tide level which can be predicted to occur under average meteorological conditions and any combination of astronomical conditions. This level may not be reached every year.

LUNAR DAY

The time of rotation of the Earth with respect to the moon, or the interval between two successive upper transits of the moon over the meridian of a place. The mean lunar day is approximately 24.84 solar hours in length, or 1.035 times as great as the mean solar day. Also called TIDAL DAY.

LUNAR TIDE

The portion of the tide that can be attributed directly to attraction to the moon.

M

MACH-STEM WAVE
Higher-than-normal wave generated when waves strike a structure at an oblique angle.

MACRO-TIDAL
Tidal range greater than 4 m.

MANAGED RETREAT
The deliberate setting back (moving landward) of the existing line of sea defense in order to obtain engineering or environmental advantages - also referred to as managed landward realignment. Sometimes refers to moving roads and utilities landward in the face of shore retreat.

MANGROVE
A tropical tree with interlacing prop roots, confined to low-lying brackish areas.

MARGIN, CONTINENTAL
A zone separating a continent from the deep-sea bottom.

MARGINAL PROBABILITY
The probability of a single variable in the context of a joint probability analysis.

MARGINAL RETURN PERIOD
The return period of a single variable in the context of a joint probability analysis.

MARGINAL SEA
The maritime belt over which a coastal state asserts sovereignty.

MARIGRAM
A graphic record of the rise and fall of the tide. The record is in the form of a curve in which time is represented by abscissas and the height of the tide by ordinates.

MARKER, REFERENCE
A mark of permanent character close to a survey station, to which it is related by an accurately measured distance and azimuth (or bearing).

MARKER, SURVEY
An object placed at the site of a station to identify the surveyed location of that station.

MARSH
(1) A tract of soft, wet land, usually vegetated by reeds, grasses and occasionally small shrubs. (2) Soft, wet area periodically or continuously flooded to a shallow depth, usually characterized by a particular subclass of grasses, cattails and other low plants.

MARSH, DIKED
A former salt marsh which has been protected by a DIKE.

MARSH, SALT
A marsh periodically flooded by salt water.

MASS TRANSPORT, SHOREWARD
The movement of water due to wave motion, which carries water through the BREAKER ZONE in the direction of wave propagation. Part of the NEARSHORE CURRENT SYSTEM.

MATTRESS
A blanket of brushwood or bamboo, poles, geotextile and reed lashed together to protect a shoreline, embankment or river/sea bed against erosion. Sometimes placed on the sea bed during JETTY construction to prevent stone from settling into soft bottom.

MEAN DEPTH
The average DEPTH of the water area between the still water level and the SHOREFACE profile from the waterline to any chosen distance seaward.

MEAN DIAMETER, GEOMETRIC
See GEOMETRIC MEAN DIAMETER.

MEAN HIGH WATER SPRINGS (MHWS)
The average height of the high water occurring at the time of spring tides.

MEAN HIGH WATER (MHW)
The average height of the high waters over a 19-year period. For shorter periods of observations, corrections are applied to eliminate known variations and reduce the results to the equivalent of a mean 19-year value. All high water heights are included in the average where the type of tide is either semidiurnal or mixed. Only the higher high water heights are included in the average where the type of tide is diurnal. So determined, mean high water in the latter case is the same as mean higher high water.

MEAN HIGHER HIGH WATER (MHHW)
The average height of the higher high waters over a 19-year period. For shorter periods of observation, corrections are applied to eliminate known variations and reduce the result to the equivalent of a mean 19-year value.

MEAN LOW WATER (MLW)
The average height of the low waters over a 19-year period. For shorter periods of observations, corrections are applied to eliminate known variations and reduce the results to the equivalent of a mean 19-year value. All low water heights are included in the average where the type of tide is either semidiurnal or mixed. Only lower low water heights are included in the average where the type of tide is diurnal. So determined, mean low water in the latter case is the same as mean lower low water.

MEAN LOW WATER SPRINGS
The average height of low waters occurring at the time of the spring tides. It is usually derived by taking a plane depressed below the half-tide level by an amount equal to one-half the spring range of tide, necessary corrections being applied to reduce the result to a mean value. This plane is used to a considerable extent for hydrographic work outside of the United States and is the plane of reference for the Pacific approaches to the Panama Canal. Frequently abbreviated to LOW WATER SPRINGS.

MEAN LOWER LOW WATER (MLLW)
The average height of the lower low waters over a 19-year period. For shorter periods of observations, corrections are applied to eliminate known variations and reduce the results to the equivalent of a mean 19-year value. Frequently abbreviated to LOWER LOW WATER.

MEAN RANGE OF TIDE
The difference in height between MEAN HIGH WATER and MEAN LOW WATER.

MEAN RISE OF THE TIDE
The height of MEAN HIGH WATER above the plane of reference or DATUM of chart.

MEAN SEA LEVEL
The average height of the surface of the sea for all stages of the tide over a 19-year period, usually determined from hourly height readings. Not necessarily equal to MEAN TIDE LEVEL. It is also the average water level that would exist in the absence of tides.

MEAN STEEPNESS
The ratio of the MEAN DEPTH to the horizontal distance over which the MEAN DEPTH was determined.

MEAN TIDE LEVEL
A plane midway between MEAN HIGH WATER and MEAN LOW WATER. Not necessarily equal to MEAN SEA LEVEL. Also HALF-TIDE LEVEL.

MEAN WATER LEVEL
The mean surface level as determined by averaging the heights of the water at equal intervals of time, usually at hourly intervals.

MEAN WAVE HEIGHT
The mean of all individual waves in an observation interval of approximately half an hour. In case of a Rayleigh-distribution 63% of the significant wave height.

MEANDERING
A single channel having a pattern of successive deviations in alignment which results in a more or less sinusoidal course.

MECHANICAL DREDGE
Mechanical plant characterized by the use of some form of bucket to excavate and raise the bottom material Normally, the *mechanical dredge* deposits material into a barge that transports it to the disposal site, but in some cases, the dredged material can be deposited directly in-water or placed on the bank immediately adjacent to the work area. Mechanical dredges may be classified into two sub-groups by how their buckets are connected to the dredge: (1) wire rope (i.e., clamshell or dragline), and (2) structurally (i.e., a backhoe).

MEDIAN DIAMETER
The diameter which marks the division of a given sand sample into two equal parts by weight, one part containing all grains larger than that diameter and the other part containing all grains smaller.

MEGARIPPLE
See SAND WAVE.

MESO-TIDAL
Tidal range between 2 m and 4 m.

METEOROLOGICAL TIDES
Tidal constituents having their origin in the daily or seasonal variation in weather conditions which may occur with some degree of periodicity.

MICRO-TIDAL
Tidal range less than 2 m.

MID-EXTREME TIDE
A plane midway between the extreme high water and the extreme LOW WATER occurring in any locality.

MIDDLE-GROUND SHOAL
A shoal formed by ebb and flood tides in the middle of the channel of the LAGOON or estuary end of an inlet.

MINERAL
A naturally occurring, inorganic, crystalline solid that has a definite chemical composition and possesses characteristic physical properties.

MINIMUM DURATION
See DURATION, MINIMUM.

MINIMUM FETCH
The least distance in which steady-state wave conditions will develop for a wind of given speed blowing a given duration of time.

MIST
Water vapor suspended in the air in very small drops finer than rain, larger than fog.

MIXED CURRENT
Type of tidal current characterized by a conspicious velocity difference between the two floods or two ebbs usually occurring each tidal day.

MIXED TIDE
A type of tide in which the presence of a diurnal wave is conspicuous by a large inequality in either the high or low water heights, with two high waters and two low waters usually occurring each tidal day. In strictness, all tides are mixed, but the name is usually applied without definite limits to the tide intermediate to those predominantly semidiurnal and those predominantly diurnal. (See Figure II-5-16.)

MOLE
In coastal terminology, a massive land-connected, solid-fill structure of earth (generally revetted), masonry, or large stone, which may serve as a breakwater or pier.

MONOCHROMATIC WAVES
A series of waves generated in a laboratory, each of which has the same length and period.

MONOLITHIC
Like a single stone or block. In coastal structures, the type of construction in which the structure's component parts are bound together to act as one.

MORAINE
An accumulation of earth, stones, etc., deposited by a glacier, usually in the form of a mound, ridge or other prominence on the terrain.

MORPHODYNAMICS
(1) The mutual interaction and adjustment of the seafloor topography and fluid dynamics involving the motion of sediment. (2) The coupled suite of mutually interdependent hydrodynamic processes, seafloor morphologies, and sequences of change.

MORPHOLOGICALLY AVERAGED
Single wave condition producing the same net longshore drift as a given proportion of the annual wave climate.

MORPHOLOGY
River/estuary/lake/seabed form and its change with time.

MOUTH
Entrance to an inland water body (e.g., river).

MUD
A fluid-to-plastic mixture of finely divided particles of solid material and water.

MUD FLAT

A level area of fine silt and clay along a shore alternately covered or uncovered by the tide or covered by shallow water.

N

NATIONAL TIDAL DATUM EPOCH (NTDE)
A period of 19 years adopted by the National Ocean Service as the period over which observations of tides are to be taken and reduced to average values for tidal datums.

NATURAL TRACER
A component of a sediment deposit that is unique to a particular source and can be used to identify the source and transport routes to a place of deposition.

NAUTICAL MILE
The length of a minute of arc, 1/21,600 of an average great circle of the Earth. Generally one minute of latitude is considered equal to one nautical mile. The accepted United States value as of 1 July 1959 is 1,852 meters (6,076.115 feet), approximately 1.15 times as long as the U.S. statute mile of 5,280 feet. Also GEOGRAPHICAL MILE.

NAVIGABLE WATERS
Waters that are either tidally-influenced or navigable in fact.

NAVIGATION PROJECT
A specific and fixed geographic area within a water body or series of water bodies that has been authorized for navigation by some group or organization (often a national government).

NEAP HIGH WATER
See NEAP TIDE.

NEAP LOW WATER
See NEAP TIDE.

NEAP RANGE
See NEAP TIDE.

NEAP TIDAL CURRENT
Tidal current of decreased velocity occurring semimonthly as the result of the moon being in quadrature.

NEAP TIDE
Tide of decreased range occurring semimonthly as the result of the moon being in quadrature. The NEAP RANGE of the tide is the average semidiurnal range occurring at the time of neap tides and is most conveniently computed from the harmonic constants. The NEAP RANGE is typically 10 to 30 percent smaller than the mean range where the type of tide is either semidiurnal or mixed and is of no practical significance where the type of tide is DIURNAL. The average height of the high waters of the neap tide is called NEAP HIGH WATER or HIGH WATER NEAPS (MHWN), and the average height of the corresponding LOW WATER is called NEAP LOW WATER or LOW WATER NEAPS (MLWN).

NEARSHORE
(1) In beach terminology an indefinite zone extending seaward from the SHORELINE well beyond the BREAKER ZONE. (2) The zone which extends from the swash zone to the position marking the start of the offshore zone, typically at water depths of the order of 20 m.

NEARSHORE BERM
Artificial berm built in shallow water using dredged material. Often, the berm is intended to renourish the adjacent and downdrift shore over time under the influence of waves and currents.

NEARSHORE CIRCULATION
The ocean circulation pattern composed of the NEARSHORE CURRENTS and the COASTAL CURRENTS.

NEARSHORE CURRENT SYSTEM

The current system caused primarily by wave action in and near the breaker zone, and which consists of four parts: the shoreward mass transport of water; longshore currents; seaward return flow, including rip currents; and the longshore movement of the expanding heads of rip currents. See also NEARSHORE CIRCULATION.

NECK

(1) The narrow strip of land which connects a peninsula with the mainland, or connects two ridges. (2) The narrow band (rip) of water flowing seaward through the surf. See also RIP CURRENT.

NESS

Roughly triangular promontory of land jutting into the sea, often consisting of mobile material, i.e. a beach form.

NETWORK

A set consisting of: (a) stations for which geometric relationships have been determined and which are so related that removal of one station from the set will affect the relationships (distances, directions, coordinates, etc.) between the other stations; and (b) lines connecting the stations to show this interdependence.

NIP

The cut made by waves in a shoreline of emergence.

NODAL ZONE

An area in which the predominant direction of the LONGSHORE TRANSPORT changes.

NODE

That part of a STANDING WAVE where the vertical motion is least and the horizontal velocities are greatest. Nodes are associated with CLAPOTIS and with SEICHE action resulting from wave reflections. Compare LOOP.

NOURISHMENT

The process of replenishing a beach. It may occur naturally by longshore transport, or be brought about artificially by the deposition of dredged materials or of materials trucked in from upland sites.

NUMERICAL MODELING

Refers to analysis of coastal processes using computational models.

O

OCEANOGRAPHY
The study of the sea, embracing and indicating all knowledge pertaining to the sea's physical boundaries, the chemistry and physics of seawater, marine biology, and marine geology.

OFFSHORE
(1) In beach terminology, the comparatively flat zone of variable width, extending from the SHOREFACE to the edge of the CONTINENTAL SHELF. It is continually submerged. (2) The direction seaward from the shore. (3) The zone beyond the nearshore zone where sediment motion induced by waves alone effectively ceases and where the influence of the sea bed on wave action is small in comparison with the effect of wind. (4) The breaker zone directly seaward of the low tide line. (See Figure A-1)

OFFSHORE BARRIER
See BARRIER BEACH.

OFFSHORE BREAKWATER
A BREAKWATER built towards the seaward limit of the littoral zone, parallel (or nearly parallel) to the shore.

OFFSHORE CURRENT
(1) Any current in the offshore zone. (2) Any current flowing away from shore.

OFFSHORE WIND
A wind blowing seaward from the land in the coastal area.

ONSHORE
A direction landward from the sea.

ONSHORE WIND
A wind blowing landward from the sea in the coastal area.

OPPOSING WIND
In wave forecasting, a wind blowing in a direction opposite to the ocean-wave advance; generally, a headwind.

ORBIT
In water waves, the path of a water particle affected by the wave motion. In deepwater waves the orbit is nearly circular, and in shallow-water waves the orbit is nearly elliptical. In general, the orbits are slightly open in the direction of wave motion, giving rise to MASS TRANSPORT. (See Figure II-1-4.)

ORBITAL CURRENT
The flow of water accompanying the orbital movement of the water particles in a wave. Not to be confused with wave-generated LITTORAL CURRENTS. (See Figure II-1-4.)

ORDINARY HIGH WATER MARK (OHWM)
That mark that will be found by examining the bed and banks and ascertaining where the presence and action of waters are so common and usual, and so long continued in all ordinary years, as to mark upon the soil a character distinct from that of the abutting upland, in respect to vegetation as that condition exists on June 1, 1971, as it may naturally change thereafter, or as it may change thereafter in accordance with permits issued by a local government. Also defined as MEAN HIGH WATER LINE (Shalowitz 1962).

ORDINARY TIDE
This expression is not used in a technical sense by the U.S. Coast and Geodetic Survey, but the word "ordinary" when applied to tides, may be taken as the equivalent of the word "mean". Thus "ordinary HIGH WATER LINE" may be assumed to be the same as "mean high water line".

ORTHOGONAL

On a wave-refraction diagram, a line drawn perpendicularly to the wave crests. Also called WAVE RAY. (See Figure II-3-4)

OSCILLATION

(1) A periodic motion backward and forward. (2) Vibration or variance above and below a mean value.

OSCILLATORY WAVE

A wave in which each individual particle oscillates about a point with little or no permanent change in mean position. The term is commonly applied to progressive oscillatory waves in which only the form advances, the individual particles moving in closed or nearly closed orbits. Compare WAVE OF TRANSLATION. See also ORBIT.

OUTCROP

A surface exposure of bare rock, not covered by soil or vegetation.

OUTFALL

A structure extending into a body of water for the purpose of discharging sewage, storm runoff, or cooling water.

OUTFLANKING

EROSION behind or around the land-based end of a GROIN, JETTY, or BREAKWATER or the terminus of a BULKHEAD, REVETMENT, or SEAWALL, usually causing failure of the structure or its function

OVERSPLASH

The water that splashes over the top of a BREAKWATER, SEAWALL, etc.

OVERTOPPING

Passing of water over the top of a structure as a result of wave runup or surge action.

OVERWASH

(1) The part of the UPRUSH that runs over the crest of a BERM or structure and does not flow directly back to the ocean or lake. (2) The effect of waves overtopping a COASTAL DEFENSE, often carrying sediment landwards which is then lost to the beach system.

P

PARAPET
A low wall built along the edge of a structure such as a SEAWALL or QUAY.

PARTICLE VELOCITY
The velocity induced by wave motion with which a specific water particle moves within a wave.

PATCH REEF
A moundlike or flat-topped organic REEF, generally less than 1 km across, frequently forming part of a larger reef complex.

PASS
In hydrographic usage, a navigable channel through a bar, REEF, or shoal, or between closely adjacent islands. On the Gulf of Mexico coast, inlets are often known as *passes* (e.g., Sabine Pass).

PEAK PERIOD
The wave period determined by the inverse of the frequency at which the wave energy spectrum reaches its maximum.

PEBBLES
Beach material usually well-rounded and between about 4 mm to 64 mm diameter. See SOIL CLASSIFICATION.

PENINSULA
An elongated body of land nearly surrounded by water and connected to a larger body of land by a neck or isthmus.

PERCHED BEACH
A beach or fillet of sand retained above the otherwise normal profile level by a submerged dike.

PERCOLATION
The process by which water flows through the interstices of a sediment. Specifically, in wave phenomena, the process by which wave action forces water through the interstices of the bottom sediment and which tends to reduce wave heights.

PERIGEAN RANGE
The average semidiurnal range occurring at the time of the PERIGEAN TIDES and most conveniently computed from the harmonic constants. It is larger than the mean range where the type of tide is either semidiurnal or mixed and is of no practical significance where the type of tide is diurnal.

PERIGEAN TIDAL CURRENTS
Tidal currents of increased velocity occurring monthly as the result of the moon being in perigee (i.e., at the point in its orbit nearest the Earth).

PERIGEAN TIDES
Tides of increased range occurring monthly as the result of the moon being in perigee.

PERIODIC CURRENT
A current caused by the tide-producing forces of the moon and the sun; a part of the same general movement of the sea that is manifested in the vertical rise and fall of the tides. See also CURRENT, FLOOD and CURRENT, EBB.

PERMANENT CURRENT
A current that runs continuously, independent of the tides and temporary causes. Permanent currents include the freshwater discharge of a river and the currents that form the general circulatory systems of the oceans.

PERMEABILITY

The property of bulk material (sand, crushed rock, soft rock in situ) which permit movement of water through its pores.

PERMEABLE GROIN

A GROIN with openings or voids large enough to permit passage of appreciable quantities of LITTORAL DRIFT through the structure.

PETROGRAPHY

The systematic description and classification of rocks.

PETROLOGY

That branch of geology which treats the scientific study of rocks.

PHASE

In surface wave motion, a point in the period to which the wave motion has advanced with respect to a given initial reference point.

PHASE INEQUALITY

Variations in the tides or tidal currents associated with changes in the phase of the Moon in relation to the Sun.

PHASE VELOCITY

Propagation velocity of an individual wave as opposed to the velocity of a wave group.

PHI GRADE SCALE

A logarithmic transformation of the Wentworth grade scale for size classifications of sediment grains based on the negative logarithm to the base 2 of the particle diameter: $= -\log_2 d$. See SOIL CLASSIFICATION.

PHOTIC ZONE

The zone extending downward from the ocean surface within which the light is sufficient to sustain photosynthesis. The depth of this layer varies with water clarity, time of year and cloud cover, but is about 100 m in the open ocean. It may be considered the Depth to which all light is filtered out except for about one percent and may be calculated as about two and one-half times the depth of a SECCHI DISK reading.

PHOTOGRAMMETRY

The science of deducing the physical dimensions of objects from measurements on images (usually photographs) of the objects.

PHOTOMOSAIC

An assemblage of photographs, each of which shows part of a region, put together in such a way that each point in the region appears once and only once in the assemblage, and scale variation is minimized.

PHREATIC LEVEL

Upper surface of an unconfined aquifer (e.g. the top sand layer in a dike) at which the pressure in the groundwater is equal to atmospheric pressure.

PHYSICAL GEOLOGY

A large division of Geology concerned with earth materials, changes of the surface and interior of the earth, and the forces that cause those changes.

PHYSICAL MODELING

Refers to the investigation of coastal or riverine processes using a scaled model.

PIER

A structure, usually of open construction, extending out into the water from the shore, to serve as a landing place, recreational facility, etc., rather than to afford coastal protection or affect the movement of water. In the Great Lakes, a term sometimes improperly applied to jetties.

PIERSON-MOSKOWITZ SPECTRUM

Wave spectrum typical of fully-developed deep water waves.

PIEZOMETRIC SURFACE

The level at which the hydrostatic water pressure in an aquifer will stand if it is free to seek equilibrium with the atmosphere. For artesian wells, this is above the ground surface.

PILE

A long, heavy timber or section of concrete or metal that is driven or jetted into the earth or seabed to serve as a support or protection.

PILING

A group of piles.

PIPING

Erosion of closed flow channels (tunnels) by the passage of water through soil; flow underneath structures, carrying away particles, may endanger the stability of the structure.

PLACER DEPOSITS

Mineral deposits consisting of dense, resistant and often economically valuable minerals which have been weathered from TERRIGENOUS rocks, transported to the sea and concentrated in marine sediments by wave or current action.

PLACER MINE

Surface mines in which valuable mineral grains are extracted from stream bar or beach deposits.

PLAIN, COASTAL

See COASTAL PLAIN.

PLANFORM

The outline or shape of a body of water as determined by the still-water line.

PLATEAU

A land area (usually extensive) having a relatively level surface raised sharply above adjacent land on at least one side; table land. A similar undersea feature.

PLEISTOCENE

An epoch of the Quaternary Period characterized by several glacial ages.

PLUNGE POINT

(1) For a plunging wave, the point at which the wave curls over and falls. (2) The final breaking point of the waves just before they rush up on the beach. (See Figure A-1)

PLUNGING BREAKER

See BREAKER.

POCKET BEACH

A beach, usually small, in a coastal reentrant or between two littoral barriers (often rocky headlands).

POINT

(1) The extreme end of a CAPE, or the outer end of any land area protruding into the water, usually less prominent than a CAPE. (2) A low profile shoreline promontory of more or less triangular shape, the top of which extends seaward.

POORLY-SORTED (POORLY-GRADED)

Said of a clastic sediment or rock that consists of particles of many sizes mixed together in an unsystematic manner so that no one size class predominates.

PORE PRESSURE

The interstitial pressure of water within a mass of soil or rock.

POROSITY

Percentage of the total volume of a soil sample not occupied by solid particles but by air and water, $\eta = V_v/V_T \times 100$.

PORT

A place where vessels may discharge or receive cargo; it may be the entire harbor including its approaches and anchorages, or only the commercial part of a harbor where the QUAYS, WHARVES, facilities for transfer of cargo, docks, and repair shops are situated. Protection may be provided by natural or artificial features.

POTENTIAL ENERGY OF WAVES

In a progressive oscillatory wave, the energy resulting from the elevation or depression of the water surface from the undisturbed level.

PRISM

See TIDAL PRISM.

PROBABILITY

The chance that a prescribed event will occur, represented by a number (p) in the range 0 - 1. It can be estimated empirically from the relative frequency (i.e. the number of times the particular event occurs, divided by the total count of all events in the class considered).

PROBABILITY DENSITY

Function specifying the distribution of a variable.

PROBABLE MAXIMUM WATER LEVEL

A hypothetical water level (exclusive of wave runup from normal wind-generated waves) that might result from the most severe combination of hydrometeorological, geoseismic, and other geophysical factors and that is considered reasonably possible in the region involved, with each of these factors considered as affecting the locality in a maximum manner.

This level represents the physical response of a body of water to maximum applied phenomena such as hurricanes, moving squall lines, other cyclonic meteorological events, tsunamis, and astronomical tide combined with maximum probable ambient hydrological conditions such as wave setup, rainfall, runoff, and river flow. It is a water level with virtually no risk of being exceeded.

PRODELTA

The part of a DELTA that is below the effective depth of wave erosion, lying beyond the delta front and sloping down into the basin into which the delta is advancing.

PROFILE, BEACH

The intersection of the ground surface with a vertical plane; typically perpendicular to the local shoreline, and may extend from the behind the DUNE line or the top of a bluff to well seaward of the breaker zone. (See Figure A-1)

PROGRESSION (of a beach)
See ADVANCE.

PROGRESSIVE WAVE
A wave that moves relative to a fixed coordinate system in a fluid. The direction in which it moves is termed the direction of wave propagation.

PROMONTORY
A high point of land projecting into a body of water; a HEADLAND.

PROPAGATION OF WAVES
The transmission of waves through water.

PROTOTYPE
In laboratory usage, the full-scale structure, concept, or phenomenon used as a basis for constructing a scale model or copy.

Q

QUARRY RUN
Waste of generally small material, in a quarry, left after selection of larger grading.

QUARRYSTONE
Any stone processed from a quarry.

QUATERNARY
(1) The youngest geologic period; includes the present time. (2) The latest period of time in the stratigraphic column, 0 – 2 million years, represented by local accumulations of glacial (PLEISTOCENE) and post-glacial (HOLOCENE) deposits which continue, without change of fauna, from the top of the Pliocene (Tertiary). The *quaternary* appears to be an artificial division of time to separate pre-human from post-human sedimentation. As thus defined, the *quaternary* is increasing in duration as man's ancestry becomes better understood.

QUAY (pronounced KEY)
A stretch of paved bank, or a solid artificial landing place parallel to the navigable waterway, for use in loading and unloading vessels.

QUICKSAND
Loose, yielding, wet sand which offers no support to heavy objects. The upward flow of the water has a velocity that eliminates contact pressures between the sand grains and causes the sand-water mass to behave like a fluid that yields easily to pressure and tends to suck down heavy objects.

R

RADAR
An instrument for determining the distance and direction to an object by measuring the time needed for radio signals to travel from the instrument to the object and back, and by measuring the angle through which the instrument's antenna has traveled.

RADIOACTIVE DATING (RADIOMETRIC DATING)
Calculating an age in years for geologic materials by measuring the presence of a short-life radioactive element (e.g., carbon-14) or a long-life element (e.g., potassium-40/argon-40). The term applies to all methods of age determination based on nuclear decay of naturally-occurring radioactive isotopes. Carbon-14 methods are often used to determine the age of peat or wood found in BARRIER ISLANDS.

RADIUS OF MAXIMUM WINDS
Distance from the eye of a hurricane, where surface and wind velocities are zero, to the place where surface windspeeds are maximum.

RAISED BEACH
A wave-cut platform, with or without a covering of beach materials, which is now raised above the present sea-level.

RANDOM WAVES
The laboratory simulation of irregular sea states that occur in nature.

RANGE OF TIDE
The difference in height between consecutive high and low waters. The MEAN RANGE is the difference between MEAN HIGH WATER and MEAN LOW WATER. The GREAT DIURNAL RANGE or DIURNAL RANGE is the difference in height between MEAN HIGHER HIGH WATER (MHHW) and MEAN LOWER LOW WATER (MLLW). Where the type of tide is diurnal, the mean range is the same as the diurnal range.

RAY, WAVE
See ORTHOGONAL.

RAYLEIGH DISTRIBUTION
A model probability distribution, commonly used in analysis of waves.

REACH
(1) An arm of the ocean extending into the land, e.g., an ESTUARY. (2) A straight section of restricted waterway that is uniform with respect to discharge, slope, and cross-section.

RECENT
(Geological) A synonym of HOLOCENE. See also QUATERNARY.

RECESSION
(1) A continuing landward movement of the shoreline. (2) A net landward movement of the shoreline over a specified time.

RECHARGE
The addition of new water to an AQUIFER or to the zone of saturation.

RECTIFICATION
The process of producing, from a tilted or oblique photograph, a photograph from which displacement caused by tilt has been removed.

RECURVED SPIT
A spit whose outer end in turned landward by current deflection, by the opposing action of two or more currents, or by WAVE REFRACTION; a HOOK.

RED TIDE
Discoloration of surface waters, most frequently in COASTAL ZONES, caused by large concentrations of microorganisms.

REEF
An offshore consolidated rock hazard to navigation, with a least depth of about 20 meters (10 fathoms) or less. Often refers to coral FRINGING REEFS in tropical waters.

REEF, ATOLL
See ATOLL.

REEF, BARRIER
See BARRIER REEF.

REEF BREAKWATER
Rubble mound of single-sized stones with a crest at or below sea level which is allowed to be (re)shaped by the waves.

REEF, FRINGING
See FRINGING REEF.

REFERENCE PLANE
The plane to which sounding and tidal data are referred. See DATUM PLANE.

REFERENCE POINT
(1) A specified location (in plan elevation) to which measurements are referred. (2) In beach material studies, a specified point within the REFERENCE ZONE.

REFERENCE STATION
A place for which tidal constants have previously been determined and which is used as a standard for the comparison of simultaneous observations at a second station. Also, a station for which independent daily predictions are given in the tide or current tables from which corresponding predictions are obtained for other stations by means of differences or factors.

REFERENCE ZONE
In regard to beach measuring procedure, the part of the FORESHORE subject to wave action (between the Limit of UPRUSH and the Limit of BACKWASH) at mid-tide stage. In areas of great tidal range a more complex definition is needed.

REFLECTED WAVE
That part of an incident wave that is returned seaward when a wave impinges on a steep beach, barrier, or other reflecting surface.

REFLECTION
The process by which the energy of the wave is returned seaward.

REFRACTION (of water waves)
(1) The process by which the direction of a wave moving in shallow water at an angle to the contours is changed: the part of the wave advancing in shallower water moves more slowly than that part still advancing in deeper water, causing the wave crest to bend toward alinement with the underwater contours. (2) The bending of wave crests by currents. (See Figure II-6-11.)

REFRACTION COEFFICIENT

The square root of the ratio of the distance between adjacent orthogonals in deep water to their distance apart in shallow water at a selected point. When multiplied by the SHOALING FACTOR and a factor for friction and percolation, this becomes the WAVE HEIGHT COEFFICIENT or the ratio of the refracted wave height at any point to the deepwater wave height. Also, the square root of the ENERGY COEFFICIENT.

REFRACTION DIAGRAM

A drawing showing positions of wave crests and/or orthogonals in a given area for a specific deepwater wave period and direction. (See Figure II-6-11.)

REGULAR WAVES

Waves with a single height, period, and direction.

RESERVOIR

An artificial lake, basin or tank in which a large quantity of water can be stored.

RESIDUAL (WATER LEVEL)

The components of water level not attributable to astronomical effects.

RESONANCE

The phenomenon of amplification of a free wave or oscillation of a system by a forced wave or oscillation of exactly equal period. The forced wave may arise from an impressed force upon the system or from a boundary condition.

RETARDATION

The amount of time by which corresponding tidal phases grow later day by day (about 50 minutes).

RETROGRESSION (of a beach)

See RECESSION.

RETURN PERIOD

Average period of time between occurrences of a given event.

REVERSING TIDAL CURRENT

A tidal current that flows alternately in approximately opposite directions with a SLACK WATER at each reversal of direction. Currents of this type usually occur in rivers and straits where the direction of flow is more or less restricted to certain channels. When the movement is towards the shore, the current is said to be flooding, and when in the opposite direction it is said to be ebbing.

REVETMENT

(1) A facing of stone, concrete, etc., to protect an EMBANKMENT, or shore structure, against erosion by wave action or currents. (2) A retaining wall. (3) Facing of stone, concrete, etc., built to protect a SCARP, EMBANKMENT or shore structure against erosion by waves of currents.

REYNOLDS NUMBER

The dimensionless ratio of the inertial force to the viscous force in fluid motion,

$$R_e = \frac{LV}{\gamma}$$

where L is a characteristic length, γ the kinematic viscosity, and V a characteristic velocity. The Reynolds number is of importance in the theory of hydrodynamic stability and the origin of turbulence.

RIA

A long, narrow inlet, with depth gradually diminishing inward. Shorter and shallower than a FJORD.

RIDGE AND RUNNEL

Beach topography consisting of sand bars that have welded to the shore during the recovery stage after a storm. At low tide, water ponds in the runnels and flows seaward through gaps in the ridge (see Figure IV-2-31).

RIDGE, BEACH

A nearly continuous mound of beach material that has been shaped by wave or other action. Ridges may occur singly or as a series of approximately parallel deposits.

RILL MARKS

Tiny drainage channels in a beach caused by the flow seaward of water left in the sands of the upper part of the beach after the retreat of the tide or after the dying down of storm waves.

RIP

A body of water made rough by waves meeting an opposing current, particularly a tidal current; often found where tidal currents are converging and sinking.

RIP CHANNEL

A channel cut by seaward flow of RIP CURRENT, usually crosses a LONGSHORE BAR.

RIP CURRENT

A strong surface current flowing seaward from the shore. It usually appears as a visible band of agitated water and is the return movement of water piled up on the shore by incoming waves and wind. With the seaward movement concentrated in a limited band its velocity is somewhat accentuated. A rip consists of three parts: the FEEDER CURRENTS flowing parallel to the shore inside the breakers; the NECK, where the feeder currents converge and flow through the breakers in a narrow band or "rip"; and the HEAD OF RIP, where the current widens and slackens outside the breaker line. A rip current is often miscalled a rip tide. Also called RIP SURF.

RIP SURF

See RIP CURRENT.

RIP TIDE

Incorrect term for RIP CURRENT.

RIPARIAN

(1) Pertaining to the banks of a body of water. (2) Of, on or pertaining to the banks of a river.

RIPPLE

(1) The ruffling of the surface of water; hence, a little curling wave or undulation. (2) A wave less than 0.05 meter (2 inches) long controlled to a significant degree by both surface tension and gravity. See CAPILLARY WAVE and GRAVITY WAVE.

RIPPLE MARKS

Undulations produced by fluid movement over sediments. Oscillatory currents produce symmetric ripples whereas a well-defined current direction produces asymmetrical ripples. The crest line of ripples may be straight or sinuous. The characteristic features of ripples depend upon current velocity, particle size, persistence of current direction and whether the fluid is air or water. Sand DUNES may be regarded as a special kind of ‘super’-ripple.

RIPPLES (bed forms)

Small bed forms with wavelengths less than 0.3 m (1 foot) and heights less than 0.03 m (0.1 foot).

RIPRAP

A protective layer or facing of quarrystone, usually well graded within wide size limit, randomly placed to prevent erosion, scour, or sloughing of an embankment or bluff; also the stone so used. The quarrystone is placed in a layer at least twice the thickness of the 50 percent size, or 1.25 times the thickness of the largest size stone in the gradation.

RISK ANALYSIS

Assessment of the total risk due to all possible environmental inputs and all possible mechanisms.

ROADSTEAD

An area of the sea used for anchorage of vessels and transhipment of cargo, usually without the protection from weather associated with harbors.

ROCK WEATHERING

Physical and mineralogical decay processes in rock brought about by exposure to climatic conditions either at the present time or in the geological past.

ROCK

(1) An aggregate of one or more minerals; or a body of undifferentiated mineral matter (e.g., obsidian). The three classes of rocks are: (a) Igneous – crystalline rocks formed from molten material. Examples are granite and basalt. (b) Sedimentary – resulting from the consolidation of loose sediment that has accumulated in layers. Examples are sandstone, shale and limestone. (c) Metamorphic – formed from preexisting rock as a result of burial, heat, and pressure. (2) A rocky mass lying at or near the surface of the water or along a jagged coastline, especially where dangerous to shipping.

ROLLER

An indefinite term, sometimes considered to denote one of a series of long-crested, large waves which roll in on a shore, as after a storm.

ROTARY CURRENT, TIDAL

A tidal current that flows continually with the direction of flow changing through all points of the compass during the tidal period. Rotary currents are usually found offshore where the direction of flow is not restricted by any barriers. The tendency for the rotation in direction has its origin in the deflecting force of the earth's rotation and, unless modified by local conditions, the change is clockwise in the Northern Hemisphere and counterclockwise in the Southern Hemisphere. The velocity of the current usually varies throughout the tidal cycle, passing through two maxima in approximately opposite directions and two minima with the direction of the current at approximately ninety degrees from the direction at the time of maximum velocity.

RUBBLE

(1) Loose angular waterworn stones along a beach. (2) Rough, irregular fragments of broken rock.

RUBBLE-MOUND STRUCTURE

A mound of random-shaped and random-placed stones protected with a cover layer of selected stones or specially shaped concrete armor units. (Armor units in a primary cover layer may be placed in an orderly manner or dumped at random.)

RUNUP, RUNDOWN

The upper and lower levels reached by a wave on a beach or coastal structure, relative to still-water level.

RUNNEL

A corrugation or trough formed in the FORESHORE or in the bottom just offshore by waves or tidal currents (see RIDGE and RUNNEL).

S

S-SLOPE BREAKWATER
Rubble mound with gentle slope around still-water level and steeper slopes above and below.

SALIENT
A bulge in the coastline projecting towards an offshore island or breakwater, but not connected to it as in the case of a TOMBOLO - see also Ness and Cusp. Developed by WAVE REFRACTION and diffraction and long shore drift.

SALINITY
Number of grams of salt per thousand grams of sea water, usually expressed in parts per thousand (symbol: ‰).

SALINITY GRADIENT
Change in salinity with expressed in parts per thousand per foot.

SALT MARSH
A marsh periodically flooded by salt water (also *tidal marsh*; *sea marsh*).

SALT-WEDGE ESTUARY
In this circulation type, the density-driven component dominates and two well-mixed layers are separated by a sharp HALOCLINE. The seawater entering the channel appears as a tongue or wedge.

SALTATION
That method of sand movement in a fluid in which individual particles leave the bed by bounding nearly vertically and, because the motion of the fluid is not strong or turbulent enough to retain them in suspension, return to the bed at some distance downstream. The travel path of the particles is a series of hops and bounds.

SAND
Sediment particles, often largely composed of quartz, with a diameter of between 0.062 mm and 2 mm, generally classified as fine, medium, coarse or very coarse. Beach sand may sometimes be composed of organic sediments such as calcareous reef debris or shell fragments.

SAND BAR
(1) See BAR. (2) In a river, a ridge of sand built to or near the surface by river currents.

SAND BYPASSING
See BYPASSING, SAND.

SAND DUNE
A DUNE formed of sand.

SAND REEF
See BAR.

SAND SPIT
A narrow sand EMBANKMENT, created by an excess of deposition at its seaward terminus, with its distal end (the end away from the point of origin) terminating in open water.

SAND WAVES
(1) Longshore sand waves are large-scale features that maintain form while migrating along the shore with speeds on the order of kilometers per year. (2) Large-scale asymmetrical bedforms in sandy river beds having high length to height ratios and continuous crestlines.

SCARP, BEACH

An almost vertical slope along the beach caused by erosion by wave action. It may vary in height from a few cm to a meter or so, depending on wave action and the nature and composition of the beach. (See Figure A-1) See also ESCARPMENT.

SCATTER DIAGRAM

A two-dimensional histogram showing the joint probability density of two variables within a data sample.

SCOUR

Removal of underwater material by waves and currents, especially at the base or toe of a shore structure.

SCOUR PROTECTION

Protection against erosion of the seabed in front of the toe.

SEA

(1) A large body of salt water, second in rank to an ocean, more or less landlocked and generally part of, or connected with, an ocean or a larger sea. Examples: Mediterranean Sea; South China Sea. (2) Waves caused by wind at the place and time of observation. (3) State of the ocean or lake surface, in regard to waves.

SEA BREEZE

A light wind blowing from the sea toward the land caused by unequal heating of land and water masses.

SEA CHANGE

(1) A change wrought by the sea. (2) A marked transformation.

SEA CLIFF

A cliff situated at the seaward edge of the coast.

SEA GRASS

Members of marine seed plants that grow chiefly on sand or sand-mud bottom. They are most abundant in water less than 9 m deep. The common types are: Eel grass (*Zostera*), Turtle grass (*Thallasia*), and Manatee grass (*Syringodium*).

SEA LEVEL

See MEAN SEA LEVEL.

SEA LEVEL RISE

The long-term trend in MEAN SEA LEVEL.

SEA PUSS

A dangerous longshore current; a rip current caused by return flow; loosely, the submerged channel or inlet through a bar caused by those currents.

SEA STATE

Description of the sea surface with regard to wave action. Also called state of sea.

SEACOAST

The coast adjacent to the sea or ocean.

SEAMOUNT

An elevation rising more than 1000 meters above the ocean floor, and of limited extent across the summit. Compare KNOLL.

SEAS

Waves caused by wind at the place and time of observation.

SEASHORE

(1) (Law) All ground between the ordinary high-water and low-water mark. (2) The shore of the sea or ocean, often used in a general sense (e.g., to visit the seashore).

SEAWALL

(1) A structure, often concrete or stone, built along a portion of a coast to prevent erosion and other damage by wave action. Often it retains earth against its shoreward face. (2) A structure separating land and water areas to alleviate the risk of flooding by the sea. Generally shore-parallel, although some reclamation SEAWALLS may include lengths that are normal or oblique to the (original) shoreline. A SEAWALL is typically more massive and capable of resisting greater wave forces than a BULKHEAD.

SECHHI DISK

Visibility disk (white and black, 30 cm diameter) used to measure the transparency of the water

SEDIMENT

(1) Loose, fragments of rocks, minerals or organic material which are transported from their source for varying distances and deposited by air, wind, ice and water. Other sediments are precipitated from the overlying water or form chemically, in place. Sediment includes all the unconsolidated materials on the sea floor. (2) The fine grained material deposited by water or wind.

SEDIMENT CELL

In the context of a strategic approach to coastal management, a length of coastline in which interruptions to the movement of sand or shingle along the beaches or near shore sea bed do not significantly affect beaches in the adjacent lengths of coastline.

SEDIMENT SINK

Point or area at which beach material is irretrievably lost from a coastal cell, such as an estuary, or a deep channel in the seabed.

SEDIMENT SOURCE

Point or area on a coast from which beach material is supplied, such as an eroding cliff, or river mouth.

SEDIMENT TRANSPORT

The main agencies by which sedimentary materials are moved are: gravity (gravity transport); running water (rivers and streams); ice (glaciers); wind; the sea (currents and LONGSHORE DRIFT). Running water and wind are the most widespread transporting agents. In both cases, three mechanisms operate, although the particle size of the transported material involved is very different, owing to the differences in density and viscosity of air and water. The three processes are: rolling or traction, in which the particle moves along the bed but is too heavy to be lifted from it; SALTATION; and suspension, in which particles remain permanently above the bed, sustained there by the turbulent flow of the air or water.

SEDIMENT TRANSPORT PATHS

The routes along which net sediment movement occurs.

SEEPAGE

The movement of water through small cracks, pores, interstices, out of a body of surface of subsurface water. The loss of water by infiltration from a canal, reservoir or other body of water or from a field. It is generally expressed as flow volume per unit of time.

SEICHE

(1) A standing wave oscillation of an enclosed waterbody that continues, pendulum fashion, after the cessation of the originating force, which may have been either seismic or atmospheric. (2) An oscillation of a fluid body in response to a disturbing force having the same frequency as the natural frequency of the fluid system. Tides are now considered to be seiches induced primarily by the periodic forces caused by the Sun and Moon. (3) In the Great Lakes area, any sudden rise in the water of a harbor or a lake whether or not it is oscillatory (although inaccurate in a strict sense, this usage is well established in the Great Lakes area).

SEISMIC REFLECTION

The return of part of the energy of seismic waves to the earth's surface after the waves bounce off an acoustic boundary (typically rock or material of different density).

SEISMIC REFRACTION

The bending of seismic waves as they pass from one material to another.

SEISMIC SEA WAVE

See TSUNAMI.

SELECTIVE SORTING

A process occurring during sediment transport that tends to separate particles according to their size, density, and shape. A *well-sorted distribution* contains a limited range of grain sizes and usually indicates that the depositional environment contains a narrow range of sediment sizes or a narrow band of depositional energy. A *poorly-sorted distribution* contains a wide range of grain sizes indicating multiple sources of sediment or a wide range of deposition energies.

SELF-SUSTAINING BEACH

A BEACH that has either natural or engineered sand retention and that can be stable through the continued supply of natural sediment sources, without any mechanical nourishment over a long period. Subsets include:

Natural or Geomorphically Self-sustaining Beaches: self-sustaining naturally without the construction of retaining structures and with no continued mechanical sand nourishment.

Anthropogenically Self-sustaining Beaches: self-sustaining by the construction of retaining structure(s) with or without initial beach fill but with no continued mechanical sand nourishment.

SEMIDIURNAL

Having a period or cycle of approximately one-half of a tidal day (12.4 hours). The predominating type of tide throughout the world is semidiurnal, with two high waters and two low waters each tidal day. The tidal current is said to be semidiurnal when there are two flood and two ebb periods each day.

SENSING, REMOTE

The response of an instrument or organism to stimuli from a distant source.

SETBACK

A required open space, specified in shoreline master programs, measured horizontally upland from an perpendicular to the ordinary high water mark.

SETUP, WAVE

Superelevation of the water surface over normal surge elevation due to onshore mass transport of the water by wave action alone.

SETUP, WIND

See WIND SETUP.

SHALLOW WATER

(1) Commonly, water of such a depth that surface waves are noticeably affected by bottom topography. It is customary to consider water of depths less than one-half the surface wavelength as shallow water. See TRANSITIONAL ZONE and DEEP WATER. (2) More strictly, in hydrodynamics with regard to progressive gravity waves, water in which the depth is less than 1/25 the wavelength.

SHALLOW WATER WAVE

A PROGRESSIVE WAVE which is in water less than 1/25 the wave length in depth.

SHEAR INSTABILITIES

Instabilities of the surf zone longshore current commonly found on beaches with barred depth profiles. These instabilities are vertical motions with little surface elevation expression. Conservation of vorticity is the restoring mechanism.

SHEAR WAVES

See SHEAR INSTABILITIES

SHEET EROSION

The removal of a thin layer of surface material, usually topsoil, by a flowing sheet of water.

SHEET FLOW

Sediment grains under high sheer stress moving as a layer that extends from the bed surface to some distance below (on the order of a few cm). Grains are transported in the direction of fluid flow.

SHEET PILE

See PILE, SHEET.

SHEET, SMOOTH

A sheet on which field control and hydrographic data such as soundings, depth curves, and regions surveyed with a wire drag are plotted before the production of a final chart.

SHELF, CONTINENTAL

See CONTINENTAL SHELF.

SHELF, INSULAR

See INSULAR SHELF.

SHINGLE

(1) Loosely and commonly, any beach material coarser than ordinary gravel, especially any having flat or flattish pebbles. (2) Strictly and accurately, beach material of smooth, well-rounded pebbles that are roughly the same size. The spaces between pebbles are not filled with finer materials. Shingle often gives out a musical sound when stepped on. The term is more widely used in Great Britain than in the United States.

SHOAL

(1) (noun) A detached area of any material except rock or coral. The depths over it are a danger to surface navigation. Similar continental or insular shelf features of greater depths are usually termed BANKS. (2) (verb) To become shallow gradually. (3) To cause to become shallow. (4) To proceed from a greater to a lesser depth of water.

SHOALING

Decrease in water depth. The transformation of wave profile as they propagate inshore.

SHOALING COEFFICIENT

The ratio of the height of a wave in water of any depth to its height in deep water with the effects of refraction, friction, and percolation eliminated. Sometimes SHOALING FACTOR or DEPTH FACTOR. See also ENERGY COEFFICIENT and REFRACTION COEFFICIENT.

SHOALING FACTOR

See SHOALING COEFFICIENT.

SHORE

The narrow strip of land in immediate contact with the sea, including the zone between high and low water lines. A shore of unconsolidated material is usually called a BEACH. (See Figure A-1). Also used in a general sense to mean the coastal area (e.g., to live at the shore). Also sometimes known as the LITTORAL.

SHORE NORMAL

A line at right-angles to the contours in the surf zone.

SHORE TERRACE

A terrace made along a COAST by the action of waves and shore currents; it may become dry land by the uplifting of the shore or the lowering of the water. Also known as *shore platform* or *wave-cut platform*.

SHOREFACE

The narrow zone seaward from the low tide SHORELINE, covered by water, over which the beach sands and gravels actively oscillate with changing wave conditions. See INSHORE (ZONE). (See Figure A-1)

SHORELINE

The intersection of a specified plane of water with the shore or beach (e.g., the high water shoreline would be the intersection of the plane of mean high water with the shore or beach). The line delineating the shoreline on National Ocean Service nautical charts and surveys approximates the mean high water line (United States).

SHORELINE MANAGEMENT

The development of strategic, long-term and sustainable coastal defense and land-use policy within a sediment cell.

SHORT-CRESTED WAVE

A wave, the crest length of which is of the same order of magnitude as the wave length. A system of short-crested waves has the appearance of hills being separated by troughs.

SIGNIFICANT WAVE

A statistical term relating to the one-third highest waves of a given wave group and defined by the average of their heights and periods. The composition of the higher waves depends upon the extent to which the lower waves are considered. Experience indicates that a careful observer who attempts to establish the character of the higher waves will record values which approximately fit the definition of the significant wave.

SIGNIFICANT WAVE HEIGHT

The average height of the one-third highest waves of a given wave group. Note that the composition of the highest waves depends upon the extent to which the lower waves are considered. In wave record analysis, the average height of the highest one-third of a selected number of waves, this number being determined by dividing the time of record by the significant period. Also CHARACTERISTIC WAVE HEIGHT.

SIGNIFICANT WAVE PERIOD

An arbitrary period generally taken as the period of the one-third highest waves within a given group. Note that the composition of the highest waves depends upon the extent to which the lower waves are considered. In wave record analysis, this is determined as the average period of the most frequently recurring of the larger well-defined waves in the record under study.

SILL

(1) A submerged structure across a river to control the water level upstream. (2) The crest of a spillway.

SILT

Sediment particles with a grain size between 0.004 mm and 0.062 mm, i.e. coarser than clay particles but finer than sand. See SOIL CLASSIFICATION.

SINUSOIDAL WAVE

An oscillatory wave having the form of a sinusoid.

SLACK TIDE (SLACK WATER)

The state of a tidal current when its velocity is near zero, especially the moment when a reversing current changes direction and its velocity is zero. Sometimes considered the intermediate period between ebb and flood currents during which the velocity of the currents is less than 0.05 meter per second (0.1 knot). See STAND OF TIDE.

SLIDE

In mass wasting, movement of a descending mass along a plane approximately parallel to the slope of the surface.

SLIP

A berthing space between two piers.

SLIP FACE

The steep, downwind slope of a DUNE; formed from loose, cascading sand that generally keeps the slope at the ANGLE OF REPOSE (about 34 deg.).

SLOPE

The degree of inclination to the horizontal. Usually expressed as a ratio, such as 1:25, indicating one unit rise in 25 units of horizontal distance; or in a decimal fraction (0.04). Also called GRADIENT.

SLOUGH

A small muddy marshland or tidal waterway which usually connects other tidal areas. See BAYOU.

SLUICE

A structure containing a gate to control the flow of water from one area to another.

SLUMP

In mass wasting, movement along a curved surface in which the upper part moves vertically downward while the lower part moves outward.

SOFT DEFENSES

Usually refers to beaches (natural or designed) but may also relate to energy-absorbing beach-control structures, including those constructed of rock, where these are used to control or redirect coastal processes rather than opposing or preventing them.

SOIL

A layer of weathered, unconsolidated material on top of bed rock; in geologic usage, usually defined as containing organic matter and being capable of supporting plant growth.

SOIL CLASSIFICATION (size)

An arbitrary division of a continuous scale of grain sizes such that each scale unit or grade may serve as a convenient class interval for conducting the analysis or for expressing the results of an analysis. There are many classifications used (see Table III-1-2).

SOLITARY WAVE

A wave consisting of a single elevation (above the original water surface), whose height is not necessarily small compared to the depth, and neither followed nor preceded by another elevation or depression of the water surfaces.

SORTING

Process of selection and separation of sediment grains according to their grain size (or grain shape or specific gravity).

SORTING COEFFICIENT

A coefficient used in describing the distribution of grain sizes in a sample of unconsolidated material. It is defined as $S_o = Q1/Q3$, where Q1 is the diameter (in millimeters) which has 75 percent of the cumulative size-frequency (by weight) distribution smaller than itself and 25 percent larger than itself, and Q3 is that diameter having 25 percent smaller and 75 percent larger than itself.

SOUND

(1) (noun) a relatively long arm of the sea or ocean forming a channel between an island and a mainland or connecting two larger bodies, as a sea and the ocean, or two parts of the same body; usually wider and more extensive than a STRAIT (e.g., Long Island Sound). (2) (verb) To measure the depth of the water.

SOUNDING

A measured depth of water. On hydrographic CHARTS the soundings are adjusted to a specific plane of reference (SOUNDING DATUM).

SOUNDING DATUM

The plane to which soundings are referred. See also CHART DATUM.

SOUNDING LINE

A line, wire, or cord used in sounding, which is weighted at one end with a plummet (sounding lead). Also LEAD LINE.

SPECIFIC GRAVITY

The ratio of the weight of unit volume of any material to the weight of unit volume of water at 4° C, $G_s = \gamma_s/\gamma_w$. Typical values of G_s for soil solids are 2.65 to 2.72.

SPILLING BREAKER

See BREAKER.

SPILLOVER LOBE

Linguoid, bar-like feature formed by ebb tidal current flow over a low area of an ebb shield.

SPILLWAY

A structure over or through a dam for discharging flood flows.

SPIT

A small point of land or a narrow shoal projecting into a body of water from the shore. (See Figure IV-1-6.)

SPOIL

Overburden or other waste material removed in mining, dredging, and quarrying.

SPOIL BANK

Artificial formation created by the deposit of dredged materials on the seabed.

SPRING RANGE

The average SEMIDIURNAL range occurring at the time of SPRING TIDES and most conveniently computed from the harmonic constants. It is larger than the MEAN RANGE where the type of tide is either SEMIDIURNAL or MIXED, and is of no practical significance where the type of tide is DIURNAL.

SPRING TIDAL CURRENTS

Tidal currents of increased velocity occurring semi-monthly as the result of the moon being new or full.

SPRING TIDE

A tide that occurs at or near the time of new or full moon (SYZYGY) and which rises highest and falls lowest from the mean sea level.

SPUR-DIKE

See GROIN.

STACK

An isolated, pillar-like rocky island isolated from a nearby headland by wave erosion; a *needle* or *chimney rock*.

STAND OF TIDE

A interval at high or low water when there is no sensible change in the height of the tide. The water level is stationary at high and low water for only an instant, but the change in level near these times is so slow that it is not usually perceptible. See SLACK TIDE.

STANDARD PROJECT HURRICANE

See HYPOTHETICAL HURRICANE.

STANDING WAVE

A type of wave in which the surface of the water oscillates vertically between fixed points, called nodes, without progression. The points of maximum vertical rise and fall are called antinodes or loops. At the nodes, the underlying water particles exhibit no vertical motion, but maximum horizontal motion. At the antinodes, the underlying water particles have no horizontal motion, but maximum vertical motion. They may be the result of two equal progressive wave trains traveling through each other in opposite directions. Sometimes called CLAPOTIS or STATIONARY WAVE.

STATION, CONTROL

A point on the ground whose horizontal or vertical location is used as a basis for obtaining locations of other points.

STATIONARY WAVE

A wave of essentially stable form which does not move with respect to a selected reference point; a fixed swelling. Sometimes called STANDING WAVE.

STEP

The nearly horizontal section which more or less divides the BEACH from the SHOREFACE.

STILL-WATER LEVEL (SWL)

The surface of the water if all wave and wind action were to cease. In deep water this level approximates the midpoint of the wave height. In shallow water it is nearer to the trough than the crest. Also called the UNDISTURBED WATER LEVEL.

STOCHASTIC

Having random variation in statistics.

STOCKPILE

Sand piled on a beach foreshore to nourish downdrift beaches by natural littoral currents or forces. See FEEDER BEACH.

STONE
Quarried or artificially-broken rock for use in construction, either as aggregate or cut into shaped blocks as dimension stone.

STONE, DERRICK
Stone heavy enough to require handling individual pieces by mechanical means, generally weighing 900 kg (1 ton) and up.

STORM SURGE
A rise above normal water level on the open coast due to the action of wind stress on the water surface. Storm surge resulting from a hurricane also includes that rise in level due to atmospheric pressure reduction as well as that due to wind stress. See WIND SETUP.

STORM TIDE
See STORM SURGE.

STRAIT
A relatively narrow waterway between two larger bodies of water (e.g., *Strait* of Gibraltar). See also SOUND.

STRAND
(1) The shore or beach of the ocean or a large lake. The land bordering any large body of water, especially a sea or an arm of the ocean. (2) WHARF, QUAY, or roadway along a water body, esp. in a city, sometimes known as a bund.

STRAND PLAIN
A prograded shore built seawards by waves and currents.

STRANDFLAT
A wave-cut platform; an elevated wave-cut terrace

STRANDING
The running aground of a ship upon a STRAND, ROCK, or bottom so that it is fast for a time.

STRANDLINE
An accumulation of debris (e.g. seaweed, driftwood and litter) cast up onto a beach, and lying along the limit of wave up rush. A shoreline above the present water level

STREAM
(1) A course of water flowing along a bed in the Earth. (2) A current in the sea formed by wind action, water density differences, etc.; e.g. the Gulf Stream. See also CURRENT, STREAM.

STREAM CURRENT
A narrow, deep and swift ocean current, such as the Gulf Stream. Opposite of DRIFT CURRENT.

STRUCTURAL GEOLOGY
The branch of geology concerned with the internal structure of bed rock and the shapes, arrangement, and interrelationships of rock units.

SUBAERIAL
Situated or occurring on or adjacent to the surface of the earth, usually meaning above the water surface.

SUBAERIAL BEACH
That part of the beach which is uncovered by water (e.g. at low tide sometimes referred to as drying beach).

SUBAQUEOUS
Existing, formed, or taking place under water; submerged

SUB-TIDAL BEACH
The part or the beach (where it exists) which extends from low water out to the approximate limit of storm erosion. The latter is typically located at a maximum water depth of 8 to 10 meters and is often identifiable on surveys by a break in the slope of the bed.

SUBCRITICAL FLOW
Flow for which the Froude number is less than unity; surface disturbances can travel upstream.

SUBDUCTION ZONE
Elongate region in which the sea floor slides beneath a continent or island arc.

SUBMARINE CANYON
V-shaped valleys that run across the CONTINENTAL SHELF and down the CONTINENTAL SLOPE.

SUBMERGENT COAST
A COAST in which formerly dry land has been recently drowned, either by land subsidence or a rise in sea level.

SUBORDINATE STATION
A tide or current station at which a short series of observations has been obtained, which is to be reduced by comparison with simultaneous observations at another station having well-determined tidal or current constants.

SUBSIDENCE
Sinking or downwarping of a part of the earth's surface.

SUBMERGED LANDS ACT
United States federal legislation that granted to the coastal states federal rights to natural resources within 3 nautical miles (up to 9 miles for Texas and the Gulf coast of Florida) of the COASTLINE).

SUBTIDAL
Below the low-water datum; thus permanently submerged.

SUPER-CRITICAL FLOW
Flow for which the Froude number is greater than unity; surface disturbances will not travel upstream.

SURF
(1) Collective term for BREAKERS. (2) The wave activity in the area between the shoreline and the outermost limit of breakers. (3) In literature, the term *surf* usually refers to the breaking waves on shore and on reefs when accompanied by a roaring noise caused by the larger waves breaking.

SURF BEAT
Irregular oscillations of the nearshore water level with periods on the order of several minutes.

SURF ZONE
The zone of wave action extending from the water line (which varies with tide, surge, set-up, etc.) out to the most seaward point of the zone (breaker zone) at which waves approaching the coastline commence breaking, typically in water depths of between 5 to 10 meters.

SURFACE GRAVITY WAVE (PROGRESSIVE)
(1) this is the term which applies to the WIND WAVES and SWELL of lakes and oceans, also called SURFACE WATER WAVE, SURFACE WAVE or DEEP WATER WAVE, (2) a progressive GRAVITY WAVE in which the disturbance is confined to the upper limits of a body of water. Strictly speaking this term applies to those progressive GRAVITY WAVES whose celerity depends only upon the wave length.

SURFACE WATER WAVE
See SURFACE GRAVITY WAVE (PROGRESSIVE).

SURGE
(1) The name applied to wave motion with a period intermediate between that of the ordinary wind wave and that of the tide, say from ½ to 60 min. It is low height, usually less than 0.9 m (3 ft). See also SEICHE. (2) In fluid flow, long interval variations in velocity and pressure, not necessarily periodic, perhaps even transient in nature. (3) see STORM SURGE.

SURGING BREAKER
See BREAKER.

SURVEY, CONTROL
A survey that provides coordinates (horizontal or vertical) of points to which supplementary surveys are adjusted.

SURVEY, HYDROGRAPHIC
A survey that has as its principal purpose the determination of geometric and dynamic characteristics of bodies of water.

SURVEY, PHOTOGRAMMETRIC
A survey in which monuments are placed at points that have been determined photogrammetrically.

SURVEY, TOPOGRAPHIC
A survey which has, for its major purpose, the determination of the configuration (relief) of the surface of the land and the location of natural and artificial objects thereon.

SUSPENDED LOAD
(1) The material moving in suspension in a fluid, kept up by the upward components of the turbulent currents or by colloidal suspension. (2) The material collected in or computed from samples collected with a SUSPENDED LOAD SAMPLER. Where it is necessary to distinguish between the two meanings given above, the first one may be called the "true suspended load."

SUSPENDED LOAD SAMPLER
A sampler which attempts to secure a sample of the water with its sediment load without separating the sediment from the water.

SUSTAINABLE BEACH
A beach area that is now and will continue to receive sufficient sediment input over a long period (years or decades) to remain stable. Such sediment input can be through either natural supplies of sediment or various forms of mechanical beach nourishment (placement by hydraulic dredge, land haul of material, nearshore deposition, etc.)

SWALE
The depression between two beach ridges.

SWASH
The rush of water up onto the beach face following the breaking of a wave. Also UPRUSH, RUNUP.

SWASH BARS

Low broad sandy bars formed by sediment in the surf and swash zones, separated by linear depressions, or RUNNELS, running parallel to the shore. Sand bodies that form and migrate across ebb-tidal shoals because of currents generated by breaking waves.

SWASH CHANNEL

(1) On the open shore, a channel cut by flowing water in its return to the present body (e.g., a rip channel). (2) A secondary channel passing through or shoreward of an inlet or river bar.

SWASH MARK

The thin wavy line of fine sand, mica scales, bits of seaweed, etc., left by the uprush when it recedes from its upward limit of movement on the beach face.

SWASH PLATFORM

Sand sheet located between the main ebb channel of a coastal inlet and an adjacent barrier island.

SWASH ZONE

The zone of wave action on the beach, which moves as water levels vary, extending from the limit of run-down to the limit of run-up.

SWELL

Wind-generated waves that have traveled out of their generating area. Swell characteristically exhibits a more regular and longer period and has flatter crests than waves within their fetch (SEAS).

SYNOPTIC CHART

A chart showing the distribution of meteorological conditions over a given area at a given time. Popularly called a weather map.

SYZYGY

The two points in the Moon's orbit when the Moon is in conjunction or opposition to the Sun relative to the Earth; time of new or full Moon in the cycle of phases.

T

T-GROIN
A GROIN built in the shape of a letter "T" with the trunk section connected to land.

TECTONIC FORCES
Forces generated from within the earth that result in uplift, movement, or deformation of part of the earth's crust.

TECTONICS
The study of the major structural features of the Earth's crust or the broad structure of a region.

TERMINAL GROIN
A GROIN, often at the end of a littoral cell or at the UPDRIFT side of an inlet, intended to prevent sediment passage into the channel beyond.

TERRACE
A horizontal or nearly horizontal natural or artificial topographic feature interrupting a steeper slope, sometimes occurring in a series.

TERRIGENOUS SEDIMENTS
Literally 'land-formed' sediment that has found its way to the sea floor. The term is applied (a) to sediments formed and deposited on land (e.g., soils, sand DUNES), and (b) to material derived from the land when mixed in with purely marine material (e.g., sand or clay in a shelly limestone).

TERRITORIAL SEA
The offshore belt in which a coastal state has exclusive jurisdiction. The territorial sea may not extend more than 12 NAUTICAL MILES from the COASTLINE.

TETRAPOD
Concrete armor unit with four stubby legs, used on breakwaters and seawalls to dissipate wave energy.

THALWEG
In hydraulics, the line joining the deepest points of an inlet or stream channel. Often serving as the boundary between two states.

THRESHOLD OF MOTION
The point at which the forces imposed on a sediment particle overcome its inertia and it starts to move.

THRESHOLD VELOCITY
The maximum orbital velocity at which the sediment on the BED begins to move as waves approach shallow water.

TIDAL CREEK
A creek draining back-barrier areas with a current generated by the rise and fall of the tide.

TIDAL CURRENT
See CURRENT, TIDAL.

TIDAL DATUM
See CHART DATUM and DATUM PLANE.

TIDAL DAY
The time of the rotation of the Earth with respect to the Moon, or the interval between two successive upper transits of the Moon over the meridian of a place, approximately 24.84 solar hours (24 hours and 50 minutes) or 1.035 times the mean solar day. (See Figure II-5-16.) Also called lunar day.

TIDAL DELTA
See DELTA.

TIDAL FLATS
(1) Marshy or muddy areas covered and uncovered by the rise and fall of the tide. A TIDAL MARSH. (2) Marshy or muddy areas of the seabed which are covered and uncovered by the rise and fall of tidal water.

TIDAL INLET
(1) A natural inlet maintained by tidal flow. (2) Loosely, any inlet in which the tide ebbs and flows. Also TIDAL OUTLET.

TIDAL MARSH
Same as TIDAL FLATS.

TIDAL PERIOD
The interval of time between two consecutive, like phases of the TIDE. (See Figure II-5-16.)

TIDAL POOL
A pool of water remaining on a beach or reef after recession of the TIDE.

TIDAL PRISM
(1) The total amount of water that flows into a harbor or out again with movement of the tide, excluding any fresh water flow. (2) The volume of water present between MEAN LOW and MEAN HIGH TIDE.

TIDAL RANGE
The difference in height between consecutive high and low (or HIGHER HIGH and LOWER LOW) waters. (See Figure II-5-16.)

TIDAL RISE
The height of tide as referred to the datum of a chart. (See Figure II-5-16.)

TIDAL RIVER
That part of a river where the water level is influenced by the tide.

TIDAL SHOALS
Shoals that accumulate near inlets due to the transport of sediments by tidal currents associated with the INLET.

TIDAL STAND
An interval at high or low water when there is no observable change in the height of the tide. The water level is stationary at high and low water for only an instant, but the change in level near these times is so slow that it is not usually perceptible.

TIDAL WAVE
(1) The wave motion of the tides. (2) In popular usage, any unusually high and destructive water level along a shore, usually referring to STORM SURGE or TSUNAMI, which are not tidal phenomena at all.

TIDALLY DRIVEN CIRCULATION
The movement of fresh water and seawater that are mixed by the sloshing back and forth of the ESTUARY in response to ocean tides.

TIDE

The periodic rising and falling of the water that results from gravitational attraction of the Moon and Sun and other astronomical bodies acting upon the rotating Earth. Although the accompanying horizontal movement of the water resulting from the same cause is also sometimes called the tide, it is preferable to designate the latter as TIDAL CURRENT, reserving the name TIDE for the vertical movement.

TIDE, DAILY RETARDATION OF

The amount of time by which corresponding tides grow later day by day (about 50 minutes). Also LAGGING.

TIDE, DIURNAL

A tide with one high water and one low water in a day. (See Figure II-5-16)

TIDE, EBB

See EBB TIDE.

TIDE, FLOOD

See FLOOD TIDE.

TIDE, MIXED

See MIXED TIDE.

TIDE, NEAP

See NEAP TIDE.

TIDE, SEMIDIURNAL

See SEMIDIURNAL TIDE.

TIDE, SLACK

See SLACK TIDE.

TIDE, SPRING

See SPRING TIDE.

TIDE STAFF

A tide gage consisting of a vertical graduated staff from which the height of the tide can be read directly. It is called a fixed staff when it is secured in place so that it cannot be easily removed. A portable staff is designed for removal from the water when not in use.

TIDE STATION

A place at which tide observations are being taken. It is called a primary tide station when continuous observations are to be taken over a number of years to obtain basic tidal data for the locality. A secondary tide station is one operated over a short period of time to obtain data for a specific purpose.

TIDE, STORM

See STORM SURGE.

TIDE TABLES

Tables which give daily predictions of the times and heights of the tide. These predictions are usually supplemented by tidal differences and constants by means of which additional predictions can be obtained for numerous other places.

TIDE, WIND

See WIND TIDE.

TIDELANDS

The zone between the MEAN HIGH WATER line and the MEAN LOW WATER line, commonly referred to as the BEACH. Waters above the tidelands are inland, being landward of the COAST LINE.

TIDES, RIP

See RIP.

TOE

Lowest part of sea- and portside BREAKWATER slope, generally forming the transition to the seabed..

TOMBOLO

A bar or spit that connects an island to the mainland or to another island. See CUSPATE SPIT. (See Figure IV-1-6.). Also applied to sand accumulation between land and a DETACHED BREAKWATER.

TONGUE

A long narrow strip of land, projecting into a body of water.

TOPOGRAPHIC MAP

A map on which elevations are shown by means of contour lines.

TOPOGRAPHY

The configuration of a surface, including its relief and the positions of its streams, roads, building, etc.

TRAINING WALL

A wall or jetty to direct current flow.

TRANSGRESSION, MARINE

The invasion of a large area of land by the sea in a relatively short space of time (geologically speaking). Although the observable result of a marine transgression may suggest an almost 'instantaneous' process, it is probable that the time taken is in reality is thousands or millions of years. The plane of marine transgression is a plane of UNCONFORMITY.

TRANSITIONAL ZONE (TRANSITIONAL WATER)

In regard to progressive gravity waves, water whose depth is less than ½ but more than 1/25 the wavelength. Often called shallow water.

TRANSLATORY WAVE

See WAVE OF TRANSLATION.

TRANSPOSED HURRICANE

See HYPOTHETICAL HURRICANE.

TRANSVERSE BAR

A bar which extends approximately right angles to shorelines.

TRANSVERSE WAVE

Waves that propagate along a sailing line of a vessel. (See Figure II-7-40)

TRENCH

A long narrow submarine depression with relatively steep sides.

TROCHOIDAL WAVE

A theoretical, progressive oscillatory wave first proposed by Gerstner in 1802 to describe the surface profile and particle orbits of finite amplitude, nonsinusoidal waves. The wave form is that of a prolate cycloid or trochoid, and the fluid particle motion is rotational as opposed to the usual irrotational particle motion for waves generated by normal forces. Compare IRROTATIONAL WAVE

TROPICAL CYCLONE

See HURRICANE

TROPICAL STORM

A tropical cyclone with maximum winds less than 34 m/sec (75 mile per hour). Compare with HURRICANE or TYPHOON (winds greater than 34 m/sec).

TROUGH

A long and broad submarine DEPRESSION with gently sloping sides.

TROUGH OF WAVE

The lowest part of a waveform between successive crests. Also, that part of a wave below still-water level.

TSUNAMI

A long-period water wave caused by an underwater disturbance such as a volcanic eruption or earthquake. Also SEISMIC SEA WAVE. Commonly miscalled "tidal wave."

TURBIDITY

(1) A condition of a liquid due to fine visible material in suspension, which may not be of sufficient size to be seen as individual particles by the naked eye but which prevents the passage of light through the liquid. (2) A measure of fine suspended matter in liquids.

TURBIDITY CURRENT

A flowing mass of sediment-laden water that is heavier than clear water and therefore flows downslope along the bottom of the sea or a lake.

TURBULENT FLOW

Any flow which is not LAMINAR, i.e., the stream lines of the fluid, instead of remaining parallel, become confused and intermingled.

TYPHOON

See HURRICANE. The term *typhoon* is applied to tropical cyclones in the western Pacific Ocean.

U

UNCONFORMITY
A surface that represents a break in the geologic record, with the rock unit immediately above it being considerably younger than the rock beneath. There are three major aspects to consider: (1) Time. An unconformity develops during a period of time in which no sediment is deposited. This concept equates deposition and time, and an unconformity represents unrecorded time. (2) Deposition. Any interruption of deposition, whether large or small in extent, is an unconformity. This aspect of unconformity pre-supposes a standard 'scale' of deposition which is complete. Major breaks in sedimentation can usually be demonstrated easily, but minor breaks may go unrecorded until highly detailed investigations are made. (3) Structure. Structurally, unconformity may be regarded as planar structures separating older rocks below from younger rocks above, representing the 'break' as defined in (1) and (2) above. A plane of unconformity may be a surface of weathering, Erosion or denudation, or a surface of non-deposition, or possibly some combination of these factors. It may be parallel to the upper strata, make an angle with the upper strata, or be irregular. Subsequent Earth movements may have folded or faulted it.

UNCONSOLIDATED
In referring to sediment grains, loose, separate, or unattached to one another.

UNDERCUTTING
Erosion of material at the foot of a cliff or bank, e.g., a sea cliff, or river bank on the outside of a meander. Ultimately, the overhang collapses, and the process is repeated.

UNDERTOW
(1) A current below water surface flowing seaward; the receding water below the surface from waves breaking on a shelving beach. (2) Actually undertow is largely mythical. As the BACKWASH of each wave flows down the BEACH, a current is formed which flows seaward. However, it is a periodic phenomenon. The most common phenomena expressed as "undertow" are actually RIP CURRENTS.

UNDERWATER GRADIENT
The slope of the sea bottom. See SLOPE.

UNDISTURBED WATER LEVEL
Same as STILL WATER LEVEL.

UNDULATION
A continuously propagated motion to and fro, in any fluid or elastic medium, with no permanent translation of the particles themselves.

UPCOAST
In United States usage, the coastal direction generally trending toward the north.

UPDRIFT
The direction opposite that of the predominant movement of littoral materials.

UPLAND
Dry land area above and landward of the ORDINARY HIGH WATER MARK (OHWM). Often used as a general term to mean high land far from the COAST and in the interior of the country.

UPLIFT
The upward water pressure on the base of a structure or pavement.

UPRUSH
The rush of water up the FORESHORE following the breaking of a wave, also called SWASH or RUNUP.

UPSTREAM

Along coasts with obliquely approaching waves there is a longshore (wave-driven) current. For this current one can define an upstream and a DOWNSTREAM direction. For example, on a beach with an orientation west-east with the sea to the north, the waves come from NW. Then the current flows from West to East. Here, *upstream* is West of the observer, and East is DOWNSTREAM of the observer.

UPWELLING

The process by which water rises from a deeper to a shallower depth, usually as a result of offshore surface water flow. It is most prominent where persistent wind blows parallel to a coastline so that the resultant Ekman transport moves surface water away from the coast.

V

VALLEY
An elongated depression, usually with an outlet, between BLUFFS or between ranges of hills or mountains.

VALLEY, SUBMARINE
A prolongation of a land valley into or across a continental or insular shelf, which generally gives evidence of having been formed by stream erosion.

VELOCITY OF WAVES
The speed at which an individual wave advances. See WAVE CELERITY.

VELOCITY PROFILE
The velocity gradient within the BOTTOM BOUNDARY LAYER, displayed as a graph of height above the bed against the velocity of the flow.

VISCOSITY (or internal friction)
That molecular property of a fluid that enables it to support tangential stresses for a finite time and thus to resist deformation. Resistance to flow.

VOID RATIO
For a sediment sample, defined as the ratio of the volume of the voids to the volume of the solids, $e = V_v/V_s$. Typical values of e for natural sands range from 0.5 to 0.8, for cohesive soils from 0.7 to 1.1.

W

WASH LOAD
Part of the suspended load with particle sizes smaller than found in the bed; it is in near-permanent suspension and transported without deposition; the amount of wash load transported through a reach does not depend on the transport capacity of the flow; the load is expressed in mass or volume per unit of time.

WASHOVER
Sediment deposited inland of a beach by overwash processes.

WATER DEPTH
Distance between the seabed and the still water level.

WATER LEVEL
Elevation of still water level relative to some datum.

WATERLINE
A juncture of land and sea. This line migrates, changing with the tide or other fluctuation in the water level. Where waves are present on the beach, this line is also known as the limit of backrush (approximately, the intersection of the land with the still-water level.)

WAVE
A ridge, deformation, or undulation of the surface of a liquid.

WAVE AGE
The ratio of wave speed to wind speed.

WAVE CELERITY
The speed of wave propagation.

WAVE CLIMATE
The seasonal and annual distribution of wave height, period and direction.

WAVE CLIMATE ATLAS
Series of maps showing the variability of wave conditions over a long coastline.

WAVE CREST
See CREST OF WAVE.

WAVE CREST LENGTH
See CREST LENGTH, WAVE.

WAVE, CYCLOIDAL
See CYCLOIDAL WAVE.

WAVE DECAY
See DECAY OF WAVES.

WAVE DIRECTION
The direction from which a wave approaches.

WAVE DIRECTIONAL SPECTRUM
Distribution of wave energy as a function of wave frequency and direction.

WAVE FORECASTING
The theoretical determination of future wave characteristics, usually from observed or predicted meteorological phenomena.

WAVE FREQUENCY
The inverse of wave period.

WAVE FREQUENCY SPECTRUM
Distribution of wave energy as a function of frequency.

WAVE, GRAVITY
See GRAVITY WAVE.

WAVE GROUP
A series of waves in which the wave direction, wavelength, and wave height vary only slightly. See also GROUP VELOCITY.

WAVE HEIGHT
The vertical distance between a crest and the preceding trough. See also SIGNIFICANT WAVE HEIGHT.

WAVE HEIGHT COEFFICIENT
The ratio of the wave height at a selected point to the deepwater wave height. The REFRACTION COEFFICIENT multiplied by the shoaling factor.

WAVE HINDCASTING
See HINDCASTING, WAVE.

WAVE, INFRAGRAVITY
See INFRAGRAVITY WAVE.

WAVE, IRROTATIONAL
See IRROTATIONAL WAVE.

WAVE, MONOCHROMATIC
See MONOCHROMATIC WAVES.

WAVE OF TRANSLATION
A wave in which the water particles are permanently displaced to a significant degree in the direction of wave travel. Distinguished from an OSCILLATORY WAVE.

WAVE, OSCILLATORY
See OSCILLATORY WAVE.

WAVE PEAK FREQUENCY
The inverse of wave peak period.

WAVE PERIOD
The time for a wave crest to traverse a distance equal to one wavelength. The time for two successive wave crests to pass a fixed point. See also SIGNIFICANT WAVE PERIOD.

WAVE, PROGRESSIVE
See PROGRESSIVE WAVE.

WAVE PROPAGATION
The transmission of waves through water.

WAVE RAY
See ORTHOGONAL.

WAVE, REFLECTED
That part of an incident wave that is returned seaward when a wave impinges on a steep beach, barrier, or other reflecting surface.

WAVE REFRACTION
See REFRACTION (of water waves).

WAVE ROSE
Diagram showing the long-term distribution of wave height and direction.

WAVE SETDOWN
Drop in water level outside of the breaker zone to conserve momentum as wave particle velocities and pressures change prior to wave breaking.

WAVE SETUP
See SETUP, WAVE.

WAVE, SINUSOIDAL
An oscillatory wave having the form of a sinusoid.

WAVE, SOLITARY
See SOLITARY WAVE.

WAVE SPECTRUM
In ocean wave studies, a graph, table, or mathematical equation showing the distribution of wave energy as a function of wave frequency. The spectrum may be based on observations or theoretical considerations. Several forms of graphical display are widely used.

WAVE, STANDING
See STANDING WAVE.

WAVE STEEPNESS
The ratio or wave height to wavelength also known as sea steepness.

WAVE TRAIN
A series of waves from the same direction.

WAVE TRANSFORMATION
Change in wave energy due to the action of physical processes.

WAVE, TROCHOIDAL
See TROCHOIDAL WAVE.

WAVE TROUGH
The lowest part of a wave form between successive crests. Also that part of a wave below still-water level.

WAVE VELOCITY
The speed at which an individual wave advances.

WAVE, WIND
See WIND WAVES.

WAVELENGTH
The horizontal distance between similar points on two successive waves measured perpendicular to the crest.

WAVES, INTERNAL
See INTERNAL WAVES.

WEIBULL DISTRIBUTION
A model probability distribution, commonly used in wave analysis.

WEIR
A low dam or wall across a stream to raise the upstream water level. Termed fixed crest weir when uncontrolled.

WEIR JETTY
A jetty with a low section or weir over which littoral drift moves into a predredged deposition basin which is then dredged periodically.

WETLANDS
Lands whose saturation with water is the dominant factor determining the nature of soil development and the types of plant and animal communities that live in the soil and on its surface (e.g. Mangrove forests).

WELL-SORTED
Clastic sediment or rock that consists of particles all having approximately the same size. Example: sand dunes.

WHARF
A structure built on the shore of a harbor, river, or canal, so that vessels may lie alongside to receive and discharge cargo and passengers.

WHITECAP
On the crest of a wave, the white froth caused by wind.

WICKER FAGGOT
Bundles of twigs or sticks, often willow, used in building earthworks or levees (traditional practice in Holland and China.). Alternate term: fascine

WIND CHOP
See CHOP.

WIND, FOLLOWING
See FOLLOWING WIND.

WIND, KATABATIC
See KATABATIC WIND

WIND, OFFSHORE
A wind blowing seaward from the land in a coastal area.

WIND, ONSHORE
A wind blowing landward from the sea in a coastal area.

WIND, OPPOSING
See OPPOSING WIND.

WIND ROSE
Diagram showing the long-term distribution of wind speed and direction.

WIND SEA
Wave conditions directly attributable to recent winds, as opposed to swell.

WIND SETDOWN
Drop in water level below the still water level on the windward ends of enclosed bodies of water and semi- enclosed bays.

WIND SETUP
On reservoirs and smaller bodies of water (1) the vertical rise in the still-water level on the leeward side of a body of water caused by wind stresses on the surface of the water; (2) the difference in still-water levels on the windward and the leeward sides of a body of water caused by wind stresses on the surface of the water. STORM SURGE (usually reserved for use on the ocean and large bodies of water).

WIND STRESS
The way in which wind transfers energy to the sea surface.

WIND TIDE
See WIND SETUP, STORM SURGE.

WIND WAVES
(1) Waves being formed and built up by the wind. (2) Loosely, any wave generated by wind.

WINDWARD
The direction from which the wind is blowing.

A-2. Sources

Bowles 1979
Bowles, J. E. 1979. *Physical and Geotechnical Properties of Soils*. McGraw Hill, New York, 465 p.

Hicks 1989
Hicks S. 1989. Tide and Current Glossary, National Ocean Service, National Oceanic and Atmospheric Administration, U.S. Department of Commerce.

Jackson and Bates (ed.) 1984
Jackson, J. A., and Bates, R. L. (editors). 1984. *Dictionary of Geological Terms,* Third Edition. Anchor Press/Doubleday, Garden City, NY

NOAA Coastal Services Center 2001
NOAA Coastal Services Center. 2001. Shoreline Mapping Web Site, Shoreline Terms, United States Department of Commerce, National Oceanic and Atmospheric Administration, National Ocean Service, Charleston, SC (http://www.csc.noaa.gov/shoreline/term.html , 30 August 2001)

Reed 2000
Reed, M. 2000. *Shore and Sea Boundaries, Volume 3, The Development of International Maritime Boundary Principles through United States Practice*. U.S. Department of Commerce, National Oceanic and Atmospheric Administration. Washington, D.C: U.S. Government Printing Office, 432 p. (Also available online at http://chartmaker.ncd.noaa.gov/hsd/shallow.htm)

***Shore Protection Manual* 1984**
Shore Protection Manual. 1984. 4th ed., 2 Vol., U.S. Army Engineer Waterways Experiment Station, U.S. Government Printing Office, Washington, D.C., 1,088 p.

Verhagen 1998
Verhagen, H. J. 1998. Glossary of Coastal Engineering Terms, Department of Hydraulic Engineering, International Institute for Infrastructural, Hydraulic, and Environmental Engineering, Delft, The Netherlands (http://www.ihe.nl/he/dicea/int01/glossary.htm , 30 August 2001)

Voight 1998
Voigt, B. 1998. Glossary of Coastal Terminology, Pub. No. 98-105, Washington State Department of Ecology, Olympia, WA (http://www.csc.noaa.gov/text/glossary.html , 30 Aug. 2001)

***Webster's Third New International Dictionary of the English Language Unabridged* 1981**
Webster's Third New International Dictionary of the English Language Unabridged. 1981. G. & C. Merriam Company, Springfield, MA.

Wiegel 1953
Wiegel, R. L. 1953. Waves, Tide, Currents, and Beaches: Glossary of Terms and List of Standard Symbols, Council on Wave Research, The Engineering Foundation, Berkeley, CA.

A-3. Acknowledgments

Editors:

Dr. Andrew Morang, Coastal and Hydraulics Laboratory, U.S. Army Engineer Research and Development Center, Vicksburg, MS.

Mr. Andre Szuwalski, Coastal and Hydraulics Laboratory, U.S. Army Engineer Research and Development Center, Vicksburg, MS (retired).

Reviewers:

Mr. John H. Lockhart, Jr., Headquarters, U.S. Army Corps of Engineers, Washington, D.C. (retired).
Mr. Orville Magoon, Coastal Zone Foundation, Middletown, CA.
Dr. Joan Oltman-Shay, Northwest Research Associates, Inc., Bellevue, WA.
Ms. Joan Pope, Coastal and Hydraulics Laboratory, U.S. Army Engineer Research and Development Center, Vicksburg, MS.

Comments or additions: Please contact Dr. Andrew Morang at tel: 601 634 2064 or email andrew.morang@erdc.usace.army.mil with comments on errors or omissions in this glossary.

Last editorial update: 24 April 2003.